A publication of the
American Pharmaceutical Association—
the National Professional Society
of Pharmacists

# JOURNAL OF PHARMACEUTICAL SCIENCES

## INDEX TO AUTHORS
## INDEX TO SUBJECTS

VOLUME 70
JANUARY TO DECEMBER, 1981

*Published monthly under the supervision of the Board of Trustees*

MARY H. FERGUSON
*Editor*

NANCY E. BROWN
*Production Editor*

JOHN PATRICK EVANS
*Copy Editor*

MICHAEL K. HAYES
*Copy Editor*

EDWARD G. FELDMANN
*Contributing Editor*

SAMUEL W. GOLDSTEIN
*Contributing Editor*

BELLE R. BECK
*Editorial Secretary*

EDWARD G. FELDMANN
*Acting Director of Publications*

EDITORIAL ADVISORY BOARD

John Autian
Norman R. Farnsworth
William J. Jusko
Herbert A. Lieberman
David E. Mann, Jr.
Ian W. Mathison
Gerald J. Papariello
Edward G. Rippie

JOURNAL OF PHARMACEUTICAL SCIENCES

JANUARY 1981
VOLUME 70 NUMBER 1

*LITERATURE SURVEY*

# Radiopharmaceuticals Used in Myocardial Imaging

**STANLEY L. MILLS *ˣ, GARO P. BASMADJIAN, and RODNEY D. ICE**

Received from the *College of Pharmacy, University of Oklahoma, Oklahoma City, OK 73190.* *Present address: Department of Medicinal Chemistry, University of Tennessee Center for the Health Sciences, Memphis, TN 38163.

**Keyphrases** □ Radiopharmaceuticals—use in myocardial imaging □ Myocardial imaging—use of radiopharmaceuticals □ Diagnostic imaging agents, myocardial—use of radiopharmaceuticals

CONTENTS

*Introduction* ..... 1
Ischemic and Infarcted Myocardium ..... 1
Approaches to Imaging Myocardial Ischemia and Infarctions ..... 1
*Cold Spot Imaging* ..... 2
Radionuclides as Inorganic Salts ..... 2
Potassium ..... 2
Rubidium ..... 2
Cesium ..... 3
Thallium 201 ..... 3
Nitrogen 13 ..... 4
Technetium 99m Complexes ..... 4
Macroaggregated Albumin ..... 4
Human Serum Albumin ..... 5
Radiolabeled Metabolites ..... 5
Fatty Acid Analogs ..... 5
β-Adrenoceptor Blocker Analogs ..... 5
Toluidine Blue Analogs ..... 5
Bretylium Analogs ..... 5
$^{13}$N-Labeled L-Asparagine ..... 6
Inert Gas Radionuclides ..... 6
*Hot Spot Imaging* ..... 6
Radionuclides as Inorganic Salts ..... 6
Gallium 67 ..... 6
Fluorine 18 ..... 6
Erbium 165 ..... 6
Technetium 99m Complexes ..... 6
Tetracycline ..... 6
Glucoheptonate ..... 6
Pyrophosphate ..... 6
Methylene Diphosphonate ..... 7
Polyphosphate ..... 7
Diphosphonate ..... 7
Ethylenediaminetetramethylenephosphonic Acid ..... 7
Imidodiphosphonate ..... 7
Radiolabeled Metabolites ..... 7
Mercurials ..... 7
Cardiac Myosin-Specific Antibodies (Fab′)$_2$ ..... 8
*References* ..... 8

## INTRODUCTION

**Ischemic and Infarcted Myocardium**—To understand fully radiopharmaceutical procedures for diagnostic evaluation of myocardial ischemia and infarction, a basic understanding of the conditions is required. Myocardial ischemia is defined as a reduced blood supply without necrosis, resulting in a reduced supply of oxygen to the myocardium. A myocardial infarction is an area within the myocardium where coagulation necrosis has occurred, or is in the process of occurring, with varied stages of repair or changes in volume.

Both acute and chronic arterial obstruction may cause myocardial infarction; however, arterial occlusion, old or new, is evident in only ~40% of the deaths associated with myocardial infarctions (1–5), the same percentage of arterial occlusions found in patients dying from causes other than myocardial infarctions (6). Occlusion of a single coronary artery in dogs rarely produces transmural infarction (7). The excellent collateral circulation that exists with interconnections of all sizes of arteries, in addition to the arteriolar–capillary plexuses of the myocardium (8), provides the heart with the ability to circumvent, to a certain extent, minor occluded vessels. However, if collateral circulation is compromised from old occlusions, old infarctions, or coronary artery disease, a thrombus producing a major occlusion may be the impetus for acute myocardial infarction (9). The ability to assess accurately the extent of damage from these occlusions, infarctions, and coronary artery diseases, along with the ability to determine the amount of improvement offered by different therapeutic modalities, is essential for improvements in therapy and prevention of acute myocardial infarction.

**Approaches to Imaging Myocardial Ischemia and Infarctions**—The purpose of identifying myocardial ischemia and acute myocardial infarction is multifold. Most important is identification of the pathological condition. To care for the patient properly, the physician must be as well informed as possible about the patient's condi-

0022-3549/81/0100-0001$01.00/0
© 1981, American Pharmaceutical Association

tion; the physician must determine first if the patient does indeed have an infarction or ischemic zone within the myocardium. Second, the physician must determine if this area is recent or if it constitutes an area where intervention probably would not result in improvement of the condition. Third, the physician must determine if the tissue surrounding the infarction, ischemic at examination, will progressively worsen and further compromise additional tissue. The accurate determination of the volume of the infarction at the time of the initial insult and of the likelihood of this area increasing with time may play a vital role in the choice of the treatment modality. If, by various means, the ischemic area and final volume of the infarction can be reduced, prognosis will be improved.

Two methods have evolved for identification of acute myocardial infarction: identifying that tissue unaffected by the present condition, which gives an indirect determination of the extent of damage (cold spot imaging), and labeling the compromised tissue and imaging it externally, which gives a direct indication of infarcted tissue (hot spot imaging).

Diagnosticians at present utilize one or both of these methods in conjunction with electrocardiograph (ECG) changes and angiographic findings to assess the patient's condition. No single procedure assesses quantitatively and/or qualitatively both myocardial ischemia and acute infarction with a high degree of accuracy.

## COLD SPOT IMAGING

**Radionuclides as Inorganic Salts**—Radionuclides for myocardial imaging generally are injected as the chloride salt in the ionic state. The biological behavior of the radionuclides of potassium, rubidium, cesium, and thallium varies with respect to dosimetry, blood clearance, duration in target organ, and target to nontarget ratios (T/NT). Isotopes of specific elements, such as potassium isotopes, demonstrate the same biological behavior. However, isotopes of a given element will not have the same dosimetry, because each isotope has different decay characteristics. Blood clearance, myocardial uptake, and T/NT ratios of isotopes should remain constant. Potassium analogs (although not in the same group in the periodic table) tend to localize in viable tissues, *e.g.*, the myocardium, to produce cold spot images of the infarcted or ischemic areas.

*Potassium*—The three isotopes of potassium that have been used in the assessment of myocardial ischemia and acute myocardial infarction are potassium 38, potassium 42, and potassium 43. Most recent research has been with potassium 43 because of better imaging characteristics; however, the high-energy $\gamma$-rays of all three isotopes result in poor quality images and excessive patient radiation dosage, limiting their use in the clinical setting on a routine basis.

Early work by Conn and Robertson (10) using potassium 42 assessed the exchange rates of potassium between coronary circulation and the myocardial interstitial fluid and between the interstitial and the intracellular fluid compartments. Sapirstein used potassium 42 in rats (11) and potassium 42 and rubidium 86 in dogs (12) to determine blood flow to specific organs and observed that 4.5 and 2.6% of the cardiac output resulted in coronary blood flow in dogs and rats, respectively. Not until Love and Smith (13) were able to develop a focusing collimator to image the hard $\gamma$-rays of potassium 42 was this isotope used to demonstrate zones of myocardial infarctions. Love *et al.* (14) later demonstrated that 71% of the potassium 42 was removed from arterial blood by the myocardium on the first pass.

Because potassium is taken up by other tissues and a small amount is maintained in the blood, low T/NT ratios were a problem. Poe (15) injected the radionuclide directly into the coronary circulation, eliminating the dilution of the radiotracer in body fluids. The results he obtained on first-pass extraction were similar to those of Love and coworkers. Holman *et al.* (16), using the same technique, observed a first-pass extraction rate of only 40%. Intracoronary artery injection, although a common procedure, should be used with caution when injecting electrolytes such as potassium. Intracoronary infusion of potassium alters repolarization and produces fibrillation (17), but no reports of repolarization with tracer quantities have been cited in the literature. Potassium 38 has been proposed as an alternative to potassium 42 and potassium 43 (18). However, with the availability of potassium 43 and suitable imaging equipment, the use of potassium 38 was not pursued (19).

With the availability of potassium 43 and its decreased shielding requirements (compared to potassium 42), decreased patient dose, and improved scanning characteristics, patient trials were initiated in 1971 (20, 21). The noninvasive technique of potassium 43 scanning compared well with traditional contrast angiograms (22–26). By imaging before and after exercise (27, 28), ischemic zones and infarcted myocardial areas were demonstrated (29, 30). This technique provided accurate, noninvasive assessment of patients with false-positive ECG exercise tests (31) and closely correlated with the reduced flow values of microspheres (32). With the use of digital computers (33) and of gated cardiac blood pool scanning (34), potassium 43 produced important diagnostic information not obtainable from other techniques.

Potassium 43 is not without its problems: the dosimetry is higher than with thallium 201 and rubidium 86 (35), the hard $\gamma$-emissions are difficult to collimate with equipment in use today, and the distribution changes after ~30 min, resulting in reduced T/NT ratios (36).

*Rubidium*—Early research on rubidium 86 (37–41) prompted Love and Burch to estimate the rate of myocardial rubidium 86 uptake (42), with and without cardiac disease (43), and to evaluate the effect of varying plasma flow rates on myocardial uptake (44). They concluded that an increased plasma flow rate increased uptake and that a decreased flow rate decreased uptake. Nolting *et al.* (45) and other investigators (46–50) reported the opposite observation, namely, an increase in rubidium 86 extraction at decreased flow rates. However, most reports supported the observation of Love and Burch that the flow rate and uptake parallel each other (44, 51–55). Conn (56, 57) showed that rubidium uptake may depend on factors other than flow rates.

Rubidium 84 was used to evaluate coronary blood flow changes (51, 58–62), but its decay characteristics preclude its use in patients. Ischemic zones and acute myocardial infarctions have been demonstrated with both rubidium 86 (63, 64) and rubidium 82 (65–67), a generator-produced radionuclide (68).

The best isotope of rubidium for scanning is rubidium 81, which has more favorable photon energies, a desirable short half-life, and economic production (69, 70). Berman and coworkers (71–73) reported better sensitivity and specificity when comparing rubidium 81 to stress ECG. Rubidium 81 scans compared favorably with intracoronary myocardial perfusion scintigrams performed with technetium 99m-labeled albumin particles (74). Rubidium 81 scintigrams (75, 76) were used to show perfusion improvement following aortocoronary bypass surgery (77). One cause of misdiagnosis in rubidium 81 perfusion scintigrams was the development of widespread collateral vessels or prior myocardial infarction (78). There is less absorbed dose with rubidium 81 than with thallium 201, with a total body dose estimate of 0.08 mrad/mCi (35), but, like potassium, the high-energy $\gamma$-emissions (Table I) are difficult to collimate and image with existing equipment (36).

*Cesium*—Cesium was first used for infarct imaging by Carr *et al.* (79, 80). Using cesium 131, they visualized myocardial infarctions in dogs and humans. Love *et al.* (81) later showed that only 22% of cesium 134 in arterial blood was removed during one passage through the heart, a value considerably less than that obtained with potassium and rubidium and supportive of earlier work on erythrocytes, which demonstrated that cesium 134 entered red blood cells more slowly than potassium or rubidium (82). Although cesium 131 has demonstrated anterior myocardial infarctions (83), it emits very low energy X-rays, which are not suitable for deeper tissue visualizations (Table I).

Cesium 129 and cesium 134m have energy emissions more suitable for imaging deeper tissues (84–86). Yano *et al.* (87) and Sodd *et al.* (88) prepared cesium 129 as a radiopharmaceutical, and the former investigators imaged patients with coronary disease and normal patients. Cesium 129 was shown to be effective in demonstrating acute myocardial infarction (89) and compared favorably to macroaggregated albumin labeled with technetium 99m (90) in flow studies. Dosimetry calculations for cesium 129 showed that it is comparable to thallium 201 with a whole body dose of 0.17 rad/mCi (35, 91). The whole body dose for cesium 129 might be reduced further by administering Prussian blue orally to inhibit the reabsorption of cesium from the gut. As with potassium and rubidium, cesium 129 emits $\gamma$-rays that are not suitable for imaging with existing equipment (Table I). Considering both the $\gamma$-ray energy and extraction rate, cesium 129 has little, if any, clinical use (92).

**Table I—Radionuclides (Potassium Analogs) Used in Myocardial Imaging** [a]

| Radionuclide | Major Emissions[b], Mev: Gamma ($\gamma$) | Positron ($\beta^+$) | Beta ($\beta^-$) | Half-Life ($t_{1/2}$) |
|---|---|---|---|---|
| Potassium 38 | 2.17 (100%) | 2.68 | — | 7.7 min |
| Potassium 42 | 1.524 (18%) | — | 3.52 | 12.35 hr |
| Potassium 43 | 0.373 (85%) | — | 1.82 (1%) | 22.4 hr |
| | 0.619 (81%) | — | 1.20 (3%) | |
| Rubidium 81 | 0.511 (64%) | 1.03 | — | 4.7 hr |
| | 0.190 (65%)[c] | | | |
| Rubidium 82 | 0.777 (9%) | 3.15 (96%) | — | 75 sec |
| Rubidium 84 | 0.88 (74%) | 1.66 | 0.91 | 33 days |
| Rubidium 86 | 1.078 (8.8%) | — | 1.78 | 18.66 days |
| Cesium 131 | X-rays; 0.029 | — | — | 9.7 days |
| Cesium 129 | 0.375 (48%) | — | — | 32.1 hr |
| | 0.416 (25%) | | | |
| Cesium 134m | 0.128 (14%) | — | 0.55 | 2.9 hr |
| Thallium 201 | 0.135 (2%) | — | — | 72 hr |
| | 0.167 (8%) | | | |
| | X-rays; 0.083 (98%) | | | |

[a] Values taken from "Radiological Health Handbook," rev. ed., Bureau of Radiological Health, Rockville, Md., 1970. [b] Positron and beta particle values are listed as maximum. [c] From daughter krypton 81m.

*Thallium 201*—Thallium is a metallic element in Group IIIA of the periodic table. Thallium 201 is administered as thallous chloride in the ionic (+1) state. Lebowitz *et al.* (93, 94) produced thallium 201 for biological distribution by irradiating a target of 99.999% pure natural thallium metal (29.5% isotopic abundance of thallium 203) with 31-Mev protons produced by the 152.4-cm Brookhaven cyclotron. The nuclear reaction is $^{203}Tl(p,3n)^{201}Pb$. The lead 201 produced has a half-life of 9.4 hr and is the parent for thallium 201.

Initial interest in the production of thallium 201 as a potential myocardial scanning agent began with work on thallium 199 by Kawana *et al.* (95). The ability of thallium to mimic potassium in the biological system was reported earlier (96–98) and may be due to the fact that the hydrated ionic radius of $Tl^+$ is between $K^+$ and $Rb^+$ in size (94), thus providing thallium 201 with the ability to enter cells through passive diffusion.

Immediately following Lebowitz's production of thallium 201, Bradley-Moore *et al.* (99) reported biodistribution studies in goats demonstrating that >3% of the injected dose localized in normal myocardium. One abnormality of thallium uptake in normal myocardium noted was nonhomogeneous uptake. Strauss *et al.* (100) found the biodistribution to be slightly less in mice, with 2.08% of the dose localized in the normal myocardium in mice. This amount compared to 1.25% for potassium 43 and 1.15% for rubidium 81 in the same 10-min interval.

Dosimetry calculated from goat (99) and rat (35) data did not correlate well, with the estimations from goat data being 20% higher for the kidneys, 40% higher for the heart, and 25% lower for the testes. This variation probably was due, in part, to the metabolic variations of species. Early patient studies (101, 102) confirmed the myocardial uptake of thallium 201 in humans. The later work indicated an effective half-life of 2.3 days and a whole body radiation dose of 162 mrad/mCi. Both reports indicated the feasibility of rapid imaging following injection of thallium 201. Atkins *et al.* (103) later reported a whole body dose of 0.21 rad/mCi following a 1-mCi injection of thallium 201. Thallium 201 has been compared, both in experimental work (104) and in review articles (35, 105, 106), to potassium 43, rubidium 81, and cesium 129. Because the ionic nature and biological properties are similar, the dosimetry (105) and biodistribution (100) of these radionuclides in animals have been analyzed. In general, due to radiation doses and current $\gamma$-camera limitations, thallium 201 appears to be the most suitable agent of this group (105).

The ability of thallium 201 to detect and localize myocardial ischemia as a result of coronary artery disease (107–111), cardiomyopathies (112–114), myocardial infarctions (101, 110, 115–117), and angina pectoris (118, 119) is well documented. Myocardial blood flow is the determining factor for initial myocardial uptake with thallium 201. The concentration of thallium 201 during the first few minutes accurately depicts well-perfused tissue

(100, 120, 121). This blood flow dependency seen on initial scans changes in a short time, and redistribution of the radiotracer occurs (122). Initially, tissues with reduced blood flow receive less thallium 201 than well-perfused tissue. Later, ischemic tissue tends to accumulate thallium 201 while well-perfused tissue loses activity (123). Animal studies (122, 123) demonstrated that within 2 hr, the concentration of tracer appeared to equalize between the normal and ischemic areas. Maseri *et al.* (118) studied the effect of redistribution of thallium 201 in patients with angina pectoris and found that the equilibrium of normal and ischemic tissue was complete within 2–4 hr. The redistribution of thallium 201 in patients with coronary artery disease appears to be complete within 4 hr and may vary depending on the extent of the disease (124).

Myocardial infarctions will not accumulate thallium 201 but appear as defects, both in the exercise and resting scintiscans. Ischemic zones surrounding infarctions appear as cold areas on the exercise scintigrams but will accumulate thallium 201 during the resting state (111). The patient, following maximal exercise stress, is injected and imaged immediately (exercise scintigram); in 4 hr, a repeat scintigram (redistribution scintigram) is made. This single-dose technique produces results similar to the double-dose exercise and rest scintigram (124).

Thallium 201 scintigrams have a high sensitivity of infarct identification within 6 hr after onset of symptoms, and optimum diagnostic information is obtained within 24 hr (110). Thallium 201 scans appear to be of little value if performed several days following the onset of symptoms (125), partly because the damage done may be irreversible. In addition, questionable and false-negative scintiscans may be obtained in patients with elevated transaminase levels (110). Ischemic regions may not, in selected cases, result in abnormal thallium 201 scans. If collateral vessels are present, a high incidence of normal-appearing scans may be produced. Rigo *et al.* (126) demonstrated that 35% of the patients with collateral blood flow failed to show stress-induced perfusion defects. Although disagreement exists (127–130), recent experimental work indicates that thallium 201 scans cannot predict the extent of ischemic tissue (131).

Myocardial uptake of thallium 201 may be enhanced or diminished by drugs currently used in the treatment of conditions associated with the heart. Hetzel *et al.* (132) demonstrated an increase in myocardial uptake of thallium 201 with bicarbonate. Hamilton *et al.* (133) produced an increase in the myocardium to background ratio by first injecting dipyridamole. Costin and Zaret (134), by first injecting propranolol, showed a 32% decrease in thallium 201 uptake, a greater reduction than the 11% decrease reported by Hamilton *et al.* (133) for the same drug.

It is difficult to differentiate between ischemic and infarcted areas and almost impossible to determine if an infarct is old or new using thallium 201 alone (135). The utilization of technetium 99m stannous pyrophosphate in conjunction with thallium 201 provides additional information essential in differentiating the ischemic tissue from acute myocardial infarctions in the presence of previously infarcted necrotic tissue (136, 137).

When imaged with current $\gamma$-cameras, the low-energy emissions of thallium 201 raise questions concerning which collimator (pinhole, converging, or high resolution) to use. Groch and Lewis (138) reported that a 75-kev converging collimator produced the best line spread function and modulation transfer function; in addition, they noted that the high-resolution collimator may not produce acceptable images unless the thallium 202 contaminant in the commercial thallium 201 is negligible. Nishiyama *et al.* (139) reported increased diagnostic accuracy with the pinhole collimator and poor lesion detectability with the converging collimator. At present, the low-energy high-resolution collimator provides the most information and is the collimator of choice in the clinical setting (108, 110, 115, 122).

Attempts to improve the diagnostic quality of thallium 201 scintiscans using computers have been reported. Graphic representation (140) and ECG synchronization (141) have been attempted to improve lesion detectability. Observer variability (142) and small infarction detection (143) may be improved by utilizing computer manipulation of data and by close attention to exercise techniques (144).

*Nitrogen 13*—Nitrogen 13, which decays by positron emission ($\beta^+$) with a 10-min half-life (145), is the only feasible radionuclide of nitrogen. Uptake studies in dogs (146–148) indicated that $^{13}N$-labeled ammonia was cleared rapidly from the blood and localized well in the myocardial tissue, although skeletal muscle, liver, kidney, and brain activity also was noted. In human subjects, researchers indicated rapid clearance from the blood (85% in 1 min), estimated a whole body dose of 5 mrad/mCi assuming uniform distribution (149), and demonstrated ischemic myocardium (150) and cold spot imaging of infarctions (151, 152).

To image the positron emissions, nitrogen 13 requires special equipment that is not available in most hospitals. In addition, the 10-min half-life of nitrogen 13 requires that the production facility and synthesizing equipment be very near the hospital (Table II).

**Technetium 99m Complexes**—*Macroaggregated Albumin*—Early attempts at myocardial scanning with macroaggregated albumin utilized iodine 131 as the ra-

**Table II—Radionuclides Used in Myocardial Imaging** [a]

| Radionuclide | Major Emissions[b], Mev: Gamma ($\gamma$) | Positron ($\beta^+$) | Beta ($\beta^-$) | Half-Life ($t_{1/2}$) |
|---|---|---|---|---|
| Nitrogen 13 | — | 1.2 | — | 10 min |
| Gallium 67 | 0.093 (40%)<br>0.184 (24%)<br>0.296 (22%) | — | — | 78 hr |
| Fluorine 18 | — | 0.635 | — | 110 min |
| Technetium 99m | 0.140 (90%) | — | — | 6.1 hr |
| Iodine 123 | 0.159 (83%) | — | — | 13.3 hr |
| Iodine 131 | 0.364 (82%) | — | 0.806 | 8.05 days |
| | 0.637 (6.8%) | — | 0.606 | |
| Xenon 127 | 0.203 (65%)<br>0.172 (22%)<br>0.375 (20%) | — | — | 36.4 days |
| Xenon 133 | 0.081 (37%) | — | 0.346 | 5.3 days |
| Krypton 81m | 0.190 (65%) | — | — | 13 sec |
| Krypton 85 | 0.514 (0.41%) | — | 0.67 | 10.8 years |
| Mercury 197 | 0.077 (18%) | — | — | 65 hr |
| Mercury 203 | 0.279 (77%) | — | 0.214 | 46.9 days |
| Erbium 165 | X-rays;<br>0.050 | — | — | 10.3 hr |

[a] Values taken from "Radiological Health Handbook," rev. ed., Bureau of Radiological Health, Rockville, Md., 1970. [b] Positron and beta particle values are listed as maximum.

diolabel. Quinn *et al.* (153) identified coronary branch occlusions in dogs, and Endo *et al.* (154) demonstrated ischemic zones in patients using macroaggregated albumin. Ashburn *et al.* (155) labeled macroggregated albumin with technetium 99m and iodine 131 and demonstrated bilateral areas of reduced blood flow in patients with coronary artery disease by injecting the $^{99m}$Tc-labeled particles into the left coronary artery and $^{131}$I-labeled particles into the right coronary artery, utilizing separate or composite images. Currently, only $^{99m}$Tc-labeled macroaggregated albumin is used due to the high radiation dose of iodine 131.

Sources of errors utilizing macroaggregated albumin have been characterized (156, 157), and improvements in labeling with technetium 99m have been reported (158). Acute myocardial infarctions have been demonstrated with macroaggregated albumin (159), but care must be taken because variations in uptake with different particle sizes have been reported (160–165). The safety of injecting radiolabeled particles (macroaggregated albumin) into the coronary arteries has been questioned (166–168), but no alterations in myocardial status have been noted. Gould *et al.* (169) observed the behavior of two injections of $^{99m}$Tc-labeled macroaggregated albumin, one in the normal state and one following vasodilation. They observed decreased tracer uptake distal to the coronary artery narrowing following vasodilation. This technique has the disadvantage of requiring surgical intervention for intracoronary artery injection and does not accurately reflect regional rates of local myocardial capillary blood flow (170).

*Human Serum Albumin*—$^{99m}$Tc-Labeled human serum albumin and computers have been used to produce multiple-gated acquisition images. A complete cardiac cycle, terminating at end systole or end diastole, is recorded for ~800 cardiac cycles (~10 min) following intravenous injection of 20 mCi of $^{99m}$Tc-labeled human serum albumin, and the cycles are summed by the computer. By viewing a full cardiac cycle, regional wall motion abnormalities can be observed (171–173). This technique may be valuable in determining the ejection fraction and end diastolic volume in patients with acute myocardial infarction (174), especially inferior wall infarctions (175). Multiple-gated acquisition images do not provide any information concerning the integrity of the myocardial blood supply, the presence of a myocardial infarction, or the age of the lesion.

**Radiolabeled Metabolites**—*Fatty Acid Analogs*—The normal myocardial tissue readily extracts fatty acids and utilizes them *via* β-oxidation as a source of energy (176–181). In myocardial tissue, oxidation appears to be the major metabolic pathway for fatty acids (182). Bragdon and Gordon (183) showed major uptake of [1-$^{14}$C]palmitic acid in muscle and liver; by feeding rats carbohydrates, they noted increased radiolabel in the heart. The extraction of [1-$^{14}$C]palmitate appears to be inversely related to the coronary blood flow; in hypoxic states, alteration in fatty acid metabolism from β-oxidation to triglyceride formation was reported (184).

Evans and coworkers first demonstrated the myocardial uptake of radioiodinated oleic acid in dogs (185) and humans (186, 187) and proposed the use of $^{131}$I-labeled oleic acid to demonstrate areas of reduced blood flow or metabolism. They demonstrated maximum uptake of label in the myocardium within 20 min. Low specific activity of the labeled fatty acid and relatively poor physical characteristics of iodine 131 limited its use.

The greatest extraction of radioiodinated fatty acids occurs in the first pass (188), and the activity of radiolabeled oleic acid analogs in the myocardium drops to ~5% at 60 min (189). Oleic acid radioiodinated by double-bond saturation is not extracted as efficiently as natural compounds (190). By terminally labeling hexadecenoic acid with iodine 123, improved imaging characteristics were observed (191, 192). The ω-labeled hexadecenoic acid has a dosimetry estimate of 0.03 rad/mCi, assuming uniform distribution and relatively pure iodine 123 (193). The ω-labeled 16-iodo-9-hexadecenoic acid is metabolized rapidly to iodoacetate and deiodinated (193). The resulting free iodide in the blood (194) increases blood background radioactivity; similar observations were made by Beierwaltes *et al.* (195) with $^{131}$I-labeled oleic acid.

With a myocardial half-life of 25 min (196), $^{123}$I-labeled hexadecenoic acid demonstrated ischemic defects in patients with coronary artery disease (196) or infarctions (197). The extraction rate of ~70% was comparable to that of potassium 43 (198). Using $^{14}$C-labeled oleic acid, Bilheimer *et al.* (199) showed that more fatty acid accumulates in the border and peripheral zones of infarction than in normal cells. Attempts at improvements in formulation (195) and labeling with other radionuclides such as carbon 11 (200, 201), fluorine 18 (202), chlorine 34m and bromine 77 (194), technetium 99m (203–205), and tellurium 123m (206–208) have not significantly improved fatty acids for myocardial scanning.

The most promising of these agents, $^{11}$C-labeled palmitic acid (209–211), will not be in routine use in the near future because of the need for specialized equipment (212). The additional problems of specific activity and formulation (213) also must be overcome for fatty acids to provide information not currently obtainable concerning acute myocardial infarctions and accompanying ischemia.

*β-Adrenoceptor Blocker Analogs*—Jiang *et al.* (214) synthesized tyramine-containing analogs of β-adrenoceptor blockers and, by labeling them with iodine 123, determined their distribution in rats as potential myocardial imaging agents. Of the four compounds synthesized, only one, a derivative of practolol, showed sufficient heart to blood ratios to be promising. The problem encountered was a myocardium to lung ratio of two, insufficient to image changes in myocardial uptake.

*Toluidine Blue Analogs*—Kang (215) proposed toluidine blue analogs as agents in infarct imaging because unlabeled toluidine blue did not concentrate as well in the infarcted tissue as in the normal tissue. However, using radioactive iodotoluidine blue, no selective uptake by the myocardium was noted by Archer *et al.* (216, 217). Carr *et al.* (218) attempted to increase the T/NT ratio by injecting a loading dose of cold toluidine blue prior to the radioactive compound. They were able to obtain a normal myocardium to blood ratio of 12:1 and an infarct to normal ratio of 0.18 (±0.31):1, which was insufficient for imaging purposes.

*Bretylium Analogs*—Counsell and coworkers (219–221) synthesized the *ortho-*, *meta-*, and *para*-analogs of bretylium, radioiodinated these compounds with iodine 125 and iodine 131, and reported results in animals, but an

increase in serum glutamic oxaloacetic transaminase levels of patients caused clinical trials to be canceled.

*$^{13}N$-Labeled L-Asparagine*—Gelbard *et al.* (222) labeled L-asparagine with nitrogen 13 and injected the purified compound into two dogs to assess organ uptake of the compound. The compound localized in the myocardium (13.7% of the injected dose), with an equal amount in the liver. Maximal uptake appeared within minutes in both organs. $^{13}N$-Labeled compounds require special equipment that is not available to most nuclear medicine departments, and no subsequent work has appeared in the literature.

**Inert Gas Radionuclides**—Although several different radioactive isotopes have been used, the technique is similar. Herd *et al.* (223), using krypton 85, studied myocardial blood flow in dogs. The technique, applied later in humans (224, 225), provided blood flow rates in myocardial tissues. Xenon 133 in solution was used by Ross *et al.* (226) because it has better decay characteristics than krypton 85 (Table I). By injecting xenon 133 following selective coronary arteriography, the myocardial blood flow and washout were recorded.

Today, the technique consists of single- (227–231) or multiple-crystal scintillation cameras (232–234) externally measuring washout curves in different regions of the myocardium following injection of xenon 133 directly into the coronary arteries. Computer analysis determines the rate constants of regional clearance from the heart muscle. No complications have been noted with this technique (235–239), and it correlates well with the flowmeter technique (240, 241). Xenon 127 has been proposed as a replacement for xenon 133. Although improved decay characteristics (Table II) result in improved imaging and dosimetry, its long half-life (36.4 days) may produce storage and disposal problems.

This drawback is not shared by krypton 81m with a half-life of 13 sec and $\gamma$-emission of 0.190 Mev (65%), which also has been proposed as a replacement for xenon 133. Produced from rubidium 81 (242–247), the krypton 81m is continuously infused in 5% dextrose into the coronary artery (248–250) directly from the generator.

## HOT SPOT IMAGING

**Radionuclides as Inorganic Salts**—*Gallium 67*—Gallium 67 localizes in inflammatory processes, resulting in a hot spot, an area containing more activity than surrounding tissue. Kramer *et al.* (251) reasoned that, since inflammation accompanies myocardial infarctions, gallium 67 might localize sufficiently to identify acute myocardial infarctions. In patients with gallium 67 localization, the uptake correlated well with conventional techniques such as ECG and angiography, but only 63% of the cases with confirmed acute myocardial infarction showed gallium 67 uptake.

*Fluorine 18*—Bonte *et al.* (252) first proposed fluorine 18 as a potential infarct-avid agent but demonstrated less uptake than with technetium 99m stannous pyrophosphate in acute myocardial infarction, a result later confirmed by Weber *et al.* (253). Cochavi *et al.* (254), using improved tomography equipment, reevaluated fluorine 18 and determined that, although sufficient uptake for imaging was noted, uptake peaked at 48–72 hr postinfarction. This delay in imaging of 48–72 hr negates the usefulness of the technique for early identification.

*Erbium 165*—Erbium 165 citrate (255) has been shown to have an affinity for myocardial infarcts in dogs with infarct to normal ratios of 2.5:1 at 2 hr, 12.5:1 at 8 hr, and 108:1 at 24 hr. However, its low-energy photopeak at 0.050 Mev with a half-life of 10 hr may preclude its use with current imaging equipment.

**Technetium 99m Complexes**—*Tetracycline*—Malek *et al.* (256), working with fluorescent identification of tetracycline in dogs, noted increased uptake of this antibiotic in acute myocardial infarctions. Holman and coworkers (257–259) labeled tetracycline with technetium 99m and attempted to identify acute myocardial infarctions directly *via* hot spot imaging. They observed maximal infarct to normal myocardium ratios of 8.4:1, requiring 24 hr for sufficient blood clearance. In 24 hr, technetium 99m has decayed four half-lives, reducing the photon yield appreciably. With a low photon yield, a 24-hr wait before imaging, and insufficient T/NT ratios, tetracycline was not pursued as an agent in acute myocardial infarction scanning.

*Glucoheptonate*—Although complete blood clearance of technetium 99m glucoheptonate is not achieved, the clearance is much more rapid than that of tetracycline. Rossman *et al.* (260) detected glucoheptonate uptake shortly after injection in animals, with acceptable infarct to normal ratios of 20:1. In subsequent studies (261–263), infarct to blood ratios were not sufficient to identify acute myocardial infarctions consistently; only one of four patients with documented acute myocardial infarctions showed diagnostic glucoheptonate scans.

*Pyrophosphate*—Bonte *et al.* (264) first reported the use of technetium 99m stannous pyrophosphate to demonstrate myocardial infarctions in closed-chest dogs. Soon thereafter, Parkey *et al.* (265) observed similar results in human patients. These early studies, followed by clinical trials performed by Holman *et al.* (266), prompted a great deal of research concerning technetium 99m pyrophosphate, currently the most widely used hot spot radiopharmaceutical for myocardial infarct imaging.

The study of Tetalman *et al.* (267), using technetium 99m pyrophosphate in 103 patients, found 68.7% true positives and 92.4% true negatives, compared with the findings of Holman *et al.* (266) of 100% true positives and 80% true negatives. Most published studies indicated true positives and true negatives within this range of values. Tetalman *et al.* (267) also indicated that a negative scan does not rule out the possibility of a recent small (<2.5 cm), subendocardial, myocardial infarct.

The ability to size acute anterior transmural myocardial infarctions in dogs accurately has been reported (268–271). Bruno *et al.* (272) reported the ability to detect infarctions of 1% of the left ventricular mass in dogs. Other experimental work with the canine model appears less encouraging. Zaret *et al.* (273) found more uptake in the border zones of acute infarctions, while Marcus *et al.* (274) discouraged the utilization of the intensity of technetium 99m pyrophosphate images for infarct sizing. Technetium 99m pyrophosphate is sequestered in bone as well as damaged myocardium, providing excellent landmarks for locating the myocardium and infarcted tissue. However, this potentially limits its ability to define the extent of the in-

farction due to labeling of the sternum and rib cage. Although pyrophosphate is a superior imaging agent, there are cases where the borders of the infarct are totally obscured by overlying bone.

In patients with inferior infarction (275) and subendocardial infarction (276, 277), the estimation of infarct size by a scintigram does not correlate well with enzyme levels. Massie *et al.* (276) reported only a 32% discrete uptake in patients with nontransmural infarction, compared with 84% of patients with a transmural infarction. The difficulty in determining the size of inferior, as well as subendocardial, infarctions has been reported (278).

The flow-dependent uptake of technetium 99m pyrophosphate (272–274, 279, 280) may limit its ability to provide accurate assessment of acute myocardial infarction size. The amount of radioactivity is inversely related to the extent of infarction after permanent occlusion and is directly related to the extent of infarction after transient occlusion (272).

The ability of technetium 99m pyrophosphate to localize in myocardial tissues following acute myocardial infarction is well documented (264–267, 281); however, other conditions also may result in myocardial uptake. Both diffuse and localized uptake have been reported with subendocardial and transmural portions of the left ventricle (267, 282–284) or the right ventricle (285). Technetium 99m pyrophosphate also will localize in old myocardial infarctions (282, 286–290), old myocardial infarctions with or without ventricular aneurysm (282, 286, 291, 292), subclinical necrosis of the myocardium (291), carcinoma invasion of the left ventricle (293), myocardial contusions (294–296), valvular calcification (297, 298), stable angina pectoris (283, 292, 299), unstable angina pectoris (267, 283, 292, 300), primary cardiomyopathy, and congestive heart failure (301, 302). In addition, technetium 99m pyrophosphate also accumulates in the myocardium following coronary artery bypass graft surgery (303), in high-energy cardioversion (304, 305), in benign and malignant breast lesions in females (306, 307), in experimental viral mild pericarditis (308), and in several cases of unknown etiology (309).

Experimentally infarcted myocardium has the potential of accumulating technetium 99m pyrophosphate within 12 hr following myocardial insult (264, 265). Because of this observation, initial patient scintigrams are obtained 12–24 hr postinfarction. In cases where the 12–24-hr postinfarct scintigram is negative, a second scintigram at 48–72 hr is recommended if acute infarction is strongly suspected (310). With the necessity for early detection and intervention, a technetium 99m pyrophosphate scintigram may be performed as early as 4 hr following the suspected injury (311). However, this approach results in a decrease in sensitivity. Images of the myocardium are usually taken 2 hr following injection of the radiopharmaceutical but may be taken as early as 90 min postinjection. If uptake is not localized, followup imaging should be done at 4 hr to allow time for blood clearance.

The mechanism of localization of technetium 99m pyrophosphate in the myocardium is unclear. Bonte and coworkers (264, 312) postulated that the phenomenon of calcium localization within the mitochondria reported by D'Agostino (313) and later by D'Agostino and Chiga (314) was the mechanism of localization. Shen and Jennings (315, 316) discussed accumulation of calcium as an index of irreversible myocardial cell damage resulting from ischemia. Dewanjee and coworkers (317, 318) proposed that the uptake of technetium 99m pyrophosphate could be due to the formation of polynuclear complexes with denatured macromolecules rather than to the formation of calcium phosphate complexes. These investigators reported most of the technetium 99m pyrophosphate activity to be associated with macromolecules rather than nuclei, mitochondria, and microsomes.

*Methylene Diphosphonate*—Following the success of pyrophosphate as a myocardial agent, virtually all bone agents have been used in an attempt to image acute myocardial infarctions. As with pyrophosphate, these agents have the disadvantage of bone uptake with varying degrees of infarct to bone ratios as well as infarct to normal myocardium ratios. Technetium 99m methylene diphosphonate has a greater affinity for infarcted myocardium, but its bone uptake is too high to prove useful. The infarct to normal ratio (27.9:1) exceeds most reports of pyrophosphate, but the infarct to bone ratio (0.4:1) does not allow sufficient visualization of myocardial damage that may lie beneath the ribs (319).

*Polyphosphate*—Polyphosphate studies in animals (320) and humans (321–323) showed good infarct to bone ratios, but optimum images were obtained 2–3 days postinfarction (323), delaying treatment.

*Diphosphonate*—Technetium 99m disphosphonate, although taken up by infarcted tissue, accumulates unevenly, preventing accurate assessment (324).

*Ethylenediaminetetramethylenephosphonic Acid*—Holman *et al.* (325), labeling ethylenediaminetetramethylenephosphonic acid with either indium 113m or technetium 99m, found the agents to be specific for infarcts. The infarct to normal ratio was 50% of published technetium 99m pyrophosphate values. Dewanjee and Kahn (326) reported good infarct to normal ratios with ethylenediaminetetramethylenephosphonic acid (40–50:1) but high bone uptake (50–57% of the injected dose).

*Imidodiphosphonate*—Preliminary work on rabbits (327) indicates that imidodiphosphonate labeled with technetium 99m has a greater infarct to normal ratio than pyrophosphate (14:1 at 1 hr and 33:1 at 6 hr). Subsequent work on rats (328) and preliminary work on 50 patients (329) indicated improved uptake over pyrophosphate, although in-depth studies have not been completed.

**Radiolabeled Metabolites**—*Mercurials*—Carr *et al.* (330) first demonstrated hot spot imaging of acute myocardial infarctions with $^{203}$Hg-labeled chlormerodrin[1] and reported 16 infarct to normal ratios greater than 15%. The initial study in dogs (330), later repeated in humans (331), was promising, but limited equipment hindered diagnostic effectiveness. Gorten *et al.* (332) also demonstrated the propensity of $^{203}$Hg-labeled chlormerodrin to localize in acute myocardial infarctions of swine. Malek *et al.* (333), using mercury 197 and mercury 203 labeling, produced a series of radiolabeled difluorescinylmercury and mono- and bis-hydroxymercurifluorescein derivatives. After improving the specific activity (334), they reported T/NT ratios of 20–77% (335). Subsequent work confirmed the

[1] Neohydrin.

infarct avidity of mercury-radiolabeled fluorescein derivatives but with varying T/NT ratios (336–338).

Recent work on structure–activity relationships of phthaleins (339) and fluoresceins (340, 341) has shown that diiodohydroxymercurifluorescein has almost six times the avidity of technetium 99m pyrophosphate for acute myocardial infarctions. $^{203}$Hg-Labeled hydroxymercurifluorescein has a T/NT ratio of 51.5(±13.5):1 and an infarct to blood ratio of 22.1(±8.1):1. Although less than the fluorescein derivatives, the ratios of the phthalein derivatives were higher than those of technetium 99m pyrophosphate, with ratios of 20.7–34.1:1 and 12.1–20.1:1, respectively (339). The structure requirements are a polycyclic organic moiety and a hydroxymercury group, with the latter (mercury 203 and mercury 197) structural requirement being more important.

The mercury-labeled compounds are hampered by poor decay characteristics (Table II) and higher absorbed radiation doses than $^{99m}$Tc-labeled compounds.

*Cardiac Myosin-Specific Antibodies (Fab′)$_2$*—Khaw *et al.* (342) showed that myocardial uptake in acute myocardial infarction tissue, resulting in a hot spot image with $^{131}$I-labeled Ab(Fab′)$_2$, was the result of antigen-antibody reactions rather than a nonspecific sequestration of proteins (343). Ab(Fab′)$_2$ uptake is very specific and inversely related to blood flow (344). Imaging must be delayed at least 48 hr following intravenous injection (345). Khaw *et al.* (346) reduced the delay in imaging by injecting the radiopharmaceutical directly into the main left coronary artery in dogs. Localization in infarcted tissue occurred within 30 min, resulting in a T/NT ratio of 34.3(±1.5):1.

Khaw *et al.* (347) recently reported formation of a bifunctional chelate labeled with Ab(Fab′)$_2$, which was labeled with gallium 68. The bifunctional chelating agent diethylenetriaminepentaacetic acid was used and tested in dogs with reported T/NT ratios as high as 100:1.

## REFERENCES


(1) R. W. P. Achor, W. D. Futch, H. B. Burchell, and J. E. Edwards, *Arch. Intern. Med.*, **98,** 162 (1956).

(2) R. S. Eliot and R. R. Streiff, *Geriatrics*, **26,** 152 (1971).

(3) J. L. Juergens, J. E. Edwards, R. W. P. Achor, and H. B. Burchell, *Arch. Intern. Med.*, **105,** 44 (1960).

(4) J. C. Ehrlich and Y. Shinohara, *Arch. Pathol.*, **78,** 432 (1964).

(5) G. Baroldi, *Am. J. Cardiol.*, **16,** 859 (1965).

(6) G. Baroldi and G. Scomazzoni, "Coronary Circulation in the Normal and Pathologic Heart," Office of the Surgeon General, Department of the Army, Washington, D.C., 1967.

(7) R. B. Jennings, *Am. J. Cardiol.*, **24,** 753 (1969).

(8) E. H. Estes, M. L. Emtman, H. B. Dixon, and D. B. Hackel, *Am. Heart J.*, **71,** 58 (1966).

(9) G. Baroldi, in "Myocardiology," E. Bajusy and G. Rona, Eds., University Park Press, Baltimore, Md., 1972, p. 399.

(10) H. L. Conn and J. S. Robertson, *Am. J. Physiol.*, **181,** 319 (1955).

(11) L. A. Sapirstein, *Circ. Res.*, **4,** 689 (1956).

(12) L. A. Sapirstein, *Am. J. Physiol.*, **193,** 161 (1958).

(13) W. D. Love and R. O. Smith, *J. Nucl. Med.*, **7,** 781 (1966).

(14) W. D. Love, Y. Ishihara, L. D. Lyon, and R. O. Smith, *Am. Heart J.*, **76,** 353 (1968).

(15) N. D. Poe, *J. Nucl. Med.*, **13,** 557 (1972).

(16) B. L. Holman, P. Eldh, D. F. Adams, M. H. Han, J. K. Poggenbery, and S. J. Adelstein, *ibid.*, **14,** 274 (1973).

(17) T. J. Regan, M. A. Harman, P. H. Lehan, W. M. Burke, and H. A. Oldewurtel, *J. Clin. Invest.*, **46,** 1657 (1967).

(18) W. G. Myers, *J. Nucl. Med.*, **14,** 359 (1973).

(19) N. D. Martin, B. L. Zaret, H. W. Strauss, H. P. Wells, and J. Albers, *Radiology*, **112,** 446 (1974).

(20) P. J. Hurley, M. Cooper, R. C. Reba, K. J. Poggenburg, and H. N. Wagner, *J. Nucl. Med.*, **12,** 516 (1971).

(21) R. J. Gorten, *ibid.*, **13,** 432 (1972).

(22) R. O. Smith, K. R. Bennett, P. H. Lehan, and H. K. Hellems, *ibid.*, **11,** 6423 (1970).

(23) K. R. Bennett, R. O. Smith, P. H. Lehan, and H. K. Hellems, *Radiology*, **120,** 117 (1972).

(24) R. R. Hall, R. L. McGowan, A. L. Bryson, M. D. Flamm, and N. D. Martin, *Circulation*, **51–52** (Suppl. II), 111 (1975).

(25) S. H. Young, A. Nishimura, J. F. Williams, and R. J. Gorten, *ibid.*, **51–52** (Suppl. II), 111 (1975).

(26) B. L. Zaret, S. C. Vlay, G. S. Freedman, S. Wolfson, and L. S. Cohen, *ibid.*, **52,** 1076 (1975).

(27) H. W. Strauss, B. L. Zaret, N. D. Martin, H. P. Wells, and M. D. Flamm, *Radiology*, **108,** 85 (1973).

(28) B. L. Zaret, H. W. Strauss, N. D. Martin, H. P. Wells, and M. D. Flamm, *N. Engl. J. Med.*, **288,** 809, (1973).

(29) B. Haider, H. A. Oldewurtel, C. B. Moschos, and T. J. Regan, *Circulation*, **53,** 115 (1976).

(30) R. E. Botti, W. J. MacIntyre, and W. H. Pritchard, *ibid.*, **47,** 486 (1973).

(31) B. L. Zaret, R. E. Stenson, N. D. Martin, H. W. Strauss, H. P. Wells, R. L. McGowan, and M. D. Flamm, *ibid.*, **43,** 1234 (1973).

(32) E. K. Prokop, H. W. Strauss, J. Shaw, B. Pitt, and H. N. Wagner, *ibid.*, **50,** 985 (1974).

(33) Y. Ishii, W. J. MacIntyre, W. H. Pritchard, and R. W. Eckstein, *Circ. Res.*, **33,** 113 (1973).

(34) P. Rigo, H. W. Strauss, and B. Pitt, *Radiology*, **115,** 387 (1975).

(35) P. A. Feller and V. J. Sodd, *J. Nucl. Med.*, **16,** 1070 (1975).

(36) H. Nishiyama, V. J. Sodd, R. J. Adolph, E. L. Saenger, J. T. Lewis, and M. Gabel, *ibid.*, **17,** 880 (1976).

(37) S. A. Threefoot, C. T. Ray, and G. E. Burch, *Am. J. Med.*, **14,** 760 (1953).

(38) W. D. Love and G. E. Burch, *J. Lab. Clin. Med.*, **41,** 351 (1953).

(39) A. Zipser and A. S. Freedberg, *Cancer Res.*, **12,** 867 (1952).

(40) A. Zipser, H. B. Pinto, and A. S. Freedberg, *J. Appl. Physiol.*, **5,** 317 (1953).

(41) W. D. Love, R. B. Romray, and G. E. Burch, *Circ. Res.*, **2,** 112 (1954).

(42) W. D. Love and G. E. Burch, *J. Clin. Invest.*, **36,** 468 (1957).

(43) W. D. Love and G. E. Burch, *Int. J. Appl. Radiat. Isot.*, **3,** 207 (1958).

(44) W. D. Love and G. E. Burch, *Circ. Res.*, **7,** 24 (1959).

(45) D. Nolting, R. Mack, E. Luthy, M. Kirsch, and C. Hogancamp, *J. Clin. Invest.*, **37,** 921 (1958).

(46) R. E. Mack, D. D. Nolting, C. E. Hogancamp, and R. J. Bing, *Am. J. Physiol.*, **197,** 1175 (1959).

(47) E. M. Renkin, *ibid.*, **197,** 1205 (1959).

(48) M. Winbury, D. Kissel, and M. Logada, in "Isotopes in Experimental Pharmacology," L. J. Roth, Ed., University of Chicago Press, Chicago, Ill., 1965, chap. 20.

(49) T. W. Moir, *Circ. Res.*, **19,** 695 (1966).

(50) A. Cohen, E. J. Zaleski, H. Baleiron, T. B. Stock, C. Chiba, and R. J. Bing, *Am. J. Cardiol.*, **19,** 556 (1967).

(51) R. J. Bing, A. Bennish, G. Bluemchen, A. Cohen, J. P. Gallagher, and E. J. Zaleski, *Circulation*, **29,** 833 (1964).

(52) L. Donato, G. Bartolomei, and R. Giordani, *ibid.*, **29,** 195 (1964).

(53) M. N. Levy and J. Martins de Oliveira, *Circ. Res.*, **9,** 96 (1961).

(54) A. Cohen, E. J. Zaleski, E. D. Luebs, and R. J. Bing, *J. Nucl. Med.*, **6,** 651 (1965).

(55) A. Cohen, J. P. Gallagher, E. Luebs, Z. Verga, J. Yamanaka, E. J. Zaleski, G. Bluemchen, and R. J. Bing, *Circulation*, **32,** 636 (1965).

(56) H. L. Conn, *Circ. Res.*, **10,** 505 (1962).

(57) H. L. Conn, *Am. J. Physiol.*, **184,** 548 (1956).

(58) S. B. Knoebel, P. L. McHenry, L. Stein, and A. Sonel, *Circulation*, **36,** 187 (1967).

(59) P. L. McHenry and S. B. Knoebel, *J. Appl. Physiol.*, **22,** 495 (1967).

(60) R. J. Bing, C. Cowan, D. Bottcher, G. Corsini, and C. G. Daniels, *J. Am. Med. Assoc.*, **205,** 79 (1968).

(61) G. Leb, F. Derntl, N. Goldschlager, G. Cowan, and R. J. Bing, *Am. J. Med. Sci.*, **257,** 203 (1969).

(62) S. B. Knoebel, P. L. McHenry, D. Roberts, and L. Stein, *Cir-*

culation, **37,** 932 (1968).
(63) E. A. Carr, W. H. Beierwaltes, A. V. Wegst, and J. D. Bartlett, *J. Nucl. Med.*, **3,** 76 (1962).
(64) H. Braselmann, U. Osswald, K. Wenzelides, and E. Seider, *Experientia*, **34,** 1478 (1978).
(65) Y. Yano and H. O. Anger, *J. Nucl. Med.*, **9,** 412 (1968).
(66) T. F. Budinger, Y. Yano, and B. Hoop, *ibid.*, **16,** 429 (1975).
(67) G. A. Beller, B. Hoop, J. A. Parker, and T. W. Smith, *Circulation*, **51–52** (Suppl. II), 111 (1975).
(68) Y. Yano, T. F. Budinger, P. Chu, P. M. Grant, A. E. Ogard, H. A. O'Brian, and B. Hoop, *J. Nucl. Med.*, **17,** 536 (1976).
(69) R. L. McGowan, N. D. Martin, B. L. Zaret, H. P. Wells, and M. D. Flamm, *Am. J. Cardiol.*, **33,** 154 (1974).
(70) N. D. Martin, B. L. Zaret, R. L. McGowan, H. P. Wells, and M. D. Flamm, *Radiology*, **111,** 651 (1974).
(71) D. S. Berman, A. F. Salel, G. L. DeNardo, and D. T. Mason, *Circulation*, **49–50** (Suppl. III), 26 (1974).
(72) *Ibid.*, **52,** 619 (1975).
(73) D. S. Berman and D. T. Mason, *Adv. Cardiol.*, **22,** 16 (1978).
(74) W. Ashburn, H. Schelbert, G. DiDonna, M. LeWinter, H. Henning, R. O'Rourke, and K. Peterson, *Circulation*, **49–50** (Suppl. III), 25 (1974).
(75) D. A. Rothbaum, H. N. Wellman, D. K. Lowe, and S. B. Knoebel, *ibid.*, **49–50** (Suppl. III), 243 (1974).
(76) R. L. McGowan, T. G. Welch, B. L. Zaret, A. L. Bryson, N. D. Martin, and M. D. Flamm, *Am. J. Cardiol.*, **38,** 422 (1976).
(77) A. J. Lurie, A. F. Salel, D. S. Berman, G. L. DeNardo, E. J. Hurley, and D. T. Mason, *Circulation*, **54** (Suppl. III), 20 (1976).
(78) E. H. Botvinick, D. M. Shames, K. M. Gershengorn, E. Carlsson, R. A. Ratshin, and W. W. Parmley, *Am. J. Cardiol.*, **39,** 364 (1977).
(79) E. A. Carr, B. J. Walker, and J. Bartlett, *J. Clin. Invest.*, **42,** 922 (1963).
(80) E. A. Carr, G. Gleason, J. Shaw, and B. Krontz, *Am. Heart J.*, **68,** 627 (1964).
(81) W. D. Love, Y. Ishihara, L. D. Lyon, and R. O. Smith, *ibid.*, **76,** 353 (1968).
(82) W. D. Love and G. E. Burch, *J. Lab. Clin. Med.*, **41,** 351 (1953).
(83) W. Burguet, G. Merchie, and H. Kulbertus, *Br. Heart J.*, **37,** 1037 (1975).
(84) D. W. Romhilt, A. B. Ashare, R. J. Adolph, N. I. Levenson, W. G. Wee, V. J. Sodd, and L. S. August, *J. Nucl. Med.*, **17,** 247 (1976).
(85) B. Gustin, D. Romhilt, R. Adolph, A. Ashare, N. Levenson, V. J. Sodd, L. S. August, and J. Kahn, *Circulation*, **51–52** (Suppl. II), 53 (1975).
(86) R. Chandra, P. Braunstein, F. Streuli, and J. Hirch, *J. Nucl. Med.*, **14,** 243 (1973).
(87) Y. Yano, D. Van Dyke, T. F. Budinger, H. O. Anger, and P. Chu, *ibid.*, **11,** 663 (1970).
(88) V. J. Sodd, J. W. Blue, and K. L. Scholz, *Phys. Med. Biol.*, **16,** 587 (1971).
(89) D. W. Romhilt, R. J. Adolph, V. J. Sodd, N. I. Levenson, L. S. August, H. Nishiyama, and R. A. Berke, *Circulation*, **48,** 1242 (1973).
(90) N. D. Poe, *Radiology*, **106,** 341 (1973).
(91) R. T. Anger and V. J. Sodd, *Phys. Med. Biol.*, **16,** 698 (1971).
(92) N. D. Poe, *J. Nucl. Med.*, **13,** 557–560 (1972).
(93) E. Lebowitz, M. W. Greene, P. Bradley-Moore, H. Atkins, A. Ansari, P. Richards, and E. Belgraves, *ibid.*, 14, 421 (1973).
(94) E. Lebowitz, M. W. Greene, R. Fairchild, P. R. Bradley-Moore, H. L. Atkins, A. N. Ansari, P. Richards, and E. Belgraves, *ibid.*, **16,** 151 (1975).
(95) M. Kawana, H. Krizek, J. Porter, K. A. Lathrop, D. Charleston, and P. V. Harper, *ibid.*, **11,** 333 (1970).
(96) L. J. Mullins and R. D. Moore, *J. Gen. Physiol.*, **43,** 759 (1960).
(97) P. J. Gehring and P. B. Hammond, *J. Pharmacol. Exp. Ther.*, **155,** 187 (1967).
(98) R. K. Barclay, W. C. Peacock, and D. A. Karnofsky, *ibid.*, **107,** 178 (1953).
(99) P. R. Bradley-Moore, E. Lebowitz, M. W. Greene, H. L. Atkins, and A. N. Ansari, *J. Nucl. Med.*, **16,** 156 (1975).
(100) H. W. Strauss, K. Harrison, J. K. Langan, E. Lebowitz, and B. Pitt, *Circulation*, **51,** 641 (1975).
(101) F. J. T. Wackers, J. B. Schoot, E. B. Sokole, G. Samson, G. J. C. Niftrik, K. I. Lie, D. Durrer, and H. J. J. Wellens, *Br. Heart J.*, **37,** 741 (1975).
(102) H. L. Atkins, A. N. Ansari, E. Lebowitz, M. W. Greene, R. Fairchild, and T. Budinger, *J. Nucl. Med.*, **16,** 513 (1975).
(103) H. L. Atkins, T. F. Budinger, A. N. Ansari, M. W. Greene, R. G. Fairchild, and K. J. Ellis, *ibid.*, **18,** 133 (1977).
(104) H. Nishiyama, V. J. Sodd, R. J. Adolph, E. L. Saenger, J. T. Lewis, and M. Gabel, *ibid.*, **17,** 880 (1976).
(105) B. L. Holman, *Circulation*, **53** (Suppl. I), 112 (1976).
(106) A. M. Weissler, *ibid.*, **57,** 645 (1978).
(107) I. K. Bailey, L. S. C. Griffith, J. Rouleau, H. W. Strauss, and B. Pitt, *ibid.*, **55,** 79 (1977).
(108) J. L. Ritchie, G. B. Trobaugh, G. W. Hamilton, K. L. Gould, K. A. Narahara, J. A. Murray, and D. L. Williams, *ibid.*, **56,** 66 (1977).
(109) E. H. Botvinick, M. R. Taradash, D. M. Shames, and W. W. Parmley, *Am. J. Cardiol.*, **41,** 43 (1978).
(110) F. J. T. Wackers, E. B. Sokole, G. Samson, J. B. Van der Schoot, K. I. Lie, K. L. Liem, and H. J. J. Wellens, *N. Engl. J. Med.*, **295,** 1 (1976).
(111) B. Pitt and H. W. Strauss, *Am. J. Cardiol.*, **37,** 797 (1976).
(112) B. H. Bulkley, J. Rouleau, H. W. Strauss, and B. Pitt, *N. Engl. J. Med.*, **293,** 1113 (1975).
(113) B. H. Bulkley, J. Rouleau, J. Q. Whitaker, H. W. Strauss, and B. Pitt, *Am. J. Cardiol.*, **37,** 125 (1976).
(114) B. H. Bulkley, G. M. Hutchins, I. Bailey, H. W. Strauss, and B. Pitt, *Circulation*, **55,** 753 (1977).
(115) G. W. Hamilton, G. B. Trobaugh, J. L. Ritchie, D. L. Williams, W. D. Weaver, and K. L. Gould, *Am. J. Cardiol.*, **39,** 347 (1977).
(116) F. J. T. Wackers, A. E. Becker, G. Samson, E. B. Sokole, J. B. Van der Schoot, A. J. T. M. Vet, K. I. Lie, D. Durrer, and H. Wellens, *Circulation*, **56,** 72 (1977).
(117) F. J. T. Wackers, K. I. Lie, E. B. Sokole, J. Res, J. B. Van der Schoot, and D. Durrer, *Am. J. Cardiol.*, **42,** 358 (1978).
(118) A. Maseri, O. Parodi, S. Severi, and A. Pesola, *Circulation*, **54,** 280 (1976).
(119) F. J. T. Wackers, K. I. Lie, L. L. Koen, E. B. Sokole, G. Samson, J. B. Van der Schoot, and D. Durrer, *ibid.*, **57,** 738 (1978).
(120) J. S. Schwartz, R. Ponto, P. Carlyle, L. Forstrom, and J. N. Cohn, *ibid.*, **57,** 332 (1978).
(121) T. M. Muller, M. L. Marcus, J. C. Ebrhardt, T. Chaudhuri, and F. M. Abbound, *ibid.*, **54,** 640 (1976).
(122) G. M. Pohost, L. M. Zir, R. H. Moore, K. A. McKusick, T. E. Guiney, and G. A. Beller, *ibid.*, **55,** 294 (1977).
(123) G. A. Beller and G. M. Pohost, *Am. J. Cardiol.*, **41,** 379 (1978).
(124) D. K. Blood, D. M. McCarthy, R. R. Sciacca, and P. J. Cannon, *Circulation*, **58,** 777 (1978).
(125) J. H. McKillop, J. G. Turner, H. W. Gray, R. G. Bessent, and W. R. Greig, *Br. Heart J.*, **40,** 870 (1978).
(126) P. Rigo, L. C. Becker, L. S. C. Griffith, P. O. Alderson, I. K. Bailey, B. Pitt, R. D. Burrow, and H. N. Wagner, *Am. J. Cardiol.*, **44,** 452 (1979).
(127) A. Lenaers, P. Block, E. Van Thiel, M. Lebedelle, P. Becquevost, F. Erbsmann, and A. M. Ermans, *J. Nucl. Med.*, **18,** 509 (1977).
(128) R. J. Wainwright, M. N. Maisey, and E. Sowton, *Br. Heart J.*, **40,** 447 (1978).
(129) B. Massie, H. Dash, E. Botvinick, B. Brundage, and D. Shames, *Am. J. Cardiol.*, **41,** 413 (1978).
(130) T. Rehn, L. Griffith, S. Achuff, B. Buckley, M. Pond, and L. Becker, *ibid.*, **41,** 413 (1978).
(131) J. H. McKillop, R. G. Murray, J. G. Turner, R. G. Bessent, A. R. Lorimer, and W. R. Greig, *J. Nucl. Med.*, **20,** 715 (1979).
(132) K. R. Hetzel, B. R. Westerman, J. L. Quinn, S. Meyers, and V. Barresi, *ibid.*, **18,** 24 (1977).
(133) G. W. Hamilton, K. A. Narahara, H. Yee, J. L. Ritchie, D. L. Williams, and K. L. Gould, *ibid.*, **19,** 10 (1978).
(134) J. C. Costin and B. L. Zaret, *ibid.*, **17,** 535 (1976).
(135) R. W. Parkey, *ibid.*, **18,** 584 (1977).
(136) R. W. Parkey, F. J. Bonte, E. M. Stokely, S. E. Lewis, K. D. Graham, L. M. Buja, and J. T. Willerson, *ibid.*, **17,** 771 (1976).
(137) H. J. Berger, A. Gottschalk, and B. L. Zaret, *Ann. Intern. Med.*, **88,** 145 (1978).
(138) M. W. Groch and G. K. Lewis, *J. Nucl. Med.*, **17,** 142 (1976).
(139) H. Nishiyama, D. W. Romhilt, C. C. Williams, R. J. Adolph, V. J. Sodd, J. W. Blue, J. T. Lewis, M. Gabel, and J. M. van der Bel-Kahn, *ibid.*, **19,** 1067 (1978).
(140) R. C. Meade, V. S. Bamrah, J. D. Horgan, P. P. Puetz, C. Kronenwetter, and E. L. Yeh, *ibid.*, **19,** 1175 (1978).
(141) G. W. Hamilton, K. A. Narahara, G. B. Trobaugh, J. L. Ritchie, and D. L. Williams, *ibid.*, **19,** 1103 (1978).

(142) G. B. Trobaugh, F. J. T. Wackers, E. B. Sokole, T. A. DeRouen, J. L. Ritchie, and G. W. Hamilton, *ibid.*, **19,** 359 (1978).
(143) J. T. Ritchie, B. L. Zaret, H. W. Strauss, B. Pitt, D. S. Berman, H. R. Schelbert, W. L. Ashburn, H. J. Berger, and G. W. Hamilton, *Am. J. Cardiol.*, **42,** 345 (1978).
(144) P. R. McLaughlin, R. P. Martin, P. Doherty, S. Daspit, M. Goris, W. Haskell, S. Lewis, J. P. Kriss, and D. C. Harrison, *Circulation,* **55,** 497 (1977).
(145) W. W. Hunter and W. G. Monahan, *J. Nucl. Med.*, **12,** 368 (1971).
(146) W. G. Monahan, R. S. Tilbury, and J. S. Laughlin, *ibid.*, **13,** 274 (1972).
(147) B. Hoop, T. W. Smith, C. A. Burnham, J. E. Correll, G. L. Brownell, and C. A. Sanders, *ibid.*, **14,** 181 (1973).
(148) T. F. Budinger, Y. Yano, and B. Hoop, *ibid.*, **16,** 429 (1975).
(149) P. V. Harper, K. A. Lathrop, H. Krizek, N. Lembares, V. Stark, and P. B. Hoffer, *ibid.*, **13,** 278 (1972).
(150) P. V. Harper, J. Al-Sadir, A. Mayorga, C. Bekerman, A. Goldbarg, N. Lembares, and K. Lathrop, *ibid.*, **14,** 405 (1973).
(151) P. V. Harper, J. Schwartz, R. N. Beck, K. A. Lathrop, N. Lembares, H. Krizek, I. Gloria, R. Dinwoodie, A. McLaughlin, V. J. Stark, C. Bekerman, P. B. Hoffer, A. Gottschalk, L. Resnekov, J. Al-Sadir, A. Mayorga, and H. L. Brooks, *Radiology,* **108,** 613 (1973).
(152) M. E. Phelps, E. J. Hoffman, R. E. Coleman, M. J. Welch, M. E. Raichle, E. S. Weiss, B. E. Sobel, and M. M. Ter-Pogossian, *J. Nucl. Med.*, **17,** 603 (1976).
(153) J. L. Quinn, M. Serratto, and P. Kezdi, *ibid.*, **7,** 107 (1966).
(154) M. Endo, T. Yamazaki, S. Konno, H. Hiratsuka, T. Akimoto, T. Tanaka, and S. Sanakibana, *Am. Heart J.*, **80,** 498 (1970).
(155) W. L. Ashburn, E. Braunwald, A. L. Simon, K. L. Peterson, and J. H. Gault, *Circulation,* **44,** 851 (1971).
(156) J. P. Archie, D. E. Fixler, D. J. Ullyot, J. I. E. Hoffman, J. R. Utley, and E. L. Carlson, *J. Appl. Physiol.*, **35,** 148 (1973).
(157) G. D. Buckburg, J. C. Luck, D. B. Payne, J. I. E. Hoffman, J. P. Archie, and D. E. Fixler, *ibid.*, **31,** 598 (1971).
(158) W. C. Eckelman, G. Meinken, and P. Richards, *J. Nucl. Med.*, **12,** 707 (1971).
(159) C. Jansen, G. C. Grames, and M. P. Judkins, in "Cardiovascular Nuclear Medicine," H. W. Strauss, B. Pitt, and A. E. James, Eds., C. V. Mosby, St. Louis, Mo., 1974, p. 211.
(160) R. J. Domenech, J. I. E. Hoffman, M. I. M. Noble, K. B. Sanders, J. R. Henson, and S. Subijanto, *Circ. Res.*, **25,** 581 (1969).
(161) G. Segre and A. Silberberg, *Nature,* **189,** 209 (1961).
(162) R. H. Phibbs and L. Doug, *Can. J. Physiol. Pharmacol.*, **48,** 415 (1970).
(163) T. Yipintsoi, W. A. Dobbs, P. D. Scanlon, T. J. Knopp, and J. B. Bassingthwaighte, *Circ. Res.*, **33,** 573 (1973).
(164) J. Utley, E. L. Carlson, J. I. E. Hoffman, H. M. Martinez, and G. D. Buckburg, *ibid.*, **34,** 391 (1974).
(165) F. R. Cobb, R. J. Bache, and J. C. Greenfield, *J. Clin. Invest.*, **53,** 1618 (1974).
(166) D. A. Weller, R. J. Adolph, H. N. Wellman, R. G. Carroll, and O. Kim, *Circulation,* **46,** 963 (1972).
(167) G. M. Grames, C. Jansen, M. P. Gander, H. C. Wieland, and M. P. Judkins, *J. Nucl. Med.*, **15,** 2 (1974).
(168) N. D. Poe, *ibid.*, **12,** 724 (1971).
(169) K. L. Gould, K. Lipscomb, and G. Hamilton, *Am. J. Cardiol.*, **33,** 87 (1974).
(170) P. J. Cannon, *Circulation,* **51,** 955 (1975).
(171) S. C. Bachrach, M. V. Green, J. S. Borer, M. A. Douglas, H. G. Ostrow, and G. S. Johnston, *J. Nucl. Med.*, **18,** 79 (1977).
(172) B. Pitt and H. W. Strauss, *N. Engl. J. Med.*, **296,** 1097 (1977).
(173) N. M. Alpert, K. A. McKusick, G. M. Pohost, R. E. Dinsmore, and M. S. Potsaid, *J. Nucl. Med.*, **15,** 1182 (1974).
(174) P. Rigo, M. Murray, H. W. Strauss, D. Taylor, D. Kelly, M. Weisfeldt, and B. Pitt, *Circulation,* **50,** 678 (1974).
(175) M. Rigo, M. Murray, D. R. Taylor, M. Weisfeldt, and D. T. Kelly, *ibid.*, **52,** 268 (1975).
(176) F. B. Ballard, W. Danforth, S. Naegle, and R. J. Bing, *J. Clin. Invest.*, **39,** 717 (1960).
(177) R. S. Gordon and A. Cherkes, *ibid.*, **35,** 206 (1956).
(178) J. C. Shipp, L. H. Opie, and D. Challoner, *Nature,* **189,** 1018 (1961).
(179) R. J. Bing, *Physiol. Rev.*, **45,** 171 (1965).
(180) L. H. Opie, *Am. Heart J.*, **76,** 685 (1968).
(181) J. R. Neely and H. E. Morgan, *Ann. Rev. Physiol.*, **36,** 413 (1974).
(182) J. R. Evans, L. H. Opie, and J. C. Shipp, *Am. J. Physiol.*, **205,** 766 (1963).
(183) J. H. Bragdon and R. S. Gordon, *J. Clin. Invest.*, **37,** 574 (1958).
(184) J. Scheuer and N. Brachfeld, *Metabolism,* **15,** 945 (1966).
(185) J. R. Evans, R. W. Gunton, and D. S. Beanlands, *Circulation,* **26,** 714 (1962).
(186) J. R. Evans, R. W. Gunton, R. G. Baker, D. S. Beanlands, and J. C. Spears, *Circ. Res.*, **16,** 1 (1965).
(187) R. W. Gunton, J. R. Evans, R. G. Baker, J. C. Spears, and D. S. Beanlands, *Am. J. Cardiol.*, **16,** 482 (1975).
(188) N. D. Poe, G. D. Robinson, and N. S. MacDonald, *J. Nucl. Med.*, **14,** 440 (1973).
(189) F. J. Bonte, K. D. Graham, and J. G. Moore, *Radiology,* **108,** 195 (1973).
(190) N. D. Poe, G. D. Robinson, and N. S. MacDonald, *Proc. Soc. Exp. Biol. Med.*, **148,** 215 (1975).
(191) G. D. Robinson and A. W. Lee, *J. Nucl. Med.*, **16,** 17 (1975).
(192) G. D. Robinson, *Int. J. Appl. Radiat. Isot.*, **28,** 149 (1977).
(193) N. D. Poe, G. D. Robinson, L. S. Graham, and N. S. MacDonald, *J. Nucl. Med.*, **17,** 1077 (1976).
(194) H. J. Machulla, G. Stöcklin, C. Kupfernagel, C. Freundlieb, A. Höck, K. Vyska, and L. E. Feinendegen, *ibid.*, **19,** 298 (1978).
(195) W. H. Beierwaltes, R. D. Ice, M. J. Shaw, and U. Y. Ryo, *ibid.*, **16,** 842 (1975).
(196) N. D. Poe, G. D. Robinson, F. W. Zielinski, W. R. Cabeen, J. W. Smith, and A. S. Gomes, *Radiology,* **124,** 419 (1977).
(197) N. D. Poe, G. D. Robinson, F. W. Zielinski, W. R. Cabeen, J. W. Smith, and A. S. Gomes, *J. Nucl. Med.*, **18,** 611 (1977).
(198) G. D. Robinson, N. D. Poe, A. Y. Lee, and C. S. Selin, *ibid.*, **15,** 528 (1974).
(199) D. W. Bilheimer, L. M. Buja, R. W. Parkey, F. J. Bonte, and J. T. Willerson, *ibid.*, **19,** 276 (1978).
(200) E. S. Weiss, E. J. Hoffman, S. A. Ahmed, M. E. Phelps, M. J. Welch, M. M. Ter-Pogossian, and B. E. Sobel, *Circulation,* **51–52** (Suppl. II), 52 (1975).
(201) E. S. Weiss, E. J. Hoffman, M. E. Phelps, M. J. Welch, M. M. Ter-Pogossian, and B. E. Sobel, *Clin. Res.*, **23,** 383A (1975).
(202) G. D. Robinson and N. S. MacDonald, *J. Nucl. Med.*, **14,** 446 (1973).
(203) S. M. Karesh, W. C. Eckelman, and R. C. Reba, *J. Pharm. Sci.*, **66,** 225 (1977).
(204) F. J. Bonte, K. D. Graham, J. G. Moore, R. W. Parkey, and G. C. Curry, *J. Nucl. Med.*, **14,** 381 (1973).
(205) E. Livni, M. A. Davis, and V. D. Warner, in "Proceedings of the Second International Symposium on Radiopharmaceuticals," Seattle, Wash., Mar. 1979.
(206) G. P. Basmadjian, S. L. Mills, G. R. Parker, A. S. Kirschner, R. D. Ice, and R. A. Magarian, *J. Nucl. Med.*, **19,** 718 (1978).
(207) S. L. Mills, G. P. Basmadjian, G. R. Parker, and R. D. Ice, *J. Lab. Comp. Radiopharm.*, in press.
(208) F. F. Knapp, K. K. Ambrose, A. P. Callahan, R. A. Grigsby, and K. J. Irgolic, in "Proceedings of the Second International Symposium on Radiopharmaceuticals," Seattle, Wash., Mar. 1979.
(209) E. J. Hoffman, M. E. Phelps, E. S. Weiss, M. J. Welch, R. E. Coleman, B. E. Sobel, and M. M. Ter-Pogossian, *J. Nucl. Med.*, **18,** 57 (1977).
(210) B. E. Sobel, E. S. Weiss, M. J. Welch, B. A. Siegel, and M. M. Ter-Pogossian, *Circulation,* **55,** 853 (1977).
(211) E. S. Weiss, S. A. Ahmed, M. J. Welch, J. R. Williamson, M. M. Ter-Pogossian, and B. E. Sobel, *ibid.*, **55,** 66 (1977).
(212) J. H. Thrall, D. P. Swanson, and D. M. Wieland, *J. Nucl. Med.*, **19,** 969 (1978).
(213) D. R. Hoogland, J. P. Weichert, S. A. Sire, M. P. Frick, L. A. Forstrom, and M. K. Loken, in "Proceedings of the Second International Symposium on Radiopharmaceuticals," Seattle, Wash., Mar. 1979.
(214) V. W. Jiang, R. E. Gibson, W. J. Rzeszotarski, W. C. Eckelman, R. C. Reba, F. Vieras, and P. O. Alderson, *J. Nucl. Med.*, **19,** 918 (1978).
(215) G. S. Kang, *ibid.*, **10,** 413 (1969).
(216) E. G. Archer, E. J. Potchen, R. Studer, and B. Siegel, *ibid.*, **10,** 386 (1969).
(217) *Ibid.*, **13,** 85 (1972).
(218) E. A. Carr, M. Carroll, W. DiGiulio, and D. C. Blair, *Am. Heart J.*, **86,** 631 (1973).
(219) R. E. Counsell, T. Yu, V. V. Ranade, and A. Buswick, *J. Med. Chem.*, **16,** 1038 (1973).

(220) E. A. Carr, R. E. Counsell, and M. Carroll, *Clin. Pharmacol. Ther.*, **14,** 132 (1973).
(221) R. E. Counsell, T. Yu, V. V. Ranade, A. A. Buswick, E. A. Carr, and M. Carroll, *J. Nucl. Med.*, **15,** 991 (1974).
(222) A. S. Gelbard, L. P. Clarke, and J. S. Laughlin, *ibid.*, **15,** 1223 (1974).
(223) J. A. Herd, M. Hollenberg, G. D. Thorburn, H. H. Kopald, and A. C. Barger, *Am. J. Physiol.*, **203,** 122 (1962).
(224) L. S. Cohen, W. C. Elliott, and R. Gorlin, *ibid.*, **206,** 997 (1964).
(225) M. D. Klein, L. S. Cohen, and R. Gorlin, *ibid.*, **209,** 705 (1965).
(226) R. S. Ross, K. Ueda, P. R. Lichtlen, and J. R. Rees, *Circ. Res.*, **15,** 28 (1964).
(227) P. J. Cannon, J. I. Haft, and P. M. Johnson, *Circulation*, **40,** 277 (1969).
(228) A. Maseri and P. Mancini, in "Myocardial Blood Flow in Man," A. Maseri, Ed., Minerva Medica, Turin, Italy, 1972, p. 219.
(229) F. J. Bonte, R. W. Parkey, E. M. Stokely, S. E. Lewis, L. D. Horwitz, and G. C. Curry, *Semin. Nucl. Med.*, **3,** 153 (1973).
(230) B. L. Holman, D. F. Adams, D. Jewitt, P. Eldh, J. Idoine, P. F. Cohn, R. Gorlin, and S. J. Adelstein, *Radiology*, **112,** 99 (1974).
(231) O. Korhola, *Acta Radiol.*, **337** (Suppl. 337), 7 (1974).
(232) P. J. Cannon, R. B. Dell, and E. M. Dwyer, *J. Clin. Invest.*, **49,** 163 (1970).
(233) *Ibid.*, **51,** 964 (1972).
(234) W. J. MacIntyre, P. J. Cannon, and W. W. Ashburn, in "Quantitative Nuclear Cardiography," R. H. Pierson, J. P. Kriss, R. H. Jones, and W. J. MacIntyre, Eds., Wiley, New York, N.Y., 1975, p. 170.
(235) P. J. Cannon, R. B. Dell, and E. M. Dwyer, *J. Clin. Invest.*, **51,** 978 (1975).
(236) E. M. Dwyer, R. B. Dell, and P. J. Cannon, *Circulation*, **48,** 924 (1973).
(237) D. H. Schmidt, M. B. Weiss, W. Casarella, E. Pollock, and P. J. Cannon, *ibid.*, **48** (Suppl. I), 64 (1973).
(238) M. B. Weiss, D. H. Schmidt, W. J. Casarella, D. L. Fowler, and P. J. Cannon, in "World Congress of Cardiology," Buenos Aires, Argentina, 1973, p. 282.
(239) M. B. Weiss, D. H. Schmidt, C. Jaffee, W. J. Casarella, K. Ellis, and P. J. Cannon, *Circulation*, **46** (Suppl. II), 235 (1972).
(240) J. B. Bassingthwaighte, T. Strandell, and D. E. Donald, *Circ. Res.*, **23,** 259 (1968).
(241) D. J. Shaw, A. Pitt, and G. C. Friesinger, *Cardiovasc. Res.*, **6,** 268 (1971).
(242) L. W. Mayron, E. Kaplan, A. M. Friedman, and J. E. Gindler, *Int. J. Appl. Radiat. Isot.*, **25,** 237 (1974).
(243) L. G. Colombetti, L. W. Mayron, E. Kaplan, W. E. Barnes, A. M. Friedman, and J. E. Gindler, *J. Nucl. Med.*, **15,** 868 (1974).
(244) E. Kaplan, L. W. Mayron, W. E. Barnes, L. G. Colombetti, A. M. Friedman, and J. E. Gindler, *ibid.*, **15,** 874 (1974).
(245) L. W. Mayron, E. Kaplan, and G. Colombetti, *Int. J. Nucl. Med. Biol.*, **2,** 40 (1975).
(246) E. Kaplan, L. W. Mayron, A. M. Friedman, J. E. Gindler, L. Frazin, J. M. Moran, H. Loeb, and R. M. Gunnar, *Am. J. Cardiol.*, **35,** 147 (1975).
(247) L. W. Mayron, A. M. Friedman, and E. Kaplan, *Int. J. Nucl. Med. Biol.*, **2,** 141 (1975).
(248) J. H. Turner, A. P. Selwyn, T. Jones, T. R. Evans, M. J. Raphael, and J. P. Lavender, *Cardiovasc. Res.*, **10,** 398 (1976).
(249) A. P. Selwyn, T. Jones, J. H. Turner, T. Pratt, J. Clark, and P. Lavender, *Circ. Res.*, **42,** 771 (1978).
(250) E. Kaplan, L. W. Mayron, A. M. Friedman, J. E. Gindler, L. Frazin, J. M. Moran, H. Loeb, and R. M. Gunnar, *Am. J. Cardiol.*, **37,** 878 (1976).
(251) R. J. Kramer, R. E. Goldstein, J. W. Hirshfeld, W. C. Roberts, G. S. Johnston, and S. E. Epstein, *ibid.*, **33,** 861 (1974).
(252) F. J. Bonte, R. W. Parkey, K. D. Graham, and J. G. Moore, *J. Nucl. Med.*, **16,** 132 (1975).
(253) P. M. Weber, D. Van Dyke, L. V. Dos Remedios, and H. O. Anger, *ibid.*, **16,** 581 (1975).
(254) S. Cochavi, G. M. Pohost, D. R. Elmaleh, and H. W. Strauss, *ibid.*, **20,** 1013 (1979).
(255) H. A. Oldewurtel, D. V. Rao, C. B. Moschos, B. Haider, and T. J. Regan, *ibid.*, **16,** 554 (1975).
(256) P. Malek, J. Kole, V. L. Zastava, F. Zak, and B. Peleska, *Cardiologia*, **42,** 303 (1963).
(257) B. L. Holman, M. K. Dewanjee, J. Idoine, C. P. Fliegel, M. A. Davis, S. Treves, and P. Eldh, *J. Nucl. Med.*, **14,** 595 (1973).
(258) B. L. Holman and F. G. Zweiman, *ibid.*, **16,** 1144 (1975).
(259) B. L. Holman, M. Lesch, F. G. Zweiman, J. Temte, B. Lown, and R. Gorlin, *N. Engl. J. Med.*, **291,** 159 (1974).
(260) D. J. Rossman, H. W. Strauss, M. E. Siegel, and B. Pitt, *J. Nucl. Med.*, **16,** 875 (1975).
(261) D. J. Rossman, J. Roulean, H. W. Strauss, and B. Pitt, *ibid.*, **16,** 980 (1975).
(262) M. Lesch, T. Tanaka, and B. L. Holman, *Circulation*, **52** (Suppl. II), 53 (1975).
(263) J. G. Jacobstein, D. R. Alonso, A. J. Roberts, P. R. Cipriano, J. R. Combes, and M. R. Post, *J. Nucl. Med.*, **18,** 413 (1977).
(264) F. J. Bonte, R. W. Parkey, K. D. Graham, J. Moore, and E. M. Stokely, *Radiology*, **110,** 473 (1974).
(265) R. W. Parkey, F. J. Bonte, S. L. Meyer, J. M. Atkins, G. L. Curry, E. M. Stokely, and J. T. Willerson, *Circulation*, **50,** 540 (1974).
(266) B. L. Holman, T. T. Tanaka, and M. Lesch, *Radiology*, **121,** 427 (1976).
(267) M. R. Tetalman, L. C. Foley, P. Crispin, C. P. Spencer, and S. P. Bishop, *ibid.*, **124,** 431 (1977).
(268) E. H. Botvinick, D. Shames, H. Lappin, J. V. Tyberg, R. Townsend, and W. W. Parmley, *Circulation*, **52,** 909 (1975).
(269) E. M. Stokely, L. M. Buja, S. E. Lewis, R. W. Parkey, F. J. Bonte, R. A. Harris, and J. T. Willerson, *J. Nucl. Med.*, **17,** 1 (1976).
(270) R. E. Coleman, M. S. Klein, S. A. Ahmad, E. S. Weiss, W. M. Buchholz, and B. E. Sobel, *Am. J. Cardiol.*, **39,** 55 (1977).
(271) B. L. Zaret, R. C. Lange, and J. C. Lee, *ibid.*, **39,** 309 (1977).
(272) F. P. Bruno, F. R. Cobb, F. Rivas, and J. K. Goodrich, *Circulation*, **54,** 71 (1976).
(273) B. L. Zaret, V. C. DiCola, R. K. Donabedian, S. Puri, S. Wolfson, G. S. Freedman, and L. S. Cohen, *ibid.*, **53,** 422 (1976).
(274) M. L. Marcus, R. J. Tomanek, J. C. Ehrhardt, R. E. Kerber, D. D. Brown, and F. M. Abbond, *ibid.*, **54,** 647 (1976).
(275) H. Henning, H. R. Schelbert, A. Righetti, W. L. Ashburn, and R. A. O'Rourke, *Am. J. Cardiol.*, **40,** 147 (1977).
(276) B. M. Massie, E. H. Botvinick, J. A. Werner, K. Chatterjee, and W. W. Parmley, *ibid.*, **43,** 186 (1979).
(277) L. R. Poliner, L. M. Buja, R. W. Parkey, F. J. Bonte, and J. T. Willerson, *Circulation*, **59,** 257 (1979).
(278) J. T. Willerson, R. W. Parkey, R. A. Harris, F. J. Bonte, E. M. Stokely, and L. M. Buja, *Clin. Res.*, **23,** 214A (1975).
(279) G. A. Beller, B. A. Khaw, E. Haber, and T. W. Smith, *Circulation*, **55,** 74 (1977).
(280) L. M. Buja, R. W. Parkey, E. M. Stokely, F. J. Bonte, and J. T. Willerson, *J. Clin. Invest.*, **57,** 1508 (1976).
(281) D. S. Berman, E. A. Amsterdam, A. F. Salel, G. L. DeNardo, G. J. Bailey, and D. T. Mason, *Circulation*, **51–52** (Suppl. II), II-53 (1975).
(282) H. G. Olson, K. P. Lyons, W. S. Aronow, W. T. Brown, and R. S. Greenfield, *ibid.*, **56,** 181 (1977).
(283) R. Prasquier, M. R. Taradash, E. H. Botvinick, D. Shames, and W. W. Parmley, *ibid.*, **55,** 61 (1977).
(284) J. T. Willerson, R. W. Parkey, F. J. Bonte, S. L. Meyer, and E. M. Stokely, *ibid.*, **51,** 436 (1975).
(285) N. Sharpe, E. Botvinick, D. Shames, K. Chatterjee, B. Massie, N. Schilles, and W. W. Parmley, *ibid.*, **53–54** (Suppl. II), II-76 (1976).
(286) M. Ahmad, J. P. Dubiel, T. A. Verdon, and R. H. Martin, *ibid.*, **53,** 833 (1976).
(287) H. Olson, K. Lyons, W. S. Aronow, J. Orlando, and J. Kyperus, *Clin. Res.*, **26,** 96A (1978).
(288) L. M. Buja, L. R. Poliner, R. W. Parkey, J. I. Pulido, D. Hutchason, M. R. Platt, L. J. Mills, F. J. Bonte, and J. T. Willerson, *Circulation*, **56,** 1016 (1977).
(289) F. R. Malin, F. D. Rollo, and E. W. Gertz, *J. Nucl. Med.*, **19,** 1111 (1978).
(290) E. H. Botvinick, D. M. Shames, D. N. Sharpe, S. C. Klausner, J. A. Werner, K. Chatterjee, and W. W. Parmley, *ibid.*, **19,** 1121 (1978).
(291) M. J. Cowley, K. Kawamura, R. B. Karp, J. A. Mantle, J. R. Logic, W. J. Rogers, R. O. Russel, C. E. Rackley, and T. N. James, *Circulation*, **53–54** (Suppl. II), II-218 (1976).
(292) M. Ahmad, J. P. Dubiel, K. W. Logan, T. A. Verdon, and R. H. Martin, *Am. J. Cardiol.*, **39,** 50 (1977).
(293) W. Harford, M. N. Weinburg, L. M. Buja, R. W. Parkey, F. J. Bonte, and J. T. Willerson, *Radiology*, **122,** 747 (1977).
(294) R. T. Go, D. B. Doty, C. L. Chiu, and J. H. Christie, *ibid.*, **116,** 107 (1975).

(295) J. Downey, R. Chagrasulis, D. Fore, and L. F. Parmley, *J. Nucl. Med.*, **18,** 1171 (1977).
(296) C. L. Chiu, J. D. Roelofs, R. T. Go, D. B. Doty, E. F. Rose, and J. H. Christie, *Radiology,* **116,** 679 (1975).
(297) A. Righetti, R. A. O'Rourke, H. Schelbert, H. Henning, T. Hardarson, P. O. Daily, W. Ashburn, and J. Ross, *Am. J. Cardiol.*, **39,** 43 (1977).
(298) J. A. Jengo, I. Mena, S. H. Joe, and J. M. Criley, *J. Nucl. Med.*, **18,** 776 (1977).
(299) J. W. Mason, R. W. Myers, E. L. Alderman, E. B. Stinson, M. L. Goris, and J. P. Kriss, *Am. J. Cardiol.*, **40,** 1 (1977).
(300) M. S. Donsky, G. C. Curry, R. W. Parkey, S. L. Meyer, F. J. Bonte, M. R. Platt, and J. T. Willerson, *Circulation,* **51–52** (Suppl. II), II-89 (1975).
(301) L. A. Gould, L. A. Perez, D. B. Hayt, C. V. Reddy, C. Blatt, and R. F. Gomprecht, *ibid.*, **49–50** (Suppl. III), III-4 (1974).
(302) L. A. Perez, D. B. Hayt, and L. M. Freeman, *J. Nucl. Med.*, **17,** 241 (1976).
(303) M. Ahmad, J. Dubiel, K. Logan, T. Verdon, and R. Martin, *Circulation,* **52** (Suppl. II), II-148 (1975).
(304) B. R. Pugh, L. M. Buja, R. W. Parkey, L. R. Poliner, E. M. Stokely, F. J. Bonte, and J. T. Willerson, *ibid.*, **54,** 399 (1976).
(305) V. C. DiCola, G. S. Freedman, S. E. Downing, and B. L. Zaret, *ibid.*, **54,** 980 (1976).
(306) I. R. McDougall and D. A. Pistenma, *Radiology,* **112,** 655 (1974).
(307) G. H. Schmitt, R. A. Holmes, A. T. Isitman, G. T. Hensley, and J. D. Lewis, *ibid.*, **112,** 733 (1974).
(308) K. Kadota, A. Matsumori, H. Kambara, and C. Kawai, *J. Nucl. Med.*, **20,** 1047 (1979).
(309) J. S. Soin, J. A. Burdine, and W. Beal, *ibid.*, **16,** 944 (1975).
(310) M. L. Marcus and R. E. Kerber, *Circulation,* **56,** 335 (1977).
(311) B. L. Holman, M. Lesch, and J. S. Alpert, *Am. J. Cardiol.*, **41,** 39 (1978).
(312) F. J. Bonte, R. W. Parkey, K. D. Graham, and J. G. Moore, *J. Nucl. Med.*, **16,** 132 (1975).
(313) A. N. D'Agostino, *Am. J. Pathol.*, **45,** 633 (1964).
(314) A. N. D'Agostino and M. Chiga, *Am. J. Clin. Pathol.*, **53,** 820 (1970).
(315) A. C. Shen and R. B. Jennings, *Am. J. Pathol.*, **67,** 441 (1972).
(316) *Ibid.*, **67,** 417 (1972).
(317) M. K. Dewanjee, P. C. Kahn, U. Dewanjee, and R. J. Connolly, *J. Nucl. Med.*, **16,** 525 (1975).
(318) M. K. Dewanjee and P. C. Kahn, *ibid.*, **17,** 639 (1976).
(319) F. G. Zwierman, B. L. Holman, A. O'Keefe, and J. Idoine, *ibid.*, **16,** 975 (1975).
(320) F. J. Bonte, R. W. Parkey, K. D. Graham, and J. G. Moore, *ibid.*, **16,** 132 (1974).
(321) P. McLaughlin, G. Coates, D. Wood, T. Cradduck, and J. Morch, *Am. J. Cardiol.*, **35,** 390 (1975).
(322) S. K. Chandarlapaty, F. Golian, and B. Befeler, *Clin. Res.*, **22,** 268A (1974).
(323) G. J. Davies, B. Fakhrai, A. Morgan, and J. R. Muir, *Br. Heart J.*, **41,** 668 (1979).
(324) W. Walsh, J. Schwartz, G. Bautovich, A. Booth, P. Harper, J. Al-Sadir, and L. Resnekov, *Clin. Res.*, **23,** 213A (1975).
(325) B. L. Holman, A. G. Jones, M. A. Davis, J. Askenazi, and P. R. Maroka, *J. Nucl. Med.*, **17,** 508 (1976).
(326) M. K. Dewanjee and P. C. Kahn, *Radiology,* **117,** 723 (1975).
(327) Z. D. Grossman, A. B. Foster, J. B. McAfee, R. Richardson, G. Subramanian, B. Markarian, G. Gagne, and D. Bassano, *J. Nucl. Med.*, **18,** 51 (1977).
(328) P. J. Ell, R. Langford, P. Pearce, D. Lui, A. T. Elliott, N. Woolf, and E. S. Williams, *Br. Heart J.*, **40,** 226 (1978).
(329) S. P. Joseph, P. J. Ell, P. Ross, R. Donaldson, A. T. Elliott, N. J. G. Brown, and E. S. Williams, *ibid.*, **40,** 234 (1978).
(330) E. A. Carr, W. H. Beierwaltes, M. E. Patno, J. D. Bartlett, and A. V. Wegst, *Am. Heart J.*, **64,** 650 (1962).
(331) E. A. Carr, E. J. Cafruny, and J. D. Bartlett, *Bull. Univ. Mich.*, **29,** 27 (1963).
(332) R. J. Gorten, L. B. Hardy, B. H. McCraw, J. R. Stokes, and G. D. Lumb, *Am. Heart J.*, **72,** 71 (1966).
(333) P. Malek, B. Vavrejn, and J. Ratusky, *Cas. Lek. Cesk.*, **105,** 1273 (1966).
(334) J. Ratusky, L. Kronrad, and P. Malek, *Radiochem. Radioanal. Lett.*, **6,** 63 (1971).
(335) P. Malek, J. Ratusky, B. Vavrejn, L. Kronrad, and J. Kole, *Nature,* **214,** 1130 (1967).
(336) P. Ramanathan, R. D. Ganatra, K. Daulatram, P. K. Sen, and M. Blau, *J. Nucl. Med.*, **12,** 641 (1971).
(337) P. J. B. Hubner, *Cardiovasc. Res.*, **4,** 509 (1970).
(338) I. L. Spar, S. M. Michaelson, V. Y. Greenhouse, and P. N. Yu, *J. Nucl. Med.*, **11,** 362 (1970).
(339) R. N. Hanson, M. A. Davis, and B. L. Holman, *ibid.*, **18,** 1211 (1977).
(340) M. A. Davis, B. L. Holman, and A. N. Carmel, *ibid.*, **17,** 911 (1976).
(341) R. N. Hanson, M. A. Davis, and B. L. Holman, *ibid.*, **18,** 803 (1977).
(342) B. A. Khaw, G. A. Beller, E. Haber, and T. W. Smith, *Clin. Res.*, **23,** 318A (1975).
(343) B. A. Khaw, G. A. Beller, E. Haber, and T. W. Smith, *J. Clin. Invest.*, **58,** 439 (1976).
(344) G. A. Beller, B. A. Khaw, E. Haber, and T. W. Smith, *Circulation,* **55,** 74 (1977).
(345) B. A. Khaw, G. A. Beller, and E. Haber, *ibid.*, **57,** 743 (1978).
(346) B. A. Khaw, H. K. Gold, R. C. Leinbach, J. T. Fallon, W. Strauss, G. M. Pohost, and E. Haber, *ibid.*, **58,** 1137 (1978).
(347) B. A. Khaw, J. T. Fallon, H. Katus, D. Elmalek, H. W. Strauss, E. Locke, G. M. Pohost, and E. Haber, *ibid.*, **59–60** (Suppl. II), 135 (1979).

# Dissolution Kinetics of Carboxylic Acids I: Effect of pH under Unbuffered Conditions

K. G. MOONEY *, M. A. MINTUN ‡, K. J. HIMMELSTEIN, and V. J. STELLA ×

Received March 24, 1980, from the *Departments of Pharmaceutical Chemistry and Chemical and Petroleum Engineering, University of Kansas, Lawrence, KS 66045.* Accepted for publication July 3, 1980. *Present address: Boehringer Ingelheim, Ridgefield, CT 06877. ‡Present address: Washington University, St. Louis, MO 63110.

**Abstract** □ The dissolution behavior of benzoic acid, 2-naphthoic acid, and indomethacin from rotating compressed disks into aqueous solutions of constant ionic strength ($\mu$ = 0.5 with potassium chloride) at 25° was investigated. The pH of the bulk aqueous medium was maintained during dissolution by means of a pH-stat apparatus. A model for the initial steady-state dissolution rate of a monoprotic carboxylic acid was derived from Fick's second law of diffusion. This model assumed that diffusion-controlled mass transport and simple, instantaneously established reaction equilibria existed across a postulated diffusion layer. Using previously determined intrinsic solubilities, pKa values, and diffusion coefficients, the model was found to predict the dissolution rates of these acids accurately as a function of the bulk solution pH. Hydroxide ion and water were the only reactive base species present in the bulk solution. The concentration profiles of all of the species across the diffusion layer were generated for a given bulk pH. Furthermore, the model generated values for the pH profile within the microclimate of the diffusion layer and the pH at the solid–solution boundary.

**Keyphrases** □ Dissolution kinetics—carboxylic acids, effect of pH under unbuffered conditions □ Carboxylic acids—dissolution kinetics, effect of pH under unbuffered conditions □ Kinetics—dissolution of carboxylic acids, effect of pH under unbuffered conditions

The purpose of this study was to examine the effect of solubility and unbuffered bulk solution pH on the dissolution kinetics of three carboxylic acids: benzoic acid (I), 2-naphthoic acid (II), and indomethacin (III). The dissolution of carboxylic acids into a basic medium represents dissolution with a simultaneous, instantaneous, reversible chemical reaction. Modeling of this system should allow determination of the solid–liquid interfacial pH and the composition of the diffusion layer (1), the unstirred liquid layer postulated to exist adjacent to the solid surface.

The dissolution kinetics of acidic compounds into a basic medium were studied initially by Brunner (2) and later by other investigators (3–7). Factors that affect the dissolution of benzoic acid, which undergoes a simultaneous chemical reaction with basic species from the bulk solution, were studied and modeled in detail by Higuchi *et al.* (5). They used the film theory of Nernst (1), which is based on Fick's laws of diffusion (8).

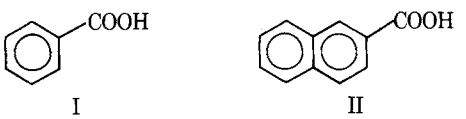


I




II

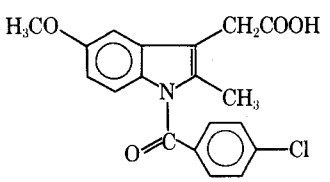


III

To investigate the initial dissolution rates of I–III over a wide range of bulk pH values without using buffers, automatic potentiometric monitoring employing a pH-stat system can be employed (9–13). This technique, combined with a rotating-disk apparatus similar to that described by Wood *et al.* (14), results in a constant dissolution surface area. The hydrodynamic theory of Levich (15) was applied to rotating disks (16, 17). From this theory, the thickness of the diffusion layer may be calculated and used in a modified Nernst (1) expression to predict initial dissolution rates (16, 17).

A simplified equation was used to describe the dissolution of acids in a basic medium (18, 19). However, this equation is derived by assuming that the bulk solution pH and the interfacial pH, $pH_0$, are identical. However, the bulk hydrogen-ion concentration is not necessarily equal to that at the solid–liquid interface or elsewhere within the diffusion layer. The interfacial pH is affected by the degree of dissociation of the acid at the interface, which is determined by the concentration and pKa of the acid. Dissociation of the acid liberates hydrogen ions, thereby lowering the pH of the diffusion layer relative to that of the bulk solution.

## THEORETICAL

The starting point for a model of dissolution of an acid in a basic medium comes from the work of Higuchi *et al.* (5). Their model was formulated around that of Nernst (1) for a diffusion-controlled process in the solution phase and postulates the existence of a diffusion layer (a region of unstirred solvent) adhering to the dissolving surface. Within this layer, all concentration gradients of reactants and products are postulated to exist as a result of diffusion and the chemical reaction between the dissolving solute and the incoming base from the bulk solution. The bulk solution is regarded as a homogeneous mixture with no concentration gradients.

Figure 1 is a pictorial representation of the model where a solid carboxylic acid, HA, dissolves at the phase boundary. At the solid–liquid interface, the boundary condition is $X = 0$ and the concentration of HA is $[HA]_0$, which is the saturated solubility of the unionized acid. The acid diffuses and simultaneously reacts with the incoming base ($B^-$) or water to give the conjugate base ($A^-$) and HB. The diffusion layer has a thickness $h$; the model specifies that, for the limit $X = h$, [HA] and $[A^-]$ are effectively zero under sink conditions.

The model also specifies that, at steady state, the acid–base reaction occurs anywhere within the diffusion layer and any equilibrium formed between the reacting species is regarded as being established instantaneously, *i.e.*, the diffusional processes are slow relative to the chemical

0022-3549/81/0100-0013$01.00/0
© 1981, American Pharmaceutical Association

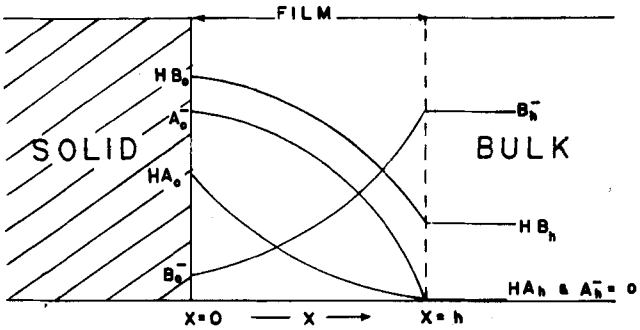


**Figure 1**—*Schematic diagram of the model of Higuchi* et al. *(5) for the dissolution of an acid, HA, into a reactive medium containing base, $B^-$ ($A^-$ and HB are products of the reaction).*

processes (reaction). Individual diffusivities for all components must be accounted for in the model.

The present model describes the dissolution of an acid in a system where the only reactive base species are hydroxide ion and water. The equilibria involved are given in Schemes I and II.

$$H_2O + HA \overset{K_a^*}{\rightleftharpoons} H_3O^+ + A^-$$

*Scheme I*

$$H_3O^+ + OH^- \rightleftharpoons 2\,H_2O$$

*Scheme II*

For simplicity, $H_3O^+$ may be regarded as hydrogen ion ($H^+$). When the equilibria are combined, they produce the situation shown in Scheme III, which also was used by Higuchi *et al.* (5).

$$HA + OH^- \overset{K_1^*}{\rightleftharpoons} H_2O + A^-$$

*Scheme III*

In the model of Higuchi *et al.* (5), only Scheme III was considered for the chemical reaction of HA with hydroxide ion. By including the equilibria of Schemes I and II, the general applicability of this model is broadened.

The equilibrium constants for Schemes I–III are given by:

$$K_a = \frac{[H^+][A^-]}{[HA]} \quad \text{(Eq. 1)}$$

$$K_w = [H^+][OH^-] \quad \text{(Eq. 2)}$$

$$K_1 = \frac{[A^-]}{[HA][OH^-]} \quad \text{(Eq. 3)}$$

where $[H_2O]$ is regarded as constant and is included in the relevant equilibrium constants and $H_3O^+$ is equivalent to $H^+$.

**Application of Fick's Laws of Diffusion to Dissolution with Simultaneous Chemical Reaction**—When a chemical reaction occurs between diffusing species, the mass balance of any species across the diffusion layer involves not only diffusion into and out of any element but also the chemical reaction, which simultaneously changes the effective concentrations of the species at any given point $X$. To account for the simultaneous chemical reaction, a reaction rate function, $\phi$, is introduced into the steady-state equations for each species. At present, this function will remain undefined. At steady state and by utilizing Fick's laws of diffusion, the following equations can be written for all of the relevant species:

$$\frac{\partial[HA]}{\partial t} = D_{HA}\frac{\partial^2[HA]}{\partial X^2} + \phi_1 = 0 \quad \text{(Eq. 4)}$$

$$\frac{\partial[OH^-]}{\partial t} = D_{OH}\frac{\partial^2[OH^-]}{\partial X^2} + \phi_2 = 0 \quad \text{(Eq. 5)}$$

$$\frac{\partial[A^-]}{\partial t} = D_A\frac{\partial^2[A^-]}{\partial X^2} + \phi_3 = 0 \quad \text{(Eq. 6)}$$

$$\frac{\partial[H^+]}{\partial t} = D_H\frac{\partial^2[H^+]}{\partial X^2} + \phi_4 = 0 \quad \text{(Eq. 7)}$$

where $\phi_{1\text{-}4}$ are the reaction rate functions. Equations 4–7 are equal to zero under steady-state conditions. When a chemical reaction occurs in the diffusion layer between species, there is a finite rate of change of flux with $X$. Alternatively, the concentration profile of a species across the diffusion layer is not represented by a simple linear relationship, as in the Noyes–Whitney model, but instead by a curve whose rate of change of the slope at any point is dependent on the reaction of that species at that point.

Independently of Eqs. 4–7, relationships between rates of change of flux for the various species can be described by mass balance equations across the diffusion layer. Therefore, by mass balance:

$$D_{HA}\frac{d^2[HA]}{dX^2} = -D_A\frac{d^2[A^-]}{dX^2} \quad \text{(Eq. 8)}$$

and:

$$D_{OH}\frac{d^2[OH^-]}{dX^2} = D_{HA}\frac{d^2[HA]}{dX^2} + D_H\frac{d^2[H^+]}{dX^2} \quad \text{(Eq. 9)}$$

Equation 8 shows that any change in the HA flux due to a chemical reaction must mean that the flux of $A^-$ changes in the opposite direction. Equation 9 states that $OH^-$, while diffusing in, will react with both HA and $H^+$ simultaneously as defined by the equilibrium constants in Schemes I and II. Hence, any change in the flux of $OH^-$ must be reflected by corresponding changes in HA and $H^+$. Comparing Eqs. 8 and 9 to Schemes I and II and Eqs. 1–7 shows that:

$$\phi_1 = -\phi_3 \quad \text{(Eq. 10)}$$

or:

$$D_A\frac{d^2[A^-]}{dX^2} = \phi_1 \quad \text{(Eq. 11)}$$

and:

$$\phi_2 = \phi_1 + \phi_4 \quad \text{(Eq. 12)}$$

Integrating Eqs. 8 and 9 once gives:

$$D_{HA}\frac{d[HA]}{dX} = D_{OH}\frac{d[OH^-]}{dX} - D_H\frac{d[H^+]}{dX} + C_1 \quad \text{(Eq. 13)}$$

$$D_{HA}\frac{d[HA]}{dX} = -D_A\frac{d[A^-]}{dX} + C_2 \quad \text{(Eq. 14)}$$

where $C_1$ and $C_2$ are constants of integration. It can be shown that $C_1$ and $C_2$ are equal by mass balance considerations based on Schemes I and III. Substituting for $C_2$ in Eq. 14 and integrating with respect to $X$ in Eqs. 13 and 14 give the following linear equations:

$$D_{HA}[HA] = D_{OH}[OH^-] - D_H[H^+] + C_1X + C_4 \quad \text{(Eq. 15)}$$

and:

$$D_{HA}[HA] = -D_A[A^-] + C_1X + C_3 \quad \text{(Eq. 16)}$$

where $C_3$ and $C_4$ are additional constants of integration.

Equations 15 and 16 must be given boundary conditions to allow evaluation of the resulting constants.

**Boundary Conditions**—

At $X = 0$:

$[HA]_0$ = solubility of HA
$[OH^-]_0$ = unknown
$[H^+]_0$ = unknown
$[A^-]_0$ = unknown

At $X = h$:

$[HA]_h$ = 0 (under sink conditions)
$[OH^-]_h$ = from bulk pH
$[H^+]_h$ = from bulk pH
$[A^-]_h$ = 0 (under sink conditions)

**Evaluation of Constants and Conditions at $X = 0$**—Utilizing these boundary conditions ($X = 0$ and $X = h$), Eqs. 15 and 16 and 2 and 3 at $X = 0$, and algebraically solving for $[H^+]_0$ yield:

$$-D_H[H^+]_0^2 + [H^+]_0(D_H[H^+]_h - D_{OH}[OH^-]_h) + K_w(D_{OH} + D_AK_1[HA]_0) = 0 \quad \text{(Eq. 17)}$$

Equation 17 is of the type:

$$az^2 + bz + c = 0 \quad \text{(Eq. 18)}$$

where:

$z = [H^+]_0$
$a = -D_H$
$b = D_H[H^+]_h - D_{OH}[OH^-]_h$

$$c = K_w(D_{OH} + D_A K_1[HA]_0)$$

the solution of which is:

$$z = \frac{-b \pm \sqrt{b^2 - 4ac}}{2a} \quad \text{(Eq. 19)}$$

By considering the possible signs of the coefficients $a$, $b$, and $c$ in Eq. 19, it may be shown that only:

$$z = \frac{-b - \sqrt{b^2 - 4ac}}{2a} \quad \text{(Eq. 20)}$$

will be the correct root. Having obtained $[H^+]_0$, all of the other unknowns, including $C_1$–$C_4$, may be calculated in a sequential manner from the preceding equations since all of the constants required in the quadratic expression (Eq. 17) are known or can be estimated.

**Expression for Total Flux of Acids at Any Given Bulk Solution pH**—The concentrations of all species at the solid–liquid interface, *i.e.*, where $X = 0$, can be calculated. An expression for the total flux of the dissolving acid is now required as a function of changing conditions in the bulk solution or at $X = h$.

Again, from Eqs. 15 and 16 and the stated boundary conditions:

$$C_1 = -\left(\frac{D_{HA}[HA]_0}{h}\right) + \frac{D_H}{h}([H^+]_h - [H^+]_0) + \frac{D_{OH}}{h}([OH^-]_0 - [OH^-]_h) \quad \text{(Eq. 21)}$$

where the right side of Eq. 21 is exactly the negative of the total flux of species across the diffusion layer. Thus:

$$J^{total} = -C_1 = \frac{D_{HA}}{h}[HA]_0 + \frac{D_H}{h}([H^+]_0 - [H^+]_h) + \frac{D_{OH}}{h}([OH^-]_h - [OH^-]_0) \quad \text{(Eq. 22)}$$

and:

$$J^{total} = J_{HA} + J_H + J_{OH} = -C_1 \quad \text{(Eq. 23)}$$

where $J^{total}$ is the total flux of HA from the solid surface at $X = 0$. Paradoxically, there is no expression relating the flux for the diffusion of $A^-$ across the diffusion layer because the fluxes of $H^+$ and $OH^-$ automatically account for that of $A^-$. Equation 22 differs from that derived by Higuchi *et al.* (5) in that it includes the terms for $[H^+]$, but it is similar to the equations of Hamlin and Higuchi (7) and Tsuji *et al.* (17).

It is important to examine some conditions where the different parts of Eq. 22 exert their influence on the total flux or dissolution rate from the solid surface.

1. The case where the bulk pH is considerably lower than the pKa of the dissolving acid, *i.e.*, $[H^+]_h \gg K_a$. Under this condition, the ionization of the acid is suppressed within the diffusion layer, making $[H^+]_0$ and $[H^+]_h$ (and, hence, $[OH^-]_0$ and $[OH^-]_h$) equal. The total flux then is given by:

$$J^{total} = \frac{D_{HA}[HA]_0}{h} \quad \text{(Eq. 24)}$$

for the case of sink conditions (*i.e.*, $[HA]_0 \gg [HA]_h$).

2. The case where the bulk solution pH is increased such that it no longer suppresses ionization in the film. Thus, HA is able to dissociate (due to interaction with water) as described by Scheme I and Eq. 1.

Hence, in pH regions around the pKa of the acid and up to neutrality in the bulk solution, the dominant form of the equation is:

$$J^{total} = \frac{D_{HA}[HA]_0}{h} + \frac{D_H}{h}([H^+]_0 - H^+]_h) \quad \text{(Eq. 25)}$$

The flux of $OH^-$ will not be zero, but, in this region, it is negligible compared to the flux of HA and $H^+$.

3. The case where the bulk solution pH is increased such that $[OH^-]_h$ approaches $[HA]_0$. The controlling factor in dissolution now is the diffusion of hydroxide ion into the diffusion layer and the reaction with HA as given by the equilibrium described in Scheme III and Eq. 3.

Thus, as HA is diffusing across the diffusion layer, the reaction with water and hydroxide ion occurs simultaneously. Hence, the total flux now is given by the full expression described in Eq. 22.

Therefore, for an accurate description of the total flux of acid where water and hydroxide ion are the only reactants in the bulk solution, it is necessary to consider $[HA]_0$, the intrinsic solubility of the acid, $K_a$, the dissociation constant of the acid, and the diffusivities of the acid, hydrogen, and hydroxide ions.

The concentrations of all of the species may be determined at any point $X$ in the diffusion layer to observe their concentration profiles. At any distance across the diffusion layer ($X = X$), Eqs. 2, 3, 15, and 16 apply. The unknowns [HA], $[A^-]$, $[OH^-]$, and $[H^+]$, without subscripts, represent the concentrations of the respective species at position $X$ in the diffusion layer. The process of solving for a particular unknown is similar to that given in the previous section for the solution at $X = 0$, except that [HA] also is an unknown. The $C_1$, $C_4$, and $C_3$ values previously were numerically determined from bulk solution boundary conditions in solving for the concentration of a species at $X = 0$.

The concentration of any one species may be solved for, but $[H^+]$ will give better insight at any particular position in the film. Hence, using Eqs. 3 and 15 to convert $[OH^-]$ to terms in $[H^+]$:

$$D_{HA}[HA] = \frac{D_{OH}K_w}{[H^+]} - D_H[H^+] + C_1X + C_4 \quad \text{(Eq. 26)}$$

To express [HA] in terms of $[H^+]$, Eqs. 3 and 16 must be used:

$$D_{HA}[HA] = \frac{-D_A[HA]K_1K_w}{[H^+]} + C_1X + C_3 \quad \text{(Eq. 27)}$$

Collecting terms in Eq. 27:

$$[HA] = (C_1X + C_3)\left(\frac{[H^+]}{D_{HA}[H^+] + D_AK_1K_w}\right) \quad \text{(Eq. 28)}$$

Equation 28 now may be substituted into Eq. 26 to give:

$$D_{HA}(C_1X + C_3)\left(\frac{[H^+]}{D_{HA}[H^+] + D_AK_1K_w}\right) = \frac{D_{OH}K_w}{[H^+]} - D_H[H^+] + C_1X + C_4 \quad \text{(Eq. 29)}$$

Multiplying Eq. 29 by $[H^+]$ $(D_{HA}[H^+] + D_AK_1K_w)$ and collecting terms give:

$$p[H^+]^3 + q[H^+]^2 + r[H^+] + s = 0 \quad \text{(Eq. 30)}$$

where:

$$p = -D_AD_{HA}$$
$$q = C_4D_{HA} - C_3D_{HA} - D_AK_1K_wD_H$$
$$r = K_w(D_{HA}D_{OH} + C_4D_AK_1 + C_1XD_AK_1)$$
$$s = D_AD_{OH}K_1K_w^2$$

The form of Eq. 30 is cubic, with the relevant coefficients being represented as $p$, $q$, $r$, and $s$ as defined. As such, Eq. 30 has three roots for $[H^+]$. The correct solution was found by the iterative method of Newton (20) utilizing a digital computer[1].

Once $[H^+]$ is calculated from Eq. 30, sequential solution of Eqs. 15, 16, 2, and 3 enables $[OH^-]$, [HA], and $[A^-]$ to be determined and the diffusion layer profiles for all species to be calculated.

**Calculation of Film Thickness ($h$)**—The Levich rotating-disk model provides a technique for following the dissolution of a solid drug from a compressed disk that maintains a constant surface area during dissolution. The Levich (15) model defines the film thickness as:

$$h = 1.612D^{1/3}\nu^{1/6}\omega^{-1/2} \quad \text{(Eq. 31)}$$

where $D$ is the diffusivity, $\nu$ is the kinematic viscosity of the medium, and $\omega$ is the angular velocity in radians per unit time.

The Levich theory used here is based on a single diffusing species with the boundary layer thickness dependent on the diffusion coefficient of that species to the one-third power (15). In the current study, there are several diffusing species with different transport properties; thus, the assumption of a constant-thickness boundary layer may not be correct where the diffusivity of a possible reaction- and flux-controlling species, *e.g.*, hydroxide ion, is significantly different from that of the acid, HA. As will be seen later, the total flux equation (Eq. 22) can collapse to where the diffusivity of hydroxide ion becomes a dominant term. Thus, the error contribution to the calculated fluxes could occur only at high pH. However, the differences in the calculated boundary layer thickness considering the differences in the diffusivities are dampened by the one-third power dependency of the thickness on diffusivity. Although it may be possible to derive a theoretical extension of the Levich approach for a multispecies system, it will be assumed that the simplified theory of a single-thickness layer presented here is reasonable considering the scope and intent of this work.

The Noyes–Whitney or Nernst–Brünner model describes the flux ($J$)

[1] Honeywell model 66/60. A copy of the procedure and program can be obtained from V. J. Stella.

of the acid under sink conditions, where no chemical reactions occur, as $J = D_{HA}C_s/h$, where $C_s$ is $[HA]_0$.

By combining this equation and Eq. 31, the following expression is obtained:

$$J = 0.62D_{HA}^{2/3}\nu^{-1/6}C_s\omega^{1/2} \quad \text{(Eq. 32)}$$

where $J$ is proportional to the square root of the rotation speed.

## EXPERIMENTAL

**Materials**—Benzoic acid[2], 2-naphthoic acid[3], and indomethacin[4] were obtained in the pure, crystalline form. Benzoic acid was used as supplied, while 2-naphthoic acid was recrystallized from 95% ethanol according to the method of Perrin *et al.* (21). Indomethacin, despite high purity, was not in a suitable form for disk formation under high compression. Using a method described by Pakula *et al.* (22), the $\alpha$-form of indomethacin was prepared, which is the lowest melting form of the compound but has been shown by Pakula *et al.* (23) to be stable.

All other chemicals were reagent grade and were not purified further.

**Solubility and pKa Determinations**—The intrinsic solubility (*i.e.*, the solubility of the undissociated species) of a monoprotic weak acid and its corresponding pKa may be determined simultaneously by measuring the total solubility of the acid as a function of pH under controlled ionic strength and temperature conditions. This method was described previously (24, 25) and is readily applied to compounds of poor aqueous solubility. This solubility method was used to determine the solubilities and pKa values of the acids at an ionic strength of 0.5 (with potassium chloride) and 25 ± 0.5° in a range of hydrochloric acid or 0.1 *M* acetate buffers.

Excess solid acid was shaken for at least 48 hr in vials containing ~10 ml of buffer at 25 ± 0.5° in a shaking water bath[5]. In all cases, 48 hr was sufficient for obtaining equilibrium solubility. Indomethacin is subject to decomposition by light and hydrolysis (26–28) in aqueous solutions. By excluding light from the vials and optimizing the equilibration time, these problems were shown to be insignificant. It was approximated from data given by previous investigators that the half-life for hydrolysis in the pH region of interest (pH 2–5) was considerably longer than the time required for equilibration during the solubility studies.

After equilibration, the solutions were filtered using a 5.0-$\mu$m membrane filter[6], and portions of the filtrate were diluted appropriately with 0.1 *M* HCl. Concentrations of all compounds were measured using a UV–visible spectrophotometer[7] with the appropriately diluted buffer solution as the reference. The wavelengths and molar absorptivity for measurement of the three acids are given in Table I. The pH of the filtrate prior to detection was measured at 25° using a combination microelectrode[8] and a pH meter[8]. All samples were run at least in duplicate.

**Determination of Dissolution Rates**—The procedure for following the initial dissolution rates of the three acids was similar to that of Tsuji *et al.* (17) and Underwood and Cadwallader (13). The apparatus (Fig. 2) was based on the rotating-disk method of Nogami *et al.* (29) and Wood *et al.* (14). It consisted of three main parts: the dissolution cell and rotating disk, the pH-stat with a measuring electrode, and the detection system for continuous monitoring of the bulk solution concentration in the dissolution cell.

The dissolution cell consisted of a water-jacketed beaker maintained at 25 ± 0.1°[9]. The dissolution medium (250 ml) was placed in the cell into which was immersed a combination pH electrode, a Plexiglas disk holder[10] with a shaft, and a titrant delivery tube. Also, two sampling tubes, which were connected to a flowthrough system, were placed in the solution at set positions to sample and return the solution during a dissolution run.

The shaft and disk holder were rotated by an overhead synchronous motor of variable speed[11] that was calibrated by a tachometer[12]. Disks of solid material, previously compressed to a precise size, were inserted into the holder to form a surface flush with that of the disk holder. The

**Table I—Spectral Characteristics of the Three Carboxylic Acids Used in Solubility Studies (25°)**

| Compound | $\lambda_{max}$, nm | $\epsilon_{molar}$ | Solvent for Measurement |
|---|---|---|---|
| Benzoic acid | 229 | 11,375 | 0.01 *M* HCl |
| 2-Naphthoic acid | 235 | 54,332 | 0.01 *M* HCl |
| Indomethacin | 264 | 17,926 | 0.01 *M* HCl or 0.1 *M* acetate buffer |

pH electrode and titrant tubing were connected to the pH-stat assembly, which continuously monitored the pH of the medium during a dissolution run and delivered titrant to maintain a predetermined pH within that medium. Once steady-state conditions were reached during a dissolution run, the titrant was delivered at a constant rate, which was dependent on the release rate of acid from the disk and the concentration of titrant used. In all cases, sodium hydroxide solution was the titrant and ranged from 0.01 to 0.5 *M*, depending on the acid and the pH being maintained.

The continuous monitoring device was a flow system with a UV spectrophotometer[13]. The spectrophotometer, equipped with a flowcell with a 1-cm path length, was set to measure the acid concentration in the bulk solution at the optimum wavelength of absorbance for each compound after standardization. A peristaltic pump[14] circulated the solution using silicon tubing of fine bore (4.1 mm o.d. × 0.76 mm i.d.); the remainder of the tubing was made of polytef[15] (1.5 mm o.d. × 0.8 mm i.d.) to reduce potential adsorption during an experiment.

When dissolution experiments were performed under acidic conditions (*i.e.*, pH 2.00), the pH-stat system was not required due to the suppression of any ionization of the dissolving acid. However, to maintain consistent hydrodynamics between runs performed at varying pH, the pH electrode and delivery tubing were not removed. To determine if the compounds dissolved by a diffusion-controlled mechanism, the dissolution rates of the acids were measured (where possible) at pH 2.00 over a range of rotation speeds.

**Disk Preparation**—Individual disks of 200–500 mg of each compound were compressed at $4.5 \times 10^3$ kg for 1 min using an IR potassium bromide pellet punch and die[16] in a hydraulic press[17]. The disks were 1.3 cm in diameter and of varying thickness, depending on the amount and compressibility of the material used. Benzoic acid and 2-naphthoic acid were compressed directly, but indomethacin presented some difficulty due to capping. The $\gamma$-polymorph of indomethacin (mp 160–162°) was the

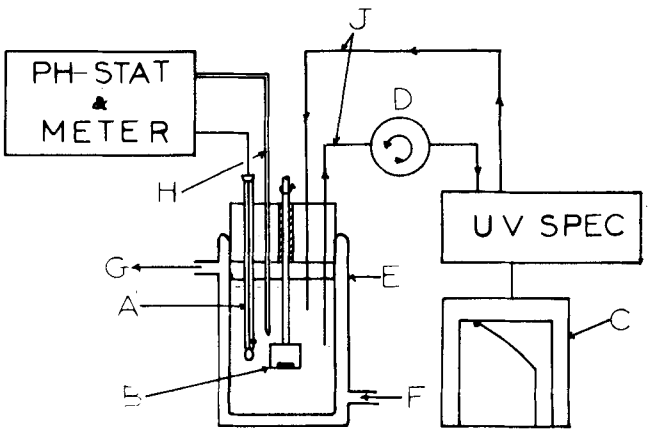


**Figure 2**—*Diagram of the rotating disk and cell, the pH-stat and concentration monitoring devices, the combination electrode (A), the Plexiglas disk holder with disk (B), the recorder for concentration* versus *time readout (C), the peristaltic pump (D), the thermostated-jacketed dissolution cell (E), the water jacket inlet (F), the water jacket outlet (G), the delivery tubing from the pH-stat (H), and the circulating tubing for the UV flowcell (J).*

[2] Fisher Scientific Co., Fair Lawn, N.J.
[3] Aldrich Chemical Co., Milwaukee, Wis.
[4] Merck Sharp & Dohme, West Point, Pa.
[5] American Optical Corp., Buffalo, N.Y.
[6] Gellman Metrical, 13 mm.
[7] Cary Instruments model 118.
[8] Radiometer Instruments, Copenhagen, Denmark.
[9] Model Fe Haake Instruments, Karlsruhe, West Germany.
[10] Manufactured at the University of Kansas.
[11] Model T2, G. K. Heller Corp., Floral Park, Long Island, N.Y.
[12] Tak-ette, Power Instruments, Skokie, Ill.
[13] Carl Zeiss, New York, N.Y.
[14] Masterflex, Cole-Parmer, Chicago, Ill.
[15] Rainin Instrument Co., Brighton, Mass.
[16] Coleman Products, England.
[17] Carver Press, Fred Carver, N.J.

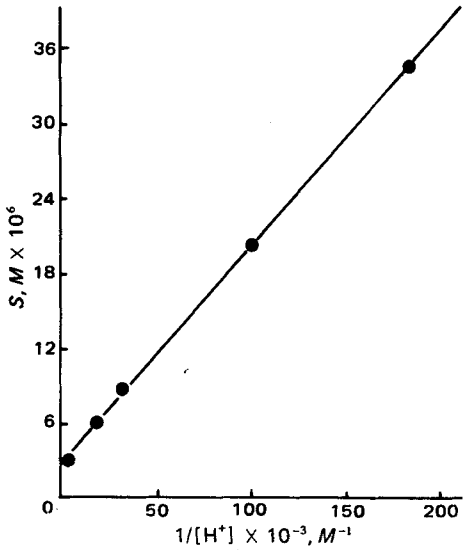


**Figure 3**—*Plot of total solubility of indomethacin at 25° versus 1/[H⁺] for equilibrated 0.1 M acetate buffers, μ = 0.5 (potassium chloride); $S_0$ is obtained from the intercept, and $K_a$ is obtained from the slope.*

worst for disk formation, while the α-form was suitable.

According to IR measurements (23) before and after compression, no appreciable amount of γ-indomethacin was formed during compression so the disks were regarded as being of uniform α-indomethacin. Where disk formation was hindered by capping and sticking, the material was compressed once, ground, and recompressed. Again, no apparent polymorphic changes were observed in the slugged α-indomethacin. It was assumed that the surface area of the disk did not change during dissolution, even though some pitting was seen with the more soluble compounds.

The rotation speed of the mounted disk was varied from 50 to 900 rpm, which corresponds to Reynolds numbers of 226–3983 as defined by:

$$Re = \frac{r^2\omega}{\nu} \qquad \text{(Eq. 33)}$$

where $Re$ is the dimensionless Reynolds number and $r$ is the radius of the disk. The Reynolds number range calculated here is well below that quoted by Levich (15) for transition from laminar to turbulent flow at the disk surface.

## RESULTS AND DISCUSSION

**Solubility and pKa**—The total solubility of a monoprotic weak acid in aqueous solution is equal to the sum of the concentrations of the species appearing in solution at equilibrium, *i.e.*:

$$S = [HA]_0 + [A^-] \qquad \text{(Eq. 34)}$$

where $S$ represents the total solubility and $[HA]_0$ and $[A^-]$ are as defined previously. Combining Eq. 34 with the $K_a$ expression for the acid yields:

$$S = [HA]_0 + \frac{K_a[HA]_0}{[H^+]} \qquad \text{(Eq. 35)}$$

where $[H^+]$ is the hydrogen-ion concentration at equilibrium. A plot of

**Table II—Measured Intrinsic Solubilities and $K_a$ Values for Benzoic Acid, 2-Naphthoic Acid, and Indomethacin at 25° (±0.5°) and an Ionic Strength of 0.5 with Potassium Chloride**

| Compound | Intrinsic Solubility ($HA_0$), $M$ | $K_a$ | pKa | $r^a$ |
|---|---|---|---|---|
| Benzoic acid | $2.16 \times 10^{-2}$ | $9.25 \times 10^{-5}$ | 4.03 | 0.9999 |
| 2-Naphthoic acid | $1.3 \times 10^{-4}$ | $9.64 \times 10^{-5}$ | 4.02 | 0.9998 |
| Indomethacin | $2.62 \times 10^{-6}$ | $6.70 \times 10^{-5}$ | 4.17 | 0.9996 |

[a] Correlation coefficient from plots of $S$ *versus* $1/[H^+]$ (Eq. 35).

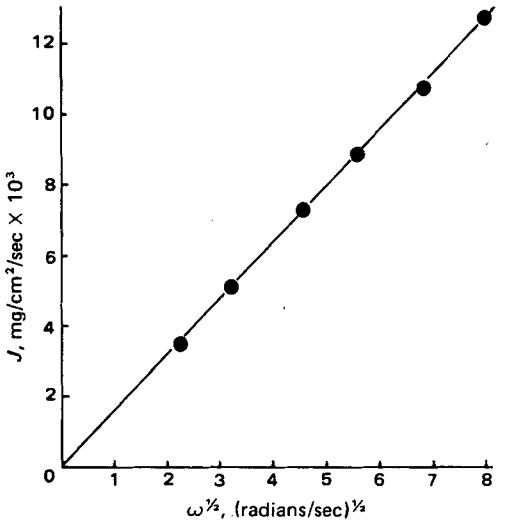


**Figure 4**—*Plot of the flux, J, of benzoic acid as a function of the square root of the rotation speed, ω, in 0.01 N HCl, μ = 0.5 (potassium chloride) at 25°.*

*S versus* $1/[H^+]$ yields an intercept of $[HA]_0$ and a slope of $K_a[HA]_0$. Dividing the intercept into the slope gives $K_a$. Figure 3 is such a plot for indomethacin. Similar plots were obtained for the other two acids, and the results are summarized in Table II.

**Dissolution Rate as Function of Rotation Speed**—The adherence to the Levich model for the dissolution of benzoic acid, 2-naphthoic acid, and indomethacin was examined. It was studied at a bulk solution pH of 2.00 for benzoic and 2-naphthoic acids. Indomethacin was too insoluble at this pH to give an accurate initial dissolution rate, especially at the lower rotation speeds. Hence, its dissolution rate study was carried out at pH 7.00.

It was assumed that the hydrodynamics at pH 7.00 were similar to those at pH 2.00. At the highest rotation speeds, an estimate of the initial dissolution rate of indomethacin was made at bulk pH 2.00. Indomethacin dissolution rates at pH 7.00, as a function of rotation speeds, were de-

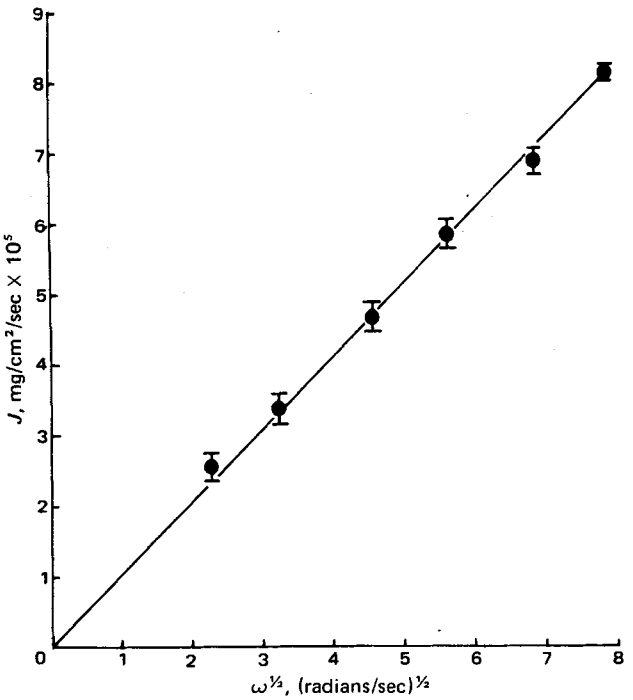


**Figure 5**—*Plot of the flux, J, of 2-naphthoic acid as a function of the square root of the rotation speed, ω, in 0.01 N HCl, μ = 0.5 (potassium chloride) at 25°. The error bars represent the standard deviation for each point.*

**Table III—Data Obtained from Plots of $J$ *versus* $\omega^{1/2}$ for Benzoic Acid, 2-Naphthoic Acid, and Indomethacin**

| Compound | Slope (Levich Plots)[a] | Calculated Diffusivity from Slope, cm²/sec | $r^b$ |
|---|---|---|---|
| Benzoic acid | $1.594 \times 10^{-3}$ | $9.6 \times 10^{-6}$ [c] | 0.9996 |
| 2-Naphthoic acid | $1.003 \times 10^{-5}$ | $6.1 \times 10^{-6}$ [c] | 0.9986 |
| Indomethacin | $4.889 \times 10^{-6}$ | $5.0 \times 10^{-6}$ [c,d] | 0.9613 |

[a] Slope = $0.62D^{2/3}\nu^{-1/6}C_s$ from Eq. 36. [b] Correlation coefficient for least-squares linear plot of $J$ *versus* $\omega^{1/2}$. [c] Using $\nu = 9.77 \times 10^{-3}$ Stokes from Ref. 31. [d] Surface pH calculated from Eq. 20.

termined with the pH-stat to maintain the bulk solution pH. It was assumed that a change in the rotation speed did not affect the mixing of the added base during dissolution. The results of the dissolution rates *versus* $\omega^{1/2}$ are given for each compound in Figs. 4–6. A summary of the slopes and diffusivities is given in Table III.

The linearity, intercepts, and slopes obtained in Figs. 4 and 5 suggest that a truly diffusion-controlled mechanism operates in the dissolution of benzoic and 2-naphthoic acids under acidic bulk pH. However, the indomethacin data do not agree with the theory in view of the pronounced nonzero intercept. The results suggest that dissolution occurs when the disk is static. The Levich theory considers only a forced-convection component due to rotation and ignores other mechanisms, such as natural convection, which may occur at low rotation speeds.

There are several possible reasons for the nonzero intercept with indomethacin. One is that the intrinsic error in the curve is large, as noted by the large standard deviations at each point, because the initial dissolution rates of indomethacin are slow and subject to greater errors than are those of the other two acids. Another possible cause is that the pH of the solution may influence the kinetics such that, with a compound as sensitive to changes in the bulk conditions as indomethacin, an additional mechanism at the surface may influence the dissolution. The possible source of this pH effect could be the assumption that the boundary layer thickness is dependent only on the diffusivity of the acid (HA) and not on the diffusivities of hydrogen and hydroxide ion, whose effects may be rotation rate dependent (see *Theoretical*). The source of an additional mechanism is unclear and was not investigated in the present study.

**Theoretical and Observed Diffusion Coefficients**—Tsuji *et al.* (17) found good agreement between diffusion coefficients derived from the Levich analysis of the dissolution rate and those determined by the diffusion cell method of Goldberg and Higuchi (30). Diffusion cell measurements were not performed for benzoic acid, 2-naphthoic acid, and indomethacin in the present study; literature values were used instead. Diffusion coefficients determined under identical conditions to those used here (25° at $\mu = 0.5$ with potassium chloride) are not found in the literature, but approximations are given in Table IV.

Flynn *et al.* (31) reviewed various ways of calculating diffusion coefficients in liquid and gaseous systems. The most commonly accepted way is to use the Stokes–Einstein equation which predicts that $D$ is proportional to $M^{-1/3}$, where $M$ is the molecular weight of the diffusing molecule.

Dayal *et al.* (34) showed that there is a good correlation between diffusivity and molecular weight to the negative one-half power of many organic compounds of pharmaceutical interest. This square root relationship would be consistent with drug molecules being planar rather than spherical.

To calculate the diffusivity from the Levich plot (Fig. 6) for indomethacin, the total concentration of ionized and unionized acid must be

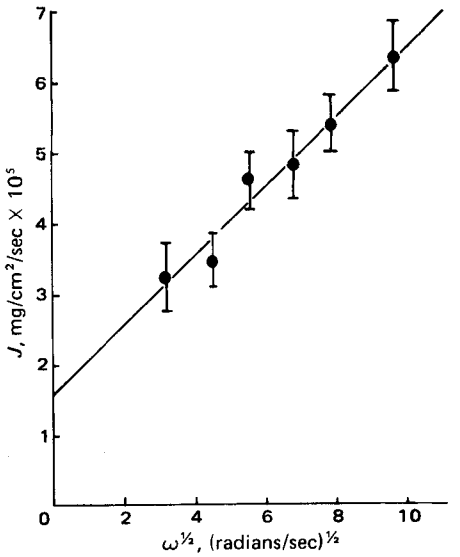


**Figure 6**—*Plot of the flux, J, of indomethacin as a function of the square root of the rotation speed, ω, in 0.5 M KCl, adjusted and maintained at pH 7.00 by a pH-stat at 25°. Error bars represent the standard deviation for each point.*

known at $X = 0$. By assuming a value of $D_A$ in Eq. 17 and also the diffusivities of $H^+$ and $OH^-$, $[H^+]_0$ for bulk pH 7.00 may be calculated. A value of $5.6 \times 10^{-6}$ cm²/sec for $D_{HA}$ was calculated from the square root relationship, using benzoic acid as the reference. Having calculated $[H^+]_0$, the total indomethacin concentration at $X = 0$ can be obtained using Eq. 35. On substitution of this value for $C_s$ into the Levich equation slope obtained from Fig. 6:

$$\text{slope} = 0.62D^{2/3}\nu^{-1/6}C_s \qquad \text{(Eq. 36)}$$

a value for the slope of $4.88 \times 10^{-6}$ is calculated. Hence, good agreement is shown between the experimental and calculated values for the slope if a $D_A$ value of $5.6 \times 10^{-6}$ cm²/sec is assumed. This substitution also was tried using the Stokes–Einstein equation as a means of estimating the indomethacin diffusivity, but it failed to give a set of values as close as those from the square root relationship. Due to the presence of swamping electrolyte in the dissolution medium (0.5 $M$ KCl) in all further calculations, the diffusivities of the conjugate bases of the acids are assumed to be equal to those of the acids.

Hydrogen and hydroxide-ion diffusivities have been discussed in the literature (32, 35–38). Many determinations have been performed using conductivity to obtain the diffusivities of the ions. However, according to Erdey-Grùz (37), care must be exercised in using diffusivity values from these sources since diffusional forces exerted on an ion in an electric field or across a potential gradient may not be identical to those in a neutral medium.

Stokes (35) determined the diffusivity of hydrochloric acid using a porous frit method and conditions similar to those employed here. He found a value of $D_H = 3.1 \times 10^{-5}$ cm²/sec at 25°, which is very close to the diffusivity of the hydroxide ion found by Higuchi *et al.* (5) in 0.75 $M$ NaCl at 25°, $D_{OH} = 2.92 \times 10^{-5}$ cm²/sec. In the present study, it will be assumed that hydrogen and hydroxide ions have equal diffusivities (ignoring the effects of dissimilar hydration and ionic geometry in solution) which approximate the value for the self-diffusion of water. The value

**Table IV—Diffusivity Data Available for Benzoic Acid, 2-Naphthoic Acid, and Indomethacin**

| Compound | Molecular Weight | $D_{exp}$[a] (25°, $\mu = 0.5$) cm²/sec | $D_{theory}$ (Stokes–Einstein), cm²/sec | $D_{theory}$[b], cm²/sec | $D_{literature}$, cm²/sec |
|---|---|---|---|---|---|
| Benzoic acid | 122.1 | $9.6 \times 10^{-6}$ | $6.63 \times 10^{-6}$ [c] | $8.90 \times 10^{-6}$ [d] | $11.0 \times 10^{-6}$ [e]<br>$12.1 \times 10^{-6}$ [e] |
| 2-Naphthoic acid | 172.2 | $6.1 \times 10^{-6}$ | $6.11 \times 10^{-6}$ [f] | $8.08 \times 10^{-6}$ [g] | — |
| Indomethacin | 357.8 | $5.6 \times 10^{-6}$ [g] | $4.80 \times 10^{-6}$ [h] | $5.60 \times 10^{-6}$ [g] | — |

[a] From Figs. 4–6. [b] Using the square root relationship. [c] Using $\rho = 1.266$ g/ml, $T = 298$°K, and $\eta = 9.97 \times 10^{-3}$ poise. [d] Using *o*-aminobenzoic acid as the reference ($D = 8.4 \times 10^{-6}$ cm²/sec) at 25° in water from Ref. 33. [e] In water at 25° ($\mu = 0$) from Refs. 5 and 22. [f] Using $\rho = 1.40$ g/ml ($T$ and $\eta$ as for benzoic acid). [g] Using benzoic acid as a comparison. [h] Using 2-naphthoic acid as a comparison.

**Table V—Initial Dissolution Rate Data for Benzoic Acid in 0.5 *M* KCl ($\mu$ = 0.5) with Varying Bulk Phase pH [a]**

| $pH_{bulk}$ | $pH_0$ [b] ($X$ = 0) | $J_{obs}$, moles/cm²/sec × $10^8$ ($\pm SD$) | $J_{theor}$ [c], moles/cm²/sec × $10^8$ |
|---|---|---|---|
| 2.00 | 2.00 | 9.39 (±0.30) | 9.06 |
| 3.00 | 2.83 | — | 9.55 |
| 4.00 | 3.05 | — | 9.93 |
| 5.00 | 3.08 | — | 9.98 |
| 6.00 | 3.08 | — | 9.99 |
| 7.00 | 3.08 | 9.60 [d] | 9.99 |
| 8.00 | 3.08 | 9.16 (±0.43) | 9.99 |
| 9.00 | 3.08 | 9.91 (±0.56) | 9.99 |
| 10.00 | 3.11 | 9.50 (±0.33) | 10.05 |
| 11.00 | 3.33 | 10.73 (±0.43) | 10.08 |
| 11.20 | 3.45 | 11.14 (±0.10) | 11.33 |
| 11.40 | 3.60 | 12.17 (±0.39) | 12.33 |
| 11.70 | 3.87 | 14.58 (±0.43) | 15.22 |
| 12.00 | 4.16 | 23.23 (±1.12) | 21.19 |
| 12.30 | 4.46 | 33.53 (±3.10) | 33.21 |
| 12.61 | 4.77 | 64.38 (±5.20) | 58.38 |
| 13.04 | 5.20 | 136.31 [d] | 141.89 |

[a] Rotation speed of the disk was 450 rpm for all dissolution rate measurements ($h = 2.31 \times 10^{-3}$ cm). [b] Calculated from Eq. 20. [c] Calculated from Eq. 22. [d] Mean taken from at least two determinations.

**Table VII—Initial Dissolution Rate Data for Indomethacin in 0.5 *M* KCl ($\mu$ = 0.5) with Varying Bulk Phase pH [a]**

| $pH_{bulk}$ | $pH_0$ [b] ($X$ = 0) | $J_{obs}$, moles/cm²/sec × $10^{12}$ ($\pm SD$) [c] | $J_{theor}$ [d], moles/cm²/sec × $10^{12}$ |
|---|---|---|---|
| 2.00 | 2.00 | 12.17 (±3.0) | 8.82 |
| 2.50 | 2.50 | — | 8.94 |
| 2.65 | 2.65 | — | 9.02 |
| 3.00 | 3.00 | 26.98 (±1.9) | 9.34 |
| 3.50 | 3.50 | — | 10.61 |
| 4.00 | 4.00 | 30.99 (±3.38) | 14.60 |
| 4.50 | 4.49 | — | 26.70 |
| 5.00 | 4.89 | 80.60 (±9.6) | 54.80 |
| 6.00 | 5.19 | 133.59 (±12.9) | 100.06 |
| 7.00 | 5.23 | 150.63 (±11.5) | 108.02 |
| 7.50 | 5.24 | 166.00 (±2.7) | 110.44 |
| 8.00 | 5.26 | 181.38 (±10.2) | 116.68 |
| 8.50 | 5.34 | 227.21 (±8.3) | 138.04 |
| 8.70 | 5.41 | 253.23 (±23.8) | 158.32 |
| 9.00 | 5.56 | 338.16 (±9.3) | 222.75 |
| 9.20 | 5.71 | — | 307.85 |
| 9.50 | 5.97 | — | 557.83 |

[a] Rotation speed of the disk was 600 rpm for all dissolution rate measurements ($h = 1.67 \times 10^{-3}$ cm). [b] Calculated from Eq. 20. [c] Standard deviation from at least three determinations. [d] Calculated from Eq. 22 and $h$ calculated from Eq. 31.

assigned to the diffusivity of hydrogen ion and hydroxide ion was $D_H = D_{OH} = 2.80 \times 10^{-5}$ cm²/sec.

**Initial Dissolution Rates as a Function of Bulk Solution pH**—The initial dissolution rates of benzoic acid, 2-naphthoic acid, and indomethacin are given in Tables V–VII. These tables include the predicted or theoretical dissolution rates based on Eq. 22. To calculate these theoretical dissolution rates for given values of $[H^+]_h$ and $[OH^-]_h$, diffusion coefficients, $[HA]_0$ values, and equilibrium constants are used as previously determined or calculated. For comparative purposes, the relative dissolution ratio, $R$, is used, which normalizes the dissolution rates of all of the acids to the rate at pH 2.00, where the undissociated species is the only diffusant; $R$ is defined by:

$$R = \frac{J}{J_0} = \left[\frac{D_{HA}[HA]_0 - D_H([H^+]_0 - [H^+]_h) + D_{OH}([OH^-]_h - [OH^-]_0)}{D_{HA}[HA]_0}\right] \quad \text{(Eq. 37)}$$

Both $R_{theor}$ (theoretical) and $R_{obs}$ (experimental) values are plotted *versus* bulk solution pH in Fig. 7. It can be seen from Eq. 37 that $R$ is independent of $h$, the diffusion layer thickness. Hence, benzoic acid and 2-naphthoic acid data obtained at 450 rpm can be compared directly to the indomethacin data obtained at 600 rpm. For the calculation of the theoretical dissolution rates, $h$, as defined by the Levich relationship, was used for each compound at its designated rotation velocity as given by Eq. 31.

Tables V–VII indicate that, in all cases, there is reasonable agreement between the theoretical and predicted quantities, $J_{theor}$, and those obtained by experiment, $J_{obs}$. The theoretical values are based entirely on equations derived previously. Only independently determined or estimated parameters (*i.e.*, $D_{HA}$ and $[HA]_0$) are used in these equations and no curve fitting actually was done.

The poorer agreement between $J_{theor}$ and $J_{obs}$ (Table VII) relative to $R_{theor}$ and $R_{obs}$ (Fig. 7) for indomethacin suggests that the value for either $D_{HA}$ or $[HA]_0$ may be off. That is, if the solubility or diffusivity of indomethacin is underestimated by ~30%, it would account for the differences noted.

Figure 8 is a plot of the pH at the solid–liquid interface, $pH_0$, calculated

**Table VI—Initial Dissolution Rate Data for 2-Naphthoic Acid in 0.5 *M* KCl ($\mu$ = 0.5) with Varying Bulk Phase pH [a]**

| $pH_{bulk}$ | $pH_0$ [b] ($X$ = 0) | $J_{obs}$, moles/cm²/sec × $10^{10}$ ($\pm SD$) [c] | $J_{theor}$ [d], moles/cm²/sec × $10^{10}$ |
|---|---|---|---|
| 2.00 | 2.00 | 4.28 (±0.18) | 4.02 |
| 2.50 | 2.50 | 4.75 (±0.01) | 4.10 |
| 2.65 | 2.65 | 4.91 (±0.25) | 4.15 |
| 3.00 | 3.00 | 4.94 (±0.13) | 4.36 |
| 3.50 | 3.49 | 5.85 (±0.17) | 5.16 |
| 4.00 | 3.91 | 7.84 (±0.34) | 7.11 |
| 4.50 | 4.15 | 10.28 (±0.64) | 9.42 |
| 5.00 | 4.24 | 11.85 (±0.15) | 10.64 |
| 6.00 | 4.28 | 13.30 (±0.40) | 11.24 |
| 7.00 | 4.28 | 13.82 (±0.61) | 11.31 |
| 8.00 | 4.29 | 13.59 (±0.43) | 11.38 |
| 8.50 | 4.29 | 14.17 (±0.97) | 11.63 |
| 9.00 | 4.32 | 14.99 (±0.24) | 12.04 |
| 9.20 | 4.35 | 16.15 (±0.56) | 12.50 |
| 9.50 | 4.41 | 18.24 (±1.07) | 13.85 |
| 10.05 | 4.69 | 27.36 (±0.70) | 22.58 |
| 10.20 | 4.80 | 34.62 (±1.45) | 28.37 |
| 10.50 | 5.07 | 56.22 (±0.92) | 49.43 |
| 10.70 | 5.27 | — | 74.90 |
| 11.00 | 5.56 | — | 144.36 |

[a] Rotation speed of the disk was 450 rpm for all dissolution rate measurements ($h = 1.99 \times 10^{-3}$ cm). [b] Calculated from Eq. 20. [c] Standard deviation from at least three determinations. [d] Calculated from Eq. 22 and $h$ calculated from Eq. 31.

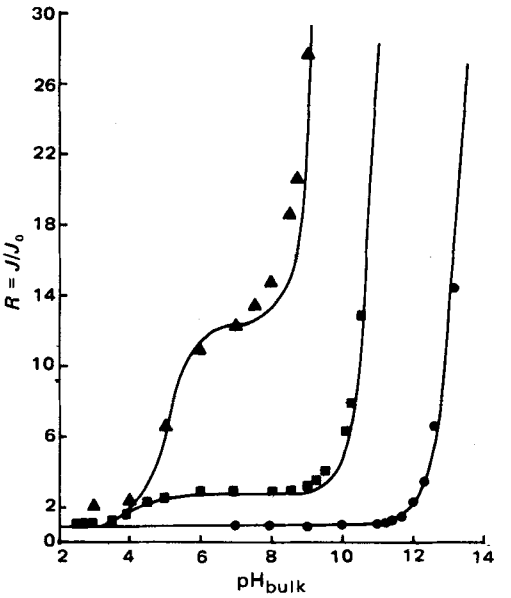


**Figure 7**—*Relative dissolution rate,* R, versus $pH_{bulk}$ *for several carboxylic acids at 25°,* $\mu$ *= 0.5 (potassium chloride) using a pH-stat to maintain constant* $pH_{bulk}$. *The solid lines are those predicted by Eq. 22, and the data points are those experimentally determined;* $J_0$ *refers to the dissolution rate at pH 2.00,* $\mu$ *= 0.5. Key:* ▲, *indomethacin;* ■, *2-naphthoic acid; and* ●, *benzoic acid.*

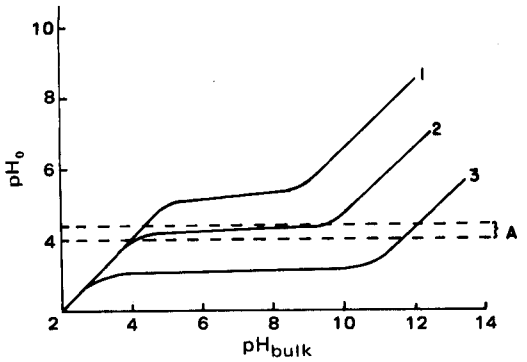


**Figure 8**—*Plot showing the relationship between the calculated pH at X = 0, $pH_0$, and $pH_{bulk}$ for the dissolution of several carboxylic acids, where water and hydroxide ion are the only bases in the dissolution medium. Key: 1, indomethacin; 2, 2-naphthoic acid; and 3, benzoic acid.*

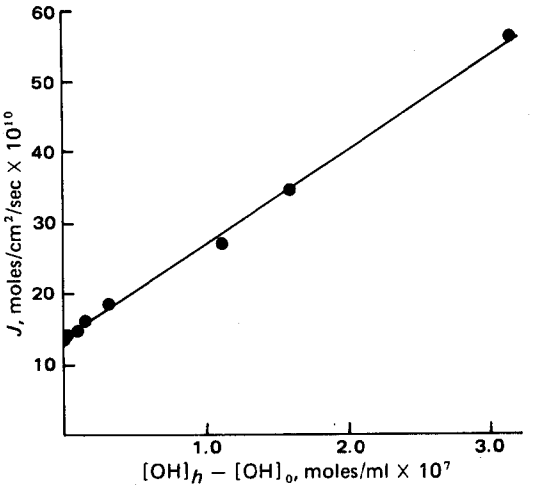


**Figure 9**—*Plot of the total dissolution rate of 2-naphthoic acid, J, as a function of the hydroxide-ion concentration difference across the diffusion layer of a rotating disk at 450 rpm.*

from Eq. 20 as a function of the bulk solution pH, $pH_{bulk}$, for each compound. In all cases, there are three clearly defined regions, which can be explained in terms of Eq. 22. The only parameters that differ between the compounds are the diffusivity ($D_{HA}$ and $D_A$) and the intrinsic solubility ($[HA]_0$), assuming that the $K_a$ values at $\mu = 0.5$ are approximately equal.

At very acidic bulk solution pH values, the pH at the solid–liquid interface equals that of the bulk because the hydrogen-ion concentration in the bulk solution is sufficient to suppress dissociation of the dissolving acids in the diffusion layer. Hence, the total concentration of the acid species at the solid–liquid interface is determined by the bulk solution pH or hydrogen-ion concentration and is the intrinsic solubility of the acid. Under these conditions, Nernst conditions exist since $pH_0$ equals $pH_{bulk}$. At lower bulk hydrogen-ion concentrations (larger $pH_{bulk}$), the acid dissociates to its conjugate base and hydrogen ions. This provides a larger total acid species concentration at $X = 0$, but hydrogen ions still limit the degree and amount of dissociation. As the bulk pH is increased or as $[H^+]_h$ decreases, benzoic acid, which is the most soluble of the acids studied, contributes to its own diffusion layer pH microenvironment at $X = 0$:

$$K_a[HA]_0 = [H^+]_0[A^-]_0 = [H^+]_0^2 \qquad \text{(Eq. 38)}$$

Alternatively, benzoic acid can be said to self-buffer the pH microenvironment of its diffusion layer. In Fig. 8, this is represented as a plateau between $pH_{bulk}$ of ~3.0 and 11.0. In this region, $pH_0$ changes very little and remains at the pH value of ~3.08. This value would be the approximate pH of a saturated benzoic acid solution in 0.5 *M* KCl at 25°. In this region, the flux expression, Eq. 22, may be approximated by:

$$J = \frac{1}{h}(D_{HA}[HA]_0 + D_H[H^+]_0) \qquad \text{(Eq. 39)}$$

Since benzoic acid self-buffers at pH ~3.0, the increase in the total benzoate species concentration at $X = 0$ over a wide range of bulk pH is only ~10% of that at bulk pH 2.00, where ionization is essentially suppressed. Therefore, the relative dissolution rate for benzoic acid changes very little in this region. 2-Naphthoic acid and indomethacin, being less soluble than benzoic acid by factors of ~$10^2$ and $10^4$, respectively, are less able to control or self-buffer the diffusion layer pH microenvironment at $X = 0$. Hence, lower hydrogen-ion concentrations in the bulk solution are required than for benzoic acid for the deviation from Nernst behavior to be observed. This change occurs at a $pH_{bulk}$ of ~4.30 for 2-naphthoic acid and at a $pH_{bulk}$ of ~5.20 for indomethacin. These pH values correspond again to those of saturated solutions of the two acids in 0.5 *M* KCl at 25°.

The plateau $pH_0$ values of 2-naphthoic acid and indomethacin correspond to 2.65 and 11.35 times, respectively, the total acid species concentration at $X = 0$ as there are at $pH_{bulk}$ 2.00. Hence, the dissolution rates of 2-naphthoic acid and indomethacin are much more sensitive to changes in the bulk solution pH. This stresses the importance of the intrinsic solubility of the acid in determining its dissolution rate dependency on pH. The $K_a$ of the acids also is important since it will determine, in combination with the intrinsic solubility, when deviation from Nernst behavior occurs with a change in bulk solution conditions.

With a further increase in the bulk solution pH, control of the dissolution rate also is affected by hydroxide ion diffusing in from the bulk solution, which reacts with the acid according to the equilibrium expression represented by Eq. 3. Thus, the total flux of the acid now includes the hydroxide-ion term, $D_{OH}([OH^-]_h - [OH^-]_0)$, because it numerically approaches the values of the other terms in the equation. A similar expression and interpretation was given by Higuchi *et al.* (5). The $pH_0$ rises at a rate that is directly dependent on the rate and amount of hydroxide ion diffusing in. Indomethacin, being poorly soluble, has little self-buffering capability and shows a sharp rise in its relative dissolution rate at a bulk pH of ~7.5. 2-Naphthoic acid is of intermediate solubility and shows a rise in its dissolution rate at a bulk pH of ~9.50 because the bulk hydroxide-ion concentration must be higher than that for indomethacin to overcome the greater self-buffering ability of 2-naphthoic acid at $X = 0$. Finally, at pH ~11.00, the considerable self-buffering capability of benzoic acid is overcome and an increase in the dissolution rate ensues with continued $pH_{bulk}$ increase.

Further information can be derived from the profiles summarized in Fig. 7 if the terminal portion of the dissolution rate *versus* $pH_{bulk}$ curve follows a limiting case of Eq. 22:

$$J = \text{constant} + \frac{D_{OH}}{h}([OH^-]_h - [OH^-]_0) \qquad \text{(Eq. 40)}$$

The $[H^+]_0 - [H^+]_h$ term in Eq. 22 is not actually constant since any change in $[OH^-]$ must give a corresponding change in $[H^+]$. However, at high bulk pH values, the hydrogen-ion term becomes negligible with respect to the hydroxide-ion term. A plot of *J versus* $[OH^-]_h - [OH^-]_0$ is shown in Fig. 9 for 2-naphthoic acid. In fact, $[OH^-]_0$ is negligible relative to $[OH^-]_h$ for all of the acids in this pH range, with a plot of *J versus* $[OH^-]_h$ having an essentially identical slope to that predicted from Eq. 40. Similar plots were made for benzoic acid and indomethacin, and the results are summarized in Table VIII.

The slopes of the three plots render values for the hydroxide-ion diffusivity that range from $2.63 \times 10^{-5}$ to $3.04 \times 10^{-5}$ cm$^2$/sec. A mean diffusivity of $2.79 \times 10^{-5}$ cm$^2$/sec was determined, and this value was chosen for $D_H$ and $D_{OH}$ in the preceding theoretical calculations. Again, the assumption was made that the boundary layer thickness, *h*, used to calculate $D_{OH}$ from the slopes in Table VIII is that calculated for the acid flux dependency on $\omega^{1/2}$. This assumption seems reasonable considering the good correlation between the experimental and calculated flux results and the consistency of the $D_{OH}$ values. Nevertheless, it is an assumption open to question.

Apart from allowing an estimate of $D_{OH}$ for this system, Eq. 40 also shows that at extremely high hydroxide-ion concentrations, the fluxes of all of the acids are identical and independent of the properties of the acid; *i.e.*, both the constant terms and $[OH^-]_0$ are negligible relative to the $[OH^-]_h$ term.

**Concentration Profiles and pH across Diffusion Layer**—Figure 10 shows idealized sections of the diffusion layer for benzoic acid, 2-naphthoic acid, and indomethacin at various bulk solution pH values. The fractional distance across the diffusion layer is calculated as $X/h$. Fractional concentrations are given by dividing the concentration of the species at $X = 0$ into that at $X = X$ in the case of HA, $A^-$, and $H^+$ or by dividing the concentration of the species at $X = h$ into that at $X = X$ for

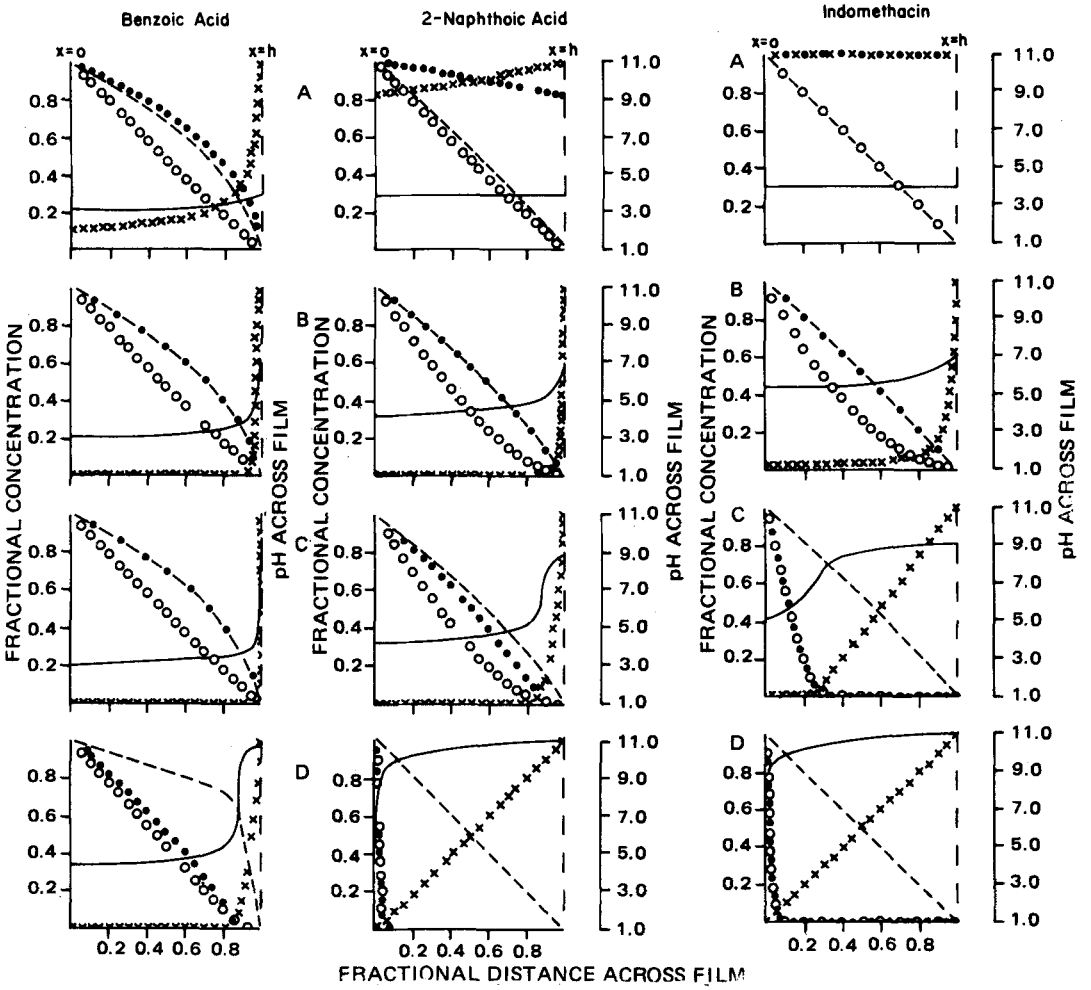


**Figure 10**—*Idealized diffusion layer cross sections for benzoic acid, 2-naphthoic acid, and indomethacin, showing the fractional concentration profiles with the fractional distance across the film as calculated from Eqs. 30 and 31. Calculated values of pH across the film in each case also are included. Key:* ○, *[HA];* – –, *[A⁻];* ●, *[H⁺];* ×, *[OH⁻];* —, *pH; A, $pH_{bulk}$ 4.00; B, $pH_{bulk}$ 7.00; C, $pH_{bulk}$ 9.00; and D, $pH_{bulk}$ 11.00.*

$OH^-$, which diffuses in the opposite direction to that of the other species. These functions normalize the data across the diffusion layer and facilitate comparison of concentration profiles for different compounds at the same bulk solution pH or for the same compound at different bulk solution pH. However, these values are useful only for comparative purposes and are obtained from the absolute data derived from Eq. 30 and its dependent equations.

The ability of benzoic acid to self-buffer the diffusion layer as $[H^+]_h$ varies is seen in Fig. 10 by observing the pH changes across the diffusion layer as a function of the bulk solution pH. Only at the rather high bulk solution pH of 11.00 does the hydroxide ion significantly affect $pH_0$ and, thus, increase the dissolution rate. 2-Naphthoic acid shows its ability to self-buffer between $pH_{bulk}$ 4.0 and 9.00, after which the diffusion of hydroxide ion begins to affect the dissolution rate. Indomethacin, as discussed previously, is less able to effect its own pH microenvironment of the diffusion layer. In this case, the bulk solution pH largely determines $pH_0$ and, therefore, the dissolution rate of the drug under these conditions.

**Table VIII—Hydroxide-Ion Diffusivity Calculated from the Slopes of the $J_{obs}$ *versus* $[OH^-]_h - [OH^-]_0$ Plots for Benzoic Acid, 2-Naphthoic Acid, and Indomethacin**

| Compound | Slope[a] × $10^8$ | $h \times 10^3$ [b], cm | $D_{OH} \times 10^5$, $cm^2/sec$ | $r$[c] |
|---|---|---|---|---|
| Benzoic acid | 1.174 | 2.29 | 2.69 | 0.9964 |
| 2-Naphthoic acid | 1.334 | 1.97 | 2.63 | 0.9987 |
| Indomethacin | 1.826 | 1.67 | 3.04 | 0.9898 |

[a] Units for $[OH^-]$ are moles per square centimeter. [b] Calculated from Eq. 31. [c] Correlation coefficient for each plot.

From the way in which the model has been developed, the diffusion layer thickness, $h$, from the Levich relationship has been taken as an absolute distance from the solid–liquid surface to where perfect mixing of the bulk solution abruptly occurs. This was shown by Levich (15), in electrochemical model systems, not to be totally correct. Rather, the concentration changes are more continuous around $X = h$. He showed that direct use of the postulated diffusion layer thickness in the Nernst relationship underestimates the true diffusion layer thickness and approximates the shape of the concentration profile. Gregory and Riddiford (39) also demonstrated that $h$ is represented more correctly by a more complex expression than that used by Levich. However, the Levich–Nernst combination is a good approximation to the real situation, as supported by the agreement between the theory and the experimental data over wide ranges of bulk solution conditions in the present study.

## CONCLUSIONS

The rotating-disk dissolution apparatus, combined with a potentiometric technique to maintain the bulk solution pH, has been demonstrated to be a convenient and precise system for the determination of dissolution rates of solid monoprotic acids into aqueous media. With minor modifications, the system is adaptable to the study of mass transport of basic compounds under similar conditions.

A theoretical approach has been presented to describe the factors that determine the dissolution rates of monoprotic acids into an unbuffered but constant pH aqueous solution where a simultaneous chemical reaction occurs with water and hydroxide ions of the bulk solution. The model adequately describes the initial dissolution rates of three carboxylic acids having a broad range of solubility properties under various pH conditions. The concept of a pH microenvironment within the diffusion layer is used

to explain the influence of several factors, such as the bulk solution pH, solubility, and diffusivity, on the dissolution rate of the acids.

## REFERENCES


(1) W. Nernst, *Z. Phys. Chem.*, **47**, 55 (1904).

(2) E. Brunner, *ibid.*, **47**, 56 (1904).

(3) C. V. King and J. S. Brodie, *J. Am. Chem. Soc.*, **59**, 1375 (1937).

(4) A. W. Hixson and S. Baum, *J. Ind. Eng. Chem.*, **36**, 528 (1944).

(5) W. I. Higuchi, E. Parrott, D. Wurster, and T. Higuchi, *J. Am. Pharm. Assoc., Sci. Ed.*, **47**, 376 (1958).

(6) W. I. Higuchi, E. Nelson, and J. G. Wagner, *J. Pharm. Sci.*, **53**, 333 (1964).

(7) W. E. Hamlin and W. I. Higuchi, *ibid.*, **55**, 205 (1966).

(8) A. Fick, *Ann. Phys.*, **94**, 59 (1855).

(9) W. H. Steinburg, H. H. Hutchins, P. G. Pick, and J. S. Lazer, *J. Pharm. Sci.*, **54**, 625 (1965).

(10) *Ibid.*, **54**, 761 (1965).

(11) A. Shah, *J. Pharm. Sci.*, **60**, 1564 (1971).

(12) J. H. Collett, J. A. Rees, and N. A. Dickinson, *J. Pharm. Pharmacol.*, **24**, 724 (1972).

(13) F. Underwood and D. Cadwallader, *J. Pharm. Sci.*, **67**, 1163 (1978).

(14) J. H. Wood, J. E. Syrato, and H. Letterman, *ibid.*, **54**, 1068 (1965).

(15) V. G. Levich, "Physico-chemical Hydrodynamics," Prentice-Hall, Englewood Cliffs, N.J., 1962.

(16) S. Prakongpan, A. H. Molokhia, K. H. Kwan, and W. I. Higuchi, *J. Pharm. Sci.*, **65**, 685 (1976).

(17) A. Tsuji, E. Nakashima, S. Hamano, and T. Yamana, *ibid.*, **67**, 1059 (1978).

(18) A. Goldberg, in "Dissolution Technology," L. J. Leeson and J. T. Carstensen, Eds., Industrial Pharmaceutical Technology Section, APhA Academy of Pharmaceutical Science, Washington, D.C., 1974.

(19) M. Gibaldi, in "The Theory and Practice of Industrial Pharmacy," L. Lachman, H. Lieberman, and J. Kanig, Eds., Lea & Febiger, Philadelphia, Pa., 1970, p. 246.

(20) B. Carnahan, H. A. Luther, and J. O. Wilkes, "Applied Numerical Methods," Wiley, New York, N.Y., 1969, p. 171.

(21) D. D. Perrin, D. R. Perrin, and W. Armarego, "Purification of Laboratory Chemicals," Pergamon, Oxford, England, 1966.

(22) R. Pakula, L. Pichnej, S. Spychala, and K. Butkiewicz, *Pol. J. Pharmacol. Pharm.*, **29**, 151 (1977).

(23) S. Spychala, K. Butkiewicz, R. Pakula, and L. Picknej, *ibid.*, **29**, 157 (1977).

(24) "Physical Pharmacy," A. N. Martin, J. Swarbrick, and A. Cammarata, Eds., Lea & Febiger, Philadelphia, Pa., 1969.

(25) E. R. Garrett and C. H. Won, *J. Pharm. Sci.*, **60**, 1801 (1971).

(26) S. Goto, W. Tseng, M. Kai, S. Aizawa, and S. Iguchi, *Yakuzaigaku*, **29**, 118 (1969).

(27) B. R. Hajratwala and J. E. Dawson, *J. Pharm. Sci.*, **66**, 27 (1977).

(28) E. Pawetczyk and B. Knitter, *Pharmazie*, **33**, 586 (1978).

(29) H. Nogami, T. Nagai, and A. Suzuki, *Chem. Pharm. Bull.*, **14**, 329 (1966).

(30) A. H. Goldberg and W. I. Higuchi, *J. Pharm. Sci.*, **57**, 1583 (1968).

(31) G. L. Flynn, S. H. Yalkowsky, and T. J. Roseman, *ibid.*, **63**, 479 (1974).

(32) R. C. Reid and T. K. Sherwood, "Properties of Gases and Liquids," McGraw-Hill, New York, N.Y., 1966.

(33) "International Critical Tables of Numerical Data, Physics, Chemistry and Technology," McGraw-Hill, New York, N.Y., 1926.

(34) S. Dayal, T. Higuchi, and I. Pitman, *J. Pharm. Sci.*, **61**, 695 (1972).

(35) R. H. Stokes, *J. Am. Chem. Soc.*, **72**, 2243 (1950).

(36) S. B. Tuwiner, "Diffusion and Membrane Technology," Reinhold, New York, N.Y., 1962, p. 378.

(37) T. Erdey-Grûz, "Transport Phenomena in Aqueous Solutions," Wiley, New York, N.Y., 1974.

(38) D. Eisenberg and W. Kauzman, "Structure and Properties of Water," Oxford University Press, New York, N.Y., 1969, pp. 217–224.

(39) D. P. Gregory and A. C. Riddiford, *J. Chem. Soc.*, **1956**, 3756.


## ACKNOWLEDGMENTS


Adapted in part from a dissertation submitted by K. G. Mooney to the University of Kansas in partial fulfillment of the Doctor of Philosophy degree requirements.

Supported by Grant GM22357 from the National Institutes of Health.


# Dissolution Kinetics of Carboxylic Acids II: Effect of Buffers


**K. G. MOONEY *, M. A. MINTUN ‡, K. J. HIMMELSTEIN, and V. J. STELLA ˣ**



Received March 24, 1980, from the *Departments of Pharmaceutical Chemistry and Chemical and Petroleum Engineering, University of Kansas, Lawrence, KS 66045.* Accepted for publication July 3, 1980.


*Present address: Boehringer Ingelheim, Ridgefield, CT 06877. ‡Present address: Washington University, St. Louis, MO 63110.



**Abstract** □ The dissolution behavior of 2-naphthoic acid from rotating compressed disks into aqueous buffered solutions of constant ionic strength ($\mu$ = 0.5 with potassium chloride) at 25° was investigated. A model was developed for the flux of a solid monoprotic carboxylic acid in aqueous buffered solutions as a function of the solution pH and the physicochemical properties of the buffer. The model assumes a diffusion layer-controlled mass transport process and a simple, instantaneously established reaction equilibrium between all reactive species (acids and bases) across the diffusion layer. Using intrinsic solubilities, pKa values, and diffusion coefficients, the model accurately predicts the dissolution of 2-naphthoic acid as a function of the bulk solution composition. The concentration profiles of all species across the diffusion layer are generated for each buffer concentration and bulk solution pH, including the pH profile within the microclimate of the diffusion layer and the pH at the solid–solution boundary.



**Keyphrases** □ Carboxylic acids—dissolution kinetics, effect of buffers □ Dissolution kinetics—carboxylic acids, effect of buffers □ Buffers—effect on dissolution kinetics of carboxylic acids


The objective of this investigation was to determine experimentally the effect of buffers on the dissolution of 2-naphthoic acid from a constant surface area pellet under controlled ionic strength ($\mu$ = 0.5 with potassium chloride), temperature (25°), and pH conditions (pH-stat). A model, an extension of one described previously (1), also was de-




0022-3549/81/0100-0022$01.00/0


© 1981, American Pharmaceutical Association

to explain the influence of several factors, such as the bulk solution pH, solubility, and diffusivity, on the dissolution rate of the acids.

## REFERENCES


(1) W. Nernst, *Z. Phys. Chem.*, **47**, 55 (1904).

(2) E. Brunner, *ibid.*, **47**, 56 (1904).

(3) C. V. King and J. S. Brodie, *J. Am. Chem. Soc.*, **59**, 1375 (1937).

(4) A. W. Hixson and S. Baum, *J. Ind. Eng. Chem.*, **36**, 528 (1944).

(5) W. I. Higuchi, E. Parrott, D. Wurster, and T. Higuchi, *J. Am. Pharm. Assoc., Sci. Ed.*, **47**, 376 (1958).

(6) W. I. Higuchi, E. Nelson, and J. G. Wagner, *J. Pharm. Sci.*, **53**, 333 (1964).

(7) W. E. Hamlin and W. I. Higuchi, *ibid.*, **55**, 205 (1966).

(8) A. Fick, *Ann. Phys.*, **94**, 59 (1855).

(9) W. H. Steinburg, H. H. Hutchins, P. G. Pick, and J. S. Lazer, *J. Pharm. Sci.*, **54**, 625 (1965).

(10) *Ibid.*, **54**, 761 (1965).

(11) A. Shah, *J. Pharm. Sci.*, **60**, 1564 (1971).

(12) J. H. Collett, J. A. Rees, and N. A. Dickinson, *J. Pharm. Pharmacol.*, **24**, 724 (1972).

(13) F. Underwood and D. Cadwallader, *J. Pharm. Sci.*, **67**, 1163 (1978).

(14) J. H. Wood, J. E. Syrato, and H. Letterman, *ibid.*, **54**, 1068 (1965).

(15) V. G. Levich, "Physico-chemical Hydrodynamics," Prentice-Hall, Englewood Cliffs, N.J., 1962.

(16) S. Prakongpan, A. H. Molokhia, K. H. Kwan, and W. I. Higuchi, *J. Pharm. Sci.*, **65**, 685 (1976).

(17) A. Tsuji, E. Nakashima, S. Hamano, and T. Yamana, *ibid.*, **67**, 1059 (1978).

(18) A. Goldberg, in "Dissolution Technology," L. J. Leeson and J. T. Carstensen, Eds., Industrial Pharmaceutical Technology Section, APhA Academy of Pharmaceutical Science, Washington, D.C., 1974.

(19) M. Gibaldi, in "The Theory and Practice of Industrial Pharmacy," L. Lachman, H. Lieberman, and J. Kanig, Eds., Lea & Febiger, Philadelphia, Pa., 1970, p. 246.

(20) B. Carnahan, H. A. Luther, and J. O. Wilkes, "Applied Numerical Methods," Wiley, New York, N.Y., 1969, p. 171.

(21) D. D. Perrin, D. R. Perrin, and W. Armarego, "Purification of Laboratory Chemicals," Pergamon, Oxford, England, 1966.

(22) R. Pakula, L. Pichnej, S. Spychala, and K. Butkiewicz, *Pol. J. Pharmacol. Pharm.*, **29**, 151 (1977).

(23) S. Spychala, K. Butkiewicz, R. Pakula, and L. Picknej, *ibid.*, **29**, 157 (1977).

(24) "Physical Pharmacy," A. N. Martin, J. Swarbrick, and A. Cammarata, Eds., Lea & Febiger, Philadelphia, Pa., 1969.

(25) E. R. Garrett and C. H. Won, *J. Pharm. Sci.*, **60**, 1801 (1971).

(26) S. Goto, W. Tseng, M. Kai, S. Aizawa, and S. Iguchi, *Yakuzaigaku*, **29**, 118 (1969).

(27) B. R. Hajratwala and J. E. Dawson, *J. Pharm. Sci.*, **66**, 27 (1977).

(28) E. Pawetczyk and B. Knitter, *Pharmazie*, **33**, 586 (1978).

(29) H. Nogami, T. Nagai, and A. Suzuki, *Chem. Pharm. Bull.*, **14**, 329 (1966).

(30) A. H. Goldberg and W. I. Higuchi, *J. Pharm. Sci.*, **57**, 1583 (1968).

(31) G. L. Flynn, S. H. Yalkowsky, and T. J. Roseman, *ibid.*, **63**, 479 (1974).

(32) R. C. Reid and T. K. Sherwood, "Properties of Gases and Liquids," McGraw-Hill, New York, N.Y., 1966.

(33) "International Critical Tables of Numerical Data, Physics, Chemistry and Technology," McGraw-Hill, New York, N.Y., 1926.

(34) S. Dayal, T. Higuchi, and I. Pitman, *J. Pharm. Sci.*, **61**, 695 (1972).

(35) R. H. Stokes, *J. Am. Chem. Soc.*, **72**, 2243 (1950).

(36) S. B. Tuwiner, "Diffusion and Membrane Technology," Reinhold, New York, N.Y., 1962, p. 378.

(37) T. Erdey-Grûz, "Transport Phenomena in Aqueous Solutions," Wiley, New York, N.Y., 1974.

(38) D. Eisenberg and W. Kauzman, "Structure and Properties of Water," Oxford University Press, New York, N.Y., 1969, pp. 217–224.

(39) D. P. Gregory and A. C. Riddiford, *J. Chem. Soc.*, **1956**, 3756.


## ACKNOWLEDGMENTS


Adapted in part from a dissertation submitted by K. G. Mooney to the University of Kansas in partial fulfillment of the Doctor of Philosophy degree requirements.

Supported by Grant GM22357 from the National Institutes of Health.


# Dissolution Kinetics of Carboxylic Acids II: Effect of Buffers


**K. G. MOONEY *, M. A. MINTUN ‡, K. J. HIMMELSTEIN, and V. J. STELLA ˣ**



Received March 24, 1980, from the *Departments of Pharmaceutical Chemistry and Chemical and Petroleum Engineering, University of Kansas, Lawrence, KS 66045.* Accepted for publication July 3, 1980.


*Present address: Boehringer Ingelheim, Ridgefield, CT 06877. ‡Present address: Washington University, St. Louis, MO 63110.



**Abstract** □ The dissolution behavior of 2-naphthoic acid from rotating compressed disks into aqueous buffered solutions of constant ionic strength ($\mu$ = 0.5 with potassium chloride) at 25° was investigated. A model was developed for the flux of a solid monoprotic carboxylic acid in aqueous buffered solutions as a function of the solution pH and the physicochemical properties of the buffer. The model assumes a diffusion layer-controlled mass transport process and a simple, instantaneously established reaction equilibrium between all reactive species (acids and bases) across the diffusion layer. Using intrinsic solubilities, pKa values, and diffusion coefficients, the model accurately predicts the dissolution of 2-naphthoic acid as a function of the bulk solution composition. The concentration profiles of all species across the diffusion layer are generated for each buffer concentration and bulk solution pH, including the pH profile within the microclimate of the diffusion layer and the pH at the solid–solution boundary.



**Keyphrases** □ Carboxylic acids—dissolution kinetics, effect of buffers □ Dissolution kinetics—carboxylic acids, effect of buffers □ Buffers—effect on dissolution kinetics of carboxylic acids


The objective of this investigation was to determine experimentally the effect of buffers on the dissolution of 2-naphthoic acid from a constant surface area pellet under controlled ionic strength ($\mu$ = 0.5 with potassium chloride), temperature (25°), and pH conditions (pH-stat). A model, an extension of one described previously (1), also was de-




0022-3549/81/0100-0022$01.00/0


© 1981, American Pharmaceutical Association

veloped that predicts the effects of solution pH and the physicochemical properties of the buffer on the dissolution of this monoprotic carboxylic acid. The model adequately predicts fluxes and the concentration profiles of all species within a postulated diffusion layer as a function of the bulk solution pH ($pH_{bulk}$) and the total buffer concentration. The results emphasize the importance of the buffer base concentration and the pKa value of the conjugate acid of the buffer on dissolution rates, but they deemphasize the direct involvement and importance of $pH_{bulk}$.

Alkaline compounds or buffers have been included in commercial tablet formulations of several acidic drugs that undergo dissolution rate-limited absorption from conventional tablets. The concept embodied in these buffered formulations is the prevention of GI irritation caused by some acidic drugs and/or the provision of a basic pH microenvironment within the diffusion layer around the dissolving acid particles to promote dissolution (2–4). Nelson (5, 6) first approached the rationale for buffered tablet formulations when he measured the dissolution rates of several solid acidic drugs in aqueous media containing various buffers at several pH values. The mechanism of this process was studied in detail by Higuchi and coworkers (7, 8). The results presented here support the use of buffered dosage forms to promote the dissolution of poorly soluble carboxylic acids.

## THEORETICAL

A model for the dissolution of an acid into an aqueous buffered medium should consider not only the diffusion layer reaction of the acid with water and hydroxide ion but also the reaction of the acid with the base component of the buffer. Hence, the number of possible chemical reactions that occur in the diffusion layer is increased because the buffer consists of a conjugate acid–base pair, which is assumed to be in rapid equilibrium with the other reactants and products.

It is assumed that the addition of buffer to the bulk solution does not change the constraints and assumptions of the previously described model (1), *i.e.*, that the dissolution of the acid (HA) into the aqueous buffer solution occurs *via* a diffusion layer-controlled process across a boundary layer of thickness $h$ as defined by the Levich rotating-disk model (9). A constant diffusion layer thickness, calculated on the basis of the diffusivity of the acid ($D_{HA}$) and regardless of the diffusivities of other species, is assumed. The limitations of this assumption were discussed earlier (1).

Within this boundary layer, all concentration gradients of the reactants and products exist as a result of diffusion and instantaneous chemical reaction between the dissolving solute and the incoming base from the bulk solution. The concentration of undissociated carboxylic acid at the solid–liquid surface ($X = 0$, where $X$ is the distance from the solid–liquid interface) always is defined by the intrinsic solubility of the acid $[HA]_0$. The bulk solution is regarded as a homogeneous mixture with no concentration gradients, and initial rates are assumed.

An additional experimental constraint is that the buffering compounds considered contain only one ionizable group. Polyprotic or polybasic compounds also may be considered in the model; however, they obviously would complicate the situation.

Figure 1 is a schematic diagram of this system. Hydroxide ion ($OH^-$) and the buffer base (B) may diffuse into the diffusion layer from the bulk solution and react with the carboxylic acid (HA) which is diffusing out. The products, also diffusing out, are the conjugate acid of the buffer ($BH^+$), the acid anion ($A^-$), and the hydrogen ion ($H^+$). The water concentration is ignored since its concentration does not change significantly as a result of these reactions.

Consider the chemical reactions within the diffusion layer as shown by Fig. 1 (Schemes I–VI).

$$H^+ + OH^- \rightleftharpoons H_2O$$
*Scheme I*

$$HA \overset{K_a^A}{\rightleftharpoons} H^+ + A^-$$
*Scheme II*

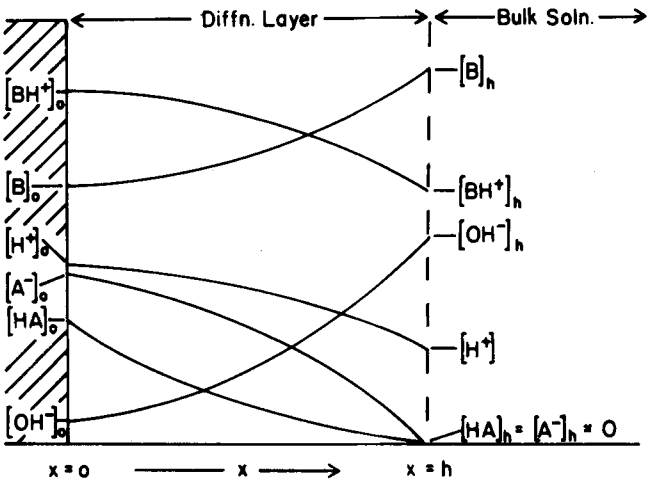


**Figure 1**—*Diagrammatic representation of a solid carboxylic acid, HA, dissolving into a reactive medium containing hydroxide ion and buffer components B and $BH^+$ with a Nernst diffusion layer existing between the solid and the bulk solution. Sink conditions exist in the bulk solution, and the products, $BH^+$, $A^-$, and $H^+$, diffuse out of the diffusion layer at a rate determined by their chemical reactivity and diffusivity.*

$$HA + OH^- \overset{K_1^*}{\rightleftharpoons} H_2O + A^-$$
*Scheme III*

$$HA + B \overset{K_2}{\rightleftharpoons} BH^+ + A^-$$
*Scheme IV*

$$BH^+ \overset{K_a^B}{\rightleftharpoons} H^+ + B$$
*Scheme V*

$$BH^+ + OH^- \overset{K_3^*}{\rightleftharpoons} H_2O + B$$
*Scheme VI*

These equilibria are described by:

$$K_w = [H^+][OH^-] \quad \text{(Eq. 1)}$$

$$K_a^A = \frac{[H^+][A^-]}{[HA]} \quad \text{(Eq. 2)}$$

$$K_1^*/[H_2O] = K_1 = \frac{[A^-]}{[HA][OH^-]} = \frac{1}{K_0^A} \quad \text{(Eq. 3)}$$

$$K_2 = \frac{[BH^+][A^-]}{[HA][B]} = \frac{K_a^A}{K_a^B} \quad \text{(Eq. 4)}$$

$$K_a^B = \frac{[H^+][B]}{[BH^+]} \quad \text{(Eq. 5)}$$

$$K_3^*/[H_2O] = K_3 = \frac{[B]}{[BH^+][OH^-]} \quad \text{(Eq. 6)}$$

For the diffusion and simultaneous chemical reaction of the individual species at steady state within the diffusion layer, Fick's laws may be applied to each species as discussed previously (1). Therefore:

$$\frac{\delta[HA]}{\delta t} = D_{HA}\frac{\delta^2[HA]}{\delta X^2} + \phi_1 = 0 \quad \text{(Eq. 7)}$$

$$\frac{\delta[A^-]}{\delta t} = D_A\frac{\delta^2[A^-]}{\delta X^2} + \phi_2 = 0 \quad \text{(Eq. 8)}$$

$$\frac{\delta[H^+]}{\delta t} = D_H\frac{\delta^2[H^+]}{\delta X^2} + \phi_3 = 0 \quad \text{(Eq. 9)}$$

$$\frac{\delta[OH^-]}{\delta t} = D_{OH}\frac{\delta^2[OH^-]}{\delta X^2} + \phi_4 = 0 \quad \text{(Eq. 10)}$$

$$\frac{\delta[B]}{\delta t} = D_B\frac{\delta^2[B]}{\delta X^2} + \phi_5 = 0 \quad \text{(Eq. 11)}$$

$$\frac{\delta[BH^+]}{\delta t} = D_{BH}\frac{\delta^2[BH^+]}{\delta X^2} + \phi_6 = 0 \quad \text{(Eq. 12)}$$

where $[N]$ represents the concentration of species $N$, $t$ is time, $X$ is distance, and $D_N$ is the diffusivity of species $N$. Each equation states that the rate of change in the concentration of $N$ with respect to time in the diffusion layer (here it is zero since steady-state conditions are assumed) is composed of a diffusional term (Fick's second law) and a chemical reaction term for the species $N$.

By observing which species react together to form particular products, a comprehensive set of species balance equations accounting for the chemical reaction may be established. Whenever a change in the flux of one species occurs due to a chemical reaction within the film, it also must be reflected by corresponding changes in the reactants and products as defined by the equilibria in Schemes I–VI. From these relationships, the following diffusion layer mass balance can be written:

$$\Delta(\text{flux } OH^- \text{ in}) + \Delta(\text{flux B in}) = \Delta(\text{flux HA out}) + \Delta(\text{flux } H^+ \text{ out}) \quad \text{(Eq. 13)}$$

Equation 13 states that the rates of change of the flux of reactants into the film, $OH^-$ and B, must equal those of the reactants coming out of the film, HA and $H^+$; $BH^+$ and $A^-$ are considered because any changes in B or HA will reflect changes in their conjugate species. Therefore:

$$D_{OH}\frac{d^2[OH^-]}{dX^2} + D_B\frac{d^2[B]}{dX^2} = D_{HA}\frac{d^2[HA]}{dX^2} + D_H\frac{d^2[H^+]}{dX^2} \quad \text{(Eq. 14)}$$

From species balance considerations, the chemical reaction terms $\phi_1$, $\phi_3$, $\phi_4$, and $\phi_5$ from Eqs. 7–12 are represented by:

$$\phi_4 + \phi_5 = \phi_1 + \phi_3 \quad \text{(Eq. 15)}$$

Any change in HA and B due to reaction automatically represents a change in their conjugate species, $A^-$ and $BH^+$. This is represented by:

$$D_{HA}\frac{d^2[HA]}{dX^2} = -\left(D_A\frac{d^2[A^-]}{dX^2}\right) \quad \text{(Eq. 16)}$$

$$D_B\frac{d^2[B]}{dX^2} = -\left(D_{BH}\frac{d^2[BH^+]}{dX^2}\right) \quad \text{(Eq. 17)}$$

Therefore, $\phi_1 = -\phi_2$ and $\phi_5 = -\phi_6$.

Equations 14, 16, and 17 are three second-order differential equations. When integrated with respect to $X$, they yield:

$$D_{HA}\frac{d[HA]}{dX} = D_{OH}\frac{d[OH^-]}{dX} + D_B\frac{d[B]}{dX} - D_H\frac{d[H^+]}{dX} + C_1 \quad \text{(Eq. 18)}$$

$$D_{HA}\frac{d[HA]}{dX} = -\left(D_A\frac{d[A^-]}{dX}\right) + C_2 \quad \text{(Eq. 19)}$$

$$D_B\frac{d[B]}{dX} = -\left(D_{BH}\frac{d[BH^+]}{dX}\right) + C_3 \quad \text{(Eq. 20)}$$

where $C_1$, $C_2$, and $C_3$ are constants of integration. If mass balance considerations are included, simplification of Eqs. 18–20 is possible because $A^-$ is a product of the reaction between HA and the combination of B, $OH^-$, and $H_2O$. However, B and $OH^-$ also react with $H^+$ in the diffusion layer. Therefore, the following identities result:

$$\Sigma\,(\text{flux of reactants in}) = (\text{flux } A^- \text{ out}) - (\text{flux } H^+ \text{ out}) \quad \text{(Eq. 21)}$$

or:

$$\Sigma\,(\text{flux of reactants in}) = \left(D_{OH}\frac{d[OH^-]}{dX} + D_B\frac{d[B]}{dX}\right) \quad \text{(Eq. 22)}$$

Remembering that fluxes into the film have positive slopes and that:

$$\text{flux } A^- \text{ out} = -\left(D_A\frac{d[A^-]}{dX}\right) \quad \text{(Eq. 23)}$$

and:

$$\text{flux } H^+ \text{ out} = -\left(D_H\frac{d[H^+]}{dX}\right) \quad \text{(Eq. 24)}$$

yields:

$$D_{OH}\frac{d[OH^-]}{dX} + D_B\frac{d[B]}{dX} = D_H\frac{d[H^+]}{dX} - D_A\frac{d[A^-]}{dX} \quad \text{(Eq. 25)}$$

From Eqs. 18 and 19, it can be seen that consistency is preserved only when $C_2 = C_1$. Therefore, Eq. 19 becomes:

$$D_{HA}\frac{d[HA]}{dX} = -\left(D_A\frac{d[A^-]}{dX}\right) + C_1 \quad \text{(Eq. 26)}$$

Further simplification may be made by substituting Eq. 20 into Eq. 18 and rearranging:

$$D_{HA}\frac{d[HA]}{dX} = C_1 + C_3 + D_{OH}\frac{d[OH^-]}{dX} - D_H\frac{d[H^+]}{dX} - D_{BH}\frac{d[BH^+]}{dX} \quad \text{(Eq. 27)}$$

Equation 26 is substituted into Eq. 27 to obtain:

$$-\left(D_A\frac{d[A^-]}{dX}\right) = D_{OH}\frac{d[OH^-]}{dX} - D_H\frac{d[H^+]}{dX} - D_{BH}\frac{d[BH^+]}{dX} + C_3 \quad \text{(Eq. 28)}$$

Consider the reactions involving $A^-$ separately. For the reaction shown in Scheme VII (Equilibrium a):

$$HA + H_2O \rightleftharpoons A^- + H_3O^+ \text{ (where } H_3O^+ = H^+\text{)}$$

*Scheme VII*

$$(\text{flux } A^- \text{ out})_a = (\text{flux } H^+ \text{ out}) \quad \text{(Eq. 29)}$$

or:

$$-\left(D_A\frac{d[A^-]}{dX}\right)_a = -\left(D_H\frac{d[H^+]}{dX}\right) \quad \text{(Eq. 30)}$$

For the reaction shown in Scheme III (Equilibrium b):

$$(\text{flux } A^- \text{ out})_b = (\text{flux } OH^- \text{ in}) \quad \text{(Eq. 31)}$$

or:

$$-\left(D_A\frac{d[A^-]}{dX}\right)_b = \left(D_{OH}\frac{d[OH^-]}{dX}\right) \quad \text{(Eq. 32)}$$

For the reaction shown in Scheme IV (Equilibrium c):

$$(\text{flux } A^- \text{ out})_c = (\text{flux } BH^+ \text{ out}) \quad \text{(Eq. 33)}$$

or:

$$-\left(D_A\frac{d[A^-]}{dX}\right)_c = -\left(D_{BH}\frac{d[BH^+]}{dX}\right) \quad \text{(Eq. 34)}$$

Hence, summing up the contributions of the three equilibria (a–c) in the diffusion layer:

$$\Sigma - \left(D_A\frac{d[A^-]}{dX}\right) = D_{OH}\frac{d[OH^-]}{dX} - D_H\frac{d[H^+]}{dX} - D_{BH}\frac{d[BH^+]}{dX} \quad \text{(Eq. 35)}$$

By comparing Eq. 35 to Eq. 28, it is seen that $C_3 = 0$. Equation 20 now becomes:

$$D_B\frac{d[B]}{dX} = -\left(D_{BH}\frac{d[BH^+]}{dX}\right) \quad \text{(Eq. 36)}$$

By integrating Eqs. 18, 26, and 36, linear equations are obtained in $X$:

$$D_{HA}[HA] = D_{OH}[OH^-] + D_B[B] - D_H[H^+] + C_1X + T_1 \quad \text{(Eq. 37)}$$

$$D_{HA}[HA] = -D_A[A^-] + C_1X + T_2 \quad \text{(Eq. 38)}$$

$$D_B[B] = -D_{BH}[BH^+] + T_3 \quad \text{(Eq. 39)}$$

where $T_1$, $T_2$, and $T_3$ are additional constants of integration.

**Application of Boundary Conditions**—To evaluate Eqs. 37–39, the following boundary conditions must be applied.

At $X = 0$:

$[HA] = [HA]_0$ (known)
$[A^-] = [A^-]_0$ (unknown)
$[H^+] = [H^+]_0$ (unknown)
$[OH^-] = [OH^-]_0$ (unknown)
$[B] = [B]_0$ (unknown)
$[BH^+] = [BH^+]_0$ (unknown)

At $X = h$:

$[HA] = [HA]_h \simeq 0$
$[A^-] = [A^-]_h \simeq 0$
$[H^+] = [H^+]_h$ (given)

$[OH^-] = [OH^-]_h$ (given)
$[B] = [B]_h$ (given)
$[BH^+] = [BH^+]_h$ (given)

Both $[HA]_h$ and $[A^-]_h$ are zero under sink conditions. Other terms ($C_1$, $T_1$, $T_2$, and $T_3$) are unknown. Applying the boundary conditions to Eqs. 37–39 at $X = 0$ results in:

$$D_{HA}[HA]_0 = D_{OH}[OH^-]_0 + D_B[B]_0 - D_H[H^+]_0 + T_1 \quad \text{(Eq. 40)}$$

$$D_{HA}[HA]_0 = -D_A[A^-]_0 + T_3 \quad \text{(Eq. 41)}$$

$$D_B[B]_0 = -D_{BH}[BH^+] + T_3 \quad \text{(Eq. 42)}$$

and at $X = h$:

$$D_H[H^+]_h = D_{OH}[OH^-]_h + D_B[B]_h + C_1h + T_1 \quad \text{(Eq. 43)}$$

$$C_1h = -T_2 \quad \text{(Eq. 44)}$$

$$D_B[B]_h = -D_{BH}[BH^+]_h + T_3 \quad \text{(Eq. 45)}$$

There are nine unknowns in these equations, providing that $[HA]_0$, the diffusivities of all species, and $h$ are known. To calculate the unknowns, three more equations are required. These are provided by the equilibrium constants given in Eqs. 1, 2, and 5.

There are now nine equations and nine unknowns. Successive substitution may be used to reduce these equations to one equation where a single unknown may be solved for. A brief summary for the solution of $[H^+]_0$ is given here.

Equation 43 is subtracted from Eq. 40 to give:

$$D_{HA}[HA]_0 = D_{OH}([OH^-]_0 - [OH^-]_h) + D_B([B]_0 - [B]_h) + D_H([H^+]_h - [H^+]_0) - C_1h \quad \text{(Eq. 46)}$$

Equation 46 was derived to eliminate $T_1$. Now $[A^-]_0$ is substituted for in Eq. 41 using Eq. 2, and $T_2$ is eliminated by using Eq. 44:

$$D_{HA}[HA]_0 = -D_A\frac{K_a^A[HA]_0}{[H^+]_0} - C_1h \quad \text{(Eq. 47)}$$

Equation 47 may now be equated to Eq. 46 to cancel $C_1h$. Substituting for $[OH^-]_0$ also results in:

$$-D_A\frac{K_a^A[HA]_0}{[H^+]_0} = \frac{D_{OH}K_w}{[H^+]_0} + D_B[B]_0 - D_H[H^+]_0 - (D_{OH}[OH^-]_h + D_B[B]_h - D_H[H^+]_h) \quad \text{(Eq. 48)}$$

To obtain $[B]_0$ in terms of $[H^+]_0$, Eqs. 42, 45, and 5 must be used:

$$T_3 = D_B[B]_0 + D_{BH}[BH^+]_0 = D_B[B]_h + D_{BH}[BH^+]_h \quad \text{(Eq. 49)}$$

Substituting for $[BH^+]_0$:

$$[B]_0 = K_a^B\left[\frac{D_B[B]_h + D_{BH}[BH^+]_h}{D_BK_a^B + D_{BH}[H^+]_0}\right] \quad \text{(Eq. 50)}$$

Equation 50 may be used to substitute for $[B]_0$ in Eq. 48 and, hence, reduce it to one with a single unknown, $[H^+]_0$. After cross-multiplication and rearrangement:

$$p[H^+]_0^3 + q[H^+]_0^2 + r[H^+]_0 + s = 0 \quad \text{(Eq. 51)}$$

where:

$p = D_HD_{BH}$
$q = D_HD_BK_a^B + D_{BH}a$
$r = D_BK_a^B(a - b) - D_AD_{BH}K_a^A[HA]_0 - D_{OH}D_{BH}K_w$
$s = -D_AD_BK_a^AK_a^B[HA]_0 - D_{OH}K_wK_a^BD_B$
$a = D_{OH}[OH^-]_h + D_B[B]_h - D_H[H^+]_h$
$b = D_B[B]_h + D_{BH}[BH^+]_h$ (also $= T_3$)

Equation 51 may be solved by the method of Newton (10). Thus, for any given conditions in the bulk solution of $[H^+]_h$, $[OH^-]_h$, $[B]_h$, and $[BH^+]_h$, $[H^+]_0$ may be determined. Once this value is obtained, the other unknowns may be successively calculated from the preceding equations. Equation 51, together with its related questions, may be solved readily using a digital computer[1].

**Expression for the Total Acid Flux**—Equation 46 may be rearranged to give an expression for the integration constant $C_1$; $C_1$ represents the negative sum of the individual fluxes across the diffusion layer and, therefore, is the negative of the total acid flux at $X = 0$ or the acid dissolution rate:

$$C_1 = -J^{total} = -1/h[D_{HA}[HA]_0 + D_H([H^+]_0 - [H^+]_h) + D_{OH}([OH^-]_h - [OH^-]_0) + D_B([B]_h - [B]_0)] \quad \text{(Eq. 52)}$$

or:

$$C_1 = -J^{total} = -(J_{HA} + J_H + J_{OH} + J_B) \quad \text{(Eq. 53)}$$

where $J_N$ is the flux of species $N$.

Therefore, by using the values of $[H^+]_0$, $[B]_0$, and $[OH^-]_0$ calculated from the preceding equations, the total flux of acid at any bulk solution pH and buffer concentration also may be calculated. Again, this problem may be included in a comprehensive computer program[1] for application to various bulk solution pH and buffer concentrations.

**Evaluation of Concentration Profiles across Diffusion Layer**—Using the Levich (9) diffusion layer thickness for a rotating disk, Eqs. 37–39 may be solved simultaneously with Eqs. 1, 2, and 5 to give the concentrations of a particular species at any point, $X$, in the diffusion layer. The substitutions required in reducing the numerous equations to one equation with a single unknown are similar to those already described, except that [HA] also must be expressed as a function of the given unknown solved. This may be done by using Eqs. 2 and 38:

$$[HA] = [H^+]\left(\frac{C_1X + T_2}{D_{HA}[H^+] + D_AK_a^A}\right) \quad \text{(Eq. 54)}$$

Now [HA] can be substituted for Eq. 37 along with a similar expression for [B], which is derived from Eqs. 39 and 5:

$$[B] = \left(\frac{K_a^BT_3}{D_BK_a^B + D_{BH}[H^+]}\right) \quad \text{(Eq. 55)}$$

Equation 37 now reads:

$$D_{HA}[H^+]\left(\frac{C_1X + T_2}{D_{HA}[H^+] + D_AK_a^A}\right) = \frac{D_{OH}K_w}{[H^+]} - D_H[H^+] + D_B\left(\frac{K_a^BT_3}{D_BK_a^B + D_{BH}[H^+]}\right) + C_1X + T_1 \quad \text{(Eq. 56)}$$

Since $C_1$, $T_2$, and $T_3$ already are known for given bulk solution conditions and $X$ is given, $[H^+]$ now is the only unknown. By algebraic rearrangement, cross-multiplication, and reduction, a quartic equation in $[H^+]$ results in the form of:

$$A[H^+]^4 + B[H^+]^3 + C[H^+]^2 + E[H^+] + F = 0 \quad \text{(Eq. 57)}$$

where:

$A = D_Hn$
$B = n(T_2 - T_1) + D_Ht$
$C = D_BD_{HA}K_a^B(C_1X + T_2 - T_3) - t(C_1X + T_1) - D_{OH}K_wn + D_Hp$
$E = -D_{OH}K_wt - p(C_1X + T_1 + T_3)$
$F = -pK_wD_{OH}$
$n = D_{HA}D_{BH}$
$t = D_{HA}D_BK_a^B + D_AD_{BH}K_a^A$
$p = D_AD_BK_a^AK_a^B$

Equation 57 can be solved by using Newton's method (10). Having obtained $[H^+]$ at any point $X$ in the film, the concentrations of the other species may be determined. If this calculation is performed at several points in the diffusion layer, then a concentration profile across this layer is described.

## EXPERIMENTAL

**Materials**—2-Naphthoic acid was from the same source as that used previously (1). Imidazole[2], acetic acid[3], sodium acetate[3] (trihydrate), morpholine[4], and potassium chloride[3] were reagent grade and were used as supplied. Hydrochloric acid[5] and sodium hydroxide[5] were obtained as standardized 1.0 *M* solutions.

**Determination of Dissolution Rates**—The apparatus for determining the dissolution rates of 2-naphthoic acid was described previously (1). In each determination, the pH-stat was used to maintain the bulk

[1] Honeywell model 66/60. A copy of the procedure and program can be obtained from V. J. Stella.

[2] Sigma Chemical Co., St. Louis, Mo.
[3] Mallinckrodt Chemicals.
[4] Matheson, Coleman and Bell.
[5] Fisher Scientific Co., Fair Lawn, N.J.

**Table I—Experimental pKa Values, Estimated Percentage Purity, and Literature Thermodynamic pKa Values for Imidazole, Morpholine, and Acetic Acid**

| Compound | pKa ($\pm SD$)[a] at $\mu$ = 0.5 (Potassium Chloride) and 25° (±0.1°) | pKa (Thermodynamic) at 25° in Water | Estimated Purity, % |
|---|---|---|---|
| Imidazole | 7.17 (±0.01) | 6.91[b] | 102.24 |
| Morpholine | 8.75 (±0.02) | 8.70[c] | 97.92 |
| Acetic acid | 4.60[b] | 4.75[b] | — |

[a] The standard deviation from at least three determinations. [b] Obtained or estimated from data in Ref. 11. [c] From Ref. 12.

**Table II—Estimated and Literature Values for the Diffusivities of Imidazole, Morpholine, and Acetic Acid, Used as Buffering Agents in the Study of 2-Naphthoic Acid Dissolution at $\mu$ = 0.5 with Potassium Chloride and 25°**

| Compound | Molecular Weight | Diffusivity, $cm^2/sec \times 10^6$ | |
|---|---|---|---|
| | | Calculated[a] | Literature (Ref.) |
| Imidazole | 68 | 8.20[b] | — |
| Morpholine | 87 | 7.00[c] | — |
| Acetic acid | 79 | 8.84[d] | 12.1[e] (14)<br>12.0[e] (15)<br>8.8[f] (16) |

[a] Using Stokes–Einstein equation (1). [b] By direct comparison with 2-naphthoic acid using the Stokes–Einstein equation. [c] A molar volume of 87 ml/mole was used, assuming the density to be 1.0 at 25°. [d] A molar volume of 38.3 ml/mole was used from Ref. 14 at 25°. [e] Extrapolated to zero acetic acid concentration ($\mu$m = 0) at 25° in water. [f] In water at 20°; other conditions not stipulated.

solution pH using 0.01–0.1 *M* NaOH, regardless of the buffer capacity of the buffer solution used.

When imidazole and morpholine were used as buffers, it was convenient to measure the absorbance of 2-naphthoic acid in the solution at 281 nm rather than at the more analytically sensitive region of 230–237 nm because the absorbance of imidazole interfered in the latter range. Furthermore, dissolution became so rapid at high buffer concentrations that the absorbance of the resulting solution quickly exceeded the range obeying the Beer–Lambert law. In acetate buffers, measurement of the dissolution rate was performed at 231 or 281 nm, depending on the buffer concentration and the pH of the dissolution medium.

In all cases, the media were adjusted to the same ionic strength ($\mu$ = 0.5) using potassium chloride. A wide range of total buffer concentrations was studied. Immediately prior to a dissolution run, the solution pH was accurately adjusted with concentrated hydrochloric acid or sodium hydroxide, and the solution then was thermally equilibrated to 25° (±0.1°). In each case, the solution used for the dissolution served as its own reference in the spectrophotometer.

2-Naphthoic acid was chosen for the investigation of buffer effects because of its intermediate aqueous solubility in the three acids used previously (1), its chemical stability, and its amenability to spectrophotometric analysis. The disks of 2-naphthoic acid were prepared as described previously (1), and all dissolution experiments were performed at disk rotation speeds of 450 rpm. Sink conditions were maintained throughout, as observed from the linear dissolution plots obtained.

**Determination of Buffer pKa Values**—The pKa values of imidazole and morpholine were measured at $\mu$ = 0.5 (potassium chloride) and 25° (±0.1°) using potentiometric titrimetry. The pKa value of acetic acid was obtained by estimation by the method of Butler (10).

## RESULTS AND DISCUSSION

The pKa values of imidazole and morpholine determined experimentally, the thermodynamic pKa values, and the estimated purity of the titrated buffers are given in Table I together with the estimated pKa for acetic acid at an ionic strength of 0.5.

**Diffusion Coefficients for Various Species**—Since the aqueous diffusion coefficients of the buffer species were not measured, literature values and estimations based on the Stokes–Einstein equation (1, 13) were used. They are summarized in Table II. The literature diffusivities (where available) differed significantly from the calculated values at 25°. The aqueous diffusivities of all weak electrolytes are strongly affected by the ionic strength of the solution and the concentration of the weak electrolyte itself. In the case of acetic acid, diffusivity values decline almost linearly with an increase in the acid concentration in the aqueous medium (14). Similar effects were noted on the diffusivity of ions in solutions of mixed electrolytes (17). Both phenomena are due to an alteration of the thermodynamic activity coefficient of the diffusant. Hence, the actual diffusivities of imidazole, morpholine, and acetic acid at $\mu$ = 0.5 (potassium chloride) and 25° in water are likely to be lower than those measured under the same conditions with $\mu$ approaching zero (infinite dilution). For this reason, the diffusivities calculated from the Stokes–Einstein equation as described previously (1) were used since these values are lower than those quoted in the literature for diffusivity in water at 25°.

**Initial Dissolution Rate of 2-Naphthoic Acid as a Function of Bulk Solution Buffer Concentration and pH**—The model discussed under *Theoretical* was tested over a wide range of bulk solution pH values and total buffer concentrations using acetic acid, imidazole, and morpholine buffers. Experimentally determined initial dissolution rates for 2-naphthoic acid ($J_{obs}$) are given in Tables III–V together with the corresponding interfacial pH ($pH_0$) calculated from Eq. 51 and theoretical initial dissolution rates ($J_{theor}$) calculated from Eq. 52. Figures 2–4 show $J_{obs}$ and $J_{theor}$ *versus* the total bulk solution buffer concentration for the three buffers used.

The agreement between the observed and predicted initial dissolution rates was good over wide ranges of bulk solution buffer concentrations and pH bulk values for all three buffer systems. The data from the acetate buffers are of particular interest since the acetic acid pKa (4.60) is similar to that of 2-naphthoic acid (4.02) and, therefore, the equilibrium constant for the reaction between the two is relatively low ($K_2$ = 3.8). Thus, the degree of catalysis of the dissolution of 2-naphthoic acid by acetate anion diffusing into the aqueous diffusion layer and reacting with dissolving acid is expected to be relatively small compared to that resulting from

**Table III—Comparison of the Observed ($J_{obs}$) and Theoretical ($J_{theor}$) Initial Dissolution Rates of 2-Naphthoic Acid in Varying Bulk Solution Acetate Buffer Concentrations at $pH_{bulk}$ 4.50, 5.00, and 6.00 ($\mu$ = 0.5 with Potassium Chloride and 25°)[a]**

| Total Bulk Solution Concentration of Acetate, *M* | $pH_{bulk}$ 4.50 | | | $pH_{bulk}$ 5.00 | | | $pH_{bulk}$ 6.00 | | |
|---|---|---|---|---|---|---|---|---|---|
| | $J_{obs}$, moles/$cm^2$/sec $\times 10^9$ | $J_{theor}$, moles/$cm^2$/sec $\times 10^9$ | $pH_0$ | $J_{obs}$, moles/$cm^2$/sec $\times 10^9$ | $J_{theor}$, moles/$cm^2$/sec $\times 10^9$ | $pH_0$ | $J_{obs}$, moles/$cm^2$/sec $\times 10^9$ | $J_{theor}$, moles/$cm^2$/sec $\times 10^9$ | $pH_0$ |
| 0.0 | 1.03 | 0.95 | 4.15 | 1.19 | 1.07 | 4.24 | 1.33 | 1.13 | 4.28 |
| 0.00025 | 1.10 | 1.01 | 4.20 | — | 1.27 | 4.35 | — | 1.49 | 4.45 |
| 0.0005 | 1.24 | 1.07 | 4.24 | — | 1.46 | 4.44 | — | 1 83 | 4.57 |
| 0.001 | 1.39 | 1.17 | 4.30 | — | 1.75 | 4.54 | — | 2.41 | 4.72 |
| 0.0025 | 1.41 | 1.32 | 4.38 | 2.50 | 2.32 | 4.70 | 3.74 | 3.67 | 4.93 |
| 0.005 | — | 1.43 | 4.42 | 3.10 | 2.81 | 4.79 | 5.20 | 5.10 | 5.09 |
| 0.01 | 1.63 | 1.51 | 4.46 | 3.45 | 3.27 | 4.87 | 7.11 | 7.07 | 5.24 |
| 0.025 | — | 1.57 | 4.48 | 3.88 | 3.75 | 4.94 | 10.67 | 10.64 | 5.42 |
| 0.05 | — | 1.60 | 4.49 | 4.16 | 3.97 | 4.97 | 13.52 | 14.17 | 5.55 |
| 0.075 | — | 1.60 | 4.49 | 4.14 | 4.06 | 4.98 | 15.95 | 16.55 | 5.62 |
| 0.10 | 1.70 | 1.61 | 4.50 | 4.10 | 4.11 | 4.98 | 18.53 | 18.23 | 5.67 |

[a] $J_{theor}$ was calculated from Eq. 52. The estimated interfacial pH ($pH_0$) for each condition was determined from Eq. 51. The rates were measured from a disk rotating at 450 rpm. Each $J_{obs}$ value is the mean from at least two runs.

**Table IV—Comparison of the Observed ($J_{obs}$) and Theoretical ($J_{theor}$) Initial Dissolution Rates of 2-Naphthoic Acid from a Disk Rotating at 450 rpm into Varying Bulk Solution Concentrations of Imidazole Buffer at $pH_{bulk}$ 6.00, 7.00, and 8.00 ($\mu$ = 0.5 with Potassium Chloride and 25°) [a]**

| Total Bulk Solution Concentration of Imidazole, $M$ | $pH_{bulk}$ 6.00 | | | $pH_{bulk}$ 7.00 | | | $pH_{bulk}$ 8.00 | | |
|---|---|---|---|---|---|---|---|---|---|
| | $J_{obs}$, moles/cm²/sec × $10^9$ | $J_{theor}$, moles/cm²/sec × $10^9$ | $pH_0$ | $J_{obs}$, moles/cm²/sec × $10^9$ | $J_{theor}$, moles/cm²/sec × $10^9$ | $pH_0$ | $J_{obs}$, moles/cm²/sec × $10^9$ | $J_{theor}$, moles/cm²/sec × $10^9$ | $pH_0$ |
| 0.0 | 1.33 | 1.13 | 4.28 | 1.38 | 1.14 | 4.28 | 1.36 | 1.15 | 4.29 |
| 0.0001 | — | 1.14 | 4.28 | 1.58 | 1.23 | 4.33 | — | 1.35 | 4.39 |
| 0.0005 | — | 1.20 | 4.31 | 2.31 | 1.66 | 4.51 | — | 2.47 | 4.73 |
| 0.001 | — | 1.27 | 4.35 | 2.89 | 2.33 | 4.70 | — | 4.13 | 4.98 |
| 0.005 | — | 1.98 | 4.61 | 9.84 | 8.50 | 5.32 | 20.84 | 17.80 | 5.65 |
| 0.01 | 3.72 | 3.02 | 4.83 | 17.44 | 15.98 | 5.61 | 38.94 | 34.06 | 5.94 |
| 0.015 | — | 4.06 | 4.98 | 24.87 | 23.02 | 5.77 | — | 49.43 | 6.10 |
| 0.0175 | — | 4.57 | 5.03 | — | 26.39 | 5.83 | 62.55 | 56.81 | 6.16 |
| 0.025 | 6.66 | 6.01 | 5.16 | 41.09 | 35.96 | 5.96 | 84.45 | 77.92 | 6.30 |
| 0.0375 | — | 8.17 | 5.30 | — | 50.35 | 6.11 | 108.96 | 110.21 | 6.45 |
| 0.04 | — | 8.57 | 5.33 | 56.51 | 53.03 | 6.13 | — | 116.30 | 6.48 |
| 0.05 | 12.12 | 10.07 | 5.40 | 67.67 | 63.16 | 6.21 | 128.88 | 139.63 | 6.56 |
| 0.0625 | — | 11.68 | 5.47 | — | 74.70 | 6.28 | 144.57 | 166.80 | 6.63 |
| 0.075 | 14.32 | 13.22 | 5.52 | 99.44 | 85.19 | 6.34 | 162.57 | 192.13 | 6.70 |
| 0.1 | 19.22 | 15.75 | 5.60 | 118.20 | 103.62 | 6.43 | 190.51 | 238.38 | 6.79 |

[a] $J_{theor}$ was calculated from Eq. 52. The estimated interfacial pH ($pH_0$) for each condition was determined from Eq. 51. Each $J_{obs}$ value is the mean from at least two runs.

**Table V—Comparison of the Observed ($J_{obs}$) and Theoretical ($J_{theor}$) Initial Dissolution Rates of 2-Naphthoic Acid from a Disk Rotating at 450 rpm into Varying Bulk Solution Concentrations of Morpholine Buffer at $pH_{bulk}$ 8.00 and 8.50 ($\mu$ = 0.5 with Potassium Chloride and 25°) [a]**

| Total Bulk Solution Concentration of Morpholine, $M$ | $pH_{bulk}$ 8.00 | | | $pH_{bulk}$ 8.50 | | |
|---|---|---|---|---|---|---|
| | $J_{obs}$, moles/cm²/sec × $10^9$ | $J_{theor}$, moles/cm²/sec × $10^9$ | $pH_0$ | $J_{obs}$, moles/cm²/sec × $10^9$ | $J_{theor}$, moles/cm²/sec × $10^9$ | $pH_0$ |
| 0.0 | 1.38 | 1.15 | 4.29 | 1.42 | 1.16 | 4.29 |
| 0.0001 | — | 1.17 | 4.30 | — | 1.23 | 4.33 |
| 0.0005 | — | 1.29 | 4.36 | — | 1.55 | 4.47 |
| 0.001 | — | 1.46 | 4.44 | — | 2.04 | 4.63 |
| 0.005 | 3.63 | 3.26 | 4.87 | 7.63 | 6.86 | 5.22 |
| 0.01 | 5.78 | 5.82 | 5.15 | 14.49 | 13.14 | 5.52 |
| 0.025 | 12.58 | 13.69 | 5.54 | 34.30 | 32.16 | 5.91 |
| 0.05 | 27.24 | 26.80 | 5.83 | 65.75 | 63.31 | 6.21 |
| 0.075 | 37.99 | 39.82 | 6.01 | 93.28 | 94.36 | 6.39 |
| 0.1 | 51.08 | 53.11 | 6.14 | — | 125.15 | 6.51 |

[a] $J_{theor}$ was calculated from Eq. 52. The estimated interfacial pH ($pH_0$) for each condition was determined from Eq. 51. Each $J_{obs}$ value is the mean from at least two determinations.

comparable concentrations of stronger bases in the bulk solution. Thus, intuitively, the basicity and acidity of the respective reacting buffer base and dissolving acid should be important in determining the initial dissolution rate, as evidenced by the presence of $K_a^A$ and $K_a^B$ in the coefficients of Eq. 51.

At constant $pH_{bulk}$, when the total buffer concentration in the bulk solution is increased, the maximum steady-state pH that can exist at the solid–liquid interface, $pH_0$, is that where $pH_0$ equals $pH_{bulk}$. This is confirmed by the data given in Table III for the acetate buffers at $pH_{bulk}$ 4.50 and 5.00 since the calculated $pH_0$ values asymptotically approach the $pH_{bulk}$ values as the total concentration of acetate buffer in the bulk solution rises.

The shape of the curves in Fig. 2 for the acetate buffers may be explained by the occurrence of a gradual change in controlling factors within the diffusion layer (which determine the 2-naphthoic acid dissolution rate) as the total bulk solution buffer concentration increases. When no buffer is present in the bulk solution and $pH_{bulk}$ is maintained only by the pH-stat, the intrinsic solubility of the acid and its degree of dissociation at the solid–liquid interface determine the dissolution rate (1). The degree of dissociation is determined by reaction with water and hydroxide ion in the diffusion layer, as is the total flux (1).

Equation 52 expresses the total flux of the same acid when buffer is present in the bulk solution, and it includes an additional term to account for any buffer base species used up in the reaction with undissociated 2-naphthoic acid, hydrogen ion, or water in the diffusion layer. As the buffer base concentration increases, the corresponding term for its flux across the diffusion layer in Eq. 52 becomes more significant than the other terms. Despite a decrease in the flux terms in $[H^+]$ and $[OH^-]$ of Eq. 52 as the effective difference in pH across the diffusion layer diminishes, the asymptotic fluxes observed in Fig. 2 at $pH_{bulk}$ 4.5 and 5.0 occur because there always is a finite difference between the buffer base concentration across the diffusion layer.

Eventually, the pH within the diffusion layer and $pH_0$ are controlled by the swamping effect of the buffer as it increases in concentration. Hence, the importance of the total buffer concentration in the bulk solution and the intrinsic solubility of the dissolving acid, $[HA]_0$, in determining the initial dissolution rate of that acid is seen.

The asymptotic fluxes were observed experimentally only with the acetate system at $pH_{bulk}$ 4.50 and 5.0, because the corresponding $pH_0$ values in the absence of buffer did not differ greatly from asymptotic values they must approach (*i.e.*, $pH_0$ 4.50 and 5.00) with increasing bulk solution acetate concentration. As observed in Table III, the relative increases in the dissolution rate in going from zero bulk solution acetate concentration to the asymptotic rate, given when $pH_0$ equals $pH_{bulk}$, were factors of 1.7 and 3.8 for $pH_{bulk}$ 4.50 and 5.0, respectively. At $pH_{bulk}$ 6.00, the total acetate concentration in the bulk solution must be much higher than that used experimentally for $pH_0$ to approach $pH_{bulk}$. Therefore, the asymptotic flux of 2-naphthoic acid is not observed at this $pH_{bulk}$ value. It should be emphasized that the shapes of these curves are highly dependent on the intrinsic solubility of the dissolving acid since this factor determines the sensitivity of the total flux to changes in the total bulk solution buffer concentration.

Figures 3 and 4 and Tables IV and V report the observed and predicted dissolution rates of 2-naphthoic acid given by inclusion of imidazole and morpholine buffers in the bulk solution as a function of $pH_{bulk}$ and buffer concentration. Similar explanations for the shapes of the curves to those given for the acetate system may be made, taking into consideration the greater basicity of these compounds and their diffusivities.

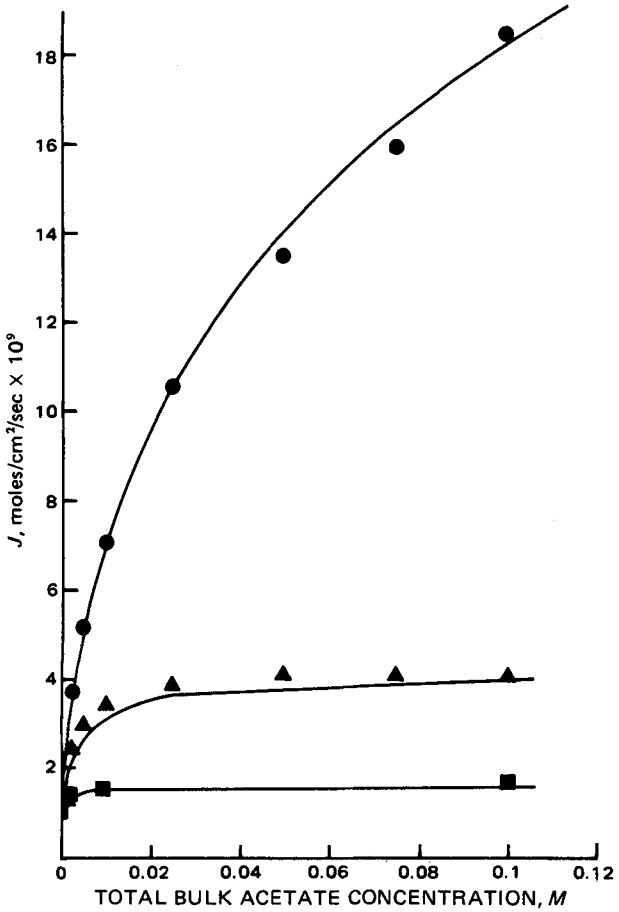


**Figure 2**—*Plot of the dissolution rate of 2-naphthoic acid from a solid disk rotating at 450 rpm into media of varying acetate buffer concentrations and $pH_{bulk}$ [$\mu$ = 0.5 (potassium chloride) at 25°]. The $pH_{bulk}$ was maintained constant by a pH-stat using 0.01 N NaOH. The solid continuous lines represent $J_{theor}$, and the symbols represent $J_{obs}$ from Table III. Key: ■, $pH_{bulk}$ 4.5; ▲, $pH_{bulk}$ 5.0; and ●, $pH_{bulk}$ 6.00.*

In view of the discussion of the shape of the plot of $J$ *versus* buffer concentration in the bulk solution plot for $pH_{bulk}$ 6.00 acetate buffer, considerable concentrations of imidazole and morpholine buffers at $pH_{bulk}$ 6–8.5 are required in the bulk solution to make $pH_0$ at the 2-naphthoic solid–liquid interface equal to $pH_{bulk}$. Hence, over normal buffer concentration ranges, the asymptotic dissolution rate of 2-naphthoic acid was not seen for these buffers at the $pH_{bulk}$ values studied.

To illustrate this point, consider the dissolution rate of 2-naphthoic acid at $pH_{bulk}$ 8.00 in the absence of imidazole or morpholine buffer. The $pH_0$ (Tables IV and V) is 4.29, and the total concentration of 2-naphthoate at $X = 0$ under these conditions may be calculated readily. The same calculation may be performed at $pH_0$ 8.00, the condition required for an asymptote, to give the corresponding total 2-naphthoate concentration at $X = 0$ when $pH_0$ and $pH_{bulk}$ are equal. The ratio of the two total concentrations of 2-naphthoate calculated to exist at $X = 0$ directly represents the expected ratio of the dissolution rates under the same conditions. The ratio of the 2-naphthoic acid dissolution rate at $pH_0$ 4.29 (zero buffer concentration) to that at $pH_0$ 8.00 (asymptotic case) is ~3400. Hence, at $pH_{bulk}$ 8.00, the asymptotic dissolution rate would be ~$4.8 \times 10^{-6}$ mole/cm²/sec, showing that a considerable imidazole or morpholine bulk solution concentration must be used to obtain this condition. The solubility and pKa of the acid also play an important role in determining the conditions at the solid–liquid interface and, therefore, also contribute in determining when the asymptotic dissolution rate is reached for given $pH_{bulk}$ values and buffer solutions.

The curvature seen in the flux *versus* buffer concentration plots (Figs. 2–4) shows that linear extrapolation of the dissolution rate data *versus* buffer concentration plots obtained at high bulk solution buffer concentrations for a given $pH_{bulk}$ is likely to give erroneous buffer-independent dissolution data. This method has been used frequently (18, 19)

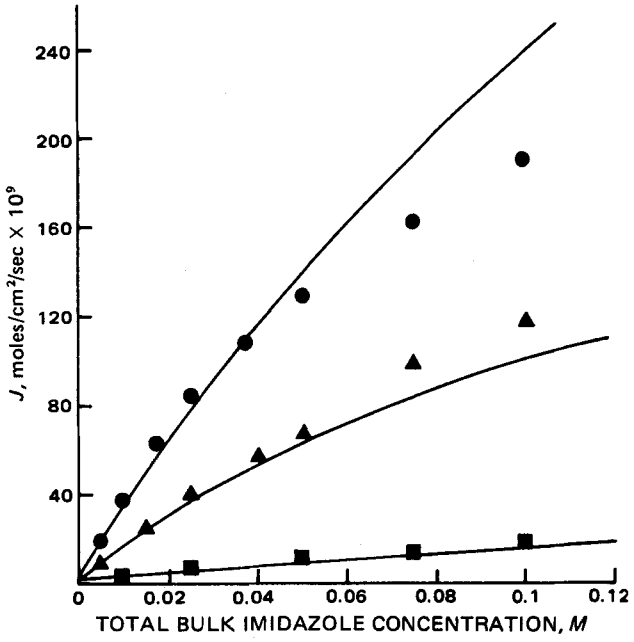


**Figure 3**—*Plot of the dissolution rate of 2-naphthoic acid from a solid disk rotating at 450 rpm into media of varying imidazole buffer concentration and $pH_{bulk}$ [$\mu$ = 0.5 (potassium chloride) at 25°]. The $pH_{bulk}$ was maintained constant by a pH-stat using 0.1 N NaOH. The solid continuous lines represent $J_{theor}$, and the symbols represent the data from Tables IV–VI. Key: ■, $pH_{bulk}$ 6.00; ▲, $pH_{bulk}$ 7.00; and ●, $pH_{bulk}$ 8.00.*

to obtain buffer-independent dissolution rates where no pH-stat is employed and the buffer capacity of the buffer solutions is assumed to be large enough to resist changes in $pH_{bulk}$ during a dissolution experiment. Referring to the imidazole data in Fig. 3, a linear least-squares fit of the four highest experimental imidazole concentrations at $pH_{bulk}$ 8.00 gives an extrapolated $J_0$ value of ~$6.4 \times 10^{-8}$ mole/cm²/sec, whereas the true $J_0$ value (as determined by the pH-stat alone) is $1.4 \times 10^{-9}$ moles/cm²/sec. Therefore, care should be taken in interpreting the intercept from extrapolated buffer dissolution data.

Dissolution rates also measured at the highest imidazole buffer concentration (0.1 $M$) without the pH-stat system operating, but otherwise

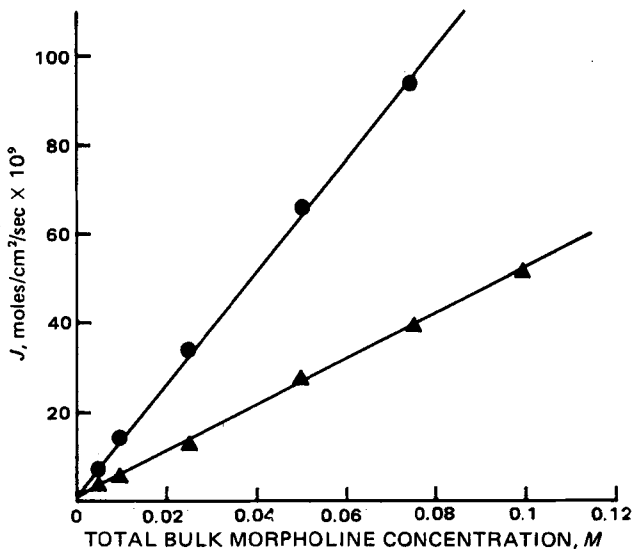


**Figure 4**—*Plot of the dissolution rate of 2-naphthoic acid from a solid disk rotating at 450 rpm into media of varying morpholine buffer concentration and $pH_{bulk}$ [$\mu$ = 0.5 (potassium chloride) at 25°]. The $pH_{bulk}$ was maintained constant by a pH-stat using 0.1 N NaOH. The solid continuous lines represent $J_{theor}$, and the symbols represent $J_{obs}$ from Table VII. Key: ▲, $pH_{bulk}$ 8.00; and ●, $pH_{bulk}$ 8.50.*

**Table VI—Concentration of Acetate Anion (Conjugate Buffer Base $[Ac^-]_h$) in the Bulk Solution and at the Solid–Liquid Interface ($[Ac^-]_0$) with Increasing Total Acetate Buffer Concentration at $pH_{bulk}$ 6.0 and the Observed Flux ($J_{obs}$) of 2-Naphthoic Acid from a Disk Rotating at 450 rpm in pH-Statted Media ($\mu$ = 0.5 with Potassium Chloride and 25°)**

| Total Buffer Concentration of Acetate, *M* | $[Ac^-]_h$, moles/cm³ × 10⁷ | $[Ac^-]_0$[a], moles/cm³ × 10⁷ | $[Ac^-]_h - [Ac^-]_0$, moles/cm³ × 10⁷ | Total Flux of 2-Naphthoic Acid ($J_{obs}$), moles/cm²/sec × 10⁹ | $pH_0$[b] |
|---|---|---|---|---|---|
| 0.0 | 0.0 | 0.0 | 0.0 | 1.33 | 4.28 |
| 0.001 | 9.62 | 5.70 | 3.92 | — | 4.72 |
| 0.0025 | 24.00 | 17.00 | 7.00 | 3.74 | 4.93 |
| 0.005 | 48.10 | 37.70 | 10.40 | 5.20 | 5.09 |
| 0.01 | 96.20 | 81.30 | 14.90 | 7.10 | 5.24 |
| 0.025 | 240.00 | 217.00 | 23.00 | 10.67 | 5.42 |
| 0.05 | 481.00 | 450.00 | 31.00 | 13.52 | 5.55 |
| 0.075 | 721.00 | 685.00 | 36.00 | 15.95 | 5.62 |
| 0.1 | 962.00 | 922.00 | 40.00 | 18.53 | 5.67 |

[a] Calculated from Eq. 50. [b] The $pH_0$ value is as defined in the text.

**Table VII—Concentration of Free Imidazole Base ($[Im]_h$) in the Bulk Solution and at the Solid–Liquid Interface ($[Im]_0$) with Increasing Total Imidazole Bulk Solution Concentration at $pH_{bulk}$ 6.0 and the Observed Flux ($J_{obs}$) of 2-Naphthoic Acid from a Disk Rotating at 450 rpm in a pH-Statted Aqueous Medium ($\mu$ = 0.5 with Potassium Chloride and 25°)**

| Total Buffer Concentration of Imidazole, *M* | $[Im]_h$, moles/cm³ × 10⁷ | $[Im]_0$[a], moles/cm³ × 10⁷ | $[Im]_h - [Im]_0$, moles/cm³ × 10⁷ | Total Flux of 2-Naphthoic Acid ($J_{obs}$), moles/cm²/sec × 10⁹ | $pH_0$[b] |
|---|---|---|---|---|---|
| 0.0 | 0.0 | 0.0 | 0.0 | 1.33 | 4.28 |
| 0.01 | 6.33 | 0.46 | 5.87 | 3.02 | 4.83 |
| 0.025 | 15.80 | 2.43 | 13.37 | 6.01 | 5.16 |
| 0.05 | 31.70 | 8.33 | 23.37 | 10.07 | 5.40 |
| 0.075 | 47.50 | 16.50 | 31.00 | 13.21 | 5.52 |
| 0.10 | 63.30 | 26.20 | 37.10 | 15.75 | 5.60 |

[a] Calculated from Eq. 50. [b] The $pH_0$ value is as defined in the text.

as described previously at $pH_{bulk}$ 7.00, did not differ significantly from those determined using the pH-stat with the same buffer solution. This finding was expected for solutions of high buffer capacity. However, in the non-pH-statted case, the $pH_{bulk}$ decreases as the buffer capacity of the dissolution media is exceeded due to dissolution of the acid. If this point is reached during a dissolution run, sink conditions may cease to exist in the bulk solution and the dissolution rate could fall accordingly (20).

**Influence of Basicity ($K_a^B$) of Buffer Base on Acid Dissolution Rate**—Tables VI and VII list the concentration of acetate anion and imidazole free base, respectively, as a function of the total buffer concentration in the bulk solution at $pH_{bulk}$ 6.0. They also list the corresponding buffer base concentrations at the solid–liquid interface (calculated from Eq. 50), the $pH_0$ (calculated from Eq. 51), the calculated buffer base concentration difference ($[B]_h - [B]_0$) across the diffusion layer, and the observed dissolution rate ($J_{obs}$) for 2-naphthoic acid. At a total buffer concentration of 0.01 *M* at $pH_{bulk}$ 6.0 for acetate and imidazole, the concentrations of buffer base in the bulk solution differ by a factor of ~15, whereas the corresponding observed dissolution rates of 2-naphthoic acid differ by a factor of only ~2.5. If the comparison is extended further to 0.1 *M* total buffer concentration, the difference in the bulk solution buffer base concentration remains the same, but the observed dissolution rates become approximately equal, as do the $pH_0$ values.

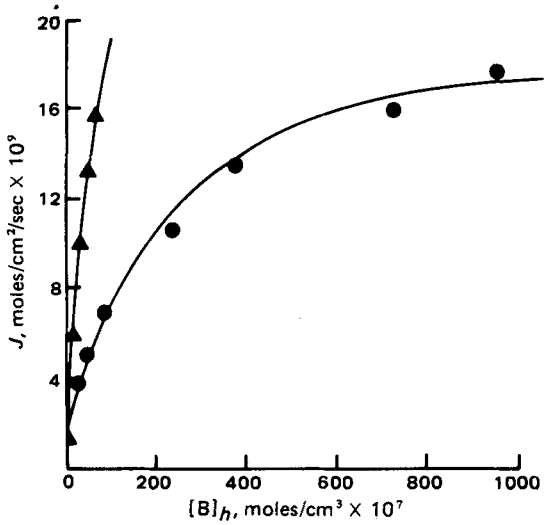


**Figure 5**—*Plot of 2-naphthoic acid dissolution rate (J)* versus *buffer base concentration in the bulk solution for acetate (●) and imidazole (▲) at $pH_{bulk}$ 6.00. The data were taken from Tables VI and VII. The symbols represent $J_{obs}$, and the continuous line represents $J_{theor}$ (given in Tables III and IV).*

These phenomena may be explained by the difference in the $K_a^B$ value between the acetate anion and imidazole (a factor of ~400), assuming that their diffusivities are approximately equal. Figure 5 shows the predicted and observed dissolution rates for 2-naphthoic acid as a function of the bulk buffer base concentration at $pH_{bulk}$ 6.00 for acetate and imidazole buffer solutions (taken from the data in Tables VI and VII). The effect of basicity in determining the extent of reaction with the dissolving acid and the proportion of buffer base in the bulk medium is observed clearly in Fig. 5 since imidazole has a much greater catalytic effect on the dissolution rate of 2-naphthoic acid for the same bulk solution buffer base concentration than does acetate. It also should be stressed that the intrinsic solubility of the dissolving acid and its $K_a^A$ are important in determining such profiles since these parameters play a significant role in describing the conditions at the solid–liquid interface, as evidenced by their presence in the coefficients *r* and *s* of Eq. 51.

An alternative way of representing the effect of the buffer base con-

**Table VIII—Regression and Correlation Data from Fig. 6 to Compute the Diffusivity ($D_B$) of the Acetate Anion and Imidazole Free Base in Aqueous Solution ($\mu$ = 0.5 with Potassium Chloride and 25°)**

| Buffer Solution at $pH_{bulk}$ 6.00 | Data from Fig. 6 (*J versus* $[B]_h - [B]_0$) | | | |
|---|---|---|---|---|
| | Slope, cm/sec | Intercept, moles/cm²/sec | $D_B$, cm²/sec | *r*[a] |
| Acetate | $4.3285 \times 10^{-3}$ | $6.3683 \times 10^{-10}$ | $8.61 \times 10^{-6}$ | 0.9962 |
| Imidazole | $4.0764 \times 10^{-3}$ | $5.86 \times 10^{-10}$ | $8.11 \times 10^{-6}$ | 0.9999 |

[a] Correlation coefficient.

**Table IX—Recalculated Data from Higuchi *et al.* (7) for Benzoic Acid Dissolving into Solutions of Sodium Acetate (with 0.75 *M* NaCl) at 25° when No pH-Stat Was Used**

| Total Bulk Solution Concentration of Acetate, *M* | Calculated[a] from $\frac{[H^+]_h}{\sqrt{K_w K_a^B/m}}$, $M \times 10^9$ | Calculated[a] $pH_{bulk}$ | Calculated[b] $pH_0$ | $J_{obs}$[c], moles/cm²/sec $\times 10^7$ | $J_{theor}$[d], moles/cm²/sec $\times 10^7$ |
|---|---|---|---|---|---|
| 0.015 | 4.09 | 8.39 | 3.76 | 1.02 | 1.13 |
| 0.05 | 2.24 | 8.65 | 4.19 | 1.75 | 1.79 |
| 0.10 | 1.59 | 8.80 | 4.41 | 2.34 | 2.52 |
| 0.15 | 1.29 | 8.88 | 4.54 | 2.82 | 3.11 |
| 0.20 | 1.12 | 8.95 | 4.62 | 3.44 | 3.63 |
| 0.25 | 1.00 | 8.99 | 4.69 | 3.82 | 4.09 |

[a] Approximate hydrogen-ion concentration for the salt of a weak acid; $K_w$ and $K_a^B$ are used as in the text, $m$ is the total concentration of the salt, and $pH_{bulk}$ is calculated from $[H^+]_h$. [b] Calculated $pH_0$ assuming that pH-stat conditions are maintained in the bulk solution (Eq. 51 was used with parameters determined for benzoic acid from Ref. 1 and acetate from Tables I and II). [c] Calculated from data given in Ref. 7. [d] Theoretical value using an equivalent diffusion layer thickness, $h = 2.82 \times 10^{-3}$ cm (1).

centration in the bulk solution on the dissolution rate of 2-naphthoic acid is to plot $J_{obs}$ *versus* $[B]_h - [B]_0$, the difference in the buffer base concentration across the diffusion layer created by the reaction therein. This plot is shown in Fig. 6 for the acetate and imidazole cases at $pH_{bulk}$ 6.00. The relationship between $J_{obs}$ and $[B]_h - [B]_0$ is approximately linear, as predicted by a modified form of Eq. 52:

$$J^{total} = \text{constant} + \frac{D_B}{h}([B]_h - [B]_0) \qquad \text{(Eq. 58)}$$

where the terms in [HA], $[H^+]$, and $[OH^-]$ represent a negligible contribution to the overall flux and may be grouped in the form of a constant. The slope of the plot of $J$ *versus* $[B]_h - [B]_0$ is $D_B/h$, thus allowing $D_B$ to be calculated if $h$ is known. The regression and correlation data for the acetate and imidazole buffers from Fig. 6 are given in Table VIII together with the calculated values of $D_B$ for both species in a solution with $\mu$ = 0.5 and at 25°. The $D_B$ values thus derived are not obtained entirely from experiment since the calculation of $[B]_0$ requires some estimate of the values of $D_B$ initially. However, close agreement is observed between assumed values (Table II) and derived values of $D_B$ (Fig. 6). Thus, consistency between theory and experiment is obtained under the conditions described, suggesting that the assumed value of $D_B$ is reasonable.

Higuchi *et al.* (7) used different bases in the dissolution media of benzoic acid in a similar study to that described here. They did not control the $pH_{bulk}$ during the dissolution experiments apart from the natural buffer capacity exerted by the added bases. In the case of benzoic acid dissolving into solutions of varying sodium acetate concentration (with 0.75 *M* NaCl as the added electrolyte and a temperature of 25°), the dissolution rate was given as a function of the acetate concentration.

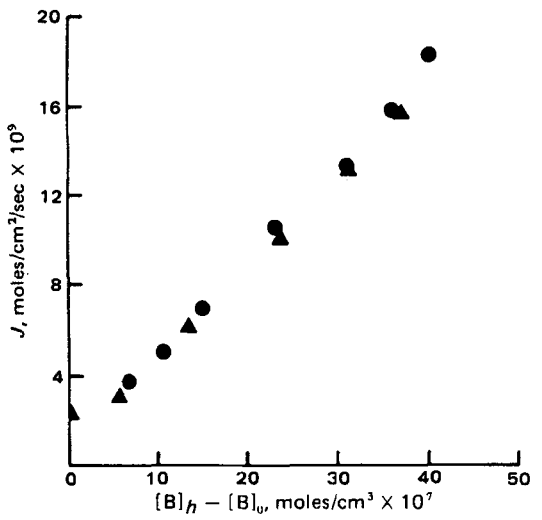


**Figure 6**—*Plot of 2-naphthoic acid dissolution rate (J)* versus *buffer base concentration difference ($[B]_h - [B]_0$) across the diffusion layer at steady state for acetate (●) and imidazole (▲) at $pH_{bulk}$ 6.00. The data were taken from Tables VI and VII. The symbols represent observed rates ($J_{obs}$). Regression and correlation data are given in Table IX.*

Disregarding the differences in ionic strength between the two studies, a theoretical initial dissolution rate of benzoic acid may be calculated from the data and methods given in Table IX[6].

The agreement between the observed and predicted $J$ values appears to be excellent. A simplified form of Eq. 52 was used by Higuchi *et al.* (7) to explain the resulting fluxes of benzoic acid in solutions of bases stronger than sodium acetate:

$$J^{total} = \frac{D_{HA}}{h}[HA]_0 + \frac{D_B}{h}[B]_h \qquad \text{(Eq. 59)}$$

Equation 59 assumes the total bulk solution buffer concentration to be equivalent to that of the base species, $[B]_h$. In the case of acetate, the equilibrium between the dissolving benzoic acid and the incoming buffer base does not favor the formation of benzoate anion as much as a similar bulk solution concentration of a stronger base, such as monohydrogen phosphate or borate. Since reaction occurs to a lesser extent with acetate ion, $[B]_h$ and $[B]_0$ are much closer in value than they would be for other stronger bases. Therefore, Eq. 58 should be used in this case rather than Eq. 59. Furthermore, Eq. 59 applies only in special cases, whereas Eqs. 52 and 58 are more general.

The reason Eq. 59 is a good approximation for the flux of benzoic acid when stronger bases than acetate anion are used is that benzoic acid is relatively water soluble (compared to 2-naphthoic acid) and maintains its pH microenvironment within the diffusion layer by the self-buffering mechanism proposed earlier (1), even when large concentrations of strong base are present in the bulk dissolution medium. As a result, for strong bases, $[B]_h$ will always be significantly greater than $[B]_0$, therefore rendering Eq. 59 applicable.

**$pH_{bulk}$ and Its Relevance to Dissolution Rates of Weak Acids**—From the data presented here for monoprotic weak acid dissolution rates in aqueous media, there are few situations where $pH_0$ equals $pH_{bulk}$. This occurs only when the acid dissociation is suppressed in the diffusion layer, when the acid is highly water insoluble, or when a base is present in the dissolution medium at such a high concentration that it swamps and controls completely the pH of the diffusion layer. The importance of the buffer base concentration in the bulk solution and the basicity of the base on the dissolution rate of weak acids cannot be overemphasized. It is extremely important that the concentration and composition of the buffer medium be stipulated in recording the dissolution rates of acids since the pH of the medium is only one of the variables (and possibly a minor variable) controlling the dissolution rate.

**Species Profiles and pH across Postulated Diffusion Layer**—Figure 7 shows the idealized sections of the diffusion layer for dissolution of 2-naphthoic acid in imidazole solutions of varying concentration and pH. The fractional distance across the diffusion layer is given by $X/h$, and the fractional concentrations of HA, $A^-$, $H^+$, and $OH^-$ are as defined previously (1). The fractional concentration of $BH^+$ is defined in a similar way to that of HA (normalized to $[BH^+]_0$), and that of B is defined in a similar way to the fractional concentration of $OH^-$ (normalized to $[B]_h$). Only the B and $BH^+$ species are shown along with the diffusion layer pH[7].

The profiles of all species within the diffusion layer are calculated using

[6] Hydrodynamic equivalence is assumed between $J_{obs}$ and $J_{theor}$ using $h = 2.82 \times 10^{-3}$ cm, derived from benzoic acid solubility data in Ref. 6 and the $D_{HA}$ value used in Ref. 1.

[7] A summary of the nonnormalized data for all species at several total bulk solution buffer concentrations and $pH_{bulk}$ values using acetate, imidazole, and morpholine can be obtained from V. J. Stella.

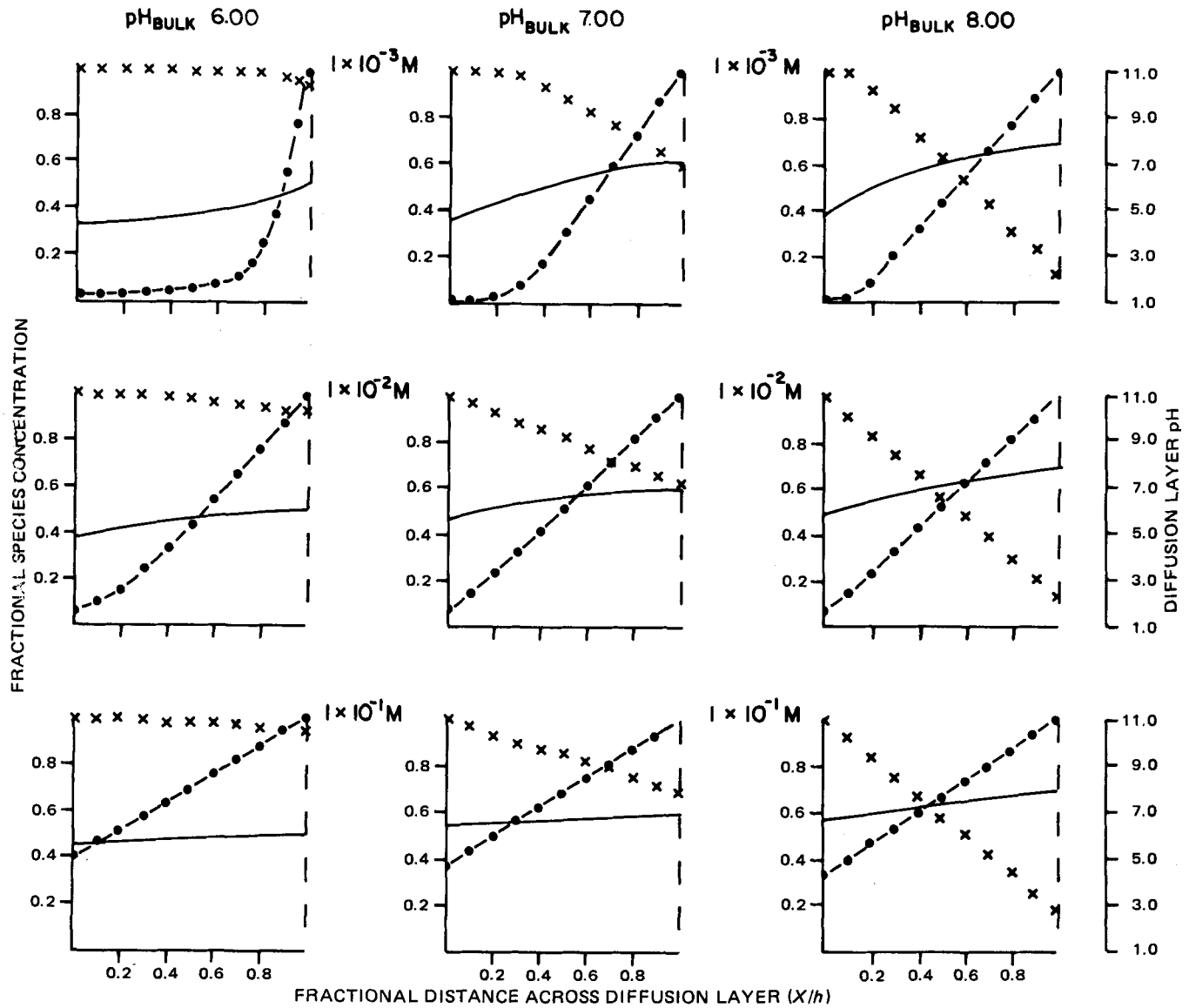


**Figure 7**—*Idealized sections across the postulated diffusion layer adjacent to the surface of dissolving 2-naphthoic acid. They depict the fractional concentration profiles of the imidazole buffer species and diffusion layer pH as a function of the changing $pH_{bulk}$ and total buffer concentration in the bulk solution. Key: ×, imidazole conjugate acid, $BH^+$; - ●, imidazole base, B; and —, pH within the diffusion layer.*

Eq. 57 and a digital computer[1]. The fractional or normalized data are misleading as given in Fig. 7 and serve only as a comparison between the different conditions tested in the bulk solution. As the total buffer concentration in the bulk solution is increased at all $pH_{bulk}$ values, the curvature in the diffusion layer pH profile becomes less pronounced since $pH_0$ approaches $pH_{bulk}$. Comparing the profiles obtained at $pH_{bulk}$ 7.00 with imidazole buffer present in the dissolution medium to those obtained with 2-naphthoic acid when no buffer is present (see Fig. 10 in Ref. 1) at the same $pH_{bulk}$, the pH within the diffusion layer shows a much less abrupt change in the buffered case.

Many investigators have used the concept of a plane of reaction within the diffusion layer moving further toward or away from the solid–liquid boundary as the reactant concentration in the bulk solution is varied. This concept has been used to explain the dissolution of benzoic acid in sodium hydroxide solutions (21, 22), implying that the reaction decreases the effective film thickness and, therefore, catalyzes the dissolution rate. Where $OH^-$ is the only base diffusing into the diffusion layer and reacting, the plane of reaction theory may be applied, as observed by the changing position in the film where an abrupt pH shift occurs when the bulk hydroxide-ion concentration is varied (1). However, this concept, as predicted by Higuchi *et al.* (7), does not apply very well to the buffered solution diffusion layers since no abrupt plane of reaction is observed due to lower reaction equilibrium constants between the acid and buffer bases than between the acid and hydroxide ion.

## CONCLUSIONS

A method of determining the initial dissolution rate of a typical solid monoprotic weak acid in the presence of buffers is demonstrated. The bulk solution pH is controlled by the buffer in combination with a pH-stat. A theoretical model, using diffusion and simultaneous, instantaneous chemical reaction of the dissolving acid with the buffer base, hydroxide ion, and water within a postulated diffusion layer, accurately predicts the dissolution rate of the acid over a wide range of bulk solution buffer concentrations and pH values.

The dissolution of 2-naphthoic acid from a compressed disk of constant surface area at constant pH, ionic strength, and temperature in acetate, imidazole, and morpholine buffers as a function of the total bulk solution buffer concentration generally is nonlinear over a wide range of buffer concentrations. Furthermore, the total acid flux may asymptotically approach the limit where $pH_0$ equals $pH_{bulk}$ with increasing total buffer concentration in the bulk solution. The approach to this condition is dependent on a complex function of the intrinsic solubility of the acid, the dissociation constants of the dissolving acid and the conjugate acid of the buffer base, the diffusivities of the reactants and products in the diffusion layer, the total concentration of the buffer in the bulk solution, and the pH of that solution.

In light of the results predicted by the model and the experimental results, the routine reporting of acid dissolution rates is meaningless

unless reference is made to the exact pH, buffer, and buffer concentrations used in the dissolution medium. Inclusion of the pKa of the buffer and acid, together with the intrinsic solubility of the acid, also is of use in interpretation of such dissolution data.

The relevance of the model presented here to the dissolution of acidic drugs from buffered tablet formulations is that, since the dissolution rate of an acidic drug is affected by the buffering effect and pH of its immediate surroundings, the incorporation of suitable buffering agents directly in tablet formulations should facilitate the release of the acidic drug from the tablet. The model certainly may assist the formulator in the choice of a buffering agent in the tablet relative to the pKa and solubility of the dissolving acid. However, direct application of the model to buffered dosage forms is difficult since the buffer must dissolve from the tablet simultaneously with the acidic drug. Furthermore, the surface area from which the dissolution occurs obviously changes during dissolution, and hydrodynamic conditions between an experiment and the *in vivo* situation are likely to differ markedly.

## REFERENCES


(1) K. G. Mooney, M. A. Mintun, K. J. Himmelstein, and V. J. Stella, *J. Pharm. Sci.*, **70**, 13 (1981).

(2) G. Levy and B. Hayes, *N. Engl. J. Med.*, **262**, 1053 (1960).

(3) G. Levy, J. R. Leonards, and J. A. Procknal, *J. Pharm. Sci.*, **54**, 1719 (1965).

(4) V. Cotty, F. Zurzola, T. Beazley, and A. Rodgers, *ibid.*, **54**, 868 (1965).

(5) E. Nelson, *J. Am. Pharm. Assoc., Sci. Ed.*, **47**, 297 (1958).

(6) *Ibid.*, **47**, 300 (1958).

(7) W. I. Higuchi, E. L. Parrott, D. E. Wurster, and T. Higuchi, *J. Am. Pharm. Assoc., Sci. Ed.*, **47**, 376 (1958).

(8) W. I. Higuchi, E. Nelson, and J. Wagner, *J. Pharm. Sci.*, **53**, 333 (1964).

(9) V. Levich, "Physicochemical Hydrodynamics," Prentice-Hall, Englewood Cliffs, N.J., 1962.

(10) B. Carnahan, H. A. Luther, and J. O. Wilkes, "Applied Numerical Methods," Wiley, New York, N.Y., 1969, p. 171.

(11) J. N. Butler, "Ionic Equilibrium, A Mathematical Approach," Addison-Wesley, Reading, Mass., 1964.

(12) A. Albert and F. Sarjeant, "Ionization Constants of Acids and Bases," Meten & Co., London, England, 1962.

(13) G. Flynn, S. H. Yalkowsky, and T. J. Roseman, *J. Pharm. Sci.*, **63**, 479 (1974).

(14) V. Vitagliano and P. A. Lyons, *J. Am. Chem. Soc.*, **78**, 4538 (1956).

(15) W. J. Albery, A. R. Greenwood, and R. F. Kibble, *Trans. Faraday Soc.*, **63**, 360 (1967).

(16) J. M. Coulson and J. F. Richardson, "Chemical Engineering," 2nd ed., vol. 1, Pergamon, New York, N.Y., 1964, p. 306.

(17) T. Erdy-Gruz, "Transport Phenomena in Aqueous Solutions," Wiley, New York, N.Y., 1974.

(18) H. K. Lee, I. H. Pitman, and T. Higuchi, *Farm. Aikak.*, **80**, 55 (1971).

(19) H. K. Lee, H. Lambert, V. J. Stella, D. Wang, and T. Higuchi, *J. Pharm. Sci.*, **68**, 288 (1979).

(20) F. L. Underwood and D. E. Cadwallader, *ibid.*, **67**, 1163 (1978).

(21) C. V. King and S. S. Brodie, *J. Am. Chem. Soc.*, **49**, 1375 (1937).

(22) A. W. Hixson and S. J. Baum, *Ind. Eng. Chem.*, **36**, 528 (1944).


## ACKNOWLEDGMENTS


Adapted in part from a dissertation submitted by K. G. Mooney to the University of Kansas in partial fulfillment of the Doctor of Philosophy degree requirements.

Supported by Grant GM22357 from the National Institutes of Health.


# Pharmacokinetic Analysis by Linear System Approach I: Cimetidine Bioavailability and Second Peak Phenomenon


**PETER VENG PEDERSEN**



Received April 28, 1980, from the *Department of Pharmacy, School of Pharmacy, University of California, San Francisco, CA 94143.* Accepted for publication July 14, 1980.



**Abstract** □ The pharmacokinetics of cimetidine were evaluated using a linear system analysis that was formulated specifically to resolve the second peak in the blood drug concentration profile after oral dosing. The analysis exemplifies a new approach to pharmacokinetic modeling, which appears to be a valuable alternative to linear compartmental or physiological modeling. The formulation of linear system analysis according to a certain interpretation of a pharmacokinetic phenomenon avoids the complexity of conventional modeling, which often obscures the significance of the kinetic parameters. The new approach should result in a more rational analysis of pharmacokinetic phenomena because the less important pharmacokinetic processes are not specifically modeled but are still accounted for in the mathematical treatment. The bioavailability of cimetidine calculated by deconvolution agrees with previous findings. The model proposed to describe the second peak after oral absorption appears to agree well with the data and the hepatic recycling reported for cimetidine.



**Keyphrases** □ Linear system approach—evaluation of pharmacokinetics of cimetidine □ Pharmacokinetics—cimetidine, evaluation by linear system approach □ Cimetidine—evaluation of pharmacokinetics by linear system approach


Pharmacokinetic phenomena have been modeled and analyzed primarily according to two classes of models: linear compartmental models and physiological models. The classical linear compartmental models frequently provide a good fit to pharmacokinetic data. However, due to the fictitious structure of these models, which often bears little relation to the true nature of the pharmacokinetic processes, the parameters estimated from such models often have no real kinetic significance. The physiological models that attempt to be more realistic by considering such factors as blood flow and elimination and distribution in various organs and tissues may provide more meaningful results. However, the great number of physiological parameters and the difficulty of obtaining accurate and reliable estimates of these parameters make this approach very difficult. Both approaches to modeling




0022-3549/81/0100-0032$01.00/0



© 1981, American Pharmaceutical Association

unless reference is made to the exact pH, buffer, and buffer concentrations used in the dissolution medium. Inclusion of the pKa of the buffer and acid, together with the intrinsic solubility of the acid, also is of use in interpretation of such dissolution data.

The relevance of the model presented here to the dissolution of acidic drugs from buffered tablet formulations is that, since the dissolution rate of an acidic drug is affected by the buffering effect and pH of its immediate surroundings, the incorporation of suitable buffering agents directly in tablet formulations should facilitate the release of the acidic drug from the tablet. The model certainly may assist the formulator in the choice of a buffering agent in the tablet relative to the pKa and solubility of the dissolving acid. However, direct application of the model to buffered dosage forms is difficult since the buffer must dissolve from the tablet simultaneously with the acidic drug. Furthermore, the surface area from which the dissolution occurs obviously changes during dissolution, and hydrodynamic conditions between an experiment and the *in vivo* situation are likely to differ markedly.

## REFERENCES


(1) K. G. Mooney, M. A. Mintun, K. J. Himmelstein, and V. J. Stella, *J. Pharm. Sci.*, **70**, 13 (1981).

(2) G. Levy and B. Hayes, *N. Engl. J. Med.*, **262**, 1053 (1960).

(3) G. Levy, J. R. Leonards, and J. A. Procknal, *J. Pharm. Sci.*, **54**, 1719 (1965).

(4) V. Cotty, F. Zurzola, T. Beazley, and A. Rodgers, *ibid.*, **54**, 868 (1965).

(5) E. Nelson, *J. Am. Pharm. Assoc., Sci. Ed.*, **47**, 297 (1958).

(6) *Ibid.*, **47**, 300 (1958).

(7) W. I. Higuchi, E. L. Parrott, D. E. Wurster, and T. Higuchi, *J. Am. Pharm. Assoc., Sci. Ed.*, **47**, 376 (1958).

(8) W. I. Higuchi, E. Nelson, and J. Wagner, *J. Pharm. Sci.*, **53**, 333 (1964).

(9) V. Levich, "Physicochemical Hydrodynamics," Prentice-Hall, Englewood Cliffs, N.J., 1962.

(10) B. Carnahan, H. A. Luther, and J. O. Wilkes, "Applied Numerical Methods," Wiley, New York, N.Y., 1969, p. 171.

(11) J. N. Butler, "Ionic Equilibrium, A Mathematical Approach," Addison-Wesley, Reading, Mass., 1964.

(12) A. Albert and F. Sarjeant, "Ionization Constants of Acids and Bases," Meten & Co., London, England, 1962.

(13) G. Flynn, S. H. Yalkowsky, and T. J. Roseman, *J. Pharm. Sci.*, **63**, 479 (1974).

(14) V. Vitagliano and P. A. Lyons, *J. Am. Chem. Soc.*, **78**, 4538 (1956).

(15) W. J. Albery, A. R. Greenwood, and R. F. Kibble, *Trans. Faraday Soc.*, **63**, 360 (1967).

(16) J. M. Coulson and J. F. Richardson, "Chemical Engineering," 2nd ed., vol. 1, Pergamon, New York, N.Y., 1964, p. 306.

(17) T. Erdy-Gruz, "Transport Phenomena in Aqueous Solutions," Wiley, New York, N.Y., 1974.

(18) H. K. Lee, I. H. Pitman, and T. Higuchi, *Farm. Aikak.*, **80**, 55 (1971).

(19) H. K. Lee, H. Lambert, V. J. Stella, D. Wang, and T. Higuchi, *J. Pharm. Sci.*, **68**, 288 (1979).

(20) F. L. Underwood and D. E. Cadwallader, *ibid.*, **67**, 1163 (1978).

(21) C. V. King and S. S. Brodie, *J. Am. Chem. Soc.*, **49**, 1375 (1937).

(22) A. W. Hixson and S. J. Baum, *Ind. Eng. Chem.*, **36**, 528 (1944).


## ACKNOWLEDGMENTS


Adapted in part from a dissertation submitted by K. G. Mooney to the University of Kansas in partial fulfillment of the Doctor of Philosophy degree requirements.

Supported by Grant GM22357 from the National Institutes of Health.


# Pharmacokinetic Analysis by Linear System Approach I: Cimetidine Bioavailability and Second Peak Phenomenon


**PETER VENG PEDERSEN**



Received April 28, 1980, from the *Department of Pharmacy, School of Pharmacy, University of California, San Francisco, CA 94143.* Accepted for publication July 14, 1980.



**Abstract** □ The pharmacokinetics of cimetidine were evaluated using a linear system analysis that was formulated specifically to resolve the second peak in the blood drug concentration profile after oral dosing. The analysis exemplifies a new approach to pharmacokinetic modeling, which appears to be a valuable alternative to linear compartmental or physiological modeling. The formulation of linear system analysis according to a certain interpretation of a pharmacokinetic phenomenon avoids the complexity of conventional modeling, which often obscures the significance of the kinetic parameters. The new approach should result in a more rational analysis of pharmacokinetic phenomena because the less important pharmacokinetic processes are not specifically modeled but are still accounted for in the mathematical treatment. The bioavailability of cimetidine calculated by deconvolution agrees with previous findings. The model proposed to describe the second peak after oral absorption appears to agree well with the data and the hepatic recycling reported for cimetidine.



**Keyphrases** □ Linear system approach—evaluation of pharmacokinetics of cimetidine □ Pharmacokinetics—cimetidine, evaluation by linear system approach □ Cimetidine—evaluation of pharmacokinetics by linear system approach


Pharmacokinetic phenomena have been modeled and analyzed primarily according to two classes of models: linear compartmental models and physiological models. The classical linear compartmental models frequently provide a good fit to pharmacokinetic data. However, due to the fictitious structure of these models, which often bears little relation to the true nature of the pharmacokinetic processes, the parameters estimated from such models often have no real kinetic significance. The physiological models that attempt to be more realistic by considering such factors as blood flow and elimination and distribution in various organs and tissues may provide more meaningful results. However, the great number of physiological parameters and the difficulty of obtaining accurate and reliable estimates of these parameters make this approach very difficult. Both approaches to modeling




0022-3549/81/0100-0032$01.00/0



© 1981, American Pharmaceutical Association

are faced with a statistical and numerical dilemma: the more complex a model becomes to consider the many kinetic factors involved and/or to get a better fit to the data, the less significant the individual parameters become.

This report discusses how linear system analysis may be applied as an alternative to other modeling approaches and how the described problems can be overcome, to some extent, by the new approach. Linear system analysis apparently has not been used in pharmacokinetic modeling because the analysis is considered and treated basically as a model-independent procedure. It is demonstrated that the linear system approach may be formulated according to a specific pharmacokinetic interpretation, without having to rely on complex pharmacokinetic or mathematical models. The formulation should result in a more rational analysis of the pharmacokinetic phenomena of interest because the pharmacokinetic processes of minor interest are not specifically modeled but are still accounted for in the mathematical treatment.

The new type of modeling is demonstrated using the pharmacokinetics of cimetidine. Since its peculiar kinetic behavior was discussed and analyzed recently using linear compartmental principles (1, 2), there should be a good basis for comparison with this conventional type of analysis.

## THEORETICAL

**Derivation**—The mathematical derivation is based on a linear system approach that involves the following basic assumptions:

1. The pharmacokinetic system is linear and time invariant (3) in the sense that the drug concentration response in the sampling region, $S$ (the blood), behaves linearly with respect to direct (intravenous) drug input (Fig. 1, part 1) and to indirect (absorption) input (Fig. 1, part 2) independent of time.
2. The characteristic response (the unit impulse response) of the sampling region is the same for direct and indirect input.

Under Assumption 1, the concentration response, $c(t)$, in $S$ is the convolution of the characteristic response, $c_\delta(t)$, and the rate of direct input, $f(t)$, into $S$:

$$c(t) = c_s(t)*f(t) = \int_0^t c_\delta(t-u)f(u)du = \int_0^t c_\delta(u)f(t-u)du \qquad \text{(Eq. 1)}$$

The characteristic response, $c_s(t)$, is determined by the transfer of drug between the sampling region, $S$, and the peripheral region, $P$[1], and by the elimination from $S$ (Fig. 1, parts 1 and 2). If the $S \leftrightarrow P$ transfer kinetics and the drug elimination kinetics do not change significantly between the direct (intravenous) input and the indirect (absorption) input, then Assumption 2 will be valid. In that case, Eq. 1 can be used to evaluate the input–response relationship in the absorption case. The vital link in this relationship, the characteristic response, $c_\delta(t)$, then can be evaluated from a direct (intravenous) drug administration (4, 5).

The current definition of bioavailability is based on the rate and extent of input into the systemic circulation (6–8). In mathematical terms, these parameters are equivalent to $f(t)$ and $\int_0^t f(t)dt$ or $\int_0^\infty f(t)dt$. The various deconvolution methods proposed to evaluate $f(t)$ from Eq. 1 were discussed previously (9–11). These methods are either inaccurate and particularly sensitive to errors in the data[2] (12) or computationally complex (9, 13, 14). However, a recently proposed deconvolution method appears to be accurate, error stable, and simple to use (5).

This method is based on an approximation (*e.g.*, least squares) of the absorption response, $c(t)$, by a sum of exponentials:

$$c(t) = \sum_{i=1}^{m} b_i e^{-\beta_i t_+} \quad \beta_i > 0 \qquad \text{(Eq. 2)}$$

where $t_+ = (t - t_{lag})_+$ and $c(0) = 0$. The characteristic response, $c_\delta(t)$, is obtained from a polyexponential approximation of the intravenous bolus response[3]:

$$c_{iv}(t) = \sum_{i=1}^{n} a_i e^{-\alpha_i t} \quad \alpha_i > 0 \qquad \text{(Eq. 3)}$$

according to:

$$c_\delta(t) = c_{iv}(t)/D_{iv} \qquad \text{(Eq. 4)}$$

where $D_{iv}$ is the intravenous bolus dose.

The cumulative amount of drug absorbed, expressed as a percentage of the dose ($D$), was derived previously (5) as:

$$PCT(t) = \frac{100}{D}\int_0^t f(t)dt = u_0 + \sum_{i=1}^{m+n-1} u_i e^{-v_i t_+} \qquad \text{(Eq. 5)}$$

and the absorption rate was derived as:

$$f(t) = \frac{D}{100}\sum_{i=1}^{m+n-1} u_i(-v_i)e^{-v_i t_+} \qquad \text{(Eq. 6)}$$

The parameters $u_0, \{u_i\}_1^{m+n-1}$ that define the input function are calculated from $\{b_i,\beta_i\}_1^m$ (Eq. 2) and $\{a_i,\alpha_i\}_1^n$ (Eq. 3) and the doses (5).

**Second Peak Phenomenon**—A previous investigation strongly suggested that the second peak observed in the oral absorption curve of cimetidine is due to a discontinuous recycling phenomenon (1). Thus, it seems appropriate to consider the oral absorption input of this drug as consisting of two components: an input, $f_A(t)$, of drug that has not been recycled and an input, $f_B(t)$, of recycled drug:

$$f(t) = f_A(t) + f_B(t) \qquad \text{(Eq. 7)}$$

This corresponds, according to the fundamental superposition principle of linear systems (3, 15), to an equivalent partitioning of the response:

$$c(t) = c_A(t) + c_B(t) \qquad \text{(Eq. 8)}$$

The input components, $f_A(t)$ and $f_B(t)$, may be estimated individually from the response components, $c_A(t)$ and $c_B(t)$, by deconvolution if these response components can be properly resolved. This seems to be the case for the oral cimetidine data because of the substantial delay in the recycling and because of the substantial magnitude of the second peak that is superimposed at the end of the primary ($A$) absorption response.

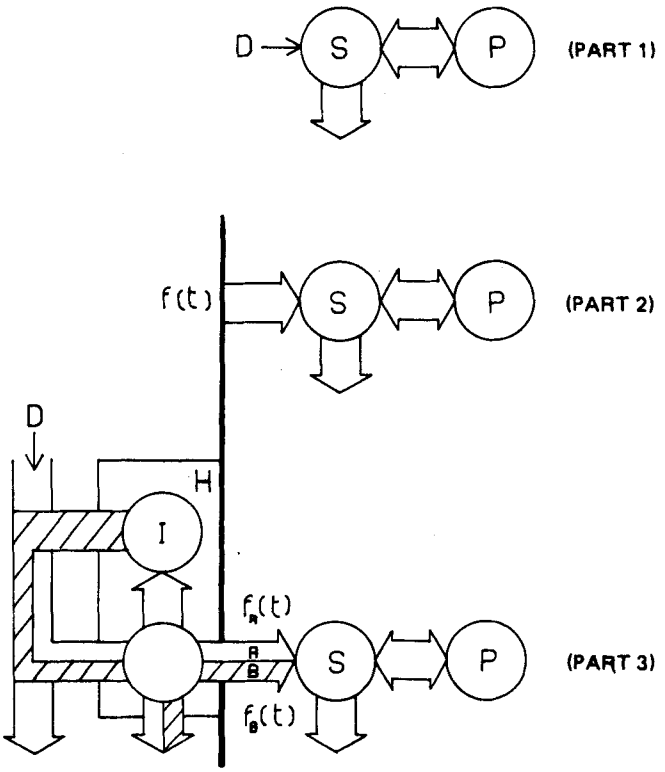


**Figure 1**—*Proposed pharmacokinetic model for cimetidine.*

[1] The treatment also is valid if the drug is eliminated from $P$.

[2] L. Z. Benet and C. W. N. Chiang, presented at the APhA Academy of Pharmaceutical Sciences, Chicago meeting, November 1977.

[3] The characteristic response can be determined readily from other types of intravenous input (5).

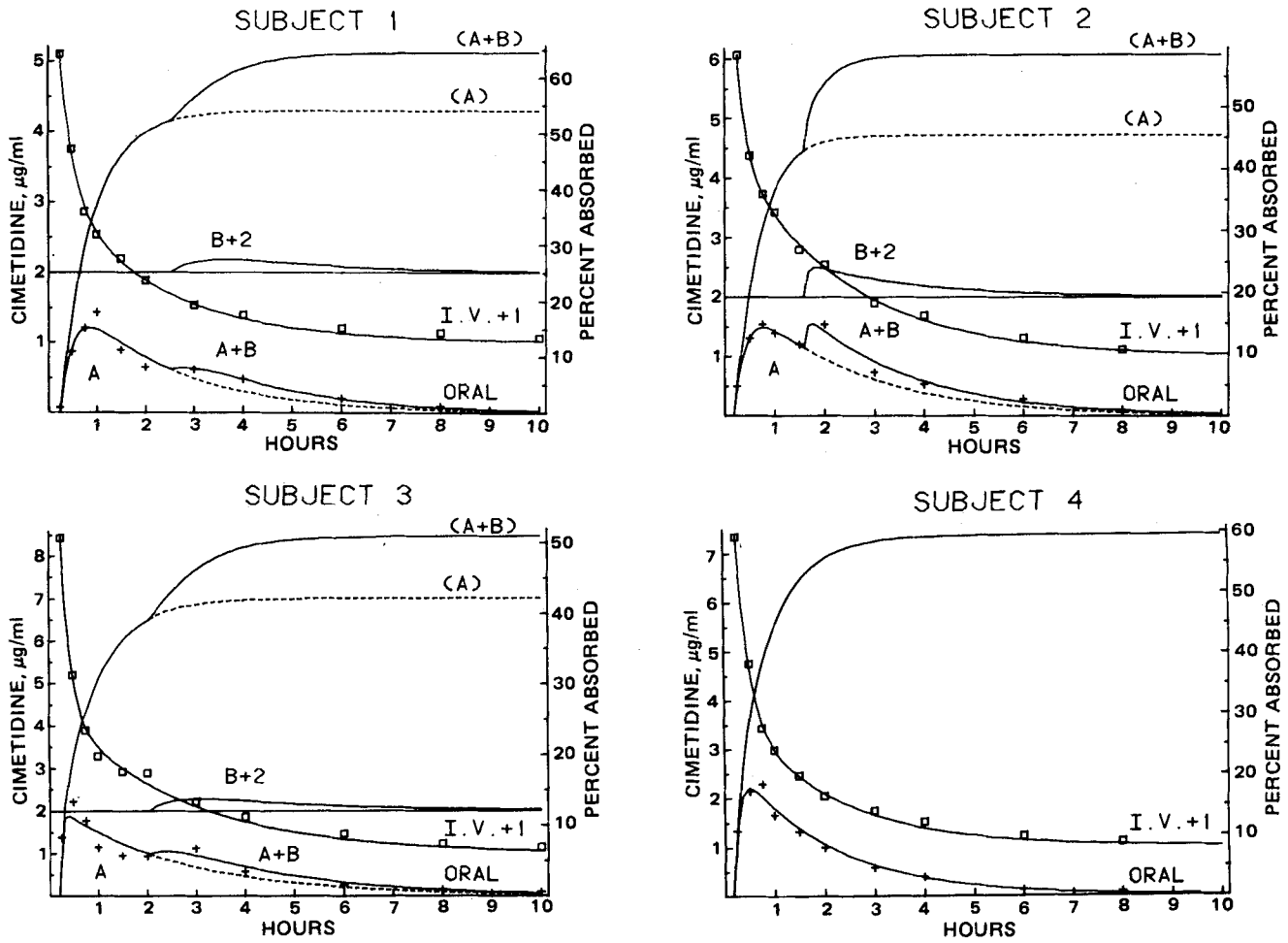


**Figure 2**—*Deconvolution of cimetidine data for Subjects 1–4. The monotonically increasing curve is the cumulative amount of input expressed as percent of the dose. The oral drug concentration–response approximation and input have been resolved into two components,* A *and* B, *where* A *is the primary input (or response) and* B *is a reabsorption component proposed according to the model in Fig. 1. The intravenous curve and data are staggered vertically one unit for clarity (I.V. + 1). The response component* B *is extracted from the oral curve and is staggered two units (*B + 2*).*

The pharmacokinetic literature has demonstrated the great utility of Eq. 2 in approximating oral absorption responses. For this reason and because of the smooth and asymptotic behavior of Eq. 2, it seems appropriate to apply Eq. 2 to resolve the absorption response in two polyexponential components:

$$c(t) = \left(\sum_{i=1}^{r} b_i e^{-\beta_i t+}\right)_A + \left(\sum_{j=1}^{s} b_j e^{-\beta_j t+}\right)_B \qquad \text{(Eq. 9)}$$

and to estimate these components by fitting their sum (Eq. 9) to the oral cimetidine data. The corresponding input components, $f_A(t)$ and $f_B(t)$, subsequently can be estimated individually by the deconvolution method, where the characteristic response is determined from the intravenous bolus data.

According to Assumption 2, the asymptotic terminal phases of the responses from the intravenous and oral administrations should agree within each subject. This specification requires that:

$$\min_i \alpha_i = \min_i (\beta_i)_A = \min_j (\beta_j)_B \qquad \text{(Eq. 10)}$$

To enforce this restriction, it is necessary to fit Eqs. 3 and 9 simultaneously to the data because of the shared parameter (Eq. 10).

The deconvolution method allows any number of exponential terms in the approximation of the characteristic response and the absorption input response. However, two exponential terms ($n = 2, r = 2, s = 2$) gave a satisfactory approximation to the data in all 12 cases (Figs. 2–4). Thus, the following equations were fitted simultaneously to the cimetidine data:

$$c_{iv}(t) = a_1 e^{-\alpha_1 t} + a_2 e^{-\alpha_2 t} \qquad \text{(Eq. 11)}$$

$$c(t) = (b_1 e^{-\beta_1 t+} + b_2 e^{-\beta_2 t+})_A + (b_1 e^{-\beta_1 t+} + b_2 e^{-\beta_2 t+})_B \qquad \text{(Eq. 12)}$$

with due consideration of the boundary conditions, $c_A(0) = 0$ and $c_B(0) = 0$:

$$(b_1 + b_2)_A = 0 \qquad \text{(Eq. 13)}$$

$$(b_1 + b_2)_B = 0 \qquad \text{(Eq. 14)}$$

If $b_1$ is defined as positive in Eq. 12, then $\beta_1 < \beta_2$ and the restriction in Eq. 10 becomes:

$$(\beta_1)_A = (\beta_1)_B = \min(\alpha_1, \alpha_2) \qquad \text{(Eq. 15)}$$

which is readily considered in the simultaneous curve fitting.

The theory (5) predicts that if $m$ exponential terms are used for the approximation of the absorption response and $n$ terms are used for the characteristic response, then the input function will consist of $m + n - 1$ exponential terms (Eqs. 5 and 6). Of these $m + n - 1$ exponential terms, $m$ has exponents (time coefficients) identical to those used in the absorption response approximation (Eq. 2). If any exponent in the absorption response approximation coincides with an exponent for the characteristic response, then the corresponding exponential term of the input function vanishes ($u \to 0$). There is one common exponent parameter (Eq. 15) in the simultaneous fitting of Eqs. 11 and 12. Thus, the number of exponential terms in the input function is $(m + n - 1) - 1 = (2 + 2 - 1) - 1 = 2$ for components $A$ and $B$[4].

In addition to a graphical presentation (Figs. 2–4) that provides the most informative picture of the absorption process, it is valuable to

[4] The $u$ values corresponding to the common exponents calculated by the computer program in Ref. 5 were zero within the accuracy of the computer computations.

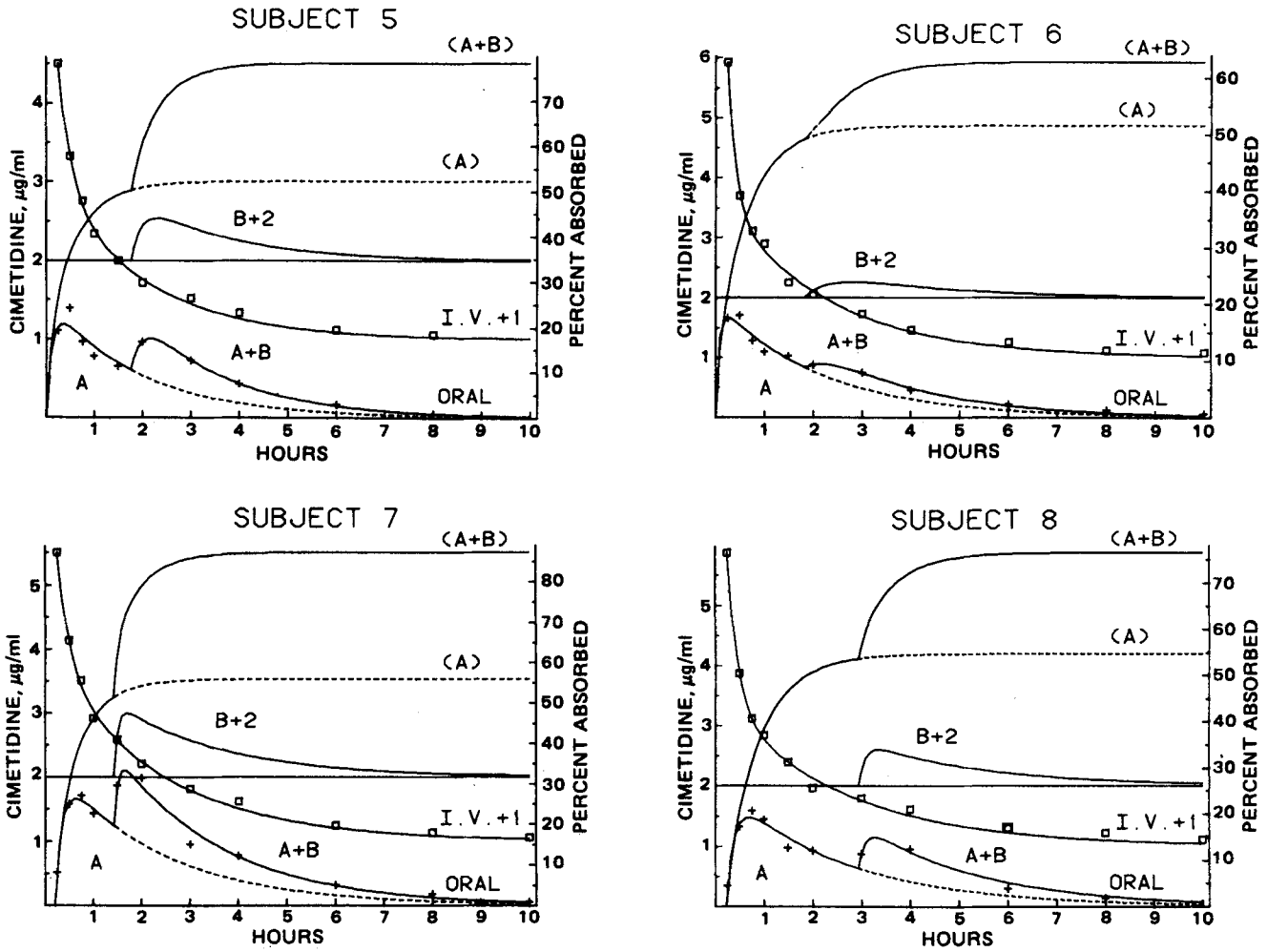


**Figure 3**—*Deconvolution of cimetidine data for Subjects 5–8. (See legend to Fig. 2.)*

quantify the rate and extent of drug input in simple terms. When Eq. 15 is satisfied, then $f(t) > 0$ for $0 < t < \infty$. Consequently, $PCT(t)$ is monotonically increasing, and the total bioavailability, expressed as percent of the dose, is ($v_i > 0$):

$$F = \lim_{t \to \infty} PCT(t) = (u_0)_A + (u_0)_B \qquad \text{(Eq. 16)}$$

The time, $t_x$ (corrected for the lag time), for a given fraction, $x$, of the total amount absorbed to be absorbed is obtained from:

$$xF - PCT(t_x + t_{lag}) = 0 \qquad \text{(Eq. 17)}$$

where $PCT(t)$ is given by Eq. 5. The absorption times, $t_{1/2}$ and $t_{0.9}$, obtained in this way are useful measures of the absorption rate.

## EXPERIMENTAL

The simultaneous fittings of Eqs. 11 and 12 to the cimetidine data were obtained using the general nonlinear regression program FUNFIT (16). The deconvolutions were done according to the algorithm and the computer program listed in Ref. 5. The absorption times, $t_{1/2}$ and $t_{0.9}$, were obtained by solving Eq. 17 using a root-finding algorithm proposed by Wilkinson (17) and improved by Brent (18). Figures 2–4 were drawn by a penplotter using computer graphics software written by the author[5].

## RESULTS AND DISCUSSION

Since the deconvolution approach makes no assumptions about the mechanism and kinetics of drug absorption or the elimination and distribution kinetics, it is a particularly powerful method. It is versatile in that it is not limited to a particular pharmacokinetic model. It is well known from the theory of linear differential equations that the input–response relationship of classical linear compartmental models can be described by the convolution integral, Eq. 1. Therefore, the deconvolution approach can be thought of as a generalization of the linear compartmental approaches in drug absorption studies. However, it is not limited to this family of models described by first-order linear differential equations. It generalizes the families of models described by linear differential equations of any kind. In fact, the convolution integral relationship (Eq. 1) can be derived for a linear response system without reference to pharmacokinetic processes modeled in differential form (3, 19). Because of the nonspecificity of the deconvolution approach, there are no restrictions, other than the basic assumptions (Assumptions 1 and 2), with respect to the interpretation or modeling of the pharmacokinetic system. The deconvolution approach should stimulate a more rational and objective evaluation of pharmacokinetics.

In the case of cimetidine, one may assume a simple pharmacokinetic model as in Fig. 1, parts 1 and 2. In the intravenous bolus administration (Fig. 1, part 1), the drug input is directly into the sampling region, $S$ (the blood). The change in the amount or concentration of drug in $S$ is due to two basic processes, elimination and reversible distribution. This change is considered in the simplest form in the model in Fig. 1, part 1, where no specific assumptions are made about the distribution kinetics ($S \leftrightarrow P$) or the elimination kinetics ($S \rightarrow$ out). In the oral administration (Fig. 1, part 2), the drug input is not directly into the sampling region. In the first-pass process, the drug is exposed to the complex kinetic mechanism of the hepatic system before it reaches $S$. However, under Assumptions 1 and 2, if the first-pass process does not significantly change the drug distribution kinetics ($S \leftrightarrow P$) or elimination kinetics from $S$, then the input can be evaluated without considering the first-pass kinetics (Fig. 1, part 2). The present deconvolution calculations of cimetidine absorption can be interpreted in this simple way (Fig. 1, parts 1 and 2).

[5] An IBM 370/148 computer was used for the calculations and the plotting.

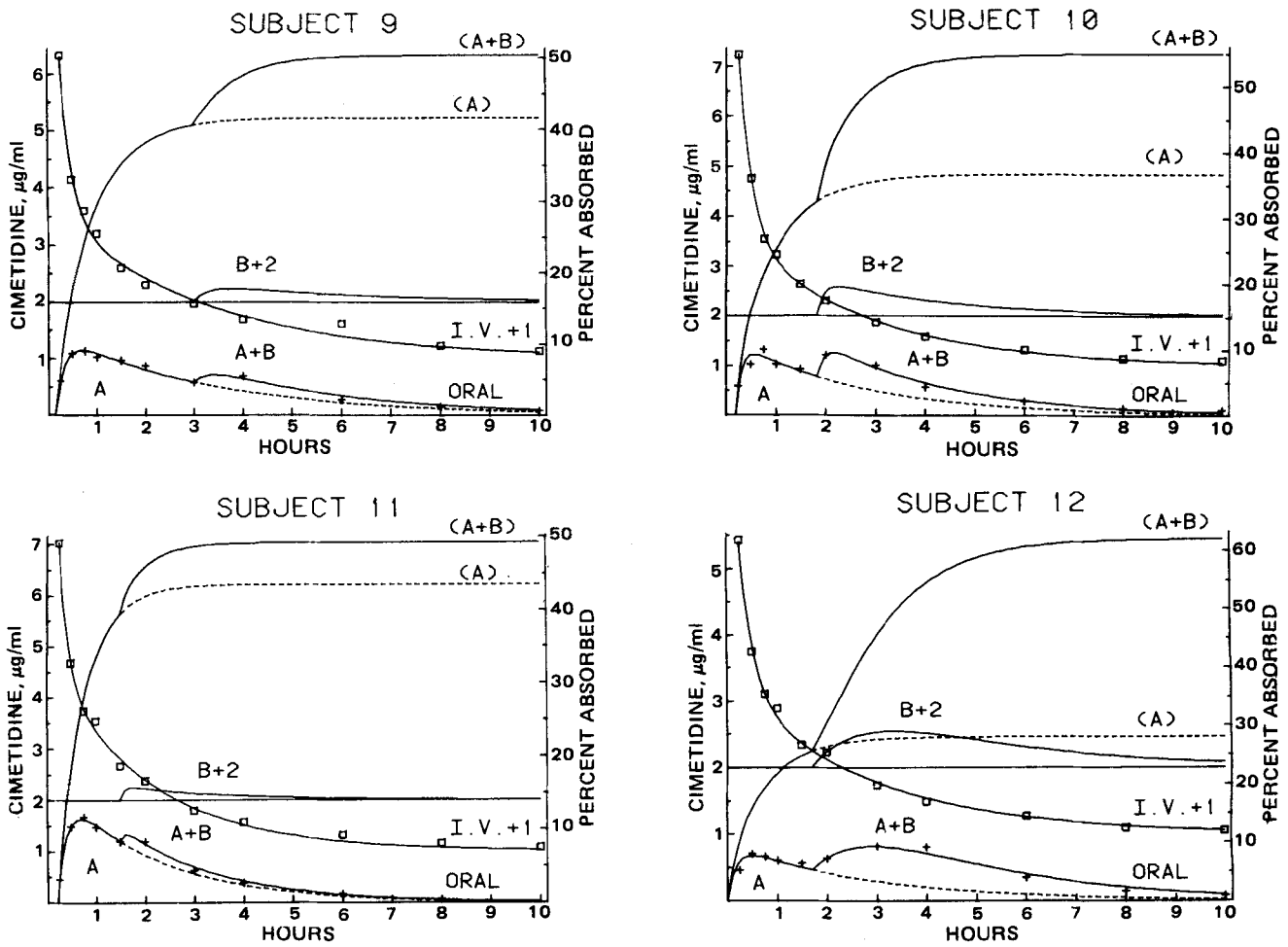


**Figure 4**—*Deconvolution of cimetidine data for Subjects 9–12. (See legend to Fig. 2.)*

The oral data show a pronounced secondary peak that a previous analysis (1) strongly suggests is a first-pass phenomenon. The following interpretation was proposed. The drug accumulates in a tissue or organ that is well perfused in the first-pass transfer. The hepatic parenchymal tissue and the bile phase appear to be the most likely storage areas. The rate of accumulation is much higher in the first-pass transfer than from the systemic circulation. The accumulation occurs by a competitive process, and absorbed elements of food seem to compete in this process. The second peak appears to be the result of a rapid release of drug and bioreversible drug compounds from the hepatic biliary system with subsequent reabsorption. This release may occur spontaneously but appears to be triggered by the intake of food.

It is of interest to quantify this proposed hepatic recycling. The pharmacokinetic model in Fig. 1, part 3, was constructed in agreement with this interpretation. This extension of the simpler model in Fig. 1, part 2, is not needed for the deconvolution calculations but is constructed to resolve the proposed drug absorption mechanism. Most of the drug ($D$) is absorbed from the GI system and is transferred to the hepatic system ($H$), where some of it is metabolized and accumulated ($I$) or passed on to the general systemic circulation ($S$) (Fig. 1, part 3). The drug accumulated in the hepatic system is released after some delay and then is reabsorbed and transferred to the systemic circulation (the shaded pathway in Fig. 1, part 3).

The extent of reaccumulation from the reabsorbed drug probably is not very significant because reabsorption appears to coincide with the intake of food (2 hr after dosing), and food apparently inhibits the hepatic drug accumulation (1). Even if the drug accumulates to the same extent after being reabsorbed, the compounded total amount (*e.g.*, 20% × 20% = 4%) most likely will not be detectable, considering the limited information density of the data. It apparently is not possible to detect any tertiary peaks in the oral data. Thus, the analysis can be appropriately limited to the primary input ($A$) and the reabsorption component ($B$) (Fig. 1, part 3), as discussed under *Theoretical*.

The simultaneous fitting of Eqs. 11 and 12 to the cimetidine data appears to give a good response approximation for all 12 subjects (Tables I and II and Figs. 2–4). The fit in the terminal phases of the oral and intravenous data is excellent for each subject, which is in agreement with Assumption 2 and Eq. 15. The cumulative input profiles for components $A$ and $B$ show asymptotic behavior, in agreement with the theory, and give a well-defined graphical representation of the extent of absorption due to $A$ and $B$ (Figs. 2–4). There is no secondary peak for Subject 4, perhaps because of a particularly slow or inhibited (nonfasting state?) hepatic drug accumulation in this subject. The good similarity between the oral response profile of Subject 4 and the $A$ response profiles of the other subjects indicates that the particular $A/B$ partitioning of the responses is a valid approach.

The average extent of primary absorption $(u_0)_A$ and reabsorption $(u_0)_B$ is 47 and 17%, respectively (Table III). The average total availability,

**Table I—Least-Squares Polyexponential Approximation of Intravenous Bolus Response (Eq. 11) [a]**

| Subject | $\alpha_1$, μg/ml | $\alpha_2$, μg/ml | $\alpha_1$, $hr^{-1}$ | $\alpha_2$, $hr^{-1}$ | $RSS^b \times 10^2$, $(\mu g/ml)^2$ |
|---|---|---|---|---|---|
| 1 | 2.30 | 5.07 | 0.479 | 3.56 | 3.96 |
| 2 | 3.69 | 7.20 | 0.449 | 5.60 | 2.54 |
| 3 | 3.60 | 15.3 | 0.395 | 5.19 | 19.1 |
| 4 | 3.08 | 10.3 | 0.523 | 4.15 | 7.92 |
| 5 | 2.18 | 3.95 | 0.531 | 3.64 | 1.67 |
| 6 | 2.78 | 11.4 | 0.464 | 6.18 | 5.37 |
| 7 | 3.05 | 4.59 | 0.449 | 3.79 | 4.11 |
| 8 | 2.55 | 8.31 | 0.407 | 4.69 | 7.15 |
| 9 | 2.66 | 7.99 | 0.318 | 4.13 | 13.6 |
| 10 | 2.87 | 9.73 | 0.388 | 3.94 | 2.64 |
| 11 | 3.83 | 9.97 | 0.506 | 5.29 | 8.74 |
| 12 | 2.31 | 5.68 | 0.365 | 3.64 | 4.76 |

[a] Fitted simultaneously with the oral absorption data (Eq. 12). [b] Residual sum of squares.

**Table II—Least-Squares Polyexponential Approximation of Absorption Response (Eq. 12) [a]**

| Subject | Component $A$ | | | Component $B$ | | | $RSS^b \times 10^2$, $(\mu g/ml)^2$ |
|---|---|---|---|---|---|---|---|
| | $b_1$, $\mu g/ml$ | $\beta_2$, $hr^{-1}$ | $t_{lag}$, hr | $b_1$, $\mu g/ml$ | $\beta_2$, $hr^{-1}$ | $t_{lag}$, hr | |
| 1 | 1.82 | 4.09 | 0.25 | 0.453 | 1.53 | 2.51 | 10.3 |
| 2 | 2.16 | 4.34 | 0.18 | 0.571 | 17.1 | 1.58 | 5.84 |
| 3 | 2.04 | 30.0 | 0.21 | 0.521 | 16.3 | 2.05 | 40.7 |
| 4 | 2.76 | 9.29 | 0.17 | — | — | — | 10.1 |
| 5 | 1.54 | 8.46 | 0 | 0.817 | 4.48 | 1.76 | 7.81 |
| 6 | 1.95 | 13.7 | 0 | 0.540 | 1.90 | 1.82 | 6.38 |
| 7 | 2.15 | 6.92 | 0.21 | 1.16 | 13.5 | 1.43 | 8.30 |
| 8 | 1.92 | 6.13 | 0.22 | 0.756 | 7.55 | 2.94 | 5.65 |
| 9 | 1.45 | 5.57 | 0.14 | 0.316 | 3.47 | 2.99 | 1.73 |
| 10 | 1.47 | 8.93 | 0.19 | 0.737 | 7.36 | 1.83 | 5.99 |
| 11 | 2.30 | 5.37 | 0.20 | 0.285 | 13.3 | 1.50 | 1.10 |
| 12 | 0.860 | 6.04 | 0 | 1.58 | 0.955 | 1.71 | 4.11 |

[a] Fitted simultaneously with the intravenous bolus data; $b_2 = -b_1$ and $\beta_1 = \alpha_1$ (Table I). [b] Residual sum of squares.

**Table III—Parameters Defining the Input Function (Eqs. 5 and 6) [a]**

| Subject | Component $A$ | | | | | Component $B$ | | | | | Total Availability, $PCT$ % |
|---|---|---|---|---|---|---|---|---|---|---|---|
| | $u_0$, % | $u_1$, % | $u_2$, % | $v_1$, $hr^{-1}$ | $v_2$, $hr^{-1}$ | $u_0$, % | $u_1$, % | $u_2$, % | $v_1$, $hr^{-1}$ | $v_2$, $hr^{-1}$ | |
| 1 | 54.0 | −4.31 | −49.7 | 4.09 | 1.44 | 10.4 | 102.7 | −113.1 | 1.53 | 1.44 | 64.4 |
| 2 | 45.5 | 10.5 | −56.0 | 4.34 | 2.19 | 13.1 | −3.95 | −9.10 | 17.1 | 2.19 | 58.6 |
| 3 | 42.3 | −9.19 | −33.1 | 30.0 | 1.31 | 8.76 | 10.4 | −19.1 | 1.99 | 1.31 | 51.1 |
| 4 | 59.6 | −12.7 | −46.9 | 9.29 | 1.36 | — | — | — | — | — | 59.6 |
| 5 | 52.2 | −16.6 | −35.6 | 8.46 | 1.64 | 26.1 | −3.47 | −22.6 | 4.49 | 1.64 | 78.3 |
| 6 | 51.6 | −8.22 | −43.4 | 13.7 | 1.59 | 11.2 | 39.0 | −50.2 | 1.90 | 1.59 | 62.8 |
| 7 | 55.9 | −16.0 | −39.9 | 6.92 | 1.78 | 31.3 | −12.2 | −19.1 | 13.5 | 1.78 | 87.2 |
| 8 | 54.7 | −5.02 | −49.7 | 6.13 | 1.41 | 21.9 | −3.07 | −18.8 | 7.55 | 1.41 | 76.6 |
| 9 | 41.7 | −4.29 | −37.4 | 5.57 | 1.27 | 8.76 | 0.812 | −9.57 | 3.47 | 1.27 | 50.5 |
| 10 | 36.8 | −7.21 | −29.6 | 8.94 | 1.20 | 18.2 | −3.07 | −15.1 | 7.36 | 1.20 | 55.0 |
| 11 | 43.5 | −0.360 | −43.1 | 5.37 | 1.83 | 5.74 | −1.39 | −4.35 | 13.3 | 1.83 | 49.2 |
| 12 | 28.0 | −5.13 | −22.9 | 6.04 | 1.31 | 34.0 | −92.4 | 58.4 | 0.955 | 1.31 | 62.0 |
| Mean | 47.15 | | | | | 17.2 | | | | | 62.9 |
| $CV$, % | 19.4 | | | | | 56.8 | | | | | 19.1 |

[a] These parameters correspond to the absorption curves in Figs. 2–4.

**Table IV—Absorption Times [a]**

| Subject | Component $A$ | | Component $B$ | | $A + B$ | |
|---|---|---|---|---|---|---|
| | $t_{1/2}$, hr | $t_{0.9}$, hr | $t_{1/2}$, hr | $t_{0.9}$, hr | $t_{1/2}$, hr | $t_{0.9}$, hr |
| 1 | 0.442 | 1.54 | 0.835 | 2.29 | 0.585 | 2.99 |
| 2 | 0.370 | 1.14 | 0.168 | 0.885 | 0.537 | 1.72 |
| 3 | 0.343 | 1.58 | 0.851 | 2.27 | 0.521 | 2.74 |
| 4 | 0.347 | 1.52 | — | — | 0.347 | 1.52 |
| 5 | 0.242 | 1.17 | 0.367 | 1.32 | 0.614 | 2.47 |
| 6 | 0.330 | 1.34 | 0.799 | 2.07 | 0.482 | 2.62 |
| 7 | 0.257 | 1.10 | 0.163 | 1.02 | 0.668 | 1.78 |
| 8 | 0.432 | 1.56 | 0.394 | 1.52 | 0.785 | 3.40 |
| 9 | 0.472 | 1.73 | 0.598 | 1.88 | 0.652 | 3.42 |
| 10 | 0.405 | 1.74 | 0.436 | 1.77 | 0.968 | 2.69 |
| 11 | 0.375 | 1.25 | 0.238 | 1.11 | 0.452 | 1.59 |
| 12 | 0.400 | 1.60 | 1.22 | 3.22 | 2.04 | 4.23 |
| Mean | 0.368 | 1.44 | 0.552 | 1.76 | 0.721 | 2.60 |
| $CV$, % | 19.0 | 15.9 | 61.4 | 39.3 | 61.8 | 32.4 |

[a] Defined by Eq. 17.

$(u_0)_A + (u_0)_B$, is 63%, which agrees closely with the availability of 61% calculated previously by the area under the curve approach (1). Cimetidine is eliminated mainly *via* the kidneys (20). This agrees closely with the 50% recovery reported previously (21), which indicates that the calculated extent of bioavailability appears to be physiologically meaningful.

A statistical comparison of the absorption rates of input components $A$ and $B$ on the basis of $t_{1/2}$ and $t_{0.9}$ (Table IV) indicates that $B$ is significantly slower than $A$ (one-tailed, paired $t$ test, $\alpha < 0.05$). The drug accumulated in the hepatic system appears to be secreted as conjugates or complexes (1). The reabsorption of the drug from these forms may involve deconjugation and decomplexation, which may explain the slower absorption than from the oral solution.

The present method of analyzing the pharmacokinetics of cimetidine and resolving the second peak phenomenon is radically different from the approach presented previously (1) and from classical linear compartmental approaches in general. The deconvolution approach has several advantages.

1. The method is more general since it does not make specific kinetic assumptions such as first-order absorption, first-order compartmental transfer, and first-order elimination processes.

2. The method is basically model independent since it does not assume a specific pharmacokinetic model with a certain compartmental structure, nor does it make specific assumptions about the nature of the kinetic processes involved.

3. Because of this model independence, the method allows a more free and rational analysis of the pharmacokinetics. The method does not postulate a specific pharmacokinetic interpretation or attempt to justify a particular model; instead, it allows a great degree of freedom in the interpretation. This approach should stimulate a more specific and rational experimental design in a future study.

4. As demonstrated for cimetidine, the deconvolution approach can

be formulated according to a specific pharmacokinetic interpretation without relying on a complex pharmacokinetic or mathematical model as in the previous study (1).

5. The deconvolution approach is computationally easier than the often complex equations of compartmental models. Considerable effort may be necessary to derive and check the equations of such models and to obtain suitable initial estimates of the often numerous microparameters for curve fitting. However, the simplicity of the equations in the deconvolution approach and the few parameters involved virtually eliminate such problems.

6. In the deconvolution approach, the input is presented in a clear comprehensible manner in terms of an input profile (Figs. 2–4), which appears to be more descriptive and detailed than classical measures of absorption such as $k_a$ and $t_{1/2(abs)}$.

7. The deconvolution approach has the important property of not requiring an extrapolation to time infinity, as required by the $AUC_0^\infty$ approach for the evaluation of the extent of bioavailability (11). In that sense, it makes fewer assumptions than the $AUC_0^\infty$ approach. It also allows a more rational and intelligent sampling design (5, 11).

The main disadvantage of the linear system approach is that it is limited to linear response systems. However, this limitation does not mean that the basic kinetic processes, such as distribution, metabolism, glomerular filtration, and drug binding that determine pharmacokinetics, need to be linear or first order. These processes most likely are of a nonlinear nature instead of the pseudolinear nature that often is assumed. However, the overall effect of the individual kinetic processes may result in a system that is well approximated linearly, so that the fundamental convolution integral relationship (Eq. 1) applies (5, 11).

The modelless nature of the linear system approach may not seem appealing if the objective of a study is to model the kinetics of specific pharmacokinetic processes. However, with some ingenuity, it may be possible to adapt the linear system approach to model and analyze a specific pharmacokinetic phenomenon, similar to what is done in this work. The linear system approach also may be combined with conventional models to simplify systems that otherwise would be rather complex. Such limited modeling approaches should be more appropriate because fewer assumptions are involved and they should lead to models of a more general nature.

The most rational approach is, if possible, not to model peripheral kinetic aspects that cannot be experimentally verified but to focus the modeling on the pharmacokinetic aspects of particular interest. If the objective is to elucidate drug input kinetics, then this can be readily accomplished using the deconvolution approach by plotting the input function according to the models considered. For example, if a plot of ln $[f(t)]$ *versus* $t$ is approximately linear, then it indicates a first-order input. Different mathematical models for the input can be considered quickly in this way. This approach is obviously more rational than is mathematical derivation with subsequent fitting of the regression equation specifically for each input model.

The equations fitted to approximate the concentration–time response in the linear system approach are empirical. There is no need to attach any specific kinetic significance to their parameters. Model-dependent approaches, however, often attempt to be kinetically significant by considering many pharmacokinetic factors. Complex models often result where the parameters of particular interest lose their practical significance because of the large total number of parameters and the low information density frequently found in pharmacokinetic data. The linear system approach is not faced with this dilemma. There is no loss in kinetic significance when the number of parameters is increased to get a more appropriate approximation of the concentration–time response.

The linear system analysis approach to evaluate pharmacokinetic phenomena seems promising. A careful formulation of this approach may offer a valuable alternative to conventional modeling. Considering the great complexity of the biological processes that determine a drug's pharmacokinetics and the often limited information density of pharmacokinetic data, it seems irrational to derive complex models to consider the many factors involved, particularly when the mechanism of many of these factors cannot be verified. It seems more rational, if possible, not to model unknown processes that are not of primary interest but instead to consider their total effect and to focus the modeling on the pharmacokinetic aspect of real concern. The linear system analysis approach offers this possibility. These principles have been exemplified in analyzing the second peak phenomenon of cimetidine.

## REFERENCES


(1) P. Veng Pedersen and R. Miller, *J. Pharm. Sci.*, **69**, 394 (1980).

(2) S. S. Walkenstein, J. W. Dubb, W. C. Randolph, W. J. Westlake, R. M. Stote, and A. P. Intoccia, *Gastroenterology*, **74**, 360 (1978).

(3) B. M. Brown, "The Mathematical Theory of Linear Systems," Chapman and Hall, London, England, 1965.

(4) P. Veng Pedersen, *J. Pharm. Sci.*, **69**, 298 (1980).

(5) P. Veng Pedersen, *J. Pharmacokinet. Biopharm.*, **8**, 463 (1980).

(6) "Guidelines for Biopharmaceutical Studies in Man," APhA Academy of Pharmaceutical Sciences, Washington, D.C., Feb. 1972.

(7) D. J. Chandos and A. R. DiSanto, "Basis of Bioavailability," Upjohn Co., Kalamazoo, Mich., 1974.

(8) "Principles and Perspectives in Drug Bioavailability," J. Blanchard, R. J. Sawchuck, and B. B. Brodie, Eds., S. Karger, Basel, Switzerland, 1979.

(9) P. Veng Pedersen, *J. Pharm. Sci.*, **69**, 305 (1980).

(10) *Ibid.*, **69**, 312 (1980).

(11) *Ibid.*, **69**, 318 (1980).

(12) J. Gamel, W. F. Rousseau, C. R. Katholi, and E. Messel, *Circ. Res.*, **32**, 516 (1973).

(13) D. Cutler, *J. Pharmacokinet. Biopharm.*, **6**, 243 (1978).

(14) H. Kiwada, K. Morita, M. Hayashi, S. Awazu, and M. Hanano, *Chem. Pharm. Bull.*, **25**, 1312 (1977).

(15) C. D. Thron, *Pharmacol. Rev.*, **26**, 3 (1974).

(16) P. Veng Pedersen, *J. Pharmacokinet. Biopharm.*, **5**, 513 (1977).

(17) J. H. Wilkinson, "Tech. Report STAN-CS-67-60," Computer Science Department, Stanford University, Stanford, Calif., 1967.

(18) R. P. Brent "Algorithms for Minimization Without Derivatives," Prentice-Hall, Englewood Cliffs, N.J., 1973.

(19) J. W. Stephenson, *Bull. Math. Biophys.*, **22**, 1 (1960).

(20) W. L. Burland, W. A. M. Duncan, T. Hesselbo, J. G. Mills, and P. C. Sharpe, *Br. J. Clin. Pharmacol.*, **2**, 481 (1975).

(21) R. Griffith, R. M. Lee, and D. C. Taylor, *Excerpta Med.*, **38**, 308 (1977).

# Prediction of Stability in Pharmaceutical Preparations XVIII: Application of High-Pressure Liquid Chromatographic Assays to Study of Nafronyl Stability and Bioanalysis

**EDWARD R. GARRETT** ˣ **and RASHMI BARBHAIYA**

Received November 30, 1979, from *The Beehive, College of Pharmacy, J. Hillis Miller Health Center, University of Florida, Gainesville, FL 32610.* Accepted for publication July 8, 1980.

**Abstract** □ Specific, sensitive, reversed-phase high-pressure liquid chromatographic assays of nafronyl (I) and its acidic metabolite and hydrolysis product (II) were developed in aqueous solutions and in biological fluids with sensitivities of 100 ng/ml using butacaine as the internal standard and spectrophotometric detection at 224 nm. Heparinized plasma can be analyzed easily in the organic phase immediately after acetonitrile denaturation. Both I and II can be extracted with haloalkane solvents, and the extracts are evaporated, reconstituted, and assayed in a minimal amount of acetonitrile. Conditions are presented that minimize the interference of II and extracted plasma components. The assay was used to determine the stability of nafronyl in aqueous solutions, to establish its log $k$–pH profiles at various temperatures, and to evaluate the Arrhenius parameters. Nafronyl is hydrolyzed by specific hydrogen-ion (15.2 kcal/mole) and hydroxide-ion (7.72 kcal/mole) catalysis of the neutral species and specific hydroxide-ion catalysis (5.91 kcal/mole) of the protonated species. The pH of maximum stability is 3.0, and pH 5.4 is the maximum that can be tolerated at 30°, with a 10% solvolysis in 3 years. The half-life of nafronyl at 30° was 7 days at pH 7, 12 hr at pH 10, and 21 min in 0.5 $N$ NaOH. Since nafronyl has a half-life of 3.2 hr in heparinized dog plasma at 25°, blood samples for pharmacokinetic studies of nafronyl must be assayed immediately after sampling. The partition coefficients of I and II determined as functions of pH permit the extraction of both compounds at pH 4.5, but only I can be extracted at pH values above 9.5.

**Keyphrases** □ Nafronyl oxalate—high-pressure liquid chromatographic analysis in stability studies □ High-pressure liquid chromatography—analysis, nafronyl oxalate, application to stability studies □ Vasodilators—nafronyl oxalate, high-pressure liquid chromatographic analysis in stability studies

When this series of stability studies was initiated 25 years ago (1), its purpose was to demonstrate the use of basic physical–chemical relations in predicting the stability of drugs over long intervals under conditions that could be present in pharmaceutical formulations. The validity of these procedures has been demonstrated fully (2, 3). Short-term studies under high temperature, high acidity and alkalinity, and other excessive stresses have permitted such predictions and have given insight into the conditions that favor the stabilization of drugs in unit dosage forms.

The objective of these investigations has been expanded to encompass those systematic studies necessary to establish optimum and valid assays for drugs and their metabolites *in vitro* and *in vivo*. Many active agents and their metabolites must be extracted selectively from pH-adjusted solutions for the assay to be valid. Their stability and partition properties as a function of pH must be known to design optimum conditions.

## BACKGROUND

The advent of the pharmacokinetic era has necessitated the determination of the time course of drugs and metabolites in living organisms for proper evaluation of effective dosage regimens and for determination of the bioavailability of the active agent from the dosage forms. Many published studies are suspect since uncritically instituted assay conditions may have transformed circulating drugs into pseudometabolites, and since the drug itself may have degraded in biological fluids and tissues stored and/or refrigerated prior to assay. A classical example, heroin, was considered recently (4), where its facile degradation in sampled plasma ($t_{1/2}$ 8 min) or upon extraction from moderately alkaline solutes could give erroneous estimates of the amounts of drugs and metabolites.

All compounds containing possibly readily hydrolyzable groups such as esters are susceptible to such erroneous analytical procedures. The development of proper methods demands a systematic study of stability as a function of pH and temperature.

Optimum conditions for extraction must be established that lead to minimal transformations during the analytical workup. The maintenance of the integrity of the drug and its metabolites must be assured for their projected storage times in sampled biological fluids and tissues.

The vasodilator and metabolic activator nafronyl [tetrahydro-$\alpha$-(1-naphthalenylmethyl)-2-furanpropanoic acid 2-(diethylamino)ethyl ester, I], also known as naftidrofuryl (5, 6), is prepared as the acid oxalate. Its smooth muscle relaxation properties and its ability to increase peripheral and cerebral blood flow and cerebral adenosine triphosphate concentrations and glucose utilization may have value in the treatment of senile brain disease (5–7). Tetrahydro-$\alpha$-(1-naphthalenylmethyl)-2-furanpropanoic acid (II), a hydrolysis product of I (Scheme I), was observed in the plasma and urine of dogs and humans (8) and rats (9) administered I. As explained by Fontaine *et al.* (8), the presumed low plasma levels of I were due to its hydrolysis by pseudocholinesterase in the plasma, with 46% of I disappearing from plasma (presumably *in vitro*) after 1 hr at 37°.

The assays in such studies were conducted after extraction with ether from biological fluids adjusted to 10% ammonia before and after hydrolysis with $\beta$-glucuronidase. The analytical method used to assay I (10) was based on ion-pair formation of I in dichloroethane with an acidic fluorescent dye in pH 5 buffer; the fluorescence of this salt due to the counteranion in dichloroethane provided estimates of the concentration of I. The sensitivity may be 0.2 $\mu$g of I/ml of dichloroethane for this nonspecific assay.

The development of proper and unique assays of I and II in biological fluids demands a thorough knowledge of the pH profile of degradation

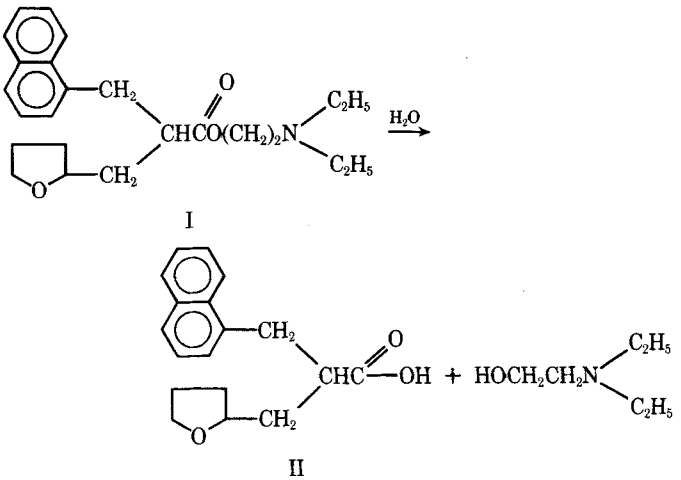


*Scheme I*

0022-3549/81/0100-0039$01.00/0
© 1981, American Pharmaceutical Association

of I to choose optimum pH values for nondegrading conditions of separation. The determination of the effective partition of I and II into appropriate organic solvents as a function of pH may permit the optimum choice of extraction conditions. The development of sensitive and specific assays of I and II in various solutions is necessary for performance of these tasks. This paper presents sensitive and specific high-pressure liquid chromatographic (HPLC) assays of I and II in buffer solutions and biological fluids. The assays are applied to the determination of the log $k$–pH stability profile of I and to the determination of the stability of I in plasma.

## EXPERIMENTAL

**Materials**—The following analytical grade materials were used: dibasic and monobasic sodium phosphates[1], dibasic and monobasic potassium phosphates[1], sodium acetate[1], acetic acid[1], volumetric concentrates of sodium hydroxide and hydrochloric acid[2], and boric acid[3]. Methylene chloride[4] was ACS grade, and acetonitrile[5] and chloroform[5] were GLC, liquid chromatographic, and UV grade. Pure I and II reference standards were used as received[6].

**Apparatus**—A high-pressure liquid chromatograph[7] equipped with a variable-wavelength UV detector[7] was used with a reversed-phase $\mu$-Bondapak alkylphenyl column[8]. Areas under the chromatogram peaks were measured by an integrator[9].

**HPLC Procedures**—Prepared solutions of sodium acetate of known molarity were adjusted to a measured pH with acetic acid. Solutions generally were 0.01–0.1 $M$, adjusted to pH values between 3.5 and 5.0. The mobile phase was a mixture of this buffer and acetonitrile (50:50 or 40:60). The flow rate of 2.5 ml/min gave a back pressure of ~2000 psi. The wavelength of the variable-wavelength detector was adjusted to 224 nm, which was the maximum absorbance of I and II; a weak absorbance at 282 nm and a negligible absorbance at 254 nm were noted. When an internal standard was used, a specified amount was dissolved in the acetonitrile used to dilute the buffer or plasma sample to be assayed. Generally, the sample was diluted to give the same percentage of acetonitrile as the mobile phase, and 25 $\mu$l of this mixture was injected. This procedure reduced the intensity of the solvent peak and its tailing.

**Kinetics of Hydrolytic Degradation of Nafronyl (I)**—*Acid Hydrolyses*—Nafronyl (I) acid oxalate (2.0 mg) was weighed accurately and dissolved in 10 ml of thermally preequilibrated 0.5, 0.4, 0.2, and 0.1 $N$ HCl ($4.223 \times 10^{-4}$ $M$), prepared from a standardized concentrate and confirmed by titration against standardized sodium hydroxide. An aliquot (100 $\mu$l) was taken immediately after dissolution and transferred to a 3.0-ml reaction vial containing 20 $\mu$l of sodium hydroxide solution, having a molarity five times greater than that of the hydrochloric acid solution used, to effect neutralization of the strong acid. A mixture of acetate buffer (pH 4.0) and acetonitrile then was added (80 $\mu$l) to adjust the pH and composition of the solution to those of the mobile phase. An aliquot (25 $\mu$l) was injected into the chromatograph under the described analytical conditions at intervals.

*Alkaline Hydrolyses*—Nafronyl (I) acid oxalate (40.0 mg) was weighed accurately and dissolved in 2.0 ml of distilled water in a 4.0-ml reaction vial to prepare the stock solution for alkaline hydrolyses. Aliquots (50 $\mu$l) from this stock solution were taken with a 50-$\mu$l syringe and dissolved in 10.0 ml of 0.01, 0.02, 0.04, and 0.05 $N$ NaOH and other solutions preequilibrated at 30° in a water bath. Similar studies were effected at other temperatures. Immediately, 100 $\mu$l of the $2.112 \times 10^{-4}$ $M$ I solution (0-hr sample) was transferred to a 2.0-ml reaction vial containing 20 $\mu$l of hydrochloric acid solution, which had a sufficient normality to neutralize the excess strong base. A mixture of 0.4 $M$ sodium acetate buffer (pH 4.0) and acetonitrile (80 $\mu$l) then was added to adjust the pH of the solution to ~4.0. Samples taken from the sodium hydroxide solutions were quenched in this manner every 5 min for the first 30 min and then every 15 min until all I was degraded to II. An aliquot of the quenched solution (25 $\mu$l) was injected into the chromatograph for the described assay.

**Studies at Intermediate pH Values**—Acetate (pH 3.4–5.4), phosphate (pH 5.6–8.2), and borate (pH 8.0–10) buffers were prepared; the ionic strength was adjusted to 0.1 with potassium chloride. The buffer solutions (10.0 ml) were preequilibrated in an oil bath at the appropriate temperature before addition of 25.0 or 50.0 $\mu$l of a solution of nafronyl (I) acid oxalate containing 20 mg/ml. Aliquots (100 $\mu$l) of the $2.101 \times 10^{-4}$ $M$ I solution were removed at different time intervals, and the pH of the solution was adjusted to 4.0 by adding 100 $\mu$l of 0.4 $M$ acetate buffer–acetonitrile. Then 25.0 $\mu$l of this solution was injected into the chromatograph.

**Stability of I in 10% Ammonia Solution**—A solution of 10% ammonia (10 ml) was preequilibrated at 30° in a water bath, and 25 $\mu$l of a solution of nafronyl (I) acid oxalate (20.0 mg/ml) was added. Aliquots of the $1.05 \times 10^{-4}$ $M$ solution of I were removed at different times. The reaction mixture was quenched to pH 4 with hydrochloric acid–acetate buffer and mixed with acetonitrile, and 25 $\mu$l was injected into the chromatograph.

**Partition Studies as Functions of pH**—An aliquot (25 $\mu$l) of a stock solution of I as the oxalate (20.00 mg/ml) was dissolved in 5.00 ml of various buffer solutions to prepare solutions of $2.101 \times 10^{-4}$ $M$ I. Chloroform (250 $\mu$l, $V_{org}$) was added to 1 ml ($V_{aq}$) of each buffer solution (99.5 $\mu$g/ml) in a 3.0-ml reaction vial. The tightly closed vial was vortexed for exactly 60 sec, and a 100-$\mu$l aliquot of the separated aqueous phase was mixed with 100 $\mu$l of a 50:50 mixture of 0.4 $M$, pH 4 acetate buffer and acetonitrile. An aliquot (25 $\mu$l) was injected into the chromatograph; an aliquot of the buffer solution prior to extraction was assayed similarly.

**HPLC Analytical Methods for I in Plasma Using Acetonitrile as Deproteinizing Agent**—*Method A*—Acetonitrile (250 $\mu$l) was added to 100 $\mu$l of heparinized human plasma spiked with I. The mixture was vortexed and centrifuged at 3000 rpm for 5 min, and then 25 $\mu$l of the acetonitrile supernate was injected into the chromatograph. The mobile phase was a mixture of 50% 0.01 $M$ sodium acetate adjusted with acetic acid to pH 3.5 and 50% acetonitrile. The flow rate was 2.5 ml/min on a $\mu$Bondapak alkylphenyl column.

The retention times for II and I were 2.76 and 7.98 min, respectively.

*Method B*—Acetonitrile (1.0 ml), containing butacaine as an internal standard, was added to 1.0 ml of heparinized human plasma spiked with I. The mixture was vortexed and centrifuged at 3000 rpm for 5 min. Then 0.8 ml of the supernate was transferred to a reaction vial and evaporated to dryness under nitrogen. The residue was reconstituted in 75 $\mu$l of acetonitrile and vortexed, and 25 $\mu$l of the solution was injected into the chromatograph.

**HPLC Analytical Methods for I in Plasma Using Haloalkane Extraction**—*Method C*—An aliquot of heparinized human plasma (2.0 ml) was extracted with 2.0 ml of chloroform, and the mixture was vortexed for 10 min and centrifuged for 5 min at 3000 rpm. The upper layer was aspirated, and 1.5 ml of the chloroform phase was evaporated to dryness. The residue was reconstituted in 100 $\mu$l of acetonitrile with vortexing, and 25 $\mu$l of the solution was injected into the chromatograph. The mobile phase consisted of 0.01 $M$ acetic acid adjusted to pH 4.0 and acetonitrile (50:50). The retention time for I was 9.62 min.

*Method D*—Aliquots (2 ml) of freshly prepared heparinized dog plasma (within 1 hr after obtainment from the dog) were adjusted to pH 3.78 with 0.35 ml of 0.2 $N$ HCl. The plasma was extracted with methylene chloride (3 ml), with 10 min of mild shaking and centrifuging for 5 min at 3300 rpm. The aqueous phase was aspirated, and 2 ml of the methylene chloride phase was evaporated to dryness under a nitrogen stream. The residue was reconstituted in 50 $\mu$l of acetonitrile containing 750 $\mu$g of butacaine sulfate/ml. The mobile phase consisted of 0.1 $M$ acetate buffer adjusted to pH 4.0 and acetonitrile (45:55).

## RESULTS AND DISCUSSION

**Reversed-Phase HPLC Assay of I and II for Degradation and Partition Studies**—The HPLC mobile phase of acetate buffer–acetonitrile (50:50) with a 224-nm UV detector and a flow rate of 2.5 ml/min provided a chromatogram (Fig. 1A) with a steady baseline and specific and sensitive quantitative analyses of I and its acid degradation product (II), with retention times of 6.66 and 3.26 min at pH 4.5 and of 8.00 and 2.79 min at pH 4.0, respectively. A series of potential internal standards was studied at pH 4.0 with the following retention times (in minutes): caffeine, 1.64; hippuric acid, 1.80; phenobarbital, 2.50; ephedrine, 2.64; codeine, 2.73; atropine, 2.92; amphetamine, 2.82; procaine, 2.51; lidocaine, 2.94; heroin, 2.90; tetracaine, 3.99; butacaine, 5.44; and papaverine, 3.60. Butacaine was selected because its retention time (5.44 min at pH 4 and 4.90 min at pH 4.5) is intermediate between those of I and II. Excellent calibration curves for assays in buffer solutions were obtained from the

[1] Mallinckrodt Chemical Works, St. Louis, MO 63160.
[2] Harleco, Philadelphia, PA 19143.
[3] J. T. Baker Chemical Co., Phillipsburg, N.J.
[4] Mallinckrodt, Paris, KY 40361.
[5] Burdick & Jackson Laboratories, Muskegon, MI 49442.
[6] Lot 1956 (I) and lot 9751 (II), Lipha Chemicals, New York, NY 10022.
[7] Model 6000A solvent delivery system and model U6K injector equipped with a model 450 variable-wavelength UV detector, Waters Associates, Milford, Mass.
[8] Waters Associates, Milford Mass.
[9] Model 3380A, Hewlett-Packard, Avondale, Pa.

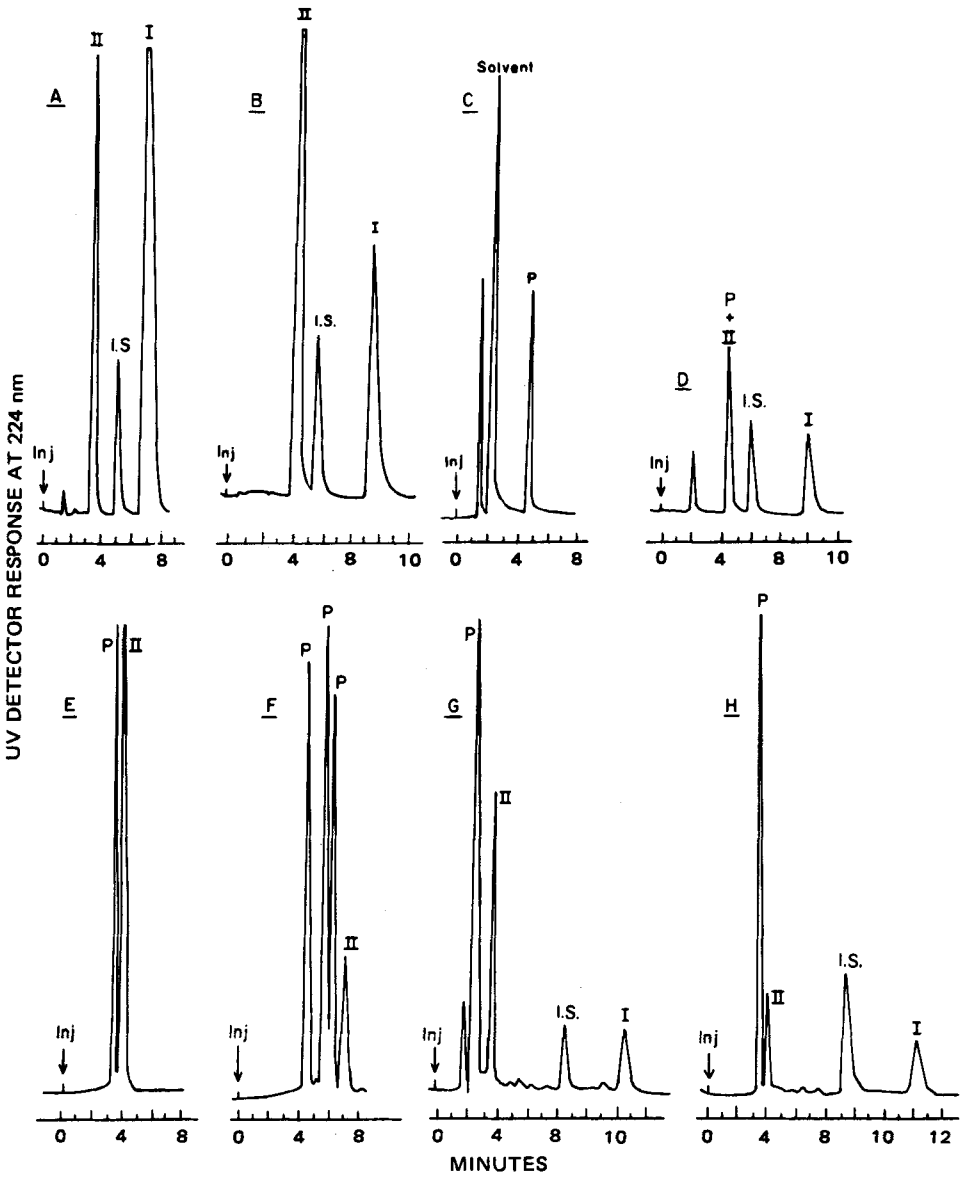


**Figure 1**—*Reversed-phase high-pressure liquid chromatograms with 224-nm detection of 25 μl of solutions of I (as acid oxalate) and its acid degradation product (II) with a butacaine sulfate internal standard (IS). Plasma interferences are labeled* P. *The flow rate was 2.2 ml/min. Key: A, aqueous solution containing 10 μg each of I, II, and the internal standard injected into a mobile phase of pH 4.5, 0.1* M *acetate buffer–acetonitrile (50:50); B, aqueous solution containing 2.5 μg each of I and II and 10 μg of the internal standard injected into the same mobile phase except in a 60:40 mixture; C, acetonitrile-reconstituted residues from Method C of plasma analysis without I and II; D, acetonitrile-reconstituted residues from Method C of plasma analysis with 5 μg of I and II/ml of plasma (the II and* P *peaks were not separated); E, separation of II and* P *peaks from acetonitrile-reconstituted residues from plasma with 2.5 μg of II/ml injected into a mobile phase of pH 3.5, 0.01* N *acetate buffer–acetonitrile (50:50) (flow rate 2.0 ml/min); F, separation of II and* P *peaks from acetonitrile-reconstituted residues from plasma with 0.5 μg of II/ml injected into a mobile phase of pH 5.0 buffer–acetonitrile (60:40) (flow rate 1.0 ml/min); and G and H, acetonitrile-reconstituted residues from plasma assays with 0.5 μg of I and II/ml of plasma injected into 0.1* N *acetate buffer–acetonitrile (55:45) (flow rate 1.5 ml/min) at pH 3.75 and 4.0, respectively.*

peak area alone (Fig. 2) so no internal standard was needed for the kinetic studies in aqueous solutions.

The standard errors of the estimates of the concentrations of I and II were 37 and 41 ng/ml, respectively, for the calibration curves prepared in the 0–2.5-μg/ml range and indicate analytical sensitivities of 100 ng/ml. The linear regression equations with standard errors of the estimates for nafronyl (I) acid oxalate are: 0–75 μg/ml, $C_I$ (±0.155) μg/ml = −0.119 (±0.080) + 1.1755 (±0.0026)$A$, $n = 7$, $r^2 = 1.000$; and 0–2.5 μg/ml, $C_I$ (±0.037) = −0.089 (±0.042) + 1.229 (±0.029)$A$, $n = 4$, $r^2 = 0.999$. For the degradation product (II), they are: 0–26 μg/ml, $C_{II}$ (±0.142) μg/ml = −0.140 (±0.068) + 0.766 (±0.005)$A$, $n = 7$, $r^2 = 1.000$; and 0–2.6 μg/ml, $C_{II}$ (±0.0408) = −0.103 (±0.034) + 0.741 (±0.017)$A$, $n = 4$, $r^2 = 0.999$, where $A$ is the relative area and was $10^{-5}$ times the actual number of area units measured. The values in parentheses are the standard errors.

The reproducibility of the assay of 10 μg/ml within and among days was challenged by assaying a refrigerated sample 10 times and then on 10 separate days. The assay of I with its standard deviation was 10.03 ± 0.23 within a day and 9.94 ± 0.50 among days; for the derived acid (II), the reproducibility was 10.07 ± 0.20 within a day and 10.09 ± 0.43 among days.

**Kinetics of I Solvolysis**—At constant pH, I degrades by an apparent first-order process. Representative semilogarithmic plots of the HPLC relative peak area for I against time are given for hydrochloric acid solutions (Fig. 3), acetate buffers (Fig. 4), phosphate and borate buffers (Fig. 5), and sodium hydroxide solutions (Fig. 6), where the apparent first-order rate constants, $k$, were obtained from the slopes in accordance with:

$$\log A = -\frac{k}{2.303}t + \log A_0 \qquad \text{(Eq. 1)}$$

where $A$ and $A_0$ are the relative peak areas at time $t$ and time zero, respectively.

The pH values for the strongly acidic and alkaline solutions were calculated from data for γ and pKw in the literature (11). The concentrations of I in alkaline solution studies had to be lowered to $2 \times 10^{-4}$ $M$ so as not to exceed the solubility of the neutral compound. Higher concentrations showed rate plots that were initially zero order. The solubility of neutral I is estimated to be 0.03–0.05 mg/ml.

**Log $k$–pH Profiles for Hydrolysis of I**—For hydrochloric acid solutions, the pH values were calculated from:

$$\text{pH} = -\log \gamma[\text{HCl}] \qquad \text{(Eq. 2)}$$

where γ is the mean activity coefficient for the hydrochloric acid solutions (11). For sodium hydroxide solutions:

$$\text{pH} = \text{pKw} - \text{pOH} = \text{pKw} + \log \gamma[\text{NaOH}] \qquad \text{(Eq. 3)}$$

where γ is the mean activity coefficient for the sodium hydroxide solution. The values of pKw = $-\log K_w$ are listed in Table I, where $K_w$ is the hydrolysis constant for water (11).

The log $k$–pH profiles for the solvolysis of I in aqueous solutions with ionic strengths (μ) of 0.1 in the buffer solutions are given in Fig. 7. They are fitted to the expression:

$$k = (k_{H^+}a_{H^+} + k_{OH}a_{OH^-})f_{(\equiv NH^+)} + k'_{OH}a_{OH^-}f_{(\equiv N)} \qquad \text{(Eq. 4)}$$

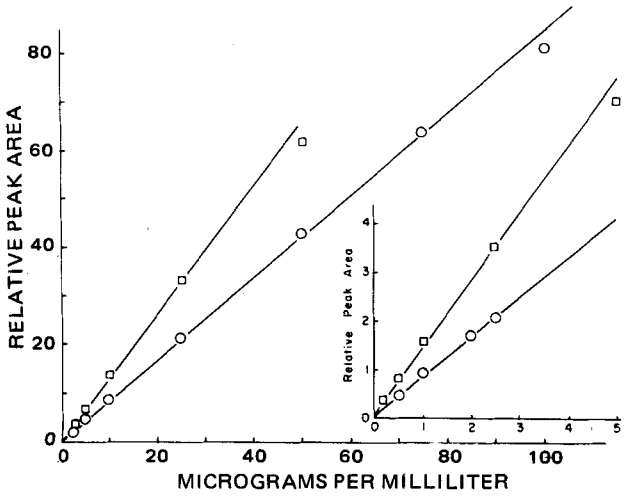


**Figure 2**—*HPLC calibration curves of relative peak area against concentration (micrograms per milliliter) for nafronyl (I) acid oxalate (○) and its derived acid (II) (□) in pH 4 acetate buffer–acetonitrile (50:50) at a flow rate of 2.5 ml/min.*

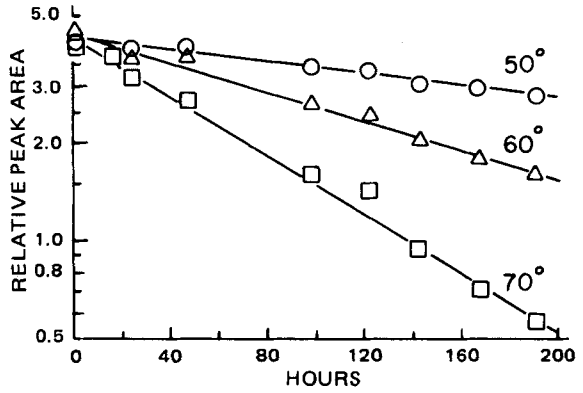


**Figure 3**—*First-order plots of HPLC relative peak area of I in 0.4* N *HCl against time. The curves are labeled with the temperature of the study.*

where the activities of the catalytic species are calculated from $a_{OH^-} = 10^{-pOH} = 10^{-(pKw-pH)}$ and $a_{H^+} = 10^{-pH}$. The fractions of protonated and nonprotonated drug are, respectively:

$$f_{(\equiv NH^+)} = a_{H^+}/(K'_a + a_{H^+}) \quad \text{(Eq. 5)}$$

and:

$$f_{(\equiv NH)} = K'_a/(K'_a + a_{H^+}) \quad \text{(Eq. 6)}$$

where $K'_a$ is the apparent dissociation constant of protonated I. The parameters for the best fits of the log $k$–pH profiles (Fig. 7) are given in Table I. These values can be substituted into Eqs. 4–6 to permit calculation of the apparent first-order rate constant under any given pH

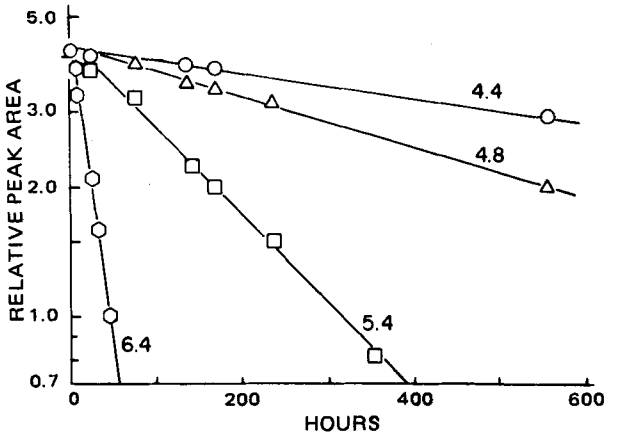


**Figure 4**—*First-order plots of HPLC relative peak area of I in acetate buffers of various pH values against time with $\mu = 0.1$ at 70.0°. The curves are labeled with the pH of the solutions.*

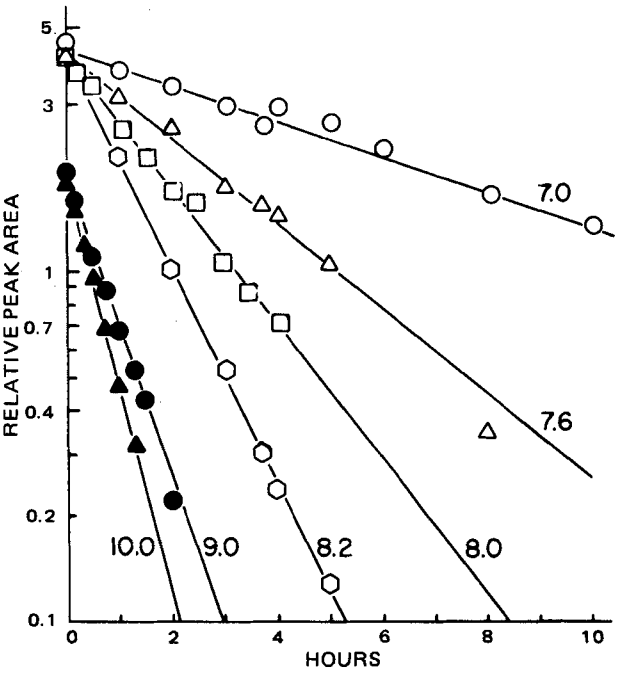


**Figure 5**—*First-order plots of HPLC relative peak area of I in phosphate and borate buffers of various pH values against time with $\mu = 0.1$ at 70.0°. The curves are labeled with the pH of the solutions.*

conditions. The temperature dependence of the rate constant for a given alkali or acid concentration or pH (Fig. 8 and Table II) also was considered in adjusting the fits for a temperature with fewer actual studies.

The log $k$–pH profile in conformity to Eq. 4 clearly showed that protonated I is hydrogen ion and hydroxide ion catalyzed, with maximum

**Table I—Parameters of Fit [a] of Log $k$–pH Profiles for the Solvolysis of I**

| Parameter | 70.0° | 60.0° | 50.0° | 30.0° |
|---|---|---|---|---|
| log $k_{OH}$ | 3.132 | 3.041 | 2.923 | 2.636 |
| $k_{OH}$, liters/mole/min | 1357 | 1100 | 837 | 433 |
| log $k'_{OH}$ | 0.180 | 0.018 | −0.140 | −0.572 |
| $k'_{OH}$, liters/mole/min | 1.510 | 1.042 | 0.724 | 0.268 |
| log $k_{H^+}$ | −3.260 | −3.523 | −3.928 | −4.611 |
| $k_{H^+}$, liters/mole/min | $5.50 \times 10^{-4}$ | $3.00 \times 10^{-4}$ | $1.18 \times 10^{-4}$ | $2.45 \times 10^{-5}$ |
| pKa′ | 7.90 | 7.90 | 7.90 | 8.20 |
| $K'_a$ | $1.259 \times 10^{-8}$ | $1.259 \times 10^{-8}$ | $1.259 \times 10^{-8}$ | $6.310 \times 10^{-9}$ |
| pKw | 12.79 | 13.02 | 13.26 | 13.83 |
| $K_w$ | $1.622 \times 10^{-13}$ | $9.550 \times 10^{-14}$ | $5.495 \times 10^{-14}$ | $1.479 \times 10^{-14}$ |

[a] Fitted to $k = (k_{H^+}a_{H^+} + k_{OH}a_{OH^-})f_{(\equiv NH^+)} + k'_{OH}a_{OH^-}f_{(\equiv N)}$, where the activities of the catalytic species are $a_{OH^-} = 10^{-pOH} = 10^{-(pKw-pH)}$ and $a_{H^+} = 10^{-pH}$, the fraction of drug that is protonated and nonprotonated, respectively, is $f_{(\equiv NH^+)} = a_{H^+}/(K'_a + a_{H^+})$ and $f_{(\equiv NH)} = K'_a/(K'_a + a_{H^+})$, and the pH values in the strongly acidic and alkaline ranges are calculated, respectively, from pH = −log γ[HCl] and pH = pKw − pOH = pKw + log γ[NaOH], where the pKw values and activity coefficients (γ) are obtained from the literature (11).

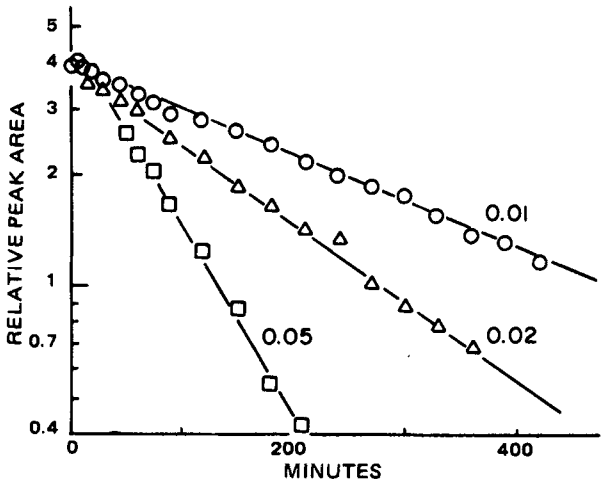


**Figure 6**—*First-order plots of HPLC relative peak area of I in sodium hydroxide solutions against time. The curves are labeled with the molarities of sodium hydroxide.*

stability at pH 3.0. Reasonable slopes of −1 and +1 were obtained for these acid and alkaline branches of the log $k$–pH curves. The plateau achieved in the pH 8–10 region indicates lessened catalytic efficiency of the hydroxide-ion attack on uncharged I with a kinetic pKa′ of ~8.0. The microscopic rate constants were determined from the intercepts of the linear segments with slopes of unity in accordance with:

$$\log k = \log k_{H^+} - \text{pH} \qquad \text{(Eq. 7)}$$

for the acid branch characterizing the hydrogen-ion attack on protonated I below pH 3, or in accordance with:

$$\log k = \log k_{OH} - \text{pH} + \text{pKw} \qquad \text{(Eq. 8)}$$

for the alkaline branch characterizing the hydroxide-ion attack on protonated I for pH 3–8, and in accordance with:

$$\log k = \log k'_{OH} - \text{pH} + \text{pKw} \qquad \text{(Eq. 9)}$$

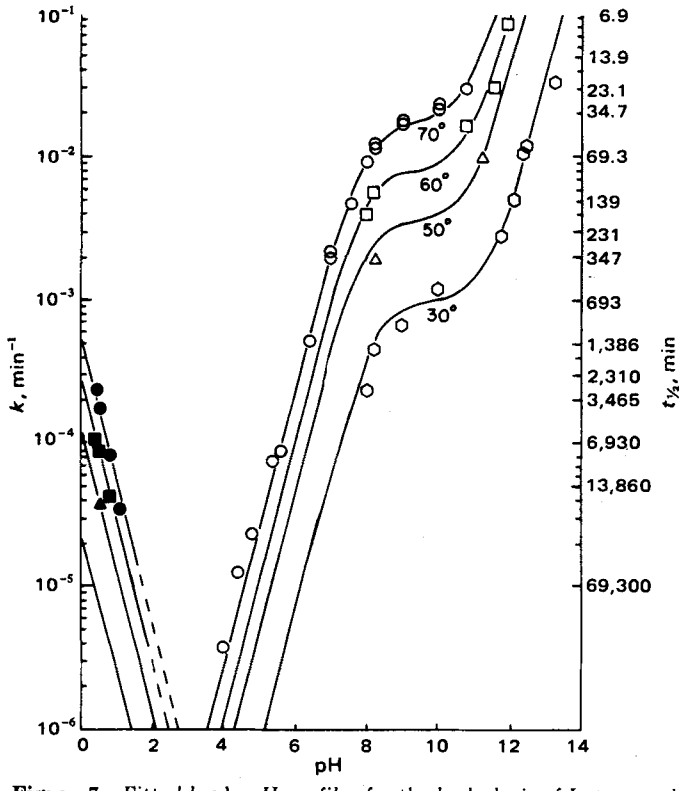


**Figure 7**—*Fitted log k–pH profiles for the hydrolysis of I at several temperatures.*

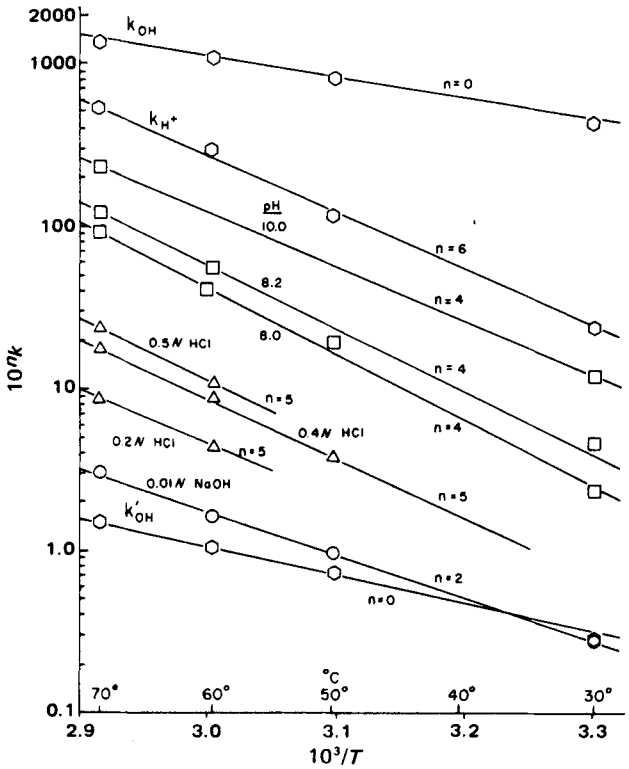


**Figure 8**—*Arrhenius plots of apparent first-order rate constants (k expressed in minutes$^{-1}$) under different pH conditions and at constant hydrochloric acid and sodium hydroxide conditions where T = 273+ °C. In addition, the Arrhenius plots are given for the microscopic catalytic constants, $k_{OH}$, $k'_{OH}$, and $k_{H^+}$, that were obtained from the fitted log k–pH profiles at the various temperatures given in Fig. 7.*

for the alkaline branch characterizing the hydroxide-ion attack on uncharged I at pH values above the plateau, pH ~11. The determined constants and the kinetic pKa′ values that define the plateaus are listed in Table I.

Other estimates of biomolecular rate constants, referenced to concentrations rather than activities, can be obtained from plots of apparent first-order rate constants against hydrochloric acid concentrations in accordance with:

$$k = k_{HCl}[HCl] \qquad \text{(Eq. 10)}$$

and the $k_{HCl}$ values were $4.44 \times 10^{-4}$ liter/mole/min at 70° and $2.16 \times 10^{-4}$ liter/mole/min at 60°. The lack of pH-independent solvolysis was indicated by the fact that these plots passed through the origin.

**Significance of Arrhenius Parameters**—The Arrhenius parameters

**Table II—Parameters for Temperature Dependence [a] of the Apparent Rate Constants for the Solvolysis of I**

| Rate Constant | Slope ($S$) | $\Delta H_a$, kcal/mole | ln $P$ |
|---|---|---|---|
| $k$ in 0.01 $M$ NaOH, min$^{-1}$ | 6098 | 12.1 | 14.25 |
| $k$ in 0.2 $M$ HCl, min$^{-1}$ | 8440 | 16.8 | 15.18 |
| $k$ in 0.4 $M$ HCl, min$^{-1}$ | 8531 | 17.0 | 16.24 |
| $k$ in 0.5 $M$ HCl, min$^{-1}$ | 7701 | 15.3 | 14.12 |
| $k$ in pH 8.0 phosphate buffer, min$^{-1}$ | 9447 | 18.9 | 23.00 |
| $k$ in pH 8.2 phosphate buffer, min$^{-1}$ | 9009 | 17.9 | 21.87 |
| $k$ in pH 9.0 borate buffer, min$^{-1}$ | 8400 | 16.7 | 20.39 |
| $k$ in pH 10.0 borate buffer, min$^{-1}$ | 7712 | 15.3 | 18.69 |
| $k_{OH}$ [b], liters/mole/min | 3886 | 7.72 | 11.74 |
| $k_{OH}$ [c], liters/mole/min | 2972 | 5.91 | 15.93 |
| $k_{H^+}$ [d], liters/mole/min | 8062 | 16.0 | 15.97 |

[a] $\ln k = \ln P - S/T = \ln P - (\Delta H_a/R)(1/T)$, where $R$ = 1.987 cal/degree and $T$ = 273+ °C. [b] Bimolecular rate constant for the attack of hydroxide-ion activity on the nonprotonated drug species as determined from the best fit of log $k$–pH profiles at the several temperatures. [c] Bimolecular rate constant for the attack of hydroxide-ion activity on the protonated drug species as determined from the best fit of log $k$–pH profiles at the several temperatures. [d] Bimolecular rate constant for the attack of hydrogen-ion activity on the protonated drug species as determined from the best fit of log $k$–pH profiles at the several temperatures.

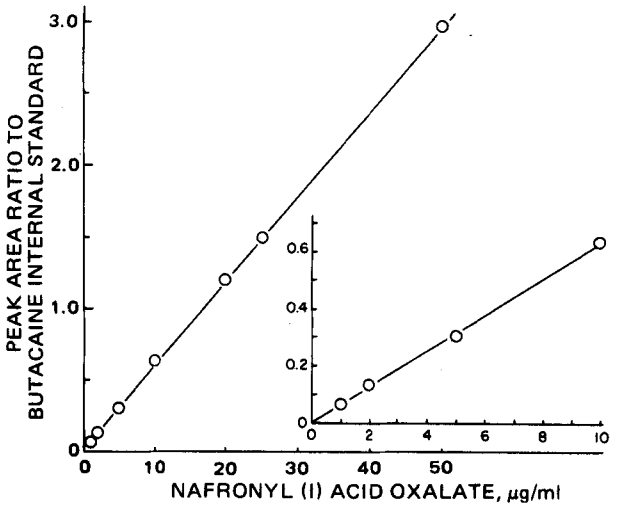


**Figure 9**—*HPLC calibration curves of the relative peak area ratio with respect to butacaine (the internal standard) against concentration (micrograms per milliliter) of nafronyl (I) acid oxalate in human plasma in pH 3.5 acetate buffer–acetonitrile (50:50); the flow rate was 2.5 ml/min.*

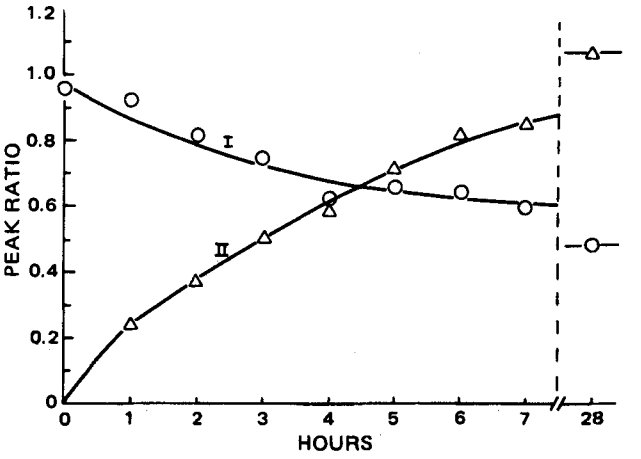


**Figure 10**—*Plots of peak area ratio of I (○) and peak height ratios of II (△) with respect to butacaine (the internal standard) against time for the degradation of I in fresh dog plasma at 24.5° with an initial concentration of 1.25 μg/ml of plasma.*

for the determined microscopic rate constants (Table II) show a higher heat of activation for the hydroxide-ion attack on the neutral species (7.72 kcal/mole) than on the coulombic charge-expedited attack on the protonated species (5.91 kcal/mole). The greater resistance of protonated I to hydrogen-ion attack is manifested by the higher heat of activation of 15.2 kcal/mole. The reasonable fits of the log $k$–pH profiles at the several temperatures were confirmed by the linearity of the Arrhenius plots for the derived constants (Fig. 8).

**Effects of Substrate Concentrations and Buffers on I Solvolysis**—Studies were conducted at several concentrations of I for given pH values, and there was no significant effect on the apparent hydrolysis rate constant. Phosphate buffer concentrations from 0.043 to 0.13 $M$ at pH 6.4 and 70° showed no significant buffer effects on the apparent first-order rate constant. There was a significant, but small, phosphate buffer effect at pH 8.1 and 70° with $\mu = 0.1$, where the $k$ ($\times 10^3$ min$^{-1}$), $[KH_2PO_4]$, and $[Na_2HPO_4]$ values were, respectively: 9.08, $9.14 \times 10^{-4}$, $1.58 \times 10^{-2}$; 10.62, $1.37 \times 10^{-3}$, $2.36 \times 10^{-2}$; and 11.64, $1.83 \times 10^{-3}$, $3.15 \times 10^{-2}$; and where:

$$K^{70°}_{pH\,8.1} = 8.52 \times 10^{-3} + 0.096\,[H_3PO_4^{2-}] \qquad \text{(Eq. 11)}$$

The half-life of I in 10% ammonia at 30° was 336 min.

**Pharmaceutical Significances of I Stability Studies**—The high solvolytic instability of I, even in mildly alkaline solutions, requires great care in the formulation of liquid and solid dosage formulations so that the microscopic environment is as acidic as possible. Alkaline lubricants and excipients should not be used, and the granulation should be kept as free of water as possible. Even at 30° and pH 7, the half-life of I in aqueous solution is predicted to be only 7 days (Fig. 7). A pH of 5.4 is the maximum that can be tolerated at 30°, with a loss of 10% of I to hydrolysis over 3 years. Thus, I must be assayed immediately and must not be stored in samples of biological tissues and fluids.

The $k$ value was calculated from:

$$k(\text{min}^{-1}) = \ln 0.1/(3 \times 365 \times 24 \times 60) = 1.46 \times 10^{-6}\ \text{min}^{-1} \qquad \text{(Eq. 12)}$$

and this rate constant is predicted to be at the pH value of 5.4 at 30° (Fig. 7). In Europe, I is distributed as the oxalate, and aqueous solutions should be pharmaceutically stable. The microscopic environment of dosage forms can be maintained at the pH of maximum stability with such an acid salt. A 0.1-mg/ml solution has a pH of 4.0 and a predicted half-life of 20 years at 30°.

Extractions of I into organic solvents may be conducted from alkalinized solutions if such extractions are performed immediately. At 30° and pH 10, the half-life of I is 12 hr but only 21 and 7 min in 0.5 and 2.5 $N$ NaOH, respectively. An extraction procedure using 10% ammonia (10) is satisfactory if it is carried out immediately, giving a half-life of 5 hr.

**Partition as a Function of pH; Application to Design of Analytical Methods**—The oil–water partition coefficient, $K$, was calculated from the observed peak areas from the HPLC analyses, in which the areas were shown to be directly proportional to concentration, by:

$$K = \frac{(A_1 - A_2)V_{aq}/V_{org}}{A_2} \qquad \text{(Eq. 13)}$$

where $A_1$ and $A_2$ are the peak areas of the aqueous phase before and after extraction, respectively, and $V_{aq}$ and $V_{org}$ are the respective volumes of the admixed buffer and chloroform solutions.

A similar procedure was used for the determination of the oil–water partition coefficient of the derived acid (II), except that the volume of chloroform used ($V_{org}$) also was 1.0 ml.

The partitioning of I into chloroform from various buffer solutions of acetate, phosphate, and borate was studied at pH 3.5, 4.4, 5.4, 6.4, 7.0, 8.0, 9.0, and 10. In all cases above pH 3.5, the partition coefficients (Eq. 1) were >100, indicating almost complete extraction. The partition coefficient was 74 at pH 3.5 and 7.7 in 0.01 $M$ HCl.

Studies of the partitioning of the acid (II) showed complete extraction

**Table III—Mobile Phases and Retention Times in HPLC Separations**

| Flow Rate, ml/min | Mobile Phase[a] pH | Mobile Phase[a] Buffer–Acetonitrile | Retention Time, min: Plasma Components | II | Butacaine | I | Adequate Separation of II and Plasma Components? |
|---|---|---|---|---|---|---|---|
| 2.0 | 4.5 | 50:50 | 3.42 | 3.24 | 4.73–4.90 | 7.04–7.15 | No |
| 2.5 | 3.5 | 50:50 | 3.45 | 4.00 | >15 | >20 | Somewhat |
| 1.0 | 5.0 | 50:50[b] | 6.95 | 6.00 | 9.14 | 12.74 | Yes |
| 1.5 | 4.0 | 55:45[c] | 3.28 | 3.6 | 8.54 | 12.83 | No |
| 1.4 | 4.0 | 55:45 | 3.33 | 4.07–4.36 | 9.40–10.00 | 14.06–14.85 | Yes |
| 1.5 | 3.75 | 55:45 | 3.66 | 4.03 | 8.37 | 12.36 | Somewhat |
| 1.0 | 5.0 | 60:40 | 6.33–6.34 | 7.05 | — | 12.52 | Yes |
| 2.5 | 4.5 | 60:40 | 4.75 | 4.65 | 6.15 | 9.90 | No |
| 2.2 | 4.5 | 60:40 | 4.74 | 4.57 | 6.00 | 9.71 | No |
| 2.5 | 3.5 | 60:40 | 11.4 | 13.0 | — | >25 | Yes |

[a] All buffer was comprised of 0.1 $M$ acetate buffer except that of last row, which was 0.01 $M$ acetate buffer. [b] Contains 1% tetrahydrofuran. [c] In this system, heparin gave a peak at 2.58 min and thiopental gave a peak at 2.80 min.

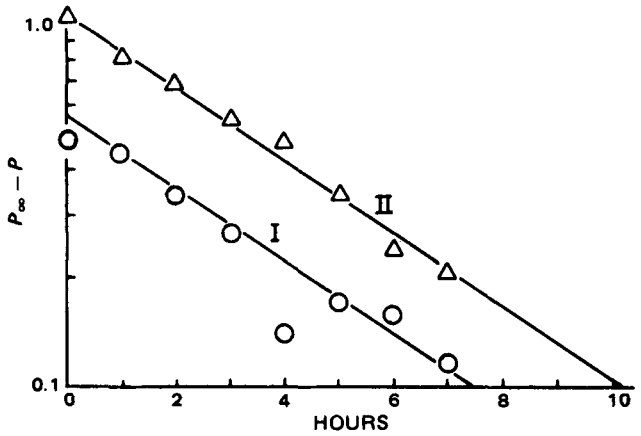


**Figure 11**—*Semilogarithmic plot of log* ($P_\infty - P$) *versus time for the loss of I and the production of II in fresh dog plasma at 24.5°. The* P *value represents peak area ratios for I and peak height ratios for II with respect to the internal standard, butacaine. The* $P_\infty$ *values were those obtained at the 28-hr assays. The half-life of I for its 50% degradation in this plasma was 3.2 hr.*

of II from acetate buffers of pH 4.5 and lower and from 0.05 *M* HCl. No II was extractable from pH 9.5 borate buffer and 10% ammonia. The oil–water partition coefficients (Eq. 1) at other pH values were 80.2 at pH 5.3, 35.1 at pH 6.2, 5.17 at pH 7.15, and 0.17 at pH 8.5. All studies except the last one (in borate buffers) were conducted in phosphate buffers.

These systematic studies on the partitioning of I from aqueous media into chloroform as a function of pH showed that I can be readily extracted over the entire pH range. Thus, there is no need to alkalinize aqueous solutions, plasma, or urine, which can lead to degradation, to extract I with efficiency. Both I and II can be extracted at pH <7, and both compounds can be analyzed simultaneously with one injection into the chromatograph. Alternatively, extraction at pH 9.5 can selectively extract I, and subsequent extraction of the acidified aqueous solution can remove the acid degradation product. HPLC analytical methods were developed using these physicochemical properties.

**HPLC Analytical Methods for I in Plasma Using Acetonitrile as Deproteinizing Agent**—Acetonitrile can be used as both a plasma deproteinizing agent and as an extraction solvent so that an aliquot of the acetonitrile fraction can be injected directly for assay. It is ideal for injection into the chromatograph since the mobile phase is a mixture of acetonitrile and acetate buffer and the intensity of the solvent peak is minimized. Methods A and B were developed using this procedure (see *Experimental*).

There were interferences from blank plasma in Method A for II, with a major plasma peak at 2.56 min under the given HPLC conditions, but not with the I peak. The calibration curves were similar to Fig. 2. The baseline of the chromatogram was linear, and the standard errors of the estimates for the 0–2.5-μg/ml range were 140 ng/ml of plasma for the peak area and 41 ng/ml for the peak heights when 100 μl of plasma was analyzed. These data indicated sensitivities of 300 and 100 ng/ml for the peak areas and peak heights, respectively, using 100 μl of plasma. The linear regression equations for the peak area ($A$) and peak height ($P$) for 0–50 μg/ml are: $C$ (±0.617) μg/ml = −0.11 (±0.27) + 4.82 (±0.06)$A$ ($n$ = 10, $r^2$ = 0.990) and $C$ (±0.23) μg/ml = −0.19 (±0.10) + 9.71 (±0.05)$P$ ($n$ = 9, $r^2$ = 0.998). For 0–2.5 μg/ml and $n$ = 4: $C$ (±0.14) μg/ml + 0.06 (±0.14) + 4.17 (±0.37)$A$ ($r^2$ = 0.9849) and $C$ (±0.041) μg/ml = −0.02 (±0.04) + 8.88 (±0.23)$P$ ($r^2$ = 0.9987). The relative area, $A$, is $10^{-6}$ times the actual area units measured. The relative peak height, $P$, is $10^{-2}$ times the actual centimeters measured. The values in parentheses are the standard errors.

The peak area ratios of I to butacaine are plotted as a function of the concentration of I in 1 ml of plasma in Fig. 9 for Method B. The standard error of the estimate was 239 ng/ml of plasma for the 0–50-μg/ml range, and it was 151 ng/ml of plasma for the 0–10-μg/ml range.

The linear regression equation for concentration ($C$ in micrograms per milliliter of plasma) against the peak area ratio (PAR) for 0–50 μg/ml is $C$ (±0.24) μg/ml = −0.28 (±0.13) + 16.99 (±0.09) PAR ($n$ = 7, $r^2$ = 0.9998). For 0–10 μg/ml, it is: $C$ (±0.15) = 0.02 (±0.12) + 15.95 (±0.34) PAR. The values in parentheses are the standard errors.

**HPLC Analytical Methods for I in Plasma Using Haloalkane Extractions**—Remarkable reproducibility was obtained for calibration curves of the peak area against the plasma concentration performed on different days by Method C. The standard error estimated for the 0–10-μg/ml range was 185 ng/ml of plasma.

The linear regression equation for concentration, expressed as micrograms per milliliter of plasma, against the relative peak area ($A$) for 0–10 μg/ml of plasma is $C$ (±0.185) μg/ml = 0.211 (±0.089) + 0.879 (±0.015)$A$ ($n$ = 9, $r^2$ = 0.9980).

The standard error estimated by Method D was 86 ng/ml of plasma for the 0–5-μg/ml range of I and 192 ng/ml of plasma for the 0–5-μg/ml range of II from the linear regression of concentration on the peak area ratio to the internal standard, butacaine. The presence of a finite intercept in the regression of II indicated a small interference from plasma constituents at the retention time of II under these analytical conditions.

The linear regression equation for concentration, expressed as micrograms per milliliter of plasma, against the peak area ratio (PAR) for 0–5 μg/ml of I is $C$ (±0.0864) μg/ml = −0.002 (±0.056) + 1.404 (±0.031) PAR ($n$ = 5, $r^2$ = 0.9985). For 0–5 μg/ml of II, it is $C$ (±0.192) μg/ml = −0.94 (±0.20) + 1.189 (±0.065) PAR ($n$ = 4, $r^2$ = 0.9946). The values in parentheses are the standard errors.

**HPLC Separation of I and Its Derived Acid (II) from Plasma Impurities and Applications to I Stability in Plasma**—The HPLC separation of I, butacaine sulfate (internal standard), and II was readily effected with a mobile phase of buffer–acetonitrile (50:50 or 60:40) where 0.01–0.10 *N* acetate buffers were used and the pH was adjusted to 3.5–5.0 (Figs. 1A and 1B and Table III).

Unfortunately, plasma has some constituents that appear close to, or concomitantly with, the retention time of II and could interfere with its assay at 224 nm. The plasma constituent extracted with chloroform or methylene chloride (Fig. 1C) produced a peak that frequently interfered with the peak of II (Figs. 1B and 1D). However, variations in the mobile phase composition did permit satisfactory separations (Figs. 1E–1H). A valid HPLC system (Fig. 1H and Method B) was chosen to analyze for the stability of 1.25 μg of nafronyl (I) oxalate/ml of freshly withdrawn heparinized dog plasma. The peak area ratio (with respect to the internal standard) calibration curves were valid for the I assay, but the peak height ratios were best for the assay of II since a slight interference with a plasma component gave a significant positive intercept in its peak area ratio calibration curve.

The peak area and height ratios of I and II are given in Fig. 10 for fresh dog plasma spiked with I at 24.5°. Appropriate semilogarithmic plots of these data are given in Fig. 11 and are consistent in their estimates of a 3.2-hr half-life for the stability of I in dog plasma. Pharmacokinetic studies where plasma samples were not assayed immediately would be suspect.

## REFERENCES

(1) E. R. Garrett and R. J. Carper, *J. Am. Pharm. Assoc., Sci. Ed.*, **44**, 515 (1955).

(2) E. R. Garrett, *J. Pharm. Sci.*, **51**, 811 (1962).

(3) E. R. Garrett, in "Advances in Pharmaceutical Sciences," vol. II, H. S. Bean, A. H. Beckett, and J. E. Carless, Eds., Academic, New York, N.Y., 1967, pp. 1–94.

(4) E. R. Garrett and T. Gürkan, *J. Pharm. Sci.*, **68**, 26 (1979).

(5) L. Fontaine, M. Grand, J. Chabert, E. Szarvasi, and M. Bayssat, *Chim. Ther.*, **3**, 463 (1968).

(6) L. Fontaine, M. Grand, E. Szarvasi, and M. Bayssat, *ibid.*, **4**, 39, (1969).

(7) A. Meynaud, M. Grand, and L. Fontaine, *Arzneim.-Forsch.*, **23**, 1431 (1973).

(8) L. Fontaine, M. Belleville, J. C. Lechevin, M. Silie, J. Delahaye, and M. Boucherat, *Chim. Ther.*, **4**, 44 (1969).

(9) H. Kitagawa, R. Nakata, and H. Yano, *Oyo Yakuri*, **7**, 1231 (1973); through *Chem. Abstr.*, **81**, 99189a (1974).

(10) M. Belleville and J C. Lechevin, *Ann. Pharm. Fr.*, **26**, 641 (1968).

(11) H. S. Harned and B. B. Owen, "The Physical Chemistry of Electrolytic Solutions," 3rd ed., Reinhold, New York, N.Y., 1958.

## ACKNOWLEDGMENTS

Supported in part by an unrestricted grant from Lipha Chemicals Inc., New York, N.Y.

The research assistance of Michael Gardner is gratefully acknowledged.

# Comparison of Quantitation Methods for L-1210 Cell Populations and Evaluation of Selected Cytotoxic Agents in Leukemic Mice

C. T. BAUGUESS ˣ, Y. Y. LEE, J. W. KOSH, and J. E. WYNN

Received December 17, 1979, from the *College of Pharmacy, University of South Carolina, Columbia, SC 29208.* Accepted for publication June 11, 1980.

**Abstract** □ A more rapid cell-counting technique using an electronic cell counter was developed as an improvement over the slower hemocytometer method. The electronic counting method produced cell counts that had a smaller standard deviation but were not significantly different from the hemocytometer method. The acetate, hexanoate, and decanoate esters of *p*-*N*,*N*-bis(2-chloroethyl)aminophenol were investigated for acute toxicity in mice, effects on survival times, and effects on L-1210 cell populations in L-1210 leukemic mice. The decanoate ester was the least toxic compound and was most effective in lengthening the lifespan of the mice. The acetate and hexanoate esters were more effective in reducing L-1210 cell populations.

**Keyphrases** □ *p*-*N*,*N*-Bis(2-chloroethyl)aminophenol—ester derivatives synthesized and evaluated for antileukemic activity and toxicity, comparison of two cell-counting methods □ Antileukemic activity—*p*-*N*,*N*-bis(2-chloroethyl)aminophenol ester derivatives, synthesis and evaluation for antileukemic activity and toxicity, comparison of two cell-counting methods

Leukemia is a malignant tumor characterized by an overproduction of leukocytes and the presence of abnormal cells in hemopoietic organs (1). The proliferating leukemia cells fill the bone marrow spaces and prevent maturation of the red blood cells. These cells spill over into widely scattered areas of the body and accumulate even in organs with no inherent blood-forming capacity such as the spleen, liver, and lymph nodes (2). Lymphoid leukemia L-1210, a form of ascitic tumor, was induced in the spleen and lymph nodes of mice by painting the skin with 3-methylcholanthrene (3). The BDA/2 strain of mice is a reliable host in which to propagate this tumor system (4). An important characteristic of L-1210 leukemia is a widely disseminated proliferation resulting in death within 8–11 days (3).

A measure of the effectiveness of a cytotoxic agent against a neoplastic disease is its ability to kill or retard tumor cell growth at a dose that is not toxic to the host. A compound can be evaluated quantitatively by measuring its ability to increase the average survival time of L-1210 leukemic mice and to reduce the number of leukemic cells.

A model series of antineoplastic agents was synthesized in these laboratories for investigating the relationship of lipophilicity and antineoplastic activity. Three representative compounds, the acetate, hexanoate, and decanoate esters of *p*-*N*,*N*-bis(2-chloroethyl)aminophenol, were selected from the series for this investigation. Cyclophosphamide was used for comparison.

The specific objectives of this investigation were to: (*a*) determine the acute toxicity as measured by the $LD_{50}$ for each compound studied, (*b*) determine the effects of each compound on L-1210 cell populations and the prolongation of life in leukemic mice, and (*c*) develop a rapid technique for the determination of tumor cell populations and compare this technique with the conventional hemocytometer method.

## EXPERIMENTAL

**Test Animals**—DBA/2 mouse strain[1], $BDF_1$ mouse strain[1], HA/ICR mouse strain[2], and L-1210 leukemic mice (tumor source)[3] were used.

**Instruments**—The necessary equipment included an electronic cell counter[4], a channelizer[4], a dilutor[4], an *x*–*y* recorder[4], a hemocytometer[5], and a microscope[6].

**Materials**—Counting diluent[4], red blood cell-lysing reagent[4], crystal violet[7], Giemsa stain[8], isotonic diluting solution[9], trypan blue[10], Wright's stain[7], and cyclophosphamide[11] were obtained commercially. The fatty acid esters of *p*-*N*,*N*-bis(2-chloroethyl)aminophenol were prepared in these laboratories, and their physical and analytical data are reported in Table I[12]. These compounds will be referred to as the acetate, hexanoate, and decanoate esters.

**Pretoxicity Testings**—Groups of two healthy (HA/ICR) male mice were injected intraperitoneally with 500, 100, 10, 1, or 0.1 mg of test drug/kg in propylene glycol to evaluate the dose range for the pharmacological screen and $LD_{50}$ determination.

**Pharmacological Screen and $LD_{50}$ Evaluation**—Five groups of six (HA/ICR) mice each were selected. A gross screen was conducted for acute toxicity, and results were recorded during the 3 hr following injection. The mice were observed and weighed every day for 21 days, and the mortalities were recorded daily. A linear regression and correlation coefficient program (5) and a graphic method (6) were applied to determine the $LD_{50}$ for each drug test.

**Transplantation Procedures**—Sterile equipment was used under aseptic conditions. DBA/2 (6–9-week-old) host mice bearing L-1210 leukemia for 6–7 days were the tumor donors; they were sacrificed under ether vapor, immersed in 0.1% benzalkonium chloride, and swabbed with 70% ethanol. A 10-ml hypodermic syringe equipped with a 20-gauge needle (flushed with heparin at 1000 USP units/ml) was inserted into the abdominal cavity of the mouse and aspirated to obtain the lymphoid leukemia L-1210 cells (7).

The leukemia cells were placed in a container over ice. One drop of ascitic fluid was prepared for microscope examination. Cell morphology was determined by staining with Wright's or Giemsa stain to differentiate the leukocytes and lymphoblasts (8). Ascitic fluid containing at least 95% lymphoblasts or lymphocytes was used for transplantation in DBA/2 mice for tumor maintenance and in $BDF_1$ mice for antileukemic studies. All inoculations of L-1210 cells were made within 1 hr after cell removal from the host mouse to ensure a viable transplant.

**Determination of Cell Counts**—*With Electronic Cell Counter*—Ascitic fluid dilutions were made using a dilutor. A 40-μl sample of ascitic fluid was diluted with 20 ml of counting diluent to make a 1:500 dilution for the white blood cell counts. A 200-μl sample of the 1:500 dilution was used to make a 1:50,000 dilution in counting diluent for the red blood cell counts. Six drops of the red blood cell-lysing reagent were added to the

[1] Jackson Laboratories.
[2] ARS/Sprague–Dawley.
[3] National Cancer Institute, National Institutes of Health, Besthesda, Md.
[4] Model ZB counter and accessories, Coulter Electronics.
[5] American Optical Co.
[6] Model RA, Carl Zeis, West Germany.
[7] Matheson, Coleman & Bell.
[8] Fisher Scientific Co.
[9] Microbiological Associates.
[10] Allied Chemical Co.
[11] Cytoxan, Mead Johnson Co.
[12] Taken in part from M. B. Caldwell, M.S. thesis, College of Pharmacy, University of South Carolina, Columbia, S.C., 1974.



0022-3549/81/0100-0046$01.00/0
© 1981, American Pharmaceutical Association

**Table I—Physical Data and Elemental Analysis for the Esters of *p*-*N*,*N*-Bis(2-chloroethyl)aminophenol**

| Derivative | Mol. Wt. | Observed Melting Point | Analysis, % Calc. | Found |
|---|---|---|---|---|
| Acetate[a,b] | 276 | Oil | C 50.53 | 50.62 |
| | | | H 5.61 | 5.28 |
| | | | N 4.93 | 4.83 |
| Hexanoate | 332 | 40.5–41° | C 57.83 | 58.02 |
| | | | H 6.93 | 6.85 |
| | | | N 4.22 | 4.12 |
| Decanoate | 388 | Semisolid | C 61.86 | 61.81 |
| | | | H 7.99 | 8.01 |
| | | | N 3.61 | 3.47 |

[a] The calculated carbon, hydrogen, and nitrogen percentages include an average of 0.5 mole of water/mole of the derivative. [b] W. C. J. Ross, G. P. Warwick, and J. J. Roberts, *J. Chem. Soc.*, **1955**, 3110.

remaining 1:500 dilution of ascitic fluid, and white blood cell counts were performed using the electronic cell counter.

After completion of the white blood cell counts, the red blood cell counts of the 1:50,000 dilution were determined. Six readings for each dilution were recorded and corrected, and the mean cell values were calculated. Peripheral blood samples, obtained by puncture of the ophthalmic venous plexus of the mouse eye using a heparinized capillary tube, were treated in a similar manner.

*With Hemocytometer*—Ascitic fluid was diluted 20-fold with a white cell-diluting fluid using a white blood cell pipet. A 1% acetic acid solution containing 0.001% trypan blue was used to establish cell viability. A hemocytometer was used to determine the cell counts (2, 9). White blood cell and red blood cell counts were recorded as the mean of the five observations in each test from ascitic or blood samples. After determining cell viability and cell counts, the ascitic fluid was diluted with isotonic diluting solution. The inoculum contained $1 \times 10^5$ tumor cells in 0.1 ml. A 1-ml tuberculin syringe equipped with a 25-gauge needle was used to inject 0.1 ml of diluted ascitic L-1210 cells into the DBA/2 or $BDF_1$ mice.

***In Vivo* Determination of Antileukemic Activities by Survival Times *versus* Cell Differentiation**—On Day 0, the tumor was implanted into $BDF_1$ male mice; the number of survivors was recorded daily during the test period. The doses used were below the $LD_{10}$ value of each test drug to minimize drug toxicity (4). The test solutions were injected within 15 min after preparation at a dose volume not to exceed 0.01 ml/g of body weight. The test drug solutions were administered intraperitoneally to each test group on Days 2 and 5. The experiment was evaluated on the day of death for the last animal in a test group or after 30 days (4).

For leukemia cell differentiation, the drugs were administered in the same manner as in the survival study; these experiments were evaluated on Day 7. The test animals were sacrificed, the ascitic fluid was collected, and the leukemia cells were counted.

## RESULTS AND DISCUSSION

The gross appearance of leukemic mice was observed after inoculation of $1 \times 10^5$ leukemia cells in six $BDF_1$ mice. The body weight, hair appearance, motor activity, food intake, and size of the abdominal cavity remained normal until around the 4th or 5th day after inoculation. After 5–6 days, the abdominal cavity appeared enlarged and distended from an accumulation of ascitic fluid. Body weight generally increased 5–10% after 7 days or by the time of death. Piloerection and alopecia were observed as the disease approached the lethal stage. Beginning on the 5th or 6th day, the leukemic mice were rejected by their healthier cage mates.

**Table II—Summary of Acute Toxicity of Cyclophosphamide and the Fatty Acid Ester Derivatives Administered Intraperitoneally to Male HA/ICR Mice**

| Drug[a] | $LD_{50}$, mg/kg | $LD_{50}$, μmoles/kg | 95% Confidence Limits, μmoles/kg | Slope, probit log dose |
|---|---|---|---|---|
| Decanoate ester | 19.7 | 55.4 | 32.31–78.4 | 2.5045 |
| Hexanoate ester | 17.7 | 53.3 | 38.19–68.43 | 3.2822 |
| Acetate ester | 14.0 | 50.8 | 30.5–70.8 | 2.4724 |
| Cylcophosphamide | 281.4 | 1078 | 880.5–1272.0 | 4.6279 |

[a] Administered in propylene glycol.

**Table III—Comparison of Doses Producing Optimal Survival Times (% T/C) of Treated L-1210 Leukemic $BDF_1$ Mice**

| Drug[a] | Dose, μmoles/kg | Mean Survival Time, days (±*SE*) Test Group | Control Group | Survival, % T/C[b] |
|---|---|---|---|---|
| Cyclophosphamide | 499.00 | 23.0 (2.5)[c] | 8.83 (0.31) | 255.6 |
| Acetate | 5.44 | 9.66 (2.74) | 8.33 (0.21) | 116.0 |
| Hexanoate | 3.01 | 10.16 (2.03) | 8.67 (0.42) | 117.3 |
| Decanoate | 4.7 | 12.0 (1.57)[d] | 8.00 (0.26) | 150.0 |

[a] Administered in propylene glycol to six mice/group. [b] The % T/C represents the ratio of the sum of number of days (T) each treated animal survives to the sum of the number of days each control animal (C) survives multiplied by 100. [c] $p < 0.01$. [d] $p < 0.05$.

The $LD_{50}$ values for the drugs were obtained by probit analysis and linear regression (Table II) (5, 6). In the HA/ICR mice, the $LD_{50}$ for the decanoate ester was 55.4 μmoles/kg. Compared to cyclophosphamide, the decanoate ester was more toxic, but it was the least toxic of the fatty acid ester derivatives. The $LD_{50}$ values for the hexanoate and acetate esters were 53.3 and 50.8 μmoles/kg, respectively. Cyclophosphamide was the least toxic compound, having an $LD_{50}$ value of 1078 μmoles/kg. This value is less than literature values (1152 and 1425 μmoles/kg), which were determined in different strains (10, 11).

The survival of treated groups (T) to untreated control groups (C) was compared. A calculated % T/C value exceeding 100% implied that the drug treatment increased the lifespan. The doses producing optimal survival in leukemic mice for cyclophosphamide and the fatty ester derivatives are summarized in Table III.

The decanoate ester produced a maximum mean survival time (% T/C) of 150% at 4.7 μmoles/kg (Table III). A small increase in survival time was observed for the hexanoate ester (Table III); the % T/C value at the optimal survival dose level of 3.01 μmoles/kg was 117%. The optimal dose for the acetate ester was 5.44 μmoles/kg, which increased the % T/C value to 116%. Significant increases in survival times (255.5%) were observed for cyclophosphamide (Tables III and IV). Two mice lived beyond 30 days, and 30% of the animals showed a complete regression of the tumor at a dose of 400 μmoles/kg. After treatment with cyclophosphamide, leukemic mice showed little evidence of ascitic tumor cells and weight loss.

**Table IV—Summary of Survival Times and Leukemia Cell Counts in Treated L-1210 $BDF_1$ Leukemic Mice**

| Drug, μmoles/kg | Survival Time, % T/C | Cells/mm³ (±*SE*)[a] Test | Control | Cell Counts, % T/C[b] |
|---|---|---|---|---|
| Cyclophosphamide | | | | |
| 685 | 152 | 2,750 (135) | 137,150 (6837) | 2.0 |
| 616 | 166 | 2,810 (722) | 107,300 (3640) | 2.6 |
| 552 | 170 | 2,700 (111) | 107,300 (3650) | 2.5 |
| 499 | 256[c] | 4,010 (44) | 137,150 (4792) | 2.9 |
| 448 | 231 | 6,800 (179) | 137,150 (4792) | 4.9 |
| Acetate ester | | | | |
| 8.15 | 95 | 46,300 (1193) | 135,750 (4784) | 34.1 |
| 7.34 | 106 | 47,000 (5718) | 135,750 (4784) | 34.6 |
| 5.44 | 115 | 66,100 (2914) | 114,175 (4573) | 57.9 |
| 3.62 | 108 | 83,600 (2475) | 114,175 (4573) | 73.2 |
| 1.81 | 102 | 88,800 (3411) | 114,175 (4573) | 77.8 |
| Hexanoate ester | | | | |
| 7.53 | 98 | 50,625 (3787) | 150,900 (7296) | 33.5 |
| 6.09 | 112 | 81,700 (2643) | 150,900 (7296) | 54.1 |
| 3.01 | 117 | 71,500 (2394) | 150,900 (7296) | 47.4 |
| 1.51 | 113 | 81,700 (2568) | 150,900 (7296) | 54.1 |
| Decanoate ester | | | | |
| 5.28 | 112 | 60,300 (2776) | 135,750 (4784) | 44.5 |
| 4.70 | 150 | 56,600 (3352) | 135,750 (4784) | 41.7 |
| 3.86 | 131 | 76,600 (2427) | 148,100 (6815) | 48.5 |
| 2.57 | 123 | 79,600 (1292) | 158,100 (7354) | 50.3 |
| 1.27 | 110 | 90,200 (2323) | 158,100 (7354) | 57.1 |

[a] Electronic cell-counting procedure. [b] The % T/C represents the ratio of cell counts test (T) to control (C) multiplied by 100. Samples taken on Day 7. [c] $p < 0.01$.

**Table V—Comparison of L-1210 Cell Counts of Ascitic Fluid from Untreated Leukemic $BDF_1$ Mice Determined on the Electronic Cell Counter or Hemocytometer on Day 7 after Intraperitoneal Inoculation of $1 \times 10^5$ Cells [a]**

| Mouse | Cell Count, cells/mm³ ± *SD* | |
|---|---|---|
| | Electronic Cell Counter | Hemocytometer |
| 1 | 130,160 ± 384.7 | 125,740 ± 1573 |
| 2 | 108,520 ± 645.8 | 113,520 ± 2570 |
| 3 | 118,880 ± 178.9 | 122,500 ± 1584 |
| 4 | 158,000 ± 1593.7 | 151,972 ± 972 |
| 5 | 108,920 ± 657.3 | 127,540 ± 1181 |
| 6 | 137,880 ± 1507.3 | 125,312 ± 2917 |

[a] Correlation coefficient = 0.943 based on the average of five individual determinations for each method ($n_1 = n_2 = 5$) and $p < 0.05$.

A difference in drug toxicity between tumor- and non-tumor-bearing animals is common (4, 12), although quantitating this difference often is difficult because the tumor may induce early death. In the higher dosage ranges, the mice died early from drug toxicity; at the lower dosages, the animals died from the tumor.

Histological determinations were conducted on leukemic mice ($BDF_1$) to note changes in the peripheral blood and ascitic fluid. The red blood cell and white blood cell counts from peripheral blood were comparable to those of the normal controls (average count of $5 \times 10^6$ and $1 \times 10^4$ cells/mm³, respectively) until about Day 5. After this time, the red blood cell counts decreased to an average of $3.9 \times 10^6$ cells/mm³. The volume of ascitic fluid in the abdominal cavity increased to ~2 ml by Day 7 or by the time of death. By Day 7, the ascitic fluid usually contained in excess of $1 \times 10^5$ leukemia cells (white blood cell)/mm³. In the normal mice, only a fraction of 1 ml of ascitic fluid having few red blood cells or white blood cells could be recovered. Autopsies were performed on normal and leukemic mice to compare the involved organs (liver, spleen, and lymph nodes). The livers became enlarged and lost the color associated with healthy organs. The lymph nodes and spleens also were enlarged. In advanced stages of leukemia, the spleens increased greatly in weight, thickness, and length.

The white blood cell counts in the antileukemic tests were obtained using both the hemocytometer and the electronic cell counter. A significant correlation between the cell counts obtained from the two methods is illustrated in Table V. The electronic cell-counting method proved to be more statistically precise, *i.e.*, smaller standard deviations. The increased speed of this method is important in that it reduces the time interval that the leukemia cells must be outside of an animal host during the transplant procedure. This maximizes the number of viable cells in the inoculum. Even though using the electronic cell counter proved to be reliable for the determination of white blood cell counts, it still was necessary to determine morphological structures and viability of the leukemia cells by microscopic examination.

The inhibitory effects on the growth rate of L-1210 leukemia cells (% T/C cell count) and the effects on survival (% T/C survival) following administration of cyclophosphamide and the fatty acid ester derivatives are summarized for the various doses in Table IV. The white blood cell counts of the ascitic fluid samples taken from the leukemic mice on Day 7 after inoculation gradually decreased when the dose was increased. A % T/C cell count ratio of <100% implies that the drug reduced the growth rate of leukemia cells.

The reduction of cell growth rates in leukemic mice receiving the fatty acid ester derivatives varied with the dose. All doses of the decanoate ester reduced the growth rate of leukemia cells. With the decanoate ester, the growth rate of leukemia cells when determined on the electronic cell counter was reduced from 57.1 (% T/C cell count) to 41.7% (Table IV) over a dosage range of 1.27–5.28 μmoles/kg, with the optimum reduction and survival occurring at 4.7 μmoles/kg. When the dose was decreased, the growth rate of leukemia cells increased (Table IV).

All doses of the hexanoate ester inhibited the growth rate of leukemia cells. The growth rate was reduced to 33.5% at 7.53 μmoles of the hexanoate ester/kg. For the hexanoate ester, the optimum cell growth inhibition was 47.4% and occurred at the optimal dose (117% T/C survival) of 3.01 μmoles/kg.

Decreased cell counts also were observed in the leukemic mice treated with the acetate ester. A 34.1% growth rate was obtained at 8.15 μmoles/kg. At the optimal level (% T/C survival) for the acetate ester of 5.44 μmoles/kg, the leukemia cell counts were depressed to 57.9%. All doses of the acetate ester inhibited the leukemic cell growth rate; however, this compound exhibited greater host toxicity.

Significant reductions in the leukemia cell populations were observed in the cyclophosphamide studies. The % T/C cell count value decreased to 2.0% (Table IV) at a dose of 685 μmoles/kg. Cyclophosphamide was included for comparison and for establishing further the reliability of the animal model in determining antileukemic activity of new agents.

Comparison of the maximum reductions in leukemia cell counts produced with cyclophosphamide and the fatty acid derivatives revealed that the hexanoate and acetate esters were effective at higher doses. At an optimal survival dose of the fatty acid esters, the decanoate ester showed a greater reduction of the leukemia cell growth rate than the hexanoate or acetate esters. The results of this study indicate that additional compounds in this series may possess antileukemic activity, and the trend suggests that a further increase in the fatty acid side chain could lead to greater reduction in toxicity and an increase in survival time.

## REFERENCES


(1) G. D. Snell, "The Physiopathology of Cancer," F. Homburger, Ed., P. B. Hoeber, New York, N.Y., 1959, p. 293.

(2) R. D. Morehead, "Human Pathology," McGraw-Hill, New York, N.Y., 1965, p. 1239.

(3) L. J. Dunham, *J. Natl. Cancer. Inst.*, **13,** 1328 (1953).

(4) B. J. Abbott, *Cancer Chemother. Rep., Part 3,* **3,** 2 (1972).

(5) Manual No. 4022 N, model 1766, Monroe Calculator Co., Moristown, N.J., 1970.

(6) L. C. Miller and M. L. Tainter, *Proc. Soc. Exp. Biol. Med.*, **57,** 261 (1944).

(7) *Jax Notes,* No. 410, Jackson Mice Co., Bar Harbor, Me., Feb. 1972.

(8) A. Joseph, E. Morholt, and P. F. Brandwein, "A Sourcebook for the Biological Sciences," Harcourt, Brace & World, New York, N.Y., 1966, p. 117.

(9) J. Berkson, T. B. Magath, and M. Hurn, *Am. J. Physiol.*, **128,** 309 (1940).

(10) M. Lane, *Cancer Res.*, **20,** 1269 (1960).

(11) W. R. Shapiro, J. I. Ausman, and D. P. Rall, *ibid.*, **30,** 2401 (1970).

(12) H. E. Skipper and L. H. Schmidt, *Cancer Chemother. Rep.*, **17,** 1 (1962).

# Inhibition of Mucopolysaccharide Sulfation

**WILLIAM O. FOYE ˣ, YUN-LING LAI-CHEN, and BHUPENDRA R. PATEL**

Received May 5, 1980, from the *Samuel M. Best Research Laboratory, Massachusetts College of Pharmacy and Allied Health Sciences, Boston, MA 02115.* Accepted for publication July 7, 1980.

**Abstract** □ A method of measuring the inhibition of sulfation in mucopolysaccharides employed the coupled enzyme system of Wortman. This procedure utilized the phenol and mucopolysaccharide sulfotransferases of beef cornea extract. Compounds tested against this system included amino acids, salicylates, 2-mercaptoethylamine and a derivative, heterocyclic ethanethiosulfuric acids, arylsulfonamidoethanethiosulfates, and several other compounds. In general, the salicylates and thiosulfates were inhibitory, with sodium 2-(4-acetamidobenzenesulfonamido)-ethanethiosulfate being the most inhibitory and 2-mercaptoethylguanidine trithiocarbonic acid the second most inhibitory. Salicylamide and allopurinol, which have been employed in kidney stone therapy, were inhibitors. Kidney stones have a mucopolysaccharide sulfate matrix, which is involved in their growth.

**Keyphrases** □ Mucopolysaccharides—inhibition of sulfation by salicylates and thiosulfates □ Salicylates—inhibition of mucopolysaccharide sulfation □ Thiosulfates—inhibition of mucopolysaccharide sulfation

Mucopolysaccharide sulfates play a role in the calcifying mechanism of most kinds of renal calculus formation (1). Boyce and Garvey investigated over 1200 renal calculi and found a matrix of mucopolysaccharide sulfates in all of them, to the extent of ~2.5% of the total weight (2). Furthermore, kidney stone formers generally have more highly sulfated mucopolysaccharides in their urine than normal (3). Other pathological conditions that are known to be associated with abnormal amounts or degrees of sulfation of mucopolysaccharides (4) include some malignant tumors (5). Abnormal amounts of mucopolysaccharide sulfates also have been observed in virus-transformed cells (6).

It therefore was considered important to find compounds that might inhibit the sulfation of mucopolysaccharides and to develop a method of measuring this inhibition. Previous studies (7) on anti-inflammatory agents showed that salicylate exerts an inhibitory effect on the sulfation of mucopolysaccharides. It also was found that several metal-binding agents, including substituted salicylates, cysteine, and 2-mercaptoethylamine and some of its derivatives, inhibited sulfation (8). Other inhibitors of this process are propylthiouracil (9), 4-methylumbelliferyl β-xyloside (10), and *p*-nitrophenyl β-xyloside (10). All of these studies were carried out with intact cartilage. However, the use of the enzyme systems involved appeared to be a more convenient and reliable method of measuring inhibition of mucopolysaccharide sulfation since use of intact cartilage requires embryonic cartilage not yet fully sulfated.

## ENZYME ASSAY

Sources of the enzyme systems known to catalyze formation of mucopolysaccharide sulfates are found in various cartilaginous tissues, including the cornea, as well as in the liver. Trials with extracts of rabbit liver, dog cornea, and beef cornea revealed that the beef corneal extracts gave the most reproducible results. Wortman (11) showed the presence of both phenol and mucopolysaccharide sulfotransferase activities in beef cornea epithelial extracts and made use of the phenol sulfotransferases (Schemes I and II) as a feeder system for the assay and characterization of mucopolysaccharide sulfotransferase (Scheme III). Although both phenol and mucopolysaccharide are sulfated in this combined assay, it appeared to be suitable for measuring mucopolysaccharide sulfation and allowed the use of a spectrophotometric procedure.

*p*-nitrophenol sulfate + 3′,5′-diphosphoadenosine
→ *p*-nitrophenol + 3′-phosphoadenosine 5′-phosphosulfate
*Scheme I*

3′-phosphoadenosine 5′-phosphosulfate + phenol
→ phenol sulfate + 3′,5′-diphosphoadenosine
*Scheme II*

3′-phosphoadenosine 5′-phosphosulfate + chondroitin
→ chondroitin sulfate + 3′,5′-diphosphoadenosine
*Scheme III*

Phenol sulfotransferase presumably carries out the reactions shown in both Schemes I and II. The overall rate of sulfate transfer is measured spectrophotometrically by the appearance of *p*-nitrophenol at 400 nm. The participation of mucopolysaccharide sulfotransferase, which also utilizes 3′-phosphoadenosine 5′-phosphosulfate as a coenzyme, assists in driving the overall reaction to the right. This process results in an increase in the change of the optical density and provides a coupled assay method for measuring mucopolysaccharide sulfation.

## RESULTS AND DISCUSSION

The activity of the coupled enzyme system in beef cornea extract over 5 hr is shown in Fig. 1. The reaction rate decreased somewhat after the 1st hr, but the reaction still was measurable after 9 hr. The changes in the optical density observed for the phenol sulfotransferase assay (Schemes I and II) and the coupled enzyme assay (Schemes I–III) over 2 hr are shown in Table I. The protein concentration of the extract varied from 0.24 to 0.84 mg/ml. The enzyme activity decreased slowly over 2 weeks; a change in the optical density (Δo.d.) of 0.104 at 2 hr was observed with freshly prepared extract, but after storage at −10° for 2 weeks, Δo.d.

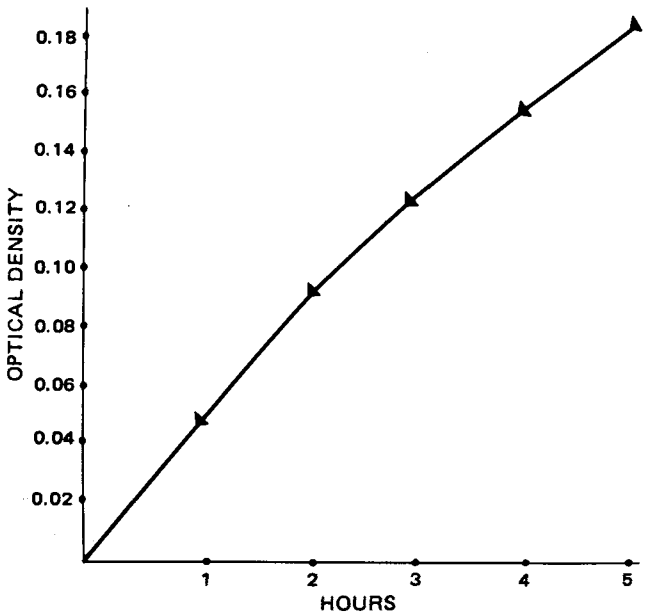


**Figure 1**—*Activity of the coupled enzyme system in beef cornea extract.*

0022-3549/81/0100-0049$01.00/0
© 1981, American Pharmaceutical Association

**Table I—Sulfate Transfer Activity of Beef Cornea Extract**

| Reaction[a] | Δo.d. at 1 hr | Δo.d. at 2 hr |
|---|---|---|
| Schemes I and II | 0.040 | 0.070 |
| Schemes I–III | 0.044 | 0.078 |

[a] Measured at pH 7.0 and 37° for transfer to chondroitin sulfate. Optical density was recorded at 400 nm.

was 0.021 at 2 hr. However, the enzyme showed no change in activity for 24 hr.

It has been found that various tissues containing sulfotransferases also contain some 3′,5′-diphosphoadenosine (12). A 3′,5′-diphosphoadenosine concentration of 2 $\mu M$ was reported as the saturation level for phenol sulfotransferase (13), whereas concentrations above 20 $\mu M$ began to be inhibitory. In this study, the decrease in the reaction rate where added 3′,5′-diphosphoadenosine was omitted from the assay system indicated the presence of 3′,5′-diphosphoadenosine in the extract. The concentration of added 3′,5′-diphosphoadenosine should not be more than $10^{-4}$ $M$ to prevent inhibition of the enzyme.

Beef cornea is known to contain arylsulfatase, which is inhibited by monobasic potassium phosphate and sodium fluoride (14). In the present study, phosphate buffer was used routinely to prevent sulfatase action. Various concentrations of chondroitin added to the enzyme system did not show appreciable differences in Δo.d. in the range of 0.05–0.5 m$M$. Although the sulfation of chondroitin was a rapid reaction in the rabbit liver system, the reaction persisted for 5 hr in the beef cornea system.

A previous investigation of inhibition of mucopolysaccharide sulfation in veal costal cartilage showed that 2-mercaptoethylamine and 2-mercaptoethylguanidine trithiocarbonate were powerful inhibitors (8), inhibiting sulfation by 90% or more. Since this degree of inhibition may have undesirable effects, particularly on bone growth, compounds with a lower degree of inhibitory activity were sought. A series of 2-mercaptoethylamine derivatives, aromatic and arylsulfonyl aminoethanethiosulfates, which should be less toxic than the thiols, was synthesized. Several salicylates and other compounds used in the previous study also were included, as well as nitrofurantoin and allopurinol, compounds found to be effective in inhibiting kidney stone growth. Results of the inhibition study are shown in Table II.

Of the salicylic acid derivatives tested, salicylic acid and salicylamide showed appreciable inhibition of sulfation and $p$-aminosalicylic acid showed some inhibition, but salicyl hydrazide showed slight stimulation of the enzyme system. These results indicate that metal-ion complexation is not a factor in the inhibition of this sulfation system. Cysteine and riboflavin both inhibited sulfation by ~20%, but nitrofurantoin gave only 5% inhibition. The latter compound showed much greater inhibition (65%) in the study using veal costal cartilage.

Allopurinol, currently used in kidney stone treatment, gave 26% inhibition. 2-Thiouracil produced 12% inhibition. 2-Mercaptoethylamine gave 27% inhibition, whereas it gave 90% inhibition in the costal cartilage system. 2-Mercaptoethylguanidine trithiocarbonate, which gave 93% inhibition in veal costal cartilage, showed 82% inhibition in the beef cornea system. At the pH (7.0) of the corneal enzyme system, much of the 2-mercaptoethylamine may have been converted to the disulfide during the observation period (2 hr).

**Table II—Inhibition of Sulfate Transfer in Beef Cornea Extract**

| Compound | Activity[a], % |
|---|---|
| None | 100 |
| Cysteine | 79 |
| Riboflavin | 80 |
| Nitrofurantoin | 95 |
| Salicylamide | 22 |
| Salicylic acid | 38 |
| Salicyl hydrazide | 109 |
| $p$-Aminosalicylic acid | 73 |
| 2-Mercaptoethylamine | 73 |
| 2-Mercaptoethylguanidine trithiocarbonic acid (17) | 18 |
| Allopurinol | 74 |
| 2-Thiouracil | 88 |
| 2-[2-(4,6-Diamino-1,3,5-triazinyl)amino]-ethanethiosulfuric acid | 75 |
| Sodium 2-(7-theophyllinyl)ethanethiosulfate | 145 |
| Sodium 2-(4-acetamidobenzenesulfonamido)-ethanethiosulfate | 0 |
| Sodium 2-(2-naphthalenesulfonamido)ethanethiosulfate | 23 |
| Sodium 2-(8-quinolinesulfonamido)ethanethiosulfate | 68 |

[a] Measured after 2 hr of incubation at 37° at a concentration of $5 \times 10^{-3}$ $M$ of the inhibitory compound, with the exceptions noted for riboflavin, nitrofurantoin, and sodium 2-(7-theophyllinyl)ethanethiosulfate. Activities of different enzyme preparations were adjusted to give a standard value.

The arylaminoethanethiosulfates were, in general, inhibitory. Sodium 2-(4-acetamidobenzenesulfonamido)ethanethiosulfate showed complete inhibition, and sodium 2-(2-naphthalenesulfonamido)ethanethiosulfate gave 77% inhibition. Sodium 2-(8-quinolinesulfonamido)ethanethiosulfate gave 32% inhibition, and 2-[2-(4,6-diamino-1,3,5-triazinyl)-amino]ethanethiosulfuric acid gave 25% inhibition. However, sodium 2-(7-theophyllinyl)ethanethiosulfate showed marked stimulation of the enzyme system. An increase in the synthesis rate of glycosaminoglycans (chondroitin and dermatan sulfates) was demonstrated in transformed fibroblast cells by the addition of theophylline (15).

It was postulated in the previous study of sulfation inhibition (8) that metal-ion complexation may be a factor since the compounds tested had the common property of metal binding and the enzyme system involved requires magnesium and possibly other metals. Not all of the compounds observed in the present study are known to be metal binding, so this postulation cannot be extended here. No other chemical property common to all of the compounds is apparent.

With compounds having hydroxyl groups, such as the salicylates and allopurinol, the possibility exists that they may act as sulfate acceptors and compete with mucopolysaccharides. It also is possible that the thiol group could function in the same manner, but the thiosulfates could enter only into possible sulfate-exchange reactions. Therefore, direct inhibition of the enzyme system involved by some form of complexation seems more likely.

## EXPERIMENTAL[1]

**Enzyme Preparation**—Wortman's method (11) was followed. Abou 75 fresh, iced beef corneas were washed with tris(hydroxymethyl)aminomethane hydrochloride buffer (0.05 $M$, pH 7.4) and then soaked in 50 ml of the buffer before homogenization. A blender[2] was used for homogenization for 30 sec, and the volume was brought to 100 ml by addition of the same buffer. The mixture was homogenized for 1 min, and the homogenate was centrifuged at 0° for 1 hr at 34,800×$g$. The supernate was collected and dialyzed against 2000 ml of 0.005 $M$ phosphate buffer with 0.5 m$M$ ethylenediaminetetraacetic acid (pH 6.5) for 1 hr in a refrigerator. The preparation was stored in a freezer.

**Sulfotransferase Assay**—The reagents were 0.6 $M$ phosphate buffer (pH 7.0), $5 \times 10^{-3}$ $M$ potassium $p$-nitrophenol sulfate, $10^{-5}$ $M$ 3′,5′-diphosphoadenosine, $10^{-4}$ $M$ chondroitin sulfate, $5 \times 10^{-3}$ $M$ phenol, and beef cornea extract.

**Method A: Assay of Phenol Sulfotransferase**—To a mixture of 0.3 ml of each reagent (except chondroitin sulfate), 0.1 ml of buffer, and 1.5 ml of distilled water in a spectrophotometric cell ($S_1$) with a 1-cm light path was added 0.5 ml of beef cornea extract to make the total volume 3 ml. After mixing, the optical density at 400 nm was recorded. The mixture was incubated in a water bath at 37° for 2 hr, and the change in the optical density at 400 nm was recorded after each hour of incubation. A blank ($S_{1'}$) was run in which phenol was replaced by water.

**Method B: Assay of Mucopolysaccharide Sulfotransferase**—The same procedure as in Method A was carried out, except that 0.3 ml of water in $S_1$ and $S_{1'}$ was replaced by chondroitin sulfate. A spectrophotometric cell ($R$) filled with 2 ml of phosphate buffer and 2 ml of water was used as the reference cell for sample cells $S_1$ and $S_{1'}$ to measure the reactions shown in Schemes I and II and Scheme I, respectively.

**Inhibition Study**—To a mixture of each reagent used in the assays and 0.1 ml of buffer in a spectrophotometric cell ($S_2$) with a 1-cm light path was added 0.3 ml of a solution of inhibitor [$5 \times 10^{-3}$ $M$, except that $0.25 \times 10^{-3}$ $M$ riboflavin and nitrofurantoin and $0.28 \times 10^{-3}$ $M$ sodium

[1] *Melting points were determined with a Mel-Temp block and are uncorrected.* IR absorption spectra were obtained with a Perkin-Elmer 457 grating spectrophotometer using potassium bromide pellets. NMR spectra were measured with a Varian T-60 spectrometer with tetramethylsilane as the internal standard. Elemental analyses were done by F. B. Strauss, Oxford, England, or by Carol K. Fitz, Carlisle, Mass. TLC was carried out using silica gel plates, and products were detected by exposure to iodine vapor or UV light. Starting substances for the syntheses were obtained from Aldrich Chemical Co., Eastman Organic Chemicals, and Fisher Scientific Co.

$p$-Nitrophenol sulfate, 3′,5′-diphosphoadenosine, and chondroitin sulfate were obtained from Sigma Chemical Co. Rabbit liver and beef cornea were obtained from Pel-Freez Biologicals. Nitrofurantoin was a gift of Eaton Laboratories, and allopurinol was a gift of Dr. Edwin L. Prien, Sr.

[2] Waring.

2-(7-theophyllinyl)ethanethiosulfate were used]. Beef cornea extract (0.5 ml) was added and mixed to give a total volume of 3 ml. The mixture was incubated in a water bath at 37°. The change in optical density at 400 nm was recorded over 2 hr. A blank ($S_{2'}$) was run in which phenol and chondroitin sulfate were replaced by water. A third cell filled with 1.0 ml of phosphate buffer, 1.7 ml of distilled water, and 0.2 ml of inhibitor (at the given concentrations) was used as a reference cell, and the previous cells ($S_2$ and $S_{2'}$) were used as sample cells. The change of optical density of each solution was recorded.

**Calculations**—The calculation of the change in the optical density (Δo.d.) of the coupled enzyme system was done as shown in the following chart, where $S_x$ is the sample cell, $S_{x'}$ is the blank cell, and $R_x$ is the reference cell.

| o.d. at 1 hr | o.d. at 2 hr | Δo.d. |
|---|---|---|
| $S_1 - S_{1'} = A$ | $S_2 - S_{2'} = a$ | $a - A$ |
| $S_1 - R_1 = B$ | $S_2 - R_2 = b$ | $b - B$ |
| $S_{1'} - R_1 = C$ | $S_{2'} - R_2 = c$ | $c - C$ |

Since $A = B - C$, $a = b - c$, and $a - A = (b - c) - (B - C) = (b - B) - (c - C)$, $a - A = (b - B) - (c - C)$.

**2-[2-(4,6-Diamino - 1,3,5 - triazinyl)amino]ethanethiosulfuric Acid**—To 13.44 g (0.075 mole) of sodium 2-aminoethanethiosulfate (16) and 2.0 g (0.05 mole) of sodium hydroxide in 100 ml of ethanol was added 7.28 g (0.05 mole) of 2-chloro-4,6-diamino-1,3,5-triazine suspended in 10 ml of ethanol with stirring over 2 hr. The mixture was refluxed for 48 hr, filtered, and evaporated to a slurry. Neutralization of the slurry with acetic acid followed by addition of ethanol gave 3.0 g (22%) of a white solid, mp 210–215°. Crystals were obtained from 95% ethanol, mp 225–228°, $R_f$ 0.375 (silica gel with benzene–methanol 8:2); IR (KBr): 3390, 3330, 3240–3120, 1200–1180 ($S_2O_3$), 1028 ($\nu$-ring), and 645 ($\beta$-ring) $cm^{-1}$.

*Anal.*—Calc. for $C_5H_{10}N_6O_3S_2$: C, 22.55; H, 3.78; N, 31.55. Found: C, 22.65; H, 4.18; N, 31.79.

**Sodium 2-(7-Theophyllinyl)ethanethiosulfate Monohydrate**—A mixture of 9.71 g (0.04 mole) of 7-(2-chloroethyl)theophylline and 11.0 g (0.045 mole) of sodium thiosulfate pentahydrate in 150 ml of ethanol–water (1:1) was refluxed with stirring for 24 hr. Flash evaporation of the solvent gave a white solid, which was extracted with 200 ml of boiling ethanol. The insoluble material was filtered, and the filtrate yielded white crystals on chilling overnight; after drying over phosphorus pentoxide for 24 hr, 7.31 g (51%) was obtained. Three recrystallizations from absolute ethanol, with drying (phosphorus pentoxide) for 24 hr and at 60° (calcium chloride) for 48 hr, gave a product that melted at 258–261°; IR (KBr): 3500, 3000, 2900, 1695 ($\nu$-ring), 1650 ($\nu$-ring), 1250–1175 ($S_2O_3$), and 1030 ($\nu$-ring) $cm^{-1}$.

*Anal.*—Calc. for $C_9H_{11}N_4NaO_5S_2 \cdot H_2O$: C, 30.00; H, 3.63; N, 15.54. Found: C, 30.30; H, 3.96; N, 15.25.

**Sodium 2-(4-Acetamidobenzenesulfonamido)ethanethiosulfate**—A suspension of 11.68 g (0.05 mole) of 4-acetamidobenzenesulfonyl chloride in 150 ml of tetrahydrofuran was added over 2 hr to a solution of 2.0 g (0.05 mole) of sodium hydroxide, 6.3 g (0.075 mole) of sodium bicarbonate, and 7.86 g (0.05 mole) of 2-aminoethanethiosulfuric acid (16) in 150 ml of ethanol at 0–5° with stirring. The mixture was stirred at room temperature for 24 hr, and the precipitate was filtered and dried. It was extracted with 300 ml of boiling 95% ethanol and filtered. After cooling overnight, the filtrate yielded a crude product, which was extracted with 100 ml of ethanol–ethyl acetate (1:1) and recrystallized four times from isopropanol. It was dried (calcium chloride) at 60° *in vacuo* for 24 hr, giving 8.65 g (46%) of a white solid, mp 155–158°; IR (KBr): 3280, 3190, 3130, 1325 ($SO_2$), 1240–1210 ($S_2O_3$), 1160 ($SO_2$), 1040 (CH), and 640 (CH) $cm^{-1}$.

*Anal.*—Calc. for $C_{10}H_{13}N_2NaO_6S_3$: C, 31.90; H, 3.48; N, 7.44. Found: C, 31.61; H, 3.85; N, 7.00.

**Sodium 2-(2-Naphthalenesulfonamido)ethanethiosulfate**—A solution of 11.33 g (0.05 mole) of 2-naphthalenesulfonyl chloride in 100 ml of tetrahydrofuran was added, with stirring, over 1 hr to a solution of 2.0 g (0.05 mole) of sodium hydroxide, 6.3 g (0.075 mole) of sodium bicarbonate, and 7.86 g (0.05 mole) of 2-aminoethanethiosulfuric acid (16) in 100 ml of 95% ethanol at 0–5°. The mixture was stirred at room temperature for 24 hr, filtered, and evaporated to a white solid. This solid was stirred with methylene chloride for 1 hr, filtered, and extracted with 100 ml of boiling absolute ethanol. The cooled filtrate gave 12.0 g (65%) of product, which was recrystallized three times from absolute ethanol and charcoal and dried (calcium chloride) at 60° for 24 hr *in vacuo*, mp 184–185°; IR (KBr): 3280, 3060, 1320 ($SO_2$), 1225–1195 ($S_2O_3$), 1155 ($SO_2$), 1025 (CH), and 635 (CH) $cm^{-1}$; NMR (deuterium oxide-$d_2$): $\delta$ 3.06–3.35 (m, 4H, $CH_2$), and 7.40–8.33 (m, 7H, ring H) ppm.

*Anal.*—Calc. for $C_{12}H_{12}NNaO_5S_3$: C, 39.01; H, 3.27; N, 3.79. Found: C, 39.17; H, 3.65; N, 3.62.

**Sodium 2-(8-Quinolinesulfonamido)ethanethiosulfate Monohydrate**—A solution of 5.69 g (0.025 mole) of 8-quinolinesulfonyl chloride in 200 ml of tetrahydrofuran was added, with stirring, over 2 hr to a solution of 1.0 g (0.025 mole) of sodium hydroxide, 2.2 g (0.026 mole) of sodium bicarbonate, and 3.39 g (0.25 mole) of 2-aminoethanethiosulfuric acid (16) in 50 ml of water at 0–5°. The mixture was stirred at room temperature for 24 hr and evaporated *in vacuo* to a white solid. The solid was extracted with 300 ml of boiling absolute ethanol and filtered. The cooled filtrate yielded 9.1 g (93%), which was recrystallized several times to give an analytical sample, mp 173–176°; IR (KBr): 3540–3500, 3280, 1335 ($SO_2$), 1230–1200 ($S_2O_3$), 1175 ($SO_2$), 1030 (CH), and 645 (CH) $cm^{-1}$; NMR (deuterium oxide-$d_2$): $\delta$ 3.0–3.40 (m, 4H, $CH_2$) and 7.45–8.45 (m, 6H, ring H) ppm.

*Anal.*—Calc. for $C_{11}H_{11}N_2NaO_5S_3 \cdot H_2O$: C, 34.02; H, 3.44; N, 7.26. Found: C, 34.40; H, 3.32; N, 7.20.

## REFERENCES


(1) P. S. Rubin and J. E. Howard, in "Transactions of the Second Conference on Metabolic Interrelations," E. C. Reifenstein, Ed., Josiah Macy, Jr. Foundation, New York, N.Y., 1950, pp. 155–166.

(2) W. H. Boyce and F. K. Garvey, *J. Urol.*, **76**, 213 (1956).

(3) W. O. Foye, H. S. Hong, C. M. Kim, and E. L. Prien, Sr., *Invest. Urol.*, **14**, 33 (1976).

(4) A. Pedrini-Mille, V. A. Pedrini, and I. V. Ponseti, *J. Lab. Clin. Med.*, **84**, 465 (1974).

(5) L. O. Sampaio, C. P. Dietrich, and O. G. Filho, *Biochim. Biophys. Acta*, **498**, 123 (1977).

(6) T. Shigematsu and L. Dmochowski, *Cancer*, **31**, 165 (1973).

(7) M. W. Whitehouse and H. Bostrom, *Biochem. Pharmacol.*, **7**, 135 (1961).

(8) W. O. Foye, M. C. M. Solis, J. W. Schermerhorn, and E. L. Prien, *J. Pharm. Sci.*, **54**, 1365 (1965).

(9) H. D. Mosier, Jr., L. C. Dearden, R. A. Jansons, and R. R. Hill, *Endocrinology*, **100**, 1644 (1977).

(10) K. D. Gibson, B. J. Segen, and J. K. Audhya, *Biochem. J.*, **162**, 217 (1977).

(11) B. Wortman, *J. Biol. Chem.*, **236**, 974 (1961).

(12) J. D. Gregory and F. Lipmann, *ibid.*, **229**, 1081 (1957).

(13) E. G. Brunngraber, *ibid.*, **233**, 472 (1958).

(14) B. Wortman, *Arch. Biochem. Biophys.*, **97**, 70 (1962).

(15) J. F. Goggins, G. S. Johnson, and I. Pastan, *J. Biol. Chem.*, **247**, 5759 (1972).

(16) W. O. Foye, Y. H. Lowe, and J. J. Lanzillo, *J. Pharm. Sci.*, **65**, 1247 (1976).

(17) W. O. Foye, J. Mickles, R. N. Duvall, and J. R. Marshall, *J. Med. Chem.*, **6**, 509 (1963).


## ACKNOWLEDGMENTS


Presented at the APhA Academy of Pharmaceutical Sciences, Washington meeting, April 1980.

Abstracted in part from the theses submitted by Y.-L. Lai-Chen and B. R. Patel to the Massachusetts College of Pharmacy and Allied Health Sciences in partial fulfillment of the Master of Science and Doctor of Philosophy degree requirements, respectively.

Supported by funds from the John R. and Marie K. Sawyer Memorial Fund, Massachusetts College of Pharmacy and Allied Health Sciences, and The Gillette Co.

# Permeation of Hairless Mouse Skin II: Membrane Sectioning Techniques and Influence on Alkanol Permeabilities

G. L. FLYNN ˣ, H. DÜRRHEIM, and W. I. HIGUCHI

Received September 1, 1979, from the *College of Pharmacy, University of Michigan, Ann Arbor, MI 48109.* Accepted for publication July 17, 1980.

**Abstract** □ The barrier properties of hairless mouse skin were examined by separating the skin into its component epidermal and dermal strata, using both mechanical and thermal techniques, and then assessing the permeability of each stratum to the homologous alkanols. The permeability data, when compared to those obtained previously for full-thickness hairless mouse skin and to new data for the permeability of the alcohols through a perfect lipid membrane, allow assignment of diffusional resistances to the respective, anatomically distinguishable membrane strata. It was found that the principal barrier for the lower alkanols is the epidermis, which contains the stratum corneum. The effective aqueous tissue resistances of the cellular and aqueous strata of full skin, the epidermis, and the dermis were estimated using sectioned skins. This resistance was much greater than that of an equivalent thickness of water. These data and methods represent a novel approach in the permeation analysis of a biological tissue and offer a means of estimating the effects of skin damage on percutaneous absorption.

**Keyphrases** □ Permeability—*n*-alkanols through hairless mouse skin strata separated by thermal and stripping techniques □ Alcohols, normal—permeation through hairless mouse skin strata separated by thermal and stripping techniques □ Skin separation techniques—separation of hairless mouse skin strata by thermal and stripping techniques, permeability of *n*-alkanols through separated strata

The skins of mammals differ widely in appearance and function (1). Even the skins of animals without prominent, terminal hair vary greatly, but all have a more fully developed epidermis with a significant outer horny or cornified layer, which functions protectively in the absence of hair. Human and hairless mouse integuments are two examples of such skins.

Cornified epithelia are unusually impermeable to both inorganic and organic chemicals (2–4). This feature of human skin limits the topical use of drugs but, at the same time, protects the body from inadvertently encountered toxins in the environment and in products of everyday use. Clearly, the delineation of barrier features and the construction of predictive models are important steps in defining topical usefulness and the risk of chemicals.

Ideally, models should be so refined that quantitative *a priori* estimates of percutaneous absorption rates based on chemical structure are possible. Some beginnings have been made in this regard (5–7), but it still is not possible to predict the permeability of a new compound unless it is related congenerically to previously studied chemicals. Furthermore, the influences of injury and disease are poorly documented. Laboratory means of assessing the effects of trauma have yet to be developed.

The purpose of the present study was to assess the permeabilities of hairless mouse skin strata, isolated by thermal and stripping techniques. Water and homologous alkanols were chosen as the permeants. By defining the diffusional resistances of each layer, especially the stratum corneum, as a function of the alkyl chain length, it should be possible to learn generally how systemic absorption as a result of stratum corneum impairment is related to the chemical structure of permeants. Gross similarities in permeability properties between hairless mouse skin and human skin make the insights relevant to humans. In this sense, the techniques developed may prove to be useful as laboratory methods for defining maximum absorption potentials and, therefore, maximum systemic toxicities of topically applied chemicals and drugs.

## EXPERIMENTAL

The present study represents a continuation of research on alkanol permeation of hairless mouse skin, for which experimental methods were described (5). The description of the experimentation details only departures from previous methods. Chemical sources, diffusion cell design and operation, and partitioning techniques also were the same as those reported previously (5).

The abdominal skins of hairless mice (HRS/J strain), 4–6 weeks old, were excised and used essentially upon receipt. The skin either was used intact or was separated into its respective strata by one of the following methods.

1. Heat treatment—The skin was separated along the epidermal–dermal junction after the abdominal surface of an anesthetized (methoxyflurane[1]) mouse was heated for 30 sec with a stream of 60° water. The animals were sacrificed, and the heat-treated skin was excised intact and separated carefully into the epidermis and dermis by raising the epidermal layer with the sharp end of a nickel spatula. Each stratum then was placed in a separate diffusion cell. The heat-separated epidermis was laid gently on the surface of normal saline solution to flatten and smooth it. This step caused the layer to unwrinkle spontaneously so that it could be lifted and placed between the cell halves if handled carefully.

2. Stripping technique—The hairless mouse skin was stripped repeatedly with cellophane tape[2]. The tape was placed firmly against the abdominal surface of an anesthetized mouse and then peeled away. This procedure was done in multiples of five strippings for up to 15 strippings and was carried out 25 times on some skins. The skin became more and more an oozing surface with each succeeding maneuver. After processing the skin, the animal was sacrificed and the skin was excised and mounted in the diffusional apparatus. The processing of the mouse skin is illustrated schematically in Fig. 1.

After positioning of the membrane in the diffusion cell, the apparatus was immersed in a 37° bath, the cell compartments were rinsed with normal saline, and the runs were conducted at 150 rpm (2). To assess boundary layer influences, polydimethylsiloxane membranes[3] were used since they provide a simple, hydrophobic membrane without internal aqueous resistance. Therefore, departure from membrane-controlled transport could be assigned totally to hydrodynamic layers at the membrane interfaces with the compartmental solutions (8, 9). The preparation of the diffusion cell after insertion of the rubber membrane was identical to that used for the skin membranes.

The permeation process, irrespective of the membrane, was tracked using radiolabeled alcohols. The permeability coefficient for each run was calculated from the pseudo-steady-state portion of the receptor compartment concentration *versus* time profile using (5):

$$P = V_R \left( \frac{dC/dt}{A\,\Delta C} \right) \qquad \text{(Eq. 1)}$$

[1] Metophase, Pitman–Moore, Washington Crossing, NJ 08560.
[2] Scotch Brand, 3M Co., Minneapolis, Minn.
[3] Silastic medical grade sheeting, 0.05 cm, Dow Corning Corp., Midland, Mich.



0022-3549/81/0100-0052$01.00/0
© 1981, American Pharmaceutical Association

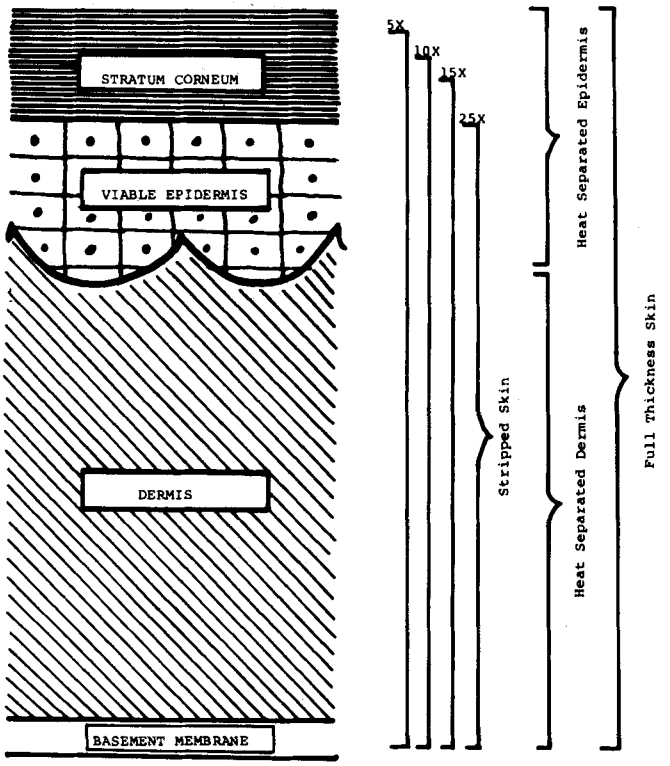


**Figure 1**—*Schematic diagram of the skin indicating the consequences of the various fractionation techniques on the processed membrane compositions. This diagram represents the structure of the mouse skin based on gross visual examination, on its physicochemical behavior as seen in permeability experiments, and on traverse histological sections viewed under the light microscope. Residuals of hair follicles seen in traverse sections are not represented.*

where $V_R$ is the receiver volume, $dC/dt$ is the steady-state rate of change in the receiver concentration (counts per minute), $A$ is the exposed cross-sectional area of the membrane, and $\Delta C$ is the concentration (counts) differential between compartments. The value of $\Delta C$ effectively is the donor concentration (counts) since the buildup of material in the receiver was never allowed to become a significant fraction of that in the donor compartment. Except as indicated, the data represent single determinations.

Some partitioning work also was done on both processed skins and the synthetic membrane. Procedural details and the method of calculation were presented previously (5).

## RESULTS AND DISCUSSION

The data for partitioning of the alcohols into full-thickness hairless mouse skin, hairless mouse epidermis, and the polydimethylsiloxane membrane from saline solution[4] are summarized in Table I. The full-thickness skin and silicone rubber membrane data are presented in Fig. 2, where the partition coefficients are plotted semilogarithmically against the alkyl chain length. Polydimethylsiloxane partitioning followed an exponential trend through the entire series, while the partitioning dependency for the tissue was biphasic. The silicone rubber dependency followed the form:

$$\log K_n = \log K_0 + \pi n \qquad \text{(Eq. 2)}$$

where $K_n$ is the partition coefficient of the homolog of chain length $n$, $\log K_0$ is the intercept of the plot on the $y$-axis corresponding to the partitioning of the hypothetical zero chain length homolog, and $\pi$ is the incremental increase in the logarithm of the partition coefficient per methylene unit. The least-squares values for these parameters are $\pi$ = 0.417 and $K_0$ = 0.029, with a correlation coefficient of 0.998. The trend predicted by Eq. 2 is the expected behavior for alkyl homologs (10–13),

[4] Sodium Chloride Irrigation (0.9%), Abbott Laboratories, North Chicago, IL 60064.

**Table I—Partitioning[a] of the Alkanols between 0.9% Saline and Full-Thickness Skin, Epidermis, and Silicone Rubber**

| Alkanol | Full-Thickness Skin[a] | Heat-Separated Epidermis[a] | Polydimethylsiloxane[a,b] |
|---|---|---|---|
| Methanol | 5.5 | — | 0.064 |
| Ethanol | 5.4 | 4.5 | 0.256 |
| *n*-Propanol | 6.0 | 4.4 | 0.612 |
| *n*-Butanol | 6.6 | 5.3 | 1.18 |
| *n*-Pentanol | 7.7 | 5.1 | 2.85 |
| *n*-Hexanol | 10.7 | 14.0 | 11.0 |
| *n*-Heptanol | 24.0 | 24.1 | 23.0 |
| *n*-Octanol | 40.8 | 68.5 | 57.7 |
| *n*-Nonanol | 86.7 | 118 | 194 |
| *n*-Decanol | — | — | 412 |

[a] The data are in grams per cubic centimeter. For silicone rubber, the $K$ values can be considered as unitless since the density of commercial polydimethylsiloxane is close to unity. [b] The slope of these data on a log $K$ *versus* alkyl chain length plot is 0.417 ($r$ = 0.998).

but the magnitude of the slope ($\pi$ value) is less than that found previously for partitioning between silicone rubber and water for a different homologous series, the alkyl *p*-aminobenzoates (0.54) (8). Based on work to be reported separately, this difference in estimates of $\pi$ appears to be related largely to differences in intermolecular interactions in the polymeric phase.

The partitioning data for the epidermis indicate that it is a two or more phase structure physicochemically, with lower alcohols exhibiting no alkyl chain length dependency but with higher homologs evidencing a marked, exponential acclivity. The same behavior was observed with the full-thickness skin. The preliminary indications are that the polar compounds

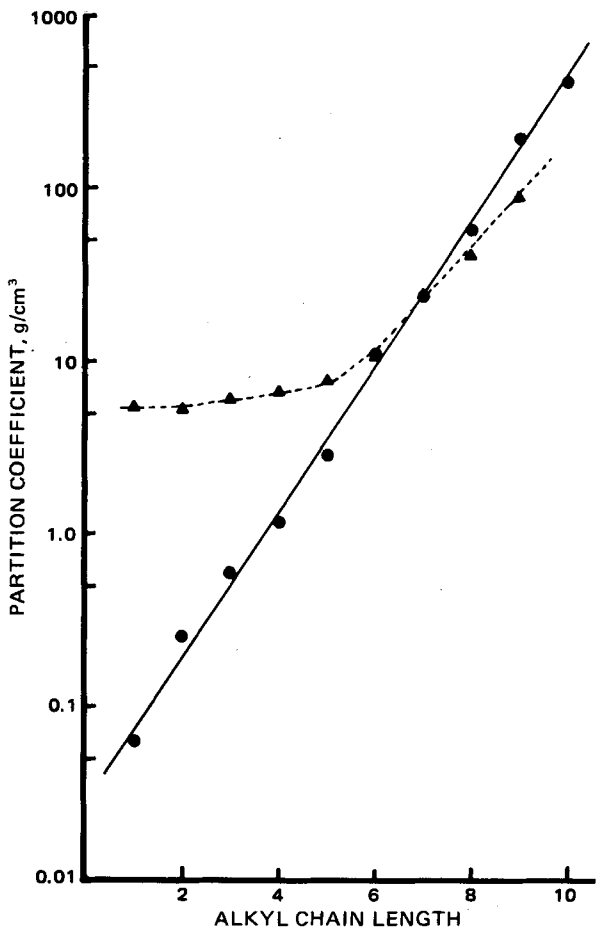


**Figure 2**—*Semilog plot of membrane–saline partition coefficients against alkyl chain length for polydimethylsiloxane (●) and for full-thickness skin (▲). The $\pi$ value (slope) for silicone rubber is 0.417. The data for the skin are biphasic with a terminal acclivity ($C_6$–$C_9$) of 0.296.*

**Table II—Permeability Data for Commercial Polydimethylsiloxane Membranes [a] at 37°**

| Alkanol | $P_n \times 10^3$, cm/hr | $D_n \times 10^6$, cm²/sec |
|---|---|---|
| Methanol | 6.8 | 1.49 |
| Ethanol | 33.5 | — |
| *n*-Propanol | 28.8 | 0.66 |
| *n*-Butanol | 56.6 | 0.68 |
| *n*-Pentanol | 123.2 | 0.61 |
| *n*-Hexanol | 301 | 0.39 |
| *n*-Heptanol | 339[b] | — |
| *n*-Octanol | 335[b] | — |
| *n*-Nonanol | 303[b] | — |
| *n*-Decanol | 315[b] | — |

[a] Silastic medical grade sheeting, Dow Corning, Midland, Mich. [b] These data are apparent values affected by membrane retention of the alkanols in the quasi-steady state and deviate significantly from expected values for a true steady state.

concentrate in the aqueous compartments of the tissue but that the nonpolar regions become the principal areas of accumulation as the compounds become more hydrophobic. The similarity between epidermal and full-thickness skin values likely means that the consequential nonpolar phase is common to both tissues.

Permeability coefficients for polydimethylsiloxane membranes are presented in Table II. These values evidence an exponential increase up to a chain length of about seven and then level off at a permeability coefficient of slightly over 0.3 cm/hr. Neglecting ethanol, which for reasons unknown does not conform to the trend[5], the exponential dependency of the $C_1$–$C_6$ data yields a value of 0.326 for $\pi$ ($r = 0.999$), which is somewhat less than the partitioning $\pi$ value. This difference in the $\pi$ value is not entirely unexpected since the permeability coefficient under membrane control is dependent on diffusivity as well as on the partition coefficient. The diffusion coefficient values for the homologs in the silicone rubber matrix decrease with increasing molecular size, which would impact on the $\pi$ constant evaluated from permeabilities in the observed fashion. Diffusivities ($D_n$) are listed in Table II for methanol through *n*-hexanol, except for ethanol. These valves were calculated from the following relationship, which assumes that the membrane is the rate-controlling barrier acting as an isotropic phase:

$$D_n = \frac{P_n h_M}{3600 K_n} \qquad \text{(Eq. 3)}$$

where $D_n$, $P_n$, and $K_n$ designate the diffusivity in square centimeters per second, the permeability coefficient in centimeters per hour, and the partition coefficient of the *n*th chain length compound, respectively, and $h_M$ is the thickness of the membrane. The factor 3600 converts the diffusion coefficient to the more conventional units of reciprocal seconds. Since the density of silicone rubber is close to one, little error is introduced in using the partition coefficients as reported, that is, in units of grams per cubic centimeter. The magnitudes of the polydimethylsiloxane diffusivities reported, $\sim 10^{-6}$ cm²/sec, are entirely reasonable.

The plateau in the permeation of polydimethylsiloxane past hexanol at first suggests the onset of boundary layer control. However, the effective boundary layer thickness based on an aqueous diffusivity for the alkanols at 37° of $1 \times 10^{-5}$ cm²/sec and a permeability coefficient of ~0.3 cm/hr is 1200 μm, which seems to be unreasonably large by a factor of three to four. Examination of the donor compartment depletion side by side with the receiver accumulation revealed that, above a chain length of six, only fractional amounts of the material entering the membrane were exiting from the other side in the pseudo-steady state.

Application of the pseudo-steady-state procedure to obtain fundamental permeation constants is based on the assumption of insignificant membrane retention of the diffusing compound during the experiments (12, 14). This condition is not achieved above a chain length of six in the polydimethylsiloxane studies due to the exponentially increasing membrane–water partition coefficient and the small volumes (1.5 ml) of the cell compartments. The capacity of the membrane for octanol relative to the aqueous phases, which is the product of its partition coefficient (57.7) and the membrane volume (0.0508-cm thickness times an area of ~0.7 cm² ≃ 0.035 cm³), is 2.0 ml, which is greater than the capacity of one of the aqueous compartments; thus, significant percentages

[5] This data point was repeated several times and always gave the same apparently high result. However, in later studies by C. R. Behl using a different lot of radiolabeled ethanol, a value of 16 was obtained, which is more consistent with the overall trend.

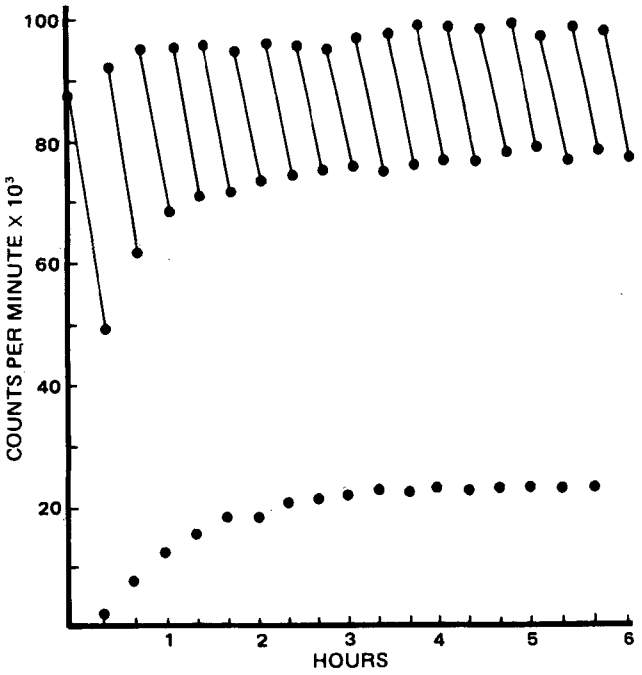


**Figure 3**—*Experimental data from the exchange procedure for* n-*octanol permeating the polydimethylsiloxane membrane at 37°. The plot is expressed in counts per minute at the beginning and end of each 20-min interval (each pair connected with a line) for the donor phase and counts per minute in the receiver at the end of each interval. It is notable that it takes about 3 hr (nine exchanges) before a steady state (plateau) is reached.*

of the higher alkanols ($n \geq 8$) remain within the membrane.

To estimate the permeability value for *n*-octanol validly and to determine the actual boundary layer effect, a procedure was developed that involved totally changing the donor and receiver cell compartment contents at fixed sampling intervals of 20 min. The donor was replaced repeatedly with a solution of the initial concentration, and the receiver was exchanged with fresh saline. This process was done in lieu of using very large compartmental volumes, which also would have neutralized the membrane retention influences, since the purpose was to assess the permeability coefficient under the same hydrodynamic conditions used for the lower alkanols.

Data for the exchange procedure are displayed in Fig. 3. The amounts (counts) in the donor compartment at the beginning and end of each interval and the amounts (counts) in the receiver at each interval termination are plotted against time. The bars on the upper set of data (donor data) join the data points for the front and back ends of a given interval. Both the upper and lower linked sets of points increase systematically to an asymptotic value, but the gap narrows to ~20,000 cpm.

**Table III—Permeability Data for Heat-Treated Skin**

| | $P_n \times 10^3$, cm/hr | | | |
|---|---|---|---|---|
| Alkanol | Full-Thickness Skin | Full-Thickness[a] Skin, Heat Treated | Heat-Separated[a] Epidermis | Heat-Separated[a] Dermis |
| Methanol | 2.6 (0.46)[b] | — | 2.3 | 318 |
| Ethanol | 4.8 (0.43) | 3.91 | 4.7 | 303 |
| *n*-Propanol | 5.4 | — | 9.7 | 289 |
| *n*-Butanol | 14.6 (0.81) | 16.2 | 16.8 | 287 |
| *n*-Pentanol | 22.0 | 39.4 | 29.3 | 285 |
| *n*-Hexanol | 48.0 (1.2) | — | 58.5 | 266[c] |
| *n*-Heptanol | 92.9 | 157 | 113 | 246 |
| *n*-Octanol | 97.2[d] (2.4) | 153[d] | 180[d] | 204[d] |
| *n*-Nonanol | 88.8[d] | 164[d] | 248[d] | 93[d] |
| *n*-Decanol | 84.5[d] | — | 233[d] | 90[d] |

[a] These results are single determinations. [b] Standard deviations of multiple runs. [c] Interpolated value. [d] These data points may be affected by membrane retention and, therefore, represent apparent *P* values under the conditions of the experiment.

**Table IV—Estimation of the Resistance of Hairless Mouse Skin Strata for the Lower Alkanols**

| Alkanol | Resistance[a], hr/cm | | | | Total Aqueous Resistance[c], % |
|---|---|---|---|---|---|
| | $R_{aq}$ | $R_{sc}$ | $R_{vt}$ | $R_{total}$[b] | |
| Methanol | 0.83 | 382 | 2.31 | 385 | 0.82 |
| Ethanol | 0.83 | 205 | 2.47 | 208 | 1.6 |
| *n*-Propanol | 0.83 | 182 | 2.63 | 185 | 1.9 |
| *n*-Butanol | 0.83 | 65 | 2.65 | 68.5 | 5.1 |
| *n*-Pentanol | 0.83 | 42 | 2.68 | 45.5 | 7.7 |
| *n*-Hexanol | 0.83 | 17 | 2.93 | 20.8 | 18.1 |

[a] Generally, $R = h/DK$ for an isotropic phase, where $h$ is the thickness, $D$ is the diffusion coefficient, and $K$ is the partition coefficient with respect to the donor compartment solution. [b] Total resistance = $1/P_n = R_{aqI} + R_{sc} + R_{vt} + R_{aqII}$, where $R_{aqI}$ and $R_{aqII}$ are the boundary layer resistances, $R_{vt}$ is the viable tissue resistance, and $R_{sc}$ is the resistance encountered in the stratum corneum. The individual resistances are obtained by difference. [c] Total aqueous resistance is $R_{aq} + R_{vt}$ (sum of the boundary layer and viable tissue resistances).

This plot indicates initial rapid membrane loading that tapers off appreciably with each succeeding interval. The receiver data demonstrate that little material diffuses across the membrane in the earliest intervals as the membrane gradient is formed; but as the membrane becomes loaded, the receiver accumulation in an interval also increases to a plateau of ~20,000 cpm.

When the amount leaving the donor compartment comes into coincidence with the amount entering the receiver, the process is effectively in a true steady state and the permeability coefficient can be calculated from either the donor or receiver data. This conclusion was reached both through computer-assisted analysis of a rigorous mathematical model written for the exchange procedure and through extensive additional experimentation, both of which were reported separately (15, 16). The permeability coefficient for octanol exceeds 1.0 cm/hr and is close to the extrapolation of the exponential trend seen for lower homologs, meaning that the permeation of octanol is substantially membrane controlled. Thus, in this diffusional system operated at a 150-rpm stirring rate, the aqueous boundary layers have a collective effective thickness of <350 μm[6]. The thickness is estimated from the permeability coefficient and from the boundary layer control relationship:

$$P = \frac{D_{AQ}}{\Sigma h_{AQ}} \qquad \text{(Eq. 4)}$$

where $D_{AQ}$ is the aqueous diffusivity ($\simeq 1 \times 10^{-5}$ cm$^2$/sec) and $\Sigma h_{AQ}$ is the total thickness of the unstirred layers. In the following analysis, a boundary layer resistance of 0.83 cm/hr, equivalent to a thickness for the hydrodynamic layers of 300 μm, is assumed. Little error is introduced using this value, even if it is inexact, since it is small and a relatively insignificant fraction of the total aqueous resistance encountered in the skin membranes.

Permeability coefficients obtained for the alkanols at 37° for full-thickness skin, heat-separated epidermis and dermis, and full-thickness skin scalded for 30 sec at 60° but not fractionated are given in Table III. These data also form the basis for Fig. 4, in which the log of the permeability coefficient is plotted against alkyl chain length. No extreme effect on permeability was produced by scalding 60° water applied to the skin for 30 sec, a treatment that was estimated to give a deep partial-thickness to full-thickness burn. When burned full-thickness skin data are compared with similar data on untreated skin, no more than a twofold increase in permeability is noted for any homolog; for ethanol and butanol, the values are not different within experimental uncertainty.

When the heat-separated epidermal data are considered side by side with the full-thickness normal and burned skin data, a striking similarity in the permeabilities for the lower homologs ($n < 8$) is seen. In all of these cases, the stratum corneum is intact, and considering all of the data, it appears to be the principal source of diffusional resistance for the polar compounds. Data on the epidermis support the observation that scalding the skin as described has no profound effect, although somewhat higher permeability coefficients for the middle homologs consistently are noted. This observation is important since the heat-separation technique has been commonly used to prepare human skin membranes for diffusional studies (17–19).

[6] Based on extensive experimental work beyond that reported here, the diffusion layers appear to be ~300 μm in total thickness (15, 16).

Considering only the full-thickness skin and epidermis, it appears as if the removal of the thick dermal matrix leads to increased permeation rates at long alkyl chain lengths, which suggests that the dermis acts as an aqueous matrix. This conclusion is somewhat tenuous, because membrane retention was not factored out of these data. By actual measurement, the epidermis is only 40 μm thick, which minimizes such concern in its case. However, the total skin is about 10 times thicker and, therefore, amounts to a significant compartment for the higher partitioning, nonpolar homologs. The data are meaningful even with the membrane retention influence included since retention would be encountered on topical application and thereby influence the quantities percutaneously absorbed. A further general conclusion is that the composite mouse tissue behaves almost identically to the excised skin of human, as evidenced in the collective studies of Scheuplein and associates (17–19).

Comparison of the heat-separated dermis data with the data for normal skin reveals that the barrier is compromised severely when the epidermis is removed. Moreover, the extent of compromise is clearly dependent on the chemical structure, largely to the extent that the permeation is stratum corneum controlled in the intact skin. Thus, methanol passed through the dermis 120 times faster than through the whole skin, while the factor for pentanol was only ~13. The risk of systemic toxicities arising from inadvertent or deliberate topical applications to broken skin is greatest with polar nonelectrolytes and salts with little capacity to breach the intact stratum corneum. Such factors should be generally evaluated for suspect agents that are to be applied to the skin (cosmetic, drug, and household product ingredients).

Since the lower alcohol homologs are not extensively membrane bound, their permeability coefficients are not altered by retention and can be further quantitatively analyzed. The value of 0.318 cm/hr for methanol through heat-separated dermis translates to a total diffusional resistance of 3.14 hr/cm (a reciprocal relationship). By a previous estimate, no more than 0.83 hr/cm of this value is attributable to boundary layers, leaving at least 2.31 hr/cm as the effective aqueous tissue resistance contributed by the dermis[7]. The dermal thickness measured by a micrometer is 350 μm, which is roughly equivalent to the thickness of the assumed boundary layers. Thus, centimeter for centimeter, the hairless mouse dermis is about three times more resistant to diffusion than water itself.

The resistance of the full-thickness skin to methanol was 385 hr/cm, and the summed boundary layer and aqueous tissue resistances were <1% of the total resistance encountered when the skin was intact. Results

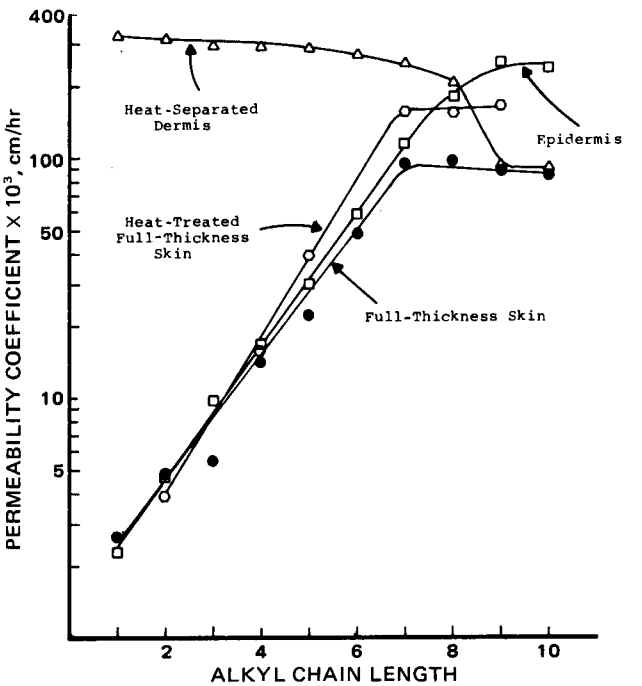


**Figure 4**—*Semilog plot of permeability coefficients for heat-processed hairless mouse membranes and normal hairless mouse skin as a function of alkyl chain length. All data were obtained at 37°.*

[7] Resistances in series are additive.

**Table V—Permeability Coefficients ($P \times 10^3$, cm/hr [a]) of the Alkanols at 37° through Stripped Skin**

| Alkanol | Number of Strippings | | | |
|---|---|---|---|---|
| | 5 | 10 | 15 | 25 |
| Methanol | 15.5 | 33.4 (38.2, 28.6) | — | 313 |
| Ethanol | 14.1 | 32.1 (36.7, 27.5) | — | 219 |
| *n*-Propanol | 13.0 | 22.2 | 130 | 218 |
| *n*-Butanol | 31.0 | 52.6 (45.2, 60.0) | 157 | 215 |
| *n*-Pentanol | 47.5 | 79.6 | — | 217 |
| *n*-Hexanol | — | — | — | 209 |
| *n*-Heptanol | — | — | — | 223 |
| *n*-Octanol | 181[b] | 197[b] | 210[b] | 225[b] |
| *n*-Nonanol | 123[b] | 126[b] | — | 133[b] |
| *n*-Decanol | — | — | — | 129[b] |

[a] Except when indicated for 10 times stripping, the results represent single determinations. [b] These data may be affected by membrane retention and, therefore, represent apparent $P$ values under the conditions of the experiment.

similarly obtained for other members of the homologous series are summarized in Table IV. The relative importance of the subepidermal layers rises rapidly with increasing alkyl chain length.

Data for the permeation of stripped skin are presented in Table V and are shown graphically in Fig. 5, which is a plot of log $P_n$ *versus* alkyl chain length. The data are in full agreement with the previous analysis, with the following added features. As might be expected, as the stratum corneum was removed (thinned), the permeability coefficients of the lower homologs increased uniformly. However, the stripping apparently caused some pitting of the skin since the increases were disproportionate for methanol and ethanol.

The lower plateau formed for five and 10 strippings is characteristic of an aqueous pore route (12). When the entire stratum corneum is removed[8] (25 strippings), the profile appears to be qualitatively similar to

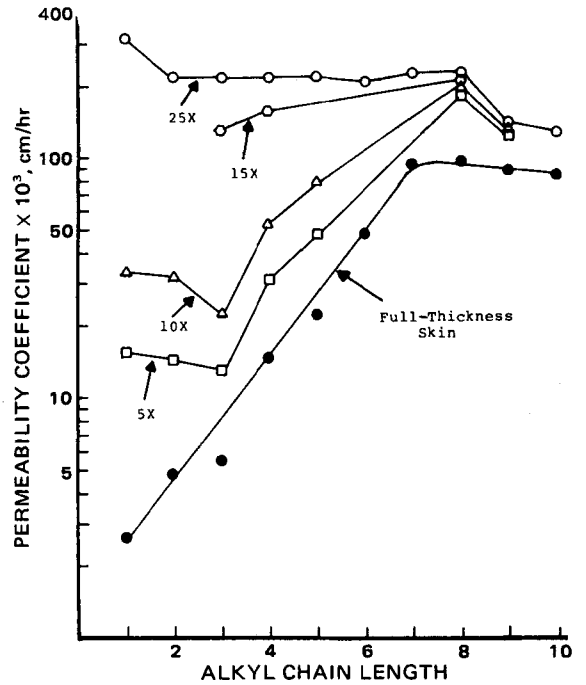


**Figure 5**—*Semilog plot of permeability coefficients for stripped hairless mouse membranes and normal hairless mouse skin as a function of alkyl chain length. All data were obtained at 37°. The skin was stripped 5, 10, 15, and 25 times.*

[8] Complete stripping was taken as the point where the surface became uniformly moist and glistening. The fact that this point represents essentially complete removal of the stratum corneum is indicated in the qualitative and quantitative parallels to heat-separated dermis.

that for heat-separated dermis. However, permeability coefficients are ~40% lower than those observed for heat-separated dermis. Several reasons can be advanced for this finding: incomplete removal of the stratum corneum so that the effective area for diffusion is somewhat reduced; the innate resistance of the viable epidermal layer, which is present with stripped skin but which is not a part of the heat-separated dermis; and damage to the dermis resulting from the heat-separation techniques. These aspects are under current laboratory investigation.

The present study further substantiates conclusions made previously (5) regarding a high degree of similarity between hairless mouse skin and human skin (17–19). Specifically, it is demonstrated that gross similarities seen histologically (20–22) translate to similarities in barrier properties. The cornified layer is the flux-determining feature for polar nonelectrolytes, and it acts as a lipid fabric in that oil–water partitioning into it is the principal determinant of the relative permeabilities of structurally similar compounds. When the stratum corneum is removed, the residual tissue offers little more than the resistance of a gelled aqueous phase to mass transfer, as was suggested by Scheuplein (18).

This study also showed how estimates of the effect of skin damage on the permeability of compounds may be roughly assessed by carefully fractionating the hairless mouse integument and determining the ratio of permeability of intact to broken skin. The more hydrophobic a compound, the closer this ratio will be to one, and, by extrapolation of the significance of the observation, the intrinsically safer the compound will be when applied to an irritated, diseased, or otherwise damaged skin surface, providing it is safe to use on intact skin in the first place.

## REFERENCES


(1) W. Montagna and R. P. Parakkal, "The Structure and Function of Skin," 3rd ed., Academic, New York, N.Y., 1974.

(2) R. J. Scheuplein and I. H. Blank, *Physiol. Rev.*, **51**, 702 (1971).

(3) A. M. Kligman, in "The Epidermis," W. Montagna and W. C. Lobitz, Eds., Academic, New York, N.Y., 1964, chap. 20.

(4) B. Idson, *J. Soc. Cosmet. Chem.*, **22**, 615 (1971).

(5) H. Dürrheim, G. L. Flynn, W. I. Higuchi, and C. R. Behl, *J. Pharm. Sci.*, **69**, 781 (1980).

(6) R. Scheuplein, in "Physics and Pathophysiology of the Skin," vol. 5, A. Jarrett, Ed., Academic, New York, N.Y., 1978, pp. 1963–1730.

(7) A. S. Michaels, S. K. Chandrasekaran, and J. E. Schaw, *AIChE J.*, **21**, 985 (1975).

(8) G. L. Flynn and S. H. Yalkowsky, *J. Pharm. Sci.*, **61**, 838 (1972).

(9) R. G. Stehle and W. I. Higuchi, *ibid.*, **56**, 1367 (1967).

(10) S. S. Davis, T. Higuchi, and J. H. Rytting, *J. Pharm. Pharmacol.*, **24**, 30P (1972).

(11) S. S. Davis, T. Higuchi, and J. H. Rytting, *Adv. Pharm. Sci.*, **4**, 63 (1974).

(12) G. L. Flynn, S. H. Yalkowsky, and T. J. Roseman, *J. Pharm. Sci.*, **63**, 479 (1974).

(13) A. Leon, C. Hansch, and D. Elkins, *Chem. Rev.*, **71**, 525 (1971).

(14) C. Barnes, *Physics*, **5**, 4 (1934).

(15) J. L. Fox, G. L. Flynn, T. Hagen, W. I. Higuchi, N. F. H. Ho, and H. Dürrheim, "Abstracts," APhA Academy of Pharmaceutical Sciences, vol. 8 (2), Nov. 1978, p. 100.

(16) G. L. Flynn, C. R. Behl, T. Kurihara, W. Smith, J. Fox, H. Dürrheim, and W. I. Higuchi, "Abstracts," APhA Academy of Pharmaceutical Sciences, vol. 9 (1), 1979, p. 97.

(17) R. J. Scheuplein, *J. Invest. Dermatol.*, **45**, 334 (1966).

(18) *Ibid.*, **48**, 79 (1967).

(19) R. J. Scheuplein and I. H. Blank, *J. Invest. Dermatol.*, **60**, 286 (1975).

(20) W. D. Steward and J. O. Runikis, *ibid.*, **49**, 159 (1967).

(21) A. J. Aguiar and M. A. Weiner, *J. Pharm. Sci.*, **58**, 210 (1969).

(22) S. J. Mann, *J. Invest. Dermatol.*, **56**, 170 (1971).


## ACKNOWLEDGMENTS


Presented at the Basic Pharmaceutics Section, APhA Academy of Pharmaceutical Sciences, New York meeting, May 1977 (Abstract 12).

Supported in part by National Institutes of Health Grant GM 24611.

# Kinetic Analysis of Relationship between Partition Coefficient and Biological Response

**EUGENE R. COOPER ˣ, BRET BERNER, and ROBERT D. BRUCE**

Received December 24, 1979, from the *Miami Valley Laboratories, Procter & Gamble Company, Cincinnati, OH 45247.* Accepted for publication June 27, 1980.

**Abstract** □ Both nonequilibrium and equilibrium models were proposed to explain the optimal biological response to a set of congeners with respect to the oil–water partition coefficient ($P$). A detailed analysis of the kinetic model proposed by Hansch demonstrates the bilinear form of the model, with the initial slope of the logarithm of the concentration for 50% receptor binding *versus* log $P$ having a slope of greater than one. This result is in contrast to the equilibrium model for an initial slope of less than one. Thus, a criterion is established for deciding whether equilibrium or nonequilibrium processes apply.

**Keyphrases** □ Partition coefficients—relationship with biological response, kinetic analysis □ Models, mathematical—relationship between partition coefficient and biological response, kinetic analysis □ Kinetics—analysis of relationship between partition coefficient and biological response

Hansch and Clayton (1) documented numerous examples of an optimal biological response to a set of congeners with respect to the oil–water partition coefficient. That is, a plot of the logarithm of the concentration at which a standard biological response is elicited *versus* the logarithm of the partition coefficient exhibits a maximum. Hansch and coworkers (2) attributed this maximum to nonequilibrium conditions resulting from transport across a series of water–oil membranes, and a kinetic model was developed to account for the maximum in the partition coefficient (2). Rather than extract model parameters from the experimental data, they fitted the data empirically with parabolic equations. While the parabolic equations have no direct relationship to the model, they are a convenient mathematical form for regression analysis.

McFarland (3) and later Kubinyi (4) employed a probability approach to account for the optimum in the partition coefficient, and they derived bilinear equations to fit the data. Higuchi and Davis (5) constructed an equilibrium model as an alternative explanation for the optimal biological response, and their model equation also has a bilinear form. Kubinyi (6) showed that bilinear equations fit the data better than parabolic equations. This finding is comforting to the model builder since none of the proposed models predicts a parabolic equation.

This paper compares the merits of the various models and proposes ways of determining whether equilibrium or nonequilibrium processes are responsible for the maximum with respect to the partition coefficient. First, the equilibrium and probability models are examined. Then the kinetic model of Hansch and coworkers (2) is examined in detail, and its bilinear form is demonstrated. The kinetic model reduces to the equilibrium model at infinite time and is consistent with what is known about transport. Difficulties in the assessment of the probability model predictions also are discussed. Time is not explicitly mentioned in the development of this model, and it appears to be a random walk-type model with probabilities obtained from the equilibrium.

## MODELS

**Equilibrium and Probability Models**—For the models considered, the arrangement of membranes can be represented as in Fig. 1. An aqueous reservoir of the active compound is in contact with a series of $n$ pairs of lipid–water membranes or compartments. In the last aqueous compartment, binding to a receptor occurs. The amount bound to the receptor is proportional to $C_{2n+1}P^{\alpha}$, where $P$ is the lipid–water partition coefficient, $C_{2n+1}$ is the concentration in the $n$th aqueous compartment, and $\alpha$ is a constant near unity that expresses a possible difference in the lipophilicity between the receptor site and the lipid compartment. Kubinyi (4) showed that the equilibrium model of Higuchi and Davis (5) could be expressed as:

$$C_r = \frac{aP^{\alpha}}{1 + \beta P} \qquad \text{(Eq. 1)}$$

where $C_r$ is the concentration at the receptor site, $a$ is a proportionality constant, and $\beta$ is the ratio of the lipid volume to the aqueous membrane volume. Kubinyi (4) modified McFarland's (3) probability model to give:

$$C_r = \frac{bP^{n}P^{\alpha}}{(1 + \beta P)^{2n}} \qquad \text{(Eq. 2)}$$

where $b$ is the proportionality constant. The slopes of log $C_r$ *versus* log $P$ predicted by these two models differ. The initial slopes are $\alpha$ and $n + \alpha$ for the equilibrium and probability models, respectively; the final slopes are $\alpha - 1$ and $\alpha - n$, respectively. In the equilibrium model, there is no unique maximum in $P$ if $\alpha = 1$.

**Kinetic Model and Solutions**—The kinetic model as represented in Fig. 1 is characterized by the water-to-lipid rate constant, $k$, by the lipid-to-water rate constant, $l$, where $P = k/l$, and by the following:

$$\frac{dC_1}{dt} = -\frac{k}{\gamma V_w} C_1 + \frac{l}{\gamma V_w} C_2 \qquad \text{(Eq. 3)}$$

$$\frac{dC_i}{dt} = \frac{k}{\beta V_w} C_{i-1} - \frac{2l}{\beta V_w} C_i + \frac{k}{\beta V_w} C_{i+1} \quad i = 2, 4, \ldots 2n \qquad \text{(Eq. 4)}$$

$$\frac{dC_i}{dt} = \frac{l}{V_w} C_{i-1} - \frac{2k}{V_w} C_i + \frac{l}{V_w} C_{i+1} \quad i = 3, 5, \ldots 2n - 1 \qquad \text{(Eq. 5)}$$

$$\frac{dC_{2n+1}}{dt} = \frac{l}{V_w} C_{2n} - \frac{k}{V_w} C_{2n+1} \qquad \text{(Eq. 6)}$$

Here $\gamma$ is the ratio of the volume of the aqueous reservoir to the volume of the aqueous compartment, $V_w$, and $\beta$ is the ratio of the volume of the lipid compartment to $V_w$. Equations 3–6 can be written in matrix notation as:

$$\dot{\mathbf{C}} = \mathcal{J} \cdot \mathbf{C} \qquad \text{(Eq. 7)}$$

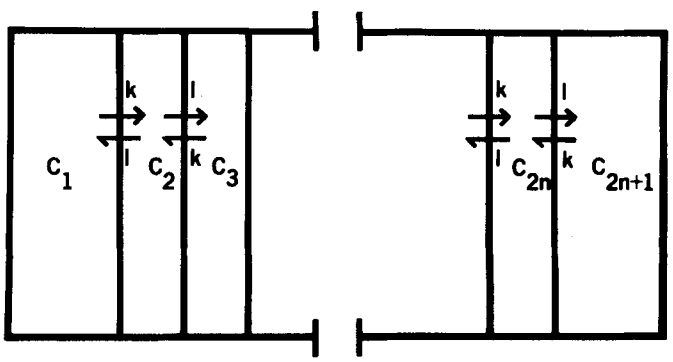


**Figure 1**—*Sequence of lipid–water barriers for transport from reservoir to receptor.*

0022-3549/81/0100-0057$01.00/0
© 1981, American Pharmaceutical Association

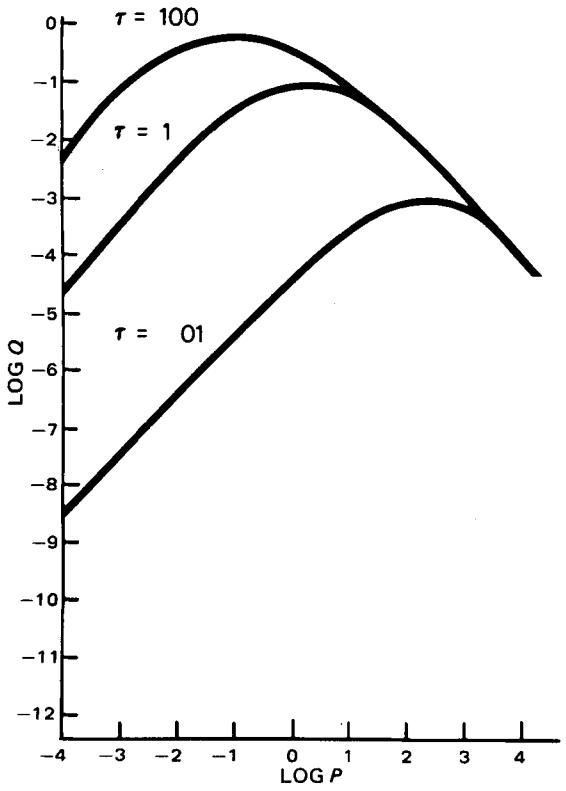


**Figure 2**—*Effect of time on Q(τ) for* n = *1, β = 1, and γ = 1.*

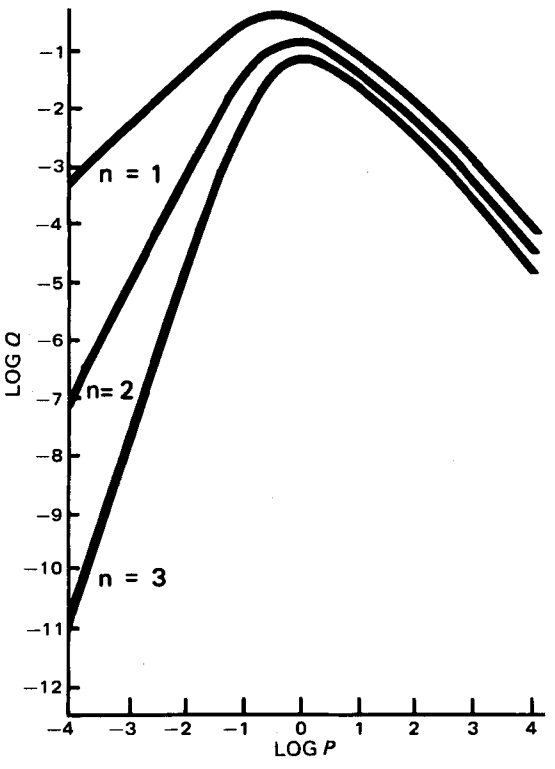


**Figure 3**—*Effect of* n *on Q(τ) for τ = 10, β = 1, and γ = 1.*

where $\dot{\mathbf{C}}$ is the time derivative of the $2n + 1$ concentrations, **C**, and $\mathcal{F}$ is the $2n + 1 \times 2n + 1$ matrix relating $\dot{\mathbf{C}}$ to **C**. If the eigenvalues of $\mathcal{F}$ are all distinct (7), then $\mathbf{C} = \mathbf{A}e^{\lambda t}$ is a solution where $\mathbf{A}_i$ is the eigenvector corresponding to the eigenvalue $\lambda_i$. The general solution for **C** is given by:

$$\mathbf{C} = \sum_{i=1}^{2n+1} f_i \mathbf{A}_i e^{\lambda_i t} \qquad \text{(Eq. 8)}$$

where the $f_i$ values are determined by the initial conditions:

$$C_1(0) = C^{(0)} \qquad \text{(Eq. 9)}$$

and:

$$C_i(0) = 0 \quad i = 2, 3, \ldots 2n + 1 \qquad \text{(Eq. 10)}$$

The quantity of interest is $C_{2n+1}(t)$, which is proportional to the amount bound at the receptor. If:

$$A^{(50)} = aP^{\alpha}C^{(50)}_{2n+1}(t) \qquad \text{(Eq. 11)}$$

where $C^{(50)}_{2n+1}(t)$ is the concentration in the receptor compartment for which half of the sites, $A^{(50)}$, are occupied, then $C_1^{(50)}(0)$, the initial concentration necessary to give half-binding at time $t$ and for the partition coefficient, $P$, can be estimated. That is:

$$C_1^{(50)}(0) = \frac{A^{(50)}}{Q_n(t)(aP^{\alpha})} \qquad \text{(Eq. 12)}$$

since $C_{2n+1}(t) = C_1(0)Q_n(t)$, where $Q_n(t)$ is independent of the initial concentration and represents the concentration fraction of initial drug in the receptor compartment. Thus, a plot of log $Q_n$ *versus* log $P$ reflects the dependence of $C_1^{50}(0)$ on $P$ except for the additional slope $\alpha$.

The solution (Eq. 8) of Eq. 7 is obtained easily for $n = 1$:

$$C_3(\tau) = C_1(0)Q_1(\tau) \qquad \text{(Eq. 13)}$$

where:

$$Q_1(\tau) = [2 + Pe^{-(P+2)\tau} - (P + 2)e^{-P\tau}]/(2P + 4) \qquad \text{(Eq. 14)}$$

For this solution, $\gamma = \beta = 1$, $V_w = 1$, and $\tau = lt$. For a short time, $Q_1(\tau)$ becomes:

$$\lim_{\tau \to 0} Q_1(\tau) = \frac{1}{2} P\tau^2 \qquad \text{(Eq. 15)}$$

which is linear in $P$ and quadratic in $\tau$. For values of $n > 1$, Eq. 8 was solved numerically (8); the results are shown in Figs. 2 and 3, where the bilinear nature of the function is clearly seen. The initial slopes ($P \ll 1$) are proportional to $n$, and the final slopes ($P \gg 1$) are all $-1$. As $\tau$ increases, the initial slopes all approach zero, the equilibrium value, and the position of the maximum with respect to $P$ decreases. The fact that all of the final slopes are $-1$ is just a consequence of equilibrium. The

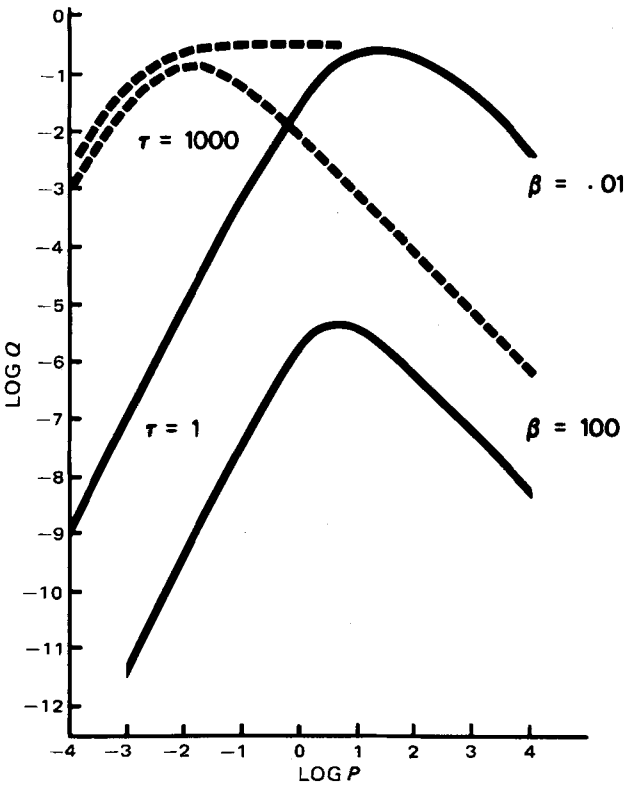


**Figure 4**—*Effect of β on Q(τ) for* n = *2 and γ = 1.*

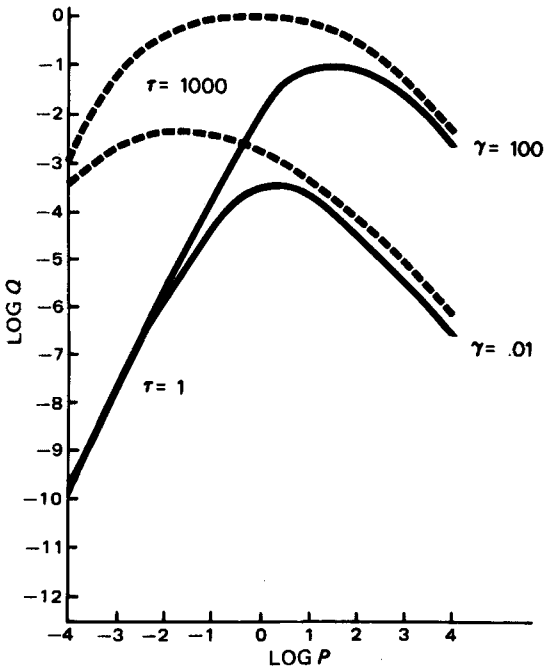


**Figure 5**—*Effect of* $\gamma$ *on* $Q(\tau)$ *for* n = 2 *and* $\beta = 1$.

position of the maximum increases only slightly with $n$. In Figs. 4 and 5, the results are shown for different values of $\beta$ and $\gamma$. The decrease in $Q(\tau)$ with an increase in the partition coefficient occurs at higher partition coefficient values for the smaller values of $\tau$. This decrease occurs at lower partition coefficient values for larger $\beta$ or smaller $\gamma$ values.

## DISCUSSION

The kinetic model accounts for transport in the steady-state approximation for diffusion across unstirred boundary layers at lipid–water interfaces, and it ignores differences in diffusion rates between the lipid phase and the aqueous phase. However, this model does approximate the effects of nonequilibrium on the concentration at the receptor site. The kinetic model predicts a time dependence for $P_{max}$, where $P_{max}$ decreases with time. The probability model and the kinetic model both predict an initial slope of $n + \alpha$ for the dependence of log $1/C_1^{50}(0)$ on log $P$, where the equilibrium model predicts an initial slope of $\alpha$. Thus, if the initial slope is greater than or equal to one, nonequilibrium processes obtain; if the slope is less than one, the equilibrium model can account for the observations. To understand the nonequilibrium models better, Kubinyi's (6) modification of Eq. 2 must be examined. He relaxed the parameter restrictions in Eq. 2 by writing:

$$C_r = \frac{bP^x}{(1 + \beta P)^y} \qquad \text{(Eq. 16)}$$

where $x$ and $y$ are freely adjustable instead of being related by $y = 2n$ ($n = 1, 2, \ldots$) and $x = n + \alpha$ where $0 \leq \alpha \leq 1$. Thus, Eq. 16 becomes a mathematical form to fit data rather than an equation to extract the model parameters $n$ and $\alpha$. Most of the data chosen by Kubinyi (6) to be fit by Eq. 16 had $x \leq 1$. This finding indicates that the equilibrium model is probably the better choice of operative process even though, with only one adjustable parameter, the data are not as well fit by Eq. 1.

Hansch and Clayton (1) summarized a variety of possible mechanisms to account for the portion of the curve that has the negative slope in log $P$. However, as they pointed out, biological data for molecules with large $P$ values are difficult to interpret because of the low water solubility. Yalkowsky and Flynn (9) showed that the maximum steady-state flux drops off as $P^{-\delta}$, where $\delta$ is similar in magnitude to $\alpha$ and is an indicator of the decrease in water solubility with increased partition coefficient. Their model is essentially one of water layers (and, hence, water solubility) controlling the transport for molecules with high partition coefficients. Since binding to the receptor is proportional to $P^{\alpha}$, one expects a final slope near zero and an initial slope of $1 + \alpha$ for cases where their model is applicable.

Since biological data are somewhat difficult to obtain and interpret for large partition coefficient values, the data for smaller partition coefficient values are interpreted most confidently. From the kinetic model analysis presented in this report, it is probable that nonequilibrium processes are involved when the initial slope is greater than one and that equilibrium processes obtain when this slope is less than unity. However, the kinetic model at longer times has a wide maximum, and the model could be stretched to fit data with initial slopes of less than one. Biological data covering a wide range of partition coefficients are needed to distinguish between nonequilibrium and equilibrium processes, especially in the small partition coefficient region.

## REFERENCES

(1) C. Hansch and J. M. Clayton, *J. Pharm. Sci.*, **62**, 1 (1973).

(2) J. T. Penniston, L. Beckett, D. L. Bentley, and C. Hansch, *Mol. Pharmacol.*, **5**, 333 (1969).

(3) J. W. McFarland, *J. Med. Chem.*, **13**, 1192 (1970).

(4) H. Kubinyi, *Arzneim.-Forsch.*, **26**, 1991 (1976).

(5) T. Higuchi and S. S. Davis, *J. Pharm. Sci.*, **59**, 1376 (1970).

(6) H. Kubinyi, *J. Med. Chem.*, **20**, 625 (1977).

(7) J. A. Jacquez, "Compartmental Analysis in Biology and Medicine," Elsevier, New York, N.Y., 1972.

(8) S. Cohen and S. C. Pieper, Speakeasy-3 Reference Manual, Level Lambda, IBM OS/VS Version, 1976.

(9) S. H. Yalkowsky and G. L. Flynn, *J. Pharm. Sci.*, **62**, 210 (1973).

# Antifertility Activity of *N*-Protected Glycine Activated Esters

**JAMES H. DREW, LARRY J. LOEFFLER ˣ, and IRIS H. HALL**

Received December 26, 1979, from the *Division of Medicinal Chemistry, School of Pharmacy, University of North Carolina, Chapel Hill, NC 27514.* Accepted for publication July 8, 1980.

**Abstract** □ A series of *N*-protected glycine activated esters was found to have antifertility activity in mice when administered intravaginally. The *N*-carbobenzoxyglycine vinyl ester and *N*-carbobenzoxyglycine 1,2-dibromoethyl ester analogs possessed the best activity in inhibiting pregnancy but were much less active when administered intraperitoneally. The acrosin enzymatic activity of sperm also was inhibited by these *N*-protected glycine activated esters, as measured by *N*-α-benzoyl-L-arginine ethyl ester and azocasein hydrolysis. The ability to inhibit *N*-α-benzoyl-L-arginine ethyl ester hydrolysis, a trypsin-like activity, appeared to have a positive correlation with antifertility activity when the agents were administered intravaginally.

**Keyphrases** □ Antifertility activity—evaluation of *N*-protected glycine activated esters □ *N*-Protected glycine activated esters—evaluation for antifertility activity □ Glycine esters—*N*-protected analogs, evaluation for antifertility activity

A number of chemical (1) and endogenous (2) agents recently were shown to inhibit the proteolytic activity of the sperm's acrosomal enzyme, acrosin (EC 3.4.21.10) and thereby reduce sperm fertilization of the ovum. Acrosin enzymatic activity is similar to trypsin proteolytic activity and thus is inhibited by trypsin inhibitors. *N*-α-Tosyl-L-lysine chloromethyl ketone administered intravaginally in sterile lubricant before coitus inhibited fertilization in rabbits (3). A series of *N*-carbobenzoxyglycine, L-leucine, and L-proline esters administered intravaginally in mice demonstrated 100% inhibition at 10 mg/kg/day, as did *N*-α-tosyl-L-lysine chloromethyl ketone and tosyl-L-phenylalanine chloromethyl ketone (4). The glycine series has been expanded to include several types of esters as well as variations in the amino protecting group, and these results are reported here.

## EXPERIMENTAL

**Chemical Synthesis**—The compounds evaluated in this study are listed in Table I. Several of the compounds were synthesized previously in this laboratory [*i.e.*, II and III (5, 6)] or elsewhere [*i.e.*, IV (7), V (8), XIV (9), and XV (10)]. Procedures for vinyl ester preparation using vinyl acetate and palladium chloride catalyst have been discussed in detail, as have those for cyanomethyl ester preparation (5, 6). The synthesis of new activated esters reported here (VI, VII, IX–XI, and XIII) was uncomplicated and involved reaction of *N*-carbobenzoxyglycine and active halogen compounds and triethylamine in ethyl acetate. In one case (VIII), the desired product was obtained using the alcohol, *N*-carbobenzoxyglycine, and *p*-toluenesulfonic acid in a standard esterification procedure. Since several compounds were difficult to purify, preparative details are included. All compounds appeared to have adequate stability when stored in a dry atmosphere, as judged by TLC and spectral methods[1].

Palladium chloride was obtained commercially[2]. *N*-Carbobenzoxyglycine *p*-nitrophenyl ester (XII), *N*-α-tosyl-L-lysine chloromethyl ketone (XVI), tosyl-L-phenylalanine chloromethyl ketone (XVII), *N*-carbobenzoxy-L-phenylalanine chloromethyl ketone (XVIII), 17-ethinyl estradiol (XIX), and diethylstilbestrol (XX) were purchased commercially[3]. The following materials were prepared as described previously: *N*-carbobenzoxyglycine vinyl ester (II) (6), *N*-carbobenzoxyglycine 1,2-dibromoethyl ester (III) (6), *N*-carbobenzoxyglycine ethyl ester (IV) (7), *N*-carbobenzoxyglycine cyanomethyl ester (V) (6), and *N*-trifluoroacetylglycine vinyl ester (XIV) (8).

N-*Carbobenzoxyglycine Acetonyl Ester (VI)*—A mixture of 1.5 g (7 mmoles) of *N*-carbobenzoxyglycine (6) and 0.8 g (8 mmoles) of triethylamine in 50 ml of tetrahydrofuran was heated to reflux. A solution of 1.0 g (7 mmoles) of bromoacetone (11) in 10 ml of tetrahydrofuran was added slowly dropwise over 1 hr. The reaction mixture then was stirred at reflux for 4 hr and cooled to room temperature, and the precipitate was collected. About 25 ml of chloroform was added to the filtrate, and this solution was washed with 20 ml of 5% HCl and dried (magnesium sulfate); the solvents were removed *in vacuo*.

The crude, oily product was purified by column chromatography, with chloroform as the eluent, to give 0.8 g (45% yield) of a white powder, mp 71–72°; IR (mineral oil): 3320 (strong) (C═O, ester), 1720 (strong) (C═O, ketone), and 1685 (strong) (C═O, carbamate) $cm^{-1}$; NMR ($CDCl_3$): δ 2.17 (s, 3H, $COCH_3$) and 4.79 (s, 2H, $OCH_2CO$). Elemental analysis (carbon, hydrogen, and nitrogen) showed a formula of $C_{13}H_{15}NO_5$.

N-*Carbobenzoxyglycine Methoxymethyl Ester (VII)*—A mixture of 2.5 g (12 mmoles) of *N*-carbobenzoxyglycine and 1.3 g (12.8 mmoles) of triethylamine in 30 ml of ethyl acetate was heated to reflux. A solution of 1.0 g (12.4 mmoles) of chloromethyl methyl ether in 25 ml of ethyl acetate was added dropwise, with stirring, over 2 hr. The reaction mixture was stirred for 3 hr at reflux and cooled, and the precipitate was filtered. The filtrate was washed with 5% HCl followed by water and dried (magnesium sulfate), and the solvents were removed *in vacuo*.

The resulting oily product was purified by column chromatography, with chloroform as the eluent, to give 1.3 g (35% yield) of pure product as an oil; IR ($CCl_4$): 3380 (strong, broad) (NH) and 1710 (strong, broad) (2 C═O) $cm^{-1}$; NMR (acetone-$d_6$): δ 3.45 (s, 3H, $OCH_3$) and 5.35 (s, 2H, $OCH_2O$).

N-*Carbobenzoxyglycine Methoxyethyl Ester (VIII)*—A mixture of 2.5 g (12 mmoles) of *N*-carbobenzoxyglycine and 0.1 g (5 mole %) of *p*-toluenesulfonic acid monohydrate in 50 ml (0.65 mole) of 2-methoxyethanol was stirred at 70° for 24 hr (12). The reaction flask was fitted to a distillation apparatus, and the accumulated water was azeotropically distilled off while fresh 2-methoxyethanol was added to the reaction flask at about the same rate at which the distillate was collected. Approximately 10 ml of the distillate was removed over 103–110°. The reaction flask then was fitted with a reflux condenser, the reaction mixture was heated at 70° for 15 hr and cooled, and the solvent plus water was removed by azeotropic evaporation with toluene *in vacuo*.

This procedure resulted in 4.0 g of an oily product, which was partitioned between 15 ml of 5% sodium bicarbonate and 25 ml of chloroform. The organic layer was removed and dried (magnesium sulfate), and the solvent was removed *in vacuo* to give 2.9 g of a crude, oily product. It was purified by column chromatography, with chloroform as the eluent. Pure product, 1.6 g (50% yield), was obtained as a colorless oil; IR ($CCl_4$): 3380 (strong, broad) (NH) and 1720 (strong, broad) (2 C═O) $cm^{-1}$; NMR (acetone-$d_6$): δ 3.4 (s, 3H, $OCH_3$), 3.6 (m, 2H, $COOCH_2CH_2O$), and 4.3 (m, 2H, $COOCH_2CH_2O$). Elemental analysis showed a formula of $C_{13}H_{17}NO_5$.

N-*Carbobenzoxyglycine Carbethoxymethyl Ester (IX)*—Compound IX was prepared in the same manner as VII using ethyl bromoacetate. Without purification by column chromatography, pure product was

[1] Melting points were determined on a Thomas-Hoover melting-point apparatus and are uncorrected. IR spectra were determined with a Perkin-Elmer 257 grating spectrophotometer. NMR spectra were measured with a Jeolco C60 HL spectrometer, and chemical shifts are reported in δ (parts per million) units relative to the internal standard tetramethylsilane, with s = singlet, d = doublet, t = triplet, and m = multiplet; *J* values are in Hertz. Data were consistent with assigned structures for all intermediates and products. Silica gel for TLC refers to Merck silica gel G. Compounds were visualized by charring with sulfuric acid (50%). Silica gel used for column chromatography was silicAR cc-7, 200–325 mesh. Elemental analyses were performed by Atlantic Microlabs, Atlanta, Ga.

[2] Engelhart Industries.

[3] Sigma Chemical Co.



*0022-3549/81/0100-0060$01.00/0*
*© 1981, American Pharmaceutical Association*

**Table I—Physical Data for Glycine Esters**

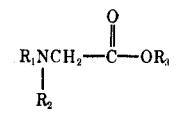

| Compound | $R_1$ | $R_2$ | $R_3$ | Yield, % | Melting Point | Crystallization Solvent | Formula | Analysis, % | Calc. | Found |
|---|---|---|---|---|---|---|---|---|---|---|
| II | Carbobenzoxy | H | $CH{=}CH_2$ | 50 | Oil | —[a] | $C_{12}H_{13}NO_4$ (5, 6) | | — | — |
| III | Carbobenzoxy | H | $CHBrCH_2Br$ | 15 | Oil | —[a] | $C_{12}H_{13}Br_2NO_4$ (5, 6) | | — | — |
| IV | Carbobenzoxy | H | $CH_2CH_3$ | 30 | 34–35° | Ethanol–water | $C_{12}H_{15}NO_4$ | | — | — |
| V | Carbobenzoxy | H | $CH_2CN$ | 70 | 69–70° | Chloroform–hexane | $C_{12}H_{12}N_2O_4$ | | — | — |
| VI | Carbobenzoxy | H | $CH_2{-}C(=O){-}CH_3$ | 45 | 71–72° | Chloroform | $C_{13}H_{15}NO_5$ | C<br>H<br>N | 58.86<br>5.70<br>5.28 | 58.88<br>5.71<br>5.27 |
| VII | Carbobenzoxy | H | $CH_2OCH_3$ | 35 | Oil | —[a] | $C_{12}H_{15}NO_5$ | C<br>H<br>N | 56.91<br>5.96<br>5.53 | 56.87<br>6.03<br>5.50 |
| VIII | Carbobenzoxy | H | $CH_2CH_2OCH_3$ | 50 | Oil | —[a] | $C_{13}H_{17}NO_5$ | C<br>H<br>N | 58.42<br>6.41<br>5.24 | 58.27<br>6.49<br>5.19 |
| IX | Carbobenzoxy | H | $CH_2{-}C(=O){-}OCH_2CH_3$ | 80 | 42–43° | —[a] | $C_{14}H_{17}NO_6$ | C<br>H<br>N | 56.95<br>5.80<br>4.74 | 56.83<br>5.86<br>4.71 |
| X | Carbobenzoxy | H | $CH(COCH_2CH_3)_2$ | 40 | Oil | —[a] | $C_{17}H_{21}NO_8$ | C<br>H<br>N | 55.58<br>5.76<br>3.81 | 55.45<br>5.81<br>3.78 |
| XI | Carbobenzoxy | H | $CH_2{-}C(=O){-}CH_3$ | 55 | Oil | —[a] | $C_{13}H_{15}NO_6$ | C<br>H<br>N | 55.51<br>5.37<br>34.14 | 55.30<br>5.41<br>4.98 |
| XIII | Tosyl | H | $CH{=}CH_2$ | 10 | 83.5–84.5° | Chloroform–hexane | $C_{11}H_{13}NO_4S$ | C<br>H<br>N | 51.75<br>5.13<br>5.49 | 51.66<br>5.16<br>5.45 |
| XIV | Trifluoroacetyl | H | $CH{=}CH_2$ | 20 | 40.5–41.5° | Chloroform–hexane | $C_6H_6F_3NO_3$ (8) | | — | — |
| XV | Phthaloyl | | $CH{=}CH_2$ | 25 | 107–108° | Chloroform–hexane | $C_{12}H_9NO_4$ (9) | | — | — |

[a] Purified by column chromatography.

obtained in an 80% yield as a colorless oil. Upon drying in a desiccator for 2 weeks, the oil solidified and was used without recrystallization, mp 42–43°; IR (mineral oil): 3320 (strong) (NH) and 1730 (strong, broad) (3 C=O) $cm^{-1}$; NMR (acetone-$d_6$): $\delta$ 1.27 (t, 3H, $J$ = 7.5, $OCH_2CH_3$), 4.24 (q, 2H, $J$ = 7.5, $OCH_2CH_3$), and 4.77 (s, 2H, $OCH_2CO$). Elemental analysis showed a formula of $C_{14}H_{17}NO_6$.

*N-Carbobenzoxyglycine Dicarbethoxymethyl Ester (X)*—Compound X was prepared in the same manner as VII using diethyl bromomalonate. The crude product was purified by column chromatography, with chloroform as the eluent, to give a yellow oil. Attempts to crystallize the product from chloroform and hexane or ethanol and water failed. Final purification was accomplished by dissolving the product in chloroform and filtering the solution hot from activated charcoal. Removal of the chloroform *in vacuo* gave a colorless oil in a 40% yield; IR ($CCl_4$): 3420 (weak, broad) (NH) and 1740 (strong, broad) (4 C=O) $cm^{-1}$; NMR (acetone-$d_6$): $\delta$ 1.27 (t, 6H, $J$ = 7.5, 2 $OCH_2CH_3$), 4.33 (q, 4H, $J$ = 7.5, 2 $OCH_2CH_3$), and 5.69 [s, 1H, $OCH(COOC_2H_5)_2$]. Elemental analysis showed a formula of $C_{17}H_{21}NO_8$.

*N-Carbobenzoxyglycine Acetoxymethyl Ester (XI)*—Compound XI was prepared in the same manner as VII using bromomethyl acetate. The crude product showed several spots on TLC; purification by column chromatography, with chloroform as the eluent, gave a product that contained one small impurity. Further purification by column chromatography, with chloroform–ethyl acetate (1:1) as the eluent, gave a 20% yield of pure product and a 35% yield of a product with the impurity. The pure product was a colorless oil: IR ($CCl_4$): 3400 (strong, broad) (NH) and 1740 (strong, broad) (3 C=O) $cm^{-1}$; NMR ($CDCl_3$): $\delta$ 2.08 (s, 3H, $COCH_3$) and 5.74 (s, 2H, $OCH_2O$). Elemental analysis showed a formula of $C_{14}H_{15}NO_6$.

*N-Tosylglycine Vinyl Ester (XIII)*—*N*-Tosylglycine (3.0 g, 13 mmoles) was subjected to the usual vinylation procedure (5) twice. The reaction mixture was worked up to give an oily product, which was very impure on TLC. Purification by column chromatography, with chloroform as the eluent, gave 0.6 g of a brown solid that still was impure on TLC. This solid was purified further by column chromatography, with chloroform–methanol (97.5:2.5) as the eluent, to give a light-brown solid, which was recrystallized from chloroform and hexane.

Pure product (0.3 g, 10% yield) was obtained as white flakes, mp 83.5–84.5°; IR (mineral oil): 3250 (moderate) (NH), 1750 (strong) (C=O), and 1645 (weak) (C=C) $cm^{-1}$; NMR ($CDCl_3$): $\delta$ 2.42 (s, 3H, $CH_3$), 3.88 (broad, d, 2H, $J$ = 4.9, $NCH_2CO$), 4.7 [ddd, 2H, $J$ (*trans*) = 13.7, $J$ (*cis*) = 6.3, $J$ (*gem*) = 2.0, $=CH_2$], 7.1 [dd, 1H, $J$ (*trans*) = 13.7, $J$ (*cis*) = 6.3, OCH=], 7.29 (d, 2H, $J$ = 8.3, aromatic), and 7.77 (d, 2H, $J$ = 8.3, aromatic). Elemental analysis (carbon, hydrogen, and nitrogen) gave a formula of $C_{11}H_{13}NO_4S$.

**Antifertility Screens**—The newly synthesized agents were tested initially for antifertility activity in $CF_1$ female mice (~28 g) in much the same manner as steroidal contraceptives. For 28 days, virgin female mice, which had been isolated for 4 weeks, were administered test compounds at 10 mg/kg/day ip (0.2 ml). Test compounds were homogenized in 1% carboxymethylcellulose to obtain a fine suspension. On Day 10, female mice were exposed to male mice (two females per male) for the remainder of the experiment. Male mice were rotated once per week to eliminate the possibility of infertility.

On Days 17–21 of gestation, the females were sacrificed, and the numbers of viable fetuses, intrauterine deaths, and implantation sites were tabulated (4, 13). 17-Ethinyl estradiol and diethylstilbestrol were used as standards. Viable fetuses were examined for teratogenic effects of these drugs by the methods outlined by Wilson (14).

For intravaginal testing, the compounds were homogenized in 40% lactose or 5% carboxymethylcellulose and administered intravaginally (0.03–0.05 ml) at 10 mg/kg/day for 28 days. A tuberculin syringe without the needle or a low-dose (0.5-ml) insulin syringe with a 1–100-$\mu$l eppendorf pipet tip modified to fit the syringe was employed. On Day 10 and on all subsequent days, females were exposed to males for 1 hr. From this point, the protocol described earlier was followed (4). Compounds XVI–XVIII were used as standard proteolytic inhibitors.

For male antifertility activity, the method of Coppola (15) was followed. Male mice (~30 g) were administered II, III, and XVIII at 10 mg/kg/day ip for 8 weeks. At the 4-, 6-, and 8-week intervals, females were exposed to the treated males for 2 weeks and then removed. The number of females pregnant 4 weeks after exposure to the males was determined for each 2-week interval.

**Enzymatic Studies**—The acrosin enzyme was isolated from the epididymides collected from 10 male $CF_1$ mice (~30 g). The epididymides were sliced in 0.25 *M* sucrose–0.001 *M* disodium ethylenediaminetetraacetate (pH 6.5). The sperm suspension was filtered through two layers of sterile cheesecloth to remove debris, then centrifuged at 600×*g* for 15

**Table II—Antifertility Activity of *N*-Protected Glycine Activated Esters in $CF_1$ Female Mice at 10 mg/kg/day**

| | Intraperitoneally | | | | Intravaginally | | | |
|---|---|---|---|---|---|---|---|---|
| Compound | *n* | Viable Fetuses per Litter | Intrauterine Deaths per Litter | Percent Pregnant | *n* | Viable Fetuses per Litter | Intrauterine Deaths per Litter | Percent Pregnant |
| I *N*-Carbobenzoxyglycine | 7 | 8.5 | 0.00 | 57 | 8 | 6.5 | 0.00 | 25 |
| II *N*-Carbobenzoxyglycine vinyl ester | 8 | 11.0 | 0.00 | 12 | 8 | 0.0 | 0.00 | 0 |
| III *N*-Carbobenzoxyglycine 1,2-dibromoethyl ester | 8 | 10.3 | 0.25 | 38 | 8 | 0.0 | 0.00 | 0 |
| IV *N*-Carbobenzoxyglycine ethyl ester | 8 | 11.4 | 0.00 | 88 | 8 | 8.0 | 0.00 | 25 |
| V *N*-Carbobenzoxyglycine cyanomethyl ester | 7 | 7.6 | 0.00 | 72 | 8 | 11.0 | 0.00 | 13 |
| VI *N*-Carbobenzoxyglycine acetonyl ester | 8 | 9.3 | 0.83 | 75 | 8 | 7.7 | 0.00 | 38 |
| VII *N*-Carbobenzoxyglycine methoxymethyl ester | 8 | 9.3 | 0.33 | 75 | 8 | 7.8 | 0.50 | 50 |
| VIII *N*-Carbobenzoxyglycine methoxyethyl ester | 8 | 9.0 | 0.25 | 57 | 8 | 8.3 | 0.75 | 50 |
| IX *N*-Carbobenzoxyglycine carbethoxymethyl ester | 8 | 10.7 | 0.67 | 38 | 8 | 1.0 | 0.00 | 13 |
| X *N*-Carbobenzoxyglycine dicarbethoxymethyl ester | 8 | 6.7 | 2.50 | 75 | 8 | 8.4 | 0.20 | 63 |
| XI *N*-Carbobenzoxyglycine acetoxymethyl ester | 8 | 8.8 | 1.80 | 50 | 8 | 10.0 | 1.30 | 50 |
| XII *N*-Carbobenzoxyglycine *p*-nitrophenyl ester | 8 | 12.8 | 0.20 | 63 | 8 | 10.0 | 0.00 | 25 |
| XIII *N*-Tosylglycine vinyl ester | 8 | 8.6 | 1.40 | 63 | 7 | 6.0 | 1.00 | 71 |
| XIV *N*-Trifluoroacetylglycine vinyl ester | 8 | 9.2 | 1.20 | 63 | 8 | 7.7 | 0.70 | 38 |
| XV *N*-Phthaloylglycine vinyl ester | 8 | 10.2 | 2.00 | 75 | 8 | 8.4 | 0.80 | 63 |
| XVI *N*-α-Tosyl-L-lysine chloromethyl ketone | 7 | 8.6 | 0.20 | 71 | 7 | 0.0 | 0.00 | 0 |
| XVII Tosyl-L-phenylalaninechloromethyl ketone | 7 | 4.5 | 0.50 | 57 | 8 | 0.0 | 0.00 | 0 |
| XVIII *N*-Carbobenzoxy-L-phenylalanine chloromethyl ketone | 8 | 11.6 | 0.14 | 88 | 8 | 9.0 | 0.00 | 38 |
| XIX 17-Ethinyl estradiol | 8 | 0.0 | 0.00 | 0 | — | — | — | — |
| XX Diethylstilbestrol | 8 | 0.0 | 0.00 | 0 | — | — | — | — |
| 1% Carboxymethylcellulose | 24 | 12.0 | 0.48 | 100 | — | — | — | — |
| 40% Lactose | — | — | — | — | 60 | 11.0 | 0.70 | 100 |
| 5% Carboxymethylcellulose | — | — | — | — | 34 | 9.6 | 0.64 | 74 |

min using a swinging bucket-type rotor head, and washed twice. The spermatozoa were resuspended in 20 ml of 0.25 *M* sucrose and frozen at −20° (9, 10).

After freeze–thawing, the tubes were agitated vigorously by vortexing for 30 sec and centrifuging at 1000×*g* for 15 min at 0°. The spermatozoa were resuspended, vortexed, and centrifuged again. The denuded spermatozoa were taken up in 5 ml of sucrose, and the pH was adjusted to 2.5 with hydrochloric acid. Acrosin was recovered in the supernate after centrifugation at 36,000×*g* for 15 min at 0° (16, 17).

Acrosin proteolytic enzymatic activity was determined by the method of Schleuning and Fritz (18). The incubation medium contained 0.7 ml of 0.1 *M* phosphate buffer (pH 7.6) and 0.3 ml of extracted crude rat acrosin, which were preincubated for 5 min at 30°. One milliliter of 2% azocasein and 1.5 μmoles of test compound in 0.2 ml of 40% lactose were added, and the mixture was incubated for 10 min at 30°. Tests were run in triplicate. The reaction was stopped with 5% trichloroacetic acid, and the mixture was centrifuged at 3500×*g* for 10 min. Absorption of the trichloroacetic acid-soluble peptides, which resulted due to the hydrolysis of azocasein, was measured at 366 nm. Enzymatic activity was calculated as the increase in absorbance per minute per milligram of protein (18, 19).

The hydrolysis of *N*-α-benzoyl-L-arginine ethyl ester, a trypsin substrate, was followed as described previously (19). Two milliliters of tris(hydroxymethyl)aminomethane, 0.3 ml of substrate, 0.1 ml of crude mouse acrosin, and 1.5 μmoles of test sample in 0.2 ml of 40% lactose were mixed, and the increase in absorbance at 253 nm was determined for 30 min. The absorbance (*A*) of the control equaled 0.320/min (18, 19). Compounds XVI–XVIII were used as proteolytic inhibitor standards.

## RESULTS AND DISCUSSION

Previous screening showed that the 1,2-dibromoethyl esters of *N*-carbobenzoxyglycine, leucine, phenylalanine, and proline afforded 100% inhibition of fertility when administered intravaginally (4). However, only *N*-carbobenzoxyglycine vinyl ester demonstrated 100% inhibition compared to leucine, phenylalanine, and proline vinyl esters. Since the vinyl esters were far less toxic (*i.e.*, $LD_{50} \geq 500$ mg/kg) than the 1,2-dibromoethyl esters, it was decided to examine other esters in the glycine series and other amino-protecting groups of the vinyl esters.

With the newly reported compounds (IV–XV), intravaginal administration compared to intraperitoneal administration at 10 mg/kg/day resulted in the best antifertility activity in mice (Table II). However, the vinyl ester analog (II) and the 1,2-dibromoethyl ester (III) of *N*-carbobenzoxyglycine still were the most active, giving 100% inhibition (Table II). The carbethoxymethyl ester (IX) and the cyanomethyl ester (V) resulted in 87% inhibition. The free acid (I), the ethyl ester (IV), and the *p*-nitrophenyl ester (XII) resulted in 75% inhibition. Administration of the methoxymethyl ester (VII) and the methoxyethyl ester (VIII) resulted in only 50% inhibition of fertility, as did the acetoxymethyl ester (XI). Examination of other amino-protecting groups of glycine vinyl esters again showed that the *N*-carbobenzoxy derivative (II) possessed the best inhibitory activity (*i.e.*, 100%) when administered intravaginally, with the *N*-trifluoroacetyl analog (XIV) having the next best inhibitory effect at 62%. The *N*-tosyl (XIII) and *N*-phthaloylglycine vinyl esters (XV) were essentially ineffective when administered intravaginally in mice.

Intraperitoneal administration of II, III, and XVII in males at 10 mg/kg/day for 8 weeks demonstrated no antifertility activity. It is believed that the enzymes of the acrosomal layer of the sperm become activated in the vaginal tract (17, 20) and are not normally active (*i.e.*, enzymes are complexed with inhibitors) in the male reproductive tract as well as in ejaculated sperm. This may account for the absence of an antifertility effect of these agents when administered to male mice, or there may be a lack of distribution of drugs to the semen and sperm after intraperitoneal administration.

Mouse acrosin enzymatic studies showed that inhibition of *N*-α-ben-

**Table III—*In Vitro* Effects of *N*-Protected Glycine Activated Esters (1.5 μmoles) on Acrosin Proteolytic Activity**

| | Inhibition, % | |
|---|---|---|
| Compound | *N*-α-Benzoyl-L-arginine Ethyl Ester Hydrolysis | Azocasein Hydrolysis |
| I | 58 ± 1.2 | 63 ± 5.3 |
| II | 91 ± 6.7 | 83 ± 3.1 |
| III | 84 ± 0.3 | 100 ± 4.2 |
| IV | 64 ± 6.5 | 55 ± 5.1 |
| VI | 62 ± 5.5 | 64 ± 11.7 |
| VII | 48 ± 10.3 | 56 ± 9.0 |
| VIII | 45 ± 11.7 | 37 ± 16.6 |
| IX | 76 ± 8.2 | 76 ± 11.2 |
| X | 42 ± 8.5 | 51 ± 15.4 |
| XI | 48 ± 14.0 | 47 ± 11.7 |
| XII | 64 ± 10.3 | 66 ± 18.8 |
| XIII | 33 ± 2.3 | 62 ± 3.9 |
| XIV | 59 ± 5.0 | 96 ± 5.4 |
| XV | 52 ± 7.1 | 67 ± 28.9 |
| XVI | 91 ± 1.2 | 100 ± 4.3 |
| XVII | 18 ± 0.6 | 100 ± 3.2 |
| XVIII | 35 ± 2.3 | 100 ± 3.8 |
| 1% Carboxymethyl cellulose | 0 ± 4 | 0 ± 6 |

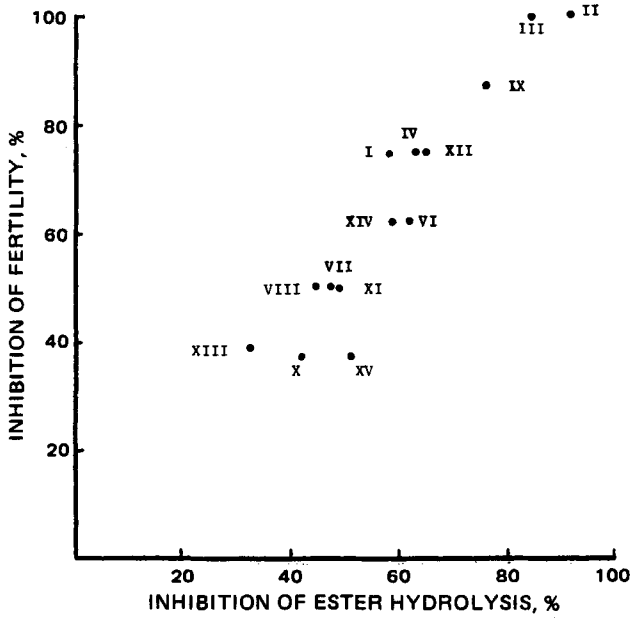


**Figure 1**—*Correlation between intravaginal antifertility activity at 10 mg/kg/day and percent inhibition of α-benzoyl-L-arginine ethyl ester hydrolysis at 1.5 μmoles.*

zoyl-L-arginine ethyl ester hydrolysis was related more directly to antifertility activity than to inhibition of azocasein hydrolytic activity (Table III). *N*-α-Benzoyl-L-arginine ethyl ester is a substrate that is readily hydrolyzed by trypsin due to its proteolytic or hydrolytic activity, whereas azocasein is a nonspecific substrate that can be hydrolyzed by several proteolytic- and esterase-type enzymes. Whereas azocasein hydrolysis was inhibited significantly by certain compounds (*i.e.*, XIV and XVIII), inhibition of azocasein hydrolysis did not appear to be positively correlated with antifertility activity. This does not preclude the possibility that these agents may inhibit other enzymatic activity of the sperm, which may contribute to the antifertility activity of these agents.

Inhibition of *N*-α-benzoyl-L-arginine ethyl ester hydrolysis by mouse acrosin preparations demonstrated a positive correlation with antifertility activity when the drug was administered intravaginally. Table II shows that those compounds that promoted >80% inhibition of *N*-α-benzoyl-L-arginine ethyl ester hydrolysis by mouse acrosin were potent fertility inhibitors, *e.g.*, I and II. Compound IX, the carbethoxymethyl ester, demonstrated 76% inhibition of *N*-α-benzoyl-L-arginine ethyl ester hydrolysis and 87% inhibition of fertility. Compounds that showed 50% inhibition of pregnancy demonstrated ~45–48% inhibition of *N*-α-benzoyl-L-arginine ethyl ester hydrolysis. Linear regression analysis showed a correlation coefficient of 0.95 between antifertility activity when administered intravaginally and reduction of *in vitro* mouse *N*-α-benzoyl-L-arginine ethyl ester hydrolysis at $p = 0.001$ (Fig. 1). When the intravaginal antifertility activity was compared to azocasein hydrolysis by mouse acrosin, a correlation coefficient of 0.68 was obtained at $p = 0.4$.

These compounds may inhibit *N*-α-benzoyl-L-arginine ethyl ester hydrolysis by conventional enzymatic inhibition mechanisms, by enzyme acylation, or by acting as a competitive substrate for the enzyme. Upon hydrolysis, II and III generate acetaldehyde or bromoacetaldehyde, which have the capability of nonreversible alkylation of the active site of the enzyme (21), thereby inhibiting its activity. Acrosin, an endopeptidase that cleaves the carboxyl bond of arginine and lysine derivatives, can be inhibited by known trypsin inhibitors. Proteolytic hydrolytic enzymatic activity is involved in sperm capacitation labilization of the external membrane of the sperm and penetration of the ovum's zona pellucida layer for fertilization. Acrosin is thought to play a vital role in the latter physiological process (4).

## REFERENCES

(1) A. K. Bhattacharyya, L. J. D. Zaneveld, B. M. Dargoje, G. F. B. Schumacher, and J. Travis, *J. Reprod. Fertil.*, **47**, 97 (1976).

(2) L. J. D. Zaneveld, R. T. Robertson, M. Kessler, and W. L. Williams, *ibid.*, **25**, 387 (1971).

(3) L. J. D. Zaneveld, R. T. Robertson, and W. L. Williams, *FEBS Lett.*, **11**, 345 (1970).

(4) I. H. Hall, J. H. Drew, Z. Sajadi, and L. J. Loeffler, *J. Pharm. Sci.*, **68**, 696 (1979).

(5) L. J. Loeffler, Z. Sajadi, and I. H. Hall, *J. Med. Chem.*, **20**, 1578 (1977).

(6) *Ibid.*, **20**, 1584 (1977).

(7) A. E. Barkdoll and W. F. Ross, *J. Am. Chem. Soc.*, **66**, 951 (1944).

(8) R. Schwyzer, M. Feurer, and B. Iselin, *Helv. Chim. Acta*, **38**, 83 (1959).

(9) F. Weygard and W. Steglich, *Angew. Chem.*, **73**, 757 (1961).

(10) M. F. Shostakovskii and E. S. Shapiro, *Akad. Nauk. SSSR* (English Translation), **1961**, 477.

(11) P. A. Levene, *Org. Synth.*, coll vol. **II**, 88 (1943).

(12) D. Theodoropoulos and L. C. Craig, *J. Org. Chem.*, **21**, 1376 (1956).

(13) B. Baggett, I. H. Hall, R. G. Boelgli, K. H. Palmer, and M. E. Wall, *Fertil. Steril.*, **21**, 60 (1970).

(14) J. C. Wilson, in "First International Conference on Congenital Malformations, General Principles in Experimental Teratology," Lippincott, Philadelphia, Pa., 1961, pp. 187–194.

(15) J. A. Coppola, *Life Sci.*, **8**, 43 (1969).

(16) C. R. Brown and E. F. Hartree, *J. Reprod. Fertil.*, **46**, 249 (1976).

(17) C. R. Brown, Z. Andani, and E. F. Hartree, *Biochem J.*, **149**, 133 (1975).

(18) W. D. Schleuning and H. Fritz, *Methods Enzymol.*, **14**, 330 (1976).

(19) G. W. Schwert and Y. Takenaka, *Biochim. Biophys. Acta*, **16**, 570 (1955).

(20) C. R. Brown and E. F. Hartree, *Hoppe-Seylers Z. Physiol. Chem.*, **356**, 1909 (1975).

## ACKNOWLEDGMENTS

The authors thank the University Research Council of the University of North Carolina at Chapel Hill for support of this research.

# Determination of Drug Stability in Aspirin Tablet Formulations by High-Pressure Liquid Chromatography

V. Y. TAGUCHI, M. L. COTTON ˣ, C. H. YATES, and J. F. MILLAR

Received April 14, 1980, from the *Pharmacy Research Department, Merck Frosst Laboratories, Pointe Claire-Dorval, Quebec H9R 4P8, Canada.* Accepted for publication July 16, 1980.

**Abstract** □ Salicylic acid and aspirin were resolved from the other salicylates in thermally degraded multicomponent tablets and determined quantitatively. The analytical method involved wetting the powdered tablet with acetic acid and diluting with chloroform to extract the drug components. Automated high-pressure liquid chromatographic analyses of filtered extracts were performed on a silica column with a mobile phase of acetic acid in heptane. The method was capable of resolving the major thermally induced transformation products in tablet formulations. It was sensitive to ~0.1 mg of salicylic acid/tablet. Good agreement with the compendial method for free salicylic acid was obtained.

**Keyphrases** □ Salicylic acid—simultaneous high-pressure liquid chromatographic analysis with aspirin in multicomponent tablets □ Aspirin—simultaneous high-pressure liquid chromatographic analysis with salicylic acid in multicomponent tablets □ High-pressure liquid chromatography—analysis, salicylic acid and aspirin multicomponent tablets □ Analgesics—aspirin and salicylic acid, high-pressure liquid chromatographic analysis in multicomponent tablets

Of the numerous methods reported for the determination of aspirin and salicylic acid in pharmaceutical preparations, few permit a simultaneous quantitative determination of both components in thermally degraded samples or have been evaluated as stability-indicating assay procedures. Free salicylic acid has been determined by column chromatography (1–3) and direct UV spectrophotometry (4, 5). Other analytical methods include fluorometry (6–8), GLC (9), and high-pressure liquid chromatography (HPLC) (10–12). Aspirin has been determined using spectrophotometry (13–15), GLC (16), NMR spectroscopy (17), nonaqueous titrimetry (18–20), TLC (21–23), and HPLC (24, 25). Aspirin and salicylic acid have been determined simultaneously by direct spectrophotometry (26), fluorometry (27), GLC (28, 29), IR spectroscopy (30), nonaqueous titrimetry (31), and HPLC (32–35).

This paper discusses an HPLC method developed for the simultaneous determination of aspirin and salicylic acid with the demonstrated precision and sensitivity required for assessing drug degradation. It is stability indicating for tablets containing aspirin stored at 50° or less. Aspirin stability can be determined either alone or in combination with drugs frequently present in analgesic formulations, such as propoxyphene, caffeine, and codeine.

## EXPERIMENTAL

**Apparatus**—The high-pressure liquid chromatograph[1] was equipped with flow control, a variable-wavelength detector, automatic sampling, an integrator–recorder, and a 10-μm microparticulate silica column[2]. Sample extracts were prepared using an ultrasonic bath[3] and filtered through chloroform-resistant membranes[4] prior to analysis.

**Reagents**—Aspirin[5], salicylic acid[6], caffeine[7], and codeine phosphate[8] were USP grade. Acetic acid[6], methanol[6], ethyl acetate[6], and acetone[6] were reagent grade. Chloroform[9], *n*-heptane[9], and trichloroethane[9] were distilled HPLC grade.

**HPLC Operating Conditions**—The mobile phase was 5% (v/v) acetic acid in *n*-heptane. The flow rate was 3.5 ml/min at 30°. The UV detector was operated at 300 nm. Instrument conditions were maintained for ~0.5 hr prior to the initial injection. Fifty microliters of either the standard or sample solution was injected onto the silica column. After use, the column was prepared for storage by flushing with *n*-heptane.

**Preparation of Sample Solutions**—For each tablet formulation, the average tablet weight was calculated by weighing 10 tablets. These tablets subsequently were pulverized to a fine powder. A quantity of powdered sample, approximately equivalent to one average tablet weight, was weighed accurately and transferred to a 100-ml volumetric flask. With the flask in an ultrasonic bath, 5 ml of acetic acid was added to wet the entire solid material. After 30 sec in the ultrasonic bath, the contents of the flask were diluted with 70 ml of chloroform, allowed to remain another 10 min in the bath, and then diluted to volume (100 ml) with chloroform.

**Preparation of Standard Solutions**—A stock solution of salicylic acid was prepared by weighing accurately ~50 mg, transferring the powder to a 100-ml volumetric flask, dissolving it in chloroform, and diluting the solution to volume with chloroform. A standard solution was prepared by weighing accurately an amount of aspirin, approximately equivalent to the labeled content of one tablet, and transferring this amount to a 100-ml volumetric flask. This solid was treated with 5 ml of acetic acid and diluted with 70 ml of chloroform in the same manner and preferably at the same time as the sample preparation. A 10.0-ml aliquot of salicylic acid stock solution was added to the aspirin solution and then diluted to volume with chloroform. Changes in aliquot size or the composition of the stock solution were made to match approximately the quantity of salicylic acid present in the standard with that in the sample if extensive degradation was anticipated.

**Chromatographic Separation and Analysis**—A standard solution was chromatographed in duplicate to check for system suitability. In a typical chromatogram, the $k'$ values for salicylic acid and aspirin were ~2 and 9, respectively. The resolution factor for salicylic acid and aspirin was preferably not less than 7 to allow for resolution from the possible degradation products. The tailing factor was <1.5 for each component.

Prior to injection, samples were filtered into appropriate vials. A standard was prepared simultaneously with two or three samples to permit frequent calibration. The quantity of salicylic acid and aspirin was determined by comparing peak areas of the sample and the external standard. The content of salicylic acid was expressed as a percentage of the label claim for aspirin.

**Identification of Degradation Products**—About 100 mg of an aspirin sample stressed at 95° for 5 weeks was dissolved in ~1 ml of chloroform and applied to a silica gel TLC plate[10] predeveloped with methanol. The plate was developed three times with 30% acetic acid in heptane, dried, and examined under UV illumination. The band ($R_f$ 0.6) between salicylic acid and the slower moving components was scraped from the plate, extracted with 5% acetic acid in chloroform, evaporated to dryness,

[1] Model 830 high-pressure liquid chromatograph with model 833 flow controller, model 834 automatic sampler, and model 837 variable-wavelength spectrophotometer, DuPont Instruments, Wilmington, Del., or model 1084 B high-pressure liquid chromatograph with variable-wavelength detector, Hewlett-Packard, Avondale, Pa.

[2] Partisil 10, 4.6 × 250 mm PXS 1025, Whatman, Clifton, N.J.

[3] Model ME 46, Mettler Electronics Corp., Anaheim, Calif.

[4] Metricel Alpha-450, Gelman Instrument Co., Ann Arbor, Mich.

[5] Dow Pharmaceuticals, Richmond Hill, Ontario, Canada.

[6] American Chemicals Ltd., Montreal, Quebec, Canada.

[7] Pfizer Co., Pointe Claire, Quebec, Canada.

[8] F. E. Cornell and Co. Ltd., Montreal, Quebec, Canada.

[9] Fisher Scientific Co., Fair Lawn, N.J.

[10] Silica gel GF, 1-mm precoated TLC plates, Analtech Inc., Newark, Del.



0022-3549/81/0100-0064$01.00/0
© 1981, American Pharmaceutical Association

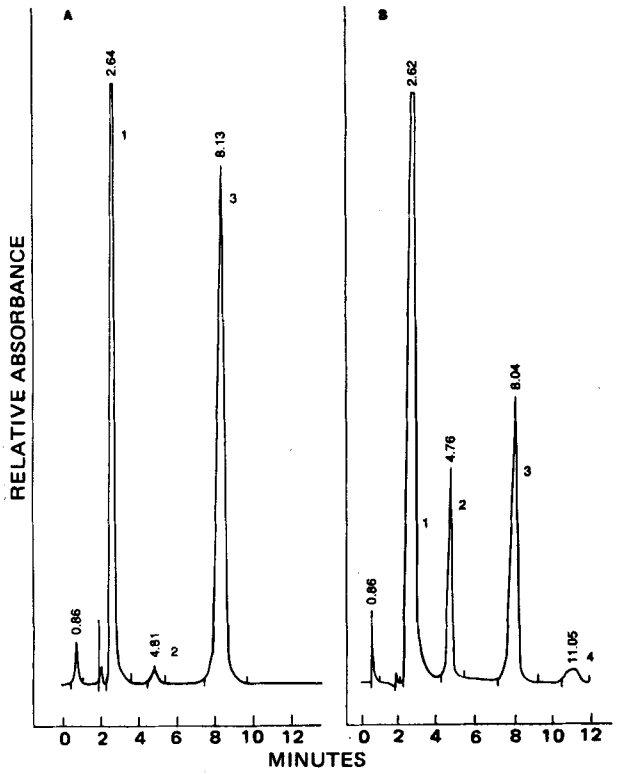


**Figure 1**—*High-pressure liquid chromatograms of aspirin tablet formulations stressed at 50° for 16 weeks (A) and at 80° for 2 weeks (B). Key: 1, salicylic acid (k′ = 2.2); 2, salicylsalicylic acid (k′ = 4.9); 3, aspirin (k′ = 9.0); and 4, acetylsalicylsalicylic acid (k′ = 12.6). The column was Partisil 10 silica, and the mobile phase was 5% acetic acid in heptane.*

and dried in a vacuum desiccator over sodium hydroxide pellets. About 10 mg was recovered from six plates. Under HPLC analytical conditions, this component eluted with a $k'$ value of 4.9, which is identical to that of the unknown compound that eluted immediately after salicylic acid (Fig. 1). The structure corresponded to salicylsalicylic acid; NMR (deuterochloroform): $\delta$ 10.4 (1H), 8.4–7.9 (2H), and 7.7–6.8 (6H), no methyl protons; mass spectrum: major ions at $m/z$ 258 ($M^{+\cdot}$), 121, and 120; UV (5% acetic acid in heptane): $\lambda_{max}$ 312 nm.

The third degradation product ($k'$ = 12.6 in Fig. 1) was not successfully isolated from TLC plates because of contamination from aspirin and other degradation products with lower $R_f$ values. Instead, 10 fractions were collected from a concentrated solution on the chromatograph. A 200-$\mu$l sample of the stressed aspirin in methanol was injected. Fractions were collected, evaporated, and dried in a vacuum desiccator over sodium hydroxide pellets. The structure corresponded to acetylsalicylsalicylic acid; mass spectrum: major ions at $m/z$ 180, 163, 138, 120, 92, and 43; UV (5% acetic acid in heptane): $\lambda_{max}$ 282 and 312 nm.

## RESULTS AND DISCUSSION

Quantitative extraction of aspirin and salicylic acid was not obtained with combinations of methanol and chloroform, probably because of adsorption on tablet excipients (36, 37). Successful drug release was achieved by initially wetting the pulverized sample with 98% formic acid, followed by dilution with chloroform (37). Aspirin hydrolysis was ~0.02%/min in the presence of the concentrated acid and 0.02%/hr after dilution with chloroform. Substitution of acetic acid in place of formic acid provided adequate drug release, similar hydrolysis rates, and reduced instrument corrosion. To compensate for aspirin hydrolysis in the sample, standards also were wetted with acetic acid and prepared at the same time as the samples.

To minimize aspirin hydrolysis, only nonaqueous mobile phases were investigated. With a mobile phase of 10% ethanol and 5% acetic acid in chloroform, a polar bonded phase column[11] resolved aspirin and salicylic acid in unstressed tablet formulations. However, inadequate resolution of the drug and its decomposition products occurred with thermally stressed formulations. Successful resolution of the latter was achieved on a silica column using acetic acid in heptane as the mobile phase (Fig. 1). Additional basic drug components commonly present in analgesic preparations, such as propoxyphene, caffeine, and codeine, were not eluted. Assays of thermally stressed samples containing various combinations of these drugs with aspirin did not indicate any interference by these additional drug components with the eluting salicylates. The HPLC column was regenerated periodically to remove the retained components by flushing with trichloroethane, ethyl acetate, acetone, methanol, and

[11] Partisil 10 PAC, 4.6 × 250 mm PXS 1025 PAC, Whatman, Clifton, N.J.

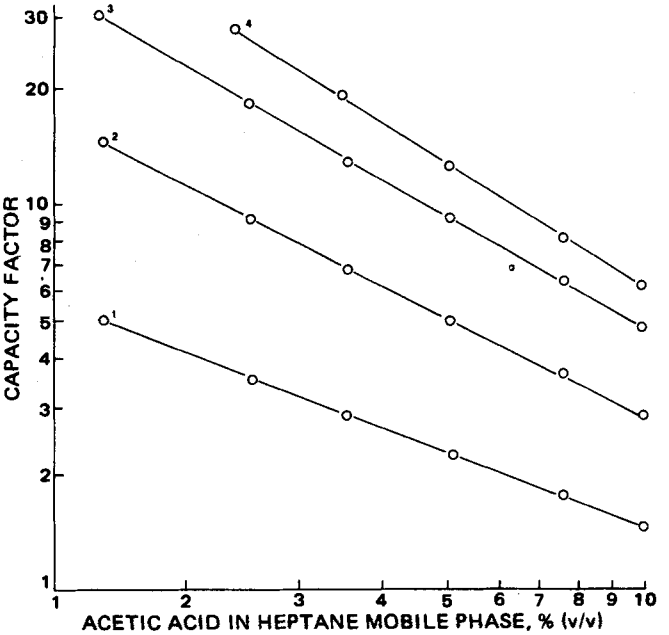


**Figure 2**—*Logarithmic correlations of capacity factors* versus *the percent of acetic acid in the mobile phase for the four salicylates. Key: 1, salicylic acid; 2, salicylsalicylic acid; 3, aspirin; and 4, acetylsalicylsalicylic acid.*

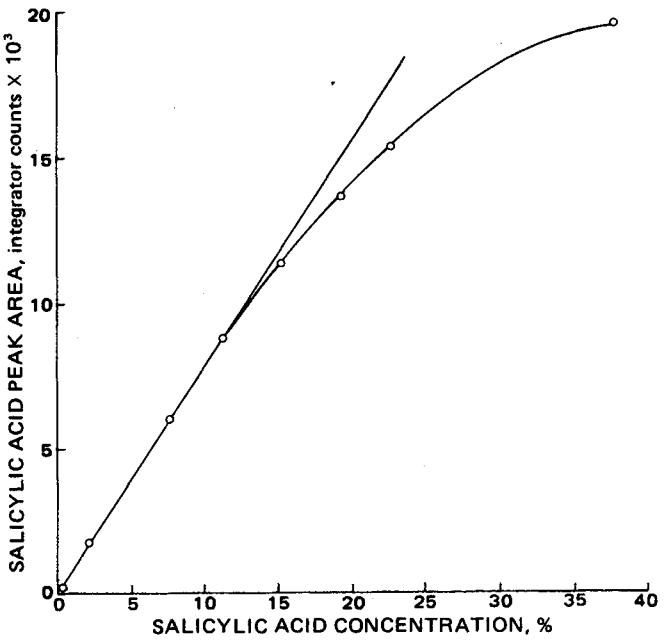


**Figure 3**—*Salicylic acid peak areas* versus *the percent of salicylic acid in standard solutions containing an increasing concentration of salicylic acid and a corresponding decreasing concentration of aspirin. In all cases, the percent of salicylic acid refers to the weight percent of salicylic acid expressed as a percentage of the label claim for aspirin. The aspirin label claim for all formulations was 650 mg.*

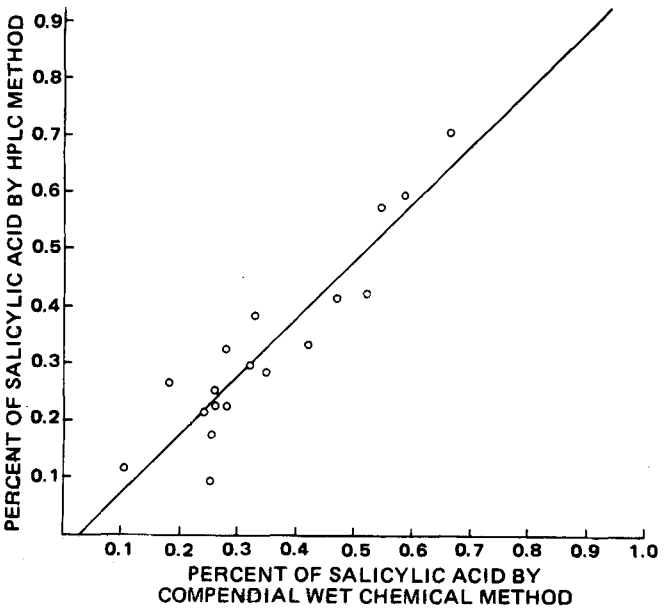


**Figure 4**—*Correlation of the HPLC salicylic acid results* versus *the wet chemical results. The latter method was based on the assay for free salicylic acid in USP XIX. With 18 data points, a slope of 1.0 ± 0.1, an intercept of −0.028 ± 0.039, and a correlation coefficient of 0.929 were calculated from the linear regression analysis.*

water and then reversing the sequence as recommended by the manufacturer.

Aspirin and three salicylate decomposition products were resolved with the silica column. In accelerated thermal stability trials, samples contained primarily salicylic acid with trace quantities of salicylsalicylic acid. Where salicylic acid concentrations were >3%, a third degradate, acetylsalicylsalicylic acid, was observed in trace quantities.

Although the time required to obtain a satisfactory chromatogram could be reduced by adding small amounts (1–2%) of a modifier, such as chloroform or ethyl acetate, to the mobile phase, no modifier was used because its presence caused dead volume interference with the salicylic acid. The presence of acetic acid was mandatory for the satisfactory elution of the acidic hydrogen-bonded species. Figure 2 illustrates the observed decrease in the capacity factors of the four components with increasing acetic acid concentrations in the heptane mobile phase.

A wavelength of 300 nm was selected for detecting the eluting components. It provided adequate sensitivity for salicylic acid and permitted the detection of salicylsalicylic acid and acetylsalicylsalicylic acid. Aspirin has a small absorptivity at 300 nm, but the absorbance was sufficient for satisfactory quantitative determination because of its large concentration. At 312 nm, the absorption maximum for salicylic acid, aspirin was difficult to detect.

The linearity of the detector response for aspirin and salicylic acid was investigated by preparing a series of samples containing decreasing amounts of aspirin and correspondingly increasing amounts of salicylic acid. Linear response was satisfactory for aspirin over the concentration

**Table I—Assay Results for Aspirin and Salicylic Acid from a Study of the HPLC Analytical Precision**

| | Aspirin, % of label claim | Salicylic Acid, %[a] |
|---|---|---|
| | 98.9 | 0.38 |
| | 97.7 | 0.38 |
| | 99.0 | 0.38 |
| | 100.3 | 0.34 |
| | 98.1 | 0.36 |
| | 99.6 | 0.39 |
| | 98.2 | 0.36 |
| | 101.1 | 0.37 |
| | 98.3 | 0.37 |
| Average | 99.0 | 0.37 |
| *SD* | 1.1 | 0.02 |

[a] The percent of salicylic acid refers to the weight percent of salicylic acid expressed as a percentage of the label claim for aspirin.

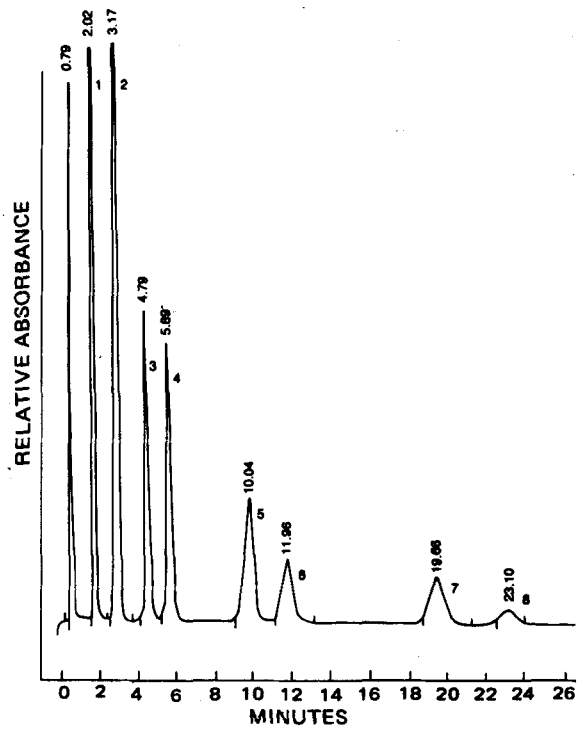


**Figure 5**—*High-pressure liquid chromatogram of aspirin stressed at 95° for 5 weeks showing the four salicylates in Fig. 1 (peaks 1–4) and the four additional components eluting at longer retention times (peaks 5–8). The column was Partisil 10 silica, and the mobile phase was 10% acetic acid in heptane.*

range of 650–300 mg. Appreciable deviations from linearity were observed for salicylic acid concentrations of 15% (98 mg/tablet) (Fig. 3). Typical assay values of <5% salicylic acid (33 mg/tablet) were well within the linear range.

A small positive intercept was obtained at zero salicylic acid concentration. Based on nine data points, a linear correlation was obtained for salicylic acid peak areas *versus* percent of salicylic acid (concentration range 0–0.36%). The correlation coefficient from the regression analysis was 1.0, and the intercept was equivalent to ~0.1% salicylic acid (0.7 mg/tablet). This amount of salicylic acid probably was generated from aspirin hydrolysis during the preparation of both the sample and the standard. As a result, a significant error was introduced when employing the external standard analytical method for samples containing <0.1% salicylic acid. Samples with 0.01–0.1% salicylic acid were assayed successfully using a linear calibration technique.

The accuracy of the HPLC method was evaluated by comparing the HPLC assay results obtained from the stressed tablet formulations containing aspirin with data obtained on the same samples using the method for free salicylic acid reported by Levine (38) and later established as a compendial method (39). The linear correlation obtained (Fig. 4) approximated a theoretical slope of 45° and a zero intercept, indicating reasonable agreement between the two methods. Based on three analysts assaying a single powdered sample on 3 different days, the HPLC data in Table I indicated good precision for both aspirin and free salicylic acid.

To demonstrate that the method was capable of detecting and resolving all major degradation products in samples from accelerated thermal stability trials, a sample of pure aspirin stressed under abnormally severe conditions (95° for 5 weeks) was examined by HPLC. In addition to the four previously identified components, four other unidentified compounds eluted later in the chromatogram with 10% acetic acid in the heptane mobile phase (Fig. 5). Traces of these four unknowns were detectable in formulations stressed at 80° for 2 weeks but were undetectable in samples stressed at 50° for 16 weeks. Only the three identified components contributed significantly to total drug degradation in the accelerated stability samples stressed at or below 50°. If the samples were exposed to more severe conditions or contained abnormal amounts of salicylic acid, increasing the acetic acid concentration in the mobile phase reduced the peak broadening and enhanced the detection of these late-eluting components.

## REFERENCES

(1) J. D. Weber and J. Levine, *J. Pharm. Sci.*, **55**, 78 (1966).
(2) J. Levine and J. D. Weber, *ibid.*, **57**, 631 (1968).
(3) D. E. Guttman and G. W. Salomon, *ibid.*, **58**, 120 (1969).
(4) R. C. Reed and W. W. David, *ibid.*, **54**, 1533 (1965).
(5) A. Badinand, J. J. Vallon, J. Cuziat, and H. Herilier, *Bull. Trav. Soc. Pharm. Lyon*, **13**, 89 (1969).
(6) N. Shane and D. Miele, *J. Pharm. Sci.*, **59**, 397 (1970).
(7) N. A. Shane and R. Stillman, *ibid.*, **60**, 114 (1971).
(8) S. Adams and J. H. McB. Miller, *J. Pharm. Pharmacol.*, **30**, 81 (1978).
(9) J. R. Watson, F. Matsui, P. M. J. McConnell, and R. C. Lawrence, *J. Pharm. Sci.*, **61**, 929 (1972).
(10) R. A. Henry and J. A. Schmit, *Chromatographia*, **1970**, 116.
(11) H. Bundgaard, *Arch. Pharm. Chemi, Sci. Ed.*, **4**, 103 (1976).
(12) S.-O. Jansson and I. Andersson, *Acta Pharm. Suec.*, **14**, 161 (1977).
(13) R. D. Deodhar, M. R. Shastri, and R. C. Mehta, *Indian J. Pharm.*, **38**, 18 (1976).
(14) E. E. Theimer and E. W. Ciurczak, *J. Pharm. Sci.*, **66**, 139 (1977).
(15) M. M. Amer, A. M. Wahbi, and M. K. Aboul-Eialah, *Bull. Fac. Pharm., Cairo Univ.*, **15**, 311 (1978).
(16) S. Patel, J. H. Perrin, and J. J. Windheuser, *J. Pharm. Sci.*, **61**, 1794 (1972).
(17) J. A. Vinson and D. M. Kozak, *Am. J. Pharm. Educ.*, **42**, 290 (1978).
(18) S.-L. Lin and M. I. Blake, *J. Pharm. Sci.*, **56**, 43 (1967).
(19) M. I. Walash, S. P. Agarwal, and M. I. Blake, *Can. J. Pharm. Sci.*, **7**, 123 (1972).
(20) M. I. Walash and M. Rizk, *Indian J. Pharm.*, **39**, 82 (1977).
(21) S. Ebel and G. Herold, *Chromatographia*, **8**, 569 (1975).
(22) C. Klein, *Isr. Pharm. J.*, **17**, 247 (1974).
(23) S. Ebel and G. Herold, *Arch. Pharm.*, **308**, 839 (1975).
(24) R. L. Stevenson and C. A. Burtis, *J. Chromatogr.*, **61**, 253 (1971).
(25) P. P. Ascione and G. P. Chrekian, *J. Pharm. Sci.*, **64**, 1029 (1975).
(26) A. W. Clayton and R. E. Thiers, *ibid.*, **55**, 404 (1966).
(27) H. Kubin and H. Gaenshirt, *Pharm. Ind.*, **38**, 224 (1976).
(28) J. F. Watson, P. Crescuolo, and F. Matsui, *J. Pharm. Sci.*, **60**, 454 (1971).
(29) S. L. Ali, *J. Chromatogr.*, **126**, 651 (1976).
(30) G. Kister, M. Ribes, J. Chanal, and A. Catterini, *Ann. Pharm. Fr.*, **34**, 215 (1976).
(31) S.-L. Lin, *J. Pharm. Sci.*, **56**, 1130 (1967).
(32) R. G. Baum and F. F. Cantwell, *Anal. Chem.*, **50**, 280 (1978).
(33) G. W. Peng, M. A. F. Gadalla, V. Smith, A. Peng, and W. L. Chiou, *J. Pharm. Sci.*, **67**, 710 (1978).
(34) R. G. Baum and F. F. Cantwell, *ibid.*, **67**, 1066 (1978).
(35) J. F. Reepmeyer and R. D. Kirchhoefer, *ibid.*, **68**, 1167 (1979).
(36) D. E. Guttman, *ibid.*, **57**, 1685 (1968).
(37) J. Levine and J. D. Weber, *ibid.*, **57**, 631 (1968).
(38) J. Levine, *ibid.*, **50**, 506 (1961).
(39) "The United States Pharmacopeia," 19th rev., Mack Publishing Co., Easton, Pa., 1975.



## ACKNOWLEDGMENTS

The authors thank Mr. J. O'Neill and Mr. P. Lamarche for technical assistance and the National Research Council of Canada for an Industrial Postdoctoral Fellowship to V. Y. Taguchi.


# Hypoglycemic Activity of Oral Hypoglycemics with Increased Hydrophilicity


**SOBHI A. SAID *x and HASAN I. AL-SHORA**



Received February 5, 1980, from the *Department of Pharmaceutics, College of Pharmacy, Riyad University, Riyad, Saudi Arabia.* Accepted for publication July 11, 1980. *On leave of absence from the Faculty of Pharmacy, Cairo University, Cairo, Egypt.



**Abstract** □ The effect of increasing the hydrophilicity of acetohexamide and tolbutamide with hydroxypropyl methylcellulose and methylcellulose on drug dissolution and hypoglycemic activity in rats was examined. The dissolution rate of both drugs was increased according to the type and concentration of the polymer. The oral absorption of both drugs was improved, as indicated by potentiation of the reduction in blood glucose in rats. The efficiency of the polymer in increasing the dissolution rates of the drugs correlated with the hydrophilicity of the polymer.



**Keyphrases** □ Hypoglycemics—improved absorption through increased hydrophilicity □ Tolbutamide—improved absorption through increased hydrophilicity □ Acetohexamide—improved absorption through increased hydrophilicity □ Absorption—tolbutamide and acetohexamide, improved absorption through increased hydrophilicity


Certain oral hypoglycemics, *e.g.*, acetohexamide and tolbutamide, are poorly water soluble and have irregular dissolution rates (1–3). Coprecipitation with povidone and solid dispersion of tolbutamide in polyethylene glycols have been utilized to increase the dissolution rate (4, 5) and bioavailability (5, 6). Inclusion of acetohexamide in cyclodextrin enhanced its dissolution and hypoglycemic activity (3).

The increased hydrophilicity of drugs, *i.e.*, the conversion of the hydrophobic surface of the drug to a hydrophilic one through treatment with a film-forming water-soluble polymer, increased the dissolution of hexobarbital (7) and the bioavailability of phenytoin (8) and griseofulvin (9). The polymers used were methylcellulose, hydroxyethyl cellulose (7), and hydroxypropyl cellulose (9).

The objective of the present study was to investigate the

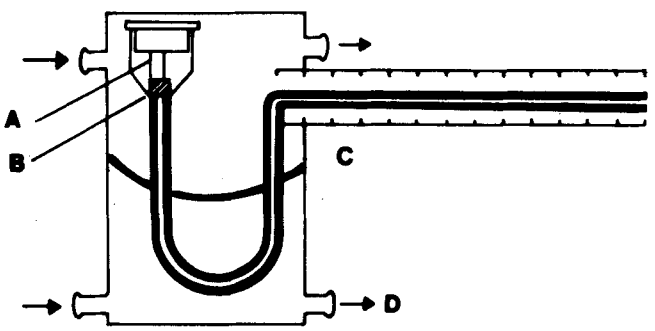


**Figure 1**—*Apparatus for measuring the uptake of dissolution fluid by drug disks. Key: A, disk stager; B, drug disk; C, graduated pipet; and D, water bath.*


*0022-3549/81/0100-0067$01.00/0*


*© 1981, American Pharmaceutical Association*

## REFERENCES

(1) J. D. Weber and J. Levine, *J. Pharm. Sci.*, **55**, 78 (1966).
(2) J. Levine and J. D. Weber, *ibid.*, **57**, 631 (1968).
(3) D. E. Guttman and G. W. Salomon, *ibid.*, **58**, 120 (1969).
(4) R. C. Reed and W. W. David, *ibid.*, **54**, 1533 (1965).
(5) A. Badinand, J. J. Vallon, J. Cuziat, and H. Herilier, *Bull. Trav. Soc. Pharm. Lyon*, **13**, 89 (1969).
(6) N. Shane and D. Miele, *J. Pharm. Sci.*, **59**, 397 (1970).
(7) N. A. Shane and R. Stillman, *ibid.*, **60**, 114 (1971).
(8) S. Adams and J. H. McB. Miller, *J. Pharm. Pharmacol.*, **30**, 81 (1978).
(9) J. R. Watson, F. Matsui, P. M. J. McConnell, and R. C. Lawrence, *J. Pharm. Sci.*, **61**, 929 (1972).
(10) R. A. Henry and J. A. Schmit, *Chromatographia*, **1970**, 116.
(11) H. Bundgaard, *Arch. Pharm. Chemi, Sci. Ed.*, **4**, 103 (1976).
(12) S.-O. Jansson and I. Andersson, *Acta Pharm. Suec.*, **14**, 161 (1977).
(13) R. D. Deodhar, M. R. Shastri, and R. C. Mehta, *Indian J. Pharm.*, **38**, 18 (1976).
(14) E. E. Theimer and E. W. Ciurczak, *J. Pharm. Sci.*, **66**, 139 (1977).
(15) M. M. Amer, A. M. Wahbi, and M. K. Aboul-Eialah, *Bull. Fac. Pharm., Cairo Univ.*, **15**, 311 (1978).
(16) S. Patel, J. H. Perrin, and J. J. Windheuser, *J. Pharm. Sci.*, **61**, 1794 (1972).
(17) J. A. Vinson and D. M. Kozak, *Am. J. Pharm. Educ.*, **42**, 290 (1978).
(18) S.-L. Lin and M. I. Blake, *J. Pharm. Sci.*, **56**, 43 (1967).
(19) M. I. Walash, S. P. Agarwal, and M. I. Blake, *Can. J. Pharm. Sci.*, **7**, 123 (1972).
(20) M. I. Walash and M. Rizk, *Indian J. Pharm.*, **39**, 82 (1977).
(21) S. Ebel and G. Herold, *Chromatographia*, **8**, 569 (1975).
(22) C. Klein, *Isr. Pharm. J.*, **17**, 247 (1974).
(23) S. Ebel and G. Herold, *Arch. Pharm.*, **308**, 839 (1975).
(24) R. L. Stevenson and C. A. Burtis, *J. Chromatogr.*, **61**, 253 (1971).
(25) P. P. Ascione and G. P. Chrekian, *J. Pharm. Sci.*, **64**, 1029 (1975).
(26) A. W. Clayton and R. E. Thiers, *ibid.*, **55**, 404 (1966).
(27) H. Kubin and H. Gaenshirt, *Pharm. Ind.*, **38**, 224 (1976).
(28) J. F. Watson, P. Crescuolo, and F. Matsui, *J. Pharm. Sci.*, **60**, 454 (1971).
(29) S. L. Ali, *J. Chromatogr.*, **126**, 651 (1976).
(30) G. Kister, M. Ribes, J. Chanal, and A. Catterini, *Ann. Pharm. Fr.*, **34**, 215 (1976).
(31) S.-L. Lin, *J. Pharm. Sci.*, **56**, 1130 (1967).
(32) R. G. Baum and F. F. Cantwell, *Anal. Chem.*, **50**, 280 (1978).
(33) G. W. Peng, M. A. F. Gadalla, V. Smith, A. Peng, and W. L. Chiou, *J. Pharm. Sci.*, **67**, 710 (1978).
(34) R. G. Baum and F. F. Cantwell, *ibid.*, **67**, 1066 (1978).
(35) J. F. Reepmeyer and R. D. Kirchhoefer, *ibid.*, **68**, 1167 (1979).
(36) D. E. Guttman, *ibid.*, **57**, 1685 (1968).
(37) J. Levine and J. D. Weber, *ibid.*, **57**, 631 (1968).
(38) J. Levine, *ibid.*, **50**, 506 (1961).
(39) "The United States Pharmacopeia," 19th rev., Mack Publishing Co., Easton, Pa., 1975.



## ACKNOWLEDGMENTS

The authors thank Mr. J. O'Neill and Mr. P. Lamarche for technical assistance and the National Research Council of Canada for an Industrial Postdoctoral Fellowship to V. Y. Taguchi.


# Hypoglycemic Activity of Oral Hypoglycemics with Increased Hydrophilicity


**SOBHI A. SAID *x and HASAN I. AL-SHORA**



Received February 5, 1980, from the *Department of Pharmaceutics, College of Pharmacy, Riyad University, Riyad, Saudi Arabia.* Accepted for publication July 11, 1980. *On leave of absence from the Faculty of Pharmacy, Cairo University, Cairo, Egypt.



**Abstract** □ The effect of increasing the hydrophilicity of acetohexamide and tolbutamide with hydroxypropyl methylcellulose and methylcellulose on drug dissolution and hypoglycemic activity in rats was examined. The dissolution rate of both drugs was increased according to the type and concentration of the polymer. The oral absorption of both drugs was improved, as indicated by potentiation of the reduction in blood glucose in rats. The efficiency of the polymer in increasing the dissolution rates of the drugs correlated with the hydrophilicity of the polymer.



**Keyphrases** □ Hypoglycemics—improved absorption through increased hydrophilicity □ Tolbutamide—improved absorption through increased hydrophilicity □ Acetohexamide—improved absorption through increased hydrophilicity □ Absorption—tolbutamide and acetohexamide, improved absorption through increased hydrophilicity


Certain oral hypoglycemics, *e.g.*, acetohexamide and tolbutamide, are poorly water soluble and have irregular dissolution rates (1–3). Coprecipitation with povidone and solid dispersion of tolbutamide in polyethylene glycols have been utilized to increase the dissolution rate (4, 5) and bioavailability (5, 6). Inclusion of acetohexamide in cyclodextrin enhanced its dissolution and hypoglycemic activity (3).

The increased hydrophilicity of drugs, *i.e.*, the conversion of the hydrophobic surface of the drug to a hydrophilic one through treatment with a film-forming water-soluble polymer, increased the dissolution of hexobarbital (7) and the bioavailability of phenytoin (8) and griseofulvin (9). The polymers used were methylcellulose, hydroxyethyl cellulose (7), and hydroxypropyl cellulose (9).

The objective of the present study was to investigate the

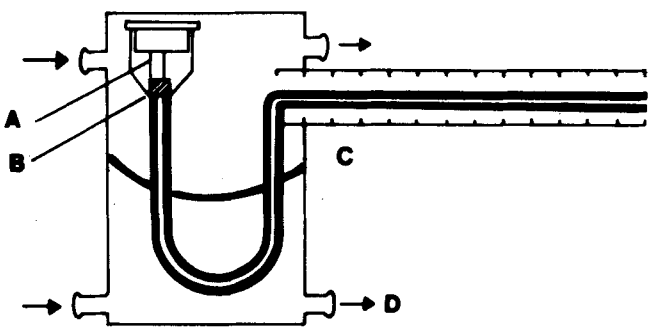


**Figure 1**—*Apparatus for measuring the uptake of dissolution fluid by drug disks. Key: A, disk stager; B, drug disk; C, graduated pipet; and D, water bath.*


*0022-3549/81/0100-0067$01.00/0*


*© 1981, American Pharmaceutical Association*

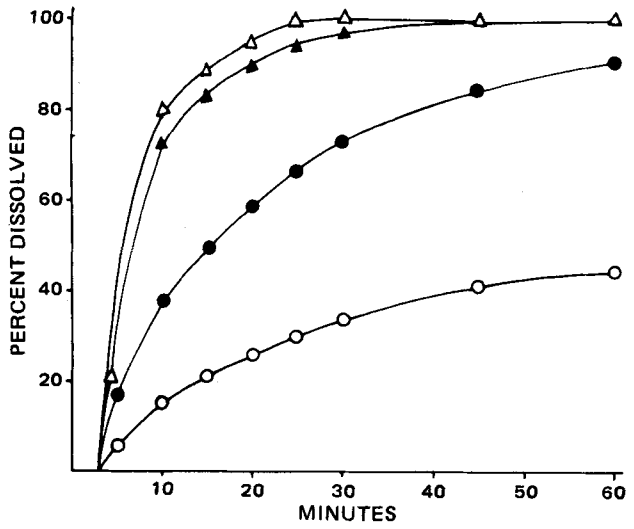


**Figure 2**—*Dissolution rate of tolbutamide untreated and treated with methylcellulose. Key:* ○, *untreated; and* ●, △, *and* ▲, *treated with 2.5, 5, and 10 ml of a 5% methylcellulose solution/20 g, respectively.*

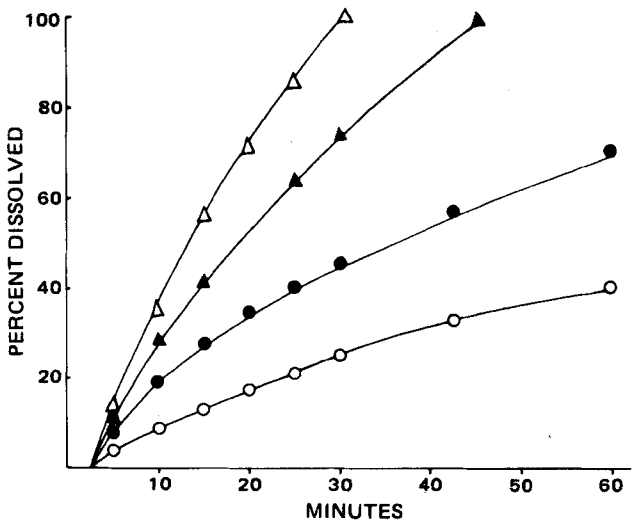


**Figure 4**—*Dissolution rate of acetohexamide untreated and treated with methylcellulose. Key:* ○, *untreated; and* ●, △, *and* ▲, *treated with 2.5, 5, and 10 ml of a 5% solution of methylcellulose/20 g, respectively.*

effects of increasing the hydrophilicity of acetohexamide (I) and tolbutamide (II) on their dissolution and oral absorption in rats. The polymers selected for increasing the hydrophilicity were hydroxypropyl methylcellulose (III) and methylcellulose (IV). The uptake of dissolution fluid by the treated and the untreated drug was measured.

## EXPERIMENTAL

**Materials**—Acetohexamide[1] (mean particle size 6 μm), tolbutamide[2] (mean particle size 7 μm), hydroxypropyl methylcellulose[3], and methylcellulose[4] were used.

**Treatment of Powders**—The dispersion of III and IV onto the surface of I and II was carried out in a small high-speed mixer[5]. The drug (20 g) was placed in the mixer with 2.5, 5, or 10 ml of a 5% aqueous solution of the polymer. Mixing was continued for 45 min and then stopped to allow removal of material adhering to the walls with a spatula. This process was repeated three times.

The resultant mass was dried *in vacuo* at 50° for 24 hr and screened through a No. 20 mesh screen. The powder then was manually filled into No. 9 capsules[5], each containing a quantity equivalent to 100 mg of the drug.

**Dissolution Testing**—The dissolution of the capsules was tested according to USP XIX (10) using the USP dissolution apparatus[5]. The dissolution medium consisted of 900 ml of the medium specified in the monograph for each drug [containing 0.01% (w/v) polysorbate 80[6]]. Samples (5 ml) were withdrawn at 10, 15, 20, 25, 30, 45, and 60 min and filtered through a membrane filter[7] (0.5-μm diameter), and their absorbances[8] were measured at 245 and 226 nm for I and II, respectively. Correction of the analysis was carried out by subtracting the absorbance, if any, due to the polymer solution to obtain the actual drug concentration. Each study was based on three dissolution tests, and the average values are reported.

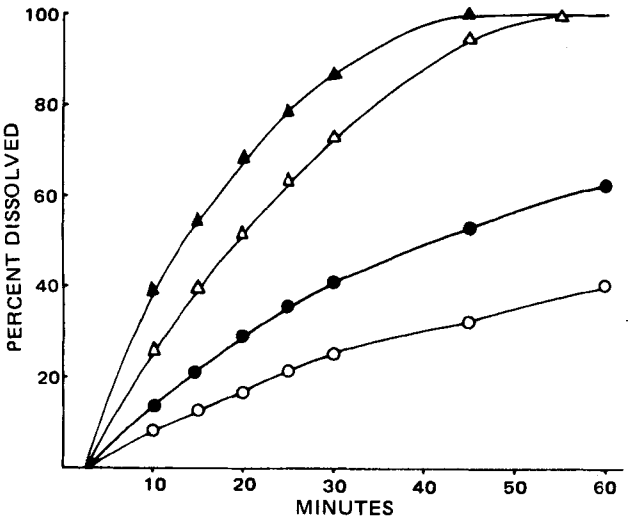


**Figure 3**—*Dissolution rate of tolbutamide untreated and treated with hydroxypropyl methylcellulose. Key:* ○, *untreated; and* ●, △, *and* ▲, *treated with 2.5, 5, and 10 ml of a 5% solution of hydroxypropyl methylcellulose/20 g, respectively.*

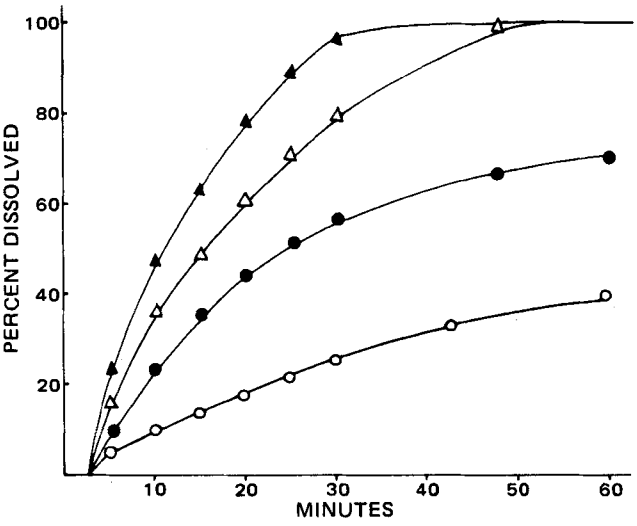


**Figure 5**—*Dissolution rate of acetohexamide untreated and treated with hydroxypropyl methylcellulose. Key:* ○, *untreated; and* ●, △, *and* ▲, *treated with 2.5, 5, and 10 ml of hydroxypropyl methylcellulose/20 g, respectively.*

[1] Eli Lilly, Indianapolis, Ind.
[2] Industriale Handelmaeatscharani, Amsterdam, The Netherlands.
[3] Al-Arabia Factory for Pharmaceuticals, Ameria, Cairo, Egypt.
[4] BDH, Poole, England.
[5] Erweka-Haeusenstamn, Kr, Offenbach, Main, West Germany.
[6] Koch-Light Laboratories, Bucks, England.
[7] Millipore Corp., Bedford, Mass.
[8] Varian Techtron UV–visible model 635.

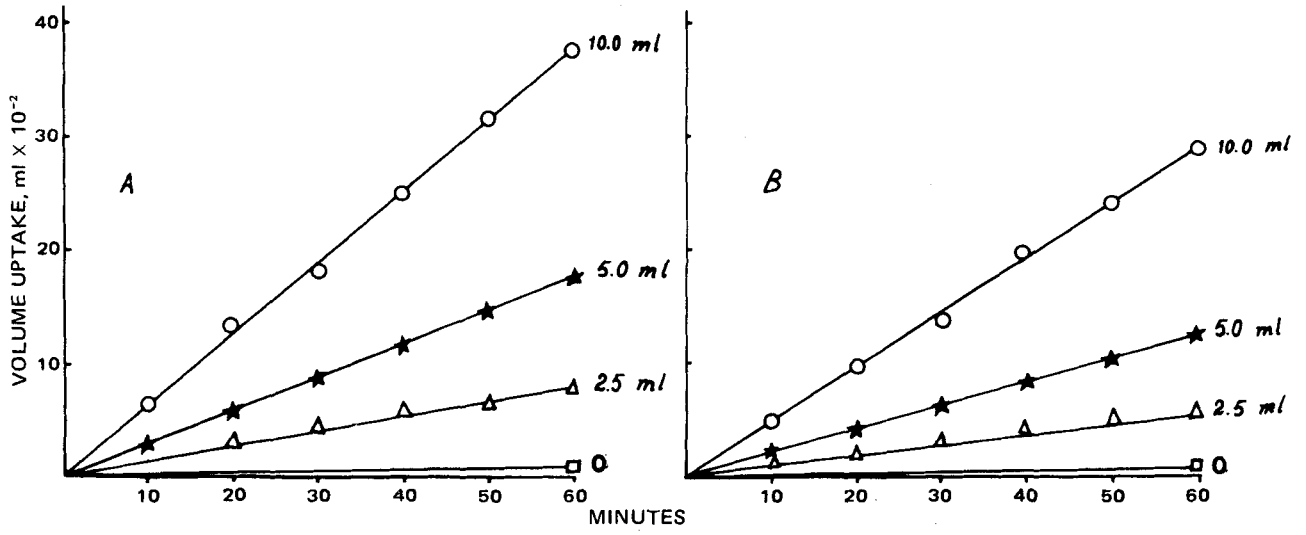


**Figure 6**—*Uptake of dissolution fluid by untreated and treated tolbutamide disks. Key: A, treated with methylcellulose; and B, treated with hydroxypropyl methylcellulose. The volumes shown were used for each 20 g of drug.*

**Disk Preparation**—The powders were compressed with a tablet machine[5] to produce disks of 200 mg, having a hardness of ~4 kg on a tablet hardness tester[5].

**Liquid Penetration**—The unidimensional penetration of the medium used for dissolution of II through disks of treated and untreated drug was carried out using the proposed apparatus (Fig. 1). The disk was fixed in position as shown. The medium used for dissolution was allowed to fill the whole capillary and just to touch the lower surface of the disk.

The movement of the liquid surface in the capillary was observed for 1 hr, and the change during each time interval was converted to volume in milliliters. The experiment was repeated with six disks of each batch. The average cumulative volume of liquid taken up by the disks was compared. The accuracy and reproducibility of the proposed technique were obtained by comparing the coefficient of variation for each batch tested.

**Hypoglycemic Activity**—The effect of orally administered acetohexamide and tolbutamide and their treated powders on the blood glucose concentration of adult male albino rats was studied. Male albino rats, 150–200 g, were fasted 24 hr before the experiment but were allowed free access to water. They were divided into six groups of 18 rats each. One group was given a suspension of II in water (1%) at a dose of 200 mg/kg. A second group was given an equal dose of II treated with a 5% solution of IV (2.5 ml/20 g). A third group was given the same dose of II treated with a solution of III (2.5 ml/20 g). The remaining three groups of rats were given treated and untreated forms of I in a similar schedule.

Each group was divided into six subgroups of three rats each. One group was sacrificed at each time interval (0.5, 1, 2, 3, 4, and 5 hr), and ~3 ml of the blood was collected from each animal. The blood samples were centrifuged at 3500 rpm for 20 min, and 0.5 ml of serum for each sample was analyzed for its glucose content[9] (11). Three animals were used as controls to determine the blood glucose level at time zero. The mean blood glucose levels of each subgroup were compared, and the differences were tested for significance using the Student *t* test.

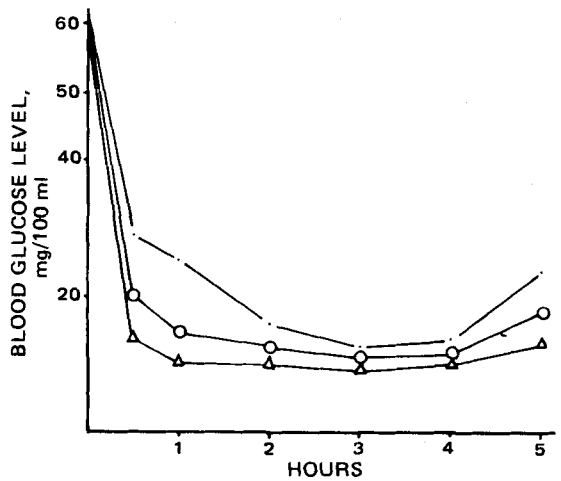


**Figure 7**—*Changes in blood glucose levels of rats after oral administration of untreated and treated tolbutamide. Key: ·, untreated; and ○ and △, treated with 5% hydroxypropyl methylcellulose and methylcellulose (2.5 ml/20 g), respectively.*

## RESULTS AND DISCUSSION

Figures 2–5 show the effect of treating the surfaces of I and II with III and IV on their dissolution from hard gelatin capsules. The treated powders exhibited faster dissolution than the nontreated drugs. Powders treated with III showed a smaller increase in dissolution than those treated with IV. The effect on the dissolution of the drugs tested increased with increasing amounts of IV from 2.5 to 5 ml/20 g. A further increase in the amount of the polymer solution to 10 ml/20 g produced a mild decrease in the dissolution. At 30 min, the average percent amounts of II dissolved were 29.8, 77.1, 99.8, and 95.5 from untreated powder and powders treated with 2.5, 5, and 10 ml of IV solution/20 g, respectively. Therefore, 5 ml of a 5% solution of IV/20 g of tolbutamide apparently is sufficient to achieve optimal hydrophilicity.

On the other hand, in the presence of III, the dissolution of II continued

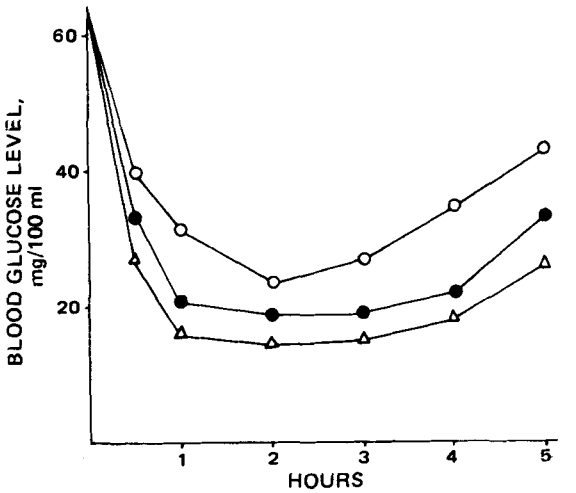


**Figure 8**—*Changes in blood glucose levels in rats after oral administration of untreated and treated acetohexamide. Key: ○, untreated; and ● and △, treated with 5% hydroxypropyl methylcellulose and methylcellulose (2.5 ml/20 g), respectively.*

[9] Automated analyzer, Boehringer, Mannheim, West Germany.

**Table I—Uptake of Dissolution Fluid by Tolbutamide Disks Prepared Using Treated Drug**

| Milliliters of Polymer Solution per 20 g of Tolbutamide | Disks Prepared from Powder Treated with *Methylcellulose* | | Disks Prepared from Powder Treated with *Hydroxypropyl* Methylcellulose | |
|---|---|---|---|---|
| | Volume Uptake, ml × $10^{-2}$ | *CV*, % | Volume Uptake, ml × $10^{-2}$ | *CV*, % |
| 2.5 | 7.5 | 1.25 | 5.5 | 1.32 |
| 5 | 17.4 | 1.12 | 12.6 | 1.22 |
| 10 | 42.5 | 1.23 | 26.8 | 1.31 |

to increase with increasing polymer concentrations within the range tested. At 30 min, the average percent amounts of II dissolved were 29.8, 72.3, 95.2, and 99.5 from untreated powder and powders treated with 2.5, 5, and 10 ml of a solution of III/20 g, respectively. The same findings were obtained with I. At 30 min, the average percent amounts of I dissolved were 22.5, 51.5, 76.3, and 96.1 from untreated powder and powders treated with 2.5, 5, and 10 ml of a solution of IV/20 g, respectively. The corresponding average percent dissolved values observed with powders treated with 2.5, 5, and 10 ml of a solution of III were 42.3, 70.2, and 95.3, respectively.

Increased dissolution of I and II by III and IV was attributed to the increased hydrophilicity of the drug particles, in accordance with the observation of Lerk *et al.* (7). However, the increase in the dissolution of I and II produced by treatment with IV seemed to decrease slightly after a certain point. This result was not observed with III in the concentration range studied and might be due to possible thermal gelation of IV at temperatures near 37° during dissolution (12).

Figure 6 shows the uptake of dissolution fluid by treated and untreated tolbutamide. Table I lists the mean cumulative volumes of fluid taken up by the untreated disks along with the coefficient of variation. The mean coefficient of variation was 1.24 ± 0.0725 (*SD*), which indicates the excellent reproducibility and accuracy of the method. It is obvious that the extent of fluid uptake by the treated powders was greater than that of the untreated powder. Also, the fluid uptake by disks of II was increased proportionally by increasing the amount of polymer used. Disks treated with IV showed a higher fluid uptake than did those treated with III. The average cumulative volumes of fluid taken up by disks of II and those prepared from powders treated with 2.5, 5, and 10 ml of a solution of IV/20 g were $0.9 \times 10^{-2}$, $9.1 \times 10^{-2}$, $17.5 \times 10^{-2}$, and $37.5 \times 10^{-2}$ ml after 60 min. The corresponding average values obtained from disks treated with 2.5, 5, and 10 ml of a solution of III/20 g were $6.5 \times 10^{-2}$, $14.2 \times 10^{-2}$, and $29.9 \times 10^{-2}$ ml. Therefore, it seems that the effects produced by III and IV on the dissolution of I and II clearly are correlated to the hydrophilic nature of the polymer, as measured by their water-absorbing ability.

The mean blood glucose concentration of 24-hr fasted rats was 62.53 mg/ml, and this amount was significantly higher than that of all of the treated groups ($p < 0.02$). Figure 7 shows the effect of I, untreated and treated with a 5% solution of III or IV (2.5 ml/20 g), on the blood glucose concentration of rats. The blood glucose concentration (milligrams per 100 ml) observed at 2 hr in rats given II treated with III was 64.2 compared to 88.3% in rats given the untreated drug. The blood glucose concentration observed at the same time in animals given II treated with IV was 74.5% compared to 52.3% in rats given the untreated drug. The reduction in the blood glucose level was greater with the treated drug than with the untreated drug and seemed more pronounced when the drug was treated with IV.

The difference between the average blood glucose concentration obtained from rats given I treated with III or IV and that obtained from rats given untreated drug was significant ($p < 0.05$) at all time intervals. Insignificant differences were calculated between the blood glucose concentrations for animals given II treated with III or IV, except at 1 and 2 hr, where a significant difference ($p < 0.05$) was observed. Figure 8 shows the effect of treated and untreated powders of I on the blood glucose concentration of rats. The mean blood glucose concentration observed at 2 hr in rats given I treated with III and IV was 82.5%; it was only 62.3% for animals given the untreated drug. Again, the differences were significant ($p < 0.05$) at all time intervals. The data show that I treated with IV exhibited a higher hypoglycemic effect than that treated with III. No significant differences were observed between values of the blood glucose concentration for rats treated with III or IV, except after 1 and 2 hr, where significant differences ($p < 0.05$) were calculated.

The increase in the dissolution of I and II after treatment with III and IV was reflected by increased drug absorption, as indicated by the greater reduction in glucose levels. Moreover, IV, which achieved higher hydrophilicity, induced better drug absorption.

Increasing hydrophilicity of the drugs by methylcellulose or hydroxypropyl methylcellulose seems better than coprecipitation with povidone or solid dispersion in polyethylene glycols. In the latter two techniques, the quantity of the polymer required to enhance the dissolution and bioavailability of tolbutamide was too high (about equal to the dose). By increasing the hydrophilicity, only a minute quantity of the polymer is required to enhance the dissolution and bioavailability of drugs.

The method of increasing the dissolution characteristics of poorly soluble drugs by increasing the hydrophilicity using a highly hydrophilic polymer may be widely applicable to other drugs.

## REFERENCES


(1) G. Levy, *Can. Med. Assoc. J.*, **88**, 98 (1963).

(2) J. G. Wagner, *Can. J. Pharm. Sci.*, **1**, 55 (1966).

(3) K. Uekama, N. Matsuo, F. Hirayama, T. Yamaguechi, Y. Imaura, and H. Ichibagase, *Chem. Pharm. Bull.*, **27**, 398 (1979).

(4) S. A. Said, H. M. El-Fatatry, and A. S. Genedi, *Austr. J. Pharm. Sci.*, **N53**, 42 (1974).

(5) H. Sekikawa, T. Naganuma, J. Fujiwara, M. Nakano, and T. Arita, *Chem. Pharm. Bull.*, **27**, 31 (1979).

(6) S. A. Said and S. F. Saad, *Austr. J. Pharm. Sci.*, **NS 4**, 4 (1945).

(7) C. F. Lerk, M. Lagas, J. T. Fellan, and P. Nauta, *J. Pharm. Sci.*, **67**, 935 (1978).

(8) C. G. Lerk, M. Lagas, L. Lie-Huen, P. Broersma, and K. Zuurman, *ibid.*, **68**, 634 (1979).

(9) J. T. Fell, R. T. Calvert, and P. Riley-Bentham, *J. Pharm. Pharmacol.*, **30**, 479 (1978).

(10) "The United States Pharmacopeia," 19th rev., Mack Publishing Co., Easton, Pa., 1975.

(11) P. Trinder, *Ann. Clin. Biochem.*, **6**, 24 (1969).

(12) J. B. Schwartz and T. P. Alvino, *J. Pharm. Sci.*, **65**, 572 (1976).


## ACKNOWLEDGMENTS


The authors thank Dr. A. H. Hikal for reviewing the manuscript, Mr. M. Hikal and Mr. Y. Hendi for technical assistance, and Mr. K. Abbas for typing the manuscript.

# Effects of Salicylate on Rectal Absorption of Theophylline

**TOSHIAKI NISHIHATA, J. HOWARD RYTTING ˣ, and TAKERU HIGUCHI**

Received May 30, 1980, from the *Pharmaceutical Chemistry Department, University of Kansas, Lawrence, KS 66045.* Accepted for publication July 17, 1980

**Abstract** □ The rectal absorption of theophylline in rats was facilitated by concurrent administration of salicylic acid or sodium salicylate. The absorption of theophylline depended on the simultaneous absorption of salicylate and increased with an increasing concentration of salicylate. Calcium and magnesium ions inhibited the effects of salicylate at pH 7.4 but not at pH 4.5. Sodium lauryl sulfate caused lasting changes in rectal absorption, whereas the effects of salicylate on absorption were observed only when salicylate was present. Strong chelating agents, such as ethylenediaminetetraacetic acid and sodium citrate did not affect the absorption of theophylline, except at very high concentrations (30%), where membrane damage was observed. Rectal drug absorption was not enhanced by vasodilation or inflammation alone since sodium nicotinate and histamine did not facilitate the disappearance of theophylline from the perfusate.

**Keyphrases** □ Theophylline—rectal absorption, effect of salicylate □ Absorption, rectal—theophylline, effects of salicylate □ Salicylate—effect on rectal absorption of theophylline

Although rectal administration of drugs is not particularly popular in the United States (~1% of all medications dispensed), it can overcome some problems associated with oral and parenteral administration. Such problems include drug inactivation in the upper GI tract or by the liver, medication of infants and debilitated patients, vomiting, and nausea. The factors that control the rate of absorption from the rectum are not fully understood. Rectal delivery also is hampered by poor and inconsistent absorption of many drugs.

Some antibiotics and polypeptides that generally are not well absorbed from the rectum have been formulated as suppositories or rectal capsules, using various surfactants as adjuvants, to enhance rectal absorption (1). However, many surfactants appear to damage the rectal membrane, which may limit their use. The present report describes studies of salicylate as an adjuvant to enhance the rectal absorption of theophylline. A preliminary report of this study was published recently (2).

## EXPERIMENTAL

**Animals**—Sprague–Dawley male rats, 275–300 g, were fasted for 16 hr prior to the experiments. During the experiment, the rats were kept on a 38° surface and were anesthetized with pentobarbital (60 mg/kg).

***In Situ* Perfusion of Rat Rectum**—These experiments were carried out by a method similar to that reported by Crommelin *et al.* (3). The rectum was exposed by an abdominal incision, and a glass cannula was inserted in the distal direction and tied firmly to keep it in position. A second cannula was inserted through the anus 1 cm inside the rectum and secured by ligation. Thus, ~2 cm of the rectum was exposed to the perfusate. The perfusate (6 ml) was circulated at a rate of 2 ml/min at 38°. Phosphate buffer (0.067 *M*) was used as the perfusate, which was adjusted, with sodium chloride to maintain an ionic strength of 0.75.

***In Vivo* Absorption Studies**—The rectum was exposed by an abdominal incision, a 0.3-ml sample of the drug solution was injected into a 2-cm section of the rectum, and the drug solution was maintained in that section by ligating the rectum with thread. After rectal administration, blood samples were collected as a function of time from a leg vein using a cannula.

In another experiment, 0.3 ml of the drug solution was injected into the rectum using a cannula, after which the anus was tied firmly to prevent leakage. After rectal administration, blood samples again were taken from a leg vein.

**Table I—Conditions for HPLC Assay [a] of Drug in the Blood and in the Perfusate**

| Compound | Mobile Phase | Flow Rate, ml/min | UV Detector Wavelength, nm |
|---|---|---|---|
| Salicylate | 0.1 *M* acetate buffer (pH 4.5)–methanol (30:70) | 1.0 | 280 |
| Theophylline | Water–propanol (95:5) | 1.5 | 280 |
| Nicotinic acid | 0.1 *M* acetate buffer (pH 4.5) | 1.0 | 284 |
| Histamine | 0.1 *M* phosphate buffer (pH 8.0)–methanol (60:40) | 1.0 | 254 |

[a] A 25-cm reversed-phase column was used.

**Assay Methods**—Theophylline, salicylate, nicotinate, and histamine were assayed by high-pressure liquid chromatography (HPLC) under the conditions shown in Table I.

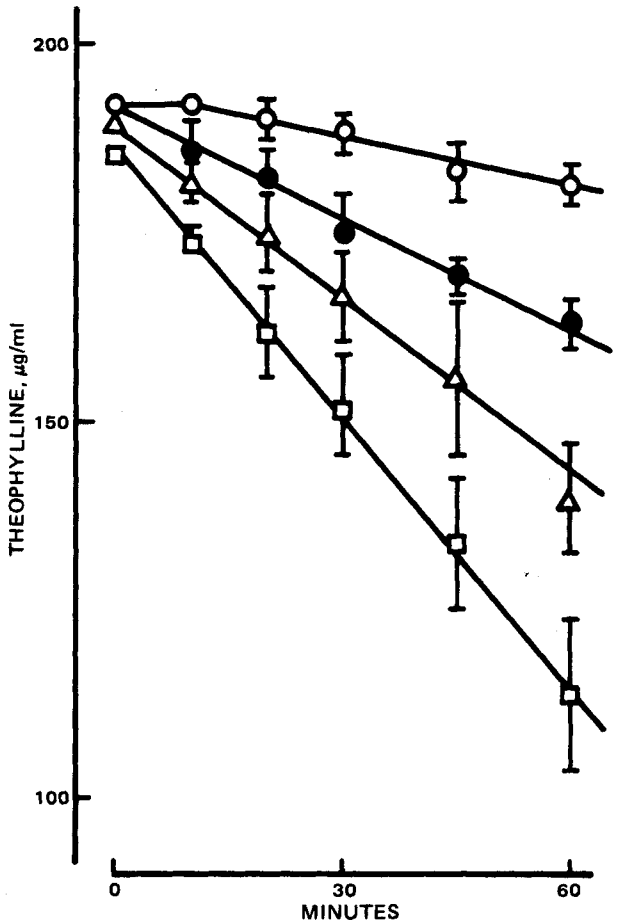


**Figure 1**—*Disappearance of theophylline from the perfusate at pH 7.4. Initial salicylate concentrations were 0 (○), 0.1 (●), 0.5 (△), and 1.0 (□)%.*

0022-3549/81/0100-0071$01.00/0
© 1981, American Pharmaceutical Association

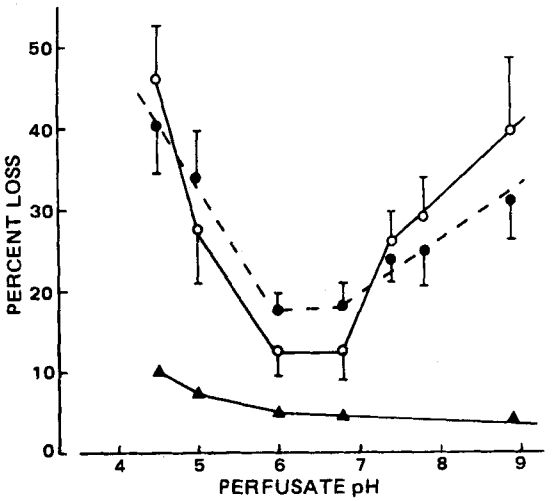


**Figure 2**—*Percent loss of salicylate or its acidic form (●) and theophylline (○ and ▲) after 1 hr from the perfusate. Initial concentrations were 0.5% sodium salicylate (●), 0.5% sodium salicylate and 200 μg of theophylline/ml (○), and 200 μg of theophylline/ml (▲). (Reproduced, with permission, from Ref. 2.)*

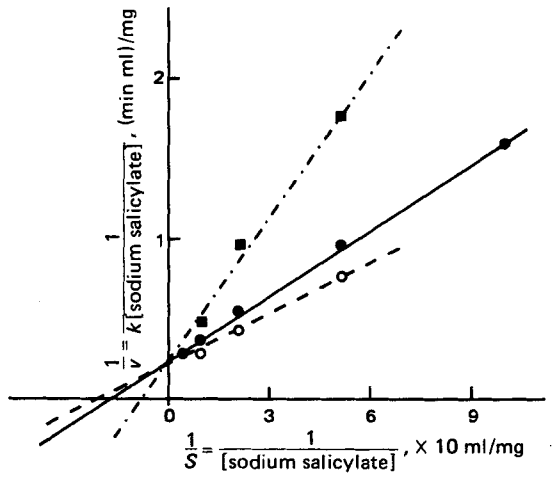


**Figure 3**—*Lineweaver–Burk plots for the disappearance of sodium salicylate at pH 6.8 (■), 7.4 (●), and 8.9 (○).*

The drug and adjuvants in blood were extracted with ether at a pH of <2.0 after deproteinization with 3.0% trichloroacetic acid. Following centrifugation, the ether layer was evaporated and the sediment was dissolved in methanol. This methanolic sample containing the drug was assayed by HPLC. The perfusate samples were assayed directly by HPLC.

The assay of ethylenediaminetetraacetic acid (I) and citrate was carried out using the turbidimetric titration method of Ogino and Hayashi (4). Ten milliliters of the sample containing I or citrate was mixed with 10 ml of 0.1% sodium lauryl sulfate. The resulting solution was maintained at 37° with mild stirring by a magnetic stirrer and was titrated with a solution of calcium chloride (equivalent to 0.1% $CaCO_3$) until precipitation of calcium lauryl sulfate was observed. A 0.02 *M* ammonium chloride–ammonium hydroxide buffer solution (pH 10.0) was used as the diluent.

## RESULTS AND DISCUSSION

**Effects of Perfusate pH and Salicylate on Disappearance of**

**Table II—Rate Constants ($k \times 10^3$, $min^{-1}$) for the Disappearance of Sodium Salicylate from the Rat Rectum as a Function of pH and Initial Salicylate Concentration [a]**

| Perfusate pH | Initial Concentration of Sodium Salicylate in Perfusate | | | | |
|---|---|---|---|---|---|
| | 0.1% | 0.2% | 0.5% | 1.0% | 2.0% |
| 4.5 | — | 8.2 ± 1.85 | 8.0 ± 1.81 | 7.6 ± 1.58 | — |
| 5.0 | — | 6.0 ± 1.05 | 6.2 ± 1.49 | 5.9 ± 1.23 | — |
| 6.0 | — | 2.6 ± 0.25 | 2.1 ± 0.19 | 2.3 ± 0.32 | — |
| 6.8 | — | 2.8 ± 0.45 | 2.0 ± 0.32 | 1.7 ± 0.23 | — |
| 7.4 | 7.1 ± 0.56 | 5.5 ± 0.48 | 3.8 ± 0.26 | 3.1 ± 0.14 | 1.9 ± 0.24 |
| 7.8 | — | 5.2 ± 0.64 | 4.1 ± 0.32 | 3.2 ± 0.30 | — |
| 8.9 | — | 6.9 ± 0.92 | 4.5 ± 0.13 | 3.9 ± 0.05 | — |

[a] Uncertainties are expressed as the standard deviation among runs (usually five or six animals).

**Table III—Effects of Magnesium and Calcium Ions on the Disappearance Rate Constants ($k \times 10^3$, $min^{-1}$) of Sodium Salicylate from the Perfusate through the Rat Rectum**

| Additive Concentration, % | Initial Concentration of Sodium Salicylate in Perfusate | | | |
|---|---|---|---|---|
| | 0.1% | 0.2% | 0.5% | 1.0% |
| Perfusate at pH 7.4 | | | | |
| None | 7.1 ± 0.6 | 5.5 ± 0.5 | 3.8 ± 0.3 | 3.1 ± 0.1 |
| Magnesium chloride 0.5 | 4.0 ± 0.2 | 3.2 ± 0.2 | 2.6 ± 0.6 | 2.4 ± 0.2 |
| Magnesium chloride 1.0 | 3.4 ± 0.3 | 2.9 ± 0.2 | 2.5 ± 0.1 | — |
| Calcium chloride 0.5 | 4.7 ± 1.0 | 3.9 ± 0.1 | 3.1 ± 0.2 | 2.5 ± 0.1 |
| Perfusate at pH 5.0 | | | | |
| None | — | 6.0 ± 1.1 | 6.2 ± 1.5 | 5.9 ± 1.2 |
| Magnesium chloride 0.5 | — | 5.8 ± 0.8 | 6.0 ± 0.9 | 5.6 ± 0.8 |
| Calcium chloride 0.5 | — | 6.1 ± 0.6 | 5.6 ± 1.0 | 5.5 ± 1.2 |

**Table IV—Effect of Magnesium and Calcium Ions on the Disappearance (Percent Lost) of Theophylline [a] after 1 hr in the Presence of Varying Amounts of Sodium Salicylate**

| Additive Concentration, % | Initial Concentration of Sodium Salicylate in Perfusate | | | | | |
|---|---|---|---|---|---|---|
| | 0% | 0.1% | 0.2% | 0.5% | 1.0% | 2.0% |
| None | 4.7 ± 0.2 | 18.3 ± 2.1 | 26.7 ± 1.9 | 29.2 ± 2.0 | 27.7 ± 4.4 | 48.1 ± 5.7 |
| Magnesium chloride 0.5 | — | 9.5 ± 0.3 | 14.9 ± 0.4 | 19.3 ± 1.1 | 24.4 ± 1.3 | — |
| Magnesium chloride 1.0 | — | 9.2 ± 0.3 | 12.2 ± 0.7 | 16.2 ± 0.7 | — | — |
| Calcium chloride 0.5 | — | 8.5 ± 0.4 | 16.9 ± 0.8 | 22.7 ± 1.3 | 29.6 ± 2.2 | — |

[a] The initial theophylline concentration was 200 μg/ml at pH 7.4.

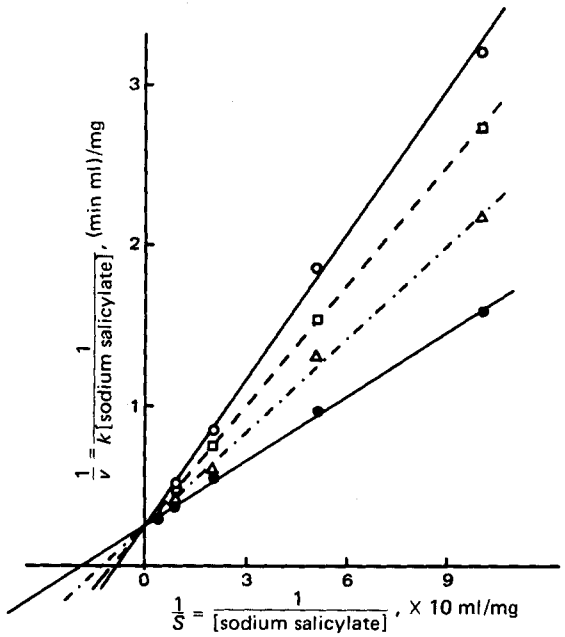


**Figure 4**—*Effects of calcium and magnesium ions on the Lineweaver–Burk plots for the disappearance of sodium salicylate at pH 7.4. The concentrations were 1.0% $MgCl_2$ (○), 0.5% $MgCl_2$ (□), and 0.5% $CaCl_2$ (△); the control also is shown (●).*

**Theophylline**—The disappearance of theophylline from the perfusate in the rat rectum in the absence of adjuvants was very slow, and the total loss of theophylline was <10% 60 min after the perfusion was begun at pH 4.5–8.9. However, a significant loss of theophylline was observed in the presence of salicylate. Figure 1 shows the disappearance of theophylline from the perfusate as a function of the salicylate concentration and time at pH 7.4. The higher the initial concentration of salicylate in the perfusate, the faster theophylline disappeared from the perfusate.

The effect of salicylate on the percent loss of theophylline from the perfusate was greater at pH values above 7.4 and below 5.0 (Fig. 2). The high loss of theophylline was accompanied by a high loss of salicylate. This result suggests that the disappearance of theophylline depends on the simultaneous disappearance of salicylate from the perfusate.

**Table V—Absolute Bioavailability of Theophylline ($F_{ab}$) as a Function of the Salicylate Concentration with and without Ligation**

| Salicylate Dose, mg/kg | Percent Bioavailability | |
|---|---|---|
| | With Ligation | Without Ligation |
| 0 | 18.2 ± 4.3 ($n$ = 6) | 35.6 ± 6.3 ($n$ = 4) |
| 1.0 | 42.2 ± 9.8 ($n$ = 6) | 37.1 ± 5.8 ($n$ = 4) |
| 2.5 | 59.3 ± 10.7 ($n$ = 6) | 60.7 ± 8.2 ($n$ = 3) |
| 3.75 | 56.8 ± 6.7 ($n$ = 6) | 74.6 ± 9.8 ($n$ = 5) |
| 7.5 | 98.6 ± 4.8 ($n$ = 8) | 96.2 ± 6.6 ($n$ = 5) |
| 15 | 97.5 ± 9.2 ($n$ = 8) | 100.3 ± 5.8 ($n$ = 5) |

**Disappearance of Salicylate from Perfusate**—The disappearance of salicylate from the perfusate appears to be a first-order process. However, in the basic pH region, the first-order disappearance followed an initial lag time. As shown in Table II, in the acidic region, the rate constant for the disappearance of salicylic acid did not depend on the initial concentration. However, in the basic region, the disappearance rate constant did depend on the initial concentration of salicylate.

In the acidic region, the disappearance of salicylic acid from the perfusate in the rectum may depend on the lipophilicity of salicylic acid, resulting in rapid distribution of salicylic acid to the rectal membrane. However, in the basic region, where the rate constant depended on the initial concentration, some type of saturable phenomenon may be involved.

Lineweaver–Burk plots obtained from the data in Table II for the basic region are shown in Fig. 3. Under these conditions, the $V_{max}$ value did

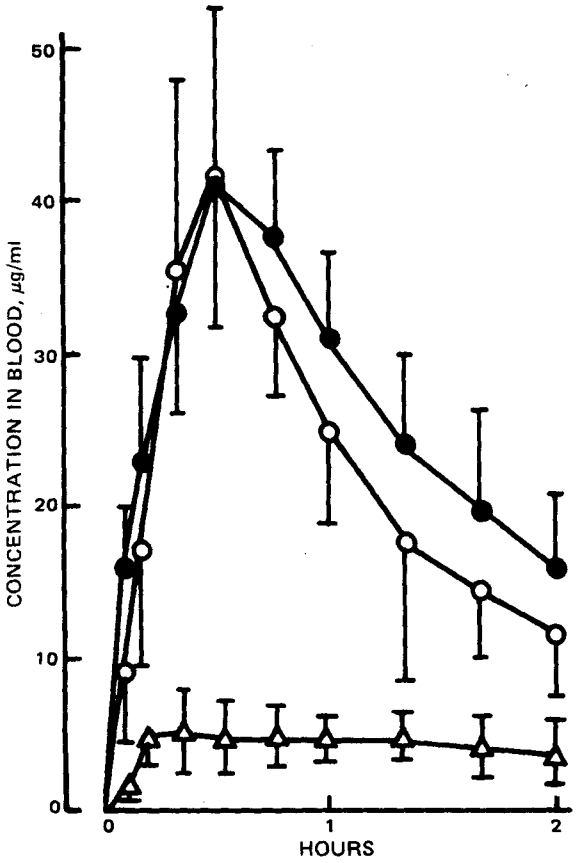


**Figure 5**—*Blood levels of theophylline (○ and △) and salicylate (●), in micrograms per milliliter, following the administration of 0.3 ml of a pH 8.0 buffer solution containing 15 mg of theophylline/kg (△) or 15 mg of theophylline and 15 mg of salicylate/kg (○ and ●) to a ligated 2-cm section of the rectum.*

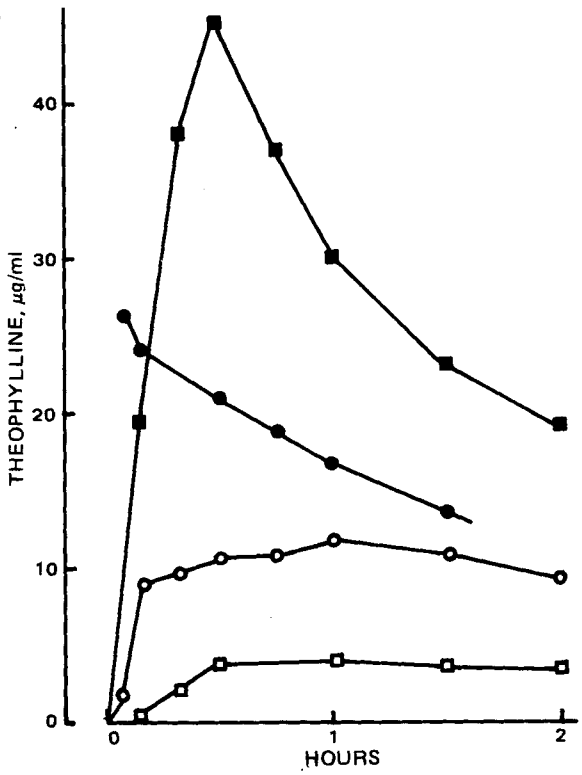


**Figure 6**—*Concentration of theophylline, in micrograms per milliliter, in blood following intravenous administration of 6 mg of theophylline/kg (●), rectal administration of 0.3 ml of a solution containing 15 mg of theophylline/kg with ligation (□) and without ligation (○), and rectal administration of 15 mg of theophylline and 15 mg of salicylate/kg without ligation (■).*

Table VI—Effect of Sodium Lauryl Sulfate on the Disappearance of Theophylline from the Rat Rectum after 1 hr as a Function of pH

| Sodium Lauryl Sulfate Concentration, % | Percent of Theophylline Lost | | | |
|---|---|---|---|---|
| | pH 4.5 | pH 6.0 | pH 7.4 | pH 8.9 |
| 0 | 9.8 ± 0.4 | 5.2 ± 0.3 | 4.7 ± 0.2 | 4.0 ± 0.1 |
| 0.5 | 10.9 ± 3.6 | 9.5 ± 1.3 | 14.2 ± 3.8 | 20.8 ± 4.4 |
| 2.0 | 12.8 ± 2.4 | 13.1 ± 1.5 | 24.7 ± 3.7 | 35.1 ± 3.4 |

not change but the $K_m$ value depended on the pH of the perfusate. This finding suggests that the disappearance of the ionic form of salicylate depends on the affinity of salicylate for some feature of the rectal membrane. At every pH value of the perfusate, the disappearance rate constant of salicylate was not affected by the presence of theophylline. This result indicates that the formation of a complex between salicylate and theophylline is not the primary factor facilitating the transport of theophylline in the presence of salicylate.

**Effect of Calcium and Magnesium Ions on Disappearance of Salicylate and Theophylline**—Since salicylate interacts with calcium and magnesium ions, the effect of these cations on the disappearance rate constant of salicylate from the perfusate through the rat rectum was studied. Addition of calcium or magnesium ions to the perfusate at pH 7.4 led to a decrease in the rate constant for salicylate disappearance (Table *III*). However, at pH 5.0, addition of calcium or magnesium ions did not affect the disappearance rate constant of salicylic acid.

This result probably means that the disappearance of salicylate in the perfusate at pH 5.0 primarily involves the nonionic form and that the disappearance process is different for the ionic and nonionic forms.

Based on the Lineweaver–Burk plots of the effect of calcium or magnesium ions at pH 7.4, these ions did not affect $V_{max}$ but led to an increase in $K_m$ (Fig. 4). This result suggests that calcium and magnesium ions competitively inhibit the binding of salicylate to some feature in the membrane. On the other hand, calcium and magnesium ions did not affect penetration of the nonionic form through the rectal membrane.

Calcium and magnesium ions did not affect the disappearance of theophylline in the absence of salicylate. At pH 7.4, the effect of salicylate on the disappearance of theophylline from the perfusate was suppressed by the presence of calcium or magnesium ions in the perfusate (Table IV). However, at pH 4.5, the effect of salicylate was not affected by calcium or magnesium ions. This observation indicates that the disappearance of theophylline probably is controlled by the disappearance of salicylate. A possible explanation is that the action of salicylate as an effective adjuvant depends on the presence of salicylate in the rectal membrane.

**Appearance of Theophylline in Rat Blood after Rectal Administration**—The absorption of theophylline into the general circulation after rectal administration to rats was studied by measuring the blood levels of theophylline as a function of time.

After the administration of 0.3 ml of pH 8.0 buffer containing 15 mg of salicylate and theophylline/kg into a 2-cm section of the rectum, the blood levels of theophylline and salicylate increased rapidly and reached maximum levels at 30 min (Fig. 5). The absorption of theophylline and salicylate occurred simultaneously.

The absolute bioavailability, $F_{ab}$, after rectal administration was calculated using the $[AUC]_0^\infty$ values corrected for intraindividual variation in the elimination rate as follows:

$$F_{ab} = \frac{[AUC]^{\infty}_{0,\text{rectal}} k_{e,\text{rectal}}\ \text{dose}_{iv}}{[AUC]^{\infty}_{0,iv} k_{e,iv}\ \text{dose}_{\text{rectal}}} \qquad \text{(Eq. 1)}$$

where $k_{e,\text{rectal}}$ and $k_{e,iv}$ are the elimination rate constants after rectal administration and intravenous injection, respectively. The elimination rate constants were determined by a linear regression analysis of the log concentration *versus* time data.

Absolute bioavailability of theophylline after rectal administration is shown in Table V and Figs. 5 and 6. Absolute bioavailability and blood levels of theophylline in solution without salicylate after rectal administration were ~20% with ligation and ~35% without ligation. Bioavailability and blood levels of theophylline without ligation were higher than with ligation. This result suggests that the effective area of the rectum available for drug absorption without ligation was larger than with ligation.

For drug solutions containing >7.5 mg of salicylate/kg, absolute bioavailabilities were 100% under both conditions. However, the bioavailability of theophylline after administration of drug solutions containing 3.75 mg of salicylate/kg was 55% with ligation and 75% without ligation. Bioavailability after giving drug solutions containing 1.0 mg of salicylate/kg was not significantly different with or without ligation of the rectum, in spite of the increase in bioavailability found in the absence of salicylate without ligation. This result may indicate that the effect of salicylate in promoting drug absorption through the rectum depends on the amount of salicylate in a limited area of the rectum.

**Comparison of a Surfactant and Salicylate**—To examine further the mechanism of rectal absorption, the relative effects of a surfactant and salicylate were studied using sodium lauryl sulfate as a surfactant. The disappearance of theophylline from the perfusate was facilitated by the presence of sodium lauryl sulfate in the perfusate (Table VI). However, as shown in Fig. 7, the presence of sodium lauryl sulfate resulted in a lasting effect, whereas the promotive effect of salicylate did not reflect a permanent change in the rectal membrane. The effect of salicylate was eliminated by washing the rectum with buffer for 5 min after pretreatment with salicylate whereas the effect of pretreatment with sodium lauryl sulfate was not eliminated by washing. This result probably indicates that the action of salicylate does not involve a lasting change in the membrane, whereas lauryl sulfate appears to damage the membrane.

**Comparison of Strong Chelating Agents with Salicylate**—Salicylate is known to interact with calcium and magnesium ions. Therefore, the action of salicylate was compared with that of ethylenediaminetetraacetic acid (I) and sodium citrate. As shown in Table VII, a 15% concentration of I or citrate did not affect the disappearance of theophylline from the perfusate. However, with very high concentrations (30%) of I or citrate in the perfusate, disappearance of theophylline from the perfusate was facilitated, but, contrary to the situation with salicylate, the perfusate developed a red color. Apparently, I and citrate produced

Table VII—Disappearance of Theophylline (Percent Lost) in the Presence of Citrate and Ethylenediaminetetraacetic Acid after 1 hr of Perfusion

| Chelating Agent | pH 7.4 | pH 8.0 |
|---|---|---|
| Citrate, 15% | 8.1 ± 0.8 | 9.7 ± 1.2 |
| Citrate, 30% | 20.3 ± 5.2 | 23.2 ± 4.6 |
| EDTA[a], 15% | 10.4 ± 3.8 | 8.5 ± 4.3 |
| EDTA, 30% | 24.8 ± 2.8 | 28.7 ± 4.6 |

[a] Ethylenediaminetetraacetic acid.

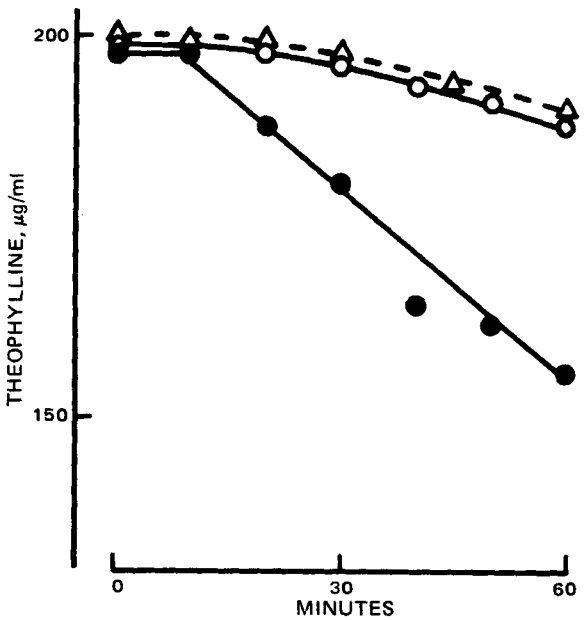


**Figure 7**—*Concentration of theophylline, in micrograms per milliliter, found in the perfusate after pretreatment of the rectum with salicylate (○) or with sodium lauryl sulfate (●). The control (△) involved no pretreatment.*

Table VIII—Effects of Nicotinic Acid and Histamine on the Disappearance of Theophylline from the Rat Rectum after 1 hr of Perfusion

| Substance | Percent Lost | | | | |
|---|---|---|---|---|---|
| | pH 4.5 | pH 6.0 | pH 6.8 | pH 7.4 | pH 8.9 |
| Theophylline only | 7.8 ± 1.5 | 5.2 ± 0.3 | — | 4.7 ± 0.2 | 4.0 ± 0.2 |
| Nicotinic acid only | 49.4 ± 1.3 | — | 4.6 ± 0.4 | 8.2 ± 3.2 | 5.5 ± 0.7 |
| Theophylline in presence of 1% nicotinic acid | 9.8 ± 2.8 | — | 5.9 ± 3.7 | 5.1 ± 0.9 | 6.1 ± 5.5 |
| Theophylline in presence of 1% histamine | 9.1 ± 4.7 | 9.1 ± 3.9 | — | 10.2 ± 3.7 | 12.2 ± 5.6 |

bleeding from the rectum, probably as a result of damage to the rectal membrane, and, thus, promoted the disappearance of theophylline from the perfusate.

Citrate and I do not appear to be absorbed from the rectum since the remaining chelating activity in the perfusate, measured according to the method of Ogino and Hayashi (4), was significant. This finding suggests that compounds that are not absorbed well themselves are not suitable adjuvants for rectal drug absorption.

**Comparison of Sodium Nicotinate and Histamine with Salicylate**—Another possible mechanism involves the effect of vasodilation and inflammation on the disappearance of theophylline from the perfusate. In this regard, the effects of nicotinate and histamine on the disappearance of theophylline were studied.

Neither histamine nor nicotinic acid significantly facilitated the disappearance of theophylline (Table VIII). At pH 4.5, the disappearance of theophylline from the perfusate was not facilitated by nicotinic acid, although nicotinate was lost from the perfusate. The action of salicylate as an adjuvant probably does not depend on vasodilation or an inflammatory action.

Mechanistically, the enhancement of rectal absorption of theophylline by salicylate still is unclear. The nonionic and ionic forms of salicylate apparently have different paths through the membrane. It is possible that salicylate reduces the lipophilicity or increases the permeability of the membrane, perhaps by interacting with some substance in the membrane, *e.g.*, calcium or magnesium ions, which may be present as structural features, and thus concurrently allows theophylline to pass through the rectal membrane.

## REFERENCES


(1) Y. Nishioka and T. Kawamura, *Yakuzaigaku*, **37**, 88 (1977).

(2) T. Nishihata, J. H. Rytting, and T. Higuchi, *J. Pharm. Sci.*, **69**, 744 (1980).

(3) D. J. A. Crommelin, J. Modderkolk, and C. J. de Blaey, *Int. J. Pharm.*, **3**, 299 (1979).

(4) K. Ogino and N. Hayashi, *Yukagaku*, **32**, 88 (1977).


## ACKNOWLEDGMENTS


Supported in part by a grant from INTERx Research Corp., Lawrence, Kans., and R. P. Scherer, North America, Detroit, Mich.

The authors thank Dr. Thomas Patton for helpful comments.


# Time Course and Disposition of Methazolamide in Human Plasma and Red Blood Cells


**W. F. BAYNE ˣ, F. T. TAO, G. ROGERS, L. C. CHU, and F. THEEUWES**



Received July 24, 1979, from *Alza Corporation, Palo Alto, CA 94304.* Accepted for publication April 11, 1980.



**Abstract** □ Methazolamide was determined in plasma, whole blood, and urine by a GLC–mass spectrometric method. Temporal patterns of methazolamide concentrations in plasma and red blood cells were obtained following single- and multiple-dose oral administration of the drug. The nonlinearity in the binding of the drug to the red blood cell carbonic anhydrase was evident from a comparison of plasma and red blood cell concentrations. The drug was cleared slowly from the red blood cells. The binding constants to the two isoenzymes of carbonic anhydrase were determined from the plasma and red blood cell concentrations and were in agreement with those determined by previous measurements. The half-life of elimination was 7.5 hr. The urinary recovery of unchanged drug was ~25% of the administered dose.



**Keyphrases** □ Methazolamide—time course and disposition in human plasma and red blood cells □ GLC–mass spectrometry—analysis, methazolamide, human plasma and red blood cells □ Distribution—methazolamide, time course and disposition in human plasma and red blood cells


Methazolamide (5-acetylimino-4-methyl-$\Delta^2$-1,3,4-thiadiazoline-2-sulfonamide) is a carbonic anhydrase inhibitor used in the treatment of glaucoma. It is the methylated analog of the tautomer of acetazolamide. Both drugs reduce the transport of ions from the secretory cells of the ciliary body into the nascent aqueous humor and decrease aqueous secretion through a local osmotic effect (1). In particular, inhibition of the carbonic anhydrase in the secretory cells of dogs reduces the bicarbonate flux (2) and sodium-ion flux (3) into the posterior chamber of the eye.

The dynamics and distribution of drug following different patterns and routes of administration have been studied much more extensively for acetazolamide than for methazolamide. All work to date on the determination of methazolamide in biological fluids and tissues has employed the indirect enzymatic method developed by Maren and coworkers (4, 5). This method is based on two facts: (*a*) the rate of hydration of carbon dioxide catalyzed by carbonic anhydrase is reduced by an inhibitor present in a biological fluid; and (*b*) the rate of hydration or, equally, the rate of formation of carbonic acid or protons directly affects the time interval required to cause a given change in pH. Although methazolamide is metabolized significantly (only 25% is recovered as unchanged drug in the urine) in contrast to acetazolamide, which is not metabolized, the metabolites appear either to be very weak inhibitors of carbonic anhydrase or to lack inhibitory potential (6).

Plasma and red blood cell concentrations and the uri-


0022-3549/81/0100-0075$01.00/0


© 1981, American Pharmaceutical Association

Table VIII—Effects of Nicotinic Acid and Histamine on the Disappearance of Theophylline from the Rat Rectum after 1 hr of Perfusion

| Substance | Percent Lost | | | | |
|---|---|---|---|---|---|
| | pH 4.5 | pH 6.0 | pH 6.8 | pH 7.4 | pH 8.9 |
| Theophylline only | 7.8 ± 1.5 | 5.2 ± 0.3 | — | 4.7 ± 0.2 | 4.0 ± 0.2 |
| Nicotinic acid only | 49.4 ± 1.3 | — | 4.6 ± 0.4 | 8.2 ± 3.2 | 5.5 ± 0.7 |
| Theophylline in presence of 1% nicotinic acid | 9.8 ± 2.8 | — | 5.9 ± 3.7 | 5.1 ± 0.9 | 6.1 ± 5.5 |
| Theophylline in presence of 1% histamine | 9.1 ± 4.7 | 9.1 ± 3.9 | — | 10.2 ± 3.7 | 12.2 ± 5.6 |

bleeding from the rectum, probably as a result of damage to the rectal membrane, and, thus, promoted the disappearance of theophylline from the perfusate.

Citrate and I do not appear to be absorbed from the rectum since the remaining chelating activity in the perfusate, measured according to the method of Ogino and Hayashi (4), was significant. This finding suggests that compounds that are not absorbed well themselves are not suitable adjuvants for rectal drug absorption.

**Comparison of Sodium Nicotinate and Histamine with Salicylate**—Another possible mechanism involves the effect of vasodilation and inflammation on the disappearance of theophylline from the perfusate. In this regard, the effects of nicotinate and histamine on the disappearance of theophylline were studied.

Neither histamine nor nicotinic acid significantly facilitated the disappearance of theophylline (Table VIII). At pH 4.5, the disappearance of theophylline from the perfusate was not facilitated by nicotinic acid, although nicotinate was lost from the perfusate. The action of salicylate as an adjuvant probably does not depend on vasodilation or an inflammatory action.

Mechanistically, the enhancement of rectal absorption of theophylline by salicylate still is unclear. The nonionic and ionic forms of salicylate apparently have different paths through the membrane. It is possible that salicylate reduces the lipophilicity or increases the permeability of the membrane, perhaps by interacting with some substance in the membrane, *e.g.*, calcium or magnesium ions, which may be present as structural features, and thus concurrently allows theophylline to pass through the rectal membrane.

## REFERENCES


(1) Y. Nishioka and T. Kawamura, *Yakuzaigaku*, **37**, 88 (1977).

(2) T. Nishihata, J. H. Rytting, and T. Higuchi, *J. Pharm. Sci.*, **69**, 744 (1980).

(3) D. J. A. Crommelin, J. Modderkolk, and C. J. de Blaey, *Int. J. Pharm.*, **3**, 299 (1979).

(4) K. Ogino and N. Hayashi, *Yukagaku*, **32**, 88 (1977).


## ACKNOWLEDGMENTS


Supported in part by a grant from INTERx Research Corp., Lawrence, Kans., and R. P. Scherer, North America, Detroit, Mich.

The authors thank Dr. Thomas Patton for helpful comments.


# Time Course and Disposition of Methazolamide in Human Plasma and Red Blood Cells


**W. F. BAYNE ˣ, F. T. TAO, G. ROGERS, L. C. CHU, and F. THEEUWES**



Received July 24, 1979, from *Alza Corporation, Palo Alto, CA 94304.* Accepted for publication April 11, 1980.



**Abstract** □ Methazolamide was determined in plasma, whole blood, and urine by a GLC–mass spectrometric method. Temporal patterns of methazolamide concentrations in plasma and red blood cells were obtained following single- and multiple-dose oral administration of the drug. The nonlinearity in the binding of the drug to the red blood cell carbonic anhydrase was evident from a comparison of plasma and red blood cell concentrations. The drug was cleared slowly from the red blood cells. The binding constants to the two isoenzymes of carbonic anhydrase were determined from the plasma and red blood cell concentrations and were in agreement with those determined by previous measurements. The half-life of elimination was 7.5 hr. The urinary recovery of unchanged drug was ~25% of the administered dose.



**Keyphrases** □ Methazolamide—time course and disposition in human plasma and red blood cells □ GLC–mass spectrometry—analysis, methazolamide, human plasma and red blood cells □ Distribution—methazolamide, time course and disposition in human plasma and red blood cells


Methazolamide (5-acetylimino-4-methyl-$\Delta^2$-1,3,4-thiadiazoline-2-sulfonamide) is a carbonic anhydrase inhibitor used in the treatment of glaucoma. It is the methylated analog of the tautomer of acetazolamide. Both drugs reduce the transport of ions from the secretory cells of the ciliary body into the nascent aqueous humor and decrease aqueous secretion through a local osmotic effect (1). In particular, inhibition of the carbonic anhydrase in the secretory cells of dogs reduces the bicarbonate flux (2) and sodium-ion flux (3) into the posterior chamber of the eye.

The dynamics and distribution of drug following different patterns and routes of administration have been studied much more extensively for acetazolamide than for methazolamide. All work to date on the determination of methazolamide in biological fluids and tissues has employed the indirect enzymatic method developed by Maren and coworkers (4, 5). This method is based on two facts: (*a*) the rate of hydration of carbon dioxide catalyzed by carbonic anhydrase is reduced by an inhibitor present in a biological fluid; and (*b*) the rate of hydration or, equally, the rate of formation of carbonic acid or protons directly affects the time interval required to cause a given change in pH. Although methazolamide is metabolized significantly (only 25% is recovered as unchanged drug in the urine) in contrast to acetazolamide, which is not metabolized, the metabolites appear either to be very weak inhibitors of carbonic anhydrase or to lack inhibitory potential (6).

Plasma and red blood cell concentrations and the uri-


0022-3549/81/0100-0075$01.00/0


© 1981, American Pharmaceutical Association

nary output of methazolamide were determined as a function of time following oral administration of the drug using a specific GLC–mass spectrometric method. The method employed the propionyl analog of methazolamide as an internal standard, methylated derivatives for chromatography, and selective-ion monitoring for detection.

## EXPERIMENTAL

**Materials**—Ethyl acetate, methylene chloride, hexane, benzene, and toluene of high purity were used as received[1]. Methyl iodide[2] was diluted with methylene chloride to prepare a 1 *M* solution, which was used to alkylate methazolamide and the internal standard.

A 0.1 *M* solution of tetrahexylammonium hydrogen sulfate, prepared in this laboratory, was used to catalyze the alkylation reaction.

A saturated aqueous solution of silver sulfate[3] was used to remove tetrahexylammonium iodide, formed during the extractive alkylation, from the organic phase (7).

A 0.5 *M* ammonium acetate buffer (pH 4.5) was prepared by titration of acetic acid with ammonium hydroxide. A 1 *M* aqueous sodium phosphate[3] solution was used for the pH adjustment of the extracted biological fluid prior to extractive alkylation.

**Synthesis of 5-Propionylimino-4-methyl-$\Delta^2$-1,3,4-thiadiazoline 2-Sulfonamide**—The hydrochloride salt of 5-imino-4-methyl-$\Delta^2$-1,3,4-thiadiazoline-2-sulfonamide (I) was formed by the acid-catalyzed hydrolysis of methazolamide. Methazolamide (1 g) was dissolved in 20 ml of ethanol and 2 ml of concentrated hydrochloric acid, and the resulting solution was heated under reflux for 1.5 hr. After cooling, the solid was filtered off and dried, resulting in 800 mg of a crystalline white material. The NMR spectrum of this material was consistent with I and showed the absence of the acetylimino group present in methazolamide.

Propionic acid (1 ml), propionic anhydride (540 mg), and I (575 mg) were heated at 120° for 2.5 hr. After cooling, 15 ml of water was added to the solution, and the mixture was extracted three times with 20 ml of ethyl acetate. The organic extract was washed with brine (20 ml), dried over anhydrous sodium sulfate, and evaporated. The crude material was dried under vacuum and recrystallized from ethyl acetate–ether to give 143 mg of the desired compound, the propionyl analog of methazolamide. The compound melted at 175–177°.

**Apparatus**—A mass spectrometer[4] was interfaced with a gas chromatograph[5]. Chromatographic columns were prepared from empty glass columns (183 cm × 2 mm i.d.), silanized, and packed with 3% OV-17 on Chromosorb W (AW, DMCS, 100–120 mesh). The column and injector temperatures were 180 and 190°, respectively. The flow rate of the carrier gas (helium) was 25 ml/min.

The methylated derivatives of methazolamide and the internal standard were detected by selective-ion monitoring of the *m/z* 249 mass fragment, which is the base peak for the methylated derivative of both methazolamide and the internal standard. The ionizing voltage was 70 ev. The retention times for the methylated derivatives of methazolamide and the internal standard were 7 and 11 min, respectively.

**Analysis of Methazolamide in Plasma and Whole Blood**—A known quantity of the internal standard in methanol was added to a 1-ml aliquot of plasma or a 0.5-ml aliquot of whole blood in a 40-ml conical centrifuge tube. Distilled water (0.5 ml) was added to the whole blood to lyse the red blood cells. Two milliliters of 0.5 *M* ammonium acetate (pH 4.5) was added to the biological fluid. Each sample was extracted twice with 10 ml of ethyl acetate by shaking the tube horizontally for 10 min and then centrifuging it to separate the organic and aqueous phases.

The combined organic extracts were taken to dryness in a second 40-ml centrifuge tube under a nitrogen stream. One milliliter of 0.1 *N* $H_2SO_4$ was added to the residue, and the aqueous solution was washed twice with 10 ml of hexane. The aqueous solution then was adjusted to pH 10 with ~150 μl of 1 *M* sodium phosphate.

Extractive methylation of methazolamide and the internal standard was effected by adding 50 μl of 0.1 *M* tetrahexylammonium hydrogen sulfate and 2.5 ml of freshly prepared methyl iodide in methylene chloride. The centrifuge tube was sealed tightly with a polytef stopper, and the contents were agitated[6] at 40° for 30 min. After centrifugation, the organic layer containing the permethylated derivatives was transferred to a 15-ml centrifuge tube and taken to dryness under a nitrogen stream. The residue was dissolved in 6 ml of benzene, and the benzene solution was washed twice with 2.5 ml of a saturated aqueous solution of silver sulfate. The retained organic layer was taken to dryness under a nitrogen stream. The residue was dissolved in toluene (100 μl), and a few microliters of the solution was injected into the GLC–mass spectrometric system.

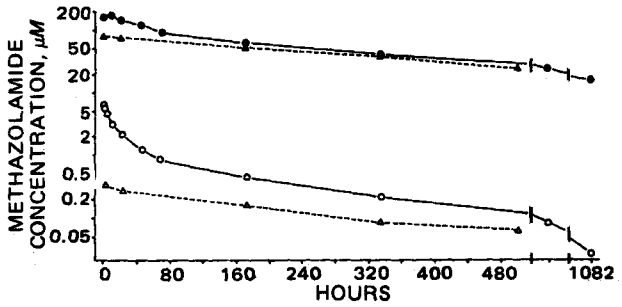


**Figure 1**—*Temporal patterns of plasma concentrations (open symbols) and red blood cell concentrations (solid symbols) for the subject administered a 50-mg tablet (△ and ▲) and for the subject administered a 150-mg solution of methazolamide (○ and ●).*

The amount of methazolamide in the biological sample was determined from the area ratio of the responses of the permethylated derivatives (methazolamide to the internal standard) and the calibration curve. The concentration of methazolamide in the red blood cells ($C_{RBC}$) was determined from:

$$C_{RBC} = \frac{C_{WB} - (1 - H)C_p}{H} \qquad \text{(Eq. 1)}$$

where $C_{WB}$ and $C_p$ are the measured concentrations of methazolamide in whole blood and plasma, respectively, and $H$ is the hematocrit.

**Analysis of Methazolamide in Urine**—Aliquots (1 ml) were analyzed using the method described for plasma and whole blood, except that the residue, when dissolved in 0.1 *N* $H_2SO_4$, was alkylated directly after adjustment to pH 10 with sodium phosphate and the hexane washes were omitted.

**Standard Curves**—A standard curve was prepared by spiking 1-ml aliquots of plasma with 0.5, 5, 50, 100, 500, 1000, and 5000 ng of methazolamide and a constant amount (250 ng) of the internal standard. The samples were prepared for GLC–mass spectrometric analysis as already described. The standard curve was obtained by plotting the area ratio of the responses of the *m/z* 249 fragments (methazolamide to the internal standard) *versus* the amount of methazolamide added. The internal standard, when derivatized, exhibited a small peak with the retention time of the methazolamide derivative. The peak area ratio of the minor peak to the major peak was 0.0025, and this ratio was used to correct the peak area ratio for the standards. Linear least-squares analysis of the data yielded a slope of $3.2 \times 10^{-3}$ and a correlation coefficient of 0.999.

Another standard curve, prepared using 0.5 ml of whole blood, had the same slope as that obtained with the spiked plasma samples.

Aliquots (1 ml) of urine were spiked with 0.1, 0.5, 1.0, 5.0, and 10 μg of methazolamide and a constant amount (1 μg) of the internal standard. The samples were prepared for analysis as already described. The slope of the standard curve using urine was 0.87, with a correlation coefficient of 0.999.

***In Vivo* Studies**—Three male subjects were administered methazolamide. Subjects 1, 2, and 3 weighed 88, 77.3, and 84 kg, respectively. Plasma and red blood cell concentrations and the cumulative urinary excretion of methazolamide were determined in single-dose studies after administration of a 50-mg methazolamide tablet to Subject 1 and after oral administration of 150 mg of methazolamide as a solution to Subject 2 and in a multiple-dose study after administration of 100-mg methazolamide tablets (three times daily) to Subject 3.

Blood from the subjects was drawn into 10-ml evacuated tubes containing heparin. The sample was divided into two parts: one part was centrifuged immediately to obtain plasma, and the other was retained for the analysis of whole blood. Hematocrits were determined. The blood samples were obtained at the times indicated in Figs. 1 and 2. Urine was

[1] Nanograde solvents, Mallinckrodt, St. Louis, Mo.
[2] Eastman Kodak Co., Rochester, N.Y.
[3] Baker Chemical Co., Phillipsburg, N.J.
[4] 1015 SL, Finnigan Corp., Sunnyvale, Calif.
[5] Model 1700, Varian Associates, Palo Alto, Calif.
[6] Evapo-Mix, Buchler Instruments, Fort Lee, N.J.

collected at variable intervals following drug administration. The pH of the urine collections obtained from the multiple-dose study was determined.

## RESULTS AND DISCUSSION

**Plasma and Red Blood Cell Concentrations (Comparison and Temporal Aspects)**—The GLC–mass spectrometric method is sensitive to <1 ng of methazolamide/ml of plasma. The sensitivity is important in the study of drug distribution between plasma and erythrocytes when the concentrations are in the nanogram and microgram per milliliter range, respectively. A typical chromatogram is shown in Fig. 3.

The temporal patterns of the plasma and red blood cell drug concentrations in the subjects administered single doses of methazolamide are presented in Fig. 1. Three hours following administration of a 50-mg tablet to Subject 1, the red blood cell and plasma drug concentrations were 19.1 (80.9 $\mu M$) and 0.078 $\mu$g/ml, respectively. With the assumption of a red blood cell volume of 2.6 liters (30 ml/kg), 49.7 mg, or nearly the entire dose, was sequestered by the red blood cells. Three hours after oral administration of 150 mg of methazolamide as a solution to Subject 2, the red blood cell and plasma drug concentrations were 36.1 (153 $\mu M$) and 1.37 $\mu$g/ml, respectively. The red blood cell drug concentration was equivalent to 84 mg or 56% of the dose present in the red blood cells. The plasma drug concentration thus varied by more than 17-fold and the red blood cell drug concentration by less than twofold for a threefold increase in the dose.

Methazolamide binds reversibly to carbonic anhydrase (8). The interaction is describable by the law of mass action. Each enzyme macromolecule has a single binding site for the drug molecule (9). Human erythrocytes have been reported to contain 156 $\mu M$ carbonic anhydrase, of which 20 $\mu M$ is the high-activity type C and 136 $\mu M$ is the low-activity type B (10). Maren *et al.* (6) reported that the total concentration of carbonic anhydrase in the human erythrocyte is variable (range 130–200 $\mu M$). Thus, the red blood cell concentration of methazolamide approaches the concentration of carbonic anhydrase in the erythrocytes following administration of the 150-mg dose but not following administration of the 50-mg tablet.

The dramatic increase in the plasma concentration for a less than twofold increase in the red blood cell concentration is a manifestation of the strong, nonlinear interaction of methazolamide with the red blood cell carbonic anhydrase. The free plasma concentration has been reported to be 45% of the total plasma concentration (11). The free drug rapidly penetrates erythrocytes (12). Therefore, the total plasma concentrations reflect the free intracellular concentrations. As the dose is increased and enzyme saturation is approached, the fraction of the dose bound to the carbonic anhydrase decreases due to the nonlinear nature of the binding. Consequently, a larger fraction of the dose is available to distribute in the total body water, and the plasma concentration increases rapidly.

The temporal patterns of the plasma and red blood cell concentrations in Subject 3, administered the multiple-dose regimen of methazolamide, are presented in Fig. 2. The plasma concentration resulting from the first 100-mg dose was insufficient to achieve a high fractional binding of the carbonic anhydrase, as judged by the reported concentrations of red blood cell carbonic anhydrase.

Repeated doses of the drug resulted in steady-state plasma concentrations of ~9.5 $\mu$g/ml (40 $\mu M$), which was much higher than the maximum plasma concentration observed in the first dosing interval (0.21 $\mu$g/ml). The red blood cell concentration at steady state was ~40 $\mu$g/ml (169 $\mu M$). Under the steady-state condition, the carbonic anhydrase in the red blood cells is near saturation since the binding constants of the isoenzymes (to be described) are much smaller than the free concentration of drug. If it is assumed that the cell water represents 63% of the volume of the red blood cells (10), the concentration of bound drug and, therefore, carbonic anhydrase was ~158 $\mu M$ [169 $\mu M$ − (0.63 × 0.45 × 40 $\mu M$)] in Subject 3.

The red blood cell concentrations appear to approach steady state significantly faster than the plasma concentrations (Fig. 2). Consideration of a simple system can demonstrate that this difference in the approach of the concentrations to their respective steady-state values is a manifestation of the strong, reversible, nonlinear interaction between the drug and carbonic anhydrase. One can imagine a system in which there is a local equilibrium between bound and free drug:

$$B = \frac{PF}{K + F} \qquad \text{(Eq. 2)}$$

where $B$ is the concentration of bound drug, $P$ is the concentration of binding sites, $F$ is the concentration of free drug, and $K$ is the dissociation

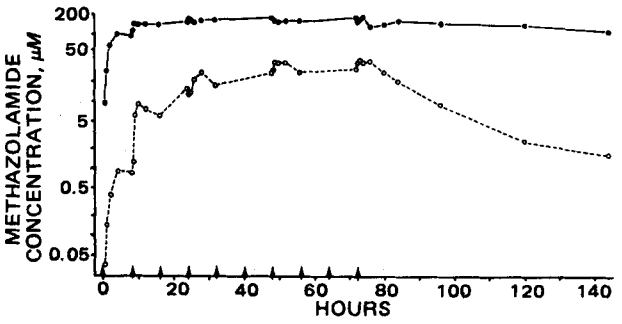


**Figure 2**—*Temporal patterns of plasma concentrations (O– –) and red blood cell concentrations (●—) for the subject administered a multiple-dose regimen.*

constant of the drug–macromolecule complex. Furthermore, it is assumed that the system is open such that the steady-state concentration of the free drug is determined by its infusion rate (mass flow) divided by the clearance of the free drug. Now at steady state:

$$B_{ss} = \frac{PF_{ss}}{K + F_{ss}} \qquad \text{(Eq. 3)}$$

Dividing Eq. 2 by Eq. 3 yields:

$$R_B = \left(\frac{\alpha + 1}{\alpha + R_F}\right) R_F \qquad \text{(Eq. 4)}$$

where $R_F = F(t)/F_{ss}$, $R_B = B(t)/B_{ss}$, and $\alpha = K/F_{ss}$.

As $R_F$ approaches 1, $R_B$ approaches 1. However, $R_B/R_F$ is always >1, except at steady state, where $R_B/R_F = 1$. In a system with strong binding and an infusion rate sufficient to ensure that $F_{ss} \gg K$, $\alpha \ll 1$. Thus, under these conditions, $R_B \simeq 1$ at times when the free concentration is an order of magnitude greater than $K$ yet substantially less than $F_{ss}$, whatever the exact temporal dependence of the free concentration on the input rate.

**Urinary Recoveries, Renal Clearances, and Total Clearances**—The amount of unchanged drug recovered in each dosing interval of the multiple-dose regimen is presented in Table I. The pH of the urine may have influenced the recovery of the drug. The pH of the urine collection and the amount of drug recovered for the sixth and ninth doses were low relative to the values for their respective preceding and following doses. Methazolamide is a weak acid with a pK value of 7.2 (12). Thus, it appears

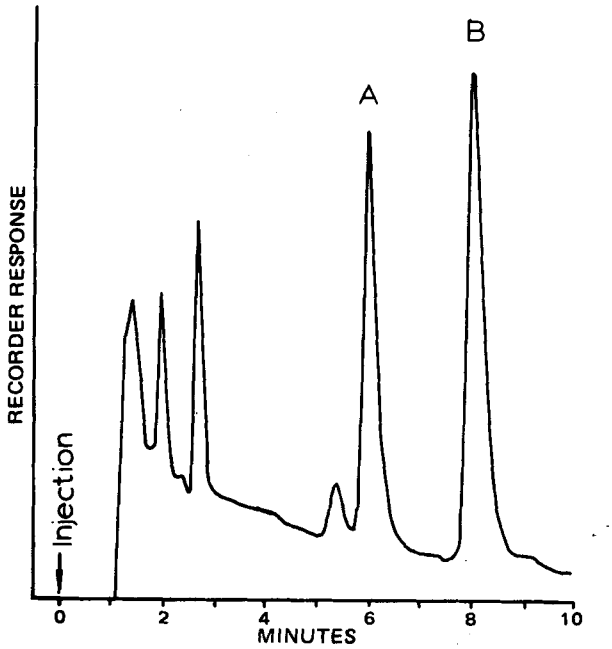


**Figure 3**—*Chromatogram of plasma sample calculated to contain 7.6 ng of methazolamide. Peaks A and B correspond to the permethylated derivatives of methazolamide and the internal standard, respectively.*

**Table I—Renal Clearances following Administration of Methazolamide**

| Dosage | Time Interval, hr (dose) | Amount Excreted, mg | pH | Volume, ml | Renal Clearance[a], ml/min |
|---|---|---|---|---|---|
| 100 mg tid | 0–8 (1) | 0.783 | 6.71 | 745 | 10.9 |
| | 8–16 (2) | 9.48 | 7.29 | 1480 | 12.3 |
| | 16–24 (3) | 11.4 | 7.20 | 1000 | 9.2[b] |
| | 24–32 (4) | 18.3 | 7.38 | 1185 | 7.6 |
| | 32–40 (5) | 19.3 | 7.24 | 1005 | 6.7[b] |
| | 40–48 (6) | 14.7 | 6.60 | 865 | |
| | 48–56 (7) | 28.6 | 6.97 | 880 | 7.2 |
| | 56–64 (8) | 22.5 | 6.62 | 840 | 5.0[b] |
| | 64–72 (9) | 11.0 | 5.70 | 350 | |
| | 72–80 (10) | 29.1 | 6.90 | 750 | 7.0 |
| | 80–144 | 53.3 | | | 8.1 |
| | 0–144 | 218.4 | | | 7.1 |
| 150 mg | 0–72 | 17.9 | | | 8.0 |
| 50 mg | 0–327 | 6.5 | | | 7.7 |

[a] Based on total plasma concentration. [b] Plasma concentration not mapped over dosing intervals 3, 5, 6, 8, and 9.

that tubular reabsorption of the drug is an important component in renal clearance. Methazolamide, in contrast to acetazolamide, is not secreted in the proximal tubules (6).

The renal clearances for the dosing intervals also are presented in Table I. The renal clearance was calculated from the amount of unchanged drug excreted during a given time interval divided by the corresponding area under the plasma curve. The area was determined using the trapezoidal approximation. The renal clearances more or less correlated with the urine pH, as they should if tubular reabsorption is important. The average renal clearances for the 50-mg, 150-mg, and 100-mg tid doses were 7.7, 8.0, and 7.1, respectively. These values are similar to the reported renal clearance (9.0 ml/min) expressed relative to the total plasma concentration (6).

Maren *et al.* (13) showed that in dogs chronically administered high doses of acetazolamide, an initial bicarbonate loss ensued, followed by a period in which the dogs became refractory to further bicarbonate loss. The pH and volumetric flow of the urine also appeared to correspond to the rate of bicarbonate excretion. Thus, a similar phenomenon may have been operative during the multiple-dose regimen of methazolamide since there appeared to be an initial increase in both the pH and the volumetric flow.

The total body clearance was estimated by subtracting from the dose the amount of drug remaining in the red blood cells (30 ml/kg) at the time of the last sampling and dividing this value by the corresponding area under the plasma curve. The contribution to the total amount of drug in the body at the last sampling time was small, as reflected in the plasma concentration (Table II). Furthermore, the contribution of the extrarenal carbonic anhydrase pool, which Maren *et al.* (6) claimed was <10% of the total pool but which Lehmann *et al.* (14), suggested was approximately equal to the red blood cell pool was neglected. Furthermore, methazolamide was reported to be well absorbed (6), and absorption was assumed to be complete. The estimated total body clearances are presented in Table II.

It is possible that along with the influence of bicarbonate excretion on the renal clearance of methazolamide, the resulting metabolic acidosis influences its metabolic clearance. Conceivably, changes in the plasma pH relative to changes in the pH of the tissue fluids could cause a redistribution of the drug, as was observed with the weak acid phenobarbital (15), and, hence, alter its clearance. Multiple-dose regimens of 25 mg bid or 50 mg bid reduced the plasma pH from 7.41 to 7.35 (16). Thus, the total clearance is at best an average over the changes of the acid–base balance caused by the drug.

The ratio of the renal clearance to the body clearance should be equal to the fraction of unchanged drug recovered in the urine, provided urine is collected for a sufficient time. The predicted fractional urinary recoveries for the 50-mg, 150-mg, and 100-mg tid doses were 0.25, 0.29, and 0.26, respectively.

In the multiple-dose study, the total amount of drug recovered in contiguous urine collections up to 216 hr was 228 mg or 23% of the administered dose (1000 mg). Excretion rates were determined for 2-hr urine collections centered at 528 and 744 hr. Linear interpolation of excretion rates between the midpoint (204 hr) of the last contiguous urine collection and those determined at 528 and 744 hr gave a total urinary recovery of 248 mg or 25% of the administered dose. This urinary recovery is similar to that reported by Maren *et al.* (6).

Much longer times would be required for urine collections following the single-dose administrations compared to the multiple-dose regimen to obtain fractional urinary recoveries similar to those predicted by the ratio of the renal and total clearances. The amount of methazolamide recovered in contiguous urine collections up to 96 hr after administration of the 150-mg dose was 19.3 mg. Based on the excretion rates determined from short-duration urine collections centered at 170, 319, and 649 hr, 39 mg (26% of the dose) would be expected to be obtained at 649 hr. Times far in excess of 649 hr would be required to obtain a reasonable estimate of the fractional urinary recovery, following administration of the 50-mg dose, solely on the basis of contiguous urine collections. The smaller the dose, the larger is the fraction of the dose that will be bound (reversibly) to the carbonic anhydrase because of the saturable nature of the binding. Thus, the smaller the dose, the longer are the periods required for most of the drug to be cleared because the enzyme effectively buffers the drug, permitting only small free concentrations of the drug to be cleared.

**Metabolites**—Approximately 75% of the dose was not accounted for as unchanged drug in the urine. Therefore, the urine was analyzed for the presence of metabolites. Deacetylated methazolamide, an intermediate in the synthesis of the internal standard, represented a possible metabolite. The type B isoenzyme of carbonic anhydrase has esterase activity (17). Hence, the isoenzyme might be expected to catalyze the hydrolysis of the acetylimino bond of methazolamide. Deacetylated methazolamide could be extracted with ethyl acetate from urine, converted to a trimethyl derivative, and detected by selective monitoring of the molecular ion ($m/z$ 236). Deacetylated methazolamide was not detected in urine collected during the multiple-dose administration to Subject 3.

Besides deacetylated methazolomide, no other metabolites were detected using mass fragmentography and the described workup.

**Methazolamide–Isoenzyme Dissociation Constants**—The plasma and red blood cell concentrations obtained following administration of the 150-mg dose of methazolamide were used to estimate the dissociation constants of the isoenzyme–methazolamide complexes. The unbound plasma concentration (45% of the total concentration) was assumed to be in equilibrium with the intracellular free concentration at all times. The mass transport coefficient for the transport of the drug across the red blood cell membrane is ~7 liters/min based on the reported rate constant of 195 $hr^{-1}$ (12). This clearance is much greater than the total body clearance, which is 60 ml/min based on the free plasma concentration. Therefore, a virtual equilibrium of drug between the plasma and intracellular water seems reasonable.

The concentration of intracellularly bound methazolamide was calculated by subtracting the product of the unbound plasma concentration and the fraction of cell water (0.63) from the total red blood cell con-

**Table II—Total Body Clearances of Methazolamide**

| Dosage | Hours | Red Blood Cell Concentration, μg/ml | Plasma Concentration, μg/ml | Total Clearance[a], ml/min |
|---|---|---|---|---|
| 100 mg tid | 744 | 4.53 | 0.019 | 27.4 |
| 150 mg | 1082 | 4.06 | 0.0076 | 27.6 |
| 50 mg | 504 | 6.49 | 0.017 | 31.3 |

[a] Based on total plasma concentration.

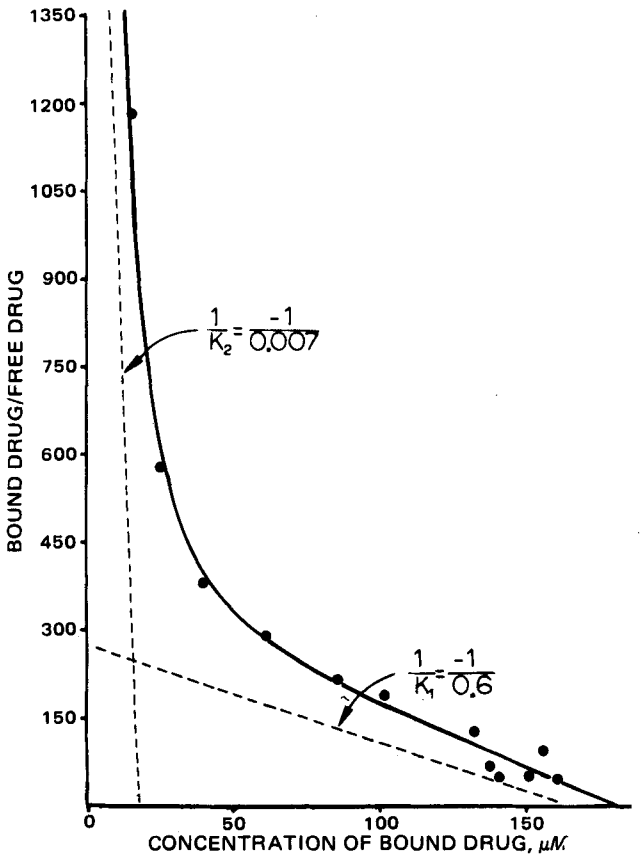


**Figure 4**—*Binding isotherm of methazolamide to red blood cells.*

centration. A Rosenthal plot (Fig. 4) was constructed by plotting the ratio of the bound drug concentration to the unbound drug concentration in the plasma against the bound drug concentration. The curvature of the plot indicates multiple binding sites for methazolamide. Since it was shown that there is one binding site per carbonic anhydrase molecule (9), the curvature may be a manifestation of the two isoenzymes of carbonic anhydrase present in the human erythrocyte. The binding curve was resolved by a graphical procedure into linear segments that reflect the two isoenzymes (18). The dissociation constants for the type B–methazolamide complex and the type C–methazolamide complex are 0.6 and 0.007 $\mu M$, respectively. The estimated concentrations of isoenzyme B and isoenzyme C are 165 and 18 $\mu M$, respectively.

The concentrations of methazolamide required to reduce the hydration rates of carbon dioxide by 50% ($I_{50}$) at 25° were reported to be 0.016 and 0.017 $\mu M$ for reactions catalyzed by the type C and type B isoenzymes, respectively (6). Since the enzyme concentrations were maintained low relative to the measured $I_{50}$ values (18), these inhibitory concentrations are similar to the dissociation constants of the respective methazolamide–enzyme complexes. The inhibitory activities of methazolamide on the carbonic anhydrase in red blood cells were similar at 4, 22, and 37° (10).

There is reasonably good agreement between the dissociation constant determined from the kinetic measurement and that determined from the binding analysis for the type C isoenzyme (0.016 and 0.007 $\mu M$, respectively). However, there is a large difference in these values for the type B isoenzyme (0.017 and 0.6 $\mu M$, respectively). Anions have been shown to reduce significantly the catalytic activity of isoenzyme B, whereas they have little effect on the catalytic activity of isoenzyme C (17). The concentration of chloride and bicarbonate ions in the red blood cell reduces the activity of isoenzyme B to 8% of that in the absence of the anions (17). Therefore, the inhibitory constant for isoenzyme B in the presence of chloride and bicarbonate ions is 0.2 $\mu M$, which is similar to the value determined from the Rosenthal plot.

The presence of the chloride and bicarbonate anions in the erythrocyte influences the distribution of the drug in the physiological situation. In principle, the same fractional inhibition of a given isoenzyme in various tissues should result at equilibrium. Thus, if 99% inhibition of the type C isoenzyme in the secretory cells of the ciliary process is achieved, a requirement for substantial intraocular pressure lowering (6), the type C isoenzyme in the erythrocyte will be 99% inhibited. However, the percent inhibition of the type B isoenzyme in the erythrocyte will be significantly less due to the presence of the anions, even though the intrinsic binding constants (binding constants in the absence of anions) of the two isoenzymes are similar.

The dissociation constant for acetazolamide and human red blood cell carbonic anhydrase (presumably type B) was determined from *in vitro* equilibration studies; a mean value of 1.6 $\mu M$ was reported (19). This value is approximately an order of magnitude larger than the $I_{50}$ value of 0.25 $\mu M$ reported by Maren *et al.* (6). This trend is exactly the same as was observed with methazolamide and, again, probably is the result of competition by the intracellular anions, yielding an apparent dissociation constant that is larger than the true dissociation constant.

**Influence of Binding on Decline in Plasma and Red Blood Cell Concentrations**—Krüger-Thiemer and coworkers (20, 21) discussed the influence of protein binding on the temporal patterns of plasma and plasma water concentrations of sulfonamide-type drugs. The diminishing steepness in the log plasma concentration–time curves was explicable in terms of the nonlinearity introduced by protein binding. The similar curvature in the temporal patterns of the plasma methazolamide concentrations is probably a manifestation of the binding of the drug to carbonic anhydrase rather than to plasma proteins. The fractional binding to plasma proteins has been reported to be constant over the therapeutic range of plasma concentrations.

The decline in plasma concentrations following the administration of the 10th dose to Subject 3 can be fitted to a model in which the distribution of the drug is rapid relative to the elimination, the elimination is proportional to the free concentration of drug, and the binding of the drug to the two isoenzymes is described by the law of mass action. Similar models were discussed by other investigators (20, 22, 23). The differential equation describing such a model is:

$$\frac{d \ln C_f}{dt} = -\frac{Q_B}{V + \frac{(1-f)}{f} V_p + \sum_{i=1}^{2} \frac{E_i K_i}{(K_i + C_f)^2}} \qquad \text{(Eq. 5)}$$

and the integrated equation is:

$$t = \frac{1}{Q_B}\left\{\left[V + \frac{(1-f)}{f} V_p\right] \ln (C_f/C_f^0) + \sum_{i=1}^{2} (E_i/K_i) \ln \times \left[\frac{C_f(K_i + C_f^0)}{C_f^0(K_i + C_f)}\right] + \sum_{i=1}^{2} E_i \frac{C_f^0 - C_f}{(K_i + C_f)(K_i + C_f^0)}\right\} \qquad \text{(Eq. 6)}$$

where $Q_B$ is the total body clearance expressed relative to the free plasma concentration, $V$ is the volume of distribution of free drug, $f$ is the fraction unbound in the plasma, $V_p$ is the volume of distribution of serum albumin (24), $E_i$ is the molar amount of isoenzyme $i$, $K_i$ is the dissociation constant of the isoenzyme $i$–drug complex, $C_f^0$ is the intial free plasma concentration, and $C_f(t)$ is the free plasma concentration at time $t$. The times for the observed plasma concentrations were evaluated using the values of the parameters shown at the bottom of Table III, varying $V$, $E_1$, and $E_2$ to obtain the best fit to Eq. 6. The predicted times and the sampling times, expressed relative to the time of the initial concentration, are presented in Table III.

**Table III—Predicted and Observed Times [a] in the Decline of Plasma Concentrations following the 10th Dose of the Multiple-Dose Regimen [b]**

| | Free Plasma Concentration, $\mu M$ | | | | | | | |
|---|---|---|---|---|---|---|---|---|
| | 18.2 | 12.2 | 9.05 | 4.10 | 1.18 | 0.743 | 0.0544 | 0.0362 |
| Calculated from Eq. 6 | 0 | 4.45 | 7.94 | 18.2 | 47.3 | 69.5 | 480 | 616 |
| Experimentally determined | 0 | 4 | 8 | 20 | 44 | 68 | 452 | 668 |

[a] Values are in hours. [b] The parameter values were: $Q_B$ = 3.5 liters/hr, $f$ = 0.45, $V$ = 30 liters, $V_p$ = 6.6 liters, $E_1$ = 500 $\mu$moles, $K_1$ = 0.6 $\mu M$, $E_2$ = 150 $\mu$moles, and $K_2$ = 0.007 $\mu M$.

The agreement between the predicted and adjusted sampling times is reasonably good. However, a volume of distribution of free drug of 30 liters rather than the volume of total body water (50 liters) was used to obtain the predicted times. Also, the total molar amount of carbonic anhydrase (650 μmoles) employed was intermediate between the amount suggested by Maren *et al.* (6) (≃400 μmoles) and the amount (≃900 μmoles) suggested by Lehmann *et al.* (14). However, recognizing the limitations of such a simple model, it nevertheless strongly suggests that carbonic anhydrase acts as the storage site for the drug.

The plasma concentrations following the administration of methazolamide in general will not decline as a simple exponential function of time, even if the drug distributes rapidly and the clearance is concentration independent. The interaction of the drug with the carbonic anhydrase masks this behavior. When the free concentrations are such that the concentration-dependent volume terms are made small relative to the concentration-independent volume terms (see denominator of Eq. 5), the plasma concentrations appear to decline in a simple exponential fashion over the initial portion of the time course. Under these conditions, the predicted half-life is 7.5 hr, using the parameters at the bottom of Table III. This predicted half-life is approximately the same as the half-life observed over the first three data points of the decline where the free plasma concentrations are large relative to $K_1$ (Fig. 2). This half-life was called the intrinsic half-life by Krüger-Thiemer *et al.* (21); in this simple model, it is the half-life for elimination not masked by the drug–macromolecular interaction.

When the free plasma concentration has declined into the range of the dissociation constant of the isoenzyme B complex, the buffering effect of the isoenzyme on the free plasma concentration becomes apparent. The ratio of the bound concentration to the free concentration increases as the plasma concentration decreases with time. The apparent volume of distribution of free drug (total amount in the body divided by the free concentration) increases as the ratio increases (23). The apparent volume of distribution of free drug ($V_{df}$) for this system is:

$$V_{df} = V + \frac{(1-f)}{f} V_p + \sum_{i}^{2} \frac{E_i}{K_i + C_i} \qquad \text{(Eq. 7)}$$

The reciprocal of the expression on the right side of Eq. 5, which can be considered as the instantaneous time constant, is not simply $V_{df}/Q_B$. At least for those times when the volume term, which is dependent on the interaction of the drug with isoenzyme 2, is negligible, the denominator in Eq. 5 can be expressed as a relatively simple function of $V_{df}$, namely:

$$V_f + \frac{K_1}{E_1}(V_{df} - V_f)^2$$

where:

$$V_f = V + \frac{(1-f)V_p}{f} \qquad \text{(Eq. 8)}$$

and:

$$V_{df} = V_f + \frac{E_1}{(K_1 + C_f)} \qquad \text{(Eq. 9)}$$

Thus, as the apparent volume of distribution increases, the instantaneous time constant increases from $V_f$ as a function of the square of the difference between the apparent volume of distribution and $V_f$. Since the instantaneous time constant increases as a function of an increase in the apparent volume of distribution, which in turn increases with a decrease in the plasma concentration, the slope of the log plasma concentration–time curve decreases strongly with a decrease in the plasma concentration in the transition region.

During the later time periods, the exceedingly slow decline in the plasma concentration is controlled by the strong binding of the drug to the type C isoenzyme. In principle, the plasma concentrations will decline exponentially as a function of time, with a half-life greatly in excess of the intrinsic half-life, when the free plasma concentration becomes small relative to the dissociation constant of the isoenzyme C–drug complex (22, 23). Plasma concentrations more than an order of magnitude less than those observed in the present study are required to observe this phenomenon.

The persistence of methazolamide in the red blood cells 1082 hr after administration of the 150-mg dose is a manifestation of the strong binding between the drug and the high activity type C carbonic anhydrase. At this time, the red blood cell concentration was 4.1 μg/ml; therefore, the red blood cells still contained 6.2% of the dose. The corresponding plasma concentration was 7.6 ng/ml (Table II). Drug is eliminated from the body very slowly, because the intracellular concentration of freely diffusible inhibitor in the erythrocytes and other tissues containing the enzyme is maintained small by the strong interaction of the drug with carbonic anhydrase.

Red blood cell and plasma concentrations were studied as a function of time in dogs administered acetazolamide intravenously (8). Although plasma concentrations were not measured directly after 24 hr because of the lack of assay sensitivity, plasma concentrations were calculated from the urinary excretion rates and the clearance. When the plasma concentration declined to a level such that the intracellular concentration of freely diffusible inhibitor was only a few percent of the total red blood cell concentration, the drug in the red blood cells acted as a source for that in the plasma. The total red blood cell concentration then declined slowly because of the small intracellular concentration of freely diffusible inhibitor.

An exceedingly slow decline ($t_{1/2}$ = 120 days) in human blood of an anticonvulsant drug, 2-amino-4-phenyl-sulphenylbenzenesulfonamide, was reported (25). The drug was shown to bind strongly to both isoenzymes of carbonic anhydrase in the human erythrocyte.

**Usefulness of Methazolamide in Comparison to Acetazolamide**—Methazolamide and acetazolamide inhibit the high activity type of carbonic anhydrase (type C) present in the ciliary body to the same degree (6). The plasma protein binding of methazolamide is significantly less than that of acetazolamide, 55 compared to 93%, respectively, in the therapeutic range of plasma concentrations (6, 11). Therefore, if the mechanism for the reduction in aqueous secretion and, hence, intraocular pressure were due solely to the inhibition of carbonic anhydrase, equal concentrations of the freely diffusible inhibitors, or a total plasma concentration of methazolamide, only 15% that of acetazolamide would be required for an equivalent response at steady state. Furthermore, since the membrane permeability of methazolamide is at least one order of magnitude greater than that of acetazolamide (12), an even greater disparity may exist in the dosage requirements with the pulsed delivery offered by conventional dosage regimens. Maren *et al.* (6) showed that methazolamide is distributed more uniformly than acetazolamide in rat tissues after oral administration of the drugs.

The systemic acidosis that results from a decrease in bicarbonate reabsorption due to the inhibition of renal carbonic anhydrase contributes to the reduction in intraocular pressure (6, 16). The resulting systemic acidosis is greater for acetazolamide than for methazolamide at equivalent plasma concentrations and was postulated to be due to the active secretion and accumulation of acetazolamide, but not methazolamide, in the proximal tubule (6).

A correlation has been demonstrated between side effects sufficiently severe to cause discontinuation of therapy and the degree of systemic acidosis (plasma carbon dioxide combining power of <21 mEq/liter; control, 27 mEq/liter) following multiple-dose regimens of either acetazolamide or methazolamide (26). The studies of Maren *et al.* (6) and Stone *et al.* (16) showed that the side effects became more severe with an increase in the acidotic state. Maren *et al.* (6) also suggested that the formation of renal stones may be due to the decrease in urinary output of citrate that occurs with an increase in systemic acidosis.

Thus, as pointed out previously (6, 16), low dose regimens of methazolamide, in which the side effects are minimized, rather than the conventional regimens of acetazolamide would be a rational therapy in patients whose intraocular pressures are controlled by the direct action of the inhibitor on the ciliary body carbonic anhydrase.

## REFERENCES


(1) T. H. Maren, *Invest. Ophthamol.*, **15**, 356 (1976).

(2) T. J. Zimmerman, L. C. Garg, B. P. Vogh, and T. H. Maren, *J. Pharmacol. Exp. Ther.*, **196**, 510 (1976).

(3) *Ibid.*, **199**, 510 (1976).

(4) T. H. Maren, V. I. Ash, and E. M. Bailey, Jr., *Bull. Johns Hopkins Hosp.*, **95**, 244 (1954).

(5) T. H. Maren, *J. Pharmacol. Exp. Ther.*, **130**, 26 (1960).

(6) T. H. Maren, J. R. Haywood, S. K. Chapman, and T. J. Zimmerman, *Invest. Ophthamol.*, **16**, 730 (1977).

(7) H. Ehrsson, *Anal. Chem.*, **46**, 922 (1974).

(8) T. H. Maren, *Biochem. Pharmacol.*, **9**, 39 (1962).

(9) J. E. Coleman, *Annu. Rev. Pharmacol.*, **15**, 221 (1975).

(10) P. J. Wistrand and P. Baathe, *Acta Pharmacol. Toxicol.*, **26**, 145 (1968).

(11) D. M. Travis, C. Wiley, and T. H. Maren, *J. Pharmacol. Exp. Ther.*, **151**, 464 (1966).

(12) L. B. Holder and S. L. Hayes, *Mol. Pharmacol.*, **1**, 266 (1968).

(13) T. H. Maren, B. C. Wadsworth, F. K. Yale, and L. G. Alonso, *Bull. Johns Hopkins Hosp.*, **96**, 277 (1954).
(14) B. Lehmann, E. Linner, and P. J. Wistrand, in "Advances in Biosciences," vol. 5, G. Raspe, Ed., Pergamon, Oxford, England, 1970, p. 197.
(15) W. J. Waddell and T. C. Butler, *J. Clin. Invest.*, **36**, 1217 (1957).
(16) R. A. Stone, T. J. Zimmerman, D. H. Shin, B. Becker, and M. Kass, *Am. J. Ophthalmol.*, **83**, 674 (1977).
(17) T. H. Maren, C. S. Rayburn, and N. E. Lidell, *Science*, **191**, 469 (1976).
(18) H. E. Rosenthal, *Anal. Biochem.*, **20**, 522 (1967).
(19) S. M. Wallace and S. Riegelman, *J. Pharm. Sci.*, **66**, 729 (1977).
(20) E. Krüger-Thiemer, *Farmaco, Sci. Ed.*, **23**, 717 (1968).
(21) E. Krüger-Thiemer, W. Diller, and P. Bunger, *Antimicrob. Agents Chemother.*, **1965**, 183 (1966).
(22) J. G. Wagner, "Biopharmaceutics and Relevant Pharmacokinetics," Drug Intelligence Publications, Hamilton, Ill., 1971.
(23) J. R. Gillette, in "Handbuch der experimentellen Pharmakologie, vol. XXVIII. Concepts in Biochemical Pharmacology," part 3, J. R. Gillette and J. R. Mitchell, Eds., Springer-Verlag, Berlin, Germany, 1975, pp. 35–85.
(24) J. R. Gillette, *Ann. N.Y. Acad. Sci.*, **266**, 6 (1973).
(25) J. Lund, J. B. Lassen, and R. F. Squires, *Acta Pharmacol. Toxicol.*, **30**, 17 (1971).
(26) D. L. Epstein and W. M. Grant, *Arch. Ophthalmol.*, **95**, 1378 (1977).

## ACKNOWLEDGMENTS

The authors thank Ms. N. Crisologo for technical assistance.

# $^{13}$C-NMR Experimental Methods for Determination of Resonance Multiplicities: *Strychnos* Alkaloids

**GARY E. MARTIN**

Received January 21, 1980, from the *Department of Medicinal Chemistry and Pharmacognosy, College of Pharmacy, University of Houston, Houston, TX 77004.* Accepted for publication July 16, 1980.

**Abstract** □ $^{13}$C-NMR spectral assignments of the *Strychnos* alkaloids brucine and strychnine have been reported by numerous investigators. One recent report contained several disparities in the assignments that were attributable to incorrect determinations of spin multiplicities. The source of the inaccuracies in the spin-multiplicity determinations of very complex molecules is discussed, and several additional techniques for the determination of these multiplicities are described that are less subject to interpretational errors than the conventional and routinely employed single-frequency off-resonance decoupling methods. These procedures are applied using brucine as a representative example.

**Keyphrases** □ $^{13}$C-NMR spectroscopy—determination of resonance multiplicities, brucine □ Brucine—determination of resonance multiplicities □ Resonance multiplicities—brucine

Several recent reports dealt with the $^{13}$C-NMR spectral assignments of strychnine, brucine, and related *Strychnos* alkaloids (1–9). The assignments in one report (8) for several resonances in both strychnine and brucine are in direct conflict to those reported previously. It is possible that errors occurred in this work that were due to the incorrect determination of spin multiplicities for the resonances in question.

The results obtained from two complementary methods that can provide unambiguous determination of the resonance multiplicities in even the most complex $^{13}$C-NMR spectra are presented using brucine as an example. These methods are alternatives to conventional single-frequency off-resonance decoupling techniques and can be executed on modern Fourier transform spectrometers with only minor modification.

## RESULTS AND DISCUSSION

A spectral parameter that is readily accessible for the pulsed Fourier transform technique and that provides an alternative method for the determination of spin multiplicities is the spin-lattice relaxation time, $T_1$ (10–12). Experimental evidence strongly supports the premise that in molecules of moderate size, the $^1$H–$^{13}$C dipolar mechanism is predominantly responsible for $^{13}$C-NMR relaxation. On this basis, for molecules that tumble at rates in excess of the motional narrowing limit (Larmor resonance frequency), the relaxation rate may be expressed as:

$$1/T_1^{DD} = N\hbar^2\gamma_C^2\gamma_H^2 r_{CH}^{-6}\tau_c \qquad \text{(Eq. 1)}$$

where $\gamma_C$ and $\gamma_H$ represent the magnetogyric ratios of the $^{13}$C and $^1$H nuclei, respectively, and $\hbar^2$ is Planck's constant. Thus, relaxation is determined by the terms $Nr_{CH}^{-6}$ and $\tau_c$, where the former term is modulated by the number of protons at specific internuclear distances (typically, relaxation is mediated by the directly attached protons, if any), while the latter term is the reorientational correlation time, typically $10^{-12}$–$10^{-10}$ sec for natural products of moderate molecular weight (*i.e.*, mol. wt. 250–1000) (13).

A further requirement is that the molecule tumble in a random fashion (isotropic), which can strictly be true only for spherical molecules or close approximations such as adamantane (14). In practice, however, the relaxation of a relatively large number of molecules has been found to conform to this simple requirement, thereby allowing the use of Eq. 1 rather than the more complex equations necessary to describe ordered (anisotropic) reorientation. This behavior leads to the very useful result that the relaxation time of a given carbon is inversely proportional to the number of directly attached protons. Thus, in relatively rigid cyclic compounds, methylene resonances are expected to undergo relaxation at a rate twice as fast as methine carbons. In contrast, methyl groups are capable of an internal reorientation in addition to the overall isotropic reorientation, which imparts a different reorientational correlation time, $\tau_i$ (referred to as $\tau_\mu$ by some investigators), typically on the order of $10^{-13}$–$10^{-11}$ sec, resulting in longer relaxation times. In the extreme case, these relaxation times can be up to three times as long as those observed for methine resonances.

In complex molecules in which large numbers of carbon resonances have substantially similar chemical shifts, thereby preventing the unambiguous interpretation of single-frequency off-resonance decoupling spin multiplicities, relaxation considerations present a viable alternative for the demonstration of this information. This consideration is especially useful where a methylene carbon bears nonequivalent (anisochronous)

0022-3549/81/0100-0081$01.00/0
© 1981, American Pharmaceutical Association

(13) T. H. Maren, B. C. Wadsworth, F. K. Yale, and L. G. Alonso, *Bull. Johns Hopkins Hosp.*, **96**, 277 (1954).
(14) B. Lehmann, E. Linner, and P. J. Wistrand, in "Advances in Biosciences," vol. 5, G. Raspe, Ed., Pergamon, Oxford, England, 1970, p. 197.
(15) W. J. Waddell and T. C. Butler, *J. Clin. Invest.*, **36**, 1217 (1957).
(16) R. A. Stone, T. J. Zimmerman, D. H. Shin, B. Becker, and M. Kass, *Am. J. Ophthalmol.*, **83**, 674 (1977).
(17) T. H. Maren, C. S. Rayburn, and N. E. Lidell, *Science*, **191**, 469 (1976).
(18) H. E. Rosenthal, *Anal. Biochem.*, **20**, 522 (1967).
(19) S. M. Wallace and S. Riegelman, *J. Pharm. Sci.*, **66**, 729 (1977).
(20) E. Krüger-Thiemer, *Farmaco, Sci. Ed.*, **23**, 717 (1968).
(21) E. Krüger-Thiemer, W. Diller, and P. Bunger, *Antimicrob. Agents Chemother.*, **1965**, 183 (1966).
(22) J. G. Wagner, "Biopharmaceutics and Relevant Pharmacokinetics," Drug Intelligence Publications, Hamilton, Ill., 1971.
(23) J. R. Gillette, in "Handbuch der experimentellen Pharmakologie, vol. XXVIII. Concepts in Biochemical Pharmacology," part 3, J. R. Gillette and J. R. Mitchell, Eds., Springer-Verlag, Berlin, Germany, 1975, pp. 35–85.
(24) J. R. Gillette, *Ann. N.Y. Acad. Sci.*, **266**, 6 (1973).
(25) J. Lund, J. B. Lassen, and R. F. Squires, *Acta Pharmacol. Toxicol.*, **30**, 17 (1971).
(26) D. L. Epstein and W. M. Grant, *Arch. Ophthalmol.*, **95**, 1378 (1977).

## ACKNOWLEDGMENTS

The authors thank Ms. N. Crisologo for technical assistance.

# $^{13}$C-NMR Experimental Methods for Determination of Resonance Multiplicities: *Strychnos* Alkaloids

**GARY E. MARTIN**

Received January 21, 1980, from the *Department of Medicinal Chemistry and Pharmacognosy, College of Pharmacy, University of Houston, Houston, TX 77004.* Accepted for publication July 16, 1980.

**Abstract** □ $^{13}$C-NMR spectral assignments of the *Strychnos* alkaloids brucine and strychnine have been reported by numerous investigators. One recent report contained several disparities in the assignments that were attributable to incorrect determinations of spin multiplicities. The source of the inaccuracies in the spin-multiplicity determinations of very complex molecules is discussed, and several additional techniques for the determination of these multiplicities are described that are less subject to interpretational errors than the conventional and routinely employed single-frequency off-resonance decoupling methods. These procedures are applied using brucine as a representative example.

**Keyphrases** □ $^{13}$C-NMR spectroscopy—determination of resonance multiplicities, brucine □ Brucine—determination of resonance multiplicities □ Resonance multiplicities—brucine

Several recent reports dealt with the $^{13}$C-NMR spectral assignments of strychnine, brucine, and related *Strychnos* alkaloids (1–9). The assignments in one report (8) for several resonances in both strychnine and brucine are in direct conflict to those reported previously. It is possible that errors occurred in this work that were due to the incorrect determination of spin multiplicities for the resonances in question.

The results obtained from two complementary methods that can provide unambiguous determination of the resonance multiplicities in even the most complex $^{13}$C-NMR spectra are presented using brucine as an example. These methods are alternatives to conventional single-frequency off-resonance decoupling techniques and can be executed on modern Fourier transform spectrometers with only minor modification.

## RESULTS AND DISCUSSION

A spectral parameter that is readily accessible for the pulsed Fourier transform technique and that provides an alternative method for the determination of spin multiplicities is the spin-lattice relaxation time, $T_1$ (10–12). Experimental evidence strongly supports the premise that in molecules of moderate size, the $^1$H–$^{13}$C dipolar mechanism is predominantly responsible for $^{13}$C-NMR relaxation. On this basis, for molecules that tumble at rates in excess of the motional narrowing limit (Larmor resonance frequency), the relaxation rate may be expressed as:

$$1/T_1^{DD} = N\hbar^2\gamma_C^2\gamma_H^2 r_{CH}^{-6}\tau_c \qquad \text{(Eq. 1)}$$

where $\gamma_C$ and $\gamma_H$ represent the magnetogyric ratios of the $^{13}$C and $^1$H nuclei, respectively, and $\hbar^2$ is Planck's constant. Thus, relaxation is determined by the terms $Nr_{CH}^{-6}$ and $\tau_c$, where the former term is modulated by the number of protons at specific internuclear distances (typically, relaxation is mediated by the directly attached protons, if any), while the latter term is the reorientational correlation time, typically $10^{-12}$–$10^{-10}$ sec for natural products of moderate molecular weight (*i.e.*, mol. wt. 250–1000) (13).

A further requirement is that the molecule tumble in a random fashion (isotropic), which can strictly be true only for spherical molecules or close approximations such as adamantane (14). In practice, however, the relaxation of a relatively large number of molecules has been found to conform to this simple requirement, thereby allowing the use of Eq. 1 rather than the more complex equations necessary to describe ordered (anisotropic) reorientation. This behavior leads to the very useful result that the relaxation time of a given carbon is inversely proportional to the number of directly attached protons. Thus, in relatively rigid cyclic compounds, methylene resonances are expected to undergo relaxation at a rate twice as fast as methine carbons. In contrast, methyl groups are capable of an internal reorientation in addition to the overall isotropic reorientation, which imparts a different reorientational correlation time, $\tau_i$ (referred to as $\tau_\mu$ by some investigators), typically on the order of $10^{-13}$–$10^{-11}$ sec, resulting in longer relaxation times. In the extreme case, these relaxation times can be up to three times as long as those observed for methine resonances.

In complex molecules in which large numbers of carbon resonances have substantially similar chemical shifts, thereby preventing the unambiguous interpretation of single-frequency off-resonance decoupling spin multiplicities, relaxation considerations present a viable alternative for the demonstration of this information. This consideration is especially useful where a methylene carbon bears nonequivalent (anisochronous)

0022-3549/81/0100-0081$01.00/0
© 1981, American Pharmaceutical Association

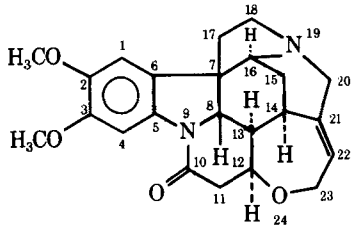

I

protons that can lead to the observation of non-first-order spin multiplets (15), which may account for the incorrect signal multiplicity of at least one resonance misassigned by Singh *et al.* (8). Circumvention of these interpretational problems by the application of relaxation phenomena has been used for various natural products, including steroids (16), terpenoids (17–21), macrolide antibiotics (22, 23), and lincomycin and its analogs (24). Furthermore, although partial relaxation data have been reported for brucine (I) (1, 2), the main application of these data was in the assignment of the quaternary carbon resonances, with no discussion of its application to spin-multiplicity determination in this compound.

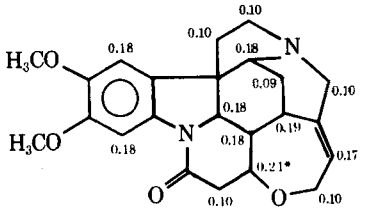

The $T_1$ relaxation data for brucine (I) are shown here for the protonated resonances. (No effort was made to incorporate the measurement of the nonprotonated carbon relaxation times.) The spin-lattice relaxation times ($T_1$) (expressed in seconds) were measured by the inversion recovery method (22) using the three-parameter nonlinear fit program (23). Examination of the average $T_1CH/T_1TH_2$ ratio gave an observed ratio of 1.82 and a calculated reorientational correlation time ($\tau_c$) of $2.5 \times 10^{-10}$ sec. While it is not always convenient or practical to determine $T_1$ relaxation times rigorously, the same multiplicity data can be inferred effectively and conveniently from a partial relaxation experiment (Fig. 1). This latter technique is particularly powerful when used in conjunction with single-frequency off-resonance decoupling, as described by Nakanishi and coworkers (18, 19). The techniques, when used in conjunction with one another, also hold promise for extending applications of relaxation behavior to include nonisotropically reorienting systems such as the retinoids (25, 26).

An additional pair of alternative techniques for the determination of spin multiplicities is the use of selective excitation, as described by Freeman and coworkers (27, 28), in conjunction with either gated decoupling (29) or single-frequency off-resonance decoupling, which was described recently by Martin *et al.* (20). In both techniques, a train of soft pulses, typically 0.5–1.0°, is applied to the sample at the precession interval of the resonance to be selectively excited. This procedure has

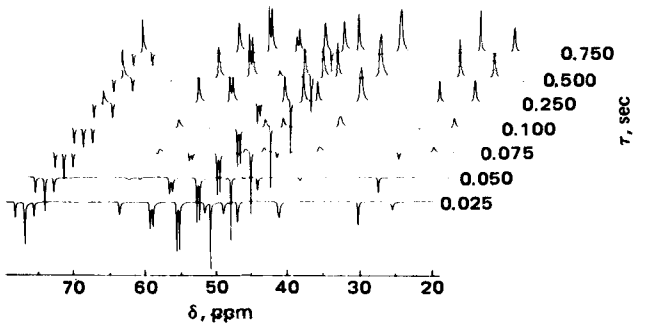


**Figure 1**—*Stack plot of a partial inversion recovery experiment showing the high-field region of brucine (I). Since relaxation is inversely proportional to the number of directly bonded protons, methylene carbons are expected to exhibit a positive inflection first ($\tau$ = 0.075 sec) followed by methine carbons ($\tau$ = 0.25 sec) and then methyl carbons. The nonprotonated C-7 resonances never become positive in this experiment.*

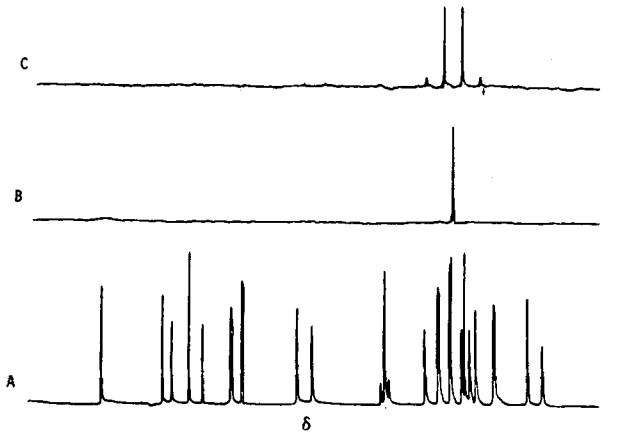


**Figure 2**—*$^{13}C$-NMR spectra of brucine. Key: A, fully decoupled $^{13}C$-NMR spectrum; B, selective excitation with full decoupling of the $OCH_3$ resonance at 55.3°; and C, selective excitation with gated decoupling of the $OCH_3$ resonance showing full spin–spin coupling, J = 144.6 Hz.*

the effect of producing a cumulative tip of the desired resonance 90° into the $x$–$y$ plane for observation. In contrast, the remaining resonances, which have different precession intervals, receive relatively little benefit from the pulse train application and thus remain as essentially unperturbed $Z$-magnetization. The net result of these two events is the acquisition of a subspectrum containing only information from the desired resonance.

By the application of selective excitation with gated decoupling, $^1H$–$^{13}C$ coupled spin multiplets were obtained for all resonances in the high-field region of the $^{13}C$-NMR spectrum of brucine (I) (Fig. 2). In all cases, the multiplicities determined by $T_1$ relaxation methods and selective excitation were in complete agreement. However, the latter method has the further advantage of providing easy experimental access to the primary $^1H$–$^{13}C$ spin-coupling constants ($^1J_{CH}$), which are otherwise inaccessible, despite their considerable diagnostic utility. These data are summarized in the structure presented here and in Table I.

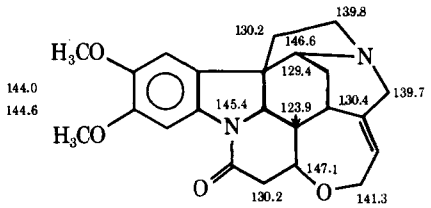

The primary coupling constants ($^1J_{CH}$) for brucine were measured by selective excitation with gated decoupling (27–30). It is certain that the resonances for C-11, C-18, and C-20, which Singh *et al.* (8) referred to as being not clear, were reported accurately by other investigators (1–7, 9).

A further point that is clarified by examination of the selectively excited $^1H$–$^{13}C$ spin-coupled subspectra is the contention by Wehrli and Nishida (13) that the assignments for C-11, C-18, and C-20 are insufficiently substantiated. Unequivocal assignment of the resonance for C-11 thus is made to the resonance at $\delta$ 41.6, based on the primary coupling constant $^1J_{C_{11}H_{11}}$ = 130.2 Hz, while C-18 and C-20 exhibit somewhat larger couplings of 139.8 and 139.7 Hz, respectively. Further discrimination between C-18 and C-20 also is possible by selective excitation, the former exhibiting considerable broadening of its spin-coupled resonance, probably as a result of couplings to the anisochronous C-17 methylene protons. This contention is supported by the observation that the two-bond coupling constants of heterocyclic systems frequently are as large as the three-bond couplings, which normally are the largest of the long-range couplings seen in $^1H$–$^{13}C$ coupled spectra. In contrast, C-20, which is positioned between N-19 and the vinyl carbon, C-21, would be expected to exhibit significantly less long-range coupling. Thus, assignment of C-18 is made to the resonance at $\delta$ 49.3, while C-20 is assigned to the resonance at $\delta$ 51.8; these assignments also are in agreement with previous reports (5–7, 9).

While considerable utility has been demonstrated for selective excitation with gated decoupling, some information is lost to the researcher

**Table I—25.158-MHz $^{13}C$-NMR Shift Assignments, Multiplicities, Relaxation Times, and Coupling Constants for Brucine**

| Carbon | $^{13}C$, $\delta$ | Multiplicity | $T_1$, sec | $^1J_{CH}$, Hz |
|---|---|---|---|---|
| 10 | 168.0 | s | — | — |
| 3 | 148.4 | s | — | — |
| 2 | 145.4 | s | — | — |
| 21 | 139.7 | s | — | — |
| 5 | 135.3 | s | — | — |
| 22 | 126.3 | d | 0.17 | — |
| 6 | 122.9 | s | — | — |
| 1 | 105.1 | d | 0.18 | — |
| 4 | 100.3 | d | 0.18 | — |
| 12 | 76.9 | d | 0.21[a] | 147.1 |
| 23 | 63.7 | t | 0.10 | 141.3 |
| 8 | 59.9 | d | 0.18 | 145.4 |
| 16 | 59.1 | d | 0.18 | 146.6 |
| $OCH_3$ | 55.7 | q | 0.84 | 144.0 |
| $OCH_3$ | 55.3 | q | 0.68 | 144.6 |
| 20 | 51.8 | t | 0.10 | 139.7 |
| 7 | 51.0 | s | — | — |
| 18 | 49.3 | t | 0.10 | 139.8 |
| 13 | 47.4 | d | 0.18 | 123.9 |
| 11 | 41.6 | t | 0.10 | 130.2 |
| 17 | 41.5 | t | 0.10 | 130.2 |
| 14 | 30.8 | d | 0.19 | 130.4 |
| 15 | 26.0 | t | 0.09 | 129.4 |

[a] Degenerate with center line of deuterochloroform triplet; relaxation time may be suspect.

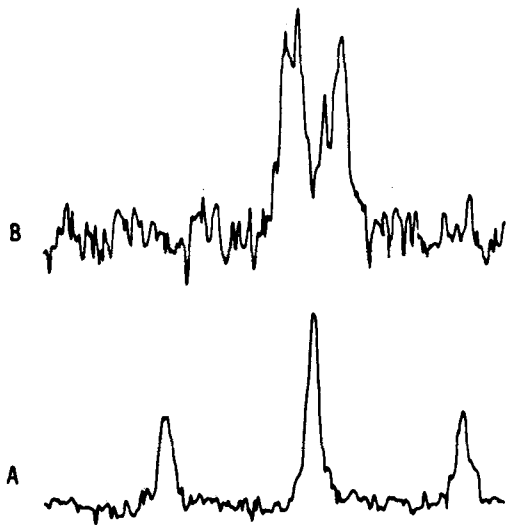


**Figure 3**—*Selective excitation in conjunction with gated decoupling of the C-15 methylene resonance at δ 26.0 (A) and single-frequency off-resonance decoupling subspectrum showing the anisochronicity of the methylene protons attached to the same carbon atom (B).*

using this technique which can be especially valuable when dealing with a molecule of unknown structure. Specifically, the lost information is that provided by the anisochronicity of methylene protons under certain circumstances (15), but it is available by conventional single-frequency off-resonance decoupling techniques. However, the advantages of single-frequency off-resonance decoupling observation with the unambiguous character of selectively excited and gated decoupled subspectra are combined in selective excitation with single-frequency off-resonance decoupling (20). The technique, in principle, is quite similar to selective excitation in the preparation of the spin system for observation. The two techniques differ in that the former employs conventional gated decoupling while the latter utilizes the collapse of the decoupling field from broad-band noise irradiation of the proton spectral window to a preselected single frequency. The net result of selective excitation method is to provide a selectively excited subspectrum with single-frequency off-resonance decoupling spectral characteristics. An illustrative example is shown in Fig. 3 for the C-15 methylene resonances, which, because of the anisochronous nature of the attached protons, may exhibit a doublet of doublets under certain decoupler conditions rather than the more conventional triplet (9, 15).

Several techniques have been described that provide the means of determining resonance spin multiplicities unambiguously. Considerable useful information in the form of primary coupling constants also is obtained, which can be of tremendous assistance in the assemblage of structural fragments into larger contiguous blocks. The errors in signal assignments such as those in the report of Singh *et al.* (8) can be completely avoided by the use of techniques that are capable of completely removing the ambiguities inherent in single-frequency off-resonance decoupling spectra of very large molecules.

## EXPERIMENTAL[1]

All $^{13}C$-NMR experiments were performed on a sample prepared by dissolving 500 mg of brucine[2] in 3.0 ml of deuterochloroform[3] and the solution was degassed with zero-grade argon[4] for 15 min followed by transfer to a 12-mm NMR tube fitted with a polytef vortex plug. All chemical shifts were referenced relative to the center line of the deuterochloroform triplet, which was taken as being 76.9 ppm downfield of tetramethylsilane. Typical instrument acquisition parameters were 5-kHz spectral observation with 8K data points (4K after transformation) and sufficient acquisitions to provide usable signal-to-noise ratios and an acquisition time of 0.8192 sec. Typical 90° pulses were obtained with a 20-sec pulse, with no effort made to optimize this pulse to the sample.

The $T_1$ relaxation studies were conducted using the inversion recovery pulse sequence (31, 32), and data reduction was accomplished with the three-parameter nonlinear fitting program (33). Selective excitation experiments were conducted using previously reported procedures and instrument modifications (20, 30).

[1] Varian Associates model XL-100-15 spectrometer system, operating at 25.158 MHz in the Fourier transform mode, equipped with a Nicolet TT-100 data system, a model TT-760 decoupler, and an NT-440 Multi-Observe Nuclei Accessory.
[2] Sigma Chemical Co., St. Louis, Mo.
[3] Aldrich Chemical Co., Milwaukee, Wis.
[4] Iweco, Houston, Tex.

## REFERENCES

(1) F. W. Wehrli, *J. Chem. Soc., Chem. Commun.*, **1973**, 379.
(2) F. W. Wehrli, *Adv. Mol. Relax. Proc.*, **6**, 139 (1974).
(3) R. Verpoorte and A. Baerheim-Svendsen, *Pharm. Weekbl.*, **111**, 745 (1976).
(4) P. R. Srinivasan and R. L. Lichter, *Org. Magn. Res.*, **8**, 198 (1976).
(5) R. Verpoorte, P. J. Hylands, and N. G. Bisset, *ibid.*, **9**, 567 (1977).
(6) J. Leung and A. J. Jones, *ibid.*, **9**, 333 (1977).
(7) E. Wenkert, A. H. T. Cheung, H. E. Gottlieb, M. C. Koch, A. Rabaron, and M. M. Plat, *J. Org. Chem.*, **43**, 1099 (1978).
(8) S. P. Singh, V. I. Steenberg, S. S. Parmar, and S. A. Farnum, *J. Pharm. Sci.*, **68**, 89 (1979).
(9) L. F. Johnson, in "Topics in Carbon-13 NMR," vol. 3, G. C. Levy, Ed., Wiley–Interscience, New York, N.Y., 1979, pp. 7–16.
(10) F. W. Wehrli and T. Wirthlin, "Interpretation of Carbon-13 NMR Spectra," Heyden and Sons, New York, N.Y., 1976, chap. 4.
(11) F. W. Wehrli, in "Topics in Carbon-13 NMR Spectroscopy," vol. 2, G. C. Levy, Ed., Wiley–Interscience, New York, N.Y., 1976, chap. 6.
(12) J. R. Lyerla, Jr., and G. C. Levy, in "Topics in Carbon-13 NMR Spectroscopy," vol. 1, G. C. Levy, Ed., Wiley–Interscience, New York, N.Y., 1974, chap. 3.
(13) F. W. Wehrli and T. Nishida, *Forschr. Chem. Org. Natur.*, **36**, 16 (1979).
(14) K. F. Kuhlman, D. M. Grant, and R. K. Harris, *J. Chem. Phys.*, **52**, 343 (1970).
(15) E. W. Hagaman, *Org. Magn. Res.*, **8**, 389 (1976).
(16) J. W. Blunt and J. B. Stothers, *ibid.*, **9**, 439 (1977).
(17) K. Nakanishi, V. P. Gullo, I. Miura, T. R. Govindacharia, and N. Vishwanathan, *J. Am. Chem. Soc.*, **95**, 6473 (1973).
(18) K. Nakanishi, J. Crouch, I. Miura, X. Dominguez, A. Zamudio, and R. Villareal, *ibid.*, **96**, 609 (1974).
(19) P. R. Zanno, I. Miura, K. Nakanishi, and D. L. Elder, *ibid.*, **97**, 1975 (1976).
(20) G. E. Martin, J. A. Matson, J. C. Turley, and A. J. Weinheimer, *ibid.*, **101**, 1888 (1979).
(21) G. E. Martin, J. A. Matson, and A. J. Weinheimer, *Tetra-*

*hedron Lett.*, **1979**, 2195.
(22) A. Neszmelyi, S. Omura, T. T. Thung, and G. Luckacs, *ibid.*, **1977**, 721.
(23) A. Neszmelyi and H. Bojarska-Dahlig, *J. Antibiot.*, **31**, 487 (1978).
(24) S. Mizsak, S. Slomp, S. D. Gero, and G. Luckacs, *Tetrahedron Lett.*, **1977**, 725.
(25) R. S. Becker, S. Berger, D. K. Dalling, D. M. Grant, and R. J. Pugmire, *J. Am. Chem. Soc.*, **96**, 7008 (1974).
(26) R. Rowan, III, and B. D. Sykes, *ibid.*, **96**, 7000 (1974).
(27) G. Bodenhausen, R. Freeman, and G. A. Morris, *J. Magn. Res.*, **23**, 171 (1976).
(28) G. A. Morris and R. Freeman, *ibid.*, **29**, 433 (1978).
(29) R. Freeman and H. D. W. Hill, *ibid.*, **5**, 278 (1971).
(30) G. E. Martin, *J. Heterocycl. Chem.*, **15**, 1539 (1978).
(31) R. L. Vold, J. S. Waugh, M. P. Klein, and D. E. Phelps, *J. Chem. Phys.*, **48**, 3831 (1968).
(32) R. Freeman and H. D. W. Hill, *ibid.*, **51**, 3140 (1969).
(33) J. Kowalewski, G. C. Levy, L. F. Johnson, and L. Palmer, *J. Magn. Res.*, **26**, 533 (1977).

**ACKNOWLEDGMENTS**

Supported by Grant E-792 from the Robert A. Welch Foundation.

## NOTES

# Synthesis and Antibacterial and Anticancer Evaluations of α-Methylene-γ-butyrolactones

**NED D. HEINDEL** ˣ **and JOHN A. MINATELLI**

Received April 7, 1980, from the *Center for Health Sciences, Lehigh University, Bethlehem, PA 18015.* Accepted for publication July 17, 1980.

**Abstract** □ Nine new α-methylene-γ-butyrolactones were synthesized by the Reformatsky condensation of ethyl α-bromomethylacrylate with ketones, aldehydes, and an epoxide. A unique spirobutyrolactone class was prepared by reaction of the zinc alkyl derivative and *N*-methylisatins. The compounds were evaluated against L-1210 and P-388 leukemia and the 9KB carcinoma of the nasopharynx. They also were screened in a microbiocidal and an antifungal assay. The spiro methylene lactone of 5-iodo-*N*-methylisatin displayed activity in the P-388, 9KB, and antifungal screens.

**Keyphrases** □ α-Methylene-γ-butyrolactones—synthesis and evaluation for antibacterial and antineoplastic activity □ Antibacterial activity, potential—evaluation of α-methylene-γ-butyrolactones □ Antineoplastic activity, potential—evaluation of α-methylene-γ-butyrolactones

Recognized as the active moiety in a wide variety of antineoplastic sesquiterpene lactones (1, 2), the α-methylene-γ-butyrolactone structure has been synthetically incorporated in numerous drug candidates in the search for anticancer activity (3, 4). Many synthetic approaches have been used (5), and new methods are reported regularly (6, 7) since many of the model substances are active.

The application of the Reformatsky method by Öhler *et al.* (8) is a facile, one-step conversion of aldehydes and ketones to the requisite lactones with the greatest potential of altering the functionality at C-5 (Scheme I). This condensation of the zinc alkyl derivative of ethyl α-bromomethylacrylate with *N*-methylisatins (II*a* and II*b*) also yields a unique class of spirolactones (V*a* and V*b*) (Scheme II). Nine lactones were synthesized in 25–59% yields using this procedure (Table I).

## EXPERIMENTAL[1]

***p*-(Pyrrolidinosulfonamido)benzaldehyde (I*d*)**—Compound I*d* was obtained by the dropwise addition of 2.78 g (39.2 mmoles) of anhydrous pyrrolidine in 10 ml of acetone to 6.00 g (19.5 mmoles) of *p*-chlorosulfonylbenzaldehyde diacetate (9) in 25 ml of acetone. The medium was stirred for 1 hr, the acetone was removed *in vacuo*, and the residue was dissolved in methylene chloride and washed with 20 ml of 10% aqueous HCl. The solvent was removed by distillation, and the crystalline diacetate was hydrolyzed by refluxing for 1 hr in a solution of 25 ml of ethanol, 25 ml of water, and 3 ml of concentrated sulfuric acid. The solution was chilled and it deposited the aldehyde as white crystals, which were filtered, recrystallized twice from ethanol, and dried *in vacuo* to yield 3.35 g (50%) of I*d*, mp 109–111°; IR (mineral oil): 1710 (C=O) $cm^{-1}$; NMR (deuterochloroform): δ 1.60–1.95 (m, 4H, $CH_2CH_2$), 3.16–3.50 (m, 4H, $CH_2NCH_2$), 8.1 (broad s, 4H, aromatic H), and 10.17 (s, 1H, CHO) ppm.

*Anal.*—Calc. for $C_{11}H_{13}NOS_3$: C, 55.19; H, 5.47; N, 5.85. Found: C, 55.16; H, 5.68; N, 5.71.

***p*-(Pyrrolidinosulfonamido)acetophenone (I*f*)**—Compound I*f* was prepared by the addition of 3.50 g (49.3 mmoles) of anhydrous pyrrolidine in 10 ml of acetone to 5.00 g (22.9 mmoles) of *p*-chlorosulfonylacetophenone (10) in 25 ml of acetone. After 2 hr of refluxing and stirring, the solution was poured into 75 ml of cold water. The resulting precipitate was collected, washed with cold water, dried *in vacuo*, and recrystallized twice from ethanol to yield 4.30 g (74%) of I*f* as pale-yellow needles, mp 142–144°; IR (mineral oil): 1690 (C=O) $cm^{-1}$; NMR (deuterochloroform): δ 1.65–2.00 (m, 4H, $CH_2CH_2$), 2.70 (s, 3H, $COCH_3$), 3.20–3.50 (m, 4H, $CH_2NCH_2$), and 7.85–8.30 (m, 4H, aromatic H) ppm.

*Anal.*—Calc. for $C_{12}H_{15}NO_3S$: C, 56.95; H, 5.97; N, 5.53. Found: C, 57.13; H, 6.16; N, 5.67.

[1] Analyses were performed by Dr. G. I. Robertson, Florham Park, N.J. Melting points were determined between glass disks on a Fisher-Johns apparatus and are uncorrected. NMR spectra were obtained on a Perkin-Elmer Hitachi R20A spectrometer and were calibrated against tetramethylsilane. IR spectra were obtained on a Perkin-Elmer 257 spectrophotometer as petroleum oil mulls.



*0022-3549/81/0100-0084$01.00/0*
*© 1981, American Pharmaceutical Association*

*hedron Lett.*, **1979**, 2195.
(22) A. Neszmelyi, S. Omura, T. T. Thung, and G. Luckacs, *ibid.*, **1977**, 721.
(23) A. Neszmelyi and H. Bojarska-Dahlig, *J. Antibiot.*, **31**, 487 (1978).
(24) S. Mizsak, S. Slomp, S. D. Gero, and G. Luckacs, *Tetrahedron Lett.*, **1977**, 725.
(25) R. S. Becker, S. Berger, D. K. Dalling, D. M. Grant, and R. J. Pugmire, *J. Am. Chem. Soc.*, **96**, 7008 (1974).
(26) R. Rowan, III, and B. D. Sykes, *ibid.*, **96**, 7000 (1974).
(27) G. Bodenhausen, R. Freeman, and G. A. Morris, *J. Magn. Res.*, **23**, 171 (1976).
(28) G. A. Morris and R. Freeman, *ibid.*, **29**, 433 (1978).
(29) R. Freeman and H. D. W. Hill, *ibid.*, **5**, 278 (1971).
(30) G. E. Martin, *J. Heterocycl. Chem.*, **15**, 1539 (1978).
(31) R. L. Vold, J. S. Waugh, M. P. Klein, and D. E. Phelps, *J. Chem. Phys.*, **48**, 3831 (1968).
(32) R. Freeman and H. D. W. Hill, *ibid.*, **51**, 3140 (1969).
(33) J. Kowalewski, G. C. Levy, L. F. Johnson, and L. Palmer, *J. Magn. Res.*, **26**, 533 (1977).

**ACKNOWLEDGMENTS**

Supported by Grant E-792 from the Robert A. Welch Foundation.

## NOTES

# Synthesis and Antibacterial and Anticancer Evaluations of α-Methylene-γ-butyrolactones

**NED D. HEINDEL** ˣ **and JOHN A. MINATELLI**

Received April 7, 1980, from the *Center for Health Sciences, Lehigh University, Bethlehem, PA 18015.* Accepted for publication July 17, 1980.

**Abstract** □ Nine new α-methylene-γ-butyrolactones were synthesized by the Reformatsky condensation of ethyl α-bromomethylacrylate with ketones, aldehydes, and an epoxide. A unique spirobutyrolactone class was prepared by reaction of the zinc alkyl derivative and *N*-methylisatins. The compounds were evaluated against L-1210 and P-388 leukemia and the 9KB carcinoma of the nasopharynx. They also were screened in a microbiocidal and an antifungal assay. The spiro methylene lactone of 5-iodo-*N*-methylisatin displayed activity in the P-388, 9KB, and antifungal screens.

**Keyphrases** □ α-Methylene-γ-butyrolactones—synthesis and evaluation for antibacterial and antineoplastic activity □ Antibacterial activity, potential—evaluation of α-methylene-γ-butyrolactones □ Antineoplastic activity, potential—evaluation of α-methylene-γ-butyrolactones

Recognized as the active moiety in a wide variety of antineoplastic sesquiterpene lactones (1, 2), the α-methylene-γ-butyrolactone structure has been synthetically incorporated in numerous drug candidates in the search for anticancer activity (3, 4). Many synthetic approaches have been used (5), and new methods are reported regularly (6, 7) since many of the model substances are active.

The application of the Reformatsky method by Öhler *et al.* (8) is a facile, one-step conversion of aldehydes and ketones to the requisite lactones with the greatest potential of altering the functionality at C-5 (Scheme I). This condensation of the zinc alkyl derivative of ethyl α-bromomethylacrylate with *N*-methylisatins (II*a* and II*b*) also yields a unique class of spirolactones (V*a* and V*b*) (Scheme II). Nine lactones were synthesized in 25–59% yields using this procedure (Table I).

## EXPERIMENTAL[1]

***p*-(Pyrrolidinosulfonamido)benzaldehyde (I*d*)**—Compound I*d* was obtained by the dropwise addition of 2.78 g (39.2 mmoles) of anhydrous pyrrolidine in 10 ml of acetone to 6.00 g (19.5 mmoles) of *p*-chlorosulfonylbenzaldehyde diacetate (9) in 25 ml of acetone. The medium was stirred for 1 hr, the acetone was removed *in vacuo*, and the residue was dissolved in methylene chloride and washed with 20 ml of 10% aqueous HCl. The solvent was removed by distillation, and the crystalline diacetate was hydrolyzed by refluxing for 1 hr in a solution of 25 ml of ethanol, 25 ml of water, and 3 ml of concentrated sulfuric acid. The solution was chilled and it deposited the aldehyde as white crystals, which were filtered, recrystallized twice from ethanol, and dried *in vacuo* to yield 3.35 g (50%) of I*d*, mp 109–111°; IR (mineral oil): 1710 (C=O) $cm^{-1}$; NMR (deuterochloroform): δ 1.60–1.95 (m, 4H, $CH_2CH_2$), 3.16–3.50 (m, 4H, $CH_2NCH_2$), 8.1 (broad s, 4H, aromatic H), and 10.17 (s, 1H, CHO) ppm.

*Anal.*—Calc. for $C_{11}H_{13}NOS_3$: C, 55.19; H, 5.47; N, 5.85. Found: C, 55.16; H, 5.68; N, 5.71.

***p*-(Pyrrolidinosulfonamido)acetophenone (I*f*)**—Compound I*f* was prepared by the addition of 3.50 g (49.3 mmoles) of anhydrous pyrrolidine in 10 ml of acetone to 5.00 g (22.9 mmoles) of *p*-chlorosulfonylacetophenone (10) in 25 ml of acetone. After 2 hr of refluxing and stirring, the solution was poured into 75 ml of cold water. The resulting precipitate was collected, washed with cold water, dried *in vacuo*, and recrystallized twice from ethanol to yield 4.30 g (74%) of I*f* as pale-yellow needles, mp 142–144°; IR (mineral oil): 1690 (C=O) $cm^{-1}$; NMR (deuterochloroform): δ 1.65–2.00 (m, 4H, $CH_2CH_2$), 2.70 (s, 3H, $COCH_3$), 3.20–3.50 (m, 4H, $CH_2NCH_2$), and 7.85–8.30 (m, 4H, aromatic H) ppm.

*Anal.*—Calc. for $C_{12}H_{15}NO_3S$: C, 56.95; H, 5.97; N, 5.53. Found: C, 57.13; H, 6.16; N, 5.67.

[1] Analyses were performed by Dr. G. I. Robertson, Florham Park, N.J. Melting points were determined between glass disks on a Fisher-Johns apparatus and are uncorrected. NMR spectra were obtained on a Perkin-Elmer Hitachi R20A spectrometer and were calibrated against tetramethylsilane. IR spectra were obtained on a Perkin-Elmer 257 spectrophotometer as petroleum oil mulls.



*0022-3549/81/0100-0084$01.00/0*
*© 1981, American Pharmaceutical Association*

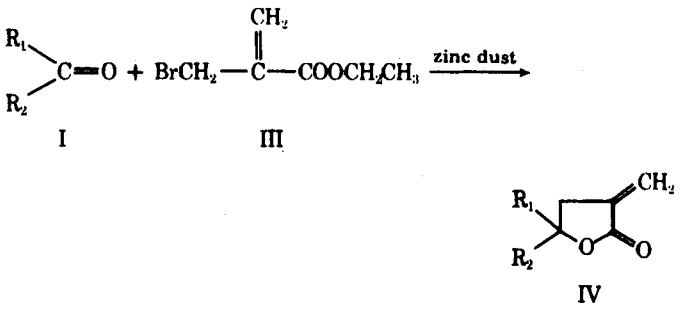

*Scheme I*

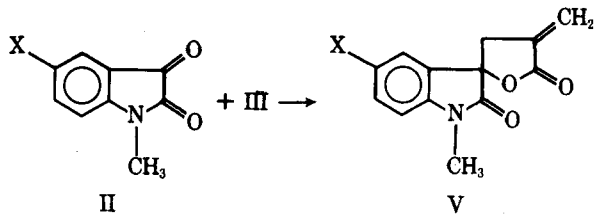

**IIa and Va**: X = H
**IIb and Vb**: X = I

*Scheme II*

Ethyl *p*-acetyl-4-phenylbutyrate (Ia) (11), *p*-(*N,N*-diethylsulfonamido)benzaldehyde (Ie) (9), *p*-(morpholinosulfonamido)benzaldehyde (Ic) (9), *N*-methylisatin (IIa) (12), and 5-iodo-*N*-methylisatin (IIb) (12) were prepared by published methods. Phenyl 2-thienyl ketone (Ib), phenylacetaldehyde (Ig), and styrene oxide were obtained commercially and were used without further purification.

**General Procedure for Synthesis of α-Methylene-γ-butyrolactones (IVa–IVg, Va, and Vb)**—A four-necked flask was fitted with a condenser with its outlet connected to a mercury bubbler, a thermometer, a dropping funnel, and a nitrogen inlet tube. The system was flame dried and charged with 25 mmoles of the requisite carbonyl compound (Ia–Ih, IIa, and IIb) or styrene oxide. To this mixture were added 25 mmoles of dry zinc dust, three crystals of iodine, and sufficient tetrahydrofuran (~10–30 ml) to effect solution of the organic component. With vigorous stirring and a constant nitrogen gas blanket, 25 mmoles of ethyl α-bromomethylacrylate (13) in 5 ml of tetrahydrofuran was added dropwise. There was an initial exothermic reaction that soon subsided.

When the addition was completed, the contents of the flask were heated at reflux for 3 hr with constant stirring, cooled, and poured into 50 ml of 10% aqueous HCl. This aqueous medium was agitated for 15 min to ensure complete hydrolysis and extracted with two 30-ml portions of methylene chloride. The extracts were washed once with water, dried over magnesium sulfate, and evaporated *in vacuo* to give the title compounds, which solidified (except IVa and IVg) from the initially oily phase. The liquids (IVa and IVg) were purified by vacuum distillation, after which IVg solidified as white needles. All solids were recrystallized from ethanol–benzene (1:1) to analytical purity; the yields, physical properties, and analytical results are given in Table I.

All products were submitted for anticancer screening in the National Cancer Institute L-1210, P-388, and 9KB assays (Table I) and for evaluation against a Gram-positive (*Staphylococcus aureus*, ATCC 6538), a Gram-negative (*Escherichia coli*, ATCC 8739), and a fungal (*Candida*

**Table I—Physical and Pharmacological Properties of Methylene Lactones**

| Compound | Melting Point (Boiling Point/mm Hg) | Yield, % | Formula | Analysis, % Calc. | Found | P-388 Leukemia[a] Dose, mg/kg | Survival | T − C Wt., g | T/C % | KB Screen[a] $ED_{50}$, μg/ml |
|---|---|---|---|---|---|---|---|---|---|---|
| IVa | (225–227°/1.9) | 33 | $C_{18}H_{22}O_4$ | C 71.50 | 71.28 | — | — | — | — | 21.0 |
| | | | | H 7.34 | 7.44 | | | | | |
| IVb | 108–110° | 25 | $C_{15}H_{12}O_2S$ | C 70.29 | 70.18 | — | — | — | — | — |
| | | | | H 4.72 | 4.96 | | | | | |
| IVc | 150–151° | 40 | $C_{15}H_{17}NO_5S$ | C 55.72 | 55.91 | 100 | 0/6 | — | T | 2.7 |
| | | | | H 5.30 | 5.50 | 50 | 4/6 | −3.7 | T | |
| | | | | N 4.33 | 4.37 | 25 | 6/6 | −0.8 | 144 | |
| | | | | | | 12.5 | 6/6 | +0.7 | 147 | |
| IVd | 112–115° | 59 | $C_{15}H_{17}NO_4S$ | C 58.62 | 58.64 | — | — | — | — | — |
| | | | | H 5.58 | 5.67 | | | | | |
| | | | | N 4.56 | 4.52 | | | | | |
| IVe | 95–98° | 52 | $C_{15}H_{19}NO_4S$ | C 58.22 | 57.98 | — | — | — | — | 15.0 |
| | | | | H 6.19 | 6.30 | | | | | |
| | | | | N 4.52 | 4.62 | | | | | |
| IVf | 142–145° | 55 | $C_{16}H_{19}NO_4S$ | C 59.80 | 59.66 | — | — | — | — | 21.0 |
| | | | | H 5.96 | 6.15 | | | | | |
| | | | | N 4.36 | 4.29 | | | | | |
| IVg | 63–64° (131–136°/0.6) | 26 | $C_{12}H_{12}O_2$ | C 76.57 | 76.44 | — | — | — | — | 27.0 |
| | | | | H 6.41 | 6.58 | | | | | |
| Va | 135–137° | 25 | $C_{13}H_{11}NO_3$ | C 68.11 | 67.85 | — | — | — | — | — |
| | | | | H 4.83 | 5.15 | | | | | |
| | | | | N 6.10 | 6.05 | | | | | |
| Vb | 157–159° | 34 | $C_{13}H_{10}INO_3$ | C 43.95 | 44.20 | 100 | 2/6 | −4.0 | T | 0.28 |
| | | | | H 2.83 | 3.03 | 50 | 3/6 | −9.3 | T | |
| | | | | N 3.94 | 3.84 | 25 | 5/6 | −2.6 | 139 | |
| | | | | | | 12.5 | 6/6 | −2.4 | 129 | |

[a] All test results were provided by the National Cancer Institute. Procedures, protocols, and data interpretation were published in R. I. Geran, N. H. Greenberg, M. M. MacDonald, A. M. Schumacher, and B. G. Abbott, *Cancer Chemother. Rep., Part 3*, 3, 7 (1972), and in "Instruction Booklet 14," Drug Evaluation Branch, Division of Cancer Treatment, National Cancer Institute, Bethesda, Md., 1978. The symbol T means the substance was too toxic for calculation of T/C % values.

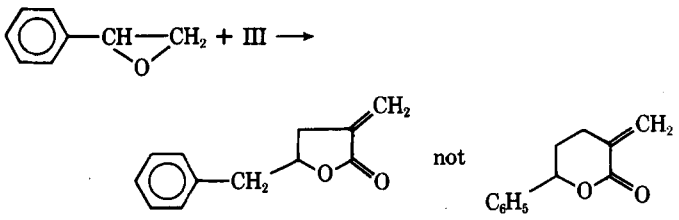

IV*g*

*Scheme III*

*albicans*, Strain 582, Rutgers University Collection) organism according to the previously published method (14).

## RESULTS AND DISCUSSION

The reaction of the Reformatsky reagent from III and styrene oxide did not yield a $\delta$-phenyl-$\alpha$-methylene-$\delta$-valerolactone as expected from ring opening of the oxide but instead gave a 26% yield of $\gamma$-benzyl-$\alpha$-methylene-$\gamma$-butyrolactone (IV*g*) (Scheme III). The mass spectrum showed intense P − 91 and 91 amu peaks corresponding to tropilium ions derived from a benzyl–carbon scission (15). Furthermore, comparison of the spectra, melting points, and mixed melting points showed that the product was identical to that obtained from phenylacetaldehyde and the zinc alkyl derivative of III. The literature contains other examples of epoxide to carbonyl rearrangements induced during Reformatsky reactions. Thus, cyclopentene oxide and cyclopentanone both gave ethyl 1-hydroxycyclopentyl acetate with ethyl $\alpha$-bromozinc acetate (16). Furthermore, $\alpha$-pinene oxide under Reformatsky conditions gave the same hydroxy ester as that derived from the carbonyl compound generated by prior rearrangement of the oxide (17).

PMR spectroscopy was useful in identifying the lactone products (IV*a*–IV*g*, V*a*, and V*b*). For all of the exocyclic methylene groups, two apparent triplets ($J$ = 3 Hz) were found at $\delta$ 6.28 ± 0.1 for the proton *anti* to the carbonyl group and at $\delta$ 5.72 ± 0.08 ppm for the proton *cis* to the carbonyl group. The C-4 methylene signals were complex multiplets at 2.6–3.8 ppm. Characteristic IR bands were found at 1660 ± 5 (C=C) and 1760 ± 5 (C=O) $cm^{-1}$ for each lactone prepared.

As was noted in other model $\alpha$-methylene-$\gamma$-butyrolactones, no active analogs were found in the L-1210 lymphoid leukemia screen (3). In addition, all of the compounds, except IV*b*, were highly toxic to the test animals and could not be evaluated accurately at doses in excess of 100 mg/kg. However, in the P-388 lymphocytic leukemia screen (ascitic fluid, intraperitoneal administration to $CDF_1$ mice), two of the analogs (IV*c* and V*b*) were evaluated, and both met the minimal activity standards of T/C > 125%. Although toxic at 50 mg/kg, IV*c* and V*b* increased the lifespan of treated animals at lower doses by 47% (T/C = 147%) and 39%, respectively. Furthermore, in the *in vitro* assay against cells derived from human carcinoma of the nasopharynx (KB) carried in cell culture, V*b* displayed potency ($ED_{50}$ = 0.28 $\mu$g/ml) in the approximate range of that observed for the sesquiterpene lactones from which these methylene lactones are modeled.

Compounds IV*b*–IV*e*, IV*g*, V*a*, and V*b* were evaluated in an antibacterial/antifungal assay in which zones of inhibition were measured from the edge of an assay disk impregnated with 4 mg of the test compound. At these concentrations, sulfamerazine gave a 17-mm zone against *E. coli* and IV*d* gave an 8-mm zone, but no other analogs tested appeared to be active. With *S. aureus*, IV*g* and V*a* both displayed 12-mm zones, while the standard sulfamerazine demonstrated a 4-mm region of inhibition. No other test compounds showed significant activity. Against *C. albicans*, for which sulfamerazine possessed negligible activity (~1-mm zone), IV*g* displayed an 18-mm zone of inhibition, and both IV*d* and V*b* demonstrated ~4-mm zones. All other analogs were inactive.

As Rosowsky *et al.* (18) found in a series of model methylene lactones, no particular correlation of structure and activity is evident from the data. The activity profile in the spiro indole methylene lactone (V*b*) should encourage further research in this class.

## REFERENCES


(1) S. M. Kupchan, *Trans. N.Y. Acad. Sci.*, **32**, 85 (1970).

(2) S. M. Kupchan, M. A. Eakin, and A. M. Thomas, *J. Med. Chem.*, **14**, 1147 (1971).

(3) G. A. Howie, P. E. Manni, and J. M. Cassady, *ibid.*, **17**, 840 (1974).

(4) J. M. Cassady, S. R. Byrn, I. K. Stamos, S. M. Evans, and A. McKenzie, *ibid.*, **21**, 815 (1978).

(5) P. A. Grieco, *Synthesis*, **1975**, 67.

(6) T. Hiyama, H. Saimoto, K. Nishio, M. Shinoda, H. Yamamoto, and H. Nozaki, *Tetrahedron Lett.*, **1979**, 2043.

(7) A. W. McCulloh and A. G. McInnes, *ibid.*, **1979**, 1963.

(8) E. Öhler, K. Reininger, and U. Schmidt, *Angew. Chem., Int. Ed., Engl.*, **9**, 457 (1970).

(9) T. P. Sychera and M. N. Shuchukina, *Sb. Statei Obschch. Khim., Akad. Nauk SSSR*, **1**, 527 (1953); through *Chem. Abstr.*, **49**, 932 (1955).

(10) C. Troeltzsch, *J. Prakt. Chem.*, **22**, 192 (1963).

(11) L. Schmid, H. Schuttes, and M. Wichtal, *Monatsh. Chem.*, **85**, 80 (1954).

(12) W. Borsche, H. Weussmann, and A. Fritzsche, *Chem. Ber.*, **57**, 1770 (1924).

(13) A. P. Ferris, *J. Org. Chem.*, **20**, 780 (1955).

(14) N. D. Heindel, C. C. Ho Ko, R. B. Birrer, and J. R. Merkel, *J. Med. Chem.*, **15**, 118 (1972).

(15) F. W. McLafferty, "Interpretation of Mass Spectra," W. A. Benjamin, New York, N.Y., 1967, p. 92.

(16) G. R. Clemo and J. Ormston, *J. Chem. Soc.*, **1933**, 362.

(17) B. A. Arbuzov, *Chem. Ber.*, **68**, 1430 (1935).

(18) A. Rosowsky, N. Papathanasopoulos, H. Lazarus, G. Foley, and E. J. Modest, *J. Med. Chem.*, **17**, 672 (1974).


## ACKNOWLEDGMENTS


Supported in part by Grant CA-22579 from the National Cancer Institute.

# PMR and $^{13}C$-NMR Spectroscopy of Tropane and *N*-Substituted Nortropane Spirohydantoins

**G. G. TRIGO ˣ, M. MARTÍNEZ, and E. GÁLVEZ**

Received April 9, 1980, from the *Department of Organic and Pharmaceutical Chemistry, School of Pharmacy, Universidad Complutense, Madrid-3, Spain.* Accepted for publication July 17, 1980.

**Abstract** □ The preferred conformations of a pharmacologically interesting series of *N*-substituted nortropane spirohydantoins were determined from PMR and $^{13}C$-NMR data to permit a structure–activity relationship study.

**Keyphrases** □ Tropane and *N*-substituted nortropane spirohydantoins—PMR and $^{13}C$-NMR spectra, determination of preferred conformation □ $^{13}C$-NMR spectroscopy—tropane and *N*-substituted nortropane spirohydantoins, determination of preferred conformation

A series of tropane and nortropane 3-spiro-5′-hydantoins, synthesized previously following the method outlined in Scheme I (1), showed anticonvulsant activity against pentylenetetrazol-induced convulsions in mice (2) and antiarrhythmic activity in rabbits previously treated with ouabain (2). Compound V is as active as procainamide in this assay. It showed an inhibitory effect on sodium transport in frog skin. As with diphenylhydantoins, it did not alter the initial inhibitory phase in the action of isoproterenol on frog skin, but it did alter subsequent stimulation (3). Furthermore, several compounds showed a local anti-inflammatory action comparable to that of indomethacin and greater than that of phenylbutazone (4).

These observations prompted the PMR and $^{13}C$-NMR study of these compounds to determine their preferred conformation in solution with the objective of establishing a structure–activity relationship.

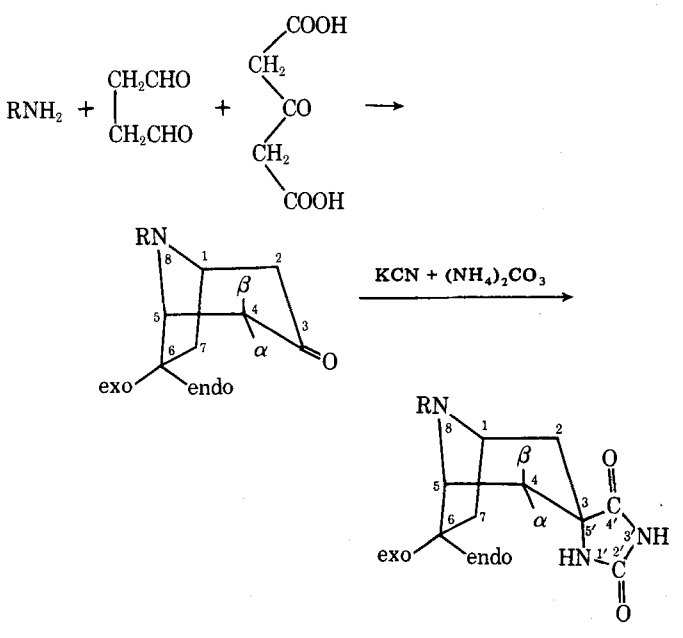


I: R = H
II: R = $CH_3$
III: R = $C_2H_5$
IV: R = *n*-$C_3H_7$
V: R = *iso*-$C_3H_7$
VI: R = *n*-$C_4H_9$
VII: R = $CH_2CH_2OH$
VIII: R = $C_6H_5$
IX: R = $CH_2C_6H_5$
X: R = $CH_2CH_2C_6H_5$

*Scheme I*

## EXPERIMENTAL

The synthesis and purification of the compounds were described previously (1). The PMR spectra were recorded at 100 MHz[1] at room temperature. The $^{13}C$-NMR spectra were determined at 20 MHz[2] and at 25.2 MHz[1] in the Fourier transform mode. The spectra were obtained at room temperature by using the deuterium resonance of the solvent (deuterium oxide) as the lock signal. Dioxane (67.4 ppm downfield relative to tetramethylsilane) was used as the reference. Both broad band decoupled and single-frequency off-resonance decoupling spectra were determined.

## RESULTS AND DISCUSSION

**PMR Spectra**—The PMR spectra of all of the spirohydantoins (Table I) displayed a fairly symmetrical two-proton band at ~4.0 ppm, which was assigned to the C-1 and C-5 hydrogens; the widths at half of the maximum height ($W_{1/2}$) of these signals were taken to measure the extent of spin coupling (5). Coupling between the C-1 and C-5 methine protons and the C-6 and C-7 methylene protons was assumed to be constant throughout the series.

The $W_{1/2}$ value for the C-1 and C-5 hydrogen signals (Table II) fell in the range of 9–11 Hz, which corresponds to a chair conformation of the piperidine ring, since the corresponding C-1 and C-5 hydrogen signals for a boat conformation are ~18 Hz (5). The chair conformation of the piperidine ring is corroborated by the values of the coupling constants $JH_{2,4\alpha}$–$H_{1,5}$ and $JH_{2,4\beta}$–$H_{1,5}$ (Table II). Furthermore, $JH_{2,4\beta}$–$H_{1,5}$ is greater than $JH_{2,4\alpha}$–$H_{1,5}$, and, therefore, the dihedral angle $H_{2,4\alpha}$–C–C–$H_{1,5}$ is greater than $H_{2,4\beta}$–C–C–$H_{1,5}$ due to a flattening of the piperidine ring.

In all of the spirohydantoins studied, there was a difference of ~0.6 ppm between the $\delta$ values corresponding to H-2$\alpha$ and H-4$\alpha$ and H-2$\beta$ and H-4$\beta$ (Table I). This difference was produced by the field effect due

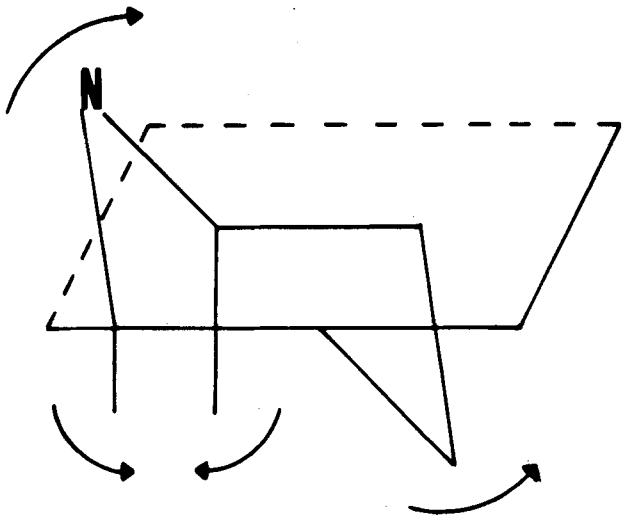


**Figure 1**—*Drawing showing piperidine linkage.*

[1] Varian XL 100 spectrometer.
[2] Varian CFT 20 spectrometer.

0022-3549/81/0100-0087$01.00/0
© 1981, American Pharmaceutical Association

**Table I—Chemical Shifts [a] of Hydrochlorides of I–X in Dimethyl Sulfoxide (Tetramethylsilane as Internal Reference)**

| Group | I | II[b] | III | IV | V | VI | VII | VIII | IX | X |
|---|---|---|---|---|---|---|---|---|---|---|
| $H_{2,4\alpha}$ | 1.83 (a) | 2.14 (a) | 1.95 (a) | 1.93 (a) | 1.9 (a) | 1.84 (a) | 1.94 (a) | 1.42 (a) | 1.93 (a) | 2.0 (a) |
| $H_{2,4\beta}$ | 2.40 (a) | 2.61 (a) | 2.46 (a) | 2.46 (a) | 2.4 (a) | 2.45 (a) | 2.6 (a) | 2.2 (a) | 2.56 (a) | 2.6 (a) |
| $H_{1,5}$ | 4.0 (b) | 4.07 (b) | 4.03 (b) | 4.10 (b) | 4.10 (b) | 3.9 (b) | 3.81 (b) | 4.26 (b) | 4.22 (b) | 4.15 (b) |
| $H_{6,7}$ | 2.13 (b) | 2.37 (c) | 2.2 (b) | 2.18 (b) | 2.18 (b) | 2.16 (b) | 2.20 (b) | 2.0 (b) | 2.32 (b) | 2.3 (b) |
| $CH\alpha$ | | 2.87 (d) | 3.06 (e) | 2.92 (f)[c] | 4.1 (c) | 2.91 (f) | 4.12 (b) | | 3.82 (b) | 3.2 |
| $CH\beta$ | | | 1.26 (f) | 1.72 (g) | 1.34 (h) | 1.64 (i)[c] | 3.08 (b) | | | 3.2 |
| $CH\gamma$ | | | | 0.9 (f) | | 1.34 (g) | | | | |
| $CH\delta$ | | | | | | 0.92 (f) | | | | |
| Aromatic | | | | | | | | 6.5–6.8 (c) | 7.4–7.6 (c) | 7.4 (d) |
| | | | | | | | | 7.0–7.2 (c) | 7.6–7.8 (c) | |

[a] a = doublet of doublets, b = wide singlet, c = multiplet, d = singlet, e = quartet, f = triplet, g = sextuplet, h = doublet, and i = quintuplet. [b] Spectra were recorded in deuterium oxide as solvent. [c] Not resolved.

**Table II—Coupling Constants of Hydrochlorides of I–X in Dimethyl Sulfoxide (Hertz Values, Tetramethylsilane as Internal Reference)**

| Identification | I[a] | II | III | IV | V | VI | VII | VIII | IX | X |
|---|---|---|---|---|---|---|---|---|---|---|
| $JH_{2,4\alpha}$–$H_{2,4\beta}$ | 14 | 16 | 16 | 15 | 16 | 16 | 16 | 14 | 14 | 14 |
| $JH_{2,4\beta}$–$H_{1,5}$ | 3 | 3 | 3 | ~3 | ~3 | 3 | ~3 | 3 | 3 | ~3 |
| $JH_{2,4\alpha}$–$H_{1,5}$ | <1 | <1 | 1 | ~1 | ~2 | 1 | ~2 | 1 | <1 | ~2 |
| $JH_{1,5}$ ($W_{1/2}$) | 9 | 9 | 10 | 9 | 10 | 9 | 10 | 9 | 9 | 11 |
| $JH_{\alpha}$–$H_{\beta}$ | | | 8 | | 6 | 8 | | | | |
| $JH_{\beta}$–$H_{\gamma}$ | | | | 8 | | 8 | | | | |
| $JH_{\gamma}$–$H_{\delta}$ | | | | | | 8 | | | | |

[a] Spectra were recorded in deuterium oxide.

to the magnetic anisotropy of the C-4′ carbonyl group, which occupies an equatorial position with regard to the piperidine ring (6, 7). This arrangement was confirmed in II by X-ray diffraction data (8).

In VIII, the signals corresponding to H-2 and H-4 were shifted toward a higher field ($\Delta\delta$ = 0.4 ppm) with respect to the other compounds of the series, as expected. However, the signal corresponding to H-1 and H-5 was deshielded ~0.3 ppm with respect to the same signal of the other compounds (Table I). This result was attributed to the field effect due to the anisotropy of the *N*-equatorial phenyl group when this group adopts the more favored conformation, which has the plane of the aromatic ring at right angles to a plane passing through the nitrogen and C-4 of the piperidine ring (9).

**$^{13}$C-NMR Spectra**—In all cases, noise-decoupled and single-frequency off-resonance decoupling spectra were obtained.

The $^{13}$C-NMR data of I, II, and X are summarized in Table III. Assignments of the carbon resonances were made by the multiplicity of signals in the single-frequency off-resonance decoupling spectra, the peak intensity of the noise-decoupled spectra, the literature data (10–14), and conventional techniques.

In all cases, the $\delta$ values of the C-2 and C-4 signals (Table III) clearly indicated the equatorial position of the radical attached to the piperidine nitrogen atom since, for an *N*-axial position, a great interaction would be apparent at C-2 and C-4 due to the steric compression between the axial C-2 and C-4 protons and the axial *N*-group, giving place to a shielding of ~20 ppm for the C-2 and C-4 atoms (13).

By comparing the C-6 and C-7 signals of I with the same carbon signals of II and X (Table III), an effect of the *N*-methyl and *N*-phenethyl groups of 1.2 and 1.7 ppm, respectively, can be deduced. The same $\gamma$-effect for the couple nortropane–tropane has a value of 3.4 ppm (10); an analogous $\gamma$-effect for 7-methylnorbornane has a value of 3.8 ppm (15). The smaller $\gamma$-effect in II and X, with respect to tropane and 7-methylnorbornane, as well as the mentioned flattening of the piperidine ring deduced in the PMR data, can be explained as follows. The linkage of the 2,6-positions of piperidine by a dimethylene bridge causes the 2,6-axial bonds to move together and the 3,5-axial bonds to diverge, while the nitrogen moves away from and C-4 moves nearer to the mean plane of the ring (Fig. 1) (16, 17). These distortions in I–X are increased by the steric compression between the ethylene bridge and the hydantoin ring.

The $\delta$ values of C-2 and C-4 in I, II, and X are in agreement with a chair conformation in the piperidine ring, with an additional shielding due to the introduction of a $\gamma$-*gauche* interaction at these carbon atoms with the NH axial proton (13). The signals of C-1 and C-5 also are in agreement with a chair conformation of the piperidine ring since the shielding effect is not observed as a consequence of eclipsing between the C-1 and C-5 and the C-2 and C-4 hydrogen atoms in the boat conformer (13).

**Table III—$^{13}$C-Chemical Shifts for Hydrochlorides of I, II, and X in Deuterium Oxide**

| Carbon Position | Multiplicity[a] | I | II | X[b] |
|---|---|---|---|---|
| 1, 5 | d | 54.33 | 63.20 | 61.35 |
| 2, 4 | t | 37.99 | 40.08 | 39.27 |
| 3 | s | 59.88 | 59.75 | 59.20 |
| 6, 7 | t | 25.29 | 24.12 | 23.63 |
| *N*-$CH_3$ | q | — | 40.88 | — |
| *N*-$CH_2CH_2$ | t | — | — | 53.30 |
| *N*-$CH_2CH_2$ | t | — | — | 31.27 |
| C-2′ | s | 159.80 | 160.80 | 159.40 |
| C-4′ | s | 180.60 | 181.09 | 179.90 |

[a] Signal multiplicity obtained from single-frequency off-resonance decoupling spectra: s = singlet, d = doublet, t = triplet, and q = quartet. [b] Aromatic: C-1, 137.3; C-2 and C-6**, 129.61; C-3 and C-5**, 132.0; and C-4, 128.24 (** Values may be interchanged).

## CONCLUSION

The results obtained by X-ray diffraction of II are in good agreement with the PMR and $^{13}$C-NMR conclusions. From the X-ray diffraction studies (8), it was deduced that: (*a*) the piperidine ring has a flattened chair conformation; (*b*) the piperidine nitrogen atom shows a pyramidal geometry, and the methyl group attached to it is in an axial position; and (*c*) the dihedral angle $C_{6,7}$–$C_{1,5}$–$N_8$ has a smaller value compared to the same dihedral angle in other tropane derivatives such as pseudotropine (17) and $\alpha$-chlorotropane monohydrate (18), which both have the *N*-methyl group in the equatorial position.

The main reason for the *N*-methyl axial position in the crystalline state of II (8) probably is to make possible the intermolecular hydrogen bonding between the N-3′ hydrogen and N-8. When II as its hydrochloride is dissolved in deuterium oxide, the *N*-methyl group occupies an equatorial position to avoid the diaxial interaction with the axial C-2 and C-4 hydrogen atoms; by consequence, the dihedral angle $C_{6,7}$–$C_{1,5}$–$N_8$ is increased to decrease the steric compression between the C-6 and C-7 *exo*-hydrogen atoms and the *N*-equatorial group.

## REFERENCES


(1) G. G. Trigo and M. Martínez, *Pharm. Mediterr.*, **10**, 643 (1974).

(2) A. García Sacristán, M. Illera, and F. Sanz Sánchez, *Arch. Farmacol. Toxicol.*, **3**, 57 (1977).

(3) M. R. Martínez Larrañaga, A. Anadón, and F. Sanz, *ibid.*, **3**, 247 (1977).

(4) S. Vindas Castro, F. Sanz Sánchez, A. García Sacristán, and M. Illera, *ibid.*, **4**, 3 (1978).

(5) A. F. Casy and J. E. Coates, *Org. Magn. Reson.*, **6**, 441 (1974).
(6) J. W. ApSimon, W. G. Craig, P. W. Demarko, D. W. Mathieson, A. K. G. Nasser, L. Saunders, and W. B. Whalley, *Chem. Commun.*, **1966**, 754.
(7) A. F. Casy, L. G. Chatten, and K. K. Khullar, *J. Chem. Soc. C*, **1969**, 2491.
(8) P. Smith-Verdier, F. Florencio, and S. García Blanco, *Acta Crystallogr.*, **B-33**, 3381 (1977).
(9) K. M. J. McErlane and A. F. Casy, *J. Chem. Soc. Perkin I*, **1972**, 339.
(10) E. Wenkert, J. S. Bindra, C. J. Chang, D. W. Cochran, and F. M. Schell, *Acc. Chem. Res.*, **7**, 46 (1974).
(11) L. Simeral and G. E. Maciel, *Org. Magn. Reson.*, **6**, 226 (1974).
(12) S. J. Daum, C. M. Martini, R. K. Kullnig, and R. L. Clark, *J. Med. Chem.*, **18**, 496 (1975).
(13) P. Hanisch, A. J. Jones, A. F. Casy, and J. E. Coates, *J. Chem. Soc. Perkin II*, **1977**, 1202.
(14) A. M. Taha and G. Rucker, *J. Pharm. Sci.*, **67**, 775 (1978).
(15) J. B. Grutzner, M. Santelat, J. B. Dence, R. A. Smith, and J. D. Roberts, *J. Am. Chem. Soc.*, **92**, 7107 (1970).
(16) E. J. Gabe and W. H. Barnes, *Acta Crystallogr.*, **16**, 796 (1963).
(17) H. Schenk, C. H. MacGillavry, S. Skolnik, and J. Laan, *ibid.*, **23**, 423 (1967).
(18) M. Vooren, H. Schenk, and C. H. MacGillavry, *ibid.*, **B-26**, 1483 (1970).

# Two-Dimensional TLC Analysis of Ginsenosides from Root of Dwarf Ginseng (*Panax trifolius* L.) Araliaceae

**TAIKWANG M. LEE and ARA DER MARDEROSIAN** ˣ

Received May 15, 1980, from the *Department of Biological Sciences, Philadelphia College of Pharmacy and Science, Philadelphia, PA 19104.* Accepted for publication July 3, 1980.

**Abstract** □ A procedure is reported for the two-dimensional TLC separation of ginsenosides from the root of *Panax trifolius* L. The solvent systems and spray reagents described are useful for the identification of ginsenosides in various species of *Panax*. The results of the separation and identification with controls of at least four ginsenosides from the root of *P. trifolius* L. are reported. The total percentage of ginsenosides was 0.0061%.

**Keyphrases** □ Ginsenosides—two-dimensional TLC analysis from root of dwarf ginseng □ *Panax trifolius* L.—two-dimensional TLC analysis of ginsenosides from root □ Ginseng, dwarf—two-dimensional TLC analysis of ginsenosides from root

Dwarf ginseng[1] is a member of the ginseng family (Araliaceae) and is distributed from southern Canada to the northern United States (1). The plant is small and delicate and has a whorl of three stalked leaves, each of which is divided into three stalkless leaflets. The plant has a small round umbel of white flowers, which develop into greenish-yellow fruits, and a round tuberous root, which grows deep in the ground.

This report describes the usefulness of two-dimensional TLC for the semimicro separation of the ginsenosides isolated from the root of dwarf ginseng (*Panax trifolius* L.).

## EXPERIMENTAL

**Plant Material**—Specimens of wild dwarf ginseng (*P. trifolius* L.) were collected on May 4, 1979, from the Tyler Arboretum, Delaware County, Pa.

**Extraction Procedure**—Ground, freeze-dried roots (18.6 g) were extracted with chloroform (150 ml) to remove pigments and lipids. The marc was air dried and extracted again with methanol (150 ml). Methanol-washed silica gel (10.0 g) was mixed well with the methanolic extract and filtered to remove impurities (2). The filtrate was combined with the methanolic silica gel washings and concentrated to 5 ml. Ten milliliters of water was added to 50 ml of the methanolic extract and then reextracted three times with water-saturated 1-butanol (60 ml total). The three butanol layers were combined and concentrated to yield the crude saponin extract (20 mg), and this extract was examined by two-dimensional TLC.

**Two-Dimensional TLC**—*Adsorbent*—Precoated silica gel 60 F-254 silanized TLC plates[2] were used (20 × 20 cm, 250-μm layer).

*Eluent Systems*—Solvents were analytical grade and were used as received[3]. Eluent A was chloroform–methanol–ethyl acetate–butanol–water (4:4:8:1:2, lower phase). Eluent B was chloroform–butanol–methanol–water (4:8:3:4, lower phase). Eluent C was chloroform–methanol–water (13:7:2, lower phase).

*Detection Reagent*—A solution of 1 ml of *p*-anisaldehyde and 1 ml of concentrated sulfuric acid diluted to 100 ml with methanol was prepared fresh daily. Plates were heated at 130° for 15 min following spraying (3).

*Standard Solutions*—Standard solutions consisted of ginsenosides[4] Ro, $Rb_1$, $Rb_2$, Rc, Rd, Re, Rf, $Rg_1$, and $Rg_2$ dissolved in methanol at a concentration of 1 mg/ml. All stock solutions were kept refrigerated (3).

*Procedure*—The concentrated crude saponins were dissolved in methanol (1 ml), and 20 μl of this solution was spotted on the bottom left corner of the plates 2.0 cm from each side. The standard solutions of 5 μl of each control ginsenoside were spotted separately 0.8 cm from each other on the bottom right and upper left, exactly 10.0 cm from the crude saponin spot. Two-dimensional TLC plates were prepared as shown in Fig. 1.

The plates were developed separately in one direction in Eluents A and B for 10 cm. After air drying for 10 min, the plates were run in the second direction using Eluent C perpendicular to the first direction for a distance of 10 cm. The $R_f$ values were calculated on the basis of a solvent front of 10.0 cm above the origin, and the relative $R_f$ values were calculated with the ginsenoside Rf as the standard.

**Quantitative Analysis**—Quantitation of the saponins of *P. trifolius* L. was performed using the spectrodensitometric procedure described previously (3). A 250-mg portion of the root was extracted, and 3.5 ml of the final 1-butanol solution was evaporated to dryness. The residue was

[1] This is the first report of continuing research on *Panax trifolius* L. All plant parts of dwarf ginseng are currently being studied in detail.

[2] Catalog No. 5601, EM Laboratories, Elmsford, NY 10523.
[3] Fisher Scientific Co., Fair Lawn, NJ 07410.
[4] Nine standard ginsenosides were obtained from Dr. J. Shoji, Showa University, Tokyo, Japan.

0022-3549/81/0100-0089$01.00/0
© 1981, American Pharmaceutical Association

(5) A. F. Casy and J. E. Coates, *Org. Magn. Reson.*, **6**, 441 (1974).
(6) J. W. ApSimon, W. G. Craig, P. W. Demarko, D. W. Mathieson, A. K. G. Nasser, L. Saunders, and W. B. Whalley, *Chem. Commun.*, **1966**, 754.
(7) A. F. Casy, L. G. Chatten, and K. K. Khullar, *J. Chem. Soc. C*, **1969**, 2491.
(8) P. Smith-Verdier, F. Florencio, and S. García Blanco, *Acta Crystallogr.*, **B-33**, 3381 (1977).
(9) K. M. J. McErlane and A. F. Casy, *J. Chem. Soc. Perkin I*, **1972**, 339.
(10) E. Wenkert, J. S. Bindra, C. J. Chang, D. W. Cochran, and F. M. Schell, *Acc. Chem. Res.*, **7**, 46 (1974).
(11) L. Simeral and G. E. Maciel, *Org. Magn. Reson.*, **6**, 226 (1974).
(12) S. J. Daum, C. M. Martini, R. K. Kullnig, and R. L. Clark, *J. Med. Chem.*, **18**, 496 (1975).
(13) P. Hanisch, A. J. Jones, A. F. Casy, and J. E. Coates, *J. Chem. Soc. Perkin II*, **1977**, 1202.
(14) A. M. Taha and G. Rucker, *J. Pharm. Sci.*, **67**, 775 (1978).
(15) J. B. Grutzner, M. Santelat, J. B. Dence, R. A. Smith, and J. D. Roberts, *J. Am. Chem. Soc.*, **92**, 7107 (1970).
(16) E. J. Gabe and W. H. Barnes, *Acta Crystallogr.*, **16**, 796 (1963).
(17) H. Schenk, C. H. MacGillavry, S. Skolnik, and J. Laan, *ibid.*, **23**, 423 (1967).
(18) M. Vooren, H. Schenk, and C. H. MacGillavry, *ibid.*, **B-26**, 1483 (1970).

# Two-Dimensional TLC Analysis of Ginsenosides from Root of Dwarf Ginseng (*Panax trifolius* L.) Araliaceae

**TAIKWANG M. LEE and ARA DER MARDEROSIAN** ˣ

Received May 15, 1980, from the *Department of Biological Sciences, Philadelphia College of Pharmacy and Science, Philadelphia, PA 19104.* Accepted for publication July 3, 1980.

**Abstract** □ A procedure is reported for the two-dimensional TLC separation of ginsenosides from the root of *Panax trifolius* L. The solvent systems and spray reagents described are useful for the identification of ginsenosides in various species of *Panax*. The results of the separation and identification with controls of at least four ginsenosides from the root of *P. trifolius* L. are reported. The total percentage of ginsenosides was 0.0061%.

**Keyphrases** □ Ginsenosides—two-dimensional TLC analysis from root of dwarf ginseng □ *Panax trifolius* L.—two-dimensional TLC analysis of ginsenosides from root □ Ginseng, dwarf—two-dimensional TLC analysis of ginsenosides from root

Dwarf ginseng[1] is a member of the ginseng family (Araliaceae) and is distributed from southern Canada to the northern United States (1). The plant is small and delicate and has a whorl of three stalked leaves, each of which is divided into three stalkless leaflets. The plant has a small round umbel of white flowers, which develop into greenish-yellow fruits, and a round tuberous root, which grows deep in the ground.

This report describes the usefulness of two-dimensional TLC for the semimicro separation of the ginsenosides isolated from the root of dwarf ginseng (*Panax trifolius* L.).

## EXPERIMENTAL

**Plant Material**—Specimens of wild dwarf ginseng (*P. trifolius* L.) were collected on May 4, 1979, from the Tyler Arboretum, Delaware County, Pa.

**Extraction Procedure**—Ground, freeze-dried roots (18.6 g) were extracted with chloroform (150 ml) to remove pigments and lipids. The marc was air dried and extracted again with methanol (150 ml). Methanol-washed silica gel (10.0 g) was mixed well with the methanolic extract and filtered to remove impurities (2). The filtrate was combined with the methanolic silica gel washings and concentrated to 5 ml. Ten milliliters of water was added to 50 ml of the methanolic extract and then reextracted three times with water-saturated 1-butanol (60 ml total). The three butanol layers were combined and concentrated to yield the crude saponin extract (20 mg), and this extract was examined by two-dimensional TLC.

**Two-Dimensional TLC**—*Adsorbent*—Precoated silica gel 60 F-254 silanized TLC plates[2] were used (20 × 20 cm, 250-μm layer).

*Eluent Systems*—Solvents were analytical grade and were used as received[3]. Eluent A was chloroform–methanol–ethyl acetate–butanol–water (4:4:8:1:2, lower phase). Eluent B was chloroform–butanol–methanol–water (4:8:3:4, lower phase). Eluent C was chloroform–methanol–water (13:7:2, lower phase).

*Detection Reagent*—A solution of 1 ml of *p*-anisaldehyde and 1 ml of concentrated sulfuric acid diluted to 100 ml with methanol was prepared fresh daily. Plates were heated at 130° for 15 min following spraying (3).

*Standard Solutions*—Standard solutions consisted of ginsenosides[4] Ro, $Rb_1$, $Rb_2$, Rc, Rd, Re, Rf, $Rg_1$, and $Rg_2$ dissolved in methanol at a concentration of 1 mg/ml. All stock solutions were kept refrigerated (3).

*Procedure*—The concentrated crude saponins were dissolved in methanol (1 ml), and 20 μl of this solution was spotted on the bottom left corner of the plates 2.0 cm from each side. The standard solutions of 5 μl of each control ginsenoside were spotted separately 0.8 cm from each other on the bottom right and upper left, exactly 10.0 cm from the crude saponin spot. Two-dimensional TLC plates were prepared as shown in Fig. 1.

The plates were developed separately in one direction in Eluents A and B for 10 cm. After air drying for 10 min, the plates were run in the second direction using Eluent C perpendicular to the first direction for a distance of 10 cm. The $R_f$ values were calculated on the basis of a solvent front of 10.0 cm above the origin, and the relative $R_f$ values were calculated with the ginsenoside Rf as the standard.

**Quantitative Analysis**—Quantitation of the saponins of *P. trifolius* L. was performed using the spectrodensitometric procedure described previously (3). A 250-mg portion of the root was extracted, and 3.5 ml of the final 1-butanol solution was evaporated to dryness. The residue was

[1] This is the first report of continuing research on *Panax trifolius* L. All plant parts of dwarf ginseng are currently being studied in detail.

[2] Catalog No. 5601, EM Laboratories, Elmsford, NY 10523.
[3] Fisher Scientific Co., Fair Lawn, NJ 07410.
[4] Nine standard ginsenosides were obtained from Dr. J. Shoji, Showa University, Tokyo, Japan.

0022-3549/81/0100-0089$01.00/0
© 1981, American Pharmaceutical Association

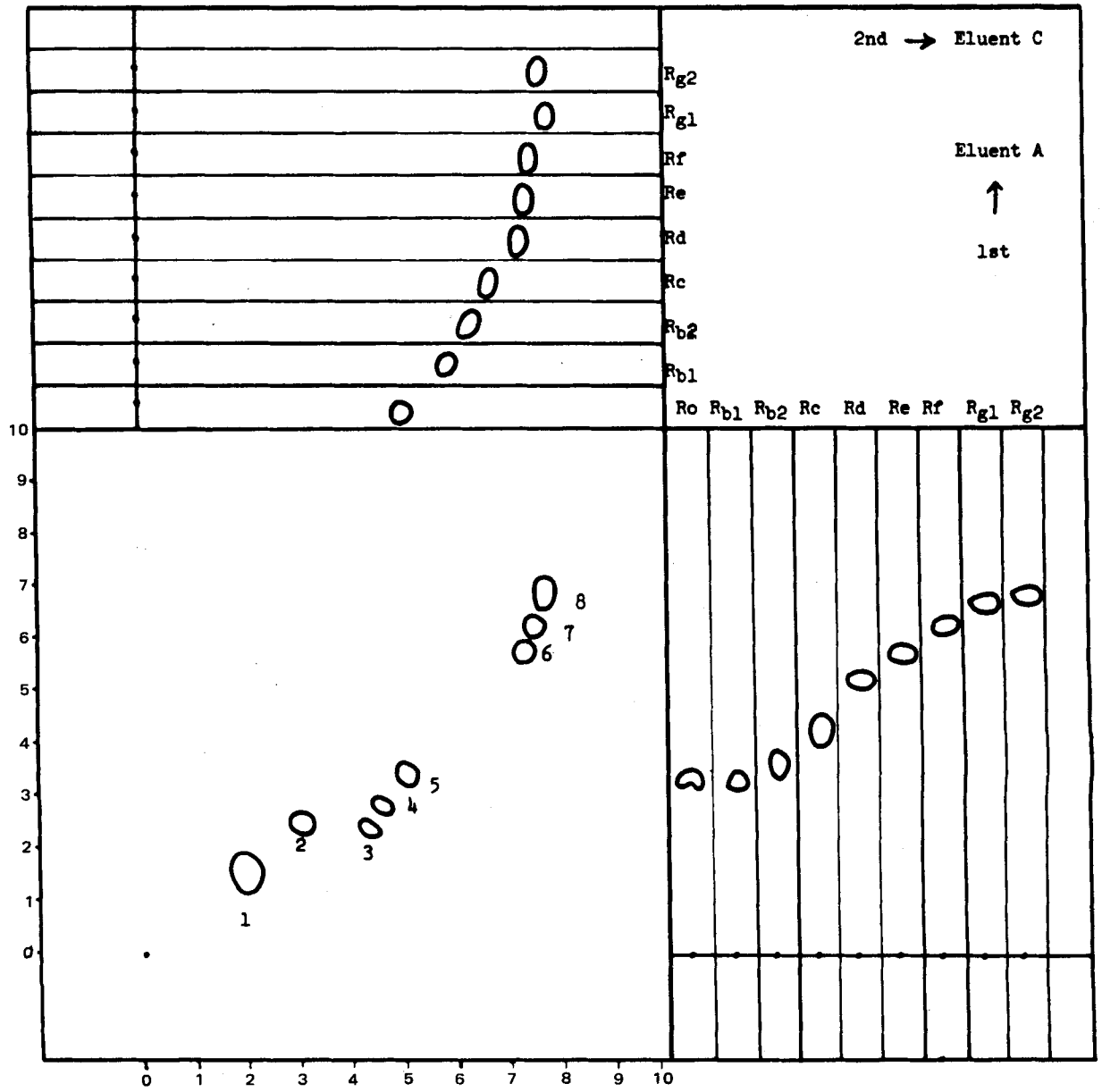


**Figure 1**—*Chromatogram of the two-dimensional identification for ginsenosides from the root of* P. trifolius *L. using Eluents A and C.*

**Table I—The $R_f$ and $RR_f$ Values and Color Reactions of the Reference and Examined Ginsenosides from the Root of *P. trifolius* L.**

| Ginsenoside[a] | Eluent A | | Eluent B | | Eluent C | | Color Reaction[c] |
|---|---|---|---|---|---|---|---|
| | $R_f$ | $RR_f$[b] | $R_f$ | $RR_f$[b] | $R_f$ | $RR_f$[b] | |
| Standards | | | | | | | |
| Ro | 0.34 | 0.55 | 0.63 | 0.74 | 0.50 | 0.68 | B |
| $Rb_1$ | 0.33 | 0.53 | 0.63 | 0.74 | 0.59 | 0.80 | V |
| $Rb_2$ | 0.37 | 0.60 | 0.64 | 0.75 | 0.63 | 0.85 | V |
| Rc | 0.42 | 0.68 | 0.69 | 0.81 | 0.67 | 0.91 | V |
| Rd | 0.52 | 0.84 | 0.78 | 0.92 | 0.72 | 0.97 | V |
| Re | 0.57 | 0.92 | 0.88 | 1.04 | 0.73 | 0.99 | G |
| Rf | 0.62 | 1.00 | 0.85 | 1.00 | 0.74 | 1.00 | G |
| $Rg_1$ | 0.66 | 1.06 | 0.98 | 1.15 | 0.77 | 1.04 | G |
| $Rg_2$ | 0.68 | 1.10 | 0.92 | 1.08 | 0.76 | 1.03 | G |
| *P. trifolius* | | | | | | | |
| 1 | 0.15 | 0.24 | 0.24 | 0.28 | 0.20 | 0.27 | G |
| 2 | 0.25 | 0.40 | 0.37 | 0.44 | 0.30 | 0.41 | G |
| 3 | 0.24 | 0.39 | 0.69 | 0.81 | 0.43 | 0.58 | G |
| 4 | 0.28 | 0.45 | 0.73 | 0.86 | 0.46 | 0.62 | G |
| 5 (Ro) | 0.34 | 0.55 | 0.63 | 0.74 | 0.50 | 0.68 | B |
| 6 (Re) | 0.57 | 0.92 | 0.88 | 1.04 | 0.73 | 0.99 | G |
| 7 (Rf) | 0.62 | 1.00 | 0.85 | 1.00 | 0.74 | 1.00 | G |
| 8 ($Rg_2$) | 0.68 | 1.10 | 0.92 | 1.08 | 0.76 | 1.03 | G |

[a] The numbers refer to the numbers given to each spot in Fig. 1. [b] Relative $R_f$ values with the ginsenoside Rf as the standard. [c] B = blue, V = violet, and G = green.

redissolved in 0.2 ml of 1-butanol, and 16 μl was applied to alternate lanes of the TLC plates[5], developed, and assayed by spectrodensitometry.

## RESULTS AND DISCUSSION

Ginseng is one of the best-known Chinese drugs and has been claimed to be useful in increasing lifespan as well as being a cure-all. The ginsenosides, abbreviated as Rx, are considered as the characteristic and active principles that account for the major biological activities of ginseng (4).

Chemically, all ginsenosides are dammarane-type triterpenoid saponins, except for Ro, which is an oleanane type. The dammarane-type compounds are classified further into two groups possessing either 20-*S*-protopanaxadiol or 20-*S*-protopanaxatriol as the sapogenin.

In this study, eight ginsenosides were found in the root of *P. trifolius* L. Of these compounds, Ro, Re, Rf, and $Rg_2$ were identified with nine of the controls. Combinations of relative $R_f$ and $RR_f$ ($R_f$ values with ginsenoside Rf as the standard) values and the specific color reactions after spraying with detection reagent facilitated identification of the ginsenosides.

Table I shows those ginsenosides ($Rb_1$, $Rb_2$, Rc, and Rd) with 20-*S*-protopanaxadiol as the sapogenin. These compounds show a violet color after spraying with the detection reagent. Those with 20-*S*-protopanaxatriol as the sapogenin (Re, Rf, $Rg_1$, and $Rg_2$) show a green color, while the oleanane-type triterpenoid saponin (Ro) yields a blue color. The ginsenosides denoted as 1–4 in Fig. 1 all were green after spraying, indicating that they are dammarane-type triterpenoid saponins with 20-*S*-protopanaxatriol as the sapogenin.

In this two-dimensional TLC procedure, identifications depend on the $R_f$ and $RR_f$ values and on color. These parameters provide a great advantage for the detection of ginsenosides, not only in the dwarf ginseng but also in other species of *Panax*.

Eight separate spots were observed by quantitative analysis, but the darkness of the spots, while sufficient for quantitation, was not sufficient for determination of the color class by this procedure. The results confirmed the presence of ginsenosides Ro, Re, Rf, and $Rg_2$ (Table II).

The identities of the remaining four saponins are unknown. The total saponin content of *P. trifolius* (including unknowns) was found to be the lowest (0.0061%) of any roots belonging to this genus that have been examined in these laboratories.

[5] Analtech Co., Newark, DE 19711.

**Table II—Individual and Total Saponin Content of *P. trifolius* Root [a]**

| Ginsenoside[b] | Individual Saponin, % | $R_f$[c] | $RR_f$[d] |
|---|---|---|---|
| 1 (Ro) | 0.0004 | 0.10 | 0.18 |
| 2 | 0.0006 | 0.25 | 0.47 |
| 3 | 0.0008 | 0.32 | 0.56 |
| 4 | 0.0012 | 0.38 | 0.67 |
| 5 (Re) | 0.0005 | 0.47 | 0.82 |
| 6 | 0.0005 | 0.51 | 0.89 |
| 7 (Rf) | 0.0008 | 0.57 | 1.00 |
| 8 ($Rg_2$) | 0.0008 | 0.63 | 1.11 |
| 9 (Sapogenins) | 0.0011 | 0.71 | 1.25 |

[a] Total saponins = 0.0061%. [b] Due to a different procedure and solvent system, the numbering of the ginsenosides does not necessarily correspond to that in Table I. [c] The solvent system was methanol–chloroform–1-butanol (1:1:1). [d] Relative $R_f$ values with ginsenoside Rf as standard.

## REFERENCES


(1) M. L. Fernald and A. C. Kinsey, "Edible Wild Plants of Eastern North America," Idlewild Press, Cornwall-on-Hudson, N.Y., 1958, p. 284.

(2) S. E. Chem and E. J. Staba, *Lloydia*, **41**, 361 (1978).

(3) L. Liberti and A. H. Der Marderosian, *J. Pharm. Sci.*, **67**, 1487 (1978).

(4) H. Otsuka, Y. Morita, Y. Ogihara, and S. Shibata, *Planta Med.*, **32**, 9 (1977).


## ACKNOWLEDGMENTS


The authors thank Dr. J. Shoji, Showa University, Tokyo, Japan, for authentic samples of ginsenosides, Mr. Robert Montgomery and Mr. John Beutler, Tyler Arboretum, Delaware County, Pa., for dwarf ginseng plant materials, and Mr. Joseph Betz, Philadelphia College of Pharmacy and Science, Philadelphia, Pa., for the spectrodensitometric analysis of the ginseng extract. They also thank Bristol Myers, Industrial Division at Syracuse, N.Y., for use of their facilities.


# Selenium–Sulfur Analogs III: Synthesis and Biodistribution of Two $^{75}$Se-Labeled 4-Substituted-1,2,3-selenadiazoles


**ROBERT N. HANSON ˣ and MICHAEL A. DAVIS**



Received March 31, 1980, from the *Departments of Medicinal Chemistry and Pharmacology, College of Pharmacy and Allied Health Professions, Northeastern University, and Department of Radiology, Joint Program in Nuclear Medicine, Harvard Medical School, Boston, MA 02115.* Accepted for publication July 11, 1980.



**Abstract** □ The $^{75}$Se-labeled 4-substituted-1,2,3-selenadiazole analogs of two drugs that inhibit the adrenocorticosteroid 11β- and 17α-hydroxylase enzymes were prepared by the [$^{75}$Se]selenious acid oxidation of the appropriate methyl ketone semicarbazones. The concentration of the radiolabeled compounds in the adrenal glands of rats over a 0.25–24-hr period was determined and compared with that in the blood, liver, and kidneys. The concentration in the adrenal glands and the target to nontarget ratios were much lower than those reported for other adrenocorticosteroid inhibitors. Therefore, these 1,2,3-selenadiazole agents do not have potential as adrenocorticosteroid imaging agents.



**Keyphrases** □ 1,2,3-Selenadiazoles—synthesis and biodistribution of radiolabeled compounds as potential adrenocorticosteroid imaging agents □ Imaging agents, potential—radiolabeled 1,2,3-selenadiazoles, synthesis and biodistribution


One current approach to the development of adrenal cortex imaging agents employs radiolabeled analogs of drugs that inhibit adrenocorticosteroid biosynthesis (1–3). Although Beierwaltes *et al.* (1–3) reported the *in vivo* visualization of the canine adrenal cortex with $^{131}$I-labeled aminophenylethylamine, their studies suggested that radiolabeled derivatives of the 11β- and 17α-hydroxylase enzyme inhibitors might be more effective. Therefore, an



© 1981, American Pharmaceutical Association

redissolved in 0.2 ml of 1-butanol, and 16 μl was applied to alternate lanes of the TLC plates[5], developed, and assayed by spectrodensitometry.

## RESULTS AND DISCUSSION

Ginseng is one of the best-known Chinese drugs and has been claimed to be useful in increasing lifespan as well as being a cure-all. The ginsenosides, abbreviated as Rx, are considered as the characteristic and active principles that account for the major biological activities of ginseng (4).

Chemically, all ginsenosides are dammarane-type triterpenoid saponins, except for Ro, which is an oleanane type. The dammarane-type compounds are classified further into two groups possessing either 20-*S*-protopanaxadiol or 20-*S*-protopanaxatriol as the sapogenin.

In this study, eight ginsenosides were found in the root of *P. trifolius* L. Of these compounds, Ro, Re, Rf, and $Rg_2$ were identified with nine of the controls. Combinations of relative $R_f$ and $RR_f$ ($R_f$ values with ginsenoside Rf as the standard) values and the specific color reactions after spraying with detection reagent facilitated identification of the ginsenosides.

Table I shows those ginsenosides ($Rb_1$, $Rb_2$, Rc, and Rd) with 20-*S*-protopanaxadiol as the sapogenin. These compounds show a violet color after spraying with the detection reagent. Those with 20-*S*-protopanaxatriol as the sapogenin (Re, Rf, $Rg_1$, and $Rg_2$) show a green color, while the oleanane-type triterpenoid saponin (Ro) yields a blue color. The ginsenosides denoted as 1–4 in Fig. 1 all were green after spraying, indicating that they are dammarane-type triterpenoid saponins with 20-*S*-protopanaxatriol as the sapogenin.

In this two-dimensional TLC procedure, identifications depend on the $R_f$ and $RR_f$ values and on color. These parameters provide a great advantage for the detection of ginsenosides, not only in the dwarf ginseng but also in other species of *Panax*.

Eight separate spots were observed by quantitative analysis, but the darkness of the spots, while sufficient for quantitation, was not sufficient for determination of the color class by this procedure. The results confirmed the presence of ginsenosides Ro, Re, Rf, and $Rg_2$ (Table II).

The identities of the remaining four saponins are unknown. The total saponin content of *P. trifolius* (including unknowns) was found to be the lowest (0.0061%) of any roots belonging to this genus that have been examined in these laboratories.

[5] Analtech Co., Newark, DE 19711.

**Table II—Individual and Total Saponin Content of *P. trifolius* Root [a]**

| Ginsenoside[b] | Individual Saponin, % | $R_f$[c] | $RR_f$[d] |
|---|---|---|---|
| 1 (Ro) | 0.0004 | 0.10 | 0.18 |
| 2 | 0.0006 | 0.25 | 0.47 |
| 3 | 0.0008 | 0.32 | 0.56 |
| 4 | 0.0012 | 0.38 | 0.67 |
| 5 (Re) | 0.0005 | 0.47 | 0.82 |
| 6 | 0.0005 | 0.51 | 0.89 |
| 7 (Rf) | 0.0008 | 0.57 | 1.00 |
| 8 ($Rg_2$) | 0.0008 | 0.63 | 1.11 |
| 9 (Sapogenins) | 0.0011 | 0.71 | 1.25 |

[a] Total saponins = 0.0061%. [b] Due to a different procedure and solvent system, the numbering of the ginsenosides does not necessarily correspond to that in Table I. [c] The solvent system was methanol–chloroform–1-butanol (1:1:1). [d] Relative $R_f$ values with ginsenoside Rf as standard.

## REFERENCES


(1) M. L. Fernald and A. C. Kinsey, "Edible Wild Plants of Eastern North America," Idlewild Press, Cornwall-on-Hudson, N.Y., 1958, p. 284.

(2) S. E. Chem and E. J. Staba, *Lloydia*, **41**, 361 (1978).

(3) L. Liberti and A. H. Der Marderosian, *J. Pharm. Sci.*, **67**, 1487 (1978).

(4) H. Otsuka, Y. Morita, Y. Ogihara, and S. Shibata, *Planta Med.*, **32**, 9 (1977).


## ACKNOWLEDGMENTS


The authors thank Dr. J. Shoji, Showa University, Tokyo, Japan, for authentic samples of ginsenosides, Mr. Robert Montgomery and Mr. John Beutler, Tyler Arboretum, Delaware County, Pa., for dwarf ginseng plant materials, and Mr. Joseph Betz, Philadelphia College of Pharmacy and Science, Philadelphia, Pa., for the spectrodensitometric analysis of the ginseng extract. They also thank Bristol Myers, Industrial Division at Syracuse, N.Y., for use of their facilities.


# Selenium–Sulfur Analogs III: Synthesis and Biodistribution of Two $^{75}$Se-Labeled 4-Substituted-1,2,3-selenadiazoles


**ROBERT N. HANSON ˣ and MICHAEL A. DAVIS**



Received March 31, 1980, from the *Departments of Medicinal Chemistry and Pharmacology, College of Pharmacy and Allied Health Professions, Northeastern University, and Department of Radiology, Joint Program in Nuclear Medicine, Harvard Medical School, Boston, MA 02115.* Accepted for publication July 11, 1980.



**Abstract** □ The $^{75}$Se-labeled 4-substituted-1,2,3-selenadiazole analogs of two drugs that inhibit the adrenocorticosteroid 11β- and 17α-hydroxylase enzymes were prepared by the [$^{75}$Se]selenious acid oxidation of the appropriate methyl ketone semicarbazones. The concentration of the radiolabeled compounds in the adrenal glands of rats over a 0.25–24-hr period was determined and compared with that in the blood, liver, and kidneys. The concentration in the adrenal glands and the target to nontarget ratios were much lower than those reported for other adrenocorticosteroid inhibitors. Therefore, these 1,2,3-selenadiazole agents do not have potential as adrenocorticosteroid imaging agents.



**Keyphrases** □ 1,2,3-Selenadiazoles—synthesis and biodistribution of radiolabeled compounds as potential adrenocorticosteroid imaging agents □ Imaging agents, potential—radiolabeled 1,2,3-selenadiazoles, synthesis and biodistribution


One current approach to the development of adrenal cortex imaging agents employs radiolabeled analogs of drugs that inhibit adrenocorticosteroid biosynthesis (1–3). Although Beierwaltes *et al.* (1–3) reported the *in vivo* visualization of the canine adrenal cortex with $^{131}$I-labeled aminophenylethylamine, their studies suggested that radiolabeled derivatives of the 11β- and 17α-hydroxylase enzyme inhibitors might be more effective. Therefore, an



© 1981, American Pharmaceutical Association

**Table I—Percent of Injected Dose per Organ of [$^{75}$Se]-I*b* following Intravenous Administration**

| Organ | 15 min | 2 hr | 6 hr | 24 hr |
|---|---|---|---|---|
| Liver | 37.62 | 36.72 | 23.62 | 14.83 |
| | 31.46–52.45[a] | 26.23–46.70 | 19.73–27.40 | 12.85–16.85 |
| Spleen | 0.29 | 0.31 | 0.57 | 0.56 |
| | 0.21–0.40 | 0.26–0.37 | 0.39–0.80 | 0.48–0.63 |
| Lungs | 7.55 | 4.99 | 2.70 | 1.84 |
| | 6.06–10.84 | 4.22–6.40 | 2.45–2.90 | 1.61–2.02 |
| Heart | 0.24 | 0.23 | 0.23 | 0.17 |
| | 0.14–0.29 | 0.20–0.26 | 0.20–0.26 | 0.13–0.21 |
| Small intestine | 13.43 | 17.20 | 5.74 | 2.92 |
| | 10.81–14.80 | 14.78–18.64 | 3.98–7.74 | 2.64–3.14 |
| Large intestine | 1.46 | 3.30 | 12.59 | 4.43 |
| | 0.88–1.83 | 1.28–7.67 | 9.52–15.13 | 2.54–6.97 |
| Kidneys | 2.02 | 4.60 | 2.86 | 2.47 |
| | 1.91–2.16 | 4.30–4.86 | 2.64–4.19 | 1.94–3.21 |
| Muscle | 14.20 | 10.73 | 17.80 | 9.45 |
| | 10.43–23.41 | 6.86–15.09 | 8.36–23.31 | 8.22–11.31 |
| Fat and fur | 15.59 | 7.90 | 9.25 | 5.31 |
| | 9.97–23.35 | 6.70–8.68 | 5.08–11.76 | 4.09–7.16 |
| Bone | 4.61 | 3.90 | 4.58 | 4.61 |
| | 2.81–6.92 | 2.68–6.86 | 3.97–5.45 | 3.98–5.82 |
| Blood | 8.42 | 9.65 | 8.10 | 6.81 |
| | 6.63–13.03 | 6.77–13.08 | 6.66–8.86 | 5.32–8.42 |
| Adrenal | 0.03 | 0.03 | 0.02 | 0.02 |
| | 0.02–0.03 | 0.02–0.04 | 0.01–0.03 | 0.01–0.03 |

[a] Mean and range for four rats.

attempt was made to utilize the structural similarity between pyridine and the 1,2,3-selenadiazole groups and the properties of selenium 75.

The 1,2,3-selenadiazolyl (I*b* and II*b*) and 1,2,3-thiadiazolyl (I*c* and II*c*) analogs of two drugs, 2-(3-pyridyl)-2-methylpropiophenone (I*a*) and 2-(3-pyridyl)-2-methyl-1-tetralone (II*a*), that inhibit the 11$\beta$- and 17$\alpha$-hydroxylase enzymes, respectively (4, 5), were prepared. In this study, I*b* and II*b* were radiolabeled and their biodistribution was determined in normal rats to evaluate their potential as adrenal cortex imaging agents. These analogs were selected rather than the thiadiazoles because they are synthesized easily and selenium 75 is readily available.

## EXPERIMENTAL

**General Method for Preparation of $^{75}$Se-Labeled 4-Substituted-1,2,3-selenadiazoles (I*b* and II*b*)**—Five millicuries (0.5 ml) of [$^{75}$Se]selenious acid in 0.5 *M* HCl was added to a solution composed of 25 $\mu$moles of the semicarbazone, 26 $\mu$moles of selenium dioxide, and 0.5 ml of acetic acid (Schemes I and II). The mixture was heated at 60° for 1 hr, cooled, diluted with 2 ml of water, and extracted with ethyl acetate. The ethyl acetate layer was evaporated, and the residue was purified by alumina column chromatography with ethyl acetate as the eluent to yield the desired product (7.5 $\mu$moles, 30%). Thin-layer radiochromatography on alumina or silica gel using ethyl acetate as the eluent indicated the presence of a single radioactive component (>98%), which comigrated with an authentic sample prepared using the same procedure but without the [$^{75}$Se]selenious acid and was characterized by IR and NMR spectroscopy[1]. The radiolabeled product was dissolved in 2.0 ml of propylene glycol. Because of the chemical instability of the 1,2,3-selenadiazoles to heat and light, it was stored at 4° in the dark for subsequent biodistribution studies.

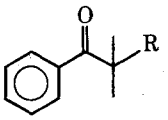

I*a*: R = 3-pyridyl
I*b*: R = 4-(1,2,3-selenadiazolyl)
I*c*: R = 4-(1,2,3-thiadiazolyl)

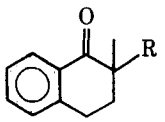

II*a*: R = 3-pyridyl
II*b*: R = 4-(1,2,3-selenadiazolyl)
II*c*: R = 4-(1,2,3-thiadiazolyl)

**Animal Studies**—The biodistribution of the radiolabeled compounds (I*b* and II*b*) was determined in outbred Wistar or Sprague–Dawley rats of either sex (150–200 g). The rats were lightly anesthetized with ether, and a propylene glycol solution of the radiopharmaceutical (0.1 ml, 7.5 $\mu$Ci) was injected into the femoral vein. Groups of three or four animals subsequently were sacrificed by ether asphyxiation at 0.25, 2.6, and 24 hr after administration.

Blood was obtained from a vein in the thoracic cavity. The organs of interest were carefully excised, weighed, and counted in a sodium iodide (Tl) $\gamma$-well scintillation counter. The data were converted to the percent of injected dose per organ. The ratios of the agent concentration (percent of injected dose per gram) in the adrenal cortex (target organ) compared with that in the liver, kidneys, and blood (nontarget organs) were calculated.

## RESULTS AND DISCUSSION

**Chemistry**—The [$^{75}$Se]selenious acid oxidation of the appropriate methyl ketone semicarbazone (6–8) provided the desired $^{75}$Se-labeled 4-substituted-1,2,3-selenadiazoles (I*b* and II*b*). Extraction with ethyl

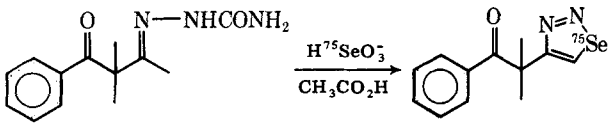


[$^{75}$Se]-I*b*

*Scheme I*

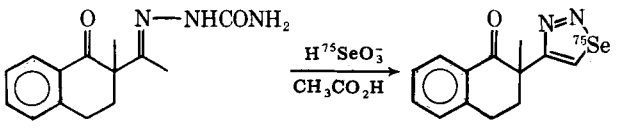


[$^{75}$Se]-II*b*

*Scheme II*

[1] The analytical data were: I*b*, IR (KBr): 1670 cm$^{-1}$; NMR ($CDCl_3$ + tetramethylsilane): $\delta$ 1.88 (6H) and 9.00 (1H); and II*b*, IR (neat): 1680 cm$^{-1}$; NMR ($CDCl_3$ + tetramethylsilane): $\delta$ 1.76 (3H) and 8.67 (1H).

Table II—Percent of Injected Dose per Organ of [$^{75}$Se]-II*b* following Intravenous Administration

| Organ | 15 min | 2 hr | 6 hr | 24 hr |
|---|---|---|---|---|
| Liver | 39.14<br>35.54–43.17[a] | 27.90<br>25.71–32.17 | 18.78<br>16.06–22.36 | 10.31<br>7.22–12.59 |
| Spleen | 0.27<br>0.20–0.32 | 0.30<br>0.27–0.37 | 0.40<br>0.27–0.50 | 0.35<br>0.21–0.53 |
| Lungs | 5.57<br>5.07–6.36 | 3.03<br>2.54–3.40 | 3.25<br>2.50–3.72 | 2.12<br>1.67–2.37 |
| Heart | 0.41<br>0.31–0.60 | 0.26<br>0.18–0.36 | 0.18<br>0.16–0.19 | 0.16<br>0.14–0.18 |
| Small intestine | 18.31<br>14.54–22.70 | 17.04<br>15.28–19.20 | 8.30<br>7.73–9.35 | 3.88<br>3.00–4.36 |
| Large intestine | 2.76<br>2.32–3.13 | 2.22<br>1.47–2.85 | 15.29<br>14.06–16.65 | 2.64<br>2.16–3.49 |
| Kidneys | 3.26<br>2.54–3.76 | 3.39<br>2.52–4.37 | 3.87<br>3.68–4.16 | 2.11<br>1.95–2.30 |
| Muscle | 9.49<br>6.72–11.40 | 15.19<br>9.53–18.91 | 16.86<br>12.34–23.32 | 9.32<br>6.48–14.38 |
| Fat and fur | 12.04<br>10.26–15.06 | 12.91<br>7.66–15.87 | 13.05<br>9.60–15.22 | 7.99<br>7.41–8.83 |
| Bone | 2.63<br>1.87–3.07 | 4.66<br>3.03–7.21 | 8.97<br>7.51–9.98 | 5.23<br>3.36–6.24 |
| Blood | 6.97<br>6.76–7.15 | 4.17<br>3.84–4.41 | 6.68<br>5.15–8.60 | 5.23<br>4.00–6.97 |
| Adrenal | 0.04<br>0.03–0.04 | 0.03<br>0.02–0.04 | 0.04<br>0.03–0.06 | 0.03<br>0.01–0.07 |

[a] Mean and range for three rats.

Table III—Adrenal Uptake and Target to Nontarget Ratios for [$^{75}$Se]-I*b* and [$^{75}$Se]-II*b*

| Time | Adrenal Uptake, % of injected dose/g | | Target to Nontarget Ratios | | | | | |
|---|---|---|---|---|---|---|---|---|
| | | | Adrenal/Kidney | | Adrenal/Liver | | Adrenal/Blood | |
| | I*b* | II*b* | I*b* | II*b* | I*b* | II*b* | I*b* | II*b* |
| 15 min | 1.07 | 0.62 | 1.07 | 0.59 | 0.30 | 0.25 | 2.10 | 2.20 |
| 2 hr | 0.65 | 1.24 | 0.27 | 0.45 | 0.19 | 0.23 | 1.25 | 2.31 |
| 6 hr | 0.57 | 1.50 | 0.40 | 0.46 | 0.26 | 0.36 | 1.08 | 1.84 |
| 24 hr | 0.75 | 1.09 | 0.47 | 0.62 | 0.37 | 0.56 | 1.42 | 1.69 |

acetate followed by column chromatographic separation gave the products, isolated in 10–30% radiochemical yield, with >98% radiochemical purity. The specific activity of the material varied from 60 to 220 mCi/mmole. The $^{75}$Se-labeled selenadiazoles were dissolved in propylene glycol and stored in the dark at 4° for use in the biodistribution study.

**Animal Studies**—The deposition and excretion patterns of [$^{75}$Se]-I*b* and [$^{75}$Se]-II*b* were similar (Tables I and II). For each agent, the liver was the primary site of localization at all time periods examined with significant percentages in the muscle, fat, and fur. Blood levels remained high over the 24-hr period, and only 50% of the label was excreted in that time. Unfortunately, the adrenal uptake of I*b* was 0.57–1.07% of the injected dose/g and that of II*b* was 0.56–1.51% of the injected dose/g, and these values are much lower than those reported for other labeled adrenocortical enzyme inhibitors (1–3). The adrenal to liver and adrenal to kidney values (Table III) for the $^{75}$Se-labeled compounds both were <1, whereas the corresponding values for the other labeled inhibitors were 2–11 and 3–20. The lack of localization and selectivity and the slow clearance of the label from the body indicate that the $^{75}$Se-labeled 4-substituted-1,2,3-selenadiazoles (I*b* and II*b*) do not possess the characteristics necessary for adrenal imaging agents.

Two factors may contribute to the failure of these compounds to localize adequately in the adrenal cortex. First, the compounds may not be sufficiently selective for the adrenal cytochrome P-450-linked hydroxylase enzymes relative to the hepatic cytochrome P-450-linked metabolic enzymes. Second, metabolism of the 1,2,3-selenadiazoles by the liver may result in the deposition in the organ of selenium 75, which is only slowly excreted.

The results of this study suggest that subsequent work should be directed toward the synthesis of more chemically stable selenium-containing compounds that possess greater selectivity for the adrenal cortex.

## REFERENCES


(1) W. H. Beierwaltes, D. M. Wieland, T. Yu, D. P. Swanson, and S. T. Mosley, *Semin. Nucl. Med.*, **8**, 5 (1978).

(2) W. H. Beierwaltes, D. M. Wieland, R. D. Ice, J. E. Seabold, S. D. Sarkar, S. P. Gill, and S. T. Mosley, *J. Nucl. Med.*, **17**, 998 (1976).

(3) W. H. Beierwaltes, D. M. Wieland, S. T. Mosley, D. P. Swanson, S. D. Sarkar, J. E. Frietas, J. H. Thrall, and K. R. Herwig, *ibid.*, **19**, 200 (1978).

(4) J. L. Napoli and R. E. Counsell, *J. Med. Chem.*, **20**, 762 (1977).

(5) W. L. Bencze and L. I. Barsky, *J. Med. Pharm. Chem.*, **5**, 1298 (1962).

(6) I. Lalezari, A. Shafiee, and M. Yalpani, *Tetrahedron Lett.*, **1969**, 5105.

(7) I. Lalezari, A. Shafiee, and S. Yazdany, *J. Pharm. Sci.*, **63**, 628 (1974).

(8) I. Lalezari, A. Shafiee, J. Khorrami, and A. Soltani, *ibid.*, **67**, 1336 (1978).


## ACKNOWLEDGMENTS


Supported in part by the Jane Coffin Child Memorial Fund and by Department of Health, Education, and Welfare Grant RR 07143, National Institutes of Health Grants HL 17739 and CA 19898, and Department of Energy Contract EY-76-S-4115.

# Formation of Thiazoles, Thiazines, and Thiadiazines from 1-Phthalazine Thiosemicarbazides as Potential Anticonvulsants

**RAAFAT SOLIMAN** *x, **M. GABR** *, **M. S. ABOUZEIT-HAR** ‡, and **F. M. SHARABI** ‡

Received August 21, 1979, from the *Department of Pharmaceutical Chemistry and the ‡Department of Pharmacology, Faculty of Pharmacy, University of Alexandria, Alexandria, Egypt. Accepted for publication July 8, 1980.

**Abstract** □ 3-Substituted-4-oxothiazolin-2-yl-(1-phthalazinyl)hydrazones, 3-substituted-4-oxo-5,6-dihydro-1,3-thiazin-2-yl-(1-phthalazinyl)hydrazones, and 2-substituted-amino-5-oxo-4-(1-phthalazinyl)-6-hydro-1,3,4-thiadiazines were prepared and tested for their anticonvulsant activity. Some compounds showed weak to moderate anticonvulsant activity.

**Keyphrases** □ Anticonvulsants, potential—thiazoles, thiazines, and thiadiazines formed from 1-phthalazine thiosemicarbazides, synthesis and evaluation for activity □ Thiazoles—synthesis from 1-phthalazine thiosemicarbazides, evaluation for anticonvulsant activity □ Thiazines—synthesis from 1-phthalazine thiosemicarbazides, evaluation for anticonvulsant activity □ Thiadiazines—synthesis from 1-phthalazine thiosemicarbazides, evaluation for anticonvulsant activity

Various pharmacological properties have been shown to be associated with thiazolidone derivatives. These properties include anticonvulsant (1–4), anesthetic (5), and hypnotic (6) activities. Anticonvulsant activity also has been reported for compounds having a hydrazino or hydrazine moiety (1, 7). These observations prompted the synthesis of 3-substituted-4-oxothiazolin-2-yl-(1-phthalazinyl)hydrazones (II and III), 3-substituted-4-oxo-5,6-dihydro-1,3-thiazin-2-yl-(1-phthalazinyl)hydrazones (IV), and 2-substituted-amino-5-oxo-4-(1-phthalazinyl)-6-hydro-1,3,4-thiadiazines (V) for evaluation of their anticonvulsant activity.

## EXPERIMENTAL[1]

The synthetic routes are illustrated in Scheme I.

**4-Substituted-1-(1-phthalazinyl)thiosemicarbazides (I)**—A solution of the appropriate isothiocyanate (0.01 mole) in ethanol (10 ml) was mixed with a solution of 1-hydrazinophthalazine hydrochloride (0.01 mole) and sodium bicarbonate (1.1 g) in ethanol (10 ml). The mixture was refluxed for 30 min, treated with sufficient hot water to dissolve the inorganic salts, and set aside overnight, after which the thiosemicarbazide was separated as crystals.

**3-Substituted -4- oxothiazolin-2-yl-(1-phthalazinyl)hydrazones (II)**—*Method A*—A solution of I (0.01 mole) and ethyl bromoacetate (0.01 mole) in ethanol (25 ml) was refluxed for 2 hr. The solvent was removed under reduced pressure, and the residue was dissolved in water and neutralized with sodium carbonate solution. The crude product obtained was recrystallized from the proper solvent.

*Method B*—To a mixture of sodium ethoxide (0.01 mole) and I (0.01 mole) in absolute ethanol (25 ml) was added dropwise, with stirring, ethyl bromoacetate (0.01 mole) in absolute ethanol (5 ml). The reaction mixture was refluxed for 1 hr and concentrated. The crude product obtained was purified by recrystallization from the proper solvent.

Compounds obtained by this method were identical with those prepared following Method A as confirmed by their melting points, mixed melting points, IR spectra, and TLC analysis (Table I).

**3 - Substituted-4-oxo-5-methylthiazolin-2-yl-(1-phthalazinyl)-hydrazones (III)**—This series of compounds was prepared following Method A, using ethyl 2-bromopropionate in place of ethyl bromoacetate (Table I).

**3-Substituted-4-oxo-5,6-dihydro -1,3- thiazin-2-yl-(1-phthalazinyl)hydrazones (IV)**—A solution of I (0.01 mole) and ethyl 3-bromopropionate (0.01 mole) in ethanol (25 ml) was refluxed for 2 hr and then concentrated and allowed to crystallize. The crude crystals were purified by recrystallization from the appropriate solvent (Table II).

**2-Substituted-amino-5-oxo -4- (1-phthalazinyl)-6-hydro-1,3,4-thiadiazines (V)**—A mixture of I (0.01 mole) and ethyl bromoacetate (0.01 mole) in concentrated hydrochloric acid (25 ml) was refluxed for 1 hr. The precipitate formed after cooling was filtered and recrystallized from absolute ethanol–ether (Table III).

## RESULTS AND DISCUSSION

**Chemistry**—The synthesis of some 4-substituted-1-(1-phthalazinyl)thiosemicarbazides (I) was reported previously. It was accomplished through the reaction between hydralazine and the appropriate isothiocyanate in ethanol.

Cyclization of thiosemicarbazides with α-halo carbonyl compounds was a subject of controversy. It was reported (9) that condensation of a thiosemicarbazide with an α-halo carbonyl compound may result in the formation of one or more five- or six-membered heterocyclic isomers. The hydrogen-ion concentration of the medium, the type of substituent present, and temperature favor the formation of specific structural isomers (10). Cyclization of a thiosemicarbazide with phenacyl bromide (11) or chloroacetone (9) might produce a thiazole, a thiazoline, or a thiadiazine. With phenacyl bromide, the stable ring was the thiadiazine, while with chloroacetone, the thiazoline was more stable (12). On the other hand, thiosemicarbazides in the presence of sodium ethoxide reacted with

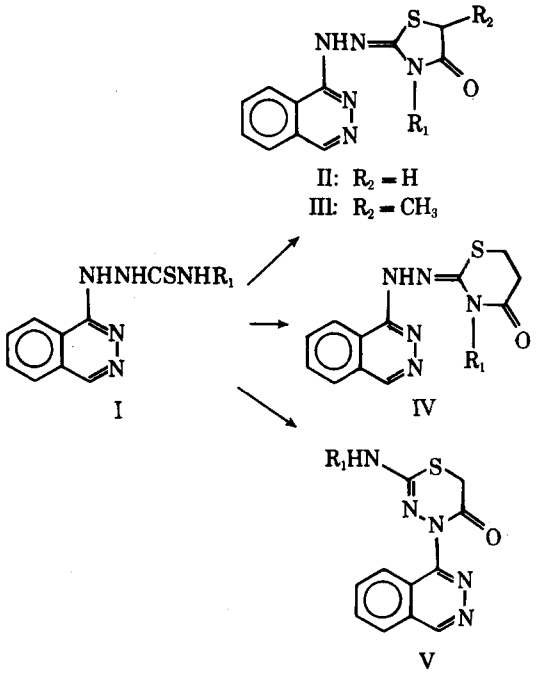


*Scheme I*

[1] Melting points were determined in open glass capillaries and are uncorrected. IR spectra were taken as Nujol mulls with a Beckman IR 4210 spectrophotometer. Microanalyses were performed at the Microanalytical Unit, Faculty of Science, University of Cairo, Cairo, Egypt.



0022-3549/81/0100-0094$01.00/0
© 1981, American Pharmaceutical Association

**Table I—3-Substituted-4-oxothiazolin-2-yl-(1-phthalazinyl)hydrazones**

| Compound | $R_1$ | $R_2$ | Yield, % | Melting Point | Formula[a] | Analysis, % Calc. | Found |
|---|---|---|---|---|---|---|---|
| IIa | $C_2H_5$ | H | 65 | 273–275° | $C_{13}H_{13}N_5OS$ | C 54.4 | 54.6 |
| | | | | | | H 4.5 | 4.4 |
| | | | | | | N 24.4 | 24.2 |
| IIb | $CH_2$=$CHCH_2$ | H | 62 | 270–271° | $C_{14}H_{13}N_5OS$ | C 56.2 | 56.6 |
| | | | | | | H 4.4 | 4.4 |
| | | | | | | N 23.4 | 23.2 |
| IIc | $CH_3(CH_2)_3$ | H | 70 | 273–274° | $C_{15}H_{17}N_5OS$ | C 57.1 | 57.4 |
| | | | | | | H 5.4 | 5.5 |
| | | | | | | N 22.2 | 22.6 |
| IId | $C_6H_{11}$ | H | 72 | 128–130° | $C_{17}H_{19}N_5OS$ | C 59.8 | 60.0 |
| | | | | | | H 5.6 | 5.8 |
| | | | | | | N 20.5 | 20.8 |
| IIe | $C_6H_5$ | H | 68 | 195–197° | $C_{17}H_{13}N_5OS$ | N 20.9 | 20.5 |
| IIf | $C_6H_5CH_2$ | H | 76 | 132–133° | $C_{18}H_{15}N_5OS$ | C 61.9 | 62.1 |
| | | | | | | H 4.3 | 4.5 |
| | | | | | | N 20.1 | 20.5 |
| IIIa | $C_2H_5$ | $CH_3$ | 66 | 150–151° | $C_{14}H_{15}N_5OS$ | C 55.8 | 56.0 |
| | | | | | | H 5.0 | 5.0 |
| | | | | | | N 23.3 | 23.5 |
| IIIb | $CH_2$=$CHCH_2$ | $CH_3$ | 60 | 130–131° | $C_{15}H_{15}N_5OS$ | C 57.5 | 57.2 |
| | | | | | | H 4.8 | 5.0 |
| | | | | | | N 22.4 | 22.5 |
| IIId | $C_6H_{11}$ | $CH_3$ | 78 | 222–224° | $C_{18}H_{21}N_5OS$ | C 60.8 | 60.5 |
| | | | | | | H 5.9 | 6.3 |
| | | | | | | N 19.7 | 19.9 |
| IIIe | $C_6H_5$ | $CH_3$ | 72 | 230–232° | $C_{18}H_{15}N_5OS$ | C 61.9 | 62.2 |
| | | | | | | H 4.3 | 4.5 |
| | | | | | | N 20.1 | 20.3 |
| IIIf | $C_6H_5CH_2$ | $CH_3$ | 80 | 147–149° | $C_{19}H_{17}N_5OS$ | C 62.8 | 62.5 |
| | | | | | | H 4.7 | 4.9 |
| | | | | | | N 19.3 | 19.6 |

[a] The IR spectra of these compounds showed a carbonyl band at 1670–1740 $cm^{-1}$ and an NH group at 3200–3400 $cm^{-1}$.

**Table II—3-Substituted-4-oxo-5,6-dihydro-1,3-thiazin-2-yl-(1-phthalazinyl)hydrazones**

| Compound | $R_1$ | Yield, % | Melting Point | Formula[a] | Analysis, % Calc. | Found |
|---|---|---|---|---|---|---|
| IVa | $C_2H_5$ | 72 | >260° | $C_{14}H_{15}N_5OS$ | C 55.8 | 55.6 |
| | | | | | H 5.0 | 4.8 |
| | | | | | N 23.3 | 23.1 |
| IVb | $CH_2$=$CHCH_2$ | 70 | 197–198° | $C_{15}H_{15}N_5OS$ | C 57.5 | 57.3 |
| | | | | | H 4.8 | 4.9 |
| | | | | | N 22.4 | 22.8 |
| IVc | $CH_3(CH_2)_3$ | 74 | 170–172° | $C_{16}H_{19}N_5OS$ | C 58.4 | 58.1 |
| | | | | | H 5.8 | 6.1 |
| | | | | | N 21.3 | 21.6 |
| IVd | $C_6H_{11}$ | 78 | 207–208° | $C_{18}H_{21}N_5OS$ | C 60.8 | 61.2 |
| | | | | | H 5.9 | 5.5 |
| | | | | | N 19.7 | 20.1 |
| IVe | $C_6H_5$ | 68 | >265° | $C_{18}H_{15}N_5OS$ | C 61.9 | 61.5 |
| | | | | | H 4.3 | 4.1 |
| | | | | | N 20.1 | 19.9 |
| IVf | $C_6H_5CH_2$ | 75 | 166–168° | $C_{19}H_{17}N_5OS$ | C 62.8 | 63.1 |
| | | | | | H 4.7 | 5.0 |
| | | | | | N 19.3 | 19.5 |

[a] The IR spectra of these compounds showed a carbonyl band at 1630–1750 $cm^{-1}$ and an NH group at 3220–3320 $cm^{-1}$.

**Table III—2-Substituted-amino-5-oxo-4-(1-phthalazinyl)-6-hydro-1,3,4-thiadiazines**

| Compound | $R_1$ | Yield, % | Melting Point | Formula | Analysis, % Calc. | Found |
|---|---|---|---|---|---|---|
| Va | $C_2H_5$ | 60 | 219–220° | $C_{13}H_{14}ClN_5OS$ | C 48.2 | 48.2 |
| | | | | | H 4.3 | 3.9 |
| | | | | | N 21.6 | 21.3 |
| Vf | $C_6H_5CH_2$ | 70 | 262–263° | $C_{18}H_{16}ClN_5OS$ | N 18.2 | 18.4 |

α-halo acids or esters to give thiazole derivatives (13, 14). Refluxing the formed 2,3-dihydrothiazole derivatives with concentrated hydrochloric acid resulted in the formation of a six-membered ring to give the hydrochloride of 2-amino-5-methyl-1,3,4-thiadiazine (10).

**Pharmacology**—The anticonvulsant activity of some representative compounds of series II–V was determined (15). Mice of both sexes (15–20 g) were divided into groups of 10, with the group weights kept as near as possible. The test compounds were suspended in aqueous carboxymethylcellulose (1% w/v) and injected intraperitoneally. Four hours after this administration, the mice were injected subcutaneously with 90 mg of pentylenetetrazol/kg. This dose produced convulsions in all untreated mice during the 1st hr following injection and caused 70% mortality during the 24-hr period.

The occurrence of seizures was observed for 60 min. An episode of

**Table IV—Anticonvulsant Activity of Thiazole, Thiazine, and Thiadiazine Derivatives of 1-Phthalazine**

| Compound | Anticonvulsant Activity, % protection[a] | Pentylenetetrazol, % mortality[b] |
|---|---|---|
| IId[c] | 70 | 20 |
| IIf | 20 | 50 |
| IIIa | 10 | 90 |
| IIIf | 40 | 50 |
| IVa | 30 | 60 |
| IVb[c] | 0 | 100 |
| IVd | 20 | 70 |
| IVe | 30 | 50 |
| IVf[c] | 10 | 90 |
| Va | 50 | 30 |

[a] Anticonvulsant activity was determined at doses of 1.0 mmole/kg, equivalent to 200 mg of meprobamate/kg, as described under *Experimental*. Meprobamate (200 mg/kg) and phenobarbital sodium (80 mg/kg) were used as standard anticonvulsants; they exerted 90–100 and 100% protection, respectively, against pentylenetetrazol-induced convulsions in mice under similar conditions. [b] Represents mortality over 24 hr in each group of animals administered pentylenetetrazol at 90 mg/kg. [c] Compounds IId, IVb, and IVf were used in doses equivalent to 50 mg of meprobamate/kg. Their corresponding $LD_{50}$ ($\pm SD$) values were 135 ± 19, 202 ± 7, and 137 ± 12 mg/kg, respectively.

clonic spasm that persisted for a minimum of 5 sec after administration of pentylenetetrazol was considered a threshold convulsion. Transient intermittent jerks and tremors were not counted. Animals devoid of threshold convulsions over 60 min were considered protected. The number of animals protected in each group was recorded, and the anticonvulsant activity of the test compounds was represented as percent protection. The mice then were observed for 24 hr, and the mortality rate in each group was recorded (Table IV). The $LD_{50}$ of some compounds was determined by the graphical method of Miller and Tainter (16).

The data presented in Table IV show that the compounds possess weak to moderate anticonvulsant activity and that the doses required for demonstration of anticonvulsant activity are very close to their corresponding toxic doses.

## REFERENCES


(1) A. K. Dimri and S. S. Parmar, *J. Heterocycl. Chem.*, **15,** 335 (1978).

(2) H. D. Troutman and L. M. Long, *J. Am. Chem. Soc.*, **70,** 3436 (1948).

(3) C. Dwinedi, T. K. Gupta, and S. S. Parmar, *J. Med. Chem.*, **15,** 553 (1972).

(4) S. P. Singh, B. Ali, T. K. Auyong, S. S. Parmar, and B. DeBoer, *J. Pharm. Sci.*, **65,** 391 (1976).

(5) A. R. Surrey, *J. Am. Chem. Soc.*, **71,** 3354 (1949).

(6) W. J. Doran and H. A. Shonle, *J. Org. Chem.*, **3,** 193 (1938).

(7) S. P. Singh, T. K. Auyong, and S. S. Parmar, *J. Pharm. Sci.*, **63,** 960 (1974).

(8) A. I. El-Sebai, M. Ragab, R. Soliman, and M. Gabr, *Pharmazie*, **31,** 436 (1976).

(9) R. C. Elderfield, "Heterocyclic Compounds," vol. 7, Wiley, New York, N.Y., 1961, p. 826.

(10) E. Campaigne and T. P. Selby, *J. Heterocycl. Chem.*, **15,** 401 (1978).

(11) P. K. Bose, *Q. J. Indian Chem. Soc.*, **1,** 51 (1924). *Ibid.*, **2,** 95 (1925).

(12) H. Beyer, *Q. Rep. Sulfur Chem.*, **1970,** 177.

(13) F. J. Wilson and R. Burns, *J. Chem. Soc.*, **1922,** 870.

(14) J. Melean and F. J. Wilson, *ibid.*, **1937,** 556.

(15) A. K. Chaturvedi, J. P. Barthwal, S. S. Parmar, and V. I. Stenberg, *J. Pharm. Sci.*, **64,** 454 (1975).

(16) L. C. Miller and M. L. Tainter, *Proc. Soc. Exp. Biol. Med.*, **57,** 261 (1944).


# Quantitative Determination of Pilocarpine, Isopilocarpine, Pilocarpic Acid, and Isopilocarpic Acid in Clinical Ophthalmic Pilocarpine Formulations by Reversed-Phase Liquid Chromatography


**A. NOORDAM, L. MAAT, and H. C. BEYERMAN** ˣ



Received November 16, 1979, from the *Laboratory of Organic Chemistry, Technische Hogeschool Delft, Julianalaan 136, 2628 BL Delft, The Netherlands.* **Accepted for publication June 24, 1980.**



**Abstract** □ A rapid and convenient reversed-phase high-performance liquid chromatographic procedure for the quantitative determination of pilocarpine and its degradation products was used to analyze 10 clinical ophthalmic pilocarpine formulations.



**Keyphrases** □ Pilocarpine—reversed-phase high-performance liquid chromatographic analysis with isopilocarpine, pilocarpic acid, and isopilocarpic acid in ophthalmic pilocarpine formulations □ High-performance liquid chromatography, reversed phase—analysis, pilocarpine, isopilocarpine, pilocarpic acid, and isopilocarpic acid in ophthalmic pilocarpine formulations


(+)-Pilocarpine {(2*S*,3*R*)-2-ethyl-3-[(1-methyl-5-imidazolyl)methyl]-4-butanolide} is an imidazole alkaloid for which a stereoselective synthesis was reported recently (1). It is used frequently in ophthalmology to relieve intraocular pressure, specifically glaucoma. For this purpose, buffered, stabilized, isotonic aqueous solutions of pilocarpine hydrochloride or nitrate usually are used (2).

In an aqueous medium, pilocarpine (I) can hydrolyze to

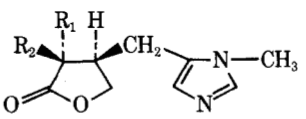

I: $R_1$ = H, $R_2$ = $C_2H_5$
II: $R_1$ = $C_2H_5$, $R_2$ = H

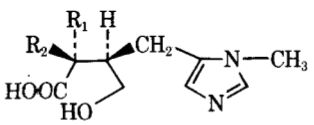

III: $R_1$ = H, $R_2$ = $C_2H_5$
IV: $R_1$ = $C_2H_5$, $R_2$ = H




*0022-3549/81/0100-0096$01.00/0*


*© 1981, American Pharmaceutical Association*

**Table IV—Anticonvulsant Activity of Thiazole, Thiazine, and Thiadiazine Derivatives of 1-Phthalazine**

| Compound | Anticonvulsant Activity, % protection[a] | Pentylenetetrazol, % mortality[b] |
|---|---|---|
| IId[c] | 70 | 20 |
| IIf | 20 | 50 |
| IIIa | 10 | 90 |
| IIIf | 40 | 50 |
| IVa | 30 | 60 |
| IVb[c] | 0 | 100 |
| IVd | 20 | 70 |
| IVe | 30 | 50 |
| IVf[c] | 10 | 90 |
| Va | 50 | 30 |

[a] Anticonvulsant activity was determined at doses of 1.0 mmole/kg, equivalent to 200 mg of meprobamate/kg, as described under *Experimental*. Meprobamate (200 mg/kg) and phenobarbital sodium (80 mg/kg) were used as standard anticonvulsants; they exerted 90–100 and 100% protection, respectively, against pentylenetetrazol-induced convulsions in mice under similar conditions. [b] Represents mortality over 24 hr in each group of animals administered pentylenetetrazol at 90 mg/kg. [c] Compounds IId, IVb, and IVf were used in doses equivalent to 50 mg of meprobamate/kg. Their corresponding $LD_{50}$ ($\pm SD$) values were 135 ± 19, 202 ± 7, and 137 ± 12 mg/kg, respectively.

clonic spasm that persisted for a minimum of 5 sec after administration of pentylenetetrazol was considered a threshold convulsion. Transient intermittent jerks and tremors were not counted. Animals devoid of threshold convulsions over 60 min were considered protected. The number of animals protected in each group was recorded, and the anticonvulsant activity of the test compounds was represented as percent protection. The mice then were observed for 24 hr, and the mortality rate in each group was recorded (Table IV). The $LD_{50}$ of some compounds was determined by the graphical method of Miller and Tainter (16).

The data presented in Table IV show that the compounds possess weak to moderate anticonvulsant activity and that the doses required for demonstration of anticonvulsant activity are very close to their corresponding toxic doses.

## REFERENCES


(1) A. K. Dimri and S. S. Parmar, *J. Heterocycl. Chem.*, **15,** 335 (1978).

(2) H. D. Troutman and L. M. Long, *J. Am. Chem. Soc.*, **70,** 3436 (1948).

(3) C. Dwinedi, T. K. Gupta, and S. S. Parmar, *J. Med. Chem.*, **15,** 553 (1972).

(4) S. P. Singh, B. Ali, T. K. Auyong, S. S. Parmar, and B. DeBoer, *J. Pharm. Sci.*, **65,** 391 (1976).

(5) A. R. Surrey, *J. Am. Chem. Soc.*, **71,** 3354 (1949).

(6) W. J. Doran and H. A. Shonle, *J. Org. Chem.*, **3,** 193 (1938).

(7) S. P. Singh, T. K. Auyong, and S. S. Parmar, *J. Pharm. Sci.*, **63,** 960 (1974).

(8) A. I. El-Sebai, M. Ragab, R. Soliman, and M. Gabr, *Pharmazie*, **31,** 436 (1976).

(9) R. C. Elderfield, "Heterocyclic Compounds," vol. 7, Wiley, New York, N.Y., 1961, p. 826.

(10) E. Campaigne and T. P. Selby, *J. Heterocycl. Chem.*, **15,** 401 (1978).

(11) P. K. Bose, *Q. J. Indian Chem. Soc.*, **1,** 51 (1924). *Ibid.*, **2,** 95 (1925).

(12) H. Beyer, *Q. Rep. Sulfur Chem.*, **1970,** 177.

(13) F. J. Wilson and R. Burns, *J. Chem. Soc.*, **1922,** 870.

(14) J. Melean and F. J. Wilson, *ibid.*, **1937,** 556.

(15) A. K. Chaturvedi, J. P. Barthwal, S. S. Parmar, and V. I. Stenberg, *J. Pharm. Sci.*, **64,** 454 (1975).

(16) L. C. Miller and M. L. Tainter, *Proc. Soc. Exp. Biol. Med.*, **57,** 261 (1944).


# Quantitative Determination of Pilocarpine, Isopilocarpine, Pilocarpic Acid, and Isopilocarpic Acid in Clinical Ophthalmic Pilocarpine Formulations by Reversed-Phase Liquid Chromatography


**A. NOORDAM, L. MAAT, and H. C. BEYERMAN** ˣ



Received November 16, 1979, from the *Laboratory of Organic Chemistry, Technische Hogeschool Delft, Julianalaan 136, 2628 BL Delft, The Netherlands.* **Accepted for publication June 24, 1980.**



**Abstract** □ A rapid and convenient reversed-phase high-performance liquid chromatographic procedure for the quantitative determination of pilocarpine and its degradation products was used to analyze 10 clinical ophthalmic pilocarpine formulations.



**Keyphrases** □ Pilocarpine—reversed-phase high-performance liquid chromatographic analysis with isopilocarpine, pilocarpic acid, and isopilocarpic acid in ophthalmic pilocarpine formulations □ High-performance liquid chromatography, reversed phase—analysis, pilocarpine, isopilocarpine, pilocarpic acid, and isopilocarpic acid in ophthalmic pilocarpine formulations


(+)-Pilocarpine {(2*S*,3*R*)-2-ethyl-3-[(1-methyl-5-imidazolyl)methyl]-4-butanolide} is an imidazole alkaloid for which a stereoselective synthesis was reported recently (1). It is used frequently in ophthalmology to relieve intraocular pressure, specifically glaucoma. For this purpose, buffered, stabilized, isotonic aqueous solutions of pilocarpine hydrochloride or nitrate usually are used (2).

In an aqueous medium, pilocarpine (I) can hydrolyze to

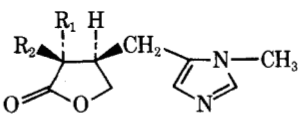

I: $R_1$ = H, $R_2$ = $C_2H_5$
II: $R_1$ = $C_2H_5$, $R_2$ = H

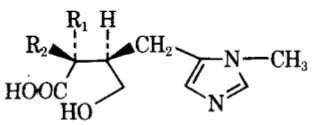

III: $R_1$ = H, $R_2$ = $C_2H_5$
IV: $R_1$ = $C_2H_5$, $R_2$ = H




*0022-3549/81/0100-0096$01.00/0*


*© 1981, American Pharmaceutical Association*

Table I—Composition of Commercially Available Ophthalmic Pilocarpine Formulations (March 1979)

| Sample | Expiration Date | Label Claim of Pilocarpine | | Pilocarpine Found, % | Relative Composition, % | | | pH Found | Additives Stated on Label |
|---|---|---|---|---|---|---|---|---|---|
| | | Form | Percent | | Pilocarpine | Isopilocarpine | Pilocarpic Acid | | |
| 1 | December 1973 | HCl | 4 | 4.3 | 95.0 | 1.5 | 3.5 | 3.5 | —[a] |
| 2 | November 1976 | HCl | 1 | 1.0 | 92.7 | 2.1 | 5.2 | 3.7 | —[a] |
| 3 | November 1976 | HCl | 1 | 1.0 | 93.0 | 2.0 | 5.0 | 3.6 | —[a] |
| 4 | May 1977 | HCl | 2 | 2.1 | 93.4 | 3.4 | 3.2 | 3.4 | —[a] |
| 5 | April 1978 | HCl | 4 | 4.2 | 96.6 | 0.7 | 2.7 | 3.2 | —[a] |
| 6 | February 22, 1979 | HCl | 2 | 1.8 | 82.3 | 5.7 | 11.3[b] | 5.5 | —[c] |
| 7 | February 16, 1979 | HCl | 4 | 4.3 | 97.5 | 0.7 | 1.8 | 2.7 | None |
| 8 | February 16, 1979 | HCl | 8 | 8.7 | 97.9 | 0.7 | 1.4 | 2.4 | None |
| 9 | — | $HNO_3$ | 2 | 2.1 | 97.7 | 1.1 | 1.2 | 6.0 | —[d,e] |
| 10 | — | $HNO_3$ | 2 | 2.2 | 97.7 | 0.8 | 1.5 | 6.0 | —[d,e] |

[a] Hydroxypropyl methylcellulose (4000 cps) at 0.5%, benzalkonium chloride at 1:25,000, phenylmercuric nitrate at 1:75,000, boric acid, sodium citrate, and distilled water. [b] The sample also contained ~0.7% isopilocarpic acid. [c] Borax–boric acid buffer at pH 6.5. [d] Lyophilized eye drops (200 mg of pilocarpine nitrate as solid matter and a vial containing 10 ml of an aqueous liquid). [e] Methylcellulose, boric acid, sodium borate, sodium chloride, thimerosal, and water.

pilocarpic acid (III) and epimerize to isopilocarpine (II), which, in turn, can hydrolyze to isopilocarpic acid (IV). The extent of the degradation depends, among other things, on pH, temperature, and time (3). Since this degradation results in deterioration of the pharmacological effect, ophthalmic aqueous pilocarpine formulations have limited stability.

Several determination methods for pilocarpine are known, including one based on $^{13}C$-NMR spectroscopy (4). (Reference 4 summarizes the existing methods and their drawbacks.) However, the application of the $^{13}C$-NMR method for the quantitative determination of pilocarpine in ophthalmic formulations is laborious and has other limitations (5, 6).

A quantitative determination was reported recently for pilocarpine and its degradation products by reversed-phase high-performance liquid chromatography (7). This report discusses the successful application of this separation method to 10 commercial, clinical ophthalmic pilocarpine formulations.

## EXPERIMENTAL

The quantitative determination is based on the separation of I–IV (7). By the use of UV detection at 215 nm instead of the refractive index, the sensitivity was improved greatly. The detection limit thus was lowered from ~6 to ~0.04 μg. The separation of I–IV was carried out within 30 min on a reversed-phase column with water–methanol (97:3) containing 5% monobasic potassium phosphate. The pH was adjusted to 2.5 with phosphoric acid. No significant difference was found with the chromatogram shown in Ref. 7, although the column contained a slightly different octadecylsilyl packing. Additives such as buffers, antiseptics, and stabilizers, which often are present in clinical formulations, did not disturb the separation.

The formulations studied had been stored unopened. When assayed (March 15, 1979), the preparations, except for Formulations 9 and 10, were past their expiration date (Table I). Starting from the concentration stated on the package, all of the formulations were diluted with water to a concentration of 1%. The diluted solutions were compared with standard solutions of a known concentration of pilocarpine hydrochloride or nitrate. The percentage of pilocarpine was found by measuring the peak height. For the determination of the relative composition, the reversed-phase high-performance liquid chromatograms were compared with those of standard mixtures of pilocarpine, isopilocarpine, pilocarpic acid, and isopilocarpic acid dissolved in water.

(+)-Pilocarpine (8) and (+)-isopilocarpine were used as their hydrochlorides. Pilocarpic acid and isopilocarpic acid were obtained by hydrolysis of pilocarpine and isopilocarpine, respectively, in 0.1 *N* aqueous NaOH. A high-performance pump was used[1]; a column (15 × 0.4 cm i.d.) packed with octadecylsilica[2] was employed with a UV detector[3] set at 215 nm. The flow rate was set at 1.5 ml/min.

## RESULTS AND DISCUSSION

The method described is superior to existing methods in many respects (accuracy, time of analysis, quantity of sample needed, and ability to determine all four compounds in one run). In addition, the method is cheap and requires little pretreatment of the sample.

The results of the analyses of the 10 pilocarpine formulations are summarized in Table I. All experiments were carried out in duplicate, and deviations were negligible. Beside pilocarpine, these formulations contained, according to their label, buffers, antiseptics, and stabilizers (Table I).

With Samples 1–5 (pH found was ~3.5), the composition was only slightly dependent on age. For Samples 6–8, no information about the additional contents was given on the package. The label of Sample 6 said that it contained borax–boric acid buffer of pH 6.5 (found pH 5.5). The relatively high pH of this sample might account for the large quantity of isopilocarpine and pilocarpic acid found. Furthermore, most, if not all, of the formulations probably initially contained an excess of pilocarpine of at least 10% over the content stated.

## REFERENCES


(1) A. Noordam, L. Maat, and H. C. Beyerman, *Rec. Trav. Chim. Pays-Bas*, **98**, 467 (1979).

(2) "The Pharmacological Basis of Therapeutics," 4th ed., L. S. Goodman and A. Gilman, Eds., Macmillan, New York, N.Y., 1970, p. 472.

(3) M. A. Nunes and E. Brochmann-Hanssen, *J. Pharm. Sci.*, **63**, 716 (1974).

(4) G. A. Neville, F. B. Hasan, and I. C. P. Smith, *Can. J. Chem.*, **54**, 2094 (1976).

(5) G. A. Neville, F. B. Hasan, and I. C. P. Smith, *J. Pharm. Sci.*, **66**, 638 (1977).

(6) G. A. Neville, F. B. Hasan, and I. C. P. Smith, *Can. J. Pharm. Sci.*, **12**, 17 (1977).

(7) A. Noordam, K. Waliszewski, C. Olieman, L, Maat, and H. C. Beyerman, *J. Chromatogr.*, **153**, 271 (1978).

(8) "Dutch Pharmacopoeia," 8th ed., Staatsuitgeverij, The Hague, The Netherlands, 1978, p. 857.


## ACKNOWLEDGMENTS


The authors thank the management of Diosynth B.V. (Apeldoorn, The Netherlands) for the gift of alkaloids, Dr. P. P. H. Alkemade for providing the ophthalmic pilocarpine formulations, and Mr. M. Makkee and Mr. C. Olieman for assistance with the analyses.


[1] Waters model 6000A pump with a model U6K injector.
[2] Nucleosil $C_{18}$, Macherey-Nagel & Co., Düren, West Germany.
[3] Pye Unicam LC3.

# Convenient Synthesis of Alkyl Esters of Urocanic Acid

**KEIICHI HONDA** ˣ **and YASUSHI NISHIJIMA**

Received August 31, 1979, from the *Cosmetics Laboratory, Kanebo, Ltd., 5-3-28 Kotobuki-cho, Odawara 250, Japan.* Accepted for publication July 15, 1980.

**Abstract** □ Ethyl, *n*-dodecyl, and *n*-hexadecyl esters of urocanic acid (4-imidazoleacrylic acid) were prepared from 4-imidazolecarboxaldehyde in satisfactory yields *via* the Wittig reaction.

**Keyphrases** □ Urocanic acid—alkyl esters, synthesis *via* Wittig reaction □ Wittig reaction—synthesis of alkyl esters of urocanic acid □ Sunscreens, potential—urocanic acid, synthesis of alkyl esters by Wittig reaction

The finding that urocanic acid (4-imidazoleacrylic acid), a metabolite of histidine, occurs in human epidermis (1) has generated interest in the possible use of the acid and its alkyl esters in cosmetics as sunscreens (2–4). *trans*-Urocanic acid, which readily isomerizes to *cis*-urocanic acid when irradiated with UV rays (5), was reported to show excellent sunlight-screening action since it has noteworthy absorption in the UV range of 240–320 nm, which is similar to the erythemal action spectrum (6). However, the utilization of urocanic acid is restricted because it is almost insoluble in oils or water unless it is derivatized to a proper salt, which, in turn, is readily removed by washing or perspiration. In contrast, most urocanic acid esters are soluble in most oils, which adds to their practical applicability.

Alkyl esters of urocanic acid generally have been synthesized by condensation of 4-imidazolecarboxaldehyde with malonic acid to give urocanic acid, which subsequently is esterified (2, 7–10). However, this two-step sequence is time consuming and deficient in overall yield. Although urocanic acid also is produced by enzymatic deamination of L-histidine (11), esterification of the acid with long-chain aliphatic alcohols is difficult due to the poor solubility of the acid in alcohols and organic solvents.

The present report describes a convenient one-step synthesis of some alkyl esters of urocanic acid from 4-imidazolecarboxaldehyde *via* the Wittig reaction.

## EXPERIMENTAL

**Spectral Measurement**—IR spectra[1] were obtained on potassium bromide disks. The PMR spectrum was recorded on a 100-MHz spectrometer[2] with tetramethylsilane as the internal standard. The chemical shifts and coupling constants are represented by $\delta$ and Hertz units, respectively. Mass spectra[3] were measured at an ionizing potential of 25 ev.

**Chromatography**—The high-performance liquid chromatograph[4] was equipped with a UV detector and a 500 × 3-mm i.d. glass column packed with vinyl acetate porous polymer gel[5]. The analyses were carried out with 0.75% (w/w) methanolic triethylamine as the eluent and naphthalene as the internal standard. The column eluates were monitored at 288 nm.

**Materials**—4-Imidazolecarboxaldehyde (I), prepared according to the procedure reported by Pyman (12), was obtained as pale-yellow crystals, mp 173–174° [lit. (13) mp 173–174°]. Diethyl carbethoxymethylphosphonate[6] (II) was obtained commercially and used without further purification. Carbethoxymethylenetriphenylphosphorane (III), mp 118–119° [lit. (14) mp 116–117°], and carbo-*n*-hexadecyloxymethylenetriphenylphosphorane (IV), mp 90–91.5° [lit. (14) mp 90–91°], were prepared by the method of Isler *et al.* (14). Carbo-*n*-dodecyloxymethylenetriphenylphosphorane (V) was prepared in an analogous manner, yielding white crystals, mp 44.5–45.5°. All melting points are uncorrected.

*Anal.*—Calc. for $C_{32}H_{41}O_2P$: C, 78.66; H, 8.46; P, 6.34. Found: C, 78.37; H, 8.47; P, 6.29.

**Preparation of Ethyl Urocanate (VI)**—*Method A*—To a stirred solution of the aldehyde (I) (1.92 g, 20 mmoles) and the phosphonate (II) (6.73 g, 30 mmoles) dissolved in 20 ml of *N,N*-dimethylformamide was added 0.96 g (40 mmoles) of sodium hydride at room temperature. After gas evolution had ceased, the mixture was heated to 95° and held at that temperature for 3 hr. After removal of the solvent at reduced pressure, the residue was acidified with 5% HCl with stirring and extracted with benzene (30 ml) to eliminate excess phosphonate.

The aqueous layer was made basic with dilute sodium bicarbonate solution and extracted with two 15-ml portions of chloroform. The combined chloroform extracts were washed with water, dried over calcium sulfate, and concentrated to afford a pale-brown oil. After dehydration[7] at 95° for 2 hr *in vacuo* and recrystallization from chloroform–petroleum ether, this oil gave 1.43 g of VI (43% yield) as white crystals, mp 81–82°; IR: 1705 (C=O) $cm^{-1}$; PMR ($CDCl_3$): $\delta$ 1.29 (t, 3H), 4.22 (q, 2H), 6.41 (d, 1H, $J$ = 16 Hz), 7.32 (s, 1H), 7.60 (d, 1H, $J$ = 16 Hz), and 7.74 (s, 1H).

*Anal.*—Calc. for $C_8H_{10}N_2O_2$: C, 57.82; H, 6.07; N, 16.86. Found: C, 57.73; H, 6.06; N, 16.89.

*Method B*—A mixture of the aldehyde (I) (1.92 g, 20 mmoles), the phosphorane (III) (8.36 g, 24 mmoles), and dimethyl sulfoxide (25 ml) was maintained at 130° for 3 hr. Evacuation of dimethyl sulfoxide *in vacuo* and similar workup gave 1.73 g (52% yield) of VI.

**Preparation of *n*-Dodecyl Urocanate (VII)**—A mixture of the aldehyde (I) (1.92 g, 20 mmoles), the phosphorane (V) (11.73 g, 24 mmoles), and dimethyl sulfoxide (25 ml) was heated at 140° for 4 hr. To the reaction mixture was added 10% HCl (10 ml), and the mother liquor was evaporated *in vacuo* to dryness. The residual paste was washed with acetone–isobutanol, suspended in hot water (10 ml), and treated with dilute sodium bicarbonate solution to give a brown oil, which gradually crystallized on standing.

The crystals were collected, washed with water, dehydrated at 80° for 2 hr *in vacuo*, and recrystallized from petroleum ether to yield 3.55 g of VII (58% yield) as white crystals, mp 61–62°; IR: 1705 (C=O) $cm^{-1}$; mass spectrum: *m/e* 306 ($M^+$, 44%), 277 (11), 179 (30), 138 (75), 122 (50), 121 (71), 95 (58), 94 (100), and 82 (59).

*Anal.*—Calc. for $C_{18}H_{30}N_2O_2$: C, 70.55; H, 9.87; N, 9.14. Found: C, 70.27; H, 9.90; N, 9.14.

In a similar manner, *n*-hexadecyl urocanate[8] (VIII) was obtained as pale-yellow crystals (54% yield), mp 55–56°; IR: 1705 (C=O) $cm^{-1}$; mass spectrum: *m/e* 362 ($M^+$, 59%), 333 (20), 179 (40), 138 (53), 122 (69), 121 (64), 95 (65), 94 (63), and 82 (100). The mass calculated for $C_{22}H_{38}N_2O_2$ was 362.2933; the mass found was 362.2945.

## RESULTS AND DISCUSSION

Although there have been several reports of the reaction of imidazolecarboxaldehydes with nucleophilic reagents (12, 15, 16), the Wittig reaction of the aldehydes generally has not been used. The reaction of 8-xanthinecarboxaldehyde, which contains the 2-imidazolecarboxal-

[1] Hitachi 215 spectrometer.
[2] Japan Electron Optics Laboratory model JNM-MH 100 instrument.
[3] Japan Electron Optics Laboratory model JMS-D 300 mass spectrometer.
[4] Hitachi 635.
[5] TSK GEL LS-140, Toyosoda Co.
[6] Aldrich Chemical Co.
[7] Ethyl urocanate is known to form a hemihydrate when isolated from aqueous media. In the present study, the crude product was dehydrated to obtain the anhydrous ester; otherwise, a mixture of the two usually was obtained. Dehydration proceeded smoothly by heating the hydrated ester at fusion temperature *in vacuo*.
[8] Gas chromatographic and mass spectrometric analyses showed that the product contained ~5% of the *n*-tetradecyl ester and 10% of the *n*-octadecyl ester.



*0022-3549/81/0100-0098$01.00/0*
*© 1981, American Pharmaceutical Association*

dehyde moiety, with carbethoxymethylenetriphenylphosphorane was reported (17). Thus, the aldehyde (I) was subjected to the reaction with the phosphonate (II) or the phosphorane (III) to yield the ethyl ester (VI) in satisfactory yield. In the reaction of I with II (Method A), 2 equivalents of sodium hydride were used, and aprotic polar solvents such as dimethyl sulfoxide and *N,N*-dimethylformamide were necessary to dissolve the sodium salt of I. The time conversion was monitored by high-performance liquid chromatography (HPLC), and I was converted to VI in a 58% yield when the reaction was carried out with 1.5 equivalents of II at 95° for 3 hr in *N,N*-dimethylformamide. The reaction rate was slower in dimethyl sulfoxide.

On the other hand, I reacted readily with resonance-stabilized ylide III (Method B) in various solvents capable of dissolving I to yield VI. However, the reaction in ethanol resulted in a lower yield than in aprotic solvents, probably due to decomposition of III by a side reaction with ethanol. Of the several solvents used, dimethyl sulfoxide and diglyme were the most suitable for this reaction. The yields of VI for the reaction in dimethyl sulfoxide and in diglyme were 66 and 63%, respectively (molar ratio of III to I of 1.2, 130°, 3 hr).

From the viewpoints of utility and facility, these results indicate that carboalkoxymethylenetriphenylphosphoranes are more appropriate for the preparation of esters of imidazoleacrylic acids containing an acidic imino hydrogen atom. Method B thus was applied to the preparation of long-chain alkyl esters. The aldehyde (I) was allowed to react with the phosphorane (V), and HPLC analysis of the reaction mixture showed the formation of *n*-dodecyl ester (VII) in a 70% yield. Similarly, I was converted, by the reaction with the phosphorane (IV), to *n*-hexadecyl ester (VIII) in 66% yield.

These esters (VI–VIII) were soluble in most oils and had an absorption maximum at 290 nm in 0.75% (w/w) triethylamine in methanol.

## REFERENCES


(1) A. Zenisek, J. A. Kral, and I. M. Hais, *Biochim. Biophys. Acta*, **18**, 589 (1955).

(2) C. Pasini, *Farmaco, Ed. Sci.*, **11**, 998 (1958).

(3) I. M. Hais and A. Zenisek, *Am. Perfum. Aromat.*, **73**(9), 26 (1959).

(4) J. H. Anglin, Jr., *Cosmet. Toiletries*, **91**, 47 (1976).

(5) S. Edelbacher and F. Heitz, *Hoppe-Seylers Z. Physiol. Chem.*, **279**, 63 (1943).

(6) R. G. Freeman, D. W. Owens, J. M. Knox, and H. T. Hudson, *J. Invest. Dermatol.*, **47**, 586 (1966).

(7) G. Barger and H. D. Dakin, *Biochem. J.*, **10**, 376 (1916).

(8) S. Akabori, S. Ose, and T. Kaneko, *Proc. Imp. Acad. (Tokyo)*, **16**, 191 (1940).

(9) Z. Horii, K. Sakurai, and K. Tomino, *Yakugaku Zasshi*, **74**, 408 (1954).

(10) N. Miyashita, Y. Emata, and M. Narita, Japanese pat. 28500 (1975).

(11) M. Tanaka and N. Nakamura, Japanese pat. 4997 (1972).

(12) F. L. Pyman, *J. Chem. Soc.*, **109**, 186 (1916).

(13) R. A. Turner, C. F. Huebner, and C. R. Scholz, *J. Am. Chem. Soc.*, **71**, 2801 (1949).

(14) O. Isler, H. Gutmann, M. Montavon, R. Rüegg, G. Ryser, and P. Zeller, *Helv. Chim. Acta*, **40**, 1242 (1957).

(15) W. Hubball and F. L. Pyman, *J. Chem. Soc.*, **121**, 21 (1928).

(16) R. G. Jones and K. C. McLaughlin, *J. Am. Chem. Soc.*, **71**, 2444 (1949).

(17) H. Bredereck and B. Föhlisch, *Chem. Ber.*, **95**, 414 (1962).


# Simultaneous Determination of Niacinamide, Pyridoxine, Riboflavin, and Thiamine in Multivitamin Products by High-Pressure Liquid Chromatography


**M. C. WALKER ˣ, B. E. CARPENTER, and E. L. COOPER**



Received February 19, 1980, from the *Control Division, The Upjohn Company, Kalamazoo, MI 49001.* Accepted for publication July 10, 1980.



**Abstract** □ A high-pressure liquid chromatographic assay was developed for the determination of four water-soluble vitamins: niacinamide, pyridoxine, thiamine, and riboflavin. The four vitamins are assayed simultaneously in multivitamin products not containing minerals. Thiamine currently is not quantitated in formulations containing minerals because it is not stable under the extraction conditions. The method was applied to the analysis of at least 12 different multivitamin products, including various formulations of sterile products, fluids, compressed tablets, and coated, compressed tablets. The method is stability indicating and is applicable to single-tablet assays.



**Keyphrases** □ Niacinamide—simultaneous high-pressure liquid chromatographic analysis with pyridoxine, riboflavin, and thiamine in multivitamin products □ Pyridoxine—simultaneous high-pressure liquid chromatographic analysis with niacinamide, riboflavin, and thiamine in multivitamin products □ Riboflavin—simultaneous high-pressure liquid chromatographic analysis with niacinamide, pyridoxine, and thiamine in multivitamin products □ Thiamine—simultaneous high-pressure liquid chromatographic analysis with niacinamide, pyridoxine, and riboflavin in multivitamin products □ Vitamins—niacinamide, pyridoxine, riboflavin, and thiamine, simultaneous high-pressure liquid chromatographic analysis in multivitamin products □ High-pressure liquid chromatography—analysis, niacinamide, pyridoxine, riboflavin, and thiamine in multivitamin products


A substantial amount of information has been published since 1970 on the use of high-pressure liquid chromatography (HPLC) for the analysis of water-soluble vitamins. An excellent review of the subject was prepared by Wittmer and Haney (1). Many of the alternative chemical and microbiological assay methods have time-consuming sample preparations and are not specific. HPLC is the preferred method for vitamin analysis, especially when the sample preparation is simple.

A recent report described the simultaneous determination of niacinamide, pyridoxine, thiamine, and riboflavin (2). Both the previously reported method and the method described in this paper use a paired-ion mobile phase system with a reversed-phase column (3).

The HPLC procedure described in this report has been used for routine analysis for 3 years. The method has been applied to 12 different multivitamin formulations, and work is continuing to add more applications. An average


*0022-3549/81/0100-0099$01.00/0*


*© 1981, American Pharmaceutical Association*

dehyde moiety, with carbethoxymethylenetriphenylphosphorane was reported (17). Thus, the aldehyde (I) was subjected to the reaction with the phosphonate (II) or the phosphorane (III) to yield the ethyl ester (VI) in satisfactory yield. In the reaction of I with II (Method A), 2 equivalents of sodium hydride were used, and aprotic polar solvents such as dimethyl sulfoxide and *N,N*-dimethylformamide were necessary to dissolve the sodium salt of I. The time conversion was monitored by high-performance liquid chromatography (HPLC), and I was converted to VI in a 58% yield when the reaction was carried out with 1.5 equivalents of II at 95° for 3 hr in *N,N*-dimethylformamide. The reaction rate was slower in dimethyl sulfoxide.

On the other hand, I reacted readily with resonance-stabilized ylide III (Method B) in various solvents capable of dissolving I to yield VI. However, the reaction in ethanol resulted in a lower yield than in aprotic solvents, probably due to decomposition of III by a side reaction with ethanol. Of the several solvents used, dimethyl sulfoxide and diglyme were the most suitable for this reaction. The yields of VI for the reaction in dimethyl sulfoxide and in diglyme were 66 and 63%, respectively (molar ratio of III to I of 1.2, 130°, 3 hr).

From the viewpoints of utility and facility, these results indicate that carboalkoxymethylenetriphenylphosphoranes are more appropriate for the preparation of esters of imidazoleacrylic acids containing an acidic imino hydrogen atom. Method B thus was applied to the preparation of long-chain alkyl esters. The aldehyde (I) was allowed to react with the phosphorane (V), and HPLC analysis of the reaction mixture showed the formation of *n*-dodecyl ester (VII) in a 70% yield. Similarly, I was converted, by the reaction with the phosphorane (IV), to *n*-hexadecyl ester (VIII) in 66% yield.

These esters (VI–VIII) were soluble in most oils and had an absorption maximum at 290 nm in 0.75% (w/w) triethylamine in methanol.

## REFERENCES


(1) A. Zenisek, J. A. Kral, and I. M. Hais, *Biochim. Biophys. Acta*, **18**, 589 (1955).

(2) C. Pasini, *Farmaco, Ed. Sci.*, **11**, 998 (1958).

(3) I. M. Hais and A. Zenisek, *Am. Perfum. Aromat.*, **73**(9), 26 (1959).

(4) J. H. Anglin, Jr., *Cosmet. Toiletries*, **91**, 47 (1976).

(5) S. Edelbacher and F. Heitz, *Hoppe-Seylers Z. Physiol. Chem.*, **279**, 63 (1943).

(6) R. G. Freeman, D. W. Owens, J. M. Knox, and H. T. Hudson, *J. Invest. Dermatol.*, **47**, 586 (1966).

(7) G. Barger and H. D. Dakin, *Biochem. J.*, **10**, 376 (1916).

(8) S. Akabori, S. Ose, and T. Kaneko, *Proc. Imp. Acad. (Tokyo)*, **16**, 191 (1940).

(9) Z. Horii, K. Sakurai, and K. Tomino, *Yakugaku Zasshi*, **74**, 408 (1954).

(10) N. Miyashita, Y. Emata, and M. Narita, Japanese pat. 28500 (1975).

(11) M. Tanaka and N. Nakamura, Japanese pat. 4997 (1972).

(12) F. L. Pyman, *J. Chem. Soc.*, **109**, 186 (1916).

(13) R. A. Turner, C. F. Huebner, and C. R. Scholz, *J. Am. Chem. Soc.*, **71**, 2801 (1949).

(14) O. Isler, H. Gutmann, M. Montavon, R. Rüegg, G. Ryser, and P. Zeller, *Helv. Chim. Acta*, **40**, 1242 (1957).

(15) W. Hubball and F. L. Pyman, *J. Chem. Soc.*, **121**, 21 (1928).

(16) R. G. Jones and K. C. McLaughlin, *J. Am. Chem. Soc.*, **71**, 2444 (1949).

(17) H. Bredereck and B. Föhlisch, *Chem. Ber.*, **95**, 414 (1962).


# Simultaneous Determination of Niacinamide, Pyridoxine, Riboflavin, and Thiamine in Multivitamin Products by High-Pressure Liquid Chromatography


**M. C. WALKER ˣ, B. E. CARPENTER, and E. L. COOPER**



Received February 19, 1980, from the *Control Division, The Upjohn Company, Kalamazoo, MI 49001.* Accepted for publication July 10, 1980.



**Abstract** □ A high-pressure liquid chromatographic assay was developed for the determination of four water-soluble vitamins: niacinamide, pyridoxine, thiamine, and riboflavin. The four vitamins are assayed simultaneously in multivitamin products not containing minerals. Thiamine currently is not quantitated in formulations containing minerals because it is not stable under the extraction conditions. The method was applied to the analysis of at least 12 different multivitamin products, including various formulations of sterile products, fluids, compressed tablets, and coated, compressed tablets. The method is stability indicating and is applicable to single-tablet assays.



**Keyphrases** □ Niacinamide—simultaneous high-pressure liquid chromatographic analysis with pyridoxine, riboflavin, and thiamine in multivitamin products □ Pyridoxine—simultaneous high-pressure liquid chromatographic analysis with niacinamide, riboflavin, and thiamine in multivitamin products □ Riboflavin—simultaneous high-pressure liquid chromatographic analysis with niacinamide, pyridoxine, and thiamine in multivitamin products □ Thiamine—simultaneous high-pressure liquid chromatographic analysis with niacinamide, pyridoxine, and riboflavin in multivitamin products □ Vitamins—niacinamide, pyridoxine, riboflavin, and thiamine, simultaneous high-pressure liquid chromatographic analysis in multivitamin products □ High-pressure liquid chromatography—analysis, niacinamide, pyridoxine, riboflavin, and thiamine in multivitamin products


A substantial amount of information has been published since 1970 on the use of high-pressure liquid chromatography (HPLC) for the analysis of water-soluble vitamins. An excellent review of the subject was prepared by Wittmer and Haney (1). Many of the alternative chemical and microbiological assay methods have time-consuming sample preparations and are not specific. HPLC is the preferred method for vitamin analysis, especially when the sample preparation is simple.

A recent report described the simultaneous determination of niacinamide, pyridoxine, thiamine, and riboflavin (2). Both the previously reported method and the method described in this paper use a paired-ion mobile phase system with a reversed-phase column (3).

The HPLC procedure described in this report has been used for routine analysis for 3 years. The method has been applied to 12 different multivitamin formulations, and work is continuing to add more applications. An average


*0022-3549/81/0100-0099$01.00/0*


*© 1981, American Pharmaceutical Association*

**Table I—Average Percent Recovery of Vitamins from Various Formulation Placebos**

| Formulation Placebo | Recovery, % Niacinamide | Pyridoxine | Riboflavin | Thiamine |
|---|---|---|---|---|
| Compressed tablet | 99.7 | 99.9 | 100.8 | 100.1 |
| Coated, compressed tablet | 100.0 | 98.8 | 101.4 | 100.2 |
| Coated, compressed tablet with minerals | 98.8 | 99.4 | 99.1 | — |

**Table II—Precision for the HPLC Determinations of Niacinamide, Pyridoxine, Riboflavin, and Thiamine**

| Dosage Form | *RSD*, % Niacinamide | Pyridoxine | Riboflavin | Thiamine |
|---|---|---|---|---|
| Injectable | 1.1 | 1.0 | 1.7 | 1.2 |
| Compressed tablet | 1.4 | 1.7 | 1.8 | 0.6 |
| Coated, compressed tablet | 1.2 | 2.0 | 1.5 | 1.8 |
| Coated, compressed tablet with minerals | 1.2 | 1.9 | 1.4 | — |

of 16 assays can be run per day. Sample preparation is minimal and involves only a one-step extraction into an internal standard solution and filtration. The method is stability indicating and is applicable to single-tablet assays.

## EXPERIMENTAL

**Chromatographic Conditions**—The equipment consisted of a suitable liquid chromatographic pump capable of operating at ~1000 psi and 1 ml/min, an automated injector with a fixed-volume 20-μl loop, a dual-wavelength (254 and 280 nm) UV detector, and a reversed-phase $C_{18}$ column[1].

**Mobile Phase**—The mobile phase contained 25% methanol and 1% acetic acid in water. The hexanesulfonic acid sodium salt concentration was adjusted to $3–8 \times 10^{-3}$ *M* to optimize chromatography and vitamin quantitation.

**Internal Standard Solution**—The internal standard solution was made up in the mobile phase to contain ~0.05 mg of *p*-hydroxybenzoic acid/ml. For multivitamin–mineral formulations, the internal standard solution also contained ~4 mg/ml of diethylenetriamine pentaacetic acid as the sodium salt.

**Reference Standard Solution**—All reference standard solutions were prepared using USP reference standards dissolved in the internal standard solution.

**Sample Preparation**—A representative number of tablets was ground to a fine powder. To an accurately weighed sample was added exactly 25.0 ml of the internal standard solution. The mixture was shaken mechanically for ~1 hr, filtered, and injected onto the column. Samples formulated with coated vitamins were heated, before shaking, at ~70° for 20 min.

## RESULTS AND DISCUSSION

To quantitate all four vitamins in one chromatographic run without changing the detector sensitivity, a dual-wavelength detection system was adopted. Figure 1 shows the absorption characteristics of the various vitamins in the mobile phase. Niacinamide, thiamine, and riboflavin usually are monitored at 254 nm; pyridoxine is quantitated at 280 nm. The linear response of the system was determined for the following vitamin concentration ranges: niacinamide, 0.21–0.50 mg/ml; pyridoxine, 0.01–0.06 mg/ml; thiamine, 0.02–0.10 mg/ml; and riboflavin, 0.018–0.042 mg/ml.

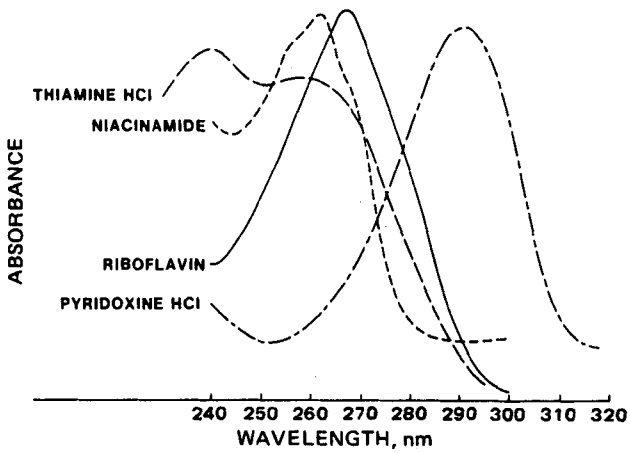


**Figure 1**—*Absorption characteristics of vitamins in the mobile phase.*

The accuracy of the methodology was established from spiked placebo recovery experiments. Results for three representative formulations are given in Table I. The percent recoveries reported for the compressed tablet, a chewable formulation, are averages of six determinations. The corresponding placebo samples were spiked in the range of 80–100% of the theoretical amount. Results for the coated compressed tablet are averages of five different placebo samples spiked with 70–120% of the theoretical amount. Averages of four replicate samples spiked at the theoretical value are reported for the multivitamin–mineral dosage form.

Reproducibility of the assay is excellent. Relative standard deviations for representative dosage forms are given in Table II. The precision data were obtained in a routine assay laboratory by several analysts over a period of at least 3 months and using at least two different columns.

Comparison between the HPLC method and current assay results for seven representative dosage forms are shown in Table III. On the average, the HPLC and available assay results agree within 2%. The HPLC results for niacinamide and pyridoxine are compared to the microbiological

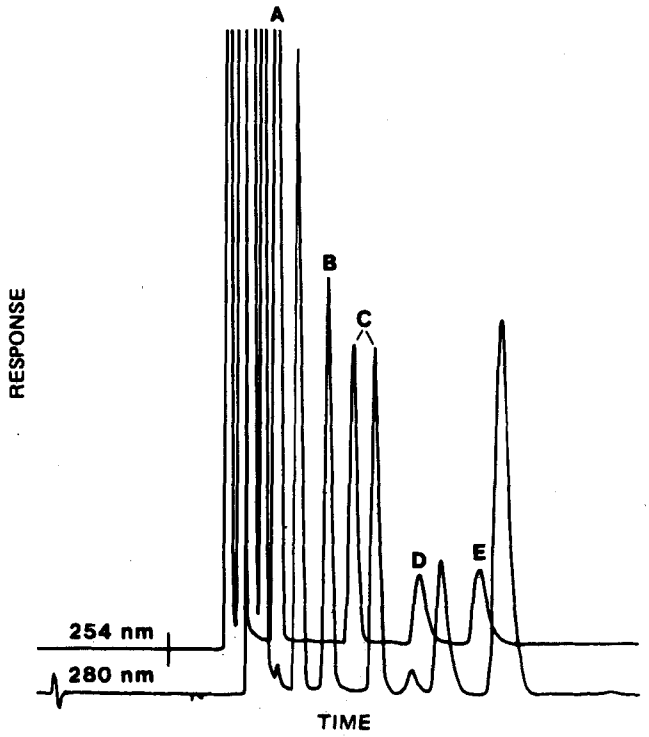


**Figure 2**—*Chromatogram of a multivitamin–mineral formulation. Niacinamide (A), p-hydroxybenzoic acid (internal standard) (C), thiamine (D), and riboflavin (E) were monitored at 254 nm. Pyridoxine (B) and the internal standard (C) were monitored at 280 nm. The mobile phase contained 25% methanol, 0.1% hexanesulfonic acid sodium salt, and 1% acetic acid.*

[1] μBondapak $C_{18}$ or equivalent, Waters Associates.

**Table III—Comparison between HPLC Method and Current Assay Results for Several Commercial Dosage Forms**

| Dosage Form | Amount of Vitamin per Tablet, mg | | | | | | | |
|---|---|---|---|---|---|---|---|---|
| | Niacinamide | | Pyridoxine | | Thiamine | | Riboflavin | |
| | HPLC | Microbiological | HPLC | Microbiological | HPLC | Chemical | HPLC | Chemical |
| Compressed tablet | | | | | | | | |
| Form A lot 1 | 21.8 | 22 | 2.18 | 2.2 | 1.94 | 1.87 | 1.92 | 1.95 |
| Form A lot 2 | 21.9 | 22 | 2.26 | 2.3 | 1.97 | 1.90 | 1.89 | 1.91 |
| Form A lot 3 | 21.7 | 22 | 2.18 | 2.1 | 2.00 | 1.90 | 1.94 | 1.91 |
| Coated compressed tablet | | | | | | | | |
| Form B lot 4 | 108 | 107 | 7.3 | 7.8 | 11.9 | 11.9 | 10.7 | 10.9 |
| Form B lot 5 | 107 | 112 | 7.2 | 7.6 | 11.5 | 11.3 | 10.7 | 10.7 |
| Form C lot 6 | 21.7 | 22.2 | 2.42 | 2.30 | 1.74 | 1.71 | 1.83 | 1.86 |
| Form C lot 7 | 21.6 | 21.6 | 2.47 | 2.50 | 1.72 | 1.74 | 1.90 | 1.96 |
| Multivitamin–mineral tablet | | | | | | | | |
| Form D lot 8 | 21.2 | 21.1 | 2.50 | 2.52 | — | — | 1.98 | 1.97 |
| Form D lot 9 | 21.5 | 21.9 | 2.50 | 2.45 | — | — | 1.90 | 1.88 |
| Form E lot 10 | 101 | 103 | 7.1 | 6.9 | — | — | 10.2 | 10.5 |
| Form E lot 11 | 104 | 109 | 7.2 | 7.0 | — | — | 10.5 | 10.7 |
| Form F lot 12 | 14.6 | 14.9 | 2.3 | 2.4 | — | — | 1.90 | 1.90 |
| Form F lot 13 | 14.9 | 15.4 | 2.4 | 2.5 | — | — | 1.87 | 1.85 |
| Form G lot 14 | 21.3 | 21.2 | 2.42 | 2.55 | — | — | 1.85 | 1.80 |
| Form G lot 15 | 20.8 | 21.8 | 2.36 | 2.50 | — | — | 1.84 | 1.87 |

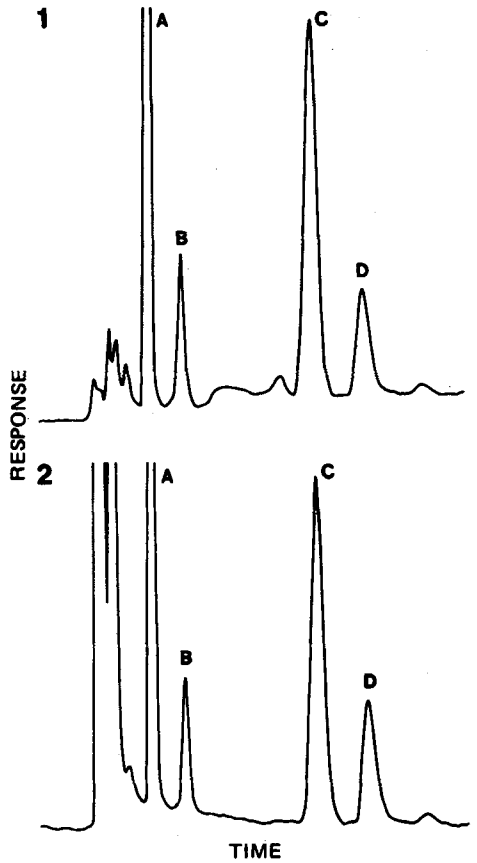


**Figure 3**—*Chromatogram of a multivitamin–mineral sample immediately after extraction with the mobile phase (1) and with the mobile phase containing 4 mg of diethylenetriamine pentaacetic acid sodium salt/ml (2). Niacinamide (A), pyridoxine (B), riboflavin (C), and thiamine (D) were monitored at 280 nm. The mobile phase contained 27% methanol, 0.14% hexanesulfonic acid sodium salt, and 1% acetic acid.*

procedure results. The current methods for thiamine and riboflavin are fluorometric assays.

For most formulations, a 30–60-min extraction of the ground tablet with the internal standard solution gave excellent recoveries. Samples containing coated vitamins must be warmed to at least the melting point of the coating to extract the vitamins completely from the gelatin matrix.

A stability problem is associated with vitamin–mineral formulations. After extraction, both ascorbic acid and thiamine are unstable in solution in the presence of minerals, especially ferrous and cupric salts. If a metal-chelating agent was not added to the extraction solution, only 60–70% of the thiamine was recovered, and four degradation product peaks appeared, which could interfere with the chromatographic run. The addition of 4 mg of diethylenetriamine pentaacetic acid sodium salt/ml increased thiamine recovery to 95%. Placebo mixtures containing both ascorbic acid and thiamine showed no chromatographic interference from excipients or degradation products. Samples of vitamin–mineral formulations were chromatographed within 24 hr of preparation. Figure 2 shows the chromatogram of a multivitamin–mineral formulation sample.

In the absence of cupric and ferrous salts, the vitamin solutions are stable for at least 2 months when stored in a refrigerator protected from light. To establish that the HPLC assay is stability indicating, vitamin solutions were subjected to accelerated degradation conditions. The decomposition peaks of riboflavin and pyridoxine do not interfere with the chromatography of the vitamins. However, thiamine degradation peaks elute with the internal standard peak. The validity of the assay for these samples was proven without including the internal standard peak in the calculations. Figure 3 shows the chromatogram of a multivitamin–mineral sample immediately after extraction with the mobile phase and with the mobile phase containing 4 mg of diethylenetriamine pentaacetic acid sodium salt/ml.

The HPLC method described here has been implemented for many different multivitamin formulations, such as injectable products, fluids, compressed tablets, and coated, compressed tablets. Work is underway to improve the recovery of thiamine from formulations containing minerals and to increase the number of applications for the assay.

## REFERENCES

(1) D. P. Wittmer and W. G. Haney, in "GLC and HPLC Analysis of Therapeutic Agents," K. Tsuji and W. Morozowitch, Eds., Dekker, New York, N.Y., 1976, chap. 36.

(2) R. L. Kirchmeier and R. P. Upton, *J. Pharm. Sci.*, **67**, 1444 (1978).

(3) "Chromatographic Applications Bulletin," Bull. 3262, Waters Associates, Milford, Mass., 1976.

## ACKNOWLEDGMENTS

Presented at the APhA Academy of Pharmaceutical Sciences, Phoenix meeting, November 1977.

# Colorimetric Determination of Thebaine in *Papaver bracteatum*

**KOSTANTIN IKONOMOVSKI**

Received May 5, 1980, from *Alkaloid Skopje, P.O. Box 8, Skopje, Yugoslavia.* Accepted for publication June 30, 1980. (Reprint requests should be directed to Howard W. Ziegler, Mallinckrodt, Inc., P.O. Box 5439, St. Louis, MO 63147.)

**Abstract** □ A rapid colorimetric test for the determination of thebaine in dried, extracted *Papaver bracteatum* is described. The method is based on the development of an orange color formed by the nitroso color reaction for phenols. The absorption peak is near 450 nm. The linear range response is from 0 to 1.0 mg of thebaine. The reproducibility of the method is quite good, making it useful for process evaluation and in a selection program for the cultivation of *P. bracteatum* for optimum thebaine content.

**Keyphrases** □ Thebaine—colorimetric determination in *Papaver bracteatum* □ *Papaver bracteatum*—colorimetric determination of thebaine in extract □ Alkaloids—thebaine, colorimetric determination in extract from *Papaver bracteatum*

A simple and rapid analytical method using small samples was needed to follow the process of thebaine isolation from *Papaver bracteatum* as well as for a selection program for the cultivation of this new alkaloidal raw material. GLC assays (1–9) have received the most attention, and high-pressure liquid chromatographic methods were reported recently (10, 11). Since not every laboratory is equipped with these rather expensive instruments, the colorimetric method described here was developed.

## BACKGROUND

When thebaine (I) is heated with mineral acids, the ether linkage in the molecule is cleaved, resulting in a phenolic hydroxyl group in position 4. Color reactions for phenols then may be used for the determination of the formed phenolic alkaloids.

Some attractive, rapid colorimetric methods (12–14) are based on conversion of thebaine to phenolic alkaloids followed by the color reaction immediately after extraction of the plant material, but they yield variable results. Pfeifer's colorimetric method (15) for the determination of morphine in *Papaver somniferum* is widely used for process control in the isolation of morphine. To develop a similar method for the determination of thebaine in *P. bracteatum*, preference was given to the nitroso color reaction for phenols (16) over the more lengthy Sakurai method (17), which relies on the formation of an ammoniacal potassium ferricyanide color complex.

Purification of the plant extracts is unavoidable. TLC separation (18, 19) followed by removal of the thebaine spot, prior to its degradation and color reaction, is time consuming. Organic solvent extraction of thebaine, often used prior to GLC assays (1, 2, 4, 5, 9), from an alkaline aqueous extract of *P. bracteatum* yields solutions pure enough for the colorimetric procedure described in this report.

## EXPERIMENTAL

**Plant Culture**—The seeds were obtained from the United Nations Narcotics Laboratory[1].

**Reagents**—All chemicals were reagent grade. The aluminum oxide was acidic[2] chromatographic grade. The thebaine standard was prepared in the laboratory with a melting point of 194° and a single TLC spot.

**Sample Preparation**—*P. bracteatum* poppy plants were chopped or broken into small pieces and dried at 105°. Dried samples were milled and screened to <1 mm (~20 mesh).

**Procedure**—Approximately 100 mg of sample was weighed accurately, mixed with 0.5 ml of water, and allowed to stand for 15 min. Acidic aluminum oxide (2 g) was added and mixed to form a dry powder. The mixture was added to a glass column (~150 × 13 mm i.d.) containing another 2 g of aluminum oxide held in place with a cotton plug. The thebaine was eluted from the column with 30 ml of 5% (v/v) acetic acid at a flow rate of ~1 ml/min into a separator. The pH of the eluate was adjusted to >11 with 10% (w/v) NaOH (~40 ml).

The aqueous phase was extracted with four 20-ml portions of chloroform, and the combined extracts were evaporated to dryness on a water bath. The residue was dissolved in 20 ml of 1 *N* HCl and heated to boiling. After cooling, the solution was transferred quantitatively to a 100-ml volumetric flask and diluted to volume with water.

Two 10-ml aliquots were transferred to each of two 50-ml volumetric flasks (larger or smaller aliquots also were used, depending on the anticipated thebaine content). One flask was diluted to 50 ml with water and used for the blank. Two milliliters of 1% (w/v) sodium nitrite was added to the second flask, which was left standing for 15 min with occasional shaking. Then 5 ml of 10% (w/v) $NH_4OH$ was added (changing the greenish-yellow color to orange), and the solution was diluted to 50 ml with water. This solution was stable for at least 20 min. The absorbance of the sample was measured against the blank, in 1-cm cells, at ~450 nm using a suitable spectrophotometer[3].

**Preparation of Thebaine Calibration Curve**—A stock standard solution was prepared by accurately weighing 100 mg of pure thebaine and transferring it to a 100-ml volumetric flask. The standard was dissolved and diluted to volume with methanol. A working standard solution was prepared by evaporating 3.0 ml of the stock standard solution to dryness on a water bath. The residue was dissolved in 20 ml of 1 *N* HCl and heated to boiling. After cooling, the solution was transferred quantitatively to a 100-ml volumetric flask and diluted to volume with water (1 ml = 0.03 mg of thebaine).

For the calibration curve, 5-, 10-, 15-, 20-, and 25-ml aliquots of the working standard solution were transferred to each of five 50-ml volumetric flasks. Two milliliters of 1% sodium nitrite was added to each flask. After the solutions stood for 15 min, with occasional shaking, the outlined procedure was followed using water for the blank. A standard calibration curve was prepared by plotting the milligrams of thebaine *versus* absorbance.

**Table I—Elution of Thebaine from Alumina Columns with Different Solvent Systems**

| Solvent System | Percent Thebaine |
|---|---|
| Methanol–ammonium hydroxide (98:2)[a] | 3.55, 3.56 |
| Chloroform–calcium hydroxide[a] | 3.55, 3.55 |
| 5% Acetic acid | |
| 20 ml | 3.58 |
| 40 ml | 3.56 |
| 60 ml | 3.58 |
| 80 ml | 3.58 |
| 100 ml | 3.56, 3.56, 3.57 |

[a] One hundred milliliters of solvent mixture.

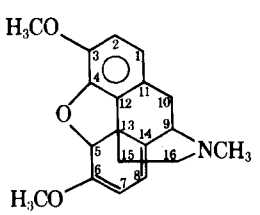


I

[1] The plant material used was the well-documented *Papaver bracteatum* Lindl.: Population Arya II, identified by Dr. P. G. Vincent (see Ref. 20).

[2] Merck 90, active acidic, Activity I.

[3] ELCO II colorimeter (Carl Zeiss) with an S49E filter (400–500 nm).



*0022-3549/81/0100-0102$01.00/0*
*© 1981, American Pharmaceutical Association*

Table II—Comparison of Thebaine Assays

| Sample[a] | Colorimetric | | GLC[b] | TLC–UV[c] |
|---|---|---|---|---|
| 1 Kavadarci capsules | 2.82 | 2.94 | 2.9 | 2.8 |
| 2 Kavadarci stems | 0.39 | 0.38 | 0.4 | 0.39 |
| 3 Kavadarci roots | 0.82 | 0.80 | 0.8 | 0.8 |
| 4 Berovo capsules | 1.83 | 1.83 | — | — |
| 5 Berovo stems | 0.21 | 0.20 | — | — |
| 6 Bitola capsules | 2.64 | 2.72 | — | — |
| 7 Sv. Nikole capsules | 3.54 | 3.50 | 3.5 | 3.44 |
| 8 Sv. Nikole stems | 0.46 | 0.46 | 0.5 | 0.46 |
| 9 Vitacevo capsules | 1.65 | 1.58 | — | — |
| 10 Vitacevo stems | 0.06 | 0.07 | — | — |
| 11 Process, Phase I | 0.20 | 0.21 | 0.2 | 0.2 |
| 12 Process, Phase II | 2.20 | 2.25 | — | — |
| 13 Process, Phase III | 0.54 | 0.52 | — | — |

[a] Samples 1–10 were obtained from plants grown in different regions of Yugoslavia. [b] From Ref. 7. [c] From Ref. 18.

## DISCUSSION

**Thebaine Degradation**—Pure thebaine was boiled with varying normalities of hydrochloric acid from 1 to 15 min and was analyzed by TLC to determine the optimum conditions for degradation. It was found that 1 *N* HCl destroyed thebaine completely when the solution was brought to a boil.

**Extraction**—Two general extraction principles for thebaine isolation from *P. bracteatum* are found in the literature: (*a*) extraction with dilute acids as a salt (2, 4, 5, 7, 9, 13, 16), and (*b*) alkalinization of the wet plant material and extraction of thebaine with an organic solvent or a mixture of solvents as the free alkaloid (1, 3, 6, 8, 12, 19, 21–24). Three solvent systems were investigated: 5% acetic acid, methanol–ammonium hydroxide (98:2), and chloroform–calcium hydroxide (0.2 g of calcium oxide was added to the sample and water in the soaking step for sample preparation).

The procedure detailed here was followed using 100 mg of sample for each experiment. In the extraction step, 100 ml of each solvent system was used. As shown in Table I, the solvent systems quantitatively extracted thebaine from *P. bracteatum*. The 5% acetic acid extraction method was chosen to avoid an evaporation step before the alkaline extraction with chloroform.

It was found experimentally that 20 ml of 5% acetic acid was sufficient for complete extraction of thebaine from 100 mg of *P. bracteatum*. Thirty milliliters was specified in the procedure so that a sufficient volume was obtained.

At least three 20-ml volumes of chloroform were needed for the removal of the degraded thebaine from an alkaline medium. A fourth extraction is recommended, especially if an emulsion is formed.

**pH Adjustment**—Most published methods recommend a pH of 9 for the alkaloid extraction step. However, emulsions form less at pH > 11. Another reason for performing the extraction at pH > 11 is to prevent the interference of any phenolic alkaloids that may be present in the poppies. TLC evaluations of *P. bracteatum* revealed a second alkaloid, believed to be alpinigenine. A third alkaloid rarely was found. The TLC spots from these two alkaloids were removed and evaluated by the described procedure. Their eluates gave no color reaction with sodium nitrite solution.

**Linearity**—The absorption peak was a broad band peaking at ~450 nm. At this wavelength, the reaction followed Beer's law between 0 and 1.0 mg of thebaine. Examination of Tables I and II indicates that the method is reproducible.

**Pigment Removal**—Some pigments eluted from the alumina columns. An attempt was made to remove pigments by acid extraction with chloroform or ether (4, 5, 18) prior to the alkaline extraction with chloroform. The same results were obtained with and without the acid extract. Most of the pigments remained in the aqueous layer after the alkaline chloroform extraction in the recommended procedure.

**Reaction Time for Color Development**—At least 10 min was required for full color development with the 1% sodium nitrite solution. The orange color took 10 min to develop fully after the addition of the 10% $NH_4OH$ and was stable for an additional 10 min. The absorbance readings must be made between 10 and 20 min after addition of the ammonium hydroxide.

## RESULTS

Samples of *P. bracteatum* plants grown in different regions of Yugoslavia were assayed by the colorimetric method described here. Samples from various process phases of thebaine isolation also were examined (Table II). For process samples, aqueous solutions were extracted directly with chloroform at pH >11. If the thebaine had been processed with organic solvents, the solvent was removed by evaporation. The residue was dissolved in 5% acetic acid, and the remainder of the procedure was followed. For comparison, some samples were assayed by a GLC method (7) and by a TLC–UV procedure (18) (Table II).

## REFERENCES


(1) J. W. Fairbairn, United Nations Secretariat, ST/SOA/SER.J/3.

(2) C. Ping and N. J. Doorenbos, United Nations Secretariat, ST/SOA/SER.J/5.

(3) F. J. Küppers, R. J. Lousberg, C. A. Bercht, and C. A. Salemink, United Nations Secretariat, ST/SOA/SER.J/8.

(4) P. G. Vincent and W. A. Gentner, United Nations Secretariat, ST/SOA/SER.J/9.

(5) R. Salkin, United Nations Secretariat, ST/SOA/SER.J/11.

(6) F. J. Küppers, C. A. Salemink, H. Grepping, L. Wuarin, and G. Meylan, United Nations Secretariat, ST/SOA/SER.J/14.

(7) United Nations Secretariat, ST/SOA/SER.J/15. Annex V.

(8) W. B. Caldwell, United Nations Secretariat, ST/SOA/SER.J/17.

(9) M. J. Duffy, P. A. Ackert, and C. F. Hiskey, United Nations Secretariat, ST/SOA/SER.J/18.

(10) D. W. Smith, T. H. Beasley, R. L. Charles, and H. W. Ziegler, *J. Pharm. Sci.*, **62**, 1691 (1973).

(11) F. Wu and R. H. Dobberstein, *J. Chromatogr.*, **140**, 65 (1977).

(12) A. Nordal, United Nations Secretariat, ST/SOA/SER.J/4.

(13) K. C. Reid, United Nations Secretariat, ST/SOA/SER.J/6.

(14) R. H. Maghssondi and A. B. Fawzi, *J. Pharm. Sci.*, **67**, 32 (1978).

(15) S. Pfeifer, *Bull. Narc.*, **10**, 18 (1958).

(16) D. C. Adamson and F. P. Handyside, *Analyst*, **70**, 305 (1945).

(17) H. Sakurai, *J. Pharm. Soc. Jpn.*, **80**, 909 (1960).

(18) J. W. Fairbairn and F. Hakim, *J. Pharm. Pharmacol.*, **25**, 353 (1973).

(19) C. J. Agasi and H. H. Bosman, United Nations Secretariat, ST/SOA/SER.J/16.

(20) P. G. Vincent, C. E. Bare, and W. A. Gentner, *J. Pharm. Sci.*, **66**, 1716 (1977).

(21) I. Lalezari, United Nations Secretariat, ST/SOA/SER.J/7.

(22) M. Capmal, United Nations Secretariat, ST/SOA/SER.J/10.

(23) J. M. Pelt and M. Lorrain, United Nations Secretariat, ST/SOA/SER.J/12.

(24) K. C. Reid, United Nations Secretariat, ST/SOA/SER.J/13.


## ACKNOWLEDGMENTS


The author thanks Howard W. Ziegler, Mallinckrodt, St. Louis, Mo., for assistance in preparing this manuscript.

# Differential Titration of Bases in Glacial Acetic Acid

THOMAS CASTELLANO, THOMAS MEDWICK ˣ, JOHN H. SHINKAI, and LEONARD BAILEY

Received April 21, 1980, from the *College of Pharmacy, Rutgers–The State University of New Jersey, Piscataway, NJ 08854.* Accepted for publication July 14, 1980.

**Abstract** □ A study of bases in acetic acid and their differential titration was carried out. The overall basicity constants for 20 bases were measured in acetic acid, and the differential titration of five binary mixtures of variable ΔpKb values in acetic acid was followed using a glass electrode–modified calomel electrode system. Agreement with literature values was good. A leveling diagram was constructed that indicated that bases stronger than aqueous pKb 10 are leveled to an acetous pKb 5.69, whereas weaker bases are not leveled but instead exhibit their own intrinsic basicity, with the acetous pKb to aqueous pKb values being linearly related (slope 1.18, correlation coefficient 0.962). A minimum acetous ΔpKb of four units is required for the satisfactory differential titration of two bases in acetic acid.

**Keyphrases** □ Bases—differential titration in glacial acetic acid □ Differential titration—bases in glacial acetic acid

Glacial acetic acid is generally considered to be a leveling solvent for bases, but some weak bases are not leveled in acetic acid. Hall (1) used a chloranil electrode system to obtain acetous half-neutralization potentials and reported a leveling diagram that was a plot of aqueous pKb values *versus* acetous base strengths calculated from half-neutralization potentials. Critchfield (2) reported a similar leveling diagram, which was a plot of aqueous pKa values *versus* acetous half-neutralization potentials, and stated that a mixture of bases may be differentially titrated if $\Delta pK_{acetous}$ is 4; however, he provided no data. Fritz (3) stated that a mixture of an aliphatic amine and an aromatic amine cannot be differentially titrated in glacial acetic acid and recommended using dioxane or acetonitrile as the solvent.

More recent work has shown that studies in glacial acetic acid are valid theoretically. Kolthoff and Bruckenstein (4) showed that accurate acetous pKb values may be calculated from neutralization potentials. These potentials can be measured with a glass electrode–modified calomel electrode system, which has been shown to function theoretically (5). This paper presents studies from which an accurate leveling diagram was constructed and from which a reliable $\Delta pK_{acetous}$ value for the differential titration of mixtures of bases in glacial acetic acid was established.

## EXPERIMENTAL

**Chemicals**—All chemicals were reagent grade and were used without further purification.

**Solutions**—Acetous perchloric acid (~0.1 *N*) was prepared according to the method of Fritz (6) and standardized against potassium biphthalate[1].

**Apparatus**—The potentials of the cells were measured using a pH meter[2] equipped with a 20-ohm (±0.05%) resister across the output resister terminals. A recorder[3] was set at 10 mv full scale and at a chart drive of 5 cm/min. The ground terminals of the pH meter, recorder, automatic constant-rate buret[4] chassis, and magnetic stirrer[5] chassis were connected to a common ground. The cell consisted of a 400-ml beaker with a ground-glass cover with openings for the electrodes and buret. The electrodes used were a glass electrode[6] (stored in distilled water) and a fiber calomel electrode[7] (stored in glacial acetic acid) modified by replacing the aqueous salt bridge solution with 0.1 *M* acetous lithium perchlorate.

**Procedures and Calculations**—The titrations were performed by dissolving ~0.6 mEq of base in 50.00 ml of glacial acetic acid. The electrodes were blotted dry and inserted into the beaker. The initial and final potentials were read from the pH meter, and the end-point potentials were taken from the acetous perchloric acid titration curve described by Medwick and Kirschner (7). The $E^{0\prime}$ value for the glass electrode, using

**Table I—Comparison of Aqueous and Acetous Basicity**

| | Compound | Aqueous pKb[a] | Acetous pKb | ΔpK | Sharpness Index[b] |
|---|---|---|---|---|---|
| 1 | Urea | 13.90 | —[c], 10.24[d] | 3.66 | — |
| 2 | Theophylline | >13 | —[c] | | — |
| 3 | 2,5-Dichloroaniline | 12.43 | 9.22, 9.17[e] 9.48[d] | 3.36 | 0.38 |
| 4 | *p*-Aminosalicylic acid | 12.22 | 8.75 | 3.47 | 2.18 |
| 5 | *p*-Aminobenzoic acid | 11.50 | 8.04 | 3.46 | 4.58 |
| 6 | Benzocaine | 11.22 | 7.53, 7.60[e] | 3.69 | 6.92 |
| 7 | Nicotinic acid | 10.87 | 7.01 | 3.86 | 4.58 |
| 8 | Isonicotinic acid | 10.74 | 6.86 | 3.88 | 7.35 |
| 9 | β-Alanine | 10.39 | 5.72 | 4.67 | 6.63 |
| 10 | Triphenylguanidine | 9.10 | 5.55, 5.57[e] | 3.55 | 12.24 |
| 11 | Phenanthroline | 9.08 | 4.86 | 4.22 | 11.84 |
| 12 | Asparagine | 8.90 | 6.57 | 2.33 | 7.76 |
| 13 | Pyridine | 8.79 | 6.21, 6.10[d] | 2.58 | 9.67 |
| 14 | *N,N*-Diethylaniline | 7.39 | 5.56[e] | 1.83 | — |
| 15 | Triethanolamine | 6.23 | 5.00 | 1.23 | 10.76 |
| 16 | Tris(hydroxymethyl)-aminomethane | 5.97 | 6.06[e] | −0.09 | — |
| 17 | Benzylamine | 4.67 | 5.95 | −1.18 | 12.24 |
| 18 | Atropine | 4.15 | 5.93[e] | −1.78 | — |
| 19 | Tribenzylamine | — | 4.87[e], 5.40[d] | — | 14.86 |
| 20 | Triethylamine | 3.25 | 5.35 | −2.10 | 9.59 |

[a] Data of Perrin (9). [b] Magnitude of the slope of the titration curve (10). [c] Compounds are not titratable in glacial acetic acid. [d] Data of Bruckenstein and Kolthoff (11). [e] Data of Medwick *et al.* (5).

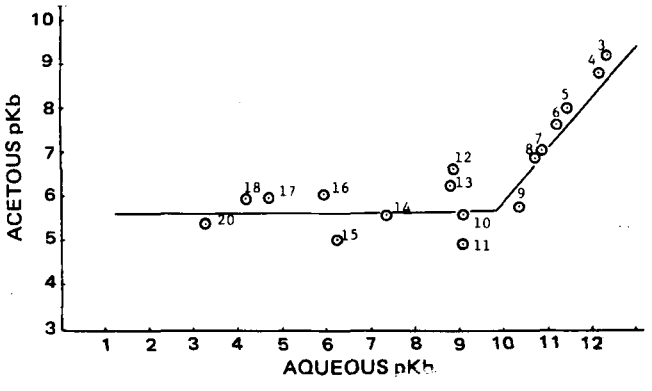


**Figure 1**—*Leveling diagram of bases showing aqueous* versus *acetous pKb values. Numbers used for each compound correspond to the numbers in Table I.*

[1] Thorn Smith, Troy, Mich.
[2] Leeds & Northrup model 7401.
[3] Leeds & Northrup Speedomax.
[4] Sargent model C.
[5] SGA Magnestir.
[6] Beckman 39099 E3.
[7] Corning 476002.



0022-3549/81/0100-0104$01.00/0
© 1981, American Pharmaceutical Association

**Table II—Analytical Results of Study of Differentiation of Bases in Glacial Acetic Acid**

| Mixture | Component, Purity[a] | $pKb_{acetous}$ | ΔpK | Sharpness Index | Recovery[a], % |
|---|---|---|---|---|---|
| 1 | Triethanolamine | 5.00 | 1.06 | — | —[b] |
| | Tris(hydroxymethyl)aminomethane | 6.06 | | — | —[b] |
| 2 | 1,10-Phenanthroline | 4.86 | 2.00 | — | —[b] |
| | Isonicotinic acid | 6.86 | | — | —[b] |
| 3 | 1,10-Phenanthroline, 102.36 ± 0.63% | 4.86 | 3.18 | 0.47 | 107.51 ± 1.06 |
| | *p*-Aminobenzoic acid, 100.93 ± 0.63% | 8.04 | | 4.99 | 93.14 ± 0.63 |
| 4 | Tribenzylamine, 101.14 ± 0.19% | 5.03 | 4.14 | 3.47 | 101.65 ± 1.05 |
| | 2,5-Dichloroaniline, 99.17 ± 0.48% | 9.17 | | 1.01 | 100.34 ± 0.40 |
| 5 | 1,10-Phenanthroline, 102.36 ± 0.63% | 4.86 | 4.31 | 3.65 | 100.84 ± 0.39 |
| | 2,5-Dichloroaniline, 99.17 ± 0.48% | 9.17 | | 1.02 | 101.11 ± 1.15 |

[a] The mean and standard deviation are given for a group of three analyses. [b] Individual analysis is not possible.

tribenzylamine[8] as the standard, and the conversions of the end-point potentials to pKb values were calculated as detailed by Medwick *et al.* (5).

## RESULTS AND DISCUSSION

Table I compares the aqueous and acetous basicity of the compounds studied. The acetous pKb values were calculated from the mean millivoltage value of three titrations. The variations in the millivoltage values ranged from 2 mv (ΔpKb = 0.04) to 13 mv (ΔpKb = 0.22). In this study, the two weakest bases, urea and theophylline, were not titratable, contrary to the report of Hall (1). Medwick and Scheisswohl (12) showed that theophylline cannot be titrated in glacial acetic acid.

The acetous pKb for urea reported by Bruckenstein and Kolthoff (11) must be considered erroneous since the titration behavior indicates that it is a weaker base than had been reported. Comparisons of other values determined by Bruckenstein and Kolthoff (11) are, with the exception of pyridine, weaker than those reported here. Comparisons of values reported by Medwick *et al.* (5) for three compounds agree very well with the results of this study, as the pK differences indicate: 2,5-dichloroaniline, ΔpK 0.05; benzocaine, ΔpK 0.07; and triphenylguanidine, ΔpK 0.02. This agreement demonstrates the excellent reproducibility of the glass electrode–modified calomel electrode system and shows its superiority to the chloranil electrode system since chloranil is subject to decomposition, precipitation, and the formation of hemiperchlorates (1).

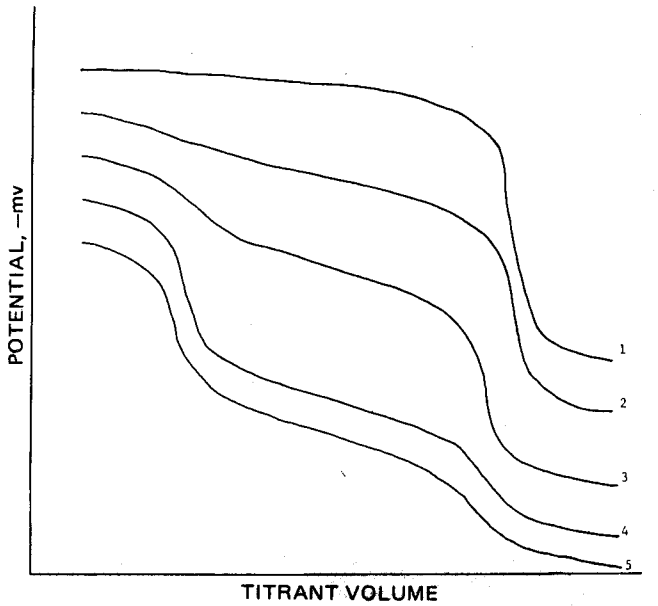


**Figure 2**—*Titrations of five different mixtures of two bases in glacial acetic acid. The individual curves are numbered to identify the mixture titrated using the same numbers as in Table II.*

[8] The melting point (uncorrected) was 93° [lit. (8) mp 92°].

The leveling diagram (Fig. 1) consists of three parts: the horizontal or leveling line, representing the value ($pKb_{acetous}$ 5.69) to which strong bases are leveled; the inflection point (9.67), theoretically 9.24, the aqueous pKb value of acetate; and the line with a slope of 1.180 (correlation coefficient 0.962). Theoretically, the slope of the line is exactly 1.00 since there is no interaction of weaker bases with either solvent, water or acetic acid, and the intrinsic basicity of each compound is observed. The scatter of points may be due to the varied sources for the aqueous pKb values.

To determine the $\Delta pKb_{acetous}$ value necessary for differential titration of bases in glacial acetic acid, five binary mixtures with differing ΔpKb values were prepared (Table II). The individual titration curves for each mixture are given in Fig. 2. When the ΔpK is two units or less, only one titration break is seen. At a ΔpK of three units, two breaks are observed, but the quality of the end-point is not very good, as seen from the sharpness index (the magnitude of the slope of the titration curve) (10), and the analytical results show overlap. When the ΔpK is greater than four units, better resolution of components and satisfactory analytical results are obtained since each titration break is sharper.

On the basis of this work, it is concluded that the minimum acetous ΔpKb for satisfactory differential titration of bases in glacial acetic acid is four units. This conclusion agrees with the statement of Critchfield (2).

## REFERENCES

(1) N. F. Hall, *J. Am. Chem. Soc.*, **52**, 5115 (1930).

(2) F. E. Critchfield, "Organic Functional Group Analysis," Macmillan, New York, N.Y., 1963, p. 11.

(3) J. S. Fritz, *Anal. Chem.*, **25**, 407 (1953).

(4) I. M. Kolthoff and S. Bruckenstein, *J. Am. Chem. Soc.*, **79**, 1 (1957).

(5) T. Medwick, G. Kaplan, and L. G. Weyer, *J. Pharm. Sci.*, **58**, 308 (1969).

(6) J. S. Fritz, "Acid-Base Titrations in Nonaqueous Solvents," G. Frederick Smith Chemical Co., Columbus, Ohio, 1951, p. 13.

(7) T. Medwick and E. Kirschner, *J. Pharm. Sci.*, **55**, 1296 (1966).

(8) "Dictionary of Organic Compounds," vol. 5, I. Heilbron *et al.*, Eds., Oxford University Press, New York, N.Y., 1965, p. 3098.

(9) "Dissociation Constants of Organic Bases in Aqueous Solution," D. D. Perrin, Ed., International Union of Pure and Applied Chemistry, Butterworth, London, England, 1965.

(10) J. N. Butler, "Ionic Equilibrium, A Mathematical Approach," Addison-Wesley, Reading, Mass., 1964, p. 158.

(11) S. Bruckenstein and I. M. Kolthoff, *J. Am. Chem. Soc.*, **78**, 2974 (1956).

(12) T. Medwick and F. Scheisswohl, *J. Pharm. Sci.*, **52**, 843 (1963).

# Analytical Determination of Purity of 1-Piperidinocyclohexanecarbonitrile and Its Hydrobromide Salt

WILLIAM H. SOINE

Received April 24, 1980, from the *Department of Pharmaceutical Chemistry, Medical College of Virginia, Richmond, VA 23298.* Accepted for publication July 17, 1980.

**Abstract** □ A common contaminant of illicit phencyclidine, 1-piperidinocyclohexanecarbonitrile (I), is a very weak base compared to tertiary amines such as phencyclidine, 1-(cyclohexenyl)piperidine, and piperidine. Compound I and its hydrobromide salt can be selectively detected and quantitated in the presence of synthetic contaminants by nonaqueous titration with perchloric acid in acetonitrile. This method allows direct assay of I under conditions where decomposition is not observed.

**Keyphrases** □ Phencyclidine—analysis of 1-piperidinocyclohexanecarbonitrile and its hydrobromide salt as synthetic contaminants □ 1-Piperidinocyclohexanecarbonitrile—nonaqueous titrimetric analysis as synthetic contaminant of phencyclidine □ Potentiometric titration—analysis of 1-piperidinocyclohexanecarbonitrile and its hydrobromide salt as synthetic contaminants of phencyclidine

Phencyclidine, a widely abused illicit drug (1), is manufactured primarily in clandestine laboratories and is reported to be contaminated with the synthetic intermediate 1-piperidinocyclohexanecarbonitrile (I) (2–7). The concern over the presence of I in illicit phencyclidine prompted the National Institute of Drug Abuse to make it available for pharmacological evaluation.

Due to the reported instability of I (3, 6–9), a convenient method for determining its purity is needed before carrying out pharmacological studies. This method also must be applicable to the assay of I·HBr, which is the preferred form for use in pharmacological studies. Compound I is unstable during TLC (8–10), GLC (3, 8–10), and mass spectrometry using electron-impact or chemical-ionization procedures (9). In addition, it does not possess a distinctive UV spectrum (10). Therefore, a volumetric method using nonaqueous titration was developed to determine the purity of I and its hydrobromide salt.

## EXPERIMENTAL

**Apparatus and Materials**—A suitable recording pH meter[1] equipped with a combination electrode[2] and coupled with a constant-volume syringe pump[3] (50-ml capacity) was used. All solvents and reagents were analytical reagent grade. Compound I was synthesized by the method of Kalir *et al.* (11) and converted to the hydrobromide salt by dissolving it in acetone followed by the slow addition of 30% HBr in acetic acid until a pH of ~2 was reached. The salt was recrystallized in chloroform–anhydrous ethanol (3:1) brought to the cloud point with anhydrous ether, mp 260–270° dec.

**Solutions**—The following reagents were used: 0.1 *N* perchloric acid in acetic acid[4], 0.1 *N* perchloric acid in dioxane, 6% (w/v) mercuric acetate in acetic acid, and 1% (w/v) methyl crystal violet in chlorobenzene.

The perchloric acid in acetic acid solution was restandardized by potentiometric titration against potassium biphthalate in acetic acid to which 2.0 ml of 6% mercuric acetate solution was added.

The perchloric acid in dioxane solution was standardized against potassium biphthalate in acetic acid.

**Determination of I or I·HBr by Direct Titration with 0.1 *N* Perchloric Acid in Acetic Acid**—An accurately weighed sample (90.0–120.0 mg) was placed in a 50-ml beaker with 20 ml of acetic acid and 2 ml of 6% mercuric acetate solution. Dissolution of I and its hydrobromide salt was effected by continuous magnetic stirring for ~10 min; occasionally, heat was applied to aid in solution. The solution, magnetically stirred, was titrated with standard 0.1 *N* perchloric acid in acetic acid. The end-point was determined from the inflection in the titration curve. When the methyl crystal violet test solution was included in the titration, appearance of the emerald-green color was found to coincide with the maximum change in the millivolt reading.

**Determination of I by Direct Titration with 0.1 *N* Perchloric Acid in Acetonitrile**—An accurately weighed sample (90.0–120.0 mg) was placed in a 50-ml beaker with 20 ml of acetonitrile. The solution, magnetically stirred, was titrated with the standard 0.1 *N* perchloric acid in dioxane. The end-point was determined from the inflection in the titration curve.

**Determination of I·HBr by Direct Titration with 0.1 *N* Perchloric Acid in Acetonitrile**—An accurately weighed sample (90.0–120.0 mg) was placed in a 50-ml beaker with 20 ml of acetonitrile and 75 μl (0.54 mmole) of triethylamine. The solution, magnetically stirred, was titrated with standard 0.1 *N* perchloric acid in dioxane. The end-point was determined from the inflection in the titration curve; I exhibited a 335-mv difference from the synthetic impurities, 1-(cyclohexenyl)piperidine (II) and piperidine (III), and triethylamine at half-neutralization.

## RESULTS AND DISCUSSION

Due to the increased interest in I because of its presence in samples of illicit phencyclidine (2–7), it seemed important to study the metabolism of I in mammals. It was necessary to convert I to a salt form so that it would exhibit good solubility in blood and serum for the development of analytical procedures. In initial experiments, significant difficulties were encountered in extracting intact I from blood. When analyzing the stock solution of I·HBr (~10 mg/ml in normal saline), piperidine was detected by GLC. The instability of I has been documented extensively (3, 6–9). Therefore, before continuing the study, it was necessary to develop a method to determine the purity of I and its hydrobromide salt.

Potential contaminants expected to be present in the hydrobromide salt of I are the hydrobromide salts of II and III. TLC was not suitable for detecting or quantitating these contaminants. Decomposition was minimized but not completely avoided using unactivated silica plates (8). During both GLC and mass spectrometry, the hydrobromide salt of I undergoes thermal decomposition to form II (2, 8, 9), a potential synthetic contaminant. A method was needed that was simple and could be carried out easily in the laboratory.

Titrimetry was the first choice since it is used frequently in the analysis of nitrogenous bases. Initially, aqueous titration of I·HBr using 0.1 *N* NaOH was attempted. Erratic results were obtained, depending on the quantity of I·HBr analyzed (80–120 mg); however, with 100.0 mg (98.0–103.0 mg), the results were reproducible and indicated the purity to be 95.3 ± 0.6% ($n$ = 3). A slight break in the titration curve at pH 8.5 was observed routinely. Since a precipitate was formed during the titration, it was possible that it was affecting the final results. Therefore, methanol–water (1:1) was used as the solvent. Titration in this solvent mixture indicated that the same sample of I·HBr was 73.7 ± 1.2% pure ($n$ = 3) (Fig. 1). These observations indicated that I decomposed during titration to liberate another base that was capable of neutralizing the hydrobromide salt.

A plausible mechanism for the decomposition of I by base is shown in Scheme I, in which 2 moles of base (cyanide and piperidine) are liberated by the decomposition of 1 mole of I. This scheme explains why aqueous

[1] Model EU-301V, Heath/Schlumberger Instruments, Benton Harbor, MI 49022.
[2] Sensorex, Westminster, CA 92683.
[3] Model 341, Orion Research, Cambridge, MA 02139.
[4] N/10, Fisher Scientific Co., Fair Lawn, NJ 07410.



0022-3549/81/0100-0106$01.00/0
© 1981, American Pharmaceutical Association

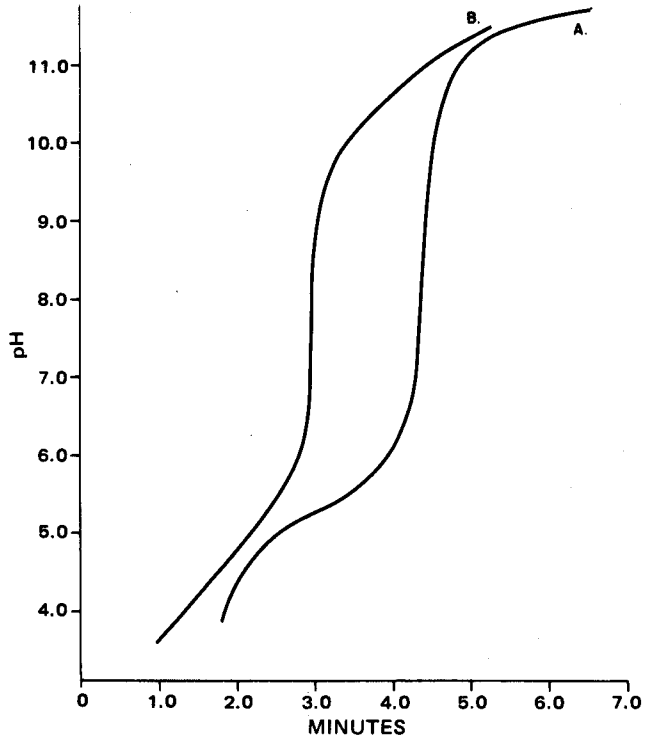


**Figure 1**—*Titration of the hydrobromide of I with 0.1* N *NaOH in water (A) and in methanol–water (1:1) (B).*

titration of I·HBr gave unrealistically low purity. In addition, since the contaminants of I·HBr are of a lower molecular weight, a sample analyzed by aqueous titration possibly could appear to be of high purity but be badly contaminated due to a balance of decomposition products and intermediates II and III.

Since aqueous titration was unsuitable, a nonaqueous titration in acetic acid was evaluated. The assay gave reproducible results and indicated that the purity was 99.9 ± 1.2% ($n$ = 7). Due to the leveling effect of acetic acid (12), the potential contaminants cannot be differentiated by titration. To determine the sensitivity of this technique, I·HBr was contaminated with III·HBr at 4.5 and 4.6% (w/w). Titration of these samples indicated a purity of 104 and 105%, respectively (theoretical purity of 103.7%). The hydrobromide of I also was contaminated with a 65:35 mixture of the hydrobromides of II and III at 8.2, 8.6, and 10.3% (w/w). Titration of these samples indicated a purity of 103.4, 103.5, and 103.9%, respectively (theoretical purities of 103.0, 103.1 and 103.7%). Nonaqueous titration of a sample of I·HBr (mol. wt. 273.2), which was contaminated with only II·HBr (mol. wt. 246.2) could not detect a 10% (w/w) contamination (theoretical purity of 101.1%).

The nonaqueous potentiometric titration of I as the free base in acetonitrile (Fig. 2) indicated that I is a much weaker base than II and III. It exhibited a 335-mv difference from II, III, and triethylamine.

Although I decomposes rapidly in aqueous solution, a rapid potentiometric titration of I·HBr was performed in a methanol–water (1:1) solution with 0.1 $N$ NaOH at 22°. The pKa obtained was 4.6. Under these conditions, phencyclidine hydrochloride precipitated from solution and no comparison was possible. Titration of I·HBr and phencyclidine hydrochloride was possible in ethylene glycol monomethyl ether–water (4:1), and the apparent pKa values were 3.3 and 8.3, respectively. It is apparent from these data that I is a much weaker base than most tertiary amines. This result was not unexpected since the pKa for $N$-cyanomethylmethylaminomethane is 4.2 in water (13).

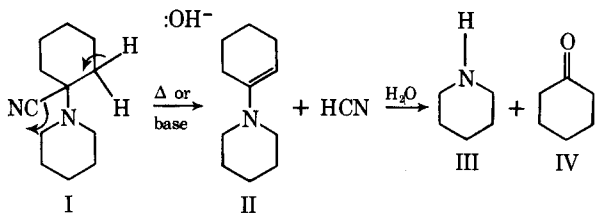


*Scheme I*

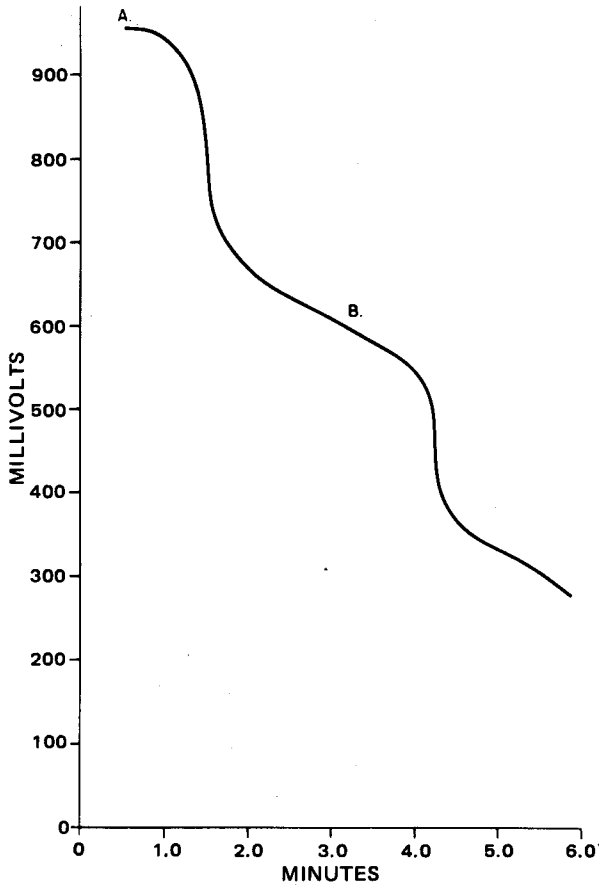


**Figure 2**—*Nonaqueous potentiometric titration of I in acetonitrile with 0.1* N *perchloric acid in dioxane. Key: A, II, III, or triethylamine; and B, I.*

Due to this difference in basicity and because I is unstable in aqueous solution, a specific nonaqueous potentiometric titration of the free base of I was developed. A closely related method allows analysis of I·HBr. If one assumes that the mechanism of decomposition of I is as outlined in Scheme I, the addition of a slight excess of a sterically hindered base (*i.e.*, triethylamine) effectively transfers the hydrobromide to the stronger base, enabling direct titration of I. This method was quite reproducible and indicated a purity of 98.4 ± 0.4% ($n$ = 6). This value is lower than that observed in the nonaqueous titration in acetic acid but is more reliable since I itself is being titrated and not the hydrobromide salt or acetate anion.

The primary advantage of nonaqueous potentiometric titration is that it enables specific and quantitative analysis of I or any salt in the presence of a mixture of amines. Previous to the development of this method, direct analysis of I under conditions in which no decomposition to II–IV could take place was not possible. This method has potential application for the quantitation of I present in illicit samples of phencyclidine to verify the results obtained using GLC, in which the thermal elimination product, II, usually is analyzed. The presence of a weak acid is expected to interfere in this type of analysis. However, preliminary identification procedures (spot tests, TLC, and GLC–mass spectrometry) would indicate the presence of such a contaminant.

## REFERENCES

(1) "Phencyclidine (PCP) Abuse: An Appraisal," R. C. Petersen and R. C. Stillman, Eds., NIDA Research Monograph 21, National Institute on Drug Abuse, Rockville, Md., 1978.

(2) W. H. Soine, W. C. Vincek, and D. T. Agee, *N. Engl. J. Med.*, **301**, 438 (1979).

(3) J. R. Ballinger and J. A. Marshman, *J. Anal. Toxicol.*, **3**, 158 (1979).

(4) E. J. Cone, W. F. Buchwald, C. W. Gorodetzky, and D. B. Vaupel, *Fed. Proc. Fed. Am. Soc. Exp. Biol.*, **38**, 435 (1979).

(5) H. G. Giles, J. A. Marshman, and E. M. Sellers, *J. Psychedelic*

*Drugs*, **7**, 397 (1975).
(6) K. Bailey, A. Y. K. Chow, R. H. Downie, and R. K. Pike, *J. Pharm. Pharmacol.*, **28**, 713 (1976).
(7) D. C. Perry, *Clin. Toxicol.*, **9**, 339 (1976).
(8) C. Helisten and A. T. Shulgin, *J. Chromatogr.*, **117**, 232 (1976).
(9) E. J. Cone, W. D. Darwin, D. Yousefnejad, and W. F. Buchwald, *ibid.*, **177**, 149 (1979).
(10) D. R. Gagne and R. K. Pike, *J. Assoc. Off. Anal. Chem.*, **60**, 32 (1977).
(11) A. Kalir, H. Edery, Z. Pelah, D. Balderman, and G. Porath, *J. Med. Chem.*, **12**, 473 (1969).
(12) J. F. Fritz, "Acid–Base Titration in Nonaqueous Solvents," Allyn & Bacon, Boston, Mass., 1973.
(13) D. D. Perrin, "Dissociation Constants of Organic Bases in Aqueous Solution," Butterworths, London, England, 1965.

**ACKNOWLEDGMENTS**

The author thanks B. J. Kline, B. van't Riet, and E. L. May for comments and advice.

## COMMUNICATIONS

# New Direct Calculation of $K_{1:1}$ and $K_{1:2}$ Complexation Constants Using Solubility Method

**Keyphrases** □ Complexation—calculation of complexation constants using solubility method, derivation of new equation □ Solubility—direct calculation of complexation constants using new equation □ Models, mathematical—equation for direct calculation of complexation constants using solubility method

*To the Editor:*

The solubility method is used frequently to determine the extent of molecular interactions between compounds. A detailed discussion of this method is available (1). In this method, a solution is maintained saturated with one component, $S$, and incremental amounts of a second complexing agent, $L$, are added. At equilibrium, the total $S$ in solution is determined. If the complexes are soluble, an increase in the solubility of $S$ is observed as a function of added $L$.

If a 1:1 complex is formed (Scheme I), complexation is represented by:

$$S + L \rightleftharpoons SL$$

*Scheme I*

$$K_{1:1} = \frac{[SL]}{S_0[L]} \quad \text{(Eq. 1)}$$

$$[S_T] = \frac{K_{1:1}S_0}{1 + K_{1:1}S_0}[L_T] + S_0 \quad \text{(Eq. 2)}$$

where $[S_T]$ is the total $S$ concentration in the solution, $S_0$ is the original solubility of $S$, $[SL]$ is the concentration of the 1:1 complex, $[L]$ is the concentration of the free complexing agent, $[L_T]$ is the total concentration of the complexing agent, and $K_{1:1}$ is the 1:1 complexation constant. The complexation constant can be determined easily and accurately from Eq. 2.

However, for a system in which both 1:1 and 1:2 complexes are formed, the 1:1 complex (Scheme I) is represented by Eqs. 1 and 2 and the 1:2 complex (Scheme II) is represented by:

$$S + 2L \rightleftharpoons SL_2$$

*Scheme II*

$$K_{1:2} = \frac{[SL_2]}{S_0[L]^2} \quad \text{(Eq. 3)}$$

where $K_{1:2}$ is the 1:2 complexation constant and $[SL_2]$ is the concentration of the 1:2 complex. The mass balance equation for $S$ becomes:

$$[S_T] = S_0 + [SL] + [SL_2] \quad \text{(Eq. 4)}$$

The combination of Eqs. 1, 3, and 4 results in:

$$[S_T] - S_0 = K_{1:1}S_0[L] + K_{1:2}S_0[L]^2 \quad \text{(Eq. 5)}$$

Since the exact amount of $[L]$ in a system is not known, it has been recognized (1–5) that Eq. 5 cannot be used directly to calculate $K_{1:1}$ and $K_{1:2}$ unless a certain assumption is made. This assumption is that $[L] = [L_T]$ or that all of the complex is in the form of either $SL$ or $SL_2$. Then the data are manipulated using several approximations to arrive at the values of $K_{1:1}$ and $K_{1:2}$.

These assumptions are totally invalid if the $SL$ and $SL_2$ concentrations are both very large. The purpose of this article is to derive an equation for calculating the two complexation constants directly and without assumptions.

Since:

$$[L_T] = [L] + [SL] + 2[SL_2] \quad \text{(Eq. 6)}$$

the combination of Eqs. 4 and 6 results in:

$$[L_T] = [L] + [SL] + 2([S_T] - S_0 - [SL]) \quad \text{(Eq. 7)}$$

and:

$$[L_T] = 2[S_T] - 2S_0 + [L] - [SL] \quad \text{(Eq. 8)}$$

Substituting for $[SL]$ in Eq. 8 using Eq. 1 gives:

$$[L_T] = 2[S_T] - 2S_0 + [L] - K_{1:1}S_0[L] \quad \text{(Eq. 9)}$$

Rearranging Eq. 9 results in:

$$[L] = \frac{[L_T] - 2([S_T] - S_0)}{1 - K_{1:1}S_0} \quad \text{(Eq. 10)}$$

Substituting this expression for $[L]$ in Eq. 5 gives:

$$[S_T] - S_0 = \frac{K_{1:1}S_0}{1 - K_{1:1}S_0}\{[L_T] - 2([S_T] - S_0)\} + \frac{K_{1:2}S_0}{(1 - K_{1:1}S_0)^2}\{[L_T] - 2([S_T] - S_0)\}^2 \quad \text{(Eq. 11)}$$

Let:

$$\frac{K_{1:1}S_0}{1 - K_{1:1}S_0} = \alpha \quad \text{(Eq. 12)}$$

and:

$$\frac{K_{1:2}S_0}{[1 - K_{1:1}S_0]^2} = \beta \quad \text{(Eq. 13)}$$



*0022-3549/81/0100-0108$01.00/0*
*© 1981, American Pharmaceutical Association*

*Drugs*, **7**, 397 (1975).
(6) K. Bailey, A. Y. K. Chow, R. H. Downie, and R. K. Pike, *J. Pharm. Pharmacol.*, **28**, 713 (1976).
(7) D. C. Perry, *Clin. Toxicol.*, **9**, 339 (1976).
(8) C. Helisten and A. T. Shulgin, *J. Chromatogr.*, **117**, 232 (1976).
(9) E. J. Cone, W. D. Darwin, D. Yousefnejad, and W. F. Buchwald, *ibid.*, **177**, 149 (1979).
(10) D. R. Gagne and R. K. Pike, *J. Assoc. Off. Anal. Chem.*, **60**, 32 (1977).
(11) A. Kalir, H. Edery, Z. Pelah, D. Balderman, and G. Porath, *J. Med. Chem.*, **12**, 473 (1969).
(12) J. F. Fritz, "Acid–Base Titration in Nonaqueous Solvents," Allyn & Bacon, Boston, Mass., 1973.
(13) D. D. Perrin, "Dissociation Constants of Organic Bases in Aqueous Solution," Butterworths, London, England, 1965.

**ACKNOWLEDGMENTS**

The author thanks B. J. Kline, B. van't Riet, and E. L. May for comments and advice.

## COMMUNICATIONS

# New Direct Calculation of $K_{1:1}$ and $K_{1:2}$ Complexation Constants Using Solubility Method

**Keyphrases** □ Complexation—calculation of complexation constants using solubility method, derivation of new equation □ Solubility—direct calculation of complexation constants using new equation □ Models, mathematical—equation for direct calculation of complexation constants using solubility method

*To the Editor:*

The solubility method is used frequently to determine the extent of molecular interactions between compounds. A detailed discussion of this method is available (1). In this method, a solution is maintained saturated with one component, $S$, and incremental amounts of a second complexing agent, $L$, are added. At equilibrium, the total $S$ in solution is determined. If the complexes are soluble, an increase in the solubility of $S$ is observed as a function of added $L$.

If a 1:1 complex is formed (Scheme I), complexation is represented by:

$$S + L \rightleftharpoons SL$$

*Scheme I*

$$K_{1:1} = \frac{[SL]}{S_0[L]} \quad \text{(Eq. 1)}$$

$$[S_T] = \frac{K_{1:1}S_0}{1 + K_{1:1}S_0}[L_T] + S_0 \quad \text{(Eq. 2)}$$

where $[S_T]$ is the total $S$ concentration in the solution, $S_0$ is the original solubility of $S$, $[SL]$ is the concentration of the 1:1 complex, $[L]$ is the concentration of the free complexing agent, $[L_T]$ is the total concentration of the complexing agent, and $K_{1:1}$ is the 1:1 complexation constant. The complexation constant can be determined easily and accurately from Eq. 2.

However, for a system in which both 1:1 and 1:2 complexes are formed, the 1:1 complex (Scheme I) is represented by Eqs. 1 and 2 and the 1:2 complex (Scheme II) is represented by:

$$S + 2L \rightleftharpoons SL_2$$

*Scheme II*

$$K_{1:2} = \frac{[SL_2]}{S_0[L]^2} \quad \text{(Eq. 3)}$$

where $K_{1:2}$ is the 1:2 complexation constant and $[SL_2]$ is the concentration of the 1:2 complex. The mass balance equation for $S$ becomes:

$$[S_T] = S_0 + [SL] + [SL_2] \quad \text{(Eq. 4)}$$

The combination of Eqs. 1, 3, and 4 results in:

$$[S_T] - S_0 = K_{1:1}S_0[L] + K_{1:2}S_0[L]^2 \quad \text{(Eq. 5)}$$

Since the exact amount of $[L]$ in a system is not known, it has been recognized (1–5) that Eq. 5 cannot be used directly to calculate $K_{1:1}$ and $K_{1:2}$ unless a certain assumption is made. This assumption is that $[L] = [L_T]$ or that all of the complex is in the form of either $SL$ or $SL_2$. Then the data are manipulated using several approximations to arrive at the values of $K_{1:1}$ and $K_{1:2}$.

These assumptions are totally invalid if the $SL$ and $SL_2$ concentrations are both very large. The purpose of this article is to derive an equation for calculating the two complexation constants directly and without assumptions.

Since:

$$[L_T] = [L] + [SL] + 2[SL_2] \quad \text{(Eq. 6)}$$

the combination of Eqs. 4 and 6 results in:

$$[L_T] = [L] + [SL] + 2([S_T] - S_0 - [SL]) \quad \text{(Eq. 7)}$$

and:

$$[L_T] = 2[S_T] - 2S_0 + [L] - [SL] \quad \text{(Eq. 8)}$$

Substituting for $[SL]$ in Eq. 8 using Eq. 1 gives:

$$[L_T] = 2[S_T] - 2S_0 + [L] - K_{1:1}S_0[L] \quad \text{(Eq. 9)}$$

Rearranging Eq. 9 results in:

$$[L] = \frac{[L_T] - 2([S_T] - S_0)}{1 - K_{1:1}S_0} \quad \text{(Eq. 10)}$$

Substituting this expression for $[L]$ in Eq. 5 gives:

$$[S_T] - S_0 = \frac{K_{1:1}S_0}{1 - K_{1:1}S_0}\{[L_T] - 2([S_T] - S_0)\} + \frac{K_{1:2}S_0}{(1 - K_{1:1}S_0)^2}\{[L_T] - 2([S_T] - S_0)\}^2 \quad \text{(Eq. 11)}$$

Let:

$$\frac{K_{1:1}S_0}{1 - K_{1:1}S_0} = \alpha \quad \text{(Eq. 12)}$$

and:

$$\frac{K_{1:2}S_0}{[1 - K_{1:1}S_0]^2} = \beta \quad \text{(Eq. 13)}$$



*0022-3549/81/0100-0108$01.00/0*
*© 1981, American Pharmaceutical Association*

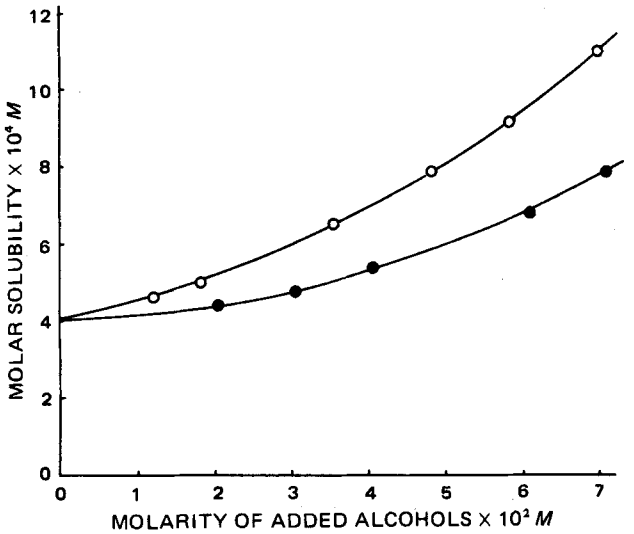


**Figure 1**—*Solubility of hydroquinone in carbon tetrachloride at 30° as a function of added alcohols. Key:* ○, *cyclohexanol; and* ●, *isobutanol.*

Equation 11 can be rewritten as:

$$[S_T] - S_0 = \alpha\{[L_T] - 2([S_T] - S_0)\} + \beta\{[L_T] - 2([S_T] - S_0)\}^2 \quad \text{(Eq. 14)}$$

Dividing both sides of Eq. 14 by $[L_T] - 2([S_T] - S_0)$ results in:

$$\frac{[S_T] - S_0}{[L_T] - 2([S_T] - S_0)} = \alpha + \beta\{[L_T] - 2([S_T] - S_0)\} \quad \text{(Eq. 15)}$$

Plots of the left side of Eq. 15 *versus* $[L_T] - 2([S_T] - S_0)$ give a straight line and both $K_{1:1}$ and $K_{1:2}$ can be calculated from the slope and the intercept. In using Eq. 15, all one needs are the easily obtainable values of $[S_T]$, $S_0$, and $[L_T]$.

It is also apparent from its derivation that Eq. 15, in contrast to Eq. 5, can be used even if the concentrations of the complex species ($SL$ and $SL_2$) are very large. However, when $SL = L$, Eq. 15 cannot be applied to calculate $K_{1:1}$ and $K_{1:2}$. The standard Eq. 5 also cannot be used for these calculations unless one assumes that $SL \gg SL_2$.

The data of Chulkaratana (5) were analyzed according to Eq. 15 to demonstrate its utility. As shown in Fig. 1, the solubility of hydroquinone in carbon tetrachloride increases nonlinearly as a function of added isobutanol and cyclohexanol (5). This increased solubility of the phenolic compound was reported to be due to the formation of 1:1 and 1:2 complexes with the added alcohols. The values for $K_{1:1}$ and $K_{1:2}$ (Table I) were calculated using a lengthy manipulation of the data. When the same data were analyzed according to Eq. 15, Fig. 2 was obtained. The values of $K_{1:1}$ and $K_{1:2}$ were calculated from the intercepts and slopes of Fig. 2 and were in good agreement with literature values (Table I).

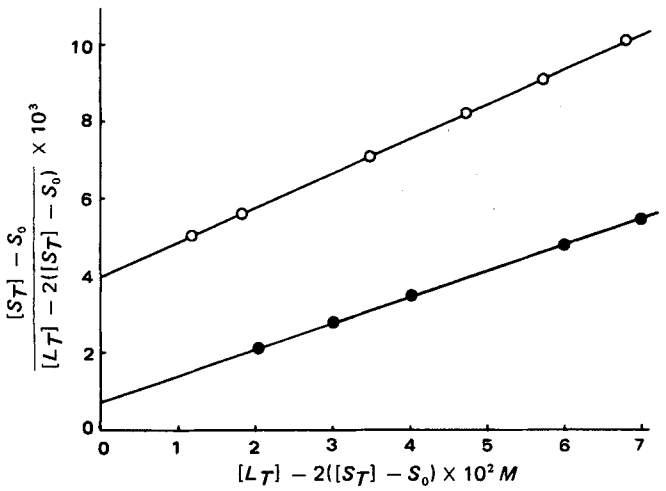


**Figure 2**—*Plots of Eq. 15 for determination of* $K_{1:1}$ *and* $K_{1:2}$ *for the hydroquinone–alcohol complex formation in carbon tetrachloride. Key:* ○, *cyclohexanol; and* ●, *isobutanol.*

**Table I—Complexation Constants of Hydroquinone in Carbon Tetrachloride–Alcohol System**

| | Values from Eq. 15 | | Literature Values | |
|---|---|---|---|---|
| | $K_{1:1}, M^{-1}$ | $K_{1:2}, M^{-2}$ | $K_{1:1}, M^{-1}$ | $K_{1:2}, M^{-2}$ |
| Cyclohexanol | 10.03 | 217.0 | 10.0 | 210.5 |
| Isobutanol | 1.83 | 169.5 | 1.75 | 167.5 |

(1) T. Higuchi and K. A. Connors, *Adv. Anal. Chem. Instr.*, **4**, 117 (1965).

(2) K. A. Connors and J. A. Mollica, Jr., *J. Pharm. Sci.*, **55**, 772 (1966).

(3) H.-L. Fung and T. Higuchi, *ibid.*, **60**, 1782 (1971).

(4) T. Higuchi, J. H. Richards, S. S. David, A. Kamada, J. P. Hou, M. Nakano, N. I. Nakano, and I. H. Pitman, *ibid.*, **58**, 661 (1969).

(5) S. Chulkaratana, Ph.D. thesis, University of Wisconsin, Madison, Wis., 1964.

*K. Iga*
*A. Hussain* ˣ
*T. Kashihara*
College of Pharmacy
University of Kentucky
Lexington, KY 40506

Received April 7, 1980.
Accepted for publication September 19, 1980.

## Plasma Area Method in Relative Bioavailability Evaluation of Drugs with Changing Biological Half-Lives

**Keyphrases** □ Bioavailability—method for drugs with changing biological half-lives, alternative calculations to plasma concentration–time curve method □ Drug absorption—relative bioavailability calculated for drugs with changing biological half-lives, compared to plasma concentration–time curve method □ Pharmacokinetics—relative bioavailability determined for drugs with changing biological half-lives, alternative method to plasma concentration–time curve method

*To the Editor:*

Both the rate and extent of absorption of a drug from dosage forms are important in biopharmaceutical and pharmacokinetic studies. An additional intravenous study often is needed to serve as a control and to obtain the disposition function of the drug (1–5). In the relative bioavailability ($F$) study of two dosage forms, the following total plasma (blood or serum) area method often is used without an intravenous study:

$$F = \frac{AUC_2\beta_2}{AUC_1\beta_1} \quad \text{(Eq. 1a)}$$

0022-3549/81/0100-0109$01.00/0
© 1981, American Pharmaceutical Association

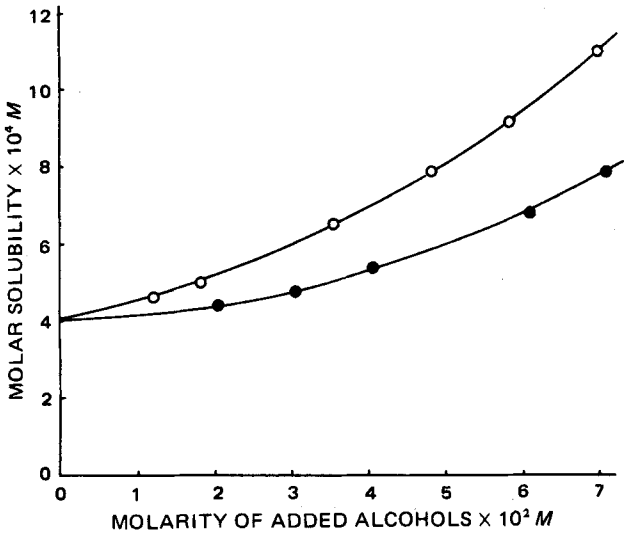


**Figure 1**—*Solubility of hydroquinone in carbon tetrachloride at 30° as a function of added alcohols. Key:* ○, *cyclohexanol; and* ●, *isobutanol.*

Equation 11 can be rewritten as:

$$[S_T] - S_0 = \alpha\{[L_T] - 2([S_T] - S_0)\} + \beta\{[L_T] - 2([S_T] - S_0)\}^2 \quad \text{(Eq. 14)}$$

Dividing both sides of Eq. 14 by $[L_T] - 2([S_T] - S_0)$ results in:

$$\frac{[S_T] - S_0}{[L_T] - 2([S_T] - S_0)} = \alpha + \beta\{[L_T] - 2([S_T] - S_0)\} \quad \text{(Eq. 15)}$$

Plots of the left side of Eq. 15 *versus* $[L_T] - 2([S_T] - S_0)$ give a straight line and both $K_{1:1}$ and $K_{1:2}$ can be calculated from the slope and the intercept. In using Eq. 15, all one needs are the easily obtainable values of $[S_T]$, $S_0$, and $[L_T]$.

It is also apparent from its derivation that Eq. 15, in contrast to Eq. 5, can be used even if the concentrations of the complex species ($SL$ and $SL_2$) are very large. However, when $SL = L$, Eq. 15 cannot be applied to calculate $K_{1:1}$ and $K_{1:2}$. The standard Eq. 5 also cannot be used for these calculations unless one assumes that $SL \gg SL_2$.

The data of Chulkaratana (5) were analyzed according to Eq. 15 to demonstrate its utility. As shown in Fig. 1, the solubility of hydroquinone in carbon tetrachloride increases nonlinearly as a function of added isobutanol and cyclohexanol (5). This increased solubility of the phenolic compound was reported to be due to the formation of 1:1 and 1:2 complexes with the added alcohols. The values for $K_{1:1}$ and $K_{1:2}$ (Table I) were calculated using a lengthy manipulation of the data. When the same data were analyzed according to Eq. 15, Fig. 2 was obtained. The values of $K_{1:1}$ and $K_{1:2}$ were calculated from the intercepts and slopes of Fig. 2 and were in good agreement with literature values (Table I).

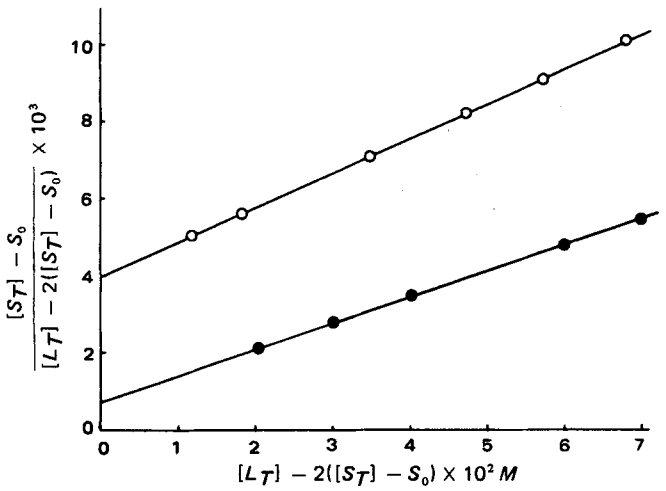


**Figure 2**—*Plots of Eq. 15 for determination of* $K_{1:1}$ *and* $K_{1:2}$ *for the hydroquinone–alcohol complex formation in carbon tetrachloride. Key:* ○, *cyclohexanol; and* ●, *isobutanol.*

**Table I—Complexation Constants of Hydroquinone in Carbon Tetrachloride–Alcohol System**

| | Values from Eq. 15 | | Literature Values | |
|---|---|---|---|---|
| | $K_{1:1}, M^{-1}$ | $K_{1:2}, M^{-2}$ | $K_{1:1}, M^{-1}$ | $K_{1:2}, M^{-2}$ |
| Cyclohexanol | 10.03 | 217.0 | 10.0 | 210.5 |
| Isobutanol | 1.83 | 169.5 | 1.75 | 167.5 |

(1) T. Higuchi and K. A. Connors, *Adv. Anal. Chem. Instr.*, **4**, 117 (1965).

(2) K. A. Connors and J. A. Mollica, Jr., *J. Pharm. Sci.*, **55**, 772 (1966).

(3) H.-L. Fung and T. Higuchi, *ibid.*, **60**, 1782 (1971).

(4) T. Higuchi, J. H. Richards, S. S. David, A. Kamada, J. P. Hou, M. Nakano, N. I. Nakano, and I. H. Pitman, *ibid.*, **58**, 661 (1969).

(5) S. Chulkaratana, Ph.D. thesis, University of Wisconsin, Madison, Wis., 1964.

*K. Iga*
*A. Hussain* ˣ
*T. Kashihara*
College of Pharmacy
University of Kentucky
Lexington, KY 40506

Received April 7, 1980.
Accepted for publication September 19, 1980.

## Plasma Area Method in Relative Bioavailability Evaluation of Drugs with Changing Biological Half-Lives

**Keyphrases** □ Bioavailability—method for drugs with changing biological half-lives, alternative calculations to plasma concentration–time curve method □ Drug absorption—relative bioavailability calculated for drugs with changing biological half-lives, compared to plasma concentration–time curve method □ Pharmacokinetics—relative bioavailability determined for drugs with changing biological half-lives, alternative method to plasma concentration–time curve method

*To the Editor:*

Both the rate and extent of absorption of a drug from dosage forms are important in biopharmaceutical and pharmacokinetic studies. An additional intravenous study often is needed to serve as a control and to obtain the disposition function of the drug (1–5). In the relative bioavailability ($F$) study of two dosage forms, the following total plasma (blood or serum) area method often is used without an intravenous study:

$$F = \frac{AUC_2\beta_2}{AUC_1\beta_1} \quad \text{(Eq. 1a)}$$

0022-3549/81/0100-0109$01.00/0
© 1981, American Pharmaceutical Association

$$F = \frac{AUC_2(t_{0.5})_1}{AUC_1(t_{0.5})_2} \quad \text{(Eq. 1b)}$$

where $AUC_1$ and $AUC_2$ are the estimated total areas (corrected to the same dose) under the plasma concentration–time curve from time zero to infinity obtained from dosage forms 1 and 2, respectively; $\beta_1$ and $\beta_2$ are the terminal exponential rate constants obtained from the studies on dosage forms 1 and 2, respectively; and $(t_{0.5})_1$ and $(t_{0.5})_2$ are the terminal biological half-lives from dosage forms 1 and 2, respectively. Equations 1*a* and 1*b* are commonly assumed to be theoretically correct and applicable to multicompartment systems.

The purpose of this communication is to consider theoretically the limitation of using Eq. 1*a* or 1*b* in a relative bioavailability study. Under certain conditions, such use might result in significant underestimations or overestimations of the relative bioavailability of the two dosage forms.

The total amount of drug absorbed into the general circulation up to infinite time ($A_b$) from a dosage can be calculated by (3):

$$A_b = AUCCl_{TB} = AUCk_{10}V_c = AUCV_{d\beta}\beta \quad \text{(Eq. 2)}$$

where $Cl_{TB}$ is the total body drug clearance, $k_{10}$ is the first-order elimination rate constant from the central compartment in the multicompartmental mammillary model system, $V_c$ is the volume of the central compartment, $V_{d\beta}$ is the apparent volume of distribution during the terminal exponential phase, and $\beta$ is the terminal exponential rate constant. Therefore, the relative bioavailability ($F$) from the two dosage forms when there is a difference in $Cl_{TB}$ between the two studies in the same subject can be calculated theoretically by:

$$F = \frac{A_{b_2}}{A_{b_1}} \quad \text{(Eq. 3a)}$$

$$F = \frac{AUC_2Cl_{TB_2}}{AUC_1Cl_{TB_1}} \quad \text{(Eq. 3b)}$$

$$F = \frac{AUC_2(k_{10})_2}{AUC_1(k_{10})_1} \quad \text{(Eq. 3c)}$$

$$F = \frac{AUC_2(V_{d\beta})_2\beta_2}{AUC_1(V_{d\beta})_1\beta_1} \quad \text{(Eq. 3d)}$$

$$F = \frac{AUC_2(V_{d\beta})_2(t_{0.5})_1}{AUC_1(V_{d\beta})_1(t_{0.5})_2} \quad \text{(Eq. 3e)}$$

It is obvious that Eqs. 3*b*–3*e* are different from Eqs. 1*a* and 1*b*. In the absence of known causes, it is reasonable to assume that in multicompartmental mammillary models, the change in $\beta$ during the two absorption studies is attributed entirely to the change in $k_{10}$ and that both the intercompartmental distribution rate constants and $V_c$ remain the same (2–6). If one accepts these assumptions, then Eqs. 1*a* and 1*b* are theoretically incorrect. The validity of Eqs. 1*a* and 1*b* is based on the assumption that the $(V_{d\beta})_1$ and $(V_{d\beta})_2$ are the same in spite of the change in $\beta$.

A hypothetical example based on reported ampicillin pharmacokinetic data (7) will be used to illustrate the influence of the change in $\beta$ on $V_{d\beta}$ and thus the relative bioavailability data. The biexponential disposition function ($A_1e^{-\alpha_1 t} + B_1e^{-\beta_1 t}$) of ampicillin was calculated from the average data in nine subjects following an intravenous bolus dose of 615 mg (7):

$$C_p(\mu g/ml) = 120.4e^{-2.4t} + 12.12e^{-0.39t} \quad \text{(Eq. 4)}$$

The $(V_{d\beta})_1$ value for ampicillin based on Eq. 4 was calculated by the standard method [*i.e.*, $(V_{d\beta})_1$ = dose/$AUC_1\beta_1$]. The new $V_{d\beta}$ value for every change in $\beta$ (±10, 20, 30, 40, 60, and 80% from the original value) was calculated by the reported method (2–5), assuming no changes in the central compartment volume and intercompartmental transfer rate constants. The new disposition function ($A_2e^{-\alpha_2 t} + B_2e^{-\beta_2 t}$) corresponding to the change in $\beta$ was calculated first. The new $V_{d\beta}$ or $(V_{d\beta})_2$ value then was calculated with:

$$(V_{d\beta})_2 = \frac{\text{dose}}{AUC_2\beta_2} \quad \text{(Eq. 5)}$$

The details for calculating the new $V_{d\beta}$ value are shown in the *Appendix*. The results of these theoretical studies are summarized in Table I. In these studies, the dose was assumed to be absorbed completely into the general circulation. The *AUC* should be independent of the administration route and absorption kinetics if the same total amount of drug is absorbed into the general circulation.

In contrast to the common notion, the data in Table I show that $V_{d\beta}$ might change markedly owing to the change in $\beta$. For example, when $\beta$ was increased by 30%, $V_{d\beta}$ increased by 134%. In the literature, a change in $V_{d\beta}$ due to a change in $\beta$ often was assumed to result from the "real" physiological change in the distribution characteristics of the drug. In these analyses, both the central compartment volume (or the apparent initial volume of distribution) and the apparent steady-state volume of distribution were assumed to remain the same despite the change in $\beta$.

The implication of these results is that the use of Eq. 1*a* or 1*b* for calculating relative bioavailability might overestimate or underestimate the true $F$ value. If it is assumed that all of the drug is absorbed from the two dosage forms, all $F$ values calculated based on Eq. 1*a* or 1*b* should be expected to be equal to 1.0 according to conventional understanding. However, this is not the case, as shown in Table I ($F$ values ranged from 0.429 to 1.919). The effect of the change in $\beta$ on $V_{d\beta}$ was reported earlier (4, 6). Nevertheless, its implication in the evaluation of relative bioavailability has not been investigated fully.

These results and discussion suggest that caution should be used in the interpretation of experimental data using Eq. 1*a* or 1*b*. These two equations are theoretically valid if the disposition kinetics of a drug can be described adequately by the one-compartment open model. The results of simulation studies with other drugs indicate that the greater the distribution phase of a drug, the less the accuracy of these equations.

**Table I—Pharmacokinetic Analysis of Ampicillin[a] Resulting from Changes in $\beta$**

| Percent Change in $\beta$ from $\beta_1$ | $AUC_2$, (hr μg)/ml | $(V_{d\beta})_2$, liters | $F^b$ |
|---|---|---|---|
| 0[c] | 81.2[d] | 19.4[e] | 1.000 |
| +10 | 61.3 | 23.4 | 0.830 |
| +20 | 43.4 | 30.3 | 0.641 |
| +30[f] | 26.8 | 45.3 | 0.429 |
| −10 | 104.1 | 16.8 | 1.154 |
| −20 | 131.3 | 15.0 | 1.293 |
| −30 | 164.8 | 13.7 | 1.420 |
| −40 | 208.1 | 12.6 | 1.537 |
| −60 | 353.9 | 11.1 | 1.743 |
| −80 | 779.4 | 10.1 | 1.919 |

[a] The disposition function from the 615-mg iv dose study (7); $C_p$ (μg/ml) = $120.4e^{-2.4t} + 12.12e^{-0.39t}$. [b] Based on Eq. 1*a*. [c] That is, $\beta = \beta_2 = 0.39\ hr^{-1}$. [d] That is, $AUC_1 = AUC_2 = 81.2$ (hr μg)/ml. [e] That is, $(V_{d\beta})_1 = (V_{d\beta})_2 = 19.4$ liters. [f] A 40% or greater change resulted in unrealistic data.

Since it is difficult to calculate $V_{d\beta}$ accurately based on plasma data from absorption studies, the use of the more correct equations, Eqs. 3*b*–3*e* is virtually impossible from a practical point of view. Therefore, Eqs. 1*a* and 1*b* can be used routinely with confidence as an approximate method for drugs whose disposition kinetics can be approximated by the one-compartment model (*e.g.*, the distribution phase accounts for <5–10%) and also for "high distribution" drugs whose changes in $\beta$ between the absorption studies are <5–10%.

These limitations might be more critical in studies involving only one or a few subjects. The errors in the relative bioavailability evaluation (overestimation and underestimation) due to the change in $\beta$ might cancel out when a larger population of subjects is used. Therefore, the use of Eq. 1*a* or 1*b* might be satisfactory under this circumstance.

The analyses (Table I) were based on the assumption that the elimination rate of the drug was proportional to its concentration in the venous plasma (almost exclusively used in bioavailability studies in humans). Such an assumption might be invalid since our recent studies showed marked arteriovenous plasma concentration differences for many drugs in dogs and rabbits (8). From a physiological point of view, the elimination rate of a drug from the body in linear pharmacokinetics should be generally proportional to its concentration in the arterial plasma and not in the venous plasma (especially for renal elimination).

The question of the theoretical validity of using venous plasma data to calculate $V_{d\beta}$ and the steady-state volume of distribution ($V_{dss}$) based on the conventionally used equations has been raised (8, 9). The implication of arteriovenous plasma concentration differences in the bioavailability evaluation of drugs with a changing terminal half-life remains to be explored. Based on the venous plasma data from absorption studies alone, there is virtually no way to characterize accurately the change in the volume of distribution of a drug in the body when there is a change in $\beta$ between the two studies. The uncertainty in the dose absorbed also contributes to the difficulty in estimating the volume of distribution.

It is of interest to note from Eq. 2 that as long as $Cl_{TB}$ remains unchanged, the dose absorbed is proportional to the $AUC$ in spite of any change in the terminal biological half-life or the apparent volume of distribution (used in a broad sense). In normal bioavailability studies in healthy subjects with strict protocols, it seems difficult to conceive that there will be any significant physiological or biochemical changes in the body that would result in a significant change in the real drug distribution characteristics and cause a noticeable change in the $AUC$ or the biological half-life. The apparent steady-state volume of distribution is a reflection of the equilibrium partition properties of the drug between various tissues and plasma. Such properties probably would not change significantly during a relatively short period.

Determination of renal clearance has been proposed as a means of estimating the change in the total body clearance in the relative bioavailability study (10). This method is particularly valuable if a drug is extensively excreted unchanged in the urine.

In view of the potential arteriovenous plasma concentration differences, it was pointed out that the timed interval method for the renal clearance measurement following a single dose might result in significant overestimation or underestimation of the true renal clearance of the drug (8, 9, 11).

Recently, a unique statistical approach for evaluating relative bioavailability studies involving a change in the terminal half-life was presented (12, 13). Perhaps, a combination of the statistical (12, 13) and renal clearance (10) approaches and the discussions presented in this communication might serve as the basis for further studies on this subject.

*Appendix*—This discussion concerns the relationship between the new disposition function ($A_2e^{-\alpha_2 t} + B_2e^{-\beta_2 t}$) and the original disposition function ($A_1e^{-\alpha_1 t} + B_1e^{-\beta_1 t}$) assuming that there is only a change in the first-order elimination rate constant from the central compartment in the two-compartment open model system when the terminal exponential rate constant changes from $\beta_1$ to $\beta_2$.

The pharmacokinetic parameters from the original disposition function obtained after intravenous dosing can be calculated by (3–5):

$$k_{21} = \frac{A_1\beta_1 + B_1\alpha_1}{A_1 + B_1} \quad \text{(Eq. A1)}$$

$$(k_{10})_1 = \frac{\alpha_1\beta_1}{k_{21}} \quad \text{(Eq. A2)}$$

$$k_{12} = \alpha_1 + \beta_1 - k_{21} - (k_{10})_1 \quad \text{(Eq. A3)}$$

$$V_c = \frac{\text{dose}}{A_1 + B_1} \quad \text{(Eq. A4)}$$

The new elimination rate constant, $(k_{10})_2$, and the new disposition function can be obtained by (3–5):

$$(k_{10})_2 = \frac{\beta_2^2 - (k_{12} + k_{21})\beta_2}{\beta_2 - k_{21}} \quad \text{(Eq. A5)}$$

$$\alpha_2 = (k_{10})_2 + k_{12} + k_{21} - \beta_2 \quad \text{(Eq. A6)}$$

$$A_2 = \frac{\text{dose}(\alpha_2 - k_{21})}{V_c(\alpha_2 - \beta_2)} \quad \text{(Eq. A7)}$$

$$B_2 = \frac{\text{dose}(k_{21} - \beta_2)}{V_c(\alpha_2 - \beta_2)} \quad \text{(Eq. A8)}$$

where $\beta_2$ is obtained from the terminal exponential phase during the absorption study.


(1) J. C. K. Loo and S. Riegelman, *J. Pharm. Sci.*, **57**, 918 (1968).

(2) "Guidelines for Biopharmaceutical Studies," APhA Academy of Pharmaceutical Sciences, Washington, D.C., 1972.

(3) A. E. Till, L. Z. Benet, and K. C. Kwan, *J. Pharmacokinet. Biopharm.*, **2**, 525 (1974).

(4) M. Gibaldi and D. Perrier, "Pharmacokinetics," Dekker, New York, N.Y., 1975.

(5) W. L. Chiou, *J. Pharm. Sci.*, **69**, 57 (1980).

(6) W. J. Jusko and M. Gibaldi, *ibid.*, **61**, 1270 (1972).

(7) G. P. Lewis and W. J. Jusko, *Clin. Pharmacol. Ther.*, **18**, 475 (1975).

(8) G. Lam and W. L. Chiou, presented at the APhA Academy of Pharmaceutical Sciences, San Antonio meeting, Nov. 1980.

(9) W. L. Chiou, "Abstracts," APhA Academy of Pharmaceutical Sciences, Washington, D.C., meeting, Apr. 1980, abstract 15.

(10) W. L. Chiou and G. Lam, *Int. J. Clin. Pharmacol. Ther. Toxicol.*, in press.

(11) K. C. Kwan and A. E. Till, *J. Pharm. Sci.*, **62**, 1494 (1973).

(12) L. B. Sheiner, R. A. Upton, J. F. Thiercelin, and S. Riegelman, in "Seminar on Biological Availability," Pharmaceutical and Chemical Manufacturer's Association of South Africa, Pretoria, South Africa, 1979, pp. 43–48.

(13) R. A. Upton, S. Riegelman, and L. B. Sheiner, presented at the APhA Academy of Pharmaceutical Sciences, Washington, D.C., meeting, Apr. 1980.

*Win L. Chiou* ˣ
*Chung Y. Lui*
*Gilbert Lam*
Department of Pharmacy
College of Pharmacy
University of Illinois at
the Medical Center
Chicago, IL 60612

Received March 4, 1980.
Accepted for publication October 23, 1980.
The authors thank Ms. Marie Zajac for her preparation of this manuscript.

# Plasma Protein Binding and Urinary Excretion of *R*- and *S*-Epimers of an Arylmalonylamino 1-Oxacephem I: In Humans

**Keyphrases** □ Stereoisomers, arylmalonylamino 1-oxacephem—new β-lactam antibacterial agent, renal clearance, plasma protein binding, humans □ Renal clearance—arylmalonylamino 1-oxacephem stereoisomers, effect of plasma protein binding, humans □ Protein binding, human plasma—arylmalonylamino 1-oxacephem stereoisomers, effect on renal clearance

*To the Editor:*

A new antibacterial agent, 7β-[2-carboxy-2-(4-hydroxyphenyl)acetamido]-7α-methoxy-3-[[(1-methyl-1*H*-tetrazol-5-yl)thio]methyl]-1-oxa-1-dethia -3- cephem-4-carboxylic acid disodium salt (I), is an arylmalonylamino 1-oxacephem derivative that was discovered and is being developed in our laboratories (1, 2). It consists of the *R*- and *S*-epimers in about a 1:1 ratio. This drug is not metabolized and almost all of the dose, ~90% or more, is excreted into the urine in humans (3, 4), ~80% is excreted into the urine in rats, and 86–90% is excreted into the urine in dogs (5, 6) when assayed by agar diffusion using *Escherichia coli* 7437 (2). This study was carried out to elucidate the behavior of the *R*- and *S*-epimers of I in the human body.

Plasma and urine samples were collected from four healthy volunteers after intravenous injection of 1 g of I. Concentrations of *R*- and *S*-epimers in the samples were determined separately by high-performance liquid chromatography [Nucleosil $10C_{18}$, using pH 6.0 ammonium acetate buffer–methanol (11.5:1) for the plasma samples and pH 6.0 phosphate buffer containing 0.005 *M* tetra-*n*-butylammonium hydroxide–methanol (75:25) for the urine samples][1]. Plasma concentration–time curves for the *R*- and *S*-epimers indicated that the *R*-epimer was eliminated faster than the *S*-epimer (Fig. 1). The time course of the concentration ratio between the *R*- and *S*-epimers in urine also showed that the excretion of the *R*-epimer was faster than that of the *S*-epimer[1]. The renal clearances calculated from these data were 65.5 ± 3.4 and 43.5 ± 3.1 ml/min/1.48 $m^2$ for the *R*- and *S*-epimers, respectively.

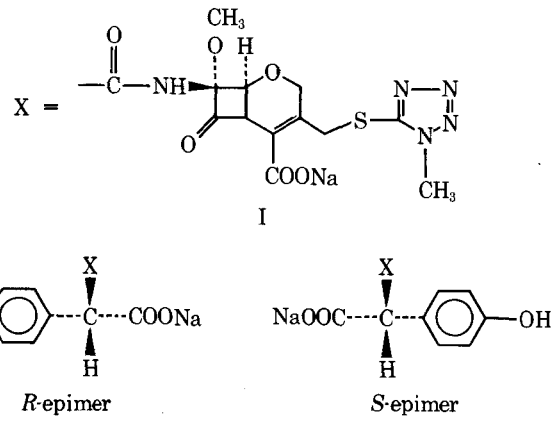


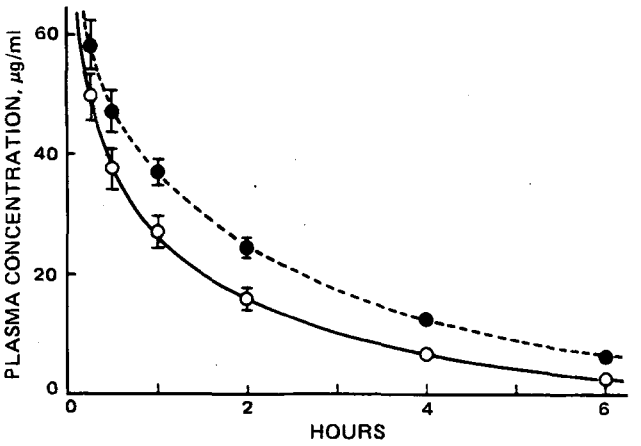


**Figure 1**—*Plasma concentration of* R- (○) *and* S- (●) *epimers after intravenous administration of I. Each data point gives the mean and standard deviation of four healthy volunteers.*

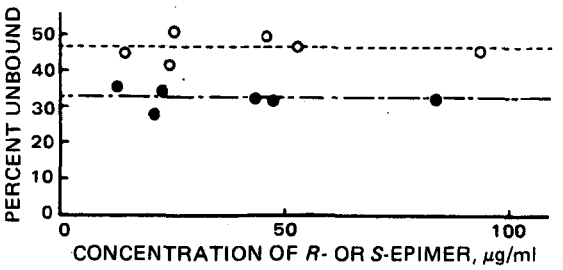


**Figure 2**—*Human plasma protein binding of* R- (○) *and* S- (●) *epimers of I. The epimer concentration includes both bound and unbound epimer.*

To investigate this difference, protein binding of these epimers was examined by ultrafiltration[2] of fresh human plasma containing I at 37°. The results indicated that the fraction of the unbound *R*-epimer was higher than that of the *S*-epimer (Fig. 2). The mean unbound ratio of the *R*-epimer was 47%, and that of the *S*-epimer was 33%.

The renal clearance of unbound *R*- and *S*-epimers calculated from these results was 140.2 ± 8.1 and 132.2 ± 7.0 ml/min/1.48 $m^2$, respectively. These two values were not significantly different.

These results suggest that the faster excretion of the *R*-epimer of I compared to the excretion of the *S*-epimer can be explained by the larger unbound fraction of the former in human plasma.

(1) M. Narisada, T. Yoshida, H. Onoue, M. Ohtani, T. Okada, T. Tsuji, I. Kikkawa, N. Haga, H. Satoh, H. Itani, and W. Nagata, *J. Med. Chem.*, 22, 757 (1979).

[1] R. Konaka, Shionogi Research Laboratories, Shionogi & Co., Fukushima-ku, Osaka 553, Japan, personal communication.
[2] Diaflo ultrafiltration membrane PM-10, Amicon Corp., Lexington, Mass.



*0022-3549/81/0100-0112$01.00/0*
*© 1981, American Pharmaceutical Association*

*Win L. Chiou* ˣ
*Chung Y. Lui*
*Gilbert Lam*
Department of Pharmacy
College of Pharmacy
University of Illinois at
the Medical Center
Chicago, IL 60612

Received March 4, 1980.
Accepted for publication October 23, 1980.
The authors thank Ms. Marie Zajac for her preparation of this manuscript.

# Plasma Protein Binding and Urinary Excretion of *R*- and *S*-Epimers of an Arylmalonylamino 1-Oxacephem I: In Humans

**Keyphrases** □ Stereoisomers, arylmalonylamino 1-oxacephem—new β-lactam antibacterial agent, renal clearance, plasma protein binding, humans □ Renal clearance—arylmalonylamino 1-oxacephem stereoisomers, effect of plasma protein binding, humans □ Protein binding, human plasma—arylmalonylamino 1-oxacephem stereoisomers, effect on renal clearance

*To the Editor:*

A new antibacterial agent, 7β-[2-carboxy-2-(4-hydroxyphenyl)acetamido]-7α-methoxy-3-[[(1-methyl-1*H*-tetrazol-5-yl)thio]methyl]-1-oxa-1-dethia -3- cephem-4-carboxylic acid disodium salt (I), is an arylmalonylamino 1-oxacephem derivative that was discovered and is being developed in our laboratories (1, 2). It consists of the *R*- and *S*-epimers in about a 1:1 ratio. This drug is not metabolized and almost all of the dose, ~90% or more, is excreted into the urine in humans (3, 4), ~80% is excreted into the urine in rats, and 86–90% is excreted into the urine in dogs (5, 6) when assayed by agar diffusion using *Escherichia coli* 7437 (2). This study was carried out to elucidate the behavior of the *R*- and *S*-epimers of I in the human body.

Plasma and urine samples were collected from four healthy volunteers after intravenous injection of 1 g of I. Concentrations of *R*- and *S*-epimers in the samples were determined separately by high-performance liquid chromatography [Nucleosil $10C_{18}$, using pH 6.0 ammonium acetate buffer–methanol (11.5:1) for the plasma samples and pH 6.0 phosphate buffer containing 0.005 *M* tetra-*n*-butylammonium hydroxide–methanol (75:25) for the urine samples][1]. Plasma concentration–time curves for the *R*- and *S*-epimers indicated that the *R*-epimer was eliminated faster than the *S*-epimer (Fig. 1). The time course of the concentration ratio between the *R*- and *S*-epimers in urine also showed that the excretion of the *R*-epimer was faster than that of the *S*-epimer[1]. The renal clearances calculated from these data were 65.5 ± 3.4 and 43.5 ± 3.1 ml/min/1.48 $m^2$ for the *R*- and *S*-epimers, respectively.

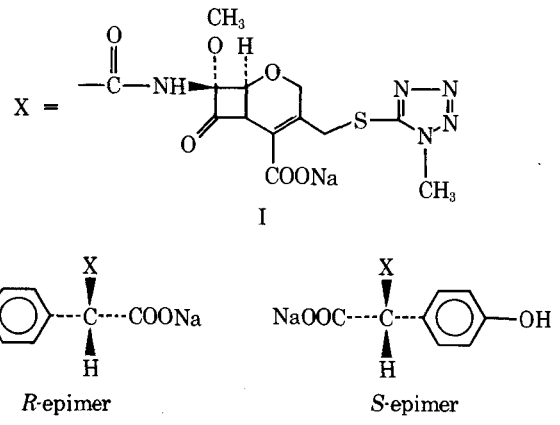


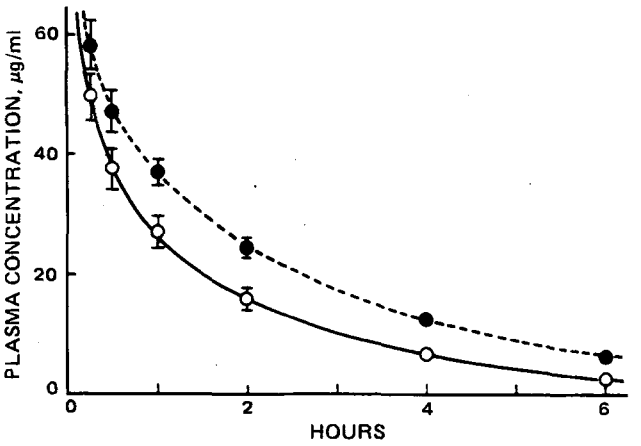


**Figure 1**—*Plasma concentration of* R- (○) *and* S- (●) *epimers after intravenous administration of I. Each data point gives the mean and standard deviation of four healthy volunteers.*

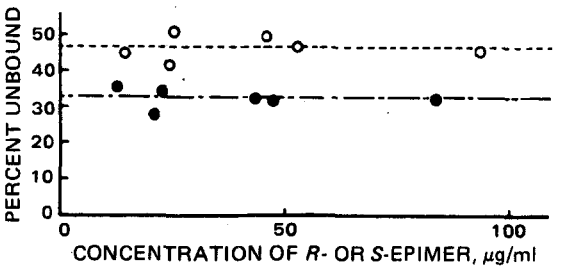


**Figure 2**—*Human plasma protein binding of* R- (○) *and* S- (●) *epimers of I. The epimer concentration includes both bound and unbound epimer.*

To investigate this difference, protein binding of these epimers was examined by ultrafiltration[2] of fresh human plasma containing I at 37°. The results indicated that the fraction of the unbound *R*-epimer was higher than that of the *S*-epimer (Fig. 2). The mean unbound ratio of the *R*-epimer was 47%, and that of the *S*-epimer was 33%.

The renal clearance of unbound *R*- and *S*-epimers calculated from these results was 140.2 ± 8.1 and 132.2 ± 7.0 ml/min/1.48 $m^2$, respectively. These two values were not significantly different.

These results suggest that the faster excretion of the *R*-epimer of I compared to the excretion of the *S*-epimer can be explained by the larger unbound fraction of the former in human plasma.

(1) M. Narisada, T. Yoshida, H. Onoue, M. Ohtani, T. Okada, T. Tsuji, I. Kikkawa, N. Haga, H. Satoh, H. Itani, and W. Nagata, *J. Med. Chem.*, 22, 757 (1979).

[1] R. Konaka, Shionogi Research Laboratories, Shionogi & Co., Fukushima-ku, Osaka 553, Japan, personal communication.
[2] Diaflo ultrafiltration membrane PM-10, Amicon Corp., Lexington, Mass.



*0022-3549/81/0100-0112$01.00/0*
*© 1981, American Pharmaceutical Association*

(2) T. Yoshida, S. Matsuura, S. Mayama, Y. Kameda, and S. Kuwahara, *Antimicrob. Agents Chemother.*, **17**, 302 (1980).
(3) J. Kurihara, K. Matsumoto, Y. Uzuka, H. Shishido, T. Nagatake, H. Yamada, T. Yoshida, T. Oguma, Y. Kimura, and Y. Tochino, in "Current Chemotherapy and Infectious Disease: Proceedings of the 11th ICC and the 19th ICAAC," vol. I, J. D. Nelson and C. Grassi, Eds., American Society for Microbiology, Washington, D.C., 1980, p. 110.
(4) H. Yamada, T. Yoshida, T. Oguma, Y. Kimura, Y. Tochino, J. Kurihara, K. Matsumoto, Y. Uzuka, H. Shishido, and T. Nagatake, *Chemotherapy (Tokyo)*, in press.
(5) S. Matsuura, T. Yoshida, K. Sugeno, Y. Harada, M. Harada, and S. Kuwahara, in "Abstracts of 18th Interscience Conference on Antimicrobial Agents and Chemotherapy," Atlanta, Ga., Oct. 1978, p. 152.
(6) T. Yoshida, Y. Kimura, and Y. Tochino, *Chemotherapy (Tokyo)*, in press.

*H. Yamada* ˣ
*T. Ichihashi*
*K. Hirano*
*H. Kinoshita*
Shionogi Research Laboratories
Shionogi & Co., Ltd.
Fukushima-ku, Osaka 553, Japan

Received May 5, 1980.
Accepted for publication September 25, 1980.

# Plasma Protein Binding and Urinary Excretion of *R*- and *S*-Epimers of an Arylmalonylamino 1-Oxacephem II: In Rats

**Keyphrases** □ Stereoisomers, arylmalonylamino 1-oxacephem—new β-lactam antibacterial agent, renal clearance, plasma protein binding, rats □ Renal clearance—new antibacterial agent, arylmalonylamino 1-oxacephem stereoisomers, effect of plasma protein binding, comparison of rat and human data □ Protein binding, rat plasma—new antibacterial agent, arylmalonylamino 1-oxacephem stereoisomers, effect on renal clearance, comparison with human data

*To the Editor:*

In Part I (1), we reported that the *R*-epimer of an arylmalonylamino 1-oxacephem derivative {7β-[2-carboxy -2- (4-hydroxyphenyl)acetamido] -7α- methoxy-3-[[(1-methyl-1*H*-tetrazol-5-yl)thio]methyl] -1- oxa-1-dethia-3-cephem-4-carboxylic acid disodium salt (I)}, a new antibacterial agent, was excreted into the urine faster than the *S*-epimer in humans. It was concluded that the phenomenon was due to the difference between the binding of human plasma protein with *R*- and *S*-epimers.

To confirm that conclusion, studies were carried out using rats in which I was not metabolized and was excreted mainly into the urine, as in humans. The extent of protein binding of the *R*- and *S*-epimers in rat plasma was measured by the same method described previously (1). Unlike in humans, there was no difference in plasma protein binding between the *R*- and *S*-epimers in rats (Fig. 1). Thus, taking into consideration our conclusion in the previous study (1), the urinary excretion rates of the *R*- and *S*-epimers in rats should be the same.

To confirm this prediction, the plasma concentration and urinary excretion rate of the *R*- and *S*-epimers after intravenous injection of I (70 mg/kg) to three rats were measured by the method described previously (1). The plasma concentration–time curves for the *R*- and *S*-epimers were the same (Fig. 2), and the renal clearance values were 0.85 ± 0.04 and 0.83 ± 0.04 ml/min/100 g for the *R*- and *S*-epimers, respectively. As expected, there was no difference in the renal clearance in rats between these epimers.

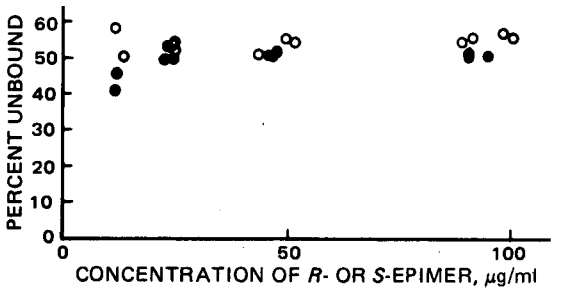


**Figure 1**—*Rat plasma protein binding of* R- (○) *and* S- (●) *epimers of I.*

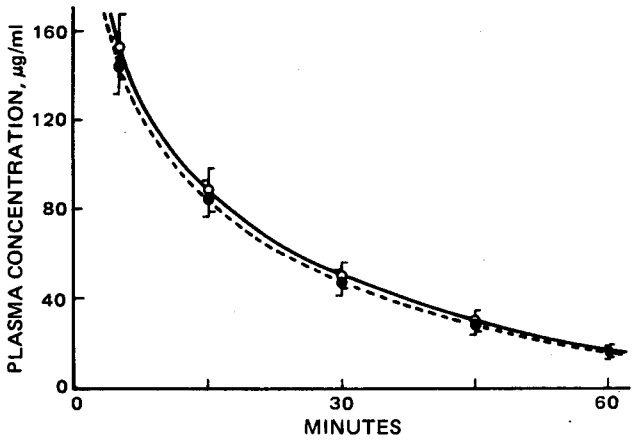


**Figure 2**—*Plasma concentration of* R- (—○) *and* S- (- -●) *epimers after intravenous administration of I. Each data point gives the mean and standard deviation of three rats.*

These stereospecific differences in plasma protein binding have been reported for other drugs (2–5) and vary between species.

*In vitro* studies[1] of the protein binding of I in dog plasma showed that the percentage of the unbound fraction of the *R*-epimer was larger than that of the *S*-epimer; these results were similar to those on human plasma protein binding. This finding suggested that urinary excretion of the *R*-epimer was faster than that of the *S*-epimer in dogs, as in humans, and this prediction was confirmed experimentally[1].

These findings support the previous conclusion that the difference in the urinary excretion rate between *R*- and *S*-epimers of I in humans is due to the difference in protein binding of human plasma between these epimers.

(1) H. Yamada, T. Ichihashi, K. Hirano, and H. Kinoshita, *J. Pharm. Sci.*, **70**, 112 (1981).
(2) D. T. Witiak and M. W. Whitehouse, *Biochem. Pharmacol.*, 18, 971 (1969).
(3) W. E. Müller and U. Wollert, *Mol. Pharmacol.*, 11, 52 (1975).
(4) A. Yacobi and G. Levy, *J. Pharmacokinet. Biopharm.*, 5, 123

[1] M. Nakamura, Shionogi Research Laboratories, Shionogi & Co., Fukushima-ku, Osaka 553, Japan, personal communication.

0022-3549/81/0100-0113$01.00/0
© 1981, American Pharmaceutical Association

(2) T. Yoshida, S. Matsuura, S. Mayama, Y. Kameda, and S. Kuwahara, *Antimicrob. Agents Chemother.*, **17**, 302 (1980).
(3) J. Kurihara, K. Matsumoto, Y. Uzuka, H. Shishido, T. Nagatake, H. Yamada, T. Yoshida, T. Oguma, Y. Kimura, and Y. Tochino, in "Current Chemotherapy and Infectious Disease: Proceedings of the 11th ICC and the 19th ICAAC," vol. I, J. D. Nelson and C. Grassi, Eds., American Society for Microbiology, Washington, D.C., 1980, p. 110.
(4) H. Yamada, T. Yoshida, T. Oguma, Y. Kimura, Y. Tochino, J. Kurihara, K. Matsumoto, Y. Uzuka, H. Shishido, and T. Nagatake, *Chemotherapy (Tokyo)*, in press.
(5) S. Matsuura, T. Yoshida, K. Sugeno, Y. Harada, M. Harada, and S. Kuwahara, in "Abstracts of 18th Interscience Conference on Antimicrobial Agents and Chemotherapy," Atlanta, Ga., Oct. 1978, p. 152.
(6) T. Yoshida, Y. Kimura, and Y. Tochino, *Chemotherapy (Tokyo)*, in press.

*H. Yamada* ˣ
*T. Ichihashi*
*K. Hirano*
*H. Kinoshita*
Shionogi Research Laboratories
Shionogi & Co., Ltd.
Fukushima-ku, Osaka 553, Japan

Received May 5, 1980.
Accepted for publication September 25, 1980.

# Plasma Protein Binding and Urinary Excretion of *R*- and *S*-Epimers of an Arylmalonylamino 1-Oxacephem II: In Rats

**Keyphrases** □ Stereoisomers, arylmalonylamino 1-oxacephem—new β-lactam antibacterial agent, renal clearance, plasma protein binding, rats □ Renal clearance—new antibacterial agent, arylmalonylamino 1-oxacephem stereoisomers, effect of plasma protein binding, comparison of rat and human data □ Protein binding, rat plasma—new antibacterial agent, arylmalonylamino 1-oxacephem stereoisomers, effect on renal clearance, comparison with human data

*To the Editor:*

In Part I (1), we reported that the *R*-epimer of an arylmalonylamino 1-oxacephem derivative {7β-[2-carboxy -2- (4-hydroxyphenyl)acetamido] -7α- methoxy-3-[[(1-methyl-1*H*-tetrazol-5-yl)thio]methyl] -1- oxa-1-dethia-3-cephem-4-carboxylic acid disodium salt (I)}, a new antibacterial agent, was excreted into the urine faster than the *S*-epimer in humans. It was concluded that the phenomenon was due to the difference between the binding of human plasma protein with *R*- and *S*-epimers.

To confirm that conclusion, studies were carried out using rats in which I was not metabolized and was excreted mainly into the urine, as in humans. The extent of protein binding of the *R*- and *S*-epimers in rat plasma was measured by the same method described previously (1). Unlike in humans, there was no difference in plasma protein binding between the *R*- and *S*-epimers in rats (Fig. 1). Thus, taking into consideration our conclusion in the previous study (1), the urinary excretion rates of the *R*- and *S*-epimers in rats should be the same.

To confirm this prediction, the plasma concentration and urinary excretion rate of the *R*- and *S*-epimers after intravenous injection of I (70 mg/kg) to three rats were measured by the method described previously (1). The plasma concentration–time curves for the *R*- and *S*-epimers were the same (Fig. 2), and the renal clearance values were 0.85 ± 0.04 and 0.83 ± 0.04 ml/min/100 g for the *R*- and *S*-epimers, respectively. As expected, there was no difference in the renal clearance in rats between these epimers.

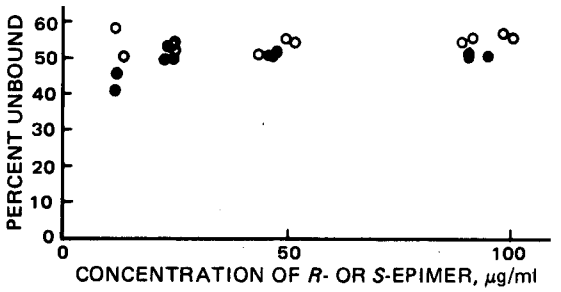


**Figure 1**—*Rat plasma protein binding of* R- (○) *and* S- (●) *epimers of I.*

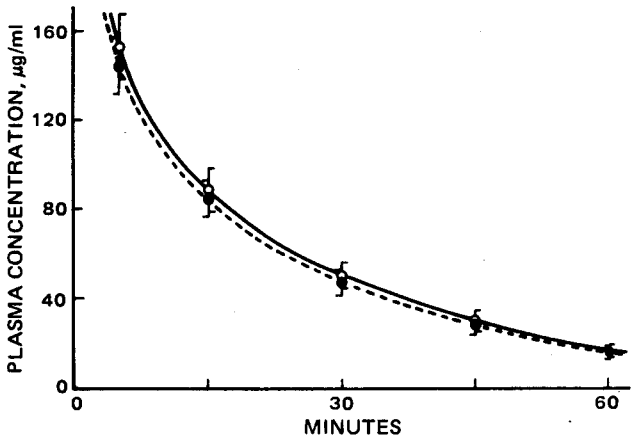


**Figure 2**—*Plasma concentration of* R- (—○) *and* S- (- -●) *epimers after intravenous administration of I. Each data point gives the mean and standard deviation of three rats.*

These stereospecific differences in plasma protein binding have been reported for other drugs (2–5) and vary between species.

*In vitro* studies[1] of the protein binding of I in dog plasma showed that the percentage of the unbound fraction of the *R*-epimer was larger than that of the *S*-epimer; these results were similar to those on human plasma protein binding. This finding suggested that urinary excretion of the *R*-epimer was faster than that of the *S*-epimer in dogs, as in humans, and this prediction was confirmed experimentally[1].

These findings support the previous conclusion that the difference in the urinary excretion rate between *R*- and *S*-epimers of I in humans is due to the difference in protein binding of human plasma between these epimers.

(1) H. Yamada, T. Ichihashi, K. Hirano, and H. Kinoshita, *J. Pharm. Sci.*, **70**, 112 (1981).
(2) D. T. Witiak and M. W. Whitehouse, *Biochem. Pharmacol.*, 18, 971 (1969).
(3) W. E. Müller and U. Wollert, *Mol. Pharmacol.*, 11, 52 (1975).
(4) A. Yacobi and G. Levy, *J. Pharmacokinet. Biopharm.*, 5, 123

[1] M. Nakamura, Shionogi Research Laboratories, Shionogi & Co., Fukushima-ku, Osaka 553, Japan, personal communication.

0022-3549/81/0100-0113$01.00/0
© 1981, American Pharmaceutical Association

(1977).
(5) W. Schmidt and E. Jähnchen, *Experientia*, **34**, 1323 (1978).

*H. Yamada* ˣ
*T. Ichihashi*
*K. Hirano*
*H. Kinoshita*
Shionogi Research Laboratories
Shionogi & Co., Ltd.
Fukushima-ku, Osaka 533, Japan

Received May 5, 1980.
Accepted for publication September 25, 1980.

## Lowering Blood Urea Nitrogen with Amino Acid Supplementation

**Keyphrases** □ Amino acids—dietary supplementation, effects on blood urea nitrogen, rats □ Colorimetry—analysis of blood urea nitrogen in rat serum, effects of dietary supplementation of amino acids □ Dietary supplements—amino acids, effects on blood urea nitrogen in rats

*To the Editor:*

Currently we are studying the effect of dietary supplementation of amino acids on alcohol metabolism. The amino acid augmentation is based on the fasting plasma profile theory (1–4).

From past work on the metabolic effects of such diets, it was found that they produce a significant decrease in serum cholesterol in rats (5) and humans (6). This observed effect was theorized to be the result of an increase in net protein utilization.

While conducting the present study, we discovered that dietary supplementation of limiting amino acids to the third level (L-lysine, L-tryptophan, and L-threonine), based on the fasting plasma profile theory, produces a significant decrease in serum blood urea nitrogen.

Twenty male Sprague–Dawley rats, 250–275 g, were randomly divided into two groups of 10 each. Following a 2-week acclimation period during which both groups were fed a standard animal diet[1], the first group was fed a diet supplemented to the third level of limiting amino acid (Table I) for 2 additional weeks while the second group was maintained on the standard diet for the same period.

On the 15th day, blood collected by orbital sinus puncture was centrifuged, and the serum was retained. Blood urea nitrogen was measured colorimetrically by means of a standard kit[2].

The serum blood urea nitrogen for the treatment group was 8.45 ± 0.36 mg/100 ml (mean ± *SEM*) while that of the control group was 15.1 ± 0.49 mg/100 ml. A Student *t* test showed a significant difference to the $p < 0.01$ level.

It is theorized that the observed effects are caused by an increase in net protein utilization when the limiting amino acids are supplemented, based on the fasting plasma profile theory, and that this increase reduces the amount of underutilized amino acids that are otherwise available for energy metabolism or storage. The end result is a decrease in the amount of nitrogenous metabolic products (wastes) in serum.

[1] Purina Laboratory Chow.
[2] Sigma Chemical Co., St. Louis, MO 63178.

**Table I—Amino Acid-Supplemented Animal Feed to the Third Level of Limiting Amino Acid**

| Ingredient | Amount, % |
|---|---|
| L-Tryptophan | 0.309 |
| L-Threonine | 0.341 |
| L-Lysine | 1.667 |
| Standard feed | 97.683 |

This type of dietary supplementation can be of invaluable assistance to those who must reduce their blood urea nitrogen levels (dialysis patients, nephrotic patients, *etc.*).

The major advantage of the augmentation of the body's amino acids based on the fasting plasma profile theory is that it removes a lot of guesswork and establishes a hard mathematical formula for preparing the diet.

(1) C. I. Jarowski, A. V. Puccini, M. Winitz, and M. C. Otey, *Agr. Biol. Chem.*, **35**, 1007 (1971).
(2) C. I. Jarowski, *ibid.*, **38**, 479 (1974).
(3) C. I. Jarowski and R. Pytelewski, *J. Pharm. Sci.*, **64**, 690 (1975).
(4) P. K. Raja and C. I. Jarowski, *ibid.*, **64**, 695 (1975).
(5) C. I. Jarowski and R. Pytelewski, *ibid.*, **64**, 690 (1975).
(6) P. K. Raja and C. I. Jarowski, *ibid.*, **64**, 694 (1975).

*Gregory M. Torre* ˣ
*Vincent D. Lynch*
*Charles I. Jarowski*
College of Pharmacy and
Allied Health Professions
St. John's University
Jamaica, NY 11435

Received June 23, 1980.
Accepted for publication October 2, 1980.

## Effect of Variation of Plasma Oleic Acid Concentration on Relative Concentration of Free and Protein Bound Warfarin

**Keyphrases** □ Warfarin—effect of plasma oleic acid concentration on free and protein bound warfarin concentration, protein binding, humans □ Protein binding—binding of warfarin to human serum albumin, effect of plasma oleic acid concentration on free and bound warfarin concentration □ Oleic acid—effect of concentration on free and protein bound warfarin concentration, humans

*To the Editor:*

Although the normal serum concentrations of free fatty acids are between 0.3 and 0.9 mmole/liter (1), pathological conditions such as diabetes, reduced renal function, cardiac infarction, and bacterial disease (2–12) can cause substantial increases in free fatty acid levels. In some cases, these levels can exceed 5 mmoles/liter. Moreover, the increasingly widespread use of intravenous fat emulsions probably is associated with significant variation in the serum concentrations of free fatty acids.

Schwartz *et al.* (13) recently demonstrated that variation in the concentration of oleic acid, a major component in the free fatty acids found in serum, can cause significant variations in the protein binding of salicylate. Similar findings concerning the effect of variation in free fatty acid concentrations on the protein binding of drugs were published previously (14–17).



*0022-3549/81/0100-0114$01.00/0*
*© 1981, American Pharmaceutical Association*

(1977).
(5) W. Schmidt and E. Jähnchen, *Experientia*, **34**, 1323 (1978).

*H. Yamada* ˣ
*T. Ichihashi*
*K. Hirano*
*H. Kinoshita*
Shionogi Research Laboratories
Shionogi & Co., Ltd.
Fukushima-ku, Osaka 533, Japan

Received May 5, 1980.
Accepted for publication September 25, 1980.

## Lowering Blood Urea Nitrogen with Amino Acid Supplementation

**Keyphrases** □ Amino acids—dietary supplementation, effects on blood urea nitrogen, rats □ Colorimetry—analysis of blood urea nitrogen in rat serum, effects of dietary supplementation of amino acids □ Dietary supplements—amino acids, effects on blood urea nitrogen in rats

*To the Editor:*

Currently we are studying the effect of dietary supplementation of amino acids on alcohol metabolism. The amino acid augmentation is based on the fasting plasma profile theory (1–4).

From past work on the metabolic effects of such diets, it was found that they produce a significant decrease in serum cholesterol in rats (5) and humans (6). This observed effect was theorized to be the result of an increase in net protein utilization.

While conducting the present study, we discovered that dietary supplementation of limiting amino acids to the third level (L-lysine, L-tryptophan, and L-threonine), based on the fasting plasma profile theory, produces a significant decrease in serum blood urea nitrogen.

Twenty male Sprague–Dawley rats, 250–275 g, were randomly divided into two groups of 10 each. Following a 2-week acclimation period during which both groups were fed a standard animal diet[1], the first group was fed a diet supplemented to the third level of limiting amino acid (Table I) for 2 additional weeks while the second group was maintained on the standard diet for the same period.

On the 15th day, blood collected by orbital sinus puncture was centrifuged, and the serum was retained. Blood urea nitrogen was measured colorimetrically by means of a standard kit[2].

The serum blood urea nitrogen for the treatment group was 8.45 ± 0.36 mg/100 ml (mean ± *SEM*) while that of the control group was 15.1 ± 0.49 mg/100 ml. A Student *t* test showed a significant difference to the $p < 0.01$ level.

It is theorized that the observed effects are caused by an increase in net protein utilization when the limiting amino acids are supplemented, based on the fasting plasma profile theory, and that this increase reduces the amount of underutilized amino acids that are otherwise available for energy metabolism or storage. The end result is a decrease in the amount of nitrogenous metabolic products (wastes) in serum.

[1] Purina Laboratory Chow.
[2] Sigma Chemical Co., St. Louis, MO 63178.

**Table I—Amino Acid-Supplemented Animal Feed to the Third Level of Limiting Amino Acid**

| Ingredient | Amount, % |
|---|---|
| L-Tryptophan | 0.309 |
| L-Threonine | 0.341 |
| L-Lysine | 1.667 |
| Standard feed | 97.683 |

This type of dietary supplementation can be of invaluable assistance to those who must reduce their blood urea nitrogen levels (dialysis patients, nephrotic patients, *etc.*).

The major advantage of the augmentation of the body's amino acids based on the fasting plasma profile theory is that it removes a lot of guesswork and establishes a hard mathematical formula for preparing the diet.

(1) C. I. Jarowski, A. V. Puccini, M. Winitz, and M. C. Otey, *Agr. Biol. Chem.*, **35**, 1007 (1971).
(2) C. I. Jarowski, *ibid.*, **38**, 479 (1974).
(3) C. I. Jarowski and R. Pytelewski, *J. Pharm. Sci.*, **64**, 690 (1975).
(4) P. K. Raja and C. I. Jarowski, *ibid.*, **64**, 695 (1975).
(5) C. I. Jarowski and R. Pytelewski, *ibid.*, **64**, 690 (1975).
(6) P. K. Raja and C. I. Jarowski, *ibid.*, **64**, 694 (1975).

*Gregory M. Torre* ˣ
*Vincent D. Lynch*
*Charles I. Jarowski*
College of Pharmacy and
Allied Health Professions
St. John's University
Jamaica, NY 11435

Received June 23, 1980.
Accepted for publication October 2, 1980.

## Effect of Variation of Plasma Oleic Acid Concentration on Relative Concentration of Free and Protein Bound Warfarin

**Keyphrases** □ Warfarin—effect of plasma oleic acid concentration on free and protein bound warfarin concentration, protein binding, humans □ Protein binding—binding of warfarin to human serum albumin, effect of plasma oleic acid concentration on free and bound warfarin concentration □ Oleic acid—effect of concentration on free and protein bound warfarin concentration, humans

*To the Editor:*

Although the normal serum concentrations of free fatty acids are between 0.3 and 0.9 mmole/liter (1), pathological conditions such as diabetes, reduced renal function, cardiac infarction, and bacterial disease (2–12) can cause substantial increases in free fatty acid levels. In some cases, these levels can exceed 5 mmoles/liter. Moreover, the increasingly widespread use of intravenous fat emulsions probably is associated with significant variation in the serum concentrations of free fatty acids.

Schwartz *et al.* (13) recently demonstrated that variation in the concentration of oleic acid, a major component in the free fatty acids found in serum, can cause significant variations in the protein binding of salicylate. Similar findings concerning the effect of variation in free fatty acid concentrations on the protein binding of drugs were published previously (14–17).



*0022-3549/81/0100-0114$01.00/0*
*© 1981, American Pharmaceutical Association*

(1977).
(5) W. Schmidt and E. Jähnchen, *Experientia*, **34**, 1323 (1978).

*H. Yamada* ˣ
*T. Ichihashi*
*K. Hirano*
*H. Kinoshita*
Shionogi Research Laboratories
Shionogi & Co., Ltd.
Fukushima-ku, Osaka 533, Japan

Received May 5, 1980.
Accepted for publication September 25, 1980.

## Lowering Blood Urea Nitrogen with Amino Acid Supplementation

**Keyphrases** □ Amino acids—dietary supplementation, effects on blood urea nitrogen, rats □ Colorimetry—analysis of blood urea nitrogen in rat serum, effects of dietary supplementation of amino acids □ Dietary supplements—amino acids, effects on blood urea nitrogen in rats

*To the Editor:*

Currently we are studying the effect of dietary supplementation of amino acids on alcohol metabolism. The amino acid augmentation is based on the fasting plasma profile theory (1–4).

From past work on the metabolic effects of such diets, it was found that they produce a significant decrease in serum cholesterol in rats (5) and humans (6). This observed effect was theorized to be the result of an increase in net protein utilization.

While conducting the present study, we discovered that dietary supplementation of limiting amino acids to the third level (L-lysine, L-tryptophan, and L-threonine), based on the fasting plasma profile theory, produces a significant decrease in serum blood urea nitrogen.

Twenty male Sprague–Dawley rats, 250–275 g, were randomly divided into two groups of 10 each. Following a 2-week acclimation period during which both groups were fed a standard animal diet[1], the first group was fed a diet supplemented to the third level of limiting amino acid (Table I) for 2 additional weeks while the second group was maintained on the standard diet for the same period.

On the 15th day, blood collected by orbital sinus puncture was centrifuged, and the serum was retained. Blood urea nitrogen was measured colorimetrically by means of a standard kit[2].

The serum blood urea nitrogen for the treatment group was 8.45 ± 0.36 mg/100 ml (mean ± *SEM*) while that of the control group was 15.1 ± 0.49 mg/100 ml. A Student *t* test showed a significant difference to the $p < 0.01$ level.

It is theorized that the observed effects are caused by an increase in net protein utilization when the limiting amino acids are supplemented, based on the fasting plasma profile theory, and that this increase reduces the amount of underutilized amino acids that are otherwise available for energy metabolism or storage. The end result is a decrease in the amount of nitrogenous metabolic products (wastes) in serum.

[1] Purina Laboratory Chow.
[2] Sigma Chemical Co., St. Louis, MO 63178.

**Table I—Amino Acid-Supplemented Animal Feed to the Third Level of Limiting Amino Acid**

| Ingredient | Amount, % |
|---|---|
| L-Tryptophan | 0.309 |
| L-Threonine | 0.341 |
| L-Lysine | 1.667 |
| Standard feed | 97.683 |

This type of dietary supplementation can be of invaluable assistance to those who must reduce their blood urea nitrogen levels (dialysis patients, nephrotic patients, *etc.*).

The major advantage of the augmentation of the body's amino acids based on the fasting plasma profile theory is that it removes a lot of guesswork and establishes a hard mathematical formula for preparing the diet.

(1) C. I. Jarowski, A. V. Puccini, M. Winitz, and M. C. Otey, *Agr. Biol. Chem.*, **35**, 1007 (1971).
(2) C. I. Jarowski, *ibid.*, **38**, 479 (1974).
(3) C. I. Jarowski and R. Pytelewski, *J. Pharm. Sci.*, **64**, 690 (1975).
(4) P. K. Raja and C. I. Jarowski, *ibid.*, **64**, 695 (1975).
(5) C. I. Jarowski and R. Pytelewski, *ibid.*, **64**, 690 (1975).
(6) P. K. Raja and C. I. Jarowski, *ibid.*, **64**, 694 (1975).

*Gregory M. Torre* ˣ
*Vincent D. Lynch*
*Charles I. Jarowski*
College of Pharmacy and
Allied Health Professions
St. John's University
Jamaica, NY 11435

Received June 23, 1980.
Accepted for publication October 2, 1980.

## Effect of Variation of Plasma Oleic Acid Concentration on Relative Concentration of Free and Protein Bound Warfarin

**Keyphrases** □ Warfarin—effect of plasma oleic acid concentration on free and protein bound warfarin concentration, protein binding, humans □ Protein binding—binding of warfarin to human serum albumin, effect of plasma oleic acid concentration on free and bound warfarin concentration □ Oleic acid—effect of concentration on free and protein bound warfarin concentration, humans

*To the Editor:*

Although the normal serum concentrations of free fatty acids are between 0.3 and 0.9 mmole/liter (1), pathological conditions such as diabetes, reduced renal function, cardiac infarction, and bacterial disease (2–12) can cause substantial increases in free fatty acid levels. In some cases, these levels can exceed 5 mmoles/liter. Moreover, the increasingly widespread use of intravenous fat emulsions probably is associated with significant variation in the serum concentrations of free fatty acids.

Schwartz *et al.* (13) recently demonstrated that variation in the concentration of oleic acid, a major component in the free fatty acids found in serum, can cause significant variations in the protein binding of salicylate. Similar findings concerning the effect of variation in free fatty acid concentrations on the protein binding of drugs were published previously (14–17).



*0022-3549/81/0100-0114$01.00/0*
*© 1981, American Pharmaceutical Association*

**Table I—Scatchard Protein Binding Parameters for Warfarin in the Presence and Absence of Linoleic, Palmitic, and Oleic Acids**

| Fatty Acid Concentration, mmoles/liter | Number of Drug Molecules Bound at Binding Sites 1 | 2 | Association Constants[a] at Binding Sites 1 | 2 |
|---|---|---|---|---|
| 0[b] | 1.95 (0.42) | 6.6 (1.6) | 7.94 (3.57) | 402 (134) |
| 0 | 2 | 7 | 6.56 (2.2) | 376 (53) |
| Linoleic acid, 2.0 | 2 | 7 | 2.54 (1.5) | 171 (61) |
| Palmitic acid, 2.0 | 2 | 7 | 0.79 (0.5) | 116 (30) |
| Oleic acid | | | | |
| 0.5 | 2 | 7 | 5.26 (0.2) | 258 (18) |
| 1.0 | 2 | 7 | 3.61 (0.4) | 214 (9) |
| 1.5 | 2 | 7 | 2.88 (0.3) | 177 (6) |
| 2.0 | 2 | 7 | 1.04 (0.2) | 115 (13) |

[a] $1\ M \times 10^{-4}$. [b] Unconstrained values; all other values reported are constrained. Values in parentheses are standard deviations.

**Table II—Estimated Percentage of Nonprotein Bound Warfarin for Serum Containing a Total Warfarin Concentration of 10 μg/liter**

| Oleic Acid Concentration, mmoles/liter | Estimated Percentage of Nonprotein Bound Warfarin |
|---|---|
| 0.0 | 1.2 |
| 0.5 | 1.6 |
| 1.0 | 2.2 |
| 1.5 | 3.0 |
| 2.0 | 7.3 |

The present paper reports the effect of variation in oleic acid concentrations on the protein binding of warfarin by human serum albumin. Warfarin was selected because it has a low therapeutic ratio for which individual patient titration is recommended (18).

The binding of warfarin[1] by human serum albumin in the presence of oleic acid concentrations of 0–2.0 mmoles/liter at pH 7.4 was examined at 37° using the continuous ultrafiltration method described previously (13). Warfarin concentrations were determined by UV spectroscopy at 308 nm. Raw experimental data were interpreted using the "constrained" Scatchard model (13).

Table I lists the Scatchard parameters for warfarin binding by human serum albumin in the presence and absence of linoleic, palmitic, and oleic acids. (The constrained values are those obtained when the maximum number of molecules bound at the different sites is restricted to integral values.) All three fatty acids caused a significant reduction in both Scatchard association constants; increasing the oleic acid concentration progressively reduced the values of the constants.

The clinical implications of the data shown in Table I are appreciated more readily from Table II in which the percentage of unbound warfarin (estimated using the results in Table I) is shown when the total serum concentration of warfarin is 10 μg/liter. The percentage of free, nonprotein bound warfarin increases almost sevenfold when the oleic acid concentration is increased from 0 to 2.0 mmoles/liter. Since there is good reason to believe that the intensity of pharmacological response is primarily a simple function of the free unbound warfarin serum concentration, these results are of considerable potential therapeutic relevance. Changes in the pathological status of patients, who have been carefully titrated for optimal warfarin therapy, are likely to result in substantial hazard if such changes are associated with variation in free fatty acid serum concentrations. Thus, patients being treated with warfarin should be retitrated whenever free fatty acid levels have changed significantly.

[1] Warfarin sodium racemic mixture, Endo Laboratories.


(1) "Fundamentals of Clinical Chemistry" N. W. Tietz, Ed., Saunders, Philadelphia, Pa., 1976.

(2) B. Persson, *Acta Med. Scand.*, **193**, 457 (1973).

(3) M. S. Losowsky and D. H. Kenward, *J. Lab. Clin. Med.*, **71**, 736 (1968).

(4) W. V. Reimoid, R. Kattermann, and E. Quellhorst, *Arch. Klin. Med.*, **216**, 384 (1969).

(5) J. C. Daubresse, G. Lerson, G. Rorive, A. S. Luyckx, and P. J. Lefebvre, *Eur. J. Clin. Invest.*, **6**, 159 (1976).

(6) A. Novarini, U. Zuliani, L. Bandini, S. Caronna, A. Montanari, and P. Perinotto, *ibid.*, **6**, 473 (1976).

(7) I. Odar-Cederlof and O. Borga, *ibid.*, **10**, 403 (1976).

(8) J. A. Moorehouse, J. Steinberg, and N. J. Rosen, *J. Clin. Endocrinol. Metab.*, **23**, 1080 (1963).

(9) P. Paul and W. L. Holmes, *Lipids*, **8**, 142 (1973).

(10) C. E. Rich, E. L. Bierman, and I. L. Schwartz, *J. Clin. Invest.*, **38**, 275 (1959).

(11) V. A. Kurien and M. F. Oliver, *Lancet*, **1**, 122 (1966).

(12) J. I. Gallin, D. Kaye, and W. M. O'Leary, *N. Engl. J. Med.*, **281**, 1081 (1969).

(13) P. A. Schwartz, D. S. Greene, and C. T. Rhodes, *J. Pharm. Sci.*, **69**, 1345 (1980).

(14) D. Rudman, T. J. Bixler, and A. E. Delrio, *J. Pharmacol. Exp. Ther.*, **176**, 261 (1971).

(15) R. Gugler, D. W. Shoeman, and D. L. Azarnoff, *Pharmacology*, **12**, 160 (1974).

(16) G. Wilding, R. C. Feldhoff, and E. S. Vesell, *Biochem. Pharmacol.*, **26**, 1143 (1977).

(17) P. D. Dawkins, J. N. McArthur, and M. J. H. Smith, *J. Pharm. Pharmacol.*, **22**, 405 (1969).

(18) "United States Pharmacopeia Dispensing Information," United States Pharmacopeial Convention, Rockville, Md., 1980.



*Peter A. Schwartz*

Brigham's & Women's Hospital
Boston, MA 02115

*Douglas S. Greene*
*C. T. Rhodes* ˣ

Department of Pharmacy
University of Rhode Island
Kingston, RI 02881



Received September 8, 1980.
Accepted for publication October 21, 1980.

## REVIEWS

**Pharmaceutical Microbiology, 2nd Ed.** Edited by W. B. HUGO and A. D. RUSSELL. Blackwell Scientific Publications. Osney Mead, Oxford OX2 0EL, England. 1980. 352 pp. 15 × 23 cm. Price $26.75 (soft cover).

The editors of this book state that: "Pharmaceutical microbiology may be defined as that part of microbiology which has a special bearing on pharmacy in all its aspects." "As this book is aimed at undergraduate pharmacy students (as well as microbiologists entering the pharmaceutical industry) we were under constraint to limit the length of the book to retain it in a defined price range."

The 21 British authors are from universities and medical schools (11 contributors), industry (nine), and government laboratories (one). The book is divided into four parts: Biology of Microorganisms, Antimicrobial Agents, Microbiological Aspects of Pharmaceutical Processing, and The Future.

In Part I, bacteria, molds and yeasts, and viruses are treated in brief chapters with sufficient detail for the purpose of this book.

Part II constitutes one-half of the book and considers the manufacture of antibiotics and immunological products, the evaluation and properties of antibiotics, disinfectants, antiseptics, and preservatives, and quality control of immunological products.

The ecology of bacteria in an industrial environment, the theory and practice of sterilization, spoilage of pharmaceutical products, and sterility testing are discussed in Part III.

Part IV is a one-page review of the outstanding problems in the fields covered in the book. Most of the references are to British journals.

The brief account of microbiological assays for antibiotic substances is a decade or two out of date with regard to both theory and practice. The nonexistent second edition of "Analytical Microbiology" was given as a reference instead of the correct citation of Volume two.

In addition to its intended audience, the book is recommended to those in the pharmaceutical industry who need a brief introduction to a very broad subject. It enables administrators to learn what their scientists have done and are or should be doing. This book is a handy general reference to the multitudinous aspects of microorganisms and antibacterial agents and their interactions. It could be as useful to those outside the pharmaceutical industry as to those inside.

*Reviewed by* Frederick Kavanagh
*829 36th St., N.W.*
*Corvallis, OR 97330*

**Concepts in Drug Metabolism, Part A.** Edited by PETER JENNER and BERNARD TESTA. (Drugs and Pharmaceutical Sciences, Vol. 10.) Dekker, 270 Madison Ave., New York, NY 10016. 1980. 409 pp. 15 × 23 cm. Price $49.50.

"Concepts in Drug Metabolism," in two multiauthored parts, presents a wide ranging collection of essays on major topics in drug metabolism and allied fields which reflect the viewpoints held by the experts in the field.

The contents of Part A are divided into seven chapters which deal with the following topics: the significance of analytical techniques in drug metabolism studies; a structural approach to selectivity in drug metabolism and disposition; mechanisms of oxidative functionalization reactions; conjugation reactions; the role of extrahepatic metabolism in drug disposition and toxicity; developmental implications; and the use of metabolite data in the evaluation of pharmacokinetics and drug action. Because each chapter was written by a different author, some overlap between the contributions has occurred. According to the editors, the authors were requested to present the reader with a wide ranging and conceptual approach to each topic. As a consequence, the chapters tend to reflect the personalities and views of the authors. The reader will find that some chapters are quite philosophical in their approach, while other chapters make use of large bodies of factual information to illustrate the underlying concepts.

"Concepts in Drug Metabolism" complements well Volume 4 of the Drugs and Pharmaceutical Sciences series, which was entitled "Drug Metabolism: Chemical and Biochemical Aspects" (1976) and was written by Testa and Jenner. Graduate students and researchers in drug metabolism in the fields of pharmacology, medicinal chemistry, toxicology, and biochemistry will find the book to be a valuable guide as well as an important source of new ideas. There are several drawbacks. With few exceptions, Part A represents a review of the literature prior to 1978. The book was published in 1980 and represents a gap of 2 years in the literature. Furthermore, although the two-volume set, in combination with the earlier book by Testa and Jenner, would make an excellent text for a graduate-level course in drug metabolism, the cost of the books tends to be prohibitive.

Part A presents an authoritative overview of vital topics and developments in drug metabolism and related areas and is highly recommended.

*Reviewed by* Sidney J. Stohs
*Department of Biomedicinal Chemistry*
*College of Pharmacy*
*University of Nebraska Medical Center*
*Omaha, NE 68105*

**Iatrogenic Diseases, 2nd Ed.** By P. F. D'ARCY and J. P. GRIFFIN. Oxford University Press, 200 Madison Ave., New York, NY 10016. 1980. 546 pp. 18 × 24 cm. Price $67.50.

The first edition of this text appeared in 1972. Other than Moser's "Diseases of Medical Progress" and "Drug Induced Diseases" by Meyler and Peck, published in 1972, there are no comprehensive books that cover adverse reactions from the perspective of this text. The book contains 26 chapters and two appendixes. The chapters are arranged by body system or site (*i.e.*, skin disease, blood dyscrasias, renal disease, and disorders of the eye).

There is a chapter on teratogenic and other possibly harmful effects of drugs in pregnancy, a chapter on drugs excreted in the breast milk, and a table of drug interactions.

The introductory chapters provide concise and informative overviews of the monitoring and epidemiology of adverse drug reactions. All major adverse reaction surveillance programs are described, and the major outcomes are highlighted. Types of reporting are categorized in an interesting and useful manner (*e.g.*, drug-oriented monitoring, disease-oriented monitoring, complication-oriented monitoring, monitoring children, and monitoring geriatrics). A well-designed tabulation provides the reader with virtually all of the studies of adverse reactions in hospitalized patients from 1964 through 1977. A nicely worded and concise description of various factors (*e.g.*, sex, age, genetics, and disease states) that may adversely affect patient responses to drugs is presented.

Each chapter is written in a crisp, authoritative, and comprehensive manner. Useful details on the pathophysiology of many drug-induced adverse reactions are presented in a logical and succinct manner. Each chapter is well referenced, apparently up through some portion of 1978.

The index is extensive, providing the reader with cross-referencing to adverse effects by drug, specific adverse effects, and broad general categories. One disadvantage to many American readers is the lack of cross-referencing of British drug names. For example, pethidine, paracetamol, rifampicin, and sulphafurazole are not cross-referenced to their U.S. counterparts (meperidine, acetaminophen, rifampin, and sulfisoxazole, respectively).

The reader will not find this book to be an encyclopedic review of adverse reactions, such as is afforded by Meyler and Herxheimer in their unexcelled offering, "Side Effects of Drugs." However, its unique approach and crisp style make it an invaluable addition to the bookshelf of the practitioner. It fills a void not covered by any other reference book of current vintage.

*Reviewed by* Fred J. Salter
*School of Pharmacy*
*Medical College of Virginia*
*Virginia Commonwealth University*
*Richmond, VA 23298*

## REVIEWS

**Pharmaceutical Microbiology, 2nd Ed.** Edited by W. B. HUGO and A. D. RUSSELL. Blackwell Scientific Publications. Osney Mead, Oxford OX2 0EL, England. 1980. 352 pp. 15 × 23 cm. Price $26.75 (soft cover).

The editors of this book state that: "Pharmaceutical microbiology may be defined as that part of microbiology which has a special bearing on pharmacy in all its aspects." "As this book is aimed at undergraduate pharmacy students (as well as microbiologists entering the pharmaceutical industry) we were under constraint to limit the length of the book to retain it in a defined price range."

The 21 British authors are from universities and medical schools (11 contributors), industry (nine), and government laboratories (one). The book is divided into four parts: Biology of Microorganisms, Antimicrobial Agents, Microbiological Aspects of Pharmaceutical Processing, and The Future.

In Part I, bacteria, molds and yeasts, and viruses are treated in brief chapters with sufficient detail for the purpose of this book.

Part II constitutes one-half of the book and considers the manufacture of antibiotics and immunological products, the evaluation and properties of antibiotics, disinfectants, antiseptics, and preservatives, and quality control of immunological products.

The ecology of bacteria in an industrial environment, the theory and practice of sterilization, spoilage of pharmaceutical products, and sterility testing are discussed in Part III.

Part IV is a one-page review of the outstanding problems in the fields covered in the book. Most of the references are to British journals.

The brief account of microbiological assays for antibiotic substances is a decade or two out of date with regard to both theory and practice. The nonexistent second edition of "Analytical Microbiology" was given as a reference instead of the correct citation of Volume two.

In addition to its intended audience, the book is recommended to those in the pharmaceutical industry who need a brief introduction to a very broad subject. It enables administrators to learn what their scientists have done and are or should be doing. This book is a handy general reference to the multitudinous aspects of microorganisms and antibacterial agents and their interactions. It could be as useful to those outside the pharmaceutical industry as to those inside.

*Reviewed by* Frederick Kavanagh
*829 36th St., N.W.*
*Corvallis, OR 97330*

**Concepts in Drug Metabolism, Part A.** Edited by PETER JENNER and BERNARD TESTA. (Drugs and Pharmaceutical Sciences, Vol. 10.) Dekker, 270 Madison Ave., New York, NY 10016. 1980. 409 pp. 15 × 23 cm. Price $49.50.

"Concepts in Drug Metabolism," in two multiauthored parts, presents a wide ranging collection of essays on major topics in drug metabolism and allied fields which reflect the viewpoints held by the experts in the field.

The contents of Part A are divided into seven chapters which deal with the following topics: the significance of analytical techniques in drug metabolism studies; a structural approach to selectivity in drug metabolism and disposition; mechanisms of oxidative functionalization reactions; conjugation reactions; the role of extrahepatic metabolism in drug disposition and toxicity; developmental implications; and the use of metabolite data in the evaluation of pharmacokinetics and drug action. Because each chapter was written by a different author, some overlap between the contributions has occurred. According to the editors, the authors were requested to present the reader with a wide ranging and conceptual approach to each topic. As a consequence, the chapters tend to reflect the personalities and views of the authors. The reader will find that some chapters are quite philosophical in their approach, while other chapters make use of large bodies of factual information to illustrate the underlying concepts.

"Concepts in Drug Metabolism" complements well Volume 4 of the Drugs and Pharmaceutical Sciences series, which was entitled "Drug Metabolism: Chemical and Biochemical Aspects" (1976) and was written by Testa and Jenner. Graduate students and researchers in drug metabolism in the fields of pharmacology, medicinal chemistry, toxicology, and biochemistry will find the book to be a valuable guide as well as an important source of new ideas. There are several drawbacks. With few exceptions, Part A represents a review of the literature prior to 1978. The book was published in 1980 and represents a gap of 2 years in the literature. Furthermore, although the two-volume set, in combination with the earlier book by Testa and Jenner, would make an excellent text for a graduate-level course in drug metabolism, the cost of the books tends to be prohibitive.

Part A presents an authoritative overview of vital topics and developments in drug metabolism and related areas and is highly recommended.

*Reviewed by* Sidney J. Stohs
*Department of Biomedicinal Chemistry*
*College of Pharmacy*
*University of Nebraska Medical Center*
*Omaha, NE 68105*

**Iatrogenic Diseases, 2nd Ed.** By P. F. D'ARCY and J. P. GRIFFIN. Oxford University Press, 200 Madison Ave., New York, NY 10016. 1980. 546 pp. 18 × 24 cm. Price $67.50.

The first edition of this text appeared in 1972. Other than Moser's "Diseases of Medical Progress" and "Drug Induced Diseases" by Meyler and Peck, published in 1972, there are no comprehensive books that cover adverse reactions from the perspective of this text. The book contains 26 chapters and two appendixes. The chapters are arranged by body system or site (*i.e.*, skin disease, blood dyscrasias, renal disease, and disorders of the eye).

There is a chapter on teratogenic and other possibly harmful effects of drugs in pregnancy, a chapter on drugs excreted in the breast milk, and a table of drug interactions.

The introductory chapters provide concise and informative overviews of the monitoring and epidemiology of adverse drug reactions. All major adverse reaction surveillance programs are described, and the major outcomes are highlighted. Types of reporting are categorized in an interesting and useful manner (*e.g.*, drug-oriented monitoring, disease-oriented monitoring, complication-oriented monitoring, monitoring children, and monitoring geriatrics). A well-designed tabulation provides the reader with virtually all of the studies of adverse reactions in hospitalized patients from 1964 through 1977. A nicely worded and concise description of various factors (*e.g.*, sex, age, genetics, and disease states) that may adversely affect patient responses to drugs is presented.

Each chapter is written in a crisp, authoritative, and comprehensive manner. Useful details on the pathophysiology of many drug-induced adverse reactions are presented in a logical and succinct manner. Each chapter is well referenced, apparently up through some portion of 1978.

The index is extensive, providing the reader with cross-referencing to adverse effects by drug, specific adverse effects, and broad general categories. One disadvantage to many American readers is the lack of cross-referencing of British drug names. For example, pethidine, paracetamol, rifampicin, and sulphafurazole are not cross-referenced to their U.S. counterparts (meperidine, acetaminophen, rifampin, and sulfisoxazole, respectively).

The reader will not find this book to be an encyclopedic review of adverse reactions, such as is afforded by Meyler and Herxheimer in their unexcelled offering, "Side Effects of Drugs." However, its unique approach and crisp style make it an invaluable addition to the bookshelf of the practitioner. It fills a void not covered by any other reference book of current vintage.

*Reviewed by* Fred J. Salter
*School of Pharmacy*
*Medical College of Virginia*
*Virginia Commonwealth University*
*Richmond, VA 23298*

## REVIEWS

**Pharmaceutical Microbiology, 2nd Ed.** Edited by W. B. HUGO and A. D. RUSSELL. Blackwell Scientific Publications. Osney Mead, Oxford OX2 0EL, England. 1980. 352 pp. 15 × 23 cm. Price $26.75 (soft cover).

The editors of this book state that: "Pharmaceutical microbiology may be defined as that part of microbiology which has a special bearing on pharmacy in all its aspects." "As this book is aimed at undergraduate pharmacy students (as well as microbiologists entering the pharmaceutical industry) we were under constraint to limit the length of the book to retain it in a defined price range."

The 21 British authors are from universities and medical schools (11 contributors), industry (nine), and government laboratories (one). The book is divided into four parts: Biology of Microorganisms, Antimicrobial Agents, Microbiological Aspects of Pharmaceutical Processing, and The Future.

In Part I, bacteria, molds and yeasts, and viruses are treated in brief chapters with sufficient detail for the purpose of this book.

Part II constitutes one-half of the book and considers the manufacture of antibiotics and immunological products, the evaluation and properties of antibiotics, disinfectants, antiseptics, and preservatives, and quality control of immunological products.

The ecology of bacteria in an industrial environment, the theory and practice of sterilization, spoilage of pharmaceutical products, and sterility testing are discussed in Part III.

Part IV is a one-page review of the outstanding problems in the fields covered in the book. Most of the references are to British journals.

The brief account of microbiological assays for antibiotic substances is a decade or two out of date with regard to both theory and practice. The nonexistent second edition of "Analytical Microbiology" was given as a reference instead of the correct citation of Volume two.

In addition to its intended audience, the book is recommended to those in the pharmaceutical industry who need a brief introduction to a very broad subject. It enables administrators to learn what their scientists have done and are or should be doing. This book is a handy general reference to the multitudinous aspects of microorganisms and antibacterial agents and their interactions. It could be as useful to those outside the pharmaceutical industry as to those inside.

*Reviewed by* Frederick Kavanagh
*829 36th St., N.W.*
*Corvallis, OR 97330*

**Concepts in Drug Metabolism, Part A.** Edited by PETER JENNER and BERNARD TESTA. (Drugs and Pharmaceutical Sciences, Vol. 10.) Dekker, 270 Madison Ave., New York, NY 10016. 1980. 409 pp. 15 × 23 cm. Price $49.50.

"Concepts in Drug Metabolism," in two multiauthored parts, presents a wide ranging collection of essays on major topics in drug metabolism and allied fields which reflect the viewpoints held by the experts in the field.

The contents of Part A are divided into seven chapters which deal with the following topics: the significance of analytical techniques in drug metabolism studies; a structural approach to selectivity in drug metabolism and disposition; mechanisms of oxidative functionalization reactions; conjugation reactions; the role of extrahepatic metabolism in drug disposition and toxicity; developmental implications; and the use of metabolite data in the evaluation of pharmacokinetics and drug action. Because each chapter was written by a different author, some overlap between the contributions has occurred. According to the editors, the authors were requested to present the reader with a wide ranging and conceptual approach to each topic. As a consequence, the chapters tend to reflect the personalities and views of the authors. The reader will find that some chapters are quite philosophical in their approach, while other chapters make use of large bodies of factual information to illustrate the underlying concepts.

"Concepts in Drug Metabolism" complements well Volume 4 of the Drugs and Pharmaceutical Sciences series, which was entitled "Drug Metabolism: Chemical and Biochemical Aspects" (1976) and was written by Testa and Jenner. Graduate students and researchers in drug metabolism in the fields of pharmacology, medicinal chemistry, toxicology, and biochemistry will find the book to be a valuable guide as well as an important source of new ideas. There are several drawbacks. With few exceptions, Part A represents a review of the literature prior to 1978. The book was published in 1980 and represents a gap of 2 years in the literature. Furthermore, although the two-volume set, in combination with the earlier book by Testa and Jenner, would make an excellent text for a graduate-level course in drug metabolism, the cost of the books tends to be prohibitive.

Part A presents an authoritative overview of vital topics and developments in drug metabolism and related areas and is highly recommended.

*Reviewed by* Sidney J. Stohs
*Department of Biomedicinal Chemistry*
*College of Pharmacy*
*University of Nebraska Medical Center*
*Omaha, NE 68105*

**Iatrogenic Diseases, 2nd Ed.** By P. F. D'ARCY and J. P. GRIFFIN. Oxford University Press, 200 Madison Ave., New York, NY 10016. 1980. 546 pp. 18 × 24 cm. Price $67.50.

The first edition of this text appeared in 1972. Other than Moser's "Diseases of Medical Progress" and "Drug Induced Diseases" by Meyler and Peck, published in 1972, there are no comprehensive books that cover adverse reactions from the perspective of this text. The book contains 26 chapters and two appendixes. The chapters are arranged by body system or site (*i.e.*, skin disease, blood dyscrasias, renal disease, and disorders of the eye).

There is a chapter on teratogenic and other possibly harmful effects of drugs in pregnancy, a chapter on drugs excreted in the breast milk, and a table of drug interactions.

The introductory chapters provide concise and informative overviews of the monitoring and epidemiology of adverse drug reactions. All major adverse reaction surveillance programs are described, and the major outcomes are highlighted. Types of reporting are categorized in an interesting and useful manner (*e.g.*, drug-oriented monitoring, disease-oriented monitoring, complication-oriented monitoring, monitoring children, and monitoring geriatrics). A well-designed tabulation provides the reader with virtually all of the studies of adverse reactions in hospitalized patients from 1964 through 1977. A nicely worded and concise description of various factors (*e.g.*, sex, age, genetics, and disease states) that may adversely affect patient responses to drugs is presented.

Each chapter is written in a crisp, authoritative, and comprehensive manner. Useful details on the pathophysiology of many drug-induced adverse reactions are presented in a logical and succinct manner. Each chapter is well referenced, apparently up through some portion of 1978.

The index is extensive, providing the reader with cross-referencing to adverse effects by drug, specific adverse effects, and broad general categories. One disadvantage to many American readers is the lack of cross-referencing of British drug names. For example, pethidine, paracetamol, rifampicin, and sulphafurazole are not cross-referenced to their U.S. counterparts (meperidine, acetaminophen, rifampin, and sulfisoxazole, respectively).

The reader will not find this book to be an encyclopedic review of adverse reactions, such as is afforded by Meyler and Herxheimer in their unexcelled offering, "Side Effects of Drugs." However, its unique approach and crisp style make it an invaluable addition to the bookshelf of the practitioner. It fills a void not covered by any other reference book of current vintage.

*Reviewed by* Fred J. Salter
*School of Pharmacy*
*Medical College of Virginia*
*Virginia Commonwealth University*
*Richmond, VA 23298*

A publication of the
American Pharmaceutical Association—
the National Professional Society
of Pharmacists

# JOURNAL OF PHARMACEUTICAL SCIENCES

## INDEX TO AUTHORS
## INDEX TO SUBJECTS

VOLUME 70
JANUARY TO DECEMBER, 1981

*Published monthly under the supervision of the Board of Trustees*

MARY H. FERGUSON
*Editor*

NANCY E. BROWN
*Production Editor*

JOHN PATRICK EVANS
*Copy Editor*

MICHAEL K. HAYES
*Copy Editor*

EDWARD G. FELDMANN
*Contributing Editor*

SAMUEL W. GOLDSTEIN
*Contributing Editor*

BELLE R. BECK
*Editorial Secretary*

EDWARD G. FELDMANN
*Acting Director of Publications*

EDITORIAL ADVISORY BOARD

John Autian
Norman R. Farnsworth
William J. Jusko
Herbert A. Lieberman
David E. Mann, Jr.
Ian W. Mathison
Gerald J. Papariello
Edward G. Rippie

JOURNAL OF PHARMACEUTICAL SCIENCES

FEBRUARY 1981
VOLUME 70 NUMBER 2

RESEARCH ARTICLES

# Evaluation of Methods for Producing Renal Dysfunction in Rats

KATHLEEN M. GIACOMINI, STEPHEN M. ROBERTS, and GERHARD LEVY ˣ

Received July 3, 1980, from the *Department of Pharmaceutics, School of Pharmacy, State University of New York at Buffalo, Amherst, NY 14260.* Accepted for publication July 28, 1980.

**Abstract** □ The following methods for producing renal dysfunction in rats were compared: single-step 5/6th nephrectomy, two-step 5/6th nephrectomy, bilateral ureteral ligation, and uranyl nitrate injection. Control groups consisted of single- and two-step sham-operated animals and animals that received an injection of normal saline solution. The methods were evaluated on the basis of the following criteria, which were assessed daily for 6 days: survival, body weight, hematocrit, serum creatinine concentration, serum urea nitrogen concentration, serum glutamic pyruvic transaminase activity, serum albumin concentration, and serum protein binding of salicylate (determined every other day). Animals with bilateral ureteral ligation survived only 2 days, and single-step 5/6th nephrectomy caused a high incidence of fatalities. Some of the methods were associated with the development of hypoalbuminemia, but no significant elevation of transaminase activity occurred. Serum protein binding of salicylate was reduced in rats with renal dysfunction. A strong positive correlation between the creatinine and urea nitrogen concentrations in the serum of animals with renal dysfunction ($r = 0.91$, $p < 0.001$) and a negative correlation between the serum albumin concentration and salicylate free fraction ($r = -0.71$, $p < 0.001$) were found. Uranyl nitrate injection has the advantages of technical simplicity, a high survival rate (no deaths in this study), and relatively consistent and sustained diminution of renal function (as reflected by serum creatinine and urea nitrogen concentrations).

**Keyphrases** □ Renal dysfunction—evaluation of methods for producing renal dysfunction □ Uranyl nitrate injection—evaluation for producing renal dysfunction

Renal dysfunction can have pronounced effects on the pharmacokinetic and pharmacodynamic characteristics of drugs (1). Because exploration of these effects in patients may be limited by ethical and practical considerations, it often becomes necessary to perform studies on animals with experimental renal dysfunction (2, 3). Several methods are available for producing renal failure or dysfunction in experimental animals (2, 4–10); they include the administration of various nephrotoxic agents (such as dichromate, uranyl nitrate, certain pigments, mercurials, and glycerol), temporary occlusion of the renal artery or intrarenal infusion of vasoconstrictors, ureteral ligation, and partial nephrectomy.

Since sequence and relative importance of the pathophysiological components of acute renal failure in patients are not clearly defined (2), it is difficult to determine which experimental method for producing renal failure in animals yields results that are most representative of the clinical condition. However, a number of practical considerations should influence the choice of the method for producing renal failure or dysfunction in experimental animals for pharmacokinetic investigations. These considerations include the time, effort, and skill required to carry out the procedure, the stability and reproducibility of renal functional impairment, the general condition and survival time of the animals, the target organ specificity of the method, changes in the hematocrit and serum albumin concentration, and changes in the serum protein binding of certain drugs (which occur clinically and are important for pharmacokinetic studies).

The purpose of this investigation was to compare and evaluate several surgical methods and one chemical method for producing renal dysfunction in rats, namely, bilateral ureteral ligation, single-step 5/6th nephrectomy, two-step 5/6th nephrectomy, and uranyl nitrate injection. Uranyl nitrate was selected because it is not a known hepatotoxin. The development of renal dysfunction was determined by daily measurement of the serum creatinine and urea nitrogen concentrations, and the correlation between these concentrations was examined. Serum glutamic pyruvic transaminase activity was measured as an index of hepatocellular damage. Hematocrit and serum albumin concentrations were monitored because these values are known to decrease in some clinical cases of renal failure (11, 12). Finally, the serum free fraction of salicylic acid was determined because the protein binding of this

0022-3549/81/0200-0117$01.00/0
© 1981, American Pharmaceutical Association

**Table I—Survival of Rats with Renal Dysfunction Induced by Various Methods [a]**

| Method | Posttreatment Day 0 | 1 | 2 | 3 | 4 | 5 | 6 |
|---|---|---|---|---|---|---|---|
| Bilateral ureteral ligation | 6/6 | 6/6 | 5/6 | 0/6 | 0/6 | 0/6 | 0/6 |
| Single-step 5/6th nephrectomy | 6/6 | 5/6 | 3/6 | 3/6 | 3/6 | 2/6 | 2/6 |
| Single-step sham-operated controls | 6/6 | 6/6 | 6/6 | 5/6 | 5/6 | 5/6 | 5/6 |
| Two-step 5/6th nephrectomy | 8/8 | 8/8 | 6/8 | 6/8 | 6/8 | 6/8 | 6/8 |
| Two-step sham-operated controls | 6/6 | 6/6 | 6/6 | 6/6 | 6/6 | 6/6 | 6/6 |
| Uranyl nitrate injection | 6/6 | 6/6 | 6/6 | 6/6 | 6/6 | 6/6 | 6/6 |
| Saline-injected controls | 4/4 | 4/4 | 4/4 | 4/4 | 4/4 | 4/4 | 4/4 |

[a] Values are given as the number of survivors remaining/original number of animals.

**Table II—Body Weight (Grams) of Rats with Experimental Renal Dysfunction and of Their Controls**

| Method | Posttreatment Day 0 | 1 | 2 | 3 | 4 | 5 | 6 |
|---|---|---|---|---|---|---|---|
| Bilateral ureteral ligation | 248 ± 21[a] (6) | 260 ± 18 (6) | 251 ± 24 (5) | — | — | — | — |
| Single-step 5/6th nephrectomy | 232 ± 19 (6) | 234 ± 21 (5) | 219 ± 12 (3) | 223 ± 16 (3) | 220 ± 23 (3) | 230, 237 (2) | 228, 238 (2) |
| Single-step sham-operated controls | 238 ± 11 (6) | 258 ± 13 (5) | 264 ± 13 (6) | 264 ± 12 (5) | 264 ± 17 (5) | 268 ± 11 (5) | 273 ± 17 (5) |
| Two-step 5/6th nephrectomy | 319 ± 18 (8) | 324 ± 17 (8) | 316 ± 16 (6) | 316 ± 25 (6) | 317 ± 31 (6) | 318 ± 27 (6) | 318 ± 30 (6) |
| Two-step sham-operated controls | 333 ± 22 (6) | 356 ± 21 (6) | 353 ± 25 (6) | 354 ± 21 (6) | 350 ± 23 (6) | 349 ± 23 (6) | 351 ± 23 (6) |
| Uranyl nitrate injection | 204 ± 16 (6) | 211 ± 8 (6) | 214 ± 15 (6) | 228 ± 16 (6) | 230 ± 16 (6) | 234 ± 14 (6) | 237 ± 15 (6) |
| Saline-injected controls | 222 ± 17 (4) | 242 ± 18 (4) | 241 ± 19 (4) | 246 ± 16 (4) | 250 ± 17 (4) | 266 ± 22 (4) | 265 ± 17 (4) |

[a] Mean ± *SD*; the number of animals is given in parentheses.

**Table III—Hematocrit (Percent) of Rats with Experimental Renal Dysfunction and of Their Controls**

| Method | Posttreatment Day 0 | 1 | 2 | 3 | 4 | 5 | 6 |
|---|---|---|---|---|---|---|---|
| Bilateral ureteral ligation | 46 ± 1[a] (6) | 46 ± 5 (6) | 44 ± 6 (5) | — | — | — | — |
| Single-step 5/6th nephrectomy | 44 ± 2 (6) | NM[b] | 37, 40 (2) | 40 ± 6 (3) | 38 ± 6 (3) | 33, 37 (2) | 32, 31 (2) |
| Single-step sham-operated controls | 44 ± 2 (5) | 46 ± 2 (4) | 42 ± 4 (6) | 36 ± 2 (5) | 35 ± 2 (5) | 35 ± 1 (5) | 34 ± 2 (5) |
| Two-step 5/6th nephrectomy | 49 ± 1 (8) | 43 ± 4 (7) | 39 ± 4 (6) | 40 ± 6 (6) | 34 ± 3 (6) | 32 ± 3 (5) | 31 ± 3 (6) |
| Two-step sham operated controls | 49 ± 2 (6) | 48 ± 2 (6) | 46 ± 2 (6) | 41 ± 1 (6) | 40 ± 1 (6) | 38 ± 1 (6) | 37 ± 1 (6) |
| Uranyl nitrate injection | 45 ± 2 (6) | 53 ± 5 (5) | 46 ± 2 (6) | 36 ± 2 (6) | 36 ± 3 (6) | 31 ± 2 (6) | 32 ± 5 (6) |
| Saline-injected controls | 44 ± 2 (4) | 50 ± 1 (4) | 45 ± 1 (4) | 37 ± 5 (4) | 36 ± 2 (4) | 32 ± 2 (4) | 36 ± 2 (4) |

[a] Mean ± *SD*; the number of animals is given in parentheses. [b] Not measured.

drug, like that of many other acidic drugs, is decreased in patients with impaired renal function (13, 14).

## EXPERIMENTAL

Male Sprague–Dawley rats, 175–400 g, were fasted overnight before treatment. Food and water were allowed *ad libitum* thereafter.

Single-step 5/6th nephrectomy was performed on six rats in the following manner. A midline incision extending from the umbilicus to just below the sternum was made under ether anesthesia. The left kidney was isolated and dissected free of the surrounding tissues. A ligature (heavy silk) was placed tightly around the upper and lower poles of the kidney so that the organ was sectioned into thirds. Care was taken not to include the ureter in the lower ligature. The upper and lower poles then were excised. If necessary, a small square of Gel Foam[1] was used to stop bleeding. The right kidney was isolated and freed by blunt dissection from the surrounding tissues. A ligature (heavy silk) was placed around the renal vessels including the ureter, the renal artery, and vein. The entire kidney then was removed. The abdomen was closed with two layers of sutures.

Two-step 5/6th nephrectomy was performed on eight animals. The procedure was identical to the preceding one except that two steps were involved. The first step, which consisted of the complete removal of the right kidney, was performed 2 weeks before the second step to allow the remaining kidney to hypertrophy. Then two-thirds of the remaining kidney was removed as described for the single-step 5/6th nephrectomy.

Bilateral ureteral ligation was performed on six animals by isolating the ureters, placing two ligatures tightly around each ureter, and cutting between the ligatures.

Uranyl nitrate, 5 mg/kg, was administered once intravenously as a 5-mg/ml solution *via* a tail vein to six rats.

There were three control groups. One group of six animals was sham operated on the same day as the bilateral ureteral-ligated rats and the single-step 5/6th-nephrectomized rats and served as the control group for both of these groups. A second group of six animals underwent two sham operations 2 weeks apart on the days of surgery of the two-step nephrectomized rats and served as their controls. A third group of four control rats was given saline solution, 1 ml/kg iv *via* a tail vein, and served as the control group for the uranyl nitrate-treated rats.

After induction of renal failure, injection of saline, or sham operation, 1 ml of blood was taken from the tail artery of each rat on Days 1, 3, and 5 and 3 ml of blood was taken on Days 0 (prior to induction of renal failure), 2, 4, and 6. Blood was taken after the second step of the procedure from the two-step nephrectomized rats and their controls. The serum was separated immediately and stored in the frozen state pending analysis. About 50–100 μl of serum from each rat was set aside daily before freezing for the determination of serum creatinine concentrations. In addition, the rats were weighed daily and the hematocrit was recorded.

Serum creatinine concentrations were measured by the Jaffe (15) reaction, and serum urea nitrogen concentrations were measured by the method of Crocker (16), both using a commercial kit[2]. Transaminase activity was determined by the enzymatic method of Wroblewski and La Due (17) with a commercial kit[3]. Total protein concentrations were measured by the method of Gornall *et al.* (18), using rat albumin as a standard. The albumin fraction was determined by serum protein electrophoresis[4], and the albumin concentration was calculated by multiplying the fraction of albumin by the total protein concentration.

[1] The Upjohn Co., Kalamazoo, Mich.

[2] Rapid-Stat, Pierce Biochemical, Rockford, Ill.

[3] Calbiochem, La Jolla, Calif.

[4] Gelman electrophoresis system, Gelman Instrument Co., Ann Arbor, Mich.

**Table IV—Serum Creatinine Concentrations (Milligrams per 100 ml) in Rats with Experimental Renal Dysfunction and in Their Controls**

| Method | Posttreatment Day | | | | | | |
|---|---|---|---|---|---|---|---|
| | 0 | 1 | 2 | 3 | 4 | 5 | 6 |
| Bilateral ureteral ligation | 1.22 ± 0.40[a] (6) | 5.78 ± 0.47 (6) | 9.33 ± 1.01 (5) | — | — | — | — |
| Single-step 5/6th nephrectomy | 0.99 ± 0.14 (6) | NM[b] | 2.68 ± 0.77 (3) | 2.83 ± 1.59 (3) | 5.03 ± 5.41 (3) | 1.18, 1.54 (2) | 1.56, 2.62 (2) |
| Single-step sham-operated controls | 1.02 ± 0.16 (6) | 1.19 ± 0.19 (5) | 0.89 ± 0.21 (6) | 1.19 ± 0.21 (5) | 1.09 ± 0.42 (5) | 0.90 ± 0.23 (5) | 0.97 ± 0.25 (5) |
| Two-step 5/6th nephrectomy | 1.11 ± 0.36 (8) | 3.05 ± 1.08 (7) | 2.91 ± 1.52 (6) | 2.81 ± 1.67 (6) | 2.29 ± 0.88 (6) | 1.81 ± 0.19 (5) | 1.95 ± 0.62 (6) |
| Two-step sham-operated controls | 0.94 ± 0.32 (6) | 1.07 ± 0.15 (6) | 0.97 ± 0.25 (6) | 1.14 ± 0.07 (6) | 1.04 ± 0.17 (6) | 0.92 ± 0.11 (6) | 0.99 ± 0.17 (6) |
| Uranyl nitrate injection | 1.08 ± 0.31 (6) | 1.48 ± 0.53 (6) | 1.78 ± 0.34 (6) | 2.25 ± 0.20 (6) | 3.26 ± 0.57 (6) | 4.00 ± 1.01 (6) | 6.84 ± 1.49 (6) |
| Saline-injected controls | 1.30 ± 0.20 (4) | 1.47 ± 0.27 (4) | 0.65 ± 0.16 (4) | 1.00 ± 0.38 (4) | 1.28 ± 0.34 (4) | 1.04 ± 0.28 (4) | 1.16 ± 0.32 (4) |

[a] Mean ± *SD*; the number of animals is given in parentheses. [b] Not measured.

**Table V—Serum Urea Nitrogen Concentrations (Milligrams per 100 ml) in Rats with Experimental Renal Dysfunction and in Their Controls**

| Method | Posttreatment Day | | | | | | |
|---|---|---|---|---|---|---|---|
| | 0 | 1 | 2 | 3 | 4 | 5 | 6 |
| Bilateral ureteral ligation | 10.8 ± 1.9[a] (6) | 149 ± 9.0 (6) | 254 ± 21.0 (5) | — | — | — | — |
| Single-step 5/6 nephrectomy | 11.4 ± 2.7 (6) | NM[b] | 57.4 ± 31.6 (3) | 46.8 ± 27.1 (3) | NM[b] | 20.3, 28.0 (2) | 32.0, 31.0 (2) |
| Single-step sham-operated controls | 9.8 ± 2.3 (6) | 15.3 ± 2.7 (5) | 12.2 ± 4.0 (6) | 8.6 ± 2.1 (5) | 16.1 ± 2.5 (5) | 9.8 ± 1.7 (5) | 9.9 ± 1.5 (5) |
| Two-step 5/6 nephrectomy | 16.1 ± 6.8 (8) | 102 ± 56 (7) | 85.5 ± 60.0 (6) | 72.0 ± 54.9 (6) | 59.6 ± 50.6 (5) | 31.4 ± 5.7 (5) | 44.0 ± 22.4 (6) |
| Two-step sham-operated controls | 10.7 ± 4.2 (6) | 13.8 ± 2.8 (6) | 17.3 ± 3.0 (6) | 17.4 ± 2.3 (6) | 14.4 ± 1.9 (6) | 14.0 ± 2.4 (6) | 13.7 ± 1.7 (6) |
| Uranyl nitrate injection | 12.1 ± 1.7 (6) | 45.0 ± 22.0 (6) | 28.7 ± 4.7 (6) | 30.4 ± 6.6 (6) | 47.6 ± 9.5 (6) | 78.2 ± 12.6 (6) | 175 ± 24 (6) |
| Saline-injected controls | 10.4 ± 1.6 (4) | 21.7 ± 2.7 (4) | 17.5 ± 2.7 (4) | 11.3 ± 1.8 (4) | 10.8 ± 1.8 (4) | 9.2 ± 1.1 (4) | 5.7 ± 1.8 (4) |

[a] Mean ± *SD*; the number of animals is given in parentheses. [b] Not measured.

The serum protein binding of salicylic acid was determined by equilibrium dialysis at 37° in plexiglass cells separated by a cellophane[5] membrane on serum samples obtained from the rats on Days 0, 2, 4, and 6. Approximately 0.5 ml of serum was dialyzed for 4 hr against an equal volume of 0.13 *M* isotonic phosphate buffer (pH 7.4) containing 300 μg of salicylic acid/ml. The salicylic acid concentration in the buffer and serum phases was assayed by the method of Brodie *et al.* (19).

## RESULTS

Animals with ligated ureters looked and acted very ill and died by the 3rd day. There was a high incidence of death following single-step 5/6th nephrectomy and a lower incidence after the two-step procedure. The uranyl nitrate-treated animals and all but one control rat survived throughout the study (Table I). Animals with renal dysfunction showed less of a gain in body weight than the controls over the 6-day study (Table II). The hematocrit decreased with time in all animals, probably due mainly to repeated blood sampling (Table III).

Serum creatinine concentrations remained stable at ~1 mg/100 ml in all control groups and increased appreciably in all animals subjected to renal injury (Table IV). The most pronounced effect occurred after ureteral ligation. Animals with particularly elevated serum creatinine concentrations after partial nephrectomy tended to expire; this fact partially accounts for the declining average creatinine concentrations in these groups on Days 5 and 6. Uranyl nitrate-treated rats exhibited a gradual and relatively consistent increase of serum creatinine concentrations with time, except for a sudden, more substantial increase from Day 5 to Day 6 (Table IV). The same tendencies were observed with respect to serum urea nitrogen concentrations, including an abrupt increase from Day 5 to Day 6 in the uranyl nitrate-treated animals (Table V). There was a strong positive correlation between the serum creatinine and urea nitrogen concentrations in the rats with renal dysfunction (Fig. 1).

Serum glutamic pyruvic transaminase activity did not increase above normal levels in any of the animals. In fact, the rats with bilateral ureteral ligation (*i.e.*, the only animals that were unable to produce urine) exhibited a remarkable decrease of transaminase activity (Table VI).

Serum albumin concentrations decreased appreciably after bilateral ureteral ligation and partial nephrectomy but did not change remarkably after uranyl nitrate injection (Table VII). Serum protein binding of sal-

[5] Average pore size of 24 Å, VWR Scientific Co., Rochester, N.Y.

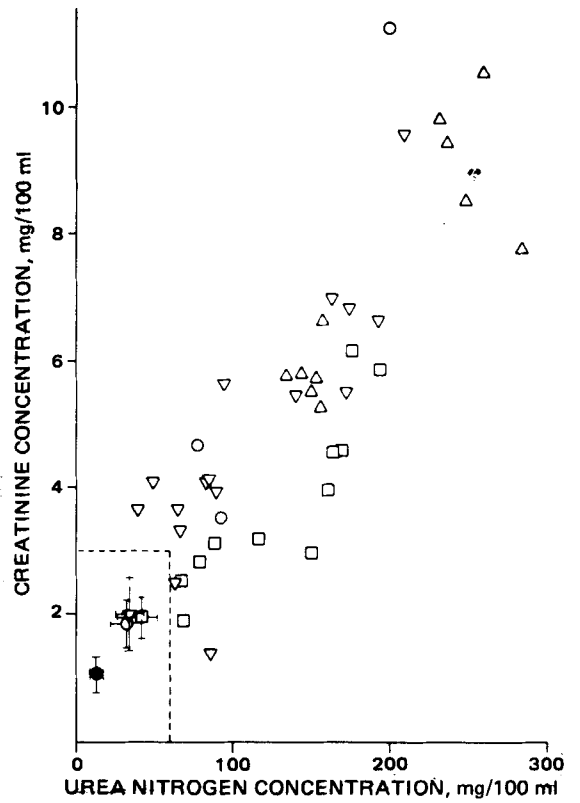


**Figure 1**—*Relationship between serum creatinine and serum urea nitrogen concentrations in rats with experimental renal dysfunction. Key:* ○, *single-step 5/6th nephrectomy;* □, *two-step 5/6th nephrectomy;* △, *bilateral ureteral ligation;* ▽, *uranyl nitrate injection; and* ●, *data from control animals (sham operated or saline injected) and from all other rats before surgery or injection of nephrotoxin. Data within the rectangle are the mean ± SD values for nine (○), 20 (□), and 20 (▽) determinations, respectively. The correlation coefficient for all except the control values is 0.913,* $p < 0.001$, $n = 90$.

**Table VI—Serum Glutamic Pyruvic Transaminase Activity (Milliunits per Milliliter) in Rats with Experimental Renal Dysfunction and in Their Controls**

| Method | Posttreatment Day | | | | | | |
|---|---|---|---|---|---|---|---|
| | 0 | 1 | 2 | 3 | 4 | 5 | 6 |
| Bilateral ureteral ligation | 13.4 ± 2.4[a] (6) | 5.8 ± 3.2 (6) | 1.0 ± 2.3 (5) | — | — | — | — |
| Single-step 5/6 nephrectomy | 17.9 ± 5.0 (6) | NM[b] | 18.5 ± 7.2 (3) | 10.6 ± 2.6 (3) | 20.6 ± 1.8 (3) | 15.4, 27.8 (2) | 9.3, 24.7 (2) |
| Single-step sham-operated controls | 16.8 ± 2.2 (6) | 18.5 ± 1.6 (5) | 21.3 ± 4.7 (6) | 15.8 ± 2.2 (5) | 15.6 ± 3.2 (5) | 16.3 ± 2.6 (5) | 17.1 ± 2.7 (5) |
| Two-step 5/6 nephrectomy | 14.6 ± 4.2 (8) | 10.7 ± 3.8 (7) | 10.3 ± 2.5 (6) | 12.5 ± 3.6 (6) | 16.5 ± 6.1 (6) | 20.6 ± 4.4 (5) | 23.8 ± 4.2 (6) |
| Two-step sham-operated controls | 11.5 ± 2.2 (6) | 17.4 ± 3.6 (6) | 23.9 ± 2.6 (6) | 23.2 ± 4.6 (6) | 23.3 ± 11.8 (6) | 23.5 ± 4.7 (6) | 26.0 ± 5.9 (6) |
| Uranyl nitrate injection | 11.3 ± 1.1 (5) | 11.2 ± 2.4 (6) | 17.8 ± 1.1 (6) | 17.0 ± 2.3 (6) | 21.6 ± 1.8 (6) | 20.8 ± 6.1 (6) | 10.8 ± 4.9 (6) |
| Saline-injected controls | 12.9 ± 1.3 (4) | 12.1 ± 1.8 (4) | 22.2 ± 3.0 (4) | 15.2 ± 3.7 (4) | 14.2 ± 3.6 (4) | 17.2 ± 2.5 (4) | 15.7 ± 2.1 (4) |

[a] Mean ± *SD*; the number of animals is given in parentheses. [b] Not measured.

**Table VII—Serum Albumin Concentrations (Grams per 100 ml) in Rats with Experimental Renal Dysfunction and in Their Controls**

| Method | Posttreatment Day | | | | | | |
|---|---|---|---|---|---|---|---|
| | 0 | 1 | 2 | 3 | 4 | 5 | 6 |
| Bilateral ureteral ligation | 3.96 ± 0.30[a] (6) | 2.73 ± 0.50 (5) | 2.58 ± 0.42 (5) | — | — | — | — |
| Single-step 5/6 nephrectomy | 3.92 ± 0.23 (5) | NM[b] | 2.41 ± 0.28 (3) | 2.44 ± 0.32 (3) | NM[b] | 3.13, 2.31 (2) | 2.98, 2.02 (2) |
| Single-step sham-operated controls | 3.78 ± 0.41 (6) | 3.75 ± 0.40 (5) | 3.61 ± 0.47 (6) | 3.50 ± 0.37 (5) | 3.58 ± 0.42 (5) | 3.51 ± 0.34 (5) | 3.72 ± 0.34 (5) |
| Two-step 5/6 nephrectomy | 5.11 ± 0.49 (8) | 2.54 ± 0.64 (7) | 2.46 ± 0.53 (6) | 2.51 ± 0.43 (6) | 2.57 ± 0.72 (6) | 2.72 ± 0.53 (5) | 2.87 ± 0.58 (6) |
| Two-step sham-operated controls | 4.31 ± 0.31 (6) | 3.53 ± 0.29 (6) | 3.34 ± 0.22 (6) | 3.30 ± 0.45 (6) | 3.26 ± 0.41 (6) | 3.35 ± 0.24 (6) | 3.51 ± 0.24 (6) |
| Uranyl nitrate injection | 3.99 ± 0.39 (6) | 4.41 ± 0.20 (6) | 3.94 ± 0.14 (6) | 3.52 ± 0.24 (6) | 3.49 ± 0.11 (4) | 3.28 ± 0.37 (6) | 3.46 ± 0.22 (5) |
| Saline-injected controls | 4.10 ± 0.19 (4) | 4.55 ± 0.33 (4) | 4.79, 4.13 (2) | 4.17 ± 0.17 (4) | 4.40 ± 0.094 (4) | 3.91 ± 0.18 (4) | 4.02 ± 0.21 (4) |

[a] Mean ± *SD*; the number of animals is given in parentheses. [b] Not measured.

**Table VIII—Serum Free Fraction (× 100) of Salicylic Acid in Rats with Experimental Renal Dysfunction and in Their Controls**

| Method | Posttreatment Day | | | |
|---|---|---|---|---|
| | 0 | 2 | 4 | 6 |
| Bilateral ureteral ligation | 34.6 ± 1.2[a] (6) | 55.3 (1) | — | — |
| Single-step 5/6 nephrectomy | 34.5 ± 5.3 (6) | 55.6 ± 16.1 (3) | 34.1 (1) | 41.5, 27.5 (2) |
| Single-step sham-operated controls | 35.2 ± 2.8 (6) | 36.3 ± 4.2 (5) | 32.8 ± 5.0 (5) | 33.6 ± 2.8 (5) |
| Two-step 5/6 nephrectomy | 32.1 ± 3.4 (5) | 51.9 ± 11.0 (5) | 59.1 ± 12.4 (6) | 52.3 ± 8.8 (5) |
| Two-step sham-operated controls | 43.8 ± 6.1 (5) | 40.4 ± 4.0 (4) | 39.4 ± 6.7 (5) | 43.2 ± 6.7 (5) |
| Uranyl nitrate injection | 33.3 ± 2.8 (6) | 33.0 ± 6.1 (5) | 43.1 ± 6.0 (6) | 47.4 ± 4.6 (6) |
| Saline-injected controls | 29.2 ± 5.5 (4) | 24.0 ± 1.9 (4) | 23.8 ± 1.8 (4) | 25.0 ± 3.6 (4) |

[a] Mean ± *SD*; the number of animals is given in parentheses.

icylic acid decreased after renal injury (Table VIII). There was a significant negative correlation between salicylic acid free fraction values and the albumin concentration in the serum, with no discernible distinction as a function of the method employed to produce renal dysfunction (Fig. 2). Weak but statistically significant positive correlations were found between salicylic acid free fractions and serum urea nitrogen concentrations ($r = 0.534$, $p < 0.001$, $n = 118$) and between salicylic acid free fractions and serum creatinine concentrations ($r = 0.477$, $p < 0.001$, $n = 121$).

## DISCUSSION

Of the methods studied, uranyl nitrate injection was the simplest for producing renal dysfunction. The method produced a significant and sustained elevation of serum creatinine and urea nitrogen concentrations and, as also found in patients, a decrease in the serum protein binding of salicylic acid. All animals survived for the duration of the study (6 days) and appeared to be in good condition. The surgical methods were more time consuming and slightly more difficult; ureteral ligation was more easily performed than partial nephrectomy. High mortality is a distinct disadvantage of the ureteral ligation and single-step 5/6th nephrectomy methods; two-step nephrectomy was associated with better survival, but the degree of renal functional impairment was more variable than after uranyl nitrate injection.

Uranyl nitrate causes necrosis of the distal portion of the proximal renal tubules. This effect is seen 4 days after injection (20). The results of this study show that renal function begins to decrease within 1 day after uranyl nitrate injection but that pronounced effects become evident on Days 5 and 6 (Tables IV and V). Decreased glomerular permeability also has been reported (21). Uranyl nitrate administration to rats has no significant effect on the cytochrome P-450 concentration and aniline hydroxylase activity in the liver but decreases hepatic aminopyrine *N*-demethylase activity (22). However, the latter also occurs after ureteral ligation and, therefore, is not a specific effect of uranyl nitrate (22). This study showed normal serum glutamic pyruvic transaminase activity after

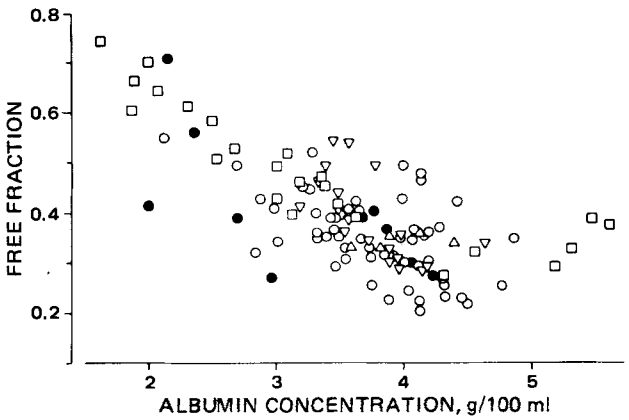


**Figure 2**—*Relationship between the free fraction of salicylic acid and the albumin concentration in the serum of rats with experimental renal dysfunction. Key: ●, single-step 5/6th nephrectomy; □, two-step 5/6th nephrectomy; △, bilateral ureteral ligation; ▽, uranyl nitrate injection; and ○, control animals. The correlation coefficient is −0.710, p < 0.001, with 113 determinations on 42 rats. This plot contains the free fraction data summdrized in Table VIII and some additional data obtained on days other than those listed in Table VIII.*

uranyl nitrate injection, indicating that there was no gross hepatocellular damage. We have no definitive explanation for the unusual decline of transaminase activity in rats with bilateral ureteral ligation; increased catabolism of the enzyme, decreased binding to serum constituents and consequent redistribution, and assay interference due to endogenous substances in these totally anuric animals may be involved[6]. Other investigators found decreased serum alkaline phosphatase activity in rats after administration of a nephrotoxic dose of cephaloridine and speculated that this result may be due to increased catabolism of the enzyme (23).

Creatinine as well as urea nitrogen concentrations in serum and renal clearances are commonly used indexes of renal function. It has been reported that "blood urea nitrogen results followed a curve virtually identical to that of the serum creatinine" in rats with transient elevation of serum creatinine concentrations associated with gentamicin-induced nephrotoxicity (24). A linear relationship between serum urea and creatinine concentrations was observed in rabbits with renal impairment induced by uranyl nitrate (25). A similar correlation was found in the present study, suggesting that experimental renal functional impairment in rats and rabbits can be assessed by measuring either creatinine or urea nitrogen. However, creatinine and urea serum concentrations or renal clearances are not always interchangeable or alternative indexes of renal function under clinical conditions since urea, but not creatinine, is partially reabsorbed from the renal tubules (26, 27). Serum concentrations of creatinine are affected by the age-dependent synthesis rate of the compound, while those of urea nitrogen may be affected by dietary protein intake. Serum urea was found to be superior to serum creatinine in the degree of the relationship to renal digoxin clearance in patients on digoxin therapy (27).

## REFERENCES


(1) J. Fabre and L. Balant, *Clin. Pharmacokinet.*, **1**, 99 (1976).

(2) N. G. Levinsky, *N. Engl. J. Med.*, **296**, 1453 (1977).

(3) S. M. Roberts and G. Levy, *J. Pharm. Sci.*, **69**, 363 (1980).

(4) W. Flamenbaum, R. J. Hamburger, M. L. Huddleston, J. Kaufman, J. S. McNeil, J. H. Schwartz, and R. Nagle, *Kidney Int.*, **10**, S-115 (1976).

(5) D. E. Oken, *Prog. Biochem. Pharmacol.*, **7**, 219 (1972).

(6) W. Flamenbaum, M. L. Huddleston, J. S. McNeil, and R. J. Hamburger, *Kidney Int.*, **6**, 408 (1974).

(7) E. E. Selkurt, *Am. J. Physiol.*, **205**, 286 (1963).

(8) R. Platt, M. H. Roscoe, and F. W. Smith, *Clin. Sci.*, **11**, 217 (1952).

(9) R. P. Fischer, E. T. Peter, and J. F. Mullane, *Arch. Surg.*, **109**, 409 (1974).

(10) H. C. Stoerk, J. H. Laragh, R. M. Aceto, and T. Budzilovich, *Am. J. Pathol.*, **58**, 51 (1970).

(11) S. B. Grossman, S. H. Yap, and D. A. Shafritz, *J. Clin. Invest.*, **59**, 869 (1977).

(12) K. M. Giacomini, T. P. Gibson, and G. Levy, *Clin. Pharmacol. Ther.*, **27**, 508 (1980).

(13) D. T. Lowenthal, W. A. Briggs, and G. Levy, *J. Clin. Invest.*, **54**, 1221 (1974).

(14) G. Levy, T. Baliah, and J. A. Procknal, *Clin. Pharmacol. Ther.*, **20**, 512 (1976).

(15) M. Jaffe, *Z. Physiol. Chem.*, **10**, 391 (1886).

(16) C. L. Crocker, *Am. J. Med. Technol.*, **33**, 361 (1963).

(17) F. Wroblewski and J. S. LaDue, *Proc. Soc. Exp. Biol. Med.*, **91**, 569 (1956).

(18) A. G. Gornall, C. J. Bardawill, and M. M. David, *J. Biol. Chem.*, **177**, 751 (1949).

(19) B. B. Brodie, S. Udenfriend, and A. F. Coburn, *J. Pharmacol. Exp. Ther.*, **80**, 114 (1944).

(20) F. A. Carone and W. G. Spector, *J. Pathol. Bacteriol.*, **80**, 55 (1960).

(21) R. C. Blantz and K. Konnen, *J. Clin. Invest.*, **55**, 621 (1975).

(22) A. P. VanPeer and F. M. Belpaire, *Arch. Int. Pharmacodyn. Ther.*, **228**, 180 (1977).

(23) E. O. Ngaha and D. T. Plummer, *Biochem. Med.*, **18**, 71 (1977).

(24) D. N. Gilbert, D. C. Houghton, W. M. Bennett, C. E. Plamp, K. Reger, and G. A. Porter, *Proc. Soc. Exp. Biol. Med.*, **160**, 99 (1979).

(25) M. J. Garcia, A. A. Dominguez-Gil, M. Cepeda, and A. Dominguez-Gil, *Int. J. Pharm.*, **5**, 117 (1980).

(26) D. B. Morgan, M. E. Carver, and R. B. Payne, *Br. Med. J.*, **2**, 929 (1977).

(27) H. Halkin, L. B. Sheiner, C. C. Peck, and K. L. Melmon, *Clin. Pharmacol. Ther.*, **17**, 385 (1975).


[6] Assay interference is unlikely since measurement of transaminase activity in mixtures of serum from normal rats and from rats with bilateral ureteral ligation yielded results consistent with the measured transaminase activity of the component serum samples and their volume ratio in the mixture.

## ACKNOWLEDGMENTS


Supported in part by Grant GM 20852 and by a postdoctoral fellowship (GM 06774 to S. M. Roberts) from the National Institute of General Medical Sciences, National Institutes of Health.

# Physicochemical Characteristics of Patent Blue Violet Dye

DAVID W. NEWTON *x, PHILIP J. BREEN, DAVID E. BROWN ‡, JOSEPH F. MACKIE, Jr., and RONALD B. KLUZA §

Received April 3, 1980, from the *Department of Pharmaceutics, Massachusetts College of Pharmacy and Allied Health Sciences, Boston, MA 02115.* Accepted for publication July 16, 1980. *Present address: Department of Pharmaceutics, College of Pharmacy, University of Nebraska Medical Center, Omaha, NE 68105. ‡Present address: Pharmacy Department, Lynn Hospital, Lynn, MA 01904. §Present address: Department of Pharmaceutics, College of Pharmacy, University of Arkansas for Medical Sciences, Little Rock, AR 72201.

**Abstract** □ Physicochemical data for patent blue violet dye (I) are reported. The pKa for protonation of the first diethylanilino group was 2.78 ± 0.03. The absorptivity values calculated for a 1% (w/v) solution of previously dried I at pH 7.4 were 1650, 170, and 250 at 638, 412, and 309 nm, respectively. A table of wavelength maxima and observed solution color as a function of pH and $H_o$ and five spectra of I at certain pH and $H_o$ values are included. The solution chemistry of I is explained, and a scheme showing its two protonated carbonium ions and its triphenylcarbinol derivative is presented. The distribution coefficients of I in *n*-octanol or chloroform and pH 7.4 phosphate buffer systems were 0.013 and 0.12, respectively. The approximate solubilities at 25° of I in six organic solvents and the solubility analysis of I in distilled water are reported. Results of the latter analysis suggest that I forms a lyotropic mesophase in high aqueous concentrations. Compound I is poorly lipid soluble. Samples of 1.000% I in 0.9% NaCl, formulated with and without 1% (v/v) benzyl alcohol and autoclaving, varied not more than 5% from the initial I content during storage in the dark and under constant fluorescent light at 25 ± 5° for 20 months. Data from the TLC of I in several eluents indicated a high degree of purity of the dye. The half-lives for the loss of color in $5 \times 10^{-4}$% I solutions in potassium hydroxide solutions of pH 13.7, 12.7, 11.3, and 10.0 were 1.2 hr, 17.0 hr, 9.5 days, and 180 days, respectively. The fraction of I bound to 4% (w/v) human serum albumin at 37° and pH 7.4 ranged from 0.05 to 0.83, corresponding to unbound I in the postdialysis concentration range of $1.7 \times 10^{-4}$ to 2.0% (w/v). A Scatchard plot of the albumin binding data of I revealed one high-affinity binding site, $K = 6235\ M^{-1}$, and five low-affinity sites, with average affinity constants of $33\ M^{-1}$. The data support the fact that the spectrophotometric determination of I at 639 ± 2 nm appears to comprise a stability-indicating assay.

**Keyphrases** □ Patent blue violet—physicochemical characteristics □ Dyes—patent blue violet, physicochemical characteristics

Patent blue violet (I) is the monosodium salt of a disulfonated triphenylmethane vital stain, which is used to delineate the patency of lymph vessels in the dorsum of the hands or feet prior to injection of an iodinized contrast medium and subsequent lymphangiography (1–3). Certain injectable formulation and nomenclature[1] problems (1), as well as some structural formula and purity discrepancies of I, have been reviewed (4).

The purpose of this study was to determine values for several physicochemical characteristics of I that pertain to its pharmaceutical analysis and unique clinical use. The concentration of I used for most research studies and all injectable solutions prepared under the investigational new drug application for administration to humans was limited to 1% (w/v) or less because higher concentrations were reported (5–8) to produce sarcomas in rodents at the sites of repeated subcutaneous injections. The usual human dose of I injected subcutaneously to assist in visualizing lymph vessels is 2–3 ml of a 1% solution normally prepared in 0.9% NaCl.

[1] Synonyms for I (as the 2,4-disulfonate) include patent blue V, blue VRS, alphazurine 2G, sulfan blue, and acid blue 1.

## EXPERIMENTAL

**Materials**—Purified patent blue violet[2] was used as received unless otherwise specified. Human serum albumin[3] and sterile water for irrigation[4] were used as received, and other reagents and solvents were analytical grade.

**Procedures**—Spectral data and the pKa titration were obtained[5] in $5 \times 10^{-4}$% solutions of I[6]. Chloroacetic acid (0.01 *M*), adjusted to the appropriate pH with 0.50 *N* NaOH or HCl, was used for samples in the pKa studies, and dilutions of 1.00 *N* KOH or $H_2SO_4$ (ACS reagent) in distilled water were used for other spectral studies. The pKa was calculated (9) using the absorbance values of I solutions determined at 638 nm:

$$\text{pKa} = \text{pH} + \log [(A_0 - A)/(A - A_+)] \qquad \text{(Eq. 1)}$$

where $A_0$ is the absorbance of the nonprotonated species[7], $A_+$ is the absorbance of the protonated species[8], and $A$ represents the absorbance values of the I solutions adjusted to pH values in the range of approximate pKa ± 1 unit.

Loss on drying was determined by placing three accurately weighed samples of ~0.5 g of I into tared glass containers with ground-glass caps unaffixed, heating at 135° for 3 hr, tightly placing the caps on the containers, allowing the samples to cool to ambient temperature in a desiccator, and determining the weight until it was constant at ±0.5 mg.

Distribution coefficients were determined with triplicate samples of $5 \times 10^{-4}$ and $5.0 \times 10^{-3}$% solutions of I in 0.1 *M* phosphate buffer (pH 7.40) previously saturated with *n*-octanol or chloroform. A 7.0-ml portion of aqueous I was transferred to a 15-ml glass tube, 7.0 ml of either *n*-octanol or chloroform saturated previously with the phosphate buffer was added, a polyethylene-lined screw cap was tightly affixed, and the tube was rotated at 45 rpm for 15 min at 25 ± 0.5° in a water bath in a bottle apparatus similar to that described previously (10). The samples were allowed to stand at 25° until phase separation occurred. The absorbance of the aqueous layer or an appropriate dilution thereof was determined at 638 nm, the concentrations of I in both phases were computed, and the lipid–aqueous distribution ratio was calculated.

The approximate solubilities of I in certain organic solvents were determined in triplicate by combining accurately weighed samples of I, ~1.5 g with 95% ethanol and 0.1 g with other solvents, with a specific volume of solvent, 5.0 ml of 95% ethanol and 50.0 ml of chloroform, ether, ethyl acetate, hexane, and toluene, in a glass tube of appropriate size. The mouths of the tubes were covered with aluminum foil, polyethylene-lined screw caps were tightly affixed, and the samples were rotated for 24 hr at 45 rpm and 25° in the bottle apparatus. The samples were filtered through a 0.45-μm membrane[9], and 1.0 ml of the 95% ethanol solution and 25.0 ml of the other solutions were evaporated and dried to constant weight in a tared dish. The weights of the solute residues then were determined to the nearest 0.1 mg.

The equilibrium phase solubility analysis of I in water for irrigation[4] was conducted as follows. Accurately weighed samples of I ranging from

[2] Product P-1888 FD, lot 4-1-1, monosodium salt, dark-green luminous powder, dye content of ~85%, mol. wt. 566.67, Sigma Chemical Co., St. Louis, Mo.

[3] Product A 9511, lot 34C-8120, mol. wt. 66,300, Sigma Chemical Co., St. Louis, Mo.

[4] Lot 89-388-DE-5, Abbott Laboratories, North Chicago, Ill.

[5] A Beckman DB-GT, Perkin-Elmer Hitachi 200, or Bausch & Lomb Spectronic 2000 double-beam spectrophotometer was used to record spectra and absorbance values.

[6] The specimen of I was previously dried to constant weight at 135°.

[7] $A_0 = 0.82$ over the pH range of 5.0–11.0 in freshly prepared solutions.

[8] $A_+ = 0$ in 2.36 *N* $H_2SO_4$ ($H_o - 0.4$).

[9] MF-Millipore, cellulose esters, Millipore Corp., Bedford, Mass.



0022-3549/81/0200-0122$01.00/0
© 1981, American Pharmaceutical Association

**Table I—Spectral Data for Patent Blue Violet (I) at $5 \times 10^{-4}$% in 0.05 *M* Phosphate Buffer (pH 7.40) at 25°**

| Wavelength, nm | Absorptivity[a] | |
|---|---|---|
| | I as Received | I Dried Previously[b] |
| 638 ± 1 | 1540 | 1650 |
| 412 ± 1 | 170 | 170 |
| 309 ± 1 | 250 | 250 |

[a] Calculated for a 1% solution of I in a 1-cm quartz cell. [b] Dried to constant weight at 135°.

~0.1 g to 5.5 g in 0.5-g increments were combined with 10.0 g of water in a 15-ml glass tube. A polytef-lined screw cap was tightly affixed, and the cap and tube neck were sealed with silicone rubber cement, which was allowed to cure under ambient conditions for 12–16 hr. The samples then were rotated at 45 rpm and 25 ± 0.5° for 24 hr. They were centrifuged at 2000 rpm for 10 min, and 7–8 ml of the supernate was removed and filtered through a 0.45-μm membrane[9]. A 5.0-ml tared flask was filled to volume (±0.1 ml) with the filtrate and weighed, and the contents were transferred quantitatively to a tared evaporating dish and dried to constant weight at 70–75° in an oven. The weights of the solute residues were recorded to the nearest 0.1 mg.

A 2.5000-g sample of I was diluted to 250.0 ml with 0.9% NaCl or 1.0% (v/v) benzyl alcohol in 0.9% NaCl. This solution was filtered through a 0.22-μm membrane[9] into clean type I glass vials[10] and sealed with rubber closures[11] and one-piece aluminum seals. Half of each lot was autoclaved at 121° and 15 psi for 30 min. Several vials from each formulation group then were stored at 25 ± 5° in the dark or 35 cm from a 15-w fluorescent bulb illuminated continuously. The absorbance at 638 nm of a sample representing each set of formulation variables was determined on six occasions during a 20-month storage period.

Solutions of I[6] at $5 \times 10^{-4}$% were prepared in 0.900, 0.090, 0.009, and $9 \times 10^{-4}$ *N* KOH and had pH values of 13.71, 12.67, 11.31, and 10.04, respectively. The solutions were stored in amber glass bottles sealed with plastic screw caps, and their absorbance at 638 nm was recorded at appropriate times to quantitate the rate of color fading of I in alkaline solution at 23 ± 2°.

Seventeen solutions of I, $2 \times 10^{-4}$–5.00% (w/v), were prepared in 0.067 *M* phosphate buffer ($\mu = 0.2$) to suppress the Donnan effect (pH 7.40 ± 0.05). A 4.00% (w/v) human serum albumin solution also was prepared in the phosphate buffer. Exactly 1.0 ml of sample solution was delivered into one side of a dialysis cell[12] partitioned by a cellulose membrane[13],

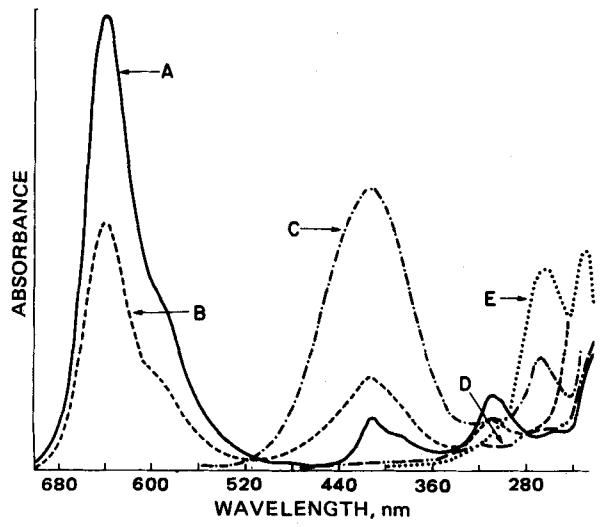


**Figure 1**—*Spectra of patent blue violet (I) at $5 \times 10^{-4}$% (A–C) or 1.0 $\times 10^{-3}$% (D and E) at specified pH or $H_o$. Key: A, pH 7.00; B, pH 2.75; C, 1.0 ≥ $H_o$ ≥ −5.8; D, −7.0 ≥ $H_o$ ≥ −10.0; and E, after 24 hr in 0.90 N KOH (pH 13.7).*

[10] Wheaton 400, 5-ml serum bottle, Wheaton Scientific, Millville, N.J.
[11] Type S-63, formulation 1816 gray butyl rubber, West Co., Millville, N.J.
[12] Constructed of plexiglass, Technilab Instrument Inc., Pequannock, N.J.
[13] Nominal pore size = 4.8 nm, impermeable to molecules with mol. wt. >6000, Technilab Instrument Inc., Pequannock, N.J.

**Table II—Observed Colors of Patent Blue Violet (I) Solutions over Certain pH and $H_o$ Ranges**

| pH or $H_o$ Range | Observed Color | Approximate Wavelength Maximum, nm[a] |
|---|---|---|
| 4.0–11.0 | Blue | 638 |
| 2.7–3.5 | Green-blue[b] | 638, 412 |
| 1.5–2.5 | Yellow-green[b] | 412 |
| −5.8–1.0[c] | Yellow | 418 |
| −10.0–−7.0[c] | Colorless | 273 |

[a] The 273-nm value was determined in 0.01% I; other values were determined in $5 \times 10^{-4}$% I. [b] Colors change from left to right corresponding to pH shifts. [c] $H_o$ values *via* dilutions of sulfuric acid.

and 1.0 ml of albumin solution was placed into the other cell compartment. The dialysis samples were incubated for 48 hr at 37 ± 1° in an oven. An accurately measured portion of I solution was removed from the cell, an appropriate dilution was made when necessary, and the absorbance at 638 nm was recorded. The percent of I bound to albumin was determined by reading the concentration of the dialyzed I solution from a linear Beer's plot for I and subtracting this value from the predialysis concentration of I.

The TLC of I was conducted with 250-μm silica gel plates[14] on which 2 μl of 0.01% methanolic I was spotted and allowed to dry before elution. The TLC plates were eluted with several single- and multicomponent solvent systems for a distance of 10.0 cm in a developing tank lined with paper to ensure saturation of the atmosphere with eluent vapor. After developing and drying under ambient conditions, the plates were observed in a chamber[15] under incandescent and UV light of ~254 and 375 nm. In some eluent systems, the TLC plate was developed a second time at a 90° angle to the first trial to assess any interaction between I and the eluent. The $R_f$ values of all samples were measured to the nearest 1.0 mm.

## RESULTS AND DISCUSSION

The structure of I shown in Scheme I is that of its recently proposed 2,5-disulfonate derivative[16] (11). However, most publications have assigned sulfonation to positions 2 and 4 (12–14). As depicted by the dotted lines, the cationic nitrogen atom exists in resonance between the two diethylanilino groups until either the diethylanilino groups are protonated (II and III) or the central carbon atom is hydroxylated (IV). The mesomerism of diamino- and triaminotriphenylmethane dyes producing quinoidal and benzenoidal (carbonium) ions *via* resonance equilibrium in aqueous solutions has been demonstrated and rationalized (12, 15–20).

Spectral data and color descriptions of I solutions are reported in Tables I and II. Figure 1 shows the spectra of several I solutions. The pKa for the equilibrium between I and II (Scheme I) was determined spectrophotometrically at 25° to be 2.78 ± 0.03 based on seven samples of pH 2.78 ± 0.56. The titration spectra exhibited an isosbestic point at 505 ± 2 nm. The protonation of one of the diethylanilino groups decreases by 50% the length of the quinoid–benzenoid resonance system in I. This result would be expected to reduce the overlapping of electron orbitals, thereby producing the hypsochromic absorbance shift from 638 to 418 ± 2 nm evidenced in Fig. 1 and Table II as the acidity of I solutions increases from pH 4 to $H_o$ −5.8. As indicated in Scheme I, the protonation of I also generates a carbonium ion (II) from the central carbon atom of the triphenylmethane molecule.

It has been shown that the second *p*-diethylamino substituent further stabilizes the already stable triphenylcarbonium (trityl) ion (20). In sulfuric acid solutions of $H_o$ −7.0 and stronger, and the second diethylanilino group of I is protonated, thereby precluding quinoidal resonance in the trityl ion (III) (15), which causes a hypsochromic shift from 418 (II) to 273 nm. The pKa for the equilibrium between II and III was not quantitated accurately, possibly because of the interfering association of the sulfonate groups, in the solutions of $H_o$ < −5.8.

Finally, the effect of ethylating the anilino nitrogens and *ortho*-sulfonating the nonanilino ring of I is to cause a bathochromic shift, as

[14] Redi-Plates, silica gel GF, 5 × 20 cm or 20 × 20 cm, Fisher Scientific Co., Fair Lawn, N.J.
[15] Model CC-20 Chromato-Vue Cabinet, Ultra-Violet Products Inc., San Gabriel, Calif.
[16] The proposed USAN is isosulfan blue.

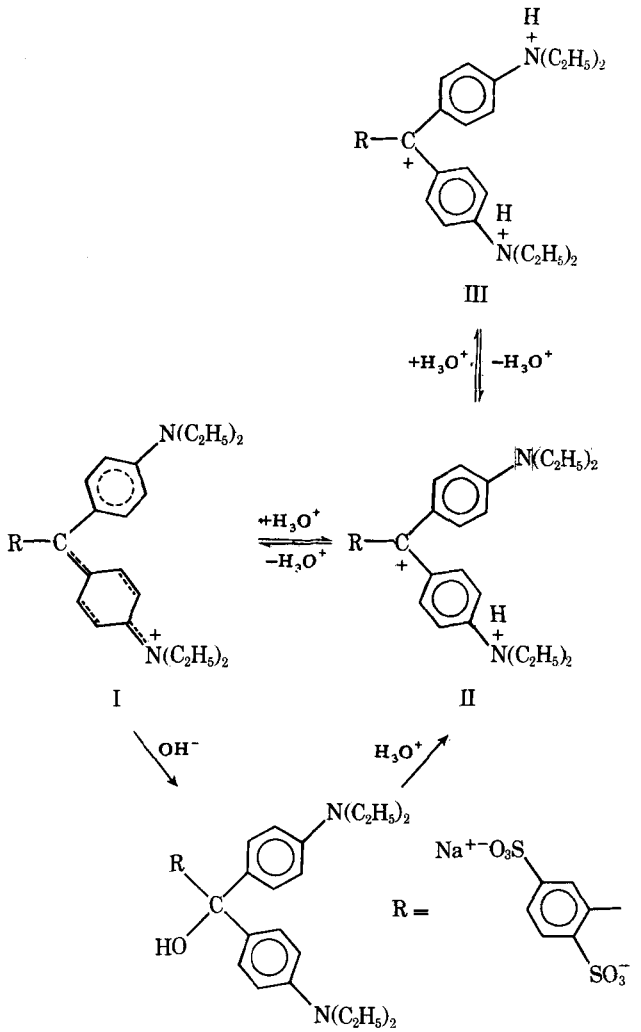

*Scheme I*

compared, for instance, to the quinoidal form of 4,4′-diaminotriphenylmethane (12, 13, 15, 20). One sulfonate group of I confers water solubility on the dye, whereas the second group forms a zwitterion with a diethylamino group during the final synthetic oxidation step (13).

Three samples of I dried at 135° to constant weight showed a loss on drying of 8.65 ± 0.15%. This weight loss apparently represents water since thin-layer chromatograms and UV spectra of ether extracts of I showed no evidence of a major starting compound, diethylaniline.

The distribution coefficients ($P$) for I in $n$-octanol–pH 7.4 buffer and chloroform–pH 7.4 buffer were 0.013 and 0.12, respectively. The experimental value of $P$ in the chloroform system was 20 times larger than that calculated using the value of $P$ obtained from the $n$-octanol system (21):

$$\log P_{\text{chloroform}} = 1.276 \log P_{n\text{-octanol}} + 0.171 \qquad \text{(Eq. 2)}$$

The poor lipophilicity of I may be attributed to its highly polar nature in solutions at physiological pH, *i.e.*, two dissociated sulfonate groups and one diethylanilinium ion. These results corroborate the microscopic observations that I enters frog capillaries *via* pores between endothelial cells and not *via* diffusion through the tissue (22) and that it does not stain the spinal cord or brain tissues of small mammals (23).

The approximate solubilities of I in several solvents are reported in Table III. As expected from its $P$ values in $n$-octanol and chloroform, I is virtually insoluble in organic solvents with low dielectric constants. The data from the phase solubility analysis of I in distilled water are illustrated in Fig. 2. This graph of solute *versus* I added appears to be analogous to that expected from a plot of a colligative property *versus* electrolyte concentration in which more extensive ion association elicits a progressive diminishing of the colligative effect (24). It is not discernible why at 25° the solubility of sodium chloride is 26.5% (w/w) (25) whereas

**Table III—Approximate Solubilities of Patent Blue Violet (I) in Various Solvents at 25°**

| Solvent | Solubility, % w/v[a] |
|---|---|
| Alcohol USP | 9.8 ± 0.4 |
| Distilled water | ≥42 |
| Chloroform | $4 \times 10^{-5}$ |
| Ether | $<1 \times 10^{-5}$ |
| Ethyl acetate | $<1 \times 10^{-5}$ |
| Hexanes | $<1 \times 10^{-5}$ |
| Toluene | $<1 \times 10^{-5}$ |

[a] A ±2% volume error in reading the meniscus of alcohol and water solutions of I.

that of I appears to exceed 37% (w/w) (Fig. 2). Furthermore, the molecular weight ratio of I to sodium chloride is 9.7. One possibility is that the commercially obtained sample of I consisted of various triphenylmethane isomers with diethylamino groups in other than just the 4,4′-positions on two of the benzene rings and/or sulfonate groups in other than positions 2 and 5 on the third ring. A mixture of such isomers could result in a phase solubility plot comprised of several linear segments (26–28). However, the following evidence appears to discredit such conjecture.

1. The data points on the curve of Fig. 2 cannot be plotted readily as a series of, for instance, three- or four-point segments, the intersections of which can be delineated clearly.

2. The precision of the pKa value, 2.78 ± 0.03, for the equilibrium between I and II (Scheme I), as well as the isosbestic point of 505 ± 2 nm for the pKa titration, indicates that the diethylamino group in only a single substituent position, *i.e.*, *para* to the central triphenylmethyl carbon atom, was protonated. The transition from I to II causes a hypsochromic shift of ~220 nm, from blue to yellow. This shift could result only from shortening of the I resonance system. Furthermore, the intense blue color of aqueous I can be attributed only to the quinoidal resonance system, which occurs when the two diethylamino groups are *para* to the central triphenylmethyl carbon atom (12, 13, 15–20). The occurrence of *meta*-quinones is highly unlikely, and the *para*-forms are more favored than the *ortho*-forms (12, 29).

3. The dialkylamino group is a highly activating, predominantly *para*-directing, stable quinoidal intermediate, which, when augmented by steric hindrance effects, virtually precludes competitive electrophilic substitution at the *ortho*- and, less likely, *meta*-positions (29). The synthesis of I requires condensing benzaldehyde-2,5-disulfonic acid with diethylaniline (13). It is ostensible that steric hindrance of the former to *ortho*- and *meta*-attack on diethylaniline should be expected.

The negative curvature of the Fig. 2 plot most likely is the result of a phenomenon involving the association of solvated solute molecules or the presence of impurity (26–28). The terms solid solutions (26, 27), liquid crystals, mesophases, and lyotropic mesomorphism have been used to define or describe these complex systems (30–34). It is relevant that the centrifuged supernates of those aqueous phase solubility analysis samples of I that exceeded ~15% (w/w) required an unusually high force on the syringe plunger to effect filtration through the 0.45-μm membrane. Furthermore, the filtered supernates of the aqueous I solubility samples,

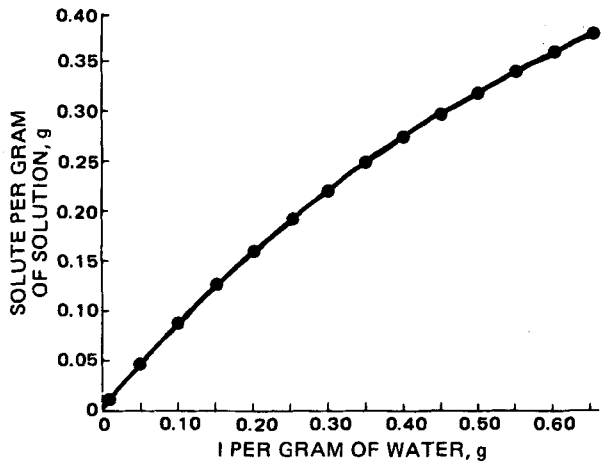


**Figure 2**—*Plot of phase solubility analysis data for patent blue violet (I) in distilled water at 25 ± 0.5°.*

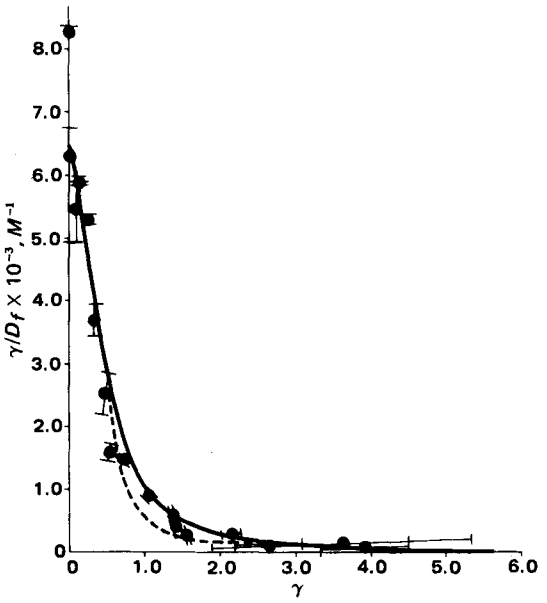


**Figure 3**—*Scatchard plot of* $\gamma/D_f$ versus $\gamma$ *for patent blue violet (I) over the concentration range of* $2 \times 10^{-4}$–*5.00% (w/v) (*$3.0 \times 10^{-6}$–*0.075* M*) I dialyzed against 4% (w/v) (*$6.03 \times 10^{-4}$ M*) human serum albumin at pH 7.4 and 37°.*

when wiped onto a tissue paper, possessed a luster and did not exhibit capillary migration, which is inherent to isotropic liquids.

Derivatives of naphthylaminedisulfonic acid have been shown to produce lyotropic mesophases in water but not in alcohol (30, 35). Furthermore, none of the aqueous and all of the alcoholic I solubility analysis samples were observed to contain undissolved solid material following both rotation at 45 rpm for 24 hr and centrifugation at 2000 rpm for 10 min. This finding suggests that the alcoholic samples consisted of two distinct phases whereas the aqueous samples were comprised of a single mesophase. Lyotropic mesophases are characterized by unusually high viscosity (30, 36) and occurrence in high concentrations of extensively hydrated solutes with large dipole moments (24, 30, 37). Because I appears to be highly dipolar (Scheme I) and its aqueous solutions were atypically viscous in concentrations exceeding the solubility of sodium chloride, it was concluded that the plot in Fig. 2 represents a lyotropic mesophase of I. Several sulfonated and other dyes have shown lyotropic mesomorphism in aqueous systems (32).

The I concentration of samples formulated with 1.000% of I with and without 1.0% (v/v) benzyl alcohol, autoclaved and not autoclaved, and stored in the dark or under continuous illumination from a fluorescent bulb varied from −0.01 to 0.04% (w/v) of I during 20 months of storage at 25 ± 5°. However, autoclaving at 121° and 15 psi for 30 min appeared to cause a 3% initial decrease in the I concentration of samples formulated with and without 1.0% (v/v) benzyl alcohol. Similarly, a decrease of ~10% in the benzyl alcohol concentration[17] was detected upon autoclaving. Interaction of I and benzyl alcohol with the rubber closures of the samples could be one reason for the decrease in the solution concentrations that resulted from autoclaving.

The half-lives for the loss of absorbance at 638 nm of $5 \times 10^{-4}$% I dissolved in 0.900, 0.090, 0.009, and $9 \times 10^{-4}$ *N* KOH at 23 ± 2° are reported in Table IV. The loss of I absorbance at 638 nm in strongly alkaline solutions was accompanied by increasing absorbance at ~265 nm and followed apparent first-order kinetics. The conversion rate of the quinoidal form of triphenylmethane dyes to their colorless carbinol or leuco bases in alkaline media is a recognized means of assessing color fastness (12, 38). Although reversible, the conversion of I to IV (Scheme I) can be rapid in strong alkali, whereas the conversion from IV to II is comparatively slow, even in more concentrated acid. For instance, $1.0 \times 10^{-3}$% I in 0.80 *N* KOH was 99.9% converted to IV in 20 hr at 23 ± 2°. However, when this solution was prepared in 3.60 *N* $H_2SO_4$ ($H_o$ −0.7, equivalent I concentration of $8.9 \times 10^{-4}$%), the dehydroxylation of IV to regenerate II required 30 days. This slowness of the triphenylcarbinol (IV) to trityl ion (II) conversion was reported elsewhere (12). Fastness to color fading of I in alkaline media is enhanced in decreasing order by the addition of a sulfonate, chloro, or methyl group *ortho* to the central triphenylmethyl carbon atom (12).

[17] Determined *via* UV absorbance at 258 nm.

**Table IV—Half-Lives for the Loss of Absorbance at 638 nm of 5 × $10^{-4}$% Patent Blue Violet (I) in Potassium Hydroxide Solutions at 23°**

| Potassium Hydroxide Concentration, *N* | pH | Half-Life |
|---|---|---|
| 0.900 | 13.7 | 1.2 hr |
| 0.090 | 12.7 | 17.0 hr |
| 0.009 | 11.3 | 9.5 days[a] |
| $9 \times 10^{-4}$ | 10.0 | 180 days[a] |

[a] One day = 24.0 hr.

It has been demonstrated that sulfonated triphenylmethane vital stains are bound to serum albumin prior to their endocytosis by macrophages (39). Furthermore, the weaker association between I and albumin compared to other dyes resulted in its more rapid clearance from, and lesser toxicity to, local tissues following repeated subcutaneous injections of 1% solutions (6).

A Scatchard plot (40–42) of the data for the binding of I to human serum albumin appears in Fig. 3. Because transmembrane equilibrium time increased proportionately with I concentration, the data were normalized to 100% equilibrium *via* the results of dialyzing I solutions against albumin-free phosphate buffer. These blank specimens also accounted for contributions of I binding to the dialysis membrane, which did not exceed 2% in any case.

The numbers of binding sites in two classes, $n_1$ and $n_2$, and their corresponding affinity constants, $K_1$ and $K_2$, were estimated by an iterative procedure of drawing ordinate ($\gamma/D_f$) and abscissa ($\gamma$) asymptotes to the original data plot (41, 43). These asymptotic lines were omitted from Fig. 3 to avoid obscuring the raw data (solid line) and fitted (dashed line) curves. One graphical iteration sufficed to produce a curve that was superimposable with a subsequent iteration of the method used (41, 43). This method normalized the raw binding data to yield the fitted curve for the special case of $n_{H1} = n_{H2} = 1$ (41, 42):

$$\gamma = \frac{n_1(K_1D_f)^{nH1}}{1 + (K_1D_f)^{nH1}} + \frac{n_2(K_2D_f)^{nH2}}{1 + (K_2D_f)^{nH2}} \qquad \text{(Eq. 3)}$$

where $\gamma$ is the molar concentration ratio of albumin-bound I to that of albumin, $D_f$ is the molar concentration of unbound I at dialysis equilibrium, $n_{H1}$ and $n_{H2}$ are the binding cooperativity or Hill coefficients, and $n_1$, $n_2$, $K_1$, and $K_2$ are the parameters described earlier. The molarity of I was based on its nominal 85% purity[2], and that of human serum albumin was based on a molecular weight of 66,300 (44, 45).

The error bars on the solid curve in Fig. 3 represent $\chi \pm 1\sigma$ for triplicate dialysis samples. These bars become more horizontal with increasing $\gamma$ because they extend radially in the direction of constant $D_f$ (41). Variability of the data tended to increase with increasing values of $\gamma/D_f$ because of the greater sensitivity of $\gamma/D_f$ to small changes in $D_f$ attributed to experimental imprecision. Several error bars at high values on the

**Table V—Fraction of Patent Blue Violet (I) Bound to 4% (w/v) Human Serum Albumin at 37° and pH 7.4 Corresponding to Concentrations of I before and after Equilibrium Dialysis**

| Fraction of I Bound | Concentration of I, % w/v | |
|---|---|---|
| | Predialysis | Postdialysis[a] |
| 0.83 | $2.0 \times 10^{-3}$ | $1.7 \times 10^{-4}$ |
| 0.79 | $3.1 \times 10^{-3}$ | $3.4 \times 10^{-4}$ |
| 0.77 | $9.8 \times 10^{-3}$ | $1.1 \times 10^{-3}$ |
| 0.76 | $4.8 \times 10^{-3}$ | $5.7 \times 10^{-4}$ |
| 0.75 | $1.95 \times 10^{-2}$ | $2.4 \times 10^{-3}$ |
| 0.68 | $3.24 \times 10^{-2}$ | $5.2 \times 10^{-3}$ |
| 0.59 | $5.23 \times 10^{-2}$ | $1.07 \times 10^{-2}$ |
| 0.48 | $7.57 \times 10^{-2}$ | $1.98 \times 10^{-2}$ |
| 0.46 | 0.1020 | $2.72 \times 10^{-2}$ |
| 0.34 | 0.2030 | 0.0068 |
| 0.26 | 0.3490 | 0.1300 |
| 0.19 | 0.4930 | 0.1980 |
| 0.13 | 0.7700 | 0.3340 |
| 0.14 | 1.0100 | 0.4350 |
| 0.09 | 1.9500 | 0.8880 |
| 0.07 | 3.2000 | 1.4800 |
| 0.05 | 4.9600 | 2.3500 |

[a] Refers to unbound I.

$\gamma$-axis could have resulted from experimental uncertainty in reading the meniscuses of I solutions exceeding 0.5% (w/v); they are colored so intensely as to preclude light transmission.

The abscissa intercept was extrapolated asymptotically to be 0.8, indicating a single class of binding site, *i.e.*, $n_1 = 1$. The total $\gamma$-axis intercept was 5.6, indicating between five and six total binding sites. Thus, by difference, the $\gamma$-axis intercept for a second class of lower affinity binding sites was 4.8, thereby indicating that five binding sites occurred in this class, *i.e.*, $n_2 = 5$. The total ordinate intercept from the fitted curve was 6400 $M^{-1}$, and $K_1$ was extrapolated asymptotically to be 6235 $M^{-1}$. The intercept for the second class of binding sites was, by difference, 165 $M^{-1}$. Thus, each of the five binding sites in the second class was assigned an average $K_2 = 33\ M^{-1}$.

It was established elsewhere that protein binding has a clinically significant effect on *in vivo* drug distribution only when $K \geq 1 \times 10^4\ M^{-1}$ (46). Therefore, it is understandable why, with $K_1 \simeq 6000$, I can be observed in the urine of lymphangiography patients within minutes after subcutaneous injection[18] (47) and has been used to measure renal clearance (48). In fact, when 5–10% (w/v) solutions of I were used in the past for lymphangiography, the rapid secretion of I into saliva and tears was regularly seen[18].

Table V lists the albumin-bound fractions of I at varying concentrations of I before and after equilibrium dialysis. A plot of the fraction of albumin-bound I *versus* the concentration of unbound I at dialysis equilibrium yielded a curve similar to the curves in Fig. 3. If the total I in a 2–3-ml injection of 1% solution were distributed in plasma and extracellular fluid, ~12 liters in an adult (49), then the I concentration *in vivo* would be in the range of $1.7 \times 10^{-4}$–$2.5 \times 10^{-4}$% (w/v), for which Table V indicates >80% of I to be albumin bound. Other brief studies of I binding to albumin appear to be clinically irrelevant because the I concentration used ranged from 0.1 to 11.0% (8, 50).

Based on derived thermodynamic parameters, it has been proposed that the binding of sulfonated dyes to albumin involves electrostatic attraction between the sulfonate anions and the cationic arginine and lysine residues of albumin as well as hydrogen bonds and van der Waals forces (51–53). The evidence for both hydrophobic and electrostatic bonding was provided in a study (51) that found no binding of a sulfonated dye to the unpolymerized amino acids arginine and lysine, whereas significant binding to bovine serum albumin and salmine occurred. Salmine is a protamine with an arginine content of 87% (51), while human serum albumin contains 23 and 58 residues of arginine and lysine per molecule, respectively (45).

Hill plots (42, 54, 55), *i.e.*, $\log (\bar{y}/1 - \bar{y})$ *versus* $\log D_f$, where $\bar{y} = \gamma/(n_1 + n_2)$, were constructed for both the 17 experimental data points on the solid curve and the 17 points on the fitted (dashed) curve corresponding to the same $D_f$ values (Fig. 3). Regression lines computed for these plots had slopes of 0.615 and 0.613 and correlation coefficients of 0.992 and 0.989, respectively. When solved for several sets of coordinates describing the locus of the fitted curve (Fig. 3), the values of the Hill coefficients in Eq. 3 were $n_{H1} = n_{H2} = 1$, which mathematically confirmed this curve to be a hyperbola. Furthermore, the condition of $n_{H1} = n_{H2} = 1$ occurs for two different classes of binding sites only when there is no cooperativity within the ligand–protein binding system (42, 54, 55). Therefore, it was concluded that neither positive nor negative cooperative binding occurred between I and human serum albumin, as evidenced by the insignificant difference between the slopes of the Hill plots of the two curves in Fig. 3; *i.e.*, the experimental (solid) data curve represents a nearly hyperbolic function where $n_{H1} = n_{H2} \simeq 1$.

The compositions of Eluents A, B, and C, used for the TLC of I, are reported in Table VI. Systems A (4) and B[19] were used in other TLC studies, and System C is similar to that reported elsewhere (56). The $R_f$ values for the TLC of I, spotted as 2 $\mu$l of a 0.01% (w/v) solution in methanol and developed over 10.0 cm, allowed to dry for 24 hr, and redeveloped at a 90° angle in Eluents A–C, are reported in Table VII. Only a single major spot, indicating a high degree of organic content purity in I, was observed following initial development in each eluent. The second development in Eluent B resulted in a 0.10-unit decrease in the $R_f$ value, which could be attributed to the formation of some IV (Scheme I) during the first trial, although only a single visible spot was observed under incandescent and UV lamps. The second TLC elution of I with Eluent C produced a second, faintly visible spot with $R_f$ 0.31, the explanation for which is not evident. However, it is apparent from Scheme I and evidence supporting it that the exposure of I to TLC eluents containing acid or alkali could produce I derivatives of different polarity.

**Table VI—Compositions of Eluents Used for TLC of Patent Blue Violet (I)**

| | Composition, parts by volume | | | | | |
|---|---|---|---|---|---|---|
| Eluent | Acetone | Acetic Acid | Ammonium Hydroxide | 1-Butanol | Ethanol | Water |
| A[a] | — | 1 | — | 4 | — | 5 |
| B | 37 | — | 19 | 37 | — | 7 |
| C | — | 1 | — | 60 | 15 | 15 |

[a] Upper phase of system used.

**Table VII—$R_f$ Values of Patent Blue Violet (I) Spotted as 2 $\mu$l of 0.01% (w/v) Methanolic Solution and Developed for 10.0 cm in Eluents A–C**

| | $R_f$ Values | |
|---|---|---|
| Eluent[a] | First Trial | Second Trial[b] |
| A | 0.26 | 0.26 |
| B | 0.58 | 0.48[c] |
| C | 0.26 | 0.26[d] and 0.31 |

[a] Compositions are listed in Table VI. [b] Developed at a 90° angle to the first trial. [c] Because of eluent volatility, the second trial was conducted with fresh eluent. [d] Major spot.

As expected from its lipophobic nature, no measurable $R_f$ values were observed when the TLC of I was conducted in the following solvents of increasing dielectric constant: toluene, ether, chloroform, and ethyl acetate. However, the TLC of I in the more polar solvents *n*-butanol, acetone, and methanol produced visible spots with $R_f$ 0.05, 0.42, and 0.72, respectively. Preliminary TLC studies showed that 2-$\mu$l spots of methanolic I solutions exceeding 0.01%, although suggested (56), elicited trailing and tailing effects which impaired the resolution of $R_f$ values. Perhaps this effect is why 2-$\mu$l samples of $5 \times 10^{-4}$% aqueous I specimens were evaluated by TLC in an earlier study (4).

## CONCLUSIONS

Based on the results of spectrophotometric studies of I solutions prepared in solvents ranging from 0.90 *N* KOH (pH 13.7) to 96% (w/w) $H_2SO_4$ ($H_o$ −10.0), the quantitative determination of I at 639 ± 2 nm appears to represent a stability-indicating assay. The results of distribution coefficient, solubility analysis, and human serum albumin binding studies corroborate other evidence suggesting that the *in vivo* distribution of I is limited to plasma and extracellular fluid. Based on the pKa for the equilibrium between I and II (Scheme I) and on the results of TLC determinations, I appears to be essentially pure with respect to its organic compound content.

## REFERENCES


(1) D. W. Newton, A. G. Rogers, C. H. Becker, and G. Torosian, *Am. J. Hosp. Pharm.*, **32**, 912 (1975).

(2) J. R. Wilder, *Surgery*, **56**, 881 (1964).

(3) J. B. Kinmonth, G. W. Taylor, and R. K. Harper, *Br. Med. J.*, **1**, 940 (1955).

(4) P. K. Hiranaka, L. M. Kleinman, E. A. Sokoloski, and H. M. Fales, *Am. J. Hosp. Pharm.*, **32**, 928 (1975).

(5) J. Hooson, P. Grasso, and S. D. Gangolli, *Br. J. Cancer*, **27**, 230 (1973).

(6) S. D. Gangolli, P. Grasso, L. Goldberg, and J. Hoosan, *Food Cosmet. Toxicol.*, **10**, 449 (1972).

(7) P. Grasso, S. D. Gangolli, L. Goldberg, and J. Hoosan, *ibid.*, **9**, 463 (1971).

(8) S. D. Gangolli, P. Grasso, and L. Goldberg, *ibid.*, **5**, 601 (1967).

(9) A. Albert and E. P. Serjeant, "The Determination of Ionization Constants," 2nd ed., Chapman and Hall, London, England, 1971, p. 45.

(10) J. C. Souder and W. C. Ellenbogen, *Drug Stand.*, **26**, 77 (1958).

(11) "Sigma Price List," Sigma Chemical Co., St. Louis, Mo., Jan. 1980, p. 450.

(12) "Organic Chemistry: An Advanced Treatise," vol. 3, H. Gilman,


[18] Dr. Francis J. Scholz, Department of Diagnostic Radiology, Lahey Clinic Foundation, Boston, Mass., personal communication.

[19] Walter C. Stern, Sigma Chemical Co., St. Louis, Mo., personal communication.

Ed., Wiley, New York, N.Y., 1953, pp. 295–305.
(13) "Rodd's Chemistry of Carbon Compounds," 2nd ed., vol. 3, part F, S. Coffey, Ed., Elsevier, New York, N.Y., 1974, pp. 129–131.
(14) R. D. Lillie, "H. J. Conn's Biological Stains," 9th ed., Williams & Wilkins, Baltimore, Md., 1977, p. 252.
(15) C. R. Bury, *J. Am. Chem. Soc.*, **57**, 2115 (1935).
(16) G. E. K. Branch and B. M. Tolbert, *ibid.*, **71**, 781 (1949).
(17) M. S. Newman and N. C. Deno, *ibid.*, **73**, 3644 (1951).
(18) R. Cigen, *Acta Chem. Scand.*, **13**, 1113 (1959).
(19) A.-M. Anthony-Barbier, P. Rumpf, and C. Viel, *Bull. Soc. Chim. Fr.*, **1959**, 1474.
(20) H. H. Freedman, in "Carbonium Ions," G. A. Olah and P. von R. Schleyer, Eds., Wiley, New York, N.Y., 1973, pp. 1501–1504, 1530–1536.
(21) A. Leo, C. Hansch, and D. Elkins, *Chem. Rev.*, **71**, 525 (1971).
(22) C. C. Michel, *J. Physiol. (London)*, **204**, 62P (1969).
(23) V. Augulis and E. B. Sigg, *Stain Technol.*, **46**, 183 (1971).
(24) A. N. Martin, J. Swarbrick, and A. Cammarata, "Physical Pharmacy," 2nd ed., Lea & Febiger, Philadelphia, Pa., 1969, pp. 178–182.
(25) "The Merck Index," 9th ed., Merck & Co., Rahway, N.J., 1976, p. MISC-69.
(26) T. J. Webb, *Anal. Chem.*, **20**, 100 (1948).
(27) W. Tarpley and M. Yudis, *ibid.*, **25**, 121 (1953).
(28) T. Higuchi and K. A. Connors, *Adv. Anal. Chem. Instrum.*, **4**, 117 (1965).
(29) J. March, "Advanced Organic Chemistry: Reactions, Mechanisms and Structure," 2nd ed., McGraw-Hill, New York, N.Y., 1977, pp. 461–464.
(30) G. W. Gray, "Molecular Structure and the Properties of Liquid Crystals," Academic, New York, N.Y., 1962, pp. 13–16.
(31) B. Jirgensons and M. E. Straumanis, "A Short Textbook of Colloid Chemistry," 2nd rev. ed., Macmillan, New York, N.Y., 1962, pp. 414, 415.
(32) G. H. Brown and W. G. Shaw, *Chem. Rev.*, **57**, 1049 (1957).
(33) A. W. Adamson, "A Textbook of Physical Chemistry," Academic, New York, N.Y., 1973, pp. 1006, 1007.
(34) E. B. Priestly, P. J. Wojtowicz, and P. Sheng, "Introduction to Liquid Crystals," Plenum, New York, N.Y., 1975, pp. 1–13.
(35) I. E. Balaban and H. King, *J. Chem. Soc.*, **1927**, 3068.
(36) A. N. Martin, J. Swarbrick, and A. Cammarata, "Physical Pharmacy," 2nd ed., Lea & Febiger, Philadelphia, Pa., 1969, pp. 537–539.
(37) H. L. Booij, in "Colloid Science," vol. 2, H. R. Kruyt, Ed., Elsevier, New York, N.Y., 1949, p. 682.
(38) R. D. Lillie, "H. J. Conn's Biological Stains," 9th ed., Williams & Wilkins, Baltimore, Md., 1977, pp. 27, 28, 246, 247.
(39) M. Kojima and Y. Imai, *Proc. Jpn. Soc. RES*, **1**, 61 (1961).
(40) G. Scatchard, *Ann. N.Y. Acad. Sci.*, **51**, 660 (1949).
(41) H. G. Weder, J. Schildkneckt, R. A. Lutz, and P. Kesselring, *Eur. J. Biochem.*, **42**, 475 (1974).
(42) G. Schwarz, *Biophys. Struct. Mech.*, **2**, 1 (1976).
(43) S. A. Berson and R. S. Yalow, *J. Clin. Invest.*, **38**, 1996 (1959).
(44) F. W. Putnam, in "The Plasma Proteins," 2nd ed., vol. 1, F. W. Putnam, Ed., Academic, New York, N.Y., 1975, pp. 63–70.
(45) T. Peters, Jr., in *ibid.*, pp. 133–181.
(46) B. K. Martin, *Nature*, **207**, 274 (1965).
(47) S. A. Threefoot, *Proc. Soc. Exp. Biol. Med.*, **103**, 780 (1960).
(48) N. Parekh, G. Popa, R. Galaske, W. Galaske, and M. Steinhausen, *Pfluegers Arch. (Eur. J. Physiol.)*, **343**, 1 (1973).
(49) R. R. Levine, "Pharmacology Drug Action and Reactions," Little, Brown, Boston, Mass., 1973, p. 100.
(50) S. A. Threefoot, *J. Appl. Physiol.*, **15**, 925 (1960).
(51) I. M. Klotz, *J. Am. Chem. Soc.*, **68**, 2299 (1946).
(52) H. J. Weder and M. H. Bickel, *J. Pharm. Sci.*, **59**, 1563 (1970).
(53) R. D. Lillie, "H. J. Conn's Biological Stains," Williams & Wilkins, Baltimore, Md., 1977, p. 24.
(54) A. V. Hill, *J. Physiol. (London)*, **40**, iv (1910).
(55) F. W. Dahlquist, *FEBS Lett.*, **49**, 267 (1974).
(56) H. Schweppe, in "The Analytical Chemistry of Synthetic Dyes," K. Venkataraman, Ed., Wiley, New York, N.Y., 1977, pp. 23–51.

**ACKNOWLEDGMENTS**

The authors thank Dr. Elton Watkins, Jr., Division of Research, Lahey Clinic Foundation, Boston, Mass., for providing the patent blue violet dye and other materials used in the investigation. They also thank Mr. Richard A. Klose, Jr., for assistance in TLC determinations, Ms. Elaine G. Howard for assistance in preparing the manuscript, and Dr. William O. Foye for critiquing parts of the *Results and Discussion* section.

# Utility of Chloranil in Assay of Naphazoline, Clemizole, Penicillin G Sodium, and Piperazine

**SAIED BELAL, M. ABDEL-HADY ELSAYED *x, MOHAMED E. ABDEL-HAMID, and HASSAN ABDINE**

Received October 15, 1979, from the *Department of Pharmaceutical Analytical Chemistry, Faculty of Pharmacy, University of Alexandria, Alexandria, Egypt.* Accepted for publication July 15, 1980. *Present address: Department of Pharmacy, University of Nigeria, Nsukka, Nigeria.

**Abstract** □ A simple and sensitive spectrophotometric method is described for the assay of naphazoline, clemizole, penicillin G sodium, and piperazine. The method was based on the formation of a charge transfer complex between these drugs as $n$-donors and chloranil, the $\pi$-acceptor. Conformity to Beer's law enabled the assay of dosage forms of these drugs. Compared with official methods, the results obtained were of equal accuracy. A more detailed investigation of the naphazoline–chloranil complex was made with respect to its composition, association constant, and free energy change.

**Keyphrases** □ Naphazoline—spectrophotometric assay in dosage forms using complex formation with chloranil □ Clemizole—spectrophotometric assay in dosage forms using complex formation with chloranil □ Penicillin G sodium—spectrophotometric assay in dosage forms using complex formation with chloranil □ Piperazine—spectrophotometric assay in dosage forms using complex formation with chloranil

Naphazoline and clemizole (antihistamines), penicillin G sodium (antibiotic), and piperazine (anthelmintic) are widely used in pharmaceutical practice. The official compendia describe a nonaqueous titration for naphazoline (1), an iodometric titration (2) and microbiological assay (3) for penicillin G sodium, and a gravimetric method (1) and nonaqueous titration (3) for piperazine. Among the methods described for the assay of naphazoline are UV

0022-3549/81/0200-0127$01.00/0
© 1981, American Pharmaceutical Association

Ed., Wiley, New York, N.Y., 1953, pp. 295–305.
(13) "Rodd's Chemistry of Carbon Compounds," 2nd ed., vol. 3, part F, S. Coffey, Ed., Elsevier, New York, N.Y., 1974, pp. 129–131.
(14) R. D. Lillie, "H. J. Conn's Biological Stains," 9th ed., Williams & Wilkins, Baltimore, Md., 1977, p. 252.
(15) C. R. Bury, *J. Am. Chem. Soc.*, **57**, 2115 (1935).
(16) G. E. K. Branch and B. M. Tolbert, *ibid.*, **71**, 781 (1949).
(17) M. S. Newman and N. C. Deno, *ibid.*, **73**, 3644 (1951).
(18) R. Cigen, *Acta Chem. Scand.*, **13**, 1113 (1959).
(19) A.-M. Anthony-Barbier, P. Rumpf, and C. Viel, *Bull. Soc. Chim. Fr.*, **1959**, 1474.
(20) H. H. Freedman, in "Carbonium Ions," G. A. Olah and P. von R. Schleyer, Eds., Wiley, New York, N.Y., 1973, pp. 1501–1504, 1530–1536.
(21) A. Leo, C. Hansch, and D. Elkins, *Chem. Rev.*, **71**, 525 (1971).
(22) C. C. Michel, *J. Physiol. (London)*, **204**, 62P (1969).
(23) V. Augulis and E. B. Sigg, *Stain Technol.*, **46**, 183 (1971).
(24) A. N. Martin, J. Swarbrick, and A. Cammarata, "Physical Pharmacy," 2nd ed., Lea & Febiger, Philadelphia, Pa., 1969, pp. 178–182.
(25) "The Merck Index," 9th ed., Merck & Co., Rahway, N.J., 1976, p. MISC-69.
(26) T. J. Webb, *Anal. Chem.*, **20**, 100 (1948).
(27) W. Tarpley and M. Yudis, *ibid.*, **25**, 121 (1953).
(28) T. Higuchi and K. A. Connors, *Adv. Anal. Chem. Instrum.*, **4**, 117 (1965).
(29) J. March, "Advanced Organic Chemistry: Reactions, Mechanisms and Structure," 2nd ed., McGraw-Hill, New York, N.Y., 1977, pp. 461–464.
(30) G. W. Gray, "Molecular Structure and the Properties of Liquid Crystals," Academic, New York, N.Y., 1962, pp. 13–16.
(31) B. Jirgensons and M. E. Straumanis, "A Short Textbook of Colloid Chemistry," 2nd rev. ed., Macmillan, New York, N.Y., 1962, pp. 414, 415.
(32) G. H. Brown and W. G. Shaw, *Chem. Rev.*, **57**, 1049 (1957).
(33) A. W. Adamson, "A Textbook of Physical Chemistry," Academic, New York, N.Y., 1973, pp. 1006, 1007.
(34) E. B. Priestly, P. J. Wojtowicz, and P. Sheng, "Introduction to Liquid Crystals," Plenum, New York, N.Y., 1975, pp. 1–13.
(35) I. E. Balaban and H. King, *J. Chem. Soc.*, **1927**, 3068.
(36) A. N. Martin, J. Swarbrick, and A. Cammarata, "Physical Pharmacy," 2nd ed., Lea & Febiger, Philadelphia, Pa., 1969, pp. 537–539.
(37) H. L. Booij, in "Colloid Science," vol. 2, H. R. Kruyt, Ed., Elsevier, New York, N.Y., 1949, p. 682.
(38) R. D. Lillie, "H. J. Conn's Biological Stains," 9th ed., Williams & Wilkins, Baltimore, Md., 1977, pp. 27, 28, 246, 247.
(39) M. Kojima and Y. Imai, *Proc. Jpn. Soc. RES*, **1**, 61 (1961).
(40) G. Scatchard, *Ann. N.Y. Acad. Sci.*, **51**, 660 (1949).
(41) H. G. Weder, J. Schildkneckt, R. A. Lutz, and P. Kesselring, *Eur. J. Biochem.*, **42**, 475 (1974).
(42) G. Schwarz, *Biophys. Struct. Mech.*, **2**, 1 (1976).
(43) S. A. Berson and R. S. Yalow, *J. Clin. Invest.*, **38**, 1996 (1959).
(44) F. W. Putnam, in "The Plasma Proteins," 2nd ed., vol. 1, F. W. Putnam, Ed., Academic, New York, N.Y., 1975, pp. 63–70.
(45) T. Peters, Jr., in *ibid.*, pp. 133–181.
(46) B. K. Martin, *Nature*, **207**, 274 (1965).
(47) S. A. Threefoot, *Proc. Soc. Exp. Biol. Med.*, **103**, 780 (1960).
(48) N. Parekh, G. Popa, R. Galaske, W. Galaske, and M. Steinhausen, *Pfluegers Arch. (Eur. J. Physiol.)*, **343**, 1 (1973).
(49) R. R. Levine, "Pharmacology Drug Action and Reactions," Little, Brown, Boston, Mass., 1973, p. 100.
(50) S. A. Threefoot, *J. Appl. Physiol.*, **15**, 925 (1960).
(51) I. M. Klotz, *J. Am. Chem. Soc.*, **68**, 2299 (1946).
(52) H. J. Weder and M. H. Bickel, *J. Pharm. Sci.*, **59**, 1563 (1970).
(53) R. D. Lillie, "H. J. Conn's Biological Stains," Williams & Wilkins, Baltimore, Md., 1977, p. 24.
(54) A. V. Hill, *J. Physiol. (London)*, **40**, iv (1910).
(55) F. W. Dahlquist, *FEBS Lett.*, **49**, 267 (1974).
(56) H. Schweppe, in "The Analytical Chemistry of Synthetic Dyes," K. Venkataraman, Ed., Wiley, New York, N.Y., 1977, pp. 23–51.

**ACKNOWLEDGMENTS**

The authors thank Dr. Elton Watkins, Jr., Division of Research, Lahey Clinic Foundation, Boston, Mass., for providing the patent blue violet dye and other materials used in the investigation. They also thank Mr. Richard A. Klose, Jr., for assistance in TLC determinations, Ms. Elaine G. Howard for assistance in preparing the manuscript, and Dr. William O. Foye for critiquing parts of the *Results and Discussion* section.

# Utility of Chloranil in Assay of Naphazoline, Clemizole, Penicillin G Sodium, and Piperazine

**SAIED BELAL, M. ABDEL-HADY ELSAYED *x, MOHAMED E. ABDEL-HAMID, and HASSAN ABDINE**

Received October 15, 1979, from the *Department of Pharmaceutical Analytical Chemistry, Faculty of Pharmacy, University of Alexandria, Alexandria, Egypt.* Accepted for publication July 15, 1980. *Present address: Department of Pharmacy, University of Nigeria, Nsukka, Nigeria.

**Abstract** □ A simple and sensitive spectrophotometric method is described for the assay of naphazoline, clemizole, penicillin G sodium, and piperazine. The method was based on the formation of a charge transfer complex between these drugs as $n$-donors and chloranil, the $\pi$-acceptor. Conformity to Beer's law enabled the assay of dosage forms of these drugs. Compared with official methods, the results obtained were of equal accuracy. A more detailed investigation of the naphazoline–chloranil complex was made with respect to its composition, association constant, and free energy change.

**Keyphrases** □ Naphazoline—spectrophotometric assay in dosage forms using complex formation with chloranil □ Clemizole—spectrophotometric assay in dosage forms using complex formation with chloranil □ Penicillin G sodium—spectrophotometric assay in dosage forms using complex formation with chloranil □ Piperazine—spectrophotometric assay in dosage forms using complex formation with chloranil

Naphazoline and clemizole (antihistamines), penicillin G sodium (antibiotic), and piperazine (anthelmintic) are widely used in pharmaceutical practice. The official compendia describe a nonaqueous titration for naphazoline (1), an iodometric titration (2) and microbiological assay (3) for penicillin G sodium, and a gravimetric method (1) and nonaqueous titration (3) for piperazine. Among the methods described for the assay of naphazoline are UV

0022-3549/81/0200-0127$01.00/0
© 1981, American Pharmaceutical Association

spectrophotometry (4), colorimetry using reagents such as bromine (5), sodium nitroprusside (6), or ceric sulfate (7), and nonaqueous titration (1, 8).

Clemizole was determined spectrophotometrically applying Glenn's method of orthogonal function (9). Penicillin G sodium was assayed by different methods, including atomic absorption spectrophotometry (10), colorimetry through hydroxamic acid formation (11), IR spectrophotometry (12), polarography (13), and titrimetric methods involving iodine (2, 14), iodine monochloride (15), mercuric ion (16), and *N*-bromosuccinimide (17) as titrants. The proposed methods for the assay of piperazine include colorimetric analyses employing ammonium reineckate (18), bromthymol blue (19), sodium β-naphthoquinone-4-sulfonate (20), and 3,5-dichloro-*p*-benzoquinonechlorimine (21), and dichlone (22), titrimetry in nonaqueous solvents (3), and indirect complexometry (23).

Substituted quinones such as 2,5-dichloroquinone (24), 7,7',8,8'-tetracyanoquinodimethane (25), and fluoranil (26) were used as π-acceptors with various electron donors to form charge transfer complexes and radical ions (27, 28). Some aromatic amines (29, 30) and amino acids (31, 32) were determined with chloranil. The present report describes the utility of chloranil for the spectrophotometric determination of naphazoline, clemizole, penicillin G sodium, and piperazine in dosage forms. In addition, the naphazoline–chloranil complex with respect to its association constant, mole ratio of reactants, and free energy change ($\Delta G°$) was investigated.

## EXPERIMENTAL

**Instruments**—A photoelectric spectrophotometer[1] with 1-cm silica or glass cells was used.

**Materials and Reagents**—Pharmaceutical grade naphazoline hydrochloride[2], clemizole hydrochloride[3], penicillin G sodium[3], and piperazine[4] were used as working standards.

*p*-Chloranil[5] was purified according to a literature method (33). The solution was prepared in chloroform ($2 \times 10^{-3}$ *M*) or dioxane (0.1 g %); the solvents were spectrograde.

**Standard Solutions**—For naphazoline and clemizole, the calculated amount (equivalent to 0.1 g of base) was dissolved in water. The solution was transferred quantitatively to a separator, alkalinized with ammonia, and extracted by shaking with five 20-ml portions of chloroform. The extracts were pooled in a 100-ml volumetric flask, and the flask was filled to volume with chloroform (1 ml contained 1 mg of the base).

For penicillin G sodium, 0.500 g of the drug was dissolved in 80% dioxane in water, and the solution was diluted quantitatively to give a concentration of 10 mg/ml.

For piperazine, 25.0 mg of the drug was placed in a 25-ml volumetric flask containing 5 ml of ethanol (95%), and the flask was shaken well before it was filled to volume with dioxane.

**Determination of Naphazoline**—For calibration, serial volumes of 1–5 ml (in 1-ml steps) of standard base solution, diluted four times to give 0.25 mg/ml, were transferred to 25-ml volumetric flasks. Sufficient chloroform was added to bring the volume to ~10 ml, and 5 ml of chloranil ($2 \times 10^{-3}$ *M* in chloroform) was added. The contents were mixed and heated in a water bath at 40 ± 1° for 24 min. The volume was brought to 25.0 ml with chloroform. The absorbance at 515 nm was measured against a blank, prepared simultaneously without naphazoline solution.

For the determination of naphazoline in eye drops, 10.0 ml (equivalent to 5.0 mg of naphazoline hydrochloride) was measured, the base was extracted as described previously with five 10-ml portions of chloroform, and the extracts were pooled in a 50-ml volumetric flask. Using ~6 ml (accurately measured) of the base solution, the procedure given for calibration of naphazoline was followed.

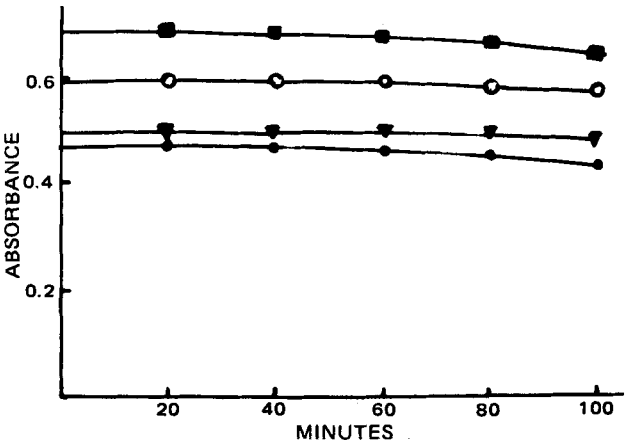


**Figure 1**—*Plot of absorbance* versus *time for complexed naphazoline (3 mg %) (○), clemizole (5 mg %) (●), penicillin G sodium (30 mg %) (▼), and piperazine (10 mg %) (■).*

**Determination of Clemizole**—For calibration, serial volumes of 2–9 ml (in 1-ml steps) of the standard solution were diluted quantitatively with chloroform to 25 ml. Exactly 1.0 ml of these diluted solutions, containing 0.08–0.36 mg, was measured into clean, dry test tubes. To each test tube were added 2.0 ml of chloranil solution (0.1 g % in dioxane) and 1.0 ml of dimethylformamide. The test tubes were maintained in a water bath at 25 ± 1° for 30 min. A blank was prepared simultaneously without clemizole solution. The absorbance was measured against the blank at 550 nm.

For the determination of clemizole in commercial tablets, 10 tablets were powdered and mixed. About 0.4 g (equivalent to two tablets) was transferred to a separator containing ~20 ml of water. The base was extracted as described with five 10-ml portions of chloroform, and the extract was diluted five times with chloroform. Exactly 1.0 ml of the diluted solution was measured, and the procedure for calibration of clemizole was followed.

**Determination of Penicillin G Sodium**—For calibration, serial volumes of 1–6 ml (in 1-ml steps) of the standard solution were transferred to 25-ml volumetric flasks and diluted quantitatively with 80% dioxane in water. Exactly 1.0 ml of the diluted solutions, containing 0.4–2.4 mg of penicillin G sodium, was measured into a series of clean, dry test tubes. To each test tube were added 2.0 ml of chloranil (0.1 g % in dioxane) and 1.0 ml of dimethylformamide. The test tubes were heated in a water bath at 40 ± 1° for 15 min. A blank was prepared simultaneously by substituting 1.0 ml of 80% dioxane in water for the penicillin G sodium solution. The absorbance was measured against the blank at 560 nm.

For the determination of penicillin G sodium in vials, the contents of one vial were dissolved in 80% dioxane in water. This solution was transferred quantitatively to a 25-ml volumetric flask and diluted 10 times with the same solvent. Using 1.0 ml of the diluted solution, the procedure for calibration of penicillin G sodium was followed.

**Determination of Piperazine**—For calibration, serial volumes of 1–5 ml of the standard solution (in 1-ml steps) were diluted in 10-ml volumetric flasks with dioxane. Exactly 1.0 ml of these solutions (equivalent to 0.1–0.5 mg) was pipetted into a series of clean, dry test tubes. Exactly 2.0 ml of chloranil (0.1 g % in dioxane) and 1.0 ml of dimethylformamide were added, and the solution was heated in a water bath at 60 ± 1° for 10 min. A blank was prepared simultaneously using 1.0 ml of dioxane instead of piperazine solution. The absorbance was measured at 540 nm against the blank.

For the determination of piperazine in powdered form, 25.0 mg of the powder was transferred to a 25-ml volumetric flask containing 5 ml of ethanol (95%). The flask was shaken well before it was filled to volume with dioxane. The solution was diluted four times with dioxane using 1.0 ml of the diluted solution, and the procedure for calibration of piperazine was followed.

**Ratio of Reactants in Naphazoline–Chloranil Complex**—Into 25-ml volumetric flasks was transferred 10 ml (varied in 1-ml steps) of an equimolar concentration ($10^{-3}$ *M*) of solutions of naphazoline and chloranil in chloroform. The procedure was continued as described for the calibration of naphazoline.

[1] Beckman model 24 double-beam spectrophotometer.
[2] Nile Co. for Pharmaceuticals and Chemical Industries.
[3] Chemical Industries Development Pharmaceutical Co.
[4] Alexandria Co. for Pharmaceutical and Chemical Industries.
[5] Pfaltz & Bauer, Stamford, Conn.

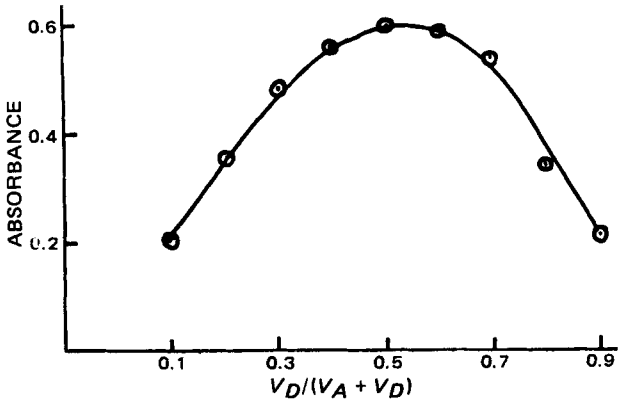


**Figure 2**—*Continuous variation plot for naphazoline–chloranil complex in chloroform ($10^{-3}$ M).*

**Determination of Association Constant and Free Energy Change**—Serial volumes of 1–5 ml of $10^{-3}$ *M* naphazoline solution (in 1-ml steps) in chloroform were transferred to 25-ml volumetric flasks. The solution was diluted with chloroform to 10 ml, and 2.0 ml of chloranil solution in chloroform ($2 \times 10^{-3}$ *M*) was added. The procedure was continued as described for the calibration of naphazoline.

## RESULTS AND DISCUSSION

In spite of their structural variation, naphazoline (I), clemizole (II), penicillin G sodium (III), and piperazine (IV) give a purple chromagen with chloranil that exhibits a strong absorption maximum at 515–560 nm, *i.e.*, in the visible region of the spectrum. These bands can be attributed to the formation of charge transfer complexes between I–IV, acting as *n*-donors (*D*) or Lewis bases, and chloranil, the $\pi$-acceptor (*A*) or Lewis acid (Scheme I).

$$\ddot{D} + A \rightarrow [\ddot{D} \frown A] \rightarrow D^+ + A^-$$

*Scheme I*

A simple general quantum mechanical theory of a 1:1 or an *n*:1 interaction of an electron donor with an electron acceptor has been proposed for the formation of the charge transfer complex. In the ground state, the two molecules are held together when they are in close proximity by forces such as van der Waals, dispersion, and hydrogen forces. Additional forces are contributed by the transfer of a small amount of charge from the donor to the acceptor. When a complex absorbs light of a suitable energy, it is raised from the ground state to the excited state. In this state, an electron that was shifted only slightly toward the acceptor is almost completely transferred. Therefore, the transfer of an electron by absorption of energy is responsible for the purple color of the formed complexes with maximum absorption at 515 nm for complexed naphazoline, 550 nm for complexed clemizole, 560 nm for complexed penicillin G sodium, and 540 nm for complexed piperazine.

Because the reaction of chloranil is known to be slow (29, 30, 32), the effect of time and temperature on the development of complexes was investigated. Maximum absorbance for the colored complexes was attained on leaving the reactant mixture in a thermostated water bath at 40° for 45 min (I), at 25° for 30 min (II), at 40° for 15 min (III), and at 60° for 10 min (IV). The complexed compounds gave absorbances that were unchanged for at least 1 hr (Fig. 1).

The slopes of the calibration curves reflect the sensitivity of the color attributed to charge transfer complex formation. The highest slope for naphazoline parallels its greatest basicity (pKa = 10.9) (34).

The other compounds, having lower pKa values, gave lower slopes compared to naphazoline. This finding indicates that the sensitivity of the developed color increases with increasing ability of the nitrogen atom to donate one of its lone pair of electrons. In penicillin G sodium (pKa = 2.8) (34), the presence of the carboxylic group and the amino group renders the compound of dual character and, therefore, gave the complex of the lowest slope.

A more detailed examination was made for the most sensitive compound, naphazoline. The decrease in absorbance per hour for complexed naphazoline followed zero-order kinetics, as determined by measuring the absorbance of the complex at 1-hr intervals for 5 hr. A plot of concentration (*C*, expressed in gram percent), calculated from the calibration graph, as a function of time (*t*, expressed in hours) gave a line with a slope of $-K$. The $K$ value was determined to be 0.000528, which indicated that the color was fading at a constant rate of 0.000528/hr.

Using Job's method of continuous variation (35), the ratio of naphazoline to chloranil equaled 1:1 (Fig. 2). This finding was anticipated by the presence of one basic or electron-donating center in the naphazoline molecule.

The absorbance of the naphazoline–chloranil complex was used to calculate the association constant using the Benesi–Hildebrand equation (36):

$$\frac{[A_0]}{A_\lambda^{AD}} = \frac{1}{\epsilon_\lambda^{AD}} + \frac{1}{K_c^{AD}\epsilon_\lambda^{AD}}\frac{1}{[D_0]} \qquad \text{(Eq. 1)}$$

where $[A_0]$ and $[D_0]$ are the total concentrations of the interacting species, $A_\lambda^{AD}$ and $\epsilon_\lambda^{AD}$ are the absorbance and molar absorptivity of the complex at 515 nm, and $K_c^{AD}$ is the association constant of the complex. On plotting the values of $[A_0]/A_\lambda^{AD}$ *versus* $1/[D_0]$, a line was obtained (Fig. 3) that is described by the following regression equation:

$$\frac{[A_0]}{A_\lambda^{AD}} = 2.0095 \times 10^{-6} + \frac{1}{[D_0]}(3.1868 \times 10^{-8}) \qquad \text{(Eq. 2)}$$

for which the regression coefficient equals 0.9997. The intercept of this line with the ordinate is $(\epsilon_\lambda^{AD})^{-1}$, and the slope equals $(\epsilon_\lambda^{AD} K_c^{AD})^{-1}$. From Eq. 2, the association constant equals 63.06. The standard free energy change (37), $\Delta G°$, of complexation is related to the association constant by:

$$\Delta G° = -2.303RT \log K \qquad \text{(Eq. 3)}$$

from which $\Delta G°$ equals −2.454 kcal.

The standard calibration graphs for naphazoline, clemizole, penicillin G sodium, and piperazine were constructed by plotting absorbance *versus* concentration (milligrams per 100 ml) calculated after addition of the chloranil solution. Conformity with Beer's law was evident in the concentration ranges of 1–5 mg % of naphazoline, 2–9 mg % of clemizole, 10–60 mg % of penicillin G sodium, and 2.5–12.5 mg % of piperazine.

Regression equations, derived using the method of least squares (38), for naphazoline, clemizole, penicillin G sodium, and piperazine are, respectively:

$$A_{515} = 0.0112 + 0.1960C \qquad \text{(Eq. 4)}$$

$$A_{550} = 0.0045 + 0.0920C \qquad \text{(Eq. 5)}$$

$$A_{560} = -0.0103 + 0.0166C \qquad \text{(Eq. 6)}$$

$$A_{540} = -0.0279 + 0.0684C \qquad \text{(Eq. 7)}$$

for which the respective regression coefficients are 0.9988, 0.9977, 0.9997, and 0.9979.

The validity of the regression equations was assessed in the determination of naphazoline in eye drops, clemizole in tablets, penicillin G sodium in vials, and piperazine in powder.

With the exception of clemizole, which was assayed by nonaqueous titration (Table I), the official methods were applied for the assay of the test compounds in powdered form (piperazine) or in dosage forms

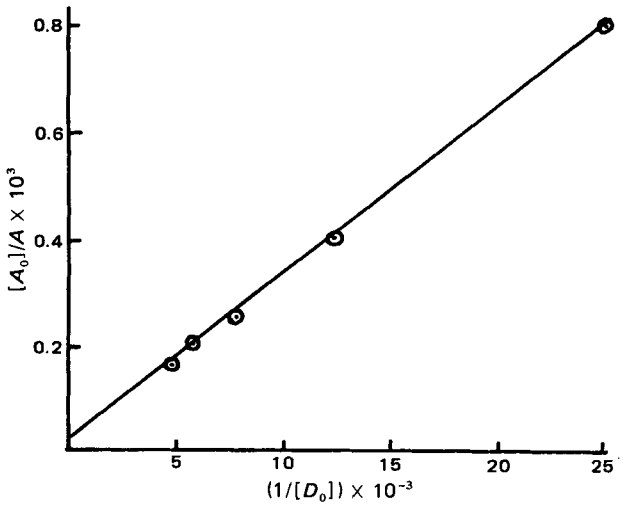


**Figure 3**—*Benesi–Hildebrand plot for naphazoline–chloranil complex in chloroform.*

**Table I—Assay Results for Dosage Forms of Naphazoline, Clemizole, Penicillin G Sodium, and Piperazine**

| Preparation | Proposed Method[a] | | | Official Method[c] | | |
|---|---|---|---|---|---|---|
| | $n$ | Assumed Concentration[b], mg % | Mean ± $SD$, % | $n$ | Assumed Concentration, mg % | Mean ± $SD$, % |
| Naphazoline drops[d] | 4 | 2.40 | 99.89 ± 0.31 (0.71) | 5 | 400.0 | 99.98 ± 0.56 (0.08) |
| Clemizole tablets[e] | 4 | 4.00 | 100.46 ± 0.93 (0.99) | 5 | 400.0 | 99.78 ± 0.46 (1.07) |
| Penicillin G sodium vial[f] | 6 | 30.00 | 100.95 ± 1.51 (1.54) | 5 | 12.0 | 100.43 ± 0.95 (1.0) |
| Piperazine powder[g] | 5 | 6.25 | 100.52 ± 0.85 (1.37) | 5 | 150.0 | 100.39 ± 0.79 (1.10) |

[a] Percent recovery in the case of naphazoline and piperazine and percent of nominal concentration in the case of the other compounds. [b] Calculated in the final dilution after the addition of chloranil. [c] Clemizole is not official in BP 1973; thus, it was assayed, as with naphazoline, by nonaqueous titration; penicillin G sodium was assayed by iodometry (2), and piperazine was assayed by nonaqueous titration (3). [d] Prepared according to Martindale (34) and contained 50 mg % of naphazoline hydrochloride. The amount of salt can be calculated from the amount of base multiplied by 1.1738. [e] Obtained commercially as Allercur tablets from Chemical Industries Development Co. (batch 641), average weight 0.19 g. Each tablet contains 20 mg of clemizole hydrochloride; the salt can be calculated by multiplying the base concentration by 1.1122. [f] Obtained commercially; each vial is stated to contain 500,000 units; 1 mg of penicillin G sodium reference standard equals 1667 units (3). [g] Analyzed powder obtained from Alexandria Co. for Pharmaceutical and Chemical Industries. The values in parentheses are calculated $t$ values for which the theoretical values at $\alpha = 0.05$ are: for $df$ 3, 3.182; for $df$ 4, 2.776; and for $df$ 5, 2.571.

(naphazoline and penicillin G sodium). The results obtained are presented in Table I. The performance of the proposed method was judged through calculation of the $t$ value. At the 95% confidence level, the calculated $t$ value did not exceed the theoretical value. Therefore, the proposed method, as with the official method, gives assay results not significantly different from the true value. This finding indicates that the methods are equally accurate.

Compared to the official methods, the proposed procedure is simpler, faster, and more sensitive. These advantages encourage its application in the analysis and quality control of drugs.

Other drugs with basic centers are expected to give similar chromophores. Amino acids and proteins also give sensitive responses (32).

## REFERENCES


(1) "British Pharmacopoeia 1973," Her Majesty's Stationery Office, London, England, 1973, p. 315.

(2) "British Pharmacopoeia 1958," Pharmaceutical Press, London, England, 1958, p. 89.

(3) "The United States Pharmacopeia," 19th rev., Mack Publishing Co., Easton, Pa., 1975, pp. 364, 386, 508.

(4) H. Abdine, A. M. Wahbi, and M. A. Korany, *J. Pharm. Pharmacol.*, **24,** 522 (1972).

(5) A. F. Moussa, *Pharmazie,* **32,** 725 (1977).

(6) A. Ismaiel and M. Twakkol, *ibid.*, **29,** 544 (1974).

(7) P. Alina and K. Elzbieta, *Acta Pol. Pharm.*, **26,** 347 (1969).

(8) S. A. Soliman, H. Abdine, and M. Morcos, *Can. J. Pharm. Sci.*, **11,** 36 (1976).

(9) H. Abdine, A. M. Wahbi, and M. A. Korany, *J. Pharm. Pharmacol.*, **24,** 518 (1972).

(10) K. Yoshiuori and N. Kougi, *Jpn. Anal.*, **24,** 742 (1975).

(11) J. H. Ford, *Anal. Chem.*, **19,** 1004 (1947).

(12) H. Weitkamp and R. Barth, *Arch. Pharm. (Weinheim, Ger.)*, **307,** 426 (1974).

(13) D. W. Hughes, A. Vilims, and W. L. Wilson, *Can. J. Pharm. Sci.*, **11,** 97 (1976).

(14) M. J. LeBelle and W. L. Wilson, *J. Pharm. Sci.*, **67,** 1495 (1978).

(15) A. Elsebai, S. M. Rida, Y. Beltagy, and M. Abdel-Khalek, *Pharmazie,* **29,** 143 (1974).

(16) B. Karlberg and U. Forsman, *Anal. Chim. Acta,* **83,** 309 (1976).

(17) J. F. Alicino, *J. Pharm. Sci.*, **65,** 300 (1976).

(18) P. D. Shirsat, *Indian J. Pharm.*, **37,** 101 (1975).

(19) V. D. Gupta, *Am. J. Hosp. Pharm.*, **33,** 283 (1976).

(20) Y. M. Dessouky and S. A. Ismaiel, *Analyst,* **99,** 482 (1974).

(21) T. R. Baggi, N. M. Surinder, and R. G. Ramana, *J. Assoc. Off. Anal. Chem.*, **57,** 1144 (1974).

(22) A. A. Abou-Auf, A. Taha, and M. B. Saidhom, *J. Pharm. Sci.*, **62,** 1700 (1973).

(23) M. S. Tawakol, S. A. Ismaiel, and M. Amer, *Pharmazie,* **31,** 609 (1976).

(24) H. Abdine, M. A. Elsayed, I. Chaaban, and M. E. Abdel-Hamid, *Analyst,* **103,** 1227 (1978).

(25) A. Taha and G. Rücker, *Arch. Pharm. (Weinheim, Ger.)*, **310,** 485 (1977).

(26) N. M. D. Brown, R. Foster, and C. A. Tyfe, *J. Chem. Soc. (R)*, **1967,** 406.

(27) R. Foster "Organic Charge Transfer Complexes," Academic, London, England, 1969, pp. 23, 33.

(28) C. N. R. Rao, S. N. Bhat, and P. C. Dwivedi, in "Applied Spectroscopy Reviews," vol. 5, E. G. Brame, Ed., Dekker, New York, N.Y., 1972, pp. 1–170.

(29) T. S. Al-Ghabsha, S. A. Rahim, and A. Townshend, *Anal. Chim. Acta,* **85,** 189 (1976).

(30) Y. Tashima, H. Hasegawa, H. Yaki, and K. Takuira, *Jpn. Anal.*, **19,** 43 (1970).

(31) J. B. Birks and M. A. Slifkin, *Nature (London)*, **197,** 42 (1963).

(32) F. Alsulimany and A. Townshend, *Anal. Chim. Acta,* **66,** 195 (1973).

(33) J. R. A. Pollock and R. Stevens "Dictionary of Organic Compounds," 4th rev., vol. 2, Eyre and Spottiswoode, London, England, 1965, p. 590.

(34) "Martindale, The Extra Pharmacopoeia," 27th ed., Pharmaceutical Press, London, England, 1977, p. xxvii.

(35) P. Job, *Ann. Chim.*, **16,** 97 (1936); through "Advanced Physicochemical Experiments," 2nd ed., Oliver and Boyd, London, England, 1964, p. 54.

(36) H. A. Benesi and J. H. Hildebrand, *J. Am. Chem. Soc.*, **71,** 2703 (1949).

(37) A. N. Martin, J. Swarbrick, and A. Cammarata, "Physical Pharmacy," 2nd ed., Lea & Febiger, Philadelphia, Pa., 1969, pp. 343, 360.

(38) E. L. Bauer, "Statistical Manual for Chemists," Academic, London, England, 1971, p. 61.

# Reversed-Phase High-Performance Liquid Chromatographic Analysis of Liothyronine Sodium and Levothyroxine Sodium in Tablet Formulations: Preliminary Studies on Dissolution and Content Uniformity

**RAO S. RAPAKA ˣ, PATRICK W. KNIGHT, and VADLAMANI K. PRASAD**

Received April 30, 1980, from the *Biopharmaceutics Laboratory, Food and Drug Administration, Washington, DC 20204.* Accepted for publication July 14, 1980.

**Abstract** □ Levothyroxine sodium was estimated from tablet formulations of levothyroxine sodium and liotrix (liothyronine sodium–levothyroxine sodium combination tablet). The procedure consisted of the addition of 3,3′,5′-triiodothyronine as the internal standard to the pulverized sample, followed by an acidic butanol extraction, evaporation, and injection onto a μBondapak reversed-phase high-performance liquid chromatographic column. The eluent was methanol–water–phosphoric acid (50:50:0.1), and the effluent was monitored by UV detection at 254 nm. A standard linear calibration curve was obtained for direct standard solutions equivalent to 18–225 μg of levothyroxine sodium/tablet. The procedure is sensitive enough for single-tablet analysis. Using this procedure, content uniformity studies were performed on liothyronine sodium tablets, levothyroxine sodium tablets, and liotrix tablets. The procedure also was adapted for conducting dissolution studies on levothyroxine sodium tablets in deionized water using the rotating-paddle method.

**Keyphrases** □ High-performance liquid chromatography—analysis, liothyronine sodium and levothyroxine sodium in tablet formulations □ Liothyronine sodium—high-performance liquid chromatographic analysis in tablet formulations □ Levothyroxine sodium—high-performance liquid chromatographic analysis in tablet formulations

In cases of hypothyroidism, a number of medications are available for thyroid replacement therapy including thyroid tablets, thyroglobulin tablets, and tablets containing synthetic amino acids, liothyronine sodium, and levothyroxine sodium. The thyroid medications are prescribed frequently, and an evaluation of the top 100 prescribed drugs in 1978 ranked a tablet dosage form containing the sodium salt of levothyroxine[1] as the 44th most frequently prescribed drug.

## BACKGROUND

The present USP procedure for the analysis of liothyronine sodium and levothyroxine sodium is based on the estimation of organic iodine (1). Procedures based on estimation of the iodine content are not specific since they do not distinguish between the various iodine-containing amino acids and, at the same time, do not distinguish between the active ingredient and the decomposition products. For the analysis of liotrix tablets (liothyronine sodium–levothyroxine sodium combination tablet), the USP method (2) consists of a laborious extraction, column chromatography, and UV determination.

Both the iodine content determination and column chromatography are insensitive and require at least 0.33–1 mg of the active ingredient for the analysis. Since the smallest dosage form of liotrix tablets contains 3.1 μg of liothyronine sodium and 12.5 μg of levothyroxine sodium, about 110 tablets are needed for a single analysis by the column chromatographic procedure. Although the USP (3) suggests content uniformity determination for all solid dosage forms that contain <50 mg of the active ingredient, a compendial requirement for content uniformity is absent for liothyronine sodium tablets, levothyroxine sodium tablets, and liotrix tablets. Furthermore, a compendial requirement for dissolution of these thyroid drugs is not imposed.

The Food and Drug Administration enacted its bioavailability and bioequivalence regulations to create a mechanism and means for establishing the bioequivalence and therapeutic equivalence of generic drug products. At present, bioequivalence of thyroid products or products containing the synthetic analogs and equivalence between the natural and synthetic products have not been established. Before undertaking bioequivalence studies, it was essential to develop simple and specific methods for the analysis of thyroid dosage forms. To perform content uniformity studies of the tablets, the required procedures must be sensitive and specific as compared to the present nonspecific iodine content assay. Moreover, content uniformity studies should be performed prior to dissolution and bioavailability studies since meaningful data can be obtained only on tablets that meet the criteria for content uniformity.

Few reports have appeared on the analysis of tablet dosage forms containing liothyronine sodium and levothyroxine sodium. Graham *et al.* (4) developed a procedure that can be applied to a tablet dosage formulation containing as low as 5 μg of liothyronine sodium or levothyroxine solution. However, this method is cumbersome and nonspecific.

A literature search for analytical methodology (5–13) revealed that previously published procedures based on TLC, paper chromatography, and column chromatography are either semiquantitative or extremely laborious and insensitive. Although some reported GLC methods (14–24) seem to have the needed sensitivity, most of the studies were done on pure synthetic mixtures or the procedures have not yet been adopted for estimation from tablets.

High-performance liquid chromatography (HPLC), a powerful analytical tool, is being used increasingly in the thyroid field (25–32). Karger and Su (25) demonstrated that thyroidal amino acids could be separated on a high-performance partition column. An instrument manufacturer (26) reported a reversed-phase HPLC method for the separation of liothyronine and levothyroxine in ~10 min. Hearn *et al.* (27) carried out a detailed investigation on qualitative separations following the method described in Ref. 26. Cieri and Illuminati (5) used HPLC to detect the presence of diiodothyronine in liothyronine sodium. Similarly, Smith and Graham (28) adapted the procedure described in Ref. 26 for estimation of impurities of diiodothyronine and triiodothyronine in pure levothyroxine samples.

Subsequent reports appeared in which the sensitivity of detection was improved (29) and in which the HPLC procedure was used in the analysis of thyroglobulin (30) or of the activity of an enzyme involved in thyroglobulin biosynthesis (31). The first adaptation of a procedure showing the feasibility of the HPLC procedure for the analysis of liothyronine sodium tablets appeared recently (32). In the present study, the procedure was investigated further for the analysis of levothyroxine sodium and liotrix tablets, for the determination of the content uniformity for liothyronine sodium, levothyroxine sodium, and liotrix tablets, and for dissolution studies on levothyroxine sodium tablets.

## EXPERIMENTAL

**Reagents and Chemicals**—Liothyronine sodium and levothyroxine sodium hexahydrate were obtained commercially[2]. 3,3′,5′-Triiodothyronine was obtained as a gift[3]. Commercial brands of liothyronine sodium tablets USP, levothyroxine sodium tablets USP, and liotrix tablets USP were purchased from a wholesale drug distributor[4]. All chemicals were

[1] Synthroid, Division of Travenol Laboratories, Deerfield, IL 60015.

[2] Sigma Chemical Co., St. Louis, Mo.

[3] Nuclear-Medical Laboratories, Dallas, Tex.

[4] The liothyronine tablets (Manufacturer A), levothyroxine sodium tablets (Manufacturers B and C), and liotrix tablets (Manufacturers D and E) were obtained from District Wholesale Co., Washington, D.C.

0022-3549/81/0200-0131$01.00/0
© 1981, American Pharmaceutical Association

reagent grade. Stock solutions of liothyronine sodium, levothyroxine sodium, and 3,3′,5′-triiodothyronine were made in 2% ammonium hydroxide in methanol at 100 μg/ml, and appropriate dilutions were made when required.

**Apparatus**—The modular high-performance liquid chromatograph consisted of a constant-flow pump[5], a loop-type injector[6], a UV detector[7], and a strip-chart recorder[8] (0.25 cm/min). Stainless steel columns[9,10], packed with fully porous 10-μm silica particles to which was chemically bonded a monomolecular layer of octadecylsilane, were obtained commercially. A stainless steel precolumn[11] (2.5 × 0.25 cm) packed with a pellicular reversed-phase material was used. Co:Pel ODS was placed in line to remove unwanted material from the sample prior to passage onto the analytical column. Dissolution studies were performed on the dissolution apparatus[12] using the USP rotating-paddle method.

**Chromatographic Conditions**—The mobile phase was methanol–water–phosphoric acid (50:50:0.1 v/v/v). Flow rates of 1.5 and 2 ml/min were used in the analyses of liothyronine sodium tablets and levothyroxine sodium and liotrix tablets, respectively. Another mobile phase that was useful was prepared by mixing methanol and 0.1 *M* ammonium acetate (pH 5.0) in a 50:50 (v/v) ratio. The flow rate was 2 ml/min (Fig. 1). The mobile phase was degassed prior to use.

**Procedure**—All of the glass vessels were silanized, and the glassware was wrapped with aluminum foil. A single tablet of levothyroxine sodium, liothyronine sodium, or liotrix or a weighed amount of ground powder of any of these tablets was taken in an erlenmeyer flask and assayed as described previously for liothyronine sodium tablets (32).

Levothyroxine sodium concentrations were determined from a standard curve. The standard curve was obtained from standard samples, each containing 50 μg of 3,3′,5′-triiodothyronine (the internal standard) and 18–225 μg of levothyroxine sodium. The standard samples were subjected to the same procedure as the tablets. The peak height ratio of levothyroxine sodium to the internal standard was plotted against the concentration of levothyroxine sodium, and a straight-line correlation was obtained ($r$ = 0.9993). A standard curve was developed similarly with liothyronine sodium and 3,3′,5′-triiodothyronine (the internal standard) to obtain a straight-line correlation ($r$ = 0.995), and liothyronine sodium concentrations were obtained from the standard curve.

**Recovery**—Known aliquots from solutions containing different concentrations of levothyroxine sodium were injected onto the high-performance liquid chromatograph, and peak heights were obtained. A straight-line correlation was obtained for the peak height as a function of concentration. Similarly, peak heights obtained from experimentally processed samples gave a straight-line correlation when plotted against concentrations. The ratio of the slopes was used to estimate the percent recovery. The recoveries for levothyroxine sodium were excellent (98–100%).

**Precision**—The precision of the method for determining levothyroxine sodium was established by analyzing standard solutions of levothyroxine sodium of several concentrations. The samples were analyzed in triplicate as described.

**Dissolution Studies on Levothyroxine Sodium**—Dissolution studies were conducted only on levothyroxine sodium tablets. The USP rotating-paddle method was used with 500 ml of deionized water as the dissolution medium at 37 ± 0.5°.

*Feasibility for Various Dosage Forms*—Dissolution studies were done at 50 rpm on four dosage forms, *i.e.*, 25, 50, 100, and 200 μg, of two commercial brands. A single sample of the dissolution medium was taken at the end of 40 min. The procedure for estimation of levothyroxine sodium in the dissolution sample will be described.

*Time Course Study*—Feasibility for the time course study was conducted on 0.5-mg levothyroxine sodium tablets. The speed of the paddles was set at 75 rpm. Samples were taken at 5, 10, 20, 40, 80, and 100 min. The dissolution samples were processed as will be described.

*Estimation of Levothyroxine Sodium*—The dissolution sample was filtered, and a known volume (50 ml for 25-, 50-, and 100-μg tablets, 25 ml for 200-μg tablets, and 10 ml for the time course of dissolution) was placed in the erlenmeyer flask. To this sample was added concentrated hydrochloric acid equivalent to 25% of the volume of the sample and 1.5 volumes of $n$-butanol. Ten micrograms of 3,3′,5′-triiodothyronine (the internal standard) also was added, and the mixture was stirred for 30 min. The mixture then was placed in a separator. The upper butanolic layer was separated and washed four times with water-saturated butanol. The washed butanolic solution was evaporated to dryness. The residue was dissolved in a known volume of 2% ammonium hydroxide in methanol (usually 200 μl), and an aliquot was injected onto the high-performance liquid chromatograph.

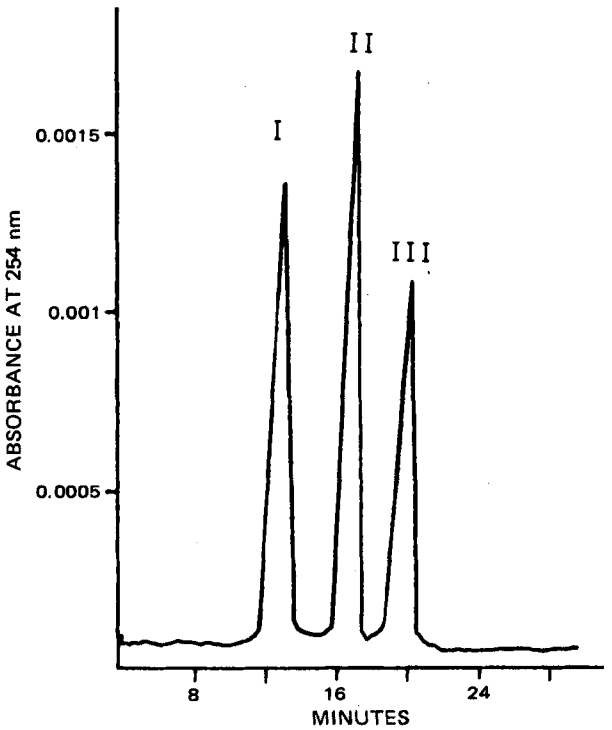


**Figure 1**—*High-performance liquid chromatogram of liothyronine (I), 3,3′,5′-triiodothyronine (II, internal standard), and levothyroxine (III) obtained on a μBondapak $C_{18}$ reversed-phase column using a mobile phase of methanol–0.1 M ammonium acetate (pH 5.0) (50:50 v/v).*

Levothyroxine sodium concentrations were determined from a standard curve obtained by plotting peak height ratios of levothyroxine sodium and the internal standard as a function of known levothyroxine sodium concentrations. These samples were subjected to the same experimental conditions as the dissolution samples from the tablets.

## RESULTS AND DISCUSSION

Several solvent systems were investigated for the HPLC analysis of the thyroidal amino acids, and methanol and ammonium acetate gave good separation of liothyronine, 3,3′,5′-triiodothyronine (the internal standard), and levothyroxine (Fig. 1). Several commercially available columns also were tried. A Partisil ODS-3[10] column gave better separation than that reported by Hearn *et al.* (27) under their given conditions (Fig. 2). However, both the μBondapak $C_{18}$ and the Partisil ODS-3 columns were satisfactory. Hence, the analysis of liothyronine sodium and levothyroxine sodium from tablets was carried out on a μBondapak $C_{18}$ column[9] and the dissolution samples of levothyroxine sodium were analyzed on a Partisil ODS-3 column[10].

**Table I—Precision of the HPLC Method for Levothyroxine Sodium from Standard Solutions**

| Total Theoretical Amount, μg | Amount Found (Range), μg | $CV^a$, % |
|---|---|---|
| 18 | 17.7 (17.5–17.8) | 1.4 |
| 27 | 26.7 (26.0–27.2) | 2.5 |
| 63 | 65.9 (64.9–66.5) | 1.3 |
| 90 | 88.5 (87.8–89.3) | 0.8 |
| 180 | 175.4 (173.0–177.6) | 1.3 |
| 225 | 228.5 (226.7–231.8) | 1.2 |

[a] $n$ = 3.

[5] Model 6000A, Waters Associates, Milford, Mass.
[6] SVOV-6, Glenco Scientific Inc., Houston, Tex.
[7] Model 440, Waters Associates, Milford, Mass.
[8] Direct-current analog recorder, Linear Instruments Corp.
[9] μBondapak $C_{18}$ column (30 cm × 3.9 mm i.d.), Waters Associates, Milford, Mass.
[10] Partisil ODS-3 column (25 cm × 4.6 mm i.d.), Whatman, Clifton, NJ.
[11] Whatman, Clifton, NJ.
[12] Model 72 S 115, Hanson Research Corp., Northridge, Calif.

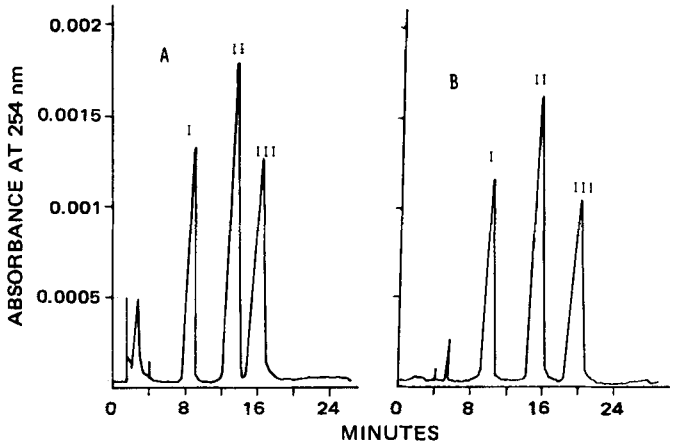


**Figure 2**—*High-performance liquid chromatograms of liothyronine (I), 3,3′,5′-triiodothyronine (II, internal standard), and levothyroxine (III) obtained on a μBondapak $C_{18}$ reversed-phase column using a mobile phase of methanol–water–phosphoric acid (50:50:0.1 v/v) (A) and of I–III obtained on a Partisil ODS-3 reversed-phase column using the same mobile phase (B).*

Levothyroxine sodium tablets were assayed following the general method described for the analysis of liothyronine sodium tablets. Analysis of levothyroxine sodium tablets by HPLC (without the internal standard) revealed that 3,3′,5′-triiodothyronine is not present in significant amounts (<2%) so it is a suitable internal standard. A straight-line correlation was obtained between the peak height ratios of levothyroxine sodium to 3,3′,5′-triiodothyronine (the internal standard) and the concentration of levothyroxine sodium. The method gave good precision (coefficient of variation of ≤2.5%) for levothyroxine sodium in the range of 18–225 μg (Table I). Similarly, good correlation was obtained between the peak height ratio of liothyronine sodium to 3,3′,5′-triiodothyronine (the internal standard) and the liothyronine sodium concentration in the range of 10–70 μg. The concentrations of liothyronine sodium and levothyroxine sodium from samples of unknown concentrations were determined from such standard curves.

Content uniformity is a general requirement in the USP for all dosage forms that contain active ingredients of 50 mg or less, provided that there is a method available for the analysis of a single tablet (3). Content uniformity assures that successive units from a given container will provide substantially equal amounts of drug. The dosage strengths that are marketed for liothyronine sodium tablets range from 5 to 50 μg; for levothyroxine sodium tablets, they range from 25 to 500 μg; and for liotrix tablets containing liothyronine sodium and levothyroxine sodium, they range from 3.1 μg of liothyronine sodium and 12.5 μg of levothyroxine sodium to 62.5 μg of liothyronine sodium and 250 μg of levothyroxine sodium.

Commercially available liothyronine sodium tablets were analyzed. In addition, for two of the dose levels, 20 tablets were pulverized, and composite powder equivalent to a single tablet was weighed and analyzed in triplicate. The analytical results are presented in Table II. The mean value of the composite material was in close agreement to the mean of the 10 individual analyses. The USP states that liothyronine sodium tablets contain an amount of liothyronine sodium equivalent to not less than 90.0% and not more than 110.0% of the labeled amount of liothyronine. Hence, the individual assay values of the tablets were reported for liothyronine and not for liothyronine sodium. If the general USP requirement for content uniformity is imposed, the individual analysis for the tablets for liothyronine should be in the range of 100 ± 15%. At both dose levels, these tablets conformed to the compendial requirements.

Individual tablet analysis of 100- and 200-μg levothyroxine sodium tablets from two manufacturers was carried out, and the results are shown in Table III. If general compendial requirements are imposed, the tablets should contain 102.5 ± 15%, *i.e.*, 87.3–117.5%, of the active ingredient. The tablets conformed to these requirements. Similarly, liotrix tablets of two commercial brands, at a single dose level, were subjected to individual tablet analysis. Liothyronine sodium and levothyroxine sodium were analyzed simultaneously. Both brands of tablets met the compendial assay requirement of 86.1–116.4% (101.25 ± 15%) of the declared value for both liothyronine sodium and levothyroxine sodium contents. The results are presented in Table IV.

The fifth supplement to USP XIX also requires that the weight ratio of levothyroxine sodium to liothyronine sodium be 4:1. The ratio in the present experiments was in the range of 3.69 ± 0.32 for tablets from one manufacturer and 3.51 ± 0.12 for tablets from another manufacturer. Thus, both firms failed to meet the ratio requirement. If both liothyronine sodium and levothyroxine sodium are allowed by the USP to be present

**Table II—Content Uniformity of Liothyronine Sodium Tablets**

| Manufacturer | Dosage Strength, μg | Individual Tablet Assay as Liothyronine, μg | Mean ± *SD* | Percent of Labeled Strength | Analysis of Composite, μg ± *SD*[a] |
|---|---|---|---|---|---|
| A | 25 | 22.1, 25.7, 21.2, 21.3, 21.9, 23.1, 23.2, 24.9, 22.8, 27.4 | 23.4 ± 2.0 | 84.9–109.4 | 23.2 ± 0.9 |
| B | 50 | 48.6, 48.1, 48.1, 50.1, 46.1, 48.1, 45.7, 40.7, 48.5, 57.0 | 47.9 ± 1.8 | 90.9–101.3 | 48.0 ± 0.4 |

[a] Average of three determinations.

**Table III—Content Uniformity of Levothyroxine Sodium Tablets USP**

| Manufacturer | Dosage Strength, μg | Individual Tablet Assay, μg | Mean (Range), μg | Mean Percent of Labeled Strength (Range) |
|---|---|---|---|---|
| B | 100 | 92.7, 97.2, 100.0, 95.7, 96.8, 101.3, 94.7, 98.2, 101.4, 102.0 | 98.0 (92.7–102.0) | 98.0 (92.7–102.0) |
| B | 200 | 188.3, 182.1, 180.8, 184.9, 201.9, 187.9, 184.9, 189.0, 196.6, 188.5 | 188.5 (180.0–201.9) | 94.2 (90.4–100.9) |
| C | 100 | 104.0, 93.6, 93.9, 94.4, 95.0, 94.6, 94.2, 89.3, 98.8, 98.9 | 95.7 (89.3–104.0) | 95.7 (89.3–104.0) |
| C | 200 | 197.5, 196.5, 187.3, 192.2, 183.2, 196.7, 196.5, 195.9, 192.3, 205.5 | 194.3 (183.2–205.5) | 97.2 (91.6–102.7) |

**Table IV—Content Uniformity of Liotrix (Liothyronine Sodium–Levothyroxine Sodium) Tablets USP**

| Manufacturer and Labeled Dosage | Liothyronine Sodium | | Levothyroxine Sodium | | Ratio of Levothyroxine Sodium to Liothyronine Sodium ± *SD* |
|---|---|---|---|---|---|
| | Mean (Individual Tablet Analysis), μg | Amount Range and Range of Percent of Labeled Strength | Mean (Individual Tablet Analysis), μg | Amount Range and Range of Percent of Labeled Strength | |
| D, 45 μg of liothyronine sodium and 180 μg of levothyroxine sodium | 48.2 (47.6, 48.8, 48.8, 48.8, 48.8, 46.7, 48.8, 47.4, 47.6, 48.8) | 46.7–48.8 μg 104.9–108.4% | 169.3 (162.0, 169.7, 171.5, 163.8, 174.4, 171.8, 168.3, 176.2, 169.7, 165.8) | 162.0–176.2 μg 90.0–97.88% | 3.51 ± 0.12 |
| E, 62.5 μg of liothyronine sodium and 250 μg of levothyroxine sodium | 64.0 (60.2, 65.2, 58.8, 66.9, 64.1, 58.2, 68.8, 69.8, 63.9, 64.2) | 58.2–69.8 μg 93.1–111.7% | 235.2 (234.6, 237.0, 237.4, 245.5, 258.1, 226.2, 249.6, 221.3, 221.3, 222.6) | 219.8–258.1 μg 87.9–103.2% | 3.69 ± 0.32 |

**Table V—Dissolution Study of Levothyroxine Sodium Tablets USP in 500 ml of Deionized Water Using 50-rpm Rotating-Paddle Method**

| Manufacturer | Dosage, μg | Average Percent Dissolved at 40 min | *SD* |
|---|---|---|---|
| B | 25 | 31.6 | 5.0 |
| | 50 | 51.1 | 5.3 |
| | 100 | 44.2 | 10.2 |
| | 200 | 60.3 | 18.7 |
| C | 25 | 58.9 | 6.2 |
| | 50 | 47.6 | 13.2 |
| | 100 | 43.3 | 7.3 |
| | 200 | 56.2 | 10.4 |

at an amount of 101.25 ± 15%, it is possible that one component may be present at the higher limit (116.4%) and the other one may be present at the lower limit (86.1%), and the tablet still may pass the content uniformity requirement. In such a case, the tablet cannot meet the 4:1 levothyroxine sodium to liothyronine sodium weight ratio requirement. For example, for a liotrix tablet containing 100 μg of levothyroxine sodium and 25 μg of liothyronine sodium, if levothyroxine sodium is present at the upper limit, 116.4% (*i.e.*, 116.4 μg of levothyroxine sodium) and liothyronine sodium is present at the lower limit, 86.1% (*i.e.*, 25 μg × 0.861 = 21.53 μg), the levothyroxine sodium to liothyronine sodium ratio would be 5.41. At the other extreme, where levothyroxine sodium is present at the lower permitted limit and liothyronine sodium is present at the higher permitted limit, the ratio is 2.95. Hence, the levothyroxine sodium to liothyronine sodium ratio could vary from 2.95 to 5.41 while still meeting the compendial requirements for content uniformity of the individual active ingredients. This point could be important for the physician prescribing these drugs, and it is recommended that the USP look into the conflicting requirements for content uniformity and the levothyroxine sodium to liothyronine sodium weight ratio.

The applicability of this new procedure for analysis of samples from the dissolution medium was investigated. The dissolution procedure was tested only on levothyroxine sodium tablets. A straight-line correlation was obtained using standard solutions of levothyroxine sodium and 3,3′,5′-triiodothyronine (the internal standard) as described under *Experimental* ($r = 0.999$; $CV = 4.5\%$ in the range of 0–20 μg of levothyroxine sodium). The feasibility of this procedure was tested on four dosage levels of levothyroxine sodium for two commercial brands, and the dissolution ranged between 30 and 60% after 40 min (Table V). The method proposed here appears to be suitable for study of the dissolution at a single time point.

This procedure also appears to be useful for time course studies of dissolution for a higher dosage of levothyroxine sodium tablets (Fig. 3). The dissolution studies and content uniformity studies were preliminary feasibility studies only, and a detailed investigation is underway.

The utility of the HPLC method for the analysis of levothyroxine sodium tablets, the determination of content uniformity of liothyronine sodium, levothyroxine sodium, and liotrix tablets, and for dissolution studies of levothyroxine sodium tablets was demonstrated. The method is simple, specific, and sensitive.

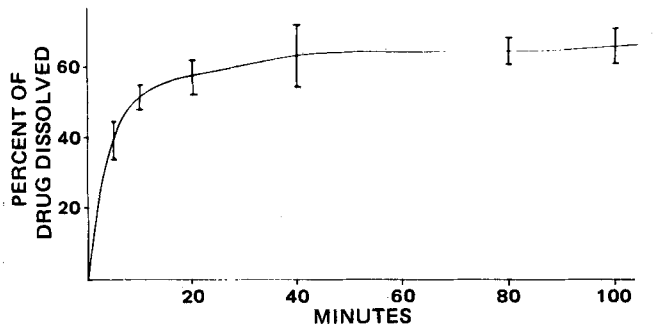


**Figure 3**—*Dissolution profile obtained for 500-μg levothyroxine sodium tablets USP in 500 ml of deionized water at 37° using the USP rotating-paddle method at 75 rpm.*

## REFERENCES


(1) "The United States Pharmacopeia," 19th rev., Mack Publishing Co., Easton, Pa., 1975, pp. 282, 286.

(2) "Fourth Supplement to the United States Pharmacopeia," 19th rev., Mack Publishing Co., Easton, Pa., 1979, p. 106.

(3) "The United States Pharmacopeia," 19th rev., Mack Publishing Co., Easton, Pa., 1975, pp. xvi, 648.

(4) J. A. Graham, D. Banes, M. E. Biesemeyer, and A. Nadakarni, *J. Pharm. Sci.*, **63,** 763 (1974).

(5) U. R. Cieri and J. C. Illuminati, *J. Assoc. Off. Anal. Chem.*, **60,** 628 (1977).

(6) M. A. Faircloth, A. D. Williams, and W. H. Florsheim, *Anal. Biochem.*, **12,** 437 (1965).

(7) M. Dobias, J. Mucha, and P. Talan, *Radiochem. Radioanal. Lett.*, **33,** 179 (1978).

(8) S. Kologlu, H. L. Schwartz, and A. C. Carter, *Endocrinology*, **78,** 231 (1966).

(9) R. Lemieux and J. M. Talmage, *J. Pharm. Pharmacol.*, **18,** 94 (1966).

(10) A. D. Williams, D. E. Freeman, and W. H. Florsheim, *J. Chromatogr.*, **45,** 371 (1969).

(11) A. D. Williams, D. E. Freeman, and W. H. Florsheim, *J. Chromatogr. Sci.*, **9,** 619 (1971).

(12) C. Peyton and C. Simon, *J. Chromatogr.*, **92,** 309 (1974).

(13) P. Thomopoulose, *Anal. Biochem.*, **65,** 600 (1975).

(14) F. Shahrokhi and C. W. Gehrke, *ibid.*, **24,** 281 (1968).

(15) N. M. Alexander and R. Scheig, *ibid.*, **22,** 187 (1968).

(16) K. Funakoshi and H. J. Cahnmann, *ibid.*, **27,** 150 (1969).

(17) E. C. Volpert, N. Kundu, and J. B. Dawidzik, *J. Chromatogr.*, **50,** 510 (1970).

(18) R. Bilouis and J. S. Windheuser, *J. Pharm. Sci.*, **62,** 274 (1973).

(19) N. N. Nihei, M. C. Gershengorn, T. Mitsuma, L. R. Stringham, A. Cordy, B. Kuchmy, and C. S. Hollander, *Anal. Biochem.*, **43,** 433 (1971).

(20) R. Docter and G. Henneman, *Clin. Chim. Acta*, **34,** 297 (1971).

(21) B. A. Petersen, R. N. Hanson, R. W. Giese, and B. L. Karger, *J. Chromatogr.*, **126,** 503 (1976).

(22) B. A. Petersen, R. W. Giese, P. R. Larsen, and B. L. Karger, *Clin. Chem.*, **23,** 1389 (1977).

(23) G. J. Manius, P. Fallon, and R. Tscherne, *Anal. Biochem.*, **87,** 496 (1978).

(24) R. O. Zimmerer, Jr., and L. T. Grady, *J. Pharm. Sci.*, **60,** 493 (1971).

(25) B. L. Karger and S. C. Su, *J. Chromatogr. Sci.*, **12,** 678 (1974).

(26) Application Highlight 19, Waters Associates, Milford, Mass., 1976.

(27) M. T. Hearn, W. S. Hancock, and C. A. Bishop, *J. Chromatogr.*, **157,** 337 (1978).

(28) D. S. Smith and J. H. Graham, *J. Assoc. Off. Anal. Chem.*, **62,** 818 (1979).

(29) F. Nachtmann, G. Knapp, and H. Spitzy, *J. Chromatogr.*, **149,** 693 (1978).

(30) N. M. Alexander and M. Nishimoto, *Clin. Chem.*, **25,** 1757 (1979).

(31) G. C. Skellern, M. Mahmoudian, and B. I. Knight, *J. Chromatogr.*, **179,** 213 (1979).

(32) R. S. Rapaka, P. W. Knight, and V. K. Prasad, *Anal. Lett.*, **12,** 1201 (1979).


## ACKNOWLEDGMENTS


The authors thank Dr. T. J. Goehl for helpful discussions. They also thank Dr. Russel Saunders, Nuclear Medical Laboratories, for the gift of 3,3′,5′-triiodothyronine.

# Synthesis of Alkylaminoalkylamides of Substituted 2-Aminopyrroles as Potential Local Anesthetic and Antiarrhythmic Agents I: α-Amines

J. WALTER SOWELL, Sr. *x, ALAN J. BLOCK ‡, MARY ELIZABETH DERRICK *§, JOHN J. FREEMAN *, JOSEPH W. KOSH *, RONALD J. MATTSON *, PHILIP F. MUBARAK *§, and PAUL A. TENTHOREY ‡¶

Received March 31, 1980, from the *College of Pharmacy, University of South Carolina, Columbia, SC 29208, and ‡Astra Research Laboratory, Framingham, MA 01701. Accepted for publication June 27, 1980. §Present address: Medical University of South Carolina, Charleston, SC 29403. ¶Present address: Bristol-Myers International Division, New York, NY 10022.

**Abstract** □ The synthesis, local anesthetic and antiarrhythmic properties, and CNS toxicity of 19 2-(2-alkylaminoalkylamido)pyrroles are described. Most of the compounds exhibited local anesthetic activity by the guinea pig wheal test, and four showed activity comparable to or greater than that of lidocaine. Most compounds also exhibited antiarrhythmic activity; five compounds had activity comparable to that of lidocaine, and one was more potent. All compounds exhibiting antiarrhythmic activity also were toxic to the central nervous system.

**Keyphrases** □ 2-(2-Alkylaminoalkylamido)pyrroles—synthesis and evaluation for local anesthetic and antiarrhythmic properties and CNS toxicity □ Antiarrhythmic agents—2-(2-alkylaminoalkylamido)pyrroles, synthesis and evaluation for activity □ Anesthetic activity—2-(2-alkylaminoalkylamido)pyrroles, synthesis and evaluation for local anesthetic activity

The success of lidocaine as a local anesthetic (1) and antiarrhythmic agent (2) has served as an impetus for the synthesis and pharmacological evaluation of numerous analogs and homologs of this drug. Modifications of the aminoacyl portion of this structure and the effects of these modifications on biological activity have been studied extensively (3–6).

Branching of the aminoacyl chain in this structure has proven to be a successful structural modification for local anesthetic and antiarrhythmic properties. From these research endeavors, prilocaine (7), etidocaine (8), mepivacaine (9), and bupivacaine (9) have been introduced as local anesthetics. More recently, tocainide (I) was synthesized (4) and currently is in the third phase of clinical trials as an orally effective antiarrhythmic agent.

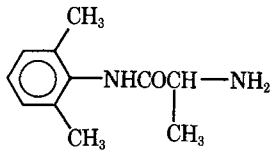

I

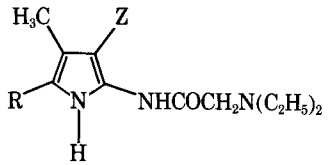

II: Z = CN
III: Z = $CONH_2$

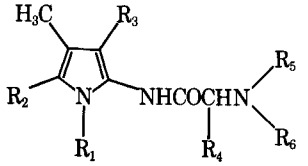

IV

In previous work directed toward heterocyclic replacement of the benzenoid ring system in lidocaine, the synthesis and local anesthetic and antiarrhythmic properties of a series of 2-diethylaminoacetamido-3-cyano-4-methyl-5-substituted pyrroles (II) and a series of the corresponding 3-carbamyl analogs (III) were studied (10, 11). The results of these studies, together with the positive results obtained from branching of the aminoacyl chain in lidocaine, prompted the synthesis and pharmacological evaluation of the alkylaminoalkylamides (IV) of various substituted 2-aminopyrroles.

## RESULTS AND DISCUSSION

**Chemistry**—The synthesis of the alkylaminoalkylamides (IV) of substituted 2-aminopyrroles is illustrated in Schemes I–III. All of the compounds possessing an asymmetric center were obtained as a racemic mixture, and no attempts were made to resolve the racemates.

Acylation of 2-amino-3-cyano-1,4,5-trimethylpyrrole (V) (12) in acetone, utilizing pyridine as a base, with 2-bromopropionyl chloride or chloroacetyl chloride gave the α-haloamide (VI*a* or VI*b*), respectively (Scheme I). The 2-(2-alkylaminopropionamido)-3-cyano-1,4,5-trimethylpyrroles (VII*a*–VII*f*) were obtained by displacement of the α-halogen in VI*a* with the appropriate primary or secondary amine. This displacement was accomplished by refluxing (2–3 hr) a solution of VI*a* in absolute ethanol with a four- to fivefold excess of the amine. 2-Diethylaminoacetamido-3-cyano-1,4,5-trimethylpyrrole (VII*g*) was obtained by reacting VI*b* with excess diethylamine by the same procedure.

In general, the free amines (VII*a*–VII*g*) were isolated by removal of the ethanol and excess unreacted amines *in vacuo*. The crude residues were dissolved in 10% HCl, the solutions were filtered, and the free amines (VII*a*–VII*g*) were extracted into chloroform after the aqueous solutions were made basic (pH 9–10) with potassium hydroxide. After the chloroform extracts were dried, the chloroform was removed *in vacuo*. The amine residues (VII*a*–VII*g*) were purified further by recrystallization (or reoiling) from cyclohexane or cyclohexane–benzene (4:1). These gummy semisolids or oils were used for hydrochloride salt formation without further purification.

The amine hydrochlorides (VIII*a*–VIII*g*) were prepared by treating an acetone solution of the free amines (VII*a*–VII*g*) with concentrated hydrochloric acid.

In the second series, 2-amino-3-cyano-4-methyl-5-substituted pyrroles (IX–XI) (13, 14) in acetone were acylated with 2-bromopropionyl chloride, utilizing pyridine as a base, to yield the corresponding α-halopropionamides (XII–XIV) (Scheme II). Nucleophilic displacement of the α-halogen with sodium azide in refluxing methanol gave the corresponding alkyl azides. Catalytic hydrogenation of the alkyl azides at 40–50 psi, utilizing 10% palladium-on-carbon as the catalyst and methanol–chloroform (100:3) as the solvent (15), gave the corresponding 2-(2-aminopropionamido)-3-cyano-4-methyl-5-substituted pyrrole hydrochlorides (XV–XVII).

Acylation of 2-amino-3-cyano-4,5-dimethylpyrrole (IX) with 2-chloropropionyl chloride by the procedure described previously gave the 2-chloropropionamide (XVIII) in a 96.1% yield (Scheme III). Compound

0022-3549/81/0200-0135$01.00/0
© 1981, American Pharmaceutical Association

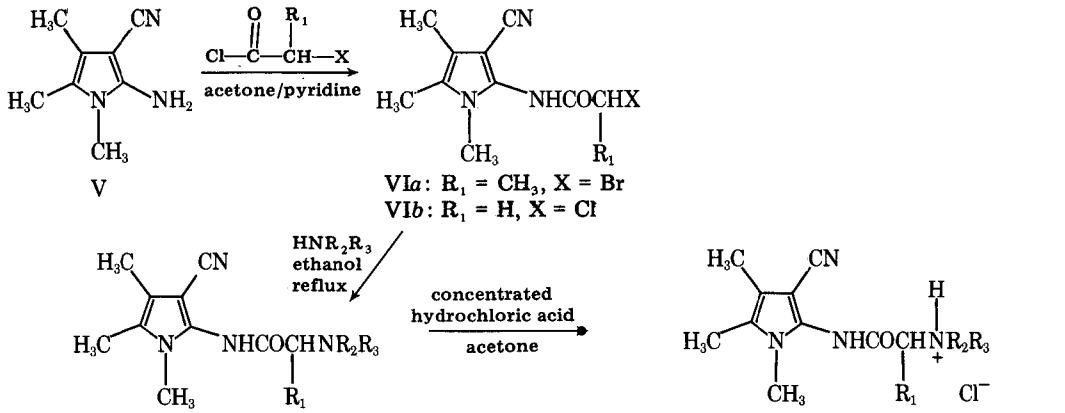


V

VI*a*: $R_1 = CH_3$, X = Br
VI*b*: $R_1$ = H, X = Cl

VII*a*: $R_1 = CH_3$, $R_2 = iso\text{-}C_4H_9$, $R_3$ = H
VII*b*: $R_1 = CH_3$, $R_2 = n\text{-}C_4H_9$, $R_3$ = H
VII*c*: $R_1 = CH_3$, $R_2 = R_3 = C_2H_5$
VII*d*: $R_1 = CH_3$, $R_2 + R_3 = -(CH_2)_4-$
VII*e*: $R_1 = CH_3$, $R_2 + R_3 = -(CH_2)_5-$
VII*f*: $R_1 = CH_3$, $R_2$ = cyclo-$C_6H_{11}$, $R_3$ = H
VII*g*: $R_1$ = H, $R_2 = R_3 = C_2H_5$

VIII*a*: $R_1 = CH_3$, $R_2 = iso\text{-}C_4H_9$, $R_3$ = H
VIII*b*: $R_1 = CH_3$, $R_2 = n\text{-}C_4H_9$, $R_3$ = H
VIII*c*: $R_1 = CH_3$, $R_2 = R_3 = C_2H_5$
VIII*d*: $R_1 = CH_3$, $R_2 + R_3 = -(CH_2)_4-$
VIII*e*: $R_1 = CH_3$, $R_2 + R_3 = -(CH_2)_5-$
VIII*f*: $R_1 = CH_3$, $R_2$ = cyclo-$C_6H_{11}$, $R_3$ = H
VIII*g*: $R_1$ = H, $R_2 = R_3 = C_2H_5$

*Scheme I*

XVIII, the corresponding 2-bromopropionamide (XII), and 2-(2-bromopropionamido)-3-cyano-4-methyl-5-isobutylpyrrole (XIII) were utilized as precursors for the synthesis of a series of 2-(2-alkylaminopropionamido)-3-cyano-4-methyl-5-substituted pyrroles (XIX*a*–XIX*e* and XXI). The synthesis of these compounds and their conversion to the corresponding hydrochloride salts (XX*a*–XX*e* and XXII) were analogous to the procedure described in Scheme I.

Hydrolysis of the nitrile (11) in XVIII in 85% phosphoric acid at 100° gave 2-(2-chloropropionamido)-3-carbamyl-4,5-dimethylpyrrole (XXIII) in a 46% yield after purification. This intermediate was utilized as a common precursor for the synthesis of the 2-(2-alkylaminopropionamido)-3-carbamyl-4,5-dimethylpyrroles (XXIV*a*–XXIV*c*) (Scheme III). The general procedure described previously was utilized in their synthesis.

The corresponding hydrochloride salts (XXV*a*–XXV*c*) were prepared by the acetone–concentrated hydrochloric acid procedure. Compound XXV*c* precipitated from acetone as white crystals; however, upon exposure to the atmosphere, the hygroscopic salt could not be isolated as a solid. After repeated attempts, the free base (XXIV*c*) was characterized.

Data for the various 2-haloalkylamides, used as precursors in this study, are given in Table I. TLC and elemental analyses were used in determining the purity of these amides. The IR and NMR spectra were consistent with the assigned structures.

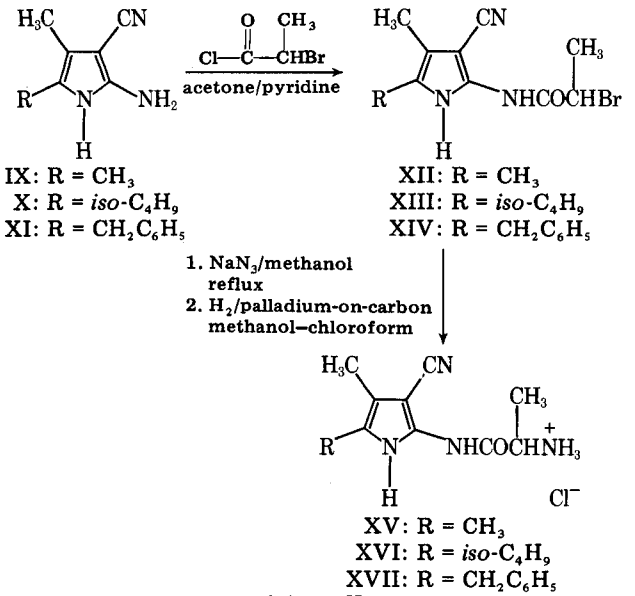


IX: R = $CH_3$
X: R = $iso\text{-}C_4H_9$
XI: R = $CH_2C_6H_5$

XII: R = $CH_3$
XIII: R = $iso\text{-}C_4H_9$
XIV: R = $CH_2C_6H_5$

XV: R = $CH_3$
XVI: R = $iso\text{-}C_4H_9$
XVII: R = $CH_2C_6H_5$

*Scheme II*

The yields, melting points, and purification data for the 2-(2-alkylaminoalkylamido)pyrroles are given in Table II. With the exception of XXIV*c*, these amines were characterized as their hydrochloride salts.

Data for the various 2-(2-alkylaminoalkylamido)pyrrole hydrochlorides are presented in Table III. The purity of these salts was determined by TLC and elemental analysis. The NMR and IR spectra were consistent with the assigned structures.

**Pharmacology**—*Local Anesthetic Activity*—Various degrees of activity were observed for all of the 2-(2-alkylaminoalkylamido)pyrrole hydrochlorides that contained the nitrile function at the 3-position (Table IV). Compounds XX*a* and XXII were comparable to lidocaine by the method employed for evaluation of local anesthetic activity. Compound XVI was slightly more active than lidocaine. The most potent compound in this series was VIII*f*, which had a duration of local anesthetic activity 1.67 times that of lidocaine when compared at a concentration of 0.125%.

Compounds XXV*a*–XXV*c*, which all possess a carbamyl function at the 3-position, were devoid of local anesthetic activity. The loss of activity may be the result of relatively low lipophilicity. Previous observations (10, 11) that pyrrole analogs of lidocaine with a 3-cyano substituent are more potent than the corresponding 3-carbamyl derivatives, except where substituents in the 5-position are large and very lipophilic, are consistent with this interpretation.

*Antiarrhythmic Activity and Acute Central Nervous System (CNS) Toxicity*—Both activities were determined in mice following subcutaneous administration of the target compounds. Respiratory arrest was induced by exposure to chloroform, and ventricular rates were measured from ECG recordings. Reduction of the incidence of ventricular tachycardia was interpreted as an antiarrhythmic effect. The presence of ataxia during the period between drug administration and exposure to chloroform was interpreted as a sign of acute CNS toxicity.

In general, the compounds listed in Table V evoked dose-dependent reductions in the incidence of tachycardia after chloroform treatment. Several compounds (VIII*a*, VIII*d*, VIII*e*, VIII*g*, and XX*b*) had a potency similar to that of lidocaine, and one compound (XVI) was more potent. Structure–activity analyses based on the limited chemical and biological information gave partially inconsistent results. While the pyrrolidinyl derivative VIII*d* with an $N^1$-methyl substituent had the lowest $ED_{50}$ value for protection among VIII*a*–VIII*g*, the corresponding compound with an $N^1$-hydrogen substituent (XX*d*) had the highest $ED_{50}$ value (together with XX*c*) among XX*a*–XX*e*. Conversely, while XX*b* was the most potent compound among XX*a*–XX*e*, the corresponding VIII*b* was not particularly potent but was very toxic. In general, pyrrole derivatives with an $N^1$-methyl substituent appear to be more potent and more toxic than those with an $N^1$-hydrogen substituent.

As with lidocaine, these compounds evoked acute CNS side effects at

**Table I—Data for 2-Haloalkylamides of Substituted 2-Aminopyrroles**

| Compound | Yield, % | Melting Point | $R_f$[a] | Recrystallization Solvent | Formula | Analysis, % | Calc. | Found |
|---|---|---|---|---|---|---|---|---|
| VI*a*[b] | 54.2 | 169–170° dec. | 0.55 | Ethanol | $C_{11}H_{14}BrN_3O$ | C | 46.49 | 47.85 |
| | | | | | | H | 4.97 | 5.12 |
| | | | | | | Br | 28.12 | 28.91 |
| | | | | | | N | 14.79 | 15.17 |
| VI*b* | 55.4 | 173–173.5° | 0.63 | Methanol | $C_{10}H_{12}ClN_3O$ | C | 53.22 | 53.10 |
| | | | | | | H | 5.36 | 5.41 |
| | | | | | | Cl | 15.71 | 15.68 |
| | | | | | | N | 18.62 | 18.58 |
| XII | 93.1 | 212–212.5° | 0.65 | Ethanol | $C_{10}H_{12}BrN_3O$ | C | 44.44 | 44.48 |
| | | | | | | H | 4.47 | 4.48 |
| | | | | | | Br | 29.60 | 29.52 |
| | | | | | | N | 15.56 | 15.56 |
| XIII[b] | 69.3 | 120–121° | 0.69 | 2-Propanol–water (2:1) | $C_{13}H_{18}BrN_3O$ | C | 50.01 | 51.49 |
| | | | | | | H | 5.81 | 5.68 |
| | | | | | | Br | 25.60 | 26.34 |
| | | | | | | N | 13.46 | 13.86 |
| XIV[b] | 87.3 | 188.5–189° | 0.71 | Ethanol | $C_{16}H_{16}BrN_3O$ | C | 55.50 | 58.51 |
| | | | | | | H | 4.66 | 4.99 |
| | | | | | | Br | 23.08 | 23.56 |
| | | | | | | N | 12.14 | 12.74 |
| XVIII | 96.1 | 190–191° dec. | 0.63 | Methanol | $C_{10}H_{12}ClN_3O$ | C | 53.22 | 53.26 |
| | | | | | | H | 5.36 | 5.39 |
| | | | | | | Cl | 15.71 | 15.68 |
| | | | | | | N | 18.62 | 18.61 |
| XXIII | 46.0 | 166.5–167° | 0.53 | Methanol | $C_{10}H_{14}ClN_3O_2$ | C | 49.28 | 49.14 |
| | | | | | | H | 5.79 | 5.83 |
| | | | | | | Cl | 14.55 | 14.49 |
| | | | | | | N | 17.24 | 17.16 |

[a] Ethyl acetate. [b] Repeated attempts to obtain correct elemental analyses for amides derived from 2-bromopropionyl chloride were unsuccessful. IR and NMR spectral data were consistent with the assigned structures, the products were homogeneous on TLC, and the products derived from the 2-bromopropionamides gave correct elemental analyses.

**Table II—Data for Substituted 2-(2-Alkylaminoalkylamido)pyrroles**

| Compound | Precursor | Yield, % | Reaction Solvent[a] | Recrystallization Solvent[b] | Melting Point | Formula |
|---|---|---|---|---|---|---|
| VII*a* | VI*a* | 90.4 | Ethanol | Cyclohexane | 110.5–111.5° | $C_{15}H_{24}N_4O$ |
| VII*b* | VI*a* | —[c] | Ethanol | Cyclohexane–benzene (5:1) | Oil | $C_{15}H_{24}N_4O$ |
| VII*c* | VI*a* | —[c] | Ethanol | Cyclohexane | Oil | $C_{15}H_{24}N_4O$ |
| VII*d* | VI*a* | —[c] | Ethanol | Cyclohexane | Oil | $C_{15}H_{22}N_4O$ |
| VII*e* | VI*a* | —[c] | Ethanol | Cyclohexane–benzene (4:1) | Oil | $C_{16}H_{24}N_4O$ |
| VII*f* | VI*a* | —[c] | Ethanol | Cyclohexane–benzene (4:1) | Oil | $C_{17}H_{26}N_4O$ |
| VII*g* | VI*b* | 62.6 | Ethanol | —[d] | Oil | $C_{14}H_{22}N_4O$ |
| XIX*a* | XII | 53.4 | *n*-Propanol | Methanol–water (4:1) | 118.5–120° | $C_{14}H_{22}N_4O$ |
| XIX*b* | XII | 42.0 | *n*-Propanol | Cyclohexane | 160–161° | $C_{14}H_{22}N_4O$ |
| XIX*c* | XII | 34.0 | Ethanol | Methanol–water (4:1) | 91.5–93° | $C_{14}H_{22}N_4O$ |
| XIX*d* | XII | 56.9 | Ethanol | Cyclohexane–benzene (1:1) | 125–127° | $C_{14}H_{20}N_4O$ |
| XIX*e* | XVIII | 68.8 | Methanol | —[d] | 120–121° | $C_{14}H_{20}N_4O_2$ |
| XXI | XIII | 75.0 | *n*-Propanol | Methanol–water (4:1) | 87–88° | $C_{18}H_{28}N_4O$ |
| XXIV*a* | XXIII | 36.0 | Ethanol | Methanol–water (9:1) | 168.5–169.5° | $C_{12}H_{22}N_4O_2$ |
| XXIV*b* | XXIII | 52.7 | Methanol | —[d] | 234–235° | $C_{14}H_{22}N_4O_3$ |
| XXIV*c*[e] | XXIII | 10.2 | Methanol | 2-Propanol–water (1:2) | 185.5–186.5° | $C_{14}H_{24}N_4O_2$ |

[a] Absolute. [b] The oils were dissolved in boiling recrystallization solvent(s), treated with activated charcoal, filtered, and collected as oils after cooling. [c] Yields were not determined for the free base. [d] Free amine suitable for hydrochloride salt formation without recrystallization. [e] *Anal.*—Calc. for XXIV*c*: C, 59.97; H, 8.63; N, 19.99. Found: C, 59.80; H, 8.65; N, 19.91.

doses that were not significantly different from those required for efficacy. While VIII*g* appeared to have some separation between protection and ataxia, there was no significant difference between the $ED_{50}$ value for ataxia and the acute $LD_{50}$ value determined in the same group of mice.

## EXPERIMENTAL

**Chemistry**[1]—*2-(2-Bromopropionamido)-3-cyano-4,5-dimethylpyrrole (XII)*—The procedure for the synthesis of XII is representative of that for VI*a*, VI*b*, XIII, XIV, and XVIII. A solution of 2-amino-3-cyano-4,5-dimethylpyrrole (IX) (27.0 g, 0.2 mole) (13) in pyridine (17.4 g, 0.22 mole) and 200 ml of acetone was stirred in an ice bath as 2-bromopropionyl chloride (37.7 g, 0.22 mole) was added dropwise. After the addition was complete, the thick slurry was stirred at room temperature for 20 min. The slurry was poured over 500 g of crushed ice, the resulting suspension was stirred until the ice had melted, and the crude product was collected by filtration.

The amide was resuspended in 300 ml of distilled water, and the insoluble product was collected by filtration and was air dried. One gram of the pale-yellow product (50.3 g, 93.1%) was recrystallized from 40 ml of absolute ethanol to yield yellow needles (homogeneous on TLC; in ethyl acetate, $R_f$ 0.65), mp 212–212.5°; IR (KBr): 3360, 3260, 3160, 3100, 3020, 2910–2700 (broad), 2210, 1670, 1620, 1510, 1470, 1440, 1360, 1230, 1210, 1170, and 700 $cm^{-1}$; NMR (dimethyl sulfoxide-$d_6$): $\delta$ 1.73 (d, 3H, $CHBrCH_3$), 1.94 (s, 3H, $CH_3$ at C-4), 2.04 (s, 3H, $CH_3$ at C-5), 4.72 (q, 1H, $CHBrCH_3$), 10.78 (s, 1H, NH), and 11.25 (s, 1H, NH) ppm. Table I gives the results of the elemental analyses.

*2-(2-Pyrrolidinopropionamido)-3-cyano-4,5-dimethylpyrrole (XIX*d*)*—The procedure for the synthesis of XIX*d* is representative of

[1] All IR spectral data were determined on a Beckman Acculab-4 spectrophotometer using the potassium bromide technique. NMR spectra were determined on a Hitachi Perkin-Elmer R24 high-resolution spectrophotometer with tetramethylsilane as the internal reference. The reported melting points were obtained using a Thomas-Hoover capillary melting-point apparatus and are uncorrected. The reported analyses of carbon, hydrogen, chlorine, and nitrogen were obtained from Atlantic Microlab, Atlanta, Ga. All thin-layer chromatograms were performed using Eastman Chromatogram sheets, type 6060 (silica gel); the sheets were developed in an iodine chamber.

**Table III—Data for Substituted 2-(2-Alkylaminoalkylamido)pyrrole Hydrochlorides**

| Compound | Yield, % | Melting Point | $R_f$ | Recrystallization Solvent | Formula | Analysis, % | Calc. | Found |
|---|---|---|---|---|---|---|---|---|
| VIII*a* | 85.0 | 226–227° dec. | 0.32[a] | Water | $C_{15}H_{25}ClN_4O$ | C | 57.59 | 57.58 |
| | | | | | | H | 8.06 | 8.08 |
| | | | | | | Cl | 11.33 | 11.33 |
| | | | | | | N | 17.91 | 17.89 |
| VIII*b* | 79.9[b] | 231.5–232° | 0.23[a] | —[c] | $C_{15}H_{25}ClN_4O$ | C | 57.59 | 57.40 |
| | | | | | | H | 8.06 | 8.08 |
| | | | | | | Cl | 11.33 | 11.28 |
| | | | | | | N | 17.91 | 17.85 |
| VIII*c* | 55.6[b] | 244.5–245° | 0.62[d] | —[c] | $C_{15}H_{25}ClN_4O$ | C | 57.59 | 57.46 |
| | | | | | | H | 8.06 | 8.07 |
| | | | | | | Cl | 11.33 | 11.32 |
| | | | | | | N | 17.91 | 17.86 |
| VIII*d* | 66.8[b] | 243.5–244.5° | 0.56[d] | —[c] | $C_{15}H_{23}ClN_4O \cdot 1.0\ H_2O$ | C | 54.78 | 54.71 |
| | | | | | | H | 7.66 | 7.66 |
| | | | | | | Cl | 10.78 | 10.74 |
| | | | | | | N | 17.04 | 17.00 |
| VIII*e* | 82.1[b] | 215.5–216.5° | 0.51[a] | 2-Propanol–hexanes (1:3) | $C_{16}H_{25}ClN_4O$ | C | 59.15 | 58.95 |
| | | | | | | H | 7.76 | 7.80 |
| | | | | | | Cl | 10.91 | 10.82 |
| | | | | | | N | 17.25 | 17.18 |
| VIII*f* | 63.9[b] | 253.5–254.5° | 0.29[a] | —[c] | $C_{17}H_{27}ClN_4O$ | C | 60.25 | 60.25 |
| | | | | | | H | 8.04 | 8.07 |
| | | | | | | Cl | 10.46 | 10.36 |
| | | | | | | N | 16.53 | 16.43 |
| VIII*g* | 81.5 | 187–187.5° | 0.35[a] | Methanol–acetone (1:9) | $C_{14}H_{23}ClN_4O$ | C | 56.27 | 56.44 |
| | | | | | | H | 7.76 | 7.84 |
| | | | | | | Cl | 11.87 | 11.82 |
| | | | | | | N | 18.75 | 18.74 |
| XV | 35.0[b] | 272–275° dec. | 0.56[d] | —[e] | $C_{10}H_{15}ClN_4O \cdot 0.55\ H_2O$ | C | 47.54 | 47.53 |
| | | | | | | H | 6.42 | 6.42 |
| | | | | | | Cl | 14.04 | 14.02 |
| | | | | | | N | 22.18 | 22.18 |
| XVI | 59.7[b] | 250° dec. | 0.57[d] | —[f] | $C_{13}H_{21}ClN_4O \cdot 1.3\ H_2O$ | C | 50.66 | 50.64 |
| | | | | | | H | 7.72 | 7.74 |
| | | | | | | Cl | 11.50 | 11.48 |
| | | | | | | N | 18.18 | 18.16 |
| XVII | 35.6[b] | 255–256° dec. | 0.59[d] | Water | $C_{16}H_{19}ClN_4O$ | C | 60.28 | 60.35 |
| | | | | | | H | 6.01 | 6.08 |
| | | | | | | Cl | 11.12 | 11.08 |
| | | | | | | N | 17.58 | 17.52 |
| XX*a* | 99.0 | 195–196° dec. | 0.52[a] | —[c] | $C_{14}H_{23}ClN_4O \cdot 1.0\ H_2O$ | C | 53.07 | 52.90 |
| | | | | | | H | 7.95 | 8.00 |
| | | | | | | Cl | 11.19 | 11.19 |
| | | | | | | N | 17.68 | 17.60 |
| XX*b* | 67.0 | 246–246.5° | 0.59[a] | —[c] | $C_{14}H_{23}ClN_4O$ | C | 56.27 | 56.33 |
| | | | | | | H | 7.76 | 7.76 |
| | | | | | | Cl | 11.87 | 11.78 |
| | | | | | | N | 18.75 | 18.80 |
| XX*c* | 95.0 | 245.5–246.5° | 0.55[a] | —[c] | $C_{14}H_{23}ClN_4O$ | C | 56.27 | 56.07 |
| | | | | | | H | 7.76 | 7.79 |
| | | | | | | Cl | 11.87 | 11.80 |
| | | | | | | N | 18.75 | 18.70 |
| XX*d* | 93.7 | 265.5–267° | 0.41[a] | —[c] | $C_{14}H_{21}ClN_4O$ | C | 56.65 | 56.56 |
| | | | | | | H | 7.13 | 7.16 |
| | | | | | | Cl | 11.95 | 11.89 |
| | | | | | | N | 18.88 | 18.81 |
| XX*e* | 81.8 | 252–253° | 0.50[a] | —[c] | $C_{14}H_{21}ClN_4O_2$ | C | 53.75 | 53.72 |
| | | | | | | H | 6.77 | 6.76 |
| | | | | | | Cl | 11.34 | 11.29 |
| | | | | | | N | 17.91 | 17.85 |
| XXII | 76.4 | 120–123° | 0.65[a] | 2-Propanol–ethyl acetate–hexane (1:1:3) | $C_{18}H_{29}ClN_4O \cdot 0.75\ H_2O$ | C | 59.00 | 59.02 |
| | | | | | | H | 8.39 | 8.44 |
| | | | | | | Cl | 9.68 | 9.68 |
| | | | | | | N | 15.29 | 15.29 |
| XXV*a* | 49.0 | 213–214° | 0.52[g] | 2-Propanol–acetone (1:5) | $C_{14}H_{23}ClN_4O_2$ | C | 53.41 | 53.58 |
| | | | | | | H | 7.36 | 7.32 |
| | | | | | | Cl | 11.26 | 11.39 |
| | | | | | | N | 17.80 | 17.88 |
| XXV*b* | 92.1 | 242–244° | 0.32[a] | Methanol–acetone (1:3.75) | $C_{14}H_{23}ClN_4O_3$ | C | 50.83 | 50.80 |
| | | | | | | H | 7.01 | 7.03 |
| | | | | | | Cl | 10.72 | 10.68 |
| | | | | | | N | 16.94 | 16.91 |
| XXV*c*[h] | — | — | — | — | — | — | — | — |

[a] Ethyl acetate. [b] Percent yield is based on the α-haloamide percursor. [c] The salt obtained was analytically pure. [d] Acetone. [e] The crystals were washed with boiling ethyl acetate and then with boiling 2-propanol. [f] The crystals were washed with boiling ethyl acetate. [g] 2-Propanol. [h] The hydrochloride salt obtained was deliquescent; therefore, elemental analysis was performed with the free base (XXIV*c*).

that of VII*a*–VII*g*, XIX*a*–XIX*e*, XXI, and XXIV*a*–XXIV*c*. A solution of XII (20.25 g, 0.075 mole) in 100 ml of absolute ethanol was stirred while pyrrolidine (21.3 g, 0.30 mole) was added. The mixture was refluxed with stirring for 6.5 hr, during which time the suspension changed to a clear brown solution. The solvent and excess amine were removed *in vacuo*, and the residue was dissolved in 100 ml of 10% HCl. The solution was

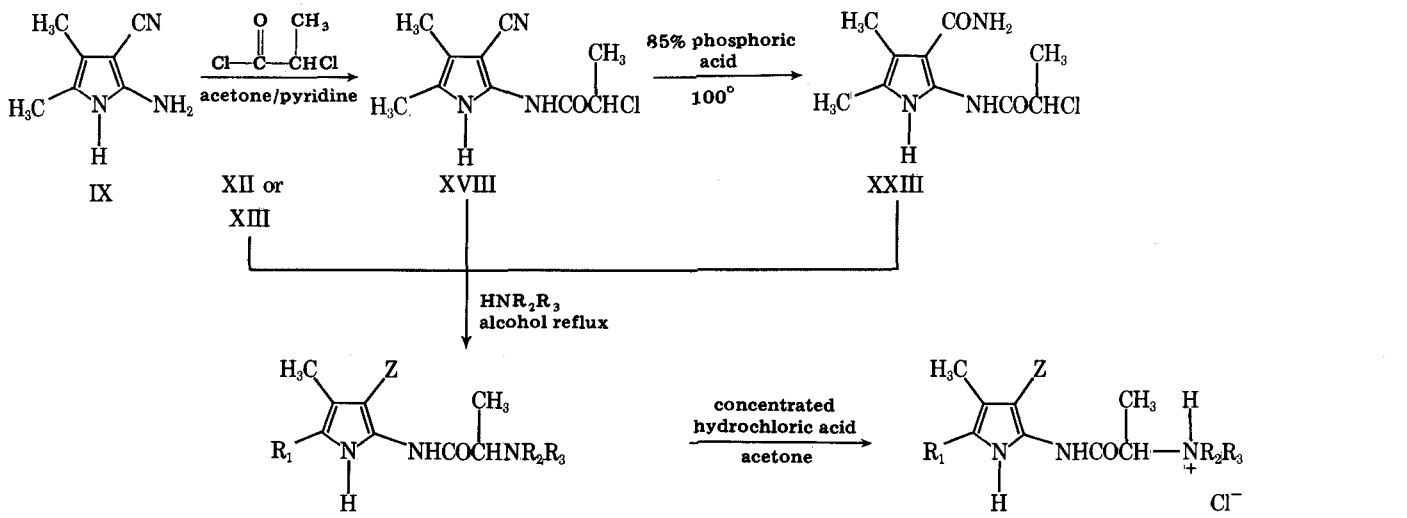


XIX*a*: $R_1 = CH_3$, $R_2 = iso\text{-}C_4H_9$, $R_3 = H$, Z = CN
XIX*b*: $R_1 = CH_3$, $R_2 = n\text{-}C_4H_9$, $R_3 = H$, Z = CN
XIX*c*: $R_1 = CH_3$, $R_2 = R_3 = C_2H_5$, Z = CN
XIX*d*: $R_1 = CH_3$, $R_2 + R_3 = -(CH_2)_4-$, Z = CN
XIX*e*: $R_1 = CH_3$, $R_2 + R_3 = -(CH_2)_2O(CH_2)_2-$, Z = CN
XXI: $R_1 = iso\text{-}C_4H_9$, $R_2 + R_3 = -(CH_2)_5-$, Z = CN
XXIV*a*: $R_1 = CH_3$, $R_2 + R_3 = -(CH_2)_4-$, Z = $CONH_2$
XXIV*b*: $R_1 = CH_3$, $R_2 + R_3 = -(CH_2)_2O(CH_2)_2-$, Z = $CONH_2$
XXIV*c*: $R_1 = CH_3$, $R_2 = R_3 = C_2H_5$, Z = $CONH_2$

XX*a*: $R_1 = CH_3$, $R_2 = iso\text{-}C_4H_9$, $R_3 = H$, Z = CN
XX*b*: $R_1 = CH_3$, $R_2 = n\text{-}C_4H_9$, $R_3 = H$, Z = CN
XX*c*: $R_1 = CH_3$, $R_2 = R_3 = C_2H_5$, Z = CN
XX*d*: $R_1 = CH_3$, $R_2 + R_3 = -(CH_2)_4-$, Z = CN
XX*e*: $R_1 = CH_3$, $R_2 + R_3 = -(CH_2)_2O(CH_2)_2-$, Z = CN
XXII: $R_1 = iso\text{-}C_4H_9$, $R_2 + R_3 = -(CH_2)_5-$, Z = CN
XXV*a*: $R_1 = CH_3$, $R_2 + R_3 = -(CH_2)_4-$, Z = $CONH_2$
XXV*b*: $R_1 = CH_3$, $R_2 + R_3 = -(CH_2)_2O(CH_2)_2-$, Z = $CONH_2$
XXV*c*: $R_1 = CH_3$, $R_2 = R_3 = C_2H_5$, Z = $CONH_2$

*Scheme III*

filtered, and the acidic filtrate was poured over 200 g of ice and alkalinized (pH 9) with 10% NaOH. A tan, gummy solid formed, which was extracted with three 40-ml portions of chloroform.

The combined chloroform extracts were washed with two 50-ml portions of saturated aqueous sodium chloride solution, and the chloroform was removed *in vacuo*. The residue was recrystallized from 60 ml of methanol–water (2:5), yielding a brown, granular solid (11.50 g, 56.9%). The crude product was recrystallized twice from 200 ml of benzene–cyclohexane (1:1), yielding a tan solid (8.2 g, 42%). This solid was suitable for hydrochloride salt formation (homogeneous on TLC; in ethyl acetate, $R_f$ 0.48), mp 125–127°. The data for the analogs are given in Table II.

*2-(2-Pyrrolidinopropionamido)-3-cyano-4,5-dimethylpyrrole Hydrochloride* (*XX*d)—The procedure given for the synthesis of XX*d* is representative of that of VIII*a*–VIII*g*, XX*a*–XX*e*, XXII, and XXV*a*–XXV*c*. The free amine (XIX*d*) (8.2 g, 0.032 mole) was dissolved in 150 ml of warm acetone and filtered, and the filtrate was treated with 3.0 ml of concentrated hydrochloric acid. The sealed flask then was placed in the freezer at −30° for 2.5 hr to yield a white powder. The salt (8.9 g, 93.7%) was collected, washed with acetone, and air dried (homogeneous on TLC; in ethyl acetate, $R_f$ 0.41), mp 265.5–267°; IR (KBr): 3300–2800 (broad), with peaks at 3140, 3030, 2940, 2800, 2660, 2200, 1690, 1610, 1575, 1540, 1460, 1300, 1255, 1190, 1120, 1085, 1060, 1040, 950, 910, 860, and 690 $cm^{-1}$; NMR (dimethyl sulfoxide-$d_6$): δ 1.56 (d, 3H, $COCHCH_3$), 2.00 (broad m, 4H, β-carbons on pyrrolidine), 1.95 (s, 3H, $CH_3$ at C-4), 2.05 (s, 3H, $CH_3$ at C-5), 3.31 (m, 4H, α-carbons on pyrrolidine), 4.25 (q, 1H, COCH), 11.35 (s, 2H, NH), and 11.55 (s, 1H, NH) ppm. Table III presents the results of the elemental analyses.

**Table IV—Local Anesthetic Activity of Substituted 2-(2-Alkylaminoalkylamido)pyrrole Hydrochlorides as Determined by the Guinea Pig Wheal Test [a]**

| Compound | Solution Concentration 1% | 0.50% | 0.25% |
|---|---|---|---|
| Lidocaine | 100 (36) | 100 (36) | 100 (31) |
| VIII*a* | 94 (34) | 89 (32) | 71 (22) |
| VIII*b* | 100 (36) | 69 (25) | 68 (21) |
| VIII*c* | 64 (23) | 50 (18) | 36 (11) |
| VIII*d* | 89 (32) | 58 (21) | 61 (19) |
| VIII*e* | 100 (36) | 47 (17) | 55 (17) |
| VIII*f* [b] | 100 (36) | 100 (36) | 116 (36) |
| VIII*g* | 92 (33) | 36 (13) | 26 (08) |
| XV | 86 (31) | 75 (27) | 45 (14) |
| XVI | 100 (36) | 100 (36) | 110 (34) |
| XVII | 100 (36) | 94 (34) | 77 (24) |
| XX*a* | 100 (36) | 89 (32) | 94 (29) |
| XX*b* | 100 (36) | 92 (33) | 48 (15) |
| XX*c* | 100 (36) | 89 (32) | 36 (11) |
| XX*d* | 33 (12) | — | — |
| XX*e* | 97 (35) | 72 (26) | 22 (07) |
| XXII | 100 (36) | 97 (35) | 97 (30) |
| XXV*a* | 3 (01) | — | — |
| XXV*b* | 0 (00) | — | — |
| XXV*c* | 3 (01) | — | — |
| Sodium chloride | 0 (00) | — | — |

[a] Values given are percent protection; the numbers in parentheses represent a sum of the number of pinpricks failing to elicit a response (skin twitch or cry) following intradermal injection of 0.25 ml of the test compound in preshaven guinea pig backs ($n$ = 2). [b] At a concentration of 0.125%, lidocaine protected against 12 pricks (100%) and VIII*f* protected against 20 pricks (167%).

**Table V—Antiarrhythmic [a] and CNS Toxic [b] Effects in Mice**

| Compound | $ED_{50}$[c], mg/kg (95% Fieller Limits) Protection | Ataxia |
|---|---|---|
| VIII*a* | 67 (47–118) | <25 |
| VIII*b* | —[d] | 21 (10–39) |
| VIII*c* | 127 (74–217)[e] | 126 (84–283) |
| VIII*d* | 28 (14–62) | 10 (5–19) |
| VIII*e* | 71 (42–120) | 39 (17–60) |
| VIII*f* | —[f] | 25 (7–41) |
| VIII*g* | 86 (24–302) | 155 (84–284) |
| XV | —[g] | —[g] |
| XVI | 26 (18–37) | 27 (18–35) |
| XVII | —[h] | —[h] |
| XX*a* | 111 (59–208)[e] | 129 (83–509) |
| XX*b* | 40 (21–59) | 35 (21–52) |
| XX*c* | 256 (176–319) | 251 (168–307) |
| XX*d* | 252 (168–307) | 252 (168–307) |
| XX*e* | 159 (73–351)[e] | 79 (13–139) |
| XXII | —[i] | —[i] |
| XXV*a* | 330 (170–641) | 159 (87–327) |
| Quinidine | 72 (61–83) | —[k] |
| Lidocaine | 48 (44–53) | 45 (40–50) |

[a] Protection against chloroform-induced tachycardia. [b] Observed prior to exposure to chloroform. [c] Subcutaneous administration. [d] At 36 mg/kg, 20% were protected; at the next higher dose of 100 mg/kg, 90% died before chloroform exposure. [e] Approximate 95% Fieller limits. [f] At 50 mg/kg, 40% were protected; at 100 mg/kg, 100% died before chloroform exposure. [g] At 200 mg/kg, 22% were protected, 22% were ataxic, and 10% were dead. [h] At 35 mg/kg, no protection or ataxia was observed. Higher doses were not soluble. [i] At 398 mg/kg, no protection or ataxia was observed. [k] No ataxia occurred at 200 mg/kg.

*2-(2-Aminopropionamido)-3-cyano-4-methyl-5-isobutylpyrrole Hydrochloride (XVI)*—The procedure for the synthesis of XVI is representative of that of XV and XVII and conforms to the method of Secrist and Loque (15).

A mixture of 2-(2-bromopropionamido)-3-cyano-4-methyl-5-isobutylpyrrole (XIII) (9.37 g, 0.03 mole) and sodium azide (2.0 g, 0.0309 mole) in absolute methanol (100 ml) was refluxed with stirring for 1.5 hr. The solution was transferred to a Parr bottle, chloroform (3.0 ml) and 10% palladium-on-carbon (1.0 g) were added, and the mixture was hydrogenated at 46 psi for 3.5 hr. (The progress of the hydrogenation was monitored by the disappearance of the azide band at 2040 $cm^{-1}$ in the IR spectrum.) The mixture was acidified and filtered, and the filtrate was reduced *in vacuo* to yield a tan solid.

This solid was treated with 100 ml of 10% HCl and warmed gently, and the insoluble salt was collected and air dried. Treatment of the solid with boiling ethyl acetate (100 ml) gave a white powder (5.1 g, 59.7%) (homogeneous on TLC; in acetone, $R_f$ 0.57; in methanol, $R_f$ 0.54), mp 250° dec.; IR (KBr): 3380, 3270, 2960, 2220, 1685, 1620, 1590, 1505, 1475, 1245, 1215, and 685 $cm^{-1}$; NMR (dimethyl sulfoxide-$d_6$): $\delta$ 0.82 (d, 6H, $J$ = 6.0 Hz, *gem*-dimethyls of isobutyl), 1.3–2.0 (m, 1H, methine of isobutyl), 1.50 [d, 3H, $J$ = 7.2 Hz, $CH(\overset{+}{N}H_3)CH_3$], 1.95 (s, 3H, methyl at C-4), 2.31 [d, 2H, $J$ = 6.0 Hz, $CH_2CH(CH_3)_2$], 4.06 [q, 1H, $J$ = 7.2 Hz, $CH(\overset{+}{N}H_3)CH_3$], 9.01 (broad s, 4H, $\overset{+}{N}H_3$ and CONH), and 11.32 (broad s, 1H, $N_1H$) ppm. Table III shows the results of the elemental analyses.

**Pharmacology**—*Local Anesthetic Activity*—The guinea pig wheal method of Bulbring and Wajda (16) was used to determine the activity. The back of the guinea pig was shaved 1 day prior to the test, and 0.25 ml of the drug solution was administered intradermally at two sites along the midline. The resulting wheals were tested by pricking the area six times with a pin at 5-min intervals for 30 min. Local anesthesia was present if the pinprick did not elicit a skin twitch. The number of pinpricks that failed to elicit a response then was recorded at each interval and compared to that of lidocaine at the same percentage concentration (Table IV).

*Antiarrhythmic Activity and CNS Toxicity*—Antiarrhythmic activity was assessed by a modification of the method by Lawson (17). Groups of 10 female mice (Charles River, CD 1), 18–24 g, were injected subcutaneously with the drug solution delivered in a volume of 0.1 ml/10 g of body weight. After 20 min, the mice were placed one at a time in an atmosphere of chloroform. Each mouse was removed when respiratory arrest occurred (~35–45 sec later) and was pinned to a cork board with dissecting needles, which also served as electrodes.

Previous experience with this procedure indicated that fibrillation was not the most prevalent arrhythmia and that a one-lead ECG was inadequate to resolve the rapid ECG events that occur after respiratory arrest in chloroform (18). Consequently, after a thoracotomy was performed, three ECGs were recorded from each mouse until 90 sec from the time it had been placed in the chloroform. Leads I and II were obtained *via* the needle electrodes, and an epicardial ECG was obtained from a wick electrode placed on the exposed surface of the right ventricle. All ECGs were displayed on a multichannel seven-pen recorder as well as on a storage oscilloscope.

Ventricular rates (beats per minute) were measured directly from the clearest ECG by counting ventricular depolarizations for several seconds and extrapolating them to beats per minute (bpm). A mouse was assumed to have a tachycardia if the 30–40-sec ECG recording contained at least 5 sec in which the ventricular rate exceeded 520 bpm or 2 sec in which the rate exceeded 600 bpm. Conversely, a mouse was protected from the arrhythmogenic effects of chloroform if these criteria were not fulfilled. Antiarrhythmic efficacy was based on the percentage of mice protected at each dose. Doses were varied by at least 0.15 log unit in an up–down fashion; the intent was to achieve a dose–response curve in which the doses evoked a low, medium, and high incidence of protection. Doses were increased until either the limits of water solubility were reached or lethal effects precluded higher doses. Thereafter, the $ED_{50}$ value for protection was calculated according to the logit $\chi^2$ method of Berkson (19).

Acute CNS toxicity was assessed during the 20-min period prior to chloroform exposure. Any mouse that displayed a staggered gait, splayed limbs, or hypertonia was assumed to have acute CNS toxicity in the form of ataxia. In general, doses were increased until at least eight animals displayed these symptoms. The $ED_{50}$ value for ataxia was also calculated according to the method of Berkson (19).

## REFERENCES


(1) T. Gordh, *Anaesthesia*, **4**, 4 (1949).

(2) J. L. Southworth, V. A. McKusick, E. C. Pierce, III, and F. L. Rawson, Jr., *J. Am. Med. Assoc.*, **143**, 717 (1950).

(3) P. Lechat, "International Encyclopedia of Pharmacology and Therapeutics, Section 8, Local Anesthetics," 1st ed., Pergamon, New York, N.Y., 1971, pp. 39–260.

(4) E. W. Byrnes, P. D. McMaster, E. R. Smith, M. R. Blair, R. N. Boyes, B. R. Duce, H. S. Feldman, G. H. Kronberg, B. H. Takman, and P. A. Tenthorey, *J. Med. Chem.*, **22**, 1171 (1979).

(5) P. D. McMaster, E. W. Byrnes, H. S. Feldman, B. H. Takman, and P. A. Tenthorey, *ibid.*, **22**, 1177 (1979).

(6) P. A. Tenthorey, R. L. DiRubio, H. S. Feldman, B. H. Takman, E. W. Byrnes, and P. D. McMaster, *ibid.*, **22**, 1182 (1979).

(7) N. M. Lofgren and C. Tegner, *Acta Chem. Scand.*, **14**, 486 (1960).

(8) H. J. F. Adams, G. H. Kronberg, and B. H. Takman, German pat. 2,162,744 (1972); through *Chem. Abstr.*, **77**, 101244c (1972).

(9) B. Ekenstam, B. Egner, and G. Pettersson, *Acta Chem. Scand.*, **11**, 1183 (1957).

(10) R. W. Johnson, T. H. Keenan, J. W. Kosh, and J. W. Sowell, Sr., *J. Pharm. Sci.*, **68**, 317 (1979).

(11) *Ibid.*, **68**, 955 (1979).

(12) R. J. Mattson and J. W. Sowell, Sr., *Synthesis*, **1979**, 217.

(13) K. Gewald, *Z. Chem.*, **1**, 349 (1961).

(14) R. W. Johnson, R. J. Mattson, and J. W. Sowell, Sr., *J. Heterocycl. Chem.*, **14**, 383 (1977).

(15) J. A. Secrist, III, and M. W. Loque, *J. Org. Chem.*, **37**, 335 (1972).

(16) E. Bulbring and I. Wajda, *J. Pharmacol. Exp. Ther.*, **85**, 78 (1945).

(17) J. W. Lawson, *ibid.*, **160**, 22 (1968).

(18) A. J. Block and J. H. Williams, *Fed. Proc. Fed. Am. Soc. Exp. Biol.*, **38**, 588 (1979).

(19) J. Berkson, *J. Am. Stat. Assoc.*, **48**, 565 (1953).


## ACKNOWLEDGMENTS


Adapted in part from theses submitted by M. E. Derrick and P. F. Mubarak to the University of South Carolina in partial fulfillment of the Master of Science degree requirements.

Supported by Astra Pharmaceutical Products.

The authors thank Ms. K. Landry and D. Charron for technical assistance.

# Two-Compartment Pharmacokinetic Models: Computer Simulations of Their Characteristics and Clinical Consequences

**FRED P. ABRAMSON**

Received May 19, 1980, from the *Department of Pharmacology, George Washington University Medical Center, Washington, DC 20037.* Accepted for publication July 17, 1980.

**Abstract** □ Computer simulations of two-compartment models of drug disposition were made. These simulations show how variations in each of the three intercompartmental rate constants are related to altered blood and tissue concentrations. Various simulations following rapid injection or continuous infusion are presented to demonstrate the general behavior of such a pharmacokinetic model. A system of drug classification based on comparative values of a drug's intercompartmental rate constants is proposed, and characteristics and consequences of each class are discussed in terms of possible therapeutic results.

**Keyphrases** □ Pharmacokinetic models—two-compartment models, computer simulations of their characteristics and clinical consequences □ Models, pharmacokinetic—two-compartment models, computer simulations of their characteristics and clinical consequences □ Drug disposition—two-compartment models, computer simulations of their characteristics and clinical consequences

At least two compartments are required in pharmacokinetic modeling: one for the drug in vascular and highly perfused tissues and one for more peripheral tissues. The physiological basis for this viewpoint was stated clearly by Riegelman *et al.* (1). Most published descriptions of the two-compartment model (2–6) have a mathematical focus to solve the simultaneous differential equations for the intercompartmental rate constants. In some cases, this approach does not provide intuitive understanding of the behavior of drugs that demonstrate two-compartment pharmacokinetics.

A series of computer simulations in which each of the three intercompartmental rate constants is varied individually has been useful in understanding and predicting the behavior of two-compartment systems. Illustrations from these simulations are presented to demonstrate the use of the method; such information is not available in textbooks or in the periodical literature.

In addition, these simulations point out situations where the conventional simplification of the two-compartment model to a one-compartment approximation may present substantial errors. These errors carry over into nomograms, which are used frequently in the calculation of adjusted doses in patients with impaired excretory capability.

## EXPERIMENTAL

An analog computer[1] was used for the simulations. The flow charts for the simulations are shown in Fig. 1. Conversions to logarithmic coordinates were performed manually.

The data are presented in arbitrary units. The time scaling can be converted from time units (TU) to any desired clock time by simple substitution. Some data are plotted in units of half-lives to emphasize the similar characteristics of drugs whose intercompartmental rate constants have similar proportionality.

The intercompartmental rate constants are given in Fig. 2. For simplicity, the drug in question is not metabolized. In this way, the disappearance of the drug from the body can be accounted for quantitatively by cumulative urinary excretion. Except for the amount of drug excreted into the urine, the overall behavior of any simulation is independent of the processes by which the drug is removed, as long as first-order kinetics are appropriate.

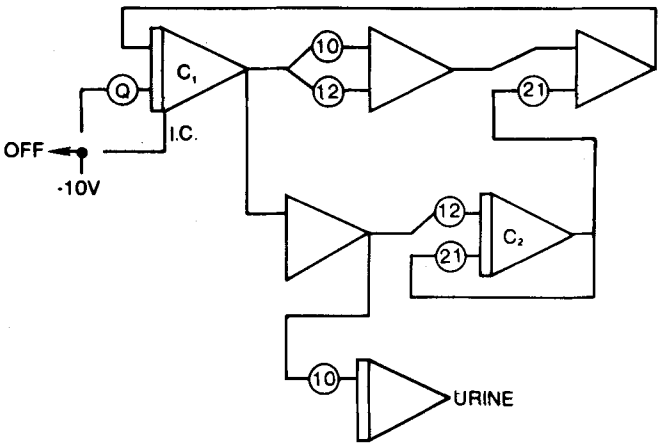


**Figure 1**—*Analog computer flow chart for two-compartment simulations, where $C_1$ and $C_2$ are the central (serum) and peripheral (tissue) compartment concentrations, respectively; 10, 12, and 21 refer to the intercompartmental rate constants seen in Fig. 2; Q represents the infusion rate; and I.C. is the initial condition on the amplifier representing $C_1$. For infusion simulations, the −10-v supply was connected through Q and turned off at an appropriate time. For simulations of intravenous dosing, the −10-v supply was attached to the initial conditions representing an instantaneous injection of drug. For one-compartment simulations, the coefficients $k_{12}$ and $k_{21}$ were set at zero.*

## RESULTS AND DISCUSSION

The parameters of a two-compartment system are characterized best following rapid intravenous administration of a drug. Figure 3 contrasts the time course of a two-compartment system with two different one-compartment simulations and demonstrates the differences in the models.

The $\beta$ value in a two-compartment model is not the same as the $k_{10}$ value in a one-compartment model. If a change in $k_{10}$ occurs for a subject, the resultant change in $\beta$ is not necessarily proportional. The behavior of a two-compartment system cannot be approximated by using the same $k_{10}$ in a one-compartment model. The steepest line in Fig. 3 makes that approximation, but its half-life is only about one-fourth of that of the two-compartment model. A one-compartment model having a $k_{10}$ equal to $\beta$ from the multicompartment system has the proper half-life but has several other differences.

The upward lines in Fig. 3 show the excretion into urine in a two-compartment system and in a one-compartment system with the same half-life. At approximately 16 TU, the distribution phase appears to be over. At that time, 49% of the drug has been excreted in the two-compartment system, while only 34% has appeared in urine in the analogous one-compartment simulation. The special behavior of the central compartment during the distribution phase is demonstrated in this comparison.

The central compartment concentration of drug is initially equal in both systems. Excretion is assumed to occur from the central compartment; thus, when $k_{10}$ in a two-compartment system is 0.10 $TU^{-1}$, there

[1] Model 580, Electronic Associates Inc., West Long Branch, N.J.

0022-3549/81/0200-0141$01.00/0
© 1981, American Pharmaceutical Association

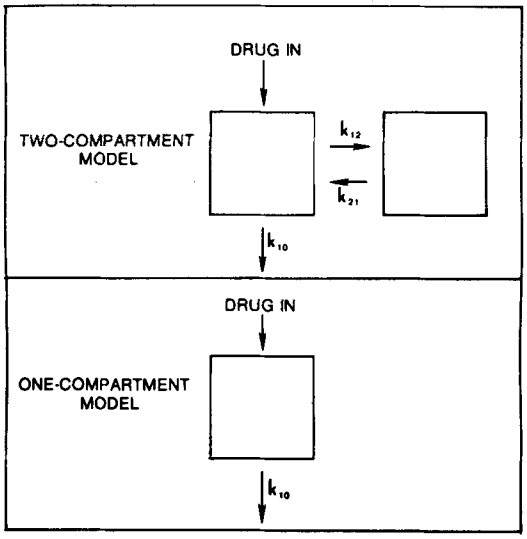


**Figure 2**—*Pharmacokinetic models used in simulations.*

is faster renal excretion than in the one-compartment simulation in Fig. 3. That $k_{10}$ value is set equal to the $\beta$ value (0.026 $TU^{-1}$) in the two-compartment system.

A high rate of drug elimination occurs during distribution, but this phase ends as sufficient drug is transferred from the central to the peripheral compartment to create an equilibrium between the two compartments. The greater the drug concentration in the peripheral compartment, the lower is the urinary excretion. Thus, in a two-compartment system, urinary excretion is initially fast but slows throughout the distribution phase. The highest concentrations of drug will reach the kidneys and the rest of the urinary tract during distribution following rapid intravenous dosing.

Another aspect of the two-compartment system is that, after distribution, drug also is contained in a tissue compartment, which may not be at the same concentration as the central compartment. In this example of a two-compartment model, the tissue concentration is 2.6 times the serum concentration. This factor is the major determinant of the smaller serum concentrations seen.

The fact that $\beta \neq k_{10}$ in a two-compartment system and the consequences with respect to drug disposition are not easily appreciated. Gibaldi and Perrier (7) demonstrated this inequality by plotting $\beta$ *versus* $k_{10}$ at several values of $k_{12}$ and $k_{21}$. A very nonlinear relationship was obvious in their plot. Figure 4 shows four sets of data for serum concentrations where only the elimination rate constant was varied.

The relationship between $\beta$ and $k_{10}$ is in the form of the solution to a binomial equation also involving $k_{12}$ and $k_{21}$ (3). The first two columns

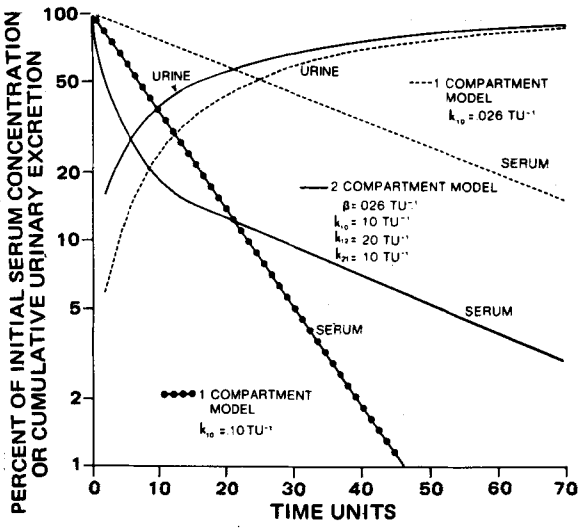


**Figure 3**—*Relationships between a two-compartment model and two one-compartment approximations following rapid intravenous administration.*

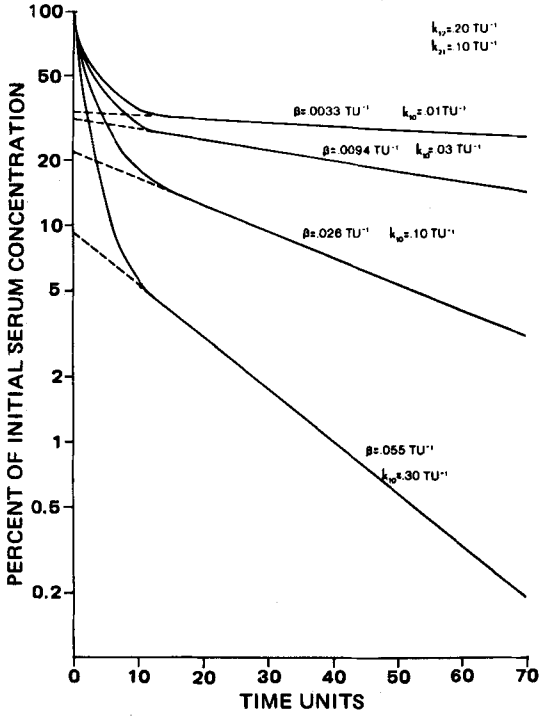


**Figure 4**—*Effects of variations in* $k_{10}$ *on the behavior of a drug exhibiting two-compartment kinetics following rapid intravenous administration;* $k_{12}$ *and* $k_{21}$ *are constant.*

of Table I show how these two parameters behave in the two-compartment simulations shown in Fig. 4. For low values of $k_{10}$, $\beta$ increases in a fairly linear fashion. As $k_{10}$ increases, it no longer is the rate-limiting step in drug elimination from the body. The relationship between $k_{21}$ and $k_{12}$ now is more important. Thus, a tripling of $k_{10}$ from 0.10 to 0.30 $TU^{-1}$ gives only a doubled $\beta$. If $k_{10}$ increased further, $\beta$ would increase at a diminishing rate. However, at all values of $k_{10}$, $k_{10}$ is greater than $\beta$. This phenomenon was observed by Juskó and Gibaldi (8), who analyzed kinetic data for penicillin G with and without probenecid. Although probenecid reduced $k_{10}$ to 46% of the control value, $\beta$ was reduced only to 78%, a clear example of how changes in $k_{10}$ do not relate linearly to changes in $\beta$.

Although there is an obvious increase in the steepness of the $\beta$-phase with increasing $k_{10}$, there also is a strong inverse relationship between $k_{10}$ and the serum concentration where the $\beta$-phase begins. Again, this is a consequence of increased drug elimination during the $\alpha$-phase. By the time that each simulation reached its $\beta$-phase (~16 TU), the percentages of drug excreted were 8, 20, 49, and 80 for $k_{10}$ values of 0.01, 0.03, 0.10, and 0.30, respectively. Thus, it is not appropriate to interpret a plasma decay curve with a pronounced $\alpha$-phase, such as that for $k_{10}$ = 0.30 $TU^{-1}$, as indicative of a large amount of drug in tissues. A large ratio between the extrapolated initial concentrations of the $\alpha$-line ($A_0$) and $\beta$-line ($B_0$) may be due to extensive tissue uptake or to extensive drug elimination during the distribution phase. Drug elimination during the $\alpha$-phase is responsible for errors in some techniques for assessing the volume of distribution, as will be discussed later.

Figure 5 illustrates how $k_{12}$ affects the disposition of a drug. Here $k_{10}$ and $k_{21}$ are held constant. The $k_{12}$ value of 0.20 $TU^{-1}$ is used again, and simulations with a larger and a smaller value also are included. Clearly, $k_{12}$ has a profound effect.

When $k_{12}$ is high, the probability increases that a drug molecule in the central compartment will enter the peripheral compartment rather than be eliminated. If increasing quantities of drug are transferred to a peripheral compartment, they will be unavailable for elimination. The overall result will be a prolonged elimination half-life. As shown in Fig. 5, when $k_{12}$ = 0.60 $TU^{-1}$, there is a rapid and extensive $\alpha$-phase. In contrast to the data shown in Fig. 4, this $\alpha$-phase represents mostly tissue distribution. When $k_{12}$ = 0.06 $TU^{-1}$, the rate of transfer to the peripheral compartment is less important and the data appear to lie closer to a single straight line, *i.e.*, more like a one-compartment model.

Similar manipulations of $k_{21}$ are seen in Fig. 6. When $k_{21}$ is rapid, the simulated serum concentrations resemble the case in Fig. 5, where $k_{12}$ was slow. In both situations, the amount of drug in the peripheral compartment is small and has little influence on the kinetics of the drug. In

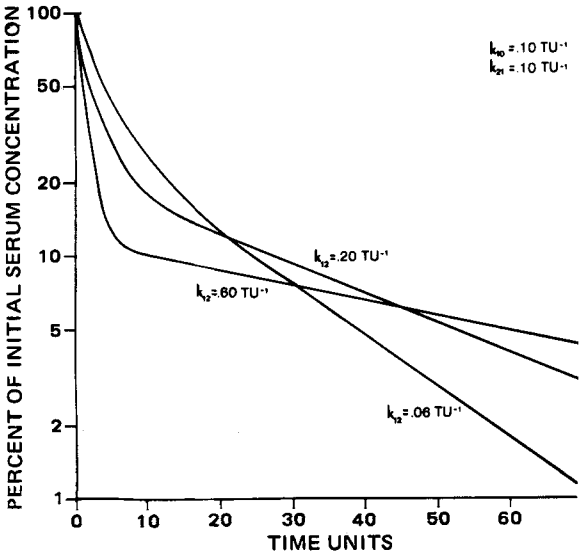


**Figure 5**—*Effects of variations in* $k_{12}$ *on the behavior of a drug exhibiting two-compartment kinetics following rapid intravenous administration;* $k_{10}$ *and* $k_{21}$ *are constant. When* $k_{12}$ *equals 0.60, 0.20, and 0.06* $TU^{-1}$, $\beta$ *equals 0.013, 0.026, and 0.047* $TU^{-1}$, *respectively.*

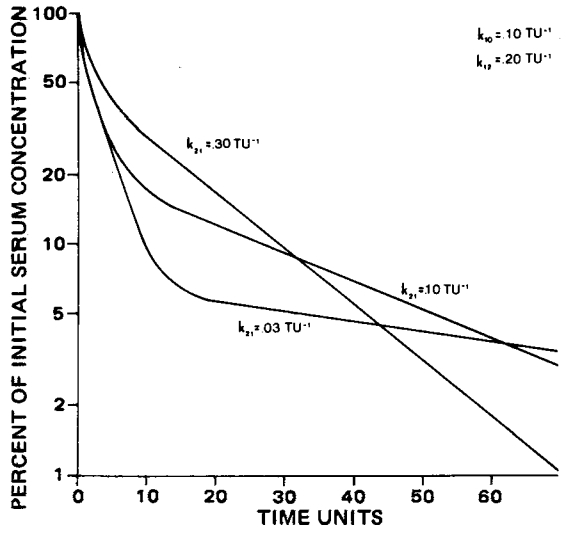


**Figure 6**—*Effects of variations in* $k_{21}$ *on the behavior of a drug exhibiting two-compartment kinetics following rapid intravenous administration;* $k_{10}$ *and* $k_{21}$ *are constant. When* $k_{21}$ *equals 0.3, 0.1, and 0.03* $TU^{-1}$, $\beta$ *equals 0.055, 0.026, and 0.0094* $TU^{-1}$, *respectively.*

this case, the drug that moved into the peripheral compartment with a rate of $k_{12}C_1$ is returned to the central compartment by the elevated rate of return, $k_{21}C_2$. This keeps the peripheral compartment from being rate limiting. In the other simulation, where $k_{21} = 0.03$ $TU^{-1}$, the peripheral compartment again is important. The overall rate of elimination, $\beta = 0.0094$ $TU^{-1}$, is greatly reduced because the drug is only slowly returned to the central compartment for elimination.

From an overall point of view, these three first-order reactions, elimination, central to peripheral transfer, and peripheral to central transfer, are seen to compete with one another in a probabilistic way. A drug molecule in the central compartment has two fates, elimination or transfer to the peripheral compartment. The rate constants for those two processes are the probabilities of their occurrence. If $k_{10}$ is three times greater than $k_{12}$, the drug has a 75% chance of being eliminated and a 25% chance of being transferred to the peripheral compartment. Once in the peripheral compartment, the drug returns to the central compartment at a rate governed by $k_{21}$, where again it is subject to the probabilities of excretion or transfer as described previously. Thus, the effect of each intercompartmental rate constant is buffered by the values of the other parameters. When all of the constants are of comparable magnitude, there will be a less than linear effect on a drug's overall kinetics for any change in a specific rate constant.

These computer simulations also permit evaluations of various ways of calculating the volume of distribution. In the computer, the actual volumes of each compartment are fixed and known. As a pharmacokinetic parameter, the volume of distribution is simply a mathematical construction to explain the relationship between the absorbed dose and the resulting blood concentration. The data in Fig. 4 can be used to examine some methods for calculating volumes of distribution. The calculation in the extrapolation method is:

$$V_d = \text{dose}/B_0 \qquad \text{(Eq. 1)}$$

while that in a two-compartment model (3) is:

$$V_{d2} = V_c[1 + k_{12}/(k_{21} - \beta)] \qquad \text{(Eq. 2)}$$

**Table I—Comparison of Volume of Distribution Calculations as a Function of Elimination Rate Constant**

| $k_{10}$ | $\beta$[a], $TU^{-1}$ | $V_{d,ext}$[b], arbitrary volume units | $V_{d2}$[b], arbitrary volume units | $f_c^*$ |
|---|---|---|---|---|
| 0.01 | 0.0033 | 3.0 | 3.1 | 0.33 |
| 0.03 | 0.0094 | 3.2 | 3.2 | 0.31 |
| 0.10 | 0.026 | 4.5 | 3.7 | 0.27 |
| 0.30 | 0.055 | 10.9 | 5.4 | 0.18 |

[a] $k_{12} = 0.20$ $TU^{-1}$ and $k_{21} = 0.10$ $TU^{-1}$. [b] Assuming a dose of 100 units and an initial concentration of 100 units/volume. Therefore, the volume of the central compartment is one volume.

Table I gives this comparison. The two-compartment equation takes into account the excess excretion during the $\alpha$-phase and correctly calculates a volume of distribution in the sense of describing the blood concentration that results from the actual amount of drug in the body. The anatomical volume of distribution is given by $V_d = V_c(1 + k_{12}/k_{21})$. Although this $V_d$ value is not a correct one to relate to observed blood concentrations except following steady-state infusions, it does describe correctly the actual volume in which the drug is distributed.

The $k_{21}/(k_{12} + k_{21})$ ratio defines the fraction of the drug in the central compartment ($f_c$) if a steady relationship is achieved between these two compartments during infusion. Because $k_{12} = 0.20$ and $k_{21} = 0.10$, $f_c = 0.10/0.30 = 0.33$ in this case. Following an intravenous bolus, the dynamic conditions lead to (2):

$$f_c^* = (k_{21} - \beta)/(k_{12} + k_{21} - \beta) \qquad \text{(Eq. 3)}$$

These data also are included in Table I. The slower the elimination phase is, the closer the dynamic $f_c^*$ approaches the static value of 0.33. In other words, there is no constant relationship between the blood concentration of a drug and its concentration in peripheral tissue. This may be important in relating blood drug concentrations to the pharmacological actions of a drug that acts in the peripheral compartment. For a drug exhibiting the characteristics of the fourth example in Table I (*i.e.*, a large $k_{10}$ relative to $k_{12}$ and $k_{21}$), the difference in the ratio of the tissue and blood concentrations between a rapid intravenous injection and a steady-state

**Table II—Intercompartmental Rate Constants for Representative Drugs**

| | $k_{10}$ | $k_{12}$ | $k_{21}$ |
|---|---|---|---|
| Class A: all constants nearly equal | | | |
| Lidocaine (9) | 0.022 $min^{-1}$ | 0.041 $min^{-1}$ | 0.029 $min^{-1}$ |
| Oxacillin (10) | 0.057 $min^{-1}$ | 0.037 $min^{-1}$ | 0.060 $min^{-1}$ |
| $\alpha$-Methyldopa (11) | 0.014 $min^{-1}$ | 0.012 $min^{-1}$ | 0.017 $min^{-1}$ |
| 5-Fluorouracil (12) | 0.18 $min^{-1}$ | 0.20 $min^{-1}$ | 0.20 $min^{-1}$ |
| Class B: $k_{12}$ more than twice $k_{10}$ or $k_{21}$ | | | |
| Diazepam (4) | 0.225 $hr^{-1}$ | 2.29 $hr^{-1}$ | 0.85 $hr^{-1}$ |
| Digoxin (13) | 0.145 $hr^{-1}$ | 0.85 $hr^{-1}$ | 0.114 $hr^{-1}$ |
| Morphine (14) | 0.100 $min^{-1}$ | 0.600 $min^{-1}$ | 0.045 $min^{-1}$ |
| Propranolol (15) | 1.5 $hr^{-1}$ | 5.9 $hr^{-1}$ | 1.3 $hr^{-1}$ |
| Doxorubicin (adriamycin) (16) | 0.48 $hr^{-1}$ | 5.1 $hr^{-1}$ | 0.29 $hr^{-1}$ |
| Class C: $k_{10}$ more than twice $k_{12}$ or $k_{21}$ | | | |
| Ampicillin (17) | 1.71 $hr^{-1}$ | 0.40 $hr^{-1}$ | 0.73 $hr^{-1}$ |
| Cytosine arabinoside (18) | 0.33 $min^{-1}$ | 0.093 $min^{-1}$ | 0.075 $min^{-1}$ |
| Cephapirin (19) | 4.2 $hr^{-1}$ | 1.09 $hr^{-1}$ | 1.28 $hr^{-1}$ |
| Class D: $k_{10}$ less than half $k_{12}$ or $k_{21}$ | | | |
| Cyclophosphamide (20) | 0.29 $hr^{-1}$ | 4.5 $hr^{-1}$ | 2.9 $hr^{-1}$ |
| Theophylline (21) | 0.31 $hr^{-1}$ | 2.7 $hr^{-1}$ | 3.1 $hr^{-1}$ |
| Warfarin (5) | 0.033 $hr^{-1}$ | 1.61 $hr^{-1}$ | 1.52 $hr^{-1}$ |
| *d*-Tubocurarine (22) | 0.017 $min^{-1}$ | 0.039 $min^{-1}$ | 0.046 $min^{-1}$ |

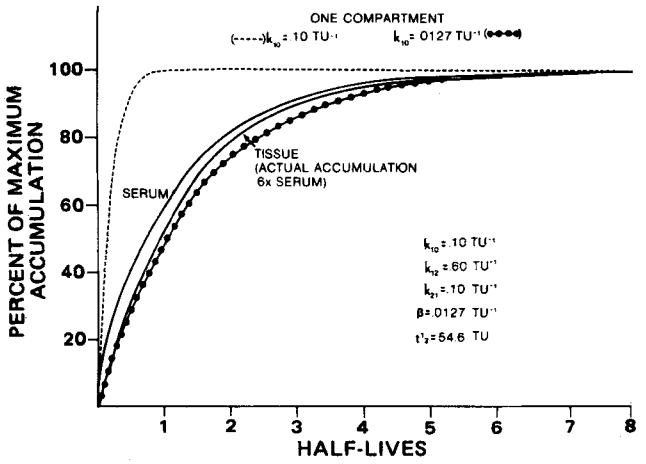


**Figure 7**—*Simulation of an intravenous infusion of a drug with a large* $k_{12}$ *compared to* $k_{10}$ *or* $k_{21}$. *Solid lines are from the two-compartment model. The dotted and dashed lines are two different one-compartment approximations. In the two-compartment data, the actual tissue concentration would be six times greater than the serum concentration at steady state.*

infusion is almost a factor of two. These observations are comparable to those published previously (8).

The concepts of these simulations may be applied by examining the intercompartmental rate constants of some representative drugs. Seventeen drugs were assigned to four classes in Table II. These data and the classification of each drug should be taken only as examples because data of this type vary greatly among individuals. The four classes represent conceptually different cases where particular parts of a two-compartment system play roles of greater or lesser importance.

Class A drugs have similar values for all three intercompartmental rate constants. The two-compartment simulation seen in Fig. 3 has such a relationship between its three rate constants as, for example, does lidocaine.

Certain drugs are known to accumulate extensively in tissues, as would be evidenced by a large $k_{12}$ compared to $k_{10}$ or $k_{21}$. Class B includes these drugs. For example, propranolol has kinetics similar to the $k_{12} = 0.60$ $TU^{-1}$ curve in Fig. 5. Class C drugs have rapid elimination rate constants compared to their intercompartmental rate constants. Ampicillin is such a drug. The lowest curve in Fig. 4 is the closest simulation to this behavior. Finally, Class D drugs, such as cyclophosphamide, have relatively low excretion rate constants. The top curve in Fig. 4 typifies a Class D drug. In this situation, as was seen in Table I, there will be a linear relationship between changes in $k_{10}$ and changes in $\beta$. There are few drugs characterized by a low $k_{21}$, as would result from slow release from tissues. This situation is more characteristic of drugs exhibiting a third compartment.

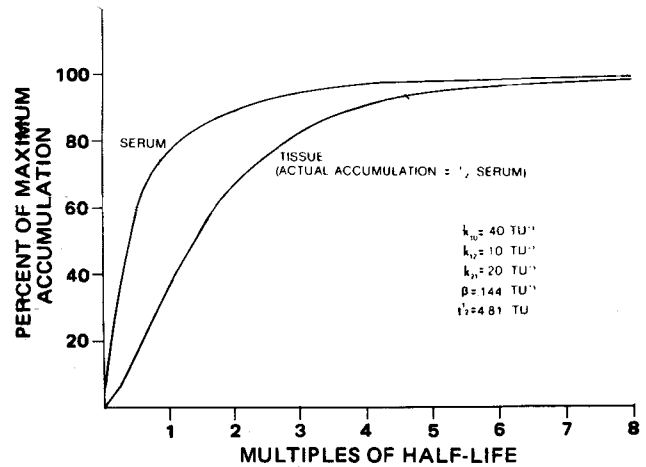


**Figure 8**—*Simulation of an intravenous infusion of a drug with a large* $k_{10}$ *compared to* $k_{12}$ *or* $k_{21}$. *The actual concentration of drug at steady state in the tissue compartment would be half of that in the serum compartment.*

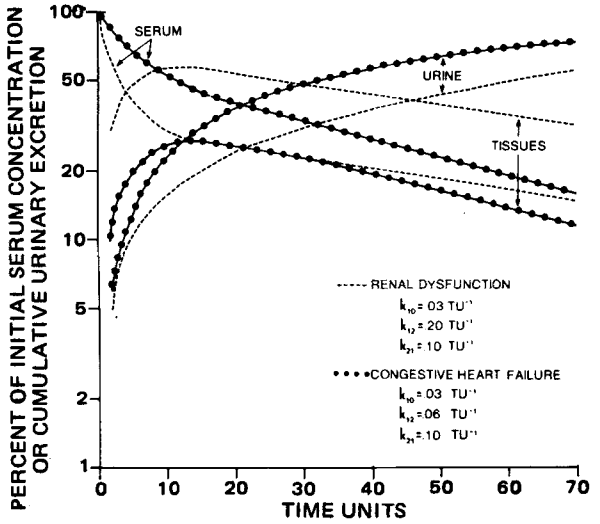


**Figure 9**—*Effects of two different disease conditions, each of which produces an equal reduction of renal drug clearance, following a rapid intravenous dose. The dashed lines represent simple renal dysfunction, and only* $k_{10}$ *is reduced from the values shown in Fig. 3. The dotted lines simulate circulatory dysfunction, which also reduced tissue perfusion.*

Although all pharmacokinetic models behave as if they were simple one-compartment systems when at steady state, as would result from a constant intravenous infusion, these classes of drugs differ in their rate of approach to equilibrium after the infusion begins. For a Class B drug, Fig. 7 shows that, despite the large amount of drug accumulation in tissue, the transfer is rapid enough that there is little difference in the rate of approach to equilibrium between the central and peripheral compartments. If one compartment is assumed using a $k_{10}$ the same as $\beta$ for the two-compartment model, the approach to equilibrium is only somewhat more rapid. However, large errors would result from assuming a one-compartment model where the overall rate of elimination was $k_{10}$, as in the top curve.

In contrast to Class B drugs, Class C drugs demonstrate what may be therapeutically important differences between the rate of accumulation in the central and peripheral compartments. Figure 8 simulates a situation where $k_{10}$ is large compared to $k_{12}$ and $k_{21}$. The serum reaches 90% of its steady state in two half-lives, while the peripheral tissue requires four half-lives to achieve an equivalent fraction of its ultimate steady-state value. Obviously, if a Class C drug had its site of action in a peripheral compartment, a much longer infusion would be needed than would be apparent from its blood kinetics.

The effects of disease states on drug disposition also have been simulated. Starting with the set of rate constants used in Fig. 3, two disease states were examined: impaired renal function and congestive heart failure. Figure 9 shows the serum and peripheral tissue concentrations as well as cumulative urinary excretion. For renal disease, the elimination rate constant was reduced from 0.10 to 0.03 $TU^{-1}$. A similar decrease in renal function was used in the congestive heart failure simulation along with an equally reduced rate of central to peripheral drug transfer: $k_{12}$ is now 0.06 $TU^{-1}$. This simulation is admittedly speculative because there are no intercompartmental rate constants in the literature that compare drug disposition in congestive heart failure and control conditions following rapid intravenous administration. The question is to what extent the peripheral to central compartment transfer is affected by congestive heart failure. This simulation assumes that this passive diffusion process will be unaltered.

Figure 9 shows that, although renal function is equally impaired, drug disposition in congestive heart failure differs markedly from renal disease not involving poor cardiac function. The reduced tissue perfusion in congestive heart failure leads to higher central compartment concentrations and more rapid urinary excretion. This simulation is for a Class A drug such as lidocaine. Thomson *et al.* (23) studied lidocaine in patients with congestive heart failure and found elevated blood concentrations compared to controls. Their data also show a reduced rate of drug elimination in both a rapidly perfused tissue compartment ($\beta$) and a deeper tissue compartment ($\gamma$). The present simulation also shows slower elimination in congestive heart failure ($\beta = 0.017$ $TU^{-1}$) than in control conditions ($\beta = 0.026$ $TU^{-1}$) but faster elimination than is seen in the

**Table III—Ampicillin Body Elimination Rate Constants in Renal Impairment Using either a One- or Two-Compartment Model**

| Percent of Renal Clearance | Impaired and Normal Ratio of Rate Constants | |
|---|---|---|
| | One-Compartment Model[a] | Two-Compartment Model[b] |
| 100 | 1.000 | 1.00 |
| 80 | 0.825 | 0.925 |
| 60 | 0.660 | 0.818 |
| 40 | 0.475 | 0.662 |
| 20 | 0.300 | 0.436 |
| 0 | 0.125 | 0.125 |

[a] One-compartment calculations use $k_e = k_{nr} + (Cl'_{cr}/Cl_{cr})k_r$ (modified from Ref. 25). [b] Two-compartment calculations use $k'_{10} = k_{10nr} + (Cl'_{cr}/Cl_{cr})k_{10r}$. $\beta = [k'_{10} + k_{12} + k_{21} - \sqrt{(k'_{10} + k_{12} + k_{21})^2 - 4k'_{10}k_{21}}]/2$.

renal dysfunction simulation ($\beta = 0.0094$ TU$^{-1}$). The latter difference results from the greater amount of the drug in the central compartment in congestive heart failure that is available for elimination.

## THERAPEUTIC IMPLICATIONS

Except for certain highly protein-bound molecules that are confined to the vasculature, such as radiopaque dyes, any drug will distribute to some peripheral tissue compartment. Thus, a two-compartment model is the simplest description of drug behavior. Whether any particular drug in any particular patient can be described suitably by a one-compartment approach is determined only by the relationships among the three intercompartmental micro rate constants. The following discussion examines some one-compartment pharmacokinetic calculations in comparison to more accurate two-compartment situations.

There are many treatments of drug dosing in renal failure (24–27). All use only one-compartment kinetics and base their adjustment of drug dosage on some measure of renal function such as decreased creatinine clearance. Because creatinine clearance measurements take place at steady state, they are truly proportional to $k_{10}$. According to the literature methods, the reduction in renal function is converted linearly into a revised elimination rate constant for the drug. The only variables are the relative importance of renal function for that drug and the extent of renal impairment. This practice is acceptable when $\beta$ and $k_{10}$ vary together in a linear fashion. As was illustrated earlier in general terms, this does not hold for all drugs.

Dettli (25) presented data showing that, for ampicillin, $k_n$ (which is $\beta$, the body elimination rate constant in normal individuals) is eight times larger than $k_{nr}$ (which is $\beta$ in patients with no renal function). From the micro rate constants in Table II for ampicillin, $\beta$ is calculated to be 0.544 hr$^{-1}$. One would expect a patient with no functioning kidneys to have $\beta$ equal to one-eighth of the normal value, or 0.068 hr$^{-1}$. To produce this $\beta$, $k_{10nr}$ must be reduced to 0.11 hr$^{-1}$. The micro rate constant for renal excretion, $k_{10r} = 1.60$ hr$^{-1}$, is found by subtracting $k_{10nr}$ from the normal $k_{10} = 1.71$ hr$^{-1}$.

Let $k'_{10}$ be the elimination micro rate constant in a subject with impaired renal excretion. This $k'_{10}$ can be used with the normal $k_{12}$ and $k_{21}$ to calculate $\beta$. The equation that relates $k'_{10}$ to renal function is:

$$k'_{10} = k_{10nr} + (Cl'_{cr}/Cl_{cr})k_{10r} \quad \text{(Eq. 4)}$$

where $Cl'_{cr}$ and $Cl_{cr}$ are the observed and normal creatinine clearances in the subject. A comparison of the body elimination rate constants for ampicillin using the one- or two-compartment method of calculation as a function of renal impairment is made in Table III. At both extremes of renal function, the methods agree. However, at intermediate degrees of renal impairment, the linear one-compartment calculation overestimates the reduction in body elimination compared to the more rigorous two-compartment model. The errors in the rate constants are translated directly into errors in dosing. With 20% renal function, the one-compartment calculation will lead to only 69% of the dose allowable from the two-compartment model.

As a Class C drug, ampicillin typifies the errors inherent in a one-compartment calculation for this group. Whenever $k_{10}$ is not the rate-limiting step, there will not be a linear relationship between $k_{10}$ and $\beta$. At the opposite end of the spectrum, the Class D drugs have an overall pharmacokinetic behavior highly dependent on $k_{10}$. There is a trivial error associated with one-compartment approximations on Class D drugs.

Dettli's data for digoxin permit a similar comparison for a Class B drug. Assuming a reduction to 50% of normal renal function, the two-compartment calculation would recommend a dose reduction of 31.5%, while the one-compartment calculation would predict 33.3%. Apparently, the relatively low value of $k_{10}$ compared to $k_{12}$ permits $k_{10}$ to be rate limiting, even with such extensive distribution to tissues.

As expected, Class A drugs behave less well than Class D drugs but better than Class C drugs. Two Class A drugs appear in Dettli's table, oxacillin and $\alpha$-methyldopa. When testing the two methods at 50% of normal renal function, the two- and one-compartment calculations predict a dosage reduction of 36.2 and 41.2% for $\alpha$-methyldopa and of 32.3 and 37.5% for oxacillin, respectively. These errors are relatively small (14–16%), but they point out that Class A drugs do not transform themselves perfectly into a one-compartment approximation. Careful pharmacokinetic experiments could suffer if a one-compartment approximation were used on a Class A drug.

In light of this classification scheme for drugs, further appreciation can be made of two reports that point out the shortcomings of one-compartment models. MacKichan *et al.* (28) showed how drug clearances of iothalamate and iodohippurate were estimated incorrectly using a one-compartment approximation. They showed graphs with a positive linear relationship between the percentage error in the clearance calculation and the endogenous creatinine clearance. They did not mention what the micro rate constants for these two substances were. The original report (29) showed that in patients with serum creatinine levels of <1.6 mg/100 ml, $k_{10}$, $k_{12}$, and $k_{21}$ were 0.54, 1.3, and 1.4 hr$^{-1}$ for iothalamate and 1.6, 1.5, and 1.1 hr$^{-1}$ for iodohippurate, respectively. In subjects with serum creatinine levels of >2.5 mg/100 ml, the micro rate constants for iothalamate were 0.15, 1.5, and 1.4 hr$^{-1}$ and for iodohippurate were 0.6, 1.8, and 1.5 hr$^{-1}$. The reduced errors reported by MacKichan *et al.* in subjects with low creatinine clearances are explained by noting that the normal sets of rate constants are all of a similar magnitude (Class A or nearly so) while those in subjects with poor renal function would qualify them for Class D, a class where the one-compartment calculations have negligible errors.

Dvorchik and Vesell (30) analyzed a number of drugs to see how the one-compartment model erred in calculations of drug clearances. They noted that for three drugs, diazepam, meperidine, and propranolol, the errors were substantially reduced in patients with hepatic cirrhosis or hypertension compared to controls. Again, in any dysfunction that reduces $k_{10}$, the drug kinetics will approach a Class D situation more closely and be appropriately handled by a one-compartment model. Because their estimates of error were based on values of $\alpha$ and $\beta$ rather than on the micro rate constants themselves, it was not clear why certain drugs behaved poorly in one-compartment calculations. The more detailed look used in the present approach shows why ampicillin is the drug most in error according to a one-compartment treatment.

In perspective, most errors caused by a one-compartment approximation will not be clinically significant. If other drugs with a narrower therapeutic range than ampicillin share its kinetic properties, then situations with clinical impact may be more frequent. The purpose of this discussion is to clarify the drug characteristics governing this decision.

The drug classification scheme in Table II points out the importance of detailed knowledge of every drug's pharmacokinetics. Only with information concerning the micro rate constants can one evaluate which pharmacokinetic approach will be valid.

In summary, computer simulations done for their own sake, rather than in the course of fitting experimental data, have been valuable in explaining the pharmacokinetic behavior of drugs described by a two-compartment model. Such understanding is useful both to the pharmacokinetics student and to persons administering drugs who will have a firsthand appreciation of various kinetic situations without having to perform the experiments.

## REFERENCES


(1) S. Riegelman, J. G. K. Loo, and M. Rowland, *J. Pharm. Sci.*, **57**, 117 (1968).

(2) M. Gibaldi and D. Perrier, "Pharmacokinetics," Dekker, New York, N.Y., 1975.

(3) R. E. Notari, "Biopharmaceutics and Pharmacokinetics," 2nd ed., Dekker, New York, N.Y., 1975.

(4) D. J. Greenblatt and J. Koch-Weser, *N. Engl. J. Med.*, **293**, 702 (1975).

(5) J. G. Wagner, "Fundamentals of Clinical Pharmacokinetics," Drug Intelligence Publications, Hamilton, Ill., 1975.

(6) E. Kruger-Thiemer, in "Handbook of Experimental Pharmacology," vol. 47, J. M. van Rossum, Ed., Springer-Verlag, New York, N.Y., 1977, pp. 63–123.

(7) M. Gibaldi and D. Perrier, *J. Pharm. Sci.*, **61**, 952 (1972).
(8) W. J. Jusko and M. Gibaldi, *ibid.*, **61**, 1270 (1972).
(9) M. Rowland, P. D. Thomson, A. Guichard, and K. L. Melmon, *Ann. N.Y. Acad. Sci.*, **179**, 383 (1971).
(10) M. Gibaldi, *J. Pharm. Sci.*, **58**, 1133 (1969).
(11) K. C. Kwan, E. L. Foltz, G. O. Breault, J. E. Baer, and J. A. Totaro, *J. Pharmacol. Exp. Ther.*, **198**, 264 (1976).
(12) E. R. Garrett, G. H. Hurst, and J. R. Green, Jr., *J. Pharm. Sci.*, **66**, 1422 (1977).
(13) E. Van der Kleijn, in "Clinical Pharmacokinetics," G. Levy, Ed., American Pharmaceutical Association, Washington, D.C., 1974, pp. 17–30.
(14) D. R. Stanski, D. J. Greenblatt, D. G. Lappas, J. Koch-Weser, and E. Lowenstein, *Clin. Pharmacol. Ther.*, **19**, 752 (1976).
(15) P. Gomeni, A. Bianchetti, R. Sega, and P. L. Morselli, *J. Pharmacokinet. Biopharm.*, **5**, 183 (1977).
(16) P. M. Wilkinson and G. E. Mawer, *Br. J. Clin. Pharmacol.*, **1**, 241 (1974).
(17) G. P. Lewis and W. J. Jusko, *Clin. Pharmacol. Ther.*, **18**, 475 (1975).
(18) R. Van Prooijen, E. Van der Kleijn, and C. Haanen, *ibid.*, **21**, 744 (1977).
(19) B. E. Cabana, D. R. Van Harken, G. H. Hottendorf, J. T. Doluisio, W. O. Griffin, Jr., D. W. A. Bourne, and C. W. Dittert, *J. Pharmacokinet. Biopharm.*, **3**, 419 (1975).
(20) J. L. Cohen, J. Y. Jao, and W. J. Jusko, *Br. J. Pharmacol.*, **43**, 677 (1971).
(21) J. G. Wagner, *Clin. Pharmacol. Ther.*, **16**, 691 (1974).
(22) M. Gibaldi, G. Levy, and W. Hayton, *Anesthesiology*, **36**, 213 (1972).
(23) P. D. Thomson, M. Rowland, and K. Melmon, *Am. Heart J.*, **82**, 417 (1971).
(24) P. Battig, K. Brune, H. Schmitt, and D. Walz, *Eur. J. Clin. Pharmacol.*, **7**, 233 (1974).
(25) L. Dettli, *Med. Clin. N. Am.*, **58**, 977 (1974).
(26) T. N. Tozer, *J. Pharmacokinet. Biopharm.*, **2**, 13 (1974).
(27) W. M. Bennett, I. Singer, T. Golper, P. Feig, and C. J. Coggins, *Ann. Intern. Med.*, **86**, 754 (1977).
(28) J. J. MacKichan, M. R. Dobrinska, P. G. Welling, and J. G. Wagner, *Clin. Pharmacol. Ther.*, **22**, 609 (1977).
(29) P. G. Welling, A. Mosegaard, M. R. Dobrinska, and P. O. Madsen, *J. Clin. Pharmacol.*, **16**, 142 (1976).
(30) B. H. Dvorchik and E. S. Vesell, *Clin. Pharmacol. Ther.*, **23**, 617 (1978).

### ACKNOWLEDGMENTS

Supported by the Renee Jordan Fund of George Washington University and National Institutes of Health Grant CA20753.

The author thanks Dr. Arnold Meltzer, Department of Electrical Engineering and Computer Sciences, George Washington University, for use of the analog computer system. He also thanks Dr. James Straw and Dr. William Eckelman for many helpful suggestions during the preparation of this manuscript.

# Ultrafiltration in Serum Protein Binding Determinations

**JOHN B. WHITLAM * and KENNETH F. BROWN ˣ**

Received January 14, 1980, from the *Department of Pharmacy, University of Sydney, Sydney, N.S.W., Australia.* Accepted for publication May 28, 1980. *Present address: Department of Pharmacy, University of Otago, Dunedin, New Zealand.

**Abstract** □ The ultrafiltration technique was evaluated theoretically and experimentally for use in clinical serum binding determinations. It is apparent from free energy considerations that the ultrafiltrate concentration approaches the true free concentration only as the pressure gradient causing flow reduces to zero. The theory presented accounts for the previously unexplained lower ultrafiltrate concentration observed at higher filtration pressures. Mathematical simulations of the molecular separation show that the ultrafiltrate concentration remains constant during filtration, and, thus, binding equilibria are not disturbed by this procedure, suggesting that an arbitrary restriction on the volume filtered is unnecessary. This finding greatly extends the value of the ultrafiltration technique in clinical binding determinations, especially for strongly bound, potent drugs where assays may be insufficiently sensitive to detect the extremely small free fractions reliably. These theoretical findings were verified experimentally by ultrafiltration of salicylate, ibuprofen, and carprofen in buffer, purified proteins, and whole serum.

**Keyphrases** □ Ultrafiltration—evaluation for use in clinical serum binding determinations □ Binding—evaluation of ultrafiltration technique for use in clinical serum binding determinations □ Salicylate—determination of serum binding by ultrafiltration □ Ibuprofen—determination of serum binding by ultrafiltration

Interest in the influence of plasma binding on drug disposition is increasing. The extent of binding partially controls drug distribution between the blood and extravascular fluids (1, 2) and may profoundly affect both hepatic and renal clearance (3, 4). Furthermore, there is ample evidence that the free fraction of drug may be substantially altered postoperatively (5), in the elderly (6), and following stress and disease (7) and, for certain drugs, may differ considerably with the plasma concentration and between individuals (8, 9).

## BACKGROUND

Reliable routine methodology for estimating the fraction of free drug in plasma and whole blood is needed. Ultrafiltration appears to be more appropriate than dialysis techniques because it can be carried out rapidly without storage or addition of potentially competitive buffer components and electrolytes. The speed with which the free fraction can be estimated after sample collection is particularly important since the levels of fatty acids produced by lipolysis of triglycerides increase on storage (10) and during dialysis (11). Nonesterified fatty acids are known to decrease the binding of drugs *in vitro* (12) and *in vivo* (13).

Among the generally recognized limitations of the ultrafiltration technique are the polarization of protein on the membrane, the uptake of small molecules by the membrane, and the change in the protein concentration with the volume filtered. Polarization may be minimized by stirring, and membrane binding may be assessed independently. However, the influence of filtration pressure in selectively altering the transport of solvent and drug molecules is not widely appreciated. Furthermore, in estimating the extent of binding by molecular filtration, it has become accepted practice to ultrafilter only a small fraction of the total sample (often <10%) to avoid disturbance of the protein binding equilibria (14–17). The subsequent difficulty in estimating extremely small amounts of ultrafiltered drug (18) often presents insurmountable analytical problems, particularly with strongly bound, low serum concentration drugs.

This report discusses two important aspects of ultrafiltration. First, the influence of filtration pressure on the ultrafiltrate drug concentration is examined theoretically. The theory presented accounts for the previously unexplained dilution of the ultrafiltrate observed at higher filtration pressures by Spector *et al.* (19). Second, it is shown theoretically and



0022-3549/81/0200-0146$01.00/0
© 1981, American Pharmaceutical Association

(7) M. Gibaldi and D. Perrier, *J. Pharm. Sci.*, **61**, 952 (1972).
(8) W. J. Jusko and M. Gibaldi, *ibid.*, **61**, 1270 (1972).
(9) M. Rowland, P. D. Thomson, A. Guichard, and K. L. Melmon, *Ann. N.Y. Acad. Sci.*, **179**, 383 (1971).
(10) M. Gibaldi, *J. Pharm. Sci.*, **58**, 1133 (1969).
(11) K. C. Kwan, E. L. Foltz, G. O. Breault, J. E. Baer, and J. A. Totaro, *J. Pharmacol. Exp. Ther.*, **198**, 264 (1976).
(12) E. R. Garrett, G. H. Hurst, and J. R. Green, Jr., *J. Pharm. Sci.*, **66**, 1422 (1977).
(13) E. Van der Kleijn, in "Clinical Pharmacokinetics," G. Levy, Ed., American Pharmaceutical Association, Washington, D.C., 1974, pp. 17–30.
(14) D. R. Stanski, D. J. Greenblatt, D. G. Lappas, J. Koch-Weser, and E. Lowenstein, *Clin. Pharmacol. Ther.*, **19**, 752 (1976).
(15) P. Gomeni, A. Bianchetti, R. Sega, and P. L. Morselli, *J. Pharmacokinet. Biopharm.*, **5**, 183 (1977).
(16) P. M. Wilkinson and G. E. Mawer, *Br. J. Clin. Pharmacol.*, **1**, 241 (1974).
(17) G. P. Lewis and W. J. Jusko, *Clin. Pharmacol. Ther.*, **18**, 475 (1975).
(18) R. Van Prooijen, E. Van der Kleijn, and C. Haanen, *ibid.*, **21**, 744 (1977).
(19) B. E. Cabana, D. R. Van Harken, G. H. Hottendorf, J. T. Doluisio, W. O. Griffin, Jr., D. W. A. Bourne, and C. W. Dittert, *J. Pharmacokinet. Biopharm.*, **3**, 419 (1975).
(20) J. L. Cohen, J. Y. Jao, and W. J. Jusko, *Br. J. Pharmacol.*, **43**, 677 (1971).
(21) J. G. Wagner, *Clin. Pharmacol. Ther.*, **16**, 691 (1974).
(22) M. Gibaldi, G. Levy, and W. Hayton, *Anesthesiology*, **36**, 213 (1972).
(23) P. D. Thomson, M. Rowland, and K. Melmon, *Am. Heart J.*, **82**, 417 (1971).
(24) P. Battig, K. Brune, H. Schmitt, and D. Walz, *Eur. J. Clin. Pharmacol.*, **7**, 233 (1974).
(25) L. Dettli, *Med. Clin. N. Am.*, **58**, 977 (1974).
(26) T. N. Tozer, *J. Pharmacokinet. Biopharm.*, **2**, 13 (1974).
(27) W. M. Bennett, I. Singer, T. Golper, P. Feig, and C. J. Coggins, *Ann. Intern. Med.*, **86**, 754 (1977).
(28) J. J. MacKichan, M. R. Dobrinska, P. G. Welling, and J. G. Wagner, *Clin. Pharmacol. Ther.*, **22**, 609 (1977).
(29) P. G. Welling, A. Mosegaard, M. R. Dobrinska, and P. O. Madsen, *J. Clin. Pharmacol.*, **16**, 142 (1976).
(30) B. H. Dvorchik and E. S. Vesell, *Clin. Pharmacol. Ther.*, **23**, 617 (1978).

### ACKNOWLEDGMENTS

Supported by the Renee Jordan Fund of George Washington University and National Institutes of Health Grant CA20753.

The author thanks Dr. Arnold Meltzer, Department of Electrical Engineering and Computer Sciences, George Washington University, for use of the analog computer system. He also thanks Dr. James Straw and Dr. William Eckelman for many helpful suggestions during the preparation of this manuscript.

# Ultrafiltration in Serum Protein Binding Determinations

**JOHN B. WHITLAM * and KENNETH F. BROWN ˣ**

Received January 14, 1980, from the *Department of Pharmacy, University of Sydney, Sydney, N.S.W., Australia.* Accepted for publication May 28, 1980. *Present address: Department of Pharmacy, University of Otago, Dunedin, New Zealand.

**Abstract** □ The ultrafiltration technique was evaluated theoretically and experimentally for use in clinical serum binding determinations. It is apparent from free energy considerations that the ultrafiltrate concentration approaches the true free concentration only as the pressure gradient causing flow reduces to zero. The theory presented accounts for the previously unexplained lower ultrafiltrate concentration observed at higher filtration pressures. Mathematical simulations of the molecular separation show that the ultrafiltrate concentration remains constant during filtration, and, thus, binding equilibria are not disturbed by this procedure, suggesting that an arbitrary restriction on the volume filtered is unnecessary. This finding greatly extends the value of the ultrafiltration technique in clinical binding determinations, especially for strongly bound, potent drugs where assays may be insufficiently sensitive to detect the extremely small free fractions reliably. These theoretical findings were verified experimentally by ultrafiltration of salicylate, ibuprofen, and carprofen in buffer, purified proteins, and whole serum.

**Keyphrases** □ Ultrafiltration—evaluation for use in clinical serum binding determinations □ Binding—evaluation of ultrafiltration technique for use in clinical serum binding determinations □ Salicylate—determination of serum binding by ultrafiltration □ Ibuprofen—determination of serum binding by ultrafiltration

Interest in the influence of plasma binding on drug disposition is increasing. The extent of binding partially controls drug distribution between the blood and extravascular fluids (1, 2) and may profoundly affect both hepatic and renal clearance (3, 4). Furthermore, there is ample evidence that the free fraction of drug may be substantially altered postoperatively (5), in the elderly (6), and following stress and disease (7) and, for certain drugs, may differ considerably with the plasma concentration and between individuals (8, 9).

## BACKGROUND

Reliable routine methodology for estimating the fraction of free drug in plasma and whole blood is needed. Ultrafiltration appears to be more appropriate than dialysis techniques because it can be carried out rapidly without storage or addition of potentially competitive buffer components and electrolytes. The speed with which the free fraction can be estimated after sample collection is particularly important since the levels of fatty acids produced by lipolysis of triglycerides increase on storage (10) and during dialysis (11). Nonesterified fatty acids are known to decrease the binding of drugs *in vitro* (12) and *in vivo* (13).

Among the generally recognized limitations of the ultrafiltration technique are the polarization of protein on the membrane, the uptake of small molecules by the membrane, and the change in the protein concentration with the volume filtered. Polarization may be minimized by stirring, and membrane binding may be assessed independently. However, the influence of filtration pressure in selectively altering the transport of solvent and drug molecules is not widely appreciated. Furthermore, in estimating the extent of binding by molecular filtration, it has become accepted practice to ultrafilter only a small fraction of the total sample (often <10%) to avoid disturbance of the protein binding equilibria (14–17). The subsequent difficulty in estimating extremely small amounts of ultrafiltered drug (18) often presents insurmountable analytical problems, particularly with strongly bound, low serum concentration drugs.

This report discusses two important aspects of ultrafiltration. First, the influence of filtration pressure on the ultrafiltrate drug concentration is examined theoretically. The theory presented accounts for the previously unexplained dilution of the ultrafiltrate observed at higher filtration pressures by Spector *et al.* (19). Second, it is shown theoretically and



0022-3549/81/0200-0146$01.00/0
© 1981, American Pharmaceutical Association

experimentally that arbitrary restriction of the volume fraction ultrafiltered is unnecessary and that the equilibrium position and ultrafiltrate concentration are unaltered, even when the protein concentration increases almost twofold. This finding greatly extends the value of ultrafiltration, particularly for clinical monitoring of binding.

## THEORY

**Free Energy Considerations: Influence of Pressure**—Modern ultrafiltration membranes do not contain pores of uniform dimensions that allow the passage of small molecules and retain the much larger binding species. The mechanism of transfer and retention is unclear. However, their characteristic of allowing free passage of the solvent and yet, at the same time, reflecting some small solute molecules (16, 20) is analogous to transfer of the drug and the solvent through traditional membranes containing heterogeneous pores and suggests the applicability of pore theory to the newer system. These membranes may even permit the passage of a small, but usually negligible, fraction of the macromolecule.

Consider a reversible interaction at equilibrium occurring in solution between a drug and protein at constant temperature and pressure. The reaction mixture is in contact with a selectively permeable membrane prior to ultrafiltration to determine the bound and free ligand concentrations (Scheme I).

$$[P] + [L] \rightleftharpoons [PL]$$

*Scheme I*

In Scheme I, $[P]$, $[L]$, and $[PL]$ are the protein, drug, and bound drug concentrations, respectively. Protein molecules with and without bound drug are unable to penetrate the membrane and, therefore, do not take part in the ultrafiltration process. The ultrafiltrate thus is produced from the interstitial solution in which the macromolecules are dispersed.

If the reaction mixture contains $m_L$ and $m_S$ moles of free drug and solvent, respectively, and the pressure on it is raised to $1 + \Delta P$ atmospheres (atm), a small volume of ultrafiltrate may be collected at 1 atm due to the pressure difference across the membrane of $\Delta P$. The ultrafiltrate contains $dm_L$ and $dm_S$ moles of drug and solvent, respectively, and the solute concentration is not necessarily the same as in the reaction mixture:

$$\frac{dm_L}{dm_S} \neq \frac{m_L}{m_S} \qquad \text{(Eq. 1)}$$

When the pressure on the reaction mixture returns to 1 atm, then the free energy ($\Delta G_1$) expended on the system to produce the ultrafiltrate is given by (21):

$$\Delta G_1 = (\bar{v}_L m_L + \bar{v}_S m_S)\Delta P \qquad \text{(Eq. 2)}$$

where $\bar{v}_L$ and $\bar{v}_S$ are the partial molal volumes of the free drug and solvent in the reaction mixture, respectively.

This free energy ($\Delta G_1$) associated with the pressure applied to accelerate filtration is available to produce changes in the composition of the ultrafiltrate compared to the composition in the interstitial solution of the reaction mixture.

On the other hand, the free energy change required to convert an infinitesimal volume of the original reaction mixture to ultrafiltrate ($\Delta G_2$) is given by (21):

$$\Delta G_2 = RT\left(dm_L \ln \frac{a_{L,uf}}{a_{L,rm}} + dm_S \ln \frac{a_{S,uf}}{a_{S,rm}}\right) \qquad \text{(Eq. 3)}$$

where $T$ is the absolute temperature, $R$ is the gas constant, and $a_{uf}$ and $a_{rm}$ are the atmospheric activities of the components of the ultrafiltrate and the reaction mixture, respectively. When the composition of the ultrafiltrate changes during filtration because the membrane is penetrated more readily by the solvent than the drug, $\Delta G_2$ is positive. When the ultrafiltrate drug concentration is identical to the free drug concentration in the reaction mixture, it follows from Eq. 3 that $\Delta G_2$ equals zero. Thus, to produce a true ultrafiltrate containing a drug concentration equal to the free concentration in the protein solution, pressure must be applied that is sufficient just to produce a finite flow rate but insufficient to supply free energy to change the ultrafiltrate composition.

Therefore, although $\Delta G_1$ must be greater than $\Delta G_2$, the ultrafiltrate drug concentration represents the free concentration most closely as the pressure gradient approaches zero.

Thus, if the membrane discriminates between solvent and drug molecules, whether on the basis of charge or dimension, then the drug concentration in the ultrafiltrate will not equal the free concentration in the original reaction mixture. The deviation will be an increasing function of the pressure gradient. This phenomenon may be explained by considering the events occurring at a particular channel through which only the solvent is able to pass. If the filtration pressure is greater than the osmotic pressure of the reaction mixture, then the solvent will pass through this pore and dilute the ultrafiltrate. In practice, this deviation may occur at pressures smaller than the osmotic pressure of the reaction mixture. The ultrafiltrate is in diffusional contact with the reaction mixture, and, thus, the pressure at which ultrafiltrate dilution occurs is simply the osmotic gradient between the reaction mixture and the ultrafiltrate.

**Mass Balance Considerations: Influence of Volume Change**—The effect of the protein and drug concentration changes that take place as a result of the reduction in volume and loss of drug in the ultrafiltrate is now considered.

Drug–protein interactions (Scheme I) often can be described by equations derived from the law of mass action. Thus, for a single class of binding sites:

$$\bar{\nu} = \frac{nKm_L}{V + Km_L} \qquad \text{(Eq. 4)}$$

where $\bar{\nu}$ is the average drug–protein molar binding ratio and $n$ is the number of sites on each protein molecule of association constant $K$. The volume of the reaction mixture is $V$, and $m_L$ is as defined previously.

It is assumed here that the ultrafiltration membrane acts as a perfect molecular sieve, completely retaining the macromolecule and neither binding nor reflecting the smaller drug molecule, such that when pressure is applied, its passage across the membrane, like that of the solvent, is unimpeded.

In the situation where a small volume ($dV$) of solution containing $dm_L$ moles of free drug is ultrafiltered through the membrane, if the new average molar binding ratio is denoted by $\bar{\nu}'$, then:

$$\bar{\nu}' = \frac{nK(m_L - dm_L)}{(V - dV) + K(m_L - dm_L)} \qquad \text{(Eq. 5)}$$

This expression can be rearranged:

$$\frac{\bar{\nu}'(V - dV)}{K} = n(m_L - dm_L) - \bar{\nu}'(m_L - dm_L) \qquad \text{(Eq. 6)}$$

Hence:

$$\frac{\bar{\nu}'}{K} = \frac{n(m_L - dm_L)}{V - dV} - \frac{\bar{\nu}'(m_L - dm_L)}{V - dV} \qquad \text{(Eq. 7)}$$

If the membrane does not differentiate between solvent and ligand molecules, then:

$$\frac{m_L - dm_L}{V - dV} = \frac{m_L}{V} \qquad \text{(Eq. 8)}$$

Substitution in Eq. 7 and rearrangement give:

$$\bar{\nu}' = \frac{nKm_L}{V(1 + Km_L/V)} = \bar{\nu} \qquad \text{(Eq. 9)}$$

It is apparent that the molar binding ratio remains constant throughout ultrafiltration, even though the protein and total drug concentrations increase markedly. Because of this constancy in $\bar{\nu}$, the drug concentration in the ultrafiltrate also will be constant and will be the same as the equilibrium free concentration in the original reaction mixture. In the treatment of the ultrafiltration process, no limitation is placed on the fraction of original reaction mixture that may be filtered. Thus, $\bar{\nu}$ and $[L]$ remain constant and independent of the volume of sample filtered. This treatment assumes constancy of both $n$ and $K$ as filtration proceeds, which may not be true at very high protein concentrations due to protein conformational change or formation of dimers or high-order macromolecular aggregates.

Similar reasoning leading to the same conclusions can be applied to more complex reaction mixtures consisting of many binding species, including proteins with more than one class of binding sites.

## EXPERIMENTAL

[$^{14}$C]Ibuprofen[1] (specific activity 13.11 ± 0.19 μCi/mg) and [$^{14}$C]carprofen[2] (specific activity 13.47 ± 0.34 μCi/mg) were used as received or diluted with unlabeled material. [$^{14}$C]Salicylic acid[3] was diluted with

[1] Boots Pure Drug Co. Ltd., Nottingham, England.
[2] Roche Pharmaceuticals, Sydney, Australia.
[3] New England Nuclear, Boston, Mass.

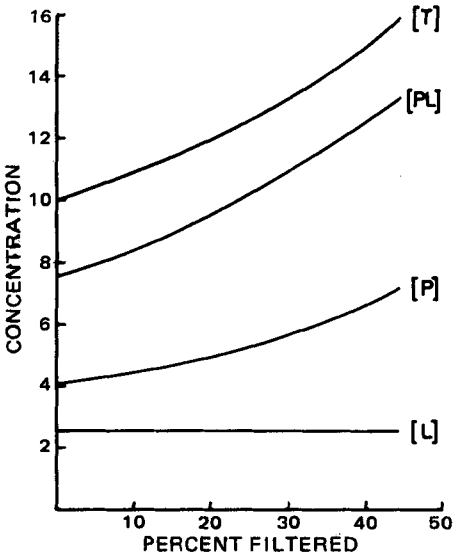


**Figure 1**—*Simulation of ultrafiltration process for hypothetical drug of binding constants* $K_1 = 10^4\,M^{-1}$ *(*$n_1 = 1$*) and* $K_2 = 10^2\,M^{-1}$ *(*$n_2 = 7$*), showing changes in the total ([T], micrograms per milliliter* $\times 10^{-1}$*), bound ([PL], micrograms per milliliter* $\times 10^{-1}$*), free ([L], micrograms per milliliter* $\times 10^{-1}$*), and protein ([P], gram percent) concentrations with the percent volume of the reaction mixture filtered.*

unlabeled compound to a specific activity of 0.144 ± 0.004 μCi/mg. Solutions were analyzed by counting $^{14}C$-labeled drug in Bray's solution to a standard deviation of <3.5% in a liquid scintillation spectrometer[4]. Correction for quenching was made using an automatic external standard technique. Quinidine sulfate[5] was assayed by fluorescence spectroscopy[6] using excitation and emission wavelengths of 245 and 375 nm, respectively.

Bovine serum albumin[7] and human serum albumin[8] were reconstituted with 0.033 *M* phosphate buffer (pH 7.4). Whole human serum was collected by venipuncture from young healthy volunteers and used immediately.

Real ultrafiltration data were obtained at ambient temperature using an 80-ml polycarbonate cell fitted with a molecular filtration membrane[9] with a surface area of 17.4 $cm^2$ stated to retain molecular weights of $>10^4$.

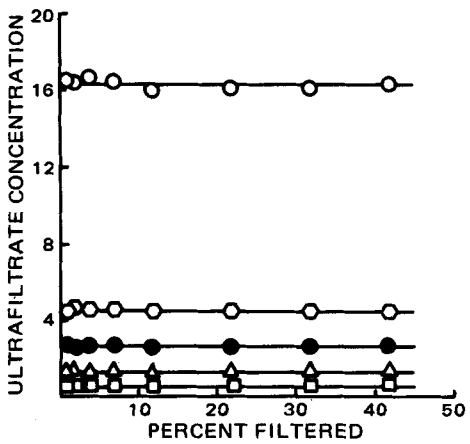


**Figure 2**—*Variation of the ultrafiltrate concentration (micrograms per milliliter* $\times 10^{-1}$*) with the percent volume filtered for salicylate in 4% bovine serum albumin (solid symbol) or whole human serum (open symbols). The initial total concentrations were 387 (○), 187 (○), 95 (△), 48 (□), and 194 (●) μg/ml.*

[4] Hewlett-Packard model 3375.
[5] BDH Laboratory Chemicals Ltd., Poole, England.
[6] Perkin-Elmer model 204.
[7] Fraction V, Sigma Chemical Co., St. Louis, Mo.
[8] Fraction V equivalent, Behringwerke AG, Marsburg, West Germany.
[9] PTGC 04710, Millipore Corp., Bedford Mass.

Solutions (25 ml) were stirred at 40 rpm during filtration under nitrogen at 10 psi. Filtrates were checked periodically for protein leakage using trichloroacetic acid. Since these membranes are quite robust, new membranes were used for each drug or macromolecular solution. Between ultrafiltrations of different concentrations of the same drug, the membrane was rinsed in several changes of phosphate buffer (pH 7.4) and 100 ml of the drug-free buffer was filtered.

The extent of drug binding to the membrane was evaluated by ultrafiltration of drugs dissolved in phosphate buffer (pH 7.4) and assay of successive aliquots of the ultrafiltrate. Concentrations were those that could reasonably be expected to be found free in serum clinically.

Ultrafiltration simulations were carried out on a programmable calculator[10] for hypothetical drugs of known binding constants. The filtration membrane was assumed to be impervious to the macromolecule and neither reflected nor bound the drug. In addition, the pressure gradient producing hydrodynamic flow was assumed to be infinitesimally small, such that any pressure artifact could be neglected. The Scatchard equation:

$$\bar{\nu} = \frac{[T] - [L]}{[P]} = \sum_{i=1}^{i=i} \frac{n_i K_i [L]}{1 + K_i [L]} \qquad \text{(Eq. 10)}$$

where $[T]$ is the total drug concentration, $[P]$, $\bar{\nu}$, $n_i$, $K_i$, and $[L]$ are as defined previously, and $i = 2$, was used to calculate the free drug concentration and, hence, the ultrafiltrate concentration for any particular total drug concentration. The algorithm for this iterative calculation was reported previously (22). The ultrafiltration process thus was simulated by allowing the unfiltered volume to decrease by small increments. Mass balance adjustments were made sequentially to account for loss of the drug to the ultrafiltrate, the reduced volume, and the increased protein concentration in the reaction mixture. Hypothetical free drug concentrations were calculated after each increment of filtered volume. Simulations were carried out for several hypothetical drugs with wide ranging binding constants.

## RESULTS AND DISCUSSION

**Influence of Pressure**—Spector *et al.* (19) observed variations of 40–75% in unbound digoxin and of 80–97% in unbound ouabain when ultrafiltration was carried out at pressures ranging from 45 to 2 psi. They were unable to explain these findings; however, it was suggested that partial blocking of the filter pores or polarization of the proteins on the filter at higher pressures might have contributed to the artifact.

A more likely explanation is that molecules of the solvent and free drug cross the membrane at different rates, and this effect is exaggerated at higher pressures, as already described. This may be supported by the observations of Kurz *et al.* (16) that membrane reflection of drug molecules increases with molecular weight; thus, the dilution artifact would be greater for the ultrafiltration of larger molecules. This concept is consistent with the data of Spector *et al.* (19) showing that the pressure effect was much greater for digoxin (mol. wt. 781) than for ouabain (mol. wt. 585).

**Influence of Volume Change**—The data presented in Fig. 1 are typical of all of the simulation data generated and are for the filtration of a drug with binding constants $K_1 = 10^4\,M^{-1}$ ($n_1 = 1$) and $K_2 = 10^2\,M^{-1}$ ($n_2 = 7$). As filtration proceeds, the total, bound drug, and protein concentrations increase markedly, but the free concentration appearing in the filtrate and, thus, the concentration ratio of bound drug to protein ($\bar{\nu}$) remain constant. This finding is of substantial relevance in clinical binding estimations since estimates of the free concentration are independent of the filtered volume.

Ultrafiltration data for various salicylate concentrations from 4% bovine serum albumin and whole human serum (Fig. 2) provide an experimental verification of the simulations. Experimentally obtained ultrafiltrate concentrations remained constant and independent of the volume fraction of the protein solution filtered up to 42% of the total volume. In these data, the percent filtered was limited to 42%; however, this limit is somewhat arbitrary. Beyond ~40% filtered, the serum became quite viscous and filtration slowed. However, if necessary, a greater fraction can be filtered. These findings are consistent with the theory. Not only does ultrafiltration not disturb binding equilibria, but a large fraction of serum may be ultrafiltered, when necessary, to compensate for a lack of assay sensitivity. Although the protein concentration was doubled throughout these experiments, this fact had no effect on the ultrafiltrate concentration, indicating the absence of any Donnan membrane error.

The ultrafiltrate concentration might be expected to deviate from the

[10] TI58, Texas Instruments, Dallas, Tex.

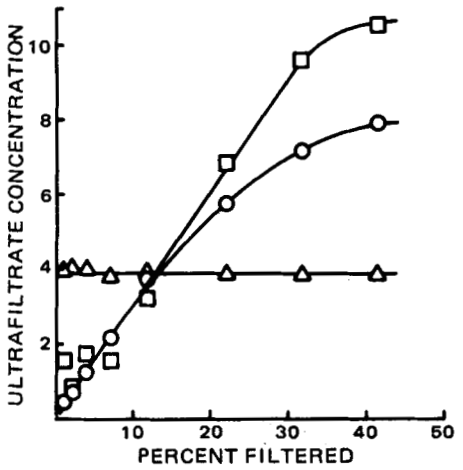


**Figure 3**—*Evaluation of membrane binding characteristics by filtration of drug in phosphate buffer (pH 7.4). Key for ultrafiltrate concentrations: △ salicylate (micrograms per milliliter × $10^{-1}$); ○, ibuprofen (micrograms per milliliter × $10^2$); and □, quinidine sulfate (micrograms per milliliter × 10). The initial concentrations were 38, 0.1, and 1.3 μg/ml, respectively.*

true free concentration if the drug binds extensively to the filtration membrane. Variable binding has been reported for various drugs and types of membranes. For example, binding was reported for phenytoin (18), salicylate (23, 24), and calcium ion (20). Some investigators reduced drug losses by minimizing the area of the membrane in contact with the reaction mixture (17). In other studies, urate (25), salicylate, acetazolamide (18), and calcium ion (26) were shown not to bind. Results from this laboratory indicate the strong binding of diazepam, quinidine sulfate, and ibuprofen to Millipore PTGC series membranes. Greater than 40% of the buffer solutions of ibuprofen and quinidine sulfate was filtered before the membrane became loaded and the ultrafiltrate concentration approached the initial drug concentration (Fig. 3). Uptake by the 17.4-$cm^2$ membrane was 0.02 μg of ibuprofen and 0.5 μg of quinidine sulfate/$cm^2$. However, this uptake would be expected to vary with the concentration of drug to be filtered if membrane binding obeys the law of mass action. Binding of salicylate to these membranes apparently is negligible (Fig. 3). Membrane binding sites probably are rapidly saturated by the much greater salicylate concentration used here to represent therapeutic free levels.

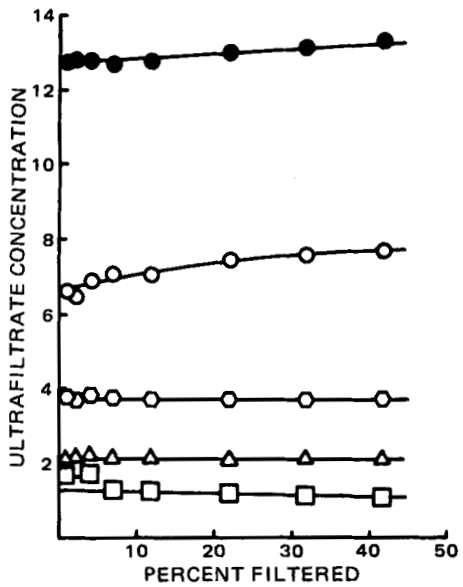


**Figure 4**—*Variation of ultrafiltrate concentration (micrograms per milliliter × $10^2$) with the percent volume filtered for ibuprofen and carprofen in 4% bovine serum albumin (solid symbol) or whole human serum (open symbols). The initial total concentrations were 4.5 (○), 2.2 (○), 1.2 (△), and 15.0 (●) μg/ml for ibuprofen and 12.7 μg/ml for carprofen (□).*

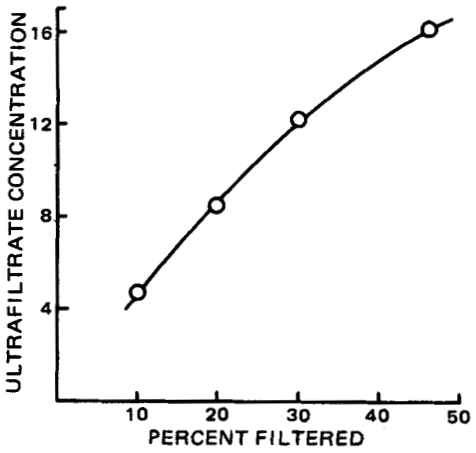


**Figure 5**—*Variation of the ultrafiltrate concentration (nanograms per milliliter) for diazepam in whole human serum at an initial total concentration of 400 ng/ml (Marianne J. Ridd, unpublished data).*

Data from the filtration of protein solutions also were obtained for the much more highly bound drug ibuprofen (Fig. 4). However, in this case, concentrations of 15.0 μg/ml in 4% bovine serum albumin and of 4.5 μg/ml in whole serum showed a slight increase in the ultrafiltrate concentration as filtration proceeded because of binding to new membranes. However, this artifact was not as great as would be predicted from the membrane binding data (Fig. 3) and would be negligible for most clinical purposes.

It is suggested that as free drug binds to the membrane, drug dissociates from the protein to reestablish the equilibrium. The net effect on the ultrafiltrate concentration thus is negligibly small when the amount of drug in the reaction mixture is much greater than that binding to the membrane. This reservoir effect may eliminate the need to correct for membrane uptake. Ultrafiltration of salicylate from 4% bovine serum albumin and whole human serum (Fig. 2), as expected, showed no membrane binding effect. It thus is probable that membrane binding is of practical importance only for extensively membrane-bound drugs where therapeutic plasma concentrations are sufficiently low that the reservoir effect is insufficient to saturate the membrane binding sites. Figure 5 shows ultrafiltration data for diazepam in whole serum at a concentration of 400 ng/ml. The marked membrane binding effect is evident from the fact that the ultrafiltrate concentration increased continuously with the volume filtered up to 45% of the 5-ml sample. At this low diazepam concentration, membrane sites are never saturated.

**Table I—Comparison of Ultrafiltration with Other Methods for Measuring Protein Binding**

| Drug | Protein | Total Concentration, μg/ml | Free Concentration, μg/ml | |
|---|---|---|---|---|
| | | | Ultrafiltration | Other[a] |
| Salicylate | 4% Bovine serum albumin | 194.15 | 26.59 | 20.96[b]* |
| | Serum | 187.62 | 44.26 | 42.90[c] |
| | Serum | 94.93 | 12.31 | 14.70[c] |
| Ibuprofen | 4% Bovine serum albumin | 14.97 | 0.13 | 0.02[d]* |
| | 1% Human serum albumin | 24.35 | 0.61 | 0.29[e]* |
| Carprofen | 1% Human serum albumin | 12.71 | 0.013 | 0.019[f]* |

[a] The asterisk indicates that the value was calculated using iterative algorithm (*cf.*, Ref. 22). [b] Dynamic dialysis: $n_1 = 1.18$, $K_1 = 2.10 \times 10^5\ M^{-1}$; and $n_2 = 5.03$, $K_2 = 1.67 \times 10^3\ M^{-1}$ (27). [c] Interpolation on serum binding profile obtained by equilibrium dialysis against plasma water (J. B. Whitlam and K. F. Brown, unpublished data). [d] Equilibrium dialysis: $n_1 = 0.92$, $K_1 = 1.37 \times 10^6\ M^{-1}$; and $n_2 = 6.66$, $K_2 = 1.94 \times 10^4\ M^{-1}$ (33). [e] Equilibrium dialysis: $n_1 = 0.80$, $K_1 = 2.73 \times 10^6\ M^{-1}$; and $n_2 = 6.27$, $K_2 = 1.95 \times 10^4\ M^{-1}$ (33). [f] Equilibrium dialysis: $n_1 = 3.53$, $K_1 = 1.39 \times 10^6\ M^{-1}$; and $n_2 = 6.31$, $K_2 = 1.28 \times 10^4\ M^{-1}$ (J. B. Whitlam and K. F. Brown, unpublished data).

The agreement between these ultrafiltration data and data obtained using dialysis procedures generally is good (Table I). Free concentrations obtained by both equilibrium dialysis and ultrafiltration of carprofen in 1% human serum albumin from a single batch are essentially identical. Free salicylate concentrations obtained by ultrafiltration of 4% bovine serum albumin solutions agree well with free concentrations obtained by calculation using binding parameters obtained previously by dynamic dialysis (27). Good agreement also was found in comparing serum free concentrations obtained by ultrafiltration with those obtained by equilibrium dialysis against plasma water.

Exact equivalence between methods would not be expected due to slight differences in experimental conditions. Different albumin batches may differ in their content of potentially displacing contaminants (28, 29). Thus, binding constants obtained for one system will not be universally applicable. In addition, binding parameter estimates may be substantially biased by the data reduction technique used (30–32). Binding constants for ibuprofen were obtained previously (33) using 1% albumin and then used in calculations for 4% albumin, assuming binding to be protein concentration independent. Protein concentration-dependent binding of drugs has been reported frequently (34, 35) and may provide a partial explanation for the observed discrepancies.

The observation that serum free concentrations determined by ultrafiltration are independent of the fraction of sample filtered should extend greatly the value of the technique. In clinical samples where free drug levels may approach the limit of detection, the ability to collect a large fraction of ultrafiltrate greatly improves the reliability of the analytical technique.

## REFERENCES


(1) M. Gibaldi and P. J. McNamara, *Eur. J. Clin. Pharmacol.*, **13,** 373 (1978).

(2) P. J. McNamara, G. Levy, and M. Gibaldi, *J. Pharmacokinet. Biopharm.*, **7,** 195 (1979).

(3) G. R. Wilkinson, in "The Effect of Disease States on Drug Pharmacokinetics," L. Z. Benet, Ed., APhA Academy of Pharmaceutical Sciences, Washington, D.C., 1976, pp. 13–32.

(4) M. Rowland, T. F. Blaschke, P. J. Meffin, and R. L. Williams, in *ibid.*, pp. 53–75.

(5) J. Elfstrom, *Clin. Pharmacokinet.*, **4,** 16 (1979).

(6) S. Wallace, B. Whiting, and J. Runcie, *Br. J. Clin. Pharmacol.*, **3,** 327 (1976).

(7) J. P. Tillement, F. Lhoste, and J. F. Giudicelli, *Clin. Pharmacokinet.*, **3,** 144 (1978).

(8) G. Levy, in "The Effect of Disease States on Drug Pharmacokinetics," L. Z. Benet, Ed., APhA Academy of Pharmaceutical Sciences, Washington, D.C., 1976, pp. 137–151.

(9) P. J. Meffin, E. W. Robert, R. A. Winkle, S. Harapat, F. A. Peters, and D. C. Harrison, *J. Pharmacokinet. Biopharm.*, **7,** 29 (1979).

(10) D. Sampson and W. J. Hensley, *Clin. Chim. Acta*, **61,** 1 (1975).

(11) O. G. Nilsen, L. Storstein, and S. Jacobsen, *Biochem. Pharmacol.*, **26,** 229 (1977).

(12) D. Rudman, T. J. Bixler, and A. E. Del Rio, *J. Pharmacol. Exp. Ther.*, **176,** 261 (1971).

(13) W. A. Craig, M. A. Evenson, and V. Ramgopal, in "The Effect of Disease States on Drug Pharmacokinetics," L. Z. Benet, Ed., APhA Academy of Pharmaceutical Sciences, Washington, D.C., 1976, pp. 125–136.

(14) I. M. Klotz, in "The Proteins," vol. I, part B, H. Neurath and K. Bailey, Eds., Academic, New York, N.Y., 1953, pp. 731, 732.

(15) J. Steinhardt and J. A. Reynolds, in "Multiple Equilibria in Proteins," B. Horecker, N. O. Kaplan, J. Marmur, and H. A. Scheraga, Eds., Academic, New York, N.Y., 1969, pp. 50–52.

(16) H. Kurz, H. Trunk, and B. Weitz, *Arzneim.-Forsch.*, **27,** 1373 (1977).

(17) K. Feldmann, *Anal. Biochem.*, **88,** 225 (1978).

(18) V. P. Shah, S. M. Wallace, and S. Riegelman, *J. Pharm. Sci.*, **63,** 1364 (1974).

(19) R. Spector, R. Vernick, and A. V. Lorenzo, *Biochem. Pharmacol.*, **22,** 2485 (1973).

(20) B. W. A. Williamson, R. C. Strange, and I. W. Percy-Robb, *Biochim. Biophys. Acta*, **543,** 397 (1978).

(21) L. B. Flexner, *J. Biol. Chem.*, **121,** 615 (1937).

(22) R. F. Mais, S. Keresztes-Nagy, J. F. Zaroslinski, and Y. T. Oester, *J. Pharm. Sci.*, **63,** 1423 (1974).

(23) C. J. Moran and W. H. C. Walker, *Biochem. Pharmacol.*, **17,** 153 (1968).

(24) R. Spector, D. T. Korkin, and A. V. Lorenzo, *J. Pharm. Pharmacol.*, **24,** 786 (1972).

(25) D. S. Campion and R. Olsen, *J. Pharm. Sci.*, **63,** 249 (1974).

(26) K. O. Pedersen, *Scand. J. Clin. Lab. Invest.*, **24,** 69 (1969).

(27) K. F. Brown and M. J. Crooks, *Biochem. Pharmacol.*, **25,** 1175 (1976).

(28) A. Saifer and L. Goldman, *J. Lipid Res.*, **2,** 268 (1961).

(29) O. G. Nilsen and S. Jacobsen, *Biochem. Pharmacol.*, **25,** 1261 (1976).

(30) B. W. Madsen and J. S. Robertson, *J. Pharm. Pharmacol.*, **26,** 807 (1974).

(31) J. H. Perrin, J. J. Vallner, and S. Wold, *Biochim. Biophys. Acta*, **371,** 482 (1974).

(32) T. W. Plumbridge, L. J. Aarons, and J. R. Brown, *J. Pharm. Pharmacol.*, **30,** 69 (1978).

(33) J. B. Whitlam, M. J. Crooks, K. F. Brown, and P. Veng Pedersen, *Biochem. Pharmacol.*, **28,** 675 (1979).

(34) S. W. Boobis and C. F. Chignell, *Biochem. Pharmacol.*, **28,** 751 (1979).

(35) L. J. Aarons, *J. Pharm. Pharmacol.*, **31,** 655 (1979).


## ACKNOWLEDGMENTS


Presented in part to the Australasian Society of Clinical and Experimental Pharmacologists, Dunedin, New Zealand, February 1979.

The authors thank Marianne J. Ridd of this laboratory for supplying the diazepam data. Radiolabeled ibuprofen and carprofen were gifts from the Boots Pure Drug Co. Ltd. and Roche Pharmaceuticals, respectively.

# Metabolism of Imipramine by Microorganisms

**CHARLES D. HUFFORD *x, GEORGE A. CAPITON *, ALICE M. CLARK *, and JOHN K. BAKER ‡**

Received June 16, 1980, from the **Department of Pharmacognosy and the* ‡*Department of Medicinal Chemistry, School of Pharmacy, University of Mississippi, University, MS 38677.* Accepted for publication July 18, 1980.

**Abstract** □ The microbial metabolism of imipramine was studied using selected fungal organisms. The major microbial metabolites were isolated, and their structures were established by spectroscopic analyses (particularly $^{13}C$-NMR) and by comparison with authentic samples. The microbial metabolites identified included 2-hydroxyimipramine, 10-hydroxyimipramine, iminodibenzyl, imipramine-*N*-oxide, and desipramine; these metabolites also have been found in mammalian metabolism studies.

**Keyphrases** □ Imipramine—microbial metabolism, identification of metabolites, fungi □ Metabolites, microbial—imipramine, identification, fungi □ Microbial metabolism—imipramine, identification of metabolites, fungi

Microorganisms possess adaptive enzymes that can be raised to high levels under suitable culture conditions or by induction. These enzymes are capable of carrying out numerous types of chemical reactions and have been utilized for microbial transformations on a wide variety of substrates (1–3).

The concept of microbial models of mammalian metabolism involves the observation that microbial metabolism often parallels mammalian metabolism (4, 5). The use of microorganisms for the study of biotransformations of drugs has been reviewed (6, 7). Numerous microbial transformation studies have involved the production of derivatives of natural product drugs with increased biological activities and/or decreased toxicities. The use of microorganisms to study drug metabolism has received far less attention, even though its potential has been noted (4–7).

Imipramine (I) is a widely used tricyclic antidepressant whose metabolism in mammals has been studied thoroughly (8–12). The metabolism of I using microorganisms was considered in this study and compared with human and mammalian metabolic studies.

## RESULTS AND DISCUSSION

Imipramine (I) was subjected to screening using 47 fungi. Of these fungi, 14 organisms were capable of metabolizing I to one or more metabolites (Table I) as indicated by TLC. Four microorganisms, *C. blakesleeana* (8688a), *M. griseo-cyanus* (1207a), *F. oxysporum* f. sp. *cepae* (11711), and *A. flavipes* (16795), were selected for preparative-scale study.

Incubation of I with stirred cultures of *C. blakesleeana* resulted in the production of two more polar metabolites, which were separated by chromatography on silica gel. Both metabolites had a molecular formula of $C_{19}H_{24}N_2O$ (mass spectrometry), and their identities were established mainly by $^{13}C$-NMR. The $^{13}C$-NMR assignments for I were made previously (13). Compound I shows only seven distinct ring carbon signals since there is an effective plane of symmetry (13), whereas each metabolite shows 14 distinct signals, indicating that the metabolites differ from imipramine in the ring carbons (the signals for the side-chain carbons are essentially the same) (Table II). One metabolite shows a singlet at 152.9 ppm, suggesting that it is hydroxylated in the aromatic ring. The most logical site of hydroxylation would be at C-2, and the $^{13}C$-NMR data are consistent with formulation of this metabolite as 2-hydroxyimipramine (II). The other metabolite shows a doublet at 70.0 ppm and a triplet at 40.2 ppm, suggesting that it is 10-hydroxyimipramine (III). The identities of both metabolites were confirmed by direct comparisons with authentic samples of II and III.

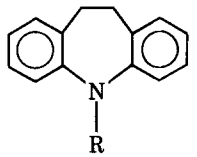

I: R = $(CH_2)_3N(CH_3)_2$
IV: R = H
V: R = $(CH_2)_3NO(CH_3)_2$
VI: R = $(CH_2)_3NHCH_3$

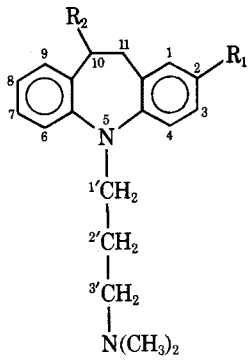

II: $R_1$ = OH, $R_2$ = H
III: $R_1$ = H, $R_2$ = OH

Preparative-scale fermentation of I using stirred cultures of *F. oxysporum* f. sp. *cepae* resulted in the production of one metabolite that was readily identified as iminodibenzyl (IV); this identification was confirmed by direct comparison with an authentic sample. Metabolism of I using shaken cultures of *A. flavipes* (16795) on a preparative scale resulted in one metabolite that was identified as imipramine-*N*-oxide (V) by comparison with an authentic sample.

The fourth microorganism chosen for preparative-scale study (stirred cultures of *M. griseo-cyanus*) produced three metabolites, two of which were identical to metabolites isolated previously (III and V). The third metabolite was shown to be desipramine (VI) by direct comparison of its hydrochloride salt with an authentic sample. These preparative-scale experiments using the four fungi allowed isolation and identification of the major microbial metabolites (II–VI) of I. The same metabolites also were detected by TLC in the screening-scale fermentation studies with the 10 additional microorganisms.

High-pressure liquid chromatographic (HPLC) procedures also were developed for the identification of the metabolites in cultures not subjected to preparative-scale study and quantitation of the metabolites in all 14 microorganisms. The retention properties of I and the metabolite standards were characterized using retention times relative to I and a retention index scale (14, 15) using HPLC System A (Table III). The retention index of drug metabolites can be estimated (15, 16) from:

$$I_m = 200\pi_x + I_{ref} \qquad \text{(Eq. 1)}$$

where $I_m$ is the retention index observed for the metabolite, $I_{ref}$ is the retention index of the reference or parent drug, and $\pi_x$ is the sum of the Hansch substituent constants (17) for the metabolite. Using this method, retention indexes of 789, 725, and 846 were calculated for II, III, and VI, respectively. These calculated values were in good agreement with the experimentally observed values (Table III). The retention indexes of IV and V were more difficult to calculate because the loss of the ionized amino group produces a retention index shift that is pH dependent.

0022-3549/81/0200-0151$01.00/0
© 1981, American Pharmaceutical Association

**Table I—Fungi Used for Screening Imipramine**

| Fungus (Number)[a] | Metabolite Production[b] |
|---|---|
| *Alternaria solani* (11078) | − |
| *Aspergillus flavipes* (1030) | + |
| *Aspergillus flavipes* (11013) | + |
| *Aspergillus flavipes* (16795) | + |
| *Aspergillus flavus* (9170) | − |
| *Aspergillus flavus* (24741) | − |
| *Aspergillus flavus* (22947) | − |
| *Aspergillus niger* (10549) | − |
| *Aspergillus niger* (11394) | − |
| *Aspergillus niger* (16888) | − |
| *Aspergillus ochraceus* (18500) | − |
| *Aspergillus parasiticus* (15517) | − |
| *Beauveria bassiana* (13144) | + |
| *Beauveria sulfurescens* (7159) | − |
| *Botrytis allii* (9435) | − |
| *Calonectria decora* (14767) | − |
| *Chaetomium cochloides* (10195) | + |
| *Cladosporium resinae* (22712) | − |
| *Cladosporium resinae f. avelleneum* (22711) | − |
| *Cunninghamella blakesleeana* (8688a) | + |
| *Cunninghamella echinulata* (NRRL 3655) | + |
| *Cunninghamella echinulata* (9244) | + |
| *Cunninghamella echinulata* (11585a) | + |
| *Cunninghamella echinulata* (11585b) | − |
| *Cunninghamella elegans* (9245) | − |
| *Curvularia lunata* (12017) | − |
| *Curvularia lunata* (13633) | − |
| *Cylindrocarpon radicicola* (11011) | − |
| *Fomes pinicola* (15341) | − |
| *Fusarium javanicum* (12575) | − |
| *Fusarium oxysporum* (7601) | − |
| *Fusarium oxysporum* f. sp. *cepae* (11711) | + |
| *Fusarium solani* var. *coeruleum* (24389) | + |
| *Mucor griseo-cyanus* (1207a) | + |
| *Penicillium adametzi* (10407) | − |
| *Penicillium chrysogenum* (9480) | − |
| *Penicillium chrysogenum* (10002) | − |
| *Penicillium frequentans* (10444) | − |
| *Penicillium oxalicum* (24784) | + |
| *Penicillium spinulosum* (16348) | − |
| *Rhizopus arrhizus* (11145) | + |
| *Rhizopus stolonifer* (6227b) | − |
| *Rhizopus stolonifer* (15441) | − |
| *Septomyxa affinis* (6737) | − |
| *Syncephalastrum racemosum* (18192) | − |
| *Whetzelinia sclerotiorum* (18015) | − |
| *Whetzelinia sclerotiorum* (24156) | − |

[a] All numbers refer to the American Type Culture Collection in Rockville, Md., unless otherwise specified. [b] Metabolite production denoted by a + indicates one or more metabolites were produced, as evidenced by TLC.

**Table II—$^{13}$C-NMR Data of Imipramine and Metabolites[a]**

| Position Assignment[b] | I[c] | II | III | IV[c] | V | VI |
|---|---|---|---|---|---|---|
| C-1 | 129.7 d | 116.1 d | 130.7 $d^1$ | 130.6 d | 130.0 d | 129.9 d |
| C-2 | 120.0 d | 152.9 s | 120.4 $d^2$ | 119.4 d | 120.0 d | 120.1 d |
| C-3 | 126.3 d | 113.2 d | 126.8 $d^3$ | 126.7 d | 126.7 d | 126.4 d |
| C-4 | 122.3 d | 121.7 $d^1$ | 122.3 $d^4$ | 118.0 d | 123.0 d | 122.5 d |
| C-4a | 148.4 s | 140.7 s | 148.9 s | 142.5 s | 147.8 s | 148.5 s |
| C-5a | 148.4 s | 148.9 s | 146.7 s | 142.5 s | 147.8 s | 148.5 s |
| C-6 | 122.3 d | 121.6 $d^1$ | 123.2 $d^4$ | 118.0 d | 123.0 d | 122.5 d |
| C-7 | 126.3 d | 126.4 d | 127.9 $d^3$ | 126.7 d | 126.7 d | 126.4 d |
| C-8 | 120.0 d | 119.0 $d^1$ | 119.9 $d^2$ | 119.4 d | 120.0 d | 120.1 d |
| C-9 | 129.7 d | 130.5 d | 130.3 $d^1$ | 130.6 d | 130.0 d | 129.9 d |
| C-9a | 134.2 s | 132.7 s | 132.2 $s^5$ | 128.6 s | 134.2 s | 134.4 s |
| C-10 | 32.3 t | 33.0 $t^2$ | 70.0 d | 34.9 t | 32.2 t | 32.4 t |
| C-11 | 32.3 t | 31.7 $t^2$ | 40.2 t | 34.9 t | 32.2 t | 32.4 t |
| C-11a | 134.2 s | 137.2 s | 134.9 $s^5$ | 128.6 s | 134.2 s | 134.4 s |
| C-1′ | 48.9 t | 48.9 t | 48.7 t | — | 47.9 t | 48.8 $t^1$ |
| C-2′ | 26.2 t | 25.7 t | 26.2 t | — | 22.4 t | 28.3 t |
| C-3′ | 57.6 t | 57.6 t | 57.6 t | — | 69.3 t | 50.0 $t^1$ |
| $N$-$CH_3$ | 45.4 q | 45.0 q | 45.2 q | — | 57.9 q | 36.5 q |

[a] All data were obtained in deuterochloroform as the free bases. [b] Based on predicted chemical shifts, literature comparisons, and single-frequency off-resonance decoupling. Assignments bearing the same numerical superscript may be interchanged. [c] The assignments for I and IV are given in Ref. 13, but the data listed are from the present study.

**Table III—Chromatographic Properties of Imipramine and Its Metabolites on HPLC System A**

| Compound | $t_R$[a] | Retention Index | $A_{254}/A_{280}$[b] |
|---|---|---|---|
| III | 0.31 | 720 | 2.53 |
| II | 0.38 | 769 | 2.06 |
| VI | 0.43 | 807 | 1.83 |
| V | 0.48 | 827 | 1.78 |
| IV | 0.72 | 871 | 0.197 |
| I | 1.00 | 1003 | 1.78 |

[a] Retention time relative to I (21 min). [b] Ratio of absorbances at 254 and 280 nm.

In complex samples, such as those obtained with the simple solvent extractions of the screening fermentation samples, it is possible that some constituents of the medium might have the same retention time as one metabolite. To minimize errors associated with this possibility, the absorbance ratio at 254 and 280 nm was measured for each standard (Table III), and these values were compared to the $A_{254}/A_{280}$ values obtained for each chromatographic peak in the fermentation extracts. With this method, the chance of an error in the identification of a metabolite peak is greatly reduced (18). Compounds I, V, and VI all had $A_{254}/A_{280}$ values near 1.79 (Table III and Fig. 1), which is consistent with their common UV chromophores. The two hydroxylated metabolites (II and III) had higher absorbance ratios, while IV showed a decrease in the ratio and a marked increase in the absorbance at 280 nm (Fig. 1).

To confirm the metabolite identifications made using HPLC System A, the metabolite extracts also were analyzed using HPLC System B, which was a normal-phase silica system. The metabolite standards generally were well resolved, and the elution order (Fig. 2) was very different from that of the reversed-phase system. Metabolite II could not be resolved from the substrate peak if the extract contained a large residual amount of the substrate.

All extracts obtained from the fermentation screening study were examined using both HPLC systems. The chromatogram of the extract of the *R. arrhizus* culture shown in Fig. 3 was typical of the results obtained with the other organisms. The yields of II, III, V, and VI in *R. arrhizus* were between 4 and 11%, and none of these chromatographic peaks was detected in the culture control. On examination of the same extract using System B (Fig. 2), the same metabolite peaks were detected. Metabolite IV was detected in the cultures of *R. arrhizus* using Systems A and B;

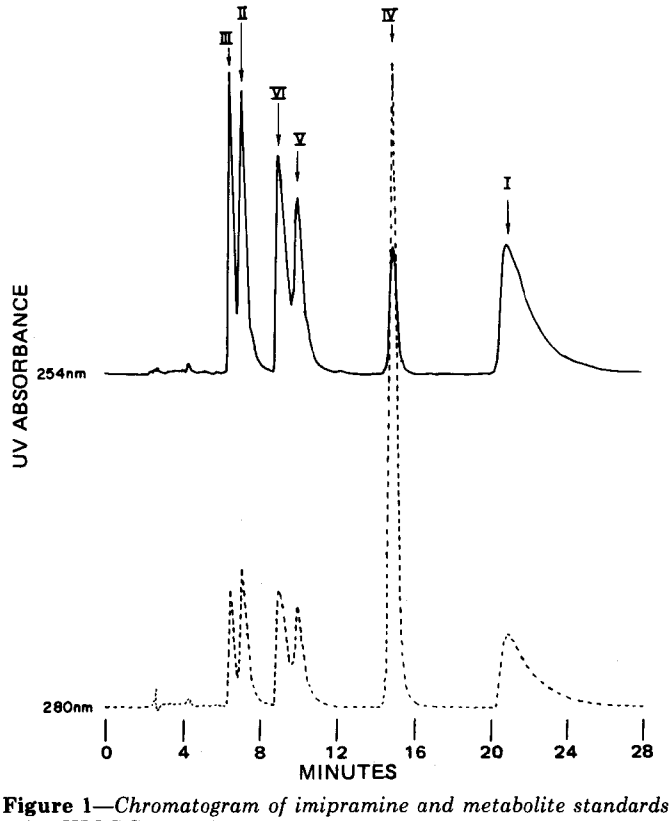


**Figure 1**—*Chromatogram of imipramine and metabolite standards using HPLC System A.*

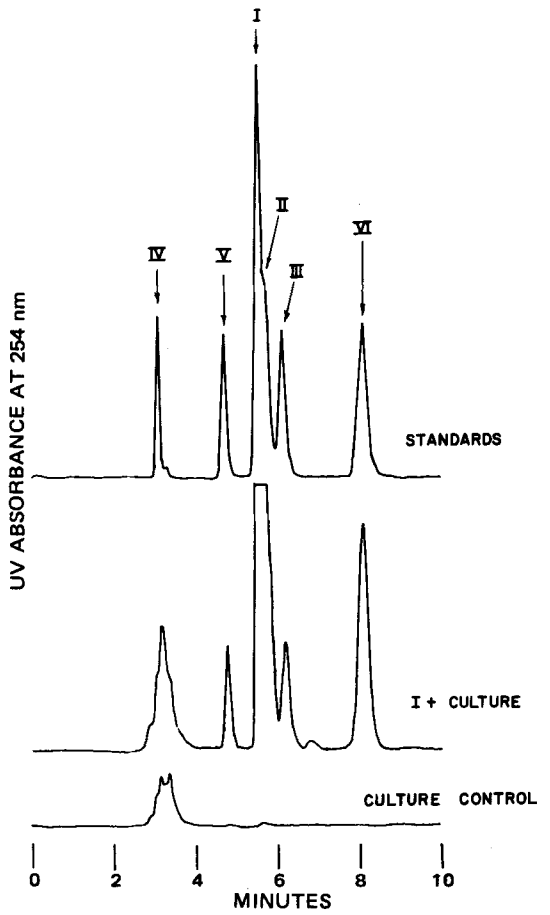


**Figure 2**—*Chromatograms of the extract of* R. arrhizus *and standards using HPLC System B. The top detector response curve was obtained from a mixture of the reference standards. The middle detector response curve was obtained from the extract of the culture containing I. The bottom detector response curve was obtained from the extract of a control culture to which I had not been added.*

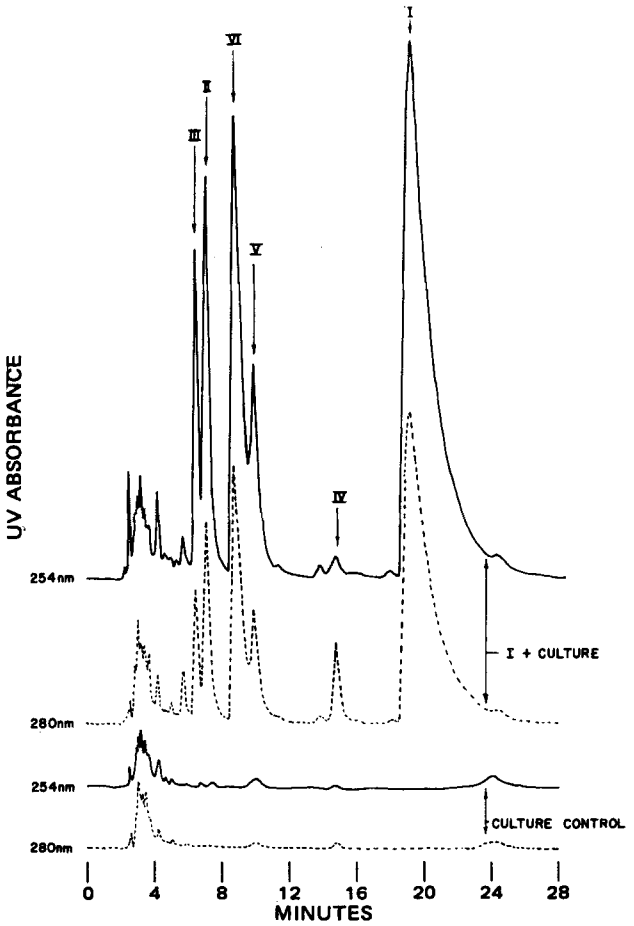


**Figure 3**—*Chromatogram of the extract of* R. arrhizus *using HPLC System A. The top two UV detector response curves were obtained from the extract of the culture containing I. The bottom two UV detector response curves were obtained from the extract of a control culture to which I had not been added.*

however, the yield of IV was not significantly greater than that found in the substrate control. Furthermore, IV was not present in the samples of I used to prepare the fermentation samples. The low levels of IV that were found in the cultures of *R. arrhizus* and most of the other organisms probably were largely due to chemical decomposition rather than metabolism. Iminodibenzyl IV also has been reported to be a microbial metabolite of *Aspergillus petrakii* (19); but since substrate controls were not conducted and since the yields were quite low, it is likely that the IV isolated here resulted from degradation and not from metabolism by *A. petrakii* (Table IV). However, in the studies with *F. oxysporum* f. sp. *cepae*, IV was consistently found at markedly higher levels than the controls, which indicates that IV was produced as a metabolite by this organism.

Using System A to quantitate metabolite production (Table IV), *F. solani*, *A. flavipes* (11013), and *A. flavipes* (16795) gave nearly quantitative conversion to the *N*-oxide (V). Moderate yields of the desmethyl metabolite also were found in the studies with *M. griseo-cyanus*, *R. arrhizus*, and *C. echinulata* (9244). Many of the organisms produced both hydroxylated metabolites; however, *M. griseo-cyanus* produced III almost exclusively, and *C. blakesleeana* produced II in the largest proportion.

An unidentified metabolite (Y) was detected in the cultures of *C. cochloides*, *C. echinulata* (3655), and *C. echinulata* (11585a); it had a retention index of 484 on System A and a retention time of 9.2 min on System B. This chromatographic peak was not detected in the substrate control or the culture control. A retention index of 529 was calculated for 10-hydroxydesmethylimipramine using Eq. 1, which was consistent with the retention index observed for Y. An $A_{254}/A_{280}$ value of 2.65 was observed for Y, which is consistent with hydroxylation at the 10-position ($A_{254}/A_{280}$ = 2.53 for III) and with *N*-demethylation (which produces no change in the ratio). Using the normal-phase HPLC system (System B), Y had a slightly longer retention time than the *N*-desmethyl metabolite (VI), and the shift in the retention time was similar to that observed between I and the 10-hydroxy metabolite (III). In the extract of the cultures of *C. cochloides*, *C. echinulata* (3655), and *C. echinulata*

**Table IV—Yields of Metabolites of Imipramine Using Microorganisms in the Screening-Scale Fermentation Studies** [a]

| Microorganism | Yield, % | | | | | |
|---|---|---|---|---|---|---|
| | I | II | III | IV | V | VI |
| *A. flavipes* (1030) | 33 | — | — | 0.9 | 8.8 | — |
| *A. flavipes* (11013) | — | — | — | 1.2 | 81 | — |
| *A. flavipes* (16795) | — | — | — | 1.3 | 87 | — |
| *B. bassiana* | 72 | 2.9 | — | 0.7 | 1.9 | 2.5 |
| *C. cochloides* [b,c] | — | 0.9 | 1.9 | 1.4 | 1.6 | 1.3 |
| *C. blakesleeana* | 72 | 10 | 6.5 | 0.7 | 3.2 | 1.4 |
| *C. echinulata* (3655) [b] | — | 16 | 28 | — | 3.9 | 3.8 |
| *C. echinulata* (9244) | 15 | 7.1 | 4.1 | 0.3 | — | 7.8 |
| *C. echinulata* (11585a) [b] | — | 6.9 | 15 | 0.1 | 1.6 | 1.6 |
| *F. oxysporum* f. sp. *cepae* | 22 | — | — | 9.3 | 0.8 | — |
| *F. solani* var. *coeruleum* | — | — | — | 1.1 | 101 | — |
| *M. griseo-cyanus* | 80 | — | 5.6 | 1.1 | — | 9.7 |
| *P. oxalicum* | 7.1 | — | 3.2 | 0.7 | 0.8 | — |
| *R. arrhizus* | 45 | 5.4 | 4.1 | 0.7 | 3.7 | 11 |
| Substrate control | 98 | — | — | 1.2 | —[d] | — |

[a] Yields are expressed as a percent conversion on a mole basis. [b] Using HPLC System A, an unknown metabolite (Y) was found having a retention index of 484 and an $A_{254}/A_{280}$ value of 2.65. The metabolite also was observed at a retention time of 9.2 min on HPLC System B. Using both HPLC systems, the metabolite peak was not detected in the culture control or the substrate control. [c] Using HPLC System A, an unknown metabolite (Z) was found having a retention index of 867 and an $A_{254}/A_{280}$ value of 1.67. The chromatographic peak was not detected in the culture control or the substrate control. [d] A trace of V was detected using HPLC System A; however, the presence of V could not be confirmed using HPLC System B.

(11585a), Y was one of the major components, the substrate was exhausted, and only moderate levels of the *N*-desmethyl and 10-hydroxylated metabolites were present. Although these findings were consistent with Y being 10-hydroxydesmethylimipramine, this hypothesis could not be verified because an authentic reference standard was not available for a direct comparison.

An additional unidentified metabolite (Z) was detected in the extract of *C. cochloides;* it was not found in either the substrate control or the culture control. Using System A, Z had a retention index of 967 ($A_{254}/A_{280}$ = 1.67). Because of the high value for the retention index and the essentially unchanged absorbance ratio, it was concluded that Z did not represent a ring hydroxylation and that it probably was modified in the side chain. Since Z was found in relatively low yields in only one microorganism, no additional studies were done with this metabolite.

## CONCLUSIONS

The microbial metabolism of imipramine (I) was studied systematically using a variety of fungi. The major metabolites identified included 2-hydroxyimipramine (II), 10-hydroxyimipramine (III), iminodibenzyl (IV), imipramine-*N*-oxide (V), and desipramine (VI). These microbial metabolites also correspond to major human and mammalian metabolites of imipramine (8–12, 20). The results of this study clearly suggest that microorganisms can be used to study drug metabolism (biotransformation), with the added advantage of producing large quantities of metabolites so that complete biological evaluation as well as complete and rigorous structural elucidation studies can be obtained.

## EXPERIMENTAL[1]

**Fermentation Screening Procedures**—Stock cultures were maintained on mycophil (BBL) agar. Preliminary screening for biotransformation products was carried out on gyrotory shakers operating at 200 rpm (room temperature) in erlenmeyer flasks (125 ml) holding 25 ml of medium. A two-stage fermentation procedure was utilized as described previously (21, 22). The fermentation medium consisted of 20 g of dextrose, 5 g of yeast extract, 5 g of peptone, 5 g of sodium chloride, and 5 g of dibasic potassium phosphate in 1000 ml of water. Imipramine hydrochloride (5 mg/culture) was added as a 5% solution in dimethylformamide.

Culture controls consisted of fermentation blanks, in which organisms were grown under identical conditions but without the substrate. Substrate controls consisted of sterile media containing the same amount of substrate and incubated under the same conditions.

**Fermentation Sampling and TLC Analysis**—The fermentations were sampled by withdrawing 5 ml of culture broth, adjusting to pH 8, and extracting with three 5-ml portions of chloroform. The chloroform layers were evaporated, and the residue was redissolved in chloroform and spotted on precoated silica gel G and aluminum oxide TLC plates (0.25 mm). The silica gel G plates were developed in ethyl acetate–methanol–ammonium hydroxide (81:15:4) and sprayed with diazotized *p*-nitroaniline followed by concentrated hydrochloric acid. The $R_f$ values were: I, 0.58 (blue); II, 0.47 (red); III, 0.40 (yellow); IV, 0.91 (yellow green); V, 0.15 (blue); and VI, 0.27 (blue). The aluminum oxide plates were developed in 2.5% methanol–chloroform and sprayed with diazotized *p*-nitroaniline followed by concentrated hydrochloric acid. The $R_f$ values were: I, 0.80 (blue); II, 0.18 (red); III, 0.46 (yellow); IV, 0.98 (green black); V, 0.08 (blue); and VI, 0.24 (blue).

**HPLC Analysis**—All quantitative analyses of the culture extracts were accomplished using HPLC System A. The mobile phase for this system was prepared using 3.3 g of dibasic potassium phosphate, 4.2 g of monobasic potassium phosphate, 0.88 ml of acetic acid, 1.2 liters of water, and 2.8 liters of methanol. A 4.6 × 250-mm octadecyl bonded phase column[2] (5-μm particles) and a mobile phase flow rate of 1.0 ml/min were used. An HPLC pump[3] and a microsyringe-loaded loop injector[4] also were used. Two UV detectors[5] were used in series (254-nm detector followed by 280-nm detector) and were calibrated using a morphine reference standard (18).

The HPLC retention indexes were made using System A, and the method was essentially the same as that reported previously (14, 15). The retention index scale was based on the relative retention of a series of 2-keto alkanes[6] ($C_3$+$C_{23}$). The retention index of a given 2-keto alkane standard was, by definition, equal to 100 times the number of carbons in the compound. Thus, 2-butanone was assigned a value of 400. The HPLC retention index of I and its metabolites was determined by interpolation of the logarithm of the capacity factors observed for the test compound and the standards.

HPLC System B consisted of a 3.9-mm × 30-cm silica column[7] with 10-μm particles. The mobile phase was prepared using methanol, 2 *N* ammonia, and 1 *N* ammonium nitrate (27:2:1); the flow rate was 1.0 ml/min.

The quantitative analyses of the microbial culture extracts were accomplished using HPLC System A. The chloroform extracts from the screening-scale fermentation studies were evaporated and then redissolved in 400 μl of methanol. Then 4 μl of the solution was chromatographed, and the peak heights were compared to those of a mixture of the standards to calculate the amount of metabolites present. The identity of each metabolite peak was verified by a comparison of the observed $A_{254}/A_{280}$ value to that of the standards and by analysis of the extracts using HPLC System B.

**Preparative-Scale Metabolism of Imipramine (I) Using *C. blakesleeana* (ATCC 8688a)**—*C. blakesleeana* was grown in 5 liters of culture medium contained in a 7.5-liter fermentor jar[8]. After a 48-hr incubation, I·HCl (1 g in 10 ml of dimethylformamide) was added to the culture. The incubation (stir rate of 200 rpm, air flow of 2 liters/min, room temperature) was continued for 20 days (no imipramine by TLC). The culture was filtered (büchner funnel), and the culture broth was adjusted to pH 7–8 and extracted with chloroform (4 × 800 ml). The combined chloroform layers were dried (sodium sulfate) and evaporated (40°) to leave 992 mg of residue. This residue was redissolved in 10 ml of chloroform and extracted thoroughly with 1% HCl (3 × 10 ml).

The combined aqueous acid extracts were adjusted to pH 8 with ammonia and extracted with chloroform (3 × 15 ml). The evaporated solution gave 591 mg of residue, which was chromatographed over silica gel (59 g, benzene–methanol–triethylamine, 93:1:6) and gave Fraction A (127 mg, pure III by TLC) and Fraction B (196 mg, pure II by TLC). It was found in later experiments that II and III could be separated more conveniently on alumina[9] using 2% methanol in chloroform.

Fraction B was crystallized from ether to give II as nearly colorless chunks (88 mg), mp 133–134° [lit. (23) mp 134–135°]; mass spectrum: $M^+$ at *m/z* 296.1901 ($C_{19}H_{24}N_2O$ requires 296.1902). The $^{13}$C-NMR data are given in Table II. Direct comparison of II with an authentic sample of 2-hydroxyimipramine (regenerated from the hydrochloride salt) showed the two samples to be identical (melting point, mixed melting point, superimposable IR spectra, TLC, and co-TLC).

Fraction A was purified further by chromatography over 122 g of alumina[9] with 1% methanol–chloroform as the eluent. A total of 30 mg of crystalline residue (III) (mp 84–86°) was obtained, $[\alpha]_D^{24}$ +3.3° (*c*, 0.7 in chloroform); mass spectrum: $M^+$ at *m/z* 296. The $^{13}$C-NMR data are given in Table II. Direct comparison of III with an authentic sample of 10-hydroxyimipramine (mp 86–88°) showed the two samples to be identical (TLC and co-TLC on silica and alumina, superimposable IR spectra, and identical $^{13}$C-NMR spectra).

**Preparative-Scale Metabolism of Imipramine (I) Using *F. oxysporum* f. sp. *cepae* (ATCC 11711)**—A total of 1 g of I·HCl was subjected to metabolism using *F. oxysporum* f. sp. *cepae* under the same fermentation conditions as described for *C. blakesleeana.* After 15 days, the culture was filtered, and the broth was adjusted to pH 7–8 and extracted with chloroform (10 × 500 ml). The combined chloroform extracts were evaporated to dryness, and the residue (326 mg) was chromatographed over alumina[9] (30 g) with benzene as the eluent. The iminodibenzyl (IV) eluted in the first few fractions followed by I (189 mg, identified by TLC and HPLC).

The fractions containing IV were combined (48 mg), and crystallization from methanol–water gave 7 mg of IV as needles, mp 106–107° [lit. (19) mp 105–107°]. Direct comparison of IV with an authentic sample of iminodibenzyl showed the two samples to be identical (melting point, mixed melting point, TLC, co-TLC, and superimposable IR spectra). The

[1] Melting points were determined on a Thomas-Hoover apparatus and are uncorrected. IR spectra were run in potassium bromide or chloroform using a Perkin-Elmer 281b spectrophotometer. The $^{13}$C-NMR spectra (15.03 MHz) were recorded in deuterochloroform on a JEOL-FX60 FT NMR spectrometer with tetramethylsilane as the internal standard. Iminodibenzyl was obtained from Aldrich Chemical Co. and was purified by crystallization from methanol–water (mp 105–107°). The melting points of the authentic samples received were determined and were: II·HCl, 186–188°; III, 86–88°; IV, 77–79°; and VI·HCl, 212–213°.

[2] Partisil PXS 5/25 ODS column, Whatman, Clifton, N.J.

[3] Model M-6000, Waters Associates, Milford, Mass.

[4] Model U6-K, Waters Associates, Milford, Mass.

[5] Model 440, Waters Associates, Milford, Mass.

[6] Analabs Inc., North Haven, Conn.

[7] μ-Porasil, Waters Associates, Milford, Mass.

[8] New Brunswick model FS 307.

[9] Woelm neutral grade I.

$^{13}$C-NMR data for IV are listed in Table II.

**Preparative-Scale Metabolism of Imipramine Using *A. flavipes* (ATCC 16795)**—*A. flavipes* was grown in 4.0 liters of medium contained in 40 500-ml erlenmeyer flasks. After a 24-hr incubation of the Stage II cultures, a total of 800 mg of I·HCl was distributed evenly among the cultures; incubation was continued for 13 days (200 rpm, room temperature). The cultures were harvested by homogenization of the whole culture, followed by filtration (through büchner funnel). The aqueous culture filtrate (pH 8) was extracted with 10 500-ml portions of chloroform, and the combined chloroform layers were dried (sodium sulfate) and evaporated *in vacuo* to leave 663 mg of a brown oily residue.

Preparative TLC of 330 mg of the residue was carried out using silica gel G plates (2.0 mm thick, 20 × 20 cm) developed in ethyl acetate–methanol–ammonium hydroxide (81:15:4). The major band, corresponding to the *N*-oxide, was located by UV light and scraped off, and the silica gel was extracted exhaustively with 10% methanol–chloroform. Evaporation of the solvent afforded 112 mg of crude V, which was crystallized from benzene–hexane as white needles, mp 76–78° [lit. (24) mp 75–79°]. Direct comparison of V with an authentic sample of imipramine-*N*-oxide showed the two samples to be identical (melting point, mixed melting point, TLC, co-TLC, and superimposable IR spectra).

**Preparative-Scale Metabolism of Imipramine (I) Using *M. griseo-cyanus* (ATCC 1207a)**—A total of 1 g of I·HCl was fed to *M. griseo-cyanus* as described for *C. blakesleeana* and worked up as described for *F. oxysporum*. The chloroform residue (664 mg) was chromatographed over alumina[9] (90 g) using chloroform followed by an increasing percentage of methanol in chloroform. A total of 496 mg of I and 45 mg of III was obtained with chloroform as the eluent (identities established by TLC and HPLC). Elution with 1% methanol–chloroform gave 30 mg of V (TLC and HPLC); 2% methanol–chloroform gave 49 mg of VI, which was converted to the hydrochloride salt (acidic ether) and crystallized from acetone as needles (10 mg), mp 211–212° [lit. (24) mp 206–208° and 214–218°]. Direct comparison of VI·HCl with an authentic sample of desipramine hydrochloride showed the two samples to be identical (melting point, mixed melting point, TLC, co-TLC, and superimposable IR spectra). The $^{13}$C-NMR data for VI are listed in Table II.

## REFERENCES


(1) W. Charney and H. L. Herzog, "Microbial Transformations of Steroids, A Handbook," Academic, New York, N.Y., 1967.

(2) H. Iizuka and A. Naito, "Microbial Transformations of Steroids and Alkaloids," University Park Press, State College, Pa., 1967.

(3) K. Kieslich, "Microbial Transformations of Non-Steroid Cyclic Compounds," George Thieme, Stuttgart, West Germany, 1976.

(4) R. V. Smith and J. P. Rosazza, *Arch. Biochem. Biophys.*, **161**, 551 (1974).

(5) R. V. Smith and J. P. Rosazza, *J. Pharm. Sci.*, **64**, 1737 (1975).

(6) R. V. Smith and J. P. Rosazza, *Biotechnol. Bioeng.*, **17**, 795 (1975).

(7) R. V. Smith, D. Acosta, Jr., and J. P. Rosazza, *Adv. Biochem. Eng.*, **5**, 69 (1977).

(8) J. V. Dingell, F. Sulser, and J. R. Gillette, *J. Pharmacol. Exp. Ther.*, **143**, 14 (1964).

(9) J. L. Crammer and B. Scott, *Psychopharmacologia*, **8**, 461 (1966).

(10) M. H. Bickel and M. Baggioline, *Biochem. Pharmacol.*, **15**, 1155 (1966).

(11) M. H. Bickel and H. J. Weder, *Arch. Int. Pharmacodyn. Ther.*, **173**, 433 (1968).

(12) J. Christiansen and L. F. Gram, *J. Pharm. Pharmacol.*, **25**, 604 (1973).

(13) R. J. Abraham, L. J. Kricka, and A. Ledwith, *J. Chem. Soc. Perkin Trans. II*, **1974**, 1648.

(14) J. K. Baker and C. Y. Ma, *J. Chromatogr.*, **169**, 107 (1979).

(15) J. K. Baker, *Anal. Chem.*, **51**, 1693 (1979).

(16) J. K. Baker, R. E. Skelton, T. N. Riley, and J. R. Bagley, *J. Chromatogr. Sci.*, **18**, 153 (1980).

(17) M. S. Tute, *Adv. Drug Res.*, **6**, 1 (1971).

(18) J. K. Baker, R. E. Skelton, and C. Y. Ma, *J. Chromatogr.*, **168**, 417 (1979).

(19) K. C. Wang and T. Yeh, *J. Taiwan Pharm. Assoc.*, **25**, 45 (1973).

(20) M. H. Bickel, *Prog. Drug. Res.*, **11**, 121 (1967).

(21) C. D. Hufford, C. C. Collins, and A. M. Clark, *J. Pharm. Sci.*, **68**, 1239 (1979).

(22) A. M. Clark and C. D. Hufford, *J. Chem. Soc. Perkin Trans. I*, **1979**, 3022.

(23) W. Schindler, *Helv. Chim. Acta*, **43**, 35 (1960).

(24) "The Merck Index," 9th ed., Merck & Co., Rahway, N.J., 1976, pp. 383, 652.


## ACKNOWLEDGMENTS


Supported in part by the Committee on Faculty Research, University of Mississippi, and the Research Institute of Pharmaceutical Sciences, School of Pharmacy, University of Mississippi.

The authors are grateful for the samples of 2-hydroxyimipramine hydrochloride, 10-hydroxyimipramine, and imipramine-*N*-oxide provided by Ciba-Geigy Corp. and desipramine hydrochloride provided by Merrell-National Laboratories. They also thank Ms. Ann Calloway and Ms. Sue Johnson for technical assistance.


# Metabolism of Phencyclidine by Microorganisms


**CHARLES D. HUFFORD *ˣ, JOHN K. BAKER ‡, and ALICE M. CLARK ***



Received June 13, 1980, from the **Department of Pharmacognosy and the* ‡*Department of Medicinal Chemistry, School of Pharmacy, University of Mississippi, University, MS 38677.* Accepted for publication July 18, 1980.



**Abstract** □ A number of microorganisms were screened for their ability to metabolize phencyclidine. Two microorganisms, *Beauveria sulfurescens* and *Cunninghamella echinulata*, produced hydroxylated metabolites, which were identified as 1-(1-phenylcyclohexyl)-4-hydroxypiperidine and 4-phenyl-4-piperidinocyclohexanol by high-pressure liquid chromatographic analysis.



**Keyphrases** □ Phencyclidine—microbial metabolism, identification of metabolites □ Metabolites, microbial—phencyclidine, identification □ Microbial metabolites—phencyclidine, identification of metabolites


Phencyclidine (I) is a commonly abused drug whose metabolism has received limited attention in mammals. Ober *et al.* (1) conducted a study of the metabolism of I in rhesus monkeys and reported some unchanged I but larger amounts of metabolites. The major metabolite present in the urine was identified as a nonphenolic dihydroxyphencyclidine. Specific structures were not proposed, but a later report (2) gave structures for those metabolites, although details were not provided. Glazko (2) also reported considerable species variation of these metabolites,


*0022-3549/81/0200-0155$01.00/0*


*© 1981, American Pharmaceutical Association*

$^{13}$C-NMR data for IV are listed in Table II.

**Preparative-Scale Metabolism of Imipramine Using *A. flavipes* (ATCC 16795)**—*A. flavipes* was grown in 4.0 liters of medium contained in 40 500-ml erlenmeyer flasks. After a 24-hr incubation of the Stage II cultures, a total of 800 mg of I·HCl was distributed evenly among the cultures; incubation was continued for 13 days (200 rpm, room temperature). The cultures were harvested by homogenization of the whole culture, followed by filtration (through büchner funnel). The aqueous culture filtrate (pH 8) was extracted with 10 500-ml portions of chloroform, and the combined chloroform layers were dried (sodium sulfate) and evaporated *in vacuo* to leave 663 mg of a brown oily residue.

Preparative TLC of 330 mg of the residue was carried out using silica gel G plates (2.0 mm thick, 20 × 20 cm) developed in ethyl acetate–methanol–ammonium hydroxide (81:15:4). The major band, corresponding to the *N*-oxide, was located by UV light and scraped off, and the silica gel was extracted exhaustively with 10% methanol–chloroform. Evaporation of the solvent afforded 112 mg of crude V, which was crystallized from benzene–hexane as white needles, mp 76–78° [lit. (24) mp 75–79°]. Direct comparison of V with an authentic sample of imipramine-*N*-oxide showed the two samples to be identical (melting point, mixed melting point, TLC, co-TLC, and superimposable IR spectra).

**Preparative-Scale Metabolism of Imipramine (I) Using *M. griseo-cyanus* (ATCC 1207a)**—A total of 1 g of I·HCl was fed to *M. griseo-cyanus* as described for *C. blakesleeana* and worked up as described for *F. oxysporum*. The chloroform residue (664 mg) was chromatographed over alumina[9] (90 g) using chloroform followed by an increasing percentage of methanol in chloroform. A total of 496 mg of I and 45 mg of III was obtained with chloroform as the eluent (identities established by TLC and HPLC). Elution with 1% methanol–chloroform gave 30 mg of V (TLC and HPLC); 2% methanol–chloroform gave 49 mg of VI, which was converted to the hydrochloride salt (acidic ether) and crystallized from acetone as needles (10 mg), mp 211–212° [lit. (24) mp 206–208° and 214–218°]. Direct comparison of VI·HCl with an authentic sample of desipramine hydrochloride showed the two samples to be identical (melting point, mixed melting point, TLC, co-TLC, and superimposable IR spectra). The $^{13}$C-NMR data for VI are listed in Table II.

## REFERENCES


(1) W. Charney and H. L. Herzog, "Microbial Transformations of Steroids, A Handbook," Academic, New York, N.Y., 1967.

(2) H. Iizuka and A. Naito, "Microbial Transformations of Steroids and Alkaloids," University Park Press, State College, Pa., 1967.

(3) K. Kieslich, "Microbial Transformations of Non-Steroid Cyclic Compounds," George Thieme, Stuttgart, West Germany, 1976.

(4) R. V. Smith and J. P. Rosazza, *Arch. Biochem. Biophys.*, **161**, 551 (1974).

(5) R. V. Smith and J. P. Rosazza, *J. Pharm. Sci.*, **64**, 1737 (1975).

(6) R. V. Smith and J. P. Rosazza, *Biotechnol. Bioeng.*, **17**, 795 (1975).

(7) R. V. Smith, D. Acosta, Jr., and J. P. Rosazza, *Adv. Biochem. Eng.*, **5**, 69 (1977).

(8) J. V. Dingell, F. Sulser, and J. R. Gillette, *J. Pharmacol. Exp. Ther.*, **143**, 14 (1964).

(9) J. L. Crammer and B. Scott, *Psychopharmacologia*, **8**, 461 (1966).

(10) M. H. Bickel and M. Baggioline, *Biochem. Pharmacol.*, **15**, 1155 (1966).

(11) M. H. Bickel and H. J. Weder, *Arch. Int. Pharmacodyn. Ther.*, **173**, 433 (1968).

(12) J. Christiansen and L. F. Gram, *J. Pharm. Pharmacol.*, **25**, 604 (1973).

(13) R. J. Abraham, L. J. Kricka, and A. Ledwith, *J. Chem. Soc. Perkin Trans. II*, **1974**, 1648.

(14) J. K. Baker and C. Y. Ma, *J. Chromatogr.*, **169**, 107 (1979).

(15) J. K. Baker, *Anal. Chem.*, **51**, 1693 (1979).

(16) J. K. Baker, R. E. Skelton, T. N. Riley, and J. R. Bagley, *J. Chromatogr. Sci.*, **18**, 153 (1980).

(17) M. S. Tute, *Adv. Drug Res.*, **6**, 1 (1971).

(18) J. K. Baker, R. E. Skelton, and C. Y. Ma, *J. Chromatogr.*, **168**, 417 (1979).

(19) K. C. Wang and T. Yeh, *J. Taiwan Pharm. Assoc.*, **25**, 45 (1973).

(20) M. H. Bickel, *Prog. Drug. Res.*, **11**, 121 (1967).

(21) C. D. Hufford, C. C. Collins, and A. M. Clark, *J. Pharm. Sci.*, **68**, 1239 (1979).

(22) A. M. Clark and C. D. Hufford, *J. Chem. Soc. Perkin Trans. I*, **1979**, 3022.

(23) W. Schindler, *Helv. Chim. Acta*, **43**, 35 (1960).

(24) "The Merck Index," 9th ed., Merck & Co., Rahway, N.J., 1976, pp. 383, 652.


## ACKNOWLEDGMENTS


Supported in part by the Committee on Faculty Research, University of Mississippi, and the Research Institute of Pharmaceutical Sciences, School of Pharmacy, University of Mississippi.

The authors are grateful for the samples of 2-hydroxyimipramine hydrochloride, 10-hydroxyimipramine, and imipramine-*N*-oxide provided by Ciba-Geigy Corp. and desipramine hydrochloride provided by Merrell-National Laboratories. They also thank Ms. Ann Calloway and Ms. Sue Johnson for technical assistance.


# Metabolism of Phencyclidine by Microorganisms


**CHARLES D. HUFFORD *ˣ, JOHN K. BAKER ‡, and ALICE M. CLARK ***



Received June 13, 1980, from the **Department of Pharmacognosy and the* ‡*Department of Medicinal Chemistry, School of Pharmacy, University of Mississippi, University, MS 38677.* Accepted for publication July 18, 1980.



**Abstract** □ A number of microorganisms were screened for their ability to metabolize phencyclidine. Two microorganisms, *Beauveria sulfurescens* and *Cunninghamella echinulata*, produced hydroxylated metabolites, which were identified as 1-(1-phenylcyclohexyl)-4-hydroxypiperidine and 4-phenyl-4-piperidinocyclohexanol by high-pressure liquid chromatographic analysis.



**Keyphrases** □ Phencyclidine—microbial metabolism, identification of metabolites □ Metabolites, microbial—phencyclidine, identification □ Microbial metabolites—phencyclidine, identification of metabolites


Phencyclidine (I) is a commonly abused drug whose metabolism has received limited attention in mammals. Ober *et al.* (1) conducted a study of the metabolism of I in rhesus monkeys and reported some unchanged I but larger amounts of metabolites. The major metabolite present in the urine was identified as a nonphenolic dihydroxyphencyclidine. Specific structures were not proposed, but a later report (2) gave structures for those metabolites, although details were not provided. Glazko (2) also reported considerable species variation of these metabolites,


*0022-3549/81/0200-0155$01.00/0*


*© 1981, American Pharmaceutical Association*

**Table I—Microorganisms Used for Screening Phencyclidine**

| Culture (Number)[a] | Metabolite Production[b] |
|---|---|
| *Arthrobacter simplex* (6946) | – |
| *Aspergillus flavipes* (1030) | – |
| *Aspergillus flavipes* (11013) | – |
| *Aspergillus flavipes* (16795) | – |
| *Aspergillus flavus* (9170) | |
| *Aspergillus flavus* (24741) | – |
| *Aspergillus niger* (10549) | – |
| *Aspergillus niger* (11394) | – |
| *Aspergillus niger* (16888) | – |
| *Aspergillus ochraceus* (18500) | – |
| *Aspergillus ochraceus* (22947) | – |
| *Aspergillus parasiticus* (15517) | – |
| *Beauveria bassiana* (13144) | – |
| *Beauveria sulfurescens* (7159) | + |
| *Botrytis allii* (9435) | – |
| *Chaetomium cochloides* (10195) | – |
| *Cladosporium resinae* (22712) | – |
| *Cunninghamella blakesleeana* (8688a) | – |
| *Cunninghamella echinulata* (NRRL 3655) | – |
| *Cunninghamella echinulata* (9244) | + |
| *Cunninghamella echinulata* (11585a) | – |
| *Cunninghamella echinulata* (11585b) | – |
| *Cunninghamella elegans* (9245) | – |
| *Curvularia lunata* (12017) | – |
| *Cylindrocarpon radicicola* (11011) | – |
| *Fomes pinicola* (15341) | – |
| *Fusarium oxysporum* (7601) | – |
| *Fusarium solani* var. *coeruleum* (24389) | – |
| *Mucor griseo-cyanus* (1207a) | – |
| *Nocardia corallina* (19070) | – |
| *Nocardia corallina* (19071) | – |
| *Nocardia corallina* (19148) | – |
| *Nocardia minima* (19150) | – |
| *Rhizopus arrhizus* (11145) | – |
| *Rhizopus stolonifer* (6227b) | – |
| *Rhizopus stolonifer* (15441) | – |
| *Streptomyces griseus* (13968) | – |
| *Streptomyces griseus* (23337) | – |
| *Streptomyces spectabilis* (27465) | – |
| *Syncephalastrum racemosum* (18192) | – |
| *Whetzelinia sclerotiorum* (18015) | – |
| *Whetzelinia sclerotiorum* (24156) | – |

[a] All cultures were obtained from the American Type Culture Collection in Rockville, Md., unless otherwise specified. [b] Metabolite production denoted by a + indicates one or more metabolites were produced, as evidenced by TLC.

with humans showing relatively large amounts of the monohydroxy metabolite. Wong and Biemann (3) tentatively identified 11 metabolites by GLC–mass spectrometry in the rat. Three of these metabolites (II*b*, III, and IV) were detected in human urine samples. Metabolites II*a* or II*b* and III also were detected in human urine samples by Lin *et al.* (4). Thus, hydroxylation of the cyclohexyl and piperidyl rings in I seems to be the major mode of mammalian metabolism. It remains to be determined whether metabolism plays a significant role in the mechanism of action and/or toxicity of I.

Smith and Rosazza (5–8) suggested that mammalian metabolism might be studied by using microbial models and cited numerous examples that show parallels between

**Table II—Chromatographic Properties of Phencyclidine and Its Metabolites on HPLC System A**

| Compound | $t_R$[a] | Retention Index | $A_{254}/A_{280}$[b] |
|---|---|---|---|
| I | 1.00 | 763 | 44.0 |
| II*a* | 0.36 | 614 | 60.8 |
| II*b* | 0.48 | 662 | 57.3 |
| III | 0.64 | 707 | 48.1 |

[a] Retention time relative to I (11 min). [b] Ratio of absorbances at 254 and 280 nm.

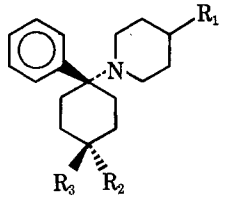


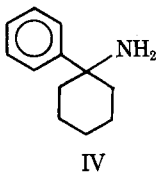


IV

I: $R_1 = R_2 = H$
II*a*: $R_1 = R_3 = H$, $R_2 = OH$
II*b*: $R_1 = R_2 = H$, $R_3 = OH$
III: $R_1 = OH$, $R_2 = R_3 = H$

mammalian and microbial metabolism. This report describes studies on the microbial metabolism of phencyclidine (I).

## RESULTS AND DISCUSSION

Of the 44 microorganisms (Table I) incubated with phencyclidine (I), only two organisms, *B. sulfurescens* (ATCC 7159) and *C. echinulata* (ATCC 9244), showed any capability to metabolize this substrate. Since TLC showed that *B. sulfurescens* produced only one metabolite, this organism was chosen for preparative-scale study.

Phencyclidine hydrochloride[1] was distributed evenly among submerged cultures of *B. sulfurescens*. After incubation for 13 days, the cultures were combined and filtered, and the aqueous culture broth was extracted with chloroform. Chromatography of the chloroform extract over alumina afforded the recovered starting material and a crystalline residue. This residue gave one spot on TLC whose $R_f$ value corresponded to that of the known hydroxylated piperidine metabolite (III). However, the $^{13}C$-NMR spectrum showed the metabolite to be a mixture of two components, which was confirmed by high-pressure liquid chromatographic (HPLC) analysis. It appeared that these two components would be difficult to separate on a preparative scale and, since authentic samples of the hydroxylated phencyclidine metabolites were available, detailed HPLC analyses were conducted.

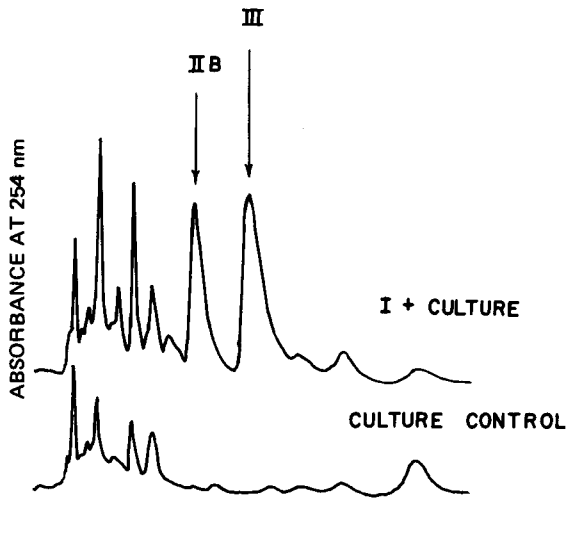


**Figure 1**—*Chromatogram of* B. sulfurescens *extract using HPLC System A. Although dual 254- and 280-nm UV detectors were used, only the response of the 254-nm detector is shown. The upper curve was obtained from the extract of the incubation mixture of I and the culture. The lower curve was obtained from the extract of the culture not containing I.*

[1] Phencyclidine (I), 1-(1-phenylcyclohexyl)-4-hydroxypiperidine (III), and 4-phenyl-4-piperidinocyclohexanol (II*a* and II*b*) were obtained from the National Institute of Drug Abuse.

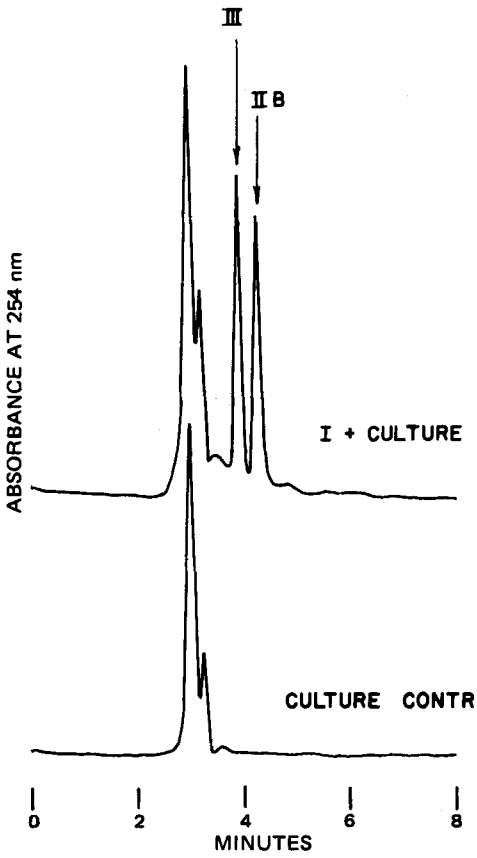


**Figure 2**—*Chromatogram of the* B. sulfurescens *extract using HPLC System B. The upper curve was obtained from the extract of the incubation mixture of I and the culture. The lower curve was obtained from the extract of the culture not containing I.*

HPLC analysis of an authentic sample of III[1] using System A showed one peak with a relative retention time of 0.64 (Table II). However, analysis of an authentic sample of 4-phenyl-4-piperidinocyclohexanol[1] using System A showed two distinct peaks with relative retention times of 0.36 and 0.48, respectively (Table II). The cyclohexyl metabolite, 4-phenyl-4-piperdinocyclohexanol, was available as a mixture of two epimers[2] (II*a* and II*b*), but their relative stereochemistry has not yet been established. The major component of this mixture corresponded to a relative retention time of 0.36 in HPLC System A and was arbitrarily assigned as II*a*. The minor component, assigned as II*b*, had a relative retention time of 0.48 in HPLC System A.

Purified extracts of *B. sulfurescens* incubated with I in a manner analogous to the preparative-scale procedure were examined using HPLC Systems A and B. In addition, the extracts of *B. sulfurescens* cultures grown under the same conditions, but without I (culture control), were analyzed and used as controls to identify any interfering peaks due to the organism or medium. With System A, two peaks not present in the culture control samples were evident (Fig. 1), with relative retention times of 0.48 and 0.64. These peaks corresponded in retention time to one isomer of the hydroxylated cyclohexyl metabolite (II*b*) and the hydroxylated piperidine metabolite (III). The identity of these metabolites was confirmed further using System B, which also showed the presence of two components, corresponding in retention times to II*b* and III (Fig. 2). In addition, the ratios of the absorbances at 254 and 280 nm for each peak in the chromatograms were consistent with the values observed for the standard samples in both systems (Table II).

The only other culture shown by TLC to produce metabolites was *C. echinulata*. Chloroform extracts of both substrate-containing and nonsubstrate-containing cultures of *C. echinulata* were concentrated on an alumina column and eluted with 1% methanol in chloroform to remove I and some of the medium constitutents. The chromatogram of the purified *C. echinulata* extract on System A (Fig. 3) clearly showed that

[2] The sample was prepared as described in the literature (4) and apparently results in an epimeric mixture, which was not separated further.

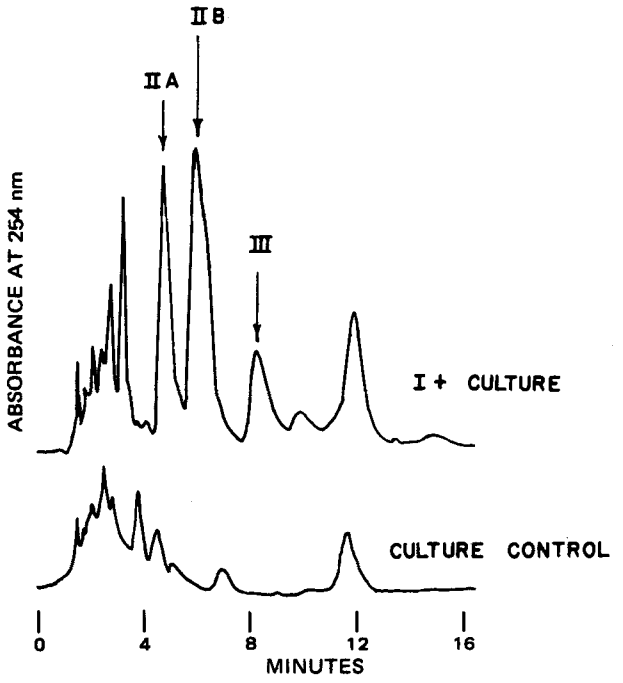


**Figure 3**—*Chromatogram of the* C. echinulata *extract using HPLC System A. The upper curve was obtained from the extract of the incubation mixture of I and the culture. The lower curve was obtained from the extract of the culture not containing I.*

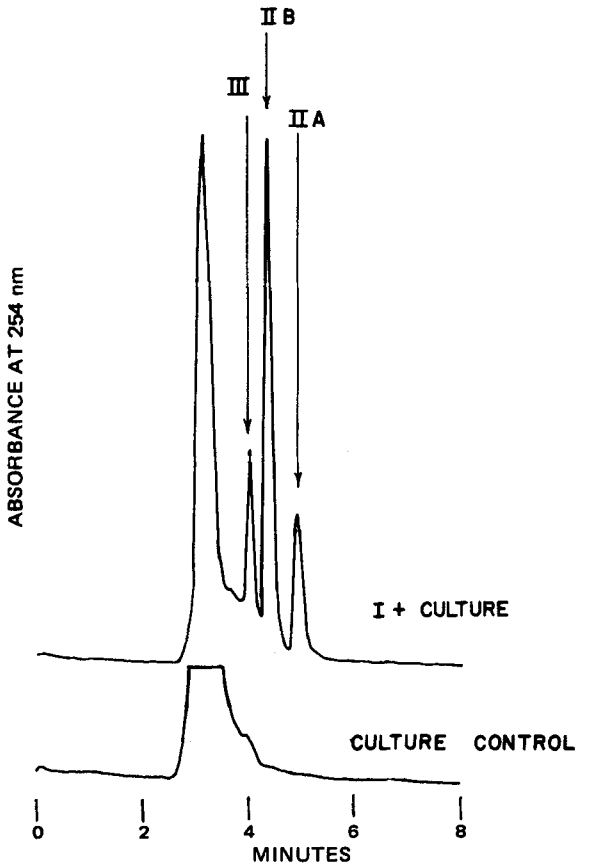


**Figure 4**—*Chromatogram of the* C. echinulata *extract using HPLC System B. The upper curve was obtained from the extract of the incubation mixture of I and the culture. The lower curve was obtained from the extract of the culture not containing I.*

metabolites II*a*, II*b*, and III were produced. This result was established further by analysis on System B (Fig. 4).

The identification of the metabolites was verified by a comparison of the absorbance ratios observed for the metabolites and the standards (Table II). The absolute quantity of each metabolite present in the alumina-purified extracts of both *B. sulfurescens* and *C. echinulata* cultures was calculated. When 15 mg of I·HCl was added to 100-ml cultures, the alumina-purified extracts of *B. sulfurescens* cultures contained 0.13 mg of II*b* and 0.19 mg of III, while purified *C. echinulata* extracts contained 0.15 mg of II*a*, 0.22 mg of II*b*, and 0.09 mg of III.

## CONCLUSIONS

It appears that both *B. sulfurescens* and *C. echinulata* produce III, which is also a metabolite in humans. GLC–mass spectral studies (3) suggested that the major mammalian metabolite is II*b* rather than II*a*; however, those findings were not confirmed by comparison to standards of proven stereochemistry. It is not possible to determine if the isomer produced by *B. sulfurescens* is the same as the reported human metabolite since the standard sample was available only as a mixture of the two isomers. *C. echinulata* appears to be less selective and produces both isomers (II*a* and II*b*).

## EXPERIMENTAL

**Fermentation Procedures**—Initial screening studies were performed to determine microorganisms capable of metabolizing phencyclidine. A total of 44 organisms (Table I) were selected[3] and were grown according to the usual two-stage fermentation procedure (9, 10) in 25 ml of medium held in 125-ml cotton-plugged erlenmeyer flasks. Phencyclidine hydrochloride was added to 24-hr second-stage cultures, which were incubated on a rotary shaker at 200 rpm and 25°. Samples of 5 ml were removed at various intervals after the substrate had been added.

Each sample was adjusted to pH ~8 with ammonium hydroxide and extracted with chloroform (3 × 5 ml), and the chloroform extracts were evaporated to dryness. The residues were redissolved in 100 μl of chloroform, and 6 μl of the solution was spotted on TLC plates. The medium used for all fermentations consisted of 10 g of dextrose, 10 g of corn steep liquor, 10 g of soya flour, 5 g of dry malt extract, 1 g of calcium chloride, and 5 g of sodium chloride in 1 liter of water. Culture controls consisted of fermentation blanks, in which the organisms were grown under identical conditions but without the substrate. Substrate controls consisted of the addition of the same amount of substrate to sterile media.

**TLC and HPLC**—Silica gel $GF_{254}$ plates were developed in either 10% acetic acid in absolute ethanol or ethyl acetate–methanol–concentrated ammonium hydroxide (85:10:5). Alumina $GF_{254}$ plates were developed in 1% methanol–chloroform. The plates were visualized under UV light and sprayed with iodoplatinate spray reagent. The $R_f$ values of I, II*a*, II*b*, and III in the 10% acetic acid in ethanol system were 0.38, 0.22, 0.22, and 0.28, respectively. Their $R_f$ values in the ethyl acetate–methanol–ammonium hydroxide (85:10:5) system were 0.80, 0.47, 0.55, and 0.55, respectively, and their $R_f$ values in the 1% methanol in chloroform (alumina) system were 0.80, 0.28, 0.28, and 0.30, respectively.

HPLC System A consisted of a 3.9-mm × 30-cm octadecyl reversed-phase column[4] with 10-μm particles. The mobile phase was prepared using 6.6 g of dibasic potassium phosphate, 8.4 g of monobasic potassium phosphate, 1.6 liters of methanol, and 2.4 liters of water; the flow rate was 2.0 ml/min. An HPLC pump[5] and a microsyringe-loaded loop injector[6] also were used. Two UV detectors[7] were used in series (254-nm detector followed by a 280-nm detector) and were calibrated using a morphine reference standard (11).

The HPLC retention indexes with HPLC System A were measured essentially as reported previously (12, 13). The retention index scale was based on the retention of the drug in question relative to a series ($C_3$–$C_{23}$) of 2-keto alkanes[8]. The retention index of a given 2-keto alkane standard was, by definition, equal to 100 times the number of carbons in the compound. Thus, 2-butanone was assigned a value of 400. The HPLC retention index of I and its metabolites was determined by interpolation of the logarithm of the capacity factors observed for the test compound and the standards.

HPLC System B consisted of a 3.9-mm × 30-cm silica column[9] with 10-μm particles. The mobile phase was prepared using methanol, 2 *N* ammonia, and 1 *N* ammonium nitrate (27:2:1); the flow rate was 1.0 ml/min.

**Preparative-Scale Metabolism of Phencyclidine (I) Using *B. sulfurescens* (ATCC 7159)**—*B. sulfurescens* (ATCC 7159) was grown in 4.0 liters of medium held in 40 500-ml cotton-plugged erlenmeyer flasks. A total of 400 mg of phencyclidine hydrochloride[1] was distributed equally among the cultures. The flasks were kept at room temperature and 200 rpm for 13 days after substrate addition. The cultures were harvested by filtration, and the aqueous culture broth (pH 8) was extracted with chloroform (3 × 2 liters). The combined chloroform layers were dried (sodium sulfate) and evaporated to dryness, yielding 341 mg of extract.

The extract was chromatographed over alumina[10] (40 g) using chloroform as the solvent. Elution with chloroform yielded a fraction containing phencyclidine (I) (137 mg), identified by TLC and $^{13}$C-NMR analyses. Elution with 1% methanol–chloroform gave a 30-mg fraction (crystalline residue) of the metabolite. The fraction showed one spot in all of the TLC systems tried but clearly was a mixture of two components (II*b* and III) as determined by HPLC and $^{13}$C-NMR spectroscopy.

## REFERENCES


(1) R. E. Ober, G. W. Gwynn, T. Chang, D. A. McCarthy, and A. J. Glazko, *Fed. Proc. Fed. Am. Soc. Exp. Biol.*, **22**, 539 (1963).

(2) A. J. Glazko, *Antimicrob. Agents Chemother.*, **3**, 660 (1966).

(3) L. K. Wong and K. Biemann, *Clin. Toxicol.*, **9**, 583 (1976).

(4) D. C. K. Lin, A. F. Fentiman, R. L. Foltz, R. D. Forney, and I. Sunshine, *Biomed. Mass Spectrom.*, **2**, 206 (1975).

(5) R. V. Smith and J. P. Rosazza, *Arch. Biochem. Biophys.*, **161**, 551 (1974).

(6) R. V. Smith and J. P. Rosazza, *J. Pharm. Sci.*, **64**, 1737 (1975).

(7) R. V. Smith and J. P. Rosazza, *Biotechnol. Bioeng.*, **17**, 75 (1975).

(8) R. V. Smith, D. Acosta, and J. P. Rosazza, *Adv. Biochem. Eng.*, **5**, 69 (1977).

(9) C. D. Hufford, C. C. Collins, and A. M. Clark, *J. Pharm. Sci.*, **68**, 1239 (1979).

(10) A. M. Clark and C. D. Hufford, *J. Chem. Soc. Perkin Trans. I*, **1979**, 3022.

(11) J. K. Baker, R. E. Skelton, and C. Y. Ma, *J. Chromatogr.*, **168**, 417 (1979).

(12) J. K. Baker and C. Y. Ma, *ibid.*, **169**, 107 (1979).

(13) J. K. Baker, *Anal. Chem.*, **51**, 1693 (1979).


## ACKNOWLEDGMENTS


Supported in part by the Committee on Faculty Research, University of Mississippi, and the Research Institute of Pharmaceutical Sciences, School of Pharmacy, University of Mississippi.


[3] Obtained from University of Mississippi School of Pharmacy culture collection.

[4] μBondapak $C_{18}$, Waters Associates, Milford, Mass.

[5] Model M-6000, Waters Associates, Milford, Mass.

[6] Model U6-K, Waters Associates, Milford, Mass.

[7] Model 440, Waters Associates, Milford, Mass.

[8] Analabs Inc., North Haven, Conn.

[9] μ-Porasil, Waters Associates, Milford, Mass.

[10] Woelm neutral grade I.

# 2,5-Diaziridinyl-3,6-bis(carboethoxyamino)-1,4-benzoquinone I: Kinetics in Aqueous Solutions by High-Performance Liquid Chromatography

G. K. POOCHIKIAN ˣ and J. C. CRADOCK

Received December 11, 1979, from the *Analytical and Product Development Section, Pharmaceutical Resources Branch, National Cancer Institute, Bethesda, MD 20205.* Accepted for publication July 18, 1980.

**Abstract** □ The application of a rapid, selective, and sensitive reversed-phase high-performance liquid chromatographic method to the analysis of 2,5-diaziridinyl-3,6-bis(carboethoxyamino)-1,4-benzoquinone (I) and its degradation products is described. The method was used to study the kinetics of degradation of I over pharmaceutically useful pH ranges. The overall reaction rate followed pseudo-first-order kinetics. The pH–rate profile demonstrated optimal stability between pH 6.0 and 6.5. The degradation behavior suggests the existence of multiple pathways. The temperature dependence of the disappearance of I also was evaluated from the regression equation derived from the Arrhenius plot.

**Keyphrases** □ 2,5-Diaziridinyl-3,6-bis(carboethoxyamino)-1,4-benzoquinone—degradation kinetics, monitoring by high-performance liquid chromatography □ Degradation—2,5-diaziridinyl-3,6-bis(carboethoxyamino)-1,4-benzoquinone, kinetics, monitoring by high-performance liquid chromatography □ High-performance liquid chromatography—analysis, 2,5-diaziridinyl-3,6-bis(carboethoxyamino)-1,4-benzoquinone, degradation kinetics

The antitumor properties of aziridinylbenzoquinone derivatives have been recognized for some time (1, 2), and these compounds were shown to induce cross-links with DNA (3). Interest in this class of compounds was renewed due to the recent demonstration of wide spectrum antitumor activity in experimental tumor systems, particularly against central nervous system (CNS) neoplasms (4, 5). 2,5-Diaziridinyl-3,6-bis(carboethoxyamino)-1,4-benzoquinone (I) was selected from a series of potential CNS antitumor agents for extensive preclinical studies and clinical trial (5). However, there have been no systematic studies reporting qualitative or quantitative data pertaining to the hydrolytic stability of this class of compounds and of this potentially useful pharmaceutical agent in particular.

The present investigation involved development of a rapid, simple, selective, and sensitive stability-indicating high-pressure liquid chromatographic (HPLC) assay for the simultaneous quantification of I and its decomposition products. Methods used previously to study the hydrolytic behavior of polyfunctional substituted aziridines were based only on the disappearance of the total aziridine moieties (6–8). The HPLC method was applied to evaluate the stability of I over a wide pH range and under various pharmaceutically applicable conditions. Decomposition products were isolated by semipreparative HPLC and characterized chemically; they are described in a separate report (9).

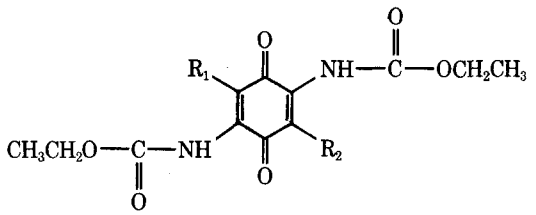

I: $R_1 = R_2 =$ –N◁

II: $R_1 =$ –N◁, $R_2 = NHCH_2CH_2OH$

III: $R_1 = R_2 = NHCH_2CH_2OH$

## EXPERIMENTAL

**Reagents**—Compound I (NSC 182986)[1] and the internal standard, 5-chloro-2-pyridinol[2], were used as received. 2-Aziridinyl-5-(2′-hydroxyethylamino)-3,6-bis(carboethoxyamino)-1,4-benzoquinone (II) and 2,5-di(2′-hydroxyethylamino)-3,6-bis(carboethoxyamino)-1,4-benzoquinone (III) were isolated by a semipreparative HPLC method from partially hydrolyzed samples of I, and their identities were verified by comparison of their retention times with those of authentic samples as well as by mass spectrometry (9). Acetonitrile[3] (distilled in glass) and distilled water were filtered through 0.45-μm solvent-resistant filters[4].

Infusion fluids were obtained commercially[5] and were utilized as received. All other chemicals were reagent grade. Initially, the influence of pH on the stability of I was studied between pH 3.0 and 8.0 using 0.01 *M* citrate–phosphate buffer (10) or 0.01 *M* phosphate buffer (11). When necessary, the pH was adjusted[6] to within 0.05 pH unit of the nominal value with either the basic or acidic component of the buffer.

**HPLC**—A modular high-pressure liquid chromatograph equipped with a constant-flow pump[7] was used to deliver the eluent at a rate of 1 ml/min to a 5-μm reversed-phase column[8] (250 × 3 mm i.d.). No attempt was made to control the column temperature. Injections were made with a rotary valve injector equipped with a 10-μl injection loop[9]. A variable-wavelength UV detector[10], set at 345 nm and 0.1 aufs deflection, was used to detect eluted compounds. The output signals were recorded with a strip-chart recorder[11].

The chromatographic mobile phase was 15% (v/v) acetonitrile in distilled water. The column pressure at a flow rate of 1 ml/min was ~2100 psi. Separations were effected isocratically at room temperature, and the chart speed was 1 cm/min. The chromatographic parameters, *i.e.*, the capacity factor ($k'$), the separation factor ($\alpha$), and the resolution ($R_s$), of various solutes were calculated from the adjusted retention volumes (12).

Peak heights were used to quantitate I and its hydrolysis products. Standard curves comparing the ratios of the peak heights of I–III to 5 μg of the internal standard exhibited linear responses ($r > 0.999$) in the working concentration range of 5–50 μg/ml. The peak heights of I–III were converted to concentrations by comparison with standard curves.

One milliliter of a freshly prepared $2.75 \times 10^{-2}$ *M* stock solution of I in *N,N*-dimethylacetamide was added to ~95 ml of the appropriate medium, and the volume was rapidly brought to 100.0 ml with the same medium. The resulting solution was shaken and filtered[4], and a zero-time

[1] Developmental Therapeutics Program, National Cancer Institute, National Institutes of Health, Bethesda, Md.
[2] Aldrich Chemical Co., Milwaukee, Wis.
[3] Burdick & Jackson Laboratories, Muskegon, Mich.
[4] Millipore Corp., Bedford, Mass.
[5] Sodium chloride injection USP (lot 64-856-DE-2), 5% dextrose injection USP (lot 51-688-DE-2), and lactated Ringer's injection USP (lot 62-458-DE-2), Abbott Laboratories, North Chicago, Ill.
[6] Beckman Zeromatic pH meter, Beckman Instruments, Irvine, Calif.
[7] Model 3500B, Spectra-Physics, Santa Clara, Calif.
[8] Spherisorb ODS (5 μm), Spectra-Physics, Santa Clara, Calif.
[9] Valco Instruments Co., Houston, Tex.
[10] Model SP 770, Spectra-Physics, Santa Clara, Calif.
[11] OmniScribe, Houston Instruments, Austin, Tex.

0022-3549/81/0200-0159$01.00/0
© 1981, American Pharmaceutical Association

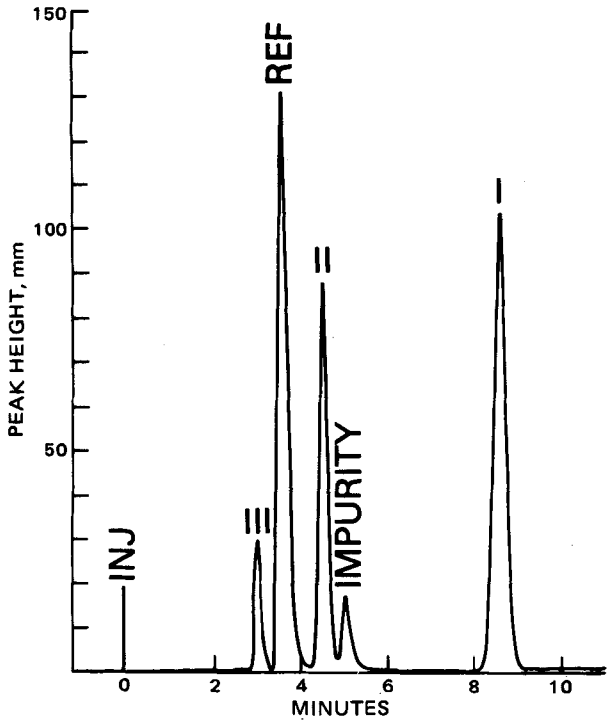


**Figure 1**—*High-performance liquid chromatogram of I–III and the internal standard (REF). The column conditions are given in the text.*

sample was assayed immediately. The remaining solution was promptly dispensed (3.0 ml) into 5-ml clean flint ampuls, sealed, and stored at 5 ± 0.1, 25 ± 0.1, 37 ± 0.1, and 50 ± 0.1° for a period not exceeding 30 days. The pH of each sample was determined prior to dilution for the assay[6].

At designated time intervals, duplicate 1.0-ml samples were removed, diluted to 2.0 ml with 15% (v/v) acetonitrile in water containing 1.0 mg of the internal standard/ml, and immediately subjected to analysis. Disappearance of I was followed beyond its second half-life. Samples were removed for analysis at a minimum of 10 different time intervals per experimental condition during each experiment.

## RESULTS AND DISCUSSION

**Solubility Studies**—Since I has poor aqueous solubility (~200 μg/ml), mixed solvent systems are required to achieve the desired concentration for intravenous injection. Although I has better solubility in ethanol (2 mg/ml), a 10% ethanolic solution did not improve its solubility. However, solutions of I ($2.75 \times 10^{-3}$ *M*) were readily prepared by dissolving 20 mg in 1 ml of *N,N*-dimethylacetamide and then diluting the solution with 19 volumes of water or buffer. Antitumor data (4) and preliminary toxicological studies[12] indicated that this concentration was adequate for preclinical and clinical studies.

**Assay Sensitivity**—Colorimetric (6, 7) and titrimetric (8) methods were reported for the quantitative determination of aziridinyl compounds. The colorimetric method is based on a comparison between a reference and a partially decomposed sample in which some aziridine moieties were destroyed. However, in the case of I, the method does not distinguish quantitatively between intact, partially reacted, or fully reacted species. The titrimetric method is based on a reaction of the ethyleneimine ring with thiosulfate ion and provides a measure of intact aziridine moieties. Likewise, no distinction can be made between a mixture of unreacted, fully decomposed polyfunctional aziridines and a mixture of partially reacted species.

In a compound with polyfunctional ethyleneimine moieties, it was expected that ring opening may not proceed simultaneously but rather in discrete steps. Development of a simple, rapid, selective, and sensitive quantitative HPLC–UV assay for I and its various decomposition products confirmed this supposition. The response curve of I was linear ($r > 0.999$) in the concentration range examined (5–50 μg/ml). Good reproducibility of the described HPLC procedure using UV detection was demonstrated when six 10-μl aliquots of a standard solution of I in the presence of II, III, and internal standard were chromatographed. The coefficient of variation of I was 0.48%, and the minimum detectable limit of I was 3 ng.

During the study, there was no noticeable loss in column performance. As a precaution, the column was reconditioned according to the manufacturer's suggestions when not in use for more than a few days.

The order of elution was III, the internal standard, II, and I (Fig. 1). A representative chromatogram of a synthetic mixture of I–III and the internal standard is shown in Fig. 1. The retention data for these substances are listed in Table I.

The retention volumes ($V_R$ in milliliters), $k'$, $\alpha$, and $R_s$ for I and various decomposition products were identical to those reported for the synthetic mixture. The impurity found in the original sample of I was identified as 2,5-diamino-2,6-dichloro-1,4-benzoquinone (IV) (9).

**Order of Reactions**—The hydration of 1-aziridinylbenzoquinones in acid solutions (13) was reported to be more rapid than that of 1-unsubstituted basic aziridines (14, 15). Such substituents on an aziridine nitrogen are expected to increase markedly the reactivity of the protonated ring; hence, these compounds more closely resemble activated aziridines than basic aziridines in their reactions. Such an activated aziridine, in addition to being sensitive to acidic reagents, also may undergo ring opening with nucleophilic reagents.

The results of the present investigation confirmed the high reactivity of I in aqueous solution. Semilog plots of residual concentrations of I *versus* time exhibited excellent linearity ($r > 0.99$) for experiments at all temperatures examined and pH 3.0–8.0. The disappearance of I followed pseudo-first-order kinetics under the conditions studied and was in accord with previous observations on aziridines (16). The degradation rate constants of I were computed by the least-squares linear regression method. Table II presents the calculated pseudo-first-order rate constants at fixed concentrations of I ($2.75 \times 10^{-4}$ *M*) and buffer (0.01 *M*) and constant temperature (25 ± 0.1°) over the pH range of 3.0–8.0. Duplicate experiments were performed for certain experimental conditions to verify the results. Rate constants from duplicate runs in these studies differed by <5%.

**Influence of pH**—The pH–rate profile for the degradation of I was constructed from the logarithm of the pseudo-first-order rate constants and the pH values at 25 ± 0.1° (Fig. 2). The buffering capacities of all of the solutions were sufficient to maintain constant pH values (±0.05) throughout the experiment, with the exception of the pH 8.0 solution. In this case, values as low as pH 7.4 were recorded.

The pH–rate profile showed a degradation minimum between pH 6.0 and 6.5 (Fig. 2). The observed results are in accord with those reported

**Table I—Retention Volume ($V_R$), Capacity Factor ($k'$), Separation Factor ($\alpha$), and Resolution ($R_s$) of Various Solutes[a]**

| Compound | $V_R$, ml | $k'$ | $\alpha$ | $R_s$ |
|---|---|---|---|---|
| III | 3.00 | 2.00 | | |
| | | | 1.33 | 2.70 |
| Internal standard | 3.65 | 2.65 | | |
| | | | 1.32 | 2.83 |
| II | 4.50 | 3.50 | | |
| | | | 1.16 | 1.66 |
| IV | 5.05 | 4.05 | | |
| | | | 1.85 | 6.08 |
| I | 8.50 | 7.50 | | |

[a] Retention data of various solutes from a 250 × 3-mm i.d. stainless steel Spherisorb ODS (5-μm particles) column; the mobile phase was 15% acetonitrile in water at a flow rate of 1 ml/min; UV detection was at 345 nm.

**Table II—Pseudo-First-Order Rate Constants for Loss of I ($2.75 \times 10^{-4}$ *M*) in Solutions at Different pH Values and 25 ± 0.1°**

| pH | $k_{obs} \times 10^2$, $day^{-1}$ |
|---|---|
| 3.0 | 763 |
| 5.0 | 62.6 |
| Unbuffered | 5.10 |
| 6.0 | 3.63 |
| 6.5 | 3.07 |
| 7.0 | 4.22 |
| 8.0 | 12.97 |

[12] R. Davis, Laboratory of Toxicology, National Cancer Institute, Bethesda, Md., personal communication.

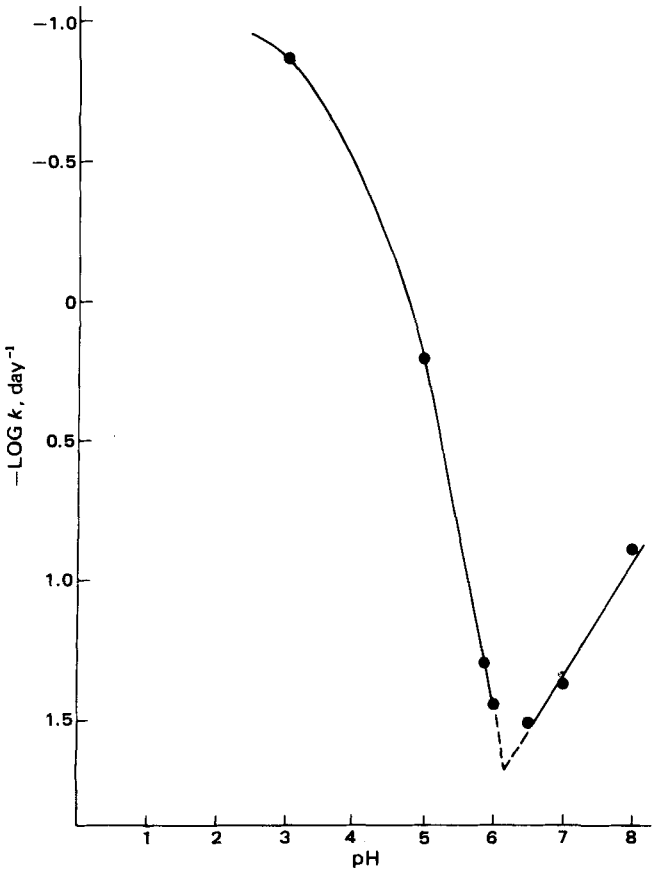


**Figure 2**—*Log* k versus *pH profile for the decomposition of I (2.75 × $10^{-4}$ M) at 25 ± 0.1°.*

for ethyleneiminoquinones, in which the hydrolysis rate of the ethyleneimino group increased with decreasing pH (2). Moreover, I in unbuffered solution (pH ~ 6) degraded faster than in pH 6.0 buffer (Table II). This accelerated decomposition of I undoubtedly was caused by the inability of the unbuffered solution to maintain a constant pH throughout the reaction (maximum decrease in pH = 0.5 unit).

The influence of the solution pH on the degradation pattern of I was dramatic. Based on the present findings, several degradation reactions appeared to be responsible for the decomposition of I in phosphate buffer (0.01 *M*). The relative importance of each reaction was dependent on the solution pH. In strongly acid solutions (pH = 1), I apparently degraded instantaneously to yield the dialcohol (III). Under alkaline conditions, the high-performance liquid chromatograms showed the presence of a hydrophilic peak at the void volume, which is characterized in a separate report (9). The intensity of this peak increased gradually as the solution pH was raised (>6), and this peak was the only degradation peak detected in the chromatogram in strongly alkaline solution. In weakly acidic solution (pH ≤ 5.0), I underwent simple, stepwise, consecutive hydrolytic cleavage of the aziridine rings to produce the monoalcohol (II) and eventually the dialcohol (III) (9). The concentration of II in such solutions of I also was pH dependent and showed a concentration maximum at ~pH 5.

**Influence of Temperature**—An Arrhenius plot of the pseudo-first-order rate constants ($k$) at varying temperatures (5 ± 0.1, 25 ± 0.1, 37 ± 0.1, and 50 ± 0.1°) in the presence of a constant phosphate buffer concentration (0.01 *M*), constant concentration of I (2.75 × $10^{-4}$ *M*), and a constant pH (6.5) is shown in Fig. 3. The apparent Arrhenius parameters for the disappearance of I were calculated from the regression equation ($r > 0.99$). The apparent activation energy was 14.0 kcal/mole, and the frequency factor ($A$) was 7.70 × $10^3$ $sec^{-1}$.

**Table III—Stability of I in Reconstituted Solution and in Various Infusion Fluids at Ambient Temperature**

| Medium | Admixture Solution pH | $T_{90}$, hr[a] |
|---|---|---|
| Reconstituted solution[b] | 6.50 | 84 |
| Lactated Ringer's injection USP[c] | 6.40 | 60 |
| Sodium chloride injection USP[c] | 6.30 | 44 |
| 5% Dextrose injection USP[c] | 5.60 | 36 |

[a] Time for 10% of the original concentration of I to disappear. [b] 2.75 × $10^{-3}$ *M* I. [c] 5.50 × $10^{-5}$ *M* I.

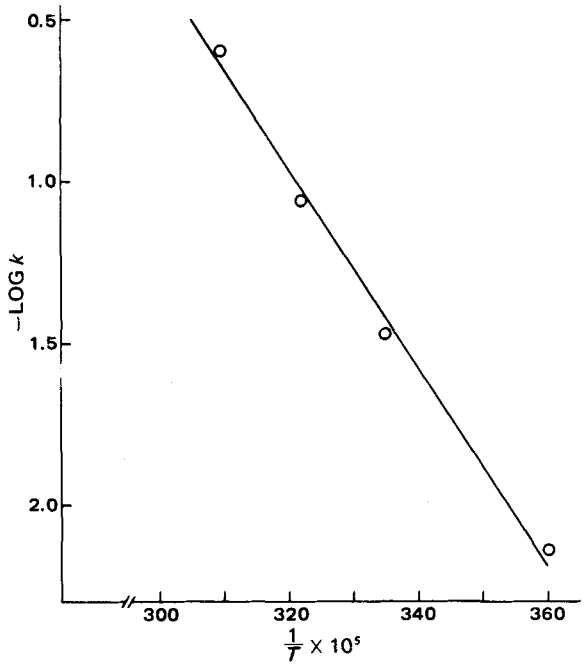


**Figure 3**—*Arrhenius plots for apparent pseudo-first-order rate constants for the disappearance of I in pH 6.5 phosphate buffer solution.*

**Stability of I in Various Infusion Fluids**—To test the compatibility of I, its degradation was followed in several commercially available infusion fluids: 5% dextrose injection USP, sodium chloride injection USP, and lactated Ringer's injection USP. A 0.5-ml portion of the stock solution of I was diluted 10-fold with 0.01 *M* phosphate buffer (pH 6.50). The resultant solution was filtered and diluted with 245 ml of infusion fluid to yield a 5.50 × $10^{-5}$ *M* solution. The admixture solutions were kept at ambient temperature (20 ± 0.5°), and the residual concentration of I and the pH were determined for at least 72 hr. The investigations usually were discontinued when the initial concentration of I had decreased by 25%.

The observed $T_{90}$ values (time for 10% decomposition of original concentration of I) at ambient temperature determined from the respective plots of concentration *versus* time are summarized in Table III. Important factors influencing the stability of I in these infusion fluids were the pH of the admixture solution, which, in turn, was dependent on the pH of the respective fluid, and the chloride concentration in the fluids (9). The chromatographic analyses of both sodium chloride and lactated Ringer's injection containing I indicated, in addition to the hydrolytic products II and III, a trace amount (<3% at $T_{90}$) of a compound identified by mass spectrometry as 2-aziridinyl-5-(2′-chloroethylamino)-3,6-bis(carboethoxyamino)-1,4-benzoquinone (VI) (9).

**Formulation Studies**—Data from the solubility and hydrolysis experiments were used to develop a stable injectable formulation of I. The hydrolysis rate of I, even within the optimal pH range (6.0–6.5), was too rapid for formulation as an aqueous solution. Instead, I was prepared as a sterile, dry product using low-temperature vacuum drying (17). Specifically, solutions of I in ethanol (3.7 × $10^{-3}$ *M*) are sterilized by filtration through 0.22-μm polytef membranes[4], dispensed into vials, and dried aseptically under low temperature in a conventional freeze drier. This product is supplied as one part of a three-component package, which also includes a sterile solution of *N,N*-dimethylacetamide and pH 6.5 sodium phosphate buffer (0.01 *M*). At the time of use, the vial contents are dissolved completely in sterile *N,N*-dimethylacetamide (0.5 ml) and then diluted with phosphate buffer (9.5 ml). Reconstituted solutions are chemically and physically stable for 84 hr at 25 ± 0.1° (Table III). This method is necessary for the convenient solution preparation since dissolution of intact I in 10% *N,N*-dimethylacetamide solution is very slow.

## REFERENCES

(1) D. R. Duvall, *Cancer Chemother. Rep.*, **8**, 156 (1960).

(2) G. Horn, *Chem. Zvesti*, **18**, 363 (1964); through *Chem. Abstr.*, **61**, 15947d (1964).

(3) M. H. Akhtar, A. Begleiter, D. Johnson, J. W. Lown, L. McLaughlin, and S. K. Sim, *Can. J. Chem.*, **53**, 2891 (1975).

(4) A. H. Khan and J. S. Driscoll, *J. Med. Chem.*, **19**, 313 (1976).

(5) F. Chou, A. H. Khan, and J. S. Driscoll, *ibid.*, **19**, 1302 (1976).

(6) J. Epstein, R. W. Rosenthal, and R. J. Ess, *Anal. Chem.*, **27**, 1435 (1955).

(7) D. H. Rosenblatt, P. Hlinka, and J. Epstein, *ibid.*, **27**, 1291 (1955).

(8) J. E. Earley, C. E. O'Rourke, L. B. Clapp, J. O. Edwards, and B. C. Lawes, *J. Am. Chem. Soc.*, **80**, 3458 (1958).

(9) G. K. Poochikian and J. A. Kelley, *J. Pharm. Sci.*, **70**, 162 (1981).

(10) T. C. McIlvaine, *J. Biol. Chem.*, **49**, 183 (1921).

(11) L. Michaelis, *ibid.*, **87**, 33 (1930).

(12) L. R. Snyder and J. J. Kirkland, "Introduction to Modern Liquid Chromatography," Wiley, New York, N.Y., 1974, p. 35.

(13) E. Bauer and H. Berg, *Chem. Zvesti*, **18**, 454 (1964); through *Chem. Abstr.*, **61**, 11375 (1964).

(14) H. Wagner and H. Berg, *J. Electroanal. Chem.*, **2**, 452 (1961).

(15) A. Anhalt and H. Berg, *ibid.*, **4**, 218 (1962).

(16) J. F. Bunnett, R. L. McDonald, and F. P. Olsen, *J. Am. Chem. Soc.*, **96**, 2855 (1974).

(17) D. W. Flamberg, D. L. Francis, S. L. Morgan, and G. F. Wickes, *Bull. Parenter. Drug Assoc.*, **24**, 209 (1970).



## ACKNOWLEDGMENTS

Presented in part at the Basic Pharmaceutics Section, APhA Academy of Pharmaceutical Sciences, Kansas City meeting, November 1979.

The authors thank Dr. J. A. Kelley, Laboratory of Medicinal Chemistry and Biology, National Cancer Institute, for the mass spectral data of II, IV, and VI and Mrs. S. Swindell for assistance in the preparation of this manuscript.


# 2,5-Diaziridinyl-3,6-bis(carboethoxyamino)-1,4-benzoquinone II: Isolation and Characterization of Degradation Products


**G. K. POOCHIKIAN *x and J. A. KELLEY ‡**



Received December 11, 1979, from the **Pharmaceutical Resources Branch and the* ‡*Laboratory of Medicinal Chemistry and Biology, National Cancer Institute, Bethesda, MD 20205.* Accepted for publication April 4, 1980.



**Abstract** □ A direct high-performance liquid chromatographic (HPLC) method was applied to monitor 2,5-diaziridinyl-3,6-bis(carboethoxyamino)-1,4-benzoquinone (I) and its degradation products in pharmaceutical vehicles at 25 ± 0.1°. At the optimal pH for stability of I, an increase in buffer concentration [phosphate and tris(hydroxymethyl)-aminomethane] or ionic strength accelerated degradation. The reaction rate in the solutions studied followed pseudo-first-order kinetics. Degradation products were characterized by mass spectrometry after isolation by semipreparative HPLC. Different degradation pathways prevailed in acidic and basic media. The acid-catalyzed reaction resulted in consecutive aziridine ring opening, while the base-catalyzed reaction led to nucleophilic displacement of the aziridine ring(s).



**Keyphrases** □ 2,5-Diaziridinyl - 3,6 - bis(carboethoxyamino)-1,4-benzoquinone—isolation and characterization of degradation products □ Degradation—2,5-diaziridinyl -3,6- bis(carboethoxyamino)-1,4-benzoquinone, isolation and characterization of degradation products □ High-performance liquid chromatography—analysis, 2,5-diaziridinyl-3,6-bis(carboethoxyamino)-1,4-benzoquinone and degradation products


The chemical behavior of a new drug in solution as well as the number and nature of degradation products and any impurities present in such a solution is always important. 2,5-Diaziridinyl-3,6 - bis(carboethoxyamino)-1,4-benzoquinone (I), a potential central nervous system (CNS) antitumor agent administered intravenously, is currently in Phase I of clinical trial. As part of a continuing study concerning the reactivity of I (1), the high-performance liquid chromatographic (HPLC) assay was applied to assess the influence of various pharmaceutical parameters (nature and concentration of the buffer, ionic strength, and storage conditions) on the stability of I in aqueous solution.

This report also describes the semipreparative HPLC isolation and the mass spectrometric structure determination of the major impurity as well as the degradation products of I generated in various pharmaceutical media. A combination of other methods (UV and NMR spectroscopy) and comparison with authentic synthetic materials also were used when sufficient sample was available.

This investigation defined the degradation behavior of I in solution with various pharmaceutically useful reagents to optimize its formulation and proper pharmaceutical use. In addition, the information accumulated here will serve as a foundation for the delineation of degradation products and metabolites of I in future pharmacokinetic studies.

## EXPERIMENTAL

**Reagents**—Compound I (NSC 182986)[1] and the internal standard, 5-chloro-2-pyridinol[2], were used as supplied. 2-Aziridinyl-5-(2′-hydroxyethanolamino)-3,6-bis(carboethoxyamino)-1,4-benzoquinone (II) and 2,5 - di(2′-hydroxyethylamino)-3,6-bis(carboethoxyamino) - 1,4-benzoquinone (III) were isolated by semipreparative HPLC from partially hydrolyzed I and were characterized as will be described. Acetonitrile[3] (distilled in glass) and distilled water were filtered through 0.45-μm

[1] Developmental Therapeutics Program, National Cancer Institute, National Institutes of Health, Bethesda, Md.

[2] Aldrich Chemical Co., Milwaukee, Wis.

[3] Burdick & Jackson Laboratories, Muskegon, Mich.




*0022-3549/81/0200-0162$01.00/0*



*© 1981, American Pharmaceutical Association*

## REFERENCES

(1) D. R. Duvall, *Cancer Chemother. Rep.*, **8**, 156 (1960).

(2) G. Horn, *Chem. Zvesti*, **18**, 363 (1964); through *Chem. Abstr.*, **61**, 15947d (1964).

(3) M. H. Akhtar, A. Begleiter, D. Johnson, J. W. Lown, L. McLaughlin, and S. K. Sim, *Can. J. Chem.*, **53**, 2891 (1975).

(4) A. H. Khan and J. S. Driscoll, *J. Med. Chem.*, **19**, 313 (1976).

(5) F. Chou, A. H. Khan, and J. S. Driscoll, *ibid.*, **19**, 1302 (1976).

(6) J. Epstein, R. W. Rosenthal, and R. J. Ess, *Anal. Chem.*, **27**, 1435 (1955).

(7) D. H. Rosenblatt, P. Hlinka, and J. Epstein, *ibid.*, **27**, 1291 (1955).

(8) J. E. Earley, C. E. O'Rourke, L. B. Clapp, J. O. Edwards, and B. C. Lawes, *J. Am. Chem. Soc.*, **80**, 3458 (1958).

(9) G. K. Poochikian and J. A. Kelley, *J. Pharm. Sci.*, **70**, 162 (1981).

(10) T. C. McIlvaine, *J. Biol. Chem.*, **49**, 183 (1921).

(11) L. Michaelis, *ibid.*, **87**, 33 (1930).

(12) L. R. Snyder and J. J. Kirkland, "Introduction to Modern Liquid Chromatography," Wiley, New York, N.Y., 1974, p. 35.

(13) E. Bauer and H. Berg, *Chem. Zvesti*, **18**, 454 (1964); through *Chem. Abstr.*, **61**, 11375 (1964).

(14) H. Wagner and H. Berg, *J. Electroanal. Chem.*, **2**, 452 (1961).

(15) A. Anhalt and H. Berg, *ibid.*, **4**, 218 (1962).

(16) J. F. Bunnett, R. L. McDonald, and F. P. Olsen, *J. Am. Chem. Soc.*, **96**, 2855 (1974).

(17) D. W. Flamberg, D. L. Francis, S. L. Morgan, and G. F. Wickes, *Bull. Parenter. Drug Assoc.*, **24**, 209 (1970).



## ACKNOWLEDGMENTS

Presented in part at the Basic Pharmaceutics Section, APhA Academy of Pharmaceutical Sciences, Kansas City meeting, November 1979.

The authors thank Dr. J. A. Kelley, Laboratory of Medicinal Chemistry and Biology, National Cancer Institute, for the mass spectral data of II, IV, and VI and Mrs. S. Swindell for assistance in the preparation of this manuscript.


# 2,5-Diaziridinyl-3,6-bis(carboethoxyamino)-1,4-benzoquinone II: Isolation and Characterization of Degradation Products


**G. K. POOCHIKIAN *x and J. A. KELLEY ‡**



Received December 11, 1979, from the **Pharmaceutical Resources Branch and the* ‡*Laboratory of Medicinal Chemistry and Biology, National Cancer Institute, Bethesda, MD 20205.* Accepted for publication April 4, 1980.



**Abstract** □ A direct high-performance liquid chromatographic (HPLC) method was applied to monitor 2,5-diaziridinyl-3,6-bis(carboethoxyamino)-1,4-benzoquinone (I) and its degradation products in pharmaceutical vehicles at 25 ± 0.1°. At the optimal pH for stability of I, an increase in buffer concentration [phosphate and tris(hydroxymethyl)-aminomethane] or ionic strength accelerated degradation. The reaction rate in the solutions studied followed pseudo-first-order kinetics. Degradation products were characterized by mass spectrometry after isolation by semipreparative HPLC. Different degradation pathways prevailed in acidic and basic media. The acid-catalyzed reaction resulted in consecutive aziridine ring opening, while the base-catalyzed reaction led to nucleophilic displacement of the aziridine ring(s).



**Keyphrases** □ 2,5-Diaziridinyl - 3,6 - bis(carboethoxyamino)-1,4-benzoquinone—isolation and characterization of degradation products □ Degradation—2,5-diaziridinyl -3,6- bis(carboethoxyamino)-1,4-benzoquinone, isolation and characterization of degradation products □ High-performance liquid chromatography—analysis, 2,5-diaziridinyl-3,6-bis(carboethoxyamino)-1,4-benzoquinone and degradation products


The chemical behavior of a new drug in solution as well as the number and nature of degradation products and any impurities present in such a solution is always important. 2,5-Diaziridinyl-3,6 - bis(carboethoxyamino)-1,4-benzoquinone (I), a potential central nervous system (CNS) antitumor agent administered intravenously, is currently in Phase I of clinical trial. As part of a continuing study concerning the reactivity of I (1), the high-performance liquid chromatographic (HPLC) assay was applied to assess the influence of various pharmaceutical parameters (nature and concentration of the buffer, ionic strength, and storage conditions) on the stability of I in aqueous solution.

This report also describes the semipreparative HPLC isolation and the mass spectrometric structure determination of the major impurity as well as the degradation products of I generated in various pharmaceutical media. A combination of other methods (UV and NMR spectroscopy) and comparison with authentic synthetic materials also were used when sufficient sample was available.

This investigation defined the degradation behavior of I in solution with various pharmaceutically useful reagents to optimize its formulation and proper pharmaceutical use. In addition, the information accumulated here will serve as a foundation for the delineation of degradation products and metabolites of I in future pharmacokinetic studies.

## EXPERIMENTAL

**Reagents**—Compound I (NSC 182986)[1] and the internal standard, 5-chloro-2-pyridinol[2], were used as supplied. 2-Aziridinyl-5-(2′-hydroxyethanolamino)-3,6-bis(carboethoxyamino)-1,4-benzoquinone (II) and 2,5 - di(2′-hydroxyethylamino)-3,6-bis(carboethoxyamino) - 1,4-benzoquinone (III) were isolated by semipreparative HPLC from partially hydrolyzed I and were characterized as will be described. Acetonitrile[3] (distilled in glass) and distilled water were filtered through 0.45-μm

[1] Developmental Therapeutics Program, National Cancer Institute, National Institutes of Health, Bethesda, Md.

[2] Aldrich Chemical Co., Milwaukee, Wis.

[3] Burdick & Jackson Laboratories, Muskegon, Mich.




*0022-3549/81/0200-0162$01.00/0*



*© 1981, American Pharmaceutical Association*

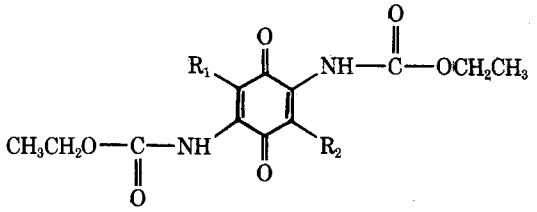

I: $R_1 = R_2 = -N\triangleleft$

II: $R_1 = NHCH_2CH_2OH$, $R_2 = -N\triangleleft$

IIa: $R_1 = NHCH_2CH_2OCOCH_3$, $R_2 = -N\triangleleft$

III: $R_1 = R_2 = NHCH_2CH_2OH$

IIIa: $R_1 = R_2 = NHCH_2CH_2OCOCH_3$

V: $R_1 = NHCH_2CH_2OH$, $R_2 = NHCH_2CH_2Cl$

VI: $R_1 = -N\triangleleft$, $R_2 = NHCH_2CH_2Cl$

VII: $R_1 = R_2 = NHCH_2CH_2Cl$

VIII: $R_1 = R_2 = OH$

IX: $R_1 = -N\triangleleft$, $R_2 = OH$

X: $R_1 = NH_2$, $R_2 = OH$

solvent-resistant filters[4]. All other chemicals were reagent grade.

**Preparation of Solutions**—Solutions of I ($2.75 \times 10^{-4}$ *M*) were prepared as described previously (1) in appropriate media at the optimum pH[5] (pH 6.5) and stored at 25 ± 0.1° under oxygen, nitrogen, or air under fluorescent lighting or in the dark. Experiments also were conducted in different concentrations (0.01, 0.1, and 0.5 *M*) of pH 6.5 phosphate buffer or tris(hydroxymethyl)aminomethane hydrochloride buffer as well as in solutions of various ionic strengths (0.016–0.70 $\mu$) obtained by the addition of sodium chloride or sodium nitrate.

For isolation of the desired benzoquinone decomposition products, solutions of I in pH 3–8 buffer were subjected to degradation at ambient temperature. Different major products were obtained in different pH solutions. Compound I also was allowed to degrade in pH 6.5 tris(hydroxymethyl)aminomethane buffer, sodium chloride solution, and at alkaline pH.

**HPLC**—A modular high-pressure liquid chromatograph consisting of a constant-flow pump[6] coupled with a rotary valve injector[7], a 10-$\mu$l injection loop, and a 5-$\mu$m reversed-phase column[8] (250 × 3 mm i.d.) was used to deliver the eluent at a rate of 1 ml/min. A variable-wavelength UV detector[9] set at 345 nm and 0.1 aufs deflection was used to detect eluted compounds. The output signals were recorded with a strip-chart recorder[10]. All chromatographic operations were performed at ambient temperature. Chromatographic conditions in the analytical mode were described previously (1).

Semipreparative separation and isolation of I and its degradation products were carried out on a 10-$\mu$m octadecylsilane column[11] (500 × 9.20 mm i.d.). The chromatographic profile of the sample was determined first on the analytical column[8]. Then an analytical injection was made on the semipreparative column, using 15% acetonitrile[3] in distilled water as the eluent at a flow rate of 5 ml/min. A concentrated solution of the sample was diluted to the proper concentration with the mobile phase and clarified through a 0.45-$\mu$m solvent-resistant filter[4] prior to injection of 250 $\mu$l onto the semipreparative column. Acetonitrile was removed under reduced pressure[12] from each collected fraction, and the residual aqueous solution was frozen immediately in dry ice and lyophilized under low temperature in a conventional freeze drier[13]. The resulting solid was subjected to further analysis.

**Mass Spectrometry**—All derivatization reactions were carried out in glass screw-capped vials[14] (3.5 ml) or Reacti-vials[14] (1.0 ml) equipped with polytef-lined rubber septums. Samples (0.3–2 mg) were trimethylsilylated by reaction with 0.45 ml of a 2:1 mixture of redistilled acetonitrile[3] and bis(trimethylsilyl)trifluoroacetamide[2] for 1–2 hr at room temperature. Acetylation was effected by reaction with 0.3 ml of a 1:2 mixture of redistilled acetic anhydride[15] and redistilled pyridine for 3 hr at room temperature. Aliquots of the derivatization mixtures were subjected to mass spectral analysis after transfer to glass capillary sample holders and *in vacuo* removal of excess reagents.

All mass spectra were obtained by direct-probe introduction of the sample into the ion source of a mass spectrometer[16] operated under data system[17] control. When the sample was known to be a mixture of compounds, fractional vaporization was used to obtain spectra of the individual components. Typical mass spectrometer (electron-impact) operating conditions were: resolution, 1000 (10% valley); ion source, 265°; electron energy, 75 ev; ionizing current, 250 $\mu$amp; and scan speed, 2 sec/decade. Accurate mass measurements (I, VIII, and X) were obtained under data system control at a scan rate of 10 sec/decade and a dynamic resolution of 5000 using perfluorokerosene as an internal reference. Probable elemental compositions of the various fragment ions were calculated using the commercially supplied data system software.

**Table I—Mass Spectra of Acetylated II and III**

| IIa Mass (Relative Intensity) | IIIa Mass (Relative Intensity) | Probable Assignment |
|---|---|---|
| 424 (3) | 484 (18) | $M^+$ |
| 378 (2) | 438 (8) | $M - CH_3CH_2OH$ |
| 351 (4) | 411 (11) | $M - CH_2OOCCH_3$ |
| 332 (1) | 392 (6) | $M - 2\,CH_3CH_2OH$ |
| 318 (4) | 378 (2) | $M - CH_3CH_2OH - CH_3COOH$ |
| 305 (4) | 365 (4) | $M - CH_3CH_2OH - CH_2OOCCH_3$ |
| 272 (10) | 332 (2) | $M - 2\,CH_3CH_2OH - CH_3COOH$ |
| — | 305 (6) | $M - CH_3CH_2OH - CH_3COOH - CH_2OOCCH_3$ |
| 87 (10) | 87 (96) | $C_4H_7O_2$ |
| 60 (25) | — | $CH_3COOH$ |
| 45 (79) | 45 (21) | $C_2H_5O^+$ |
| 43 (100) | 43 (100) | $CH_3C{\equiv}O^+$ |
| 31 (84) | 31 (40) | $CH_2{=}O^+H$ |
| 29 (10) | 29 (50) | $C_2H_5^+$ |

**General Methods**—Melting points[18] were determined in open glass capillaries and are uncorrected. UV spectra were obtained with a scanning UV–visible spectrophotometer[19]. NMR spectra were recorded[20] in deuterated dimethyl sulfoxide (containing 1% tetramethylsilane)[21]. Microanalyses[22] for carbon, hydrogen, and nitrogen were within 0.4% of the calculated values.

*2,5-Di(2-hydroxyethylamino)-3,6-bis(carboethoxyamino)-1,4-benzoquinone (III)*—Compound I (0.5 g, 1.37 mmoles) was dissolved in *N,N*-dimethylacetamide (20 ml), and the resulting solution was diluted with water (225 ml). The solution was adjusted to pH 3 with 0.1 *N* aqueous HCl and stirred at ambient temperature for 24 hr. The reaction was followed to completion by HPLC, and the resulting solution was freeze dried. Recrystallization of the solid from benzene gave III as red crystals, 0.45 g (82%), mp 182–184°; UV (water–acetonitrile, 85:15): $\lambda_{max}$ 343 (log $\epsilon$ 4.27) and 237 (3.94) nm; NMR (dimethyl sulfoxide-$d_6$): $\delta$ 1.20 (t, 6H, 2 $CH_3$), 3.40–3.70 (m, 8H, 2 $NCH_2CH_2O$), 4.05 (q, 4H, 2 $CH_2CH_3$), 4.05 (s, 2H, 2 OH), 7.30 (s, 2H, 2 NH), and 7.90 (s, 2H, 2 NH of amide) ppm. The mass spectral data (acetylated) are given in Table I.

*Anal.*—Calc. for $C_{16}H_{24}N_4O_8$: C, 48.00; H, 6.04; N, 13.99. Found: C, 48.20; H, 6.08; N, 13.69.

*2,5 - Dihydroxy - 3,6 - bis(carboethoxyamino) - 1,4 - benzoquinone (VIII)*—Compound I (0.18 g, 0.5 mmole) dissolved in *N,N*-dimethylacetamide (8 ml) was diluted with 50 ml of 0.02 *N* aqueous NaOH. The resulting solution was stirred overnight at room temperature and filtered. The filtrate was acidified with dilute hydrochloric acid and extracted into chloroform. The extracts were dried (sodium sulfate), filtered, and con-

[4] Millipore, Bedford, Mass.
[5] Beckman Zeromatic pH meter, Beckman Instruments, Irvine, Calif.
[6] Model 3500B, Spectra-Physics, Santa Clara, Calif.
[7] Valco Instruments Co., Houston, Tex.
[8] Spherisorb ODS (5 $\mu$m), Spectra-Physics, Santa Clara, Calif.
[9] Model SP 770, Spectra-Physics, Santa Clara, Calif.
[10] OmniScribe, Houston Instruments, Austin, Tex.
[11] Partisil M9, Whatman Inc., Clifton, N.J.
[12] Buchi Rotavapor-R, Brinkmann Instruments, Westbury, N.Y.
[13] 10-MRSA Freezemobile, Virtis Co., Gardiner, N.Y.
[14] Pierce Chemical Co., Rockford, Ill.
[15] B & A, Morristown, N.J.
[16] DuPont 21-492B, DuPont Instruments, Monrovia, Calif.
[17] VG 2040, VG Data Systems, Altrincham, Cheshire, England.
[18] Thomas-Hoover Uni-Melt apparatus, A. H. Thomas, Philadelphia, Pa.
[19] Cary 15 recording spectrophotometer, Varian Associates, Monrovia, Calif.
[20] T-60 spectrometer, Varian Associates, Palo Alto, Calif.
[21] Silanor, Merck & Co., Rahway, N.J.
[22] National Institute of Arthritis, Metabolism, and Digestive Diseases, National Institutes of Health, Bethesda, Md.

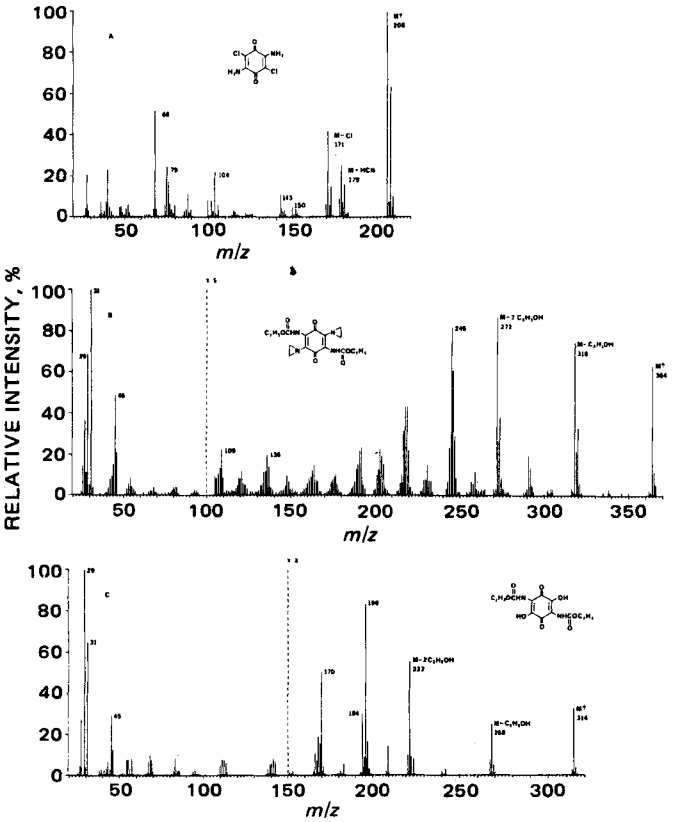


**Figure 1**—*Direct-probe electron-impact mass spectrum of IV (A), I isolated by HPLC (B), and VIII (C).*

centrated under reduced pressure. Recrystallization of the residue from methanol–water yielded VIII as reddish crystals, 0.125 g (80%), mp 197–200° dec.; UV (methanol): $\lambda_{max}$ 304 (log $\epsilon$ 4.06) nm; NMR (dimethyl sulfoxide-$d_6$): $\delta$ 1.25 (t, 6H, 2 $CH_3$), 4.03 (q, 4H, 2 $CH_2CH_3$), 4.58 (broad, 2H, 2 OH), and 8.10 (s, 2H, 2 NH) ppm. The mass spectrum is shown in Fig. 1C.

*Anal.*—Calc. for $C_{12}H_{14}N_2O_8$: C, 45.86; H, 4.49; N, 8.91. Found: C, 46.10; H, 4.68; N, 8.62.

## RESULTS AND DISCUSSION

**Separation and Identification of Hydrolysis Products of I**—The isolation and identification of the major impurity associated with I and the degradation products generated in various pharmaceutical media were accomplished by semipreparative HPLC and mass spectrometry. The retention order of I and its degradation products on the semipreparative column was identical to that of the analytical column. When desired, the retention times were adjusted by varying the proportion of the organic component of the eluent.

Molecular ion peaks were present in the mass spectra of all compounds examined, and the mass spectral fragmentation patterns allowed determination of the various functional groups present. When needed, derivatization by acetylation or silylation was employed to increase the volatility of selected degradation products for direct-probe analysis. Acetylation was preferred over silylation, even though the persilylated derivatives were much more volatile, because the former procedure added much less mass to the molecular weight of the derivative and the structural features were delineated more clearly in the mass spectrum.

The mass spectrum of the most abundant HPLC-isolated impurity of I[23] indicated an apparent molecular weight of 206 and the 9:6:1 isotopic pattern indicative of two chlorine atoms (Fig. 1A). Comparison of this mass spectrum with that of an authentic sample of 2,5-diamino-3,6-dichloro-1,4-benzoquinone[24] (IV), a synthetic intermediate of I, confirmed the identity. The mass spectrum of IV was unusual in that the successive losses of two molecules of carbon monoxide were not as prominent as in other 1,4-benzoquinones (2). These ions were observed at *m/z* 178 (M − CO) and 150 (M − 2 CO), but the loss of hydrocyanic acid from the intact molecule (*m/z* 179) was more pronounced. There was no fission into two halves, as is commonly observed with other 1,4-benzoquinones, but fission with hydrogen transfer did occur to give an ion at *m/z* 104 containing one chlorine atom. Loss of hydrogen chloride from this fragment produced an ion of *m/z* 68. The peak at *m/z* 75 probably was due to elimination of 1-amino-2-chloroacetylene with concomitant charge retention.

The mass spectrum of I (Fig. 1B) served as a model for interpreting the mass spectra of the degradation products. In addition to a molecular ion ($M^+$) peak of moderate intensity at *m/z* 364, the most noticeable feature of this spectrum was the successive loss of two ethanol molecules at *m/z* 318 (M − $CH_3CH_2OH$) and 272 (M − 2 $CH_3CH_2OH$), an indication of *N*-substituted ethyl carbamates (3). Compound I was not very volatile and required probe temperatures at or greater than its 230° melting and decomposition point (4) before a recognizable spectrum could be obtained. Thus, the successive losses of ethanol probably occurred thermally as well as during electron impact. Metastable peaks were observed for the transformation, but the low mass portion of the spectrum (below *m/z* 50) was identical to the spectrum of ethanol (5).

When the amount of I was low and there was appreciable water or another hydrogen radical source in the mass spectrometer inlet system or ionization chamber, an appreciable M + 2 peak was observed. This peak has been commonly observed in the mass spectra of other 1,4-benzoquinones and represents formation of the analogous hydroquinone (2). Therefore, the moderately intense A + 2 peaks observed for both *m/z* 318 and 272 probably were due to hydroquinone formation from the isocyanoquinones resulting from thermal decomposition of I with use of the resultant ethanol as a hydrogen radical source. Thus, the peaks at *m/z* 318 and 272 probably represented fragment ions as well as molecular ions produced by thermal decomposition. The other peaks in the spectrum then could be interpreted as resulting from further fragmentation of these ions. Thus, *m/z* 136 would represent fission of the bis(isocyano)quinone of mass 272 into halves, while *m/z* 109 might result from loss of an ethoxy radical from the acetylene formed by 1,3-cleavage of I.

Compound III, the major and ultimate degradation product of I in acidic media, was isolated by HPLC and characterized as 2,5-di(2′-hydroxyethylamino)-3,6-bis(carboethoxyamino)-1,4-benzoquinone. The acetylated derivative (III*a*) was more volatile and exhibited less thermal decomposition than the parent compound. The mass spectral analysis of III*a* clearly indicated its molecular weight (*m/z* 484) as well as all pertinent structural features (Table I). Successive losses of ethanol indicated intact *N*-substituted ethyl carbamate moieties (3), while loss of 73 amu (*e.g.*, *m/z* 411, M − $CH_2OCOCH_3$) was characteristic of an acetate of a primary alcohol. The high mass end of the spectrum (*m/z* > 300) could be explained by the appropriate combination of the losses of ethanol (46 amu), acetic acid (60 amu), and ·$CH_2OCOCH_3$ (73 amu). As with I, peaks from ethanol were superimposed on the low mass portion of the spectrum (*m/z* < 50). NMR and elemental analyses of the synthetically obtained III (see *Experimental*) supported the mass spectral data.

Compound II was the second major degradation product of I detected in acidic to neutral media. The concentration of II was pH dependent and had a maximum at pH ~ 5. Mass spectrometry suggested that II was 2-aziridinyl-5-(2′-hydroxyethylamino)-3,6-bis(carboethoxyamino)-1,4-benzoquinone, the intermediate hydrolytic product. Acetylation was employed to make a more volatile derivative, and the mass spectrum of II*a* corroborated the proposed structure (Table I). A molecular ion was evident at *m/z* 424, and most of the structural features present in III*a* also were indicated.

**Buffer Effect**—The analytical HPLC method described previously (1) was applied to evaluate the effect of various pharmaceutical media at the optimal pH on the degradation rate of I. The pseudo-first-order rate constants for the disappearance of I in aqueous solutions of pH 3.0–8.0 (1) do not necessarily reflect the hydrolysis rate of aziridine rings since anions present in the solution may compete with water molecules for the protonated aziridines. Water is sufficiently acidic to provide a very low concentration of aziridinium ion, which then undergoes reaction with the various nucleophilic reagents present at rates corresponding to the nucleophilicity of the reagent.

The catalytic effect of the buffer systems was determined at constant temperature (25 ± 0.1°), pH (6.5 ± 0.05), ionic strength (1.0), and concentration of I ($2.75 \times 10^{-4}$ *M*) in various strengths (0.01, 0.1, and 0.5 *M*) of phosphate or tris(hydroxymethyl)aminomethane buffer. The disappearance rate of I followed pseudo-first-order kinetics with respect to

[23] The amount of IV was 1.5% (w/w); $\lambda_{max}$ (acetonitrile–water, 25:75) 338 (log $\epsilon$ 4.45).

[24] Provided by Dr. J. S. Driscoll, National Cancer Institute, National Institutes of Health, Bethesda, Md.

**Table II—Pseudo-First-Order Rate Constants for Loss of I ($2.75 \times 10^{-4}$ *M*) in Various Concentrations of pH 6.5 Phosphate and Tris(hydroxymethyl)aminomethane Buffer at 25 ± 0.1°**

| Total Buffer Concentration, *M* | $K_{obs} \times 10^2$, $day^{-1}$ | |
|---|---|---|
| | Phosphate Buffer | Tris(hydroxymethyl)aminomethane Buffer |
| 0.01 | 3.07 | 3.20 |
| 0.1 | 5.07 | 5.23 |
| 0.5 | 12.64 | 13.36 |

**Table III—Retention Volume ($V_R$), Capacity Factor ($k'$), Separation Factors ($\alpha$), and Resolution ($R_s$) of Various Solutes [a]**

| Compound | $V_R$, ml | $k'$ | $\alpha$ | $R_s$ |
|---|---|---|---|---|
| I | 8.50 | 7.50 | | |
| | | | 1.23 | 2.53 |
| V | 10.20 | 9.20 | | |
| | | | 1.96 | 6.96 |
| VI | 19.00 | 18.00 | | |
| | | | 2.28 | 8.22 |
| VII | 42.00 | 41.00 | | |

[a] Retention data of various solutes from a 250 × 3-mm i.d. stainless steel Spherisorb ODS (5-μm particles) column; the mobile phase was 15% acetonitrile in water at a flow rate of 1 ml/min; UV detection was at 345 nm.

its concentration. The reaction rate constants were computed by the least-squares method. Plots of the observed rate constant of the reactions *versus* buffer concentration showed a direct increase in the disappearance rate of I with an increasing concentration of either buffer (Table II).

Examination of the chromatogram of degraded solutions of I indicated that the reaction is partially a function of phosphate ion. Increased buffer concentration intensified the hydrophilic peak at the void volume while it decreased peaks corresponding to the hydrolytic products (II and III) in the chromatogram. The catalytic effect of phosphate buffer on unsubstituted aziridines (6–9) and its derivatives (10, 11) was observed previously. The present study confirmed similar observations. Increasing the pH of the 0.01 *M* phosphate buffer (*i.e.*, dibasic ion concentration of the phosphate buffer) increased the intensity of the unretained peak in the chromatogram. At pH 8.0, only I and this peak were observed.

In spite of their corresponding rates for the disappearance of I (Table II), the nature and relative proportion of the degradation products of I in similar concentrations of tris(hydroxymethyl)aminomethane and phosphate buffer systems were noticeably different. In tris(hydroxymethyl)aminomethane buffer solutions, beside the hydrolysis products (II and III), additional decomposition products (V–VII) were detected, which increased with increasing buffer concentration. Table III summarizes the chromatographic retention volumes ($V_R$ in milliliters), capacity factors ($k'$), separation factors ($\alpha$), and resolution ($R_s$) of V–VII. These products also were observed in sodium chloride solution and will be described further.

Aziridinylbenzoquinone (I) in tris(hydroxymethyl)aminomethane buffer (pH 6.5 ± 0.05) led, apart from the cleavage reactions, to the displacement of one or both aziridine residues and the formation of 2,5-dihydroxy-3,6-bis(carboethoxyamino)-1,4-benzoquinone (VIII) or 2-aziridinyl-5-hydroxy-3,6-bis(carboethoxyamino)-1,4-benzoquinone (IX). Both compounds were detected as a single peak in the void volume of the chromatogram. Only partial separation of these compounds could be achieved, even with water as the mobile phase. Mass spectral analysis employing controlled fractional vaporization indicated that the mixture consisted of VIII and IX in approximately equal proportions. The NMR and elemental analyses of VIII (see *Experimental*) confirmed the structure suggested by mass spectrometry.

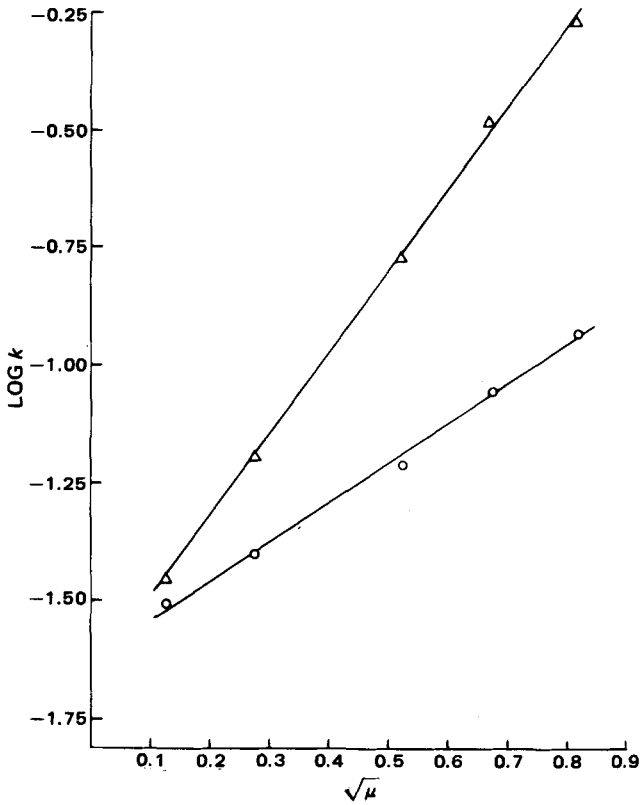


**Figure 2**—*Bronsted–Bjerrum plot of the logarithm of the observed rate constants* versus *μ. The ionic strength was controlled with sodium chloride (△) or sodium nitrate (○).*

The generation of the degradation products under mild conditions prompted an investigation of the reactivity of I with basic nucleophiles. Compound I in the presence of dilute sodium hydroxide generated a similar peak in the high-performance liquid chromatogram. HPLC monitoring of this reaction showed an instantaneous decrease of >90% in the concentration of I upon addition of sodium hydroxide. The molecular weight of this new compound appeared to be 314, 50 amu less than I (Fig. 1C). Accurate mass measurement of the major peaks in this spectrum allowed generation of a self-consistent set of fragment ion elemental compositions (Table IV), which indicated that this compound was VIII. Similarly, treatment of I with equimolar ammonium hydroxide followed by lyophilization resulted almost exclusively in 2-amino-5-hydroxy-3,6-bis(carboethoxyamino)-1,4-benzoquinone (X). This compound possessed a mass spectrum that exhibited the same neutral losses as that of VIII and in which most of the major peaks were shifted 1 amu lower (Table IV). Direct replacement of the aziridine groups in similar 1,4-benzoquinone derivatives was observed after treatment with alkylamines (12–15) or sodium hydroxide (16). The ease of replacement depended on the basicity of the reagent and the nature of the other substituents present in the quinone (17). Thus, the primary mode of decomposition of I under basic conditions involves direct displacement of one or both aziridine moieties.

**Primary Salt Effect**—An investigation of the disappearance rate of I as a function of ionic strength was carried out to determine the influence of electrolytes. To conduct these studies, solutions were prepared at constant pH (6.5 ± 0.05), concentration of I ($2.75 \times 10^{-4}$ *M*), phosphate

**Table IV—Accurate Mass Measurement of Selected Ions in the Mass Spectra of the Basic Degradation Products of I**

| Structural Assignment | VIII | | | X | | |
|---|---|---|---|---|---|---|
| | Nominal Mass | Accurate Mass | Elemental Composition | Nominal Mass | Accurate Mass | Elemental Composition |
| $M^+$ | 314 | 314.078 | $C_{12}H_{14}N_2O_8$ | 313 | 313.081 | $C_{12}H_{15}N_3O_7$ |
| $M - CH_3CH_2OH$ | 268 | 268.035 | $C_{10}H_8N_2O_7$ | 267 | 267.045 | $C_{10}H_9N_3O_6$ |
| $M - 2\,CH_3CH_2OH$ | 222 | 221.992 | $C_8H_2N_2O_6$ | 221 | 221.004 | $C_8H_3N_3O_5$ |
| $M - C_2H_4 - CO_2 - CH_3CH_2OH$ | 196 | 196.007 | $C_7H_4N_2O_5$ | 195 | 195.018 | $C_7H_5N_3O_4$ |
| $M - 2\,CH_3CH_2OH - CO$ | 194 | 193.992 | $C_7H_2N_2O_5$ | 193 | 193.009 | $C_7H_3N_3O_4$ |

**Table V—Mass Spectra of Ring-Opened One-Armed Mustards**

| VI Mass (Relative Intensity) | VII Mass (Relative Intensity) | Probable Assignment |
|---|---|---|
| 400 (13) | 436 (13) | $M^+$ |
| 364 (29) | 400 (4) | M − HCl |
| 354 (7) | 390 (7) | M − $CH_3CH_2OH$ |
| 351 (14) | 387 (25) | M − $CH_2Cl$ |
| — | 364 (21) | M − 2 HCl |
| 305 (13) | 341 (9) | M − $CH_2Cl$ − $CH_3CH_2OH$ |
| 318 (37) | 318 (26) | 364 − $CH_3CH_2OH$ |
| 272 (21) | 272 (17) | 364 − 2 $CH_3CH_2OH$ |
| 245 (28) | 245 (17) | 272 − $C_2H_3$ |
| 45 (41) | 45 (37) | $C_2H_5O^+$ |
| 36 (65) | 36 (100) | $HCl^+$ |
| 31 (76) | 31 (71) | $CH_2{=}O^+H$ |
| 29 (100) | 29 (85) | $C_2H_5^+$ |

buffer concentration (0.01 *M*), and temperature (25 ± 0.1°) but at varying ionic strengths. The ionic strength was controlled by the addition of sodium chloride or sodium nitrate.

The results are shown in Fig. 2. The logarithm of $K_{obs}$ is plotted *versus* $\sqrt{\mu}$ according to the method of Bronsted and Bjerrum (18). These plots resulted in straight lines ($r > 0.970$), indicating that the reaction was dependent on the ionic strength ($\sqrt{\mu}$). However, the disappearance rate of I was 1.1- to 4.6-fold faster in the presence of sodium chloride than in sodium nitrate due to the nucleophilic attack of the chloride ion on the aziridine ring(s) (19), producing, in addition to the hydrolysis products, the one-armed mustards (V–VII) in significant proportions (Table III).

Compound VII was identified as 2,5-di(2′-chloroethylamino)-3,6-bis(carboethoxyamino)-1,4-benzoquinone by mass spectral analysis (Table V). Obvious losses of ethanol (*m/z* 390) and the chloromethylene radical (*m/z* 387) from the molecular ion (*m/z* 436) plus the characteristic isotopic pattern of two chlorine atoms (*e.g.*, *m/z* 436) allowed definition of the key structural features of VII. Comparison with the mass spectrum of an authentic sample[24] confirmed this structural assignment.

Degradation product VI was identified as the derivative of I in which only one aziridine ring was opened by chloride-ion attack, namely, 2-aziridinyl-5-(2′-chloroethylamino)-3,6-bis(carboethoxyamino)-1,4-benzoquinone. The mass spectral fragmentation is similar to that of VII, except for the molecular ion peak (*m/z* 400) and the presence of only one chlorine atom (Table V).

The mass spectral analysis of V suggested the presence of 2-(2′-chloroethylamino) - 5-(2′-hydroxyethylamino)-3,6-bis(carboethoxyamino)-1,4-benzoquinone. This degradation product was identified tentatively on the basis of an apparent molecular ion peak at *m/z* 418, displaying the characteristic isotope pattern of a single chlorine, as well as fragment peaks at *m/z* 387 (M − $CH_2OH$) and 369 (M − $CH_2Cl$).

**Oxygen and Light Effect**—Identical solutions of I ($2.75 \times 10^{-4}$ *M*) were stored for 3 weeks in 0.01 *M* phosphate buffer (pH 6.5) under oxygen, nitrogen, and air at 25 ± 0.1°. Similar solutions were exposed to fluorescent light or kept in the dark at the same temperature. When assayed periodically, no difference was observed among the pseudo-first-order rate constants for the disappearance of I in these solutions as well as among the proportions of its degradation products. These observations, coupled with the reproducibility of the observed rate constants at various times and their strict adherence to pseudo-first-order kinetics, suggest nucleophilic (hydrolytic) rather than oxidative breakdown of I in aqueous solution.

**Degradation Patterns of I**—Although this study does not permit definitive judgments on the detailed mechanisms of degradation of I throughout the pH range studied, it does demonstrate that I is subject to both general acid and base catalysis. Several reactions appear to be responsible for the degradation of I, the relative importance of each being dependent on both the buffer species and the form of I present in solution.

At pH 3, the diaminoalcohol (III) was the major hydrolytic product; in solutions between pH 3 and 7, both II and III were present in varying amounts. Once the ethyleneimine was protonated, it became the primary target of nucleophilic attack by water or other nucleophiles to produce the respective degradation products. Ring opening by water or halogen acids is among the oldest and most often reported reaction for aziridines (20). At pH 3.0, the chromatogram of I at various time intervals provides conclusive evidence that hydrolysis constitutes the only degradative pathway through a two-step sequential mechanism since a total of 1 mole of II plus III appears for each mole of I consumed.

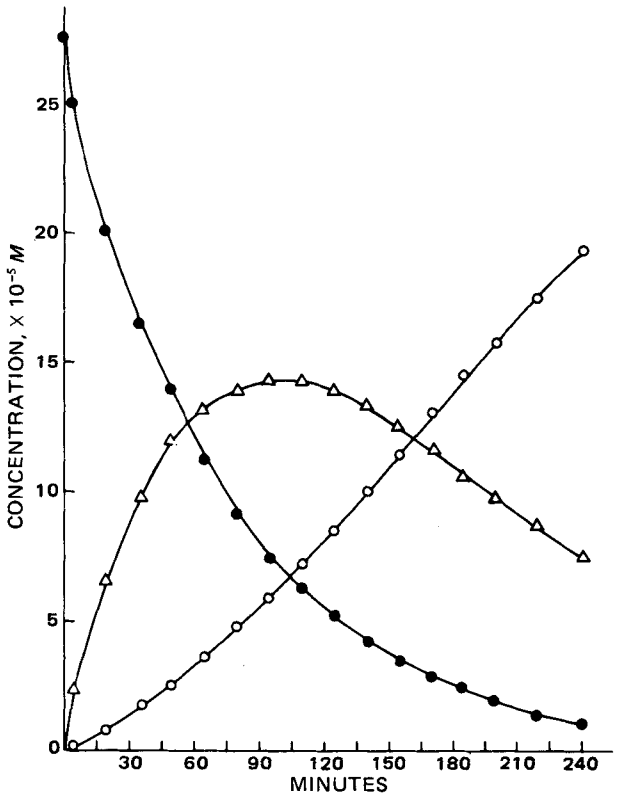


**Figure 3**—*Concentration–time curves for I (●), II (△), and III (○) at 25 ± 0.1° and pH 3.0.*

A typical plot of the hydrolysis of I and the appearance of II and III at pH 3.0 and 25 ± 0.1° is presented in Fig. 3. The rapid decrease of I is accompanied by an increase in II, which reaches a maximum value after 100 min and then decreases in an approximately linear fashion. After a lag period of 20 min, the concentration of III rises gradually. This pattern suggests two consecutive first-order reactions:

$$I \xrightarrow{K_1} II \xrightarrow{K_2} III$$

where $K_1$ and $K_2$ are pseudo-first-order rate constants. Several methods (21, 22) have been described for the determination of the second rate constant of consecutive first-order reactions using dimensionless parameters and variables. With the method of Jensen and Lamb (22), $K_2$ was $1.11 \times 10^{-3}$ ($min^{-1}$) while $K_1$ was $5.29 \times 10^{-3}$ ($min^{-1}$).

The data obtained from the degradation of I in solutions ranging from weakly acidic to weakly alkaline cannot be treated likewise. The pseudo-first-order disappearance rates of I in these solutions are not conclusive evidence that ring-cleavage hydrolysis constitutes the only degradative pathway since new compounds are generated as the pH of the solution is raised. This additional degradation mode of I in solution, unlike acid-catalyzed solvolysis, involves the displacement of one or both aziridine moieties by nucleophiles. This decomposition pattern of I becomes its major degradation route in basic media.

## REFERENCES

(1) G. K. Poochikian and J. C. Cradock, *J. Pharm. Sci.*, **70**, 159 (1981).

(2) K. P. Zeller, in "The Chemistry of the Quinoid Compounds," S. Patai, Ed., Wiley, New York, N.Y., 1974, pp. 231–256.

(3) H. Budzikiewicz, C. Djerassi, and D. H. Williams, "Mass Spectrometry of Organic Compounds," Holden-Day, San Francisco, Calif., 1967, p. 500.

(4) A. H. Khan and J. S. Driscoll, *J. Med. Chem.*, **19**, 313 (1976).

(5) K. Biemann, "Mass Spectrometry: Organic Chemical Applications," McGraw-Hill, New York, N.Y., 1962, p. 73.

(6) J. G. Pomonis, R. F. Severson, P. A. Hermes, R. G. Zaylskie, and A. C. Terranova, *Anal. Chem.*, **43**, 1709 (1971).

(7) H. N. Christensen, *J. Biol. Chem.*, **135**, 399 (1940).
(8) Y. Sanno and K. Tanaka, *Chem. Pharm. Bull.*, **8**, 753 (1960); through *Chem. Abstr.*, **55**, 15501 (1960).
(9) Y. S. Tsizin and N. A. Preobrazhenskii, *J. Gen. Chem. USSR* (English translation), **33**, 2800 (1963).
(10) M. Beroza and A. B. Borkovec, *J. Med. Chem.*, **7**, 44 (1964).
(11) D. Lalka and T. J. Bardos, *J. Pharm. Sci.*, **62**, 1294 (1973).
(12) A. N. Makarova and A. Y. Berlin, *J. Gen. Chem. USSR* (English translation), **29**, 3919 (1959).
(13) *Ibid.*, **29**, 659 (1959).
(14) A. Y. Berlin and A. N. Makarova, *J. Gen. Chem. USSR* (English translation), **30**, 1411 (1960).
(15) A. N. Makarova and A. Y. Berlin, *ibid.*, **31**, 2193 (1961).
(16) *Ibid.*, **34**, 3073 (1964).
(17) A. N. Makarova, V. S. Martynov, and A. Y. Berlin, *J. Gen. Chem. USSR* (English translation), **33**, 1601 (1963).
(18) V. K. LaMer, *Chem. Rev.*, **10**, 179 (1932).
(19) B. Cohen, E. R. Van Artsdalen, and J. Harris, *J. Am. Chem. Soc.*, **80**, 3458 (1958).
(20) A. N. Makarova and A. Y. Berlin, *J. Gen. Chem. USSR* (English translation), **31**, 2193 (1961).
(21) A. A. Frost and R. G. Pearson, "Kinetics and Mechanism," 2nd ed., Wiley, New York, N.Y., 1961, p. 166.
(22) E. H. Jensen and D. J. Lamb, *J. Pharm. Sci.*, **53**, 402 (1964).

**ACKNOWLEDGMENTS**

Presented in part at the Basic Pharmaceutics Section, APhA Academy of Pharmaceutical Sciences, Kansas City meeting, November 1979.

The authors thank Mr. J. C. Cradock and Dr. J. S. Driscoll, National Cancer Institute, for helpful discussions and Mrs. S. Swindell for assistance in the preparation of this manuscript.

# Simultaneous GLC Analysis of Aspirin and Nonaspirin Salicylates in Pharmaceutical Tablet Formulations

**ROBERT N. GALANTE ˣ, JOHN C. EGOVILLE, ANTHONY J. VISALLI, and DAHYABHAI M. PATEL**

Received June 6, 1980, from the *Analytical and Physical Chemistry Department, Research and Development, William H. Rorer, Inc., Fort Washington, PA 19034.* Accepted for publication July 25, 1980.

**Abstract** □ The analysis of aspirin and nonaspirin salicylates in buffered and plain tablet formulations employing nearly nonaqueous extraction is described. The results obtained compare favorably with those obtained from USP procedures. A simultaneous assay for aspirin and nonaspirin salicylates in buffered tablets involves the use of an acidified chromatographic siliceous earth column for the separation of the aspirin and nonaspirin salicylates from various buffers or antacids. The column is eluted with chloroform, and the aspirin and nonaspirin salicylates are analyzed by GLC as their trimethylsilyl derivatives. The methods described here have definite advantages over USP XX procedures, and the buffered aspirin tablet procedure also is adaptable to aspirin formulations containing codeine, acetaminophen, propoxyphene, caffeine, and many antihistamines.

**Keyphrases** □ Aspirin—simultaneous GLC analysis with nonaspirin salicylates in tablet formulations □ Salicylates, nonaspirin—simultaneous GLC analysis with aspirin in tablet formulations □ GLC—analysis, aspirin and nonaspirin salicylates in tablet formulations

The GLC analysis of aspirin and nonaspirin salicylates in solid pharmaceutical dosage forms and biological fluids has been reported (1–18). The extraction of nonaspirin salicylates from various buffers is accomplished by the current USP procedure; however, the USP procedure for the analysis of aspirin does not effectively free aspirin from aged tablets containing calcium, aluminum, and magnesium buffers. Complexation of aspirin and nonaspirin salicylates with buffers has been reported (19–22). The current USP spectrophotometric procedures for aspirin tablets may not separate impurities such as acetylsalicylsalicylic acid and acetylsalicylic acid anhydride (23–27). Analysis of aspirin and nonaspirin salicylates by high-pressure liquid chromatography (HPLC) also has been reported (28–35). Mobile phases and extractions employing methanol and water, even in small quantities, result in unavoidable hydrolysis of aspirin, thereby giving variable and nonreproducible quantitation of salicylic acid.

The buffered aspirin tablet procedure described here enables the extraction of both aspirin and nonaspirin salicylates from excipients and buffers in a virtually nonaqueous procedure, thereby keeping hydrolysis of aspirin to a minimum.

## EXPERIMENTAL

**Materials**—Aspirin USP reference standard (GLC purity 99.95%), salicylic acid USP reference standard (GLC purity 100.0%), chromatographic siliceous earth prepared by the USP procedure, propylparaben USP, and *N,O*-bis(trimethylsilyl)acetamide were used. Chloroform and hydrochloric acid were reagent grade.

**Simultaneous GLC Analysis of Aspirin and Nonaspirin Salicylates in Buffered Tablets**—*Internal Standard Solution*—About 425 mg of propylparaben USP was diluted to 100 ml with chloroform and mixed.

*Aspirin Standard Preparation*—About 125 mg of aspirin USP reference standard was weighed accurately, transferred to a 50-ml volumetric flask, diluted to volume with chloroform, and mixed. The standard preparation was derivatized within 2 hr of preparation.

*Salicylic Acid Standard Preparation*—About 15 mg of salicylic acid USP reference standard was weighed accurately, transferred to a 200-ml volumetric flask, diluted to volume with chloroform, and mixed.

*Assay Preparation*—The average tablet weight of 20 tablets was determined, and the tablets were ground to a fine powder. Without delay, a portion of the ground tablets equivalent to 500 mg of aspirin was transferred to a small beaker containing 3.0 g of acid-washed chromatographic siliceous earth. The powders were mixed with a glass rod, 2.0 ml of 6 *N* HCl was added, and the powders were mixed again with the glass rod. The mixture was transferred to a 20 × 2.5-cm chromatographic column, and the beaker was dry washed with 1.0 g of siliceous earth (glass wool was used at both ends of the column).

The column was packed uniformly and eluted with successive portions of chloroform *via* the sample beaker at the rate of ~10 ml/min. About 150 ml of the eluate was collected in a 200-ml volumetric flask. The tip

0022-3549/81/0200-0167$01.00/0
© 1981, American Pharmaceutical Association

(7) H. N. Christensen, *J. Biol. Chem.*, **135**, 399 (1940).
(8) Y. Sanno and K. Tanaka, *Chem. Pharm. Bull.*, **8**, 753 (1960); through *Chem. Abstr.*, **55**, 15501 (1960).
(9) Y. S. Tsizin and N. A. Preobrazhenskii, *J. Gen. Chem. USSR* (English translation), **33**, 2800 (1963).
(10) M. Beroza and A. B. Borkovec, *J. Med. Chem.*, **7**, 44 (1964).
(11) D. Lalka and T. J. Bardos, *J. Pharm. Sci.*, **62**, 1294 (1973).
(12) A. N. Makarova and A. Y. Berlin, *J. Gen. Chem. USSR* (English translation), **29**, 3919 (1959).
(13) *Ibid.*, **29**, 659 (1959).
(14) A. Y. Berlin and A. N. Makarova, *J. Gen. Chem. USSR* (English translation), **30**, 1411 (1960).
(15) A. N. Makarova and A. Y. Berlin, *ibid.*, **31**, 2193 (1961).
(16) *Ibid.*, **34**, 3073 (1964).
(17) A. N. Makarova, V. S. Martynov, and A. Y. Berlin, *J. Gen. Chem. USSR* (English translation), **33**, 1601 (1963).
(18) V. K. LaMer, *Chem. Rev.*, **10**, 179 (1932).
(19) B. Cohen, E. R. Van Artsdalen, and J. Harris, *J. Am. Chem. Soc.*, **80**, 3458 (1958).
(20) A. N. Makarova and A. Y. Berlin, *J. Gen. Chem. USSR* (English translation), **31**, 2193 (1961).
(21) A. A. Frost and R. G. Pearson, "Kinetics and Mechanism," 2nd ed., Wiley, New York, N.Y., 1961, p. 166.
(22) E. H. Jensen and D. J. Lamb, *J. Pharm. Sci.*, **53**, 402 (1964).

**ACKNOWLEDGMENTS**

Presented in part at the Basic Pharmaceutics Section, APhA Academy of Pharmaceutical Sciences, Kansas City meeting, November 1979.

The authors thank Mr. J. C. Cradock and Dr. J. S. Driscoll, National Cancer Institute, for helpful discussions and Mrs. S. Swindell for assistance in the preparation of this manuscript.

# Simultaneous GLC Analysis of Aspirin and Nonaspirin Salicylates in Pharmaceutical Tablet Formulations

**ROBERT N. GALANTE ˣ, JOHN C. EGOVILLE, ANTHONY J. VISALLI, and DAHYABHAI M. PATEL**

Received June 6, 1980, from the *Analytical and Physical Chemistry Department, Research and Development, William H. Rorer, Inc., Fort Washington, PA 19034.* Accepted for publication July 25, 1980.

**Abstract** □ The analysis of aspirin and nonaspirin salicylates in buffered and plain tablet formulations employing nearly nonaqueous extraction is described. The results obtained compare favorably with those obtained from USP procedures. A simultaneous assay for aspirin and nonaspirin salicylates in buffered tablets involves the use of an acidified chromatographic siliceous earth column for the separation of the aspirin and nonaspirin salicylates from various buffers or antacids. The column is eluted with chloroform, and the aspirin and nonaspirin salicylates are analyzed by GLC as their trimethylsilyl derivatives. The methods described here have definite advantages over USP XX procedures, and the buffered aspirin tablet procedure also is adaptable to aspirin formulations containing codeine, acetaminophen, propoxyphene, caffeine, and many antihistamines.

**Keyphrases** □ Aspirin—simultaneous GLC analysis with nonaspirin salicylates in tablet formulations □ Salicylates, nonaspirin—simultaneous GLC analysis with aspirin in tablet formulations □ GLC—analysis, aspirin and nonaspirin salicylates in tablet formulations

The GLC analysis of aspirin and nonaspirin salicylates in solid pharmaceutical dosage forms and biological fluids has been reported (1–18). The extraction of nonaspirin salicylates from various buffers is accomplished by the current USP procedure; however, the USP procedure for the analysis of aspirin does not effectively free aspirin from aged tablets containing calcium, aluminum, and magnesium buffers. Complexation of aspirin and nonaspirin salicylates with buffers has been reported (19–22). The current USP spectrophotometric procedures for aspirin tablets may not separate impurities such as acetylsalicylsalicylic acid and acetylsalicylic acid anhydride (23–27). Analysis of aspirin and nonaspirin salicylates by high-pressure liquid chromatography (HPLC) also has been reported (28–35). Mobile phases and extractions employing methanol and water, even in small quantities, result in unavoidable hydrolysis of aspirin, thereby giving variable and nonreproducible quantitation of salicylic acid.

The buffered aspirin tablet procedure described here enables the extraction of both aspirin and nonaspirin salicylates from excipients and buffers in a virtually nonaqueous procedure, thereby keeping hydrolysis of aspirin to a minimum.

## EXPERIMENTAL

**Materials**—Aspirin USP reference standard (GLC purity 99.95%), salicylic acid USP reference standard (GLC purity 100.0%), chromatographic siliceous earth prepared by the USP procedure, propylparaben USP, and *N,O*-bis(trimethylsilyl)acetamide were used. Chloroform and hydrochloric acid were reagent grade.

**Simultaneous GLC Analysis of Aspirin and Nonaspirin Salicylates in Buffered Tablets**—*Internal Standard Solution*—About 425 mg of propylparaben USP was diluted to 100 ml with chloroform and mixed.

*Aspirin Standard Preparation*—About 125 mg of aspirin USP reference standard was weighed accurately, transferred to a 50-ml volumetric flask, diluted to volume with chloroform, and mixed. The standard preparation was derivatized within 2 hr of preparation.

*Salicylic Acid Standard Preparation*—About 15 mg of salicylic acid USP reference standard was weighed accurately, transferred to a 200-ml volumetric flask, diluted to volume with chloroform, and mixed.

*Assay Preparation*—The average tablet weight of 20 tablets was determined, and the tablets were ground to a fine powder. Without delay, a portion of the ground tablets equivalent to 500 mg of aspirin was transferred to a small beaker containing 3.0 g of acid-washed chromatographic siliceous earth. The powders were mixed with a glass rod, 2.0 ml of 6 *N* HCl was added, and the powders were mixed again with the glass rod. The mixture was transferred to a 20 × 2.5-cm chromatographic column, and the beaker was dry washed with 1.0 g of siliceous earth (glass wool was used at both ends of the column).

The column was packed uniformly and eluted with successive portions of chloroform *via* the sample beaker at the rate of ~10 ml/min. About 150 ml of the eluate was collected in a 200-ml volumetric flask. The tip

0022-3549/81/0200-0167$01.00/0
© 1981, American Pharmaceutical Association

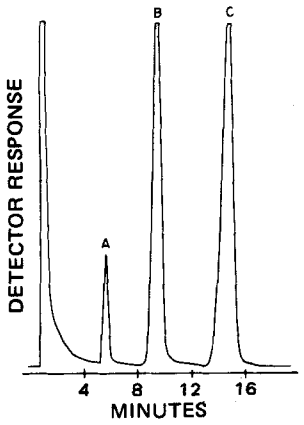


**Figure 1**—*Gas chromatogram of the trimethylsilyl derivatives of salicylic acid (a), aspirin (b), and the internal standard, propylparaben (c), for buffered aspirin tablets.*

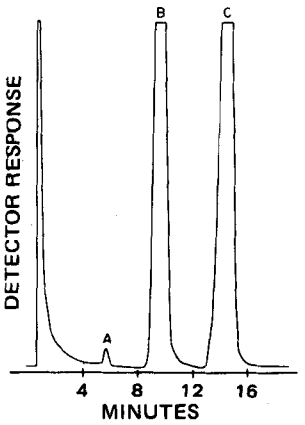


**Figure 2**—*Gas chromatogram of the trimethylsilyl derivatives of salicylic acid (a), aspirin (b), and the internal standard, propylparaben (c), for aspirin tablets.*

of the column was rinsed with chloroform, and the flask was brought to volume and mixed. The chloroform elution was conducted within 30 min of column packing, and the powdered tablets were sampled within 1 hr of grinding.

*Procedure*—Aliquots (2.0 ml) of the aspirin standard preparation, the salicylic acid standard preparation, and the assay preparation were transferred to separate reaction vials. A 1.0-ml aliquot of the internal standard solution was added to each vial. The contents of all of the vials were derivatized using 250 μl of *N,O*-bis(trimethylsilyl)acetamide with vigorous mixing for 30 sec.

All vials were vented and heated at 60° for ~15 min and then cooled to room temperature for subsequent injection into the gas chromatograph. (The derivatized solutions are stable for 4 days in airtight containers.) The gas chromatograph[1] was equipped with a flame-ionization detector and an electronic integrator[2]. The glass column typically was 180 cm × 2 mm and was packed with 3% phenyl methyl silicone liquid phase (OV-17) on 100–120-mesh chromatographic silanized siliceous earth[3].

The temperatures of the injection port, column, and detector were 180, 120, and 140°, respectively. The carrier gas was nitrogen at a flow rate of ~35 ml/min. Relative retention times for the trimethylsilyl derivatives of salicylic acid, aspirin, and propylparaben were 0.36, 0.63, and 1.0, respectively (Fig. 1). In a suitable chromatogram, the resolution factor was not <2.0 between any two peaks, and the relative standard deviation was not >2.0 for five replicate injections of the standard preparation. At the completion of each sample chromatogram, the column temperature was raised to 240° for 3 min to purge the column of tablet excipients.

*Calculations*—The quantities (in milligrams) of aspirin and salicylic acid in the portion taken for the assay preparation were calculated by the same formula, $100C(R_u/R_s)$, in which $C$ is the concentration (in milligrams per 2.0 ml) of the appropriate USP reference standard in the standard preparation and $R_u$ and $R_s$ are the ratios of the peak areas of the corresponding analyte to those of the internal standard obtained with the assay preparation and the standard preparation, respectively.

**Simultaneous GLC Analysis of Aspirin and Nonaspirin Salicylates in Aspirin Tablets**—*Internal Standard Solution*—About 1.7 g of propylparaben USP was diluted to 100 ml with chloroform and mixed.

*Aspirin Standard Preparation*—About 100 mg of aspirin USP reference standard was weighed accurately and transferred to a 50-ml glass-stoppered flask.

*Salicylic Acid Standard Preparation*—About 30 mg of salicylic acid USP reference standard was weighed accurately, transferred to a 100-ml volumetric flask, diluted to volume with chloroform, and mixed. A 1.0-ml aliquot was transferred to a 50-ml glass-stoppered flask.

*Assay Preparation*—The average tablet weight of 20 tablets was determined, and the tablets were ground to a fine powder. A portion of the ground tablets equivalent to 100 mg of aspirin was transferred to a 50-ml glass-stoppered flask.

*Procedure*—A 5.0-ml aliquot of the internal standard solution and 15 ml of chloroform were transferred to each 50-ml glass-stoppered flask containing the standards and assay preparations. All solutions were shaken mechanically for exactly 3 min and filtered. Without delay, a 2.0-ml portion of each solution was derivatized with 300 μl of *N,O*-bis(trimethylsilyl)acetamide, shaken for 30 sec, and heated at 60° for ~15 min. The GLC analysis (Fig. 2) was conducted as described for the buffered aspirin tablets.

*Calculations*—The quantity (in milligrams) of aspirin in the portion taken for the assay preparation was calculated from $C(R_u/R_s)$, in which $C$ is the concentration (in milligrams) of the USP reference standard in the standard preparation and $R_u$ and $R_s$ are the ratios of the peak areas of the corresponding analyte to those of the internal standard obtained with the assay preparation and the standard preparation, respectively. The nonaspirin salicylates were determined on a pass or fail 0.3% limit standard.

## RESULTS AND DISCUSSION

**Linearity and Precision**—The response linearity for the described GLC methods was suitable for the entire assay range. The precision on multiple injections into the chromatograph was ±0.45% for the aspirin analysis and ±1.0% for the nonaspirin salicylate analysis.

**Assay Specificity**—Recoveries of aspirin and salicylic acid mixtures from the chromatographic siliceous earth column averaged 99.9 and 99.8%, respectively. None of the commercial products analyzed produced any GLC interference. A comparison of the GLC analysis to the USP procedure for buffered aspirin tablets and plain aspirin tablets is shown in Tables I and II, respectively. Table III shows the results of the GLC analysis of aspirin tablets containing aluminum and magnesium hydroxides.

Because of the good response linearity of the salicylic acid trimethylsilyl derivative, the actual percentages were calculated from a single-point

**Table I—Assay Results on Commercial Buffered Aspirin Tablets**

| Product | Aspirin, % of claim | | Nonaspirin Salicylates, % | |
|---|---|---|---|---|
| | GLC Method | USP Method | GLC Method | USP Method |
| A | 98.3 | 96.5 | 0.68 | 0.58 |
| B | 98.2 | 98.2 | 0.73 | 0.75 |
| C | 97.8 | 98.1 | 0.60 | 0.57 |
| D | 93.1 | 94.5 | 0.41 | 0.36 |
| E | 95.7 | 93.5 | 1.55 | 1.48 |
| *SD*[a] | 1.51 | | 0.045 | |

[a] Standard deviation of the GLC method compared to the USP method.

**Table II—Commercial Aspirin Tablets**

| Product | Aspirin, % of claim | | Nonaspirin Salicylates, % | |
|---|---|---|---|---|
| | GLC Method | USP Method | GLC Method | USP Method |
| F | 100.2 | 99.3 | <0.3 | <0.3 |
| G | 100.5 | 100.9 | <0.3 | <0.3 |
| H | 99.4 | 96.9 | <0.3 | <0.3 |
| I | 102.0 | 99.8 | <0.3 | <0.3 |
| J | 99.5 | 98.4 | <0.3 | <0.3 |
| *SD*[a] | 1.15 | | | |

[a] Standard deviation of the GLC method compared to the USP method.

[1] Hewlett-Packard model 7620A.
[2] Hewlett-Packard model 3370A.
[3] Applied Science Laboratories, State College, Pa.

**Table III—GLC Assay Results on Aspirin Tablets Containing Magnesium and Aluminum Hydroxides**

| Lot | Age | Aspirin, % of claim | Nonaspirin Salicylates, % |
|---|---|---|---|
| 1 | 1 week | 98.4 | 0.18 |
| 2 | 2 weeks | 99.4 | 0.23 |
| 3 | 2 weeks | 98.3 | 0.25 |
| 4 | 2 weeks | 99.1 | 0.28 |
| 5 | 3 weeks | 97.5 | 0.33 |
| 6 | 3 weeks | 98.5 | 0.26 |
| 7 | 4 weeks | 101.6 | 0.28 |
| 8 | 5 weeks | 100.5 | 0.45 |
| 9 | 6 weeks | 100.6 | 0.47 |
| 10 | 6 weeks | 100.9 | 0.26 |
| 11 | 3 years | 98.5 | 0.89 |
| 12 | 3 years | 96.3 | 0.95 |
| 13 | 3 years | 98.0 | 0.80 |
| 14 | 4 years | 99.2 | 0.77 |
| 15 | 4 years | 98.2 | 0.99 |
| 16 | 4 years | 98.4 | 0.82 |
| *SD*[a] | | 1.21 | 0.032 |

[a] Average standard deviation of duplicate analyses.

standard in the analysis of buffered tablets. The average aspirin assay for 21 determinations of buffered tablets by the GLC and USP procedures was 98.4 and 98.7%, respectively. The same values for 21 analyses of the nonaspirin salicylates were 0.58 and 0.58%, respectively. Plain aspirin tablets were determined on a pass or fail 0.3% limit standard. Analysis of aspirin in combination with codeine, caffeine, acetaminophen, propoxyphene, and many antihistamines, although not reported here, gave good results by a modified GLC procedure as described for buffered aspirin tablets.

**Hydrolysis of Aspirin**—Chromatographic siliceous earth has been used extensively as a partitioning medium for aspirin analysis (36–42). The USP employs this material with a ferric chloride–urea reagent to complex salicylic acid. The use of siliceous earth in the procedure described here is not as a partitioning medium but rather as a distribution and absorption medium. In this study, 2.0 ml of 6 *N* HCl was used for all commercial tablets tested. In practice, the acid strength can be adjusted so that it is in slight excess of the amount needed to neutralize the buffers in the tablet.

The siliceous earth incorporated with the 6 *N* HCl and the ground tablet distributes the drug over a large surface area and adsorbs the buffers on the acidified surface, releasing the aspirin and nonaspirin salicylates to the chloroform eluent. The 2.0 ml of 6 *N* HCl is retained on the siliceous earth surface and has the capacity to solubilize ~7 mg of the 500 mg of aspirin sample taken for assay. However, the buffers and tablet excipients, together with the siliceous earth, adsorb the available acid, thereby minimizing hydrolysis. The extraction is virtually nonaqueous, and the aspirin is out of solution.

A previous report described the hydrolysis and kinetics of aspirin in relation to solution and concentration, giving a much lower hydrolysis rate of the drug out of solution (43). The hydrolysis rate of aspirin induced by the siliceous earth column was determined to be ~0.06% for 30 min. In practice, the chloroform elution was conducted within 15 min of column packing. Texts (44, 45) and review articles (46, 47) have detailed the decomposition, hydrolysis, and kinetics of aspirin with a list of over 300 references.

## CONCLUSIONS

Multiple analyses of aspirin and nonaspirin salicylates in solid pharmaceutical dosage forms have been difficult and time consuming by the USP procedures. The USP procedure is stability indicating for nonaspirin salicylates but not for aspirin. The GLC procedures described here are less time consuming and lend themselves to multiple analysis on a gas chromatograph equipped with an automatic injector. In practice, a chemist can prepare 15–20 samples daily employing the buffered aspirin tablet procedure and up to 40 samples daily with the plain aspirin tablet procedure. Beside the savings in analytical costs, these procedures are stability indicating and adaptable to many pharmaceutical solid dosage forms of aspirin.

## REFERENCES


(1) J. G. Nikelly, *Anal. Chem.*, **36**, 2248 (1964).

(2) R. C. Crippen and H. C. Freimuth, *ibid.*, **36**, 273 (1964).

(3) R. N. Galante, A. J. Visalli, and D. M. Patel, *J. Pharm. Sci.*, **68**, 1494 (1979).

(4) E. B. Dechene, L. H. Booth, and M. J. Caughey, *J. Pharm. Pharmacol.*, **21**, 678 (1969).

(5) B. H. Thomas, G. Solomonraj, and B. B. Coldwell, *ibid.*, **25**, 201 (1973).

(6) P. H. Ko, *J. Pharm. Sci.*, **66**, 731 (1977).

(7) M. J. Rance, B. J. Jordan, and J. D. Nichols, *J. Pharm. Pharmacol.*, **27**, 425 (1975).

(8) S. Patel, J. H. Perrin, and J. J. Windheuser, *J. Pharm. Sci.*, **61**, 1794 (1972).

(9) L. J. Walter, D. F. Biggs, and R. T. Coutts, *ibid.*, **63**, 1754 (1974).

(10) C. H. Morris, J. E. Christian, R. R. Landolt, and W. G. Hansen, *ibid.*, **59**, 270 (1970).

(11) J. R. Watson, P. Crescuolo, and F. Matsui, *ibid.*, **60**, 454 (1971).

(12) A. J. Hoffman and H. I. Mitchell, *ibid.*, **52**, 305 (1963).

(13) S. L. Ali, *Z. Anal. Chem.*, **27**, 365 (1976).

(14) S. L. Ali, *Chromatographia*, **8**, 33 (1975).

(15) Z. I. El-Darawy and Z. M. Mobarak, *Pharmazie*, **27**, 738 (1972).

(16) T. Inoue and M. Koibuchi, *Eisei Kagaku*, **19**, 18 (1973).

(17) J. R. Watson, F. Matsui, P. M. J. McConnell, and R. C. Lawrence, *J. Pharm. Sci.*, **61**, 929 (1972).

(18) M. Rowland and S. Riegelman, *ibid.*, **56**, 717 (1967).

(19) D. E. Guttman and G. W. Salomon, *ibid.*, **58**, 120 (1969).

(20) D. E. Guttman, *ibid.*, **57**, 1685 (1968).

(21) J. Levine and J. D. Weber, *ibid.*, **57**, 631 (1968).

(22) S. S. Kornblum and M. A. Zoglio, *ibid.*, **56**, 1569 (1967).

(23) S. L. Ali, *J. Chromatogr.*, **126**, 651 (1976).

(24) E. Saito, H. Ogata, T. Shibazaki, A. Ejima, and T. Inoue, *Eisei Shikensho Hokoku*, **95**, 1 (1977).

(25) H. D. Spitz, *J. Chromatogr.*, **140**, 131 (1977).

(26) A. L. De Weck, *Int. Arch. Allergy*, **41**, 393 (1971).

(27) M. G. Quaglia, *Farmaco, Ed. Prat.*, **34**, 126 (1978).

(28) P. P. Ascione and G. P. Chrekian, *J. Pharm. Sci.*, **64**, 1029 (1975).

(29) R. G. Baum and F. F. Cantwell, *ibid.*, **67**, 1066 (1978).

(30) P. J. Twitchett, A. E. P. Gorvin, and A. C. Moffat, *J. Chromatogr.*, **120**, 359 (1976).

(31) D. Blair, B. H. Rumack, and R. G. Peterson, *Clin. Chem.*, **24**, 1543 (1978).

(32) R. L. Stevenson and C. A. Burtis, *J. Chromatogr.*, **61**, 253 (1971).

(33) V. D. Gupta, *J. Pharm. Sci.*, **69**, 110 (1980).

(34) *Ibid.*, **69**, 113 (1980).

(35) G. W. Peng, M. A. F. Gadalla, V. Smith, A. Peng, and W. L. Chiou, *J. Pharm. Sci.*, **67**, 710 (1978).

(36) J. D. Weber, *J. Assoc. Off. Anal Chem.*, **48**, 1151 (1965).

(37) J. Levine, *J. Pharm. Sci.*, **50**, 506 (1961).

(38) J. D. Weber and J. Levine, *ibid.*, **55**, 78 (1966).

(39) A. R. Green, *Australas. J. Pharm. Sci.*, **45**, 588 (1964).

(40) J. R. Luber, A. J. Visalli, and D. M. Patel, *J. Pharm. Sci.*, **68**, 780 (1979).

(41) A. L. Jacobs, A. E. Dilatush, S. Weinstein, and J. J. Windheuser, *ibid.*, **55**, 893 (1966).

(42) "The United States Pharmacopeia," 19th rev., Mack Publishing Co., Easton, Pa., 1975, p. 38.

(43) K. C. James, *J. Pharm. Pharmacol.*, **10**, 363 (1958).

(44) K. Florey, "Analytical Profiles of Drug Substances," vol. 8, Academic, New York, N.Y., 1979.

(45) A. Pryde and M. T. Gilbert, "Applications of High Performance Liquid Chromatography," Wiley, New York, N.Y., 1979.

(46) C. A. Kelly, *J. Pharm. Sci.*, **59**, 1053 (1970).

(47) S. L. Ali, *Pharm. Ztg.*, **121**, 201 (1976).

# Extended Solubility Approach: Solubility Parameters for Crystalline Solid Compounds

**ALFRED MARTIN *x and JENS CARSTENSEN ‡**

Received February 22, 1980, from the **Drug Dynamics Institute, College of Pharmacy, University of Texas, Austin, TX 78712,* and the ‡*School of Pharmacy, University of Wisconsin, Madison, WI 53706.* Accepted for publication July 16, 1980.

**Abstract** □ A method is suggested to obtain solubility parameters for crystalline solid compounds, involving a quadratic equation based on the original Scatchard–Hildebrand solubility expression. The geometric mean, $\delta_1\delta_2$, of the Hildebrand approach is replaced by $w_{12} = K\delta_1\delta_2$, and $\log \alpha_2/(V_2\phi_2^2/2.3RT)$ is regressed against $\delta_1$ in a second-degree power series for parabens and benzoic acid in a series of normal alcohols. The method provides reasonable solubility parameters for the solid solutes and affords a convenient calculation of the solubility of drugs in a homologous series of solvents.

**Keyphrases** □ Solubility parameters—calculation for crystalline solids □ Parabens—calculation of solubility parameters in normal alkanols □ Solids, crystalline—calculation of solubility parameters

Solution theory (1) begins with the well-known relation:

$$-\log X_2 = -\log X_2^i + \log \alpha_2 \qquad \text{(Eq. 1)}$$

where $X_2$ is the solute mole fraction solubility, $X_2^i$ is the ideal solubility of the solid, and $\alpha_2$ is the solute activity coefficient. According to regular solution theory as formulated by Hildebrand and Scott (1) and Scatchard (2), the logarithm of the activity coefficient is written as:

$$\log \frac{a_2^s}{X_2} = \log \alpha_2 = \frac{V_2\phi_1^2}{2.303RT}(w_1 + w_2 - 2w_{12}) \qquad \text{(Eq. 2)}$$

where $a_2^s$ is the activity of the solid solute referenced to the pure supercooled liquid and equals $X_2^i$ for an ideal solution, $V_2$ is the molar volume of the solute (subscript 2), $\phi_1$ is the volume fraction of the solvent (subscript 1), $R$ is the molar gas constant, $T$ is the absolute temperature at which the study is conducted, $w_1$ and $w_2$ are the cohesive energy densities of the solvent and solute, and $w_{12}$ is the adhesion energy density of the solute–solvent pair. The square roots of the energy densities are known as solubility parameters, $\delta_i$, and may be obtained from the energy or heat of vaporization per cubic centimeter:

$$\delta_i^2 = w_i = \frac{\Delta E^v}{V_i} = \frac{\Delta H^v - RT}{V_i} \qquad \text{(Eq. 3)}$$

In regular solution theory, it is assumed that the solute–solvent interaction energy, $w_{12}$, may be expressed as the geometric mean of the solvent, $w_1$, and the solute, $w_2$:

$$w_{12} = (w_1w_2)^{1/2} = \delta_1\delta_2 \qquad \text{(Eq. 4)}$$

Substitution of the geometric mean into Eq. 2 yields the logarithmic activity coefficient of the Hildebrand–Scatchard solubility equation:

$$\log \alpha_2 = A(\delta_1^2 + \delta_2^2 - 2\delta_1\delta_2) = A(\delta_1 - \delta_2)^2 \qquad \text{(Eq. 5)}$$

where $A$ equals $V_2\phi_1^2/(2.303RT)$.

## THEORETICAL

Solubility parameters of crystalline compounds usually have been obtained from solubility measurements. Equation 2 shows that when the drug is dissolved in a solvent of the same $\delta$ value, *i.e.*, when $w_1 = w_2$, the right-hand term of Eq. 2 approaches (but does not ordinarily equal) zero.

**Table I—Heats of Fusion of the Parabens**

| Compound | Melting Point | Apparent $\Delta H_m$ (Ref. 4) | $\Delta H_m^f$ [a] |
|---|---|---|---|
| Methylparaben | 399.7 °K | 4352 | 5400 |
| Ethylparaben | 389.7 °K | 4243 | 6100 |
| Propylparaben | 369.7 °K | 4026 | 6250 |
| Butylparaben | 343.2 °K | 3737 | 6410 |

[a] Values obtained from the United States Pharmacopeial Laboratories.

Then:

$$\log X_2 = \log a_2^s = \log X_2^i \qquad \text{(Eq. 6)}$$

signifying that the drug is dissolved to form a nearly ideal solution, one in which maximum solubility is obtained, barring solvation effects. When a pure solvent or solvent mixture is found that yields a nearly ideal solution, characterized by a peak in the solubility profile (plot of $X_2$ *versus* $\delta_1$), it can be assumed that the solute solubility parameter, $\delta_2$, is equal to the solubility parameter of the solvent system.

This peak solubility approach to finding $\delta_2$ values for drugs and other crystalline compounds has been used in several investigations (3–5). A similar procedure, involving the observation of maximum swelling, is used in the plastics industry to obtain solubility parameters of polymers. The method has its shortcomings, particularly when a sharp, single maximum value is not observed in the solubility curve. Additional methods for obtaining $\delta_2$ values of solids therefore would be of considerable value, not only for predicting solubilities but also in dosage form design, bioavailability studies, and studies designed to investigate pharmaceutical solutions on a theoretical basis.

Modification of the activity term of Eq. 5 provides another approach for calculating $\delta_2$ values for crystalline compounds. In solutions ordinarily of interest to the pharmaceutical scientist, semipolar drugs are dissolved in nonpolar and polar solvents, and the geometric mean seldom can be assumed to apply. However, $w_{12}$ and $\delta_1\delta_2$ may be related by introducing a proportionality constant, $K$ (6):

$$w_{12} = K\delta_1\delta_2 \qquad \text{(Eq. 7)}$$

Equation 5 then becomes:

$$\log \alpha_2 = A(\delta_1^2 + \delta_2^2 - 2K\delta_1\delta_2) \qquad \text{(Eq. 8)}$$

Rearrangement of Eq. 8 yields:

$$\frac{\log \alpha_2}{A} = \delta_2^2 - (2K\delta_2)\delta_1 + \delta_1^2 \qquad \text{(Eq. 9)}$$

which suggests a power series of $\log \alpha_2/A$ in $\delta_1$ (7–9)[1].

If a solid drug such as benzoic acid is dissolved in a number of solvents of a particular class, such as the normal alcohols, it should be possible to regress the experimentally obtained quantity, $\log (a_2^s/X_2)/A = (\log \alpha_2)/A$, against $\delta_1$ in a second-degree power series:

$$(\log \alpha_2)/A = B + C\delta_1 + D\delta_1^2 \qquad \text{(Eq. 10)}$$

By this procedure, one may obtain the solubility parameter $\delta_2$ of crystalline compounds such as drugs, excipients, and biochemicals found in polar pharmaceutical solutions.

## RESULTS AND DISCUSSION

It is assumed that $\log \alpha_2$ is known from experimental solubility mea-

[1] See G. Cavé, R. Kothari, F. Puisieux, A. Martin, and J. T. Carstensen, *Int. J. Pharm.*, 5, 267 (1980).



*0022-3549/81/0200-0170$01.00/0*
*© 1981, American Pharmaceutical Association*

**Table II—Coefficients of the Quadratic Equation for (Log $\alpha_2$)/$A$ Regressed on Solubility Parameters of Parabens and Benzoic Acid in $n$-Alkanols [a] at 25 °**

| Compound | Data from Ref. 4 | | | Data from Ref. 10 | | | Combination of Refs. 4 and 10 | | |
|---|---|---|---|---|---|---|---|---|---|
| | $B_1$ | $C_1$ | $D_1$ | $B_2$ | $C_2$ | $D_2$ | $B_3$ | $C_3$ | $D_3$ |
| Methylparaben | 186.411994 | −33.477824 | 1.495773 | 70.477644 | −11.539949 | 0.466753 | 63.444455 | −10.524791 | 0.430560 |
| Ethylparaben | 143.159953 | −25.763854 | 1.134002 | 75.774512 | −12.834344 | 0.520475 | 70.173648 | −12.018541 | 0.491099 |
| Propylparaben | 78.085942 | −14.104458 | 0.618690 | 39.692531 | −6.805210 | 0.276630 | 39.192279 | −6.809410 | 0.279553 |
| Butylparaben | 49.701722 | −8.027767 | 0.285181 | 67.542467 | −10.479523 | 0.363866 | 61.081553 | −9.519539 | 0.328528 |
| Benzoic acid | 449.521048 | −79.852095 | 3.546044 | — | — | — | — | — | — |

[a] The compounds were studied in methanol, ethanol, propanol, butanol, hexanol, octanol, and decanol.

**Table III—Solute Solubility Parameter and $K$ Value Obtained from Quadratic Equation of Table II and Eqs. 13 and 14**

| Compound | Data from Ref. 4 | | Data from Ref. 10 | | Combined Results from Refs. 4 and 10 | |
|---|---|---|---|---|---|---|
| | $\delta_2$ | $K$ | $\delta_2$ | $K$ | $\delta_2$ | $K$ |
| Methylparaben | 11.16 | 1.00244 | 12.29 | 1.00602 | 12.14 | 1.00686 |
| Ethylparaben | 11.24 | 1.01103 | 12.07 | 1.02184 | 11.95 | 1.02365 |
| Propylparaben | 11.23 | 1.01462 | 11.98 | 1.02685 | 11.84 | 1.02860 |
| Butylparaben | 13.20 | 1.06615 | 13.62 | 1.05694 | 13.64 | 1.06254 |
| Benzoic acid | 11.26 | 1.00002 | — | — | — | — |

surements, together with an estimate of $X_2^i$, which usually is obtained by measuring the heat of fusion and the melting point of the compound by differential scanning calorimetry (8, 10) or differential thermal analysis (11). The values of $A$, $V_1$, $V_2$, and $\delta_1$ also are assumed to be known. Restaino and Martin (4) determined the heats of fusion for the $p$-hydroxybenzoic acid esters relative to the heat of fusion of benzoic acid, and Alexander *et al.* (10) used these results in a later study. However, basing the heats of fusion on the literature value of benzoic acid was incorrect[2].

The laboratories of the United States Pharmacopeial Convention supply reference standards for the parabens and have performed differential scanning calorimetry tests on these esters. The heats of fusion and melting points for the parabens are found in Table I[3]. These values were used in the present study to calculate ideal solubility for methyl-, ethyl-, propyl-, and butylparabens by employing the following equations (8):

$$\Delta H_m^f / T_m = \Delta S_m^f \qquad \text{(Eq. 11)}$$

$$\log X_2^i = \frac{\Delta S_m^f}{R} \log \frac{T}{T_m} \qquad \text{(Eq. 12)}$$

where $\Delta H_m^f$ and $\Delta S_m^f$ are the heat and entropy of fusion at the melting point, respectively; $R$ is the ideal gas constant; and $T$ and $T_m$ are the temperature of the experiment and the melting temperature of the compound in degrees Kelvin, respectively.

In two studies (4, 10), the mole fraction solubility of a series of parabens was determined in normal alcohols at 25 °C. Restaino and Martin (4) began the solvent series with propanol, while Alexander *et al.* (10) started with methanol and ethanol. These investigators omitted pentanol and added decanol. Because of the different choice of solvents in the two studies, different regression equations would be expected. The two sets of data yielded quadratic equations, the coefficients of which are shown in Table II for methyl-, ethyl-, propyl-, and butylparabens. The solute solubility parameter, $\delta_2$, and the proportionality constant, $K$, are calculated as follows. The coefficients of the quadratic expressions of Table II correspond to the terms $B$, $C$, and $D$ in Eq. 10. Referring to Eq. 9, it is observed that $B/D$ corresponds to $\delta_2^2$ and that $C/D$ corresponds to $-2K\delta_2$. Therefore:

$$B/D = \delta_2^2 \qquad \text{(Eq. 13)}$$

$$-\frac{C/D}{2\delta_2} = K \qquad \text{(Eq. 14)}$$

The solute solubility parameter is calculated using Eq. 13 with the values of $B$ and $D$ found in Table II. The $\delta_2$ value then is combined with the coefficients $C$ and $D$ of Eq. 14 to obtain $K$. The values of $\delta_2$ (Table III) correspond well (except in the case of butylparaben) with those obtained by the maximum solubility method (4). In the peak solubility method, methylparaben, ethylparaben, propylparaben, and benzoic acid had solubility parameters of 11–11.5; butylparaben exhibited a more diffuse maximum solubility, with a $\delta_2$ of ~11–12.

The solubilities given by Restaino and Martin (4) differ by ~10% from those of Alexander *et al.* (10), and such differences must be accepted in solubility work when results are obtained in different laboratories. To investigate a larger series of solvents, the separate results of the two studies were combined and a single regression equation was obtained for each solute of the paraben series. Using the regression coefficients of Table II, the $\delta_2$ and $K$ values from Refs. 4 and 10 and the combined calculations are recorded in Table III. The $\delta_2$ values from the combined calculations are reasonable when compared with those obtained by using the solubility data of Ref. 4 or 10 independently and when checked against $\delta_2$ values obtained by other methods. The values for butylparaben were somewhat larger than expected.

Figure 1 shows the solubility of methyl- and propylparabens in the $n$-alkanols. For methylparaben, the solubility of which is plotted against $\delta_2$ for the eight normal alcohols, the resulting $\delta_2$ values from Refs. 4 and 10 are not in complete agreement. The peak solubilities from Ref. 4 result in a solubility parameter for methylparaben of 11.16, which falls between

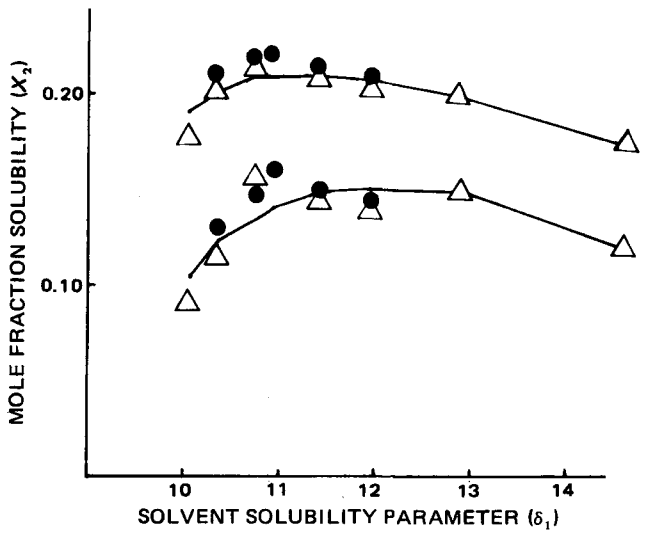


**Figure 1**—*Mole fraction solubility of methylparaben (lower curve) and propylparaben (upper curve) in* n*-alkanols ranging from decanol ($\delta_2$ = 10) to methanol ($\delta_2$ = 14.5). Key: ●, solubility data from Ref. 4; △, solubility data from Ref. 10; and —, calculated solubility line using the appropriate combined quadratic equation (Table II) and Eq. 16. The lines were obtained by connecting points of back-calculated solubilities at each solvent δ value.*

[2] A. Beerbower, Industrial Consultant, San Diego, Calif., Mar. 1980, personal communication.

[3] Provided by L. T. Grady and S. Sun, United States Pharmacopeial Convention, Rockville, Md.

that of pentanol (10.9) and butanol (11.4), where maximum solubility is observed. Alexander *et al.* (10) omitted pentanol and included ethanol and methanol. Figure 1 shows that this choice of solvents shifted the peak of the combined back-calculation curve of Refs. 4 and 10 to the right, yielding a maximum solubility at a $\delta_1$ value of ~12. Accordingly, a regression of log $\alpha_2/A$ *versus* $\delta_1$ employing the data of Ref. 10 yields a $\delta_2$ value of 12.29 from methylparaben, and the combined regression equation gives $\delta_2 = 12.14$.

The combined results of Tables II and III appear to follow the values of Alexander *et al.* (10) for $\delta_2$ for the various parabens and correspond to the $K$ values relative to the data of Alexander *et al.* (10) more closely than the results of Restaino and Martin (4). For the present, one would choose the combined regression equation to obtain reasonable solubilities of the parabens in normal alcohols. However, the most satisfactory approach would be repetition of the study, including all of the solvents of Restaino and Martin (4) and Alexander *et al.* (10) so that the solubilities determined by the two groups of investigators, employing different solvent series, would not bias the results. Figure 1 also shows the solubilities of propylparaben in the series of *n*-alkanols together with the back-calculated curve. In this case, similar $\delta_2$ values (Table III) were obtained from Restaino and Martin (4), Alexander *et al.* (10), and the combined results of the two groups.

As shown in Table III, the $K$ value for benzoic acid in the series of normal alcohols is unity. This finding indicates that $w_{12} = \delta_1\delta_2$; therefore, use of the Hildebrand–Scatchard equation, involving a geometric mean, should provide reasonable solubility values for benzoic acid in the *n*-alkanols.

The present method alters the activity coefficient term of the solubility equation (Eq. 2) in the following ways. In modifying the regression equation to make it correspond to the quadratic form of Eq. 9, the terms involving solubility parameters were divided by $D$, the coefficient associated with $\delta_1^2$. This process may be considered as a normalization procedure, utilized to provide coefficients of unity for $\delta_1^2$ and $\delta_2^2$. Since the right side of Eq. 10 is divided by $D$, the left side must be treated in the same way:

$$\frac{(\log \alpha_2)/A}{D} = \frac{B}{D} + \frac{C}{D}\delta_1 + \frac{D}{D}\delta_1^2 \qquad \text{(Eq. 15)}$$

The complete solubility equation (Eqs. 1 and 2) then becomes:

$$-\log X_2 = -\log X_2^i + DA(\delta_1^2 + \delta_2^2 - 2K\delta_1\delta_2) \qquad \text{(Eq. 16)}$$

Multiplication of $A$ by $D$ in Eq. 16 may be considered to yield an empirical coefficient, $A'$, associated with the solubility parameter term of Eq. 16. The case of ethylparaben dissolved in *n*-propanol (4, 10) is taken to illustrate the calculations involved. Employing the combined quadratic expression of Table II:

$$\delta_2^2 = \frac{B}{D} = 142.891 \qquad \text{(Eq. 17)}$$

$$\delta_2 = 11.95 \qquad \text{(Eq. 18)}$$

$$K = -\frac{C/D}{2\delta_2} = 1.02365 \qquad \text{(Eq. 19)}$$

These values of $\delta_2$ and $K$ are found in Table III. With $-\log X_2^i = 0.91589$, $\delta_1 = 11.9$ from Ref. 4, $D$ from Table II = 0.491099, $A = V_2\phi_1^2/2.303RT = 0.053570$, and $A' = (0.491099)(0.053570) = 0.026308$, one writes:

$$-\log X_2 = 0.91589 + 0.026308[(11.95)^2 + (11.9)^2 - 2(1.02365)(11.95)(11.9)] \qquad \text{(Eq. 20)}$$

$$-\log X_2 = 0.73902 \qquad \text{(Eq. 21)}$$

with $X_2$(calc) = 0.182 and $X_2$(obs) = 0.171 (4) and 0.176 (10).

The calculated values for the solubility using $\delta_2$, $K$, and $A'$ are within 5–25% of the observed solubility. The method was tested with polar drugs, such as the methyl xanthines, in different mixtures of polar solvents, and the results were less satisfactory; $\delta_2$ values sometimes are obtained that do not correspond well with values obtained from the peak solubility method[4].

In an earlier study[1], a somewhat different regression method was employed using the results of Restaino and Martin (4) to obtain estimates of $\delta_2$ and the molar volume of the solute, $V_2$. Satisfactory $\delta_2$ values were calculated, but the method failed to produce reasonable $V_2$ values. This result may have been due to the creation, through regression methodology, of an empirical $A'$ term, as noted, which involves the molar volume of the solute.

## CONCLUSION

The present approach provides a convenient means of obtaining solubility parameters and $K$ values from solubility data for parabens in normal alkanols. It yields a normalization parameter, $D$, which provides unit coefficients for $\delta_1^2$ and $\delta_2^2$, and $D$ is multiplied by the $A$ term of the solubility equation ($AD = A'$) to yield the correct value of log $\alpha_2$. The log $\alpha_2$ calculated in this way, together with the ideal solubility of a drug, provides good estimates of the solubility of paraben derivatives in a series of normal alcohols. In studies to be reported later, the method gave satisfactory results for drugs in hydrocarbons and less acceptable values in binary mixtures of polar solvents.

## REFERENCES


(1) J. H. Hildebrand and R. L. Scott, "The Solubility of Nonelectrolytes," Dover, New York, N.Y., 1964.

(2) G. Scatchard, *Chem. Rev.*, **8**, 321 (1931).

(3) M. J. Chertkoff and A. Martin, *J. Am. Pharm. Assoc., Sci. Ed.*, **49**, 444 (1960).

(4) F. A. Restaino and A. Martin, *J. Pharm. Sci.*, **53**, 636 (1964).

(5) K. C. James, C. T. Ng, and P. R. Noyce, *ibid.*, **65**, 656 (1976).

(6) E. E. Walker, *J. Appl. Chem.*, **2**, 470 (1952).

(7) A. Martin, J. Newburger, and A. Adjei, *J. Pharm. Sci.*, **68**(10), IV (1979).

(8) *Ibid.*, **69**, 487 (1980).

(9) A. Adjei, J. Newburger, and A. Martin, *J. Pharm. Sci.*, **69**, 659 (1980).

(10) K. S. Alexander, J. W. Mauger, H. Petersen, Jr., and A. N. Paruta, *ibid.*, **66**, 42 (1977).

(11) C. Sungwoo and H. Eisen, *ibid.*, **60**, 238 (1971).


## ACKNOWLEDGMENTS


Funds for the study were obtained from the professorship provided to A. Martin by Coulter R. Sublett.

The authors thank A. N. Paruta for permission to use the data of Ref. 10. They also thank A. Adjei for assistance and Terri Shrode for secretarial support.


[4] A. Martin, unpublished results.

# Calculating Number and Surface Area of Liposomes in Any Suspension

**CHARLES PIDGEON and C. ANTHONY HUNT** ˣ

Received May 23, 1980, from the *School of Pharmacy, University of California, San Francisco, CA 94143.* Accepted for publication August 1, 1980.

**Abstract** □ Simple formulas for calculating the total surface area and number of liposomes in any liposome population are presented. The necessary parameters for calculating these values are the encapsulation ratio (or efficiency) of the population, the partial specific volume of the lipids used to prepare the liposomes, and an estimate of the frequency distribution of the population. When tested on theoretical liposome populations, excellent results are obtained regardless of the heterogeneity of the population.

**Keyphrases** □ Liposomes—simple formulas for calculating number and surface area of liposomes, heterogeneous populations □ Drug delivery systems, potential—liposomes, simple formulas for calculating number and surface area □ Models, mathematical—simple formulas for calculating number and surface area of liposomes

Liposome is the generic term for any lipid bilayer vesicle that traps a volume of water, regardless of its size, composition, and number of lamellae (Fig. 1). In part, because of their ability to entrap and transport drugs *in vivo*, liposomes have been studied extensively.

The disposition properties of intravenously injected liposomes are complicated and depend in part on size (1), dose (2–4), charge (1, 4), number of particles, and total surface area. Pharmacological experiments based solely on the number of particles and total surface area have not been pursued because these parameters are not easily estimated for a given vesicle population. Although dose and size taken together are related to the number of particles and surface area, the tendency of liposome populations to be heterogeneous allows for differences in number and surface area for any given total lipid dose. Even for homogeneously sized vesicles, the relationships among dose, size, number, and surface area are ambiguous.

Methods for estimating the number of particles and surface area for solid spheres are available (5, 6), but liposomes are not solid spheres. A method is presented here for calculating the number and total surface area for any liposome population given the liposome encapsulation efficiency, an estimate of the liposome frequency *versus* radius distribution, and the total effective volume of lipid used to prepare the vesicles.

## THEORETICAL

Any given liposome population, whether artificially generated or real, may be classified into one of three categories: a homogeneous population, a fixed-lamella, variable-radius population, or a heterogeneous population. The liposomes in a homogeneous population are the same in every parameter, *i.e.*, radius, surface area, and number of layers if multilamellar. An example of this type of population is unilamellar liposomes that have been sized carefully (6). A fixed-lamella, variable-radius population is similar to a homogeneous population in that the lipid bilayer and water layer thicknesses are the same in all liposomes, but the number of repeating water–lipid layers and, consequently, the liposome radii vary between liposomes. In contrast, a heterogeneous liposome population is the most diverse; every liposome parameter can differ within and between vesicles.

The properties of each population can be rigorously described

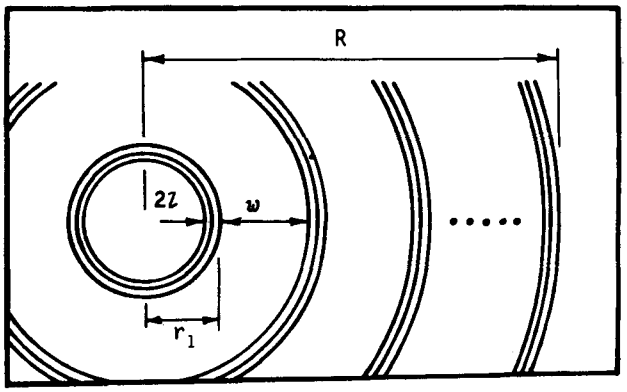


**Figure 1**—*Schematic drawing of liposome structure. Each multilamellar liposome consists of* n *lamellae, each of which is composed of a lipid bilayer of thickness 2l. Each lamella alternates with water layers of average thickness* w*; the core lamella forms a unilamellar liposome of radius* $r_1$ *(Eq. 19).*

mathematically. The volume of water encapsulated in a unilamellar (single-layered) liposome, $VW_1$, is:

$$VW_1 = \frac{4}{3}\pi R^3 - VL_1 \qquad \text{(Eq. 1)}$$

where $VL_1$ is the volume of lipid in the single-layered liposome and $R$ is the effective outside radius. If a second layer of water and lipid is added, then:

$$VW_2 = \frac{4}{3}\pi R^3 - VL_2 \qquad \text{(Eq. 2)}$$

where $VW_2$ is the volume of water encapsulated in a bilamellar liposome and $VL_2$ is the volume of lipid required for its formation. Equation 2 can be generalized for a $n$-lamellar liposome (Fig. 1) as:

$$VW_n = \frac{4}{3}\pi R^3 - VL_n \qquad \text{(Eq. 3)}$$

In a homogeneous population, the values of $VW_n$ and $VL_n$ are identical between vesicles. Therefore, multiplying Eq. 3 by the number of liposomes in the population, $N$, gives the total volume of trapped water $TVW$:

$$TVW = NVW_n = N\frac{4}{3}\pi R^3 - NVL_n = N\frac{4}{3}\pi R^3 - TVL \qquad \text{(Eq. 4)}$$

where $TVL$ is the total effective volume of lipid used to prepare the liposome population. $TVL$, in turn, is calculated from:

$$TVL = \bar{v}M(\overline{MW}) \qquad \text{(Eq. 5)}$$

where $\bar{v}$ is the partial specific volume, $M$ is the number of moles, and $\overline{MW}$ is the average molecular weight of the hydrated lipids. Dividing Eq. 4 by Eq. 5 and defining the encapsulation ratio (or efficiency), $E$, as the ratio of the entrapped water volume to the total volume of lipid yield:

$$E = \frac{\frac{4}{3}\pi NR^3}{TVL} - 1 \qquad \text{(Eq. 6)}$$

Solving Eq. 6 for $N$ gives:

$$N = \frac{(E+1)TVL}{\frac{4}{3}\pi R^3} \qquad \text{(Eq. 7)}$$

Equation 7 is derived for a homogeneous population of liposomes where

0022-3549/81/0200-0173$01.00/0
© 1981, American Pharmaceutical Association

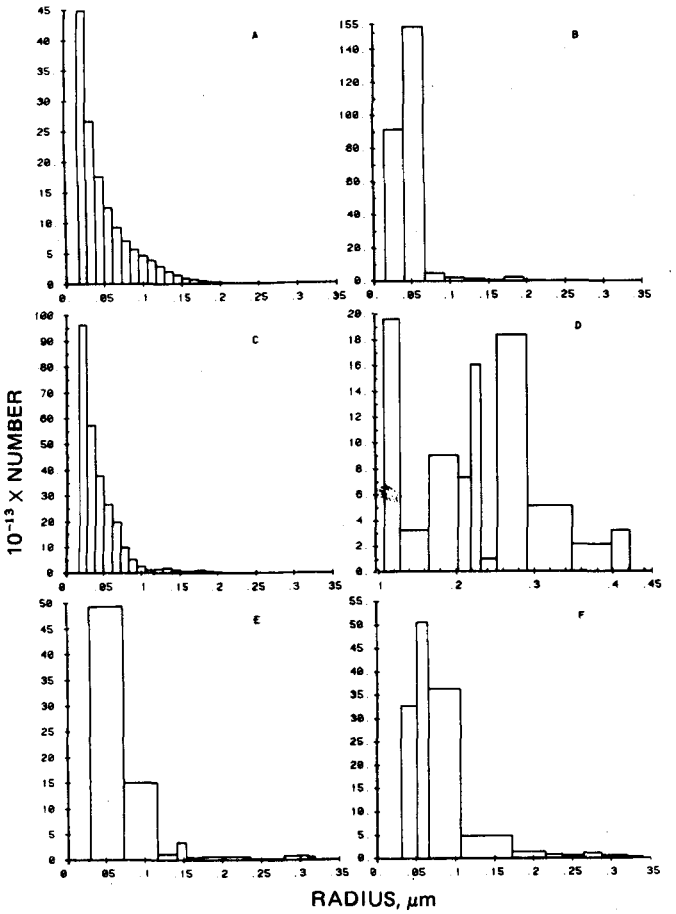


**Figure 2**—*Frequency* versus *radius for six hypothetical liposome populations used to illustrate the validity of Eqs. 15 and 18. In each frame, the number of liposomes in each subpopulation of fixed radius is indicated. Each liposome population is composed of 1 mmole of lipid, and each bar represents a homogeneous subpopulation. The variable liposomal parameters used to construct each population were described in the text. Key: A,* w = *7.4 nm and* $r_1$ = *22.5 nm, with* n *ranging from one to 18 in steps of one; B,* w = *92.5 nm and* $r_1$ = *15 nm, with* n *ranging from two to 18 in steps of two; C,* w = *7.4 nm and* $r_1$ = *22.5 nm, with* n *ranging from one to 18 in steps of one; D,* w *ranges from 7.4 to 333 nm and* $r_1$ *ranges from 15 to 100 nm, with* n *ranging from eight to 15 (values shown on the ordinate are reduced by a factor of 10); E,* w *ranges from 7.4 to 333 nm and* $r_1$ *ranges from 15 to 80 nm, with* n *ranging from two to 18; and F,* w *ranges from 7.4 to 259 nm and* $r_1$ *ranges from 15 to 80 nm with* n *ranging from two to 14.*

every liposome parameter is identical between liposomes. If many homogeneous subpopulations are combined to give a heterogeneous population or a fixed-lamella, variable-radius population, Eq. 7 will hold for each $i$th subpopulation and can be rewritten as:

$$N_i = \frac{(E_i + 1)TVL_i}{\frac{4}{3}\pi R_i^3} \qquad \text{(Eq. 8)}$$

Rearranging Eq. 8 and summing the subpopulations up to the $k$th population give:

$$\frac{4}{3}\pi \sum_{i=1}^{k} N_i R_i^3 = \sum_{i=1}^{k} (E_i + 1)TVL_i = \sum_{i=1}^{k} E_i TVL_i + \sum_{i=1}^{k} TVL_i \qquad \text{(Eq. 9)}$$

Recognizing that $\Sigma_{i=1}^{k} TVL_i$ is the total volume of lipid in the entire population, one can write Eq. 9 as:

$$\frac{\frac{4}{3}\pi \sum_{i=1}^{k} N_i R_i^3}{TVL} = \frac{\sum_{i=1}^{k} E_i TVL_i}{TVL} + 1 \qquad \text{(Eq. 10)}$$

Since $TVL_i/TVL$ is the mole fraction, $x_i$, of lipid in the $i$th population,

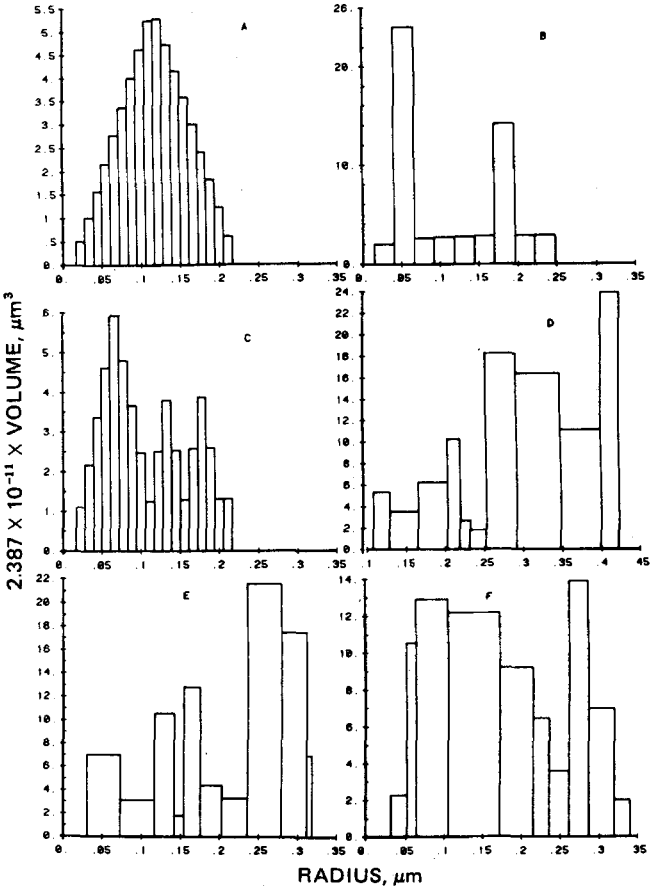


**Figure 3**—*Volume* versus *radius for the same liposome populations shown in Fig. 2 (*$10^{-10}/[(4/3)\pi] = 2.387 \times 10^{-11}$*). Each bar gives the total volume in cubic micrometers (*$10^{11}$ $\mu m^3$ = *0.1 ml) of a homogeneous subpopulation of fixed radius.*

Eq. 10 can be rewritten as:

$$\frac{\frac{4}{3}\pi \sum_{i=1}^{k} N_i R_i^3}{TVL} = \sum_{i=1}^{k} x_i E_i + 1 \qquad \text{(Eq. 11)}$$

The encapsulation efficiency of the entire population, $E_p$, is equal to $\Sigma_{i=1}^{k} x_i E_i$; therefore, Eq. 11 reduces to:

$$\sum_{i=1}^{k} N_i R_i^3 = \frac{(E_p + 1)TVL}{\frac{4}{3}\pi} \qquad \text{(Eq. 12)}$$

Dividing both sides of Eq. 12 by $\Sigma_{i=1}^{k} N_i = N_p$ and rearranging give:

$$N_p = \frac{(E_p + 1)TVL}{\left(\frac{4}{3}\pi \sum_{i=1}^{k} N_i R_i^3\right) \Big/ \sum_{i=1}^{k} N_i} \qquad \text{(Eq. 13)}$$

where the term $(4/3)\pi\Sigma_{i=1}^{k} N_i R_i^3$ is the total volume of all liposomes in the entire population; therefore, $[(4/3)\pi\Sigma_{i=1}^{k} N_i R_i^3]/\Sigma_{i=1}^{k} N_i$ is the average volume per liposome. This average volume can be calculated directly from a frequency *versus* radius distribution of the population obtained from electron micrographs (7). It follows that the liposome with the average volume will have a radius $r_{\bar{v}}$ as is given in:

$$\frac{\frac{4}{3}\pi \sum_{i=1}^{k} N_i R_i^3}{\sum_{i=1}^{k} N_i} = \frac{4}{3}\pi r_{\bar{v}}^3 \qquad \text{(Eq. 14)}$$

Substitution of Eq. 14 into Eq. 13 gives:

$$N_p = \frac{(E_p + 1)TVL}{\frac{4}{3}\pi r_{\bar{v}}^3} \qquad \text{(Eq. 15)}$$

Equation 15 allows the total number of liposomes to be calculated for any

**Table I—Typical Example [a] of a Complete Set of Properties for Homogeneous Liposome Subpopulations**

| $n$ | $R$, μm | $10^5\ vl_n$, μm³ | $10^5\ VL_n$, μm³ | $10^5\ vw_n$, μm³ | $10^5\ VW_n$, μm³ | $E$ | $10^{-14}\ N$ | $10^{-13}\ TSA$, μm² | $10^{-12}\ TVW$, μm³ |
|---|---|---|---|---|---|---|---|---|---|
| 1 | 0.0225 | 1.99 | 1.99 | 2.78 | 2.78 | 1.4 | 404 | 25.7 | 1.12 |
| 2 | 0.0336 | 4.69 | 6.68 | 6.43 | 9.21 | 1.38 | 120 | 17.0 | 1.11 |
| 3 | 0.0447 | 8.54 | 15.2 | 13.0 | 22.2 | 1.46 | 52.7 | 13.2 | 1.17 |
| 4 | 0.0558 | 13.5 | 28.8 | 21.8 | 44.0 | 1.53 | 27.9 | 10.9 | 1.23 |
| 5 | 0.0669 | 19.7 | 48.4 | 33.0 | 77.0 | 1.59 | 16.6 | 9.32 | 1.27 |
| 6 | 0.0780 | 26.9 | 75.4 | 46.4 | 123 | 1.64 | 10.6 | 8.13 | 1.31 |
| 7 | 0.0891 | 35.4 | 111 | 62.1 | 185 | 1.67 | 7.24 | 7.22 | 1.34 |
| 8 | 0.1002 | 45.0 | 156 | 80.1 | 265 | 1.70 | 5.15 | 6.50 | 1.37 |
| 9 | 0.1113 | 55.7 | 211 | 100 | 366 | 1.73 | 3.79 | 5.91 | 1.39 |
| 10 | 0.1224 | 67.6 | 279 | 123 | 489 | 1.75 | 2.87 | 5.41 | 1.41 |
| 11 | 0.1335 | 80.6 | 360 | 148 | 637 | 1.77 | 2.23 | 5.00 | 1.42 |
| 12 | 0.1446 | 94.7 | 454 | 175 | 812 | 1.79 | 1.76 | 4.64 | 1.43 |
| 13 | 0.1557 | 110 | 564 | 204 | 1020 | 1.80 | 1.42 | 4.33 | 1.44 |
| 14 | 0.1668 | 126 | 691 | 236 | 1250 | 1.81 | 1.16 | 4.06 | 1.45 |
| 15 | 0.1779 | 144 | 835 | 270 | 1520 | 1.82 | 0.961 | 3.82 | 1.46 |
| 16 | 0.1890 | 163 | 998 | 307 | 1830 | 1.83 | 0.804 | 3.61 | 1.47 |
| 17 | 0.2001 | 182 | 1180 | 345 | 2180 | 1.84 | 0.680 | 3.42 | 1.48 |
| 18 | 0.2112 | 204 | 1380 | 386 | 2560 | 1.85 | 0.579 | 3.25 | 1.48 |

[a] Each row gives the properties of a homogeneous, $n$-lamellar liposome population composed of 1 mmole of lipid ($8.0226 \times 10^{11}$ μm³). For this example, $w$, the thickness of each water layer ($n > 1$) is fixed at 7.4 nm; the outside radius of the innermost liposome is fixed at 22.5 nm. The column headings are defined in the text.

type of liposome population whenever valid measures of the parameters on either side of Eq. 14 can be obtained.

A similar expression can be obtained for calculating the total surface area of the population. Rearranging Eqs. 12 and 15 to:

$$\sum_{i=1}^{k} 4\pi N_i R_i^3 = 3(E_p + 1)TVL = 4\pi N_p r_{\bar{v}}^3 \qquad \text{(Eq. 16)}$$

and dividing by the total surface area of the population, $TSA_p$, gives:

$$\eta = \frac{r_{\bar{v}}^3}{r_{\bar{s}}^2} = \frac{3(E_p + 1)TVL}{TSA_p} = \frac{\sum_{i=1}^{k} 4\pi N_i R_i^3}{\sum_{i=1}^{k} 4\pi N_i R_i^2} \qquad \text{(Eq. 17)}$$

where:

$$TSA_p = \sum_{i=1}^{k} 4\pi N_i R_i^2 = 4\pi N_p r_{\bar{s}}^2$$

and $r_{\bar{s}}$ is the radius of the liposome with the average surface area and $\eta = r_{\bar{v}} = r_{\bar{s}}$ for a homogeneous population. Solving for $TSA_p$ and canceling terms give:

$$TSA_p = \frac{3(E_p + 1)TVL}{\left(\sum_{i=1}^{k} N_i R_i^3\right) \Big/ \sum_{i=1}^{k} N_i R_i} = \frac{3(E_p + 1)TVL}{\eta} \qquad \text{(Eq. 18)}$$

Thus, to calculate $N_p$ and $TSA_p$ for any liposome population, only four parameters ($E_p$, $TVL$, $r_{\bar{s}}$, and $r_{\bar{v}}$) are needed.

## RESULTS

**Data Generation**—Data to test Eqs. 15 and 18 were generated from lipid molecular parameters reported by Mason and Huang (8) for phosphatidylcholine liposomes. Briefly, data generation involved specifying the outside radius of the first lamella and the length of the lipid molecule and then calculating the volume of lipid and the volume of water in the liposome. The remaining liposome parameters were calculated, then another layer of water and lipid was added, and the same calculations were performed. Data tables thus were generated with 18 rows, each row corresponding to a homogeneous population of liposomes composed of 1 mmole of phospholipid. All liposome input and output parameters, along with the method of calculation, are outlined here.

The outside radius, $R$, in micrometers of any liposome (Fig. 1) is given by:

$$R = r_1 + (n - 1)(2l + w) \qquad \text{(Eq. 19)}$$

where $r_1$ is the outside radius of the first lamella (*i.e.*, the outside radius of the innermost liposome in a multilamellar liposome), $n$ is the number of lamella or lipid layers, $l$ is the average length of a lipid molecule (it is also one-half of the lipid bilayer thickness), and $w$ is the water layer thickness (only when $n \geq 2$).

The volume, in cubic micrometers, of lipid in the $n$th lamella or lipid layer, $vl_n$, is:

$$vl_n = \frac{4}{3}\pi[R^3 - (R - 2l)^3] \qquad \text{(Eq. 20)}$$

The volume, in cubic micrometers, of lipid in any $n$-lamellar liposome, $VL_n$, is:

$$VL_n = \sum_{i=1}^{n} vl_i \qquad \text{(Eq. 21)}$$

The volume of water in the $n$th aqueous compartment or layer, $vw_n$, is:

$$vw_n = \frac{4}{3}\pi\{[r_1 + (n - 1)w + 2l(n - 2)]^3 - [r_1 + (n - 2)w + (n - 2)2l]^3\} \qquad \text{(Eq. 22)}$$

The volume of water in any $n$-lamellar liposome, $VW_n$, is:

**Table II—Example [a] of Subpopulation Parameter Values Used to Construct Heterogeneous Liposome Populations**

| $10^4\ w$, μm | $10^4\ r_1$, μm | $n$ | $R$, μm | $10^{-14}\ N_i$ | $10^{-13}\ TSA_i$, μm² | $10^{-12}\ TVW_i$, μm³ | $X_i$ | $X_i\ 10^{-14}\ N_i$ | $X_i\ 10^{-13}\ TSA_i$, μm² | $X_i\ 10^{-11}\ TVW_i$, μm³ |
|---|---|---|---|---|---|---|---|---|---|---|
| 74 | 300 | 2 | 0.041 | 73.9 | 15.7 | 1.35 | 0.044 | 3.25 | 0.698 | 0.600 |
| 74 | 800 | 5 | 0.224 | 0.854 | 5.40 | 3.24 | 0.067 | 0.057 | 0.360 | 2.16 |
| 92.5 | 225 | 10 | 0.139 | 2.27 | 5.51 | 1.75 | 0.200 | 0.454 | 1.10 | 3.50 |
| 92.5 | 1400 | 6 | 0.205 | 0.974 | 5.12 | 2.69 | 0.111 | 0.108 | 0.569 | 2.99 |
| 111 | 150 | 4 | 0.059 | 28.3 | 12.5 | 1.68 | 0.178 | 5.03 | 2.22 | 2.99 |
| 111 | 2200 | 3 | 0.250 | 1.06 | 8.27 | 6.08 | 0.022 | 0.024 | 0.184 | 1.35 |
| 148 | 150 | 4 | 0.071 | 20.5 | 12.8 | 2.21 | 0.178 | 3.64 | 2.28 | 3.93 |
| 148 | 1000 | 14 | 0.341 | 0.231 | 3.37 | 3.02 | 0.022 | 0.005 | 0.075 | 0.670 |
| 185 | 300 | 12 | 0.274 | 0.505 | 4.77 | 3.56 | 0.133 | 0.067 | 0.636 | 4.75 |
| 259 | 1800 | 5 | 0.298 | 0.594 | 6.64 | 5.81 | 0.044 | 0.026 | 0.295 | 2.58 |
| Population value | | | | | | | 1.0 | 12.7 | 8.417 | 25.52 |

[a] These data are for population $F$ and correspond to Figs. 2F and 3F. This heterogeneous population is composed of 10 homogeneous subpopulations (each corresponding to one of the 10 rows and one bar in Figs. 1 and 2), where their relative proportion in the total population ($X_i$) is randomly selected. The total lipid concentration in each final heterogeneous population is 1 m$M$.

**Table III—Comparison of Actual Values of the Total Number and Total Surface Area with Values Calculated Using Eqs. 15 and 18, Respectively, for the Six Liposome Populations Shown in Figs. 2 and 3**

| Population | $r_{\bar{v}}$, μm | $\eta$, μm | $E_p$ | Actual Value of $N_p$ | Calculated Value of $N_p$ | Actual Value of $TSA_p$, μm² | Calculated Value of $TSA_p$, μm² |
|---|---|---|---|---|---|---|---|
| A | 0.0714 | 0.098 | 1.71 | $1.41 \times 10^{15}$ | $1.42 \times 10^{15}$ | $6.64 \times 10^{13}$ | $6.56 \times 10^{13}$ |
| B | 0.0604 | 0.079 | 1.96 | $2.58 \times 10^{15}$ | $2.57 \times 10^{15}$ | $9.04 \times 10^{13}$ | $9.00 \times 10^{13}$ |
| C | 0.0579 | 0.080 | 1.66 | $2.62 \times 10^{15}$ | $2.62 \times 10^{15}$ | $7.99 \times 10^{13}$ | $8.00 \times 10^{13}$ |
| D | 0.2272 | 0.260 | 4.19 | $8.48 \times 10^{13}$ | $8.48 \times 10^{13}$ | $4.79 \times 10^{13}$ | $4.80 \times 10^{13}$ |
| E | 0.1072 | 0.156 | 3.64 | $7.21 \times 10^{14}$ | $7.21 \times 10^{14}$ | $7.14 \times 10^{13}$ | $7.16 \times 10^{13}$ |
| F | 0.0857 | 0.119 | 3.18 | $1.27 \times 10^{15}$ | $1.27 \times 10^{15}$ | $8.42 \times 10^{13}$ | $8.40 \times 10^{13}$ |

$$VW_n = \sum_{i=1}^{n} vw_i \qquad \text{(Eq. 23)}$$

The total volume of lipid used is given by Eq. 5 and by:

$$TVL = (6.023 \times 10^{23})Ml\alpha \qquad \text{(Eq. 24)}$$

where $M$ is the number of moles of lipid used and $\alpha$ is the area per lipid molecule.

Approximately 3500 homogeneous liposome populations were generated. A typical set of homogeneous liposome populations with the number of lamella ranging from one to 18 is given in Table I.

Fixed-lamella, variable-radius populations were generated by combining an entire data table such as Table I. Each row of the table was generated using 1 mmole of lipid. So that the final fixed-lamella, variable-radius population also would contain only 1 mmole of lipid, each row in the table was multiplied by $X_i$, the fraction of the total lipid contained in the $i$th homogeneous subpopulation, where $\Sigma X_i = 1$ for each fixed-lamella, variable-radius population. Three examples of such populations are included in Figs. 2 and 3.

Since $w$ and $r_1$ in Eq. 19 are constant in any one data table, combining rows from different data tables allows generation of heterogeneous populations composed of $i$ homogeneous populations. Again, $X_i$ is the fraction of the total lipid contained in the $i$th homogeneous population (values of $X_i$ were selected at random). Table II is an example of one heterogeneous population in Figs. 2 and 3.

**Testing of Eqs. 15 and 19**—Six heterogeneous populations were generated (Figs. 2 and 3). Each population was treated as if it were a sample of a larger population. For each population, the total volume of lipid, $TVL$, was the same and was calculated from Eq. 5, where $\bar{v} = 1$ ml/g $= 10^{12}$ μm³/g, $M = 10^{-3}$ (or 1 mmole), and $\overline{MW} = 802.26$ g/mole; thus, $TVL = 8.0226 \times 10^{11}$ μm³/mmole. The encapsulation ratio, $E_p$, for each population was calculated as the ratio of $TVW$ to $TVL$, $r_{\bar{v}}$ was calculated from Eq. 14, and $\eta$ was calculated from Eq. 17. Actual and calculated values of $N_p$ and $TSA_p$ for the six liposome populations in Figs. 2 and 3 are compared in Table III.

## DISCUSSION

Whenever liposomes are used as drug delivery systems, either *in vivo* or *in vitro*, the number and surface area of the liposomes should be known. These parameters can be calculated using Eqs. 15 and 18. Number and surface area values from Eqs. 15 and 18 are theoretically exact as was demonstrated in Table III, regardless of the population heterogeneity. However, experimental estimates of the parameters $E_p$, $TVL$, $r_{\bar{v}}$, and $r_{\bar{s}}$ will have associated error, which will be reflected in the final values of number and surface area. Thus, how the estimates of the four dependent variables in Eqs. 15 and 18 are obtained should be discussed. It is assumed that estimates of number and surface area within 90% of the actual values can be obtained and are adequate for most purposes.

The encapsulation ratio is defined as the ratio of the total volume of trapped water to the total volume of lipid. Typically, however, the encapsulation ratio is measured relative to some solute; *e.g.*, $X$% of an aqueous glucose solution is encapsulated by $Y$ moles of lipid. When it is known that the solute does not interact with the lipid bilayer, the general assumption is that the encapsulated concentration of solute is the same as in the original solution; therefore, the encapsulated volume of aqueous phase can be calculated directly. For inert solutes, this assumption is generally reasonable. The exceptions are small unilamellar liposomes (8) and poorly hydrated multilamellar liposomes in which the water of hydration, which may exclude the solute somewhat, is a significant fraction of the total encapsulated aqueous phase. This should not be the case as long as $E_p \geq 1.0$.

The value of the partial specific volume of the hydrated lipids (Eq. 5) will never be significantly less than or greater than unity. For example, the value for phosphatidylcholine is 0.98 (8). A reasonable assumption is that $\bar{v} = 1$ (9, 10), even though the area and volume per molecule in mixed lipid liposomes can vary substantially. Thus, the total volume of lipid can be approximated reasonably by the total mass of lipid used, regardless of the molecular weights of the component lipids.

An estimate of the frequency *versus* size distribution is essential for these calculations. This estimate can be obtained by electron microscopy using either negative stain or freeze–fracture techniques. Olson *et al.* (7) showed that both procedures give essentially the same frequency *versus* size distributions over a wide range of liposome diameters. (They also discussed the limitations of both techniques.) Estimates of both $r_{\bar{v}}$ and $\eta$ are obtained directly from the electron photomicrographs of the liposome sample. An estimate of $r_{\bar{v}}$ also can be obtained using laser light-scattering techniques (11). The value of $r_{\bar{v}}$ is calculated using Eq. 14, and the value of $\eta$ is calculated from:

$$\eta = \frac{\sum_{i=1}^{k} N_i R_i^3}{\sum_{i=1}^{k} N_i R_i^2} \qquad \text{(Eq. 25)}$$

where $k$ is the sample size.

## REFERENCES


(1) R. L. Juliano and D. Stamp, *Biochem. Biophys. Res. Commun.*, **63**, 651 (1975).

(2) D. H. Haynes and C. H. Kang, *Ann. N.Y. Acad. Sci.*, **308**, 440 (1978).

(3) G. Gregoriadis, E. D. Neerunjum, and R. Hunt, *Life Sci.*, **21**, 357 (1977).

(4) H. K. Kimelberg and E. G. Mayhew, *Crit. Rev. Toxicol.*, **6**, 25 (1978).

(5) J. M. DallaValle, "Micromeritics," 2nd ed., Pitman, New York, N.Y., 1948, pp. 41–95.

(6) C. Orr and J. M. DallaValle, "Fine Particle Measurement," Macmillan, New York, N.Y., 1959, pp. 13–42.

(7) F. Olson, C. A. Hunt, F. C. Szoka, W. J. Vail, and D. Papahadjopoulos, *Biochim. Biophys. Acta*, **557**, 9 (1979).

(8) J. T. Mason and C. Huang, *Ann. N.Y. Acad. Sci.*, **308**, 29 (1978).

(9) G. C. Newman and C. Huang, *Biochemistry*, **14**, 3363 (1975).

(10) C. Huang and J. P. Charlton, *J. Biol. Chem.*, **246**, 2555 (1971).

(11) J. C. Selser, Y. Yeh, and R. J. Baskin, *Biophys. J.*, **16**, 337 (1976).


## ACKNOWLEDGMENTS


Supported in part by Public Health Service Grants GM-24612 and GM-26691.

The authors thank Mark Bosworth, Robert Abra, and D. Papahadjopoulos for helpful discussions and Elma P. Belenson for help in preparing this manuscript.

All calculations were obtained with the PROPHET computer system sponsored by the Chemical/Biological Information-Handling Program, Division of Research Resources, National Institutes of Health.

# High-Performance Liquid Chromatographic Determination of Hydrocortisone Cypionate: Method Development and Characterization of Chromatographic Behavior

**J. W. MUNSON** [x] **and T. D. WILSON** [*]

Received May 2, 1980, from *Quality Control, The Upjohn Company, Kalamazoo, MI 49001.* Accepted for publication August 1, 1980. [*]Present address: Vick Research and Development, Mt. Vernon, NY 10553.

**Abstract** □ A reversed-phase high-performance liquid chromatographic method for hydrocortisone cypionate bulk drug and oral solution was developed that avoids the use of a heated column as described in USP XX. A study of the effect of the organic modifier concentration on the capacity factor suggests that mixed partition and adsorption phenomena are responsible for the retention of several steroids when acetonitrile is used in the mobile phase. Evidence is presented that hydrogen bonding of the solute molecule with silane hydroxyl groups may be responsible for the adsorption.

**Keyphrases** □ Hydrocortisone cypionate—high-performance liquid chromatographic analysis, bulk drug and oral solution, chromatographic behavior evaluated □ High-performance liquid chromatography—hydrocortisone cypionate in bulk and oral solution, chromatographic behavior evaluated □ Adsorption—effect of organic modifier on steroid retention, high-performance liquid chromatographic analysis of hydrocortisone cypionate

Hydrocortisone cypionate[1] (21-cyclopentylpropionyl ester of hydrocortisone, I) is described in USP XX (1) and is marketed as an oral suspension[2]. The compendial assay for potency requires a 1-m column packed with macroparticulate octadecylsilane and heated to 60°. Under the conditions employed in this method [mobile phase of 25% (v/v) methanol in water], the analyte does not elute in a convenient time at 25°. Although heating to 60° allows for an acceptable analysis time, it is inconvenient since a column oven capable of accepting a 1-m column is necessary.

A stability-indicating assay was developed that utilizes a microparticulate octadecylsilane column at ambient temperatures. The chromatographic behavior of I along with other nonpolar steroids was examined. Evidence is provided that suggests that the separations are not governed totally by partition mechanisms.

## BACKGROUND

Hydrocortisone cypionate (I) is derived from the condensation of hydrocortisone alcohol and a cyclopentylpropionic acid derivative. Consequently, hydrocortisone represents a potential process impurity. Furthermore, hydrocortisone is a potential degradation product arising from ester hydrolysis. The C-11 oxidation product, cortisone cypionate (II), is another potential degradation product. The conversion of 11$\beta$-ols to 11-ones by air oxidation in the crystalline state first was observed in C-20-epimeric 11$\beta$-hydroxy-17,20-acetonido-21-acetates (III) (2).

In this study, it was observed that the 21-acetoxy group was necessary for air oxidation of the 11$\beta$-ol since the corresponding 21-ol was stable. This phenomenon also was observed in samples of hydrocortisone 21-*tert*-butyrate, hydrocortisone 21-valerate, hydrocortisone 21-stearate, and hydrocortisone 21-cypionate (3). However, oxidation of the 11$\beta$-ol was not observed or induced in aged samples (15–17 years old) of the 21-pivalyl, acetyl, and propionyl esters of hydrocortisone. The crystalline steroid form played a major role in sensitivity to air oxidation. Consequently, a stability-indicating assay should distinguish between hydrocortisone cypionate and its possible degradation products, hydrocortisone and cortisone cypionate.

The retention of nonpolar steroids, such as I and II, in reversed-phase high-performance liquid chromatographic (HPLC) systems generally is held to be due to the distribution of the analyte between the stationary and mobile phases. In such cases, the capacity factor, $k'$ (also called the capacity ratio), is given by:

$$k' = \frac{[X]_s}{[X]_m}\frac{V_s}{V_m} \qquad \text{(Eq. 1)}$$

where $[X]_s$ and $[X]_m$ represent the analyte concentration in the stationary and mobile phases, respectively, and $V_s$ and $V_m$ are the total volumes of each phase in the column. This equation assumes ideal behavior in dilute solutions and, hence, neglects activity coefficients. Solubility parameter theory (4, 5) states that the distribution of the analyte between the two phases is related to the Hildebrand solubility parameters of the analyte ($\delta_x$), stationary ($\delta_s$), and mobile ($\delta_m$) phases and to the total volume of the analyte ($\overline{V}_x$) as shown by:

$$\log\frac{[X]_s}{[X]_m} = \overline{V}_x\frac{[(\delta_x-\delta_m)^2-(\delta_s-\delta_x)^2]}{2.3RT} \qquad \text{(Eq. 2)}$$

where $R$ is the gas constant and $T$ is the absolute temperature.

The $\delta$ values vary linearly with the solvent composition for binary solvent mixtures. Thus, the solubility parameter for the mobile phase can be expressed as:

$$\delta_m = \delta_a + (\delta_b - \delta_a)C \qquad \text{(Eq. 3)}$$

where $\delta_a$ and $\delta_b$ are the solubility parameters of the two components of the solvent mixtures and $C$ is the concentration (mole fraction) of solvent $b$ in this mixture (solvent $b$ is the stronger solvent in terms of eluting power). Substitution of Eq. 3 into Eq. 2 gives:

$$\log k' = \log\frac{V_s}{V_m} + \frac{\overline{V}_x}{2.3RT}[(\delta_x-\delta_a)^2-(\delta_s-\delta_x)^2] - \frac{2\overline{V}_x}{2.3RT}(\delta_x-\delta_a)(\delta_b-\delta_a)C + \frac{\overline{V}_x}{2.3RT}(\delta_b-\delta_a)^2C^2 \qquad \text{(Eq. 4)}$$

By assuming that the term containing the $C^2$ term can be ignored, a first-order approximation can be written as:

$$k' = k_0'10^{-nc} \qquad \text{(Eq. 5)}$$

where $k_0'$ and $n$ are constants that contain the terms $V_s$, $V_m$, $\overline{V}_x$, $\delta_x$, $\delta_a$, $\delta_s$, and $2.3RT$ (6).

Equation 5 suggests that a plot of $\log k'$ *versus* $C$ will be linear with a slope of $-n$ and an intercept of $\log k_0'$. This behavior was observed in a study of the elution of 2-ethyl-9,10-anthraquinone, chloronaphthalene, halogenated benzenes, fused-ring aromatics, and phthalate esters using methanol–water and dioxane–water mobile phases (7).

## EXPERIMENTAL

**Materials**—Medroxyprogesterone acetate, hydrocortisone cypionate (I), hydrocortisone, hydrocortisone acetate, and methylprednisolone acetate were USP or NF quality. Cortisone cypionate (II) was generated *in situ* from an aged sample of I. Fractions of the eluate containing the II peak were collected and dried. Electron-impact mass spectrometry of the residue gave a molecular ion at $m/z$ 484, consistent with that of II. Methanol and acetonitrile were glass distilled[3]. Deionized water was used for all mobile phases.

**Mobile Phases**—All mobile phases were prepared by measuring the

[1] Currently described as cortisol cypionate in USP XX.
[2] Fluid CORTEF, The Upjohn Co.
[3] Burdick & Jackson, Muskegon, Mich.

0022-3549/81/0200-0177$01.00/0
© 1981, American Pharmaceutical Association

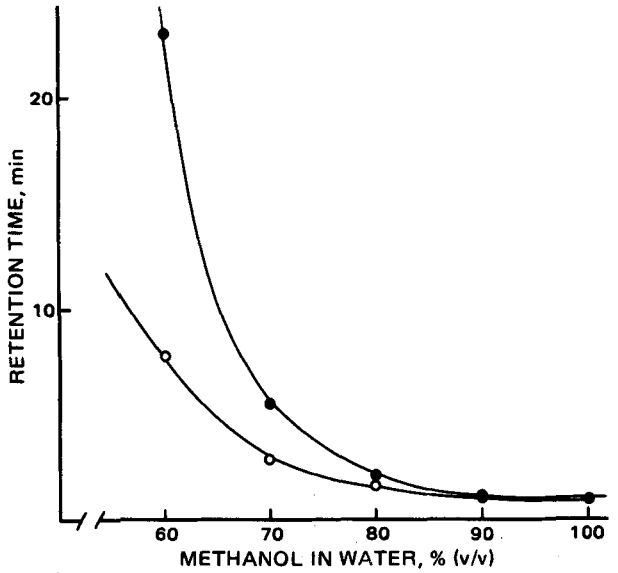


**Figure 1**—*Effect of the methanol concentration (percent volume to volume) in the mobile phase on the retention times of hydrocortisone cypionate (●) and medroxyprogesterone acetate (○).*

required quantity of the organic modifier in a 1-liter graduated cylinder followed by the addition of water to ~95% of the final volume. The mixtures then were allowed to equilibrate to room temperature before the final adjustment to volume was made. Degassing of the mobile phases was not necessary. To determine the mole fraction of the organic modifier in the mobile phase, water was added from a container of known volume so that volume changes due to mixing could be taken into account.

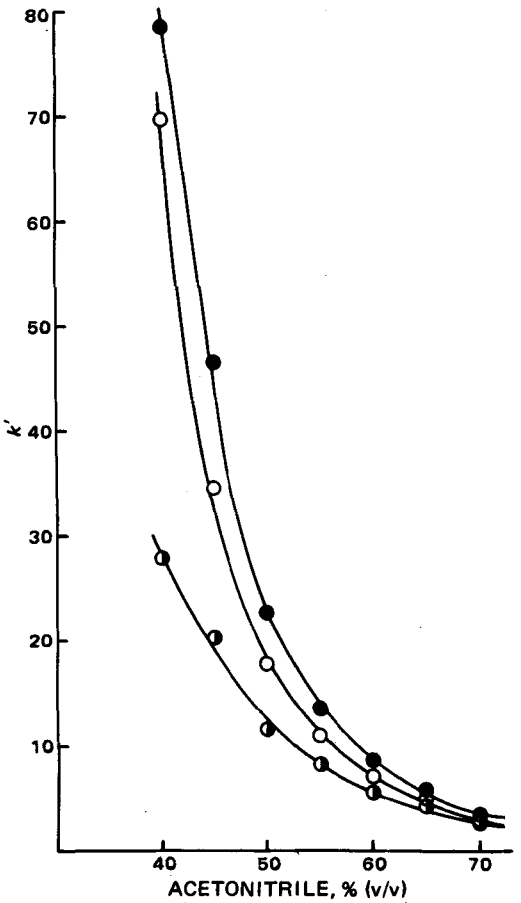


**Figure 2**—*Effect of the acetonitrile concentration on the capacity factors for medroxyprogesterone acetate (◑), hydrocortisone cypionate (○), and cortisone cypionate (●).*

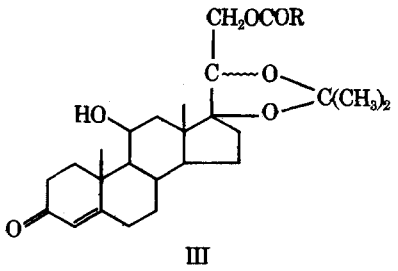


III

**Instrumentation**—The HPLC system was described previously (8).

**Quantitative Procedure for I in Oral Suspensions**—A volume of the suspension, equivalent to 12–15 mg of I, was transferred accurately to a suitable container. The internal standard solution (15.0 ml, 0.4 mg of medroxyprogesterone acetate in acetonitrile/ml) was added, and the solution was shaken for 90 min. The phases were allowed to separate, and 25-μl aliquots of the clear supernate were chromatographed using a mobile phase of 50% (v/v) acetonitrile in water at a flow rate of ~2.0 ml/min. Samples of bulk drug were analyzed by mixing an accurately weighed quantity of drug (~15 mg) with 15.0 ml of the internal standard. Calculations are based on the measurement of the peak height ratios of a sample preparation to those of a standard preparation.

## RESULTS AND DISCUSSION

The initial purpose of this study was to develop a stability-indicating method that did not require a 1-m column heated to 60°. A study of the retention times of medroxyprogesterone acetate and I as a function of the methanol concentration in the mobile phase (at ambient temperatures) is shown in Fig. 1. While adequate resolution of the internal standard (medroxyprogesterone acetate) and I could be achieved at methanol concentrations of 65–70% (v/v), II was not even partially resolved from I until the methanol concentration was lowered to 50% (v/v). However, analysis times became prohibitively long with the microparticulate (10 μm) octadecylsilane[4] column (30 cm × 4 mm). At this point, methanol as an organic modifier was abandoned in favor of acetonitrile.

Acetonitrile gave adequate resolution of I, II, and the internal standard at a 50% (v/v) concentration (the initial concentration examined). A more

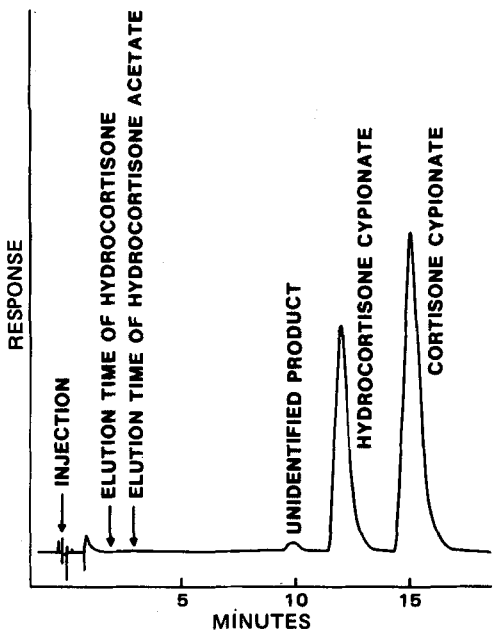


**Figure 3**—*Chromatographic tracing of hydrocortisone cypionate and cortisone cypionate showing the elution times of hydrocortisone and hydrocortisone acetate. Under these conditions, medroxyprogesterone acetate eluted at 8.8 min.*

[4] μBondapak $C_{18}$, Waters Associates, Milford, Mass.

**Table I—Linear Regression Data for Plot of log $k'$ *versus* log $C$ for Medroxyprogesterone Acetate, Hydrocortisone Cypionate (I), and Cortisone Cypionate (II)**

| Compound | Concentration of Acetonitrile in Mobile Phase | | | | | |
|---|---|---|---|---|---|---|
| | Percent (Volume to Volume) | | | Mole Fraction | | |
| | Slope | Intercept | Correlation Coefficient | Slope | Intercept | Correlation Coefficient |
| Medroxyprogesterone acetate | −4.08 | 8.00 | 0.9981 | −2.60 | −0.489 | 0.9986 |
| I | −5.40 | 10.47 | 0.9985 | −3.44 | −0.780 | 0.9948 |
| II | −5.56 | 10.82 | 0.9991 | −3.55 | −0.763 | 0.9981 |

complete study on the effect of the acetonitrile concentration indicated that adequate separations and reasonable retention times could be achieved between 45 and 55% (v/v) (Fig. 2). For example, under the final analytical conditions chosen (50% acetonitrile–water), II eluted within 20 min (Fig. 3). A plot of log $k'$ *versus* acetonitrile concentration (percent volume to volume) shows nonlinear behavior (Fig. 4). Equation 5 predicts that this plot should be linear. A similar plot using mole fraction on the $x$-axis displayed the same behavior. The data then were plotted in a log–log fashion. Excellent linearity was achieved (Table I) for acetonitrile expressed both as percent (volume to volume) and mole fraction. The same linear correlation of log $k'$ *versus* $C$ was obtained on two different columns from the same manufacturer.

To characterize further the correlations observed, a similar study was performed on three more polar steroids: hydrocortisone, hydrocortisone acetate, and methylprednisolone acetate. The plot of log $k'$ *versus* acetonitrile concentration (percent volume to volume) in the mobile phase for these three steroids is shown in Fig. 5. Once again, distinct curvature is observed whereas the data plotted as log $k'$ *versus* log $C$ give an excellent linear fit (Table II). These data suggest mechanisms other than retention by partitioning between the two phases.

A study using methanol as the organic modifier was performed to make sure that the observed behavior was not an artifact of the columns. In this case, excellent correlations of log $k'$ *versus* methanol concentration (percent volume to volume) were obtained (Fig. 6 and Table III). This behavior is as predicted by Eq. 5.

The behavior observed for acetonitrile is similar to many instances observed for adsorption chromatography. In adsorption chromatography, the distribution coefficient in a binary solvent system has been described as:

$$\log D_{ab} = \log D_a + \bar{\alpha} A_s(\epsilon_a^0 - \epsilon_{ab}^0) \qquad \text{(Eq. 6)}$$

where $D_{ab}$ is the distribution coefficient in the binary solvent system, $D_a$ is the distribution coefficient in a single solvent system $a$, $\bar{\alpha}$ is a measure of the adsorbent activity, $A_s$ is the molecular area of the adsorbed sample molecule on the adsorbent surface, and $\epsilon^0$ is the solvent strength parameter describing the influence of the solvent on adsorption (9). The term $\epsilon^0$ is independent of the nature of the adsorbent and the sample. Solvent $b$ is assumed to be a much stronger eluent than $a$ ($\epsilon_b^0 > \epsilon_a^0$).

Equation 6 was manipulated and simplifed to give:

$$k' = k_0' C^{-n} \qquad \text{(Eq. 7)}$$

where $k'$ is the capacity factor in the binary solvent system, $k_0'$ is the capacity factor in solvent system $b$, and $n$ is $A_s/n_b$ ($n_b$ is the effective molecular area of an adsorbed solvent molecule $b$). The relationship expressed in Eq. 7 was verified for lumisterol, tachysterol, calciferol, and ergosterol on Lichrosorb ALOX T with $n$-propanol–$n$-heptane mobile phases (10); indole alkaloids on silica with methylene chloride–diethylamine, chloroform–methanol, $n$-hexane–tetrahydrofuran, and tetrahydrofuran–methanol mobile phases (11); and steroids on silica with mobile phases consisting of 21 different binary mixtures (12).

The data presented in this paper suggest that the separation of steroids on certain microparticulate octadecylsilanes may not be due entirely to partitioning mechanisms and that adsorption phenomena may play a role. If so, adsorption phenomena would influence the degree of resolution obtained from such columns with differing carbon coverages of the silica surface. Therefore, different methods of bonding alkyl chains to the surface may give different chromatographic behavior for the same analytes with the same mobile phase when columns from different manufacturers are used. Thus, it is expected that the behavior observed in this study may not be found with columns that have a higher percentage of the silanol sites derivatized. The observed behavior is probably typical of column materials with a low carbon load (<10%).

The facile separation of I and II in mobile phases containing acetonitrile can be rationalized by considering an adsorption phenomenon. In some bonded octadecylsilane columns, only a small percentage of the silane hydroxyl groups on the particle surface are bonded covalently to the octadecylsilane group. Consequently, there may be numerous free silanol groups that can interact by hydrogen bonding with the mobile phase and analytes. In methanol–water mobile phases, all solvent molecules have the capacity for hydrogen bonding both as donors and acceptors. Thus, it is expected that interaction of the analyte molecules with the hydroxyl group is essentially swamped by the interaction of the mo-

**Table II—Linear Regression Data for Plot of log $k'$ *versus* log $C$[a] for Hydrocortisone, Hydrocortisone Acetate, and Methylprednisolone Acetate**

| Compound | Slope | Intercept | Correlation Coefficient |
|---|---|---|---|
| Hydrocortisone | −2.73 | 4.50 | 0.9984 |
| Hydrocortisone acetate | −3.53 | 6.23 | 0.9993 |
| Methylprednisolone acetate | −4.05 | 7.20 | 0.9995 |

[a] Concentration of acetonitrile in the mobile phase (percent volume to volume).

**Table III—Linear Regression Data for Plot of log $k'$ *versus* $C$[a] for Hydrocortisone, Hydrocortisone Acetate, and Methylprednisolone Acetate**

| Compound | Slope | Intercept | Correlation Coefficient |
|---|---|---|---|
| Hydrocortisone | −0.047 | 2.79 | 0.9982 |
| Hydrocortisone acetate | −0.057 | 3.31 | 0.9997 |
| Methylprednisolone acetate | −0.054 | 3.71 | 0.9987 |

[a] Concentration of methanol in the mobile phase (percent volume to volume).

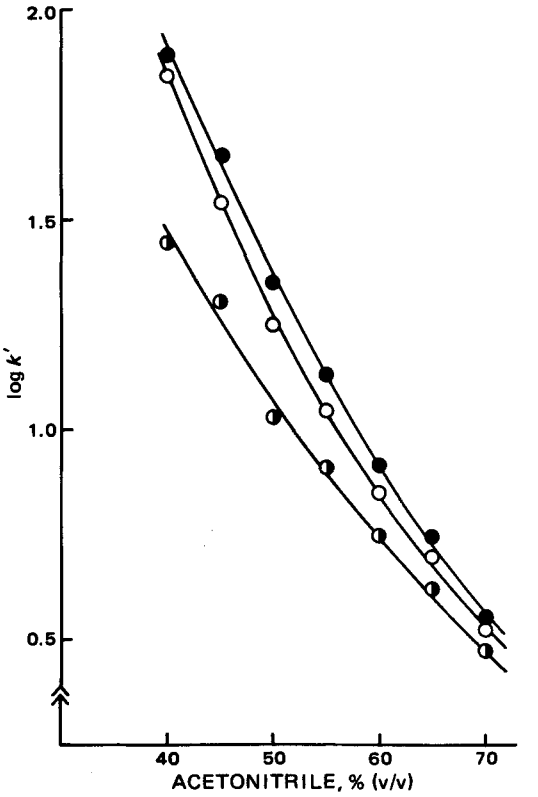


**Figure 4**—*Relationship of log* k′ *(capacity factor) and acetonitrile concentration for the steroids described in Fig. 2.*

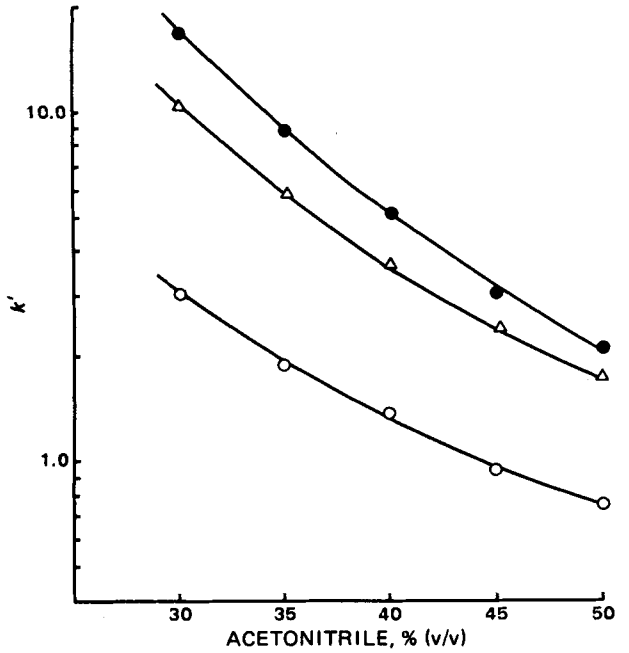


**Figure 5**—*Relationship of log* k′ *and acetonitrile concentration for hydrocortisone (○), hydrocortisone acetate (△), and methylprednisolone acetate (●).*

bile phase and these hydroxyl groups. Consequently, with methanol–water mobile phases, retention by adsorption mechanisms should not be evident. This behavior was confirmed for hydrocortisone, hydrocortisone acetate, and methylprednisolone (Fig. 7).

On the other hand, acetonitrile is an aprotic solvent and does not participate in hydrogen bonding. At high acetonitrile concentrations, a solvent environment can be created such that hydrogen bonding of the analytes with the silane hydroxyl groups will not be overcome by interactions with the solvents. This is apparently the case for I and II in the mobile phases that contain high concentrations of acetonitrile (in water). In Fig. 4, the curvature is more distinct at higher acetonitrile concentrations. Interaction of both I and II with the silane hydroxyl groups favor their separation since I contains a hydroxyl group at the 11-position while II possesses a keto group at the 11-position. While the 11-hydroxyl group of I can act as a hydrogen bond acceptor, it is expected that the carbonyl oxygen of the 11-keto group of II may be a stronger hydrogen bond acceptor because of the partial polarization of the carbonyl double bond. Thus, the greater retention of II in acetonitrile–water mixtures is reasonable based on these considerations.

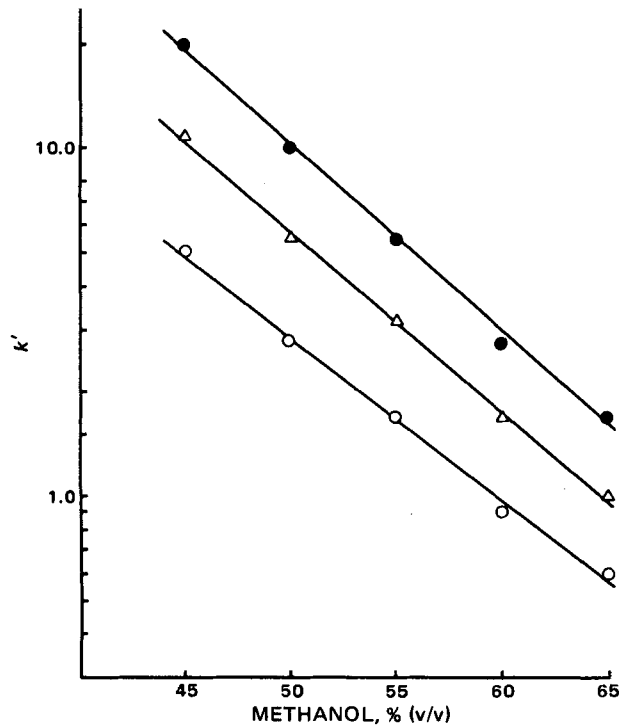


**Figure 6**—*Relationship of log* k′ *and the methanol concentration for the steroids described in Fig. 5.*

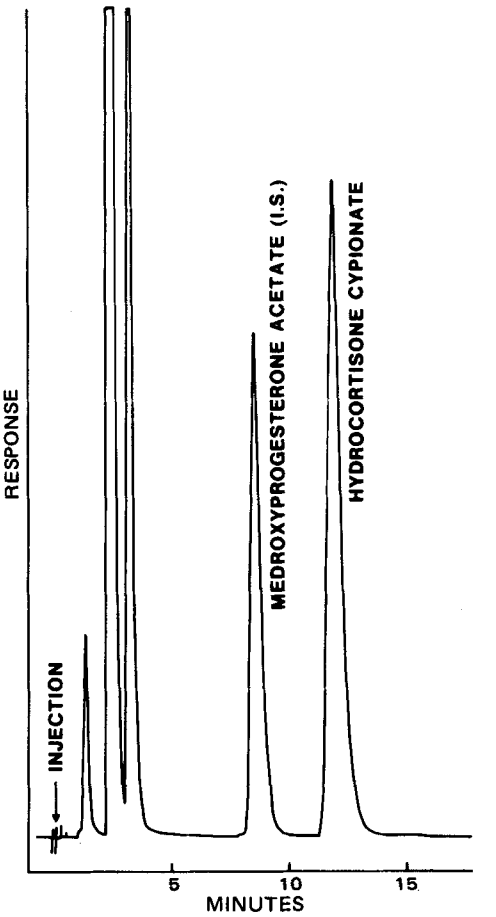


**Figure 7**—*Chromatographic tracing of typical sample preparation obtained from the oral suspension.*

To develop and validate an analytical method for I, a mobile phase of 50% (v/v) acetonitrile in water was chosen. This mobile phase gave adequate resolution of the analyte, internal standard, potential impurities, and degradation products within a reasonable time (Fig. 3). The unidentified product was present only in the aged sample of I and would not interfere with the internal standard peak that eluted at 9 min.

A chromatographic tracing of a typical sample preparation is shown in Fig. 7. The excipient peaks eluted early and did not interfere. Recovery from a spiked placebo was excellent (Table IV). The spiking levels ranged from 68 to 131% of the labeled amount of I. Replicate analyses of a single lot of oral suspension gave a mean value of 13.3 mg/5 ml with a relative standard deviation of 0.6% ($n$ = 6). Several lots of an aged product (>5 years old) were assayed and were in good agreement with theory (97–101%). Cortisone cypionate was not detected in any sample (detection limit of 0.3%), indicating that conversion by oxidation does not occur in an aqueous environment.

**Table IV—Recovery of Hydrocortisone Cypionate (I) from Spiked Placebo**

| Amount Added, mg/5 ml | Amount Found, mg/5 ml | Recovery, % |
|---|---|---|
| 9.05 | 9.11 | 100.7 |
| 10.39 | 10.39 | 100.0 |
| 13.52 | 13.50 | 99.8 |
| 15.11 | 15.03 | 99.5 |
| 17.57 | 17.42 | 99.1 |
| Mean | | 99.8 |

This method was applied to bulk drug samples, giving a relative standard deviation of <0.4% ($n = 5$).

In summary, the method presented here is rapid, stability indicating, precise, and accurate, and it is experimentally simpler than current compendial assays.

## REFERENCES


(1) "The United States Pharmacopeia," 20th rev., Mack Publishing Co., Easton, Pa., 1980.

(2) M. L. Lewbart, *Nature*, **222**, 663 (1963).

(3) G. Brenner, F. E. Roberts, A. Hoinowski, J. Budavari, B. Powell, D. Hinkley, and E. Schoenewaldt, *Angew. Chem., Int. Ed.*, **8**, 975 (1969).

(4) L. R. Snyder, in "Modern Practice of Liquid Chromatography," J. J. Kirkland, Ed., Wiley-Interscience, New York, N.Y., 1971, pp. 131–142.

(5) J. H. Hildebrand and R. L. Scott, "The Solubility of Non-Electrolytes," 3rd ed., Dover, New York, N.Y., 1964.

(6) P. Jandera and J. Churacek, *J. Chromatogr.*, **91**, 207 (1974).

(7) J. A. Schmit, R. A. Henry, R. C. Williams, and J. F. Dieckman, *J. Chromatogr. Sci.*, **9**, 645 (1971).

(8) E. J. Kubiak and J. W. Munson, *J. Pharm. Sci.*, **69**, 152 (1980).

(9) L. R. Snyder, "Principles of Adsorption Chromatography," Dekker, New York, N.Y., 1968.

(10) P. Jandera, M. Janderova, and J. Churacek, *J. Chromatogr.*, **148**, 79 (1978).

(11) S. Hara, N. Yamauchi, C. Nakae, and S. Saki, *Anal. Chem.*, **52**, 33 (1980).

(12) S. Hara, Y. Fujii, M. Hirasawa, and S. Miyamoto, *J. Chromatogr.*, **149**, 143 (1978).


## ACKNOWLEDGMENTS


The authors thank W. F. Beyer for the hydrocortisone cypionate sample that contained cortisone cypionate.


# Initial Rate Studies of Hydrolysis and Acyl Migration in Methylprednisolone 21-Hemisuccinate and 17-Hemisuccinate


**BRADLEY D. ANDERSON** ˣ **and VANESSA TAPHOUSE**



Received April 7, 1980, from *The Upjohn Company, Kalamazoo, MI 49001.* Accepted for publication July 25, 1980.



**Abstract** □ The degradation of methylprednisolone 21-succinate in aqueous solution was examined as a function of pH at 25° by monitoring the initial rates of product formation. In addition to hydrolysis, acyl migration from the 21-hydroxyl group to the 17-hydroxyl group was found to be an important reaction. The 17-succinate was isolated, and its decomposition to the 21-succinate was followed by the initial rate method. Direct hydrolysis of the 17-ester was much slower than the 17 → 21 acyl migration under alkaline conditions. From the rate constants for the forward and reverse acyl migration, it may be concluded that the 21-ester is thermodynamically more stable, even though its alkaline hydrolysis is faster. The hydrolysis of the 21-ester and the reversible rearrangement are subject to intramolecular catalysis by the terminal carboxyl group, for which a kinetic pKa value of 4.5–4.6 was estimated.



**Keyphrases** □ Methylprednisolone—17- and 21-succinates, hydrolysis and acyl migration, initial rate studies □ Hydrolysis—methylprednisolone 17- and 21-succinates, initial rate studies □ Degradation—methylprednisolone 17- and 21-succinates, hydrolysis and acyl migration, initial rate studies


Methylprednisolone 21-succinate (sodium salt[1]) is a soluble prodrug of methylprednisolone used as an injectable corticoid in acute hypersensitivity and dermatological conditions. Solubilization is achieved through the use of the ionizable hemisuccinate moiety, which is cleaved *in vivo* to release the active parent compound.

Previous studies of the kinetic behavior of this compound and similar compounds in aqueous solution generally focused on the hydrolytic cleavage of the ester linkage. Hydrolysis usually is regarded as the major degradation pathway of 21-steroid esters (1–3), followed by further decomposition *via* several routes (2, 4, 5). These kinetic studies were based on the results of nonspecific analytical methods such as the consumption of base (1) or extraction coupled with the blue tetrazolium assay (2) for measuring reaction rates.

In this study, the kinetics of methylprednisolone 21-hemisuccinate degradation were reexamined using a highly sensitive and specific high-performance liquid chromatographic (HPLC) technique. By monitoring the initial rates of product formation, data could be obtained easily at room temperature (25°) and at pH values where the reactions are quite slow. As a result of the improved analytical methodology, the role of acyl migration in the aqueous solution degradation of this steroid 21-ester and the isomeric 17-ester could be explored in addition to the hydrolysis reaction.

## EXPERIMENTAL

**HPLC Analysis**—A modular high-performance liquid chromatographic system consisting of an automated sample injector[2], a constant-flow pump[3] operated at 0.9–1.4 ml/min, a reversed-phase column[4] packed with 10-μm Lichrosorb RP-18[5], a variable-wavelength UV detector[6] operated at 248 nm, and a digital integrator[7] was used for all kinetic studies. The mobile phase contained 33% acetonitrile[8] and 67% water buffered at pH 5.2–5.4 with 0.05 *M* acetate buffer.

Under these chromatographic conditions, methylprednisolone 17-hemisuccinate was eluted first, followed by methylprednisolone and then by methylprednisolone 21-hemisuccinate. As will be discussed later, the retention times of the esters changed dramatically with small changes in the pH. Detector response, measured either as the peak area or peak height, was linear for all solution components over the concentration range of interest.

[1] Solu-Medrol (methylprednisolone sodium succinate), The Upjohn Co.

[2] Wisp model 710A, Waters Associates, Milford, Mass.
[3] Model 110A, Altex Scientific, Berkeley, Calif.
[4] Brownlee Laboratories, Berkeley, Calif.
[5] E. Merck, Darmstadt, West Germany.
[6] Altex/Hitachi model 153-00, Altex Scientific, Berkeley, Calif.
[7] Model 3380A, Hewlett-Packard, Avondale, Pa.
[8] Burdick & Jackson Laboratories, Muskegon, Mich.


0022-3549/81/0200-0181$01.00/0


© 1981, American Pharmaceutical Association

This method was applied to bulk drug samples, giving a relative standard deviation of <0.4% ($n = 5$).

In summary, the method presented here is rapid, stability indicating, precise, and accurate, and it is experimentally simpler than current compendial assays.

## REFERENCES


(1) "The United States Pharmacopeia," 20th rev., Mack Publishing Co., Easton, Pa., 1980.

(2) M. L. Lewbart, *Nature*, **222**, 663 (1963).

(3) G. Brenner, F. E. Roberts, A. Hoinowski, J. Budavari, B. Powell, D. Hinkley, and E. Schoenewaldt, *Angew. Chem., Int. Ed.*, **8**, 975 (1969).

(4) L. R. Snyder, in "Modern Practice of Liquid Chromatography," J. J. Kirkland, Ed., Wiley-Interscience, New York, N.Y., 1971, pp. 131–142.

(5) J. H. Hildebrand and R. L. Scott, "The Solubility of Non-Electrolytes," 3rd ed., Dover, New York, N.Y., 1964.

(6) P. Jandera and J. Churacek, *J. Chromatogr.*, **91**, 207 (1974).

(7) J. A. Schmit, R. A. Henry, R. C. Williams, and J. F. Dieckman, *J. Chromatogr. Sci.*, **9**, 645 (1971).

(8) E. J. Kubiak and J. W. Munson, *J. Pharm. Sci.*, **69**, 152 (1980).

(9) L. R. Snyder, "Principles of Adsorption Chromatography," Dekker, New York, N.Y., 1968.

(10) P. Jandera, M. Janderova, and J. Churacek, *J. Chromatogr.*, **148**, 79 (1978).

(11) S. Hara, N. Yamauchi, C. Nakae, and S. Saki, *Anal. Chem.*, **52**, 33 (1980).

(12) S. Hara, Y. Fujii, M. Hirasawa, and S. Miyamoto, *J. Chromatogr.*, **149**, 143 (1978).


## ACKNOWLEDGMENTS


The authors thank W. F. Beyer for the hydrocortisone cypionate sample that contained cortisone cypionate.


# Initial Rate Studies of Hydrolysis and Acyl Migration in Methylprednisolone 21-Hemisuccinate and 17-Hemisuccinate


**BRADLEY D. ANDERSON** ˣ **and VANESSA TAPHOUSE**



Received April 7, 1980, from *The Upjohn Company, Kalamazoo, MI 49001.* Accepted for publication July 25, 1980.



**Abstract** □ The degradation of methylprednisolone 21-succinate in aqueous solution was examined as a function of pH at 25° by monitoring the initial rates of product formation. In addition to hydrolysis, acyl migration from the 21-hydroxyl group to the 17-hydroxyl group was found to be an important reaction. The 17-succinate was isolated, and its decomposition to the 21-succinate was followed by the initial rate method. Direct hydrolysis of the 17-ester was much slower than the 17 → 21 acyl migration under alkaline conditions. From the rate constants for the forward and reverse acyl migration, it may be concluded that the 21-ester is thermodynamically more stable, even though its alkaline hydrolysis is faster. The hydrolysis of the 21-ester and the reversible rearrangement are subject to intramolecular catalysis by the terminal carboxyl group, for which a kinetic pKa value of 4.5–4.6 was estimated.



**Keyphrases** □ Methylprednisolone—17- and 21-succinates, hydrolysis and acyl migration, initial rate studies □ Hydrolysis—methylprednisolone 17- and 21-succinates, initial rate studies □ Degradation—methylprednisolone 17- and 21-succinates, hydrolysis and acyl migration, initial rate studies


Methylprednisolone 21-succinate (sodium salt[1]) is a soluble prodrug of methylprednisolone used as an injectable corticoid in acute hypersensitivity and dermatological conditions. Solubilization is achieved through the use of the ionizable hemisuccinate moiety, which is cleaved *in vivo* to release the active parent compound.

Previous studies of the kinetic behavior of this compound and similar compounds in aqueous solution generally focused on the hydrolytic cleavage of the ester linkage. Hydrolysis usually is regarded as the major degradation pathway of 21-steroid esters (1–3), followed by further decomposition *via* several routes (2, 4, 5). These kinetic studies were based on the results of nonspecific analytical methods such as the consumption of base (1) or extraction coupled with the blue tetrazolium assay (2) for measuring reaction rates.

In this study, the kinetics of methylprednisolone 21-hemisuccinate degradation were reexamined using a highly sensitive and specific high-performance liquid chromatographic (HPLC) technique. By monitoring the initial rates of product formation, data could be obtained easily at room temperature (25°) and at pH values where the reactions are quite slow. As a result of the improved analytical methodology, the role of acyl migration in the aqueous solution degradation of this steroid 21-ester and the isomeric 17-ester could be explored in addition to the hydrolysis reaction.

## EXPERIMENTAL

**HPLC Analysis**—A modular high-performance liquid chromatographic system consisting of an automated sample injector[2], a constant-flow pump[3] operated at 0.9–1.4 ml/min, a reversed-phase column[4] packed with 10-μm Lichrosorb RP-18[5], a variable-wavelength UV detector[6] operated at 248 nm, and a digital integrator[7] was used for all kinetic studies. The mobile phase contained 33% acetonitrile[8] and 67% water buffered at pH 5.2–5.4 with 0.05 *M* acetate buffer.

Under these chromatographic conditions, methylprednisolone 17-hemisuccinate was eluted first, followed by methylprednisolone and then by methylprednisolone 21-hemisuccinate. As will be discussed later, the retention times of the esters changed dramatically with small changes in the pH. Detector response, measured either as the peak area or peak height, was linear for all solution components over the concentration range of interest.

[1] Solu-Medrol (methylprednisolone sodium succinate), The Upjohn Co.

[2] Wisp model 710A, Waters Associates, Milford, Mass.
[3] Model 110A, Altex Scientific, Berkeley, Calif.
[4] Brownlee Laboratories, Berkeley, Calif.
[5] E. Merck, Darmstadt, West Germany.
[6] Altex/Hitachi model 153-00, Altex Scientific, Berkeley, Calif.
[7] Model 3380A, Hewlett-Packard, Avondale, Pa.
[8] Burdick & Jackson Laboratories, Muskegon, Mich.


0022-3549/81/0200-0181$01.00/0


© 1981, American Pharmaceutical Association

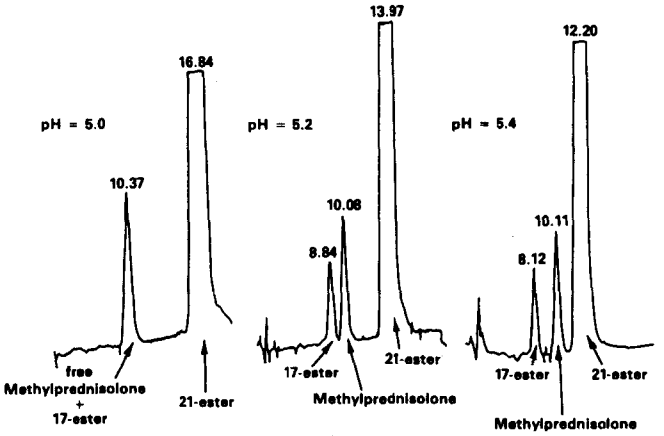


**Figure 1**—*Effect of mobile phase pH on the resolution of methylprednisolone and methylprednisolone 17-hemisuccinate in the presence of high concentrations of 21-hemisuccinate. The flow rate was 1.3 ml/min, and the detector sensitivity was 0.16 absorbance unit/10-mv output. Other chromatographic conditions are reported in the text.*

**Standard Solutions**—Standard solutions of methylprednisolone and methylprednisolone 17- and 21-succinates were prepared at concentrations of $1.0 \times 10^{-6}$–$1.0 \times 10^{-5}$ *M*, depending on the samples being analyzed. These solutions were prepared at pH 3–4 in 0.01 *M* ionic strength buffer (6) and were stable for at least 1 day at 25°.

**Kinetic Studies**—Solutions of methylprednisolone 21- or 17-succinate were prepared, at concentrations in the range of $1.0$–$6.0 \times 10^{-4}$ *M* in 0.01 *M* ionic strength buffers (6), by one of the following two methods:

1. An amount of the ester stock solution in dimethylformamide of known concentration and density was weighed accurately into a 25-ml volumetric flask and diluted with buffer to 25 ml.

2. An amount of the ester was weighed accurately, transferred to a 25-ml volumetric flask, dissolved in 200 μl of dimethylformamide, and then diluted to 25 ml with buffer.

All solutions contained <1% dimethylformamide. The time of preparation and the exact pH were recorded. Samples were maintained at 25° in a constant-temperature water bath or in the sample compartment of the automatic sampler, which was modified to maintain a constant temperature of 25 ± 0.6° in the compartment.

Samples for HPLC analysis were injected directly using the conditions described previously. In general, at least five data points prior to 3% degradation of the starting material were obtained. Product concentrations generally were determined using the ratio of the peak areas of the sample and standard. However, when very high precision was desired, peak heights were preferable.

**Isolation of Methylprednisolone 17-Hemisuccinate**—Although an additional impurity in methylprednisolone 21-succinate solutions had been observed previously by HPLC and some evidence suggested that it was the 17-succinate[9], the compound had not been isolated in sufficient quantity for conclusive structural elucidation. Furthermore, relatively pure 17-hemisuccinate was needed for use as a standard for the kinetic studies.

Methylprednisolone 21-hemisuccinate (3 g) was dissolved in 100 ml of deionized water by adjusting the pH to ~7.5 with dilute sodium hydroxide. The solution was heated to 60–70°, and the pH was maintained at 7.5 by occasional addition of dilute sodium hydroxide. Formation of the unknown product and free methylprednisolone were monitored by HPLC. After 1 day, the unknown appeared to reach a maximum concentration of ~12% of the initial starting material (by peak areas).

After cooling, the solution was acidified (acetic acid) and extracted with three 100-ml portions of ethyl acetate. The organic layers were combined, and the solvent was removed on a rotary evaporator. The viscous residue was redissolved in a solution of 40% acetonitrile and 60% aqueous buffer containing 0.05 *M* acetic acid, which was adjusted to pH 5.2 with potassium hydroxide. This solution was injected onto a reversed-phase preparative system[10] and eluted with a mobile phase of the same composition as the sample solvent. At a flow rate of 18 ml/min, the fraction containing the desired product eluted in ~13 min. This fraction was acidified (acetic acid) and extracted with three equal-volume portions of ethyl acetate.

The organic extracts were combined and dried (anhydrous sodium sulfate), and the solvent was evaporated to a few milliliters. Several portions of acetonitrile were added and evaporated, using a rotary evaporator to pull off residual acetic acid. The final residue was dissolved in a small volume (~20 ml) of ethyl acetate, filtered, and added dropwise to a large volume of hexane (~500 ml), with rapid stirring, to give 175 mg of a white precipitate[11]. This material was collected and dried overnight at 60° in a high vacuum and was shown by HPLC to contain no detectable methylprednisolone and <1% 21-succinate, mp 143° dec.[11].

*Anal.*—Calc. for $C_{26}H_{34}O_8$: C, 65.8; H, 7.22. Found: C, 65.69; H, 7.57.

The mass spectrum of the trimethylsilylated derivative of the unknown was reasonable for the 17-hemisuccinate but was not conclusive. A peak at *m/z* 587 corresponding to loss of $CH_2OSi(CH_3)_3$ from the molecular ion would not be expected from the 21-hemisuccinate or from an intermediate hemi-ortho ester unless decomposition occurred, but this peak is reasonable for the 17-ester, which has a $CH_2OH$ group.

Noise-decoupled $^{13}C$-NMR spectroscopy showed a downfield shift in the quaternary C-17 from δ 88.68 for the 21-hemisuccinate to δ 94.48 for the unknown and an upfield shift of the 21-carbon from δ 67.68 to 65.58. Moreover, no quaternary carbons were observed in the region expected for a carbon bonded to three oxygens, eliminating the unlikely possibility that the unknown was the hemi-ortho ester, the existence of which has been postulated (7).

The kinetic behavior of the unknown strongly supports the assigned structure.

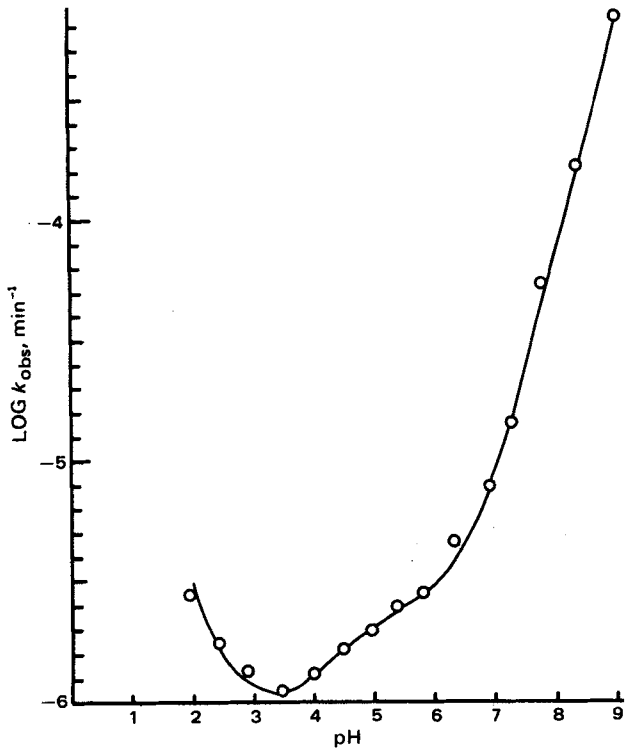


**Figure 2**—*Plot of hydrolysis rate as a function of pH for methylprednisolone 21-hemisuccinate in aqueous buffers at 25°. Key: O, experimental data; and —, theoretical curve.*

## RESULTS AND DISCUSSION

**Reversed-Phase HPLC Determination of Methylprednisolone 21-Hemisuccinate and Its Degradation Products**—Previous studies of soluble steroid degradation generally focused on the hydrolysis reaction and failed to address acyl migration. Presumably, the analytical methods used were not specific for the 17-ester in the presence of the 21-ester. Although normal-phase chromatographic methods for the separation of methylprednisolone (II) and the 17-hemisuccinate (III) from methylprednisolone 21-hemisuccinate (I) (Scheme I) have been developed (8), a reversed-phase method was considered as more desirable for

[9] H. J. Rodriguez, L. E. Fox, and W. F. Beyer, The Upjohn Co., Kalamazoo, MI 49001, internal communications.

[10] Two size B RP-8 Lobar (E. Merck, Darmstadt, West Germany) columns were employed.

[11] In a repetition of the synthesis, crystallization occurred in ethyl acetate prior to the precipitation step. The crystallized material exhibited a melting point of 175.0–178.5°.

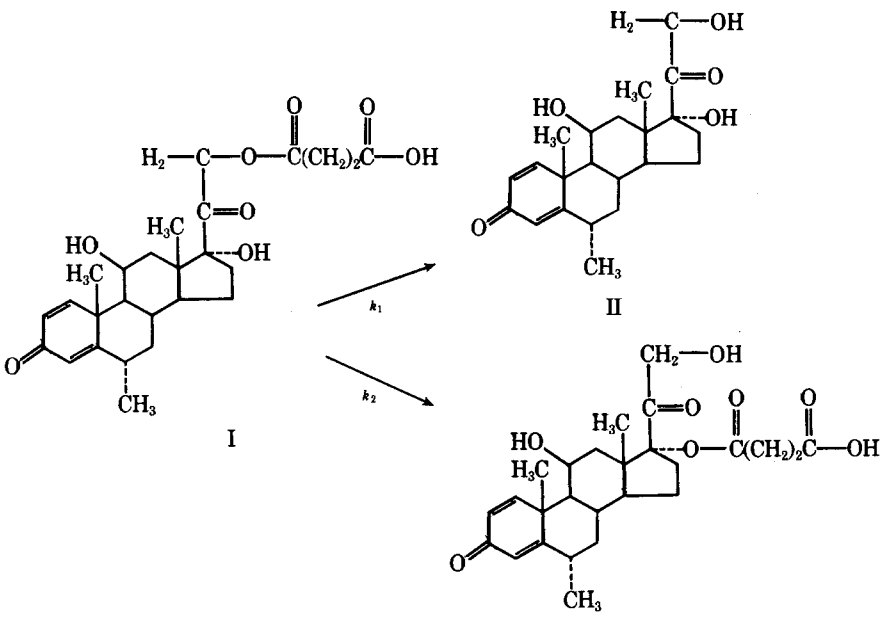

*Scheme I—Initial reaction pathways in the degradation of methylprednisolone 21-hemisuccinate*

kinetic studies since it would allow direct injection of an aqueous solution without time-consuming extraction during which further degradation could occur.

A recent report that described a reversed-phase HPLC procedure for the components of interest failed to mention the 17-hemisuccinate (9). Those investigators reported the use of a mobile phase containing 2% acetic acid. In the present study, it was found that the pH of the mobile phase is important. Figure 1 shows the effects of relatively small changes in pH on the resolution of the three solution components. As expected, the retention times of the hemisuccinate isomers can be varied relative to that of free methylprednisolone. At pH 5.0, the 17-hemisuccinate peak merged with the free methylprednisolone peak. In the previously reported method (9), the peaks for the 17-ester and free methylprednisolone probably merged.

**Kinetic Studies**—*Advantage of Initial Rate Method*—Because the reaction rates are very slow at room temperature and at pH values near neutrality, most earlier studies were carried out at high temperature and at pH values where reaction rates were well above the minimum in the pH–rate profile so that reactions could be followed conveniently for several half-lives. When the reactions are followed for several half-lives, other competing side reactions, such as oxidation of the dihydroxyacetone side chain (4) and D-homo rearrangement (10), complicate the kinetics.

To obtain the complete pH–rate profile at room temperature in a reasonable time and to avoid the mathematical complications brought about by consecutive reactions when following kinetics over several half-lives, initial rates of product formation were monitored. Prior to 2–3% degradation, the concentration of the reactant can be considered constant so that product formation rates are constant. The free alcohol and 17-ester form at rates that are independent of the presence of each other in initial rate studies.

*Determination of Reaction Order*—Both the hydrolysis reaction and the acyl migration from the 21-position were shown to be first order with respect to methylprednisolone 21-hemisuccinate. In the initial rate studies, the reactions shown in Scheme I occur. In Scheme I, $k_1$ and $k_2$ represent pseudo-first-order rate constants. Although the 21 → 17 rearrangement is reversible, the reverse reaction rate is negligible early in the approach to equilibrium. Since I can be considered constant during the time frame of interest, the reaction order can be determined by varying the initial concentration of I. Reaction rates were found to be a linear function of the initial concentration of I, indicating that these reactions are first order in I. Rate constants at various concentrations of I and at three pH values are shown in Table I. As expected, the rate constants do not change significantly with the concentration of I in the dilute region.

**Table I—Rate Constants at Various Dilute Concentrations of Methylprednisolone 21-Hemisuccinate (I)**

| pH | Concentration, $M \times 10^4$ | $k_1$, $min^{-1}$ | $k_2$, $min^{-1}$ |
|---|---|---|---|
| 7.30 | 1.94 | $(1.5 \pm 0.8) \times 10^{-5}$ | $(2.4 \pm 0.9) \times 10^{-5}$ |
| 7.30 | 4.10 | $(1.6 \pm 0.3) \times 10^{-5}$ | $(2.9 \pm 0.3) \times 10^{-5}$ |
| 7.30 | 5.91 | $(1.5 \pm 0.1) \times 10^{-5}$ | $(2.6 \pm 0.2) \times 10^{-5}$ |
| 5.82 | 2.08 | $(3.6 \pm 0.6) \times 10^{-6}$ | $(1.3 \pm 0.2) \times 10^{-5}$ |
| 5.82 | 3.24 | $(2.7 \pm 0.2) \times 10^{-6}$ | $(1.1 \pm 0.1) \times 10^{-5}$ |
| 5.82 | 4.15 | $(3.0 \pm 0.3) \times 10^{-6}$ | $(1.2 \pm 0.03) \times 10^{-5}$ |
| 4.02 | 0.968 | $(1.6 \pm 0.2) \times 10^{-6}$ | $(3.7 \pm 0.3) \times 10^{-6}$ |
| 4.02 | 1.28 | $(1.7 \pm 0.1) \times 10^{-6}$ | $(3.6 \pm 0.1) \times 10^{-6}$ |
| 4.02 | 2.00 | $(1.4 \pm 0.1) \times 10^{-6}$ | $(3.2 \pm 0.3) \times 10^{-6}$ |

*Hydrolysis of Methylprednisolone 21-Hemisuccinate*—The pH–rate profile for the hydrolysis of methylprednisolone 21-succinate is shown in Fig. 2. From the shape of the curve, it is evident that more than one mechanism must be invoked to account for the hydrolysis at different pH values. The line drawn in Fig. 2 represents the theoretical curve based on the relationship:

$$k_1 = \frac{k_{H^+}^{hyd}[H^+]^2 + k_{H_2O}^{hyd}[H^+] + k_{OH^-}^{hyd}K_w + k'^{hyd}_{OH^-}[OH^-]K_a}{[H^+] + K_a} \quad \text{(Eq. 1)}$$

Values for the rate constants at 25° were estimated using a least-squares computer-fitting technique (11) and are listed in Table II with values representing 95% confidence limits. A pKa of 4.54 was assumed based on the results of curve fitting of the acyl migration data (to be presented later).

The value obtained for $k'^{hyd}_{OH^-}$ is close to that calculated for a similar system (1). The $k'^{hyd}_{OH^-}$ value represents specific hydroxide-ion-catalyzed hydrolysis of the succinate anion and is the most important term at pH values above 6.5.

Between pH 4.1 and 6.5, the dominant term in the hydrolysis is hydroxide-ion attack on the unionized ester or the kinetically equivalent water attack on the anion. Mechanistically, the increase in the rate over that predicted from $k'^{hyd}_{OH^-}$ as the pKa is approached can be interpreted as being due to one or more of the following reactions: (*a*) intramolecular nucleophilic catalysis by the anion, (*b*) intramolecular general base catalysis of attack by water, (*c*) intramolecular general acid catalysis of

**Table II—Rate Constants for Hydrolysis of Methylprednisolone 21-Hemisuccinate in Water at 25°**

| Parameter | Rate Constant | 95% Confidence Limit |
|---|---|---|
| $k'^{hyd}_{OH^-}$ | 74 liters/mole/min | ±14 liters/mole/min |
| $k'^{hyd}_{OH^-}$ | $7.2 \times 10^3$ liters/mole/min | $\pm 1.7 \times 10^3$ liters/mole/min |
| $k^{hyd}_{H_2O}$ | $1.0 \times 10^{-6}$ $min^{-1}$ | $\pm 0.34 \times 10^{-6}$ $min^{-1}$ |
| $k^{hyd}_{H^+}$ | $2.0 \times 10^{-4}$ liter/mole/min | $\pm 1.2 \times 10^{-4}$ liter/mole/min |

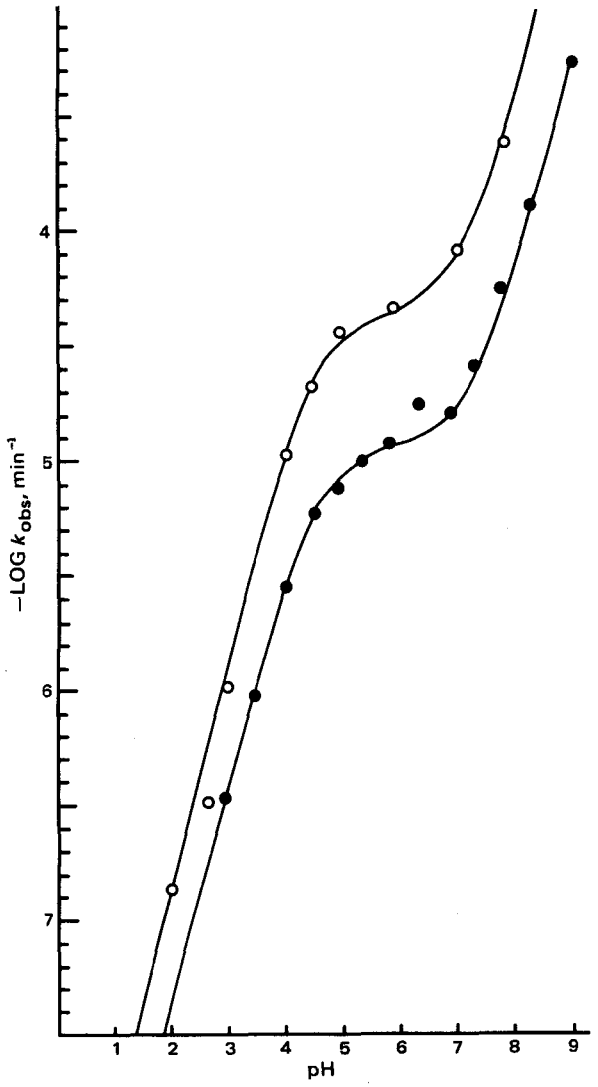


**Figure 3**—*Plot of rearrangement rate as a function of pH for the migration of the hemisuccinate moiety from the 17 → 21 position (○) and from the 21 → 17 position (●) in aqueous buffers at 25°.*

attack by hydroxide ion, and (*d*) repulsion of hydroxide ion by the negatively charged carboxylate which decreases as the pKa is approached. The present study does not differentiate between these kinetically equivalent mechanisms.

Although intramolecular nucleophilic attack by the terminal carboxylate was shown to occur in some monoesters of dicarboxylic acids (12), evidence supporting this mechanism in the present case is not available. Fersht and Kirby (13) showed that the borderline between intramolecular general base and nucleophilic catalysis lies in the region where the pKa of the leaving group is 5.5–6.5 units more basic than the pKa of the attacking nucleophile. Based on the estimations that the apparent pKa of the C-17 side chain of methylprednisolone probably is near 11 due to enolization (14) and that the pKa of the terminal carboxylic acid group is 4.5, methylprednisolone 21-succinate apparently lies on the borderline between the general base and nucleophilic mechanisms. Intramolecular general acid catalysis also cannot be ruled out. In fact, this mechanism appears to be the most reasonable mode of catalysis of acyl migration.

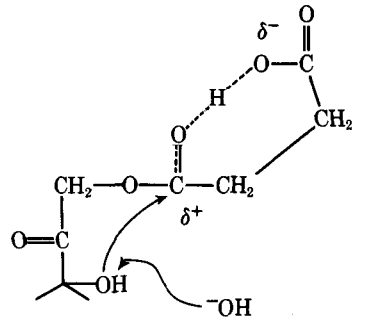

*Scheme II—General acid-specific base catalysis*

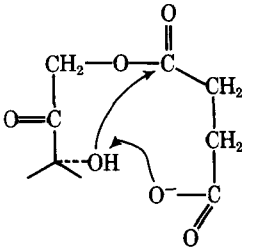

*Scheme III—General base catalysis*

**Acyl Migration in Methylprednisolone Hemisuccinate**—*21 → 17 Acyl Migration*—Although acyl migration in steroid esters was reported previously (15, 16), the present investigators are not aware of any quantitative data on acyl migration from the 21-hydroxyl group to the highly hindered 17-hydroxyl group. In spite of the fact that the 17-hydroxyl group is in a sterically crowded environment, the 21 → 17 rearrangement is quite facile. The pH–rate profile for the rearrangement of the hemisuccinate moiety from the 21-hydroxyl group to the 17-hydroxyl group is shown in Fig. 3. The initial rate of 21 → 17 acyl migration is faster than hydrolysis at pH values between 3.6 and 7.4. The theoretical curve drawn in Fig. 3 represents the following relationship:

$$k_2 = \frac{k_{OH^-}^{21\rightarrow 17} K_w + k_{OH^-}^{\prime 21\rightarrow 17} K_a [OH^-]}{[H^+] + K_a} \qquad \text{(Eq. 2)}$$

Estimates of the second-order rate constants $k_{OH^-}^{21\rightarrow 17}$ and $k_{OH^-}^{\prime 21\rightarrow 17}$ and the acid dissociation constant $K_a$ were obtained by applying a least-squares computer-fitting technique (11) to the rate data *versus* pH. These values are listed in Table III along with 95% confidence limits.

Intramolecular catalysis represents an acceleration of ~600-fold in the rearrangement. This acceleration is significantly greater (by a factor of ~6) than the intramolecular catalysis observed previously in the hydrolysis and accounts for the fact that the initial rate of acyl migration is faster than hydrolysis between pH 3.6 and 7.4. Two possible mechanisms may account for this acceleration (Schemes II and III). Intramolecular general acid catalysis involves the formation of a six-membered ring (assuming a linear hydrogen bond), while general base catalysis requires the formation of a 10-membered ring. On this basis, general acid catalysis is more likely.

Repulsion of hydroxide ion by the anion probably can be ruled out due to the magnitude of the rate enhancement. Nucleophilic catalysis, which is a possible mechanism in hydrolysis, is not possible in the rearrangement.

*17 → 21 Acyl Migration*—Also shown in Fig. 3 is the pH–rate profile for the rearrangement of the succinate from the 17-hydroxyl group to the

**Table III—Kinetically Determined pKa Values for Methylprednisolone Succinate Esters and Rate Constants for 21 → 17 and 17 → 21 Acyl Migration in Water at 25°**

| Compound | Parameter | Parameter Value | 95% Confidence Limit |
|---|---|---|---|
| 21-Succinate | pKa | 4.54 | ±0.19 |
| | $k_{OH^-}^{21\rightarrow 17}$ | $3.5 \times 10^4$ liters/mole/min | $\pm 0.9 \times 10^4$ liters/mole/min |
| | $k_{OH^-}^{\prime 21\rightarrow 17}$ | 59 liters/mole/min | ±16 liters/mole/min |
| 17-Succinate | pKa | 4.62 | ±0.13 |
| | $k_{OH^-}^{17\rightarrow 21}$ | $1.2 \times 10^5$ liters/mole/min | $\pm 0.2 \times 10^5$ liters/mole/min |
| | $k_{OH^-}^{\prime 17\rightarrow 21}$ | 290 liters/mole/min | ±100 liters/mole/min |

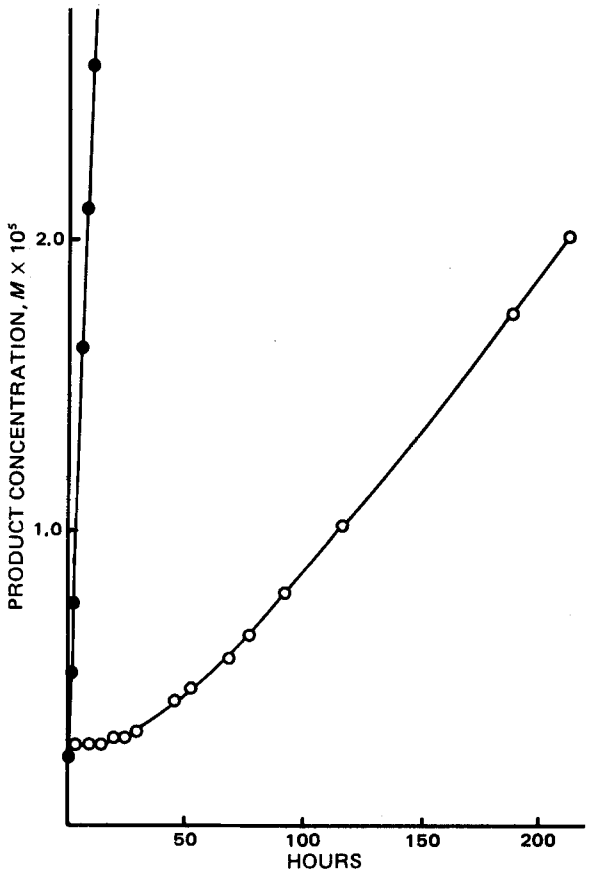


**Figure 4**—*Appearance of free methylprednisolone (○) and 21-ester (●) versus time in a solution containing 4 × 10⁻⁴ M methylprednisolone 17-hemisuccinate buffered at pH 7.2 at 25°.*

21-hydroxyl group. Except for their vertical position, the curves are virtually superimposable. An equation identical to Eq. 2 but with the pseudo-first-order rate constant $k_{-2}$ and second-order rate constants $k_{OH^-}^{17\rightarrow 21}$ and $k_{OH^-}^{\prime 17\rightarrow 21}$ can be used to describe the 17 → 21 rearrangement. Table III lists the computer-determined best values for the second-order rate constants and the kinetically determined pKa for the 17-succinate.

**Relative Stabilities of Methylprednisolone 17- and 21-Succinates**—A true equilibrium between the 17 and 21-succinates never is attained in aqueous solution due to rapid hydrolysis. However, from a comparison of the migration rate constants in Table III, the relative thermodynamic stability of the two isomers can be estimated.

In the rearrangement reaction, the transition state is the same for both the forward and reverse acyl migration by the principle of microscopic reversibility (17), so that the ratio of the migration rates depends only on the relative reactant stabilities. From Table III, this ratio ($k_{OH^-}^{17\rightarrow 21}/k_{OH^-}^{21\rightarrow 17}$ or $k_{OH^-}^{\prime 17\rightarrow 21}/k_{OH^-}^{\prime 21\rightarrow 17}$) is ~3–5, indicating that the 21-succinate is thermodynamically more stable by 650–950 cal/mole.

The 21-succinate is an ester of a primary hydroxyl group, while the 17-succinate, being an ester of a tertiary hydroxyl group, is more hindered. If the difference in ester stability observed is due to a steric effect, the 21-ester is expected to be favored. The relatively small difference seen suggests that steric hindrance affects the ground-state stability of these compounds to only a minor extent.

Even though the 21-ester is thermodynamically more stable, it hydrolyzes much faster than the 17-ester. Direct hydrolysis of the 17-succinate does not appear to be an important reaction, at least under alkaline conditions. Figure 4 shows the concentrations of free methylprednisolone and its 21-hemisuccinate formed as a function of time in a solution of the 17-hemisuccinate buffered at pH 7.2. A lag time is clearly apparent in the formation of free methylprednisolone, suggesting that hydrolysis occurs after 21-ester formation. This evidence indicates that the reaction shown in Scheme IV applies to these systems.

It is apparent that steric effects on the relative rates of hydrolysis of these esters are pronounced. Steric effects are known to be important in hydrolysis reactions, because the transition state involving the formation of a tetrahedral intermediate is more crowded than the initial state and

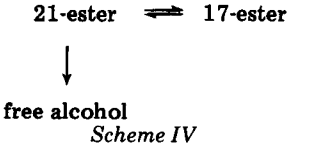


*Scheme IV*

is more highly ordered since two molecules have combined to form one (18). From a consideration of steric parameters of alkyl substituents at the oxygen in acetate esters (19), base-catalyzed hydrolysis rates of primary alkyl acetates are expected to be faster than hydrolysis of tertiary alkyl acetates by a factor of >100. Thus, the hydrolysis of the 17-hemisuccinate is expected to be quite slow, as was observed in this study.

## CONCLUSIONS

Because current analytical techniques are superior in sensitivity and specificity to those used in the past for drug degradation studies, reevaluation of earlier data may be useful. A reexamination of the aqueous degradation of methylprednisolone 21-hemisuccinate serves as an example.

A specific HPLC method for determining low levels of methylprednisolone and methylprednisolone 17-hemisuccinate in the presence of the 21-hemisuccinate was developed. Initial rate kinetic studies of the degradation of methylprednisolone 21-hemisuccinate in aqueous solution at 25° showed that degradation proceeds by parallel first-order reactions in the initial phase. Although hydrolysis is a significant reaction at all pH values, reversible acyl migration dominates at pH 3.6–7.4. Therefore, acyl migration is more important in such systems than previously was recognized.

## REFERENCES

(1) E. R. Garrett, *J. Pharm. Sci.*, **51**, 445 (1962). E. R. Garrett, *J. Med. Pharm. Chem.*, **5**, 112 (1962).

(2) J. W. Mauger, A. N. Paruta, and R. J. Gerraughty, *J. Pharm. Sci.*, **58**, 574 (1969).

(3) R. Yamamoto, S. Fujisawa, and M. Kawamura, *Yakugaku Zasshi*, **91**, 855 (1971).

(4) D. E. Guttmann and P. D. Meister, *J. Am. Pharm. Assoc., Sci. Ed.*, **47**, 773 (1958).

(5) K. J. Kripiliani and D. L. Sorby, *J. Pharm. Sci.*, **56**, 687 (1967).

(6) D. D. Perrin, *Aust. J. Chem.*, **16**, 572 (1963).

(7) V. Stella, in "Prodrugs as Novel Drug Delivery Systems," T. Higuchi and V. Stella, Eds., American Chemical Society, Washington, D.C., 1975, chap. 1.

(8) W. F. Beyer, "Abstracts," vol. 9, APhA Academy of Pharmaceutical Sciences, Washington, D.C., 1979, p. 130.

(9) M. D. Smith and D. J. Hoffman, *J. Chromatogr.*, **168**, 163 (1979).

(10) L. F. Fieser and M. Fieser, "Steroids," Reinhold, New York, N.Y., 1951, chap. 18.

(11) S. L. Morgan and S. N. Deming, *Anal. Chem.*, **46**, 1170 (1974).

(12) A. J. Kirby and A. R. Fersht, in "Progress in Bioorganic Chemistry," E. J. Kaiser and F. J. Kezdy, Eds., vol. 1, Wiley, New York, N.Y., 1971.

(13) A. R. Fersht and A. J. Kirby, *J. Am. Chem. Soc.*, **90**, 5818 (1968).

(14) J. Hansen and H. Bundgaard, *Arch. Pharm. Chem., Sci. Ed.*, **7**, 135 (1979).

(15) L. F. Fieser and M. Fieser, "Steroids," Reinhold, New York, N.Y., 1951, p. 680.

(16) Y. W. Yip and A. Li Wan Po, *J. Pharm. Pharmacol.*, **31**, 400 (1979).

(17) L. P. Hammett, "Physical Organic Chemistry," McGraw-Hill, New York, N.Y., 1970, p. 142.

(18) A. J. Kirby, in "Comprehensive Chemical Kinetics," vol. 10, C. H. Bamford and C. F. H. Tipper, Eds., Elsevier, Amsterdam, The Netherlands, 1972, p. 139.

(19) M. Charton, *J. Org. Chem.*, **42**, 3531 (1977).

## ACKNOWLEDGMENTS

The authors acknowledge the work of many people at The Upjohn Co., Kalamazoo, Mich., who played a role in the demonstration of acyl migration discussed in this report, including H. J. Rodriguez, L. E. Fox, W.

F. Beyer, and S. Nail. They also thank J. R. Boal for assistance in interpretation of the mass spectral data and S. Mizsak for interpretation of the $^{13}C$-NMR data.

V. Taphouse participated in this study through a senior independent research program sponsored jointly by The Upjohn Co. and Kalamazoo College, Kalamazoo, Mich.

# Fluorometric Determination of Tetracyclines in Small Blood and Tissue Samples

**C. van den BOGERT and A. M. KROON ˣ**

Received May 27, 1980, from the *Laboratory of Physiological Chemistry, State University School of Medicine, Bloemsingel 10, 9712 KZ Groningen, The Netherlands.* Accepted for publication July 25, 1980.

**Abstract** □ A reported fluorometric method to determine tetracyclines in biological material was modified to determine low levels of the antibiotics when using only small amounts of starting material. The method is applicable to tissue distribution studies in small experimental animals and also can be used for serial determinations in blood samples of these animals and for biopsy material. The tetracyclines are extracted in the presence of ethylenediaminetetraacetic acid, and the phosphate precipitation steps are omitted. This omission makes the procedure considerably less time consuming. The recoveries of the tetracyclines, oxytetracycline and doxycycline, are ~80–100%. The values obtained by this method were consistent with those from microbiological assays, and its reliability was shown further in a comparison with the fate of radioactive tetracycline.

**Keyphrases** □ Tetracyclines—fluorometric determination in small blood and tissue samples □ Oxytetracycline—fluorometric determination in small blood and tissue samples □ Doxycycline—fluorometric determination in small blood and tissue samples □ Fluorometry—analysis, tetracyclines in small blood and tissue samples

Several methods are available to determine the amount of tetracycline in biological material. Microbiological assays often are preferred even though their precision is low and data can be obtained only after prolonged incubation (1).

Spectrophotometric methods (2) are insensitive, and interference from other material cannot always be excluded. High-pressure liquid chromatography (HPLC) (3) and polarographic analysis (4) of tetracyclines also have been described, but they require special equipment. Fluorometric analysis is relatively simple and specific for the tetracyclines (5, 6).

## BACKGROUND

Studies have been made of the inhibition of mitochondrial protein synthesis by tetracyclines and the consequences of this inhibition on the functional activity of cells, tissues, and whole animals (7–10). Because of the many other possible effects of tetracyclines, which occur mainly at drug concentrations much higher than those at which mitochondrial protein synthesis is impaired, careful control of tetracycline levels and amounts is necessary in such studies.

For these reasons, the fluorometric method described by Poiger and Schlatter (6) was selected for measurement of tetracycline concentrations in tissues and serum samples of rats after prolonged drug administration. This method is based on buffer extraction of tetracyclines from blood and tissue samples. After deproteinization and elimination of phosphates, the tetracyclines are extracted into an organic solvent as ion-pairs with calcium and trichloroacetate ions. Fluorescence of the tetracyclines is induced by the addition of a base and magnesium ions. The method gives reproducible results, although the recoveries are low—on the order of 35–40% for tetracycline and chlortetracycline. Only for oxytetracycline was 60% recovery from serum recorded (6).

A major disadvantage of the method is the large quantity of material required (3 ml of serum or 2 g of tissue). Therefore, the amounts of tetracyclines in blood and tissue samples of experimental animals such as mice and rats are difficult to determine with this method. By critical evaluation of the various steps of the method, it was possible to modify it in a way that allows the detection of small amounts of the tetracyclines in as little as 0.2 ml of serum or 50 mg (wet weight) of tissue.

## EXPERIMENTAL

**Chemicals and Antibiotics**—All chemicals were analytical grade. Oxytetracycline[1] (as hydrochloride), doxycycline[2] (as hydrochloride), and [7-$^3$H-(N)]tetracycline[3] (0.94 Ci/mmole) were used as obtained.

**Experimental Animals and Preparation of Homogenates**—In all recovery studies, after the addition of tetracyclines (oxytetracycline, doxycycline, or tetracycline), rat tissue homogenates or serum samples were incubated for 20 min at 37° to obtain maximal binding. Tissue homogenates were prepared in saline using a glass–polytef homogenizer.

**Extraction of Tetracyclines**—Two milliliters of 0.1 *M* glycine–hydrochloric acid (pH 2) was added per milliliter of a 20% homogenate or dilutions thereof or per milliliter of serum with a known tetracycline content. Proteins were precipitated by the addition of 2 ml of 1 *M* trichloroacetic acid. The mixture was shaken vigorously and then centrifuged. Four milliliters of the supernate was mixed with 1.2 ml of a solution containing sodium acetate (2 *M*) and lead nitrate (0.06 *M*) and allowed to stand for 45 min at room temperature before centrifugation. Then 0.85 ml of saturated potassium iodide solution was added to 5 ml of the supernate, and the mixture was left for 15 min. After centrifugation, 5 ml of the supernate was mixed with 50 μl of 1 *M* calcium chloride and saturated with sodium chloride.

The pH was adjusted to 9.5 with concentrated ammonia. After addition of 3 ml of ethyl acetate, the tetracycline was extracted by shaking the mixture for 1.5 min. Deviations from this general procedure will be indicated.

**Fluorescence Measurements**—Fluorescence of tetracyclines extracted into the organic layer was induced by adding 0.5 ml of a solution containing 200 mg of barbital sodium and 600 mg of magnesium acetate in 100 ml of methanol to 3 ml of the ethyl acetate extract just prior to the measurement of fluorescence. When small amounts of tissue or serum were used, 1 ml of water, treated as for a sample containing tetracycline, was a suitable blank. In other cases, a sample of tissue or serum without tetracycline was used as a blank because of the background fluorescence.

After reading the fluorescence of a sample, a known amount of tetracycline was added to the cell to calculate the recovery of tetracycline from the sample.

Fluorescence measurements were carried out on a fluorescence spectrophotometer[4] equipped with a xenon arc lamp. The spectral bandwidth was 10 nm for both excitation and emission. The instrument settings were 400 nm for excitation and 505 nm for emission.

[1] Vendarcin, Gist-Brocades, Delft, The Netherlands.
[2] Pfizer Inc., Brussels, Belgium.
[3] New England Nuclear, Dreiech, West Germany.
[4] Perkin-Elmer MPF-43, Charles Goffin, Maastricht-de Bilt, The Netherlands.



0022-3549/81/0200-0186$01.00/0
© 1981, American Pharmaceutical Association

F. Beyer, and S. Nail. They also thank J. R. Boal for assistance in interpretation of the mass spectral data and S. Mizsak for interpretation of the $^{13}C$-NMR data.

V. Taphouse participated in this study through a senior independent research program sponsored jointly by The Upjohn Co. and Kalamazoo College, Kalamazoo, Mich.

# Fluorometric Determination of Tetracyclines in Small Blood and Tissue Samples

**C. van den BOGERT and A. M. KROON ˣ**

Received May 27, 1980, from the *Laboratory of Physiological Chemistry, State University School of Medicine, Bloemsingel 10, 9712 KZ Groningen, The Netherlands.* Accepted for publication July 25, 1980.

**Abstract** □ A reported fluorometric method to determine tetracyclines in biological material was modified to determine low levels of the antibiotics when using only small amounts of starting material. The method is applicable to tissue distribution studies in small experimental animals and also can be used for serial determinations in blood samples of these animals and for biopsy material. The tetracyclines are extracted in the presence of ethylenediaminetetraacetic acid, and the phosphate precipitation steps are omitted. This omission makes the procedure considerably less time consuming. The recoveries of the tetracyclines, oxytetracycline and doxycycline, are ~80–100%. The values obtained by this method were consistent with those from microbiological assays, and its reliability was shown further in a comparison with the fate of radioactive tetracycline.

**Keyphrases** □ Tetracyclines—fluorometric determination in small blood and tissue samples □ Oxytetracycline—fluorometric determination in small blood and tissue samples □ Doxycycline—fluorometric determination in small blood and tissue samples □ Fluorometry—analysis, tetracyclines in small blood and tissue samples

Several methods are available to determine the amount of tetracycline in biological material. Microbiological assays often are preferred even though their precision is low and data can be obtained only after prolonged incubation (1).

Spectrophotometric methods (2) are insensitive, and interference from other material cannot always be excluded. High-pressure liquid chromatography (HPLC) (3) and polarographic analysis (4) of tetracyclines also have been described, but they require special equipment. Fluorometric analysis is relatively simple and specific for the tetracyclines (5, 6).

## BACKGROUND

Studies have been made of the inhibition of mitochondrial protein synthesis by tetracyclines and the consequences of this inhibition on the functional activity of cells, tissues, and whole animals (7–10). Because of the many other possible effects of tetracyclines, which occur mainly at drug concentrations much higher than those at which mitochondrial protein synthesis is impaired, careful control of tetracycline levels and amounts is necessary in such studies.

For these reasons, the fluorometric method described by Poiger and Schlatter (6) was selected for measurement of tetracycline concentrations in tissues and serum samples of rats after prolonged drug administration. This method is based on buffer extraction of tetracyclines from blood and tissue samples. After deproteinization and elimination of phosphates, the tetracyclines are extracted into an organic solvent as ion-pairs with calcium and trichloroacetate ions. Fluorescence of the tetracyclines is induced by the addition of a base and magnesium ions. The method gives reproducible results, although the recoveries are low—on the order of 35–40% for tetracycline and chlortetracycline. Only for oxytetracycline was 60% recovery from serum recorded (6).

A major disadvantage of the method is the large quantity of material required (3 ml of serum or 2 g of tissue). Therefore, the amounts of tetracyclines in blood and tissue samples of experimental animals such as mice and rats are difficult to determine with this method. By critical evaluation of the various steps of the method, it was possible to modify it in a way that allows the detection of small amounts of the tetracyclines in as little as 0.2 ml of serum or 50 mg (wet weight) of tissue.

## EXPERIMENTAL

**Chemicals and Antibiotics**—All chemicals were analytical grade. Oxytetracycline[1] (as hydrochloride), doxycycline[2] (as hydrochloride), and [7-$^3$H-(N)]tetracycline[3] (0.94 Ci/mmole) were used as obtained.

**Experimental Animals and Preparation of Homogenates**—In all recovery studies, after the addition of tetracyclines (oxytetracycline, doxycycline, or tetracycline), rat tissue homogenates or serum samples were incubated for 20 min at 37° to obtain maximal binding. Tissue homogenates were prepared in saline using a glass–polytef homogenizer.

**Extraction of Tetracyclines**—Two milliliters of 0.1 *M* glycine–hydrochloric acid (pH 2) was added per milliliter of a 20% homogenate or dilutions thereof or per milliliter of serum with a known tetracycline content. Proteins were precipitated by the addition of 2 ml of 1 *M* trichloroacetic acid. The mixture was shaken vigorously and then centrifuged. Four milliliters of the supernate was mixed with 1.2 ml of a solution containing sodium acetate (2 *M*) and lead nitrate (0.06 *M*) and allowed to stand for 45 min at room temperature before centrifugation. Then 0.85 ml of saturated potassium iodide solution was added to 5 ml of the supernate, and the mixture was left for 15 min. After centrifugation, 5 ml of the supernate was mixed with 50 μl of 1 *M* calcium chloride and saturated with sodium chloride.

The pH was adjusted to 9.5 with concentrated ammonia. After addition of 3 ml of ethyl acetate, the tetracycline was extracted by shaking the mixture for 1.5 min. Deviations from this general procedure will be indicated.

**Fluorescence Measurements**—Fluorescence of tetracyclines extracted into the organic layer was induced by adding 0.5 ml of a solution containing 200 mg of barbital sodium and 600 mg of magnesium acetate in 100 ml of methanol to 3 ml of the ethyl acetate extract just prior to the measurement of fluorescence. When small amounts of tissue or serum were used, 1 ml of water, treated as for a sample containing tetracycline, was a suitable blank. In other cases, a sample of tissue or serum without tetracycline was used as a blank because of the background fluorescence.

After reading the fluorescence of a sample, a known amount of tetracycline was added to the cell to calculate the recovery of tetracycline from the sample.

Fluorescence measurements were carried out on a fluorescence spectrophotometer[4] equipped with a xenon arc lamp. The spectral bandwidth was 10 nm for both excitation and emission. The instrument settings were 400 nm for excitation and 505 nm for emission.

[1] Vendarcin, Gist-Brocades, Delft, The Netherlands.
[2] Pfizer Inc., Brussels, Belgium.
[3] New England Nuclear, Dreiech, West Germany.
[4] Perkin-Elmer MPF-43, Charles Goffin, Maastricht-de Bilt, The Netherlands.



0022-3549/81/0200-0186$01.00/0
© 1981, American Pharmaceutical Association

Table I—Recovery of [$^3$H]Tetracycline Measured after Every Step of the Fluorometric Determination Procedure where 10 μg of [$^3$H]Tetracycline Was Added/5 ml of Homogenate (20% w/v)

| Step in Procedure | Recovery, % 0.25 ml of Homogenate | 10 ml of Homogenate |
|---|---|---|
| After trichloroacetic acid precipitation | 71 | 32 |
| After lead phosphate precipitation | 100 | 87 |
| After lead iodide precipitation | 91 | 93 |
| After ethyl acetate extraction | 43 | 81 |
| Counting of radioactivity (net recovery) | 28 | 25 |
| Fluorometric measurement (net recovery) | 22 | 30 |

**Microbiological Assay**—The tetracycline content of the tetracycline solutions was determined microbiologically by measuring the growth inhibition of *Bacillus cereus* D220 (11).

**Radioactivity Measurements**—Tritiated tetracycline was used in some experiments. Radioactivity was counted in a liquid scintillation counter using various scintillators on xylene basis[5].

## RESULTS AND DISCUSSION

**Recovery Studies with Labeled Tetracycline**—To gain insight into the causes of the low recoveries found with the method of Poiger and Schlatter (6), the recovery of tritiated tetracycline after each step of the procedure was investigated. The method was applied to small (0.25-ml) and large (10-ml) amounts of a 20% (w/v) liver homogenate containing 10 μg of [$^3$H]tetracycline/g (wet weight) of tissue.

A considerable amount of tetracycline was coprecipitated with the proteins, reducing the recovery in the supernate, especially if large amounts of homogenate were used (Table I). An important loss also was observed in the extraction of tetracycline into ethyl acetate; the reduced recovery in this step seemed to be inversely proportional to the amount of tissue present. Table I also shows that the values for the recovery based on the radioactivity and fluorescence measurements agree rather well. This finding indicates that the tetracycline is not decomposed during the procedure.

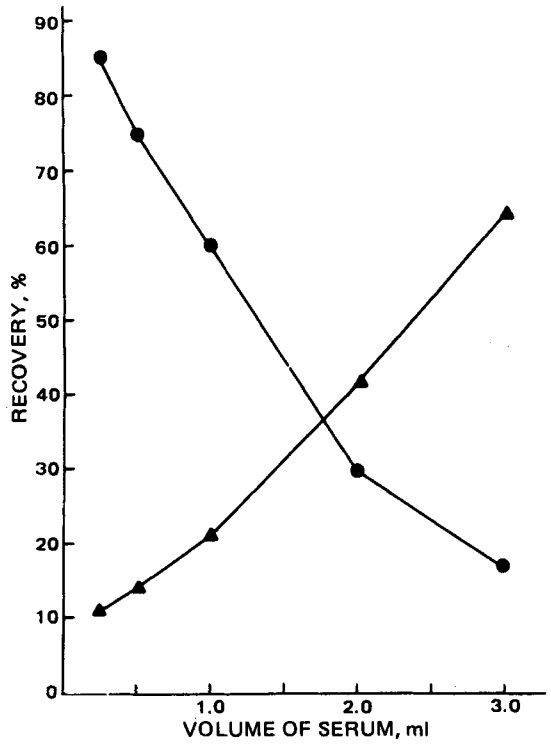


**Figure 1**—*Percentage recovery of 1 μg of oxytetracycline added to various amounts of human serum. Key: ●, recovery in the presence of 75 mM ethylenediaminetetraacetic acid during glycine treatment of the samples; and ▲, recovery without the addition of ethylenediaminetetraacetic acid.*

[5] Lipoluma and Hydroluma, J. T. Baker Chemicals, B. V. Deventer, The Netherlands.

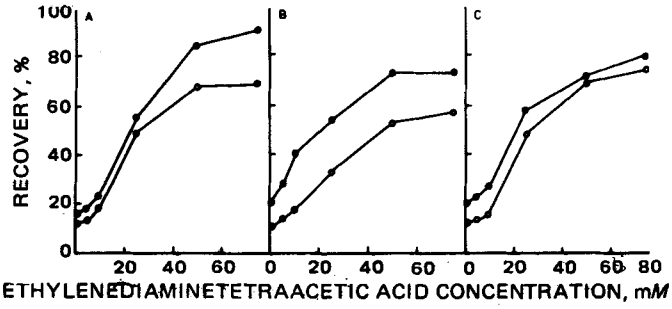


**Figure 2**—*Recovery of 0.1 μg of oxytetracycline (●) or 0.1 μg of doxycycline (▲) added to 0.2 ml of human serum (A), 0.25 ml of rat liver homogenate (20% w/v) (B), and 0.25 ml of rat kidney homogenate (20% w/v) (C). Recovery was measured in the presence of varying amounts of ethylenediaminetetraacetic acid.*

**Modification of the Poiger and Schlatter Method**—Various mechanisms such as chelation have been proposed for the binding of tetracyclines, especially to proteins (12). Addition of ethylenediaminetetraacetic acid during the first extraction may influence these processes and improve the efficiency of the extraction as well. However, the presence of ethylenediaminetetraacetic acid also influences other steps in the procedure. Because of its chelating properties, addition of ethylenediaminetetraacetic acid results in the removal of lead ions. Precipitation of lead phosphate or lead iodide thus is counteracted if enough ethylenediaminetetraacetic acid is added. The presence of lead ions as well as of phosphates inhibits the extraction of tetracyclines into ethyl acetate. Especially in samples containing only a little phosphate, excess lead may not be removed completely after the addition of potassium iodide. This condition may lead to a lower recovery. Therefore, the effects of ethylenediaminetetraacetic acid on the recovery of tetracyclines from serum and tissues were investigated under various conditions.

Figure 1 shows this effect for 1 μg of oxytetracycline added to various amounts of human serum. Ethylenediaminetetraacetic acid was added to the homogenate to give a final concentration of 75 m*M* together with the glycine. To measure the recovery of 1 μg of oxytetracycline added to 2 ml of serum, only 3 ml of the supernate after trichloroacetic acid precipitation was used. Before the addition of ethyl acetate, the calcium chloride concentration was raised to 150 m*M* to compensate for the high ethylenediaminetetraacetic acid content of the samples. Excess calcium chloride was used not only in the ethylenediaminetetraacetic acid-treated samples but also in the untreated ones. Recoveries varied with the amount of serum used (Table I). Ethylenediaminetetraacetic acid clearly improved the recovery, especially at the lower serum concentrations. Small amounts of serum and various organ homogenates incubated with doxycycline or oxytetracycline showed similar high recoveries if ethylenediaminetetraacetic acid was present during the glycine treatment (Fig. 2).

Figure 3 shows the result of treatment with ethylenediaminetetraacetic acid at increasing concentrations, measured immediately after trichloroacetic acid precipitation, for different samples containing 0.1 μg of [$^3$H]tetracycline. The presence of ethylenediaminetetraacetic acid im-

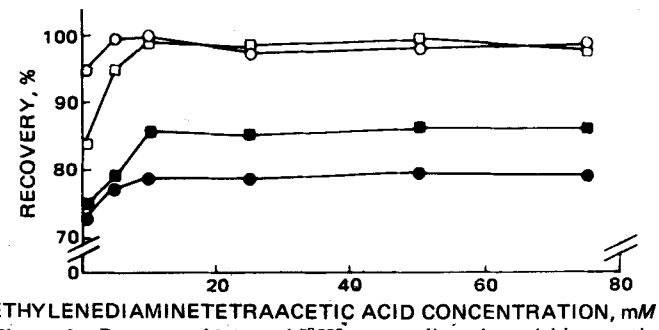


**Figure 3**—*Recovery of 0.1 μg of [$^3$H]tetracycline after trichloroacetic acid precipitation added to 0.1 ml of human serum (○), 1.0 ml of human serum (●), 0.25 ml of rat liver homogenate (20% w/v) (□), and 0.5 ml of rat liver homogenate (20% w/v) (■).*

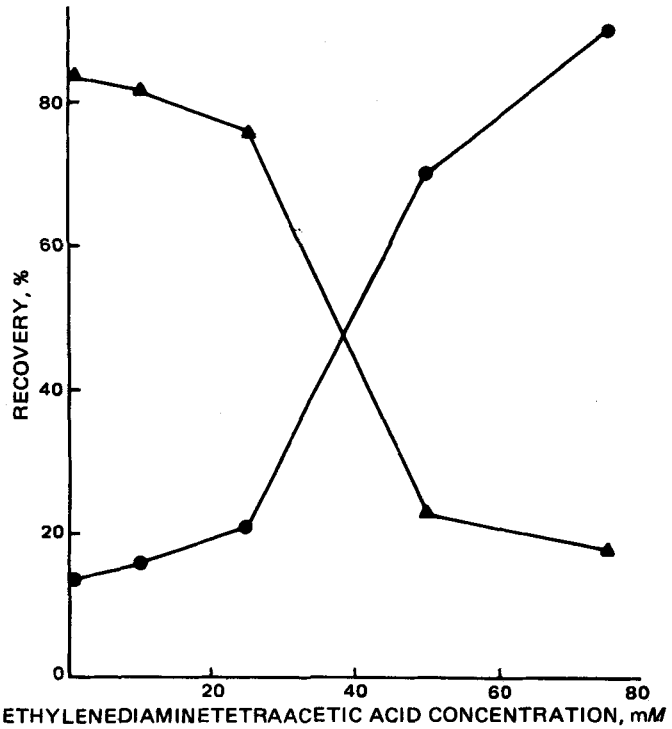


**Figure 4**—*Recovery of 1 μg of doxycycline/ml of distilled water or phosphate buffer at different ethylenediaminetetraacetic acid concentrations. Key: ●, distilled water; and ▲, 75 mM potassium phosphate buffer (pH 7.1).*

proved the recovery in this step in both serum and tissue but only to a small extent. The increase of ~10% was already reached at 10 m*M* ethylenediaminetetraacetic acid. Figure 3 also illustrates that the recovery was lower if more biological material was used.

Figure 4 shows the effect of ethylenediaminetetraacetic acid on the recovery of doxycycline in the presence and absence of 75 m*M* phosphate. Recovery was lowered from 80 to ~20% by the addition of ethylenediaminetetraacetic acid in the presence of phosphate but was raised from 15 to 90% in the absence of phosphate. It can be concluded that in the presence of phosphate and the absence of ethylenediaminetetraacetic acid, a large proportion of the lead ions are removed as lead phosphate, resulting in little lead iodide precipitation and negligible interference of phosphate or lead during the ethyl acetate extraction. In the presence of ethylenediaminetetraacetic acid and phosphate, the phosphate cannot be removed because of chelation of the lead ions. However, removal of phosphate is necessary because it strongly inhibits the extraction of tetracyclines into ethyl acetate (6).

On the other hand, small amounts of tissue or serum contain little phosphate. The excess lead ions that are not precipitated as lead phosphate now inhibit the extraction of tetracyclines into ethyl acetate. This implies that potassium iodide does not completely remove the lead ions. Addition of ethylenediaminetetraacetic acid seems to be more successful, resulting in much better recovery. Table II confirms these conclusions: the presence of ethylenediaminetetraacetic acid does improve the recovery from small amounts of liver homogenate but has no net effect on the recovery from large amounts.

In summary, it is obvious that the use of small samples of biological material, which contain little phosphate, to determine the tetracycline content of a particular sample offers several advantages, especially if the phosphate-precipitating steps are omitted. The procedure is less time consuming because of the omission of the phosphate-removing steps. Recoveries are between 80 and 100%. The high recoveries are the result of the low amount of trichloroacetic acid-precipitated material, which reduces the quantity of coprecipitated tetracycline, and of the avoidance of any loss caused by the unnecessary phosphate-precipitating steps.

The reliability of the modified method is indicated by the comparison of recoveries obtained by fluorometric and radioactivity counting measurements (Tables I and II). The recoveries were identical. A comparison of the amount of oxytetracycline measured fluorometrically and microbiologically is shown in Fig. 5.

Solutions of oxytetracycline in 0.9% NaCl at different pH values were

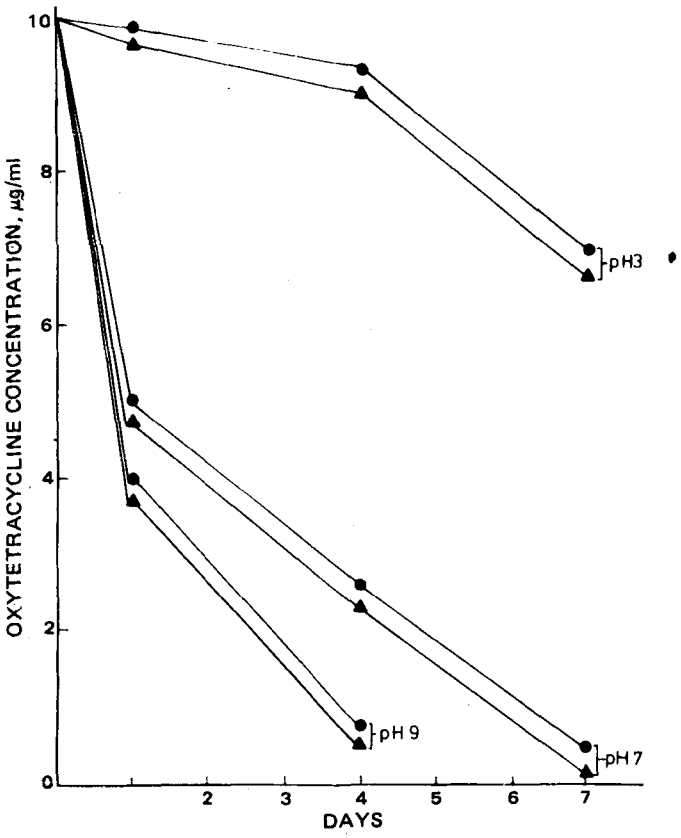


**Figure 5**—*Stability of solutions of different pH values containing 10 μg of oxytetracycline/ml. Key: ●, fluorometric assay; and ▲, microbiological assay.*

protected against light and kept at 20° for several days. The amount of oxytetracycline was determined fluorometrically and microbiologically on Days 1, 4, and 7 after preparation of the solutions.

Oxytetracycline values obtained fluorometrically are slightly elevated compared to those of the microbiological measurements, but the decrease in the oxytetracycline content is comparable. The stability of oxytetracycline depends on the pH of the solution (Fig. 5). Tetracycline solutions should be prepared fresh daily, unless it is possible to use an acid solution. For example, in tissue distribution studies, solutions of tetracyclines at pH 2 seemed to be suitable (and stable) in continuous intravenous infusions for up to 4 days. The comparable results obtained by the microbiological, fluorometric, and radioactivity assays suggest that the modified fluorometric determination gives fully reliable results in this type of study.

Böcker and Estler (13, 14) recently described a sensitive HPLC method for the determination of tetracyclines. The method presented in this paper has approximately the same sensitivity. It also is fast, and many samples can be handled at the same time. The HPLC method is more specific in that it discriminates among the various tetracyclines and their breakdown products. However, for most purposes such specificity is not required since a mixture of tetracyclines seldom is used. In the case of treatment with rolitetracycline, tetracycline can be formed. However,

**Table II—Recovery of [$^3$H]Tetracycline Measured in the Presence of Ethylenediaminetetraacetic Acid after Every Step of the Fluorometric Determination Procedure where 10 μg of [$^3$H]Tetracycline Was Added/5 ml of Homogenate (20% w/v)**

| Step in Procedure | Recovery, % 0.25 ml of Homogenate | Recovery, % 10 ml of Homogenate |
|---|---|---|
| After trichloroacetic acid precipitation | 94 | 41 |
| After lead phosphate precipitation | 100 | 100 |
| After lead iodide precipitation | 92 | 91 |
| After ethyl acetate extraction | 85 | 38 |
| Counting of radioactivity (net recovery) | 77 | 17 |
| Fluorometric measurement (net recovery) | 75 | 13 |

the antibacterial action of both antibiotics is similar. Moreover, the breakdown products comprise only a small (nondetectable) fraction of the tetracyclines after *in vivo* administration (14). In many cases, the fluorometric method, as presented here, may become the method of choice.

## REFERENCES


(1) "Methods of Analysis of the Association of Official Analytical Chemists," 12th ed., Association of Official Analytical Chemists, Washington, D.C., 1975.

(2) P. P. Ascione, J. B. Zagar, and G. P. Chrekian, *J. Pharm. Sci.*, **56**, 1396 (1967).

(3) A. P. de Leenheer and H. J. C. F. Nelis, *ibid.*, **68**, 999 (1979).

(4) L. G. Chatten, R. E. Moskalyk, R. A. Locock, and K.-S. Huang, *ibid.*, **65**, 1315 (1976).

(5) K. W. Kohn, *Anal. Chem.*, **33**, 362 (1961).

(6) H. Poiger and C. Schlatter, *Analyst*, **101**, 802 (1976).

(7) H. de Vries and A. M. Kroon, *Biochim. Biophys. Acta*, **204**, 531 (1970).

(8) W. P. Gijzel, M. Strating, and A. M. Kroon, *Cell Differ.*, **1**, 191 (1972).

(9) W. P. Gijzel and A. M. Kroon, *J. Mol. Med.*, **3**, 157 (1978).

(10) J. A. Leezenberg, H. Wesseling, and A. M. Kroon, *Eur. J. Clin. Pharmacol.*, **16**, 237 (1979).

(11) J. Hoette and A. P. Struyk, *J. Lab. Clin. Med.*, **51**, 638 (1959).

(12) H. Zia and J. C. Price, *J. Pharm. Sci.*, **65**, 226 (1976).

(13) R. Böcker and C. J. Estler, *Arzneim.-Forsch.*, **29**, 1690 (1979).

(14) *Ibid.*, **29**, 1693 (1979).


## ACKNOWLEDGMENTS


Supported by a grant from the Dutch Organization for the Advancement of Pure Research, ZWO.

The authors thank Mr. E. H. J. Dontje and Mr. J. J. Wybenga for technical assistance.


# Sepiolite, a Potential Excipient for Drugs Subject to Oxidative Degradation


**MARIA C. HERMOSIN *, JUAN CORNEJO *, JOE L. WHITE *, and STANLEY L. HEM ‡×**



Received May 5, 1980, from the *Departments of *Agronomy and ‡Industrial and Physical Pharmacy, Purdue University, West Lafayette, IN 47907.* Accepted for publication July 29, 1980.



**Abstract** □ Sepiolite, a member of the fibrous mineral group of clays, is relatively free of surface ferric iron and does not accelerate significantly the oxidative degradation of hydrocortisone. The compatibility of sepiolite with drugs that can undergo oxidative degradation is in sharp contrast to the catalytic effect of attapulgite, another fibrous mineral, which contains a significant amount of surface ferric iron and which therefore accelerates oxidative degradation. Sepiolite adsorbs hydrocortisone by a weak adsorption mechanism, which was shown by IR spectroscopy to be chiefly due to hydrogen bonding. However, accelerated oxidative degradation of the adsorbed hydrocortisone does not occur. Maximum adsorption occurs at pH 7–8.5. Desorption occurs readily by washing with water. Sepiolite has similar rheological properties to attapulgite. The results of this study suggest that sepiolite may be useful as a pharmaceutical excipient for drugs that undergo oxidative degradation.



**Keyphrases** □ Sepiolite—potential as excipient for drugs subject to oxidative degradation □ Excipients—potential of sepiolite as excipient for drugs subject to oxidative degradation □ Clays—sepiolite, potential as excipient for drugs subject to oxidative degradation □ Adsorption—sepiolite, potential excipient evaluated for use with drugs subject to oxidative degradation


A recent study (1) demonstrated that hydrocortisone is adsorbed weakly by attapulgite and subsequently undergoes oxidative degradation, catalyzed by both adsorbed iron oxides and hydroxides as well as by structural ferric iron at the clay surface. Other clays such as montmorillonite (2–4) and hectorite (5, 6) promote the oxidation of organic compounds. Surface-adsorbed contaminants or structural ferric iron at the clay surface have been suggested as being responsible for the oxidation of organic materials by these clays.

## BACKGROUND

Attapulgite, which frequently is termed palygorskite in clay mineralogy literature, is a member of the fibrous mineral group of clays. The fibrous minerals are similar to the smectite group of clays, which includes montmorillonite, hectorite, and saponite, since they are 2:1 type minerals consisting of a layer of magnesium octahedra sandwiched between two silica tetrahedral sheets. However, their properties are significantly different from the smectite group since crystal growth is limited to the C-dimension, resulting in ribbons of the 2:1 layer attached at their longitudinal edges. A cross section of the fiber gives a checkerboard arrangement of ribbons and voids with no possibility of expansion. In addition, the fibrous minerals have little or no true cation-exchange capacity. However, because of the very thin nature of the ribbons, the external surface area is moderately high. Fibrous minerals also are very porous due to the channels between the ribbons. However, little adsorption occurs within the pores since the dimensions of the pores can accommodate only small molecules such as water, ammonia, and lower alcohols (7).

Sepiolite also belongs to the fibrous mineral group of clays and has an ideal formula, external surface area, internal surface, and channel dimensions that are very similar to attapulgite (Table I). However, there is a striking difference in the ferric iron content of natural samples. Sepiolite samples contain much less ferric iron than is found in attapulgite samples. Since the surface ferric iron is responsible for catalyzing the oxidative degradation, it was decided to investigate the effect of sepiolite on the oxidative degradation of hydrocortisone. In addition, since sepiolite has not been mentioned as a pharmaceutical excipient or as a GI adsorbent, the rheological properties of sepiolite suspensions were compared to attapulgite suspensions to determine if sepiolite could be considered for such use.

## EXPERIMENTAL

**Materials**—All chemicals were official or reagent grade. The vallecas sepiolite studied was obtained from a deposit near Madrid, Spain, and was used as received. X-ray diffractograms indicated that sepiolite was the major mineral present, although a small amount of calcite also was found. The total iron content was determined by hydrofluoric acid dissolution (8).

**Hydrocortisone Assay**—A high-pressure liquid chromatographic (HPLC) method that was recommended for the analysis of hydrocortisone tablets (9) was modified slightly for this study. The liquid chro-



© 1981, American Pharmaceutical Association

the antibacterial action of both antibiotics is similar. Moreover, the breakdown products comprise only a small (nondetectable) fraction of the tetracyclines after *in vivo* administration (14). In many cases, the fluorometric method, as presented here, may become the method of choice.

## REFERENCES


(1) "Methods of Analysis of the Association of Official Analytical Chemists," 12th ed., Association of Official Analytical Chemists, Washington, D.C., 1975.

(2) P. P. Ascione, J. B. Zagar, and G. P. Chrekian, *J. Pharm. Sci.*, **56**, 1396 (1967).

(3) A. P. de Leenheer and H. J. C. F. Nelis, *ibid.*, **68**, 999 (1979).

(4) L. G. Chatten, R. E. Moskalyk, R. A. Locock, and K.-S. Huang, *ibid.*, **65**, 1315 (1976).

(5) K. W. Kohn, *Anal. Chem.*, **33**, 362 (1961).

(6) H. Poiger and C. Schlatter, *Analyst*, **101**, 802 (1976).

(7) H. de Vries and A. M. Kroon, *Biochim. Biophys. Acta*, **204**, 531 (1970).

(8) W. P. Gijzel, M. Strating, and A. M. Kroon, *Cell Differ.*, **1**, 191 (1972).

(9) W. P. Gijzel and A. M. Kroon, *J. Mol. Med.*, **3**, 157 (1978).

(10) J. A. Leezenberg, H. Wesseling, and A. M. Kroon, *Eur. J. Clin. Pharmacol.*, **16**, 237 (1979).

(11) J. Hoette and A. P. Struyk, *J. Lab. Clin. Med.*, **51**, 638 (1959).

(12) H. Zia and J. C. Price, *J. Pharm. Sci.*, **65**, 226 (1976).

(13) R. Böcker and C. J. Estler, *Arzneim.-Forsch.*, **29**, 1690 (1979).

(14) *Ibid.*, **29**, 1693 (1979).


## ACKNOWLEDGMENTS


Supported by a grant from the Dutch Organization for the Advancement of Pure Research, ZWO.

The authors thank Mr. E. H. J. Dontje and Mr. J. J. Wybenga for technical assistance.


# Sepiolite, a Potential Excipient for Drugs Subject to Oxidative Degradation


**MARIA C. HERMOSIN *, JUAN CORNEJO *, JOE L. WHITE *, and STANLEY L. HEM ‡×**



Received May 5, 1980, from the *Departments of *Agronomy and ‡Industrial and Physical Pharmacy, Purdue University, West Lafayette, IN 47907.* Accepted for publication July 29, 1980.



**Abstract** □ Sepiolite, a member of the fibrous mineral group of clays, is relatively free of surface ferric iron and does not accelerate significantly the oxidative degradation of hydrocortisone. The compatibility of sepiolite with drugs that can undergo oxidative degradation is in sharp contrast to the catalytic effect of attapulgite, another fibrous mineral, which contains a significant amount of surface ferric iron and which therefore accelerates oxidative degradation. Sepiolite adsorbs hydrocortisone by a weak adsorption mechanism, which was shown by IR spectroscopy to be chiefly due to hydrogen bonding. However, accelerated oxidative degradation of the adsorbed hydrocortisone does not occur. Maximum adsorption occurs at pH 7–8.5. Desorption occurs readily by washing with water. Sepiolite has similar rheological properties to attapulgite. The results of this study suggest that sepiolite may be useful as a pharmaceutical excipient for drugs that undergo oxidative degradation.



**Keyphrases** □ Sepiolite—potential as excipient for drugs subject to oxidative degradation □ Excipients—potential of sepiolite as excipient for drugs subject to oxidative degradation □ Clays—sepiolite, potential as excipient for drugs subject to oxidative degradation □ Adsorption—sepiolite, potential excipient evaluated for use with drugs subject to oxidative degradation


A recent study (1) demonstrated that hydrocortisone is adsorbed weakly by attapulgite and subsequently undergoes oxidative degradation, catalyzed by both adsorbed iron oxides and hydroxides as well as by structural ferric iron at the clay surface. Other clays such as montmorillonite (2–4) and hectorite (5, 6) promote the oxidation of organic compounds. Surface-adsorbed contaminants or structural ferric iron at the clay surface have been suggested as being responsible for the oxidation of organic materials by these clays.

## BACKGROUND

Attapulgite, which frequently is termed palygorskite in clay mineralogy literature, is a member of the fibrous mineral group of clays. The fibrous minerals are similar to the smectite group of clays, which includes montmorillonite, hectorite, and saponite, since they are 2:1 type minerals consisting of a layer of magnesium octahedra sandwiched between two silica tetrahedral sheets. However, their properties are significantly different from the smectite group since crystal growth is limited to the C-dimension, resulting in ribbons of the 2:1 layer attached at their longitudinal edges. A cross section of the fiber gives a checkerboard arrangement of ribbons and voids with no possibility of expansion. In addition, the fibrous minerals have little or no true cation-exchange capacity. However, because of the very thin nature of the ribbons, the external surface area is moderately high. Fibrous minerals also are very porous due to the channels between the ribbons. However, little adsorption occurs within the pores since the dimensions of the pores can accommodate only small molecules such as water, ammonia, and lower alcohols (7).

Sepiolite also belongs to the fibrous mineral group of clays and has an ideal formula, external surface area, internal surface, and channel dimensions that are very similar to attapulgite (Table I). However, there is a striking difference in the ferric iron content of natural samples. Sepiolite samples contain much less ferric iron than is found in attapulgite samples. Since the surface ferric iron is responsible for catalyzing the oxidative degradation, it was decided to investigate the effect of sepiolite on the oxidative degradation of hydrocortisone. In addition, since sepiolite has not been mentioned as a pharmaceutical excipient or as a GI adsorbent, the rheological properties of sepiolite suspensions were compared to attapulgite suspensions to determine if sepiolite could be considered for such use.

## EXPERIMENTAL

**Materials**—All chemicals were official or reagent grade. The vallecas sepiolite studied was obtained from a deposit near Madrid, Spain, and was used as received. X-ray diffractograms indicated that sepiolite was the major mineral present, although a small amount of calcite also was found. The total iron content was determined by hydrofluoric acid dissolution (8).

**Hydrocortisone Assay**—A high-pressure liquid chromatographic (HPLC) method that was recommended for the analysis of hydrocortisone tablets (9) was modified slightly for this study. The liquid chro-



© 1981, American Pharmaceutical Association

**Table I—Comparison of Formula and Dimensions of Sepiolite and Attapulgite**

| | Sepiolite | Attapulgite |
|---|---|---|
| Ideal formula | $(OH_2)_4(OH)_4Mg_8Si_{12}O_{30}8H_2O$[a] | $(OH_2)_4(OH)_2Mg_5Si_8O_{20}4H_2O$[b] |
| Natural sample formula | $(OH_2)_4(OH)_4(Si_{11.92}Al_{0.08})(Al_{0.52}Fe^{3+}_{0.02})(Mg_{6.98}Fe^{2+}_{0.08})$[c] | $(OH_2)_4(OH)_2(Si_{0.83}Al_{0.17})(Al_{1.36}Ti_{0.07}Fe^{3+}_{0.37})(Fe^{2+}_{0.03}Mg_{1.98})$[b] |
| External surface area, $m^2/g$ | 400[d] | 280[d] |
| Internal surface area, $m^2/g$ | 500[d] | 635[d] |
| Channel dimensions, Å | $3.7 \times 10.6$[d] | $3.7 \times 6.4$[d] |

[a] K. Brauner and A. Preisinger, *Tschermaks Mineral Petrogr. Mitt.*, **6**, 120 (1956). [b] W. F. Bradley, *Am. Miner.*, **25**, 405 (1940). [c] J. L. Ahlrichs, C. Serna, and J. M. Serratosa, *Clays Clay Miner.*, **23**, 119 (1975). [d] Reference 7.

matograph[1] was equipped with a UV detector operating at 254 nm and a 20-μl injector loop[2]. A commercially packed octadecylsilane[3] column was used with acetonitrile–water (35:65) as the mobile phase. The operating parameters were: flow rate, 1 ml/min; pressure, 1000–1200 psi; temperature, ambient; and UV attenuator, 0.02 aufs. Linear calibration curves were used to quantify the hydrocortisone content of the aqueous phase, while the relative concentration of the observed degradation products was characterized by peak heights.

Changes in the A-ring of hydrocortisone were monitored by UV spectrometry at 254 nm.

**IR Analysis**—Self-supporting films were prepared for IR analysis[4] by pipetting appropriate volumes of either sepiolite or hydrocortisone–sepiolite suspensions onto polyethylene terephthalate[5] and air drying at room temperature (10).

Hydrocortisone was prepared for IR analysis as a potassium bromide pellet.

**Kinetic Studies**—The sepiolite concentration was selected as representative of the range of clay usually used in pharmaceuticals; the hydrocortisone concentration was chosen to be below the solubility limit, 280 μg/ml at 25° (11), to ensure complete solubility during the kinetic studies. Thus, 300 mg of sepiolite was mixed with 25 ml of an aqueous solution of hydrocortisone (200 μg/ml) in a 50-ml stoppered centrifuge tube. The pH was adjusted with hydrochloric acid to pH 8.4 to compare the chemical stability of hydrocortisone in the presence of sepiolite with the results reported previously (1) for hydrocortisone–attapulgite suspensions. The samples were aged in a constant-temperature shaker bath at 23°. At appropriate intervals, aliquots were taken and centrifuged at 6000 rpm, and the supernate was filtered and analyzed by HPLC and UV spectrometry. The pH was 8.4 at each sampling.

Aqueous solutions of hydrocortisone (200 μg/ml) adjusted to pH 8.4 with sodium hydroxide were aged with the hydrocortisone–sepiolite suspensions and served as controls.

**Adsorption Isotherm**—Hydrocortisone–sepiolite suspensions were prepared as described, except that hydrocortisone concentrations of 1–200 μg/ml were used. The suspensions were equilibrated in the constant-temperature shaker bath at 23° for 24 hr. The amount of hydrocortisone adsorbed was calculated from the change in the hydrocortisone concentration of the supernate after equilibration as determined by HPLC assay and UV spectrometry at 254 nm.

Desorption studies were performed by recovering the equilibrated sepiolite from the adsorption study and resuspending the sepiolite in sufficient water, adjusted to pH 8.4, to achieve the original sepiolite concentration. After equilibration for 30 min in the constant-temperature shaker bath at 23°, the procedure was repeated to give sepiolite samples, which were washed one, two, or three times. The hydrocortisone concentration desorbed in each washing was determined by HPLC.

**Effect of pH on Adsorption**—Eight hydrocortisone–sepiolite suspensions were prepared at pH 2.4, 3.2, 5.3, 6.8, 7.8, 8.5, 9.2, and 9.8 by adding 20 ml of a hydrocortisone stock solution (250 μg/ml) to 300 mg of sepiolite. Each suspension was adjusted to the desired pH with hydrochloric acid or sodium hydroxide. The suspensions were diluted to 25 ml with water to produce sepiolite suspensions containing 200 μg of hydrocortisone/ml. The suspensions were equilibrated for 24 hr in the constant-temperature shaker bath at 23°. The concentration of hydrocortisone adsorbed was determined as described under *Adsorption Isotherm*.

**Viscosity Measurement**—The rheological properties of 1 and 2% sepiolite suspensions were compared to 1 and 2% attapulgite suspensions using a rotational viscometer[6] with spindle 1. The suspensions were prepared by sonicating each suspension for 1 min.

## RESULTS AND DISCUSSION

Hydrocortisone exhibited very slow degradation in aqueous solution at pH 8.4, which is consistent with previously reported stability results (1, 12, 13). In a sepiolite suspension, the hydrocortisone content of the aqueous phase decreased from 200 to 125 μg/ml during the 1st hr and very slowly during the next 170 hr (Fig. 1). As noted in Fig. 1, identical stability results were obtained by HPLC and UV analysis.

The previously reported (1) degradation profile of hydrocortisone in an attapulgite suspension as determined by HPLC analysis also is shown in Fig. 1. The initial decrease in the hydrocortisone content as a result of interaction with attapulgite was less than was observed in the presence of sepiolite. However, the hydrocortisone content of the aqueous phase of the attapulgite suspension decreased substantially during the entire 170 hr of the study. Furthermore, except for a small initial decrease, UV spectroscopy showed no change in the hydrocortisone concentration when the hydrocortisone–attapulgite suspensions were aged at 23, 38, 50, and 69° (1).

The HPLC and UV analyses of the hydrocortisone–sepiolite suspensions suggested that hydrocortisone is adsorbed by sepiolite, producing

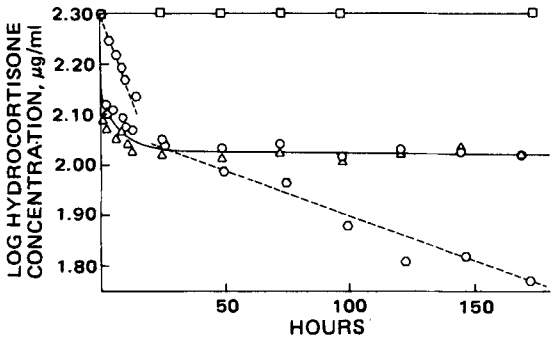


**Figure 1**—*Change in hydrocortisone concentration of aqueous phase (theory = 200 μg/ml) during aging at pH 8.4 and 23°. Key: □, hydrocortisone solution determined by HPLC; △, sepiolite suspension determined by HPLC; ○, sepiolite suspension determined by UV spectrometry; and ○, attapulgite suspension determined by HPLC from Ref. 1.*

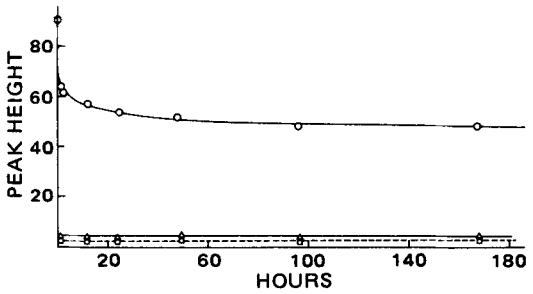


**Figure 2**—*Relative concentration of hydrocortisone and degradation products in sepiolite suspensions at pH 8.4 during aging at 23°. Key: ○, hydrocortisone; △, degradation product with a retention time of 2.5 min; and □, degradation product with a retention time of 11 min.*

[1] Model ALC 202, Waters Associates, Framingham, Mass.
[2] Rheodyne, Berkeley, Calif.
[3] Partisil-10 ODS, Whatman Inc., Clifton, N.J.
[4] Model 180, Perkin-Elmer Corp., Norwalk, Conn.
[5] Mylar.
[6] Model RVT, Brookfield Engineering Laboratories, Stoughton, Mass.

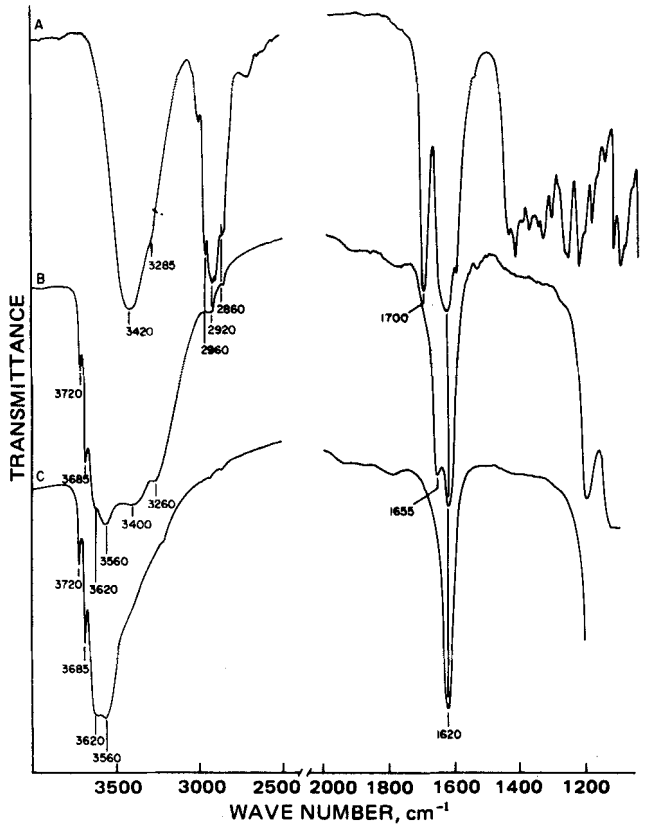


**Figure 3**—*IR spectra of hydrocortisone in a potassium bromide pellet (A), a film of equilibrated hydrocortisone–sepiolite suspension at pH 8.4 (B), and a film of sepiolite (C).*

an immediate decrease in the hydrocortisone concentration. However, little degradation of hydrocortisone appears to occur in the sepiolite suspension. This hypothesis is confirmed by analysis of the peaks appearing in the high-pressure liquid chromatogram. With the HPLC system used, hydrocortisone has a retention time of 8 min, while the two initial degradation products of hydrocortisone have retention times of 2.5 and 11 min (1). The peak height of the hydrocortisone peak dropped initially for the sepiolite suspension but changed relatively little on aging (Fig. 2). However, the peak height for the peaks corresponding to the two initial degradation products was very low and increased only slightly on aging. Thus, in contrast to the hydrocortisone–attapulgite suspension (1), it does not appear that hydrocortisone degrades very rapidly in the presence of sepiolite. The initial decrease in the hydrocortisone concentration seems to be due to adsorption of hydrocortisone by sepiolite rather than to accelerated degradation of hydrocortisone.

The adsorption of hydrocortisone by sepiolite was examined by IR spectroscopy. Figure 3A shows the IR spectrum of hydrocortisone in a potassium bromide pellet. The IR spectrum of sepiolite is shown in Fig. 3C. The IR spectrum of the hydrocortisone–sepiolite suspension at pH 8.4 (Fig. 3B) shows the hydroxyl stretching vibration of sepiolite at 3720 and 3685 $cm^{-1}$. Water displayed asymmetric hydroxyl stretching bands at 3620 and 3560 $cm^{-1}$ and a hydroxyl bending vibration at 1620 $cm^{-1}$. Hydrocortisone absorption bands were evident at 3400, 3260, 2960, 2920, 2860, and 1655 $cm^{-1}$. The IR spectrum of hydrocortisone–sepiolite

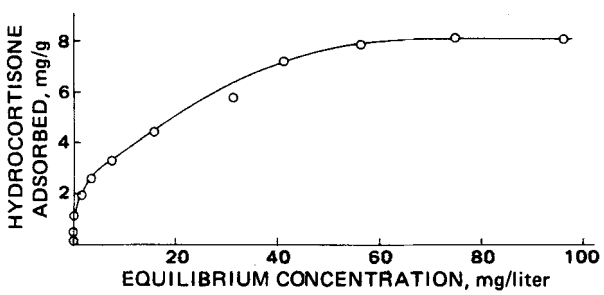


**Figure 4**—*Adsorption isotherm for hydrocortisone by sepiolite.*

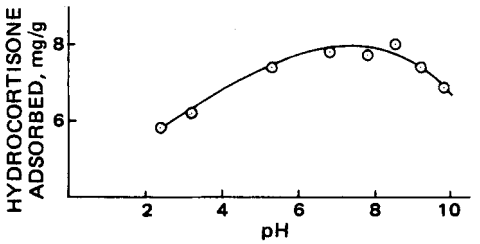


**Figure 5**—*Effect of pH on adsorption of hydrocortisone by sepiolite.*

supports a weak adsorption mechanism. Generally, adsorption due to hydrogen bonding can be detected by shifts in the absorption bands of participating functional groups. Some hydroxyl groups of hydrocortisone might be expected to take part in hydrogen bonding with the clay surface. Evidence for hydrogen bonding is seen in the shift of the hydroxyl stretching vibrations of hydrocortisone at 3420 and 3285 $cm^{-1}$ to 3400 and 3260 $cm^{-1}$ in the presence of sepiolite. In addition, the carbonyl stretching vibration of the C-17 hydrocortisone side chain was shifted from 1700 to 1655 $cm^{-1}$ as a result of interaction with sepiolite. The shift of these groups to a lower frequency suggests that hydrogen bonding is the principal adsorption mechanism, although van der Waals forces also may contribute. The fact that the CH-stretching vibrations at 2960, 2920, and 2860 $cm^{-1}$ were not shifted in the presence of sepiolite suggests that the energy of interaction with sepiolite is similar to the intermolecular bonding in hydrocortisone. The IR spectrum clearly shows significant adsorption of hydrocortisone by sepiolite. This finding also is in sharp contrast to the interaction of hydrocortisone with attapulgite, where no change in the IR spectrum was observed after interaction with hydrocortisone (1).

To evaluate the amount of hydrocortisone adsorbed by sepiolite, the adsorption isotherm at pH 8.4 was determined (Fig. 4). The isotherm is of the L or Langmuir type according to the classification of Giles *et al.* (14), who, along with Knight and Tomlinson (15), suggested that this type of isotherm indicates a specific interaction between the adsorbate and the adsorption sites. The adsorption data were applied to both the theoretical Langmuir isotherm equation and the empirical Freundlich equation. The adsorption data gave a good linear fit with both the Langmuir and Freundlich isothermal plots ($r$ = 0.9901 and 0.9937, respectively). The maximum adsorption of hydrocortisone by sepiolite as determined by the slope of the Langmuir plot was 8.75 mg/g.

The adsorption of hydrocortisone by sepiolite is pH dependent (Fig. 5). Maximum adsorption occurred between pH 7 and 8.5. It is hypothesized that the surface Si-OH groups of sepiolite are uncharged in this pH range. Thus, interaction occurs most strongly between the neutral hydrocortisone molecule and the neutral sepiolite surface.

Desorption studies also confirmed that hydrocortisone is adsorbed weakly by sepiolite since it was desorbed readily by washing with water at pH 2.9, 6.8, or 9.8 (Table II).

The rheograms of 1 and 2% sepiolite suspensions are very similar to the rheograms of 1 and 2% attapulgite suspensions, suggesting that sepiolite could be used in place of attapulgite as a pharmaceutical excipient (Fig. 6).

The minimal effect of sepiolite on the oxidative degradation of hydrocortisone in comparison to the catalytic effect of attapulgite is consistent with the small amount of iron (0.3%) present in the sepiolite

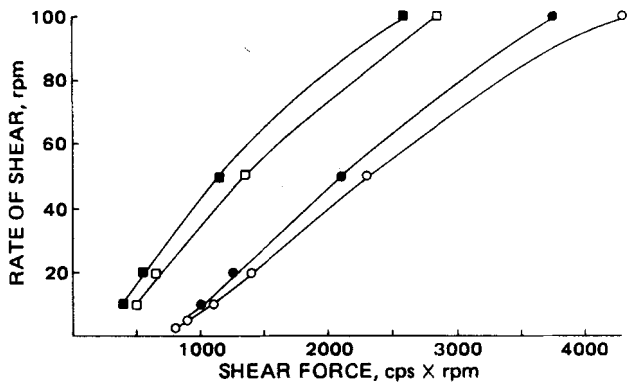


**Figure 6**—*Rheograms of sepiolite and attapulgite suspensions. Key: ■, 1% sepiolite; □, 2% sepiolite; ●, 1% attapulgite; and ○, 2% attapulgite.*

Table II—Desorption from Hydrocortisone–Sepiolite Suspensions by Washing with Water

| pH | Hydrocortisone Adsorbed, mg/g | Hydrocortisone Desorbed, mg/g | | |
|---|---|---|---|---|
| | | First Wash | Second Wash | Third Wash |
| 2.9 | 5.75 | 1.03 | 0.63 | 0.60 |
| 6.8 | 7.91 | 3.17 | 1.45 | 0.86 |
| 9.8 | 6.69 | 1.50 | 0.88 | 0.80 |

sample compared to the iron content of the attapulgite studied previously (2.6%). The oxidative degradation of hydrocortisone is affected minimally by sepiolite, although significant adsorption occurs. Adsorption of hydrocortisone by sepiolite can be explained by the high external surface area of sepiolite (400 $m^2/g$). However, attapulgite also has a significant external surface area (280 $m^2/g$), but no adsorption of hydrocortisone by attapulgite was observed by IR spectroscopy (1). It is hypothesized that the contact time needed for adsorption is greater than the contact time needed for the ferric iron-catalyzed oxidative degradation. Thus, in clays with a high ferric iron content, oxidative degradation is the predominant reaction. However, in clays such as sepiolite with a low ferric iron content and, therefore, a much smaller catalytic effect, the major reaction is adsorption.

The results of this study strongly suggest that sepiolite should be considered for use in pharmaceuticals. It has a very similar structure to attapulgite but a greater external surface area, which suggests that sepiolite will have excellent properties as a GI adsorbent. In addition, sepiolite is a desirable clay for use as a pharmaceutical excipient since its low ferric iron content means that it is compatible with drugs such as hydrocortisone that degrade by oxidative degradation. In addition, the reversible nature of the adsorption of hydrocortisone by sepiolite suggests that the bioavailability of neutral drugs will not be affected significantly by interaction with sepiolite. Finally, the rheological properties of sepiolite suspensions are very similar to attapulgite suspensions.

## REFERENCES


(1) J. Cornejo, M. C. Hermosin, J. L. White, G. E. Peck, and S. L. Hem, *J. Pharm. Sci.*, **69**, 945 (1980).

(2) K. Kumada and H. Kato, *Soil Sci. Plant Nutr.*, **16**, 195 (1970).

(3) T. D. Thompson and W. F. Moll, Jr., *Clays Clay Miner.*, **21**, 337 (1973).

(4) B. K. G. Theng, "The Chemistry of Clay-Organic Reactions," Adam Hilger, London, England, 1974, pp. 263, 264.

(5) D. H. Solomon, B. C. Loft, and A. J. Swift, *Clay Miner.*, **7**, 389 (1968).

(6) M. B. McBride, *Clays Clay Miner.*, **27**, 224 (1979).

(7) C. J. Serna and G. E. Van Scoyoc, in "Proceedings of the International Clay Mineral Conference–1978," V. C. Farmer and M. M. Mortland, Eds., Elsevier, Amsterdam, The Netherlands, 1979, pp. 197–206.

(8) C. B. Roth, M. L. Jackson, E. G. Lotse, and J. K. Syers, *Isr. J. Chem.*, **6**, 361 (1968).

(9) "Analysis of Pharmaceutical Products," Waters Associates, Milford, Mass., 1976, p. 9.

(10) L. S. Porubcan, C. J. Serna, J. L. White, and S. L. Hem, *J. Pharm. Sci.*, **67**, 1081 (1978).

(11) "The Merck Index," 9th ed., Merck & Co., Rahway, N.J., 1976, p. 629.

(12) T. Takubo, T. Tadaka, and T. Sauwai, *Yakuzaigaku*, **22**, 66 (1962).

(13) I. H. Pitman, T. Higuchi, M. Alton, and R. Wiley, *J. Pharm. Sci.*, **61**, 918 (1972).

(14) C. H. Giles, T. H. MacEwan, S. N. Nakhwa, and D. Smith, *J. Chem. Soc.*, **1960**, 2973.

(15) B. A. G. Knight and T. E. Tomlinson, *J. Soil Sci.*, **18**, 233 (1967).


## ACKNOWLEDGMENTS


J. Cornejo gratefully acknowledges the support of the United States–Spanish Joint Committee for Scientific and Technical Cooperation.

This report is Journal Paper 8056, Purdue University Agricultural Experiment Station, West Lafayette, IN 47907.


# Synthesis and Anticonvulsant Activity of Racemic 2-Amino-*N*-substituted Succinimide Derivatives


**A. MICHAEL CRIDER ˣ, THOMAS M. KOLCZYNSKI, and DAVID L. MISKELL**



Received June 16, 1980, from the *College of Pharmacy, University of Toledo, Toledo, OH 43606.* Accepted for publication July 25, 1980.



**Abstract** □ Several derivatives of (*R,S*)-2-amino-*N*-substituted succinimides were synthesized and evaluated in mice against seizures produced by electroshock and pentylenetetrazol. The most active compound against both electroshock- and pentylenetetrazol-induced seizures was (*R,S*)-*N*-benzyl-2-(methanesulfamido)succinimide.



**Keyphrases** □ 2-Amino-*N*-substituted succinimide derivatives—synthesis and evaluation for anticonvulsant activity □ Anticonvulsant activity—2-amino-*N*-substituted succinimide derivatives, synthesis and evaluation for activity □ Structure–activity relationships—2-amino-*N*-substituted succinimide derivatives, synthesis and evaluation for anticonvulsant activity


Many epileptic seizures cannot be controlled by currently available anticonvulsants. Furthermore, those individuals whose seizures are controlled often tolerate harmful side effects (1). The development of carbamazepine and valproic acid has improved seizure protection for epileptics, of whom only 50% were completely protected by previously marketed antiepileptic drugs. Despite the beneficial effects of these drugs, new anticonvulsants with more selective action and less toxicity are needed (2).

## BACKGROUND

In the development of new anticonvulsants, most attention has been centered on the ureide structure (I). Three succinimides, phensuximide, methsuximide, and ethosuximide, that contain this basic structure are used in the treatment of petit mal epilepsy (3).

Witiak *et al.* (4) reported the synthesis and anticonvulsant activity of




*0022-3549/81/0200-0192$01.00/0*


*© 1981, American Pharmaceutical Association*

Table II—Desorption from Hydrocortisone–Sepiolite Suspensions by Washing with Water

| pH | Hydrocortisone Adsorbed, mg/g | Hydrocortisone Desorbed, mg/g | | |
|---|---|---|---|---|
| | | First Wash | Second Wash | Third Wash |
| 2.9 | 5.75 | 1.03 | 0.63 | 0.60 |
| 6.8 | 7.91 | 3.17 | 1.45 | 0.86 |
| 9.8 | 6.69 | 1.50 | 0.88 | 0.80 |

sample compared to the iron content of the attapulgite studied previously (2.6%). The oxidative degradation of hydrocortisone is affected minimally by sepiolite, although significant adsorption occurs. Adsorption of hydrocortisone by sepiolite can be explained by the high external surface area of sepiolite (400 $m^2/g$). However, attapulgite also has a significant external surface area (280 $m^2/g$), but no adsorption of hydrocortisone by attapulgite was observed by IR spectroscopy (1). It is hypothesized that the contact time needed for adsorption is greater than the contact time needed for the ferric iron-catalyzed oxidative degradation. Thus, in clays with a high ferric iron content, oxidative degradation is the predominant reaction. However, in clays such as sepiolite with a low ferric iron content and, therefore, a much smaller catalytic effect, the major reaction is adsorption.

The results of this study strongly suggest that sepiolite should be considered for use in pharmaceuticals. It has a very similar structure to attapulgite but a greater external surface area, which suggests that sepiolite will have excellent properties as a GI adsorbent. In addition, sepiolite is a desirable clay for use as a pharmaceutical excipient since its low ferric iron content means that it is compatible with drugs such as hydrocortisone that degrade by oxidative degradation. In addition, the reversible nature of the adsorption of hydrocortisone by sepiolite suggests that the bioavailability of neutral drugs will not be affected significantly by interaction with sepiolite. Finally, the rheological properties of sepiolite suspensions are very similar to attapulgite suspensions.

## REFERENCES


(1) J. Cornejo, M. C. Hermosin, J. L. White, G. E. Peck, and S. L. Hem, *J. Pharm. Sci.*, **69**, 945 (1980).

(2) K. Kumada and H. Kato, *Soil Sci. Plant Nutr.*, **16**, 195 (1970).

(3) T. D. Thompson and W. F. Moll, Jr., *Clays Clay Miner.*, **21**, 337 (1973).

(4) B. K. G. Theng, "The Chemistry of Clay-Organic Reactions," Adam Hilger, London, England, 1974, pp. 263, 264.

(5) D. H. Solomon, B. C. Loft, and A. J. Swift, *Clay Miner.*, **7**, 389 (1968).

(6) M. B. McBride, *Clays Clay Miner.*, **27**, 224 (1979).

(7) C. J. Serna and G. E. Van Scoyoc, in "Proceedings of the International Clay Mineral Conference–1978," V. C. Farmer and M. M. Mortland, Eds., Elsevier, Amsterdam, The Netherlands, 1979, pp. 197–206.

(8) C. B. Roth, M. L. Jackson, E. G. Lotse, and J. K. Syers, *Isr. J. Chem.*, **6**, 361 (1968).

(9) "Analysis of Pharmaceutical Products," Waters Associates, Milford, Mass., 1976, p. 9.

(10) L. S. Porubcan, C. J. Serna, J. L. White, and S. L. Hem, *J. Pharm. Sci.*, **67**, 1081 (1978).

(11) "The Merck Index," 9th ed., Merck & Co., Rahway, N.J., 1976, p. 629.

(12) T. Takubo, T. Tadaka, and T. Sauwai, *Yakuzaigaku*, **22**, 66 (1962).

(13) I. H. Pitman, T. Higuchi, M. Alton, and R. Wiley, *J. Pharm. Sci.*, **61**, 918 (1972).

(14) C. H. Giles, T. H. MacEwan, S. N. Nakhwa, and D. Smith, *J. Chem. Soc.*, **1960**, 2973.

(15) B. A. G. Knight and T. E. Tomlinson, *J. Soil Sci.*, **18**, 233 (1967).


## ACKNOWLEDGMENTS


J. Cornejo gratefully acknowledges the support of the United States–Spanish Joint Committee for Scientific and Technical Cooperation.

This report is Journal Paper 8056, Purdue University Agricultural Experiment Station, West Lafayette, IN 47907.


# Synthesis and Anticonvulsant Activity of Racemic 2-Amino-*N*-substituted Succinimide Derivatives


**A. MICHAEL CRIDER ˣ, THOMAS M. KOLCZYNSKI, and DAVID L. MISKELL**



Received June 16, 1980, from the *College of Pharmacy, University of Toledo, Toledo, OH 43606.* Accepted for publication July 25, 1980.



**Abstract** □ Several derivatives of (*R,S*)-2-amino-*N*-substituted succinimides were synthesized and evaluated in mice against seizures produced by electroshock and pentylenetetrazol. The most active compound against both electroshock- and pentylenetetrazol-induced seizures was (*R,S*)-*N*-benzyl-2-(methanesulfamido)succinimide.



**Keyphrases** □ 2-Amino-*N*-substituted succinimide derivatives—synthesis and evaluation for anticonvulsant activity □ Anticonvulsant activity—2-amino-*N*-substituted succinimide derivatives, synthesis and evaluation for activity □ Structure–activity relationships—2-amino-*N*-substituted succinimide derivatives, synthesis and evaluation for anticonvulsant activity


Many epileptic seizures cannot be controlled by currently available anticonvulsants. Furthermore, those individuals whose seizures are controlled often tolerate harmful side effects (1). The development of carbamazepine and valproic acid has improved seizure protection for epileptics, of whom only 50% were completely protected by previously marketed antiepileptic drugs. Despite the beneficial effects of these drugs, new anticonvulsants with more selective action and less toxicity are needed (2).

## BACKGROUND

In the development of new anticonvulsants, most attention has been centered on the ureide structure (I). Three succinimides, phensuximide, methsuximide, and ethosuximide, that contain this basic structure are used in the treatment of petit mal epilepsy (3).

Witiak *et al.* (4) reported the synthesis and anticonvulsant activity of




*0022-3549/81/0200-0192$01.00/0*


*© 1981, American Pharmaceutical Association*

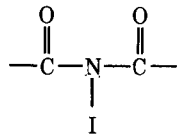

I

chiral 2-amino-*N*-benzyl-substituted succinimides. The most potent anticonvulsant activity against maximal electroshock was observed with the enantiomorphic imides II and III. However, no stereoselective differences in anticonvulsant activity were observed with the (*S*)-II and (*R*)-III enantiomorphs.

The purpose of this investigation was to evaluate the anticonvulsant activity of 2-amino-*N*-substituted succinimide derivatives in which the lipophilicity of the groups on the nitrogen and at the 2-position was varied. The relationship between log *p* of the compound and anticonvulsant activity was discussed previously (5, 6).

Sulfonamide or urea derivatives of (*R,S*)-2-amino-*N*-(*n*-propyl)-succinimide hydrochloride (VII) and (*R,S*)-2-amino-*N*-benzylsuccinimide hydrochloride (VIII) are described. These derivatives were chosen because both the size and the lipophilicity of the substituent could be varied easily. Additionally, previous investigators showed that nitrogen-containing substituents at the 2-position of the succinimide ring imparted good anticonvulsant activity (7). Based on the findings of Witiak *et al.* (4), no attempt was made to prepare the individual enantiomorphs of the compounds.

## RESULTS AND DISCUSSION

The succinimide derivatives (V–XI) were prepared as shown in Scheme I, and the physical properties of the (*R,S*)-2-ureido-*N*-substituted succinimides (IX*a*–IX*j*) are given in Table I.

The anticonvulsant activity of V–XI is shown in Table II. Only VI, VIII, IX*d*, and XI ($ED_{50}$ = 288) exhibited activity in the maximal electroshock seizure (MES) test. Witiak *et al.* (4) reported the anticonvulsant activity of the individual enantiomorphs of VI. It is surprising that the polar compounds VIII and XI exhibited activity against MES. Only VIII was active against MES at 4 hr after administration. Several succinimide derivatives (V, VI, VIII, IX*c*, IX*h*–IX*j*, X, and XI) were active against subcutaneous pentylenetetrazol-induced seizures. Compound VIII showed activity at 300 mg/kg (four out of four mice protected) at 0.5 hr after administration. The $ED_{50}$ of the sulfonamide XI was 120 mg/kg at the time of the peak effect (0.5 hr). Both VIII and XI ($TD_{50}$ = 422) exhibited significant toxicity in the rotorod test. Among the ureas, IX*c* appeared to be the most active. To observe activity against subcutaneous pentylenetetrazol-induced seizures in the urea series, a propyl, butyl, or 2-chloroethyl group on one of the urea nitrogens is necessary.

It appears that the 2-amino-*N*-benzylsuccinimide derivatives are more active than the corresponding 2-amino-*N*-(*n*-propyl)succinimides. The introduction of a urea substituent into the 2-position of the succinimide ring does not impart significant activity. The activity of (*R,S*)-2-amino-*N*-benzylsuccinimide hydrochloride (VIII) and (*R,S*)-*N*-benzyl-2-(methanesulfamido)succinimide (XI) against both maximal electroshock seizure and subcutaneous pentylenetetrazol-induced seizure is interesting since they are quite polar and are expected to penetrate the blood–brain barrier poorly. Further work is in progress to evaluate the anticonvulsant activity of VIII and XI as well as to prepare other hydrophilic derivatives related to these two compounds.

## EXPERIMENTAL[1]

**(*R,S*)-*N*-Acetylaspartic Acid (IV)**—Compound IV was prepared by the method of Barker (8) in an 83% yield, mp 163–165° [lit. (8) mp 139–140°].

**(*R,S*)-2-Acetamido-*N*-(*n*-propyl)succinimide (V)**—A mixture of IV (23.0 g, 0.13 mole) and *n*-propylamine (15.5 g, 0.26 mole) was heated to 210°. Water was removed during heating *via* a Dean–Stark trap. The reaction mixture was cooled to yield a dark-brown oil. The oil was taken up into chloroform (100 ml) and chromatographed on a silica gel column

[1] Melting points were determined on a Fisher-Johns melting-point apparatus and are uncorrected. IR spectra were recorded as potassium bromide pellets with a Perkin-Elmer 137 spectrophotometer. NMR spectra were recorded on a Varian EM 360A spectrometer. Chemical shifts are reported in parts per million (δ) relative to tetramethylsilane (1%) as the internal standard. Analytical data were obtained from Micro-Analysis Inc., Wilmington, Del. TLC was performed on precoated silica gel plastic sheets (Macherey-Nagel). Column chromatography was carried out using MN-Kieselgel (70–325 mesh) as the adsorbent.

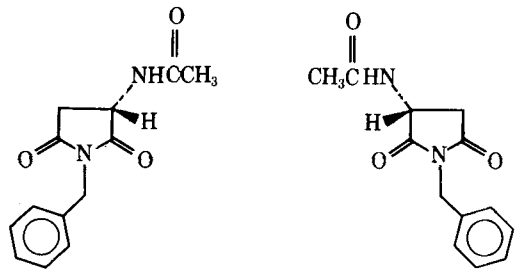

II III

with chloroform–ethanol (8:2) as the solvent. Evaporation of the solvent gave 13.4 g (52%) of a light-tan solid. Recrystallization from chloroform–hexane gave an analytically pure product, mp 104–106°; IR (KBr): 3400 (NH), 1785 (C=O, imide), 1710 (C=O, imide), and 1670 (C=O, amide) $cm^{-1}$; NMR ($CDCl_3$): δ 0.90 (t, 3H, *J* = 7 Hz, $NCH_2CH_2CH_3$), 1.60 (m, 2H, $NCH_2CH_2CH_3$), 2.03 (s, 3H, $NCOCH_3$), 2.57–3.60 (m, 4H, ring $CH_2$ and $NCH_2$), 4.27 (m, 1H, ring CH), and 7.17 (d, 2H, NHCO).

*Anal.*—Calc. for $C_9H_{14}N_2O_3$: C, 54.52; H, 7.13; N, 14.13. Found: C, 54.27; H, 7.22; N, 13.96.

**(*R,S*)-2-Acetamido-*N*-benzylsuccinimide (VI)**—Compound VI was prepared from IV (20.0 g, 0.11 mole) and benzylamine (12.2 g, 0.11 mole) in the same manner as described for the synthesis of V. Recrystallization from ethanol–ethyl acetate gave analytically pure material, mp 172–174° [lit. (4) mp of the (*R*)- or (*S*)-enantiomer 171–175°]; IR (KBr): 3400 (NH), 1785 (C=O, imide), 1710 (C=O, imide), and 1667 (C=O, amide) $cm^{-1}$.

*Anal.*—Calc. for $C_{13}H_{14}N_2O_3$: C, 63.39; H, 5.74; N, 11.38. Found: C, 63.16; H, 5.60; N, 11.35.

**(*R,S*)-2-Amino-*N*-(*n*-propyl)succinimide Hydrochloride (VII)**—A suspension of V (3.00 g, 0.15 mole) in 27 ml of 6 *N* HCl was refluxed for 0.5 hr until a clear solution was obtained. The reaction mixture was cooled, made basic with 8 *N* $NH_4OH$, and extracted with two 75-ml portions of chloroform. The combined chloroform extracts were dried (sodium sulfate), filtered, and evaporated under reduced pressure to afford a light-yellow oil. The oil was taken up into absolute ethanol and converted to a crystalline hydrochloride derivative. Recrystallization from

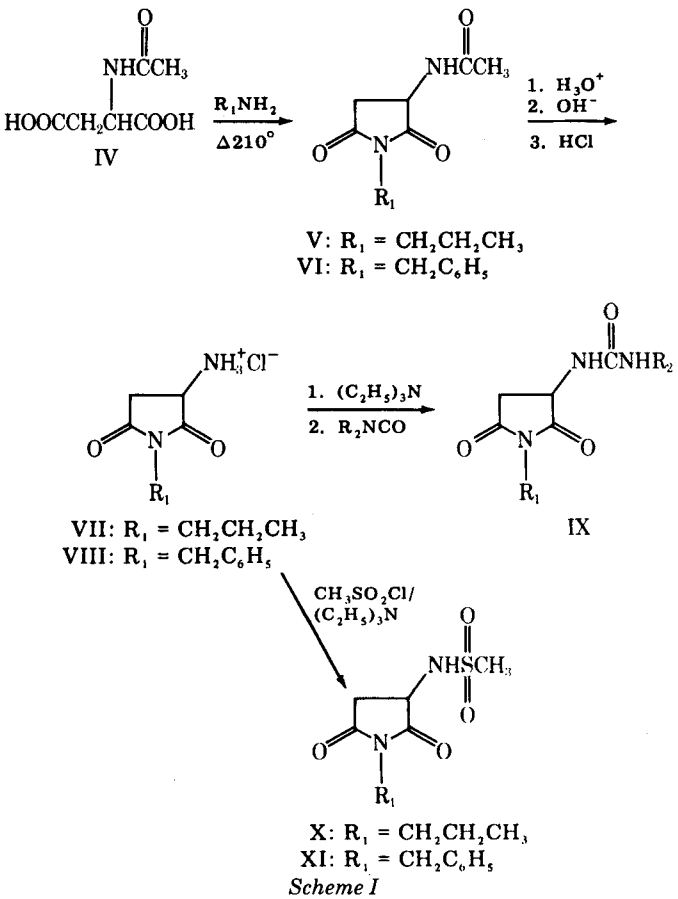

*Scheme I*

**Table I—Physical Properties of (*R,S*)-2-Ureido-*N*-substituted Succinimides (IX)**

| Compound | $R_1$ | $R_2$ | Melting Point | Yield, % | Recrystallization Solvent[a] | Formula | Analysis, % | Calc. | Found |
|---|---|---|---|---|---|---|---|---|---|
| IX*a* | $CH_2CH_2CH_3$ | $CH_3$ | 117–118° | 43 | A | $C_9H_{15}N_3O_3$ | C | 50.68 | 50.70 |
| | | | | | | | H | 7.10 | 7.20 |
| | | | | | | | N | 19.71 | 19.60 |
| IX*b* | $CH_2CH_2CH_3$ | $CH_2CH_3$ | 84–87° | 57 | A | $C_{10}H_{17}N_3O_3$ | C | 52.84 | 52.81 |
| | | | | | | | H | 7.55 | 7.58 |
| | | | | | | | N | 18.49 | 18.50 |
| IX*c* | $CH_2CH_2CH_3$ | $CH_2CH_2CH_3$ | 102–104° | 52 | A | $C_{11}N_{19}N_3O_3$ | C | 54.74 | 54.55 |
| | | | | | | | H | 7.95 | 8.04 |
| | | | | | | | N | 17.42 | 17.31 |
| IX*d* | $CH_2CH_2CH_3$ | $CH_2CH_2CH_2CH_3$ | 101–102° | 68 | A | $C_{12}H_{21}N_3O_3$ | C | 56.43 | 56.29 |
| | | | | | | | H | 8.31 | 8.39 |
| | | | | | | | N | 16.46 | 16.33 |
| IX*e* | $CH_2CH_2CH_3$ | $CH_2CH_2Cl$ | 133–135° | 62 | A | $C_{10}H_{16}ClN_3O_3$ | C | 45.88 | 46.13 |
| | | | | | | | H | 6.17 | 6.15 |
| | | | | | | | N | 16.06 | 16.24 |
| IX*f* | $CH_2C_6H_5$ | $CH_3$ | 163–165° | 69 | B | $C_{13}H_{15}N_3O_3$ | C | 59.75 | 59.70 |
| | | | | | | | H | 5.80 | 5.83 |
| | | | | | | | N | 16.08 | 16.32 |
| IX*g* | $CH_2C_6H_5$ | $CH_2CH_3$ | 139–141° | 49 | B | $C_{14}H_{17}N_3O_3$ | C | 61.07 | 61.37 |
| | | | | | | | H | 6.24 | 6.24 |
| | | | | | | | N | 15.26 | 15.39 |
| IX*h* | $CH_2C_6H_5$ | $CH_2CH_2CH_3$ | 147–149° | 70 | A | $C_{15}H_{19}N_3O_3$ | C | 62.26 | 62.42 |
| | | | | | | | H | 6.63 | 6.59 |
| | | | | | | | N | 14.52 | 14.50 |
| IX*i* | $CH_2C_6H_5$ | $CH_2CH_2CH_2CH_3$ | 145–147° | 62 | A | $C_{16}H_{21}N_3O_3$ | C | 63.34 | 63.56 |
| | | | | | | | H | 6.99 | 6.98 |
| | | | | | | | N | 13.85 | 14.06 |
| IX*j* | $CH_2C_6H_5$ | $CH_2CH_2Cl$ | 191–194° | 71 | B | $C_{14}H_{16}ClN_3O_3$ | C | 54.27 | 54.37 |
| | | | | | | | H | 5.23 | 5.50 |
| | | | | | | | N | 13.57 | 13.50 |

[a] A = acetone–ether, and B = acetone.

**Table II—Anticonvulsant Activity of Succinimide Derivatives**

| Compound | MES Activity[a] 0.5 hr | MES Activity[a] 4 hr | sc Met Activity[a,b] 0.5 hr | sc Met Activity[a,b] 4 hr | Toxicity[c] |
|---|---|---|---|---|---|
| V | – | – | + (1/4) | – | 0/4 |
| VI | + | – | ++ (2/4) | – | 0/4 |
| VII | – | – | – | – | 0/4 |
| VIII | ++ (4/4) | + (1/4) | ++ (4/4) | – | 4/4 at 600 mg/kg |
| IX*a* | – | – | – | – | 0/4 |
| IX*b* | – | – | – | – | 0/4 |
| IX*c* | – | – | ++ (3/4) | – | 0/4 |
| IX*d* | + | – | + (2/4) | – | 3/4 at 600 mg/kg |
| IX*e* | – | – | – | – | 0/4 |
| IX*f* | – | – | – | – | 0/4 |
| IX*g* | – | – | – | – | 0/4 |
| IX*h* | – | – | +++ (1/4) | – | 0/4 |
| IX*i* | – | – | ++ (1/4) | – | 0/4 |
| IX*j* | – | – | +++ (1/4) | – | 0/4 |
| X | – | – | ++ (4/4) | | 0/4 |
| XI | 288[d] (217–310)[e,f] | – | 120[d] (90–166)[e,f] | – | 422[g] (390–457)[e,f] |
| Phensuximide | 112[d] (104–131)[e,f] | | 50 (21–65)[e,f] | | 232[g] (187–267)[e,f] |

[a] +++, ++, and + signify activity at 100, 300, and 600 mg/kg, respectively; – denotes no activity observed at 600 mg/kg. [b] Numbers in parentheses indicate the number of animals protected against sc Met-induced seizures or maximal electroshock-induced seizures. [c] Number of animals exhibiting neurotoxicity as determined by the rotorod test. [d] $ED_{50}$. [e] The 95% confidence limits. [f] Determined at time of the peak effect (0.5 hr). [g] $TD_{50}$.

absolute ethanol–ether gave 1.68 g (58%) of a white solid, mp 207–208°; IR (KBr): 2750 ($NH_3^+$), 1785 (C=O, imide), and 1710 (C=O, imide) $cm^{-1}$; NMR ($D_2O$): δ 0.80 (t, 3H, $J$ = 7 Hz, $NCH_2CH_2CH_3$), 1.57 (m, 2H, $NCH_2CH_2CH_3$), 2.60–3.63 (m, 4H, ring $CH_2$ and $NCH_2$), and 4.47 (m, 1H, ring CH).

*Anal.*—Calc. for $C_7H_{13}ClN_2O_2$: C, 43.63; H, 6.81; N, 14.54. Found: C, 46.61; H, 6.73; N, 14.53.

**(*R,S*)-2-Amino-*N*-benzylsuccinimide Hydrochloride (VIII)**—Compound VIII was prepared, as described for VII, from VI (3.12 g, 0.13 mole) and 27 ml of 6 *N* HCl. Workup in the normal manner gave 1.84 g (71%) of the free base, mp 67–68°. The hydrochloride was prepared and recrystallized from absolute ethanol to give analytically pure material, mp 217.5–219°; IR (KBr): 2750 ($NH_3^+$), 1785 (C=O, imide), and 1710 (C=O, imide) $cm^{-1}$; NMR (dimethyl sulfoxide-$d_6$): δ 2.90–3.17 (m, 3H, ring $CH_2$ and CH), 4.57 (s, 2H, $NCH_2$), 7.40 (s, 5H, $C_6H_5$), and 9.20 (s, 3H, $NH_3^+$).

*Anal.*—Calc. for $C_{11}H_{13}ClN_2O_2$: C, 54.88; H, 5.45; N, 11.64. Found: C, 55.15; H, 5.38; N, 11.65.

**(*R,S*)-2-Ureido-*N*-substituted Succinimides (IX*a*–IX*j*)**—The synthesis of (*R,S*)-2-[3-(2-chloroethyl)ureido]-*N*-(*n*-propyl)succinimide (IX*e*) is representative of the general method. The amine hydrochloride (VII) (2.00 g, 0.010 mole) and triethylamine (1.05 g, 0.010 mole) in 50 ml of tetrahydrofuran were stirred for a few minutes and treated with 2-chloroethyl isocyanate[2] (1.10 g, 0.010 mole). The reaction mixture was stirred overnight and filtered to remove the precipitated triethylamine hydrochloride. The filtrate was removed under reduced pressure to yield a white solid. Recrystallization of the solid from acetone–ether gave 1.45 g (62%) of analytically pure product, mp 133–135°; IR (KBr): 3320 (NH), 1785 (C=O, imide), 1710 (C=O, imide), and 1670 (C=O, urea) $cm^{-1}$; NMR ($CDCl_3$): δ 0.87 (t, 3H, $J$ = 6 Hz, $NCH_2CH_2CH_3$), 1.47 (m, 2H, $NCH_2CH_2CH_3$), 2.30–3.72 (m, 8H, $NCH_2CH_2CH_3$, ring $CH_2$, and $CH_2CH_2Cl$), 4.40 (m, 1H, ring CH), and 6.37–6.87 (m, 2H, NHCONH).

*Anal.*—Calc. for $C_{10}H_{16}ClN_3O_3$: C, 45.88; H, 6.17; N, 16.06. Found: C, 46.13; H, 6.15; N, 16.24.

**(*R,S*)-2-Methanesulfamido-*N*-(*n*-propyl)succinimide (X)**—A

[2] Eastman Kodak.

solution of VII as the free base (1.96 g, 0.013 mole) in 50 ml of tetrahydrofuran was treated with triethylamine (1.27 g, 0.013 mole), followed by the dropwise addition of methanesulfonyl chloride (1.43 g, 0.013 mole). The reaction mixture was stirred at room temperature for 4 hr and filtered to remove the precipitated triethylamine hydrochloride. The filtrate was evaporated under reduced pressure to yield a light-yellow oil. Column chromatography of the oil using silica gel as the adsorbent and chloroform–methanol (9:1) as the solvent gave, after evaporation of the solvents, 0.77 g (26%) of a white crystalline solid. An analytical sample was obtained by recrystallization from chloroform–hexane to give white crystals, mp 82–83°; IR (KBr): 3300 (NH), 1785 (C=O, imide), 1710 (C=O, imide), and 1150 ($SO_2$) $cm^{-1}$; NMR: δ 0.90 (t, 3H, $J$ = 6 Hz, $NCH_2CH_2CH_3$), 1.60 (m, 2H, $NCH_2CH_2CH_3$), 2.40–3.67 (m, including s at 3.13, 7H, $SO_2CH_3$), 4.47 (m, 1H, ring CH), and 5.77 (s, 1H, NH).

*Anal.*—Calc. for $C_8H_{14}N_2O_4S$: C, 41.01; H, 6.03; N, 11.96. Found: C, 41.19; H, 5.90; N, 12.22.

**(*R,S*)-*N*-Benzyl-2-(methanesulfamido)succinimide (XI)**—Compound XI was synthesized from VIII as the free base (1.00 g, 0.005 mole), triethylamine (0.496 g, 0.005 mole), and methanesulfonyl chloride (0.561 g, 0.005 mole) in 50 ml of tetrahydrofuran in the same manner as described for X. Recrystallization of the solid product from chloroform–hexane gave 0.729 g (57%) of analytically pure product, mp 118–121°; IR (KBr): 3300 (NH), 1785 (C=O, imide), 1710 (C=O, imide), and 1150 ($SO_2$) $cm^{-1}$; NMR ($CDCl_3$): δ 2.50 (m, including s at 3.10, 5H, $SO_2CH_3$), 4.10–4.77 (m, including s at 4.63, 3H, $NCH_2C_6H_5$), 5.77 (d, 1H, NH), and 7.33 (s, 5H, $C_6H_5$).

*Anal.*—Calc. for $C_{12}H_{14}N_2O_4S$: C, 51.04; H, 5.01; N, 9.92. Found: C, 50.97; H, 4.91; N, 10.08.

**Pharmacological Testing**[3]—Three tests were performed: the maximal electroshock seizure test (MES), the subcutaneous pentylenetetrazol seizure threshold test (sc Met), and the rotorod test to evaluate neurotoxicity[4].

All tests were performed on male Carworth Farms No. 1 mice. All compounds were tested at 30, 100, 300, and 600 mg/kg at 30 min and 4 hr after intraperitoneal administration. Four animals were injected with each dose. After 30 min, each animal was examined for toxicity in the rotorod test. Immediately thereafter, anticonvulsant activity was evaluated by subjecting one mouse to the MES test and another to the sc Met test. The same tests were repeated 4 hr later on the two remaining mice.

All compounds were solubilized in either 0.9% NaCl or 30% polyethylene glycol 400 and administered intraperitoneally in a volume of 0.01 ml/g. The $ED_{50}$ and $TD_{50}$ values and their confidence limits were determined by the method of Litchfield and Wilcoxon (11). The MES activity is defined as abolition of the hindlimb tonic extensor component of the maximal electroshock seizure elicited in mice with a 60-Hz alternating current of 50 mamp delivered for 0.1 sec *via* corneal electrodes. The sc Met activity is defined as failure to observe even a threshold seizure (a single episode of clonic spasms of at least 5 sec).

[3] All compounds were tested for anticonvulsant activity by the Antiepileptic Drug Development Program administered by the Section on Epilepsy, National Institutes of Health, Bethesda, MD 20014. The compounds were evaluated using the Anticonvulsant Screening Project test systems (9, 10).

[4] Neurological toxicity is defined as failure of an animal to remain for 1 min on a rod rotating at 6 rpm.

## REFERENCES


(1) R. L. Krall, J. K. Penry, H. J. Kupferburg, and E. A. Swinyard, *Epilepsia*, **19**, 393 (1978).

(2) R. L. Krall, J. K. Penry, B. G. White, H. J. Kupferburg, and E. A. Swinyard, *ibid.*, **19**, 409 (1978).

(3) J. A. Vida and E. H. Gerry, in "Medicinal Chemistry—A Series of Monographs," vol. 15, G. DeStevens, Ed., Academic, New York, N.Y., 1977, p. 189.

(4) D. T. Witiak, B. R. Vishnuvajjala, W. L. Cook, J. A. Minatelli, T. K. Gupta, and M. C. Gerald, *J. Med. Chem.*, **20**, 801 (1977).

(5) M. H. Hussain and E. J. Lien, *ibid.*, **14**, 138 (1971).

(6) E. J. Lien, R. C. H. Liao, and H. G. Shinouda, *J. Pharm. Sci.*, **68**, 463 (1979).

(7) M. J. Kornet, A. M. Crider, and E. O. Magarian, *J. Med. Chem.*, **20**, 405 (1977).

(8) C. C. Barker, *J. Chem. Soc.*, **1953**, 453.

(9) Anticonvulsant Screening Project, Antiepileptic Drug Development Program, National Institutes of Health, DHEW Publication No. (NIH) 76-1093, Bethesda, Md., 1976.

(10) E. A. Swinyard, W. C. Brown, and L. S. Goodman, *J. Pharmacol. Exp. Ther.*, **106**, 319 (1952).

(11) J. T. Litchfield and F. Wilcoxon, *ibid.*, **96**, 99 (1949).


## ACKNOWLEDGMENTS


The authors thank Mr. Gill D. Gladding for arranging anticonvulsant testing through the Antiepileptic Drug Development Program administered by the National Institutes of Health.


# First-Pass Effect: Nonlinear Concept Comprising an Explicit Solution of Integrated Michaelis–Menten Equation


**FRIEDER KELLER ˣ and JÜRGEN SCHOLLE**



Received January 24, 1980, from the *Freie Universität, Klinikum Steglitz, Medizinische Klinik, Nephrologie, Hindenburgdamm 30, 1000 Berlin 45, Germany.* Accepted for publication August 6, 1980.



**Abstract** □ The first-pass effect results from metabolism during the first liver passage of a drug given by mouth. The metabolism is described by the Michaelis–Menten equation, but the integrated form of the Michaelis–Menten equation has no explicit solution for concentration and its handling requires a computer. However, the presented nonlinear equation of the first-pass effect is an explicit integration of the Michaelis–Menten equation and involves only general mathematics. However, the problem of evaluating the Michaelis–Menten constants $V_m$ and $K_m$ is not resolved. Therefore, linear equations are also derived, which correspond to previous clearance models.



**Keyphrases** □ Pharmacokinetics—first-pass effect, nonlinear approach to solution of Michaelis–Menten equation □ First-pass effect—nonlinear approach to solution of integrated Michaelis–Menten equation □ Michaelis–Menten kinetics—first-pass effect, nonlinear approach □ Clearance—first-pass effect, nonlinear approach to solution of integrated Michaelis–Menten equation


First-pass effect is defined as the reduced systemic bioavailability resulting from metabolism during the first liver passage of an orally administered drug (Fig. 1) (1). The mathematical description of this effect usually is based on first-order compartment or clearance models (1–3). However, metabolism follows nonlinear kinetics


*0022-3549/81/0200-0195$01.00/0*


*© 1981, American Pharmaceutical Association*

solution of VII as the free base (1.96 g, 0.013 mole) in 50 ml of tetrahydrofuran was treated with triethylamine (1.27 g, 0.013 mole), followed by the dropwise addition of methanesulfonyl chloride (1.43 g, 0.013 mole). The reaction mixture was stirred at room temperature for 4 hr and filtered to remove the precipitated triethylamine hydrochloride. The filtrate was evaporated under reduced pressure to yield a light-yellow oil. Column chromatography of the oil using silica gel as the adsorbent and chloroform–methanol (9:1) as the solvent gave, after evaporation of the solvents, 0.77 g (26%) of a white crystalline solid. An analytical sample was obtained by recrystallization from chloroform–hexane to give white crystals, mp 82–83°; IR (KBr): 3300 (NH), 1785 (C=O, imide), 1710 (C=O, imide), and 1150 ($SO_2$) $cm^{-1}$; NMR: δ 0.90 (t, 3H, $J$ = 6 Hz, $NCH_2CH_2CH_3$), 1.60 (m, 2H, $NCH_2CH_2CH_3$), 2.40–3.67 (m, including s at 3.13, 7H, $SO_2CH_3$), 4.47 (m, 1H, ring CH), and 5.77 (s, 1H, NH).

*Anal.*—Calc. for $C_8H_{14}N_2O_4S$: C, 41.01; H, 6.03; N, 11.96. Found: C, 41.19; H, 5.90; N, 12.22.

**(*R,S*)-*N*-Benzyl-2-(methanesulfamido)succinimide (XI)**—Compound XI was synthesized from VIII as the free base (1.00 g, 0.005 mole), triethylamine (0.496 g, 0.005 mole), and methanesulfonyl chloride (0.561 g, 0.005 mole) in 50 ml of tetrahydrofuran in the same manner as described for X. Recrystallization of the solid product from chloroform–hexane gave 0.729 g (57%) of analytically pure product, mp 118–121°; IR (KBr): 3300 (NH), 1785 (C=O, imide), 1710 (C=O, imide), and 1150 ($SO_2$) $cm^{-1}$; NMR ($CDCl_3$): δ 2.50 (m, including s at 3.10, 5H, $SO_2CH_3$), 4.10–4.77 (m, including s at 4.63, 3H, $NCH_2C_6H_5$), 5.77 (d, 1H, NH), and 7.33 (s, 5H, $C_6H_5$).

*Anal.*—Calc. for $C_{12}H_{14}N_2O_4S$: C, 51.04; H, 5.01; N, 9.92. Found: C, 50.97; H, 4.91; N, 10.08.

**Pharmacological Testing**[3]—Three tests were performed: the maximal electroshock seizure test (MES), the subcutaneous pentylenetetrazol seizure threshold test (sc Met), and the rotorod test to evaluate neurotoxicity[4].

All tests were performed on male Carworth Farms No. 1 mice. All compounds were tested at 30, 100, 300, and 600 mg/kg at 30 min and 4 hr after intraperitoneal administration. Four animals were injected with each dose. After 30 min, each animal was examined for toxicity in the rotorod test. Immediately thereafter, anticonvulsant activity was evaluated by subjecting one mouse to the MES test and another to the sc Met test. The same tests were repeated 4 hr later on the two remaining mice.

All compounds were solubilized in either 0.9% NaCl or 30% polyethylene glycol 400 and administered intraperitoneally in a volume of 0.01 ml/g. The $ED_{50}$ and $TD_{50}$ values and their confidence limits were determined by the method of Litchfield and Wilcoxon (11). The MES activity is defined as abolition of the hindlimb tonic extensor component of the maximal electroshock seizure elicited in mice with a 60-Hz alternating current of 50 mamp delivered for 0.1 sec *via* corneal electrodes. The sc Met activity is defined as failure to observe even a threshold seizure (a single episode of clonic spasms of at least 5 sec).

[3] All compounds were tested for anticonvulsant activity by the Antiepileptic Drug Development Program administered by the Section on Epilepsy, National Institutes of Health, Bethesda, MD 20014. The compounds were evaluated using the Anticonvulsant Screening Project test systems (9, 10).

[4] Neurological toxicity is defined as failure of an animal to remain for 1 min on a rod rotating at 6 rpm.

## REFERENCES


(1) R. L. Krall, J. K. Penry, H. J. Kupferburg, and E. A. Swinyard, *Epilepsia*, **19**, 393 (1978).

(2) R. L. Krall, J. K. Penry, B. G. White, H. J. Kupferburg, and E. A. Swinyard, *ibid.*, **19**, 409 (1978).

(3) J. A. Vida and E. H. Gerry, in "Medicinal Chemistry—A Series of Monographs," vol. 15, G. DeStevens, Ed., Academic, New York, N.Y., 1977, p. 189.

(4) D. T. Witiak, B. R. Vishnuvajjala, W. L. Cook, J. A. Minatelli, T. K. Gupta, and M. C. Gerald, *J. Med. Chem.*, **20**, 801 (1977).

(5) M. H. Hussain and E. J. Lien, *ibid.*, **14**, 138 (1971).

(6) E. J. Lien, R. C. H. Liao, and H. G. Shinouda, *J. Pharm. Sci.*, **68**, 463 (1979).

(7) M. J. Kornet, A. M. Crider, and E. O. Magarian, *J. Med. Chem.*, **20**, 405 (1977).

(8) C. C. Barker, *J. Chem. Soc.*, **1953**, 453.

(9) Anticonvulsant Screening Project, Antiepileptic Drug Development Program, National Institutes of Health, DHEW Publication No. (NIH) 76-1093, Bethesda, Md., 1976.

(10) E. A. Swinyard, W. C. Brown, and L. S. Goodman, *J. Pharmacol. Exp. Ther.*, **106**, 319 (1952).

(11) J. T. Litchfield and F. Wilcoxon, *ibid.*, **96**, 99 (1949).


## ACKNOWLEDGMENTS


The authors thank Mr. Gill D. Gladding for arranging anticonvulsant testing through the Antiepileptic Drug Development Program administered by the National Institutes of Health.


# First-Pass Effect: Nonlinear Concept Comprising an Explicit Solution of Integrated Michaelis–Menten Equation


**FRIEDER KELLER ˣ and JÜRGEN SCHOLLE**



Received January 24, 1980, from the *Freie Universität, Klinikum Steglitz, Medizinische Klinik, Nephrologie, Hindenburgdamm 30, 1000 Berlin 45, Germany.* Accepted for publication August 6, 1980.



**Abstract** □ The first-pass effect results from metabolism during the first liver passage of a drug given by mouth. The metabolism is described by the Michaelis–Menten equation, but the integrated form of the Michaelis–Menten equation has no explicit solution for concentration and its handling requires a computer. However, the presented nonlinear equation of the first-pass effect is an explicit integration of the Michaelis–Menten equation and involves only general mathematics. However, the problem of evaluating the Michaelis–Menten constants $V_m$ and $K_m$ is not resolved. Therefore, linear equations are also derived, which correspond to previous clearance models.



**Keyphrases** □ Pharmacokinetics—first-pass effect, nonlinear approach to solution of Michaelis–Menten equation □ First-pass effect—nonlinear approach to solution of integrated Michaelis–Menten equation □ Michaelis–Menten kinetics—first-pass effect, nonlinear approach □ Clearance—first-pass effect, nonlinear approach to solution of integrated Michaelis–Menten equation


First-pass effect is defined as the reduced systemic bioavailability resulting from metabolism during the first liver passage of an orally administered drug (Fig. 1) (1). The mathematical description of this effect usually is based on first-order compartment or clearance models (1–3). However, metabolism follows nonlinear kinetics


*0022-3549/81/0200-0195$01.00/0*


*© 1981, American Pharmaceutical Association*

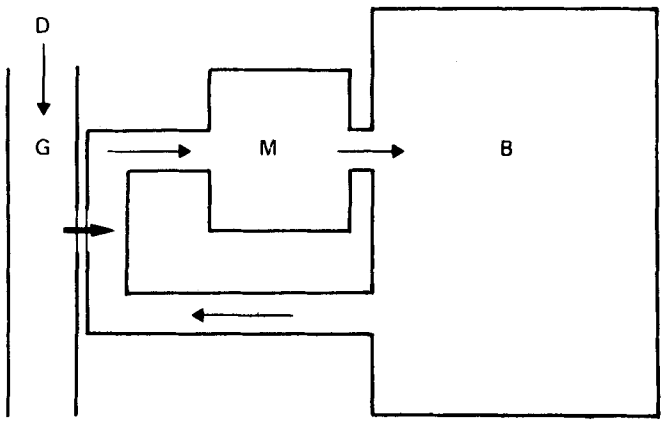


**Figure 1**—*Scheme of the first-pass effect. The amount given as the oral dose (D) equals the amount in the gut (G) plus the amount that is metabolized by the liver plus the amount that reaches the systemic circulation (B).*

described by the Michaelis–Menten equation (4):

$$\frac{dC}{dt} = \frac{V_m C}{K_m + C} \qquad \text{(Eq. 1)}$$

These first-order models are only valid under the condition $C \ll K_m$. A model that is independent of this premise will be deduced here from the Michaelis–Menten equation.

## THEORY

Absorption of a dose ($D$) from the intestinal tract is supposed to be a first-order process (2):

$$\frac{dG}{dt} = -K_a G \qquad \text{(Eq. 2)}$$

Therefore, the amount in the gut ($G$) diminishes in an exponential fashion with a constant absorption rate ($K_a$):

$$G = D \exp(-K_a t) \qquad \text{(Eq. 3)}$$

At every time interval in the circulation of portal blood ($T$ = 1 min), a fractional amount ($M$) is absorbed and transported into the liver:

$$M = \frac{dG}{dt} T \qquad \text{(Eq. 4)}$$

This actually absorbed amount becomes metabolized by liver enzymes, and this metabolism follows Michaelis–Menten kinetics. The Michaelis–Menten constants ($V_{\overline{m}}$, $K_{\overline{m}}$) are described here in mass rate terms:

$$\frac{dM}{dt} = \frac{V_{\overline{m}} M}{K_{\overline{m}} + M} \qquad \text{(Eq. 5)}$$

The difference between the absorbed and the metabolized amount is the rate at which the drug enters the systemic circulation ($dB/dt$):

$$\frac{dB}{dt} = \frac{dG}{dt} - \frac{dM}{dt} \qquad \text{(Eq. 6)}$$

The integrated rate reveals the systemically available amount ($B$):

$$B = \int_0^t \frac{dB}{dt}\, dt \qquad \text{(Eq. 7)}$$

The relation between the systemically available ($B$) and the applied amount ($D$) expresses the bioavailability factor ($F$):

$$F = \frac{B}{D} \qquad \text{(Eq. 8)}$$

$$F = \int_{t_1}^{t_2} \left[ K_a \exp(-K_a t) - \frac{V_{\overline{m}} K_a T \exp(-K_a t)}{K_{\overline{m}} + D K_a T \exp(-K_a t)} \right] dt \qquad \text{(Eq. 9)}$$

The solution of this integral (5) comprises an explicit solution of the Michaelis–Menten equation:

$$F = \exp(-K_a t_1) - \exp(-K_a t_2) - \frac{V_{\overline{m}}}{D} \left[ t_2 - t_1 + \frac{1}{K_a} \ln \frac{D K_a T + K_{\overline{m}} \exp(K_a t_1)}{D K_a T + K_{\overline{m}} \exp(K_a t_2)} \right] \qquad \text{(Eq. 10)}$$

Unfortunately, this integral shows no convergency. Therefore, the initial ($t_1$) and final ($t_2$) conditions must be defined:

$$t_1 = 0 \qquad \text{(Eq. 11)}$$

$$t_2 = 10 \ln(2)/K_a \qquad \text{(Eq. 12)}$$

The final condition ($t_2$) is given by the time [10 half-lives of absorption = $10 \ln(2)/K_a$], where >99% of the applied amount ($D$) has already been absorbed from the gut. So the first-pass effect ($F$) or the bioavailability of a metabolized drug can be described as a nonlinear process:

$$F = 1 - \frac{V_{\overline{m}}}{D K_a} \left[ 10 \ln(2) + \ln \frac{D K_a T + K_{\overline{m}}}{D K_a T + K_{\overline{m}} \exp[10 \ln(2)]} \right] \qquad \text{(Eq. 13)}$$

For the calculation of the nonlinear first-pass effect, the constant parameters ($V_{\overline{m}}$, $K_{\overline{m}}$, and $K_a$) have to be determined *in vivo*. This evaluation is possible using computers. The integrated Michaelis–Menten equation has been computer fitted to the plasma concentration decline of phenytoin and ethanol (6–10). The parameters ($V_m$ and $K_m$) derived from the plasma concentration decline can be related to the mass rate terms ($V_{\overline{m}}$ and $K_{\overline{m}}$). The concentration decline ($dC/dt$) is the mass rate ($dM/dt$) per volume of distribution ($V_d$):

$$\frac{dC}{dt} = \frac{dM}{dt} \Big/ V_d \qquad \text{(Eq. 14)}$$

The concentration ($C$) submitted to metabolism is the amount ($M$) in the liver blood volume ($V_l$):

$$C = \frac{M}{V_l} \qquad \text{(Eq. 15)}$$

The concentration rate terms and mass rate terms are related *via* the volume of distribution ($V_d$) and the liver blood volume ($V_l$):

$$\frac{V_{\overline{m}}}{V_m} = \left( \frac{K_{\overline{m}} + C V_l}{K_m + C} \right) \frac{V_d}{V_l} \qquad \text{(Eq. 16)}$$

The substrate mass ($K_{\overline{m}}$) equals the concentration at the half-maximal metabolism rate ($K_m$) in the liver blood volume ($V_l$):

$$K_{\overline{m}} = K_m V_l \qquad \text{(Eq. 17)}$$

So the mass rate of metabolism ($V_{\overline{m}}$) can be derived (based on Eq. 16) from the concentration rate term ($V_m$), which is determined from the plasma concentration decline ($dC/dt$):

$$V_{\overline{m}} = V_m V_d \qquad \text{(Eq. 18)}$$

The first-pass effect can be evaluated (Eq. 13) if the maximal metabolism velocity expressed as a concentration rate term ($V_m$), the concentration at the half-maximal metabolism rate ($K_m$), the volume of distribution ($V_d$), and the liver blood volume ($V_l$) have been determined from plasma concentration data. These parameters ($V_m$, $K_m$, and $K_a$) can be evaluated only by computer. For an overall determination of these parameters ($V_m$, $K_m$, and $K_a$), simplified equations can be derived and applied without advanced computer equipment.

Nonlinear Michaelis–Menten kinetics can be schematically divided into three sections (Fig. 2):

1. The initial part follows zero-order kinetics, showing linearity in the nontransformed plot, and is defined by $C \gg K_m$ or $M \gg K_{\overline{m}}$.
2. The final part follows first-order kinetics, showing linearity in the semilogarithmic plot, and is defined by $C \ll K_m$ or $M \ll K_{\overline{m}}$.
3. The intermediate part shows no linearity.

For the zero-order part, the Michaelis–Menten equation may be simplified (Eq. 19) (2) and the maximal metabolism rate ($V_m$) can be determined from the concentration decline (Eq. 20):

$$-\frac{dC}{dt} = V_m \qquad \text{(Eq. 19)}$$

$$V_m = \frac{C_1 - C_2}{t_1 - t_2} \qquad \text{(Eq. 20)}$$

For the first-order part, the Michaelis–Menten equation also may be simplified (2):

$$-\frac{dC}{dt} = \frac{V_m}{K_m} C = \frac{\ln(2)}{T/2} C \qquad \text{(Eq. 21)}$$

Therefore, $K_m$ can be derived from the elimination half-life ($T/2$) of the

first-order process:

$$K_m = V_m \frac{T/2}{\ln(2)} \qquad \text{(Eq. 22)}$$

The absorption rate constant ($K_a$) is often unknown also; its calculation takes some computer assistance (11), but a simplified evaluation of $K_a$ is given by the time in which the maximal concentration is reached after oral dosing (Eq. 23 derived from the Bateman function):

$$\ln(K_a) - K_a t_{max} = \ln\left[\frac{\ln(2)}{T/2}\right] - \frac{\ln(2)}{T/2} t_{max} \qquad \text{(Eq. 23)}$$

The solution for $K_a$ needs a stepwise iteration, but it can be done by any desk calculator.

After determination of $V_m$ (according to Eq. 20), the $K_m$ value can be derived from a linear kinetic model (Eq. 22). The term $K_m$ also can be determined from the intrinsic hepatic clearance ($Cl_{int}$) (3, 12, 13). The following parameters are the terms of the authors [$V_{max} = V_{\bar{m}}$, $K_M = K_m$, $K_e = \ln(2)/(T/2)$, $C_{L,u} = C_{HV}$, and $Cl_H = Cl_1$]:

$$\frac{dM}{dt} = K_e M \qquad \text{(Eq. 24)}$$

$$\frac{dM}{dt} = K_e V_d C_S \qquad \text{(Eq. 25)}$$

$$\frac{dM}{dt} = Cl_H C_S \qquad \text{(Eq. 26)}$$

$$\frac{dM}{dt} = Cl_{int} C_{HV} \qquad \text{(Eq. 27)}$$

$$\frac{dM}{dt} = \frac{V_{\bar{m}} C_{HV}}{K_m + C_{HV}} \qquad \text{(Eq. 28)}$$

$$\frac{dM}{dt} = \frac{Q Cl_H C_{HV}}{Q - Cl_H} \qquad \text{(Eq. 29)}$$

$$K_{Mapp} = K_M + C_{L,u} = V_{max}\left(\frac{1}{Cl_1} - \frac{1}{Q}\right) \qquad \text{(Eq. 30)}$$

## EXAMPLES AND DISCUSSION

Bioavailability generally is measured by comparison of the different areas under the concentration–time curves ($AUC$) after oral and intravenous dosing (2).

But the $AUC$ method only gives rough data on bioavailability. It gives no insight into the underlying process.

If the bioavailability is reduced because of metabolism during the first liver passage, nonlinear enzyme kinetics have to be assumed. The evaluation of the first-pass effect requires the use of the troublesome Michaelis–Menten equation. The present equation of the first-pass effect comprises an explicit solution of the integrated Michaelis–Menten equation. This approach may be of some value, particularly since it requires only general mathematics (Eq. 13).

The validity of this equation of the first-pass effect can be illustrated by examples, to which the parameters ($V_m$, $K_m$, $K_a$, $V_d$, and $F$) are referred in the literature (6, 8–10, 14–18). The first-pass effect calculated by this equation shows good agreement with the values calculated by computer (Table I).

The present equation of the first-pass effect has two questionable premises (Eq. 13). First, it reflects only the amount actually absorbed from the intestine (Eq. 4). It disregards the amount that has already reached the systemic circulation.

The substrate to be metabolized consists of the actually absorbed, as well as the already systemically available, amount. The already systemically available amount competes with the actually absorbed amount for the receptor, so the first-pass effect will be overestimated if enzyme saturation is reached. Enzyme saturation will be reached particularly after multiple dosing where cumulation of the drug in the body occurs.

Therefore, after multiple dosing, a higher bioavailability generally has to be expected than after a single dose of a drug subjected to first-pass metabolism (19). The present equation does not yet give the solution for this problem, but it may be a step toward the correct description. The case of enzyme induction, also relevant in steady-state kinetics, is not covered by the present equation.

The second limitation of the present concept may be the assumption that absorption from the intestine follows first-order kinetics, but this simplification may be legitimate (7, 11, 20).

These questionable premises are also involved in other concepts of the

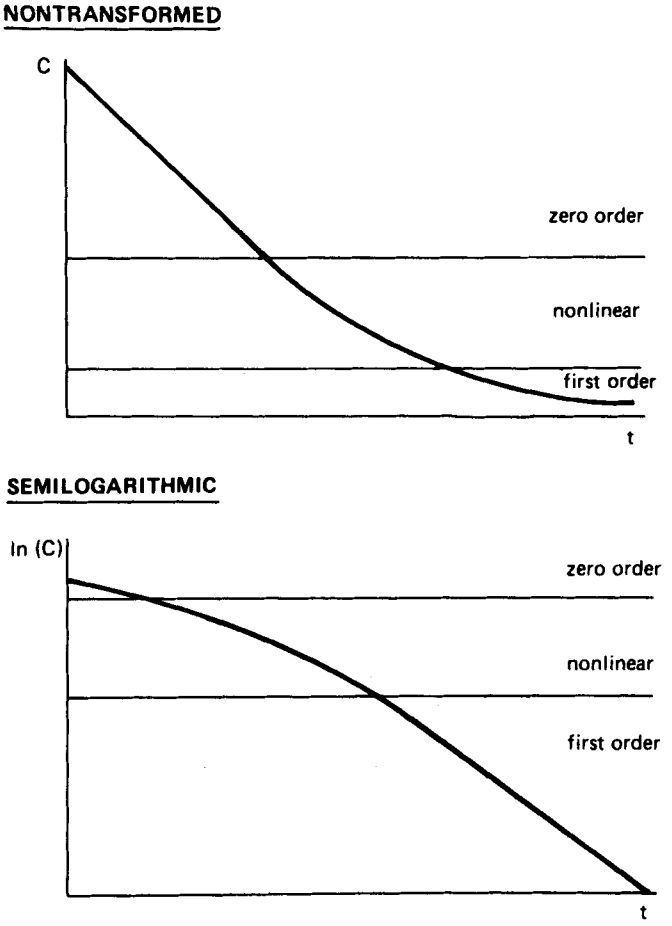


**Figure 2**—*Nontransformed and semilogarithmic graphs of the concentration decline in saturable pharmacokinetics with zero-order, nonlinear, and first-order parts.*

first-pass effect. This fact becomes evident if $C \ll K_m$ or if first-order kinetics are valid. Then the present concept (Eq. 9) can be transformed to the conventional clearance concepts (1, 3).

For first-order kinetics, there may be the simplified integration (of Eq. 9):

$$F = K_a\left(1 - \frac{V_{\bar{m}}}{K_{\bar{m}}} T\right)\left[\frac{\exp(-K_a t_2)}{K_a} - \frac{\exp(-K_a t_1)}{K_a}\right] \qquad \text{(Eq. 31)}$$

and for $t_1 = 0$, $t_2 = \infty$:

$$F = 1 - \frac{V_{\bar{m}}}{K_{\bar{m}}} T \qquad \text{(Eq. 32)}$$

**Table I—Bioavailability ($F$) of Phenytoin and Ethanol Calculated by the Present Concept (Eq. 13) Compared with the Values Referred to in the Literature**

| Drug | Parameter | | |
|---|---|---|---|
| | Literature | Calculated[a] | Equation |
| Phenytoin (6, 8, 14–18) | $V_m$ = 0.4 mg/(liters × hr) | $V_{\bar{m}}$ = 18 mg/hr | 17 |
| | $K_m$ = 11 mg/liter | $K_{\bar{m}}$ = 16.5 mg | 18 |
| | $K_a$ = 0.4 $hr^{-1}$ | | |
| | $V_d$ = 45 liters | | |
| | $F$ = 0.98 | $F$ = 0.98 | 13 |
| Ethanol (9, 10) | $V_m$ = 0.202 g/(liters × hr) | $V_{\bar{m}}$ = 8.9 g/hr | 17 |
| | $K_m$ = 0.818 g/liter | $K_{\bar{m}}$ = 0.123 g | 18 |
| | $K_a = k_e$ = 10 $hr^{-1}$ | | |
| | $V_d$ = 44 liters | | |
| 45 g | $F$ = 1.0 | $F$ = 0.92 | 13 |
| 11.3 g | $F$ = 0.785 | $F$ = 0.78 | 13 |

[a] The liver blood volume is considered constant ($V_l$ = 1.5 liters).

In the case of first-order kinetics, the elimination half-life ($T/2$) is related to the metabolism constants ($V_m$ and $K_m$) (2):

$$\frac{V_m}{K_m} = \frac{\ln(2)}{T/2} \quad \text{(Eq. 33)}$$

and the following deduction can be assumed (considering Eqs. 17, 18, and 32):

$$F = 1 - \frac{\ln(2)}{T/2}\frac{V_d}{V_l}T \quad \text{(Eq. 34)}$$

$$F = 1 - \frac{\text{systemic clearance}}{\text{hepatic blood flow}} \quad \text{(Eq. 35)}$$

$$F = \frac{Cl_H F}{Q(1-F)} \quad \text{(Eq. 36)}$$

$$F = \frac{Cl_H}{Cl_{\text{int}}} \quad \text{(Eq. 37)}$$

$$F = \frac{Q(1-F)}{Cl_{i(\text{tot})}} \quad \text{(Eq. 38)}$$

$$F = \frac{Q}{Q - Cl_{i(\text{tot})}} \quad \text{(Eq. 39)}$$

The conventional clearance concepts of the first-pass effect in terms of the authors (1, 3, 12, 19) can be derived from the present concept under the special condition of first-order kinetics.

## APPENDIX 1: NOMENCLATURE

$C$ = concentration
$t$ = time
$t_{max}$ = $t$ at maximal $C$
$V_m$ = maximal metabolism rate (concentration rate term)
$V_{\bar{m}}$ = maximal metabolism rate (mass rate term)
$K_m$ = Michaelis constant or concentration at $V_m/2$
$K_{\bar{m}}$ = Michaelis constant or mass at $V_{\bar{m}}/2$
$V_l$ = liver blood volume
$T$ = circulation time of $V_l$ ($T$ = 1 min for $V_l$ = 1.5 liters)
$V_d$ = volume of distribution
$K_a$ = absorption rate constant
$T/2$ = elimination half-life
$D$ = dose
$G$ = amount in GI tract
$M$ = absorbed amount
$B$ = amount in systemic circulation
$F$ = bioavailability factor
exp( ) = $e$-function of ( )
ln( ) = logarithmus numeralis from ( )
$Cl$ = clearance

## APPENDIX 2

The nonlinear equation of the first-pass effect (Eq. 13) is derived in the following way:

$$-\frac{dG}{dt} = K_a G \quad \text{(Eq. A1)}$$

$$G = D\exp(-K_a t) \quad \text{(Eq. A2)}$$

The (−) sign changes to a (+) sign since the decrease of the GI amount ($-dG/dt$) is the increase of the absorbed amount ($+dG/dt$), which is further considered:

$$\frac{dG}{dt} = K_a D\exp(-K_a t) \quad \text{(Eq. A3)}$$

$$M = \frac{dG}{dt}T \quad \text{(Eq. A4)}$$

$$\frac{dM}{dt} = \frac{V_{\bar{m}}M}{K_{\bar{m}} + M} \quad \text{(Eq. A5)}$$

$$\frac{dB}{dt} = \frac{dG}{dt} - \frac{dM}{dt} \quad \text{(Eq. A6)}$$

$$\frac{dB}{dt} = K_a D\exp(-K_a t) - \frac{V_{\bar{m}}M}{K_{\bar{m}} + M} \quad \text{(Eq. A7)}$$

$$\frac{dB}{dt} = K_a D\exp(-K_a t) - \frac{V_{\bar{m}}\frac{dG}{dt}T}{K_{\bar{m}} + \frac{dG}{dt}T} \quad \text{(Eq. A8)}$$

$$\frac{dB}{dt} = K_a D\exp(-K_a t) - \frac{V_{\bar{m}}K_a DT\exp(-K_a t)}{K_{\bar{m}} + K_a DT\exp(-K_a t)} \quad \text{(Eq. A9)}$$

$$B = \int_0^t \frac{dB}{dt}dt \quad \text{(Eq. A10)}$$

$$F = \frac{B}{D} = \int_0^t \left[K_a\exp(-K_a t) - \frac{V_{\bar{m}}K_a T}{K_{\bar{m}}\exp(K_a t) + K_a DT}\right]dt \quad \text{(Eq. A11)}$$

## REFERENCES


(1) M. Rowland, *J. Pharm. Sci.*, **61**, 70 (1972).
(2) M. Gibaldi and D. Perrier, "Pharmacokinetics," Dekker, New York, N.Y., 1975.
(3) G. R. Wilkinson and D. G. Shand, *Clin. Pharmacol. Ther.*, **18**, 377 (1975).
(4) L. Michaelis and M. L. Menten, *Biochem. Z.*, **49**, 333 (1913).
(5) J. S. Gradshteyn and J. M. Ryzhik, "Table of Integrals, Series and Products," Academic, New York, N.Y., 1965.
(6) N. Gerber and J. G. Wagner, *Res. Commun. Chem. Pathol. Pharmacol.*, **3**, 455 (1972).
(7) L. Martis and R. H. Levy, *J. Pharmacokinet. Biopharm.*, **1**, 283 (1973).
(8) G. E. Mawer, M. M. Rodgers, A. J. Robins, and S. B. Lucas, *Br. J. Clin. Pharmacol.*, **1**, 162 (1974).
(9) P. K. Wilkinson, A. J. Sedman, E. Sakmar, R. H. Earhart, D. J. Weidler, and J. G. Wagner, *Clin. Pharmacol. Ther.*, **19**, 213 (1975).
(10) P. K. Wilkinson, A. J. Sedman, E. Sakmar, D. R. Kay, and J. G. Wagner, *J. Pharmacokinet. Biopharm.*, **5**, 207 (1977).
(11) J. G. Wagner, "Fundamentals of Clinical Pharmacokinetics," Drug Intelligence Publications, Hamilton, Ill., 1975.
(12) A. S. Nies, D. G. Shand, and G. R. Wilkinson, *Clin. Pharmacokinet.*, **1**, 135 (1976).
(13) K. S. Pang, M. Rowland, and T. N. Tozer, *Drug Metab. Disp.*, **6**, 197 (1978).
(14) R. A. Buchanan, A. W. Kinkel, J. R. Goulet, and T. C. Smith, *Neurology*, **22**, 126 (1972).
(15) W. J. Jusko, J. R. Koup, and G. Alvan, *J. Pharmacokinet. Biopharm.*, **4**, 327 (1976).
(16) E. Martin, T. N. Tozer, L. B. Sheiner, and S. Riegelman, *ibid.*, **5**, 579 (1977).
(17) G. Franke, M. Zschiesche, and H. Hüller, *Int. J. Clin. Pharmacol. Biopharm.*, **16**, 410 (1978).
(18) P. J. Neuvonen, *Clin. Pharmacokinet.*, **4**, 91 (1979).
(19) A. J. J. Wood, K. Carr, R. E. Vestal, S. Belcher, G. R. Wilkinson, and D. G. Shand, *Br. J. Clin. Pharmacol.*, **6**, 345 (1978).
(20) M. Rowland, S. Riegelman, P. A. Harris, and S. D. Sholkoff, *J. Pharm. Sci.*, **61**, 379 (1972).

# Syntheses and Biological Evaluation of 2- and 9-Aminobenzonorbornenes as Conformationally Rigid Analogs of Amphetamines

L. E. WOOD, R. DANIELS, L. BAUER, and J. E. GEARIEN ˣ

Received May 15, 1980, from the *Department of Medicinal Chemistry, University of Illinois at the Medical Center, Chicago, IL 60680.* Accepted for publication August 13, 1980.

**Abstract** □ Isomers of the 2- and 9-aminobenzonorbornenes were prepared as rigid analogs of amphetamine and were employed to study the conformational requirements of indirectly acting sympathomimetic agents. Of this series of isomeric amines, the *exo*-2 and *anti*-9 isomers closely resemble the fully extended conformation of amphetamine. The other two amines, the *endo*-2 and *syn*-9 isomers, conformationally resemble the folded conformation of amphetamine. The isomers that resemble the extended conformation of amphetamine increased the spontaneous motor activity in mice while the isomers resembling the folded form either decreased or had no effect on motor activity. These compounds also were studied for their ability to accelerate the efflux of tritiated norepinephrine from vesicular and nonvesicular storage sites of isolated perfused rabbit atria; either α-methyl-*p*-tyrosine- or reserpine-pretreated rabbits were used. Amphetamine and the *exo*-2 and *anti*-9 isomers of aminobenzonorbornene could accelerate norepinephrine efflux from either compartment while the *endo*-2 and *syn*-9 isomers could accelerate the efflux from only the nonvesicular compartment at the concentrations studied. Fenfluramine and methylphenidate also were studied for their ability to accelerate efflux. Fenfluramine and methylphenidate resembled the aminobenzonorbornenes that correspond to the folded conformation of amphetamine in their ability to accelerate the efflux from nonvesicular storage. However, fenfluramine also resembled amphetamine and the aminobenzonorbornenes corresponding to the extended conformation of amphetamine in its ability to accelerate efflux from vesicular storage sites. The response to methylphenidate was similar to that of the aminobenzonorbornenes resembling the folded conformation of amphetamine.

**Keyphrases** □ Aminobenzonorbornenes—syntheses and biological evaluation as conformationally rigid analogs of amphetamines □ Amphetamines—syntheses and biological evaluation of the 2- and 9-aminobenzonorbornenes as conformationally rigid analogs □ Conformational requirements—indirectly acting sympathomimetic agents, syntheses and biological evaluation of the 2- and 9-aminobenzonorbornenes as amphetamine analogs

Amphetamine is a unique drug with respect to its simple structure and multiple pharmacological effects. Its wide spectrum of biological activity may be ascribed to its structural resemblance to several neurotransmitters such as norepinephrine, dopamine, and serotonin. One structural feature common to all of these compounds is an amino group separated by two carbon atoms from an aromatic ring. Free rotation about the two carbon atoms of such an ethylamine side chain permits amphetamine to assume suitable conformations to interact with various receptors in neurons associated with these neurotransmitters.

## BACKGROUND

A conformational energy map of amphetamine, generated by Pullman *et al.*[1] (1), shows three energetically equivalent minima. One minimum corresponds to the fully extended form of amphetamine where the nitrogen atom is pointed away from the aromatic ring, and the other two minima correspond to folded forms of amphetamine where the nitrogen is rotated toward the aromatic ring (1).

Another major investigation concerning the conformation of phenethylamine derivatives was that by Weintraub and Hopfinger (2). They employed empirical potential functions, which take into account several aspects that are neglected in the quantum mechanical calculations such as solvent effects and the conformational dependence on the ionization state of the molecule. Their work is in agreement with that of Pullman *et al.* (1) in that the same two basic conformations, extended and folded, are predicted.

However, the work by Weintraub and Hopfinger suggests that the most probable conformation of amphetamine for a given ionization state of the amine nitrogen depends on the interaction with aqueous solvent. They calculated that the most stable conformation for unionized amphetamine in a vacuum is the folded form. However, for the charged molecule in aqueous media, their calculations predict a strong preference for the extended conformation (2). These findings of the conformational preference of amphetamine are in agreement with the results of Neville *et al.* (3), whose PMR study of amphetamine in aqueous solution showed the molecule to be in the extended form.

While such mathematical methods can provide a theoretical model for the preferred conformation of a molecule, certain aspects cannot be included in these calculations. One such aspect concerns the lack of knowledge concerning the precise nature of the drug–receptor interaction. Hence, the effects of the receptor on the drug conformation cannot be determined. The molecular level local environmental conditions also are unknown and, therefore, cannot be considered.

These limitations of theoretical methods for the determination of conformations clearly suggest a study of the biological activities of rigid analogs of amphetamine. The two major centers of the amphetamine molecule that are implicated most frequently in receptor interactions are the amino group and the aromatic ring. The distance between these two parts of the amphetamine molecule for each predicted stable conformation, as well as the corresponding distance for the 2- and 9-aminobenzonorbornenes, is shown in Table I.

The use of rigid analogs of a pharmacologically active compound can yield information about the stereochemical requirements for a molecule to elicit the biological response. In the case of amphetamine and its derivatives, the wide variety of physiological effects observed for these compounds may be due partially to the ability of the ethylamine chain to assume various conformations, permitting interaction with many types of receptors. To study the conformational requirements for the biological activity of amphetamine, the 2- and 9-aminobenzonorbornenes were designed and synthesized as conformationally rigid analogs of amphetamine. These compounds are strictly rigid, offer only a minimal addition to the molecular weight and size of the amphetamine molecule, and have

**Table I—Atomic Parameters for Amphetamine and the Isomeric 2- and 9-Aminobenzonorbornenes**

| Compound | $D_1$[a], Å | $D_2$[b], Å |
|---|---|---|
| Amphetamine[c] | | |
| Extended conformation | 5.11 | 1.24 |
| Folded conformation | 3.82 | 2.14 |
| 2-Aminobenzonorbornenes[d] | | |
| *exo*-Isomer, I | 5.1 | 1.7 |
| *endo*-Isomer, II | 3.7 | 2.5 |
| 9-Aminobenzonorbornenes[d] | | |
| *anti*-Isomer, III | 4.8 | 0.7 |
| *syn*-Isomer, IV | 3.6 | 2.3 |

[a] Distance from the center of the aromatic ring to the amino nitrogen. [b] Distance from the plane of the aromatic ring to the amino nitrogen. [c] Distances as calculated by Pullman *et al.* (1). [d] Distances measured using Dreiding models.

[1] Using a refined all-valence-electrons procedure, designated as the PCILO method (perturbative configurational interaction using localized orbitals).

0022-3549/81/0200-0199$01.00/0
© 1981, American Pharmaceutical Association

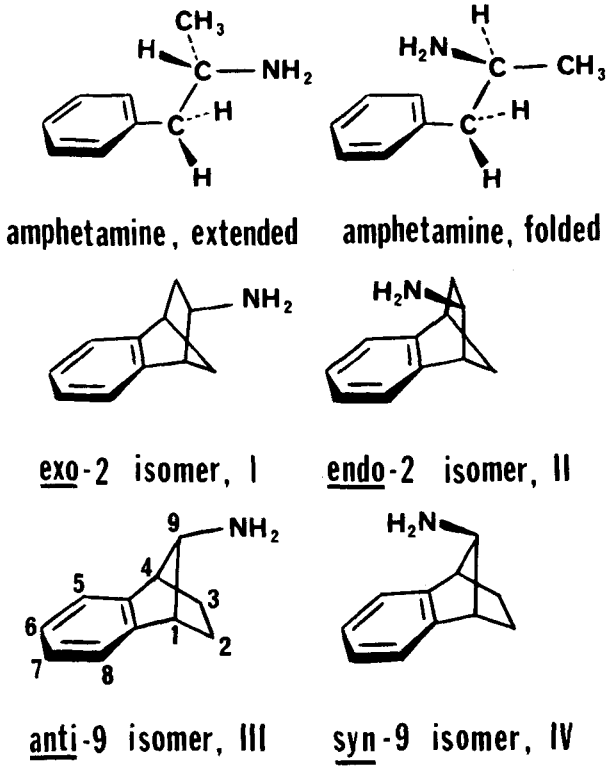


**Figure 1**—*Steric relationships between the 2- and 9-aminobenzonorbornenes and the stable conformers of amphetamine. The numbering of the benzonorbornene ring systems is shown on the* anti-*9 isomer.*

two isomers closely related conformationally to the folded form of amphetamine and two isomers closely related to the extended conformation of amphetamine. The relationship of these compounds to the predicted stable conformations of amphetamine is shown in Table I and Fig. 1. A preliminary account of this study was reported previously (4).

## EXPERIMENTAL

**Chemical**[2]—exo-*2-Aminobenzonorbornene (I) Hydrochloride*—To a mixture of sodium borohydride (0.78 g, 0.02 mole) and benzonorbornadiene (5) (7.1 g, 0.05 mole) in diglyme (25 ml) at 0° (under nitrogen) was added dropwise, over 10 min, boron trifluoride etherate (3.90 g, 0.03 mole). The mixture then was stirred at 25° for 3 hr under nitrogen. A slurry of hydroxylamine *O*-sulfonic acid (10 g, 0.09 mole) in diglyme (45 ml) was added, and stirring was continued for 18 hr at 100°. The amber solution was decanted from insoluble material, treated with concentrated hydrochloric acid (20 ml) and water (200 ml), and extracted with ether (3 × 75 ml). The aqueous layer was made strongly alkaline with sodium hydroxide (15 g) and extracted with ether (3 × 75 ml).

The ether extract was washed with water (100 ml) and dried over anhydrous sodium sulfate. The solvents were removed *in vacuo*, first at 60° (50 torr) and then at 55° (0.5 torr), leaving *exo*-2-aminobenzonorbornene as a yellow oil (2.3 g, 30%); PMR: δ 1.15–2.08 (complex m, 4H, H-3 and H-9), 1.43 (s, 2H, exchangeable with deuterium oxide, $NH_2$), 2.80–3.10 (complex m, 2H, bridgehead protons), 3.17–3.36 (complex m, 1H, *endo*-H-2), and 7.04 (m, 4H, aromatic protons); mass spectrum: *m/z* (relative intensity) 159 ($M^+$, 17) and 116 (100). This amine was reportedly prepared by another method, but no experimental details or structure proof was given (6).

A solution of the amine (2.30 g) in anhydrous ether (50 ml) was treated with dry hydrogen chloride. The salt was collected and recrystallized quantitatively from absolute methanol–anhydrous ether (3:150 ml), mp 278–281° (sealed tube).

*Anal.*—Calc. for $C_{11}H_{14}ClN$: C, 67.52; H, 7.26; N, 7.16. Found: C, 67.69; H, 7.27; N, 7.12.

*2-Benzonorbornenone Oxime*—To a solution of hydroxylamine hydrochloride (1.86 g, 0.03 mole) and sodium acetate (2.79 g, 0.04 mole) in water (8 ml) were added 2-benzonorbornenone (7, 8) (3 g, 0.02 mole) and enough ethanol to effect dissolution (5 ml). This mixture was heated on a steam bath for 20 min. After cooling, the formed precipitate (2.4 g) was collected, and the mother liquor was extracted with chloroform (2 × 25 ml) to give an additional 0.6 g of the crude oxime. Recrystallization from ethanol (~7 ml) furnished the pure product (2.91 g, 89%), mp 118–119.5°; PMR: δ 1.95–2.95 (complex m, 4H, H-3 and H-9), 3.49–3.70 (m, 1H, H-4), 3.85–3.95 (m, 1H, H-1), 7.00–7.41 (m, 4H, aromatic protons), and 7.45–8.00 (m, 1H, exchangeable with deuterium oxide, N–OH); mass spectrum: *m/z* (relative intensity) 173 ($M^+$, 58), 116 (46), and 115 (100).

*Anal.*—Calc. for $C_{11}H_{11}NO$: C, 76.30; H, 6.43; N, 8.09. Found: C, 76.44; H, 6.40; N, 8.24.

endo-*2-Aminobenzonorbornene (II) Hydrochloride*—Sodium (2.5 g, 0.28 g atom) was added (in four pieces) to a stirred solution of the oxime (1.73 g, 0.01 mole) in 1-propanol (250 ml) over 45 min. After the sodium was consumed, the solvent was removed *in vacuo*. The thick residue was diluted with water (500 ml) and extracted with ether (3 × 100 ml). The ether extract was dried over anhydrous sodium sulfate and evaporated *in vacuo* to give the amine (1.42 g, 90%) as an oil; PMR: δ 0.37–0.68 (m, 1H, *endo*-H-3), 0.98 (s, 2H, exchangeable with deuterium oxide, $NH_2$), 1.61–1.92 (complex m, 2H, H-9), 2.05–2.56 (complex m, 1H, *exo*-H-3), 3.03–3.28 (complex m, 2H, bridgehead protons), 3.43–3.78 (complex m, 1H, *exo*-H-2), and 6.95–7.33 (m, 4H, aromatic protons); mass spectrum: *m/z* (relative intensity) 159 ($M^+$, 17) and 116 (100). This amine has been reported, but no experimental details or structure proof was provided (9).

The amine was converted to its hydrochloride as already described, mp 220–223°.

*Anal.*—Calc. for $C_{11}H_{14}ClN$: C, 67.52; H, 7.26; N, 7.16. Found: C, 67.78; H, 7.26; N, 7.28.

*9-Benzonorbornenone Oxime*—To a solution of hydroxylamine hydrochloride (2.82 g, 0.04 mole) and sodium acetate (4.20 g, 0.05 mole) in water (12 ml) were added 9-benzonorbornenone (10, 11) (4.50 g, 0.02 mole) and enough ethanol to effect dissolution (~10 ml). This mixture was heated on a steam bath for 4 hr, cooled, and extracted with ether (3 × 25 ml). The ether extract was washed with water, dried over anhydrous magnesium sulfate, and evaporated *in vacuo* to give 9-benzonorbornenone oxime as a thick amber oil. This oil could not be crystallized readily and thus was used in subsequent reactions without further purification.

syn-*9-Aminobenzonorbornene (IV) and* anti-*9-Aminobenzonorbornene (III) Hydrochlorides*—Sodium (16 g, 0.7 g atom) was added in three pieces to a solution of 9-benzonorbornenone oxime (4.00 g, 0.023 mole) in 1-propanol (600 ml) over 1.5 hr. After the sodium was consumed completely, the mixture was cooled and acidified with concentrated hydrochloric acid, and the solvents were removed *in vacuo*. The residue was diluted with water (200 ml) and extracted with benzene to remove neutral and acidic substances. The aqueous layer was made basic with sodium hydroxide and extracted with benzene.

The benzene extract was dried over anhydrous magnesium sulfate and evaporated *in vacuo* to give a mixture of *syn*-9 and *anti*-9-amines (3.16 g, 86%). This mixture was dissolved in formic acid (150 ml) and treated with acetic anhydride (150 ml) over 10 min, followed by a 3-hr reflux to prepare the corresponding formamides. Removal of the solvents *in vacuo* gave the formamides (3.47 g, 93%); PMR: δ 7.86 and 8.10 (s, ~0.5H each, CHO).

This formamide mixture was chromatographed on a column of silica gel[3] (600 g) prepared in benzene. The *syn*-9-amide (1.39 g) was eluted with benzene–ether (2:1, ~1.5 liters) and recrystallized from 2-propanol, mp 129–131°; PMR: δ 1.01–1.33 (m, 2H, *endo*-H-2 and *endo*-H-3), 1.92–2.29 (m, 2H, *exo*-H-2 and *exo*-H-3), 3.27 (m, 2H, bridgehead protons), 4.14–4.29 (m, 1H, *anti*-H-9), 5.19–5.95 (broad s, 1H, NH), 7.17 (m, 4H, aromatic protons), and 7.86 (s, 1H, CHO); mass spectrum: *m/z* (relative intensity) 188 ($M^+ + 1$, 3), 187 ($M^+$, 9), and 142 (100).

*Anal.*—Calc. for $C_{12}H_{13}NO$: C, 76.97; H, 7.00; N, 7.48. Found: C, 77.15; H, 7.02; N, 7.39.

The *anti*-9-amide (1.77 g) also was eluted with benzene–ether (2:1, ~2

[2] Melting points below 240° were determined on a Thomas-Hoover Unimelt apparatus and are uncorrected, and those over 240° were determined on a Mel-Temp apparatus and are uncorrected. Analyses were performed by Micro-Tech Laboratories, Skokie, Ill. PMR spectra were obtained in deuterochloroform on a Varian A-60 spectrometer equipped with a Nicolet TT-7 Fourier transform accessory. Chemical shifts are reported in parts per million (δ) downfield from tetramethylsilane as the internal standard. Mass spectra (at 70 ev) were obtained by Richard Dvorak using a Hitachi Perkin-Elmer RMU-D6 single-focusing mass spectrometer.

[3] J. T. Baker Chemical Co., 60–200 mesh.

liters) and recrystallized from ethanol, mp 133.5–135°; PMR: δ 1.11–1.36 (m, 2H, *endo*-H-2 and *endo*-H-3), 1.86–2.17 (m, 2H, *exo*-H-2 and *exo*-H-3), 3.28 (m, 2H, bridgehead protons), 3.85–3.96 (m, 1H, *syn*-H-9), 6.17–6.70 (broad s, 1H, NH), 7.14 (m, 4H, aromatic protons), and 8.10 (s, 1H, CHO); mass spectrum: *m/z* (relative intensity) 188 ($M^+ + 1$, 3), 187 ($M^+$, 9), and 142 (100).

*Anal.*—Calc. for $C_{12}H_{13}NO$: C, 76.97; H, 7.00; N, 7.48. Found: C, 77.19; H, 7.08; N, 7.45.

A solution of the *syn*-9-formamide (1.0 g) in 10% HCl (30 ml) was heated under reflux for 1 hr. The aqueous solution was extracted with ether (3 × 25 ml), made basic with sodium hydroxide pellets (with cooling), and extracted with benzene (3 × 50 ml). The benzene extract was dried over anhydrous magnesium sulfate and evaporated *in vacuo* to give *syn*-9-aminobenzonorbornene quantitatively; PMR: δ 0.87–1.33 (complex m, 2H, *endo*-H-2 and *endo*-H-3), 0.98 (s, 2H, exchangeable with deuterium oxide, $NH_2$), 1.80–2.18 (complex m, 2H, *exo*-H-2 and *exo*-H-3), 2.97–3.13 (complex m, 2H, bridgehead protons), 3.29 (s, 1H, *anti*-H-9), and 7.06–7.30 (m, 4H, aromatic protons); mass spectrum: *m/z* (relative intensity) 159 ($M^+$, 18) and 128 (100).

The amine was converted to its hydrochloride as already described, mp 344–346° (sealed tube).

*Anal.*—Calc. for $C_{11}H_{14}ClN$: C, 67.52; H, 7.26; N, 7.16. Found: C, 67.79; H, 7.26; N, 7.05.

The *anti*-9-formamide (1.0 g) was hydrolyzed as already described to yield *anti*-9-aminobenzonorbornene quantitatively; PMR: δ 1.02–1.40 (complex m, 2H, *endo*-H-2 and *endo*-H-3), 1.24 (s, 2H, exchangeable with deuterium oxide, $NH_2$), 1.87–2.27 (complex m, 2H, *exo*-H-2 and *exo*-H-3), 2.97–3.20 (m, 3H, *syn*-H-9 and bridgehead protons), and 7.14 (m, 4H, aromatic protons), in good agreement with the literature data (12, 13); mass spectrum: *m/z* (relative intensity) 159 ($M^+$, 35) and 128 (100).

The hydrochloride was prepared as already described, mp 298–302° (sealed tube) [lit. (12) mp > 240°].

*Anal.*—Calc. for $C_{11}H_{14}ClN$: C, 67.52; H, 7.26; N, 7.16. Found: C, 67.60; H, 7.22; N, 7.11.

**Biological**[4]—*Evaluation of Effect on Motor Activity*—The effect of the 2- and 9-aminobenzonorbornenes on spontaneous motor activity was determined using groups of five female ICR mice (17–22 g). Three circular activity cages, each containing six photocells, were used. To eliminate error due to any difference in sensitivity of the photocells, each dose of each compound was tested once in each cage and the values were averaged. All drugs and controls were administered intraperitoneally in a dose volume of 1–1.5 ml/100 g of weight. The aminobenzonorbornene hydrochlorides were administered as isotonic saline solutions.

Control animals were treated with appropriate volumes of isotonic saline. Controls were carried out each testing day in each cage and averaged. The cages were dark inside, and ambient noise levels were kept to a minimum. Counting began immediately after injection and was continued for 30 min.

*Evaluation of Ability to Accelerate Efflux of Tritiated Norepinephrine from Isolated Perfused Rabbit Atria*—The experiment was designed to measure the ability of the aminobenzonorbornenes (and several known sympathomimetics) to accelerate the efflux of tritium-labeled norepinephrine from isolated perfused rabbit atria. The technique represents a modification of that reported by Paton (14).

Adult male New Zealand rabbits, 1.8–3.0 kg, were pretreated with either reserpine (2.0 mg/kg sc, 18 hr; 1.0 mg/kg iv, 1 hr) or D,L-α-methyl-*p*-tyrosine (250 mg/kg ip, 9 hr). The animals were killed by a blow on the neck, and their hearts then were excised rapidly. The atria were isolated and cut into six pieces of ~35 mg each. The pieces then were mounted on fine hooks (prepared by bending the needles of standard 1-ml tuberculin syringes), which held the tissues and also delivered a constant stream of oxygen to any medium into which the tissues were placed.

The atrial dissection was performed under constantly oxygenated medium (100% oxygen) at 25°, and all subsequent incubations were done at 37°. The medium had the following composition: 140 m*M* NaCl, 5 m*M* KCl, 1.5 m*M* $CaCl{\cdot}H_2O$, 1.2 m*M* $MgSO_4$, 10 m*M* tris(hydroxymethyl)-aminomethane (pH 7.4), and 10 m*M* D-glucose. Edetate disodium dihydrate (ethylenediaminetetraacetic acid disodium salt dihydrate) ($3 \times 10^{-5}$ *M*) and sodium ascorbate ($1 \times 10^{-4}$ *M*) were added to the medium to prevent norepinephrine oxidation. To inhibit catechol *O*-methyltransferase, the medium contained $1 \times 10^{-4}$ *M* tropolone (14).

Once the atrial pieces were mounted onto the hooks, they were allowed to stand in the medium for 30 min to equilibrate. Then the tissue pieces were incubated for 30 min in medium that contained pargyline ($5 \times 10^{-4}$ *M*) to inhibit monoamine oxidase. The tissues then were transferred to fresh medium for 30 min to wash out the excess pargyline and were incubated in medium containing $5.8 \times 10^{-7}$ *M* tritiated norepinephrine for 1 hr. The tissues then were transferred every 5 min successively through a series of 21 tubes, each containing 5 ml of fresh medium. The compounds studied were present from 60 to 100 min during which efflux was measured. Amphetamine, methylphenidate, isomer I, and isomer III were studied at $5 \times 10^{-5}$ *M*; fenfluramine, isomer II, and isomer IV were studied at $1 \times 10^{-4}$ *M*. At the end of the efflux period, the tissues were placed into scintillation vials containing 1 ml of tissue solubilizer at 37°. Once the tissues were solubilized, the tissue solubilizer was neutralized with acetic acid, 10 ml of liquid scintillation cocktail was added, and the total tritium content was determined.

One-milliliter portions of all efflux media (tubes 1–21) were added to scintillation vials, 10 ml of scintillation cocktail was added, and the tritium content was determined. In all cases, the scintillation counting was done after the vials had been cooled and dark adapted. The average counting efficiency was 40%.

The tritiated norepinephrine content ($A_t$) of the tissue at various times was calculated by adding successively, in reverse order, the amount of tritiated norepinephrine released into each tube during efflux to that remaining in the tissue at the end of the experiment. Efflux was expressed as a rate coefficient ($f$) in minutes$^{-1}$:

$$f = \frac{\Delta A}{\Delta t A_t} \qquad \text{(Eq. 1)}$$

where $\Delta A$ represents the decays per minute (dpm) lost in the time interval $\Delta t$ (5 min) and $A_t$ is the amount of tritiated norepinephrine (dpm) in the tissue at the midpoint of the time interval $\Delta t$.

## RESULTS

**Effect of 2- and 9-Aminobenzonorbornenes on Spontaneous Motor Activity**—The effects of the aminobenzonorbornenes on spontaneous motor activity are shown in Fig. 2. Isomers I and III increased motor activity while II decreased motor activity. The *syn*-9 isomer (IV) did not significantly affect motor activity. The effect of dextroamphetamine sulfate also was studied by the same procedure for direct comparison to the aminobenzonorbornenes. The $ED_{50}$ of dextroamphetamine sulfate was 0.55 mg/kg, and the maximal response was similar to that obtained for *anti*-9-aminobenzonorbornene.

**Acceleration of Efflux of Tritiated Norepinephrine from Isolated Perfused Rabbit Atria**—The results are shown in Figs. 3 and 4 in which the calculated rate coefficient is plotted against time. In Fig. 3A, the entire efflux period is plotted. In all subsequent figures, only the efflux from 35 to 105 min after labeling is shown. In all cases, the portion of the graph not included is similar to that of Fig. 3A.

All four 2- and 9-aminobenzonorbornene isomers accelerated the efflux of tritiated norepinephrine from neurons of reserpine-treated animals. Isomers I and III exhibited effects similar in magnitude and duration to those caused by amphetamine. There was a peak response in the first tube (55–60 min), which contained the most tritiated norepinephrine after efflux, after which the amount of tritiated norepinephrine released into each tube approached control levels.

Isomers II and IV were comparatively much less potent at the concentration studied. These isomers were also similar to each other in magnitude and duration of response. They were, however, considerably different from I and III in the time course of response. Whereas I and III caused an immediate maximal response which rapidly fell back toward control levels, it took several tubes for II and IV (55–70 min) before the maximal response was noted; and once this maximum level was reached, it was maintained for the duration of efflux. This finding was similar to the results obtained for fenfluramine and methylphenidate.

When the animals were pretreated with α-methyl-*p*-tyrosine, I and III, as well as amphetamine, again produced an immediate maximal response. The magnitude and time course of the response caused by I and III were similar to these caused by amphetamine. In contrast to reserpine pretreatment, the response did not fall rapidly after the immediate maximum but declined only slightly from the maximal response during the remainder of efflux.

Isomers II and IV were much less potent at accelerating the efflux of

[4] Injectable reserpine (Serpasil) was purchased from Ciba Pharmaceutical Co. Pargyline hydrochloride and D,L-α-methyl-*p*-tyrosine were purchased from Sigma Chemical Co. The α-methyl-*p*-tyrosine was administered as a suspension in corn oil. NCS tissue solubilizer was purchased from Amersham/Searle. Tritiated L-norepinephrine (5.8 Ci/mmole, NET-377) was purchased from New England Nuclear. All scintillation counting was done in 22-mm glass vials (Research Products International Corp., Elk Grove Village, Ill., No. 121053, polyethylene-lined caps) with a Packard model 2425 Tri-Carb liquid scintillation spectrometer. The scintillation cocktail was Packard Insta-Gel (6002177).

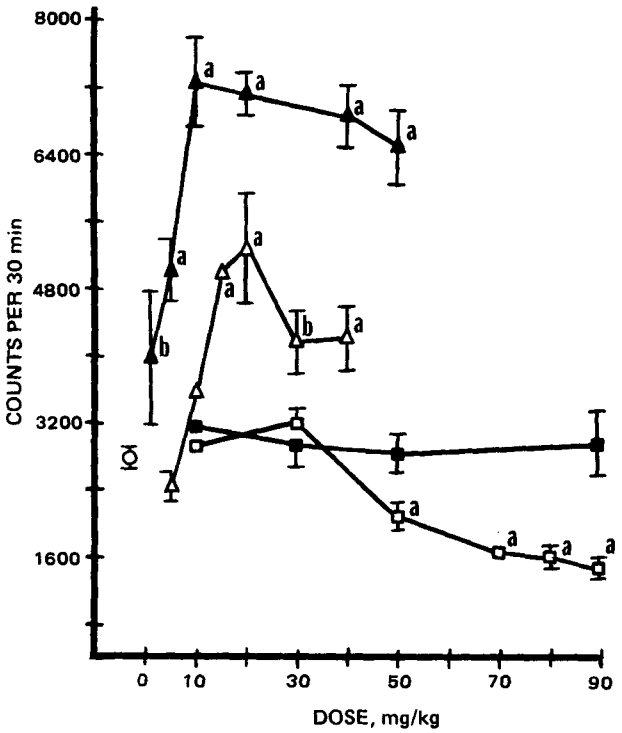


**Figure 2**—*Effect of the isomeric aminobenzonorbornenes on the spontaneous motor activity of mice. The data are expressed as counts per 30 min* versus *various doses of the compounds; the procedures are described under* Experimental. *Each point represents the mean of three experiments of five mice each (±SEM), except the control value (○) where* n = *33. Key: △, isomer I; □, isomer II; ▲, isomer III; and ■, isomer IV.*

tritiated norepinephine from atria of α-methyl-*p*-tyrosine-pretreated rabbits. They did produce a very slight immediate increase in efflux, which then decreased to nearly control levels. Fenfluramine was approximately as effective at accelerating the efflux of tritiated norepinephrine from α-methyl-*p*-tyrosine-pretreated tissues as from reserpine-pretreated tissue. Methylphenidate resembled II and IV in that it was capable of accelerating the efflux of tritiated norepinephrine from reserpine-pretreated tissues but not from α-methyl-*p*-tyrosine-pretreated tissues.

## DISCUSSION

Of the aminobenzonorbornenes studied, only isomers that resemble the extended conformation of amphetamine (I and III) increased the spontaneous motor activity of mice. These results are consistent with an earlier study which led to the conclusion that the extended conformation is critical for an agent of this type to cause an increase in motor activity (15). That isomer II decreased motor activity while IV had no effect on it is in general agreement with previous studies in which rigid and semirigid analogs that resembled the folded conformation of amphetamine either decreased or had no effect on motor activity (15, 16).

It is generally accepted that functionally distinct compartmentation of stored norepinephrine exists in adrenergic neurons. This compartmentation is believed to consist primarily of a reserpine-sensitive vesicular store and a reserpine-resistant extravesicular (cytoplasmic) store (17–21). The cytoplasmic level of accumulated norepinephrine normally is regulated by vesicular storage (17) and by deamination by monoamine oxidase (22–24). Therefore, inhibition of these processes provides a means of increasing the size of the cytoplasmic store. In the present study, the ability of the isomers of aminobenzonorbornene to accelerate the efflux of tritiated norepinephrine from these two major compartments was studied. By using pargyline-treated atrial tissue from reserpine-pretreated rabbits, a primarily cytoplasmic store was obtained. A primarily vesicular storage was obtained by using atrial tissue from α-methyl-*p*-tyrosine-pretreated rabbits. Although pargyline also was used in the α-methyl-*p*-tyrosine cases, the evidence indicates the lack of a significant cytoplasmic store.

In another recent study using rigid analogs of amphetamine and a

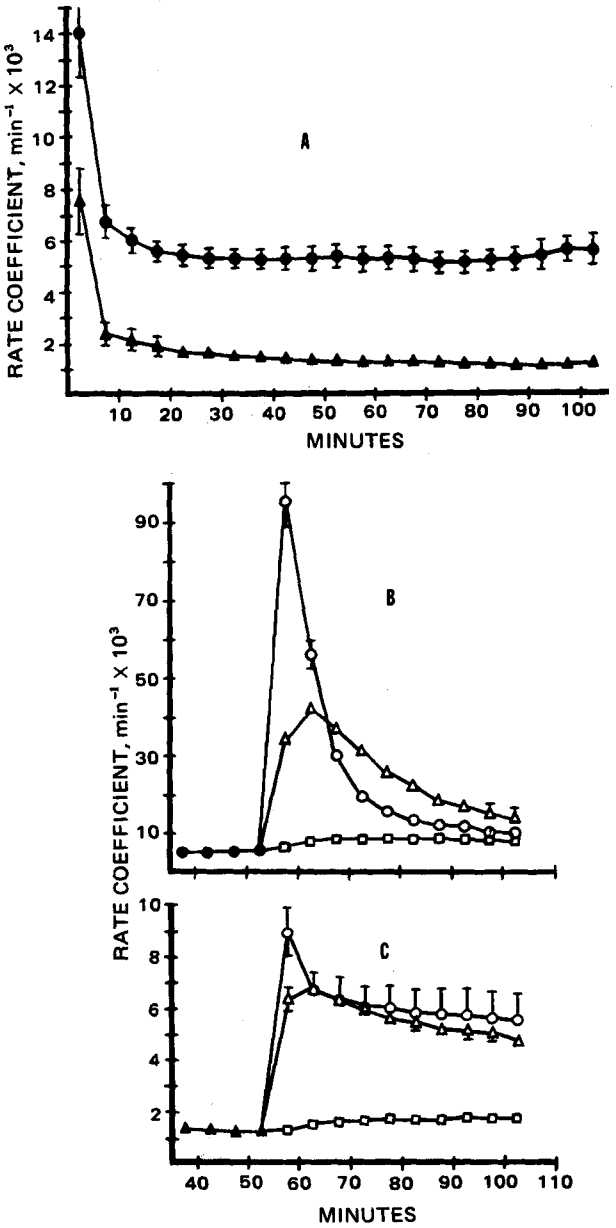


**Figure 3**—*Efflux of tritiated norepinephrine from isolated perfused rabbit atria; the procedures are described under* Experimental. *Key for graph A, controls* (n = *5):* ●, *reserpine pretreatment; and* ▲, *α-methyl-*p*-tyrosine pretreatment. Key for graph B, reserpine pretreatment* (n = *3), and graph C, α-methyl-*p*-tyrosine pretreatment* (n = *3):* ○, *amphetamine, 5* × $10^{-5}$ M; △, *fenfluramine, 1* × $10^{-4}$ M; *and* □, *methylphenidate, 5* × $10^{-5}$ M.

similar experimental protocol, it was concluded that the fully extended form of amphetamine is involved in the displacement of norepinephrine from the cytoplasmic compartment while conformational mobility, or a conformation not approximated by either reported isomer, is required for displacement from the vesicular compartment.(25).

In the present study, all of the aminobenzonorbornenes were capable of accelerating the efflux of tritiated norepinephrine from reserpine-pretreated tissue. This finding indicated that each amine was capable of entering the neurons. The difference in the manner in which these rigid analogs accelerate the efflux of tritiated norepinephrine may reflect different types of tritiated norepinephrine storage with different stereochemical sensitivities and/or different modes of entry (for the test compounds) into the neurons (active transport *versus* passive diffusion). The curve shape and the magnitude of maximal response for methylphenidate were similar to those of II and IV. This fact may indicate that the stable conformation of methylphenidate resembles the folded form of amphetamine.

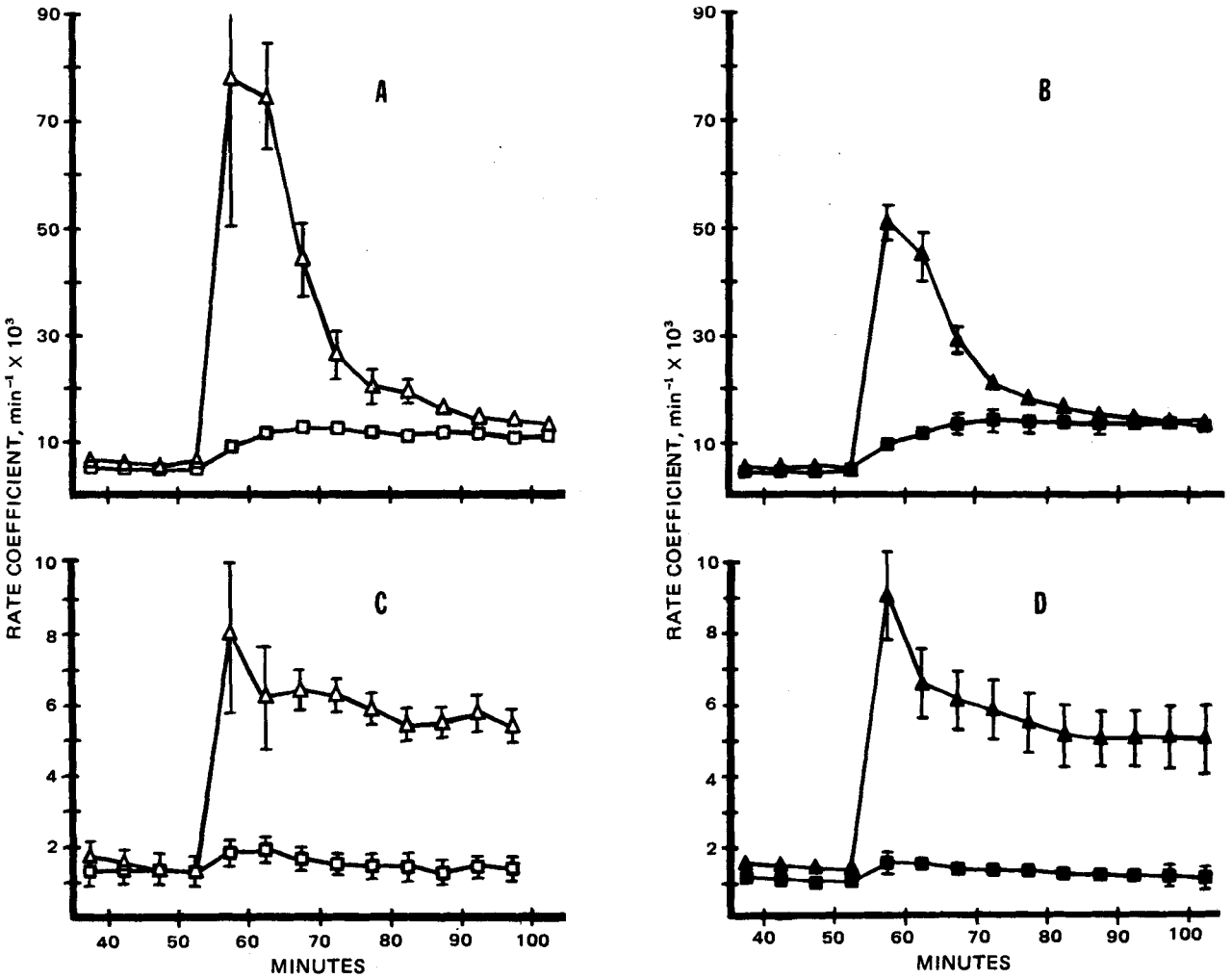


**Figure 4**—*Efflux of tritiated norepinephrine from isolated perfused rabbit atria (n = 3); the procedures are described under* Experimental. *Graphs A and B are for reserpine pretreatment, and graphs C and D are for α-methyl-*p*-tyrosine pretreatment. Key: △, isomer I, 5 × 10⁻⁵ M; □, isomer II, 1 × 10⁻⁴ M; ▲, isomer III, 5 × 10⁻⁵ M; and ■, isomer IV, 1 × 10⁻⁴ M.*

When the tissue used for these studies was taken from animals pretreated with α-methyl-*p*-tyrosine, the results were quite different. Again, rigid analogs resembling the extended form of amphetamine were able to release tritiated norepinephrine. Also the shape of the curve and the magnitude of the response were similar for each compound (I and III and amphetamine). The analogs resembling the folded conformation, however, were unable to release tritiated norepinephrine significantly from the tissue of α-methyl-*p*-tyrosine-treated animals. The use of the two pretreatments (reserpine *versus* α-methyl-*p*-tyrosine) to give either predominantly cytoplasmic or vesicular storage of the perfused tritiated norepinephrine indicates that release from the vesicular storage has more rigid stereochemical requirements than release from cytoplasmic (reserpine insensitive) sites. The extended conformation of amphetamine appears to be necessary for release from the vesicular sites while either the extended or the folded forms may cause the release from cytoplasmic sites. That methylphenidate again resembles II and IV, this time in its inability to accelerate efflux from α-methyl-*p*-tyrosine-pretreated tissues, further indicates that the stable conformation of methylphenidate may resemble the folded form of amphetamine.

It was reported that fenfluramine causes a decrease in motor activity except in animals pretreated with a monoamine oxidase inhibitor, in which case fenfluramine is nearly equipotent with amphetamine in increasing motor activity (26). In comparing the efflux data for these two compounds, one possible explanation for this phenomenon may be seen. Both compounds have similar curves for releasing tritiated norepinephrine from α-methyl-*p*-tyrosine-pretreated animals with the exception that amphetamine shows a slight maximal response, which then falls rapidly to a constant level of efflux, while fenfluramine comes to this level immediately and declines only slightly from this level. However, in reserpine-pretreated tissue, amphetamine shows a much stronger initial response than does fenfluramine. This ability of fenfluramine to release tritiated norepinephrine from vesicles as effectively as amphetamine, while not being as effective at releasing tritiated norepinephrine from cytoplasmic sites, would cause the norepinephrine released from vesicles, by fenfluramine, to have a greater exposure to intraneuronal monoamine oxidase than that released by amphetamine. If the level of norepinephrine in the cytoplasm and the level of deaminated metabolites of norepinephrine inside the neuron have a biochemical role in the neuron, it can be seen how compounds that can displace norepinephrine from cytoplasmic sites but not from vesicular sites (and vice versa) may derive some pharmacological effects *via* alteration of the normal level of these metabolites and nonvesicular norepinephrine.

## REFERENCES

(1) B. Pullman, J.-L. Coubeils, P. Courrière, and J.-P. Gervois, *J. Med. Chem.*, **15**, 17 (1972).

(2) H. J. R. Weintraub and A. J. Hopfinger, *J. Theor. Biol.*, **41**, 53 (1973).

(3) G. A. Neville, R. Deslauriers, B. J. Blackburn, and I. C. Smith, *J. Med. Chem.*, **14**, 717 (1971).

(4) L. E. Wood, *Res. Commun. Chem. Pathol. Pharmacol.*, **21**, 169 (1978).

(5) G. Wittig and E. Knauss, *Chem. Ber.*, **91**, 895 (1958).

(6) P. Burn, P. A. Crooks, and J. M. H. Rees, *J. Pharm. Pharmacol., 12-Suppl.*, **28**, 80P (1976).

(7) P. D. Bartlett and W. P. Giddings, *J. Am. Chem. Soc.*, **82**, 1240 (1960).

(8) D. J. Sandman, K. Mislow, W. P. Giddings, J. Dirlam, and G. C. Hanson, *ibid.*, **90**, 4877 (1968).

(9) K. R. Bharucha, D. Ajdukovic, V. Pavilanis, and A. C. MacKay, U.S. pat. 3,932,512 (1976); through *Chem. Abstr.*, **84**, 135372c.
(10) P. F. Ranken and M. A. Battiste, *J. Org. Chem.*, **36**, 1996 (1971).
(11) R. Muneyuki and H. Tanida, *ibid.*, **31**, 1988 (1966).
(12) H. Tanida, T. Tsuji, and T. Irie, *ibid.*, **31**, 3941 (1966).
(13) J. Ehrenfreund and E. Zbiral, *Justus Liebigs Ann. Chem.*, **1973**, 290.
(14) D. M. Paton, *Br. J. Pharmacol.*, **49**, 614 (1973).
(15) E. E. Smissman and T. L. Pazdernik, *J. Med. Chem.*, **16**, 14 (1973).
(16) *Ibid.*, **16**, 18 (1973).
(17) N. Weiner, P. R. Draskoczy, and W. R. Burack, *J. Pharmacol. Exp. Ther.*, **137**, 47 (1962).
(18) M. J. Antonaccio and C. B. Smith, *ibid.*, **188**, 654 (1974).
(19) J. R. Crout, A. J. Muskus, and U. Trendelenburg, *Br. J. Pharmacol.*, **18**, 600 (1962).
(20) L.-O. Farnebo, *Biochem. Pharmacol.*, **20**, 2715 (1971).
(21) R. F. Furchgott, S. M. Kirpekar, M. Rieder, and A. Schwab, *J. Pharmacol. Exp. Ther.*, **142**, 39 (1963).
(22) A. Giachetti and R. A. Hollenbeck, *Br. J. Pharmacol.*, **58**, 497 (1976).
(23) A. Giachetti and P. R. Shore, *Biochem. Pharmacol.*, **15**, 607 (1966).
(24) L. L. Iversen, J. Glowinski, and J. Axelrod, *J. Pharmacol. Exp. Ther.*, **150**, 173 (1965).
(25) J. A. Ruth, G. L. Grunewald, and C. O. Rutledge, *ibid.*, **204**, 615 (1978).
(26) R. J. Ziance, I. G. Sipes, W. J. Kinnard, Jr., and J. P. Buckley, *ibid.*, **180**, 110 (1972).

## ACKNOWLEDGMENTS

Abstracted in part from a dissertation submitted by L. E. Wood to the University of Illinois in partial fulfillment of the Doctor of Philosophy degree requirements.

# Theophylline Magnesium Salicylate, a New Xanthine Compound

**R. H. BARRY, H. RUBIN *, J. B. JOHNSON, and J. H. LAZARUS ˣ**

Received February 19, 1980, from the *Pharmaceutical R&D Department, Hoffmann-La Roche Inc., Nutley, NJ 07110.* Accepted for publication August 1, 1980. *Present address: Block Drug Co., Jersey City, NJ 07302.

**Abstract** □ Interaction of 1 mole of magnesium salicylate and 2 moles of theophylline in water precipitated a crystalline compound, identified as theophylline magnesium salicylate pentahydrate from analytical and supportive physicochemical data. Similarly, barium salicylate and theophylline produced theophylline barium salicylate. No precipitates were formed with calcium salicylate or strontium salicylate under the same conditions. Theophylline magnesium salicylate is not a mixture of components and differs in composition from the known theophylline calcium salicylate dihydrate. Unlike the latter compound, it is not alkaline.

**Keyphrases** □ Theophylline magnesium salicylate—synthesis and properties □ Xanthines—theophylline magnesium salicylate, synthesis and properties

The methylxanthines theobromine, theophylline, and caffeine have been used to stimulate the central nervous system, to promote diuresis, and for their cardiovascular effects. While investigating theophylline as a diuretic component for a proprietary product, an insoluble product resulted from the interaction of magnesium salicylate and theophylline. This paper describes the preparation and properties of theophylline magnesium salicylate, a crystalline compound not previously reported.

## BACKGROUND

Theobromine, theophylline, and caffeine are used medically as single entities, as soluble amine salts, or as the so-called double salts with alkali or alkaline earth metal salts of organic acids such as acetic, gluconic, benzoic, and salicylic acids. These double salts, believed by some to be definite compounds and by others to be simply mixtures, were prepared either to solubilize the xanthine (*e.g.*, theophylline sodium acetate and caffeine sodium benzoate) or to make insoluble products (*e.g.*, theobromine and theophylline calcium salicylates); the latter type of compound is claimed to be tolerated better in the GI tract than the parent xanthine.

Various methods have been described for the preparation of the xanthine double salts with alkali or alkaline earth metal salts of organic acids. For example, the soluble compound theophylline sodium acetate is made by heating together 1 equivalent each of theophylline and sodium hydroxide, mixing them with 1 equivalent of aqueous sodium acetate, and evaporating the mixture to dryness (1). Theobromine sodium salicylate is made in a similar fashion (2). Theobromine and theophylline calcium salicylates are prepared according to a 1925 patent (3) by dissolving the xanthine in aqueous sodium hydroxide, adding a solution of sodium salicylate followed by solutions of calcium chloride and ammonium hydroxide, and removing and drying the precipitate. The two insoluble calcium salicylate double salts are described as having the following compositions:

1. For the neutral double salt, $(C_7H_7N_4O_2)Ca(C_6H_4OHCO_2)_2Ca$. The present authors believe this empirical formula to be in error because the formula should be $(C_7H_7N_4O_2)_2Ca(C_6H_4OHCO_2)_2Ca$ or simply $(C_7H_7N_4O_2)Ca(C_6H_4OHCO_2)$ since a subsequent patent (4) indicated that the compound contains one atom of calcium and 1 mole each of theobromine and salicylic acid.
2. For the basic double salt, $(C_7H_7N_4O_2)_2Ca(C_6H_4OHO_2Ca)_2$.

The aforementioned patents also stated that the analogous strontium double salts can be made in a similar fashion.

Another patent (5), issued in 1949 for the same manufacturer as the previously cited patents, contained only one example for the preparation of neutral theobromine calcium salicylate[1] (by reacting theobromine calcium and salicylic acid), which is assigned the formula $(C_7H_7N_4O_2)$-$Ca(C_6H_4OHCO_2)\cdot H_2O$. The corresponding theophylline calcium salicylate[2] is the double salt of calcium salicylate and calcium theophylline in equimolecular proportions or $(C_7H_7N_4O_2)Ca(C_6H_4OHCO_2)\cdot 2H_2O$ (6). Both theobromine and theophylline calcium salicylates are slightly soluble in water and are alkaline (7–9).

This description of the formula and preparation of theophylline cal-

[1] Theocalcin, Knoll.
[2] Phyllicin, Knoll.



*0022-3549/81/0200-0204$01.00/0*
*© 1981, American Pharmaceutical Association*

(9) K. R. Bharucha, D. Ajdukovic, V. Pavilanis, and A. C. MacKay, U.S. pat. 3,932,512 (1976); through *Chem. Abstr.*, **84**, 135372c.
(10) P. F. Ranken and M. A. Battiste, *J. Org. Chem.*, **36**, 1996 (1971).
(11) R. Muneyuki and H. Tanida, *ibid.*, **31**, 1988 (1966).
(12) H. Tanida, T. Tsuji, and T. Irie, *ibid.*, **31**, 3941 (1966).
(13) J. Ehrenfreund and E. Zbiral, *Justus Liebigs Ann. Chem.*, **1973**, 290.
(14) D. M. Paton, *Br. J. Pharmacol.*, **49**, 614 (1973).
(15) E. E. Smissman and T. L. Pazdernik, *J. Med. Chem.*, **16**, 14 (1973).
(16) *Ibid.*, **16**, 18 (1973).
(17) N. Weiner, P. R. Draskoczy, and W. R. Burack, *J. Pharmacol. Exp. Ther.*, **137**, 47 (1962).
(18) M. J. Antonaccio and C. B. Smith, *ibid.*, **188**, 654 (1974).
(19) J. R. Crout, A. J. Muskus, and U. Trendelenburg, *Br. J. Pharmacol.*, **18**, 600 (1962).
(20) L.-O. Farnebo, *Biochem. Pharmacol.*, **20**, 2715 (1971).
(21) R. F. Furchgott, S. M. Kirpekar, M. Rieder, and A. Schwab, *J. Pharmacol. Exp. Ther.*, **142**, 39 (1963).
(22) A. Giachetti and R. A. Hollenbeck, *Br. J. Pharmacol.*, **58**, 497 (1976).
(23) A. Giachetti and P. R. Shore, *Biochem. Pharmacol.*, **15**, 607 (1966).
(24) L. L. Iversen, J. Glowinski, and J. Axelrod, *J. Pharmacol. Exp. Ther.*, **150**, 173 (1965).
(25) J. A. Ruth, G. L. Grunewald, and C. O. Rutledge, *ibid.*, **204**, 615 (1978).
(26) R. J. Ziance, I. G. Sipes, W. J. Kinnard, Jr., and J. P. Buckley, *ibid.*, **180**, 110 (1972).

## ACKNOWLEDGMENTS

Abstracted in part from a dissertation submitted by L. E. Wood to the University of Illinois in partial fulfillment of the Doctor of Philosophy degree requirements.

# Theophylline Magnesium Salicylate, a New Xanthine Compound

**R. H. BARRY, H. RUBIN *, J. B. JOHNSON, and J. H. LAZARUS ˣ**

Received February 19, 1980, from the *Pharmaceutical R&D Department, Hoffmann-La Roche Inc., Nutley, NJ 07110.* Accepted for publication August 1, 1980. *Present address: Block Drug Co., Jersey City, NJ 07302.

**Abstract** □ Interaction of 1 mole of magnesium salicylate and 2 moles of theophylline in water precipitated a crystalline compound, identified as theophylline magnesium salicylate pentahydrate from analytical and supportive physicochemical data. Similarly, barium salicylate and theophylline produced theophylline barium salicylate. No precipitates were formed with calcium salicylate or strontium salicylate under the same conditions. Theophylline magnesium salicylate is not a mixture of components and differs in composition from the known theophylline calcium salicylate dihydrate. Unlike the latter compound, it is not alkaline.

**Keyphrases** □ Theophylline magnesium salicylate—synthesis and properties □ Xanthines—theophylline magnesium salicylate, synthesis and properties

The methylxanthines theobromine, theophylline, and caffeine have been used to stimulate the central nervous system, to promote diuresis, and for their cardiovascular effects. While investigating theophylline as a diuretic component for a proprietary product, an insoluble product resulted from the interaction of magnesium salicylate and theophylline. This paper describes the preparation and properties of theophylline magnesium salicylate, a crystalline compound not previously reported.

## BACKGROUND

Theobromine, theophylline, and caffeine are used medically as single entities, as soluble amine salts, or as the so-called double salts with alkali or alkaline earth metal salts of organic acids such as acetic, gluconic, benzoic, and salicylic acids. These double salts, believed by some to be definite compounds and by others to be simply mixtures, were prepared either to solubilize the xanthine (*e.g.*, theophylline sodium acetate and caffeine sodium benzoate) or to make insoluble products (*e.g.*, theobromine and theophylline calcium salicylates); the latter type of compound is claimed to be tolerated better in the GI tract than the parent xanthine.

Various methods have been described for the preparation of the xanthine double salts with alkali or alkaline earth metal salts of organic acids. For example, the soluble compound theophylline sodium acetate is made by heating together 1 equivalent each of theophylline and sodium hydroxide, mixing them with 1 equivalent of aqueous sodium acetate, and evaporating the mixture to dryness (1). Theobromine sodium salicylate is made in a similar fashion (2). Theobromine and theophylline calcium salicylates are prepared according to a 1925 patent (3) by dissolving the xanthine in aqueous sodium hydroxide, adding a solution of sodium salicylate followed by solutions of calcium chloride and ammonium hydroxide, and removing and drying the precipitate. The two insoluble calcium salicylate double salts are described as having the following compositions:

1. For the neutral double salt, $(C_7H_7N_4O_2)Ca(C_6H_4OHCO_2)_2Ca$. The present authors believe this empirical formula to be in error because the formula should be $(C_7H_7N_4O_2)_2Ca(C_6H_4OHCO_2)_2Ca$ or simply $(C_7H_7N_4O_2)Ca(C_6H_4OHCO_2)$ since a subsequent patent (4) indicated that the compound contains one atom of calcium and 1 mole each of theobromine and salicylic acid.
2. For the basic double salt, $(C_7H_7N_4O_2)_2Ca(C_6H_4OHO_2Ca)_2$.

The aforementioned patents also stated that the analogous strontium double salts can be made in a similar fashion.

Another patent (5), issued in 1949 for the same manufacturer as the previously cited patents, contained only one example for the preparation of neutral theobromine calcium salicylate[1] (by reacting theobromine calcium and salicylic acid), which is assigned the formula $(C_7H_7N_4O_2)$-$Ca(C_6H_4OHCO_2)\cdot H_2O$. The corresponding theophylline calcium salicylate[2] is the double salt of calcium salicylate and calcium theophylline in equimolecular proportions or $(C_7H_7N_4O_2)Ca(C_6H_4OHCO_2)\cdot 2H_2O$ (6). Both theobromine and theophylline calcium salicylates are slightly soluble in water and are alkaline (7–9).

This description of the formula and preparation of theophylline cal-

[1] Theocalcin, Knoll.
[2] Phyllicin, Knoll.



*0022-3549/81/0200-0204$01.00/0*
*© 1981, American Pharmaceutical Association*

**Table I—Analysis of Theophylline Magnesium Salicylate**

| | Found, % | Calculated, % $(I)_2Mg(II)_2 \cdot 5H_2O$ | (I)Mg(II) | $(I)Mg(II) \cdot 3H_2O$ |
|---|---|---|---|---|
| Theophylline (I) | 47.60 | 47.98 | 52.59 | 45.43 |
| Salicylate (II) as salicylic acid | 36.20 | 36.70 | 40.31 | 34.83 |
| Magnesium | 3.28 | 3.26 | 7.10 | 6.13 |
| Water (Karl Fischer method) | 12.80 | 12.06 | — | 13.61 |
| Total | 99.88 | 100.00 | 100.00 | 100.00 |

**Table II—Analysis of Theophylline Barium Salicylate**

| | Found, % | Calculated, % $(I)_2Ba(II)_2$ | (I)Ba(II) |
|---|---|---|---|
| Theophylline (I) | 46.6 | 46.6 | 39.49 |
| Salicylate (II) as salicylic acid | 35.7 | 35.7 | 30.23 |
| Barium | 17.8 | 17.7 | 30.28 |
| Total | 100.1 | 100.0 | 100.00 |

cium salicylate is cited in detail because it will be shown that theophylline magnesium salicylate differs from its calcium analog, both in its composition and in the manner of its preparation.

## EXPERIMENTAL

**Theophylline Magnesium Salicylate Pentahydrate**—Magnesium salicylate tetrahydrate[3] $[(C_6H_4OHCOO)_2Mg \cdot 4H_2O]$ (37.1 g, 0.1 mole) was dissolved in 480 ml of distilled water and warmed to 40°. Anhydrous theophylline[4] ($C_7H_8N_4O_2$) (36.0 g, 0.2 mole) was added and stirred until it dissolved. The resulting solution was filtered rapidly and allowed to stand, upon which precipitation of a white crystalline solid occurred. After standing for several hours, the precipitate was filtered off and washed quickly with three 15-ml portions of cold (5°) distilled water. The precipitate was dried at 70° for 6 hr. The product yield was 61.8 g. The analytical results are shown in Table I.

**Theophylline Barium Salicylate**—To compare the behavior of barium salicylate under reaction conditions similar to those used for the preparation of theophylline magnesium salicylate, 43 g (0.1 mole) of barium salicylate monohydrate[5] was dissolved in 250 ml of water, and 36 g (0.2 mole) of theophylline was dissolved in the solution. After standing for 1 day, the precipitated solid was filtered off and dried *in vacuo* for 6 hr at 70°. The yield was ~50 g. The analysis of the dried product is shown in Table II.

**Attempts to Prepare Strontium and Calcium Analogs of Theophylline Magnesium Salicylate**—Strontium salicylate[5] (19.9 g, 0.05 mole) was dissolved in 400 ml of water, and 18.0 g (0.1 mole) of theophylline was dissolved in this solution. No precipitation occurred on standing for several hours. Only a small amount of solid formed overnight in the refrigerator, and it was identified as theophylline by its melting point and mixed melting point with an authentic sample.

Calcium salicylate[5] (17.5 g, 0.05 mole) was dissolved in 588 ml of water, and 18.0 g (0.1 mole) of theophylline was dissolved in this solution. No precipitate formed on standing at room temperature; on standing in the refrigerator overnight, a small amount of solid deposited and was identified as theophylline.

No attempts were made to evaporate the aqueous solutions of theophylline, strontium, and calcium salicylates and to identify the residues since the principal aim was to determine if the reactants would readily yield precipitates under the same conditions employed for the reaction between magnesium and barium salicylates and theophylline.

**Preparation of Magnesium Analog of Theophylline Calcium Salicylate Dihydrate**—Since the cited patent literature discloses processes for making double salts of theobromine and theophylline by reacting these xanthines and their calcium or strontium salts with an equivalent molecular quantity of basic or neutral calcium or strontium salicylate, a similar procedure was used to make the analogous magnesium double salt. A solution of 37 g (0.1 mole) of magnesium salicylate tetrahydrate in 458 ml of water was placed in a blender. To this solution were added 19.45 g (0.1 mole) of magnesium hydroxide (as the 30% paste[6]) and 36 g (0.2 mole) of anhydrous theophylline, and the mixture was dispersed thoroughly. The resultant slurry was evaporated to dryness over a steam bath and then ground to a powder to yield 75 g. The analysis of the powder is given in Table III.

**Table III—Analysis of the Magnesium Analog of Theophylline Calcium Salicylate Dihydrate**

| | Found, % | Calculated, % $(I)Mg(II) \cdot 3H_2O$ | $(I)_2Mg(II)_2 \cdot 5H_2O$ |
|---|---|---|---|
| Theophylline (I) | 45.6 | 45.54 | 47.98 |
| Salicylate (II) as salicylic acid | 35.4 | 34.66 | 36.70 |
| Magnesium | 6.1 | 6.15 | 3.26 |
| Water (Karl Fischer method) | 13.9 | 13.65 | 12.06 |
| Total | 101.0 | 100.00 | 100.00 |

**Physical Data**—To support the fact that theophylline magnesium salicylate is a definite crystalline compound and not a physical mixture of its components, UV and IR spectrograms, X-ray powder diffraction data, and thermograms were evaluated.

The UV spectrogram of theophylline magnesium salicylate pentahydrate was compared to the spectra of magnesium salicylate and theophylline, and no significant structural changes could be deduced.

The IR spectrum obtained[7] from a physical mixture in mineral oil containing 2 moles of theophylline and 1 mole of magnesium salicylate was essentially the sum of the spectra of theophylline and magnesium salicylate (Fig. 1). This finding was confirmed by grinding theophylline in mineral oil and then adding magnesium salicylate to it. The spectrum from this suspension was identical to the spectrum of the physical mixture. In contrast, the IR spectrum of theophylline magnesium salicylate pentahydrate (Fig. 2) differed from that of the physical mixture. Beside the difference in the NH stretching region (3120 $cm^{-1}$), the carbonyl band at 1715 $cm^{-1}$ in the physical mixture was not present in the spectrum of theophylline magnesium salicylate.

X-ray diffraction measurements were made to compare theophylline magnesium salicylate, a physical mixture of theophylline and magnesium salicylate in a 2:1 molar ratio, and the individual components. The samples, positioned in a Bakelite holder, were placed in the sample compartment of a spectrogoniometer[8] arranged in the diffractometry mode and irradiated with CuK radiation. The diffraction patterns from 5 to 20° 2$\theta$ were obtained. The relative peak intensities were calculated, and the interplanar $d$ spacings corresponding to the diffraction peaks were calculated using a trigonometric package program[9] adapted to determine 2$\theta$ values from $d$ values and to determine $d$ values from 2$\theta$ values. Only the data from the physical mixture and theophylline magnesium

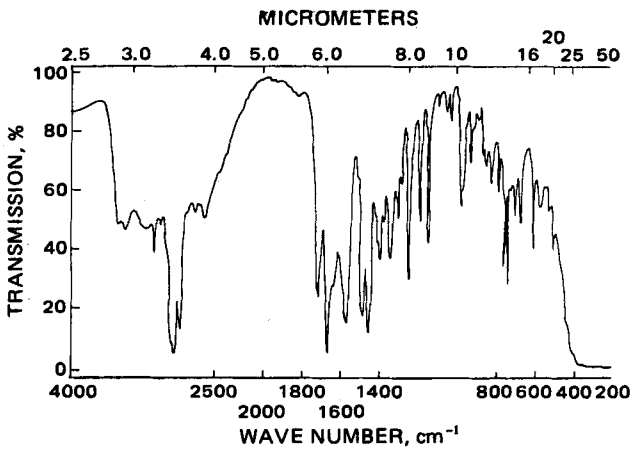


**Figure 1**—*IR spectrogram of a physical mixture of theophylline and magnesium salicylate in a 2:1 molar ratio.*

[3] S. B. Penick & Co.
[4] Ganes Chemical Works.
[5] Pfaltz and Bauer.
[6] Hydromagma, Merck.
[7] Perkin-Elmer model 283.
[8] General Electric GE XRD-6.
[9] Wang Laboratories.

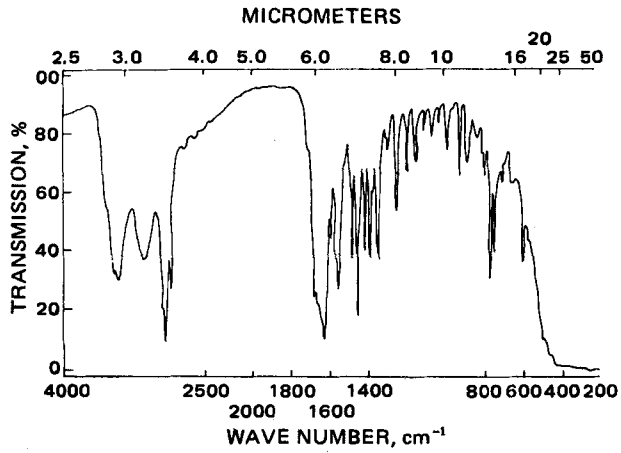


**Figure 2**—*IR spectrogram of theophylline magnesium salicylate.*

salicylate are shown in Table I and Figs. 3 and 4. The diffraction data show that theophylline magnesium salicylate is a true compound that exists in a crystalline form different from its components and a physical mixture of each component.

Thermograms (Fig. 5) were obtained with magnesium salicylate, theophylline, a 2:1 theophylline–magnesium salicylate mixture, and theophylline magnesium salicylate using a scanning calorimeter[10]. Thermal transitions occurred in theophylline and magnesium salicylate at 283 and 117–118°, respectively. Only one thermal transition, at 139–140°, occurred with theophylline magnesium salicylate. Upon cooling, this melt again was subjected to thermal analysis, and one transition at 139–140° was found. The 2:1 molar mixture of components showed two bands, one corresponding to magnesium salicylate at 118° and another at 139–140°. The latter band probably arises from a reaction between the two components in the molten state to form theophylline magnesium salicylate.

**Pharmacological Data on Theophylline Magnesium Salicylate**—The acute oral toxicity in mice (72 hr) was determined as: theophylline magnesium salicylate, 665 ± 35 mg/kg; anhydrous theophylline, 460 ± 35 mg/kg; and magnesium salicylate, 1200 ± 53 mg/kg.

The toxicity appears to be a summation of the toxicities of the theophylline and magnesium salicylate entities of the compound, which is not unexpected since the compound contains ~48% theophylline and 40% magnesium salicylate. When the compound was given intravenously to a dog at 4 mg/kg, it showed a slight but transient elevation of blood pressure. In the inflamed rat paw test (10), the compound given orally

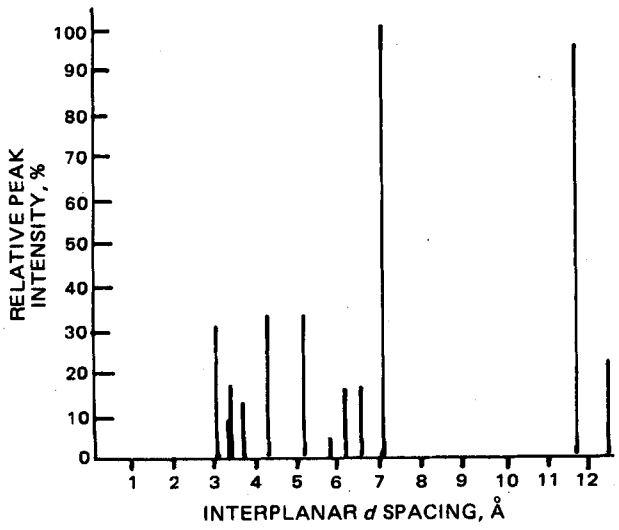


**Figure 3**—*X-ray diffraction data showing relative peak intensities of a 2:1 molar physical mixture of theophylline and magnesium salicylate.*

[10] Perkin-Elmer DSC-1B.

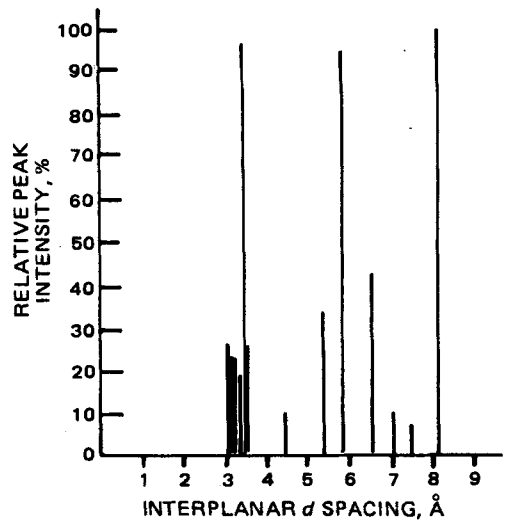


**Figure 4**—*X-ray diffraction data showing relative peak intensities corresponding to interplanar* d *spacings of theophylline magnesium salicylate.*

at 200 mg/kg showed the expected salicylate (anti-inflammatory and antipyretic) effects of moderate duration (2–3 hr).

## RESULTS AND DISCUSSION

As indicated by the data in Table I, the precipitated product conformed most nearly to the pentahydrate. When 0.5–2.0 moles of magnesium salicylate was reacted with 1 mole of theophylline under similar conditions, the precipitated solids, after drying, showed analyses quite similar to those reported here, indicating that the insoluble product in each case was $(I)_2Mg(II)_2{\cdot}5H_2O$. The substance was a white, bitter, crystalline compound containing ~48% theophylline, 40% magnesium salicylate, and 12% water of hydration. It had no definite melting point and was sparingly soluble in water (~2% at 25°) and in ethanol (~1% at 25°). One-percent solutions were slightly acidic (pH 6). The dried product conformed to the formula $(I)_2Ba(II)_2$ (Table II).

From the data in Table III, the product made by this procedure can be approximated to be theophylline magnesium salicylate trihydrate, which is the magnesium analog of theophylline calcium salicylate dihydrate. A 1% aqueous dispersion of this product had a pH of 8.4. This product does not appear to have been reported in the literature, and it has a different composition than the crystalline theophylline magnesium salicylate pentahydrate described earlier in this report.

The known theophylline calcium salicylate was stated earlier as being composed of calcium theophylline $[Ca(C_7H_7N_4O_2)_2]$ and calcium salicylate in molecular proportions, or it could be represented by the simple

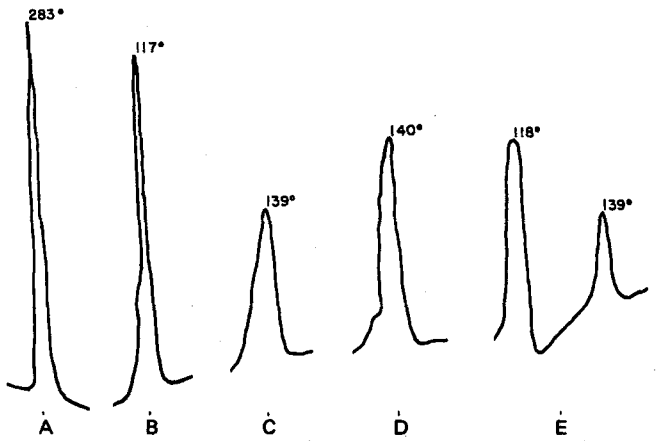


**Figure 5**—*Thermograms of theophylline (A), magnesium salicylate (B), theophylline magnesium salicylate (C), cooled melt of theophylline magnesium salicylate (D), and a 2:1 molar mixture of theophylline and magnesium salicylate.*

**Table IV—Analysis of Commercial Theophylline Calcium Salicylate**

| | Found, % | Calculated, % (I)Ca(II)·$2H_2O$ | Calculated, % $(I)_2Ca(II)_2$ |
|---|---|---|---|
| Theophylline (I) | 43.9 | 45.66 | 53.27 |
| Salicylate (II) as salicylic acid | 34.1 | 34.94 | 40.77 |
| Calcium | 10.2 | 10.21 | 5.96 |
| Water (Karl Fischer method) | 11.8 | 9.19 | — |
| Total | 100.0 | 100.00 | 100.00 |

formula $(C_7H_7N_4O_2)Ca(C_6H_4OHCO_2)$. To ascertain with certainty that this formula was correct for theophylline calcium salicylate, a commercial sample[2] of this product was analyzed. The results are given in Table IV. These results confirm that theophylline calcium salicylate can be represented by the formula $(C_7H_8N_4O_2)Ca(C_6H_4OHCO_2)\cdot 2H_2O$.

From the foregoing experimental data, it is evident that theophylline magnesium salicylate pentahydrate is a crystalline compound that differs in composition from its calcium analog, theophylline calcium salicylate dihydrate. Moreover, theophylline magnesium salicylate shows a slightly acidic reaction in water, in contrast to the alkaline character of the theophylline and theobromine calcium salicylates and to many of the so-called double salts derived from the reaction of these xanthines with metal salts of organic acids. While the alkali metal salts of salicylic acid usually combine with the xanthines to yield water-soluble complexes, the alkaline earth metal salicylates usually yield insoluble complexes. However, calcium and strontium salicylates did not yield precipitates with theophylline under the present experimental conditions, whereas magnesium and barium salicylates produced theophylline derivatives with similar compositions.

A French patent (11) disclosed the preparation of a double salt of theophylline with barium salicylate for which the formula $(C_7H_8N_4O_2)_2Ba(C_7H_5O_3)_2$ or $(I)_2Ba(II)_2$ was given. According to the patent, this compound was made by dissolving theophylline in an aqueous solution of barium salicylate, filtering, and then evaporating the filtrate to dryness *in vacuo*. The resulting compound was said to be easily soluble in water. From the present experiments using barium salicylate and theophylline, the resultant product readily precipitated from the aqueous solution of the reactants, and it was only sparingly soluble in water. Analysis of the product showed it to conform to the formula $(I)_2Ba(II)_2$ (Table V). Although the French patent assigned this formula to their product, the inventors had to resort to evaporation *in vacuo* to obtain it. Moreover, the same patent assigned the formula $(C_8H_{10}N_4O_2)$-$Ba(C_7H_5O_3)_2$ or (caffeine)Ba(salicylate)$_2$ to the double salt of caffeine and barium salicylate (prepared in similar fashion as the theophylline double salt). Since analyses were not given in this patent for either the theophylline or caffeine barium salicylates, it is not clear how the inventors arrived at their formulas.

**Table V—X-Ray Diffraction Patterns for a 2:1 Molar Ratio Mixture of Theophylline and Magnesium Salicylate (A) and Theophylline Magnesium Salicylate (B)**

| A | | | B | | |
|---|---|---|---|---|---|
| $2\theta$ | $d$, Å | $I/I_1$ | $2\theta$ | $d$, Å | $I/I_1$ |
| 7.14° | 12.3803 | 23 | 10.89° | 3.1241 | 100 |
| 7.57° | 11.6780 | 96 | 11.83° | 7.4806 | 8 |
| 12.57° | 7.0418 | 100 | 12.55° | 7.0530 | 11 |
| 13.47° | 6.5733 | 17 | 13.52° | 6.5491 | 43 |
| 14.32° | 6.1849 | 17 | 15.25° | 5.8098 | 95 |
| 15.27° | 5.8022 | 5 | 16.52° | 5.3659 | 24 |
| 17.19° | 5.1582 | 34 | 19.79° | 4.4860 | 11 |
| 20.28° | 4.3787 | 34 | 25.25° | 3.5270 | 27 |
| 24.12° | 3.6896 | 13 | 25.92° | 3.4373 | 97 |
| 25.54° | 3.4876 | 18 | 26.97° | 3.3058 | 19 |
| 26.39° | 3.3772 | 10 | 28.12° | 3.1732 | 24 |
| 28.85° | 3.0945 | 32 | 29.02° | 3.0768 | 27 |

The diversity of opinion concerning the nature of the interaction of xanthines with the metal salts of organic acids, variously referred to as double salts, mixtures, or complexes, has long been recognized (12). The complexation of salicylic acid and its sodium salt with caffeine (13, 14), theobromine (13), and theophylline (15, 16) has been studied extensively, and a good review of the literature on caffeine complexation was given by Stamm (17) in 1969. The relative roles of such factors as hydrophobic binding, hydrogen bonding, and donor–acceptor forces were considered in these publications. The factors involved in the formation of theophylline magnesium salicylate await further exploration.

## REFERENCES


(1) R. Eder, J. Buchi, H. Fluck, and H. Kasermann, "Kommentar zur Pharmacopoeia Helvetica," Editio Quinta, Selbstverlag Des Schweiz, Apotheker-Vereins, Zurich, Switzerland, 1947, p. 823.

(2) "Pharmacopoeia Helvetica," Editio Quinta, Eidgenossische Drucksacken und Material Zentrale, Bern, Switzerland, 1953, p. 1010.

(3) U.S. pat. 1,547,698 (1925).

(4) British pat. 241,266 (1925).

(5) German pat. 835,146 (1949). See also Ref. 2, p. 1017.

(6) "The Merck Index," 9th ed., Merck & Co., Rahway, N.J., 1976, p. 9006.

(7) *Ibid.*, pp. 8998, 9006.

(8) "Remington's Practice of Pharmacy," 12th ed., Mack Publishing Co., Easton, Pa., 1961, p. 1106.

(9) "Husa's Pharmaceutical Dispensing," 5th ed., E. W. Martin, Ed., Mack Publishing Co., Easton, Pa., 1959, pp. 462, 463.

(10) L. O. Randall and J. J. Selitto, *Arch. Int. Pharmacodyn. Ther.*, **111**, 409 (1957).

(11) French pat. 360,909 (1925).

(12) "United States Dispensatory," 24th ed., A. Osol and G. Farrar, Eds., Lippincott, Philadelphia, Pa., 1947, p. 1206.

(13) M. Blake and L. Harris, *J. Am. Pharm. Assoc., Sci. Ed.*, **41**, 521, 524, 527 (1952).

(14) T. Higuchi and D. Zuck, *ibid.*, **42**, 138 (1953).

(15) T. Higuchi and A. Drubulis, *J. Pharm. Sci.*, **50**, 905 (1961).

(16) T. Higuchi and F. Pisano, *ibid.*, **53**, 644 (1964).

(17) H. Stamm, *Arch. Pharm.*, **302**, 174 (1969).


## ACKNOWLEDGMENTS


Presented at the Basic Pharmaceutics Section, APhA Academy of Pharmaceutical Sciences, Hollywood, Fla. meeting, November 1978.

The authors thank Dr. P. K. Bhattacharyya for the IR spectrograms, D. Stewart for the X-ray diffraction data, and M. Sarli for the preparation of the figures.

# Routine Quality Evaluation of Benzodiazepine Drugs to USP–NF Specifications

**D. B. BLACK, R. C. LAWRENCE, E. G. LOVERING, and J. R. WATSON ˣ**

Received May 5, 1980, from the *Pharmaceutical Chemistry Division, Drug Research Laboratories, Health Protection Branch, Ottawa, Ontario, Canada K1A 0L2.* Accepted for publication August 7, 1980.

**Abstract** □ A GLC procedure was developed for the evaluation of diazepam, chlordiazepoxide, and flurazepam formulations to USP–NF specifications for drug content, content uniformity, impurities, and identity by retention times and peak areas. The polyimide column, instrument zone temperatures, gas flows, internal standard solution, extraction solvent, and auxiliary equipment were the same for each drug. No derivatization of the samples was required. The GLC assay values (mean of 10 individual dosage units) for diazepam and flurazepam products were in good agreement with the results obtained by the pharmacopeial composite assays. With chlordiazepoxide capsules, when the levels of the two pharmacopeial impurities determined by GLC were added to the GLC assay results (mean of 10), the aggregate values were consistent with the drug content results found by the nonspecific USP method. The procedure can be made sensitive to impurity levels of ~0.01% for 2-amino-5-chlorobenzophenone and to ~0.2% for 7-chloro-1,3-dihydro-5-phenyl-2*H*-1,4-benzodiazepin-2-one 4-oxide. With the equipment used, the estimated potential outputs in lots per working day for a complete quality profile (drug content, content uniformity, purity, and identity) were seven for chlordiazepoxide if no impurity test was required, five if such a test was required, eight for diazepam, and seven for flurazepam.

**Keyphrases** □ Benzodiazepines—routine quality evaluation for adherence to USP–NF specifications □ Diazepam—routine evaluation of content, uniformity, impurities, and identity by retention times and peak areas □ Chlordiazepoxide—routine evaluation of content, uniformity, impurities, and identity by retention times and peak areas □ Flurazepam—routine evaluation of content, uniformity, impurities, and identity by retention times and peak areas □ GLC—routine evaluation of benzodiazepines

Pharmacopeial test procedures for drug quality generally tend to be tedious and time (money) consuming, and assay methods occasionally lack specificity. Even within the same chemical family of drugs, such methods sometimes require different experimental techniques and apparatus. Compendial procedures, which are legal standards not necessarily designed for speed and efficiency, may not be compatible with the needs of control laboratories that must routinely perform identity, purity, content uniformity, and drug content tests on a large number of drug products.

Most recently published GLC and high-pressure liquid chromatographic (HPLC) methods for benzodiazepines are concerned with their analysis in biological media only (1–10). New procedures reported for the determination of these drugs in pharmaceutical dosage forms include HPLC (11–13), fluorometry (14), and automated polarography (15). However, most of these methods are not suitable for moderate to large-scale drug quality screening programs.

This paper describes a semiautomated multifunctional GLC procedure for the evaluation of three benzodiazepine drugs (chlordiazepoxide, diazepam, and flurazepam) to USP–NF specifications (16, 17) for drug content, content uniformity, impurities, and identity by retention times and peak areas.

## EXPERIMENTAL

**Material and Equipment**—The following were used: chlordiazepoxide hydrochloride[1] (USP reference standard), 7-chloro-1,3-dihydro-5-phenyl-2*H*-1,4-benzodiazepin-2-one 4-oxide[1] (II) (USP reference standard), 2-amino-5-chlorobenzophenone[1] (III) (USP reference standard), diazepam[1] (USP reference standard), flurazepam hydrochloride[1] (NF reference standard), dicyclohexyl phthalate[2] (95–99%), toluene[3] (ACS reagent grade, distilled in glass), sodium hydrogen carbonate[4] (analytical reagent), 1 *N* HCl, Acculute solution[5], screw-capped tubes[6] (19 × 150 mm), variable-speed mechanical horizontal shaking apparatus[7], and a 3/4-h.p. centrifuge, 5000 rpm maximum[8].

**Solutions**—The internal standard solution was dicyclohexyl phthalate in toluene, accurately prepared to contain ~0.25 mg/ml. The stock solution of II was accurately prepared in the internal standard solution to contain ~0.2 mg/ml, and the stock solution of III was accurately prepared in the internal standard solution to contain ~0.02 mg/ml.

The diazepam stock solution was accurately prepared in the internal standard solution to contain ~0.5 mg/ml. The sodium bicarbonate (sodium hydrogen carbonate) solution was prepared in water to contain ~5% (w/v).

**GLC System**—The gas chromatograph[9] (flame-ionization detector) was fitted with a coiled glass column, 0.91 m × 6 mm o.d. (2 mm i.d.), firmly packed with 3% Poly I-110 on Gas Chrom Q[10] (80–100 mesh) and vibrated so that no cracks or deadspaces were evident. The column was conditioned overnight at 250° with a nitrogen flow of 35 ml/min. Experimental temperature conditions were: column, 250°; injector port, 250°; and detector, 250°. The gas flows were: nitrogen, 29 ml/min; hydrogen, 30 ml/min; and air, 300 ml/min. The maximum loads injected onto the column were ~0.5 μg for chlordiazepoxide and diazepam and 1.5 μg for flurazepam.

The detector output signal was fed to a digital microprocessor, which automatically computed the required information in the preinstructed format. Appropriate slope sensitivity and attenuation settings were entered *via* the keyboard terminal prior to analyses.

**Chlordiazepoxide Hydrochloride Analysis**—*Preparation and GLC of Chlordiazepoxide Calibration Solutions*—For each dosage level (5, 10, and 25 mg/capsule), a corresponding standard solution containing a similar amount of drug was prepared daily as required. About 5, 10, or 25 mg of chlordiazepoxide hydrochloride was weighed accurately into a screw-capped tube. Distilled water (2 ml), sodium bicarbonate (2 ml), and the internal standard solution (20.0 ml) were added, the contents of the tube were mechanically shaken vigorously for 10 min, and the solution was centrifuged at 3000 rpm for 10 min. To prevent column overloading, the organic layer resulting from the extraction of the 25-mg calibration solution was diluted 2:5 with the internal standard solution. A portion of the final organic layer was transferred to a sample vial[11], which was capped[11] immediately and placed in the sampling tray. About 1 μl of solution was injected in duplicate into the gas chromatograph. The run time was 10 min.

*GLC Analysis of Capsule Preparations for Content Uniformity*—The

[1] USP–NF Reference Standards, Rockville, Md.
[2] K & K Laboratories, Plainview, N.Y.
[3] Caledon Laboratories Ltd., Georgetown, Ontario, Canada.
[4] BDH Chemicals Ltd., Toronto, Ontario, Canada.
[5] Anachemia Chemicals Ltd., Montreal, Quebec, Canada.
[6] O. H. Johns Glass Co. Ltd., Toronto, Ontario, Canada.
[7] Eberbach Corp., Ann Arbor, Mich.
[8] International Equipment Co., Needham Heights, Mass.
[9] Hewlett-Packard 5840A series reporting gas chromatograph with automatic liquid sampler model 7671A.
[10] Applied Science Laboratories, State College, Pa.
[11] Hewlett-Packard, 1 ml, clear glass with caps (11 mm) and a hand capper (10 mm).



*0022-3549/81/0200-0208$01.00/0*
*© 1981, American Pharmaceutical Association*

**Table I—GLC Data on Benzodiazepine Compounds on Polyimide Column**

| Compound | Retention Time, min | Relative[a] Response Factor | CV, % | Number of Data Points | Weight Range[b] Examined, mg |
|---|---|---|---|---|---|
| Chlordiazepoxide hydrochloride | 4.1[c] | 1.2411 | 1.5 | 4 | 5.3–25.5 |
| II | 5.3 | 2.49[illegible]1 | 2.8 | 3 | 1.0–1.8 |
| III | 1.0 | 1.07[illegible]1 | 6.1 | 3 | 0.035–0.088 |
| Diazepam | 2.7 | 1.0715 | 1.5 | 3 | 2.1–10.4 |
| Flurazepam dihydrochloride | 4.8[c] | 1.4777 | 1.1 | 3 | 11.2–30.3 |

[a] Relative to the internal standard (dicyclohexyl phthalate, retention time of 1.7 min). [b] Amount extracted into 20.0 ml of the internal standard solution. [c] Eluted as the free base.

**Table II—GLC *versus* Pharmacopeial Assay Results for 10-mg Chlordiazepoxide Hydrochloride Capsules**

| Formulation | Manufacturer | Percent of Label Claim, GLC, I[b] C.U.[a] Range | I[b] CV, % | Mean[c] | II[d] | III[e] | Total | USP XIX[f] |
|---|---|---|---|---|---|---|---|---|
| 1 | A | 84.4–91.7 | 2.4 | 89.4 | 7.1 | 0.02 | 96.6 | 96.2 |
| 2 | B | 97.2–106.9 | 3.0 | 101.6 | 0.7 | 0 | 102.3 | 105.9 |
| 3 | C | 93.0–107.5 | 4.4 | 97.7 | 3.4 | 0 | 101.1 | 99.8 |
| 4 | F | 93.6–105.5 | 4.0 | 99.3 | 1.7 | 0 | 101.0 | 98.9 |
| 5 | G | 93.8–105.0 | 3.6 | 98.2 | 1.2 | 0 | 99.4 | 97.4 |

[a] Content uniformity of 10 individual dosage units. [b] Chlordiazepoxide hydrochloride. [c] Mean of 10 content uniformity values. [d] Pharmacopeial II impurity. [e] Pharmacopeial III impurity. [f] Composite assay on 10 capsules.

**Table III—GLC *versus* Pharmacopeial Assay Results for Diazepam Tablets**

| Formulation | Dosage Level, mg/unit | Manufacturer | Percent of Label Claim, GLC, C.U.[a] Range | CV, % | Mean[b] | USP XIX[c] |
|---|---|---|---|---|---|---|
| 1 | 10 | B | 98.6–100.7 | 0.6 | 99.4 | 101.0 |
| 2 | 2 | D | 84.6–113.4 | 8.1 | 97.6 | 98.6 |
| 3 | 5 | H | 99.0–108.9 | 3.1 | 105.9 | 105.2 |
| 4 | 10 | F | 96.1–99.2 | 1.1 | 97.9 | 96.4 |
| 5 | 5 | I | 97.5–106.3 | 2.7 | 100.4 | 104.0 |
| 6 | 10 | J | 96.3–100.8 | 1.6 | 98.3 | 100.4 |
| 7 | 5 | K | 89.5–102.3 | 4.6 | 97.9 | 96.5 |

[a] Content uniformity of 10 individual dosage units. [b] Mean of 10 content uniformity values. [c] Composite assay on 10 powdered tablets.

contents of each of 10 individual capsules were emptied into separate screw-capped tubes labeled 1–10. The contents of each tube were subjected to the same extraction and chromatographic procedures as described for the calibration solutions. For each sample solution, the amount of chlordiazepoxide hydrochloride present, expressed as a percentage of the label claim, was calculated automatically with reference to a calibration solution of approximately the same concentration and chromatographed just prior to the analysis of each batch of 10 dosage units. The mean of the 10 individual results was used as the assay value.

*Preparation and GLC of II and III Impurity Calibration Solutions*—Various volumes of the stock II and III impurity solutions were pipetted into three separate screw-capped tubes (A–C), each containing about 50 mg of chlordiazepoxide hydrochloride, accurately weighed. The volumes added corresponded to the following impurity levels based on the weight of chlordiazepoxide hydrochloride: A, 2.0% of II and 0.08% of III; B, 2.8% of II and 0.12% of III; and C, 4.0% of II and 0.20% of III. In each tube, the volume of the internal standard required for a total volume of 20.0 ml of organic solution then was added with water (2 ml) and sodium bicarbonate (2 ml). A blank containing ~50 mg of chlordiazepoxide hydrochloride, accurately weighed, the internal standard solution (20.0 ml), water (2 ml), and sodium bicarbonate (2 ml) also was prepared.

Each mixture was shaken mechanically for 10 min and then centrifuged at 3000 rpm for 10 min. Exactly 10.0 ml of each of the four respective organic layers and 1 *N* HCl (2 ml) were pipetted into separate screw-capped tubes, the contents were shaken mechanically for 5 min, and the solution was centrifuged at 3000 rpm for 10 min. An aliquot of each of the four organic layers was chromatographed.

*GLC Determination of II and III Impurities in Capsule Formulations*—Prior to the determination of II and III, the contents of 20 capsules were emptied, thoroughly mixed, and accurately weighed. An amount of powder equivalent to ~50 mg of chlordiazepoxide hydrochloride was accurately weighed into a screw-capped tube. The internal standard solution (20.0 ml), water (2 ml), and sodium bicarbonate (2 ml) were added, and the contents were subjected to the same bicarbonate–acid double-extraction procedure already described.

About 1 μl of the final organic layer was injected into the gas chromatograph, and the run time was set at 10 min. For each sample, the II and III levels were calculated with reference to the impurity calibration solution closest to the concentration of impurities estimated by inspection of the assay chromatogram and were expressed as a percentage of the drug label claim.

**Diazepam Analysis**—*Preparation and GLC of Diazepam Calibration Solutions*—The stock diazepam (0.5 mg/ml and 10 mg/20 ml) was successively diluted with the internal standard solution to give solutions of 0.25 mg/ml (5 mg/20 ml) and 0.1 mg/ml (2 mg/20 ml), respectively. About 1 μl of each of the three solutions (including the stock solution) was injected into the gas chromatograph set in the automatic mode with a run time of 5 min.

*GLC Analysis of Tablet Preparations for Content Uniformity*—Ten tablets (2, 5, or 10 mg/tablet) were selected at random, and each was placed in a separate screw-capped tube and crushed to a fine powder with a blunt-end stirring rod (10 mm in diameter). Exactly 20.0 ml of the internal standard solution was pipetted into each tube, after which the contents were mechanically shaken vigorously for 10 min and then centrifuged at 3000 rpm for 10 min. A 1-μl portion of each supernate was chromatographed with a run time set at 5 min. For each sample, the amount of diazepam present, expressed as a percentage of the label claim, was calculated automatically with reference to a calibration solution of approximately the same concentration. The mean of the 10 individual results was used as the assay value.

**Flurazepam Dihydrochloride Analysis**—*Preparation and GLC of Flurazepam Calibration Solutions*—For each dosage level (15 and 30 mg/capsule), a corresponding standard solution containing a similar amount of drug was prepared daily as required. About 15 or 30 mg of flurazepam dihydrochloride was weighed accurately into a screw-capped tube. Distilled water (2 ml), sodium bicarbonate solution (2 ml), and the internal standard solution (20 ml) were added, the contents of the tube

were mechanically shaken vigorously for 10 min, and then the solution was centrifuged at 3000 rpm for 10 min. A 1-$\mu$l portion of the organic layer was chromatographed with a run time of 10 min.

*GLC Analysis of Capsule Preparations for Content Uniformity*—The contents of each of 10 individual capsules were emptied into separate screw-capped tubes labeled 1–10. The contents of each tube were subjected to the same extraction and chromatographic procedure as described for the calibration solutions. For each sample, the amount of flurazepam dihydrochloride present, expressed as a percentage of the label claim, was calculated automatically with reference to a calibration solution of approximately the same concentration. The mean of the 10 individual results was used as the assay value.

## DISCUSSION

In selecting an appropriate column for this work, the criteria adopted were that the three drugs, their associated impurities, and the internal standard (dicyclohexyl phthalate) should all be eluted quickly as single sharp peaks and should require no derivatization. Poly I-110, a polyimide nonsilicone polymer suitable for the separation of a variety of amine-type drugs and necessitating no pretreatment of the functional groups with derivatizing agents, was the phase of choice. The capacity of the column was ~0.5 $\mu$g for chlordiazepoxide and diazepam and ~1.5 $\mu$g for flurazepam. While Poly I-110 is claimed to be stable to 275°, some deterioration in column performance, evidenced by darkening of the packing material and peak broadening, particularly with chlordiazepoxide, was noted after 3–4 weeks of operation at 250°. When these symptoms were observed, the column was replaced. Zone temperatures and gas flow conditions were chosen to achieve optimum elution characteristics and minimum run times of the drugs, and instrument settings were adjusted for maximum quantitation accuracy.

Relevant GLC data on the compounds eluted from the polyimide column are listed in Table I. The internal standard was eluted as a sharp, symmetrical peak at 1.7 min and did not interfere with any peak of interest. Detector linearity was established for each drug over weight ranges that approximated the dosage level ranges encountered in their commercial formulations. The associated coefficients of variation for chlordiazepoxide, diazepam, and flurazepam were 1.5, 1.5, and 1.1%, respectively, indicating that any of these calibration solutions would be satisfactory for the analysis of that drug at any of its dosage levels (Table I). Nonetheless, to minimize error, the calibration solutions were prepared to about the same concentration as the sample solutions.

Compounds II and III were studied at concentrations equivalent to levels of 2.0–3.6 and 0.07–0.18% of the weight of chlordiazepoxide hydrochloride, respectively. The USP limits for these impurities in commercial capsules of chlordiazepoxide hydrochloride are 3.0 and 0.1%, respectively. Only trace amounts of chlordiazepoxide were observed in each impurity calibration solution, and no II and III were detected in the blank sample. The toluene layer was back-extracted with 1 *N* HCl to remove the potentially interfering parent drug. Compounds II and III are not soluble in 1 *N* HCl and were extracted completely into toluene since neither was detected in the residual aqueous layer. While the response factor coefficient of variation values were higher for II and III (2.8 and 6.1%, respectively) than for the drugs, the quantitation errors would be small (certainly much less than those of the USP TLC test) considering the low levels of these compounds usually encountered in formulations.

**Drug Content and Content Uniformity**—The USP limits for chlordiazepoxide hydrochloride and diazepam in commercial capsules and tablets, respectively, and the NF limits for flurazepam in capsule preparations are 90.0–110.0% of the labeled amount of drug. All chlordiazepoxide formulations listed in Table II met the USP requirement when analyzed by the nondiscriminating USP spectrophotometric procedure, but Formulation 1 fell just outside (89.4%) the lower limit when assayed by the GLC method. This product, several years old and containing >7% of II, was chosen to illustrate the greater specificity of the GLC procedure. When the levels of II and III determined by GLC were added to the GLC assay results, the aggregates were in good agreement with the respective USP values. All diazepam products met the compendial assay requirements and gave consistent results by both procedures (Table III). One flurazepam product (15-mg capsules) was examined and afforded values of 96.2% with the GLC procedure and 95.9% with the NF XIV spectrophotometric method.

In the present chromatographic method, the mean of 10 content uniformity values was taken as the assay result. In the pharmacopeial situation, this method of calculating drug content may not be justified since the content uniformity test often entails direct dissolution of the dosage unit in a suitable solvent, leading to possible excipient interference and overestimation of the drug content.

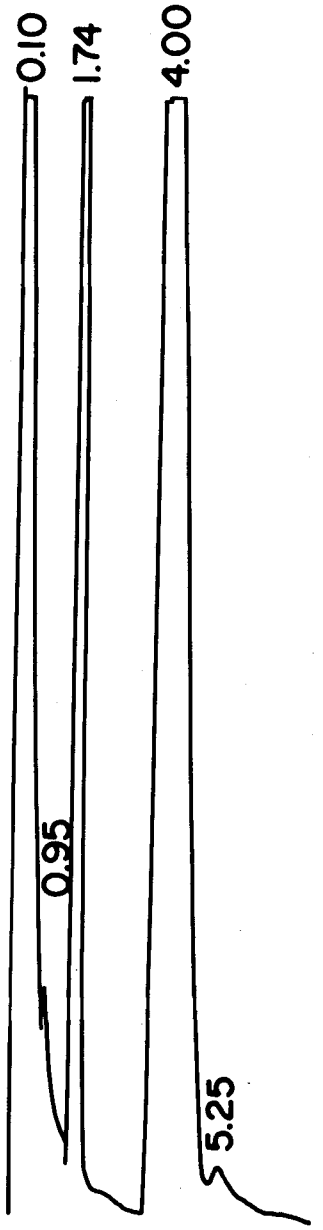


**Figure 1**—*Chromatogram of a reference impurities assay solution (10 mg of chlordiazepoxide hydrochloride spiked with 3.0% of II and 0.1% of III). The peaks are 0.95 min for III, 1.7 min for the internal standard, 4.0 min for chlordiazepoxide, and 5.25 min for II.*

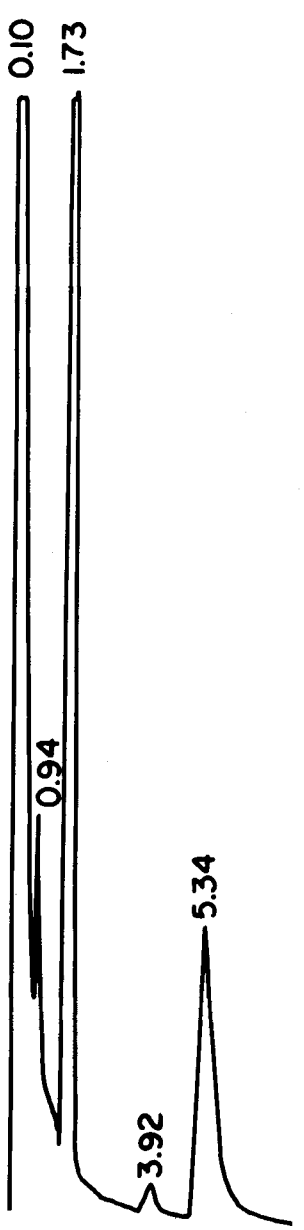


**Figure 2**—*Chromatogram of an impurities calibration solution at the USP limit for II (3.0%) and III (0.1%). The peaks are 0.94 min for III, 1.7 min for the internal standard, 3.9 min for residual chlordiazepoxide, and 5.34 min for II.*

Content uniformity results were evaluated in terms of the USP–NF specifications for tablets and capsules. One diazepam tablet, Formulation 2 (Table III), gave a value of 84.6%, but 20 additional tablets were not assayed. A satisfactory range of 91.8–101.5% of the label claim was obtained for the flurazepam formulation.

**Purity**—The USP monograph for chlordiazepoxide hydrochloride capsules includes a TLC test for the related Compounds II and III, and this test must be applied to every formulation since the impurity levels cannot be estimated from the other pharmacopeial tests performed. In the GLC method, the assay chromatogram provides important preliminary information on the product purity and eliminates the impurity test for formulations for which no extraneous peaks are observed. This pro-

cedure can result in considerable savings in cost and time over the duration of the drug screening. In judging whether or not an impurity test is required, comparison is made with a reference impurities assay chromatogram (Fig. 1). In the present work, the GLC determination of II and III was carried out on all capsule formulations. A larger amount of chlordiazepoxide hydrochloride was used for the impurities test to increase the concentrations of II and III in the final solution to afford increased peak areas and improved accuracy.

The data given in Table II show that, by the GLC procedure, Formulations 1 (7.1% of II) and 3 (3.4% of II) failed to comply with the USP purity requirement of 3.0% of II. Impurity III was detected at a level of 0.02% in Formulation 1 but was not observed in others. The products were old samples selected to demonstrate the merits of the GLC method and are not representative of the quality of chlordiazepoxide capsule preparations currently on the market. A chromatogram of an impurity calibration solution containing the maximum levels of II and III allowed in the USP monograph for chlordiazepoxide hydrochloride capsules is shown in Fig. 2.

**Identity**—USP identity tests for chlordiazepoxide hydrochloride capsules and diazepam tablets involve nonspecific UV absorbance scans of the assay solutions and chemical tests on aliquots of the sample powders. The NF identity of flurazepam in capsule formulations is confirmed by these tests and also by an IR trace of a carbon disulfide extract of the drug. While this test is highly specific, it can be time consuming if numerous samples are to be monitored.

In the GLC procedure, identity was established during the analytical run by comparing the retention time and peak area of the drug in the sample solution with those of the reference standard in the calibration solution, the latter having been prepared at the concentration assumed for the sample solution. The probability of an artifact compound in a formulation labeled to contain the drug of interest having coincident retention time and peak area to those of the reference standard is considered remote. This manner of confirming the identity of the drug is suitable for screening programs, and it is not only quicker than the pharmacopeial tests but also is generally more specific and allows verification of the identity of the drug in each dosage unit. However, in rare instances where the identity of the product might be questioned or otherwise still be in doubt, absolute identification of the drug can be confirmed by IR spectroscopy.

## REFERENCES


(1) R. C. Basalt, C. B. Stewart, and S. J. Franch, *J. Anal. Toxicol.*, 1, 10 (1977).

(2) J. Besic, M. Grims, I. Sernhorst-Staresinic, I. Beus, and J. Rulnjevic, *Acta Pharm. Jugosl.*, **26**, 99 (1976).

(3) J. P. Cano, J. Guintrand, C. Aubert, and A. Viala, *Arzneim.-Forsch.*, **27**, 338 (1977).

(4) J. L. Ferguson and D. J. Couri, *J. Anal. Toxicol.*, 1, 171 (1977).

(5) B. E. Pape and M. A. Ribick, *J. Chromatogr.*, **136**, 127 (1977).

(6) G. J. G. Parry and D. G. Ferry, *ibid.*, **128**, 166 (1976).

(7) D. M. Rutherford, *ibid.*, **137**, 439 (1977).

(8) J. A. F. de Silva, I. Bekersky, C. V. Puglisi, M. A. Brooks, and R. E. Winefeld, *Anal. Chem.*, **48**, 10 (1976).

(9) A. J. Bugge, *J. Chromatogr.*, **128**, 111 (1976).

(10) K. Harzer and R. J. Barchet, *ibid.*, **132**, 83 (1977).

(11) L. C. Bailey, *Am. J. Pharm. Educ.*, **42**, 63 (1978).

(12) A. G. Butterfield, F. F. Matsui, S. J. Smith, and R. W. Sears, *J. Pharm. Sci.*, **66**, 684 (1977).

(13) M. Emery and J. Kowto, *ibid.*, **68**, 1185 (1979).

(14) J. T. Stewart and J. L. Williamson, *Anal. Chem.*, **48**, 1182 (1976).

(15) W. Lund and L. Opheim, *Anal. Chim. Acta*, **88**, 275 (1977).

(16) "The United States Pharmacopeia," 19th rev., Mack Publishing Co., Easton, Pa., 1975, pp. 80, 136.

(17) "The National Formulary," 14th ed., Mack Publishing Co., Easton, Pa., pp. 292, 293.


## ACKNOWLEDGMENTS


The authors thank the staff of the Health Protection Branch, Ontario Regional Laboratories, Toronto, Ontario, Canada, for performing the compendial assays on the diazepam formulations, and Mrs. F. Matsui and Mr. D. Robertson, Drug Research Laboratories, Health Protection Branch, Ottawa, Ontario, Canada, for helpful suggestions.


# Stability-Indicating Assay for Hydrochlorothiazide


**S. L. DANIELS and A. J. VANDERWIELEN** ˣ



Received June 9, 1980, from *Product Control II, The Upjohn Company, Kalamazoo, MI 49001.* Accepted for publication August 6, 1980.



**Abstract** □ A stability-indicating method for determining hydrochlorothiazide in tablet formulations and in the bulk form is described. Hydrochlorothiazide is dissolved or extracted using methanol. An aliquot of the solution, containing sulfadiazine as an internal standard, is chromatographed on a 10-$\mu$m $C_{18}$ column with an aqueous mobile phase containing 5% methanol as the modifier. The pH is adjusted to about 4.5 with acetic acid. The method gave accurate results for nine lots (four different suppliers) of tablets and two bulk drug lots (two different suppliers). The assay has a relative standard deviation of about 1%. The method can also be used as a test for impurities in hydrochlorothiazide. The data in this study indicate that the test should give accurate results for impurities between 0.1 and 5%.



**Keyphrases** □ Hydrochlorothiazide—stability-indicating high-pressure liquid chromatographic method □ Degradation—stability-indicating high-pressure liquid chromatographic assay of hydrochlorothiazide □ High-pressure liquid chromatography—stability-indicating assay of hydrochlorothiazide


Hydrochlorothiazide is a common diuretic. It is used as an antihypertensive by itself and in combination with other compounds. It is available in a wide range of dosage forms (25–100-mg tablets) and in combination tablets (*e.g.*, hydrochlorothiazide and guanethidine).

The assay listed in USP XIX is a titration with sodium methoxide. This method cannot distinguish hydrochlo-

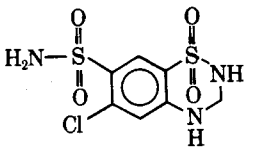

I

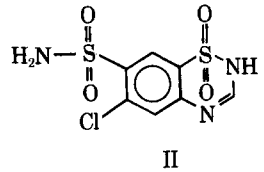

II

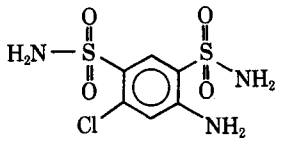

III


0022-3549/81/0200-0211$01.00/0


© 1981, American Pharmaceutical Association

cedure can result in considerable savings in cost and time over the duration of the drug screening. In judging whether or not an impurity test is required, comparison is made with a reference impurities assay chromatogram (Fig. 1). In the present work, the GLC determination of II and III was carried out on all capsule formulations. A larger amount of chlordiazepoxide hydrochloride was used for the impurities test to increase the concentrations of II and III in the final solution to afford increased peak areas and improved accuracy.

The data given in Table II show that, by the GLC procedure, Formulations 1 (7.1% of II) and 3 (3.4% of II) failed to comply with the USP purity requirement of 3.0% of II. Impurity III was detected at a level of 0.02% in Formulation 1 but was not observed in others. The products were old samples selected to demonstrate the merits of the GLC method and are not representative of the quality of chlordiazepoxide capsule preparations currently on the market. A chromatogram of an impurity calibration solution containing the maximum levels of II and III allowed in the USP monograph for chlordiazepoxide hydrochloride capsules is shown in Fig. 2.

**Identity**—USP identity tests for chlordiazepoxide hydrochloride capsules and diazepam tablets involve nonspecific UV absorbance scans of the assay solutions and chemical tests on aliquots of the sample powders. The NF identity of flurazepam in capsule formulations is confirmed by these tests and also by an IR trace of a carbon disulfide extract of the drug. While this test is highly specific, it can be time consuming if numerous samples are to be monitored.

In the GLC procedure, identity was established during the analytical run by comparing the retention time and peak area of the drug in the sample solution with those of the reference standard in the calibration solution, the latter having been prepared at the concentration assumed for the sample solution. The probability of an artifact compound in a formulation labeled to contain the drug of interest having coincident retention time and peak area to those of the reference standard is considered remote. This manner of confirming the identity of the drug is suitable for screening programs, and it is not only quicker than the pharmacopeial tests but also is generally more specific and allows verification of the identity of the drug in each dosage unit. However, in rare instances where the identity of the product might be questioned or otherwise still be in doubt, absolute identification of the drug can be confirmed by IR spectroscopy.

## REFERENCES


(1) R. C. Basalt, C. B. Stewart, and S. J. Franch, *J. Anal. Toxicol.*, 1, 10 (1977).

(2) J. Besic, M. Grims, I. Sernhorst-Staresinic, I. Beus, and J. Rulnjevic, *Acta Pharm. Jugosl.*, **26**, 99 (1976).

(3) J. P. Cano, J. Guintrand, C. Aubert, and A. Viala, *Arzneim.-Forsch.*, **27**, 338 (1977).

(4) J. L. Ferguson and D. J. Couri, *J. Anal. Toxicol.*, 1, 171 (1977).

(5) B. E. Pape and M. A. Ribick, *J. Chromatogr.*, **136**, 127 (1977).

(6) G. J. G. Parry and D. G. Ferry, *ibid.*, **128**, 166 (1976).

(7) D. M. Rutherford, *ibid.*, **137**, 439 (1977).

(8) J. A. F. de Silva, I. Bekersky, C. V. Puglisi, M. A. Brooks, and R. E. Winefeld, *Anal. Chem.*, **48**, 10 (1976).

(9) A. J. Bugge, *J. Chromatogr.*, **128**, 111 (1976).

(10) K. Harzer and R. J. Barchet, *ibid.*, **132**, 83 (1977).

(11) L. C. Bailey, *Am. J. Pharm. Educ.*, **42**, 63 (1978).

(12) A. G. Butterfield, F. F. Matsui, S. J. Smith, and R. W. Sears, *J. Pharm. Sci.*, **66**, 684 (1977).

(13) M. Emery and J. Kowto, *ibid.*, **68**, 1185 (1979).

(14) J. T. Stewart and J. L. Williamson, *Anal. Chem.*, **48**, 1182 (1976).

(15) W. Lund and L. Opheim, *Anal. Chim. Acta*, **88**, 275 (1977).

(16) "The United States Pharmacopeia," 19th rev., Mack Publishing Co., Easton, Pa., 1975, pp. 80, 136.

(17) "The National Formulary," 14th ed., Mack Publishing Co., Easton, Pa., pp. 292, 293.


## ACKNOWLEDGMENTS


The authors thank the staff of the Health Protection Branch, Ontario Regional Laboratories, Toronto, Ontario, Canada, for performing the compendial assays on the diazepam formulations, and Mrs. F. Matsui and Mr. D. Robertson, Drug Research Laboratories, Health Protection Branch, Ottawa, Ontario, Canada, for helpful suggestions.


# Stability-Indicating Assay for Hydrochlorothiazide


**S. L. DANIELS and A. J. VANDERWIELEN** ˣ



Received June 9, 1980, from *Product Control II, The Upjohn Company, Kalamazoo, MI 49001.* Accepted for publication August 6, 1980.



**Abstract** □ A stability-indicating method for determining hydrochlorothiazide in tablet formulations and in the bulk form is described. Hydrochlorothiazide is dissolved or extracted using methanol. An aliquot of the solution, containing sulfadiazine as an internal standard, is chromatographed on a 10-$\mu$m $C_{18}$ column with an aqueous mobile phase containing 5% methanol as the modifier. The pH is adjusted to about 4.5 with acetic acid. The method gave accurate results for nine lots (four different suppliers) of tablets and two bulk drug lots (two different suppliers). The assay has a relative standard deviation of about 1%. The method can also be used as a test for impurities in hydrochlorothiazide. The data in this study indicate that the test should give accurate results for impurities between 0.1 and 5%.



**Keyphrases** □ Hydrochlorothiazide—stability-indicating high-pressure liquid chromatographic method □ Degradation—stability-indicating high-pressure liquid chromatographic assay of hydrochlorothiazide □ High-pressure liquid chromatography—stability-indicating assay of hydrochlorothiazide


Hydrochlorothiazide is a common diuretic. It is used as an antihypertensive by itself and in combination with other compounds. It is available in a wide range of dosage forms (25–100-mg tablets) and in combination tablets (*e.g.*, hydrochlorothiazide and guanethidine).

The assay listed in USP XIX is a titration with sodium methoxide. This method cannot distinguish hydrochlo-

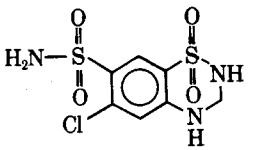

I

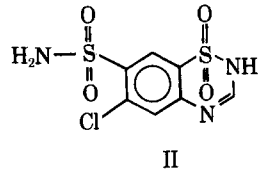

II

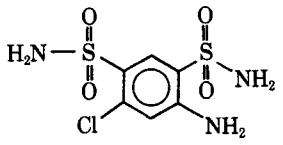

III


0022-3549/81/0200-0211$01.00/0


© 1981, American Pharmaceutical Association

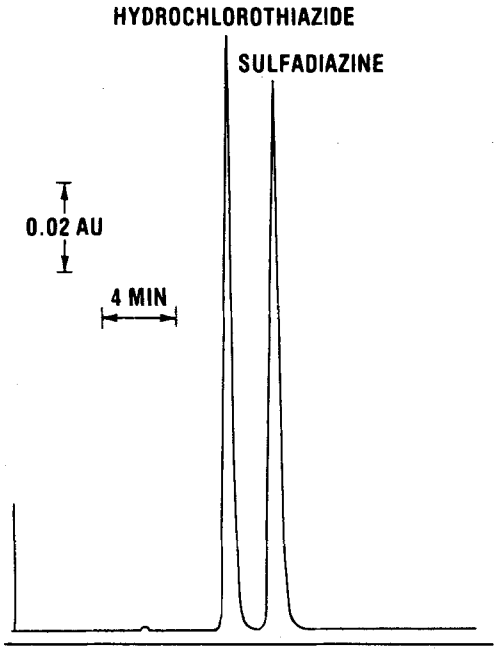


**Figure 1**—*Typical chromatogram for the hydrochlorothiazide assay. The mobile phase is 5% methanol in water at pH 4.5.*

rothiazide (I) from likely degradation and process impurities such as chlorothiazide (II) and 4-amino-6-chloro-1,3-benzenedisulfonamide (III).

Liquid chromatographic methods for quantitating thiazides have been developed for tablet formulations (1) and the determination of hydrochlorothiazide in serum, plasma, and urine (2, 3). This report describes a new reversed-phase high-pressure liquid chromatographic (HPLC) method that is specific for hydrochlorothiazide and has adequate sensitivity for the determination of impurities.

## EXPERIMENTAL

**Materials**—Sulfanilamide[1], chlorothiazide[1] (II), hydrochlorothiazide[2,3] (I), sulfadiazine[1], and 4-amino-6-chloro-1,3-benzenedisulfonamide[1] (III) were obtained in pure form and dissolved in methanol for chromatography and spectroscopy. Solvents and reagents were commercial analytical grade. Tablets from four sources[2–5] were used.

**Chromatographic Conditions**—A liquid chromatograph[6] with a low volume septumless injector, a fixed-wavelength detector[7] (254 nm), and a minicomputer[8] were used. Commercial 10-[9] and 5-$\mu$m[10] $C_{18}$ columns (30 cm × 4 mm i.d.) were used at ambient temperature. The mobile phase consisted of 5% (v/v) methanol in double-distilled water. The pH was adjusted to 4.5–5.0 with 0.1 *M* acetic acid, and then the solution was filtered and deaerated. The flow rate was adjusted to 2.0 ml/min.

**Internal Standard Solution**—A solution of methanol containing ~0.7 mg of sulfadiazine/ml was used.

**Standard Preparation**—About 20 mg of USP hydrochlorothiazide reference standard[1] was weighed accurately, and 10.0 ml of internal standard solution was added.

**Sample Preparation**—*Tablets*—Ten tablets were weighed accurately, and the average tablet weight was determined before they were crushed gently using a mortar and pestle. An amount equivalent to about 20 mg of hydrochlorothiazide was weighed, 10.0 ml of internal standard solution was added, and the solution was shaken for 35–40 min. The solution was filtered or centrifuged to remove the particulate matter.

*Bulk Drug*—The samples were prepared in the same way as the reference standard.

*Impurities Test*—About 10.0 mg of sample was weighed, and 10 ml of reagent grade methanol was added.

**Procedure**—The sample or standard preparation, 6–10 $\mu$l, was chromatographed using conditions described. The reference standard was run in duplicate at the beginning and end of the run and between every seventh sample. The detector attenuation was set at 0.2–0.5 aufs. To observe the impurities on a 10-mv recorder, the attenuation was adjusted to 0.01 aufs.

**Calculations**—*Tablets*—The hydrochlorothiazide (I) content, expressed in milligrams per tablet, is calculated from:

$$I = (R_{sam}/R_{std}) \times (W_{std}/W_{sam}) \times (F1/F3) \times F2 \times P \quad \text{(Eq. 1)}$$

where:

$R_{sam}$ = ratio of hydrochlorothiazide peak height to internal standard peak height in sample preparation
$R_{std}$ = ratio of hydrochlorothiazide reference standard peak height to internal standard peak height in standard preparation
$W_{std}$ = weight of hydrochlorothiazide reference standard in milligrams
$W_{sam}$ = weight of sample in milligrams
$F1$ = volume of internal standard used in sample preparation in milliliters
$F2$ = average tablet weight in milligrams
$F3$ = volume of internal standard used in standard preparation in milliliters
$P$ = purity of hydrochlorothiazide reference standard expressed as a decimal

*Bulk Drug*—The percent hydrochlorothiazide is found using:

$$I = (R_{sam}/R_{std}) \times (W_{std}/W_{sam}) \times (F1/F3) \times P \times 100 \quad \text{(Eq. 2)}$$

*Impurities Test*—The content of the impurities in the sample, expressed as percent by weight, is calculated from:

$$\text{impurities} = \frac{H_3R_3 + H_2R_2 + \ldots H}{H_1 + H_3R_3 + H_2R_2 + \sum H} \times 100 \quad \text{(Eq. 3)}$$

where:

$H_3$ = height of 4-amino-6-chloro-1,3-benzenedisulfonamide (III) peak
$R_3$ = response factor for III (about 0.3 on a weight basis)
$H_2$ = height of chlorothiazide (II) peak
$R_2$ = response factor for II (about 1.6 on a weight basis)
$H_1$ = height of hydrochlorothiazide peak
$H$ = height of any unknown peaks

**Recovery Studies**—Recovery studies were performed by adding 10–30 mg of I to 180 mg of a placebo mix. If no placebo mix was available, 13–50 mg of I was added to the crushed tablet mix. The samples were then treated as described under *Sample Preparation*.

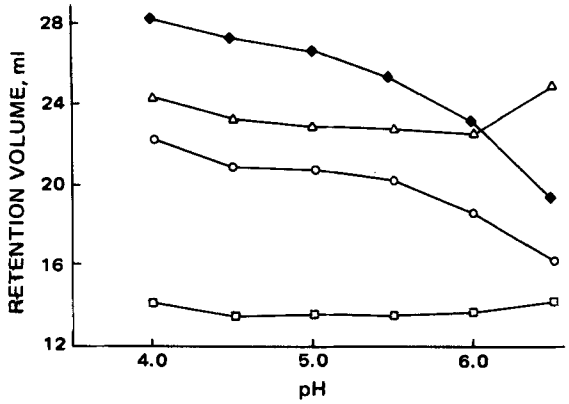


**Figure 2**—*Effect of pH on the retention volume of I (△), IV (♦), II (○), and III (□) in water–methanol (95:5).*

[1] United States Pharmacopeial Convention, Rockville, Md.
[2] Abbott Laboratories, North Chicago, Ill.
[3] Ciba Pharmaceutical Co., Summit, N.J.
[4] Barr Laboratories, Northvale, N.J.
[5] The Upjohn Co., Kalamazoo, Mich.
[6] ALC 202, Waters Associates, Milford, Mass.
[7] Model 440, Waters Associates, Milford, Mass.
[8] PDP11-40, Digital Equipment Corp., Marlborough, Mass.
[9] $\mu$Bondapak $C_{18}$, Waters Associates, Milford, Mass.
[10] Ultrasphere ODS, Altex Scientific, Berkeley, Calif.

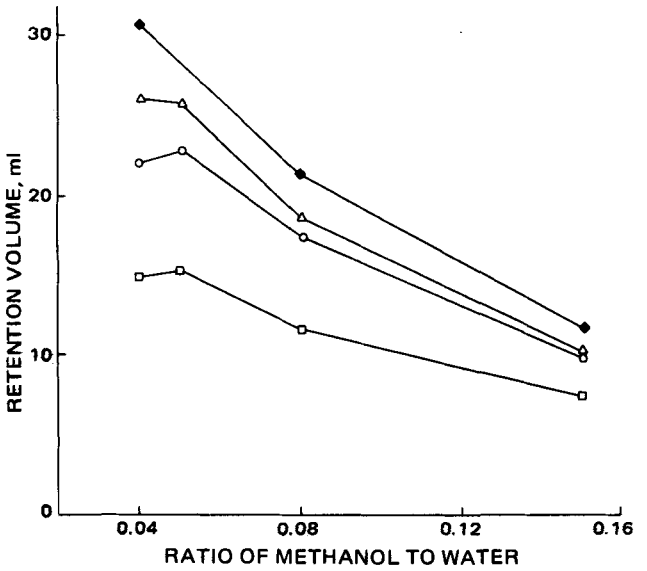


**Figure 3**—*Effect of methanol concentration on the retention volume of I (△), IV (♦), II (○), and III (□) at pH 5.*

**Response Factors**—Samples of II and III were weighed and added to 10 mg of I (accurately weighed). These mixtures were dissolved in about 10 ml of methanol. The samples were then chromatographed under the conditions described. The response factors were calculated using:

$$R = \frac{Wt_{sam}}{Wt_I} \times \frac{X_I}{X_{sam}} \qquad \text{(Eq. 4)}$$

where:

$Wt_{sam}$ = weight of a sample of II or III in milligrams
$Wt_I$ = weight of I in milligrams
$X_{sam}$ = height or area of II or III peak
$X_I$ = height or area of I peak

## RESULTS

**Chromatography and Specificity**—The mobile phase was adjusted to obtain good retention of hydrochlorothiazide (I) and baseline separation of the sulfadiazine (IV) internal standard. The chromatogram of I and IV (Fig. 1) indicates that, under the recommended experimental conditions, the method is free of interference and gives symmetrical chromatographic peaks. Apparently, none of the excipients was extracted into the methanol during the I extraction step. In fact, no peaks were observed when the placebo was extracted with methanol for 30 min. The placebo sample was rerun at a much higher sensitivity (0.01 aufs), and only a small peak due to the methanol solvent (at about 2-ml retention volume) was observed.

During the search for the optimum chromatographic conditions, it was observed that pH had a pronounced effect on the retention volume of the internal standard (IV), especially between pH 5 and 6. Therefore, a study was done to determine the effect of pH on I, IV, and the two known impurities of I (II and III). The results (Fig. 2) indicate that the pH has a definite effect on all compounds except III. Its retention volume remained about the same between pH 4 and 6.5. The order of elution of I and IV reversed between 6 and 6.5. Between pH 4 and 5, the relative retention times of all compounds remained about the same. It is recommended that the pH be kept between these values for reproducibility.

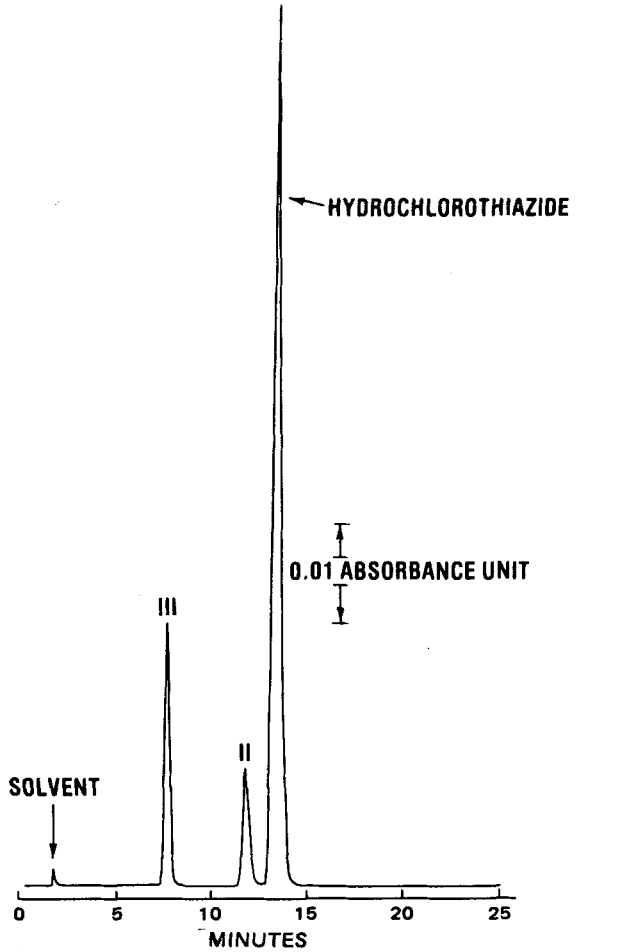


**Figure 4**—*Chromatogram of hydrochlorothiazide spiked with 7% III and 17% II.*

Methanol was used as the organic modifier for the aqueous mobile phase. The retention data obtained by chromatographing I–IV are shown in Fig. 3. The results, when plotted as the ratio of methanol to water, are about linear up to a point corresponding to 4% methanol in water. This level of methanol gave the best combination of resolution and analytical results. Assay specificity was tested by chromatographing a mixture of I–III (Fig. 4).

Several other benzenesulfonamides were chromatographed to test further the method specificity. The results in Table I indicate that there are large differences in retention volume even for closely related compounds. Sulfamerazine differs from sulfadiazine only by one methyl group on the heterocyclic ring. These data also illustrate that the procedure is highly specific.

The chromatographic method was also tested by performing the assay with a different column. Table II and Fig. 5 show the results obtained on a 5-μm $C_{18}$ column compared to the results normally obtained on the 10-μm column. The retention times for the 5-μm column were longer,

**Table I—Specificity of the HPLC Method**

| Compound | Retention Volume, ml | Capacity Factor[a] |
|---|---|---|
| Guanadrel sulfate | 3.6 | — |
| Sulfanilamide | 6.8 | 0.9 |
| III | 15.4 | 3.2 |
| II | 23.0 | 5.4 |
| I | 26.0 | 6.2 |
| IV | 35.5 | 8.9 |
| Sulfamerazine | 68.8 | 18.0 |

[a] Void volume is 3.6 ml; capacity factor = (volume − void volume)/void volume.

**Table II—Comparison of Chromatography on a 10- and 5-μm Column**

| Parameter | $C_{18}$[a], 10 μm[b] | $C_{18}$[c], 5 μm[d] |
|---|---|---|
| IV retention time, min | 16.5 ± 0.4 | 22.1 ± 0.3 |
| I retention time, min | 12.1 ± 0.2 | 16.6 ± 0.1 |
| Theoretical plates[e] | 1080 ± 130 | 3150 ± 580 |
| Resolution[f] | 2.7 ± 0.2 | 3.2 ± 0.2 |

[a] μBondapak $C_{18}$, Waters Associates, Milford, Mass. [b] Average of 59 values; error is 2 *SD*. [c] Ultrasphere ODS, Altex Scientific, Berkeley, Calif. [d] Average of nine values; error is 2 *SD*. [e] Theoretical plates = $5.54\ (T/w)^2$. [f] Resolution = $[2|T_1 - T_2|]/1.67\ (w_1 + w_2)$, where $T$ is the retention time and $w$ is the peak width at half height.

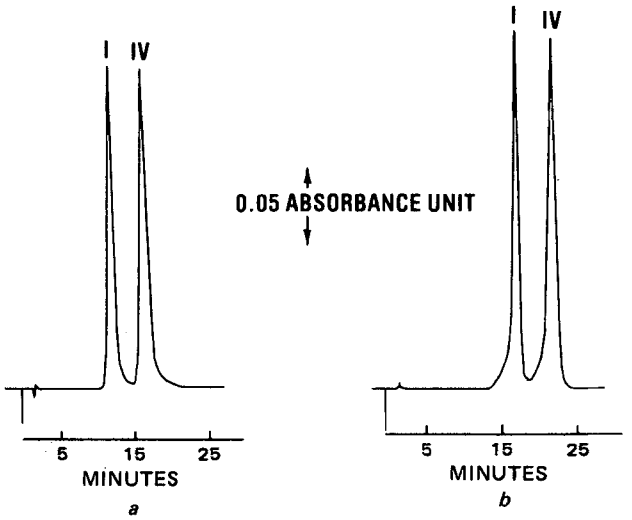


**Figure 5**—*Separation of I and IV on 10-μm (a) and 5-μm (b) $C_{18}$ reversed-phase columns.*

resulting in more theoretical plates, but there was essentially no increase in the resolution. In fact, on a new 10-μm $C_{18}$ column, the resolution between hydrochlorothiazide and the internal standard was 3.9. However, the data do serve to illustrate the ruggedness of the chromatographic conditions.

**Recovery and Linearity**—The effectiveness of the extraction step was tested by adding I to the powdered placebo mixture (Table III). A plot of the amount of I added *versus* the amount of I recovered indicates that the slope is 1 (0.97 ± 0.02) within experimental error and that the intercept is 0 (0.25 ± 0.31). These data, a correlation coefficient of 0.999, and complete recovery of I (99.1 ± 1.7%) show that the assay is linear and accurate between 50 and 150% of the tablet formulations (25 mg of I/225-mg tablet) tested.

The method was further tested by spiking several different formulations with additional I. Fifty percent of the label amount was added to three different formulations (from two different manufacturers) containing 25, 50, and 100 mg of I. The results (Table IV) indicate that complete recovery was obtained for all three formulations. The validity of the measurement was tested by changing the concentration of I relative to the internal standard (IV). Eight 8-μl aliquots (concentration range was 0.76–3.06 mg of I/ml) were chromatographed. The plots of both height and area ratio of I/IV *versus* the amount of I were linear (correlation coefficients > 0.98) and showed no bias (intercepts were 0 ± 2 *SD*).

**Table III—Hydrochlorothiazide (I) Extraction Study**

| Sample | Amount of I Added, mg | Amount of I Recovered, mg | Recovery, % |
|---|---|---|---|
| | Samples Extracted 30 min | | |
| 100% Std. | 20.3 | 20.1 | 99.0 |
| 100% Std.[a] | 20.3 | 20.6 | 101.7 |
| 100% Std. | 20.4 | 19.7 | 96.7 |
| 100% Std.[a] | 20.4 | 19.9 | 97.7 |
| 50% Std. | 9.8 | 9.9 | 101.1 |
| 80% Std. | 16.4 | 16.4 | 99.8 |
| 90% Std. | 18.7 | 18.4 | 98.2 |
| 110% Std. | 22.8 | 22.2 | 97.4 |
| 120% Std. | 24.0 | 23.4 | 97.5 |
| 150% Std. | 30.6 | 30.3 | 99.2 |
| Average | | | 99.1 |
| *RSD* | | | 1.7 |
| | Samples Extracted 45 min | | |
| 50% Std. | 10.4 | 10.5 | 101.0 |
| 100% Std. | 20.8 | 20.7 | 99.5 |
| 150% Std. | 30.1 | 29.4 | 97.7 |
| 80% Std. | 16.7 | 16.5 | 98.8 |
| Average | | | 99.2 |
| *RSD* | | | 1.4 |

[a] Repeat of previous standard.

**Table IV—Standard Addition Results for Tablet Formulations**

| Unspiked I per Tablet, mg | Amount of I Added, mg | Measured I per Tablet, mg | Recovery, %[a] |
|---|---|---|---|
| 24.4 | 13.1 | 37.5 | 99.8 |
| 50.2 | 26.7 | 76.3 | 99.2 |
| 97.5 | 50.2 | 144.3 | 97.7 |

[a] Percent recovery = [measured I/(unspiked I + added I)] × 100.

**Table V—Response Factors for Known Impurities**

| Impurity Concentration, % by weight | Response Factor | |
|---|---|---|
| | Area | Height |
| III | | |
| 0.3 | 0.46 | 0.28 |
| 2.5 | 0.50 | 0.29 |
| 7.1 | 0.54 | 0.31 |
| Average | 0.50 | 0.29 |
| *RSD*, % | 8 | 5 |
| II | | |
| 0.5 | 1.66 | 1.56 |
| 4.6 | 1.84 | 1.61 |
| 16.8 | 2.03 | 1.76 |
| Average | 1.84 | 1.64 |
| *RSD*, % | 10 | 6 |

These results indicate that the assay is accurate over a fourfold concentration range.

A study of I–III was performed to determine their absorptivity at 254 nm. The results show that the most sensitive region was between 220 and 226 nm. However, at 254 nm, all three compounds had adequate absorptivity. Since the absorptivities of these compounds differed, it was necessary to determine response factors for II and III relative to I. As shown in Table V, response factors based on peak height and peak area were determined. Since peak height appears to give the more precise data, it is the recommended parameter for quantitative measurements. Although there was a definite concentration effect on the response factor, this effect was significant only at concentrations much higher than would ever be expected in pure I (Table VI).

The detector (UV at 254 nm) gave linear responses for II and III between 0.01 and 5 μg with a correlation coefficient of 0.99 or better. The intercept for both II and III was 0 ± 1 *SD*. The normal injection volume

**Table VI—Hydrochlorothiazide Impurities: Recovery Study**

| Compound | Amount Added, % (w/w) | Amount Observed, % (w/w) | Recovery, % (w/w) |
|---|---|---|---|
| III | 0.28 | 0.30 | 109.0 |
| | 2.50 | 2.56 | 102.4 |
| | 7.11 | 6.91 | 97.2 |
| II | 0.51 | 0.52 | 102.9 |
| | 4.60 | 4.58 | 99.6 |
| | 16.80 | 16.09 | 95.8 |
| | 50.00 | 45.29 | 90.6 |

**Table VII—Hydrochlorothiazide Assay Results for Tablet Formulations**

| Formulation | Label per Tablet, mg | Average Tablet Weight, mg | Tablet Potency | | Percent of Label |
|---|---|---|---|---|---|
| | | | Amount, mg/tablet | *RSD*, % | |
| 1A | 25.0[a] | 224 | 23.6 | 0.5 | 94.4 |
| 1A-1 | 25.0[a] | 224 | 23.8[b] | 0.6 | 95.2 |
| 1B | 25.0[a] | 224 | 24.0 | 1.2 | 96.0 |
| 2 | 25.0 | 101 | 24.9 | 0.4 | 99.6 |
| 3A | 25.0[c] | 296 | 24.4 | 1.0 | 97.6 |
| 3B | 50.0 | 302 | 49.2 | 0.6 | 98.4 |
| 3C | 100.0 | 348 | 97.5 | 1.0 | 97.5 |
| 4A | 25.0 | 85 | 25.7 | 1.1 | 102.8 |
| 4B | 25.0 | 86 | 24.4 | 0.4 | 97.6 |
| 4C | 50.0 | 171 | 50.2 | 2.8 | 100.4 |

[a] Tablets also contained 10 mg of guanadrel sulfate. [b] Results obtained using the 5-μm column. [c] Tablets also contained 10 mg of guanethidine sulfate.

**Table VIII—Hydrochlorothiazide Assay Results for Bulk Drug Lots**

| Lot | Assay (Peak Height)[a] % | Assay (Peak Height)[a] *RSD* | Assay (Peak Area)[a] % | Assay (Peak Area)[a] *RSD* | USP Assay |
|---|---|---|---|---|---|
| A | 98.7 | 0.7 | 98.6 | 1.6 | 100.7 |
| B | 98.2 | 0.8 | 98.0 | 0.9 | 101.4 |
| C | 98.8 | 0.6 | 98.6 | 1.3 | 99.8 |
| D | 100.0 | 1.1 | 100.3 | 1.4 | 100.3 |
| E | 97.8 | 0.8 | 97.3 | 1.6 | 100.0 |
| F | 98.0 | 1.1 | 98.4 | 1.1 | 99.9 |
| G | 97.7 | 1.8 | 98.2 | 1.8 | 99.5 |
| H | 97.6 | 0.6 | 96.4 | 1.4 | 100.5 |

[a] Calculated on the anhydrous basis; the results are averages of at least five determinations.

**Table IX—Effects of Injection Size and Sample Age**

| Day | Run | Amount Injected[a], μl | Hydrochlorothiazide Recovered, mg |
|---|---|---|---|
| 1 | 19 | 8 | 23.7 |
| 2 | 22 | 8 | 23.8 |
| | 24 | 10 | 23.6 |
| | 25 | 6 | 23.9 |
| | 26 | 6 | 23.6 |
| 3 | 29 | 8 | 23.5 |
| Mean | | | 23.7 |
| *RSD*, % | | | 0.6 |

[a] Concentration = 2 mg/ml.

for the impurities test of about 10 μl of a 1-mg/ml preparation corresponds to 10 μg. The data indicate that the test should give accurate results for impurities between 0.1 and 5%. At higher levels, the response factors used would have to be redetermined. Therefore, the method can be used to determine the purity of bulk hydrochlorothiazide.

## DISCUSSION

The method was tested by assaying nine lots of tablets from the four suppliers. Three samples were obtained from each lot and prepared as indicated under *Experimental*. Two aliquots of each sample were chromatographed. The results (Table VII) indicate that the method gives accurate results for the various formulations since there is good agreement with the label concentrations in all cases.

The results also indicate that the assay has good precision. A statistical evaluation of the variability (4), using a $\chi^2$ distribution at the 95% confidence level, indicates that the true relative standard deviation is between 0.7 and 1.1% using peak height. The results for eight lots of bulk drug from two suppliers are listed in Table VIII. The data indicate that the pooled relative standard deviation is about 1.1% for the peak height measurement. This value is in good agreement with the assay precision found for the products listed. The results in Table VIII indicate that equivalent results are obtained using peak height or peak area. However, peak area measurements resulted in less precise results (pooled *RSD* = 1.5%). The purity of the lots examined was 97.5–98.5%, except for Lots D and H. For the very pure Lot D (100% by HPLC and USP methods; 99.9% by summation of minor impurities), there was excellent agreement between the HPLC and USP XIX methods; for all other lots, the USP method gave higher results.

**Table X—Stability of Hydrochlorothiazide (I)**

| Sample | Impurities[a], % III | Unknown | Total |
|---|---|---|---|
| Initial assay[b] | 0.04 | ND[c] | 0.04 |
| 3 months at room temperature (10 mg/ml in methanol) | 1.52 | ND | 1.52 |
| 1 hr at 100° | 0.09 | ND | 0.09 |
| 4 days at 100° | 0.11 | ND | 0.11 |
| 16 hr in 0.1 *N* HCl (aqueous) | 0.28 | 1.54 | 1.82 |
| 16 hr in 0.1 *N* NaOH (aqueous) | 0.13 | 0.94 | 1.07 |

[a] Chlorothiazide (II) was not detected in any of these samples. [b] Average of five assays where impurity was detected. [c] None detected.

The HPLC results indicate that some impurities in hydrochlorothiazide (I) may interfere with the USP method for the following reasons:

1. The HPLC impurity test and the other impurity tests listed in USP XIX indicate that Lot H has impurities present at 1% or more, yet the USP assay gave a purity value of 100.5%.
2. The USP assay is a sodium methoxide titration, which would not distinguish I from II and III.
3. All results using the USP method were 100% or larger, suggesting a positive bias.

A study of injection size and sample stability was performed. The data (Table IX) indicate that 6–10-μl aliquots give accurate and precise results over 3 days. Hydrochlorothiazide stability was examined under several conditions. The data given in Table X show that I is very stable in the powdered form. No significant degradation was observed when the dry powder was kept at 100° for 4 days. Even under severe conditions such as in 0.1 *N* HCl, I only degraded at a rate of about 0.1%/hr. A sample left at room temperature in methanol for 3 months produced about 1.5% III. This result shows that III is a degradation compound of I and that the method is stability indicating.

## REFERENCES

(1) A. G. Butterfield, E. G. Lovering, and R. W. Sears, *J. Pharm. Sci.*, **67**, 651 (1978).

(2) M. J. Cooper, A. R. Sinaiko, M. W. Anders, and B. L. Mirkin, *Anal. Chem.*, **48**, 1110 (1976).

(3) E. Redalieu, U. V. Tipnis, and W. E. Wagner, Jr., *J. Pharm. Sci.*, **67**, 726 (1978).

(4) A. H. Bower and G. J. Lieberman, "Engineering Statistics," Prentice Hall, Englewood Cliffs, N.J., 1959.

## ACKNOWLEDGMENTS

The authors thank A. D. Kellerman for analyzing many of the tablet formulations used to test the method.

# Progestin Permeation through Polymer Membranes V: Progesterone Release from Monolithic Hydrogel Devices

**S. Z. SONG, J. R. CARDINAL ˣ, S. H. KIM, and S. W. KIM**

Received April 2, 1979, from the *Department of Pharmaceutics, College of Pharmacy, University of Utah, Salt Lake City, UT 84112.* Accepted for publication August 1, 1980.

**Abstract** □ Progesterone release from monolithic devices prepared from various copolymers of poly(hydroxyethyl methacrylate) and poly(methoxyethoxyethyl methacrylate) or poly(methoxyethyl methacrylate) was examined. In general, plots of the fraction of drug released *versus* (time)$^{1/2}$ were linear during the early stages of drug release. This behavior is similar to that found for drugs released from hydrophobic polymers such as polydimethyl siloxane. However, for some release curves using the hydrogels, a breakpoint appeared during the early stages of drug release. These breakpoints were due to the effects of water absorption by these polymers. From analyses of permeability coefficients, it was demonstrated that release rates also were dependent on the initial drug load and the equilibrium water content of the polymer. These conclusions were verified from cross-membrane diffusion studies on films depleted of their initial drug load. In conjunction with this work, the aqueous solubility of progesterone was determined by several methods; an average value of 38 μg/ml at 23° was obtained.

**Keyphrases** □ Hydrogels—progesterone permeation, release from monolithic devices of various comonomer compositions evaluated □ Progesterone—permeation through hydrogel membranes □ Delivery devices, controlled—hydrogel membranes, progesterone permeation

Poly(hydroxyethyl methacrylate), a synthetic hydrogel, was first synthesized by Wichterle and Lim in 1960 (1). This polymer and many of its derivatives have been investigated extensively for possible biomedical applications (2). Among these uses are controlled-release drug delivery (3–7). Toward this end, this laboratory has been involved with studies on the mechanisms of solute transport through hydrogels (8–10). These studies have demonstrated that hydrogels are permeable to solutes that are only slightly soluble in water (*e.g.*, steroids) and to water-soluble solutes including both electrolytes and nonelectrolytes. It was shown that the transport mechanisms depend on solute size, the aqueous solubility of the solute, polymer hydration, and the nature and concentration of the cross-linking agent.

Recently, attention has been devoted to the role of polymerization conditions on the transport mechanisms and rate (11). Hydrogel films may be prepared under various conditions of temperature, initiator concentration, additive concentration, and solvent concentration and type. A study in this laboratory (11) demonstrated that permeability and partition coefficients for progesterone in poly(hydroxyethyl methacrylate) were independent of the nature and concentration of the solvents employed (*e.g.*, water, ethanol, and *tert*-butanol).

In this study, progesterone release from monolithic hydrogel devices was examined as a function of polymer composition, initial drug load, and initiator concentration. Planar and rod-shaped hydrogel devices were prepared from poly(hydroxyethyl methacrylate) and some of its derivatives. Progesterone was added to the monomer solution prior to polymerization. In all cases, polymerizations were carried out in the absence of a solvent, and the concentration of progesterone exceeded its saturation solubility when these devices were fully hydrated. Analyses of data obtained from the release of progesterone from rod-shaped monolithic devices and from transport studies on drug-depleted films revealed that: (*a*) permeability coefficients were dependent on the initial drug load, (*b*) initial release rates were dependent on the rate of water uptake by the devices, and (*c*) steady-state release rates were dependent on polymer hydration.

## EXPERIMENTAL

**Materials**—Hydroxyethyl methacrylate[1] was a highly purified sample (9) and was used as received. Methoxyethyl methacrylate and methoxyethoxyethyl methacrylate were synthesized from methyl methacrylate[2] by transesterification with the appropriate alcohol. Azobis(methylisobutyrate) was synthesized by the method of Mortimer (12).

Progesterone[3] and [1,2-$^3$H]progesterone[4] were used as received. TLC analyses, with 20% (v/v) ethyl acetate in toluene as the developing reagent, indicated that the progesterone was pure. Only one spot was detectable under UV light. Radiolabeled progesterone had the same $R_f$ value as the unlabeled material with >95% of the detectable activity associated with the primary spot. The remaining radioactivity was distributed uniformly on the plate.

**Methods**—Rod-shaped monolithic hydrogel devices were prepared in a polyethylene mold by polymerization at 60° for 24 hr. Azobis(methylisobutyrate), at a concentration of 7.84 mmoles/liter of the monomer, was used as the initiator. Prior to polymerization, a mixture of labeled and unlabeled progesterone was dissolved in the monomer to obtain a homogeneous solution. The maximum concentration utilized approximated the saturation solubility of a drug in the monomer. The dimensions of the dried devices used in the experiments were ~4 (height) × ~0.5 (diameter) cm.

Planar monolithic hydrogel devices were prepared using similar techniques, except only unlabeled drug was utilized. The thickness of the dried samples was ~0.03 cm.

Progesterone release studies on the rod-shaped devices were conducted at room temperature (23 ± 1.0°) in a 1-liter beaker containing 900 ml of deionized water. All release experiments were performed in duplicate. To reduce boundary layer effects, the aqueous phase was stirred continuously at 1600 rpm by externally mounted, constant-speed synchronous motors. The devices were supported in the cell *via* metallic holders made from nickel–chrome wire. At selected intervals, usually every hour in root time, the medium was replaced with fresh deionized water. Under these conditions, the progesterone concentration in the aqueous phase was far below saturation (<10% of the saturation solubility) so that sink conditions were maintained. The amount of progesterone released was determined by withdrawing ~0.5 ml of sample in triplicate. These samples were weighed in tared vials, 10 ml of scintillation fluid[5] was added, and the concentration was determined using a scintillation counter[6].

Water influx experiments were performed on rod-shaped monolithic devices prepared in a fashion analogous to that described, except that the labeled drug was omitted. At selected intervals, the devices were re-

[1] Courtesy of Hydron Laboratories, New Brunswick, N.J.
[2] Aldrich Chemical Co., Milwaukee, Wis.
[3] Steraloids Inc., Pauling, N.Y.
[4] New England Nuclear, Boston, Mass.
[5] Formula 950A, New England Nuclear, Boston, Mass.
[6] Model 3385, Packer Instrument Co., Downers Grove, Ill.



0022-3549/81/0200-0216$01.00/0
© 1981, American Pharmaceutical Association

moved from the water bath and weighed. Surface water was removed with tissue paper prior to weighing.

Permeability coefficients were determined on the planar devices in an all-glass diffusion cell at room temperature (23 ± 1°) (8, 9). Prior to these permeation experiments, the films were depleted of the initial drug load by placing them in a large volume of water. The aqueous phase was stirred continuously and exchanged at regular intervals. Drug release was followed by UV spectroscopic measurements. Film thicknesses were determined with a lightwave micrometer[7]. The water content of the hydrated films was determined as described previously (8).

Partition coefficients, $K_d$, defined as the ratio of the drug concentration in the film and in the bulk aqueous phase, were determined by a solution depletion technique (8) in which 20 ml of progesterone was allowed to equilibrate with a known volume of polymer. The aqueous phase contained both labeled and unlabeled drug. Adsorption of the drug onto glass and the initial aqueous phase concentration of the drug did not affect the values obtained.

Three methods were utilized to determine the aqueous solubility of progesterone. In the first method, a rod-shaped hydrogel matrix device containing labeled and unlabeled drug was placed in an aqueous solution in a covered beaker. The aqueous phase was stirred continuously, and the concentration was checked repeatedly until a constant value was reached.

The second method was similar to the first, except that several rod-shaped hydrogel devices containing both labeled and unlabeled drug were placed in an open beaker. The aqueous phase was stirred continuously. The volume of the aqueous phase decreased over time. The aqueous phase concentration was monitored until a steady-state value was reached. At this time, the aqueous phase was passed through a glass membrane filter until successive portions produced the same value.

In the third method, excess solid progesterone was added to a beaker containing ~1 liter of water. This solution was sonified for ~6 hr. The solution was allowed to cool and then was left undisturbed for 2 days. The resulting supernate was filtered through a glass filter, and the concentration was determined by UV spectroscopy.

## RESULTS AND DISCUSSION

**Progesterone Release from Monolithic Hydrogel Devices**—The release of medicaments from monolithic devices has been investigated extensively (4, 13–16). Equations that describe the release rate based on Fick's laws have been developed for several common shapes (13, 16). For rod-shaped monolithic devices prepared from polydimethyl siloxane, Roseman (14) showed that time release profiles could be described by the following equation:

$$(1 - F) \ln (1 - F) + F = Kt \qquad \text{(Eq. 1)}$$

where:

$$K = \frac{4C_s D}{C_0 r_0^2} \qquad \text{(Eq. 2)}$$

and:

$F$ = fraction released at time $t$ (seconds) = $M_t/M_\infty$
$M_t$ = amount of drug released (milligrams) at time $t$
$M_\infty$ = total amount of drug released (milligrams) at infinite time
$C_s$ = saturation solubility of drug in polymer (milligrams per cubic centimeter)
$C_0$ = initial drug concentration in matrix (milligrams per cubic centimeter)
$r_0$ = radius of the cylinder (centimeters)
$D$ = diffusion coefficient (square centimeters per second)

When $F$ is plotted *versus* the square root of time using Eq. 1, a nonlinear relationship results such that increasing negative deviations from linearity occur over time (14). At early times, Eq. 1 can be simplified to (14):

$$F = \frac{M_t}{M_\infty} = \left(\frac{8C_s Dt}{C_0 r_0^2}\right)^{1/2} \qquad \text{(Eq. 3)}$$

From Eq. 3, it is apparent that a plot of $F$ *versus* $t^{1/2}$ should be linear during the early stages of drug release and that the release rate should be dependent on the saturation solubility of the drug in the polymer, its diffusion coefficient in the polymer, and the radius of the device. These

[7] Van Kueren Co., Watertown, Mass.

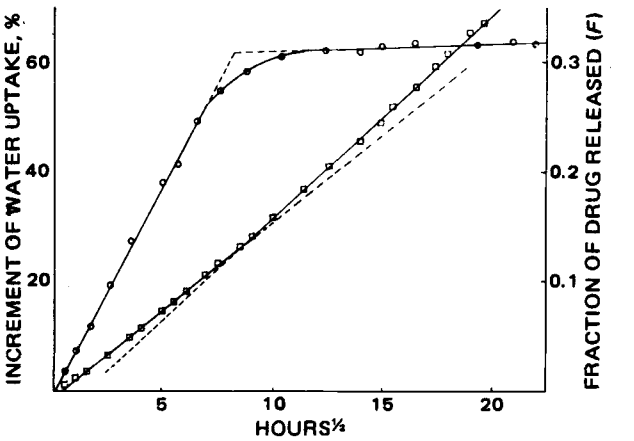


**Figure 1**—*Plots of water uptake (○) and fraction of drug released (□) versus* $t^{1/2}$ *for poly(hydroxyethyl methacrylate) with an initial drug load of 16% (w/w).*

conclusions were verified experimentally for such hydrophobic polymers as polydimethyl siloxane (13, 14).

Figures 1 and 2 are plots of $F$ *versus* $t^{1/2}$ for progesterone release from rod-shaped hydrogel devices. A breakpoint in these release curves is clearly evident during the early stages. The existence of these breakpoints was confirmed from plots of $\Delta M_t/\Delta t$ *versus* $t$. This function is constant in each case until ~8 hr in root time. At longer times, $\Delta M_t/\Delta t$ again is constant but its value is somewhat greater.

Also given in Figs. 1 and 2 are plots of the water uptake of these devices (defined as the increased weight of hydrated polymer per initial weight of the nonhydrated device) *versus* the square root of time. The breakpoints in these curves correspond with those in the drug release curve. Based on this finding, it may be inferred that the influx of water affects the initial release rate of the drug. From the observed smaller slope in the drug release curve prior to the breakpoint, it may be concluded that drug release is slower during the early stages of release.

Since hydration of these devices occurs simultaneously with drug release, it is difficult to define precisely the reasons for this initial decreased release rate. The situation is complicated further by the fact that the existence of these breakpoints in the drug release profiles was not observed universally. In other systems examined (Table I), which differed in the initial drug load or in the monomer composition, breakpoints in the drug release profiles were not found. Of particular interest was the fact that a breakpoint was not observed in the system prepared with methoxyethoxyethyl methacrylate. This device has the highest equilibrium water content; therefore, it was expected that release from this device would be most affected by water uptake.

Some insight into the events that control release was obtained from visual inspection of the devices during hydration. As noted, these monolithic devices were prepared by dissolving progesterone in the monomer and then polymerizing. Subsequent to polymerization, the devices are

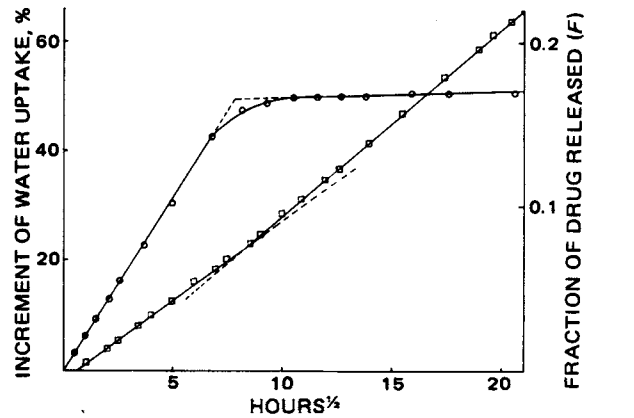


**Figure 2**—*Plots of water uptake (○) and fraction of drug released (□) versus* $t^{1/2}$ *for a copolymer of methoxyethoxyethyl methacrylate and hydroxyethyl methacrylate (monomer mole ratio of 2:1). The initial progesterone load was 9.1% (w/w).*

**Table I—Release Characteristics for Progesterone from Monolithic Hydrogel Devices**

| System | Monomers[a] | Initial Drug Load, % (w/w) | Permeability $\times 10^6$, cm²/sec | Slope of Water Influx Plot, $hr^{-1/2}$ | Water Saturation Time, $hr^{1/2}$ | $Q \times 10^5$, cm/sec | Appearance of Breakpoint |
|---|---|---|---|---|---|---|---|
| 1 | M | 7.8 | 3.64 | 0.44 | 14 | 3.91 | No |
| 2 | 67% M, 33% H | 9.1 | 2.01 | 0.78 | 8.2 | 5.56 | Yes |
| 3 | H | 16.7 | 1.55 | 0.60 | 8 | 5.09 | Yes |
| 4 | H | 13.0 | 1.22 | 0.63 | 9.5 | 4.18 | No |
| 5 | H | 9.1 | 1.05 | 0.65 | 7.5 | 3.35 | No |
| 6 | H | 4.8 | 0.88 | 0.67 | 7.5 | 2.30 | No |
| 7 | 80% H, 20% O | 9.1 | 0.61 | 0.34 | 8.0 | 1.34 | No |
| 8 | 67% H, 33% O | 9.1 | 0.44 | 0.46 | 8.5 | 1.53 | No |

[a] M is methoxyethoxyethyl methacrylate, H is hydroxyethyl methacrylate, and O is methoxyethyl methacrylate.

**Table II—Comparison of Permeation Parameters from Monolithic Devices and Drug-Depleted Films**

| Monomers[a] | Initial Drug Load, % (w/w) | $P \times 10^6$ (from Matrix) | $P \times 10^6$ (from Cross-Membrane) | $W_f$ (with Drug) | $W_f$ (after Drug Depletion) | $K_d$ | $D^b \times 10^8$, cm²/sec | $D^c \times 10^8$, cm²/sec |
|---|---|---|---|---|---|---|---|---|
| M | 7.8 | 3.64 | — | 0.38 | — | 130[d] | 2.80 | — |
| 67% M, 33% H | 9.1 | 2.01 | 1.84 | 0.36 | 0.54 | 141 | 1.43 | 1.30 |
| H | 16.7 | 1.55 | 1.50 | 0.34 | 0.43 | 130 | 1.19 | 1.15 |
| H | 13.0 | 1.22 | — | 0.35 | — | 129[d] | 0.95 | — |
| H | 9.1 | 1.05 | 1.05 | 0.35 | 0.43 | 143 | 0.73 | 0.73 |
| H | 4.8 | 0.88 | 0.88 | 0.35 | 0.43 | 127 | 0.69 | 0.69 |
| 80% H, 20% O | 9.1 | 0.61 | 0.57 | 0.24 | 0.37 | 212 | 0.29 | 0.27 |
| 67% H, 33% O | 9.1 | 0.44 | — | 0.25 | — | 192[d] | 0.23 | — |

[a] M is methoxyethoxyethyl methacrylate, H is hydroxyethyl methacrylate, and O is methoxyethyl methacrylate. [b] From matrix release studies. [c] From cross-membrane studies. [d] For polymer with 0% initial drug load.

clear, which suggests that progesterone is dispersed molecularly in the polymer matrix. Upon contact with water, progesterone located at the outer portion of the device precipitates. This zone of precipitation proceeds inwardly with time. More importantly, the time required for completion of this process appears to coincide with the breakpoints in the water uptake curves. This finding implies that the outer regions, where progesterone precipitation has occurred, must be fully hydrated, or nearly so, at very early times. This result is significant since drug release occurs from this region during the early stages.

The following information may be concluded concerning drug release during the early stages: (*a*) solute release occurs only from the outermost regions of the devices, (*b*) the parameters that normally affect release (*e.g.*, solubility of drug in the matrix, partitioning, and hydration) are probably constant, and (*c*) water influx occurs *via* diffusion through this outer hydrated region. Previous work (9, 10) demonstrated that both water transport and the permeation of steroids occur predominately within the water-filled channels or pores of the hydrogels. This observation suggests that during the early stages of release, a counterflow of solute and solvent must occur in these water-filled channels. This counterflow could affect the release rate by providing an additional resistance to flow. The magnitude of this effect should be dependent on the relative rates of drug efflux and water influx.

An empirical parameter, $Q$, will be developed to serve as a semiquantitative measure of the magnitudes of these crossflows. The magnitude of $Q$ will be compared with the experimental results obtained from the drug release curves.

The rate of drug efflux from monolithic devices during the early stages of release is given by Eq. 3. The amount of drug released at infinite time, $M_\infty$, is given by $\pi r_0^2 h C_0$. Substitution of this value for $M_\infty$ in Eq. 3 gives:

$$M_t = (8\pi^2 h^2 D C_0 C_s r_0^2 t)^{1/2} \quad \text{(Eq. 4)}$$

or by substitution of the permeability coefficient, $P$, for $DK_d$:

$$M_t = (8\pi^2 h^2 r_0^2 C_0 C_w P t)^{1/2} \quad \text{(Eq. 5)}$$

Differentiation of Eq. 5 gives the release rate:

$$\frac{dM_t}{dt} = (2\pi^2 h^2 r_0^2 C_0 C_w P) t^{-1/2} \quad \text{(Eq. 6)}$$

For the various devices investigated, the values of $h$, $r_0$, and $C_w$ are constant. Therefore, the relative drug release rate can be expressed by $(dM_t/dt) \alpha \sqrt{C_0 P}$. The permeability coefficients were obtained *via* Eqs. 1 and 2. For systems that produced a breakpoint, $P$ was obtained from the slope of the line above the breakpoint. The values of $P$ are listed in Table I.

The relative rate of drug efflux from the various devices should be dependent on $C_0$ and $P$ $[(dM_t/dt) \alpha \sqrt{C_0 P}]$. This relative release rate also should be dependent on the relative rate of water uptake by the devices. Equations that quantitatively state the water influx rate by devices with cylindrical geometry have not been developed. However, it is apparent that the relative rates must be proportional to the slope, $\beta$, of a water uptake *versus* $t^{1/2}$ plot.

It was hypothesized that drug release should be affected by the relative rates of solute and solvent crossflows in the water-filled channels or pores of the device. The magnitude of these crossflows should be proportional to the product of the relative rates of drug efflux and water influx. Therefore, the empirical parameter, $Q$, is defined as the product of these relative rates:

$$Q = \beta \sqrt{P C_0} \quad \text{(Eq. 7)}$$

where $\beta$ is a measure of the relative rate of water influx. This semiempirical parameter should provide a relative measure of the effects of water uptake on the release of solutes from hydrogel devices.

The $Q$ values (Table I) range from $1.33 \times 10^{-5}$ to $5.56 \times 10^{-5}$ cm/sec. However, a breakpoint in the drug release curve arises only when $Q$ is $> \sim 5 \times 10^{-6}$ cm/sec. Thus, as the magnitude of the solute and solvent crossflows increases (as measured by $Q$), breakpoints occur in the drug release curve. This situation can also explain the lack of a breakpoint in the drug release curve for methoxyethoxyethyl methacrylate since the water uptake rate by this device is relatively slow (Table I). The magnitude of the counterflow of solute and solvent is small; thus, a breakpoint in the drug release profile is not observed.

**Progesterone Transport in Drug-Depleted Films**—In the development of the permeability coefficients listed in Table I, the aqueous solubility of the solute, progesterone, in water must be known. For the present study, a value of 38 μg/ml was utilized based on the average value obtained from the three techniques described for the measurement of the aqueous solubility. This value is substantially higher than that of 12.6 μg/ml given by Roseman (14) and that of 27 μg/ml given by Sundarum and Kincl (17). Both of these values were obtained at 37°, whereas the value used in this study was obtained at 23°.

This uncertainty in the value for the aqueous solubility of progesterone

leads to a considerable uncertainty in the $P$ values listed in Table I. Thus, a second method was developed to determine progesterone permeability in the monolithic devices. When permeability is assessed from studies of the transfer rate of solute across a thin film, the $P$ values can be obtained directly from plots of a concentration variable *versus* time. It was shown previously (9) that when the solute has a high film–water partition coefficient, the following equation can be utilized to obtain the permeability coefficient:

$$\ln\left(\frac{C_3 - C_4}{C_1 - C_2}\right) = \frac{-2AP}{Vl}(t_{ss} - t_{oss}) \qquad \text{(Eq. 8)}$$

where:

$V$ = compartment volumes (176 ml)
$C_1$ = concentration in Compartment I at onset of steady state ($t_{oss}$)
$C_2$ = concentration in Compartment II at onset of steady state
$C_3$ = concentration in Compartment I at $t_{ss}$ (anytime during steady state)
$C_4$ = concentration in Compartment II at $t_{ss}$
$A$ = membrane area (14.2 $cm^2$)
$l$ = wet membrane thickness

Table II is a summary of the values of $P$, $D$, and $K_d$ obtained from measurements on hydrogel films. These films were prepared with the initial drug loadings listed in Table II and then subsequently were depleted of drug prior to the permeation experiments. The $P$ values obtained *via* this method are in excellent agreement with those obtained from the progesterone release studies with rod-shaped devices.

This agreement between the $P$ values obtained from the release studies and the transport studies provides further evidence that the aqueous solubility of progesterone is close to 38 μg/ml. In fact, this combined method for the determination of the permeability may be excellent for the determination of the solubility of slightly soluble solutes in aqueous solution.

Sufficient data are available in the paper by Roseman (14) to estimate the aqueous solubility of progesterone at 37° using this technique. Roseman reported diffusion coefficients in polydimethyl siloxane of $16.5 \times 10^{-7}$ $cm^2$/sec (estimated from matrix release studies) and $4.50 \times 10^{-7}$ $cm^2$/sec (obtained from membrane transport studies). With these values and 0.572 mg/ml for $C_s$ and 50.2 for $K_d$, the aqueous solubility of progesterone is 42 μg/ml *via* Eq. 5. This result is in good agreement with that obtained in the present study.

The permeation parameters shown in Tables I and II may be utilized to understand the various factors that control the release of solutes from monolithic hydrogel devices.

From a comparison of the $P$ values with the equilibrium water contents, $W_f$, it is apparent that permeability increases as the equilibrium water content of the polymer increases. This conclusion is consistent with previous results (8, 9). The $K_d$ values shown in Table I obtained on the depleted films are also consistent with the previous work, suggesting that the incorporation of drug into the device with its subsequent precipitation does not affect the equilibrium solubility of progesterone in the polymer matrix.

However, drug incorporation is not without effect on the transport properties of the matrix. This effect is demonstrated by the comparison of $P$ values obtained from transport studies (with no added drug) with those obtained in the presence of drug. In each case, the permeability of the drug-filled polymers is greater. This effect is proportional to the initial drug load, as demonstrated by studies with devices prepared from hydroxyethyl methacrylate. As the initial drug load decreases, the permeability decreases and approaches the value obtained from films prepared without drug. This result may indicate that the ultimate precipitation of progesterone in the matrix devices affects the average pore size of the matrix phase. Previous work (8, 9) demonstrated that the pore mechanism dominates progesterone permeation in hydrogels of the type utilized in the present study. It is expected that the presence of solid drug particles would affect the formation of these pores and, therefore, lead to the observed increases in permeability.

## REFERENCES


(1) O. Wichterle and D. Lim, *Nature*, **185**, 117 (1960).

(2) B. D. Ratner and A. S. Hoffman, in "Hydrogels for Medical and Related Applications," ACS Symposium Series 31, J. D. Andrade, Ed., American Chemical Society, Washington, D.C., 1976, p. 1.

(3) J. M. Anderson, T. Koinis, T. Nelson, M. Horst, and D. S. Love, in *ibid.*, p. 167.

(4) Y. W. Chien and E. P. K. Lau, *J. Pharm. Sci.*, **65**, 488 (1976).

(5) R. H. Abrahams and S. H. Ronel, *J. Biomed. Mater. Res.*, **9**, 355 (1975).

(6) S. Hosaka, H. Ozawa, and H. Tanzawa, *J. Appl. Polym. Sci.*, **23**, 2089 (1979).

(7) L. Olanoff, T. Koinis, and J. M. Anderson, *J. Pharm. Sci.*, **68**, 1147 (1979).

(8) G. M. Zentner, J. R. Cardinal, and S. W. Kim, *ibid.*, **67**, 1352 (1978).

(9) G. M. Zentner, J. R. Cardinal, J. Feijen, and S. Z. Song, *ibid.*, **68**, 970 (1979).

(10) S. W. Kim, J. R. Cardinal, S. Wisniewski, and G. M. Zentner, in "Water in Polymers," ACS Symposium Series 127, S. P. Rowland, Ed., American Chemical Society, Washington, D.C., 1980, p. 347.

(11) G. M. Zentner, J. R. Cardinal, and D. E. Gregonis, *J. Pharm. Sci.*, **68**, 794 (1979).

(12) G. A. Mortimer, *J. Org. Chem.*, **30**, 1632 (1964).

(13) T. J. Roseman and W. I. Higuchi, *J. Pharm. Sci.*, **59**, 353 (1970).

(14) T. J. Roseman, *ibid.*, **61**, 46 (1972).

(15) Y. W. Chien, H. J. Lambert, and D. E. Grant, *ibid.*, **63**, 365 (1974).

(16) J. Cobby, M. Mayersohn, and G. C. Walker, *ibid.*, **63**, 725 (1974).

(17) K. Sundarum and F. A. Kincl, *Steroids*, **12**, 517 (1968).


## ACKNOWLEDGMENTS


Presented in part at the APhA Academy of Pharmaceutical Sciences, Phoenix meeting, November 1977.

Supported by National Institutes of Health Grant HD-09791-03.

The authors thank Dr. D. E. Gregonis, Dr. J. D. Andrade, and Dr. C. Anderson for their contributions.

# High-Pressure Liquid Chromatographic Determination of Viloxazine in Human Plasma and Urine

**ROBERTA GILLILAN and WILLIAM D. MASON** ˣ

Received May 19, 1980, from the *Pharmacokinetics Laboratory, Schools of Pharmacy and Medicine, University of Missouri–Kansas City, Kansas City, MO 64108.* Accepted for publication July 30, 1980.

**Abstract** □ A rapid, specific, high-pressure liquid chromatographic method is presented for the determination of viloxazine in plasma and urine. This method employs the high sensitivity of fluorescence detection with selective extraction and reversed-phase chromatography to measure concentrations as low as 25 ng/ml of plasma and 1.0 μg/ml of urine. Known metabolites of viloxazine do not interfere with the analysis, and experience with several hundred samples in a bioavailability study demonstrated the applicability and reliability of the method.

**Keyphrases** □ Viloxazine—high-pressure liquid chromatographic analysis, human plasma and urine □ High-pressure liquid chromatography—analysis, viloxazine, human plasma and urine □ Antidepressants—viloxazine, high-pressure liquid chromatographic analysis, human plasma and urine

Viloxazine hydrochloride [2-(2-ethoxyphenoxymethyl)tetrahydro-1,4-oxazine hydrochloride, ICI 58,834] is a psychotropic drug with antidepressant activity; its clinical pharmacology was summarized by Bayliss and Duncan (1). It was reported that viloxazine is absorbed completely and metabolized extensively following oral administration to human volunteers (2).

Previous procedures for the determination of viloxazine in plasma and urine employed GLC with electron-capture detection (3) following extraction and conversion to the heptafluorobutyrate or labeling with carbon 14 in combination with TLC (2). Although the GLC methods can be sufficiently specific and sensitive for pharmacokinetic and bioavailability studies, they are relatively complex and require a demanding prechromatographic derivatization.

The procedure reported here combines a selective two-step extraction with the separative capability of high-pressure liquid chromatography (HPLC) and the sensitivity of fluorescence detection. The method is rapid, is easily automated, employs an internal standard, separates the drug metabolites, and is of sufficient sensitivity (25-ng/ml plasma detection limit) for pharmacokinetic studies.

**Table I—Retention Times for Viloxazine, Dextrorphan, and Viloxazine Metabolites**

| Compound | Code Number[a] | Retention Time, min | Retention Time Relative to Viloxazine, min |
|---|---|---|---|
| Viloxazine | 58834 | 8.2 | 1.00 |
| Dextrorphan | — | 6.7 | 0.81 |
| *o*-Hydroxyviloxazine | 60169 | 3.0 | 0.36 |
| 2-(2-Ethoxyphenoxymethyl)-2,3,5,6-tetrahydro-5-oxo-1,4-oxazine | 69322 | 7.4 | 0.90 |
| *n*-Methylviloxazine | 70098 | 16.0 | 1.95 |
| *m*-Hydroxyviloxazine | 71928 | 2.6 | 0.31 |
| *p*-Hydroxyviloxazine | 71976 | 3.0 | 0.36 |

[a] Taken from Ref. 2.

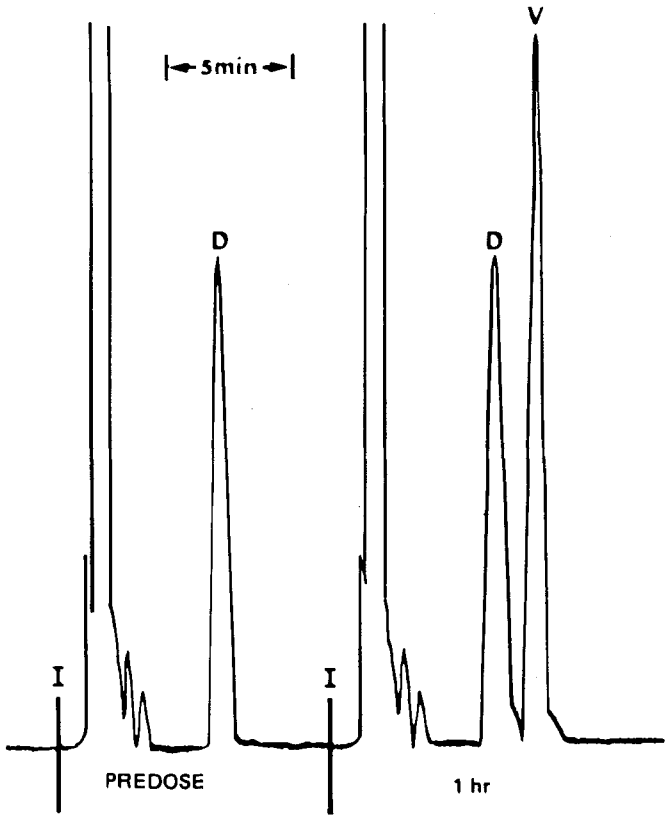


**Figure 1**—*High-pressure liquid chromatograms (excitation at 220 nm, no filter) of extracts before dosing and 1 hr after a 50-mg dose. Key: I, injection; D, dextrorphan; and V, viloxazine.*

## EXPERIMENTAL

**Materials**—*n*-Butanol[1], *n*-butyl chloride[1], acetonitrile[1], triethylamine[2], dibasic sodium phosphate[3], phosphoric acid[4], and acetic acid[4] were used as received. Water was deionized and then distilled. Dextrorphan[5] (3-hydroxy-*N*-methylmorphinan), viloxazine[6], and the metabolites[6] of viloxazine were used as received.

[1] UV grade, Burdick & Jackson Laboratories, Muskegon, Mich.
[2] Reagent grade, Aldrich Chemical Co., Milwaukee, Wis.
[3] Reagent grade, Fisher Scientific Co., Fair Lawn, N.J.
[4] Reagent grade, Mallinckrodt, Paris, Ky.
[5] Hoffmann–La Roche Laboratories, Nutley, N.J.
[6] ICI Americas, Wilmington, Del.



0022-3549/81/0200-0220$01.00/0
© 1981, American Pharmaceutical Association

**Table II—Accuracy and Precision**

| | Concentration, ng/ml | | | | | | | | | |
|---|---|---|---|---|---|---|---|---|---|---|
| | 50.0 | 100.0 | 150.0 | 200.0 | 250.0 | 300.0 | 400.0 | 600.0 | 800.0 | 1000.0 |
| *n* | 9 | 27 | 10 | 24 | 11 | 20 | 30 | 27 | 23 | 16 |
| Mean | 54.7 | 100.9 | 153.3 | 193.2 | 247.9 | 297.2 | 391.8 | 587.1 | 804.5 | 1026.0 |
| *SD* | 5.1 | 5.5 | 8.8 | 8.2 | 16.0 | 15.3 | 17.9 | 27.4 | 35.4 | 73.4 |
| *CV*, % | 9.3 | 5.4 | 5.7 | 4.2 | 6.4 | 5.1 | 4.5 | 4.7 | 4.4 | 7.1 |

**Apparatus**—The HPLC system consisted of an automatic injector[7], a high-pressure pump[8], a bonded-phase column[9], and a fluorescence detector[10].

**Chromatographic Parameters**—Although several mobile phases were evaluated, the system containing 17.5% acetonitrile, 6 m*M* triethylamine, and 0.20 *M* phosphate buffer at pH 3.2 was optimal in this laboratory. The phosphate buffer was filtered through a 0.45-μm filter prior to mixing, as were all other reagent solutions. A flow rate of 1.3 ml/min at ambient temperature (usually 22°) was employed in most studies. Aliquots of 50–100 μl of the back-extraction were injected directly onto the column.

**Analytical Procedure**—*Plasma*—A 0.50-ml aliquot of plasma was pipetted into a 15-ml centrifuge tube and adjusted to pH 10.4 by adding 50 μl of saturated sodium carbonate solution. Eight milliliters of 10% *n*-butanol in butyl chloride containing 25 ng of dextrorphan/ml was added, and the capped tube was vortexed 1 min and then centrifuged. The upper organic phase was transferred to a second 15-ml centrifuge tube containing 300 μl of 1.0% acetic acid. The second tube was vortexed and centrifuged, and the upper organic layer was discarded. The acetic acid solution was injected into the HPLC system.

*Urine*—Twenty microliters of well-mixed urine was diluted with 0.5 ml of 0.139 *M* dibasic sodium phosphate buffer (pH 10.5) in a 15-ml centrifuge tube. This diluted aliquot was subjected to the same procedure as the plasma samples.

## RESULTS AND DISCUSSION

Table I lists the retention times of viloxazine, dextrorphan, and the known unconjugated metabolites of viloxazine. All of the tested compounds were resolved from one another and the normal components of plasma and urine. The 8.3-min retention time for viloxazine allows a convenient processing of five or six samples per hour. Figure 1 shows chromatograms for two samples, one obtained prior to dosing and the other obtained 1 hr after a 50-mg oral dose. Although the metabolites do chromatograph and are detectable when injected directly onto the column, they do not extract efficiently and are not detected in plasma and urine.

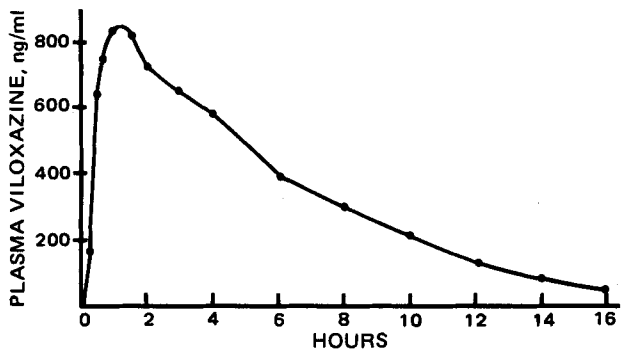


**Figure 2**—*Viloxazine concentration* versus *time curve in a human subject following a single 50-mg dose.*

The peak height ratio of viloxazine to dextrorphan varies linearly with the concentration of viloxazine added to pooled plasma. A typical standard curve obtained by assaying samples with 0, 50, 100, 150, 200, 250, 300, 400, 600, 800, and 1000 ng/ml had a linear regression coefficient of 0.999, a slope of 515.8 ng/ml, and an intercept of 11.6 ng/ml, where the peak height ratio was the abscissa and the viloxazine concentration was the ordinate. During the analysis of several hundred samples over 4 months, the slope and intercept values of frequent standard curves remained within ±20% of these stated values.

The precision and accuracy of the method are demonstrated in Table II. The analysis of 10 aliquots of a 50-ng/ml standard, assayed in batch, had a coefficient of variation of 9.7%, while a similarly processed 300-ng/ml standard gave a 6.9% coefficient of variation. When processing large numbers of samples, 25 ng/ml in plasma and 1 μg/ml in urine are practical lower limits of detection.

During the analysis of 576 plasma samples in duplicate from 12 healthy volunteers in a bioavailability study, no chromatographic peaks were observed to interfere with either viloxazine or dextrorphan. Figure 2 presents the plasma viloxazine concentration–time curve for one typical subject following a single 50-mg dose. The method clearly is sufficiently sensitive to describe the plasma curve in this dose range. Urine samples (252) from the same study also were assayed in duplicate, and no interfering chromatographic peaks were observed. The findings of the bioavailability study will be presented in a subsequent report.

As with most chromatographic procedures, the exact mobile phase composition required and the limits of detection will vary with the particular column and matrix of the sample. In this laboratory, the described method works well with several similar columns and for samples obtained from healthy volunteers. However, modifications may be required to achieve optimal separations in diseased patients, especially those receiving multidrug therapy. When the same column was used, the day-to-day change in the slope of the standard curve was <±1%; however, larger changes of up to 5% were observed when a different column was installed. Fortunately, properly maintained columns will allow several hundred determinations.

[7] WISP 710A, Waters Associates, Milford, Mass.
[8] Model 6000A, Waters Associates, Milford, Mass.
[9] Altex Scientific Inc., Berkeley, Calif.
[10] SPF 970, Schoeffel, Westwood, N.J.

## REFERENCES

(1) P. F. C. Bayliss and S. M. Duncan, *Br. J. Clin. Pharmacol.*, **1**, 431 (1974).

(2) D. E. Case and P. R. Reeves, *Xenobiotica*, **5**, 113 (1975).

(3) D. E. Case, *J. Pharm. Pharmacol.*, **25**, 800 (1973).

# Bonding Mechanisms and Hysteresis Areas in Compression Cycle Plots

**J. T. CARSTENSEN *x, JEAN-PAUL MARTY ‡, F. PUISIEUX ‡, and HATEM FESSI ‡**

Received February 25, 1980, from the **School of Pharmacy, University of Wisconsin, Madison, WI 53706,* and the ‡*Faculté de Pharmacie, Université de Paris-Sud, 92290 Châtenay-Malabry, France.* Accepted for publication August 1, 1980.

**Abstract** □ It was shown previously that if compression of a powder is treated in an analogous manner to the compression of a nonporous solid, a plot of the transmitted pressure *versus* the applied pressure should have a hysteresis area that is linear with respect to the maximally applied pressure if plastic deformation occurs. However, if brittle fracture occurs, the area should be quadratically related to the maximally applied pressure. A series of compounds expected to yield by plastic deformation was tested, and they were found to give the quadratic relationship. Thus, it is indicated experimentally that the assumptions made in general in treating compression cycles may be partially invalid.

**Keyphrases** □ Powders—compression cycles at various maximum pressures for substances expected to undergo plastic deformation □ Tablet manufacture—compression cycles at various maximum pressures for substances expected to undergo plastic deformation □ Compression cycles—compression at various maximum pressures of substances expected to undergo plastic deformation

In tablet manufacture, a powder or granulation is placed within a die and then compressed between two punches. The process can be considered as being composed of five stages (1):

1. The particles rearrange so that the powder attains its closest packing.
2. The particles then deform elastically.
3. At stresses or pressures above the elastic limits, the particles either deform plastically or fracture. Either process is assumed to lead to bonding between the particles and, therefore, to tablet formation (2).
4. The upper punch is released, and the stresses relax.
5. The tablet is ejected.

If the die wall pressure ($F$) or lower punch pressure ($P'$) in Stages 1–4 is monitored as a function of the upper punch pressure ($P$), then a compression cycle results.

## BACKGROUND

Long (3) and Leigh *et al.* (4) analyzed the theoretical relationships $P' = f(P)$ and $F = f(P)$ and arrived at relationships that have been useful in investigating the physics of powder compression. Carstensen (5) and Carstensen and Toure (6) applied the suggested model, which involves an analogy between the behavior of a nonporous mass and the powder in question, to treatment of the areas of the hysteresis loops described by the functions $P' = f(P)$ and $F = f(P)$. They cautioned that the assumptions used might be unrealistic in some aspects and concluded that if the assumptions held, then bonding by plastic deformation should lead to a linear relationship between the hysteresis area ($A$) and the maximally applied pressure ($P_m$):

$$A = a'P_m + b' \qquad \text{(Eq. 1)}$$

If brittle fracture occurred, then the relationship would be:

$$A = c + bP_m + aP_m^2 \qquad \text{(Eq. 2)}$$

or if $c$ and $b$ were small, it would be simply:

$$\ln A = 2 \ln P_m + \ln a \qquad \text{(Eq. 3)}$$

where $a$, $b$, and $c$ are constants. One interesting note in the few available cases is that sodium chloride appears to bond by brittle fracture rather than by plastic deformation, as has been generally assumed.

The aims of the present study were to test the compression cycles at various maximum pressures for substances that are expected to deform plastically beyond the elastic limit and to test which equation (Eq. 1 or 2) is valid.

**Table I—Regression Values for Cycle Areas ($A$) as a Function of Maximum Pressure ($P^*$) According to Eq. 4**

| Formula | Correlation Coefficient | $\alpha$ | $\beta$ |
|---|---|---|---|
| Polyvinyl chloride | 0.998 | 1.90 | −1.66 |
| Polyvinyl chloride and excipients[a] | 0.998 | 1.82 | −0.79 |
| Polyvinyl alcohol | 0.996 | 1.94 | −1.67 |
| Polyvinyl alcohol and excipients[a] | 0.998 | 2.2 | −3.0 |
| Polyvinyl alcohol–polyvinyl chloride copolymer | 0.983 | 2.13 | −2.83 |
| Polyvinyl alcohol–polyvinyl chloride copolymer (50%) and excipients[a] | 0.998 | 1.94 | −1.68 |
| Polyvinyl alcohol–polyvinyl chloride copolymer (60%) and excipients[a] | 0.999 | 2.05 | −2.24 |
| Polyvinyl alcohol–polyvinyl chloride copolymer (70%) and excipients[a] | 0.998 | 2.15 | −2.81 |
| Polyvinyl alcohol–polyvinyl chloride copolymer (80%) and excipients[a] | 0.999 | 1.97 | −1.99 |

[a] The excipients were as stated in the text; the granulation liquid was isopropanol, except in the last case where methylene chloride was used.

## EXPERIMENTAL

The compositions of the tablets are shown in Table I. In three cases, the polymers (polyvinyl alcohol[1], polyvinyl chloride[2], and a copolymer of the two compounds[3]) were compressed as they were. The particle sizes of the polymers were 250–400, <5, and 80–125 μm, respectively. In the remaining cases, granulations of the polymers were used consisting of 20% diphenhydramine hydrochloride, 1.5% povidone, 50% polymer (unless stated otherwise) and an amount of tribasic calcium phosphate (*q.s.*). With the copolymer, a series of compositions was compressed with increased polymer content (60 and 70%).

The granulations were prepared by mixing the powders without povidone and then granulating them with a 3.75% solution of povidone in either isopropanol or methylene chloride. The granulation was dried at 60° for 15 min in a small fluid bed drier[4]. Then the granulation was passed through an oscillating granulator with a 1-mm screen opening, after which the 0.2–0.8-mm fraction was separated out by screening and used for compression.

Compression was carried out on a single-punch tablet machine[5] equipped with strain gauges and operated at a speed that gave a cycle time of 1/60 sec; 0.5 g of powder or granulation was used for the compression, and 12-mm flat-faced punches were employed. Data were reduced to sets of corresponding $P$ and $P'$ values, and a hysteresis plot (Fig. 1) was made for each. Areas of the hysteresis loops were determined with a planimeter.

## RESULTS AND DISCUSSION

A typical set of compression cycles (with three different maximal

[1] Rhodopas, H, Rhone-Poulenc, France.
[2] Pevikon, 637P, Seppic, Paris, France.
[3] 15 PVA85PVC, Solvic, Solvay, France.
[4] Glatt, Basel, Switzerland.
[5] Frogerais type AO, Societe Edmond Frogerais, Vitry-sur-Seine, France.



0022-3549/81/0200-0222$01.00/0
© 1981, American Pharmaceutical Association

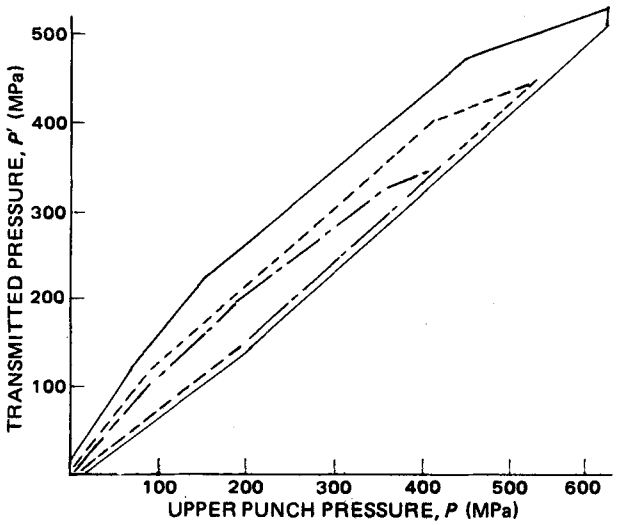


**Figure 1**—*Pressure cycles at three maximal pressures for polyvinyl alcohol–polyvinyl chloride copolymer (60%) and excipients. Two other cycles at other maximal pressures are not shown for pictorial clarity.*

pressures) is shown for one formulation (copolymer and excipients) in Fig. 1. Five maximal pressures were employed in each case, but only three are shown for pictorial clarity. Each point of an individual cycle is the mean of six experimental determinations, so each cycle is an average cycle; the standard deviation of a sample of six points was ~4%. In all cases, the areas ($A$) of the hysteresis loops were plotted *versus* the maximal pressure, $P^*$, resulting in relations of the type:

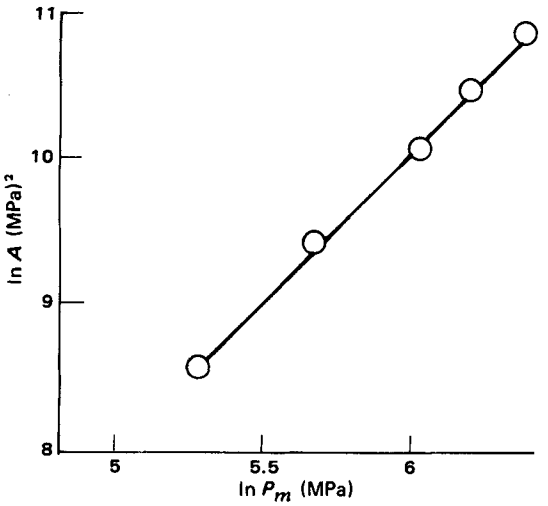


**Figure 2**—*Areas of the hysteresis loops of Fig. 1 plotted according to Eq. 4.*

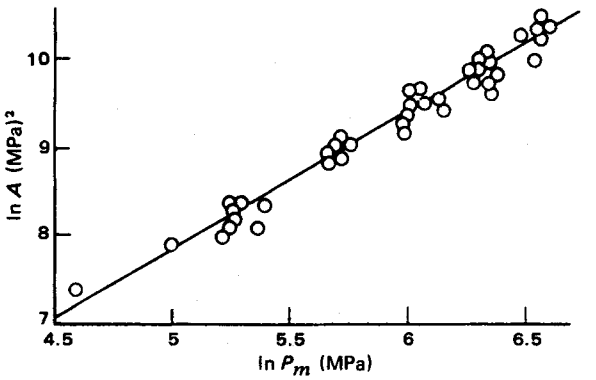


**Figure 3**—*All of the experimental hysteresis loop areas plotted according to Eq. 4.*

$$\ln A = \alpha \ln P_m + \beta \qquad \text{(Eq. 4)}$$

The data from the formulation in Fig. 1 are plotted in this fashion in Fig. 2, and the linearity is obvious. The slopes and intercepts obtained by least-squares fitting are shown in Table I. All of the slopes are close to 2. The fact that the plots are similar for all of the compositions is not surprising since the polymers can be expected to exhibit comparable behavior due to their chemical similarity. The fact that the data are comparable allowed graphical presentation of all of the experimental (area) data on one plot (Fig. 3).

The surprising feature is that the quadratic relationship:

$$A = aP^2_{max} \qquad \text{(Eq. 5)}$$

occurs, as predicted for brittle fracture. Polymers intuitively should give rise to plastic deformation, and Eq. 1 (the linear relationship) should hold rather than Eq. 2 (or Eq. 3). Carstensen and Toure (6) pointed out that some assumptions made in conventional modeling of compression cycles may be unrealistic. The solid is highly porous at the onset of the cycle and slightly porous to nonporous (practically in some cases) at the end but, by analogy, is compared to a solid, nonporous body at all stages. Equations 1 and 2, therefore, are no more valid than the assumptions made; and since the polymers used here probably do not bond by brittle fracture, it may be assumed that one or more of the assumptions made in deriving the conventional cycle equations (whether for the individual line segments or for the areas) are unrealistic.

## REFERENCES

(1) J. T. Carstensen, "Pharmaceutics of Solids and Solid Dosage Forms," Wiley, New York, N.Y., 1977, pp. 154, 155.

(2) E. N. Hiestand, presented at the International Conference on Powder Technology and Pharmacy, Basel, Switzerland, June 1978.

(3) W. M. Long, *Powder Metall.*, **6**, 73 (1960).

(4) S. Leigh, J. E. Carless, and B. W. Burt, *J. Pharm. Sci.*, **56**, 888 (1967).

(5) J. T. Carstensen, "Mechanical Properties and Rate Processes in Solid Pharmaceuticals," Academic, New York, N.Y., 1980.

(6) J. T. Carstensen and P. Toure, *Powder Technol.*, **26**, 199 (1980).

# Chlorothiazide Absorption from Solution and Tablet Dosage Forms in Dogs

**WILLIAM F. EBLING *, ANDREW F. MURRO *, FRANK J. VOELKER *, DENNIS E. RESETARITS *, and THEODORE R. BATES ‡x**

Received March 18, 1980, from the **Department of Pharmaceutics, School of Pharmacy, State University of New York at Buffalo, Amherst, NY 14260,* and the ‡*Department of Pharmaceutics, School of Pharmacy, University of Pittsburgh, Pittsburgh, PA 15261.* Accepted for publication July 30, 1980.

**Abstract** □ The bioavailability of an aqueous solution of chlorothiazide and three commercially available chlorothiazide tablets was assessed in adult mongrel dogs. In two crossover urinary excretion studies, six fasting dogs received single 500-mg doses of chlorothiazide as an aqueous solution, one 500-mg originator tablet on two separate occasions (Tablets A-1 and A-2), two 250-mg originator tablets (Tablet B), or one 500-mg generic tablet (Tablet C). 6-Amino-4-chlorobenzene-1,3-disulfonamide (chloraminophenamide), a pharmacologically active hydrolysis product of chlorothiazide, was not detected in any urine sample. Urinary recoveries of chlorothiazide after oral administration, expressed as the mean (range) percent of the dose, were only 22.0 (8.41–33.9), 15.7 (10.2–25.0), 20.7 (7.25–31.0), 18.5 (8.72–33.2), and 21.9% (6.69–41.1%) for the aqueous solution and Tablets A-1, A-2, B, and C, respectively. Considerable interindividual variation and some intraindividual variation were observed. No statistically significant difference in bioavailability existed among the aqueous solution and Tablets A-2 and B, between Tablets A-1 and C, and between Tablets A-1 and A-2.

**Keyphrases** □ Chlorothiazide—bioavailability from tablets and aqueous solution, dogs □ Bioavailability—chlorothiazide, absorption from aqueous solution and tablets, dogs □ Diuretics—chlorothiazide, bioavailability from aqueous solution and tablets, dogs

Chlorothiazide is a diuretic used in the treatment of hypertension, congestive heart failure, and other edematous conditions in animals and humans (1). After intravenous administration to dogs (2–4) and humans (5–7), chlorothiazide is excreted rapidly and completely in the urine as unchanged drug. In contrast, urinary recoveries ranging from only 13 to 32% (percent of dose) have been observed in humans after oral administration of 250–1000 mg of chlorothiazide as tablets (6–9) or as an aqueous solution of the sodium salt (6). Absorption of chlorothiazide in dogs also is poor and variable and apparently is dose dependent at oral doses comparable to those used in the treatment of edematous conditions (4). Thus, the dog appears to be a good animal model for studies designed to assess the influence of physicochemical and physiological factors on chlorothiazide absorption.

The purpose of the present study was to determine the effect of the dosage form and the dosage form formulation on chlorothiazide absorption.

**Table I—Experimental Designs for Chlorothiazide Absorption Studies in Mongrel Dogs [a]**

| Dog | Body Weight, kg | Study I Week 1 | Study I Week 2 | Study II Week 1 | Study II Week 2 | Study II Week 3 |
|---|---|---|---|---|---|---|
| 1 | 17.0 | C | A-1 | AS | B | A-2 |
| 4 | 18.5 | C | A-1 | AS | B | A-2 |
| 5 | 19.7 | C | A-1 | B | A-2 | AS |
| 8 | 18.1 | A-1 | C | B | A-2 | AS |
| 9 | 16.6 | A-1 | C | A-2 | AS | B |
| 10 | 21.8 | A-1 | C | A-2 | AS | B |

[a] Each item within the matrix corresponds to a specific formulation. Tablets A-1 and A-2 represent 500-mg tablets (Merck Sharp and Dohme) administered on two separate occasions, Tablet B represents two 250-mg tablets (Merck Sharp and Dohme), Tablet C is one 500-mg tablet (Econo-Rx), and AS is the aqueous solution containing 500 mg of chlorothiazide as the sodium salt.

## EXPERIMENTAL

**Materials**—Chlorothiazide[1], sulfadiazine[2], acetonitrile[3], and ethyl acetate[4] were used as received.

Commercial 250- and 500-mg chlorothiazide tablets[5] manufactured by the originator of the drug product and a generic 500-mg chlorothiazide tablet[6] were obtained commercially. An aqueous solution dosage form of chlorothiazide sodium was prepared immediately prior to use. The 250-mg originator tablet, the 500-mg originator tablet, the 500-mg generic tablet, and the aqueous solution were assayed for their drug content by HPLC and were found to contain 99.5 ± 2.3, 99.4 ± 1.8, 94.1 ± 3.1, and 99.6 ± 1.0% [mean ($n$ = 6) ± $SD$] of the labeled amount of chlorothiazide. All other chemicals and solvents were reagent grade.

**Absorption Studies**—Six unanesthetized mongrel dogs (five male and one female), 16.6–21.8 kg (mean 18.6 kg), were fasted with water *ad libitum* for 16–18 hr prior to and for 24 hr after drug administration. Between 8:00 and 9:00 am, each animal received, in two crossover studies (Table I), single 500-mg oral doses of chlorothiazide as one 500-mg originator tablet on two separate occasions (Tablets A-1 and A-2), two 250-mg originator tablets (Tablet B), one 500-mg generic tablet (Tablet C), and 50 ml of an aqueous solution of chlorothiazide sodium. A 1-week washout period was allowed between drug administrations.

Quantitative urine collections were made at 0–12, 12–24, 24–48, 48–72, and 72–96 hr after chlorothiazide administration, and the pH and volume of each collection were recorded. On a separate occasion, 24-hr blank urine specimens were collected from each dog. An aliquot of all specimens was stored at −20° until it was assayed.

The specific HPLC method of Lin and Benet (7) for the quantitative determination of chlorothiazide in urine was used. The original method was modified as described previously (4, 10) to include an extraction step and sulfadiazine as the internal standard.

Differences among more than two mean urinary excretion values were evaluated statistically by an analysis of variance for crossover (Latin square) design, and differences between any two means were compared using either Tukey's multiple-range test or the Student $t$ test for paired samples (11).

## RESULTS AND DISCUSSION

There is general agreement that the extent of absorption of thiazide diuretics is assessed best from cumulative urinary excretion data (12–17).

No statistical difference in the urine pH or urine volume existed among the five study conditions. As demonstrated previously (4), chlorothiazide was excreted quantitatively and uniformly in the urine after administration of 50- and 250-mg iv doses of chlorothiazide to four of the six dogs used in the present investigation. Thus, chlorothiazide elimination *via* active renal tubular and biliary secretion (2, 3) apparently occurs in a linear fashion over this dosage range.

The mean cumulative percent of the chlorothiazide dose (based on

[1] Supplied by Merck Sharp and Dohme, West Point, Pa.
[2] American Pharmaceutical Co., New York, N.Y.
[3] High-pressure liquid chromatographic (HPLC) grade, Burdick & Jackson Laboratories, Muskegon, Mich.
[4] Reagent grade, Fisher Scientific Co., Rochester, N.Y.
[5] Diuril tablets, Merck Sharp and Dohme.
[6] Econo-Rx tablets (Bolar). These tablets were from the same lot as those used in the human chlorothiazide bioavailability study performed by Straughn *et al.* (9) and were supplied by these investigators.



*0022-3549/81/0200-0224$01.00/0*
*© 1981, American Pharmaceutical Association*

**Table II—Mean Urinary Excretion of Chlorothiazide in Dogs as a Function of Time after Administration of a 500-mg Oral Dose as Two Different 500-mg Chlorothiazide Tablets**

| Hours | Mean Cumulative Percentage of Dose Excreted ($n = 6$) ± $SD$ | |
|---|---|---|
| | Tablet A-1[a] | Tablet C[b] |
| 0 | 0 | 0 |
| 12 | 8.06 ± 4.1 | 9.88 ± 5.2 |
| 24 | 10.2 ± 4.4 | 11.9 ± 7.3 |
| 48 | 15.3 ± 4.8 | 18.8 ± 8.9 |
| 72 | 15.7 ± 5.1 | 21.8 ± 11.4 |
| 96 | 15.7 ± 5.1 | 21.9 ± 11.7 |

[a] Tablet A-1 represents one 500-mg tablet (Merck Sharp and Dohme) (Trial 1). [b] Tablet C represents one 500-mg tablet (Econo-Rx).

**Table III—Mean Urinary Excretion of Chlorothiazide in Dogs as a Function of Time after Administration of a 500-mg Oral Dose as an Aqueous Solution, One 500-mg Tablet, and Two 250-mg Tablets**

| Hours | Mean Cumulative Percentage of Dose Excreted ($n = 6$) ± $SD$ | | |
|---|---|---|---|
| | Aqueous Solution[a] | Tablet A-2[b] | Tablet B[c] |
| 0 | 0 | 0 | 0 |
| 12 | 9.30 ± 4.4 | 10.3 ± 4.8 | 4.63 ± 4.3 |
| 24 | 11.7 ± 2.4 | 12.3 ± 5.8 | 9.29 ± 5.4 |
| 48 | 16.5 ± 4.6 | 19.4 ± 7.2 | 16.5 ± 7.8 |
| 72 | 21.3 ± 7.5 | 20.1 ± 7.1 | 18.4 ± 7.7 |
| 96 | 22.0 ± 8.0 | 20.7 ± 6.9 | 18.5 ± 7.8 |

[a] Sodium salt. [b] Tablet A-2 represents one 500-mg tablet (Merck Sharp and Dohme) (Trial 2). [c] Tablet B represents two 250-mg tablets (Merck Sharp and Dohme).

assay results) excreted unchanged in the urine at each sampling time after oral administration of the four test dosage forms is shown in Tables II and III. Under all study conditions, plateau excretion values were reached within 48–72 hr, indicating that the experimental period selected was more than adequate to assess the excretion and, thereby, the absorption characteristics of chlorothiazide. As reflected by the high standard deviation associated with each mean excretion value, the urinary excretion rate of chlorothiazide from each dosage form tested showed considerable interindividual variation. This finding is consistent with that observed after oral administration of various brands of chlorothiazide tablets to humans (6, 8, 9).

Thiazide diuretics undergo hydrolysis *in vivo* to 6-amino-4-chlorobenzene-1,3-disulfonamide (I), which is absorbed and excreted in the urine of humans and possesses diuretic activity (18). Although the extent of hydrolysis in humans is greatest for the more potent thiazide diuretics (*e.g.*, cyclothiazide and methyclothiazide) (18), it was important to determine whether I and chlorothiazide were coexcreted in the urine of dogs. HPLC analyses[7] revealed that I was not present in any urine specimen.

Similar to the situation found in humans (6, 8, 9), the extent of chlorothiazide bioavailability in dogs was quite low and variable, regardless of the dosage form and dosage form formulation used (Tables IV and V). Although no statistically significant difference in bioavailability existed between the originator 500-mg tablet (Tablet A-1) and the generic 500-mg tablet (Tablet C), Tablet C appeared to be absorbed more erratically (Table IV). In contrast, Tablets A-1 and C have been reported to be bioinequivalent in humans (9). This apparent species difference may be due to the fact that the human urinary excretion studies were terminated in 24 hr (9), even though chlorothiazide excretion reportedly continues for at least 48 hr in humans (12). It also is possible that the bioavailability estimates for Tablets A-1 and C in humans (9) are in error due to variable interferences from urinary constituents in the modified Bratton–Marshall colorimetric method employed by these investigators (10, 12, 19).

A comparison of the 96-hr urinary recovery values for each dog after administration of Tablet A on two separate occasions (Tablets A-1 and A-2) reveals that the absorption of chlorothiazide also is subject to some intraindividual variation (Tables IV and V). The lack of a significant difference in the mean cumulative 96-hr urinary recovery among the

[7] Under the chromatographic conditions employed (4, 10), the retention times for I, sulfadiazine, and chlorothiazide were 5.25, 5.61, and 6.97 min, respectively.

**Table IV—Extent of Chlorothiazide Bioavailability in Dogs after Administration of a 500-mg Oral Dose as Two Different 500-mg Chlorothiazide Tablets**

| Dog | Cumulative 96-hr Urinary Excretion of Chlorothiazide, mg | |
|---|---|---|
| | Tablet A-1[a] | Tablet C[b] |
| 1 | 61.1 | 43.7 |
| 4 | 125.2 | 169.3 |
| 5 | 107.0 | 122.2 |
| 8 | 51.1 | 83.4 |
| 9 | 59.3 | 33.5 |
| 10 | 68.1 | 205.7 |
| Mean | 78.6 | 109.6 |
| *SD* | 25.4 | 58.3 |
| *CV*, % | 32 | 53 |
| Paired *t* test | NS[c] ($p > 0.05$) | |

[a] Tablet A-1 represents one 500-mg tablet (Merck Sharp and Dohme) (Trial 1). [b] Tablet C represents one 500-mg tablet (Econo-Rx). [c] Not significant.

**Table V—Extent of Chlorothiazide Bioavailability in Dogs after Administration of a 500-mg Oral Dose as an Aqueous Solution, One 500-mg Tablet, and Two 250-mg Tablets**

| Dog | Cumulative 96-hr Urinary Excretion of Chlorothiazide, mg | | |
|---|---|---|---|
| | Aqueous Solution[a] | Tablet A-2[b] | Tablet B[c] |
| 1 | 76.7 | 95.1 | 43.6 |
| 4 | 122.8 | 155.2 | 108.4 |
| 5 | 150.5 | 103.6 | 113.8 |
| 8 | 97.2 | 93.3 | 72.1 |
| 9 | 40.1 | 36.2 | 49.9 |
| 10 | 169.7 | 136.2 | 165.8 |
| Mean | 109.5 | 103.3 | 92.3 |
| *SD* | 40.6 | 34.7 | 39.1 |
| *CV*, % | 37 | 34 | 42 |

Statistical significance: difference among three oral treatments (analysis of variance for crossover design)
NS[d], $p > 0.05$ ($F = 2.96$; $df = 2,8$)[e]

[a] Sodium salt. [b] Tablet A-2 represents one 500-mg tablet (Merck Sharp and Dohme) (Trial 2). [c] Tablet B represents two 250-mg tablets (Merck Sharp and Dohme). [d] Not significant. [e] Critical $F$ value for two and eight degrees of freedom at the 5% level is 4.46.

aqueous solution and the originator 250- and 500-mg tablets (Tablets B and A-2) indicates that chlorothiazide absorption is affected minimally by the nature of the dosage form administered, provided that the dosage form is well formulated.

The results of this study show that at an oral dose comparable to that used in the treatment of edematous conditions in dogs, the absorption of chlorothiazide is variable and incomplete, regardless of whether the drug is administered as an aqueous solution or tablet dosage form. Since the maximum solubility of chlorothiazide at pH 1.0 and 6.2 is 417 and 655 mg/liter, respectively (4), poor drug absorption may have resulted from slow dissolution[8] of the drug due to the high oral dose (500 mg) to solubility ratio employed or from the existence of an active or other capacity-limited intestinal transport process for chlorothiazide (4).

## REFERENCES


(1) E. A. Swinyard, in "Remington's Pharmaceutical Sciences," Mack Publishing Co., Easton, Pa., 1975, p. 896.

(2) J. E. Baer, H. L. Leedy, A. V. Brooks, and K. H. Beyer, *J. Pharmacol. Exp. Ther.*, **125**, 295 (1959).

(3) K. H. Beyer, *Ann. N.Y. Acad. Sci.*, **71**, 363 (1958).

(4) D. E. Resetarits and T. R. Bates, *J. Pharmacokinet. Biopharm.*, **7**, 463 (1979).

(5) H. R. Brettell, J. K. Aikawa, and G. S. Gordon, *Arch. Intern. Med.*, **106**, 57 (1960).

(6) M. C. Meyer and A. B. Straughn, *Curr. Ther. Res.*, **22**, 573 (1977).


[8] Upon contacting the acidic gastric fluids, chlorothiazide probably precipitates from the aqueous solution of the sodium salt. Thus, a dissolution step precedes the absorption of chlorothiazide from the solution dosage form.

(7) E. T. Lin and L. Z. Benet, "Abstracts," APhA Academy of Pharmaceutical Sciences, vol. 8(1), 1978, p. 194.
(8) R. E. Kauffman and D. L. Azarnoff, *Clin. Pharmacol. Ther.*, **14**, 886 (1973).
(9) A. B. Straughn, A. P. Melikian, and M. C. Meyer, *J. Pharm. Sci.*, **68**, 1099 (1979).
(10) D. E. Resetarits and T. R. Bates, *ibid.*, **68**, 126 (1979).
(11) G. W. Snedecor and W. G. Cochran, "Statistical Methods," 6th ed., Iowa State University Press, Ames, Iowa, 1967, pp. 91–119.
(12) V. P. Shah, P. Sojka, V. K. Prasad, and B. E. Cabana, *Curr. Ther. Res.*, **24**, 366 (1978).
(13) B. Beermann, M. Groschinsky-Grind, and A. Rosen, *Clin. Pharmacol. Ther.*, **19**, 531 (1976).
(14) B. Beermann and M. Groschinsky-Grind, *Eur. J. Clin. Pharmacol.*, **12**, 297 (1977).
(15) B. Beermann, M. Groschinsky-Grind, and B. Lindstrom, *ibid.*, **11**, 203 (1977).
(16) B. Beermann and M. Groschinsky-Grind, *ibid.*, **13**, 385 (1978).
(17) *Ibid.*, **13**, 125 (1978).
(18) H. W. Murphy, *J. Pharm. Sci.*, **68**(7), iv (1979).
(19) J. P. Hunt, V. P. Shah, V. K. Prasad, and B. E. Cabana, "Abstracts," APhA Academy of Pharmaceutical Sciences, vol. 8(1), 1978, p. 195.

**ACKNOWLEDGMENTS**

Presented in part at the Basic Pharmaceutics Section, APhA Academy of Pharmaceutical Sciences, Washington meeting, April 1980.

Supported in part by Grant GM 20852 from the National Institutes of Health, Bethesda, Md.

# Evidence for Metabolic Inertness of Doxycycline

**H. J. C. F. NELIS and A. P. De LEENHEER ˣ**

Received January 16, 1980, from the *Laboratoria voor Medische Biochemie en voor Klinische Analyse, R.U.G., De Pintelaan 135, B-9000 Gent, Belgium.* Accepted for publication July 17, 1980.

**Abstract** □ Several conflicting observations in the literature raised considerable doubt about the metabolic fate of doxycycline, which, like other tetracyclines, has been claimed to be metabolically inert. A double liquid chromatographic approach was used in an attempt to demonstrate the polar metabolites and/or conjugates in excreta of human volunteers who ingested the drug. Both ion-exchange and reversed-phase chromatography failed to reveal significant by-products in urine and feces, except for minor amounts of 4-epidoxycycline. In addition, enzymatic hydrolysis procedures did not present any evidence of the conjugates. Thus, the different excretion behavior of doxycycline, compared to other analogs, cannot be explained in terms of increased metabolism.

**Keyphrases** □ Doxycycline—tetracycline analog, metabolic fate, analysis, human urine and feces □ Liquid chromatography—analysis, doxycycline in human urine and feces □ Antibacterials—doxycycline, metabolic fate, analysis in human urine and feces

It is generally accepted that tetracycline antibiotics are not metabolized in the human body (1–4). However, considerable doubt still exists concerning the fate of the more lipophilic derivatives (5, 6). A study with $^3$H-labeled doxycycline failed to reveal by-products in excreta, but a rather poor chromatographic technique had been used (7).

Some investigators noted a dramatic decrease in the half-life of the drug following coadministration of typical enzyme-inducing substances, including barbiturates (8), antiepileptics (9, 10), and ethanol (11). This observation was explained in terms of accelerated doxycycline metabolism and led to speculation concerning the formation of conjugates (10). However, other investigators did not support these views and questioned the reliability of the effect (12). Furthermore, an unidentified, biologically inactive fraction is claimed to occur in feces (13–15) and might be due to intestinally formed metabolites.

The lack of suitable chromatographic techniques has hampered the unambiguous settling of these controversial observations. This paper reports the use of liquid chromatography for detecting possible doxycycline by-products in human urine and feces. In addition, enzymatic hydrolysis was carried out in order not to overlook conjugates. Although a similar approach allowed demonstration of minocycline metabolites in urine (16), strong evidence is presented here for the metabolic inertness of doxycycline.

## EXPERIMENTAL

**Chromatography**—Two liquid chromatographs[1], equipped with a sample valve[2] and a variable-wavelength detector[3] operated at 350 nm, were used. The first column (10 × 0.46 cm) consisted of a strong cation-exchange material[4] and was utilized with a 38:62 (v/v) mixture of ethanol–0.1 *M* citrate buffer (pH 4.6) containing 0.05% edetate disodium as the eluent. A reversed-phase system, previously reported for the quantitative determination of doxycycline in human serum and urine (17), was applied to feces samples as well.

**Collection of Excreta**—A single 200-mg doxycycline dose was administered orally to human volunteers just after a light breakfast. Urine was collected over the following 24 hr. Three days after administration, feces samples were taken. Blank samples were obtained before drug intake.

**Extraction of Urine and Feces**—Urine samples were extracted with ethyl acetate as described previously (17).

Feces (0.8 g) were homogenized in 0.2 *M* HCl (12 ml) using a high-speed mixer[5]. After centrifugation, a 1-ml aliquot of the supernate was neutralized with 1 *M* NaOH and buffered with 1 ml of phosphate–sulfite buffer (pH 6) (17). Extraction was performed with 10 ml of ethyl acetate. The organic layer was evaporated to dryness[6], and the residue was redissolved in 1 ml of the chromatographic solvent of either the reversed-phase or the ion-exchange system. Finally, 20–100 μl was injected onto the columns. Alternatively, feces were homogenized in 0.2 *M* acetate buffer (pH 5) and processed in a similar way.

**Hydrolysis Procedures**—Urine samples and feces homogenates were adjusted to pH 5 using acetic acid and 2 *M* NaOH, respectively. Then, they were incubated at 37° with the arylsulfatase–glucuronidase enzyme

[1] Model 8500, Varian Associates, Palo Alto, Calif.
[2] Model CV-6-UHPa-N60, Valco Instruments Co., Houston, Tex.
[3] Varichrom, Varian Associates, Palo Alto, Calif.
[4] Nucleosil SA, 5 μm, Machery & Nagel, Düren, West Germany.
[5] Virtis S 23, Virtis Research Equipment, Gardiner, N.Y.
[6] Rotary Evapo Mix, Büchler Instruments, Fort Lee, N.J.



0022-3549/81/0200-0226$01.00/0
© 1981, American Pharmaceutical Association

(7) E. T. Lin and L. Z. Benet, "Abstracts," APhA Academy of Pharmaceutical Sciences, vol. 8(1), 1978, p. 194.
(8) R. E. Kauffman and D. L. Azarnoff, *Clin. Pharmacol. Ther.*, **14**, 886 (1973).
(9) A. B. Straughn, A. P. Melikian, and M. C. Meyer, *J. Pharm. Sci.*, **68**, 1099 (1979).
(10) D. E. Resetarits and T. R. Bates, *ibid.*, **68**, 126 (1979).
(11) G. W. Snedecor and W. G. Cochran, "Statistical Methods," 6th ed., Iowa State University Press, Ames, Iowa, 1967, pp. 91–119.
(12) V. P. Shah, P. Sojka, V. K. Prasad, and B. E. Cabana, *Curr. Ther. Res.*, **24**, 366 (1978).
(13) B. Beermann, M. Groschinsky-Grind, and A. Rosen, *Clin. Pharmacol. Ther.*, **19**, 531 (1976).
(14) B. Beermann and M. Groschinsky-Grind, *Eur. J. Clin. Pharmacol.*, **12**, 297 (1977).
(15) B. Beermann, M. Groschinsky-Grind, and B. Lindstrom, *ibid.*, **11**, 203 (1977).
(16) B. Beermann and M. Groschinsky-Grind, *ibid.*, **13**, 385 (1978).
(17) *Ibid.*, **13**, 125 (1978).
(18) H. W. Murphy, *J. Pharm. Sci.*, **68**(7), iv (1979).
(19) J. P. Hunt, V. P. Shah, V. K. Prasad, and B. E. Cabana, "Abstracts," APhA Academy of Pharmaceutical Sciences, vol. 8(1), 1978, p. 195.

**ACKNOWLEDGMENTS**

Presented in part at the Basic Pharmaceutics Section, APhA Academy of Pharmaceutical Sciences, Washington meeting, April 1980.

Supported in part by Grant GM 20852 from the National Institutes of Health, Bethesda, Md.

# Evidence for Metabolic Inertness of Doxycycline

**H. J. C. F. NELIS and A. P. De LEENHEER ˣ**

Received January 16, 1980, from the *Laboratoria voor Medische Biochemie en voor Klinische Analyse, R.U.G., De Pintelaan 135, B-9000 Gent, Belgium.* Accepted for publication July 17, 1980.

**Abstract** □ Several conflicting observations in the literature raised considerable doubt about the metabolic fate of doxycycline, which, like other tetracyclines, has been claimed to be metabolically inert. A double liquid chromatographic approach was used in an attempt to demonstrate the polar metabolites and/or conjugates in excreta of human volunteers who ingested the drug. Both ion-exchange and reversed-phase chromatography failed to reveal significant by-products in urine and feces, except for minor amounts of 4-epidoxycycline. In addition, enzymatic hydrolysis procedures did not present any evidence of the conjugates. Thus, the different excretion behavior of doxycycline, compared to other analogs, cannot be explained in terms of increased metabolism.

**Keyphrases** □ Doxycycline—tetracycline analog, metabolic fate, analysis, human urine and feces □ Liquid chromatography—analysis, doxycycline in human urine and feces □ Antibacterials—doxycycline, metabolic fate, analysis in human urine and feces

It is generally accepted that tetracycline antibiotics are not metabolized in the human body (1–4). However, considerable doubt still exists concerning the fate of the more lipophilic derivatives (5, 6). A study with $^3$H-labeled doxycycline failed to reveal by-products in excreta, but a rather poor chromatographic technique had been used (7).

Some investigators noted a dramatic decrease in the half-life of the drug following coadministration of typical enzyme-inducing substances, including barbiturates (8), antiepileptics (9, 10), and ethanol (11). This observation was explained in terms of accelerated doxycycline metabolism and led to speculation concerning the formation of conjugates (10). However, other investigators did not support these views and questioned the reliability of the effect (12). Furthermore, an unidentified, biologically inactive fraction is claimed to occur in feces (13–15) and might be due to intestinally formed metabolites.

The lack of suitable chromatographic techniques has hampered the unambiguous settling of these controversial observations. This paper reports the use of liquid chromatography for detecting possible doxycycline by-products in human urine and feces. In addition, enzymatic hydrolysis was carried out in order not to overlook conjugates. Although a similar approach allowed demonstration of minocycline metabolites in urine (16), strong evidence is presented here for the metabolic inertness of doxycycline.

## EXPERIMENTAL

**Chromatography**—Two liquid chromatographs[1], equipped with a sample valve[2] and a variable-wavelength detector[3] operated at 350 nm, were used. The first column (10 × 0.46 cm) consisted of a strong cation-exchange material[4] and was utilized with a 38:62 (v/v) mixture of ethanol–0.1 *M* citrate buffer (pH 4.6) containing 0.05% edetate disodium as the eluent. A reversed-phase system, previously reported for the quantitative determination of doxycycline in human serum and urine (17), was applied to feces samples as well.

**Collection of Excreta**—A single 200-mg doxycycline dose was administered orally to human volunteers just after a light breakfast. Urine was collected over the following 24 hr. Three days after administration, feces samples were taken. Blank samples were obtained before drug intake.

**Extraction of Urine and Feces**—Urine samples were extracted with ethyl acetate as described previously (17).

Feces (0.8 g) were homogenized in 0.2 *M* HCl (12 ml) using a high-speed mixer[5]. After centrifugation, a 1-ml aliquot of the supernate was neutralized with 1 *M* NaOH and buffered with 1 ml of phosphate–sulfite buffer (pH 6) (17). Extraction was performed with 10 ml of ethyl acetate. The organic layer was evaporated to dryness[6], and the residue was redissolved in 1 ml of the chromatographic solvent of either the reversed-phase or the ion-exchange system. Finally, 20–100 μl was injected onto the columns. Alternatively, feces were homogenized in 0.2 *M* acetate buffer (pH 5) and processed in a similar way.

**Hydrolysis Procedures**—Urine samples and feces homogenates were adjusted to pH 5 using acetic acid and 2 *M* NaOH, respectively. Then, they were incubated at 37° with the arylsulfatase–glucuronidase enzyme

[1] Model 8500, Varian Associates, Palo Alto, Calif.
[2] Model CV-6-UHPa-N60, Valco Instruments Co., Houston, Tex.
[3] Varichrom, Varian Associates, Palo Alto, Calif.
[4] Nucleosil SA, 5 μm, Machery & Nagel, Düren, West Germany.
[5] Virtis S 23, Virtis Research Equipment, Gardiner, N.Y.
[6] Rotary Evapo Mix, Büchler Instruments, Fort Lee, N.J.



0022-3549/81/0200-0226$01.00/0
© 1981, American Pharmaceutical Association

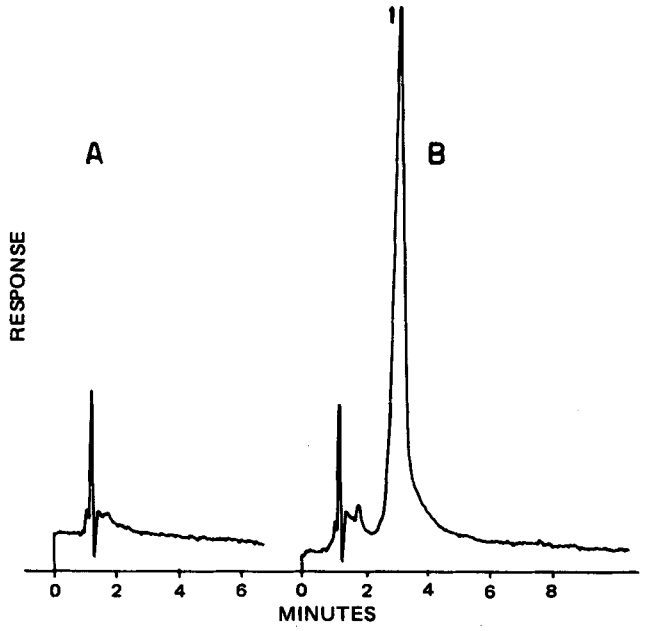


**Figure 1**—*Chromatograms of a blank urine extract (A) and a urine extract obtained after doxycycline administration (B). Peak 1 is doxycycline. A 10 × 0.46-cm Nucleosil SA (5 μm) column was used, and the mobile phase was ethanol–0.1 M citrate buffer (pH 4.6) with 0.05% edetate disodium (38:62 v/v) at a flow rate of 1 ml/min.*

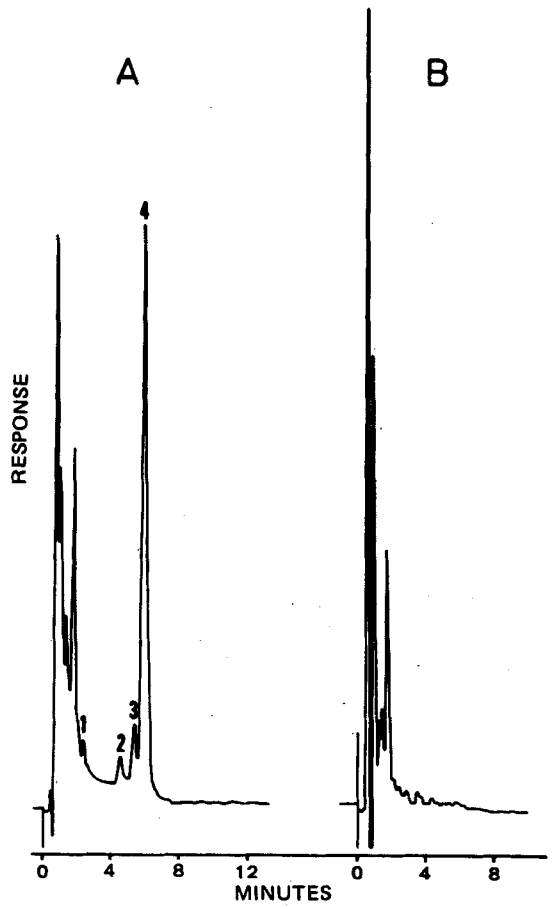


**Figure 2**—*Chromatograms of urine obtained from a volunteer who ingested 200 mg of doxycycline (A) and a blank urine chromatogram (B). Key: 1, unidentified doxycycline by-product; 2, unidentified peak; 3, 4-epidoxycycline; and 4, doxycycline. A 10 × 0.2-cm Lichrosorb RP8 (5 μm) column was used, and the mobile phase was acetonitrile–0.1 M citric acid (24:76 v/v) at a flow rate of 0.5 ml/min.*

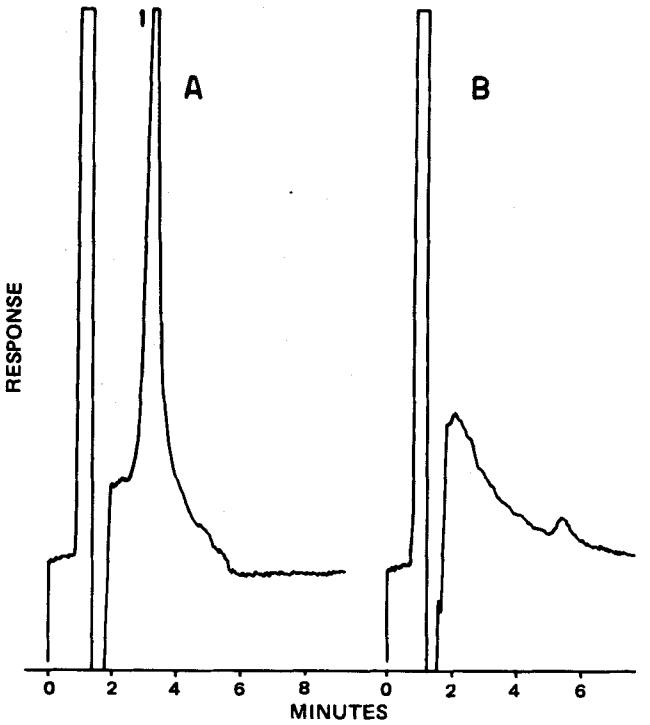


**Figure 3**—*Chromatograms of a feces extract obtained after doxycycline administration (A) and of a blank feces extract (B). Peak 1 is doxycycline. Conditions were the same as in Fig. 1.*

complex from *Helix pomatia*[7] (200 μl of the enzyme solution/ml) for 48 hr. Reference samples containing no enzyme were kept simultaneously under the same conditions. Feces samples homogenized in the acetate buffer were incubated without pretreatment.

## RESULTS

**Urine**—Injection of urine extracts onto the ion-exchange column yielded one large doxycycline peak (Fig. 1). The chromatographic pattern in the reversed-phase system (Fig. 2) was more composite but also did not show significant additional peaks. The retention time of the principal accompanying peak (peak 3) corresponded to that of 4-epidoxycycline. Unfortunately, its spectrometric characteristics were difficult to determine because of a coeluting compound. For an unknown reason, the epimer eluted as an extremely distorted peak from the ion-exchange column. This could explain its absence in urine chromatograms obtained on this particular column. Direct injection of undiluted urine did not reveal additional doxycycline-related peaks in the chromatograms, nor did detection at other wavelengths (270 and 430 nm).

After incubation with hydrolyzing enzymes, no increase of the doxycycline peak was observed when compared to reference samples.

**Feces**—A chromatogram of a feces extract obtained on the ion-exchange column showed a single doxycycline peak (Fig. 3). Reversed-phase chromatograms (Fig. 4) again illustrated the absence of major additional peaks. A peak corresponding to 4-epidoxycycline was barely detectable (peak 2). Peak 1 probably was an artifact since it has been observed in serum, urine, and fresh standard solutions as well (17). Results were confirmed by direct injection of the homogenates without extraction.

## DISCUSSION

Application of two liquid chromatographic techniques in combination with hydrolysis procedures strongly suggests the absence of polar doxycycline metabolites and conjugates in urine. Components that are more polar than doxycycline normally will elute before doxycycline from a reversed-phase column. A minor extra peak probably is attributable to

[7] Solution in water (Boehringer, Mannheim, West Germany); glucuronidase activity was 5.2 units/ml (38°, phenolphthalein monoglucuronide as the substrate); arylsulfatase activity was 2.6 units/ml (38°, phenolphthalein disulfate as the substrate).

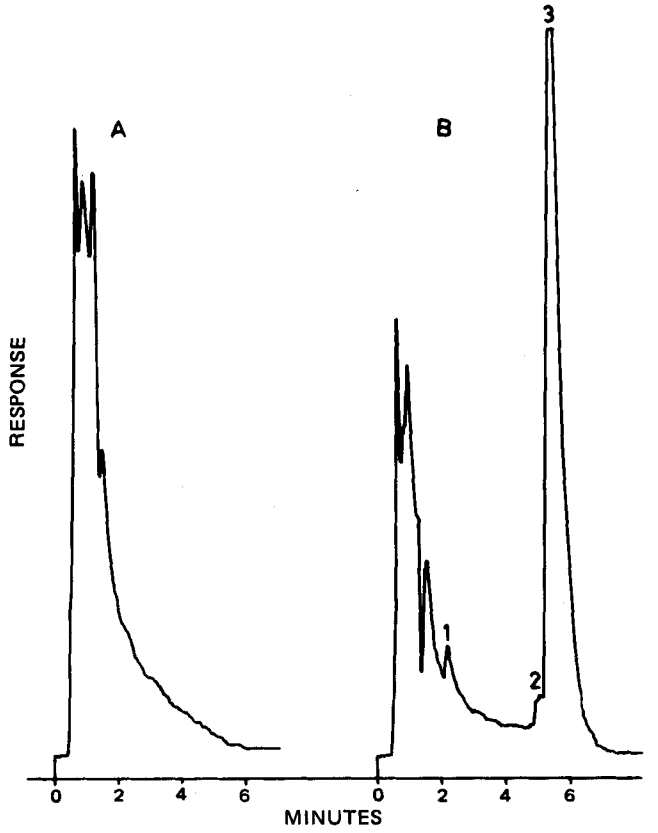


**Figure 4**—*Chromatograms of a blank feces extract (A) and a feces extract obtained after doxycycline administration (B). Key: 1, unidentified doxycycline by-product; 2, 4-epidoxycycline; and 3, doxycycline. Conditions were the same as in Fig. 2.*

4-epidoxycycline. Its presence is not unlikely because a weakly acidic medium is known to catalyze epimerization (18).

Thus, the lower urinary doxycycline levels, compared to those of the classical tetracyclines, are not due to the presence of biologically inactive metabolites but rather are caused by increased tubular reabsorption (19), which is in agreement with the stronger lipophilic character of the drug.

Doxycycline is claimed to be excreted in the feces by direct diffusion through the intestinal wall (13, 14); biliary excretion seems to be of minor importance (12). Because no extra peaks were detected, the exact nature of the biologically inactive fecal fraction, if present, cannot be elucidated easily using chromatographic techniques. The observation of the present investigators indirectly supports the currently accepted theory of the chelate formation between doxycycline and divalent cations leading to partial biological deactivation (20). Homogenization of feces in hydrochloric acid releases doxycycline from the complex. The need for a relatively strong acid to recover all fecal doxycycline is documented (13). The quasi-absence of the epimeric form can be rationalized in terms of the less favorable pH medium in the intestine. The possibility of hydrolysis of labile conjugates in the strong acid prior to enzymatic attack was not considered because homogenization in the less aggressive acetate buffer yielded the same results.

Because the existence of metabolites was not indicated, the interaction between doxycycline and certain drugs cannot be explained in terms of enzyme induction. On the other hand, displacement of the drug from plasma proteins might be the mechanism involved. Although doxycycline, unlike other analogs, is excreted *via* an alternative intestinal pathway, metabolism is not a supplementary factor distinguishing the drug from the classical tetracyclines.

## REFERENCES

(1) R. G. Kelly and D. A. Buyske, *J. Pharmacol. Exp. Ther.*, **130**, 144 (1960).

(2) R. G. Kelly, L. A. Kanegis, and D. A. Buyske, *ibid.*, **134**, 320 (1961).

(3) H. J. Eisner and R. J. Wulf, *ibid.*, **142**, 122 (1963).

(4) H. Swarz, *Méd. Chir. Dig.*, **5**, 323 (1976).

(5) H. Macdonald, R. G. Kelly, E. S. Allen, J. F. Noble, and L. A. Kanegis, *Clin. Pharmacol. Ther.*, **14**, 852 (1973).

(6) J. R. Brown and D. S. Ireland, "Advances in Pharmacology and Chemotherapy," vol. 15, Academic, New York, N.Y., 1978, pp. 186–189.

(7) F. Ritzl, M. Schoog, A. Höck, and F. E. Feinendegen, *Proc. Int. Congr. Chemother. 7th*, **1**, 35 (1972).

(8) P. J. Neuvonen and O. Penttilä, *Br. Med. J.*, **1**, 535 (1974).

(9) O. Penttilä, P. J. Neuvonen, K. Aho, and R. Lehtovaara, *ibid.*, **2**, 470 (1974).

(10) P. J. Neuvonen, O. Penttilä, R. Lehtovaara, and K. Aho, *Eur. J. Clin. Pharmacol.*, **9**, 147 (1975).

(11) P. J. Neuvonen, O. Penttilä, M. Roos, and J. Tirkkonen, *Int. J. Clin. Pharmacol.*, **14**, 303 (1976).

(12) K. Alestig, *Scand. J. Infec. Dis.*, **6**, 265 (1974).

(13) M. Schach von Wittenau and T. M. Twomey, *Chemotherapy*, **16**, 217 (1971).

(14) W. A. Mahon, G. E. Johnson, M. F. Kelly, and S. S. A. Fenton, *Rev. Can. Biol.*, **32**, 107 (1973).

(15) J. Fabre, P. Kalfopoulos, and M. Rudhardt, *Proc. Int. Congr. Chemother. 7th*, **1**, 29 (1972).

(16) A. P. De Leenheer and H. J. C. F. Nelis, *J. Pharm. Sci.*, **68**, 1527 (1979).

(17) *Ibid.*, **68**, 999 (1979).

(18) J. R. D. McCormick, S. M. Fox, L. S. Smith, B. A. Bitler, J. Reichenthal, V. E. Origoni, W. H. Muller, R. Winterbottom, and A. P. Doerschuk, *J. Am. Chem. Soc.*, **79**, 2849 (1957).

(19) J. M. Jaffe, J. L. Colaizzi, R. I. Poust, and R. H. McDonald, *J. Pharmacokinet. Biopharm.*, **1**, 267 (1973).

(20) M. Schach von Wittenau, *Opusc. Med.*, **33**, 5 (1974).

## ACKNOWLEDGMENTS

Supported by the National Research Foundation.

Doxycycline and 4-epidoxycycline were provided by Dr. Gordts, Medical Department, Pfizer, Inc., Brussels, Belgium.

# GLC Assay for Lidocaine in Human Plasma

**F. E. KARCH ˣ and K. F. CHMIELEWSKI**

Received June 4, 1980, from the *School of Medicine and Dentistry, University of Rochester, Rochester, NY 14642.* Accepted for publication August 27, 1980.

**Abstract** □ A simple, rapid, and highly sensitive method for the GLC analysis of plasma lidocaine is described. Mepivacaine hydrochloride is added as the internal standard; the plasma is deproteinated and centrifuged, and the supernate is alkalinized and extracted into a small volume of carbon disulfide. The column is connected to a flame-ionization detector, and the column oven temperature is programmed from 130 to 260°. Plasma lidocaine concentrations between 0.04 and 8.0 μg/ml can be measured accurately, and there is no interference from the monoethylglycinexylidide or glycinexylidide metabolites of lidocaine or from many commonly used drugs and diagnostic agents. The sensitivity, simplicity, and speed of this assay are important in pharmacokinetic studies of lidocaine.

**Keyphrases** □ Lidocaine—GLC assay in human plasma □ GLC—analysis, lidocaine in human plasma □ Anesthetics, local—lidocaine, GLC assay in human plasma

Several methods for measuring plasma lidocaine have been described, but many have limited usefulness in pharmacokinetic studies. Some require lengthy extractions (1–5), which reduce the number of samples that can be analyzed in a day. Other methods lack the sensitivity needed for measuring low concentrations of lidocaine (6–8), and one method requires a benzene extraction step with the attendant hazards of benzene exposure (9). Kline and Martin (10) reported a GLC lidocaine assay that avoided complex extractions and provided reasonable sensitivity. However, the method had not been evaluated systematically for interference from other commonly used drugs, and the sensitivity was not adequate for the present study.

This paper reports efforts to improve the assay sensitivity of the Kline and Martin method and to evaluate the method for interference from commonly used medications.

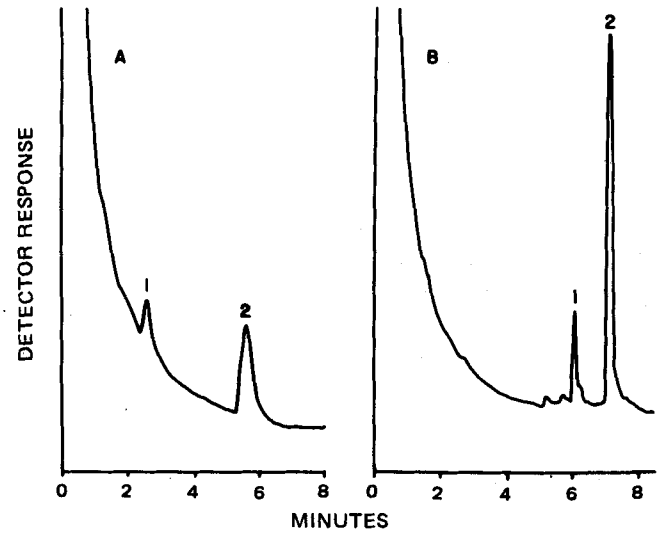


**Figure 1**—*GLC plasma lidocaine determination using 4 μl of carbon disulfide-extracted plasma containing 325 ng of lidocaine/ml (1) and mepivacaine (2) as the internal standard. Determinations were from the same sample. Key: A, chromatogram using the isothermal method described by Kline and Martin (10); and B, chromatogram using a programmed oven temperature operation from 130 to 260°.*

## EXPERIMENTAL

**Reagents**—Lidocaine hydrochloride monohydrate[1], mepivacaine hydrochloride[2], analytical reagent grade trichloroacetic acid[3], carbon disulfide[3], and sodium hydroxide[3] were used as provided. Lidocaine concentrations are expressed as the free base.

**Apparatus**—A gas chromatograph[4] equipped with oven temperature programming capability and a flame-ionization detector was fitted with a 1.8-m × 2-mm i.d. glass column, packed with 3% OV-17 on 100–120-mesh Gas Chrom Q. The operating temperatures were 200 and 280° for the injector and detector, respectively. The column oven temperature was programmed for an initial 1-min hold at 130°, and then the oven temperature was raised 24°/min to 260° and held for 4 min. The carrier gas (nitrogen) and hydrogen flow rates were 45 and 30 ml/min, respectively. A 2-mv recorder[5] was used.

**Procedure**—To a 12-ml glass centrifuge tube were added 1 ml of plasma, 2 ml of mepivacaine hydrochloride (1 μg/ml in water) as the internal standard, and 1 ml of 1.8 *N* trichloroacetic acid; the solution then was mixed gently on a vortex mixer for 10 sec. After the tube was centrifuged at 2200 rpm for 10 min, the supernate was removed and centrifuged for 10 min.

The final supernate was transferred to a clear 13-ml glass-stoppered centrifuge tube, and 1 ml of 5 *N* NaOH and 100 μl of carbon disulfide were added. After vigorous vortexing for 45 sec, the tube was centrifuged for 10 min; then 4 μl of the carbon disulfide layer was injected onto the GLC column.

**Interference Study**—To test for interference from lidocaine metabolites or commonly used drugs, plasma samples were spiked with one of the following: monoethylglycinexylidide[1] (1 or 5 μg/ml), glycinexylidide[1] (1 or 5 μg/ml), acetaminophen (20 μg/ml), aminophylline (100 μg/ml), aspirin (100 or 200 μg/ml), atropine (0.2 μg/ml), bretylium tosylate (70 μg/ml), chlordiazepoxide (3 μg/ml), cimetidine (5 μg/ml), diazepam (2.5 μg/ml), diazoxide (60 μg/ml), digoxin (2 ng/ml), dobutamine (0.2 or 0.5 μg/ml), dopamine (0.7 μg/ml), ethacrynic acid (20 μg/ml), furosemide (20 μg/ml), heparin (2 units/ml), hydralazine (1 μg/ml), hydrocortisone (200 μg/ml), indocyanine green (10 or 20 μg/ml), isoproterenol (10 ng/ml), meperidine (1 μg/ml), methadone (1 μg/ml), methyldopa (50 μg/ml), methylprednisolone (10 μg/ml), morphine (0.1 μg/ml), nitroglycerin (0.1 μg/ml), nitroprusside (0.2 μg/ml), norepinephrine (10 ng/ml), ouabain (1 ng/ml), pentazocine (0.2 μg/ml), pentobarbital (20 μg/ml), phenytoin (20 μg/ml), physostigmine (0.4 μg/ml), procainamide (6 μg/ml), prochlorperazine (1 μg/ml), propranolol (0.2 or 1.0 μg/ml), quinidine (3.75 or 8.0 μg/ml), trimethaphan (1 μg/ml), or warfarin (10 μg/ml).

## RESULTS AND DISCUSSION

**Comparison with Published Method**—Kline and Martin (10) described a simple, rapid GLC assay for plasma lidocaine that was quite satisfactory for measuring usual therapeutic lidocaine levels. One problem, however, is that the lidocaine peak comes off the column during the rapid decline phase of the solvent front (Fig. 1A). Sensitivity with the Kline–Martin technique is limited to ~250 ng of lidocaine/ml of plasma. To improve sensitivity while retaining the simplicity of the extraction, oven temperature programming was employed. This modification clearly separates the lidocaine and internal standard peaks from the solvent front and improves peak resolution and peak height (Fig. 1). With the oven

[1] Gift from Astra Research Laboratory, Framingham, Mass.
[2] Gift from Sterling-Winthrop Research Institute, Rensselaer, N.Y.
[3] Scientific Products, Rochester, N.Y.
[4] Model 900, Perkin-Elmer Corp., Norwalk, Conn.
[5] Speedomax X/L 680, Leeds & Northrup Co., North Wales, Pa.

0022-3549/81/0200-0229$01.00/0
© 1981, American Pharmaceutical Association

**Table I—Lidocaine GLC Assay Precision with Column Oven Temperature Programming**

| Actual Plasma Lidocaine Concentration, μg/ml | Measured Lidocaine Concentration, μg/ml |
|---|---|
| 4.00 | 4.01 ± 0.13 (21)[a] |
| 1.62 | 1.61 ± 0.04 (15) |
| 0.16 | 0.17 ± 0.01 (15) |
| 0.08 | 0.08 ± 0.01 (18) |
| 0.04 | 0.04 ± 0.002 (14) |

[a] Mean ± *SE* (*n*).

temperature programming modification, plasma lidocaine concentrations as low as 30 ng/ml can be measured. The retention times for lidocaine and mepivacaine (internal standard) are 6.0 and 7.1 min, respectively.

**Calibration Curve**—Calibration curves were constructed with the ratio of lidocaine–mepivacaine peak heights plotted along the ordinate and the lidocaine concentration plotted along the abscissa. Initially, curves were developed by spiking blank plasma with 0.03, 0.08, 0.16, 0.40, 0.80, 1.60, 4.0, and 8.0 μg of lidocaine/ml and analyzing the samples as described. Calibration data were fit to a single straight line using a least-squares regression[6] with $r = 0.994$. Despite the apparent fit, the calculated regression line did not coincide adequately with the observed peak height ratios for low lidocaine concentrations. Instead, the calibration curves were described best by two straight lines: one for lidocaine concentrations above 0.8 μg/ml and another for concentrations below 0.8 μg/ml.

The calculated correlation coefficients and equations were $r = 0.994$, ratio = 2.121 [lidocaine concentration (μg/ml)] − 1.04 for the upper range, and $r = 0.999$, ratio = 1.149 [lidocaine concentration (μg/ml)] + 0.05 for the lower range. Curves prepared from aqueous standards (same procedure but without the first two centrifugations) were the same as those using plasma standards; therefore, aqueous standards were used for daily calibration.

**Precision**—Assay precision was evaluated by analyzing multiple plasma samples spiked with 0.04, 0.08, 0.16, 1.62, or 4.00 μg of lidocaine/ml (Table I). Over this concentration range, assay precision was quite satisfactory.

**Interference**—Neither the monoethylglycinexylidide or glycinexylidide lidocaine metabolites nor any of the tested drugs produced interfering peaks or alterations in the lidocaine–mepivacaine (internal standard) peak height ratios with this method. Meperidine (1 μg/ml) generated a sharp peak with a peak height almost 75% as large as the internal standard, but the meperidine peak (retention time of 5.1 min) eluted before the lidocaine and mepivacaine peaks and did not interfere with the lidocaine assay.

**Conclusions**—The GLC lidocaine assay reported by Kline and Martin (10) is a simple and rapid method; however, the sensitivity is not adequate for many pharmacokinetic studies. Incorporating column oven temperature programming improved the assay sensitivity so that plasma lidocaine concentrations as low as 40 ng/ml could be measured readily. The modification retains the simplicity, speed, and sample capacity of the original method.

[6] TI Program ST 1-08, Texas Instruments Inc., Dallas, Tex.

## REFERENCES


(1) J. B. Keenaghan, *Anesthesiology*, **29**, 110 (1968).

(2) K. K. Adjepon-Yamoah and L. F. Prescott, *J. Pharm. Pharmacol.*, **26**, 889 (1974).

(3) E. Naito, M. Matsuki, and K. Shimoji, *Anesthesiology*, **47**, 466 (1977).

(4) G. Caille, J. Lelorier, Y. Latour, and J. G. Besner, *J. Pharm. Sci.*, **66**, 1383 (1977).

(5) E. Zybler-Katz, L. Granit, and M. Levy, *Clin. Chem.*, **24**, 1573 (1978).

(6) C. B. Walberg, *J. Anal. Toxicol.*, **2**, 121 (1978).

(7) L. J. Haywood, K. Claiborne, and C. Walberg, *Am. J. Cardiol.*, **43**, 360 (1979).

(8) D. P. Lehane, P. J. Wissert, P. Menyharth, A. L. Levy, and M. A. Kukucka, *Clin. Chem.*, **25**, 614 (1979).

(9) H. B. Hucker and S. C. Stauffer, *J. Pharm. Sci.*, **65**, 926 (1976).

(10) B. J. Kline and M. F. Martin, *ibid.*, **67**, 887 (1978).


## ACKNOWLEDGMENTS


Supported in part by U.S. Public Health Service Grant RR-05403.


# COMMUNICATIONS

## Specific Radioimmunoassay for Flunitrazepam


**Keyphrases** □ Flunitrazepam—quantitation by radioimmunoassay, compared with electron-capture GLC, human plasma □ Radioimmunoassay—quantitation of flunitrazepam, compared with electron-capture GLC, human plasma □ Hypnotic agents—flunitrazepam, quantitation by radioimmunoassay, human plasma


*To the Editor:*

Flunitrazepam[1] [5-(2-fluorophenyl)-1,3-dihydro-1-methyl-7-nitro-2*H*-1,4-benzodiazepin-2-one, I], a benzodiazepine derivative, is clinically effective as a hypnotic when administered orally in the 0.5–2-mg dose range and may be administered parenterally, usually in combination with other drugs, for the induction of anesthesia (1, 2). Flunitrazepam has been marketed for several years in Europe and is presently under clinical evaluation in the United States.

In humans, I is completely metabolized; apart from intact I, the major metabolites found in plasma are the *N*-desmethyl and 7-amino derivatives (3). However, intact I is primarily responsible for the hypnotic activity of the drug (3) and has a half-life of 20–36 hr on chronic administration (4, 5).

Electron-capture GLC has been the method of choice

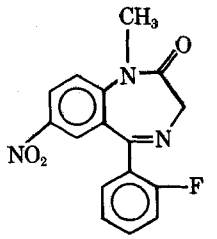


I

[1] Rohypnol, Hoffmann–La Roche.




*0022-3549/81/0200-0230$01.00/0*



*© 1981, American Pharmaceutical Association*

**Table I—Lidocaine GLC Assay Precision with Column Oven Temperature Programming**

| Actual Plasma Lidocaine Concentration, μg/ml | Measured Lidocaine Concentration, μg/ml |
|---|---|
| 4.00 | 4.01 ± 0.13 (21)[a] |
| 1.62 | 1.61 ± 0.04 (15) |
| 0.16 | 0.17 ± 0.01 (15) |
| 0.08 | 0.08 ± 0.01 (18) |
| 0.04 | 0.04 ± 0.002 (14) |

[a] Mean ± *SE* (*n*).

temperature programming modification, plasma lidocaine concentrations as low as 30 ng/ml can be measured. The retention times for lidocaine and mepivacaine (internal standard) are 6.0 and 7.1 min, respectively.

**Calibration Curve**—Calibration curves were constructed with the ratio of lidocaine–mepivacaine peak heights plotted along the ordinate and the lidocaine concentration plotted along the abscissa. Initially, curves were developed by spiking blank plasma with 0.03, 0.08, 0.16, 0.40, 0.80, 1.60, 4.0, and 8.0 μg of lidocaine/ml and analyzing the samples as described. Calibration data were fit to a single straight line using a least-squares regression[6] with $r = 0.994$. Despite the apparent fit, the calculated regression line did not coincide adequately with the observed peak height ratios for low lidocaine concentrations. Instead, the calibration curves were described best by two straight lines: one for lidocaine concentrations above 0.8 μg/ml and another for concentrations below 0.8 μg/ml.

The calculated correlation coefficients and equations were $r = 0.994$, ratio = 2.121 [lidocaine concentration (μg/ml)] − 1.04 for the upper range, and $r = 0.999$, ratio = 1.149 [lidocaine concentration (μg/ml)] + 0.05 for the lower range. Curves prepared from aqueous standards (same procedure but without the first two centrifugations) were the same as those using plasma standards; therefore, aqueous standards were used for daily calibration.

**Precision**—Assay precision was evaluated by analyzing multiple plasma samples spiked with 0.04, 0.08, 0.16, 1.62, or 4.00 μg of lidocaine/ml (Table I). Over this concentration range, assay precision was quite satisfactory.

**Interference**—Neither the monoethylglycinexylidide or glycinexylidide lidocaine metabolites nor any of the tested drugs produced interfering peaks or alterations in the lidocaine–mepivacaine (internal standard) peak height ratios with this method. Meperidine (1 μg/ml) generated a sharp peak with a peak height almost 75% as large as the internal standard, but the meperidine peak (retention time of 5.1 min) eluted before the lidocaine and mepivacaine peaks and did not interfere with the lidocaine assay.

**Conclusions**—The GLC lidocaine assay reported by Kline and Martin (10) is a simple and rapid method; however, the sensitivity is not adequate for many pharmacokinetic studies. Incorporating column oven temperature programming improved the assay sensitivity so that plasma lidocaine concentrations as low as 40 ng/ml could be measured readily. The modification retains the simplicity, speed, and sample capacity of the original method.

[6] TI Program ST 1-08, Texas Instruments Inc., Dallas, Tex.

## REFERENCES


(1) J. B. Keenaghan, *Anesthesiology*, **29**, 110 (1968).

(2) K. K. Adjepon-Yamoah and L. F. Prescott, *J. Pharm. Pharmacol.*, **26**, 889 (1974).

(3) E. Naito, M. Matsuki, and K. Shimoji, *Anesthesiology*, **47**, 466 (1977).

(4) G. Caille, J. Lelorier, Y. Latour, and J. G. Besner, *J. Pharm. Sci.*, **66**, 1383 (1977).

(5) E. Zybler-Katz, L. Granit, and M. Levy, *Clin. Chem.*, **24**, 1573 (1978).

(6) C. B. Walberg, *J. Anal. Toxicol.*, **2**, 121 (1978).

(7) L. J. Haywood, K. Claiborne, and C. Walberg, *Am. J. Cardiol.*, **43**, 360 (1979).

(8) D. P. Lehane, P. J. Wissert, P. Menyharth, A. L. Levy, and M. A. Kukucka, *Clin. Chem.*, **25**, 614 (1979).

(9) H. B. Hucker and S. C. Stauffer, *J. Pharm. Sci.*, **65**, 926 (1976).

(10) B. J. Kline and M. F. Martin, *ibid.*, **67**, 887 (1978).


## ACKNOWLEDGMENTS


Supported in part by U.S. Public Health Service Grant RR-05403.


# COMMUNICATIONS

## Specific Radioimmunoassay for Flunitrazepam


**Keyphrases** □ Flunitrazepam—quantitation by radioimmunoassay, compared with electron-capture GLC, human plasma □ Radioimmunoassay—quantitation of flunitrazepam, compared with electron-capture GLC, human plasma □ Hypnotic agents—flunitrazepam, quantitation by radioimmunoassay, human plasma


*To the Editor:*

Flunitrazepam[1] [5-(2-fluorophenyl)-1,3-dihydro-1-methyl-7-nitro-2*H*-1,4-benzodiazepin-2-one, I], a benzodiazepine derivative, is clinically effective as a hypnotic when administered orally in the 0.5–2-mg dose range and may be administered parenterally, usually in combination with other drugs, for the induction of anesthesia (1, 2). Flunitrazepam has been marketed for several years in Europe and is presently under clinical evaluation in the United States.

In humans, I is completely metabolized; apart from intact I, the major metabolites found in plasma are the *N*-desmethyl and 7-amino derivatives (3). However, intact I is primarily responsible for the hypnotic activity of the drug (3) and has a half-life of 20–36 hr on chronic administration (4, 5).

Electron-capture GLC has been the method of choice

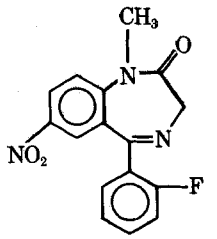


I

[1] Rohypnol, Hoffmann–La Roche.




*0022-3549/81/0200-0230$01.00/0*



*© 1981, American Pharmaceutical Association*

for the determination of the low nanogram concentrations of I in plasma following administration of therapeutic doses to humans (6, 7). However, none of the reported procedures can approach the simplicity, sensitivity, and speed of radioimmunoassay. We now report a specific and sensitive radioimmunoassay for I that permits its quantitation directly in plasma or blood.

To obtain antibodies to I, an immunogen first was prepared by covalently coupling 3-hemisuccinyloxyflunitrazepam to bovine serum albumin using the mixed anhydride procedure of Erlanger *et al.* (8). The resulting conjugate consisted of 18 moles of the hapten coupled to 1 mole of albumin. Rabbits were immunized intradermally, and the antiserum with the highest titer (1:3000 dilution) of antibodies to I was used.

The radioligand used for the assay was [*methyl*-$^3$H]-flunitrazepam[2] with a specific activity of 87.5 Ci/mmole. Prior to use, radiolabeled I was purified by TLC on silica gel with chloroform–acetone (4:1) as the solvent system.

The radioimmunoassay was carried out in a manner identical to that described recently for diazepam (9). A logit–log calibration curve for I was linear from 15 to 1000 pg/tube; thus, a working limit of sensitivity of 0.15 ng/ml was obtained using 0.1 ml of plasma. This value represents about a fivefold increase in sensitivity compared to electron-capture GLC techniques. However, for routine analysis of plasma and blood from subjects receiving chronic therapeutic doses of I, such sensitivity is unnecessary and a 10-$\mu$l sample is more appropriate for analysis. The intra- and interassay coefficients of variation did not exceed 10% over a range of 1.65–10 ng of I/ml in a selection of random clinical samples.

The antiserum specificity was determined initially by its cross-reactivity with the known metabolites of I present in blood and with the benzodiazepine drugs, diazepam, *N*-desmethyldiazepam, flurazepam, and nitrazepam. For each compound tested, cross-reactivity was <1% relative to I (100%); this finding demonstrated that the 1-methyl, 7-nitro, and 2′-fluoro groups on the hapten were potent antigenic determinants and indicated that the antiserum was highly specific for I.

Further evidence for the specificity of the radioimmunoassay procedure was obtained by comparison with an electron-capture GLC method (7). The joint determinations for I in 20 plasma and 12 whole blood samples from subjects who received a 2-mg dose of the drug were subjected to linear regression analysis by a method that takes into account differences in the precision of both analytical procedures (10). The correlation coefficient, regression line slope, and $y$-intercept were 0.98, 0.93, and 0.13, respectively, over a range of 0.5–18 ng/ml. Furthermore, the two groups of data were not significantly different ($p > 0.05$) using a $t$ test. These statistical parameters indicate that the radioimmunoassay and electron-capture GLC methods yield equivalent results.

(1) R. Piret and J. C. Devoghel, *J. Int. Med. Res.*, **2**, 370 (1974).
(2) E. Wickstrom, *Anaesthesist*, **23**, 90 (1974).
(3) G. Wendt, in "Bisherige Erfahrungen mit Rohypnol (Flunitrazepam) in der Anasthesiologie und Intensivtherapie," W. Hugin, G. Hossli, and M. Gemperle, Eds., F. Hoffmann–La Roche, Basel, Switzerland, 1976, pp. 27–38.
(4) E. Wickstrom, R. Amrein, P. Haefelfinger, and D. Hartmann, *Eur. J. Clin. Pharmacol.*, **17**, 189 (1980).
(5) H. Boxenbaum, H. Postmanter, T. Macasieb, K. Geitner, R. Weinfeld, J. Moore, A. Darragh, D. O'Kelly, L. Weissman, and S. Kaplan, *J. Pharmacokinet. Biopharm.*, **6**, 283 (1978).
(6) J. Cano, J. Guintrand, C. Aubert, and A. Viala, *Arzneim.-Forsch.*, **27**, 338 (1977).
(7) J. A. F. de Silva and I. Bekersky, *J. Chromatogr.*, **99**, 447 (1974).
(8) B. F. Erlanger, F. Borek, S. M. Beiser, and S. Lieberman, *J. Biol. Chem.*, **234**, 1090 (1959).
(9) R. Dixon and T. Crews, *J. Anal. Toxicol.*, **2**, 210 (1978).
(10) M. G. Kendall and A. Stuart, "The Advanced Theory of Statistics," vol. 2, 3rd ed., Hafner, New York, N.Y., 1973, pp. 391–406.

*Ross Dixon* ˣ
*William Glover*
*James Earley*
Hoffmann–La Roche Inc.
Nutley, NJ 07110

Received August 1, 1980.
Accepted for publication November 3, 1980.

[2] New England Nuclear, Boston, MA 02118.

## Calcium Binding by Arteriographic Contrast Media

**Keyphrases** □ Arteriographic contrast media—calcium binding, effect of additives in media on calcium binding *in vitro* □ Calcium—binding in plasma by arteriographic contrast media, effect of additives in media □ Diatrizoate meglumine sodium—arteriographic contrast medium, effect on calcium binding □ Binding—calcium to ionic arteriographic contrast media, effect of additives

*To the Editor:*

Selective coronary arteriography with common ionic contrast media is associated with a decrease of myocardial force, which was suggested to be due to decreased ionized calcium levels in the blood perfusing the myocardium (1, 2). This depressant action has been attributed exclusively to the potent calcium-binding ligands added to contrast media for anticoagulation, stabilization, and buffering (1–3). The calcium-binding properties of contrast media have not yet been reported.

To investigate the basis for the reduction of ionized calcium levels, fixed quantities of diluted contrast media were titrated with increasing amounts of calcium chloride *in vitro*. The following contrast media were evaluated: ioxaglate meglumine sodium[1] (59% sodium and methylglucamine *N*-(2-hydroxyethyl)-2,4,6-triiodo-5-{2-[2,4,6-triiodo-3-(*N*-methylacetamido)-5-(methylcarbonyl)-benzamido]acetamido} isophthalamic acid, I), lysine diatrizoate[2] [80% L-lysine 3,5-bis(acetamido)-2,4,6-triiodobenzoate, II], diatrizoate meglumine sodium[3] [76% sodium and methylglucamine 3,5-bis(acetamido)-2,4,6-triiodobenzoate, III], and diatrizoate meglumine sodium[4] with 0.32% sodium citrate and 0.04% edetate disodium [(ethylenedinitrilo)tetraacetic acid disodium salt] (IV).

[1] Hexabrix, Byk Gulden, Konstanz, West Germany.
[2] Peritrast-400, Dr. Franz Köhler Chemie, Alsbach, Bergstrasse, West Germany.
[3] Urografin-76, Schering AG, Berlin/Bergkamen, West Germany.
[4] Renografin-76, Squibb, Princeton, N.J.

0022-3549/81/0200-0231$01.00/0
© 1981, American Pharmaceutical Association

for the determination of the low nanogram concentrations of I in plasma following administration of therapeutic doses to humans (6, 7). However, none of the reported procedures can approach the simplicity, sensitivity, and speed of radioimmunoassay. We now report a specific and sensitive radioimmunoassay for I that permits its quantitation directly in plasma or blood.

To obtain antibodies to I, an immunogen first was prepared by covalently coupling 3-hemisuccinyloxyflunitrazepam to bovine serum albumin using the mixed anhydride procedure of Erlanger *et al.* (8). The resulting conjugate consisted of 18 moles of the hapten coupled to 1 mole of albumin. Rabbits were immunized intradermally, and the antiserum with the highest titer (1:3000 dilution) of antibodies to I was used.

The radioligand used for the assay was [*methyl*-$^3$H]-flunitrazepam[2] with a specific activity of 87.5 Ci/mmole. Prior to use, radiolabeled I was purified by TLC on silica gel with chloroform–acetone (4:1) as the solvent system.

The radioimmunoassay was carried out in a manner identical to that described recently for diazepam (9). A logit–log calibration curve for I was linear from 15 to 1000 pg/tube; thus, a working limit of sensitivity of 0.15 ng/ml was obtained using 0.1 ml of plasma. This value represents about a fivefold increase in sensitivity compared to electron-capture GLC techniques. However, for routine analysis of plasma and blood from subjects receiving chronic therapeutic doses of I, such sensitivity is unnecessary and a 10-$\mu$l sample is more appropriate for analysis. The intra- and interassay coefficients of variation did not exceed 10% over a range of 1.65–10 ng of I/ml in a selection of random clinical samples.

The antiserum specificity was determined initially by its cross-reactivity with the known metabolites of I present in blood and with the benzodiazepine drugs, diazepam, *N*-desmethyldiazepam, flurazepam, and nitrazepam. For each compound tested, cross-reactivity was <1% relative to I (100%); this finding demonstrated that the 1-methyl, 7-nitro, and 2′-fluoro groups on the hapten were potent antigenic determinants and indicated that the antiserum was highly specific for I.

Further evidence for the specificity of the radioimmunoassay procedure was obtained by comparison with an electron-capture GLC method (7). The joint determinations for I in 20 plasma and 12 whole blood samples from subjects who received a 2-mg dose of the drug were subjected to linear regression analysis by a method that takes into account differences in the precision of both analytical procedures (10). The correlation coefficient, regression line slope, and $y$-intercept were 0.98, 0.93, and 0.13, respectively, over a range of 0.5–18 ng/ml. Furthermore, the two groups of data were not significantly different ($p > 0.05$) using a $t$ test. These statistical parameters indicate that the radioimmunoassay and electron-capture GLC methods yield equivalent results.

(1) R. Piret and J. C. Devoghel, *J. Int. Med. Res.*, **2**, 370 (1974).
(2) E. Wickstrom, *Anaesthesist*, **23**, 90 (1974).
(3) G. Wendt, in "Bisherige Erfahrungen mit Rohypnol (Flunitrazepam) in der Anasthesiologie und Intensivtherapie," W. Hugin, G. Hossli, and M. Gemperle, Eds., F. Hoffmann–La Roche, Basel, Switzerland, 1976, pp. 27–38.
(4) E. Wickstrom, R. Amrein, P. Haefelfinger, and D. Hartmann, *Eur. J. Clin. Pharmacol.*, **17**, 189 (1980).
(5) H. Boxenbaum, H. Postmanter, T. Macasieb, K. Geitner, R. Weinfeld, J. Moore, A. Darragh, D. O'Kelly, L. Weissman, and S. Kaplan, *J. Pharmacokinet. Biopharm.*, **6**, 283 (1978).
(6) J. Cano, J. Guintrand, C. Aubert, and A. Viala, *Arzneim.-Forsch.*, **27**, 338 (1977).
(7) J. A. F. de Silva and I. Bekersky, *J. Chromatogr.*, **99**, 447 (1974).
(8) B. F. Erlanger, F. Borek, S. M. Beiser, and S. Lieberman, *J. Biol. Chem.*, **234**, 1090 (1959).
(9) R. Dixon and T. Crews, *J. Anal. Toxicol.*, **2**, 210 (1978).
(10) M. G. Kendall and A. Stuart, "The Advanced Theory of Statistics," vol. 2, 3rd ed., Hafner, New York, N.Y., 1973, pp. 391–406.

*Ross Dixon* ˣ
*William Glover*
*James Earley*
Hoffmann–La Roche Inc.
Nutley, NJ 07110

Received August 1, 1980.
Accepted for publication November 3, 1980.

[2] New England Nuclear, Boston, MA 02118.

## Calcium Binding by Arteriographic Contrast Media

**Keyphrases** □ Arteriographic contrast media—calcium binding, effect of additives in media on calcium binding *in vitro* □ Calcium—binding in plasma by arteriographic contrast media, effect of additives in media □ Diatrizoate meglumine sodium—arteriographic contrast medium, effect on calcium binding □ Binding—calcium to ionic arteriographic contrast media, effect of additives

*To the Editor:*

Selective coronary arteriography with common ionic contrast media is associated with a decrease of myocardial force, which was suggested to be due to decreased ionized calcium levels in the blood perfusing the myocardium (1, 2). This depressant action has been attributed exclusively to the potent calcium-binding ligands added to contrast media for anticoagulation, stabilization, and buffering (1–3). The calcium-binding properties of contrast media have not yet been reported.

To investigate the basis for the reduction of ionized calcium levels, fixed quantities of diluted contrast media were titrated with increasing amounts of calcium chloride *in vitro*. The following contrast media were evaluated: ioxaglate meglumine sodium[1] (59% sodium and methylglucamine *N*-(2-hydroxyethyl)-2,4,6-triiodo-5-{2-[2,4,6-triiodo-3-(*N*-methylacetamido)-5-(methylcarbonyl)-benzamido]acetamido} isophthalamic acid, I), lysine diatrizoate[2] [80% L-lysine 3,5-bis(acetamido)-2,4,6-triiodobenzoate, II], diatrizoate meglumine sodium[3] [76% sodium and methylglucamine 3,5-bis(acetamido)-2,4,6-triiodobenzoate, III], and diatrizoate meglumine sodium[4] with 0.32% sodium citrate and 0.04% edetate disodium [(ethylenedinitrilo)tetraacetic acid disodium salt] (IV).

[1] Hexabrix, Byk Gulden, Konstanz, West Germany.
[2] Peritrast-400, Dr. Franz Köhler Chemie, Alsbach, Bergstrasse, West Germany.
[3] Urografin-76, Schering AG, Berlin/Bergkamen, West Germany.
[4] Renografin-76, Squibb, Princeton, N.J.

0022-3549/81/0200-0231$01.00/0
© 1981, American Pharmaceutical Association

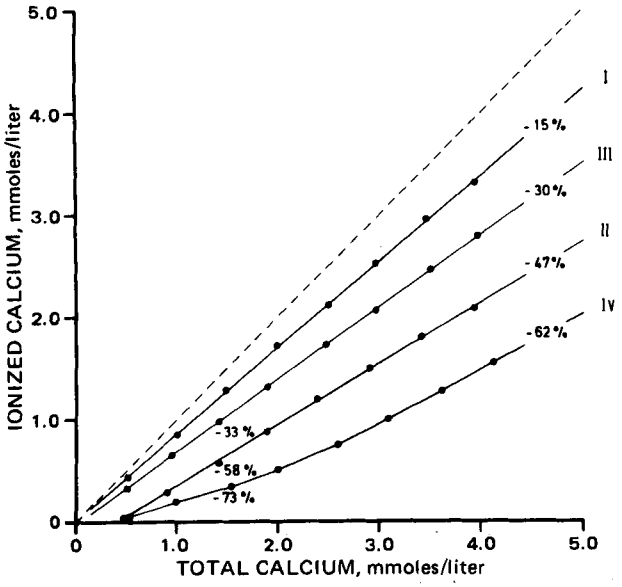


**Figure 1**—*Binding of added ionized calcium by contrast media (two parts) in a physiological saline solution (0.9% NaCl, seven parts). The roman numerals refer to contrast media (see text). Percentage values denote the reduction of ionized calcium levels below the total calcium content of 1.5 and 4.0 mmoles/liter. The expected line (i.e., no binding of ionized calcium) is shown as a dashed line with a slope of 1.*

The presence or absence of additives and their amounts were not analyzed; the compositions are given as presented in the manufacturer's data.

Total calcium content was determined by the fluorometric method[5] with correction for any edetate disodium present. Ionized calcium levels were measured by a calcium-sensitive flow-through electrode[6]. The reduction of ionized calcium levels below the expected line (Fig. 1) is consistent with calcium binding.

The shift in the lysine diatrizoate (II) titration curve, as well as the shift and the bend at 2 mmoles of total calcium/liter in one of the diatrizoate meglumine sodium (IV) curves, is believed to be due to the saturation of the calcium-chelating additives present in these contrast media (*e.g.*, 3.2 mg of citrate/ml and 0.4 mg of edetate disodium/ml in IV). The near-zero intercepts on the abscissa of the titration curves for ioxaglate meglumine sodium (I) and diatrizoate meglumine sodium (III) suggest a lack of large amounts of potent calcium-binding ligands in these contrast media. Deviations of the slopes of individual titration curves from the expected line after saturation of disodium edetate and citrate binding sites, or without any chelating additives present, indicate that calcium chelation is primarily an inherent property of ionic contrast media and not that of the additives.

The association constants ($K_0$) of radiopaque ligands ($L$) with calcium have been calculated on the basis of a 1:1 association by:

$$K_0 = \frac{[CaL]}{[Ca][L]} \qquad \text{(Eq. 1)}$$

Log $K_0$ values were 0.36 for the diatrizoate–calcium complex and 0.28 for the ioxaglate–calcium complex. However, the calculations do not necessarily signify the stability constants for well-defined chemical structures since the stoichiometry is not known. Values are below the known stability constants of human plasma protein–calcium complexes [log $K_0 \simeq$ 2–7 (4)]. Nevertheless, when the opacifying bolus is injected intracoronarily, the contrast molecules are more concentrated than the protein fraction in plasma and thus cause a marked reduction of plasma ionized calcium levels.

[5] Corning calcium analyzer 940, Vogel, Giessen, West Germany.
[6] Nova 2, Union Carbide, Newton, Mass.

(1) J. B. Caulfield, L. Zir, and J. W. Harthorne, *Circulation*, **52**, 119 (1975).
(2) C. B. Higgins and W. Schmidt, *ibid.*, **58**, 512 (1978).
(3) R. S. Frech, *Invest. Radiol.*, **10**, 323 (1975).
(4) R. J. P. Williams, in "Calcium-Binding Proteins and Calcium Function," R. H. Wasserman, R. A. Corradino, E. Carafoli, R. H. Kretsinger, D. H. MacLennan, and F. L. Siegel, Eds., North-Holland, New York, N.Y., 1977, pp. 3–12.

*H. G. Wolpers* ˣ
*D. H. Hunneman*
*M. Stellwaag*
*G. Hellige*
Physiological Institut I
Department of Experimental Cardiology
University of Göttingen
Humboldtallee 7, D-3400 Göttingen
Federal Republic of Germany

Received July 17, 1980.
Accepted for publication November 10, 1980.
Supported by the Deutsche Forschungsgemeinschaft, SFB 89-Kardiologie Göttingen.

## Effect of Sampling Probe Size on Dissolution of Tableted Drug Samples

**Keyphrases** □ Dissolution rates—effect of sampling probe size on dissolution rate of tableted drug samples, USP paddle method □ Dissolution testing systems—various sampling probe sizes evaluated for effect on dissolution rate of tableted drug samples □ Hydrodynamics—dissolution rates affected by sampling probe size, USP paddle method

*To the Editor:*

When *in vitro* dissolution rates were determined using the USP paddle method (1), some tablet formulations consistently gave higher dissolution rates when sampled with an automated sampling system than when sampled manually. This difference was traced to turbulence caused by the filter-tipped probes used in automated sampling. With the automated system used in this laboratory, the probes are suspended in the dissolution medium during the entire test.

**Table I—Effect of Sampling Probes on Dissolution Rate**

| Probe | Probe Volume, mm³ | Dissolution[a], % of label claim | Increase in Dissolution, % |
|---|---|---|---|
| None | — | 41.4 | — |
| 1 | 44 | 41.4 | 0 |
| 2 | 177 | 43.0 | 1.6 |
| 3 | 466 | 45.1 | 3.7 |
| 4 | 706 | 46.4 | 5.0 |
| 5 | 877 | 48.4 | 7.0 |

[a] Average of 12 tablets.



*0022-3549/81/0200-0232$01.00/0*
*© 1981, American Pharmaceutical Association*

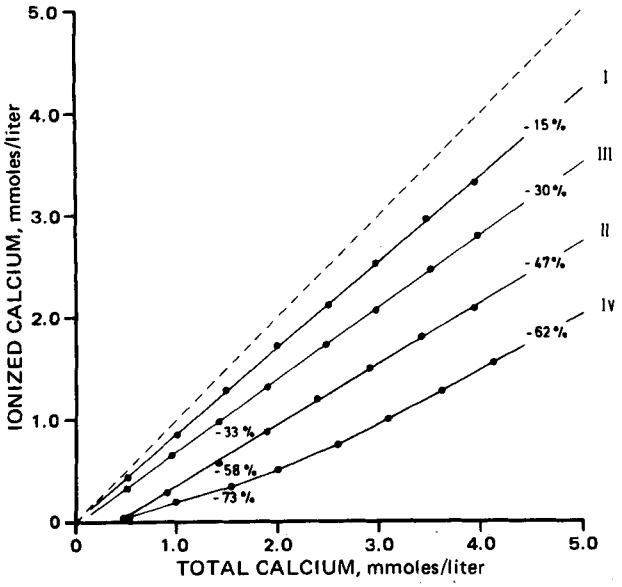


**Figure 1**—*Binding of added ionized calcium by contrast media (two parts) in a physiological saline solution (0.9% NaCl, seven parts). The roman numerals refer to contrast media (see text). Percentage values denote the reduction of ionized calcium levels below the total calcium content of 1.5 and 4.0 mmoles/liter. The expected line (i.e., no binding of ionized calcium) is shown as a dashed line with a slope of 1.*

The presence or absence of additives and their amounts were not analyzed; the compositions are given as presented in the manufacturer's data.

Total calcium content was determined by the fluorometric method[5] with correction for any edetate disodium present. Ionized calcium levels were measured by a calcium-sensitive flow-through electrode[6]. The reduction of ionized calcium levels below the expected line (Fig. 1) is consistent with calcium binding.

The shift in the lysine diatrizoate (II) titration curve, as well as the shift and the bend at 2 mmoles of total calcium/liter in one of the diatrizoate meglumine sodium (IV) curves, is believed to be due to the saturation of the calcium-chelating additives present in these contrast media (*e.g.*, 3.2 mg of citrate/ml and 0.4 mg of edetate disodium/ml in IV). The near-zero intercepts on the abscissa of the titration curves for ioxaglate meglumine sodium (I) and diatrizoate meglumine sodium (III) suggest a lack of large amounts of potent calcium-binding ligands in these contrast media. Deviations of the slopes of individual titration curves from the expected line after saturation of disodium edetate and citrate binding sites, or without any chelating additives present, indicate that calcium chelation is primarily an inherent property of ionic contrast media and not that of the additives.

The association constants ($K_0$) of radiopaque ligands ($L$) with calcium have been calculated on the basis of a 1:1 association by:

$$K_0 = \frac{[CaL]}{[Ca][L]} \qquad \text{(Eq. 1)}$$

Log $K_0$ values were 0.36 for the diatrizoate–calcium complex and 0.28 for the ioxaglate–calcium complex. However, the calculations do not necessarily signify the stability constants for well-defined chemical structures since the stoichiometry is not known. Values are below the known stability constants of human plasma protein–calcium complexes [log $K_0 \simeq$ 2–7 (4)]. Nevertheless, when the opacifying bolus is injected intracoronarily, the contrast molecules are more concentrated than the protein fraction in plasma and thus cause a marked reduction of plasma ionized calcium levels.

[5] Corning calcium analyzer 940, Vogel, Giessen, West Germany.
[6] Nova 2, Union Carbide, Newton, Mass.

(1) J. B. Caulfield, L. Zir, and J. W. Harthorne, *Circulation*, **52**, 119 (1975).
(2) C. B. Higgins and W. Schmidt, *ibid.*, **58**, 512 (1978).
(3) R. S. Frech, *Invest. Radiol.*, **10**, 323 (1975).
(4) R. J. P. Williams, in "Calcium-Binding Proteins and Calcium Function," R. H. Wasserman, R. A. Corradino, E. Carafoli, R. H. Kretsinger, D. H. MacLennan, and F. L. Siegel, Eds., North-Holland, New York, N.Y., 1977, pp. 3–12.

*H. G. Wolpers* ˣ
*D. H. Hunneman*
*M. Stellwaag*
*G. Hellige*
Physiological Institut I
Department of Experimental Cardiology
University of Göttingen
Humboldtallee 7, D-3400 Göttingen
Federal Republic of Germany

Received July 17, 1980.
Accepted for publication November 10, 1980.
Supported by the Deutsche Forschungsgemeinschaft, SFB 89-Kardiologie Göttingen.

## Effect of Sampling Probe Size on Dissolution of Tableted Drug Samples

**Keyphrases** □ Dissolution rates—effect of sampling probe size on dissolution rate of tableted drug samples, USP paddle method □ Dissolution testing systems—various sampling probe sizes evaluated for effect on dissolution rate of tableted drug samples □ Hydrodynamics—dissolution rates affected by sampling probe size, USP paddle method

*To the Editor:*

When *in vitro* dissolution rates were determined using the USP paddle method (1), some tablet formulations consistently gave higher dissolution rates when sampled with an automated sampling system than when sampled manually. This difference was traced to turbulence caused by the filter-tipped probes used in automated sampling. With the automated system used in this laboratory, the probes are suspended in the dissolution medium during the entire test.

**Table I—Effect of Sampling Probes on Dissolution Rate**

| Probe | Probe Volume, mm³ | Dissolution[a], % of label claim | Increase in Dissolution, % |
|---|---|---|---|
| None | — | 41.4 | — |
| 1 | 44 | 41.4 | 0 |
| 2 | 177 | 43.0 | 1.6 |
| 3 | 466 | 45.1 | 3.7 |
| 4 | 706 | 46.4 | 5.0 |
| 5 | 877 | 48.4 | 7.0 |

[a] Average of 12 tablets.



*0022-3549/81/0200-0232$01.00/0*
*© 1981, American Pharmaceutical Association*

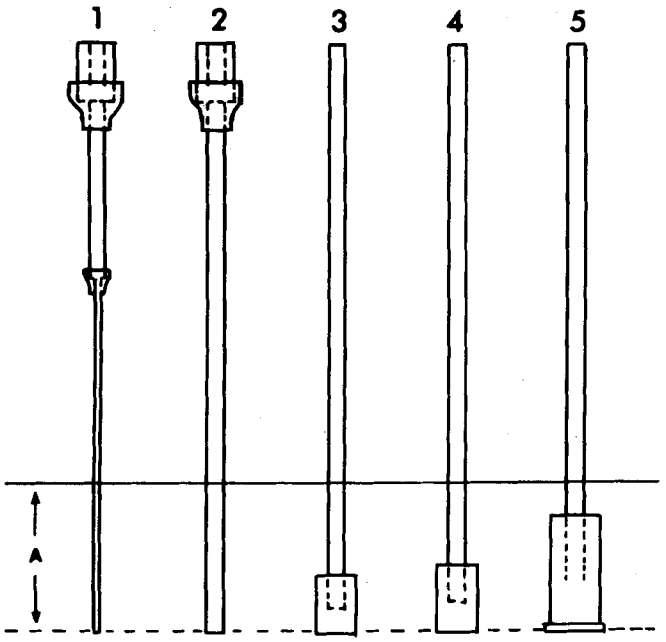


**Figure 1**—*Sampling probes, showing immersion depth (A).*

To reduce probe interference, five probe designs (Fig. 1) were tested with a six-place dissolution apparatus. All of the probes were constructed in this laboratory. Probes 3 and 4 were used early in the dissolution work. Probe 5 was designed to be similar to probes used in some commercial dissolution equipment. Probe 1 was the result of the laboratory's search for a probe with minimum interference in the dissolution test. Probe 2 was chosen to give an intermediate size between Probes 1 and 3. All probes were constructed from 3-mm o.d. glass tubing. The tip of Probe 1 was a 1.3-mm o.d. melting-point capillary. Commercially available filters were used. The 5-mg prednisone tablets used for the test were from a sample known to give different results depending on the presence or absence of a sample probe during the test.

One probe was suspended in each of five dissolution vessels, and the sixth vessel was used without a probe. The probes were placed halfway between the vessel wall and the paddle shaft, with the probe tip 25 mm below the liquid surface (approximately halfway between the liquid surface and the top of the paddle). The dissolution test was conducted for 30 min; samples then were withdrawn with a syringe for analysis by the USP (2) procedure. The test was repeated, and then the probes were moved to different vessels. This procedure was repeated until all probes were tested in duplicate in each vessel. This experimental design eliminated interference from sources other than the probes.

The data (Table I) show that there was a direct relationship between the displacement volume of the sampling probe and the increase in dissolution rate for the sample used. With the tablets used in this study, no effect on the observed dissolution rate was noted from Probe 1. However, the presence of any foreign object disturbs the hydrodynamics of the dissolution medium, and it is possible that the results from other, more sensitive samples could be influenced by the use of Probe 1.

The results show that the displacement volumes of sampling probes used with automated samplers should be as small as possible to reduce interference with the dissolution test.

(1) "The United States Pharmacopeia," 20th rev., United States Pharmacopeial Convention, Rockville, Md., 1980, p. 959.

(2) *Ibid.*, p. 655.

*Clyde E. Wells*

National Center for Drug Analysis
1114 Market Street
St. Louis, MO 63101

Received April 3, 1980.
Accepted for publication November 14, 1980.

# BOOKS

## REVIEWS

**Pharmacy: A Profession in Search of a Role.** By JACK ROBBINS. Navillus Publishing Corp. 1979. 143 pp. 15 × 23 cm. Price $14.95. (Available from Technomic Publishing Co., 265 Post Rd. W., Westport, CT 06880.)

The title of this book is both provocative and ambiguous. Readers seeking a definitive statement of the professional status or role of the pharmacist will not find it, nor will they find an expression of the need for clinical pharmacy, specialists, or new directions for the future.

Most of this book (large type, liberal white space) is devoted to an objective presentation of a 1975 mail survey of pharmacists. The study attempts to "correlate the dynamic changes in pharmacy during the past half century with the various modes which pharmacists have adopted to make their role expectations more consonant with their performance" and "to incorporate social–psychological theory in order to better understand the motivations underlying pharmacists' various adaptation modes." Theories (including role theory, role conflict and adaptation, and professionalization) are presented in easily understood language and context. Although a more in-depth discussion might be preferred, this approach is rational, laudable, and worthwhile in an area that too often is merely descriptive.

Chapter 5, Generational Effects: Younger *versus* Older Pharmacists, is especially intriguing to the reader seeking insight into the direction of future change. Chapter 8, Role Conflict and Social Change, is excellent and expands on the familiar business–professional conflict, reporting both the extent and direction of conflict within the context of practice changes.

Given the emphasis and style, chapter titles, acknowledgments, and cautious conclusions and projected future trends, one suspects that the book originally was a dissertation, a suspicion heightened by a citation of the same title by the same author in *Dissertation Abstracts* (1977). The dissertation subtitle, Functional and Psychological Adaptations of Pharmacists to Technological and Social Changes During the Past 50 Years, is descriptive of the contents. Exclusion of the survey instrument and the inadequate literature search (for example, no citations after 1976) will disappoint the researcher.

The foreword indicates that the book should be read by social scientists, pharmacy educators, individual pharmacy practitioners, pharmacy association executives, other health-care practitioners and organizations, members of Congress, and health-care planners and administrators. Such a broad appeal is unlikely to satisfy anyone completely.

The book should be of interest to pharmacy school administrators and pharmaceutical industry executives and employees whose market is practicing pharmacists. Chapter 4, Opinions About the Industry and

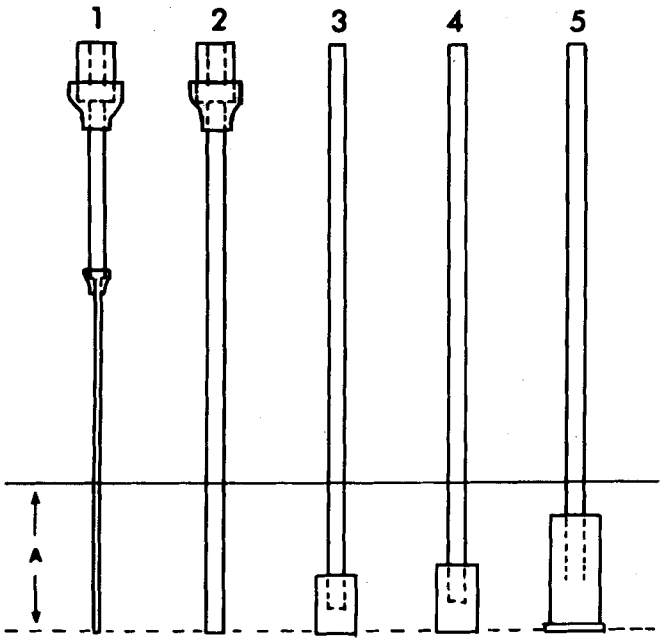


**Figure 1**—*Sampling probes, showing immersion depth (A).*

To reduce probe interference, five probe designs (Fig. 1) were tested with a six-place dissolution apparatus. All of the probes were constructed in this laboratory. Probes 3 and 4 were used early in the dissolution work. Probe 5 was designed to be similar to probes used in some commercial dissolution equipment. Probe 1 was the result of the laboratory's search for a probe with minimum interference in the dissolution test. Probe 2 was chosen to give an intermediate size between Probes 1 and 3. All probes were constructed from 3-mm o.d. glass tubing. The tip of Probe 1 was a 1.3-mm o.d. melting-point capillary. Commercially available filters were used. The 5-mg prednisone tablets used for the test were from a sample known to give different results depending on the presence or absence of a sample probe during the test.

One probe was suspended in each of five dissolution vessels, and the sixth vessel was used without a probe. The probes were placed halfway between the vessel wall and the paddle shaft, with the probe tip 25 mm below the liquid surface (approximately halfway between the liquid surface and the top of the paddle). The dissolution test was conducted for 30 min; samples then were withdrawn with a syringe for analysis by the USP (2) procedure. The test was repeated, and then the probes were moved to different vessels. This procedure was repeated until all probes were tested in duplicate in each vessel. This experimental design eliminated interference from sources other than the probes.

The data (Table I) show that there was a direct relationship between the displacement volume of the sampling probe and the increase in dissolution rate for the sample used. With the tablets used in this study, no effect on the observed dissolution rate was noted from Probe 1. However, the presence of any foreign object disturbs the hydrodynamics of the dissolution medium, and it is possible that the results from other, more sensitive samples could be influenced by the use of Probe 1.

The results show that the displacement volumes of sampling probes used with automated samplers should be as small as possible to reduce interference with the dissolution test.

(1) "The United States Pharmacopeia," 20th rev., United States Pharmacopeial Convention, Rockville, Md., 1980, p. 959.

(2) *Ibid.*, p. 655.

*Clyde E. Wells*

National Center for Drug Analysis
1114 Market Street
St. Louis, MO 63101

Received April 3, 1980.
Accepted for publication November 14, 1980.

# BOOKS

## REVIEWS

**Pharmacy: A Profession in Search of a Role.** By JACK ROBBINS. Navillus Publishing Corp. 1979. 143 pp. 15 × 23 cm. Price $14.95. (Available from Technomic Publishing Co., 265 Post Rd. W., Westport, CT 06880.)

The title of this book is both provocative and ambiguous. Readers seeking a definitive statement of the professional status or role of the pharmacist will not find it, nor will they find an expression of the need for clinical pharmacy, specialists, or new directions for the future.

Most of this book (large type, liberal white space) is devoted to an objective presentation of a 1975 mail survey of pharmacists. The study attempts to "correlate the dynamic changes in pharmacy during the past half century with the various modes which pharmacists have adopted to make their role expectations more consonant with their performance" and "to incorporate social–psychological theory in order to better understand the motivations underlying pharmacists' various adaptation modes." Theories (including role theory, role conflict and adaptation, and professionalization) are presented in easily understood language and context. Although a more in-depth discussion might be preferred, this approach is rational, laudable, and worthwhile in an area that too often is merely descriptive.

Chapter 5, Generational Effects: Younger *versus* Older Pharmacists, is especially intriguing to the reader seeking insight into the direction of future change. Chapter 8, Role Conflict and Social Change, is excellent and expands on the familiar business–professional conflict, reporting both the extent and direction of conflict within the context of practice changes.

Given the emphasis and style, chapter titles, acknowledgments, and cautious conclusions and projected future trends, one suspects that the book originally was a dissertation, a suspicion heightened by a citation of the same title by the same author in *Dissertation Abstracts* (1977). The dissertation subtitle, Functional and Psychological Adaptations of Pharmacists to Technological and Social Changes During the Past 50 Years, is descriptive of the contents. Exclusion of the survey instrument and the inadequate literature search (for example, no citations after 1976) will disappoint the researcher.

The foreword indicates that the book should be read by social scientists, pharmacy educators, individual pharmacy practitioners, pharmacy association executives, other health-care practitioners and organizations, members of Congress, and health-care planners and administrators. Such a broad appeal is unlikely to satisfy anyone completely.

The book should be of interest to pharmacy school administrators and pharmaceutical industry executives and employees whose market is practicing pharmacists. Chapter 4, Opinions About the Industry and

Selected Companies, may hold particular interest for the latter group. For other readers, the chapter is an unnecessarily lengthy digression from the theme. The book deserves library space and would be a useful addition to a reading list for an introductory pharmacy course.

*Reviewed by* H. John Baldwin
*Behavioral and Administrative Pharmacy*
*School of Pharmacy*
*West Virginia University*
*Morgantown, WV 26506*

---

**Analytical Procedures for Therapeutic Drug Monitoring and Emergency Toxicology.** By RANDALL C. BASELT. Biomedical Publications, P.O. Box 495, Davis, CA 95616. 1980. 316 pp. 18 × 26 cm. Price $35.00.

It is a realistic world that we work in, but one that is governed by idealistic regulatory agencies. As this compilation of analytical methods points out, one can only generate the "numbers" with the available equipment afforded by his or her employer. For example, you cannot determine the blood level of phencyclidine by nitrogen-specific GLC if all you have available is a dual-beam spectrophotometer. On the other hand, you will never achieve the sensitivity needed for phencyclidine detection using a dual-beam spectrophotometer. Baselt is realistic in pointing out that not all laboratories are equally equipped and that one may have to sacrifice some accuracy for speed, depending on the situation.

The book presents alphabetically a series of potential quantitative methods for 84 drugs and some general screening procedures. The drugs and chemicals included are those generally encountered by the clinical chemist and analytical toxicologist. For example, GLC procedures are given for ibuprofen, ketamine, and methylphenidate. Three methods are given for the oral hypoglycemics. Blood levels in the therapeutic and toxic ranges are given for each drug.

The introduction could have included some guidelines for the interpretation of the blood levels given for therapeutic, toxic, and lethal concentrations. Consideration must be given to whether these levels were obtained from human or animal data. Also, lethal levels may be those reported from only a single, isolated case or may represent a minimum lethal level. Consideration also must be given to any disease states or tolerance the person may have to a particular drug.

In general, the book lacks any specific indications of the factors that affect blood drug levels. The book deserves consideration and will serve as a reference in any forensic or clinical laboratory. It is useful for new laboratories or for laboratories that are expanding the number of tests they perform. It also gives important information concerning the equipment and supplies necessary in establishing an analytical toxicology laboratory.

The greatest utility of this book will be for analytical toxicologists, pathologists, and medical technologists in a large teaching hospital where emphasis is placed on therapeutic drug monitoring.

*Reviewed by* Charles L. Winek
*Duquesne University*
*Pittsburgh, PA 15219*

---

**How to Write and Publish a Scientific Paper.** By ROBERT A. DAY. ISI Press, 325 Chestnut St., Philadelphia, PA 19106. 1979. 160 pp. Price $8.95.

This valuable and witty book was written by a managing editor with 25 years of experience. Until this year, he was managing editor for the journals published by the American Society for Microbiology. The first 15 of the 26 chapters deal with the preparation of the different elements of a manuscript, beginning with a definition of a scientific paper and ending with where and how to submit the manuscript. The next two chapters describe the review and publishing processes. Chapter 22 is on ethics, rights, and permissions. The next three chapters discuss the use and misuse of English.

I recommend the book to authors and editors. If authors would learn its lessons, editors would return fewer manuscripts to be rewritten due to poor style. Perhaps editors should enclose a copy of the book with returned manuscripts! The book should be required reading for those who prepare internal documents in our institutions—academic, corporate, and governmental.

The next edition should have a chapter on footnotes, one on the metric system, and one directed to the typist. Manuscripts are received with footnotes typed single spaced at the bottom of the page. Too many authors of documents do not know how to abbreviate the metric or English system of units. The appendix on accepted abbreviations in this book gives the abbreviations for cubic centimeter, gram, and liter but not for milliliter. Typists must receive on-the-job training in manuscript preparation; their schools do not teach them, nor apparently do their employers.

*Reviewed by* Frederick Kavanagh
*829 36th St., N.W.*
*Corvallis, OR 97330*

---

## NOTICES

*Stabilitätsprüfung in der Pharmazie: Theorie und Praxis.* By W. GRIMM and G. SCHEPKY. Editio Cantor, D-7960 Aulendorf, West Germany. 1980. 397 pp. 16 × 24 cm. (*In German.*)

*Les Cosmétiques.* By H. THIERS. Masson Publishing USA, 14 E. 60th St., New York, NY 10022. 1980. 340 pp. 16 × 24 cm. (*In French.*)

*Casarett and Doull's Toxicology—The Basic Science of Poisons, 2nd Ed.* Edited by JOHN DOULL, CURTIS D. KLAASSEN, and MARY O. AMDUR. Macmillan, 866 Third Ave., New York, NY 10022. 1980. 778 pp. 17 × 26 cm. Price $29.95.

*The Renin–Angiotensin System.* Edited by J. ALAN JOHNSON and RALPH R. ANDERSON. (Advances in Experimental Medicine and Biology, Vol. 130.) Plenum, 227 W. 17th St., New York, NY 10011. 291 pp. 16 × 25 cm.

*Neurochemistry and Biochemical Pharmacology.* Edited by K. F. TIPTON. (International Review of Biochemistry, Vol. 26.) University Park Press, 233 E. Redwood St., Baltimore, MD 21202. 1980. 314 pp. 16 × 23.5 cm. Price $29.50.

*Recent Developments in Chromatography and Electrophoresis, 10.* Edited by ALBERTO FRIGERIO and MALCOLM McCAMISH. (Analytical Chemistry Symposia Series, Vol. 3.) 1980. 342 pp. 16 × 24 cm. Price $68.25.

*Advances in Chromatography, Vol. 18.* Edited by J. CALVIN GIDDINGS, ELI GRUSHKA, JACK CAZES, and PHYLLIS R. BROWN. Dekker, 270 Madison Ave., New York, NY 10016. 1980. 292 pp. 15 × 23 cm. Price $38.50.

*Fundamentals of Human Lymphoid Cell Culture.* By J. LESLIE GLICK. Dekker, 270 Madison Ave., New York, NY 10016. 1980. 157 pp. 14 × 23 cm. Price $22.50.

*IARC Monographs on the Evaluation of the Carcinogenic Risk of Chemicals to Humans, Vol. 22: Some Non-Nutritive Sweetening Agents.* International Agency for Research on Cancer. 1980. 208 pp. 17 × 24 cm. Price $15.00. (Distributed by the World Health Organization, 1211 Geneva 27, Switzerland.)

*WHO Expert Committee on Specifications for Pharmaceutical Preparations, 27th Report.* (Technical Report Series, No. 645.) World Health Organization, 1211 Geneva 27, Switzerland. 1980. 53 pp. 14 × 20 cm. Price Sw. fr. 4.

*Lithium Effects on Granulopoiesis and Immune Function.* Edited by ARTHUR H. ROSSOF and WILLIAM A. ROBINSON. (Advances in Experimental Medicine and Biology, Vol. 127.) Plenum, 227 W. 17th St., New York, NY 10011. 1980. 475 pp. 16 × 25 cm. Price $47.50.

*Vitamin D: Molecular Biology and Clinical Nutrition.* Edited by ANTHONY W. NORMAN. (Basic and Clinical Nutrition, Vol. 2.) Dekker, 270 Madison Ave., New York, NY 10016. 1980. 800 pp. 15 × 23 cm. Price $85.00.

*Reagents for Organic Synthesis, Vol. 8.* By MARY FIESER. Wiley, 605 Third Ave., New York, NY 10016. 1980. 602 pp. 15 × 23 cm. Price $36.00.

*Trends in Enzyme Histochemistry and Cytochemistry.* (Ciba Foundation Symposium 73.) Excerpta Medica, P. O. Box 1126, 1000 BC Amsterdam, The Netherlands. 1980. 114 pp. 15 × 24 cm. Price $53.75.

---

## NEW JOURNALS

*Journal of Pharmacy.* M. AMIN, Chief Editor. Faculty of Pharmacy, University of the Punjab, Lahore, Pakistan. 1980. 68 pp. 18 × 25 cm.

Selected Companies, may hold particular interest for the latter group. For other readers, the chapter is an unnecessarily lengthy digression from the theme. The book deserves library space and would be a useful addition to a reading list for an introductory pharmacy course.

*Reviewed by* H. John Baldwin
*Behavioral and Administrative Pharmacy*
*School of Pharmacy*
*West Virginia University*
*Morgantown, WV 26506*

---

**Analytical Procedures for Therapeutic Drug Monitoring and Emergency Toxicology.** By RANDALL C. BASELT. Biomedical Publications, P.O. Box 495, Davis, CA 95616. 1980. 316 pp. 18 × 26 cm. Price $35.00.

It is a realistic world that we work in, but one that is governed by idealistic regulatory agencies. As this compilation of analytical methods points out, one can only generate the "numbers" with the available equipment afforded by his or her employer. For example, you cannot determine the blood level of phencyclidine by nitrogen-specific GLC if all you have available is a dual-beam spectrophotometer. On the other hand, you will never achieve the sensitivity needed for phencyclidine detection using a dual-beam spectrophotometer. Baselt is realistic in pointing out that not all laboratories are equally equipped and that one may have to sacrifice some accuracy for speed, depending on the situation.

The book presents alphabetically a series of potential quantitative methods for 84 drugs and some general screening procedures. The drugs and chemicals included are those generally encountered by the clinical chemist and analytical toxicologist. For example, GLC procedures are given for ibuprofen, ketamine, and methylphenidate. Three methods are given for the oral hypoglycemics. Blood levels in the therapeutic and toxic ranges are given for each drug.

The introduction could have included some guidelines for the interpretation of the blood levels given for therapeutic, toxic, and lethal concentrations. Consideration must be given to whether these levels were obtained from human or animal data. Also, lethal levels may be those reported from only a single, isolated case or may represent a minimum lethal level. Consideration also must be given to any disease states or tolerance the person may have to a particular drug.

In general, the book lacks any specific indications of the factors that affect blood drug levels. The book deserves consideration and will serve as a reference in any forensic or clinical laboratory. It is useful for new laboratories or for laboratories that are expanding the number of tests they perform. It also gives important information concerning the equipment and supplies necessary in establishing an analytical toxicology laboratory.

The greatest utility of this book will be for analytical toxicologists, pathologists, and medical technologists in a large teaching hospital where emphasis is placed on therapeutic drug monitoring.

*Reviewed by* Charles L. Winek
*Duquesne University*
*Pittsburgh, PA 15219*

---

**How to Write and Publish a Scientific Paper.** By ROBERT A. DAY. ISI Press, 325 Chestnut St., Philadelphia, PA 19106. 1979. 160 pp. Price $8.95.

This valuable and witty book was written by a managing editor with 25 years of experience. Until this year, he was managing editor for the journals published by the American Society for Microbiology. The first 15 of the 26 chapters deal with the preparation of the different elements of a manuscript, beginning with a definition of a scientific paper and ending with where and how to submit the manuscript. The next two chapters describe the review and publishing processes. Chapter 22 is on ethics, rights, and permissions. The next three chapters discuss the use and misuse of English.

I recommend the book to authors and editors. If authors would learn its lessons, editors would return fewer manuscripts to be rewritten due to poor style. Perhaps editors should enclose a copy of the book with returned manuscripts! The book should be required reading for those who prepare internal documents in our institutions—academic, corporate, and governmental.

The next edition should have a chapter on footnotes, one on the metric system, and one directed to the typist. Manuscripts are received with footnotes typed single spaced at the bottom of the page. Too many authors of documents do not know how to abbreviate the metric or English system of units. The appendix on accepted abbreviations in this book gives the abbreviations for cubic centimeter, gram, and liter but not for milliliter. Typists must receive on-the-job training in manuscript preparation; their schools do not teach them, nor apparently do their employers.

*Reviewed by* Frederick Kavanagh
*829 36th St., N.W.*
*Corvallis, OR 97330*

---

## NOTICES

*Stabilitätsprüfung in der Pharmazie: Theorie und Praxis.* By W. GRIMM and G. SCHEPKY. Editio Cantor, D-7960 Aulendorf, West Germany. 1980. 397 pp. 16 × 24 cm. (*In German.*)

*Les Cosmétiques.* By H. THIERS. Masson Publishing USA, 14 E. 60th St., New York, NY 10022. 1980. 340 pp. 16 × 24 cm. (*In French.*)

*Casarett and Doull's Toxicology—The Basic Science of Poisons, 2nd Ed.* Edited by JOHN DOULL, CURTIS D. KLAASSEN, and MARY O. AMDUR. Macmillan, 866 Third Ave., New York, NY 10022. 1980. 778 pp. 17 × 26 cm. Price $29.95.

*The Renin–Angiotensin System.* Edited by J. ALAN JOHNSON and RALPH R. ANDERSON. (Advances in Experimental Medicine and Biology, Vol. 130.) Plenum, 227 W. 17th St., New York, NY 10011. 291 pp. 16 × 25 cm.

*Neurochemistry and Biochemical Pharmacology.* Edited by K. F. TIPTON. (International Review of Biochemistry, Vol. 26.) University Park Press, 233 E. Redwood St., Baltimore, MD 21202. 1980. 314 pp. 16 × 23.5 cm. Price $29.50.

*Recent Developments in Chromatography and Electrophoresis, 10.* Edited by ALBERTO FRIGERIO and MALCOLM McCAMISH. (Analytical Chemistry Symposia Series, Vol. 3.) 1980. 342 pp. 16 × 24 cm. Price $68.25.

*Advances in Chromatography, Vol. 18.* Edited by J. CALVIN GIDDINGS, ELI GRUSHKA, JACK CAZES, and PHYLLIS R. BROWN. Dekker, 270 Madison Ave., New York, NY 10016. 1980. 292 pp. 15 × 23 cm. Price $38.50.

*Fundamentals of Human Lymphoid Cell Culture.* By J. LESLIE GLICK. Dekker, 270 Madison Ave., New York, NY 10016. 1980. 157 pp. 14 × 23 cm. Price $22.50.

*IARC Monographs on the Evaluation of the Carcinogenic Risk of Chemicals to Humans, Vol. 22: Some Non-Nutritive Sweetening Agents.* International Agency for Research on Cancer. 1980. 208 pp. 17 × 24 cm. Price $15.00. (Distributed by the World Health Organization, 1211 Geneva 27, Switzerland.)

*WHO Expert Committee on Specifications for Pharmaceutical Preparations, 27th Report.* (Technical Report Series, No. 645.) World Health Organization, 1211 Geneva 27, Switzerland. 1980. 53 pp. 14 × 20 cm. Price Sw. fr. 4.

*Lithium Effects on Granulopoiesis and Immune Function.* Edited by ARTHUR H. ROSSOF and WILLIAM A. ROBINSON. (Advances in Experimental Medicine and Biology, Vol. 127.) Plenum, 227 W. 17th St., New York, NY 10011. 1980. 475 pp. 16 × 25 cm. Price $47.50.

*Vitamin D: Molecular Biology and Clinical Nutrition.* Edited by ANTHONY W. NORMAN. (Basic and Clinical Nutrition, Vol. 2.) Dekker, 270 Madison Ave., New York, NY 10016. 1980. 800 pp. 15 × 23 cm. Price $85.00.

*Reagents for Organic Synthesis, Vol. 8.* By MARY FIESER. Wiley, 605 Third Ave., New York, NY 10016. 1980. 602 pp. 15 × 23 cm. Price $36.00.

*Trends in Enzyme Histochemistry and Cytochemistry.* (Ciba Foundation Symposium 73.) Excerpta Medica, P. O. Box 1126, 1000 BC Amsterdam, The Netherlands. 1980. 114 pp. 15 × 24 cm. Price $53.75.

---

## NEW JOURNALS

*Journal of Pharmacy.* M. AMIN, Chief Editor. Faculty of Pharmacy, University of the Punjab, Lahore, Pakistan. 1980. 68 pp. 18 × 25 cm.

Selected Companies, may hold particular interest for the latter group. For other readers, the chapter is an unnecessarily lengthy digression from the theme. The book deserves library space and would be a useful addition to a reading list for an introductory pharmacy course.

*Reviewed by* H. John Baldwin
*Behavioral and Administrative Pharmacy*
*School of Pharmacy*
*West Virginia University*
*Morgantown, WV 26506*

---

**Analytical Procedures for Therapeutic Drug Monitoring and Emergency Toxicology.** By RANDALL C. BASELT. Biomedical Publications, P.O. Box 495, Davis, CA 95616. 1980. 316 pp. 18 × 26 cm. Price $35.00.

It is a realistic world that we work in, but one that is governed by idealistic regulatory agencies. As this compilation of analytical methods points out, one can only generate the "numbers" with the available equipment afforded by his or her employer. For example, you cannot determine the blood level of phencyclidine by nitrogen-specific GLC if all you have available is a dual-beam spectrophotometer. On the other hand, you will never achieve the sensitivity needed for phencyclidine detection using a dual-beam spectrophotometer. Baselt is realistic in pointing out that not all laboratories are equally equipped and that one may have to sacrifice some accuracy for speed, depending on the situation.

The book presents alphabetically a series of potential quantitative methods for 84 drugs and some general screening procedures. The drugs and chemicals included are those generally encountered by the clinical chemist and analytical toxicologist. For example, GLC procedures are given for ibuprofen, ketamine, and methylphenidate. Three methods are given for the oral hypoglycemics. Blood levels in the therapeutic and toxic ranges are given for each drug.

The introduction could have included some guidelines for the interpretation of the blood levels given for therapeutic, toxic, and lethal concentrations. Consideration must be given to whether these levels were obtained from human or animal data. Also, lethal levels may be those reported from only a single, isolated case or may represent a minimum lethal level. Consideration also must be given to any disease states or tolerance the person may have to a particular drug.

In general, the book lacks any specific indications of the factors that affect blood drug levels. The book deserves consideration and will serve as a reference in any forensic or clinical laboratory. It is useful for new laboratories or for laboratories that are expanding the number of tests they perform. It also gives important information concerning the equipment and supplies necessary in establishing an analytical toxicology laboratory.

The greatest utility of this book will be for analytical toxicologists, pathologists, and medical technologists in a large teaching hospital where emphasis is placed on therapeutic drug monitoring.

*Reviewed by* Charles L. Winek
*Duquesne University*
*Pittsburgh, PA 15219*

---

**How to Write and Publish a Scientific Paper.** By ROBERT A. DAY. ISI Press, 325 Chestnut St., Philadelphia, PA 19106. 1979. 160 pp. Price $8.95.

This valuable and witty book was written by a managing editor with 25 years of experience. Until this year, he was managing editor for the journals published by the American Society for Microbiology. The first 15 of the 26 chapters deal with the preparation of the different elements of a manuscript, beginning with a definition of a scientific paper and ending with where and how to submit the manuscript. The next two chapters describe the review and publishing processes. Chapter 22 is on ethics, rights, and permissions. The next three chapters discuss the use and misuse of English.

I recommend the book to authors and editors. If authors would learn its lessons, editors would return fewer manuscripts to be rewritten due to poor style. Perhaps editors should enclose a copy of the book with returned manuscripts! The book should be required reading for those who prepare internal documents in our institutions—academic, corporate, and governmental.

The next edition should have a chapter on footnotes, one on the metric system, and one directed to the typist. Manuscripts are received with footnotes typed single spaced at the bottom of the page. Too many authors of documents do not know how to abbreviate the metric or English system of units. The appendix on accepted abbreviations in this book gives the abbreviations for cubic centimeter, gram, and liter but not for milliliter. Typists must receive on-the-job training in manuscript preparation; their schools do not teach them, nor apparently do their employers.

*Reviewed by* Frederick Kavanagh
*829 36th St., N.W.*
*Corvallis, OR 97330*

---

## NOTICES

*Stabilitätsprüfung in der Pharmazie: Theorie und Praxis.* By W. GRIMM and G. SCHEPKY. Editio Cantor, D-7960 Aulendorf, West Germany. 1980. 397 pp. 16 × 24 cm. (*In German.*)

*Les Cosmétiques.* By H. THIERS. Masson Publishing USA, 14 E. 60th St., New York, NY 10022. 1980. 340 pp. 16 × 24 cm. (*In French.*)

*Casarett and Doull's Toxicology—The Basic Science of Poisons, 2nd Ed.* Edited by JOHN DOULL, CURTIS D. KLAASSEN, and MARY O. AMDUR. Macmillan, 866 Third Ave., New York, NY 10022. 1980. 778 pp. 17 × 26 cm. Price $29.95.

*The Renin–Angiotensin System.* Edited by J. ALAN JOHNSON and RALPH R. ANDERSON. (Advances in Experimental Medicine and Biology, Vol. 130.) Plenum, 227 W. 17th St., New York, NY 10011. 291 pp. 16 × 25 cm.

*Neurochemistry and Biochemical Pharmacology.* Edited by K. F. TIPTON. (International Review of Biochemistry, Vol. 26.) University Park Press, 233 E. Redwood St., Baltimore, MD 21202. 1980. 314 pp. 16 × 23.5 cm. Price $29.50.

*Recent Developments in Chromatography and Electrophoresis, 10.* Edited by ALBERTO FRIGERIO and MALCOLM McCAMISH. (Analytical Chemistry Symposia Series, Vol. 3.) 1980. 342 pp. 16 × 24 cm. Price $68.25.

*Advances in Chromatography, Vol. 18.* Edited by J. CALVIN GIDDINGS, ELI GRUSHKA, JACK CAZES, and PHYLLIS R. BROWN. Dekker, 270 Madison Ave., New York, NY 10016. 1980. 292 pp. 15 × 23 cm. Price $38.50.

*Fundamentals of Human Lymphoid Cell Culture.* By J. LESLIE GLICK. Dekker, 270 Madison Ave., New York, NY 10016. 1980. 157 pp. 14 × 23 cm. Price $22.50.

*IARC Monographs on the Evaluation of the Carcinogenic Risk of Chemicals to Humans, Vol. 22: Some Non-Nutritive Sweetening Agents.* International Agency for Research on Cancer. 1980. 208 pp. 17 × 24 cm. Price $15.00. (Distributed by the World Health Organization, 1211 Geneva 27, Switzerland.)

*WHO Expert Committee on Specifications for Pharmaceutical Preparations, 27th Report.* (Technical Report Series, No. 645.) World Health Organization, 1211 Geneva 27, Switzerland. 1980. 53 pp. 14 × 20 cm. Price Sw. fr. 4.

*Lithium Effects on Granulopoiesis and Immune Function.* Edited by ARTHUR H. ROSSOF and WILLIAM A. ROBINSON. (Advances in Experimental Medicine and Biology, Vol. 127.) Plenum, 227 W. 17th St., New York, NY 10011. 1980. 475 pp. 16 × 25 cm. Price $47.50.

*Vitamin D: Molecular Biology and Clinical Nutrition.* Edited by ANTHONY W. NORMAN. (Basic and Clinical Nutrition, Vol. 2.) Dekker, 270 Madison Ave., New York, NY 10016. 1980. 800 pp. 15 × 23 cm. Price $85.00.

*Reagents for Organic Synthesis, Vol. 8.* By MARY FIESER. Wiley, 605 Third Ave., New York, NY 10016. 1980. 602 pp. 15 × 23 cm. Price $36.00.

*Trends in Enzyme Histochemistry and Cytochemistry.* (Ciba Foundation Symposium 73.) Excerpta Medica, P. O. Box 1126, 1000 BC Amsterdam, The Netherlands. 1980. 114 pp. 15 × 24 cm. Price $53.75.

---

## NEW JOURNALS

*Journal of Pharmacy.* M. AMIN, Chief Editor. Faculty of Pharmacy, University of the Punjab, Lahore, Pakistan. 1980. 68 pp. 18 × 25 cm.

Selected Companies, may hold particular interest for the latter group. For other readers, the chapter is an unnecessarily lengthy digression from the theme. The book deserves library space and would be a useful addition to a reading list for an introductory pharmacy course.

*Reviewed by* H. John Baldwin
*Behavioral and Administrative Pharmacy*
*School of Pharmacy*
*West Virginia University*
*Morgantown, WV 26506*

---

**Analytical Procedures for Therapeutic Drug Monitoring and Emergency Toxicology.** By RANDALL C. BASELT. Biomedical Publications, P.O. Box 495, Davis, CA 95616. 1980. 316 pp. 18 × 26 cm. Price $35.00.

It is a realistic world that we work in, but one that is governed by idealistic regulatory agencies. As this compilation of analytical methods points out, one can only generate the "numbers" with the available equipment afforded by his or her employer. For example, you cannot determine the blood level of phencyclidine by nitrogen-specific GLC if all you have available is a dual-beam spectrophotometer. On the other hand, you will never achieve the sensitivity needed for phencyclidine detection using a dual-beam spectrophotometer. Baselt is realistic in pointing out that not all laboratories are equally equipped and that one may have to sacrifice some accuracy for speed, depending on the situation.

The book presents alphabetically a series of potential quantitative methods for 84 drugs and some general screening procedures. The drugs and chemicals included are those generally encountered by the clinical chemist and analytical toxicologist. For example, GLC procedures are given for ibuprofen, ketamine, and methylphenidate. Three methods are given for the oral hypoglycemics. Blood levels in the therapeutic and toxic ranges are given for each drug.

The introduction could have included some guidelines for the interpretation of the blood levels given for therapeutic, toxic, and lethal concentrations. Consideration must be given to whether these levels were obtained from human or animal data. Also, lethal levels may be those reported from only a single, isolated case or may represent a minimum lethal level. Consideration also must be given to any disease states or tolerance the person may have to a particular drug.

In general, the book lacks any specific indications of the factors that affect blood drug levels. The book deserves consideration and will serve as a reference in any forensic or clinical laboratory. It is useful for new laboratories or for laboratories that are expanding the number of tests they perform. It also gives important information concerning the equipment and supplies necessary in establishing an analytical toxicology laboratory.

The greatest utility of this book will be for analytical toxicologists, pathologists, and medical technologists in a large teaching hospital where emphasis is placed on therapeutic drug monitoring.

*Reviewed by* Charles L. Winek
*Duquesne University*
*Pittsburgh, PA 15219*

---

**How to Write and Publish a Scientific Paper.** By ROBERT A. DAY. ISI Press, 325 Chestnut St., Philadelphia, PA 19106. 1979. 160 pp. Price $8.95.

This valuable and witty book was written by a managing editor with 25 years of experience. Until this year, he was managing editor for the journals published by the American Society for Microbiology. The first 15 of the 26 chapters deal with the preparation of the different elements of a manuscript, beginning with a definition of a scientific paper and ending with where and how to submit the manuscript. The next two chapters describe the review and publishing processes. Chapter 22 is on ethics, rights, and permissions. The next three chapters discuss the use and misuse of English.

I recommend the book to authors and editors. If authors would learn its lessons, editors would return fewer manuscripts to be rewritten due to poor style. Perhaps editors should enclose a copy of the book with returned manuscripts! The book should be required reading for those who prepare internal documents in our institutions—academic, corporate, and governmental.

The next edition should have a chapter on footnotes, one on the metric system, and one directed to the typist. Manuscripts are received with footnotes typed single spaced at the bottom of the page. Too many authors of documents do not know how to abbreviate the metric or English system of units. The appendix on accepted abbreviations in this book gives the abbreviations for cubic centimeter, gram, and liter but not for milliliter. Typists must receive on-the-job training in manuscript preparation; their schools do not teach them, nor apparently do their employers.

*Reviewed by* Frederick Kavanagh
*829 36th St., N.W.*
*Corvallis, OR 97330*

---

## NOTICES

*Stabilitätsprüfung in der Pharmazie: Theorie und Praxis.* By W. GRIMM and G. SCHEPKY. Editio Cantor, D-7960 Aulendorf, West Germany. 1980. 397 pp. 16 × 24 cm. (*In German.*)

*Les Cosmétiques.* By H. THIERS. Masson Publishing USA, 14 E. 60th St., New York, NY 10022. 1980. 340 pp. 16 × 24 cm. (*In French.*)

*Casarett and Doull's Toxicology—The Basic Science of Poisons, 2nd Ed.* Edited by JOHN DOULL, CURTIS D. KLAASSEN, and MARY O. AMDUR. Macmillan, 866 Third Ave., New York, NY 10022. 1980. 778 pp. 17 × 26 cm. Price $29.95.

*The Renin–Angiotensin System.* Edited by J. ALAN JOHNSON and RALPH R. ANDERSON. (Advances in Experimental Medicine and Biology, Vol. 130.) Plenum, 227 W. 17th St., New York, NY 10011. 291 pp. 16 × 25 cm.

*Neurochemistry and Biochemical Pharmacology.* Edited by K. F. TIPTON. (International Review of Biochemistry, Vol. 26.) University Park Press, 233 E. Redwood St., Baltimore, MD 21202. 1980. 314 pp. 16 × 23.5 cm. Price $29.50.

*Recent Developments in Chromatography and Electrophoresis, 10.* Edited by ALBERTO FRIGERIO and MALCOLM McCAMISH. (Analytical Chemistry Symposia Series, Vol. 3.) 1980. 342 pp. 16 × 24 cm. Price $68.25.

*Advances in Chromatography, Vol. 18.* Edited by J. CALVIN GIDDINGS, ELI GRUSHKA, JACK CAZES, and PHYLLIS R. BROWN. Dekker, 270 Madison Ave., New York, NY 10016. 1980. 292 pp. 15 × 23 cm. Price $38.50.

*Fundamentals of Human Lymphoid Cell Culture.* By J. LESLIE GLICK. Dekker, 270 Madison Ave., New York, NY 10016. 1980. 157 pp. 14 × 23 cm. Price $22.50.

*IARC Monographs on the Evaluation of the Carcinogenic Risk of Chemicals to Humans, Vol. 22: Some Non-Nutritive Sweetening Agents.* International Agency for Research on Cancer. 1980. 208 pp. 17 × 24 cm. Price $15.00. (Distributed by the World Health Organization, 1211 Geneva 27, Switzerland.)

*WHO Expert Committee on Specifications for Pharmaceutical Preparations, 27th Report.* (Technical Report Series, No. 645.) World Health Organization, 1211 Geneva 27, Switzerland. 1980. 53 pp. 14 × 20 cm. Price Sw. fr. 4.

*Lithium Effects on Granulopoiesis and Immune Function.* Edited by ARTHUR H. ROSSOF and WILLIAM A. ROBINSON. (Advances in Experimental Medicine and Biology, Vol. 127.) Plenum, 227 W. 17th St., New York, NY 10011. 1980. 475 pp. 16 × 25 cm. Price $47.50.

*Vitamin D: Molecular Biology and Clinical Nutrition.* Edited by ANTHONY W. NORMAN. (Basic and Clinical Nutrition, Vol. 2.) Dekker, 270 Madison Ave., New York, NY 10016. 1980. 800 pp. 15 × 23 cm. Price $85.00.

*Reagents for Organic Synthesis, Vol. 8.* By MARY FIESER. Wiley, 605 Third Ave., New York, NY 10016. 1980. 602 pp. 15 × 23 cm. Price $36.00.

*Trends in Enzyme Histochemistry and Cytochemistry.* (Ciba Foundation Symposium 73.) Excerpta Medica, P. O. Box 1126, 1000 BC Amsterdam, The Netherlands. 1980. 114 pp. 15 × 24 cm. Price $53.75.

---

## NEW JOURNALS

*Journal of Pharmacy.* M. AMIN, Chief Editor. Faculty of Pharmacy, University of the Punjab, Lahore, Pakistan. 1980. 68 pp. 18 × 25 cm.

A publication of the
American Pharmaceutical Association—
the National Professional Society
of Pharmacists

# JOURNAL OF PHARMACEUTICAL SCIENCES

## INDEX TO AUTHORS
## INDEX TO SUBJECTS

VOLUME 70
JANUARY TO DECEMBER, 1981

*Published monthly under the supervision of the Board of Trustees*

MARY H. FERGUSON
*Editor*

NANCY E. BROWN
*Production Editor*

JOHN PATRICK EVANS
*Copy Editor*

MICHAEL K. HAYES
*Copy Editor*

EDWARD G. FELDMANN
*Contributing Editor*

SAMUEL W. GOLDSTEIN
*Contributing Editor*

BELLE R. BECK
*Editorial Secretary*

EDWARD G. FELDMANN
*Acting Director of Publications*

EDITORIAL ADVISORY BOARD

John Autian
Norman R. Farnsworth
William J. Jusko
Herbert A. Lieberman
David E. Mann, Jr.
Ian W. Mathison
Gerald J. Papariello
Edward G. Rippie

JOURNAL OF PHARMACEUTICAL SCIENCES

MARCH 1981
VOLUME 70 NUMBER 3

RESEARCH ARTICLES

# Kinetics of *trans*-Cinnamic Anhydride Reactions Catalyzed by Pyridine, 4-Dimethylaminopyridine, and *N*-Methylimidazole

**SHU-FEN LIN and KENNETH A. CONNORS** ˣ

Received June 27, 1980, from the *School of Pharmacy, University of Wisconsin, Madison, WI 53706.* Accepted for publication August 19, 1980.

**Abstract** □ The kinetics of hydrolysis of *trans*-cinnamic anhydride and of its reactions with hydroxy compounds were studied in the presence of pyridine, 4-dimethylaminopyridine, and *N*-methylimidazole as catalysts. The absolute rates of the catalyzed hydrolysis decreased with increasing acetonitrile content (decreasing solvent polarity), but the catalytic efficiency of *N*-methylimidazole and 4-dimethylaminopyridine relative to pyridine increased as the solvent polarity decreased. The relative catalytic rates for the cinnamoylation of *n*-propanol in acetonitrile were 1:259:16,000 for pyridine, *N*-methylimidazole, and 4-dimethylaminopyridine, respectively.

**Keyphrases** □ Kinetics—hydrolysis of *trans*-cinnamic anhydride catalyzed by pyridine, 4-dimethylaminopyridine, and *N*-methylimidazole □ *trans*-Cinnamic anhydride—hydrolysis kinetics catalyzed by pyridine, 4-dimethylaminopyridine, and *N*-methylimidazole □ Hydrolysis kinetics—*trans*-cinnamic anhydride, catalyzed by pyridine, 4-dimethylaminopyridine, and *N*-methylimidazole

The cinnamoyl group, $C_6H_5CH{=}CHCO$, is a powerful chromophore and, therefore, of analytical interest. A quantitative method for aliphatic amines (1, 2) is based on their reaction with *trans*-cinnamic anhydride to give the corresponding cinnamamides. These reactions are rapid and quantitative, but aromatic amines and alcohols, which are relatively weak nucleophiles, react too slowly for practical use of the published procedure.

Pyridine is a widely used acylation catalyst; recently, the more powerful 4-dimethylaminopyridine (3, 4) and *N*-methylimidazole (5, 6) have been introduced as catalysts for analytical acetylations. Therefore, the application of these catalysts to the cinnamoylation of aromatic amines and alcohols may be of analytical utility. This paper describes kinetic measurements on the hydrolysis of cinnamic anhydride and its reactions with some hydroxy compounds using pyridine, 4-dimethylaminopyridine, and *N*-methylimidazole as the catalysts.

## EXPERIMENTAL

**Materials**—*trans*-Cinnamic anhydride was prepared by a modified published procedure (7). A mixture of 30 g of *trans*-cinnamic acid and 50 g of acetic anhydride, protected from atmospheric moisture, was refluxed for 2 hr. Acetic acid and acetic anhydride were removed by distillation, and the solid residue was recrystallized three times from benzene, in the presence of activated charcoal, to give colorless needles, mp 136–137° [lit. (7) mp 136°]. The molar absorptivity in acetonitrile solution at $\lambda_{max}$ 294 nm was $4.23 \times 10^4$ [lit. (8) $4.32 \times 10^4$].

Pyridine[1] and *N*-methylimidazole[2] were used directly. 4-Dimethylaminopyridine[2] was recrystallized from petroleum ether, mp 113° [lit. (9) mp 112–113°]. Acetonitrile[3] was a spectrophotometric grade solvent. Phenol[4] was recrystallized from benzene, mp 40.9° [lit. (10) mp 40.85°]. Alcohols were reagent grade products and were used directly. Buffers were prepared from reagent grade materials and water that was redistilled from alkaline permanganate in an all-glass system. Ionic strength was brought to a constant value with potassium chloride.

**Procedures**—*Hydrolysis Kinetics*—All kinetic runs were carried out at 25.0°. The ionic strength in the hydrolysis studies was 0.10 *M*. The rate measurements were made in one of three ways, depending on the reaction half-life. If the half-life was <2 min, 50 μl of $3.3 \times 10^{-5}$ *M trans*-cinnamic anhydride in acetonitrile was stirred rapidly into 3.0 ml of the aqueous buffer contained in a rectangular 1-cm spectrophotometer cell positioned in the spectrophotometer[5] cell compartment. Absorbance, monitored at 305 nm, was recorded as a function of time beginning within 10 sec of initiation of the reaction.

For reactions with half-lives of 2–15 min, 2.0 ml of $1.7 \times 10^{-4}$ *M* cinnamic anhydride in acetonitrile was delivered into 50.0 ml of aqueous buffer. The mixed solution was transferred to a 10-cm cell for absorbance measurements at 305 nm. With both procedures, the data were interpreted by means of plots of log $(A_t - A_\infty)$ *versus* $t$, where $A_t$ is the absorbance at time $t$ and $A_\infty$ is the absorbance when the reaction is essentially complete (at least 10 half-lives). From the slopes of the linear plots, the apparent first-order rate constants were evaluated.

[1] Fisher Scientific Co.
[2] Aldrich Chemical Co.
[3] Burdick & Jackson Laboratories.
[4] Mallinckrodt Chemical Works.
[5] Cary model 14.

0022-3549/81/0300-0235$01.00/0
© 1981, American Pharmaceutical Association

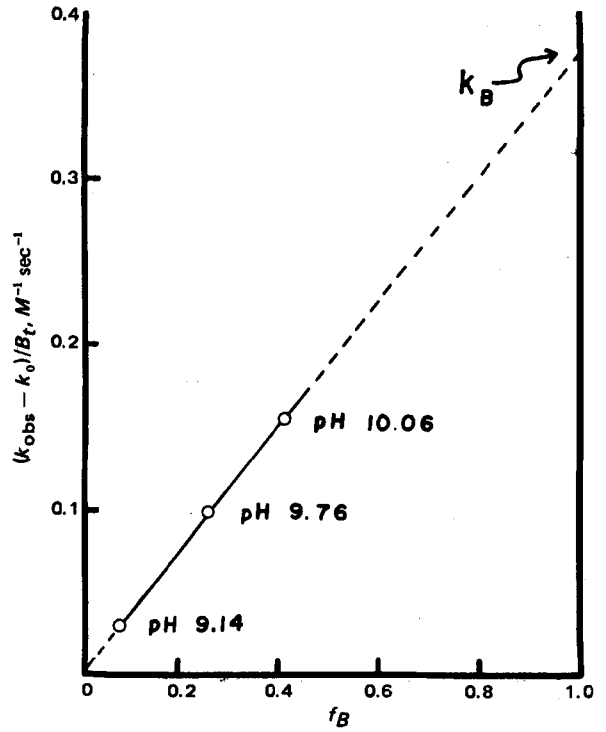


**Figure 1**—*Plot according to Eq. 4 for* trans-*cinnamic anhydride hydrolysis in carbonate buffers at 25°.*

If the half-life was >15 min, an initial rate method was used. The absorbance of the reaction mixture (prepared as for reactions having half-lives of 2–15 min) at 305 nm was a linear function of time initially. By writing the rate equation as $V_0 = k_{obs}C_A^0$ at essentially zero time, $k_{obs}$ can be calculated as the ratio of the initial rate $V_0$ (in moles per liter second) to the initial anhydride concentration $C_A^0$. The initial rate $V_0$ is obtained from the initial slope $V_0'$ of absorbance *versus* time by $V_0 = V_0'/b(\epsilon_R - 2\epsilon_p)$, where $b$ is the path length and $\epsilon_R$ and $\epsilon_p$ are the molar absorptivities of reactant cinnamic anhydride and product cinnamic acid anion, respectively. At 305 nm, $\epsilon_R = 3.60 \times 10^4$ and $\epsilon_p = 1.34 \times 10^3$.

*Esterification Kinetics*—Appropriate volumes of acetonitrile solutions of the hydroxy compound and the catalyst (the volumes depend on the reactivities of the hydroxy compound and the catalyst) were mixed in a beaker. An acetonitrile solution of cinnamic anhydride was added, and the absorbance was followed at 305 nm in a 1-cm cell.

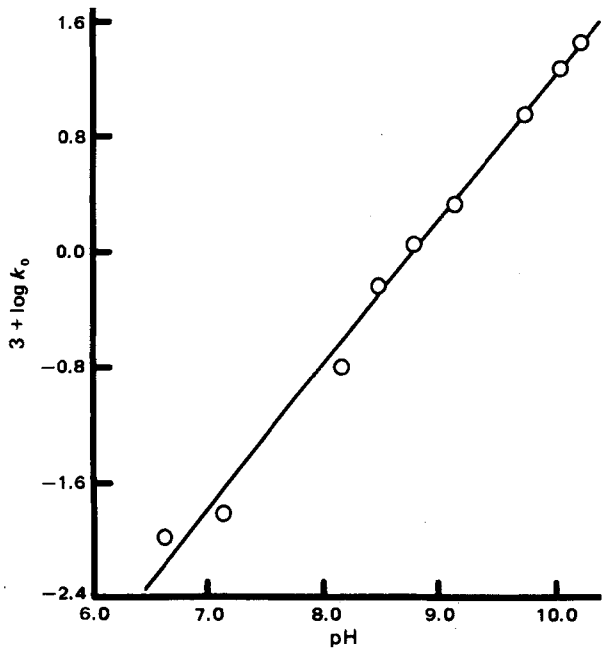


**Figure 2**—*The pH-rate profile for the hydrolysis of* trans-*cinnamic anhydride at 25°, ionic strength 0.10* M, *and zero buffer concentration. Data were taken from Table I.*

**Table I—Rate Constants for Hydrolysis of *trans*-Cinnamic Anhydride at 25°**

| pH | Buffer | $10^3 k_0$, sec$^{-1}$ | $k_B$, $M^{-1}$ sec$^{-1}$ |
|---|---|---|---|
| 10.23 | Carbonate | 29.07 | 0.381[a] |
| 10.06 | Carbonate | 18.84 | |
| 9.76 | Carbonate | 8.95 | |
| 9.14 | Carbonate | 2.14 | |
| 8.80 | Tris(hydroxymethyl)-aminomethane | 1.13 | 0.332[a] |
| 8.48 | Tris(hydroxymethyl)-aminomethane | 0.582 | |
| 8.17 | Tris(hydroxymethyl)-aminomethane | 0.158 | |
| 7.14 | Phosphate | 0.0160 | 0.00254[a] |
| 6.64 | Phosphate | 0.0111 | |

[a] Mean values.

## RESULTS AND DISCUSSION

**Cinnamic Anhydride Hydrolysis Kinetics**—The hydrolysis reaction shown in Scheme I:

$$(C_6H_5CH{=}CHCO)_2O + H_2O \rightarrow 2\ C_6H_5CH{=}CHCOOH$$

*Scheme I*

is accompanied by a decrease in absorbance at 305 nm. Pseudo-first-order kinetics were observed at constant pH, temperature, and ionic strength. Reproducibility was excellent, as indicated by this typical result at pH 8.8 (mean ± *SD*): $k_{obs} = 6.75 \pm 0.04 \times 10^{-3}$ sec$^{-1}$ ($n = 3$).

**Buffer Catalysis and pH–Rate Profile**—The pseudo-first-order rate constants were measured as a function of total buffer concentration at constant pH, temperature (25°), and ionic strength (0.10 *M*), over the pH range of 6.64–10.23 in phosphate, tris(hydroxymethyl)aminomethane, and carbonate buffers. The rate constants increased with buffer concentration and were interpreted as follows. Letting $k_{obs}$ represent the observed pseudo-first-order rate constant:

$$k_{obs} = k_0 + k_B[B] + k_A[A] \qquad \text{(Eq. 1)}$$

where [A] and [B] are the molar concentrations of buffer species in the conjugate acid and base forms, respectively, $k_A$ and $k_B$ are the second-order rate constants for buffer catalysis by $A$ and $B$, respectively, and $k_0$ is the first-order rate constant for hydrolysis at zero buffer concentrations, with the entire equation referring to constant pH. The buffer species concentrations can be related to the total buffer concentration $B_t$ by:

$$[A] = f_A B_t \qquad \text{(Eq. 2)}$$

$$[B] = f_B B_t \qquad \text{(Eq. 3)}$$

where $f_A$ and $f_B$ are the fractions of buffer in the indicated form. Combining Eqs. 1–3 gives:

$$\frac{k_{obs} - k_0}{B_t} = k_A + (k_B - k_A)f_B \qquad \text{(Eq. 4)}$$

If the experiment is carried out at several pH values (with the same buffer), a plot of $(k_{obs} - k_0)/B_t$ against $f_B$ is predicted to be linear, with

**Table II—Rate Constants for Catalyzed Hydrolysis of Cinnamic Anhydride at pH 8.45 and 25°**

| Catalyst | $10^4 C_t$[a], $M$ | $10^4$ [C], $M$ | $10^3 k_{obs}$, sec$^{-1}$ | $k_C$, $M^{-1}$ sec$^{-1}$ |
|---|---|---|---|---|
| Pyridine | 12.1 | 12.1 | 8.60 | 2.77 |
| | 19.4 | 19.4 | 10.28 | 2.60 |
| | 24.2 | 24.2 | 11.85 | 2.72 |
| *N*-Methylimidazole | 2.94 | 2.79 | 9.06 | 13.69 |
| | 4.90 | 4.64 | 11.60 | 13.70 |
| | 6.86 | 6.51 | 14.09 | 13.61 |
| 4-Dimethylamino-pyridine | 0.117 | 0.00639 | 6.48 | $1.88 \times 10^3$ |
| | 0.195 | 0.01073 | 7.42 | $1.99 \times 10^3$ |
| | 0.274 | 0.01507 | 8.27 | $1.97 \times 10^3$ |

[a] Total catalyst concentration.

**Table III—Catalytic Rate Constants for the Hydrolysis of Cinnamic Anhydride at 25°**

| pH | $k_C$, $M^{-1}$ sec$^{-1}$ | | |
|---|---|---|---|
| | Pyridine | *N*-Methylimidazole | 4-Dimethylaminopyridine |
| 8.45 | 2.70 | 13.66 | $1.95 \times 10^3$ |
| 8.78 | 3.02 | 14.22 | $1.85 \times 10^3$ |
| 9.17 | 3.75 | 14.95 | $1.82 \times 10^3$ |

intercepts of $k_A$ when $f_B = 0$ and of $k_B$ when $f_B = 1$. The quantity $k_0$ is obtained at each pH by plotting $k_{obs}$ *versus* $B_t$ and extrapolating to $B_t = 0$; the fraction $f_B$ is calculated with $f_B = K_a/([H^+] + K_a)$, where $K_a$ is the buffer acid dissociation constant.

The thermodynamic pKa values of bicarbonate, protonated tris(hydroxymethyl)aminomethane, and monobasic potassium phosphate at 25° are 10.33, 8.06, and 7.20, respectively (11). The apparent pKa values at ionic strength 0.10 *M*, calculated by Davies' method (12), are 10.22, 8.18, and 7.09, respectively. Plots of $k_{obs}$ *versus* $B_t$ at constant pH were linear. Figure 1 shows the plot according to Eq. 4 for carbonate buffer, showing negligible catalytic effect by the conjugate acid form of the buffer. The same behavior was observed for the other buffers. Since $k_A = 0$, Eq. 1 shows that $k_B$ also can be evaluated by plotting $k_{obs}$ *versus* [B]. Table I summarizes these studies, listing the $k_0$ and $k_B$ values found.

The $k_B$ quantities for carbonate and phosphate probably describe a general base catalysis of the hydrolysis, but $k_B$ for tris(hydroxymethyl)-aminomethane undoubtedly includes a nucleophilic attack on the anhydride since the absorption spectrum of the reaction product is not identical with that of the expected product cinnamic acid.

Figure 2 is a pH–rate profile for the anhydride hydrolysis. The slope of 1.00 shows the expected first-order dependence on the hydroxide ion. From the relationship $k_0 = k_{OH}a_{OH}$, the second-order rate constant for alkaline hydrolysis of cinnamic anhydride is $k_{OH} = 169\ M^{-1}$ sec$^{-1}$.

**Catalysis by Pyridine, 4-Dimethylaminopyridine, and *N*-Methylimidazole**—The hydrolysis of cinnamic anhydride catalyzed by pyridine, 4-dimethylaminopyridine, and *N*-methylimidazole was studied in carbonate, tris(hydroxymethyl)aminomethane, and phosphate buffer. The catalyzed reaction was first order in the conjugate base form of the catalyst. Therefore, at any given pH, the observed pseudo-first-order rate constant is given by:

$$k_{obs} = k_0 + k_B[B] + k_C[C] \qquad \text{(Eq. 5)}$$

where $k_C$ is the catalytic rate constant and [C] is the molar concentration of the base form of the catalyst. Since $k_0$ and $k_B$ are known, $k_C$ can be calculated. The pKa values at 0.10 *M* ionic strength and 25° are 5.29 for pyridine, 9.68 for 4-dimethylaminopyridine (11), and 7.19 for *N*-methylimidazole (13). Table II gives typical results, showing the constancy of $k_C$ and its reproducibility, at several catalyst concentrations. The $k_C$ values obtained at several pH values are listed in Table III.

In view of the reproducibility of $k_C$ at a given pH (Table II), the data of Table III indicate a pH dependency of $k_C$ for pyridine and *N*-methylimidazole. Over the limited pH range studied, $k_C$ can be described by $2.45 + 8.5 \times 10^4\ a_{OH}\ M^{-1}$ sec$^{-1}$, $13.50 + 1.01 \times 10^5\ a_{OH}\ M^{-1}$ sec$^{-1}$, and $1.87 \times 10^3\ M^{-1}$ sec$^{-1}$ for pyridine, *N*-methylimidazole, and 4-dimethylaminopyridine, respectively.

Although the mechanisms of these reactions have not yet been elucidated, it appears probable, based on the similar acetic anhydride reaction (14), that the catalysis occurs *via* the formation of an intermediate as shown for *N*-methylimidazole in Schemes II and III.

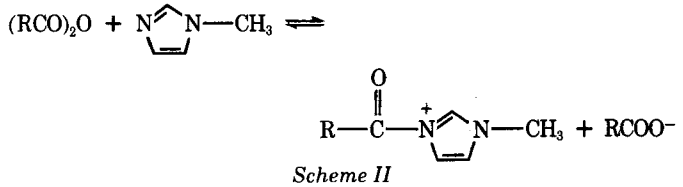

*Scheme II*

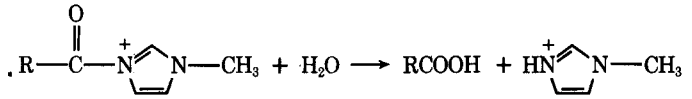

*Scheme III*

The pH-independent component of $k_C$ describes the attack of water on the intermediate, whereas the pH-dependent component represents the attack by hydroxide ion. The magnitudes of the latter quantity, particularly for 4-dimethylaminopyridine, are uncertain because of the restricted pH range studied.

**Table IV—Effect of Acetonitrile on the Catalytic Rate Constant for the Hydrolysis of Cinnamic Anhydride [a,b]**

| Acetonitrile Content, % v/v | $k_C$, $M^{-1}$ sec$^{-1}$ | | |
|---|---|---|---|
| | Pyridine | *N*-Methylimidazole | 4-Dimethylaminopyridine |
| 3.9 | 3.51 | 13.89 | $1.96 \times 10^3$ |
| 13.5 | 1.89 | 10.53 | $1.91 \times 10^3$ |
| 23.1 | 0.90 | 6.22 | $1.73 \times 10^3$ |
| 32.8 | 0.40 | 3.70 | $1.46 \times 10^3$ |
| 42.4 | 0.17 | 1.96 | $0.86 \times 10^3$ |

[a] At pH 8.86 and 25°; the buffer contained 0.004 *M* protonated tris(hydroxymethyl)aminomethane, 0.017 *M* of the buffer base, and 0.096 *M* KCl. [b] The concentrations of catalysts in their base forms were: pyridine, $1.21 \times 10^{-3}$ *M*; *N*-methylimidazole, $2.89 \times 10^{-4}$ *M*; and 4-dimethylaminopyridine, $1.38 \times 10^{-6}$ *M*.

**Table V—Third-Order Rate Constants for *N*-Methylimidazole-Catalyzed Reaction of Cinnamic Anhydride with Hydroxy Compounds in Acetonitrile at 25° [a]**

| Hydroxy Compound [b] | $10^2 k_3$, $M^{-2}$ sec$^{-1}$ | |
|---|---|---|
| | Mean | *SD* [c] |
| Phenol | 96.4 | 0.1 |
| Isoamyl alcohol | 10.7 | 0.2 |
| *n*-Amyl alcohol | 9.22 | 0.04 |
| Isobutyl alcohol | 7.88 | 0.05 |
| *n*-Butyl alcohol | 3.47 | 0.06 |
| *n*-Propyl alcohol | 3.24 | 0.03 |
| Isopropyl alcohol | 0.72 | 0.03 |
| *sec*-Butyl alcohol | 0.65 | 0.09 |
| *tert*-Butyl alcohol | 0.58 | 0.03 |

[a] Initial anhydride concentration was $2.67 \times 10^{-5}$ *M*. [b] Initial phenol concentration was 0.105 *M*, initial alcohol concentrations were 1.02–2.37 *M*, and the catalyst concentration was 0.14–1.12 *M*. [c] Six determinations for *n*-propyl alcohol; three determinations for the other compounds.

**Medium Effects**—The alkaline hydrolysis rate of cinnamic anhydride was decreased sharply by the addition of acetonitrile to the aqueous medium, as illustrated by these pseudo-first-order rate constants ($10^3$ $k_{obs}$/sec$^{-1}$) at 25° in a pH 8.86 buffer in the absence of added acetonitrile: 3.9% acetonitrile, 6.14; 13.5%, 3.72; 23.1%, 1.74; 32.8%, 0.96; and 42.4%,

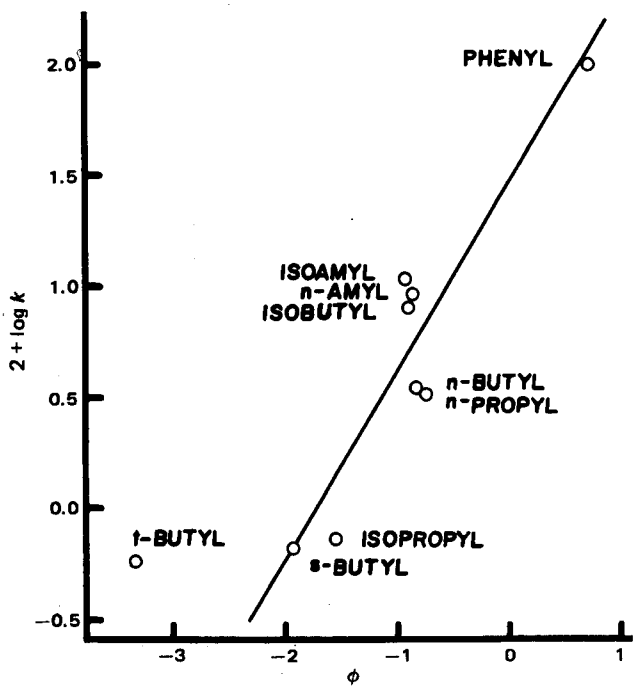


**Figure 3**—*Correlation of rates of cinnamoylation of hydroxy compounds (Table V) with substituent constant ϕ (17).*

**Table VI—Relative Catalytic Effectiveness of *N*-Methylimidazole and 4-Dimethylaminopyridine in Some Acylation Reactions (Pyridine = 1.00)**

| Reactants | Solvent | Relative Rate | |
|---|---|---|---|
| | | *N*-Methylimidazole | 4-Dimethylaminopyridine |
| Cinnamic anhydride + water | 3.9% aqueous acetonitrile | 3.96 | 558 |
| Cinnamic anhydride + water | 13.5% aqueous acetonitrile | 5.57 | 1011 |
| Cinnamic anhydride + water | 23.1% aqueous acetonitrile | 6.91 | 1922 |
| Cinnamic anhydride + water | 32.8% aqueous acetonitrile | 9.25 | 3650 |
| Cinnamic anhydride + water | 42.4% aqueous acetonitrile | 11.5 | 5058 |
| Cinnamic anhydride + *n*-propanol | Acetonitrile | 259 | $1.6 \times 10^4$ |
| Acetic anhydride + isopropanol[a] | *N,N*-Dimethylformamide | 362 | $1.7 \times 10^4$ |

[a] Taken from Ref. 18.

0.60. Higher acetonitrile concentrations were not studied because of buffer insolubility.

The second-order catalytic rate constant $k_C$ was measured for pyridine, *N*-methylimidazole, and 4-dimethylaminopyridine in water–acetonitrile mixtures (Table IV). All of the constants decreased as the organic component of the solvent increased, with the decrease being relatively greater the weaker the catalyst. This behavior (*i.e.*, reduction in reactivity as the solvent polarity decreases) indicates that the transition state is more polar than the initial state of the rate-determining step of the reaction. Rate-limiting formation of the onium-ion intermediate in Scheme II is consistent with this result.

This dependence of the rate on solvent polarity observed with the catalyzed hydrolysis of cinnamic anhydride in mixed aqueous solvents contrasts with the finding (15) that the rate of the *N*-methylimidazole-catalyzed reaction of acetic anhydride with isopropanol is relatively insensitive to solvent polarity for a series of organic solvents.

**Cinnamoylation of Hydroxy Compounds**—Kinetic studies of the reaction of cinnamic anhydride with *n*-propanol catalyzed by *N*-methylimidazole in acetonitrile solution showed that it was first order in the alcohol and in the catalyst. Therefore, the pseudo-first-order rate constant for the loss of anhydride may be written as:

$$k_{obs} = k_3[\text{alcohol}][\text{catalyst}] \qquad \text{(Eq. 6)}$$

Table V lists $k_3$ values for the *N*-methylimidazole-catalyzed cinnamoylation of some hydroxy compounds.

For *n*-propanol, $k_3$ was also measured with pyridine and 4-dimethylaminopyridine as the catalysts, yielding $1.25 \pm 0.003 \times 10^{-4}\ M^{-2}\,\text{sec}^{-1}$ for pyridine and $2.01 \pm 0.01\ M^{-2}\,\text{sec}^{-1}$ for 4-dimethylaminopyridine.

The $k_3$ values of Table V correlate roughly with the basicity of the hydroxy compound as measured by the pKa of the conjugate acid $ROH_2^+$(16). They are not correlated well by the Taft polar substituent constant $\sigma^*$ perhaps because of a steric influence. Robinson and Matheson (17) defined a substituent constant $\phi$, which includes the steric effect in the alkyl portion of esters. Figure 3 shows the correlation of $k_3$ values with $\phi$. The equation of the regression line is:

$$\log k_3 = 0.844\phi - 0.56 \qquad \text{(Eq. 7)}$$

with correlation coefficient $r^2 = 0.93$ and a standard deviation about the regression line of 0.28 log $k$ unit. (The value for *tert*-butyl alcohol is not included in the regression.) In general, this acylation reaction is faster for primary alcohols than for branched alcohols, probably for steric reasons; among the primary alcohols, the reaction rates parallel alcohol basicity.

**Relative Catalytic Activity**—Table VI collects relative rate data for several acylation reactions in various solvents for pyridine, *N*-methylimidazole, and 4-dimethylaminopyridine. For each entry (line) in Table VI, the relative rate is expressed as the ratio $k_C$ (catalyst)/$k_C$ (pyridine) for that particular reaction and solvent.

In summary, the most important findings were that the reaction rate decreases as the solvent polarity decreases and that the catalytic activities of *N*-methylimidazole and of 4-dimethylaminopyridine relative to pyridine increase as the solvent polarity decreases. Both observations are consistent with the formation of the ionic onium intermediates (Scheme II). The intermediates formed from *N*-methylimidazole and 4-dimethylaminopyridine are capable of extensive charge delocalization relative to the acylpyridinium intermediate. As the solvent polarity decreases, the transition state leading to the intermediate is destabilized for all catalysts, but this effect is greatest for pyridine. Thus, the relative rate increases for the more powerful catalysts. This finding is indirect evidence for the intermediacy of the onium ion.

## REFERENCES


(1) W. H. Hong and K. A. Connors, *Anal. Chem.*, **40**, 1273 (1968).

(2) K. A. Connors and W. H. Hong, *Anal. Chim. Acta*, **43**, 334 (1968).

(3) K. A. Connors and K. S. Albert, *J. Pharm. Sci.*, **62**, 845 (1973).

(4) E. L. Rowe and S. M. Machkovech, *ibid.*, **66**, 273 (1977).

(5) N. K. Pandit and K. A. Connors, *Anal. Chem.*, **50**, 1542 (1978).

(6) R. Wachowiak and K. A. Connors, *ibid.*, **51**, 27 (1979).

(7) J. D. M. Simpson and S. S. Isrealstam, *J. S. Afr. Chem. Inst.*, **2**, 170 (1949).

(8) W. H. Hong, Ph.D. thesis, University of Wisconsin, Madison, Wis., 1969, p. 16.

(9) G. Höfle, W. Steglich, and H. Vorbrüggen, *Angew. Chem. Int. Ed. Engl.*, **17**, 569 (1978).

(10) D. D. Perrin, W. L. F. Armarego, and D. R. Perrin, "Purification of Laboratory Chemicals," Pergamon, Oxford, England, 1966.

(11) D. D. Perrin, "Dissociation Constants of Organic Bases in Aqueous Solution," Butterworths, London, England, 1965.

(12) C. W. Davies, *J. Chem. Soc.*, **1938**, 2093.

(13) N. C. Li, J. M. White, and E. Doody, *J. Am. Chem. Soc.*, **76**, 6219 (1954).

(14) A. R. Fersht and W. P. Jencks, *ibid.*, **92**, 5432 (1970).

(15) N. K. Pandit, A. O. Obaseki, and K. A. Connors, *Anal. Chem.*, **52**, 1678 (1980).

(16) W. Gerrard and E. D. Macklen, *Chem. Rev.*, **59**, 1105 (1959).

(17) J. R. Robinson and L. E. Matheson, *J. Org. Chem.*, **34**, 3630 (1969).

(18) N. K. Pandit, M.S. thesis, University of Wisconsin, Madison, Wis., 1978.


## ACKNOWLEDGMENTS


Supported by National Science Foundation Grant CHE78-06603.

# Optimal Perfusion Rate Determined for *In Situ* Intestinal Absorption Studies in Rats

**PAUL M. SAVINA, A. E. STAUBUS ˣ, T. S. GAGINELLA, and D. F. SMITH**

Received June 9, 1980, from the *College of Pharmacy, Ohio State University, Columbus, OH 43201.* Accepted for publication August 13, 1980.

**Abstract** □ Iopanoic acid was used as a model compound to study the effects of the intestinal perfusion rate on the mean absorption clearance. Absorption of iopanoic acid followed first-order kinetics, with a first-order absorption rate constant ($k_a$) linearly dependent on the dry intestinal weight. An absorption clearance–time plot revealed three phases. Phase I represented an equilibration phase, Phase II was a uniform phase, and Phase III was a physiological deterioration of the animal under prolonged anesthesia. The variability in the observations during Phase II of the absorptive clearance–time profiles was assessed statistically, and the minimum occurred at 9.9 μl/sec (0.594 ml/min). The relation between the coefficient of variance ($CV$) and the perfusion rate is given by $CV = (-5.52 \times 10^{-5})Q^3 + (2.78 \times 10^{-3})Q^2 - (3.87 \times 10^{-2})Q + 0.243$, where $Q$ is the perfusion rate through the intestinal lumen. These studies demonstrate that an optimal flow rate exists for minimizing the variability in *in situ* absorption studies. The dependency of the absorption clearance on the intestinal perfusion rate appears to conform to the convective diffusion model.

**Keyphrases** □ Iopanoic acid—absorption from *in situ* rat small intestine, optimal perfusion rate determined □ Absorption, GI—iopanoic acid from *in situ* rat small intestine, optimal perfusion rate determined □ Models, pharmacokinetic—convective diffusion model, relationship between intestinal absorption clearance and intestinal perfusion rate, rats □ Perfusion rate—optimum, *in situ* intestinal absorption studies, rats

Drug absorption studies have utilized animal models and employed both *in vitro* and *in vivo* techniques. The clinical ramification of these studies is the delineation of the factors influencing drug absorption so as to maximize drug therapy from the standpoint of drug dosing, efficacy, and safety.

Results from *in vivo* studies often lack reproducibility. This problem may be due to a lack of attention on experimental design or the physiological conditions of the animal preparation (1). Factors that influence both solute absorption and transmucosal fluid movement include the constituents of the perfusates (1), pH (2–8), and bile salts (9–11). The flow rate through the intestine also significantly affects the absorption rate. The flow rate influenced the calcium absorption rate in dogs (12), and the *in vivo* perfusion method was used to determine the effect of flow rate on glucose absorption in rats (13). In another study (14), the perfusion load could predict glucose absorption in humans. Other studies (3, 4) investigated the effects of flow rates and other lumenal factors influencing vitamins $A_1$ and $K_1$ absorption. In addition, the possible mechanisms by which changes in flow rate might affect drug absorption were studied (15).

Although each of these studies led to recommendations for the optimal experimental design for drug absorption studies, virtually no work has been reported on the effects of flow rates on the variability of absorption. Maintaining the variability at a minimum is important for valid comparisons between agents that may alter normal absorption. This study was designed to determine an optimal flow rate at which variability in the mean absorption clearance of a model compound, iopanoic acid, could be minimized during *in situ* experiments.

## EXPERIMENTAL

All chemicals were analytical reagent grade and were used as received. A modified Krebs buffer constituted the working isosmotic buffer, in which the iopanoic acid perfusion solution was prepared, and was composed of 25 m*M* $NaHCO_3$, 1.2 m*M* $KH_2PO_4$, 1.2 m*M* $MgSO_4$, 4.7 m*M* KCl, and 118.4 m*M* NaCl. The iopanoic acid perfusion solution was prepared by stirring excess iopanoic acid[1] with 1 liter of the buffer and filtering through a büchner funnel. The filtrate concentration of iopanoic acid was adjusted to 1.8 μmoles/ml, and the resultant pH was 7.8 as measured on a pH meter[2].

Male albino Sprague–Dawley rats[3], 200–300 g, were maintained in fully accredited animal care facilities[4] on a 12-hr light cycle at 72 °F (11.1 °C) and 50% humidity for at least 1 week prior to use. The animals received food[5] and water *ad libitum* but were fasted 12–16 hr before each experiment. Longer fasting times were not used to avoid possible deviations in absorption (16).

The surgical procedure was similar to that described by Schanker *et al.* (6). Anesthesia was induced by injection of urethan (1.5 mg/kg ip). A midventral abdominal incision extending 5–6 cm posteriorly to the pectoris minor was made, and the small intestine was exposed. The jejunum was located, and a small incision was made 6–8 cm below the ligament of Trietz. Care was taken not to cut through the segment completely. A similar incision was made 30 cm aboral to the first. The segment then was gently flushed with 30–40 ml of modified Krebs buffer until the effluent was clear and the segment was free of waste and debris. The flushing process was slow so as not overly to expand the intestine and cause damage due to high hydrostatic pressure.

The ends of the segment were cannulated with the needle adaptor end of a sterilized Travenol extension set and secured with encircling 00 surgical silk sutures fitted through the mesentary proper, between two branches of the superior mesenteric vein. The free end of the extension set cannulating the upper portion of the segment was attached to a Lambda infusion pump[6], while the free end of the extension set cannulating the distal portion of the segment extended along the ventral surface of the rat into a 10-ml graduated cylinder. The intestinal segment then was placed within the abdominal cavity carefully to avoid crimping and kinking of the segment, which would lead to subsequent obstruction. The body temperature of the animal was maintained at 37° by a heating lamp and a constant-temperature device[7] regulated by a thermister probe placed within the abdominal cavity. The abdominal incision, as well as any exposed intestine, then was covered with gauze sponges moistened with warmed buffer and changed throughout the study to ensure a clean moist cover.

The cannulated jejunal segments ranged from 20 to 30 cm in length and were perfused with iopanoic acid at one of the following flow rates: 2.1 μl/sec (0.126 ml/min), 3.1 μl/sec (0.186 ml/min), 4.2 μl/sec (0.252 ml/min), 8.3 μl/sec (0.498 ml/min), 12.5 μl/sec (0.75 ml/min), 16.7 μl/sec (1.002 ml/min), and 20.5 μl/sec (1.23 ml/min) for 240–300 min. Drainage from the segment to the collecting cylinder was achieved by gravity. Samples were taken every 30 min for the perfusion rate of 2.1 μl/sec and

[1] Telepaque, Sterling-Winthrop, Rensselaer, N.Y.
[2] Model 12, Corning Glass Works, Corning, N.Y.
[3] Laboratory Supply Co., Indianapolis, Ind.
[4] American Association for the Accreditation of Laboratory Animal Care.
[5] Purina Rodent Laboratory Chow 5001.
[6] Model 1301, Harvard Apparatus Co., Millis, Mass.
[7] Thermistemp, model 74, Yellow Springs Instrument Co., Yellow Springs, Ohio.

0022-3549/81/0300-0239$01.00/0
© 1981, American Pharmaceutical Association

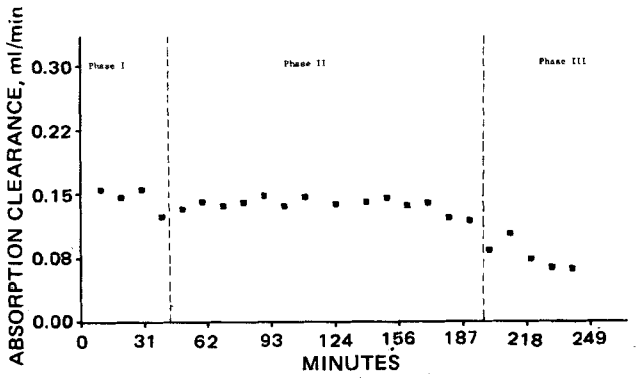


**Figure 1**—*Relationship between the intestinal absorption clearance ($Cl_A$) and time for iopanoic acid to perfuse at a rate of 9.9 μl/sec. The broken vertical lines delineate the three distinct phases within a particular study. Phase I represents an equilibration phase, Phase II is the phase of uniform clearance from which all comparisons are made, and Phase III is indicative of a physiological deterioration of the animal under prolonged anesthesia.*

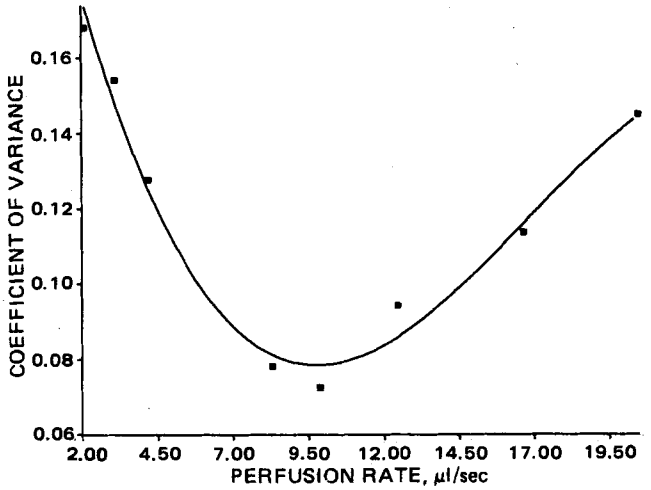


**Figure 2**—*NONLIN computer fit for the third-order polynomial function relating the mean coefficient of variance in the absorption clearance and the intestinal perfusion rate.*

every 15 min for 3.1 μl/sec to ensure adequate volume collection for accuracy in the assay and in volume determination. Eight-minute intervals were used for sample collection at the flow rate of 20.5 μl/sec so as not to exceed the capacity of the collecting cylinders. Sample collection intervals of every 10 min were used for the other flow rates.

The volume at the end of each time interval was recorded, and the sample was mixed on a vortex mixer[8] to ensure a homogeneous solution. A 2-ml aliquot then was placed in a 2.5-ml polystyrene vial[9] and assayed for total iodine content by fluorescence excitation analysis (17). A standard curve was constructed by plotting the ratio ($NK\alpha/NC$) against known concentrations of iodine, prepared by dissolving appropriate amounts of sodium iodide[10] in demineralized, double-distilled water to yield concentrations of 0.0, 0.25, 0.5, 1.0, 1.5, and 5.0 $\mu M$/ml.

Standard curves were constructed routinely to verify the reliability of the assay. At no point was the correlation coefficient ($r$) less than 0.999. During the analysis of a set of samples from one experiment, standard samples were run periodically as a check for deviation in the standard curve. Most checks were within ±2%. A deviation of 4% or greater was considered unacceptable, and a new standard curve was constructed. In such cases, the analysis was repeated starting from the first sample assayed using the previous standard curve.

At the end of the experiment, the animal was sacrificed and the intestinal segment was placed in an aluminum dish and oven dried at 110° for 48 hr. The dried intestine was weighed[11] accurately, and all clearance values were normalized to 100 mg of dry weight. The relationship between clearance and the dry intestinal weight was linear.

Absorption clearance ($Cl_A$) for each collection period was calculated using:

$$Cl_A = \left[\frac{C_{in} - C_{out}}{C_{in}}\right]\mathring{V} \qquad \text{(Eq. 1)}$$

where $\mathring{V}$ is the measured perfusion flow for that collection period, $C_{in}$ is the iopanoic acid concentration in buffer entering the gut segment, and $C_{out}$ is the iopanoic acid concentration collected leaving the gut segment during the collection period.

## RESULTS AND DISCUSSION

Iopanoic acid is a poorly absorbed cholecystographic agent. Its poor absorption has been implicated as the cause of some failures encountered during an initial examination since, upon repeat administration or doubling of the dose, 30% of those subjects with initial inadequate visualization showed excellent visualization (18–20). Therefore, nonvisualization must be confirmed by repeat examination or upon doubling of the dose at a future date before disease or obstruction can be considered a viable diagnosis.

Since absorption of iopanoic acid must be maximized to produce a desired effect, it was selected as a model compound to suggest a method of decreasing variability in the data collected, thereby giving more credence to the results of comparative treatments made to influence drug absorption and to delineate absorption mechanisms. Iopanoic acid also provides a quick, sensitive, and uncomplicated assay with essentially no manipulation involved.

The absorption clearance was measured and plotted as a function of time. A representative absorption clearance–time course is shown in Fig. 1. These clearance profiles have three distinct phases or sections. Phase I, lasting about 60–70 min, generally exhibited an apparent decrease in clearance with time; this result could be due to equilibration of water transport and failure to flush out totally the residual wash solution remaining within the segment at the start of the perfusion. Schanker *et al.* (6) reported a similar phenomenon during the initial phase of their absorption experiments. Podesta and Mettrick (21) also allowed a 20-min equilibration period in their perfusion experiments.

Phase II, characterized by relatively uniform clearance values from 40 to 180 min (and in some cases 240 min), was followed by a third phase of clearance. Phase III was attributed to a deterioration in the physiological condition of the rat under prolonged anesthesia. In separate studies, it was determined that back-diffusion of iopanoic acid from the blood to the lumen and its binding to the gut mucosa did not occur.

The scatter or variability of the data in Phase II of the clearance–time profiles appeared to be flow rate dependent. High scatter seemed to be associated with the fast and slow flow rates; low scatter was associated with intermediate flow rates. To discern the actual relationship, the mean coefficient of variance at each flow rate was calculated and plotted as a function of the flow rate (Fig. 2). The resultant plot resembled a parabolic function. The data were fitted subsequently to a series of polynomial functions as well as hyperbolic, logarithmic, exponential, and root functions. The equation giving the best fit and minimum sum of squares is:

$$Y = (-5.19 \times 10^{-5})x^3 + (2.65 \times 10^{-3})x^2 - (3.7 \times 10^{-2})x + 0.24 \qquad \text{(Eq. 2)}$$

where $x$ is the flow rate (microliters per second) and $Y$ is the coefficient of variance.

Solving the quadratic differential yielded a root of 9.89 for the minimum value. Six rat studies were conducted at the calculated optimal flow rate (9.9 μl/sec), predicted to provide the minimum coefficient of variance for the aborption clearance. These results gave the predicted minimum coefficient of variance (Table I). The results of the least-squares nonlinear regression analysis by Marquardt's gradient–expansion method (22) are given in Table II. The data obtained from the flow rate experiment performed at 9.9 μl/sec (0.594 ml/min) were added to the results of the previous studies and again fitted to a series of polynomial functions. The final equation from the least-squares fit is given by Eq. 3 and was verified by successfully fitting the data using NONLIN (23):

$$Y = (-5.52 \times 10^{-5})x^3 + (2.784 \times 10^{-3})x^2 - (3.87 \times 10^{-2})x + 0.243 \qquad \text{(Eq. 3)}$$

[8] Bronwill, VWR Scientific, Brisbone, Calif.
[9] Sherwood Medical Industries, St. Louis, Mo.
[10] Mallinckrodt.
[11] Mettler H542 balance.

**Table I—Mean Coefficient of Variance and Standard Deviation of Absorption Clearance at Different Perfusion Rates**

| Perfusion Rate, μl/sec | $n$ | Mean Coefficient of Variance | Standard Deviation between Experiments |
|---|---|---|---|
| 2.1 | 4 | 0.1682 | 0.0339 |
| 3.1 | 8 | 0.1541 | 0.0568 |
| 4.2 | 5 | 0.1278 | 0.0394 |
| 8.3 | 5 | 0.0781 | 0.0182 |
| 9.9 | 6 | 0.0754 | 0.0164 |
| 12.5 | 6 | 0.0942 | 0.0252 |
| 16.7 | 7 | 0.1137 | 0.0355 |
| 20.5 | 7 | 0.1450 | 0.0170 |

The dependence of the coefficient of variance on flow seems to follow this polynomial relationship. From this relationship, the flow at which the coefficient of variance was minimized could be calculated. Thus, the optimal flow rate, which minimized the variability in the data, was determined to be 9.9 μl/sec (0.594 ml/min).

The magnitude of the mean absorption clearance within the uniform phase (Phase II) was also dependent on the flow rate (Fig. 3) as noted previously (24). The higher flow rates produced higher absorption clearance values, which will be discussed.

An analysis for determining significant differences between the coefficients of variance at each flow rate was performed. Since multiple comparisons were to be made, the linear contrast method, Fisher's protected least signficant difference (25), was selected over multiple $t$ tests to minimize the overall error rate. The overall error rate to $t$ test comparisons is given by:

$$\text{overall error rate} = 1 - (1 - \alpha)^c \qquad \text{(Eq. 4)}$$

The term $\alpha$ is a value between 0 and 1 and denotes the probability of incurring type I errors (falsely rejecting the null hypothesis), and c is the number of comparisons made. Thus, the error rate increases with an increasing number of comparisons. Therefore, if multiple comparisons between the eight flow rates are made, the probability of falsely rejecting the null hypothesis (the means of the coefficients of variance at two flow rates are equal) on at least one $t$ test becomes quite large. The calculated $F$ ratio (6.36) is much larger than the tabulated value (3.3) at $\alpha = 0.01$. The least signficant difference ($LSD$) for each comparison was calculated by:

$$LSD = t_{\alpha/2}\sqrt{S^2w\left(\frac{1}{N_i} + \frac{1}{N_j}\right)} \qquad \text{(Eq. 5)}$$

where $t_{\alpha/2}$ denotes the tabulated critical $t$ value for a two-tailed test, $N_i$ and $N_j$ are the respective sample sizes, and $S^2w$ is the mean square within samples obtained from a one-way analysis of variance.

The results of the $LSD$ were: ($a$) 9.9 and 8.3 μl/sec were significantly less than 2.1, 3.1, 4.2, and 20.5 μl/sec at $p < 0.01$ and significantly less than 16.7 μl/sec at $p < 0.05$; ($b$) 12.5 μl/sec was significantly less than 2.1, 3.1, and 20.5 μl/sec at $p < 0.005$; and ($c$) 16.7 μl/sec was significantly less than 2.1 μl/sec at $p < 0.005$ and significantly less than 3.1 μl/sec at $p < 0.05$.

**Table II—Nonlinear Least-Squares Regression Analysis [a] for the Mean Coefficient of Variance *versus* Flow Rate Curve**

| $X$ [b] | $Y$(obs) [c] | $Y$(calc) [c] | Deviation |
|---|---|---|---|
| 2.1 | 0.1682 | 0.1735 | −0.0053 |
| 3.1 | 0.1541 | 0.1482 | 0.0060 |
| 4.2 | 0.1278 | 0.1255 | 0.0023 |
| 8.3 | 0.0781 | 0.0822 | −0.0041 |
| 9.9 | 0.0754 | 0.0794 | −0.0040 |
| 12.5 | 0.0942 | 0.0868 | 0.0074 |
| 16.7 | 0.1137 | 0.1165 | −0.0028 |
| 20.5 | 0.1450 | 0.1445 | 0.0048 |

weighting = 1
variance = $411.42 \times 10^{-7}$
standard deviation = 0.0064
correlation coefficient = 0.9904
$r$-square = 0.9804
sum of squares of error = $164.57 \times 10^{-6}$
percent error reduction = 99.8

[a] By Marquardt's gradient–expansion method (22). [b] Flow rate, microliters per second. [c] Coefficient of variance.

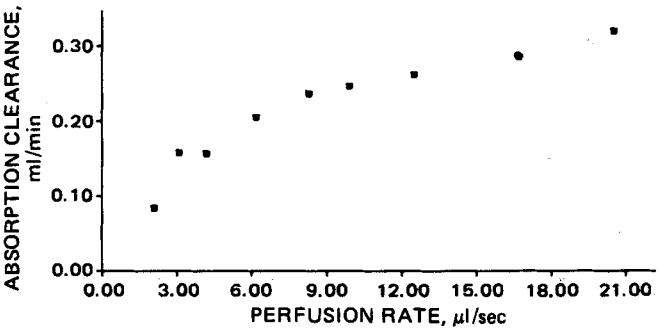


**Figure 3**—*Relationship between the mean absorption clearance and the intestinal perfusion rate.*

No significant difference was observed among 8.3, 9.9, and 12.5 μl/sec ($p > 0.1$). The coefficient of variance for 16.7 μl/sec did not differ significantly from the coefficient of variance for 12.5 μl/sec but was significantly different from 8.3 and 9.9 μl/sec at $p < 0.01$. Because of this latter result, the optimal flow rate, which could aid in the experimental design and improve the results of subsequent absorption studies, should be between 8 and 10 μl/sec rather than between 8 and 13 μl/sec.

*In vivo* work by Hollander and coworkers (2, 3), who used flow rates of 0.5, 1.0, 2.5, 5.0, and 10.0 ml/min to study their effect on vitamin $A_1$ and vitamin $K_1$ absorption, tends to support the present work. Use of their data to calculate a coefficient of variance reveals that the minimum coefficient of variance occurred at 0.5 ml/min (8.3 μl/sec). The maximum variability occurred between 1.0 and 2.5 ml/min. Koezumi *et al.* (26), using flow rates of 2.5, 5.0, 6.5, and 10.0 ml/min to study the absorption rate of unionized sulfamerazine, reported data that, by our calculations, revealed low coefficient of variance values. Rates above 1.5 ml/min become, in a sense, nonphysiological, and the decrease in or the low coefficient of variance values become an artifact of the high perfusion rate. Such high rates do not allow for subtle intralumenal influences normally affecting drug transport across the mucosal barrier. These large values for the absorption rate increase the denominator in the calculation of the coefficient of variance, thereby making it small and reflecting perhaps the efficiency of the pump delivering the perfusate.

The convective diffusion model of Nelson and Shah (27–29) was selected to describe the effects of flow rates on the absorption clearance. Originally used to describe the drug dissolution rate (27, 28) and later membrane transport (29), the model gives the equation for the dissolution rate ($R$) across the surface of a rectangle of length $L$ and width $b$ as:

$$R = 0.808D^{2/3}C_0\alpha^{1/3}bL^{2/3} \qquad \text{(Eq. 6)}$$

where $D$ is the diffusivity, $C_0$ is the solubility (usually given as the initial concentration in the donor phase), and $\alpha$ represents the shear rate adjacent to the planes for flow between two parallel planes and is defined as:

$$\alpha = \frac{6Q}{H^2W} \qquad \text{(Eq. 7)}$$

where $Q$ is the volumetric flow rate and $H$ and $W$ are the height and width of the channel in the diffusion cell, respectively. If a cylinder is considered to be a good approximation of the intestinal membrane surface, the corresponding equation for the absorption rate ($R$) is:

$$R = 0.808D^{2/3}C_0\alpha^{1/3}2\pi rL^{2/3} \qquad \text{(Eq. 8)}$$

The initial concentration in the perfusing solution ($C_0$) changes as a result of absorption. To account for absorption and the subsequent concentration gradient, the "logarithmic mean," $(C_0 - C_z)/\ln(C_0/C_z)$, was used as the best average for laminar flow through a solute-permeable tube (30). Dividing Eq. 8 by this logarithmic mean for the concentration results in the absorption clearance expression:

$$Cl_A = 0.808D^{2/3}\alpha^{1/3}2\pi rL^{2/3} \qquad \text{(Eq. 9)}$$

The shear rate ($\alpha$), relating the linear velocity with the distance away from the surface over which the flow occurs (Eq. 7), is for flow between two planes; however, a similar expression can be derived for the shear rate through a cylinder. If it is assumed that the intestinal segment is long enough to avoid end effects, the velocity distribution for a liquid under steady laminar flow through the cylinder of length $L$ and radius $r$ is a parabolic function given by (31):

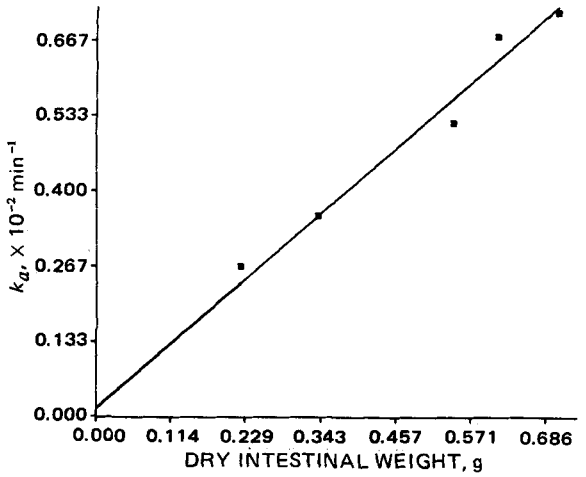


**Figure 4**—*Linear relationship between the first-order absorption rate constant ($k_a$) and the dry intestinal weight. The correlation coefficient of the regression line is 0.9933 with a corresponding slope of 0.01 (g min)$^{-1}$. The intercept of 0.0001 was not statistically different from zero ($p < 0.05$).*

$$V_z = \frac{\Delta P r^2}{4\eta L}\left[1 - \left(\frac{r'}{r}\right)^2\right] \qquad \text{(Eq. 10)}$$

where $\eta$ is the viscosity that is the proportionality constant relating the shear rate and the shearing stress and $\Delta P$ is the pressure drop over the intestinal segment and represents the combined effect of static pressure and gravitational force. The volumetric flow rate ($Q$) is given by the well-known Hagen–Poiseuille law (31):

$$Q = \frac{\pi(\Delta P)r^4}{8\eta L} \qquad \text{(Eq. 11)}$$

Differentiating the velocity with respect to $r'$, the radial distance from the parabolic maximum velocity (center of the tube), results in an expression for the shear rate given by:

$$\alpha = \frac{dV_z}{dr'} = \left(\frac{-\Delta P}{2\eta L}\right)r' \qquad \text{(Eq. 12)}$$

Since the concern is with stress against the absorbing surface, this point of maximal stress occurs where $r'$ equals the radius $r$. Solving Eq. 11 for $\Delta P$ and substituting into Eq. 12 give an expression relating the shear rate and the volumetric flow rate for laminar flow through a tube:

$$\alpha = \frac{4Q}{\pi r^3} \qquad \text{(Eq. 13)}$$

Winne (32) reported that the length and intralumenal radius of the perfused segment were not altered when the perfusion rate was varied from 0.1 to 0.5 ml/min. Lewis and Fordtran (15) showed that the intralumenal pressure did not change when the perfusion rate was raised from 1 to 10 ml/min. These reports indicate that the radius can be considered a constant over the range of rates used.

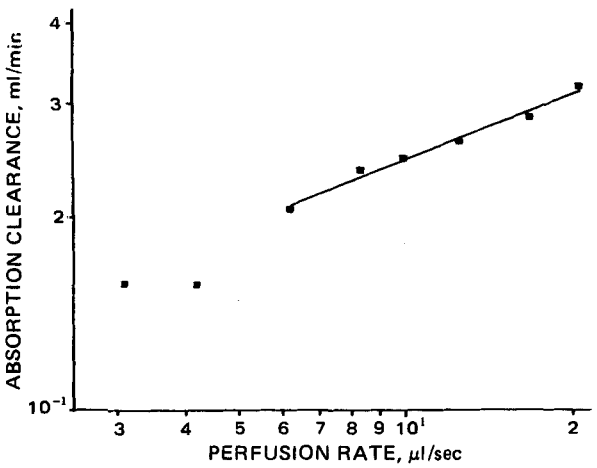


**Figure 5**—*Log–log plot of the absorption clearance as a function of the intestinal perfusion rate in accord with the convective diffusion model.*

The linear relationship between $Cl_A$ and the dry intestinal weight, previously mentioned, was also noted between the first-order absorption rate constant and the dry intestinal weight (Fig. 4). This figure suggests that, on normalization, the only variable becomes the flow rate. By combining constants, Eq. 9 reduces to a simplified format exemplified by:

$$Cl_A = NQ^{1/3} \qquad \text{(Eq. 14)}$$

where $N$ is the constant product of all other terms.

In accord with Eq. 14, a plot of log $Cl_A$ *versus* log $Q$ should result theoretically in a straight line with a thoretical slope of 0.33. The experimental results are plotted in Fig. 5. The resulting slope is 0.339 with a correlation coefficient of 0.992 for rates between 6.2 and 20.5 µl/sec. This experimental slope value indicates excellent correlation with the theoretical value for the convective diffusion model hypothesis. Even when the rates of 3.1 and 4.2 µl/sec are included in the statistical analysis, the resultant least-squares slope of 0.388 still is in reasonable accord with the model. The slight deviation from theory on addition of the lower flow rates may be the result of longer resident times within the segment, possibly reflecting more complex absorption phenomena resulting from the invaginations between villi not accounted for in the simple cylinder shape assumption.

The literature abounds with discussions on the aqueous diffusion layer adjacent to the mucosal wall and its influence on the absorptive process. The convective diffusion model not only accounts for simple diffusion through this layer but allows for fluid flow and convection, which has been very useful in modeling the absorptive process for iopanoic acid in these studies. The increase in clearance with increasing flow rate probably was due to increased shear adjacent to the membrane, which increased the concentration gradient normal to it, since the surface area does not seem to be greatly affected (32) until rates above 10 ml/min are used (15).

In summary, the present studies suggest that there is a singular region in which the flow rate in an *in situ* perfusion system maximizes the reliability of the data collected. Minimizing the coefficient of variance lends more credence to observed data, providing more reliable parameters for comparative studies.

Knowing the optimal flow rate at which to perform perfusion experiments *in vivo* will permit more precise comparisons of the effects of modifying agents (*e.g.*, ions, nutrients, bile salts, and other drugs) on mucosal transport of a given solute.

## REFERENCES

(1) S. Kitazawa, M. Ishizir, and E. Arakawa, *Chem. Pharm. Bull.*, **24**, 3169 (1976).

(2) D. Hollander, E. Rim, and K. S. Muralidhara, *Am. J. Physiol.*, **232**, E69 (1977).

(3) D. Hollander and K. S. Muralidhara, *ibid.*, **232**, E471 (1977).

(4) C. A. M. Hogben, D. J. Tocco, B. B. Brodie, and L. S. Schanker, *J. Pharmacol. Exp. Ther.*, **125**, 275 (1959).

(5) C. A. M. Hogben, L. S. Schanker, D. J. Tocco, and B. B. Brodie, *ibid.*, **120**, 540 (1957).

(6) L. S. Schanker, D. J. Tocco, B. B. Brodie, and C. A. M. Hogben, *ibid.*, **123**, 81 (1958).

(7) L. S. Schanker, P. A. Shore, B. B. Brodie, and C. A. M. Hogben, *ibid.*, **120**, 528 (1957).

(8) P. A. Shore, B. B. Brodie, and C. A. M. Hogben, *ibid.*, **119**, 361 (1957).

(9) S. Feldman and M. Gibaldi, *Proc. Soc. Exp. Biol. Med.*, **132**, 1031 (1969).

(10) K. Kakemi, H. Sezaki, R. Konishi, T. Kimura, and M. Murakami, *Chem. Pharm. Bull.*, **18**, 275 (1970).

(11) T. S. Gaginella, P. Bass, J. H. Perrin, and J. J. Vallner, *J. Pharm. Sci.*, **62**, 1121 (1973).

(12) C. F. Cramer and T. A. Haqq, *Can. J. Biochem. Physiol.*, **41**, 127 (1963).

(13) A. M. Dawson and H. B. McMichael, *Proc. Phys. Soc.*, **2–3**, 13P (1968).

(14) C. D. Holdsworth and A. M. Dawson, *Clin. Sci.*, **27**, 371 (1964).

(15) L. D. Lewis and J. S. Fordtran, *Gastroenterology*, **68**, 1509 (1975).

(16) J. T. Doluisio, G. H. Tan, N. F. Billups, and L. Diamond, *J. Pharm. Sci.*, **58**, 1200 (1969).

(17) J. L. Kaufman, J. Nelson, and D. Price, *IEEE Trans. Nucl. Sci.*

*NS*, **20**, 402 (1973).
(18) R. M. Taketa, R. N. Berk, J. H. Lang, E. C. Lasser, and C. R. Dunn, *Am. J. Roentgenol.*, **114**, 767 (1972).
(19) L. E. Goldberger, R. N. Berk, J. H. Lang, and P. M. Loeb, *Invest. Radiol.*, **9**, 16 (1974).
(20) H. D. Rosembaum, *Am. J. Roentgenol.*, **82**, 1011 (1959).
(21) R. B. Podesta and D. F. Mettrick, *Am. J. Physiol.*, **232**, E62 (1977).
(22) P. R. Bevington, "Data Reduction and Error Analysis for the Physical Sciences," McGraw-Hill, New York, N.Y., 1969, p. 235.
(23) C. M. Metzler, "NONLIN, A Computer Program for Parameter Estimation in Non-Linear Situations," Upjohn Co., Kalamazoo, Mich., 1969.
(24) I. Komiya, J. Y. Park, A. Kamani, N. F. H. Ho, and W. I. Higuchi, "Abstracts," vol. 9 (2), APhA Academy of Pharmaceutical Sciences, Washington, D.C., 1979, p. 84.
(25) L. Ott, "An Introduction to Statistical Methods and Data Analysis," Wadsworth Publishing, Belmont, Calif., 1977, p. 384.
(26) T. Koezumi, T. Arita, and K. Kakemi, *Chem. Pharm. Bull.*, **12**, 421 (1964).
(27) K. G. Nelson and A. C. Shah, *J. Pharm. Sci.*, **64**, 610 (1975).
(28) A. C. Shah and K. G. Nelson, *ibid.*, **64**, 1518 (1975).
(29) K. G. Nelson and A. C. Shah, *ibid.*, **66**, 137 (1977).
(30) D. Winne and I. Markgraf, *Naunyn-Schmiedebergs Arch. Pharmacol.*, **309**, 271 (1979).
(31) R. B. Bird, W. E. Stewart, and E. N. Lightfoot, "Transport Phenomena," Wiley, New York, N.Y., 1960, p. 42.
(32) D. Winne, *Naunyn-Schmiedebergs Arch. Pharmacol.*, **307**, 265 (1979).

**ACKNOWLEDGMENTS**

Presented in part at the Basic Pharmaceutics Section, APhA Academy of Pharmaceutical Sciences, Washington meeting, April 1980.

The authors thank Ms. Sue Sheffield for her skilled secretarial assistance.

# Mixing of Pharmaceutical Solids II: Evaluation of Multicomponent Mixing of Cohesive Powders in Cylindrical Shear Mixer

**Z. T. CHOWHAN ˣ, E. E. LINN, and LI-HUA CHI**

Received November 1, 1979, from *Syntex Research, Palo Alto, CA 94304.* Accepted for publication August 14, 1980.

**Abstract** □ The mixing of three organic carboxylic acids with micronized lactose, all cohesive in nature, was studied using a cylindrical shear mixer. Three mixing indexes ($s/\sigma_A$, $s/\sigma_R$, and the Ashton–Valentin mixing index) were used to evaluate mixing of the three drugs with lactose. The results suggested that maximum homogeneity was reached after 45 min of mixing. However, different mixing indexes showed different sensitivity to homogeneity of the individual components. The mixing index $s/\sigma_A$, which is based on setting standard specifications, appears to provide a better evaluation of homogeneity of individual components compared to the mixing indexes based on complete random mixing theory. The latter did not approach unity for any drug component used in this study. These results suggested that mixing of cohesive powders is a complex process and cannot be explained fully by simple theory based on complete random mixing.

**Keyphrases** □ Mixing—of multicomponent cohesive powders, evaluation of homogeneity using three mixing indexes based on statistical analysis □ Powders—multicomponent mixing of cohesive powders, evaluation of homogeneity using three mixing indexes based on statistical analysis □ Carboxylic acids—cohesive powders mixed with lactose for homogeneity evaluation, evaluation of three mixing indexes based on statistical analysis □ Dosage forms, design—multicomponent mixing of cohesive powders to determine homogeneity of individual components, three mixing indexes evaluated

The mixing of a cohesive drug with cohesive, noncohesive, and free-flowing excipients was studied previously (1) using two types of mixers, cylindrical shear and V-shaped tumbling. Most mixing studies use binary systems, and mixing indexes based on statistical analysis are used to evaluate homogeneity. However, many practical situations in dosage form design require mixing several powders. Although most multicomponent mixing has been studied theoretically (2–6), one practical multicomponent system used 10% phenobarbital, 1% secobarbital, 1% butobarbital, and 88% lactose (7–9).

The multicomponent mixing of cohesive powders is one of the most difficult and complex powder mixing systems. None of the reported mixing studies have dealt with this powder mixing system.

This paper reports the mixing of cohesive powders of three organic carboxylic acids and an excipient in a cylindrical shear mixer. The results were evaluated by the mixing indexes based on complete random mixing and on standard specifications described previously (10, 11).

## EXPERIMENTAL

**Materials**—Three organic carboxylic acids, 7-methylsulfinyl-2-xanthone carboxylic acid (I), 7-methylthio-2-xanthone carboxylic acid (II), and 5-isopropoxy-7-methylthio-2-xanthone carboxylic acid (III), and mestranol were at least 99% pure[1]. USP grade lactose[2] was micronized[3]. Component I was micronized, and II and III were used as received. Methanol[4] was spectra grade, and polysorbate 80[5] was USP grade. All other chemicals were analytical grade unless specified otherwise.

**Physical Properties**—The particle-size distributions of I–III were determined[6] by electronic counting. The vehicle was a saturated solution of the compound in 0.6% HCl containing 0.018% polysorbate 80. The filtered vehicle was used to disperse the drug powder.

The particle-size distribution of the micronized lactose was determined[7] by automatic sedimentation, using photoextinction to measure the apparent projected area at decreasing sedimentation depths with increasing time.

The densities of the organic carboxylic acids were determined by the density matching method of Oster and Yamamoto (12). Mixtures of

[1] Institute of Organic Chemistry, Syntex Research, Palo Alto, CA 94304.
[2] Lactose regular, Foremost Food Co., San Francisco, CA 94104.
[3] Jet Pullverizer Co., Palmyra, N.J.
[4] Mallinckrodt Chemical Works, St. Louis, MO 63160.
[5] ICI America, Atlas Chemical Division, Wilmington, Del.
[6] Coulter counter model TA, Coulter Electronics, Hialeah, FL 33010.
[7] Sedigraph-L Micromeretics Instrument Corp., Norcross, Ga.

0022-3549/81/0300-0243$01.00/0
© 1981, American Pharmaceutical Association

*NS*, **20**, 402 (1973).
(18) R. M. Taketa, R. N. Berk, J. H. Lang, E. C. Lasser, and C. R. Dunn, *Am. J. Roentgenol.*, **114**, 767 (1972).
(19) L. E. Goldberger, R. N. Berk, J. H. Lang, and P. M. Loeb, *Invest. Radiol.*, **9**, 16 (1974).
(20) H. D. Rosembaum, *Am. J. Roentgenol.*, **82**, 1011 (1959).
(21) R. B. Podesta and D. F. Mettrick, *Am. J. Physiol.*, **232**, E62 (1977).
(22) P. R. Bevington, "Data Reduction and Error Analysis for the Physical Sciences," McGraw-Hill, New York, N.Y., 1969, p. 235.
(23) C. M. Metzler, "NONLIN, A Computer Program for Parameter Estimation in Non-Linear Situations," Upjohn Co., Kalamazoo, Mich., 1969.
(24) I. Komiya, J. Y. Park, A. Kamani, N. F. H. Ho, and W. I. Higuchi, "Abstracts," vol. 9 (2), APhA Academy of Pharmaceutical Sciences, Washington, D.C., 1979, p. 84.
(25) L. Ott, "An Introduction to Statistical Methods and Data Analysis," Wadsworth Publishing, Belmont, Calif., 1977, p. 384.
(26) T. Koezumi, T. Arita, and K. Kakemi, *Chem. Pharm. Bull.*, **12**, 421 (1964).
(27) K. G. Nelson and A. C. Shah, *J. Pharm. Sci.*, **64**, 610 (1975).
(28) A. C. Shah and K. G. Nelson, *ibid.*, **64**, 1518 (1975).
(29) K. G. Nelson and A. C. Shah, *ibid.*, **66**, 137 (1977).
(30) D. Winne and I. Markgraf, *Naunyn-Schmiedebergs Arch. Pharmacol.*, **309**, 271 (1979).
(31) R. B. Bird, W. E. Stewart, and E. N. Lightfoot, "Transport Phenomena," Wiley, New York, N.Y., 1960, p. 42.
(32) D. Winne, *Naunyn-Schmiedebergs Arch. Pharmacol.*, **307**, 265 (1979).

**ACKNOWLEDGMENTS**

Presented in part at the Basic Pharmaceutics Section, APhA Academy of Pharmaceutical Sciences, Washington meeting, April 1980.

The authors thank Ms. Sue Sheffield for her skilled secretarial assistance.

# Mixing of Pharmaceutical Solids II: Evaluation of Multicomponent Mixing of Cohesive Powders in Cylindrical Shear Mixer

**Z. T. CHOWHAN ˣ, E. E. LINN, and LI-HUA CHI**

Received November 1, 1979, from *Syntex Research, Palo Alto, CA 94304.* Accepted for publication August 14, 1980.

**Abstract** □ The mixing of three organic carboxylic acids with micronized lactose, all cohesive in nature, was studied using a cylindrical shear mixer. Three mixing indexes ($s/\sigma_A$, $s/\sigma_R$, and the Ashton–Valentin mixing index) were used to evaluate mixing of the three drugs with lactose. The results suggested that maximum homogeneity was reached after 45 min of mixing. However, different mixing indexes showed different sensitivity to homogeneity of the individual components. The mixing index $s/\sigma_A$, which is based on setting standard specifications, appears to provide a better evaluation of homogeneity of individual components compared to the mixing indexes based on complete random mixing theory. The latter did not approach unity for any drug component used in this study. These results suggested that mixing of cohesive powders is a complex process and cannot be explained fully by simple theory based on complete random mixing.

**Keyphrases** □ Mixing—of multicomponent cohesive powders, evaluation of homogeneity using three mixing indexes based on statistical analysis □ Powders—multicomponent mixing of cohesive powders, evaluation of homogeneity using three mixing indexes based on statistical analysis □ Carboxylic acids—cohesive powders mixed with lactose for homogeneity evaluation, evaluation of three mixing indexes based on statistical analysis □ Dosage forms, design—multicomponent mixing of cohesive powders to determine homogeneity of individual components, three mixing indexes evaluated

The mixing of a cohesive drug with cohesive, noncohesive, and free-flowing excipients was studied previously (1) using two types of mixers, cylindrical shear and V-shaped tumbling. Most mixing studies use binary systems, and mixing indexes based on statistical analysis are used to evaluate homogeneity. However, many practical situations in dosage form design require mixing several powders. Although most multicomponent mixing has been studied theoretically (2–6), one practical multicomponent system used 10% phenobarbital, 1% secobarbital, 1% butobarbital, and 88% lactose (7–9).

The multicomponent mixing of cohesive powders is one of the most difficult and complex powder mixing systems. None of the reported mixing studies have dealt with this powder mixing system.

This paper reports the mixing of cohesive powders of three organic carboxylic acids and an excipient in a cylindrical shear mixer. The results were evaluated by the mixing indexes based on complete random mixing and on standard specifications described previously (10, 11).

## EXPERIMENTAL

**Materials**—Three organic carboxylic acids, 7-methylsulfinyl-2-xanthone carboxylic acid (I), 7-methylthio-2-xanthone carboxylic acid (II), and 5-isopropoxy-7-methylthio-2-xanthone carboxylic acid (III), and mestranol were at least 99% pure[1]. USP grade lactose[2] was micronized[3]. Component I was micronized, and II and III were used as received. Methanol[4] was spectra grade, and polysorbate 80[5] was USP grade. All other chemicals were analytical grade unless specified otherwise.

**Physical Properties**—The particle-size distributions of I–III were determined[6] by electronic counting. The vehicle was a saturated solution of the compound in 0.6% HCl containing 0.018% polysorbate 80. The filtered vehicle was used to disperse the drug powder.

The particle-size distribution of the micronized lactose was determined[7] by automatic sedimentation, using photoextinction to measure the apparent projected area at decreasing sedimentation depths with increasing time.

The densities of the organic carboxylic acids were determined by the density matching method of Oster and Yamamoto (12). Mixtures of

[1] Institute of Organic Chemistry, Syntex Research, Palo Alto, CA 94304.
[2] Lactose regular, Foremost Food Co., San Francisco, CA 94104.
[3] Jet Pullverizer Co., Palmyra, N.J.
[4] Mallinckrodt Chemical Works, St. Louis, MO 63160.
[5] ICI America, Atlas Chemical Division, Wilmington, Del.
[6] Coulter counter model TA, Coulter Electronics, Hialeah, FL 33010.
[7] Sedigraph-L Micromeretics Instrument Corp., Norcross, Ga.

0022-3549/81/0300-0243$01.00/0
© 1981, American Pharmaceutical Association

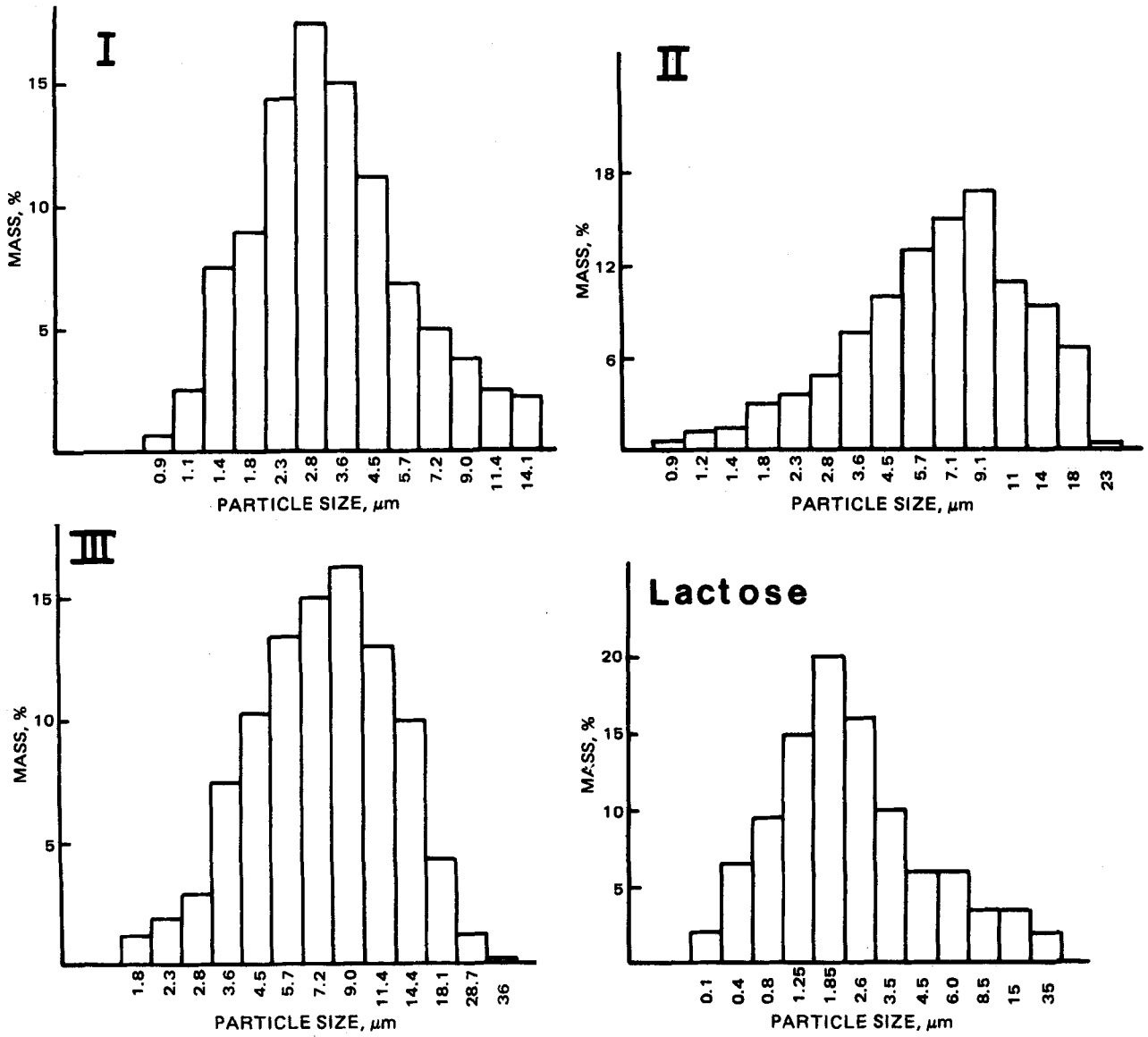


**Figure 1**—*Particle-size distribution of I, II, III, and lactose.*

hexane and carbon tetrachloride were prepared, and the powder was placed in the test tubes containing these solvent mixtures to pinpoint the density range. The powder density was determined by matching with the solvent mixture. The density of the final solvent was determined by weighing the solvent in a liquid pycnometer, which was calibrated with water at room temperature. The density of the lactose was obtained from the literature.

**Mixing**—The mixing was carried out in a cylindrical shear mixer equipped with a stainless steel blade. The cylindrical drum was rotated at a desired speed controlled by a speed regulator. The axis of rotation coincided with the axis of the cylindrical drum. The multicomponent system consisted of micronized lactose and the three carboxylic acids (I, 12%; II, 6%; and III, 2%). The loading was carried out through the same side of the mixer, and each component was dilated during loading.

The mixer was rotated at 60 rpm throughout the study. Twenty spot samples, 20 mg each, were withdrawn from six different locations of the powder bed at each time interval.

The samples were individually weighed, extracted with methanol, and assayed for I–III by high-performance liquid chromatography (HPLC) using mestranol as the internal standard.

**Assay of I–III in Mixture**—The samples of the powder mixtures were dissolved and extracted in methanol. Residual lactose was removed by filtration through a 0.8-μm pore diameter filter[8]. The first 15 ml of the filtered solution was discarded to account for any adsorption of the solute to the membrane filter. To an aliquot of the filtrate, an aliquot of mestranol in methanol was added and appropriately diluted before injection. The injection volume was 100 μl. The high-pressure liquid chromatograph was equipped with a fixed-wavelength UV detector at 280 nm. Separation was accomplished on a Spherisorb ODS, 10-μm, reversed-phase column (25 cm × 4.6 mm).

The mobile phase was 60% methanol and 1% acetic acid in distilled water. The eluent was filtered through a 2.0-μm filter[8] and degassed prior to use. The flow rate was adjusted to 1 ml/min (~1500 psi).

Calibration curves were prepared for solutions containing I–III and mestranol in the mobile phase. A linear relationship was obtained for I, II, and III over ranges of 1–7.0, I–4.0, and 0.1–1.2 μg/ml, respectively.

Method reproducibility was checked by injecting 20 samples from the same stock solution prepared from the accurately weighed amount of I–III and lactose in the same proportion as used in the mixing studies.

## RESULTS AND DISCUSSION

The particle-size distributions of I–III and lactose are given in Fig. 1. Table I gives the mass median diameter, density, effective particle weight, and total number of particles in a sample of all components in the mixture. The classification of powders into cohesive and noncohesive powders was based largely on the particle-size distribution, because simple measurements such as the angle of repose did not differentiate between these

[8] Metricel membrane filter.

**Table I—Particle Properties of Mixing Components**

| Property | I | II | III | Lactose |
|---|---|---|---|---|
| Mass median diameter, μm | 3.06 | 7.23 | 6.40 | 2.10 |
| Density, g/ml | 1.53 | 1.50 | 1.40 | 1.53 |
| Effective mean particle weight, μg | $0.147 \times 10^{-3}$ | $0.799 \times 10^{-3}$ | $0.65 \times 10^{-3}$ | $0.821 \times 10^{-3}$ |
| Total number of particles in sample | $2.79 \times 10^{8}$ | $4.78 \times 10^{7}$ | $6.93 \times 10^{6}$ | $4.275 \times 10^{11}$ |
| Cohesion | Cohesive | Cohesive | Cohesive | Cohesive |

powders (1). Since the mass median diameter of all mixing components used was <10 μm, all powders were classified qualitatively as cohesive.

Figure 2 gives the chromatogram showing the separation of I–III and the internal standard. The observed retention times for I, II, mestranol, and III were 6, 10, 13, and 16 min, respectively. The error due to the method was determined, and the variance of the method was 0.0029, 0.00064, and 0.00031% for I, II, and III, respectively. This error was small and was considered negligible. Since the sampling error is difficult to determine and the error due to the impurities is very small, they were neglected also. The total error in powder mixing experiments is generally attributed to the error in the analytical method, sampling, impurities, and mixing:

$$S_t^2 = S_a^2 + S_s^2 + S_i^2 + S_m^2 \qquad \text{(Eq. 1)}$$

where $S^2$ represents sampling variance and subscripts $t$, $a$, $s$, $i$, and $m$ represent total, analytical method, sampling, impurities, and mixing, respectively.

For simplicity, the total error in these studies is attributed to the error due to mixing.

The sample standard deviation $s$ was obtained experimentally from the results of 20 samples. With the assumption of a normal distribution, the acceptable standard deviation $\sigma_A$ with a 99.7% confidence level within ±10 and ±15% of the mean $X$ was calculated from:

$$\pm 3\sigma_A = \pm 0.1X = (\text{tolerance} \times \text{mean}) \qquad \text{(Eq. 2a)}$$

$$\pm 3\sigma_A = \pm 0.15X = (\text{tolerance} \times \text{mean}) \qquad \text{(Eq. 2b)}$$

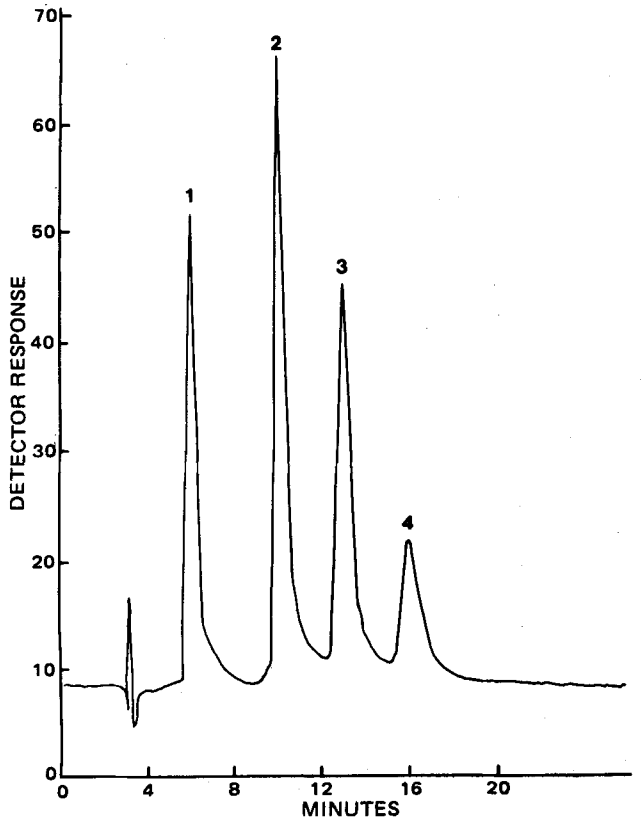


**Figure 2**—*Chromatogram of I–III from a mixture containing mestranol as the internal standard. Detector response was at 0.04 aufs. Key: 1, I; 2, II; 3, mestranol; and 4, III.*

The acceptable standard deviation $\sigma_A$ may be fixed at any desired tolerance, for example, 15% within the mean. The sample standard deviation $s$ is obtained from the mixing experiments. The mixing index $s/\sigma_A$ approaches acceptability as the sample standard deviation approaches $\sigma_A$.

Figure 3 gives the results of $s/\sigma_A$ as a function of the mixing time. As mixing approached acceptability, the ratio of the sample standard deviations and the acceptable standard deviation $\sigma_A$ approached unity. The $s/\sigma_A$ for I, which was at the highest concentration, approached unity after ~35 min of mixing. When mixing was continued, the $s/\sigma_A$ remained below unity. The $s/\sigma_A$ for II approached acceptable homogeneity after ~45 min of mixing. Component III, which was at the lowest concentration in the mixture, approached acceptability only after 75 min of mixing.

The results in Fig. 3 clearly indicate that homogeneity in a multicomponent cohesive system is very dependent on the concentration of the individual components[9]. The component at the highest concentration in the mixture appeared to approach the acceptability range at the fastest rate, and the component at the lowest concentration was slowest in approaching the acceptability range. Since the degree of mixedness in a multicomponent system is dependent on the concentration of individual components, it is important to monitor the homogeneity of individual

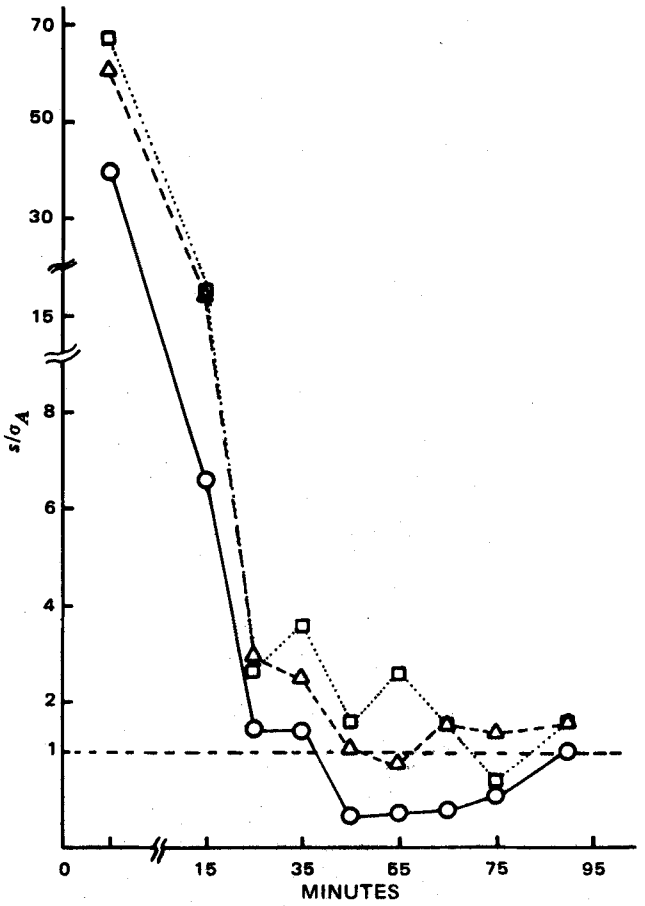


**Figure 3**—*Plots of* $s/\sigma_A$ *versus mixing time, showing the mixing of I (○), II (△), and III (□). The* $\sigma_A$ *was calculated at ±10% tolerance with a 99.7% confidence level.*

[9] Such a concentration effect has largely been ignored in the past except for one brief study (13). It has not been reported for multicomponent mixtures.

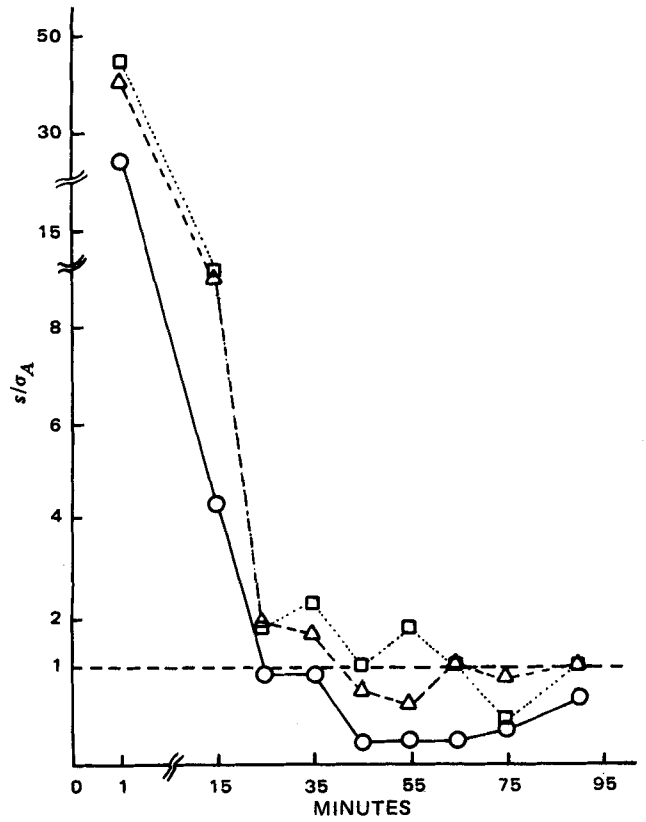


**Figure 4**—*Plots of* $s/\sigma_A$ versus *mixing time, showing the mixing of I (○), II (△), and III (□). The* $\sigma_A$ *was calculated at ±15% tolerance with a 99.7% confidence level.*

components to reach an acceptability range for all components in the mixture. It is obvious from the results in Fig. 3 that the mixture did not pass the 10% acceptable limit on standard deviation at any time point because the mixing index for at least one of the three components did not approach the acceptability range.

Figure 4 gives the results of the $s/\sigma_A$ mixing index tested according to the USP criterion of ±15% for content uniformity at the 99.7% confidence level. All three components approached acceptable homogeneity

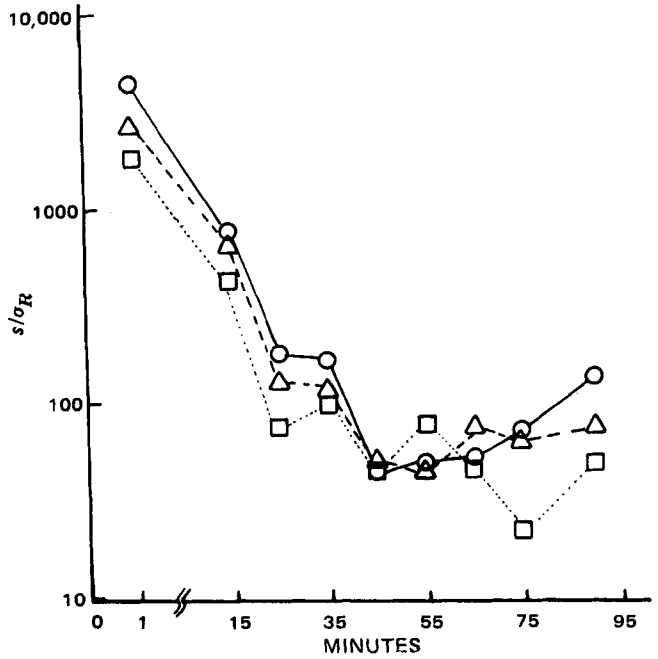


**Figure 5**—*Plots of* $s/\sigma_R$ versus *mixing time, showing the mixing of I (○), II (△), and III (□).*

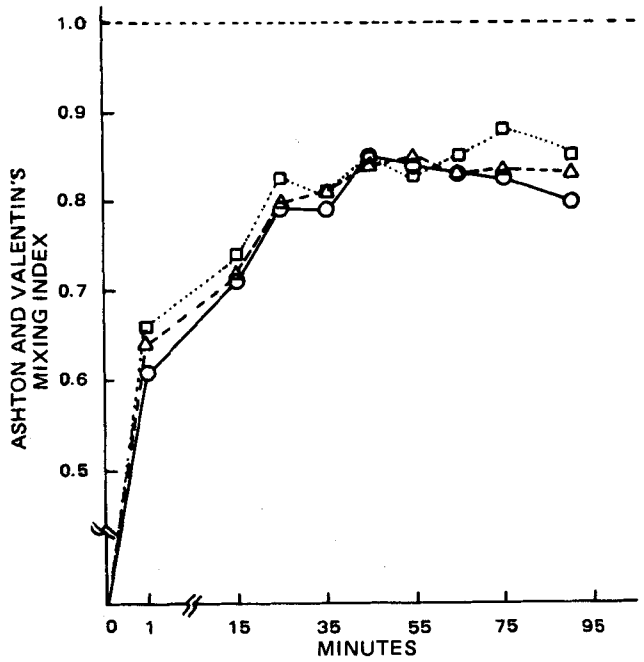


**Figure 6**—*Plots of* $(\log \sigma_0^2 - \log S^2)/(\log \sigma_0^2 - \log \sigma_R^2)$ versus *mixing time, showing the mixing of I (○), II (△), and III (□).*

after mixing for 45, 75, and 90 min.

Mixing processes are generally considered as random in nature. Over 30 different mixing indexes were reviewed by Fan *et al.* (14). For a fully randomized two-component system of identical densities and particle sizes, the standard deviation was given (11) by:

$$\sigma_R = \left(\frac{pq}{N}\right)^{1/2} \qquad \text{(Eq. 3)}$$

where $p$ and $q$ are the proportions of two components, $N$ is the number of particles in the unit of scrutiny, and $\sigma_R$ is in a unit of fraction of particles.

Poole *et al.* (15) modified an expression (16) to account for the particle-size distribution of a binary system:

$$\sigma_R = \left\{pq \Big/ \left[\frac{W}{q(\Sigma fw)_p + p(\Sigma fw)_q}\right]\right\}^{1/2} \qquad \text{(Eq. 4)}$$

where $\Sigma(fw)$ is the effective mean particle weight of that ingredient denoted by the subscript and $W$ is the mass of the sample taken from a mix. Stange (5) extended this form to a multicomponent system:

$$\sigma_{R,p}^2 = \frac{p^2}{W}\left[\left(\frac{1-p}{p}\right)^2 p(\Sigma fw)_p + q(\Sigma fw)_q + r(\Sigma fw)_r + \cdots\right] \qquad \text{(Eq. 5)}$$

The ratio of the sample standard deviation and $\sigma_R$ obtained from Eq. 5 is plotted *versus* mixing time in Fig. 5. As expected from the results of a binary system (1), this index was not suitable for evaluating mixing of multicomponents that are all cohesive.

Ashton and Valentin (17) proposed the following mixing index (Eq. 6), which is more sensitive to variations of mixedness in its entire span ranging from the completely segregated state to completely mixed state:

$$Mu^2 = \frac{\log \sigma_0^2 - \log S^2}{\log \sigma_0^2 - \log \sigma_R^2} \qquad \text{(Eq. 6)}$$

where $\sigma_0^2$, $S^2$, and $\sigma_R^2$ are the variances in the initial, intermediate, and ultimate random conditions, respectively. Figure 6 gives the plots of this mixing index as a function of the mixing time. All three components approached maximum homogeneity on mixing for ~45 min, after which some segregation tendency was noticeable with two components.

The analyses of mixing data of multicomponent cohesive powders by the mixing indexes based on complete random mixing theory and on setting standard specifications suggested that the maximum attainable homogeneity was reached after 45 min of mixing. The two analyses show different sensitivity to the homogeneity of individual components. The mixing index $s/\sigma_A$, which is based on setting standard specifications, appears to provide a better evaluation of homogeneity of individual

components compared to the mixing index based on complete random mixing theory. The mixing indexes based on complete random mixing do not approach unity for any of the three drug components used in this study. These results suggest that mixing of cohesive powders is a complex process and cannot be fully explained by simple theory based on complete random mixing.

The analyses of multicomponent mixing were based on fundamental statistical concepts. The mixing index based on standard specifications provides satisfactory evaluation of mixing multicomponent cohesive powders. The mixing index of Ashton and Valentin (17) may be used to evaluate multicomponent mixing systems of the type described in this paper, although it has some disadvantages.

Recently, Wang *et al.* (2) applied multivariate statistical analysis to the mixing process and to a mixture of multicomponent solid particles. They used three types of lucite spherical particles which had identical properties except color. Since it is an interesting approach for evaluating multicomponent mixing, future work directed in this vein using a more practical multicomponent system would elucidate the understanding of mixing.

## REFERENCES


(1) Z. T. Chowhan and E. E. Linn, *Powder Technol.*, **24**, 237 (1979).

(2) R. H. Wang, L. T. Fan, and J. R. Too, *ibid.*, **21**, 171 (1978).

(3) L. T. Fan and J. R. Too, *ibid.*, **22**, 205 (1979).

(4) D. Buslik, *Bull. Am. Soc. Testing Mater.*, **165**, 66 (1950).

(5) K. Stange, *Chem. Ing. Tech.*, **35**, 580 (1963).

(6) N. Harnby, *Chem. Eng.*, **214**, CE270 (1967).

(7) P. Cook and J. A. Hersey, *Powder Technol.*, **9**, 257 (1974).

(8) P. C. Cook and J. A. Hersey, *Austr. J. Pharm Sci.*, **NS3**, 49 (1974).

(9) J. A. Hersey, P. Cook, M. Smyth, E. A. Bishop, and E. A. Clarke, *J. Pharm. Sci.*, **63**, 408 (1974).

(10) J. A. Hersey, *J. Pharm. Pharmacol., Suppl.*, **19**, 168S (1979).

(11) P. M. C. Lacey, *Trans. Inst. Chem. Eng.*, **21**, 53 (1943).

(12) G. Oster and M. Yamamoto, *Chem. Rev.*, **63**, 257 (1963).

(13) J. T. Carstensen and M. R. Patel, *Powder Technol.*, **17**, 273 (1977).

(14) L. T. Fan, S. J. Chen, and C. A. Watson, *Ind. Eng. Chem. Process Des. Dev.*, **62**, 53 (1970).

(15) K. R. Poole, R. F. Taylor, and G. P. Wall, *Trans. Inst. Chem. Eng.*, **42**, T305 (1964).

(16) K. Stange, *Chem. Ing. Tech.*, **26**, 129 (1954).

(17) M. D. Ashton and F. H. H. Valentin, *Trans. Inst. Chem. Eng.*, **44**, T166 (1966).


# Mixing of Pharmaceutical Solids III: Multivariate Statistical Analysis of Multicomponent Mixing


**Z. T. CHOWHAN ˣ and LI-HUA CHI**



Received November 1, 1979, from *Syntex Research, Palo Alto, CA 94304.* Accepted for publication August 12, 1980.



**Abstract** □ The multicomponent mixing for cohesive powders was evaluated by multivariate statistical methods. Tests were carried out for the sampling technique, completely random state and completely segregated state. Hotelling's statistics were not helpful in testing the practical sampling technique. Comparisons of the mixing indexes based on univariate and multivariate statistics indicated excellent consistency in optimizing mixing time. Neither mixing index approached unity because cohesive powders do not reach a completely random state. The multivariate mixing index was smaller than the univariate indexes largely due to interparticular forces among small cohesive particles.



**Keyphrases** □ Mixing—of multicomponent cohesive powders, evaluation of homogeneity using multivariate statistical analysis □ Powders—multicomponent mixing of cohesive powders, evaluation of homogeneity using multivariate statistical analysis □ Dosage forms, design—multicomponent mixing of cohesive powders to determine homogeneity of mixture, comparison of univariate and multivariate statistical analyses


Theories concerning the state of mixedness of solids generally deal with univariate statistical analysis of the sample standard deviation and the theoretical standard deviation (1–6). However, almost all processes of experimentation, data collection, and observations are multivariate in nature. Multivariate analysis deals with summarization, representation, and interpretation of data sampled from populations where the variables yield measures of more than one characteristic (7–9). In pharmaceutical practice, the drug(s) and excipient(s) being mixed vary in their particle-size distribution, inter- and intraparticular forces, mixing composition, shape, *etc.* From a statistical viewpoint, analysis of heterogeneous solid mixtures using the univariate statistical approach does not account for the interactions and statistical dependency of individual components.

Recently, Wang *et al.* (10) applied multivariate statistical analysis to the mixing process and to a mixture of multicomponent solid particles. They used three types of spherical particles with identical properties except color.

The mixing of three organic carboxylic acids with micronized lactose, all cohesive in nature, was studied (11) using a cylindrical shear mixer. The results were evaluated by the mixing indexes based on univariate statistics. This paper analyzes the previous experimental results using multivariate statistical methods. Comparisons of the results of the mixing indexes based on univariate statistics (6) and multivariate statistics (10) indicate excellent consistency in optimizing mixing time for mixing multicomponent cohesive powders. Due to interparticular forces among small cohesive particles, the resulting multivariate mixing index was smaller than the univariate index of individual components. Neither mixing index approached unity, indicating that the mixing of cohesive powders is not completely random.

## THEORETICAL

In the univariate normal distribution, measurement of the effect is evaluated through independent random events. The problems arising in the multivariate populations are mostly straightforward analogies of the problems arising in univariate populations. For a single variable, the


0022-3549/81/0300-0247$01.00/0


© 1981, American Pharmaceutical Association

components compared to the mixing index based on complete random mixing theory. The mixing indexes based on complete random mixing do not approach unity for any of the three drug components used in this study. These results suggest that mixing of cohesive powders is a complex process and cannot be fully explained by simple theory based on complete random mixing.

The analyses of multicomponent mixing were based on fundamental statistical concepts. The mixing index based on standard specifications provides satisfactory evaluation of mixing multicomponent cohesive powders. The mixing index of Ashton and Valentin (17) may be used to evaluate multicomponent mixing systems of the type described in this paper, although it has some disadvantages.

Recently, Wang *et al.* (2) applied multivariate statistical analysis to the mixing process and to a mixture of multicomponent solid particles. They used three types of lucite spherical particles which had identical properties except color. Since it is an interesting approach for evaluating multicomponent mixing, future work directed in this vein using a more practical multicomponent system would elucidate the understanding of mixing.

## REFERENCES


(1) Z. T. Chowhan and E. E. Linn, *Powder Technol.*, **24**, 237 (1979).

(2) R. H. Wang, L. T. Fan, and J. R. Too, *ibid.*, **21**, 171 (1978).

(3) L. T. Fan and J. R. Too, *ibid.*, **22**, 205 (1979).

(4) D. Buslik, *Bull. Am. Soc. Testing Mater.*, **165**, 66 (1950).

(5) K. Stange, *Chem. Ing. Tech.*, **35**, 580 (1963).

(6) N. Harnby, *Chem. Eng.*, **214**, CE270 (1967).

(7) P. Cook and J. A. Hersey, *Powder Technol.*, **9**, 257 (1974).

(8) P. C. Cook and J. A. Hersey, *Austr. J. Pharm Sci.*, **NS3**, 49 (1974).

(9) J. A. Hersey, P. Cook, M. Smyth, E. A. Bishop, and E. A. Clarke, *J. Pharm. Sci.*, **63**, 408 (1974).

(10) J. A. Hersey, *J. Pharm. Pharmacol., Suppl.*, **19**, 168S (1979).

(11) P. M. C. Lacey, *Trans. Inst. Chem. Eng.*, **21**, 53 (1943).

(12) G. Oster and M. Yamamoto, *Chem. Rev.*, **63**, 257 (1963).

(13) J. T. Carstensen and M. R. Patel, *Powder Technol.*, **17**, 273 (1977).

(14) L. T. Fan, S. J. Chen, and C. A. Watson, *Ind. Eng. Chem. Process Des. Dev.*, **62**, 53 (1970).

(15) K. R. Poole, R. F. Taylor, and G. P. Wall, *Trans. Inst. Chem. Eng.*, **42**, T305 (1964).

(16) K. Stange, *Chem. Ing. Tech.*, **26**, 129 (1954).

(17) M. D. Ashton and F. H. H. Valentin, *Trans. Inst. Chem. Eng.*, **44**, T166 (1966).


# Mixing of Pharmaceutical Solids III: Multivariate Statistical Analysis of Multicomponent Mixing


**Z. T. CHOWHAN ˣ and LI-HUA CHI**



Received November 1, 1979, from *Syntex Research, Palo Alto, CA 94304.* Accepted for publication August 12, 1980.



**Abstract** □ The multicomponent mixing for cohesive powders was evaluated by multivariate statistical methods. Tests were carried out for the sampling technique, completely random state and completely segregated state. Hotelling's statistics were not helpful in testing the practical sampling technique. Comparisons of the mixing indexes based on univariate and multivariate statistics indicated excellent consistency in optimizing mixing time. Neither mixing index approached unity because cohesive powders do not reach a completely random state. The multivariate mixing index was smaller than the univariate indexes largely due to interparticular forces among small cohesive particles.



**Keyphrases** □ Mixing—of multicomponent cohesive powders, evaluation of homogeneity using multivariate statistical analysis □ Powders—multicomponent mixing of cohesive powders, evaluation of homogeneity using multivariate statistical analysis □ Dosage forms, design—multicomponent mixing of cohesive powders to determine homogeneity of mixture, comparison of univariate and multivariate statistical analyses


Theories concerning the state of mixedness of solids generally deal with univariate statistical analysis of the sample standard deviation and the theoretical standard deviation (1–6). However, almost all processes of experimentation, data collection, and observations are multivariate in nature. Multivariate analysis deals with summarization, representation, and interpretation of data sampled from populations where the variables yield measures of more than one characteristic (7–9). In pharmaceutical practice, the drug(s) and excipient(s) being mixed vary in their particle-size distribution, inter- and intraparticular forces, mixing composition, shape, *etc.* From a statistical viewpoint, analysis of heterogeneous solid mixtures using the univariate statistical approach does not account for the interactions and statistical dependency of individual components.

Recently, Wang *et al.* (10) applied multivariate statistical analysis to the mixing process and to a mixture of multicomponent solid particles. They used three types of spherical particles with identical properties except color.

The mixing of three organic carboxylic acids with micronized lactose, all cohesive in nature, was studied (11) using a cylindrical shear mixer. The results were evaluated by the mixing indexes based on univariate statistics. This paper analyzes the previous experimental results using multivariate statistical methods. Comparisons of the results of the mixing indexes based on univariate statistics (6) and multivariate statistics (10) indicate excellent consistency in optimizing mixing time for mixing multicomponent cohesive powders. Due to interparticular forces among small cohesive particles, the resulting multivariate mixing index was smaller than the univariate index of individual components. Neither mixing index approached unity, indicating that the mixing of cohesive powders is not completely random.

## THEORETICAL

In the univariate normal distribution, measurement of the effect is evaluated through independent random events. The problems arising in the multivariate populations are mostly straightforward analogies of the problems arising in univariate populations. For a single variable, the


0022-3549/81/0300-0247$01.00/0


© 1981, American Pharmaceutical Association

central limit theorem leads to the univariate normal distribution; for several variables, the general limit theorem leads to the multivariate normal distribution. The suitable methods of analysis are based mainly on the standard operations of matrix algebra.

For a univariate normal distribution, variable $Y$ was taken from the normal distribution $N$:

$$Y \sim N(\mu, \sigma^2) \quad \text{(Eq. 1)}$$

where $\mu$ is the population mean and $\sigma^2$ is the population variance.

To test if the sample mean $\overline{X}$ is equal to the hypothetical population mean $\mu_0$, $t$ statistics is used:

$$t = (N)^{1/2} \frac{(\overline{X} - \mu_0)}{S} \quad \text{(Eq. 2)}$$

where $N$ is the number of observations in the sample and $S$ is the sample standard deviation.

In the multivariate statistics, a vector random variable $Y$, which is a $p$-element vector, and $T^2$ statistics proposed by Hotelling are used:

$$T^2 = N(\overline{Y} - \mu_0)'S^{-1}(\overline{Y} - \mu_0) \quad \text{(Eq. 3)}$$

where $\overline{Y}$ is the mean vector of a sample of $N$ number, $S$ is the sample variance–covariance matrix that is the unbiased estimation of the dispersion, and the prime is the transpose of the matrix.

**Multivariate Test of Sampling Technique**—In sampling a $p$-variate normal population, it is assumed that:

$$Y_i' \sim N_p(\mu, \Sigma) \quad \text{(Eq. 4)}$$

$$Y_1' = [y_{11} \quad y_{12} \quad \dots \quad y_{1p}] \quad \text{(Eq. 5)}$$

$$\begin{matrix} Y_2' = [y_{21} & y_{22} & \dots & y_{2p}] \\ \vdots & \vdots & \vdots & \vdots\vdots\vdots \\ Y_N' = [y_{N1} & y_{N2} & \dots & y_{Np}] \end{matrix} \quad \text{(Eq. 6)}$$

or:

$$Y' = \begin{bmatrix} y_{11} & y_{12} & \dots & y_{1p} \\ y_{21} & y_{22} & \dots & y_{2p} \\ \vdots & \vdots & \vdots\vdots\vdots & \\ y_{N1} & y_{N2} & \dots & y_{Np} \end{bmatrix} \quad \text{(Eq. 7)}$$

where $\mu$ is the sample mean vector, $\Sigma$ is the variance–covariance matrix, and $Y_i'$ is the $p$-vector random variable where $i = 1, 2, \dots N$.

Next, the null hypothesis $H_0$ ($\mu = \mu_0$) is tested against the alternative hypothesis $H_1$ ($\mu \neq \mu_0$). The most likely estimator of the centroid is an unbiased estimator and is given by:

$$\overline{Y} = \frac{1}{N}\left(\sum_{i=1}^{N} Y_i\right) \quad \text{(Eq. 8)}$$

The most likely estimator of the dispersion or variance–covariance matrix $S$ is given by:

$$S = \frac{1}{N-1}\sum_{i=1}^{N}(Y_i - \overline{Y})(Y_i - \overline{Y})' \quad \text{(Eq. 9)}$$

If the Hotelling statistics $T^2 > T^2_{\alpha(p,N-1)}$, the null hypothesis that the mean has not been significantly biased at level $\alpha$ is rejected. Thus, $T^2_{\alpha(p,N-1)}$ denotes the upper $\alpha$ percentage point of the $T^2$ distribution.

The rejection of the null hypothesis $H_0$, $\mu = \mu_0$, indicates that the sample mean is significantly different from the population mean. This result could be due to improper location and spacing of the spot samples, bias during sampling, or a peculiar segregation tendency that favored the concentration of one material in some small area.

**Multivariate Test for Completely Random and Completely Segregated States**—The criterion in multivariate analysis is to determine if the variance–covariance matrix of the mixture is significantly different from that of a completely random state. The test for a completely segregated state could be performed in a similar fashion.

Given $Y_1'$, $Y_2'$, and $Y_N'$ as observation vectors of the $p + 1$ component from $Np(\mu, \Sigma)$, the most likely ratio criterion for testing the null hypothesis $H_0$:

$$\Sigma = \Sigma_0 \quad \text{(Eq. 10)}$$

against the alternative hypothesis $H_1$ ($\Sigma \neq \Sigma_0$), where $\Sigma_0$ is the specified variance–covariance matrix as given by (12):

$$\lambda_1 = \left(\frac{e}{N}\right)^{1/2(pN)} |B\Sigma_0^{-1}|^{1/2(N)} e^{-1/2(tr)(B\Sigma_0^{-1})} \quad \text{(Eq. 11)}$$

where $B = \sum_{i=1}^{N}(Y_i - \overline{Y})(Y_i - \overline{Y})'$.

It was shown (12) that:

$$\mathbf{X} = -2 \ln \lambda_1 \quad \text{(Eq. 12a)}$$

$$\mathbf{X} = pN(\ln N - 1) - N \ln |B\Sigma_0^{-1}| + tr(B\Sigma_0^{-1}) \quad \text{(Eq. 12b)}$$

is distributed approximately as a $\chi^2$ random variable with $p(p + 1)/2$ degrees of freedom when $H_0$ is true. Thus, the null hypothesis is rejected at the significance level $\alpha$ if $\mathbf{X} > x^2_\alpha(p(p + 1)/2)$.

For the spot sample of size $N$ taken from a completely random mixture, the particles in the mixture are expected to be randomly distributed. Assume the random variables $(\mathbf{X}_1, \mathbf{X}_2 \dots \mathbf{X}_{p+1})$ for a mixture of $(p + 1)$ components, where $\mathbf{X}_j$ is the number of $j$ components occurring among the $n$ repetition of the event. Hence, $\mathbf{X}_j = n_j$, $n_j = 0, 1, \dots, n$, and:

$$x_j = \frac{\mathbf{X}_j}{n} \quad \text{(Eq. 13)}$$

where $x_j$ denotes the number proportion of type $j$ particles in the mixture. The probability of a spot sample to contain $n_1$ particles of type 1, $n_2$ particles of type 2, and $n_{(p+1)}$ particles of type $(p + 1)$ was given as the probability function:

$$P(\mathbf{X}_1 = n_1, \mathbf{X}_2 = n_2 \dots \mathbf{X}_{(p+1)} = n_{p+1}) = \frac{n!}{n_1!\, n_2! \dots n_{p+1}!} c_1^{n_1} c_2^{n_2} \dots c_{p+1}^{n(p+1)} \quad \text{(Eq. 14)}$$

where:

$$\sum_{i=1}^{p+1} n_i = n$$

$$\sum_{i=1}^{p+1} c_i = 1$$

and $c_i$ is the fraction concentration of component $i$ in the mixture. In a four-component system, $n_1 + n_2 + n_3 + n_4 = n$ and $c_1 + c_2 + c_3 + c_4 = 1$.

These random variables, $\mathbf{X}_1, \mathbf{X}_2, \dots \mathbf{X}_{(p+1)}$, with the function given above have a multinomial probability distribution that is a generalization of the binomial distribution. The mean, variance, and covariance of the probability density (13), respectively, are:

$$E(\mathbf{X}_j) = nC_j \quad \text{(Eq. 15)}$$

$$VAR(\mathbf{X}_j) = nC_j(1 - C_j) \quad \text{(Eq. 16)}$$

$$COV(\mathbf{X}_i, \mathbf{X}_j) = -nC_iCj \quad \text{(Eq. 17)}$$

Hence, for a completely random state, $\Sigma_r$ may be expressed as:

$$\Sigma_r = \frac{1}{n}\begin{bmatrix} c_1(1-c_1) & -c_1c_2 & \dots & -c_1c_p \\ -c_1c_2 & c_2(1-c_2) & \dots & -c_2c_p \\ \vdots & \vdots & \vdots\vdots\vdots & \\ -c_1c_p & -c_2c_p & \dots & c_p(1-c_p) \end{bmatrix} \quad \text{(Eq. 18)}$$

In the completely segregated state, particles of the same kind aggregate together. The variance–covariance matrix for the completely segregated state is:

$$VAR(x_i) = c_i(1 - c_i) \quad \text{(Eq. 19)}$$

$$COV(x_i, x_j) = -c_ic_j \quad \text{(Eq. 20)}$$

For a completely segregated state, $\Sigma_s$ can be expressed as:

$$\Sigma_s = \begin{bmatrix} c_1(1-c_1) & -c_1c_2 & \dots & -c_1c_p \\ -c_1c_2 & c_2(1-c_2) & \dots & -c_2c_p \\ \vdots & \vdots & \vdots\vdots\vdots & \\ -c_pc_1 & -c_pc_2 & \dots & c_p(1-c_p) \end{bmatrix} \quad \text{(Eq. 21)}$$

**Multivariate Mixing Index for Multicomponent Mixture**—Wang *et al.* (10) proposed a mixing index for a multicomponent mixture that can range between 0 and 1, based on the value of the determinant of the variance–covariance matrix at the completely segregated state and that at the completely random state:

$$Mm = \frac{(\ln |\Sigma_s| - \ln |S|)^{1/2}}{(\ln |\Sigma_s| - \ln |\Sigma_r|)^{1/2}} \quad \text{(Eq. 22)}$$

where:

$|S|$ = determinant of sample variance–covariance matrix
$|\Sigma_s|$ = determinant of variance–covariance matrix at completely segregated state

**Table I—Sample Mean and Standard Deviation**

| Number | Mixing Time, min | | Mean Recovery ± *SD* |
|---|---|---|---|
| 1 | 1 | I | 0.1535 ± 0.1583 |
| | | II | 0.0926 ± 0.1233 |
| | | III | 0.0320 ± 0.04507 |
| 2 | 15 | I | 0.1237 ± 0.0266 |
| | | II | 0.0640 ± 0.0305 |
| | | III | 0.0224 ± 0.0104 |
| 3 | 25 | I | 0.1182 ± 0.0058 |
| | | II | 0.0594 ± 0.0060 |
| | | III | 0.0199 ± 0.0018 |
| 4 | 35 | I | 0.1210 ± 0.0058 |
| | | II | 0.0602 ± 0.0051 |
| | | III | 0.0203 ± 0.0024 |
| 5 | 45 | I | 0.1208 ± 0.0015 |
| | | II | 0.0607 ± 0.0023 |
| | | III | 0.0205 ± 0.0011 |
| 6 | 55 | I | 0.1192 ± 0.0016 |
| | | II | 0.0601 ± 0.0019 |
| | | III | 0.0202 ± 0.0018 |
| 7 | 65 | I | 0.1205 ± 0.0017 |
| | | II | 0.0601 ± 0.0033 |
| | | III | 0.0201 ± 0.0011 |
| 8 | 75 | I | 0.1178 ± 0.0023 |
| | | II | 0.0596 ± 0.0029 |
| | | III | 0.0196 ± 0.00048 |
| 9 | 90 | I | 0.1179 ± 0.0043 |
| | | II | 0.0606 ± 0.0033 |
| | | III | 0.0200 ± 0.0011 |

$|\Sigma_r|$ = determinant of variance–covariance matrix at completely random state

## RESULTS AND DISCUSSION

The experimental results of the multicomponent mixing (11) are summarized in Table I. As the mixing time increased, the mean composition of the individual components became closer to the theoretical values until plateau values were reached. The standard deviations decreased up to 45 min of mixing time, after which the standard deviation increased or decreased depending on the individual components.

To test for the sampling technique, the null hypothesis $H_0$:

$$\begin{bmatrix}\mu_1\\ \mu_2\\ \mu_3\end{bmatrix} = \begin{bmatrix}0.12\\ 0.06\\ 0.02\end{bmatrix} \quad \text{(Eq. 23)}$$

was tested against the alternative hypothesis $H_1$:

$$\begin{bmatrix}\mu_1\\ \mu_2\\ \mu_3\end{bmatrix} \neq \begin{bmatrix}0.12\\ 0.06\\ 0.02\end{bmatrix} \quad \text{(Eq. 24)}$$

For the first time point:

$$Y_1 = \begin{bmatrix}0.408\\ 0.1062\\ 0.0272\end{bmatrix} \quad \text{(Eq. 25a)}$$

$$Y_2 = \begin{bmatrix}0.2832\\ 0.2916\\ 0.0332\end{bmatrix} \quad \text{(Eq. 25b)}$$

$$\vdots$$

$$Y_{20} = \begin{bmatrix}0.0468\\ 0.0042\\ 0.0028\end{bmatrix} \quad \text{(Eq. 25c)}$$

$$Y' = \begin{bmatrix}0.408 & 0.1062 & 0.0272\\ 0.2832 & 0.2916 & 0.0332\\ 0.2664 & 0.2346 & 0.0510\\ 0.4044 & 0.3576 & 0.0910\\ 0.4836 & 0.3690 & 0.1474\\ 0.1392 & 0.1440 & 0.1446\\ 0.1596 & 0.0702 & 0.0134\\ 0.1752 & 0.0852 & 0.0212\\ 0.144 & 0.0828 & 0.0154\\ 0.0408 & 0.0696 & 0.0156\\ 0.0204 & 0.0036 & 0.0009\\ 0.0186 & 0.0066 & 0.0019\\ 0.0138 & 0.0027 & 0.0482\\ 0.0216 & 0.0036 & 0.0009\\ 0.0126 & 0.0027 & 0.0001\\ 0.0264 & 0.0057 & 0.0010\\ 0.0198 & 0.0045 & 0.0128\\ 0.0270 & 0.0033 & 0.0113\\ 0.3855 & 0.0039 & 0.0003\\ 0.0468 & 0.0042 & 0.0028\end{bmatrix} \quad \text{(Eq. 25d)}$$

with a sample mean of:

$$\overline{Y} = \frac{1}{N}\left(\sum_{i=1}^{N} Y_i\right) = \frac{1}{20}\left(\begin{bmatrix}0.408\\ 0.1062\\ 0.0272\end{bmatrix} + \begin{bmatrix}0.2832\\ 0.2916\\ 0.0332\end{bmatrix} + \cdots \begin{bmatrix}0.0468\\ 0.0042\\ 0.0028\end{bmatrix}\right) = \begin{bmatrix}0.1535\\ 0.0926\\ 0.0320\end{bmatrix} \quad \text{(Eq. 26)}$$

The sample variance–covariance matrix is:

$$S = \frac{1}{N-1}\sum_{i=1}^{N}(Y_i - \overline{Y})(Y_i - \overline{Y})' \quad \text{(Eq. 27a)}$$

$$S = \frac{1}{19}\sum_{i=1}^{20}(Y_i - \overline{Y})(Y_i - \overline{Y})' \quad \text{(Eq. 27b)}$$

$$S = \begin{bmatrix}0.2505\times10^{-1} & 0.1529\times10^{-1} & 0.3910\times10^{-2}\\ 0.1529\times10^{-1} & 0.1520\times10^{-1} & 0.4126\times10^{-2}\\ 0.3910\times10^{-2} & 0.4126\times10^{-1} & 0.2032\times10^{-2}\end{bmatrix} \quad \text{(Eq. 27c)}$$

$$S^{-1} = \begin{bmatrix}0.1040\times10^{3} & -0.112\times10^{3} & 0.2733\times10^{2}\\ -0.1120\times10^{3} & 0.2673\times10^{3} & -0.3271\times10^{2}\\ 0.2733\times10^{2} & -0.3271\times10^{3} & 0.1104\times10^{4}\end{bmatrix} \quad \text{(Eq. 28)}$$

$$T^2 = N(\overline{Y} - \mu_0)'S^{-1}(\overline{Y} - \mu_0) \quad \text{(Eq. 29a)}$$

$$T^2 = 20 \times \left(\begin{bmatrix}0.1535\\ 0.0926\\ 0.0320\end{bmatrix} - \begin{bmatrix}0.12\\ 0.06\\ 0.02\end{bmatrix}\right)' S^{-1} \left(\begin{bmatrix}0.1535\\ 0.0926\\ 0.0320\end{bmatrix} - \begin{bmatrix}0.12\\ 0.06\\ 0.02\end{bmatrix}\right) \quad \text{(Eq. 29b)}$$

$$T^2 = 20 \times [0.0335 \quad 0.0326 \quad 0.0120]\, S^{-1} \begin{bmatrix}0.0335\\ 0.0326\\ 0.0120\end{bmatrix} \quad \text{(Eq. 29c)}$$

$$T^2 = 20 \times 0.0811 \quad \text{(Eq. 29d)}$$

$$T^2 = 1.6217 \quad \text{(Eq. 29e)}$$

$$T^2_{0.05(3,19)} = 10.729 > 1.6217 \quad \text{(Eq. 30)}$$

Thus, $H_0$ was accepted.

Table II gives the results of the sampling technique test. Comparison of the data in Tables I and II indicates that the smaller the difference in the mean vector from the initial composition, the larger the Hotelling statistic value is. As the mixing time increased, the Hotelling statistic

**Table II—Test of the Sampling Technique**

| Mixing Time, min | Hotelling's $T^2$ | Acceptance of $H_0$ | Variance–Covariance | | | Determinant |
|---|---|---|---|---|---|---|
| 1 | 1.6217 | Yes | $0.2505 \times 10^{-1}$ | $0.1529 \times 10^{-1}$ | $0.3910 \times 10^{-2}$ | $0.1333 \times 10^{-6}$ |
| | | | $0.1529 \times 10^{-1}$ | $0.1520 \times 10^{-1}$ | $0.4126 \times 10^{-2}$ | |
| | | | $0.3910 \times 10^{-2}$ | $0.4126 \times 10^{-2}$ | $0.2032 \times 10^{-2}$ | |
| 15 | 1.1159 | Yes | $0.7064 \times 10^{-3}$ | $0.7618 \times 10^{-3}$ | $0.1843 \times 10^{-3}$ | $0.455 \times 10^{-11}$ |
| | | | $0.7618 \times 10^{-3}$ | $0.9299 \times 10^{-3}$ | $0.2036 \times 10^{-3}$ | |
| | | | $0.1843 \times 10^{-3}$ | $0.2036 \times 10^{-3}$ | $0.1078 \times 10^{-3}$ | |
| 25 | 3.0466 | Yes | $0.3323 \times 10^{-4}$ | $0.2648 \times 10^{-4}$ | $0.5387 \times 10^{-5}$ | $0.111 \times 10^{-14}$ |
| | | | $0.2648 \times 10^{-4}$ | $0.3584 \times 10^{-4}$ | $0.4664 \times 10^{-5}$ | |
| | | | $0.5387 \times 10^{-4}$ | $0.4664 \times 10^{-5}$ | $0.3148 \times 10^{-5}$ | |
| 35 | 0.8262 | Yes | $0.3397 \times 10^{-4}$ | $0.2159 \times 10^{-4}$ | $0.7391 \times 10^{-5}$ | $0.1496 \times 10^{-14}$ |
| | | | $0.2159 \times 10^{-4}$ | $0.2563 \times 10^{-4}$ | $0.1849 \times 10^{-5}$ | |
| | | | $0.7391 \times 10^{-5}$ | $0.1849 \times 10^{-5}$ | $0.599 \times 10^{-5}$ | |
| 45 | 8.4767 | Yes | $0.2319 \times 10^{-5}$ | $-0.4899 \times 10^{-7}$ | $0.5543 \times 10^{-6}$ | $0.1263 \times 10^{-16}$ |
| | | | $-0.4899 \times 10^{-7}$ | $0.5282 \times 10^{-5}$ | $0.8504 \times 10^{-6}$ | |
| | | | $0.5543 \times 10^{-6}$ | $0.8504 \times 10^{-6}$ | $0.1304 \times 10^{-5}$ | |
| 55 | 5.2375 | Yes | $0.2608 \times 10^{-5}$ | $-0.3062 \times 10^{-6}$ | $0.6129 \times 10^{-6}$ | $0.3022 \times 10^{-16}$ |
| | | | $-0.3062 \times 10^{-6}$ | $0.3571 \times 10^{-5}$ | $-0.7514 \times 10^{-6}$ | |
| | | | $0.6129 \times 10^{-6}$ | $-0.7514 \times 10^{-6}$ | $0.3552 \times 10^{-6}$ | |
| 65 | 1.8884 | Yes | $0.2750 \times 10^{-5}$ | $0.3027 \times 10^{-6}$ | $-0.8375 \times 10^{-7}$ | $0.3558 \times 10^{-16}$ |
| | | | $0.3027 \times 10^{-6}$ | $0.1077 \times 10^{-4}$ | $-0.2977 \times 10^{-6}$ | |
| | | | $-0.8375 \times 10^{-7}$ | $-0.2977 \times 10^{-6}$ | $0.1215 \times 10^{-5}$ | |
| 75 | 31.2681 | No | $0.5323 \times 10^{-5}$ | $0.4861 \times 10^{-5}$ | $0.9437 \times 10^{-6}$ | $0.1343 \times 10^{-17}$ |
| | | | $0.4861 \times 10^{-5}$ | $0.8507 \times 10^{-5}$ | $0.8758 \times 10^{-6}$ | |
| | | | $0.9437 \times 10^{-6}$ | $0.8758 \times 10^{-6}$ | $0.2293 \times 10^{-6}$ | |
| 90 | 7.5040 | Yes | $0.1832 \times 10^{-4}$ | $0.4772 \times 10^{-5}$ | $0.1489 \times 10^{-5}$ | $0.1295 \times 10^{-15}$ |
| | | | $0.4772 \times 10^{-5}$ | $0.1092 \times 10^{-4}$ | $0.2353 \times 10^{-5}$ | |
| | | | $0.1489 \times 10^{-5}$ | $0.2353 \times 10^{-5}$ | $0.1251 \times 10^{-5}$ | |

value increased so that a value of 31.268 was obtained at 75 min. This finding resulted in the rejection of the null hypothesis, indicating that the sample mean is not equal to the theoretical composition. However, the data at 75 min of mixing indicated that the sample mean was very close to the theoretical mean. If it is assumed that:

$$y_1 = y_2 = y_3 \ldots y_{20} \qquad \text{(Eq. 31)}$$

then:

$$Y_i = \overline{Y} \qquad \text{(Eq. 32)}$$

This leads to a variance–covariance of zero. Hence, $T^2$ is infinitely large and the Hotelling statistic $T^2$ would be $>>> T^2_{\alpha(p,n-1)}$. Hence, the null hypothesis ($\mu = \mu_0$) would be rejected at any given $\mu_0$ except when $\mu_0 = \mu$.

This procedure leads to the conclusion that when there is small variance between 20 samples, the small differences between the sample mean vector and the theoretical mean ($\mu_0$) would tend to reject the null hypothesis when it should accept it. This result also could be due to the interactions between the mix components and the mixer, which were not accounted for in this analysis.

Thus, the Hotelling statistics is sensitive to small errors introduced in the theoretical composition of the three components during weighing, which could lead to false rejection of the best time points in evaluating powder homogeneity.

At early time points, the significant differences between the sample mean and theoretical mean were offset by the large value of the determinant of the variance–covariance matrix, leading to acceptance of the null hypothesis.

**Table III—Test of Completely Segregated and Completely Random State**

| Mixing Time, min | Statistic **X** | | Statistic **X** | |
|---|---|---|---|---|
| | Random State | Rejection of $H_0$ | Segregated State | Rejection of $H_0$ |
| 1 | $0.548 \times 10^{13}$ | Yes | $0.9114 \times 10^{2}$ | Yes |
| 15 | $0.2585 \times 10^{12}$ | Yes | $0.2846 \times 10^{3}$ | Yes |
| 25 | $0.9852 \times 10^{10}$ | Yes | $0.4504 \times 10^{3}$ | Yes |
| 35 | $0.9493 \times 10^{10}$ | Yes | $0.4444 \times 10^{3}$ | Yes |
| 45 | $0.1520 \times 10^{10}$ | Yes | $0.5399 \times 10^{3}$ | Yes |
| 55 | $0.2194 \times 10^{10}$ | Yes | $0.5225 \times 10^{3}$ | Yes |
| 65 | $0.2286 \times 10^{10}$ | Yes | $0.5192 \times 10^{3}$ | Yes |
| 75 | $0.1883 \times 10^{10}$ | Yes | $0.5847 \times 10^{3}$ | Yes |
| 90 | $0.3710 \times 10^{10}$ | Yes | $0.4934 \times 10^{3}$ | Yes |

To test for the completely random state after 1 min of mixing, Eq. 18 gives:

$$\Sigma_r = \frac{1}{4.275 \times 10^{11}} \begin{bmatrix} 0.12 \times 0.88 & -0.12 \times 0.06 & -0.12 \times 0.02 \\ -0.06 \times 0.12 & 0.06 \times 0.94 & -0.06 \times 0.02 \\ -0.02 \times 0.12 & -0.06 \times 0.02 & 0.02 \times 0.98 \end{bmatrix} \qquad \text{(Eq. 33}a\text{)}$$

$$\Sigma_r = \begin{bmatrix} 2.47 \times 10^{-13} & -1.68 \times 10^{-14} & -5.61 \times 10^{-15} \\ -1.68 \times 10^{-14} & 1.32 \times 10^{-13} & -2.81 \times 10^{-15} \\ -5.61 \times 10^{-15} & -2.81 \times 10^{-15} & 4.58 \times 10^{-14} \end{bmatrix} \qquad \text{(Eq. 33}b\text{)}$$

To investigate if a completely random state was reached after 1 min of mixing at 60 rpm, the null hypothesis $H_0$ is tested:

$$\Sigma = \Sigma_r = \begin{bmatrix} 2.47 \times 10^{-13} & -1.68 \times 10^{-14} & -5.61 \times 10^{-15} \\ -1.68 \times 10^{-14} & 1.32 \times 10^{-13} & -2.81 \times 10^{-15} \\ -5.61 \times 10^{-15} & -2.81 \times 10^{-15} & 4.58 \times 10^{-14} \end{bmatrix} \qquad \text{(Eq. 34)}$$

against the alternative hypothesis $H_1$ ($\Sigma \neq \Sigma_r$).

From Eq. 12*b*:

$$\mathbf{X} = 3 \times 20 \times (\ln 20 - 1) - 20 \times \ln |B\Sigma_0^{-1}| + tr(B\Sigma_0^{-1}) \qquad \text{(Eq. 35)}$$

and:

$$x^2_{0.05}\left(\frac{3(3+1)}{2}\right) = 12.6 \qquad \text{(Eq. 36)}$$

since:

$$\mathbf{X} = 0.548 \times 10^{13} > 12.6 \qquad \text{(Eq. 37)}$$

the null hypothesis is rejected, and the mixture did not attain a completely random state after 1 min of mixing at a significance level of 0.05.

To test for the completely segregated state from Eqs. 19 and 20:

$$\Sigma_s = \begin{bmatrix} 0.1056 & -0.0072 & -0.0024 \\ -0.0072 & 0.0564 & -0.0012 \\ -0.0024 & -0.0012 & 0.0196 \end{bmatrix} \qquad \text{(Eq. 38)}$$

To investigate if the mixture remained completely segregated after

**Table IV—Comparisons between Univariate and Multivariate Mixing Indexes**

| Mixing Time, min | Univariate (Eq. 42) | Multivariate (Eq. 22) |
|---|---|---|
| 1 | 0.61 | 0.2901 |
| | 0.64 | |
| | 0.66 | |
| 15 | 0.71 | 0.4606 |
| | 0.72 | |
| | 0.74 | |
| 25 | 0.79 | 0.5619 |
| | 0.80 | |
| | 0.83 | |
| 35 | 0.79 | 0.5586 |
| | 0.81 | |
| | 0.81 | |
| 45 | 0.85 | 0.6094 |
| | 0.84 | |
| | 0.85 | |
| 55 | 0.845 | 0.6005 |
| | 0.85 | |
| | 0.83 | |
| 65 | 0.84 | 0.5988 |
| | 0.83 | |
| | 0.85 | |
| 75 | 0.83 | 0.6319 |
| | 0.83 | |
| | 0.88 | |
| 90 | 0.80 | 0.5852 |
| | 0.83 | |
| | 0.85 | |

1 min of mixing, the null hypothesis $H_0$ is tested:

$$\Sigma = \Sigma_s = \begin{bmatrix} 0.1056 & -0.0072 & -0.0024 \\ -0.0072 & 0.0564 & -0.0012 \\ -0.0024 & -0.0012 & 0.0196 \end{bmatrix} \quad \text{(Eq. 39)}$$

against the alternative hypothesis $H_1$ ($\Sigma \neq \Sigma_s$).

Equation 12*b* gives:

$$\mathbf{X} = 0.9114 \times 10^2 \quad \text{(Eq. 40)}$$

since:

$$\mathbf{X} = 0.914 \times 10^2 > 12.6 \quad \text{(Eq. 41)}$$

The null hypothesis $H_0$ is rejected.

Table III gives the results of these two states as a function of mixing time. At early mixing times, the value of the **X** statistics for testing complete randomness decreased. At later mixing times, a major change in **X** statistics did not occur, indicating that the powder system used in this study was unable to reach a completely random state. This finding confirms earlier (11, 14) results that cohesive powders do not reach a state of complete randomness.

For testing the segregation state, the **X** statistics also increased at the initial mixing times. After 1 min of mixing, segregation tendency was not observable (Table III). Wang *et al.* (10) showed that large spherical particles segregated after 2 min of mixing. Thus, the segregation tendency is largely dependent on the physical properties of the system.

The results of the mixing index of Ashton and Valentin (6) were reported previously (11). This mixing index based on univariate statistical analysis (Eq. 42) is similar to that proposed by Wang *et al.* (10), which is based on multivariate analysis (Eq. 22):

$$M_u^2 = \frac{\ln \sigma_0^2 - \ln S^2}{\ln \sigma_0^2 - \ln \sigma_r^2} \quad \text{(Eq. 42)}$$

where $\sigma_0^2$, $S^2$, and $\sigma_r^2$ are the variances in the initial, intermediate, and ultimate random conditions, respectively.

Comparisons of the mixing indexes based on univariate and multivariate analyses are given in Table IV. The powders in the multicomponent heterogeneous system interact with each other and are affected by other components before an optimized mixed state is reached. The interparticular dependency among the particles of each component was considered through the variance–covariance matrix, and the results were a scalar quantity instead of the three individual quantities. Due to the interparticular forces among the small cohesive particles, the resulting multivariate mixing index is expected to be smaller than the univariate mixing indexes of individual components. The values of both mixing indexes increased with mixing time until there was a very small change. The results suggest that an optimized mixing time was ~45–55 min, which is consistent using both approaches.

## REFERENCES


(1) P. M. C. Lacy, *Trans. Inst. Chem. Eng.*, **21**, 53 (1943).

(2) L. T. Fan and R. H. Wang, *Powder Technol.*, **11**, 27 (1975).

(3) K. Stange, *Chem. Ing. Tech.*, **35**, 580 (1963).

(4) *Ibid.*, **26**, 129 (1954).

(5) K. R. Poole, R. F. Taylor, and G. P. Wall, *Trans. Inst. Chem. Eng.*, **42**, T305 (1964).

(6) M. D. Ashton and F. H. H. Valentin, *ibid.*, **44**, T166 (1966).

(7) D. F. Morrison, "Multivariate Statistical Methods," McGraw-Hill, New York, N.Y., 1976.

(8) N. H. Timm, "Multivariate Analysis with Application in Education and Psychology," Brooks/Cole Publishing, Monterey, Calif., 1975.

(9) C. Y. Kramer, "A First Course in Methods of Multivariate Analysis," Virginia Polytechnic Institute, Blacksburg, Va., 1972.

(10) R. H. Wang, L. T. Fan, and J. R. Too, *Powder Technol.*, **21**, 171 (1978).

(11) Z. T. Chowhan, E. E. Linn, and L.-H. Chi, *J. Pharm. Sci.*, **70**, 243 (1981).

(12) T. W. Anderson, "An Introduction to Multivariate Statistical Analysis," Wiley, New York, N.Y., 1958.

(13) M. Fisz, "Probability Theory and Mathematical Statistics," Wiley, New York, N.Y., 1963.

(14) Z. T. Chowhan and E. E. Linn, *Powder Technol.*, **24**, 237 (1979).

# Protein Binding and Erythrocyte Partitioning of the Antirheumatic Proquazone

**ANDRÉ ROOS and PETER H. HINDERLING** ˣ

Received January 14, 1980, from the *Department of Pharmacology, Biocenter, University of Basel, 4056 Basel, Switzerland.* Accepted for publication October 29, 1980.

**Abstract** □ The kinetics of proquazone, a new nonacidic nonsteroidal anti-inflammatory drug, were investigated by equilibrium dialysis and red blood cell partitioning methods on human blood and its subcompartments: erythrocytes, plasma, and plasma water. The binding of this lipophilic compound to plasma proteins and albumin was high (98%) and was not concentration dependent or altered in the presence of large concentrations of metabolites. The plasma protein binding of proquazone increased with increasing pH. The apparent solubility of the hydrophobic drug was largely increased in buffers in which albumin was admixed in high concentrations. Albumin as a biological solubilizer permits intravenous administration of significantly larger amounts of the drug. The erythrocyte–buffer partition coefficient averaged 5.5 and was pH dependent. Equilibrium between red blood cells and the buffer was obtained quickly after drug addition (<2 min). The erythrocyte–plasma partition coefficient value of 0.09 indicated that only unbound drug partitions into red cells.

**Keyphrases** □ Proquazone—erythrocyte partitioning and equilibrium dialysis methods evaluated for determination of plasma protein binding of drug □ Protein binding—proquazone in human plasma, erythrocyte partitioning and equilibrium dialysis methods evaluated □ Anti-inflammatory agents—proquazone, erythrocyte partitioning and equilibrium dialysis methods evaluated for determination of proquazone binding to plasma proteins

Proquazone[1], a new anti-inflammatory compound (1, 2), exhibits antiphlogistic activities in animals and humans comparable to those of classical, nonsteroidal anti-inflammatory compounds (1–4). Its primary therapeutic indications are thought to be in the treatment of rheumatoid arthritis, osteoarthritis, and gouty arthritis (5, 6). However, proquazone differs chemically from other representatives of this drug class. It is a quinazolinone derivative (I) and a weak base[2]. Proquazone is strongly lipophilic[3] with low aqueous solubility[4].

The performance and analysis of the pharmacokinetics of highly lipophilic compounds may cause special problems. Intravenous experiments have not been performed with proquazone. Its low water solubility necessitates either administration of smaller dosages in aqueous solution or higher dosages dissolved in large and, thus, toxic quantities of solubilizers (*e.g.*, glycerolformal[5]). Preliminary pharmacokinetic experiments with proquazone administered orally to healthy subjects showed that this drug is metabolized extensively[5]. The metahydroxy- (II), methylhydroxymetahydroxy (III), methylhydroxy- (IV), and carboxylic acid (V) metabolites were identified as major metabolites in humans[5].

The primary aim of this study was to determine proquazone kinetics *in vitro* in the blood subcompartments: plasma, plasma water, and erythrocytes. The results are

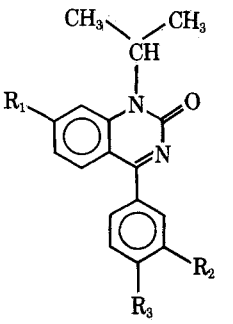

I: $R_1 = CH_3$, $R_2 = R_3 = H$
II: $R_1 = CH_3$, $R_2 = OH$, $R_3 = H$
III: $R_1 = CH_2OH$, $R_2 = OH$, $R_3 = H$
IV: $R_1 = CH_2OH$, $R_2 = R_3 = H$
V: $R_1 = COOH$, $R_2 = R_3 = H$

prerequisites for a proper delineation of the pharmacokinetics of the drug *in vivo*. Another aim was to develop an appropriate nontoxic intravenous dosage form for the administration of sufficiently large proquazone dosages so that its intravenous kinetics could be determined using the fluorometric assay developed[6].

## EXPERIMENTAL

**Reagents**—Proquazone[1] (I), [$^{14}$C]proquazone[1] ($^{14}$C-I), and metahydroxy[1] (II), 7-methylhydroxymetahydroxy[1] (III), 7-methylhydroxy[1] (IV), and 7-carboxylic acid[1] (V) metabolites were used. The specifically labeled $^{14}$C-I ([4-*phenyl*-3,5-$^{3}$H]proquazone) had a specific activity of 79.0 μCi/mg. Its radiochemical purity exceeded 96% in three different TLC systems: chloroform–methanol (95:5) developed on silica gel[7], ethyl acetate developed on silica gel[7], and ether developed on silica gel[7].

Heparinized (5 USP units/ml) blood and human plasma with known protein fractions were obtained from healthy volunteers (Subjects A–I), who had no prior drug intake. Human albumin[8,9] and hemoglobin[10] were purchased. A human albumin solution used for blood volume expansion in the treatment of shock was obtained from a hospital pharmacy[11]. Different 0.067 *M* phosphate buffers (8) were prepared to which sodium chloride was added to give an osmolarity of 0.300 Osmol (pH 6.60–8.00). The ionic strength of the buffers varied between 0.19 and 0.27. The phosphate buffers were used for preparation of the erythrocyte buffer suspensions and the albumin and hemoglobin solutions.

**Instruments**—Hematocrits of erythrocyte suspensions were determined with a centrifuge[12]. A two-chamber dialysis apparatus with chamber volumes of 1.2 ml each, separated by a membrane[13], was used for equilibrium dialysis of plasma and the albumin and hemoglobin solutions. Ultrafiltration of the albumin solutions was effected with high-flux cone membranes[14].

**Liquid Scintillation Counting**—Plasma, plasma water, and buffer

[1] Biarison, Sandoz Ltd. and Wander Ltd., Switzerland.
[2] An apparent pKa of 1.1 was obtained for proquazone in methyl ether cellulose in water (70:30 v/v) by the titrimetric method of Albert and Serjeant (7).
[3] An octanol–water partition coefficient of 13.2 was obtained for proquazone at a pH of 1.2 for the aqueous phase and room temperature.
[4] Proquazone solubility in water is ≤0.1% (g/v).
[5] Unpublished data.
[6] Lower level of sensitivity in plasma and urine is 10 ng/ml; to be published.
[7] Silica gel 60 $F_{254}$, 250 μm, Merck, Darmstadt, West Germany.
[8] Fraction V, fatty acid free, No. A-1887, Miles Laboratories, Elkhart, Ind.
[9] Fraction V, fatty acid free, No. A-1887, Sigma Chemical Co., St. Louis, Mo.
[10] Type IV, crystallized twice, No. H-7379, Sigma Chemical Co., St. Louis, Mo.
[11] Twenty percent (g/v) human albumin SRK, Berne, Switzerland.
[12] Readacrit, Clay Adams, Division of Becton–Dickinson, Parsippany, N.J.
[13] Cuprophane, Technicon Ltd., Zürich, Switzerland.
[14] Centriflo 50 membrane ultrafilters with conical supports and tubes, Amicon Corp., Lexington, Mass.



*0022-3549/81/0300-0252$01.00/0*
*© 1981, American Pharmaceutical Association*

were assayed for radioactivity directly or after combustion. The radioactivity in erythrocytes was measured by liquid scintillation counting[15] only after hemolysis and combustion. Hemolysis was induced by keeping the samples frozen at −20° for 2 hr. Combustion was effected with a sample oxidizer[16]. The efficiency of combustion was monitored by simultaneous processing of biological samples spiked with known amounts of radioactivity.

Aliquots (100–500 μl) of plasma, plasma water, and buffer were transferred to liquid scintillation vials to which 3 ml of liquid scintillation fluid[17] was then added. After the contents were mixed thoroughly, the vials were kept at 37° for 2 hr to allow the water to dissolve in the liquid scintillation fluid. Replicate samples of 100–500 μl of buffer, plasma, and hemolyzed erythrocytes were oxidized to tritiated water, which was subsequently dissolved in Bray's liquid scintillation fluid[18] (9). The vials were kept for 2 hr at 4° in the dark prior to counting. The measured radioactivity was corrected for background and loss of efficiency by relation to an external standard. Separate quench curves were constructed for the two liquid scintillation fluids.

**Protein Binding of I**—Equilibrium dialysis, erythrocyte partitioning, and ultrafiltration were used for the determination of $^{14}$C-I binding to proteins. The techniques used in equilibrium dialysis were described previously (10). Dialysis of the protein solutions spiked with $^{14}$C-I was performed against buffer for 4 hr. Preliminary experiments showed that complete equilibration of free drug in both chambers of the apparatus occurred during this time. All experiments were performed at 37° at pH 7.35–7.45 unless otherwise specified.

The protein binding of $^{14}$C-I was investigated in healthy subjects (Subjects A–I). Subjects A–F also participated in the pharmacokinetic study[19]. The albumin and globulin contents of all plasma were determined (11, 12) and were within the physiological ranges of 42–54 and 23–31 g/liter, respectively (13). The plasma protein binding of $^{14}$C-I was studied over the 50–50,000-ng/ml range found for the drug in pharmacokinetic studies after intravenous dosages of 75 and 122 mg and oral dosages of 300 and 900 mg. The plasma protein binding of $^{14}$C-I in the presence of Metabolites II–V was investigated at a total metabolite to drug ratio of 20:1.

Since the pH in inflamed tissue reportedly varies (14, 15), the plasma protein binding of $^{14}$C-I was investigated in the pH range of 6.60–8.30. These experiments were performed in the presence and absence of II–V. The influence of temperature on plasma protein binding of $^{14}$C-I was investigated at 37 and 22°. The albumin binding of $^{14}$C-I was studied at various albumin concentrations (0.5–50 mg/ml, 7.25–725 × $10^{-6}$ mole/liter) and $^{14}$C-I concentrations (60–60,000 ng/ml, 2.16–3370 × $10^{-8}$ mole/liter). The purpose of these experiments was to determine the binding parameters of $^{14}$C-I at an albumin concentration where the binding of $^{14}$C-I is clearly saturable and to investigate the binding of $^{14}$C-I at albumin concentrations comparable to those in the interstitial and synovial fluids (16–18). All of these experiments were performed at 37°, and the pH was maintained at 7.35–7.45 unless otherwise specified. Constancy of the pH was ascertained by measurement before and after dialysis.

**Solubility Analysis and Protein Binding of I**—Preliminary experiments established that the concentrated albumin (dissolved in buffer) could be employed as a "biological solubilizer" for the hydrophobic drug, I. These experiments indicated that the drug was highly bound to albumin at "physiological" albumin concentrations (40–50 mg/ml) and that the bound amounts of I were augmented significantly when the volumes or concentrations of the albumin solution were increased. Quick estimates of the maximum amounts of I soluble in albumin solutions at 22° were obtained by determining the concentrations of I in increasingly concentrated albumin solutions that just provoked microscopically visible drug precipitation. These I concentrations ranged between 4.0 and 5.0 mg/ml of albumin solution (200 mg/ml). This protein concentration was the highest that could be safely given intravenously.

For more definitive determinations of quasimaximum dosages for intravenous application, a centrifugal method and modified ultrafiltration were employed. With the centrifugation method, test tubes were filled with 5 ml of albumin solution (200 mg/ml) spiked with $^{14}$C-I dissolved in glycerolformal (2–4% v/v) to give final $^{14}$C-I concentrations of 1.6, 2.4, and 3.2 mg/ml. After mixing for several hours at 22°, the solutions were centrifuged at 6000×*g* for 10 min. Five consecutive aliquots (1 ml) then were taken, starting from the top and proceeding to the bottom of the tubes. The radioactivity in each aliquot was measured separately. Supersaturation of the albumin solution and precipitations of $^{14}$C-I would lead to significantly increased activities in the aliquots from the bottom of the tubes.

In the modified ultrafiltration procedure, unbound concentrations of $^{14}$C-I were determined in albumin solutions (174 mg/ml) spiked with $^{14}$C-I in glycerolformal (4% v/v) to yield total drug concentrations of 3.0 mg/ml. A solubility "reserve" could be estimated from the difference between the known maximal concentration of $^{14}$C-I soluble in aqueous solution and the unbound concentration of $^{14}$C-I found with the albumin solution. Ultrafiltration was preferred over equilibrium dialysis because of potential bias in drug binding estimates at high protein concentrations with the latter method. Net transport of water from the buffer to the protein-containing chambers as a result of an osmotic pressure difference may lead to a considerable decrease in the effective protein concentration during equilibrium dialysis. Ultrafiltration experiments were performed at 22° with a pH 6.8 human albumin solution[9].

The original ultrafiltration procedure (19) was modified slightly. Presaturation of the cone membranes with $^{14}$C-I was necessary after preliminary experiments demonstrated significant concentration-dependent and saturable membrane binding of $^{14}$C-I. All cone membranes used in the final experiments thus were presaturated routinely with I by filtration of the albumin solution to one-tenth of the volume after spiking with the appropriate concentration of $^{14}$C-I. Successful saturation of the membranes was demonstrated when cones that were repetitively (one to six times) filled with fresh albumin solution spiked with 3.0 mg of $^{14}$C-I/ml showed constant recoveries in the second to sixth filtrate after 10 filtrations. The 10th filtrate of the albumin solutions was reached after centrifugation for 10 min at 2500×*g*. Complementation of the ultrafiltration procedure by equilibrium dialysis proved to be necessary after the filtrates were shown to contain albumin in concentrations that bound $^{14}$C-I significantly. The true unbound concentrations of $^{14}$C-I in the filtrates could be determined in the buffer chambers after they were subjected to equilibrium dialysis.

**Erythrocyte Partitioning of I**—The determination of the erythrocyte partitioning of $^{14}$C-I was performed in erythrocyte–buffers and erythrocyte–plasma suspensions having constant hematocrits of 40%. Erythrocytes for suspension in buffer were obtained by centrifugation of fresh whole blood. After removal of the upper layer containing the buffy coat, the red blood cells were washed twice with twice the volume of 0.9% NaCl solution and once with twice the volume of buffer. After further centrifugation, aliquots of erythrocytes were added to the buffer to yield hematocrits of 40%. Erythrocyte–plasma suspensions were obtained similarly. The buffy coat was removed from plasma after centrifugation of blood. The erythrocytes obtained were resuspended in plasma without prior washing.

The red cell–buffer partitioning of $^{14}$C-I was studied over a concentration range of 50–5000 ng/ml in the presence and absence of unlabeled Metabolites II–V. The ratio of total metabolite to drug was 20:1. All experiments were performed at 37° at pH 7.30–7.45 unless otherwise

**Table I—Percentage of Plasma Unbound Proquazone, $\varphi$, in the Presence and Absence of Its Metahydroxy, Methylhydroxymetahydroxy, Methylhydroxy, and Carboxylic Acid Metabolites in Plasma from Subject F**

| Total Plasma Proquazone Concentration ($C_p$), ng/ml | Dialysis | $\varphi$ | Mean ± *SD* ($n$ = 3) |
|---|---|---|---|
| 50 | 1 | 1.65 | |
| | 2 | 1.69 | 1.68 ± 0.023 |
| | 3 | 1.69 | |
| 300 | 1 | 1.78 | |
| | 2 | 1.79 | 1.78 ± 0.058 |
| | 3 | 1.78 | |
| 300[a] | 1 | 1.85 | |
| | 2 | 1.82 | 1.84 ± 0.015 |
| | 3 | 1.84 | |
| 2500 | 1 | 1.86 | |
| | 2 | 1.80 | 1.81 ± 0.050 |
| | 3 | 1.76 | |
| 5000 | 1 | 1.74 | |
| | 2 | 1.75 | 1.74 ± 0.058 |
| | 3 | 1.74 | |
| Overall mean ± *SD* ($n$ = 15) | | | 1.77 ± 0.061 |

[a] The concentration ratio, 20, is the sum of unlabeled metabolites to labeled proquazone.

[15] Packard Tri-Carb 3280 and 3255, Packard Instruments, Downers Grove, Ill.
[16] Model 4101, Intertechnique, Plaisir, France.
[17] Instagel, Packard-Becker, BV, Groningen, The Netherlands.
[18] Bray's solution: 700 ml of 1,4-dioxane, 300 ml of toluene, 20 g of naphthalene, and 7 g of butyl 2-phenyl-5-(4-biphenyl)-1,3,4-oxadiazole.
[19] P. H. Hinderling and A. Roos, to be published.

**Table II—Percentage of Plasma Unbound Proquazone, $\varphi$, in the Presence and Absence of Its Metahydroxy, Methylhydroxymetahydroxy, Methylhydroxy, and Carboxylic Acid Metabolites in Plasma of Subjects A–F**

| Total Plasma Proquazone Concentration ($C_p$), ng/ml | Percentage of Plasma Unbound Proquazone, $\varphi$ | | | | | |
|---|---|---|---|---|---|---|
| | Subject A | Subject B | Subject C | Subject D | Subject E | Subject F |
| 300 | 1.96 ± 0.070 | 1.82 ± 0.046 | 1.95 ± 0.015 | 2.09 ± 0.082 | 2.04 ± 0.053 | 1.78 ± 0.006 |
| 300[a] | 2.04 ± 0.036 | — | — | — | — | 1.84 ± 0.015 |
| 5000 | 2.06 ± 0.040 | 1.99 ± 0.026 | 2.12 ± 0.067 | 2.29 ± 0.010 | 2.05 ± 0.055 | 1.74 ± 0.006 |
| Overall mean | 2.02 | 1.90 | 2.04 | 2.19 | 2.05 | 1.79 |
| *SD* | ± 0.063 | ± 0.101 | ± 0.099 | ± 0.120 | ± 0.049 | ± 0.044 |
| *n* | 9 | 6 | 6 | 6 | 6 | 9 |

[a] The concentration ratio, 20, is the sum of unlabeled metabolites to labeled proquazone.

specified. The constancy of pH was ascertained by the equivalency of the values obtained at the start and finish of the experiments. The erythrocyte–buffer partition coefficient of $^{14}$C-I in the suspensions was determined at 10, 30, 60, and 90 min after addition of I. In another experiment, the partitioning of $^{14}$C-I was studied systematically as a function of time over 140 min; the apparent partition coefficient was determined at 2, 4, 6, 9, 14, 20, 90, 120, and 140 min following addition of I.

In other experiments, the erythrocyte partitioning of $^{14}$C-I was studied as a function of pH. Red blood cell–buffer suspensions were prepared at pH values of 6.60, 6.90, 7.20, and 7.50, and the partitioning of $^{14}$C-I then was determined 30 and 60 min after I addition. The concentrations of $^{14}$C-I were determined in both phases of the suspensions, in the apparent red blood cell phase and in the true buffer or plasma phase. Aliquots were taken and centrifuged at 2500×*g* at intervals of 0.5–5 min, and the true buffer or plasma phases were removed. Hematocrits were determined in the remaining apparent erythrocyte phases; they ranged between 60 and 95%.

The binding of $^{14}$C-I to hemoglobin was investigated since slight hemolysis occurred in the erythrocyte–buffer partitioning experiments. The hemoglobin concentrations then were measured routinely[20] and ranged between 0 and 25 mg/ml (0–3.62 × $10^{-5}$ mole/liter). If no corrections were applied for the hemoglobin-bound $^{14}$C-I in the buffer phase, then the partition coefficients for the drug would be underestimated.

Erythrocyte partitioning was also employed as an alternative method for measuring the plasma protein binding of $^{14}$C-I. For comparison, the protein binding of $^{14}$C-I in plasma of Subject I was assayed simultaneously by partitioning and equilibrium dialysis.

## RESULTS AND DISCUSSION

**Protein Binding of Proquazone[21] (I)**—The percentage of drug unbound to plasma protein, albumin, or hemoglobin, $\varphi$, was calculated according to:

$$\varphi = 10^2 - \beta = 10^2\left(1 - \frac{C_b}{C_t}\right) = 10^2\left(\frac{C_u}{C_t}\right) \qquad \text{(Eq. 1)}$$

The binding of $^{14}$C-I to plasma protein and albumin at "physiological" concentrations of 70 and 50 mg/ml of albumin was relatively large. The $^{14}$C-I concentration-independent $\varphi$ value amounted to only 2% on the average (Tables I and II). The $\varphi$ value was unaltered by the presence of large concentrations of Metabolites II–V (Tables I and II). There was a remarkably small variability of $\varphi$ for a given individual plasma. The maximum intersubject difference in $\varphi$ for the subjects tested was 18% (Table II). Equivalent $\varphi$ values were obtained for $^{14}$C-I (50–50,000 ng/ml) with plasma and albumin (50 mg/ml). On the average, $\varphi$ was 1.99 ± 0.155 ($n$ = 36) and 1.98 ± 0.113 ($n$ = 6), respectively. Large concentrations of metabolites did not influence the binding of $^{14}$C-I to albumin [$\varphi$ = 1.97 ± 0.120 ($n$ = 2)].

These results indicated that $^{14}$C-I was bound predominantly to the albumin fraction in plasma. The extent of plasma protein binding was clearly pH dependent (Fig. 1). There was an apparent linear relationship between $\varphi$ and pH. The $\varphi$ values at pH 7.80 averaged 1.40 but were 2.30 at pH 7.00. This difference was equivalent to a 40% rise in concentration of the pharmacologically active unbound drug species when the pH was lowered by 0.80 unit. The pH-dependent binding characteristics of $^{14}$C-I were not influenced by the presence of large concentrations of II–V (Fig. 1). These findings may be clinically relevant if proquazone binding to synovial and interstitial proteins are similarly pH dependent. It has been reported that the pH is low and the protein content is increased in chronically inflamed synovial tissues and fluids (15, 16).

The plasma protein binding of $^{14}$C-I (5000 ng/ml) was temperature independent between 22 and 37°: $\varphi$ (37°) = 2.04 ± 0.171 ($n$ = 18) and $\varphi$ (22°) = 2.05 ± 0.071 ($n$ = 2). A gradual decrease of the albumin concentrations from 50 to 0.5 mg/ml (725–7.25 × $10^{-6}$ mole/liter) with a constant concentration of $^{14}$C-I (300 or 50,000 ng/ml, 1.08 or 18.0 × $10^{-7}$ mole/liter) brought a gradual increase of $\varphi$ (Table III). The $\varphi$ value was identical for both $^{14}$C-I concentrations at a given albumin concentration in the range between 10.0 and 50.0 mg/ml (14.5–72.5 × $10^{-5}$ mole/liter) (Table III). Scatchard plots with an apparent positive slope (Fig. 2) characterized the binding behavior of I when the protein concentration was varied within the range of 7.25–72.5 × $10^{-5}$ mole/liter. At the lowest albumin concentration of 0.5 mg/ml (7.25 × $10^{-6}$ mole/liter), $\varphi$ clearly varied with the $^{14}$C-I concentrations, and the binding was saturable (Table III and Fig. 3).

Proquazone is a lipophilic compound. Extensive binding to plasma protein and albumin has been reported for other lipophilic drugs (21, 22). Proquazone is a weak base with an apparent pKa of 1.1. Its unionized species largely prevails at the pH range studied. The compound posesses two partial charges in the quinazolinone ring: a negative charge at the oxygen of the carbonyl group and a positive charge at the adjacent nitrogen. The decrease of $\varphi$ with increasing pH suggests that hydrophobic rather than electrostatic forces or hydrogen bonds are involved in the binding of $^{14}$C-I, even though the decrease of $\varphi$ at higher pH values exceeds the increase of the unionized drug species. Alternatively, a pH- or ionic strength-induced conformational change of plasma protein (albumin) resulting in a larger affinity for the drug may be involved. There is evidence that albumin is a flexible molecule which can undergo reversible conformational alterations (23, 24). Another rationalization may be that

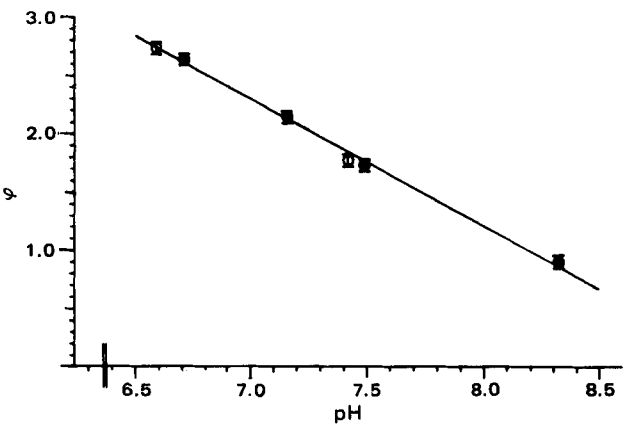


**Figure 1**—*Apparent pH dependency of percentage of plasma unbound proquazone, $\varphi$, in the presence (○) and absence of its metahydroxy, methylhydroxymetahydroxy, methylhydroxy, and carboxylic acid metabolites (●). Values of mean (±SD) (vertical bars) of two experiments performed at each pH level are given. Blood of Subject I was used.*

[20] Hemoglobin after transformation to hemiglobin cyanid was determined spectrophotometrically (20). Calibration curves were set up with Dade HiCN-Standards of Merz & Dade AG, Berne, Switzerland.

[21] The values for $\varphi$, unless otherwise specified, were normalized for pH 7.40 according to the experimentally obtained relationship between $\varphi$ and pH (Fig. 1).

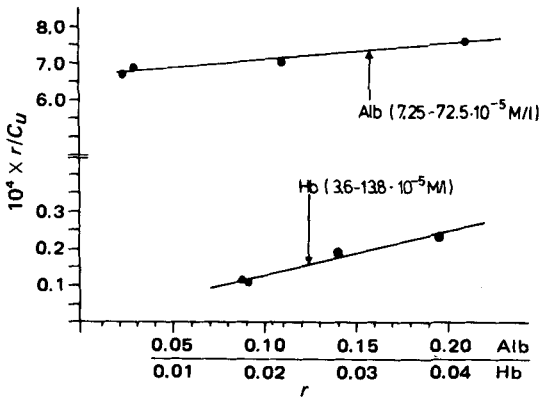


**Figure 2**—*Classical Scatchard plots of* $r/C_u$ *against* r *with apparent positive slopes for proquazone binding to albumin and hemoglobin. Total concentration of proquazone was 5000 ng/ml (1.80 × 10$^{-5}$ mole/liter). Coefficients and standard errors of linear regressions were for the binding of* $^{14}$*C-I to albumin:* $r/C_u = 6.67 \times 10^4 (\pm 3.81 \times 10^2) + 4.48 \times 10^4 (\pm 3.15 \times 10^3)r$ *(coefficient of determination = 0.999); the slope was statistically significantly different from zero [two-sided* t *test:* $t (\alpha = 0.005) = 14.09$, $t_{calc} = 14.21$*]. Coefficients and standard errors of linear regressions were for the binding of* $^{14}$*C-I to hemoglobin:* $r/C_u = 1.05 \times 10^2 (\pm 4.35) + 5.81 \times 10^4 (\pm 1.59 \times 10^3)r$ *(coefficient of determination = 0.999); the slope was statistically significantly different from zero [two-sided* t *test:* $t (\alpha = 0.001) = 31.60$, $t_{calc} = 36.63$*].*

a pH- or ionic strength-catalyzed molecular segregation of the protein occurs with an increase of binding surface (25). The $^{14}$C-I concentration-independent plasma protein (albumin) binding indicates that there is an abundance of accessible binding sites, which could also explain the observed constancy of $\varphi$ at high concentration ratios of metabolites to parent drug.

The lowering of albumin concentrations from 50 to 5 mg/ml increased $\varphi$ but to a lesser extent than was expected. The affinity of albumin for $^{14}$C-I at lower protein concentrations (40–10 mg/ml) was clearly larger than at physiological concentrations (50 mg/ml) (Fig. 2). A further decrease in the albumin concentration (0.5 mg/ml) brought a reduction in the affinity for $^{14}$C-I. The binding of $^{14}$C-I became concentration dependent and saturable (Fig. 3). These findings can be explained by reversible conformational changes (23, 24) or molecular segregation (24) of albumin induced either by dilution or by an increased concentration ratio of the phosphate buffer to the protein. Phosphate buffer was shown to interfere with the binding of small molecules (26). Binding data should not be viewed as a result of the interaction of a ligand and a protein molecule only.

The possible influence of the buffer, its ionic strength and composition, must be evaluated critically. However, there is little choice of buffers that have electrolytic compositions similar to biological fluids and can be used

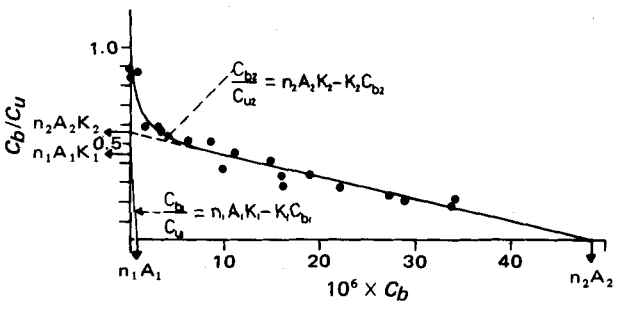


**Figure 3**—*Modified Scatchard plot for proquazone binding to albumin (0.5 mg/ml = 7.25 × 10$^{-6}$ mole/liter). Total concentrations of proquazone ranged between 50 and 60,000 ng/ml (= 2.16 × 10$^{-8}$–3.37 × 10$^{-5}$ mole/liter). Graphical analysis according to Rosenthal (35) on the premise of the existence of two independent classes of binding sites was performed. Two straight lines,* $C_{b_1}/C_u = n_1A_1K_1 - K_1C_{b_1}$ *and* $C_{b_2}/C_u = n_2A_2K_2 - K_2C_{b_2}$*, with the slopes of* $-K_1$ *and* $-K_2$*, the respective intercepts on the abscissa of* $n_1A_1$ *and* $n_2A_2$*, and the respective intercepts on the ordinate of* $n_1A_1K_1$ *and* $n_2A_2K_2$ *were obtained. The determined apparent binding parameters for proquazone were* $K_1 = 2.0 \times 10^6$ *liters/mole,* $K_2 = 1.25 \times 10^4$ *liters/mole,* $n_1 = 0.027$*, and* $n_2 = 6.35$*.*

**Table III—Albumin Concentration Dependency of the Percentage of Unbound Proquazone, $\varphi$**

| Total Proquazone Concentration ($C_p$), ng/ml | Albumin, mg/ml | $\varphi$, mean ± *SD* ($n$ = 2) |
|---|---|---|
| 300 | 50 | 2.08 ± 0.099 |
| 5000 | | 2.01 ± 0.064 |
| 300 | 40 | 2.44 ± 0.028 |
| 5000 | | 2.46 ± 0.035 |
| 300 | 10 | 8.81 ± 0.120 |
| 5000 | | 8.87 ± 0.028 |
| 5000 | 5 | 15.33 ± 0.410 |
| 300 | 0.5 | 60.60 ± 1.56 |
| 5000 | | 65.69 ± 1.44 |

in the biologically significant pH range (27). A buffer such as tromethamine interferes with the binding of small molecules (28). The potential impact of contaminants on binding data also should be considered (29). The apparent affinity changes of albumin observed at lowered concentrations are not likely to be due to contaminants or fatty acids found in commercial albumin preparations (29). If this were the case, a decrease in the concentration ratio of contaminant to drug by either lowering the albumin content or increasing the drug concentration should have an equivalent effect on the apparent affinity of the albumin for $^{14}$C-I. However, changes in affinity were observed only after dilution of albumin; an increase of the apparent affinity was seen at concentrations between 50 and 5 mg/ml; a decrease of the apparent affinity occurred at 0.5 mg/ml.

Similar apparent affinity increases for $^{14}$C-I were observed with differently diluted hemoglobin solutions (9.5–2.5 mg/ml, 13.8–3.60 × 10$^{-5}$ mole/liter) that were spiked with $^{14}$C-I to give total concentrations of 300 or 5000 ng/ml. The binding data of $^{14}$C-I were characterized by Scatchard plots with positive slopes (Fig. 2). The same rationalizations may be inferred to explain the results presented for the albumin data.

**Protein Binding and Solubility Analysis of I**—The results of the centrifugation method indicated that $^{14}$C-I at total concentrations of 1.6, 2.4, and 3.2 μg/ml was completely dissolved in albumin (200 mg/ml). The radioactivity present in aliquots obtained from the bottom of the tubes was not different from that of the three upper aliquots and was (expressed in percent of the mean activities of the upper three aliquots) 104.1, 99.8, and 101.7% for 1.6, 2.4, and 3.2 μg/ml, respectively, of $^{14}$C-I.

The percentage of true unbound $^{14}$C-I ($\varphi_{true}$) in ultrafiltration and equilibrium dialysis with total concentrations of 3.0 mg of $^{14}$C-I/ml of albumin (200 mg/ml) was calculated according to:

$$\varphi_{true} = \frac{\varphi^{UF'}\varphi^{ED}}{10^2} \qquad \text{(Eq. 2)}$$

where $\varphi^{UF'}$ is the apparent percentage of unbound $^{14}$C-I in the ultrafiltration procedure and $\varphi^{ED}$ is the true percentage of unbound $^{14}$C-I in the equilibrium dialysis method. The $\varphi^{UF'}$ value was obtained from:

$$\varphi^{UF'} = \frac{C_u^{UF'}}{C_t^{UF}} \qquad \text{(Eq. 3)}$$

where $C_u^{UF'}$ and $C_t^{UF}$ correspond to the apparent unbound concentration of $^{14}$C-I in the filtrate and to the total concentration of $^{14}$C-I in the spiked solution prior to filtration, respectively. The $\varphi^{ED}$ value was similarly obtained from:

$$\varphi^{ED} = \frac{C_u^{ED}}{C_t^{ED}} \qquad \text{(Eq. 4)}$$

where $C_u^{ED}$ and $C_t^{ED}$ represent the albumin unbound concentration of $^{14}$C-I in the dialysate and the total concentration of $^{14}$C-I in the albumin solution after dialysis at equilibrium, respectively.

The mean value (±*SD*) for $\varphi_{true}$ in four different experiments was 10.0 ± 0.53. Accordingly, the true unbound concentration of $^{14}$C-I in the original albumin solution was 0.3 mg/ml, a value considerably smaller than the $^{14}$C-I solubility in aqueous solution (≤1 mg/ml).

Based on these data, it was concluded that $^{14}$C-I could be safely given by the intravenous route in a total concentration of 3.0 mg/ml in albumin (200 mg/ml).

**Erythrocyte Partitioning of Proquazone**[22]—The erythrocyte-

[22] The values of $P_{E/B}$ were corrected for binding of $^{14}$C-I to hemoglobin in buffer. The hemoglobin resulted from slight hemolysis of erythrocytes suspended in buffer. The hemoglobin concentrations in buffer ranged between 0 and 25 mg/ml, and the percentage of $^{14}$C-I bound to hemoglobin varied between 0 and 10%. The $P_{E/B}$ values were not normalized for pH 7.40.

**Table IV—Erythrocyte–Buffer Partition Coefficient ($P_{E/B}$) and Erythrocyte–Plasma Partition Coefficient ($P_{E/P}$) of Proquazone in the Presence and Absence of Its Metahydroxy, Methylhydroxymetahydroxy, Methylhydroxy, and Carboxylic Acid Metabolites in Blood of Subject F**

| Total "Blood" Proquazone Concentration ($C_{bl}$), ng/ml | $P_{E/B}$, mean ± $SD$ ($n$ = 4) | $P_{E/P}$, mean ± $SD$ ($n$ = 4) |
|---|---|---|
| 50 | 5.33 ± 0.172 | 0.086 ± 0.020 |
| 300 | 5.71 ± 0.351 | 0.089 ± 0.019 |
| 300[a] | 5.60 ± 0.286 | 0.100 ± 0.018 |
| 2500 | 5.57 ± 0.183 | 0.094 ± 0.015 |
| 5000 | 5.53 ± 0.201 | 0.094 ± 0.018 |
| Overall mean | 5.55 ± 0.254 | 0.093 ± 0.017 |

[a] The concentration ratio, 20, is the sum of unlabeled metabolites to labeled proquazone.

buffer partition coefficient, $P_{E/B}$, was defined (30) as:

$$P_{E/B} = \frac{C_e}{C_u} \quad \text{(Eq. 5)}$$

where $C_e$ and $C_u$ correspond to the true erythrocyte and buffer (plasma water) concentrations of $^{14}$C-I, respectively, after equilibration. Analogously, the erythrocyte–plasma partition coefficient, $P_{E/P}$, is:

$$P_{E/P} = \frac{C_e}{C_t} \quad \text{(Eq. 6)}$$

where $C_t$ represents the total (bound and unbound) concentration of $^{14}$C-I in plasma after equilibration.

In the centrifugation method, $C_u$ or $C_t$ was measured in buffer or plasma after centrifugal separation. The apparent erythrocyte concentration ($C_{e'}$) was measured in the remaining concentrated erythrocyte suspension. The hematocrit ($Hc'$) of these suspensions was measured, and the true erythrocyte concentration of $^{14}$C-I ($C_e$) was determined for the erythrocyte–buffer and erythrocyte–plasma suspensions, respectively, from:

$$C_e = \frac{C_{e'} - [(1 - Hc')C_u]}{Hc'} \quad \text{(Eq. 7a)}$$

$$C_e = \frac{C_{e'} - [(1 - Hc')C_t]}{Hc'} \quad \text{(Eq. 7b)}$$

The red blood cell partitioning of $^{14}$C-I from buffer was large. The $P_{E/B}$ value averaged 5.5 (Tables IV and V), which is characteristic for lipophilic compounds (21, 31). The apparent red blood cell partitioning of $^{14}$C-I from plasma was much smaller and averaged 0.09 (Table IV). The $P_{E/B}$ and $P_{E/P}$ values were not dependent on the concentration of $^{14}$C-I within the range studied (50–50,000 ng/ml). There was good reproducibility of $P_{E/B}$ values in individual blood samples and red blood cell suspensions (Tables IV and V). The maximum percent interindividual difference in $P_{E/B}$ was 7% in the blood samples from the subjects (Table V). The red blood cell partitioning of $^{14}$C-I was invariant in the presence of a large concentration ratio of total metabolites to parent drug (Tables IV and V). The extent of the red blood cell partitioning from buffer clearly depended on the pH of the suspensions. The $P_{E/B}$ value increased apparently linearly with increasing pH (Fig. 4) and was ($n$ = 2) 4.72 (±0.100), 5.05 (±0.108), 5.40 (±0.219), and 5.80 (±0.176) at pH 6.62, 6.91, 7.23, and 7.53, respectively. This increase was equivalent to a 23% increase of the erythrocyte concentration of $^{14}$C-I within the pH 6.62–7.53 range.

The $P_{E/B}$ value was invariant with time at the four pH levels studied (Fig. 4). Equilibration of $^{14}$C-I between erythrocytes and buffer was rapid and completed in <2 min after addition of I at pH 7.4. The ratio of the erythrocyte concentration to the buffer concentration was time independent from 2 to 140 min after spiking, with the $P_{E/B}$ value remaining constant at 5.23 ± 0.142 ($n$ = 9). This finding suggested that all partitioning values of $^{14}$C-I obtained in these studies represented equilibrium values. A rapid attainment of equilibrium between red blood cells and buffer or plasma is consistent with the strongly lipophilic properties of $^{14}$C-I (32). The large $P_{E/B}$ value of 5.5 found for $^{14}$C-I indicated that there is an additional binding to, or greater solubility in, the red blood cells than can be accounted for by the assumption that the volume of the erythrocytes contained only an aqueous phase, wherein $^{14}$C-I has the same chemical activity in buffer or plasma water. Red blood cell structures, which reportedly bind drug quantitatively, are hemoglobin (32), the membrane (33), and the enzyme carbonic anhydrase (34). The observed pH-dependent binding of $^{14}$C-I to red blood cell structures is comparable to that to plasma proteins described earlier. Similar rationalizations may be given to explain both of these findings.

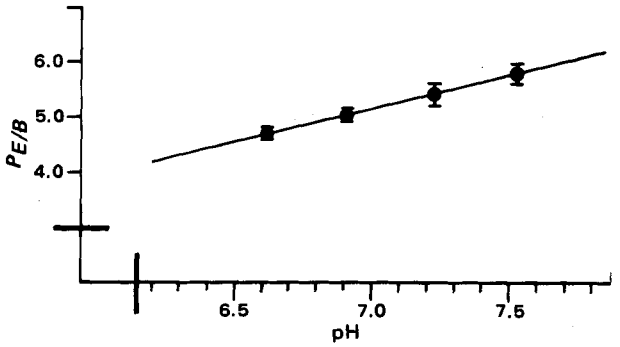


**Figure 4**—*Apparent pH dependency of the erythrocyte–buffer partition coefficient ($P_{E/B}$) of proquazone. Mean (±SD) (vertical bars) of four experiments performed at each PH level are given. Blood of Subject I was used.*

The results obtained for $^{14}$C-I with proteins and erythrocytes indicate that studies of the binding kinetics of highly bound ligands may be useful in detecting and quantifying conformation and aggregation changes of extracellular and cellular macromolecules.

If only the plasma unbound drug partitioned into red blood cells, estimates of $\varphi$ could be obtained from the erythrocyte partitioning method. The value of $\varphi$ was defined in Eq. 1. If Eqs. 5 and 6 are solved for $C_u$ and $C_t$, respectively, and the resulting expressions are substituted into Eqs. 7a and 7b, upon rearrangement Eq. 8 is obtained:

$$\varphi = 10^2 \left(\frac{P_{E/P}}{P_{E/B}}\right) \quad \text{(Eq. 8)}$$

and $\varphi$ can be calculated directly from the erythrocyte–buffer and erythrocyte–plasma partition coefficients. The usefulness of the red cell partitioning method for protein binding determinations was demonstrated by the equivalent results obtained with this method and with equilibrium dialysis. On the average, constant $\varphi$ values of 1.68 ± 0.255 ($n$ = 20) and of 1.77 ± 0.026 ($n$ = 15) were obtained with red cell partitioning and equilibrium dialysis, respectively, for the concentration range of 50–5000 ng of $^{14}$C-I/ml. The close agreement of the binding data obtained with the two methods confirms that only unbound drug partitions into red blood cells. However, the precision of equilibrium dialysis was clearly greater than that of the partitioning method.

## REFERENCES

(1) R. V. Coombs, R. P. Dauna, M. Denzer, G. E. Hardtmann, B. Huegi, G. Koletar, H. Ott, E. Jukniewicz, J. W. Perrine, E. I. Takesue, and J. H. Trapold, *J. Med. Chem.*, **16**, 1237 (1973).

(2) G. E. Hardtmann, B. Huegi, G. Koletar, S. Kroin, H. Ott, J. W. Perrine, and E. I. Takesue, *ibid.*, **17**, 636 (1974).

(3) E. I. Takesue, J. W. Perrine, and J. H. Trapold, *Arch. Int. Phar-*

**Table V—Erythrocyte–Buffer Partition Coefficient of Proquazone ($P_{E/B}$) in the Presence and Absence of Its Metahydroxy, Methylhydroxymetahydroxy, Methylhydroxy, and Carboxylic Acid Metabolites in Blood of Subjects A–F**

| Total "Blood" Proquazone Concentration ($C_{bl}$), ng/ml | $P_{E/B}$, mean ± $SD$ ($n$ = 4) | | | | | |
|---|---|---|---|---|---|---|
| | Subject A | Subject B | Subject C | Subject D | Subject E | Subject F |
| 300 | 5.34 ± 0.223 | 5.19 ± 0.079 | 5.76 ± 0.289 | 5.57 ± 0.415 | 5.80 ± 0.758 | 5.71 ± 0.351 |
| 300[a] | 5.90 ± 0.340 | — | — | — | — | 5.59 ± 0.284 |
| 5000 | 5.31 ± 0.537 | 5.25 ± 0.118 | 5.53 ± 0.346 | 4.96 ± 0.279 | 5.25 ± 0.556 | 5.23 ± 0.201 |
| Overall mean ± $SD$ | 5.51 ± 0.493 | 5.22 ± 0.998 | 5.64 ± 0.320 | 5.26 ± 0.460 | 5.52 ± 0.681 | 5.63 ± 0.274 |

[a] The concentration ratio, 20, is the sum of unlabeled metabolites to labeled proquazone.

*macodyn. Ther.*, **221**, 122 (1976).
(4) U. Gubler and M. Baggiolini, *Scand. J. Rheumatol., Suppl.*, **21**, 8 (1978).
(5) R. Allan and M. Bleicher, *J. Int. Med Res.*, **5**(4), 253 (1977).
(6) M. Nissilä and A. Kajander, *Scand. J. Rheumatol., Suppl.*, **21**, 36 (1978).
(7) A. Albert and E. P. Serjeant, "The Determination of Ionization Constants," Chapman and Hall, London, England, 1962, p. 9.
(8) "Documenta Geigy, Scientific Tables," 7th ed., K. Diem and C. Lentner, Eds., Geigy Pharmaceuticals, Ardsley, N.Y., 1975, p. 281.
(9) G. A. Bray, *Anal. Biochem.*, **1**, 279 (1960).
(10) P. H. Hinderling, *Agents Actions*, **7**, 379 (1977).
(11) L. T. Skeggs, Jr., and H. Hochstrasser, *Clin. Chem.*, **10**, 918 (1964).
(12) C. B. Laurell and B. G. Johanssen, *Scand. J. Clin. Lab. Invest.*, **29**, 7 (1972).
(13) "Documenta Geigy, Scientific Tables," 7th ed., K. Diem and C. Lentner, Eds., Geigy Pharmaceuticals, Ardsley, N.Y., 1975, p. 582.
(14) K. H. Falchuk, E. J. Goetze, and J. P. Kulka, *Am. J. Med.*, **49**, 223 (1970).
(15) N. A. Cummings and G. L. Norby, *Arthritis Rheum.*, **9**, 47 (1966).
(16) "Documenta Geigy, Scientific Tables," 7th ed., K. Diem and C. Lentner, Eds., Geigy Pharmaceuticals, Ardsley, N.Y., 1975, p. 641.
(17) L. Sunblad, E. Jonsson, and E. Nettelbladt, *Nature*, **192**, 1192 (1961).
(18) W. F. Ganong, "Review of Medical Physiology," 4th ed., Lange Medical Publications, Los Altos, Calif., 1969.
(19) P. H. Hinderling, J. Brès, and E. R. Garrett, *J. Pharm. Sci.*, **63**, 1684 (1974).
(20) O. W. van Assenfeldt, W. G. Zijlstra, and E. J. van Kampen, *Proc. K. Ned. Akad. Wet. Ser.*, **C73**, 104 (1970).
(21) D. Kurata and G. R. Wilkinson, *Clin. Pharmacol. Ther.*, **16**, 355 (1974).
(22) G. H. Evans and D. G. Shand, *ibid.*, **14**, 494 (1973b).
(23) G. Weber and L. B. Young, *J. Biol. Chem.*, **239**, 1424 (1964).
(24) J. F. Foster, in "The Plasma Proteins," F. Putnam, Ed., Academic, New York, N.Y., 1960, p. 232.
(25) D. Shen and M. Gibaldi, *J. Pharm. Sci.*, **63**, 1698 (1974).
(26) I. M. Klotz and J. M. Urquhart, *J. Phys. Colloid Chem.*, **53**, 100 (1949).
(27) M. J. Cho, A. G. Mitchell, and M. Pernarowski, *J. Pharm. Sci.*, **60**, 196 (1971).
(28) M. J. Crooks and K. F. Brown, *ibid.*, **62**, 1904 (1973).
(29) C. J. Bowner and W. E. Lindup, *ibid.*, **67**, 1193 (1978).
(30) E. R. Garrett and H. J. Lambert, *ibid.*, **62**, 550 (1973).
(31) L. B. Jellet and D. G. Shand, *Pharmacologist*, **15**, 245 (1973).
(32) L. S. Schanker, J. M. Johanssen, and J. J. Jeffrey, *Am. J. Physiol.*, **207**, 503 (1964).
(33) U. Abshagen, H. Kewitz, and N. Rietbrock, *Naunyn-Schmiedebergs Arch. Pharmakol.*, **270**, 105 (1971).
(34) W. Dieterle, J. Wagner, and J. W. Faigle, *Eur. J. Clin. Pharmacol.*, **10**, 37 (1976).
(35) H. E. Rosenthal, *Anal. Biochem.*, **20**, 525 (1967).

### ACKNOWLEDGMENTS

Supported in part by a grant provided by Sandoz Ltd., Basel, Switzerland.

# Simultaneous Determination of Imipramine, Desipramine, and Their 2-Hydroxy Metabolites in Plasma by Ion-Pair Reversed-Phase High-Performance Liquid Chromatography with Amperometric Detection

**RAYMOND F. SUCKOW** ˣ **and THOMAS B. COOPER**

Received March 21, 1980, from *Rockland Research Institute, Orangeburg, NY 10962.* Accepted for publication August 14, 1980.

**Abstract** □ An ion-pair reversed-phase high-performance liquid chromatographic (HPLC) method, using an electrochemical detector, is presented for the simultaneous and rapid quantitation of imipramine, desipramine, and their 2-hydroxylated metabolites in plasma. The drugs are extracted from 1 ml of plasma at pH 9.7 with ether, back-extracted into 0.1 *M* HCl, and reextracted into ether following alkalinization. An efficient electrochemical oxidation reaction at the detector electrode affords a low detection level of ~5 ng/ml in a mobile phase of acetonitrile–acetate buffer (40:60) containing 0.005 *M* heptanesulfonate. Patient data are presented as correlations between the plasma level of each hydroxy metabolite and its respective parent compound. The method is applicable to the laboratory experienced in HPLC.

**Keyphrases** □ Imipramine—simultaneous determination with desipramine and their 2-hydroxy metabolites, ion-pair reversed-phase high-performance liquid chromatography □ Desipramine—simultaneous determination with imipramine and their 2-hydroxy metabolites, ion-pair reversed-phase high-performance liquid chromatography □ High-performance liquid chromatography—simultaneous determination of imipramine, desipramine, and their 2-hydroxy metabolites

Considerable interest exists in the relationship between the plasma concentration of tricyclic antidepressant drugs and the therapeutic outcome or side effects, and this subject was reviewed recently (1, 2). There seems to be a consensus that there is a therapeutic range for nortriptyline and a minimum effective level for imipramine plus desipramine in patients with "endogenous-type depression"; a therapeutic range also was suggested for desipramine (3). Data for amitriptyline, however, are much more controversial (4), and other tricyclic antidepressants have not been studied adequately.

## BACKGROUND

Until recently, the role of the hydroxylated metabolites of the tricyclic antidepressant drugs has been largely ignored, because it was assumed (erroneously) that these metabolites were not psychoactive, did not cross the blood–brain barrier, and were rapidly excreted. Christianssen and Gram (5) demonstrated that these hydroxylated metabolites were present in the central nervous system in an acute overdose case. Several studies demonstrated considerable quantities of unconjugated and conjugated hydroxy metabolites of tricyclic antidepressants in the plasma of treated patients (6–11).

It is now known that the hydroxy metabolites of imipramine have strong cardiovascular activity (12, 13) and are essentially equipotent to the parent compound in the blockade of norepinephrine and 5-hydrox-

0022-3549/81/0300-0257$01.00/0
© 1981, American Pharmaceutical Association

*macodyn. Ther.*, **221**, 122 (1976).
(4) U. Gubler and M. Baggiolini, *Scand. J. Rheumatol., Suppl.*, **21**, 8 (1978).
(5) R. Allan and M. Bleicher, *J. Int. Med Res.*, **5**(4), 253 (1977).
(6) M. Nissilä and A. Kajander, *Scand. J. Rheumatol., Suppl.*, **21**, 36 (1978).
(7) A. Albert and E. P. Serjeant, "The Determination of Ionization Constants," Chapman and Hall, London, England, 1962, p. 9.
(8) "Documenta Geigy, Scientific Tables," 7th ed., K. Diem and C. Lentner, Eds., Geigy Pharmaceuticals, Ardsley, N.Y., 1975, p. 281.
(9) G. A. Bray, *Anal. Biochem.*, **1**, 279 (1960).
(10) P. H. Hinderling, *Agents Actions*, **7**, 379 (1977).
(11) L. T. Skeggs, Jr., and H. Hochstrasser, *Clin. Chem.*, **10**, 918 (1964).
(12) C. B. Laurell and B. G. Johanssen, *Scand. J. Clin. Lab. Invest.*, **29**, 7 (1972).
(13) "Documenta Geigy, Scientific Tables," 7th ed., K. Diem and C. Lentner, Eds., Geigy Pharmaceuticals, Ardsley, N.Y., 1975, p. 582.
(14) K. H. Falchuk, E. J. Goetze, and J. P. Kulka, *Am. J. Med.*, **49**, 223 (1970).
(15) N. A. Cummings and G. L. Norby, *Arthritis Rheum.*, **9**, 47 (1966).
(16) "Documenta Geigy, Scientific Tables," 7th ed., K. Diem and C. Lentner, Eds., Geigy Pharmaceuticals, Ardsley, N.Y., 1975, p. 641.
(17) L. Sunblad, E. Jonsson, and E. Nettelbladt, *Nature*, **192**, 1192 (1961).
(18) W. F. Ganong, "Review of Medical Physiology," 4th ed., Lange Medical Publications, Los Altos, Calif., 1969.
(19) P. H. Hinderling, J. Brès, and E. R. Garrett, *J. Pharm. Sci.*, **63**, 1684 (1974).
(20) O. W. van Assenfeldt, W. G. Zijlstra, and E. J. van Kampen, *Proc. K. Ned. Akad. Wet. Ser.*, **C73**, 104 (1970).
(21) D. Kurata and G. R. Wilkinson, *Clin. Pharmacol. Ther.*, **16**, 355 (1974).
(22) G. H. Evans and D. G. Shand, *ibid.*, **14**, 494 (1973b).
(23) G. Weber and L. B. Young, *J. Biol. Chem.*, **239**, 1424 (1964).
(24) J. F. Foster, in "The Plasma Proteins," F. Putnam, Ed., Academic, New York, N.Y., 1960, p. 232.
(25) D. Shen and M. Gibaldi, *J. Pharm. Sci.*, **63**, 1698 (1974).
(26) I. M. Klotz and J. M. Urquhart, *J. Phys. Colloid Chem.*, **53**, 100 (1949).
(27) M. J. Cho, A. G. Mitchell, and M. Pernarowski, *J. Pharm. Sci.*, **60**, 196 (1971).
(28) M. J. Crooks and K. F. Brown, *ibid.*, **62**, 1904 (1973).
(29) C. J. Bowner and W. E. Lindup, *ibid.*, **67**, 1193 (1978).
(30) E. R. Garrett and H. J. Lambert, *ibid.*, **62**, 550 (1973).
(31) L. B. Jellet and D. G. Shand, *Pharmacologist*, **15**, 245 (1973).
(32) L. S. Schanker, J. M. Johanssen, and J. J. Jeffrey, *Am. J. Physiol.*, **207**, 503 (1964).
(33) U. Abshagen, H. Kewitz, and N. Rietbrock, *Naunyn-Schmiedebergs Arch. Pharmakol.*, **270**, 105 (1971).
(34) W. Dieterle, J. Wagner, and J. W. Faigle, *Eur. J. Clin. Pharmacol.*, **10**, 37 (1976).
(35) H. E. Rosenthal, *Anal. Biochem.*, **20**, 525 (1967).

### ACKNOWLEDGMENTS

Supported in part by a grant provided by Sandoz Ltd., Basel, Switzerland.

# Simultaneous Determination of Imipramine, Desipramine, and Their 2-Hydroxy Metabolites in Plasma by Ion-Pair Reversed-Phase High-Performance Liquid Chromatography with Amperometric Detection

**RAYMOND F. SUCKOW** ˣ **and THOMAS B. COOPER**

Received March 21, 1980, from *Rockland Research Institute, Orangeburg, NY 10962.* Accepted for publication August 14, 1980.

**Abstract** □ An ion-pair reversed-phase high-performance liquid chromatographic (HPLC) method, using an electrochemical detector, is presented for the simultaneous and rapid quantitation of imipramine, desipramine, and their 2-hydroxylated metabolites in plasma. The drugs are extracted from 1 ml of plasma at pH 9.7 with ether, back-extracted into 0.1 *M* HCl, and reextracted into ether following alkalinization. An efficient electrochemical oxidation reaction at the detector electrode affords a low detection level of ~5 ng/ml in a mobile phase of acetonitrile–acetate buffer (40:60) containing 0.005 *M* heptanesulfonate. Patient data are presented as correlations between the plasma level of each hydroxy metabolite and its respective parent compound. The method is applicable to the laboratory experienced in HPLC.

**Keyphrases** □ Imipramine—simultaneous determination with desipramine and their 2-hydroxy metabolites, ion-pair reversed-phase high-performance liquid chromatography □ Desipramine—simultaneous determination with imipramine and their 2-hydroxy metabolites, ion-pair reversed-phase high-performance liquid chromatography □ High-performance liquid chromatography—simultaneous determination of imipramine, desipramine, and their 2-hydroxy metabolites

Considerable interest exists in the relationship between the plasma concentration of tricyclic antidepressant drugs and the therapeutic outcome or side effects, and this subject was reviewed recently (1, 2). There seems to be a consensus that there is a therapeutic range for nortriptyline and a minimum effective level for imipramine plus desipramine in patients with "endogenous-type depression"; a therapeutic range also was suggested for desipramine (3). Data for amitriptyline, however, are much more controversial (4), and other tricyclic antidepressants have not been studied adequately.

## BACKGROUND

Until recently, the role of the hydroxylated metabolites of the tricyclic antidepressant drugs has been largely ignored, because it was assumed (erroneously) that these metabolites were not psychoactive, did not cross the blood–brain barrier, and were rapidly excreted. Christianssen and Gram (5) demonstrated that these hydroxylated metabolites were present in the central nervous system in an acute overdose case. Several studies demonstrated considerable quantities of unconjugated and conjugated hydroxy metabolites of tricyclic antidepressants in the plasma of treated patients (6–11).

It is now known that the hydroxy metabolites of imipramine have strong cardiovascular activity (12, 13) and are essentially equipotent to the parent compound in the blockade of norepinephrine and 5-hydrox-

0022-3549/81/0300-0257$01.00/0
© 1981, American Pharmaceutical Association

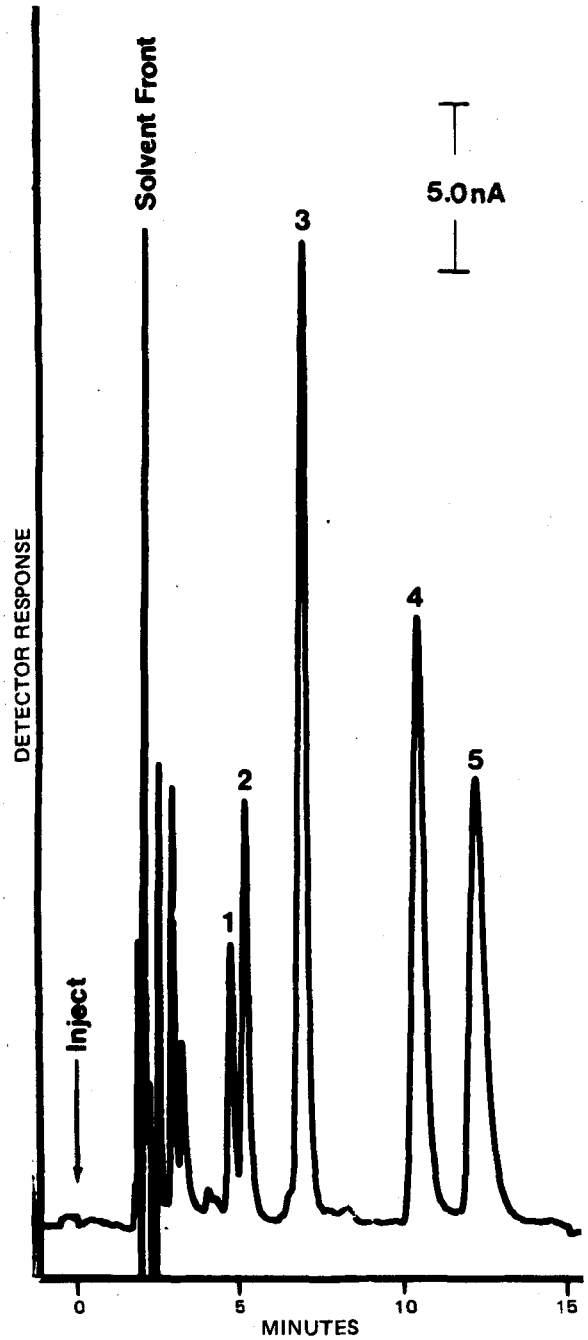


**Figure 1**—*Sample chromatogram of a 1-ml spiked plasma extract containing 25 ng of 2-hydroxydesipramine (1), 25 ng of 2-hydroxyimipramine (2), 100 ng of 8-hydroxyclomipramine (3), 50 ng of desipramine (4), and 50 ng of imipramine (5). One-half (50 μl) of the reconstituted extract was injected.*

ytryptophan receptors in rat brain slices, and isolated synaptosomal fractions (14–17). Also, the specificity of the respective hydroxylated metabolites is maintained, *e.g.*, 2-hydroxydesipramine was 100 times more potent in inhibiting norepinephrine than 5-hydroxytryptophan accumulation. These metabolites are present in the plasma in the same order of magnitude as the primary and secondary amines (10, 11). These data indicate that examination of the hydroxy metabolites may give insight into the clinical efficacy–side-effect relationship to the plasma drug levels.

The methods of analysis of the tricyclic antidepressants and their metabolites were reviewed recently (18). All methods involving high-performance liquid chromatography (HPLC) employed UV detection at various wavelengths. However, most of these methods suffer from poor resolution of the metabolites, interfering endogenous substances, or analysis time lasting >15 min. An assay for imipramine, desipramine,

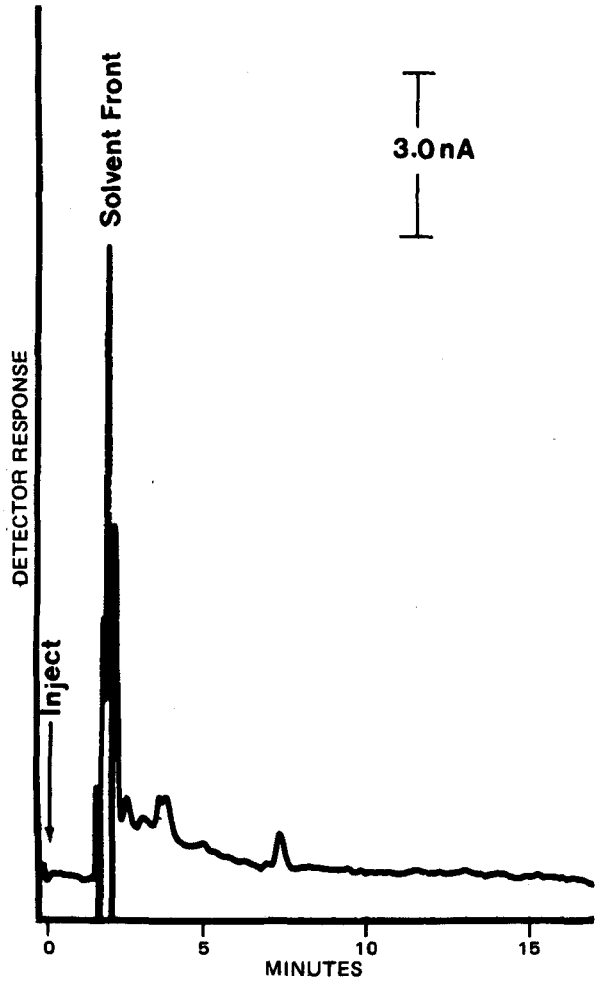


**Figure 2**—*Sample chromatogram of a 1-ml blank plasma extract. One-half (50 μl) of the reconstituted extract was injected.*

and their 2-hydroxylated metabolites in plasma was reported using a fluorescence detector and achieving a 1-ng/ml low level of detection (19). However, silica columns, as used in the preceding method, may deteriorate quickly when used at pH > 7.

Therefore, an assay was developed using ion-pair reversed-phase HPLC with amperometric detection for the rapid, sensitive, and simultaneous quantitations of imipramine, desipramine, and their 2-hydroxylated metabolites in plasma.

## EXPERIMENTAL

**Reagents**—Acetonitrile[1] was HPLC grade. Ether[1] was distilled prior to use. Acetic acid[1], sodium acetate[1], sodium carbonate[1], and sodium bicarbonate[1] were ACS reagent grade. Sodium heptanesulfonate[2] was used as received. Distilled water was passed through a water purification system[3] before use.

**Apparatus**—A high-performance liquid chromatograph[4] with a 2-ml syringe loading injector[5] was used. Chromatography was performed on a reversed-phase column[6]. The detector system consisted of a thin-layer flow-through electrochemical cell[7] with glassy carbon as the working and auxiliary electrodes and a silver–silver chloride reference electrode. The working electrode was directly opposite to the auxiliary electrode in the detector cell. This configuration was essential for increasing the linearity by several orders of magnitude to drug concentrations of >1 μg/ml. The potential and current response were monitored by an amperometric

[1] Fisher Scientific Co., Fair Lawn, N.J.
[2] Eastman Kodak Co., Rochester, N.Y.
[3] Milli-Q, Millipore Corp., Bedford, Mass.
[4] Model ALC/GPC 204, Waters Associates, Milford, Mass.
[5] UK6, Waters Associates, Milford, Mass.
[6] μBondapak $C_{18}$ (30 × 0.39 cm i.d.), Waters Associates, Milford, Mass.
[7] TL-5A, BioAnalytical Systems, West Lafayette, Ind.

**Table I—Recovery of Imipramine, Desipramine, 2-Hydroxyimipramine, and 2-Hydroxydesipramine (50 ng/ml Each) from 1 ml of Plasma**

| Compound | Recovery, % | SD | CV, % |
|---|---|---|---|
| 2-Hydroxyimipramine | 76 | 2.9 | 3.8 |
| 2-Hydroxydesipramine | 60 | 1.7 | 2.8 |
| Imipramine | 89 | 5.8 | 6.5 |
| Desipramine | 84 | 4.6 | 5.6 |

controller[8] and recorder[9], interfaced with a laboratory data acquisition system[10].

**Standards**—Stock solutions of imipramine hydrochloride[11] (1.13 mg/ml), desipramine hydrochloride[12] (1.13 mg/ml), 2-hydroxydesipramine free base[13] (1 mg/ml), and 2-hydroxyimipramine free base[13] (1 mg/ml) were prepared in methanol. The internal standard, 8-hydroxyclomipramine free base[13] (1 mg/ml), also was prepared in methanol.

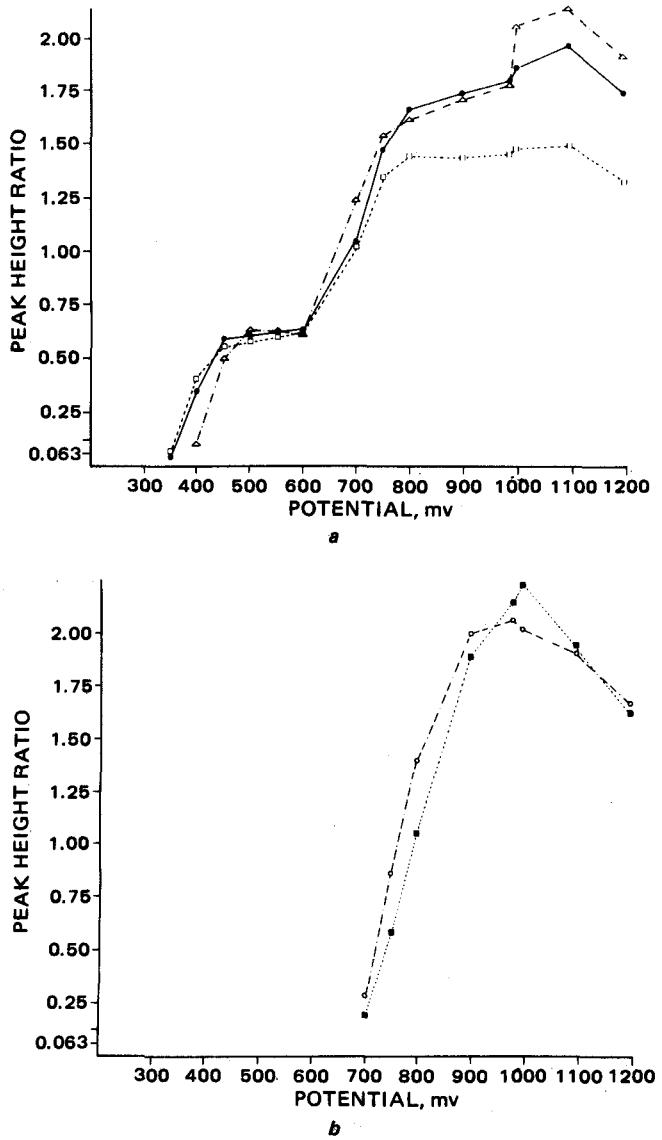


**Figure 3**—(a) *Plot of the peak height ratio against the potential* (versus *silver–silver chloride) for 2-hydroxyimipramine* (●), *2-hydroxydesipramine* (□), *and 8-hydroxyclomipramine* (△). *(b) Plot of the peak height ratio against the potential* (versus *silver–silver chloride) for desipramine* (○) *and imipramine* (■). *The chromatographic conditions were the same as described previously.*

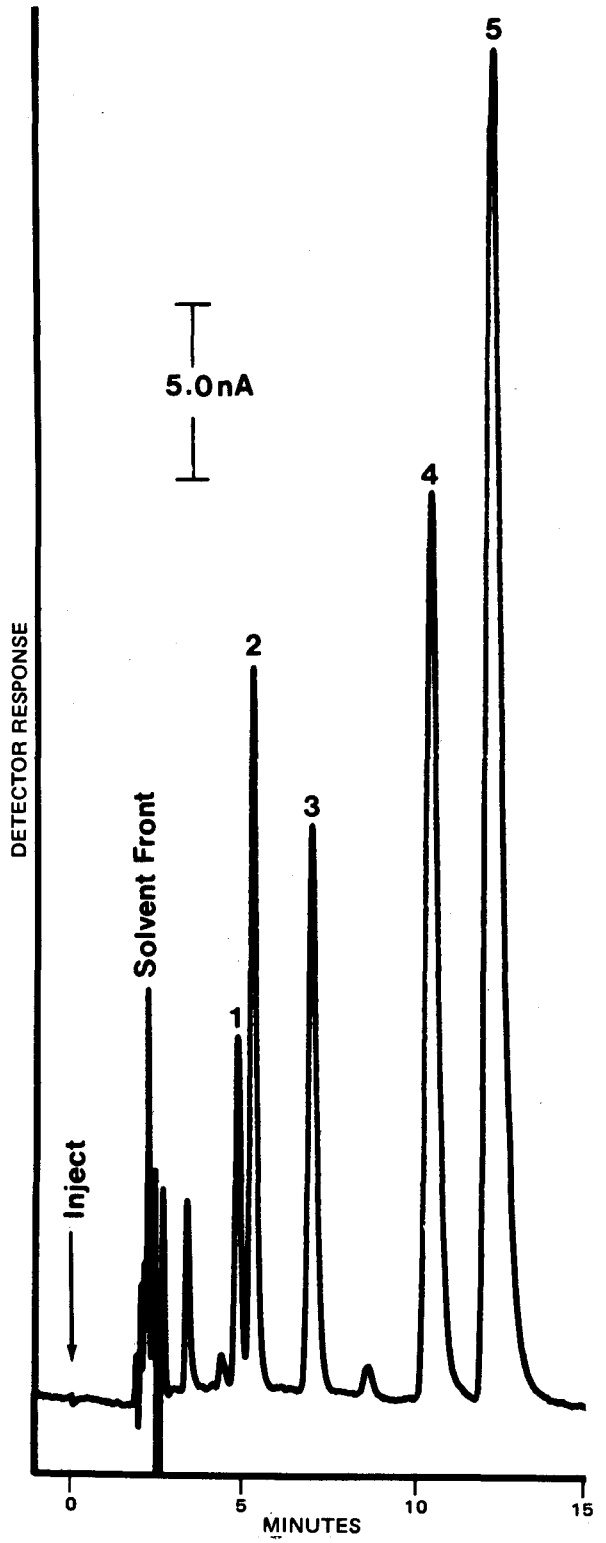


**Figure 4**—*Sample chromatogram of a 1-ml plasma sample from a patient receiving imipramine. One-quarter (25 μl) of the reconstituted extract was injected. The plasma levels were: 2-hydroxydesipramine (1), 54 ng; 2-hydroxyimipramine (2), 74 ng; internal standard (3); desipramine (4), 129 ng; and imipramine (5), 267 ng.*

[8] Metrohm V/A detector 611, Brinkmann Instruments, Westbury, N.Y.
[9] Houston Omniscribe model B5217B-2, Houston Instruments, Austin, Tex.
[10] Digital PDP/11/34 "Peak II" system, Digital Equipment Corp., Maynard, Mass.
[11] Ciba-Geigy Corp., Ardsley, N.Y.
[12] USV Pharmaceutical Corp., Tuckahoe, N.Y.
[13] A gift of Dr. Albert A. Manian, National Institute of Mental Health, National Institutes of Health, Rockville, Md.

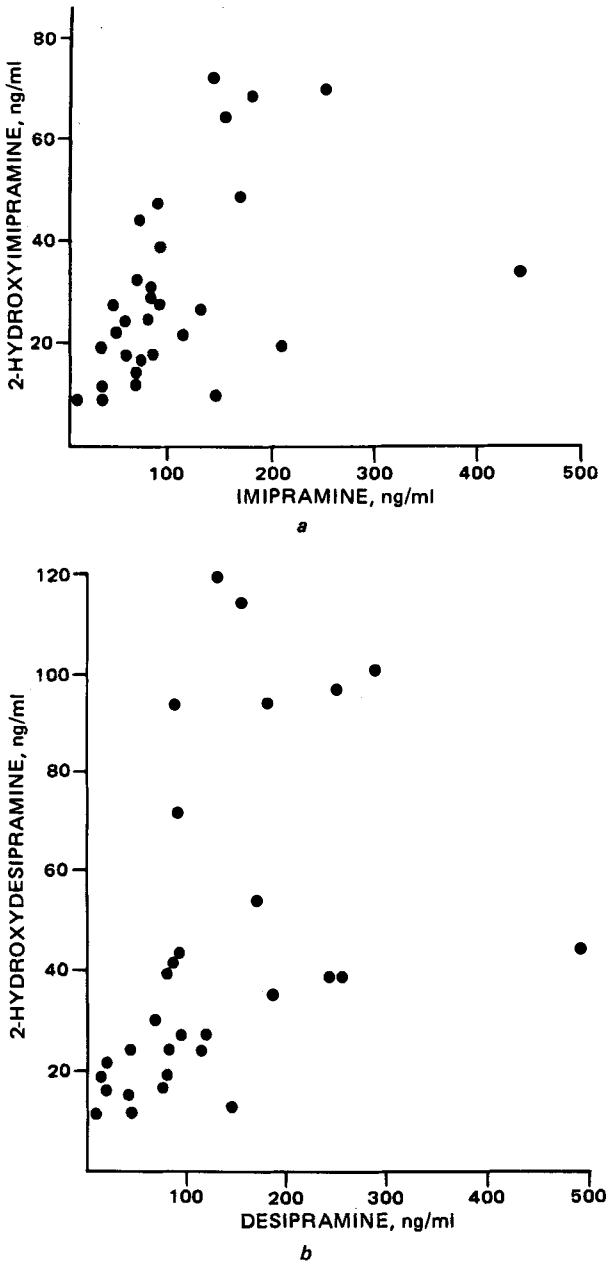


**Figure 5**—*(a) Relationship between plasma imipramine and 2-hydroxyimipramine levels in 30 randomly selected patients (r = 0.46). (b) Relationship between plasma desipramine and 2-hydroxydesipramine levels in the same patients (r = 0.40).*

Standard curves were prepared by the addition of the standards to drug-free plasma to give final concentrations of 25–400 ng of imipramine and desipramine/ml and of 10–200 ng of each of the 2-hydroxy metabolites.

**Extraction**—To 1.0 ml of plasma standard or unknown, 1.0 ml of water, 50 μl (100 ng) of the internal standard, and 1.0 ml of 0.6 *M* carbonate buffer (pH 9.7) were added in specially washed glassware[14]. Extraction was carried out by the addition of 8 ml of freshly distilled ether, and the solution was shaken and centrifuged for 15 min. The ether layer then was qualitatively transferred to 15-ml tapered centrifuge tubes containing 1.2 ml of 0.1 *M* HCl. After shaking and centrifuging for 10 min, the top layer was aspirated and the aqueous layer was transferred to 3-ml tapered, glass-stoppered, minicentrifuge tubes.

Neutralization resulted from the addition of 0.5 ml of 0.6 *M* carbonate buffer (pH 9.7). Ether (0.8 ml) was added, and the solution was shaken for 5 min and centrifuged for 5 min. The lower aqueous layer was discarded, and the ether layer was transferred to 1.0-ml reaction vials[15] and evaporated to dryness under a nitrogen stream at room temperature. The extract was reconstituted with 100 μl of the mobile phase, and the vial was capped.

**Chromatographic Conditions**—The mobile phase consisted of 0.1 *M* acetate buffer (pH 4.2) and acetonitrile (60:40). The paired-ion sodium heptanesulfonate (0.005 *M*) was added, and the mixture was filtered[16] and degassed prior to use. The flow rate was 1.3 ml/min, and the temperature was ambient. The effluent was monitored through the detector cell at a potential of +1.05 v *versus* the silver–silver chloride reference electrode.

**Quantitation**—All determinations were performed by calculating the peak height ratios of each compound to the internal standard. A standard curve was run with each set of samples.

## RESULTS AND DISCUSSION

Imipramine, desipramine, and their 2-hydroxylated metabolites were quantitated simultaneously in plasma. Each chromatogram took <15 min to elute all five compounds (Fig. 1).

The absolute sensitivity of this method was 1 ng injected for all four compounds (signal to noise ≃3). In practical terms, however, the lowest quantifiable levels were ~5 ng/ml of plasma. The blank plasma extracts showed no interfering endogenous substances (Fig. 2). This result was due to a careful sample cleanup, selectivity of the electrochemical detector, and the nature of the nonpolar bonded reversed phase, which eluted most hydrophilic biological material quickly.

The absolute recovery was checked by preparing a solution containing 50 ng of each 2-hydroxy metabolite, imipramine, and desipramine. The internal standard was added to five aliquots, and the sample was injected directly into the chromatograph. Then 1.0 ml of plasma was added to five additional aliquots, and the samples were processed routinely except for the internal standard, which was added to the vials after the samples were evaporated to dryness. The difference between the standard and the internal standard in the processed samples compared to the direct-injection sample gives a measure of the overall recovery (Table I).

The precision of the reported procedure was determined by spiking 10 1.0-ml aliquots of drug-free plasma with 25 ng of 2-hydroxyimipramine, 2-hydroxydesipramine, and 50 ng of imipramine and desipramine. After the addition of 100 ng of internal standard, each aliquot was processed as already described. The resulting coefficient of variation for each compound was 3.1% for 2-hydroxyimipramine, 8.7% for 2-hydroxydesipramine, 3.6% for imipramine, and 4.0% for desipramine.

8-Hydroxyclomipramine was chosen as the internal standard because of its structural similarity to all four compounds, its relative retention time, and its sensitive detector response. Its isomer, 2-hydroxyclomipramine, also may be used since the retention times differ by <1 min and it does not interfere with the assay.

Several drugs were tested using this assay to determine potential interference. When patient samples were tested, some high-dose major tranquilizers such as chlorpromazine, thioridazine, prochlorperazine, and loxapine did interfere with either the parent drug or, more frequently, the more polar metabolites. Low-dose major tranquilizers such as fluphenazine, perphenazine, and haloperidol and their metabolites are found therapeutically in very low concentrations in plasma and did not present significant interference problems.

Other tricyclic antidepressants such as nortriptyline, its 10-hydroxy metabolite, and protriptyline were not detected electrochemically but did appear on a simultaneous chromatogram with a UV detector. Amitriptyline and its 10-hydroxy metabolite were detected electrochemically but did not display a substantial response, as compared to the simultaneous UV run chromatogram. The benzodiazepines frequently are administered as adjuvants in these affective disorders and could interfere if UV detection were used. However, none of the benzodiazepines tested (chlordiazepoxide, diazepam, and flurazepam) is electrochemically active under the prevailing conditions. It would be prudent, however, to examine the medication profile of a patient prior to this assay (as with any other) to anticipate possible interferences.

The tricyclic antidepressant compounds containing the dibenzcycloheptane nucleus (*e.g.*, amitriptyline and nortriptyline) are devoid of, or have little, electrochemical reactivity under the described conditions. Therefore, the sensitivity of the electrochemically active dibenzazepine tricyclic antidepressants probably is due, at least in part, to the presence

[14] All glassware was treated as reported previously (20).

[15] Reactivials, Pierce Chemical Co., Rockford, Ill.

[16] Millipore type FH, 0.5 μm, Millipore Corp., Bedford, Mass.

of the ring nitrogen. A mechanism of electrochemical oxidation of these dibenzazepines seems best described by a two-step, three-electron ECE[17] process (21). The first step involves the transfer of one electron to form a radical, followed by dimerization. This compound then is oxidized further by an overall two-electron process at a more negative potential.

To determine the optimum positive potential for the five compounds used in this assay, current–potential curves were generated by injecting a standard solution of these compounds in methanol into the chromatograph at various potentials. A fixed-wavelength UV detector[18] (254 nm) was used as an "internal standard," connected in series preceding the electrochemical detector cell. The peak heights from the electrochemical response at various potentials were compared to the corresponding peak height from the UV detector response. These ratios were plotted against potentials. Figure 3*a* indicates that the 2-hydroxylated metabolites undergo oxidation at potentials more negative than the parent compound, probably due to the presence of the ring hydroxyl group. A second wave corresponds to the oxidation of the parent compounds (Fig. 3*b*).

Substantial levels of the 2-hydroxy metabolites can be found in patients receiving imipramine (Fig. 4). The relationships of the plasma concentrations of imipramine and desipramine to their respective 2-hydroxy metabolites are shown in Figs. 5*a* and 5*b*, respectively. These data show only a weak correlation, indicating the wide interindividual variations in the metabolic rates and pathways. A similar relationship between nortriptyline and 10-hydroxynortriptyline in plasma was reported with a somewhat stronger correlation ($r = 0.63$) (10).

These relationships may explain, in part, the variability in therapeutic response to the tricyclic antidepressants. Therefore, plasma level studies of these agents should include the active hydroxy metabolites when comparing the plasma levels and clinical efficacy and/or side effects.

## REFERENCES


(1) L. F. Gram, *Commun. Psychopharmacol.*, **2**, 373 (1978).

(2) S. C. Risch, L. Y. Huey, and D. S. Janowsky, *J. Clin. Psychiatr.*, **40**, 5, 58 (1979).

(3) R. O. Friedel, R. C. Veith, V. Bloom, and R. J. Bielski, *Commun. Psychopharmacol.*, **3**, 81 (1979).

(4) D. S. Robinson, T. B. Cooper, C. L. Ravaris, J. O. Ives, A. Nies, D. Bartlett, and K. P. Lamborn, *Psychopharmacology*, **63**, 223 (1979).

(5) J. Christianssen and L. F. Gram, *J. Pharm. Pharmacol.*, **25**, 604 (1973).

(6) V. E. Ziegler, B. T. Co, J. R. Taylor, P. J. Clayton, and J. T. Biggs, *Clin. Pharmacol. Ther.*, **19**, 795 (1976).

(7) P. Kragh-Sorenson, O. Borga, M. Garle, L. Bolvig-Hansen, C. E. Hansen, E. F. Hvidberg, N. E. Larsen, and F. Sjoqvist, *Eur. J. Clin. Pharmacol.*, **11**, 479 (1977).

(8) G. Alvan, O. Borga, M. Lind, L. Palmer, and B. Siwers, *ibid.*, **11**, 219 (1977).

(9) S. Nakano and L. E. Hollister, *Clin. Pharmacol. Ther.*, **23**, 199 (1978).

(10) L. Bertilsson, B. Melstrom, and F. Sjoqvist, *Life Sci.*, **25**, 1285 (1979).

(11) W. Z. Potter, H. Calil, A. Zavadil, W. Jusko, J. Sutfin, and J. Rapaport, *Clin. Pharmacol. Ther.*, **25**, 242 (1979).

(12) B. S. Jandhyala, M. L. Steenberg, J. M. Perel, A. A. Manian, and J. P. Buckley, *Eur. J. Pharmacol.*, **42**, 403 (1977).

(13) R. D. Wilkerson, *J. Pharmacol. Exp. Ther.*, **205**, 666 (1978).

(14) R. E. Heikkila, S. S. Holdfinger, and H. Orlansky, *Res. Commun. Chem. Pathol. Pharmacol.*, **13**, 237 (1976).

(15) B. Siwers, S. Borg, A. D'Elia, G. Lundlin, G. Plym-Forshell, H. Raotman, and G. Roman, *Acta Psychiatr. Scand.*, **55**, 21 (1977).

(16) J. I. Javid, J. M. Perel, and J. M. Davis, *Life Sci.*, **24**, 21 (1979).

(17) W. Z. Potter, H. M. Calil, A. A. Manian, A. P. Zavadil, and F. K. Goodwin, *Biol. Psychiatr.*, **14**, 601 (1979).

(18) B. A. Scroggins, K. P. Maguire, T. R. Norman, and G. D. Burrows, *Clin. Chem.*, **26**, 5 (1980).

(19) T. A. Sutfin and W. J. Jusko, *J. Pharm. Sci.*, **68**, 703 (1979).

(20) T. B. Cooper, D. S. Robinson, and A. Nies, *Commun. Psychopharmacol.*, **2**, 505 (1978).

(21) S. N. Frank and A. J. Bard, *J. Electrochem. Soc.*, **122**, 898 (1975).


[17] An electron-transfer step followed by a chemical reaction and a second electron-transfer step.

[18] Model 440, Waters Associates, Milford, Mass.

## ACKNOWLEDGMENTS


Supported in part by Public Health Service Grant RR 05651-10 from the Department of Health and Human Services.

R. F. Suckow is currently a research associate in the Analytical Psychopharmacology Laboratory Postdoctoral Program at Rockland Research Institute.

# Kinetics of Aspirin, Salicylic Acid, and Salicyluric Acid following Oral Administration of Aspirin as a Tablet and Two Buffered Solutions

**WILLIAM D. MASON** ˣ **and NATHANIEL WINER**

Received May 15, 1980, from the *Pharmacokinetics Laboratory, Schools of Pharmacy and Medicine, University of Missouri-Kansas City, Kansas City, MO 64108.* Accepted for publication August 21, 1980.

**Abstract** □ Twelve fasting normal volunteers received three aspirin dosage forms in a single-dose, complete crossover study; the plasma and urine levels of aspirin, salicylic acid, and salicyluric acid were measured for 10 hr. The three dosage forms were an unbuffered tablet, an effervescent solution with 16 mEq of buffer, and an effervescent solution with 34 mEq of buffer. Significant differences in the absorption rate were observed, with the solution having 16 mEq of buffer being fastest, the solution having 34 mEq of buffer being intermediate, and the tablet being slowest. These differences are attributed to gastric emptying rates and tablet dissolution. Urine pH and renal clearance for all three acid compounds are influenced by the buffer during the first 2 hr following dosing but not later. Area under the curve comparisons suggest that ~20% more aspirin reaches the general circulation intact following the tablet but that the total amount of salicylate absorbed is not different. Further studies are required to select the optimal buffer content to provide rapid absorption with minimal sodium dose and urine alkalinization.

**Keyphrases** □ Aspirin—tablet and two buffered solutions, kinetics following oral administration, salicylic acid and salicyluric acid levels and kinetics □ Salicylic acid—kinetics following oral administration of aspirin as tablet and two buffered solutions □ Salicyluric acid—kinetics following oral administration of aspirin as tablet and two buffered solutions □ Absorption kinetics—aspirin in tablet and two buffered solutions □ Buffer—effect on aspirin kinetics

Aspirin is the drug of choice when a mild analgesic–antipyretic is required, and it is also a primary agent in the chronic management of rheumatic fever, rheumatoid arthritis, and osteoarthritis. Following oral administration, rapid absorption is necessary to provide rapid onset of effects and to reduce the contact time with the gastric mucosa.

**Table I—Mean Plasma Aspirin Data and Computed Parameters**

| Parameter | Mean ± *SD*, μg/ml[a] | | |
|---|---|---|---|
| | T | S-16 | S-34 |
| Time, min | | | |
| 5 | 0.8 ± 1.0[c] | 2.5 ± 3.1[c] | 1.7 ± 2.2[c] |
| 10 | 2.9 ± 3.3[c] | 7.5 ± 6.2[c] | 4.8 ± 4.5[c] |
| 15 | 4.8 ± 4.2[c] | 12.0 ± 7.3[d] | 8.4 ± 6.6[cd] |
| 20 | 5.9 ± 4.0[c] | 13.0 ± 5.8[e] | 9.5 ± 6.1[d] |
| 30 | 8.8 ± 3.8[c] | 9.5 ± 2.8[c] | 9.6 ± 2.2[c] |
| 45 | 7.0 ± 2.8[c] | 5.1 ± 1.8[c] | 5.8 ± 2.0[c] |
| 60 | 4.9 ± 1.3[d] | 2.7 ± 0.9[c] | 2.9 ± 1.1[c] |
| 90 | 2.9 ± 1.2[d] | 0.8 ± 0.4[c] | 0.9 ± 0.4[c] |
| 120 | 1.3 ± 0.7[d] | 0.3 ± 0.2[c] | 0.3 ± 0.2[c] |
| Area under curve to 120 min, (mg min)/liter | 518.0 ± 104.8[d] | 494.0 ± 85.3[d] | 450.0 ± 75.4[c] |
| Time of maximum concentration, min | 35.0 ± 12.7[e] | 22.1 ± 9.5[c] | 27.5 ± 9.7[d] |
| Maximum concentration, mg/liter | 9.6 ± 3.7[c] | 16.4 ± 4.7[e] | 12.6 ± 4.5[d] |
| Area under curve to infinity, (mg min)/liter | 582 ± 86[d] | 506 ± 89[d] | 465 ± 78[a] |
| *MRT*, min | 63 ± 16[c] | 38 ± 9.9[d] | 41 ± 9.0[d] |
| *MAT*[b], min | 38 ± 13[c] | 15 ± 10[d] | 19 ± 8.1[d] |
| *VRT*, hr | 29 ± 16[c] | 13 ± 6.6[d] | 13 ± 7.1[d] |
| *VAT*[b], hr | 20 ± 15[c] | 4.6 ± 5.8[d] | 4.6 ± 7.0[d] |

[a] A common letter following the standard deviation indicates no significant difference ($p < 0.05$) (17). [b] The *MAT* defined in the discussion corresponds to the $MRT_g$ in Ref. 13, and *VAT* corresponds to the $VRT_g$.

## BACKGROUND

A recent review (1) indicated that prolonged and repeated contact of aspirin alters the gastric membrane to allow hydrogen-ion back-diffusion, which results in irritation, bleeding, and, possibly, ulceration. As the pH of the stomach contents is raised, gastric irritation and bleeding decrease. This finding is consistent with reports (2, 3) that administering aspirin in sufficient buffer to reduce the acidity of gastric fluids reduces occult blood loss.

Other studies (4–6) showed that aspirin absorption through the stomach is negligible at alkaline pH and increases (to ~11% of the dose) when administered in an unbuffered or acid solution. Reducing the acid content of the stomach speeds gastric emptying, which reduces the residence time for aspirin in the stomach (7). Thus, administration of aspirin as a buffered solution provides more rapid delivery to the primary absorption site (*i.e.*, the intestine) while reducing the potential for adverse effects on the gastric membrane. Martin (8) reviewed aspirin kinetics and the influence of formulation factors on aspirin absorption.

It is desirable to optimize the amounts of buffer components to provide rapid absorption and to reduce irritation with minimal alkalinization of urine and sodium intake. Since previous studies (2, 3, 9) measured the total salicylate in plasma, the efect of buffering on the bioavailability of unhydrolyzed aspirin is not known. In this study, plasma and urine aspirin, salicylic acid, and salicyluric acid were quantitated by high-pressure liquid chromatography (HPLC) following aspirin administration in two different effervescent buffered solutions and as unbuffered tablets to 12 fasting normal volunteers.

## EXPERIMENTAL

**Dosage Forms**—Three commercially available dosage forms were used to provide approximately equal doses of aspirin. They were two plain tablets[1], each containing 325 mg of aspirin (T); one effervescent tablet[2] containing 640 mg of aspirin, 1.825 g of sodium bicarbonate, and 1.079 g of citric acid (16 mEq of buffer) (S-16); and two effervescent tablets[3], each containing 324 mg of aspirin, 1.904 g of sodium bicarbonate, and 1.0 g of citric acid (34 mEq of buffer) (S-34).

**Subjects**—Twelve healthy male volunteers, 21–29 years old and 61.4–81.4 kg, were screened by a comprehensive physical examination, complete blood chemistry, urinalysis, and complete blood count and differential. All were free of any active disease, such as flu, and from the use of any medication for 14 days prior to the study. None of the subjects had a history of GI disease or surgery.

**Method**—A Latin-square design for three treatments in 12 subjects over three consecutive Saturdays was employed. A 10-hr fast preceded dosing and continued 4 hr postdosing except for water. At approximately 7 am, predose urine and blood samples were obtained, and a single dose of aspirin with 240 ml of water was administered. The effervescent tablets were dissolved in 140 ml of water 3 min prior to dosing, and then the mixture was swallowed. The glass was rinsed with 100 ml of water, which also was swallowed. Following dosing, 100 ml of water was administered at 1, 2, and 3 hr, and a uniform meal was served after the 4-hr sample. Subjects remained standing or sitting through the day, and exercise was limited to walking about the room.

[1] Bayer aspirin, Glenbrook Laboratories, Division of Sterling Drug, New York, N.Y.
[2] Aspirvess, Miles Laboratories, Elkhart, Ind.
[3] Alka-Seltzer, Miles Laboratories, Elkhart, Ind.



*0022-3549/81/0300-0262$01.00/0*
*© 1981, American Pharmaceutical Association*

**Table II—Mean Plasma Salicylic Acid Data**

| Parameter | Mean ± SD, μg/ml[a] T | S-16 | S-34 |
|---|---|---|---|
| Time | | | |
| 5 min | 0.7 ± 0.6[b] | 2.5 ± 3.0[b] | 2.3 ± 2.3[b] |
| 10 min | 2.7 ± 2.9[b] | 9.4 ± 8.4[b] | 7.5 ± 6.6[bc] |
| 15 min | 6.2 ± 5.4[b] | 18.0 ± 12.4[b] | 15.3 ± 11.9[c] |
| 20 min | 9.1 ± 6.0[b] | 25.9 ± 13.9[b] | 21.6 ± 14.3[c] |
| 30 min | 17.9 ± 7.7[b] | 34.5 ± 11.9[b] | 33.0 ± 12.2[c] |
| 45 min | 27.3 ± 11.3[b] | 37.2 ± 7.3[b] | 39.1 ± 7.3[c] |
| 1 hr | 31.6 ± 12.8[b] | 38.3 ± 7.2[b] | 40.0 ± 6.3[c] |
| 1.5 hr | 37.7 ± 10.1[b] | 36.1 ± 6.2[b] | 38.2 ± 5.0[b] |
| 2 hr | 38.0 ± 8.1[b] | 34.8 ± 5.6[b] | 34.6 ± 3.7[b] |
| 3 hr | 33.9 ± 6.9[c] | 29.7 ± 5.1[b] | 29.8 ± 4.9[b] |
| 4 hr | 30.2 ± 6.5[c] | 25.2 ± 5.5[b] | 25.6 ± 4.8[b] |
| 6 hr | 21.4 ± 6.4[c] | 17.1 ± 4.8[b] | 18.1 ± 5.3[b] |
| 8 hr | 14.2 ± 6.2[c] | 10.6 ± 4.7[b] | 11.5 ± 4.6[b] |
| 10 hr | 8.4 ± 4.7[c] | 6.7 ± 3.9[b] | 7.4 ± 3.7[bc] |
| Area under curve to 10 hr, (mg hr)/liter | 230 ± 56.6[c] | 210 ± 44.9[b] | 216 ± 40.9[bc] |
| Time of maximum concentration, hr | 1.9 ± 0.4[c] | 1.0 ± 0.5[b] | 1.0 ± 0.4[b] |
| Maximum concentration, mg/liter | 39.8 ± 8.9[b] | 40.3 ± 6.8[b] | 41.2 ± 6.0[b] |
| Area under curve to infinity, (mg hr)/liter | 282 ± 104[c] | 244 ± 71.8[b] | 253 ± 63.2[b] |

[a] A common letter following the standard deviation indicates no significant difference ($p < 0.05$) by ANOVA and least-significant difference method (17).

**Table III—Mean Plasma Salicyluric Acid Data**

| Parameter | Mean ± SD, μg/ml[a] T | S-16 | S-34 |
|---|---|---|---|
| Time | | | |
| 5 min | 0.0 ± 0.0[b] | 0.0 ± 0.0[b] | 0.0 ± 0.0[b] |
| 10 min | 0.0 ± 0.1[b] | 0.2 ± 0.2[b] | 0.2 ± 0.2[b] |
| 15 min | 0.2 ± 0.2[b] | 0.4 ± 0.3[b] | 0.4 ± 0.4[b] |
| 20 min | 0.4 ± 0.2[b] | 0.7 ± 0.4[b] | 0.6 ± 0.4[b] |
| 30 min | 0.7 ± 0.3[b] | 1.0 ± 0.4[b] | 0.9 ± 0.5[b] |
| 45 min | 1.1 ± 0.4[b] | 1.4 ± 0.6[b] | 1.2 ± 0.6[b] |
| 1 hr | 1.2 ± 0.4[b] | 1.5 ± 0.8[b] | 1.4 ± 0.7[b] |
| 1.5 hr | 1.4 ± 0.5[b] | 1.6 ± 0.8[b] | 1.5 ± 0.6[b] |
| 2 hr | 1.5 ± 0.5[b] | 1.7 ± 0.9[b] | 1.5 ± 0.6[b] |
| 3 hr | 1.5 ± 0.5[b] | 1.6 ± 0.9[b] | 1.4 ± 0.4[b] |
| 4 hr | 1.4 ± 0.5[b] | 1.5 ± 0.7[b] | 1.3 ± 0.4[b] |
| 6 hr | 1.3 ± 0.3[b] | 1.3 ± 0.7[b] | 1.2 ± 0.2[b] |
| 8 hr | 1.0 ± 0.2[b] | 0.9 ± 0.6[b] | 0.8 ± 0.2[b] |
| 10 hr | 0.6 ± 0.1[b] | 0.6 ± 0.4[b] | 0.6 ± 0.1[b] |
| Area under curve to 10 hr, (mg hr)/liter | 11.5 ± 2.9[b] | 12.3 ± 6.4[b] | 10.9 ± 2.9[b] |
| Time of maximum concentration, hr | 2.9 ± 1.6[b] | 1.7 ± 0.4[b] | 2.4 ± 1.3[b] |
| Maximum concentration, mg/liter | 1.6 ± 0.5[b] | 1.8 ± 0.9[b] | 1.5 ± 0.6[b] |

[a] A common letter following the standard deviation indicates no significant difference ($p < 0.05$) (17).

Blood was drawn into chilled vacuum containers[4] *via* an indwelling catheter at 5, 10, 15, 20, 30, and 45 min and at 1, 2, 3, 4, 6, 8, and 10 hr. Plasma was separated by centrifugation at 1764×*g* within 20 min of collection. All urine was collected at 2-hr intervals over 10 hr, the pH and volume were measured, and an acidified aliquot was saved for analysis. All samples were frozen at −30° and assayed within 2 weeks of collection by the HPLC method described previously (10).

## RESULTS

As shown in Tables I–III, plasma aspirin, salicylic acid, and salicyluric acid levels rose more rapidly following the solutions than following the tablet; the solution containing 16 mEq of buffer was fastest. The rank order and profile projected in the tables are the same in 11 of the 12 subjects, except that the two tablets occasionally showed two or three maxima.

Urine pH ranged between 5.8 and 7.4, and the urine flow rate averaged 108 ± 58 ml/hr for the 170 samples collected at 2-hr intervals. Over 10 hr, urinary excretion of aspirin, salicylic acid, and salicyluric acid (in aspirin equivalents) accounted for 1.06–1.52, 5.4–10.9, and 55.2–56.9% of the dose (Table IV). Projected to infinite time, salicyluric acid accounted for 64–69% of the aspirin dose, which is consistent with an earlier report (11). The mean renal salicylurate clearance of 35.7 liters/hr (595 ml/min) is somewhat higher than that reported earlier (11, 12), which may be due to the young subjects whose prestudy creatinine clearances all exceeded 120 ml/min.

Significant ($p < 0.05$) differences in urine pH and the renal clearance of aspirin and salicylic acid occurred only during the first 2 hr, and salicyluric acid clearance was not significantly affected. Multiple linear regression analysis provided a negative correlation of aspirin and salicylic acid renal clearance with the urine hydronium-ion concentration and no significant correlation with the urine flow rate or plasma drug concentration. Salicylurate renal clearance did not correlate with urine hydronium-ion concentration, urine flow rate, or plasma salicylurate or plasma salicylate concentrations.

Statistical moments as described by Yamaoka *et al.* (13) were used to estimate the mean residence time in the body and GI tract ($MRT$ and $MRT_g$) and the corresponding variances ($VRT$ and $VRT_g$) for aspirin. These parameters were computed for each dose for each subject, assuming first-order elimination from a single compartment.

Linear regression of the natural logarithm of the last three measured plasma concentrations of each curve was used to estimate the apparent half-life and to compute the area to infinite time. For each subject, the smallest apparent half-life was taken as an estimate of the one-compartment elimination half-life and used for subsequent statistical moment computations. This approach resulted in an elimination half-life of 15.6 ± 2.7 (mean ± *SD*) min for the 12 subjects, which closely approximates the 14.9-min half-life reported for intravenous aspirin (14). Averages of the mean residence times and variances are presented in Table I. These parameters provide a quantitative estimate of the relative absorption rate without reference to an absorption model and also reflect the more consistent plasma curve obtained following ingestion of solutions in comparison to the tablet.

## DISCUSSION

The combination of a specific HPLC analysis with sample handling and extraction procedures allows a detailed evaluation of plasma and urine aspirin, salicylic acid, and salicyluric acid levels following a tablet and two effervescent solutions. The solution with 16 mEq of buffer was the most rapidly absorbed, with the solution containing 34 mEq of buffer and the tablet following in that order.

The gastric emptying rate was measured[5] for the two solutions following a similar protocol by recovery of the gastric contents, and gastric emptying was observed with both to be about five times faster than occurs when the same volume of water is taken in the fasting state (7).

There are several possible methods of analysis for the aspirin absorption rate. One could utilize the Wagner–Nelson equation (15) to analyze the plasma aspirin or salicylate concentration–time curves. However, this approach presumes that a single-body compartment model applies to these data. Both compounds exhibit biexponential disposition, and salicylate–salicylurate data indicate that the salicylate is eliminated by one or more capacity-limited processes. A further analysis of the apparent percent absorbed–time curves, which could be obtained from such an analysis, requires certain presumptions, *e.g.*, that either first- or zero-order absorption kinetics apply. An alternative is to compare the peak time or concentrations. However, this approach leads only to a rank correlation and is open to serious errors due to difficulties in accurate estimation of the peak time and/or concentration from the available data.

Therefore, the application of the mean residence time approach recently introduced by Yamaoka *et al.* (13) was explored. It was shown[6] recently that relative mean absorption time ($MAT$) values can be calculated from oral data using the terminal rate constant in the calculation. In this approach, a drug exactly exhibiting one-compartment first-order elimination would have an $MRT_{iv}$ equal to:

[4] Vacutainer BD, 278-069, 7.0 ml containing 14 mg of potassium oxalate and 17.5 mg of sodium fluoride.

[5] J. N. Hunt, School of Medicine, Baylor University, Houston, Tex., personal communication.

[6] S. Riegelman and P. Collier, School of Pharmacy, University of California, San Francisco, Calif., personal communication.

**Table IV—Mean Urine pH and Renal Clearance of Aspirin, Salicylic Acid, and Salicyluric Acid [a]**

| Period, hr | Treatment | pH, mean ± *SD* | Renal Clearance, liters/hr: Aspirin, mean ± *SD* | Salicylic Acid, mean ± *SD* | Salicyluric Acid, mean ± *SD* |
|---|---|---|---|---|---|
| Predose | T | 5.93 ± 0.28 | — | — | — |
| | S-16 | 5.93 ± 0.24 | — | — | — |
| | S-34 | 5.91 ± 0.31 | — | — | — |
| | | NS[b] | | | |
| 0–2 | T | 5.72 ± 0.44[c] | 0.84 ± 0.48[c] | 0.054 ± 0.071[c] | 33.6 ± 6.5[c] |
| | S-16 | 5.89 ± 0.48[cd] | 1.21 ± 0.54[c] | 0.141 ± 0.138[cd] | 32.7 ± 8.6[c] |
| | S-34 | 6.42 ± 0.58[d] | 1.50 ± 0.69[a] | 0.304 ± 0.243[d] | 37.2 ± 7.3[c] |
| 2–4 | T | 6.01 ± 0.58[c] | — | 0.113 ± 0.155[c] | 36.2 ± 5.0[c] |
| | S-16 | 6.48 ± 0.63[d] | — | 0.204 ± 0.180[c] | 34.4 ± 8.5[c] |
| | S-34 | 6.59 ± 0.48[d] | — | 0.199 ± 0.160[c] | 37.5 ± 4.5[c] |
| 4–6 | T | 5.93 ± 0.50[c] | — | 0.086 ± 0.080[c] | 33.5 ± 7.4[c] |
| | S-16 | 6.24 ± 0.48[c] | — | 0.156 ± 0.095[c] | 34.4 ± 9.4[c] |
| | S-34 | 6.31 ± 0.52[c] | — | 0.116 ± 0.104[c] | 37.7 ± 6.3[c] |
| 6–8 | T | 6.31 ± 0.46[c] | — | 0.276 ± 0.289[c] | 35.1 ± 6.3[c] |
| | S-16 | 6.52 ± 0.56[c] | — | 0.260 ± 0.149[c] | 36.2 ± 8.9[c] |
| | S-34 | 6.53 ± 0.51[c] | — | 0.234 ± 0.185[c] | 36.8 ± 4.2[c] |
| 8–10 | T | 6.30 ± 0.41[c] | — | 0.211 ± 0.140[c] | 37.5 ± 5.0[c] |
| | S-16 | 6.69 ± 0.42[c] | — | 0.342 ± 0.159[c] | 36.6 ± 9.6[c] |
| | S-34 | 6.77 ± 0.30[c] | — | 0.310 ± 0.167[c] | 36.4 ± 9.7[c] |
| Aspirin equivalents excreted in 10 hr, mg | T | — | 6.87 ± 3.64 | 34.8 ± 29.8 | 364.8 ± 89.5 |
| | S-16 | — | 9.69 ± 4.34 | 6.4 ± 68.7 | 353.3 ± 85.8 |
| | S-34 | — | 9.91 ± 5.11 | 70.6 ± 65.7 | 368.7 ± 110 |
| Percent of aspirin dose in 10 hr | T | — | 1.06 ± 0.56 | 5.4 ± 4.6 | 56.3 ± 13.8 |
| | S-16 | — | 1.51 ± 0.67 | 10.1 ± 10.7 | 55.2 ± 13.4 |
| | S-34 | — | 1.52 ± 0.78 | 10.9 ± 10.1 | 56.9 ± 16.9 |

[a] A common letter following the standard deviation indicates no significant difference ($p < 0.05$) (17). [b] NS = not significant.

$$MRT_{iv} = 1/k \quad \text{(Eq. 1)}$$

When administered orally with a first-order absorption rate constant of $k_a$, the drug would exhibit an $MRT_{oral}$ of:

$$MRT_{oral} = \frac{1}{k_a} + \frac{1}{k} \quad \text{(Eq. 2)}$$

The mean absorption time could be estimated as:

$$MAT = MRT_{oral} - MRT_{iv} \quad \text{(Eq. 3a)}$$

or:

$$MAT = \left(\frac{1}{k_a} + \frac{1}{k}\right) - \frac{1}{k} = \frac{1}{k_a} \quad \text{(Eq. 3b)}$$

if one could estimate the elimination rate constant from the fall-off curve.

Since absorption disposition after intravenous administration probably exhibits two-compartment body kinetics (*2CBM*), a small error is involved in the *MAT* estimate. Riegelman and Collier[6] showed that the $MRT_{iv}$ value for a drug exhibiting two-compartment body kinetics exactly equals:

$$(MRT_{iv})_{2CBM} = \frac{1}{\alpha} - \frac{1}{k_{21}} + \frac{1}{\beta} \quad \text{(Eq. 4)}$$

Thus, when one calculates the *MAT* values using Eq. 1, one obtains a value equivalent to:

$$MAT_{exact} = MAT_{uncorr} + \left(\frac{1}{\alpha} - \frac{1}{k_{21}}\right) \quad \text{(Eq. 5)}$$

For aspirin, the magnitude of the correction assuming two-compartment body kinetics can be estimated from the intravenous studies of Rowland and Riegelman (14) to be 4.5 min on the average. If one presumes that disposition does not change significantly between studies, this negative correction should be added to the relative or uncorrected *MAT* values listed in Table I. The resultant *MAT* values are not dependent on any particular input kinetics but probably represent the time for 63% of the dose to be absorbed.

The computed mean residence times for aspirin in the GI tract (*MAT* values) of 15 ± 10, 19 ± 8.1, and 38 ± 13 min for S-16, S-34, and T, respectively, indicate a statistically significant increased $MRT_g$ value for the tablet. These results probably reflect the rate at which aspirin leaves the stomach and enters the intestine and the continued dissolution of the tablets. With the more acid gastric environment, the tablet is emptied more slowly into the intestine, and the potential for gastric absorption and irritation is greater than with the two buffered solutions. Although *in vitro* experiments showed the aspirin tablets to be ~90% dissolved in 5 min, *in vivo* some solid aspirin particles may exist for a longer time and even be emptied into the intestine.

Pharmacokinetic studies showed that aspirin solutions are absorbed completely and that ~60% reaches the general circulation unhydrolyzed (16). In the present study, two findings suggest that the amount of total salicylate (*i.e.*, aspirin plus salicylic acid) absorbed is equivalent for the three dosage forms. First, the total salicyluric acid excreted over 10 hr was essentially equal for all dosage forms (Table IV). Second, the areas under the plasma salicylate curve following the three treatments were within an 11% range, which may be attributed to the differences in renal clearance. The area under the curve for aspirin was 20% higher following the tablet than following the solution with 34 mEq of buffer, a difference not attributable to the small difference in renal clearance of aspirin associated with the two dosage forms. Thus, following the tablet, ~20% less aspirin was hydrolyzed prior to and/or during absorption when compared to the buffered solutions. If ~60% of the aspirin reaches the general circulation unhydrolyzed following the tablet, then ~50% does so following the effervescent solutions. This difference may result from a partial hydrolysis at the elevated pH associated with the buffered solution. Alternatively, part of the aspirin from the tablet may escape metabolism in the intestinal mucosa by being absorbed through the stomach.

An interesting observation is that the effervescent solution with 34 mEq of buffering agent and 648 mg of aspirin in a two-tablet dose contains more buffering than is required for rapid aspirin absorption in the fasting subject. Since this dosage form is commonly employed to treat the combined symptoms of headache and gastric hyperacidity, the 34 mEq of buffering may not be excessive. The effects of food on the absorption rate from buffered solutions are currently under study and may reveal different buffering requirements than were observed in the fasting stomach. However, for patients requiring only an analgesic effect, it may be advantageous to employ a solution with less buffering to obtain rapid absorption with a low sodium dose.

## REFERENCES


(1) B. M. Rothschild, *Clin. Pharmacol. Ther.*, **26**, 145 (1979).

(2) J. R. Leonards and G. Levy, *Arch. Intern. Med.*, **129**, 457 (1972).

(3) J. R. Leonards and G. Levy, *Clin. Pharmacol. Ther.*, **10**, 571 (1969).

(4) C. A. M. Hogben, L. S. Schanker, D. J. Tocco, and B. B. Brodie, *J. Pharmacol. Exp. Ther.*, **120**, 540 (1957).
(5) A. R. Cooke and J. N. Hunt, *Am. J. Dig. Dis.*, **15**, 95 (1970).
(6) A. R. Cooke and J. N. Hunt, *Guys Hosp. Rep.*, **120**, 221 (1971).
(7) J. N. Hunt, *Am. J. Dig. Dis.*, **8**, 885 (1963).
(8) B. K. Martin, *Adv. Pharm. Sci.*, **3**, 107 (1971).
(9) J. R. Leonards, *Clin. Pharmacol. Ther.*, **4**, 476 (1963).
(10) E. N. Amick and W. D. Mason, *Anal. Lett.*, **12**, 629 (1979).
(11) G. Levy, *J. Pharm. Sci.*, **54**, 959 (1965).
(12) D. Schacter and J. Manis, *J. Clin. Invest.*, **37**, 800 (1958).
(13) K. Yamaoka, T. Nakagawa, and T. Uno, *J. Pharmacokinet. Biopharm.*, **6**, 547 (1978).
(14) M. Rowland and S. Riegelman, *J. Pharm. Sci.*, **57**, 1313 (1968).
(15) J. Wagner, "Fundamentals of Clinical Pharmacokinetics," Drug Intelligence Publications, Hamilton, Ill., 1975, chap. 4.
(16) M. Rowland, L. Z. Benet, and S. Riegelman, *J. Pharm. Sci.*, **61**, 379 (1972).
(17) J. C. R. Li, "Statistical Inference," vol. 1, Edwards Brothers, Ann Arbor, Mich., 1964, p. 265.

# Anthracycline Assay by High-Pressure Liquid Chromatography

**STEVEN D. AVERBUCH *, THEODORE T. FINKELSTEIN ‡, SUSAN E. FANDRICH ‡, and STEVEN D. REICH ‡§¶x**

Received January 28, 1980, from the **Northwestern University Medical School, Chicago, IL 60611*, the ‡*Upstate Medical Center, State University of New York, Syracuse, NY 13210*, and §*Bristol Laboratories, Syracuse, NY 13201.* Accepted for publication August 14, 1980. ¶Present address: Division of Clinical Pharmacology, Department of Medicine, University of Massachusetts Medical School, Worcester, MA 01605.

**Abstract** □ A general method of analysis of anthracycline concentrations was developed. Drug is extracted from plasma with organic solvent and separated from metabolites by high-pressure liquid chromatography on an aminocyanosilica column. Detection and quantitation are by the endogenous fluorescence of compounds having an intact tetracyclic ring structure. Limits of sensitivity are 5, 1, and 5 ng/ml of plasma for doxorubicin, carubicin, and marcellomycin, respectively. The assay can be used for studying the aldo–keto reductase and reductive glycosidase reactions with anthracyclines as the substrates and for the evaluation of the clinical pharmacology or pharmacodynamics of various doxorubicin analogs.

**Keyphrases** □ Anthracyclines—doxorubicin, carubicin, daunorubicin, and marcellomycin, high-pressure liquid chromatographic analysis, dog plasma □ High-pressure liquid chromatography—analysis of doxorubicin, carubicin, daunorubicin, and marcellomycin in dog plasma □ Antineoplastic activity, potential—high-pressure liquid chromatographic analysis of anthracyclines in dog plasma, doxorubicin, carubicin, daunorubicin, and marcellomycin

Doxorubicin (adriamycin) is the best known of several hundred characterized anthracyclines. It has a broad spectrum of activity, so it is widely used in cancer therapy. However, because of significant acute and chronic toxicities, there is a constant search for active anthracyclines with less severe or less frequent adverse effects.

Several anthracycline analogs have reached the clinical stage of development. Daunorubicin (daunomycin, cerubidine), for example, was shown to be useful in the treatment of leukemia (1) and is now commercially available. Carubicin (carminomycin), an anthracycline that was developed and clinically tested in the Soviet Union (2), is being evaluated in the United States and Europe. Aclacinomycin A, a drug from Japan, is being evaluated in Europe (3) and tested clinically in the United States. Another anthracycline, marcellomycin, appears to be relatively nontoxic to white cells in animals (4) and is now undergoing toxicity studies in preparation for clinical testing.

A simple, rapid, inexpensive method of analysis of anthracycline concentrations in biological fluids is needed not only for comparative studies of pharmacokinetics and pharmacodynamics but also for the clinical monitoring of patients receiving doxorubicin analogs. A method for determining parent drug concentrations for various anthracyclines including doxorubicin, daunorubicin, carubicin, and marcellomycin has been developed. The method employs drug extraction with an organic solvent followed by high-pressure liquid chromatography (HPLC) with fluorescence detection. *In vitro* enzyme studies and *in vivo* pharmacokinetic investigations can be performed using this assay.

## EXPERIMENTAL

**Reagents and Drugs**—Purified doxorubicin[1], daunorubicin[1], carubicin[2], marcellomycin[2], rudolphomycin[2], and aclacinomycin A[2] were used for assay development. Clinical grade doxorubicin[3] and carubicin[2] were used in animal studies. Adriamycinol and daunorubicinol were obtained by reduction of the parent compound with aldo–keto reductase according to the procedure of Felsted *et al.* (5). Carminomycinol was prepared by borohydride reduction according to a modified procedure of Povarov *et al.* (6).

Aglycones were prepared by acid hydrolysis at elevated temperature (7). Deoxyaglycones of doxorubicin and adriamycinol were produced by reaction of the parent compound with microsomal enzymes in the presence of reduced nicotinamide-adenine dinucleotide phosphate (NADPH) under anaerobic conditions (8). Solvents were reagent grade or better, and degassing was not necessary. Water was glass distilled.

**Instruments**—Volume measurements were made with automatic pipets[4]. The high-pressure liquid chromatograph included an injection port[5] and a single-piston pump[6] with electronic damping. The column (25 cm × 4.6 mm i.d.) was packed with 10-μm aminocyanosilica[7]. The detection unit consisted of a filter-type fluorometer[8] with an emission filter of bandwidth 560–570 nm and an excitation filter of bandwidth

[1] Adria Laboratories, Dublin, Ohio.
[2] Bristol Laboratories, Syracuse, N.Y.
[3] Adriamycin, Adria Laboratories, Dublin, Ohio.
[4] Digital Pipetman, Rainin Instrument Co., Brighton, Mass.
[5] Model 7210, Rheodyne, Berkeley, Calif., or model U6K, Waters Associates, Milford, Mass.
[6] Model 110, Altex, Rainin Instrument Co., Brighton, Mass.
[7] Partisil-10 PAC, Whatman, Clifton, N.J.
[8] Spectra-Glo, Gilson Medical Electronics, Middleton, Wis.

0022-3549/81/0300-0265$01.00/0
© 1981, American Pharmaceutical Association

(4) C. A. M. Hogben, L. S. Schanker, D. J. Tocco, and B. B. Brodie, *J. Pharmacol. Exp. Ther.*, **120**, 540 (1957).
(5) A. R. Cooke and J. N. Hunt, *Am. J. Dig. Dis.*, **15**, 95 (1970).
(6) A. R. Cooke and J. N. Hunt, *Guys Hosp. Rep.*, **120**, 221 (1971).
(7) J. N. Hunt, *Am. J. Dig. Dis.*, **8**, 885 (1963).
(8) B. K. Martin, *Adv. Pharm. Sci.*, **3**, 107 (1971).
(9) J. R. Leonards, *Clin. Pharmacol. Ther.*, **4**, 476 (1963).
(10) E. N. Amick and W. D. Mason, *Anal. Lett.*, **12**, 629 (1979).
(11) G. Levy, *J. Pharm. Sci.*, **54**, 959 (1965).
(12) D. Schacter and J. Manis, *J. Clin. Invest.*, **37**, 800 (1958).
(13) K. Yamaoka, T. Nakagawa, and T. Uno, *J. Pharmacokinet. Biopharm.*, **6**, 547 (1978).
(14) M. Rowland and S. Riegelman, *J. Pharm. Sci.*, **57**, 1313 (1968).
(15) J. Wagner, "Fundamentals of Clinical Pharmacokinetics," Drug Intelligence Publications, Hamilton, Ill., 1975, chap. 4.
(16) M. Rowland, L. Z. Benet, and S. Riegelman, *J. Pharm. Sci.*, **61**, 379 (1972).
(17) J. C. R. Li, "Statistical Inference," vol. 1, Edwards Brothers, Ann Arbor, Mich., 1964, p. 265.

# Anthracycline Assay by High-Pressure Liquid Chromatography

**STEVEN D. AVERBUCH *, THEODORE T. FINKELSTEIN ‡, SUSAN E. FANDRICH ‡, and STEVEN D. REICH ‡§¶x**

Received January 28, 1980, from the **Northwestern University Medical School, Chicago, IL 60611*, the ‡*Upstate Medical Center, State University of New York, Syracuse, NY 13210*, and §*Bristol Laboratories, Syracuse, NY 13201.* Accepted for publication August 14, 1980. ¶Present address: Division of Clinical Pharmacology, Department of Medicine, University of Massachusetts Medical School, Worcester, MA 01605.

**Abstract** □ A general method of analysis of anthracycline concentrations was developed. Drug is extracted from plasma with organic solvent and separated from metabolites by high-pressure liquid chromatography on an aminocyanosilica column. Detection and quantitation are by the endogenous fluorescence of compounds having an intact tetracyclic ring structure. Limits of sensitivity are 5, 1, and 5 ng/ml of plasma for doxorubicin, carubicin, and marcellomycin, respectively. The assay can be used for studying the aldo–keto reductase and reductive glycosidase reactions with anthracyclines as the substrates and for the evaluation of the clinical pharmacology or pharmacodynamics of various doxorubicin analogs.

**Keyphrases** □ Anthracyclines—doxorubicin, carubicin, daunorubicin, and marcellomycin, high-pressure liquid chromatographic analysis, dog plasma □ High-pressure liquid chromatography—analysis of doxorubicin, carubicin, daunorubicin, and marcellomycin in dog plasma □ Antineoplastic activity, potential—high-pressure liquid chromatographic analysis of anthracyclines in dog plasma, doxorubicin, carubicin, daunorubicin, and marcellomycin

Doxorubicin (adriamycin) is the best known of several hundred characterized anthracyclines. It has a broad spectrum of activity, so it is widely used in cancer therapy. However, because of significant acute and chronic toxicities, there is a constant search for active anthracyclines with less severe or less frequent adverse effects.

Several anthracycline analogs have reached the clinical stage of development. Daunorubicin (daunomycin, cerubidine), for example, was shown to be useful in the treatment of leukemia (1) and is now commercially available. Carubicin (carminomycin), an anthracycline that was developed and clinically tested in the Soviet Union (2), is being evaluated in the United States and Europe. Aclacinomycin A, a drug from Japan, is being evaluated in Europe (3) and tested clinically in the United States. Another anthracycline, marcellomycin, appears to be relatively nontoxic to white cells in animals (4) and is now undergoing toxicity studies in preparation for clinical testing.

A simple, rapid, inexpensive method of analysis of anthracycline concentrations in biological fluids is needed not only for comparative studies of pharmacokinetics and pharmacodynamics but also for the clinical monitoring of patients receiving doxorubicin analogs. A method for determining parent drug concentrations for various anthracyclines including doxorubicin, daunorubicin, carubicin, and marcellomycin has been developed. The method employs drug extraction with an organic solvent followed by high-pressure liquid chromatography (HPLC) with fluorescence detection. *In vitro* enzyme studies and *in vivo* pharmacokinetic investigations can be performed using this assay.

## EXPERIMENTAL

**Reagents and Drugs**—Purified doxorubicin[1], daunorubicin[1], carubicin[2], marcellomycin[2], rudolphomycin[2], and aclacinomycin A[2] were used for assay development. Clinical grade doxorubicin[3] and carubicin[2] were used in animal studies. Adriamycinol and daunorubicinol were obtained by reduction of the parent compound with aldo–keto reductase according to the procedure of Felsted *et al.* (5). Carminomycinol was prepared by borohydride reduction according to a modified procedure of Povarov *et al.* (6).

Aglycones were prepared by acid hydrolysis at elevated temperature (7). Deoxyaglycones of doxorubicin and adriamycinol were produced by reaction of the parent compound with microsomal enzymes in the presence of reduced nicotinamide-adenine dinucleotide phosphate (NADPH) under anaerobic conditions (8). Solvents were reagent grade or better, and degassing was not necessary. Water was glass distilled.

**Instruments**—Volume measurements were made with automatic pipets[4]. The high-pressure liquid chromatograph included an injection port[5] and a single-piston pump[6] with electronic damping. The column (25 cm × 4.6 mm i.d.) was packed with 10-μm aminocyanosilica[7]. The detection unit consisted of a filter-type fluorometer[8] with an emission filter of bandwidth 560–570 nm and an excitation filter of bandwidth

[1] Adria Laboratories, Dublin, Ohio.
[2] Bristol Laboratories, Syracuse, N.Y.
[3] Adriamycin, Adria Laboratories, Dublin, Ohio.
[4] Digital Pipetman, Rainin Instrument Co., Brighton, Mass.
[5] Model 7210, Rheodyne, Berkeley, Calif., or model U6K, Waters Associates, Milford, Mass.
[6] Model 110, Altex, Rainin Instrument Co., Brighton, Mass.
[7] Partisil-10 PAC, Whatman, Clifton, N.J.
[8] Spectra-Glo, Gilson Medical Electronics, Middleton, Wis.

0022-3549/81/0300-0265$01.00/0
© 1981, American Pharmaceutical Association

380–480 nm equipped with a 15-μl flowcell. Chromatograms were recorded on a chart recorder with an electronic integrating channel[9].

**Assay of Plasma Samples**—Plasma, obtained from heparinized blood, was taken from storage at −10° or colder and warmed to room temperature. Samples then were vortexed rapidly or sonicated to disperse the cryoprecipitate. Aliquots (1.0 ml) were transferred to 15-ml tubes[10], and a small volume (20 μl) of the internal standard in aqueous solution was added. The internal standard consisted of an anthracycline with a convenient retention time that did not interfere with the peaks secondary to the test drug or its metabolites. Table I lists the internal standards used with the various test compounds.

To each plasma sample, two volumes of chloroform–isopropanol (1:1 v/v) solution were added. The mixture was vortexed for 20 sec, saturating quantities of ammonium sulfate were added, and the mixture was vortexed again. The tubes were centrifuged at 2650×*g* for 30 min, and the upper organic layer was removed and placed in clear, glass tubes. The organic solvent was evaporated under a nitrogen gas stream in a temperature-controlled water bath at 37°. The residue was analyzed immediately or stored at −40° until the next day. The residues were dissolved in 50 μl of the mobile phase just prior to injection into the chromatograph.

The column was conditioned before the first injection of the day by eluting with chloroform–methanol (1:1) at 1.5 ml/min for 30 min and then with the mobile phase of chloroform–methanol–acetic acid–water (80:20:2:3) at the operating flow rate of 3.5 ml/min for 30 min. This conditioning was reversed for the shutdown procedure, and a final wash of 100% methanol for 30 min at 1.5 ml/min was used. A constant flow rate of 3.5 ml/min was maintained during analysis at a column head pressure of 2700–4500 psi. When pressure greater than 4500 psi was encountered, the filter frits at the input end of the column were changed.

Standards encompassing the range of concentrations expected from plasma samples were run at the beginning of each day. Standards were prepared by spiking pooled dog plasma with the test drug and internal standard and carrying them through the assay. Peak heights of the test drug and internal standard were compared directly without correction for retention time or by comparison of the area under the peaks. Peaks were sharp so little difference between these methods was noted. Peak heights were normalized by dividing the peak height by the relative gain of the fluorescence detector. This procedure required changing the sensitivity setting when peaks started to go off scale.

***In Vitro* Metabolism Studies**—Enzyme kinetic studies of daunorubicin reductase (aldo–keto reductase) and daunorubicin reductive glycosidase (cytochrome P-450 reductase) were performed according to Bachur and associates (5, 8, 9), except that TLC was replaced by HPLC separation. The method involved incubation of the substrate with reduced nicotinamide-adenine dinucleotide phosphate in a suitable buffer with the enzyme. The product of the aldo–keto reductase reaction was adriamycinol when doxorubicin was the substrate. When the reductive glycosidase was incubated under anaerobic conditions, deoxyadriamycin aglycone was the product. The reaction was stopped by thorough mixing with *n*-butanol and saturating quantities of solid sodium chloride.

An aliquot (usually 20 μl) of the butanol layer, which extracted drug and metabolites, was injected directly into the chromatograph. The normalized peak height secondary to the fluorescence of the major metabolite was expressed as a fraction of the summation of all normalized peak heights. This fraction was multiplied by the initial amount of substrate to give the quantity of product formed. Since the tetracyclic ring structure of the anthracycline remains intact following either enzymatic conversion, it was assumed that the molar fluorescence of the substrate and products was the same and that no significant quantities of nonfluorescent products were formed.

## RESULTS AND DISCUSSION

The retention times of various anthracyclines and other fluorescent compounds are given in Table II. Because of slight changes in retention times with column maturation, authentic samples of compounds were sometimes injected into the column to confirm that a particular peak was due to the drug or metabolites and not to a spurious peak secondary to an unknown fluorescent plasma constituent.

Standard curves for doxorubicin, carubicin, and marcellomycin were linear over the range tested when four or five concentration points were used. The standard curve for doxorubicin with daunorubicin (250 ng/ml) as the internal standard was linear to 1250 ng/ml with a correlation coefficient of 0.997 for the best-fit line. The doxorubicin curve can be based on the area under the peak or normalized peak heights with similar results. The doxorubicin–daunorubicin system was reproducible from day to day with an average standard curve slope of 2.54 and a coefficient of variation of 10% ($n = 4$).

The standard curve for carubicin with doxorubicin (400 ng/ml) as the internal standard was linear to 50 ng/ml with a correlation coefficient of 0.994 for five concentration points done in triplicate. The marcellomycin standard curve was prepared using doxorubicin (400 ng/ml) as the internal standard and was linear to 100 ng/ml with a correlation coefficient of 0.991 for four concentration points done in triplicate. Standard curves for carubicin and marcellomycin were as reproducible as those for doxorubicin. Usually standard curves were generated at the beginning of test runs using three to five samples. Limits of sensitivity were 5, 1, and 5 ng/ml of plasma for doxorubicin, carubicin, and marcellomycin, respectively.

Plasma disappearance curves of doxorubicin and carubicin are shown in Fig. 1. Each curve was generated by giving the drug to a dog by rapid intravenous injection and obtaining plasma samples at timed intervals. Although the doxorubicin dose was 12-fold that of carubicin, plasma concentrations of doxorubicin at later time points were about 25 times higher than carubicin levels. The slopes of the terminal phases of both drugs in the two dogs appeared similar with half-lives of ~20 hr.

The enzyme kinetics of daunorubicin reductase and reductive glycosidase are shown in Figs. 2 and 3, respectively. The reactions were linear with respect to time over 15 min when protein concentrations were <1.5 mg/ml for the reductase and <0.4 mg/ml for the glycosidase. A Lineweaver–Burk reciprocal plot for the daunorubicin reductase also is shown in Fig. 2. The value obtained for the $K_m$ of this enzyme was approximately the same as was reported previously (5).

The use of HPLC with fluorescence detection for the isolation and separation of anthracyclines is an established technique (10–19). Many methods described in the literature involve multistep extraction procedures, lack sensitivity, use expensive instrumentation, or require gradient elution. The method described in this paper is actually the extraction method used by Benjamin *et al.* (20) and the HPLC methodology of Harris and Gudauskas (11). The instrumentation was chosen on the basis of simplicity, reproducibility, and cost. Since fluorescence detection is

**Table I—Internal Standards Used with Test Compounds in the Anthracycline Assay**

| Test Compound | Internal Standard (Concentration) |
|---|---|
| Doxorubicin | Daunorubicin (250 ng/ml) or carubicin (50 ng/ml) |
| Daunorubicin | Doxorubicin (250 ng/ml) |
| Marcellomycin | Doxorubicin (400 ng/ml) |
| Aclacinomycin A | Doxorubicin (400 ng/ml) |
| Carubicin | Doxorubicin (400 ng/ml) |

**Table II—Retention Times for Various Anthracyclines and Other Fluorescent Compounds**[a]

| Compound | Retention Time, min |
|---|---|
| Solvent front | 0.5 |
| Adriamycin aglycone | 0.5 |
| Carminomycin aglycone | 0.5 |
| Daunorubicin aglycone | 0.5 |
| Pyrromycinone | 0.5 |
| Quinine sulfate | 0.8 |
| Acridine | 1.0 |
| Aclacinomycin A | 1.1 |
| Pyrromycin | 1.7 |
| Bleomycin | 2.0 |
| Marcellomycin | 2.0 |
| Daunorubicin | 2.2 |
| Rudolphomycin | 2.2 |
| Carubicin | 2.3 |
| Proflavin | 2.4 |
| Puromycin | 2.5 |
| Musettamycin | 2.6 |
| Carminomycinol | 3.3 |
| Doxorubicin | 3.9 |
| Adriamycinol | 4.5 |
| Quinidine sulfate | 4.8 |

[a] The column was Whatman Partisil-10 PAC, the eluting solvent was chloroform–methanol–acetic acid–water (80:20:2:3), and the flow rate was 3.5 ml/min.

[9] Linear No. 252, Serco, Deerfield, Ill.
[10] Corex, Kimble Products.

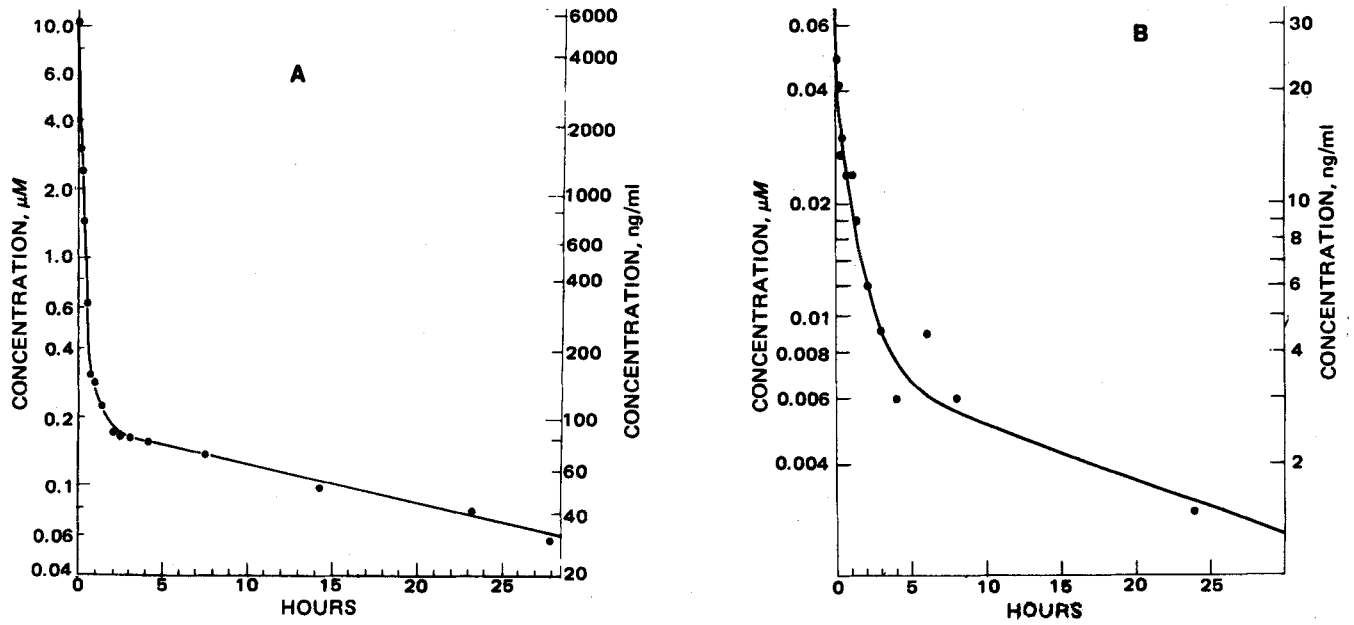


**Figure 1**—*Plasma disappearance curves for anthracyclines given to a dog as a bolus intravenous injection. Key: A, doxorubicin (90 mg/m²); and B, carubicin (7.5 mg/m²).*

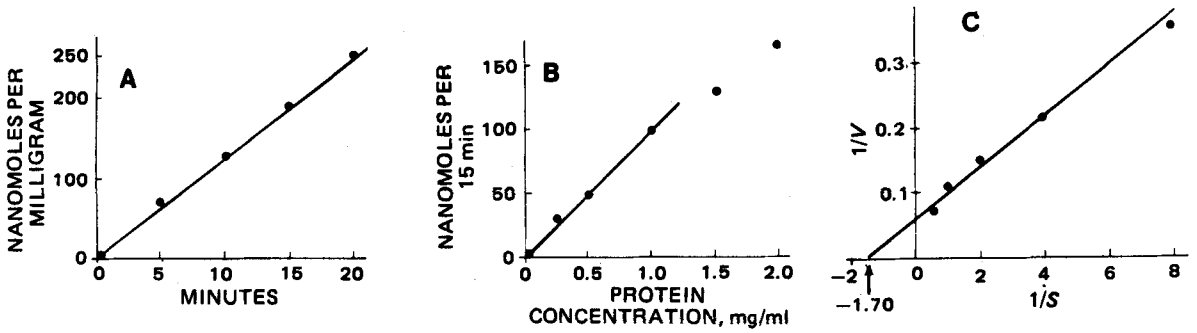


**Figure 2**—*Kinetics of the aldo–keto reductase enzyme with daunorubicin as the substrate. Final concentrations in 0.5 ml were 0.05 M phosphate buffer (pH 7.4), 1 × 10⁻³ M NADPH, 0–2 mg of protein/ml, and 1 × 10⁻³ M daunorubicin. Key: A, nanomoles of daunorubicinol per milligram of protein formed versus time; B, nanomoles of daunorubicinol formed per 15 min versus protein concentration; and C, Lineweaver–Burk reciprocal plot ($K_m$ = 59 μM).*

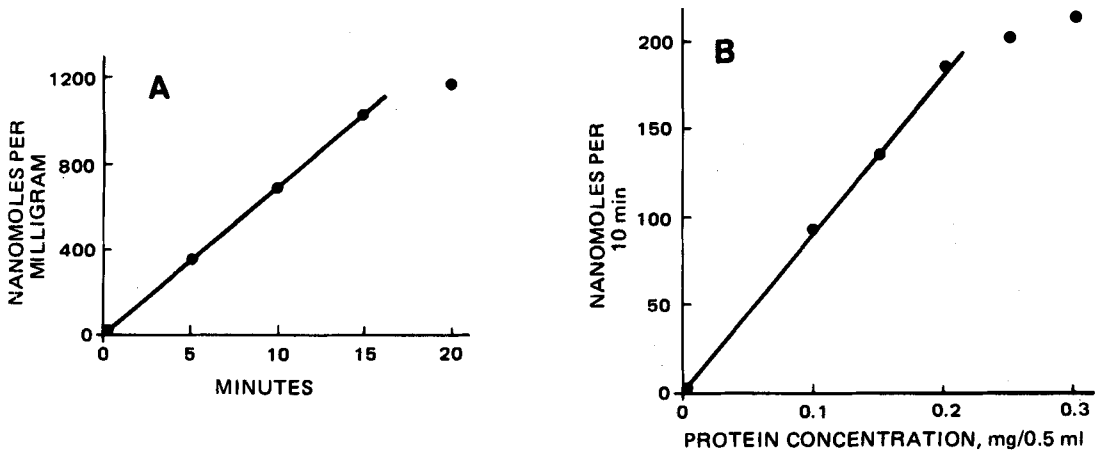


**Figure 3**—*Kinetics of reductive glycosidase with daunorubicin as the substrate. Final concentrations in 0.5 ml were 0.05 M phosphate buffer (pH 7.4), 1 × 10⁻³ M NADPH, 0–0.6 mg of protein/ml, and 1 × 10⁻³ M daunorubicin. Key: A, nanomoles of deoxydaunomycinone per milligram of protein formed versus time; and B, nanomoles of deoxydaunomycinone formed per 10 min versus protein concentration.*

not sensitive to pressure changes, the pulsation caused by the single-piston pump used in this system does not affect the chromatogram.

One disadvantage of this method is that the number of samples that can be processed is limited to about six or seven per hour since 6–10 min is required between injections. However, it takes about the same time to develop, scrape, and quantify materials on TLC plates, and TLC of doxorubicin may cause artifactual metabolite concentration values (21). Another disadvantage is that aglycones cannot be readily quantified from

plasma since aglycones of the drug and metabolites are not well resolved and elute near the solvent front, where there are high levels of nonspecific fluorescence due to plasma constituents.

Aglycone separation is not a problem in the *in vitro* assays since there are few interfering substances. Separation of aglycones from deoxyaglycones can be accomplished for most anthracyclines using the aminocyanosilica column if a less polar mobile phase is used. The parent compound, however, will have a longer retention time under these conditions.

Marcellomycin is an anthracycline with a three-sugar chain linked by a glycosidic bond to pyrromycione (22). Mussettamycin and pyrromycin are the di- and monosaccharides in this series, respectively. As can be seen from Table II, these four anthracyclines can be separated easily by this system.

The relative peak heights of test compounds compared to doxorubicin in this HPLC system depend on three major factors: (*a*) the molar fluorescence of the compounds at the excitation–emission bandwidths used in the fluorescence detector, (*b*) the extraction efficiency of the chloroform–isopropanol solvent, and (*c*) the retention time of the compound. Since retention times of the compounds are short, there is not much spreading of peak widths so the third factor does not influence peak heights substantially. However, the other two factors are important since the relative fluorescence of carubicin is ~2.5–3 times that of doxorubicin in this system. For example, 50 ng of carubicin/ml produces a peak height that is ~33% of that due to 400 ng of doxorubicin/ml. This result means that the fluorescence due to 50 ng of carubicin is equivalent to that due to 132 ng of doxorubicin/ml. Since the standard curve for carubicin is linear, it is not necessary to determine if this greater relative fluorescence is due to differences in molar fluorescence or to extraction efficiency. The relative fluorescence of doxorubicin, daunorubicin, and marcellomycin appears to be comparable when these drugs are extracted from pooled plasma.

The examples reported here demonstrate the usefulness and versatility of HPLC to anthracycline research. There is good evidence that doxorubicin toxicity can be predicted on the basis of elevated drug exposure or the area under the plasma concentration curve (23). If this observation holds for anthracycline analogs, then drug monitoring could warn against toxicity during early clinical trials. This HPLC system would then be useful in obtaining concentrations within a reasonable time with accuracy and reproducibility.

## REFERENCES


(1) P. H. Wiernik, *Clin. Haematol.*, **7**, 259 (1978).

(2) S. T. Crooke, *J. Med.*, **8**, 295 (1977).

(3) G. Mathe, M. Bayssas, J. Gouveia, D. Dantchev, P. Ribaud, D. Machover, J. L. Misset, L. Schwarzenberg, C. Jasmin, and M. Hayat, *Cancer Chemother. Pharmacol.*, **1**, 259 (1978).

(4) W. T. Bradner and M. Misiek, *J. Antibiot.*, **30**, 519 (1977).

(5) R. L. Felsted, M. Gee, and N. R. Bachur, *J. Biol. Chem.*, **249**, 3672 (1974).

(6) L. S. Povarov, V. A. Shorin, V. S. Bazhanov, and N. G. Shepelevtseva, *Antibiotiki*, **21**, 1008 (1976).

(7) N. R. Bachur, *J. Pharmacol. Exp. Ther.*, **177**, 575 (1971).

(8) N. R. Bachur and M. Gee, *ibid.*, **197**, 681 (1976).

(9) S. D. Reich and N. R. Bachur, *Cancer Res.*, **36**, 3803 (1976).

(10) J. J. Langone, H. Van Vunakis, and N. R. Bachur, *Biochem. Med.*, **12**, 283 (1975).

(11) P. A. Harris and G. Gudauskas, "Application Note for Waters Associates," Waters Associates, Milford, Mass., 1976.

(12) R. Hulhoven and J. P. Desager, *J. Chromatogr.*, **125**, 369 (1976).

(13) S. Eksborg and H. Ehrsson, *ibid.*, **153**, 211 (1978).

(14) S. Eksborg, *ibid.*, **149**, 225 (1978).

(15) M. Israel, W. J. Pegg, P. M. Wilkinson, and M. B. Garnick, *J. Liq. Chromatogr.*, **1**, 795 (1978).

(16) B. Andersson, M. Beran, B. Eberhardsson, S. Eksborg, and P. Slanini, *Cancer Chemother. Pharmacol.*, **2**, 159 (1979).

(17) R. Baurain, D. Deprez-de Campeneere, and A. Trouet, *Anal. Biochem.*, **94**, 112 (1979).

(18) J. H. Peters and J. F. Murray, Jr., *J. Liq. Chromatogr.*, **2**, 45 (1979).

(19) P. M. Wilkinson, M. Israel, W. J. Pegg, and E. Frei, III, *Cancer Chemother. Pharmacol.*, **2**, 121 (1979).

(20) R. S. Benjamin, C. E. Riggs, Jr., and N. R. Bachur, *Cancer Res.*, **37**, 1416 (1977).

(21) S. D. Reich, F. Steinberg, N. R. Bachur, C. E. Riggs, Jr., R. Goebel, and M. Berman, *Cancer Chemother. Pharmacol.*, **3**, 125 (1979).

(22) D. E. Nettleton, Jr., W. T. Bradner, J. A. Bush, A. B. Coon, J. E. Moseley, R. W. Myllymaki, F. A. O'Herron, R. H. Schreiber, and A. L. Vulcano, *J. Antibiot.*, **30**, 525 (1977).

(23) N. R. Bachur, C. E. Riggs, Jr., M. R. Green, J. J. Langone, H. Van Vunakis, and L. Levine, *Clin. Pharmacol. Ther.*, **21**, 70 (1977).


## ACKNOWLEDGMENTS


Supported by grants from the American Cancer Society, Illinois Division, and 5S07RR05402-18 from the U.S. Public Health Service and by gifts from Adria Laboratories and Bristol Laboratories.

S. D. Averbuch was a recipient of a Pharmaceutical Manufacturers Association Foundation Medical Student Research Fellowship.

The authors thank Dr. George Okita, Dr. Paula Stern, Dr. Thomas Gibson, Dr. Robert Smyth, and Dr. Stanley Crooke for support and suggestions, Dr. John Schurig for supplying plasma samples from the dog treated with carubicin, Constance Gonczy for technical assistance, and Sue Briggs, Gail Monopoli, and Dan Mullen for help in manuscript preparation.


## ADDENDUM TO ANTHRACYCLINE ASSAY BY HIGH-PRESSURE LIQUID CHROMATOGRAPHY: MODIFICATION OF MOBILE PHASE FOR AMINOCYANOSILICA COLUMNS USED FOR ANTHRACYCLINE ASSAY


(Prepared by Steven D. Reich[1x], Lorraine Martinez[1], Walter W. Krehel[2], and J. Robert Bickler[2].


Received June 9, 1980. Accepted for publication August 14, 1980.)


High-pressure liquid chromatography (HPLC) is an efficient technique for the separation and quantification of anthracycline antibiotics. Various assay procedures have been described, including several that employ an aminocyanosilica column[3] (1–3). Users of this column should be aware that a modification in the manufacturing process for the packing material has changed the properties of this column with respect to anthracycline assay. Although the change improved the uniformity of the columns without significantly altering retention times of standard test compounds or the number of theoretical plates, the affinity of the packing for anthracyclines was decreased. No other problems secondary to the change have been reported to the manufacturer.

**Table AI—Retention Times for Several Compounds [a]**

| Compound | Retention Time, min |
|---|---|
| Solvent front | 1.3 |
| Acridine | 1.3 |
| Aclacinomycin A | 1.3 |
| Carubicin | 3.0 |
| Quinidine sulfate | 3.3 |
| Daunorubicin | 3.6 |
| Puromycin | 3.6 |
| Quinine sulfate | 3.8 |
| Carminomycinol | 4.0 |
| Proflavin | 4.0 |
| Daunorubicinol | 4.8 |
| Doxorubicin | 6.3 |

[a] The column was Whatman Partisil PXS 10/25 PAC (lot 100320), the mobile phase was hexane–ethylene chloride–methanol–acetic acid–water (40:40:10:4:1), and the flow rate was 3.0 ml/min.

Those columns[3] manufactured prior to May 24, 1979, separate doxorubicin (adriamycin), adriamycinol, adriamycin aglycones, daunorubicin, and daunorubicinol with a mobile phase of choloform–methanol–acetic acid–water (80:20:2:3). Columns manufactured after May 1979 (lots 100302 and higher) require a modification in the mobile phase to separate these compounds; hexane–ethylene chloride–methanol–acetic acid–water (40:40:10:4:1) at a flow rate of 3.0 ml/min can be used without loss of separation or sensitivity compared to the old system.

To document that the new system can be used for assay of doxorubicin and other anthracyclines, standard curves for doxorubicin and carubicin (carminomycin) were prepared in plasma. Daunorubicin (50 ng/ml) and


[1] Division of Clinical Pharmacology, Department of Medicine, University of Massachusetts Medical School, Worcester, MA 01605.

[2] Whatman, Clifton, NJ 07014.
[3] Partisil-10 PAC, Whatman, Clifton, NJ 07014.

doxorubicin (150 ng/ml) were used as the internal standards, respectively. Samples were assayed according to the procedure of Averbuch *et al.* (3), except that new columns (lot 100302) were used with the hexane–ethylene chloride–methanol–acetic acid–water mobile phase system. The assay sensitivity (signal strength of >2.5 times baseline noise) was 5 and 1 ng/ml, respectively. In both cases, the response was linear to 200 ng/ml (highest concentration tested). The correlation coefficient for six points was >0.99 for both assays. Retention times for several anthracyclines and other fluorescent compounds were determined (Table AI).

The aminocyanosilica column is effective in separating highly polar compounds and is almost free of solvent memory. It is unfortunate that a change in silica gel manufacture caused a substantial change in operating characteristics with respect to the anthracycline assay. However, if the appropriate mobile phase is used, depending on lot number, then this column continues to be useful to anthracycline research.

(1) P. A. Harris and B. Gudauskas, in "Whatman Liquid Chromatography Product Guide," Bull. 123, Whatman, Clifton, N.J., 1977, p. 22.

(2) M. Israel, W. I. Pegg, P. M. Wilkinson, and M. B. Garnick, *J. Liq. Chromatogr.*, **1**, 795 (1978).

(3) S. D. Averbuch, T. T. Finkelstein, S. E. Fandrich, and S. D. Reich, *J. Pharm. Sci.*, **70**, 265 (1981).

Supported by Grant IN-129 from the American Cancer Society.

# Effect of Surfactant on Tetracycline Absorption across Everted Rat Intestine

**LOYD V. ALLEN, Jr. *x, R. S. LEVINSON ‡, CASEY ROBINSON *, and ANDREW LAU ***

Received January 28, 1980, from the **College of Pharmacy, Health Sciences Center, University of Oklahoma, Oklahoma City, OK 73190,* and the ‡*Arnold & Marie Schwartz College of Pharmacy, Long Island University, Brooklyn, NY 11201.* Accepted for publication August 18, 1980.

**Abstract** □ Absorption of tetracycline hydrochloride (500 μg/ml) from oxygenated modified Krebs buffer in randomized everted rat jejunal segments was determined alone and in the presence of calcium, polysorbate 80, and calcium plus polysorbate 80. Surfactant increased absorption of tetracycline in the presence and absence of calcium, with 0.01% (w/v) polysorbate 80 increasing transfer to the greatest extent of the concentrations examined (0.005, 0.01, 0.05, 0.1, and 1%); tetracycline hydrochloride + 12.5 m*M* $CaCl_2$, 143 ± 45 μg/ml; tetracycline hydrochloride + polysorbate 80, 389 ± 18 μg/ml; tetracycline hydrochloride + 12.5 m*M* $CaCl_2$ + polysorbate 80, 255 ± 31 μg/ml. On the premise that the effective surfactant concentration is similar to the critical micelle concentration, an absorption mechanism based on micellar solubilization is postulated.

**Keyphrases** □ Tetracycline—absorption, effect of polysorbate 80, everted rat intestine □ Polysorbate 80—effect on tetracycline absorption across everted rat intestine □ Surfactants—effect of polysorbate 80 on tetracycline absorption across everted rat intestine

Tetracycline is a widely used antibiotic. Its serum level should not fall below the minimum inhibitory concentration (MIC), usually between 0.1 and 1.5 μg/ml, for most bacterial strains. Occasionally, this concentration is difficult to maintain due to decreased absorption caused by other drugs or divalent and trivalent cations present in the GI tract (1–3). The intestinal absorption of most tetracyclines is rapid but incomplete, and the absorption mechanism is poorly understood (4, 5).

Physicochemical interactions in the gut are not uncommon and, at least pharmacokinetically, seem to be the most important form of interaction affecting the absorption of tetracycline derivatives. Chelation of tetracycline with polyvalent cations, which has been well documented, is the most common reaction that decreases tetracycline absorption. In addition to forming direct tetracycline–metal complexes, tetracycline binds to both nucleic acids and proteins, with the binding mediated by divalent cations such as zinc, calcium, and magnesium.

Recently, the role of endogenous and exogenous surfactants in drug absorption experiments was explored (6, 7). In some instances, the addition of surfactants enhanced drug absorption (8).

Since decreased tetracycline absorption presents a clinical problem, often requiring alteration of food and medications, a method of optimizing tetracycline absorption to avoid the present restrictions would be valuable. Surfactants may enhance tetracycline absorption to an acceptable level, even in the presence of divalent ions; if so, they may prove to be a valuable additive to oral dosage forms.

This investigation determined the effects of surfactants on tetracycline absorption from the rat everted gut sac to obtain information on the enhancement of tetracycline transport and the tetracycline transport mechanism.

## EXPERIMENTAL

**Intestine Preparation**—An everted intestinal sac technique (9, 10) was used. The solution on the inside of the sac is referred to as the serosal solution, and the solution in which it is incubated is called the mucosal solution.

Seven male white Holtzman rats, 175–200 g, were fasted overnight (20–24 hr), but water was not withheld prior to the experiment. The animals were anesthetized with ether and then killed by stunning and cervical fracture. The jejunum was removed and rinsed immediately with several portions of cold normal saline and everted on a thin glass rod. After eversion, the jejunum was washed in cold normal saline and cut into seven segments of 5-cm length. Segments of the rat intestine were selected randomly for the different treatment groups.

Sacs of everted intestine were prepared by tying one end tightly and the other end loosely with fine thread. Then 0.5 ml of buffer was introduced inside the sac with a 1-ml syringe fitted with a blunt needle. The loose ligature was tightened, and the buffer-filled sacs then were transferred immediately to 25-ml erlenmeyer flasks containing 15 ml of buffer mixed with tetracycline hydrochloride[1], 0.5 g/liter with or without the additives. Control sacs were placed in buffer alone. The other five sacs were incubated in buffer to which 0.005, 0.01, 0.05, 0.1, or 1% (w/v) pol-

[1] Lot 6 X090-71000, Pfizer Laboratories, New York, N.Y.

0022-3549/81/0300-0269$01.00/0
© 1981, American Pharmaceutical Association

plasma since aglycones of the drug and metabolites are not well resolved and elute near the solvent front, where there are high levels of nonspecific fluorescence due to plasma constituents.

Aglycone separation is not a problem in the *in vitro* assays since there are few interfering substances. Separation of aglycones from deoxyaglycones can be accomplished for most anthracyclines using the aminocyanosilica column if a less polar mobile phase is used. The parent compound, however, will have a longer retention time under these conditions.

Marcellomycin is an anthracycline with a three-sugar chain linked by a glycosidic bond to pyrromycione (22). Mussettamycin and pyrromycin are the di- and monosaccharides in this series, respectively. As can be seen from Table II, these four anthracyclines can be separated easily by this system.

The relative peak heights of test compounds compared to doxorubicin in this HPLC system depend on three major factors: (*a*) the molar fluorescence of the compounds at the excitation–emission bandwidths used in the fluorescence detector, (*b*) the extraction efficiency of the chloroform–isopropanol solvent, and (*c*) the retention time of the compound. Since retention times of the compounds are short, there is not much spreading of peak widths so the third factor does not influence peak heights substantially. However, the other two factors are important since the relative fluorescence of carubicin is ~2.5–3 times that of doxorubicin in this system. For example, 50 ng of carubicin/ml produces a peak height that is ~33% of that due to 400 ng of doxorubicin/ml. This result means that the fluorescence due to 50 ng of carubicin is equivalent to that due to 132 ng of doxorubicin/ml. Since the standard curve for carubicin is linear, it is not necessary to determine if this greater relative fluorescence is due to differences in molar fluorescence or to extraction efficiency. The relative fluorescence of doxorubicin, daunorubicin, and marcellomycin appears to be comparable when these drugs are extracted from pooled plasma.

The examples reported here demonstrate the usefulness and versatility of HPLC to anthracycline research. There is good evidence that doxorubicin toxicity can be predicted on the basis of elevated drug exposure or the area under the plasma concentration curve (23). If this observation holds for anthracycline analogs, then drug monitoring could warn against toxicity during early clinical trials. This HPLC system would then be useful in obtaining concentrations within a reasonable time with accuracy and reproducibility.

## REFERENCES


(1) P. H. Wiernik, *Clin. Haematol.*, **7**, 259 (1978).

(2) S. T. Crooke, *J. Med.*, **8**, 295 (1977).

(3) G. Mathe, M. Bayssas, J. Gouveia, D. Dantchev, P. Ribaud, D. Machover, J. L. Misset, L. Schwarzenberg, C. Jasmin, and M. Hayat, *Cancer Chemother. Pharmacol.*, **1**, 259 (1978).

(4) W. T. Bradner and M. Misiek, *J. Antibiot.*, **30**, 519 (1977).

(5) R. L. Felsted, M. Gee, and N. R. Bachur, *J. Biol. Chem.*, **249**, 3672 (1974).

(6) L. S. Povarov, V. A. Shorin, V. S. Bazhanov, and N. G. Shepelevtseva, *Antibiotiki*, **21**, 1008 (1976).

(7) N. R. Bachur, *J. Pharmacol. Exp. Ther.*, **177**, 575 (1971).

(8) N. R. Bachur and M. Gee, *ibid.*, **197**, 681 (1976).

(9) S. D. Reich and N. R. Bachur, *Cancer Res.*, **36**, 3803 (1976).

(10) J. J. Langone, H. Van Vunakis, and N. R. Bachur, *Biochem. Med.*, **12**, 283 (1975).

(11) P. A. Harris and G. Gudauskas, "Application Note for Waters Associates," Waters Associates, Milford, Mass., 1976.

(12) R. Hulhoven and J. P. Desager, *J. Chromatogr.*, **125**, 369 (1976).

(13) S. Eksborg and H. Ehrsson, *ibid.*, **153**, 211 (1978).

(14) S. Eksborg, *ibid.*, **149**, 225 (1978).

(15) M. Israel, W. J. Pegg, P. M. Wilkinson, and M. B. Garnick, *J. Liq. Chromatogr.*, **1**, 795 (1978).

(16) B. Andersson, M. Beran, B. Eberhardsson, S. Eksborg, and P. Slanini, *Cancer Chemother. Pharmacol.*, **2**, 159 (1979).

(17) R. Baurain, D. Deprez-de Campeneere, and A. Trouet, *Anal. Biochem.*, **94**, 112 (1979).

(18) J. H. Peters and J. F. Murray, Jr., *J. Liq. Chromatogr.*, **2**, 45 (1979).

(19) P. M. Wilkinson, M. Israel, W. J. Pegg, and E. Frei, III, *Cancer Chemother. Pharmacol.*, **2**, 121 (1979).

(20) R. S. Benjamin, C. E. Riggs, Jr., and N. R. Bachur, *Cancer Res.*, **37**, 1416 (1977).

(21) S. D. Reich, F. Steinberg, N. R. Bachur, C. E. Riggs, Jr., R. Goebel, and M. Berman, *Cancer Chemother. Pharmacol.*, **3**, 125 (1979).

(22) D. E. Nettleton, Jr., W. T. Bradner, J. A. Bush, A. B. Coon, J. E. Moseley, R. W. Myllymaki, F. A. O'Herron, R. H. Schreiber, and A. L. Vulcano, *J. Antibiot.*, **30**, 525 (1977).

(23) N. R. Bachur, C. E. Riggs, Jr., M. R. Green, J. J. Langone, H. Van Vunakis, and L. Levine, *Clin. Pharmacol. Ther.*, **21**, 70 (1977).


## ACKNOWLEDGMENTS


Supported by grants from the American Cancer Society, Illinois Division, and 5S07RR05402-18 from the U.S. Public Health Service and by gifts from Adria Laboratories and Bristol Laboratories.

S. D. Averbuch was a recipient of a Pharmaceutical Manufacturers Association Foundation Medical Student Research Fellowship.

The authors thank Dr. George Okita, Dr. Paula Stern, Dr. Thomas Gibson, Dr. Robert Smyth, and Dr. Stanley Crooke for support and suggestions, Dr. John Schurig for supplying plasma samples from the dog treated with carubicin, Constance Gonczy for technical assistance, and Sue Briggs, Gail Monopoli, and Dan Mullen for help in manuscript preparation.


## ADDENDUM TO ANTHRACYCLINE ASSAY BY HIGH-PRESSURE LIQUID CHROMATOGRAPHY: MODIFICATION OF MOBILE PHASE FOR AMINOCYANOSILICA COLUMNS USED FOR ANTHRACYCLINE ASSAY


(Prepared by Steven D. Reich[1x], Lorraine Martinez[1], Walter W. Krehel[2], and J. Robert Bickler[2].


Received June 9, 1980. Accepted for publication August 14, 1980.)


High-pressure liquid chromatography (HPLC) is an efficient technique for the separation and quantification of anthracycline antibiotics. Various assay procedures have been described, including several that employ an aminocyanosilica column[3] (1–3). Users of this column should be aware that a modification in the manufacturing process for the packing material has changed the properties of this column with respect to anthracycline assay. Although the change improved the uniformity of the columns without significantly altering retention times of standard test compounds or the number of theoretical plates, the affinity of the packing for anthracyclines was decreased. No other problems secondary to the change have been reported to the manufacturer.

**Table AI—Retention Times for Several Compounds [a]**

| Compound | Retention Time, min |
|---|---|
| Solvent front | 1.3 |
| Acridine | 1.3 |
| Aclacinomycin A | 1.3 |
| Carubicin | 3.0 |
| Quinidine sulfate | 3.3 |
| Daunorubicin | 3.6 |
| Puromycin | 3.6 |
| Quinine sulfate | 3.8 |
| Carminomycinol | 4.0 |
| Proflavin | 4.0 |
| Daunorubicinol | 4.8 |
| Doxorubicin | 6.3 |

[a] The column was Whatman Partisil PXS 10/25 PAC (lot 100320), the mobile phase was hexane–ethylene chloride–methanol–acetic acid–water (40:40:10:4:1), and the flow rate was 3.0 ml/min.

Those columns[3] manufactured prior to May 24, 1979, separate doxorubicin (adriamycin), adriamycinol, adriamycin aglycones, daunorubicin, and daunorubicinol with a mobile phase of choloform–methanol–acetic acid–water (80:20:2:3). Columns manufactured after May 1979 (lots 100302 and higher) require a modification in the mobile phase to separate these compounds; hexane–ethylene chloride–methanol–acetic acid–water (40:40:10:4:1) at a flow rate of 3.0 ml/min can be used without loss of separation or sensitivity compared to the old system.

To document that the new system can be used for assay of doxorubicin and other anthracyclines, standard curves for doxorubicin and carubicin (carminomycin) were prepared in plasma. Daunorubicin (50 ng/ml) and


[1] Division of Clinical Pharmacology, Department of Medicine, University of Massachusetts Medical School, Worcester, MA 01605.

[2] Whatman, Clifton, NJ 07014.
[3] Partisil-10 PAC, Whatman, Clifton, NJ 07014.

doxorubicin (150 ng/ml) were used as the internal standards, respectively. Samples were assayed according to the procedure of Averbuch *et al.* (3), except that new columns (lot 100302) were used with the hexane–ethylene chloride–methanol–acetic acid–water mobile phase system. The assay sensitivity (signal strength of >2.5 times baseline noise) was 5 and 1 ng/ml, respectively. In both cases, the response was linear to 200 ng/ml (highest concentration tested). The correlation coefficient for six points was >0.99 for both assays. Retention times for several anthracyclines and other fluorescent compounds were determined (Table AI).

The aminocyanosilica column is effective in separating highly polar compounds and is almost free of solvent memory. It is unfortunate that a change in silica gel manufacture caused a substantial change in operating characteristics with respect to the anthracycline assay. However, if the appropriate mobile phase is used, depending on lot number, then this column continues to be useful to anthracycline research.

(1) P. A. Harris and B. Gudauskas, in "Whatman Liquid Chromatography Product Guide," Bull. 123, Whatman, Clifton, N.J., 1977, p. 22.

(2) M. Israel, W. I. Pegg, P. M. Wilkinson, and M. B. Garnick, *J. Liq. Chromatogr.*, **1**, 795 (1978).

(3) S. D. Averbuch, T. T. Finkelstein, S. E. Fandrich, and S. D. Reich, *J. Pharm. Sci.*, **70**, 265 (1981).

Supported by Grant IN-129 from the American Cancer Society.

# Effect of Surfactant on Tetracycline Absorption across Everted Rat Intestine

**LOYD V. ALLEN, Jr. *x, R. S. LEVINSON ‡, CASEY ROBINSON *, and ANDREW LAU ***

Received January 28, 1980, from the **College of Pharmacy, Health Sciences Center, University of Oklahoma, Oklahoma City, OK 73190,* and the ‡*Arnold & Marie Schwartz College of Pharmacy, Long Island University, Brooklyn, NY 11201.* Accepted for publication August 18, 1980.

**Abstract** □ Absorption of tetracycline hydrochloride (500 μg/ml) from oxygenated modified Krebs buffer in randomized everted rat jejunal segments was determined alone and in the presence of calcium, polysorbate 80, and calcium plus polysorbate 80. Surfactant increased absorption of tetracycline in the presence and absence of calcium, with 0.01% (w/v) polysorbate 80 increasing transfer to the greatest extent of the concentrations examined (0.005, 0.01, 0.05, 0.1, and 1%); tetracycline hydrochloride + 12.5 m*M* $CaCl_2$, 143 ± 45 μg/ml; tetracycline hydrochloride + polysorbate 80, 389 ± 18 μg/ml; tetracycline hydrochloride + 12.5 m*M* $CaCl_2$ + polysorbate 80, 255 ± 31 μg/ml. On the premise that the effective surfactant concentration is similar to the critical micelle concentration, an absorption mechanism based on micellar solubilization is postulated.

**Keyphrases** □ Tetracycline—absorption, effect of polysorbate 80, everted rat intestine □ Polysorbate 80—effect on tetracycline absorption across everted rat intestine □ Surfactants—effect of polysorbate 80 on tetracycline absorption across everted rat intestine

Tetracycline is a widely used antibiotic. Its serum level should not fall below the minimum inhibitory concentration (MIC), usually between 0.1 and 1.5 μg/ml, for most bacterial strains. Occasionally, this concentration is difficult to maintain due to decreased absorption caused by other drugs or divalent and trivalent cations present in the GI tract (1–3). The intestinal absorption of most tetracyclines is rapid but incomplete, and the absorption mechanism is poorly understood (4, 5).

Physicochemical interactions in the gut are not uncommon and, at least pharmacokinetically, seem to be the most important form of interaction affecting the absorption of tetracycline derivatives. Chelation of tetracycline with polyvalent cations, which has been well documented, is the most common reaction that decreases tetracycline absorption. In addition to forming direct tetracycline–metal complexes, tetracycline binds to both nucleic acids and proteins, with the binding mediated by divalent cations such as zinc, calcium, and magnesium.

Recently, the role of endogenous and exogenous surfactants in drug absorption experiments was explored (6, 7). In some instances, the addition of surfactants enhanced drug absorption (8).

Since decreased tetracycline absorption presents a clinical problem, often requiring alteration of food and medications, a method of optimizing tetracycline absorption to avoid the present restrictions would be valuable. Surfactants may enhance tetracycline absorption to an acceptable level, even in the presence of divalent ions; if so, they may prove to be a valuable additive to oral dosage forms.

This investigation determined the effects of surfactants on tetracycline absorption from the rat everted gut sac to obtain information on the enhancement of tetracycline transport and the tetracycline transport mechanism.

## EXPERIMENTAL

**Intestine Preparation**—An everted intestinal sac technique (9, 10) was used. The solution on the inside of the sac is referred to as the serosal solution, and the solution in which it is incubated is called the mucosal solution.

Seven male white Holtzman rats, 175–200 g, were fasted overnight (20–24 hr), but water was not withheld prior to the experiment. The animals were anesthetized with ether and then killed by stunning and cervical fracture. The jejunum was removed and rinsed immediately with several portions of cold normal saline and everted on a thin glass rod. After eversion, the jejunum was washed in cold normal saline and cut into seven segments of 5-cm length. Segments of the rat intestine were selected randomly for the different treatment groups.

Sacs of everted intestine were prepared by tying one end tightly and the other end loosely with fine thread. Then 0.5 ml of buffer was introduced inside the sac with a 1-ml syringe fitted with a blunt needle. The loose ligature was tightened, and the buffer-filled sacs then were transferred immediately to 25-ml erlenmeyer flasks containing 15 ml of buffer mixed with tetracycline hydrochloride[1], 0.5 g/liter with or without the additives. Control sacs were placed in buffer alone. The other five sacs were incubated in buffer to which 0.005, 0.01, 0.05, 0.1, or 1% (w/v) pol-

[1] Lot 6 X090-71000, Pfizer Laboratories, New York, N.Y.

0022-3549/81/0300-0269$01.00/0
© 1981, American Pharmaceutical Association

doxorubicin (150 ng/ml) were used as the internal standards, respectively. Samples were assayed according to the procedure of Averbuch *et al.* (3), except that new columns (lot 100302) were used with the hexane–ethylene chloride–methanol–acetic acid–water mobile phase system. The assay sensitivity (signal strength of >2.5 times baseline noise) was 5 and 1 ng/ml, respectively. In both cases, the response was linear to 200 ng/ml (highest concentration tested). The correlation coefficient for six points was >0.99 for both assays. Retention times for several anthracyclines and other fluorescent compounds were determined (Table AI).

The aminocyanosilica column is effective in separating highly polar compounds and is almost free of solvent memory. It is unfortunate that a change in silica gel manufacture caused a substantial change in operating characteristics with respect to the anthracycline assay. However, if the appropriate mobile phase is used, depending on lot number, then this column continues to be useful to anthracycline research.

(1) P. A. Harris and B. Gudauskas, in "Whatman Liquid Chromatography Product Guide," Bull. 123, Whatman, Clifton, N.J., 1977, p. 22.

(2) M. Israel, W. I. Pegg, P. M. Wilkinson, and M. B. Garnick, *J. Liq. Chromatogr.*, **1**, 795 (1978).

(3) S. D. Averbuch, T. T. Finkelstein, S. E. Fandrich, and S. D. Reich, *J. Pharm. Sci.*, **70**, 265 (1981).

Supported by Grant IN-129 from the American Cancer Society.

# Effect of Surfactant on Tetracycline Absorption across Everted Rat Intestine

**LOYD V. ALLEN, Jr. *x, R. S. LEVINSON ‡, CASEY ROBINSON *, and ANDREW LAU ***

Received January 28, 1980, from the **College of Pharmacy, Health Sciences Center, University of Oklahoma, Oklahoma City, OK 73190,* and the ‡*Arnold & Marie Schwartz College of Pharmacy, Long Island University, Brooklyn, NY 11201.* Accepted for publication August 18, 1980.

**Abstract** □ Absorption of tetracycline hydrochloride (500 μg/ml) from oxygenated modified Krebs buffer in randomized everted rat jejunal segments was determined alone and in the presence of calcium, polysorbate 80, and calcium plus polysorbate 80. Surfactant increased absorption of tetracycline in the presence and absence of calcium, with 0.01% (w/v) polysorbate 80 increasing transfer to the greatest extent of the concentrations examined (0.005, 0.01, 0.05, 0.1, and 1%); tetracycline hydrochloride + 12.5 m*M* $CaCl_2$, 143 ± 45 μg/ml; tetracycline hydrochloride + polysorbate 80, 389 ± 18 μg/ml; tetracycline hydrochloride + 12.5 m*M* $CaCl_2$ + polysorbate 80, 255 ± 31 μg/ml. On the premise that the effective surfactant concentration is similar to the critical micelle concentration, an absorption mechanism based on micellar solubilization is postulated.

**Keyphrases** □ Tetracycline—absorption, effect of polysorbate 80, everted rat intestine □ Polysorbate 80—effect on tetracycline absorption across everted rat intestine □ Surfactants—effect of polysorbate 80 on tetracycline absorption across everted rat intestine

Tetracycline is a widely used antibiotic. Its serum level should not fall below the minimum inhibitory concentration (MIC), usually between 0.1 and 1.5 μg/ml, for most bacterial strains. Occasionally, this concentration is difficult to maintain due to decreased absorption caused by other drugs or divalent and trivalent cations present in the GI tract (1–3). The intestinal absorption of most tetracyclines is rapid but incomplete, and the absorption mechanism is poorly understood (4, 5).

Physicochemical interactions in the gut are not uncommon and, at least pharmacokinetically, seem to be the most important form of interaction affecting the absorption of tetracycline derivatives. Chelation of tetracycline with polyvalent cations, which has been well documented, is the most common reaction that decreases tetracycline absorption. In addition to forming direct tetracycline–metal complexes, tetracycline binds to both nucleic acids and proteins, with the binding mediated by divalent cations such as zinc, calcium, and magnesium.

Recently, the role of endogenous and exogenous surfactants in drug absorption experiments was explored (6, 7). In some instances, the addition of surfactants enhanced drug absorption (8).

Since decreased tetracycline absorption presents a clinical problem, often requiring alteration of food and medications, a method of optimizing tetracycline absorption to avoid the present restrictions would be valuable. Surfactants may enhance tetracycline absorption to an acceptable level, even in the presence of divalent ions; if so, they may prove to be a valuable additive to oral dosage forms.

This investigation determined the effects of surfactants on tetracycline absorption from the rat everted gut sac to obtain information on the enhancement of tetracycline transport and the tetracycline transport mechanism.

## EXPERIMENTAL

**Intestine Preparation**—An everted intestinal sac technique (9, 10) was used. The solution on the inside of the sac is referred to as the serosal solution, and the solution in which it is incubated is called the mucosal solution.

Seven male white Holtzman rats, 175–200 g, were fasted overnight (20–24 hr), but water was not withheld prior to the experiment. The animals were anesthetized with ether and then killed by stunning and cervical fracture. The jejunum was removed and rinsed immediately with several portions of cold normal saline and everted on a thin glass rod. After eversion, the jejunum was washed in cold normal saline and cut into seven segments of 5-cm length. Segments of the rat intestine were selected randomly for the different treatment groups.

Sacs of everted intestine were prepared by tying one end tightly and the other end loosely with fine thread. Then 0.5 ml of buffer was introduced inside the sac with a 1-ml syringe fitted with a blunt needle. The loose ligature was tightened, and the buffer-filled sacs then were transferred immediately to 25-ml erlenmeyer flasks containing 15 ml of buffer mixed with tetracycline hydrochloride[1], 0.5 g/liter with or without the additives. Control sacs were placed in buffer alone. The other five sacs were incubated in buffer to which 0.005, 0.01, 0.05, 0.1, or 1% (w/v) pol-

[1] Lot 6 X090-71000, Pfizer Laboratories, New York, N.Y.

0022-3549/81/0300-0269$01.00/0
© 1981, American Pharmaceutical Association

**Table I—Effect of Different Polysorbate 80 Concentrations on Tetracycline Absorption across Everted Rat Gut Sac**

| Treatment | Tetracycline Absorbed, μg/ml |
|---|---|
| Tetracycline | 241 ± 25[a] |
| Tetracycline + 0.005% (w/v) polysorbate 80 | 283 ± 19 |
| Tetracycline + 0.01% (w/v) polysorbate 80 | 345 ± 23 |
| Tetracycline + 0.05% (w/v) polysorbate 80 | 333 ± 14 |
| Tetracycline + 0.1% (w/v) polysorbate 80 | 315 ± 25 |
| Tetracycline + 1% (w/v) polysorbate 80 | 283 ± 28 |

[a] Mean ± *SE*.

**Table II—Effect of Calcium Chloride on Inhibition of Tetracycline Transfer in Everted Rat Gut Sac**

| Treatment | Tetracycline Transferred, μg/ml |
|---|---|
| Tetracycline | 251 ± 25[a] |
| Tetracycline + 12.5 m*M* $CaCl_2$ | 143 ± 45 |
| Tetracycline + polysorbate 80 | 389 ± 18 |
| Tetracycline + 12.5 m*M* $CaCl_2$ + polysorbate 80 | 255 ± 31 |

[a] Mean ± *SE*.

ysorbate 80[2] had been added. The solutions were gassed with oxygen, and the flasks were stoppered, transferred into a shaker-incubator[3], and incubated at 37° for 1 hr. They were taken out and opened, and the contents were placed into tubes for later tetracycline determination. The mucosal solution pH never rose above 7.7.

The buffer was pH 7.4 modified Krebs bicarbonate buffer free of calcium and magnesium as described by Mayersohn and Gibaldi (11). It contained, in millimolar concentrations: NaCl, 122; KCl, 5; $KH_2PO_4$, 1; and $NaHCO_3$, 26. The mucosal and serosal solutions were identical except for the presence of drug and surfactant in the mucosal solution.

Two kinds of experiments were done. In one, tetracycline absorption in the presence of calcium and surfactant was studied; the other involved the kinetics of surfactant effects on the passive transfer of tetracycline across the everted rat intestine. In the first, the mucosal solutions, except in one control experiment, contained 0.5 mg of tetracycline/ml. The solutions to which five sacs per rat were exposed were: (*a*) tetracycline alone; (*b*) tetracycline with calcium chloride, 12.5 m*M*; (*c*) tetracycline with surfactant, 0.01% (w/v) polysorbate 80; (*d*) tetracycline with both calcium chloride and polysorbate 80; and (*e*) control, containing only buffer.

**Fluorometric Assays**—The fluorometric assays were performed by a modification of the method of Hall (12). To the contents of each sac, 0.5 ml of 0.1 *M* HCl was added and mixed thoroughly. Then 0.5 ml of 0.75 *M* aluminum chloride[4] was added, and the tubes again were mixed thoroughly by shaking. After incubating for 15 min at room temperature, fluorescence was measured in a spectrophotofluorometer[5] at 400-nm excitation and 465-nm emission. A fluorescence standard curve was obtained by plotting fluorescence intensity against calibrator concentrations and computing the line of best fit by least-squares regression analysis ($y = 750x + 45$, $r = 0.99$). Means and standard errors of each group were determined in each experiment. Lines of best fit and correlation coefficients were determined, and the differences in transfer were compared by the Student *t* test (using *t* independent with one-tail comparisons).

The second group of experiments were carried out as follows. Eight gut sacs were prepared from each rat intestine. Twelve rats were divided into two groups of six rats each. One group had only 0.5 mg of tetracycline/ml in the mucosal solution. The other group had 0.01% (w/v) polysorbate 80 in addition to tetracycline. Sacs then were incubated in the shaker-bath for preassigned times. At 5, 10, 20, 30, 40, 50, and 60 min, one sac was removed from the shaker bath for fluorometric assay to determine the amount of tetracycline transferred during each period.

The reciprocal of tetracycline concentration and the log of tetracycline concentration were plotted against time to determine whether the absorption followed first- or second-order kinetics.

[2] Lot 11-78297, Tween 80, Sargent-Welch Scientific Co., Skokie, Ill.
[3] Shaker-bath model 50, GLA Precision Scientific Co., Chicago, Ill.
[4] Lot 45,572, J. T. Baker Chemical Co., Phillipsburg, N.J.
[5] Aminco-Bowman, American Instrument Co., Silver Spring, Md.

## RESULTS

**Effect of Different Polysorbate 80 Concentrations on Tetracycline Absorption across Everted Rat Gut Sac**—In the presence of polysorbate 80, tetracycline movement across the intestine increased ~20–40% (Table I). The intestinal transfer rate of tetracycline increased inversely with the concentration of polysorbate 80 added. The surfactant concentration that enhanced tetracycline absorption the most across the intestine appeared to be 0.01%. A 55% increase ($p < 0.05$) in transport was observed when compared with tetracycline alone in the incubation medium after 60 min (Table II). Each difference was significantly different from tetracycline alone ($p < 0.05$) except for the 1% (w/v) concentration.

**Tetracycline Transfer across Everted Rat Gut Sac in Presence of Calcium and Surfactant**—Calcium chloride decreased tetracycline transfer across the intestine by 43.0% ($p < 0.05$) in the absence of surfactant and by 34.4% ($p < 0.05$) in the presence of surfactant. With calcium reducing the intestinal transfer of tetracycline and surfactant enhancing it, tetracycline transferred in the presence of both calcium and surfactant together was approximately normal (Table II).

**Effect of Polysorbate 80 on Tetracycline Transfer across Everted Rat Intestine**—Two kinetic studies were conducted on the data obtained on the effects of polysorbate 80 on tetracycline absorption across rat everted gut sacs. In the first, the data were plotted as a first-order reaction. In this experiment, the time for peak absorption was 60 min (Fig. 1), with further prolongation of incubation resulting in decreased absorption. Therefore, 60 min was selected as the maximal time plotted. Results of this plot correlated well with theoretical requirements of a first-order process (Fig. 1). A straight line was obtained, and computation of the correlation coefficient of the line by linear regression gave an *r* value of 0.975.

To determine goodness-of-linear-fit for second-order kinetics, the same data on tetracycline absorption were tested as a second-order kinetic process, resulting in a correlation coefficient of 0.487; thus, the goodness-of-linear-fit for a second-order process was poor.

## DISCUSSION

The mechanism of intestinal tetracycline absorption has yet to be elucidated. The results of Pindell *et al.* (4) suggested that tetracycline is absorbed by passive diffusion. However, Levine *et al.* (5) observed that tetracycline absorption might not occur by passive diffusion alone.

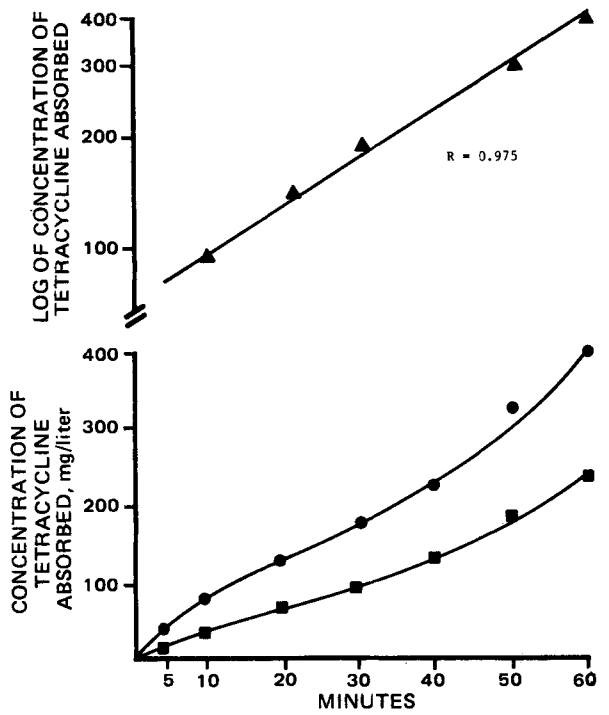


**Figure 1**—*Effect of 0.01% (w/v) polysorbate 80 on tetracycline absorption across the everted gut sac. Key:* ■, *tetracycline alone;* ●, *tetracycline with polysorbate 80 (0.01% w/v); and* ▲, *tetracycline with polysorbate 80 (0.01% w/v).*

Banerjee and Chakrabarti (10) suggested that the mechanism was not active transport or simple passive diffusion. They postulated that tetracycline was absorbed as its zwitterion and shared a common route with glucosamine. Glucosamine has been shown to be carrier mediated *via* facilitated passive diffusion.

Tetracycline exists mainly as the charged species over the entire pH range of the alimentary tract. Perrin and Vallner (13) stated that tetracycline is therapeutically active when given orally and, therefore, must be absorbed as a charged species. These investigators showed that tetracycline and its derivatives can be absorbed from the rat stomach as the protonated species apparently by passive diffusion. In their studies, the absorption was linked to the surface activity of tetracycline rather than to its lipid solubility. The greater the surface activity of the tetracycline derivative, the higher was the absorption rate.

In the present study, to determine further the mechanism of intestinal tetracycline absorption, dextrose was excluded from the incubation medium to eliminate or reduce greatly any active transport processes. Since absorption took place regardless of this energy source deficiency, tetracycline was transferred across the intestine by methods other than active transport.

Intestinal tetracycline absorption, when polysorbate 80 was added to the medium, was enhanced at every polysorbate 80 concentration except at 1%, with 0.01% causing optimum absorption. This low concentration approximates the critical micelle concentration (CMC) of polysorbate 80 in physiological fluids, and this finding suggests an influence of micelle formation on tetracycline absorption. The CMC for polysorbate 80 solutions was reported for distilled water (14) as $0.6 \times 10^{-4}$ *M*. Further evidence of micelle-mediated absorption can be seen as a surface tension decrease during micelle formation and as an interfacial absorption increase. Above the CMC, surface tension remains relatively constant; therefore, less enhancement of tetracycline absorption at the higher polysorbate 80 concentrations tends to indicate the necessity of micelles for absorption. This postulation is in agreement with Perrin and Vallner's (13) surface activity absorption relationship and further substantiates the previous suggestion that tetracycline absorption is passive.

The enhancing effect by polysorbate 80 on tetracycline absorption may be due to the increase in drug solubility and the low viscosity in the medium. Both could be the end results of micelle formation in the medium. Said *et al.* (8) noted that the increased solubility and absorption of griseofulvin was achieved in aqueous solution by surfactant addition. Shozo *et al.* (15) found that tetracycline was better absorbed from low viscosity than from high viscosity media.

In these studies, pH probably had little effect on absorption since pH was controlled closely. The initial pH was 7.4; at the end of the experiments, it did not exceed 7.7. Tetracycline has three pKa values (16). The amount of the unionized species at pH 7.4 is $8 \times 10^{-5}$ *M* for the group with a pKa of 3.3, $5.6 \times 10^{-7}$ *M* for the group with a pKa of 7.7, and $3.5 \times 10^{-5}$ *M* for the group with a pKa of 9.7, assuming a 1 *M* solution of total tetracycline. The ratio of the completely unionized molecules to the ionized molecules was $5.72 \times 10^{-7}$. It is unlikely that this small number of molecules could contribute much to the intestinal tetracycline transfer. Therefore, solubilization of the ionized form seems to be involved in the enhanced absorption.

It is also unlikely that the differences in the media pH contributed to differences in absorption. One reason is that the pH changes were random and could not have influenced absorption in a single direction. Another reason is that the ratio of molecules existing in the unionized forms in either case seems to be negligibly small (at pH of 7.4, $2.2 \times 10$; at pH of 7.7, $1.8 \times 10$). Thus, pH should have little effect on absorption. *In vivo*, however, the effects of pH changes may be more important.

The addition of polysorbate 80 probably does not alter any chelation between tetracycline and calcium because chelation is a direct drug–metal reaction (17). The lower tier of the tetracycline molecule contains binding sites that chelate readily with calcium to form six-membered rings. Although calcium reduced intestinal tetracycline transfer in the presence of surfactant, tetracycline was transferred in the presence of both calcium and surfactant. This result may have been due to increased tetracycline solubility, which made more drug available for absorption despite the fact that some drug had become less available due to chelation with calcium.

To reconfirm and elucidate the fact that polysorbate 80 exerts an effect on tetracycline that is absorbed, the absorption data were treated as first- and second-order reactions. A straight line was obtained on only the first-order reaction plot.

Hence, although from the previous discussion one would think that the micelle is intimately involved in tetracycline transfer across everted gut, the micelle apparently does not act as a kinetic partner with tetracycline. If it did, a second-order kinetic plot would be linear. The linearity of the first-order plot indicated a monomolecular passive transfer that is dependent only on a single species: tetracycline. This result is possible if tetracycline is picked up into the micelle and diffused out of the micelle in a purely physical fashion. The micelle then could act as a corridor for tetracycline diffusion.

## REFERENCES


(1) G. Gothoni, P. J. Neuvonen, M. Mattila, and R. Hackman, *Acta Med. Scand.*, **191**, 409 (1972).

(2) J. M. Jaffe, J. L. Colaizzi, R. I. Poust, and R. H. McDonald, Jr., *J. Pharmacokinet. Biopharm.*, **1**, 267 (1973).

(3) P. J. Neuvonen and O. Penttila, *Eur. J. Clin. Pharmacol.*, **7**, 361 (1974).

(4) M. Pindell, K. M. Cull, K. M. Doran, and H. L. Dickison, *J. Pharmacol. Exp. Ther.*, **125**, 287 (1959).

(5) R. Levine, D. Waitzona, and C. Squires, "Topics in Medicinal Chemistry," vol. 4, Wiley, New York, N.Y., 1971, p. 41.

(6) K. J. Humphrey, G. Richardson, and C. T. Rhodes, *J. Pharm. Pharmacol.*, **20**, 45 (1968).

(7) B. Cox, J. H. Collett, and R. Withington, *ibid.*, **26**, 34 (1974).

(8) S. Said, H. Mahrous, and A. Kassem, *Infection*, **4**, 49 (1976).

(9) T. Wilson and G. Wiseman, *J. Physiol.*, **23**, 116 (1954).

(10) S. Banerjee and K. Chakrabarti, *J. Pharm. Pharmacol.*, **28**, 133 (1976).

(11) M. Mayersohn and M. Gibaldi, *J. Pharm. Sci.*, **60**, 225 (1971).

(12) D. Hall, *J. Pharm. Pharmacol.*, **28**, 420 (1976).

(13) J. Perrin and J. Vallner, *ibid.*, **22**, 758 (1970).

(14) J. M. N. Gillan and A. T. Florence, *ibid., Suppl.*, **25**, 137P (1973).

(15) M. Shozo, E. Hitomi, N. Tanekazu, and A. Takaichi, *Chem. Pharm. Bull.*, **25**, 1186 (1977).

(16) J. Colaizzi and P. Klink, *J. Pharm. Sci.*, **58**, 1184 (1969).

(17) P. J. Neuvonen, *Drug*, **11**, 45 (1976).

# Stability of *N*-Formimidoylthienamycin in Aqueous Solution

**GEORGE B. SMITH ˣ and ERWIN F. SCHOENEWALDT**

Received March 25, 1980, from *Merck Sharp & Dohme Research Laboratories, Rahway, NJ 07065.* Accepted for publication August 26, 1980.

**Abstract** □ The stability of *N*-formimidoylthienamycin in aqueous solution at 25 and 40° was determined. In pH 5–8 nonnucleophilic inert buffers, pseudo-first-order ring opening was observed with dilute solutions (1 or 2 mg/ml initially). At higher initial concentrations, a second-order reaction also was evident. The rate data were compared with literature data for various cephalosporins and penicillins.

**Keyphrases** □ *N*-Formimidoylthienamycin—stability in aqueous solution at 25 and 40° □ Stability—*N*-formimidoylthienamycin in aqueous solution, reaction kinetics, compared to other β-lactam antibiotics □ Kinetics—stability of *N*-formimidoylthienamycin in aqueous solution □ β-Lactam antibiotics—stability of *N*-formimidoylthienamycin in aqueous solution

Thienamycin (I) is a new β-lactam antibiotic, discovered in culture broths of *Streptomyces* MA4297 (1). Although a detailed kinetic study of thienamycin has not been made, it is known to decompose in dilute aqueous solution by apparent first-order reaction and has its greatest stability at neutral pH. However, the decomposition accelerates as the antibiotic concentration is increased (1). This behavior is believed to be due to aminolysis of the β-lactam by the primary amine of a second thienamycin molecule. Analogous reactions of 6-aminopenicillanic acid (2) and ampicillin (3) have been reported. *N*-Formimidoylthienamycin (II) was designed to mitigate this bimolecular reaction (4).

The present study determined the stability of II in aqueous solution; the results are related to data for other β-lactam antibiotics.

## EXPERIMENTAL

**Materials**—2-(*N*-Morpholino)ethanesulfonic acid[1], 3-(*N*-morpholino)propanesulfonic acid[1], monobasic potassium phosphate[2], and 50% sodium hydroxide solution[3] were used for buffers.

The $^{13}C$-NMR, PMR, and IR spectra were consistent with the structure of II monohydrate (4).

*Anal.*—Calc. for $C_{12}H_{17}N_3O_4S \cdot H_2O$: C, 45.41; H, 6.04; N, 13.25; S, 10.08. Found: C, 45.11; H, 6.14; N, 13.09; S, 10.07.

**TLC**—Aged aqueous solutions of II were examined by TLC as follows. Solution aliquots containing ~50 μg of solute were loaded onto 250-μm silica gel GF[4] plates. The plates were developed in a saturated chamber with toluene–acetone–*n*-butanol–acetic acid–water (1:1:1:1:1) and were viewed under short- and long-wavelength UV lights.

**Kinetic Runs**—Aqueous buffer solutions of monobasic potassium phosphate, 2-(*N*-morpholino)ethanesulfonic acid (pKa 6.15), and 3-(*N*-morpholino)propanesulfonic acid (pKa 7.2) were adjusted to the desired pH with concentrated aqueous sodium hydroxide. These buffers, to be used as solvents for kinetic runs, were prepared at the reaction temperatures.

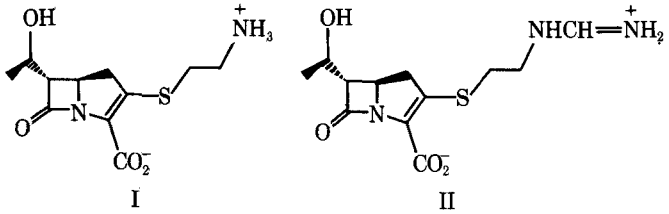

I



II

Compound II was weighed into 3-ml glass reaction vials equipped with open-top screw caps and silicone septa. Each reaction vial contained 1–30 mg of II and 1 ml of buffer. Nitrogen containing <10 ppm of oxygen was used to protect the reaction solutions from air.

Each kinetic run was initiated by adding nitrogen-purged buffer to the screw-capped vial. The vial was closed immediately and purged with a subsurface nitrogen stream injected through the septum with a 25-gauge syringe needle. A second needle through the septum served as the vent. The vials were stored in constant-temperature water baths.

Aliquots (100 μl) of the reaction solutions were removed periodically with a microsyringe equipped with a 25-gauge needle. The reaction vials were purged with nitrogen while aliquots were removed. The aliquots were diluted quantitatively to UV concentration, 0.2 μmole of II/ml initially, with 0.1 *M*, pH 7, 3-(*N*-morpholino)propanesulfonic acid, which had been purged with nitrogen; the UV spectra then were recorded[5]. Then 0.1 ml of 0.2 *M* aqueous hydroxylamine hydrochloride[2] was mixed with 3 ml of each diluted aliquot (hydroxylamine concentration of 6.5 μmoles/ml). The UV spectra were recorded again after the hydroxylamine mixtures had aged for 20 min at room temperature. (Hydroxylamine hydrochloride was used for all kinetic runs except the preliminary runs with phosphate buffer.)

## RESULTS AND DISCUSSION

**Reaction of II and Phosphate**—In preliminary runs with pH 7.2 phosphate buffer, a complex reaction was evident by direct UV assay of the solutions exposed to air. After a weakening of the II spectrum initially (absorbance maximum at 297 nm), a consecutive reaction was apparent with the appearance of absorbance peaks at 308 and 270 nm, and the reaction solutions turned brown. The consecutive reaction was due to oxygen. With air excluded, the solutions remained nearly colorless, and pseudo-first-order behavior was observed. The UV spectra of II and its product with oxygen excluded are shown in Fig. 1 as curves A and B, respectively.

Curve B was observable only if the reaction mixture had been purged with nitrogen initially and during aliquot removal and only if the buffer used for dilution had been purged with nitrogen. Then the entire absorbance curve could be recorded twice (about 10 min) before the peaks at 308 and 270 nm appeared as the result of exposing the cell to room air.

The results of four runs with pH 7.2 phosphate buffer at 23° are shown in Fig. 2. The percent of the initial II unreacted, measured at 300 nm, is plotted on the logarithmic scale *versus* reaction time. The reaction was first order with respect to II, as shown by the linear log plots for the runs under nitrogen. Furthermore, the half-life was unchanged when the initial II concentration was halved from 6 to 3 m*M*. When the phosphate concentration was reduced from 1 to 0.5 *M*, the half-life doubled. This result means that II hydrolysis was catalyzed by phosphate and that essentially all of the reaction observed in these runs was due to phosphate. The apparent initial rate for the run unprotected from air was about the same as that for the runs under nitrogen. However, the final spectrum used to calculate the rate could be obtained only when air was excluded.

**Analytical Methods**—After the runs with phosphate buffer, kinetic data for unreacted II were obtained by hydroxylamine UV assay. When diluted aliquots of hydrolysis mixtures were treated with hydroxylamine, ~90% of the II absorbance was extinguished, but the absorbances of the hydrolysis products obtained in the presence or absence of oxygen were unaffected. The loss of absorbance at 300 nm, measured on treatment

[1] Calbiochem.
[2] Merck.
[3] Baker.
[4] Analtech.
[5] Cary model 14, Varian Associates.



0022-3549/81/0300-0272$01.00/0
© 1981, American Pharmaceutical Association

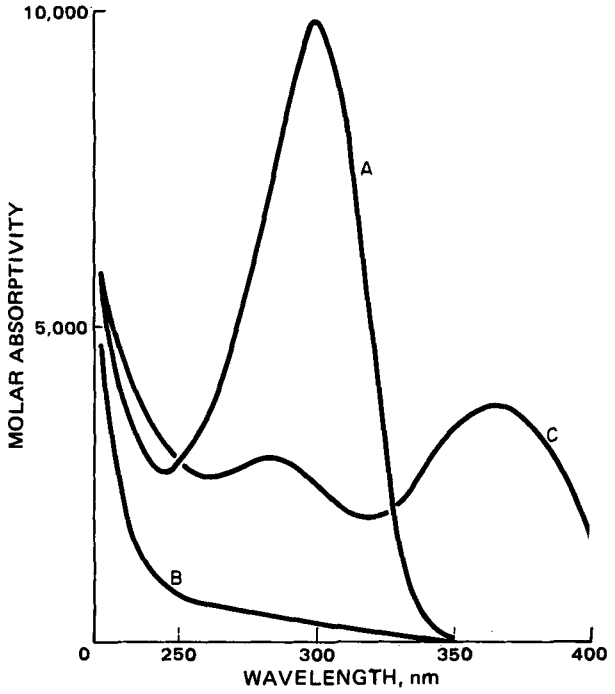


**Figure 1**—*UV spectra measured with 0.1* M, *pH 7, 3-(*N*-morpholino)-propanesulfonic acid buffer as the UV solvent. Key: A, II; B, decomposition product formed in pH 7.2 phosphate buffer protected from air; and C, decomposition product formed in pH 5 or 6 2-(*N*-morpholino)-ethanesulfonic acid buffer.*

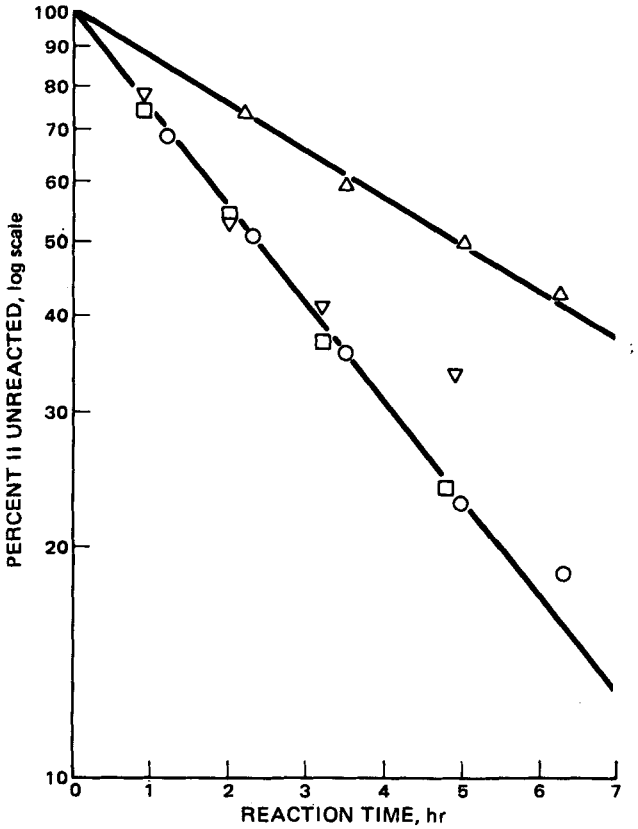


**Figure 2**—*Stability of II in pH 7.2 phosphate buffer at 23°. Key:* ○, *6 mM substrate in 1.00* M *buffer under nitrogen;* △, *6 mM substrate in 0.50* M *buffer under nitrogen;* □, *3 mM substrate in 1.00* M *buffer under nitrogen; and* ▽, *6 mM substrate in 1.00* M *buffer unprotected from air.*

with hydroxylamine, was proportional to the concentration of unreacted β-lactam.

Although the hydroxylamine UV assay for II was adequate and did not require oxygen exclusion, all kinetic runs were performed with oxygen excluded so that the direct UV assay data could be used. In every run, the transition from the initial spectrum of II to that of the product appeared as a simple one-step reaction, although the product UV spectra, always measured at pH 7, varied depending on the reaction pH (discussion to follow). Although not completely stable by UV assay, the products were more stable than the starting material, and the reaction rates were calculated readily from the crude UV data. Good agreement of the rate data obtained by the two UV methods was observed.

**Reaction Products**—The UV assays provided measurements of the concentration of II during reaction but did not characterize the products. Brief studies by Fourier transform IR spectroscopy (FTIR) and TLC revealed that hydrolysis of II led to complex product mixtures.

Opening of the β-lactam ring was observed by FTIR of unbuffered aqueous II, 5 mg/ml. The disappearance of the β-lactam band at 1774 $cm^{-1}$ was not accompanied by appearance of any distinct features in the spectrum.

Decomposition of an aqueous solution of II (5 mg/ml), adjusted to pH 4 with trifluoroacetic acid, was monitored by TLC. This procedure was done at pH 4 because the consecutive reaction with oxygen at higher pH, evident by UV assay, did not occur at pH 4. Even so, several degradates were apparent in short-wavelength UV light by fluorescence quenching and in long-wavelength UV light by fluorescence. Therefore, the slow, rate-determining opening of the β-lactam ring in the absence of oxygen, for which the kinetics are described later, preceded the relatively rapid formation of many unidentified degradates.

**Table I—Apparent First-Order Rates in Nonnucleophilic Buffers**

| Buffer pH | $k_{pH}$, $hr^{-1}$, at 25° | | $k_{pH}$, $hr^{-1}$, at 40° | |
|---|---|---|---|---|
| | Observed | Calculated | Observed | Calculated |
| 5.0[a] | 0.0315 | 0.0318 | 0.111 | 0.113 |
| 5.5[a] | 0.0139 | 0.0128 | 0.0533 | 0.0465 |
| 6.0[a] | 0.0069 | 0.0069 | 0.0257 | 0.0257 |
| 6.5[a] | 0.0048 | 0.0050 | 0.0169 | 0.0197 |
| 6.5[b] | 0.0048 | 0.0050 | 0.0169 | 0.0197 |
| 7.0[b] | 0.0040 | 0.0047 | 0.0169 | 0.0197 |
| 7.5[b] | 0.0055 | 0.0054 | 0.0262 | 0.0255 |
| 8.0[b] | 0.0083 | 0.0082 | 0.0462 | 0.0461 |

[a] 2-(*N*-Morpholino)ethanesulfonic acid. [b] 3-(*N*-Morpholino)propanesulfonic acid.

**Rate–pH Profiles for II at Low Concentration**—Kinetic runs with nonnucleophilic 2-(*N*-morpholino)ethanesulfonic acid at pH 5.0, 5.5, 6.0, and 6.5 and 3-(*N*-morpholino)propanesulfonic acid at pH 6.5, 7.0, 7.5, and 8.0 were performed at 25 and 40°. Each buffer was used at 0.5 and 1.0 *M* with an initial II concentration of 3 or 6 m*M*, *i.e.*, 1 or 2 mg/ml. Kinetic data for these runs were accumulated over 1 week since the reaction mixtures had half-lives of several days. Then the reaction mixtures were stored at 60° to hasten completion of the reactions, and the final UV spectra were recorded at pH 7. (The products were quite stable by UV assay.)

The final UV spectra for runs at 40° were about the same as those for runs at 25° at the corresponding pH values. The final UV spectrum with the pH 8 buffer was the same as that observed with pH 7.2 phosphate buffer (Fig. 1, curve B). The product formed at pH 8, like that formed in pH 7.2 phosphate, gave absorbance peaks at 308 and 270 nm upon exposure to air. The final UV spectra for runs with buffers at pH 5–6 denoted a different product (Fig. 1, curve C). An isosbestic point at 328 nm was observed. By UV assay, the product formed in pH 5–6 buffers, unlike the pH 8 product, was stable to air at pH 5 or 7, with or without added phosphate. The final spectra for reactions at pH 6–8 were intermediate between curves B and C of Fig. 1.

At low initial II concentration, pseudo-first-order decomposition was observed. Plots of log (percent of II unreacted) *versus* time were linear, similar to the runs under nitrogen shown in Fig. 2; at each pH, the apparent rate constant was measurably the same with initial II concentrations of 1 and 2 mg/ml. The reaction rates were independent of the nonnucleophilic buffer concentrations; *i.e.*, at each pH, the reaction rate was about the same in 0.5 or 1.0 *M* buffer. Thus, the rate effect of ionic strength was insignificant. Moreover, the rates with 2-(*N*-morpholino)-ethanesulfonic acid and 3-(*N*-morpholino)propanesulfonic acid at pH 6.5 were about the same.

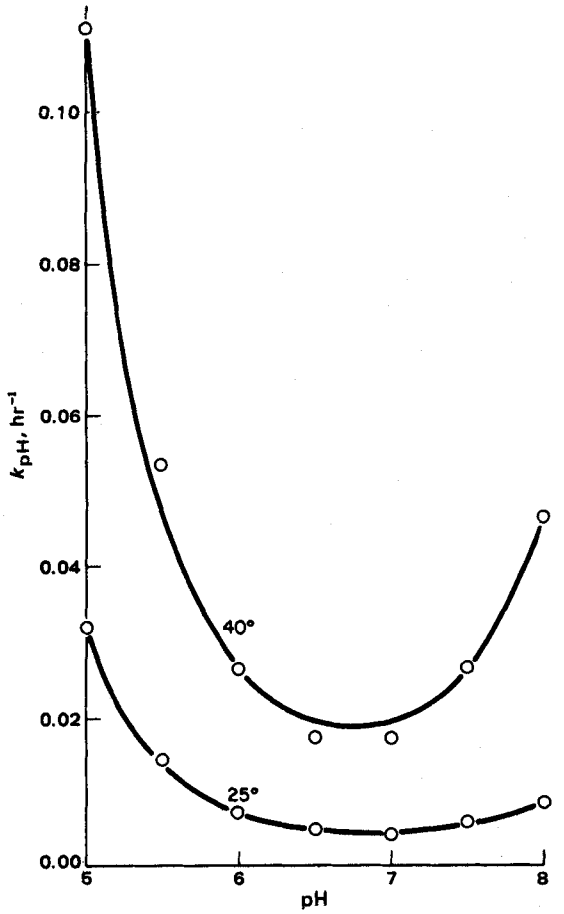


**Figure 3**—*The pH profiles of pseudo-first-order rate constants: data points (○) and least-squares curves calculated according to Eq. 1 (—).*

The apparent pseudo-first-order rate constants observed at 25 and 40° are listed in Table I. At each temperature, II was most stable at neutral pH, *i.e.*, pH ~ 7.0 at 25° and pH ~ 6.75 at 40° [$K_W = 10^{-14.00}$ at 25° and $K_W = 10^{-13.53}$ at 40° (5)]. The rate–pH profiles were consistent with:

$$k_{pH} = k_H a_H + k_0 + k_{OH}(K_W/a_H) \qquad \text{(Eq. 1)}$$

where $k_{pH}$ is the apparent first-order rate constant at a given pH; $k_H$ and $k_{OH}$ are the second-order rate constants for the hydrogen-ion-catalyzed degradation and hydroxide-ion-catalyzed degradation, respectively; $k_0$ is the first-order rate constant for spontaneous or water-catalyzed degradation; $K_W$ is the dissociation constant of water; and $a_H$ is the hydrogen-ion activity as measured by the glass electrode. The least-squares reactivities for each reaction at the two temperatures were determined, according to Eq. 1, by nonlinear regression. The calculated pseudo-first-order rate constants, $k_{pH}$, were in good agreement with the observed values (Table I). The observed $k_{pH}$ data points are shown in Fig. 3 with the calculated $k_{pH}$ curves. The least-squares reactivities of hydrogen ion, water, and hydroxide ion and the Arrhenius activation energies are listed in Table II.

**Stability of II at High Concentration**—Slow pseudo-first-order reaction of II in the nonnucleophilic, inert buffers had been observed at initial II concentrations of 1 and 2 mg/ml. Any competitive second-order reaction of II must have been very slow relative to the first-order reaction. Therefore, to detect any second-order reaction, the initial II concentration was varied under conditions at which the pseudo-first-order reaction was minimal, pH 7.0 at 25° and pH 6.75 at 40°.

**Table II—Calculated Reactivities and Activation Energies in Nonnucleophilic Buffers**

| Parameter | $k_H$, $M^{-1}$ hr$^{-1}$ | $k_0$, hr$^{-1}$ | $k_{OH}$, $M^{-1}$ hr$^{-1}$ |
|---|---|---|---|
| Least-squares reactivity at 40° | 9730 | 0.01565 | 10,300 |
| Least-squares reactivity at 25° | 2780 | 0.00403 | 4,150 |
| $E_a$, kcal/mole | 15.5 | 16.8 | 11.2 |

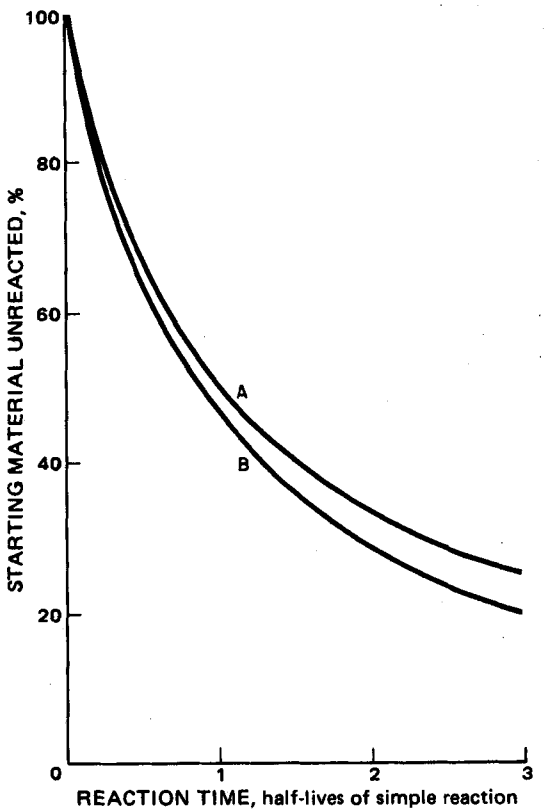


**Figure 4**—*Calculated time course of second-order reactions. Key: A, simple second-order reaction; and B, second-order reaction involving oligomers.*

At each temperature, a series of kinetic runs was performed with initial II concentrations of 1.8, 3, 6, 15, and 30 mg/ml (0.006, 0.01, 0.02, 0.05, and 0.1 *M*, respectively) in 1 *M* 3-(*N*-morpholino)propanesulfonic acid. In each series, the decomposition rates, as shown by plots of percent II unreacted *versus* reaction time, were progressively more rapid at higher initial concentration. Furthermore, the product UV spectra, measured at pH 7, included progressively more high wavelength absorbance (peak wavelength at ~365 nm, which is similar to that observed with low initial II concentrations at pH 5–6) for runs at higher initial concentration. This trend of product compositions was not due to pH shifts. The pH of all reaction solutions remained the same as the pH of the buffer used.

Thus, competitive first- and second-order reactions of II were observed. The second-order reaction was treated as dimerization in that the second-order rate was evaluated according to:

$$-dA/dt = k_{pH}A + k_2A^2 \qquad \text{(Eq. 2)}$$

where $A$ represents the II concentration. The reaction product, however, was not identified.

The assumed dimerization of II is complex in that oligomers higher than a dimer can form. Presumably, this reaction involves attack by the amidine group of one II molecule on the β-lactam group of another. Since the resulting dimer has one amidine group and one β-lactam group, it could react further; a trimer, tetramer, *etc.*, could form. However, solvent attack on the β-lactams of these oligomers would hinder their propagation.

Results of kinetic studies of condensation polymerization reactions show that the chemical reactivity of a functional group usually does not depend on the size of the molecule to which it is attached (6). At any stage of polymerization, the reactivity of every like functional group is the same. Furthermore, the rate constant for a given reaction step usually remains constant throughout polymerization. Consequently, polymerization can be regarded as a reaction between functional groups, of constant reactivity, without differentiation in regard to molecular size.

Accordingly, a second-order oligomerization was simulated in which all products had the reactivity of the monomeric starting material toward each other and toward unreacted monomer. The concentration dependence of the starting material on reaction time is shown in Fig. 4 with the

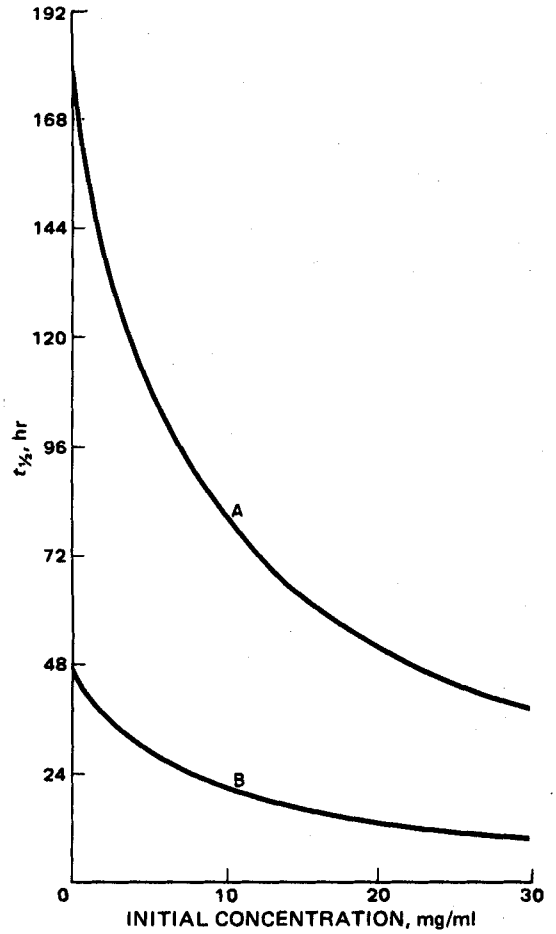


**Figure 5**—*Half-life at neutral pH* versus *initial II concentration. Key: A, reactions at 25° and pH 7.00; and B, reactions at 40° and pH 6.75.*

corresponding curve for a simple second-order dimerization.

The initial reaction rates are equal since only monomer initially is present in both reactions. The calculated effect of oligomers on the monomer is slight. For example, 53% of the monomer reacts in the complex reaction in the same time that 50% reacts in the simple reaction. Therefore, Eq. 2 is a good approximation.

The change of variable $y = 1/A$ reduces Eq. 2 to linear form:

$$dy - k_{pH}y\,dt = k_2\,dt \qquad \text{(Eq. 3)}$$

The integrating factor $e^{-k_{pH}t}$ affords integration to (7):

$$\left(\frac{1}{A} + \frac{k_2}{k_{pH}}\right) e^{-k_{pH}t} = \left(\frac{1}{A_0} + \frac{k_2}{k_{pH}}\right) \qquad \text{(Eq. 4)}$$

where $A$ represents the II concentration and $A_0$ represents the initial concentration.

For each series of runs in which the initial II concentration was varied, the pseudo-first-order rate constant value, $k_{pH}$ (observed at low initial concentration), was substituted in Eq. 4. Then the second-order rate constant value, $k_2$, was adjusted to fit the UV assay data.

The dimer, the first oligomerization product, predominated among the oligomers for several half-lives of the monomer in the simulated oligomerization with all rate constants being equal. As already mentioned, when two monomers react, one of the two β-lactams remains intact. Consequently, the rate measured by UV assay should be very nearly one-half of the actual rate. Therefore, the $k_2$ value was calculated as twice the value corresponding to the UV data.

The $k_2$ values so calculated were 0.2 $M^{-1}$ hr$^{-1}$ at pH 7.0 and 25° and 0.8 $M^{-1}$ hr$^{-1}$ at pH 6.75 and 40°. The corresponding Arrhenius activation energy was about 17 kcal/mole. The effect of the second-order reaction on II stability is shown by the plots of half-life *versus* initial concentration (Fig. 5).

Two more series of runs were performed similarly at 25° with initial II concentrations of 1.8–30 mg/ml in 1 *M* 2-(*N*-morpholino)ethanesulfonic acid (pH 6) and in 1 *M* 3-(*N*-morpholino)propanesulfonic acid (pH

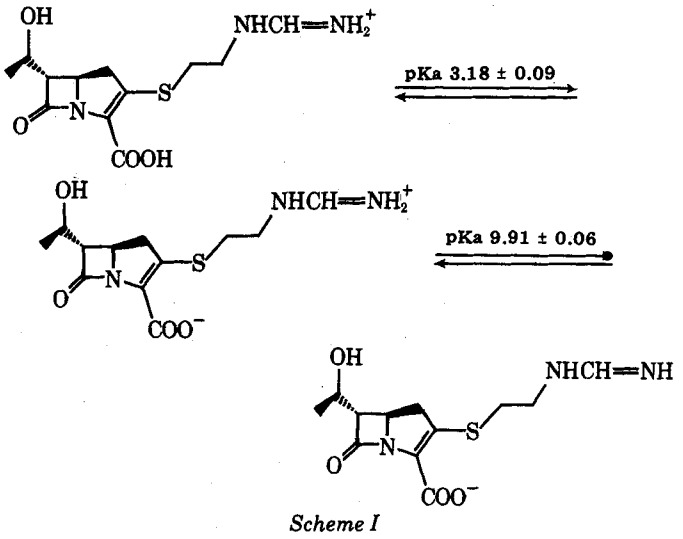


*Scheme I*

8). The second-order rate constant of ~0.2 $M^{-1}$ hr$^{-1}$, the value found at pH 7 and 25°, also was found at pH 6 and 8. The product UV spectra of the runs at pH 6 were all similar to curve C in Fig. 1, and those at pH 8 were all similar to curve B in Fig. 1. (All UV spectra were measured at pH 7.) In the runs at high initial II concentration, these different products formed largely from the second-order reaction, whose rate was pH independent. This fact supports the earlier conclusion that rate-determining β-lactam opening, even in the absence of oxygen, precedes the rapid formation of several products whose composition is pH dependent (see *Reaction Products*).

Compound II exists in ionic equilibria (Scheme I) for which the pKa values, obtained by analyzing titration curves, are as shown. According to these pKa data, about 0.01, 0.1, and 1% of the amidine nitrogen are unprotonated at pH 6, 7, and 8, respectively. One might expect the sec-

**Table III—Reactivities with Hydrogen Ion, Water, and Hydroxide Ion at 35°**

| β-Lactam Antibiotic | $k_H$, $M^{-1}$ hr$^{-1}$ | $10^3k_0$, hr$^{-1}$ | $10^{-2}k_{OH}$, $M^{-1}$ hr$^{-1}$ |
|---|---|---|---|
| II | 6500 | 10.1 | 77 |
| Penicillins | | | |
| Penicillin G | 601 | 0.90 | 11.9 |
| Carbenicillin | 52.2 | 2.04 | 12.1 |
| Cloxacillin | 35.6 | 0.94 | 13.4 |
| Propicillin | 30.7 | 0.89 | 17.3 |
| Cyclacillin | 4.61 | 2.49 | 11.0 |
| Ampicillin | 1.82 | 0.75 | 25.7 |
| Cephalosporins | | | |
| Cephalothin | 0.172 | 10.9 | 10.6 |
| III*a* | 0.238 | 21.0 | 9.08 |
| III*b* | 0.206 | 18.7 | 8.56 |
| III*c* | 0.186 | 11.4 | 8.45 |
| III*d* | 0.265 | 7.06 | 9.55 |
| IV*a* | — | 0.270 | 1.43 |
| IV*b* | — | — | 1.33 |
| IV*c* | — | 0.270 | 1.56 |
| IV*d* | — | — | 1.52 |

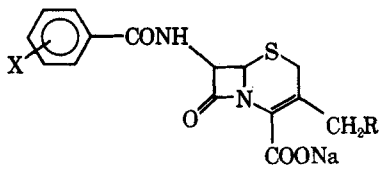


III*a*: R = $OCOCH_3$, X = 4-$CH_3$
III*b*: R = $OCOCH_3$, X = H
III*c*: R = $OCOCH_3$, X = 4-Cl
III*d*: R = $OCOCH_3$, X = 4-$NO_2$
IV*a*: R = H, X = 4-$CH_3$
IV*b*: R = H, X = H
IV*c*: R = H, X = 4-Cl
IV*d*: R = H, X = 4-$NO_2$

**Table IV—Reactivities with Monobasic Phosphate Anion**

| β-Lactam Antibiotic | $k_{HPO_4^{2-}}$, $M^{-1}$ hr$^{-1}$ | Temperature | Reference |
|---|---|---|---|
| II | 0.58 | 23° | — |
| Ampicillin | 0.166 | 35° | 11 |
| Carbenicillin | 0.064 | 35° | 11 |
| Cloxacillin | 0.092 | 35° | 11 |
| Cyclacillin | 0.355 | 35° | 11 |
| Methicillin | 0.087 | 35° | 11 |
| | 2.0 | 75° | 12 |
| Oxacillin | 0.073 | 35° | 11 |
| Penicillin G | 0.078 | 35° | 11 |
| | 0.82 | 60° | 13 |
| Phenethicillin | 0.094 | 35° | 11 |
| Propicillin | 0.128 | 35° | 11 |
| Sulbenicillin | 0.078 | 35° | 11 |
| 6-(α-Toluenesulfonamido)-penicillanic acid | 0.030 | 35° | 11 |

ond-order reaction to involve attack by the nucleophilic unprotonated amidine nitrogen of one II molecule on the β-lactam of another. The fact that the second-order rate constant is pH independent rules out predominant attack by this nucleophile and is consistent with attack by the protonated amidine nitrogen. However, this fact allows the reactivity of the unprotonated amidine to be the greater. The apparent second-order rate still could be essentially independent of pH because of the relatively large amounts of protonated amidine present at pH 6–8.

**Stability Comparison of II and Other β-Lactam Antibiotics**—The stability of penicillins and cephalosporins in aqueous solution has been described extensively. Stabilities at 35° and $\mu = 0.5$ were summarized by Yamana and Tsuji (8) in terms of Eq. 1. The II reactivities are shown in Table III with some penicillin and cephalosporin data. (The reactivities of II at 25 and 40°, shown in Table II, were interpolated to 35° by means of the Arrhenius equation.)

The reactivities of II with hydrogen ion, water, and hydroxide ion are all significantly greater than those of penicillin G. The other penicillins listed in Table III have smaller $k_H$ values than penicillin G since they are designed to avoid intramolecular rearrangement in acidic solution. Their reactivities with water and hydroxide ion are about the same as those of penicillin G.

Cephalothin and the other cephalosporins with the 3-acetoxymethylene group are less reactive with hydrogen ion than are the penicillins, but they exhibit reactivities with water comparable to that of II and with hydroxide ion comparable to those of the penicillins. The reactivities of these cephalosporins, however, are due mainly to the 3-substituent (for which II and the penicillins have no counterpart), as shown by the lower reactivities of the corresponding deacetoxycephalosporins.

Furthermore, II is more reactive with phosphate than the penicillins, and the cephalosporins are essentially unreactive with phosphate. Phosphate buffers have been used as inert media for rate studies of cephalosporins (9). Moreover, the apparent first-order rate constant for the degradation of cefoxitin at 25°, measured in this laboratory at pH 7 and $\mu = 0.5$ in agreement with the published value of 0.00246 hr$^{-1}$ (10), was the same with nonnucleophilic 3-(*N*-morpholino)propanesulfonic acid buffers as with phosphate buffers of 0.01–0.25 *M*.

**Table V—$\Sigma_N$ and *D* Values Determined from X-Ray Crystallographic Data**

| Compound | $\Sigma_N$ | *D*, Å | Reference |
|---|---|---|---|
| *N*-Acetylthienamycin methyl ester | 325.9° | 0.49 | 14 |
| Penicillin V | 337° | 0.40 | 14 |
| Ampicillin | 339° | 0.38 | 14 |
| 6-Aminopenicillanic acid | 343° | 0.32 | 14 |
| Cephalosporin C | 345° | 0.32 | 15 |
| Cephaloridine | 350.7° | 0.24 | 14 |
| 7-Phenylacetamido-7-methoxy-3-methyl-3-cephem-*tert*-butyl ester | 356.7° | 0.15 | 14 |
| $\Delta^2$-Cephem | 359.3° | 0.06 | 15 |

The reactivity of II with phosphate at 23° (Fig. 2) is compared with literature data for various penicillins at $\mu = 0.5$ and at 35° and higher temperatures in Table IV. In the present study, the reactivity of II with phosphate was measured only at pH 7.2 and 23°, using 0.50 *M* phosphate ($\mu = 1$) or 1.00 *M* phosphate ($\mu = 2$). The same rate constant was observed at the two phosphate concentrations. The reactivity of II with $HPO_4^{2-}$ (Table IV) was calculated from the observed rates with the assumption that $H_2PO_4^-$ is inert or much less reactive than $HPO_4^{2-}$. (This assumption holds true for the penicillins, according to the references given in Table IV.)

The degradations of the penicillins and cephalosporins in aqueous solution are complex and, consequently, cannot be compared easily with the degradation of II in general terms. Nevertheless, the reactivities in Tables III and IV fall into three distinct groups. Compound II is more reactive than the penicillins which, in turn, are more reactive than the deacetoxycephalosporins. This distinction reflects the relative strains of the nuclei as shown by the X-ray crystallographic data in Table V. The table includes values for the sum of the bond angles about the β-lactam ring nitrogen, $\Sigma_N$, and the distance of the nitrogen atom from the plane of the three attached carbon atoms, *D*.

## REFERENCES


(1) J. S. Kahan, F. M. Kahan, R. Goegelman, S. A. Currie, M. Jackson, E. O. Stapley, T. W. Miller, A. K. Miller, D. Hendlin, S. Mochales, S. Hernandez, H. B. Woodruff, and J. Birnbaum, *J. Antibiot.*, **32**, 1 (1979).

(2) N. H. Grant, D. E. Clark, and H. E. Alburn, *J. Am. Chem. Soc.*, **84**, 876 (1962).

(3) H. Bundgaard and C. Larsen, *J. Chromatogr.*, **132**, 51 (1977).

(4) W. J. Leanza, K. J. Wildonger, T. W. Miller, and B. G. Christensen, *J. Med. Chem.*, **22**, 1435 (1979).

(5) "CRC Handbook of Chemistry and Physics," 48th ed., Chemical Rubber Co., Cleveland, Ohio, 1967, p. D-92.

(6) P. J. Flory, "Principles of Polymer Chemistry," Cornell University Press, Ithaca, N.Y., 1953, chap. 3.

(7) H. T. H. Piaggio, "Differential Equations," Open Court Publishing, LaSalle, Ill., 1948, p. 18.

(8) T. Yamana and A. Tsuji, *J. Pharm. Sci.*, **65**, 1563 (1976).

(9) A. B. Taylor, *J. Chem. Soc.*, **1965**, 7020.

(10) E. R. Oberholtzer and G. S. Brenner, *J. Pharm. Sci.*, **68**, 863 (1979).

(11) T. Yamana, A. Tsuji, and Y. Mizukami, *Chem. Pharm. Bull.*, **22**, 1186 (1974).

(12) M. A. Schwartz, E. Bara, I. Rubycz, and A. P. Granatek, *J. Pharm. Sci.*, **54**, 149 (1965).

(13) P. Finholt, G. Jürgensen, and H. Kristiansen, *ibid.*, **54**, 387 (1965).

(14) G. Albers-Schönberg, B. H. Arison, O. D. Hensens, J. Hirshfield, K. Hoogsteen, E. A. Kaczka, R. E. Rhodes, J. S. Kahan, F. M. Kahan, R. W. Ratcliffe, E. Walton, L. J. Ruswinkle, R. B. Morin, and B. G. Christensen, *J. Am. Chem. Soc.*, **100**, 6491 (1978).

(15) J. G. Gleason, T. F. Buckley, K. G. Holden, D. B. Bryan, and P. Siler, *ibid.*, **101**, 4730 (1979).


## ACKNOWLEDGMENTS


The authors thank Dr. G. Albers-Schönberg, Dr. G. S. Brenner, Mr. F. M. Kahan, Mrs. J. S. Kahan, Dr. S. H. Pines, and Dr. K. E. Wilson for helpful discussions. They also thank Mr. J. A. Bolognese for the least-squares calculations, Dr. J. A. McCauley for pKa data, and Mrs. E. S. Otterbein for FTIR spectroscopy.

# Structural Functions of the Sweet Pharmacophore

**G. G. BIRCH *, S. Z. DZIEDZIC *§x, R. S. SHALLENBERGER ‡, and M. G. LINDLEY ‡¶**

Received February 26, 1980, from the **National College of Food Technology, University of Reading, Weybridge, Surrey KT13 ODE, England,* and the ‡*New York State Agriculture Experiment Station, Cornell University, Geneva, NY 14456.* Accepted for publication August 18, 1980. §Present address: Department of Food Science, University of Reading, Reading, RG1 5AQ, Berks., England. ¶Present address: Tate and Lyle Ltd., Philip Lyle Memorial Research Laboratory, Reading, RG6 2XB, Berks., England.

**Abstract** □ The relative sweetness, onset times, and durations of response of D-glucose, D-xylose, D-quinovose, D-galactose, L-arabinose, and D-fucose were determined at four temperatures. The results can be interpreted by simple concepts of intramolecular hydrogen bonding which indicate that the so-called γ-function of the tripartite AH,B,γ sweet pharmacophore plays little or no part in sugar sweetness. Probably the Lemieux effect (intramolecular hydrogen bonding between the hydroxymethyl substituent and the 4-hydroxy group) is of overriding importance in determining sugar sweetness, and the separate features of intensity and time of response indicate distinct functions of chemoreception. The absence of a γ-function in simple hydrophilic molecules such as glucose has already been emphasized. This function distinguishes them from the artificial sweeteners such as saccharin, which may be 500 times or more sweeter than sucrose, depending on their stereostructure and lipophilicity.

**Keyphrases** □ Sweet pharmacophore—structural function, relative sweetness of six sugars tested □ Sugars—relative sweetness, onset time, and duration of response determined for six sugars, structural functions of the sweet pharmacophore □ Structure–activity relationships—structural functions of six sugars evaluated for sweetness

The AH,B,γ concept of the sweet pharmacophore (1, 2) has been invoked recently (3, 4) to explain differences in sweetness elicited by structurally related molecules. The pharmacophore may be considered (5) as a scalene triangle with the acid function (AH) and the basic function (B) at two of the apexes while the lipophilic function (γ) is at the third apex. The γ-function may be important for sweetness intensity in molecules, such as the aminonitrobenzenes, that have a highly lipophilic character. Its role in sugar molecules is likely to be minimal.

## BACKGROUND

Stepwise chemical modification of glucopyranoside molecules (3, 4, 6) indicated that the 3,4-α-glycol is probably the primary AH,B unit. Therefore, the only likely location of the γ-function is the methylene group at C-6 of hexopyranosides.

The galactopyranosides differ from the glucopyranosides only in the configuration of the hydroxyl group at C-4, and their primary AH,B units (O–O interorbital spacings of 2.86 Å) therefore are intrinsically equivalent to the glucopyranosides. However, in galactopyranosides, the hydroxyl group at C-4 forms an intramolecular bond with the ring oxygen and thus is less available than the hydroxyl at C-4 of the glucopyranosides to bind with the taste receptor. Galacto-type structures are generally less sweet than gluco types, although the interplay of hydrogen bonding that governs the sweetness is temperature dependent.

Another type of hydrogen bond that underlies the sweetness of sugars is the intramolecular hydrogen bond between the hydroxymethylene group of glucose (and galactose) and the C-4 hydroxyl. This enhances (5) the acidity of the C-4 hydroxyl proton and has been termed the Lemieux effect (7). Whether such an effect elevates or depresses sweetness in a molecule depends on the molecular structure and temperature. Hydrogen bonds may rupture as the temperature is increased so that effects ascribable solely to their interplay diminish.

Kier (2) and Holtje and Kier (8) explained the contribution of the third dispersion binding moiety to sweet taste and underlined its importance in molecules such as saccharin, neohesperidin dihydrochalcone, and nitroanilines, which are 500–3000 times sweeter than sucrose. Since the low order of sweetness in sugars probably is due to the absence of an effective γ-function, it is of structural interest to modify the γ-effect. Recently, the temporal factor in the sweet response has excited some interest (9, 10), and the persistence of the response has been attributed to an ordered localized concentration of stimulus molecules at or near the receptor. Such a local concentration of molecules may be attributable to the γ-function of the sweet pharmacophore, because the persistence of most simple sugars is similar. Alteration of the γ-function of sugar molecules (*e.g.*, by removal of the oxygen of the hydroxymethyl) would increase lipophilicity and might increase sweetness and persistence. On the other hand, removal of the hydroxymethyl would eliminate the Lemieux effect, in which case the sweetness would diminish.

To explore these fine differences in analogous sugar structures, the sweetness and persistence of six structural analogs in the gluco and galacto series of sugars were investigated. Relative sweetness and persistence values were determined at four temperatures to elucidate the importance of hydrogen bonding in the sweet response.

## EXPERIMENTAL

6-Deoxy-α-D-methylglucoside (methyl α-D-quinovopyranoside, I) and D-quinovose (6-deoxy-α-D-glucose, II) were prepared by a series of well-documented procedures in carbohydrate chemistry. D-Glucose (III), D-xylose (IV), D-galactose (V), L-arabinose (VI), D-fucose (VII) α-D-methylglucoside (methyl α-D-glucopyranoside, VIII), and α-D-methylxyloside (methyl α-D-xylopyranoside, IX) were purchased[1] commercially. All compounds were purified by repeated crystallizations before use.

The assessors were selected and trained according to well-established procedures (11). This training involved recognition of suprathreshold levels of the four basic tastes and ranking of different sucrose concentrations.

Equimolar (0.5 *M*) solutions were used, prepared 15 hr prior to tasting so that mutarotational effects were similar. The order of temperatures and presentation was randomized.

**Intensity Determinations**—Ten panelists were presented with 3-ml samples in sealed glass vials equilibrated to the temperature of tasting. Prior to assessment, panelists were required to rinse their mouths continuously for 20 sec with rinse water provided at that temperature. A method of category scaling (0–10) was used. Panelists were presented with an internal standard (5) and were asked to score the sweetness of the other two solutions accordingly. Two-digit random numbers were used. Tastings were duplicated, *i.e.*, 20 judgments for each compound at each temperature. Continual reference could be made to the standard, provided the mouth was rinsed between tastings. Significance was determined by the Student *t* test.

**Temporal Determinations**—Immediately before tasting, 12 panelists were asked to rinse their mouths continuously for 20 sec at the specific temperature under examination. At any sitting, three randomly chosen solutions were administered; 50 μl[2] was placed onto the tip of the extended tongue. Panelists communicated visually the onset and persistence of the sweet taste, which were recorded on a stopwatch. Panelists waited at least 2 min before taking the next sample. The results were calculated as an analysis of variance, 4 × 6 × 12 "2 off" unreplicated experiment (*i.e.*, four temperatures, six sugars, 12 panelists). The 95% confidence lists are indicated in all figures by two times the standard error of the mean.

## RESULTS AND DISCUSSION

Figure 1 shows the three galacto analogs and the sweetness of L-arab-

[1] Sigma Chemical Co. Poole, Dorset, England.
[2] Oxford dispenser.

0022-3549/81/0300-0277$01.00/0
© 1981, American Pharmaceutical Association

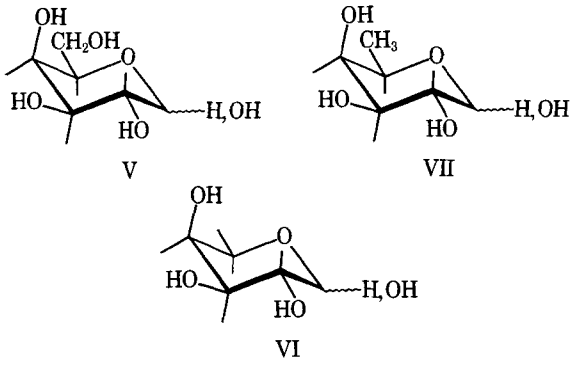


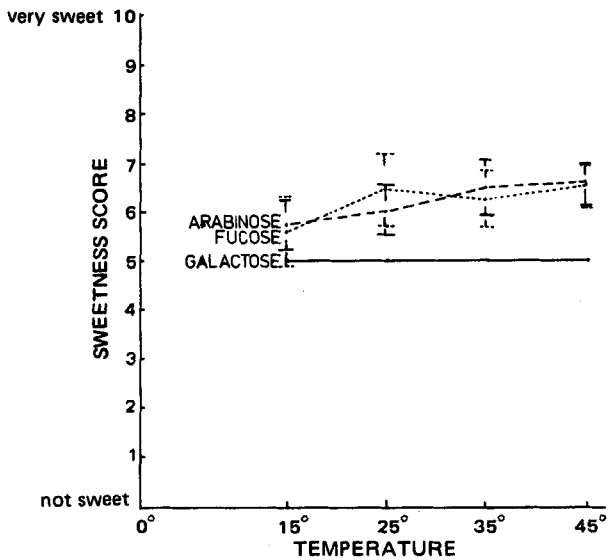


**Figure 1**—*Sweetness of D-fucose and L-arabinose compared to D-galactose (5) at 15, 25, 35, and 45°. Vertical bars represent the standard error of the mean.*

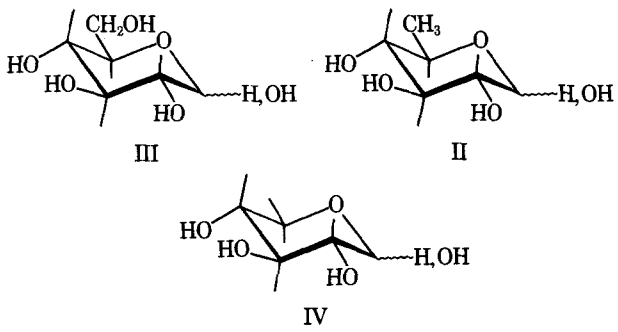


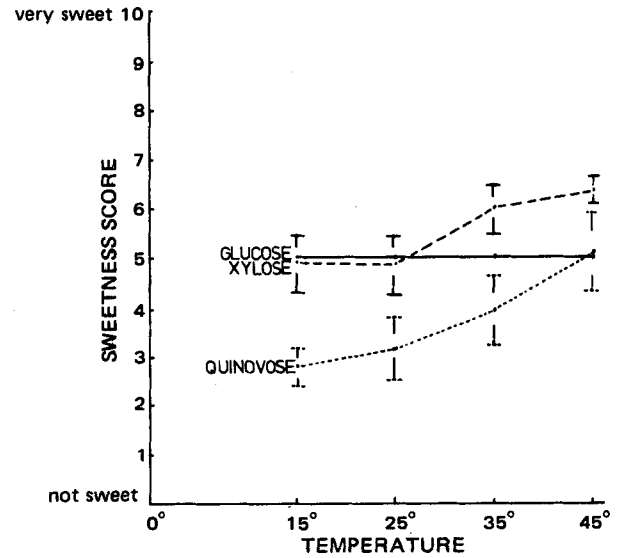


**Figure 2**—*Sweetness of D-quinovose and D-xylose compared to D-glucose (5) at 15, 25, 35, and 45°. Vertical bars represent the standard error of the mean.*

inose and D-fucose compared to D-galactose (which was given the value 5.0 at each of the four temperatures, 15, 25, 35, and 45°). Both L-arabinose and D-fucose were sweeter than D-galactose throughout this temperature range; this finding is attributable to the two intramolecular hydrogen bonds in the latter sugar. The relative sweetness of L-arabinose and D-fucose increased with increasing temperature because more energy was needed to rupture the doubly intramolecularly hydrogen-bonded galactose molecule. Although D-fucose possesses a $\gamma$-function and L-arabinose does not, there was no significant difference in the sweetness of these two sugars throughout the temperature range. This finding illustrates the lack of importance of the $\gamma$-site in these analogous structures and emphasizes the overriding property of intramolecular hydrogen bonding and the Lemieux effect, which depresses galactose sweetness.

Figure 2 shows the three gluco analogs and the sweetness of D-xylose and D-quinovose compared to D-glucose over the same temperature range. D-Xylose had a similar sweetness to D-glucose at the lower temperatures, but xylose became significantly sweeter at higher temperatures. Both molecules have the same AH,B system at the 3,4-$\alpha$-glycol group, but presumably D-xylose, being the smaller molecule, is more sterically favored by the receptor at the higher temperatures. At the lower temperatures, D-glucose undergoes the Lemieux effect, which enhances the acidity of the 4-hydroxy proton and, hence, increases sweetness so that it becomes similar to that of xylose. D-Quinovose has no Lemieux effect (being devoid of a C-4 oxygen) and was significantly less sweet than glucose at lower temperatures. Only at higher temperatures, when the Lemieux effect is no longer operational due to rupture of all intramolecular hydrogen bonds, did D-glucose and D-quinovose become sterically and sensorically equivalent. The $\gamma$-site exerted no noticeable effect in any of these results. If it had, D-quinovose would have been sweeter than D-glucose at the higher temperatures.

In a third experiment, the $\alpha$-D-methylglycosides of the three gluco analogs were tested over the same temperature range. The resulting curves (Fig. 3) were similar to those of the free sugars (Fig. 2); this finding underlines the lack of involvement of the anomeric center.

Shallenberger and Lindley (5) reported the dimensions of the scalene triangle (Fig. 4), which specifiy the tripartite sweet pharmacophore. In the gluco and galacto analogs studied, the favored conformation of all six analogs confines the $\gamma$-site to C-6 of the hexoses. However, 6-deoxyglucose (quinovose) was less sweet than glucose or xylose at all but the highest temperature studied (Fig. 2), and the same exact pattern was repeated in the glycosides (Fig. 3). Only with 6-deoxygalactose (fucose) was there any increase of sweetness compared with the parent hexose. However, this result can be explained by the doubly intramolecularly hydrogen-bonded galactose structure (Fig. 1) as discussed earlier. Furthermore, fucose had the same sweetness as arabinose, in which the $\gamma$-site is absent. Thus, the $\gamma$-site is not of major importance in the relative sweetness of these analogous structures.

It was pointed out recently (10) that the temporal factors in sweetness (*i.e.*, onset time and duration of response) may be related to the approach, alignment, and localized concentration of the stimulus molecules in chemoreception. Sugars differ from many artificial sweeteners in that their durations decrease with increasing temperature, and this behavior may be a result of their ineffective $\gamma$-sites. If the approach of a stimulus molecule to a sweet receptor governs the onset time and the localized concentration governs the duration of response, it is possible that both may be affected by changes in temperature.

Figure 5 shows that the mean onset time of response of all six sugars decreased with increasing temperature, while Fig. 6 shows that their mean duration likewise decreased. These results are both significant ($p < 0.001$) and agree with those of Larson-Powers and Pangborn (12) for sucrose.

The onset time may be a simple function of temperature-dependent diffusion whereas the duration may represent the accession of sapid molecules to localized concentrations or stores. Thus, the negative temperature effect again reflects the absence of an effective $\gamma$-function. The present results also indicate that quinovose had a longer duration of sweetness than the other sugars at all temperatures tested, but there were no other obvious structural differences between the sugars that could have affected their temporal response.

If the $\gamma$-site of the sweet pharmacophore is viewed as a function that

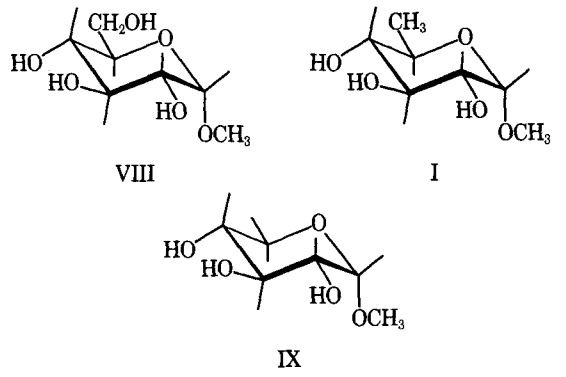


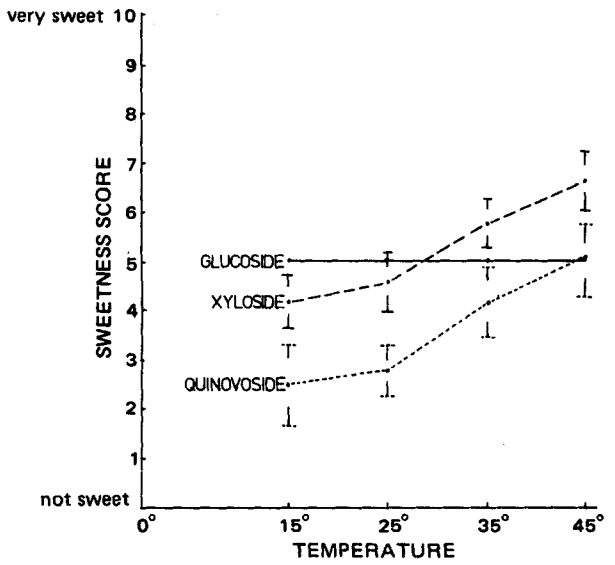


**Figure 3**—*Sweetness of methyl α-D-xylopyranoside and methyl α-D-quinopyranoside compared to methyl α-D-glucopyranoside at 15, 25, 35, and 45°. Vertical bars represent the standard error of the mean.*

facilitates the accession of stimulus molecules to receptors, 6-deoxyhexoses might show high sweetness intensities and long durations. However, there is no reason to believe that a long duration of response (high localized concentration) should demand a high intensity (occupation of receptors); a more accurate concept of taste chemoreception may involve the distinction of these factors as separate mechanisms (9, 10). Therefore, the observation that quinovose has a longer duration but a lower intensity of sweetness than glucose could be due to its enhanced

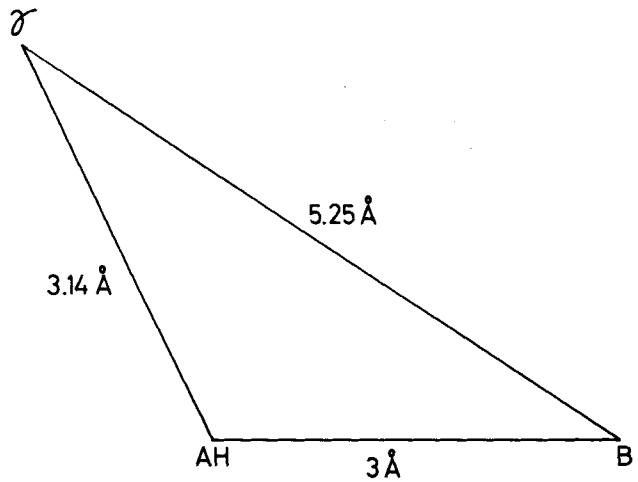


**Figure 4**—*Dimensions of tripartite sweet pharmacophore represented by scalene triangle (5).*

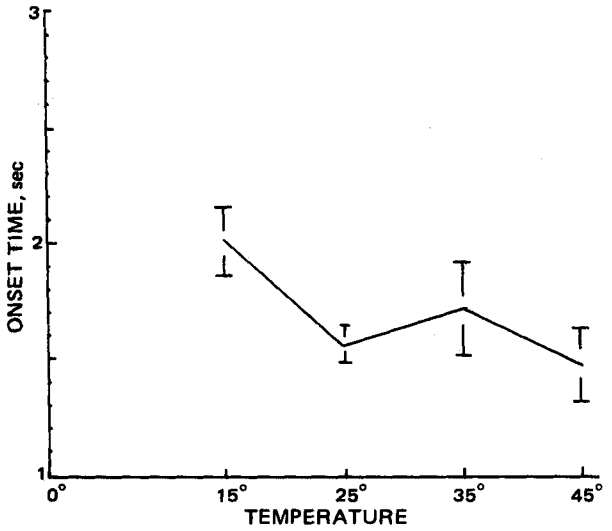


**Figure 5**—*Mean onset time of sweetness of six analogs at 15, 25, 35, and 45°. Vertical bars represent the standard error of the mean.*

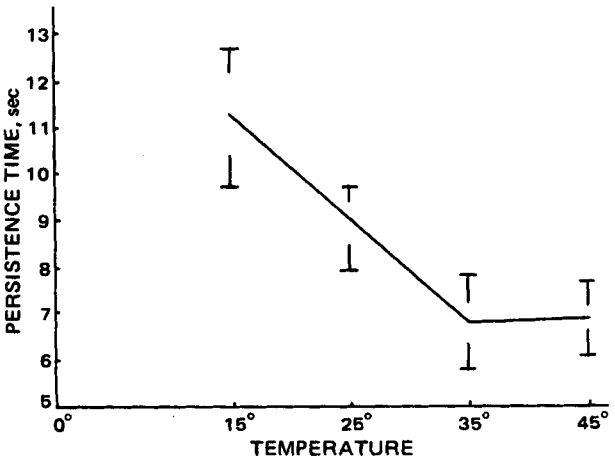


**Figure 6**—*Mean persistence time (i.e., duration) of sweetness of six analogs at 15, 25, 35, and 45°. Vertical bars represent the standard error of the mean.*

localized concentration at or near the same number of receptors as glucose.

## CONCLUSION

Studies of a conformationally and configurationally defined class of sweeteners such as the sugars can result in particular deductions about the sweet pharmacophore. The results reported here underline the dominant role of hydrogen bonding in the sweetness of sugars and offer an explanation of the relative effects of analogous structures. Both intensity and time factors in the sweetness response depend on temperature and may contribute jointly to an understanding of the chemoreception of taste.

Although Kier's (2) γ-function appears to be virtually absent in normal sugar structures, it may be enhanced in 6-deoxyglucose. A more refined and detailed function of the γ-site is postulated in that the latter may govern the approach, alignment, and localized concentrations of sweetener molecules at or near the receptor. These results confirm Kier's (2) original stipulations about the third binding site and extend the concept of the sweet pharmacophore to include intensity–time interactions of the sweet response.

## REFERENCES

(1) R. S. Shallenberger and T. E. Acree, *Nature*, **216**, 480 (1967).
(2) L. B. Kier, *J. Pharm. Sci.*, **61**, 1394 (1972).
(3) G. G. Birch, *Crit. Rev. Food Sci. Nutr.*, **8**, 57 (1976).

(4) G. G. Birch, in "Olfaction and Taste," 6th ed., J. Le Magnen and P. MacLeod, Eds., IRL, London, England, 1977, p. 27.
(5) R. S. Shallenberger and M. G. Lindley, *Food Chem.*, **2**, 145 (1977).
(6) G. G. Birch and C. K. Lee, *J. Food Sci.*, **39**, 947 (1974).
(7) R. U. Lemieux and J. T. Brewer, in "Carbohydrates in Solution," H. S. Isbell, Ed., Advances in Chemistry Series 117, American Chemical Society, Washington, D.C., 1973, p. 121.
(8) H. D. Holtje and L. B. Kier, *J. Pharm. Sci.*, **63**, 1722 (1974).
(9) G. G. Birch and C. K. Lee, in "Developments in Sweeteners," C. A. M. Hough, K. J. Parker, and A. J. Vlitos, Eds., Applied Science, London, England, 1979, p. 165.
(10) G. G. Birch, in "Carbohydrate Sweeteners in Foods and Nutrition," P. Koivistoinen and L. Hyvönen, Eds., Academic, London, England, 1980, pp. 61–75.
(11) H. W. Spencer, in "Sweetness and Sweeteners," G. G. Birch, L. F. Green, and C. B. Coulson, Eds., Applied Science, London, England, 1971, p. 112.
(12) N. Larson-Powers and R. M. Pangborn, *J. Food Sci.*, **43**, 41 (1978).

# Crystal Structure and Solid-State Behavior of Aspirin Anhydride Crystals

**STEPHEN R. BYRN** ˣ **and P. Y. SIEW**

Received May 2, 1980, from the *Department of Medicinal Chemistry and Pharmacognosy, School of Pharmacy and Pharmacal Sciences, Purdue University, West Lafayette, IN 47906.* Accepted for publication August 15, 1980.

**Abstract** □ The crystal structure and solid-state behavior of aspirin anhydride were determined using single-crystal X-ray techniques and microscopic examination of the reacting crystals. The crystal structure and solid-state conformation of aspirin anhydride were similar to those of related compounds. The crystal packing of aspirin anhydride allows the initial product of the solid-state reaction to be predicted; however, this prediction could not be tested because the thermal degradation products reported in the literature appear to be those obtained from reaction in a liquid state.

**Keyphrases** □ Aspirin anhydride—determination of crystal structure and solid-state behavior, X-ray crystallography and microscopy of reacting crystals □ Crystal structure—aspirin anhydride, determination of solid-state behavior of crystals □ Degradation, thermal—aspirin anhydride end-products, crystal structure and solid-state behavior of aspirin anhydride determined

The use of crystallographic data to explain the products of solid-state reactions has provided insight into these reactions and the factors controlling them (1–3). However, few studies have been conducted to determine the relationship between the crystal structure and the degradation products of pharmaceuticals. The aim of this study was to investigate the products of the true solid-state reaction of aspirin anhydride in terms of the crystal packing. It is hoped that such studies will lay the groundwork for understanding drug degradation in the solid state and how to prevent this degradation.

This investigation involved a microscopic study of the behavior of solid aspirin anhydride during heating and determined the crystal structure of aspirin anhydride using single-crystal X-ray techniques. It was found that solid aspirin anhydride liquefies during reaction even at 50°.

## EXPERIMENTAL

**Preparation of Aspirin Anhydride**—Aspirin anhydride was prepared following literature procedures for the reaction of acetylsalicylic acid with ethyl chloroformate (4, 5). When 10 g of acetylsalicylic acid was mixed with 6.2 g of ethyl chloroformate with cooling, ~4 g of crystals formed, mp 79–81°. Subsequent structure determination showed these crystals to be aspirin anhydride.

**Crystal Properties of Aspirin Anhydride ($C_{18}H_{14}O_7$, mol. wt. = 342.31)**—The crystals were tetragonal with a = 8.457(1), c = 23.166(6) Å, V = 1656.85 Å$^3$, z = 4, $\rho_{calc}$ = 1.372 g/cm$^3$, $\mu$ (20°, CuK$\alpha$, $\lambda$ = 1.5418 Å) = 9.176 cm$^{-1}$; systematic absences $00l$, $l \neq 4n$; $h00$ ($0k0$), $h \neq 2n$ ($k \neq 2n$); space group $P4_12_12$ or $P4_32_12$. The structure was determined assuming space group $P4_12_12$.

**Data Collection**—A crystal of 0.49 × 0.48 × 0.20 mm$^3$ was obtained from absolute ethanol by cooling and was aligned with its long axis parallel to the $\phi$ direction of a Picker four-angle diffractometer. The $\phi$ direction thus was parallel to the $a$ axis. Intensity data were collected with CuK$\alpha$ radiation and a scintillation counter for the reciprocal octant $hkl$ to a $2\theta$ maximum of 133.85° using a $\theta/2\theta$ scan of 2.4° and a scan speed of 30 sec/degree. Background readings were taken for 10 sec at each end of the scan range. During the data collection (120 hr), the decay of two reference reflections was only 6.7%.

Equivalent reflections in the two semioctants $hkl$ ($h > k$) and $khl$ ($h < k$) were averaged using a discrepancy factor $R$ of 0.067. If:

$$\frac{|I(hkl) - I(khl)|}{[I(hkl)I(khl)]^{1/2}} \leq R$$

the average was taken; otherwise, the reflection with the larger net count was retained. The total number of independent reflections was 946, 645 of which satisfied the criterion $F > 3\sigma(F)$ and were considered to be observed. Lorentz polarization corrections were applied to all data. No absorption correction was made.

**Structure Determination and Refinement**—The 100 reflections of the largest $E$-forming 843 $\Sigma_2$ relationships were sorted with respect to the strength of the phase reliability given by the equation $\sigma_h = 2\sigma_3\sigma_2^{-3/2}|E_h|(s_h^2 + c_h^2)^{1/2}$, where the symbols are defined by Karle and Karle (6). The convergence method was applied to generate 64 starting sets which, upon multiple-tangent refinement, yielded sets of phases with various figures of merit (7). An $E$-map calculated from the set of phases with the highest figure of merit revealed the positions of 12 of the 13 nonhydrogen atoms. The remaining atom was the oxygen atom.

Full matrix least-squares techniques were used to refine the structure. A weighting scheme ($w^{-1} = (|F_{obs} - B|/A)^2 + 1$, where $A$ = 2.5 and $B$ = 11.3) was also used. Refinement with nonhydrogen atoms proceeded smoothly to an $R$ of 0.105 and a $wR$ of 0.080. A difference Fourier map then revealed the positions of five of the seven hydrogen atoms, and the other two methyl hydrogen atom positions were calculated. The refinement holding the hydrogen atoms invariant with a temperature factor of $B_{overall}$ + 1 then proceeded smoothly to an $R$ of 0.085 and a $wR$ of 0.074. Release of the constraints on the hydrogen atoms resulted in improvement of the $R$ factor to 0.082 and chemically reasonable positions for the aromatic hydrogen atoms but unreasonable positions for the methyl hydrogen atoms; thus, these positions were recalculated, and the final



0022-3549/81/0300-0280$01.00/0
© 1981, American Pharmaceutical Association

(4) G. G. Birch, in "Olfaction and Taste," 6th ed., J. Le Magnen and P. MacLeod, Eds., IRL, London, England, 1977, p. 27.
(5) R. S. Shallenberger and M. G. Lindley, *Food Chem.*, **2**, 145 (1977).
(6) G. G. Birch and C. K. Lee, *J. Food Sci.*, **39**, 947 (1974).
(7) R. U. Lemieux and J. T. Brewer, in "Carbohydrates in Solution," H. S. Isbell, Ed., Advances in Chemistry Series 117, American Chemical Society, Washington, D.C., 1973, p. 121.
(8) H. D. Holtje and L. B. Kier, *J. Pharm. Sci.*, **63**, 1722 (1974).
(9) G. G. Birch and C. K. Lee, in "Developments in Sweeteners," C. A. M. Hough, K. J. Parker, and A. J. Vlitos, Eds., Applied Science, London, England, 1979, p. 165.
(10) G. G. Birch, in "Carbohydrate Sweeteners in Foods and Nutrition," P. Koivistoinen and L. Hyvönen, Eds., Academic, London, England, 1980, pp. 61–75.
(11) H. W. Spencer, in "Sweetness and Sweeteners," G. G. Birch, L. F. Green, and C. B. Coulson, Eds., Applied Science, London, England, 1971, p. 112.
(12) N. Larson-Powers and R. M. Pangborn, *J. Food Sci.*, **43**, 41 (1978).

# Crystal Structure and Solid-State Behavior of Aspirin Anhydride Crystals

**STEPHEN R. BYRN** ˣ **and P. Y. SIEW**

Received May 2, 1980, from the *Department of Medicinal Chemistry and Pharmacognosy, School of Pharmacy and Pharmacal Sciences, Purdue University, West Lafayette, IN 47906.* Accepted for publication August 15, 1980.

**Abstract** □ The crystal structure and solid-state behavior of aspirin anhydride were determined using single-crystal X-ray techniques and microscopic examination of the reacting crystals. The crystal structure and solid-state conformation of aspirin anhydride were similar to those of related compounds. The crystal packing of aspirin anhydride allows the initial product of the solid-state reaction to be predicted; however, this prediction could not be tested because the thermal degradation products reported in the literature appear to be those obtained from reaction in a liquid state.

**Keyphrases** □ Aspirin anhydride—determination of crystal structure and solid-state behavior, X-ray crystallography and microscopy of reacting crystals □ Crystal structure—aspirin anhydride, determination of solid-state behavior of crystals □ Degradation, thermal—aspirin anhydride end-products, crystal structure and solid-state behavior of aspirin anhydride determined

The use of crystallographic data to explain the products of solid-state reactions has provided insight into these reactions and the factors controlling them (1–3). However, few studies have been conducted to determine the relationship between the crystal structure and the degradation products of pharmaceuticals. The aim of this study was to investigate the products of the true solid-state reaction of aspirin anhydride in terms of the crystal packing. It is hoped that such studies will lay the groundwork for understanding drug degradation in the solid state and how to prevent this degradation.

This investigation involved a microscopic study of the behavior of solid aspirin anhydride during heating and determined the crystal structure of aspirin anhydride using single-crystal X-ray techniques. It was found that solid aspirin anhydride liquefies during reaction even at 50°.

## EXPERIMENTAL

**Preparation of Aspirin Anhydride**—Aspirin anhydride was prepared following literature procedures for the reaction of acetylsalicylic acid with ethyl chloroformate (4, 5). When 10 g of acetylsalicylic acid was mixed with 6.2 g of ethyl chloroformate with cooling, ~4 g of crystals formed, mp 79–81°. Subsequent structure determination showed these crystals to be aspirin anhydride.

**Crystal Properties of Aspirin Anhydride ($C_{18}H_{14}O_7$, mol. wt. = 342.31)**—The crystals were tetragonal with a = 8.457(1), c = 23.166(6) Å, V = 1656.85 Å$^3$, z = 4, $\rho_{calc}$ = 1.372 g/cm$^3$, $\mu$ (20°, CuK$\alpha$, $\lambda$ = 1.5418 Å) = 9.176 cm$^{-1}$; systematic absences $00l$, $l \neq 4n$; $h00$ ($0k0$), $h \neq 2n$ ($k \neq 2n$); space group $P4_12_12$ or $P4_32_12$. The structure was determined assuming space group $P4_12_12$.

**Data Collection**—A crystal of 0.49 × 0.48 × 0.20 mm$^3$ was obtained from absolute ethanol by cooling and was aligned with its long axis parallel to the $\phi$ direction of a Picker four-angle diffractometer. The $\phi$ direction thus was parallel to the $a$ axis. Intensity data were collected with CuK$\alpha$ radiation and a scintillation counter for the reciprocal octant $hkl$ to a $2\theta$ maximum of 133.85° using a $\theta/2\theta$ scan of 2.4° and a scan speed of 30 sec/degree. Background readings were taken for 10 sec at each end of the scan range. During the data collection (120 hr), the decay of two reference reflections was only 6.7%.

Equivalent reflections in the two semioctants $hkl$ ($h > k$) and $khl$ ($h < k$) were averaged using a discrepancy factor $R$ of 0.067. If:

$$\frac{|I(hkl) - I(khl)|}{[I(hkl)I(khl)]^{1/2}} \leq R$$

the average was taken; otherwise, the reflection with the larger net count was retained. The total number of independent reflections was 946, 645 of which satisfied the criterion $F > 3\sigma(F)$ and were considered to be observed. Lorentz polarization corrections were applied to all data. No absorption correction was made.

**Structure Determination and Refinement**—The 100 reflections of the largest $E$-forming 843 $\Sigma_2$ relationships were sorted with respect to the strength of the phase reliability given by the equation $\sigma_h = 2\sigma_3\sigma_2^{-3/2}|E_h|(s_h^2 + c_h^2)^{1/2}$, where the symbols are defined by Karle and Karle (6). The convergence method was applied to generate 64 starting sets which, upon multiple-tangent refinement, yielded sets of phases with various figures of merit (7). An $E$-map calculated from the set of phases with the highest figure of merit revealed the positions of 12 of the 13 nonhydrogen atoms. The remaining atom was the oxygen atom.

Full matrix least-squares techniques were used to refine the structure. A weighting scheme ($w^{-1} = (|F_{obs} - B|/A)^2 + 1$, where $A$ = 2.5 and $B$ = 11.3) was also used. Refinement with nonhydrogen atoms proceeded smoothly to an $R$ of 0.105 and a $wR$ of 0.080. A difference Fourier map then revealed the positions of five of the seven hydrogen atoms, and the other two methyl hydrogen atom positions were calculated. The refinement holding the hydrogen atoms invariant with a temperature factor of $B_{overall}$ + 1 then proceeded smoothly to an $R$ of 0.085 and a $wR$ of 0.074. Release of the constraints on the hydrogen atoms resulted in improvement of the $R$ factor to 0.082 and chemically reasonable positions for the aromatic hydrogen atoms but unreasonable positions for the methyl hydrogen atoms; thus, these positions were recalculated, and the final



0022-3549/81/0300-0280$01.00/0
© 1981, American Pharmaceutical Association

**Table I—Final Parameters (Estimated Standard Deviation) x,y,z × $10^4$, $U_{ij}$ × $10^3$ Å$^2$, Temperature Factors = exp[$-2\pi^2(a^{*2}h^2U\cdots + \cdots + 2b^*c^*klU_{23})$]**

| Atom | x | y | z | $U_{11}$ | $U_{22}$ | $U_{33}$ | $U_{12}$ | $U_{13}$ | $u_{23}$ |
|---|---|---|---|---|---|---|---|---|---|
| O-1 | 1516 (4) | $x$ | 0 | 56 (2) | $u_{11}$ | 115 (4) | −5 (3) | $-u_{23}$ | 19 (2) |
| O-2 | 3471 (5) | 2484 (5) | 552 (2) | 69 (2) | 58 (2) | 100 (3) | −1 (2) | 1 (2) | −13 (2) |
| O-3 | 4499 (4) | 261 (5) | 1356 (2) | 48 (2) | 96 (3) | 67 (2) | −2 (2) | 2 (2) | −17 (2) |
| O-4 | 6920 (5) | 649 (6) | 1014 (2) | 65 (3) | 95 (3) | 99 (3) | −12 (3) | 19 (3) | −11 (2) |
| C-1 | 3240 (6) | −305 (6) | 446 (2) | 49 (3) | 55 (3) | 57 (3) | −11 (3) | 2 (2) | −4 (3) |
| C-2 | 4136 (6) | −806 (7) | 913 (2) | 51 (3) | 73 (4) | 49 (3) | −11 (3) | 3 (3) | −7 (3) |
| C-3 | 4616 (7) | −2355 (7) | 979 (2) | 59 (3) | 70 (4) | 74 (3) | −3 (4) | 2 (3) | 10 (3) |
| C-4 | 4154 (8) | −3464 (7) | 580 (3) | 78 (4) | 61 (4) | 91 (4) | 7 (3) | 8 (4) | 4 (4) |
| C-5 | 3233 (8) | −3030 (6) | 119 (3) | 78 (4) | 52 (3) | 72 (4) | −9 (3) | 1 (3) | −7 (3) |
| C-6 | 2780 (6) | −1464 (7) | 60 (2) | 62 (3) | 68 (4) | 56 (3) | −4 (3) | −3 (3) | −3 (3) |
| C-7 | 2824 (6) | 1347 (7) | 351 (2) | 47 (3) | 51 (3) | 74 (4) | −13 (3) | 10 (3) | −10 (3) |
| C-8 | 5947 (7) | 957 (7) | 1356 (3) | 65 (4) | 69 (4) | 62 (3) | 13 (3) | −1 (3) | 1 (3) |
| C-9 | 6083 (8) | 2086 (9) | 1843 (3) | 84 (5) | 104 (5) | 86 (4) | −24 (4) | 1 (4) | −26 (4) |

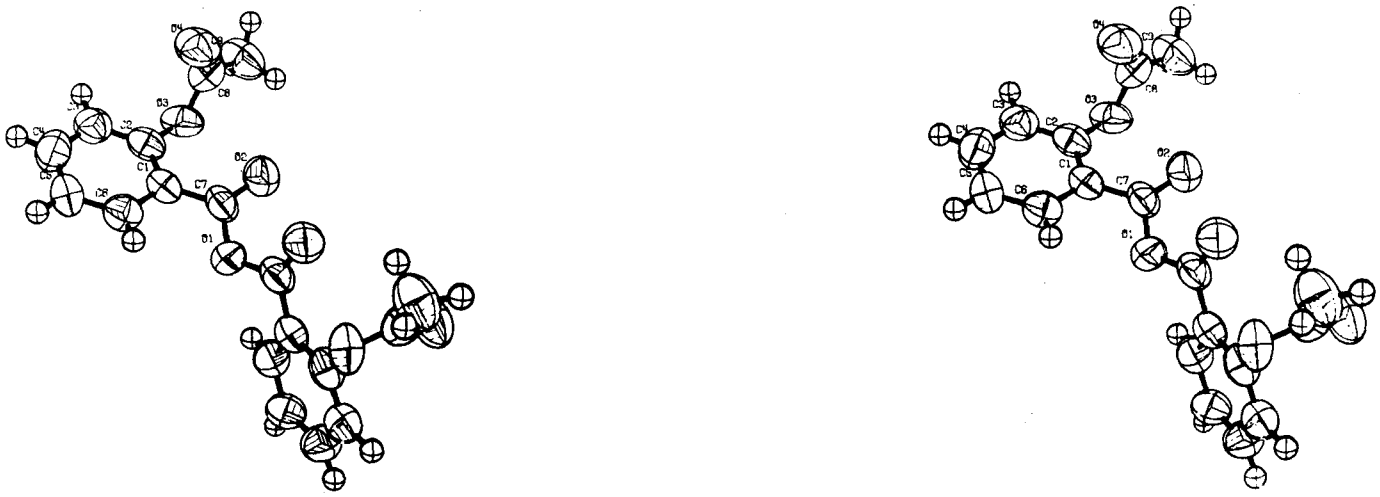

**Figure 1**—*View of aspirin anhydride along the (018) direction. The ellipsoids are drawn with a probability of 60% and the isotropic spheres of the hydrogen atoms with the arbitrary radius of 0.147 Å.*

refinement was performed holding the hydrogen atom positions and temperature factors constant. The final $R$ was 0.082 and $wR$ was 0.065. Table I lists the final atomic positions and temperature factors.

Figure 1 gives a stereoscopic view of the aspirin anhydride molecule along the (018) direction. The molecule has point group symmetry C-2 with the unique oxygen atom situated on the diad axis of the crystal structure.

Figure 2 shows a stereoscopic drawing of the crystal packing of aspirin anhydride.

Tables II and III list the bond lengths and angles in aspirin anhydride.

Table IV describes the deviation of atoms C-7, O-2, O-3, and O-1 from the best plane through the ring atoms C-1 through C-6. The plane through these six ring atoms gives a $\chi^2$ of 14.94, indicating a probability of <0.01 that these atoms are planar.

Table V lists the dihedral angles for the various atoms. In addition, the angle of twist of the anhydride, *i.e.*, the angle between the plane through C-7, O-1, and O-2 and the plane through C-7′, O-2′, and O-1 was 54°. Table VI lists the contacts of less than 3.5 Å.

The solid-state behavior of aspirin anhydride crystals grown from ethanol was studied. Single crystals were heated on a hot stage at various temperatures. Liquefication was observed at all temperatures. Even at the lowest temperature (50°), liquefication occurred after 11 days.

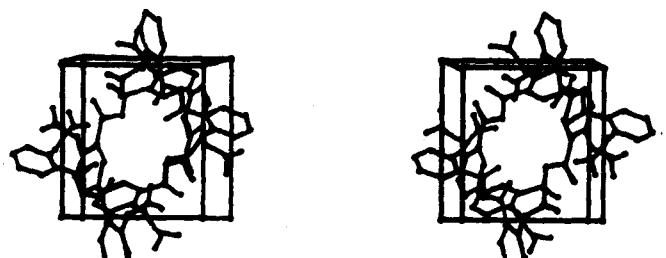

**Figure 2**—*Stereoscopic view of the crystal packing of aspirin anhydride. The origin is at the bottom left with a across and b vertical.*

## DISCUSSION

The general molecular geometry of aspirin anhydride is consistent with that of other anhydrides such as *p*-bromobenzoic anhydride (8) in that

**Table II—Bond Lengths and Important Intramolecular Contacts in Aspirin Anhydride with Standard Deviations in Parentheses**

| Atom | Bond | Atom | Bond |
|---|---|---|---|
| O-1–C-7 | 1.380 (6) | C-2–C-3 | 1.380 (9) |
| O-2–C-7 | 1.202 (7) | C-3–C-4 | 1.374 (9) |
| O-3–C-2 | 1.400 (7) | C-4–C-5 | 1.371 (9) |
| O-3–C-8 | 1.359 (7) | C-5–C-6 | 1.385 (8) |
| O-4–O-8 | 1.172 (7) | C-8–C-9 | 1.483 (9) |
| C-1–C-2 | 1.387 (7) | C-7–O-4 | 3.835 (7) |
| C-1–C-6 | 1.382 (7) | C-8–O-2 | 3.084 (7) |
| C-1–C-7 | 1.457 (8) | O-2–C-7′ | 2.772 (7) |

**Table III—Bond Angles in Aspirin Anhydride with Standard Deviations in Parentheses**

| Atom | Bond | Atom | Bond |
|---|---|---|---|
| C-7′–O-1–C-7 | 120.9 (4) | C-1–C-2–C-3 | 122.5 (5) |
| O-1–C-7–O-2 | 120.7 (5) | C-3–C-2–O-3 | 117.8 (5) |
| O-1–C-7–C-1 | 112.5 (4) | C-2–O-3–C-8 | 118.5 (4) |
| O-2–C-7–C-1 | 126.8 (5) | C-2–C-3–C-4 | 119.3 (5) |
| C-7–C-1–C-2 | 122.9 (5) | C-3–C-4–C-5 | 120.2 (6) |
| C-7–C-1–C-6 | 121.0 (5) | C-4–C-5–C-6 | 119.3 (5) |
| C-2–C-1–C-6 | 116.1 (5) | C-5–C-6–C-1 | 122.5 (5) |
| C-1–C-2–O-3 | 119.6 (5) | | |

**Table IV—Deviation of All Atoms of Aspirin Anhydride from the Best Plane through the Ring Atoms C-1 through C-6**

| Atom | Deviation from Plane, Å |
|---|---|
| C-1 | −0.015 |
| C-2 | 0.013 |
| C-3 | −0.004 |
| C-4 | −0.004 |
| C-5 | 0.002 |
| C-6 | 0.007 |
| O-1 | 0.360 |
| O-2 | −0.471 |
| O-3 | 0.144 |
| O-4 | 2.030 |
| C-7 | −0.095 |
| C-8 | −0.974 |
| C-9 | −0.639 |

**Table V—Dihedral Angles in Degrees for Aspirin Anhydride**

| Atom | Angle |
|---|---|
| O-3–C-2–C-1–C-7 | 8.5 (8) |
| C-2–C-1–C-7–O-2 | 19.9 (9) |
| C-2–C-1–C-7–O-1 | −158.4 (5) |
| C-6–C-1–C-7–O-1 | 23.1 (7) |
| C-6–C-1–C-7–O-2 | −158.6 (5) |
| C-2–O-3–C-8–C-9 | 177.9 (5) |
| C-2–O-3–C-8–O-4 | −3.2 (8) |
| C-1–C-2–O-3–C-8 | −99.4 (6) |
| C-3–C-2–O-3–C-8 | 84.4 (6) |
| C-6–C-1–C-2–O-3 | −172.9 (5) |
| C-3–C-2–C-1–C-6 | 3.2 (8) |
| C-3–C-2–C-1–C-7 | −175.4 (5) |

**Table VI—Contact Distances ≤3.5 Å Involving Nonhydrogen Atoms**

| Atoms | Distance |
|---|---|
| O-2···C-3 ($\frac{1}{2} - x, \frac{1}{2} + y, \frac{1}{4} - z$) | 3.446 (7) |
| O-2···C-4 (x, y + 1, z) | 3.476 (7) |
| O-2···C-5 (y + 1, x, $\bar{z}$) | 3.402 (7) |
| O-4···C-5 (y + 1, x, $\bar{z}$) | 3.414 (8) |
| O-4···C-6 (y + 1, x, $\bar{z}$) | 3.362 (7) |

the geometry is *syn* rather than *anti*. However, the crystal packing of aspirin anhydride is different from that of *p*-bromobenzoic anhydride. The bond lengths, angles, and torsion angles are consistent with those of the related acetylsalicylic acid and salicylic acid. The crystal packing indicates that a particular product should predominate during solid-state reaction; however, published studies indicate that numerous products are formed (4), probably because liquefication occurs during the reaction.

**Bond Lengths and Angles**—The bond lengths (Table II) are within $2\sigma$ of those of acetylsalicylic acid (9) except for the bond lengths involving the carboxyl group of the anhydride: C-7–O-1 is 1.380(6) in aspirin anhydride *versus* 1.29 in aspirin; C-7–O-2 is 1.202(7) in aspirin anhydride *versus* 1.24 in aspirin; and C-7–C-1 is 1.457(8) in aspirin anhydride *versus* 1.50 in aspirin. Similarly, the bond lengths of aspirin anhydride are within $2\sigma$ of those for salicylic acid (10), except for C-7–O-2 and C-7–O-1, which are 1.23 and 1.31 in salicylic acid, respectively.

The bond angles in aspirin anhydride differ from those in aspirin and salicylic acid only around the anhydride and acetyl groups. The angles in aspirin anhydride *versus* aspirin that differ by more than 2° ($2\sigma$) are: C-7–C-1–C-2, 122.9 *versus* 125; O-2–C-7–C-1, 126.8 *versus* 118; O-2–C-7–O-1, 120.7 *versus* 123; and O-1–C-7–C-1, 112.5 *versus* 119. For aspirin anhydride *versus* salicylic acid, the angles that differ by more than 2° ($2\sigma$) are: C-7–C-1–C-2, 122.9 *versus* 120; C-6–C-1–C-2, 116.1 *versus* 119; C-1–C-2–C-3, 122.5 *versus* 120; O-2–C-7–C-1, 126.8 *versus* 123; and O-1–C-7–C-1, 112.5 *versus* 116.

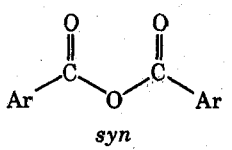

*syn*

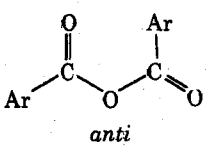

*anti*

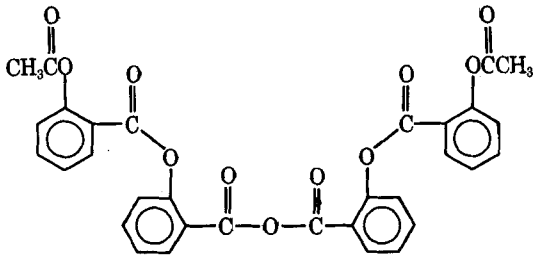

I

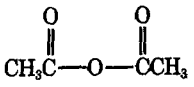

II

None of these differences in bond lengths or angles are major, and they probably reflect the slightly different electronic and steric requirements of the anhydride *versus* the acid functionality.

**Molecular Conformation and Torsion Angles**—Aspirin anhydride adapts a nonplanar *syn*-conformation instead of the *anti*-conformation that might be expected to be more planar. The angle of twist of the car-

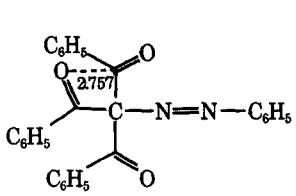

III

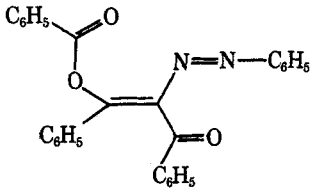

IV

*Scheme I—Benzoyl transfer reactions of phenylazotribenzoylmethane (III).*

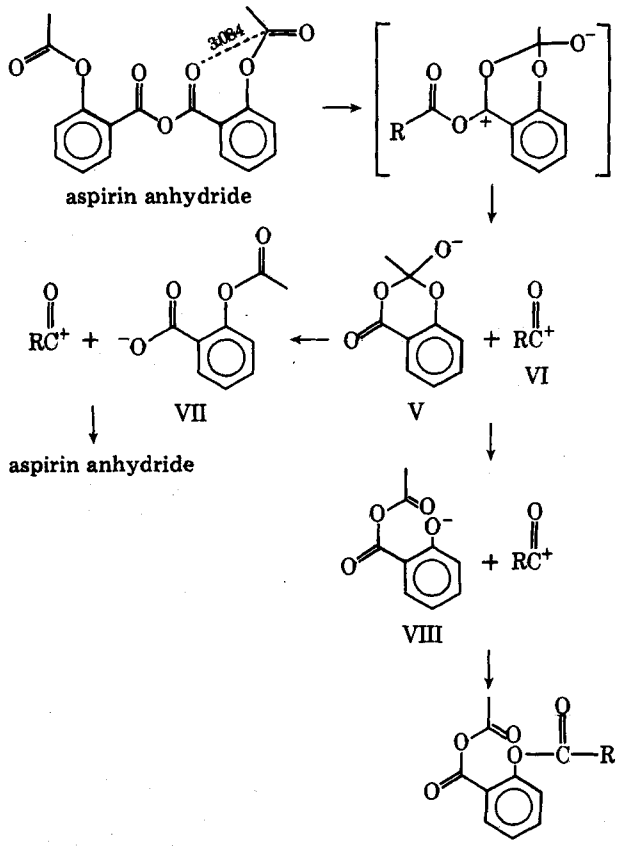


*Scheme II—Possible acyl transfer reaction in solid aspirin anhydride.*

bonyl groups with respect to each other is 54°. A similar *syn*-conformation is observed in *p*-bromobenzoic anhydride crystals. The anhydride group in aspirin anhydride is twisted from the plane of the benzene ring significantly more than is the acid group in either acetylsalicylic acid or salicylic acid. In aspirin, the C-2–C-1–C-7–O-2 torsion angle is −2°; in salicylic acid, it is 1°, in aspirin anhydride, it is 19.9(9)°. The acetyl group is rotated about the C-2–O-3 bond in both aspirin anhydride and acetylsalicylic acid. The torsion angle C-1–C-2–O-3–C-8 is 99.4° in aspirin anhydride and 86° in aspirin.

**Solid-State Reactions and Crystal Packing**—The following generalizations can be made concerning the solid-state thermal reactions of aspirin anhydride (4):

1. Water contamination increases the thermal instability of aspirin anhydride.

2. Thoroughly dried, high-purity aspirin anhydride has enhanced thermal stability.

3. Removal of the aspirin anhydride degradation products (*i.e.*, acetic acid and acetic anhydride) by a stream of heated air inhibits liquefication and stabilizes aspirin anhydride.

4. The thermal degradation products include all possible mixed anhydrides from acyl and benzoyl transfer reactions; however, the end-products are I and II (4). It is likely that the end-products observed are due to the reaction in both the solid and liquid states.

The crystal packing of aspirin anhydride was investigated to see if any predictions concerning the products of the solid-state reactions can be made. In particular, the crystal packing was investigated to see if the formation of a single acyl or benzoyl transfer product could be predicted.

The O···C=O intramolecular contacts are listed in Table II. No intramolecular O···C=O contacts of <4.0 Å were observed. The intramolecular contacts are within the normal range of O···C=O interactions (11) but are not unusually short since the shortest intramolecular interaction reported by Burgi *et al.* was 2.58 Å (11). In addition, the conversion of the yellow form of phenylazotribenzoylmethane (III) to α-phenylazo-β-benzoyloxybenzolacetophenone (IV) involves a benzoyl migration in a case where the O···C=O distance is 2.757 Å (12). In aspirin anhydride, the shortest O···C=O distance is 2.772 Å; however, rearrangement involving this contact regenerates aspirin anhydride. Acyl transfer involving the next closest contact (3.084 Å) leads to V and VI (or the equivalent radicals; Scheme II), which degrades to VII and VIII. If VI and VII recombine, aspirin anhydride is regenerated; if VIII and VI combine, IX is formed. Thus, a true solid-state reaction with cage recombination would be expected to yield IX.

Indeed, IX was synthesized and found to give the same degradation products as aspirin anhydride (4). Thus, the decomposition products of aspirin anhydride are completely consistent with crystal packing. However, a true solid-state reaction is expected to yield only IX. The fact that other products are isolated indicates that other reactions also occur. This finding is reasonable since liquefication of aspirin anhydride crystals occurs even at 50°. Careful study of the initial stages of aspirin anhydride degradation is in order, perhaps using high-pressure liquid chromatography, to see if IX is an initial product in aspirin anhydride degradation.

In summary, this paper illustrates the predictions and insight into the degradation of solid pharmaceuticals that can be gained by a combined X-ray crystallographic and photomicrographic study. Future studies of the degradation of solid pharmaceuticals will involve application of these techniques and should lead to both a better understanding of the solid-state degradation of pharmaceuticals and to improved methods of stabilization of pharmaceuticals.

## REFERENCES


(1) S. R. Byrn, *J. Pharm. Sci.*, **65**, 1 (1976).

(2) D. Y. Curtin and I. C. Paul, *Science*, **187**, 19 (1975).

(3) M. D. Cohen and B. S. Green, *Chem. Br.*, **490**, (1973).

(4) E. R. Garrett, E. L. Schumann, and M. F. Grostic, *J. Am. Pharm. Assoc., Sci. Ed.*, **48**, 684 (1959).

(5) A. Einhour and R. Seuffert, *Chem. Ber.*, **43**, 2990 (1910).

(6) J. Karle and I. L. Karle, *Acta Crystallogr.*, **21**, 849 (1966).

(7) G. Germain, P. Main, and M. M. Wolfson, *ibid.*, **B26**, 274 (1970).

(8) C. S. McCammon and J. Trotter, *ibid.*, **17**, 1333 (1964).

(9) P. J. Wheatley, *J. Chem. Soc.*, **1964**, 6036.

(10) M. Sundaralingam and L. H. Jensen, *Acta Crystallogr.*, 18 1053 (1965).

(11) H. G. Burgi, J. D. Dunitz, and E. Shefter, *ibid.*, **B30**, 1517 (1974).

(12) D. B. Pendergrass, D. Y. Curtin, and I. C. Paul, *J. Am. Chem. Soc.*, **94**, 8722 (1972).


## ACKNOWLEDGMENTS


Supported by National Institute of Health Grant GM-21174.

# Comparisons of Rotamer Populations of Nialamide, Azaperone, and Chloroquine in Solid State and in Solution

**GERALD P. MIGLIACCIO * and STEPHEN R. BYRN ˣ**

Received May 15, 1980, from the *Department of Medicinal Chemistry and Pharmacognosy, School of Pharmacy and Pharmacal Sciences, Purdue University, West Lafayette, IN 47907.* Accepted for publication August 15, 1980. *Present address: Antibiotic Recovery Department, Pfizer, Inc., Groton, CT 06340.

**Abstract** □ IR and NMR spectroscopy were combined with previously published X-ray crystallographic data to determine the solution conformations of the $-(CH_2)_n-$ fragments of nialamide, azaperone, and chloroquine. The solution conformation of these compounds then was compared to the solid-state conformation. In addition, the limits of the IR–X-ray method are discussed. This paper shows that a combination of IR, NMR, and X-ray crystallographic data can lead to a complete picture of the conformations available to drugs. In addition, the danger of using solid-state conformational data alone to make pharmacological suggestions is illustrated.

**Keyphrases** □ Nialamide—comparison of rotamer populations in solid state and in solution, conformation determined by IR and NMR spectroscopy and X-ray crystallography □ Azaperone—comparison of rotamer populations in solid state and in solution, IR and NMR spectroscopic and X-ray crystallographic determinations of conformation □ Chloroquine—comparison of rotamer populations in solid state and in solution, IR and NMR spectroscopic and X-ray crystallographic determination of conformation □ Conformation—in solid state and in solution, azaperone, nialamide, chloroquine

An understanding of the relationship between the conformation of a flexible drug at the receptor and its conformation in the liquid (solution) and solid state is a major goal of molecular pharmacology.

## BACKGROUND

A relationship (1) between the proportion of rapidly equilibrating conformers in solution and biological activity has been proposed for histamine, antihistamines, acetylcholine and its analogs, and several hormones (1–10). For example, the ability of histamine to stimulate two distinct biological responses initially was suggested to be due to the presence of *gauche*- and *trans*-conformers (1). The observation that ethylenediamine antihistamines blocked only one of these responses was attributed to their preference for the *trans*-conformation (2). However, more recent studies led to other suggestions, including the conclusion that there is no clearcut conformation–activity relationship for histamine and its derivatives (3, 4).

A relationship between the solid-state conformation about the phenyl–piperidine bond and analgesic potency was suggested (8), and the solid-state conformation of anticonvulsant drugs was suggested to be related to their activity (9).

Finally, the most stable conformer of several drugs in solution was suggested to be the one bound to the receptor (11). This suggestion led to numerous attempts to correlate differences in the proportion of the most stable conformers with activity.

In contrast to these suggestions, it was postulated that rapid substrate isomerism should not affect enzymatic reaction rates (12). Furthermore, rapid substrate isomerism had no effect on the rate of chymotrypsin-catalyzed hydrolysis of DL-thiazoline (13), and the enzyme thermolysin bound the lowest energy solution conformer of one dipeptide inhibitor and the highest energy solution conformer of a second dipeptide inhibitor[1].

In addition to these examples of the trapping of a rotamer by a receptor, there are numerous examples of the separation of a rotamer from a mixture of rotamers by crystallization (14–22). For example, crystallization results in the trapping of a single rotamer of chlorocyclohexane (14), tetramethylthiatane (15), cyclo-gly-gly-*d*-ala-*d*-ala-gly-gly (16, 17), isobutyramide (18), 3′-isopropyo-3,5-diiodo-*l*-thyronine (19), 1,4-diphenyl-1,4-dithiabutane-1,4-dioxide (20), and histamine (21). In addition, the phenomenon of conformational polymorphism was reviewed (22). Conformational polymorphism occurs when a compound crystallizes in different conformations in different polymorphs.

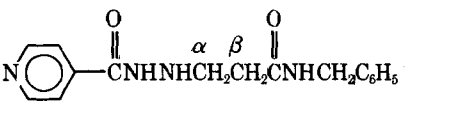

I

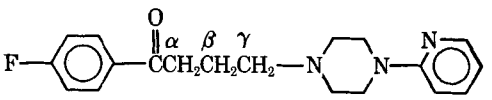

II

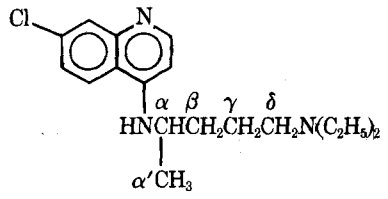

III

These reports show that crystallization can result in the selection of one rotamer from a mixture; thus, the development of methods for investigating whether crystallization results in the trapping of one of a mixture of rotamers is an important step toward understanding the relationship (if any) between the solid-state, solution, and receptor-bound conformations of a drug. This paper reports studies aimed at developing such an understanding. Three flexible drugs were chosen for investigation using an extension of the IR–X-ray method (21): nialamide (I), a monoamine oxidase inhibitor (23); azaperone (II), a sedative neuroleptic (24); and chloroquine (III), an antimalarial (25).

## EXPERIMENTAL

**Apparatus and Spectra**—All IR spectra were analyzed as solids in potassium bromide pellets or as solutions in 0.5-mm sodium chloride cells[2]. Preliminary NMR spectra were measured on 60-, 80-, or 90-MHz spectrometers[3]. All samples then were analyzed on a 360-MHz superconducting Fourier transform spectrometer[4]. All spectra were analyzed by computer[5].

**Chemicals**—Chloroquine was obtained as the diphosphate salt[6]. It was used without further purification in aqueous solution and was converted to the free base for analysis in organic solvents according to a literature method (26). The diphosphate salt (25 g) was dissolved in distilled water (500 ml). The free base was separated by addition of 0.1 *N* NaOH (200 ml). A white viscous solution formed and was extracted with methylene chloride (4 × 100 ml). The extract was dried over anhydrous sodium sulfate for 1 hr with stirring. This solution then was filtered, and

[1] T. L. Shieh and S. R. Byrn, unpublished data.

[2] Beckman IR4230 spectrometer.

[3] Varian EM-360 or FT-80 and Perkin-Elmer R-32, 90 MHz.

[4] Nicolet Technology Corp. (at the Purdue University Regional Biochemical Magnetic Resonance Laboratory).

[5] Purdue University CDC computer system.

[6] Sigma Chemical Co.



*0022-3549/81/0300-0284$01.00/0*
*© 1981, American Pharmaceutical Association*

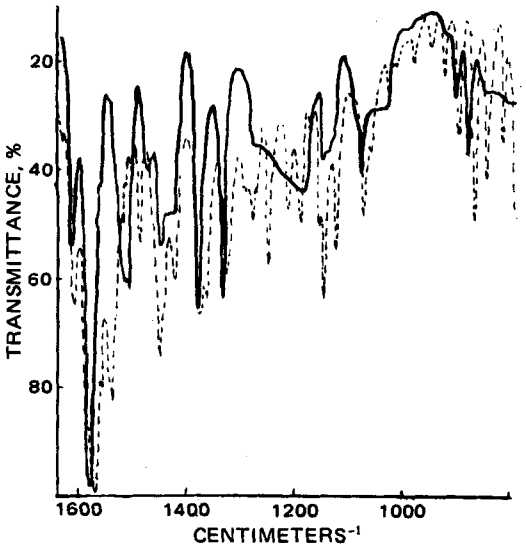


**Figure 1**—*Solid (---) and solution ($CHCl_3$) (—) IR spectra of chloroquine.*

the methylene chloride was removed by vacuum distillation. A yellow oil remained, which crystallized after 12 hr, mp 86–88°.

**Solutions**—All IR solutions were prepared with spectral grade chloroform. Concentrations were adjusted to maximize the signal in the fingerprint region.

The following solvents[7] were used for NMR studies: chloroform-$d_1$ (99.8 atom % D), acetone-$d_6$ (99.5 atom % D), dimethyl sulfoxide-$d_6$ (99.5 atom % D), deuterium oxide (99.7 atom % D), and pyridine-$d_5$ (99 atom % D). Tetramethylsilane was used as the internal standard in organic solvents. In deuterium oxide, the chemical shifts were usually reported relative to the HDO resonance position.

The following solution concentrations were used: 10–30 mg/0.5 ml for the 60- and 90-MHz spectra, 5–10 mg for the 80-MHz spectra, and 2–3 mg for the 360-MHz spectra. All solutions were filtered with a fritted-glass filter and were placed immediately in 5-mm tubes.

**Computer Analysis**—Chemical shifts were extracted from the spectra, and representative coupling constants were submitted to the LAOCN3 computer program (27). These calculated frequencies then were assigned to experimentally observed frequencies. The same input data along with those assignments then were submitted to LAOCN3. Calculated chemical shifts and coupling constants were produced that best fit the experimental spectrum. After most assignments were made, the calculated spectral data were submitted as input data to LAOCN3 and the process was repeated until a suitable simulation was obtained.

## RESULTS

**Chloroquine**—The IR spectra of chloroquine in solution and in the solid state are shown in Fig. 1. The 360-MHz NMR spectrum of chloroquine in acetone gave the following data: 0.98 (t, 6H), 1.32 (d, 3H), 1.60 (m, 3H), 1.80 (m, 1H), 2.07 [m, $(CH_2H)_2CO$], 2.42 (t, 2H), 2.47 (m, 4H), 3.30 (s, $H_2O$), 3.93 (m, 1H), 6.49 (d, 1H), 6.60 (d, 1H), 7.37 (dd, 1H), 7.88 (d, 1H), 8.25 (d, 1H), and 8.47 (d, 1H) ppm.

The region of interest is the aliphatic portion of the spectrum, and the following assignments were made for that area. The triplet at 0.98 ppm was assigned to the methyl protons of the ethyl group, and the multiplet at 2.47 ppm was assigned to the methylene protons of this group. The methylene protons adjacent to the nitrogen on $C_\delta$ were assigned to the triplet at 2.42 ppm. The multiplet at 1.60 ppm was from the two $C_\gamma$ protons and one $C_\beta$ proton, while the other $C_\beta$ proton was assigned to the multiplet at 1.80 ppm. The multiplet at 3.93 ppm was assigned to the $C_\alpha$ proton, and the doublet at 1.32 ppm was assigned to the $C_{\alpha'}$ methyl protons.

LAOCN3 analysis gave the following set of vicinal coupling constants: $J_{\alpha,\beta} = 8.28$ Hz, $J_{\alpha,\beta'} = 8.28$ Hz, $J_{\beta,\gamma} = 8.77$ Hz, $J_{\beta',\gamma} = 7.35$ Hz, and $J_{\gamma,\delta} = 5.92$ Hz. The simulated spectrum obtained from these coupling constants and the observed spectrum are shown in Fig. 2.

These coupling constants can be used to estimate the population of

[7] Aldrich Chemical Co.

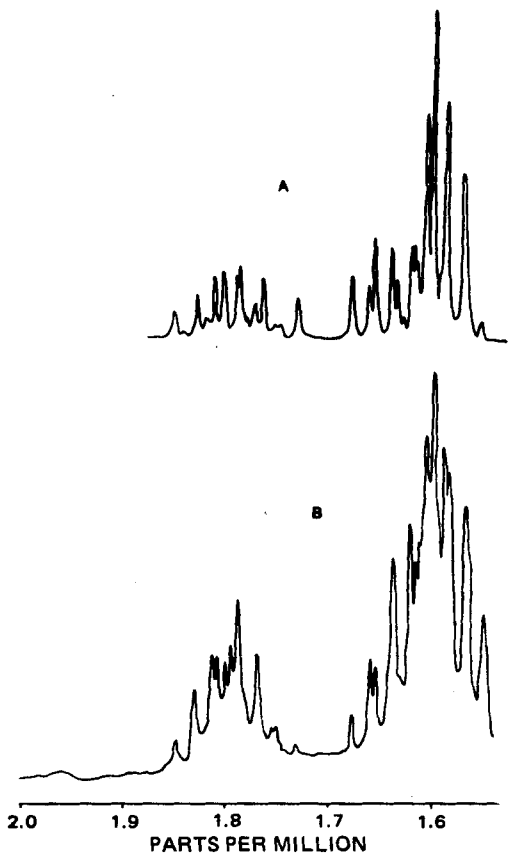


**Figure 2**—*Observed (B) and simulated (A) 360-MHz spectra of chloroquine in the range of 550–675 Hz. The simulated spectrum was obtained from the LAOCN3 stick plot. A 1.5-Hz linewidth was used.*

rotamers according to published procedures (28–31). The conformation about the $\alpha$–$\beta$ bond can be approximated using Eqs. 1–3 and Scheme I as derived by Abraham and Pachler (28):

$$N_1 = \frac{J_{\alpha\beta} - J_g}{J_t - J_g} \qquad \text{(Eq. 1)}$$

$$N_2 = \frac{J_{\alpha\beta'} - J_g}{J_t - J_g} \qquad \text{(Eq. 2)}$$

$$N_3 = 1 - N_1 - N_2 \qquad \text{(Eq. 3)}$$

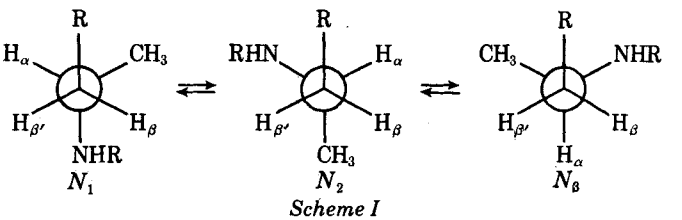


*Scheme I*

In these equations, $N_1$, $N_2$, and $N_3$ are the populations of the rotamers shown and $J_t = 13.11$ Hz and $J_g = 3.63$ Hz. Solving these equations gives $N_1 = N_2 = 0.49$ and $N_3 = 0.02$. While these numbers should be considered as estimates due to the assumptions involved, the sterically hindered conformer $N_3$ is obviously energetically unfavorable.

The conformation about the $\beta$–$\gamma$ bond can be determined using the following procedure (28–30). Let $N = J_{\beta\gamma} + J_{\beta'\gamma}$ and $L = J_{\beta\gamma} - J_{\beta'\gamma}$. Since it is impossible to differentiate $J_{\beta\gamma}$ and $J_{\beta'\gamma}$, $L$ can have either a positive or negative value. The equation $\frac{1}{2}N + \frac{1}{6}L = 17.97 - 0.80\Sigma E$ can be used to determine whether $L$ is positive or negative. The value of $\Sigma E$ is calculated with the assumption that $L$ is both positive and negative and $\Sigma E$ is calculated from tables provided in the literature (32). Usually, a clear indication that $L$ is positive or negative is obtained. If $L$ is positive, the *gauche*-rotamers predominate; if $L$ is negative, the *trans*-rotamers predominate. If $L$ is zero, there is a nearly equal proportion of all rotamers. For the $\beta$–$\gamma$ bond, $N = 16.12$ and $L = \pm 1.42$. This small value of

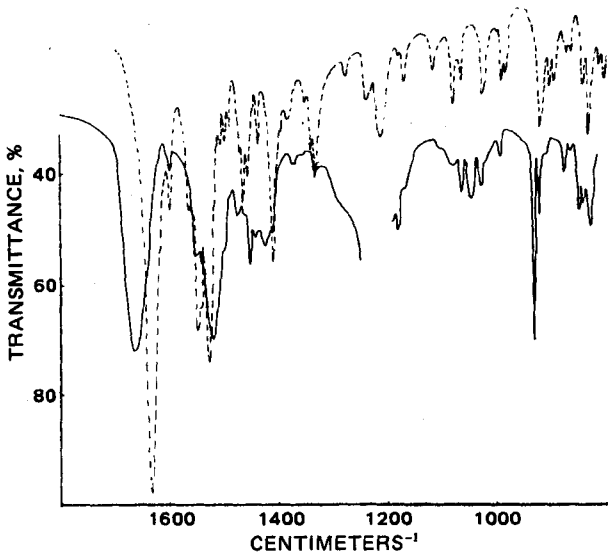


**Figure 3**—*IR spectra of nialamide in the solid state (- - -) and in solution ($CHCl_3$) (——).*

$L$ indicates that the *gauche*- and *trans*-rotamers are of nearly equal energy. If $L$ is positive, $\Sigma E$ is calculated to be 12.09; if $L$ is negative, $\Sigma E$ is calculated to be 12.69. The theoretical $\Sigma E$ is 14.00. Since $L$ may be negative, this exercise indicates that the *trans*-rotamer may be of slightly lower energy than the *gauche*-rotamers.

The conformation about the $\gamma$–$\delta$ bond can be analyzed in the same way. In this case, $L = 0$, indicating that the *gauche*- and *trans*-isomers are of equal energy.

**Nialamide**—The IR spectra of nialamide (I) in the solid state and in solution can be compared in Fig. 3. The 80-MHz NMR spectrum of nialamide in pyridine gave the following data: 2.85 (t, 2H), 3.66 (t, 2H), 4.68 (d, 2H), and 5.17 (s) ppm. The triplets at 2.85 and 3.66 ppm were assigned to the methylene protons on $C_\beta$ and $C_\alpha$, respectively. The doublet at 4.68 ppm was assigned to the benzyl protons. The broad singlet at 5.17 ppm was thought to be due to all of the nitrogen protons in the molecule. The coupling constant for $J_{\alpha,\beta}$ was 6.5 Hz. This coupling constant gave $L = 0$ and indicates that all three rotamers are equally populated in the absence of the deceptively simple catastrophe.

**Azaperone**—Figure 4 shows the comparison of the solid and solution IR spectra of azaperone. The 90-MHz NMR spectrum in chloroform gave the following data: 2.00 (m, 2H), 2.45 (t, 2H), 2.55 (t, 4H), 3.00 (t, 2H), and 3.49 (t, 4H) ppm. The multiplet at 2.00 ppm was assigned to the $C_\beta$ methylene protons. The signals due to the $C_\gamma$ and $C_\alpha$ methylene protons were determined to be the triplets at 2.45 and 3.00 ppm, respectively. The triplets at 2.55 and 3.49 ppm were assigned to the piperazinyl protons. The coupling constants were $J_{\beta,\gamma} = 7.0$ Hz and $J_{\alpha,\beta} = 7.1$ Hz. These data indicate that $L = 0$ for both the $\beta,\gamma$ and $\alpha,\beta$ bonds, thus suggesting that the *gauche*- and *trans*-rotamers are of equal energy.

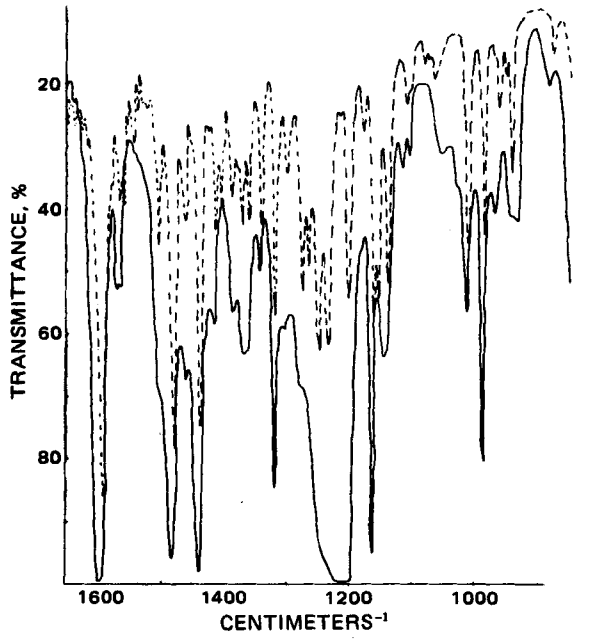


**Figure 4**—*IR spectra of azaperone in the solid state (- - -) and in solution ($CHCl_3$). (——)*

## DISCUSSION

Comparison of the IR spectra of azaperone (II) in the solid state and in solution (Fig. 4) indicates that the solid and solution conformations are the same. An extremely good correlation can be seen between peak positions as well as between relative intensities. Since the *trans*-rotamer about both the $\alpha$–$\beta$ and $\beta$–$\gamma$ bond is frozen in the solid, this rotamer probably predominates in solution. However, the NMR spectrum of azaperone is characteristic of a rapidly rotating $A_2B_2$ system about both the $C_\alpha$–$C_\beta$ bond axis and the $C_\beta$–$C_\gamma$ bond axis. The coupling constants produce rotamer percentages that indicate (within experimental error) that the molecule exists one-third of the time as each rotamer about each bond. In other words, the molecule is rapidly rotating and there is no preference for any one of the three rotamers. In addition, theoretical calculations of the populations of the rotamers of butyrophenones related to azaperone showed that the *gauche*- and *trans*-conformers about the $\beta$–$\gamma$ and $\gamma$–$\delta$ bonds were nearly equally populated (33). If it is rotating rapidly, it would be impossible for the solid-state conformation to be the same as the solution conformation; thus, the general utility of the IR–X-ray method must be questioned.

The earlier analysis of methapyrilene intensifies this contradiction (21). Comparison of the solid-state and solution IR spectra indicates the same results as with azaperone; the conformations in both states should be the same. Once again, the NMR spectrum is in disagreement. The methylene protons of methapyrilene produce two triplets in chloroform solution, indicative of rapid rotation. The NMR results for diphenhydramine in chloroform also indicate that the *gauche*- and *trans*-rotamers are of nearly equal energy; however, in this case, the solid-state and solution spectra are different, substantiating these results (21) and indicating that the solid-state and solution conformations are different.

To investigate these contradictions, the peaks in the fingerprint region of the IR spectrum were characterized. The theory behind the IR–X-ray method (21) states that conformational changes are reflected by changes in the absorption frequency of a given vibration. Only vibrations that are intimately involved with rotations about the ethane fragment or that come in close contact with it upon rotational change reflect any conformational change. Therefore, it is necessary to decide whether the fingerprint region contains enough absorbances that can reliably reflect conformational change or whether the region is dominated by absorbances of rigid structural components whose vibrations are not significantly affected by rotation.

Characterization of the azaperone IR spectrum leads to the finding that most major absorbances are due to rigid structural components. They dominate the entire region and mask any absorbances due to the ethane fragment. For example, three positions of absorbance of the fluorobenzene component are at 1600, 1480, and 1160 $cm^{-1}$. These peaks are all dominating in the fingerprint region. Many more absorbances can be assigned to the fluorobenzene portion of the molecule along with contributions from the pyridine and piparazine ring systems. Actually, most peaks in the IR spectrum are due to these three components. Likewise, it is evident that the absorbances in the methapyrilene IR spectrum cannot reflect changes in conformation. These absorbances can be attributed to the pyridine and thiophene portions of the molecule. Thus, in these cases, the IR–X-ray method probably is unreliable.

Similar characterizations of the IR spectra of nialamide (I), diphenhydramine, and chloroquine (III) provide different results. The IR spectra of nialamide indicate that the solid and solution conformations differ, and the NMR data are in agreement with these results. Once again, equal proportion of rotamers about the ethane fragment is found in solution while the crystal structure shows that the *gauche*-rotamer is trapped in the solid state (24). Some major spectral lines are due to pyridine. The phenyl ring contributes only a small number of sharp absorbances to the spectrum. Therefore, there is a sufficient number of spectral lines to reflect conformational change, and the method is valid. Similar results for diphenhydramine explain the agreement between the IR and NMR data. The two phenyl rings create little interference in the IR spectrum, and once again the analysis is valid.

The quinoline ring system of chloroquine is similar to the phenyl ring in contributing a few sharp peaks to the IR spectrum; thus, the IR–X-ray

method is valid for analysis of this compound. Indeed, the IR spectra of chloroquine in the solid state and in solution are quite different. This result is confirmed by comparison of the NMR data and the crystal structure. The NMR data indicate that rotamers $N_1$ and $N_2$ predominate for the $\alpha$–$\beta$ bond while nearly an equal proportion of rotamers exists for the $\beta$–$\gamma$ and $\gamma$–$\delta$ bonds. In the solid state, the crystal structure shows that rotamer $N_2$ is frozen for the $\alpha$–$\beta$ bond, the *trans*-rotamer is frozen for the $\beta$–$\gamma$ bond, and the *gauche*-rotamer is frozen for the $\gamma$–$\beta$ bond.

In addition, the solution conformation of chloroquine was determined without shift reagents and the results of this analysis were similar to those obtained with shift reagents (26), indicating that the shift reagent did not greatly alter the conformation of chloroquine.

In the NMR experiment, many of the compounds produced sets of triplets with coupling constants that indicate equal proportions of rotamers. These spectra may be deceptively simple (28), which would make the NMR results unreliable. Deceptively simple means that there is more than one set of chemical shifts and coupling constants that could produce the same NMR spectrum; therefore, there could be different proportions of rotamers. To ensure the reliability of the NMR data, this problem is attacked using nialamide as the example. If the two triplets in the nialamide spectrum arose from a conformation that was strongly preferred due to intramolecular or intermolecular interaction, this conformation probably would be similar to the conformation that is frozen upon crystallization. By taking the hydrogen atom coordinates from the crystal structure, the solid-state dihedral angles can be calculated using the BONDLA computer program (34). Solid-state coupling constants then are determined from the Karplus equation and are: $J_{\alpha,\beta} = 2.97$ Hz, $J_{\alpha,\beta'} = 7.23$ Hz, $J_{\alpha',\beta} = 12.8$ Hz, and $J_{\alpha',\beta'} = 3.31$ Hz. These coupling constants produce a complex *AA'BB'*-simulated NMR spectrum, which has little resemblance to the experimentally observed spectrum. Therefore, the NMR technique apparently is reliable.

In conclusion, these results indicate that if a compound contains two or more heteroatomic rings, any IR spectral changes due to conformational changes probably are masked by the absorption of these ring systems. The fingerprint region of the IR spectrum for all compounds containing rigid structures must be characterized prior to the use of the IR–X-ray method to ensure its validity.

This paper also shows how a combination of IR and NMR spectroscopy and X-ray crystallography can be used to provide a complete picture of the conformational features of drugs. In addition, the study illustrates the importance of comparing solid-state and solution conformations before making pharmacological suggestions based on the conformation in the solid state. In nialamide, azaperone, and chloroquine, the solid-state conformation represents only one of several nearly equally energetic solution conformers, which clearly shows that the conformer frozen in the solid state cannot be assumed to be the pharmacologically active or lowest energy solution conformer.

## REFERENCES


(1) L. B. Kier, *J. Med. Chem.*, **16,** 616 (1973).

(2) G. R. Clark and G. J. Palenik, *J. Am. Chem. Soc.*, **94,** 4005 (1972). N. S. Ham, *J. Pharm. Sci.*, **60,** 1764 (1971).

(3) C. R. Ganellin, E. S. Pepper, G. N. J. Port, and W. G. Richards, *J. Med. Chem.*, **16,** 610 (1973). C. R. Ganellin, G. N. J. Port, and W. G. Richards, *ibid.*, **16,** 616 (1973). C. R. Ganellin, *ibid.*, **16,** 620 (1973).

(4) N. S. Ham, A. F. Casy, and R. R. Ison, *J. Med. Chem.*, **16,** 470 (1973).

(5) R. W. Baker, C. H. Clothia, P. J. Pauling, and T. J. Petcher, *Nature (London)*, **230,** 439 (1970).

(6) E. Shefter, in "Cholinergic Ligand Interactions," D. J. Triggle, J. F. Moran, and E. A. Barnard, Eds., Academic, New York, N.Y., 1971.

(7) A. Makriyannis, R. J. Sullivan, and H. G. Mautner, *Proc. Natl. Acad. Sci. USA*, **69,** 3416 (1972). P. Partington, J. Feeney, and A. S. V. Burger, *Mol. Pharmacol.*, **8,** 269 (1972).

(8) P. S. Portoghese, Z. S. Gomaa, D. L. Larson, and E. Shefter, *J. Med. Chem.*, **16,** 199 (1973).

(9) N. Camerman and H. Camerman, *J. Am. Chem. Soc.*, **94,** 8553 (1972).

(10) R. H. Davis, B. Sheard, and P. J. Taylor, *J. Pharm. Sci.*, **68,** 397 (1979).

(11) L. B. Kier, "Molecular Orbital Theory in Drug Research," Academic, New York, N.Y., 1971. L. B. Kier, *J. Pharm. Pharmacol.*, **21,** 93 (1969).

(12) D. E. Koshland, Jr., and K. E. Neet, *Ann. Rev. Biochem.*, **37,** 379 (1972).

(13) M.-A. Coletti-Previero, F. Kraicsovits, and A. Previero, *FEBS Lett.*, **37,** 93 (1973).

(14) F. R. Jensen and C. H. Bushweller, *J. Am. Chem. Soc.*, **91,** 3223 (1969).

(15) F. R. Jensen, G. Bhat, L. J. Letendre, J. A. Brunelle, H. S. Bilofsky, H. Ruben, D. H. Templeton, and A. Zalkin, *ibid.*, **97,** 65 (1974).

(16) A. E. Tonelli and A. I. Brewster, *ibid.*, **94,** 2851 (1972).

(17) I. L. Karle, J. W. Gibson, and J. Karle, *ibid.*, **92,** 3755 (1970).

(18) C. Cohen-Addad and J. P. Cohen-Addad, *J. Chem. Soc., Perkin II*, **1978,** 168.

(19) J. K. Fawcett, N. Camerman, and A. Camerman, *J. Am. Chem. Soc.*, **98,** 587 (1976).

(20) A. L. Ternay, Jr., J. Lin, T. Sutliff, S. S. C. Chu, and B. Chung, *J. Org. Chem.*, **43,** 3024 (1978).

(21) S. R. Byrn, C. W. Graber, and S. L. Midland, *ibid.*, **41,** 2283 (1976).

(22) J. L. Bernstein and A. T. Hagler, *J. Am. Chem. Soc.*, **100,** 673 (1978).

(23) J. Lopez de Lerman, S. Garcia-Blanco, J. Foyos, and J. G. Rodriguez, *Acta Crystallogr.*, **B33,** 2311 (1977).

(24) M. H. J. Koch, G. Germain, J. P. Declerq, and M. VanMeerssche, *ibid.*, **B33,** 1975 (1977).

(25) C. Courseille, B. Busetta, and M. Hospital, *Cryst. Struct. Commun.*, **2,** 283 (1973).

(26) N. S. Angerman, S. S. Danyluk, and T. A. Victor, *J. Am. Chem. Soc.*, **94,** 7137 (1972).

(27) A. A. Bothner-By and S. M. Castellano, in "Computer Programs for Chemistry," vol. I, D. F. Detar, Ed., Benjamin, New York, N.Y., 1968, p. 10.

(28) R. J. Abraham and K. G. R. Pachler, *Mol. Phys.*, **7,** 165 (1964).

(29) R. J. Abraham and G. Gatti, *J. Chem. Soc., B*, **1969,** 961.

(30) R. J. Cushley and H. G. Mautner, *Tetrahedron*, **26,** 2151 (1970).

(31) K. G. R. Pachler, *Spectrochim. Acta*, **19,** 2085 (1963).

(32) M. L. Huggins, *J. Am. Chem. Soc.*, **75,** 4123 (1953).

(33) J. P. Tollenaere, H. Moerells, and M. H. J. Koch, *Eur. J. Med. Chem.*, **12,** 199 (1977).

(34) "The X-Ray System," version of June 1972 (updated 1974), Technical Report TR-192 of the Computer Science Center, University of Maryland, June 1972.


## ACKNOWLEDGMENTS


Supported by Grant ES00929.

The authors thank the Purdue University Regional Biochemical Magnetic Resonance Laboratory, supported by Grant RR01077, for the 360-MHz spectra. They also thank John Kozlowski of this Department for valuable assistance in obtaining some spectra.

# Densification of Powders by Concavo-Convex Roller Compactor

EUGENE L. PARROTT

Received May 23, 1980, from the *Division of Pharmaceutics, College of Pharmacy, University of Iowa, Iowa City, IA 52242.* Accepted for publication August 28, 1980.

**Abstract** □ By means of a concavo-convex roller compactor, several pharmaceutical powders were compressed into sheets or flakes, which then were reduced in size by an oscillating granulator to form compacted granules. Several properties (bulk density, drop density, repose angle, and flow rate) of the powders and compacted granules were determined and compared. The primary effect of the roller compactor was to increase the bulk density without a significant change in flowability. Two materials compacted at five pressures demonstrated that the bulk and drop density are linearly related to the logarithm of compaction pressure.

**Keyphrases** □ Powders—densification by concavo-convex roller compactor, effects on flowability □ Compacted granules—densification of powders by a concavo-convex roller compactor, effect on flowability □ Density—effects of a concavo-convex roller compactor

For many years, dry granulation by compression has been used to form granules of materials that are sensitive to moisture or heat. Dry granulation consists of compacting powder to form a slug with a heavy duty, rotary tablet press or a solid strip using a roller compactor and then reducing its size by milling or screening to achieve a desired granule. The advantages of the roller compactor over the tablet press slugging process include greater production capacity, more control over pressure and dwell time, and no need for lubrication of the powder (1). The powder is force fed by a variable-speed screw feeder to the nip of two counter-rotating rollers, which deaerate and compress the powder into a sheet or flake. The pressure may be varied by control of hydraulic cylinders, which apply the force to a roller. The pressure required varies with the material and the desired density of the granule. The roller compactor may be used for densification of powders for encapsulation, for making a granulation for direct tableting, and for producing a directly compressible excipient that can be blended with the active ingredients.

In the conventional flat roller compactor in which the angle of the inner wall slope of the rim is zero, an adequate supply of powder is not delivered to the gripping and compressing zone by the screw feeder because the stationary side seals act as a resistance to the powder flow. A rectangular aperture chute fitted at the end of the feed screw has been suggested to provide a more uniform supply of powder to the rollers; however, it does not prevent the compression pressure from being greater toward the middle of the width of the rollers than toward the edges (2).

This study demonstrated the usefulness of a concavo-convex roller compactor to increase the density of several pharmaceutical powders and measured some pharmaceutical characteristics of these compacted granules.

## EXPERIMENTAL

**Bulk Materials and Their Properties**—The powders, purchased in bulk, were acetaminophen USP, aminobenzoic acid, precipitated calcium carbonate USP, dibasic calcium phosphate dihydrate USP, granular dicalcium phosphate[1], hydrous lactose[2], light magnesium carbonate USP, sulfadiazine USP, and sulfisoxazole USP. Each powder was transferred by a spatula into a 100-ml cylindrical graduate, and the volume and weight of the powder were determined. The bulk density is the quotient of the weight and volume. Each graduate containing the powder then was dropped five times from a height of 5 cm onto a wooden surface. The volume and weight of the powder were determined, and the quotient was defined as the drop density.

The repose angle was measured by placing the bulk powder in a funnel and allowing the powder to be discharged until the circumference of a circular dish with a radius $r$ was just touched by the pile of powder formed (3). The height $h$ of the pile was measured. The response angle $\phi$ is defined by $\phi = \tan^{-1} h/r$.

The flow rate in grams per second was determined in a flowmeter with a 1.905-cm circular orifice (4). The particle-size distribution was determined by a suitable nest of sieves in a sonic sifter[3]. For materials anticipated to be 200 mesh, a sedimentation technique was employed with an Andreasen pipet[4].

**Compaction**—The powder was compacted in a concavo-convex roller compactor[5] using grooved rollers. The pressure was adjusted and measured by means of a gauge incorporated into the hydraulic system of the compactor. The speeds of the feed screw and the rollers were adjusted for each powder so that compacted strips or flakes were produced and the current of the roller ammeter did not exceed 2 amp. The flakes and

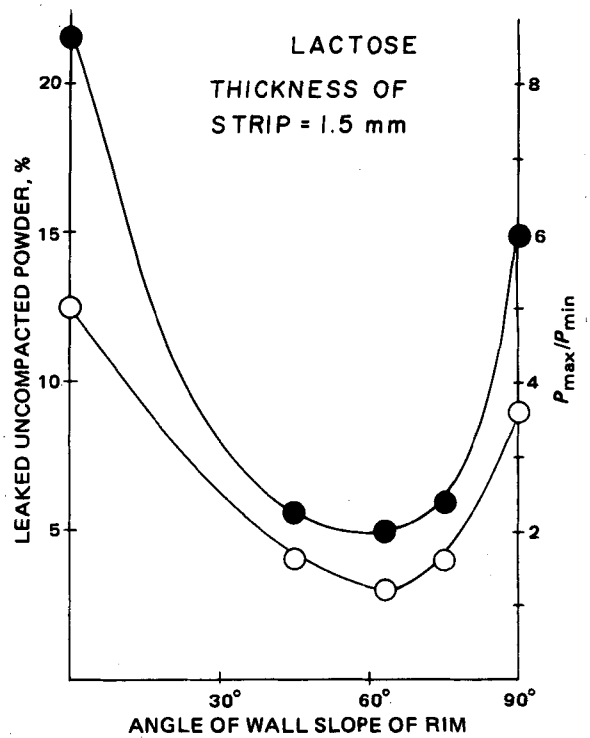


**Figure 1**—*Percent leakage and pressure distribution in relation to wall slope of rim. Key: ●, leakage; and ○, $P_{max}/P_{min}$. (Reproduced, with permission, from Ref. 2.)*

[1] Emcompress, Edward Mendell Co., Carmel, NY 10512.
[2] Spray dried, Foremost Foods Co., San Francisco, CA 44104.
[3] Allen-Bradley, Milwaukee, Wis.
[4] Fisher Scientific Co., Chicago, IL 60143.
[5] Freund Model Mini, Vector Corp., Marion, IA 52302.



0022-3549/81/0300-0288$01.00/0
© 1981, American Pharmaceutical Association

**Table I—Pharmaceutical Properties of Selected Powders**

| Bulk Material | Bulk Density, g/cm³ | Drop Density, g/cm³ | Repose Angle | Flow Rate, g/sec | Median Size, μm |
|---|---|---|---|---|---|
| Acetaminophen | 0.360 | 0.458 | 46.8° | Blocked | 45[a] |
| Aminobenzoic acid | 0.334 | 0.470 | 46.8° | Blocked | 130[a] |
| Calcium carbonate, precipitated | 0.267 | 0.322 | 41.6° | Blocked | 23[a] |
| Dibasic calcium phosphate dihydrate | 0.695 | 0.746 | 40.4° | Blocked | 23[a] |
| Dicalcium phosphate, granular[b] | 0.890 | 0.925 | 33.4° | 66.8 | 160 |
| Lactose, hydrous | 0.633 | 0.774 | 31.9° | 44.6 | 160 |
| Magnesium carbonate, light | 0.152 | 0.168 | 44.3° | Blocked | 3[a] |
| Sulfadiazine | 0.296 | 0.314 | 52.9° | Blocked | 80[a] |
| Sulfisoxazole | 0.368 | 0.430 | 51.5° | Blocked | 70[a] |

[a] Sedimentation by Andreasen pipet. [b] Emcompress.

**Table II—Pharmaceutical Properties of Granules Compacted at 140 kg/cm² and Passed through 1-mm Screen in an Oscillating Granulator**

| Compacted Granules | Bulk Density, g/cm³ | Drop Density, g/cm³ | Repose Angle | Flow Rate, g/sec | Median Size, μm | Crushing Load[a], g |
|---|---|---|---|---|---|---|
| Acetaminophen | 0.567 | 0.646 | 43.0° | Blocked | 700 | <15 |
| Aminobenzoic acid | 0.491 | 0.586 | 43.7° | Blocked | 600 | 39.3 (13.3)[b] |
| Calcium carbonate, precipitated | 0.657 | 0.835 | 38.7° | Blocked | 680 | 34.6 (9.2) |
| Dibasic calcium phosphate dihydrate | 0.943 | 1.215 | 44.3° | Blocked | 580 | 29.9 (9.7) |
| Dicalcium phosphate, granular[c] | 0.939 | 1.115 | 36.2° | Blocked | 440 | — |
| Lactose, hydrous | 0.697 | 0.809 | 40.5° | Blocked | 480 | 33.5 (15.4) |
| Magnesium carbonate, light | 0.460 | 0.565 | 38.6° | Pulsating[d] | 670 | 30.9 (9.0) |
| Sulfadiazine | 0.592 | 0.712 | 41.6° | Pulsating[d] | 730 | 80.0 (32.5) |
| Sulfisoxazole | 0.610 | 0.735 | 40.2° | Blocked | 730 | 40.1 (11.7) |

[a] Average of 10 determinations on 18/20-mesh size fraction. [b] Standard deviation in parentheses. [c] Emcompress. [d] From 20.2 to 32.8 g/sec.

any uncompacted powder were separated using a 10-mesh sieve, and the finer material was returned to the hopper. The densified compact was processed by an oscillating granulator[6] fitted with a 1.0-mm screen. The physical properties of the resulting granules of the compact were measured as described previously.

**Crushing Load**—By means of sieves, a 18/20-mesh size fraction (920 μm ± 10%) of each compacted granule was collected. A viewing port was cut near the end of a 100-ml syringe from which the tip had been removed (5). A granule was placed on a flat metal platform, and the syringe was vertically fitted over it. A hollow plunger was gently lowered into the supporting syringe until its flat face contacted the granule. Mercury was dispensed at a given rate from a separator into the hollow plunger until the granule fractured. The crush load was the sum of the weight of the plunger and the mercury it contained.

## RESULTS AND DISCUSSION

Within the past 5 years, a roller compactor with a concavo-convex roller pair, which maintains their mutual fit while rotating, has been marketed. In the design, the height of the rim and the slope of the inner wall determine the amount of powder to be gripped and compressed. The presence of the additional inner walls of the rims means a greater area of powder is in contact with the roller, and increased powder is subjected to the roller frictional drive in the region of the side seals. This feature counteracts the side seal effect. Thus, the proper selection of the rimmed roller design provides that: (*a*) an adequate supply of powder is delivered into the gripping and compression zone to form a compacted strip and (*b*) this powder is conveyed fully into the narrowest part of the roller gap, essentially eliminating the influence of the side seals.

Satisfying these two conditions may depend on the physical properties of the powder; however, in practice, an angle of 65° for the inner wall slope of the rims or flanges and a ridge height of 7 mm provide uniform compression pressure if proper adjustments are made in the operating conditions such as roller gap, speed of screw feed, and speed of rollers. The influence of the angle of the rim wall slope on the distribution of pressure across the width of the roller and the leakage of power is shown in Fig. 1. The ratio, $P_{max}/P_{min}$, of the maximal and minimal pressures across the width of the rollers represents a nonuniformity index.

By means of a concavo-convex roller pair similar to that shown in Fig. 2, eight compounds with a median diameter ranging from 3 to 160 μm

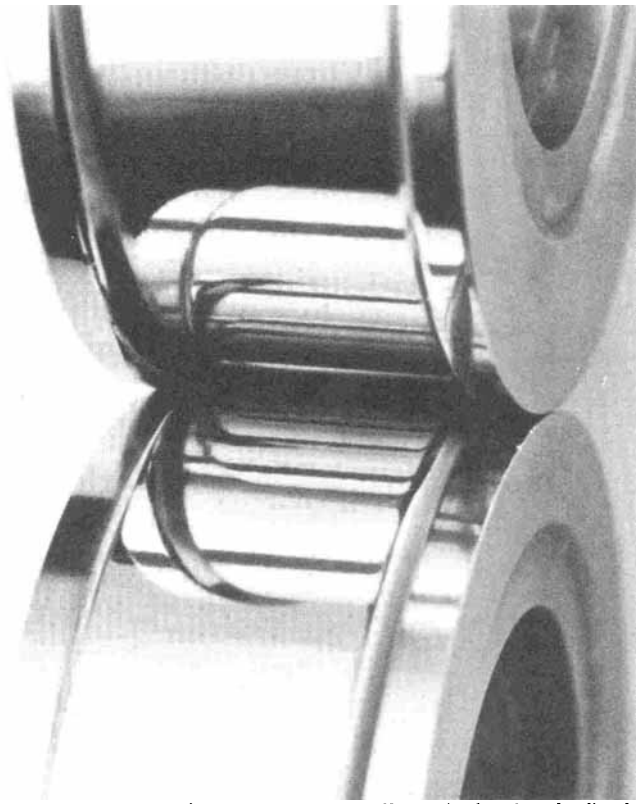

**Figure 2**—*A smooth concavo-convex roller pair showing the fit of the rollers and the wall slope of 65°.*

[6] Type FGS, Erweka-Apparatebau, GmbH, Heusenstamm Kr., Offenbach/Main, West Germany.

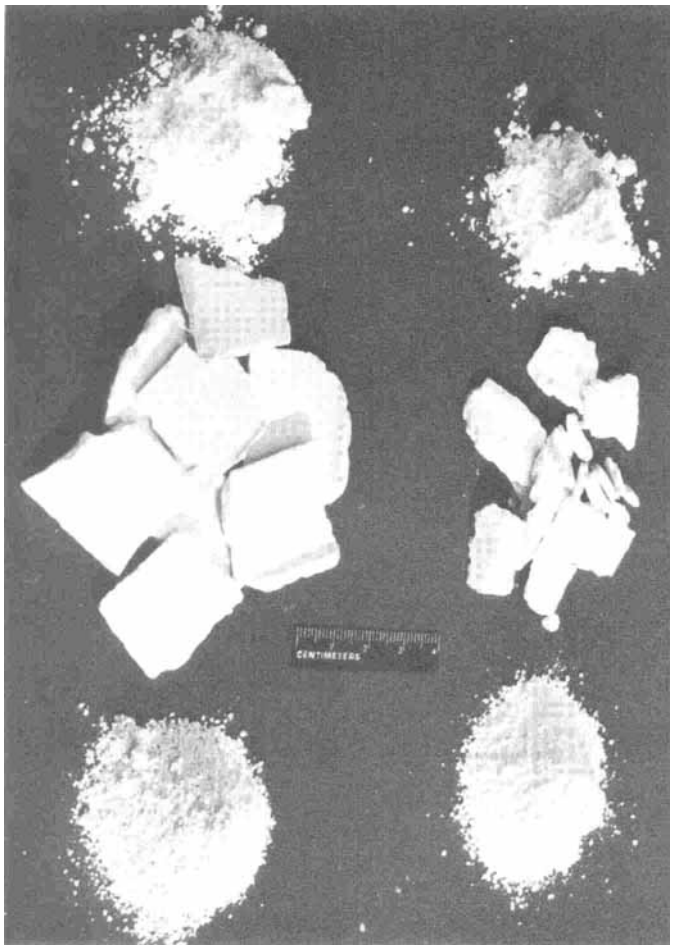

**Figure 3**—*Bulk and roller compacted materials. The upper piles are the bulk powders, the middle samples are the flakes of compacted materials, and the lower piles are the compacted granules prepared by passing the flakes through a 1.0-mm screen in an oscillating granulator. Aminobenzoic acid is on the left, and sulfadiazine is on the right.*

were compacted under a pressure of 140 kg/cm$^2$. The powders listed in Table I were compacted into sheets or flakes as shown in Fig. 3 for aminobenzoic acid and sulfadiazine.

Since the roller compactor is used to densify powders to be encapsulated or tableted, the sheets or flakes were reduced to a size common to these operations by means of an oscillating granulator fitted with a 1.0-mm screen. The median diameter of the compacted granule shown in Table II was determined by the 50% size read from a plot of the size against percent less than the stated size as determined experimentally by sieve analysis. A composite of these plots (Fig. 4) shows that the compacted granules (except lactose and dicalcium phosphate dihydrate) had a median diameter of ~700 μm. Lactose and dicalcium phosphate dihydrate were fragmented during compression (6, 7). The flakes of lactose and dicalcium phosphate dihydrate may have been fractured due to their brittle nature during processing in the oscillating granulator to produce a smaller median diameter than the other materials.

The crushing load or the weight in grams required to fracture a granule was determined (Table II). The crushing load for lactose granules prepared by roller compaction was 33.5 g. The crushing loads for lactose granules prepared by wet granulation were 33.9, 116, and 358.8 g for 1, 3, and 5%, respectively, of povidone as a binding agent (3). Although the

**Table III—Comparison of Bulk Density, Drop Density, and Repose Angle of Powder and Compacted Granules**

| Material | Ratio of Bulk Density of Compacted Granule to Bulk Density of Powder | Ratio of Drop Density of Compacted Granule to Drop Density of Powder | Change in Repose Angle |
|---|---|---|---|
| Acetaminophen | 1.57 | 1.41 | −3.8° |
| Aminobenzoic acid | 1.47 | 1.25 | −3.1° |
| Calcium carbonate | 2.46 | 2.59 | −2.9° |
| Dibasic calcium phosphate dihydrate | 1.35 | 1.63 | +3.9° |
| Dicalcium phosphate, granular[a] | 1.05 | 1.20 | +2.8° |
| Lactose, hydrous | 1.10 | 1.04 | +8.6° |
| Magnesium carbonate | 3.03 | 3.36 | −5.7° |
| Sulfadiazine | 2.00 | 2.27 | −11.3° |
| Sulfisoxazole | 1.66 | 1.71 | −11.3° |

[a] Emcompress.

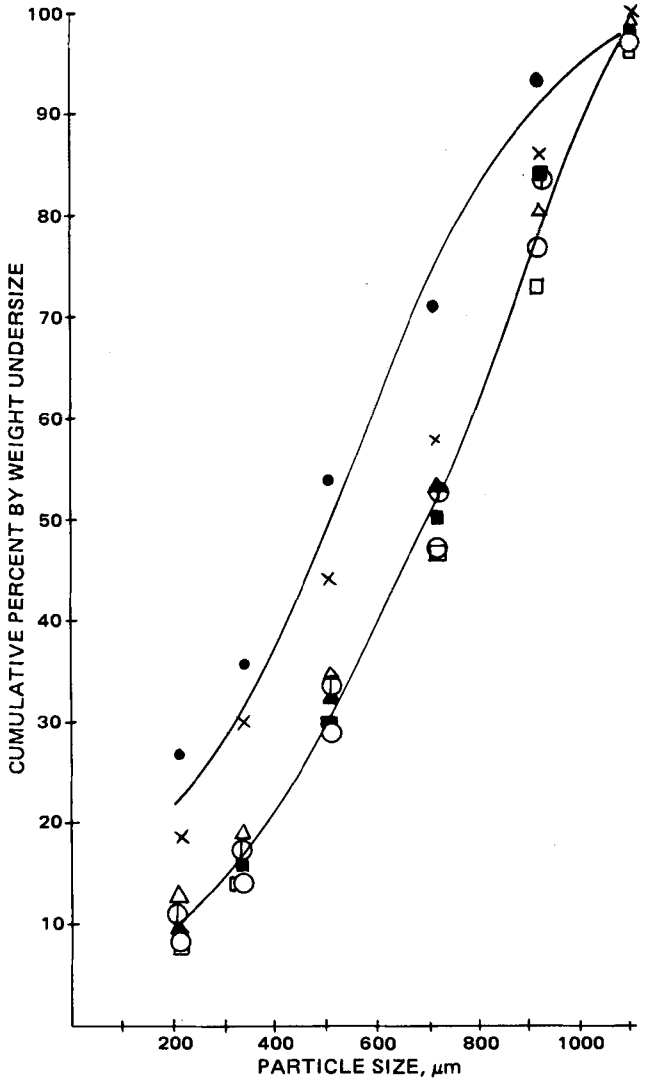


**Figure 4**—*Particle-size distribution of compacted granules. Key: ■, acetaminophen; ⊕, aminobenzoic acid; △, calcium carbonate; ×, dibasic calcium phosphate; ●, lactose; ▲, magnesium carbonate; □, sulfadiazine; and ○, sulfisoxazole.*

**Table IV—Effect of Compaction Pressure on Bulk Density**

| Pressure, kg/cm$^2$ | Density, g/cm$^3$ | | | |
|---|---|---|---|---|
| | Calcium Carbonate | | Magnesium Carbonate | |
| | Bulk | Drop | Bulk | Drop |
| 50 | 0.477 | 0.577 | 0.311 | 0.385 |
| 70 | 0.551 | 0.674 | 0.328 | 0.415 |
| 90 | 0.547 | 0.697 | 0.370 | 0.463 |
| 110 | 0.609 | 0.784 | 0.396 | 0.489 |
| 140 | 0.657 | 0.835 | 0.460 | 0.565 |

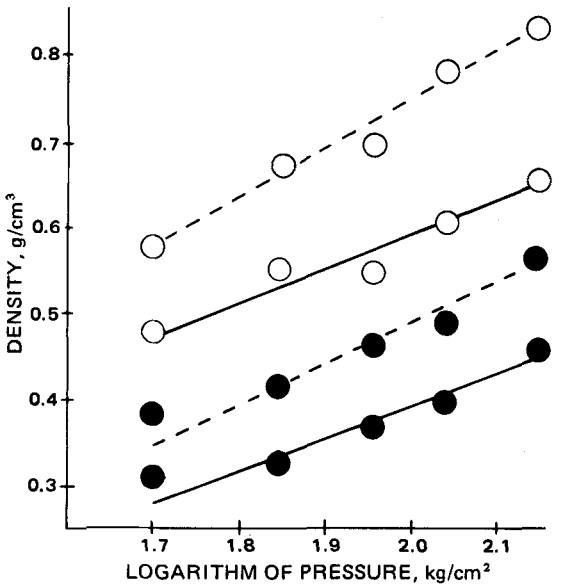


**Figure 5**—*Relationship of bulk and drop densities to logarithm of roller pressure. Key: ○, calcium carbonate; ●, magnesium carbonate; —, bulk density; and ---, drop density.*

crushing loads for lactose and dibasic calcium phosphate dihydrate were similar, the magnitude did not differ markedly from that of the materials. Thus, no correlation is apparent between the size of the material passed through the oscillating granulator and the crushing load of the compacted granules. In pharmaceutical processes, a property of a material is often influenced by the physicochemical nature of the material in addition to the process itself. Even more emphatically than the variation of the particle-size distribution, the effect of the nature of the material is demonstrated by phenacetin, which did not compact in the pressure range of 50–140 kg/cm$^2$.

As shown in Table III, the bulk density of the compacted granules was double to triple that of the bulk density of the powder for calcium carbonate, magnesium carbonate, and sulfadiazine. For acetaminophen, aminobenzoic acid, dibasic calcium phosphate dihydrate, and sulfisoxazole, the bulk density of the compacted granules was increased ~50% more than that of the bulk powder. Essentially the same relationship was demonstrated between the drop density of the compacted granules and that of the powder.

The primary effect of compaction was to increase the bulk density; little or no effect was shown on flowability. A decrease in the repose angle is intuitively associated with improved flowability. Although the repose angle for six materials was less after the materials were compacted, the compacted granules still possessed poor mobility. Only magnesium carbonate and sulfadiazine were discharged from the flowmeter, and their flow was a pulsating one. The repose angle increased for dibasic calcium phosphate dihydrate and hydrous lactose. For the hydrous lactose and granular dicalcium phosphate[1], which were marketed as readily flowable materials, the flow rate decreased from 44.6 and 66.8 g/sec, respectively, to a blockage in the flowmeter, indicating that compaction had destroyed the desired flowability.

Calcium carbonate and magnesium carbonate were selected to study the influence of compaction pressure on bulk density, because they had the smallest median diameters and lowest bulk densities. The bulk and drop densities of these materials compacted at five pressures are given in Table IV; clearly, the density increased as the compaction pressure increased. As shown in Fig. 5, there was a linear relationship between the bulk and drop density and the logarithm of compaction pressure.

## REFERENCES

(1) W. C. Gunsel and J. L. Kanig, in "The Theory and Practice of Industrial Pharmacy," L. Lachman, H. A. Lieberman, and J. L. Kanig, Eds., Lea & Febiger, Philadelphia, Pa., 1976, p. 337.

(2) Y. Funakoshi, T. Asogawa, and E. Satake, *Drug Dev. Ind. Pharm.*, **3**, 555 (1977).

(3) E. L. Parrott and W. Saski, "Experimental Pharmaceutics," 4th ed., Burgess, Minneapolis, Minn., 1977, p. 21.

(4) F. Q. Danish and E. L. Parrott, *J. Pharm. Sci.*, **60**, 548 (1971).

(5) P. Jarosz, Ph.D. thesis, University of Iowa, Iowa City, Iowa, 1980.

(6) J. A. Hersey, J. E. Ress, and E. T. Cole, *J. Pharm. Sci.*, **62**, 2060 (1973).

(7) J. S. Hardman and B. A. Lilley, *Nature*, **228**, 353 (1970).

# High-Pressure Liquid Chromatographic Determination of Chlorothiazide and Hydrochlorothiazide in Plasma and Urine: Preliminary Results of Clinical Studies

**R. H. BARBHAIYA ˣ, T. A. PHILLIPS, and P. G. WELLING**

Received July 8, 1980, from the *School of Pharmacy, University of Wisconsin, Madison, WI 53706.* Accepted for publication August 27, 1980.

**Abstract** □ High-pressure liquid chromatographic procedures were developed for the determination of chlorothiazide and hydrochlorothiazide in plasma and urine. The plasma assay incorporates a preextraction procedure that eliminates interference by endogenous substances. Chromatography is carried out on an octadecyl reversed-phase column. Mobile phases are 15% methanol in 0.01 *M* acetic acid for plasma and 4% acetonitrile in 0.01 *M* sodium perchlorate, adjusted to pH 4.6, for urine. At a flow rate of 2.5 ml/min, the retention times for chlorothiazide and hydrochlorothiazide are 3.5 and 4.6 min for plasma and 10.5 and 13.5 min for urine, respectively. Preliminary results of a clinical study in fasting male volunteers showed that the plasma levels and urinary excretion rate of chlorothiazide peaked at 1–2 hr following a 500-mg oral dose and subsequently declined irregularly. On the other hand, the plasma levels and urinary excretion rate of hydrochlorothiazide peaked at 2–3 hr following a 50-mg oral dose and subsequently declined in biphasic fashion. Urinary excretion rates of both chlorothiazide and hydrochlorothiazide closely resemble their concentration profiles in plasma.

**Keyphrases** □ Chlorothiazide—simultaneous high-pressure liquid chromatographic determinations with hydrochlorothiazide, plasma and urine □ Hydrochlorothiazide—simultaneous high-pressure liquid chromatographic determinations with chlorothiazide, plasma and urine □ High-pressure liquid chromatography—simultaneous determinations of chlorothiazide and hydrochlorothiazide, plasma and urine

Chlorothiazide and hydrochlorothiazide, two thiazide diuretics, are used commonly for treatment of hypertension, congestive heart failure, and other edematous conditions. The spectrophotometric methods originally used to measure these compounds in urine (1–4) are based on derivatizations involving the Bratton–Marshall reaction

0022-3549/81/0300-0291$01.00/0
© 1981, American Pharmaceutical Association

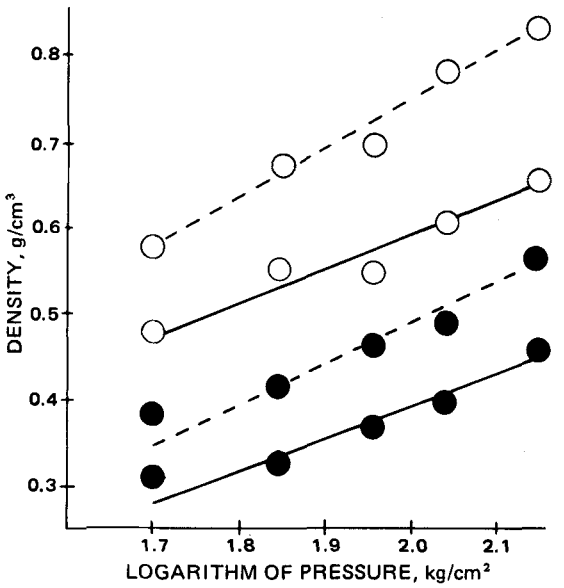


**Figure 5**—*Relationship of bulk and drop densities to logarithm of roller pressure. Key: ○, calcium carbonate; ●, magnesium carbonate; —, bulk density; and ---, drop density.*

crushing loads for lactose and dibasic calcium phosphate dihydrate were similar, the magnitude did not differ markedly from that of the materials. Thus, no correlation is apparent between the size of the material passed through the oscillating granulator and the crushing load of the compacted granules. In pharmaceutical processes, a property of a material is often influenced by the physicochemical nature of the material in addition to the process itself. Even more emphatically than the variation of the particle-size distribution, the effect of the nature of the material is demonstrated by phenacetin, which did not compact in the pressure range of 50–140 kg/cm$^2$.

As shown in Table III, the bulk density of the compacted granules was double to triple that of the bulk density of the powder for calcium carbonate, magnesium carbonate, and sulfadiazine. For acetaminophen, aminobenzoic acid, dibasic calcium phosphate dihydrate, and sulfisoxazole, the bulk density of the compacted granules was increased ~50% more than that of the bulk powder. Essentially the same relationship was demonstrated between the drop density of the compacted granules and that of the powder.

The primary effect of compaction was to increase the bulk density; little or no effect was shown on flowability. A decrease in the repose angle is intuitively associated with improved flowability. Although the repose angle for six materials was less after the materials were compacted, the compacted granules still possessed poor mobility. Only magnesium carbonate and sulfadiazine were discharged from the flowmeter, and their flow was a pulsating one. The repose angle increased for dibasic calcium phosphate dihydrate and hydrous lactose. For the hydrous lactose and granular dicalcium phosphate[1], which were marketed as readily flowable materials, the flow rate decreased from 44.6 and 66.8 g/sec, respectively, to a blockage in the flowmeter, indicating that compaction had destroyed the desired flowability.

Calcium carbonate and magnesium carbonate were selected to study the influence of compaction pressure on bulk density, because they had the smallest median diameters and lowest bulk densities. The bulk and drop densities of these materials compacted at five pressures are given in Table IV; clearly, the density increased as the compaction pressure increased. As shown in Fig. 5, there was a linear relationship between the bulk and drop density and the logarithm of compaction pressure.

## REFERENCES

(1) W. C. Gunsel and J. L. Kanig, in "The Theory and Practice of Industrial Pharmacy," L. Lachman, H. A. Lieberman, and J. L. Kanig, Eds., Lea & Febiger, Philadelphia, Pa., 1976, p. 337.

(2) Y. Funakoshi, T. Asogawa, and E. Satake, *Drug Dev. Ind. Pharm.*, **3**, 555 (1977).

(3) E. L. Parrott and W. Saski, "Experimental Pharmaceutics," 4th ed., Burgess, Minneapolis, Minn., 1977, p. 21.

(4) F. Q. Danish and E. L. Parrott, *J. Pharm. Sci.*, **60**, 548 (1971).

(5) P. Jarosz, Ph.D. thesis, University of Iowa, Iowa City, Iowa, 1980.

(6) J. A. Hersey, J. E. Ress, and E. T. Cole, *J. Pharm. Sci.*, **62**, 2060 (1973).

(7) J. S. Hardman and B. A. Lilley, *Nature*, **228**, 353 (1970).

# High-Pressure Liquid Chromatographic Determination of Chlorothiazide and Hydrochlorothiazide in Plasma and Urine: Preliminary Results of Clinical Studies

**R. H. BARBHAIYA ˣ, T. A. PHILLIPS, and P. G. WELLING**

Received July 8, 1980, from the *School of Pharmacy, University of Wisconsin, Madison, WI 53706.* Accepted for publication August 27, 1980.

**Abstract** □ High-pressure liquid chromatographic procedures were developed for the determination of chlorothiazide and hydrochlorothiazide in plasma and urine. The plasma assay incorporates a preextraction procedure that eliminates interference by endogenous substances. Chromatography is carried out on an octadecyl reversed-phase column. Mobile phases are 15% methanol in 0.01 *M* acetic acid for plasma and 4% acetonitrile in 0.01 *M* sodium perchlorate, adjusted to pH 4.6, for urine. At a flow rate of 2.5 ml/min, the retention times for chlorothiazide and hydrochlorothiazide are 3.5 and 4.6 min for plasma and 10.5 and 13.5 min for urine, respectively. Preliminary results of a clinical study in fasting male volunteers showed that the plasma levels and urinary excretion rate of chlorothiazide peaked at 1–2 hr following a 500-mg oral dose and subsequently declined irregularly. On the other hand, the plasma levels and urinary excretion rate of hydrochlorothiazide peaked at 2–3 hr following a 50-mg oral dose and subsequently declined in biphasic fashion. Urinary excretion rates of both chlorothiazide and hydrochlorothiazide closely resemble their concentration profiles in plasma.

**Keyphrases** □ Chlorothiazide—simultaneous high-pressure liquid chromatographic determinations with hydrochlorothiazide, plasma and urine □ Hydrochlorothiazide—simultaneous high-pressure liquid chromatographic determinations with chlorothiazide, plasma and urine □ High-pressure liquid chromatography—simultaneous determinations of chlorothiazide and hydrochlorothiazide, plasma and urine

Chlorothiazide and hydrochlorothiazide, two thiazide diuretics, are used commonly for treatment of hypertension, congestive heart failure, and other edematous conditions. The spectrophotometric methods originally used to measure these compounds in urine (1–4) are based on derivatizations involving the Bratton–Marshall reaction

0022-3549/81/0300-0291$01.00/0
© 1981, American Pharmaceutical Association

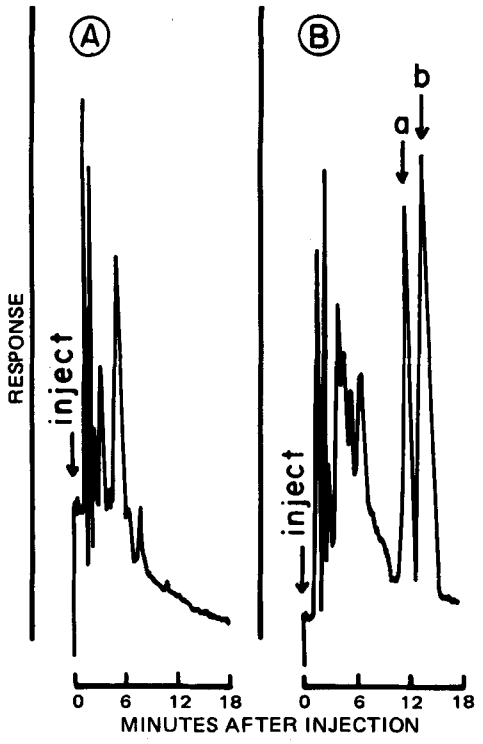


**Figure 1**—*Chromatograms from urine containing no drugs (A) and urine containing 15 μg of I/ml (a in B) and 18 μg of II/ml (b in B).*

and suffer from interference by endogenous urinary constituents (5, 6); TLC with direct fluorometric detection (7) and GLC procedures (8–10) are time consuming. The GLC procedures also involve complex extraction procedures and derivatization.

High-pressure liquid chromatographic (HPLC) assays were recently introduced for hydrochlorothiazide (11–13) and chlorothiazide (14). One method requires gel filtration to remove plasma components (11), while another uses no internal standard and requires injection of a sodium hydroxide solution into the liquid chromatograph, which can reduce the column life (12). None of the methods used the $\lambda_{max}$ of 228 nm for plasma chlorothiazide and hydrochlorothiazide estimations, possibly because of interference by endogenous substances; therefore, maximum assay sensitivity has not been achieved. This limitation is particularly important for plasma where thiazide concentrations are low.

New rapid and sensitive assays for chlorothiazide and hydrochlorothiazide in plasma and urine, together with preliminary plasma level and urinary excretion data for these compounds in human volunteers, are reported in this paper.

## EXPERIMENTAL

**Extraction from Urine**—To 1 ml of urine were added 60 μl of a 300-μg/ml aqueous solution of chlorothiazide or hydrochlorothiazide, each compound acting as the internal standard for the other, 1.5 ml of 0.01 *M* acetate buffer (pH 5.0), and 10 ml of ethyl acetate. After shaking for 10 min and centrifugation at 3000×*g* for 3 min, 8 ml of ethyl acetate was transferred to a clean tube and evaporated to dryness under nitrogen at room temperature. The residue was reconstituted in 75 μl of methanol by vortexing, and 20 μl was injected into the chromatograph.

**Extraction from Plasma**—To 2 ml of plasma were added 100 μl of a 40-μg/ml aqueous solution of the internal standard hydroflumethiazide and 4 ml of toluene. After shaking for 10 min and centrifugation for 3 min, the toluene layer was aspirated and discarded. To the remaining solution were added 0.5 ml of 0.01 *M* acetate buffer (pH 3.8) and 5 ml of ethyl acetate. After shaking for 10 min and centrifugation for 3 min, 3.5–4.0 ml of ethyl acetate was transferred to a clean tube, evaporated to dryness, and reconstituted in 75 μl of methanol; then 20 μl was injected into the chromatograph.

**Chromatography**—The HPLC system consisted of a solvent pump[1], a fixed-volume (20-μl) sample injection valve[2], a 10-μm particle size reversed-phase octadecyl column[3] (30 cm × 4 mm), and a variable-wavelength UV detector[4] set at 228 nm for plasma and at 278 nm for urine. All chromatograms were recorded at a chart speed of 10 cm/hr.

Mobile phases were 4% acetonitrile in 0.01 *M* sodium perchlorate, adjusted to pH 4.6 with 0.01 *M* perchloric acid for urine, and 15% methanol in 0.01 *M* acetic acid for plasma. The flow rate was 2.5 ml/min in both assays. Concentrations were determined by the method of peak height ratios.

**Clinical Study**—Single doses of 500 mg of chlorothiazide[5] (I) and 50 mg of hydrochlorothiazide[6] (II) were administered to three healthy male volunteers[7]. Subjects fasted overnight before drug administration and continued fasting until 4 hr postdosing. All doses were administered at 8 am; the tablets were swallowed whole with 240 ml of water. Blood samples (10 ml) were taken from a forearm vein into heparinized tubes[8] immediately before dosing and serially through 48 or 34 hr postdosing for I or II, respectively. Urines were collected quantitatively through 48 or 60 hr postdosing for I or II, respectively. The blood and urine collection times conformed to larger clinical protocols for both compounds[7]. Plasma and urine samples were stored at −20° until they were assayed, usually within 1 week.

**Reagents**—Human plasma for assay development and standardization was purchased[9]. Human drug-free urine was obtained from male donors as required. Chlorothiazide[10] (I), hydrochlorothiazide[10] (II), and hydroflumethiazide[11] (III) of reference standard quality and methanol[12], acetonitrile[12], acetic acid[13], sodium perchlorate[14], and perchloric acid[15] of analytical grade quality were used as received.

**Table I—Day-to-Day Reproducibility of the Assay for Chlorothiazide and Hydrochlorothiazide in Urine [a]**

| Concentration in Urine, μg/ml | Found, μg/ml | Recovery, % | *CV*, % |
|---|---|---|---|
| | Chlorothiazide | | |
| 2 | 2.04 | 102 | 6.7 |
| 5 | 5.04 | 101 | 5.6 |
| 10 | 10.0 | 100 | 4.9 |
| 20 | 20.2 | 101 | 6.2 |
| 50 | 51.2 | 102 | 4.7 |
| 100 | 102.3 | 102 | 6.3 |
| | Hydrochlorothiazide | | |
| 2 | 2.01 | 101 | 5.9 |
| 5 | 4.95 | 99 | 9.1 |
| 10 | 9.7 | 97 | 4.3 |
| 20 | 19.0 | 95 | 5.5 |
| 50 | 51.8 | 104 | 8.4 |
| 100 | 100.5 | 101 | 6.5 |

[a] $n$ = 10 for all concentrations.

## RESULTS AND DISCUSSION

**Assays**—Both chlorothiazide (I) and hydrochlorothiazide (II) are excreted from the body extensively as unchanged drug in urine (14, 15), and the urinary concentration of both compounds is higher than in plasma. Urine analysis requires specific methods to distinguish the

[1] Model 110, Altex Scientific, Berkeley, Calif.
[2] Model 210, Altex Scientific, Berkeley, Calif.
[3] MCH-10 Micropak, Varian Associates, Palo Alto, Calif.
[4] Hitachi model 100-10, Altex Scientific, Berkeley, Calif.
[5] Lot 559-197, 250-mg tablets, Lederle, Pearl River, N.Y.
[6] Lot B 0686, Hydrodiuril, 50-mg tablets, Merck Sharp and Dohme, West Point, Pa.
[7] These dosages were part of more extensive bioavailability studies, which will be reported separately.
[8] Vacutainer, Becton–Dickinson, Rutherford, N.J.
[9] American Red Cross, Madison, Wis.
[10] Merck Sharp and Dohme, West Point, Pa.
[11] Bristol Laboratories, Syracuse, N.Y.
[12] Burdick & Jackson, Muskegon, Mich.
[13] Allied Chemical Corp., Morristown, N.J.
[14] Fisher Scientific Co., Fair Lawn, N.J.
[15] J. T. Baker Chemical Co., Phillipsburg, N.J.

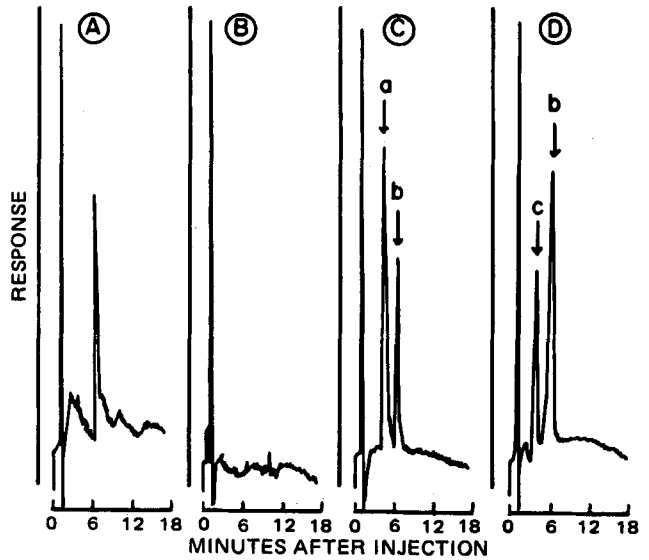


**Figure 2**—*Chromatograms from plasma containing no drugs and assayed without a toluene preextraction step. (A), plasma containing no drugs and assayed with a toluene preextraction step (B), plasma containing 400 ng of II/ml (a in C) and 2 μg of III/ml (b in C), and plasma containing 200 ng of I/ml (c in D) and 2 μg of III/ml (b in D).*

thiazide from interfering substances (5, 6). In addition to specificity, plasma analysis requires high assay sensitivity to measure the low drug concentrations. The assays described here are specific and sensitive for I and II in human urine and plasma following single or repeated doses.

Typical chromatograms obtained from blank urine and from urine containing I and II are shown in Fig. 1. Retention times for I and II from urine were 10.5 and 13.5 min, respectively, and the response was linear for both compounds in the range of 2–100 μg/ml, with a coefficient of variation of <10%. Standard curves obtained from repeated determinations were $y = 0.040 + 0.0598x$, $r = 0.999$, $n = 35$, for I and $y = 0.024 + 0.0712x$, $r = 0.996$, $n = 35$, for II. The day-to-day reproducibility of the urine assays, determined on 10 occasions during 2 months, is shown in Table I.

Typical chromatograms obtained from blank plasma, with and without toluene preextraction, and from plasma containing I, II, and hydroflumethiazide (III), are given in Fig. 2. Retention times for I, II, and III from plasma were 3.5, 4.6, and 6.0 min, respectively, and the response was linear for I and II concentrations of 10–750 ng/ml, with a coefficient of variation of <10%. Standard curves obtained from repeated determinations were $y = 0.007 + 0.0032x$, $r = 0.999$, $n = 35$, for I and $y = 0.023 + 0.004x$, $r = 0.999$, $n = 35$, for II. The day-to-day reproducibility of the plasma assays determined on 10 occasions during 2 months is shown in Table II. In the urine assays, I and II could be separated from each other by using 4% acetonitrile in 0.01 *M* sodium perchlorate (pH 4.6) as the mobile phase. Therefore, they were used as internal standards for each other. Interference by endogenous substances was not a major problem with the urine assays, and clear chromatograms were obtained with the detector set at 278 nm.

The low levels of I and II that occur in plasma compared to urine required some procedural modifications to obtain the required assay sensitivity and selectivity. A toluene preextraction step removed interfering peaks due to endogenous plasma components but did not remove I–III, which are sparingly soluble in toluene. Assay sensitivity was improved further by setting the detector at 228 nm, the $\lambda_{max}$ for both I and II, and also by using methanol–acetic acid as the mobile phase. Both I and II absorb UV light at 228 nm to a greater extent in this solvent than in acetonitrile–sodium perchlorate. Effective separation of I and II could not

**Table II—Day-to-Day Reproducibility of the Assays for Chlorothiazide and Hydrochlorothiazide in Plasma [a]**

| Concentration in Plasma, ng/ml | Found, ng/ml | Recovery, % | *CV*, % |
|---|---|---|---|
| | Chlorothiazide | | |
| 10 | 9.9 | 99 | 5.8 |
| 25 | 24.3 | 97 | 5.5 |
| 50 | 49.0 | 98 | 6.0 |
| 100 | 99.6 | 100 | 6.2 |
| 500 | 508 | 102 | 5.7 |
| 750 | 746 | 99 | 4.4 |
| | Hydrochlorothiazide | | |
| 10 | 10.0 | 100 | 6.7 |
| 20 | 19.3 | 96 | 6.7 |
| 50 | 50.6 | 101 | 6.9 |
| 100 | 99.0 | 99 | 6.2 |
| 250 | 254 | 102 | 5.4 |
| 500 | 498 | 100 | 4.2 |
| 750 | 750 | 100 | 1.7 |

[a] $n = 10$ for all concentrations.

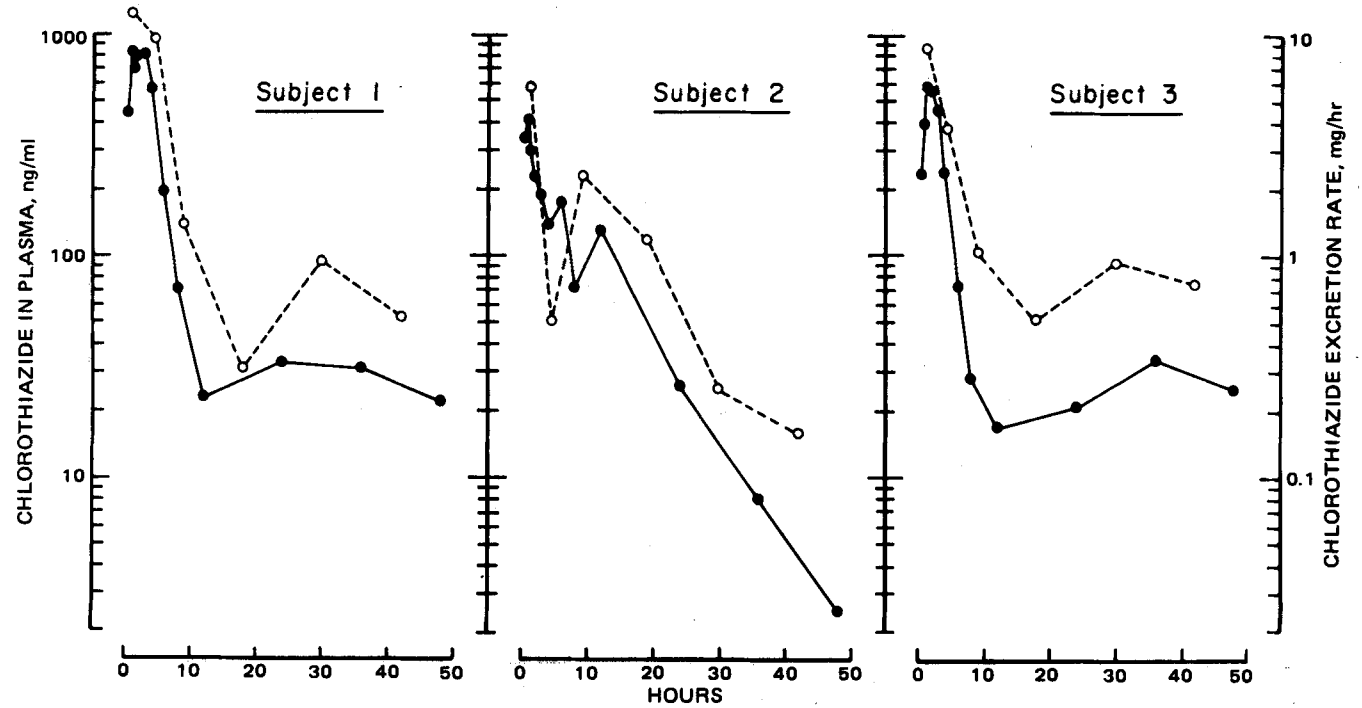


**Figure 3**—*Plasma levels (●) and urinary excretion rates (○) for I in three subjects following a single 500-mg oral dose.*

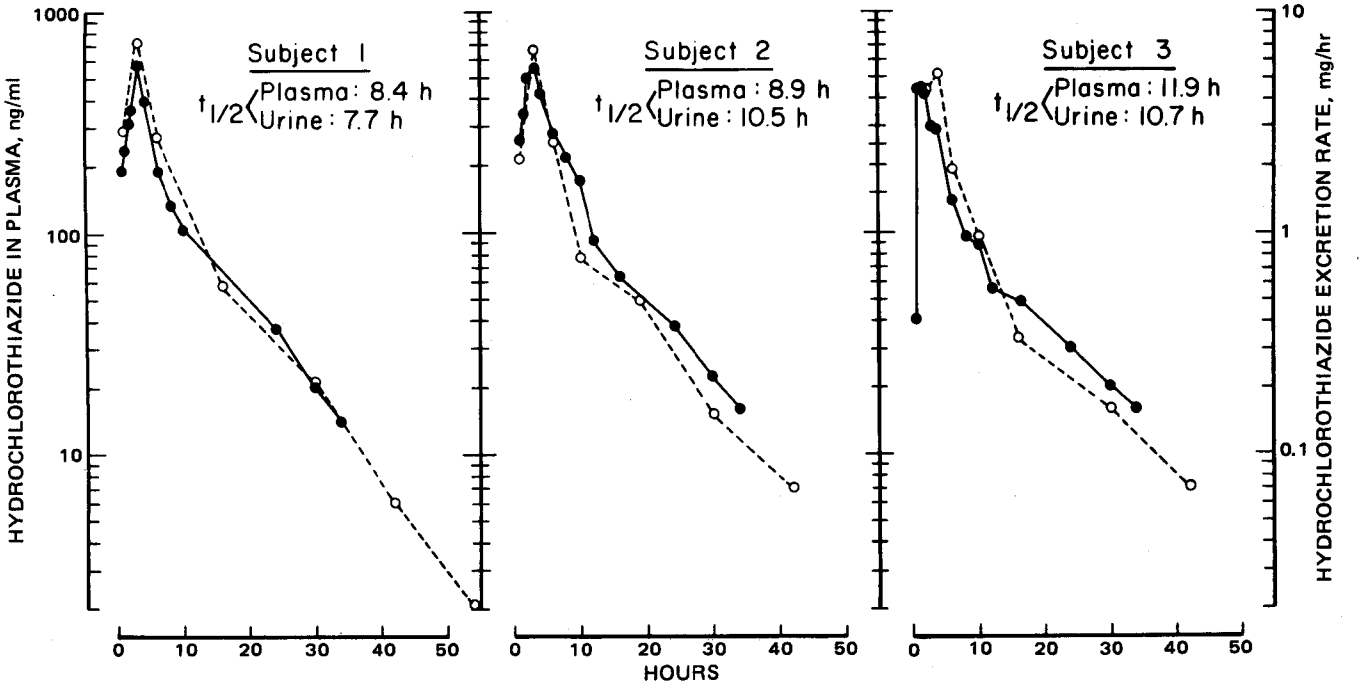


**Figure 4**—*Plasma levels (●) and urinary excretion rates (○) for II in three subjects following a single 50-mg oral dose.*

be achieved using methanol–acetic acid, but both compounds did separate from III. Therefore, III was used as the internal standard in the assays for I and II in plasma.

**Clinical Studies**—Individual plasma levels of I and II, each drug being administered to three subjects, are shown in Figs. 3 and 4, respectively.

The I profiles were similar in the three individuals. Peak plasma I levels of 420–850 ng/ml were achieved 1–2 hr following a single 500-mg dose. Drug levels then declined rapidly until 8–12 hr postdosing, at which time they became irregular, exhibiting a saw-toothed effect in two subjects while declining to lower levels in the other subject.

The II profiles were also similar in the three individuals but quite different from the plasma profiles obtained with I. Peak plasma II levels of 450–550 ng/ml were achieved 2–3 hr following a single 50-mg dose. Drug levels then declined rapidly until 10–12 hr postdosing and continued to decline at a slower monoexponential rate. The terminal plasma half-lives, which were measurable for II, were 8.4, 8.9, and 11.9 hr in the three subjects.

While the reason for the different behavior of I and II in human plasma is not known, the types of profiles reported here have been observed routinely in subjects receiving these drugs in this laboratory[16] and have been reported by others. The rapid initial loss of orally dosed I from plasma followed by variable drug levels was reported recently (14), while biphasic elimination of plasma II with an apparently prolonged drug distribution phase was reported at dose levels similar to those used in this study (15).

The cumulative 48-hr urinary recovery of I accounted for only 10.4, 19.0, and 13.9% of the dose in the three subjects, while 87.8, 79.3, and 74.4% of II were recovered in 60-hr urine. High urinary recovery of II and low recovery of I also are consistent with previous observations (14, 15).

To compare the kinetics of urinary recovery with the rate of drug loss from plasma, the individual urinary excretion rates of both compounds were calculated at the midpoint of each urine collection interval; the values were plotted on a semilogarithmic scale along with the plasma drug profiles in Figs. 3 and 4.

Comparison of the data indicates similarity in the individual plasma levels and urinary excretion rates for both I and II. Details of plasma levels and urinary excretion of these two compounds in a larger number of subjects will be reported in detail, together with pharmacokinetic analysis. However, these preliminary observations are of interest in view of the limited pharmacokinetic information available for the thiazide diuretics and their identification as compounds with actual or potential bioequivalence problems (16). These results are important also in view of the nonproportionality that has been reported between urinary recovery of I and the administered dose (14, 17) and the good correlations reported between dose size and resulting plasma II levels (15). There is clearly a high correlation between plasma levels and urinary excretion kinetics of both I and II, and these relationships are being examined further at different dose levels.

The methods described here are sufficiently sensitive to detect plasma levels of I for 48 hr and II for 34 hr and to measure urinary excretion of both compounds for 48–60 hr after oral doses of 500 and 50 mg of I and II, respectively. The procedure for plasma has marked advantages over previous methods (11–13) in both sensitivity and specificity. Degradation of II, which may occur in other procedures (12, 13) where sodium hydroxide solutions are used for back-extraction or reconstitution, is avoided by eliminating the use of alkaline solutions. Although the procedures are different in urine and plasma, the use of identical extraction and chromatographic conditions for both compounds in plasma and urine makes the methods simple, accurate, and convenient for pharmacokinetic studies.

[16] R. H. Barbhaiya and P. G. Welling, unpublished data.

## REFERENCES

(1) J. E. Baer, H. L. Leidy, A. V. Brooks, and K. H. Beyer, *J. Pharmacol. Exp. Ther.*, **125**, 295 (1959).

(2) H. Sheppard, T. F. Mowles, and A. J. Plummer, *J. Am. Pharm. Assoc., Sci. Ed.*, **49**, 722 (1960).

(3) M. C. Meyer and A. B. Straughn, *Curr. Ther. Res.*, **22**, 573 (1977).

(4) D. Suria, *Clin. Biochem.*, **11**, 222 (1978).

(5) D. E. Resetarits and T. R. Bates, *J. Pharm. Sci.*, **68**, 126 (1979).

(6) J. P. Hunt, V. P. Shah, V. K. Prasad, and B. Cabana, *Anal. Lett.*, **13**, 135 (1980).

(7) M. Schafer, H. G. Geissler, and E. Mulshler, *J. Chromatogr.*, **143**, 615 (1977).

(8) B. Lindstrom and M. Molander, *ibid.*, **114**, 459 (1975).

(9) E. Redalieu, V. V. Tipnis, and W. E. Wagner, *J. Pharm. Sci.*, **67**, 726 (1978).

(10) W. J. A. VandenHeuvel, V. F. Gruber, R. W. Walker, and F. J. Wolf, *ibid.*, **64**, 1309 (1975).

(11) A. S. Christopherson, K. E. Rasmussen, and B. Salvesen, *J. Chromatogr.*, **132**, 91 (1977).

(12) M. J. Cooper, A. R. Sinaiko, M. W. Anders, and B. L. Mirkin, *Anal. Chem.*, **48**, 1110 (1976).

(13) W. T. Robinson and L. Cosyns, *Clin. Biochem.*, **11**, 172 (1978).

(14) V. P. Shah, V. K. Prasad, B. E. Cabana, and P. Sojka, *Curr. Ther. Res.*, **24**, 366 (1978).
(15) B. Beermann and M. Groschinsky-Grind, *Eur. J. Clin. Pharmacol.*, **12**, 297 (1977).
(16) Department of Health, Education, and Welfare Publication (FDA) 76-3009, **4**, 11 (1976).
(17) A. B. Straughn, A. P. Melikan, and M. C. Meyer, *J. Pharm. Sci.*, **68**, 1099 (1979).

ACKNOWLEDGMENTS

Supported by National Institutes of Health Grant GM 20327.

# Pharmacokinetic Evidence for Possible Renal Accumulation of Model Organic Anions in Rats

**JANARDAN B. NAGWEKAR ˣ and JOO WHA CHEON**

Received May 30, 1980, from the *Pharmaceutics Division, College of Pharmacy and Allied Health Professions, Wayne State University, Detroit, MI 48202.* Accepted for publication August 27, 1980.

**Abstract** □ The urinary excretion and blood level kinetics of *p*-methylbenzoylformic acid (I) after intravenous infusion for 1 hr were studied in rats. The determined first-order half-lives were compared with those determined in studies in which a single intravenous dose of I was administered rapidly to rats that previously were infused with normal saline for 1 hr. While the blood $t_{1/2}$ or body clearance of I determined in the 1-hr infusion studies was similar to that determined in the single intravenous dose studies, the urinary $t_{1/2}$ of I determined in the 1-hr infusion studies was significantly greater than that determined in the single intravenous dose studies. In infusion studies where the half-lives of I were determined in the presence of renal tubular secretion inhibitor, DL-tropic acid (II), the ratio of (urinary $t_{1/2})_{\text{II present}}$/(urinary $t_{1/2})_{\text{II absent}}$ was almost twice the ratio of (blood $t_{1/2})_{\text{II present}}$/(blood $t_{1/2})_{\text{II absent}}$. The urinary $t_{1/2}$ value of I determined after infusion for only 10 min was intermediate between values obtained in the single intravenous dose studies and the 1-hr infusion studies. These data provide pharmacokinetic evidence to support the hypothesis that I and other organic anions temporarily accumulate in the surface-lying renal tubular cells after a single intravenous dose, but they tend to penetrate into the deeper renal tubular cells upon intravenous infusion, with depth of penetration increasing with increasing infusion time.

**Keyphrases** □ Renal accumulation—*p*-methylbenzoylformic acid, pharmacokinetics, rats □ *p*-Methylbenzoylformic acid—model organic compound used for determination of renal accumulation, pharmacokinetics □ Pharmacokinetics—renal accumulation of model organic anions, rats

Recent studies (1) in rats showed that the biological half-lives of mandelic acid, benzoylformic acid, and several of their *para*-alkylated homologs, including *p*-methylbenzoylformic acid (I), determined from urinary excretion data are longer than those determined from blood level data following a single intravenous dose. In the presence of a simultaneously administered intravenous dose of DL-tropic acid (II), a competitive inhibitor of renal tubular secretion of these compounds, the urinary half-lives were disproportionately longer than the blood half-lives. The ratios of (urinary $t_{1/2}$/blood $t_{1/2}$) determined for these compounds in the presence of II were greater than such ratios determined in the absence of II. The longer urinary half-lives were attributed to the retention or detention of these compounds in the renal tubular membranes during secretion.

## BACKGROUND

Several reports (2–4) indicated that cellular trapping of organic anions, such as *p*-aminohippurate and phenolsulfonphthalein, occurs during their renal tubular secretion in mammals. Recent *in vitro* rat kidney slice uptake studies (4, 5) showed that *p*-aminohippurate accumulates mainly in the proximal renal tubules, and the volume of renal tubules that absorb the compound increases with incubation time and its concentration in the medium. Also, in the presence of renal tubular secretion inhibitors, a redistribution of accumulation of *p*-aminohippurate occurred and further uptake took place in the deeper proximal renal tubules (6).

The purpose of this study was to obtain pharmacokinetic evidence in support of the proposed hypotheses concerning the retention/detention and distribution of organic anions in the renal tubules by studying blood level kinetics and urinary excretion kinetics of I in rats after intravenous infusion for 1 hr, both in the absence and presence of II. Therefore, the specific objectives of the study were to demonstrate that:

1. The (urinary $t_{1/2})_{\text{infusion}}$ of I determined in the infusion study is longer than its (urinary $t_{1/2})_{\text{single iv dose}}$ determined in the single intravenous dose study.
2. The (blood $t_{1/2})_{\text{infusion}}$ of I is similar to its (blood $t_{1/2})_{\text{single iv dose}}$.
3. The ratio of (urinary $t_{1/2}$/blood $t_{1/2})_{\text{infusion}}$ of I obtained in the presence of II is greater than that obtained in the absence of II.
4. The urinary $t_{1/2}$ determined after infusing I for 1 hr is longer than that determined after infusing it for 10 min.

Compound I (pKa 3.3) was used as a model organic anion because it is neither metabolized, bound to plasma proteins, nor reabsorbed from the renal tubules of rats (1). Furthermore, the entire administered dose of I is eliminated renally (which includes renal tubular secretion), and it follows one-compartment open model kinetics (1).

## EXPERIMENTAL

**Materials**—*p*-Methylbenzoylformic acid, mp 97–99°, was synthesized by the method of Kindler *et al.* (7). DL-Tropic acid[1], mp 116–118°, and pentobarbital sodium[2] (USP grade) were also used.

**Apparatus and Analytical Procedure**—The GLC[3] procedures used for the quantitative determination of I in rat urine and blood were essentially the same as described previously (1, 8).

**Surgical Preparation of Rats**—Sprague–Dawley male rats, 170–230 g (a majority weighed ~200 g), were used in the blood level kinetic studies and urinary excretion kinetic studies. Food, but not water, was withheld from the rats 12–14 hr prior to the study and during it. Each rat was prepared surgically for infusion of the isotonic solution of I (1.75 mg/ml), with or without II, *via* a femoral vein.

A rat was anesthetized with pentobarbital sodium (40 mg/kg ip) and placed on an animal board. A small amount of ether was used to anesthetize the rats completely. The limbs were tied to the animal board, and hair between the left leg and abdomen was shaved off with an electric clipper; the shaved part was cleaned with 70% (v/v) ethanol. The skin between the left leg and the midline was cut open to expose a femoral vein, which was isolated from the femoral artery and femoral nerve. The femoral vein was cannulated with polyethylene tubing[4] (0.028 cm i.d.,

[1] Aldrich Chemical Co., Milwaukee, Wis.
[2] Merck & Co., Rahway, N.J.
[3] Hewlett-Packard model 5720A gas chromatograph.
[4] Intramedic (PE-10), Clay Adams, Division of Becton–Dickenson Co., Parsippany, N.J.

0022-3549/81/0300-0295$01.00/0
© 1981, American Pharmaceutical Association

(14) V. P. Shah, V. K. Prasad, B. E. Cabana, and P. Sojka, *Curr. Ther. Res.*, **24**, 366 (1978).
(15) B. Beermann and M. Groschinsky-Grind, *Eur. J. Clin. Pharmacol.*, **12**, 297 (1977).
(16) Department of Health, Education, and Welfare Publication (FDA) 76-3009, **4**, 11 (1976).
(17) A. B. Straughn, A. P. Melikan, and M. C. Meyer, *J. Pharm. Sci.*, **68**, 1099 (1979).

ACKNOWLEDGMENTS

Supported by National Institutes of Health Grant GM 20327.

# Pharmacokinetic Evidence for Possible Renal Accumulation of Model Organic Anions in Rats

**JANARDAN B. NAGWEKAR ˣ and JOO WHA CHEON**

Received May 30, 1980, from the *Pharmaceutics Division, College of Pharmacy and Allied Health Professions, Wayne State University, Detroit, MI 48202.* Accepted for publication August 27, 1980.

**Abstract** □ The urinary excretion and blood level kinetics of *p*-methylbenzoylformic acid (I) after intravenous infusion for 1 hr were studied in rats. The determined first-order half-lives were compared with those determined in studies in which a single intravenous dose of I was administered rapidly to rats that previously were infused with normal saline for 1 hr. While the blood $t_{1/2}$ or body clearance of I determined in the 1-hr infusion studies was similar to that determined in the single intravenous dose studies, the urinary $t_{1/2}$ of I determined in the 1-hr infusion studies was significantly greater than that determined in the single intravenous dose studies. In infusion studies where the half-lives of I were determined in the presence of renal tubular secretion inhibitor, DL-tropic acid (II), the ratio of (urinary $t_{1/2})_{\text{II present}}$/(urinary $t_{1/2})_{\text{II absent}}$ was almost twice the ratio of (blood $t_{1/2})_{\text{II present}}$/(blood $t_{1/2})_{\text{II absent}}$. The urinary $t_{1/2}$ value of I determined after infusion for only 10 min was intermediate between values obtained in the single intravenous dose studies and the 1-hr infusion studies. These data provide pharmacokinetic evidence to support the hypothesis that I and other organic anions temporarily accumulate in the surface-lying renal tubular cells after a single intravenous dose, but they tend to penetrate into the deeper renal tubular cells upon intravenous infusion, with depth of penetration increasing with increasing infusion time.

**Keyphrases** □ Renal accumulation—*p*-methylbenzoylformic acid, pharmacokinetics, rats □ *p*-Methylbenzoylformic acid—model organic compound used for determination of renal accumulation, pharmacokinetics □ Pharmacokinetics—renal accumulation of model organic anions, rats

Recent studies (1) in rats showed that the biological half-lives of mandelic acid, benzoylformic acid, and several of their *para*-alkylated homologs, including *p*-methylbenzoylformic acid (I), determined from urinary excretion data are longer than those determined from blood level data following a single intravenous dose. In the presence of a simultaneously administered intravenous dose of DL-tropic acid (II), a competitive inhibitor of renal tubular secretion of these compounds, the urinary half-lives were disproportionately longer than the blood half-lives. The ratios of (urinary $t_{1/2}$/blood $t_{1/2}$) determined for these compounds in the presence of II were greater than such ratios determined in the absence of II. The longer urinary half-lives were attributed to the retention or detention of these compounds in the renal tubular membranes during secretion.

## BACKGROUND

Several reports (2–4) indicated that cellular trapping of organic anions, such as *p*-aminohippurate and phenolsulfonphthalein, occurs during their renal tubular secretion in mammals. Recent *in vitro* rat kidney slice uptake studies (4, 5) showed that *p*-aminohippurate accumulates mainly in the proximal renal tubules, and the volume of renal tubules that absorb the compound increases with incubation time and its concentration in the medium. Also, in the presence of renal tubular secretion inhibitors, a redistribution of accumulation of *p*-aminohippurate occurred and further uptake took place in the deeper proximal renal tubules (6).

The purpose of this study was to obtain pharmacokinetic evidence in support of the proposed hypotheses concerning the retention/detention and distribution of organic anions in the renal tubules by studying blood level kinetics and urinary excretion kinetics of I in rats after intravenous infusion for 1 hr, both in the absence and presence of II. Therefore, the specific objectives of the study were to demonstrate that:

1. The (urinary $t_{1/2})_{\text{infusion}}$ of I determined in the infusion study is longer than its (urinary $t_{1/2})_{\text{single iv dose}}$ determined in the single intravenous dose study.
2. The (blood $t_{1/2})_{\text{infusion}}$ of I is similar to its (blood $t_{1/2})_{\text{single iv dose}}$.
3. The ratio of (urinary $t_{1/2}$/blood $t_{1/2})_{\text{infusion}}$ of I obtained in the presence of II is greater than that obtained in the absence of II.
4. The urinary $t_{1/2}$ determined after infusing I for 1 hr is longer than that determined after infusing it for 10 min.

Compound I (pKa 3.3) was used as a model organic anion because it is neither metabolized, bound to plasma proteins, nor reabsorbed from the renal tubules of rats (1). Furthermore, the entire administered dose of I is eliminated renally (which includes renal tubular secretion), and it follows one-compartment open model kinetics (1).

## EXPERIMENTAL

**Materials**—*p*-Methylbenzoylformic acid, mp 97–99°, was synthesized by the method of Kindler *et al.* (7). DL-Tropic acid[1], mp 116–118°, and pentobarbital sodium[2] (USP grade) were also used.

**Apparatus and Analytical Procedure**—The GLC[3] procedures used for the quantitative determination of I in rat urine and blood were essentially the same as described previously (1, 8).

**Surgical Preparation of Rats**—Sprague–Dawley male rats, 170–230 g (a majority weighed ~200 g), were used in the blood level kinetic studies and urinary excretion kinetic studies. Food, but not water, was withheld from the rats 12–14 hr prior to the study and during it. Each rat was prepared surgically for infusion of the isotonic solution of I (1.75 mg/ml), with or without II, *via* a femoral vein.

A rat was anesthetized with pentobarbital sodium (40 mg/kg ip) and placed on an animal board. A small amount of ether was used to anesthetize the rats completely. The limbs were tied to the animal board, and hair between the left leg and abdomen was shaved off with an electric clipper; the shaved part was cleaned with 70% (v/v) ethanol. The skin between the left leg and the midline was cut open to expose a femoral vein, which was isolated from the femoral artery and femoral nerve. The femoral vein was cannulated with polyethylene tubing[4] (0.028 cm i.d.,

[1] Aldrich Chemical Co., Milwaukee, Wis.
[2] Merck & Co., Rahway, N.J.
[3] Hewlett-Packard model 5720A gas chromatograph.
[4] Intramedic (PE-10), Clay Adams, Division of Becton–Dickenson Co., Parsippany, N.J.

0022-3549/81/0300-0295$01.00/0
© 1981, American Pharmaceutical Association

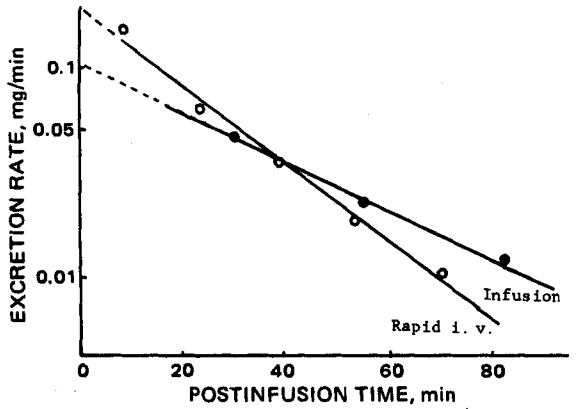


**Figure 1**—*Typical semilogarithmic urinary excretion plots obtained for I after its rapid intravenous administration of a single dose to a rat previously infused with normal saline for 1 hr (○) and after continuous intravenous infusion into a rat for 1 hr (●).*

0.061 cm o.d.). The inserted end of the cannula and the vein were tied together to keep the cannula in the vein. The surgically opened area was closed with clips using a clip applier[5].

The surgical procedure took ~20 min. The rat generally regained consciousness within 30 min after the cannulation. The rat then was placed in an acrylic restraining cage and usually was ready for infusion ~1 hr after cannulation.

**Urinary Excretion Studies**—The urinary excretion kinetics of I were studied under the following four conditions:

1. Compound I was infused into the rat for 1 hr at 0.2275 mg/0.13 ml/min. This infusion rate was chosen to produce, at the end of the 1-hr infusion, a blood concentration that would be close to the initial blood concentration produced following rapid intravenous administration of a single dose of 22 mg/kg as reported previously (1). Six rat studies were performed.

2. The rat was infused with normal saline for 1 hr at 0.092 ml/min, immediately followed by a rapid intravenous infusion of a single dose of 4.4 mg of I contained in 2 ml. This study served as a control for that described in Condition 1. Four rat studies were performed.

3. Compound I was infused into the rat for 1 hr at 0.2275 mg/0.13 ml/min in the presence of II. The infusion rate of II, which was contained in the same solution of I, was 4.55 mg/0.13 ml/min. The II infusion rate was chosen to produce, at the end of the 1-hr infusion, a blood concentration that would be similar to the initial blood concentration produced following rapid intravenous administration of a single dose of 100 mg/kg as reported previously (1). There was no need to conduct a separate single intravenous dose control study for this portion of the study (see *Discussion*). Five rat studies were performed.

4. The rat was infused first with normal saline at 0.13 ml/min for 50 min, followed by the I infusion at 0.5562 mg/0.13 ml/min for 10 min. The I infusion rate was chosen to produce, at the end of the 10-min infusion, a blood concentration that would be similar to that at the end of the 1-hr infusion as described in Condition 1. Five rat studies were performed.

All solutions used in Conditions 1–4 were isotonic and were adjusted to pH 7.4. Immediately after the prolonged or rapid infusion of I, the outer cannula was cut at a point ~1 cm from the skin, and the cannula opening was sealed with a flame. The rat then was transferred to a urine collection cage (9), and urine samples were collected according to the procedure described previously (9).

**Blood Studies**—The blood level kinetics of I were studied under the following conditions:

1. Compound I was infused into the rat for 1 hr at 0.2275 mg/0.13 ml/min. As described previously (8, 10), only one blood sample was obtained from a given rat upon its decapitation at a predetermined time. On a given day, altogether three blood I levels were determined from three different rats decapitated at 10, 20, and 30 min postinfusion. The procedure used for collecting blood samples was the same as described previously (8). Fifteen rat studies were performed. There was no need to conduct a separate single intravenous dose control study for this phase (see *Discussion*).

2. Compound I was infused into the rat for 1 hr at 0.2275 mg/0.13 ml/min in the presence of II. The infusion rate of II, which was contained in the same solution of I, was 4.55 mg/0.13 ml/min, as explained under the urinary excretion studies. The procedure for obtaining blood samples and the number of blood samples obtained from rats were identical to that described under Condition 1. Fifteen rat studies were performed. There was no need to conduct a separate single intravenous dose control study for this phase (see *Discussion*).

[5] Autoclips and autoclip applier, Clay Adams, Division of Becton–Dickenson Co., Parsippany, N.J.

## RESULTS

**Urinary Excretion Kinetics of I after 1-hr Infusion**—Since the urinary excretion of I is an apparent first-order process after a single intravenous dose in the 2.0–9.7-mg/rat range (1), and since, as shown later, I disappearance from the blood after the 1-hr infusion occurs monoexponentially, the urinary excretion of the compound after a 1-hr infusion can be expected to occur by a first-order process (Fig. 1). The data were treated according to:

$$\log(\Delta D_e/\Delta t) = \log k_{ex} D_0 - (k_{ex} t/2.303) \qquad \text{(Eq. 1)}$$

where $\Delta D_e/\Delta t$ is the urinary excretion rate of I at time $t$, the midpoint of the urine collection period; $D_0$ is the amount of I in the body at the time of discontinuation of infusion; and $k_{ex}$ is a first-order rate constant for urinary excretion of the compound, which is essentially equivalent to the rate constant of I elimination since renal excretion is the only process by which I is eliminated intact from the body.

In constructing an individual infusion plot for each rat (Fig. 1), the first data point was ignored and is not shown since the urine sample collected within 10 min after the discontinuation of infusion very likely contained an amount of I greater than that expected. The reason for this belief was that the rat seldom urinated immediately prior to or after the discontinuation of infusion.

According to Eq. 1, the rate constant of urinary excretion was calculated from the slope ($-k_{ex}/2.303$) of the straight line of each plot obtained by least-squares regression. The urinary $t_{1/2}$ was calculated from $t_{1/2} = 0.693/k_{ex}$. The mean $k_{ex}$ of I was $0.0281 \pm 0.0042$ min$^{-1}$, and the average urinary $t_{1/2}$ was 24.7 min.

**Urinary Excretion Kinetics of I after Single Intravenous Dose in Control Study**—Since the single intravenous dose urinary excretion kinetic studies of I conducted previously (1) did not involve continuous infusion of normal saline for 1 hr, those studies cannot be assumed (without evidence) to serve as the control for such studies after continuous infusion for 1 hr. Therefore, to provide an appropriate control, the urinary excretion kinetics of I were studied after administering a single intravenous dose to each rat, immediately after infusing the rat with normal saline for 1 hr. The typical urinary excretion data obtained in this control study are shown in Fig. 1. The mean $k_{ex}$ of I was $0.0430 \pm 0.0034$ min$^{-1}$, which was significantly different ($p < 0.01$) from that obtained in the 1-hr infusion study. The average urinary $t_{1/2}$ of I was 16.2 min.

**Urinary Excretion Kinetics of I after 1-hr Infusion in Presence of II**—These excretion studies in the postinfusion period determined the urinary $t_{1/2}$ of I after blocking its renal tubular secretion with II. Both I and II were contained in the same solution, and the infusion rate of II or the concentration of II was 20 times greater than that of I to inhibit completely the renal tubular secretion of I. The typical apparent first-order urinary excretion data obtained for I are shown in Fig. 2. The mean

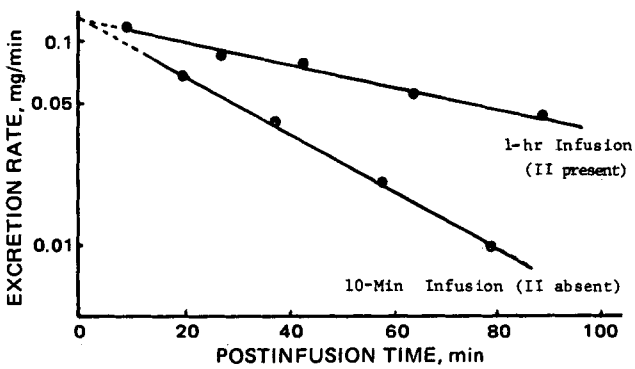


**Figure 2**—*Typical semilogarithmic urinary excretion plots obtained for I after its continuous intravenous infusion into a rat for 1 hr in the presence of II (●) and after its continuous intravenous infusion in the absence of II for 10 min into a rat previously infused with normal saline for 50 min (⊖).*

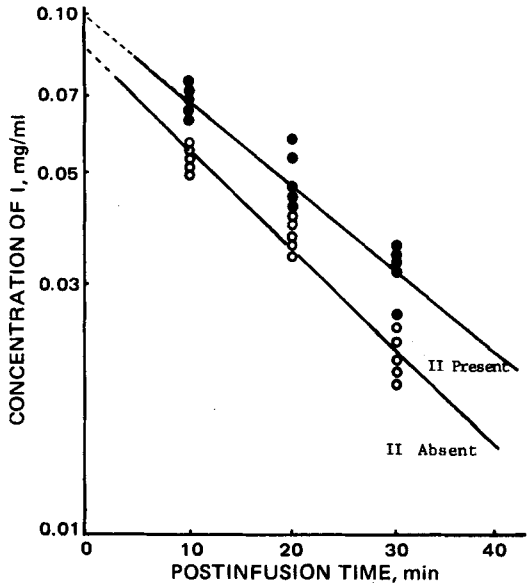


**Figure 3**—*Postinfusion blood levels of I in the absence (○) and presence (●) of II. Each data point represents the concentration of I noted in a given rat, as explained in the text.*

$k_{ex}$ of I was 0.0122 ± 0.0012 $min^{-1}$, which was significantly lower ($p < 0.001$) than that observed in the absence of II in the 1-hr infusion study. The average urinary $t_{1/2}$ of I was 57.0 min.

**Urinary Excretion Kinetics of I after 10-min Infusion**—These excretion studies determined the effect of the infusion time on the urinary $t_{1/2}$ of I. The typical apparent first-order urinary excretion data obtained for I are shown in Fig. 2. The mean $k_{ex}$ of I was 0.0399 ± 0.0049 $min^{-1}$, which was significantly greater ($p < 0.01$) than that observed in the 1-hr infusion study. The average urinary $t_{1/2}$ of I was 17.3 min.

**Blood Level Kinetics of I after 1-hr Infusion in Absence of II**—It was shown previously (8, 10) that the blood levels of I decline monoexponentially after a rapid intravenous administration of a single dose. The blood levels of I obtained in the postinfusion period also declined monoexponentially (Fig. 3), and these data are treated according to the following first-order equation:

$$\log C' = \log C'_0 - (K_{el}t/2.303) \qquad \text{(Eq. 2)}$$

where $C'$ is the I concentration at time $t$ in the postinfusion period, $C'_0$ is the I concentration at the time of discontinuation of infusion, and $K_{el}$ is the first-order rate constant of elimination or excretion of I. The $K_{el}$ of I was calculated from the slope ($-K_{el}/2.303$) of the least-squares straight line. The blood $t_{1/2}$ of the compound was calculated from $t_{1/2} = 0.693/K_{el}$.

The apparent volume of distribution, $V_d$, of I was calculated from:

$$V_d = \frac{k_0}{C'_0 K_{el}}(1 - e^{-K_{el}T}) \qquad \text{(Eq. 3)}$$

where $k_0$ is the infusion rate and $C'_0$ is the I concentration at time $T$ of discontinuation of infusion. The value of $C'_0$ was obtained by extrapolating back to zero time the least-squares straight line obtained in Fig. 3. The values of the various pharmacokinetic parameters are listed in Table I.

**Blood Level Kinetics of I after 1-hr Infusion in Presence of II**—The apparent monoexponential decline of blood levels of I in the presence of II was observed (Fig. 3). The pharmacokinetic parameters calculated are listed in Table I.

## DISCUSSION

**Comparison of Urinary $t_{1/2}$ and Blood $t_{1/2}$ of I**—In the previous single intravenous dose studies of I (1, 8, 10), the rats were not infused with normal saline for 1 hr; however, 5 ml of normal saline was injected intraperitoneally into each rat 20 min prior to intravenous I administration. Therefore, if any substantial difference were to occur between the I half-life determined in the single intravenous dose studies reported previously (1, 8, 10) and that determined in the present single dose studies of the saline-infused (control) rats, such a difference probably would be due to the surgical trauma and infusion procedure employed in the infusion studies.

**Table I—Pharmacokinetic Parameters Determined for I from Postinfusion Blood Level Data Obtained in the Absence and Presence of II**

| | Without II | With II |
|---|---|---|
| Pharmacokinetic parameter | | |
| $C'_0$, mg/ml | 0.0842 | 0.0995 |
| $K_{el}$, $min^{-1}$ | 0.0443 | 0.0373 |
| $t_{1/2}$, min | 15.6[a] | 18.5[a] |
| $V_d$, ml/kg | 281.1 | 273.0 |
| Body clearance, ml $min^{-1}$ $kg^{-1}$ | 12.5 | 10.2 |
| Measures of fit | | |
| Coefficient of determination ($r^2$) | 0.996 | 0.996 |
| Correlation coefficient | 0.998 | 0.998 |

[a] For comparison, the blood $t_{1/2}$ values obtained for I in previous (8, 10) single intravenous dose studies in nonsurgical rats in the absence and presence of II were 14.1 and 16.9 min, respectively.

However, the average urinary $t_{1/2}$ (16.2 min) of I determined in the control rats was similar to that (16.7 min) reported previously (1) in the nonsurgical rats after administration of a single intravenous dose of I. Furthermore, the urinary $t_{1/2}$ (17.3 min) of I determined after infusing it for 10 min into rats, which were already infused with normal saline for 50 min, was not substantially greater than that determined in the previous single intravenous dose studies (1) performed in the nonsurgical rats. Additionally, the blood $t_{1/2}$ (15.6 min) and the body clearance (12.5 ml/min/kg) of I determined in the infusion studies also were similar (14.1 min; 12.1 ml/min/kg) to those noted for I in the previous (8) single intravenous dose studies in nonsurgical rats.

These observations suggested that the surgery and infusion procedures have little or no effect on the I half-lives and that the values of the urinary and blood half-lives obtained for I in the previous single intravenous dose studies in the nonsurgical rats can be used as the control values for the present study.

**Comparison of Ratios of Urinary $t_{1/2}$ and Blood $t_{1/2}$ Values of I in Absence and Presence of II**—The average blood $t_{1/2}$ or urinary $t_{1/2}$ of I in the presence of II was greater than that determined in the absence of II in the single intravenous dose study and in the infusion study. However, while the increase in blood $t_{1/2}$ of I observed in the infusion study with II was similar to that noted in the single intravenous dose study (Table I), the increase in the urinary $t_{1/2}$ of I observed in the presence of II in the infusion study was 1.8 times greater than that noted in the single intravenous dose study. Therefore, the increase observed in the blood $t_{1/2}$ of I in the presence of II either in the single intravenous dose study or in the infusion study primarily reflects the effect of inhibition of renal tubular secretion of I by II. However, the greater increase observed in the urinary $t_{1/2}$ of I in the presence of II in the infusion study, as compared to that observed in the single intravenous dose study, cannot be attributed merely to the inhibition of renal tubular secretion of I by II. Other factors such as retention or detention of I in the renal tubular membranes (1) and its distribution into the deeper tissues of the kidney (5, 6) may be responsible for this phenomenon.

Therefore, to reveal the role of these factors, although indirectly, the various ratios of the I half-lives were evaluated. Previous studies (1) with I and other model organic anions showed that the values of all four ratios listed in Table II were greater than unity for the organic anions. This

**Table II—Various Ratios of Urinary $t_{1/2}$ and Blood $t_{1/2}$ Values Obtained in Infusion Studies and Single Intravenous Dose Studies of I in the Absence and Presence of II**

| Ratio | Infusion | Single Intravenous Dose |
|---|---|---|
| $\left(\frac{\text{urinary } t_{1/2}}{\text{blood } t_{1/2}}\right)_{\text{II absent}}$ | 1.58 | 1.18 |
| $\left(\frac{\text{urinary } t_{1/2}}{\text{blood } t_{1/2}}\right)_{\text{II present}}$ | 3.08 | 1.24 |
| $\frac{(\text{urinary } t_{1/2})_{\text{II present}}}{(\text{urinary } t_{1/2})_{\text{II absent}}}$ | 2.26 | 1.25 |
| $\frac{(\text{blood } t_{1/2})_{\text{II present}}}{(\text{blood } t_{1/2})_{\text{II absent}}}$ | 1.19 | 1.20 |

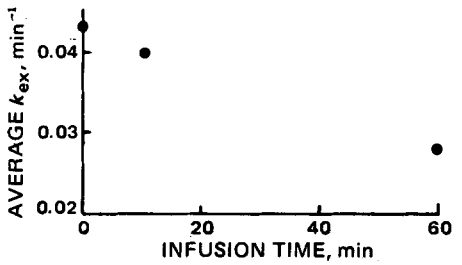


**Figure 4**—*Plot showing the effect of continuous intravenous infusion time on the postinfusion* $k_{ex}$ *of I in rats.*

analysis led to the proposal (1) that once the organic anions entered the renal tubular membranes, they probably did not diffuse back into the blood compartment and that the renal tubular membranes did not constitute a part of the blood compartment or the peripheral tissue compartment for anions associated with multicompartment disposition characteristics.

The data for I (Table II) clearly indicate that, while the ratios of (blood $t_{1/2}$ with II/blood $t_{1/2}$ without II) observed in the infusion studies was practically identical to that noted in the single intravenous dose studies, the ratio of (urinary $t_{1/2}$ with II/urinary $t_{1/2}$ without II) observed in the infusion studies was almost two times greater than that in the single intravenous dose studies. Therefore, the possible accumulation of I in the renal tubular membranes was not only more pronounced when administered by continuous infusion but such retention occurred only in the eliminating organ, the kidney. The urinary $t_{1/2}$ data in Table II also prompted the suggestion that I diffuses into the deeper tissues in the kidney. This hypothesis appears to be supported by the fact that the ratio of the ratios expressed as (urinary $t_{1/2}$/blood $t_{1/2})_{\text{infusion}}$/(urinary $t_{1/2}$/blood $t_{1/2})_{\text{single iv dose}}$ observed for I in the presence of II was almost two times greater than that observed in the absence of II.

**Effect of Infusion Time on $k_{ex}$ of I**—As pointed out earlier, the $k_{ex}$ value of I in the 10-min infusion study was $0.0399 \pm 0.0049$ $min^{-1}$, which was significantly ($p < 0.01$) greater than that observed in the 1-hr infusion study. However, this $k_{ex}$ value was significantly smaller than that of I determined in the single intravenous dose study only at a 75% confidence limit. There appears to be a trend to suggest that $k_{ex}$ of I decreases with increasing infusion time (Fig. 4). Since the excretion rate constants of I were not determined at additional infusion times, it is not known whether a relationship between $k_{ex}$ of I and its infusion time is linear over the infusion time of 0–60 min.

**Possible Mechanism**—The effect of length of the infusion period on the urinary $t_{1/2}$ or $k_{ex}$ of I observed in the present study is parallel to the effect of length of the incubation period on the depth of uptake of *p*-aminohippurate by the rat kidney slice studies of Wedeen and Weiner (4–6). The mechanism they proposed, which accounts for the intrarenal distribution and localization of tritiated *p*-aminohippurate in the rat kidney slices, was that the uptake of this anion occurs primarily in the surface-lying tubules during the shorter incubation period but that the uptake occurs in the tubules in the deeper tissue region during prolonged incubation. It also was demonstrated (6) that, in the presence of even the nonmetabolic competitive inhibitors, although no uptake of *p*-aminohippurate occurred in the surface-lying tubules of the cortical slices, its uptake proceeded into the deeper proximal tubules.

In view of the proposed mechanisms (4–6), it seems reasonable to assume that I penetrates into the deeper lying proximal renal tubules upon its intravenous infusion for 1 hr and, because of its increased residence time in the kidney, results in a prolonged urinary $t_{1/2}$. Furthermore, in the presence of II, I probably is able to gain access to further deeper lying renal tubules, resulting in a prolonged urinary $t_{1/2}$.

Therefore, it may be hypothesized that I tends to accumulate temporarily in the surface-lying renal tubular cells after the administration of a single intravenous dose but that it tends to penetrate into the deeper renal tubular cells upon intravenous infusion, with the depth of cortical tissue involved in its uptake increasing with increasing infusion time. Consequently, uptake of the compound in the deeper lying tubules, together with its temporary retention in the renal tubular membranes during secretion, is reflected in the longer apparent half-life of the compound when determined from the urinary excretion data than when determined from the blood level data.

**Practical Significance of Study**—As noted previously (1), the apparent biological half-lives of drugs sometimes are longer in humans when determined from urinary excretion data than when determined from blood level data. The previous (1) and present studies with model organic anions suggest that if drugs that are subject to renal tubular secretion exhibit a greater urinary $t_{1/2}$ than blood $t_{1/2}$, it may be due to their accumulation in the renal tubular membranes and penetration into the deeper lying cortical renal tubules, especially in chronic drug therapy. Such pharmacokinetic disposition of some drugs may result in nephrotoxicity caused by interference by drug molecules in the integrity of the membrane structure and normal metabolic functions of tubular cells. Therefore, if a drug is suspected to be nephrotoxic, comparison of its urinary $t_{1/2}$ and blood $t_{1/2}$ values in test subjects may help to detect this possibility.

## REFERENCES

(1) Y. M. Amin and J. B. Nagwekar, *J. Pharm. Sci.*, **65**, 1341 (1976).

(2) A. D. Bains, C. W. Gottschalk, and W. E. Lassiter, *Am. J. Physiol.*, **214**, 703 (1968).

(3) E. H. Barany, *Acta Pharmacol. Toxicol.*, **35**, 309 (1974).

(4) R. P. Wedeen and B. Weiner, *Kidney Int.*, **3**, 205 (1973).

(5) *Ibid.*, **3**, 214 (1973).

(6) R. P. Wedeen and B. Weiner, *Am. J. Physiol.*, **226**, 953 (1974).

(7) K. Kindler, W. Metzendorf, and D. Y. Kevok, *Chem. Ber.*, **76B**, 308 (1943).

(8) Y. M. Amin and J. B. Nagwekar, *J. Pharm. Sci.*, **64**, 1804 (1975).

(9) E. J. Randinitis, M. Barr, H. C. Wormser, and J. B. Nagwekar, *ibid.*, **59**, 806 (1970).

(10) Y. M. Amin and J. B. Nagwekar, *ibid.*, **64**, 1813 (1975).

## ACKNOWLEDGMENTS

Abstracted in part from a thesis submitted by J. W. Cheon to Wayne State University in partial fulfillment of the Master of Science degree requirements.

# Pharmacokinetics of Procainamide and *N*-Acetylprocainamide in Rats

**BURDE L. KAMATH ˣ, CHII-MING LAI, SURINDER D. GUPTA, MANZER J. DURRANI, and AVRAHAM YACOBI**

Received May 5, 1980, from the *Pharmaceutical Development Department, Research and Medical Affairs, American Critical Care, McGaw Park, IL 60085.* Accepted for publication September 2, 1980.

**Abstract** □ The pharmacokinetics of distribution and elimination of procainamide and its major metabolite, *N*-acetylprocainamide, were studied in rats. Eight rats were selected randomly, and each received intravenously $^{14}$C-labeled procainamide hydrochloride (75 mg/kg) or $^{14}$C-labeled *N*-acetylprocainamide hydrochloride (86 mg/kg) according to a two-way crossover design. Serial blood samples were withdrawn for 8 hr, and cumulative urine and feces were collected for 48 hr. The plasma concentration–time relationships of procainamide and *N*-acetylprocainamide were characterized by one- and two-compartment open models, respectively. A pseudo-three-compartment model was necessary to characterize the time course of *N*-acetylprocainamide in plasma formed after administration of procainamide. The biological half-lives of procainamide and *N*-acetylprocainamide averaged 0.66 and 2.1 hr, respectively. The urinary excretion profiles of these drugs and the ratio of their biological half-lives in rats were similar to those in humans.

**Keyphrases** □ Pharmacokinetics—procainamide and *N*-acetylprocainamide, rat blood, urine, and feces, compared with human data □ Procainamide—and metabolite *N*-acetylprocainamide, pharmacokinetic study in rat urine, blood, and feces, compared with human data □ *N*-Acetylprocainamide—metabolite of procainamide, pharmacokinetic study in rats, compared with human data □ Metabolism—procainamide and *N*-acetylprocainamide, pharmacokinetics in rats, compared with human data □ Models, pharmacokinetic—procainamide and *N*-acetylprocainamide metabolism in rats, compared with human data

*N*-Acetylprocainamide (acecainide, II) has been identified as the major metabolite of procainamide (I) in humans (1). It was found to be as potent as I in suppressing chloroform-induced ventricular fibrillation in mice (2). Various investigations have confirmed the antiarrhythmic efficacy of II in isolated tissues (3, 4), animals (4, 5), and humans (6–9). The most significant difference between these two drugs is that patients on chronic I therapy developed lupus erythematosus while those on II did not (8–10). The longer half-life of II offers another advantage over I; the average half-life of I is 3 hr (11), and that of II is 6.0 hr or longer in humans (12, 13).

In humans, ~50% of a I dose was excreted unchanged in urine and 7–34% was acetylated to II (11), whereas II was excreted mainly unchanged (12). In dogs, 50–67% of I was excreted unchanged in urine and no II was found (14, 15). In monkeys, I was extensively metabolized to II and a small portion of the dose (2.1%) was excreted unchanged in urine (15). In rats, 34% of a 50-mg/kg dose of I was excreted unchanged in urine, 38% was converted to II, and the rest was eliminated as unidentified metabolites (16). In the same study, 72% of a 50-mg/kg dose of II was excreted unchanged in urine. The biotransformation of I to II and the elimination of II in rats are qualitatively similar to those in humans.

The purposes of the present investigation were: (*a*) to study the comparative pharmacokinetics of I and II in the same rat, (*b*) to develop a pharmacokinetic model that describes the formation and elimination of II after administration of a single dose of I intravenously, and (*c*) to confirm the suitability of the rat model for pharmacokinetic studies of I and its metabolite II.

## EXPERIMENTAL

$^{14}$C-Labeled procainamide[1] (32.0 μCi/mg) and $^{14}$C-labeled *N*-acetylprocainamide[1] (23.1 μCi/mg) as hydrochloride salts were diluted with unlabeled drugs[2]. The final specific activities of the administered procainamide hydrochloride (I) and *N*-acetylprocainamide hydrochloride (II) were 0.561 and 0.775 μCi/mg, respectively.

Eight male Charles River CD rats[3], 250–450 g, were randomly selected and kept in the individual metabolism cages during the study. Each animal received I (75 mg/kg) and II (86 mg/kg) intravenously according to a two-way crossover design. Four of the eight rats received I first while the other four received II. One day before drug administration, a cannula was surgically inserted into the jugular vein of each rat under light ether anesthesia. The preparation of the cannulas and the surgical procedure were described previously (17).

The drug solutions were administered intravenously through the jugular cannula after an overnight fast. Water was freely available at all times. Serial blood samples (0.4 ml each) were withdrawn at 0, 0.25, 0.5, 0.75, 1, 1.5, 2, 3, 4, 6, and 8 hr after drug administration. After each withdrawal, 0.4–0.5 ml of normal saline containing 1% heparin solution was infused to replace the lost volume. Plasma was separated and frozen immediately. Urine and feces were collected for 48 hr and frozen until they were assayed. Three to 7 days elapsed before the second phase of the study was performed.

**Analytical Methods**—The total radioactivity in urine was determined directly *via* a liquid scintillation counter[4]. The total radioactivity in the feces was measured after homogenization[5] and combustion in an oxidizer[6]. The I and II concentrations in plasma and urine were determined by a specific high-pressure liquid chromatographic method (18).

**Data Analysis**—The plasma concentration–time plots of I and II for each rat were fitted to mono- and biexponential equations, respectively, using nonlinear least-squares regression analysis[7]. The time course of formation and elimination of II after I administration was fitted to a pseudo-three-compartment open model (see *Appendix*). In this model, the pharmacokinetics of I are characterized by a one-compartment open model with two routes of elimination, an acetylation route and a nonacetylation route. The elimination of II is described by a two-compartment open model. Convergence was defined as a relative change in the residual sum of squares $<10^{-8}$. Data in all functions were weighed by the reciprocal of the square of each observation. The parameter estimates of each exponential equation were used to calculate rate constants describing the individual model (19) (see *Appendix*).

## RESULTS

Table I summarizes the elimination of procainamide (I) and *N*-acetylprocainamide (II) in urine and feces 48 hr after intravenous administration of either drug. After dosing with I, 84 and 5% of the total administered radioactivity were eliminated in urine and feces, respectively. Of the amount recovered in urine, 49% was unchanged I and 20% was II. As much as 31% was excreted in an unidentified form. After dosing with II, 90.5 and 3.2% of the total administered radioactivity were eliminated in urine and feces, respectively. Of the amount recovered in urine,

[1] New England Nuclear, Boston, Mass.
[2] Arnar-Stone Laboratories, McGaw Park, Ill.
[3] Charles River Breeding Laboratories, Wilmington, Mass.
[4] Model 2425, Packard Instrument Co., Downers Grove, Ill.
[5] Polytron homogenizer, Brinkmann Instruments, Westbury, N.Y.
[6] Model B306, Packard Instrument Co., Downers Grove, Ill.
[7] NLIN procedure, Statistical Analysis System, SAS Institute, Raleigh, N.C.

0022-3549/81/0300-0299$01.00/0
© 1981, American Pharmaceutical Association

**Table I—Elimination of Procainamide (I) and *N*-Acetylprocainamide (II) in Urine and Feces in 48 hr**

| | Percent of I Dose | | | | Percent of II Dose | | |
|---|---|---|---|---|---|---|---|
| | Urine | | | Feces, | Urine | | Feces, |
| Rat | Unchanged I | II | Total Radioactivity | Total Radioactivity | Unchanged II | Total Radioactivity | Total Radioactivity |
| 1 | 36.8 | 15.7 | 77.4 | 3.4 | 69.4 | 91.3 | 2.2 |
| 2 | 51.4 | 15.6 | 82.9 | 8.5 | 62.2 | 71.8 | 4.2 |
| 3 | 24.5 | 14.5 | 71.0 | 2.9 | 76.1 | 90.4 | 1.1 |
| 4 | 51.2 | 22.4 | 98.1 | 2.4 | 67.4 | 94.1 | 1.3 |
| 5 | 41.8 | 14.9 | 89.1 | 6.7 | 67.0 | 92.3 | 1.9 |
| 6 | 36.4 | 15.3 | 83.3 | 1.9 | 71.1 | 95.1 | 4.0 |
| 7 | 42.5 | 19.6 | 93.0 | 7.3 | 81.9 | 90.8 | 7.7 |
| 8 | 43.5 | 14.5 | 78.3 | 6.0 | 89.4 | 98.3 | 2.8 |
| Mean | 41.0 | 16.6 | 84.1 | 4.9 | 73.1 | 90.5 | 3.2 |
| *SD* | 8.7 | 2.9 | 8.9 | 2.5 | 8.9 | 8.0 | 2.2 |

80% of the dose was unchanged II and the remainder was unidentified. Only traces of I were found in the urine of three rats after II administration.

Figure 1 depicts the time course of the plasma concentrations of I and II following administration of each drug in a representative animal. Table II lists the mean pharmacokinetic parameters and constants that describe the model computer fit for I (one-compartment model), II (two-compartment model), and the *N*-acetylated metabolite of I (pseudo-three-compartment model). The pseudo-three-compartment model (Scheme I) was derived by combining the pharmacokinetic models used to fit the individual data observed for I and II as unchanged drugs (see *Appendix*).

The metabolite data from seven rats fit quite well (correlation coefficient of ≥0.95) to the proposed model. There were not sufficient data from the eighth animal. On the average, there was excellent agreement between the pharmacokinetic parameters of II obtained by the two-compartment open model after administration of II and by the pseudo-three-compartment model after administration of I. The mean elimination half-life of the *N*-acetylated metabolite of I was 2.22 hr, which was almost identical to that obtained after administration of II to the same rats. The formation rate constant of II ($k_f$) from I in seven rats averaged 0.254 $hr^{-1}$.

Table III shows the comparative values of the biological half-life, volume of distribution, and renal clearance of I and II in individual rats. The biological half-life of II was 2.13 hr, about three times longer than that of I (0.658 hr). There was little difference in the values of the volume of distribution of either drug. The renal clearance of I was 1.92 liters/hr/kg (32 ml/min/kg), twice as large as that of II, 0.880 liter/hr/kg (14.7 ml/min/kg).

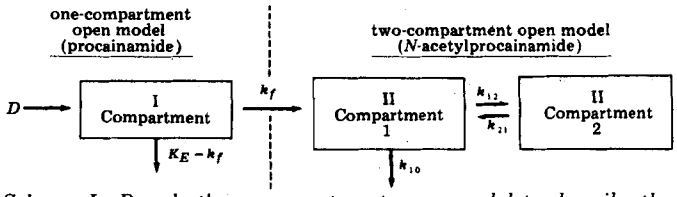


*Scheme I—Pseudo-three-compartment open model to describe the formation and elimination of the* N*-acetylated metabolite of procainamide in the rat.*

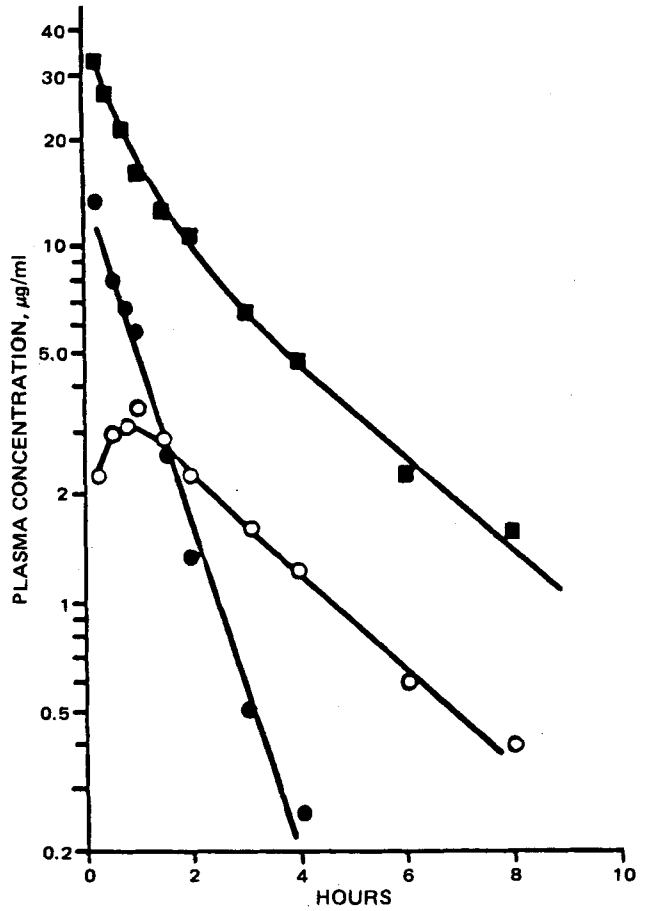


**Figure 1**—*Typical semilogarithmic plot of plasma concentrations of drugs* versus *time following intravenous administration of procainamide (●) and* N*-acetylprocainamide (■) in one rat. The open circles (○) show the time course of the* N*-acetylated metabolite of procainamide.*

## DISCUSSION

There was no appreciable change (>10%) in the hematocrit between the initial samples of the two crossover phases. In addition, there was no difference in the pharmacokinetics of either drug between the two phases

**Table II—Parameters Describing the Pharmacokinetics of Procainamide (I) and *N*-Acetylprocainamide (II) in Rats**

| | | II | |
|---|---|---|---|
| Parameter | I, One-Compartment Open Model ($n$ = 8) | Pseudo-Three-Compartment Model[a] ($n$ = 7) | Two-Compartment Open Model[b] ($n$ = 8) |
| $K_E$, $hr^{-1}$ | 1.10 (0.05)[c] | — | — |
| $\alpha$, $hr^{-1}$ | — | 2.70 (0.77) | 2.52 (0.38) |
| $\beta$, $hr^{-1}$ | — | 0.327 (0.025) | 0.333 (0.017) |
| Half-life, hr | 0.66 (0.04) | 2.22 (0.20) | 2.13 (0.13) |
| $k_{12}$, $hr^{-1}$ | — | — | 0.983 (0.237) |
| $k_{21}$, $hr^{-1}$ | — | — | 0.971 (0.134) |
| $k_{10}$, $hr^{-1}$ | — | — | 0.900 (0.102) |
| $k_{ex}$, $hr^{-1}$ | 0.448 (0.052) | — | 0.657 (0.081) |
| $k_{mu}$, $hr^{-1}$ | 0.181 (0.020)[d] | — | — |
| $k_f$, $hr^{-1}$ | 0.248[d] | 0.254 (0.044) | — |
| $V_C$, liters/kg | — | — | 1.46 (0.19) |
| $V_{d(\beta)}$, liters/kg | 4.60 (0.57) | — | 3.82 (0.54) |
| $Cl_p$, liters/hr/kg | 4.84 (0.53) | — | 1.24 (0.12) |
| $Cl_r$, liters/hr/kg | 1.92 (0.17) | 0.919 (0.096) | 0.880 (0.059) |

[a] Data obtained for II formed after administration of I. [b] Data describing the time course of unchanged drug after intravenous administration of II. [c] Data in parentheses show the standard error of the mean. [d] The $k_{mu}$ value represents the excretion of *N*-acetylated metabolite of I in urine. The $k_f$ value was calculated using a correction factor to account for the amount of II eliminated as metabolites. This factor was obtained from the II data and is 73%.

Table III—Comparisons of Biological Half-Life ($t_{1/2}$), Apparent Volume of Distribution ($V_d$), and Renal Clearance ($Cl_r$) of Procainamide (I) and *N*-Acetylprocainamide (II) in Individual Rats

| Rat | $t_{1/2}$, hr | | | $V_d$, liters/kg | | $Cl_r$, liters/hr/kg | |
|---|---|---|---|---|---|---|---|
| | I | II | Ratio | I | II | I | II |
| 1 | 0.831 | 2.10 | 2.53 | 5.93 | 3.18 | 1.82 | 0.730 |
| 2 | 0.550 | 2.92 | 5.31 | 3.90 | 7.40 | 2.53 | 1.09 |
| 3 | 0.646 | 1.86 | 2.88 | 7.48 | 3.71 | 1.97 | 1.05 |
| 4 | 0.536 | 1.94 | 3.62 | 4.03 | 4.10 | 2.67 | 0.986 |
| 5 | 0.800 | 2.00 | 2.50 | 5.43 | 3.06 | 1.97 | 0.711 |
| 6 | 0.648 | 2.38 | 3.67 | 4.45 | 3.76 | 1.74 | 0.779 |
| 7 | 0.592 | 2.04 | 3.45 | 2.45 | 2.48 | 1.22 | 0.691 |
| 8 | 0.664 | 1.72 | 2.59 | 3.15 | 2.86 | 1.43 | 1.00 |
| Mean | 0.658 | 2.13 | 3.32 | 4.60 | 3.82 | 1.92 | 0.919 |
| *SD* | 0.107 | 0.37 | 0.94 | 1.61 | 1.53 | 0.48 | 0.272 |

of the crossover study. Therefore, it can be assumed that the withdrawal of blood during the first phase did not affect the pharmacokinetics during the second phase.

Procainamide (I) is metabolized partially to *N*-acetylprocainamide (II) in rats but is excreted mainly unchanged (~50% of the dose) in the urine. On a qualitative basis, there is a similarity in the elimination of I in humans and rats. However, in contrast to the finding in humans, there was no indication of a bimodal distribution of I acetylation in rats. This finding is in agreement with the observation made by Cerna *et al.* (20). *N*-Acetylprocainamide is excreted primarily unchanged in urine. A fraction of both I and II doses was eliminated in the urine as unidentified polar compounds. No attempt was made to separate or characterize these metabolites, which appear to be unextractable in organic solvents and may consist of congregate forms of the drug.

A small portion (3–5%) of the intravenous dose of both drugs was eliminated in the feces, indicating biliary secretion. If the drugs enter enterohepatic cycling, the magnitude of the biliary excretion should be larger than that indicated by the feces data.

To describe the time course of II formed after I administration in rats, a pseudo-three-compartment open model was derived. This approach was possible by combining the one-compartment open model and two-compartment open model characterizing the pharmacokinetics of I and II, respectively. The link between the two models is $k_f$, the rate constant for I acetylation in the body. Since there was almost no deacetylation of the metabolite, it was assumed that the $k_f$ represents the rate constant of nonreversible acetylation.

Because a portion of the II dose was eliminated as an unknown metabolite, its urinary excretion rate constant after administration of I probably will be smaller than $k_f$. This possibility was verified by the value of $k_{mu}$, which represents the renal excretion of the *N*-acetylated metabolite but not its formation rate as described by $k_f$. When the value of $k_{mu}$ (0.181 $hr^{-1}$) was corrected for the percent of II eliminated as an unidentified metabolite, the rate constant was 0.248 $hr^{-1}$, which was almost identical to that of $k_f$ (0.254 $hr^{-1}$). Furthermore, one may calculate that only 73% of the *N*-acetylated metabolite of I would be eliminated as such in rats. This value is in excellent agreement with the observed value of urinary excretion after administration of II.

A discrepancy between the results of this study and those described previously (16) with respect to the half-life and volume of distribution of II was noted. This difference was addressed previously (21) and was attributed mainly to the use of inadequate blood sampling to characterize the pharmacokinetics of II and the inappropriate method of calculating the volume of distribution.

This investigation of comparative pharmacokinetics in rats showed that the biological half-life of II is about three times longer than that of I in rats. A ratio between 2 and 3 also has been demonstrated in humans. The volume of distribution of these drugs is quite similar. The renal clearance of I (32 ml/min/kg) is twice as large as that for II (15 ml/min/kg). These values are larger than the glomerular filtration rate of 8.0 ml/min/kg (22) in 200-g rats, which indicates that active processes are taking place in urinary excretion of either drug.

In summary, the elimination of I and II when given individually to rats can be described by one- and two-compartment open models. A pseudo-three-compartment model was developed to fit the plasma II concentrations that form following I administration to rats. The results show that the pharmacokinetics and metabolism of I and II are qualitatively similar in both humans and rats. *N*-Acetylprocainamide has a half-life two or three times longer than that of procainamide in both humans and rats. The percentages of unchanged drug and the metabolites excreted in urine following administration of either drug are qualitatively similar in both species.

## APPENDIX

The concentration of *N*-acetylprocainamide (II) in plasma ($C_p$) at time $t$ after procainamide (I) administration can be fitted to:

$$C_p = Pe^{-K_E t} + A'e^{-\alpha t} + B'e^{-\beta t} \quad \text{(Eq. A1)}$$

where the parameters $P$, $A'$, $B'$, $K_E$, $\alpha$, and $\beta$ characterize the three-exponential equation, and:

$D$ = intravenously administered dose
$K_E$ = apparent first-order elimination rate constant for I
$k_f$ = formation rate constant for II
$k_{12}$ and $k_{21}$ = intercompartmental distribution rate constants for II
$k_{10}$ = apparent first-order elimination rate constant from central compartment for II
$V_C$ = apparent volume of central compartment for II

The area under the plasma concentration *versus* time curve ($AUC$) is given by:

$$AUC = \frac{P}{K_E} + \frac{A'}{\alpha} + \frac{B'}{\beta} \quad \text{(Eq. A2)}$$

The individual pharmacokinetic parameters and constants are defined as follows:

$$P = \frac{K_f D(K_E - k_{21})}{V_C(\beta - K_E)(K_E - \alpha)} \quad \text{(Eq. A3)}$$

$$A' = \frac{k_f D(\alpha - k_{21})}{V_C(\alpha - \beta)(K_E - \alpha)} \quad \text{(Eq. A4)}$$

$$B' = \frac{k_f D(\beta - k_{21})}{V_C(\alpha - \beta)(\beta - K_E)} \quad \text{(Eq. A5)}$$

$$P + A' + B' = 0 \quad \text{(Eq. A6)}$$

$$\alpha + \beta = k_{12} + k_{21} + k_{10} \quad \text{(Eq. A7)}$$

$$\alpha\beta = k_{21}k_{10} \quad \text{(Eq. A8)}$$

$$k_{21} = \frac{B'K_E(\alpha - \beta) + P\beta(\alpha - K_E)}{B'(\alpha - \beta) + P(\alpha - K_E)} \quad \text{(Eq. A9)}$$

$$k_{12} = \alpha + \beta - k_{21} - k_{10} \quad \text{(Eq. A10)}$$

$$k_{10} = \frac{\alpha\beta}{k_{21}} \quad \text{(Eq. A11)}$$

$$k_f = \frac{V_C K_E k_{10} AUC}{D} \quad \text{(Eq. A12)}$$

## REFERENCES


(1) J. Dreyfuss, J. J. Ross, and E. C. Schreiber, *Arzneim.-Forsch.*, **21**, 948 (1971).

(2) D. E. Drayer, M. M. Reidenberg, and R. W. Sevy, *Proc. Soc. Exp. Biol. Med.*, **146**, 358 (1974).

(3) H. Refsum, K. Frislid, P. K. M. Lunde, and K. H. Landmark, *Eur. J. Pharmacol.*, **33**, 47 (1975).

(4) E. E. Bagwell, T. Walle, D. E. Drayer, M. M. Reidenberg, and J. K. Pruett, *J. Pharmacol. Exp. Ther.*, **197**, 38 (1976).

(5) R. F. Minchin, K. F. Ilet, and J. W. Paterson, *Eur. J. Pharmacol.*, **47**, 51 (1978).

(6) J. Elson, J. M. Strong, W.-K. Lee, and A. J. Atkinson, Jr., *Clin. Pharmacol. Ther.*, **17**, 134 (1975).

(7) W.-K. Lee, J. M. Strong, R. F. Kehoe, J. S. Dutcher, and A. J. Atkinson, Jr., *ibid.*, **19**, 508 (1976).
(8) J. J. L. Lertora, A. J. Atkinson, Jr., W. Kushner, M. J. Nevin, W. K. Lee, C. Jones, and F. R. Schmid, *ibid.*, **25**, 273 (1979).
(9) G. P. Stec, J. J. L. Lertora, A. J. Atkinson, Jr., M. J. Nevin, W. Kushner, C. Jones, F. R. Schmid, and J. Askenazi, *Ann. Intern. Med.*, **90**, 800 (1979).
(10) R. Lahita, J. Kluger, D. E. Drayer, D. Koffler, and M. M. Reidenberg, *Clin. Res.*, **27**, 235A (1979).
(11) E. Karlsson, *Clin. Pharmacokinet.*, **3**, 97 (1978).
(12) J. M. Strong, J. S. Dutcher, W.-K. Lee, and A. J. Atkinson, Jr., *J. Pharmacokinet. Biopharm.*, **3**, 223 (1975).
(13) D. M. Roden, S. B. Reele, S. B. Higgins, G. R. Wilkinson, R. F. Smith, J. A. Oates, and R. L. Woosley, *Am. J. Cardiol.*, **46**, 463 (1980).
(14) D. T. Baer and J. C. Barkus, Jr., *Res. Commun. Chem. Path. Pharmacol.*, **17**, 333 (1977).
(15) J. Dreyfuss, J. T. Bigger, Jr., A. I. Cohn, and E. C. Schreiber, *Clin. Pharmacol. Ther.*, **13**, 366 (1972).
(16) D. W. Schneck, K. Grove, F. O. Dewitt, R. A. Shiroff, and A. H. Hayes, Jr., *J. Pharmacol. Exp. Ther.*, **204**, 219 (1978).
(17) P. G. Harms and S. R. Ojeda, *J. Appl. Phys.*, **36**, 391 (1974).
(18) C. M. Lai, B. L. Kamath, Z. M. Look, and A. Yacobi, *J. Pharm. Sci.*, **69**, 982 (1980).
(19) M. Gibaldi and D. Perrier, "Drugs and the Pharmaceutical Sciences, Vol. 1, Pharmacokinetics," Dekker, New York, N.Y., 1975.
(20) J. Cerna, Z. Zidek, and I. Janku, *J. Pharm. Pharmacol.*, **31**, 711 (1979).
(21) B. L. Kamath and A. Yacobi, *J. Pharm. Sci.*, **69**, 864 (1980).
(22) E. M. Renkin and J. P. Gilmore, in "Handbook of Physiology. Section 8: Renal Physiology," J. Orloff, R. W. Berliner, and S. R. Geiger, Eds., American Physiological Society, Washington, D.C., 1973, pp. 185–248.

# Electrophoretic Properties of Sulfamethoxazole Microcapsules and Gelatin–Acacia Coacervates

**H. TAKENAKA, Y. KAWASHIMA ˣ, and S. Y. LIN**

Received November 21, 1979, from the *Gifu College of Pharmacy, Mitahora, Gifu 502, Japan.* Accepted for publication September 2, 1980.

**Abstract** □ The electrophoretic properties of sulfamethoxazole microcapsules and the coacervates prepared by gelatin–acacia coacervation were investigated. The effects of the parameters in the microcapsule preparation, such as the coacervation pH, amount of formaldehyde used for hardening, and drying method of the coacervates, on the ζ-potential of the resultant microcapsules were clarified. The Büchner effect was observed in coacervates in an electric field, which indicated that the coacervate wall was flexible. The ζ-potential *versus* pH curves of the coacervates appeared on the upper side of the plain sulfamethoxazole, while those of the microcapsules dried conventionally shifted to the lower side due to denaturation of the gelatin in the microcapsule wall, which occurred during drying. Spray drying increased the denaturation of gelatin, which imparted a negative charge to the spray-dried microcapsules. Formalization of the coacervates refined the electrophoretic behavior of the microcapsules, depending on the amount of formaldehyde used. The ζ-potential of the plain sulfamethoxazole also was measured in the simulated coacervation solution to analyze the mechanism of coacervation electrophoretically.

**Keyphrases** □ Sulfamethoxazole—microcapsules and coacervates, electrophoretic properties compared □ Gelatin–acacia coacervates—sulfamethoxazole microcapsules and coacervates compared electrophoretically □ Microcapsules, acacia–gelatin—sulfamethoxazole, electrophoretic properties compared □ Coacervation, acacia–gelatin—sulfamethoxazole coacervates and microcapsules compared electrophoretically

Much attention has been paid to the electrophoretic properties of microcapsules because they are decisive parameters in stabilizing suspensions compounded with microcapsules (1). In addition, to prepare a microcapsule containing living cell fluid for use as an artificial cell, it is necessary to simulate the electrophoretic properties of the microcapsule as well as other properties such as elasticity, mechanical strength, and permeability (2).

Measurement of the ζ-potential of microcapsules is one way to assess their electrophoretic properties. The ζ-potential of microcapsules prepared by an interfacial polycondensation method was measured, and the effect of the pH medium on these properties was reported (3). The ζ-potential of gelatin–acacia coacervates, excluding the core material, also was determined (4). However, the electrophoretic properties of gelatin–acacia microcapsules containing the core material were not exhaustively investigated.

In the present study, ζ-potentials of gelatin–acacia coacervates and microcapsules prepared by drying were measured. One aim of the study was to elucidate the parameters that affect the electrophoretic properties of the coacervates and microcapsules. The amount of formaldehyde used for hardening, the coacervation pH, and the drying method of the coacervate droplets were assumed to be the parameters affecting this property. Another purpose was to manifest the coacervation process electrophoretically by measuring the changes in the ζ-potentials of plain sulfamethoxazole particles and gelatin–acacia coacervates during processing.

## EXPERIMENTAL

**Materials**—The test samples used to measure the ζ-potential were micronized sulfamethoxazole[1], gelatin–acacia coacervate droplets, and dried gelatin–acacia microcapsules of sulfamethoxazole. The gelatin–acacia coacervates of sulfamethoxazole were prepared as described earlier (5, 6). The coacervation pH was adjusted to 2.05–4.2. The coacervate droplets were formalized with 0, 30, and 50 ml of formaldehyde.

The conventional method of drying the coacervates (using warm air at 40°) and a spray drying technique were adopted. Spray drying of the slurries containing coacervate droplets was conducted using a centrifugal wheel atomizer driven at 40,000 rpm at 140 ± 10°. The preparation procedures of the microcapsules are shown in Fig. 1.

The microcapsules used for measuring the ζ-potential were characterized by the following micromeritic properties: geometric mean diameter of 8.5–28.5 μm, wall thickness of 0.75–1.31 μm, and particle density of 1.02–1.19 g/cm³ (7).

**Dispersion Medium**—The dispersion media used to measure the

[1] Micronized to <6 μm by a jet micronizer, Shionogi Pharmaceuticals Co., Osaka, Japan.



0022-3549/81/0300-0302$01.00/0
© 1981, American Pharmaceutical Association

(7) W.-K. Lee, J. M. Strong, R. F. Kehoe, J. S. Dutcher, and A. J. Atkinson, Jr., *ibid.*, **19**, 508 (1976).
(8) J. J. L. Lertora, A. J. Atkinson, Jr., W. Kushner, M. J. Nevin, W. K. Lee, C. Jones, and F. R. Schmid, *ibid.*, **25**, 273 (1979).
(9) G. P. Stec, J. J. L. Lertora, A. J. Atkinson, Jr., M. J. Nevin, W. Kushner, C. Jones, F. R. Schmid, and J. Askenazi, *Ann. Intern. Med.*, **90**, 800 (1979).
(10) R. Lahita, J. Kluger, D. E. Drayer, D. Koffler, and M. M. Reidenberg, *Clin. Res.*, **27**, 235A (1979).
(11) E. Karlsson, *Clin. Pharmacokinet.*, **3**, 97 (1978).
(12) J. M. Strong, J. S. Dutcher, W.-K. Lee, and A. J. Atkinson, Jr., *J. Pharmacokinet. Biopharm.*, **3**, 223 (1975).
(13) D. M. Roden, S. B. Reele, S. B. Higgins, G. R. Wilkinson, R. F. Smith, J. A. Oates, and R. L. Woosley, *Am. J. Cardiol.*, **46**, 463 (1980).
(14) D. T. Baer and J. C. Barkus, Jr., *Res. Commun. Chem. Path. Pharmacol.*, **17**, 333 (1977).
(15) J. Dreyfuss, J. T. Bigger, Jr., A. I. Cohn, and E. C. Schreiber, *Clin. Pharmacol. Ther.*, **13**, 366 (1972).
(16) D. W. Schneck, K. Grove, F. O. Dewitt, R. A. Shiroff, and A. H. Hayes, Jr., *J. Pharmacol. Exp. Ther.*, **204**, 219 (1978).
(17) P. G. Harms and S. R. Ojeda, *J. Appl. Phys.*, **36**, 391 (1974).
(18) C. M. Lai, B. L. Kamath, Z. M. Look, and A. Yacobi, *J. Pharm. Sci.*, **69**, 982 (1980).
(19) M. Gibaldi and D. Perrier, "Drugs and the Pharmaceutical Sciences, Vol. 1, Pharmacokinetics," Dekker, New York, N.Y., 1975.
(20) J. Cerna, Z. Zidek, and I. Janku, *J. Pharm. Pharmacol.*, **31**, 711 (1979).
(21) B. L. Kamath and A. Yacobi, *J. Pharm. Sci.*, **69**, 864 (1980).
(22) E. M. Renkin and J. P. Gilmore, in "Handbook of Physiology. Section 8: Renal Physiology," J. Orloff, R. W. Berliner, and S. R. Geiger, Eds., American Physiological Society, Washington, D.C., 1973, pp. 185–248.

# Electrophoretic Properties of Sulfamethoxazole Microcapsules and Gelatin–Acacia Coacervates

**H. TAKENAKA, Y. KAWASHIMA ˣ, and S. Y. LIN**

Received November 21, 1979, from the *Gifu College of Pharmacy, Mitahora, Gifu 502, Japan.* Accepted for publication September 2, 1980.

**Abstract** □ The electrophoretic properties of sulfamethoxazole microcapsules and the coacervates prepared by gelatin–acacia coacervation were investigated. The effects of the parameters in the microcapsule preparation, such as the coacervation pH, amount of formaldehyde used for hardening, and drying method of the coacervates, on the ζ-potential of the resultant microcapsules were clarified. The Büchner effect was observed in coacervates in an electric field, which indicated that the coacervate wall was flexible. The ζ-potential *versus* pH curves of the coacervates appeared on the upper side of the plain sulfamethoxazole, while those of the microcapsules dried conventionally shifted to the lower side due to denaturation of the gelatin in the microcapsule wall, which occurred during drying. Spray drying increased the denaturation of gelatin, which imparted a negative charge to the spray-dried microcapsules. Formalization of the coacervates refined the electrophoretic behavior of the microcapsules, depending on the amount of formaldehyde used. The ζ-potential of the plain sulfamethoxazole also was measured in the simulated coacervation solution to analyze the mechanism of coacervation electrophoretically.

**Keyphrases** □ Sulfamethoxazole—microcapsules and coacervates, electrophoretic properties compared □ Gelatin–acacia coacervates—sulfamethoxazole microcapsules and coacervates compared electrophoretically □ Microcapsules, acacia–gelatin—sulfamethoxazole, electrophoretic properties compared □ Coacervation, acacia–gelatin—sulfamethoxazole coacervates and microcapsules compared electrophoretically

Much attention has been paid to the electrophoretic properties of microcapsules because they are decisive parameters in stabilizing suspensions compounded with microcapsules (1). In addition, to prepare a microcapsule containing living cell fluid for use as an artificial cell, it is necessary to simulate the electrophoretic properties of the microcapsule as well as other properties such as elasticity, mechanical strength, and permeability (2).

Measurement of the ζ-potential of microcapsules is one way to assess their electrophoretic properties. The ζ-potential of microcapsules prepared by an interfacial polycondensation method was measured, and the effect of the pH medium on these properties was reported (3). The ζ-potential of gelatin–acacia coacervates, excluding the core material, also was determined (4). However, the electrophoretic properties of gelatin–acacia microcapsules containing the core material were not exhaustively investigated.

In the present study, ζ-potentials of gelatin–acacia coacervates and microcapsules prepared by drying were measured. One aim of the study was to elucidate the parameters that affect the electrophoretic properties of the coacervates and microcapsules. The amount of formaldehyde used for hardening, the coacervation pH, and the drying method of the coacervate droplets were assumed to be the parameters affecting this property. Another purpose was to manifest the coacervation process electrophoretically by measuring the changes in the ζ-potentials of plain sulfamethoxazole particles and gelatin–acacia coacervates during processing.

## EXPERIMENTAL

**Materials**—The test samples used to measure the ζ-potential were micronized sulfamethoxazole[1], gelatin–acacia coacervate droplets, and dried gelatin–acacia microcapsules of sulfamethoxazole. The gelatin–acacia coacervates of sulfamethoxazole were prepared as described earlier (5, 6). The coacervation pH was adjusted to 2.05–4.2. The coacervate droplets were formalized with 0, 30, and 50 ml of formaldehyde.

The conventional method of drying the coacervates (using warm air at 40°) and a spray drying technique were adopted. Spray drying of the slurries containing coacervate droplets was conducted using a centrifugal wheel atomizer driven at 40,000 rpm at 140 ± 10°. The preparation procedures of the microcapsules are shown in Fig. 1.

The microcapsules used for measuring the ζ-potential were characterized by the following micromeritic properties: geometric mean diameter of 8.5–28.5 μm, wall thickness of 0.75–1.31 μm, and particle density of 1.02–1.19 g/cm³ (7).

**Dispersion Medium**—The dispersion media used to measure the

[1] Micronized to <6 μm by a jet micronizer, Shionogi Pharmaceuticals Co., Osaka, Japan.



0022-3549/81/0300-0302$01.00/0
© 1981, American Pharmaceutical Association

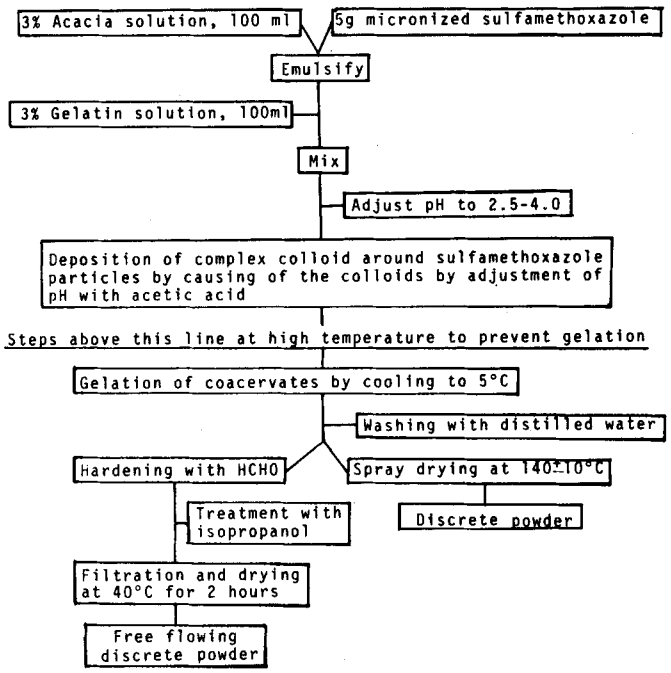


**Figure 1**—*Processing of microencapsulation of sulfamethoxazole by gelatin–acacia complex coacervation.*

ζ-potential were distilled water, the equilibrium coacervation solution, and the buffer solution with pH values of 2.5–9.5 and a constant ionic strength of 0.1.

**Electrophoretic Mobility Measurements**—The electrophoretic mobility of the test samples was measured[2]. The test particles, weighing ~10 mg, were dispersed in the required medium that was thermally controlled at 23° and were fed into the electrophoretic cell. The specific conductance of each medium was measured to select the most suitable voltage to apply across the electrophoresis cell.

The mobilities of 20 particles were measured for each batch, and the electrophoretic mobility was the average value of three batches. The experimental variations are indicated by the standard deviation bars in the figures. The ζ-potentials were calculated by inserting the mobilities into the Helmholtz–Smoluchowski equation:

$$\zeta = 9.0 \times 10^4 \left(\frac{4\P \eta u}{D}\right) \qquad \text{(Eq. 1)}$$

where $\zeta$ is the ζ-potential (millivolts), $\eta$ is the viscosity of the suspending liquid (poises), $D$ is the dielectric constant of the suspending liquid, and $u$ is the electrophoretic mobility of the suspended solid (micrometers per second per volt per centimeter). The factor $9.0 \times 10^4$ converts electrostatic units and micrometers to practical electrical units and centimeters, respectively.

**ζ-Potential Measurement of Sulfamethoxazole Particles**—To elucidate the change in the electrophoretic property of sulfamethoxazole particles during formation of the gelatin–acacia coacervates, the ζ-potential of sulfamethoxazole particles was measured in the medium adjusted to simulate the coacervation procedure (Fig. 1). Five grams of sulfamethoxazole particles was suspended in 200 ml of distilled water and in 200 ml of acacia–gelatin solution (3%) thermally controlled at 50° with stirring at 620 rpm.

The pH of each suspension was adjusted gradually to 2.5–4.0 by dropwise addition of diluted acetic acid. The particles were filtered after the suspension was cooled to 5.0° by immersion in a water bath. A portion of the separated particles was redispersed in the filtrate of each suspension, and the ζ-potentials were measured.

## RESULTS AND DISCUSSION

**ζ-Potential of Sulfamethoxazole Particles**—The pH profiles of the ζ-potential of sulfamethoxazole strongly depended on the type of polymer contained in an acetic acid solution (Fig. 2); the curves showed a positive

[2] Zeter-Meter, New York, NY 10028.

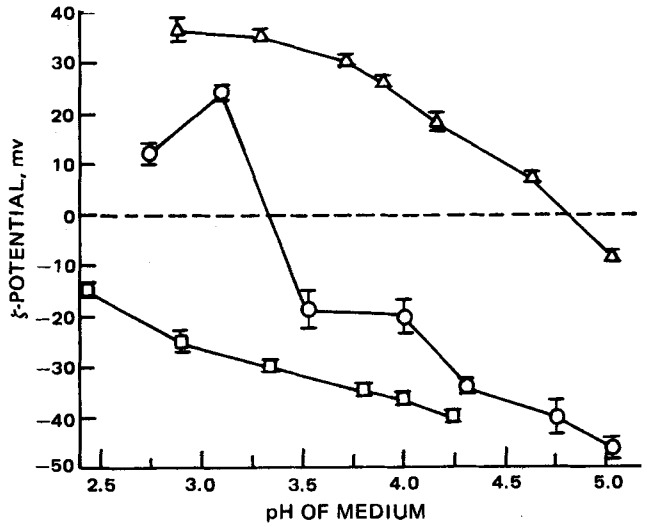


**Figure 2**—*ζ-Potential of sulfamethoxazole particles in acetic acid solution containing acacia and gelatin. Key (composition of medium): ○, acetic acid; □, acetic acid and acacia; and △, acetic acid and gelatin.*

charge at the lower pH range of 3.35 but a negative charge at the higher range. The apparent isoelectric point of sulfamethoxazole in this system was determined to be 3.35, which is slightly lower than the literature value of 3.8. This difference may be due to adsorption of acetate ions onto the sulfamethoxazole particle, which converts the surface charge slightly to the negative.

The ζ-potential in gelatin solution revealed a positive charge at pH 2.88–4.8. The pH value of 4.8, which intercepted the line of $\zeta = 0$, coincided with the isoelectric point of the gelatin used in this study. This result indicated that the gelatin molecules were adsorbed onto the sulfamethoxazole particles and formed a protective film around them. Thus, the particles with adsorbed gelatin molecules could behave as a gelatin molecule.

The ζ-potential of sulfamethoxazole in acacia solution was negative, which resembled the electrophoretic behavior of acacia. The absolute values of the ζ-potential decreased slightly with decreasing pH values, which can be attributed to the conversion of acacia from the salt form (such as calcium, magnesium, and potassium arabiate) to the free acid form.

The filtered sulfamethoxazole particles were redispersed directly, without washing, in distilled water for measuring the ζ-potential. Other measurements were made using particles washed with 100 ml of distilled water after filtration (Fig. 3). The ζ-potential of the washed particles from acetic acid solution was −30 mv in distilled water with a pH of 4.48–4.52. The absolute values of the ζ-potential in distilled water was slightly lower than in the acetic acid solution with a corresponding pH. This finding

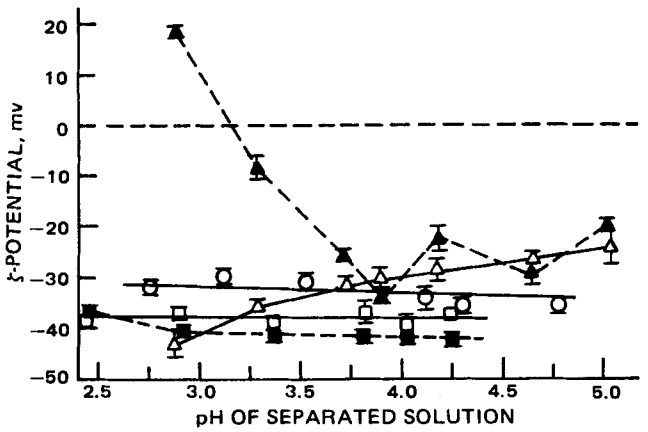


**Figure 3**—*Effect of washing on the ζ-potential of the sulfamethoxazole particle in distilled water. Key (type of separated solution): ■ and □, acacia without washing and washed with 100 ml of water, respectively; ▲ and △, gelatin without washing and washed with 100 ml of water, respectively; and ○, acetic acid washed with 100 ml of water.*

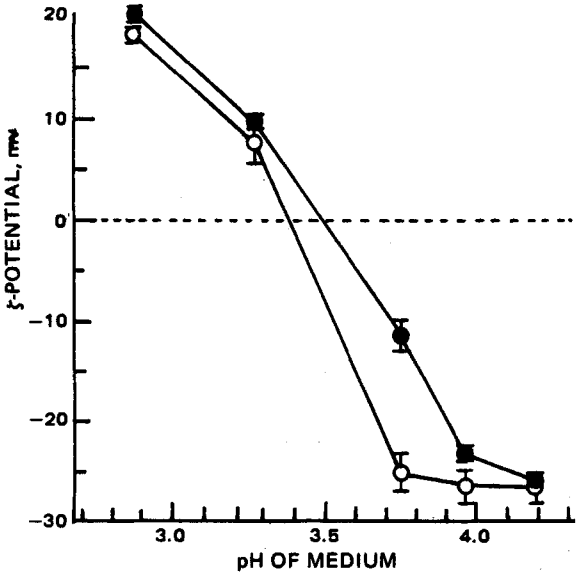


**Figure 4**—*ζ-Potential of the coacervate in the supernate of the coacervation solution. Key: ○, original sulfamethoxazole; and ●, coacervate.*

indicated the release of acetate ions from the particle surface by washing.

The washing effect also reflected on the ζ-potentials of particles separated from acacia and gelatin solutions. The difference in the ζ-potential curves of particles in gelatin solution before and after washing is seen in Fig. 3. Little difference was found at pH 4.0–5.0, which indicated stronger adsorption of gelatin onto the particle than at lower pH. These results suggest that, during preparation of coacervates by the present method, acacia molecules first are adsorbed onto sulfamethoxazole particles and then the coacervates are formed on the particle surface by adding gelatin and adjusting to the required pH.

**ζ-Potential of Coacervate Droplets of Sulfamethoxazole**—The ζ-potentials of the coacervate droplets were measured in the supernate of the coacervation solution and compared with those of the plain sulfamethoxazole particle. In an electric field, the coacervate droplets were deformed to an ellipsoid, the short axis of which was parallel to the direction of the electric field. This phenomenon, the Büchner effect (8), indicated that the coacervate wall was flexible.

Although the ζ-potential *versus* pH curve of the coacervates was above that of plain sulfamethoxazole, the form of the profile was almost the same (Fig. 4). This result suggests that the electrophoretic property of coacervates is affected by the encapsulated sulfamethoxazole. The pH profile of sulfamethoxazole almost coincided with the profile in the acetic acid solution (Fig. 2), suggesting that adsorption of the polymer to the particle was slight and that the polymer did not exist in the supernate. This finding proved that a complete phase separation occurred.

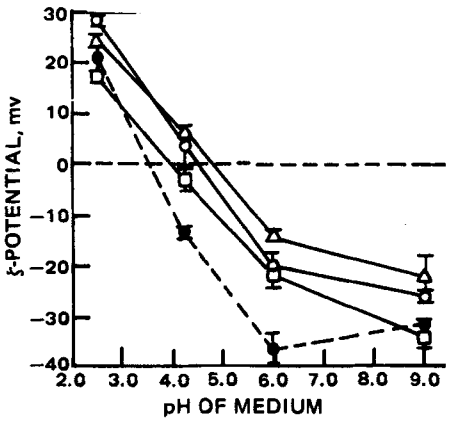


**Figure 6**—*Effect of coacervation pH on the ζ-potential of coacervates in the buffer solution. The buffer medium was μ 0.1. Key (coacervation pH): △, 2.5; ○, 3.5; and □, 4.0. The original sulfamethoxazole is indicated by a solid dot (●).*

The unformalized coacervate droplets were removed from the system with various pH values and were redispersed in distilled water. The change in the ζ-potential of the coacervates was derived by replacing the medium resembling the plain sulfamethoxazole adsorbed with gelatin (Figs. 3 and 5). This gelatin-like property of the coacervates suggests that the adsorbed gelatin on the particle surface can determine the electrochemical property of the coacervate. The formalized coacervate showed almost the same change in the ζ-potential as appeared in the unformalized coacervate. This result suggests that the gelatin was not denatured by formalization at this stage.

The coacervates removed from the system at various pH values were washed sufficiently with distilled water and were redispersed in the buffer solution, which was adjusted to various pH values and a constant ionic strength of 0.1. The pH profile of ζ-potentials of the coacervates and plain sulfamethoxazole in buffer are represented in Fig. 6. The ζ-potential *versus* pH curves of the coacervates appeared mainly on the upper side relative to the plain particles. These results indicate that the electrical property of gelatin–acacia coacervates is controlled by gelatin and the encapsulated core material. With decreasing coacervation pH, the pH

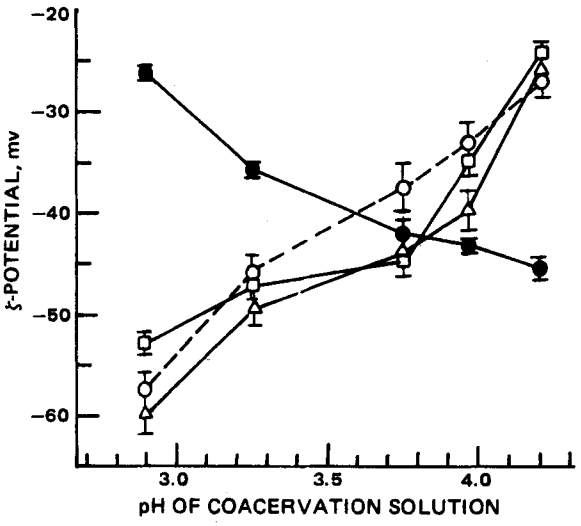


**Figure 5**—*Effect of washing on the ζ-potential of the coacervate in distilled water. Key: □, formalized coacervate with 15 ml of formaldehyde and washing with 1200 ml of water; ●, unformalized coacervate without washing; △, unformalized coacervate washed with 100 ml of water; and ○, unformalized coacervate washed with 1200 ml of water.*

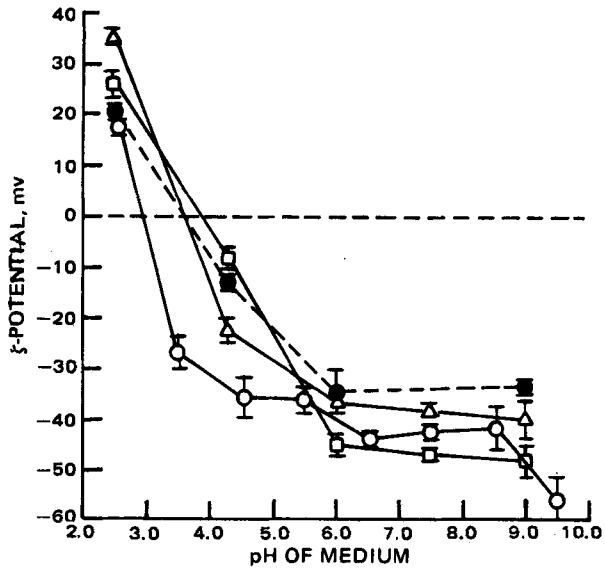


**Figure 7**—*Effect of coacervation pH on the ζ-potential of microcapsules in the buffer solution. The buffer medium was μ 0.1. Key (coacervation pH): △, 2.5; ○, 3.5; and □, 4.0. The original sulfamethoxazole is indicated by a solid dot (●).*

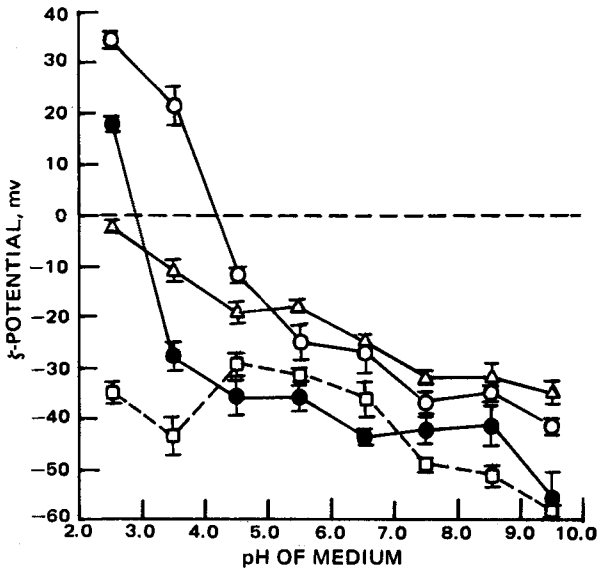


**Figure 8**—*Effect of formalization and spray drying on the ζ-potential of microcapsules in buffer solution. The buffer medium was μ 0.1. Key (milliliters of formaldehyde used): ●, 0; ○, 30; and △, 50. The spray-dried microcapsules are indicated by an open box (□).*

profile of the ζ-potential shifted more to the right, and the isoelectric point moved toward that of gelatin. The ζ-potential–pH profile of the coacervate prepared at pH 2.5 almost coincided with that of gelatin.

**ζ-Potential of Microcapsules**—The unformalized microcapsules prepared by drying the coacervates in the conventional way were dispersed in the coacervation medium adjusted to the required pH. The distinct difference in the pH profiles of the microcapsules from those of the corresponding coacervates is illustrated in Fig. 7. All of the curves moved to the left of the plain particles. This result was due to the denaturation of gelatin in the microcapsule wall which occurred during drying. Because of the gelatin denaturation, the contribution of acacia compared to that of gelatin became dominant, resulting in the negative charge.

The ζ-potential in the buffer solution *versus* pH curves of the microcapsules prepared at pH 3.5 was a function of the amount of formaldehyde used for hardening (Fig. 8). Upon formalizing with 30 ml of formaldehyde, the ζ-potential curve shifted to the upper side relative to that of the unformalized microcapsule. This result might be due to liberation of acacia from the microcapsule wall, which was induced by formalization. Thies (9) reported that glutaraldehyde treatment liberated acacia from gelatin–acacia coacervates. The release of acacia from the microcapsule wall caused the electrical equilibrium on the microcapsule surface to become unbalanced. The gelatin remaining in the microcapsule wall imparted a positive charge to the microcapsule, whereas stronger formalization, *e.g.*, 50 ml of formaldehyde, pushed the ζ-potential curve to the negative side for all of the pH ranges. In this case, the denaturation of gelatin compared to the liberation of acacia contributed to the negative conversion of the ζ-potential. The electrical property of the microcapsule was determined by a balance of the two actions. The spray-dried microcapsules revealed negative ζ-potentials at pH 2.5–9.5. The pH profile of the spray-dried microcapsules as seen in Fig. 8 resembled that of acacia in Fig. 2. The denaturation of gelatin, which occurred during drying, led to this result. The denaturation of gelatin in the microcapsule wall and the liberation of acacia from the wall were the main parameters used to determine the electrical properties of the microcapsules.

**Conclusion**—The mechanism of coacervation with gelatin and acacia was elucidated electrochemically, and the parameters that affected the electrophoretic properties of the microcapsules were found by measuring the ζ-potential of plain sulfamethoxazole, coacervates, and microcapsules.

Coacervation occurred on the surface of the sulfamethoxazole particle with adsorbed acacia, as shown by the fact that the ζ-potential–pH profile of the coacervates coincided with that of gelatin.

The Büchner effect appeared when the coacervates were in an electric field, thus indicating that the wall of coacervates was flexible.

With decreasing coacervation pH, the ζ-potential–pH curve of the coacervate became closer to that of gelatin and eventually coincided with it at pH 2.0.

The denaturation of gelatin caused by formaldehyde did not occur at the coacervation stage but during the succeeding drying process, which completed the hardening of the microcapsules.

Used as a hardening agent, formaldehyde can release acacia from the coacervate and denature the gelatin left in the microcapsule, thus determining the ζ-potentials of the formalized microcapsules. When the amount of formaldehyde was insufficient or sufficient for denaturing the gelatin, the ζ-potential of the formalized microcapsules became higher or lower, respectively, than that of the unformalized microcapsules.

The gelatin in the coacervates was denatured during spray drying, which depressed the ζ-potentials of the dried microcapsules.

## REFERENCES

(1) J. B. Kayes, *J. Pharm. Pharmacol.*, **29**, 199 (1977).

(2) T. M. S. Chang, "Artificial Cell," Charles C Thomas, Springfield, Ill., 1972.

(3) M. Shiba, Y. Kawano, S. Tomioka, M. Koishi, and T. Kondo, *Kolloid-Z. Z. Polym.*, **249**, 1056 (1971).

(4) H. G. Bungenberg de Jong and W. A. L. Dekker, *Kolloidchem. Beih.*, **43**, 143 (1935). *Ibid.*, **44**, 213 (1936).

(5) B. K. Green and L. Schleicher, U.S. pats. 2,730,456 and 2,730,457 (1956).

(6) L. A. Luzzi and R. J. Gerraughty, *J. Pharm. Sci.*, **53**, 429 (1964).

(7) H. Takenaka, Y. Kawashima, and S. Y. Lin, *ibid.*, **69**, 513 (1980).

(8) L. de Ruiter and H. G. Bungenberg de Jong, *Proc. Ned. Akad. Wet.*, **50**, 1189 (1947).

(9) C. Thies, *J. Colloid Interface Sci.*, **44**, 133 (1973).

# Semiautomated Assay for Indapamide in Biological Fluids

**PETER E. GREBOW ˣ, JO A. TREITMAN, ANNE K. YEUNG *, and MARTHA M. JOHNSTON**

Received June 13, 1980, from the *Biochemistry and Drug Disposition Department, USV Pharmaceutical Corporation, Tuckahoe, NY 10707.* Accepted for publication September 4, 1980. *Present address: Lederle Laboratories, Pearl River, NY 10965.

**Abstract** □ A sensitive fluorescence procedure for the determination of indapamide in plasma and whole blood was developed. The procedure requires preextraction of the biological sample followed by continuous-flow analysis. The assay is sensitive to indapamide levels of 25 ng/ml in plasma and blood. A linear response from 25 to 200 ng/ml is observed. The procedure also can be used to measure urinary levels of indapamide. The assay has been used to obtain whole blood and plasma level curves from subjects receiving 2.5 mg of indapamide.

**Keyphrases** □ Indapamide—semiautomated assay in biological fluids □ Fluorometry—analysis, indapamide in plasma, whole blood, and urine □ Antihypertensives—semiautomated assay of indapamide in biological fluids

Indapamide[1] [4-chloro-*N*-(2-methyl-1-indolinyl)-3-sulfamoylbenzamide, I] is a new and potent antihypertensive agent (1–4) undergoing extensive multicenter clinical studies in the United States. The drug is well tolerated and efficacious at single daily doses of 2.5 mg in patients with mild to moderate hypertension.

A fluorometric procedure for the measurement of I in urine was described previously (5). A semiautomated method for the measurement of I levels in plasma and blood now has been developed to support clinical pharmacology studies. A procedure for whole blood was necessary since I is taken into the red cells *in vitro* within 5 min of incubation at a ratio to plasma of approximately 9:1 (6). These fluorescence procedures require preextraction of drug from the biological sample followed by continuous-flow analysis. Urine samples also can be analyzed by a modification of the method for plasma. The procedure is capable of analyzing 10 biological samples/hr.

## EXPERIMENTAL

**Materials and Instruments**—All fluorescence measurements were done using a spectrophotofluorometer[2] equipped with a flowcell. Tubings[3,4] resistant to organic solvents were used for organic solutions. Lysis of blood was accomplished with a sonifier[5] equipped with a cup horn[6].

Indapamide[7] (I) was used without further purification. A stock solution of I in methanol (100 μg/ml) was used to prepare standards for the calibration curves in the different biological fluids. Methanol, ethylene dichloride, and *n*-heptane were distilled in glass[8]. Formaldehyde[9], 37% solution, was filtered prior to use. Tromethamine[10] (II) and all other reagents[9] were analytical reagent grade. Anhydrous ether[9] was preextracted twice with 0.1 *N* NaOH (ether–sodium hydroxide, 2:3 v/v) on the day of use. The buffer used for the continuous-flow system was 0.05 *M* II, pH 8.5. A solution of 0.1 *N* NaOH and 1.0 *M* NaCl was used for the final aqueous extraction in the continuous-flow system.

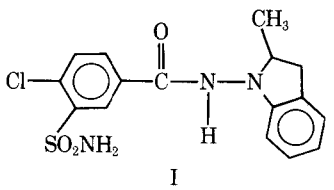


I

**Whole Blood Assay**—Whole blood samples (10 ml) were lysed by sonication for 5 min with a sonifier equipped with a water-jacketed cup horn. A 3.0-ml aliquot of each sample was pipetted into a polytef-lined, screw-capped culture tube (16 × 150 mm), and I was extracted into 6.0 ml of ether. The ethereal layer was transferred to a 15-ml conical tube and evaporated to dryness[11] under a gentle nitrogen stream at 30°. The dried extract was stored at −20° until analysis on the continuous-flow system.

Prior to analysis, each sample was reconstituted in 0.75 ml of heptane and vortexed vigorously. Three milliliters of 0.5 *M* II buffer was added, and the samples were vortexed and centrifuged. Approximately 1 ml of the aqueous phase was transferred to a sample cup, and the solution was sampled automatically at a rate of 10 samples/hr with a sample-to-wash ratio of 1:6. Figure 1 is a diagram of the continuous-flow system for the measurement of whole blood concentrations of I. The drug was extracted from the sample into ethylene dichloride, heptane was added, and the organic phase was mixed with a solution of 0.1 *N* NaOH and 1.0 *M* NaCl. The alkaline solution was heated in three 10.6-ml heating coils immersed in a 75° oil bath.

After addition of formaldehyde (5), the fluorescence of I was measured in a flowcell with an integral debubbler. The spectrophotofluorometer was set at an excitation wavelength of 284 nm and an emission wavelength of 356 nm; the photomultiplier slit was adjusted to 2 mm. The baseline was adjusted to approximately zero, with all of the reagents pumped through their respective lines and water pumped through the sample line. The change in the relative fluorescence intensity was measured by subtracting the baseline value from the peak height of each I sample.

Standards ranging from 25 to 400 ng of I/ml were prepared in duplicate and assayed with the samples. A standard was assayed approximately every fifth sample cup.

To determine the precision of the assay, I standards of 100 ng/ml ($n$ = 19) or 200 ng/ml ($n$ = 20) in whole blood were prepared on the day of assay and assayed as unknown samples over 2 months.

**Plasma Assay**—The procedure used for I in plasma was identical to that used for whole blood except that sample lysis was not necessary.

**Urine Assay**—The ether extracts of urine samples were washed with 8 ml of a 0.1 *M* sodium phosphate buffer, pH 7.4, prior to being evaporated to dryness. In all other steps, the assay of urine samples for I was identical to that for plasma samples.

**Assay of Clinical Specimens**—Samples of whole blood and plasma were obtained from healthy adult male subjects given an oral solution of 2.5 mg of I. Samples were taken at 0.5, 1.0, 2.0, 3.0, 4.0, and 6.0 hr after dosing.

## RESULTS AND DISCUSSION

As described in detail previously (5), a fluorescent product with excitation and emission wavelengths of 284 and 356 nm, respectively, is produced when indapamide (I) is heated in an alkaline solution. The described procedures employ the same principles as those of the previously described method for determining the concentration of I in urine but with considerable modification.

**Assay Conditions**—Ether, which was used previously, is not readily amenable to continuous-flow systems due to its high volatility. Thus,

[1] USV 2555.
[2] Aminco-Bowman flowcell of Suprasil quartz with an integral debubbler (4 mm o.d.), American Instrument Co., Silver Spring, Md.
[3] AutoAnalyzer sampler IV, proportioning pump III, temperature controller, AA II manifold, and Acidflex pump tubing (used for organic solutions), Technicon Instruments Corp., Tarrytown, N.Y.
[4] Scientific Instruments Corp., Pleasantville, N.Y.
[5] Model 185 cell disruptor, Branson Sonic Power Co., Danbury, Conn.
[6] Heat Systems-Ultrasonics, Plainview, N.Y.
[7] USV Laboratories, Tuckahoe, N.Y.
[8] Burdick & Jackson Laboratories, Muskegon, Mich.
[9] Fisher Chemical, Fair Lawn, N.J.
[10] Sigma Chemical Co., St. Louis, Mo.
[11] N-Evap, Organomation Associates, Shrewsbury, Mass.



0022-3549/81/0300-0306$01.00/0
© 1981, American Pharmaceutical Association

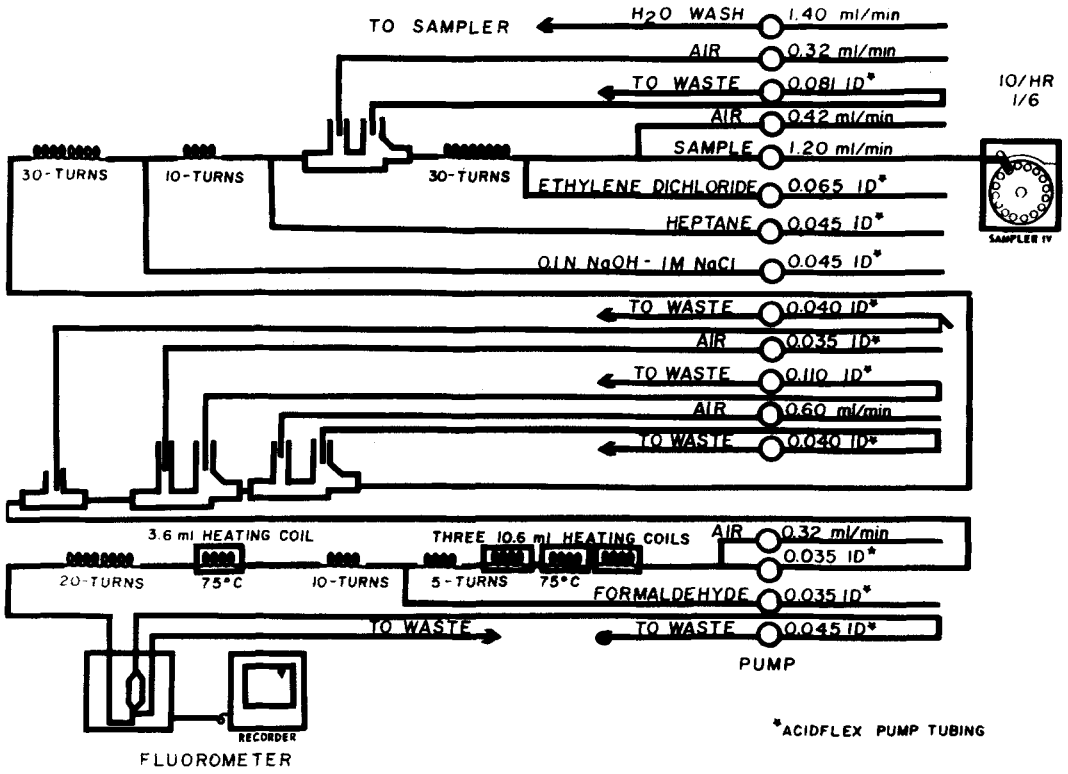


**Figure 1**—*Continuous-flow system for the measurement of indapamide concentrations in preextracted biological samples.*

ethylene dichloride was selected as the solvent since it also efficiently extracted I from biological fluids. This change in solvent necessitated the following modifications of the extraction procedure. Indapamide was extracted from biological fluids at physiological pH instead of pH 2. On-line separation of an organic–aqueous mixture is achieved more effectively when a four-point phase separator is used rather than a five-point phase separator. Addition of heptane to the ethylene dichloride–water mixture reversed the relative specific gravities of the organic and aqueous phase and thus permitted the use of the four-point phase separator. A three-point glass fitting was used just prior to the heating coils to prevent any small organic droplets from reaching these coils. Any introduction of organic material into the heating coils would drastically disturb the hydraulics of the system.

Due to the endogenous proteinaceous material present in plasma and whole blood and the sensitivity requirements of the assay, it was not possible to sample blood or plasma directly. Nor was it possible to sample an organic extract since evaporation over time would be a problem. Therefore, the samples were extracted with ether, evaporated to dryness, and stored at −20°. In this state, the samples were stable for at least 48 hr. The use of heptane to dissolve the residue from the extracts initially was necessary since endogenous materials that coextracted with I into ether were not soluble in the aqueous buffer.

**Standard Curves**—A typical chart recording for whole blood standards is shown in Fig. 2. A linear response for 25–400 ng of I/ml was observed for whole blood standards. Since the plasma I levels were proportionately lower, standards only up to 200 ng/ml were assayed. These solutions also showed a linear response. The net fluorescence intensities obtained for each concentration of I in plasma and whole blood are shown in Table I. Similar results were obtained for urine samples. A comparison of standards prepared with human plasma and whole blood and dog plasma and whole blood showed no difference. Thus, either source was used for the standards.

Standards of 100 and 200 ng of I/ml in whole blood were assayed as unknown samples. The 19 100-ng/ml standards were assayed to be 104.7 ± 14.1 ng/ml (mean ± *SD*), and the 20 200-ng/ml standards were assayed to be 208.9 ± 28.1 ng/ml (mean ± *SD*).

**Sensitivity**—Plasma and whole blood samples from 15 human subjects were assayed for I using the described procedure. The predose samples, as well as samples obtained during the day from subjects administered a placebo, gave an indication of the variability of the plasma and whole blood banks. The resultant fluorescence intensities were calculated to

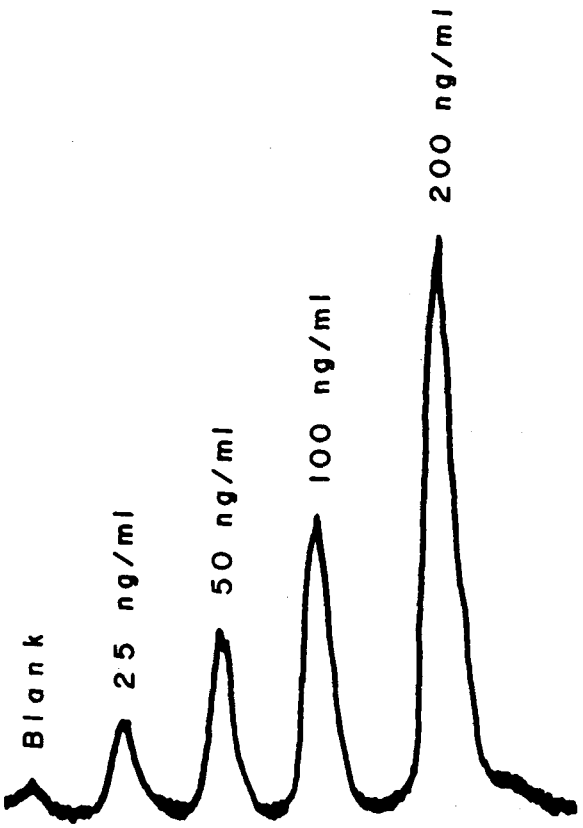


**Figure 2**—*Chart tracing for a blood standard curve.*

**Table I—Fluorescence Intensities of Indapamide Standards in Whole Blood and Plasma**

| Sample | Indapamide Concentration, ng/ml | | | | |
|---|---|---|---|---|---|
| | 25 | 50 | 100 | 200 | 400 |
| Plasma | 5.6 ± 1.2[a] | 11.5 ± 1.8 | 21.8 ± 4.6 | 45.4 ± 5.4 | — |
| Blood | 5.3 ± 0.2 | 8.9 ± 1.4 | 18.9 ± 1.4 | 37.1 ± 1.4 | 72.4 ± 8.8 |

[a] Mean ± *SD* ($n$ = 4).

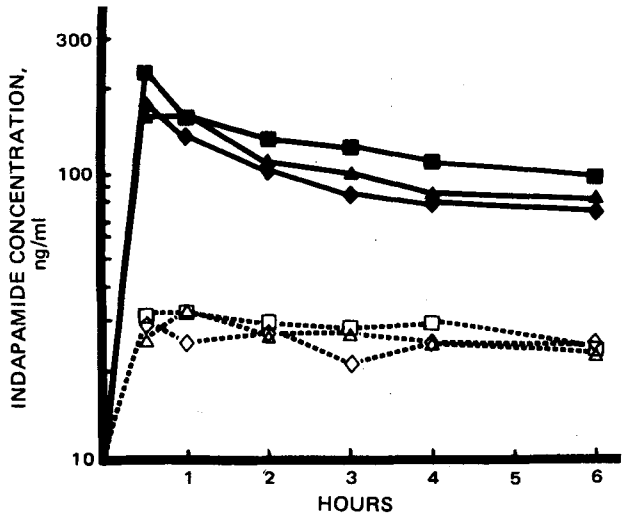


**Figure 3**—*Blood (■, ▲, ♦) and plasma (□, △, ◇) concentrations of indapamide following oral administration of 2.5 mg of indapamide to three subjects.*

be 2.0 ± 4.4 and 6.5 ± 5.7 ng/ml (mean ± *SD*) of apparent I, respectively. Based on these values, the sensitivity limit was considered to be ~20 ng of I/ml in both plasma and whole blood. A similar sensitivity limit was determined for urine samples.

**Specificity**—The specificity of the previous procedure for the measurement of unchanged I in urine was examined by high-pressure liquid chromatography (HPLC) and TLC (5). Blood concentrations of I from human subjects given the drug were measured both by the method described in this report and by an HPLC method that is under development. There was no significant difference between the measured I concentrations from the two procedures.

**Applicability to Clinical Samples**—The plasma and whole blood concentrations of I from three subjects who received an oral dose of 2.5 mg of I are shown in Fig. 3. The described procedure is adequate for monitoring the I concentrations in these media.

This method has several advantages over the previous method (5). The number of samples assayed per day is approximately doubled. The sensitivity is improved because of the better reproducibility of a continuous-flow system. In particular, a stable baseline is obtainable since the flowcell is not manipulated between samples as is a normal fluorescence cell during a manual procedure.

## REFERENCES

(1) G. Onesti, D. Lowenthal, M. Affirme, C. Swartz, J. Shirk, R. Mann, and E. Schultz, *Clin. Pharmacol. Ther.*, **21**, 113 (1977).

(2) P. Hatt and J. Lebrond, *Curr. Med. Res. Opin.*, **3**, 138 (1975).

(3) P. Millier and P. Tcherdakoff, *ibid.*, **3**, 9 (1975).

(4) S. Witchitz, H. Elguedri, J. Giudicelli, A. Kamoun, and P. Chiche, *Therapie*, **29**, 109 (1974).

(5) P. Grebow, J. Treitman, and A. Yeung, *J. Pharm. Sci.*, **67**, 1117 (1978).

(6) D. Campbell, A. Taylor, Y. Hopkins, and J. Williams, *Curr. Med. Res. Opin. (Suppl. 1)*, **5**, 13 (1977).

# Sulfoconjugation and Glucuronidation of Salicylamide in Isolated Rat Hepatocytes

**MASAHIRO KOIKE, KOICHI SUGENO, and MASAHARU HIRATA** ˣ

Received February 28, 1980, from *Shionogi Research Laboratories, Shionogi & Co., Ltd., Fukushima-ku, Osaka, 553 Japan.* Accepted for publication September 4, 1980.

**Abstract** □ Sulfoconjugation and glucuronidation of salicylamide by isolated hepatocytes were examined with various concentrations of salicylamide and sodium sulfate. The ratio of sulfate to glucuronide formed changed markedly, depending on the concentrations of salicylamide and inorganic sulfate in the medium. The apparent $K_m$ value of sulfoconjugation for salicylamide was 0.006 m*M*, while its $V_{max}$ value varied depending on the concentration of inorganic sulfate (*e.g.*, 2.1 and 0.5 nmoles/min/$10^6$ cells at 1.2 and 0.5 m*M* inorganic sulfate, respectively). The $K_m$ and $V_{max}$ values of glucuronidation for salicylamide were 0.19 m*M* and 1.28 nmoles/min/$10^6$ cells, respectively, in the absence of sodium sulfate. Glucuronidation was suppressed in the presence of inorganic sulfate. The suppression could be attributable to the competitive consumption of salicylamide by sulfotransferase. Additional *in vivo* experiments revealed that an extra amount of salicylamide markedly lowered the blood inorganic sulfate levels of rats. The significance of the finding is discussed in conjunction with the variation of the $V_{max}$ value of sulfoconjugation with the inorganic sulfate concentration.

**Keyphrases** □ Salicylamide—sulfoconjugation and glucuronidation □ Hepatocytes, rat—sulfoconjugation and glucuronidation of salicylamide □ Sulfate, inorganic—effect on conjugation and glucuronidation of salicylamide □ Conjugation—salicylamide, effect of inorganic sulfate

Numerous phenolic compounds are competitively metabolized *in vivo* to their conjugates by glucuronidation with uridine diphosphate (UDP) glucuronic acid and sulfoconjugation with 3′-phosphoadenosine-5′-phosphosulfate. In many cases, the sulfate is formed mainly at a low dosage while the glucuronide predominates at a high dosage (1–3).

This dose-dependent reversal of the sulfate/glucuronide ratio was explained by Levy and Matsuzawa (1) as follows. Blood inorganic sulfate can be consumed temporarily if a large amount of phenolic drug is administered and the 3′-phosphoadenosine-5′-phosphosulfate available for sulfoconjugation is limited, leading to a lower proportion of sulfate in the total conjugates. In fact, capacity-limited suppression of the sulfoconjugation can be overcome by simultaneous administration of drugs and sodium sulfate or cysteine to the subjects (4, 5). However, Weitering *et al.* (6) reported that the injection of phenol to rats did not lower the inorganic sulfate levels enough to elucidate the phenomenon. They emphasized that the reversed conjugation ratio found in *in vivo* experiments could be attributable to the different $K_m$ values of sulfotransferase and UDPglucuronyltransferase.

The problems underlying these controversial proposals may be settled by a simpler *in vitro* experiment using an isolated hepatocyte system. Isolated hepatocytes maintain



*0022-3549/81/0300-0308$01.00/0*
*© 1981, American Pharmaceutical Association*

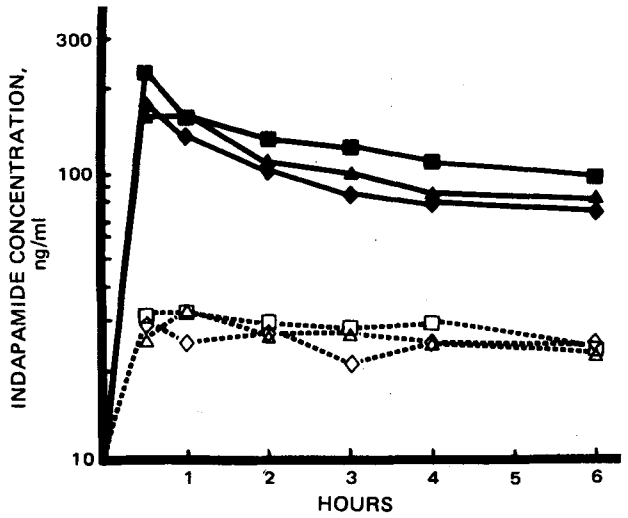


**Figure 3**—*Blood (■, ▲, ♦) and plasma (□, △, ◇) concentrations of indapamide following oral administration of 2.5 mg of indapamide to three subjects.*

be 2.0 ± 4.4 and 6.5 ± 5.7 ng/ml (mean ± *SD*) of apparent I, respectively. Based on these values, the sensitivity limit was considered to be ~20 ng of I/ml in both plasma and whole blood. A similar sensitivity limit was determined for urine samples.

**Specificity**—The specificity of the previous procedure for the measurement of unchanged I in urine was examined by high-pressure liquid chromatography (HPLC) and TLC (5). Blood concentrations of I from human subjects given the drug were measured both by the method described in this report and by an HPLC method that is under development. There was no significant difference between the measured I concentrations from the two procedures.

**Applicability to Clinical Samples**—The plasma and whole blood concentrations of I from three subjects who received an oral dose of 2.5 mg of I are shown in Fig. 3. The described procedure is adequate for monitoring the I concentrations in these media.

This method has several advantages over the previous method (5). The number of samples assayed per day is approximately doubled. The sensitivity is improved because of the better reproducibility of a continuous-flow system. In particular, a stable baseline is obtainable since the flowcell is not manipulated between samples as is a normal fluorescence cell during a manual procedure.

## REFERENCES

(1) G. Onesti, D. Lowenthal, M. Affirme, C. Swartz, J. Shirk, R. Mann, and E. Schultz, *Clin. Pharmacol. Ther.*, **21**, 113 (1977).

(2) P. Hatt and J. Lebrond, *Curr. Med. Res. Opin.*, **3**, 138 (1975).

(3) P. Millier and P. Tcherdakoff, *ibid.*, **3**, 9 (1975).

(4) S. Witchitz, H. Elguedri, J. Giudicelli, A. Kamoun, and P. Chiche, *Therapie*, **29**, 109 (1974).

(5) P. Grebow, J. Treitman, and A. Yeung, *J. Pharm. Sci.*, **67**, 1117 (1978).

(6) D. Campbell, A. Taylor, Y. Hopkins, and J. Williams, *Curr. Med. Res. Opin. (Suppl. 1)*, **5**, 13 (1977).

# Sulfoconjugation and Glucuronidation of Salicylamide in Isolated Rat Hepatocytes

**MASAHIRO KOIKE, KOICHI SUGENO, and MASAHARU HIRATA** ˣ

Received February 28, 1980, from *Shionogi Research Laboratories, Shionogi & Co., Ltd., Fukushima-ku, Osaka, 553 Japan.* Accepted for publication September 4, 1980.

**Abstract** □ Sulfoconjugation and glucuronidation of salicylamide by isolated hepatocytes were examined with various concentrations of salicylamide and sodium sulfate. The ratio of sulfate to glucuronide formed changed markedly, depending on the concentrations of salicylamide and inorganic sulfate in the medium. The apparent $K_m$ value of sulfoconjugation for salicylamide was 0.006 m*M*, while its $V_{max}$ value varied depending on the concentration of inorganic sulfate (*e.g.*, 2.1 and 0.5 nmoles/min/$10^6$ cells at 1.2 and 0.5 m*M* inorganic sulfate, respectively). The $K_m$ and $V_{max}$ values of glucuronidation for salicylamide were 0.19 m*M* and 1.28 nmoles/min/$10^6$ cells, respectively, in the absence of sodium sulfate. Glucuronidation was suppressed in the presence of inorganic sulfate. The suppression could be attributable to the competitive consumption of salicylamide by sulfotransferase. Additional *in vivo* experiments revealed that an extra amount of salicylamide markedly lowered the blood inorganic sulfate levels of rats. The significance of the finding is discussed in conjunction with the variation of the $V_{max}$ value of sulfoconjugation with the inorganic sulfate concentration.

**Keyphrases** □ Salicylamide—sulfoconjugation and glucuronidation □ Hepatocytes, rat—sulfoconjugation and glucuronidation of salicylamide □ Sulfate, inorganic—effect on conjugation and glucuronidation of salicylamide □ Conjugation—salicylamide, effect of inorganic sulfate

Numerous phenolic compounds are competitively metabolized *in vivo* to their conjugates by glucuronidation with uridine diphosphate (UDP) glucuronic acid and sulfoconjugation with 3′-phosphoadenosine-5′-phosphosulfate. In many cases, the sulfate is formed mainly at a low dosage while the glucuronide predominates at a high dosage (1–3).

This dose-dependent reversal of the sulfate/glucuronide ratio was explained by Levy and Matsuzawa (1) as follows. Blood inorganic sulfate can be consumed temporarily if a large amount of phenolic drug is administered and the 3′-phosphoadenosine-5′-phosphosulfate available for sulfoconjugation is limited, leading to a lower proportion of sulfate in the total conjugates. In fact, capacity-limited suppression of the sulfoconjugation can be overcome by simultaneous administration of drugs and sodium sulfate or cysteine to the subjects (4, 5). However, Weitering *et al.* (6) reported that the injection of phenol to rats did not lower the inorganic sulfate levels enough to elucidate the phenomenon. They emphasized that the reversed conjugation ratio found in *in vivo* experiments could be attributable to the different $K_m$ values of sulfotransferase and UDPglucuronyltransferase.

The problems underlying these controversial proposals may be settled by a simpler *in vitro* experiment using an isolated hepatocyte system. Isolated hepatocytes maintain



*0022-3549/81/0300-0308$01.00/0*
*© 1981, American Pharmaceutical Association*

biochemically and structurally organized functions and allow easier kinetic study than *in vivo* systems (2). Their ability to generate endogenous cosubstrates as well as to catalyze sequential reactions is particularly useful for drug conjugation studies (7). In view of its established metabolic routes and clinical importance (1, 8), salicylamide was chosen as a model, and its conjugation in isolated hepatocytes was studied. Attention was focused on the effect of inorganic sulfate on conjugation at high and low salicylamide concentrations.

## EXPERIMENTAL

**Materials**—The following materials were obtained commercially: collagenase[1] (*Clostridium histolyticum*), bovine serum albumin[2] (demineralized), amino acid mixture[3] (without L-glutamate), β-glucuronidase–arylsulfatase[4] (*Helix pomatia*, 9.3 IU of β-glucuronidase/ml, 5.9 IU of arylsulfatase/ml), β-glucuronidase[5] (calf, 13,000 UF/ml), salicylamide[6], and 2,6-dichloro-4-nitrophenol[7]. All other chemicals were reagent grade.

**Preparation of Isolated Hepatocytes**—Suspensions of isolated hepatocytes were prepared from male Wistar rats, 250–300 g, fed *ad libitum*, as described by Moldéus *et al.* (9). The oxygenator and buffer reservoir were jacketed for thermostatic control at 37°, and 13 m*M* *N*-2-hydroxyethylpiperazine-*N'*-2-ethanesulfonic acid[8] and penicillin[9] (400 IU/ml) were added to the buffers (10). The yield of each preparation was 5–6 × $10^8$ cells/liver, and the viability of fresh cells was 98–99% according to the lactic dehydrogenase latency test (9). The values were unchanged for 5 hr if the cells were suspended in albumin containing Krebs–Henseleit buffer at 4° saturated with 95% $O_2$–5% $CO_2$.

**Incubation of Isolated Hepatocytes**—Prior to incubation, the cells were washed twice with pH 7.4 Krebs–Henseleit buffer in which magnesium sulfate was replaced by magnesium chloride. To eliminate possible adsorption and binding of salicylamide conjugates (11), bovine serum albumin was not included in the buffer, although this omission caused deterioration of the cell viability to 95–96%. The cell suspension (7–15 ml/flask) was incubated in a rotating round-bottom flask at 37° under a stream of oxygen–carbon dioxide with 2 × $10^6$ cells/ml unless specified otherwise. For the kinetic studies, different amounts of salicylamide and sodium sulfate were added to Krebs–Henseleit buffer, in which magnesium sulfate was replaced by magnesium chloride and supplemented with 10 m*M* glucose, amino acid mixture, *N*-2-hydroxyethylpiperazine-*N'*-2-ethanesulfonic acid, and penicillin.

The viability of the isolated hepatocytes was checked periodically with the lactic dehydrogenase latency test (90–92% after 40 min of incubation). At intervals, samples were transferred to test tubes and boiled for 1 min to terminate the reaction. After centrifugation for 20 min at 2000 rpm, 1 ml of supernate was used for the conjugate determination.

**Determination of Salicylamide Conjugates**—Salicylamide sulfate and glucuronide were analyzed by the modified method of Veresh *et al.* (12) and Houston and Levy (13). One milliliter of sample was combined with 1.5 ml of 0.1 *M* acetate buffer (pH 5.0) and 6 ml of ethylene dichloride in a 12-ml glass-stoppered test tube, which was shaken vigorously for 15 min and centrifuged for 15 min at 2000 rpm. After removal of the organic layer by suction, 5 ml of ethylene dichloride was added to the tube and the extraction was repeated.

Subsequently, two parts of a 1-ml portion from the upper layer were taken into two tubes, one for the determination of glucuronide (Tube A) and the other for the determination of sulfate (Tube B). Salicylamide glucuronide was determined by adding 0.5 ml of β-glucuronidase and 1 ml of 0.1 *M* acetate buffer (pH 5.0) to Tube A and incubating for 40 hr at 37°. Salicylamide released by the enzymic hydrolysis was extracted with 6 ml of ethylene dichloride by shaking. After centrifugation, 4-ml portions of the organic layer were transferred to a test tube containing 5 ml of 0.1 *M* carbonate buffer (pH 11), which was shaken for 15 min and centrifuged for 10 min at 2000 rpm. The amount of salicylamide in the aqueous layer was determined fluorometrically using 325 and 420 nm for excitation and emission, respectively.

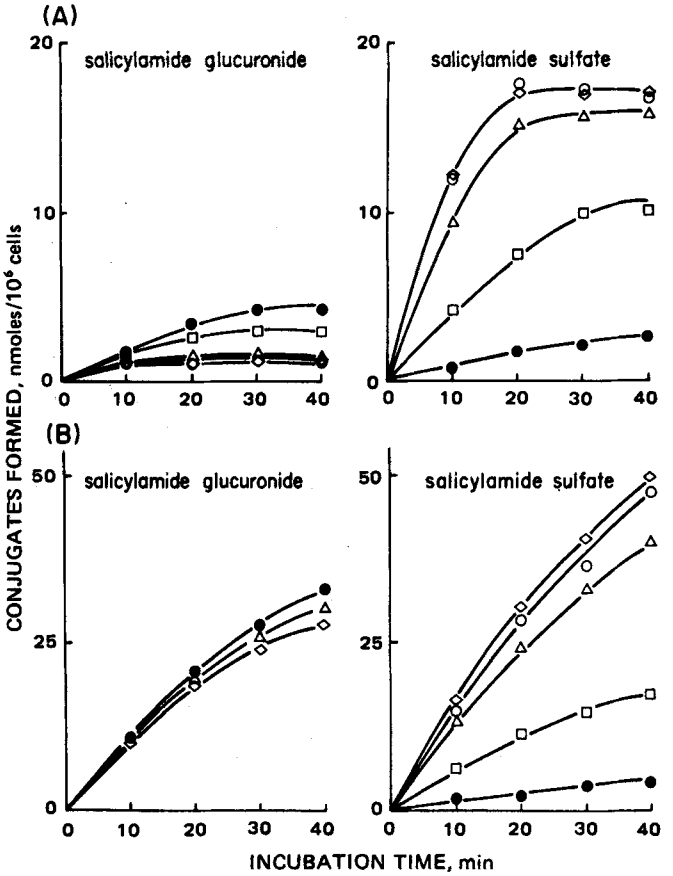


**Figure 1**—*Time courses of sulfoconjugation and glucuronidation of salicylamide in isolated rat hepatocytes at 0.05 m*M *(A) and 0.4 m*M *(B) salicylamide. Incubation was performed as described in the text in the absence (●) or presence of 0.1 (□), 0.5 (△), 1.2 (○), or 3.0 (◇) m*M *sodium sulfate.*

Next, the amount of salicylamide sulfate was determined by adding 0.1 ml of β-glucuronidase–arylsulfatase and 1 ml of 0.1 *M* acetate buffer (pH 5.0) to Tube B and incubating for 40 hr at 37°. By the same procedures used for Tube A, the total amount of salicylamide sulfate and glucuronide was determined, and the amount of the sulfate was calculated by subtracting the values obtained for Tube A from those for Tube B. Blank values were obtained in the same way, except that boiled liver cells were used. Incubation of isolated hepatocytes with different amounts of salicylamide and sodium sulfate was repeated two to three times, and the reproducibility was confirmed.

**Assay of Inorganic Sulfate in Rat Serum**—Male Wistar rats, 320–370 g, were anesthetized with pentobarbital sodium[10] before polyethylene tubing[11] was introduced into their right external jugular veins. Immediately after withdrawal of 2 ml of blood, 50 mg of salicylamide[12]/kg was administered. Subsequently, at 15-min intervals, 2 ml of blood was collected *via* the cannula and then centrifuged for 30 min at 4000 rpm using a serum separation aid[13]. The amount of inorganic sulfate in the serum was analyzed by turbidometry as described by Weitering *et al.* (6). Prior to the drug administration studies, it was confirmed that inclusion of 1 m*M* salicylamide in the serum, taken from an untreated rat, would not interfere with the determination of inorganic sulfate.

## RESULTS AND DISCUSSION

The time courses of sulfoconjugation and glucuronidation of salicylamide by isolated hepatocytes at 0.05 and 0.4 m*M* salicylamide and

[1] Boehringer Mannheim GmbH., West Germany.
[2] Povite Producten N.V., Amsterdam, The Netherlands.
[3] Gibco minimal essential medium amino acid mixture (without L-glutamate), Grand Island Biochemical Co., Grand Island, N.Y.
[4] Calbiochem, San Diego, Calif.
[5] Tokyo Zoki Chemical Co., Tokyo, Japan.
[6] Nakarai Chemicals, Kyoto, Japan.
[7] Tokyo Kasei Co., Tokyo, Japan.
[8] Hepes, Nakarai Chemicals, Kyoto, Japan.
[9] Penicillin G potassium, Meiji Seika Co., Tokyo, Japan.
[10] Somnopentyl, Pitman-Moore, Washington Crossing, N.J.
[11] Intramedic PE60, Clay Adams, Parsippany, N.J.
[12] Salicylamide was dissolved in 1 *N* NaOH, and the pH was adjusted to 9.0 with hydrochloric acid. The final concentration of salicylamide was 20 mg/ml.
[13] Separaid, HATCO International, Los Angeles, Calif.

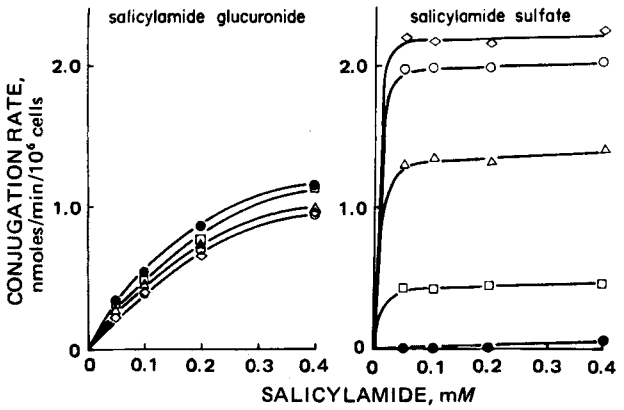


**Figure 2**—*Effect of salicylamide concentrations on the rate of salicylamide conjugation in isolated hepatocytes. The cells (1 × 10⁶ cells/ml) were incubated for 7 min at 37° with 3.0 (◇), 1.2 (○), 0.5 (△), or 0.1 (□) mM sodium sulfate or without (●) sodium sulfate.*

various inorganic sulfate concentrations are shown in Fig. 1. Apparently, a larger amount of salicylamide sulfate formed as the sodium sulfate concentration increased, whereas glucuronidation was suppressed at higher inorganic sulfate concentrations. Although the levels of conjugation varied, similar patterns of time courses were observed with the incubation system containing 0.1 or 0.2 m*M* salicylamide (not shown). An appreciable amount of salicylamide sulfate also was produced in the system without sodium sulfate, presumably due to the use of amino acids (*e.g.*, cysteine and methionine) in the medium as the source of sulfate, although the presence of contaminative inorganic sulfate in the cell isolation medium could not be ruled out. The ratio of conjugates, sulfate to glucuronide, changed markedly depending on the salicylamide concentration. For example, with 1.2 m*M* sodium sulfate, the sulfate to glucuronide ratio in a 10-min period decreased from 15 to 1.2 if the salicylamide concentration was increased from 0.05 to 0.4 m*M*.

Figure 2 shows the kinetics of conjugation by a 7-min incubation of isolated liver cells in the presence of different amounts of salicylamide and inorganic sulfate. The sulfoconjugation rate reached a maximum at low salicylamide concentration, while the glucuronidation rate increased progressively with increasing salicylamide concentrations. The effects of sodium sulfate on the two conjugation reactions were contrasting. The sulfoconjugation was accelerated by increasing inorganic sulfate, indicating the simultaneous increase of 3′-phosphoadenosine-5′-phosphosulfate, the cosubstrate for the conjugation, within the liver cells. On the other hand, the glucuronidation was suppressed by inorganic sulfate.

The reciprocal plots of [salicylamide glucuronide] against the reciprocal

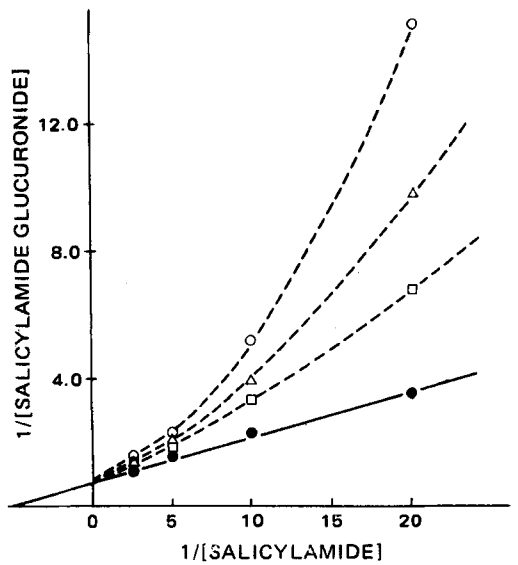


**Figure 3**—*Double reciprocal plots of salicylamide concentration (millimolar) against salicylamide glucuronide formed (nanomoles per minute per 10⁶ cells). The illustration was based on Fig. 2. The sodium sulfate concentration was 1.2 (○), 0.5 (△), 0.1 (□), or 0 (●) m*M.

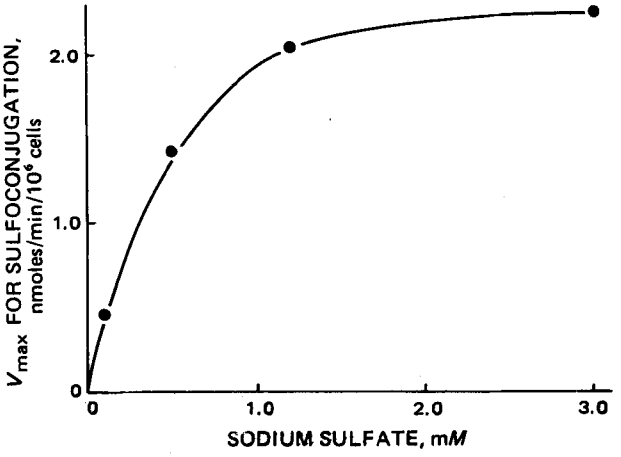


**Figure 4**—*Dependency of $V_{max}$ values of salicylamide sulfoconjugation on inorganic sulfate concentrations.*

of [salicylamide] in the absence of sodium sulfate produced a straight line (Fig. 3), and the $K_m$ and $V_{max}$ values of glucuronidation for salicylamide were estimated to be 0.19 m*M* and 1.28 nmoles/min/10⁶ cells, respectively. Concave curves produced in the presence of sodium sulfate indicate the inhibitory effect of inorganic sulfate on glucuronidation. The effect was less pronounced at higher salicylamide concentrations and was not appreciable at $V_{max}$, as indicated by the intersection of the lines on the vertical axis (Fig. 3). Although inorganic sulfate appeared to interfere with glucuronidation in an unusual manner, inhibition by inorganic sulfate has not been reported to the knowledge of the authors.

Anomalous kinetics of salicylamide glucuronidation in the presence of sodium sulfate can be interpreted alternatively on the basis of localization and $K_m$ differences of sulfotransferase and UDPglucuronyltransferase in isolated hepatocytes (14). The deviation from a straight line in Lineweaver–Burk (15) plots with increasing sodium sulfate concentration was probably due to the preferential use of salicylamide by sulfotransferase. When the concentration of salicylamide was low and that of inorganic sulfate was high, a large proportion of salicylamide, incorporated into the liver cells, could be used by sulfotransferase (which has a low $K_m$ value for the drug) in cytosol. Therefore, the actual concentration of salicylamide available for glucuronyltransferase in the endoplasmic reticulum would have been much lower than the amount added to the medium. However, if the salicylamide concentration was high, the reaction rate of sulfotransferase would reach a maximum level, thus leaving some substrate for glucuronidation. Therefore, the ratio of sulfate to glucuronide conjugates would decrease as the substrate concentration increased.

Since an isolated hepatocyte system functions like an *in vivo* system in many respects (2, 16), this interpretation may be more likely. The apparent $K_m$ and $V_{max}$ values of sulfoconjugation for inorganic sulfate were 0.47 m*M* and 2.62 nmoles/min/10⁶ cells, respectively, as calculated

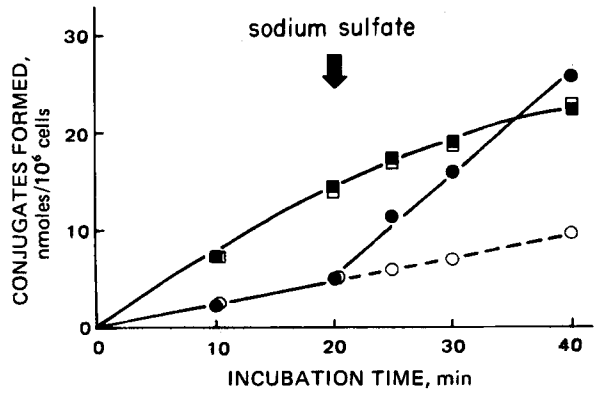


**Figure 5**—*Time courses of salicylamide conjugations: response to the increasing sulfate concentration from 0.1 to 1.2 m*M*. Isolated liver cells were incubated in the presence of 0.4 m*M* salicylamide and 0.1 m*M* sodium sulfate (○ and □). After 20 min of incubation, the concentration of sodium sulfate was increased to 1.2 m*M* (● and ■). Key: ○, ●, salicylamide sulfate; and □, ■, salicylamide glucuronide.*

**Table I—Effect of a High Dose [a] of Salicylamide on Rat Serum Inorganic Sulfate**

| Minutes after Injection | $n$ [b] | Sulfate Concentration [c], m$M$ |
|---|---|---|
| 0 | 7 | 0.72 ± 0.04 |
| 15 | 7 | 0.33 ± 0.08 |
| 30 | 7 | 0.16 ± 0.08 |
| 45 | 6 | 0.25 ± 0.12 |
| 60 | 4 | 0.43 ± 0.08 |

[a] Fifty milligrams of salicylamide/kg was intravenously administered. [b] Number of animals. [c] Mean sulfate concentration ± *SD*.

from typical Lineweaver–Burk plots. Since the $K_m$ value of sulfoconjugation for salicylamide was very small, it was obtained with plots of $[S]/V$ *versus* $[S]$ ($S$, salicylamide; $V$, the rate of sulfoconjugation) (14) and was 0.006 m$M$ when calculated by the least-squares method. The $V_{max}$ values of sulfoconjugation for salicylamide varied, depending on the sodium sulfate concentration (Fig. 4). The effect of inorganic sulfate on $V_{max}$ was remarkable at concentrations lower than 1.2 m$M$, indicating that the variation of inorganic sulfate in biological fluid would produce profound effects on sulfoconjugation of the drug *in vivo* since the level of inorganic sulfate in human serum is reported to vary from 0.2 to 0.7 m$M$ (17).

Another feature of conjugation was a quick response of the sulfoconjugation reaction to exogenous inorganic sulfate (Fig. 5), suggesting rapid incorporation of inorganic sulfate into liver cells and biotransformation to its active form, 3′-phosphoadenosine-5′-phosphosulfate (18). This finding supports the clinical utility of sodium sulfate for reducing acute toxicity of certain drugs (5, 19, 20).

To study the postulated depletion of blood inorganic sulfate by ingestion of a large amount of phenolic drug (1), 50 mg of salicylamide/kg iv was injected to anesthetized rats, and the inorganic sulfate levels in blood serum were analyzed for 60 min (Table I). The inorganic sulfate concentration decreased to as low as 22% of the initial blood level 30 min after the administration and then gradually recovered. This recovery could have been attained by the formation of inorganic sulfate from amino acids and the release of inorganic sulfate from various tissues (21). The analytical procedure using barium chloride (6) seems to be pertinent in this study since similar results were reproduced by isotachophoretic assay of inorganic sulfate in the blood samples (not shown). Thus, the data in Table I and Fig. 4 show that the $V_{max}$ values of salicylamide sulfoconjugation at 0.7 (initial blood level) and 0.16 m$M$ inorganic sulfate (30 min after the injection) were 1.68 and 0.62 nmole/min/$10^6$ cells, respectively, which implies at most a 60% reduction of the sulfoconjugation reaction by an extreme salicylamide overdosage.

An additional experiment confirmed the effect of 2,6-dichloro-4-nitrophenol, an *in vivo* sulfoconjugation inhibitor (22), on sulfoconjugation of salicylamide in isolated hepatocytes. The conjugation was terminated instantaneously by 0.05 m$M$ 2,6-dichloro-4-nitrophenol added to the system 10 min after incubation of the cells with 0.1 m$M$ salicylamide and 1.2 m$M$ sodium sulfate, whereas glucuronidation was slightly enhanced (not shown).

In conclusion, kinetic studies of the salicylamide metabolism using isolated hepatocytes allowed rational interpretation of previous conflicting *in vivo* observations on the metabolism of phenolic drugs, where dose-dependent fluctuation of the sulfate to glucuronide ratio was characteristic (1–3, 23). Available evidence suggests that at a low salicylamide dosage, a large proportion of the drug entering the cells is consumed preferentially by sulfotransferase in the cytosol and the effective salicylamide concentration for microsomal UDPglucuronyltransferase becomes very low. Consequently, the ratio of sulfate to glucuronide should be large. At high dosage, however, the ratio decreases because a larger amount of the drug is accessible to glucuronyltransferase, and glucuronidation occurs more actively. Furthermore, the observed variation of the $V_{max}$ value of sulfoconjugation for salicylamide, depending on the inorganic sulfate concentration, and the reduction of blood inorganic sulfate levels by the administration of salicylamide will, in combination, give rise to the capacity-limited suppression of sulfoconjugation of the drug *in vivo*.

## REFERENCES


(1) G. Levy and T. Matsuzawa, *J. Pharmacol. Exp. Ther.*, **156,** 285 (1967).

(2) S. Orrenius, B. Andersson, B. Jernström, and P. Moldéus, in "Conjugation Reactions in Drug Biotransformation," A. Aitio, Ed., Elsevier/North-Holland Biochemical Press, Amsterdam, The Netherlands, 1978, p. 273.

(3) H. Büch, G. Karachristiandis, and W. Rüdinger, *Arch. Exp. Pathol. Pharmakol.*, **251,** 107 (1965).

(4) G. Levy and H. Yamada, *J. Pharm. Sci.*, **60,** 215 (1971).

(5) R. E. Galinsky, J. T. Slattery, and G. Levy, *ibid.*, **68,** 803 (1979).

(6) J. G. Weitering, K. R. Krijgsheld, and G. J. Mulder, *Biochem. Pharmacol.*, **28,** 757 (1979).

(7) B. Andersson, M. Berggren, and P. Moldéus, *Drug Metab. Dispos.*, **6,** 611 (1978).

(8) B. Testa and P. Jenner, "Drug Metabolism," Dekker, New York, N.Y., 1976, p. 194.

(9) P. Moldéus, J. Högberg, and S. Orrenius, in "Methods in Enzymology," vol. 52, S. Fleischer and L. Packer, Eds., Academic, New York, N.Y., p. 60.

(10) J. Högberg and A. Kristoferson, *Eur. J. Biochem.*, **74,** 77 (1977).

(11) M. D. Burk and S. Orrenius, *Biochem. Pharmacol.*, **27,** 1533 (1978).

(12) S. A. Veresh, F. S. Hom, and J. J. Miskel, *J. Pharm. Sci.*, **60,** 1092 (1971).

(13) J. B. Houston and G. Levy, *J. Pharmacol. Exp. Ther.*, **198,** 284 (1976).

(14) G. J. Mulder and A. H. Hagedoorn, *Biochem. Pharmacol.*, **23,** 2101 (1974).

(15) M. Dixon and E. C. Webb, "Enzyme," Longmans, Green, London, England, 1964, p. 67.

(16) R. Billing, R. E. McMahon, J. Ashmore, and S. R. Wagle, *Drug. Metab. Dispos.*, **5,** 518 (1977).

(17) H. A. Harper, "Review of Physiological Chemistry," 12th ed., Maruzen, Tokyo, Japan, 1969, p. 214.

(18) G. J. Mulder and E. Scholtens, *Biochem. J.*, **172,** 247 (1978).

(19) I. Smith and P. D. Michell, *ibid.*, **142,** 189 (1974).

(20) J. T. Slattery and G. Levy, *Clin. Pharmacol. Ther.*, **25,** 184 (1979).

(21) G. J. Mulder and K. Keulemans, *Biochem. J.*, **176,** 959 (1978).

(22) G. J. Mulder and E. Scholtens, *ibid.*, **165,** 553 (1977).

(23) T. A. Slotkin, V. DiStefano, and W. Y. W. Au, *J. Pharmacol. Exp. Ther.*, **173,** 26 (1970).


## ACKNOWLEDGMENTS


The authors thank Mr. I. Ikeuchi for performing the isotachophoretic analyses of the blood samples.

# Kit Preparation of Radioiodinated *o*-Iodohippuran

**GEORGE H. HINKLE ˣ, GARO P. BASMADJIAN, ALAN S. KIRSCHNER *, and RODNEY D. ICE**

Received June 16, 1980, from the *College of Pharmacy, University of Oklahoma, Oklahoma City, OK 73190.* Accepted for publication September 5, 1980. *Present address: Arnold & Marie Schwartz College of Pharmacy, Long Island University, Brooklyn, NY 11201.

**Abstract** □ The purpose of this study was to evaluate a kit preparation for radioiodinated *o*-iodohippuran (I). All ingredients, excluding the radionuclide, were packaged in a ready-to-use kit for easy, quick formulation. Electrophoresis was utilized to evaluate the radiochemical purity of the labeled product and indicated that the radiolabeling technique provided a product with >95% radiochemical purity. Biodistribution studies in rats and rabbits provided an indication of the tissue distribution and localization of the radiopharmaceutical. Computer-generated renogram curves plotted from γ-camera images of rabbits showed the equivalency of the $^{131}$I-labeled I and $^{123}$I-labeled I to the commercially available radiopharmaceutical.

**Keyphrases** □ *o*-Iodohippuran, radioiodinated—kit preparation evaluated and compared with commercial products, biodistribution studies in rats and rabbits □ Radiopharmaceuticals—*o*-iodohippuran labeled with iodine 123 and with iodine 131, kit preparation method developed and compared with commercial products, biodistribution studies in rats and rabbits □ Biodistribution—radioiodinated *o*-iodohippuran in rats and rabbits, kit preparation of radiopharmaceutical developed and compared with commercial products

*o*-Iodohippurate sodium (I) radiolabeled with iodine 131 is used extensively for the noninvasive assessment of kidney function. Diagnostic information regarding renal blood flow, urinary tract patency, and urine flow may be obtained quickly and easily.

The clinical significance of a renal study with radioiodinated I may be improved by using iodine 123 rather than iodine 131 (1–5). The short physical half-life (13 hr) of iodine 123 and its pure γ-photon emission decrease the absorbed radiation dose per millicurie to the patient compared to iodine 131 (6). In addition, iodine 123 produces improved images with nuclear medicine instrumentation compared to iodine 131. The γ-photons emitted from iodine 131 are too energetic to be detected efficiently by the instrumentation generally used today. However, the 0.159 Mev γ-photons emitted from iodine 123 are detected more efficiently using a γ-camera and thus provide better counting statistics.

The relatively short physical half-life is a disadvantage in the use of iodine 123. The radiopharmaceutical, *i.e.*, $^{123}$I-labeled I, must be prepared at the institution where it will be used to make the agent economically feasible. Thus, the preparation method must be in the form of a radiopharmaceutical kit similar to kits used to prepare $^{99m}$Tc-labeled radiopharmaceuticals. Previous means for producing radioiodinated I (4, 7–15) involved extensive radiochemical synthetic and purification methods that do not allow the agent to be prepared easily at the site of use.

A rapid method for exchanging iodine 125 with the nonradioactive iodine in I was presented recently (16). The objectives of this research were to modify that method (16) to produce $^{123}$I-labeled I in kit form and to evaluate its biological distribution in animals.

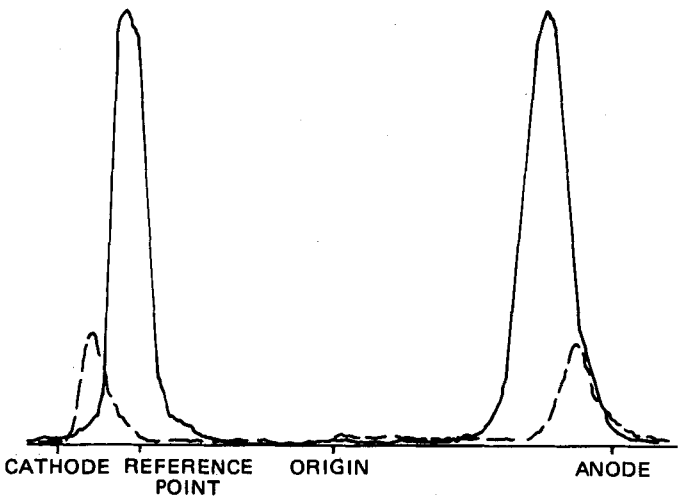


**Figure 1**—*Radiochromatogram scans of electrophoresis strips of sodium [$^{131}$I]iodide (—) and sodium [$^{123}$I]iodide (– –) showing the movement of radioiodine in this form toward the anode.*

## EXPERIMENTAL

**Materials**—*o*-Iodohippuric acid[1] was extracted three times with benzene (17) to remove traces of *o*-iodobenzoic acid (II), which competes with I for radioiodine during the exchange reaction (16). Melting-point determination and high-pressure liquid chromatographic (HPLC) analysis indicated that extraction effectively removed traces of II from I.

A solution of 50 mg of anhydrous copper sulfate in 10 ml of distilled water further enhanced the labeling of I by preferentially binding to any remaining II. Phosphate buffer was prepared by dissolving 6.185 g of dibasic sodium phosphate in 100 ml of distilled water.

Sodium [$^{131}$I]iodide was obtained commercially[2]. The 0.1 *N* NaOH solution of the sodium [$^{123}$I]iodide[3] was reduced to pH 3–7 with 0.5 *N* HCl prior to radioiodination of I.

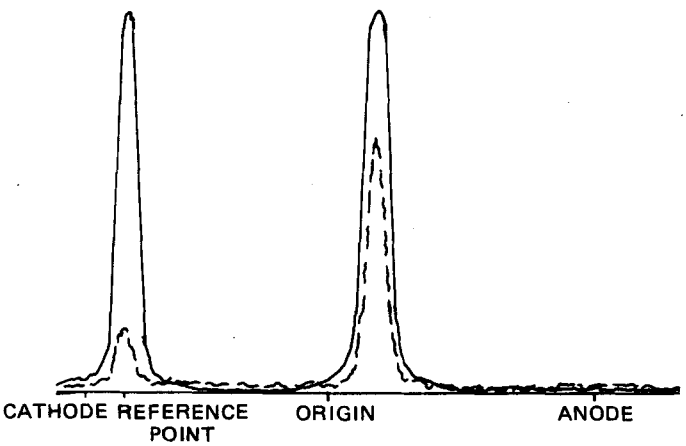


**Figure 2**—*Radiochromatogram scans of electrophoresis strips of $^{131}$I-labeled I (—) and $^{123}$I-labeled I (– –) showing the movement of the labeled compound.*

[1] Aldrich Chemical Co., Milwaukee, Wis.
[2] Mallinckrodt Nuclear, St. Louis., Mo., and E. R. Squibb & Sons, Princeton, N.J.
[3] Crocker Nuclear Laboratory, Davis, CA 95616.



0022-3549/81/0300-0312$01.00/0
© 1981, American Pharmaceutical Association

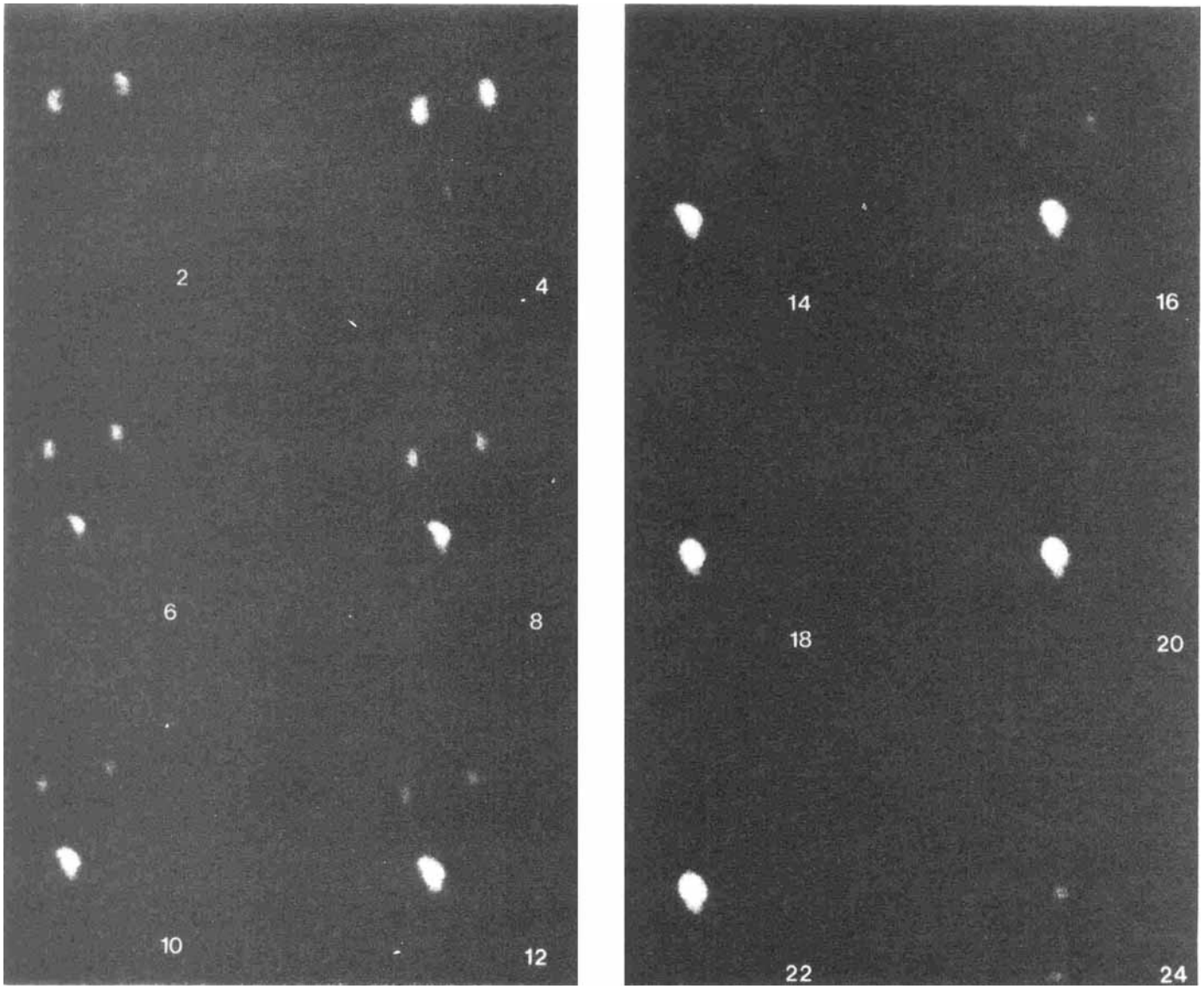


**Figure 3**—*γ-Camera image of rabbit biodistribution of kit-prepared $^{123}$I-labeled I. Each frame represents 2 min of elapsed time.*

**Lyophilization**—To prepare 10 lyophilized vials, 50 mg of purified I was dissolved in 1 ml of absolute ethanol, and 6 ml of distilled water was added. One milliliter of the copper sulfate–distilled water solution (5 mg/ml) was added to bring the final volume to 10 ml. Aliquots (1 ml) were filtered through a 0.22-μm filter[4] into 10-ml serum vials. The solutions were frozen rapidly with solid carbon dioxide lyophilized[5] for 24 hr, and the vials were stoppered and sealed. Each vial contained 5 mg of I and 0.5 mg of copper sulfate in lyophilized form.

**Preparation of Radioiodinated I**—From 0.5 to 5.0 mCi of radioiodine (either sodium [$^{123}$I]iodide or sodium [$^{131}$I]iodide) was added to the vial containing the lyophilized I and copper sulfate. The vial was autoclaved[6] for 15 min at 120–130° and allowed to cool at room temperature. Phosphate buffer (2 ml) was added to precipitate the copper as copper phosphate and to raise the pH to 7–8. Then the solution was passed through a 0.22-μm filter[4] into a clean 10-ml evacuated serum vial. The total activity was measured in a dose calibrator[7], and the specific concentration was calculated.

**Radiochemical Purity**—A sample of radioiodinated I was placed on the center of a cellulose polyacetate electrophoresis strip[8]. A similar sample of radioiodinated sodium iodide was placed on a second strip as a control. In addition, a third strip was spotted with a small amount of radioiodinated II. The strips were placed in an electrophoresis chamber[8] containing tromethamine–barbital–barbital sodium buffer[8] (pH 8.8, ionic strength 0.06). The voltage was set at 275 v and allowed to run for 15 min. Then the strips were removed from the chamber and allowed to air dry. A small amount of radioactive material was placed on the cathode end of each strip as a reference point, and the position of radioactivity on each strip was determined with a radiochromatogram scanner[9].

**Biodistribution**—Five millicuries of $^{123}$I-labeled I was prepared as described, and the radiochemical purity was determined by electrophoresis.

Normal male Sprague–Dawley rats, 300–400 g, were weighed and anesthetized with chloroform. A dose (0.1 ml) of $^{123}$I-labeled I then was administered intravenously into the femoral vein following a femoral vein cutdown procedure.

Two rats were sacrificed at 1, 2, 5, 10, and 30 min following injection. Duplicate samples of blood, liver, heart, small intestines, kidneys, fat, and testes were removed from each rat, weighed, and placed in counting tubes.

A standard for counting was prepared by diluting 0.1 ml of the preparation to 100 ml with saline. Each tube, except the tubes containing kidney samples, were counted in an automatic γ-counter[10] for 1 min. A 0.1-ml aliquot of the standard was placed before and after each set of

[4] Millipore.
[5] Labconco Freeze-Dry, Labconco Corp., Kansas City, Mo.
[6] Model 1250 Labclave, Ritter Sybron Corp., Rochester, N.Y.
[7] Model CRC-10R radioisotope calibrator, Capintec Inc., Mount Vernon, N.Y.
[8] Gelman, Ann Arbor, Mich.
[9] Model 930, Vangard Systems, Stamford, Conn.
[10] Gamma 300, Beckman Instruments, Fullerton, Calif.

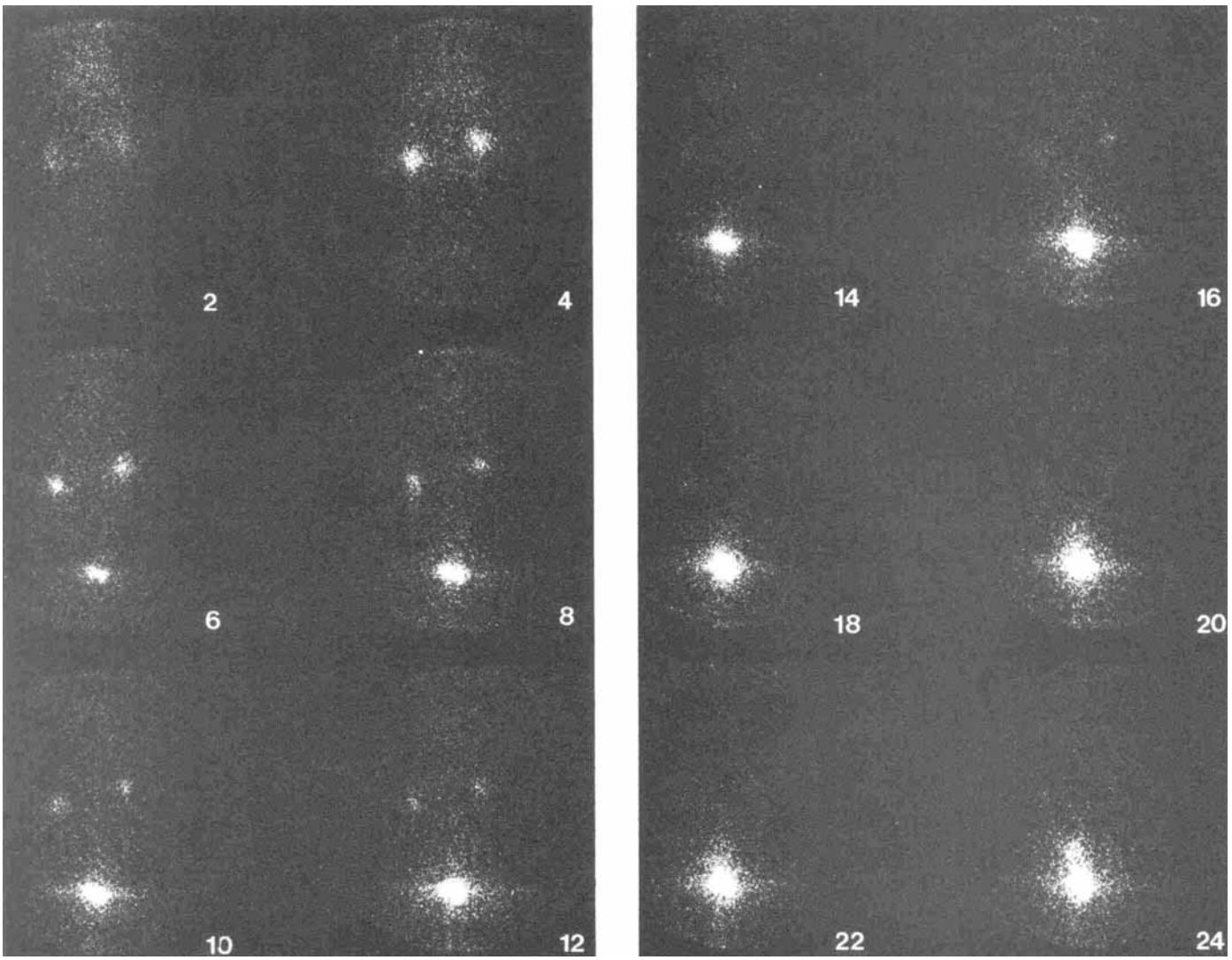


**Figure 4**—*γ-Camera image of rabbit biodistribution of kit-prepared $^{131}I$-labeled I. Each frame represents 2 min of elapsed time.*

tissue samples from a given rat. Kidney samples were counted ~39 hr after the other samples because of the extremely high levels of radioactivity, which would have caused an error in the results due to resolving time losses.

The tissue levels of radioactivity are described as percent of kilogram dose per gram (% kg dose/g) (18):

$$\%\ \text{kg dose/g} = \frac{\text{cpm in tissue/g of tissue}}{\text{cpm in dose/kg wt. of animal}} \times 100\% \quad \text{(Eq. 1)}$$

where cpm in dose = cpm in diluted dose × 1000.

**Rabbit Studies**—White, female, New Zealand rabbits were anesthetized using a combination of xylazine[11] (10 mg/kg) and ketamine[12] (35 mg/kg) injected intramuscularly. The rabbits were injected intravenously with 0.1–0.5 mCi of $^{123}I$-labeled I prepared by the kit method or $^{131}I$-labeled I obtained commercially[13] or prepared from a kit. The γ-camera[14] images were taken 2 min apart for 30 min. Renogram curves were obtained through the use of a computer interphased with the γ-camera.

## RESULTS

**Radiochemical Purity**—The pH of the radioiodine solution used in preparing the radiopharmaceutical was found to be important. Commercially available sodium [$^{131}I$]iodide solutions have pH values of 3–7, which is acceptable. However, the sodium [$^{123}I$]iodide utilized in this study was supplied in 0.1 *N* NaOH. The pH of this radioiodine solution must be ≤7 to label I efficiently using the kit described.

Electrophoresis was an efficient method for evaluating the radiochemical purity of radioiodinated I. Figure 1 illustrates the expected migration of $^{131}I^-$ and $^{123}I^-$ toward the anode. Both $^{131}I$-labeled I and $^{123}I$-labeled I also traveled toward the anode (Fig. 2) with an $R_I$- of ~0.3–0.4, identical to that of commercially available $^{131}I$-labeled I. Radioiodinated II traveled toward the anode with an $R_I$- of 0.17. This finding illustrates the system's ability to separate between the radioiodinated I and the radioiodinated II impurity. Greater than 95% radiochemical purity was achieved utilizing the kit method in the preparation of these agents.

Electrophoresis of the two radiolabeled compounds at various times after preparation indicated that the radiopharmaceutical was stable for at least 10 days when stored at room temperature.

**Biodistribution**—The $^{123}I$-labeled I prepared by the kit method (Table I) was cleared rapidly from the blood. Kidney concentration of radioactivity reached a maximum between 1 and 5 min after injection and then declined rapidly. Radioactivity in organs other than the kidneys was low relative to the kidneys. Free radioiodine localizes to a large extent in the intestine (19). The relatively low concentration of radioactivity in the small intestine indicated good *in vivo* stability of $^{123}I$-labeled I.

**Rabbit Studies**—Of major concern in the development of a new method of preparing a radiopharmaceutical that is available commercially is that the nuclear medicine images obtained are similar or improved. To evaluate this point, rabbits were injected with commercially available

[11] Chemagro, Kansas City, Mo.
[12] Bristol Laboratories, Syracuse, N.Y.
[13] Mallinckrodt Nuclear, St. Louis, Mo.
[14] LFOV, Searle, Chicago, Ill.

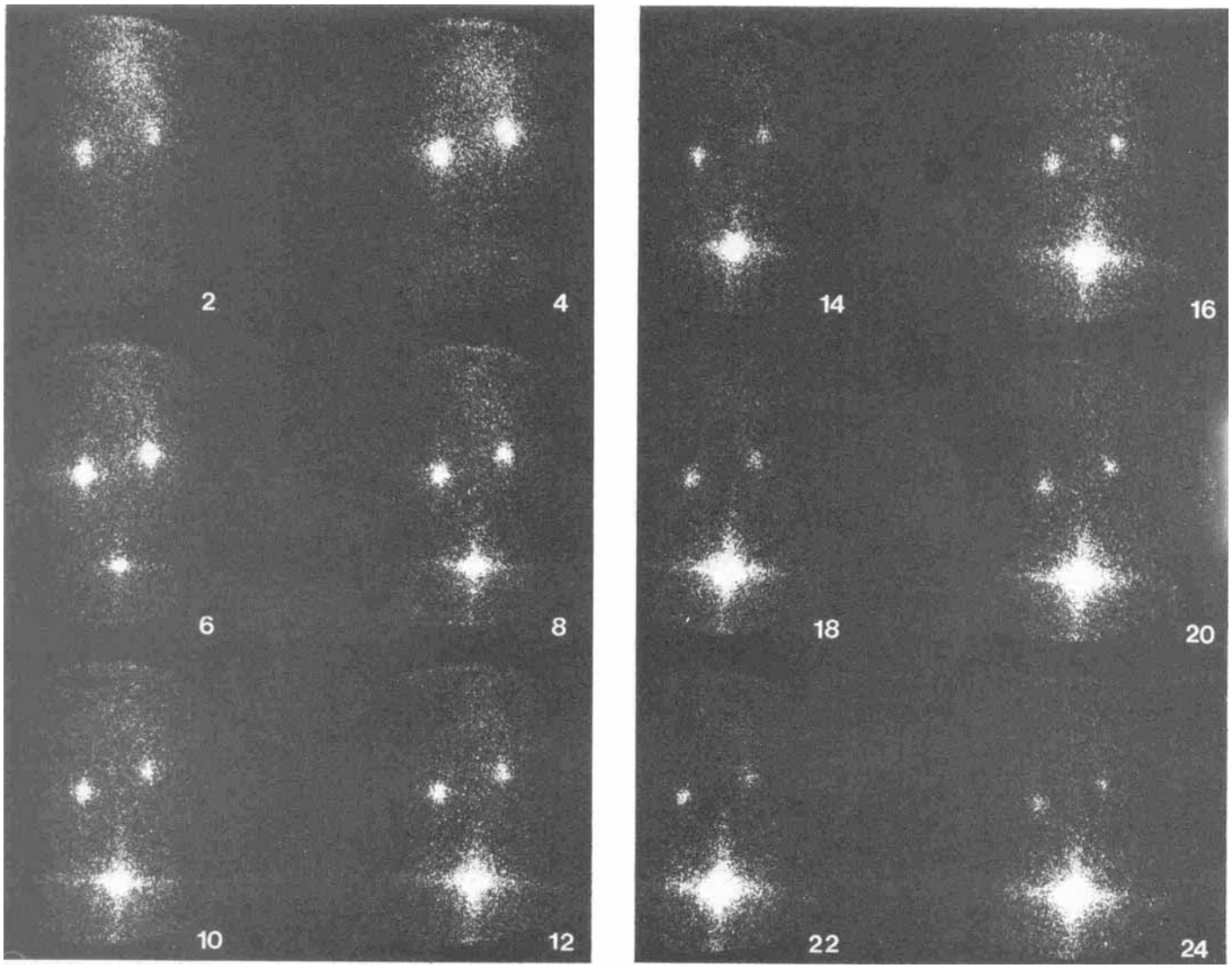


**Figure 5**—*γ-Camera image of rabbit biodistribution of commercially available $^{131}I$-labeled I. Each frame represents 2 min of elapsed time.*

$^{131}I$-labeled I and kit-prepared $^{131}I$-labeled I and $^{123}I$-labeled I. The images obtained using standard nuclear medicine instrumentation and procedures were comparable with all three preparations (Figs. 3–5).

Kidneys were seen within the first 2 min after injection. Urinary bladder was visible within 4–6 min following injection. At 20 min, all of the radioactivity appeared to have localized in the urinary bladder with faint shadows of the kidneys visible. The nonvisualization of the thyroid supports the conclusion that an *in vivo* stable product is formed. The images obtained with $^{123}I$-labeled I (Fig. 3) were superior to those obtained with $^{131}I$-labeled I (Fig. 4) prepared by the kit method and $^{131}I$-labeled I (Fig. 5) obtained commercially. This improved imaging was due to the higher photon flux and the more efficiently detected γ-photon of iodine 123. Renograms (Fig. 6) generated by computer accumulation of the distribution of radioactivity also were comparable with all three preparations.

## DISCUSSION

The kit method for preparing $^{123}I$-labeled I and $^{131}I$-labeled I yields a radiochemically pure agent. The method is quick and easy, with the final product obtained 60 min after the addition of radioiodine to the reaction vial.

The radiopharmaceutical kit consists of: (*a*) a 10-ml sterile, pyrogen-free, evacuated vial containing 5 mg of purified I and 0.5 mg of copper sulfate in lyophilized form; (*b*) a 3-ml disposable glass syringe containing 2 ml of dibasic sodium phosphate buffer (6.185 g/100 ml); (*c*) a 0.22-μm sterile disposable filter; (*d*) a 10-ml sterile, pyrogen-free, evacuated serum vial; and (*e*) a 5-ml syringe.

The γ-camera images of rabbits and computer-generated renograms following intravenous injection of the kit preparation were of excellent quality and comparable to those following intravenous injection of

**Table I—Tissue Distribution [a] of [$^{123}I$]-*o*-Iodohippuran in Rats**

| Minutes after Injection | Blood | Kidneys | Liver | Heart | Small Intestine | Testes | Fat |
|---|---|---|---|---|---|---|---|
| 1 | 0.650 | 2.69 | 0.330 | 0.187 | 0.092 | 0.041 | 0.020 |
| 2 | 0.508 | 2.75 | 0.337 | 0.191 | 0.141 | 0.036 | 0.036 |
| 5 | 0.188 | 1.56 | 0.130 | 0.064 | 0.048 | 0.033 | 0.031 |
| 10 | 0.109 | 0.822 | 0.067 | 0.032 | 0.027 | 0.019 | 0.012 |
| 30 | 0.046 | 0.170 | 0.020 | 0.010 | 0.036 | 0.009 | 0.010 |

[a] Mean percent of kilogram dose per gram.

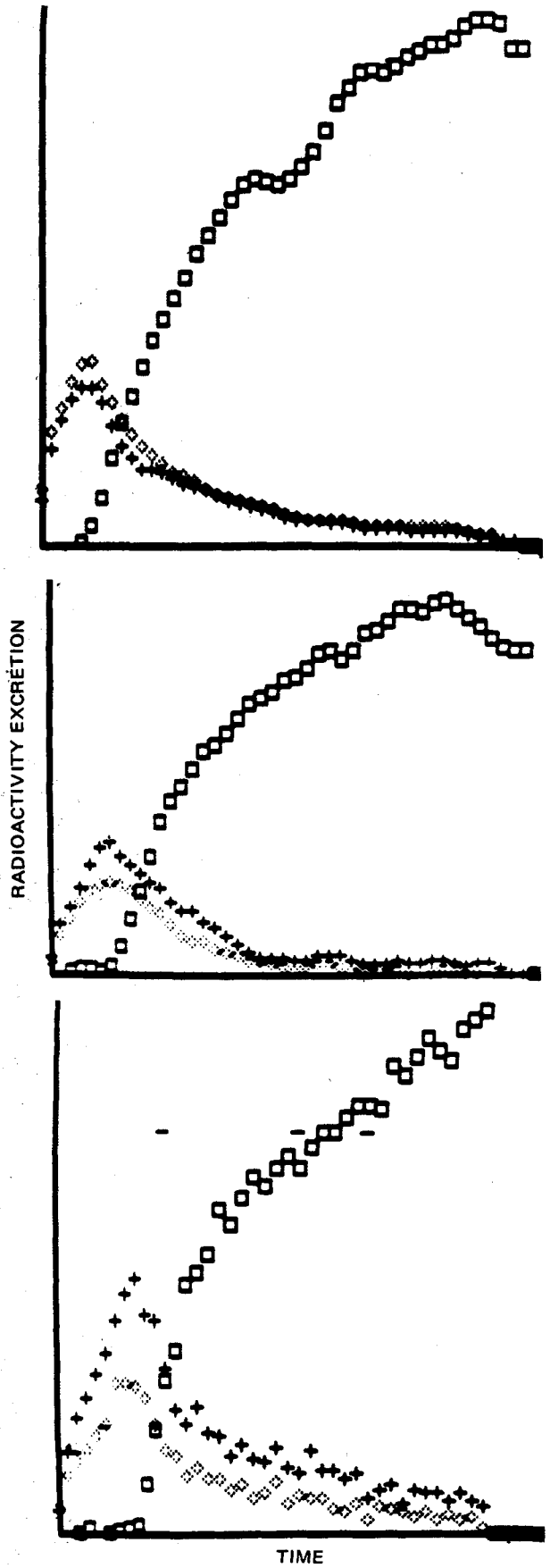


**Figure 6**—*Renogram curves showing the excretion of $^{123}I$-labeled I prepared by the kit method (top), $^{131}I$-labeled I prepared by the kit method (middle), and $^{131}I$-labeled I obtained commercially (bottom). Each point on a line represents 30 sec of elapsed time. The squares represent the radioactivity in the bladder while the crosses and diamonds represent the radioactivity in each kidney.*

commercially obtained $^{131}I$-labeled I.

This method for preparing radioiodinated I, especially $^{123}I$-labeled I, will be evaluated for human use. It would allow nuclear pharmacies and nuclear medicine units to prepare $^{123}I$-labeled I at the site of use and thus reduce the cost of the agent, reduce the radiation dose to the patient, and improve the clinical evaluation.

## REFERENCES

(1) A. T. Elliott and K. E. Britton, *Int. J. Appl. Radiat. Isotopes*, **29**, 571 (1978).

(2) R. W. Kenny, D. M. Ackery, J. S. Fleming, B. A. Goddard, and R. W. Grant, *Br. J. Radiol.*, **48**, 481 (1975).

(3) M. D. Short, H. I. Glass, G. D. Chisholm, P. Vernon, and D. J. Silvester, *ibid.*, **46**, 289 (1973).

(4) F. W. Zielinski, F. E. Holly, G. D. Robinson, Jr., and L. R. Bennett, *Radiology*, **125**, 753 (1977).

(5) K. E. Britton, in "Medical Radionuclide Imaging," vol. II, International Atomic Energy Agency, Vienna, Austria, 1977, p. 401.

(6) W. G. Myers, H. O. Anger, J. F. Lamb, and H. S. Winchell, in "Radiopharmaceuticals and Labelled Compounds," vol. I, International Atomic Energy Agency, Vienna, Austria, 1973, p. 249.

(7) P. J. Robbins and D. L. Fortman, *J. Nucl. Med.*, **12**, 459 (1971).

(8) A. P. Wolf, D. R. Christman, J. S. Fowler, and R. M. Lambrecht, in "Radiopharmaceuticals and Labelled Compounds," vol. I, International Atomic Energy Agency, Vienna, Austria, 1973, p. 345.

(9) A. E. A. Mitta, A. Fraga, and N. Veall, *Int. J. Appl. Radiat. Isotopes*, **12**, 146 (1961).

(10) R. S. Mani and R. J. V. Prabakaran, *Curr. Sci.*, **1**, 16 (1966).

(11) M. L. Thakur, B. M. Chauser, and R. F. Hudson, *Int. J. Appl. Radiat. Isotopes*, **26**, 319 (1975).

(12) K. E. Scheer and W. M. Borst, *Nucl. Med.*, **2**, 193 (1961).

(13) M. Tubis, E. Posnick, and R. A. Nordyke, *Proc. Soc. Exp. Biol. Med.*, **103**, 497 (1960).

(14) L. J. Anghileri, *Int. J. Appl. Radiat. Isotopes*, **15**, 95 (1964).

(15) H. Elias, C. H. Arnold, and G. Kloss, *ibid.*, **24**, 463 (1973).

(16) P. M. Wanek, H. B. Hupf, and H. A. O'Brien, Jr., *J. Nucl. Med.*, **18**, 638 (1977).

(17) W. Hartrodt, *Nucl. Med.*, **4**, 423 (1965).

(18) A. S. Kirschner, R. D. Ice, and W. H. Beierwaltes, *J. Nucl. Med.*, **16**, 248 (1975).

(19) M. Berman, L. E. Braverman, J. Burke, L. Groot, K. R. McCormack, T. H. Oddie, R. H. Rohrer, H. N. Wellman, and E. M. Smith, *ibid.*, **16**, 857 (1975).

# Semiaqueous Potentiometric Determinations of Apparent $pKa_1$ Values for Benzothiadiazines and Detection of Decomposition during Solubility Variation with pH Studies

**U. G. HENNIG, R. E. MOSKALYK, L. G. CHATTEN ˣ, and S. F. CHAN**

Received May 19, 1980, from the *Faculty of Pharmacy and Pharmaceutical Sciences, University of Alberta, Edmonton, Alberta, Canada T6G 2N8.* Accepted for publication September 9, 1980.

**Abstract** □ Apparent acidity constants obtained for various benzothiadiazine diuretics by semiaqueous potentiometric titrations gave satisfactory agreement with many values obtained by aqueous potentiometry. One suitable method for determining the acidity constants of sparingly soluble drugs, the solubility variation with pH technique, does not take into account instability problems. The preparation of decomposition products and the TLC analysis of sample solutions at various time intervals during solubility studies of methyclothiazide and bendroflumethiazide indicated that decomposition takes place during agitation and equilibration. This decomposition in buffers of pH 8 and higher was confirmed with the acidified *p*-dimethylaminobenzaldehyde test for primary aromatic amines.

**Keyphrases** □ Benzothiadiazines—apparent $pKa_1$ values, semiaqueous potentiometry, detection of decomposition □ Diuretics—benzothiadiazines, semiaqueous potentiometric determination of apparent $pKa_1$ values, detection of decomposition □ $pKa_1$ values, apparent—benzothiadiazines, semiaqueous potentiometric determination □ Decomposition—benzothiadiazines, solubility variation with pH studies □ Potentiometry, semiaqueous—benzothiadiazines, determination of apparent $pKa_1$ values

In searching for the most suitable method of determining the dissociation constants of the benzothiadiazine diuretics, the utility and applicability of previously reported methods were examined first. Potentiometry in aqueous media has been commonly used in the determination of pKa values (1); however, the low aqueous solubility of benzothiadiazines precludes the use of water as the sole solvent. In such instances of solubility problems, potentiometry in mixed solvent systems has been used (2). In addition, Ågren and Bäck (3) employed the solubility variation with pH technique in determining the first acidic ionization constant of bendroflumethiazide. Their experimental conditions seemed to favor significant decomposition, which they did not appear to take into account.

The first part of this investigation was the determination of apparent $pKa_1$ values for various benzothiadiazine diuretics, and the second phase concerned the effect of pH on the stability of representative benzothiadiazines during the solubility pKa determination procedure.

## EXPERIMENTAL

**Reagents and Buffers**—All chemicals and reagents were either ACS or reagent grade, unless otherwise specified. Buffers were prepared with glass-distilled and deionized water free of carbon dioxide. Sorensen's (4) borate and glycine buffers were used.

**Reference Standards**—Purification of the selected benzothiadiazines was achieved by recrystallization to a constant melting point from ethanol and ethanol–water mixtures.

**Semiaqueous Potentiometric Determination of Apparent $pKa_1$ Values by Extrapolation Technique**—The apparent $pKa_1$ values of various benzothiadiazines were determined by the method of Chatten

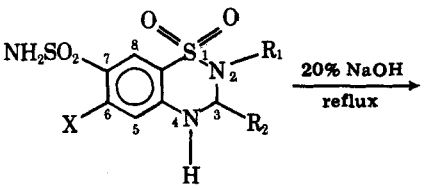


I: $R_1$ = H, $R_2$ = benzyl, X = $CF_3$
II: $R_1$ = $CH_3$, $R_2$ = $CH_2Cl$, X = Cl

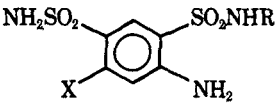

III: R = H, X = $CF_3$
IV: R = $CH_3$, X = Cl

*Scheme I*

*et al.* (5) using acetone–water mixtures. Four concentrations of each benzothiadiazine (0.0005, 0.001, 0.0015, and 0.002 *M*) were prepared from 0.02 *M* acetone stock solutions. The acetone–water ratios were 5:45, 10:40, 15:35, and 20:30 ml, respectively. The solutions were titrated with 0.05 *N* NaOH, and the pH was measured[1] after the addition of each 0.1-ml increment of titrant. The apparent $pKa_1$ values then were obtained by the usual extrapolation techniques (2, 5).

**Preparation of Reference Decomposition Products**[2]—The decomposition products of bendroflumethiazide (I) and methyclothiazide (II) were prepared (Scheme I) by dissolving 1 g of the parent compound in 30 ml of 20% NaOH solution. The mixtures were refluxed for 2 hr, allowed to stand for 20 hr, and then acidified to pH 4 with 6 *N* HCl. The resulting precipitates were separated by vacuum filtration, washed with distilled water, and recrystallized from water to a constant melting point. The identity of the products (III and IV) was confirmed with IR and mass spectra.

*4-Amino-6-trifluoromethyl-1,3-benzenedisulfonamide (III)*—Compound III was prepared from bendroflumethiazide (I), giving fine white crystals (yield 0.52 g or 68.0%), mp 245–247° dec. [lit. (6) mp 246–247°].

*4-Amino-2-chloro-5-(methylsulfamyl)benzenesulfonamide (IV)*—Compound IV was prepared from methyclothiazide (II), giving fine, off-white crystals (yield 0.61 g or 72.6%), mp 170° dec. [lit. (6) mp 168–170°].

**Solubility Determinations**—An excess of pure drug was shaken with a constant volume of buffer and agitated[3] at constant temperature for 15 min. After 5 min of equilibration, the suspensions were filtered[4] and the clear filtrate was centrifuged[5]. The pH[1] of each solution then was obtained, and the absorbances[6] for II were read at 267 nm.

[1] Fisher Accumet model 320 expanded-scale pH meter fitted with glass and calomel electrodes.

[2] Melting points were determined using a Thomas-Hoover capillary apparatus and are uncorrected. IR spectra were recorded on a Perkin-Elmer 267 grating IR spectrometer as potassium bromide disks. Mass spectra were taken on a Hewlett-Packard 5981A spectrometer.

[3] Dubnoff metabolic shaking incubator (GCA/Precision Scientific) maintained at 25 ± 1°.

[4] Whatman No. 1 filter paper.

[5] Servall automatic-refrigerated centrifuge maintained at 25 ± 1° (15,000 rpm for 10 min).

[6] Beckman model 25 spectrophotometer.

0022-3549/81/0300-0317$01.00/0
© 1981, American Pharmaceutical Association

**Table I—Comparison of the Apparent Acidity Constants ($pKa_1$) of Certain Benzothiadiazines Obtained by Semiaqueous Potentiometric Titration with Literature Values**

| Benzothiadiazine | Literature[a] | Semiaqueous Potentiometric Titration |
|---|---|---|
| Flumethiazide | 6.44 (13) | 6.3 |
| Hydrochlorothiazide | 7.0 (14), 7.9 (15), 8.6 (16), 8.8 (13) | 8.7 |
| Hydroflumethiazide | 8.9 (14), 8.45 (13) | 8.5 |
| Cyclothiazide | — | 8.8 |
| Trichloromethiazide | — | 6.9 |
| Methyclothiazide (II) | — | 9.5 |
| Polythiazide | — | 9.1 |

[a] Aqueous potentiometric titrimetry.

*Methyclothiazide (II)*—After the initial solubility determination in 25 ml of glycine buffer, the procedure was repeated at 1-hr intervals for 6 hr and then again at 24 hr. Once decomposition was detected at pH 8.6, 9.0, and 9.4, the suspensions stood at room temperature for 22 days without agitation.

*Bendroflumethiazide (I)*—An excess of pure drug was shaken with 10 ml of borate buffer at pH 8.4, 9.0, and 9.6 and agitated[3] continuously for 3 hr (3, 7) at constant temperature.

**Detection of Decomposition by TLC**—The II suspensions were monitored for decomposition at 0.25, 0.5, 0.75, 1, 2, 3, and 24 hr and also at 22 days following the initial exposure to the buffers. The I suspensions were monitored at the same time intervals for up to 3 hr.

At the appropriate interval, a 50-$\mu$l aliquot of each sample was removed and diluted to 150 $\mu$l with acetone. The acetone–water aliquot then was applied to a silica gel-coated chromatographic sheet[7] and developed in ethyl acetate–benzene (8:2) (8–10). The sheets were examined under shortwave (254-nm) UV light[8] and then sprayed with acidified *p*-dimethylaminobenzaldehyde[9].

## RESULTS AND DISCUSSION

Most benzothiadiazine diuretics are sparingly soluble in water, and a nonaqueous solvent must be added to ensure that the compounds remain in solution. Thus, semiaqueous potentiometry is a logical choice for investigating acidity constants if apparent values for relative acidities must be obtained rapidly. The term "relative acidities" refers to the apparent ionization constants obtained in semiaqueous media for a particular series of structurally related compounds (11). Dissociation constants obtained by potentiometric titration in semiaqueous media are not thermodynamically rigorous because there is no satisfactory way of correlating activity coefficients in different solvent systems. The liquid junction potential between two solvents also is a problem. Many references attest to these difficulties (*e.g.*, 1, 11, 12).

The apparent $pKa_1$ values obtained by potentiometric titrations of selected benzothiadiazines in water–acetone mixtures are given in Table I and are compared with literature values. Despite the problems outlined previously, the apparent values obtained for the $pKa_1$ of several benzothiadiazines by semiaqueous potentiometric titrimetry compare favorably with those reported for aqueous potentiometry. This finding clearly suggests that the method is useful as a comparative means for structurally related compounds such as the benzothiadiazine diuretics, and it can provide accurate relative acidity constants.

Close *et al.* (6) observed that boiling certain benzothiadiazines with alkali readily promoted opening of the thiadiazine ring system. This type of hydrolysis was studied by Mollica *et al.* (16, 17) who investigated these effects on hydrochlorothiazide at 60° in 1 *N* NaOH. Accordingly, an experiment was designed in this laboratory to study the effect of pH on the stability of representative benzothiadiazine diuretics under the conditions outlined for the solubility variation with pH method of determining pKa values.

The investigation was initiated with the preparation of reference decomposition products that were obtained by alkaline hydrolysis of bendroflumethiazide (I) and methyclothiazide (II). Substitution at the 3-position affects the overall reaction rate (16); but when 3-substituted benzothiadiazines are refluxed in 20% NaOH, complete hydrolysis to produce the corresponding benzenedisulfonamide (III or IV) can be expected.

[7] Eastman chromagram developing apparatus and sheets (silica gel adsorbent with fluorescent indicator).

[8] Ultraviolet lamp, Applied Science Laboratories.

[9] *p*-Dimethylaminobenzaldehyde (1 g), dissolved in 95% ethanol to provide a 1% solution, was acidified by the addition of 10 ml of concentrated hydrochloric acid (9, 10).

**Table II—$R_f$ Values for Representative Benzothiadiazines and Their Decomposition Products in Ethyl Acetate–Benzene (8:2)**

| Compound | $R_f$ Value | Color Formed with Acidified *p*-Dimethylaminobenzaldehyde |
|---|---|---|
| Hydrochlorothiazide | 0.17 | — |
| I | 0.68 | — |
| II | 0.60 | — |
| III | 0.36 | Lemon yellow |
| IV | 0.46 | Lemon yellow |

TLC analysis provided $R_f$ values for both parent compounds (I and II) and the decomposition products (III and IV) (Table II). The presence of the primary aromatic amino group was confirmed by the Schiff base formation with acidified *p*-dimethylaminobenzaldehyde.

The UV spectra of the decomposition products are similar to those of the parent 3,4-saturated benzothiadiazines because the basic chromophore has not been altered sufficiently to effect a change in the wavelength of maximum absorption. Conversion of the basic amino group to a free aromatic amine may cause a shift of only a few nanometers to a longer wavelength, and this change is insufficient to distinguish between the parent 3,4-saturated benzothiadiazines and their decomposition products. Baer *et al.* (18) examined the UV absorption spectra of chlorothiazide, a 3,4-unsaturated benzothiadiazine, and its decomposition product obtained in a basic medium and observed a 30-nm shift in the wavelength of maximum absorbance.

Since the 3,4-saturated benzothiadiazines and their decomposition products have similar UV absorption spectra, the use of UV spectrophotometry to measure quantitatively the drug content of samples in the solubility variation with pH technique will not detect any decomposition taking place in the basic buffers. The pKa value ultimately derived from the solubility data may be that of the decomposition product or, more likely, a mixture of the parent benzothiadiazine and its hydrolysis product.

Samples of methyclothiazide (II) and bendroflumethiazide (I) in buffers of pH > 9 were obtained from the solubility studies and analyzed by TLC. The results of the analysis indicated the presence of the benzothiadiazines and their decomposition products, as confirmed by the $R_f$ values and the color reaction with acidified *p*-dimethylaminobenzaldehyde spray reagent. From this reaction, an interesting and unexpected result was noted. After application of the acidified *p*-dimethylaminobenzaldehyde, violet spots appeared at the same $R_f$ values as I and II, and the color intensity of these spots increased with increasing pH values for the buffers.

The aqueous samples from the solubility studies were diluted with

**Table III—Absorbance Changes for Methyclothiazide (II) Relative to Equilibration–Agitation Periods**

| pH | Hours[a] | Absorbance at 267 nm | | |
|---|---|---|---|---|
| | | Sample 1 | Sample 2 | Sample 3 |
| 8.6 | 0.5 | 1.138 | 1.146 | 1.198 |
| | 1.0 | 1.220 | 1.231 | 1.277 |
| | 3.0 | 1.277 | 1.298 | 1.338 |
| | 4.0 | 1.297 | 1.318 | 1.354 |
| | 5.0 | 1.303 | 1.320 | 1.372 |
| | 6.0 | 1.337 | 1.343 | 1.390 |
| | 24.0 | 1.410 | 1.416 | 1.440 |
| | 528.0 | 0.105 | 0.105 | 0.110 |
| 9.0 | 1.0 | 0.938 | 0.842 | 0.893 |
| | 2.0 | 1.152 | 1.040 | 1.088 |
| | 3.0 | 1.263 | 1.133 | 1.171 |
| | 4.0 | 1.346 | 1.239 | 1.254 |
| | 5.0 | 1.412 | 1.333 | 1.324 |
| | 6.0 | 1.400 | 1.393 | 1.435 |
| | 24.0 | 1.516 | 1.571 | 1.597 |
| | 26.0 | 1.711 | 1.715 | 1.697 |
| | 28.0 | 1.790 | 1.808 | 1.745 |
| | 528.0 | 0.175 | 0.202 | 0.178 |
| 9.4 | 3.0 | 1.799 | 1.850 | 1.890 |
| | 528.0 | 0.243 | 0.280 | 0.232 |

[a] The absorbance values at 22 days of equilibration are for diluted samples (0.1 ml of filtrate plus 2.9 ml of the appropriate buffer).

acetone before they were spotted on the TLC plates, whereas the I and II reference standards were dissolved in ethyl acetate prior to TLC analysis. Since the violet color was not produced with samples from the ethyl acetate stock solutions, it can be postulated that the acidified *p*-dimethylaminobenzaldehyde only reacts with the benzothiadiazines in their ionized form. The color only appeared when buffers of pH > 9 (the region following the first pKa) were used in the solubility studies. The violet color faded soon after its development, indicating an unstable complex.

Schiff base formation with primary aromatic and aliphatic amines yields yellow, orange-red, or brown products. The only record of a violet color that the authors could find was that of the reaction of pyrrole with *p*-dimethylaminobenzaldehyde (19), and the product rearranged into a quinoidal form. The type of colored complex formed between the benzothiadiazines and *p*-dimethylaminobenzaldehyde is difficult to postulate without further work since there is no apparent record of Schiff base formation with the nitrogen of a sulfonamido group.

Decomposition during the solubility studies was evident from the TLC analyses of the solutions performed at various times. Monitoring of the solubility samples by TLC indicated that detectable decomposition had occurred after 1 hr of agitation at pH 8.6, 9.0, and 9.4 for II and at pH 8.4, 9.0, and 9.6 for I. In addition to that of the parent benzothiadiazine, a spot was visible under shortwave (254-nm) UV light that had the same $R_f$ value as the corresponding reference decomposition product (either III or IV). The spots did not react visibly with acidified *p*-dimethylaminobenzaldehyde because of the low concentration of the particular decomposition product present in the samples at that time. The color formed, and the intensity increased, as the time of exposure of the benzothiadiazines to the basic buffers was extended.

At pH 8.6 for II and at 8.4 for I, the degradation products at 1 hr of exposure were visible only under shortwave UV light; but after 3 hr of exposure, faint-yellow spots appeared upon application of acidified *p*-dimethylaminobenzaldehyde. Upon further exposure of the drugs to the basic buffers, the color of the spots increased in intensity.

If equilibration is considered to be complete when any further change in the drug concentration is <3% (1, 20), the 3-hr limit of agitation time set by Green (7) and used by Ågren and Bäck (3) is not adequate for either I or II. As shown by Table III, the concentration of II was still changing significantly once decomposition had started. The decomposition of I also began before the 3-hr agitation had been completed.

Although solubility variation with pH is an ideal method for determining thermodynamic pKa values for sparingly soluble compounds (20), the technique is not suitable for the benzothiadiazine diuretics. Under the conditions of the method, the decomposition of these drugs occurs before equilibration has been achieved. Work is continuing in this laboratory on the determination of pKa values for these compounds by other methods.

## REFERENCES


(1) A. Albert and E. P. Serjeant, "The Determination of Ionization Constants: A Laboratory Manual," Chapman and Hall, London, England, 1971.

(2) L. G. Chatten and L. E. Harris, *Anal. Chem.*, **34**, 1495 (1962).

(3) A. Ågren and T. Bäck, *Acta Pharm. Suec.*, **10**, 223 (1973).

(4) K. Diem and C. Lentner, "Documenta Geigy Scientific Tables," 7th ed., J. R. Geigy S. A., Basel, Switzerland, 1970, pp. 280–282.

(5) L. G. Chatten, R. E. Moskalyk, R. A. Locock, and F. J. Schaefer, *J. Pharm. Sci.*, **63**, 1294 (1974).

(6) W. J. Close, L. R. Swett, L. E. Brady, J. H. Short, and M. Vernsten, *J. Am. Chem. Soc.*, **82**, 1132 (1960).

(7) A. L. Green, *J. Pharm. Pharmacol.*, **19**, 10 (1966).

(8) P. J. Smith and T. S. Hermann, *Anal. Biochem.*, **22**, 134 (1968).

(9) B. G. Osborne, *J. Chromatogr.*, **70**, 190 (1972).

(10) D. Sohn, J. Simon, M. A. Hanna, G. Ghali, and R. Tolba, *ibid.*, **87**, 570 (1973).

(11) R. F. Cookson, *Chem. Rev.*, **74**, 5 (1974).

(12) L. Z. Benet and J. E. Goyan, *J. Pharm. Sci.*, **56**, 665 (1967).

(13) A. Essig, *Am. J. Physiol.*, **201**, 303 (1961).

(14) "The Merck Index," 9th ed., Merck & Co., Rahway, N.J., 1976, pp. 4674, 4686.

(15) "The Merck Index," 8th ed., Merck & Co., Rahway, N.J., 1968, p. 541.

(16) J. A. Mollica, C. R. Rehm, J. B. Smith, and H. K. Govan, *J. Pharm. Sci.*, **60**, 1380 (1971).

(17) J. A. Mollica, C. R. Rehm, and J. B. Smith, *ibid.*, **58**, 635 (1969).

(18) J. E. Baer, H. L. Leidy, A. V. Brooks, and K. H. Beyer, *J. Pharmacol. Exp. Ther.*, **125**, 295 (1959).

(19) F. Feigl, "Spot Tests in Organic Analysis," 7th ed., Elsevier, Amsterdam, The Netherlands, 1966, pp. 381, 382.

(20) C. C. Peck and L. Z. Benet, *J. Pharm. Sci.*, **67**, 12 (1978).


## ACKNOWLEDGMENTS


U. G. Hennig gratefully acknowledges the research scholarship provided by Pfizer Co., and S. F. Chan thanks the Medical Research Council of Canada for a summer studentship.

The authors acknowledge the reference standards generously supplied by the following manufacturers: Abbott Laboratories, Bristol Laboratories of Canada, CIBA Pharmaceutical Co., Eli Lilly and Co., Merck Sharp & Dohme Canada, Pfizer Co., A. H. Robins Co., Schering Corp., and E. R. Squibb and Sons of Canada. The authors also thank Dr. R. J. Flanagan for the mass spectra.

# High-Performance Liquid Chromatographic Assay of Perhexiline Maleate in Plasma

J. D. HOROWITZ *, P. M. MORRIS ‡, O. H. DRUMMER ‡, A. J. GOBLE *, and W. J. LOUIS ‡x

Received June 9, 1980, from the *Department of Cardiology and the ‡Department of Clinical Pharmacology, University of Melbourne, Austin Hospital, Heidelberg, 3084, Victoria, Australia. Accepted for publication September 9, 1980.

**Abstract** □ A sensitive assay is described for the calcium antagonist perhexiline maleate. Alkalinized plasma was extracted with *n*-hexane, the organic phase was evaporated, and the residue was dansylated prior to analysis by reversed-phase high-performance liquid chromatography using a fluorescence detector. Perhexiline was resolved from its mono- and dihydroxylated metabolites, and the limit of sensitivity was 5 ng of perhexiline/ml. This limit represents approximately 100 times the sensitivity of the previously described GLC assay. Single-dose pharmacokinetic studies were performed with 150- and 300-mg oral doses of perhexiline maleate in five patients with severe angina pectoris and impaired left ventricular function. Peak plasma perhexiline levels occurred 3–6 hr after drug ingestion in four patients and after 12–18 hr in the fifth patient. The mean elimination half-life, measured 24 hr after drug ingestion, varied with plasma perhexiline concentration. It was 11.2 ± 2.1 hr after the 150-mg dose and 19.1 ± 2.8 hr after the 300-mg dose. The mean ratio of areas under the concentration–time curve for the 300- *versus* 150-mg doses was 5.3:1, suggesting that hepatic metabolism of perhexiline may be saturable and that the bioavailability of perhexiline is dose dependent.

**Keyphrases** □ Perhexiline maleate—high-performance liquid chromatographic assay, human plasma □ High-performance liquid chromatography—analysis, perhexiline in human plasma □ Vasodilators, coronary—perhexiline, high-performance liquid chromatographic analysis in human plasma

Perhexiline maleate, a calcium antagonist, is used as a prophylactic antianginal drug (1, 2) and shows promise as an antiarrhythmic agent (3). In spite of the impressive therapeutic efficacy of perhexiline, its clinical use has remained limited largely due to the occurrence, with long-term use, of severe adverse effects such as peripheral neuropathy and hepatotoxicity (4).

This paper reports the development of a sensitive high-performance liquid chromatographic (HPLC) assay for perhexiline maleate in plasma and its application to the study of single-dose pharmacokinetics of perhexiline in patients with severe angina pectoris.

The data suggest that the bioavailability of perhexiline is dose dependent. This information may be of value in avoiding toxic drug levels.

## EXPERIMENTAL

**Instrumentation**—Assays were carried out using a constant-flow, high-performance liquid chromatograph[1] equipped with a solvent delivery system[2], a universal injector[3], and a filter fluorescence detector[4] operating with standard excitation[5] and emission[6] filters corresponding to nominal wavelengths of 360 and 510 nm, respectively. The stainless steel column (30 cm long × 3.7 mm i.d.) was prepacked[7].

**Reagents**—Perhexiline maleate [2-(2,2-dicyclohexylethyl)piperidine maleate, I], the internal standard hexadiline hydrochloride [1,1-dicyclohexyl-2-(2-piperidyl)ethylene hydrochloride, II], and a mixture of the 4-monohydroxy and 4,4′-dihydroxy metabolites of perhexiline were used[8]. The derivatizing reagent was dansyl chloride[9]. *n*-Hexane, cyclohexane, benzene, methylene chloride, ethyl acetate[10], ether[11], and dimethyl sulfoxide[12] were analytical reagent grade, and methanol was HPLC grade[1].

**Standard Solutions**—Standard solutions of perhexiline maleate (2 μg/ml) and hexadiline hydrochloride (1.4 μg/ml) were prepared by dissolving pure drug in dimethyl sulfoxide (2 ml) and diluting the resultant solutions to 250 ml with 0.1 *N* HCl. All solutions were stable when stored at −20° for 30 days.

**Extraction**—Tris(hydroxymethyl)aminomethane buffer (0.5 ml, 2 *M*, pH 8.75), hexadiline (0.1 ml), and *n*-hexane (7 ml) were added to 1.0 ml of plasma in a polypropylene tube[13]. Each sample then was mixed[14] for 1 min and centrifuged at 3000 rpm for 15 min. The upper *n*-hexane layer was transferred to a polypropylene tube and evaporated to dryness under nitrogen at 60°. Sodium bicarbonate solution (0.1 ml, 0.1 *M*, pH 10) and dansyl chloride (0.1 ml, 0.01 *M*) in acetone were added to the remaining residue and mixed[14].

The derivatization was allowed to proceed for 20 min at 37°. Each tube was extracted with 3 ml of *n*-hexane by mixing[14] for 20 sec. Following a quick centrifugation (1 min) to separate the phases, the *n*-hexane layer was transferred to another clean polypropylene tube and evaporated to dryness at 60° under nitrogen. The dry residue was stable for 7 days when stored at −20°.

Each sample was reconstituted in 0.1 ml of mobile phase prior to chromatography.

**Chromatography**—The injection volumes were 50 μl. The mobile phase was methanol–water (92.5:7.5) maintained at a flow rate of 1.2 ml/min with a back pressure of 1000 psi. The retention time for both the mono- and dihydroxylated metabolites was 5.3 min whereas the retention times for hexadiline and perhexiline were 13.7 and 15.7 min, respectively.

**Quantitation**—Standard curves for the determination of perhexiline maleate were prepared by spiking drug-free plasma samples. The curve used for the estimation of perhexiline levels following single-dose pharmacokinetic studies was in the range of 0–5000 ng/ml.

Recoveries from spiked plasma samples were obtained by comparing the peak height of perhexiline after extraction with the corresponding peak height obtained on the same amount of perhexiline chromatographed from a dansylated stock solution.

The perhexiline maleate concentrations in unknown plasma were determined from a graph in which the peak height ratios of perhexiline to the internal standard (hexadiline) were plotted against the concentrations of known standards.

**Patients and Sampling Procedure**—Five patients (68–75 years old), suffering from severe angina pectoris for which perhexiline administration was clearly indicated, were studied after obtaining written consent. After an overnight fast, 150 mg of perhexiline maleate was given as a single dose. Patients continued to fast for 3 hr after ingestion. Immediately prior to the 150-mg dose and at 0, 0.5, 1, 1.5, 2, 2.5, 3, 3.5, 4, 5, 6, 8, 12, 18, and 24 hr, 10-ml blood samples were taken from an indwelling catheter in a forearm vein and placed in heparinized tubes for assay of plasma perhexiline concentrations. Samples were centrifuged immediately to separate the plasma, which was stored frozen at −20° until it was assayed.

Forty-eight hours after the first dose, a second dose of 300 mg of per-

[1] Waters Associates, Chippendale, Sydney, Australia, 2008.
[2] Model 6000A, Waters Associates.
[3] Model U6K, Waters Associates.
[4] Fluorichrom, Varian Pty. Ltd., Victoria, Australia, 3170.
[5] No. 7-54 and 7-50, Varian Pty. Ltd.
[6] No. 4-76 and 3-71, Varian Pty. Ltd.
[7] μBondapak $C_{18}$, Waters Associates.
[8] Merrell-National Laboratories, Cincinnati, Ohio.
[9] Sigma Chemical Co., St. Louis, Mo.
[10] Merck, Darmstadt, West Germany.
[11] May and Baker, Melbourne, Australia.
[12] Mallinckrodt, St. Louis, Mo.
[13] Size 15P, Disposable Products, Melbourne, Australia.
[14] Vortex mixer.



0022-3549/81/0300-0320$01.00/0
© 1981, American Pharmaceutical Association

**Table I—Recovery of Perhexiline Maleate from Plasma with Various Solvents**

| Solvent | Mean Recovery, % |
|---|---|
| *n*-Hexane | 40 |
| Cyclohexane | 23 |
| Benzene | 26 |
| Methylene chloride[a] | 40 |
| Ether[b] | 60 |
| Ethyl acetate[b] | 75 |

[a] Peaks interfered with detection of perhexiline metabolites. [b] Peaks interfered with determination of perhexiline.

hexiline maleate was given under the same conditions, and the study was repeated.

**Pharmacokinetic Analysis**—For single-dose pharmacokinetic studies, plasma concentration–time data were fitted to a polyexponential equation using a nonlinear least-squares regression analysis computer program (5). Pharmacokinetic parameter estimates were obtained for the computer program AUTOAN 2 NONLIN (6), assuming first-order absorption and elimination. Equations generated by this program contained two or more exponentials and included a possible lag time.

The area under the concentration–time curve was calculated by the trapezoidal method and extrapolated to infinity by dividing the final concentration point by the slope of the terminal phase.

## RESULTS AND DISCUSSION

Previous investigators experienced difficulty with the development of a sensitive and specific assay for perhexiline. Studies with radiolabeled perhexiline did not differentiate between perhexiline and its hydroxylated metabolites (7). Because of the low recovery of perhexiline due to extraction and the tendency of perhexiline, a weakly basic lipophilic drug, to adsorb to laboratory glassware, the sensitivity of the GLC assay was limited to plasma drug concentrations above 500 ng/ml (8).

The HPLC assay reported here resolved perhexiline from its mono- and dihydroxylated metabolites with a lower limit of sensitivity of 5 ng/ml. Perhexiline has no natural absorption properties in the UV or visible regions. However, under suitable reaction conditions, derivatization of the secondary amine nitrogen in the piperidine ring of perhexiline by the highly reactive fluorophore dansyl chloride for 20 min at 37° resulted in complete conversion of perhexiline to a highly absorptive dansylated compound. Free dansyl chloride elutes with the solvent front on HPLC. However, preliminary separation of the perhexiline dansylate from most of the unreacted dansyl chloride using hexane extraction reduced the solvent front and resulted in a cleaner chromatogram.

Figure 1 illustrates typical chromatograms obtained after extraction of blank plasma (Fig. 1*a*) and of plasma from a patient treated with perhexiline (Fig. 1*b*). The peak at 15.7 min in Fig. 1*b* represents a plasma perhexiline concentration of 200 ng/ml. Endogenous peaks in blank plasma emerged before the hexadiline and perhexiline peaks. The mono- and dihydroxylated metabolites of perhexiline were not resolved under the conditions employed. However, by altering the mobile phase to methanol–water (80:20, v/v), adequate separation of these metabolites was obtained. Thus, simultaneous assay of individual metabolites and perhexiline also would be feasible under nonisocratic conditions using a solvent programmer.

Lignocaine, procainamide, digoxin, propranolol, verapamil, disopyramide, hydralazine, prazosin, and metoclopramide were examined for possible interference. None of these drugs produced peaks that emerged simultaneously with perhexiline, hexadiline, or the hydroxylated metabolites of perhexiline.

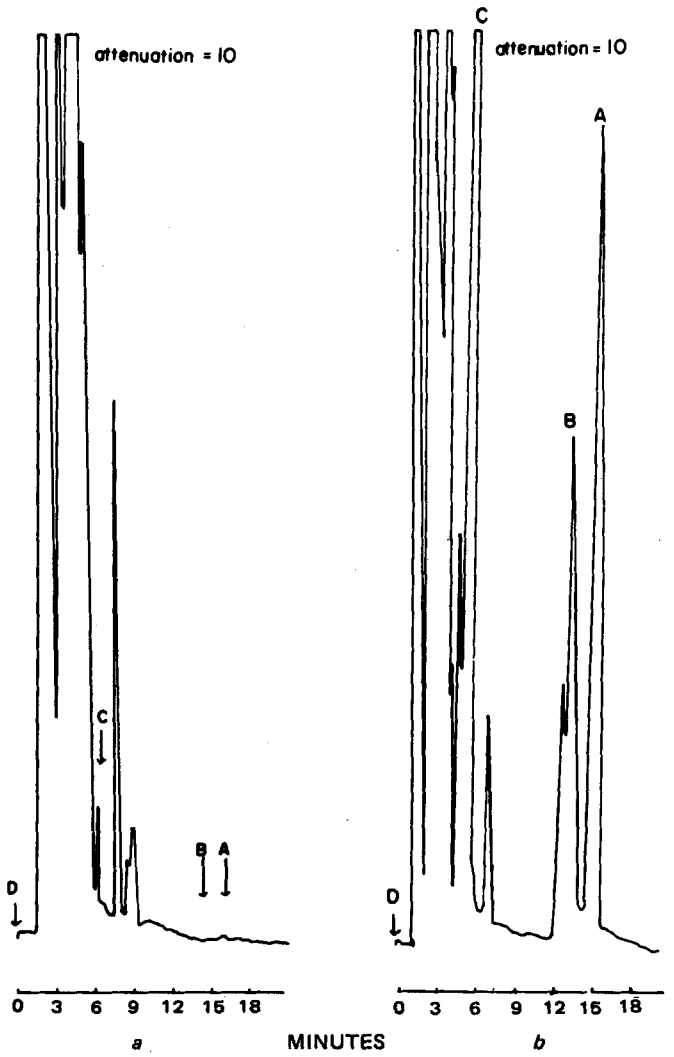


**Figure 1**—*High-performance liquid chromatograms for a blank extract (a) and for an extract of a plasma sample obtained from a patient receiving a daily dose of 100 mg of perhexiline (b). (Perhexiline concentration = 200 ng/ml.) Key: A, perhexiline; B, hexadiline; C, hydroxylated perhexiline metabolites; and D, injection.*

The component eluting just before the internal standard is believed to be a contaminant of hexadiline since it appears when only hexadiline is chromatographed and is not present in chromatograms devoid of hexadiline. The height of this additional peak was a constant fraction of that of the hexadiline peak and did not affect quantitation of perhexiline.

Of a number of solvents selected to extract perhexiline from alkalinized plasma (Table I), only *n*-hexane was satisfactory. This solvent gave an extraction efficiency, measured throughout the assay, of 40 ± 3%. Other

**Table II—Summary of Perhexiline Pharmacokinetics**

| | | 150-mg Dose | | | | 300-mg Dose | | | | |
|---|---|---|---|---|---|---|---|---|---|---|
| Patient | Age, years | Time to Peak, hr | Peak Concentration, ng/ml | *AUC*, (ng hr)/ml | $t_{1/2}$[a], hr | Time to Peak, hr | Peak Concentration, ng/ml | *AUC*, (ng hr)/ml | $t_{1/2}$[a], hr | $\frac{AUC_{300}}{AUC_{150}}$ |
| 1 | 73 | 2.5 | 82 | 810 | 14.0 | 4.2 | 348 | 5260 | 18.0 | 6.49 |
| 2 | 68 | 4.5 | 22 | 490 | 12.0 | 4 | 144 | 1740 | 23.5 | 3.55 |
| 3 | 75 | 6 | 116 | 1190 | 4.5 | 3 | 438 | 7110 | 9.5 | 5.97 |
| 4 | 68 | 12 | 65 | 1850 | 16.5 | 18 | 234 | 6240 | 26.0 | 3.37 |
| 5 | 70 | 6 | 49 | 690 | 9.0 | 6 | 204 | 5020 | 18.5 | 7.27 |
| Mean | 70.7 | 6.2 | 66.8 | 1010 | 11.2 | 7.0 | 274 | 5110 | 19.1 | 5.33 |
| *SE* | 1.1 | 1.6 | 15.8 | 240 | 2.1 | 2.8 | 52.8 | 920 | 2.8 | 0.79 |

[a] At 24 hr.

solvents gave better recoveries (ether and ethyl acetate), but they also extracted other compounds from the plasma eluting in the region of perhexiline and the hydroxylated metabolites. This effect precluded their use as alternative extraction solvents.

The threshold of detection of perhexiline maleate in plasma corresponding to a peak height three times that of baseline noise was 5 ng/ml. The coefficient of variation for replicate assays of a pooled plasma sample containing 150 ng of perhexiline/ml was studied over 21 days and was 8.5% ($n$ = 8) while that for replicate assays performed on the same day was 2.8% ($n$ = 5).

Calibration curves for the peak height ratio of perhexiline to hexadiline were linear over a perhexiline concentration range of 0–5000 ng/ml. The use of disposable polypropylene tubes minimized inaccuracies due to adsorption of perhexiline onto glass surfaces.

Limited pharmacokinetic treatment of the single-dose studies in patients with angina pectoris was performed (Table II). There was a lag time of 1.0–2.5 hr before detectable concentrations of perhexiline appeared in plasma. Absorption rates of perhexiline varied, and peak drug concentrations occurred 3–6 hr after ingestion of the tablets in four of the five patients. In Patient 4, peak drug concentrations were delayed, occurring 12 hr after ingestion of the 150-mg dose and 18 hr after the 300-mg dose. However, peak levels for this patient were close to the mean of all five subjects for both the 150- and 300-mg doses. Peak concentrations of perhexiline after ingestion of the 300-mg doses were 4.3 times greater than those after the 150-mg dose.

The elimination half-life of perhexiline as determined 24 hr after drug ingestion appeared to be concentration dependent, increasing from ~18 hr with the 150-mg doses to 24 hr after the 300-mg dose. Patient 4, who had delayed absorption, also exhibited a prolonged elimination half-life at 24 hr compared to the other subjects. This patient was not excluded from the analysis since the data merely highlight the variable absorption of this drug and do not modify the conclusions concerning nonlinear kinetics. Because the mean ratio of the areas under the plasma concentration–time ($AUC$) curve for the 300- *versus* 150-mg doses in all patients was 5.3:1, nonlinear elimination kinetics clearly applied.

Possible contributions of variable plasma protein binding to the nonlinearity of perhexiline elimination kinetics are currently under investigation. Preliminary results do not reveal saturation of protein binding within the perhexiline concentration range encountered in these studies.

The results suggest that the elimination pharmacokinetics of perhexiline are nonlinear and that hepatic hydroxylation is saturable, resulting in variable systemic availability of orally administered perhexiline. Similar saturability of metabolism previously was demonstrated for alcohol (9), lorcainide (10), phenytoin (11), and fluorouracil (12). Drugs that demonstrate this phenomenon need great attention to dosage since it is often easy to move from therapeutic to toxic plasma levels with small changes in dose.

## REFERENCES


(1) L. N. Roberts and G. P. Mason, *J. Clin. Pharmacol.*, **12**, 342 (1972).

(2) W. P. Garson, R. C. Gülin, and D. N. Phear, *Postgrad. Med. J., Suppl. 3*, **49**, 90 (1973).

(3) T. G. Pickering and L. Goulding, *Br. Heart J.*, **40**, 851 (1978).

(4) J. D. Horowitz and M. L. Mashford, *Med. J. Aust.*, **1**, 485 (1979).

(5) C. M. Metzler, "NONLIN. A Computer Program for Parameter Estimation in Non-Linear Situation," Upjohn Co., Kalamazoo, Mich., 1979.

(6) J. G. Wagner, in "Fundamentals of Clinical Pharmacokinetics," Drug Intelligence Publications, Hamilton, Ill., 1975, p. 437.

(7) G. J. Wright, G. A. Leeson, A. V. Zeiger, and J. F. Lang, *Postgrad. Med. J., Suppl. 3*, **49**, 8 (1973).

(8) J. F. Lang, R. A. Okerholm, J. B. Thiele, B. J. Walker, and G. J. Wright, "A Simplified Method (Modified) for the Analysis of Perhexiline in Human Plasma," Merrell-National Laboratories, Cincinnati, Ohio, 1978.

(9) F. Lundquist and H. Wolthers, *Acta Pharmacol. Toxicol.*, **14**, 265 (1958).

(10) E. Jähnchen, H. Bechtold, W. Kasper, F. Kersting, H. Just, J. Heykants, and T. Meinertz, *Clin. Pharmacol. Ther.*, **26**, 187 (1979).

(11) N. Gerber and J. G. Wagner, *Res. Commun. Chem. Pathol. Pharmacol.*, **3**, 455 (1972).

(12) N. Christophidis, F. J. E. Vajda, I. Lucas, O. Drummer, W. J. Moon, and W. J. Louis, *Clin. Pharmacokinet.*, **3**, 330 (1978).


## ACKNOWLEDGMENTS


Supported by the National Health and Medical Research Council of Australia and Richardson-Merrell.

# Effect of Sulfadimethoxine on Thiopental Distribution and Elimination in Rats

**HSIU YING YU, YASUFUMI SAWADA, YUICH SUGIYAMA, TATSUJI IGA, and MANABU HANANO ˣ**

Received February 22, 1980, from the *Faculty of Pharmaceutical Sciences, University of Tokyo, Bunkyo-ku, Tokyo, Japan.* Accepted for publication September 8, 1980.

**Abstract** □ The effect of sulfadimethoxine on the distribution and elimination of thiopental was examined by comparing the change in the steady-state volume of distribution ($V_{ss}$) determined from both *in vivo* plasma elimination and *in vitro* serum and tissue binding studies in rats. The plasma disappearance of thiopental after a 12-mg/kg iv dose followed a biexponential decline in both the control and sulfadimethoxine-treated rats. The plasma thiopental concentrations under the steady-state plasma sulfadimethoxine concentration (500 μg/ml) were significantly lower than those of the control rats. In the sulfadimethoxine-treated rats, the pharmacokinetic parameter $\beta$ significantly decreased while $V_{ss}$ significantly increased to 3.6-fold that of the control rats. With sulfadimethoxine, a significant increase was observed in the apparent dissociation constant ($K_d$) of thiopental to serum protein by equilibrium dialysis, but the total number of binding sites was not altered. The *in vitro* serum free fraction of thiopental was increased to about 2.6-fold in the presence of sulfadimethoxine. The free fraction of thiopental in the main distribution tissues (liver, muscle, and adipose) was determined by equilibrium dialysis with and without sulfadimethoxine. No significant changes were observed in the presence of sulfadimethoxine. The calculated $V_{ss}$, determined by the free fractions from *in vitro* binding experiments, also showed a significant increase. The ratio of $V_{ss}$ with sulfadimethoxine to that of the control rats was 2.8. The total clearance did not change, but the intrinsic clearance decreased to one-half of that of the control rats due to the increase of the serum free fraction by sulfadimethoxine. It was concluded that sulfadimethoxine caused a displacement of thiopental in plasma protein binding, which significantly increased the free fraction of thiopental, and this result may explain the significant increase of $V_{ss}$ and the decrease of both $\beta$ and intrinsic clearance. Tissue binding of thiopental, however, was unaffected by sulfadimethoxine.

**Keyphrases** □ Sulfadimethoxine—effect on elimination and distribution of thiopental in rats, *in vitro* and *in vivo* studies □ Thiopental—elimination and distribution in rats, effect of sulfadimethoxine on thiopental metabolism, *in vitro* and *in vivo* studies □ Metabolism—effect of sulfadimethoxine on thiopental metabolism in rats, *in vitro* and *in vivo* studies

The apparent volume of distribution and total body clearance are influenced by age, disease, and drug–drug interaction. These changes are based on alterations in plasma and/or tissue binding, metabolism, and hepatic blood flow (1–5). The volume of distribution at steady state ($V_{ss}$) can be expressed by:

$$V_{ss} = V_p + (f_p/f_t)V_t \qquad \text{(Eq. 1)}$$

where $V_p$ is the plasma volume, $V_t$ is the volume of the other body tissues, and $f_p$ and $f_t$ are the fractions of the drug present in unbound form in the plasma and tissue, respectively (6, 7). Equation 1 shows that $V_{ss}$ is influenced by alterations in $f_p$ or $f_t$ due to the displacement of protein-bound drug. When metabolism is the rate-determining step of drug elimination, total body clearance ($Cl_{tot}$) can be expressed by:

$$Cl_{tot} \simeq f_p Cl_{int} \qquad \text{(Eq. 2)}$$

where $Cl_{int}$ is the intrinsic clearance of unbound drug (7). Equation 2 shows that both the increase in $f_p$, due to displacement by the second drug, and the change in $Cl_{int}$, due to metabolic inhibition or induction, may affect $Cl_{tot}$.

The present study determined the effect of sulfadimethoxide on the distribution and elimination of thiopental by comparing the changes of $V_{ss}$, which were determined from both *in vivo* plasma elimination and *in vitro* serum and tissue binding studies. The change of $Cl_{int}$ also is discussed.

## EXPERIMENTAL

Adult male Wistar rats[1], 245–280 g, were used. Under light ether anesthesia, the femoral vein and artery were cannulated with polyethylene tubing[2]. Cannulated rats were kept in restraining cages under normal housing conditions for 1 day prior to the experiments. All animals were fasted overnight (~15 hr) but had water *ad libitum* before the experiments. After a loading dose of 200 mg of sulfadimethoxine[3]/kg, 41.3 mg/kg/hr was infused through the femoral vein cannula for 3 hr with a constant-rate infusion pump[4]; with this dosage, steady-state concentrations of sulfadimethoxine (500 μg/ml) were obtained within 20–35 min after the beginning of the infusion.

At 50 min after the initiation of infusion, the rats were given 12 mg of thiopental[5]/kg in saline through the other femoral vein cannula over a 5-sec interval with a 500-μl syringe. Blood samples (0.25 ml) then were obtained at 1, 5, 10, 15, 30, 45, 60, 90, 120, 150, and 180 min in heparinized polyethylene centrifuge tubes[6]. The body temperature was kept at 37° by a heat lamp. Plasma was separated by centrifugation for 20 sec in a tabletop microfuge[6] and assayed for thiopental by the method of Brodie *et al.* (8). Sulfadimethoxine in plasma did not interfere with the assay of thiopental. The method of Tsuda and Matsunaga (9) was employed for the assay of sulfadimethoxine in plasma. The thiopental concentration data for individual animals were fitted to the equation $C_t = Ae^{-\alpha t} + Be^{-\beta t}$ for the plasma concentration $C_t$ at time $t$ by nonlinear least-squares regression (10). Pharmacokinetic constants (Table I) were determined from the biexponential equation constants, *i.e.*, $A$, $\alpha$, $B$, and $\beta$, using conventional equations (11).

Serum was separated from the blood, obtained through the carotid artery, by centrifugation for 10 min at 3000 rpm after standing for 60 min at room temperature. The serum free thiopental fraction was determined by equilibrium dialysis at 37° for 16 hr using semimicrocells[7] and a semipermeable membrane[8] against 0.05 *M* isotonic tromethamine–hydrochloric acid buffer (pH 7.4), containing 0.05–0.5 m*M* thiopental and 2.4 m*M* sulfadimethoxine. The protein binding of thiopental to serum and tissues was unchanged between 16 and 20 hr of dialysis at 37°.

Previous studies in this laboratory compared binding data of thiopental determined from equilibrium dialysis at 37° for 20 hr and from flow dialysis, but the difference between the two methods was insignificant (12). The effect of dialysis on the serum binding of thiopental also was examined at 37° for 24 hr with polarization analysis (13) using 1-anilino-8-naphthalenesulfonate and compared with the dialysis at 4° for 24 hr, but no denaturation of proteins after dialysis was observed. The sulfadimethoxine concentration in the protein chamber after dialysis was in the

[1] Nihon Seibutsu Zairyo, Tokyo, Japan.
[2] Type PE-10 (for femoral vein) and PE-50 (for femoral artery), Clay Adams, Becton–Dickinson Co., Parsippany, N.J.
[3] Daiichi Pharmaceutical Industries Co., Tokyo, Japan.
[4] Natsume Seisakusho Co., Tokyo, Japan.
[5] Tanabe Pharmaceutical Industries, Osaka, Japan.
[6] Beckman Instruments, Fullerton, Calif.
[7] Kokugo-gomu Co., Tokyo, Japan.
[8] Type 36/32, Visking Co., Chicago, Ill.

0022-3549/81/0300-0323$01.00/0
© 1981, American Pharmaceutical Association

Table I—Thiopental Pharmacokinetics in Rats[a]

| Rat | Body Weight, g | $A$, μg/ml | $\alpha$, $min^{-1}$ | $B$, μg/ml | $\beta$, $min^{-1}$ | $k_{12}$, $min^{-1}$ | $k_{21}$, $min^{-1}$ | $k_{el}$, $min^{-1}$ | $V_1$, ml/kg | $V_{ss}$, ml/kg | $V_{d\beta}$, ml/kg | $AUC$, (μg min)/ml | $Cl_{tot}$[b], ml/(min kg) | $Cl_{int}$[c], ml/(min kg) |
|---|---|---|---|---|---|---|---|---|---|---|---|---|---|---|
| **Without Sulfadimethoxine** | | | | | | | | | | | | | | |
| 1 | 250 | 269.7 | 21.03 | 15.2 | 0.007 | 19.774 | 1.126 | 0.138 | 42.1 | 782.3 | 787.8 | 2060.0 | 5.83 | |
| 2 | 270 | 24.7 | 0.27 | 14.5 | 0.007 | 0.155 | 0.104 | 0.017 | 306.3 | 762.7 | 793.9 | 2291.3 | 5.24 | |
| 3 | 245 | 49.7 | 3.00 | 22.6 | 0.009 | 2.063 | 0.944 | 0.030 | 166.0 | 524.1 | 528.0 | 2445.6 | 4.91 | |
| Mean | 255 | 114.7 | 8.10 | 17.4 | 0.008 | 7.330 | 0.724 | 0.062 | 171.5 | 689.7 | 703.2 | 2265.6 | 5.33 | 38.4 |
| ±SE | 7.6 | 77.8 | 6.51 | 2.6 | 0.001 | 6.253 | 0.315 | 0.038 | 76.3 | 83.0 | 87.6 | 112.1 | 0.27 | |
| **With Sulfadimethoxine** | | | | | | | | | | | | | | |
| 11 | 250 | 6.0 | 0.26 | 6.1 | 0.003 | 0.125 | 0.132 | 0.006 | 989.3 | 1926.2 | 1946.4 | 2201.8 | 5.45 | |
| 12 | 280 | 6.6 | 0.08 | 5.4 | 0.002 | 0.038 | 0.036 | 0.005 | 1003.3 | 2071.6 | 2143.5 | 2433.0 | 4.93 | |
| 13 | 245 | 133.9 | 2.32 | 6.1 | 0.005 | 2.101 | 0.105 | 0.119 | 85.7 | 1794.1 | 1885.2 | 1178.1 | 10.18 | |
| 14 | 265 | 12.1 | 0.27 | 2.8 | 0.001 | 0.212 | 0.052 | 0.007 | 808.1 | 4129.1 | 4221.4 | 2030.4 | 5.91 | |
| Mean | 260 | 39.7 | 0.73 | 5.1[d] | 0.003[d] | 0.619 | 0.081 | 0.034 | 721.6 | 2480.2[d] | 2549.1[d] | 1960.8 | 6.62 | 17.9 |
| ±SE | 9.1 | 31.4 | 0.53 | 0.8 | 0.001 | 0.495 | 0.023 | 0.028 | 216.6 | 552.5 | 560.1 | 273.6 | 1.20 | |

[a] Pharmacokinetic parameters were calculated by conventional equations (11) using biexponential equation constants from plasma disappearance curves. [b] Total clearance ($Cl_{tot}$) was calculated using $Cl_{tot}$ = dose/$AUC$. [c] Intrinsic clearance ($Cl_{int}$) was calculated using $Cl_{tot} = (Q_H s f_p Cl_{int})/(Q_H s + f_p Cl_{int})$, where $Q_H$ is the hepatic blood flow of 59.1 ml/min/kg (15), $f_p$ is the plasma free fraction, $s$ is the blood-to-plasma distribution ratio, and $Cl_{tot}$ is the total clearance. The hematocrit value was 0.45. [d] Significantly different from the control rats ($p < 0.05$).




**Figure 1**—*Plasma disappearance curves of thiopental after 12 mg/kg iv. Each point and vertical bar represent the mean and standard error of three or four rats. Curves were calculated by the SALS method (10) using a digital computer. Key:* ●, *plasma concentration of control rats;* ○, *plasma concentration of sulfadimethoxine-treated rats, which were infused with sulfadimethoxine (41.3 mg/kg/hr) after a loading dose of 200 mg/kg; and* □, *concentration of sulfadimethoxine.*

same range as that of the *in vivo* steady-state concentration of sulfadimethoxine (500 μg/ml) in plasma.

Liver, abdominal muscle, and adipose tissues were excised after the carotid artery bleeding. A 50% liver homogenate and a 25% muscle homogenate were prepared in 0.05 *M* tromethamine–hydrochloric acid buffer (pH 7.4) using a homogenizer[9]. The adipose homogenate was used without dilution and predialysis, but the liver and muscle homogenates were predialyzed against 0.05 *M* tromethamine–hydrochloric acid buffer (pH 7.4) at 4° for 24 hr. Equilibrium dialysis was performed on these three tissue homogenates at 37° for 16 hr, using 1 ml of buffer and 1 ml of each homogenate. The initial concentrations of thiopental in the buffer solution were 0.1 m*M* for the liver and muscle homogenates and 0.5 m*M* for adipose homogenate, and the initial concentration of sulfadimethoxine was 2 m*M* for all homogenates. After dialysis, the concentrations of both unbound thiopental and sulfadimethoxine in the buffer solution were determined as already described.

The unbound (free) fraction ($f$) in serum or tissue homogenate was calculated by:

$$C_{in} - 2C_f = C_b \qquad \text{(Eq. 3)}$$

$$\frac{C_f}{C_f + pC_b} = f \qquad \text{(Eq. 4)}$$

where $C_{in}$ is the initial concentration in the buffer solution, $C_f$ is the concentration of unbound drug in the buffer solution after dialysis, $C_b$ is the concentration of bound drug in serum or tissue after dialysis, and $p$ is the dilution factor for the tissue homogenate. In this study, $p = 1$ for the serum and adipose homogenates, $p = 2$ for the liver homogenate, and $p = 4$ for the muscle homogenate.

The blood-to-plasma distribution ratio ($s$) of thiopental was determined to calculate the intrinsic clearance ($Cl_{int}$). The blood was incubated with 5 μg/ml of thiopental at 37° for 20 min with and without sulfadimethoxine. The blood sulfadimethoxine concentration was 454 μg/ml (corresponding to the *in vivo* plasma concentration of 500 μg/ml). After centrifugation, an aliquot of the plasma was removed and the concentration of thiopental was determined as already described. An analytical blank without substrate was determined in the same manner. The hemolysis during incubation was negligible.

[9] Silverson Co., Bucks, United Kingdom.

Table II—*In Vitro* Thiopental Free Fraction in Rat Tissues[a]

| Tissue | Control Rats | Sulfadimethoxine-Treated Rats[b] 1 m*M* | 2 m*M* |
|---|---|---|---|
| Liver[b] | 0.076 ± 0.004[c] | 0.064 ± 0.009[c] | 0.075 ± 0.004[c] |
| Muscle[d] | 0.101 ± 0.014 | 0.105 ± 0.016 | 0.114 ± 0.017 |
| Adipose[e] | 0.011 ± 0.003 | 0.008 ± 0.001 | 0.008 ± 0.001 |

[a] The free fraction was determined by equilibrium dialysis. [b] $n = 3$. [c] Mean ± *SE*. [d] $n = 6$–12. [e] $n = 4$ or 5.

All means are presented with their standard error (mean ± *SE*). The Student *t* test was utilized to determine a significant difference between control and sulfadimethoxine-treated rats with $p = 0.05$ as the minimal level of significance.

## RESULTS

The plasma disappearance of thiopental after intravenous administration of 12 mg/kg is shown in Fig. 1. The disappearance of thiopental followed biexponential curves in both the control and sulfadimethoxine-treated rats. The plasma sulfadimethoxine concentration was kept at a constant level of 500 μg/ml during the 3-hr sampling period. The plasma thiopental concentrations in rats under constant infusion of sulfadimethoxine were significantly lower than those in controls without sulfadimethoxine. The pharmacokinetic constants were computed by a nonlinear iterative least-squares method (10) and are listed in Table I. In the sulfadimethoxine-treated rats, a significant decrease was observed in $\beta$ while a significant increase (3.6-fold of the control rats) was observed in $V_{ss}$. The total (body) clearance, however, did not change significantly.

Scatchard plots of thiopental binding to serum protein obtained from equilibrium dialysis are shown in Fig. 2. In both experiments, *i.e.*, with and without sulfadimethoxine, there was no evidence for the existence of more than one class of binding site in the concentration range tested, which corresponds to the *in vivo* plasma concentration range of thiopental after intravenous administration of 12 mg/kg. The apparent dissociation constant ($K_d$) of thiopental was 0.1 m*M*, and the total number of binding sites (binding capacity) was 0.6 m*M*. In the presence of 500 μg/ml of sulfadimethoxine, a typical competitive inhibition was observed, and $K_d$ was increased to 0.4 m*M*, but the binding capacity was not altered.

The serum free fraction ($f_p$) of thiopental showed nonlinearity in the concentration range studied with and without sulfadimethoxine; therefore, the mean values of $f_p$ obtained from the *in vivo* mean plasma concentration of thiopental for 3 hr, *i.e.*, 0.035 m*M* for the control without sulfadimethoxine and 0.014 m*M* in the presence of sulfadimethoxine, were used to calculate the intrinsic clearance of unbound drug ($Cl_{int}$) using the *in vivo* total body clearance. The $f_p$ of thiopental increased from 0.153 to 0.402 with sulfadimethoxine. The blood-to-plasma distribution ratios ($s$) were 0.922 for the control and 1.382 for the sulfadimethoxine-treated rats. Using these ratios and the hepatic blood flow obtained from the literature (14), the *in vivo* intrinsic clearance ($Cl_{int}$) of thiopental was calculated (Table I). With sulfadimethoxine, the $Cl_{int}$ was decreased to about one-half that of the control rats. The *in vivo* free fractions of thiopental at 30 min ($\beta$-phase) after intravenous administration of 12 mg of thiopental/kg determined by ultrafiltration were 0.131 for the control rats and 0.269 for the sulfadimethoxine-treated rats. A remarkable increase in the free fraction was observed in the sulfadimethoxine-treated rats.

The free fraction of thiopental to the mainly distributed tissue homogenates (*i.e.*, liver, muscle, and adipose tissues) (8) was determined by equilibrium dialysis, and the *in vitro* apparent volume of distribution [$V_{ss(in\ vitro)}$] was calculated by:

$$V_{ss(in\ vitro)} = V_p + \frac{f_p}{f_l} V_l + \frac{f_p}{f_m} V_m + \frac{f_p}{f_a} V_a \qquad \text{(Eq. 5)}$$

where $f$ is the free fraction of thiopental in each tissue, $V$ is the anatomical plasma and tissue volumes, and the subscripts $p$, $l$, $m$, and $a$ denote plasma, liver, muscle, and adipose, respectively. In this study, reported values (14) of 44 ml/kg for both $V_p$ and $V_l$ and of 500 ml/kg for $V_m$ were used, but the value of 40 ml/kg for $V_a$ was experimentally determined. In spite of the presence of sulfadimethoxine, alterations of the free fraction of thiopental binding to liver, muscle, and adipose homogenates were insignificant, suggesting that sulfadimethoxine does not alter the binding of thiopental to these tissues (Table II).

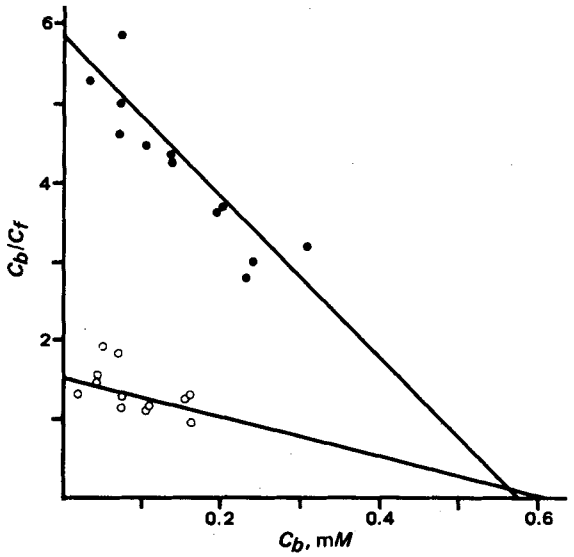


**Figure 2**—*Scatchard plot of data for the binding of thiopental to rat serum with (○) and without (●) sulfadimethoxine. Equilibrium dialysis was performed at 37° for 16 hr against 0.05 M isotonic tromethamine–hydrochloric acid buffer (pH 7.4) containing 0.05–0.5 m*M *thiopental. The concentration of sulfadimethoxine was 2.4 m*M*. Lines were fitted by a linear least-squares regression.*

The mean apparent volumes of distribution ($V_{ss}$) calculated from each plasma disappearance curve were 689.7 ± 83.0 ml/kg for the control rats and 2480.2 ± 552.5 ml/kg for the sulfadimethoxine-treated rats (Table I); $V_{ss(in\ vitro)}$ values, calculated by Eq. 5 from the *in vitro* binding studies for the main distribution tissues (*i.e.*, liver, muscle, and adipose), were 1442 ml/kg for the control rats and 4083 ml/kg for the sulfadimethoxine-treated rats. The ratio of $V_{ss(in\ vitro)}$ with sulfadimethoxine to that of the control was 2.8, which seems to be comparable to the ratio of 3.6 from the *in vivo* experiments.

## DISCUSSION

The importance of tissue binding on drug distribution and elimination as well as plasma binding has been emphasized recently (6, 15, 16). In this study, the effect of sulfadimethoxine on the elimination and distribution of thiopental was examined in both plasma disappearance and *in vitro* serum and tissue binding studies in an attempt to predict the drug interaction from *in vitro* binding data.

In plasma protein binding, a typical displacement of thiopental by sulfadimethoxine was observed (Fig. 2); but in tissue binding, no significant difference was observed in the free fraction of thiopental with or without sulfadimethoxine (Table II). This finding suggests that sulfadimethoxine does not alter the binding of thiopental to these tissues. The possible reasons for this discrepancy would be that thiopental is bound mainly to albumin in plasma but is bound in part to albumin in tissues but mainly to lipid or other macromolecules, which have nonspecific binding activities, due to the high lipophilicity of thiopental.

The overestimation of $V_{ss(in\ vitro)}$ compared to values from the plasma disappearance curves (Table I) might be due to underestimation of the free fraction of thiopental in tissue binding (Table II). In this study, diluted (25–50%) homogenates were used for liver and muscle binding studies, and this approach may cause the underestimation of the free fraction of thiopental due to the protein concentration dependency in the thiopental binding. Recently, Fichtl *et al.* (17) reported that the displacement of thiopental by phenylbutazone was not revealed in tissue binding using rabbit muscle homogenate. With respect to the displacement of thiopental in plasma binding by sulfadimethoxine, little has been reported, and only the displacement of tolbutamide binding to the plasma protein by sulfadimethoxine in sheep was reported (18). Thus, the increase in $V_{ss}$ in the presence of sulfadimethoxine might be explained by the alteration of plasma binding of thiopental. Furthermore, a significant difference also was shown in $V_{d_\beta}$ between the control and sulfadimethoxine-treated rats (Table I), which also can be explained by the alteration of the plasma binding of thiopental.

The possibility of inhibition in the metabolism of thiopental by sulfadimethoxine also should be considered. Previously, the inhibition in the microsomal oxidation of tolbutamide by sulfaphenazole was reported

(19). In this study, in the presence of sulfadimethoxine, the $Cl_{int}$ of thiopental also decreased to one-half that of the control rats (Table I). These findings suggest that the inhibition in thiopental metabolism might be affected by sulfadimethoxine.

The values for the tissue binding reported in this paper are only relative; they are not absolute. Further elaborate studies are necessary for the precise evaluation of tissue binding.

## REFERENCES


(1) R. A. Branch and D. G. Shand, *Clin. Pharmacokinet.*, **1**, 264 (1976).

(2) R. K. Roberts, G. R. Wilkinson, R. A. Branch, and S. Schenker, *Gastroenterology*, **75**, 479 (1978).

(3) J. W. Kraus, P. V. Desmond, J. P. Marshall, R. F. Johnson, S. Schenker, and G. R. Wilkinson, *Clin. Pharmacol. Ther.*, **24**, 411 (1978).

(4) L. Kangas, E. Iisalo, J. Kanto, V. Lehtinen, S. Pynnonen, I. Ruikka, J. Salmin, M. Sillanpaa, and E. Syvalahti, *Eur. J. Clin. Pharmacol.*, **15**, 163 (1979).

(5) R. E. Vestal, A. J. J. Wood, R. A. Branch, D. G. Shand, and G. R. Wilkinson, *Clin. Pharmacol. Ther.*, **26**, 8 (1979).

(6) J. R. Gillette, *Ann. N.Y. Acad. Sci.*, **179**, 43 (1971).

(7) G. R. Wilkinson and D. G. Shand, *Clin. Pharmacol. Ther.*, **18**, 377 (1975).

(8) B. B. Brodie, L. C. Mark, E. M. Papper, P. A. Lief, E. Bernstein, and E. A. Rovenstine, *J. Pharmacol. Exp. Ther.*, **98**, 85 (1950).

(9) K. Tsuda and S. Matsunaga, *J. Pharm. Soc. Jpn.*, **62**, 362 (1942).

(10) T. Nakagawa, Y. Koyanagi, and H. Togawa, "SALS, a Computer Program for Statistical Analysis with Least Squares Fitting," Library Program of the University of Tokyo Computer Center, Tokyo, Japan, 1978.

(11) M. Gibaldi and D. Perrier, "Pharmacokinetics," Dekker, New York, N.Y., 1975.

(12) Y. Igari, Y. Sugiyama, S. Awazu, and M. Hanano, *J. Pharm. Sci.*, in press.

(13) S. K. Chakrabarti, *Biochem. Pharmacol.*, **27**, 729 (1978).

(14) R. L. Dedrick, D. S. Zaharko, and R. J. Lutz, *J. Pharm. Sci.*, **62**, 882 (1973).

(15) M. Gibaldi, G. Levy, and P. McNamara, *Clin. Pharmacol. Ther.*, **24**, 1 (1978).

(16) P. Conway, M. Valentovic, and K. Bachmann, *Res. Commun. Chem. Pathol. Pharmacol.*, **26**, 309 (1979).

(17) B. Fichtl, H. Kurz, I. Wachter, and Z. Ziegler, *Naunyn-Schmiedebergs Arch. Pharmacol.*, **302**, R2 (1978).

(18) J. J. Thiessen and M. Rowland, *J. Pharm. Sci.*, **66**, 1063 (1977).

(19) Y. H. Lin, S. Awazu, and M. Hanano, *J. Pharm. Dyn.*, **2**, 273 (1979).


## ACKNOWLEDGMENTS


Supported by a grant-in-aid for scientific research provided by the Ministry of Education.

H. Y. Yu thanks Shionogi Pharmaceutical Industries Co. for support.


# NOTES

# Effects of Imide Analogs on Enzymes Required for Cholesterol and Fatty Acid Synthesis


**IRIS H. HALL ˣ, JAMES M. CHAPMAN, Jr., and GEORGE H. COCOLAS**



Received March 20, 1980, from the *Division of Medicinal Chemistry, School of Pharmacy, University of North Carolina, Chapel Hill, NC 27514.* Accepted for publication August 21, 1980.



**Abstract** □ Twelve imide analogs were examined for their ability to lower serum cholesterol and triglyceride levels in mice. Potent activity was observed for compounds containing a phthalimide or saccharin ring structure. The ability to lower serum cholesterol appears to be related to the ability to suppress acetyl-CoA synthetase activity. The availability of acetyl-CoA in the cytoplasm is a key regulatory component for cholesterol and fatty acid synthesis. The capacity to reduce serum triglycerides was related directly to the ability of the compound to inhibit acetyl-CoA carboxylase activity, the regulatory enzyme of fatty acid synthesis.



**Keyphrases** □ Imide analogs—effects on enzymes required for cholesterol and fatty acid synthesis, serum cholesterol and triglyceride levels, mice □ Cholesterol synthesis—effects of 12 imide analogs on related enzymes □ Fatty acid synthesis—effects of 12 imide analogs on related enzymes □ Triglyceride levels—effects of imide analogs on enzymes required for cholesterol and fatty acid synthesis


The antihyperlipidemic effects of potassium phthalimide and *N*-substituted phthalimides at 20 mg/kg/day in rodents were reported previously (1). Side-chain lengths of four carbon atoms or their equivalent for the *N*-substituted acids, esters, and ketones resulted in the greatest inhibition. β-Hydroxy-β-methylglutaryl-CoA reductase activity was not affected by these agents significantly, but inhibition of acetyl-CoA synthetase activity was related directly to the ability to lower serum lipids. Furthermore, the agents appeared to accelerate cholesterol excretion in the feces. No toxic or teratogenic effects were noted for these compounds, *i.e.*, $LD_{50} \geq 2$ g/kg.

The present study involves variation of the type of nucleus and the side chain to improve antihyperlipidemic activity and examination of the enzymes involved early in cholesterol and triglyceride synthesis for inhibition by these agents.

## EXPERIMENTAL

Twelve compounds were selected for this study (Table I). Phthalimide[1] (I), succinimide[1] (III), 1,8-naphthalimide[2] (V), saccharin[3] (VII), dibutyl phthalate[4] (X), and the standard, acetazolamide[5], were purchased commercially.

[1] Kodak Co.
[2] Aldrich Chemical Co.
[3] Ruger Chemical Co.
[4] Matheson, Coleman and Bell.
[5] Lederle Laboratories.




*0022-3549/81/0300-0326$01.00/0*


*© 1981, American Pharmaceutical Association*

(19). In this study, in the presence of sulfadimethoxine, the $Cl_{int}$ of thiopental also decreased to one-half that of the control rats (Table I). These findings suggest that the inhibition in thiopental metabolism might be affected by sulfadimethoxine.

The values for the tissue binding reported in this paper are only relative; they are not absolute. Further elaborate studies are necessary for the precise evaluation of tissue binding.

## REFERENCES


(1) R. A. Branch and D. G. Shand, *Clin. Pharmacokinet.*, **1**, 264 (1976).

(2) R. K. Roberts, G. R. Wilkinson, R. A. Branch, and S. Schenker, *Gastroenterology*, **75**, 479 (1978).

(3) J. W. Kraus, P. V. Desmond, J. P. Marshall, R. F. Johnson, S. Schenker, and G. R. Wilkinson, *Clin. Pharmacol. Ther.*, **24**, 411 (1978).

(4) L. Kangas, E. Iisalo, J. Kanto, V. Lehtinen, S. Pynnonen, I. Ruikka, J. Salmin, M. Sillanpaa, and E. Syvalahti, *Eur. J. Clin. Pharmacol.*, **15**, 163 (1979).

(5) R. E. Vestal, A. J. J. Wood, R. A. Branch, D. G. Shand, and G. R. Wilkinson, *Clin. Pharmacol. Ther.*, **26**, 8 (1979).

(6) J. R. Gillette, *Ann. N.Y. Acad. Sci.*, **179**, 43 (1971).

(7) G. R. Wilkinson and D. G. Shand, *Clin. Pharmacol. Ther.*, **18**, 377 (1975).

(8) B. B. Brodie, L. C. Mark, E. M. Papper, P. A. Lief, E. Bernstein, and E. A. Rovenstine, *J. Pharmacol. Exp. Ther.*, **98**, 85 (1950).

(9) K. Tsuda and S. Matsunaga, *J. Pharm. Soc. Jpn.*, **62**, 362 (1942).

(10) T. Nakagawa, Y. Koyanagi, and H. Togawa, "SALS, a Computer Program for Statistical Analysis with Least Squares Fitting," Library Program of the University of Tokyo Computer Center, Tokyo, Japan, 1978.

(11) M. Gibaldi and D. Perrier, "Pharmacokinetics," Dekker, New York, N.Y., 1975.

(12) Y. Igari, Y. Sugiyama, S. Awazu, and M. Hanano, *J. Pharm. Sci.*, in press.

(13) S. K. Chakrabarti, *Biochem. Pharmacol.*, **27**, 729 (1978).

(14) R. L. Dedrick, D. S. Zaharko, and R. J. Lutz, *J. Pharm. Sci.*, **62**, 882 (1973).

(15) M. Gibaldi, G. Levy, and P. McNamara, *Clin. Pharmacol. Ther.*, **24**, 1 (1978).

(16) P. Conway, M. Valentovic, and K. Bachmann, *Res. Commun. Chem. Pathol. Pharmacol.*, **26**, 309 (1979).

(17) B. Fichtl, H. Kurz, I. Wachter, and Z. Ziegler, *Naunyn-Schmiedebergs Arch. Pharmacol.*, **302**, R2 (1978).

(18) J. J. Thiessen and M. Rowland, *J. Pharm. Sci.*, **66**, 1063 (1977).

(19) Y. H. Lin, S. Awazu, and M. Hanano, *J. Pharm. Dyn.*, **2**, 273 (1979).


## ACKNOWLEDGMENTS


Supported by a grant-in-aid for scientific research provided by the Ministry of Education.

H. Y. Yu thanks Shionogi Pharmaceutical Industries Co. for support.


# NOTES

# Effects of Imide Analogs on Enzymes Required for Cholesterol and Fatty Acid Synthesis


**IRIS H. HALL ˣ, JAMES M. CHAPMAN, Jr., and GEORGE H. COCOLAS**



Received March 20, 1980, from the *Division of Medicinal Chemistry, School of Pharmacy, University of North Carolina, Chapel Hill, NC 27514.* Accepted for publication August 21, 1980.



**Abstract** □ Twelve imide analogs were examined for their ability to lower serum cholesterol and triglyceride levels in mice. Potent activity was observed for compounds containing a phthalimide or saccharin ring structure. The ability to lower serum cholesterol appears to be related to the ability to suppress acetyl-CoA synthetase activity. The availability of acetyl-CoA in the cytoplasm is a key regulatory component for cholesterol and fatty acid synthesis. The capacity to reduce serum triglycerides was related directly to the ability of the compound to inhibit acetyl-CoA carboxylase activity, the regulatory enzyme of fatty acid synthesis.



**Keyphrases** □ Imide analogs—effects on enzymes required for cholesterol and fatty acid synthesis, serum cholesterol and triglyceride levels, mice □ Cholesterol synthesis—effects of 12 imide analogs on related enzymes □ Fatty acid synthesis—effects of 12 imide analogs on related enzymes □ Triglyceride levels—effects of imide analogs on enzymes required for cholesterol and fatty acid synthesis


The antihyperlipidemic effects of potassium phthalimide and *N*-substituted phthalimides at 20 mg/kg/day in rodents were reported previously (1). Side-chain lengths of four carbon atoms or their equivalent for the *N*-substituted acids, esters, and ketones resulted in the greatest inhibition. β-Hydroxy-β-methylglutaryl-CoA reductase activity was not affected by these agents significantly, but inhibition of acetyl-CoA synthetase activity was related directly to the ability to lower serum lipids. Furthermore, the agents appeared to accelerate cholesterol excretion in the feces. No toxic or teratogenic effects were noted for these compounds, *i.e.*, $LD_{50} \geq 2$ g/kg.

The present study involves variation of the type of nucleus and the side chain to improve antihyperlipidemic activity and examination of the enzymes involved early in cholesterol and triglyceride synthesis for inhibition by these agents.

## EXPERIMENTAL

Twelve compounds were selected for this study (Table I). Phthalimide[1] (I), succinimide[1] (III), 1,8-naphthalimide[2] (V), saccharin[3] (VII), dibutyl phthalate[4] (X), and the standard, acetazolamide[5], were purchased commercially.

[1] Kodak Co.
[2] Aldrich Chemical Co.
[3] Ruger Chemical Co.
[4] Matheson, Coleman and Bell.
[5] Lederle Laboratories.




*0022-3549/81/0300-0326$01.00/0*


*© 1981, American Pharmaceutical Association*

**Table I—Physical Properties of Imides Tested for Antihyperlipidemic Effects**

| | Compound | Molecular Weight | Observed bp/mp* | Literature bp/mp | Reference |
|---|---|---|---|---|---|
| I | Phthalimide | 147.1 | 235–236° | 232–235° | 13 |
| II | 1-*N*-Phthalimidobutan-3-one | 217.2 | 114–116° | 111–113° | 2 |
| III | Succinimide | 99.1 | 122–124° | 123–125° | 14 |
| IV | 1-*N*-Succinimidobutan-3-one | 169.2 | 50–52° | 53.5–55.5° | 2 |
| V | 1,8-Naphthalimide | 197.2 | 296–299° | 285–298° | 15 |
| VI | 1-*N*-(1,8-Naphthalimido)butan-3-one | 267.3 | 154–156° | — | — |
| VII | Saccharin | 183.2 | 225–229° | 228.8–229.7° | 16 |
| VIII | 1-*N*-(*o*-Benzosulfimido)butan-3-one | 253.3 | 120–122° | 116–117.5° | 2 |
| IX | 3-*N*-Phthalimidopropionic acid | 219.2 | 152–153° | 151° | 3 |
| X | Dibutyl phthalate | 278.3 | — | 340°/76 mm | 17 |
| XI | 1-*N*-Phthalimidopropan-2-one | 203.2 | 123–124° | 122.9–123.5° | 18 |
| XII | *N*-*n*-Butylphthalimide | 203.2 | 110–116°/0.12 mm | 100–104°/0.03 mm | 5 |
| | Acetazolamide | 222.3 | 255° | 258–259° | 19 |

1-*N*-Phthalimidobutan-3-one (II, mp 114–116°), 1-*N*-succinimidobutan-3-one (IV, mp 50–52°), and 1-*N*-(*o*-benzosulfimido)butan-3-one (VIII, mp 120–122°) were prepared by the method of Irai *et al.* (2).

1-*N*-(1,8-Naphthalimido)butan-3-one (VI) was prepared by the following procedure. 1,8-Naphthalimide (9.86 g, 0.05 mole) was added to 300 ml of ethyl acetate containing a catalytic amount of sodium ethoxide. The suspension was heated at 60°, and 7.01 g (0.10 mole) of methyl vinyl ketone was added over 20 min. The resulting reaction mixture was refluxed for 5 hr, cooled, and washed with two 150-ml portions of 5% NaOH. The solvent was removed *in vacuo*, and the resulting yellow solid was recrystallized from ethanol to yield 3.1 g of VI, mp 154–156°; IR: 1695 and 1660 $cm^{-1}$ (C=O stretch); NMR: $\delta$ 8.1 (m, 6H, aromatic), 4.55 (t, 2H, $N-CH_2$), 2.95 (t, 2H, $CH_2C$), and 2.28 (s, 3H, $CH_3$).

*Anal.*—Calc. for $C_{16}H_{13}NO_3$: C, 71.89; H, 4.90. Found: C, 72.00; H, 4.84.

3-*N*-Phthalimidopropionic acid (IX) was synthesized by the method of Chodroff *et al.* (3), mp 152–153°. 1-*N*-Phthalimidopropan-2-one (XI) was synthesized by adapting the procedure of Abdel-Monem *et al.* (4),

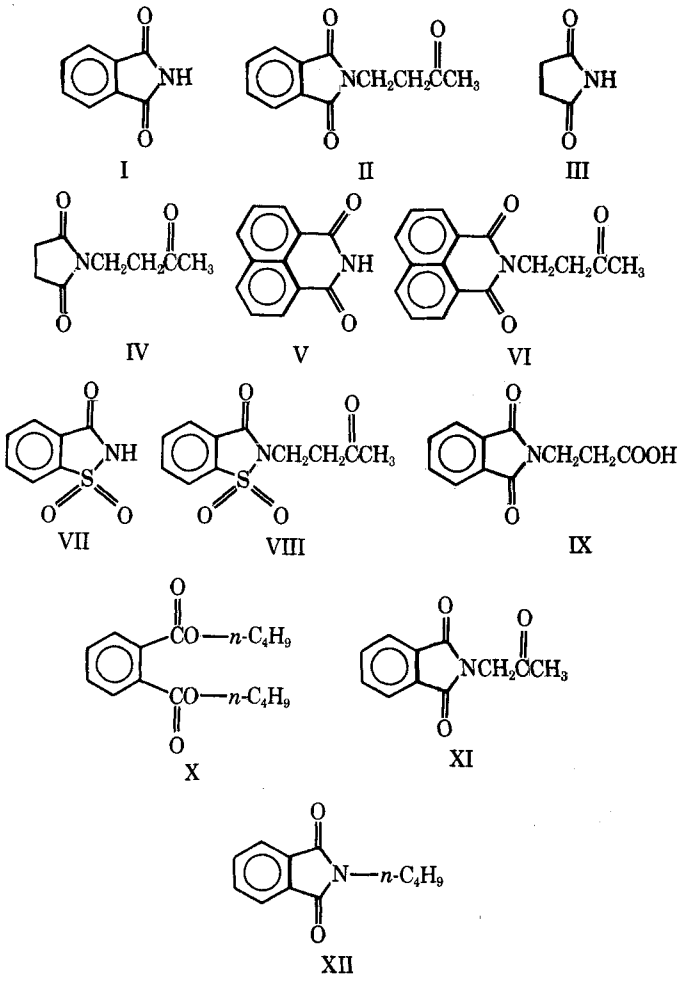


**Table II—Effects of Imide Analogs on Serum Cholesterol and Triglyceride Levels of Male Mice ($n = 6$)**

| Compound | Percent of Control: Serum Cholesterol, Day 9 | Percent of Control: Serum Cholesterol, Day 16 | Percent of Control: Serum Triglyceride, Day 14 |
|---|---|---|---|
| I | 63 ± 13[a] | 57 ± 7[a] | 44 ± 8[a] |
| II | 67 ± 11[a] | 63 ± 7[a] | 58 ± 7[a] |
| III | 78 ± 9[a] | 73 ± 12[b] | 68 ± 7[a] |
| IV | 90 ± 9 | 88 ± 7 | 79 ± 15 |
| V | 81 ± 6[a] | 61 ± 7[a] | 87 ± 12 |
| VI | 94 ± 12 | 86 ± 9[b] | 54 ± 15[a] |
| VII | 68 ± 11[a] | 67 ± 10[a] | 51 ± 16[a] |
| VIII | 60 ± 8[a] | 62 ± 6[a] | 51 ± 7[a] |
| IX | 74 ± 10[a] | 55 ± 12[a] | 58 ± 9[a] |
| X | 89 ± 10 | 91 ± 12 | 74 ± 10[a] |
| XI | 80 ± 16 | 67 ± 12[a] | 48 ± 10[a] |
| XII | 72 ± 11[a] | 54 ± 6[a] | 82 ± 10 |
| Acetazolamide | 82 ± 13 | 77 ± 10 | 79 ± 15 |
| Carboxymethylcellulose, 1% | 100 ± 5[c] | 100 ± 6[d] | 100 ± 6[e] |

[a] $p \leq 0.001$. [b] $p \leq 0.005$, Student $t$ test. [c] 118 mg % of control value. [d] 122 mg % of control value. [e] 137 mg % of control value.

mp 123–124°, and *N*-*n*-butylphthalimide (XII) was prepared according to the procedure of Sterk *et al.* (5), bp 110–116°/0.12 mm.

Compounds were tested at 20 mg/kg/day ip in male $CF_1$ mice (~30 g). On Days 9 and 16, blood was collected by tail vein bleeding. Serum cholesterol was determined by the Liebermann–Burchard reaction (6). A separate group of mice was bled on Day 14, and their serum triglyceride levels were determined using a commercial kit[6].

Compounds were tested *in vitro* at 2.5 μmoles for their effects on the enzymatic activity of a 10% liver homogenate prepared in 0.25 *M* sucrose and 0.001 *M* (ethylenedinitrilo)tetraacetic acid at pH 7.2. Adenosine triphosphate citrate-lyase activity was measured by the method of Hoffmann *et al.* (7). Acetyl-CoA synthetase activity was determined by the method of Goodridge (8).

The acetyl-CoA formed from both enzymatic assays was coupled with hydroxylamine to produce acetyl hydroxylmate, which was measured at 540 nm. Acetyl-CoA carboxylase activity was measured by a literature method (9), utilizing sodium [$^3$H]bicarbonate (6.2 mCi/mmole) after 30 min of incubation at 37° for enzyme polymerization (10). Fatty acid synthetase was determined by a literature method (11), utilizing [2'-$^{14}$C]malonyl-CoA (37.5 mCi/mmole) incorporation into fatty acids.

## RESULTS AND DISCUSSION

Compounds that contained the phthalimide or saccharin nucleus were more active in lowering serum cholesterol levels after 16 days of dosing than the succinimide (III and IV) derivatives or the naphthalimide derivative (VI) (Table II). Compounds XII and IX afforded the best anticholesterolemic activities followed by V, VIII, II, and VII (significant at $p \leq 0.001$). The commonly used industrial plasticizer (X) resulted in a loss of the analog's ability to lower serum cholesterol.

Serum triglyceride levels also were reduced by the imide analogs after 2 weeks of dosing. Compounds I and XI gave the best antitriglyceride activity followed by VII, VIII, VI, II, IX, III, and X (significant at $p \leq$

[6] Fisher, Hycel Triglyceride Test (1975), Hycel Inc.

**Table III—*In Vitro* Effects of Imide Analogs on Enzymes of Cholesterol and Triglyceride Synthetic Pathways in Mice ($n$ = 6)**

| Compound | Percent of Control, $\bar{x} \pm SD$ | | | |
|---|---|---|---|---|
| | Acetyl-CoA Synthetase | Citrate-lyase | Acetyl-CoA Carboxy-lase | Fatty Acid Synthetase |
| I | 70 ± 8[a] | 42 ± 6[a] | 8 ± 4[a] | 105 ± 8 |
| II | 53 ± 12[a] | 34 ± 4[a] | 17 ± 3[a] | 109 ± 7 |
| III | 74 ± 6[a] | 38 ± 3[a] | 87 ± 7 | 98 ± 9 |
| IV | 58 ± 6[a] | 38 ± 7[a] | 100 ± 5 | 81 ± 7[b] |
| V | 63 ± 9[a] | 66 ± 6[a] | 106 ± 6 | 86 ± 8 |
| VI | 88 ± 5[b] | 60 ± 5[a] | 59 ± 8[a] | 103 ± 4 |
| VII | 61 ± 7[a] | 65 ± 6[a] | 9 ± 2[a] | 93 ± 5 |
| VIII | 74 ± 9[a] | 47 ± 8[a] | 12 ± 3[a] | 104 ± 7 |
| IX | 57 ± 10[a] | 87 ± 6[b] | 18 ± 4[a] | 107 ± 7 |
| X | 87 ± 8[b] | 82 ± 7[a] | 54 ± 5[a] | 110 ± 8 |
| XI | 58 ± 7[a] | 76 ± 4[a] | 24 ± 4[a] | 91 ± 9 |
| XII | 44 ± 11[a] | 72 ± 9[a] | 76 ± 3[a] | 75 ± 10[b] |
| Acetazolamide | 66 ± 4[a] | 66 ± 7[a] | 13 ± 2[a] | 82 ± 6[b] |
| Carboxymethyl-cellulose, 1% | 100 ± 5[c] | 100 ± 4[d] | 100 ± 7[e] | 100 ± 7[f] |

[a] $p \leq 0.001$. [b] $p \leq 0.005$, Student $t$ test. [c] 28.5 mg of acetyl-CoA formed/g of wet tissue/30 min. [d] 30.5 mg of citrate hydrolyzed/g of wet tissue/30 min. [e] 32,010 dpm/g of wet tissue/30 min. [f] 37,656 dpm/g of wet tissue/30 min.

0.001). These agents were not toxic at the doses employed, and no side effects were noted.

An attempt was made to correlate the antihyperlipidemic activity with the ability to inhibit enzymatic activities at key biochemical sites early in the synthesis of cholesterol and fatty acids (Table III). The ability to lower serum cholesterol levels correlated positively with the ability to suppress liver acetyl-CoA synthetase activity ($r = 0.86$, $p = 0.001$, using the means of each test group[7]). The ability to suppress acetyl-CoA carboxylase activity correlated positively with the lowering of serum triglycerides ($r = 0.84$, $p = 0.001$). The ability to inhibit citrate-lyase activity, although inhibited by I–IV and VIII which caused >50% inhibition, did not correlate with the ability to lower the serum cholesterol or triglycerides levels. The imide derivatives had no effect on fatty acid synthetase activities except in isolated cases such as IV, V, and XII. Both acetyl-CoA synthetase and citrate-lyase regulate the availability of acetyl-CoA in the cytoplasm for the synthesis of both cholesterol and fatty acids for the synthesis of triglycerides. Acetyl-CoA carboxylase is the regulatory enzyme in the synthesis of fatty acids, which subsequently are required in triglyceride synthesis. In this assay, the carboxylase enzyme must be polymerized for optimum activity (10). Highest inhibition by the imide compounds was observed when test compounds were added to the incubation medium prior to polymerization. However, significant inhibition was observed even if the compounds were added after polymerization, *e.g.*, I, II, VIII, and IX caused 76, 62, 42, and 70% inhibition of the carboxylase activity, respectively.

These studies demonstrate pellucidly the antihyperlipidemic effects of imides. Compared to available standard pharmacological agents, these agents are potent in their ability to lower serum lipids at a relatively low dose with no observable deleterious side effects. These compounds offer unique ways to regulate lipid synthesis which have not been reported previously.

[7] Pearson-product-moment coefficient of correlation ($r$); probability determined by the Student $t$ test (12).

## REFERENCES


(1) J. M. Chapman, G. H. Cocolas, and I. H. Hall, *J. Med. Chem.*, **22**, 1399 (1979).

(2) H. Irai, S. Shima, and N. Murata, *Kogyo Kagaku Zasshi*, **62**, 82 (1959); through *Chem. Abstr.*, **58**, 5659b (1963).

(3) S. Chodroff, R. Kapp, and C. O. Beckmann, *J. Am. Chem. Soc.*, **69**, 256 (1947).

(4) M. M. Abdel-Monem, N. E. Newton, and C. E. Weeks, *J. Med. Chem.*, **17**, 447 (1974).

(5) L. Sterk, J. Hasko, and K. Nador, *Arzneim.-Forsch.*, **18**, 798 (1968).

(6) A. T. Ness, J. V. Pastewka, and A. C. Peacock, *Clin. Chim. Acta*, **10**, 229 (1964).

(7) M. Hoffmann, L. Weiss, and O. H. Wieland, *Anal. Biochim.*, **84**, 441 (1978).

(8) A. G. Goodridge, *J. Biol. Chem.*, **248**, 4218 (1973).

(9) M. D. Greenspan and J. M. Lowenstein, *ibid.*, **243**, 6273 (1968).

(10) T. P. Cao and S. Rous, *Life Sci.*, **22**, 2067 (1978).

(11) R. O. Brady, R. M. Bradley, and E. G. Trams, *J. Biol. Chem.*, **235**, 3093 (1960).

(12) G. W. Snedecor, "Statistical Methods," Iowa State College Press, Ames, Iowa, 1956.

(13) W. A. Noyes and P. K. Porter, *Org. Synth.*, coll. vol. **I**, 457 (1932).

(14) H. T. Clarke and L. D. Behr, *ibid.*, coll. vol. **II**, 562 (1943).

(15) A. E. Porai-Koshits and I. S. Pavlushenko, *J. Gen. Chem. (USSR)*, **17**, 1739 (1947); through *Chem. Abstr.*, **42**, 5893a (1948).

(16) "The Merck Index," 9th ed., Merck & Co., Rahway, N.J., 1976, p. 8075.

(17) *Ibid.*, p. 1574.

(18) R. E. Lancaster, Jr., and C. A. Vanderwerf, *J. Org. Chem.* **23**, 1208 (1958).

(19) R. O. Roblin, Jr., and J. W. Clapp, *J. Am. Chem. Soc.*, **72**, 4890 (1950).


# Thermal Hardness Coefficient of Tablets


**EUGENE L. PARROTT**



Received May 7, 1980, from the *Division of Pharmaceutics, College of Pharmacy, University of Iowa, Iowa City, IA 52242.* Accepted for publication September 2, 1980.



**Abstract** □ The hardness of 10 commercial compressed tablets was measured at −25, 0, 24, and 50°. The hardness is relatively insensitive to temperature change within normal storage and handling temperatures. Consequently, no temperature control is needed in measuring tablet hardness. Nonconventional (sustained-release) tablets behave differently.



**Keyphrases** □ Tablets—determination of hardness at various temperatures □ Hardness—tablets, effects of temperature □ Temperature—effect on hardness coefficient of tablets


Carbon steel and martensitic steels have low mechanical strength at low temperatures. With the exception of tetrafluoroethylene resin, plastics are embrittled at low temperatures (1). In the cryopulverizing process, the material to be comminuted has its temperature lowered so that it changes from a ductile to a brittle solid (2, 3). All materials are not embrittled by chilling; copper, aluminum, nickel, and most solid–solution alloys of these metals are strong at low temperatures.

In pharmaceutics, the brittleness or resistance to crushing is known as hardness, which is defined as the compression force that, when applied diametrically, just causes the tablet to fracture. Although no official standards




*0022-3549/81/0300-0328$01.00/0*



*© 1981, American Pharmaceutical Association*

**Table III—*In Vitro* Effects of Imide Analogs on Enzymes of Cholesterol and Triglyceride Synthetic Pathways in Mice ($n$ = 6)**

| Compound | Percent of Control, $\bar{x} \pm SD$ | | | |
|---|---|---|---|---|
| | Acetyl-CoA Synthetase | Citrate-lyase | Acetyl-CoA Carboxy-lase | Fatty Acid Synthetase |
| I | 70 ± 8[a] | 42 ± 6[a] | 8 ± 4[a] | 105 ± 8 |
| II | 53 ± 12[a] | 34 ± 4[a] | 17 ± 3[a] | 109 ± 7 |
| III | 74 ± 6[a] | 38 ± 3[a] | 87 ± 7 | 98 ± 9 |
| IV | 58 ± 6[a] | 38 ± 7[a] | 100 ± 5 | 81 ± 7[b] |
| V | 63 ± 9[a] | 66 ± 6[a] | 106 ± 6 | 86 ± 8 |
| VI | 88 ± 5[b] | 60 ± 5[a] | 59 ± 8[a] | 103 ± 4 |
| VII | 61 ± 7[a] | 65 ± 6[a] | 9 ± 2[a] | 93 ± 5 |
| VIII | 74 ± 9[a] | 47 ± 8[a] | 12 ± 3[a] | 104 ± 7 |
| IX | 57 ± 10[a] | 87 ± 6[b] | 18 ± 4[a] | 107 ± 7 |
| X | 87 ± 8[b] | 82 ± 7[a] | 54 ± 5[a] | 110 ± 8 |
| XI | 58 ± 7[a] | 76 ± 4[a] | 24 ± 4[a] | 91 ± 9 |
| XII | 44 ± 11[a] | 72 ± 9[a] | 76 ± 3[a] | 75 ± 10[b] |
| Acetazolamide | 66 ± 4[a] | 66 ± 7[a] | 13 ± 2[a] | 82 ± 6[b] |
| Carboxymethyl-cellulose, 1% | 100 ± 5[c] | 100 ± 4[d] | 100 ± 7[e] | 100 ± 7[f] |

[a] $p \leq 0.001$. [b] $p \leq 0.005$, Student $t$ test. [c] 28.5 mg of acetyl-CoA formed/g of wet tissue/30 min. [d] 30.5 mg of citrate hydrolyzed/g of wet tissue/30 min. [e] 32,010 dpm/g of wet tissue/30 min. [f] 37,656 dpm/g of wet tissue/30 min.

0.001). These agents were not toxic at the doses employed, and no side effects were noted.

An attempt was made to correlate the antihyperlipidemic activity with the ability to inhibit enzymatic activities at key biochemical sites early in the synthesis of cholesterol and fatty acids (Table III). The ability to lower serum cholesterol levels correlated positively with the ability to suppress liver acetyl-CoA synthetase activity ($r = 0.86$, $p = 0.001$, using the means of each test group[7]). The ability to suppress acetyl-CoA carboxylase activity correlated positively with the lowering of serum triglycerides ($r = 0.84$, $p = 0.001$). The ability to inhibit citrate-lyase activity, although inhibited by I–IV and VIII which caused >50% inhibition, did not correlate with the ability to lower the serum cholesterol or triglycerides levels. The imide derivatives had no effect on fatty acid synthetase activities except in isolated cases such as IV, V, and XII. Both acetyl-CoA synthetase and citrate-lyase regulate the availability of acetyl-CoA in the cytoplasm for the synthesis of both cholesterol and fatty acids for the synthesis of triglycerides. Acetyl-CoA carboxylase is the regulatory enzyme in the synthesis of fatty acids, which subsequently are required in triglyceride synthesis. In this assay, the carboxylase enzyme must be polymerized for optimum activity (10). Highest inhibition by the imide compounds was observed when test compounds were added to the incubation medium prior to polymerization. However, significant inhibition was observed even if the compounds were added after polymerization, *e.g.*, I, II, VIII, and IX caused 76, 62, 42, and 70% inhibition of the carboxylase activity, respectively.

These studies demonstrate pellucidly the antihyperlipidemic effects of imides. Compared to available standard pharmacological agents, these agents are potent in their ability to lower serum lipids at a relatively low dose with no observable deleterious side effects. These compounds offer unique ways to regulate lipid synthesis which have not been reported previously.

[7] Pearson-product-moment coefficient of correlation ($r$); probability determined by the Student $t$ test (12).

## REFERENCES


(1) J. M. Chapman, G. H. Cocolas, and I. H. Hall, *J. Med. Chem.*, **22**, 1399 (1979).

(2) H. Irai, S. Shima, and N. Murata, *Kogyo Kagaku Zasshi*, **62**, 82 (1959); through *Chem. Abstr.*, **58**, 5659b (1963).

(3) S. Chodroff, R. Kapp, and C. O. Beckmann, *J. Am. Chem. Soc.*, **69**, 256 (1947).

(4) M. M. Abdel-Monem, N. E. Newton, and C. E. Weeks, *J. Med. Chem.*, **17**, 447 (1974).

(5) L. Sterk, J. Hasko, and K. Nador, *Arzneim.-Forsch.*, **18**, 798 (1968).

(6) A. T. Ness, J. V. Pastewka, and A. C. Peacock, *Clin. Chim. Acta*, **10**, 229 (1964).

(7) M. Hoffmann, L. Weiss, and O. H. Wieland, *Anal. Biochim.*, **84**, 441 (1978).

(8) A. G. Goodridge, *J. Biol. Chem.*, **248**, 4218 (1973).

(9) M. D. Greenspan and J. M. Lowenstein, *ibid.*, **243**, 6273 (1968).

(10) T. P. Cao and S. Rous, *Life Sci.*, **22**, 2067 (1978).

(11) R. O. Brady, R. M. Bradley, and E. G. Trams, *J. Biol. Chem.*, **235**, 3093 (1960).

(12) G. W. Snedecor, "Statistical Methods," Iowa State College Press, Ames, Iowa, 1956.

(13) W. A. Noyes and P. K. Porter, *Org. Synth.*, coll. vol. **I**, 457 (1932).

(14) H. T. Clarke and L. D. Behr, *ibid.*, coll. vol. **II**, 562 (1943).

(15) A. E. Porai-Koshits and I. S. Pavlushenko, *J. Gen. Chem. (USSR)*, **17**, 1739 (1947); through *Chem. Abstr.*, **42**, 5893a (1948).

(16) "The Merck Index," 9th ed., Merck & Co., Rahway, N.J., 1976, p. 8075.

(17) *Ibid.*, p. 1574.

(18) R. E. Lancaster, Jr., and C. A. Vanderwerf, *J. Org. Chem.* **23**, 1208 (1958).

(19) R. O. Roblin, Jr., and J. W. Clapp, *J. Am. Chem. Soc.*, **72**, 4890 (1950).


# Thermal Hardness Coefficient of Tablets


**EUGENE L. PARROTT**



Received May 7, 1980, from the *Division of Pharmaceutics, College of Pharmacy, University of Iowa, Iowa City, IA 52242.* Accepted for publication September 2, 1980.



**Abstract** □ The hardness of 10 commercial compressed tablets was measured at −25, 0, 24, and 50°. The hardness is relatively insensitive to temperature change within normal storage and handling temperatures. Consequently, no temperature control is needed in measuring tablet hardness. Nonconventional (sustained-release) tablets behave differently.



**Keyphrases** □ Tablets—determination of hardness at various temperatures □ Hardness—tablets, effects of temperature □ Temperature—effect on hardness coefficient of tablets


Carbon steel and martensitic steels have low mechanical strength at low temperatures. With the exception of tetrafluoroethylene resin, plastics are embrittled at low temperatures (1). In the cryopulverizing process, the material to be comminuted has its temperature lowered so that it changes from a ductile to a brittle solid (2, 3). All materials are not embrittled by chilling; copper, aluminum, nickel, and most solid–solution alloys of these metals are strong at low temperatures.

In pharmaceutics, the brittleness or resistance to crushing is known as hardness, which is defined as the compression force that, when applied diametrically, just causes the tablet to fracture. Although no official standards




*0022-3549/81/0300-0328$01.00/0*



*© 1981, American Pharmaceutical Association*

Table I—Average (±*SD*) Hardness of Tablets in Kilopounds at Various Temperatures (±1°)

| Product | −25° | 0° | 24° | 50° |
|---|---|---|---|---|
| A[a] | 9.7 ± 1.3[b] | 8.2 ± 1.2 | 9.0 ± 0.9 | 7.1 ± 0.9 |
| B[c] | 6.7 ± 1.1 | 6.3 ± 1.1 | 6.0 ± 1.2 | 5.0 ± 1.4 |
| C[d] | 7.5 ± 0.8 | 6.5 ± 0.6 | 6.6 ± 0.6 | 4.5 ± 0.4 |
| D[e] | 7.1 ± 2.4 | 6.5 ± 2.2 | 6.7 ± 1.7 | 5.8 ± 1.3 |
| E[f] | 7.4 ± 0.7 | 6.6 ± 0.8 | 7.0 ± 1.0 | 6.0 ± 1.0 |
| F[g] | 7.2 ± 0.8 | 8.6 ± 0.8 | 9.0 ± 0.8 | 6.2 ± 0.5 |
| G[h] | 15.3 ± 2.2 | 13.6 ± 2.2 | 11.2 ± 1.1 | 5.0 ± 0.6 |

[a] Belladenal, Sandoz, lot 241 A 8473 (July 1984). [b] Average of 10 measurements. [c] Furadantin (50 mg), Norwich-Eaton, lot 02276 (August 1984). [d] Hydergine, Sandoz, lot 764 Y 6460 (July 1981). [e] Methotrexate, Lederle, lot 513-418 (May 1982). [f] P-A-C Compound, Upjohn, lot 670GK (March 1982). [g] PBZ Lontabs (50 mg), lot 11172 (September 1981). [h] Tedral SA, Warner-Chilcott, lot 2210V075A (July 1980).

Table II—Average (±*SD*) Hardness of Tablets in Kilograms[a] at Various Temperatures (±1°)

| Product | −25° | 0° | 24° | 50° |
|---|---|---|---|---|
| H[b] | 19.9 ± 0.4[c] | 19.7 ± 0.3 | 19.4 ± 0.6 | 20.0 ± 0.2 |
| I[d] | 19.8 ± 0.4 | 19.3 ± 1.5 | 17.9 ± 1.9 | 20.2 ± 0.3 |
| J[e] | 19.3 ± 0.4 | 19.9 ± 0.2 | 18.5 ± 0.6 | 19.6 ± 0.6 |

[a] Pfizer hardness tester. [b] Gris-PEG, Dorsey, lot L77207 (February 1981). [c] Average of 10 measurements. [d] Tenuate Dospan, Merrell, lot 155BB (January 1984). [e] Tral Gradumet, Abbott, lot 53988AF26 (April 1980).

exist to measure or express the hardness of compressed tablets, hardness is a universally used manufacturing specification for inprocess control and batch evaluation. The embrittlement of compressed tablets at temperatures (−25–50°) likely to be encountered in handling, shipment, and storage is of interest.

## EXPERIMENTAL

Ten commercial products were arbitrarily selected without regard to the medicinal compound. The tablets were placed in separate amber glass vials at ambient temperature and humidity. Tablets were stored in a freezer at −25° for 20 hr, in an oven at 50° for 20 hr, or in an ice bath at 0° for 8 hr. Tablets were removed from the constant-temperature chambers and immediately measured by means of a motor-driven hardness tester[1], which applied force at a constant rate. A manual hardness tester[2] was used only when the hardness exceeded the scale on the motor-driven tester. For each product, 10 tablets were measured.

## RESULTS AND DISCUSSION

The mean hardness and standard deviation of seven commercial tablets at −25, 0, 24, and 50° are shown in Table I. The mean hardness and standard deviation as determined by the manual hardness tester permits comparison of hardness at various temperatures (Table II).

Inspection of Table I suggests a slight decrease in hardness as the temperature was increased (~−0.02 kilopound/degree) for Products A–E. The sustained-release tablets (F and G) were softest at the highest temperature. Wax-like ingredients (carnauba wax and stearyl alcohol), which impart a sustained-release pattern, probably soften and become more plastic as the temperature rises from room temperature to 50°; this effect decreased the hardness by 50% for Tablet G. Since the exact formulations are unknown, speculation on the form of the curves serves no useful purpose. However, the results confirm that for nonconventional (sustained-release) tablets, one would not necessarily anticipate a constant value of the thermal hardness coefficient as was demonstrated for the conventional tablets.

In the temperature range studied, Products H–J had a thermal hardness coefficient of zero (Table II). In these products, the medicinal compound is held within a matrix. For example, in Product J, the hexocyclium methylsulfate exists within the channels and pores of a water-insoluble matrix of methyl acrylate and methyl methacrylate, which maintains a constant hardness at the usual temperatures of handling and storage.

## REFERENCES

(1) "Chemical Engineers' Handbook," 4th ed., R. H. Perry, C. H. Chilton, and S. D. Kirkpatrick, Eds., McGraw-Hill, New York, N.Y., 1963, pp. 12–40.

(2) M. W. Biddulph, *Conserv. Recycling*, **1**, 281 (1977).

(3) J. H. Bilbrey, Jr., and E. G. Valdez, *Cryog. Eng.*, **20**, 411 (1975).

[1] Schleuniger model 2E/205, Vector Corp., Marion, IA 52302.
[2] Pfizer Co., New York, NY 10017.

# Dry Column Chromatographic Procedure for Rapid Concentration of Biological Activity in Natural Products Fractionation

**GERARD C. HOKANSON ˣ and NANCY J. MATYUNAS**

Received June 13, 1980, from the *College of Pharmacy and Allied Health Professions, Wayne State University, Detroit, MI 48202.* Accepted for publication August 28, 1980.

**Abstract** □ A dry column chromatographic procedure is described. It allows for the rapid concentration of biologically active materials in natural products fractionation. The potential value of the technique is described, utilizing as an example the separation of an anticancer active fraction obtained from *Euphorbia cyparissias*.

**Keyphrases** □ Column chromatography, dry—rapid concentration of biological activity, natural products fractionation □ *Euphorbia cyparissias*—separation of anticancer active fraction, dry column chromatography □ Separation—biological activity in natural products, dry column chromatography

One of the largest and most successful plant screening programs in recent years has been coordinated by the U.S. National Cancer Institute to discover new naturally occurring tumor inhibitors (1–3). As part of this effort, this laboratory established an extensive program to screen the higher plants of southeastern Michigan for anticancer activity and to isolate active plant constituents. As with all work of this type, the successful completion of fractionation studies depends largely on the rapid concentration of active materials into simplified fractions so that maximal effort can be directed toward purification of active plant components. To facilitate this process, a method was sought that would rapidly indicate which plant constituents were responsible for activity observed with crude plant extracts.

0022-3549/81/0300-0329$01.00/0
© 1981, American Pharmaceutical Association

Table I—Average (±*SD*) Hardness of Tablets in Kilopounds at Various Temperatures (±1°)

| Product | −25° | 0° | 24° | 50° |
|---|---|---|---|---|
| A[a] | 9.7 ± 1.3[b] | 8.2 ± 1.2 | 9.0 ± 0.9 | 7.1 ± 0.9 |
| B[c] | 6.7 ± 1.1 | 6.3 ± 1.1 | 6.0 ± 1.2 | 5.0 ± 1.4 |
| C[d] | 7.5 ± 0.8 | 6.5 ± 0.6 | 6.6 ± 0.6 | 4.5 ± 0.4 |
| D[e] | 7.1 ± 2.4 | 6.5 ± 2.2 | 6.7 ± 1.7 | 5.8 ± 1.3 |
| E[f] | 7.4 ± 0.7 | 6.6 ± 0.8 | 7.0 ± 1.0 | 6.0 ± 1.0 |
| F[g] | 7.2 ± 0.8 | 8.6 ± 0.8 | 9.0 ± 0.8 | 6.2 ± 0.5 |
| G[h] | 15.3 ± 2.2 | 13.6 ± 2.2 | 11.2 ± 1.1 | 5.0 ± 0.6 |

[a] Belladenal, Sandoz, lot 241 A 8473 (July 1984). [b] Average of 10 measurements. [c] Furadantin (50 mg), Norwich-Eaton, lot 02276 (August 1984). [d] Hydergine, Sandoz, lot 764 Y 6460 (July 1981). [e] Methotrexate, Lederle, lot 513-418 (May 1982). [f] P-A-C Compound, Upjohn, lot 670GK (March 1982). [g] PBZ Lontabs (50 mg), lot 11172 (September 1981). [h] Tedral SA, Warner-Chilcott, lot 2210V075A (July 1980).

Table II—Average (±*SD*) Hardness of Tablets in Kilograms[a] at Various Temperatures (±1°)

| Product | −25° | 0° | 24° | 50° |
|---|---|---|---|---|
| H[b] | 19.9 ± 0.4[c] | 19.7 ± 0.3 | 19.4 ± 0.6 | 20.0 ± 0.2 |
| I[d] | 19.8 ± 0.4 | 19.3 ± 1.5 | 17.9 ± 1.9 | 20.2 ± 0.3 |
| J[e] | 19.3 ± 0.4 | 19.9 ± 0.2 | 18.5 ± 0.6 | 19.6 ± 0.6 |

[a] Pfizer hardness tester. [b] Gris-PEG, Dorsey, lot L77207 (February 1981). [c] Average of 10 measurements. [d] Tenuate Dospan, Merrell, lot 155BB (January 1984). [e] Tral Gradumet, Abbott, lot 53988AF26 (April 1980).

exist to measure or express the hardness of compressed tablets, hardness is a universally used manufacturing specification for inprocess control and batch evaluation. The embrittlement of compressed tablets at temperatures (−25–50°) likely to be encountered in handling, shipment, and storage is of interest.

## EXPERIMENTAL

Ten commercial products were arbitrarily selected without regard to the medicinal compound. The tablets were placed in separate amber glass vials at ambient temperature and humidity. Tablets were stored in a freezer at −25° for 20 hr, in an oven at 50° for 20 hr, or in an ice bath at 0° for 8 hr. Tablets were removed from the constant-temperature chambers and immediately measured by means of a motor-driven hardness tester[1], which applied force at a constant rate. A manual hardness tester[2] was used only when the hardness exceeded the scale on the motor-driven tester. For each product, 10 tablets were measured.

## RESULTS AND DISCUSSION

The mean hardness and standard deviation of seven commercial tablets at −25, 0, 24, and 50° are shown in Table I. The mean hardness and standard deviation as determined by the manual hardness tester permits comparison of hardness at various temperatures (Table II).

Inspection of Table I suggests a slight decrease in hardness as the temperature was increased (~−0.02 kilopound/degree) for Products A–E. The sustained-release tablets (F and G) were softest at the highest temperature. Wax-like ingredients (carnauba wax and stearyl alcohol), which impart a sustained-release pattern, probably soften and become more plastic as the temperature rises from room temperature to 50°; this effect decreased the hardness by 50% for Tablet G. Since the exact formulations are unknown, speculation on the form of the curves serves no useful purpose. However, the results confirm that for nonconventional (sustained-release) tablets, one would not necessarily anticipate a constant value of the thermal hardness coefficient as was demonstrated for the conventional tablets.

In the temperature range studied, Products H–J had a thermal hardness coefficient of zero (Table II). In these products, the medicinal compound is held within a matrix. For example, in Product J, the hexocyclium methylsulfate exists within the channels and pores of a water-insoluble matrix of methyl acrylate and methyl methacrylate, which maintains a constant hardness at the usual temperatures of handling and storage.

## REFERENCES

(1) "Chemical Engineers' Handbook," 4th ed., R. H. Perry, C. H. Chilton, and S. D. Kirkpatrick, Eds., McGraw-Hill, New York, N.Y., 1963, pp. 12–40.

(2) M. W. Biddulph, *Conserv. Recycling*, **1**, 281 (1977).

(3) J. H. Bilbrey, Jr., and E. G. Valdez, *Cryog. Eng.*, **20**, 411 (1975).

[1] Schleuniger model 2E/205, Vector Corp., Marion, IA 52302.
[2] Pfizer Co., New York, NY 10017.

# Dry Column Chromatographic Procedure for Rapid Concentration of Biological Activity in Natural Products Fractionation

**GERARD C. HOKANSON ˣ and NANCY J. MATYUNAS**

Received June 13, 1980, from the *College of Pharmacy and Allied Health Professions, Wayne State University, Detroit, MI 48202.* Accepted for publication August 28, 1980.

**Abstract** □ A dry column chromatographic procedure is described. It allows for the rapid concentration of biologically active materials in natural products fractionation. The potential value of the technique is described, utilizing as an example the separation of an anticancer active fraction obtained from *Euphorbia cyparissias*.

**Keyphrases** □ Column chromatography, dry—rapid concentration of biological activity, natural products fractionation □ *Euphorbia cyparissias*—separation of anticancer active fraction, dry column chromatography □ Separation—biological activity in natural products, dry column chromatography

One of the largest and most successful plant screening programs in recent years has been coordinated by the U.S. National Cancer Institute to discover new naturally occurring tumor inhibitors (1–3). As part of this effort, this laboratory established an extensive program to screen the higher plants of southeastern Michigan for anticancer activity and to isolate active plant constituents. As with all work of this type, the successful completion of fractionation studies depends largely on the rapid concentration of active materials into simplified fractions so that maximal effort can be directed toward purification of active plant components. To facilitate this process, a method was sought that would rapidly indicate which plant constituents were responsible for activity observed with crude plant extracts.

0022-3549/81/0300-0329$01.00/0
© 1981, American Pharmaceutical Association

**Table I—Separation Results and Biological Activity of Fractions Obtained from Dry Column Chromatography of *E. cyparissias* Chloroform Fraction**

| Fraction | Band Position[a], cm | Weight[b], mg | Elution Solvent[c] | PS Activity, best % T/C (Dosage, mg/kg) | KB Activity, $ED_{50}$, μg/ml |
|---|---|---|---|---|---|
| Ethanol extract | — | — | — | 147 (12.5) | 30 |
| Chloroform fraction | — | — | — | 141 (4) | 7.5 |
| A | Eluted | 43 | Benzene–hexane (1:1) | 105 (1) | 70 |
| B | 0–8 | 40 | Benzene–hexane (3:1) | 109 (2) | 70 |
| C | 8–12 | 27 | Benzene | 108 (4) | 2.2 |
| D | 12–24 | 54 | Benzene–chloroform (1:1) | 100 (2) | 23 |
| E | 24–28 | 20 | Benzene–chloroform (15:85) | 123 (0.5) | 17 |
| F | 28–40 | 48 | Chloroform | 115 (2) | 29 |
| G | 40–44 | 60 | Chloroform | 115 (2) | 26 |
| H | 44–56 | 27 | Chloroform–methanol (98:2) | 135 (1) | 28 |
| I | 56–60 | 189 | Chloroform–methanol (9:1) | 119 (4) | 70 |

[a] Position of band from bottom of a 60-cm column. [b] Amount recovered from a 525-mg sample. [c] Solvent required to obtain similar materials *via* gradient-elution column chromatography on a separate 9-g sample.

Various methods have been described for the fractionation of anticancer active plant extracts (3, 4). Unfortunately, conventional techniques may require considerable time and effort before work can be focused on active fractions. One method that has not been utilized extensively in natural products fractionation is dry column chromatography, although procedures have been available (5–8). Dry column chromatography usually is employed to scale-up preparative TLC procedures in the final purification of materials. Because dry column chromatographic procedures can be performed in one afternoon, the method is ideal for initial fractionation. Complex mixtures may be separated into 10 or more fractions whose bioassay may provide a clue to the material responsible for the observed anticancer activity. Larger scale procedures then may be utilized to prepare sufficient quantities of the active fraction for purification and structural analysis.

The described dry column procedure has been successfully employed in the preliminary analysis of several plants including *Euphorbia cyparissias* L. (Euphorbiaceae), which is presented here as an example[1].

## EXPERIMENTAL

**Materials and General Procedures**—TLC was performed on precoated silica gel plates[2], developed in chloroform–ether (95:5) and visualized by spraying with 3% ceric sulfate in 3 *N* $H_2SO_4$, followed by heating at 110° for 10 min. Dry column chromatography utilized silica gel[3] packed into 4-cm (flat) nylon tubing[4]. Silica gel activity on the Brockmann scale (9) was analyzed using *p*-dimethylaminoazobenzene[5] according to established procedures (6). Column chromatography was performed on silica gel 60[6] (70–230 mesh). Plant material[7] was collected from selected areas of southeastern lower Michigan, air dried, and milled to a fine powder.

**Extraction and Preliminary Fractionation**—Dried and milled *E. cyparissias* (all plant parts), 520 g, was macerated in ethanol (95%) at room temperature for 24 hr. Following filtration of the plant material and concentration of the filtrate *in vacuo*, the ethanolic extract (97.4 g) was partitioned between equal volumes of chloroform and water. Separation of the organic layer and concentration *in vacuo* yielded 34.3 g of a dark-green tar (chloroform fraction).

**Dry Column Chromatography**—An 80-cm length of nylon tubing was sealed at one end by folding the tubing several times and stapling. Holes were punched above the seal, allowing for drainage and escape of air during column packing, and a small pad of glass wool was inserted above the holes. Silica gel (175 g) was added in six or seven portions, and the column was compacted by sharply tapping or vibrating the sides while firmly grasping the column just above the adsorbent layer. Following addition of the final portion of adsorbent and compacting as before, the top of the column was uniformly compressed by inserting an inverted stopper (of the same approximate diameter as the column) attached to a glass rod and exerting pressure on the top of the column.

The sample to be chromatographed, 525 mg of the chloroform fraction, was dissolved in chloroform and added to 2 g of diatomaceous earth[8]. The resulting mixture, evaporated to dryness *in vacuo*, was ground to a powder in a mortar and added to the top of the column. Following compression of the sample layer from the top, the column was completed by the addition of a 2–3-cm layer of sand. The prepared column, measuring ~2.5 × 60 cm, was supported by inserting a piece of open glass tubing into the open end and clamping the glass and nylon tubing together. Two additional clamps were added further down the column for support.

Column development was effected by adding the developing solvent (chloroform–ether, 95:5) under a constant liquid head of 3–5 cm. Separation of pigmented bands was observed within the first 10–15 cm, with further separation achieved as development continued. Additional solvent was added until yellow pigmented materials, moving with the solvent front, eluted from the column. The total development time was ~45 min, requiring 450 ml of solvent.

Immediately upon completion of column development, the column was laid on its side and sliced into 15 4-cm bands. Following extraction of adsorbent fractions with ether–methanol combinations, filtration, and concentration of the filtrates *in vacuo*, the extracted materials were compared by TLC and similar fractions were combined. Separation results and data from subsequent biological assay[9] are summarized in Table I.

**Gradient Elution Column Chromatography**—A 9-g sample of the chloroform fraction was chromatographed on 450 g of silica gel, eluting with combinations of hexane, benzene, chloroform, and methanol. A total of 165 fractions (125 ml each) was collected and combined on the basis of TLC behavior. Solvents required to elute materials similar to dry column chromatographic fractions are indicated in Table I.

## RESULTS

As indicated in Table I, an ethanolic extract of *E. cyparissias* possessed activity in the P-388 (PS) lymphocytic leukemia *in vivo* assay in mice (an active fraction possesses a percent T/C value of ≥130). Following solvent partitioning between chloroform and water, the activity was shown to reside in the chloroform fraction, which also demonstrated activity in the 9KB carcinoma of the nasopharynx *in vitro* assay (activity is indicated by $ED_{50}$ values of ≤20 μg/ml for crude fractions and of ≤4 μg/ml for purified materials). TLC analysis of the active chloroform fraction indicated

[1] Complete details concerning *E. cyparissias* fractionation and structural work on isolated materials will be published.
[2] Analtech.
[3] Woelm Pharma, Eschwege, West Germany.
[4] Universal Scientific.
[5] Aldrich Chemical Co.
[6] E. Merck, Darmstadt, West Germany.
[7] The plant material was identified as *Euphorbia cyparissias* L. (Euphorbiaceae) by Dr. C. M. Rogers, Department of Biology, Wayne State University. A voucher specimen (No. 16218) is preserved in the Wayne State University Department of Biology Herbarium.
[8] Celite, Fisher Scientific Co.
[9] Extracts and fractions were tested under the auspices of the Developmental Therapeutics Program, National Cancer Institute (10).

it to be a complex mixture, containing a minimum of 20 components. No information was available to indicate which component was responsible for the observed activity.

The results of dry column separation of the chloroform fraction indicated the presence of at least two active materials (Table I), a higher $R_f$ fraction (Fraction C) possessing *in vitro* KB activity and a more polar fraction (Fraction H) possessing PS activity. While certain additional fractions possessed marginal KB activity, subsequent fractionation efforts were directed at the two most active materials. With biological data available from dry column chromatographic analysis, larger scale gradient-elution column chromatographic procedures could be aimed specifically at the resupply of the active materials.

## DISCUSSION

The complex nature of the biologically active *E. cyparissias* chloroform fraction presented a formidable challenge to the dry column chromatographic technique. Although all components of this mixture were not separated completely (some fractions contain more than one component), useful separation was achieved and, on the basis of dry column chromatographic results, subsequent efforts could be directed toward a limited group of materials possessing bioactivity. The value of the dry column technique in the preliminary analysis of a complex active fraction thus was demonstrated. In examples not presented here, pure materials could be isolated and their activity determined directly from the dry column procedure.

In certain investigations involving the fractionation of biologically active plant or fermentation extracts, a previously isolated active material may be presumed to be responsible for the observed activity based on phytochemical or chemotaxonomic information. Much effort may be saved in these instances by employing the dry column chromatographic procedure as the initial fractionation step. If the $R_f$ of the material is known, the corresponding dry column chromatographic band can be obtained and analyzed for activity as well as for the presence of the known compound.

As indicated in Table I, a developing solvent for dry column chromatographic analysis can be utilized that will produce results roughly similar to those obtained from extensive column chromatographic procedures. By employing dry column procedures first, however, careful liquid chromatographic techniques need only be employed to separate components of active fractions, allowing inactive materials to be collected together. Thus, some time, effort, and expense of conventional techniques may be saved.

The described dry column technique represents only minor modification of previously described dry column chromatographic techniques. Although such methods have not been heavily utilized by the natural product chemist, they should become increasingly important in improving the efficiency and speed of fractionation efforts.

## REFERENCES


(1) S. A. Schepartz, *Cancer Treat. Rep.*, **60**, 975 (1976).

(2) H. Umezawa, in "Methods of Cancer Research," vol. 16, V. T. DeVita, Jr., and H. Busch, Eds., Academic, New York, N.Y., 1979, p. 43.

(3) M. Suffness and J. Douros, in *ibid.*, p. 73.

(4) M. E. Wall, M. C. Wani, and H. Taylor, *Cancer Treat. Rep.*, **60**, 1011 (1976).

(5) P. R. Ocken, *J. Lipid Res.*, **10**, 460 (1969).

(6) B. Loev and M. M. Goodman, in "Progress in Separation and Purification," vol. 3, E. S. Perry and C. J. Van Oss, Eds., Wiley–Interscience, New York, N.Y., 1970, p. 73.

(7) F. M. Rabel, in "Ultrapurity," M. Zief and R. Speights, Eds., Dekker, New York, N.Y., 1972, p. 157.

(8) B. P. Engelbrecht and K. A. Weinberger, *Am. Lab.*, **9**, 71 (1977).

(9) H. Brockmann and H. Schodder, *Chem. Ber.*, **74B**, 73 (1941).

(10) R. L. Geran, N. H. Greenberg, M. M. MacDonald, A. M. Schumacher, and B. J. Abbott, *Cancer Chemother. Rep., Part 3*, **3**, 1 (1972).


## ACKNOWLEDGMENTS


Supported in part by a research grant from the Comprehensive Cancer Center of Metropolitan Detroit.

The authors thank Dr. C. M. Rogers for assistance in identifying plant specimens, Dr. H. N. Abramson and Ms. J. A. Hokanson for assistance in plant collection, and Mr. J. L. Lane and Mr. C. M. McIntyre for technical assistance in conducting the investigation.


# Absorption of Orally Administered Sodium Sulfate in Humans


**DAVID M. COCCHETTO and GERHARD LEVY ˣ**



Received June 23, 1980, from the *Department of Pharmaceutics, School of Pharmacy, State University of New York at Buffalo, Amherst, NY 14260.* Accepted for publication August 28, 1980.



**Abstract** □ Sodium sulfate can be used to enhance the conjugation of phenolic drugs with sulfate and to treat hypercalcemia. It is thought that sulfate ion is absorbed slowly and incompletely from the digestive tract. The purposes of this investigation were to determine the absorption of a large amount of sodium sulfate (18.1 g as the decahydrate, equivalent to 8.0 g of the anhydrous salt) and to compare the bioavailability when this amount is administered orally to normal subjects as a single dose and as four equally divided hourly doses. The 72-hr urinary recovery of free sulfate following single and divided doses was 53.4 ± 15.8 and 61.8 ± 7.8%, respectively (mean ± *SD*, $n=5$, $p > 0.2$). The single dose produced severe diarrhea while the divided doses caused only mild or no diarrhea. Thus, a large amount of sodium sulfate, when administered orally in divided doses over 3 hr, is well tolerated and is absorbed to a significant extent. Orally administered sodium sulfate may be useful for the early treatment of acetaminophen overdose.



**Keyphrases** □ Sodium sulfate—absorption after oral administration, single and divided doses, bioavailability, humans □ Acetaminophen—use of sodium sulfate for early treatment of toxicity, absorption of orally administered sodium sulfate, single and divided doses □ Bioavailability—sodium sulfate, comparison of single and divided doses, role in treatment of acetaminophen toxicity


Humans and animals have a limited capacity to conjugate phenolic drugs with sulfate (1–5). The limiting factor is the availability of sulfate ion rather than its activation or the transfer of activated sulfate to the acceptor molecule (3, 5). Sulfate ion is acquired by the body partly as such from dietary sources and partly by oxidation of cysteine and methionine (6). The possibility of enhancing the formation of phenolic sulfates by direct administration of inorganic sulfate was first proposed in 1876 and has been demonstrated by several investigators (6, 7). Typically,


0022-3549/81/0300-0331$01.00/0


© 1981, American Pharmaceutical Association

it to be a complex mixture, containing a minimum of 20 components. No information was available to indicate which component was responsible for the observed activity.

The results of dry column separation of the chloroform fraction indicated the presence of at least two active materials (Table I), a higher $R_f$ fraction (Fraction C) possessing *in vitro* KB activity and a more polar fraction (Fraction H) possessing PS activity. While certain additional fractions possessed marginal KB activity, subsequent fractionation efforts were directed at the two most active materials. With biological data available from dry column chromatographic analysis, larger scale gradient-elution column chromatographic procedures could be aimed specifically at the resupply of the active materials.

## DISCUSSION

The complex nature of the biologically active *E. cyparissias* chloroform fraction presented a formidable challenge to the dry column chromatographic technique. Although all components of this mixture were not separated completely (some fractions contain more than one component), useful separation was achieved and, on the basis of dry column chromatographic results, subsequent efforts could be directed toward a limited group of materials possessing bioactivity. The value of the dry column technique in the preliminary analysis of a complex active fraction thus was demonstrated. In examples not presented here, pure materials could be isolated and their activity determined directly from the dry column procedure.

In certain investigations involving the fractionation of biologically active plant or fermentation extracts, a previously isolated active material may be presumed to be responsible for the observed activity based on phytochemical or chemotaxonomic information. Much effort may be saved in these instances by employing the dry column chromatographic procedure as the initial fractionation step. If the $R_f$ of the material is known, the corresponding dry column chromatographic band can be obtained and analyzed for activity as well as for the presence of the known compound.

As indicated in Table I, a developing solvent for dry column chromatographic analysis can be utilized that will produce results roughly similar to those obtained from extensive column chromatographic procedures. By employing dry column procedures first, however, careful liquid chromatographic techniques need only be employed to separate components of active fractions, allowing inactive materials to be collected together. Thus, some time, effort, and expense of conventional techniques may be saved.

The described dry column technique represents only minor modification of previously described dry column chromatographic techniques. Although such methods have not been heavily utilized by the natural product chemist, they should become increasingly important in improving the efficiency and speed of fractionation efforts.

## REFERENCES


(1) S. A. Schepartz, *Cancer Treat. Rep.*, **60**, 975 (1976).

(2) H. Umezawa, in "Methods of Cancer Research," vol. 16, V. T. DeVita, Jr., and H. Busch, Eds., Academic, New York, N.Y., 1979, p. 43.

(3) M. Suffness and J. Douros, in *ibid.*, p. 73.

(4) M. E. Wall, M. C. Wani, and H. Taylor, *Cancer Treat. Rep.*, **60**, 1011 (1976).

(5) P. R. Ocken, *J. Lipid Res.*, **10**, 460 (1969).

(6) B. Loev and M. M. Goodman, in "Progress in Separation and Purification," vol. 3, E. S. Perry and C. J. Van Oss, Eds., Wiley–Interscience, New York, N.Y., 1970, p. 73.

(7) F. M. Rabel, in "Ultrapurity," M. Zief and R. Speights, Eds., Dekker, New York, N.Y., 1972, p. 157.

(8) B. P. Engelbrecht and K. A. Weinberger, *Am. Lab.*, **9**, 71 (1977).

(9) H. Brockmann and H. Schodder, *Chem. Ber.*, **74B**, 73 (1941).

(10) R. L. Geran, N. H. Greenberg, M. M. MacDonald, A. M. Schumacher, and B. J. Abbott, *Cancer Chemother. Rep., Part 3*, **3**, 1 (1972).


## ACKNOWLEDGMENTS


Supported in part by a research grant from the Comprehensive Cancer Center of Metropolitan Detroit.

The authors thank Dr. C. M. Rogers for assistance in identifying plant specimens, Dr. H. N. Abramson and Ms. J. A. Hokanson for assistance in plant collection, and Mr. J. L. Lane and Mr. C. M. McIntyre for technical assistance in conducting the investigation.


# Absorption of Orally Administered Sodium Sulfate in Humans


**DAVID M. COCCHETTO and GERHARD LEVY ˣ**



Received June 23, 1980, from the *Department of Pharmaceutics, School of Pharmacy, State University of New York at Buffalo, Amherst, NY 14260.* Accepted for publication August 28, 1980.



**Abstract** □ Sodium sulfate can be used to enhance the conjugation of phenolic drugs with sulfate and to treat hypercalcemia. It is thought that sulfate ion is absorbed slowly and incompletely from the digestive tract. The purposes of this investigation were to determine the absorption of a large amount of sodium sulfate (18.1 g as the decahydrate, equivalent to 8.0 g of the anhydrous salt) and to compare the bioavailability when this amount is administered orally to normal subjects as a single dose and as four equally divided hourly doses. The 72-hr urinary recovery of free sulfate following single and divided doses was 53.4 ± 15.8 and 61.8 ± 7.8%, respectively (mean ± *SD*, $n=5$, $p > 0.2$). The single dose produced severe diarrhea while the divided doses caused only mild or no diarrhea. Thus, a large amount of sodium sulfate, when administered orally in divided doses over 3 hr, is well tolerated and is absorbed to a significant extent. Orally administered sodium sulfate may be useful for the early treatment of acetaminophen overdose.



**Keyphrases** □ Sodium sulfate—absorption after oral administration, single and divided doses, bioavailability, humans □ Acetaminophen—use of sodium sulfate for early treatment of toxicity, absorption of orally administered sodium sulfate, single and divided doses □ Bioavailability—sodium sulfate, comparison of single and divided doses, role in treatment of acetaminophen toxicity


Humans and animals have a limited capacity to conjugate phenolic drugs with sulfate (1–5). The limiting factor is the availability of sulfate ion rather than its activation or the transfer of activated sulfate to the acceptor molecule (3, 5). Sulfate ion is acquired by the body partly as such from dietary sources and partly by oxidation of cysteine and methionine (6). The possibility of enhancing the formation of phenolic sulfates by direct administration of inorganic sulfate was first proposed in 1876 and has been demonstrated by several investigators (6, 7). Typically,


0022-3549/81/0300-0331$01.00/0


© 1981, American Pharmaceutical Association

**Table I—Urinary Excretion of Free Sulfate by Normal Men after Oral Administration of 18 g of Sodium Sulfate Decahydrate in Single and Divided Doses**

| Subject | Age, years | Body Weight, kg | Baseline Excretion Rate, mmoles/24 hr[a] | Cumulative Percent of Dose Excreted | | | | | |
|---|---|---|---|---|---|---|---|---|---|
| | | | | Single Dose | | | Divided Dose[b] | | |
| | | | | 24 hr | 48 hr | 72 hr | 24 hr | 48 hr | 72 hr |
| PM | 25 | 79 | 22.9 ± 2.9 | 24.5 | 27.1 | 38.8 | 37.2 | 49.7 | 57.2 |
| DC | 25 | 66 | 16.7 ± 1.2 | 40.7 | 62.9 | 71.5 | 44.6 | 52.8 | 63.2 |
| DS | 34 | 77 | 24.3 ± 6.5 | 55.2 | 65.3 | 68.9 | 48.3 | 60.0 | 69.3 |
| UW | 36 | 74 | 25.0 ± 6.4 | 44.4 | 49.0 | 39.4 | 59.8 | 60.4 | 68.4 |
| SR | 28 | 66 | 13.0 ± 2.1 | 17.3 | 43.0 | 48.5 | 27.9 | 42.5 | 50.8 |
| Mean | | | | 36.4 | 49.5 | 53.4 | 43.5[c] | 53.1[c] | 61.8[c] |
| *SD* | | | | 15.4 | 15.6 | 15.8 | 12.0 | 7.5 | 7.8 |

[a] Mean ± *SD*, $n = 3$ consecutive days. [b] Four equally divided doses administered at hourly intervals. [c] Not significantly different ($p > 0.1$) from corresponding value after single dose.

sodium sulfate has been administered parenterally but it has also been effective when given orally in small doses (3, 6).

## BACKGROUND

It may be desirable under certain circumstances to administer relatively large doses of sodium sulfate orally, provided that it can be ascertained that the sulfate ion is absorbed reasonably well. For example, intravenous administration of >100 g of sodium sulfate decahydrate to adults is considered to be an effective and relatively safe treatment for hypercalcemia (8). Parenteral administration of sodium sulfate enhances the conjugation of large doses of acetaminophen to acetaminophen sulfate in rats and thereby accelerates drug elimination (5). Overdoses of acetaminophen may cause serious and sometimes fatal hepatotoxicity, apparently due to the formation of one or several quantitatively minor but highly reactive metabolites (9). It is reasonable to assume that enhanced formation of acetaminophen sulfate by a parallel and competing pathway will reduce the formation of hepatotoxic metabolite(s) and thereby reduce the toxicity of acetaminophen (10). In fact, parenteral administration of sodium sulfate reduced the acute toxicity of acetaminophen in mice (11).

Oral administration of a tracer dose of sodium [$^{35}$S]sulfate to normal men resulted in the recovery of ~80% of the radiolabel in the 24-hr urine, compared to a recovery of ~86% following intravenous injection of the same dose (12). However, the intestinal absorption of sulfate ion occurs by active transport, at least in rats, hamsters, and rabbits (13), and, therefore, is subject to saturation. Large doses of sodium sulfate (~15 g of the decahydrate in adults) are used as an osmotic cathartic on the basis that sulfate ion is only slowly and incompletely absorbed (14). No report concerning the actual bioavailability of sodium sulfate administered in such large doses to humans was found.

In view of the potential therapeutic usefulness of systemic sodium sulfate, particularly for reducing or preventing acetaminophen toxicity (10, 11), the absorption of a relatively large amount of sodium sulfate was determined following oral administration to human volunteers as a single large dose and as four equally divided hourly doses.

## EXPERIMENTAL

Five healthy men, who had given their written informed consent, participated in the study. They collected all urine for three separate 24-hr periods for determination of baseline free sulfate output. They then received 18.1 g of sodium sulfate USP (the decahydrate, equivalent to 8.00 g of anhydrous sodium sulfate) orally on two occasions, at least 1 week apart. At these times, the subjects fasted overnight and consumed a low fat breakfast in the morning. They then emptied their bladder and ingested the sodium sulfate dissolved in 50 ml of warm water, either as a single dose or in four equally divided hourly doses. They ate lunch, and their subsequent meals and fluid intake were not restricted or controlled. All urine was collected in sterile plastic bags over 0–24, 24–48, and 48–72 hr. The urines were frozen immediately after collection, pending assay.

The concentration of free (inorganic) sulfate was determined by the method of Häkkinen and Häkkinen (15), which involves precipitation of urinary calcium as the oxalate (to avoid assay interference), precipitation of free sulfate as the barium salt by addition of barium chloranilate, and spectrophotometric assay of the liberated chloranilic acid. Total sulfate (*i.e.*, the sum of free and organically bound sulfate) was determined by the same procedure following acid hydrolysis at 80° (15). The procedures were performed in quadruplicate; one reaction mixture was used to prime the filter paper, which then was used to filter the other three. Results of the three assays were averaged (coefficient of variation usually was ≃5%).

## RESULTS

The results are summarized in Table I. The baseline individual average excretion rate of inorganic sulfate ranged from 13 to 25 mmoles/24 hr and was relatively constant (coefficient of variation of 7–27%). The individuals with the lowest body weight (DC and SR) exhibited the lowest baseline values. Compared with the amount of sodium sulfate taken by the subjects (56.3 mmoles), the baseline excretion rate of inorganic sulfate was substantial.

The baseline excretion rate of free sulfate was not affected by relatively large changes in urine flow rate, but the baseline excretion rate of total sulfate (and, therefore, of organically bound sulfate) increased essentially linearly with increasing urine flow rate (Fig. 1). This differential effect of the urine flow rate also was observed after sodium sulfate administration.

The cumulative amounts of free sulfate excreted in the urine 24, 48, and 72 hr after sodium sulfate administration (*i.e.*, the sum of endogenous and exogenous free sulfate excretion) were significantly larger than the amounts of free sulfate excreted during the same lengths of time in control experiments ($p < 0.01$ by paired $t$ test). The average urinary recovery of administered sulfate, calculated as the 72-hr excretion of free sulfate minus the baseline excretion, averaged 53.4% from the single dose and 61.8% from the divided doses. There was considerably less interindividual variation in urinary recovery of free sulfate from the divided doses (Table I).

All subjects experienced severe diarrhea after the single dose of sodium sulfate, starting typically after 2 hr and lasting up to 24 hr. The same amount of sodium sulfate taken in four equal hourly doses produced either no diarrhea or mild diarrhea of short duration. No other adverse effects were reported.

## DISCUSSION

Sodium [$^{35}$S]sulfate has been used extensively in tracer doses to estimate extracellular fluid volume in humans (12, 16–18). Typically, plasma sulfur 35-derived radioactivity declines biexponentially after intravenous injection, with a terminal apparent half-life of ~4 hr (17). The apparent volume of distribution is usually ~20% of the body volume (12, 17, 18); the renal clearance is ~35 ml/min/1.73 m$^2$ (16, 17), *i.e.*, approximately one-third of the glomerular filtration rate. Since sulfate ion is not appreciably bound to plasma proteins, the difference between its renal clearance and the glomerular filtration rate is probably due to renal tubular reabsorption. The renal tubular reabsorption of sulfate is capacity limited (19). However, the urinary excretion of free sulfate is apparently not urine flow rate dependent, at least in the flow rate range encountered in this study (Fig. 1). That is not so with respect to organically bound (ethereal) sulfate; total nonradioactive sulfate in the urine is, therefore, not a suitable index of sulfate absorption.

Urinary recovery of sulfur 35 activity in humans after administration of a tracer dose of sodium [$^{35}$S]sulfate was ~38% of an oral dose in 5 hr (18), and ~86% in 24 hr (12) and 95% within 5 days (17) after an intravenous dose. It was also reported that 90–100% of a 117-g iv dose of nonradioactive sodium sulfate decahydrate was excreted in the urine within 1 day, but no details were given (8). More than 92% of the radioactivity excreted in the urine within 4 hr after intravenous injection of

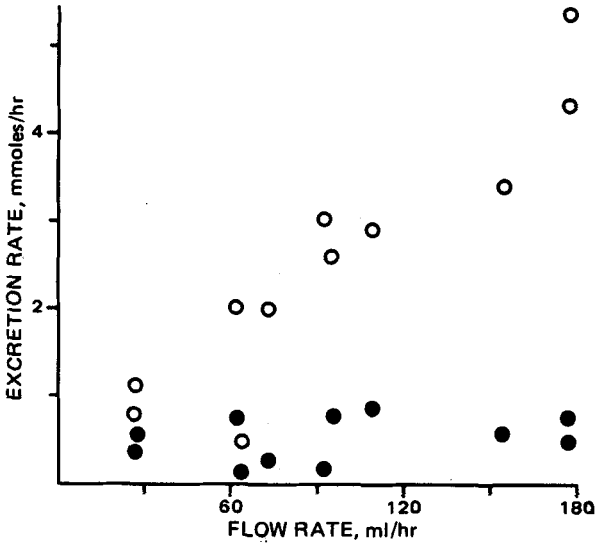


**Figure 1**—*Relationship between urine flow rate and baseline excretion rate of free (●) and total (○) sulfate for Subject DC. Urine was collected every 2–3 hr for 24 hr.*

sodium [$^{35}$S]sulfate is free sulfate, *i.e.*, sulfate ion which could be precipitated as benzidine sulfate (16).

The baseline excretion of free sulfate in the urine (*i.e.*, excretion without administration of a sulfate salt) is affected by the diet, particularly by the intake of proteins and green vegetables (6, 20). Most sulfur excretion is in the form of inorganic sulfate (20, 21). The average baseline urinary excretion rate of free sulfate by normal men is ~22 mmoles/day (22). This rate is substantial when compared with the dose of sodium sulfate used in the present study (56.3 mmoles). Ideally, therefore, the drug should have been administered together with $^{35}$S-labeled sodium sulfate, but it was considered inadvisable to expose the volunteers to sulfur 35, particularly without first attempting to perform the study without radioactive sulfate. This conservative approach was justified by the results. The individual 72-hr urinary recoveries were reasonably consistent, especially after administration of sodium sulfate in divided doses (Table I). Cumulative recovery increased progressively over 3 days, except for Subject UW following the single dose[1]. Thus, the relatively large amount of drug administered and the relatively consistent baseline excretion rate of free sulfate made it possible to conduct this investigation without radioactive tracer.

Considering its pronounced cathartic effect, the single large dose of sodium sulfate was surprisingly well absorbed. However, the same is true in rats. Oral administration of ~250 mg of sodium [$^{35}$S]sulfate/kg to adult male rats resulted in the recovery of 73.7% of the administered radioactivity in the urine, compared with a recovery of 76.7% after intraperitoneal injection (7). Another investigator administered oral doses of 0.35, 0.70, 1.41, and 2.0 g/kg to adult male and female rats and recovered 57–74% of the radioactivity in urine over 72 hr, with no apparent relationship between the dose and urinary recovery (23). The same investigator determined that the median effective laxative dose of sodium sulfate in rats was 1.6 g/kg and that a dose of 1.22 g/kg had no laxative effect, while a dose of 2.8 g/kg was 100% effective by his criteria (23). Thus, the relative bioavailability of sodium sulfate in rats was not affected by the degree of catharsis, which also reflects the relative intestinal motility or transit rate. Our results in men were similar: there was no statistically significant difference in the urinary recovery of free sulfate after administration of a large amount of sodium sulfate as a single dose (which produced severe diarrhea) or in divided doses (which produced little or no diarrhea).

In conclusion, oral administration of sodium sulfate is a viable means of introducing large amounts of free sulfate into the systemic circulation. We also found, in an unpublished study, that sodium sulfate is not significantly adsorbed onto activated charcoal. The latter is effective in inhibiting the absorption of acetaminophen (24). Administration of as little as 2 g of acetaminophen to healthy men caused depletion of endogenous sulfate as reflected by reduced urinary excretion of free sulfate and endogenous sulfate conjugates (25), while administration of sodium sulfate enhanced conjugation of acetaminophen with sulfate in humans and animals (3, 5, 25) and reduced the acute toxicity of acetaminophen in animals (11). Consequently, the combined use of sodium sulfate and activated charcoal, both being widely available home remedies, for the initial treatment of acetaminophen overdose deserves clinical investigation. However, pending such investigation, this treatment is not advocated for routine use and should certainly not take the place of presently accepted therapy.

[1] An apparent decrease in the urinary recovery of free sulfate, as observed in Subject UW from 48 to 72 hr (Table I), can occur if the baseline excretion rate determined in the drug-free control period is higher than the excretion rate of endogenous free sulfate after sodium sulfate administration.

## REFERENCES

(1) G. Levy and T. Matsuzawa, *J. Pharmacol. Exp. Ther.*, **156**, 285 (1967).

(2) G. Levy and H. Yamada, *J. Pharm. Sci.*, **60**, 215 (1971).

(3) J. B. Houston and G. Levy, *ibid.*, **65**, 1218 (1976).

(4) J. B. Houston and G. Levy, *J. Pharmacol. Exp. Ther.*, **198**, 284 (1976).

(5) R. E. Galinsky, J. T. Slattery, and G. Levy, *J. Pharm. Sci.*, **68**, 803 (1979).

(6) I. Smith and P. D. Mitchell, *Biochem. J.*, **142**, 189 (1974).

(7) D. D. Dziewiatkowski, *J. Biol. Chem.*, **178**, 389 (1949).

(8) Z. H. Chakmakjian and J. E. Bethune, *N. Engl. J. Med.*, **275**, 862 (1966).

(9) J. A. Hinson, in "Reviews in Biochemical Toxicology," vol. 2, E. Hodgson, J. R. Bend, and R. M. Philpot, Eds., Elsevier/North-Holland, New York, N.Y., 1980, pp. 103–129.

(10) J. T. Slattery and G. Levy, *Clin. Pharmacol. Ther.*, **25**, 184 (1979).

(11) J. T. Slattery and G. Levy, *Res. Commun. Chem. Pathol. Pharmacol.*, **18**, 167 (1977).

(12) J. H. Bauer, *J. Appl. Physiol.*, **40**, 648 (1976).

(13) C. Anast, R. Kennedy, G. Volk, and L. Adamson, *J. Lab. Clin. Med.*, **65**, 903 (1965).

(14) "The Pharmacological Basis of Therapeutics," L. S. Goodman and A. Gilman, Eds., Macmillan, New York, N.Y., 1975, chap. 49.

(15) I. P. T. Häkkinen and L. M. Häkkinen, *Scand. J. Clin. Lab. Invest.*, **11**, 294 (1959).

(16) M. Walser, D. W. Seldin, and A. Grollman, *J. Clin. Invest.*, **32**, 299 (1953).

(17) R. J. Ryan, L. R. Pascal, T. Inoye, and L. Bernstein, *ibid.*, **35**, 1119 (1956).

(18) P. Omvik, R. C. Tarazi, and E. L. Bravo, *Kidney Int.*, **15**, 71 (1979).

(19) H. W. Smith, "The Kidney," Oxford University Press, New York, N.Y., 1951, pp. 121–126.

(20) T. R. Ittyerah, *Clin. Chim. Acta*, **25**, 365 (1969).

(21) D. B. Papadopoulou, *Clin. Chem.*, **3**, 257 (1957).

(22) "Documenta Geigy, Scientific Tables," K. Diem and C. Lentner, Eds., J. R. Geigy S. A., Basel, Switzerland, 1970, p. 663.

(23) K. Hwang, *Arch. Int. Pharmacodyn. Ther.*, **163**, 302 (1966).

(24) G. Levy and J. B. Houston, *Pediatrics*, **58**, 432 (1976).

(25) H. Büch, W. Rummel, K. Pfleger, C. Eschrich, and N. Texter, *Naunyn-Schmiedebergs Arch. Pharmakol. Exp. Pathol.*, **259**, 276 (1968).

## ACKNOWLEDGMENTS

Supported in part by Grant GM 19568 from the National Institute of General Medical Sciences, National Institutes of Health.

# Degradation of Propildazine in Water

**PAOLO VENTURA, FRANCESCO PARRAVICINI, LUCA SIMONOTTI, RICCARDO COLOMBO, and GIORGIO PIFFERI ***

Received March 26, 1980, from the *Laboratories for Biomedical Research, ISF, 20090 Trezzano s/N, Milan, Italy.* Accepted for publication August 28, 1980.

**Abstract** □ Propildazine degradation in water at pH 7.4 was studied under aerobic conditions. Three main products were isolated by column chromatography and identified on the basis of IR, UV, and NMR spectroscopy and mass spectrometry and by comparison with synthetic samples. Drug disappearance in water was monitored by UV spectroscopy and was concentration, pH, temperature, and oxygen dependent. Propildazine degradation also was followed in methanol at various pH values.

**Keyphrases** □ Propildazine—degradation in water, ionization constants, pKa determination, identification of degradation products □ Antihypertensive agents—propildazine, degradation in water, identification of degradation products □ Degradation—propildazine in water and methanolic solutions, determination of products

Propildazine (I) is a new antihypertensive drug. Because of its potent peripheral vasodilatory action (1, 2), it has been subjected to pharmacological screening (3–5) and clinical trials (6–10). Compound I can be stored easily as the dihydrochloride, but its conjugated bases (monohydrochloride and free base) are, like hydralazine (11), unstable. Therefore, good characterization and understanding of the stability of I in solution are needed for pharmacokinetic and preformulation studies.

This study identified the major degradation products resulting from the hydrolysis of I at pH 7.4; in addition, estimates were made of its hydrolysis in aqueous buffers at pH 6.0, 7.4, and 9.0 at 26 and 37°. Isolation of the degradation products was carried out by preliminary column chromatography and subsequent monitoring by TLC. New structures were elucidated by IR, UV, NMR, and mass spectral techniques. For analytical purposes (12), decomposition of I in methanolic solution was also followed.

## EXPERIMENTAL

**Materials**—All chemicals were reagent grade. Distilled water was used for preparing aqueous solutions[1]. Spectrophotometric grade methanol was used for UV determinations. The identity and purity of I were verified by IR[2], UV[3], NMR[4], and mass[5] spectra, melting point (215–218° dec.), elemental analysis, and TLC [silica gel plates[6] buffered at pH 5; eluent of acetone–0.1 *N* HCl (70:10); $R_f$ 0.68].

**Determination of Ionization Constants**—The pKa values of propildazine were determined at 25°. A 10-ml sample of a $3.7 \times 10^{-3}$ *M* solution of I in water was titrated with 0.01 *N* NaOH ($CO_2$ free). The change in pH as a function of the titrant delivered was monitored by a pH meter[7] equipped with a glass electrode.

The pKa values were estimated to be 3.2 (amine group) and 7.1 (hydrazine group).

**Hydrolytic Degradation**—A solution of 2 g (7.4 mmoles) of I in 2 liters of pH 7.4 phosphate buffer was incubated in daylight at 26°. The degradation of I was monitored by UV detection at 244 nm, and the incubation was stopped after 14 days when the maximum absorbance was obtained. The aqueous solution was evaporated *in vacuo*, and the residue was dried over phosphorus pentoxide, triturated with methanol, and filtered. The solvent was removed, and the resulting syrupy liquid was passed through a silica gel column using methanol–chloroform (2:98) as the eluent. The collected fractions were examined by TLC on silica gel plates developed with chloroform–methanol (80:20).

**Preparation of Standards**—*3-[(2-Hydroxypropyl)methylamino]-pyridazine (II)*—To a solution of 2 g of 3-chloro-6-[(2-hydroxypropyl)methylamino]pyridazine (1) in 40 ml of methanol was added 200 mg of 5% palladium-on-charcoal. The reduction was performed at room temperature under hydrogen (1.3 atm). The catalyst was filtered, the solvent was evaporated, and the residue was treated with alkali and extracted with chloroform.

The extract was dried and the solvent was evaporated to give an oil. This oil was distilled at 150°/0.8 mm Hg to yield 0.84 g (51%) of a pale-yellow oil; IR (liquid film): 3350 (OH) and 1595, 1500, and 805 (pyridazine moiety) $cm^{-1}$; UV (methanol): maxima at 251 and 332 nm; NMR ($CDCl_3$): δ 8.43 (dd, $J$ = 1.5 and 4.5 Hz), 7.2 (dd, $J$ = 4.5 and 9.5 Hz), 6.93 (dd, $J$ = 1.5 and 9.5 Hz, aromatic H), 4.7 (broad OH), 4.19 (m, $CH$–OH), 3.60 (d, $J$ = 5.3 Hz, N–$CH_2$), 3.14 (s, $NCH_3$), and 1.22 (d, $J$ = 6 Hz, $CHCH_3$) ppm; mass spectra (70 ev, 1.5 mamp): *m/z* 167 (23%, $M^+$), 122 (100, [M – $CH_3CHOH]^+$), 109 (37), and 94 (26).

*Anal.*—Calc. for $C_8H_{13}N_3O$: C, 57.46; H, 7.83; N, 25.12. Found: C, 57.59; H, 7.84; N, 25.34.

*3-[(2-Hydroxypropyl)methylamino]pyridazine-6-one (III)*—A solution of 2 g (10 mmoles) of 3-chloro-6-[(2-hydroxypropyl)methylamino]pyridazine (1) and dry potassium acetate (1.18 g, 0.12 mmole) in 20 ml of acetic acid was refluxed for 4 hr. The solvent was removed *in vacuo*, and the residue was hydrolyzed in boiling 10% HCl for 1 hr. The solution was made alkaline with ammonium hydroxide and evaporated *in vacuo*. The resulting oil was passed through a silica gel column and

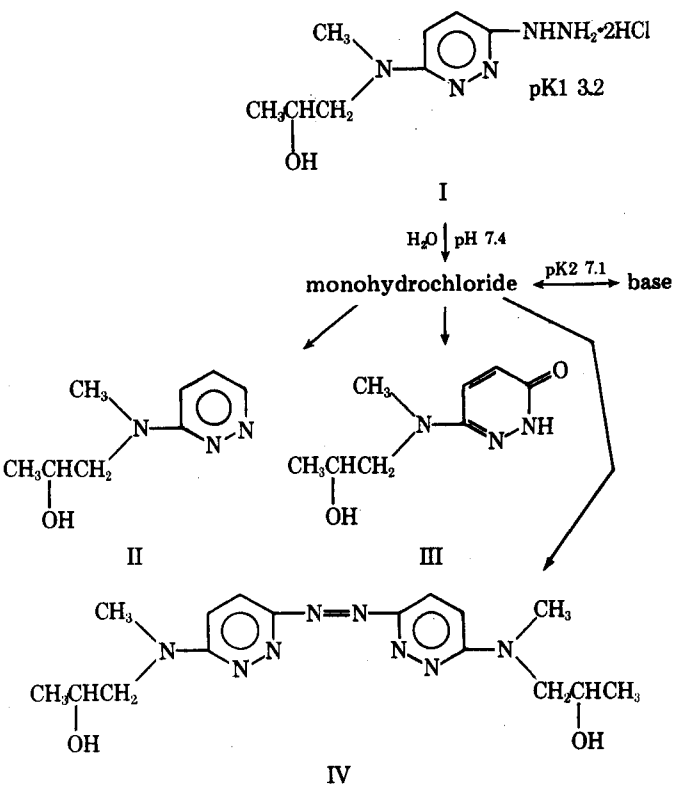


*Scheme I—Proposed degradation pattern of propildazine in aqueous solution.*

[1] Buffers Normex, Carlo Erba, Milan, Italy.
[2] Perkin-Elmer model 177 spectrophotometer.
[3] Beckman DB-GT spectrophotometer.
[4] Perkin-Elmer model R 12 B spectrometer (60 MHz).
[5] Varian MAT model 112 spectrometer.
[6] Silica gel 60-$F_{254}$, Merck, Darmstadt, West Germany.
[7] Corning model 7.



*0022-3549/81/0300-0334$01.00/0*
*© 1981, American Pharmaceutical Association*

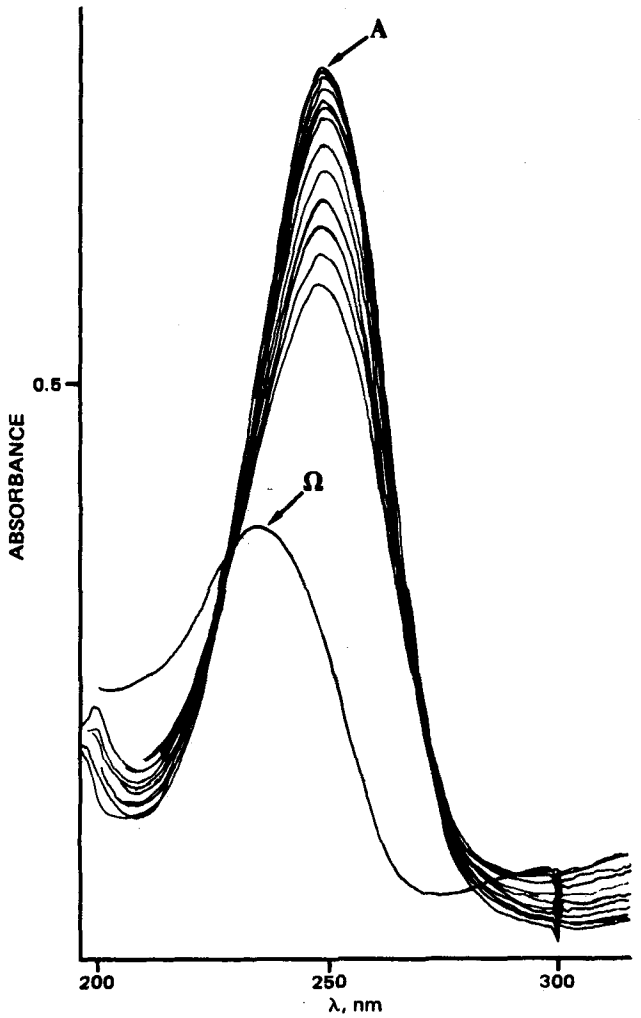


**Figure 1**—*Representative UV absorption spectra of propildazine (pH 7.4, 3.7 × 10⁻⁵ M, 26°) at different times. Key: A, t = 0; and Ω, 10 times the half-life.*

eluted with chloroform–methanol (95:5) to give 0.46 g (25%) of III as a white powder, mp 152–154°, from ether–methanol (90:10); IR (mineral oil): 3260 (OH), 1685 (C=O), and 1600, 1550, and 843 (pyridazine moiety) $cm^{-1}$; UV (water): maxima at 245 and 352 nm; NMR (dimethyl sulfoxide-$d_6$): δ 12.00 (NH), 7.47 and 6.75 (*AB*q, $J_{AB}$ = 10.2 Hz, aromatic H), 4.70 (d, $J$ = 4.7 Hz, CH-*OH*), 3.87 (m, *CH*OH), 3.22 (d, $J$ = 6 Hz, N-$CH_2$), 2.93 (s, $NCH_3$), and 1.05 (d, $J$ = 6 Hz, $CHCH_3$) ppm; mass spectra (70 ev, 1.5 mamp): *m/z* 183 (17%, $M^+$), 138 (100, [M − $CH_3CHOH]^+$), 125 (5), and 110 (22).

*Anal.*—Calc. for $C_8H_{13}N_3O_2$: C, 52.44; H, 7.15; N, 22.93. Found: C, 52.45; H, 7.17; N, 22.89.

*3 - [(2 - Hydroxypropyl)methylamino]-6-isopropylidenehydrazinopyridazine Hydrochloride (V)*—A suspension of I (2.7 g, 10 mmoles) in 50 ml of ethanol was stirred with sodium bicarbonate powder (1.68 g, 20 mmoles) under nitrogen at room temperature for 2 hr. Salts were removed, and the solvent was evaporated *in vacuo*. The resulting syrupy liquid was treated with acetone (15 ml) and cooled to yield 1.85 g (68%) of V as a yellow powder, mp 115–120° dec.; IR (mineral oil): 3420 (OH), 3350 (NH), 1645, 1570, 1520, and 830 (pyridazine moiety) $cm^{-1}$; UV (methanol): maxima at 368 and 280 nm; NMR (dimethyl sulfoxide-$d_6$): δ 8.00 (s, aromatic H), 3.95 (m, CH), 3.43 (d, $J$ = 5.3 Hz, N-$CH_2$), 3.08 (s, N-$CH_3$), 2.10 and 2.07 [s, $C(CH_3)_2$], and 1.09 (d, $J$ = 6.0, CH-$CH_3$) ppm; mass spectrum (70 ev, 1.5 mamp): *m/z* 237 (16%, $M^+$), 222 (100, [M − $CH_3]^+$), and 192 (28, [M − $CH_3CHOH]^+$).

*Anal.*—Calc. for $C_{11}H_{19}N_5O{\cdot}HCl$: C, 48.26; H, 7.36; Cl, 12.95; N, 25.58. Found: C, 48.31; H, 7.37; Cl, 12.92; N, 25.54.

**Degradations**—The aqueous solutions of I (3.7 × $10^{-5}$ *M*, 3.7 × $10^{-4}$ *M*, and 3.7 × $10^{-3}$ *M*) were prepared in phosphate (pH 6.0 and 7.4) and borate (pH 9.0) buffers. The ionic strength was adjusted to 0.13 with potassium chloride. The reaction flasks were kept in a constant-temperature water bath in the dark at 37 or 26°. Aliquots of the solution were withdrawn periodically, and the UV spectra were scanned from 350 to 200 nm. The methanolic solutions of I (1.85 × $10^{-5}$ *M*, 3.7 × $10^{-5}$ *M*, and 3.7 × $10^{-4}$ *M*) were prepared in 1 *N* methanolic HCl, in methanol, and in 0.9 *M* methanolic trimethylamine and maintained in the dark at room temperature. The degradative behavior of these solutions was verified by following the change of their UV spectra as a function of time.

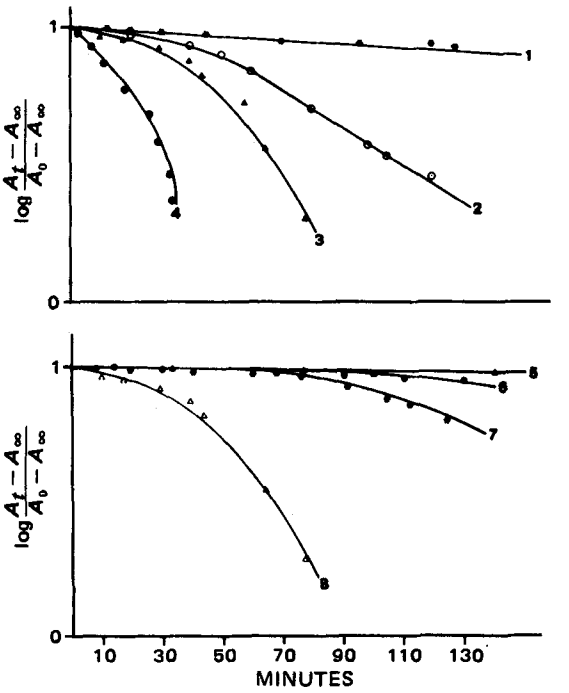


**Figure 2**—*Profiles of logarithmic normalized absorption (254 nm) versus time. Top: Degradation at different oxidative and pH conditions (c 3.7 × $10^{-5}$ M, 37°). Key: 1, anaerobic conditions, pH 7.4; 2, aerobic conditions, pH 6.0; 3, aerobic conditions, pH 7.4; and 4, aerobic conditions, pH 9. Bottom: Degradation at different concentrations and temperatures (aerobic conditions, pH 7.4). Key: 5, c 3.7 × $10^{-3}$ M, 37°; 6, c 3.7 × $10^{-4}$ M, 37°; 7, c 3.7 × $10^{-5}$ M, 26°; and 8, c 3.7 × $10^{-5}$ M, 37°.*

## RESULTS AND DISCUSSION

Three main degradation products, A–C, were isolated on column chromatography (Scheme I).

**Compound A**—The $R_f$ value (0.51) of this oily compound and the IR, UV, NMR, and mass spectra were identical with those of the synthetic standard II.

**Compound B**—The isolated product had an $R_f$ 0.22, and the melting point was undepressed (150–153°) in admixture with the synthetic sample III. The spectral data were consistent with the assigned structure.

**Compound C**—After the separation of B, the eluate was concentrated, and the oily residue was crystallized from chloroform–methanol to afford a bright-yellow product, mp 219–223°, $R_f$ 0.24.

*Anal.*—Calc. for $C_{16}H_{24}N_8O_2$: C, 53.32; H, 6.71; N, 31.08. Found: C, 53.38; H, 6.72; N, 31.02.

The spectra in the UV and visible high region showed an absorption maximum at 420 nm, which shifted to 365 nm after catalytic reduction with palladium-on-charcoal at room temperature and normal pressure. The IR spectra exhibited bands at 3380 $cm^{-1}$ (OH stretching) and at 1590, 1490, 845, and 837 $cm^{-1}$, characteristic of a substituted pyridazine ring. Moreover, the proton resonances in dimethyl sulfoxide solution confirmed the presence of the same side chain already observed in I and II, while the *AB* quartet at 7.84 and 7.33 ($J$ = 10 Hz) was consistent with a 3,6-disubstituted pyridazine structure.

The mass spectrum indicated the presence of a molecular ion at *m/z* 362, corresponding to the reduced hydrazo derivative of IV. This result may be due to reduction of IV by moisture in the mass spectrometer source (13). When deuterium oxide was introduced, peaks at *m/z* 363 and 364 were observed contemporaneously; the fragmentation pattern with peaks at *m/z* 332 and 278 ruled out isotopic substitution on the side chain. All of these data and the elemental analysis were in agreement with the unusual proposed structure bis-3-[6-(2-hydroxypropyl)methylaminopyridazine]diazene (IV).

Propildazine degradation in water was monitored by following the change in absorbance ($A$) at 254 nm as a function of time. Two isosbestic points at 233 and 279 nm were observed (Fig. 1). The logarithms of the normalized difference in the absorbance ($A_t - A_\infty / A_0 - A_\infty$, $A_\infty$ being calculated after about 10 half-lives) were plotted against time (Fig. 2). The resulting profiles are clearly concentration (curves 5, 6, and 8), pH (curves 2–4), and temperature (curves 7 and 8) dependent. Moreover, the behavior at pH 7.4, using water bubbled with nitrogen and maintained under nitrogen, showed that oxygen also plays a significant role in the hydrolytic degradation of I (curves 1 and 3).

Propildazine is stable in acidic methanolic solution (0.1 $N$ methanolic HCl, $\lambda_{max}$ 254 nm unvaried after 2 days), while it is rapidly degraded in methanolic trimethylamine. Moreover, in methanol concentrations of $10^{-5}$ $M$, I showed a UV spectrum that rapidly changed its maximum from 259 to 280 nm. This variation was due to trace amounts of acetone present in the spectroscopic grade methanol which reacted with I. In fact, I is a very strong carbonyl group scavenger, giving rise to the corresponding hydrazone 3-isopropylidenehydrazine-6-[(2-hydroxypropyl)methylamino]pyridazine (V) (see *Experimental*).

It is worthwhile to remember the importance of *in vivo* hydrazone formation (14, 15) to explain the prolonged antihypertensive effect of hydralazine-like compounds.

## REFERENCES


(1) G. Pifferi, F. Parravicini, C. Carpi, and L. Dorigotti, *J. Med. Chem.*, **18**, 741 (1975).

(2) *Drugs of the Future*, **1**, 290 (1976).

(3) L. Dorigotti, R. Rolandi, and C. Carpi, *Pharmacol. Res. Commun.*, **8**, 295 (1976).

(4) L. Dorigotti, C. Semeraro, and C. Carpi, 7th Congress S.S.F.A., Varese, Italy, 1977.

(5) L. Dorigotti, C. Carpi, G. Bertoli, and P. L. Mariani, 7th International Congress of Pharmacology, Paris, France, 1978, Abstract 2693.

(6) C. Bianchini, L. Terzoli, U. Cornelli, C. Sala, G. Leonetti, and A. Zanchetti, 7th Congress S.S.F.A., Varese, Italy, 1977.

(7) R. Ripa, G. Abbondati, B. Frisoni, and G. Tripodi, *Minerva Cardioangiol.*, **23**, 735 (1975).

(8) R. Ripa, G. Abbondati, B. Frisoni, E. Farabegoli, and G. Tripodi, *ibid.*, **23**, 901 (1975).

(9) R. Pellegrini and G. Abbondati, *Farmaco, Ed. Prat.*, **32**, 19 (1977).

(10) R. Ripa, G. Tripodi, and B. Frisoni, *Arch. Med. Intern.*, **29**, 17 (1977).

(11) Z. H. Israili and P. G. Dayton, *Drug Metab. Rev.*, **6**, 283 (1977), and references cited therein.

(12) P. Ventura, M. Zanol, M. Visconti, and G. Pifferi, *J. Chromatogr.*, **161**, 237 (1978).

(13) S. Ukai, K. Hirose, A. Tatematsu, and T. Goto, *Tetrahedron Lett.*, **49**, 4999 (1967).

(14) K. D. Haegele, A. J. McLean, P. du Souich, K. Barron, J. Laquer, J. L. McNay, and O. Carrier, *Br. J. Clin. Pharmacol.*, **5**, 489 (1978).

(15) A. J. McLean, K. Barron, P. du Souich, K. D. Haegele, J. L. McNay, O. Carrier, and A. Briggs, *J. Pharmacol. Exp. Ther.*, **205**, 418 (1978).


## ACKNOWLEDGMENTS


The authors thank Dr. Maura Moggia and Dr. Marco Visconti for help in the preparation of this manuscript.


# High-Pressure Liquid Chromatography of Nadolol and Other β-Adrenergic Blocking Drugs


**BHUPENDRA R. PATEL, JOEL J. KIRSCHBAUM ˣ, and RAYMOND B. POET**



Received June 23, 1980, from the *Squibb Institute for Medical Research, New Brunswick, NJ 08903.* Accepted for publication September 3, 1980.



**Abstract** □ A high-pressure liquid chromatographic assay was developed for the analysis of the β-adrenergic blocking agent nadolol as a bulk material or formulated in a tablet. Other β-adrenergic blocking drugs such as acebutolol, alprenolol, atenolol, metoprolol, oxprenolol, pindolol, practolol, propranolol, sotalol, and timolol can be chromatographed in this system. An ethylsilane column and a mobile phase consisting of 35% methanol–65% aqueous 0.0005 $M$ hydrochloric acid–0.05 $M$ sodium chloride are used. Detection is either at 254 nm with a fixed UV wavelength detector or at the peak maximum of 220 nm with a variable-wavelength detector. As exemplified by nadolol, the drug content can be quantitated with or without atenolol as an internal standard.



**Keyphrases** □ Nadolol—high-pressure liquid chromatographic analysis □ β-Adrenergic blockers—high-pressure liquid chromatographic analysis □ High-pressure liquid chromatography—analysis, nadolol and 10 other β-adrenergic agents


β-Adrenergic blocking drugs are presently being used for the treatment of diseases characterized by excess sympathetic nervous activity (1). These illnesses range from cardiac arrhythmia, sinus tachycardia, angina pectoris, hypertension, and migraine to anxiety, essential tremor, alcoholism, and drug dependence.

A high-pressure liquid chromatographic (HPLC) assay was developed for nadolol, *cis*-5-[3-((1,1-dimethylethyl)amino)-2-hydroxypropoxyl] - 1,2,3,4 - tetrahydro-2,3-naphthalenediol, a potent β-adrenergic blocking drug, both as bulk material and in tablets. The chromatographic system also elutes other β-adrenergic blocking agents such as acebutolol, alprenolol, atenolol, metoprolol, oxprenolol, pindolol, practolol, propranolol, sotalol, and timolol at convenient retention times. An analytical profile on nadolol was published previously (2). Nadolol was determined in tablets using colorimetry (3) and in serum using GLC–mass spectrometry (4) or fluorometry (5).

The reported chromatographic procedures are mainly for β-adrenergic blocking agents in body fluids: propranolol in plasma (6–11), atenolol in plasma (12, 13), alprenolol in serum (14), oxprenolol in blood or plasma (15, 16) and in liver tissue (17), acebutolol in serum (18), and practolol in plasma and urine (19). Presumably, these methods could be modified for bulk and formulated material.

## EXPERIMENTAL

**Materials**—Acebutolol[1], alprenolol[2], atenolol[3], metoprolol[4], nadolol[5], oxprenolol[4], pindolol[6], practolol[7], propranolol[5], sotalol[8], and timolol[9] were

[1] May and Baker.
[2] Astra Pharmaceuticals.
[3] Stuart Pharmaceuticals.
[4] Ciba-Geigy.
[5] E. R. Squibb and Sons.
[6] Sandoz Pharmaceuticals.
[7] Ayerst Laboratories.
[8] Mead Johnson.
[9] Merck & Co.




0022-3549/81/0300-0336$01.00/0


© 1981, American Pharmaceutical Association

Propildazine degradation in water was monitored by following the change in absorbance ($A$) at 254 nm as a function of time. Two isosbestic points at 233 and 279 nm were observed (Fig. 1). The logarithms of the normalized difference in the absorbance ($A_t - A_\infty / A_0 - A_\infty$, $A_\infty$ being calculated after about 10 half-lives) were plotted against time (Fig. 2). The resulting profiles are clearly concentration (curves 5, 6, and 8), pH (curves 2–4), and temperature (curves 7 and 8) dependent. Moreover, the behavior at pH 7.4, using water bubbled with nitrogen and maintained under nitrogen, showed that oxygen also plays a significant role in the hydrolytic degradation of I (curves 1 and 3).

Propildazine is stable in acidic methanolic solution (0.1 $N$ methanolic HCl, $\lambda_{max}$ 254 nm unvaried after 2 days), while it is rapidly degraded in methanolic trimethylamine. Moreover, in methanol concentrations of $10^{-5}$ $M$, I showed a UV spectrum that rapidly changed its maximum from 259 to 280 nm. This variation was due to trace amounts of acetone present in the spectroscopic grade methanol which reacted with I. In fact, I is a very strong carbonyl group scavenger, giving rise to the corresponding hydrazone 3-isopropylidenehydrazine-6-[(2-hydroxypropyl)methylamino]pyridazine (V) (see *Experimental*).

It is worthwhile to remember the importance of *in vivo* hydrazone formation (14, 15) to explain the prolonged antihypertensive effect of hydralazine-like compounds.

## REFERENCES


(1) G. Pifferi, F. Parravicini, C. Carpi, and L. Dorigotti, *J. Med. Chem.*, **18**, 741 (1975).

(2) *Drugs of the Future*, **1**, 290 (1976).

(3) L. Dorigotti, R. Rolandi, and C. Carpi, *Pharmacol. Res. Commun.*, **8**, 295 (1976).

(4) L. Dorigotti, C. Semeraro, and C. Carpi, 7th Congress S.S.F.A., Varese, Italy, 1977.

(5) L. Dorigotti, C. Carpi, G. Bertoli, and P. L. Mariani, 7th International Congress of Pharmacology, Paris, France, 1978, Abstract 2693.

(6) C. Bianchini, L. Terzoli, U. Cornelli, C. Sala, G. Leonetti, and A. Zanchetti, 7th Congress S.S.F.A., Varese, Italy, 1977.

(7) R. Ripa, G. Abbondati, B. Frisoni, and G. Tripodi, *Minerva Cardioangiol.*, **23**, 735 (1975).

(8) R. Ripa, G. Abbondati, B. Frisoni, E. Farabegoli, and G. Tripodi, *ibid.*, **23**, 901 (1975).

(9) R. Pellegrini and G. Abbondati, *Farmaco, Ed. Prat.*, **32**, 19 (1977).

(10) R. Ripa, G. Tripodi, and B. Frisoni, *Arch. Med. Intern.*, **29**, 17 (1977).

(11) Z. H. Israili and P. G. Dayton, *Drug Metab. Rev.*, **6**, 283 (1977), and references cited therein.

(12) P. Ventura, M. Zanol, M. Visconti, and G. Pifferi, *J. Chromatogr.*, **161**, 237 (1978).

(13) S. Ukai, K. Hirose, A. Tatematsu, and T. Goto, *Tetrahedron Lett.*, **49**, 4999 (1967).

(14) K. D. Haegele, A. J. McLean, P. du Souich, K. Barron, J. Laquer, J. L. McNay, and O. Carrier, *Br. J. Clin. Pharmacol.*, **5**, 489 (1978).

(15) A. J. McLean, K. Barron, P. du Souich, K. D. Haegele, J. L. McNay, O. Carrier, and A. Briggs, *J. Pharmacol. Exp. Ther.*, **205**, 418 (1978).


## ACKNOWLEDGMENTS


The authors thank Dr. Maura Moggia and Dr. Marco Visconti for help in the preparation of this manuscript.


# High-Pressure Liquid Chromatography of Nadolol and Other β-Adrenergic Blocking Drugs


**BHUPENDRA R. PATEL, JOEL J. KIRSCHBAUM ˣ, and RAYMOND B. POET**



Received June 23, 1980, from the *Squibb Institute for Medical Research, New Brunswick, NJ 08903.* Accepted for publication September 3, 1980.



**Abstract** □ A high-pressure liquid chromatographic assay was developed for the analysis of the β-adrenergic blocking agent nadolol as a bulk material or formulated in a tablet. Other β-adrenergic blocking drugs such as acebutolol, alprenolol, atenolol, metoprolol, oxprenolol, pindolol, practolol, propranolol, sotalol, and timolol can be chromatographed in this system. An ethylsilane column and a mobile phase consisting of 35% methanol–65% aqueous 0.0005 $M$ hydrochloric acid–0.05 $M$ sodium chloride are used. Detection is either at 254 nm with a fixed UV wavelength detector or at the peak maximum of 220 nm with a variable-wavelength detector. As exemplified by nadolol, the drug content can be quantitated with or without atenolol as an internal standard.



**Keyphrases** □ Nadolol—high-pressure liquid chromatographic analysis □ β-Adrenergic blockers—high-pressure liquid chromatographic analysis □ High-pressure liquid chromatography—analysis, nadolol and 10 other β-adrenergic agents


β-Adrenergic blocking drugs are presently being used for the treatment of diseases characterized by excess sympathetic nervous activity (1). These illnesses range from cardiac arrhythmia, sinus tachycardia, angina pectoris, hypertension, and migraine to anxiety, essential tremor, alcoholism, and drug dependence.

A high-pressure liquid chromatographic (HPLC) assay was developed for nadolol, *cis*-5-[3-((1,1-dimethylethyl)amino)-2-hydroxypropoxyl] - 1,2,3,4 - tetrahydro-2,3-naphthalenediol, a potent β-adrenergic blocking drug, both as bulk material and in tablets. The chromatographic system also elutes other β-adrenergic blocking agents such as acebutolol, alprenolol, atenolol, metoprolol, oxprenolol, pindolol, practolol, propranolol, sotalol, and timolol at convenient retention times. An analytical profile on nadolol was published previously (2). Nadolol was determined in tablets using colorimetry (3) and in serum using GLC–mass spectrometry (4) or fluorometry (5).

The reported chromatographic procedures are mainly for β-adrenergic blocking agents in body fluids: propranolol in plasma (6–11), atenolol in plasma (12, 13), alprenolol in serum (14), oxprenolol in blood or plasma (15, 16) and in liver tissue (17), acebutolol in serum (18), and practolol in plasma and urine (19). Presumably, these methods could be modified for bulk and formulated material.

## EXPERIMENTAL

**Materials**—Acebutolol[1], alprenolol[2], atenolol[3], metoprolol[4], nadolol[5], oxprenolol[4], pindolol[6], practolol[7], propranolol[5], sotalol[8], and timolol[9] were

[1] May and Baker.
[2] Astra Pharmaceuticals.
[3] Stuart Pharmaceuticals.
[4] Ciba-Geigy.
[5] E. R. Squibb and Sons.
[6] Sandoz Pharmaceuticals.
[7] Ayerst Laboratories.
[8] Mead Johnson.
[9] Merck & Co.




0022-3549/81/0300-0336$01.00/0


© 1981, American Pharmaceutical Association

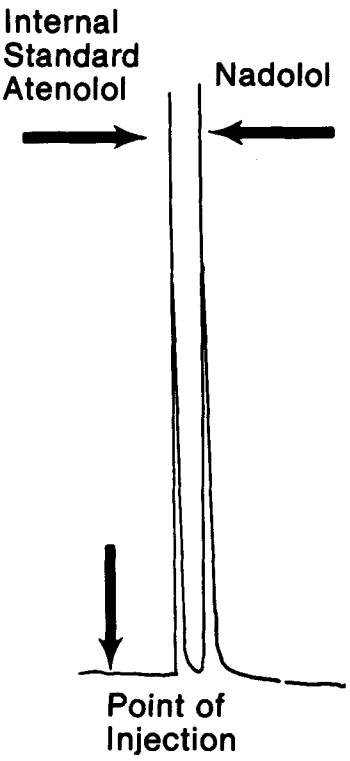


**Figure 1**—*High-pressure liquid chromatogram of nadolol with atenolol as an internal standard. The void volume was at ~3 min, atenolol eluted in ~4.5 min, and nadolol eluted in ~6 min. Detection was at 254 nm.*

used as received. Distilled water was double distilled and stored in glass. HPLC grade methanol, ACS reagent grade sodium chloride, and concentrated hydrochloric acid were obtained commercially[10].

**Apparatus**—A pump[11] capable of maintaining a constant flow at 200–2000 psig delivered degassed mobile phase at a flow rate of 1.2 ml/min. A precision loop injector[12], with a nominal capacity of 20 μl, was attached to a reversed-phase, ethylsilane (RP-2), 10-μm, 250-mm long × 4.6-mm i.d. prepacked column[13] through an inlet filter[14]. The column outlet was connected to a fixed-wavelength detector[15] with the peak maximum at 254 nm or to a variable-wavelength monitor[16] set at 220 nm. The strip-chart recorders[17], 25 cm, had input capability for receiving the detector output. The system was washed with methanol–water (1:1) at the end of the day.

**Mobile Phase**—The mobile phase was 35% methanol–65% aqueous 0.0005 *M* hydrochloric acid–0.05 *M* sodium chloride. One milliliter of 0.1 *M* HCl was added to ~1200 ml of double-distilled water in a 2-liter glass-stoppered graduated cylinder, and then 5.84 g of sodium chloride was added. The solution was mixed to dissolve the salt, and then 700 ml of methanol was added and mixed. The volume was adjusted with additional double-distilled water, and the solution was mixed and then filtered through a medium-porosity sintered-glass funnel. The apparent pH was ~4.5.

**Standard or Bulk Drug Solution**—A solution containing 0.2 mg of nadolol standard or bulk drug/ml of mobile phase was used.

**Tablet Analysis**—A ground tablet, equivalent to ~50 mg of drug, was weighed accurately into a 250-ml volumetric flask. Nadolol was extracted into 200 ml of the mobile phase by ultrasonicating the flask for 15 min. The volume of the solution was adjusted to the 250-ml mark with additional mobile phase. The solution was filtered through a 0.45-μm solvent inert filter or was centrifuged.

**Tablet Analysis Using Internal Standard**—Each 20.0 ml of tablet extract and standard solution, containing 0.5 mg of nadolol/ml, was fortified with 5.0 ml of atenolol solution (1.2 mg/ml in mobile phase) as an internal standard.

**System Suitability Test**—A solution containing nadolol and atenolol (0.4 and 0.24 mg/ml, respectively, in the mobile phase) was injected. The resolution, $R_s$, should be above 1.7 for the two peaks and is calculated

[10] Fisher Scientific.
[11] Altex model 110A or Waters M6000.
[12] Rheodyne model 7010.
[13] LiChrosorb, E. Merck.
[14] Rheodyne model 7362.
[15] Altex model 153 or Chromatronix model 220.
[16] Schoeffel model 770 or Varian Varichrome.
[17] Linear Inc.

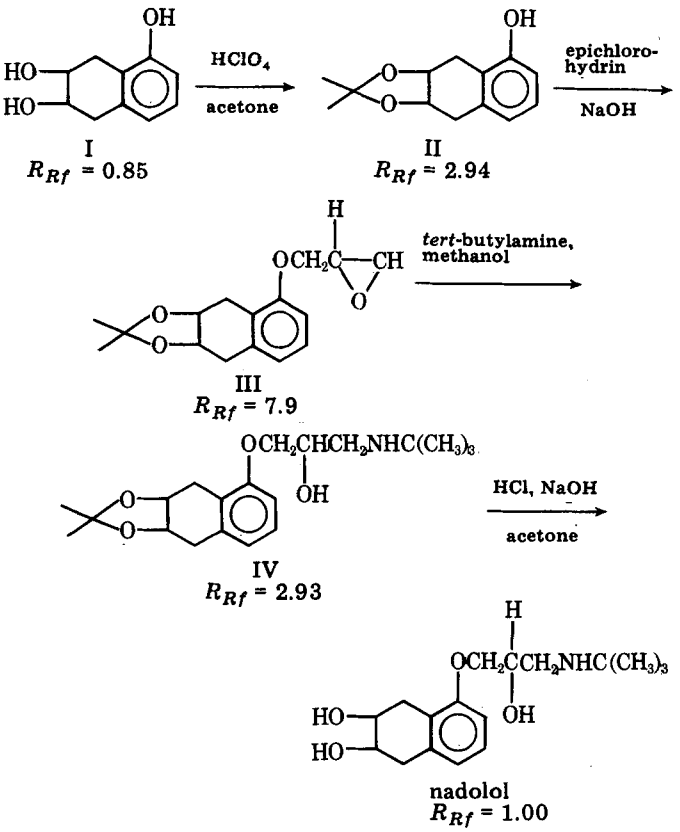


*Scheme I—Relative retention times ($R_{Rf}$) or α of the intermediates in the synthesis of nadolol.*

using the formula $R_s = 2(t_2 - t_1)/(w_1 + w_2)$, where $t_1$ and $t_2$ are the retention times and $w_1$ and $w_2$ are the respective peak widths expressed in the same units.

## RESULTS AND DISCUSSION

Nadolol tablets with potencies of 40–320 mg were analyzed with and without an internal standard. Figure 1 shows a sample chromatogram of nadolol when atenolol was used as an internal standard. The mean peak heights of atenolol and nadolol, using the recommended procedure, were 12.98 and 13.25 cm with relative standard deviations of 0.5 and 0.4%, respectively, for seven repetitive injections. When the ratios of peak heights of nadolol to atenolol were calculated, the series gave a relative standard deviation of 0.4%, which was insignificant.

The use of an internal standard is not necessary if the chromatograph is equipped with a precision loop injector. However, the nadolol–atenolol solution is recommended for the system suitability test. Nadolol tablets were analyzed using HPLC as well as TLC on silica gel plates developed with acetone–chloroform–2 *M* ammonium hydroxide (8:1:1). The results obtained by the two techniques were similar with an average difference of 1% and served to validate the two methods. When the tablets were analyzed with or without atenolol as an internal standard, the results did not vary by more than 1%. Recoveries of nadolol added to placebo formulations were 100.4 and 100.6%. UV detector responses for nadolol at 220 and 254 nm were linear for concentrations of 0.025–0.2 μg/ml and passed through the origin. Detection at 220 nm was ~25 times more sensitive than at 254 nm, but no impurities were detected in the standard at either wavelength.

Scheme I gives the structures of the synthetic intermediates and their relative retention times ($R_{Rf}$ or α of nadolol = 1.0), demonstrating the selectivity of the chromatographic system. Several possible impurities were synthesized. When added to a solution of nadolol and injected into the chromatographic system, all were completely resolved, showing that the method is stability indicating.

The retention times relative to nadolol for 10 other β-adrenergic blocking drugs are presented in Table I. If desired, minor modifications can be made in the mobile phase and flow rate to optimize the retention time and peak shape. For example, to quantitate propranolol (as the hydrochloride), 15% more methanol was added to the mobile phase to halve the retention time to ~8 min. Five repetitive injections gave an

**Table I—Retention Times of β-Adrenergic Blocking Agents Compared to Nadolol**

| Compound | Structure | $R_{Rf}$ |
|---|---|---|
| Acebutolol | 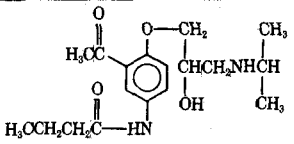 | 1.50 |
| Alprenolol | 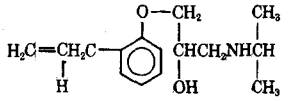 | 4.68 |
| Atenolol | 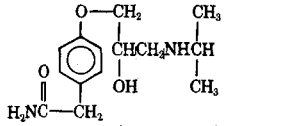 | 0.65 |
| Metoprolol | 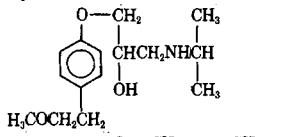 | 1.75 |
| Nadolol | 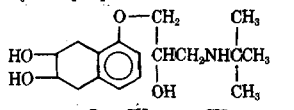 | 1.00 |
| Oxprenolol | 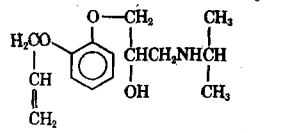 | 2.7 |
| Pindolol | 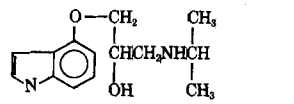 | 1.29 |
| Practolol | 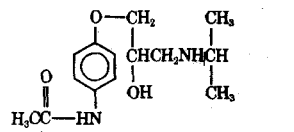 | 0.80 |
| Propranolol | 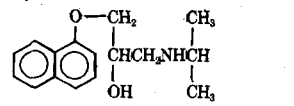 | 2.7 |
| Sotalol | 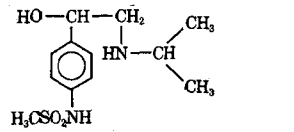 | 1.38 |
| Timolol | 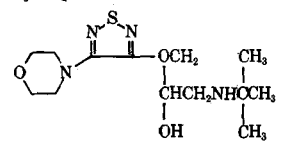 | 1.45 |

[a] Retention time of agent divided by nadolol retention time.

average peak height of 9.47 cm ($RSD$ = 0.5%). The response to various concentrations from 0.025 to 0.2 μg/ml was linear and passed through the origin. The relative standard deviation of the normalized response was 0.5%. The experimentally observed relative retention times (Table I) can be used to calculate Hansch π values. A straight line was found, as was predicted previously (20), for atenolol, practolol, metoprolol, oxprenolol, and alprenolol.

Although use of an ethylsilane (RP-2) column is recommended, a reasonable peak shape for nadolol may be obtained with an octylsilane (RP-8) column. A broader peak with longer retention was obtained with an octadecylsilane (RP-18) column. Although RP-18 columns give higher theoretical plate counts with nadolol, the peaks are sharper and more symmetrical with RP-2 columns.

In conclusion, nadolol and 10 other β-adrenergic blocking agents are analyzable by one HPLC system. One agent may be used as an internal standard for another.

## REFERENCES


(1) R. Clarkson, H. Tucker, and J. Wale, "Annual Reports in Medicinal Chemistry," Academic, New York, N.Y., 1975, pp. 10, 51.

(2) K. Florey and L. Slusarek, "Analytical Profiles of Drug Substances," vol. 9, Academic, New York, N.Y., 1980, pp. 455–486.

(3) E. Ivashikiv, *J. Pharm. Sci.*, **67**, 1024 (1978).

(4) P. T. Funke, M. F. Malley, E. Ivashkiv, and A. I. Cohen, *ibid.*, **67**, 653 (1978).

(5) E. Ivashkiv, *ibid.*, **66**, 1168 (1977).

(6) A. M. Taburet, A. A. Taylor, J. R. Mitchell, D. E. Rollins, and J. L. Pool, *Life Sci.*, **24**, 209 (1979).

(7) S. Caccia, G. Guiso, M. Ballabio, and P. DePonte, *J. Chromatogr.*, **172**, 457 (1979).

(8) G. Nygard, W. H. Shelver, and S. K. Wahba Khalil, *J. Pharm. Sci.*, **68**, 379 (1979).

(9) K. Y. Lee, D. Nurok, and A. Zlatkis, *J. Chromatogr.*, **158**, 403 (1978).

(10) R. L. Nation, G. W. Peng, and W. L. Chiou, *ibid.*, **145**, 429 (1978).

(11) E. Disalle, K. M. Baker, S. R. Bareggi, W. D. Watkins, C. A. Chidsey, A. Frigerio, and P. L. Morselli, *ibid.*, **84**, 347 (1973).

(12) O. H. Weddle, E. N. Amick, and W. D. Mason, *J. Pharm. Sci.*, **67**, 1033 (1978).

(13) B. Scales and P. B. Copsey, *J. Pharm. Pharmacol.*, **27**, 430 (1975).

(14) K. O. Borg, M. Gabrielsson, and T. E. Joensson, *Acta Pharm. Suec.*, **11**, 313 (1974).

(15) D. B. Jack and W. Reiss, *J. Chromatogr.*, **88**, 173 (1974).

(16) S. F. Tsuei, J. Thomas, and R. G. Moore, *ibid.*, **181**, 135 (1980).

(17) J. S. Oliver and A. A. Watson, *Med. Sci. Law*, **17**, 279 (1977).

(18) J. M. Steyn, *J. Chromatatogr.*, **120**, 465 (1976).

(19) J. P. Desager and C. Harvengt, *J. Pharm. Pharmacol.*, **27**, 52 (1975).

(20) J. K. Baker, *Anal. Chem.*, **51**, 1693 (1979).


## ACKNOWLEDGMENTS


The authors express their appreciation to Dr. G. Brewer and Dr. K. Florey for their encouragement and suggestions. They also thank Mrs. L. Kerr and Mrs. M. Iko for their technical assistance and Ms. R. Fox for the synthetic intermediates and compounds related to nadolol. They are grateful to Mr. H. Roberts and Ms. E. Proctor for their TLC data and to Dr. John K. Baker, University of Mississippi, for his astute reading of this manuscript and for calculating the Hansch π values.

# Antihyperlipidemic Activity of Amine Cyanoboranes, Amine Carboxyboranes, and Related Compounds

**I. H. HALL *x, M. K. DAS ‡, F. HARCHELROAD, Jr. ‡, P. WISIAN-NEILSON ‡, A. T. McPHAIL ‡, and B. F. SPIELVOGEL ‡**

Received May 16, 1980, from the *Division of Medicinal Chemistry, School of Pharmacy, University of North Carolina, Chapel Hill, NC 27514, and the ‡Paul M. Gross Chemical Laboratory, Duke University, Durham, NC 27706. Accepted for publication September 10, 1980.

**Abstract** □ A series of amine cyanoboranes and amine carboxyboranes were observed to be antihyperlipidemic agents in mice; *i.e.*, they lowered serum cholesterol and triglyceride levels significantly. These compounds appeared to inhibit lipid synthesis in the early stages. The ability to lower serum cholesterol levels appeared to correlate with the suppression of the regulatory enzyme of cholesterol synthesis, β-hydroxy-β-methylglutaryl-CoA reductase activity. The reduction of serum triglycerides correlated with the ability of the borane compound to suppress liver fatty acid synthetase activity.

**Keyphrases** □ Amine carboxyboranes—borane analogs of α-amino acids, evaluation for antihyperlipidemic activity, mice □ Amine cyanoboranes—borane analogs of α-amino acids, evaluation for antihyperlipidemic activity, mice □ Antihyperlipidemic activity—effects of amine cyanoboranes and amine carboxyboranes on serum cholesterol and triglyceride levels in mice

The antineoplastic (1) and anti-inflammatory (2) activities of a series of amine cyanoboranes, amine carboxyboranes (boron analogs of amino acids), and related analogs in mice were reported previously. While studying the metabolic effects of the cyanoborane derivatives in Ehrlich ascites cells, it was noted that a number of these analogs significantly reduced the activity of the regulatory enzymes of cholesterol synthesis. For example, trimethylamine cyanoborane reduced the enzymatic activity of β-hydroxy-β-methylglutaryl-CoA reductase activity by 25%. This observation suggested that the amine cyanoborane and amine carboxyborane analogs should be screened for antihyperlipidemic effects. Those studies are now reported.

## EXPERIMENTAL

**Compounds**—The following reagents were purchased: *tert*-butylamine borane[1] [$(CH_3)_3CNH_2{\cdot}BH_3$] (I), morpholine borane[1] [$O(CH_2CH_2)_2NH{\cdot}BH_3$] (II), trimethylamine borane[2] [$(CH_3)_3N{\cdot}BH_3$] (III), and dimethylamine borane[2] [$(CH_3)_2NH{\cdot}BH_3$] (IV). Trimethylamine cyanoborane [$(CH_3)_3N{\cdot}BH_2CN$] (V), dimethylamine cyanoborane [$(CH_3)_2NH{\cdot}BH_2CN$] (VI), trimethylamine-*N*-ethylamidoborane [$(CH_3)_3N{\cdot}BH_2C(O)N(CH_2CH_3)H$] (VII), trimethylamine carboxyborane [$(CH_3)_3N{\cdot}BH_2COOH$] (VIII), trimethylamine iodoborane [$(CH_3)_3N{\cdot}BH_2I$] (IX), and hexakis(ammonia cyanoborane)sodium iodide {$[Na(NH_3{\cdot}BH_2CN)_6]I$} (X) were prepared by procedures outlined previously (1).

Likewise, the following were prepared by previously outlined procedures (2): *N,N,N′,N′*-tetramethylethylenediamine-bis(cyanoborane) $[CH_2N(CH_3)_2{\cdot}BH_2CN]_2$ (XI), *N,N,N′,N′*-tetramethylethylenediamine-bis(carboxyborane) $[CH_2N(CH_3)_2{\cdot}BH_2COOH]_2$ (XII), *N,N,N′,N′*-tetramethylethylenediamine-bis(*N*-ethylamidoborane) $[CH_2N(CH_3)_2{\cdot}BH_2C(O)NHCH_2CH_3]_2$ (XIII), *N*-methylmorpholine cyanoborane $[O(CH_2CH_2)_2N(CH_3)_2{\cdot}BH_2CN]$ (XIV), pyridine cyanoborane ($C_5H_5N{\cdot}BH_2CN$) (XV), pyridine carboxyborane ($C_5H_5N{\cdot}BH_2COOH$) (XVI), ammonia cyanoborane ($NH_3{\cdot}BH_2CN$) (XVII), trimethylamine carboethoxyborane $[(CH_3)_3N{\cdot}BH_2COOCH_2CH_3]$ (XVIII), 3-dimethylaminoproprionitrile cyanoborane $[NCCH_2CH_2N(CH_3)_2{\cdot}BH_2CN]$ (XIX), and ethylenediamine-bis(cyanoborane) $(CH_2NH_2{\cdot}BH_2CN)_2$ (XX).

Ammonia carboxyborane ($NH_3{\cdot}BH_2COOH$) (XXI), the boron analog of glycine, was prepared by an amine-displacement reaction on $(CH_3)_3N{\cdot}BH_2COOH$ with liquid ammonia (3). Similarly, methylamine carboxyborane ($CH_3NH_2{\cdot}BH_2COOH$) (XXII) and dimethylamine carboxyborane [$(CH_3)_2NH{\cdot}BH_2COOH$] (XXIII) were prepared by amine-displacement reactions on $(CH_3)_3N{\cdot}BH_2COOH$ with the appropriate amine (4). Sodium dimethylaminohydroborate [$Na(CH_3)_2NBH_3$] (XXIV) was obtained commercially[3].

**Serum Antihyperlipidemic Effects**—$CF_1$ male mice (~30 g) were fed rodent laboratory food with water *ad libitum* during the experiment. Drugs were suspended in 1% carboxymethylcellulose–water and homogenized. Doses were calculated on weekly weights of the mice (5). Test compounds were administered at 20 mg/kg/day ip. On Days 9 and 16, blood was collected by tail vein bleeding in alkali-free, nonheparinized microcapillary tubes and centrifuged 3 min to obtain the serum. Duplicate 30-μl samples of nonhemolyzed serum were used to determine the serum cholesterol levels (milligram percent) by a modification of the Liebermann–Burchard reaction (6). A separate group of mice were bled on Day 14, and their serum triglyceride levels (milligram percent) were determined by using 25-μl samples (7).

**Enzymatic Assays**—Compounds were tested *in vitro* at $10^{-5}$ *M* concentrations for their effects on enzymatic activity of a 10% liver homogenate prepared in 0.25 *M* sucrose and 0.001 *M* ethylenediaminetetraacetic acid, pH 7.2. Adenosine triphosphate citrate-lyase activity was measured by the method of Hoffmann *et al.* (8). Acetyl-CoA synthetase activity was determined by the method of Goodridge (9). The acetyl-CoA formed from each enzymatic reaction was coupled with hydroxylamine to produce acetohydroxamide, which was measured at 540 nm. Acetyl-CoA carboxylase activity was measured by the method of Greenspan and Lowenstein (10), utilizing sodium-[$^3$H]bicarbonate (6.2 mCi/mmole) after 30 min of incubation at 37° for polymerization of the enzymes (11).

Fatty acid synthetase activity was determined by the method of Brady *et al.* (12), utilizing [2′-$^{14}$C]malonyl-CoA (37.5 mCi/mmole) incorporated into newly synthesized fatty acids. [$^{14}$C]Acetate (57.8 mCi/mmole) incorporation into cholesterol (β-hydroxy-β-methylglutaryl-CoA reductase activity) was measured as described by Haven *et al.* (13) and extracted by the method of Wada *et al.* (14).

## RESULTS AND DISCUSSION

The amine cyanoborane and amine carboxyborane compounds significantly reduced serum cholesterol levels in mice after 16 days of dosing (Table I). Compound XXI demonstrated the best inhibitory effect by causing 56% reduction of serum cholesterol at 20 mg/kg/day. Compounds IV, VII, and VIII caused >40% inhibition while I, II, X, XV, XVIII, XXII, and XXIII caused >30% inhibition of serum cholesterol levels. The serum triglyceride levels also were lowered after 14 days of treatment with the borane derivatives; V, XVIII, XXII, and XXIV caused >40% reduction. Compounds VII, VIII, IX, XII, and XV–XIX reduced the serum triglyceride levels at least 30%, whereas II and XXIII caused a 20% reduction.

With *in vitro* enzymatic assays, it was demonstrated that acetyl-CoA synthetase activity was suppressed >50% by II and XV and 40% by IV, V, X, XVI, XVIII, XIX, XXII, and XXIV (Table II). Compounds VIII, IX, XVII, XX, and XXIII caused at least 30% inhibition. Citrate-lyase activity was inhibited at least 30% by VI, XIV, and XV and 20% by II, III, V, IX–XI, XVII, and XVIII. β-Hydroxy-β-methylglutaryl-CoA reductase activity was inhibited 62% by XXI and 50% by IV. Compounds V, VIII, XI–XV, XVIII, XX, and XXIII suppressed this enzymatic activity by

[1] Alfa Products.
[2] Aldrich Chemical Co.
[3] Callery Chemical Co.

0022-3549/81/0300-0339$01.00/0
© 1981, American Pharmaceutical Association

**Table I—Effects of Boron Analogs on Serum Lipids in Mice ($n = 8$)**

| Compound | Formula | Dose, mg/kg | Percent of Control, $\bar{x} \pm SD$ Serum Cholesterol Day 9 | Serum Cholesterol Day 16 | Serum Triglyceride, Day 14 |
|---|---|---|---|---|---|
| I | $(CH_3)_3CNH_2{\cdot}BH_3$ | 10 | $77 \pm 5^a$ | $64 \pm 8^a$ | $90 \pm 7$ |
| II | $O(CH_2CH_2)_2NH{\cdot}BH_3$ | 20 | $67 \pm 6^a$ | $64 \pm 5^a$ | $74 \pm 9^a$ |
| III | $(CH_3)_3N{\cdot}BH_3$ | 20 | $91 \pm 7^b$ | $70 \pm 3^a$ | $85 \pm 5^a$ |
| IV | $(CH_3)_2NH{\cdot}BH_3$ | 20 | $71 \pm 4^a$ | $58 \pm 5^a$ | $88 \pm 11$ |
| V | $(CH_3)_3N{\cdot}BH_2CN$ | 20 | $92 \pm 8^a$ | $72 \pm 6^a$ | $58 \pm 9^a$ |
| VI | $(CH_3)_2NH{\cdot}BH_2CN$ | 20 | $88 \pm 5^b$ | $72 \pm 7^a$ | $98 \pm 9$ |
| VII | $(CH_3)_3N{\cdot}BH_2C(O)NHCH_2CH_3$ | 20 | $81 \pm 5^a$ | $58 \pm 6^a$ | $64 \pm 7^a$ |
| VIII | $(CH_3)_3N{\cdot}BH_2COOH$ | 20 | $68 \pm 6^a$ | $51 \pm 6^a$ | $61 \pm 5^a$ |
| IX | $(CH_3)_3N{\cdot}BH_2I$ | 20 | $100 \pm 7$ | $85 \pm 5^a$ | $65 \pm 8^a$ |
| X | $[Na][NH_3{\cdot}BH_2(CN)]_6]I$ | 20 | $88 \pm 6^b$ | $64 \pm 5^a$ | — |
| XI | $[CH_2N(CH_3)_2{\cdot}BH_2CN]_2$ | 20 | $88 \pm 6^b$ | $73 \pm 7^a$ | $89 \pm 7^b$ |
| XII | $[CH_2N(CH_3)_2{\cdot}BH_2COOH]_2$ | 20 | $95 \pm 4$ | $89 \pm 5^c$ | $89 \pm 10$ |
| XIII | $[CH_2N(CH_3)_2{\cdot}BH_2C(O)NHCH_2CH_3]_2$ | 20 | $100 \pm 3$ | $90 \pm 4^c$ | $68 \pm 6^a$ |
| XIV | $O(CH_2CH_2)_2NCH_3{\cdot}BH_2CN$ | 5 | $84 \pm 7^a$ | $73 \pm 8^a$ | $95 \pm 11$ |
| XV | $C_5H_5N{\cdot}BH_2CN$ | 5 | $81 \pm 8^a$ | $66 \pm 3^a$ | $70 \pm 7^a$ |
| XVI | $C_5H_5N{\cdot}BH_2COOH$ | 5 | $82 \pm 4^a$ | $71 \pm 5^a$ | $60 \pm 8^a$ |
| XVII | $NH_3{\cdot}BH_2CN$ | 5 | $89 \pm 7^b$ | $85 \pm 5^a$ | $64 \pm 4^a$ |
| XVIII | $(CH_3)_3N{\cdot}BH_2COOCH_2CH_3$ | 20 | $76 \pm 7^a$ | $64 \pm 6^a$ | $57 \pm 5^a$ |
| XIX | $NCCH_2CH_2N(CH_3)_2{\cdot}BH_2CN$ | 20 | $98 \pm 6$ | $76 \pm 7$ | $66 \pm 9$ |
| XX | $(CH_2NH_2{\cdot}BH_2CN)_2$ | 5 | $83 \pm 7^a$ | $96 \pm 7^a$ | $84 \pm 4^a$ |
| XXI | $NH_3{\cdot}BH_2COOH$ | 20 | $56 \pm 5$ | $44 \pm 6$ | $101 \pm 10$ |
| XXII | $CH_3NH_2{\cdot}BH_2COOH$ | 20 | $66 \pm 5^a$ | $66 \pm 5^a$ | $55 \pm 6^a$ |
| XXIII | $(CH_3)_2NH{\cdot}BH_2COOH$ | 20 | $65 \pm 6^a$ | $63 \pm 4^a$ | $77 \pm 8^a$ |
| XXIV | $Na(CH_3)_2NBH_3$ | 20 | $74 \pm 4^a$ | $74 \pm 5^a$ | $59 \pm 9^a$ |
| Carboxymethylcellulose (1%) | | | $100 \pm 5^e$ | $100 \pm 6^e$ | $100 \pm 8^f$ |

[a] $p \leq 0.001$. [b] $p \leq 0.025$. [c] $p \leq 0.010$. [d] 115 mg %. [e] 118 mg %. [f] 130 mg %.

**Table II—*In Vitro* Effects of Boron Analogs on Regulatory Enzymes of Cholesterol and Triglyceride Synthesis**

| Compound | Percent of Control, $\bar{x} \pm SD$ Acetyl-CoA Synthetase | Citrate-lyase | β-Hydroxy-β-methylglutaryl CoA Reductase | Acetyl-CoA Carboxylase | Fatty Acid Synthetase |
|---|---|---|---|---|---|
| I | $78 \pm 6^a$ | $97 \pm 6$ | $79 \pm 8^a$ | $95 \pm 6$ | $100 \pm 10$ |
| II | $43 \pm 5^a$ | $79 \pm 5^a$ | $118 \pm 9$ | $82 \pm 7^b$ | $92 \pm 9^a$ |
| III | $77 \pm 8^a$ | $72 \pm 6^a$ | $74 \pm 8^a$ | $86 \pm 7^c$ | $79 \pm 10^b$ |
| IV | $59 \pm 7^a$ | $96 \pm 7$ | $50 \pm 5^a$ | $83 \pm 6^b$ | $98 \pm 9$ |
| V | $50 \pm 7^a$ | $79 \pm 8^a$ | $64 \pm 7^a$ | $100 \pm 9$ | $64 \pm 7^a$ |
| VI | $71 \pm 8^a$ | $67 \pm 7^a$ | $106 \pm 8^a$ | $100 \pm 4$ | $77 \pm 8^a$ |
| VII | — | — | — | — | — |
| VIII | $60 \pm 9^a$ | $100 \pm 8$ | $61 \pm 9^a$ | $100 \pm 5$ | $62 \pm 5^d$ |
| IX | $69 \pm 5^a$ | $77 \pm 5^a$ | $89 \pm 7^c$ | $79 \pm 6^a$ | $76 \pm 7^a$ |
| X | $50 \pm 7^a$ | $71 \pm 7^a$ | $74 \pm 8^a$ | — | — |
| XI | $76 \pm 5^a$ | $70 \pm 6^a$ | $58 \pm 6^a$ | $103 \pm 8$ | $100 \pm 9$ |
| XII | $89 \pm 8^c$ | $99 \pm 5$ | $62 \pm 4^a$ | $106 \pm 7$ | $100 \pm 11$ |
| XIII | $80 \pm 9^a$ | $80 \pm 7^a$ | $64 \pm 6^a$ | $113 \pm 7$ | $65 \pm 8^a$ |
| XIV | $77 \pm 7^a$ | $67 \pm 7^a$ | $62 \pm 5^a$ | $118 \pm 9$ | $89 \pm 7^c$ |
| XV | $49 \pm 6^a$ | $67 \pm 8^a$ | $58 \pm 7^a$ | $78 \pm 8^b$ | $102 \pm 8$ |
| XVI | $50 \pm 4^a$ | $86 \pm 4^a$ | $72 \pm 8^a$ | $82 \pm 5^b$ | $92 \pm 6$ |
| XVII | $61 \pm 7^a$ | $78 \pm 10^a$ | $74 \pm 7^a$ | $94 \pm 6$ | $100 \pm 11$ |
| XVIII | $55 \pm 8^a$ | $72 \pm 5^a$ | $61 \pm 6^a$ | $65 \pm 4^a$ | $92 \pm 9$ |
| XIX | $54 \pm 5^a$ | $94 \pm 6$ | $78 \pm 6^a$ | $100 \pm 7$ | $87 \pm 8^c$ |
| XX | $66 \pm 6^a$ | $102 \pm 5$ | $56 \pm 5^a$ | $100 \pm 7$ | $99 \pm 10$ |
| XXI | — | $100 \pm 4$ | $38 \pm 7^a$ | $101 \pm 8$ | $70 \pm 7^a$ |
| XXII | $55 \pm 7^a$ | $100 \pm 8$ | $100 \pm 8$ | $40 \pm 6^a$ | $72 \pm 7^a$ |
| XXIII | $63 \pm 4^a$ | $100 \pm 11$ | $60 \pm 5^a$ | $75 \pm 5^a$ | $83 \pm 9^c$ |
| XXIV | $53 \pm 7^a$ | $93 \pm 9$ | $87 \pm 4^a$ | $101 \pm 8$ | $100 \pm 10$ |
| Carboxymethylcellulose (1%) | $100 \pm 5^d$ | $100 \pm 4^e$ | $100 \pm 4^f$ | $100 \pm 7^g$ | $100 \pm 6^h$ |

[a] $p \leq 0.001$. [b] $p \leq 0.010$. [c] $p \leq 0.025$. [d] 28.5 mg of acetyl-CoA formed/g of wet tissue in 30 min. [e] 30.5 mg of citrate hydrolyzed/g of wet tissue in 30 min. [f] 1,142,065 dpm/g of wet tissue in 60 min. [g] 32,010 dpm/g of wet tissue in 30 min. [h] 37,656 dpm/g of wet tissue in 30 min.

at least 35%; I, III, X, XVI, XVII, and XIX suppressed this activity by 20%. Acetyl-CoA carboxylase activity was inhibited >20% by IX, XV, and XXIII, whereas XXII caused 60% inhibition of enzymatic activity. Fatty acid synthetase activity was suppressed >30% by V, VIII, and XIII and 20% by III, VI, IX, XXI, and XXII.

The ability to lower serum cholesterol levels appeared to correlate positively with the suppression of the regulatory enzyme of cholesterol synthesis, β-hydroxy-β-methylglutaryl-CoA reductase. For example, XXI lowered serum cholesterol levels and β-hydroxy-β-methylglutaryl-CoA reductase activity maximally. Compound IV followed the same pattern. The ability to lower serum triglyceride levels appeared to correlate positively with the inhibition of fatty acid synthetase activity, as seen with V, VIII, and XIII. Fatty acid synthetase is required for fatty acid synthesis, which is needed for triglyceride synthesis. Specific boron analogs inhibited acetyl-CoA carboxylase, the regulatory enzyme of fatty acid synthesis, and adenosine triphosphate citrate-lyase, a hydrolytic enzyme needed for the cleavage of citrate from the mitochondria to acetyl-CoA. However, the inhibition of neither enzyme seemed to correlate directly with the ability of the boron analogs to suppress serum cholesterol and triglyceride levels.

The ability to lower acetyl-CoA synthetase enzymatic activity appeared to be linked to both the ability to lower serum cholesterol and triglyceride levels, as observed with II, IV, V, VIII, XV, XVI, XVIII, and XXII–XXIV. Acetyl-CoA synthetase is required in the activation of acetate in the cytoplasm for the synthesis of cholesterol and fatty acids. Thus, it was demonstrated that the amine cyanoborane and carboxyborane an-

alogs were potent antihyperlipidemic agents in mice by suppressing both cholesterol and triglyceride levels. The probable site of action of the boron analogs is in the early synthesis of lipids.

### REFERENCES

(1) I. H. Hall, C. O. Starnes, B. F. Spielvogel, P. Wisian-Neilson, M. K. Das, and L. Wojnowich, *J. Pharm. Sci.*, **68**, 685 (1979).

(2) I. H. Hall, C. O. Starnes, A. T. McPhail, P. Wisian-Neilson, M. K. Das, F. Harchelroad, Jr., and B. F. Spielvogel, *ibid.*, **69**, 1025 (1980).

(3) B. F. Spielvogel, M. K. Das, A. T. McPhail, K. D. Onan, and I. H. Hall, *J. Am. Chem. Soc.*, **102**, 6343 (1980).

(4) B. F. Spielvogel, in "Boron Chemistry," R. W. Parry and G. Kodama, Eds., Pergamon, New York, N.Y., 1980, p. 119.

(5) I. H. Hall and G. L. Carlson, *J. Med. Chem.*, **19**, 1257 (1976).

(6) A. T. Ness, J. V. Pastewka, and A. C. Peacock, *Clin. Chim. Acta*, **10**, 229 (1964).

(7) J. M. Chapman, G. H. Cocolas, and I. H. Hall, *J. Med. Chem.*, **22**, 1399 (1980).

(8) G. Hoffmann, L. Weiss, and O. H. Wieland, *Anal. Biochem.*, **84**, 441 (1978).

(9) A. G. Goodridge, *J. Biol. Chem.*, **248**, 4318 (1973).

(10) M. D. Greenspan and J. M. Lowenstein, *ibid.*, **243**, 6273 (1968).

(11) T. P. Cas and S. Rous, *Life Sci.*, **22**, 2067 (1978).

(12) R. O. Brady, R. M. Bradley, and E. G. Trams, *J. Biol. Chem.*, **235**, 3093 (1960).

(13) G. T. Haven, J. R. Krzemien, and T. T. Nguyen, *Res. Commun. Chem. Pathol. Pharmacol.*, **6**, 253 (1960).

(14) F. Wada, K. Hirata, and Y. Sakamato, *J. Biochem.*, **65**, 171 (1969).

# Inhibition of Histidine Decarboxylase by Imidazole Derivatives

**JAMES L. KELLEY ˣ, ED W. McLEAN, and CARL A. MILLER**

Received July 9, 1980, from *Wellcome Research Laboratories, Research Triangle Park, NC 27709.* Accepted for publication September 17, 1980.

**Abstract** □ A series of 4-imidazolylmethyl arylsulfides, sulfoxides, and sulfones and two carbon isosteres of 4-imidazolylmethylphenyl sulfide (I) were synthesized and tested for inhibition of histidine decarboxylase from rat stomach. None of these analogs of I met the criterion of a potent and specific inhibitor of histidine decarboxylase.

**Keyphrases** □ Imidazoles, 4-substituted—synthesis and evaluation for inhibition of histidine decarboxylase □ Histidine decarboxylase—inhibition, synthesis and evaluation of 4-substituted imidazoles □ Structure–activity relationships—synthesis and evaluation of 4-substituted imidazoles for inhibition of histidine decarboxylase

Due to the implication of histamine in many physiological processes (1, 2), there has been interest in regulating its *de novo* biosynthesis by inhibiting histidine decarboxylase (EC 4.1.1.22) (3–7). A specific and potent inhibitor of this enzyme would be important as a new type of antihistamine and as a useful research tool. The authors previously reported on some derivatives of histidine as candidate inhibitors of histidine decarboxylase from rat stomach (3, 4). This paper summarizes the synthesis and evaluation of some 4-substituted imidazoles as inhibitors of this pharmacologically important enzyme.

## DISCUSSION

The imidazolyl sulfides in Table I were prepared by reaction of the appropriate 4-imidazolylalkyl chloride with a mercaptan by a modification of a literature method (7, 8). Oxidation of I or II with hydrogen peroxide gave the sulfoxides VI and VIII or sulfones VII and IX. If the reactions were heated, partial decomposition occurred and the yields were diminished. Application of the Wittig reaction to 4-(*N*-triphenylmethyl)imidazolecarboxaldehyde (4), followed by removal of the trityl group and catalytic hydrogenation, gave IV and V.

Inhibition of histidine decarboxylase was measured as described previously (3). The inhibition obtained with I and II was in close agreement with reported values (7). Varying the nature of the bridge between the imidazole and phenyl rings resulted in a loss in inhibition relative to I (II–IX in Table II). Insertion of nitrogen in the phenyl ring (X and XI) also was deleterious to activity. Substitution of a methyl group on the bridge (XII) gave some enhancement in inhibition with an $I_{50}$ of $4.7 \pm 0.3 \times 10^{-5}$ *M*. Extending the chain length (XIII and XIV) resulted in a loss in inhibition.

In conclusion, several alterations in the structure of I were made, but none of the analogs met the criteria of a potent and specific inhibitor of histidine decarboxylase.

## EXPERIMENTAL[1]

Each analytical sample had spectral data compatible with its assigned structure and moved as a single spot on TLC. The analytical samples gave combustion values for carbon, hydrogen, and nitrogen within 0.4% of the theoretical values.

**4-Imidazolylmethylphenyl Sulfide Hydrochloride (I)**—*Method A*—To an ice bath-cooled solution of 3.24 g (60.0 mmoles) of sodium methoxide in 100 ml of ethanol was added 6.15 ml (60.0 mmoles) of thiophenol, followed by the addition of 4.45 g (29.0 mmoles) of 4-chloromethylimidazole hydrochloride (8, 9) in 25 ml of ethanol. After 1 hr, the ice bath was removed, and the reaction was stirred at ambient temperature for several hours. The mixture was filtered, and the filtrates were spin evaporated *in vacuo*.

The residue was dissolved in 10% HCl and extracted with ether to remove the excess thiol. The aqueous solution was adjusted to pH 8–9 with 1 *M* NaOH and extracted with ether. The combined extracts were washed with water and brine and then dried. Spin evaporation gave an oil, which was converted to the solid hydrochloride and recrystallized.

*Method B*—The reaction was carried out with an equimolar quantity of mercaptan. The reaction mixture was spin evaporated to give a residue. This residue was dissolved in chloroform, washed with water, dried, and reevaporated prior to hydrochloride formation.

**4-Imidazolylmethylphenyl Sulfone Hydrochloride (VII): *Method C***—A solution of 3.13 g (13.8 mmoles) of I and 15 ml of 30% aqueous hydrogen peroxide in 20 ml of acetic acid was stirred at ambient temperature for 20 hr. The reaction was poured over 200 ml of ether containing 10 ml of hydrogen chloride-saturated ethanol, and the mixture was stirred vigorously to induce the oil to solidify. The solvent was decanted from the semisolid, a moderate amount of ethanol was added, and the mixture was stirred until a crystalline solid was formed. The product was collected, washed with ether, and recrystallized.

**1-(4-Imidazolyl)-2-phenylethylene Hydrochloride (IV)**—To a

[1] Melting points were taken in capillary tubes on a Mel-Temp block and are uncorrected.

0022-3549/81/0300-0341$01.00/0
© 1981, American Pharmaceutical Association

alogs were potent antihyperlipidemic agents in mice by suppressing both cholesterol and triglyceride levels. The probable site of action of the boron analogs is in the early synthesis of lipids.

### REFERENCES

(1) I. H. Hall, C. O. Starnes, B. F. Spielvogel, P. Wisian-Neilson, M. K. Das, and L. Wojnowich, *J. Pharm. Sci.*, **68**, 685 (1979).

(2) I. H. Hall, C. O. Starnes, A. T. McPhail, P. Wisian-Neilson, M. K. Das, F. Harchelroad, Jr., and B. F. Spielvogel, *ibid.*, **69**, 1025 (1980).

(3) B. F. Spielvogel, M. K. Das, A. T. McPhail, K. D. Onan, and I. H. Hall, *J. Am. Chem. Soc.*, **102**, 6343 (1980).

(4) B. F. Spielvogel, in "Boron Chemistry," R. W. Parry and G. Kodama, Eds., Pergamon, New York, N.Y., 1980, p. 119.

(5) I. H. Hall and G. L. Carlson, *J. Med. Chem.*, **19**, 1257 (1976).

(6) A. T. Ness, J. V. Pastewka, and A. C. Peacock, *Clin. Chim. Acta*, **10**, 229 (1964).

(7) J. M. Chapman, G. H. Cocolas, and I. H. Hall, *J. Med. Chem.*, **22**, 1399 (1980).

(8) G. Hoffmann, L. Weiss, and O. H. Wieland, *Anal. Biochem.*, **84**, 441 (1978).

(9) A. G. Goodridge, *J. Biol. Chem.*, **248**, 4318 (1973).

(10) M. D. Greenspan and J. M. Lowenstein, *ibid.*, **243**, 6273 (1968).

(11) T. P. Cas and S. Rous, *Life Sci.*, **22**, 2067 (1978).

(12) R. O. Brady, R. M. Bradley, and E. G. Trams, *J. Biol. Chem.*, **235**, 3093 (1960).

(13) G. T. Haven, J. R. Krzemien, and T. T. Nguyen, *Res. Commun. Chem. Pathol. Pharmacol.*, **6**, 253 (1960).

(14) F. Wada, K. Hirata, and Y. Sakamato, *J. Biochem.*, **65**, 171 (1969).

# Inhibition of Histidine Decarboxylase by Imidazole Derivatives

**JAMES L. KELLEY ˣ, ED W. McLEAN, and CARL A. MILLER**

Received July 9, 1980, from *Wellcome Research Laboratories, Research Triangle Park, NC 27709.* Accepted for publication September 17, 1980.

**Abstract** □ A series of 4-imidazolylmethyl arylsulfides, sulfoxides, and sulfones and two carbon isosteres of 4-imidazolylmethylphenyl sulfide (I) were synthesized and tested for inhibition of histidine decarboxylase from rat stomach. None of these analogs of I met the criterion of a potent and specific inhibitor of histidine decarboxylase.

**Keyphrases** □ Imidazoles, 4-substituted—synthesis and evaluation for inhibition of histidine decarboxylase □ Histidine decarboxylase—inhibition, synthesis and evaluation of 4-substituted imidazoles □ Structure–activity relationships—synthesis and evaluation of 4-substituted imidazoles for inhibition of histidine decarboxylase

Due to the implication of histamine in many physiological processes (1, 2), there has been interest in regulating its *de novo* biosynthesis by inhibiting histidine decarboxylase (EC 4.1.1.22) (3–7). A specific and potent inhibitor of this enzyme would be important as a new type of antihistamine and as a useful research tool. The authors previously reported on some derivatives of histidine as candidate inhibitors of histidine decarboxylase from rat stomach (3, 4). This paper summarizes the synthesis and evaluation of some 4-substituted imidazoles as inhibitors of this pharmacologically important enzyme.

## DISCUSSION

The imidazolyl sulfides in Table I were prepared by reaction of the appropriate 4-imidazolylalkyl chloride with a mercaptan by a modification of a literature method (7, 8). Oxidation of I or II with hydrogen peroxide gave the sulfoxides VI and VIII or sulfones VII and IX. If the reactions were heated, partial decomposition occurred and the yields were diminished. Application of the Wittig reaction to 4-(*N*-triphenylmethyl)imidazolecarboxaldehyde (4), followed by removal of the trityl group and catalytic hydrogenation, gave IV and V.

Inhibition of histidine decarboxylase was measured as described previously (3). The inhibition obtained with I and II was in close agreement with reported values (7). Varying the nature of the bridge between the imidazole and phenyl rings resulted in a loss in inhibition relative to I (II–IX in Table II). Insertion of nitrogen in the phenyl ring (X and XI) also was deleterious to activity. Substitution of a methyl group on the bridge (XII) gave some enhancement in inhibition with an $I_{50}$ of $4.7 \pm 0.3 \times 10^{-5}$ *M*. Extending the chain length (XIII and XIV) resulted in a loss in inhibition.

In conclusion, several alterations in the structure of I were made, but none of the analogs met the criteria of a potent and specific inhibitor of histidine decarboxylase.

## EXPERIMENTAL[1]

Each analytical sample had spectral data compatible with its assigned structure and moved as a single spot on TLC. The analytical samples gave combustion values for carbon, hydrogen, and nitrogen within 0.4% of the theoretical values.

**4-Imidazolylmethylphenyl Sulfide Hydrochloride (I)**—*Method A*—To an ice bath-cooled solution of 3.24 g (60.0 mmoles) of sodium methoxide in 100 ml of ethanol was added 6.15 ml (60.0 mmoles) of thiophenol, followed by the addition of 4.45 g (29.0 mmoles) of 4-chloromethylimidazole hydrochloride (8, 9) in 25 ml of ethanol. After 1 hr, the ice bath was removed, and the reaction was stirred at ambient temperature for several hours. The mixture was filtered, and the filtrates were spin evaporated *in vacuo*.

The residue was dissolved in 10% HCl and extracted with ether to remove the excess thiol. The aqueous solution was adjusted to pH 8–9 with 1 *M* NaOH and extracted with ether. The combined extracts were washed with water and brine and then dried. Spin evaporation gave an oil, which was converted to the solid hydrochloride and recrystallized.

*Method B*—The reaction was carried out with an equimolar quantity of mercaptan. The reaction mixture was spin evaporated to give a residue. This residue was dissolved in chloroform, washed with water, dried, and reevaporated prior to hydrochloride formation.

**4-Imidazolylmethylphenyl Sulfone Hydrochloride (VII): *Method C***—A solution of 3.13 g (13.8 mmoles) of I and 15 ml of 30% aqueous hydrogen peroxide in 20 ml of acetic acid was stirred at ambient temperature for 20 hr. The reaction was poured over 200 ml of ether containing 10 ml of hydrogen chloride-saturated ethanol, and the mixture was stirred vigorously to induce the oil to solidify. The solvent was decanted from the semisolid, a moderate amount of ethanol was added, and the mixture was stirred until a crystalline solid was formed. The product was collected, washed with ether, and recrystallized.

**1-(4-Imidazolyl)-2-phenylethylene Hydrochloride (IV)**—To a

[1] Melting points were taken in capillary tubes on a Mel-Temp block and are uncorrected.

0022-3549/81/0300-0341$01.00/0
© 1981, American Pharmaceutical Association

**Table I—4-Substituted Imidazoles**

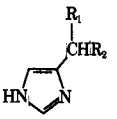

| Compound | $R_1$ | $R_2$ | Method | Yield, % | Melting Point | Formula | | Analysis, % Calc. | Found |
|---|---|---|---|---|---|---|---|---|---|
| I | H | $SC_6H_5$ | A | 77 | 124–125°[a,b] | $C_{10}H_{10}N_2S$·HCl | C | 53.0 | 53.2 |
| | | | | | | | H | 4.89 | 4.91 |
| | | | | | | | N | 12.4 | 12.5 |
| II | H | $SCH_2C_6H_5$ | A | 57[a] | 143–144°[c] | $C_{11}H_{12}N_2S$·HCl | C | 54.9 | 54.6 |
| | | | | | | | H | 5.44 | 5.46 |
| | | | | | | | N | 11.6 | 11.8 |
| III | H | $CH_2SC_6H_5$ | A[d] | 73 | 108–109°[e] | $C_{11}H_{12}N_2S$·HCl | C | 54.9 | 54.5 |
| | | | | | | | H | 5.44 | 5.45 |
| | | | | | | | N | 11.6 | 11.7 |
| IV | | $=CHC_6H_5$ | Exp. | 48 | 98–110°[a] | $C_{11}H_{10}N_2$·HCl | C | 63.9 | 63.7 |
| | | | | | | | H | 5.37 | 5.37 |
| | | | | | | | N | 13.6 | 13.5 |
| V | H | $CH_2C_6H_5$ | Exp. | 99 | 147–149°[a] | $C_{11}H_{12}N_2$·HCl | C | 63.3 | 63.4 |
| | | | | | | | H | 6.28 | 6.22 |
| | | | | | | | N | 13.4 | 13.8 |
| VI | H | $S(O)C_6H_5$ | C[f] | 78[a] | 155–157° | $C_{10}H_{10}N_2OS$·HCl | C | 49.5 | 49.8 |
| | | | | | | | H | 4.57 | 4.59 |
| | | | | | | | N | 11.5 | 11.5 |
| VII | H | $S(O)_2C_6H_5$ | C | 69[g] | 217–225° | $C_{10}H_{10}N_2O_2S$·HCl | C | 46.4 | 46.5 |
| | | | | | | | H | 4.29 | 4.35 |
| | | | | | | | N | 10.8 | 11.0 |
| VIII | H | $S(O)CH_2C_6H_5$ | C[f] | 86 | 181–182°[a] | $C_{11}H_{12}N_2OS$·HCl | C | 51.5 | 51.6 |
| | | | | | | | H | 5.10 | 5.24 |
| | | | | | | | N | 10.9 | 11.0 |
| IX | H | $S(O)_2CH_2C_6H_5$ | C | 72[g] | 228–233° eff. | $C_{11}H_{12}N_2O_2S$·HCl | C | 48.4 | 48.3 |
| | | | | | | | H | 4.80 | 4.97 |
| | | | | | | | N | 10.3 | 10.5 |
| X | H | *S*-Pyridin-2-yl | B | 52 | 218–219° dec.[a] | $C_9H_9N_3S$·2HCl | C | 40.9 | 41.0 |
| | | | | | | | H | 4.20 | 4.29 |
| | | | | | | | N | 15.9 | 15.8 |
| XI | H | *S*-Pyrimidin-2-yl | B | 48 | 147–149° eff.[a] | $C_8H_8N_4S$·HCl·$H_2O$ | C | 38.9 | 39.0 |
| | | | | | | | H | 4.49 | 4.49 |
| | | | | | | | N | 22.7 | 22.4 |
| XII | $CH_3$ | $SC_6H_5$ | A[h] | 52[a] | 124–126° | $C_{11}H_{12}N_2S$·HCl | C | 54.9 | 54.6 |
| | | | | | | | H | 5.44 | 5.54 |
| | | | | | | | N | 11.6 | 11.6 |
| XIII | $CH_2CH_3$ | $SC_6H_5$ | A[h,i] | 46 | 71–72°[j] | $C_{12}H_{14}N_2S$ | C | 66.0 | 66.0 |
| | | | | | | | H | 6.46 | 6.49 |
| | | | | | | | N | 12.8 | 12.9 |
| XIV | $(CH_2)_5CH_3$ | $SC_6H_5$ | A[h,k] | 29 | 64–65°[j] | $C_{16}H_{22}N_2S$ | C | 70.0 | 69.6 |
| | | | | | | | H | 8.08 | 8.15 |
| | | | | | | | N | 10.2 | 10.6 |

[a] Recrystallized from ethanol–ether. [b] Lit. (7) mp 124–125°. [c] Lit. (7) mp 142–143°. [d] For the preparation of the starting 4-(2-chloroethyl)imidazole, see Refs. 11 and 12. [e] Recrystallized from acetonitrile. [f] Only a 10% molar excess of 30% hydrogen peroxide was used. [g] Recrystallized from ethanol. [h] For preparation of the starting chloroalkylimidazoles, see Ref. 4. [i] Purified as oxalic acid salt prior to neutralization. [j] Recrystallized from ethyl acetate–hexane. [k] Purified by column chromatography on Florisil as free base.

stirred mixture of 6.66 g (17.1 mmoles) of benzyltriphenylphosphonium chloride (10) and 5.70 g (16.8 mmoles) of 4-(*N*-triphenylmethyl)imidazolecarboxaldehyde (4) in 150 ml of ethanol was added 1.30 g (2.41 mmoles) of sodium methoxide in 20 ml of ethanol. After 23 hr at ambient temperature, the reaction was diluted with 400 ml of water and extracted with three 75-ml portions of chloroform. The combined extracts were washed with 50 ml of water and 50 ml of brine, dried, and spin evaporated *in vacuo*.

The residual syrup was dissolved in a minimum of hot ethyl acetate and introduced on a column of magnesium silicates[2] (65 g, 31 cm × 2.4 cm) in hexane. After the column had cooled, it was eluted with hexane. The first 200 ml of eluate, which contained the triphenylphosphine oxide free product, was spin evaporated *in vacuo* to give a syrup. This syrup was triturated under hexane to give a white solid (60% yield, 4.10 g) of 1-[4-(*N*-triphenylmethyl)imidazolyl]-2-phenylethylene (XV) as a mixture of *cis*- and *trans*-isomers, which was used without further purification.

A solution of 4.05 g (10.1 mmoles) of XV, 20 ml of tetrahydrofuran, and 30 ml of 6 *M* HCl was heated on a steam bath for 3 hr. The reaction was cooled, spin evaporated *in vacuo*, and diluted with 50 ml of water. The solids were removed by filtration and washed with water. The combined filtrates and washes were spin evaporated *in vacuo* to give an oil, which crystallized under ether. The compound was a mixture of the *cis*- and *trans*-isomers and appeared as two spots on TLC in chloroform–ethanol (9:1) on silica gel plates.

**4-(2-Phenethyl)imidazole Hydrochloride (V)**—A mixture of 1.05 g (5.08 mmoles) of IV, 100 ml of ethanol, and 100 mg of 10% palladium-on-carbon was shaken in the presence of hydrogen at 2–3 atm for 0.5 hr.

**Table II—Inhibition of Histidine Decarboxylase[a]**

| Compound | Inhibition at $10^{-4}$ *M*, % |
|---|---|
| I | 69 |
| II | 40 |
| III | 35 |
| IV | 21 |
| V | 5 |
| VI | 7 |
| VII | 43 |
| VIII | 7 |
| IX | 6 |
| X | 34 |
| XI | 6 |
| XII | 84 |
| XIII | 54 |
| XIV | 31 |

[a] The enzyme from rat stomach was assayed with 0.24 m*M* [*carboxyl*-$^{14}$C]-L-histidine as previously described (3).

[2] Florisil.

The reaction was filtered and spin evaporated *in vacuo* to give white crystals. These crystals were collected, washed with ether, and recrystallized.

## REFERENCES


(1) D. M. Shepherd and D. MacKay, *Prog. Med. Chem.*, **5**, 199 (1967).

(2) J. P. Green, in "Medicinal Chemistry," part II, A. Burger, Ed., Wiley–Interscience, New York, N.Y., 1970, p. 1633.

(3) J. L. Kelley, C. A. Miller, and H. L. White, *J. Med. Chem.*, **20**, 506 (1977).

(4) J. L. Kelley, C. A. Miller, and E. W. McLean, *ibid.*, **20**, 721 (1977).

(5) J. I. DeGraw, J. Engstrom, M. Ellis, and H. L. Johnson, *ibid.*, **20**, 1671 (1977).

(6) E. E. Smissman and J. A. Weis, *ibid.*, **14**, 945 (1971).

(7) L. R. Swett and T. O. Yellin, *ibid.*, **13**, 968 (1970).

(8) P. M. Ruoff and R. C. Scott, *J. Am. Chem. Soc.*, **72**, 4950 (1950).

(9) B. Robinson and D. M. Shepherd, *J. Chem. Soc.*, **1961**, 5037.

(10) K. Friedrich and H.-G. Henning, *Chem. Ber.*, **92**, 2756 (1959).

(11) R. A. Turner, *J. Am. Chem. Soc.*, **71**, 3476 (1949).

(12) C. F. Huebner, *ibid.*, **73**, 4667 (1951).


## ACKNOWLEDGMENTS


The authors thank Dr. Helen L. White and her staff for the enzyme inhibition results and Dr. B. S. Hurlbert and his staff for the elemental analyses and NMR spectra.


# Effects of Chronic Emetine Treatment on Mitochondrial Function


**MICHAEL A. DUBICK * and WILLIAM C. T. YANG ˣ**



Received March 10, 1980, from the *Department of Pharmacology and Nutrition, School of Medicine, University of Southern California, Los Angeles, CA 90033.* Accepted for publication September 8, 1980. *Present address: Department of Nutrition, University of California, Davis, CA 95616.



**Abstract** □ Emetine has long been recognized as a cardiotoxic drug, but its mechanism remains unknown. Since many studies reported an effect of emetine on cardiac metabolism, permanent damage to the heart could result from such treatment. To investigate this action of emetine in relation to the cardiotoxicity seen after a therapeutic regimen, New Zealand albino rabbits were given 2 mg/kg/day ip of emetine for 9 days. Heart and liver mitochondrial metabolism was assessed polarographically using pyruvate, pyruvate plus malate, or succinate as the substrate. Heart mitochondrial metabolism was reduced in emetine-treated rabbits in comparison to the normal controls. However, the metabolic activity of the pair-fed control group was equally reduced. Only the liver mitochondrial metabolism of the pair-fed control group was reduced in relation to the normal controls, while the liver mitochondrial metabolism of emetine-treated rabbits remained unchanged. These data indicated that the reduction in heart mitochondrial metabolism resulted from the inanition induced by the chronic emetine treatment and not from a primary effect of the drug.



**Keyphrases** □ Emetine—effects of chronic treatment on heart and liver mitochondrial metabolism □ Mitochondrial function—effects of chronic emetine treatment □ Cardiotoxicity—effects of chronic emetine treatment on mitochondrial function


Emetine remains important in the treatment of amebiasis. Its role, however, has been reduced to an alternative drug choice, primarily because of its numerous side effects, the most serious affecting the cardiovascular system. Many studies reported adverse effects of high concentrations of emetine on cardiac metabolism (1–4), although the mechanism of this cardiotoxicity remains unknown.

## BACKGROUND

In a series of experiments, rats injected with ~2 mg/kg/day of emetine for 14–17 days showed a reduction in heart homogenate respiration with butyrate, β-hydroxybutyrate, citrate, α-ketoglutarate, malate, pyruvate, or lactate as the substrate (5–7). Since no effects were observed on the liver homogenate respiration, Appelt and Heim (5–7) concluded that emetine appeared to be selectively toxic to the heart. However, they reported that animals chronically treated with emetine reduced their food intake and lost weight. Since pair-fed controls were not included in their study, their conclusion must be reevaluated.

Few studies investigated the action of emetine on mitochondrial metabolism, but two reports indicated that therapeutic doses of emetine may affect heart mitochondria. Brink *et al.* (8) found a reduction in oxygen uptake and [$^{14}$C]carbon dioxide formation from glucose, pyruvate, and palmitate. If these effects are not secondary to the reduced contractility observed, a reduction in heart mitochondrial metabolism must be postulated. Pearce *et al.* (9) described the mitochondrion as the primary structure in the cardiac cell to be affected morphologically in response to therapeutic doses of emetine in dogs.

Since metabolic changes in the heart could indicate cardiac damage, further study of emetine is important in the overall evaluation of the cardiotoxicity seen clinically. Thus, heart mitochondrial metabolism was assessed in rabbits treated with therapeutic doses of emetine. Since emetine is toxic to the heart yet exerts a major therapeutic effect in the liver, liver mitochondrial metabolism was studied for comparison with the heart.

## EXPERIMENTAL

Male New Zealand albino rabbits were given 2 mg/kg/day ip of emetine hydrochloride for 9 days. Since emetine-treated animals ate less, pair-fed controls were included to exclude effects due to inanition. Normal controls were fed *ad libitum*, and water was freely available to all groups.

Heart mitochondria were prepared as described previously (10). After removal of the heart, a piece of ventricle was removed and prepared for electron microscopy according to techniques outlined by Hayat (11). Rabbit liver mitochondria were prepared similarly. The homogenization and suspending media consisted of 0.25 *M* sucrose plus 1 m*M* ethylenediaminetetraacetic acid (pH 7.2).

Heart and liver mitochondrial metabolism was studied polarographically with an oxygraph. Pyruvate (5 m*M*), pyruvate (5 m*M*) plus malate (0.1 m*M*), and succinate (5 m*M*) were the substrates. The reaction medium for the heart mitochondrial studies contained 0.25 *M* mannitol, 10 m*M* KCl, 10 m*M* tris(hydroxymethyl)aminomethane hydrochloride, 0.1 m*M* ethylenediaminetetraacetic acid, and 5 m*M* phosphate buffer (pH 7.2). The reaction medium for the liver studies consisted of 0.25 *M* sucrose, 0.1 m*M* KCl, and 10 m*M* tris(hydroxymethyl)aminomethane phosphate buffer (pH. 7.2). Small volumes of concentrated adenine diphosphate and magnesium chloride were added to reach final concen-


*0022-3549/81/0300-0343$01.00/0*


*© 1981, American Pharmaceutical Association*

The reaction was filtered and spin evaporated *in vacuo* to give white crystals. These crystals were collected, washed with ether, and recrystallized.

## REFERENCES


(1) D. M. Shepherd and D. MacKay, *Prog. Med. Chem.*, **5**, 199 (1967).

(2) J. P. Green, in "Medicinal Chemistry," part II, A. Burger, Ed., Wiley–Interscience, New York, N.Y., 1970, p. 1633.

(3) J. L. Kelley, C. A. Miller, and H. L. White, *J. Med. Chem.*, **20**, 506 (1977).

(4) J. L. Kelley, C. A. Miller, and E. W. McLean, *ibid.*, **20**, 721 (1977).

(5) J. I. DeGraw, J. Engstrom, M. Ellis, and H. L. Johnson, *ibid.*, **20**, 1671 (1977).

(6) E. E. Smissman and J. A. Weis, *ibid.*, **14**, 945 (1971).

(7) L. R. Swett and T. O. Yellin, *ibid.*, **13**, 968 (1970).

(8) P. M. Ruoff and R. C. Scott, *J. Am. Chem. Soc.*, **72**, 4950 (1950).

(9) B. Robinson and D. M. Shepherd, *J. Chem. Soc.*, **1961**, 5037.

(10) K. Friedrich and H.-G. Henning, *Chem. Ber.*, **92**, 2756 (1959).

(11) R. A. Turner, *J. Am. Chem. Soc.*, **71**, 3476 (1949).

(12) C. F. Huebner, *ibid.*, **73**, 4667 (1951).


## ACKNOWLEDGMENTS


The authors thank Dr. Helen L. White and her staff for the enzyme inhibition results and Dr. B. S. Hurlbert and his staff for the elemental analyses and NMR spectra.


# Effects of Chronic Emetine Treatment on Mitochondrial Function


**MICHAEL A. DUBICK * and WILLIAM C. T. YANG ˣ**



Received March 10, 1980, from the *Department of Pharmacology and Nutrition, School of Medicine, University of Southern California, Los Angeles, CA 90033.* Accepted for publication September 8, 1980. *Present address: Department of Nutrition, University of California, Davis, CA 95616.



**Abstract** □ Emetine has long been recognized as a cardiotoxic drug, but its mechanism remains unknown. Since many studies reported an effect of emetine on cardiac metabolism, permanent damage to the heart could result from such treatment. To investigate this action of emetine in relation to the cardiotoxicity seen after a therapeutic regimen, New Zealand albino rabbits were given 2 mg/kg/day ip of emetine for 9 days. Heart and liver mitochondrial metabolism was assessed polarographically using pyruvate, pyruvate plus malate, or succinate as the substrate. Heart mitochondrial metabolism was reduced in emetine-treated rabbits in comparison to the normal controls. However, the metabolic activity of the pair-fed control group was equally reduced. Only the liver mitochondrial metabolism of the pair-fed control group was reduced in relation to the normal controls, while the liver mitochondrial metabolism of emetine-treated rabbits remained unchanged. These data indicated that the reduction in heart mitochondrial metabolism resulted from the inanition induced by the chronic emetine treatment and not from a primary effect of the drug.



**Keyphrases** □ Emetine—effects of chronic treatment on heart and liver mitochondrial metabolism □ Mitochondrial function—effects of chronic emetine treatment □ Cardiotoxicity—effects of chronic emetine treatment on mitochondrial function


Emetine remains important in the treatment of amebiasis. Its role, however, has been reduced to an alternative drug choice, primarily because of its numerous side effects, the most serious affecting the cardiovascular system. Many studies reported adverse effects of high concentrations of emetine on cardiac metabolism (1–4), although the mechanism of this cardiotoxicity remains unknown.

## BACKGROUND

In a series of experiments, rats injected with ~2 mg/kg/day of emetine for 14–17 days showed a reduction in heart homogenate respiration with butyrate, β-hydroxybutyrate, citrate, α-ketoglutarate, malate, pyruvate, or lactate as the substrate (5–7). Since no effects were observed on the liver homogenate respiration, Appelt and Heim (5–7) concluded that emetine appeared to be selectively toxic to the heart. However, they reported that animals chronically treated with emetine reduced their food intake and lost weight. Since pair-fed controls were not included in their study, their conclusion must be reevaluated.

Few studies investigated the action of emetine on mitochondrial metabolism, but two reports indicated that therapeutic doses of emetine may affect heart mitochondria. Brink *et al.* (8) found a reduction in oxygen uptake and [$^{14}$C]carbon dioxide formation from glucose, pyruvate, and palmitate. If these effects are not secondary to the reduced contractility observed, a reduction in heart mitochondrial metabolism must be postulated. Pearce *et al.* (9) described the mitochondrion as the primary structure in the cardiac cell to be affected morphologically in response to therapeutic doses of emetine in dogs.

Since metabolic changes in the heart could indicate cardiac damage, further study of emetine is important in the overall evaluation of the cardiotoxicity seen clinically. Thus, heart mitochondrial metabolism was assessed in rabbits treated with therapeutic doses of emetine. Since emetine is toxic to the heart yet exerts a major therapeutic effect in the liver, liver mitochondrial metabolism was studied for comparison with the heart.

## EXPERIMENTAL

Male New Zealand albino rabbits were given 2 mg/kg/day ip of emetine hydrochloride for 9 days. Since emetine-treated animals ate less, pair-fed controls were included to exclude effects due to inanition. Normal controls were fed *ad libitum*, and water was freely available to all groups.

Heart mitochondria were prepared as described previously (10). After removal of the heart, a piece of ventricle was removed and prepared for electron microscopy according to techniques outlined by Hayat (11). Rabbit liver mitochondria were prepared similarly. The homogenization and suspending media consisted of 0.25 *M* sucrose plus 1 m*M* ethylenediaminetetraacetic acid (pH 7.2).

Heart and liver mitochondrial metabolism was studied polarographically with an oxygraph. Pyruvate (5 m*M*), pyruvate (5 m*M*) plus malate (0.1 m*M*), and succinate (5 m*M*) were the substrates. The reaction medium for the heart mitochondrial studies contained 0.25 *M* mannitol, 10 m*M* KCl, 10 m*M* tris(hydroxymethyl)aminomethane hydrochloride, 0.1 m*M* ethylenediaminetetraacetic acid, and 5 m*M* phosphate buffer (pH 7.2). The reaction medium for the liver studies consisted of 0.25 *M* sucrose, 0.1 m*M* KCl, and 10 m*M* tris(hydroxymethyl)aminomethane phosphate buffer (pH. 7.2). Small volumes of concentrated adenine diphosphate and magnesium chloride were added to reach final concen-


*0022-3549/81/0300-0343$01.00/0*


*© 1981, American Pharmaceutical Association*

**Table I—Effect of Chronic Emetine Treatment on Pyruvate [a] Oxidation by Heart Mitochondria [b]**

| | Initial Rate | State 3 | Magnesium Chloride | State 3 | RC Ratio | ADP:O Ratio |
|---|---|---|---|---|---|---|
| Normal control ($n$ = 10) | 27.5 ± 3.4 | 433.3 ± 49.2 | 202.2 ± 15.0<br>135.6 ± 12.1 | 523.7 ± 47.8 | 12.8 ± 0.4<br>3.4 ± 0.3[c] | 3.1 ± 0.1<br>3.6 ± 0.2[c] |
| Pair-fed control ($n$ = 8) | 18.7 ± 1.6[d] | 306.0 ± 22.5[d] | 147.6 ± 16.4[d]<br>106.8 ± 11.3 | 351.9 ± 24.8[e] | 11.2 ± 0.6<br>3.0 ± 0.3[c] | 3.2 ± 0.2<br>3.8 ± 0.1[c] |
| Emetine treated[f] ($n$ = 8) | 18.2 ± 1.5[d] | 271.0 ± 9.3[e] | 137.4 ± 8.7[e]<br>96.4 ± 3.7[e] | 324.0 ± 14.4[e] | 10.9 ± 0.5<br>3.3 ± 0.2[c] | 3.3 ± 0.2<br>3.7 ± 0.2[c] |

[a] Includes 0.1 m$M$ malate. [b] Mean ± $SE$ expressed as $n$ atoms of oxygen consumed per minute per milligram of mitochondrial protein. [c] After the addition of 1.4 m$M$ $MgCl_2$. [d] $p < 0.05$ from normal control. [e] $p \ll 0.05$ from normal control. [f] Given 2 mg/kg/day ip for 9 days.

**Table II—Effect of Chronic Emetine Treatment on Succinate Oxidation by Heart Mitochondria [a]**

| | Initial Rate | State 3 | Magnesium Chloride | State 3 | RC Ratio | ADP:O Ratio |
|---|---|---|---|---|---|---|
| Normal control ($n$ = 8) | 119.7 ± 12.0 | 656.0 ± 43.9 | 359.7 ± 23.2 | 764.8 ± 74.4[b] | 4.6 ± 0.2 | 2.3 ± 0.1 |
| Pair-fed control ($n$ = 3) | 92.6 ± 8.7 | 508.3 ± 48.1 | 347.6 ± 33.7 | 523.5 ± 69.1 | 3.9 ± 0.5 | 2.5 ± 0.2 |
| Emetine treated[c] ($n$ = 3) | 83.4 ± 5.3[d] | 466.9 ± 28.9 | 310.7 ± 40.7 | 506.9 ± 15.2[d] | 4.4 ± 0.3 | 2.6 ± 0.1 |

[a] Mean ± $SE$ expressed as $n$ atoms of oxygen consumed per minute per milligram of mitochondrial protein. [b] $n$ = 4. [c] Given 2 mg/kg/day ip for 9 days. [d] $p < 0.05$ from normal control.

trations of 0.3 and 1.4 m$M$, respectively. All reactions were run at 28°. Protein determination was by the method of Lowry *et al.* (12).

## RESULTS

With pyruvate plus malate or pyruvate alone as the substrate, the respiration rates of heart mitochondria isolated from the pair-fed control and emetine-treated rabbits were significantly lower than those recorded from normal control mitochondria (Table I). (Since both results were similar, only those with pyruvate plus malate are shown). This same trend was observed with succinate, but only the initial rate and postmagnesium State 3 respiration rates were significantly lower in the emetine-treated group than in the normal control group (Table II). In both cases, the respiration rates of mitochondria isolated from the pair-fed control group did not differ from the rates observed in the emetine-treated group. Also, as shown in Tables I and II, the respiratory control (RC) and adenosine 5′-phosphate–oxygen (ADP:O) ratios did not differ significantly in any of the three groups.

Liver mitochondria responded differently than heart mitchondria to chronic emetine treatment with all substrates used. Liver mitochondria from the pair-fed control rabbits, respiring in the presence of pyruvate plus malate or pyruvate alone, had significantly lower State 3 respiration rates than did both the normal control and emetine-treated mitochondria (Table III). In addition, the premagnesium RC ratio was significantly lower in the pair-fed control group than in the normal control group. With succinate as the substrate, only the premagnesium State 3 rate was significantly lower in the pair-fed control group in comparison to both the normal control and emetine-treated groups (Table IV). With any substrate used, the emetine-treated rabbits maintained mitochondrial respiration at normal control levels (Tables III and IV). No differences were detected in the ADP:O ratios in all liver mitochondrial preparations.

## DISCUSSION

The results from the present experiments with heart mitochondria agreed with preliminary experiments using $\alpha$-ketoglutarate as the substrate (13). In addition, they were similar to those obtained by Appelt and Heim (5–7) with rats and by Hanasono (14) with rabbits. The only discrepancy was that Appelt and Heim (6) observed no difference between control and emetine-treated heart homogenate respiration with succinate as the substrate. Our results on the reduced respiration of rabbit heart mitochondria with succinate as the substrate agreed with those of Hanasono using rabbit heart homogenates (14). The discrepancy may be due to species differences. Nevertheless, the major observation from this study was that although heart mitochondrial respiration in the emetine-treated group was reduced in comparison to the normal control group, respiration in the pair-fed control group was equally reduced. This finding indicated that the apparent depressive effects of emetine on heart mitochondrial respiration were not due to a direct action of the drug but were secondary to the nutritional state of the animal.

Other evidence to support this hypothesis comes from work by Gold and coworkers (15, 16). In rats semistarved or totally starved for 7 days, the activities of myocardial enzymes, including those found in the mitochondria, were reduced.

**Table III—Effect of Chronic Emetine Treatment of Pyruvate [a] Oxidation by Liver Mitochondria [b]**

| | Initial Rate | State 3 | Magnesium Chloride | State 3 | RC Ratio | ADP:O Ratio |
|---|---|---|---|---|---|---|
| Normal control ($n$ = 10) | 8.3 ± 1.0 | 38.9 ± 2.4 | 22.1 ± 1.4 | 55.9 ± 3.3 | 3.8 ± 0.3<br>3.4 ± 0.3[c] | 3.2 ± 0.2<br>3.5 ± 0.3[c] |
| Pair-fed control ($n$ = 8) | 6.2 ± 0.5 | 24.4 ± 1.3[d,e] | 17.9 ± 0.8 | 34.3 ± 3.0[d,e] | 2.8 ± 0.1[d]<br>2.6 ± 0.3[c] | 3.7 ± 0.2<br>3.5 ± 0.0[c] |
| Emetine treated[f] ($n$ = 7) | 6.3 ± 0.5 | 35.8 ± 2.5 | 19.2 ± 1.1 | 51.8 ± 4.3 | 3.5 ± 0.2<br>2.9 ± 0.2[c] | 3.4 ± 0.2<br>3.6 ± 0.2[c] |

[a] Plus 0.1 m$M$ malate. [b] Mean ± $SE$ expressed as $n$ atoms of oxygen consumed per minute per milligram of mitochondrial protein. [c] After the addition of 1.4 m$M$ $MgCl_2$. [d] $p \ll 0.05$ from normal control. [e] $p \ll 0.05$ from emetine-treated rabbits. [f] Given 2 mg/kg/day ip for 9 days.

**Table IV—Effect of Chronic Emetine Treatment on Succinate Oxidation by Liver Mitochondria [a]**

| | Initial Rate | State 3 | Magnesium Chloride | State 3 | RC Ratio | ADP:O Ratio |
|---|---|---|---|---|---|---|
| Normal control ($n$ = 10) | 17.3 ± 1.6 | 66.3 ± 4.6 | 31.3 ± 2.0 | 61.87 ± 4.04 | 3.6 ± 0.2 | 2.4 ± 0.1 |
| Pair-fed control ($n$ = 8) | 11.1 ± 0.8[b] | 45.3 ± 1.7[c] | 26.5 ± 1.1 | 59.0 ± 3.9 | 3.3 ± 0.2 | 2.4 ± 0.1 |
| Emetine treated[d] ($n$ = 3) | 17.2 ± 2.3 | 74.8 ± 5.3 | 33.3 ± 3.3 | 78.0 ± 5.4 | 3.8 ± 0.2 | 2.3 ± 0.1 |

[a] Mean ± $SE$ expressed as $n$ atoms of oxygen consumed per minute per milligram of mitochondrial protein. [b] $p \ll 0.05$ from normal control. [c] $p \ll 0.05$ from normal control and emetine-treated rabbits. [d] Given 2 mg/kg/day ip for 9 days.

Independent of the substrate used, the RC and ADP:O ratios were similar in all three groups. This finding indicated that neither emetine nor malnutrition affected the coupling of oxidation to phosphorylation or the oxidative phosphorylation process, respectively.

The results from the liver mitochondrial studies also agreed with the findings of Appelt and Heim (6, 7). Since the respiration rates were lower only in the pair-fed control group in comparison to the normal control group, liver mitochondrial metabolism apparently was reduced by malnutrition. This effect was overcome in the emetine-treated rabbits.

Basically, it seemed that liver mitochondria were less susceptible to the effects of inanition than heart mitochondria. This result was consistent with observations in semistarved rats (17) and probably reflects the higher metabolic rates and energy requirement of the heart.

As with heart mitochondria, emetine treatment did not affect oxidative phosphorylation in liver mitochondria. Since no consistent effects on the RC ratio were observed in the pair-fed control group, mitochondrial coupling probably was not significantly affected by malnutrition.

In the present experiments, the heart mitochondria from emetine-treated rabbits appeared unaltered, except for a slight swelling of the cristae, when examined under the electron microscope. However, these observations appeared to reflect metabolic effects. Similar morphological findings also were noted by Hatt *et al.* (18) in rats chronically treated with emetine, but they differed from the results of Pearce *et al.* (9) and may reflect species differences. As seen by the treatment schedule used by Pearce's group, the dog may be more sensitive to the actions of emetine than the rat and rabbit.

Thus, the results of these experiments indicate that chronic therapeutic doses of emetine produced no direct detrimental effect on heart mitochondrial metabolism. Any effects observed were secondary to the inanition induced by chronic treatment. The different response noted in liver mitochondria probably reflected the different metabolic states of the heart and liver, as well as the unique metabolic response of the liver during semistarvation or starvation (19). Thus, it appears unlikely that metabolic damage to the myocardium will result from chronic therapeutic doses of emetine. This view agrees with the clinical observation that after therapeutic doses of emetine, most patients recover from cardiovascular side effects without any compromise in cardiac function.

## REFERENCES


(1) R. Deitrich and H. Heim, *J. Pharm. Sci.*, **45**, 512 (1956).

(2) A. Marino and S. Magliulo, *Arch. Int. Pharmacodyn. Ther.*, **132**, 331 (1961).

(3) H. Heim, H. Froede, and V. Erwin, *J. Pharmacol. Exp. Ther.*, **137**, 107 (1962).

(4) S. Imam, V. Rao, and K. Kar, *Biochem. Pharmacol.*, **21**, 3089 (1972).

(5) G. Appelt and H. Heim, *J. Pharm. Sci.*, **53**, 108 (1964).

(6) *Ibid.*, **54**, 1621 (1965).

(7) *Ibid.*, **57**, 1428 (1968).

(8) A. Brink, J. Kotze, S. Muller, and A. Lochner, *J. Pharmacol. Exp. Ther.*, **165**, 251 (1969).

(9) M. Pearce, R. Bulloch, and M. Murphy, *Arch. Pathol.*, **91**, 8 (1971).

(10) W. C. T. Yang and M. Dubick, *Life Sci.*, **21**, 1171 (1977).

(11) M. A. Hayat, "Basic Electron Microscopy," Van Nostrand-Reinhold, New York, N.Y., 1972, pp. 5, 6.

(12) O. Lowry, N. Rosenbrough, A. Farr, and R. Randall, *J. Biol. Chem.*, **193**, 265 (1951).

(13) M. A. Dubick and W. C. T. Yang, *Toxicol. Appl. Pharmacol.*, **54**, 311 (1980).

(14) G. Hanasono, Master's thesis, University of Southern California, Los Angeles, Calif., 1966.

(15) A. J. Gold and L. C. Costello, *Am. J. Physiol.*, **227**, 1336 (1974).

(16) A. J. Gold and S. R. Yaffe, *J. Nutr.*, **108**, 410 (1978).

(17) A. J. Gold and L. C. Costello, *ibid.*, **105**, 208 (1975).

(18) P. Y. Hatt, B. Swynghedauw, and J. C. Hayat, *Ann. N.Y. Acad. Sci.*, **160**, 799 (1969).

(19) S. Gaetani, A. M. Paolucci, M. A. Spadoni, and G. Tomasssi, *J. Nutr.*, **84**, 173 (1964).


# COMMUNICATIONS

## General Equation for Assessing Drug Removal by Extracorporeal Devices


**Keyphrases** □ Pharmacokinetics—general equation for measurement of drug removal by extracorporeal devices □ Extracorporeal devices—general equation for measurement of drug removal □ Drug removal—by extracorporeal devices, general equation


*To the Editor:*

The efficiency of extracorporeal drug removal commonly is measured as dialysance or dialysis clearance. Such terms, however, do not correlate directly with the amount of drug removed by the device. Previous investigators (1, 2) proposed an alternative parameter, $f$, defined as the fraction of drug in the body at the start of extracorporeal drug removal (EDR) that is removed by the device. This fraction is the product of the fraction of total elimination that EDR represents and the fraction of drug lost by all elimination routes during EDR and is given by:

$$f = \frac{Cl_D}{Cl + Cl_D}\left[1 - e^{[-(Cl+Cl_D)/V]t}\right] \qquad \text{(Eq. 1)}$$

where $Cl_D$ is the EDR clearance, $Cl$ is the total body clearance in the absence of EDR, $V$ is the apparent volume of distribution of the drug, and $t$ is the duration of EDR.

Equation 1 assumes one-compartment pharmacokinetics; thus, for most drugs, it may yield inaccurate estimates of the fraction of drug removed by an extracorporeal device. An alternative general equation that can be used for drugs following single or multicompartment kinetics is developed in this communication.

Consider the mass balance equation:

$$X_S = X_D + X_{el} + X_f \qquad \text{(Eq. 2)}$$

where $X_S$ and $X_f$ are the amounts of drug in the body at the beginning and the end of EDR, respectively, and $X_D$ and $X_{el}$ are the amounts of drug eliminated by EDR and by the body during EDR, respectively. Equation 2 may be expressed as:

$$X_S = Cl_D AUC_1 + ClAUC_1 + ClAUC_2 \qquad \text{(Eq. 3)}$$

where $AUC_1$ is the area under the plasma concentration–time curve during EDR and $AUC_2$ is the area under the


0022-3549/81/0300-0345$01.00/0


© 1981, American Pharmaceutical Association

Independent of the substrate used, the RC and ADP:O ratios were similar in all three groups. This finding indicated that neither emetine nor malnutrition affected the coupling of oxidation to phosphorylation or the oxidative phosphorylation process, respectively.

The results from the liver mitochondrial studies also agreed with the findings of Appelt and Heim (6, 7). Since the respiration rates were lower only in the pair-fed control group in comparison to the normal control group, liver mitochondrial metabolism apparently was reduced by malnutrition. This effect was overcome in the emetine-treated rabbits.

Basically, it seemed that liver mitochondria were less susceptible to the effects of inanition than heart mitochondria. This result was consistent with observations in semistarved rats (17) and probably reflects the higher metabolic rates and energy requirement of the heart.

As with heart mitochondria, emetine treatment did not affect oxidative phosphorylation in liver mitochondria. Since no consistent effects on the RC ratio were observed in the pair-fed control group, mitochondrial coupling probably was not significantly affected by malnutrition.

In the present experiments, the heart mitochondria from emetine-treated rabbits appeared unaltered, except for a slight swelling of the cristae, when examined under the electron microscope. However, these observations appeared to reflect metabolic effects. Similar morphological findings also were noted by Hatt *et al.* (18) in rats chronically treated with emetine, but they differed from the results of Pearce *et al.* (9) and may reflect species differences. As seen by the treatment schedule used by Pearce's group, the dog may be more sensitive to the actions of emetine than the rat and rabbit.

Thus, the results of these experiments indicate that chronic therapeutic doses of emetine produced no direct detrimental effect on heart mitochondrial metabolism. Any effects observed were secondary to the inanition induced by chronic treatment. The different response noted in liver mitochondria probably reflected the different metabolic states of the heart and liver, as well as the unique metabolic response of the liver during semistarvation or starvation (19). Thus, it appears unlikely that metabolic damage to the myocardium will result from chronic therapeutic doses of emetine. This view agrees with the clinical observation that after therapeutic doses of emetine, most patients recover from cardiovascular side effects without any compromise in cardiac function.

## REFERENCES


(1) R. Deitrich and H. Heim, *J. Pharm. Sci.*, **45**, 512 (1956).

(2) A. Marino and S. Magliulo, *Arch. Int. Pharmacodyn. Ther.*, **132**, 331 (1961).

(3) H. Heim, H. Froede, and V. Erwin, *J. Pharmacol. Exp. Ther.*, **137**, 107 (1962).

(4) S. Imam, V. Rao, and K. Kar, *Biochem. Pharmacol.*, **21**, 3089 (1972).

(5) G. Appelt and H. Heim, *J. Pharm. Sci.*, **53**, 108 (1964).

(6) *Ibid.*, **54**, 1621 (1965).

(7) *Ibid.*, **57**, 1428 (1968).

(8) A. Brink, J. Kotze, S. Muller, and A. Lochner, *J. Pharmacol. Exp. Ther.*, **165**, 251 (1969).

(9) M. Pearce, R. Bulloch, and M. Murphy, *Arch. Pathol.*, **91**, 8 (1971).

(10) W. C. T. Yang and M. Dubick, *Life Sci.*, **21**, 1171 (1977).

(11) M. A. Hayat, "Basic Electron Microscopy," Van Nostrand-Reinhold, New York, N.Y., 1972, pp. 5, 6.

(12) O. Lowry, N. Rosenbrough, A. Farr, and R. Randall, *J. Biol. Chem.*, **193**, 265 (1951).

(13) M. A. Dubick and W. C. T. Yang, *Toxicol. Appl. Pharmacol.*, **54**, 311 (1980).

(14) G. Hanasono, Master's thesis, University of Southern California, Los Angeles, Calif., 1966.

(15) A. J. Gold and L. C. Costello, *Am. J. Physiol.*, **227**, 1336 (1974).

(16) A. J. Gold and S. R. Yaffe, *J. Nutr.*, **108**, 410 (1978).

(17) A. J. Gold and L. C. Costello, *ibid.*, **105**, 208 (1975).

(18) P. Y. Hatt, B. Swynghedauw, and J. C. Hayat, *Ann. N.Y. Acad. Sci.*, **160**, 799 (1969).

(19) S. Gaetani, A. M. Paolucci, M. A. Spadoni, and G. Tomasssi, *J. Nutr.*, **84**, 173 (1964).


# COMMUNICATIONS

## General Equation for Assessing Drug Removal by Extracorporeal Devices


**Keyphrases** □ Pharmacokinetics—general equation for measurement of drug removal by extracorporeal devices □ Extracorporeal devices—general equation for measurement of drug removal □ Drug removal—by extracorporeal devices, general equation


*To the Editor:*

The efficiency of extracorporeal drug removal commonly is measured as dialysance or dialysis clearance. Such terms, however, do not correlate directly with the amount of drug removed by the device. Previous investigators (1, 2) proposed an alternative parameter, $f$, defined as the fraction of drug in the body at the start of extracorporeal drug removal (EDR) that is removed by the device. This fraction is the product of the fraction of total elimination that EDR represents and the fraction of drug lost by all elimination routes during EDR and is given by:

$$f = \frac{Cl_D}{Cl + Cl_D}\left[1 - e^{[-(Cl+Cl_D)/V]t}\right] \qquad \text{(Eq. 1)}$$

where $Cl_D$ is the EDR clearance, $Cl$ is the total body clearance in the absence of EDR, $V$ is the apparent volume of distribution of the drug, and $t$ is the duration of EDR.

Equation 1 assumes one-compartment pharmacokinetics; thus, for most drugs, it may yield inaccurate estimates of the fraction of drug removed by an extracorporeal device. An alternative general equation that can be used for drugs following single or multicompartment kinetics is developed in this communication.

Consider the mass balance equation:

$$X_S = X_D + X_{el} + X_f \qquad \text{(Eq. 2)}$$

where $X_S$ and $X_f$ are the amounts of drug in the body at the beginning and the end of EDR, respectively, and $X_D$ and $X_{el}$ are the amounts of drug eliminated by EDR and by the body during EDR, respectively. Equation 2 may be expressed as:

$$X_S = Cl_D AUC_1 + ClAUC_1 + ClAUC_2 \qquad \text{(Eq. 3)}$$

where $AUC_1$ is the area under the plasma concentration–time curve during EDR and $AUC_2$ is the area under the


0022-3549/81/0300-0345$01.00/0


© 1981, American Pharmaceutical Association

**Table I—Comparison of Methods of Estimating the Fraction of Sotalol in the Body Removed by Hemodialysis [a]**

| Time of Dialysis, hr | $AUC_1$, mg/liter/hr | $AUC_2$, mg/liter/hr | $f$ Eq. 1 | $f$ Eq. 4 | $f$ Eq. 5 |
|---|---|---|---|---|---|
| 1–7 | 5.87 | 6.77 | 0.17 | 0.26 | 0.26 |
| 12–18 | 1.75 | 3.67 | 0.17 | 0.20 | 0.20 |

[a] Pharmacokinetic parameters taken from Refs. 3 and 4; $Cl$ = 140 ml/min, $V$ = 136 liters, and $Cl_D$ = 105 ml/min, with an intravenous bolus dose of 160 mg.

plasma concentration–time curve from the termination of EDR to infinity.

The fraction of drug in the body at the start of EDR that is removed by the device is given by:

$$f = \frac{X_D}{X_S} \qquad \text{(Eq. 4)}$$

which, from Eq. 3, may be expressed as:

$$f = \frac{Cl_D AUC_1}{(Cl + Cl_D)AUC_1 + ClAUC_2} \qquad \text{(Eq. 5)}$$

To test the validity of Eq. 5, plasma concentrations of sotalol, a β-adrenergic receptor blocking agent, were simulated by computer. Pharmacokinetic parameters describing the time course of this drug in the body were obtained from Sundquist *et al.* (3). Hemodialysis was started and terminated at 1 and 7 hr, respectively, following intravenous bolus administration. In a second simulation, dialysis was started and terminated at 12 and 18 hr following drug administration. A dialysis clearance, $Cl_D$, for sotalol of 105 ml/min was estimated from the study by Tjandramaga *et al.* (4). Areas under the plasma concentration–time curve were estimated using the trapezoidal rule.

By employing Eq. 4, $f$ was determined directly using the simulated amounts in the plasma and tissue compartments at the beginning of dialysis, $X_S$, and the amount of drug removed by dialysis, $X_D$. The value of $f$ obtained was compared with that obtained using Eqs. 1 and 5 (Table I).

Sotalol pharmacokinetics can be described by a two-compartment model with a distribution phase of ~10 hr. When dialysis is performed during the distribution phase of the drug, use of Eq. 1 underestimates the fraction of drug removed by dialysis. When dialysis is conducted in the postdistributive phase, the prediction of $f$ using Eq. 1 improves but still underestimates this parameter. Regardless of the time of dialysis relative to drug administration, Eq. 5 accurately predicts the fraction of drug removed from the body.

Equation 5 provides a valid means of determining the fraction of drug removed by EDR. It is more general than Eq. 1 in that it can be applied to drugs following multicompartment pharmacokinetics regardless of the time of EDR relative to drug administration. The clearance values are easily obtained. Proper use of the equation requires that the final plasma sample be obtained during the terminal log-linear phase of the plasma drug concentration curve and that the slope of this linear phase be determined to estimate $AUC_2$ accurately.

(1) P. R. Gwilt and D. Perrier, *Clin. Pharmacol. Ther.*, **24**, 154 (1978).

(2) S. Takki, J. G. Gambertoglio, D. H. Honda, and T. N. Tozer, *J. Pharmacokinet. Biopharm.*, **5**, 427 (1978).

(3) H. Sundquist, M. Antilla, A. Simon, and J. W. Reich, *J. Clin. Pharmacol.*, **19**, 557 (1979).

(4) T. B. Tjandramaga, J. Thomas, R. Verbeek, R. Verbesselt, R. Verberckmoes, and P. J. De Schepper, *Br. J. Clin. Pharmacol.*, **3**, 259 (1976).

*Peter R. Gwilt*
School of Pharmacy
Ferris State College
Big Rapids, MI 49307

Received July 8, 1980.
Accepted for publication November 13, 1980.

## Novel Source of Ubiquitous Phthalates as Analytical Contaminant

**Keyphrases** □ Plasticizers—phthalate, analytical contaminant □ Mass spectrometry—detection of phthalate esters by selected-ion monitoring □ Phthalates—interference with oxprenolol assay using GLC with electron-capture detection □ Contaminants—phthalates, interference in drug assays using electron-capture detection

*To the Editor:*

The ubiquitous distribution of the phthalate ester plasticizers in the environment is well known, and they are frequently encountered in samples processed in biomedical laboratories. Although the analyst can often identify phthalate plasticizers in biological samples, it is not always clear whether the plasticizer is a genuine contaminant in the specimen or an analytical artifact (1). Phthalates are readily leached into blood stored in plastic containers (2), and collecting blood specimens with evacuated tubes (3) or some plastic syringes (1) can result in contamination with phthalates or other plasticizers.

In addition to their ubiquity, the phthalates manifest two other frustrating properties for the analyst. First, the range of phthalate esters used commercially ensures that a phthalate will cochromatograph with many analytes of interest such as barbiturates (4), disopyramide (5), and long-chain fatty acids (6). Second, although the phthalate esters contain no halogen atoms, they show good response factors to the electron-capture detector (7), which ensures that even nanogram quantities may interfere in trace level determinations of some compounds.

The range of reported sources of phthalates as analytical contaminants is impressive, but we recently encountered a novel and unexpected source that could be of importance to analysts using electron-capture detection for trace level assay of drugs.

To carry out low dose bioavailability studies with oxprenolol, a sensitive assay for this β-blocking drug in plasma was required. An assay by GLC with electron-capture detection, using heptafluorobutyryl derivatives of oxprenolol and the internal standard (metoprolol), was investigated. However, assay blanks invariably contained a spurious peak with a retention time almost equivalent to that of derivatized oxprenolol. A phthalate plasticizer was suspected, so meticulous care was taken to ensure that no plastic materials came in contact with any glassware, reagents, or specimens used. The contaminant persisted, and one of the offending blanks was subjected to GLC–mass spectrometric analysis to confirm the presence of the suspected phthalate. No confirmation could be established



0022-3549/81/0300-0346$01.00/0
© 1981, American Pharmaceutical Association

**Table I—Comparison of Methods of Estimating the Fraction of Sotalol in the Body Removed by Hemodialysis [a]**

| Time of Dialysis, hr | $AUC_1$, mg/liter/hr | $AUC_2$, mg/liter/hr | $f$ Eq. 1 | $f$ Eq. 4 | $f$ Eq. 5 |
|---|---|---|---|---|---|
| 1–7 | 5.87 | 6.77 | 0.17 | 0.26 | 0.26 |
| 12–18 | 1.75 | 3.67 | 0.17 | 0.20 | 0.20 |

[a] Pharmacokinetic parameters taken from Refs. 3 and 4; $Cl$ = 140 ml/min, $V$ = 136 liters, and $Cl_D$ = 105 ml/min, with an intravenous bolus dose of 160 mg.

plasma concentration–time curve from the termination of EDR to infinity.

The fraction of drug in the body at the start of EDR that is removed by the device is given by:

$$f = \frac{X_D}{X_S} \qquad \text{(Eq. 4)}$$

which, from Eq. 3, may be expressed as:

$$f = \frac{Cl_D AUC_1}{(Cl + Cl_D)AUC_1 + ClAUC_2} \qquad \text{(Eq. 5)}$$

To test the validity of Eq. 5, plasma concentrations of sotalol, a β-adrenergic receptor blocking agent, were simulated by computer. Pharmacokinetic parameters describing the time course of this drug in the body were obtained from Sundquist *et al.* (3). Hemodialysis was started and terminated at 1 and 7 hr, respectively, following intravenous bolus administration. In a second simulation, dialysis was started and terminated at 12 and 18 hr following drug administration. A dialysis clearance, $Cl_D$, for sotalol of 105 ml/min was estimated from the study by Tjandramaga *et al.* (4). Areas under the plasma concentration–time curve were estimated using the trapezoidal rule.

By employing Eq. 4, $f$ was determined directly using the simulated amounts in the plasma and tissue compartments at the beginning of dialysis, $X_S$, and the amount of drug removed by dialysis, $X_D$. The value of $f$ obtained was compared with that obtained using Eqs. 1 and 5 (Table I).

Sotalol pharmacokinetics can be described by a two-compartment model with a distribution phase of ~10 hr. When dialysis is performed during the distribution phase of the drug, use of Eq. 1 underestimates the fraction of drug removed by dialysis. When dialysis is conducted in the postdistributive phase, the prediction of $f$ using Eq. 1 improves but still underestimates this parameter. Regardless of the time of dialysis relative to drug administration, Eq. 5 accurately predicts the fraction of drug removed from the body.

Equation 5 provides a valid means of determining the fraction of drug removed by EDR. It is more general than Eq. 1 in that it can be applied to drugs following multicompartment pharmacokinetics regardless of the time of EDR relative to drug administration. The clearance values are easily obtained. Proper use of the equation requires that the final plasma sample be obtained during the terminal log-linear phase of the plasma drug concentration curve and that the slope of this linear phase be determined to estimate $AUC_2$ accurately.

(1) P. R. Gwilt and D. Perrier, *Clin. Pharmacol. Ther.*, **24**, 154 (1978).

(2) S. Takki, J. G. Gambertoglio, D. H. Honda, and T. N. Tozer, *J. Pharmacokinet. Biopharm.*, **5**, 427 (1978).

(3) H. Sundquist, M. Antilla, A. Simon, and J. W. Reich, *J. Clin. Pharmacol.*, **19**, 557 (1979).

(4) T. B. Tjandramaga, J. Thomas, R. Verbeek, R. Verbesselt, R. Verberckmoes, and P. J. De Schepper, *Br. J. Clin. Pharmacol.*, **3**, 259 (1976).

*Peter R. Gwilt*
School of Pharmacy
Ferris State College
Big Rapids, MI 49307

Received July 8, 1980.
Accepted for publication November 13, 1980.

## Novel Source of Ubiquitous Phthalates as Analytical Contaminant

**Keyphrases** □ Plasticizers—phthalate, analytical contaminant □ Mass spectrometry—detection of phthalate esters by selected-ion monitoring □ Phthalates—interference with oxprenolol assay using GLC with electron-capture detection □ Contaminants—phthalates, interference in drug assays using electron-capture detection

*To the Editor:*

The ubiquitous distribution of the phthalate ester plasticizers in the environment is well known, and they are frequently encountered in samples processed in biomedical laboratories. Although the analyst can often identify phthalate plasticizers in biological samples, it is not always clear whether the plasticizer is a genuine contaminant in the specimen or an analytical artifact (1). Phthalates are readily leached into blood stored in plastic containers (2), and collecting blood specimens with evacuated tubes (3) or some plastic syringes (1) can result in contamination with phthalates or other plasticizers.

In addition to their ubiquity, the phthalates manifest two other frustrating properties for the analyst. First, the range of phthalate esters used commercially ensures that a phthalate will cochromatograph with many analytes of interest such as barbiturates (4), disopyramide (5), and long-chain fatty acids (6). Second, although the phthalate esters contain no halogen atoms, they show good response factors to the electron-capture detector (7), which ensures that even nanogram quantities may interfere in trace level determinations of some compounds.

The range of reported sources of phthalates as analytical contaminants is impressive, but we recently encountered a novel and unexpected source that could be of importance to analysts using electron-capture detection for trace level assay of drugs.

To carry out low dose bioavailability studies with oxprenolol, a sensitive assay for this β-blocking drug in plasma was required. An assay by GLC with electron-capture detection, using heptafluorobutyryl derivatives of oxprenolol and the internal standard (metoprolol), was investigated. However, assay blanks invariably contained a spurious peak with a retention time almost equivalent to that of derivatized oxprenolol. A phthalate plasticizer was suspected, so meticulous care was taken to ensure that no plastic materials came in contact with any glassware, reagents, or specimens used. The contaminant persisted, and one of the offending blanks was subjected to GLC–mass spectrometric analysis to confirm the presence of the suspected phthalate. No confirmation could be established



0022-3549/81/0300-0346$01.00/0
© 1981, American Pharmaceutical Association

when the mass spectrometer was operated in the full-scan mode. However, when the sample was analyzed in the more sensitive selected-ion mode, with the mass spectrometer focussed only on ions of mass 149 and 167, which are prominent in the spectrum of bis(2-ethylhexyl) phthalate (8), the presence of this compound was indicated.

Careful reassessment of the entire oxprenolol assay revealed that the only plastic material used was about 2 m of polyvinyl chloride tubing attached to a Pasteur pipet; it was employed to blow nitrogen over the tubes in a water bath for solvent removal. When this polyvinyl chloride tubing was replaced with polytetrafluoroethylene tubing, clean blanks were achieved.

(1) M. T. Rosseel and M. G. Bogaert, *J. Pharm. Pharmacol.*, **28**, 942 (1976).
(2) R. J. Jaeger and R. J. Rubin, *Lancet*, **1**, 151 (1970).
(3) A. W. Missen and S. J. Dickson, *Clin. Chem.*, **20**, 1247 (1974).
(4) W. D. Hooper, D. K. Dubetz, M. J. Eadie, and J. H. Tyrer, *J. Chromatogr.*, **110**, 206 (1975).
(5) D. K. Dubetz, N. N. Brown, W. D. Hooper, M. J. Eadie, and J. H. Tyrer, *Br. J. Clin. Pharmacol.*, **6**, 279 (1978).
(6) C. Geisler, A. R. Swanson, L. Zieve, and M. W. Anders, *Clin. Chem.*, **25**, 308 (1979).
(7) C. S. Giam, H. S. Chan, and G. S. Neff, *Anal. Chem.*, **47**, 2225 (1975).
(8) M. P. Friocourt, D. Picart, and H. H. Floch, *Biomed. Mass. Spectrom.*, **7**, 193 (1980).

*Wayne D. Hooper* ˣ
*Maree T. Smith*
Department of Medicine of Queensland University
Royal Brisbane Hospital
Herston Qld 4029, Australia

Received October 14, 1980.
Accepted for publication December 10, 1980.

## Effects of Spermine and Spermidine on Gastric Emptying in Rats

**Keyphrases** □ Spermine—effects on gastric emptying in rats, structure–activity relationships □ Spermidine—effects on gastric emptying in rats, structure–activity relationships □ Structure–activity relationships—spermidine and spermine, effects on gastric emptying in rats

*To the Editor:*

Spermine and spermidine have been intensively studied with regard to their function in cellular metabolism and, more recently, their role in normal and neoplastic growth (1). These biogenic amines were reported (2) to occur in relatively high concentrations in the GI tract, but no precise physiological role has been attributed to them.

Recently, we reported that a branched-chain polyethyleneamine (mol. wt. >600) greatly inhibited gastric emptying in the rat while an isomeric linear version of this same polymer was essentially inactive (3). Since the repeating unit in both branched and linear polyethyleneimine is somewhat similar to that of spermine and spermidine, we decided to measure the effect of spermine, spermidine, and related small molecule polyamines on the stomach emptying rate in the rat.

**Table I—Effects of Polyamines on Gastric Emptying in the Rat**

| Compound | Molecular Weight | Dose, mg/kg po | Inhibition at 4 hr, %[a] |
|---|---|---|---|
| Diethylenetriamine | 103 | 250 | 0 |
| Triethylenetetramine | 146 | 250 | 0 |
| $N,N^1$-Bis(3-aminopropyl)piperazine | 200 | 250 | 23 |
| (*N*-Aminoethyl)-1,4-diaminobutane | 131 | 250 | 36 |
| Spermidine | 145 | 250 | 87 |
| Polyethyleneimine (commercial product) | >40,000 | 250 | 92 |
| Polyethyleneimine (linear) | >10,000 | 250 | 11 |

[a] Resin bead method; see Ref. 3

The results of initial studies (Table I) indicate that the naturally occurring polyamines, spermine and spermidine, are highly effective in reducing gastric emptying in the rat. Certain closely related commercially available polyamines, such as diethylenetriamine and triethylenetetramine, are completely inactive. Other analogs such as (*N*-aminoethyl)-1,4-diaminobutane and $N,N^1$-bis(3-aminopropyl)piperazine have weak activity.

The structure–activity (inhibition of gastric emptying) of these compounds may be summarized as follows:

$$H_2N(CH_2)_mNH(CH_2)_nNH(CH_2)_mNH_2$$

$m = 3, n = 4$ spermine (very active)
$m = 2, n = 2$ triethylenetetramine (inactive)

$$H_2N(CH_2)_mNH(CH_2)_nNH_2$$

$m = 3, n = 4$ spermidine (very active)
$m = 2, n = 4$ *N*-aminoethyl-1,4-diaminobutane (low activity)
$m = 2, n = 2$ diethylenetriamine (inactive)

$m = 3$ $N,N^1$-bis(3-aminopropyl)piperazine (low activity)

These results indicate that gastric emptying inhibition in the rat by both polymeric and low molecular weight polyamines is clearly dependent on chemical structure. The reason for this structural specificity is not known. The results suggest, however, that endogenous spermine and spermidine may have some unrecognized GI secretomotor activity that can be duplicated by conformationally similar synthetic materials.

(1) D. H. Russell, "Polyamines in Normal and Neoplastic Growth," Raven, New York, N.Y., 1973.
(2) H. Tabor and C. Tabor, *Pharmacol. Rev.*, **16**, 245 (1964).
(3) S. Melamed, G. R. Carlson, J. N. Moss, E. J. Belair, and M. F. Tansy, *J. Pharm. Sci.*, **66**, 899 (1977).

*E. J. Belair* *
*G. R. Carlson*
*S. Melamed*
*J. N. Moss*
Research Laboratories
Rohm and Haas Company
Spring House, PA 19477
*M. F. Tansy* ˣ
Department of Physiology and Biophysics
Health Sciences Center
Temple University
Philadelphia, PA 19140

Received November 5, 1980.
Accepted for publication December 8, 1980.
* Present address: Adria Laboratories, Columbus, OH 43216.

0022-3549/81/0300-0347$01.00/0
© 1981, American Pharmaceutical Association

when the mass spectrometer was operated in the full-scan mode. However, when the sample was analyzed in the more sensitive selected-ion mode, with the mass spectrometer focussed only on ions of mass 149 and 167, which are prominent in the spectrum of bis(2-ethylhexyl) phthalate (8), the presence of this compound was indicated.

Careful reassessment of the entire oxprenolol assay revealed that the only plastic material used was about 2 m of polyvinyl chloride tubing attached to a Pasteur pipet; it was employed to blow nitrogen over the tubes in a water bath for solvent removal. When this polyvinyl chloride tubing was replaced with polytetrafluoroethylene tubing, clean blanks were achieved.

(1) M. T. Rosseel and M. G. Bogaert, *J. Pharm. Pharmacol.*, **28**, 942 (1976).
(2) R. J. Jaeger and R. J. Rubin, *Lancet*, **1**, 151 (1970).
(3) A. W. Missen and S. J. Dickson, *Clin. Chem.*, **20**, 1247 (1974).
(4) W. D. Hooper, D. K. Dubetz, M. J. Eadie, and J. H. Tyrer, *J. Chromatogr.*, **110**, 206 (1975).
(5) D. K. Dubetz, N. N. Brown, W. D. Hooper, M. J. Eadie, and J. H. Tyrer, *Br. J. Clin. Pharmacol.*, **6**, 279 (1978).
(6) C. Geisler, A. R. Swanson, L. Zieve, and M. W. Anders, *Clin. Chem.*, **25**, 308 (1979).
(7) C. S. Giam, H. S. Chan, and G. S. Neff, *Anal. Chem.*, **47**, 2225 (1975).
(8) M. P. Friocourt, D. Picart, and H. H. Floch, *Biomed. Mass. Spectrom.*, **7**, 193 (1980).

*Wayne D. Hooper* ˣ
*Maree T. Smith*
Department of Medicine of Queensland University
Royal Brisbane Hospital
Herston Qld 4029, Australia

Received October 14, 1980.
Accepted for publication December 10, 1980.

## Effects of Spermine and Spermidine on Gastric Emptying in Rats

**Keyphrases** □ Spermine—effects on gastric emptying in rats, structure–activity relationships □ Spermidine—effects on gastric emptying in rats, structure–activity relationships □ Structure–activity relationships—spermidine and spermine, effects on gastric emptying in rats

*To the Editor:*

Spermine and spermidine have been intensively studied with regard to their function in cellular metabolism and, more recently, their role in normal and neoplastic growth (1). These biogenic amines were reported (2) to occur in relatively high concentrations in the GI tract, but no precise physiological role has been attributed to them.

Recently, we reported that a branched-chain polyethyleneamine (mol. wt. >600) greatly inhibited gastric emptying in the rat while an isomeric linear version of this same polymer was essentially inactive (3). Since the repeating unit in both branched and linear polyethyleneimine is somewhat similar to that of spermine and spermidine, we decided to measure the effect of spermine, spermidine, and related small molecule polyamines on the stomach emptying rate in the rat.

**Table I—Effects of Polyamines on Gastric Emptying in the Rat**

| Compound | Molecular Weight | Dose, mg/kg po | Inhibition at 4 hr, %[a] |
|---|---|---|---|
| Diethylenetriamine | 103 | 250 | 0 |
| Triethylenetetramine | 146 | 250 | 0 |
| $N,N^1$-Bis(3-aminopropyl)piperazine | 200 | 250 | 23 |
| (*N*-Aminoethyl)-1,4-diaminobutane | 131 | 250 | 36 |
| Spermidine | 145 | 250 | 87 |
| Polyethyleneimine (commercial product) | >40,000 | 250 | 92 |
| Polyethyleneimine (linear) | >10,000 | 250 | 11 |

[a] Resin bead method; see Ref. 3

The results of initial studies (Table I) indicate that the naturally occurring polyamines, spermine and spermidine, are highly effective in reducing gastric emptying in the rat. Certain closely related commercially available polyamines, such as diethylenetriamine and triethylenetetramine, are completely inactive. Other analogs such as (*N*-aminoethyl)-1,4-diaminobutane and $N,N^1$-bis(3-aminopropyl)piperazine have weak activity.

The structure–activity (inhibition of gastric emptying) of these compounds may be summarized as follows:

$$H_2N(CH_2)_mNH(CH_2)_nNH(CH_2)_mNH_2$$

$m = 3, n = 4$ spermine (very active)
$m = 2, n = 2$ triethylenetetramine (inactive)

$$H_2N(CH_2)_mNH(CH_2)_nNH_2$$

$m = 3, n = 4$ spermidine (very active)
$m = 2, n = 4$ *N*-aminoethyl-1,4-diaminobutane (low activity)
$m = 2, n = 2$ diethylenetriamine (inactive)

$m = 3$ $N,N^1$-bis(3-aminopropyl)piperazine (low activity)

These results indicate that gastric emptying inhibition in the rat by both polymeric and low molecular weight polyamines is clearly dependent on chemical structure. The reason for this structural specificity is not known. The results suggest, however, that endogenous spermine and spermidine may have some unrecognized GI secretomotor activity that can be duplicated by conformationally similar synthetic materials.

(1) D. H. Russell, "Polyamines in Normal and Neoplastic Growth," Raven, New York, N.Y., 1973.
(2) H. Tabor and C. Tabor, *Pharmacol. Rev.*, **16**, 245 (1964).
(3) S. Melamed, G. R. Carlson, J. N. Moss, E. J. Belair, and M. F. Tansy, *J. Pharm. Sci.*, **66**, 899 (1977).

*E. J. Belair* *
*G. R. Carlson*
*S. Melamed*
*J. N. Moss*
Research Laboratories
Rohm and Haas Company
Spring House, PA 19477
*M. F. Tansy* ˣ
Department of Physiology and Biophysics
Health Sciences Center
Temple University
Philadelphia, PA 19140

Received November 5, 1980.
Accepted for publication December 8, 1980.
* Present address: Adria Laboratories, Columbus, OH 43216.

0022-3549/81/0300-0347$01.00/0
© 1981, American Pharmaceutical Association

## REVIEWS

**Essentials of Drug Product Quality: Concepts and Methodology.** By MAHMOUD M. ABDEL-MONEM and JAMES G. HENKEL. C. V. Mosby, 11830 Westline Industrial Drive, St. Louis, MO 63141. 1978. 274 pp. 20 × 25 cm. Price $14.95.

This text, according to the preface, is designed for first professional year pharmacy students. It is unique in two respects: (*a*) it attempts to integrate the elements of quality assurance of drugs and drug products with the accompanying methodology (directed toward both the drug product and the drug in biological fluid); and (*b*) it employs a format and style designed to support the use of the personalized system of instruction (PSI). PSI is described as "characterized by a mastery learning requirement, student self-pacing within the course, the use of proctors for immediate grading of tests taken by students for each unit (chapter), and infrequent lectures." Nevertheless, the format should lend itself well to a more traditional mode of instruction. In this regard, each of the 21 chapters begins with a list of performance objectives for the student and closes with a more than ample list of study questions and practice problems. The writing generally is very readable and lucid.

The first three chapters provide a well-planned, coherent treatment of the principles of drug product selection and include an introduction to dosage forms, the history and purpose of the official compendia, the role played by the FDA in drug product quality assurance, and drug product selection based on pharmaceutical equivalence and bioequivalence. However, some instructors may desire more depth in the treatment of dosage forms and bioequivalence. The treatment of the basis, application, and interpretation of official tests for unit-to-unit variation and uniformity (Chapter 2) is especially well done. However, the few sentences devoted to the dissolution test in Chapter 3 are incomplete and superficial. Chapters 4 and 5, which discuss data analysis and significance testing, are especially noteworthy.

The preface suggests that the analytical methodology chosen to be discussed (Chapters 6–20) is that supporting the quality assurance of drugs and states that the "important analytical methods" are covered. This philosophy apparently influenced the selection of topics, which include ionic equilibria ($K_{sp}$ and acid–base chemistry) (two chapters), solvent extraction principles (one chapter), gravimetric analysis (one chapter), volumetric analysis (acid–base and redox) (two chapters), spectrometry (UV, colorimetry, IR, fluorescence, and mass spectrometry) (five chapters), chromatography (column, TLC, GLC, and HPLC) (three chapters), and radioactivity (one chapter). The emphasis is on the analysis of organic drugs and less on inorganic substances, as evidenced by the absence of precipitation and complexometric titrations among the volumetric techniques discussed and the omission of the analysis of heavy-metal ions among the gravimetric techniques. Also, electrochemical techniques are ignored, although cursory consideration is given to redox potentials in the section on redox titrations and potentiometric end-point determination is referred to in some examples of titrimetric analysis.

Each subject begins with a review of chemical principles at an elementary, general chemistry level. However, the scope often is limited. For example, amphiprotic salts and polyprotic acids are not dealt with in the chapter on acid–base equilibria, the use of acid–base titrimetry in the analysis of esters by saponification is discussed but a related application to the acylation of alcohols is not, and although chemically bonded stationary phases in HPLC are considered, formal allusion to reversed-phase methodology, one of the fastest growing techniques applied to drug analysis, is absent. However, the chapters on spectrometric and chromatographic methods are particularly well presented and provide the best depth of coverage of any of the topics discussed.

Among the most useful components of the chapters on methodology are the examples given to illustrate the principles. These examples, taken primarily from USP XIX and NF XIV, form an essential part of the textual material of the chapter since, in many cases, information or methodology may be presented here that is not dealt with in the main part of the chapter. Similar examples from the compendia also are offered as problems in the study guide found at the end of each chapter.

Chapter 21 deals with the use of the scientific literature and is followed by an appendix reviewing elementary mathematical operations (significant figures, exponents, powers, roots, and logarithms).

In summary, this is a generally well-written and well-designed text that uniquely incorporates principles of drug product selection, quality assurance, and analytical methodology. As such, the text could find application in a modern pharmacy curriculum; however, supplementation may be needed in certain areas. The major portion of the text provides a survey at the elementary level of certain methodology applied to the analysis of organic drugs. For more detailed and more comprehensive coverage of these topics, one of the more standard texts in pharmaceutical or analytical chemistry may be more appropriate.

*Reviewed by* Larry L. Augsburger
*Department of Pharmaceutics*
*and*
S. Edward Krikorian
*Department of Medicinal Chemistry/Pharmacognosy*
*School of Pharmacy*
*University of Maryland*
*Baltimore, MD 21201*

---

**The Basis of Medicinal Chemistry: Burger's Medicinal Chemistry, 4th Ed., Part I.** Edited by MANFRED E. WOLFF. Wiley, 605 Third Ave., New York, NY 10016. 1980. 497 pp. 17 × 25 cm. Price $29.50.

Part I is the first of a three-volume work containing 12 chapters. This multiauthored text presents underlying principles of medicinal chemistry and includes new areas and topics representing the changes in the pharmaceutical sciences since the last edition. The authors, chosen by the editor, are considered to be authorities in their field. The topics are reminiscent of those in the "Principles of Drug Action: The Basis of Pharmacology, 2nd ed.," by A. Goldstein, L. Aronow, and S. M. Kalman.

The 12 subjects covering 478 pages in this volume were selected apparently on the basis of their broad appeal. They include an introductory chapter dealing with a historical account of medicinal chemistry; one chapter on Drug Absorption, Distribution, and Elimination; two chapters on metabolism, Drug Biotransformation—Oxidation, Reduction, Hydrolytic and Conjugation Reactions and Chemical and Biological Factors Influencing Drug Biotransformation; three chapters based on drug–receptor interactions, Receptor Theories and Dose–Response Relationships, Drug–Receptor Geometry, and The Nature of the Drug–Receptor Bond; three chapters on the methods of drug design, Guidelines for Drug and Analog Design, Approaches to the Rational Design of Enzyme Inhibitors, and QSAR; and two chapters covering Drug Allergy and Chemical Carcinogenesis. The chapters on metabolism, drug–receptor interactions, and drug design were particularly interesting.

With well-written chapters, a thorough and updated literature coverage in most chapters (3451 references of which 1337 are in the introductory chapter) for further investigation, and a comprehensive subject index, this book accomplishes its purpose as a secondary source for the biologist and medicinal chemist in industry and academia. This text can be recommended as a useful reference to graduate students for an advanced course in medicinal chemistry and other disciplines (biochemistry, pharmacology, biophysics, microbiology, and bio-organic). Most researchers in these areas will find this book to be a useful addition to their library.

*Reviewed by* Robert A. Magarian
*Department of Medicinal Chemistry*
*College of Pharmacy*
*Health Sciences Center*
*University of Oklahoma*
*Oklahoma City, OK 73190*

---

**Handbook of Basic Pharmacokinetics, 2nd ed.** By WOLFGANG A. RITSCHEL. Drug Intelligence Publications, Hamilton, IL 62341. 1980. 454 pp. 11 × 19 cm. Price $19.50.

The author views this book not as a textbook but rather as a collection of pharmacokinetic facts. The book meets this definition well. It is a comprehensive collection of important facts necessary to the understanding of pharmacokinetics.

This edition has new sections on dosage adjustment in the elderly and

## REVIEWS

**Essentials of Drug Product Quality: Concepts and Methodology.** By MAHMOUD M. ABDEL-MONEM and JAMES G. HENKEL. C. V. Mosby, 11830 Westline Industrial Drive, St. Louis, MO 63141. 1978. 274 pp. 20 × 25 cm. Price $14.95.

This text, according to the preface, is designed for first professional year pharmacy students. It is unique in two respects: (*a*) it attempts to integrate the elements of quality assurance of drugs and drug products with the accompanying methodology (directed toward both the drug product and the drug in biological fluid); and (*b*) it employs a format and style designed to support the use of the personalized system of instruction (PSI). PSI is described as "characterized by a mastery learning requirement, student self-pacing within the course, the use of proctors for immediate grading of tests taken by students for each unit (chapter), and infrequent lectures." Nevertheless, the format should lend itself well to a more traditional mode of instruction. In this regard, each of the 21 chapters begins with a list of performance objectives for the student and closes with a more than ample list of study questions and practice problems. The writing generally is very readable and lucid.

The first three chapters provide a well-planned, coherent treatment of the principles of drug product selection and include an introduction to dosage forms, the history and purpose of the official compendia, the role played by the FDA in drug product quality assurance, and drug product selection based on pharmaceutical equivalence and bioequivalence. However, some instructors may desire more depth in the treatment of dosage forms and bioequivalence. The treatment of the basis, application, and interpretation of official tests for unit-to-unit variation and uniformity (Chapter 2) is especially well done. However, the few sentences devoted to the dissolution test in Chapter 3 are incomplete and superficial. Chapters 4 and 5, which discuss data analysis and significance testing, are especially noteworthy.

The preface suggests that the analytical methodology chosen to be discussed (Chapters 6–20) is that supporting the quality assurance of drugs and states that the "important analytical methods" are covered. This philosophy apparently influenced the selection of topics, which include ionic equilibria ($K_{sp}$ and acid–base chemistry) (two chapters), solvent extraction principles (one chapter), gravimetric analysis (one chapter), volumetric analysis (acid–base and redox) (two chapters), spectrometry (UV, colorimetry, IR, fluorescence, and mass spectrometry) (five chapters), chromatography (column, TLC, GLC, and HPLC) (three chapters), and radioactivity (one chapter). The emphasis is on the analysis of organic drugs and less on inorganic substances, as evidenced by the absence of precipitation and complexometric titrations among the volumetric techniques discussed and the omission of the analysis of heavy-metal ions among the gravimetric techniques. Also, electrochemical techniques are ignored, although cursory consideration is given to redox potentials in the section on redox titrations and potentiometric end-point determination is referred to in some examples of titrimetric analysis.

Each subject begins with a review of chemical principles at an elementary, general chemistry level. However, the scope often is limited. For example, amphiprotic salts and polyprotic acids are not dealt with in the chapter on acid–base equilibria, the use of acid–base titrimetry in the analysis of esters by saponification is discussed but a related application to the acylation of alcohols is not, and although chemically bonded stationary phases in HPLC are considered, formal allusion to reversed-phase methodology, one of the fastest growing techniques applied to drug analysis, is absent. However, the chapters on spectrometric and chromatographic methods are particularly well presented and provide the best depth of coverage of any of the topics discussed.

Among the most useful components of the chapters on methodology are the examples given to illustrate the principles. These examples, taken primarily from USP XIX and NF XIV, form an essential part of the textual material of the chapter since, in many cases, information or methodology may be presented here that is not dealt with in the main part of the chapter. Similar examples from the compendia also are offered as problems in the study guide found at the end of each chapter.

Chapter 21 deals with the use of the scientific literature and is followed by an appendix reviewing elementary mathematical operations (significant figures, exponents, powers, roots, and logarithms).

In summary, this is a generally well-written and well-designed text that uniquely incorporates principles of drug product selection, quality assurance, and analytical methodology. As such, the text could find application in a modern pharmacy curriculum; however, supplementation may be needed in certain areas. The major portion of the text provides a survey at the elementary level of certain methodology applied to the analysis of organic drugs. For more detailed and more comprehensive coverage of these topics, one of the more standard texts in pharmaceutical or analytical chemistry may be more appropriate.

*Reviewed by* Larry L. Augsburger
*Department of Pharmaceutics*
*and*
S. Edward Krikorian
*Department of Medicinal Chemistry/Pharmacognosy*
*School of Pharmacy*
*University of Maryland*
*Baltimore, MD 21201*

---

**The Basis of Medicinal Chemistry: Burger's Medicinal Chemistry, 4th Ed., Part I.** Edited by MANFRED E. WOLFF. Wiley, 605 Third Ave., New York, NY 10016. 1980. 497 pp. 17 × 25 cm. Price $29.50.

Part I is the first of a three-volume work containing 12 chapters. This multiauthored text presents underlying principles of medicinal chemistry and includes new areas and topics representing the changes in the pharmaceutical sciences since the last edition. The authors, chosen by the editor, are considered to be authorities in their field. The topics are reminiscent of those in the "Principles of Drug Action: The Basis of Pharmacology, 2nd ed.," by A. Goldstein, L. Aronow, and S. M. Kalman.

The 12 subjects covering 478 pages in this volume were selected apparently on the basis of their broad appeal. They include an introductory chapter dealing with a historical account of medicinal chemistry; one chapter on Drug Absorption, Distribution, and Elimination; two chapters on metabolism, Drug Biotransformation—Oxidation, Reduction, Hydrolytic and Conjugation Reactions and Chemical and Biological Factors Influencing Drug Biotransformation; three chapters based on drug–receptor interactions, Receptor Theories and Dose–Response Relationships, Drug–Receptor Geometry, and The Nature of the Drug–Receptor Bond; three chapters on the methods of drug design, Guidelines for Drug and Analog Design, Approaches to the Rational Design of Enzyme Inhibitors, and QSAR; and two chapters covering Drug Allergy and Chemical Carcinogenesis. The chapters on metabolism, drug–receptor interactions, and drug design were particularly interesting.

With well-written chapters, a thorough and updated literature coverage in most chapters (3451 references of which 1337 are in the introductory chapter) for further investigation, and a comprehensive subject index, this book accomplishes its purpose as a secondary source for the biologist and medicinal chemist in industry and academia. This text can be recommended as a useful reference to graduate students for an advanced course in medicinal chemistry and other disciplines (biochemistry, pharmacology, biophysics, microbiology, and bio-organic). Most researchers in these areas will find this book to be a useful addition to their library.

*Reviewed by* Robert A. Magarian
*Department of Medicinal Chemistry*
*College of Pharmacy*
*Health Sciences Center*
*University of Oklahoma*
*Oklahoma City, OK 73190*

---

**Handbook of Basic Pharmacokinetics, 2nd ed.** By WOLFGANG A. RITSCHEL. Drug Intelligence Publications, Hamilton, IL 62341. 1980. 454 pp. 11 × 19 cm. Price $19.50.

The author views this book not as a textbook but rather as a collection of pharmacokinetic facts. The book meets this definition well. It is a comprehensive collection of important facts necessary to the understanding of pharmacokinetics.

This edition has new sections on dosage adjustment in the elderly and

## REVIEWS

**Essentials of Drug Product Quality: Concepts and Methodology.** By MAHMOUD M. ABDEL-MONEM and JAMES G. HENKEL. C. V. Mosby, 11830 Westline Industrial Drive, St. Louis, MO 63141. 1978. 274 pp. 20 × 25 cm. Price $14.95.

This text, according to the preface, is designed for first professional year pharmacy students. It is unique in two respects: (*a*) it attempts to integrate the elements of quality assurance of drugs and drug products with the accompanying methodology (directed toward both the drug product and the drug in biological fluid); and (*b*) it employs a format and style designed to support the use of the personalized system of instruction (PSI). PSI is described as "characterized by a mastery learning requirement, student self-pacing within the course, the use of proctors for immediate grading of tests taken by students for each unit (chapter), and infrequent lectures." Nevertheless, the format should lend itself well to a more traditional mode of instruction. In this regard, each of the 21 chapters begins with a list of performance objectives for the student and closes with a more than ample list of study questions and practice problems. The writing generally is very readable and lucid.

The first three chapters provide a well-planned, coherent treatment of the principles of drug product selection and include an introduction to dosage forms, the history and purpose of the official compendia, the role played by the FDA in drug product quality assurance, and drug product selection based on pharmaceutical equivalence and bioequivalence. However, some instructors may desire more depth in the treatment of dosage forms and bioequivalence. The treatment of the basis, application, and interpretation of official tests for unit-to-unit variation and uniformity (Chapter 2) is especially well done. However, the few sentences devoted to the dissolution test in Chapter 3 are incomplete and superficial. Chapters 4 and 5, which discuss data analysis and significance testing, are especially noteworthy.

The preface suggests that the analytical methodology chosen to be discussed (Chapters 6–20) is that supporting the quality assurance of drugs and states that the "important analytical methods" are covered. This philosophy apparently influenced the selection of topics, which include ionic equilibria ($K_{sp}$ and acid–base chemistry) (two chapters), solvent extraction principles (one chapter), gravimetric analysis (one chapter), volumetric analysis (acid–base and redox) (two chapters), spectrometry (UV, colorimetry, IR, fluorescence, and mass spectrometry) (five chapters), chromatography (column, TLC, GLC, and HPLC) (three chapters), and radioactivity (one chapter). The emphasis is on the analysis of organic drugs and less on inorganic substances, as evidenced by the absence of precipitation and complexometric titrations among the volumetric techniques discussed and the omission of the analysis of heavy-metal ions among the gravimetric techniques. Also, electrochemical techniques are ignored, although cursory consideration is given to redox potentials in the section on redox titrations and potentiometric end-point determination is referred to in some examples of titrimetric analysis.

Each subject begins with a review of chemical principles at an elementary, general chemistry level. However, the scope often is limited. For example, amphiprotic salts and polyprotic acids are not dealt with in the chapter on acid–base equilibria, the use of acid–base titrimetry in the analysis of esters by saponification is discussed but a related application to the acylation of alcohols is not, and although chemically bonded stationary phases in HPLC are considered, formal allusion to reversed-phase methodology, one of the fastest growing techniques applied to drug analysis, is absent. However, the chapters on spectrometric and chromatographic methods are particularly well presented and provide the best depth of coverage of any of the topics discussed.

Among the most useful components of the chapters on methodology are the examples given to illustrate the principles. These examples, taken primarily from USP XIX and NF XIV, form an essential part of the textual material of the chapter since, in many cases, information or methodology may be presented here that is not dealt with in the main part of the chapter. Similar examples from the compendia also are offered as problems in the study guide found at the end of each chapter.

Chapter 21 deals with the use of the scientific literature and is followed by an appendix reviewing elementary mathematical operations (significant figures, exponents, powers, roots, and logarithms).

In summary, this is a generally well-written and well-designed text that uniquely incorporates principles of drug product selection, quality assurance, and analytical methodology. As such, the text could find application in a modern pharmacy curriculum; however, supplementation may be needed in certain areas. The major portion of the text provides a survey at the elementary level of certain methodology applied to the analysis of organic drugs. For more detailed and more comprehensive coverage of these topics, one of the more standard texts in pharmaceutical or analytical chemistry may be more appropriate.

*Reviewed by* Larry L. Augsburger
*Department of Pharmaceutics*
*and*
S. Edward Krikorian
*Department of Medicinal Chemistry/Pharmacognosy*
*School of Pharmacy*
*University of Maryland*
*Baltimore, MD 21201*

---

**The Basis of Medicinal Chemistry: Burger's Medicinal Chemistry, 4th Ed., Part I.** Edited by MANFRED E. WOLFF. Wiley, 605 Third Ave., New York, NY 10016. 1980. 497 pp. 17 × 25 cm. Price $29.50.

Part I is the first of a three-volume work containing 12 chapters. This multiauthored text presents underlying principles of medicinal chemistry and includes new areas and topics representing the changes in the pharmaceutical sciences since the last edition. The authors, chosen by the editor, are considered to be authorities in their field. The topics are reminiscent of those in the "Principles of Drug Action: The Basis of Pharmacology, 2nd ed.," by A. Goldstein, L. Aronow, and S. M. Kalman.

The 12 subjects covering 478 pages in this volume were selected apparently on the basis of their broad appeal. They include an introductory chapter dealing with a historical account of medicinal chemistry; one chapter on Drug Absorption, Distribution, and Elimination; two chapters on metabolism, Drug Biotransformation—Oxidation, Reduction, Hydrolytic and Conjugation Reactions and Chemical and Biological Factors Influencing Drug Biotransformation; three chapters based on drug–receptor interactions, Receptor Theories and Dose–Response Relationships, Drug–Receptor Geometry, and The Nature of the Drug–Receptor Bond; three chapters on the methods of drug design, Guidelines for Drug and Analog Design, Approaches to the Rational Design of Enzyme Inhibitors, and QSAR; and two chapters covering Drug Allergy and Chemical Carcinogenesis. The chapters on metabolism, drug–receptor interactions, and drug design were particularly interesting.

With well-written chapters, a thorough and updated literature coverage in most chapters (3451 references of which 1337 are in the introductory chapter) for further investigation, and a comprehensive subject index, this book accomplishes its purpose as a secondary source for the biologist and medicinal chemist in industry and academia. This text can be recommended as a useful reference to graduate students for an advanced course in medicinal chemistry and other disciplines (biochemistry, pharmacology, biophysics, microbiology, and bio-organic). Most researchers in these areas will find this book to be a useful addition to their library.

*Reviewed by* Robert A. Magarian
*Department of Medicinal Chemistry*
*College of Pharmacy*
*Health Sciences Center*
*University of Oklahoma*
*Oklahoma City, OK 73190*

---

**Handbook of Basic Pharmacokinetics, 2nd ed.** By WOLFGANG A. RITSCHEL. Drug Intelligence Publications, Hamilton, IL 62341. 1980. 454 pp. 11 × 19 cm. Price $19.50.

The author views this book not as a textbook but rather as a collection of pharmacokinetic facts. The book meets this definition well. It is a comprehensive collection of important facts necessary to the understanding of pharmacokinetics.

This edition has new sections on dosage adjustment in the elderly and

the obese and physiological and pathological factors that influence drug response. A section on correlating clinical response with drug disposition has been added. There also is a new chapter on bioavailability and bioequivalence.

Definitions are presented as a glossary in the first chapter. The processes of liberation, absorption, distribution, metabolism, and elimination are described in Chapter 2. Histological features of organs and cell membranes and drug–receptor interactions are considered in Chapters 3–5.

Absorption mechanisms (Chapter 6), physicochemical principles, including pKa values and partition coefficients (Chapters 7–9), and a physiological discussion of the GI tract and the circulatory system (Chapters 10 and 11) are presented.

Protein binding (Chapter 12), drug metabolism (Chapter 13), and drug elimination (Chapter 14) are mentioned, and drug reabsorption in the kidneys and biliary recycling are presented in Chapter 15.

The next section of the book (Chapters 16–26) deals with mathematical descriptions of various compartmental models. Included are one- and two-compartment models with intravenous and oral dosing. The determination of rate constants by noncomputer techniques is included with a discussion of volumes of distribution. Concentrations after single and multiple doses are calculated. Methods for calculating and using the area under the curve and urine data are presented. Dosage adjustment for children, elderly, and obese patients are presented, as are methods used to calculate dosage regimens for desired results.

The final chapters of the book (Chapters 27–31) deal with the effect of physiological factors on drug response and disposition, nonlinear pharmacokinetics, curve fitting, clinical response correlations with disposition, and bioavailability and bioequivalence. The appendix gives 14 pages of pharmacokinetic information for various drugs.

This book covers many of the topics discussed in an undergraduate biopharmaceutics course and of interest to a clinical pharmacist. Each topic is covered briefly but comprehensively. Both students and practicing pharmacists should find this book to be a very useful aid in understanding and using pharmacokinetic principles.

*Reviewed by* David Bourne
*Division of Pharmaceutics and Pharmaceutical Analysis*
*University of Kentucky*
*Lexington, KY 40506*

---

**Pharmaceutical Dosage Forms: Tablets Vol. 1.** Edited by HERBERT A. LIEBERMAN and LEON LACHMAN. Dekker, 270 Madison Ave., New York, NY 10016. 1980. 490 pp. 18 × 25.5 cm. Price $59.75. (A special introductory price of $29.75 is available on orders of five or more copies in the United States and Canada.)

This book is the first in a three-volume treatise designed to examine in detail all phases of tablet technology, from initial development to final quality assurance. In the first volume, each chapter develops from an introduction through to the present pharmaceutical practice. Fourteen authors contributed to this first volume of eight chapters, and they, along with those listed for the other two volumes, represent an illustrious selection of experts in this area.

Chapter I, entitled Preformulating Testing, is an excellent review of all the physical pharmacy testing necessary to characterize a new drug substance. Three excellent case studies are presented. The second chapter, entitled Tablet Formulation and Design, demonstrates how a suitable drug formulation should be developed based on available preformulation knowledge. Compressed Tablets comprises Chapter III in which each unit process step is reviewed, and the advantages and disadvantages of the techniques and excipients available are discussed in detail.

The final five chapters are entitled Compression-Coated and Layer Tablets; Effervescent Tablets; Special Tablets: Sublingual and Buccal Tablets; Chewable Tablets; and Medicated Lozenges. For each, the processing steps and alternatives are reviewed along with details of typical formulations.

The remaining two volumes promise to discuss each unit process in detail. Each chapter in Volume 1 is, however, complete within itself. When publication is completed, this series will be considered as the definitive state of the art. If, as the title implies, further volumes on capsules, liquids, and semisolids follow, this series will become the encyclopedia of pharmaceutical technology. Anyone actively involved in tablet formulation will require access to this series. However, anyone involved in formulation development or evaluation will also find this series to be of great value. It deserves to be the definitive reference for academic use.

*Reviewed by* John H. Wood
*School of Pharmacy*
*Medical College of Virginia*
*Virginia Commonwealth University*
*Richmond, VA 23298*

---

**Drug Level Monitoring—Analytical Techniques, Metabolism, and Pharmacokinetics.** By WOLFGANG SADÉE and GEERTRUIDA C. M. BEELEN. Wiley, 605 Third Ave., New York, NY 10016. 495 pp. 15 × 23 cm. Price $35.00.

This book is divided into essentially two parts. The first part consists of brief, generalized chapters on drug metabolism, pharmacokinetics, clinical pharmacokinetics and therapeutic drug level monitoring, and analytical techniques. Of these four chapters, the work on analytical techniques is the most extensive.

The second section consists of drug monographs for 102 drugs which were chosen on the basis of being currently measured in clinical pharmacokinetic laboratories, being representative of a class of chemical or pharmacological agents, and/or belonging to the following major classes: antimicrobials, anticancer drugs, antiepileptics, cardiovascular drugs, psychotropic drugs, analgesics, and drugs of abuse. Each monograph contains a brief description of the therapeutic and toxic concentration ranges, metabolism, analogous compounds, and analytical techniques. The last section of each monograph briefly describes the various analytical methods (with pertinent references) that have been employed. References in this section are current to 1978. However, an addendum at the end of the book updates the references through October 1979.

The chapters that appear in the first part of this book are far too brief and cursory to be of value to anyone unfamiliar with the given area. Two pages on the topic of pharmacokinetics is hardly worth the effort. In addition, the treatment of the various analytical techniques is quite unbalanced. Spectroscopic methods such as UV and visible spectroscopy, colorimetry, and fluorescence are given as much coverage as high-performance liquid chromatography, although the latter method is of much greater utility in monitoring blood levels of drugs. Greater coverage of the more important methods at the expense of the less important ones might have been a better approach.

The section containing drug monographs provides a wealth of information and important references. In most cases, some details are given on the most suitable methods.

Despite the shortcomings of the initial chapters, this book will be valuable to anyone engaged in drug level monitoring. Since the book provides a good survey of the pertinent literature, it can serve as an excellent starting point in searching for the best assay for a given drug level monitoring project.

*Reviewed by* James W. Munson
*The Upjohn Company*
*Kalamazoo, MI 49001*

---

**Clinical Pharmacology, 24th ed.** Edited by RONALD H. GIRWOOD. Macmillan, 866 Third Ave., New York, NY 10022. 1980. 608 pp. 15 × 23 cm. Price $29.95.

First published in 1884 in Great Britain, *Clinical Pharmacology* appears to be designed to acquaint medical and paramedical professionals with a relatively complete compilation of currently used drugs. Following two chapters devoted to discussions of Mechanisms Involved in Drug Action and Adverse Drug Reactions are 16 additional chapters that address antimicrobials, analgesics, autonomic and CNS drugs, cardiovascular drugs, drugs affecting the respiratory system, drugs affecting the alimentary system, drugs acting on the kidney, endocrine drugs, vitamins, hematinics, anticoagulants, cancer chemotherapy, heavy metals, and drug treatment of skin disorders. Chapter 19, An International Guide to Proprietary Names, provides a cross-listing of generic names from the trade names of drugs marketed both in Europe and the United States.

Written by one of the six contributing authors, each chapter introduces the drug category, describes the physical or chemical characteristics of

the obese and physiological and pathological factors that influence drug response. A section on correlating clinical response with drug disposition has been added. There also is a new chapter on bioavailability and bioequivalence.

Definitions are presented as a glossary in the first chapter. The processes of liberation, absorption, distribution, metabolism, and elimination are described in Chapter 2. Histological features of organs and cell membranes and drug–receptor interactions are considered in Chapters 3–5.

Absorption mechanisms (Chapter 6), physicochemical principles, including pKa values and partition coefficients (Chapters 7–9), and a physiological discussion of the GI tract and the circulatory system (Chapters 10 and 11) are presented.

Protein binding (Chapter 12), drug metabolism (Chapter 13), and drug elimination (Chapter 14) are mentioned, and drug reabsorption in the kidneys and biliary recycling are presented in Chapter 15.

The next section of the book (Chapters 16–26) deals with mathematical descriptions of various compartmental models. Included are one- and two-compartment models with intravenous and oral dosing. The determination of rate constants by noncomputer techniques is included with a discussion of volumes of distribution. Concentrations after single and multiple doses are calculated. Methods for calculating and using the area under the curve and urine data are presented. Dosage adjustment for children, elderly, and obese patients are presented, as are methods used to calculate dosage regimens for desired results.

The final chapters of the book (Chapters 27–31) deal with the effect of physiological factors on drug response and disposition, nonlinear pharmacokinetics, curve fitting, clinical response correlations with disposition, and bioavailability and bioequivalence. The appendix gives 14 pages of pharmacokinetic information for various drugs.

This book covers many of the topics discussed in an undergraduate biopharmaceutics course and of interest to a clinical pharmacist. Each topic is covered briefly but comprehensively. Both students and practicing pharmacists should find this book to be a very useful aid in understanding and using pharmacokinetic principles.

*Reviewed by* David Bourne
*Division of Pharmaceutics and Pharmaceutical Analysis*
*University of Kentucky*
*Lexington, KY 40506*

---

**Pharmaceutical Dosage Forms: Tablets Vol. 1.** Edited by HERBERT A. LIEBERMAN and LEON LACHMAN. Dekker, 270 Madison Ave., New York, NY 10016. 1980. 490 pp. 18 × 25.5 cm. Price $59.75. (A special introductory price of $29.75 is available on orders of five or more copies in the United States and Canada.)

This book is the first in a three-volume treatise designed to examine in detail all phases of tablet technology, from initial development to final quality assurance. In the first volume, each chapter develops from an introduction through to the present pharmaceutical practice. Fourteen authors contributed to this first volume of eight chapters, and they, along with those listed for the other two volumes, represent an illustrious selection of experts in this area.

Chapter I, entitled Preformulating Testing, is an excellent review of all the physical pharmacy testing necessary to characterize a new drug substance. Three excellent case studies are presented. The second chapter, entitled Tablet Formulation and Design, demonstrates how a suitable drug formulation should be developed based on available preformulation knowledge. Compressed Tablets comprises Chapter III in which each unit process step is reviewed, and the advantages and disadvantages of the techniques and excipients available are discussed in detail.

The final five chapters are entitled Compression-Coated and Layer Tablets; Effervescent Tablets; Special Tablets: Sublingual and Buccal Tablets; Chewable Tablets; and Medicated Lozenges. For each, the processing steps and alternatives are reviewed along with details of typical formulations.

The remaining two volumes promise to discuss each unit process in detail. Each chapter in Volume 1 is, however, complete within itself. When publication is completed, this series will be considered as the definitive state of the art. If, as the title implies, further volumes on capsules, liquids, and semisolids follow, this series will become the encyclopedia of pharmaceutical technology. Anyone actively involved in tablet formulation will require access to this series. However, anyone involved in formulation development or evaluation will also find this series to be of great value. It deserves to be the definitive reference for academic use.

*Reviewed by* John H. Wood
*School of Pharmacy*
*Medical College of Virginia*
*Virginia Commonwealth University*
*Richmond, VA 23298*

---

**Drug Level Monitoring—Analytical Techniques, Metabolism, and Pharmacokinetics.** By WOLFGANG SADÉE and GEERTRUIDA C. M. BEELEN. Wiley, 605 Third Ave., New York, NY 10016. 495 pp. 15 × 23 cm. Price $35.00.

This book is divided into essentially two parts. The first part consists of brief, generalized chapters on drug metabolism, pharmacokinetics, clinical pharmacokinetics and therapeutic drug level monitoring, and analytical techniques. Of these four chapters, the work on analytical techniques is the most extensive.

The second section consists of drug monographs for 102 drugs which were chosen on the basis of being currently measured in clinical pharmacokinetic laboratories, being representative of a class of chemical or pharmacological agents, and/or belonging to the following major classes: antimicrobials, anticancer drugs, antiepileptics, cardiovascular drugs, psychotropic drugs, analgesics, and drugs of abuse. Each monograph contains a brief description of the therapeutic and toxic concentration ranges, metabolism, analogous compounds, and analytical techniques. The last section of each monograph briefly describes the various analytical methods (with pertinent references) that have been employed. References in this section are current to 1978. However, an addendum at the end of the book updates the references through October 1979.

The chapters that appear in the first part of this book are far too brief and cursory to be of value to anyone unfamiliar with the given area. Two pages on the topic of pharmacokinetics is hardly worth the effort. In addition, the treatment of the various analytical techniques is quite unbalanced. Spectroscopic methods such as UV and visible spectroscopy, colorimetry, and fluorescence are given as much coverage as high-performance liquid chromatography, although the latter method is of much greater utility in monitoring blood levels of drugs. Greater coverage of the more important methods at the expense of the less important ones might have been a better approach.

The section containing drug monographs provides a wealth of information and important references. In most cases, some details are given on the most suitable methods.

Despite the shortcomings of the initial chapters, this book will be valuable to anyone engaged in drug level monitoring. Since the book provides a good survey of the pertinent literature, it can serve as an excellent starting point in searching for the best assay for a given drug level monitoring project.

*Reviewed by* James W. Munson
*The Upjohn Company*
*Kalamazoo, MI 49001*

---

**Clinical Pharmacology, 24th ed.** Edited by RONALD H. GIRWOOD. Macmillan, 866 Third Ave., New York, NY 10022. 1980. 608 pp. 15 × 23 cm. Price $29.95.

First published in 1884 in Great Britain, *Clinical Pharmacology* appears to be designed to acquaint medical and paramedical professionals with a relatively complete compilation of currently used drugs. Following two chapters devoted to discussions of Mechanisms Involved in Drug Action and Adverse Drug Reactions are 16 additional chapters that address antimicrobials, analgesics, autonomic and CNS drugs, cardiovascular drugs, drugs affecting the respiratory system, drugs affecting the alimentary system, drugs acting on the kidney, endocrine drugs, vitamins, hematinics, anticoagulants, cancer chemotherapy, heavy metals, and drug treatment of skin disorders. Chapter 19, An International Guide to Proprietary Names, provides a cross-listing of generic names from the trade names of drugs marketed both in Europe and the United States.

Written by one of the six contributing authors, each chapter introduces the drug category, describes the physical or chemical characteristics of

the obese and physiological and pathological factors that influence drug response. A section on correlating clinical response with drug disposition has been added. There also is a new chapter on bioavailability and bioequivalence.

Definitions are presented as a glossary in the first chapter. The processes of liberation, absorption, distribution, metabolism, and elimination are described in Chapter 2. Histological features of organs and cell membranes and drug–receptor interactions are considered in Chapters 3–5.

Absorption mechanisms (Chapter 6), physicochemical principles, including pKa values and partition coefficients (Chapters 7–9), and a physiological discussion of the GI tract and the circulatory system (Chapters 10 and 11) are presented.

Protein binding (Chapter 12), drug metabolism (Chapter 13), and drug elimination (Chapter 14) are mentioned, and drug reabsorption in the kidneys and biliary recycling are presented in Chapter 15.

The next section of the book (Chapters 16–26) deals with mathematical descriptions of various compartmental models. Included are one- and two-compartment models with intravenous and oral dosing. The determination of rate constants by noncomputer techniques is included with a discussion of volumes of distribution. Concentrations after single and multiple doses are calculated. Methods for calculating and using the area under the curve and urine data are presented. Dosage adjustment for children, elderly, and obese patients are presented, as are methods used to calculate dosage regimens for desired results.

The final chapters of the book (Chapters 27–31) deal with the effect of physiological factors on drug response and disposition, nonlinear pharmacokinetics, curve fitting, clinical response correlations with disposition, and bioavailability and bioequivalence. The appendix gives 14 pages of pharmacokinetic information for various drugs.

This book covers many of the topics discussed in an undergraduate biopharmaceutics course and of interest to a clinical pharmacist. Each topic is covered briefly but comprehensively. Both students and practicing pharmacists should find this book to be a very useful aid in understanding and using pharmacokinetic principles.

*Reviewed by* David Bourne
*Division of Pharmaceutics and Pharmaceutical Analysis*
*University of Kentucky*
*Lexington, KY 40506*

---

**Pharmaceutical Dosage Forms: Tablets Vol. 1.** Edited by HERBERT A. LIEBERMAN and LEON LACHMAN. Dekker, 270 Madison Ave., New York, NY 10016. 1980. 490 pp. 18 × 25.5 cm. Price $59.75. (A special introductory price of $29.75 is available on orders of five or more copies in the United States and Canada.)

This book is the first in a three-volume treatise designed to examine in detail all phases of tablet technology, from initial development to final quality assurance. In the first volume, each chapter develops from an introduction through to the present pharmaceutical practice. Fourteen authors contributed to this first volume of eight chapters, and they, along with those listed for the other two volumes, represent an illustrious selection of experts in this area.

Chapter I, entitled Preformulating Testing, is an excellent review of all the physical pharmacy testing necessary to characterize a new drug substance. Three excellent case studies are presented. The second chapter, entitled Tablet Formulation and Design, demonstrates how a suitable drug formulation should be developed based on available preformulation knowledge. Compressed Tablets comprises Chapter III in which each unit process step is reviewed, and the advantages and disadvantages of the techniques and excipients available are discussed in detail.

The final five chapters are entitled Compression-Coated and Layer Tablets; Effervescent Tablets; Special Tablets: Sublingual and Buccal Tablets; Chewable Tablets; and Medicated Lozenges. For each, the processing steps and alternatives are reviewed along with details of typical formulations.

The remaining two volumes promise to discuss each unit process in detail. Each chapter in Volume 1 is, however, complete within itself. When publication is completed, this series will be considered as the definitive state of the art. If, as the title implies, further volumes on capsules, liquids, and semisolids follow, this series will become the encyclopedia of pharmaceutical technology. Anyone actively involved in tablet formulation will require access to this series. However, anyone involved in formulation development or evaluation will also find this series to be of great value. It deserves to be the definitive reference for academic use.

*Reviewed by* John H. Wood
*School of Pharmacy*
*Medical College of Virginia*
*Virginia Commonwealth University*
*Richmond, VA 23298*

---

**Drug Level Monitoring—Analytical Techniques, Metabolism, and Pharmacokinetics.** By WOLFGANG SADÉE and GEERTRUIDA C. M. BEELEN. Wiley, 605 Third Ave., New York, NY 10016. 495 pp. 15 × 23 cm. Price $35.00.

This book is divided into essentially two parts. The first part consists of brief, generalized chapters on drug metabolism, pharmacokinetics, clinical pharmacokinetics and therapeutic drug level monitoring, and analytical techniques. Of these four chapters, the work on analytical techniques is the most extensive.

The second section consists of drug monographs for 102 drugs which were chosen on the basis of being currently measured in clinical pharmacokinetic laboratories, being representative of a class of chemical or pharmacological agents, and/or belonging to the following major classes: antimicrobials, anticancer drugs, antiepileptics, cardiovascular drugs, psychotropic drugs, analgesics, and drugs of abuse. Each monograph contains a brief description of the therapeutic and toxic concentration ranges, metabolism, analogous compounds, and analytical techniques. The last section of each monograph briefly describes the various analytical methods (with pertinent references) that have been employed. References in this section are current to 1978. However, an addendum at the end of the book updates the references through October 1979.

The chapters that appear in the first part of this book are far too brief and cursory to be of value to anyone unfamiliar with the given area. Two pages on the topic of pharmacokinetics is hardly worth the effort. In addition, the treatment of the various analytical techniques is quite unbalanced. Spectroscopic methods such as UV and visible spectroscopy, colorimetry, and fluorescence are given as much coverage as high-performance liquid chromatography, although the latter method is of much greater utility in monitoring blood levels of drugs. Greater coverage of the more important methods at the expense of the less important ones might have been a better approach.

The section containing drug monographs provides a wealth of information and important references. In most cases, some details are given on the most suitable methods.

Despite the shortcomings of the initial chapters, this book will be valuable to anyone engaged in drug level monitoring. Since the book provides a good survey of the pertinent literature, it can serve as an excellent starting point in searching for the best assay for a given drug level monitoring project.

*Reviewed by* James W. Munson
*The Upjohn Company*
*Kalamazoo, MI 49001*

---

**Clinical Pharmacology, 24th ed.** Edited by RONALD H. GIRWOOD. Macmillan, 866 Third Ave., New York, NY 10022. 1980. 608 pp. 15 × 23 cm. Price $29.95.

First published in 1884 in Great Britain, *Clinical Pharmacology* appears to be designed to acquaint medical and paramedical professionals with a relatively complete compilation of currently used drugs. Following two chapters devoted to discussions of Mechanisms Involved in Drug Action and Adverse Drug Reactions are 16 additional chapters that address antimicrobials, analgesics, autonomic and CNS drugs, cardiovascular drugs, drugs affecting the respiratory system, drugs affecting the alimentary system, drugs acting on the kidney, endocrine drugs, vitamins, hematinics, anticoagulants, cancer chemotherapy, heavy metals, and drug treatment of skin disorders. Chapter 19, An International Guide to Proprietary Names, provides a cross-listing of generic names from the trade names of drugs marketed both in Europe and the United States.

Written by one of the six contributing authors, each chapter introduces the drug category, describes the physical or chemical characteristics of

the obese and physiological and pathological factors that influence drug response. A section on correlating clinical response with drug disposition has been added. There also is a new chapter on bioavailability and bioequivalence.

Definitions are presented as a glossary in the first chapter. The processes of liberation, absorption, distribution, metabolism, and elimination are described in Chapter 2. Histological features of organs and cell membranes and drug–receptor interactions are considered in Chapters 3–5.

Absorption mechanisms (Chapter 6), physicochemical principles, including pKa values and partition coefficients (Chapters 7–9), and a physiological discussion of the GI tract and the circulatory system (Chapters 10 and 11) are presented.

Protein binding (Chapter 12), drug metabolism (Chapter 13), and drug elimination (Chapter 14) are mentioned, and drug reabsorption in the kidneys and biliary recycling are presented in Chapter 15.

The next section of the book (Chapters 16–26) deals with mathematical descriptions of various compartmental models. Included are one- and two-compartment models with intravenous and oral dosing. The determination of rate constants by noncomputer techniques is included with a discussion of volumes of distribution. Concentrations after single and multiple doses are calculated. Methods for calculating and using the area under the curve and urine data are presented. Dosage adjustment for children, elderly, and obese patients are presented, as are methods used to calculate dosage regimens for desired results.

The final chapters of the book (Chapters 27–31) deal with the effect of physiological factors on drug response and disposition, nonlinear pharmacokinetics, curve fitting, clinical response correlations with disposition, and bioavailability and bioequivalence. The appendix gives 14 pages of pharmacokinetic information for various drugs.

This book covers many of the topics discussed in an undergraduate biopharmaceutics course and of interest to a clinical pharmacist. Each topic is covered briefly but comprehensively. Both students and practicing pharmacists should find this book to be a very useful aid in understanding and using pharmacokinetic principles.

*Reviewed by* David Bourne
*Division of Pharmaceutics and Pharmaceutical Analysis*
*University of Kentucky*
*Lexington, KY 40506*

---

**Pharmaceutical Dosage Forms: Tablets Vol. 1.** Edited by HERBERT A. LIEBERMAN and LEON LACHMAN. Dekker, 270 Madison Ave., New York, NY 10016. 1980. 490 pp. 18 × 25.5 cm. Price $59.75. (A special introductory price of $29.75 is available on orders of five or more copies in the United States and Canada.)

This book is the first in a three-volume treatise designed to examine in detail all phases of tablet technology, from initial development to final quality assurance. In the first volume, each chapter develops from an introduction through to the present pharmaceutical practice. Fourteen authors contributed to this first volume of eight chapters, and they, along with those listed for the other two volumes, represent an illustrious selection of experts in this area.

Chapter I, entitled Preformulating Testing, is an excellent review of all the physical pharmacy testing necessary to characterize a new drug substance. Three excellent case studies are presented. The second chapter, entitled Tablet Formulation and Design, demonstrates how a suitable drug formulation should be developed based on available preformulation knowledge. Compressed Tablets comprises Chapter III in which each unit process step is reviewed, and the advantages and disadvantages of the techniques and excipients available are discussed in detail.

The final five chapters are entitled Compression-Coated and Layer Tablets; Effervescent Tablets; Special Tablets: Sublingual and Buccal Tablets; Chewable Tablets; and Medicated Lozenges. For each, the processing steps and alternatives are reviewed along with details of typical formulations.

The remaining two volumes promise to discuss each unit process in detail. Each chapter in Volume 1 is, however, complete within itself. When publication is completed, this series will be considered as the definitive state of the art. If, as the title implies, further volumes on capsules, liquids, and semisolids follow, this series will become the encyclopedia of pharmaceutical technology. Anyone actively involved in tablet formulation will require access to this series. However, anyone involved in formulation development or evaluation will also find this series to be of great value. It deserves to be the definitive reference for academic use.

*Reviewed by* John H. Wood
*School of Pharmacy*
*Medical College of Virginia*
*Virginia Commonwealth University*
*Richmond, VA 23298*

---

**Drug Level Monitoring—Analytical Techniques, Metabolism, and Pharmacokinetics.** By WOLFGANG SADÉE and GEERTRUIDA C. M. BEELEN. Wiley, 605 Third Ave., New York, NY 10016. 495 pp. 15 × 23 cm. Price $35.00.

This book is divided into essentially two parts. The first part consists of brief, generalized chapters on drug metabolism, pharmacokinetics, clinical pharmacokinetics and therapeutic drug level monitoring, and analytical techniques. Of these four chapters, the work on analytical techniques is the most extensive.

The second section consists of drug monographs for 102 drugs which were chosen on the basis of being currently measured in clinical pharmacokinetic laboratories, being representative of a class of chemical or pharmacological agents, and/or belonging to the following major classes: antimicrobials, anticancer drugs, antiepileptics, cardiovascular drugs, psychotropic drugs, analgesics, and drugs of abuse. Each monograph contains a brief description of the therapeutic and toxic concentration ranges, metabolism, analogous compounds, and analytical techniques. The last section of each monograph briefly describes the various analytical methods (with pertinent references) that have been employed. References in this section are current to 1978. However, an addendum at the end of the book updates the references through October 1979.

The chapters that appear in the first part of this book are far too brief and cursory to be of value to anyone unfamiliar with the given area. Two pages on the topic of pharmacokinetics is hardly worth the effort. In addition, the treatment of the various analytical techniques is quite unbalanced. Spectroscopic methods such as UV and visible spectroscopy, colorimetry, and fluorescence are given as much coverage as high-performance liquid chromatography, although the latter method is of much greater utility in monitoring blood levels of drugs. Greater coverage of the more important methods at the expense of the less important ones might have been a better approach.

The section containing drug monographs provides a wealth of information and important references. In most cases, some details are given on the most suitable methods.

Despite the shortcomings of the initial chapters, this book will be valuable to anyone engaged in drug level monitoring. Since the book provides a good survey of the pertinent literature, it can serve as an excellent starting point in searching for the best assay for a given drug level monitoring project.

*Reviewed by* James W. Munson
*The Upjohn Company*
*Kalamazoo, MI 49001*

---

**Clinical Pharmacology, 24th ed.** Edited by RONALD H. GIRWOOD. Macmillan, 866 Third Ave., New York, NY 10022. 1980. 608 pp. 15 × 23 cm. Price $29.95.

First published in 1884 in Great Britain, *Clinical Pharmacology* appears to be designed to acquaint medical and paramedical professionals with a relatively complete compilation of currently used drugs. Following two chapters devoted to discussions of Mechanisms Involved in Drug Action and Adverse Drug Reactions are 16 additional chapters that address antimicrobials, analgesics, autonomic and CNS drugs, cardiovascular drugs, drugs affecting the respiratory system, drugs affecting the alimentary system, drugs acting on the kidney, endocrine drugs, vitamins, hematinics, anticoagulants, cancer chemotherapy, heavy metals, and drug treatment of skin disorders. Chapter 19, An International Guide to Proprietary Names, provides a cross-listing of generic names from the trade names of drugs marketed both in Europe and the United States.

Written by one of the six contributing authors, each chapter introduces the drug category, describes the physical or chemical characteristics of

the drug, briefly addresses the mode of action of the drug(s), lists the pharmaceutical preparations available with the recommended dosage, discusses the pharmacodynamic properties of the drug(s) in an uncomplicated fashion, and describes the indications for use and adverse effects (toxicological and allergic). When appropriate, antidotal measures, drug interactions, and contraindications are included.

The book is not a complete treatis on pharmacology and should not be expected to replace general pharmacology texts. Neither does it provide an indepth discourse on the pathological signs or symptoms of diseases or their most appropriate therapeutic approach. It is an easily read introduction into each of these areas. As an aid in using the book as a reference in clinical pharmacology and therapeutics, the index lists the drugs, disease states, pathological conditions, and organisms responsible for infectious pathological diseases. The fact that the book is written and published in the United Kingdom does not detract from its potential, but perhaps limited, usefulness by U.S. pharmacists.

*Reviewed by* A. E. Wade
*Department of Pharmacology*
*School of Pharmacy*
*University of Georgia*
*Athens, GA 30601*

---

**The Organic Chemistry of Drug Synthesis, Vol. 2.** By DANIEL LEDNICER and LESTER A. MITSCHER. Wiley, 605 Third Ave., New York, NY 10016. 1980. 526 pp. 15 × 23 cm. Price $28.00.

This book is Volume 2 in a series and apparently will be followed by future volumes as generic names are granted. Together, Volumes 1 and 2 include syntheses for compounds granted a generic name by the USAN Council through 1976.

In making a comparison between Volumes 1 and 2, one notices immediately that the latter volume is easier to read because of the darker type and greater spacing between lines. This volume, although not errorless, appears to contain fewer mistakes than the previous one. The final 13 pages contain Errata for Volume 1.

As the title implies, the major focus is on organic chemistry (particularly, drug synthesis), with appropriate brief mention of the associated pharmacological action. The authors have done a good job illustrating the reaction mechanisms for many synthetic pathways while keeping details to a minimum. Historical sidelights (*e.g.*, cortisone story on p. 176 and LSD story on p. 476) also enliven the reading.

This volume contains 16 chapters as opposed to 22 in Volume 1. Most of the same chapter headings are carried over in Volume 2. Deletions include: Chapter 1, Introduction; Chapter 2, A Case Study in Molecular Manipulation: The Local Anesthetics; Chapter 7, Arylethylenes and Their Reduction Products (no mention of diethylstilbestrol or its derivatives in Volume 2); Chapter 11, Tetracyclines (this material is incorporated into Chapter 7, Polycyclic Aromatic and Hydroaromatic Compounds); Chapter 12, Acyclic Compounds (new material is found in Chapter 1, Monocyclic and Acyclic Aliphatic Compounds); and Chapter 19, Phenothiazines (incorporated into Chapter 14, Heterocycles Fused to Two Benzene Rings). In addition to the chapter headings for various types of aliphatic, aromatic, and heterocyclic compounds, the chapters on steroids, morphinoids, benzodiazepines, and $\beta$-lactam antibiotics are retained. Changes in chapter organization were necessitated by the relative amounts of new work. Volume 2 contains several examples of antineoplastic drug syntheses, which were lacking in the previous volume. The valuable Cross Index of Drugs also is retained.

This book fills a previous void since medicinal chemistry texts sometimes must slight the presentation of drug synthesis. This reviewer finds it to be a valuable contribution, which should be particularly useful to practicing medicinal and organic chemists as well as to students of these disciplines.

*Reviewed by* Milton J. Kornet
*College of Pharmacy*
*University of Kentucky*
*Lexington, KY 40506*

---

## NOTICES

*Elsevier's Dictionary of Pharmaceutical Science and Techniques, Vol. 2: Materia Medica.* In Six Languages. By A. SLIOSBERG. Elsevier/North-Holland, 52 Vanderbilt Ave., New York, NY 10017. 1980. 552 pp. 15 × 22 cm. Price $122.00.

*Lecture Notes in Chemistry, Vol. 15. Steric Fit in Quantitative Structure–Activity Relations.* By ALEXANDRU T. BALABAN, ADRIAN CHIRIAC, IOAN MOTOC, and ZENO SIMON. Springer-Verlag New York, 44 Hartz Way, Secaucus, NJ 07094. 1980. 178 pp. 16 × 24 cm. Price $17.50.

*Handbook of Biological Psychiatry, Part III: Brain Mechanisms and Abnormal Behavior—Genetics and Neuroendocrinology.* Vol. 1. Edited by HERMAN M. VAN PRAAG, MALCOLM H. LADER, OLE J. RAFAELSEN, and EDWARD J. SACHAR. Dekker, 270 Madison Ave., New York, NY 10016. 1980. 383 pp. 15 × 23 cm. Price $29.50.

*Reviews of Physiology, Biochemistry and Pharmacology, Vol. 87.* Edited by R. H. ADRIAN *et al.* Springer-Verlag New York, 44 Hartz Way, Secaucus, NJ 07094. 1980. 232 pp. 16 × 24 cm. Price $51.90.

*Progress in Medicinal Chemistry, Vol. 17.* Edited by G. P. ELLIS and G. B. WEST. Elsevier/North-Holland, 52 Vanderbilt Ave., New York, NY 10017. 1980. 280 pp. 14 × 21 cm. Price $64.00.

*A Clinician's Guide to Research Design.* By GERALD GOLDSTEIN. Nelson-Hall, 111 N. Canal St., Chicago, IL 60606. 1980. 280 pp. 13 × 21 cm. Price $24.95.

*Biomedical Polymers. Polymeric Materials and Pharmaceuticals for Biomedical Use.* Edited by EUGENE P. GOLDBERG and AKIO NAKAJIMA. Academic, 111 Fifth Ave., New York, NY 10003. 1980. 457 pp. 15 × 23 cm.

*Marijuana Research Findings: 1980. NIDA Research Monograph 31.* Edited by ROBERT C. PETERSEN. 1980. 221 pp. 14 × 23 cm. (Distributed by U.S. Dept. of Health & Human Services, Public Health Service, Alcohol, Drug Abuse, and Mental Health Administration, 5600 Fishers Lane, Rockville, MD 20857.)

the drug, briefly addresses the mode of action of the drug(s), lists the pharmaceutical preparations available with the recommended dosage, discusses the pharmacodynamic properties of the drug(s) in an uncomplicated fashion, and describes the indications for use and adverse effects (toxicological and allergic). When appropriate, antidotal measures, drug interactions, and contraindications are included.

The book is not a complete treatis on pharmacology and should not be expected to replace general pharmacology texts. Neither does it provide an indepth discourse on the pathological signs or symptoms of diseases or their most appropriate therapeutic approach. It is an easily read introduction into each of these areas. As an aid in using the book as a reference in clinical pharmacology and therapeutics, the index lists the drugs, disease states, pathological conditions, and organisms responsible for infectious pathological diseases. The fact that the book is written and published in the United Kingdom does not detract from its potential, but perhaps limited, usefulness by U.S. pharmacists.

*Reviewed by* A. E. Wade
*Department of Pharmacology*
*School of Pharmacy*
*University of Georgia*
*Athens, GA 30601*

---

**The Organic Chemistry of Drug Synthesis, Vol. 2.** By DANIEL LEDNICER and LESTER A. MITSCHER. Wiley, 605 Third Ave., New York, NY 10016. 1980. 526 pp. 15 × 23 cm. Price $28.00.

This book is Volume 2 in a series and apparently will be followed by future volumes as generic names are granted. Together, Volumes 1 and 2 include syntheses for compounds granted a generic name by the USAN Council through 1976.

In making a comparison between Volumes 1 and 2, one notices immediately that the latter volume is easier to read because of the darker type and greater spacing between lines. This volume, although not errorless, appears to contain fewer mistakes than the previous one. The final 13 pages contain Errata for Volume 1.

As the title implies, the major focus is on organic chemistry (particularly, drug synthesis), with appropriate brief mention of the associated pharmacological action. The authors have done a good job illustrating the reaction mechanisms for many synthetic pathways while keeping details to a minimum. Historical sidelights (*e.g.*, cortisone story on p. 176 and LSD story on p. 476) also enliven the reading.

This volume contains 16 chapters as opposed to 22 in Volume 1. Most of the same chapter headings are carried over in Volume 2. Deletions include: Chapter 1, Introduction; Chapter 2, A Case Study in Molecular Manipulation: The Local Anesthetics; Chapter 7, Arylethylenes and Their Reduction Products (no mention of diethylstilbestrol or its derivatives in Volume 2); Chapter 11, Tetracyclines (this material is incorporated into Chapter 7, Polycyclic Aromatic and Hydroaromatic Compounds); Chapter 12, Acyclic Compounds (new material is found in Chapter 1, Monocyclic and Acyclic Aliphatic Compounds); and Chapter 19, Phenothiazines (incorporated into Chapter 14, Heterocycles Fused to Two Benzene Rings). In addition to the chapter headings for various types of aliphatic, aromatic, and heterocyclic compounds, the chapters on steroids, morphinoids, benzodiazepines, and $\beta$-lactam antibiotics are retained. Changes in chapter organization were necessitated by the relative amounts of new work. Volume 2 contains several examples of antineoplastic drug syntheses, which were lacking in the previous volume. The valuable Cross Index of Drugs also is retained.

This book fills a previous void since medicinal chemistry texts sometimes must slight the presentation of drug synthesis. This reviewer finds it to be a valuable contribution, which should be particularly useful to practicing medicinal and organic chemists as well as to students of these disciplines.

*Reviewed by* Milton J. Kornet
*College of Pharmacy*
*University of Kentucky*
*Lexington, KY 40506*

---

## NOTICES

*Elsevier's Dictionary of Pharmaceutical Science and Techniques, Vol. 2: Materia Medica.* In Six Languages. By A. SLIOSBERG. Elsevier/North-Holland, 52 Vanderbilt Ave., New York, NY 10017. 1980. 552 pp. 15 × 22 cm. Price $122.00.

*Lecture Notes in Chemistry, Vol. 15. Steric Fit in Quantitative Structure–Activity Relations.* By ALEXANDRU T. BALABAN, ADRIAN CHIRIAC, IOAN MOTOC, and ZENO SIMON. Springer-Verlag New York, 44 Hartz Way, Secaucus, NJ 07094. 1980. 178 pp. 16 × 24 cm. Price $17.50.

*Handbook of Biological Psychiatry, Part III: Brain Mechanisms and Abnormal Behavior—Genetics and Neuroendocrinology.* Vol. 1. Edited by HERMAN M. VAN PRAAG, MALCOLM H. LADER, OLE J. RAFAELSEN, and EDWARD J. SACHAR. Dekker, 270 Madison Ave., New York, NY 10016. 1980. 383 pp. 15 × 23 cm. Price $29.50.

*Reviews of Physiology, Biochemistry and Pharmacology, Vol. 87.* Edited by R. H. ADRIAN *et al.* Springer-Verlag New York, 44 Hartz Way, Secaucus, NJ 07094. 1980. 232 pp. 16 × 24 cm. Price $51.90.

*Progress in Medicinal Chemistry, Vol. 17.* Edited by G. P. ELLIS and G. B. WEST. Elsevier/North-Holland, 52 Vanderbilt Ave., New York, NY 10017. 1980. 280 pp. 14 × 21 cm. Price $64.00.

*A Clinician's Guide to Research Design.* By GERALD GOLDSTEIN. Nelson-Hall, 111 N. Canal St., Chicago, IL 60606. 1980. 280 pp. 13 × 21 cm. Price $24.95.

*Biomedical Polymers. Polymeric Materials and Pharmaceuticals for Biomedical Use.* Edited by EUGENE P. GOLDBERG and AKIO NAKAJIMA. Academic, 111 Fifth Ave., New York, NY 10003. 1980. 457 pp. 15 × 23 cm.

*Marijuana Research Findings: 1980. NIDA Research Monograph 31.* Edited by ROBERT C. PETERSEN. 1980. 221 pp. 14 × 23 cm. (Distributed by U.S. Dept. of Health & Human Services, Public Health Service, Alcohol, Drug Abuse, and Mental Health Administration, 5600 Fishers Lane, Rockville, MD 20857.)

the drug, briefly addresses the mode of action of the drug(s), lists the pharmaceutical preparations available with the recommended dosage, discusses the pharmacodynamic properties of the drug(s) in an uncomplicated fashion, and describes the indications for use and adverse effects (toxicological and allergic). When appropriate, antidotal measures, drug interactions, and contraindications are included.

The book is not a complete treatis on pharmacology and should not be expected to replace general pharmacology texts. Neither does it provide an indepth discourse on the pathological signs or symptoms of diseases or their most appropriate therapeutic approach. It is an easily read introduction into each of these areas. As an aid in using the book as a reference in clinical pharmacology and therapeutics, the index lists the drugs, disease states, pathological conditions, and organisms responsible for infectious pathological diseases. The fact that the book is written and published in the United Kingdom does not detract from its potential, but perhaps limited, usefulness by U.S. pharmacists.

*Reviewed by* A. E. Wade
*Department of Pharmacology*
*School of Pharmacy*
*University of Georgia*
*Athens, GA 30601*

---

**The Organic Chemistry of Drug Synthesis, Vol. 2.** By DANIEL LEDNICER and LESTER A. MITSCHER. Wiley, 605 Third Ave., New York, NY 10016. 1980. 526 pp. 15 × 23 cm. Price $28.00.

This book is Volume 2 in a series and apparently will be followed by future volumes as generic names are granted. Together, Volumes 1 and 2 include syntheses for compounds granted a generic name by the USAN Council through 1976.

In making a comparison between Volumes 1 and 2, one notices immediately that the latter volume is easier to read because of the darker type and greater spacing between lines. This volume, although not errorless, appears to contain fewer mistakes than the previous one. The final 13 pages contain Errata for Volume 1.

As the title implies, the major focus is on organic chemistry (particularly, drug synthesis), with appropriate brief mention of the associated pharmacological action. The authors have done a good job illustrating the reaction mechanisms for many synthetic pathways while keeping details to a minimum. Historical sidelights (*e.g.*, cortisone story on p. 176 and LSD story on p. 476) also enliven the reading.

This volume contains 16 chapters as opposed to 22 in Volume 1. Most of the same chapter headings are carried over in Volume 2. Deletions include: Chapter 1, Introduction; Chapter 2, A Case Study in Molecular Manipulation: The Local Anesthetics; Chapter 7, Arylethylenes and Their Reduction Products (no mention of diethylstilbestrol or its derivatives in Volume 2); Chapter 11, Tetracyclines (this material is incorporated into Chapter 7, Polycyclic Aromatic and Hydroaromatic Compounds); Chapter 12, Acyclic Compounds (new material is found in Chapter 1, Monocyclic and Acyclic Aliphatic Compounds); and Chapter 19, Phenothiazines (incorporated into Chapter 14, Heterocycles Fused to Two Benzene Rings). In addition to the chapter headings for various types of aliphatic, aromatic, and heterocyclic compounds, the chapters on steroids, morphinoids, benzodiazepines, and $\beta$-lactam antibiotics are retained. Changes in chapter organization were necessitated by the relative amounts of new work. Volume 2 contains several examples of antineoplastic drug syntheses, which were lacking in the previous volume. The valuable Cross Index of Drugs also is retained.

This book fills a previous void since medicinal chemistry texts sometimes must slight the presentation of drug synthesis. This reviewer finds it to be a valuable contribution, which should be particularly useful to practicing medicinal and organic chemists as well as to students of these disciplines.

*Reviewed by* Milton J. Kornet
*College of Pharmacy*
*University of Kentucky*
*Lexington, KY 40506*

---

## NOTICES

*Elsevier's Dictionary of Pharmaceutical Science and Techniques, Vol. 2: Materia Medica.* In Six Languages. By A. SLIOSBERG. Elsevier/North-Holland, 52 Vanderbilt Ave., New York, NY 10017. 1980. 552 pp. 15 × 22 cm. Price $122.00.

*Lecture Notes in Chemistry, Vol. 15. Steric Fit in Quantitative Structure–Activity Relations.* By ALEXANDRU T. BALABAN, ADRIAN CHIRIAC, IOAN MOTOC, and ZENO SIMON. Springer-Verlag New York, 44 Hartz Way, Secaucus, NJ 07094. 1980. 178 pp. 16 × 24 cm. Price $17.50.

*Handbook of Biological Psychiatry, Part III: Brain Mechanisms and Abnormal Behavior—Genetics and Neuroendocrinology.* Vol. 1. Edited by HERMAN M. VAN PRAAG, MALCOLM H. LADER, OLE J. RAFAELSEN, and EDWARD J. SACHAR. Dekker, 270 Madison Ave., New York, NY 10016. 1980. 383 pp. 15 × 23 cm. Price $29.50.

*Reviews of Physiology, Biochemistry and Pharmacology, Vol. 87.* Edited by R. H. ADRIAN *et al.* Springer-Verlag New York, 44 Hartz Way, Secaucus, NJ 07094. 1980. 232 pp. 16 × 24 cm. Price $51.90.

*Progress in Medicinal Chemistry, Vol. 17.* Edited by G. P. ELLIS and G. B. WEST. Elsevier/North-Holland, 52 Vanderbilt Ave., New York, NY 10017. 1980. 280 pp. 14 × 21 cm. Price $64.00.

*A Clinician's Guide to Research Design.* By GERALD GOLDSTEIN. Nelson-Hall, 111 N. Canal St., Chicago, IL 60606. 1980. 280 pp. 13 × 21 cm. Price $24.95.

*Biomedical Polymers. Polymeric Materials and Pharmaceuticals for Biomedical Use.* Edited by EUGENE P. GOLDBERG and AKIO NAKAJIMA. Academic, 111 Fifth Ave., New York, NY 10003. 1980. 457 pp. 15 × 23 cm.

*Marijuana Research Findings: 1980. NIDA Research Monograph 31.* Edited by ROBERT C. PETERSEN. 1980. 221 pp. 14 × 23 cm. (Distributed by U.S. Dept. of Health & Human Services, Public Health Service, Alcohol, Drug Abuse, and Mental Health Administration, 5600 Fishers Lane, Rockville, MD 20857.)

A publication of the
American Pharmaceutical Association—
the National Professional Society
of Pharmacists

# JOURNAL OF PHARMACEUTICAL SCIENCES

## INDEX TO AUTHORS
## INDEX TO SUBJECTS

VOLUME 70
JANUARY TO DECEMBER, 1981

*Published monthly under the supervision of the Board of Trustees*

MARY H. FERGUSON
*Editor*

NANCY E. BROWN
*Production Editor*

JOHN PATRICK EVANS
*Copy Editor*

MICHAEL K. HAYES
*Copy Editor*

EDWARD G. FELDMANN
*Contributing Editor*

SAMUEL W. GOLDSTEIN
*Contributing Editor*

BELLE R. BECK
*Editorial Secretary*

EDWARD G. FELDMANN
*Acting Director of Publications*

EDITORIAL ADVISORY BOARD

John Autian
Norman R. Farnsworth
William J. Jusko
Herbert A. Lieberman
David E. Mann, Jr.
Ian W. Mathison
Gerald J. Papariello
Edward G. Rippie

JOURNAL OF PHARMACEUTICAL SCIENCES

APRIL 1981
VOLUME 70 NUMBER 4

*SYMPOSIUM*

*The articles appearing in this section were presented at the Fourth International Symposium on Microencapsulation, sponsored by the West Virginia University School of Pharmacy and the University of Miami Institute for Molecular and Cellular Evolution.*

# Microencapsulation of Living Cells and Tissues

**FRANKLIN LIM ˣ and RICHARD D. MOSS**

Received August 2, 1979, from the *Medical College of Virginia, Virginia Commonwealth University, Richmond, VA 23298.* Accepted for publication February 6, 1980.

**Abstract** □ A new microencapsulation procedure involving an all-aqueous phase system was developed. Viable cells or tissues were suspended in sodium alginate droplets, which then were gelled by calcium chloride solution. A permanent, semipermeable membrane was formed on the surface layer of the temporary gel capsules by treatment with a solution of polylysine. Finally, true living cell-containing microcapsules were produced by "liquefying" the gel within the microcapsules through calcium-ion removal by simple ion exchange. Microencapsulated living cells and tissues continued to grow and flourish. In tissue culture medium, microencapsulated rat pancreatic islets continued to release insulin and remained sensitive to glucose and theophylline stimulation, responding with a typical physiological biphasic insulin-release pattern for over 2 months. Microencapsulation of other viable cells and tissues such as red blood cells, hepatoma cells, sperm cells, and pancreatic endocrine tissues also was successful.

**Keyphrases** □ Semipermeability—membranes of microencapsulated viable hepatoma cells and microencapsulated viable pancreatic islets □ Pancreatic islets—viability within microcapsule demonstrated by insulin release pattern and histological staining □ Microencapsulation—symposium, preparation of viable microencapsulated hepatoma cells and pancreatic islets, semipermeable membranes

Microencapsulation is a process in which small, discrete, solid materials, liquid droplets, or gases are completely enveloped by an intact membrane. The functions of the capsular membrane are to protect the material within and to control the flow of materials, inside and outside, across the membrane.

## BACKGROUND

Microcapsules may possess impermeable or semipermeable membranes, depending on how and why the materials are encapsulated. Research and development in semipermeable microcapsules, pioneered by Chang (1, 2), have recently multiplied greatly, especially in the biomedical field. Important materials encapsulated include activated carbon granules, ion-exchange resins, enzymes, cofactors, hormones, proteins, antigens, and antiserums (1–6). Semipermeable microcapsules containing microbial cells also have been reported (7, 8). However, they were used as sources of enzyme activities, and the cells were not viable. As far as the present authors know, no viable mammalian cells have been microencapsulated.

The current state of the art for preparing semipermeable microcapsules involves at least one of two harsh conditions: (*a*) contact of the aqueous phase, where the cells are located, with at least one organic solvent phase; and (*b*) heating during the process. However, both conditions must be avoided for cells to stay viable during and after microencapsulation.

The present report describes a simple all-aqueous phase system that successfully microencapsulates viable mammalian cells and tissues.

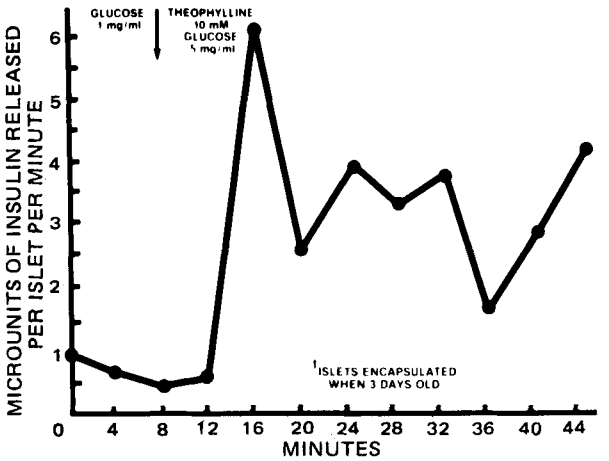


**Figure 1**—*Insulin release pattern of 27-day-old microencapsulated rat islets by perfusion.*

0022-3549/81/0400-0351$01.00/0
© 1981, American Pharmaceutical Association

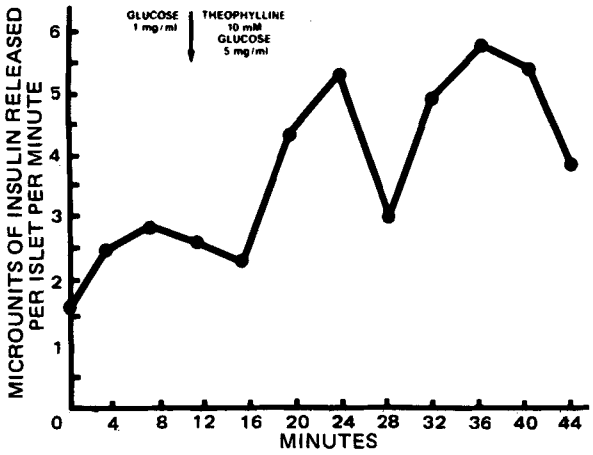


**Figure 2**—*Insulin release pattern of 27-day-old rat islets by perfusion.*

## EXPERIMENTAL

**Microencapsulation**—The hepatoma cells[1] or pancreatic islets[2] first were uniformly suspended in a 0.6% sodium alginate[3] solution prepared in saline. Droplets containing either cells or islets were produced by extrusion through a capillary tip and dropped into a beaker containing 1.5% $CaCl_2$ solution. The calcium ions caused immediate gelling of each droplet. The temporary microcapsules thus formed were harvested by decantation and were processed further to impart a permanent semipermeable membrane by suspension in a 0.02% polylysine[3] solution for 3–5 min. Before the cell- or islet-containing microcapsules were transferred into tissue culture medium[4], the alginate gel inside the capsules was "liquefied" in isotonic sodium citrate solution at pH 7.2 for 5 min.

**Cell Culture Studies**—Cell- and islet-containing microcapsules, as well as the corresponding nonencapsulated cells and islets used as controls, were cultured at 37° in disposable, plastic tissue culture flasks[5] containing the culture medium with 9% fetal bovine serum and 20 mg of gentamicin/ml.

Viability and growth of the cultures were monitored through an inverted microscope and by histological stains on microscopic sections.

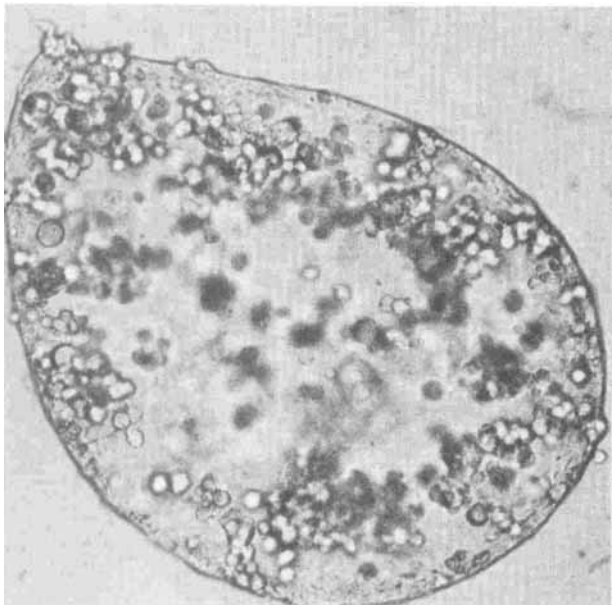

**Figure 3**—*Hepatoma cells growing inside a microcapsule, Day 1 (270×).*

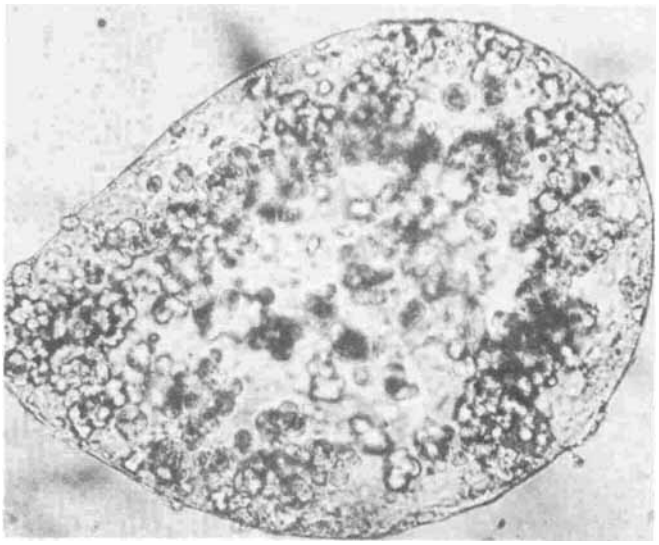

**Figure 4**—*The same microcapsule, Day 2 (same magnification).*

For insulin production and release studies, a perfusion system similar to that used by Lacy *et al.* (9) was assembled and used inside a 37° walkin incubating room. Samples were collected at 2- and 4-min intervals. Baseline insulin release was obtained with 100 mg/100 ml of glucose in the perfusing culture medium, while stimulation studies were carried out with medium containing 500 mg/100 ml of glucose and 10 m*M* of theophylline.

## RESULTS AND DISCUSSION

Perfusion studies with 10 islets and 10 microencapsulated islets (Figs. 1 and 2) showed that the amounts of insulin released per islet per minute upon stimulation by a combination of high glucose (5 mg/ml) and theophylline (10 m*M*) were comparable between the two groups. However, at 24 days, the control islets showed a high level of baseline insulin release (1 mg/ml) and a somewhat abnormal-looking stimulation–response pattern. In contrast, the microencapsulated islets produced a reasonably low level of baseline insulin release and a typical, biphasic stimulation–response pattern.

Abundance and continuation of cell proliferation were evident in all microencapsulated cells and tissues (Figs. 3–8). Viable and healthy B cells

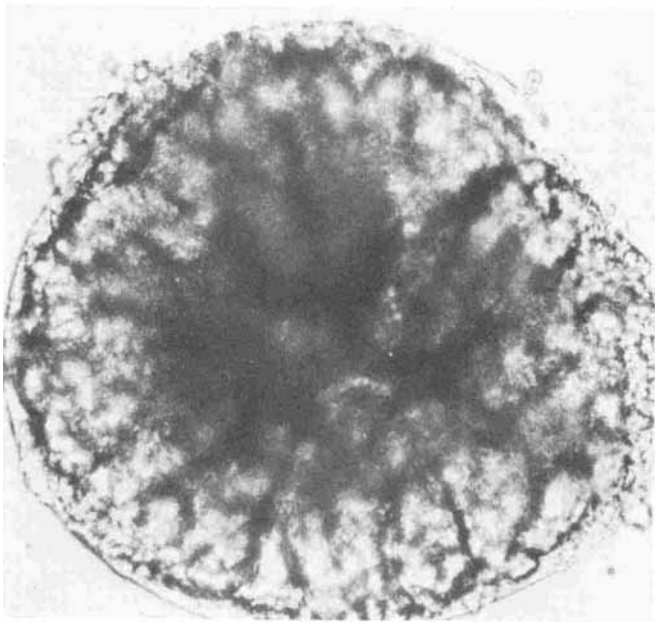

**Figure 5**—*The same microcapsule, Day 9 (same magnification). Note the increase in size due to stretching of the membrane by the overcrowded cells.*

[1] Hepatoma cells were freshly grown and provided by Dr. Richard Carchman's laboratory, Department of Pharmacology, Medical College of Virginia, Virginia Commonwealth University, Richmond, Va.

[2] Three- to 6-day-old pancreatic islets were supplied by Dr. Anthony Sun, Connaught Laboratories.

[3] Sigma Chemicals Co., St. Louis, Mo.

[4] Medium CMRL-1969, Connaught Laboratories, Toronto, Canada.

[5] Falcon flasks, Flow Laboratories, McLean, Va.

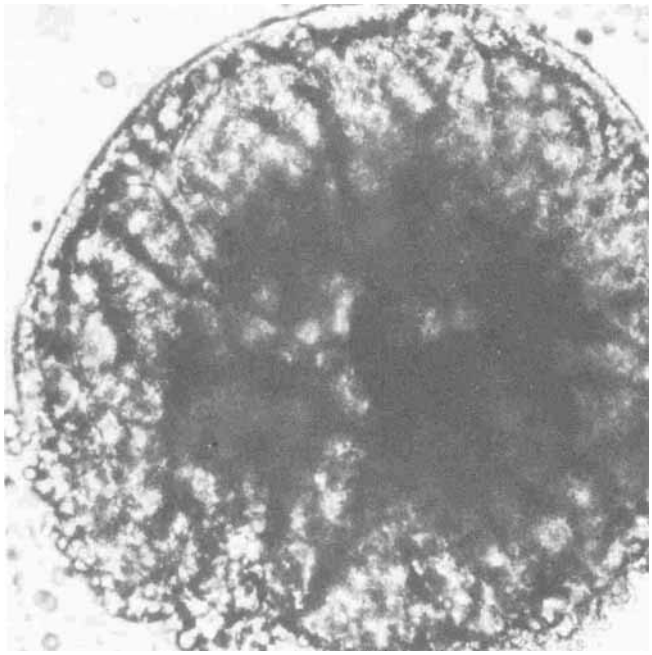

**Figure 6**—*The same microcapsule, Day 10 (same magnification). Note the continuing increase in size and the definite sign of bursting of the microcapsule.*

were noted in the microscopic sections of microencapsulated islets stained with hematoxylin–eosin and with aldehyde–fuchsin (Figs. 9 and 10). Control islets showed signs of degeneration, including progressive B-cell degranulation, at the end of 3 weeks. On the other hand, microencapsulated islets flourished for over 8 weeks, with more cell proliferation and good insulin production and release.

Microencapsulated hepatoma cells appeared to grow and multiply in suspension at about the same rate as the nonencapsulated control group (doubling time of ~24 hr). Final photomicrographs (Figs. 3–7) of the same microcapsules taken through the tissue culture flask showed that overcrowding hepatoma cells first stretched the capsular membrane before finally bursting the capsule at Day 10.

The significance and advantages of maintaining cultures of viable cells or tissues within semipermeable microcapsules are numerous:

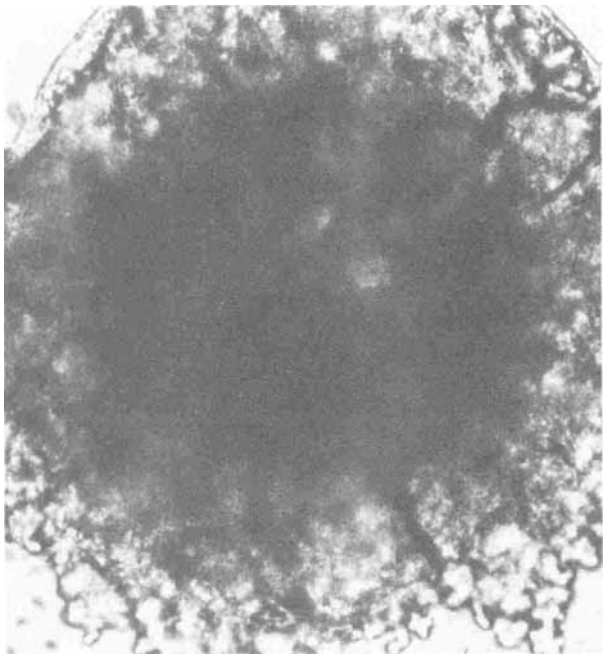

**Figure 7**—*The same microcapsule, Day 11 (same magnification). Note the further increase in size and the complete bursting of the microcapsule.*

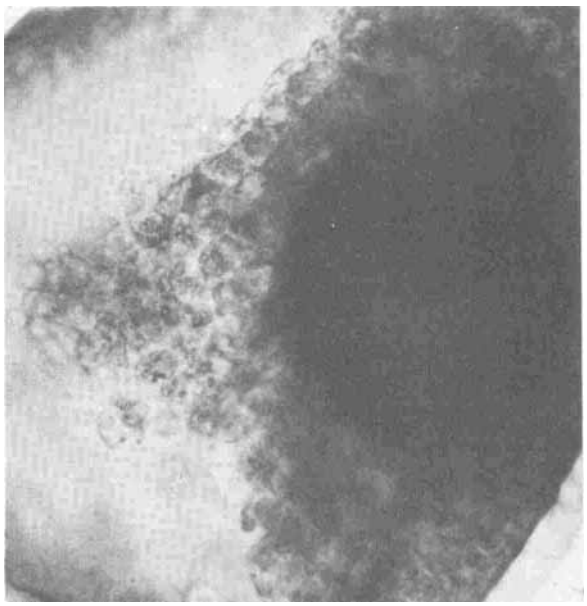

**Figure 8**—*Five-week-old microencapsulated rat islet. Note the number of cells proliferated from the islet.*

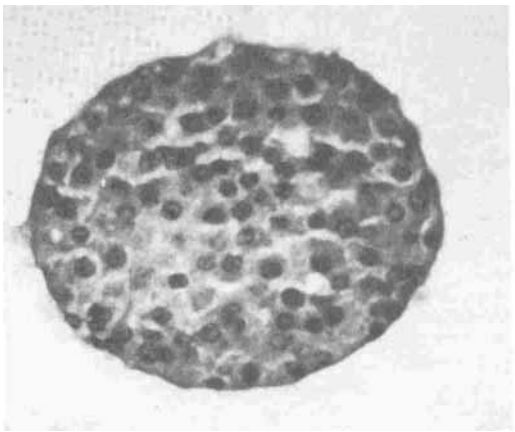

**Figure 9**—*Paraffin section of microencapsulated islet stained with hematoxylin–eosin.*

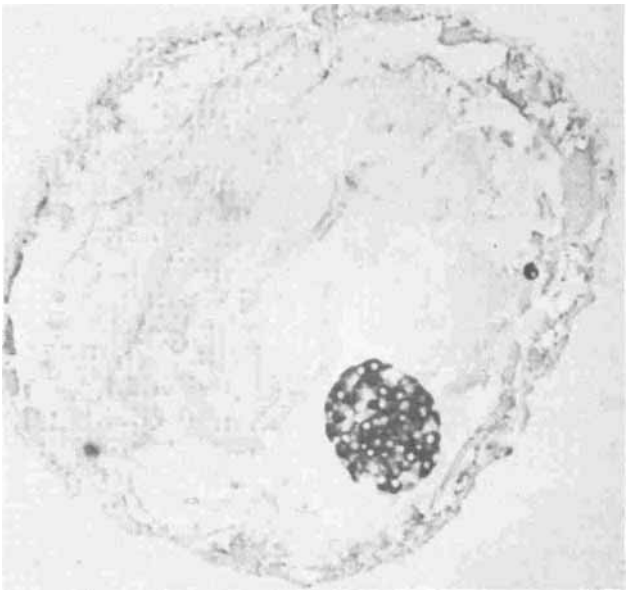

**Figure 10**—*Paraffin section of microencapsulated islet stained with aldehyde–fuchsin.*

1. The microcapsules can be used as individual microculture flasks, making it easier to handle and manipulate culture cells, especially when they are used as an investigative tool in the study of cell metabolism and regulation and the dynamics of hormone action and production.

2. The immediate cell environment can be made more similar to solid tissue density and biochemical characteristics and, therefore, more physiological and natural.

3. *In vivo* and *in vitro* sterile conditions are easier to maintain since bacterial and viral cells cannot cross the capsular membrane.

4. When microencapsulated cells or tissues are used as injectable prostheses or implantable (or *ex vivo*) artificial organs, it should be possible to specify the capsular membrane's permeability range to suit a particular use such as prevention of immune rejection or toxin removal.

Specifically, the microencapsulated islet appears to have great potential as a better and simpler implantable and, possibly, physiologically disposable artificial pancreatic endocrine organ for the treatment of diabetes. Preliminary animal studies have begun to give encouraging results.

## REFERENCES


(1) T. M. S. Chang, "Artificial Cells," Charles C Thomas, Springfield, Ill., 1972.

(2) T. M. S. Chang, "Biomedical Applications of Immobilized Enzymes and Proteins," vol. 1, Plenum, New York, N.Y., 1977, pp. 69–104.

(3) F. Lim and R. D. Moss, in "Microencapsulation, New Techniques and Applications," T. Kondo, Ed., Techno, Tokyo, Japan, 1978, pp. 167–178.

(4) F. Lim and R. D. Moss, *Clin. Chem.*, **24**, 1040 (1978). *Ibid.*, **25**, 1071 (1979).

(5) "Microencapsulation, Processes and Applications," J. E. Vandegaar, Ed., Plenum, New York, N.Y., 1973.

(6) "Microencapsulation," J. R. Nixon, Ed., Dekker, New York, N.Y., 1976.

(7) K. Mosbach and R. Mosbach, *Acta Chem. Scand.*, **20**, 2807 (1966).

(8) R. R. Mohan and N. N. Li, *Biotechnol. Bioeng.*, **17**, 1137 (1975).

(9) P. E. Lacy, E. H. Finke, S. Conant, and S. Naber, *Diabetes*, **25**, 484 (1976).


## ACKNOWLEDGMENTS


Supported by a research grant from Damon Diagnostic, Needham Heights, Mass.

The authors thank Mrs. Beverly Lockwood and Mrs. Caroline Coe for their technical assistance and the Histology Laboratory of the Pathology Department for preparation and staining of the microscopic sections.


# Preparation of Hemolysate-Loaded Poly($N^{\alpha}$,$N^{\epsilon}$-L-lysinediylterephthaloyl) Nanocapsules


**MASAYUKI ARAKAWA and TAMOTSU KONDO** ˣ



Received August 2, 1979, from the *Faculty of Pharmaceutical Sciences, Science University of Tokyo, Shinjuku-ku, Tokyo, Japan 162.* Accepted for publication January 10, 1980.



**Abstract** □ Poly($N^{\alpha}$,$N^{\epsilon}$-L-lysinediylterephthaloyl) capsules containing hemolysate were prepared in the nanometer range by an interfacial polymerization technique using electrocapillary emulsification to obtain very fine hemolysate droplets for encapsulation. The effects of temperature, emulsifier concentration, and the applied potential on the size distribution of the polyamide capsules were investigated. The polyamide capsules prepared under proper conditions have an average diameter of ~500 nm.



**Keyphrases** □ Poly($N^{\alpha}$,$N^{\epsilon}$-L-lysinediylterephthaloyl) microcapsules—containing hemolysate, prepared by interfacial polymerization using electrocapillary emulsification □ Electrocapillary emulsification—synthesis of poly($N^{\alpha}$,$N^{\epsilon}$-L-lysinediylterephthaloyl) microcapsules containing hemolysate, effect of temperature, emulsifier concentration, and applied potential on polyamide capsule-size distribution □ Microencapsulation—symposium, preparation of nanograde-sized polyamide microcapsules containing hemolysate, effect of temperature, emulsifier concentration, and applied potential on capsule-size distribution


Previous studies on poly($N^{\alpha}$,$N^{\epsilon}$-L-lysinediylterephthaloyl) microcapsules containing hemolysate were carried out with the aim of using them as artificial red blood cells (1–3). Most of the encapsulated hemoglobin molecules retained their oxygen absorbability while catalase and carbonic anhydrase lost some of their enzymatic activities during encapsulation; suspensions of the microcapsules exhibited flow properties similar to those of blood unless the capsule concentration exceeded 30% by volume. Because of their relatively large size (mean diameter of 10 μm) and low deformability in shear flows, the microcapsules were not expected to pass through capillary blood vessels. Thus, an attempt was made to prepare much smaller capsules loaded with hemolysate that could pass through capillary blood vessels.

When a potential difference that is higher than a critical value, the critical voltage of emulsification, is applied to an oil–water interface, the interfacial tension is reduced almost to zero and spontaneous emulsification occurs, due to the interfacial fluctuation, in the absence of surfactant or in the presence of a very small amount (4, 5). The emulsions thus formed are monodisperse and stable, with the average particle diameter being <200 nm. The necessary condition for this electrocapillary emulsification is that the ionic strength, and hence the reciprocal double-layer thickness, of the inner phase be higher than that of the outer phase. Because of the difficulty in obtaining hemolysate droplets of <1 μm by conventional mechanical emulsification processes, the electrocapillary emulsification technique seems to be promising.

The present paper describes the preparation of poly($N^{\alpha}$,$N^{\epsilon}$-L-lysinediylterephthaloyl) capsules in the nanometer range containing sheep hemolysate by interfacial polymerization using electrocapillary emulsification to obtain very fine hemolysate droplets for encapsulation. Factors influencing the capsule size also are described. In addition, the effect of the applied potential on the enzymatic activities of catalase and carbonic anhydrase in the hemolysate droplets is reported.

## EXPERIMENTAL

**Apparatus for Electrocapillary Emulsification**—Figure 1 shows the schematic diagram of the apparatus used for electrocapillary emul-




0022-3549/81/0400-0354$01.00/0


© 1981, American Pharmaceutical Association

1. The microcapsules can be used as individual microculture flasks, making it easier to handle and manipulate culture cells, especially when they are used as an investigative tool in the study of cell metabolism and regulation and the dynamics of hormone action and production.

2. The immediate cell environment can be made more similar to solid tissue density and biochemical characteristics and, therefore, more physiological and natural.

3. *In vivo* and *in vitro* sterile conditions are easier to maintain since bacterial and viral cells cannot cross the capsular membrane.

4. When microencapsulated cells or tissues are used as injectable prostheses or implantable (or *ex vivo*) artificial organs, it should be possible to specify the capsular membrane's permeability range to suit a particular use such as prevention of immune rejection or toxin removal.

Specifically, the microencapsulated islet appears to have great potential as a better and simpler implantable and, possibly, physiologically disposable artificial pancreatic endocrine organ for the treatment of diabetes. Preliminary animal studies have begun to give encouraging results.

## REFERENCES


(1) T. M. S. Chang, "Artificial Cells," Charles C Thomas, Springfield, Ill., 1972.

(2) T. M. S. Chang, "Biomedical Applications of Immobilized Enzymes and Proteins," vol. 1, Plenum, New York, N.Y., 1977, pp. 69–104.

(3) F. Lim and R. D. Moss, in "Microencapsulation, New Techniques and Applications," T. Kondo, Ed., Techno, Tokyo, Japan, 1978, pp. 167–178.

(4) F. Lim and R. D. Moss, *Clin. Chem.*, **24**, 1040 (1978). *Ibid.*, **25**, 1071 (1979).

(5) "Microencapsulation, Processes and Applications," J. E. Vandegaar, Ed., Plenum, New York, N.Y., 1973.

(6) "Microencapsulation," J. R. Nixon, Ed., Dekker, New York, N.Y., 1976.

(7) K. Mosbach and R. Mosbach, *Acta Chem. Scand.*, **20**, 2807 (1966).

(8) R. R. Mohan and N. N. Li, *Biotechnol. Bioeng.*, **17**, 1137 (1975).

(9) P. E. Lacy, E. H. Finke, S. Conant, and S. Naber, *Diabetes*, **25**, 484 (1976).


## ACKNOWLEDGMENTS


Supported by a research grant from Damon Diagnostic, Needham Heights, Mass.

The authors thank Mrs. Beverly Lockwood and Mrs. Caroline Coe for their technical assistance and the Histology Laboratory of the Pathology Department for preparation and staining of the microscopic sections.


# Preparation of Hemolysate-Loaded Poly($N^{\alpha}$,$N^{\epsilon}$-L-lysinediylterephthaloyl) Nanocapsules


**MASAYUKI ARAKAWA and TAMOTSU KONDO** ˣ



Received August 2, 1979, from the *Faculty of Pharmaceutical Sciences, Science University of Tokyo, Shinjuku-ku, Tokyo, Japan 162.* Accepted for publication January 10, 1980.



**Abstract** □ Poly($N^{\alpha}$,$N^{\epsilon}$-L-lysinediylterephthaloyl) capsules containing hemolysate were prepared in the nanometer range by an interfacial polymerization technique using electrocapillary emulsification to obtain very fine hemolysate droplets for encapsulation. The effects of temperature, emulsifier concentration, and the applied potential on the size distribution of the polyamide capsules were investigated. The polyamide capsules prepared under proper conditions have an average diameter of ~500 nm.



**Keyphrases** □ Poly($N^{\alpha}$,$N^{\epsilon}$-L-lysinediylterephthaloyl) microcapsules—containing hemolysate, prepared by interfacial polymerization using electrocapillary emulsification □ Electrocapillary emulsification—synthesis of poly($N^{\alpha}$,$N^{\epsilon}$-L-lysinediylterephthaloyl) microcapsules containing hemolysate, effect of temperature, emulsifier concentration, and applied potential on polyamide capsule-size distribution □ Microencapsulation—symposium, preparation of nanograde-sized polyamide microcapsules containing hemolysate, effect of temperature, emulsifier concentration, and applied potential on capsule-size distribution


Previous studies on poly($N^{\alpha}$,$N^{\epsilon}$-L-lysinediylterephthaloyl) microcapsules containing hemolysate were carried out with the aim of using them as artificial red blood cells (1–3). Most of the encapsulated hemoglobin molecules retained their oxygen absorbability while catalase and carbonic anhydrase lost some of their enzymatic activities during encapsulation; suspensions of the microcapsules exhibited flow properties similar to those of blood unless the capsule concentration exceeded 30% by volume. Because of their relatively large size (mean diameter of 10 μm) and low deformability in shear flows, the microcapsules were not expected to pass through capillary blood vessels. Thus, an attempt was made to prepare much smaller capsules loaded with hemolysate that could pass through capillary blood vessels.

When a potential difference that is higher than a critical value, the critical voltage of emulsification, is applied to an oil–water interface, the interfacial tension is reduced almost to zero and spontaneous emulsification occurs, due to the interfacial fluctuation, in the absence of surfactant or in the presence of a very small amount (4, 5). The emulsions thus formed are monodisperse and stable, with the average particle diameter being <200 nm. The necessary condition for this electrocapillary emulsification is that the ionic strength, and hence the reciprocal double-layer thickness, of the inner phase be higher than that of the outer phase. Because of the difficulty in obtaining hemolysate droplets of <1 μm by conventional mechanical emulsification processes, the electrocapillary emulsification technique seems to be promising.

The present paper describes the preparation of poly($N^{\alpha}$,$N^{\epsilon}$-L-lysinediylterephthaloyl) capsules in the nanometer range containing sheep hemolysate by interfacial polymerization using electrocapillary emulsification to obtain very fine hemolysate droplets for encapsulation. Factors influencing the capsule size also are described. In addition, the effect of the applied potential on the enzymatic activities of catalase and carbonic anhydrase in the hemolysate droplets is reported.

## EXPERIMENTAL

**Apparatus for Electrocapillary Emulsification**—Figure 1 shows the schematic diagram of the apparatus used for electrocapillary emul-




0022-3549/81/0400-0354$01.00/0


© 1981, American Pharmaceutical Association

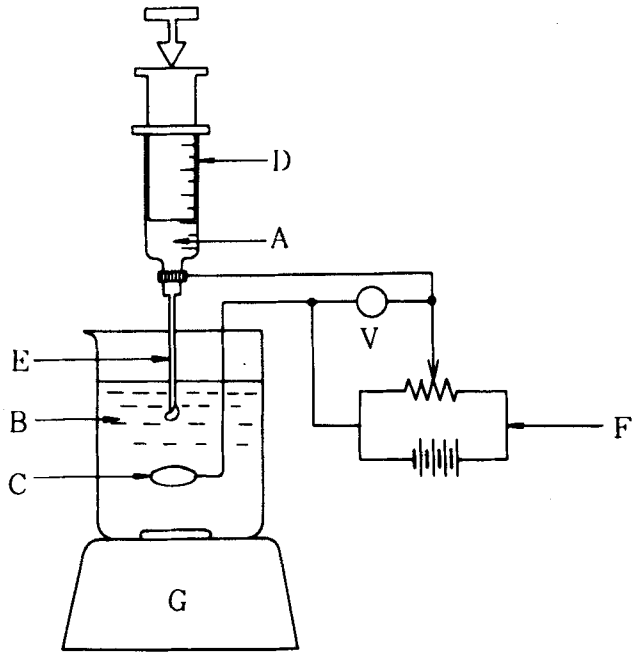


**Figure 1**—*Schematic diagram of the apparatus for electrocapillary emulsification.*

sification. The aqueous phase (A) in a syringe (D) was introduced into the oil phase (B) by driving a motor through a needle (E), which also was used as an electrode. This electrode and a platinum electrode (C) in the oil phase were connected to a variable dc supply (F), the potential of which is measured by a voltmeter (V). The container of the oil phase was surrounded by ice (low temperature) or water (room temperature), and the content was stirred continuously by a magnetic stirrer (G).

**Preparation of Hemolysate-Loaded Polyamide Capsules**—The aqueous phase to be encapsulated contained sheep hemolysate (~10% as hemoglobin), 0.4 *M* L-lysine, and 0.45 *M* sodium carbonate. The oil phase consisted of three volumes of cyclohexane and one volume of chloroform in which terephthaloyl dichloride, tetraethylammonium chloride, and sorbitan trioleate were dissolved. The concentration of terephthaloyl dichloride was 0.04 *M*. The quaternary ammonium salt gave electroconductivity to the oil phase, and its concentration was $1.5 \times 10^{-4}$ *M*.

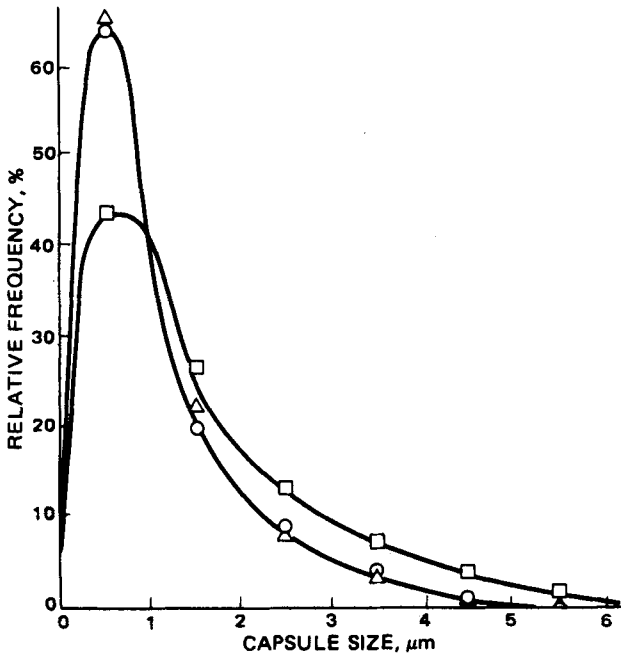


**Figure 2**—*Effect of aqueous phase addition rate on the size distribution of polyamide capsules. Key:* ○, *0.003 ml/min;* △, *0.015 ml/min; and* □, *0.10 ml/min.*

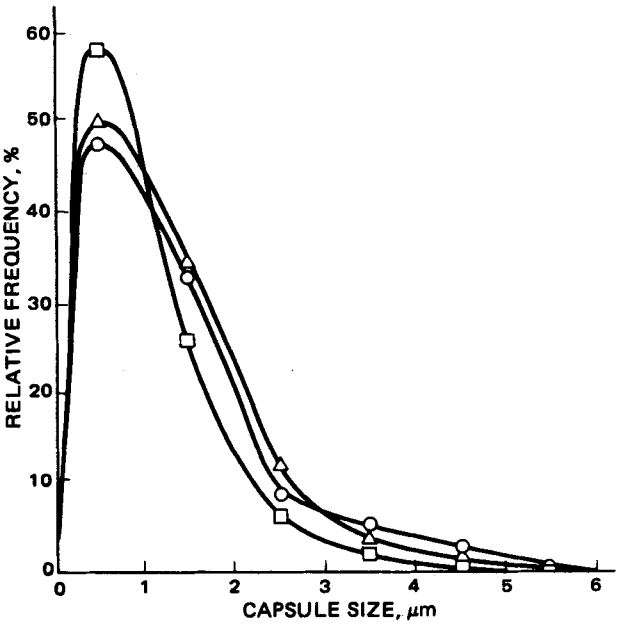


**Figure 3**—*Effect of emulsifier concentration on the size distribution of polyamide capsules. Key:* ○, *3% (v/v);* △, *5% (v/v); and* □, *10% (v/v).*

The aqueous phase (1 ml) was introduced through the needle to 50 ml of the oil phase in a beaker. The addition was made at a constant rate under the influence of an applied potential between the electrodes, which were separated by ~5 mm. The oil phase was gently stirred during the addition. Since the applied potential was always above a critical value, spontaneous emulsification occurred and a shower of fine hemolysate droplets was formed. The applied potential was positive on the aqueous phase side with respect to the oil phase throughout this work.

On the surface of each droplet, polycondensation took place between L-lysine and terephthaloyl dichloride to form a poly($N^{\alpha}$,$N^{\epsilon}$-L-lysinediylterephthaloyl) membrane. The hydrogen chloride formed as a reaction by-product was neutralized immediately by the alkali in the aqueous phase. The polyamide capsules thus formed were centrifuged at 1000 rpm for 3 min. The separated capsules were dispersed in water with the aid of poly(oxyethylene) sorbitan monolaurate, a dispersing agent.

**Capsule-Size Measurement**—A portion of the aqueous capsule dispersion diluted with distilled water was withdrawn and placed on a hemocytometer and photographed under an optical microscope. In some cases, the capsule size also was measured by an electronic particle counter[1] or a scanning electron microscope.

**Enzyme Activity Measurement**—Catalase activity in the sheep hemolysate droplets dispersed in the organic phase was estimated by determining by means of iodometry at 4° and pH 7.4 the amount of hydrogen peroxide decomposed by the enzyme in the hemolysate supernate obtained after centrifuging the dispersion.

Similarly, the enzymatic activity of carbonic anhydrase in the hemolysate supernate was estimated by measuring the change in pH as a function of time in the presence of a large excess of carbon dioxide at 4° after breaking down the dispersion.

## RESULTS

**Capsule-Size Distribution**—As the rate of addition of the aqueous phase increased, the capsule-size distribution curve widened and the relative frequency of large capsules increased. Figure 2 shows the size distribution curves of the polyamide capsules prepared under a constant applied potential (1000 v), a fixed emulsifier concentration (5%), and different rates of addition of the aqueous phase into the oil phase.

An increase in the emulsifier concentration made the capsule-size distribution slightly narrower and sharper if the emulsifier concentration was higher than 1%, the minimum value needed for continuous emulsification to occur. Figure 3 shows the effect of the emulsifier concentration on the size distribution of the polyamide capsules prepared at an applied potential of 1000 v and a rate of aqueous phase addition of 0.015 ml/min.

[1] Coulter counter, Coulter Industrial Sales, Elmhurst, Ill.

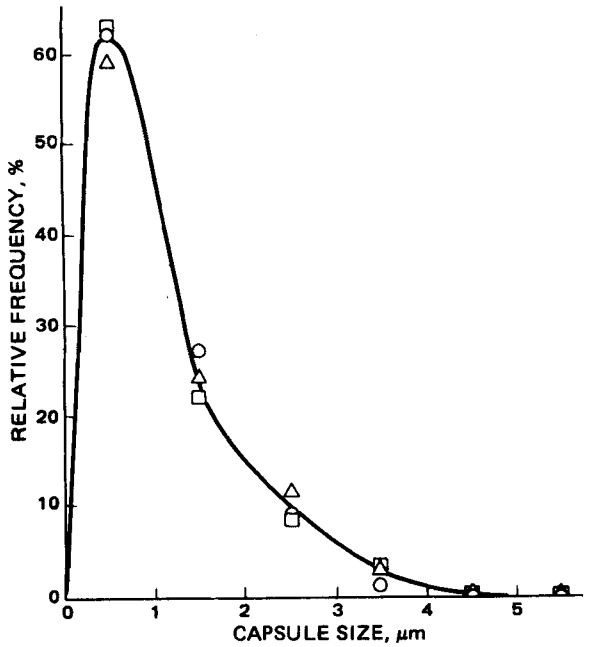


**Figure 4**—*Effect of applied potential on the size distribution of polyamide capsules. Key:* ○, *200 v;* △, *500 v; and* □, *1000 v.*

No significant effect of applied potential on the size distribution was observed provided that the potential was higher than the critical voltage of emulsification, which was <200 v for the system studied in this work (Fig. 4). The emulsifier concentration and the rate of addition of the aqueous phase were fixed at 5% and 0.015 ml/min, respectively.

The capsule-size distribution was affected favorably by increasing temperature. Capsules prepared at high temperature had a narrower and sharper size distribution than those prepared at low temperature. Figure 5 shows the size distribution curves of the capsules prepared at different temperatures using a 5% emulsifier concentration, a 1000-v applied potential, and a 0.015-ml/min rate of addition.

**Enzymatic Activity**—Since low concentrations of sorbitan trioleate did not prevent catalase and carbonic anhydrase in the hemolysate from losing enzymatic activity, the emulsifier in electrocapillary emulsification was used at 5%, which was high enough to minimize reduction in the activities caused by contact with the organic solvent.

With increasing applied potential, the enzymatic activity of catalase in the hemolysate initially decreased and then leveled off (Fig. 6). Similar results were obtained with carbonic anhydrase in the hemolysate droplets (Fig. 7).

Enzymatic activities of encapsulated catalase and carbonic anhydrase were kept at ~60% of the original values (immediately after encapsulation) after 40 days of storage in a refrigerator.

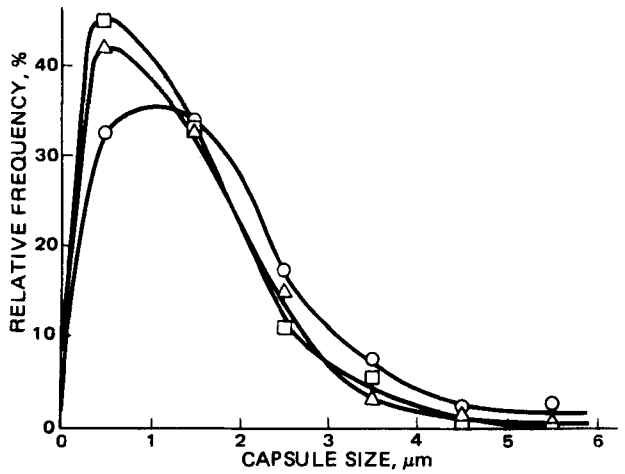


**Figure 5**—*Effect of temperature on the size distribution of polyamide capsules. Key:* ○, *2°;* △, *20°; and* □, *40°.*

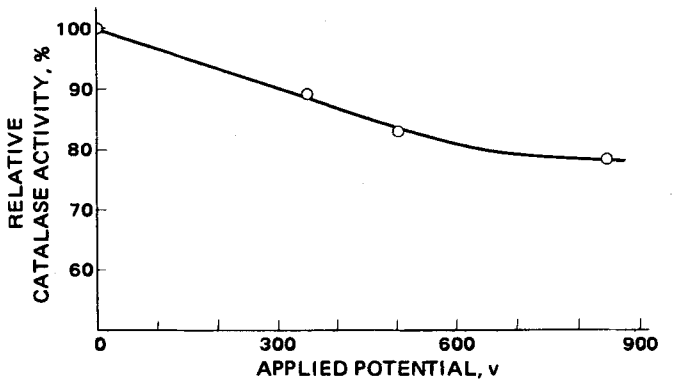


**Figure 6**—*Effect of applied potential on catalase activity in hemolysate.*

## DISCUSSION

An increase in the addition rate of the hemolysate probably increases the drop size and the drop formation rate due to gravity acting on the drops being formed at the tip of the needle. This result causes incomplete electrocapillary emulsification, which leads to capsules with a broad size distribution. Consequently, to obtain capsules with a narrow size distribution and a small mean diameter, the rate at which hemolysate is introduced into the oil phase should be lower than a certain definite value.

In general, the emulsifier concentration is important in preparing an emulsion with a narrow and sharp size distribution. However, the role of emulsifier in this case is to prevent coalescence of primary hemolysate droplets formed in electrocapillary emulsification, rather than allowing the aqueous phase to disperse easily as fine droplets into the oil phase, since the interfacial tension is almost zero due to the applied potential. Therefore, the emulsifier concentration should only be enough to cover the surface of the primary droplets.

Since the interfacial tension between the hemolysate and the organic phase is lowered almost to zero by an applied potential that is higher than the critical voltage of emulsification in the presence of a small amount of emulsifier, there is no significant effect of the applied potential on the size distribution when the potential is increased beyond the critical value.

Several factors are affected by temperature change. The interfacial fluctuation increases as the temperature rises, which leads to formation of hemolysate droplets of smaller size at high temperature than those obtained at low temperature. However, this effect will not be significant if a sufficiently high potential is applied to the interface and a small amount of emulsifier is present.

The rise in temperature also decreases the viscosity of the oil phase, suggesting that hemolysate droplets coalesce to form larger drops through collision of the primary droplets. This effect is countered by the formation of a polymer membrane on the surface of the primary droplets. The rate of polymer formation is dependent on the temperature and transfer of water-soluble reactant into the oil phase from the aqueous phase. These factors can affect the capsule size to a considerable extent (6).

Transfer of L-lysine is affected by the emulsifier concentration in the oil phase and temperature (Fig. 8). At a fixed concentration of sorbitan

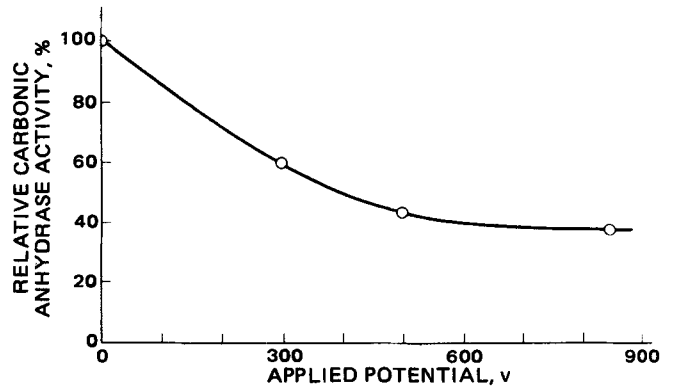


**Figure 7**—*Effect of applied potential on carbonic anhydrase activity in hemolysate.*

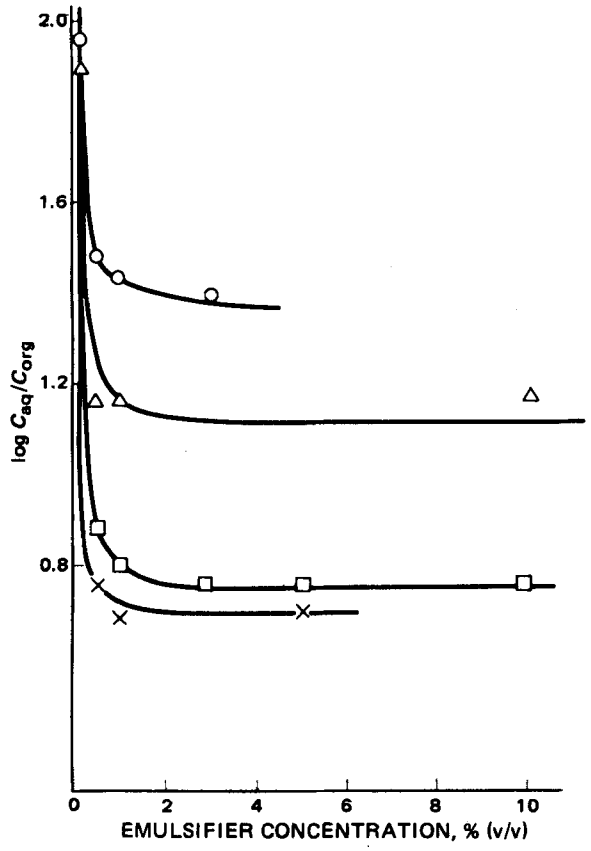


**Figure 8**—*Transfer of L-lysine into the oil phase from the aqueous phase as a function of temperature and emulsifier concentration. Key: ○, 20°, 800 v; △, 20°, 1000 v; □, 20°, 1000 v, stirred; and ×, 2°, 1000 v.*

trioleate, transfer of the amino acid is more noticeable at low temperature than at high temperature. However, since the amino acid concentration in the oil phase is determined a few minutes after the completion of emulsification, only cumulative values of the amino acid concentration are given in the the figure. In other words, no useful information is obtained from these data on the rate of transfer of the amino acid in a very short period, which presumably will be high at high temperature. In addition, the rate of polycondensation also will be high at high temperature. Therefore, it is not unreasonable to expect that the capsule-size distribution becomes narrower and sharper as temperature rises if a small amount of emulsifier is present to promote the amino acid transfer.

Based on the previous discussion, hemolysate-loaded polyamide capsules with an average diameter of ~500 nm can be prepared. Figure 9 gives an example of a scanning electron micrograph of the capsules.

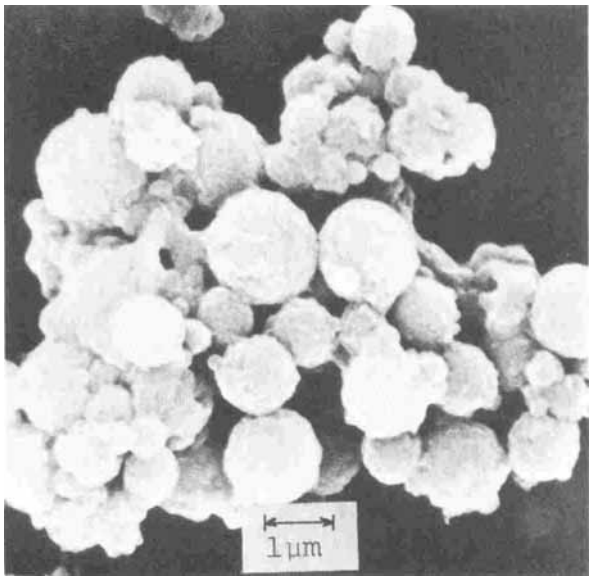


**Figure 9**—*Scanning electron micrograph of polyamide capsules.*

Application of electric potential to the interface between the aqueous and oil phases causes an oriented adsorption of the enzymes at the interface. The adsorption should increase the chance for the enzymes to contact the organic solvent and lose their activities (7).

## REFERENCES

(1) T. Kondo, M. Arakawa, and B. Tamamushi, in "Microencapsulation," J. R. Nixon, Ed., Dekker, New York, N.Y., 1976, p. 163.

(2) M. Arakawa, T. Kondo, and B. Tamamushi, *Biorheology*, **12**, 57 (1975).

(3) M. Arakawa and T. Kondo, *Can. J. Physiol. Pharmacol.*, **55**, 1378 (1977).

(4) A. Watanabe, K. Higashitsuji, and K. Nishizawa, in "Colloidal Dispersion and Micellar Behavior," K. L. Mittal, Ed., American Chemical Society, Washington, D.C., 1975, p. 97.

(5) A. Watanabe, K. Higashitsuji, and K. Nishizawa, *J. Colloid Interface Sci.*, **64**, 278 (1978).

(6) Y. Shigeri, M. Koishi, T. Kondo, M. Shiba, and S. Tomioka, *Can. J. Chem.*, **48**, 2047 (1970).

(7) T. Kondo and N. Muramatsu, in "Microencapsulation," J. R. Nixon, Ed., Dekker, New York, N.Y., 1976, p. 67.

## ACKNOWLEDGMENTS

The authors thank Miss I. Inoue and Mr. K. Go for skillful experimental assistance.

# Preparation of Egg Albumin Microcapsules and Microspheres

**TAKAFUMI ISHIZAKA, KENJI ENDO, and MASUMI KOISHI** ˣ

Received August 2, 1979, from the *Faculty of Pharmaceutical Sciences, Science University of Tokyo, 12, Ichigaya Funakawara-machi, Shinjuku-ku, Tokyo, Japan.* Accepted for publication April 29, 1980.

**Abstract** □ Protein microspheres and microcapsules containing fine hydrophilic particles (spherical silica gel beads, iron hydrous oxide-modified nylon 12, or phenacetin) were prepared by using water-soluble egg albumin, which is heat-coagulable at 50–80°. The size and size distribution of the microspheres and microcapsules formed and the microencapsulation percentage of fine particles were determined, and the factors affecting them were studied. Favorable conditions are suggested to obtain phenacetin-containing microcapsules in high yield.

**Keyphrases** □ Albumin, egg—preparation of microcapsules and microspheres containing fine hydrophilic particles of silica gel beads, iron hydrous oxide-modified nylon 12, and phenacetin, heat coagulation method □ Silica gel, spherical beads—preparation of microcapsules and microspheres of silica gel beads using egg albumin, heat coagulation method □ Phenacetin—preparation of microcapsules and microspheres of phenacetin using egg albumin, heat coagulation method □ Microencapsulation—symposium, preparation of microcapsules and microspheres containing fine hydrophilic particles of silica gel beads, modified nylon 12, and phenacetin using water-soluble egg albumin, heat coagulation method, evaluation of factors affecting size, size distribution, and percent of microencapsulated particles

Interest in the application of microcapsules to many industrial fields is increasing, and application to the modification of drugs has been studied, but many problems remain. Nixon and Walker (1) reported the release of sulfadiazine from microcapsules prepared by simple gelatin coacervation, and Luzzi *et al.* (2) investigated the prolonged release of nylon microcapsules prepared by emulsion polymerization. Zolle *et al.* (3) prepared radiolabeled albumin microspheres to study blood circulation in humans and animals.

Sugibayashi *et al.* (4) studied the drug-carrier property of albumin microspheres in chemotherapy and the preparation and tissue distribution of microsphere-entrapped [6-$^3$H]fluorouracil in mice. Kramer (5) investigated albumin microspheres containing an anticancer agent as vehicles for achieving specificity in drug delivery.

Widder *et al.* (6) reported the preparation and characterization of a novel delivery system for water-soluble drugs. The system consisted of albumin microspheres (average of 1 μm in diameter) containing ultrafine magnetic particles, magnetite (ferrosoferric oxide), and a prototype drug, doxorubicin hydrochloride.

This paper reports the microencapsulation of fine hydrophilic particles and drug using a metabolizable protein, albumin, as the membrane material.

## EXPERIMENTAL

**Materials**—Isooctane, dibasic potassium phosphate, monobasic sodium phosphate dodecahydrate, acetic acid, and sodium acetate were reagent grade. Phenacetin JP[1] (*p*-acetophenetidide) was ground with an agate mortar and then classified with stainless steel sieves. Powder, 250–300 mesh (specific gravity 1.275), was used for microencapsulation.

Egg albumin[2] was used following some purification. Albumin was dissolved in pH 8.0, 0.1 *N* $KH_2PO_4$–0.1 *N* $Na_2HPO_4$ (1:16 v/v). The solution was filtered[3] after centrifugation at 16,000×*g* for 30 min to remove undissolved material, and the solution concentrations were ~5, 10, and 20% (w/w).

Spherical porous silica gel beads[4] [Brunauer, Emmett, and Teller (BET) specific surface area, 420 $m^2/g$; mean pore size, 80 Å; specific gravity, 2.127; and mean diameter, 52.5 ± 12.7 μm] and nylon 12 spheres[5] (BET specific surface area, 1.0 $m^2/g$; specific gravity, 1.02; and mean diameter, 3 μm) modified with iron hydrous oxide also were used as core materials. Iron hydrous oxide (iron hydrosol) was used to modify the surface of the nylon 12 spheres to enhance their wettability by aqueous albumin solution. Iron hydrous oxide settles from solution onto such hydrophobic surfaces as those of polyethylene, polytef, and paraffin, rendering the surfaces hydrophilic (7). Once deposited and dried, these colloid particles have a high degree of adherence to the substrate surface.

**Preparation of Iron Hydrous Oxide Solution**—Twenty-five milliliters of an aqueous 10% (w/w) ferric chloride solution was added to 200 ml of boiling water, and boiling was continued for 3 min. After cooling to room temperature, the solution was treated with 40 ml of an anion-exchange resin[6] and stirred for 5 min. The iron hydrous oxide solution obtained was used for surface modification of nylon 12 spheres.

**Preparation of Microcapsules and Microspheres**—Albumin microcapsules and microspheres were prepared by a modification of the method used by Farhadieh (8).

To 100 ml of isooctane containing 0.1, 0.5, 1.0, or 5.0% (v/v) sorbitan trioleate as an emulsifier in a three-necked flask was added, with stirring, 15 ml of 5, 10, or 20% (w/w) egg albumin solution or the albumin solution containing solid powders [silica gel beads (1.063, 2.126, or 3.190 g)], iron hydrous oxide-modified nylon 12 (2.250 g), and phenacetin (1.912, 2.854, or 3.825 g) as the core materials. After 10 min with continuous stirring, the flask was immersed in a water bath at 50° for 5 min and then at 75–85° for 10 min to denature the egg albumin. The resultant dispersion was cooled to room temperature.

The particles separated by decantation were mixed with 100 ml of isooctane, and this mixture was agitated gently for 1 hr. The separated particles again were dispersed into 10 ml of pH 4.7 acetate buffer solution,

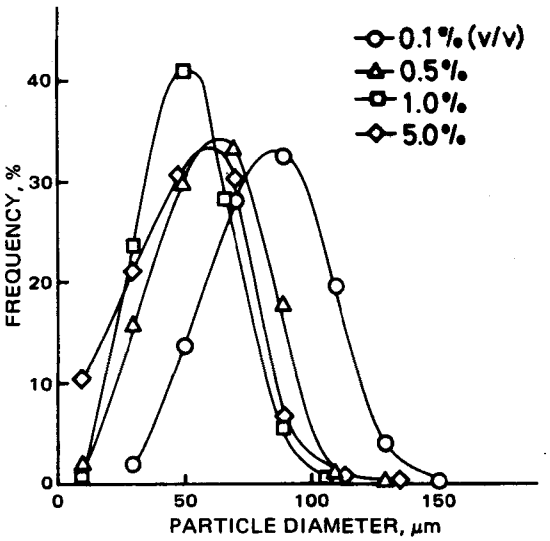


**Figure 1**—*Effect of sorbitan trioleate concentration on size distribution of albumin microspheres dispersed in isooctane. The albumin concentration was 10% (w/w) at a speed setting of 512 rpm.*

[1] Hoei Pharmaceutical Co., Tokyo, Japan.
[2] Tokyo Kasei Kogyo Co., Tokyo, Japan.
[3] No. 7 paper filter, Toyo Roshi Kaisha, Tokyo, Japan.
[4] Iatrobeads, Iatron Laboratories, Tokyo, Japan.
[5] Toyo Rayon Co., Tokyo, Japan.
[6] Amberlite IRA-410, Japan Organo Co., Tokyo, Japan.



0022-3549/81/0400-0358$01.00/0
© 1981, American Pharmaceutical Association

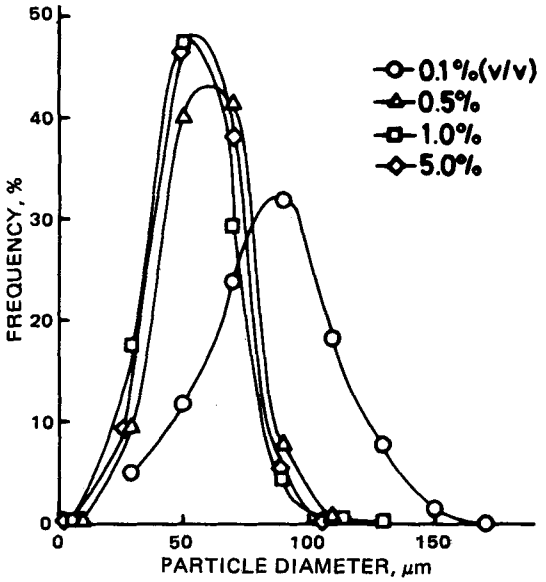


**Figure 2**—*Effect of sorbitan trioleate concentration on size distribution of albumin microspheres dispersed in 2.0% (v/v) polyoxyethylene sorbitan monolaurate solution. The albumin concentration was 10% (w/w) at a speed setting of 512 rpm.*

consisting of 0.1 *N* acetic acid–0.1 *N* sodium acetate (1:1 v/v) and 10% (v/v) polyoxyethylene sorbitan monolaurate, with vigorous agitation. Then the dispersion was diluted with the same buffer solution to make the concentration of polyoxyethylene sorbitan monolaurate 2.0% (v/v).

The total numbers of microcapsules and microspheres ranging from 1000 to 2500 were measured by projecting their photomicrographs on a screen. Size measurements were performed in isooctane and then in 2.0% (v/v) polyoxyethylene sorbitan monolaurate solution after treating the capsules with acetate buffer. Each film strip was projected onto a large section of paper by a slide projector[7], and the enlarged images of the microcapsules and microspheres were measured to the nearest 1.0 μm. The scales in the micrometer were used for calibration. If the contour of projected images was of a complex or indistinct shape, these images were not measured. Then calculations were made on the mean length diameter, size distribution, and standard deviation.

**Measurements of Viscosity and Interfacial Tension**—Relative viscosity of albumin solutions was measured at 25° with an Ubbelohde viscosimeter. The pendant drop method (9) was used for measuring the interfacial tension between albumin solution and 5.0% (v/v) sorbitan trioleate solution in isooctane (10).

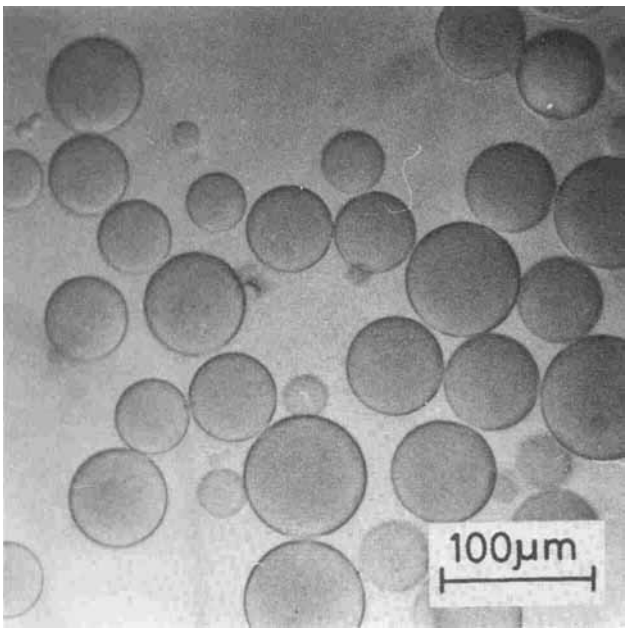


**Figure 3**—*Photomicrograph of albumin microspheres in isooctane.*

[7] Color Cabin, Cabin Industry Co., Tokyo, Japan.

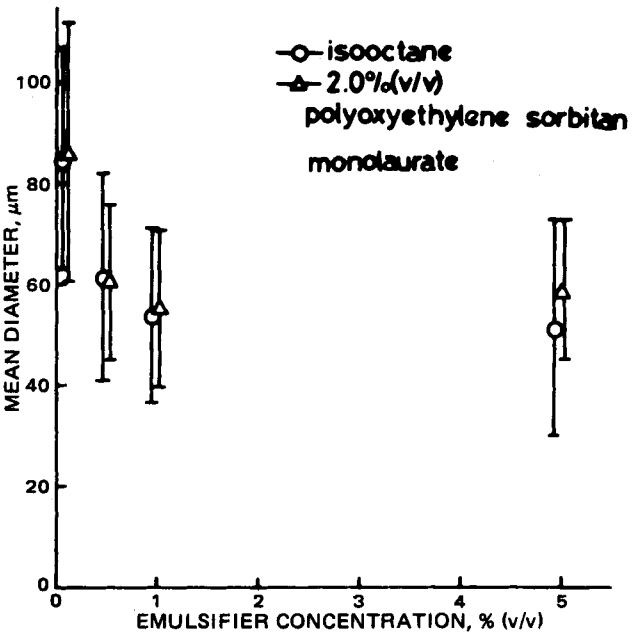


**Figure 4**—*Effect of sorbitan trioleate concentration on the mean diameter of albumin microspheres dispersed in isooctane and in 2.0% (v/v) polyoxyethylene sorbitan monolaurate solution. The albumin concentration was 10% (w/w) at a speed setting of 512 rpm.*

## RESULTS AND DISCUSSION

**Size Distribution and Mean Size**—The size distribution of the albumin microspheres was strongly affected by the sorbitan trioleate concentration, mechanical agitation, and albumin concentration in the first step of the preparation.

Figures 1 and 2 show the effect of the sorbitan trioleate concentration

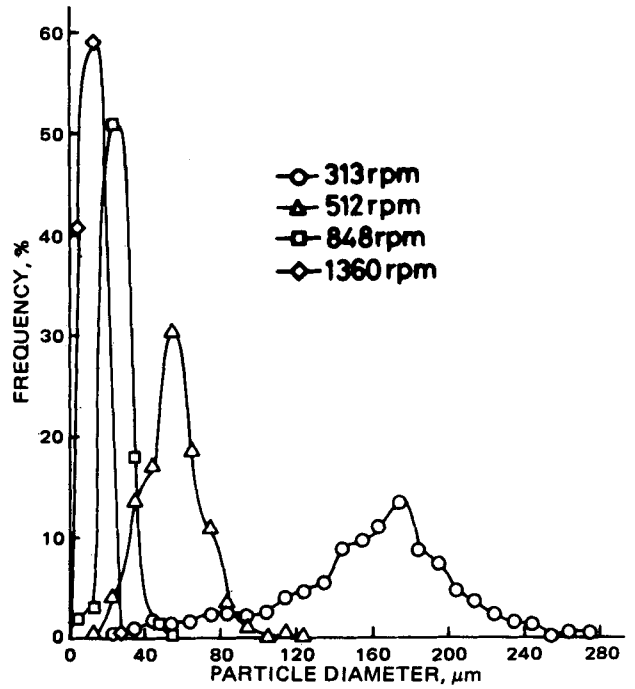


**Figure 5**—*Effect of stirring speed on size distribution of albumin microspheres dispersed in 2.0% (v/v) polyoxyethylene sorbitan monolaurate solution. The albumin concentration was 10% (w/w), and the emulsifier was 1.0% (v/v) sorbitan trioleate.*

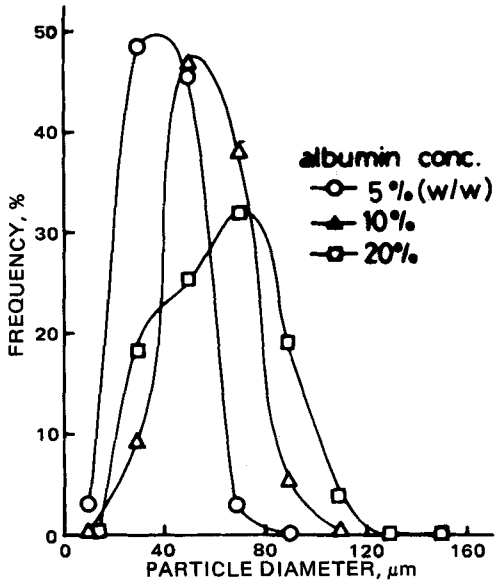


**Figure 6**—*Effect of albumin concentration on size distribution of microspheres dispersed in 2.0% (v/v) polyoxyethylene sorbitan monolaurate solution. The emulsifier was 1.0% (v/v) sorbitan trioleate at a speed setting of 512 rpm.*

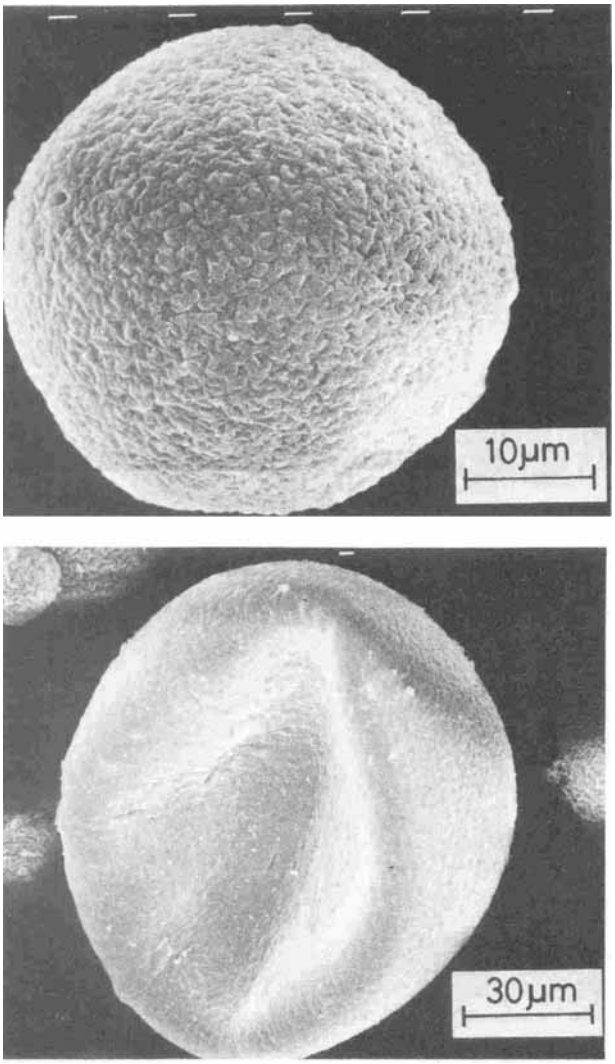


**Figure 7**—*Scanning electron micrographs of albumin microcapsules containing phenacetin.*

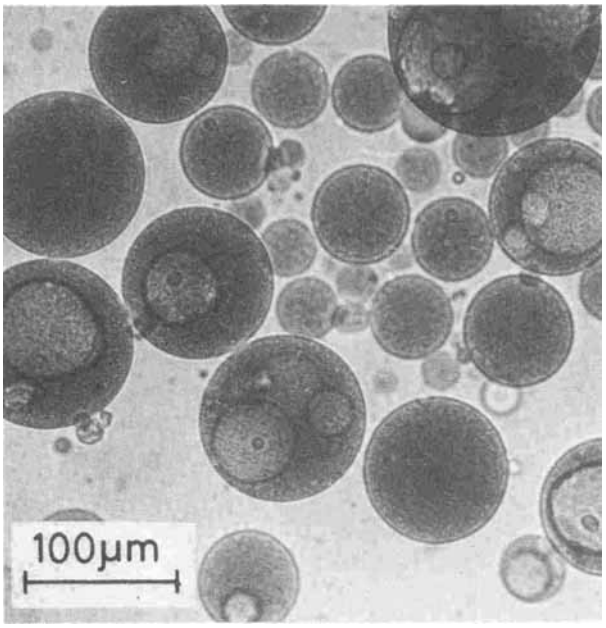


**Figure 8**—*Photomicrograph of albumin microcapsules containing silica gel beads in isooctane.*

on the size distribution of the microspheres prepared from 10% (w/w) albumin solution at 512 rpm. The size distribution curve, obtained from the photographs taken in isooctane and in 2.0% (v/v) polyoxyethylene sorbitan monolaurate solution, distinctly shifted toward the lesser particle diameter with increasing sorbitan trioleate concentration up to 0.5%, above which no appreciable shift was observed. Typical albumin microspheres dispersed in isooctane are shown in Fig. 3.

Figure 4 shows the relationship of the mean length diameter and its standard deviation of albumin microspheres prepared at different sorbitan trioleate concentrations. A decrease in the mean diameter was apparent with increasing sorbitan trioleate concentration. There are no observable differences in diameter between those measured in isooctane and in 2.0% (v/v) polyoxyethylene sorbitan monolaurate solution. The results indicate that albumin microspheres were formed tightly by heat denaturation and, thus, the spheres did not swell in the surfactant solution.

Figure 5 shows the size distributions of the microspheres in 2.0% (v/v) polyoxyethylene sorbitan monolaurate solution prepared at various stirring speeds. The size distribution curve clearly became narrower and

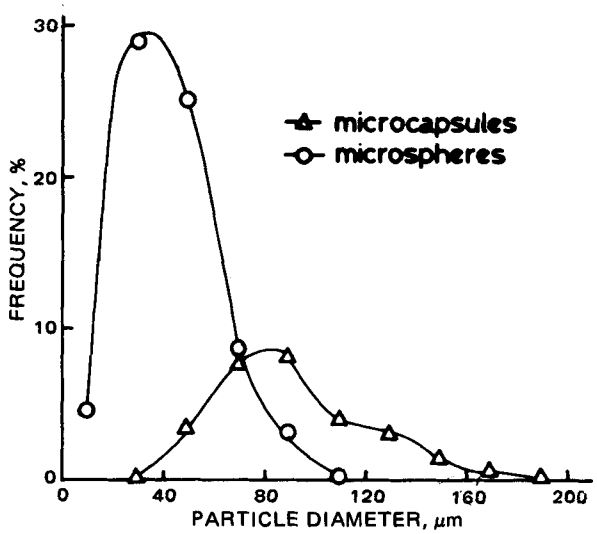


**Figure 9**—*Size distribution of albumin microcapsules containing silica gel beads dispersed in isooctane. The volume ratio of silica gel beads to albumin solution was 1:9, and the weight of beads was 3.190 g. The albumin concentration was 10% (w/w), and the emulsifier was 1.0% (v/v) sorbitan trioleate. The speed setting was at 512 rpm. The microspheres contained no silica gel beads.*

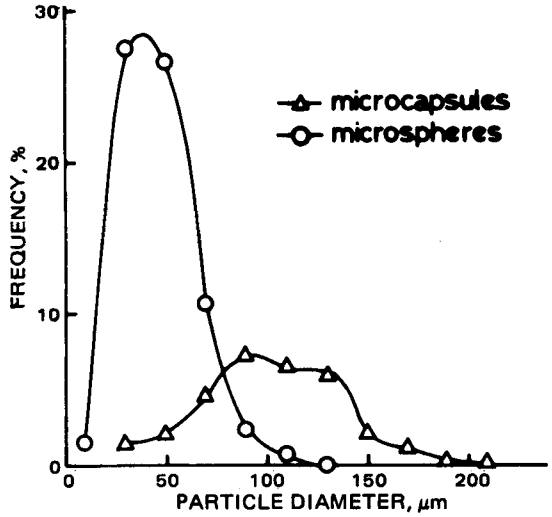


**Figure 10**—*Size distribution of albumin microcapsules containing silica gel beads dispersed in isooctane. The volume ratio of silica gel beads to albumin solution was 1:14, and the weight of beads was 2.126 g. The albumin concentration was 20% (w/w), and the emulsifier was 1.0% (v/v) sorbitan trioleate. The speed setting was at 512 rpm. The microspheres contained no silica gel beads.*

sharper with increased stirring speed. Similar results were reported by Koishi *et al.* (11) on the size of polyphthalamide microcapsules prepared by the interfacial polycondensation method. The size distribution curve of albumin microspheres in 2.0% (v/v) polyoxyethylene sorbitan monolaurate solution prepared using 5,10, and 20% (w/w) albumin solutions clearly became broader with increasing albumin concentration (Fig. 6).

These results indicate that the size distribution of the microspheres depends mainly on the size distribution of the droplets of albumin dispersed in isooctane during preparation. The changes in the dispersed phase caused by an increase in albumin concentration, interfacial tension between dispersed phase (albumin solution) and dispersing medium (sorbitan trioleate solution in isooctane), and viscosity of albumin solution seem to influence the size distribution of the albumin droplets. The results on the interfacial tension and relative viscosity of the albumin solution (Table I) show that the increase in viscosity of the dispersed phase is certainly a major influence on the size distribution. Albumin microspheres prepared using 20% (w/w) albumin solution (Fig. 6) had an unsymmetrical size distribution. Namely, subdivision of globules of 20% (w/w) albumin, dispersed in isooctane, into many smaller sizes is prevented by the large increase in the resistance to deformation of the globules brought about by high interfacial viscosity due to the high relative viscosity of the protein solution (Table I).

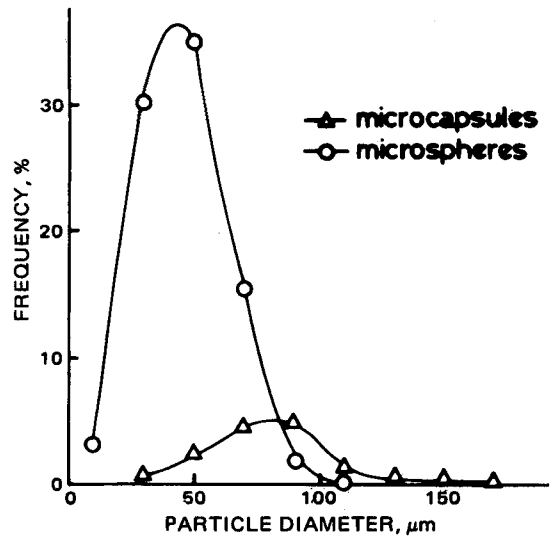


**Figure 11**—*Size distribution of albumin microcapsules containing silica gel beads dispersed in isooctane. The volume ratio of silica gel beads to albumin solution was 1:14, and the weight of beads was 2.126 g. The albumin concentration was 20% (w/w), and the emulsifier was 1.0% (v/v) sorbitan trioleate. The speed setting was at 848 rpm. The microspheres contained no silica gel beads.*

**Table I—Interfacial Tensions between Albumin Solutions and 5.0% (v/v) Sorbitan Trioleate Solution in Isooctane and the Viscosities of Albumin Solutions**

| Albumin, % (w/w) | Relative Interfacial Tension[a] | Relative Viscosity |
|---|---|---|
| 0 | 0.051 | 1.02 |
| 5 | 0.024 | 1.43 |
| 10 | 0.026 | 2.07 |
| 20 | 0.027 | 5.00 |

[a] The ratio of the interfacial tension between two phases to the surface tension of water.

**Microencapsulation of Powder Particles**—Figure 7 show scanning-electron micrographs of the surface appearances of albumin mi-

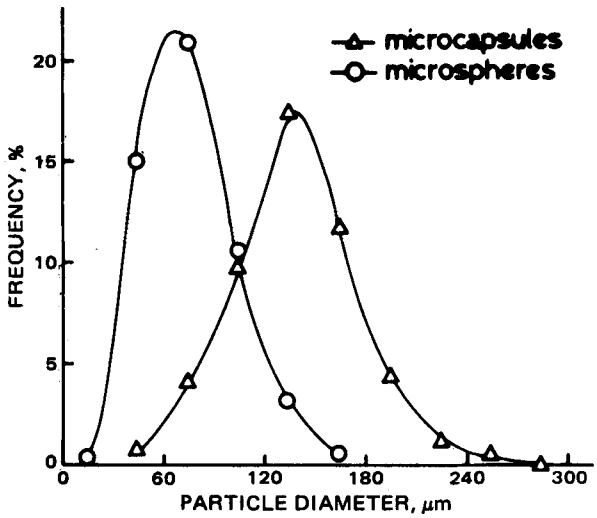


**Figure 12**—*Size distribution of albumin microcapsules containing silica gel beads dispersed in isooctane, prepared at the volume ratio of silica gel beads to albumin solution of 1:29, and the weight of beads was 1.063 g. The albumin concentration was 20% (w/w), and the emulsifier was 1.0% (v/v) sorbitan trioleate. The speed setting was at 512 rpm. The microspheres contained no silica gel beads.*

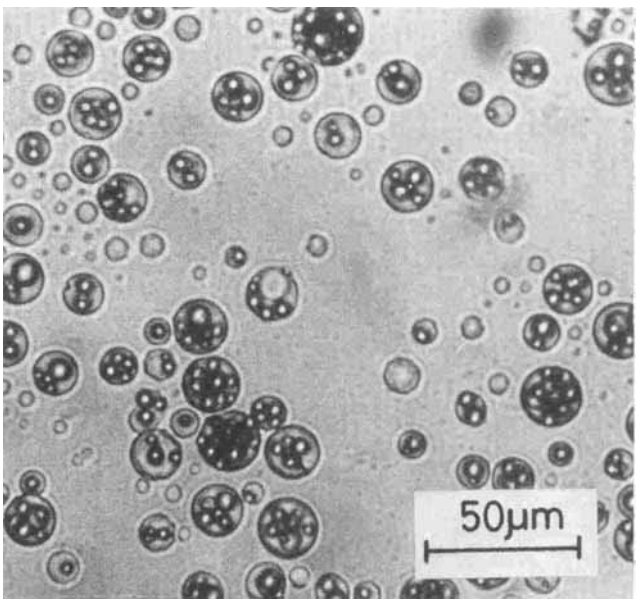


**Figure 13**—*Photomicrograph of albumin microcapsules containing iron hydrous oxide-modified nylon 12 particles in isooctane.*

Table II—Mean Diameter ($d$), Standard Deviation ($\delta$), and Microencapsulation Percentage ($P_m$) of Albumin Microcapsules Dispersed in Isooctane, Prepared by Using Silica Gel Beads as a Core Material

| Albumin, % (w/w) | Volume Ratio[a] | Weight of Silica Gel Beads Used, g | Speed Setting, rpm | Sorbitan Trioleate, % (v/v) | Microcapsule Containing Silica Gel Beads | | | Microcapsule Containing No Silica Gel Beads | | | Mean Value[b] | | $P_m$[c], % |
|---|---|---|---|---|---|---|---|---|---|---|---|---|---|
| | | | | | $d$, μm | $\delta$, μm | Number, $M_1$ | $d$, μm | $\delta$, μm | Number, $M_2$ | $d$, μm | $\delta$, μm | |
| 10 | 1:9 | 3.190 | 512 | 1.0 | 92.1 | 30.2 | 288 | 43.3 | 17.8 | 705 | 57.5 | 31.2 | 29.0 |
| 20 | 1:14 | 2.126 | 512 | 1.0 | 101.6 | 33.6 | 329 | 46.3 | 17.6 | 749 | 63.2 | 34.8 | 30.5 |
| 20 | 1:14 | 2.126 | 848 | 1.0 | 79.1 | 24.4 | 353 | 46.0 | 16.5 | 2146 | 50.7 | 21.2 | 14.1 |
| 20 | 1:29 | 1.063 | 512 | 1.0 | 138.7 | 37.2 | 950 | 76.2 | 26.8 | 967 | 107.2 | 45.0 | 49.6 |

[a] Silica gel beads to albumin solution. [b] Calculated from total size distribution. [c] Microencapsulation percentage: $M_1/(M_1 + M_2) \times 100$.

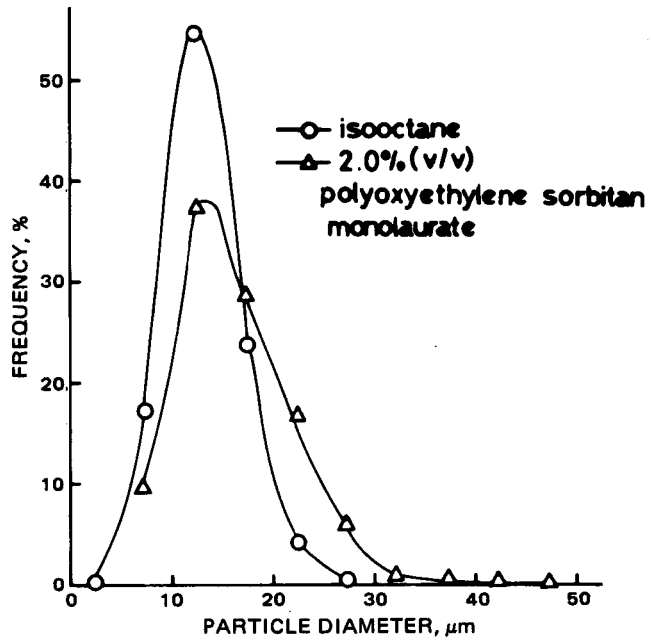


**Figure 14**—*Size distribution of albumin microcapsules containing iron hydrous oxide-modified nylon 12 particles prepared at the volume ratio of iron hydrous oxide-modified nylon 12 to albumin solution of 1:5.6, and the weight of beads was 2.250 g. Microcapsules were dispersed in isooctane or 2.0% (v/v) polyoxyethylene sorbitan monolaurate. The albumin concentration was 10% (w/w), and the emulsifier was 5.0% (v/v) sorbitan trioleate. The speed setting was at 1360 rpm.*

crocapsules containing fine phenacetin particles. After the microcapsules were suspended in 2.0% (v/v) polyoxyethylene sorbitan monolaurate solution, the suspension was poured slowly, stepwise, into sufficient ethanol. The suspension then was dried under reduced pressure at room temperature. Finally, the dried microcapsules were vacuum coated with gold in an ion coater[8].

Silica gel beads were microencapsulated as fine hydrophilic particles. Typical examples of the microcapsules dispersed in isooctane are shown in Fig. 8. Uncovered beads and racemose aggregates of albumin and beads together with microcapsules were found. Figures 9–12 show the size distributions of the microcapsules containing silica gel beads dispersed

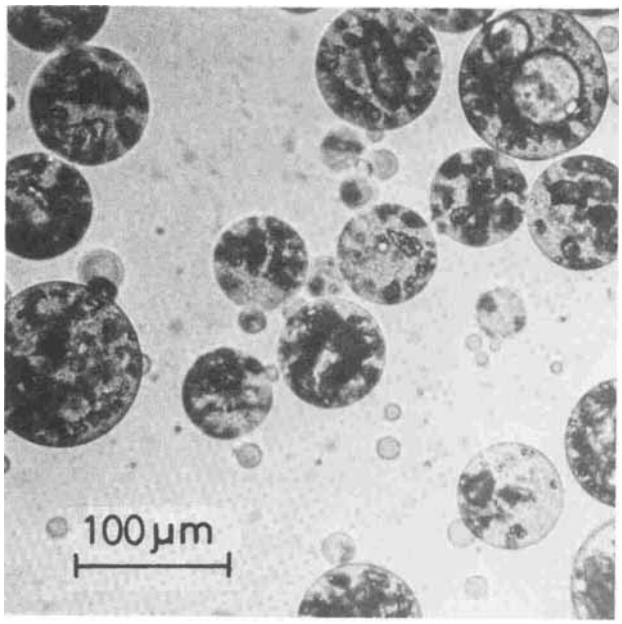


**Figure 15**—*Photomicrograph of albumin microcapsules containing phenacetin in isooctane.*

[8] JEC 1100, JEOL Ltd., Tokyo, Japan.

Table III—Mean Diameter ($d$) and Standard Deviation ($\delta$) of Microcapsules Containing Phenacetin, Prepared by Using 10% (w/w) Albumin and 5.0% (v/v) Sorbitan Trioleate at a Speed Setting of 512 rpm

| Volume Ratio[a] | Weight of Phenacetin Used, g | In Isooctane | | In 2.0% (v/v) Polyoxyethylene Sorbitan Monolaurate Solution | | |
|---|---|---|---|---|---|---|
| | | $d$, μm | $\delta$, μm | $d$, μm | $\delta$, μm | $P_m$[b], % |
| 1:9 | 1.912 | 50.4 | 25.6 | 59.3 | 26.4 | 100 |
| 1:5.7 | 2.854 | 48.1 | 25.8 | 38.8 | 19.1 | 100 |
| 1:4 | 3.825 | 57.7 | 33.4 | 53.1 | 26.9 | 100 |

[a] Phenacetin to albumin solution. [b] Microencapsulation percentage.

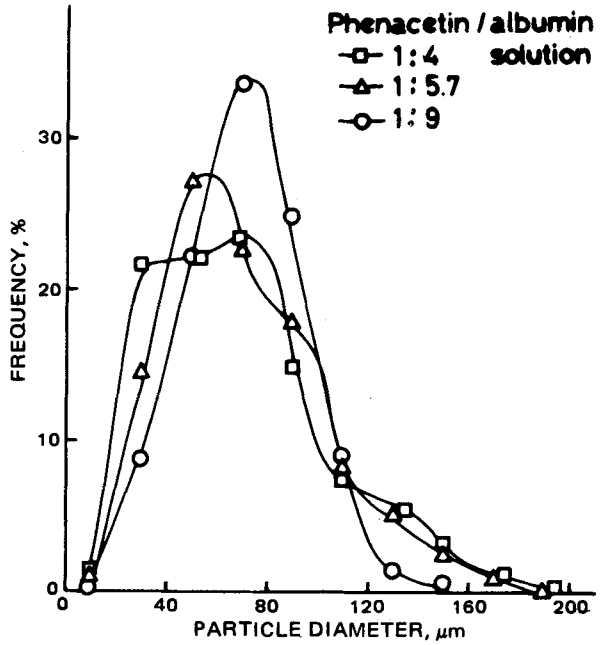


**Figure 16**—*Size distribution of albumin microcapsules containing phenacetin dispersed in isooctane, prepared at volume ratios of phenacetin to albumin solution of 1:9, 1:5.7, and 1:4 (weight of nylon 12 was 1.912, 2.854, and 3.825 g, respectively). The albumin concentration was 10% (w/w), and the emulsifier was 5.0% (v/v) sorbitan trioleate. The speed setting was at 512 rpm.*

in isooctane. Table II summarizes the mean diameter, standard deviation, and microencapsulation percentage (percentage of the number of microcapsules containing beads and not containing beads).

The mean diameters of albumin microcapsules containing silica gel beads were always about two times larger than those of the microcapsules containing no beads. The size distribution of the microcapsules containing silica gel beads shifted toward the larger particle diameter and broadened over a wide range as compared with that of the capsules containing no beads (Figs. 9–12). Broadening of the size distribution was caused by the size of silica gel beads (mean diameter of 52.5 ± 12.7 μm) and the viscosity increase of the albumin solution containing beads. However, the number of beads in each microcapsule also depended on the factors described previously (Fig. 8).

Typical microspheres and microcapsules containing iron hydrous oxide-modified nylon particles dispersed in isooctane are shown in Fig. 13. The percentage of modified nylon particles that were microencapsulated was ~70%.

Figure 14 shows the size distribution curves of the albumin microcapsules containing modified nylon particles in isooctane and in 2.0% (v/v) polyoxyethylene sorbitan monolaurate solution. The mean diameter and its standard deviation of the microcapsules in isooctane were 13.3 and 3.7 μm, respectively. Furthermore, the mean diameter was slightly larger for the microcapsules than for the microspheres (~10.0 μm).

**Microencapsulation of Phenacetin**—Phenacetin particles, 49–63 μm in diameter, were encapsulated. Typical albumin microcapsules containing phenacetin dispersed in isooctane are shown in Fig. 15. The size distribution of these albumin microcapsules prepared at three volume ratios of albumin solution to phenacetin is shown in Fig. 16. Table III summarizes the mean diameter and its standard deviation of the albumin microcapsules.

The mean diameter did not vary appreciably with the volume ratio of albumin to phenacetin, and the size distribution curves of the capsules were similar to each other. Furthermore, phenacetin was encapsulated completely in contrast with the silica gel beads, as seen from the $P_m$ values in Table III. The marked difference in the percentage of microencapsulation between silica gel beads having a high porous surface and crystalline phenacetin are due to differences in: (*a*) the surface chemical properties such as hydrophilicity, porosity, surface area, and specific gravity, and (*b*) the adsorption amount of albumin or the adhesiveness of albumin thin film, formed by denaturation, onto the surface of solid particles. These problems will be discussed in a future paper.

## REFERENCES


(1) J. R. Nixon and S. E. Walker, *J. Pharm. Pharmacol.*, **23**, 147S (1971).

(2) L. A. Luzzi, M. A. Zoglio, and H. V. Maulding, *J. Pharm. Sci.*, **59**, 338 (1970).

(3) I. Zolle, B. A. Rhodes, and H. N. Wagner, Jr., *Int. J. Appl. Radiat. Isotop.*, **21**, 155 (1970).

(4) K. Sugibayashi, Y. Morimoto, T. Nadai, Y. Kato, A. Hasegawa, and T. Arita, *Chem. Pharm. Bull.*, **27**, 204 (1979).

(5) P. A. Kramer, *J. Pharm. Sci.*, **63**, 1646 (1974).

(6) K. Widder, G. Flouret, and A. Senyei, *ibid.*, **68**, 79 (1979).

(7) J. T. Kenney, W. P. Townsend, and J. A. Emerson, *J. Colloid Interface Sci.*, **42**, 589 (1973).

(8) B. Farhadieh (to Abbott Laboratories), U.S. pat. 3,922,379 (1975).

(9) J. M. Andreas, E. A. Hauser, and W. B. Tucker, *J. Phys. Chem.*, **42**, 1001 (1938).

(10) A. J. I. Ward and L. H. Regan, *J. Colloid Interface Sci.*, **66**, 195 (1978).

(11) M. Koishi, N. Fukuhara, and T. Kondo, *Chem. Pharm. Bull.*, **17**, 804 (1969).


## ACKNOWLEDGMENTS


The authors thank Iatron Laboratories for providing Iatrobeads.

# Microencapsulation and Fabrication of Fuel Pellets for Inertial Confinement Fusion

**R. L. NOLEN, Jr., and L. B. KOOL** ˣ

Received August 2, 1979, from *KMS Fusion, Inc., Ann Arbor, MI 48104.* Accepted for publication March 12, 1980.

**Abstract** □ Various microencapsulation techniques were evaluated for fabrication of thermonuclear fuel pellets for use in existing experimental facilities studying inertial confinement fusion and in future fusion-power reactors. Coacervation, spray drying, *in situ* polymerization, and physical microencapsulation methods were employed. Highly spherical, hollow polymeric shells were fabricated ranging in size from 20 to 7000 μm. *In situ* polymerization microencapsulation with poly(methyl methacrylate) provided large shells, but problems with local wall defects still must be solved. Extension to other polymeric systems met with limited success. Requirements for inertial confinement fusion targets are described, as are the methods that were used.

**Keyphrases** □ Fuel pellets—fabrication and microencapsulation, various microencapsulation techniques, glasses, and polymers compared □ Polymers—shell fabrication, fuel pellets, various microencapsulation techniques compared □ Microencapsulation—symposium, various microencapsulation techniques compared, glass and polymeric shells, microencapsulation of fuel pellets

The use of high-energy pulsed lasers to compress matter to extremely high densities (*e.g.*, 1000 times its solid density) has been studied for some time (1). By compression of deuterium and of deuterium and tritium mixtures, thermonuclear fusion reactions are expected to be initiated for practical, commercial energy production. In principle, extremely high compression, with consequent heating, initiates fusion. Further heating by alpha-particles (whose range is drastically reduced by the compressed fuel) increases the reaction rates of deuterium and tritium to sustain and enhance the burn. High-energy (14.1 Mev) neutrons generated by these deuterium–tritium fusions become available as a usable source of nuclear energy to be exploited by capture in a heat-transfer medium such as lithium or by radionuclear chemistry for direct production of gaseous fuels such as hydrogen or methane.

## DISCUSSION

Large-scale release of fusion energy has occurred on earth but only in the uncontrolled action of thermonuclear weapons. In attempts to employ high compression for the controlled release of thermonuclear energy, confinement difficulties arise because the material being compressed escapes before useful work can be performed. These confinement difficulties are diminished if compression is accomplished rapidly to take advantage of inertial confinement.

Experiments were conducted in these laboratories utilizing implosion experiments with spherical pellets. In a laser-driven implosion, the pellet surface is heated by the laser and ablated away while the cold inner surface is driven inward, thereby conserving momentum and causing compression of the fuel and subsequent thermonuclear fusion.

Target pellets are produced by filling hollow spherical shells of glass or polymer with deuterium or a deuterium–tritium mixture, taking advantage of the shell's permeability to hydrogen at elevated temperatures. Since these pellets are microcapsules, utilization and extension of existing microencapsulation technology are desirable to solve problems in the fabrication of microscopic, highly spherical, hollow shells that fulfill the stringent requirements of inertial confinement fusion.

**Glass Shells**—Glasses and polymers, because of uniquely suitable properties, are the principal shell materials chosen for inertial confinement fusion targets. Although considerable progress has been made in utilizing these properties, many areas for improvement remain. Glasses have extremely high tensile strengths, ~$7 \times 10^2$ kgf/mm$^2$ (~1,000,000 psi), when formed under carefully controlled experimental conditions. Therefore, one could expect to make glass shells of high tensile strength, ~$1.4 \times 10^2$ kgf/mm$^2$ (~200,000 psi) or higher.

A most important quality of glasses is the extremely low permeability at ambient temperature, which allows gas retention times in targets ranging from hours for silica to years for soda lime glasses. Permeability increases exponentially with temperature, however, allowing relatively rapid filling to equilibrium pressure at elevated temperatures (~10 hr

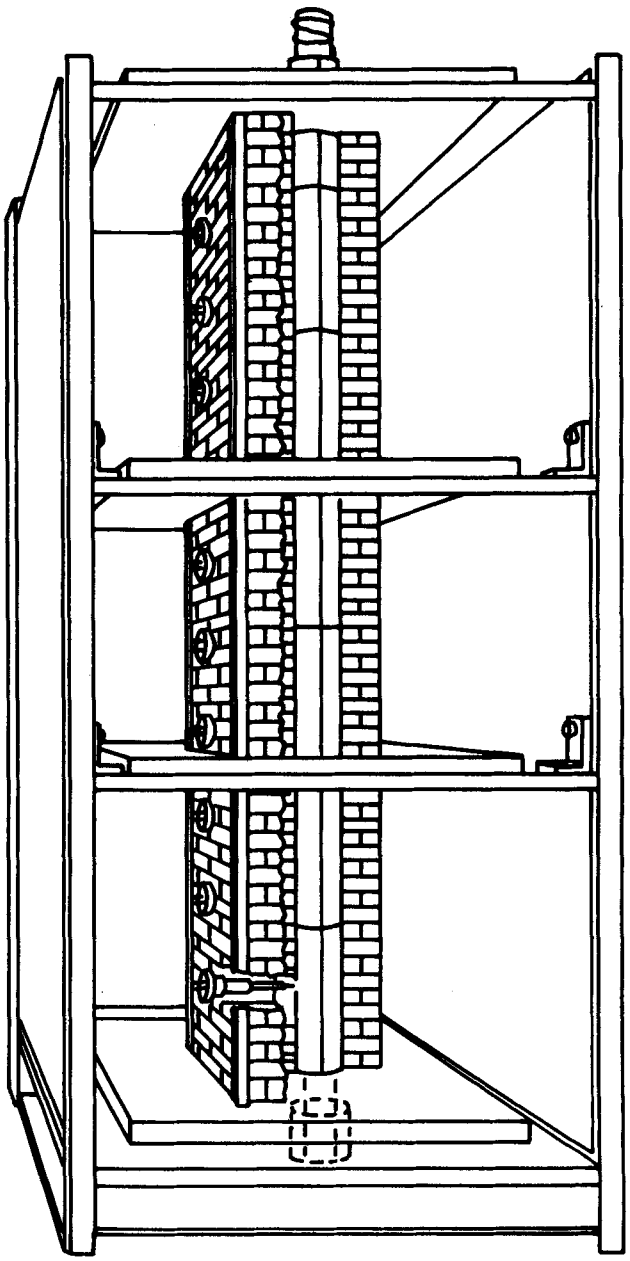

**Figure 1**—*Glass-shell-blowing tower furnace. Coiled wire resistors in clamshell heaters surround an inner mullite tube (7.0 cm i.d. × 2.1 m long). The tube end is terminated in a container of water. Temperature maximum was 1250° (±10° for 1.3 m).*



*0022-3549/81/0400-0364$01.00/0*
*© 1981, American Pharmaceutical Association*

for soda lime at 673 °K). The amorphous nature of glass permits easy fabrication of hollow shells. The large range of viscosities through which a glass proceeds helps to control the formation and freezing of the glass to produce a hollow shell configuration.

Another important property of glass is its ability to withstand low-energy ionizing radiation (such as tritium beta-particles) for extended periods without serious loss of strength.

**Gel Synthesis**—Microscopic glass shells suitable for use in targets for inertial confinement fusion research can be produced by at least two techniques. The first method utilizes the phenomenon known as glass reboil. Reboil can occur in glass that was manufactured to contain dissolved gases or gas-generating species that are produced or released when the glass is reheated to temperatures above its original forming temperature. For bulk glass, the resultant product of such a treatment is a foamed structure. If the glass is in particulate form, the reboil phenomenon can result in the formation of glass shells (2).

The second technique uses a solution-derived dried gel as the glass shell starting material. A blowing agent is incorporated in the solid gel during the solution stage prior to gelation. As described in a patent (3), a gel, derived from a water–glass-type solution, first is converted into particulate form and subsequently is heated in a furnace where glass shells are formed. The preparation of such gels from water or water–alcohol solutions of chemicals convertible to metal oxides was probably first reported by Roy (4) who employed them as precursors for glasses and synthetic minerals. The gel approach to glass manufacture is costly compared to conventional glass-forming techniques, but its unique characteristics make it attractive as the basis for additional research on glass shells (5, 6).

The gel is cured by heating for 14 hr at ~55°. The product then is air dried to remove most solvents and reaction by-products and finally is vacuum dried at 100°. The resulting particles, 0.1–1.0 cm in size, are crushed and sieved. This crushed and sieved material will be referred to as "metal–organic gel."

The gel technique and the dried particulates it provides have disadvantages as well as advantages. The disadvantages include: (*a*) restrictions on glass composition arising from incompatibility of certain metal–organic reagent combinations; (*b*) the metastable state of the solutions, which requires careful control of reaction parameters to obtain homogeneous gels instead of precipitates with their accompanying segregation of glass precursor components; and (*c*) the presence of residual organic groups, which can result in the production of carbon in the glass shell, which is not removed during fabrication.

Important advantages are: (*a*) the variability of glass composition through any of three variations of the basic technique; (*b*) the capability of combining all glass precursors in a solution and thus achieving mixing on a molecular scale, an important consideration when producing individual gel particles weighing only nanograms; and (*c*) the homogeneous incorporation of a blowing agent. Carbon, converted to carbon dioxide in the drop tower, is the likely source of the blowing agent in the gel technique. Homogeneous distribution of carbon throughout the dried gel seems highly probable since the carbon undoubtedly arises from residual ethoxy groups trapped in the silicon–oxygen–silicon network during gelation.

Glass shells are fabricated in a vertical tubular furnace or tower furnace (Fig. 1). The bottom of the mullite tube is sealed by immersion in water. This arrangement effectively prevents undesirable updrafts in the furnace tube and serves as a convenient collection medium for glass shells produced in the tube.

The shell fabrication procedure involves adding 20–30 mg of metal–organic gel at the top of the tower intermittently. Time intervals are varied from 0.25 to 1.0 min, depending on gel size. Shells formed in the furnace are collected and subsequently washed with water, washed and floated in isopropyl alcohol, and then dried.

**Polymeric Shells**—Glass shells are the most commonly used fuel containers because their physical properties are nearly ideal. Glass exhibits very low permeability, high tensile strength, optical clarity, a high melting point, abrasion resistance, and chemical durability, and it can be formed easily into shells.

Polymeric shells offer the following alternatives in physical properties that could be useful in the design of future laser fusion targets:

1. Organic polymers are considerably less dense than glass or metal.
2. Polymers can be copolymerized and blended to produce a wide range of physical properties and compositions.
3. Polymers offer the potential for low cost, high volume fabrication of shells.

A polymer must satisfy a number of prerequisites to be useful as a container for inertial confinement fuel. Since a target must contain the gaseous fuel until illumination by the driver, low permeability to hydrogen isotopes is essential. Permeability coefficients range from $1.4 \times 10^{-14}$ mole (standard temperature and pressure) $m/m^2$-SPa for poly(propylene) to $3.0 \times 10^{-2}$ mole (standard temperature and pressure) $m/m^2$-SPa for silica (7). Some polymers exhibit characteristics similar to those of glass, but only a few exhibit permeability coefficients that approach those of glass [silica is ~100 times less permeable than poly(vinyl alcohol) at 293 °K].

Since shells usually are pressurized with 10 atm (1 MPa) of gaseous fuel, the shell material must have sufficient tensile strength to withstand the stress of high internal pressure. The tensile strength of poly(methyl methacrylate), representative of most common plastics, is 7 $kgf/mm^2$; that of heat-treated poly(vinyl alcohol) is 110 $kgf/mm^2$ (8).

Elongation is another important property affecting the selection of polymers because of its relation to the dimensional stability of pressurized pellets. Elongation values range from 4% for poly(methyl methacrylate) to 600% for poly(vinyl alcohol) with water present. Typically, the elongation of fully hydrolyzed poly(vinyl alcohol) is 250%; however, with proper heat treatment, its elongation can be held to <2% (8). Typical glass elongation is 3% at break (8). Thus, heat-treated poly(vinyl alcohol) shells kept at a relative humidity of <5% can have elongations comparable to glass shells.

The ideal polymer must satisfy the conditions of high strength, low permeability to hydrogen, and low elongation. Poly(vinyl alcohol) satisfies these criteria better than any polymer investigated. Although most experiments have used poly(vinyl alcohol), considerable research has been devoted to chemical synthesis of new monomers and subsequent polymers such as polymethylol[1]. Polymethylol has certain properties and characteristics superior to those of poly(vinyl alcohol); but since polymethylol is not soluble in useful solvents, it is not suitable for established shell fabrication methods. Some polymers cannot be spray dried or microencapsulated, and polymethylol appears to be one of them.

Two techniques to fabricate polymer shells were developed. These two techniques, spray drying and *in situ* polymerization microencapsulation, will be described.

*Spray Drying*—The spray-drying method of polymer shell fabrication involves spraying a solution of polymer and volatile solvent into a large, heated chamber. This method was developed initially to produce minute solid particles and was modified to produce hollow shells. Shell formation involves atomizing a polymer solution, thus forming droplets which, upon heating, concentrate and encapsulate a mixture of solvent, air, and atomizing gas. These various encapsulants form the inner cavity but diffuse through the shell wall upon expansion of the capsule when heated. Mass spectral analysis of the residual gas in polymer shells revealed only trace quantities of the solvent vapor.

The drying chamber consists of a square box (3.66 m high × 1.22 m × 1.22 m) constructed of galvanized steel sheet and insulated with 10.2 cm of fiber glass. Sixteen 1.5-m long electrical resistance heaters are affixed at regular intervals along the inside walls and supply heat to the chamber. Thermocouples are positioned at three different locations within the chamber to record the temperature profile. The 3.66-m chamber is of sufficient height to provide time for falling droplets within the size range of interest to be dried.

The atomizer[2] utilizes a high-velocity jet of gas as the atomization medium. The polymer solution is fed into the gas stream, which imparts shearing force to the solution to form droplets. This atomizer is designed to provide maximum variability in atomizing solutions over a wide range of viscosities. Interchangeable atomizer heads were employed in this study to accommodate the large range of viscosities and to produce droplets of predictable and reproducible size. The atomizer uses compressed gas to form the high velocity atomizing jet. The flow rates of the solution and gas are variable. Various polymers have been spray dried, of which nine have produced acceptable shells. Table I lists these polymers, their characteristic sizes, and their gas retention times.

Because the physical properties of polymers vary greatly, shells were produced under unique conditions for each polymer. Poly(methyl methacrylate) and polycarbonate, for example, form high quality shells quite readily. Both are hard, glassy, amorphous polymers, which form solutions of moderate viscosity in low boiling solvents. Poly(vinyl alcohol) and carboxymethylcellulose sodium form shells only under precisely controlled temperature and solution composition. Both polymers are water soluble, and their solutions are difficult to atomize because of high

[1] Polymethylol is poly(vinyl alcohol) with a hydroxyl group on each carbon atom.

[2] The atomizer is a modified version of the A-CUADF automatic airbrush manufactured by Paasche Airbrush Co.

**Table I—Spray-Dried Polymeric Shells**

| Polymer[a] | Mean Diameter, μm | Mean Wall Thickness, μm | Maximum Diameter, μm | Maximum Aspect Ratio | $R_t$[b], hr | Gas[c] |
|---|---|---|---|---|---|---|
| PVA (10 lots) | 56–116 | 1.2–2.9 | 182 | 134 | 32.0<br>28.0 | $D_2$<br>DT |
| PMMA (two lots) | 96–567 | 1.6–2.0 | 744 | 402 | <0.5 | $D_2$ |
| CMC | 83 | 2.2 | 108 | 78 | 35.0<br>15.0 | $D_2$<br>DT |
| VAVB | 85 | 2.2 | 132 | 55 | <0.5 | $D_2$ |
| SAL | 90 | 4.6 | 112 | 25 | <0.5 | $D_2$ |
| PVF | 98 | 4.0 | 124 | 49 | <0.5 | $D_2$ |
| PC | 112 | 2.4 | 142 | 71 | <0.5 | $D_2$ |
| PVB | 90 | 2.7 | 116 | 59 | <0.5 | $D_2$ |
| HPM | 67 | 1.2 | 92 | 85 | <0.5 | $D_2$ |
| PS | 123 | 3.9 | 184 | 54 | <0.5 | $D_2$ |

[a] PC = polycarbonate. PVA = poly(vinyl alcohol). PMMA = poly(methyl methacrylate). CMC = carboxymethylcellulose sodium. VAVB = poly[(vinyl alcohol)-co(vinyl butyral)], 80% of which is butyral. SAL = poly[(styrene)-co(allyl alcohol)]. PVF = poly(vinyl formal). HPM = poly(2-hydroxypropyl methacrylate). PS = polystyrene. [b] Time for pressure to drop to 80% of $P_0$ = 1 MPa. [c] $D_2$ = deuterium, and DT = deuterium–tritium mixture.

viscosity. Furthermore, water is difficult to remove quickly because of its high heat capacity and heat of vaporization.

A polymer solution that is too dilute forms solid beads or thin, collapsed shells. If a polymer solution is too concentrated or if the polymer has a high molecular weight (>100,000), the shear forces provided by the atomizing gas are insufficient, and long filaments result. For example, when high molecular weight poly(methyl methacrylate) is sprayed from dilute solution, only very fine fibers are obtained because of the high viscosity of the solution. If the atomized polymer is very crystalline, the polymer precipitates when sprayed, and no hollow particles are formed. When a solution of low molecular weight polyethylene in toluene is sprayed, opaque solid beads are formed. This polyethylene is highly crystalline and precipitates instead of forming a film.

The parameters of shell formation involved in spray drying a variety of polymers were investigated. The method can produce shells ranging from 20 to 740 μm. The size of a shell produced from a given droplet can be estimated (9):

$$D_2 = D_1\left(\frac{d}{\rho d_s}\right)^{1/3} \qquad \text{(Eq. 1)}$$

where $D_2$ is the droplet diameter, $D_1$ is the capsule diameter, $d$ is the capsule density, $d_s$ is the solution density, and $\rho$ is the weight fraction of the polymer solution.

The spray-drying method is versatile, and a broad range of shell sizes can be fabricated from numerous polymers. Many shells can be fabricated easily in a short time. The hardware is relatively safe to operate and easy to maintain, and the equipment and process can be integrated into an automatic system.

*Coacervation Microencapsulation*—Microcapsules containing a liquid internal phase have been considered both as possible fusion pellets and as expansible precursors of hollow shells. The patent literature is replete with descriptions of microencapsulation systems that produce liquid-containing microcapsules using coacervation microencapsulation.

Coacervated microcapsules generally exhibit sphericity and surface finish that are unsatisfactory for fusion pellets. Extensive experimentation with a urea–formaldehyde coacervation system has not yielded acceptable sphericity or surface finish.

In Situ *Polymerization Microencapsulation*—Another patent (10) described a process for producing thermoplastic microcapsules containing a liquid blowing agent. Heating of the microcapsules causes them to expand and form hollow particles. In this method, a solution is prepared consisting of a monomer, a free radical polymerization initiator, a low boiling liquid (used in the internal phase and as a solvent for the monomer and initiator), and additives (for tailoring molecular weight by chain transfer). This solution is added to an immiscible aqueous phase containing surfactants and a colloidal antiagglomerating agent.

Upon mechanical agitation, the monomer solution is dispersed as suspended droplets in the aqueous medium. The initiator causes the monomer to polymerize as a film on the outer surface of the droplet, thus forming a thin wall. As polymerization continues, the film thickens and grows internally while the internal phase is encapsulated. This process continues, and the capsule wall thickens until all of the monomer and/or initiator is consumed.

After the polymerization process, the capsules are separated from the aqueous phase, washed, and sorted. When a capsule is heated above the glass transition point of the polymer, the capsules expand to form hollow shells due to the liquid–gas transition of the internal phase. The gaseous vapors of the internal phase escape by permeation as the wall thickness decreases and are replaced by air shortly after expansion, as verified by mass spectroscopy of the shell contents.

## EXPERIMENTAL

All *in situ* polymerization microencapsulation experiments were run in a 1-liter resin kettle equipped with a variable-speed impeller, condenser, and nitrogen inlet. The resin kettle was immersed in a constant-temperature water bath.

The aqueous phase consisted of 300 ml of distilled water, 0.5 g of colloidal silica[3], 3 g of 5% surfactant[4], and 1 g of 2.5% sodium dichromate. The pH was adjusted to 4 with dilute hydrochloric acid.

The oil phase consisted of 100 g of methyl methacrylate, 35 g of neohexane (internal phase), 0.5 ml of dichlorodimethylsilane, and 1.42 g of free radical polymerization initiator[5]. This mixture was maintained at 35° in a constant-temperature bath.

The two phases were mixed vigorously at ~5000 rpm for 1 min; then agitation was stopped. After 2 hr, the reaction temperature started to rise because of autoacceleration. Ice was added to the kettle, and gentle agitation was provided to maintain a temperature below 37°. After 8 hr, capsules were isolated by filtration and washed several times. Capsules expanded upon heating in an oven at 175° for 5 min and then were placed in a 100° oven for several hours to allow out-permeation of the internal phase vapor.

## RESULTS

The experimental procedure produced shells of 100–7000 μm. The size and wall thickness were controlled by the size of the stable droplet formed in the aqueous solution and the relative amounts of monomer and internal phase.

A narrow distribution of stable droplet sizes is obtained by using limited coalescence (10). In limited coalescence, colloidal particles, which are dispersed in the aqueous phase, collect on the surface of the suspended droplets. Droplets that are substantially covered by colloids are stable to coalescence. In a given droplet dispersion, the total droplet surface area is a function of the total volume of the dispersed liquid and the diameter of the droplets. In limited coalescence, the nonaqueous phase is dispersed as small droplets until they reach a critical limiting size, which depends on the amount of colloid present. The average size of a stable droplet is related directly to the aqueous phase composition by (10):

$$D = \frac{\pi dtV}{kW} \qquad \text{(Eq. 2)}$$

where $D$ is the average diameter of the stabilized droplets in centimeters, $t$ is the colloidal particle thickness in centimeters, $V$ is the volume of the droplet phase in cubic centimeters, $k$ is the swelling ratio of the colloid, $d$ is the dry density of the solid colloid in grams per cubic centimeter, and $W$ is the weight of solid colloid suspending agent in grams.

A more useful scaling relationship is (10):

$$D_1W_1 = D_2W_2 \qquad \text{(Eq. 3)}$$

This equation means that if a weight ($W_1$) of colloid producing capsules of average diameter ($D_1$) has been determined experimentally, the procedure can be tailored to produce capsules of another diameter ($D_2$) simply by adjusting the amount of colloid in the aqueous phase to an amount ($W_2$) in accordance with the ratio of diameters.

Early successful *in situ* polymerization microencapsulation experiments produced shells with poor inner surface uniformity. Upon microscopic examination, there appeared to be small polymer particles that were not incorporated into the wall. Apparently, a high molecular weight polymer formed late in polymerization after the capsule wall had appreciably hardened and thus could not merge with the wall. This hypothesis was supported in experiments with dichlorodimethylsilane, a potent polymerization chain transferring agent. With this agent, the amount of inner surface roughness decreased appreciably. Further im-

[3] Ludox, DuPont.
[4] Hyonic LA-90, Diamond Shamrock.
[5] VaZo 33W, DuPont.

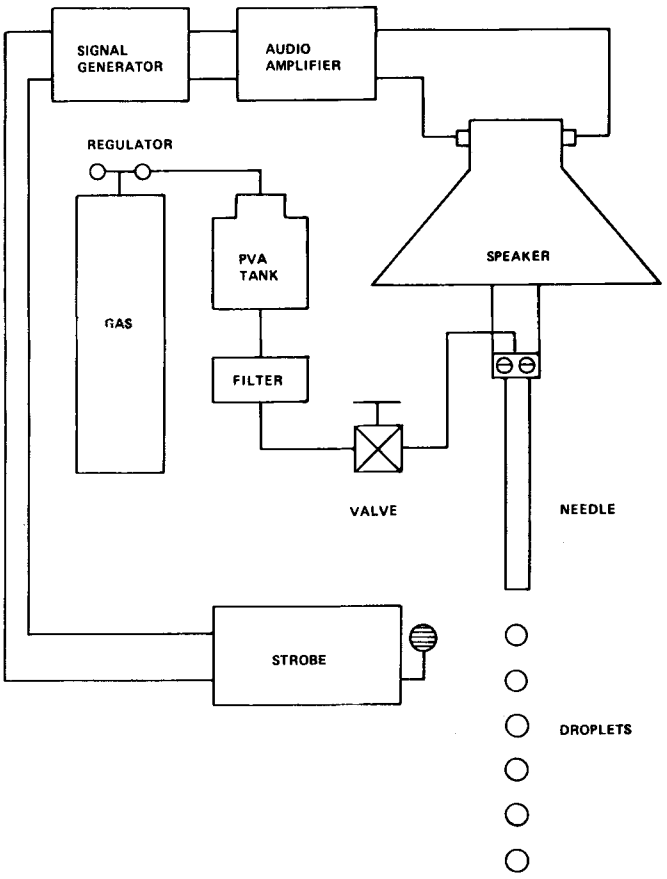


**Figure 2**—*Schematic diagram of droplet generator. [PVA = poly(vinyl alcohol).]*

provements may be achieved by modifying the polymerization kinetics.

Further polymeric shell research will be aimed at improving sphericity and increasing sizes. To this end, a device known as an acoustically modulated fluid jet has been designed and built (Fig. 2.) It is capable of producing uniformly sized droplets of polymer solution or melt. The solution to the problem of producing large (5 mm), hollow, spherical polymeric pellets will likely be solved through an understanding of uniform droplet production.

## REFERENCES

(1) J. Nuckolls, L. Wood, A. Thiessen, and G. Zimmerman, *Nature*, **239**, 139 (1972).

(2) W. R. Beck and D. L. O'Brien (to Minnesota Mining and Manufacturing Co.), U.S. pat. 3,365,315 (Apr. 28, 1968).

(3) F. Veatch, H. E. Alford, and R. D. Croft (to Standard Oil Co.), U.S. pat. 3,030,215 (Apr. 17, 1962).

(4) R. Roy, *J. Am. Ceram. Soc.*, **39**, 145 (1956).

(5) R. G. Budrick, F. T. King, A. J. Martin, R. L. Nolen, Jr., and D. E. Solomon (to KMS Fusion), U.S. pat. 4,017,290 (Apr. 12, 1977).

(6) R. G. Budrick, F. T. King, R. L. Nolen, Jr., and D. E. Solomon, (to KMS Fusion), U.S. pat. 4,021,253 (May 3, 1977).

(7) "Polymer Handbook," 2nd ed., J. Brandrup and E. H. Immergut, Eds., Wiley, New York, N.Y., 1975, p. 299.

(8) W. J. Roff, J. R. Scott, and J. Pacitti, "Handbook of Common Polymers," CRC Press, Cleveland, Ohio, 1971, p. 602.

(9) F. L. Veatch and R. B. Bruhans (to Standard Oil Co.), U.S. pat. 2,797,201 (June 25, 1957).

(10) D. D. Morehouse and R. J. Tetreault (to Dow Chemical Co.), U.S. pat. 3,615,972 (Oct. 26, 1971).

## ACKNOWLEDGMENTS

Supported in part by the U.S. Department of Energy under Contracts EY-76-C-02-2709, ES-77-C-02-4149, ED-78-C-08-1598, and DE-AC08-78DP40030.

This report was prepared for the Department of Energy under Contract DE-AC08-78DP40030.

# Long-Term Studies of Microencapsulated and Adsorbed Influenza Vaccine Nanoparticles

**JÖRG KREUTER** *x **and EKKE LIEHL** ‡

Received August 2, 1979, from the **Department of Pharmaceutical Technology, Swiss Federal Institute of Technology, Clausiusstr. 25, CH-8092 Zürich, Switzerland*, and the ‡*Sandoz Forschungsinstitut Gesellschaft M. B. H., Vienna, Austria.* Accepted for publication March 13, 1980.

**Abstract** □ Incorporation of antigens into nanometer-sized polymer particles was recently shown to lead to a good adjuvant effect. An optimal antibody response with killed influenza virus antigens was achieved with 0.5% poly(methyl methacrylate). Long-term experiments showed prolonged antibody response of polymer adjuvants with incorporated or adsorbed influenza virus. Adsorption also yielded an optimal adjuvant effect with 0.5% poly(methyl methacrylate). The antibody response was accompanied by protection of the mice against infection with mice-adapted influenza virus. In addition, the polymer vaccines were more stable against temperature inactivation than were vaccines with aluminum hydroxide or without adjuvants.

**Keyphrases** □ Vaccine, influenza—virus antigen incorporated into and adsorbed onto polymer nanoparticles, vaccines with and without adjuvant compared for protection in mice and against heat inactivation □ Polymers—poly(methyl methacrylate) and aluminum hydroxide used as adjuvants in influenza vaccine, effect of polymer on protection against influenza in mice and heat inactivation □ Microencapsulation—symposium, incorporation of influenza virus antigens into polymer nanoparticles compared with their adsorption onto polymer nanoparticles, vaccines with and without adjuvant evaluated for protection against influenza in mice and heat inactivation

Nanocapsules or nanoparticles, first described a few years ago (1–4), are nanometer-sized delivery systems for biologically active materials. This biologically active material may be totally or partially encapsulated, or it may be attached to these particles by adsorption or through chemical bonding.

At present, there are three distinctly different methods for nanoparticle production (1). The first method is micelle polymerization (2). In this process, polymerization is carried out in micelles or micelle-like structures in which the biologically active material and the polymerizable material are present.

0022-3549/81/0400-0367$01.00/0
© 1981, American Pharmaceutical Association

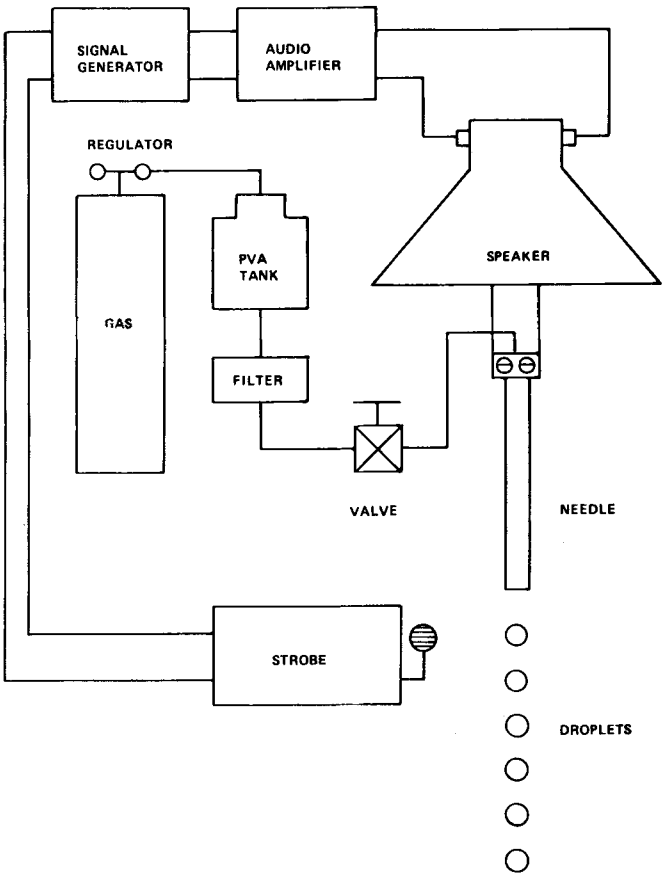


**Figure 2**—*Schematic diagram of droplet generator. [PVA = poly(vinyl alcohol).]*

provements may be achieved by modifying the polymerization kinetics.

Further polymeric shell research will be aimed at improving sphericity and increasing sizes. To this end, a device known as an acoustically modulated fluid jet has been designed and built (Fig. 2.) It is capable of producing uniformly sized droplets of polymer solution or melt. The solution to the problem of producing large (5 mm), hollow, spherical polymeric pellets will likely be solved through an understanding of uniform droplet production.

## REFERENCES

(1) J. Nuckolls, L. Wood, A. Thiessen, and G. Zimmerman, *Nature*, **239**, 139 (1972).

(2) W. R. Beck and D. L. O'Brien (to Minnesota Mining and Manufacturing Co.), U.S. pat. 3,365,315 (Apr. 28, 1968).

(3) F. Veatch, H. E. Alford, and R. D. Croft (to Standard Oil Co.), U.S. pat. 3,030,215 (Apr. 17, 1962).

(4) R. Roy, *J. Am. Ceram. Soc.*, **39**, 145 (1956).

(5) R. G. Budrick, F. T. King, A. J. Martin, R. L. Nolen, Jr., and D. E. Solomon (to KMS Fusion), U.S. pat. 4,017,290 (Apr. 12, 1977).

(6) R. G. Budrick, F. T. King, R. L. Nolen, Jr., and D. E. Solomon, (to KMS Fusion), U.S. pat. 4,021,253 (May 3, 1977).

(7) "Polymer Handbook," 2nd ed., J. Brandrup and E. H. Immergut, Eds., Wiley, New York, N.Y., 1975, p. 299.

(8) W. J. Roff, J. R. Scott, and J. Pacitti, "Handbook of Common Polymers," CRC Press, Cleveland, Ohio, 1971, p. 602.

(9) F. L. Veatch and R. B. Bruhans (to Standard Oil Co.), U.S. pat. 2,797,201 (June 25, 1957).

(10) D. D. Morehouse and R. J. Tetreault (to Dow Chemical Co.), U.S. pat. 3,615,972 (Oct. 26, 1971).

## ACKNOWLEDGMENTS

Supported in part by the U.S. Department of Energy under Contracts EY-76-C-02-2709, ES-77-C-02-4149, ED-78-C-08-1598, and DE-AC08-78DP40030.

This report was prepared for the Department of Energy under Contract DE-AC08-78DP40030.

# Long-Term Studies of Microencapsulated and Adsorbed Influenza Vaccine Nanoparticles

**JÖRG KREUTER** *x **and EKKE LIEHL** ‡

Received August 2, 1979, from the **Department of Pharmaceutical Technology, Swiss Federal Institute of Technology, Clausiusstr. 25, CH-8092 Zürich, Switzerland*, and the ‡*Sandoz Forschungsinstitut Gesellschaft M. B. H., Vienna, Austria.* Accepted for publication March 13, 1980.

**Abstract** □ Incorporation of antigens into nanometer-sized polymer particles was recently shown to lead to a good adjuvant effect. An optimal antibody response with killed influenza virus antigens was achieved with 0.5% poly(methyl methacrylate). Long-term experiments showed prolonged antibody response of polymer adjuvants with incorporated or adsorbed influenza virus. Adsorption also yielded an optimal adjuvant effect with 0.5% poly(methyl methacrylate). The antibody response was accompanied by protection of the mice against infection with mice-adapted influenza virus. In addition, the polymer vaccines were more stable against temperature inactivation than were vaccines with aluminum hydroxide or without adjuvants.

**Keyphrases** □ Vaccine, influenza—virus antigen incorporated into and adsorbed onto polymer nanoparticles, vaccines with and without adjuvant compared for protection in mice and against heat inactivation □ Polymers—poly(methyl methacrylate) and aluminum hydroxide used as adjuvants in influenza vaccine, effect of polymer on protection against influenza in mice and heat inactivation □ Microencapsulation—symposium, incorporation of influenza virus antigens into polymer nanoparticles compared with their adsorption onto polymer nanoparticles, vaccines with and without adjuvant evaluated for protection against influenza in mice and heat inactivation

Nanocapsules or nanoparticles, first described a few years ago (1–4), are nanometer-sized delivery systems for biologically active materials. This biologically active material may be totally or partially encapsulated, or it may be attached to these particles by adsorption or through chemical bonding.

At present, there are three distinctly different methods for nanoparticle production (1). The first method is micelle polymerization (2). In this process, polymerization is carried out in micelles or micelle-like structures in which the biologically active material and the polymerizable material are present.

0022-3549/81/0400-0367$01.00/0
© 1981, American Pharmaceutical Association

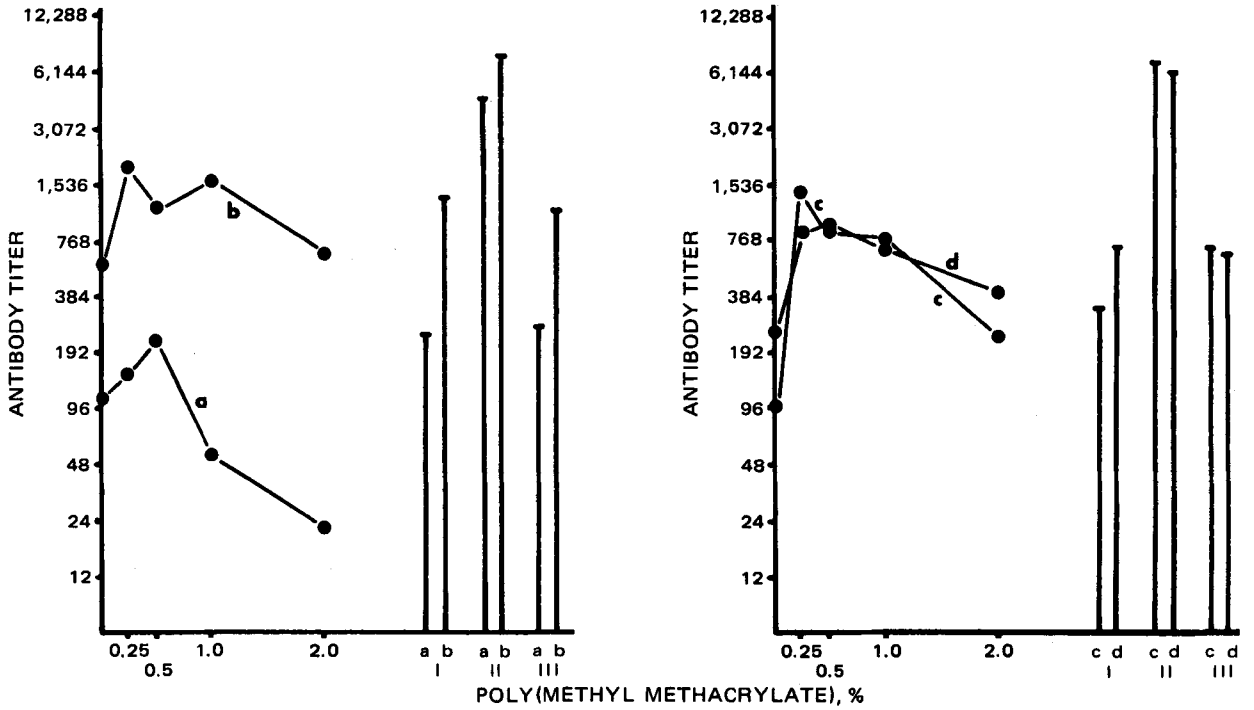


**Figure 1**—*Influence of increasing amounts of poly(methyl methacrylate) after antigen incorporation into the polymer on the antibody response after 4 (a), 8 (b), 12 (c), and 20 (d) weeks in guinea pigs. Boosting occurred after 4 weeks with fluid vaccines. The following adjuvants were used in addition: I, 0.1% aluminum hydroxide; II, Freund's complete adjuvant; and III, 0.5% methyl methacrylate + 0.5% acrylamide copolymer. The antigen was 400 IU of B/Hongkong 8/73 whole virions. For variabilities, see Table I. (Reproduced, with permission, from Ref. 3.)*

The second process involves polymerization of an aqueous solution of a polymerizable monomer (3, 5). During polymerization, the biologically active material is incorporated into the polymer particles due to interactions with the monomer or the polymer prior to or during polymerization. These interactions were demonstrated by the fact that 30% more monomer was clearly soluble in a virus suspension containing 3600 hemagglutinating units/ml than in a corresponding phosphate-buffered saline without virus (6). These 3600 hemagglutinating units correspond to 700 IU (international units), which approximates the content of various commercial vaccines.

The third process utilizes the rolling-up phenomenon of macromolecules (7). This conformational change occurs during the addition of a desolvating agent to a diluted solution of macromolecules. The rolled-up macromolecules entrap the biologically active material and may be hardened (for instance, with aldehydes) if gelatin is used as the macromolecule.

This report focuses on the second process, which is useful for vaccination when poly(methyl methacrylate) is used as the polymer (3).

## EXPERIMENTAL

**Virus**—$A_2$/Hongkong/1/68 influenza virus (X-31 strain) was grown in 11-day-old fertile chicken eggs as described by Hoyle (8). The virus was purified and concentrated by density zonal centrifugation followed by dialysis against pH 7.2 phosphate-buffered saline. The final suspension was inactivated with 0.1% formaldehyde. The hemagglutinin content (9) was determined as described by Wood *et al.* (10).

The challenge virus, $A_2$/Hongkong/1/68 influenza virus, was adapted to mice by multiple passages through mouse lungs.

**Influenza Subunits**—The subunits containing hemagglutinin and neuraminidase were prepared as described by Bachmayer and coworkers (11, 12).

**Table I—Antibody Titers (HI Titers) and Corresponding $Log_2$ of Guinea Pig Serum**

| Adjuvant | Parameter | Weeks 4 | 8 | 12 | 20 |
|---|---|---|---|---|---|
| 0.25% I | HI titer | 146 | 1871 | 1360 | 838 |
| | $\log_2 \bar{x} \pm SD$ | 7.19 ± 0.84 | 10.87 ± 1.15 | 10.41 ± 1.32 | 9.71 ± 0.99 |
| 0.5% I | HI titer | 218 | 1136 | 843 | 891 |
| | $\log_2 \bar{x} \pm SD$ | 7.77 ± 0.98 | 10.51 ± 1.09 | 9.72 ± 1.17 | 9.80 ± 0.99 |
| 1.0% I | HI titer | 52.3 | 1607 | 768 | 709 |
| | $\log_2 \bar{x} \pm SD$ | 5.71 ± 1.55 | 10.65 ± 0.82 | 9.58 ± 0.91 | 9.47 ± 0.78 |
| 2.0% I | HI titer | 21.3 | 657 | 234 | 402 |
| | $\log_2 \bar{x} \pm SD$ | 4.41 ± 1.51 | 9.36 ± 1.93 | 7.87 ± 1.58 | 8.65 ± 1.86 |
| Fluid | HI titer | 105 | 568 | 96 | 241 |
| | $\log_2 \bar{x} \pm SD$ | 6.71 ± 1.63 | 9.15 ± 1.56 | 6.58 ± 1.63 | 7.91 ± 1.00 |
| 0.1% $Al(OH)_3$ | HI titer | 237 | 1287 | 340 | 709 |
| | $\log_2 \bar{x} \pm SD$ | 7.89 ± 1.08 | 10.33 ± 0.87 | 8.41 ± 1.12 | 9.47 ± 1.05 |
| Freund's adjuvant | HI titer | 4420 | 7492 | 7042 | 6144 |
| | $\log_2 \bar{x} \pm SD$ | 12.11 ± 0.62 | 12.87 ± 0.59 | 12.78 ± 0.66 | 12.58 ± 1.08 |
| 0.5% I + 0.5% polyacrylamide | HI titer | 265 | 1105 | 704 | 644 |
| | $\log_2 \bar{x} \pm SD$ | 8.05 ± 1.07 | 10.11 ± 0.94 | 9.46 ± 0.67 | 9.33 ± 1.26 |

[a] For vaccination scheme and specification of vaccines, see Fig. 1.

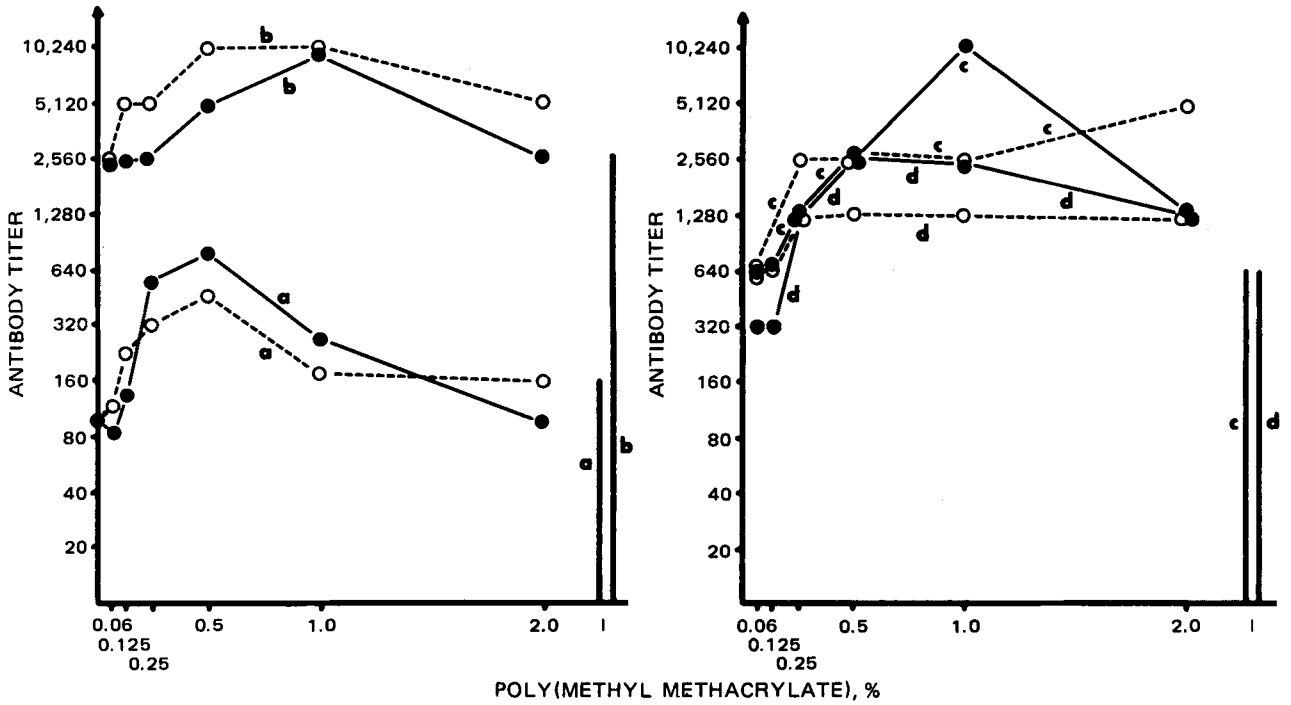


**Figure 2**—*Influence of different contents of poly(methyl methacrylate) on the antibody response of mice after 28 (a), 36 (b), 64 (c), and 92 (d) days. Boosting occurred after 28 days with the same vaccine as was used in the primary vaccination. Key: — ●, incorporation into poly(methyl methacrylate); - - - ○, adsorption onto poly(methyl methacrylate); and |, adsorption onto 0.2% aluminum hydroxide.*

**Monomer**—Methyl methacrylate[1] was purified from polymerization inhibitors by the methods described by Riddle (13) and Tessmar (14).

**Incorporation of Antigen into Poly(methyl methacrylate) (I) Nanoparticles**—Methyl methacrylate was dissolved in the antigen suspension and then polymerized with γ-rays (0.5 mrad) using a cobalt 60 source.

**Adsorption of Antigen to I Nanoparticles**—The monomer was polymerized as described; however, pH 7.2 phosphate-buffered saline was used instead of the antigen suspension. The resulting particles were centrifuged (680×*g* for 15 min) and resuspended in the antigen suspension after being washed three times with pH 7.2 phosphate-buffered saline.

**Animals**—Female NMRI mice[2], 20–24 g, were used.

**Influence of I Content on Antibody Response**—Whole influenza virions were used as the antigen. The vaccines had a hemagglutinin content of 630 IU/ml. Fourteen groups of 10 mice each received 0.1 ml/mouse, using one of the following adjuvant preparations: fluid without adjuvant; fluid incorporated into 0.06, 0.125, 0.25, 0.5, 1.0, and 2.0% I; fluid adsorbed onto 0.06, 0.125, 0.25, 0.5, 1.0, and 2.0% I; and fluid adsorbed onto 0.2% aluminum hydroxide.

The mice were boosted after 28 days with the same vaccine as was used in the primary vaccination. Blood was taken before boosting and after 36, 64, and 92 days.

**Effect of Boosting on Antibody Response**—Influenza subunits with a hemagglutinin content of 630 IU/ml were used as the antigen. Four groups of 20 mice each received 0.1 ml/mouse im. The following adjuvant preparations were used: fluid without adjuvant, fluid incorporated into 0.5% I, fluid adsorbed onto 0.5% I, and fluid adsorbed onto 0.2% aluminum hydroxide.

After 21 days, 10 mice of each group were boosted with the same vaccines as were used in the primary vaccination. Blood was taken after 21, 28, 42, 70, 125, and 180 days.

**Antibody Determiation**—The antibody determination was performed with the hemagglutination test, using the microtiter method (15, 16) in U plates with a 0.5% chicken erythrocyte suspension. Serum was pooled before determination.

**Heat Stability**—Whole influenza virions were used as the antigen. The vaccines had a hemagglutinin content of 21 IU/ml and were incorporated into 0.5% I, adsorbed onto 0.5% I, adsorbed onto 0.2% aluminum hydroxide, or without adjuvant. Each vaccine preparation was stored for 0, 15, 30, 60, 120, and 240 hr at 40°. Then 24 groups (four vaccines, six storage times) of 20 mice each received 0.1 ml/mouse of one vaccine preparation that had been stored for one of the specified time periods. One group of 20 mice served as a nonvaccinated control group. Twenty-eight days after immunization, the mice were challenged by spray infection with 50 times the $LD_{50}$ value of the homologous mouse-adapted virus as described by Schulman and Kilbourne (17). The $LD_{50}$ value of the challenge virus suspension was calculated according to Reed and Muench (18). Infection of the mice was recorded up to 9 days after the challenge, and the percentage of morbidity (lung lesions) was calculated.

## RESULTS AND DISCUSSION

**Influence of Poly(methyl methacrylate) (I) Content on Antibody Response**—For vaccination purposes, it is desirable not to coat the viral antigen completely but to incorporate it partially into the particles so the antigen can react with the immunocompetent cells of the immunized host. The extent of coating can be monitored by the monomer content before polymerization (3). This effect is illustrated in Fig. 1.

Four weeks after vaccination of guinea pigs, the optimal antibody response was obtained with 0.5% I (3). After the 4-week blood samples were taken, all animals were boosted with a fluid vaccine. After 8 weeks and particularly after 12 and 20 weeks, the differences in antibody response between 0.5% vaccines and vaccines with a higher polymer content decreased more and more. The cause for this decrease could be polymer decomposition. Thus, more antigen would be exposed to the immunocompetent cells of the host and result in a prolonged immunostimulation. Indications of polymer decomposition were found recently[3]. Another reason for the decrease in differences between these vaccines could be that much less antigen is necessary to provoke a booster-type immune response compared with a primary vaccination.

Since the effectiveness of an immunization can depend on the animal species used, it was of interest to determine if the results obtained with guinea pigs could be reproduced in mice. Immunization of mice with influenza virus antigens seems to be relevant for adjuvant testing not only because the antibody response can be determined but because the protection after infection with live virus can be measured. Figure 2 shows the influence of different contents of I on the antibody response of mice. After 28 days, an optimum at 0.5% polymer was observed with influenza virions incorporated into nanoparticles and with virions adsorbed to

[1] Fluka AG, Buchs, Switzerland.
[2] Versuchstier-Zuchtanstalt Willy Gassner, Sulzfeld, Austria.
[3] Unpublished results.

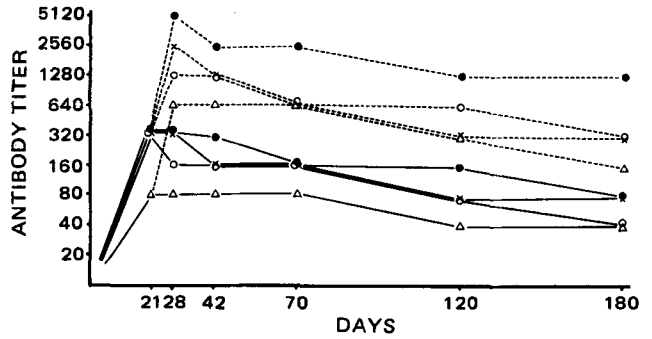


**Figure 3**—*Effect of boosting on the antibody response of mice. Key: —, unboosted groups; - - -, boosting after 21 days with the same vaccine as was used in the primary vaccination; ●, incorporation into 0.5% poly(methyl methacrylate); ○, adsorption onto 0.5% poly(methyl methacrylate); ×, adsorption onto 0.2% aluminum hydroxide; and △, fluid vaccine without adjuvant.*

nanoparticles. The optimum after incorporation shifted to 1% polymer after 36 and 64 days. The differences in antibody titers between the different polymer concentrations decreased after extended time with the incorporated and the adsorbed products. With the adsorbed products, the differences between the optimal and other polymer concentrations, however, were not as distinct as with the incorporated product. Both polymer vaccines were superior to aluminum hydroxide if optimal polymer concentrations were used.

It can be concluded that the antibody response in mice against influenza vaccines tested in these experiments is similar to the antibody response in guinea pigs. Moreover, when influenza is adsorbed onto nanoparticles, the antibody response is not as dependent on polymer content as it is after incorporation. However, incorporation into optimal polymer contents, in general, yielded higher antibody titers than adsorption. On the other hand, adsorption onto empty nanoparticles has the advantages that one batch of particles can be used with different antigens and that more drastic polymerization methods may be employed that otherwise would destroy the antigen.

**Effect of I Adjuvants on Secondary Antibody Response**—The effect of revaccination is shown in Fig. 3. Influenza incorporated into I always yielded the highest antibody response, whereas adsorption onto I and aluminum hydroxide yielded approximately the same response.

**Mice Protection**—Mice protection experiments are advantageous in that they can show the cooperation of all immune mechanisms following stimulation by vaccination and not only one immune mechanism, namely, antibody response. Although protection data obtained with mice

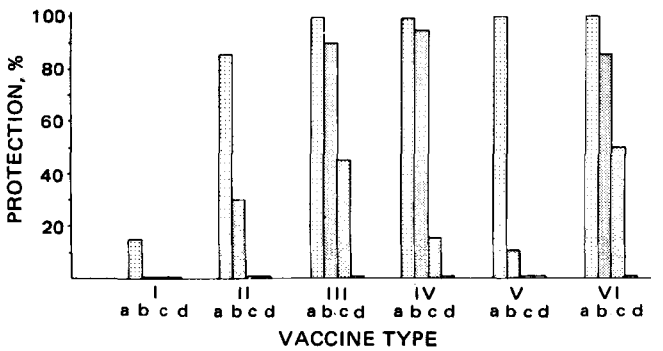


**Figure 4**—*Protection against mortality after immunization with $A_2$/Hongkong/1/68 (hemagglutinin content of the undiluted vaccine of 500 IU/ml) and challenge with 50 times the $LD_{50}$ value of homologous mouse-adapted virus. The following vaccine preparations were used: Group I, incorporation of the undiluted vaccine into 0.5% poly(methyl methacrylate) and dilution together with the polymer; Group II, adsorption of the undiluted vaccine onto 0.5% poly(methyl methacrylate) and dilution together with the polymer; Group III, incorporation of the previously diluted vaccine into 0.5% poly(methyl methacrylate); Group IV, adsorption of the previously diluted vaccine onto 0.5% poly(methyl methacrylate); Group V, fluid vaccine without adjuvants; and Group VI, adsorption of the previously diluted vaccine onto 0.2% aluminum hydroxide. The vaccine dilutions were 1:50 (a), 1:500 (b), 1:5000 (c), and 1:50,000 (d). Levels of significance are shown in Table II.*

**Table II—Levels of Significance of Protection against Mortality after Immunization with $A_2$/Hongkong/1/68 and Challenge with 50 Times the $LD_{50}$ Value of Homologous Mouse-Adapted Virus Using the $\chi^2$ Test of Snedecor and Cochran (20)**

| Vaccine[a] | Dilution | Statistical Significance of Protection |
|---|---|---|
| I | 1:50 | NS[b] |
| | 1:500 | NS |
| | 1:5000 | NS |
| | 1:50,000 | NS |
| II | 1:50 | $p < 0.001$ |
| | 1:500 | $p < 0.05$ |
| | 1:5000 | NS |
| | 1:50,000 | NS |
| III | 1:50 | $p < 0.001$ |
| | 1:500 | $p < 0.001$ |
| | 1:5000 | $p < 0.01$ |
| | 1:50,000 | NS |
| IV | 1:50 | $p < 0.001$ |
| | 1:500 | $p < 0.001$ |
| | 1:5000 | $p < 0.01$ |
| | 1:50,000 | NS |
| V | 1:50 | $p < 0.001$ |
| | 1:500 | NS |
| | 1:5000 | NS |
| | 1:50,000 | NS |
| VI | 1:50 | $p < 0.001$ |
| | 1:500 | $p < 0.001$ |
| | 1:5000 | $p < 0.001$ |
| | 1:50,000 | NS |

[a] For vaccine number identification, see Fig. 4. [b] Not significant.

may not always be relevant for humans, they seem to correlate quite well with the effectiveness of the vaccines in humans; therefore, the mice protection model is widely used (17).

One disadvantage of mice protection experiments is that the mice cannot be vaccinated with the same antigen content contained in commercial vaccines since the protection is too good to differentiate between efficient and less efficient vaccines. For this reason, the vaccines have to be diluted.

Figure 4 shows the effect of dilution on six different vaccines. The experimental procedures were reported previously (19). The levels of significance (Table II) were calculated using the method of Snedecor and Cochran (20). The vaccines were diluted 1:50, 1:500, 1:5000, and 1:50,000. Group V represents the four dilutions of the fluid vaccine without adjuvants. In Group VI, 0.2% aluminum hydroxide was added to each dilution. In Group IV, 0.5% I nanoparticles were added by adsorption onto each

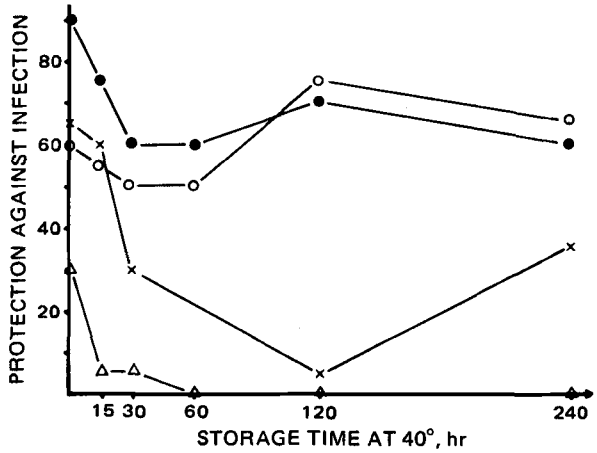


**Figure 5**—*Stability of vaccines against heat inactivation showing protection of mice against morbidity after immunization with vaccines that were stored at 40° for different time periods. The vaccines contained the following adjuvants: ●, incorporation into 0.5% poly(methyl methacrylate); ○, adsorption onto 0.5% poly(methyl methacrylate); ×, adsorption onto 0.2% aluminum hydroxide; and △, fluid vaccine without adjuvants. The mice were challenged with 50 times the $LD_{50}$ value of homologous mice-adapted virus. Levels of significance are shown in Table III. The influence of heat inactivation tested by the 6 × 2 contingency table is shown in Table IV.*

**Table III—Stability of Vaccines against Heat Inactivation: Levels of Significance of the Protection of Mice against Morbidity after Immunization with Vaccines that Were Stored at 40° for Different Times [a]**

| Vaccine | Storage Time at 40°, hr | | | | | |
|---|---|---|---|---|---|---|
| | 0 | 15 | 30 | 60 | 120 | 240 |
| 0.5% Poly(methyl methacrylate) incorporation | $p < 0.001$ | $p < 0.001$ | $p < 0.001$ | $p < 0.001$ | $p < 0.001$ | $p < 0.001$ |
| 0.5% Poly(methyl methacrylate) adsorption | $p < 0.001$ | $p < 0.001$ | $p < 0.01$ | $p < 0.01$ | $p < 0.001$ | $p < 0.001$ |
| 0.2% Aluminum hydroxide adsorption | $p < 0.001$ | $p < 0.001$ | $p < 0.05$ | $p < 0.01$ | NS[b] | $p < 0.05$ |
| Fluid without adjuvant | $p < 0.05$ | NS | NS | NS | NS | NS |

[a] Levels of significance were determined using the $\chi^2$ test. [b] Not significant.

**Table IV—Effect of Heat Inactivation on the Stability of Vaccines Determined Using a 6 × 2 Contingency Table with $\chi^2$ Test and Evaluation of Linear Regression [a] (21)**

| | Degrees of Freedom | 0.5% Poly(methyl methacrylate) Incorporation, $\chi^2$ | 0.5% Poly(methyl methacrylate) Adsorption, $\chi^2$ | 0.2% Aluminum Hydroxide Adsorption, $\chi^2$ | Fluid without Adjuvant, $\chi^2$ |
|---|---|---|---|---|---|
| Regression | 1 | 4.77* | 0.50 NS | 10.13*** | 13.27*** |
| Rest | 4 | 2.93 NS | 3.07 NS | 10.67* | 8.50 NS |
| Total | 5 | 7.70 NS | 3.57 NS | 20.80*** | 21.77*** |

[a] * = $p < 0.05$, *** = $p < 0.001$, and NS = not significant.

dilution; in Group III, each dilution was incorporated into 0.5% I nanoparticles.

In contrast to the latter two groups, in Group II the concentrated, undiluted vaccine was adsorbed onto 0.5% nanoparticles; in Group I, the undiluted vaccine was incorporated into 0.5% nanoparticles. Both vaccines then were diluted 1:50, 1:500, 1:5000, and 1:50,000. By this procedure the polymer was diluted together with the vaccine, resulting in 50- to 50,000-fold lower polymer concentrations in the final vaccine than in Groups III and IV. The resulting protection after adsorption onto polymer in Group II was equivalent to that of the fluid vaccine (Group V), whereas incorporation into the nanoparticles in Group I yielded much lower protection. Possibly too much antigen was covered by the polymer so that little or no immune stimulation resulted. These low polymer concentrations yielded no adjuvant effect. In contrast, incorporation of the previously diluted vaccine into 0.5% polymer resulted in good protection, as can be seen in Group III.

This experiment demonstrated that mice protection experiments have to be designed carefully and that the correct dilution as well as the correct dilution procedure has to be selected.

**Heat Stability**—Figure 5 and Table III show the heat stability of the vaccines tested in mice protection experiments. The vaccines were kept at 40° for 0, 15, 30, 60, 120, and 240 hr. The vaccines with adjuvants were more immunogenic than the fluid vaccine; after heating, the I vaccines were better than the aluminum hydroxide vaccine. For this reason, the nanoparticle vaccines, especially the adsorbed vaccine that is totally stable against heat inactivation (Table IV), hold promise for use when cooling conditions are not optimal.

## CONCLUSIONS

Adsorption and incorporation of influenza virus antigen into nanoparticles yielded very effective vaccines. Their effectiveness was especially pronounced in long-term experiments. This result could be demonstrated by measurement of antibodies in mice and guinea pigs. The effectiveness was clearly dependent on the polymer content, especially after incorporation. With an optimal polymer content of 0.5%, incorporation yielded vaccines that were superior to all other products tested with the exception of Freund's complete adjuvant, which, however, is too toxic for vaccination. In addition, the polymer vaccines were more stable against heat inactivation than aluminum hydroxide-adjuvanted and fluid vaccines.

## REFERENCES


(1) J. Kreuter, *Pharm. Acta Helv.*, **53**, 33 (1978).

(2) G. Birrenbach and P. P. Speiser, *J. Pharm. Sci.*, **65**, 1763 (1976).

(3) J. Kreuter and P. P. Speiser, *Infect. Immun.*, **13**, 204 (1976).

(4) P. P. Speiser, in "Microencapsulation: New Techniques and Application," T. Kondo, Ed., Techno Inc., Tokyo, Japan, 1979, p. 245.

(5) J. Kreuter, R. Mauler, H. Gruschkau, and P. P. Speiser, *Exp. Cell. Biol.*, **44**, 12 (1976).

(6) J. Kreuter and P. P. Speiser, *J. Pharm. Sci.*, **65**, 1624 (1976).

(7) J. J. Marty, R. C. Oppenheim, and P. P. Speiser, *Pharm. Acta Helv.*, **53**, 17 (1978).

(8) L. Hoyle, in "Virology Monographs," vol. 4, S. Gard, C. Hallauer, and K. F. Meyer, Eds., Springer Verlag, New York, N.Y., 1968, p. 26.

(9) *Ibid.*, p. 89.

(10) J. M. Wood, G. C. Schild, R. W. Newman, and V. Seagroatt, *J. Biol. Stand.*, **5**, 237 (1977).

(11) H. Bachmayer, E. Liehl, and G. Schmidt, *Postgrad. Med. J.*, **52**, 360 (1976).

(12) H. Bachmayer, *Intervirology*, **5**, 260 (1975).

(13) E. H. Riddle, "Monomeric Acrylic Esters," Reinhold, New York, N.Y., 1954, p. 15.

(14) K. Tessmar, in "Methoden der Organischen Chemie," (Houben-Weyl), vol. XIV/1, E. Müller, Ed., Makromolekulare Stoffe, G. Thieme Verlag, Stuttgart, West Germany, 1961, p. 1037.

(15) J. L. Sever, *J. Immunol.*, **88**, 320 (1962).

(16) D. F. Palmer, W. R. Dowdle, M. P. Coleman, and G. C. Schild, "Advanced Laboratory Techniques for Influenza Diagnosis," Immunology Series No. 6, U.S. Department of Health, Education, and Welfare, Public Health Service, Center of Disease Control, Bureau of Laboratories, Atlanta, Ga., 1975.

(17) J. L. Schulman and E. D. Kilbourne, *J. Exp. Med.*, **118**, 257 (1963).

(18) L. J. Reed and H. Muench, *Am. J. Hyg.*, **27**, 493 (1938).

(19) J. Kreuter and E. Liehl, *Med. Microbiol. Immunol.*, **165**, 111 (1978).

(20) G. W. Snedecor and W. G. Cochran, "Statistical Methods," Iowa State University Press, Ames, Iowa, 1971, p. 327.

(21) L. Sachs, "Statistische Auswertungsmethoden," Springer Verlag, New York, N.Y., 1968, p. 458.

# Influences of Matrixes on Nylon-Encapsulated Pharmaceuticals

**JAMES W. McGINITY ˣ, ALFRED MARTIN, GEORGE W. CUFF, and ALAN B. COMBS**

Received August 2, 1979, from the *Drug Dynamics Institute, College of Pharmacy, University of Texas, Austin, TX 78712.* Accepted for publication December 12, 1979.

**Abstract** □ The preparation and properties of nylon microcapsules containing three different matrixes (formalized gelatin, calcium alginate, and calcium sulfate) are described. Microcapsules containing each matrix were dense and free flowing and could be made of very small diameter by controlling the stirring speed during nylon formation. The preparation of microcapsules containing calcium alginate employed freeze-drying procedures. Lyophilization was not necessary with the formalized gelatin and calcium sulfate systems. Various representative drugs (anionic, cationic, nonionic, quaternary, and amphoteric compounds) were used in the formulation studies. The effects of pH, matrix, and encapsulated species on retention of drug in the microcapsules are described. In addition, the surface morphology of the microcapsules was examined using scanning electron microscopy.

**Keyphrases** □ Nylon microcapsules—preparation and properties, various matrixes and drugs, effects of pH, matrix, and encapsulated species on retention of drug during formulation □ Matrix, microcapsules—formalized gelatin, calcium alginate, and calcium sulfate, influence of matrixes on properties of nylon-encapsulated pharmaceuticals □ Microencapsulation—symposium, influence of matrixes on properties of nylon-encapsulated pharmaceuticals

The preparation of dense, free flowing, drug-containing microcapsules can improve certain physical characteristics of formulations such as compressibility and flow. In addition, the microencapsulation process has been utilized to modify drug release, to improve drug stability, and to permit the mixing and storage of reactive or incompatible materials (1). The types of wall materials and preparation methods of microcapsules were reviewed extensively by Madan (2). Microcapsules can range in diameter from nanometers to millimeters, depending on the material to be encapsulated and the ultimate product use. Microcapsules for oral preparations have been prepared with nonbiodegradable membranes including nylon (3–6), ethylcellulose (7–9), cellulose acetate phthalate (10), polystyrene, and cellulose nitrate (11). *dl*-Polylactic acid (12) and albumin (13–16) have been employed as membranes for biodegradable microcapsules for injectable preparations.

## BACKGROUND

Nylon is a polyamide formed from the reaction of a diamine and a diacid halide. Since several different types of nylon can be formed by altering the carbon chain length or configuration in the amine or diacid and since each alteration may change the permeability of the resultant film, nylons seem to offer an excellent array of possibilities for the microencapsulation of pharmaceuticals (17). However, the application of nylon to microcapsules has generally been limited to the encapsulation of large molecules such as proteins and enzymes. For example, Chang and coworkers (18–20) formulated and used encapsulated enzymes to treat enzyme deficiencies. The microencapsulated enzymes are immobilized and are prevented from leaking out of the capsule, thereby preventing hypersensitivity or other immunological reactions. However, the enzymes can act on small molecule substrates, which can dialyze across the semipermeable nylon membrane (21). Pharmaceuticals that have been encapsulated in nylon include pentobarbital sodium (3, 6), phenothiazines (4), and sulfathiazole sodium (5, 22).

The present investigators (5, 22) employed a nylon membrane to encapsulate sulfathiazole sodium as a soluble model compound. The encapsulation essentially combined the nylon microencapsulation technique of Chang *et al.* (19) with the gelatin micropellet method of Tanaka *et al.* (23). The resulting microcapsules consisted of drug embedded in a core of formalized gelatin surrounded by a nylon membrane. Microcapsules containing a solid matrix within the nylon membrane are easily separable by light trituration, following the drying step. In contrast, drug-containing capsules with no matrix tend to stick together, and levigation procedures to separate the capsules often damage the microcapsules. In addition, matrix-containing particles are dense and gritty and do not adhere together. These capsules have excellent flow properties and can be made of very small diameter by controlling the stirring speed during nylon formation.

In the present study, several different pharmaceuticals were encapsulated using the nylon technique. In addition to formalized gelatin, two other matrixes, calcium sulfate hemihydrate and calcium alginate, were investigated. The efficiency of the process with respect to the drug content inside the microcapsules was measured by assaying the dried microcapsules and the external organic medium employed. The surface morphology of the resulting microcapsules was examined by scanning electron microscopy.

## EXPERIMENTAL

**Materials**—The following were used: chloroform[1], cyclohexane[1], gelatin USP[1], formalin[1] (formaldehyde solution USP, 37%), 1,6-hexamethylenediamine[2], sebacyl chloride[2], caffeine[2], theobromine[2], sulfathiazole sodium[3], methantheline bromide[4], benzalkonium chloride[5], phenytoin[6], diphenhydramine hydrochloride[6], diazepam[7], theophylline[8], morphine sulfate[9], sodium alginate[10], and calcium sulfate hemihydrate[11].

**Preparation of Microcapsules**—Nylon-coated microcapsules containing matrixes of formalized gelatin, calcium sulfate, and calcium alginate were prepared. The microcapsules were formulated to contain a matrix-to-drug ratio of 2:1. The content of matrix chosen represents the amount needed to provide a workable viscosity of the aqueous phase during microcapsule preparation.

For the preparation of formalin-treated nylon gelatin microcapsules, 30 ml of aqueous 0.4 *M* hexamethylenediamine solution was added to an equal aqueous volume containing 5 g of gelatin and 2.5 g of drug. This solution was emulsified in 300 ml of an organic phase (cyclohexane–chloroform, 4:1) using a suitable mixer[12]. A nylon membrane was formed at the interface of the emulsified droplets by the slow addition of 1.2 ml of sebacyl chloride in 300 ml of the organic phase. The reaction vessel then was cooled to 5° in an ice bath. Next, 10 ml of 37% formalin was added to harden the gelatin matrix, and the reaction vessel was maintained at 5° for 12 hr. The microcapsules then were separated from the organic phase and dried at 37° to constant weight.

Nylon microcapsules containing a calcium sulfate matrix were prepared similarly. Initially, 7.5 ml of the hexamethylenediamine solution was added to 10 g of calcium sulfate hemihydrate and 5 g of drug. The addition of 3.5 ml of water to this mixture resulted in 20 ml of thick suspen-

[1] Fisher Scientific Co., Fair Lawn, N.J.
[2] Eastman, Rochester, N.Y.
[3] Mallinckrodt, St. Louis, Mo.
[4] Searle and Co., San Juan, Puerto Rico.
[5] Winthrop Laboratories, New York, N.Y.
[6] Parke-Davis and Co., Detroit, Mich.
[7] Hoffmann-La Roche, Nutley, N.J.
[8] Knoll Pharmaceuticals, New York, N.Y.
[9] Merck & Co., Rahway, N.J.
[10] Kelcosol, Kelco Co., Chicago, Ill.
[11] Plaster of Paris.
[12] Eppenbach.



0022-3549/81/0400-0372$01.00/0
© 1981, American Pharmaceutical Association

**Table I—Partitioning of Drug between Microcapsules and the Organic Phase [a]**

| Drug | Formalized Gelatin | Calcium Sulfate | Calcium Alginate |
|---|---|---|---|
| Sulfathiazole sodium | >99:1 | >99:1 | ≥99:1 |
| Sodium salicylate | ≥99:1 | ≥99:1 | ≥99:1 |
| Methantheline bromide | —[b] | —[b] | —[b] |
| Benzalkonium chloride | —[b] | —[b] | —[b] |
| Phenytoin | >99:1 | >99:1 | ≥99:1 |
| Diazepam | 90:10 | 75:25 | 88:12 |
| Caffeine | 75:25 | 66:34 | 75:25 |
| Theophylline | 69:31 (>99:1)[c] | —[b] | ≥99:1 |
| Theobromine | >99:1 | >99:1 | >99:1 |
| Diphenhydramine hydrochloride | 56:44 | 41:59 | 40:60 |
| Morphine sulfate | 85:15 | 96:4 | 95:5 |

[a] Expressed as the ratio of percent drug found in microcapsules to percent drug found in the organic phase. The amounts of drug originally formulated into microcapsules containing matrixes of formalized gelatin, calcium sulfate, and calcium alginate were 2.5, 5, and 1.25 g, respectively. [b] Microcapsules did not form. [c] Absence of formalin.

sion, and this suspension was emulsified in 300 ml of organic phase. The addition of 0.3 ml of sebacyl chloride contained in 300 ml of organic phase resulted in the formation of nylon-coated microcapsules. The capsules were allowed to stand at room temperature for 12 hr and then were separated from the organic phase. The microcapsules were allowed to dry undisturbed at 30° for 1 week.

To prepare nylon microcapsules containing a matrix of calcium alginate, 30 ml of the hexamethylenediamine solution was added initially to 30 ml of an aqueous solution containing 2.5 g of sodium alginate and 1.25 g of drug. This aqueous mixture then was emulsified in 300 ml of the organic phase. Nylon was formed by the slow addition of 1.2 ml of sebacyl chloride contained in 300 ml of organic phase. Calcium alginate was formed by the addition of 5 ml of saturated calcium chloride solution to the reaction mixture. Following the removal of 90% of the organic phase, the slurry of microcapsules was frozen using dry ice–acetone. Lyophilization for 2 days followed. The microcapsules then were stored at room temperature in a desiccator. Lyophilization prevented the microcapsules from sticking together during drying. The calcium alginate matrix should only be used for calcium-compatible drugs.

**Electron Scanning Microscopy**—The microcapsules were coated under an argon atmosphere with ~200 Å of gold–palladium using a cold sputter module in a high-vacuum evaporator equipped with an omnirotary stage. Samples were examined with a scanning electron microscope[13] using 20,000–30,000 kv.

**Analysis of Microcapsules and Organic Phase**—The amount of drug remaining in the microcapsules after formulation was determined by extracting the particles in an aqueous pH-adjusted medium for 12 hr. To determine the amount of drug that had partitioned into the organic phase during formulation, 100-ml volumes of this phase were evaporated to dryness and reconstituted with an aqueous medium of the appropriate pH to facilitate rapid drug dissolution. The drug concentration in both the microcapsules and the organic phase was determined spectrophotometrically at the wavelength of maximal absorbance for each drug.

## RESULTS AND DISCUSSION

The inclusion of hard matrixes such as formalized gelatin, calcium sulfate, and calcium alginate inside nylon coatings resulted in the formation of dense, free flowing, spherical microcapsules. In all cases, >95% of the finished solid product was present as intact microcapsules. Nylon microcapsules containing these matrixes were formulated with anionic, cationic, quaternary, amphoteric, and nonionic compounds to determine the versatility of this process (Table I).

The nylon membrane is formed *in situ* by interfacial polymerization. Morgan and Kwolek (24) showed that nylon, like most water-insensitive polymers, forms and grows on the organic solvent side of the interface. These workers found that the strongest nylon membrane was formed when the ratio of amide to diacid was approximately 1.8:1. However, the excess of diamine in the aqueous phase resulted in an alkaline pH inside the microcapsule after the nylon membrane was formed. Studies with the formalized gelatin matrix containing phenolphthalein showed that the pH was >9 prior to the addition of formalin. The addition of 10 ml of formalin to microcapsules containing phenol red in a gelatin matrix resulted in a slightly acidic pH inside the microcapsule. Since formalin was not added to nylon capsules containing calcium sulfate and calcium alginate, the pH of the microcapsule remained alkaline due to the excess quantities of the amine and the calcium salt.

[13] Model 1000, Advanced Metals Research, Burlington, Mass.

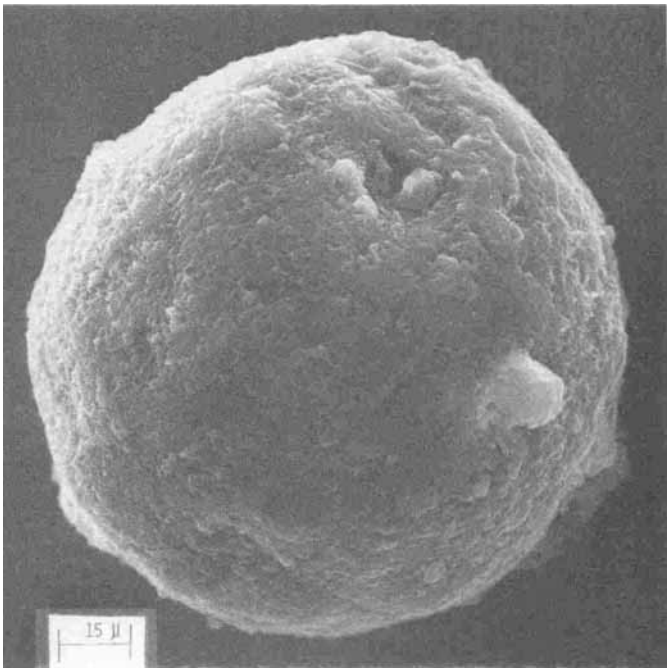


**Figure 1**—*Scanning electron micrograph of a formalin-treated nylon gelatin microcapsule containing morphine sulfate.*

For several drugs, the pH inside the microcapsule influenced the ionic character of the encapsulated drug. To determine the extent of partitioning into the organic phase, the microcapsules and organic phase were assayed for drug content; the ratio of drug in the capsule to the amount of drug partitioned into the organic phase at equilibrium is shown in Table I. Equilibrium conditions were established rapidly with all of the drugs studied. As expected with anionic drugs, little sulfathiazole sodium and sodium salicylate appeared in the organic phase.

Great difficulty was experienced in encapsulating the quaternary drugs, methantheline bromide and benzalkonium chloride, in nylon; in each

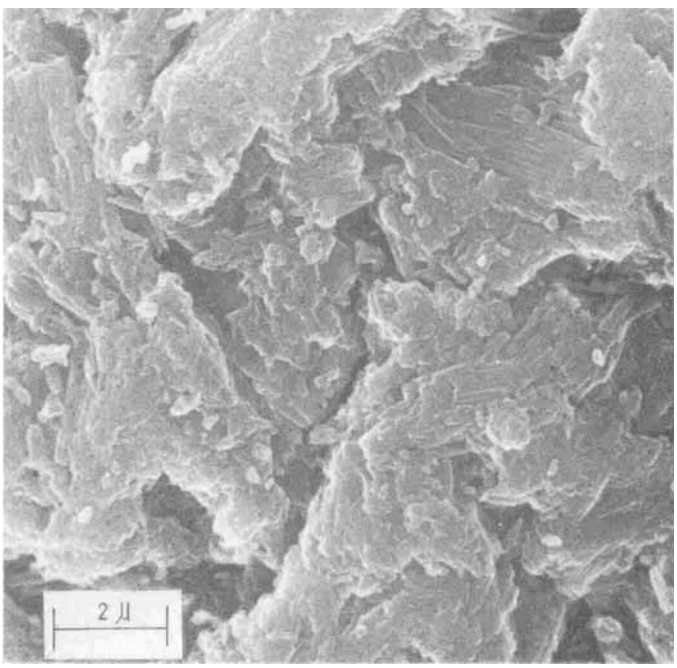


**Figure 2**—*Scanning electron micrograph of the microcapsule surface in Fig. 1.*

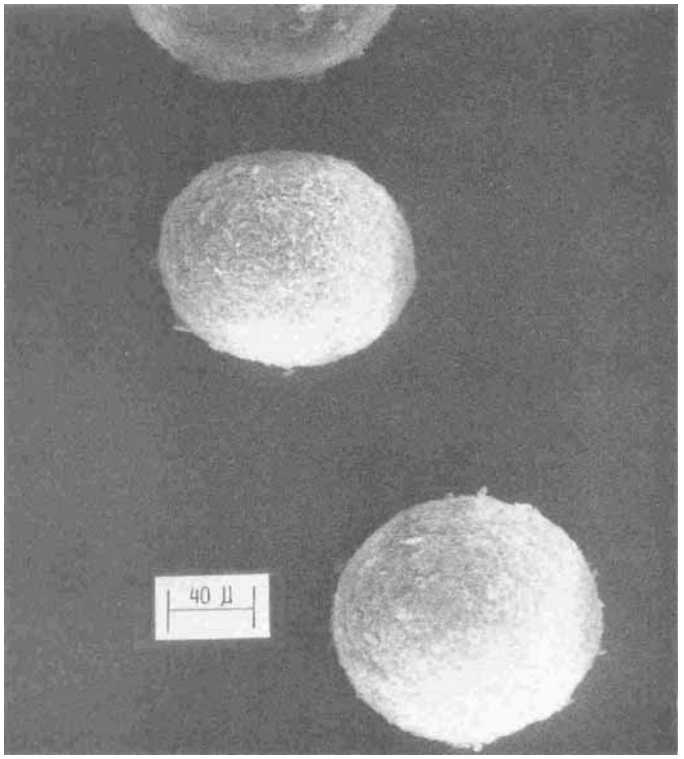


**Figure 3**—*Scanning electron micrograph of nylon microcapsules containing morphine sulfate in a calcium alginate matrix (lyophilized for 2 days).*

case, microcapsules were not formed. Preliminary studies showed that another quaternary compound, pralidoxime iodide, could be encapsulated in nylon with a formalized gelatin matrix, although the capsules were sticky and difficult to separate. Quaternary compounds apparently interfere with the reaction to form nylon.

Both phenytoin and diazepam formed suspensions in the aqueous phase containing hexamethylenediamine and the matrix components. Phenytoin can form a sodium salt at very high pH, so a small amount of a diamine salt may have formed in the hexamethylenediamine solution.

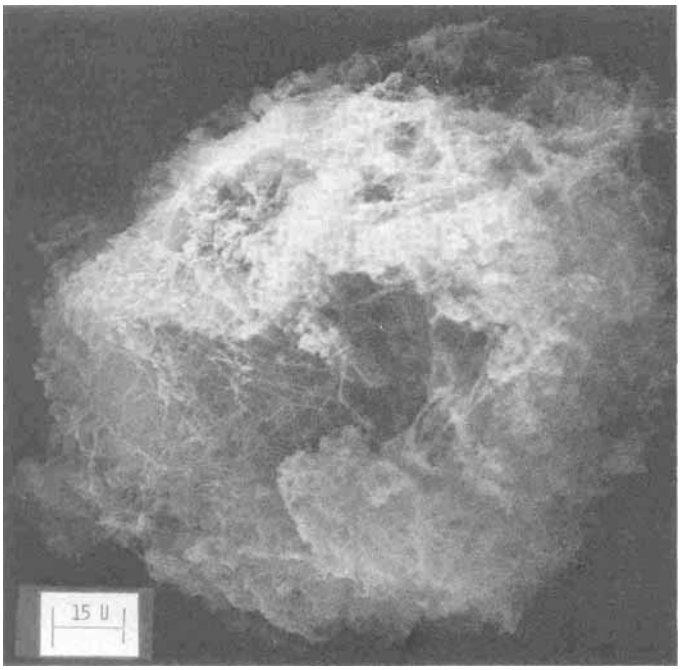


**Figure 4**—*Scanning electron micrograph of a nylon microcapsule containing morphine sulfate in a calcium alginate matrix (lyophilized for 5 days).*

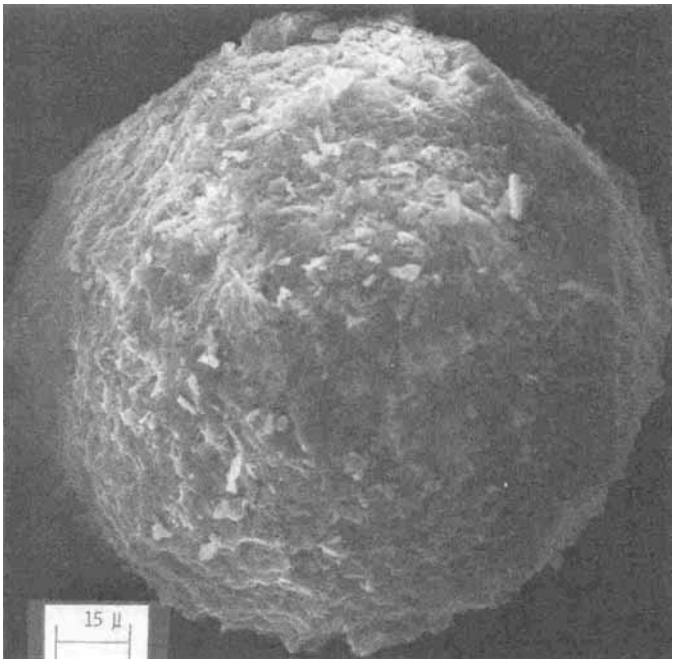


**Figure 5**—*Scanning electron micrograph of a nylon microcapsule containing morphine sulfate in a calcium sulfate matrix.*

Negligible quantities of drug were recovered in the organic phase, probably due to the very low solubility of phenytoin in both cyclohexane and chloroform. This was not the case with diazepam. Its yellow color was quite noticeable in the organic phase, and analysis confirmed the partitioning of the drug from the microcapsules.

Interesting results were seen with both the xanthine derivatives and the cationic drugs. The three xanthine derivatives included caffeine, theophylline, and theobromine. The caffeine and theobromine data can be explained on the basis of the relative drug solubilities in the organic phase. Caffeine has a solubility of 1 g in 5.5 ml of chloroform whereas theobromine is practically insoluble in both chloroform and cyclohexane. Theophylline microcapsules did not form when the matrix was calcium sulfate. The addition of theophylline to the calcium sulfate suspension and amine solution resulted in a very thick suspension, which was diluted with a small quantity of water. However, on addition to the organic phase, the aqueous suspension of calcium sulfate and theophylline did not emulsify in the organic phase and adhered strongly to the sides of the glass vessel and the stainless steel stirring apparatus, thus preventing the formation of microcapsules. The addition of formalin solution to the gelatin–theophylline microcapsules significantly decreased the amount of drug remaining in the capsules.

The two basic drugs studied were diphenhydramine hydrochloride and morphine sulfate. Small quantities of morphine were recovered in the organic phase. However, significant partitioning of the drug from the microcapsules was found only with the antihistamine due to its high solubility in chloroform.

The amount of drug remaining after the preparation of microcapsules containing the calcium alginate matrix was dependent on the volume of saturated calcium chloride used to form the calcium alginate. Calcium chloride solution was added to the reaction vessel following the formation of the nylon membrane. The electrolyte diffused into and reacted with the sodium alginate matrix. Since excess electrolyte stays in the aqueous phase, the percentage composition of drug in the microcapsules increases as the volume of calcium chloride solution decreases. When 10, 5, and 1 ml of saturated calcium chloride were added to alginate microcapsules containing sulfathiazole sodium, 7.35, 12.57, and 17.98% of drug were in the microcapsules, respectively.

Scanning electron micrographs of nylon microcapsules containing morphine sulfate and the three different matrixes are shown in Figs. 1–6. A microcapsule containing the formalized gelatin matrix is shown in Figs. 1 and 2. The surface appears to be rough and porous with a plate-like structure. However, these surface photographs do not indicate the inner structural features of the membrane, which may exhibit different morphology at the matrix interface. No drug particles were seen on the surface of the microcapsules. Nylon microcapsules containing calcium alginate were very similar to the formalized gelatin capsules (Fig. 3). As previously

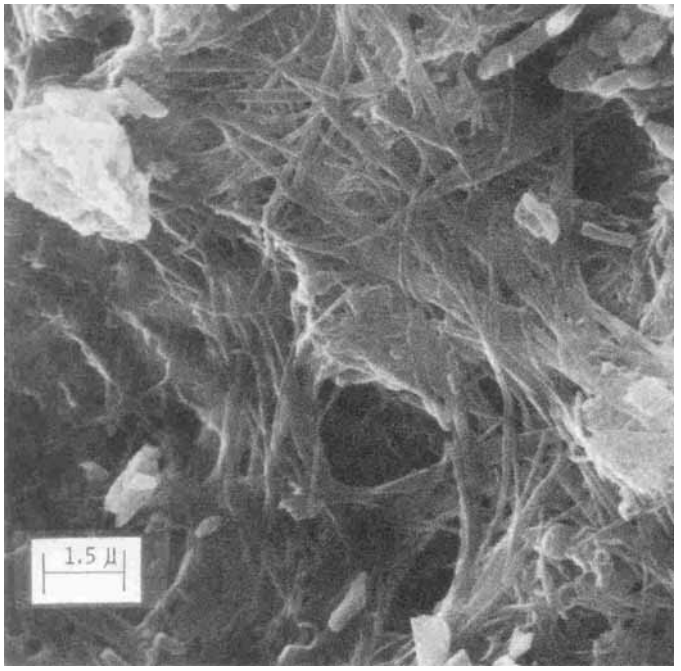


**Figure 6**—*Scanning electron micrograph of the microcapsule surface in Fig. 5.*

mentioned, the calcium alginate microcapsules were lyophilized for 2 days. Lyophilization for longer than 4 days resulted in disruption of the nylon membrane and loss of the matrix (Fig. 4). Figures 5 and 6 show morphine-containing microcapsules with a calcium sulfate matrix. The presence of calcium sulfate crystals on the surface is quite evident in Fig. 6. The surface appears to be very porous and fibrous in comparison to the other capsules.

Calcium sulfate hemihydrate (known as plaster of Paris) is formed by heating the dihydrate material (gypsum) (Scheme I).

$$2(CaSO_4 \cdot 2H_2O) \rightleftharpoons (CaSO_4)_2 \cdot H_2O + 3H_2O$$

*Scheme I*

When mixed with water, the equilibrium is reversed and the plaster sets to form a mass of gypsum crystals. The setting results in an increase in volume, which causes the nylon membrane to stretch. This expansion of the matrix helps explain the fibrous appearance of the nylon membrane in Fig. 6. The plate-like surface features seen with the formalized gelatin and calcium alginate matrixes and the fibrous structure seen with the calcium sulfate matrix differ markedly from the pitted surface of the nylon microcapsules containing polyoxyethylene glycol 400 shown by Jenkins and Florence (25).

In summary, the nylon encapsulation technique is applicable to a wide range of pharmaceuticals. Two major problems include drug partitioning into the organic phase and the possibility of decreased drug stability as a result of the alkaline pH inside the capsules. Preliminary results suggested that both problems may be overcome by altering the composition of the organic solvents and by adding small quantities of dilute acid to the reaction vessel following the formation of the nylon membrane. Future efforts will be directed toward optimizing the formulation to improve the retention of drugs that partition into the organic phase. The microcapsules also will be examined for their dissolution behavior, sustained release, and drug stabilizing properties and for the separation of incompatible ingredients.

## REFERENCES

(1) J. A. Bakan and F. D. Sloan, *Drug Cosmet. Ind.*, **110**, 34 (Mar. 1972).

(2) P. L. Madan, *Pharm. Technol.*, **2**, 24 (Aug. 1978).

(3) L. A. Luzzi, M. A. Zoglio, and H. V. Maulding, *J. Pharm. Sci.*, **59**, 338 (1970).

(4) A. F. Florence and A. W. Jenkins, in "Microencapsulation," J. R. Nixon, Ed., Dekker, New York, N.Y., 1976, pp. 39–55.

(5) J. W. McGinity, A. B. Combs, and A. N. Martin, *J. Pharm. Sci.*, **64**, 889 (1975).

(6) M. D. DeGennaro, B. B. Thompson, and L. A. Luzzi, in "Controlled Release Polymeric Formulations," D. R. Paul and F. F. Harris, Eds., American Chemical Society, Washington, D.C., 1976, pp. 195–207.

(7) J. R. Nixon, I. Jalsenjak, C. F. Nicolaidou, and M. Harris, *Drug Dev. Ind. Pharm.*, **4**, 117 (1978).

(8) S. Motycka and J. G. Nairn, *J. Pharm. Sci.*, **68**, 211 (1979).

(9) T. Kondo, in "Surface and Colloidal Science," vol. 10, E. Matijevic, Ed., Plenum, New York, N.Y., 1978, pp. 1–43.

(10) H. P. Merkle and P. Speiser, *J. Pharm. Sci.*, **62**, 1444 (1973).

(11) P. L. Madan, *Pharm. Technol.*, **2**, 31 (Feb. 1978).

(12) H. Mason, C. Thies, and T. J. Cicero, *J. Pharm. Sci.*, **65**, 847 (1976).

(13) P. A. Kramer, *ibid.*, **63**, 1646 (1974).

(14) K. J. Widder, A. E. Senyei, and D. G. Scarpelli, *Proc. Soc. Exp. Biol. Med.*, **58**, 141 (1978).

(15) A. Senyei, K. Widder, and G. Czerlinski, *J. Appl. Phys.*, **49**, 3578 (1978).

(16) K. Widder, G. Flouret, and A. Senyei, *J. Pharm. Sci.*, **68**, 79 (1979).

(17) L. A. Luzzi, in "Microencapsulation," J. R. Nixon, Ed., Dekker, New York, N.Y., 1976, pp. 193–206.

(18) T. M. S. Chang, *Science*, **146**, 524 (1964).

(19) T. M. S. Chang, F. C. MacIntosh, and S. G. Mason, *Can. J. Physiol. Pharmacol.*, **44**, 115 (1966).

(20) T. M. S. Chang, *Nature*, **229**, 117 (1971).

(21) T. M. S. Chang and M. J. Poznansky, *J. Biomed. Mater. Res.*, **2**, 187 (1968).

(22) J. W. McGinity, A. B. Combs, and A. Martin, in "Microencapsulation—New Techniques and Applications," T. Kondo, Ed., Techno Inc., Tokyo, Japan, 1979, pp. 57–77.

(23) N. Tanaka, S. Takino, and I. Utsumi, *J. Pharm. Sci.*, **52**, 664 (1963).

(24) P. W. Morgan and S. L. Kwolek, *J. Polym. Sci.*, **40**, 299 (1959).

(25) A. W. Jenkins and A. T. Florence, *J. Pharm. Pharmacol.*, **25**, 57P (1973).

## ACKNOWLEDGMENTS

The authors thank Dr. Garry Cole for the scanning electron micrographs.

# *In Vitro* and *In Vivo* Release of Microencapsulated Chlorothiazide

**J. R. NIXON**

Received August 2, 1979, from the *Department of Pharmacy, Chelsea College, University of London, Manresa Road, London SW3, England.* Accepted for publication December 20, 1979.

**Abstract** □ Microcapsules of chlorothiazide were prepared by the complex coacervate technique using gelatin and acacia as the wall-forming materials. The release of drug from the microcapsules and compressed tablets of microcapsules were studied *in vitro* and *in vivo*. *In vitro* dissolution was characterized by a rapid release of drug followed by a slower, more sustained release. The effects of pH and concentration are discussed. *In vivo* release of drug was determined from urine, and the volume of urine passed was studied.

**Keyphrases** □ Chlorothiazide—*in vitro* and *in vivo* release rates evaluated from plain tablets, compressed tablets of microcapsules, and microcapsules □ Gelatin–acacia coacervates—chlorothiazide, *in vitro* and *in vivo* release rates evaluated from compressed tablets of microcapsules, plain tablets, and microcapsules □ Microencapsulation—symposium, chlorothiazide release rates evaluated from plain tablets, compressed tablets of microcapsules, and microcapsules *in vitro* and *in vivo*

The preparation of gelatin–acacia microcapsules containing water-insoluble drugs is well known (1), although the number of modifications to the basic technique (2), in particular to the extraction of a fine powder, still precludes setting up a simple general method. The dosage forms in which microcapsules are used usually are not specified, although their use as suspensions, powders, and tablets all have been suggested (3, 4). Most published data regarding dissolution is from *in vitro* work (5–8), but some *in vivo* studies have been reported (9). Few attempts have been made to compare the performance of different formulations of the same microcapsules and to correlate *in vivo–in vitro* properties within and between preparations.

The present work attempts to investigate how chlorothiazide behaves when it is microencapsulated and formulated as powder and tableted dosage forms.

## BACKGROUND

Chlorothiazide and related compounds are diuretics that reduce the reabsorption of electrolyte from the renal tubules and, therefore, increase the excretion of sodium and chloride ions and, as a consequence, water.

Unmicroencapsulated diuretics given orally may produce diuresis after 2 hr; this diuresis can be maintained for up to 12 hr, although a more normal time is from 5 to 9 hr. Tolerance does not develop, and this diuretic may be used over a long period. Because of the long continuous activity, continuous administration usually is not needed; after an initial dose of 1 or 2 g, it is sufficient to give maintenance doses, which rarely exceed 1 g every few days.

Mild symptoms of discomfort have been reported for chlorothiazide and occasionally there are more serious toxic effects, particularly with patients suffering from diabetes and hepatic disorders (10–12). As with many materials given as tablets, ulceration of the gut is possible, particularly when the drug is in the form of a layered tablet that contains potassium chloride as a potassium supplement. The use of supplementary potassium with chlorothiazide is recommended, and the preparation of potassium chloride microcapsules is reported elsewhere. Subsequently, it is hoped that both types of microcapsules can be combined into a single dosage form that will allow a more sustained chlorothiazide diuretic effect and prevent gut ulceration due to the potassium chloride.

As a reasonable reference compound to study *in vivo*, chlorothiazide has a number of advantages. It allows measurement of urinary excretion rates (metabolism is not an important factor in the elimination of thiazide from the body), the rate of flow of urine and changes in the total urine volume, and changes in the elimination of sodium and potassium.

## EXPERIMENTAL

**Preparation of Microcapsules**—The microcapsules were prepared by gelatin coacervate techniques outlined previously (13, 14). With complex gelatin–acacia coacervates, it was immaterial whether the drug was dispersed in the gelatin or acacia prior to mixing (15, 16). Extraction was carried out by treating the mixture with formaldehyde solution (formalin), filtering, washing with isopropanol, and drying in a stream of air. The recovery was between 86 and 92%, and the mean size of the microcapsules was 73 μm with 80% of the sizes between 5 and 136 μm.

**Preparation of Tablets of Chlorothiazide Microcapsules**—These tablets were compressed in a single-punch hand compressor which had a 30-sec compression and a 10-sec rest under compression, followed by a 10-sec stage during which compression was released. In all cases, flat punches were used making 5-mm diameter tablets. The weight of the microcapsules was 250 mg for each tablet, and compression varied between 0.5 and 5 tonnes.

**Determination of Chlorothiazide**—*Microcapsules*—To determine the amount of chlorothiazide in the microcapsules, they were extracted with either water at pH 10 or isopropanol. In both cases, a 500-mg charge of the microcapsules was refluxed for 10–15 min at 100° with water or at 80° with isopropanol. The normal spectrophotometric assay at 513 nm was performed. The system was refluxed for an additional 15 min with fresh solvent to be certain that all chlorothiazide had been extracted.

*Urine*—Protein-free urine samples were obtained by diluting 1 ml with 4 ml of 20% *p*-toluenesulfonic acid and diluting to 20 ml with water. Five milliliters of this solution was heated in a water bath for 30 min with 1 ml of 3.75 *N* NaOH, during which chlorothiazide was hydrolyzed to a 6-aminodisulfonamide along with any conjugates present.

After this hydrolysis step, the assay followed the Bratton–Marshall method for sulfonamides. Five milliliters of the cooled solution was acidified with hydrochloric acid, sodium nitrite was added to diazotize the amine, and the tube was left in ice for 3 min. The excess nitrous acid was destroyed by ammonium sulfamate, and the solution was allowed to stand at room temperature for 5 min. The diazonium salt was coupled with *N*-(1-naphthyl)ethylenediamine hydrochloride, and the color developed after 10 min was read spectrophotometrically at 513 nm. The standard solutions for comparison were made from chlorothiazide in 4% *p*-toluenesulfonic acid.

***In Vitro* Dissolution**—The *in vitro* release from chlorothiazide microcapsules was studied using 250 mg of microcapsules containing either 163.7 or 95.6 mg of drug. This quantity was dispersed in 2 liters of water at 37° and adjusted to pH 2, 5, 7, or 9 with hydrochloric acid or sodium hydroxide. The stirring rate was 100 rpm.

***In Vivo* Dissolution**—The *in vivo* dissolution of the drug from the microcapsules was studied by giving 27 healthy volunteers on three separate occasions either plain chlorothiazide tablets, microcapsules, or tableted microcapsules. All dosages contained 500 mg of chlorothiazide, and 1 week elapsed between a repeat dose of drug to any subject. The normal volume of urine over 3 days was monitored for the subjects prior to taking the preparation, and all urines were assayed to ensure that a positive assay for chlorothiazide did not exist. No special diet was used, and sodium and potassium intake was not monitored or supplemented.

## RESULTS AND DISCUSSION

The results of the *in vitro* dissolutions are shown in Figs. 1 and 2. All samples at different pH values showed the familiar pattern of a rapid initial release followed by a slower sustained release. With all samples other than those at pH 2, ~50–60% of the drug was released within 20 min for the higher chlorothiazide concentration. However, with the lower



0022-3549/81/0400-0376$01.00/0
© 1981, American Pharmaceutical Association

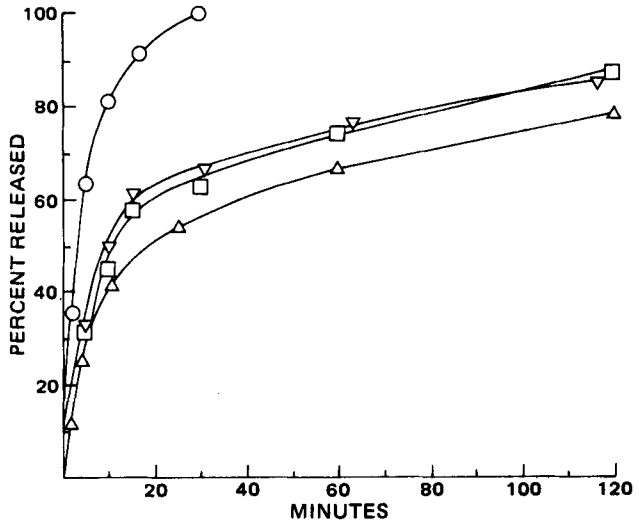


**Figure 1**—*Effect of pH on the* in vitro *release of chlorothiazide from formaldehyde solution-treated gelatin–acacia microcapsules. The concentration of chlorothiazide was 65.48% in a charge of 250 mg in 2 liters of water at 37°. Key:* ○, *pH 2;* ▽, *pH 5;* □, *pH 7; and* △, *pH 9.*

concentration, the change in the release rate was more gradual, and it was difficult to discern any break that could be regarded as the start of a sustained, or slower release, stage.

With both high and low concentrations of drug in the microcapsules, the fastest release was at pH 2; and since the microcapsules had been formaldehyde solution treated, it appears that this treatment did not produce any enteric coating effect. This observation suggests that *in vivo* the bulk of the drug would be released in and absorbed from the stomach. Also shown in Fig. 2 is the rate of solubility of the unencapsulated drug in water. Although the dissolution rate from the microcapsules at pH 2 was rapid, there was a slight delay in release when compared with the dissolution rate of raw drug.

Figure 3 shows the percentage released as a function of both pH and the percentage of drug in the microcapsules. A linear relationship existed between the percentage of drug present and the quantity released. In the first 30 min, irrespective of the pH other than pH 2, a higher percentage of drug was released from those microcapsules containing the larger percentages. This result was not unexpected because, with the method of manufacture employed, these microcapsules have the thinnest protective wall. However, after 60 min, the core content appeared to have little effect on the total percentage of drug released, except at pH 9 where the microcapsules with the highest content of chlorothiazide were releasing a higher total percentage of drug than the thicker walled, lower drug content ones.

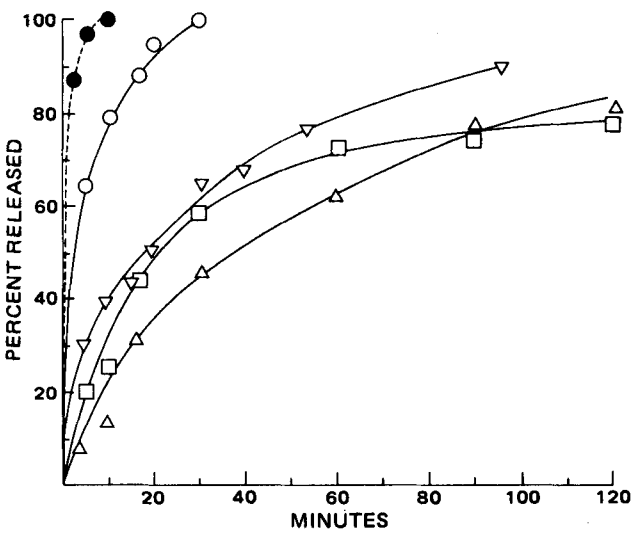


**Figure 2**—*Effect of pH on the* in vitro *release of chlorothiazide from formaldehyde solution-treated gelatin–acacia microcapsules. The concentration of chlorothiazide was 38.24% in a charge of 250 mg in 2 liters of water at 37°. Key:* ○, ●, *pH 2;* ▽, *pH 5;* □, *pH 7;* △, *pH 9;* ○, ▽, □, △, *microcapsules; and* ●, *raw drug.*

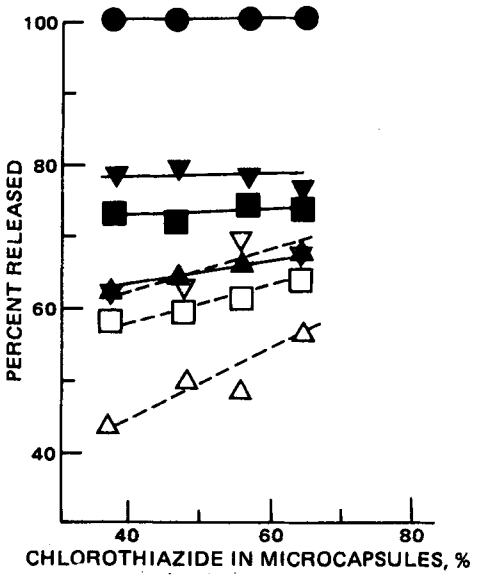


**Figure 3**—*Effect of pH and drug concentration on the* in vitro *release of chlorothiazide from a charge of 250 mg of microcapsules at 37°. Key:* ●, *pH 2;* ▽, ▼, *pH 5;* □, ■, *pH 7;* △, ▲, *pH 9;* ●, ▲, ■, ▼, *60 min; and* △, □, ▽, *30 min.*

The *in vitro* release rate of tablets of microcapsules is shown in Fig. 4. *In vitro* dissolution tests, carried out as described previously, showed a much slower release from the compressed microcapsules. Contrary to expectation, the tablets did not disintegrate and were still present as definite entities at the end of the 2-hr *in vitro* experiments. The effect of pressure followed the expected norm; as with the uncompressed material, release into acidic pH was far more rapid than in pH 9. As with the uncompressed microcapsules, higher drug concentrations seemed to lead to a more rapid total release, although the difference was not so noticeable as in the early release from uncompressed material. Separate, detailed studies into the compression characteristics of microcapsules are being conducted.

Figure 5 shows the mean urine excretion found with all subjects up to 28 hr. The subjects measured the volume of urine passed and retained a sample for subsequent analysis. The normal, nondiuretic-induced condition for the subjects showed a fairly steady increase in total urine passed throughout the day. As expected, this volume was lower at all times than after diuretic dosage. A standard tablet of nonmicroencap-

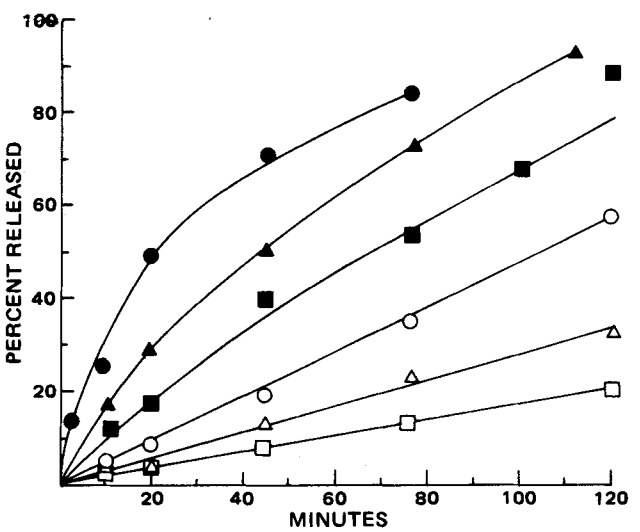


**Figure 4**—*Effect of pH and compression pressure on the* in vitro *release of chlorothiazide from tableted microcapsules. The concentration of chlorothiazide was 65.48% in a charge of one 250-mg tablet in 2 liters of water at 37°. Key:* ●, ▲, ■, *pH 2;* ○, △, □, *pH 9;* ○, ●, *0.5 tonne of pressure;* △, ▲, *3 tonnes of pressure; and* □, ■, *5 tonnes of pressure.*

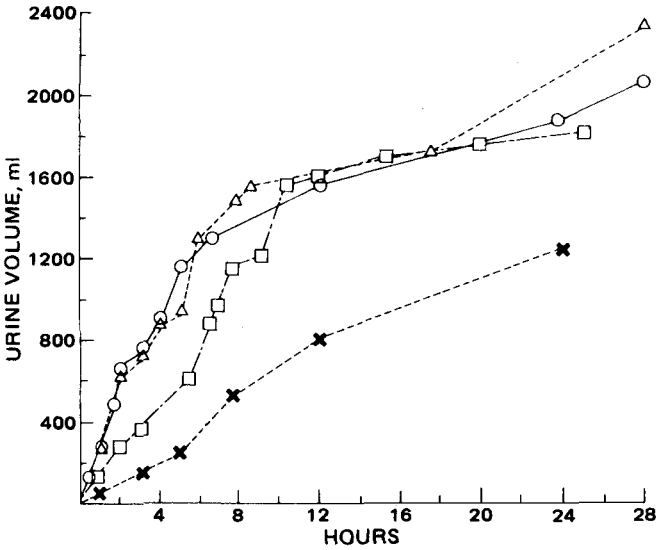


**Figure 5**—*Mean volume of urine passed after ingestion of 500 mg of chlorothiazide in various dosage forms. Key: ×, control; ○, standard tablet; △, microcapsules; and □, tableted microcapsules. Tablet compression pressure was 5 tonnes.*

sulated chlorothiazide produced a steady rapid release of urine over the first 2 hr when compared with the nondosed control state. This release fell slightly but rose again after the midday meal. About 10 hr after ingestion of the tablet, the rate of urine production followed approximately the normal condition.

Microencapsulated drug was given in both tableted and powder forms. The microencapsulated tablet showed a urine production intermediate between that produced by the nondosed and normal tablet-dosed form. The urine production increased after 5 hr, probably corresponding to increased release of chlorothiazide from the tablet because of either diffusion or disintegration. After 5 hr, the tablet would be expected to progress to the more alkaline region of the small intestine, where the formaldehyde solution-treated microcapsules should disintegrate more than in the acidic conditions of the stomach. However, the *in vitro* dissolution data showed a more rapid release of drug under acidic conditions. Therefore, under *in vivo* conditions, it may take time for tableted microcapsules to build up a high diuretic concentration in the body and to exert a marked diuretic effect, even though drug is released from the moment of ingestion. After 10 hr, the amount of urine produced was approximately the same as that resulting from the standard tablet.

Nontableted microcapsules showed no significant difference in urine production over a normal tablet, indicating that the drug dose had been released rapidly in the acidic pH conditions of the stomach and was available almost immediately. This result was expected from the *in vitro* dissolution data, which showed 100% release of the drug within a period far shorter than the normal stomach-emptying time.

All doses of the drug were small when compared with the normal therapeutic dose, but the same pattern probably is obtained with initial doses of up to 2 g of chlorothiazide.

To determine how much drug was excreted, urine samples were assayed by the modified Bratton–Marshall method. The urinary concentration of drug followed the same pattern as the urine production from a given formulation (Fig. 6). Thus, with microcapsules of chlorothiazide and ordinary tablets, there was a rapid buildup of drug excreted in the urine; after 10 hr, there was little further increase. With the tableted microcapsules, only slightly less chlorothiazide was excreted over the first 2 hr, but the mean urine production from this dosage form was smaller. However, after 2 hr, there was significantly less drug in the urine from the tableted microcapsules. This was still the case after 10 hr, although

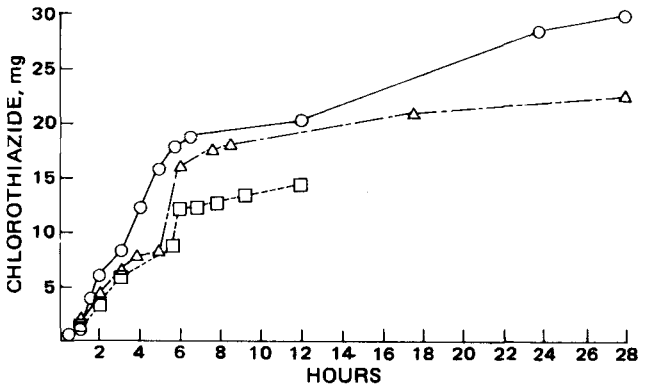


**Figure 6**—*Release of chlorothiazide in urine after a 500-mg dose. Key: ○, standard tablet; △, microcapsules; and □, tableted microcapsules. Tablet compression pressure was 5 tonnes.*

the urine production curves had shown that there was no significant difference in urine production with any formulation after this time.

Only a fraction of the drug (<10%) was found in the urine, indicating either significant body retention of the drug or very incomplete absorption from the GI tract.

There is a potassium loss from the body during the use of chlorothiazide, and studies on the use of microencapsulated potassium chloride incorporated with microencapsulated chlorothiazide are underway. This work is being extended to a study of the physical characteristics involved in tableting microcapsules. So that there is only one microcapsule formulation to investigate, the water-soluble potassium chloride is encapsulated in a gelatin–acacia coacervate, which normally is restricted to use with water-insoluble drugs.

## REFERENCES

(1) L. A. Luzzi, *J. Pharm. Sci.*, **59**, 1367 (1970).

(2) B. K. Green and L. Schleicher, U.S. pat. 2,730,456 (1956).

(3) M. Calanchi, in "Microencapsulation," J. R. Nixon, Ed., Dekker, New York, N.Y., 1976, p. 93.

(4) I. Jalsenjak, C. F. Nicolaidou, and J. R. Nixon, *J. Pharm. Pharmacol.*, **28**, 912 (1976).

(5) A. T. Florence and A. W. Jenkins, in "Microencapsulation," J. R. Nixon, Ed., Dekker, New York, N.Y., 1976, p. 37.

(6) E. Rosen, T. Ellison, P. Tannenbaum, S. M. Free, and A. P. Crosley, Jr., *J. Pharm. Sci.*, **56**, 365 (1967).

(7) L. A. Luzzi and G. J. Gerraughty, *ibid.*, **53**, 429 (1964). *Ibid.*, **56**, 634, 1174 (1967).

(8) J. A. Bakan and J. L. Anderson, in "Theory and Practice of Industrial Pharmacy," 2nd ed., L. Lachman, H. A. Lieberman, and J. L. Kanig, Eds., Lea & Febiger, Philadelphia, Pa., 1976, p. 420.

(9) V. de Sabata, in "Microencapsulation," J. R. Nixon, Ed., Dekker, New York, N.Y., 1976, p. 143.

(10) D. N. S. Kerr, A. E. Read, and S. Sherlock, *Lancet*, **1**, 1221 (1959).

(11) E. Paloyan, M. Forland, and J. R. Pickleman, *J. Am. Med. Assoc.*, **210**, 1243 (1969).

(12) B. S. Schifrin, W. N. Spellacy, and W. A. Little, *Obstet. Gynecol.*, **34**, 215 (1969).

(13) B. R. Matthews, Ph.D. thesis, London University, London, England, 1975.

(14) A. Nouh, Ph.D. thesis, London University, London, England, (1978).

(15) J. R. Nixon and A. Nouh, *Drug Devp. Ind. Pharm.*, **4**, 275 (1978).

(16) J. R. Nixon and A. Nouh, *J. Pharm. Pharmacol.*, **30**, 533 (1978).

# Sustained-Release Drug Delivery System I: Coated Ion-Exchange Resin System for Phenylpropanolamine and Other Drugs

Y. RAGHUNATHAN ˣ, L. AMSEL, O. HINSVARK, and W. BRYANT

Received August 2, 1979, from the *Pharmaceutical Division, Pennwalt Corporation, Rochester, NY 14623.* Accepted for publication December 18, 1979.

**Abstract** □ Ion-exchange resin–drug complexes have been used to formulate sustained-release products of acidic and basic drugs. However, sustained release may be difficult to achieve due to many variables. A novel technique is reported that minimizes these variables by providing a polymeric film coating to the ion-exchange resin–drug complex particles, making drug release from these particles diffusion controlled. Direct application of an atomized polymer solution to the fluidized ion-exchange resin–drug complex particles was ineffective in controlling drug release since the coating came off in the dissolution medium due to swelling and fracturing of the particles. Pretreatment of the ion-exchange resin–drug complex particles with an agent such as polyethylene glycol was essential for the particles to retain their geometry and coating during dissolution. With divinylbenzenesulfonic acid resin complexed with phenylpropanolamine as a model, mixtures of ethylcellulose-coated and uncoated resin–drug complex particles were prepared. These mixtures gave varying drug release profiles that showed rank-order correlation with plasma concentration profiles obtained in bioavailability studies with suspension dosage forms.

**Keyphrases** □ Phenylpropanolamine—microencapsulated with ion-exchange resin, new sustained-release delivery system, effect of particle size, coating, and dosage form on bioavailability □ Drug delivery systems—sustained release of phenylpropanolamine, ion-exchange resin–drug complex □ Microencapsulation—symposium, sustained-release delivery system for phenylpropanolamine, coated ion-exchange resin–drug complex

Ion exchangers are solid and suitably insolubilized high-molecular weight polyelectrolytes that can exchange their mobile ions of equal charge with the surrounding medium. The resulting ion exchange is reversible and stoichiometric, with the displacement of one ionic species by another on the exchanger (1). The commercial availability of insoluble exchange resins having one functional group caught the attention of pharmaceutical scientists and resulted in several patents (2–10).

Keating (2) listed the following advantages of adsorbing basic nitrogen-containing drugs onto sulfonic acid cation-exchange resins and using them in dosage forms: (*a*) prolong availability by releasing the drug from the complex over 12 hr in the GI tract; (*b*) reduce toxicity by slowing drug absorption; (*c*) increase stability by protecting the drug from hydrolysis or other degradative changes in the GI tract; (*d*) improve palatability; and (*e*) enable formulation of liquid and solid sustained-release dosage forms.

## BACKGROUND

Schlichting (11) evaluated carbinoxamine–resin complexes of polystyrenesulfonic acid (pK 1.3), phenol formaldehydesulfonic acid (pK 1.3), polyacrylic acid (pK 5.2), polymethacrylic acid (pK 6.0), polyacrylic acid–sulfonic acid (7:3 ratio), and polystyrene phosphonate (pK 3.2). The polystyrene sulfonic acid salt of the drug showed the most retardation in the release of carbinoxamine. Increased resin cross-linking also decreased the dissolution rate. Resins with a pK value of 5.2 and greater showed no retardation of dissolution.

Koff (5) described the use of coating with castor wax to improve the palatability and stability of a highly acidic cation-exchange resin complexed with amotropine. Macek *et al.* (6) improved the gritty and astringent taste of finely divided polystyrene divinylbenzene copolymer anion-exchange resin intended for swallowing by coating the particles with an acrylic polymer cross-linked with allyl sucrose. Borodkin and Sundberg (7, 8) coated 72–147-μm particles of polymethacrylic acid–ion-exchange complexes of basic drugs with an ethylcellulose–hydroxypropyl methylcellulose (4:1) mixture using an air suspension coater to overcome the bitterness of the drugs.

Clark (9) applied the enteric-coating agent cellulose acetate phthalate on 0.1–1-mm diameter pellets of cation-exchange adsorbate of drugs in a coating pan. No dissolution data were presented.

Jungmann (10) spray dried a slurry of codeine–resin adsorbate in a solution of the coating agent, a copolymer of acrylic acid esters and methacrylic acid esters modified with ammonium groups. At 13.3% drug load and 20% level of coating, the 2-hr release was ~70%.

In an attempt to formulate sustained-release dosage forms of phenylpropanolamine using the sulfonic acid cationic resin system, sufficient retardation in drug release could not be obtained. Application of a diffusion barrier coating on the resin–drug complex was attempted using an air suspension technique. This report presents the results of this work.

## EXPERIMENTAL

**Materials**—*Resins*—A gel-type divinylbenzenesulfonic acid cation-exchange resin consisting of spherical particles (590–840 μm) was used as the model large-particle resin[1]. The model small-particle resin was obtained by grinding these spherical particles[2]; these particles ranged in size from 37 to 150 μm. These resins are approved for pharmaceutical use by the Food and Drug Administration.

*Drugs*—Phenylpropanolamine, a sympathomimetic amine drug [biological half-life of 3.9 hr in humans, pK of 9.4 (12)] was the first drug used in this coating investigation. Other drugs used were dextromethorphan, pseudoephedrine, ephedrine, and phentermine. The results obtained with phenylpropanolamine and dextromethorphan are reported here. These drugs were obtained either as bases or their salts from standard suppliers of pharmacopeial quality drugs.

*Coating Materials*—Ethylcellulose 50 cps[3] was selected as the model diffusion barrier material. A refined vegetable oil[4] was used as a plasticizer.

*Auxiliary Agents*—Polyethylene glycol 4000[5] was selected to help retain resin geometry during coating and dissolution.

*Solvents*—The coating solvent was either ethanol or methylene chloride–acetone. These solvents were obtained from reliable commercial supplies of highest purity.

*Water*—Water was either distilled or deionized as indicated.

**Equipment**—*Coating Equipment*—The coating experiments were carried out using an air suspension coating apparatus[6].

*Dissolution Test Apparatus*—The dissolution assembly[7] was essentially the same as described in USP XIX (13).

**Procedure for Phenylpropanolamine[8]–Resin Complex**—Five hundred milliliters of 0.1 *N* HCl was added to a 1-liter vessel[9] (16 cm high

[1] Amberlite IR-120, Rohm & Haas Co., Philadelphia, PA 19105.
[2] Amberlite XE-69 (also known as IRP-69), Rohm & Haas Co., Philadelphia, PA 19105.
[3] NF grade, Dow Chemical Co., Midland, Mich.
[4] Durkee Foods Division, SCM Corp., Rockville Center, NY 11570.
[5] Union Carbide Co., New York, NY 10017.
[6] Wurster, Dairy Equipment Corp., Madison, Wis.
[7] Model 72 R 115, Hanson Research Corp., Northridge, CA 91324.
[8] The following material describes the procedures for phenylpropanolamine dissolution. Other drugs were similarly tested spectrophotometrically at suitable wavelengths using appropriate amounts of samples.
[9] Kimble Glass Co., Division of Owens-Illinois, Montclair, NJ 07042.

0022-3549/81/0400-0379$01.00/0
© 1981, American Pharmaceutical Association

× 10 cm i.d.). A three-bladed polyethylene propeller stirrer (2.5-cm blade size) was positioned just below the surface of the dissolution medium and rotated at 50 rpm. The temperature of the medium was allowed to rise to 37 ± 0.5°. A filtering device, consisting of an ~1-cm syringe filter holder[10] with a small cotton plug, enabled the dissolution medium to filter into a glass tube from which it was pumped through a polyethylene tube into a 1-cm path flow-through cell of an eight-channel recording spectrophotometer[11] and back to the dissolution vessel for continuous monitoring and recording on a moving chart. The assembly was set up to monitor and record six samples and one standard every 5 min at 257 nm and 0.5*A* attenuation.

Samples of phenylpropanolamine–resin complex equivalent to 90.6 mg (60 mg for a 5-cm cell) of phenylpropanolamine were added to each dissolution vessel. A phenylpropanolamine standard was run simultaneously. The drug in solution then was expressed as a percentage of the total drug present in the resin complex particles. Earlier experiments were carried out with a two-channel spectrophotometer[12] using a 5-cm flow-through cell at 60 rpm.

**Procedure for Phenylpropanolamine–Resin Complex Dosage Forms**—*Capsules*—The contents of a single capsule (containing resin complex product equivalent to 30.2 mg of phenylpropanolamine) were emptied into 168 ml of 0.1 *N* HCl contained in the dissolution vessel, and dissolution started. Several such dissolution runs were set up. The tests were carried out as described previously without the spectrophotometric monitoring. Dissolution was terminated at 0.5, 1, 3, and 5 hr, and the samples were immediately filtered free of the resin particles through medium-porosity sintered-glass funnels. The filtrates were assayed for phenylpropanolamine by the GLC technique to be described.

*Suspensions*—Fifteen milliliters of the suspension (containing resin complex product equivalent to 90.6 mg of phenylpropanolamine) was transferred to a medium-porosity sintered-glass funnel and washed free of the vehicle with two 30-ml quantities of distilled water. The resin then was transferred quantitatively to the dissolution vessel with 450 ml of distilled water; then 1 *N* HCl (50 ml) was added, and dissolution was started. Several such dissolution runs were set up and completed as described under *Capsules*. The filtrates were assayed for phenylpropanolamine by GLC.

**GLC Assay for Phenylpropanolamine**—Fifty milliliters of the filtered dissolution medium was added to a 125-ml separator, and 2 ml of 10% NaOH was added and mixed. This mixture then was extracted with four portions of chloroform (20, 10, 8, and 8 ml); the chloroform layers were collected in a 50-ml volumetric flask, and the volume was adjusted. Two microliters of the sample or of a similarly prepared standard (126 μg/ml) was injected in a suitable gas chromatograph[13] for potency assay. The 183-cm × 2-mm glass[14] column was packed with 3% OV-225 on 100–120-mesh Gas Chrom Q, and the flow rate of the helium carrier gas was 40 ml/min. The column oven was maintained at 190°, the injection port temperature was 220°, and the flame-ionization detector was at 290°.

**Determination of Water Uptake Time**—Five grams of the resin or resin mixture was packed lightly in a 25-ml graduated cylinder with tapping. The initial volume of the mixture was noted. Deionized water (4 ml) was delivered to the top of the packed surface from a pipet held 2 cm away from the surface. The time, in seconds, required for the water layer to disappear completely was noted. At least two determinations were done for each mixture.

**Apparent Specific Volume Determination**—

1. Five grams of the resin was placed in a 15-ml graduated centrifuge tube. The tube was tapped to allow the resin to settle. When no more settling was noticed, the volume of the resin was noted, and the apparent specific volume of the resin was calculated.

2. Distilled water (10 ml) was added to the 15-ml centrifuge tube containing 5 g of the resin, and the contents were shaken and allowed to settle for 12 hr at either 23 or 97°. The volume of the resin then was determined, and the apparent specific volume of the resin was calculated for each temperature.

3. Melted polyethylene glycol 4000 (10 ml) was added to a centrifuge tube containing 5 g of the resin, and the contents were shaken and allowed to settle for 12 hr at 97°. The volume of the resin then was determined, and the apparent specific volume was calculated.

**Microscopic Examination**—The particles were examined using a low-power binocular microscope (objective ×3 and eyepiece ×10).

**Particle-Size Determination**—Two grams of the sample was placed on the top screen of a nest of suitable sieves[15], and the sifter was agitated for 15 min. The weight of the fractions retained on the screens was obtained. Particle sizes (*d*) at specific weight percents (16, 50, and 84) were obtained from a log probability plot of the data as described by Edmundson (14). These particle sizes are described later as *d*16, *d*50, and *d*84.

**Preparation of Resin–Drug Complexes**—The resin–drug complexes were prepared by the batch process as described by Keating (2).

The gel-type divinylbenzenesulfonic acid cation-exchange resin (either the large or small particle type) of hydrogen form was slurried in deionized water. Phenylpropanolamine base or any drug in its basic form was added to the resin slurry with agitation. The resin–drug complex was formed by the addition reaction. It was washed free of any unreacted drug with deionized water and dried in a fluid bed drier or tray drier at 60°. The dried, small particle resin–drug complex then was screened through a 60-mesh screen. The large particle resin–drug complex was screened through a 10-mesh screen. A drug load of ~33% was obtained with phenylpropanolamine using either resin.

The gel-type divinylbenzenesulfonic acid cation-exchange resin (either the large or small particle type) of sodium form was slurried in deionized water. Phenylpropanolamine hydrochloride or any drug in its salt form was added to the resin slurry with agitation. The resin–drug complex was formed by the exchange reaction. It was washed free of the exchanged salt and any free drug with deionized water. The washed resin–drug complex was dried and screened as described for a drug in its basic form. A drug load of ~25% was obtained with phenylpropanolamine using the fine particle resin.

**Polyethylene Glycol Treatment of Resin–Drug Complex**—The resin–drug complex was transferred to a suitable mixer and mixed with an aqueous solution of polyethylene glycol 4000. The ratio of drug–resin complex to polyethylene glycol 4000 varied from 4:1 to 5:1, depending on the resin–drug complex. The polyethylene glycol 4000-treated large particle resin–drug complex was used for coating directly. The treated fine particle resin–drug complex was dried in a fluid bed drier or tray drier to a moisture content of ~6% and then was screened through a 60-mesh screen before being coated.

**Preparation of Coated Resin–Drug Complex**—The polyethylene glycol 4000-treated resin–drug complex (core material) was transferred to a suitable coating apparatus[6]. A 15.24-cm coater handled ~500–600 g of the core material; a 45.72-cm coating apparatus could handle 15–25 kg. The core material then was coated with ethylcellulose–vegetable oil (2.5:1) in methylene chloride–acetone (10:1). Smaller batches were coated using ethanol as the solvent. The coated materials were screened using vibratory screens.

**Preparation of Resin–Drug Complex Mixtures**—The drug release rates and assays on the mixture components, *i.e.*, the phenylpropanolamine–resin complex (or any other resin–drug complex) and the coated phenylpropanolamine–resin complex (or any other coated resin–drug complex) were obtained. The ratio of the mixture components required for a desired drug release profile was calculated. Resin–drug complex mixtures were prepared by mixing suitable quantities of coated and uncoated resin–drug complexes. The resin–drug complex mixture was assayed for drug content and drug release rate to determine its suitability for sustained-release dosage form preparation.

**Preparation of Capsule Dosage Forms**—The fine particle resin–drug complex mixture was mixed with excipients and other drug–resin complexes (if any). The mix then was filled into suitable capsules using a capsule-filling machine. The phenylpropanolamine–resin complex mixture was mixed with excipients and chlorpheniramine–resin complex and filled into No. 3 capsules.

Each capsule contained the equivalent of 37.5 mg of phenylpropanolamine hydrochloride and 4 mg of chlorpheniramine maleate. The adult sustained-release dose was designed as two capsules to be taken every 12 hr, providing drugs equivalent to 75 mg of phenylpropanolamine hydrochloride and 8 mg of chlorpheniramine maleate. The large particle resin–drug complex mixtures were used similarly in the preparation of capsules in earlier developmental work.

**Preparation of Suspension Dosage Forms**—The fine particle resin–drug complex mixture and other resin–drug complexes (if any) were suspended in a palatable, flavored vehicle containing suitable suspending agents. Phenylpropanolamine–resin complex mixture and chlorpheniramine–resin complex were suspended in a fruit-flavored vehicle. Each

[10] Millipore Corp., Bedford, MA 01730.
[11] Model 25, Beckman Instruments Co., Irvine, CA 92664.
[12] Model DK-2A, Beckman Instruments Co., Irvine, CA 92664.
[13] Model 7610A, Hewlett-Packard, Avondale, PA 19311.
[14] Pyrex.

[15] Allen Bradley sonic sifter, Fisher Scientific Co., Pittsburgh, PA 15219.

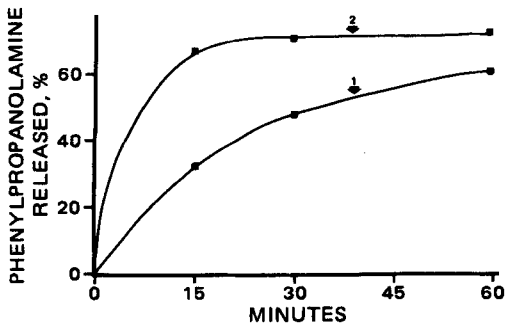


**Figure 1**—*Mean release profile of phenylpropanolamine in 0.1 N HCl at 60 rpm. Key: 1, uncoated large particle phenylpropanolamine–resin complex; and 2, uncoated fine particle phenylpropanolamine–resin complex.*

5 ml of this flavored and palatable suspension contained the equivalent of 37.5 mg of phenylpropanolamine hydrochloride and 4 mg of chlorpheniramine maleate. The adult sustained-release dose was designed as 10 ml to be taken every 12 hr, which is equivalent to 75 mg of phenylpropanolamine hydrochloride and 8 mg of chlorpheniramine maleate.

**Bioavailability Studies**—Details of the bioavailability protocols were reported elsewhere (15).

## RESULTS AND DISCUSSION

**Variables Affecting Drug Release from Resin–Drug Complex Particles**—Figure 1 shows the effect of particle-size differences on the release of phenylpropanolamine in 0.1 *N* HCl uncoated large resin–drug complex particles (590–800 μm) and uncoated, irregularly shaped resin–drug complex particles with *d*50 of 80–95 μm. The drug loads in the two resin–drug complexes were ~33%. About 48% drug release was observed in 30 min from the large resin–drug complex particles, whereas 72% was released in the same time from the finer resin–drug particles.

Figure 2 shows the comparative release in 0.1 *N* HCl of phenylpropanolamine and chlorpheniramine from fine particle resin–drug complexes containing a 25% drug load. Drug release from the chlorpheniramine–resin complex was only 7.5% in 2 hr, indicating that the equilibrium concentration for this complex in 0.1 *N* HCl was low. Release of phenylpropanolamine, on the other hand, from its resin complex was ~82% in the same time, indicating a high equilibrium concentration for this drug at 0.1 *M* ionic concentration. Increasing the ionic concentration to 0.4 *M* shifted the equilibrium concentration toward more complete drug release with the chlorpheniramine–resin complex (Fig. 3); ~72% chlorpheniramine was released in 2 hr. About 98% phenylpropanolamine was released from its resin complex in 2 hr in a 0.4 *M* dissolution medium.

Chlorpheniramine was completely bioavailable from this resin–drug complex in the present study. However, the significant difference observed in the *in vitro* release of chlorpheniramine due to ionic concentrations was not reflected *in vivo* (15). This result was perhaps due to the continuous absorption of released drug into the blood, resulting in a lower GI drug concentration, which, in turn, permitted more drug release. It was perhaps also due to the higher ionic concentration in the GI tract and to the continuous passage of the resin through the GI tract.

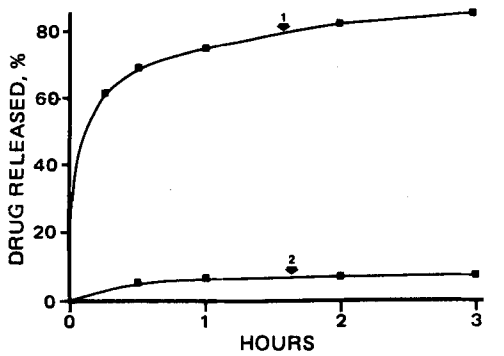


**Figure 2**—*Mean release profile of phenylpropanolamine and chlorpheniramine in 0.1 N HCl at 50 rpm. Key: 1, uncoated fine particle phenylpropanolamine–resin complex; and 2, uncoated fine particle chlorpheniramine–resin complex.*

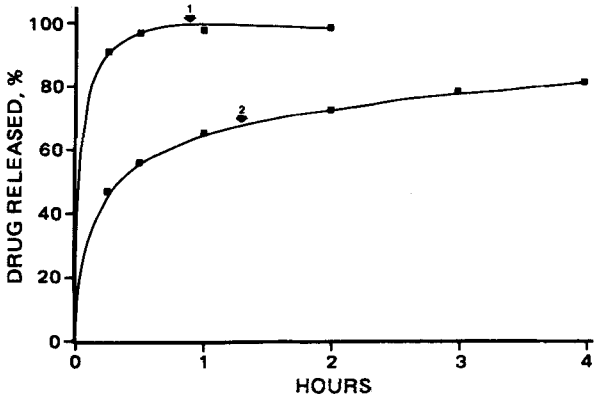


**Figure 3**—*Mean release profile of phenylpropanolamine and chlorpheniramine in 0.4 M KCl solution at 50 rpm. Key: 1, uncoated fine particle phenylpropanolamine–resin complex; and 2, uncoated fine particle chlorpheniramine–resin complex.*

**Coating Studies**—The results indicated the need for a diffusion barrier coating for the phenylpropanolamine–resin complex to modify the drug release profile, particularly with the fine particle drug–resin complex, essential for formulation of a sustained-release liquid dosage form.

Ethylcellulose 50 cps NF was selected as the diffusion barrier film since it is commercially available in pharmaceutical grade. Preliminary studies with the agent indicated the need for a plasticizer to improve film toughness.

Coating by spray drying a suspension of the fine particle resin–drug complex using a coating solution of ethylcellulose in methylene chloride was attempted. The process did not provide efficient coating, and no retardation of drug release was noticed. Therefore, a fluid bed technique was tried using the coating apparatus[6]. Initial experiments were carried out with the large particle phenylpropanolamine–resin complex.

The gel-type divinylbenzenesulfonic acid resins (both the large and fine particles) swell when placed in water and shrink in volume when dried. This property was a disadvantage for obtaining a good diffusion barrier coating on the resin–drug complex particles. The coating peeled from the particles as soon as they were suspended in the dissolution medium because they absorbed the medium too rapidly and became swollen. Attempts to coat the particles in the wet stage (and the swollen form) failed because the particles did not fluidize satisfactorily in the coating apparatus. They also lost water to air by evaporation during fluidization and coating and thus ended up being in their shrunken state. Maintenance of high humidity in the coating chamber helped but did not overcome the problem of fluidization. In any case, the coated particles did not show significant retardation in drug release.

Therefore, it was thought necessary to fill the resin–drug complex matrix, at least partially, with an agent that had hydroalcoholic properties, was a solid and relatively nonvolatile, and was water miscible. The polyethylene glycols and sugars seemed to possess these properties. Polyethylene glycol 4000 was tried as a treatment agent initially, and it improved the coating efficiency and thereby retarded drug release. Other

**Table I—Water Uptake Time for Fine Particle Phenylpropanolamine–Resin Complex Pretreated with Various Agents**

| Agent | Percent Added | Water Uptake Time[a], sec | Water Layer at End of Time |
|---|---|---|---|
| No additive | 0 | 36 | None |
| Polyethylene glycol 4000 | 2 | 208 | None |
| | 20 | 1149 | Present |
| Propylene glycol | 20 | >240 | Present |
| Mannitol | 20 | 96 | None |
| Lactose, anhydrous | 20 | 108 | None |
| Methylcellulose | 2 | 330 | None |
| | 20 | >600 | Present |
| Gelatin | 2 | 20 | None |
| | 20 | 23 | None |
| Talc | 20 | 73 | None |

[a] Uptake time (mean value) for 4 ml of water by 5 g of mixture gently packed in a 25-ml graduated cylinder.

**Table II—Apparent Specific Volume of Fine Particle Resins or Resin–Drug Complex in Various Media**

| Material | Medium | Temperature | Apparent Specific Volume, ml/g | Increase in Volume over Volume in Air at Same Temperature, % |
|---|---|---|---|---|
| Fine particle resin | Air | 23° | 1.380 | — |
| | Air | 97° | 1.460 | — |
| | Water | 23° | 1.750 | 26.8 |
| | Water | 97° | 2.100 | 43.8 |
| | Polyethylene glycol 4000 | 97° | 1.480 | 1.4 |
| Fine particle phenylpropanolamine–resin complex | Air | 23° | 1.458 | — |
| | Water | 23° | 1.875 | 28.6 |
| Fine particle phenylpropanolamine–resin complex treated with polyethylene glycol 4000 | Air | 23° | 1.620 | — |
| | Water | 23° | 1.750 | 8.0 |

**Table III—Water Uptake Time for Ethylcellulose-Coated Large and Small Particle Phenylpropanolamine–Resin Complex**

| Agent | Water Uptake Time[a], sec | Water Layer at End of Time |
|---|---|---|
| Large particle complex | | |
| Without polyethylene glycol 4000 | 192 | None |
| With polyethylene glycol 4000 | 580 | None |
| Small particle complex | | |
| Without polyethylene glycol 4000 | 511 | None |
| With polyethylene glycol 4000 | 1800 | Present |

[a] Uptake time (mean value) for 4 ml of water by 5 g of material gently packed in a 25-ml graduated cylinder.

agents were screened for their suitability for mixing with the resin–drug complex particles by determining their effects on the water uptake time of the resins. Additional studies were carried out with phenylpropanolamine–resin complex treated with polyethylene glycol 4000 to understand the mechanism.

Table I gives the water uptake times for various agents mixed with fine particle phenylpropanolamine–resin complex. Polyethylene glycol 4000, propylene glycol, and methylcellulose increased the water uptake times significantly. Talc, mannitol, and lactose provided some increase. Of the agents tested, polyethylene glycol 4000 retarded the water uptake time the most. Gelatin appeared to decrease the water uptake time.

Table II gives the apparent specific volumes in air and in water for the fine particle resin and the corresponding resin–drug complex of phenylpropanolamine pretreated with polyethylene glycol 4000. The untreated fine particle resin increased in volume in water by 26.8% at 23° and by 43.3% at 97°. The same resin, when placed in melted polyethylene glycol 4000 at 97°, showed an increase of only 1.4% in volume. The fine particle phenylpropanolamine–resin complex treated with 20% polyethylene glycol increased in volume by only 8% when placed in water compared to the 28.6% increase of the untreated material.

Microscopic examination of the coated and uncoated resin–drug complex particles was made. Large particles of phenylpropanolamine–resin complex were spherical in shape. These uncoated particles wetted

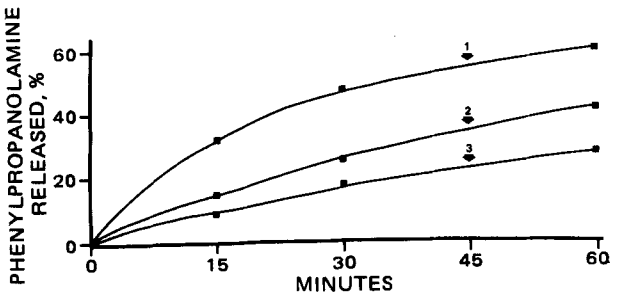


**Figure 4**—*Mean release profile of phenylpropanolamine in 0.1 N HCl at 60 rpm. Key: 1, uncoated large particle phenylpropanolamine; 2, ethylcellulose-coated large particle phenylpropanolamine–resin complex without polyethylene glycol 4000 treatment; and 3, ethylcellulose-coated large particle phenylpropanolamine–resin complex with polyethylene glycol 4000 treatment. The coating level was 5.7% ethylcellulose.*

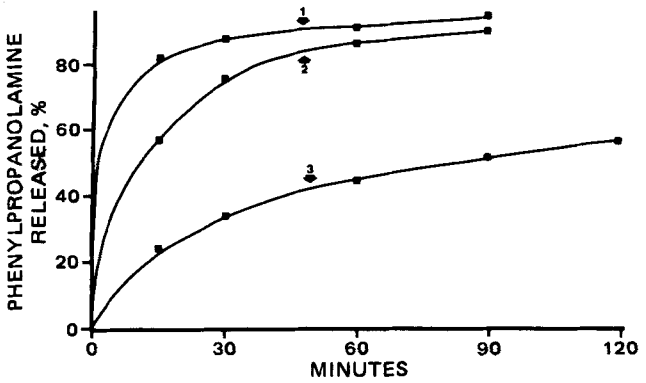


**Figure 5**—*Mean release profile of phenylpropanolamine in 0.1 N HCl at 60 rpm. Key: 1, uncoated fine particle phenylpropanolamine–resin complex; 2, ethylcellulose-coated fine particle phenylpropanolamine–resin complex without polyethylene glycol 4000 treatment; and 3, ethylcellulose-coated fine particle phenylpropanolamine–resin complex with polyethylene glycol 4000 treatment. The coating level was 11.4% ethylcellulose.*

easily with water and enlarged in diameter. The ethylcellulose-coated particles were also spherical. They did not wet with water easily, nor did they change in shape or size significantly. The fine particle phenylpropanolamine–resin complex and the corresponding ethylcellulose-coated particles behaved like the spherical resin–drug particles. The coated particles were pretreated with polyethylene glycol.

Table III presents the water uptake times observed with ethylcellulose-coated resin–drug complex particles with and without polyethylene glycol pretreatment. The water uptake times observed for the pretreated particles were much larger than those for untreated particles. These results agree with the microscopic observations.

**Drug Release from Coated Resin–Drug Complexes**—Figures 4 and 5 show the drug release profiles observed with ethylcellulose-coated phenylpropanolamine–resin complex particles with and without polyethylene glycol 4000 treatment. About 28 and 42% of phenylpropanolamine were released in 1 hr from the coated, treated large particle phenylpropanolamine–resin complex and coated, untreated particles, respectively. These particles were coated with 5.7% ethylcellulose. About 45 and 87% of phenylpropanolamine were released in 1 hr from the coated, fine particle phenylpropanolamine–resin complex treated with polyethylene glycol 4000 and those untreated, respectively. These particles were coated with 11.4% ethylcellulose. The effect of polyethylene glycol

**Table IV—Phenylpropanolamine Release in 0.1 *N* HCl from Coated and Uncoated Fine Particle Phenylpropanolamine–Resin Complex Used in Mixtures Listed in Table V**

| Time Lapsed, hr | Percent Released: Coated (Lot 825-594PD) | Coated (Lot 846-715PD) | Uncoated (Lot 842-349RC) |
|---|---|---|---|
| 0.5 | 22.9 | 27.5 | 70.3 |
| 1.0 | 31.4 | 40.6 | 76.0 |
| 2.0 | 37.3 | 54.9 | 79.1 |
| 3.0 | 42.7 | 61.8 | 80.5 |

**Table V—Phenylpropanolamine Release in 0.1 *N* HCl from Phenylpropanolamine–Resin Complex Mixtures Used in Bioavailability Test Suspensions**

| Time Lapsed, hr | Percent Released | | | | | | | | | |
|---|---|---|---|---|---|---|---|---|---|---|
| | Mixture Lot 850-201-PD[a] (Mixture Components: 846-715/842-349; Ratio, % coated to uncoated: 82.5:17.5) | | Mixture Lot 850-202PD[b] (Mixture Components: 846-715/842-349; Ratio, % coated to uncoated: 65:35) | | Mixture Lot 850-203PD[c] (Mixture Components: 846-715/842-349; Ratio, % coated to uncoated: 45:55) | | Mixture Lot 850-204PD[d] (Mixture Components: 846-715/842-349; Ratio, % coated to uncoated: 75:25) | | Mixture Lot 843-988PD[e] (Mixture Components: 825-594/842-349; Ratio, % coated to uncoated: 83:17) | |
| | Calc. | Obs. | Calc. | Obs. | Calc. | Obs. | Calc. | Obs. | Calc. | Obs. |
| 0.5 | 35.0 | 37.6 | 42.5 | 42.7 | 51.1 | 57.6 | 38.2 | 40.3 | 30.9 | 26.4 |
| 1.0 | 46.8 | 48.8 | 53.0 | 52.5 | 60.1 | 63.9 | 49.5 | 50.1 | 39.0 | 37.7 |
| 2.0 | 59.1 | 59.7 | 63.4 | 58.8 | 68.2 | 73.0 | 61.0 | 60.7 | 44.4 | 47.2 |
| 3.0 | 65.1 | 66.5 | 68.4 | 64.6 | 72.1 | 77.9 | 66.4 | 65.7 | 49.1 | 51.0 |
| 5.0 | — | 72.6 | — | 69.9 | — | 84.4 | — | 72.8 | — | 56.0 |
| 6.0 | — | 75.8 | — | 72.2 | — | 87.2 | — | 74.6 | — | 58.0 |

[a] Used in Suspension D. [b] Used in Suspension B. [c] Used in Suspension C. [d] Used in Suspension A. [e] Used in Suspension E.

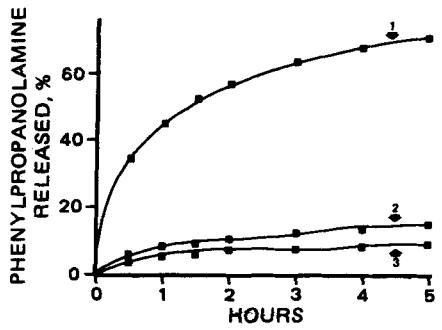


**Figure 6**—*Mean release profile of phenylpropanolamine in 0.1* N *HCl at 60 rpm from fine particle phenylpropanolamine–resin complex at various coating levels of ethylcellulose. Key: 1, 11.4%; 2, 21.0%; and 3, 28.25%.*

4000 pretreatment is evident in the slower drug release from these coated particles.

Figure 6 shows the effect of ethylcellulose coating levels on the release of phenylpropanolamine from the coated fine particle drug–resin complex. The drug release at the end of 2 hr was 57, 10, and 7.0% with ethylcellulose coating levels of 11.4, 21.0, and 28.3%, respectively. The effect of the coating levels in retarding drug release is evident.

Figure 7 shows the drug release from ethylcellulose-coated and uncoated fine particle dextromethrophan–resin complex. The coated particles were pretreated with polyethylene glycol 4000. Retardation of drug release in the coated particles was seen.

**Effect of Coating on Particle Size**—The coated fine particle phenylpropanolamine–resin complex particles were generally between 40 and 200 mesh (74–420 μm). For example, a 30-kg batch coated with 11.4% ethylcellulose in a 45.72-cm coating apparatus had particle-size values for *d*16, *d*50, and *d*84 of 184, 123, and 82 μm, respectively. The corresponding *d*16, *d*50, and *d*84 values for uncoated fine particle phenylpropanolamine–resin complex particles were 140, 94, and 61 μm, respectively.

**Drug Release from Dosage Forms**—Mixtures of coated and uncoated fine particle phenylpropanolamine–resin complex were prepared with desirable release profiles. Tables IV and V show the release of phenylpropanolamine from the components and several mixtures used in the preparation of Suspensions A–E for bioavailability studies. The observed release values for the mixtures are in close agreement with the values calculated by adding proportionate release values of components of the mixtures, indicating that mixing of coated and uncoated resin–drug complex is a reliable technique for obtaining desired release profiles.

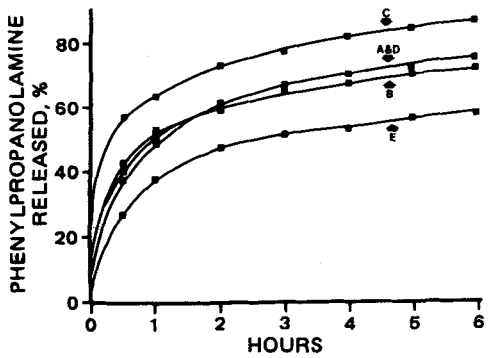


**Figure 8**—*Mean release profile of phenylpropanolamine from mixtures of varying ratios of coated and uncoated fine particle phenylpropanolamine–resin complex in 0.1* N *HCl at 50 rpm. Key: A, mixture lot 850-204PD used in Suspension A; B, mixture lot 850-202PD used in Suspension B; C, mixture lot 850-203PD used in Suspension C; D, mixture lot 850-201PD used in Suspension D; and E, mixture lot 843-998PD used in Suspension E.*

Figure 8 presents graphically the drug release profiles of the mixtures.

Figure 9 shows the release of phenylpropanolamine from Suspensions A, C, and E made with mixtures shown in Fig. 8. Good agreement of the drug release profiles between the mixtures and the corresponding suspension dosages is seen.

Figure 10 shows the release of phenylpropanolamine from one experimental production batch of capsules and suspensions after storage for

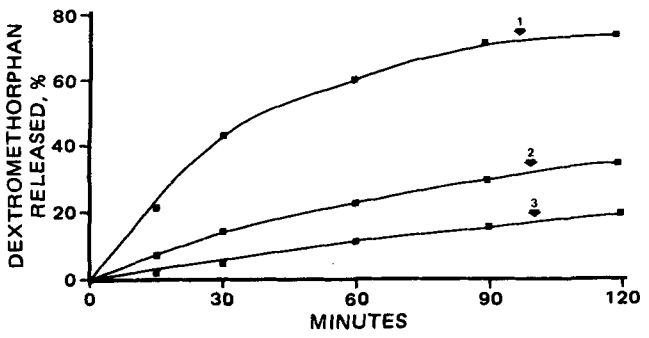


**Figure 7**—*Mean release profile of dextromethorphan in 0.1* N *HCl at 60 rpm from fine particle dextromethorphan–resin complex at various coating levels of ethylcellulose. Key: 1, uncoated; 2, 6.22% ethylcellulose; and 3, 8.93% ethylcellulose.*

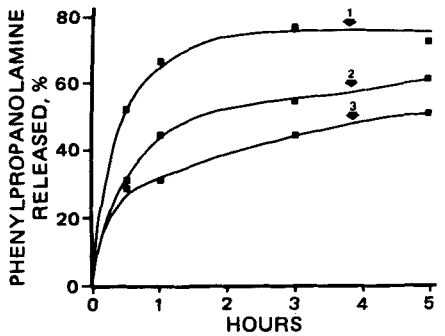


**Figure 9**—*Mean release profile of phenylpropanolamine from Suspensions A, C, and E in 0.1* N *HCl at 50 rpm. Key: 1, Suspension C; 2, Suspension A; and 3, Suspension E.*

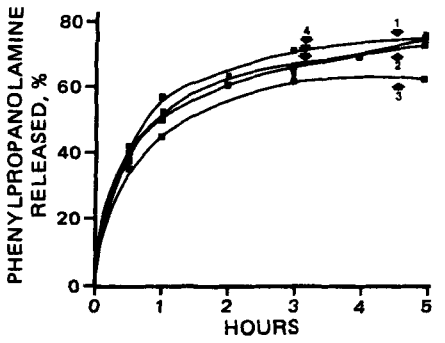


**Figure 10**—*Mean release profile of phenylpropanolamine from dosage forms in 0.1 N HCl at 50 rpm. Key: 1, capsule lot 855-101PD after 647 days; 2, mixture lot 850-204PD used in Suspension A; 3, suspension lot 847-576PD after 669 days; and 4, mixture lot 846-748PD (initial value at 60 rpm) used in the experimental production batches of capsules and suspensions.*

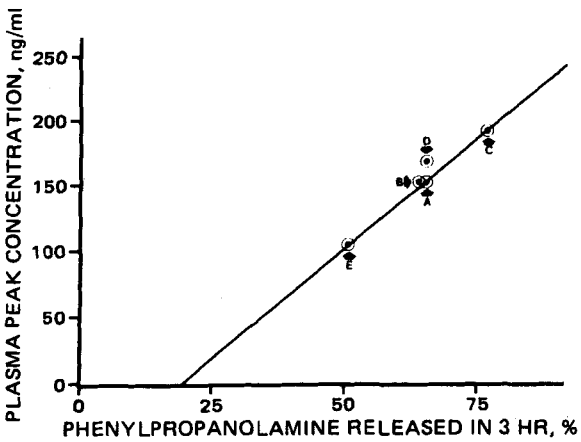


**Figure 11**—*Relationship between the mean peak plasma concentration for phenylpropanolamine (obtained with Suspensions A–E) and mean 3-hr drug release values for mixtures used in these suspensions as given in Table V.*

647 and 669 days, respectively. The drug release profiles of the mixture used in Suspension A in the bioavailability studies as well as the mixture used in the preparation of the experimental batches are included. Good agreement of the drug release profiles between the mixtures and dosage forms is seen.

**Bioavailability Studies**—The results of the bioavailability studies were discussed elsewhere (15).

Plasma concentrations of phenylpropanolamine and chlorpheniramine obtained from capsules and suspension dosage forms made with coated and uncoated mixtures of fine particle phenylpropanolamine–resin complex and fine particle chlorpheniramine–resin complex administered once every 12 hr for 2 weeks (dosage equivalent to 75 mg of phenylpropanolamine hydrochloride and 8 mg of chlorpheniramine maleate) were not significantly different from those obtained with a solution of the drugs administered once every 6 hr (in doses of 37.5 mg of phenylpropanolamine hydrochloride and 4 mg of chlorpheniramine maleate). The resin complex products were sustained-release products providing effective plasma concentrations for 12 hr.

In the variable profile bioavailability study with suspensions of phenylpropanolamine–resin complex mixtures listed in Table V, Suspension C gave the highest plasma phenylpropanolamine peak concentration while Suspension E gave the lowest. Figure 11 shows a plot of the 3-hr *in vitro* release values of phenylpropanolamine for the mixtures *versus* the peak plasma concentrations obtained with Suspensions A–E. There is good correlation between phenylpropanolamine release and plasma peak concentration. Similar correlations were obtained with plots of drug release for 0.5, 1, 2, and 5 hr against the peak plasma concentrations. The areas under the plasma concentration curves and the time to peak obtained with these products also showed rank-order correlation.

The results suggest that a desired plasma concentration profile of phenylpropanolamine may be obtained by mixing coated and uncoated phenylpropanolamine–resin complex in suitable ratios to produce specific drug release profiles. These correlations have been used to help establish product specifications for the finished dosage forms.

## REFERENCES

(1) K. Dorfner, "Ion Exchangers, Properties and Applications," 3rd ed., Ann Arbor Science Publishers, Ann Arbor, Mich., 1972, p. 2.

(2) J. W. Keating, U.S. pat. 2,990,332 (1961).

(3) J. W. Keating, U.S. pat. 3,143,465 (1964).

(4) E. E. Hays, U.S. pat. 3,035,979 (1962).

(5) A. Koff, U.S. pat. 3,138,525 (1964).

(6) T. J. Macek, C. E. Sloop, and D. R. Stauffer, U.S. pat. 3,499,960 (1970).

(7) S. Borodkin and D. P. Sundberg, U.S. pat. 3,594,470 (1971).

(8) S. Borodkin and D. P. Sundberg, *J. Pharm. Sci.*, **60**, 1523 (1971).

(9) C. A. Clark, British pat. 1,218,102 (1971).

(10) P. W. Jungmann, German pat. 2,246,037 (1975).

(11) D. A. Schlichting, *J. Pharm. Sci.*, **51**, 134 (1962).

(12) "Perspectives in Clinical Pharmacy," D. E. Francke and H. A. K. Whitney, Eds., Drug Intelligence, Hamilton, Ill., 1972, pp. 315, 357.

(13) "The United States Pharmacopeia," 19th rev., Mack Publishing Co., Easton, Pa., 1975, p. 651.

(14) I. C. Edmundson, in "Advances in Pharmaceutical Sciences," H. S. Bean, A. H. Beckett, and J. E. Carless, Eds., Academic, London, England, 1967, p. 95.

(15) O. Hinsvark, W. Bryant, J. Giering, L. Amsel, and Y. Raghunathan, "Abstracts of Papers," Fourth International Symposium on Microencapsulation, Miami Beach, Fla. meeting, Mar. 26–30, 1979.

## ACKNOWLEDGMENTS

The authors gratefully acknowledge the excellent technical assistance of Mr. P. Attaldo, Mr. L. Duncan, Mrs. J. Hubsch, and Mr. P. Emo.

# Microencapsulation of Methylglyoxal and Two Derivatives

**YASUO NOZAWA and SIDNEY W. FOX** ×

Received August 10, 1979, from the *Laboratory of the National Foundation for Cancer Research, Institute for Molecular and Cellular Evolution, University of Miami, Coral Gables, FL 33134.* Accepted for publication January 22, 1980.

**Abstract** □ Microcapsules of methylglyoxal, methylglyoxal bis(guanylhydrazone), and methylglyoxal–ascorbic acid condensation complex were prepared and release curves were determined. The effect of various concentrations of hydrochloric acid on the decomposition of the ascorbic acid complex was investigated.

**Keyphrases** □ Methylglyoxal—preparation of microcapsules of methylglyoxal, methylglyoxal bis(guanylhydrazone), or methylglyoxal–ascorbic acid complex, decomposition in aqueous solution □ Release—of microcapsules of methylglyoxal, methylglyoxal bis(guanylhydrazone), or methylglyoxal–ascorbic acid complex, decomposition in aqueous solution □ Microencapsulation—symposium, preparation of microcapsules of methylglyoxal and derivatives for gradual release in aqueous solution

In Szent-Györgyi's model for tumorgenesis, the sequence of reactions is: (*a*) methylglyoxal (I) or a related compound interferes with cell division, (*b*) release of glyoxalase I by an oncogenic agent reduces the I concentration, and (*c*) cell division then proceeds unhindered (1). Aside from using inhibitors of glyoxalase I (2–5), one may attempt to reestablish control of cell division by administering I or suitable derivatives.

Compound I, the bis(guanylhydrazone) of I (II) (6), and the methylglyoxal–ascorbate condensation product (III) (7) inhibited the growth of Ehrlich ascites tumor cells in mice[1]. Since the toxicity of I and that of complexes with I generally is high (8), such compounds have been microencapsulated for gradual release.

Although the prospects for gradual release are not promising due to the high solubility of each compound in water, gradual release from such microencapsulated products has been observed.

## EXPERIMENTAL

**Production of Microcapsules**—A 20% methylene chloride solution of polymethyl methacrylate[2] (very high molecular weight) was emulsified (5:1) with an aqueous solution of I or either derivative by stirring on an homogenizer[3] at a setting of 2.5 (2–5 min). To this solution was added 10 parts of a 1% solution of gelatin[4] (or polyaminoacid), and the original water/oil emulsion was converted to a (water/oil)water emulsion by stirring at a setting of 4 (~10 min). This emulsion was stirred magnetically for 5–6 hr at room temperature. Compound II was purchased[2].

In each case, the product was sifted through a 500-mesh sieve[5] and then centrifuged at 4000 rpm to a paste.

**Stability of III**—Compound III[6] was unstable under all conditions but less so at high acidity. Its decomposition rate was tested in various concentrations of hydrochloric acid. Compound III (3.9 mg) was allowed to stand for various periods in 50 ml of each hydrochloric acid concentration (Fig. 1). The entire experiment was shielded from light.

**Release Experiments**—For release of I, 8 g of the moist paste of I microcapsules was stirred magnetically in 500 ml of 4.6% HCl. Release was complete at ~175 hr. Samples of the clarified fluid were monitored at 270 nm.

For release of II, 1 g of paste was used. The receiving solution was 500 ml of water adjusted to pH 3 with hydrochloric acid. The wavelength for analysis was 280 nm.

For III, 6 g of paste was stirred into 500 ml of 4.6% HCl; the release was monitored at 240 nm.

The 4.6% HCl was used for I because high acidity is required to inhibit the rapid polymerization that occurs otherwise[7]. The decomposition observed with III (Fig. 1), which is also attenuated by concentrated hydrochloric acid, is perhaps related mechanistically to the decomposition of I. Concentrated hydrochloric acid was unnecessary to stabilize II, in which both carbonyl groups are derivatized.

No control experiments on the relative rate of solution of I or II in the absence of microcapsules are reported; I and II are highly soluble in the receiving solution, and they dissolve momentarily. Compound III is more slowly soluble; its rate of solution is approximately twice as great as its rate of release.

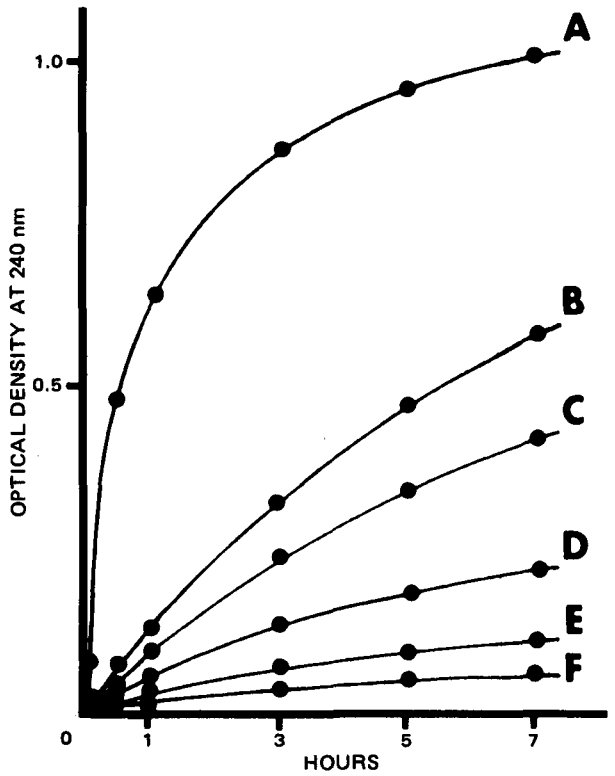


**Figure 1**—*Decomposition of methylglyoxal–ascorbic acid complex (III). Key: A, pH 3; B, 0.95% HCl; C, 1.6% HCl; D, 2.3% HCl; E, 6.9% HCl; and F, 11.5% HCl.*

## RESULTS AND DISCUSSION

The decomposition of III is shown in Fig. 1. The high acidities required to stabilize III suggest the need for extensive study of its physical properties should this compound prove to have pharmacological activity.

Figure 2 shows microcapsules of I and indicates that they are typical

[1] T. F. Slater, Brunel University, Brunel, England, personal communication.
[2] Aldrich Chemical Co., Metuchen, N.J.
[3] Sorvall Omni-Mixer, Newtown, Conn.
[4] Swine skin type 1, ~300 bloom, Sigma Chemical Co., St. Louis, Mo.
[5] W. S. Tyler Co., Mentor, Ohio.
[6] Gift from Dr. Gabor Fodor, West Virginia University, Morgantown, W.Va.
[7] P. Gascoyne, Marine Biological Laboratory, Woods Hole, Mass., personal communication.

0022-3549/81/0400-0385$01.00/0
© 1981, American Pharmaceutical Association

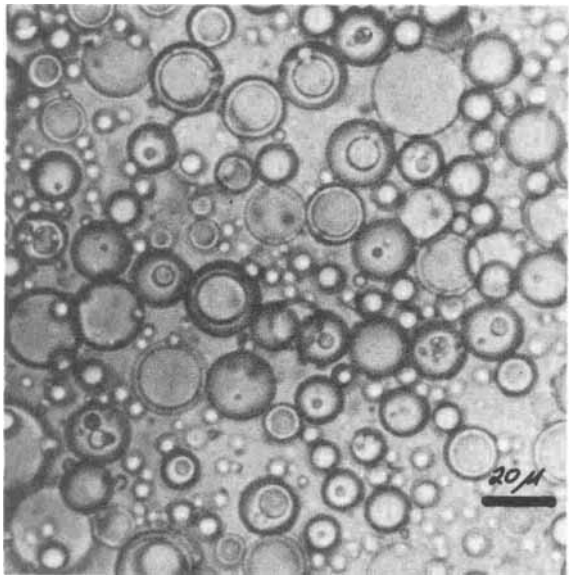


**Figure 2**—*Microcapsules containing methylglyoxal (I).*

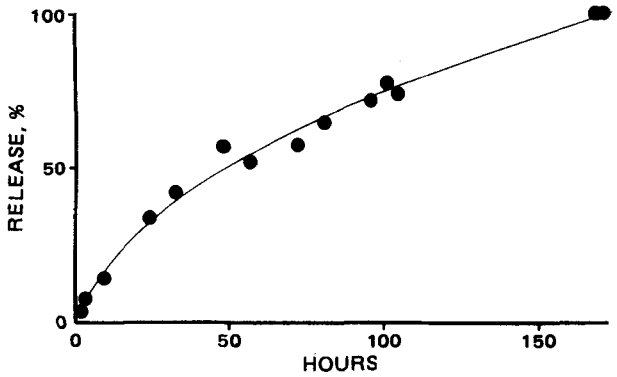


**Figure 3**—*Release of methylglyoxal (I).*

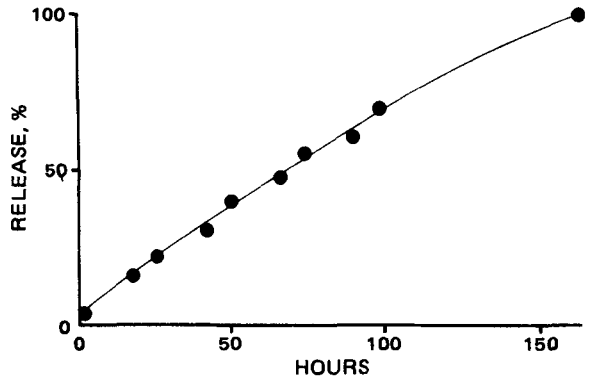


**Figure 4**—*Release of methylglyoxal bis(guanylhydrazone) (II).*

microcapsules. The microcapsules of II and III are visibly indistinguishable from those of I.

The release curve for I is shown in Fig. 3. The release curves for II and III are given in Figs. 4 and 5, respectively.

Microencapsulation of I, II, or III was accomplished, despite their considerable aqueous solubility. There are several possible explanations for the capture of these compounds.

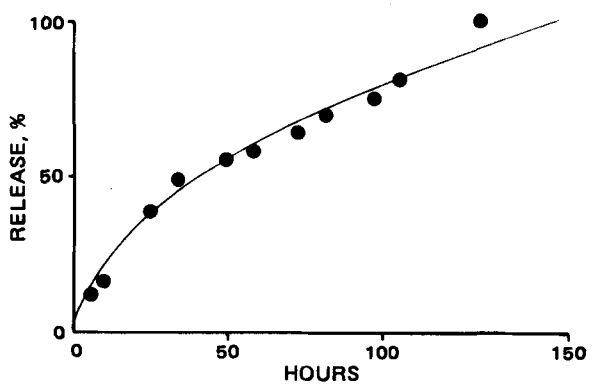


**Figure 5**—*Release of methylglyoxal–ascorbic acid condensation product (III).*

One inferred influence is gross physical entrapment of the type common to all microencapsulation. However, this entrapment is insufficient to delay release of many water-soluble compounds.

The encapsulated material may be caught within the meshwork resulting from the interdigitation of branched macromolecules, such as with amylopectin (9). Such a structure also was proposed for collagen (10), from which is obtained gelatin, which is often used in microcapsules.

Another explanation depends on a loose kind of bond that could be anticipated from the interaction of a dicarbonyl compound with special groups in the gelatin. Since II and III do not have free carbonyl groups, the meshwork explanation is more general and is in accord with the similar release curves observed for I–III. Moreover, the leaching of solid from a network structure is easily visualized. The probable mechanism thus includes physical entrapment by walls of microcapsules and entrapment within the lacunae provided by a meshwork of branched macromolecules.

## REFERENCES

(1) A. Szent-Györgyi, *Int. J. Quantum Chem. Quantum Biol. Symp.*, **4**, 179 (1977).

(2) S. W. Fox, R. M. Syren, and C. R. Windsor, in "Submolecular Biology and Cancer," G. E. W. Wostenholme, D. W. Fitzsimons, and J. Whelan, Eds., Ciba Foundation Press, London, England, 1979, p. 175.

(3) R. Vince and W. B. Wadd, *Biochem. Biophys. Res. Commun.*, **35**, 593 (1969).

(4) R. Vince, S. Daluge, and W. B. Wadd, *J. Med. Chem.*, **14**, 402 (1971).

(5) C. Silipo and C. Hansch, *Farmaco, Ed. Sci.*, **34**, 3 (1979).

(6) S. N. Pathak, C. W. Porter, and C. Dave, *Cancer Res.*, **37**, 2246 (1977).

(7) G. Fodor, R. Mujumdar, and J. Butterick, in "Submolecular Biology and Cancer," G. E. W. Wostenholme, D. W. Fitzsimons, and J. Whelan, Eds., Ciba Foundation Press, London, England, 1979, p. 165.

(8) T. F. Slater, in *ibid.*, p. 169.

(9) K. H. Meyer, "Natural and Synthetic High Polymers," Interscience, New York, N.Y., 1950, p. 468.

(10) N. P. Stimler and M. L. Tanzer, *Adv. Exp. Biol. Med.*, **86B**, 675 (1977).

## ACKNOWLEDGMENTS

Supported by Grant NGR-10-007-008 of the National Aeronautics and Space Administration.

The authors thank Mr. Charles R. Windsor for experimental repetitions.

This report is Contribution 333 of the Institute for Molecular and Cellular Evolution.

Y. Nozawa was on leave from Shizoku College of Pharmacy.

# Specific Cell Binding Using Staphylococcal Protein A Magnetic Microspheres

KENNETH J. WIDDER *x, ANDREW E. SENYEI ‡, HAIM OVADIA §, and PHILIP Y. PATERSON §

Received August 2, 1979, from the *Department of Pathology, Duke University Medical Center, Durham, NC 27710, the ‡Department of Obstetrics and Gynecology, University of California Irvine, Orange, CA 92668, and the §Department of Microbiology-Immunology, Northwestern University Medical and Dental Schools, Chicago, IL 60611. Accepted for publication January 9, 1980.

**Abstract** □ Protein A, a protein derived from *Staphylococcus aureus*, was incorporated into the matrix of magnetic albumin microspheres. Because staphylococcal protein A binds most subclasses of immunoglobulin G through their Fc portions, immunoglobulin may be rapidly bound to microspheres without chemical coupling agents or a diaminoheptane spacer group. Microspheres so prepared bind specifically to a given cell type when incubated *in vitro* with a heterogeneous cell population. The use of these microspheres as a drug carrier capable of cellular specificity as well as their ability to isolate homogeneous cell populations rapidly is discussed.

**Keyphrases** □ Carriers, drug—magnetic microspheres synthesized with immunological specificity, incorporation of staphylococcal protein A into microsphere matrix, cell binding studies *in vitro* □ Staphylococcal protein A—incorporation into microsphere matrix, immunological specificity □ Microencapsulation—symposium, magnetic microspheres synthesized with immunological specificity through incorporation of staphylococcal protein A, immunoglobulin G–blood cell binding studies

The ability to impart *in vivo* specificity to particulate drug carriers is desirable to restrict efficacious, yet toxic, chemotherapeutic agents to desired tissues. Specificity has been achieved either by magnetic restriction of a particulate drug carrier at an *in vivo* target site (1) or by immunological methods (2). Magnetic localization results in specific regional restriction of the carrier, with the subsequent release of entrapped drug into surrounding tissue; immunological methods of targeting drug carriers are capable of theoretically selecting the desired cell type without necessarily being restricted to a specific body area. Combining these two modalities may prove beneficial in the treatment of metastatic and unresectable malignancies.

Conventional means of coupling immunoglobulin to solid carriers involve chemical coupling agents (3–5) and require considerable time for chemical reaction and purification of products. In most cases, it also is necessary to have a diaminoheptane spacer group chemically coupled to the carrier prior to the antibody linkage procedure (3, 4). Subsequent orientation of the covalently bound immunoglobulin is random, resulting in only a percentage of immunoglobulin capable of interacting with the desired antigen.

Staphylococcal protein A was incorporated into the matrix of magnetically responsive albumin microspheres in these laboratories. Because staphylococcal protein A can bind the Fc portion of most subclasses of immunoglobulin G (IgG) (6), specific immunoglobulin directed against a desired cell surface antigen can be coupled to the microspheres by a simple nonchemical incubation. This procedure results in the proper molecular orientation of the IgG molecule so that the bound antibody is capable of antigen interaction.

This paper describes the *in vitro* immunological specificity of these microspheres in the separation of chicken red blood cells from a mixture of chicken and sheep red blood cells and, in a different system, the immunoglobulin-bearing lymphocytes from a spleen cell suspension.

## EXPERIMENTAL

**Preparation of Microspheres**—Microspheres were prepared by a modification of methods described previously (7). Essentially, a phase-separation emulsion–polymerization method was employed. A 0.5-ml aqueous suspension containing 190 mg of dry material was made consisting of 66% human serum albumin[1], 19% ferrosoferric oxide[2], and 15% staphylococcal protein A[3]. Cottonseed oil[4] (60 ml) was added to this suspension, and the emulsion was homogenized by sonication[5] for 1 min at 60 w. The homogenate then was added to 200 ml of constantly stirred cottonseed oil at 120–125° for 10 min. Resultant microspheres were washed free of oil by adding excess anhydrous ether[6] and centrifuging[7] for 15 min at 2000×*g*. After the fourth wash, the microspheres were allowed to air dry and were stored at 4° until they were used.

**Coupling of Immunoglobulin to Microspheres**—Microspheres (0.5 mg) were suspended in 0.2 ml of 0.154 *N* NaCl with 0.1% polysorbate 80[8] (I). To this suspension was added 0.5 mg of normal rabbit IgG, rabbit anti-chicken red blood cells[9], fluorescein isothiocyanate-conjugated rabbit anti-rat immunoglobulin[10], or rabbit anti-rat immunoglobulin[10], and the mixture was incubated at 37° for 40 min. Excess immunoglobulin was removed by centrifugation with excess I at 10,000×*g* for 5 min.

**Labeling of Chicken and Sheep Red Blood Cells**—Aliquots of chicken or sheep red blood cells were labeled with chromium 51 to assess the extent of the microsphere immunological specificity as well as cell integrity. Labeling was performed by incubating $1 \times 10^8$ chicken red blood cells suspended in 0.2 ml of Hanks balanced salt solution containing 2.5% heat-inactivated fetal calf serum with 100 μCi of sodium [$^{51}$Cr]-chromate[11] for 90 min at 37°. Sheep red blood cells were treated similarly except that they were incubated overnight at 37°.

**Separation of Cells**—Microspheres bearing immunoglobulin directed against specific cellular antigens were used to isolate cells exhibiting these antigens from heterogeneous cell populations utilizing the magnetic property of the microspheres (8).

*Red Cell Separation*—Microspheres (0.5 mg) bearing either rabbit anti-chicken red blood cells or normal rabbit IgG were suspended in 0.2 ml of I. To this suspension was added a mixture of $1 \times 10^6$ chicken red blood cells and $1 \times 10^6$ sheep red blood cells in 0.2 ml of Hanks balanced salt solution. Depending on the experimental group, either the chicken or sheep red blood cells were labeled with chromium 51. After incubation with the microspheres for 30 min at 37°, the cells were exposed to a 4000-gauss (gradient = 1500 gauss/cm) magnetic field applied to the side of the reaction vessel. Both the supernatant and pellet fractions were counted for chromium 51 γ-emission[12]. Control labeled cells incubated in I were counted for chromium 51 to assess spontaneous release.

*Lymphocyte Separation*—A suspension of spleen cells was obtained

[1] Sigma Chemical Co.
[2] Magnetite ($Fe_3O_4$) in aqueous suspension, Ferrofluidics Corp.
[3] Sigma Chemical Co.
[4] Sargent-Welch.
[5] Branson sonifier model 185.
[6] Mallinckrodt Chemicals.
[7] Sorvall model RC-5.
[8] Tween 80, Sigma Chemical Co.
[9] Cappel Laboratories.
[10] The IgG fraction was predominantly anti-IgG as determined by immunoelectrophoresis, Miles Laboratories.
[11] $Na_2{}^{51}CrO_4$, 1 mCi/ml, Amersham.
[12] Beckman model 8000 γ-counter.

0022-3549/81/0400-0387$01.00/0
© 1981, American Pharmaceutical Association

**Table I—Separation of Chicken Red Blood Cells (CRBC) and Sheep Red Blood Cells (SRBC) Using Rabbit Anti-Chicken Red Blood Cells Coupled to Staphylococcal Protein A Magnetic Microspheres**

| Antibody Coupled to Microspheres | Type of Cell Suspension | Percent of $^{51}$Cr-Labeled Red Blood Cells Bound to Microsphere | Percent of CRBC in Supernate |
|---|---|---|---|
| Rabbit anti-CRBC (IgG fraction) | $^{51}$Cr-labeled CRBC ($1 \times 10^6$) and SRBC ($1 \times 10^6$) | 97.8 | 0.26 |
| Rabbit anti-CRBC (IgG fraction) | $^{51}$Cr-labeled SRBC ($1 \times 10^6$) and CRBC ($1 \times 10^6$) | 9.5 | 0.33 |
| Normal rabbit IgG | $^{51}$Cr-labeled CRBC ($3 \times 10^6$) and SRBC ($1 \times 10^6$) | 10.0 | 90 |

by teasing rat spleen (Lewis rats) in Hanks balanced salt solution with 10% heat-inactivated fetal calf serum. After washing three times with Hanks balanced salt solution, the cells were overlaid on Ficoll–Hypaque (specific gravity of 1.072) and centrifuged at 1200×*g* for 25 min at 25° to eliminate the red blood cells and nonviable monocytes. The resultant interface band was removed and assessed for viability by trypan blue dye exclusion.

Rabbit anti-rat immunoglobulin, normal rabbit IgG, and rabbit anti-chicken red blood cells were coupled to 0.5 mg of staphylococcal protein A microspheres (0.5 mg of IgG/0.5 mg of microspheres) as described previously. Splenocytes ($2 \times 10^6$) suspended in Hanks balanced salt solution with 2.5% heat-inactivated fetal calf serum were added to the IgG-bearing microspheres. Mixtures were incubated for 2.5 hr at 4°. Cells with adherent microspheres were separated magnetically, and resultant cells in the supernates were analyzed for viability. The number of residual immunoglobulin-bearing cells was determined by incubating cells in the supernate for 20 min at 37° with fluorescein isothiocyanate-conjugated rabbit anti-rat immunoglobulin.

**Immunological Sensitivity**—The sensitivity of the microspheres for cellular interaction and subsequent magnetic removal from suspension was tested in two systems. Serial dilutions of microspheres bearing rabbit anti-chicken red blood cells were made, and $1 \times 10^6$ chicken red blood cells labeled with chromium 51 were added to each dilution. Incubation of the microspheres and cells was carried out for 30 min at 37°. Cells with adherent microspheres were removed magnetically, and both pellet and supernatant fractions were assessed for chromium 51 activity.

In addition, serial dilutions of the microspheres coupled with rabbit anti-human IgG[13] were made, and $5 \times 10^6$ human peripheral lymphocytes were added to each dilution[14]. The mixture was incubated for 1 hr at 4°, after which cells with adherent microspheres were removed magnetically. Supernatant cells were assessed for the presence of surface immunoglobulin by incubation with fluorescein isothiocyanate-conjugated rabbit anti-human IgG[13] for 20 min at 37° and analyzed by fluorescence microscopy.

## RESULTS AND DISCUSSION

A qualitative assessment of microsphere capacity for IgG binding was determined by incubating staphylococcal protein A microspheres with fluorescein isothiocyanate-conjugated rabbit and anti-rat immunoglobulin. The apparent diffuse surface fluorescence of the microspheres suggested that staphylococcal protein A was available on the microsphere surface for IgG binding. Moreover, despite the fact that staphylococcal protein A was an integral part of the microsphere matrix, it was oriented on the microsphere surface in such a manner as to retain its ability to bind IgG, as determined by the presence of fluorescence.

Results of the red cell separation are shown in Table I. Using $^{51}$Cr-labeled chicken red blood cells, when a mixture of $1 \times 10^6$ chicken red blood cells and $1 \times 10^6$ sheep red blood cells was incubated with 0.5 mg of staphylococcal protein A microspheres bearing rabbit anti-chicken red blood cells, 97.8% of the chromium 51 label was associated with the cells removed magnetically from suspension. The percentage of residual chicken red blood cells remaining in the supernate after magnetic isolation of cells was 0.26%, as judged by light microscopy. Nonspecific adherence of sheep red blood cells was determined by labeling them with chromium 51. Based on the chromium 51 counts, 9.5% of the label was associated with the microsphere fraction after magnetic separation of the mixture.

In addition, when normal rabbit IgG was coupled to the microspheres, an immunoglobulin unrelated to either chicken or sheep red blood cells (again 10% nonspecific adherence) was present. This minimal nonspecific adherence may be due to bound cross-reactive rabbit IgG based on shared antigens between microbes and mammalian cells (9). Because of the selective interaction of the anti-chicken red blood cell-bearing microspheres for chicken red blood cells, a highly purified and enriched sheep red blood cell population was generated.

Similar good specificity and separation were obtained when microspheres were used to separate immunoglobulin-bearing lymphocytes from a suspension of spleen cells. Between 43 and 51% of the starting splenocytes were immunoglobulin bearing, as determined by fluorescein isothiocyanate-conjugated anti-rat immunoglobulin binding to cells. When rabbit anti-rat immunoglobulin was coupled to staphylococcal protein A microspheres and subsequently incubated with $2 \times 10^6$ splenocytes, only 0.5% of immunoglobulin-bearing splenocytes remained in the supernate after magnetic removal of cells with adherent microspheres (Fig. 1). Moreover, when these microspheres were incubated with $2 \times 10^6$ thymocytes (normally containing 4–6% immunoglobulin-bearing lymphocytes), no immunoglobulin-bearing cells could be detected in the supernate representing 100% separation of immunoglobulin-bearing cells from nonimmunoglobulin-bearing cells. No loss of cellular viability was noted in any experimental group. To control for nonspecific adherence, normal rabbit IgG and rabbit anti-chicken red blood cells were coupled to the microspheres and incubated with the splenocytes. After magnetic separation of cells, 47 and 44% of the splenocytes in the supernate were

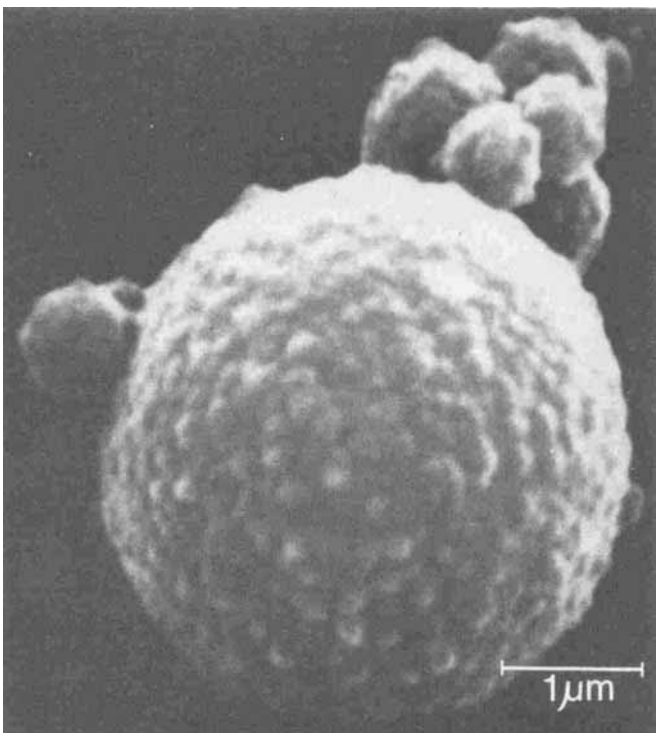


**Figure 1**—*Scanning electron micrograph of a rat lymphocyte with adherent microspheres (1 μm) on its surface. The micrograph is representative of cells obtained after coincubation of staphylococcal protein A microspheres bearing rabbit anti-rat immunoglobulin and splenocytes and subsequent magnetic isolation of microsphere–cell complexes.*

[13] Antiheavy and light chains, Cappel Laboratories.

[14] Lymphocytes were prepared similarly to the rat splenocytes; 15–30% of circulating peripheral lymphocytes are immunoglobulin bearing.

immunoglobulin bearing, respectively. These figures correlate well with the known number of immunoglobulin-bearing splenocytes (44–51%) and demonstrate minimal nonspecific adherence.

To determine the immunological sensitivity of the microspheres, two different systems were tested. It was found that 100% of the chicken red blood cells was magnetically removed from suspension when $\geq 104$ μg of microspheres was incubated with $1 \times 10^6$ chicken red blood cells. One milligram of staphylococcal protein A microspheres coupled with rabbit anti-human IgG effectively depleted all immunoglobulin-bearing human peripheral lymphocytes from a suspension containing $\leq 80 \times 10^6$ cells. These values demonstrate the capacity of staphylococcal protein A microspheres to separate a large number of cells rapidly and effectively *via* immunological means.

The ability of staphylococcal protein A microspheres to bind several different antiserums, which can confer a high degree of immunological specificity *in vitro*, was presented in this paper. Because magnetic microspheres can be used as drug carriers (1), it is proposed that with the addition of staphylococcal protein A to the microsphere matrix, tumor-specific antibody could be bound rapidly, resulting in a carrier capable of area-specific drug delivery and tumor-cell specificity. Thus, drug action could be limited solely to the desired cell population.

Because antibody coupling is rapid and easily performed, it is ideally suited for cell separation. No spacer group has to be coupled to the microspheres prior to antibody coupling. Moreover, no chemical coupling agents are used, which allows the reutilization of valuable antiserums. Since most IgG subclasses can bind staphylococcal protein A microspheres, this system may be valuable in rapid protein and enzyme purification. This system also may be useful as a mechanism for automated radioimmunoassays.

## REFERENCES


(1) K. J. Widder, A. E. Senyei, and D. G. Scarpelli, *Proc. Soc. Exp. Biol. Med.*, **158**, 141 (1978).

(2) G. Gregoriadis and E. D. Neerunjun, *Biochem. Biophys. Res. Commun.*, **65**, 537 (1975).

(3) R. S. Molday, S. P. S. Yen, and A. Rembaum, *Nature*, **268**, 437 (1977).

(4) P. L. Kronick, G. L. Campbell, and K. Joseph, *Science*, **200**, 1074 (1978).

(5) J. Antoine, T. Ternynck, M. Rodrigot, and S. Avrameas, *Immunochemistry*, **15**, 443 (1978).

(6) A. Forsgren and J. Sjöquist, *J. Immunol.*, **97**, 822 (1966).

(7) K. Widder, G. Flouret, and A. Senyei, *J. Pharm. Sci.*, **68**, 79 (1979).

(8) A. Senyei, K. Widder, and G. Czerlinski, *J. Appl. Phys.*, **49**, 3578 (1978).

(9) G. F. Springer, *Prog. Allergy*, **15**, 9 (1971).


## ACKNOWLEDGMENTS


The authors thank Dr. R. Radvany, Dr. N. Ponzio, and Dr. C. Whitacre for advice and assistance.


# *In Vivo* Kinetics of Magnetically Targeted Low-Dose Doxorubicin


**ANDREW E. SENYEI *¶x, STEVEN D. REICH ‡, CONSTANCE GONCZY §, and KENNETH J. WIDDER ***



Received August 2, 1979, from the **Department of Pathology and the Cancer Center and the* ‡*Departments of Pharmacology and Medicine and the Cancer Center, Northwestern University Medical School, Chicago, IL 60611*, and §*Calbiochem-Behring Corporation, San Diego, CA 92112.* Accepted for publication July 29, 1980.


¶Present address: Department of Obstetrics and Gynecology, University of California Irvine Medical Center, Orange, CA 92668.



**Abstract** □ The *in vivo* kinetics of low-dose doxorubicin (0.05 mg/kg), entrapped in a carrier and magnetically targeted, were characterized in a rat tail model. Tissue concentrations of doxorubicin at a preselected target site and in various organs were followed over time. As late as 60 min postinjection, 3.7 μg/g of drug was found at the target site with no detectable drug levels found in any organ. In comparison, a 100-fold higher dose (5.0 mg/kg iv) of free doxorubicin yielded drug concentrations of 1.8 μg/g at the target site and 15.0 μg/kg in the pooled organs. Therefore, 1% of the free intravenous dose targeted magnetically yielded approximately twice the local doxorubicin concentration at a preselected target site with no detectable systemic distribution. Magnetic targeting of particulate drug carriers to localized disease sites is suggested as an efficient method of obtaining high local drug concentrations and may reduce many unwanted side effects from unrestricted systemic circulation.



**Keyphrases** □ Microspheres, magnetic—as drug carriers, doxorubicin, *in vivo* □ Carriers, drug—doxorubicin-bearing magnetic microspheres, *in vivo* □ Doxorubicin—*in vivo* fate of localized low dose, kinetics □ Delivery, drug—magnetic microspheres as drug carriers, doxorubicin, *in vivo* □ Microencapsulation—symposium, doxorubicin-bearing magnetic microspheres, *in vivo* fate of localized low dose


Current approaches to enhancing the tumoricidal activity of antineoplastic agents involve combining them with various carriers in the hope of favorably altering their systemic distribution. Early work by Chang (1), who encapsulated proteins and enzymes to develop artificial organs, suggested that drugs also may be encapsulated in carriers. The current targeting of drug carriers such as liposomes (2) or natural cells (3) depends on a moderate to marked enhancement of the endocytic activity (4) exhibited by some solid tumors. Other modalities for enhancing drug concentration at known tumor sites include regional perfusion, hyperthermia, and local installation and implantation of drugs. However, most of these modalities have met with limited clinical success (5).

A biophysical approach to targeting chemotherapeutic agents to known tumor sites was described recently (6). The system utilizes magnetically responsive albumin microspheres as the carrier for entrapped doxorubicin. The application of an extracorporeal magnetic field over a selected body area results in accumulation of the carrier containing the entrapped drug at the target site. The synthesis (7), magnetic responsiveness (8), and *in vivo* distribution (6) of the carrier at one time period postinjection were described previously. However, the correlation of carrier distribution with doxorubicin distribution over time was not examined. In this report, the levels of doxorubicin obtained at different time intervals at a preselected target site are characterized. In addition, a low dose (0.05


0022-3549/81/0400-0389$01.00/0


© 1981, American Pharmaceutical Association

immunoglobulin bearing, respectively. These figures correlate well with the known number of immunoglobulin-bearing splenocytes (44–51%) and demonstrate minimal nonspecific adherence.

To determine the immunological sensitivity of the microspheres, two different systems were tested. It was found that 100% of the chicken red blood cells was magnetically removed from suspension when $\geq 104$ μg of microspheres was incubated with $1 \times 10^6$ chicken red blood cells. One milligram of staphylococcal protein A microspheres coupled with rabbit anti-human IgG effectively depleted all immunoglobulin-bearing human peripheral lymphocytes from a suspension containing $\leq 80 \times 10^6$ cells. These values demonstrate the capacity of staphylococcal protein A microspheres to separate a large number of cells rapidly and effectively *via* immunological means.

The ability of staphylococcal protein A microspheres to bind several different antiserums, which can confer a high degree of immunological specificity *in vitro*, was presented in this paper. Because magnetic microspheres can be used as drug carriers (1), it is proposed that with the addition of staphylococcal protein A to the microsphere matrix, tumor-specific antibody could be bound rapidly, resulting in a carrier capable of area-specific drug delivery and tumor-cell specificity. Thus, drug action could be limited solely to the desired cell population.

Because antibody coupling is rapid and easily performed, it is ideally suited for cell separation. No spacer group has to be coupled to the microspheres prior to antibody coupling. Moreover, no chemical coupling agents are used, which allows the reutilization of valuable antiserums. Since most IgG subclasses can bind staphylococcal protein A microspheres, this system may be valuable in rapid protein and enzyme purification. This system also may be useful as a mechanism for automated radioimmunoassays.

## REFERENCES


(1) K. J. Widder, A. E. Senyei, and D. G. Scarpelli, *Proc. Soc. Exp. Biol. Med.*, **158**, 141 (1978).

(2) G. Gregoriadis and E. D. Neerunjun, *Biochem. Biophys. Res. Commun.*, **65**, 537 (1975).

(3) R. S. Molday, S. P. S. Yen, and A. Rembaum, *Nature*, **268**, 437 (1977).

(4) P. L. Kronick, G. L. Campbell, and K. Joseph, *Science*, **200**, 1074 (1978).

(5) J. Antoine, T. Ternynck, M. Rodrigot, and S. Avrameas, *Immunochemistry*, **15**, 443 (1978).

(6) A. Forsgren and J. Sjöquist, *J. Immunol.*, **97**, 822 (1966).

(7) K. Widder, G. Flouret, and A. Senyei, *J. Pharm. Sci.*, **68**, 79 (1979).

(8) A. Senyei, K. Widder, and G. Czerlinski, *J. Appl. Phys.*, **49**, 3578 (1978).

(9) G. F. Springer, *Prog. Allergy*, **15**, 9 (1971).


## ACKNOWLEDGMENTS


The authors thank Dr. R. Radvany, Dr. N. Ponzio, and Dr. C. Whitacre for advice and assistance.


# *In Vivo* Kinetics of Magnetically Targeted Low-Dose Doxorubicin


**ANDREW E. SENYEI *¶x, STEVEN D. REICH ‡, CONSTANCE GONCZY §, and KENNETH J. WIDDER ***



Received August 2, 1979, from the **Department of Pathology and the Cancer Center and the* ‡*Departments of Pharmacology and Medicine and the Cancer Center, Northwestern University Medical School, Chicago, IL 60611*, and §*Calbiochem-Behring Corporation, San Diego, CA 92112.* Accepted for publication July 29, 1980.


¶Present address: Department of Obstetrics and Gynecology, University of California Irvine Medical Center, Orange, CA 92668.



**Abstract** □ The *in vivo* kinetics of low-dose doxorubicin (0.05 mg/kg), entrapped in a carrier and magnetically targeted, were characterized in a rat tail model. Tissue concentrations of doxorubicin at a preselected target site and in various organs were followed over time. As late as 60 min postinjection, 3.7 μg/g of drug was found at the target site with no detectable drug levels found in any organ. In comparison, a 100-fold higher dose (5.0 mg/kg iv) of free doxorubicin yielded drug concentrations of 1.8 μg/g at the target site and 15.0 μg/kg in the pooled organs. Therefore, 1% of the free intravenous dose targeted magnetically yielded approximately twice the local doxorubicin concentration at a preselected target site with no detectable systemic distribution. Magnetic targeting of particulate drug carriers to localized disease sites is suggested as an efficient method of obtaining high local drug concentrations and may reduce many unwanted side effects from unrestricted systemic circulation.



**Keyphrases** □ Microspheres, magnetic—as drug carriers, doxorubicin, *in vivo* □ Carriers, drug—doxorubicin-bearing magnetic microspheres, *in vivo* □ Doxorubicin—*in vivo* fate of localized low dose, kinetics □ Delivery, drug—magnetic microspheres as drug carriers, doxorubicin, *in vivo* □ Microencapsulation—symposium, doxorubicin-bearing magnetic microspheres, *in vivo* fate of localized low dose


Current approaches to enhancing the tumoricidal activity of antineoplastic agents involve combining them with various carriers in the hope of favorably altering their systemic distribution. Early work by Chang (1), who encapsulated proteins and enzymes to develop artificial organs, suggested that drugs also may be encapsulated in carriers. The current targeting of drug carriers such as liposomes (2) or natural cells (3) depends on a moderate to marked enhancement of the endocytic activity (4) exhibited by some solid tumors. Other modalities for enhancing drug concentration at known tumor sites include regional perfusion, hyperthermia, and local installation and implantation of drugs. However, most of these modalities have met with limited clinical success (5).

A biophysical approach to targeting chemotherapeutic agents to known tumor sites was described recently (6). The system utilizes magnetically responsive albumin microspheres as the carrier for entrapped doxorubicin. The application of an extracorporeal magnetic field over a selected body area results in accumulation of the carrier containing the entrapped drug at the target site. The synthesis (7), magnetic responsiveness (8), and *in vivo* distribution (6) of the carrier at one time period postinjection were described previously. However, the correlation of carrier distribution with doxorubicin distribution over time was not examined. In this report, the levels of doxorubicin obtained at different time intervals at a preselected target site are characterized. In addition, a low dose (0.05


0022-3549/81/0400-0389$01.00/0


© 1981, American Pharmaceutical Association

Table I—*In Vivo* Distribution of $^{125}$I-Labeled Magnetic Microspheres [a]

| Time Magnetic Field Was Applied, min | Liver | Lungs | Spleen | Kidneys | Heart | Tail Segment 1 | 2 | 3 | 4 |
|---|---|---|---|---|---|---|---|---|---|
| 5 | 7 | 4 | 5 | 0 | 0 | 0 | 0 | 47 | 0 |
| 15 | 6 | 4 | 5 | 0 | 0 | 0 | 0 | 45 | 0 |
| 30 | 6 | 6 | 8 | 0 | 0 | 0 | 0 | 45 | 0 |
| 60 | 8 | 6 | 8 | 0 | 0 | 0 | 0 | 44 | 0 |
| Control | 13 | 6 | 10 | 0 | 0 | 0 | 0 | 0 | 0 |

[a] Values are expressed as counts per minute × $10^2$ per gram of wet weight of tissue and represent an average of two animals. The control consisted of microsphere infusion without the application of a magnetic field. The level of detectability was $3 \times 10^2$ cpm/g. Values were rounded to the nearest 100, with zero indicating that counts were either not present or below the level of detectability. Tail Section 3 was chosen as the target area.

mg/kg) of magnetically targeted doxorubicin and a 100-fold higher free intravenous dose are examined with respect to the target and whole body distribution.

## EXPERIMENTAL

**Preparation of Microspheres**—The synthesis and characterization of magnetic microspheres bearing doxorubicin hydrochloride[1] were described previously (7). The emulsion polymerization method was carried out as follows. An aqueous solution was prepared containing 250 mg of human serum albumin[2], 32 mg of bulk, purified, lactose-free doxorubicin hydrochloride, 72 mg of magnetite[3], and 0.028 mCi of $^{125}$I-labeled bovine serum albumin[4] in 1 ml of distilled water. A 0.5-ml aliquot of this suspension was homogenized with 30 ml of cottonseed oil[5] by sonication[6] (100 w) for 1 min at 4°. The homogenate then was added dropwise to 100 ml of stirred (1600 rpm) cottonseed oil, which was preheated to 145°.

After 10 min of heating, the microspheres were washed free of the oil by centrifugation in anhydrous ether. After three washes, the ether was removed and the microspheres were stored in the dark at 4° until time of use. Prior to injection, the microspheres were resuspended in 0.1% polysorbate 80–saline[7] and washed once by centrifugation to remove any surface adherent drug. The microspheres contained 26.4 μg of doxorubicin/mg of microspheres and had a specific activity of 33,100 cpm/mg after suspension.

**Animal Model**—Female Sprague–Dawley rats, 300 g, were anesthetized with methoxyflurane, and the ventral caudal artery at the base of the tail was exposed for catheterization as described previously (6). The femoral vein was used for intravenous administration. The tail was demarcated into four equal sections, with Section 1 being proximal and Section 4 being the most distal. Tail Section 3 was the target site and was placed between the poles of a bipolar magnet[8]. The magnet exerted a field of 8000 Oe with a gradient of ±4 kOe within Section 3, and minimal or no magnetic fields were detected in adjacent segments.

A dose of 0.05 mg of doxorubicin/kg encapsulated in microspheres was infused in the ventral caudal artery in Section 1 at 0.6 ml/min by a constant-flow syringe pump[9]. The magnetic field at the target site was left in position for 5, 15, 30, or 60 min, after which the animal was immediately sacrificed by intracardiac injection of saturated potassium chloride. Control infusions consisted of 0.05 mg of free doxorubicin/kg *via* the caudal artery and 5.0 mg of free doxorubicin/kg iv, after which the animals were sacrificed at the cited time intervals in the manner described.

**Tissue Analysis**—Tissue extraction of doxorubicin was accomplished by a modification of a literature method (9). At the selected times, animals were dissected rapidly; the heart, liver, lungs, kidneys, spleen, and the four separate tail sections were frozen immediately at −60°. The excised organs and tail sections were examined for microsphere content by determining iodine 125 activity in a well-type γ-counter[10]. Two animals were used for each time point.

The organs were weighed and homogenized[11] in a 5% HCl solution in ethanol at 4° for 2 min. However, the tail skin sections were treated overnight in 0.5 *N* acetic acid at 4° to facilitate collagen solubilization and subsequent homogenization. Previous experiments showed that treatment of doxorubicin with 0.5 *N* acetic acid under these conditions did not significantly alter its fluorescence characteristics. The tissue homogenates were centrifuged[12] at 10,000×*g*, and the supernates were examined for total fluorescence using a spectrophotofluorometer[13].

Since the 0.05-mg/kg dose delivered in encapsulated form did not yield detectable drug concentrations in the individual organs, pooling of the organs was necessary.

In addition, quick-frozen sections of the tail skin segments were examined by fluorescence microscopy[14] according to the method of Egorin *et al.* (10). The characteristic orange-red fluorescence of doxorubicin in and surrounding small arterioles and capillaries of the rat tail skin was evaluated.

## RESULTS AND DISCUSSION

Table I shows the *in vivo* distribution of $^{125}$I-labeled microspheres at different times postinjection. Tail Section 3, the target area, contained a significantly higher concentration of microspheres than the surrounding tail segments. Moreover, in comparison to the liver and spleen, which are the normal sites for sequestration of particulate carriers, the target site had approximately a ninefold higher concentration of carrier. No discernible carrier redistribution was noted over the time periods studied. This finding is significant in that analysis of drug distribution was not complicated by this variable. The usual time required for 50% clearance of nonmagnetic microspheres varied from 2 to 8 hr, depending on the extent of matrix stabilization (11, 12).

The determination of doxorubicin content in the individual organs was not possible for the 0.05-mg/kg dose in either the free or encapsulated form because of the low levels attained after systemic distribution. However, the 5.0-mg/kg free dose showed individual organ values in agreement with values reported previously (13). Pooling of the individual organs of low-dose-treated animals still yielded barely detectable levels of doxorubicin but permitted a comparison between the 0.05- and 5-mg/kg doses.

Figure 1 shows the amount of doxorubicin found at 5 and 60 min postinjection in the 0.05-mg/kg carrier-delivered dose *versus* the free 5-mg/kg iv dose. Microsphere-delivered doxorubicin resulted in a target site concentration of 4.2 μg of doxorubicin/g of tissue at 5 min, which decreased to 3.7 μg/g at 60 min. In comparison, the 100-fold higher dose of 5 mg/kg resulted in a tissue concentration of 6.2 μg/g at the target site at 5 min, after which it rapidly decreased to only 1.8 μg/g at 60 min. Intermediate values between 5 and 60 min decreased in nonlinear fashion.

The rapid plasma disappearance of free doxorubicin is in agreement with current concepts of doxorubicin kinetics. Doxorubicin plasma decay curves follow a three-phase pattern (14). The half-life of the first phase is ~10 min and represents rapid tissue uptake. The other two phases represent redistribution and metabolism and vary from species to species (15).

Figure 1 also compares concentrations of free doxorubicin and magnetically localized low-dose doxorubicin in the pooled organs. Essentially nondetectable levels of doxorubicin were present in the pooled organs with the low carrier-delivered dose at both 5 and 60 min postinjection, whereas the free dose showed 15 and 8 μg/g at 5 and 60 min, respectively. With respect to correlating drug distribution with carrier distribution, the theoretically predicted doxorubicin concentration at the target site, based on iodine 125 counts of the carrier, is 3.5 μg of doxorubicin/g at 60

[1] Adriamycin, Adria Laboratories.
[2] Sigma Chemical Co.
[3] Ferrosoferric oxide ($Fe_3O_4$) in aqueous suspension (MO-I), Ferrofluidics Corp.
[4] Specific activity of 1.51 mCi/mg, New England Nuclear.
[5] Sargent–Welch.
[6] Branson sonifier model 185.
[7] Tween 80 (Sigma Chemical Co.) in 0.154 *N* NaCl.
[8] No. 70,752, Edmund Scientific.
[9] Model 341, Sage Instruments.
[10] Packard model 578.
[11] Sorvall Omni-Mixer.
[12] Sorvall RC-2B.
[13] Aminco SPF-125S (excitation at 470 nm, and emission at 586 nm).
[14] Leitz Ortholux microscope with KP490 excitation and K530 barrier filters.

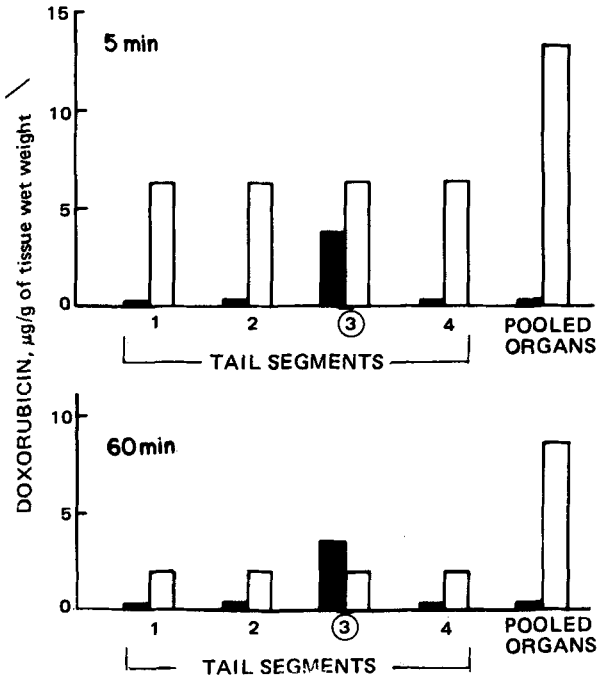


**Figure 1**—*Doxorubicin tissue concentration was determined spectrophotofluorometrically after infusion of either 5 mg of free doxorubicin/kg iv (□) or 0.05 mg of doxorubicin/kg encapsulated in magnetic microspheres via the caudal artery (■). Each value represents the average of two animals.*

min whereas the actual value found by spectrophotofluorometric methods was 3.7 μg/g.

The doxorubicin assay employed in these experiments was limited to determining the total tissue fluorescence. Adriamycinol, an active metabolite, accounts for a percentage of the total fluorescence. However, this metabolite, which is produced by the action of an ubiquitous intracellular aldo–keto oxidoreductase, is minimally active in rats in comparison to humans or monkeys (15). The magnetic sequestration of carrier-delivered doxorubicin from systemic circulation thus could be beneficial in eliminating many of the known acute and chronic toxic side effects. Although the data indicate a good correlation between carrier and drug distribution, the question of bioavailability of carrier-delivered doxorubicin has yet to be determined in a tumor model test system. However, analysis *in situ* by fluorescence microscopy of the microspheres 30 min postinjection at the target site suggested a radial diffusion of doxorubicin from the microspheres into the surrounding tissues. The rapid cellular uptake of doxorubicin that occurs as early as 0.5 min postinjection (10) should facilitate its diffusion into the cells once it is released from the microspheres.

In conclusion, magnetic targeting of chemotherapeutic agents to known sites of disease should be feasible with many currently available antitumor agents. As late as 60 min postinjection, 1% of a free intravenous dose of doxorubicin magnetically localized resulted in almost twice the local tissue concentration than was achieved by a 100-fold higher intravenous dose. The bioavailability of the localized drug is currently under investigation in a tumor model system.

## REFERENCES

(1) T. M. Chang, *Trans. Am. Soc. Intern. Organs*, **12**, 13 (1966).

(2) G. Gregoriadis and B. D. Ryman, *Biochem. J.*, **124**, 58 (1971).

(3) D. A. Tyrrell and B. D. Ryman, *Biochem. Soc. Trans.*, **4**, 677 (1976).

(4) G. Gregoriadis and E. D. Neerunjun, *Res. Commun. Chem. Pathol.*, in press.

(5) K. J. Widder, A. E. Senyei, and D. F. Ranney, in "Advances in Pharmacology and Chemotherapy," S. Garattini, A. Goldin, F. Hawking, I. J. Kopin, and R. J. Schnitzer, Eds., vol. 16, Academic, New York, N.Y., 1979, p. 213.

(6) K. J. Widder, A. E. Senyei, and D. G. Scarpelli, *Proc. Soc. Exp. Biol. Med.*, **158**, 141 (1978).

(7) K. J. Widder, G. Flouret, and A. E. Senyei, *J. Pharm. Sci.*, **68**, 79 (1979).

(8) A. E. Senyei, K. J. Widder, and G. Czerlinski, *J. Appl. Phys.*, **49**, 3578 (1978).

(9) N. R. Bachur, A. L. Moore, J. G. Bernstein, and A. Liu, *Cancer Chemother. Rep.*, **54**, 89 (1970).

(10) M. J. Egorin, R. C. Hildebrand, E. F. Cimino, and N. R. Bachur, *Cancer Res.*, **34**, 2243 (1974).

(11) B. A. Rhodes, I. Zolle, J. W. Buchanan, and H. N. Wagner, Jr., *Radiology*, **92**, 1453 (1969).

(12) V. M. Petrier, T. R. Bochkovz, D. G. Khachirov, and S. V. Seryi, *Med. Radiol.*, **21**, 39 (1976).

(13) N. R. Bachur, M. J. Egorin, and R. C. Hildebrand, *Biochem. Med.* **8**, 352 (1973).

(14) S. D. Reich, *Pharmacol. Ther. Part C*, **2**, 239 (1978).

(15) P. M. Wilkinson, M. Israel, W. J. Pegg, and E. Frei, III, *Cancer Chemother. Pharmacol.*, **2**, 121 (1979).

## ACKNOWLEDGMENTS

Supported in part by the Northwestern University Cancer Center, the Department of Pathology, and the American Cancer Society, Illinois Division.

The authors thank Dr. Raja Bahu for preparation of the specimens for fluorescence microscopy and Leila Schneitzer for preparation of the manuscript.

# Preparation and Release Characteristics of Potassium Chloride Microcapsules

**M. S. HARRIS**

Received August 2, 1979, from the *Department of Pharmacy, Chelsea College, University of London, Manresa Road, London SW3 6LX, England.* Accepted for publication October 16, 1980.

**Abstract** □ The release characteristics of potassium chloride were studied when it was coated with a selection of polymers; from the results obtained, a suitable batch was microencapsulated using a gelatin–gum arabic coacervate system. The microencapsulated product offers better controlled release for this drug when compared to standard tablet and powder forms.

**Keyphrases** □ Potassium chloride—preparation and release characteristics of microcapsules □ Polymers—various polymers and waxes investigated for microencapsulation of potassium chloride □ Microencapsulation—symposium, preparation and release characteristics of potassium chloride microcapsules □ Drug release—potassium chloride microcapsules, preparation and release characteristics

The satisfactory control of drugs in tablet or powder form from protective membranes is often difficult to achieve (1, 2). The present work investigated the microencapsulation of a material that is usually given in a

0022-3549/81/0400-0391$01.00/0
© 1981, American Pharmaceutical Association

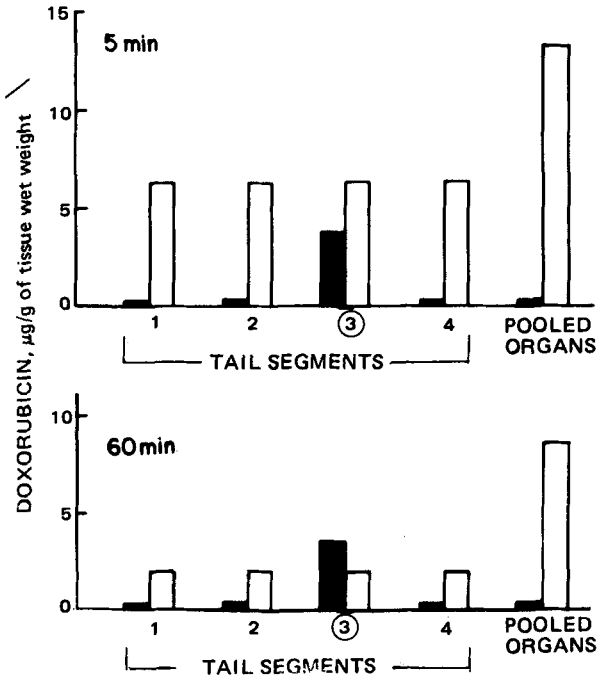


**Figure 1**—*Doxorubicin tissue concentration was determined spectrophotofluorometrically after infusion of either 5 mg of free doxorubicin/kg iv (□) or 0.05 mg of doxorubicin/kg encapsulated in magnetic microspheres via the caudal artery (■). Each value represents the average of two animals.*

min whereas the actual value found by spectrophotofluorometric methods was 3.7 μg/g.

The doxorubicin assay employed in these experiments was limited to determining the total tissue fluorescence. Adriamycinol, an active metabolite, accounts for a percentage of the total fluorescence. However, this metabolite, which is produced by the action of an ubiquitous intracellular aldo–keto oxidoreductase, is minimally active in rats in comparison to humans or monkeys (15). The magnetic sequestration of carrier-delivered doxorubicin from systemic circulation thus could be beneficial in eliminating many of the known acute and chronic toxic side effects. Although the data indicate a good correlation between carrier and drug distribution, the question of bioavailability of carrier-delivered doxorubicin has yet to be determined in a tumor model test system. However, analysis *in situ* by fluorescence microscopy of the microspheres 30 min postinjection at the target site suggested a radial diffusion of doxorubicin from the microspheres into the surrounding tissues. The rapid cellular uptake of doxorubicin that occurs as early as 0.5 min postinjection (10) should facilitate its diffusion into the cells once it is released from the microspheres.

In conclusion, magnetic targeting of chemotherapeutic agents to known sites of disease should be feasible with many currently available antitumor agents. As late as 60 min postinjection, 1% of a free intravenous dose of doxorubicin magnetically localized resulted in almost twice the local tissue concentration than was achieved by a 100-fold higher intravenous dose. The bioavailability of the localized drug is currently under investigation in a tumor model system.

## REFERENCES

(1) T. M. Chang, *Trans. Am. Soc. Intern. Organs*, **12**, 13 (1966).

(2) G. Gregoriadis and B. D. Ryman, *Biochem. J.*, **124**, 58 (1971).

(3) D. A. Tyrrell and B. D. Ryman, *Biochem. Soc. Trans.*, **4**, 677 (1976).

(4) G. Gregoriadis and E. D. Neerunjun, *Res. Commun. Chem. Pathol.*, in press.

(5) K. J. Widder, A. E. Senyei, and D. F. Ranney, in "Advances in Pharmacology and Chemotherapy," S. Garattini, A. Goldin, F. Hawking, I. J. Kopin, and R. J. Schnitzer, Eds., vol. 16, Academic, New York, N.Y., 1979, p. 213.

(6) K. J. Widder, A. E. Senyei, and D. G. Scarpelli, *Proc. Soc. Exp. Biol. Med.*, **158**, 141 (1978).

(7) K. J. Widder, G. Flouret, and A. E. Senyei, *J. Pharm. Sci.*, **68**, 79 (1979).

(8) A. E. Senyei, K. J. Widder, and G. Czerlinski, *J. Appl. Phys.*, **49**, 3578 (1978).

(9) N. R. Bachur, A. L. Moore, J. G. Bernstein, and A. Liu, *Cancer Chemother. Rep.*, **54**, 89 (1970).

(10) M. J. Egorin, R. C. Hildebrand, E. F. Cimino, and N. R. Bachur, *Cancer Res.*, **34**, 2243 (1974).

(11) B. A. Rhodes, I. Zolle, J. W. Buchanan, and H. N. Wagner, Jr., *Radiology*, **92**, 1453 (1969).

(12) V. M. Petrier, T. R. Bochkovz, D. G. Khachirov, and S. V. Seryi, *Med. Radiol.*, **21**, 39 (1976).

(13) N. R. Bachur, M. J. Egorin, and R. C. Hildebrand, *Biochem. Med.* **8**, 352 (1973).

(14) S. D. Reich, *Pharmacol. Ther. Part C*, **2**, 239 (1978).

(15) P. M. Wilkinson, M. Israel, W. J. Pegg, and E. Frei, III, *Cancer Chemother. Pharmacol.*, **2**, 121 (1979).

## ACKNOWLEDGMENTS

Supported in part by the Northwestern University Cancer Center, the Department of Pathology, and the American Cancer Society, Illinois Division.

The authors thank Dr. Raja Bahu for preparation of the specimens for fluorescence microscopy and Leila Schneitzer for preparation of the manuscript.

# Preparation and Release Characteristics of Potassium Chloride Microcapsules

**M. S. HARRIS**

Received August 2, 1979, from the *Department of Pharmacy, Chelsea College, University of London, Manresa Road, London SW3 6LX, England.* Accepted for publication October 16, 1980.

**Abstract** □ The release characteristics of potassium chloride were studied when it was coated with a selection of polymers; from the results obtained, a suitable batch was microencapsulated using a gelatin–gum arabic coacervate system. The microencapsulated product offers better controlled release for this drug when compared to standard tablet and powder forms.

**Keyphrases** □ Potassium chloride—preparation and release characteristics of microcapsules □ Polymers—various polymers and waxes investigated for microencapsulation of potassium chloride □ Microencapsulation—symposium, preparation and release characteristics of potassium chloride microcapsules □ Drug release—potassium chloride microcapsules, preparation and release characteristics

The satisfactory control of drugs in tablet or powder form from protective membranes is often difficult to achieve (1, 2). The present work investigated the microencapsulation of a material that is usually given in a

0022-3549/81/0400-0391$01.00/0
© 1981, American Pharmaceutical Association

**Table I—Release Data for Potassium Chloride from Various Coatings prior to Microencapsulation**

| Coating Material | Drug Released with Time, % | |
|---|---|---|
| | 2 min | 5 min |
| Cellulose acetate phthalate | 42 | 80 |
| Cellulose acetate phthalate and wax coat | 20 | 48 |
| Cellulose acetate phthalate over wax matrix | 37 | 71 |
| Hydroxypropyl methylcellulose | 90 | 100 |
| Hydroxypropyl methylcellulose and wax coat | 30 | 65 |
| Hydroxypropyl methylcellulose over wax matrix | 30 | 66 |
| Cellulose acetate phthalate–ethylcellulose (1:1) | 40 | 70 |
| Cellulose acetate phthalate–ethylcellulose (4:1) | 70 | 90 |
| Ethylcellulose | 56 | 84 |
| Cellulose acetate phthalate–ethylcellulose (1:1) and wax coat | 40 | 68 |
| Ethylcellulose and wax coat | 28 | 67 |

slow-release form. Potassium chloride was chosen because it presents the risk that a large initial dose, or continuing smaller doses, will result in ulceration of the gut and in other side effects (3–8).

## BACKGROUND

It was anticipated that a protective membrane around the drug crystals could result in a more satisfactory controlled release than is possible with conventional tableted forms, which often incorporate film polymers or sugar protective membranes in their outer portion. The gelatin–acacia coacervate microcapsule (9) was chosen as the protective membrane system because many of the coating technique parameters can be controlled. This system is normally limited to use with water-insoluble drugs. To coat a water-soluble drug with this coacervate membrane, the crystalline material first must be protected from the aqueous environment.

A selection of polymers and waxes possessing both enteric and nonenteric properties was researched for this preliminary coat. They had to offer sufficient protection to the potassium chloride crystals and retard solution time to allow coating by the coacervate. Drug coated with these polymers did not constitute a microcapsule. The gelatin–acacia coacervate coat was required for connection with tableting studies on other diuretic drugs.

## EXPERIMENTAL

**Materials**—The polymers and solvents were cellulose acetate phthalate[1] in ethanol–acetone, hydroxypropyl methylcellulose[2] in ethanol–chloroform, cellulose acetate butyrate[3] in propylene glycol–acetone, and ethylcellulose[4] in ethanol. All concentrations were kept at 8% (w/v). Carnauba wax and stearic acid were used in the wax investigations. Materials for microencapsulation were acacia BP and gelatin acid (Bloom 250) at a concentration of 2% (w/v). The solvent was distilled water.

**Polymer Coating of Crystals**—Potassium chloride, previously dried at 80° for 30 min, was placed in a spray-coating pan and several polymer coats were applied. The first coat consisted of 25 ml of 8% polymer solution with a 50-g charge of potassium chloride. This coat was dried for 5 min in hot air at 60°. Subsequent coats (10 ml) of polymer solution were added and dried to give a total weight increase of 10–16%.

**Wax Coating of Crystals**—A combination of carnauba wax (10 g) and stearic acid (5 g) was melted, and the potassium chloride (100 g) was dispersed to give a uniform coat. This mixture was allowed to cool slowly in a revolving coating pan. Discrete pellets of wax-coated drug were obtained.

**Polymer and Wax Coating of Crystals**—The two previous methods were combined. The polymer-coated particles were subsequently wax treated to give up to 30% increase in weight.

**Microencapsulation of Coated Crystals**—Equal volumes of acacia and gelatin were prepared at a concentration of 2% in distilled water. The acacia solution was stirred at ~280 rpm at 41°, and the membrane-coated potassium chloride crystals were introduced. The gelatin solution, also at 41°, was added, and the pH was adjusted to 3.9. After satisfactory coating, formaldehyde was added, and the system was cooled to 5° to fix the coat. The microcapsules then were filtered and dried with ether. The extent of potassium chloride leakage was measured by flame photometry.

**Potassium Chloride Assay**—A flame photometer was calibrated using standard solutions of potassium chloride in distilled water. The solutions consisted of 50, 40, 30, 20, and 10 mg of potassium chloride dissolved in 1 liter of distilled water.

In dissolution studies, the sample was diluted 1 in 10 prior to passing through the photometer. Six independent readings were taken on each sample. To determine the total quantity of potassium chloride in the coated crystals and microcapsules, necessary for expressing the percent released, a 50-mg sample was refluxed with water prior to flame photometry.

**Dissolution Studies**—*Preliminary Studies of Polymer-Wax-Coated Crystals*—The *in vitro* dissolution of the coated crystals was studied at pH 2.0 using 2 liters of dissolution medium at 37° and 500 mg of coated drug. The stirrer speed was 100 rpm. Suitable aliquots were taken at 1-min intervals, diluted where necessary, and assayed for potassium chloride content.

In Vitro *Dissolution of Microcapsules*—A similar technique was used for the microcapsules. Five hundred milligrams of the microcapsules containing 310 mg of potassium chloride was dispersed in 2 liters of water adjusted to pH 2.0 with hydrochloric acid. Suitable aliquots were taken, diluted where necessary, and assayed for drug content using the flame photometer.

In Vivo *Studies on Coacervate-Coated Potassium Chloride*—A baseline for potassium chloride in urine was determined in four healthy volunteers over 48 hr. No special dietary instructions were given other than the avoidance of alcoholic drinks. Subsequently, 1 g of microcapsules containing 620 mg of potassium chloride in powder form was given. Urine samples were collected, measured, and assayed over 6 hr.

## RESULTS AND DISCUSSION

Prior to microencapsulation by the gelatin–acacia coacervate system, it was necessary to protect the water-soluble potassium chloride from the aqueous environment. Cellulose acetate phthalate was chosen initially because its enteric properties prevent solution at the acidic pH of coacervation. The coated material was assayed for active content and contained an average of 86% potassium chloride. The total input of core material could be accounted for within the coated crystals.

The *in vitro* dissolution of the coated crystals was studied at pH 2.0 prior to microencapsulation. Table I shows that 42% of the drug was released after 2 min and that 80% was released after 5 min. This rapid release from cellulose acetate phthalate-coated potassium chloride was due in part to the large surface area available for solution and to the fact that cellulose acetate phthalate acts as a permeable membrane in the presence of ionic solutions. Under these pH conditions, it releases potassium chloride rapidly.

Although the coated particles do not provide any delayed action, they were to be used as a basis for microencapsulation because the gelatin–acacia coacervate forms almost immediately and incorporation of the coated crystals is complete before potassium chloride leaches out. In this way, it is possible to microencapsulate a water-soluble drug within a gelatin–acacia coacervate coat.

When the normal microencapsulation process (7) was attempted, microscopic observation showed numerous small coacervate droplets. Some drug had been encapsulated, but a high percentage had gone into solution, causing salting-out effects on the coacervate. A decrease in the turbidity of the system also indicated a gradual loss of coacervate, although it was not destroyed completely. This result is similar to the influences of electrolytes on the complex coacervate system reported previously (10, 11).

Loss of drug was expected to be excessive. However, the microencapsulation was continued, formaldehyde was added prior to cooling the system to 5°, and the microcapsules were extracted in the usual way.

Assay of these microcapsules yielded only a 12% potassium chloride content. The remainder was in the separated aqueous phase, so all of the drug was accounted for. Subsequent attempts to improve the quantity encapsulated were equally unsatisfactory. Large inputs, because of the increased aqueous potassium chloride concentrations that resulted, produced complete destruction of the coacervate. Attempts to use oil

[1] Eastman Kodak Co., Rochester, NY 14650.
[2] Imperial Chemical Industries, Nobel Division, Stevenston Ayrshire, Scotland.
[3] Eastman Chemical Products.
[4] British Drug Houses, Poole, Dorset, England.

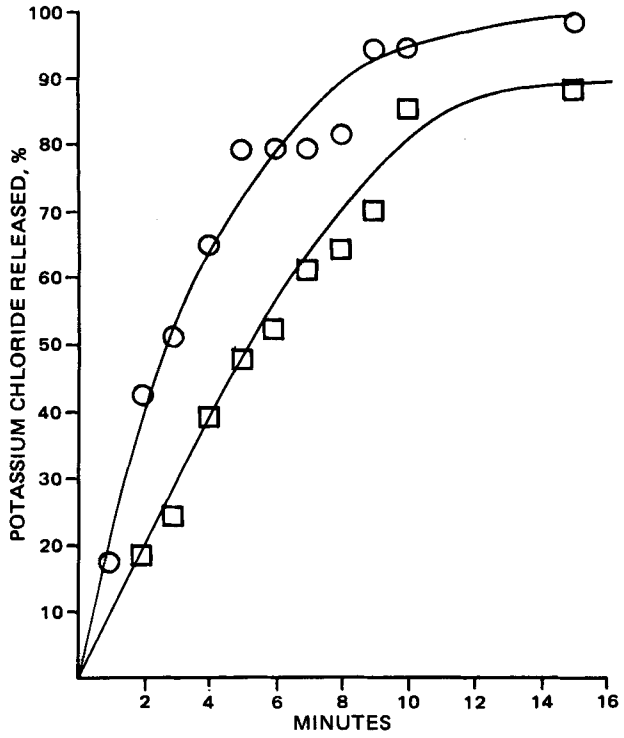


**Figure 1**—*Release of potassium chloride from cellulose acetate phthalate membrane and cellulose acetate phthalate membrane with outer wax coat at pH 2.0 in 2 liters at 37°. Key: ○, cellulose acetate phthalate membrane over potassium chloride, and □, cellulose acetate phthalate membrane and outer wax coat over potassium chloride.*

suspensions of the coated drug were equally unproductive.

A coating formulation employing cellulose acetate phthalate was unsatisfactory. Additional coating to retard water penetration through the polymer membrane was desirable, and carnauba wax and stearic acid were investigated. The carnauba wax would retard water penetration, and the stearic acid would act as a lubricant, which would prevent aggregation of the wax-coated particles. Both compounds also show enteric properties. The increase in weight due to this extra coating was 30%.

An *in vitro* dissolution test was performed at pH 2.0 to study the release characteristics in acidic conditions. Figure 1 shows that the application of a carnauba wax–stearic acid–cellulose acetate phthalate coat retarded drug dissolution. After 5 min, 48% of the drug was released compared to 80% with only a coat of cellulose acetate phthalate. However, when microencapsulation was attempted, except at a low potassium chloride concentration, further additions of wax coats to the polymer did not significantly improve either the percent of potassium chloride encapsulated or the release characteristics.

In a final attempt to use cellulose acetate phthalate, potassium chloride was incorporated in the wax matrix, resulting in larger sized particles. These particles were film coated with the same polymer concentration as was used previously. Dissolution at pH 2.0 was studied. Table I shows that 71% of the drug was released after 5 min. This procedure was less satisfactory than the previous applications of a wax coat applied to a polymer-covered particle and, therefore, would not be expected to produce satisfactory microcapsules.

Since successful microencapsulation was not achieved with any of the cellulose acetate phthalate-coated particles, different polymer coatings were studied. It was hoped that they would show a slower drug release in the presence of aqueous ionic systems.

Cellulose acetate butyrate (17% butyrate) was investigated, but release from this polymer was significantly faster than with cellulose acetate phthalate. With hydroxypropyl methylcellulose, release was rapid but slightly slower than with the cellulose acetate butyrate. Drug release was 100% after 4 min when a simple polymer-coated particle was studied. A carnauba wax–stearic acid coat to this system produced a 65% release of drug after 5 min of dissolution. Potassium chloride incorporated in a wax matrix and film coated with hydroxypropyl methylcellulose produced a slightly slower release of drug than cellulose acetate phthalate but not to any significant extent.

Although some of the polymer formulations retained large quantities of potassium chloride during the important first few minutes of coacervation, none produced satisfactory microcapsules due to the salt effect. Thus, a more hydrophobic preliminary coating was needed. Ethylcellulose was investigated because it is more hydrophobic than cellulose acetate phthalate but will mix with the latter. It was expected to improve the release characteristics and produce a smaller salt effect.

Three formulations were prepared using four parts of cellulose acetate phthalate to one part of ethylcellulose, equal parts of both polymers, and ethylcellulose alone; the overall polymer concentrations were unchanged from those used previously. The functioning of these multipolymer systems could be compared with that of the cellulose acetate phthalate coats.

Partial *in vitro* dissolutions at pH 2.0 are shown in Table I. A mixture of the two polymers (1:1) offered the slowest release. However, the batch containing ethylcellulose alone was not significantly faster, and these two systems were studied further by coating with a wax matrix.

The batch containing ethylcellulose plus a wax coat released 67% of the drug after 5 min, and that containing the mixed polymers and wax coat released 68% (Table I). Both formulations showed similar release. However, the batch containing ethylcellulose and a wax coat released potassium chloride more slowly in the initial stages, and it was this batch that subsequently produced a satisfactory microcapsule. Although the cellulose acetate phthalate formulation had a slower release when given a wax coat (Table I), it could not be used because of problems arising during coacervation due to the ionic environment.

Before subjecting the ethylcellulose–wax-coated drug to the complex coacervate system, possible changes in the microencapsulation process itself were considered. The objective was to introduce the coated cores to the coacervate system in such a way as to ensure that they had a protective gelatin–acacia membrane surrounding them before the potassium chloride concentration leached into the equilibrium liquid could suppress coacervation. Reduction of coacervate volumes to a total of 100 ml produced a suitable handling level at the extraction stage. With the small bench quantities used in this investigation, only about 30 sec was required for the core material to be incorporated within the coacervate. Reduction of temperature to fix this coat and prevent drug diffusion from the microcapsules could be rapid; at 25°, formaldehyde was added. On reaching 5°, the microcapsules were filtered and dried with ether. The core content of potassium chloride obtained corresponded to 61% of the initial input.

The *in vitro* dissolution of these microcapsules at pH 2.0 is shown in

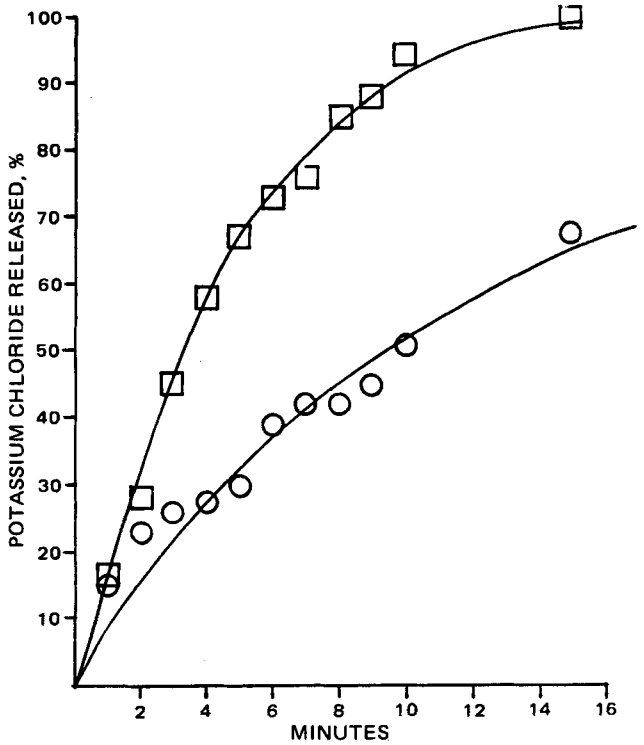


**Figure 2**—*Release of potassium chloride from microcapsules of ethylcellulose–wax-coated potassium chloride and release from unmicroencapsulated potassium chloride at pH 2.0 in 2 liters at 37°. Key: ○, microcapsules; and □, nonmicrocapsules.*

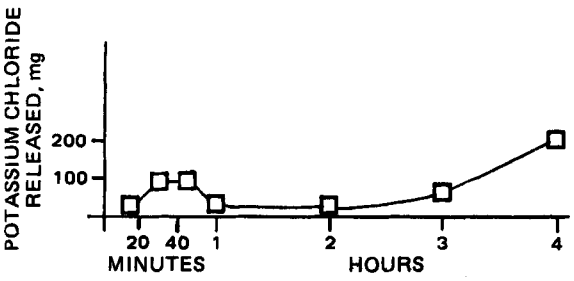


**Figure 3**—*Mean differential release of potassium chloride.*

Fig. 2 along with the release characterstics of the ethylcellulose–wax-coated potassium chloride. The microencapsulated material had a slower release under these *in vitro* conditions. The total potassium chloride was released from the microcapsules after 1 hr.

The *in vivo* performances of these microcapsules is being investigated. Several delivery systems are being studied including tableting, and preliminary results show a significant delayed release of potassium chloride in some cases. Some preliminary *in vivo* release results are shown in Fig. 3 where the mean differential release of potassium chloride microcapsules prior to any formulatory processes is plotted. Over the first 30–40 min after administration of the microencapsulated drug, there was a significant increase in released potassium chloride above that found under normal excretory conditions. It is believed that this increase corresponds to loosely held potassium chloride associated with the wall of the microcapsule, possibly in solid solution. This initial release shows a quiescent period when the drug is probably diffusing toward the outside of the capsule but the potassium chloride found in urine is only that normally excreted. After 2 hr, the differential potassium chloride begins to show a progressive increase as the drug in the center of the microcapsule diffuses out.

In summary, whether a drug is water soluble or not, it can be microencapsulated using the gelatin–gum arabic coacervate system. This system has many advantages due to the wide range of controllable parameters that the system allows.

## REFERENCES

(1) G. K. Noren, G. K. Korpi, and G. J. England, *J. Appl. Polym. Sci.*, **24**, 2369 (1979).

(2) L. N. Sansom, R. W. Milne, and D. Cooper, *Eur. J. Clin. Pharmacol.*, **16**, 417 (1979).

(3) J. I. Kanig, *Drug Stand.*, **22**, 113 (1954).

(4) U.S. Department of Health, Education, and Welfare, cited in *Pharm. J.*, **2**, 183 (1965).

(5) B. R. McAvoy, *Br. Med. J.*, **4**, 164 (1974).

(6) F. Sandor, *J. R. Coll. Gen. Pract.*, **26**, 595 (1976).

(7) R. L. Tanner and A. Cordano, *J. Pharmacol. Exp. Ther.*, **204**, 240 (1978).

(8) B. P. Block and M. B. Thomas, *J. Pharm. Pharmacol., Suppl.*, **30**, 70p (1978).

(9) J. R. Nixon, S. A. H. Khalil, and J. E. Carless, *J. Pharm. Pharmacol.*, **18**, 409 (1966). *Ibid.*, **20**, 348, 528 (1968).

(10) H. G. Bungenberg De Jong, E. G. Haskam, and L. H. V. D. Brandhof-Schaegen, *Proc. K. Ned. Akad. Wet.*, **44**, 1104 (1941).

(11) N. Yashida and C. Thies, *J. Colloid Interface Sci.*, **24**, 29 (1967).

# Effect of Caffeine on Circulating Theophylline Levels in Beagle Dogs

F. L. S. TSE *x, K. H. VALIA, D. W. SZETO, T. J. RAIMONDO, and B. KOPLOWITZ

Received August 18, 1980, from the *College of Pharmacy, Rutgers–The State University, Piscataway, NJ 08854.* Accepted for publication October 2, 1980. *Present address: Sandoz Pharmaceuticals, East Hanover, NJ 07936.

**Abstract** □ The pharmacokinetic interactions of caffeine with theophylline were examined in two beagle dogs by administering 100 mg of aminophylline intravenously, 3 weeks before and immediately after repeated oral doses of caffeine. Serial plasma samples were analyzed for caffeine and theophylline simultaneously by high-performance liquid chromatography. Upon multiple oral dosing, 100 mg every 12 hr for 7 days, the caffeine half-life increased slightly in one dog but decreased in the other. As predicted from single-dose data, caffeine accumulation in plasma after repeated doses was slight, while plasma levels of the *N*-demethylated metabolite, theophylline, rose to about three times the initial values. After rapid intravenous doses of aminophylline, the theophylline half-life was 5–7 hr, which decreased slightly when the drug was administered concomitantly with caffeine during steady state of caffeine. The theophylline volume of distribution (0.75 liter/kg) was unaffected by caffeine. On the other hand, an acute aminophylline injection prolonged the elimination half-life and increased the apparent volume of distribution of caffeine, causing little overall change in its plasma clearance. The results suggested that interactions between theophylline and caffeine may be attributed to changes in drug distribution and drug elimination characteristics.

**Keyphrases** □ Caffeine—pharmacokinetic interactions with theophylline □ Theophylline—pharmacokinetic interaction with caffeine □ Plasma clearance—plasma caffeine levels, plasma theophylline levels

The bronchodilator theophylline is eliminated from the human body primarily by metabolism. Approximately 90% of the dose is metabolized by the liver *via* oxidative and demethylation reactions to 3-methylxanthine, 1,3-dimethyluric acid, and 1-methyluric acid (1). The plasma half-life of theophylline in humans is ~6 hr after intravenous (2) or oral (3) dosing, and kinetic indexes in asthmatics and healthy adults are similar (4).

The effect of concurrent administration of other drugs on theophylline disposition has been examined to some extent. Piafsky *et al.* (5) observed *in vivo* induction of theophylline metabolism in humans by phenobarbital, although others (6) reported decreased or unchanged theophylline clearance after phenobarbital therapy. Allopurinol, a xanthine oxidase inhibitor, blocks the conversion of 1-methylxanthine to 1-methyluric acid but has no significant effect on the overall theophylline clearance (7, 8).

In a recent study, Monks *et al.* (9) reported a decrease in the theophylline elimination half-life in subjects on a methylxanthine-free diet. These authors suggested that, since theophylline and the dietary methylxanthines share common metabolic pathways, they may compete with one another for the same enzymes, thus resulting in suppressed theophylline metabolism. On the other hand, caffeine was shown to increase enzyme synthesis in rat liver (10), which could enhance drug metabolism.

The present study concerned caffeine pharmacokinetics in the dog after single and multiple oral doses of caffeine tablets for 1 week. The effect of steady-state blood levels of caffeine on theophylline disposition was examined by administering aminophylline intravenously, 3 weeks before and immediately after the caffeine multiple-dosing regimen. Changes in the pharmacokinetic profile of caffeine due to an acute aminophylline injection were also analyzed.

## EXPERIMENTAL

A 1-year-old male (Dog A, 11.4 kg) beagle dog and a 2-year-old female (Dog B, 11.7 kg) beagle dog were used. The dogs were fasted overnight before and 4 hr after each drug dose in the single-dosing experiments and the first and last dose in the multiple-dosing experiments. During an experiment, dogs were initially placed in a restraining sling to facilitate accurate drug administration and blood sample collection.

**Single Intravenous Aminophylline**—Each dog received a single 100-mg aminophylline[1] (85% theophylline) dose by bolus injection into a front leg vein. Serial 5-ml blood samples were collected in 10-ml heparinized tubes[2] during 24 hr after dosing. Plasma was separated by centrifugation and stored at −20° prior to assay.

**Multiple Oral Caffeine**—Multiple caffeine regimens were started 3 weeks after the initial aminophylline dose. Each dog received one 100-mg tablet of caffeine[3] twice daily at 9:00 am and 9:00 pm for 8 days. Tablets were administered by placing them on the posterior portion of the tongue so that they were not fractured before being swallowed and were followed by 5 ml of water. A predose blood sample was taken before each morning dose, and serial blood samples were collected during the 12 hr after the morning doses on Days 1 and 8.

**Concurrent Aminophylline and Caffeine**—On the day after the multiple caffeine experiments (Day 9), each dog received orally a 100-mg caffeine tablet at 9:00 am, followed immediately by an intravenous injection of 100 mg of aminophylline. Blood samples were collected immediately before and serially during 24 hr after dosing.

**Plasma Assay**—Plasma concentrations of theophylline and caffeine were determined in 1-ml samples by the high-performance liquid chromatographic (HPLC) assay of Valia *et al.* (11). Samples were prepared as described previously, but the chromatographic conditions were modified slightly. A 10-μm μBondapak $C_{18}$ column[4] was used in conjunction with a chromatograph[5] equipped with a spectrophotometric detector[6]. The mobile phase was 10% acetonitrile–0.01 *M* acetate buffer (pH 4). The column temperature and the solvent temperature were ambient. A flow rate of 1.5 ml/min was used, yielding an operating pressure of 1500 psi. The spectrophotometric detector had a 15.6-μl cell volume and was operated at 280 nm.

[1] Aminophylline Injection USP, 25 mg/ml, Gibco/Invenex, Chagrin Falls, Ohio.
[2] Vacutainer, Becton-Dickinson, Rutherford, N.J.
[3] NoDoz, Bristol-Myers, New York, N.Y.
[4] Waters Associates, Milford, Mass.
[5] Model 244, Waters Associates, Milford, Mass.
[6] Model 440, Waters Associates, Milford, Mass.

0022-3549/81/0400-0395$01.00/0
© 1981, American Pharmaceutical Association

**Table I—Pharmacokinetic Parameters of Caffeine after Single and Repeated Oral Doses**

| Parameter | Dog A | | Dog B | |
|---|---|---|---|---|
| | Day 1 | Day 8 | Day 1 | Day 8 |
| $k_a$, $hr^{-1}$ | 1.29 | 0.71 | 1.76 | 0.72 |
| | (−0.17–2.75)[a] | (0.45–0.97) | (0.79–2.74) | (0.19–1.25) |
| $t_{1/2,abs}$[b], hr | 0.54 | 0.97 | 0.39 | 0.96 |
| $k_{el}$, $hr^{-1}$ | 0.18 | 0.15 | 0.13 | 0.21 |
| | (−0.013–0.37) | (0.11–0.20) | (0.067–0.20) | (0.086–0.34) |
| $t_{1/2}$[c], hr | 3.84 | 4.52 | 5.16 | 3.23 |
| $FD/V$, μg/ml | 16.0 | 19.1 | 12.3 | 18.0 |
| | (6.09–25.9) | (13.8–24.4) | 9.34–15.3) | (7.80–28.2) |
| $t_0$, hr | 0.083 | —[d] | 0.027 | — |
| | (−0.10–0.27) | | (0.062–0.12) | |
| $r^2$[e] | 0.82 | 0.96 | 0.94 | 0.91 |
| $AUC^{0\to\infty}$[f], (μg hr)/ml | 88.9 | — | 94.6 | — |
| $AUC^{0\to12}$[g], (μg hr)/ml | — | 122 | — | 83.8 |
| $C_{max}$[h], μg/ml | 11.6 | 15.6 | 9.97 | 12.0 |
| $t_{max}$[i], hr | 1.84 | 2.44 | 1.61 | 2.23 |

[a] The 95% confidence limits. [b] Half-time of absorption = $0.693/k_a$. [c] Half-life of elimination by all routes = $0.693/k_{el}$. [d] Not calculated. [e] Coefficient of determination = $(\Sigma \text{ obs}^2 - \Sigma \text{ dev}^2)/\Sigma \text{ obs}^2$. [f] Area under plasma level–time curve = $FD/Vk_{el}$. [g] Obtained by trapezoidal rule.

[h] Peak height:

$$\text{Day 1} = \frac{FD}{V}\left(\frac{k_a}{k_{el}}\right)^{k_{el}/(k_{el}-k_a)}$$

$$\text{Day 8} = \frac{FD}{V}\left(\frac{1}{1-e^{-k_{el}\tau}}\right)\left[\frac{k_a(1-e^{-k_{el}\tau})}{k_{el}(1-e^{-k_a\tau})}\right]^{k_{el}/(k_{el}-k_a)}$$

[i] Time of peak height:

$$\text{Day 1} = \ln\left(\frac{k_a}{k_{el}}\right)\Big/(k_a - k_{el}) + t_0$$

$$\text{Day 8} = \ln\left[\frac{k_a(1-e^{-k_{el}\tau})}{k_{el}(1-e^{-k_a\tau})}\right]\Big/(k_a - k_{el})$$

**Table II—Pharmacokinetic Parameters of Theophylline after Single Intravenous Doses of Aminophylline Alone or during Steady State of Caffeine**

| Parameter | Dog A | | | Dog B | | |
|---|---|---|---|---|---|---|
| | Aminophylline | Aminophylline + Caffeine | | Aminophylline[b] | Aminophylline + Caffeine | |
| | | Corrected[a] | Uncorrected | | Corrected | Uncorrected[b] |
| $k_{el}$, $hr^{-1}$ | 0.098 | 0.11 | 0.05 | —[c] | 0.17 | — |
| $t_{1/2}$, hr | 7.10 | 6.08 | 13.7 | — | 4.03 | — |
| $D/V$, μg/ml | 9.96 | 9.96 | 17.5 | — | 8.56 | — |
| $V$, liter/kg | 0.75 | 0.75 | 0.43 | — | 0.85 | — |
| $r^2$[d] | 0.99 | 0.97 | 0.96 | — | 0.99 | — |
| $k_{12}$, $hr^{-1}$ | — | — | — | 3.62 | — | 8.17 |
| | | | | (0.80–6.44) | | (−23.4–39.7) |
| $k_{21}$, $hr^{-1}$ | — | — | — | 5.20 | — | 9.97 |
| | | | | (3.05–7.35) | | (2.17–17.8) |
| $k_{el}$, $hr^{-1}$ | — | — | — | 0.24 | — | 0.16 |
| | | | | (0.19–0.29) | | (−0.067–0.38) |
| $\alpha$, $hr^{-1}$ | — | — | — | 8.92 | — | 18.2 |
| $t_{1/2,\alpha}$[e], hr | — | — | — | 0.078 | — | 0.038 |
| $\beta$, $hr^{-1}$ | — | — | — | 0.14 | — | 0.086 |
| $t_{1/2,\beta}$[f], hr | — | — | — | 4.94 | — | 8.10 |
| $D/V_1$, μg/ml | — | — | — | 16.5 | — | 24.2 |
| | | | | (13.5–19.6) | | (−10.2–58.6) |
| $V_1$, liter/kg | — | — | — | 0.44 | — | 0.30 |
| $V_{ss}$[g], liter/kg | — | — | — | 0.74 | — | 0.55 |
| $R^2$ | — | — | — | 1.00 | — | 1.00 |
| $Cl_p$[h], ml/min/kg | 1.22 | 1.42 | 0.36 | 1.76 | 2.43 | 0.78 |
| $AUC^{0\to\infty}$[i], (μg hr)/ml | 102 | 90.5 | 350 | 68.8 | 50.4 | 151 |

[a] Calculated using observed plasma theophylline concentration minus the theophylline formed as metabolite of caffeine. [b] Obtained by analyses using two-compartment model. [c] Not relevant. [d] Correlation coefficient. [e] Half-life of rapid phase of decline in plasma levels = $0.693/\alpha$. [f] $0.693/\beta$. [g] $V_{ss} = V_1(1 + k_{12}/k_{21})$. [h] Plasma clearance = $Vk_{el}$ in one-compartment model and $V_1k_{el}$ in two-compartment model. [i] Area under plasma level–time curve = $D/Cl_p$.

Complete peak resolution was obtained for caffeine, theophylline, and the internal standard, β-hydroxyethyltheophylline, with retention times of 9.6, 5.6, and 6.5 min, respectively. Other xanthines did not interfere. The limit of detection was 1 μg/ml for both theophylline and caffeine. Linear regressions of the peak height ratios of drug to internal standard *versus* plasma drug levels of 1, 5, 10, 25, and 50 μg/ml were described by the equations $y = 0.066x + 0.013$ ($n = 20, r = 1.00$) for theophylline and $y = 0.036x + 0.016$ ($n = 20, r = 1.00$) for caffeine.

**Pharmacokinetic Analysis**—Plasma caffeine levels after oral doses were fitted to the pharmacokinetic one-compartment open model with first-order absorption and elimination. Plasma caffeine concentrations, $C$, at any time, $t$, after a single dose are described by:

$$C = \frac{FD}{V}\left(\frac{k_a}{k_a - k_{el}}\right)[e^{-k_{el}(t-t_0)} - e^{-k_a(t-t_0)}] \qquad \text{(Eq. 1)}$$

where $F$ is the fraction of the dose, $D$, absorbed; $V$ is the apparent distribution volume of caffeine in the body; $k_a$ and $k_{el}$ are first-order rate constants for absorption and elimination, respectively; and $t_0$ is the lag time between dosing and the appearance of drug in the circulation. During steady state following multiple dosing, plasma caffeine concentrations, $C^\infty$, were fitted to (12):

$$C^\infty = \frac{FD}{V}\left(\frac{k_a}{k_a - k_{el}}\right)\left(\frac{e^{-k_{el}t}}{1-e^{-k_{el}\tau}} - \frac{e^{-k_at}}{1-e^{-k_a\tau}}\right) \qquad \text{(Eq. 2)}$$

where $\tau$ is the dosing interval and equals 12 hr in each case.

Except in two cases, plasma theophylline levels after rapid intravenous doses of aminophylline appeared to obey one-compartment open model kinetics and were analyzed by linear regression (13). Attempts to fit these data to the two-compartment model resulted in greater errors in parameter values with no improvement in the coefficients of determination. In the two situations where the two-compartment model was adequate, plasma theophylline concentrations, $C_1$, were described by (12):

$$C_1 = \frac{D}{V_1(\alpha - \beta)}[(\alpha - k_{21})e^{-\alpha t} + (k_{21} - \beta)e^{-\beta t}] \qquad \text{(Eq. 3)}$$

where $V_1$ is the volume of the central compartment and $\alpha$ and $\beta$ are composite rate constants depending on $k_{el}$ and the first-order rate constants, $k_{12}$ and $k_{21}$, governing the transfer of drug between compartments:

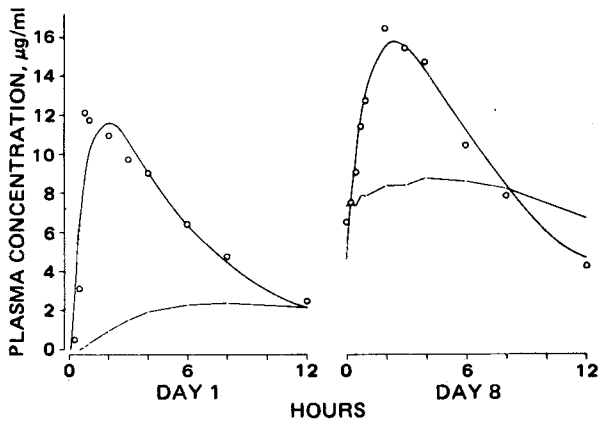


**Figure 1**—*Plasma levels of caffeine (○) and theophylline (– –) in Dog A after the morning dose on Days 1 and 8 during a 100-mg caffeine twice daily regimen. The curves for caffeine are computer derived.*

$$\begin{matrix}\alpha \\ \beta\end{matrix} = \tfrac{1}{2}\{(k_{12} + k_{21} + k_{el}) \pm [(k_{12} + k_{21} + k_{el})^2 - 4k_{21}k_{el}]^{1/2}\} \quad \text{(Eq. 4)}$$

Individual data sets were fitted to the appropriate equations by iterative least-squares methods using the program NONLIN[7] (14).

Pharmacokinetic parameters obtained from single-dose (Day 1) caffeine data were used to predict drug accumulation characteristics upon multiple dosing. Predicted parameter values were compared with those observed in the Day 8 experiment.

## RESULTS

Plasma concentration–time data after single and multiple oral doses of caffeine to Dogs A and B are presented in Figs. 1 and 2, respectively. Results of pharmacokinetic analyses are given in Table I. Following single 100-mg tablet doses, caffeine appeared in plasma almost immediately, reaching peak levels of 11.6 and 9.97 μg/ml in 1–2 hr. Elimination half-lives were 3.84 hr in Dog A and 5.16 hr in Dog B. Accordingly, steady-state concentrations should be achieved in 1 day, and this projection was confirmed by the caffeine levels observed in the daily predose plasma samples.

Upon multiple dosing, caffeine absorption was slower in both dogs, as reflected by the prolonged absorption half-times and delayed peak times. The half-life was increased slightly after repeated dosing in Dog A but was decreased in Dog B. The value of $FD/V$ was higher on Day 8 in each case. The area under the curve increased significantly in Dog A, but the change in Dog B was slight. The accumulation factor, $R$, calculated by the ratio of $C_{max}$ on Day 8 to that on Day 1, was 1.34 for Dog A and 1.20 for Dog B; $R$ values predicted from Day 1 data alone, using $R = 1/[(1 - e^{-k_{el}\tau})(1 - e^{-k_a\tau})]$, were 1.13 and 1.25 for Dogs A and B, respectively.

In humans, caffeine is metabolized in part by $N$-demethylation to theophylline (15). This route was shown to exist in dogs also in the present study. After a single 100-mg oral dose of caffeine, detectable plasma theophylline levels appeared in 45 min, reaching a plateau of ~2 μg/ml at 4 hr. The sustained nature of plasma theophylline in this case precluded the accurate calculation of its elimination rate. The accumulation factors obtained by the ratio of observed values of $C_{max}$ on Day 8 and Day 1 were 3.67 and 2.66 for Dogs A and B, respectively.

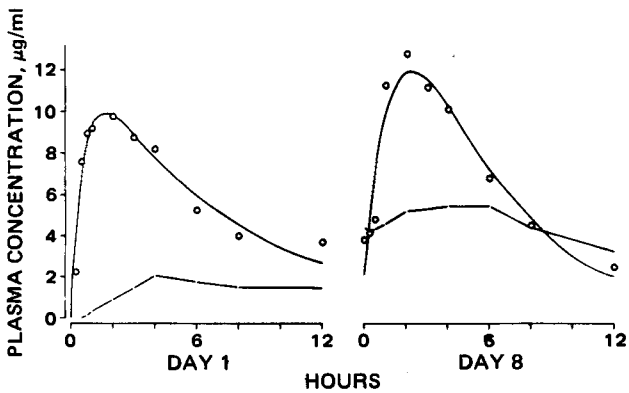


**Figure 2**—*Plasma levels of caffeine (○) and theophylline (– –) in Dog B after the morning dose on Days 1 and 8 during a 100-mg caffeine twice daily regimen.*

[7] An IBM 370/168 digital computer at the Rutgers Computer Center for Informational Services was used.

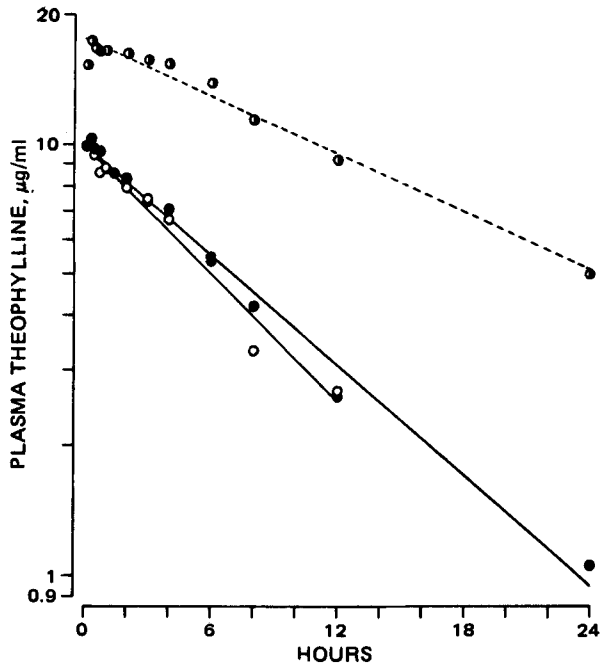


**Figure 3**—*Plasma theophylline levels in Dog A after 100 mg of aminophylline was intravenously administered alone (●) or during steady state of caffeine, with data corrected (○) and uncorrected (◑) for theophylline derived from caffeine, respectively.*

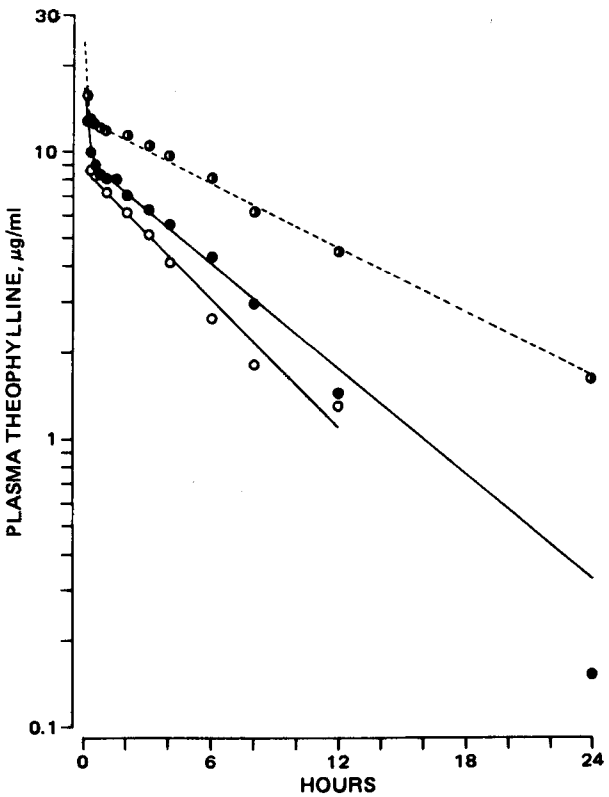


**Figure 4**—*Plasma theophylline levels in Dog B after 100 mg of aminophylline was intravenously administered alone (●) or during steady state of caffeine, with data corrected (○) and uncorrected (◑) for theophylline derived from caffeine, respectively.*

**Table III—Pharmacokinetic Parameters of Caffeine after an Oral Dose during Steady State with Concomitant Aminophylline Injection**

| Parameter | Dog A | Dog B |
|---|---|---|
| $k_a$, $hr^{-1}$ | 1.67 (1.30–2.05) | 8.82 (6.97–10.7) |
| $t_{1/2,abs}$, hr | 0.41 | 0.079 |
| $k_{el}$, $hr^{-1}$ | 0.12 (0.10–0.13) | 0.14 (0.13–0.16) |
| $t_{1/2}$, hr | 5.95 | 4.89 |
| $FD/V$, μg/ml | 13.7 (11.9–15.6) | 11.1 (10.3–11.9) |
| $r^2$ | 0.98 | 0.99 |
| $AUC^{0\to12}$, (μg hr)/ml | 116 | 77.5 |
| $C_{max}$, μg/ml | 15.0 | 12.8 |
| $t_{max}$, hr | 1.52 | 0.45 |

Figures 3 and 4 describe plasma theophylline concentrations following bolus intravenous injections of 100 mg of aminophylline to Dogs A and B, respectively. While theophylline kinetics were being examined after simultaneous administration with the final dose of caffeine in the multiple caffeine dosing experiment, it was realized that caffeine metabolism resulted in sufficiently high theophylline levels to interfere with interpretation of data from the intravenous dose. Therefore, corrected plasma theophylline levels from the aminophylline injection (Day 9) were estimated by deducting from observed values the theophylline concentrations at the same sampling time on the previous day (Day 8). This procedure was justified by the observed theophylline concentrations in the daily predose plasma samples, which showed that this metabolite also had reached steady state. Both corrected and uncorrected theophylline data were analyzed, and the results of the pharmacokinetic analyses are shown in Table II.

Except for a short initial period (15 min) of rapid decline in plasma levels in two cases, theophylline pharmacokinetics were described adequately by the one-compartment open model. Despite its higher initial concentration in Dog B (16.5 μg/ml, compared to 9.96 μg/ml in Dog A), theophylline appeared to distribute into virtually identical overall spaces in Dogs A ($V$ = 0.75 liter/kg) and B ($V_{ss}$ = 0.74 liter/kg). Elimination half-lives of 7 and 5 hr were observed in Dogs A and B, respectively.

Pharmacokinetic analysis of corrected theophylline data showed that a concomitant dose of aminophylline with caffeine at steady state of caffeine resulted in little or no change in the apparent distribution volume of theophylline in the two dogs. However, the half-life was shortened by ~1 hr in each dog. The increase in the elimination rate was reflected also in changes in the plasma clearance and area under the curve values. As expected, analysis of the uncorrected data led to much higher initial plasma theophylline concentrations (17.5 μg/ml in Dog A and 24.2 μg/ml in Dog B) and longer half-lives (13.7 and 8.10 hr in Dogs A and B, respectively).

Pharmacokinetic parameters of caffeine after concomitant caffeine and aminophylline doses on Day 9 are given in Table III. Comparison with the Day 8 data in Table I indicated that the injection of aminophylline resulted in faster absorption of caffeine from the oral dose (larger $k_a$ and smaller $t_{max}$ in both dogs), although $C_{max}$ values were almost unchanged. These results also are shown in Figs. 5 and 6 for Dogs A and B, respectively. Aminophylline increased the elimination half-life of caffeine but

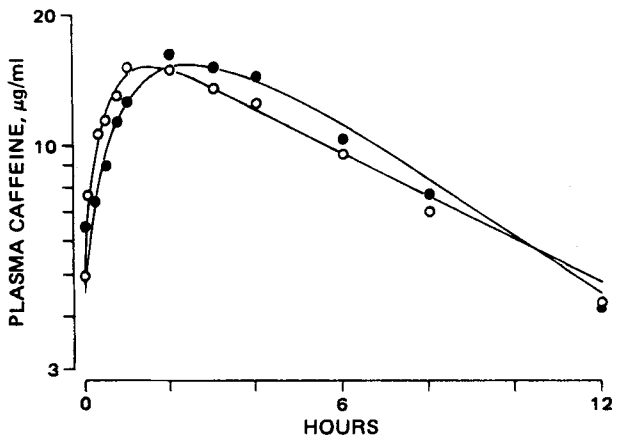


**Figure 5**—*Steady-state plasma caffeine levels in Dog A after oral administration of 100 mg of caffeine, with (○) and without (●) a concomitant dose of intravenous aminophylline.*

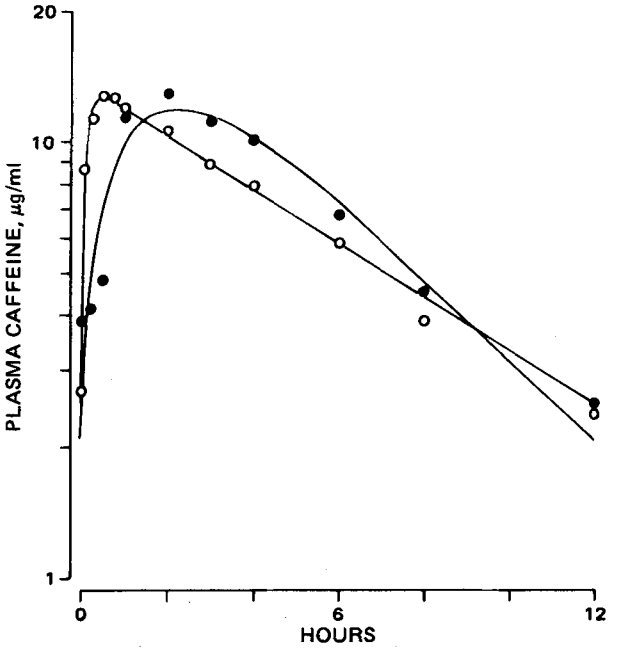


**Figure 6**—*Steady-state plasma caffeine levels in Dog B after oral administration of 100 mg of caffeine, with (○) and without (●) a concomitant dose of intravenous aminophylline.*

decreased the $FD/V$ values so that the area under the plasma caffeine level–time curve during a dose interval was virtually unaffected.

## DISCUSSION

The caffeine half-life determined after single oral doses to dogs was 4–5 hr, similar to that observed in humans (15). However, longer half-life values (6.4–9.1 hr) were reported in a more recent study in three healthy nonsmokers (16). Intersubject variation in caffeine kinetics was apparent in the present study. This variation and the limited number of dogs used made it difficult to evaluate the effect of repeated dosing on caffeine pharmacokinetic properties. With the dosage regimen employed, which was equivalent to about 1 cup of coffee every 12 hr, there was limited accumulation of caffeine in the circulation. On the other hand, plasma levels of the $N$-demethylated metabolite, theophylline, rose to nearly 9 and 6 μg/ml in Dogs A and B, respectively, about three times the concentrations after the initial dose. These figures were higher than those reported in humans given comparable doses of caffeine (15). Therefore, subjects must refrain from caffeine-containing beverages before participating in theophylline disposition studies, despite recent advancements in analytical technology that permit simultaneous determination of caffeine and theophylline in biological fluids.

The decline in plasma theophylline levels after intravenous dosing appeared to be biphasic, although the distribution phase was so rapid that a one-compartment model was adequate for data analysis in four of the six cases tested. This characteristic behavior was reported by others (6, 17). The theophylline half-life in dogs after single doses was similar to that in humans. When given concomitantly with caffeine during steady state of caffeine, theophylline showed slight increases in its elimination rate, probably due to metabolic enzyme activity stimulated by the repeated caffeine doses. The distribution volume (0.75 liter/kg) of theophylline was unaltered by caffeine.

No explanation was apparent for the more rapid absorption of caffeine when given simultaneously with intravenous aminophylline. Starr *et al.* (18) reported that aminophylline increased cardiac output in humans by 26% and also may enhance blood flow through the GI tract. Further studies are being conducted to elucidate this phenomenon. Aminophylline prolonged the elimination half-life of caffeine, presumably by competing with caffeine for the same enzymes. Aminophylline also increased the apparent distribution volume of caffeine (assuming constant $F$), probably by displacing caffeine from plasma protein binding sites. Thus, theophylline appeared to have a stronger affinity than caffeine for drug metabolizing enzymes as well as for plasma proteins. In humans, theophylline is 60–70% plasma protein bound (19, 20), compared to ~15% in the case of caffeine (21). Because of changes in $V$ and $k_{el}$ in opposite di-

rections, the overall plasma clearance of caffeine was virtually unaffected by acute aminophylline administration.

The need for establishing dosage guidelines for safe intravenous administration of theophylline has been stressed (22). Theophylline has a narrow therapeutic index of 10–20 μg/ml, and the risk of toxicity, including seizures and death, increases as serum concentrations exceed this range. In asthmatic patients receiving chronic theophylline therapy, routine monitoring of serum drug levels is recommended. Interactions of theophylline with other exogenous compounds may influence the therapeutic outcome of this drug. For example, methylxanthines such as caffeine and theobromine, present in various common beverages and foods, were shown to inhibit theophylline metabolism in humans (9). In the present study, the theophylline half-life in beagle dogs actually decreased after multiple doses of caffeine, probably due to enzyme induction by the latter. Nevertheless, plasma theophylline levels were elevated and sustained as a result of metabolic conversion of administered caffeine to theophylline.

These observations may suggest the need to reduce theophylline maintenance doses in asthmatics who are chronic coffee drinkers. Caution is also warranted in treatment with theophylline in breast-fed infants, who may be exposed to methylxanthines in the milk (23, 24). Recently it has become evident that theophylline is biotransformed to caffeine by *N*-methylation in the premature newborn infant (25–28), which further complicates theophylline–caffeine interactions. This metabolic pathway was not observed in adult humans (25) and dogs in the present study.

## REFERENCES


(1) J. W. Jenne, H. T. Nagasawa, and R. D. Thompson, *Clin. Pharmacol. Ther.*, **19,** 375 (1976).

(2) P. W. Trembath and S. W. Boobis, *ibid.*, **26,** 654 (1979).

(3) P. G. Welling, L. L. Lyons, W. A. Craig, and G. A. Trochta, *ibid.*, **17,** 475 (1975).

(4) P. G. Welling, J. Domoradzki, J. A. Sims, and C. E. Reed, *J. Clin. Pharmacol.*, **16,** 43 (1976).

(5) K. M. Piafsky, D. S. Sitar, and R. I. Ogilvie, *Clin. Pharmacol. Ther.*, **22,** 336 (1977).

(6) R. I. Ogilvie, *Clin. Pharmacokinet.*, **3,** 267 (1978).

(7) J. J. Grygiel, L. M. H. Wing, J. Farkas, and D. J. Birkett, *Clin. Pharmacol. Ther.*, **26,** 660 (1979).

(8) S. Vozeh, J. R. Powell, G. C. Cupit, S. Riegelman, and L. B. Sheiner, *ibid.*, **27,** 194 (1980).

(9) T. J. Monks, J. Caldwell, and R. L. Smith, *ibid.*, **26,** 513 (1979).

(10) C. Mitoma, T. J. Sorich, II, and S. E. Neubauer, *Life Sci.*, **7,** 145 (1968).

(11) K. H. Valia, C. A. Hartman, N. Kucharczyk, and R. D. Sofia, *J. Chromatogr.*, **221,** 170 (1980).

(12) M. Gibaldi and D. Perrier, "Pharmacokinetics," Dekker, New York, N.Y., 1975, pp. 52, 110.

(13) F. L. S. Tse and P. G. Welling, *J. Pharm. Sci.*, **66,** 1751 (1977).

(14) C. M. Metzler, G. L. Elfring, and A. J. McEwen, *Biometrics*, **30,** 562 (1974).

(15) S. Sved, R. D. Hossie, and I. J. McGilveray, *Res. Commun. Chem. Pathol. Pharmacol.*, **13,** 185 (1976).

(16) J. Descotes, J. L. Brazier, M. Ollagnier, and J.-Cl. Evreux, *Thérapie*, **34,** 619 (1979).

(17) J. P. Rosen, M. Danish, M. C. Ragni, C. L. Saccar, S. J. Yaffe, and H. I. Lecks, *Pediatrics*, **64,** 248 (1979).

(18) I. Starr, C. J. Gamble, A. Margolies, J. S. Donal, Jr., N. Joseph, and E. Eagle, *J. Clin. Invest.*, **16,** 799 (1937).

(19) R. Koysooko, E. F. Ellis, and G. Levy, *Clin. Pharmacol. Ther.*, **15,** 454 (1974).

(20) K. F. Simons, F. E. R. Simons, C. J. Briggs, and L. Lo, *J. Pharm. Sci.*, **68,** 252 (1979).

(21) J. Axelrod and J. Reichenthal, *J. Pharmacol. Exp. Ther.*, **107,** 519 (1953).

(22) "FDA Drug Bulletin," vol. 10, no. 1, Food and Drug Administration, Rockville, Md., Feb. 1980, pp. 4–6.

(23) B. H. Resman, H. P. Blumenthal, and W. J. Jusko, *J. Pediatr.*, **91,** 477 (1977).

(24) J. T. Wilson, R. D. Brown, D. R. Cherek, J. W. Dailey, B. Hilman, P. C. Jobe, B. R. Manno, J. E. Manno, H. M. Redetzki, and J. J. Stewart, *Clin. Pharmacokinet.*, **5,** 1 (1980).

(25) C. Bory, P. Baltassat, M. Porthault, M. Bethenod, A. Frederich, and J. V. Aranda, *J. Pediatr.*, **94,** 988 (1979).

(26) H. S. Bada, N. N. Khanna, S. M. Somani, and A. A. Tin, *ibid.*, **94,** 993 (1979).

(27) M. J. Boutroy, P. Vert, R. J. Royer, P. Monin, and M. J. Royer-Morrot, *ibid.*, **94,** 996 (1979).

(28) F. E. R. Simons, F. R. Friesen, and K. J. Simons, *Am. J. Dis. Child.*, **134,** 39 (1980).


# Nonsteroidal Estrogens and Antiestrogens: Biological Activity of Cyclopropyl Analogs of Stilbene and Stilbenediol


**J. THOMAS PENTO *x, ROBERT A. MAGARIAN *, ROBERT J. WRIGHT *, M. MARGARET KING ‡, and ERIC J. BENJAMIN ***



Received September 25, 1979, from the **College of Pharmacy, University of Oklahoma, Health Sciences Center, Oklahoma City, OK 73190*, and the ‡*Oklahoma Medical Research Foundation, Oklahoma City, OK 73104.* Accepted for publication November 30, 1979.



**Abstract** □ The estrogenic, antiestrogenic, and receptor binding activity of a series of cyclopropyl analogs of stilbene and stilbenediol were determined using the uterotropic assay in the mouse and the receptor binding assay with rat uterine cytosol. One compound, 1,1-dichloro-*cis*-2,3-diphenylcyclopropane (II), displayed antiestrogenic activity *in vivo* with a low affinity for the estrogen receptor *in vitro* and showed tumor remission activity on 7,12-dimethylbenz(*a*)anthracene-induced estrogen-dependent rat mammary tumors. Compounds VIII, IV, and V (in that order) exhibited the greatest estrogenic activity in the mouse and the greatest receptor binding activity *in vitro*. Compound VIII exhibited antifertility activity in the mouse.



**Keyphrases** □ Estrogenic activity—cyclopropyl analogs of stilbene and stilbenediol, mice □ Antiestrogenic activity—cyclopropyl analogs of stilbene and stilbenediol, mice □ Receptor binding activity—cyclopropyl analogs of stilbene and stilbenediol □ Stilbene and stilbenediol—cyclopropyl analogs, pharmacological activity in mice and rats


Various rigid ring systems have been used to lock functional groups into desired conformations to study receptor interactions (1, 2). The cyclopropane ring is a relatively new structure to be employed synthetically to produce a fixed stereochemical configuration with minimal steric interference in potential medicinal agents (3–5). Magarian and Benjamin (6) reported the preparation of a series of stilbene and stilbenediol derivatives (Table I) containing



*© 1981, American Pharmaceutical Association*

rections, the overall plasma clearance of caffeine was virtually unaffected by acute aminophylline administration.

The need for establishing dosage guidelines for safe intravenous administration of theophylline has been stressed (22). Theophylline has a narrow therapeutic index of 10–20 μg/ml, and the risk of toxicity, including seizures and death, increases as serum concentrations exceed this range. In asthmatic patients receiving chronic theophylline therapy, routine monitoring of serum drug levels is recommended. Interactions of theophylline with other exogenous compounds may influence the therapeutic outcome of this drug. For example, methylxanthines such as caffeine and theobromine, present in various common beverages and foods, were shown to inhibit theophylline metabolism in humans (9). In the present study, the theophylline half-life in beagle dogs actually decreased after multiple doses of caffeine, probably due to enzyme induction by the latter. Nevertheless, plasma theophylline levels were elevated and sustained as a result of metabolic conversion of administered caffeine to theophylline.

These observations may suggest the need to reduce theophylline maintenance doses in asthmatics who are chronic coffee drinkers. Caution is also warranted in treatment with theophylline in breast-fed infants, who may be exposed to methylxanthines in the milk (23, 24). Recently it has become evident that theophylline is biotransformed to caffeine by *N*-methylation in the premature newborn infant (25–28), which further complicates theophylline–caffeine interactions. This metabolic pathway was not observed in adult humans (25) and dogs in the present study.

## REFERENCES


(1) J. W. Jenne, H. T. Nagasawa, and R. D. Thompson, *Clin. Pharmacol. Ther.*, **19,** 375 (1976).

(2) P. W. Trembath and S. W. Boobis, *ibid.*, **26,** 654 (1979).

(3) P. G. Welling, L. L. Lyons, W. A. Craig, and G. A. Trochta, *ibid.*, **17,** 475 (1975).

(4) P. G. Welling, J. Domoradzki, J. A. Sims, and C. E. Reed, *J. Clin. Pharmacol.*, **16,** 43 (1976).

(5) K. M. Piafsky, D. S. Sitar, and R. I. Ogilvie, *Clin. Pharmacol. Ther.*, **22,** 336 (1977).

(6) R. I. Ogilvie, *Clin. Pharmacokinet.*, **3,** 267 (1978).

(7) J. J. Grygiel, L. M. H. Wing, J. Farkas, and D. J. Birkett, *Clin. Pharmacol. Ther.*, **26,** 660 (1979).

(8) S. Vozeh, J. R. Powell, G. C. Cupit, S. Riegelman, and L. B. Sheiner, *ibid.*, **27,** 194 (1980).

(9) T. J. Monks, J. Caldwell, and R. L. Smith, *ibid.*, **26,** 513 (1979).

(10) C. Mitoma, T. J. Sorich, II, and S. E. Neubauer, *Life Sci.*, **7,** 145 (1968).

(11) K. H. Valia, C. A. Hartman, N. Kucharczyk, and R. D. Sofia, *J. Chromatogr.*, **221,** 170 (1980).

(12) M. Gibaldi and D. Perrier, "Pharmacokinetics," Dekker, New York, N.Y., 1975, pp. 52, 110.

(13) F. L. S. Tse and P. G. Welling, *J. Pharm. Sci.*, **66,** 1751 (1977).

(14) C. M. Metzler, G. L. Elfring, and A. J. McEwen, *Biometrics*, **30,** 562 (1974).

(15) S. Sved, R. D. Hossie, and I. J. McGilveray, *Res. Commun. Chem. Pathol. Pharmacol.*, **13,** 185 (1976).

(16) J. Descotes, J. L. Brazier, M. Ollagnier, and J.-Cl. Evreux, *Thérapie*, **34,** 619 (1979).

(17) J. P. Rosen, M. Danish, M. C. Ragni, C. L. Saccar, S. J. Yaffe, and H. I. Lecks, *Pediatrics*, **64,** 248 (1979).

(18) I. Starr, C. J. Gamble, A. Margolies, J. S. Donal, Jr., N. Joseph, and E. Eagle, *J. Clin. Invest.*, **16,** 799 (1937).

(19) R. Koysooko, E. F. Ellis, and G. Levy, *Clin. Pharmacol. Ther.*, **15,** 454 (1974).

(20) K. F. Simons, F. E. R. Simons, C. J. Briggs, and L. Lo, *J. Pharm. Sci.*, **68,** 252 (1979).

(21) J. Axelrod and J. Reichenthal, *J. Pharmacol. Exp. Ther.*, **107,** 519 (1953).

(22) "FDA Drug Bulletin," vol. 10, no. 1, Food and Drug Administration, Rockville, Md., Feb. 1980, pp. 4–6.

(23) B. H. Resman, H. P. Blumenthal, and W. J. Jusko, *J. Pediatr.*, **91,** 477 (1977).

(24) J. T. Wilson, R. D. Brown, D. R. Cherek, J. W. Dailey, B. Hilman, P. C. Jobe, B. R. Manno, J. E. Manno, H. M. Redetzki, and J. J. Stewart, *Clin. Pharmacokinet.*, **5,** 1 (1980).

(25) C. Bory, P. Baltassat, M. Porthault, M. Bethenod, A. Frederich, and J. V. Aranda, *J. Pediatr.*, **94,** 988 (1979).

(26) H. S. Bada, N. N. Khanna, S. M. Somani, and A. A. Tin, *ibid.*, **94,** 993 (1979).

(27) M. J. Boutroy, P. Vert, R. J. Royer, P. Monin, and M. J. Royer-Morrot, *ibid.*, **94,** 996 (1979).

(28) F. E. R. Simons, F. R. Friesen, and K. J. Simons, *Am. J. Dis. Child.*, **134,** 39 (1980).


# Nonsteroidal Estrogens and Antiestrogens: Biological Activity of Cyclopropyl Analogs of Stilbene and Stilbenediol


**J. THOMAS PENTO *x, ROBERT A. MAGARIAN *, ROBERT J. WRIGHT *, M. MARGARET KING ‡, and ERIC J. BENJAMIN ***



Received September 25, 1979, from the **College of Pharmacy, University of Oklahoma, Health Sciences Center, Oklahoma City, OK 73190*, and the ‡*Oklahoma Medical Research Foundation, Oklahoma City, OK 73104.* Accepted for publication November 30, 1979.



**Abstract** □ The estrogenic, antiestrogenic, and receptor binding activity of a series of cyclopropyl analogs of stilbene and stilbenediol were determined using the uterotropic assay in the mouse and the receptor binding assay with rat uterine cytosol. One compound, 1,1-dichloro-*cis*-2,3-diphenylcyclopropane (II), displayed antiestrogenic activity *in vivo* with a low affinity for the estrogen receptor *in vitro* and showed tumor remission activity on 7,12-dimethylbenz(*a*)anthracene-induced estrogen-dependent rat mammary tumors. Compounds VIII, IV, and V (in that order) exhibited the greatest estrogenic activity in the mouse and the greatest receptor binding activity *in vitro*. Compound VIII exhibited antifertility activity in the mouse.



**Keyphrases** □ Estrogenic activity—cyclopropyl analogs of stilbene and stilbenediol, mice □ Antiestrogenic activity—cyclopropyl analogs of stilbene and stilbenediol, mice □ Receptor binding activity—cyclopropyl analogs of stilbene and stilbenediol □ Stilbene and stilbenediol—cyclopropyl analogs, pharmacological activity in mice and rats


Various rigid ring systems have been used to lock functional groups into desired conformations to study receptor interactions (1, 2). The cyclopropane ring is a relatively new structure to be employed synthetically to produce a fixed stereochemical configuration with minimal steric interference in potential medicinal agents (3–5). Magarian and Benjamin (6) reported the preparation of a series of stilbene and stilbenediol derivatives (Table I) containing



*© 1981, American Pharmaceutical Association*

**Table I—Estrogenic, Antiestrogenic, and Receptor Binding Activity of the Cyclopropyl Analogs**

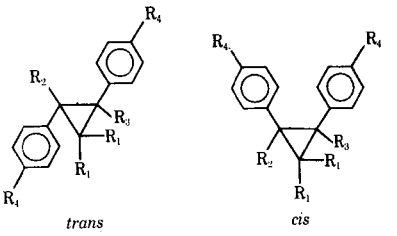


| Compound | Configuration | $R_1$ | $R_2$ | $R_3$ | $R_4$ | Relative Uterotropic Activity[a] | Antiestrogenic Activity[b] | Relative Receptor Binding Activity[c] |
|---|---|---|---|---|---|---|---|---|
| Estradiol | | | | | | 100 | —[d] | 100 |
| I | *trans* | Cl | H | H | H | —[d] | —[d] | 0.02 |
| II | *cis* | Cl | H | H | H | —[d] | 36 μg | 0.0086 |
| III | *trans* | H | $C_2H_5$ | $C_2H_5$ | $OCH_3$ | —[d] | —[d] | 0.4 |
| IV | *trans* | Cl | $C_2H_5$ | $C_2H_5$ | OH | 1.63 | —[e] | 48.6 |
| V | *trans* | Cl | $C_2H_5$ | $C_2H_5$ | $OCOCH_3$ | 1.57 | —[e] | 3.6 |
| VI | *trans* | Cl | H | H | $OCH_3$ | —[d] | —[d] | 0.0038 |
| VII | *trans* | Cl | $C_2H_5$ | $C_2H_5$ | $OCH_3$ | —[d] | —[d] | 0.049 |
| VIII | *trans* | H | $C_2H_5$ | $C_2H_5$ | OH | 2.55 | —[e] | 9.1 |
| IX | *cis* | H | H | H | H | —[d] | —[d] | 0.0045 |
| X | *trans* | H | H | H | H | —[d] | —[d] | 0.0064 |

[a] Activity expressed as a percentage of estradiol activity according to Bliss (10). [b] Dose of analog that would produce a 50% reduction in the uterotropic response to 0.04 μg of estradiol. [c] (Concentration of estradiol that displaced 70% [$^3$H]estradiol/concentration of analog that displaced 70% [$^3$H]estradiol) × 100. [d] No response. [e] Not tested.

the cyclopropyl moiety in place of the double bond to produce conformationally rigid, isomeric structures with substituent groups above and below the plane of the cyclopropane ring. This configuration is in contrast to the coplanar structure of the parent series, such as in the stilbenediol derivative *trans*-diethylstilbestrol, where resonance interactions and minimal steric interference tend to hold the two aromatic rings and connecting ethylene carbons in the same plane. It was anticipated that this new stereochemical conformation in the stilbene and stilbenediol series might produce antiestrogenic activity by preventing estrogens from expressing their full effects on estrogen target tissue and thus could be used to probe estrogen receptor events (6).

These compounds were studied to provide additional insight into the steric requirements of the ligand that binds to the estrogen receptor since the molecular shape of the ligand determines antiestrogenic activity (7). They also served as a basis for obtaining structural information for the design of new antiestrogens. The present study examined the cyclopropyl analogs not only for estrogenic, antiestrogenic, and receptor binding activity but also for antifertility and antineoplastic activities.

## EXPERIMENTAL

**Uterotropic Assay for Estrogenic and Antiestrogenic Activity**—The assay for estrogenic activity was a modification (8) of the method of Rubin *et al.* (9). Immature Swiss–Webster mice, 10–14 g (~21 days old), were distributed randomly into groups of five or six mice each. Estradiol and the test compounds were dissolved separately in sesame oil and administered subcutaneously in a volume of 0.1 ml. Control animals were treated with the same volume of sesame oil alone.

All animals were treated daily for 3 consecutive days. On the 4th day, the animals were sacrificed; the uteri were dissected carefully, blotted lightly, and weighed to the nearest 0.1 mg. Body weights also were recorded. Estradiol was used in the dosage range of 0.01–0.04 μg (total dose) as the assay standard. Each cyclopropyl analog was examined over a dosage range of 1–25 μg (total dose).

The uterotropic assay also was used to evaluate the antiestrogenic activity of the test compounds that did not produce an estrogenic response in the previous assay. The antiestrogenic assay was conducted as described for estrogenic activity, except that each animal in the cyclopropyl analog treatment groups received a standard stimulating dose of estradiol (0.04 μg). The test compounds and estradiol were administered separately at different injection sites to minimize possible physical interaction or reduce absorption of either compound. Antiestrogenic activity was measured as a decrease in the estradiol-stimulated uterotropic response in groups that received both the test compound and estradiol as compared to a group treated with estradiol alone.

A line of best fit was plotted for each compound that produced an estrogenic or antiestrogenic response. Regression analysis was used to calculate each line. The slope of the response to each analog was compared to the slope of the estradiol response to determine parallelism. The relative uterotropic activity of each compound was expressed as a percentage of the estradiol activity according to the method of Bliss (10).

**Histological Preparation and Examination**—Mouse uterine tissue was fixed in 10% formaldehyde, embedded in paraffin, sectioned on a microtome, and stained with hematoxylin–eosin. Slides were examined with a compound light microscope, and measurements were made on each cross section at several levels along the uterine horn. These measurements included: (*a*) the total uterine horn diameter or thickness at two points, and (*b*) the endometrial thickness at two points as measured from the endometrial–myometrial border to the maximum invagination of the endometrium into the uterine horn lumen. Photomicrographs of uterine horn cross sections and epithelial linings were taken with a camera[1] attached to a compound light microscope.

**Antifertility Assay**—Adult (8-week-old) Swiss–Webster mice were used in the antifertility assay, which was a modification of the method of Wani *et al.* (11). The female mice were randomized into dosage groups containing eight mice per group. The test compounds were dissolved in sesame oil and administered by subcutaneous injection in a total volume of 0.1 ml. The control group received an equal volume of sesame oil.

The female mice were dosed daily for 23 consecutive days. Males of known fertility were caged with the females (one male per four females) from treatment Days 8 to 20. During this period, the females were checked for vaginal plugs; body weights were recorded weekly. The females were sacrificed on Day 27, and the uterine horns were examined for the number of fetuses and any gross malformation. In addition, the fetal weights were recorded.

**Antineoplastic Assay**—In this study, 50-day-old female Sprague–Dawley rats received a single oral dose of 10 mg of 7,12-dimethylbenz(*a*)anthracene dissolved in 1 ml of corn oil *via* a stomach tube. The animals were examined and palpated for tumors at weekly intervals until tumors were detected. Animals that displayed tumors of 1–3 cm in their largest diameter were included. The rats were distributed into experimental groups on the basis of the total tumor volume and number so that

[1] Polaroid Land Instrument ED-10.

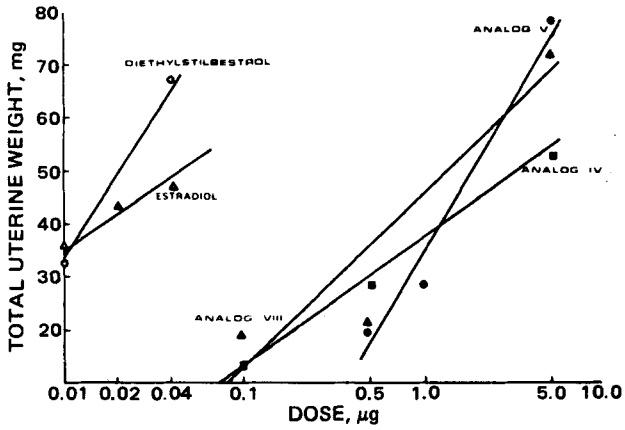


**Figure 1**—*Uterotropic activity of the active cyclopropyl analogs. Each point represents the mean uterine weight from five or six mice.*

each group contained approximately the same mean tumor volume and mean number at the beginning of treatment. Rats in the ovariectomized group had both ovaries removed 1 day prior to treatment.

Analog II was dissolved in olive oil at a concentration of 1.2 mg/ml. The treatment group received 0.6 mg of II (0.5 ml sc) three times per week, and the control group received an equal volume of olive oil. The dose of II was doubled after the 3rd week of therapy. Tumor size was determined twice weekly in all groups using a vernier caliper to measure the major and minor diameters of each tumor. Tumor volume was calculated based on an ellipsoid tumor shape ($V = 4/3\pi r_1^2 r_2$, where $r_1$ is the minor tumor radius) (12).

**Receptor Binding Assay**—A modification of the competitive receptor binding assay method of Korenman was used (13). Uteri were removed from female Sprague–Dawley rats weighing ~250 g. The uteri were cleaned of connective tissue and homogenized in 5 volumes (w/v) of ice-cold tromethamine buffer containing 0.02 *M* tromethamine hydrochloride, 0.0015 *M* disodium ethylenediaminetetraacetate, and 0.25 *M* sucrose; the pH was adjusted to 7.4. The tissue was homogenized using a motor-driven ground-glass tissue homogenizer placed in an ice water bath. The homogenate was centrifuged at 100,000×*g* for 1 hr at 4° using a swinging bucket rotor[2] on an ultracentrifuge[3].

The supernate (cytosol) was used immediately after preparation in the receptor binding assay. Incubations were conducted for 20 hr at 4° in a total volume of 0.5 ml of tromethamine buffer containing 100–150 μl of uterine cytosol, 0.01 μCi of 2,4,6,7-(*n*)-[$^3$H]17β-estradiol[4] (327 mCi/mg), and various concentrations of the test compounds. Each test compound was assayed at three concentrations over a range of $10^{-4}$–$10^{-6}$ *M* for the cyclopropyl analogs and of $10^{-7}$–$10^{-9}$ *M* for the estradiol standard. The test compounds were dissolved in ethanol; in all cases, the final ethanol concentration was <2% of the incubation medium.

At the end of incubation, the cytosol-bound [$^3$H]estradiol was separated from the unbound [$^3$H]estradiol by the addition of 0.5 ml of dextran-coated charcoal solution (tromethamine buffer containing 0.05% dextran 70 and 0.5% activated charcoal[5]). The assay tubes were vortexed and centrifuged at 500×*g* for 15 min. The [$^3$H]estradiol concentration of a 0.5-ml aliquot of the supernate was determined by liquid scintillation spectrometry using an aqueous compatible scintillation medium[6]. Counting times were adjusted automatically to obtain a counting error of <1% using a liquid scintillation counter[7]. The [$^3$H]estradiol displacement for each test compound was determined by linear regression analysis and plotted graphically. The relative receptor binding activity of each analog was determined using the following ratio: (concentration of unlabeled estradiol producing 70% displacement of [$^3$H]estradiol/concentration of cyclopropyl analog producing 70% displacement of [$^3$H]estradiol) × 100.

## RESULTS

Each compound was tested initially in the uterotropic assay. Compounds IV, V, and VIII produced uterotropic response curves that were

[2] Beckman model SW 27.1.
[3] Beckman model L5-65.
[4] Amersham Corp.
[5] Norite A, Sigma Chemical Co.
[6] Aquasol-2, New England Nuclear.
[7] Beckman model LS-100C.

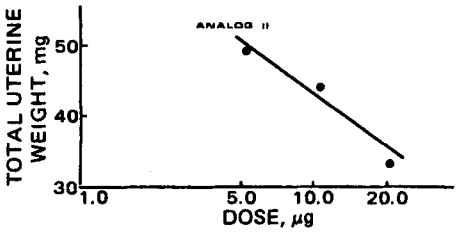


**Figure 2**—*Antiestrogenic activity of II. Each point represents the mean uterine weight from five or six mice.*

parallel to the estradiol curve (Fig. 1). The relative estrogenic activity of these analogs was VIII > IV > V. These compounds produced 1.5–2.5% of the uterotropic response of estradiol on a molecular weight basis (Table I). Diethylstilbestrol, a synthetic nonsteroidal estrogen containing the stilbenediol moiety, was equipotent to estradiol in the uterotropic assay (Fig. 1). Cyclopropyl analogs that displayed no estrogenic activity in the uterotropic assay were tested further for antiestrogenic activity. Only II produced an antiestrogenic response (Fig. 2 and Table I).

Since the uterotropic response is a nonspecific measure of estrogenic activity, the uteri were examined histologically to confirm the estrogenic nature of the uterotropic response. Estradiol and the cyclopropyl analogs (IV and VIII) significantly ($p < 0.001$) increased uterine diameter and endometrial thickness, which represented a specific estrogenic response (Table II).

The cyclopropyl analogs were tested for receptor binding activity and compared to the estradiol standard. All of the analogs were capable of displacing [$^3$H]estradiol from the estrogen receptor. However, IV, VIII, and V (in that order) displayed the greatest binding activity, from 4 to 50% of the receptor binding activity produced by estradiol on a molecular weight basis (Fig. 3 and Table I).

The estrogen (VIII) and the antiestrogen (II) were tested for antifertility activity using estradiol as a standard antifertility agent. Both estradiol and VIII exhibited good antifertility activity (Table III). The antiestrogen (II) produced no antifertility effect; however, one female in this treatment group had pups that were markedly underdeveloped, with a total fetal weight of 0.9 g/10 pups as compared to the group mean of 7.5 g/10.3 pups.

The antitumor activity of the antiestrogen (II) was examined using the 7,12-dimethylbenz(*a*)anthracene-induced mammary tumor assay in the rat. The tumor data were expressed as both the tumor volume per animal (Fig. 4) and the tumor number per animal (Fig. 5). Ovariectomy produced a slightly greater reduction in tumor volume during the first 3 weeks of treatment, while tumor volume in the treated group remained essentially unchanged. Castration has been reported to cause regression of 7,12-dimethylbenz(*a*)anthracene-induced tumors (14) and was employed in the present study to verify the estrogen-dependent nature of the tumors in the rats. The number of tumors per animal increased in all three groups

**Table II—Histological Examination of Uterine Tissue**

| Compound | Dose, μg | Uterine Diameter (Mean ± *SD*), mm | Endometrial Thickness (Mean ± *SD*), mm |
|---|---|---|---|
| Control | 0.0 | 0.56 ± 0.15 | 0.16 ± 0.04 |
| Estradiol | 0.04 | 1.42 ± 0.24[a] | 0.49 ± 0.15[a] |
| IV | 5.0 | 1.53 ± 0.19[a] | 0.48 ± 0.12[a] |
| VIII | 5.0 | 1.30 ± 0.15[a] | 0.40 ± 0.07[a] |

[a] Significantly different from control ($p < 0.001$).

**Table III—Antifertility Activity of Active Estrogenic and Antiestrogenic Cyclopropyl Analogs**

| Compound | Daily Dose, μg | Animals per Pregnant Group | Implants per Mouse (Mean ± *SD*) | Fetal Weight per Group (Mean ± *SD*), g |
|---|---|---|---|---|
| Control | 0.0 | 6/8 | 11.2 ± 3.25 | 7.5 ± 3.33 |
| Estradiol | 0.033 | 0/8 | 0 | —[a] |
| II | 16.7 | 6/8 | 10.3 ± 1.86 | 7.5 ± 5.07 |
| VIII | 4.2 | 0/8 | 0 | —[a] |

[a] No response.

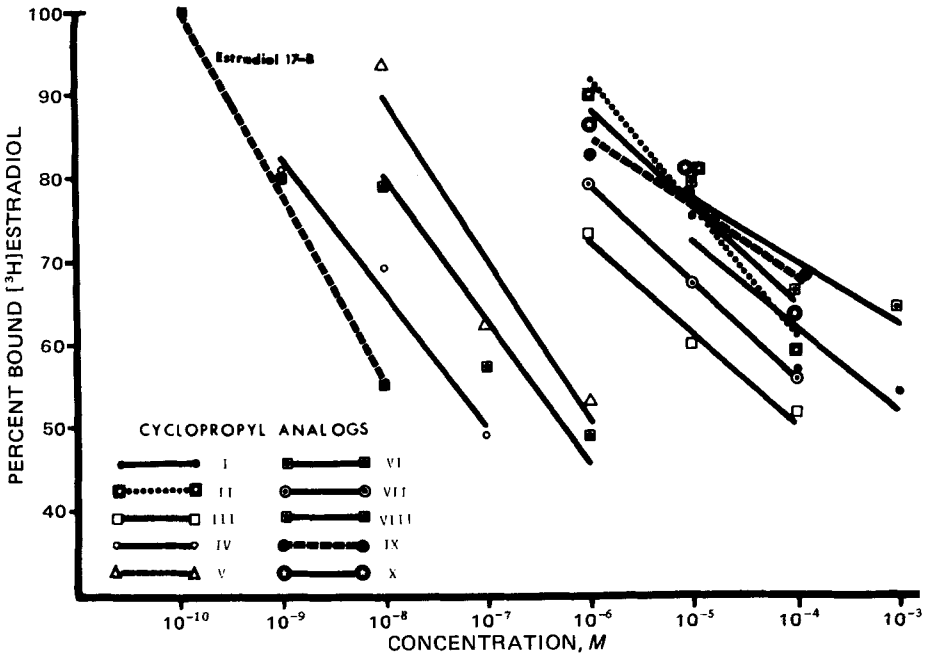


**Figure 3**—*Uterine receptor binding activity of the cyclopropyl analogs. Each point represents the mean of two or three separate determinations.*

during the treatment period; however, both ovariectomy and II reduced tumor incidence to approximately the same extent as compared to the control group. The total weight gain during treatment in the control and treated groups was not significantly different, suggesting that the antitumor activity of II was not the result of a general toxic effect of the compound. At the end of treatment, all animals were sacrificed, and the tumors were verified histologically to be adenocarcinomas.

## DISCUSSION

The objective of this study was to compare the pharmacological effects of the various stilbene and stilbenediol analogs in which the cyclopropyl moiety locked functional groups into a fixed stereochemical configuration to examine structure–activity relationships. Analogs included 1,1-dichloro-*cis*- and *trans*-2,3-diarylcyclopropanes and *trans*-2,3-diarylcyclopropanes along with *p*-hydroxyphenyl, *p*-acetoxyphenyl, and *p*-methoxyphenyl substituents and combinations with 2,3-diethyl substituents. Other compounds include reduced analogs (without the *gem*-dichloro groups) of *cis*- and *trans*-1,2-dicyclopropanes and *trans*-1,2-diarylcyclopropanes with *p*-methoxyphenyl and *p*-hydroxyphenyl groups in combination with 2,3-diethyl substituents.

The cyclopropyl moiety in place of the double bond in stilbene and stilbenediol produces a conformationally rigid, planar structure with group attachments above and below the cyclopropyl ring, as compared to the coplanar configuration of stilbene and stilbenediol. The present study indicates that the cyclopropyl analogs retain the ability to bind to the estrogen receptor and produce an estrogenic response; however, estrogenic activity is significantly reduced. Further estrogenic and receptor binding activity is modified by various functional group attachments and conformation of the cyclopropyl derivative. Accordingly, the phenyl rings in the cyclopropyl analogs are not in the same plane, and the hydrophobic attachment to the receptor is not expected to be as great as in the olefin analogs, thereby reducing binding affinity between the ligand and the receptor.

An examination of Table I reveals that the test compounds that produce estrogenic activity *in vivo* contain either *trans*-hydroxyphenyl groups (IV and VIII) or *trans*-acetoxyphenyl groups in combination with *trans*-ethyl groups (V). The cyclopropyl derivative of diethylstilbestrol (VIII) was the most potent estrogenic analog *in vivo;* IV, the *gem*-dichloro derivative, and V, the *trans*-acetoxyphenyl-*gem*-dichloro derivative, were approximately equipotent and less active than VIII. The *gem*-dichloro moiety thus appears to decrease estrogenic activity *in vivo*. The acetate group was reported to be hydrolyzed to the hydroxyl group in the body (11). Consequently, V may be metabolized to IV *in vivo*. However, both the hydroxyl and acetate groups are capable of hydrogen bonding, which is known to be important for significant receptor interaction and initiation of the estrogenic response (15).

Only the *gem*-dichloro cyclopropyl analog of *cis*-stilbene (II) displayed

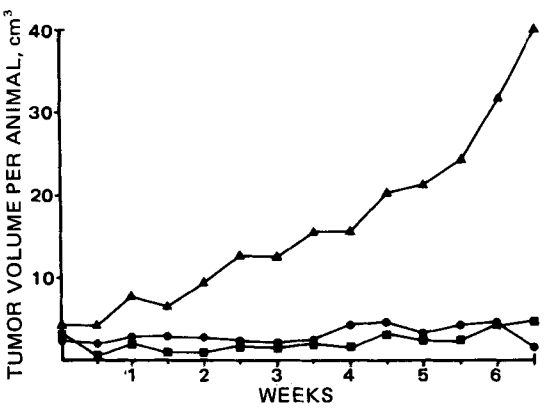


**Figure 4**—*Influence of II and ovariectomy on 7,12-dimethylbenz(a)anthracene-induced mammary tumor volume. The control group contained four rats, the II-treated group contained five rats, and the ovariectomized group contained three rats. Each point represents the mean tumor volume per animal. Key:* ▲, *control;* ●, *treated; and* ■, *ovariectomized.*

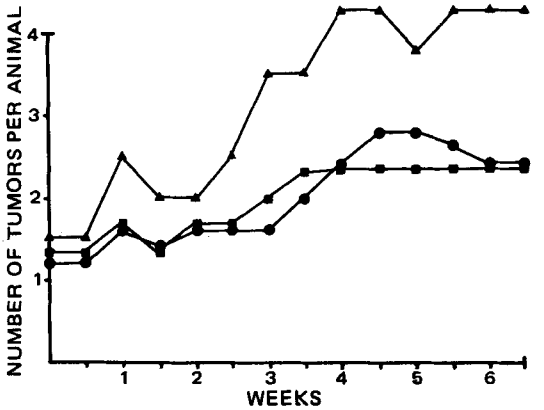


**Figure 5**—*Influence of II and ovariectomy on 7,12-dimethylbenz(a)anthracene-induced mammary tumor number per animal. The control group contained four rats, the II-treated group contained five rats, and the ovariectomized group contained three rats. Each point represents the mean tumor number per animal. Key:* ▲, *control;* ●, *treated; and* ■, *ovariectomized.*

significant antiestrogenic activity *in vivo*. Thus, the *cis*-configuration and *gem*-dichloro substitution appear to be important for antiestrogenic activity in the cyclopropyl series since neither the *trans*-isomer (I) nor the reduced compound (IX) was antiestrogenic in this study.

An examination of receptor binding activity in Fig. 3 and Table I indicates that various structural modifications significantly alter estrogen binding activity. The structure–activity relationships revealed by this series of cyclopropyl analogs are:

1. Replacement of hydroxyl groups with *O*-methyl groups decreases receptor binding activity (compare III with VIII and IV with VII). The importance of free hydroxyl groups for the production of estrogenic activity was demonstrated with other stilbenediol derivatives (16, 17).
2. The absence of *trans*-ethyl groups decreases receptor binding activity (compare VI with VII).
3. The *trans*-configuration produces a slightly greater binding affinity than the *cis*-configuration (compare I with II and IX with X).
4. The *gem*-dichloro substitution generally increases receptor binding activity (compare I with X, IV with VIII, and II with IX). However, the *gem*-dichloro substitution together with *p*-methoxy substitution decreases binding affinity (compare III with VII), perhaps due to a steric interaction of these bulky groups that interfere with access to the receptor site.

Receptor binding activity paralleled *in vivo* estrogenic activity in this series of compounds, except VIII, which displayed the most potent estrogenic activity *in vivo* and the second greatest receptor affinity *in vitro*. This result may be explained by the fact that receptor binding and the initiation of an estrogenic response are two separate events and have been dissociated in the *in vitro* receptor binding assay due to the isolation of the receptor complex. Korenman (13) demonstrated previously that the relative binding affinity of steroidal estrogens paralleled uterotropic activity.

It is difficult to make structure–activity conclusions based on this limited series of analogs. Other members of the cyclopropyl series are being synthesized and evaluated for biological activity. However, the information obtained from this study will guide the design of other members of this series. It appears from the results that the *gem*-dichloro analogs with *cis*-phenyl rings hold the greatest promise for antiestrogenic activity.

This study also indicates that the cyclopropyl analogs of stilbene and stilbenediol may become useful in the treatment of estrogen-dependent tumors and as potential antifertility agents. Antifertility agents with fewer side effects and more effective antineoplastic therapy for breast and uterine cancer clearly are needed. However, synthesis of the complete series of cyclopropyl analogs and thorough evaluation of these compounds will be required. Thus, the design, development, and biological evaluation of these potential therapeutic agents are in progress.

## REFERENCES


(1) E. E. Smissman, W. L. Nelson, J. B. La Pidus, and J. L. Day, *J. Med. Chem.*, **9**, 458 (1966).

(2) P. D. Armstrong, J. G. Cannon, and J. P. Long, *Nature*, **220**, 65 (1968).

(3) A. Burger, in "Progress in Drug Research," vol. 15, E. Jucker and A. Birkhauser, Eds., Birkhäuser, Basel, Switzerland, 1971.

(4) J. G. Cannon, *J. Med. Chem.*, **13**, 1037 (1970).

(5) *Ibid.*, **15**, 71 (1972).

(6) R. A. Magarian and E. J. Benjamin, *J. Pharm. Sci.*, **64**, 1626 (1975).

(7) V. C. Jordan, C. J. Dix, K. E. Naylor, G. Prestwich, and L. Rowsby, *J. Toxicol. Environ. Health*, **4**, 363 (1978).

(8) J. T. Pento, R. J. Wright, R. A. Magarian, and A. F. Hoge, *J. Endocrinol.*, **78**, 287 (1978).

(9) B. L. Rubin, A. S. Dorfman, L. Black, and R. I. Dorfman, *Endocrinology*, **49**, 429 (1951).

(10) C. I. Bliss, "The Statistics of Bioassay," Academic, New York, N.Y., 1952.

(11) M. C. Wani, D. H. Rector, H. D. Christensen, G. L. Kimmel, and C. D. Cook, *J. Med. Chem.*, **18**, 982 (1975).

(12) E. R. De Sombre and L. Y. Arbogast, *Cancer Res.*, **34**, 1971 (1974).

(13) S. G. Korenman, *Steroids*, **13**, 163 (1969).

(14) D. P. Griswald and C. H. Green, *Cancer Res.*, **30**, 819 (1970).

(15) L. Terenius, *Acta Pharmacol. Toxicol.*, **31**, 449 (1972).

(16) E. C. Dodds, *Nature*, **142**, 34 (1938).

(17) M. Rubin and H. Wishinsky, *J. Am. Chem. Soc.*, **66**, 1948 (1944).


## ACKNOWLEDGMENTS


The tumor study was supported in part by Grant ES 01789 to M. M. King.

The authors gratefully acknowledge the technical assistance of Annette Owens, Robert Heffington, Fred Horton, and John Johnson.


# First-Pass Metabolism of Ethinyl Estradiol in Dogs and Rats


**S. HIRAI, A. HUSSAIN ˣ, M. HADDADIN, and R. B. SMITH ***



Received May 9, 1980, from the *College of Pharmacy, University of Kentucky, Lexington, KY 40506.* Accepted for publication September 17, 1980. *Present address: The Upjohn Company, Kalamazoo, MI 49001.



**Abstract** □ The contraceptive steroid ethinyl estradiol was extensively metabolized when given orally in solution to dogs. It was thought at first that metabolism occurred exclusively in the liver. However, use of standard equations to predict the oral bioavailability of drugs known to be metabolized by hepatic first pass resulted in significantly higher values than those obtained experimentally. To rationalize the data and to determine whether ethinyl estradiol also is metabolized in the gut wall during absorption, metabolism in rats was studied. The drug was administered in solution intraduodenally, intraportally, and intravenously as a bolus and by first-order infusion. The results indicate that, in rats, 40% of the drug is metabolized by the gut wall and 79% of the drug in the portal blood is metabolized by the liver after intraduodenal administration.



**Keyphrases** □ Ethinyl estradiol—first-pass metabolism in dogs and rats, gut wall metabolism in rats □ Bioavailability—ethinyl estradiol, first-pass metabolism in rats and dogs, gut wall metabolism in rats □ Metabolism—ethinyl estradiol in rats and dogs, first-pass metabolism and possible gut wall metabolism


The natural contraceptive steroids such as progesterone and estradiol are not effective orally due to their extensive metabolism in the GI tract during absorption and to hepatic first-pass metabolism (1, 2). Although introduction of the ethinyl group at the 17α-position renders the compound stable toward metabolic attack by 17α-hydroxylase, ethinyl estradiol, like estradiol, contains a phenolic hydroxyl group at the 3-position that is subject to sulfate and


*0022-3549/81/0400-0403$01.00/0*


*© 1981, American Pharmaceutical Association*

significant antiestrogenic activity *in vivo*. Thus, the *cis*-configuration and *gem*-dichloro substitution appear to be important for antiestrogenic activity in the cyclopropyl series since neither the *trans*-isomer (I) nor the reduced compound (IX) was antiestrogenic in this study.

An examination of receptor binding activity in Fig. 3 and Table I indicates that various structural modifications significantly alter estrogen binding activity. The structure–activity relationships revealed by this series of cyclopropyl analogs are:

1. Replacement of hydroxyl groups with *O*-methyl groups decreases receptor binding activity (compare III with VIII and IV with VII). The importance of free hydroxyl groups for the production of estrogenic activity was demonstrated with other stilbenediol derivatives (16, 17).
2. The absence of *trans*-ethyl groups decreases receptor binding activity (compare VI with VII).
3. The *trans*-configuration produces a slightly greater binding affinity than the *cis*-configuration (compare I with II and IX with X).
4. The *gem*-dichloro substitution generally increases receptor binding activity (compare I with X, IV with VIII, and II with IX). However, the *gem*-dichloro substitution together with *p*-methoxy substitution decreases binding affinity (compare III with VII), perhaps due to a steric interaction of these bulky groups that interfere with access to the receptor site.

Receptor binding activity paralleled *in vivo* estrogenic activity in this series of compounds, except VIII, which displayed the most potent estrogenic activity *in vivo* and the second greatest receptor affinity *in vitro*. This result may be explained by the fact that receptor binding and the initiation of an estrogenic response are two separate events and have been dissociated in the *in vitro* receptor binding assay due to the isolation of the receptor complex. Korenman (13) demonstrated previously that the relative binding affinity of steroidal estrogens paralleled uterotropic activity.

It is difficult to make structure–activity conclusions based on this limited series of analogs. Other members of the cyclopropyl series are being synthesized and evaluated for biological activity. However, the information obtained from this study will guide the design of other members of this series. It appears from the results that the *gem*-dichloro analogs with *cis*-phenyl rings hold the greatest promise for antiestrogenic activity.

This study also indicates that the cyclopropyl analogs of stilbene and stilbenediol may become useful in the treatment of estrogen-dependent tumors and as potential antifertility agents. Antifertility agents with fewer side effects and more effective antineoplastic therapy for breast and uterine cancer clearly are needed. However, synthesis of the complete series of cyclopropyl analogs and thorough evaluation of these compounds will be required. Thus, the design, development, and biological evaluation of these potential therapeutic agents are in progress.

## REFERENCES


(1) E. E. Smissman, W. L. Nelson, J. B. La Pidus, and J. L. Day, *J. Med. Chem.*, **9**, 458 (1966).

(2) P. D. Armstrong, J. G. Cannon, and J. P. Long, *Nature*, **220**, 65 (1968).

(3) A. Burger, in "Progress in Drug Research," vol. 15, E. Jucker and A. Birkhauser, Eds., Birkhäuser, Basel, Switzerland, 1971.

(4) J. G. Cannon, *J. Med. Chem.*, **13**, 1037 (1970).

(5) *Ibid.*, **15**, 71 (1972).

(6) R. A. Magarian and E. J. Benjamin, *J. Pharm. Sci.*, **64**, 1626 (1975).

(7) V. C. Jordan, C. J. Dix, K. E. Naylor, G. Prestwich, and L. Rowsby, *J. Toxicol. Environ. Health*, **4**, 363 (1978).

(8) J. T. Pento, R. J. Wright, R. A. Magarian, and A. F. Hoge, *J. Endocrinol.*, **78**, 287 (1978).

(9) B. L. Rubin, A. S. Dorfman, L. Black, and R. I. Dorfman, *Endocrinology*, **49**, 429 (1951).

(10) C. I. Bliss, "The Statistics of Bioassay," Academic, New York, N.Y., 1952.

(11) M. C. Wani, D. H. Rector, H. D. Christensen, G. L. Kimmel, and C. D. Cook, *J. Med. Chem.*, **18**, 982 (1975).

(12) E. R. De Sombre and L. Y. Arbogast, *Cancer Res.*, **34**, 1971 (1974).

(13) S. G. Korenman, *Steroids*, **13**, 163 (1969).

(14) D. P. Griswald and C. H. Green, *Cancer Res.*, **30**, 819 (1970).

(15) L. Terenius, *Acta Pharmacol. Toxicol.*, **31**, 449 (1972).

(16) E. C. Dodds, *Nature*, **142**, 34 (1938).

(17) M. Rubin and H. Wishinsky, *J. Am. Chem. Soc.*, **66**, 1948 (1944).


## ACKNOWLEDGMENTS


The tumor study was supported in part by Grant ES 01789 to M. M. King.

The authors gratefully acknowledge the technical assistance of Annette Owens, Robert Heffington, Fred Horton, and John Johnson.


# First-Pass Metabolism of Ethinyl Estradiol in Dogs and Rats


**S. HIRAI, A. HUSSAIN ˣ, M. HADDADIN, and R. B. SMITH ***



Received May 9, 1980, from the *College of Pharmacy, University of Kentucky, Lexington, KY 40506.* Accepted for publication September 17, 1980. *Present address: The Upjohn Company, Kalamazoo, MI 49001.



**Abstract** □ The contraceptive steroid ethinyl estradiol was extensively metabolized when given orally in solution to dogs. It was thought at first that metabolism occurred exclusively in the liver. However, use of standard equations to predict the oral bioavailability of drugs known to be metabolized by hepatic first pass resulted in significantly higher values than those obtained experimentally. To rationalize the data and to determine whether ethinyl estradiol also is metabolized in the gut wall during absorption, metabolism in rats was studied. The drug was administered in solution intraduodenally, intraportally, and intravenously as a bolus and by first-order infusion. The results indicate that, in rats, 40% of the drug is metabolized by the gut wall and 79% of the drug in the portal blood is metabolized by the liver after intraduodenal administration.



**Keyphrases** □ Ethinyl estradiol—first-pass metabolism in dogs and rats, gut wall metabolism in rats □ Bioavailability—ethinyl estradiol, first-pass metabolism in rats and dogs, gut wall metabolism in rats □ Metabolism—ethinyl estradiol in rats and dogs, first-pass metabolism and possible gut wall metabolism


The natural contraceptive steroids such as progesterone and estradiol are not effective orally due to their extensive metabolism in the GI tract during absorption and to hepatic first-pass metabolism (1, 2). Although introduction of the ethinyl group at the 17α-position renders the compound stable toward metabolic attack by 17α-hydroxylase, ethinyl estradiol, like estradiol, contains a phenolic hydroxyl group at the 3-position that is subject to sulfate and


*0022-3549/81/0400-0403$01.00/0*


*© 1981, American Pharmaceutical Association*

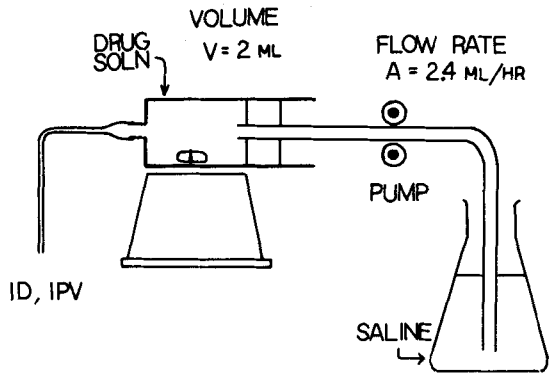


**Figure 1**—*Apparatus used to administer first-order infusion intraportally and intraduodenally.*

glucuronide conjugation in both humans and animals (3, 4).

In this study, the extent of the GI and hepatic first-pass metabolism of ethinyl estradiol in dogs and rats was investigated.

## EXPERIMENTAL

**Materials**—Radiolabeled ethinyl [6,7-$^3$H(N)]estradiol[1] (57.2 Ci/mmole) and nonradiolabeled ethinyl estradiol[2] were used as supplied. All other solvents and reagents were analytical reagent grade.

**Dog Experiment**—Three female beagle dogs, ~10 kg, were used. Prior to drug administration, the dogs were fasted overnight with water *ad libitum*. Then, 35 μg of ethinyl estradiol/dog (100 μCi/dog) was administered on separate occasions as an intravenous solution (dissolved in 1 ml of 5% ethanol–saline) and an oral solution (dissolved in 5 ml of 1% ethanol–water). The oral administration was followed immediately with 45 ml of water.

After administration, 3 ml of blood was withdrawn from the cubital vein periodically. After centrifugation, 0.1 ml of plasma was analyzed for total radioactivity, and 0.5 ml of plasma was analyzed for unchanged ethinyl estradiol according to the method described later. Urine was collected for up to 48 hr after administration, and 0.1-ml urine samples were analyzed for total radioactivity and unchanged steroid.

**Rat Experiment**—Male Sprague–Dawley rats, ~270 g, were anesthetized with pentobarbital sodium (50 mg/kg). For intraduodenal and intraportal administrations, the abdomen was opened through a midline incision. A polyethylene tube[3] was attached to one end of the shank of a 23-gauge needle[4], the other end of which was inserted directly into the duodenum or the hepatic portal vein and fixed with an adhesive agent[5]. The tube was extended to the exterior of the animal prior to closure of the abdomen with sutures. To collect periodic blood samples, the femoral artery was cannulated with a polyethylene tube (PE-50) attached to a syringe filled with heparinized saline (100 units/ml).

For bolus administration, 3.5 μg of ethinyl estradiol/kg was administered in 0.1 ml of 5% ethanol–saline into the femoral vein, the hepatic portal vein, or the duodenum. First-order infusions of the drug (3.5 μg/kg), simulating oral absorption, were given *via* the hepatic portal vein and the duodenum at a rate constant of 1.2 $hr^{-1}$ ($t_{1/2}$ = 0.58 hr) over 4 hr (Fig. 1) according to the method of Ronfeld and Benet (5). After drug administration, 0.2-ml samples of blood were removed periodically from the femoral artery and analyzed for unchanged steroid.

**Assays for Total Radioactivity and Unchanged Ethinyl Estradiol**—The total radioactive steroid in the plasma and urine was measured by diluting the samples directly with 10 ml of a commercial scintillant[6] and counting the radioactivity using a liquid scintillation spectrometer[7].

Unchanged ethinyl estradiol in plasma and urine was determined as follows. One milliliter of 0.01 *N* HCl was added to the sample, and the mixture was extracted with 6 ml of benzene–heptane (2:3 v/v). Five milliliters of the organic phase was transferred to the scintillation vial and evaporated to dryness with a nitrogen stream. The radioactivity was determined according to the procedure for the total radioactive steroid.

To confirm that only unchanged steroid was measured, the benzene–heptane extracts were concentrated by evaporation with a nitrogen stream and spotted on TLC silica gel HF precoated plates[8]. After development in three solvent systems (benzene–ethanol, 9:1 v/v; benzene–ethyl acetate, 4:1 v/v; and cyclohexane–acetone, 4:1 v/v), the plates were air dried and divided into 1-cm sections. Each section was scraped into 10 ml of scintillation cocktail and counted.

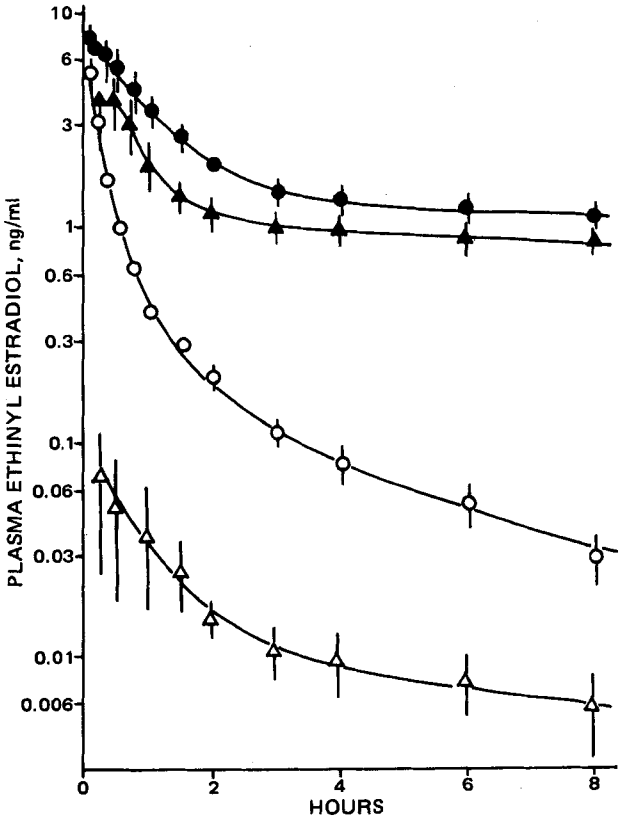


**Figure 2**—*Mean plasma levels of total activity and unchanged ethinyl estradiol for intravenous and oral solutions. Key:* ● *and* ▲, *total activity of intravenous and oral solutions, respectively; and* ○ *and* △, *unchanged ethinyl estradiol as intravenous and oral solutions, respectively.*

## RESULTS AND DISCUSSION

Plasma samples extracted with benzene–heptane after intravenous and oral administration of $^3$H-labeled ethinyl estradiol to rats and dogs resulted in a single spot corresponding to that of ethinyl estradiol in all TLC systems used. This finding indicates that benzene–heptane extracts only the unchanged fraction of ethinyl estradiol.

Plasma levels, as a function of time, of the total radioactivity and unchanged ethinyl estradiol after intravenous and oral administration of ethinyl estradiol solution to dogs is shown in Fig. 2. The plasma level of unchanged steroid following oral administration was significantly lower than that following intravenous administration, although the plasma level of total radioactivity following either administration was nearly the same. These data strongly indicate that ethinyl estradiol, given orally, is metabolized extensively during or after absorption in dogs. The half-lives of the initial and terminal phases of the plasma level curve of unchanged steroid after the intravenous administration were graphically estimated to be about 15 and 180 min, respectively.

Table I shows the urinary recovery of total radioactivity and unchanged ethinyl estradiol after intravenous and oral administration to dogs. The percent urinary recovery of total radioactivity and unchanged steroid after both routes of administration were almost the same. These urinary recovery data and the plasma total radioactivity data shown in Fig. 2

[1] New England Nuclear, Boston, Mass.
[2] Sigma Chemical Co., St. Louis, Mo.
[3] Clay Adams, Parsippany, N.J.
[4] Jelco Laboratories, Raritan, N.J.
[5] Super Glue-3, Woodhill Permatex, Cleveland, Ohio.
[6] Insta-Gel, Packard Instrument Co., Downers Grove, Ill.
[7] Model 3255 Tri-Carb, Packard Instrument Co., Downers Grove, Ill.
[8] Analtech Inc., Newark, Del.

**Table I—Urinary Recovery (Percent of Dose) of Total Radioactivity and Unchanged Ethinyl Estradiol after Intravenous and Oral Adminstration in Three Beagle Dogs [a]**

| Dog | Intravenous | | Oral | |
|---|---|---|---|---|
| | Total | Unchanged | Total | Unchanged |
| IJ96 | 18.5 | 0.54 | 21.2 | 0.32 |
| NJ06 | 22.3 | 0.38 | 17.6 | 0.21 |
| JO96 | 24.0 | 0.63 | 22.0 | 0.40 |
| Mean | 21.6 | 0.51 | 20.2 | 0.31 |
| ±*SE* | 1.6 | 0.07 | 1.3 | 0.05 |

[a] The urine collection period was 0–48 hr, and the dose was 35 μg/dog (100 μCi/dog).

suggest that the drug is completely absorbed from the GI tract. Based on the recovery of radioactivity, ethinyl estradiol was shown by Reed *et al.* (6) to be rapidly and completely absorbed from the GI tract.

For a drug that is completely absorbed and eliminated exclusively by hepatic metabolism, oral bioavailability can be predicted using the equation derived by Rowland (7):

$$\theta = 1 - \frac{f_m D_{iv}}{V_{bl}[H/K_p + (1 - H)]AUC_{iv}} \quad \text{(Eq. 1)}$$

where $f_m$ is the fraction of the dose metabolized in the liver on intravenous administration, $V_{bl}$ is the liver blood flow, $H$ is the hematocrit, $K_p$ is the apparent partition coefficient of the drug between plasma and erythrocytes, $D_{iv}$ is the dose, and $AUC_{iv}$ is the area under the curve for intravenous administration. This equation has been applied with reasonable success to predict the oral bioavailability of propranolol (8) and nortriptyline (9) in humans.

The fraction of unchanged steroid in the urine after intravenous administration was very small (0.5% of the dose). Therefore, the renal clearance was almost negligible. In one study in dogs, the drug was completely absorbed after oral administration. If it is assumed that ethinyl estradiol is metabolized exclusively by the liver, then $f_m = 1$, and Eq. 1 can be used to predict the bioavailability of the drug after oral administration (7). Since $H$ is known to be 0.4 and $K_p$ (for ethinyl estradiol) was determined experimentally in these laboratories to be >500, $H/K_p$ is almost zero. By using the value of $V_{bl}$ in dogs of 51 ml/min/kg (10), the predicted oral bioavailability was calculated and compared to the experimental values.

Table II shows the area under the curve for the unchanged drug after intravenous and oral administration of ethinyl estradiol to dogs and the comparison of the experimentally determined and predicted values. The observed availability (0.075) was much lower than the predicted value (0.222). Such a difference could not be attributed to incomplete absorption of ethinyl estradiol from the GI tract since the total plasma radioactivity and urinary recovery data from the two routes of administration were almost the same. Since the predicted availability was calculated based on the assumption that drug metabolism occurred only in the liver, the differences between the predicted and observed availability after oral administration may be due to metabolism of the drug on its passage through the gut wall, which Eq. 1 does not take into account.

To estimate the extent of gut wall and liver metabolism of ethinyl estradiol, studies were undertaken with rats. Solutions of the drug were administered as an intraportal, intraduodenal, or intravenous bolus. To simulate oral absorption, the drug was also administered intraportally and intraduodenally by first-order infusion.

Figures 3 and 4 show the mean blood levels of unchanged ethinyl estradiol after bolus and first-order infusion, respectively. The drug blood levels after intraduodenal administration were significantly lower than those after intraportal or intravenous administration.

The bioavailability following intraportal and intraduodenal administration can be compared to intravenous administration using the following relationships (11, 12):

$$\frac{AUC_{ipv}}{AUC_{iv}} = 1 - F_l \quad \text{(Eq. 2)}$$

$$\frac{AUC_{id}}{AUC_{iv}} = (1 - F_l)(1 - F_g) \quad \text{(Eq. 3)}$$

where $AUC_{ipv}$, $AUC_{id}$, and $AUC_{iv}$ are the areas under the blood level curves when the drug is given intraportally, intraduodenally, and intravenously, respectively, and $F_g$ and $F_l$ are the fractions of the drug metabolized in the gut wall and the liver, respectively.

**Table II—Area under Curve Values after Intravenous and Oral Administration of Ethinyl Estradiol and Oral Bioavailability in Three Beagle Dogs [a]**

| Dog | *AUC*, (ng hr)/ml | | Bioavailability | |
|---|---|---|---|---|
| | Intravenous | Oral | Observed [b] | Predicted [c] |
| IJ96 | 2.554 | 0.310 | 0.121 | 0.253 |
| NJ06 | 2.594 | 0.106 | 0.041 | 0.183 |
| JO96 | 2.254 | 0.147 | 0.065 | 0.231 |
| Mean | 2.467 | 0.188 | 0.075 | 0.222 |
| ±*SE* | 0.107 | 0.063 | 0.024 | 0.021 |

[a] The dose was 35 μg/dog (100 μCi/dog). [b] Observed bioavailability was obtained from $AUC_{po}/AUC_{iv}$. [c] Predicted bioavailability calculated from Eq. 1.

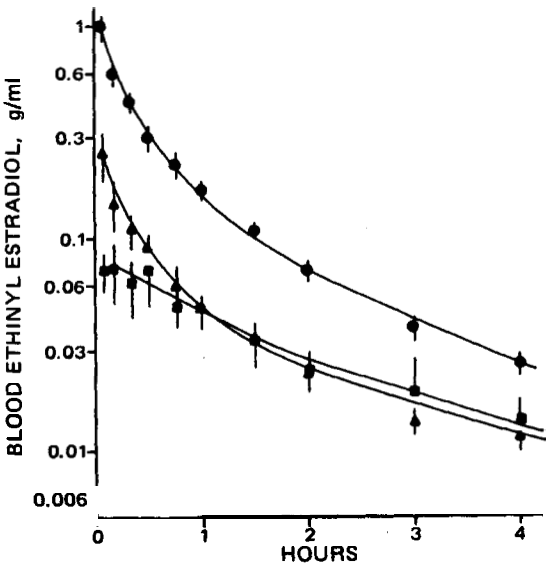


**Figure 3**—*Mean blood levels of unchanged ethinyl estradiol after bolus intravenous (●), bolus intraportal (▲), and bolus intraduodenal (■) administration of 3.5 μg/kg in rats.*

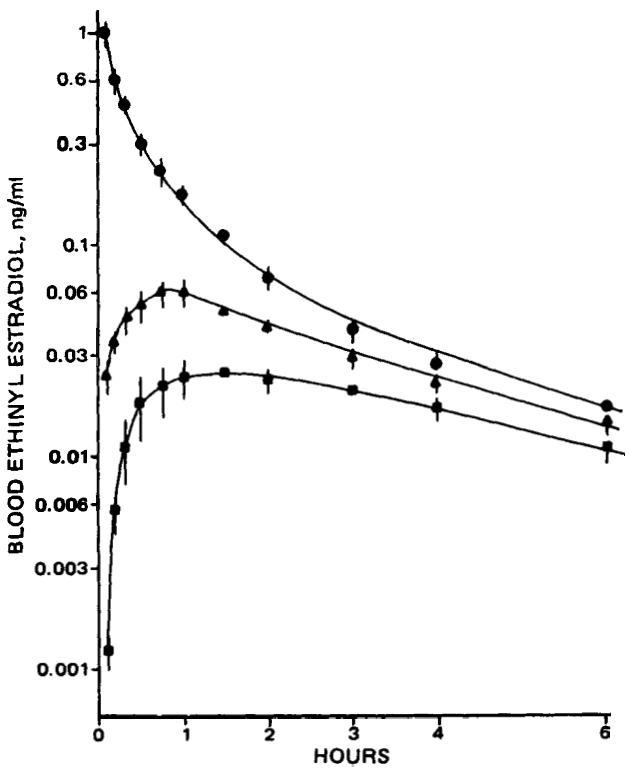


**Figure 4**—*Mean blood levels of unchanged ethinyl estradiol after bolus intravenous (●), first-order intraportal (▲), and first-order intraduodenal (■) administration of 3.5 μg/kg in rats.*

Table III—$AUC$, $F_g$, and $F_l$ Values Obtained from Intraduodenal, Intraportal, and Intravenous Administration in Rats [a]

| Route | $AUC_{id}$ | $AUC_{ipv}$ | $AUC_{iv}$ | Intraduodenal/Intravenous | Intraportal/Intravenous | $F_g$ | $F_l$ |
|---|---|---|---|---|---|---|---|
| First-order infusion [b] | 9.0 ± 1.2 | 15.0 ± 1.1 | – | 0.129 | 0.215 | 0.399 | 0.785 |
| Bolus | 10.8 ± 2.0 | 13.0 ± 2.9 | 69.6 ± 6.4 | 0.155 | 0.186 | 0.169 | 0.814 |

[a] The ethinyl estradiol dose was 3.5 μg/kg (100 μCi/kg), and the $AUC$ values are expressed in nanogram minutes per milliliter from zero time to infinity and are the mean ± $SE$ ($n$ = 3). [b] $K$ = 1.2 $hr^{-1}$, $t_{1/2}$ = 0.58 hr.

From Eq. 2:

$$F_l = 1 - \frac{AUC_{ipv}}{AUC_{iv}} \quad \text{(Eq. 4)}$$

Substitution of Eqs. 2 and 4 into Eq. 3 yields:

$$F_g = 1 - \frac{AUC_{id}AUC_{iv}}{AUC_{iv}AUC_{ipv}} = 1 - \frac{AUC_{id}}{AUC_{ipv}} \quad \text{(Eq. 5)}$$

Table III shows the $AUC$, $F_g$, and $F_l$ values obtained from intraduodenal, intraportal, and intravenous administration of ethinyl estradiol in rats at a dose of 3.5 μg/kg. The results indicate that 40% of the drug was metabolized by the gut wall ($F_g$) and that 79% of the drug in the portal blood was metabolized by the liver ($F_l$) before reaching the systemic circulation after first-order infusion. The $F_l$ value after bolus administration was almost the same as that after first-order infusion, whereas the $F_g$ value was significantly different. The difference could be due to the saturation of the metabolizing enzyme in the gut wall after bolus intraduodenal administration.

The results of this study indicate that, in the rat, the oral contraceptive steroid, ethinyl estradiol, is extensively metabolized in both the gut wall and the liver. In view of this finding, differences between the predicted and observed availability after oral administration of the drug to dogs also may be due to metabolism of the drug in the gut wall.

To compare the $F_g$ and the $F_l$ values in rats with those in dogs, the $F_g$ and $F_l$ values in dogs were estimated by:

$$F_l = 1 - \text{(predicted bioavailability)} \quad \text{(Eq. 6)}$$

$$F_g = 1 - \frac{\text{(observed bioavailability)}}{\text{(predicted bioavailability)}} \quad \text{(Eq. 7)}$$

The $F_l$ value in dogs was 0.78, which was close to that found in rats (0.78–0.81). The $F_g$ value in dogs was 0.66, which was significantly greater than that found in rats (0.17 from a bolus administration and 0.40 from a first-order infusion).

The difference in the $F_g$ value between the two animal species may be due to factors such as stomach emptying, rate of absorption, and the amount of enzymes in the GI tract.

## REFERENCES


(1) C. Longcope and K. I. H. Williams, *J. Clin. Endocrinol. Metab.*, **38**, 602 (1974).

(2) "The Pharmacological Basis of Therapeutics," 5th ed., L. S. Goodman and A. Gilman, Eds., Macmillan, New York, N.Y., 1975, chap. 68.

(3) E. D. Helton, M. C. Williams, and J. W. Goldzieher, *Steroids*, **27**, 851 (1976).

(4) M. J. Reed and K. Fotherby, *J. Steroid Biochem.*, **6**, 121 (1975).

(5) R. A. Ronfeld and L. Z. Benet, *J. Pharm. Sci.*, **66**, 178 (1977).

(6) M. J. Reed, K. Fotherby, and S. J. Steele, *J. Endocrinol.*, **55**, 351 (1972).

(7) M. Rowland, *J. Pharm. Sci.*, **61**, 70 (1972).

(8) M. Gibaldi, *ibid.*, **60**, 1338 (1971).

(9) *Ibid.*, **64**, 1036 (1975).

(10) L. A. Saperstein, *Am. J. Physiol.*, **193**, 161 (1958).

(11) M. K. Cassidy and J. B. Houston, *J. Pharm. Pharmacol.*, **32**, 57 (1980).

(12) S. Pang and J. R. Gillette, *J. Pharm. Sci.*, **67**, 703 (1978).


# Terpenoids Biotransformation in Mammals III: Biotransformation of α-Pinene, β-Pinene, Pinane, 3-Carene, Carane, Myrcene, and *p*-Cymene in Rabbits


**T. ISHIDA *x, Y. ASAKAWA ‡, T. TAKEMOTO ‡, and T. ARATANI §**



Received December 24, 1979, from the **Hiroshima Institute of Technology, Itsukaichi, Hiroshima 738, Japan*, the ‡*Institute of Pharmacognosy, Tokushima-Bunri University, Tokushima 770, Japan*, and the §*Faculty of Integrated Arts and Sciences, Hiroshima University, Hiroshima 730, Japan.* Accepted for publication September 25, 1980.



**Abstract** □ The biotransformation of (+)-, (−)-, and (±)-α-pinenes, (−)-β-pinene (nopinene), (−)-*cis*-pinane, (+)-3-carene, (−)-*cis*-carane, myrcene, and *p*-cymene in rabbits was investigated. The major metabolites were as follows: (−)-*trans*-verbenol from (+)-, (−)-, and (±)-α-pinenes; (−)-10-pinanol and (−)-1-*p*-menthene-7,8-diol from (−)-β-pinene; (−)-α-terpineol and (−)-*trans*-sobrerol from (−)-*cis*-pinane; (−)-*m*-mentha-4,6-dien-8-ol, 3-caren-9-ol, (−)-3-carene-9-carboxylic acid, and 3-carene-9,10-dicarboxylic acid from (+)-3-carene; carane-9,10-dicarboxylic acid from (−)-*cis*-carane; and myrcene-3(10)-glycol, myrcene-1,2-glycol, uroterpenol, and *p*-cymene-9-carboxylic acid from *p*-cymene. These metabolisms include allylic oxidation, epoxidation, stereoselective *gem*-dimethyl hydroxylation and its oxidation, cleavage of a conjugated double bond by epoxidation, and regioselective oxidation, some of which are not found usually in chemical reactions, and due to which various new compounds were determined. This biotransformation of the monoterpene hydrocarbons gave some insect pheromones in high yield.



**Keyphrases** □ Biotransformation—neutral and acidic metabolites of α-pinene, β-pinene, pinane, 3-carene, carane, myrcene, and *p*-cymene in rabbits □ Metabolites, neutral and acidic—biotransformation of α-pinene, β-pinene, pinane, 3-carene, carane, myrcene, and *p*-cymene in rabbits □ Terpenoids—α-pinene, β-pinene, pinane, 3-carene, carane, myrcene, and *p*-cymene, neutral and acidic metabolites, biotransformation in rabbits


In many countries, plants with mono-, di-, or sesquiterpenoids are used as folk medicine. Medicinal plants with essential oils can be found in many pharmacopeias. The pharmaceutical activities of mono- and sesquiterpenoids were reviewed (1), and it was reported that turpentine oil containing α-pinene, β-pinene, 3-carene, and myrcene is




*0022-3549/81/0400-0406$01.00/0*


*© 1981, American Pharmaceutical Association*

Table III—$AUC$, $F_g$, and $F_l$ Values Obtained from Intraduodenal, Intraportal, and Intravenous Administration in Rats [a]

| Route | $AUC_{id}$ | $AUC_{ipv}$ | $AUC_{iv}$ | Intraduodenal/Intravenous | Intraportal/Intravenous | $F_g$ | $F_l$ |
|---|---|---|---|---|---|---|---|
| First-order infusion [b] | 9.0 ± 1.2 | 15.0 ± 1.1 | – | 0.129 | 0.215 | 0.399 | 0.785 |
| Bolus | 10.8 ± 2.0 | 13.0 ± 2.9 | 69.6 ± 6.4 | 0.155 | 0.186 | 0.169 | 0.814 |

[a] The ethinyl estradiol dose was 3.5 μg/kg (100 μCi/kg), and the $AUC$ values are expressed in nanogram minutes per milliliter from zero time to infinity and are the mean ± $SE$ ($n$ = 3). [b] $K$ = 1.2 $hr^{-1}$, $t_{1/2}$ = 0.58 hr.

From Eq. 2:

$$F_l = 1 - \frac{AUC_{ipv}}{AUC_{iv}} \quad \text{(Eq. 4)}$$

Substitution of Eqs. 2 and 4 into Eq. 3 yields:

$$F_g = 1 - \frac{AUC_{id}AUC_{iv}}{AUC_{iv}AUC_{ipv}} = 1 - \frac{AUC_{id}}{AUC_{ipv}} \quad \text{(Eq. 5)}$$

Table III shows the $AUC$, $F_g$, and $F_l$ values obtained from intraduodenal, intraportal, and intravenous administration of ethinyl estradiol in rats at a dose of 3.5 μg/kg. The results indicate that 40% of the drug was metabolized by the gut wall ($F_g$) and that 79% of the drug in the portal blood was metabolized by the liver ($F_l$) before reaching the systemic circulation after first-order infusion. The $F_l$ value after bolus administration was almost the same as that after first-order infusion, whereas the $F_g$ value was significantly different. The difference could be due to the saturation of the metabolizing enzyme in the gut wall after bolus intraduodenal administration.

The results of this study indicate that, in the rat, the oral contraceptive steroid, ethinyl estradiol, is extensively metabolized in both the gut wall and the liver. In view of this finding, differences between the predicted and observed availability after oral administration of the drug to dogs also may be due to metabolism of the drug in the gut wall.

To compare the $F_g$ and the $F_l$ values in rats with those in dogs, the $F_g$ and $F_l$ values in dogs were estimated by:

$$F_l = 1 - \text{(predicted bioavailability)} \quad \text{(Eq. 6)}$$

$$F_g = 1 - \frac{\text{(observed bioavailability)}}{\text{(predicted bioavailability)}} \quad \text{(Eq. 7)}$$

The $F_l$ value in dogs was 0.78, which was close to that found in rats (0.78–0.81). The $F_g$ value in dogs was 0.66, which was significantly greater than that found in rats (0.17 from a bolus administration and 0.40 from a first-order infusion).

The difference in the $F_g$ value between the two animal species may be due to factors such as stomach emptying, rate of absorption, and the amount of enzymes in the GI tract.

## REFERENCES


(1) C. Longcope and K. I. H. Williams, *J. Clin. Endocrinol. Metab.*, **38**, 602 (1974).

(2) "The Pharmacological Basis of Therapeutics," 5th ed., L. S. Goodman and A. Gilman, Eds., Macmillan, New York, N.Y., 1975, chap. 68.

(3) E. D. Helton, M. C. Williams, and J. W. Goldzieher, *Steroids*, **27**, 851 (1976).

(4) M. J. Reed and K. Fotherby, *J. Steroid Biochem.*, **6**, 121 (1975).

(5) R. A. Ronfeld and L. Z. Benet, *J. Pharm. Sci.*, **66**, 178 (1977).

(6) M. J. Reed, K. Fotherby, and S. J. Steele, *J. Endocrinol.*, **55**, 351 (1972).

(7) M. Rowland, *J. Pharm. Sci.*, **61**, 70 (1972).

(8) M. Gibaldi, *ibid.*, **60**, 1338 (1971).

(9) *Ibid.*, **64**, 1036 (1975).

(10) L. A. Saperstein, *Am. J. Physiol.*, **193**, 161 (1958).

(11) M. K. Cassidy and J. B. Houston, *J. Pharm. Pharmacol.*, **32**, 57 (1980).

(12) S. Pang and J. R. Gillette, *J. Pharm. Sci.*, **67**, 703 (1978).


# Terpenoids Biotransformation in Mammals III: Biotransformation of α-Pinene, β-Pinene, Pinane, 3-Carene, Carane, Myrcene, and *p*-Cymene in Rabbits


**T. ISHIDA *x, Y. ASAKAWA ‡, T. TAKEMOTO ‡, and T. ARATANI §**



Received December 24, 1979, from the **Hiroshima Institute of Technology, Itsukaichi, Hiroshima 738, Japan*, the ‡*Institute of Pharmacognosy, Tokushima-Bunri University, Tokushima 770, Japan*, and the §*Faculty of Integrated Arts and Sciences, Hiroshima University, Hiroshima 730, Japan.* Accepted for publication September 25, 1980.



**Abstract** □ The biotransformation of (+)-, (−)-, and (±)-α-pinenes, (−)-β-pinene (nopinene), (−)-*cis*-pinane, (+)-3-carene, (−)-*cis*-carane, myrcene, and *p*-cymene in rabbits was investigated. The major metabolites were as follows: (−)-*trans*-verbenol from (+)-, (−)-, and (±)-α-pinenes; (−)-10-pinanol and (−)-1-*p*-menthene-7,8-diol from (−)-β-pinene; (−)-α-terpineol and (−)-*trans*-sobrerol from (−)-*cis*-pinane; (−)-*m*-mentha-4,6-dien-8-ol, 3-caren-9-ol, (−)-3-carene-9-carboxylic acid, and 3-carene-9,10-dicarboxylic acid from (+)-3-carene; carane-9,10-dicarboxylic acid from (−)-*cis*-carane; and myrcene-3(10)-glycol, myrcene-1,2-glycol, uroterpenol, and *p*-cymene-9-carboxylic acid from *p*-cymene. These metabolisms include allylic oxidation, epoxidation, stereoselective *gem*-dimethyl hydroxylation and its oxidation, cleavage of a conjugated double bond by epoxidation, and regioselective oxidation, some of which are not found usually in chemical reactions, and due to which various new compounds were determined. This biotransformation of the monoterpene hydrocarbons gave some insect pheromones in high yield.



**Keyphrases** □ Biotransformation—neutral and acidic metabolites of α-pinene, β-pinene, pinane, 3-carene, carane, myrcene, and *p*-cymene in rabbits □ Metabolites, neutral and acidic—biotransformation of α-pinene, β-pinene, pinane, 3-carene, carane, myrcene, and *p*-cymene in rabbits □ Terpenoids—α-pinene, β-pinene, pinane, 3-carene, carane, myrcene, and *p*-cymene, neutral and acidic metabolites, biotransformation in rabbits


In many countries, plants with mono-, di-, or sesquiterpenoids are used as folk medicine. Medicinal plants with essential oils can be found in many pharmacopeias. The pharmaceutical activities of mono- and sesquiterpenoids were reviewed (1), and it was reported that turpentine oil containing α-pinene, β-pinene, 3-carene, and myrcene is




*0022-3549/81/0400-0406$01.00/0*


*© 1981, American Pharmaceutical Association*

**Table I—Orally Administered Monoterpene Hydrocarbons and Yields of Metabolites [a]**

| Compound | Administered Dose, g | Metabolite, g | |
|---|---|---|---|
| | | Neutral | Acidic as Methyl Ester |
| (+)-α-Pinene | 10.0 (560)[b] | 0.318 | —[c] |
| (−)-α-Pinene | 8.0 (440) | 1.423 | 3.0 |
| (±)-α-Pinene | 10.0 (560) | 1.199 | —[c] |
| (−)-β-Pinene | 12.0 (670) | 0.753 | 1.0 |
| (−)-*cis*-Pinane | 18.0 (670) | 1.040 | 0.35 |
| (+)-3-Carene | 26.0 (670) | 2.159 | 2.6 |
| (−)-*cis*-Carane | 12.0 (670) | 1.014 | 2.0 |
| Myrcene | 19.0 (670) | 4.00 | 0.8 |
| *p*-Cymene | 2.0 (670)[d] | 0.20 | 0.20 |

[a] Six male rabbits were administered one dose (<12 g/six rabbits) or repeated doses (>12 g/six rabbits). [b] The values in parentheses mean the maximum dose in milligrams per kilogram in each case. [c] Not measured. [d] Only one rabbit was used.

irritating to the skin, is used as a rubefacient and a liniment, and has choleretic activity. Other monoterpenoids have expectorant (1,8-cineol, bornyl acetate, and phellandrenes) or diuretic (diosphenol and terpinen-4-ol in juniper oil) properties. In addition, some sesquiterpenoids show anticancer, analeptic, antibiotic, and anthelmintic properties.

Terpenoid biotransformation in mammals was studied on camphor (2, 3), cedrol (4, 5), patchoulol (6), limonene (7, 8), α-pinene (9), β-pinene (9), and 1,8-cineol (10, 11). These biotransformation products gave enzymatically specific metabolites, that is, regioselective or stereoselective hydroxylated, carboxylated, or reduced metabolites. It is expected that these metabolites become the starting materials in organic synthesis. Moreover, biotransformation of terpenoids is expected to give a new method for optical separation of racemic isomers or to give biologically active substances such as pheromones, cosmetic fragrances, and food additives. It is also interesting to compare the metabolism of terpenoids in mammals with that in microorganisms with regard to enzymatic systems.

During the investigation of structure–activity relationships among metabolites and administered terpenoids in mammals (12, 13), the metabolites of naturally occurring monoterpene hydrocarbons, (+)-, (−)-, and (±)-α-pinenes, (−)-β-pinene, (+)-3-carene, myrcene, and *p*-cymene were studied. Two saturated monoterpene hydrocarbons, (−)-*cis*-pinane and (−)-*cis*-carane, were also studied for comparison.

## EXPERIMENTAL[1]

**Administered Monoterpene Hydrocarbons**—The administered monoterpene hydrocarbons are listed in Table I.

[1] A Shimadzu GC-6A gas chromatograph equipped with both a hydrogen flame-ionization detector and a thermal-conductivity detector was used. For the detection of neutral metabolites, the following conditions were used unless stated otherwise: a 0.26-mm × 2-m glass column packed with 5% OV-1 on Diasolid L (60–80 mesh) or 5% Thermon 1000 on Chromosorb W (80–100 mesh, AW-DMCS), an injection temperature of 250°, a column temperature of 100–250°, a program rate of 10°/min, a detector temperature of 250°, and nitrogen gas at 40 ml/min. For preparative purposes, the same size glass column of 5% Thermon 1000 was used under the same conditions. GLC–mass spectrometric analyses were performed at 70 ev using a 2-mm × 3-m column packed with OV-1 or OV-17 (5%) with temperature programmed at 50–250° at 5°/min and helium at 30 ml/min on a Shimadzu LKB 9000B. TLC plates of silica gel 60 (0.25 cm) F-254 were used, and the spots were observed by UV light (254 nm), 50% $H_2SO_4$ or iodine vapor. The $^1$H-NMR spectra were recorded with Hitachi R-22 (90 MHz) and Varian T-60 (60 MHz) spectrometers. The $^{13}$C-NMR spectra were conducted on a Hitachi R-42 FT spectrometer. IR spectra were obtained with a Hitachi 215 spectrophotometer, and UV spectra were recorded on a Shimadzu US 200S spectrophotometer. The solvents used for spectral determinations were tetramethylsilane–deuterochloroform ($^1$H-NMR of 90 and 60 MHz and $^{13}$C-NMR of 90 MHz) and chloroform ([α]$_D$ and IR) unless stated otherwise.

**Table II—Optical Rotations and Purities of Verbenols Obtained from Optically Active α-Pinenes**

| [α]$_D$ of Administered α-Pinenes | Verbenols as Metabolites | |
|---|---|---|
| | [α]$_D$ | Purity[a], % |
| +22.0° | ±0° | 67.2 |
| −30.9° | −31.2° | 98.9 |
| ±0.0° | −11.3° | 67.5 |

[a] The purities were obtained from the GLC of the neutral metabolites.

**Animals and Dosing**—Six male albino rabbits[2] (2–3 kg) were starved for 2 days before the experiment. Monoterpene hydrocarbons were suspended in water (100 ml) containing polysorbate 80[3] (0.1 g) and were homogenized well. This solution (20 ml) was administered to each rabbit through a stomach tube followed by water (20 ml). This dose of monoterpene corresponds to 400–700 mg/kg. The animals were housed in individual stainless steel metabolism cages and were allowed rabbit food[4] and water *ad libitum*. The urine was collected daily for 3 days after drug administration and stored at 0–5° until time of analysis.

**Extraction and Fractionation of Urinary Metabolites**—The urine was centrifuged to remove feces[5] and hairs at 0°, and the supernate was used for the experiments. The urine was adjusted to pH 4.7[6] with acetate buffer and incubated with β-glucuronidase–arylsulfatase (3 ml/1000 ml of the fresh urine) at 37° for 48 hr, followed by continuous ether extraction for 48 hr. The ether extracts were washed with 5% $NaHCO_3$ and 5% NaOH to remove the acidic and phenolic fractions, respectively, and dried (magnesium sulfate). Ether was evaporated under reduced pressure to give neutral metabolites. The yields are shown in Table I.

The neutral metabolites were chromatographed on a column containing 100 g of silicic acid (200 mesh). Elution was started with *n*-hexane, and *n*-hexane–ethyl acetate mixtures (95:5, 90:10, 85:15, 70:30, and 50:50) were used as subsequent eluents. The acidic metabolites were recovered from the sodium bicarbonate layer by acidification with 5% HCl, followed by ether extraction. The ether extracts were esterified with diazomethane in ether or with dimethyl sulfate in the presence of potassium carbonate in anhydrous acetone. These esters of the acidic metabolites also were chromatographed in the same manner as the neutral metabolites.

**Determination and Identification of Urinary Metabolites**—Purification by silicic acid gave pure metabolites. When necessary, metabolites were isolated by preparative TLC or GLC. Structure determination or identification was based on spectral data and chemical transformations.

## RESULTS

**Metabolites of (+)-, (−)-, and (±)-α-Pinenes**—From each α-pinene, the same three metabolites were identified as follows.

*Verbenol and Myrtenol*—IR and $^1$H-NMR spectra of the main urinary metabolites of (−)-α-pinene (I) agreed well with those of (−)-*trans*-verbenol (II), with a 98.9% purity from the GLC peak area of the neutral metabolite (15). All spectral data of the acetylation and oxidation products of this main metabolite also agreed with those of (−)-*trans*-verbenyl acetate and (−)-verbenone, respectively. The yields (purities by GLC) and the optical rotations of the verbenols obtained from (+)-, (−)-, and (±)-α-pinenes are listed in Table II. The minor urinary metabolites of each α-pinene were identified as myrtenol (III) by comparison of $R_t$ (GLC) and $R_f$ (TLC) values with those of an authentic sample prepared from (−)-α-pinene. The yields of III were 14.9, 0.9, and 9.3% by GLC from (+)-, (−)-, and (±)-α-pinenes, respectively.

*Myrtenic Acid (IV) as Methyl Ester*—As the acidic metabolite from (+)-, (−)-, and (±)-α-pinenes, methyl myrtenate (IV*a*)[7] was isolated in each case; mass spectrum: *m/z* (%) 180 ($M^+$, $C_{11}H_{16}O_2$, 6), 165 (16), 137 (75), 105 (base), and 93 (81); $^1$H-NMR[8] (90 MHz): δ 6.80 (m, 1H), 3.71 (s, 3H), 1.33 (s, 3H), and 0.80 (s, 3H) (16).

**Metabolites of (−)-β-Pinene**—Four neutral and one acidic metabolites were isolated from (−)-β-pinene (V).

[2] Japanese White, Miyamoto Jikken Dobutsu, Hiroshima, Japan.
[3] Tween 80.
[4] Oriental RC-4.
[5] In this experiment, feces were not analyzed.
[6] The pH value for enzymatic hydrolysis by β-glucuronidase was variously reported. In this experiment, pH 4.7 was adopted following the method of LUU Bang *et al.* (4). More recently, pH 6.0 was recommended for the hydrolysis by β-glucuronidase (14).
[7] Compound IV*a* is the methyl ester of IV in Scheme I.
[8] m = multiplet, s = singlet, d = doublet, t = triplet, q = quartet, ss = sharp singlet, bs = broad singlet, and b = broad.

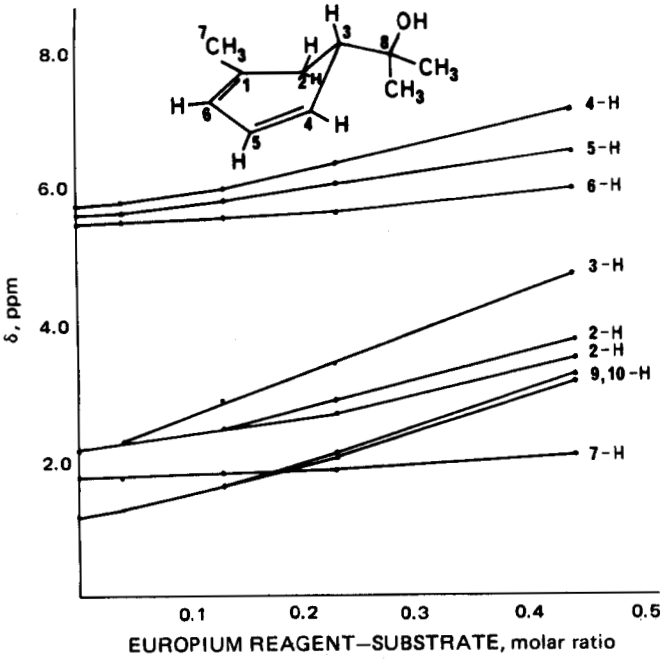


**Figure 1**—*Lanthanide-induced shifts with europium reagent in the* $^1$*H-NMR spectrum of* m-*cymene-4,6-dien-8-ol (XXIII).*

*(+)*-trans-*Pinocarveol (VI) (11%)*[9]—$[\alpha]_D$ +28.2° (*c*, 1.42); mass spectrum: *m/z* (%) 134 ($M^+ - H_2O$, 37), 119 (38), 109 (38), 92 (base), 83 (77), 70 (69), 55 (76), and 41 (50); IR: $\nu$ 3580 and 3350 cm$^{-1}$. These data compared well with the reported values of (+)-*trans*-pinocarveol (17). All spectral data of the derived pinocarvone [$[\alpha]_D$ +28.6° (*c*, 0.35)] were coincident with literature values (18).

*(−)*-trans-*10-Pinanol (VII) (39%)*—$[\alpha]_D$ −21.4° (*c*, 1.68); mass spectrum: *m/z* (%) 154 ($M^+$, $C_{10}H_{18}O$, 9), 139 (base), 121 (40), 83 (85), 64 (69), and 55 (33); IR: $\nu$ 3400 cm$^{-1}$; $^1$H-NMR: $\delta$ 3.47 (s, 2H), 1.23 (s, 3H), and 0.88 (s, 3H). These spectral data revealed this alcohol to be (−)-*trans*-10-pinanol (VII) (19, 20). Its acetate showed IR: $\nu$ 1720 cm$^{-1}$; $^1$H-NMR: $\delta$ 4.10 (s, 2H), 2.12 (s, 3H), 1.26 (s, 3H), and 0.96 (s, 3H).

*(−)-1-*p-*Menthene-7,8-diol (VIII) (30%)*—$[\alpha]_D$ −33.3° (*c*, 0.83); mass spectrum: *m/z* (%) 152 ($M^+ - H_2O$, 21), 137 (6), 121 (19), 109 (32), 94 (26), 93 (27), 79 (base), 59 (88), and 43 (32); IR: $\nu$ 3650, 3450, 1365, 1230, 1035, and 910 cm$^{-1}$; $^1$H-NMR: $\delta$ 5.67 (bs, 1H), 3.95 (2H, $w_{1/2}$ = 3 Hz), and 1.20 (s, 6H). The derived monoacetate showed $[\alpha]_D$ − 51.2° (*c*, 5.4); IR: $\nu$ 3500, 1720, 1240, 1020, and 920 cm$^{-1}$; $^1$H-NMR: $\delta$ 5.75 (bs, 1H), 4.48 (s, 2H), 2.08 (s, 3H), and 1.20 (s, 6H). Furthermore, the derived aldehyde of IX showed $[\alpha]_D$ −65.4° (*c*, 0.46); $^1$H-NMR: $\delta$ 11.10 (s, 1H), 6.75 (s, 1H), and 1.27 (s, 6H). The spectral data established this metabolite to be VIII, which was prepared by Sato (21).

*(−)-α-Terpineol (IX) (5%)*—$[\alpha]_D$ −51.0° (*c*, 1.57); mass spectrum: *m/z* (%) 154 (not appeared, $M^+$), 136 ($C_{10}H_{16}$, $M^+ - H_2O$, 30), 121 (33), 107 (5), 93 (50), 81 (36), 79 (17), 68 (19), 67 (20), and 59 (base); IR: $\nu$ 3400 cm$^{-1}$; $^1$H-NMR: $\delta$ 5.43 (bs, 1H), 1.67 (bs, 3H), and 1.22 (s, 6H) (22).

As an acidic metabolite of (−)-$\beta$-pinene, myrtenic acid (IV) was identified by GLC–mass spectrometry as its methyl ester.

**Metabolites of (−)-*cis*-Pinane**—In (−)-*cis*-pinane (X), three neutral compounds were isolated as alcohols and four as derivatives. No acidic metabolites were identified from GLC–mass spectrometry.

*(−)-α-Terpineol (IX) (43%)*—$[\alpha]_D$ −46.3° (*c*, 1.77); mass spectrometry, IR and $^1$H-NMR spectra, and $[\alpha]_D$ agreed well with those of (−)-$\alpha$-terpineol biotransformed from (−)-$\beta$-pinene.

*(−)*-trans-*Sobrerol (XIV) (6%)*—$[\alpha]_D$ −68.8° (*c*, 0.8); mass spectrum: *m/z* (%) 152 ($M^+ - H_2O$, $C_{10}H_{16}O$, 7), 137 (11), 119 (18), 109 (base), 94 (69), and 79 (93); IR: $\nu$ 3300, 1460, 1440, 1380, 1175, 1150, 1030, and 905 cm$^{-1}$; $^1$H-NMR (90 MHz): $\delta$ 5.27 (bs, 1H), 3.93 [m, 1H, C*H*(OH)], 1.66 (s, 3H), 1.27 (s, 3H), and 1.21 (s, 3H). The signal at $\delta$ 3.93 was replaced by deuterium oxide. These spectral data were easily assigned to XIV.

trans-*Carveol (XV)*—Mass spectrum: *m/z* (%) 152 ($M^+$, $C_{10}H_{16}O$, 1), 134 ($M^+ - H_2O$, 32), 119 (base), 105 (11), 91 (77), 77 (20), and 65 (12) (23).

In addition to IX, XIV, and XV, one fraction that was difficult to isolate was oxidized with Jones reagent. The preparative GLC of the oxidation products resulted in the isolation of four compounds, (−)-3-pinanone, (−)-4-pinanone, verbenone, and a lactonic compound, which were not found among the original metabolites.

*(−)-3-Pinanone*—$[\alpha]_D$ −5.42° (*c*, 2.02); mass spectrum: *m/z* (%) 152 ($M^+$, $C_{10}H_{16}O$, 19), 110 (18), 95 (48), 83 (96), 69 (base), and 55 (92); IR: $\nu$ 1705 cm$^{-1}$; $^1$H-NMR: $\delta$ 1.32 (s, 3H), 1.21 (d, 3H, $J$ = 7 Hz), and 0.89 (s, 3H) (24).

*(−)-4-Pinanone*—$[\alpha]_D$ −27.9° (*c*, 1.67); mass spectrum: *m/z* (%) 152 ($M^+$, $C_{10}H_{16}O$, 12), 137 (14), 109 (32), 95 (64), and 83 (base); IR: $\nu$ 1705 cm$^{-1}$; $^1$H-NMR: $\delta$ 1.33 (s, 3H), 1.15 (d, 3H, $J$ = 6.5 Hz), and 1.00 (s, 3H) (24).

*Verbenone*—Mass spectrum: *m/z* (%) 150 ($M^+$, 43); IR: $\nu$ 1685 and 1622 cm$^{-1}$; $^1$H-NMR: $\delta$ 5.72 (m, 1H), 2.02 (m, 3H), 1.52 (s, 3H), and 1.03 (s, 3H) (15).

The three alcohols, 3-pinanol (XI), 4-pinanol (XII), and verbenol (XIII), were recognized as neutral metabolites from (−)-*cis*-pinane. The lactonic compound (XVI) gave the following spectra: mass spectrum: *m/z* (%) 184 ($M^+$, $C_{10}H_{16}O_3$, trace), 169 ($M^+ - CH_3$, 3), 166 ($M^+ - 18$, 19), 151 (11), 127 (11), 123 (8), 111 (27), 98 (35), 83 (11), 82 (15), 81 (7), 69 (9), 68 (10), 55 (17), and 43 (base); IR: $\nu$ 1765, 1720, 1380, and 1360 cm$^{-1}$; $^1$H-NMR (90 MHz): $\delta$ 2.43 (q, 4H, $J$ = 14 and 8 Hz, $A_2B_2$), 2.16 (4H), 1.46 (s, 3H), and 1.28 (s, 3H). These spectral data suggest the presence of a $\gamma$-lactone having a *gem*-dimethyl group. The comparison of these data with the authentic spectra of homoterpenyl methyl ketone (XVI) showed good agreement (25, 26). This lactone might be derived by Jones oxidation from $\alpha$-terpineol or sobrerol.

**Neutral Metabolites of (+)-3-Carene**—In (+)-3-carene (XVII), two neutral compounds were isolated, one of which is a new compound. In addition, a third neutral metabolite was identified by comparison with an authentic sample as a front shoulder in the GLC of the main neutral metabolite.

*(−)-*m-*Mentha-4,6-dien-8-ol (XXIII) (71.8%)*—The IR spectrum of the main metabolite showed the same pattern in 1660 and 1598 cm$^{-1}$ as occidentalol having a *cis*-conjugated diene in the six-membered ring. Other spectral data agreed with those of XXIII, $[\alpha]_D$ −116.1° (*c*, 1.08); mass spectrum: *m/z* (%) 152 ($M^+$, $C_{10}H_{16}O$, 1), 134 ($M^+ - H_2O$, 40), 119 (base), and 91 (71); IR (liquid film): $\nu$ 3400, 3050, 1720, 1660, and 1598 cm$^{-1}$; $^1$H-NMR (90 MHz): $\delta$ 5.83–5.67 (total 3H), 1.80 (s, 3H), and 1.22 (ss, 6H). A lanthanide-induced shift was also studied to confirm this structure (Fig. 1).

The following three derivatives of XXIII also gave the same spectral data as the reported ones (27):

1. 3,5-Dinitrobenzoate. The dienol (XXIII) (36.2 mg) and 3,5-dinitrobenzoyl chloride (85.6 mg) were dissolved in pyridine (1.0 ml) and allowed to stand overnight at 5°. The reaction mixture was treated in the usual manner, and 3,5-dinitrobenzoate (84.5 mg) was obtained: $[\alpha]_D$ −25.6° (*c*, 2.03); IR (liquid film): $\nu$ 3100, 1720, 1622, 1600, and 1540 cm$^{-1}$.

2. Maleic anhydride adduct. The dienol (XXIII) (61.6 mg) and maleic anhydride (40.4 mg) were dissolved in anhydrous benzene (10 ml), and the reaction mixture was refluxed at 90° for 1.5 hr. The product was obtained from the neutral fraction (51.7 mg), mp 142°, $[\alpha]_D$ −63.3° (*c*, 2.10); IR: $\nu$ 3100, 1845, 1775, 1370, 1260, 1050, 880, and 860 cm$^{-1}$.

3. Acetate. IR (liquid film): $\nu$ 1720 and 1240 cm$^{-1}$.

m-*Cymen-8-ol (XXIV)*—A front shoulder was included in the GLC peak of XXIII, and one set of unshifted protons was observed in the field of aromatic protons in the lanthanide-induced shift experiment of XXIII. On the other hand, 3-carene (XVII) was oxidized according to the method of Dauben *et al.* (28), and XXIV was obtained as one product. The comparison of $^1$H-NMR data and the GLC retention time indicated the shoulder to be XXIV; mass spectrum: *m/z* (%) 150 ($M^+$, $C_{10}H_{14}O$, 1), 135 (10), 132 (98), 117 (base), 115 (47), 92 (53), 91 (75), 77 (16), and 65 (30); $^1$H-NMR: $\delta$ 7.40–6.85 (total 4H), 2.35 (s, 3H), and 1.55 (s, 6H) (29).

*3-Caren-9-ol (XVIII) (10.5%)*—Mass spectrum of the secondary major neutral metabolite of 3-carene showed the molecular ion of $C_{10}H_{16}O$ at *m/z* 152, and its IR spectrum showed a hydroxyl absorption at 3350 cm$^{-1}$. The $^1$H-NMR spectrum showed the hydroxymethylene protons at 3.33 and an allylic methyl group at 1.62 ppm. These results indicate that one *gem*-dimethyl group was hydroxylated. This alcohol was easily changed to its acetate with acetic anhydride in pyridine, and it was clear that this alcohol was a primary one.

The determination of which methyl group was metabolized was based on the comparison of the $^1$H-NMR signals of the *gem*-dimethyl groups

[9] The value in the parentheses means the relative ratio of identified metabolites in the chromatogram of the neutral portions. The ratio of acidic metabolites in GLC cannot be given because the acidic fraction contained many acidic and phenolic metabolites originating from normal urine of rabbits.

**Table III—Chemical Shifts (in Hertz) of Methyl Protons of 3-Carene and 3-Caren-9-ol**

| | 3-Carene (30) | 3-Caren-9-ol | Difference[a] |
|---|---|---|---|
| C-8 methyl | 48 | 52.8 | 4.8 |
| C-9 methyl | 64 | — | 11.2 |

[a] This value means the difference of the chemical shift (in Hertz) of methyl protons between these two compounds.

with those of 3-carene (Table III). In this table, the signal at 52.8 Hz can be reasonably assigned as the C-8 methyl group on the basis of the small difference (4.8 Hz) from the C-8 methyl group of 3-carene (30). As the result, this metabolite was determined to be XVIII, $[\alpha]_D$ −17.9° (*c*, 0.6); mass spectrum: *m/z* (%) 152 ($M^+$, $C_{10}H_{16}O$, 2), 134 ($M^+ - H_2O$, 18), 121 (25), 119 (38), 108 (21), 105 (24), 93 (47), 91 (76), 78 (base), 77 (41), and 67 (22); IR (liquid film): $\nu$ 3350, 1720, 1430, 1370, 1240, 1020, 820, and 780 $cm^{-1}$; $^1$H-NMR: $\delta$ 5.27 (bs, 1H), 3.33 (s, 2H), 2.17 (OH, 1H), 1.62 (bt, 3H), and 0.88 (s, 3H).

*3-Caren-9-ol Acetate*—Compound XVIII (61.8 mg) was acetylated with acetic anhydride in pyridine, and an acetate (41.6 mg) was obtained; mass spectrum: *m/z* (%) 194 ($M^+$, $C_{12}H_{18}O_2$, 7), 150 (10), 134 (50), 132 (45), 119 (base), 105 (35), 93 (48), 92 (36), 91 (36), 79 (33), and 43 (76); IR: $\nu$ 1720, 1600, 1450, 1380, 1360, 1240, and 1020 $cm^{-1}$; $^1$H-NMR (90 MHz): $\delta$ 5.22 (bs, 1H), 3.80 (s, 2H), 2.04 (s, 3H), 1.60 (s, 3H), and 0.84 (s, 3H).

**Acidic Metabolites of (+)-3-Carene**—The acidic metabolites of 3-carene (XVII) were esterified with diazomethane in ethereal solution; three compounds were isolated, and their structures were determined. In addition, one metabolite was estimated on the basis of the mass spectrum.

*3-Carene-9-carboxylic Acid (XIX) as Methyl Ester*—The major acidic metabolite showed *m/z* 180 of $C_{11}H_{16}O_2$ as a molecular ion. The presence of one methyl ester group (1720 $cm^{-1}$ and 3.62 ppm) was suggested from its spectrum. The position of the carbomethoxyl group was determined to be C-9 on the basis of the lanthanide-induced shift experiment (Fig. 2). According to the increase of europium reagent, two methine protons (H-1 and H-6) on the cyclopropane ring and the C-9 carbomethoxymethyl group (9-$CO_2CH_3$) slanted more sharply than the C-8 methyl group on the cyclopropane ring. This result suggests the metabolized methyl group of *gem*-dimethyl orients to an *exo*-configuration against the cyclohexenyl ring. Hence, this methyl ester was determined to be methyl 3-carene-9-carboxylate (XIX*a*). Other signals in $^1$H-NMR agreed with those of 3-carene, and the conformation of this monoester is shown in Fig. 2. Thus,

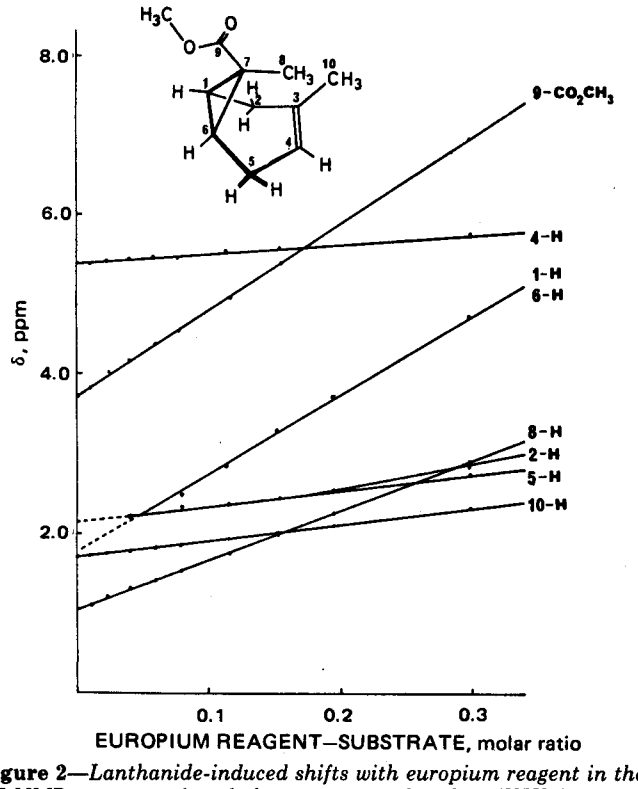


**Figure 2**—*Lanthanide-induced shifts with europium reagent in the $^1$H-NMR spectrum of methyl 3-carene-9-carboxylate (XIXa).*

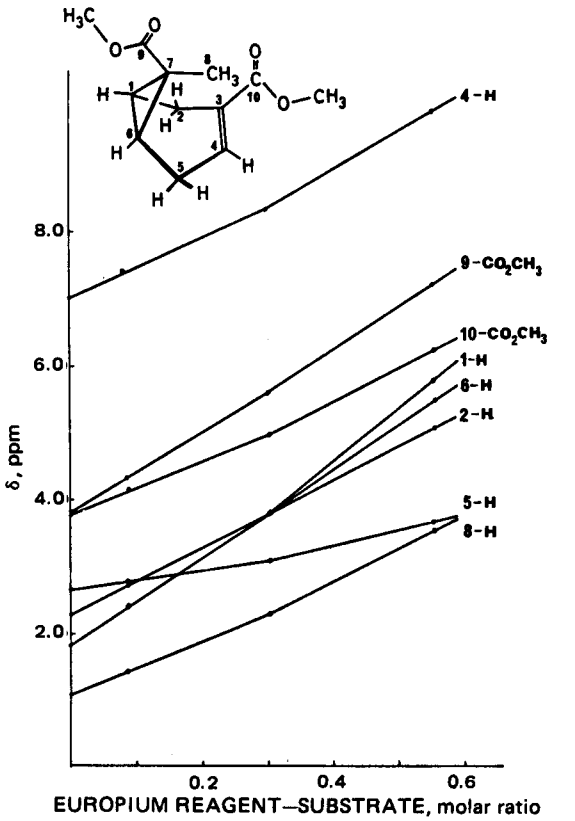


**Figure 3**—*Lanthanide-induced shifts with europium reagent in the $^1$H-NMR spectrum of dimethyl 3-carene-9,10-dicarboxylate (XXIIa).*

the formation of a primary alcohol, 3-caren-9-ol (XVIII), is suspected from the acidic metabolite, methyl 3-carene-9-carboxylate (XIX*a*), $[\alpha]_D$ +8.94° (*c*, 2.6); mass spectrum: *m/z* (%) 180 ($C_{11}H_{16}O_2$, 15), 121 (23), 112 (base), 105 (35), and 93 (29); IR: $\nu$ 1720, 1260, and 1120 $cm^{-1}$; $^1$H-NMR (90 MHz): $\delta$ 5.24 (bs, 1H), 3.62 (s, 3H), 2.70–1.60 (6H), 1.60 (s, 3H), and 1.02 (s, 3H).

*(−)-3-Carene-9-carboxylic Acid (XIX)*—The ester (XIX*a*) (120.5 mg) was hydrolyzed with 1% KOH in ethanol refluxing for 2 hr, and the free acid (XIX) (30.7 mg) was obtained, $[\alpha]_D$ −3.26° (*c*, 4.3); UV: $\lambda_{max}^{ethanol}$ 208 (log $\epsilon$ 3.5) nm; IR: $\nu$ 3500–2300, 1680, and 1260 $cm^{-1}$; $^1$H-NMR: $\delta$ 10.95 (b, 1H, COOH), 5.23 (bs, 1H), 1.62 (bs, 3H), 1.03 (s, 3H), and 1.23 and 1.00 (dt, 2H, $J$ = 5 Hz, cyclopropane). Furthermore, XIX*a* was converted into XVIII (10.2 mg) with aluminum lithium hydride (25 mg) in ether. Thus, the structure of this acid was determined.

*3-Carene-9,10-dicarboxylic Acid (XXII) as Dimethyl Ester*—The secondary major acidic metabolite showed the parent peak at *m/z* 224 of $C_{12}H_{16}O_4$, and the IR spectrum revealed the presence of an ester group at 1720 $cm^{-1}$. In the $^1$H-NMR spectrum, in comparison with that of 3-carene, disappearence of the signal of an allylic methyl group and the appearance of new signals at 3.72 and 3.36 ppm assignable to two methyl groups of ester groups were observed. The lanthanide-induced shift in $^1$H-NMR of this compound is shown in Fig. 3. Increasing amounts of europium reagent caused the shift of one methyl group at 3.72 ppm to the lower field. This shift pattern looks like that of an esteric methyl group of XIX*a*, suggesting the identity of the position of one carboxyl group in XXII with the carboxyl group of XIX*a*. This diester was reduced to an alcohol to give 3-carene-9,10-diol. In the IR spectrum of this diol, the absorption near 3320 $cm^{-1}$ was shifted to 3400 $cm^{-1}$ as the temperature increased. In addition, the absorption at 3525 $cm^{-1}$ disappeared with increasing dilution with carbon tetrachloride.

These results mean that the diol is hydrogen bonded intermolecularly (dimerically) and not intramolecularly. Thus, the relative configuration of two hydroxyl groups in 3-carene-9,10-diol was concluded as being in the *anti*-position in the model. This result indicates that the positions of the carboxylated carbon atoms of 3-carene in rabbits are C-9 and C-10. Consequently, the structure of dimethyl 3-carene-9,10-dicarboxylate (XXII*a*) was established: $[\alpha]_D$ −7.33° (*c*, 2.7); UV: $\lambda_{max}^{ethanol}$ 223 (log $\epsilon$ 3.8) nm; mass spectrum: *m/z* (%) 224 ($M^+$, $C_{12}H_{16}O_4$, 17), 193 (25), 192 (23), 164 (15), 133 (40), 112 (base), and 105 (78); IR: $\nu$ 1720, 1680, 1460, 1440,

Table IV—$^{13}$C-NMR Spectral Data of Metabolites or Derivatives (Parts per Million from Tetramethylsilane)

| Metabolite | C-1 | C-2 | C-3 | C-4 | C-5 | C-6 | C-7 | C-8 | C-9 | C-10 | 9-$CO_2CH_3$ | 10-$CO_2CH_3$ |
|---|---|---|---|---|---|---|---|---|---|---|---|---|
| 9,10-Dimethoxy-3-carene | 21.07[a] d | 21.07 t | 128.06 s | 137.22 d | 18.60 t | 20.00[a] d | 25.25 s | 7.41 q | 167.30 s | 176.15 s | 51.95 q | 51.59 q |
| 1,4,4-Trimethylcycloheptan-1-ol | 73.19 s | 36.51 t | 34.74 t | 32.93 s | 43.30 t | 19.26 t | 45.07 t | 31.55 q | 30.43[a] q | 30.54[a] q | — | — |
| Reported values[b] | 73.6 | 37.1 | 35.3 | 33.5 | 44.0 | 19.8 | 45.7 | 31.2 | 31.1 | 31.1 | | |
| Myrcene-3(10)-glycol | 115.30 t | 140.88 d | 76.35 s | 36.90 t | 22.07 t | 124.31 d | 132.29 s | 25.73 q | 17.71 q | 68.95 t | — | — |
| Linalool reported values[c] | 111.6 | 146.3 | 72.9 | 43.0 | 28.1 | 125.5 | 131.0 | 25.9 | 17.8 | 23.2 | — | — |

[a] Means the alternative value. [b] The values of 1,4,4-trimethylcycloheptan-1-ol in Ref. 33. [c] The values of linalool in Ref. 34.

1340, 1315, 1260, 1198, 1160, 1140, 1095, 1060, 1010, and 890 $cm^{-1}$; $^1$H-NMR (90 MHz): $\delta$ 6.88 (q, 1H), 3.72 (s, 3H, 9-$CO_2CH_3$), 3.64 (s, 3H, 10-$CO_2CH_3$), 1.00 (s, 3H, 8-$CCH_3$), and 3.0–1.6 (6H). The $^{13}$C-NMR spectral data are shown in Table IV, and these values also support the structure of XXIIa.

*3-Carene-9,10-dicarboxylic Acid (XXII)*—This diester (XXIIa) (35 mg) was hydrolyzed in 5% KOH in ethanol with refluxing for 1 hr to give a diacid (XXII) (29 mg), mp 163.5° (ethanol); UV: $\lambda_{max}^{ethanol}$ 290 (log $\epsilon$ 4.23) nm; IR: $\nu$ 1690 and 1220 $cm^{-1}$. This diacid was not soluble in deuterochloroform at room temperature.

*3-Carene-9,10-diol*—The diester (XXIIa) (33.1 mg) was dissolved in anhydrous ether and stirred with aluminum lithium hydride (15.4 mg) for 1 hr under nitrogen gas at room temperature to give a diol (20.3 mg); mass spectrum: *m/z* (%) 168 ($M^+$, $C_{10}H_{16}O_2$, 23), 150 (8), 132 (14), 119 (62), 91 (99), 79 (base), and 77 (41); IR: $\nu$ 3350, 1710, 1695, 1430, 1265, and 1030 $cm^{-1}$; $^1$H-NMR (acetone-$d_6$): $\delta$ 5.53 (bm, 1H), 3.90 (s, 2H, =C-$CH_2$OH), 3.30 (s, 2H, $CH_2$OH), 2.83 (two OH), and 0.87 (5H, 8-$CH_3$ and two cyclopropane protons).

*3-Carene-9,10-diol Diacetate*—3-Carene-9,10-diol (77.6 mg) was acetylated with acetic anhydride (0.5 ml) and pyridine (1 ml) to give a diacetate (42.9 mg), $[\alpha]_D$ +8.4° (c, 4.0); mass spectrum: *m/z* (%) 252 ($M^+$, $C_{14}H_{20}O_4$, 1), 192 (3), 132 (78), 117 (base), 91 (53), and 43 (52); IR: $\nu$ 1740, 1370, 1240, and 1035 $cm^{-1}$; $^1$H-NMR: $\delta$ 5.67 (m, 1H), 4.47 (s, 2H, 10-$CH_2$), 3.85 (s, 2H, 9-$CH_2$), 2.08 (s, 6H, two $CO_2CH_3$), 0.87 (s, 3H, 8-$CH_3$), and 1.00–0.87 (2H, cyclopropane).

*3-Carene-10-carboxylic Acid (XXI) as Methyl Ester*—A minor acidic metabolite was isolated from the near fraction of XIXa, and it was identified as methyl chaminate (XXIa) from the spectral data, $[\alpha]_D$ +3.88° (c, 2.57); UV: $\lambda_{max}^{ethanol}$ 220 (log $\epsilon$ 3.6) nm; mass spectrum: *m/z* (%) 180 ($M^+$, $C_{11}H_{16}O_2$, 37), 137 (78), 121 (53), and 105 (base); IR: $\nu$ 1710, 1650, 1250, and 1070 $cm^{-1}$; $^1$H-NMR (90 MHz): $\delta$ 6.90 (m, 1H, 4-CH), 3.73 (s, 3H, 10-$CO_2CH_3$), 2.80–1.8 (4H), 1.8–1.5 (2H, cyclopropane), 1.06 (s, 3H, 9-$CH_3$), and 0.73 (s, 3H, 8-$CH_3$) (31, 32).

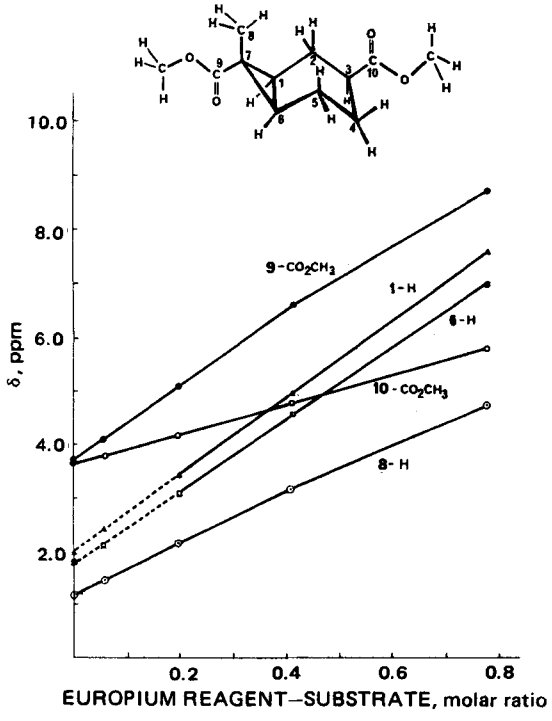


**Figure 4**—*Lanthanide-induced shifts with europium reagent in the $^1$H-NMR spectrum of dimethyl 3-carane-9,10-dicarboxylate (XXVIIIa).*

*3-Caren-10-ol*—Methyl chaminate (XXIa) (45.0 mg) was reduced with aluminum lithium hydride (15.3 mg) at 0° to give an allylic alcohol (39.5 mg); $^1$H-NMR: $\delta$ 5.50 (bs, 1H), 3.93 (bs, 2H, $CH_2$OH), 1.00 (s, 3H, 9-$CH_3$), and 0.73 (s, 3H, 8-$CH_3$).

*3-Caren-10-ol-9-carboxylic Acid (XX) as Methyl Ester*—In addition to the three acidic metabolites, one acidic compound was estimated by GLC–mass spectrometric analysis. This compound has the molecular ion at *m/z* 196, meaning $C_{11}H_{16}O_3$. From this molecular formula and the base peak of *m/z* 112, two structures can be proposed as metabolites, methyl 3-caren-10-ol-9-carboxylate and methyl 3-caren-9-ol-10-carboxylate. The mass spectrum of the compound did not show the same cracking pattern, even partially, as XVIII and XXIa. Thus, methyl 3-caren-10-ol-9-carboxylate (XXa) seems to be reasonable; mass spectrum: *m/z* (%) 196 ($M^+$, $C_{11}H_{16}O_3$, 2), 181 (4), 167 (13), 165 (8), 153 (6), 137 (12), 136 (13), 135 (17), 121 (20), 119 (19), 112 (base), 107 (33), 95 (20), 93 (27), 91 (24), and 79 (18).

**Metabolites of (−)-*cis*-Carane**—The neutral metabolites of (−)-*cis*-carane (XXVII) were acetylated, and one compound was isolated as the acetate; its structure remains to be established. One compound that resisted acetylation was isolated by TLC and identified as 1,4,4-trimethylcycloheptan-1-ol (XXX) from the spectral data (33).

*1,4,4-Trimethylcycloheptan-1-ol (XXX)*—$[\alpha]_D$ −14.4° (c, 2.2); mass spectrum: *m/z* (%) 156 ($M^+$, $C_{10}H_{20}O$, 1), 141 (41), 123 (39), and 71 (base); IR (liquid film): $\nu$ 3375, 2960, 2860, 1470, 1375, 1365, 1110, 930, and 865 $cm^{-1}$; $^1$H-NMR: $\delta$ 1.20 (s, 3H) and 0.87 (s, 6H). The $^{13}$C-NMR data support the structure (XXX) (Table IV).

*Carane-9,10-dicarboxylic Acid (XXVIII) as Dimethyl Ester*—Acidic metabolites of carane in acetone were refluxed with dimethyl sulfate in the presence of sodium bicarbonate, and the neutral products were separated into pure compounds by preparative GLC. Compound XXVIII showed the parent peak at *m/z* 226 of $C_{12}H_{18}O_4$ in mass spectrum, and other spectral data (1740 $cm^{-1}$; 3.60 and 3.63 ppm) showed the loss of the secondary methyl group of carane and the appearance of two carbomethoxyl groups. The positions and the orientations of the metabolized methyl groups were determined by the lanthanide-induced shift experiment (Fig. 4). According to the lanthanide increase, two carbomethoxyl groups showed two completely different slopes, indicating the stereochemically separated position of these two groups. One group was tertiary, and the other was secondary. One carbomethoxyl group showed the same sharp slant as the two cyclopropane protons, and one *tert*-methyl group of the three-membered ring slanted more sharply. Hence, dimethyl 3-carane-9,10-dicarboxylate (XXVIIIa) was established.

Moreover, the hydrogenation of dimethyl 3-carene-9,10-dicarboxylate (XXIIa) (75.2 mg) in the presence of palladium-on-charcoal at room temperature for 1 day gave only one product, whose spectrum agreed with that of the diester from carane. This finding means that hydrogen attacks the unsaturated diester from the less-hindered lower side and, thus, the 10-$CO_2CH_3$ group orients toward the equatorial axis (Fig. 4); XXVIIIa: $[\alpha]_D$ −17.3° (c, 1.5); mass spectrum: *m/z* (%) 226 ($M^+$, $C_{12}H_{18}O_4$, 6), 194 (87), 167 (10), 166 (39), 151 (12), 135 (85), 134 (50), and 107 (base); IR (liquid film): $\nu$ 1740, 1438, 1310, 1265, 1195, 1170, 1135, 1110, 1010, and 770 $cm^{-1}$; $^1$H-NMR: $\delta$ 3.63 (s, 3H), 3.60 (s, 3H), and 1.19 (s, 3H).

**Metabolites of Myrcene**—Three neutral and two esterified acidic metabolites of myrcene (XXXI) were isolated chromatographically.

*Myrcene-3(10)-glycol (XXXII) (40.7%)*—The main neutral metabolite showed the molecular ion at *m/z* 170 of $C_{10}H_{18}O_2$ in the mass spectrum. This alcohol (3380 $cm^{-1}$) was converted into the monoacetate (1735 $cm^{-1}$) with a hydroxyl group remaining (3655 and 3500 $cm^{-1}$). Consequently, it was shown that the major metabolite of myrcene has

two hydroxyl groups. Furthermore, this diol was changed to a conjugated ketone (UV: $\lambda_{max}^{ethanol}$ 215 nm) with activated manganese dioxide in acetone. The parent peak of the ketone appeared at *m/z* 138 of $C_9H_{14}O$, indicating the loss of one carbon atom. The $^1$H-NMR spectral data of this ketone showed *ABC*- or *AMX*-type olefinic three protons with the signals of an isopropenyl group. These facts ruled out the presence of methyl ketone in this conjugated ketone. Thus, the positions of the two hydroxyl groups were determined to be C-3 and C-10.

The $^{13}$C-NMR spectrum (Table IV) of XXXII, which corresponds to that of linalool (34), further supports the structure of XXXII. The diol also was converted into its acetonide to confirm the 1,2-glycol. Compound XXXII showed $[\alpha]_D$ ±0° (*c*, 2.9); mass spectrum: *m/z* (%) 170 ($M^+$, $C_{10}H_{18}O_2$, trace), 152 (4), 139 (24), 121 (47), and 69 (base); IR: $\nu$ 3380, 3090, 1450, 1380, 1260, 1200, 1195, 1150, 1140, 1000, 930, 842, and 838 cm$^{-1}$; $^1$H-NMR (90 MHz): $\delta$ 5.82 (q, 1H, $J_{XA}$ = 17.5 Hz, $J_{XM}$ = 10.0 Hz), 5.35 (q, 1H, $J_{AX}$ = 17.5 Hz, $J_{AM}$ = 2.0 Hz), 5.20 (q, 1H, $J_{MX}$ = 10.0 Hz, $J_{MA}$ = 2.0 Hz), 5.10 (bt, 1H, $J$ = 6.0 and 1.8 Hz), 3.47 (s, 2H, $CH_2O$, $w_{1/2}$ = 5 Hz), 2.55 (s, 2H, two OH), 1.67 (s, 3H, $w_{1/2}$ = 3.5 Hz, 9-$CH_3$), and 1.59 (s, 3H, 8-$CH_3$); $^1$H-NMR (dimethyl sulfoxide-$d_6$): $\delta$ 5.87 (1H, $J_{XA}$ = 17.0 Hz, $J_{XB}$ = 10.0 Hz), 5.17 (1H, $J_{AX}$ = 17.0 Hz, $J_{AB}$ = 3.0 Hz), 4.97 (1H, $J_{BX}$ = 10.0 Hz, $J_{BA}$ = 3.0 Hz), 4.37 (bt, 1H, $J$ = 6.0 Hz, $CH_2OH$), 4.17 (bs, 1H, *tert*-OH), 3.23 (bs, 2H, $w_{1/2}$ = 4.2 Hz, $CH_2O$), 1.63 (s, 3H), and 1.55 (s, 3H). By the addition of deuterium oxide to this solution, the signals at 4.37 and 4.17 ppm were lost, and the peak at 3.23 became sharp ($w_{1/2}$ = 2 Hz).

*Myrcene-3(10)-glycol-10-acetate*—Mass spectrum: *m/z* (%) 194 ($M^+$ − $H_2O$, trace), 152 (1), 139 (19), 134 (56), 119 (78), 87 (10), 83 (22), 69 (base), 55 (49), 43 (77), and 41 (22); IR: $\nu$ 3655, 3500, 3075, 2950, 2910, 2845, 1735, 1640, 1450, 1410, 1380, 1260, 1240, 1145, 1100, 1040, 993, 913, and 850 cm$^{-1}$; $^1$H-NMR: $\delta$ 6.00–4.93 (4H), 4.05 (q, 2H, $J$ = 15.0 and 11.0 Hz, $CH_2OCOCH_3$), 2.10 (s, 3H), 1.72 (s, 3H, 9-$CH_3$), and 1.63 (s, 3H, 8-$CH_3$).

*10-Normyrcen-3-one*—The glycol (XXXII) (105.1 mg) was dissolved in petroleum ether (5 ml) containing activated manganese dioxide (0.5 g) and stirred for 3 days at room temperature. The products were purified by column chromatography to give a ketone (16.9 mg); mass spectrum: *m/z* (%) 138 ($M^+$, $C_9H_{14}O$, 7), 123 (25), 95 (53), 55 (base), and 41 (46); IR: $\nu$ 2960, 2920, 2850, 1700 (weak), 1680, 1620, 1422, 1380, 1360, 1182, 1098, 990, 965, and 818 cm$^{-1}$; $^1$H-NMR: $\delta$ 6.36–6.22 (2H, *AMX*), 5.77 (q, 1H, $J$ = 8.0 and 4.0 Hz, AM*X*), 5.10 (bt, 1H, $J$ = 7.0 Hz, 6-CH), 2.93–1.93 (4H), 1.67 (s, 3H, 9-$CH_3$), and 1.60 (s, 3H, 8-$CH_3$).

*Acetonide of XXXII*—The glycol (XXXII) (38.3 mg) was dissolved in anhydrous acetone (5 ml) containing anhydrous cupric sulfate (28.2 mg) and stirred for 21 hr at room temperature. After filtration of the reaction mixture, acetone was evaporated under reduced pressure to give 15.9 mg of an acetonide; mass spectrum: *m/z* (%) 195 ($M^+$ − 15, $C_{12}H_{19}O_2$, 3) and 69 (base); $^1$H-NMR: $\delta$ 6.10–4.93 (4H), 2.62 (2H, $CH_2O$), 1.67 (s, 3H), 1.60 (s, 3H), and 1.27 [ss, 6H, $C(CH_3)_2$]; IR: $\nu$ 1360–1380 (very strong) cm$^{-1}$.

*Myrcene-1,2-glycol (XXXIV) (20.8%)*—The mass spectrum of the second neutral metabolite, $C_{10}H_{18}O_2$ ($M^+$, 170), showed the presence of a dimethyl allyl group [1.73, 1.63 (s, each 3H), and 5.13 (m, 1H); *m/z* 69 (base)] and an *exo*-cyclic methylene group [4.97 and 5.13 (s, each 1H) ppm]. The IR spectrum revealed hydroxyl absorption at 3575 and 3450 cm$^{-1}$. This alcohol was converted into its diacetate (1735 cm$^{-1}$), whose $^1$H-NMR showed two sets of route protons of primary and secondary acetoxyl groups (4.14, 2H, and 5.38, 1H). The presence of the two hydroxyl groups of XXXIV was determined further by $^1$H-NMR in dimethyl sulfoxide-$d_6$, namely, the signals of 4.63 (d) and 4.38 (t), assignable to CH(*OH*) and $CH_2OH$, respectively, which disappeared upon the addition of deuterium oxide. Thus, it was confirmed that the vinyl group of myrcene was metabolized to a glycol, and the formation of 1,2-glycol acetonide strongly supports this determination.

The biotransformed XXXIV showed the same $^1$H-NMR spectrum as that of the synthetic one (35); $[\alpha]_D$ ±0° (*c*, 2.5); mass spectrum: *m/z* (%) 170 ($M^+$, $C_{10}H_{18}O_2$, 1), 152 (2), 121 (8), 119 (11), 109 (21), 101 (17), 95 (13), 85 (12), 81 (12), 79 (11), 70 (12), and 69 (base); IR: $\nu$ 3575, 3400, 1010, 910, and 840 cm$^{-1}$; $^1$H-NMR: $\delta$ 5.13 and 4.97 (s, each 1H, =$CH_2$), 5.13 (m, 1H, C=CH), 4.17 [m, 1H, C*H*(OH)], 3.63 (m, 2H, $CH_2OH$), 1.70 (s, 3H, 9-$CH_3$), and 1.63 (s, 3H, 8-$CH_3$); $^1$H-NMR (dimethyl sulfoxide-$d_6$): $\delta$ 4.63 [d, 1H, $J$ = 5 Hz, CH(*OH*)] and 4.38 (t, 1H, $J$ = 6 Hz, $CH_2OH$), which were replaceable with deuterium oxide.

*Diacetate of XXXIV*—The 1,2-glycol (19.3 mg) was acetylated in the usual manner to give the diacetate (13.2 mg), $[\alpha]_D$ −0.08° (*c*, 2.5); mass spectrum: *m/z* (%) 194 ($M^+$ − 60, $C_{12}H_{18}O_2$, 4), 151 (10), 134 (86), and 119 (base); IR: $\nu$ 3020, 1735, 1650, 980, 950, and 915 cm$^{-1}$; $^1$H-NMR (90 MHz): $\delta$ 5.38 [q, 1H, $J$ = 7.5 and 4.0 Hz, =C–C*H*($OCOCH_3$)], 5.09 and 4.97 (s, each 1H, =$CH_2$), 5.20–4.90 (bs, 1H, =CH), 4.17 and 4.14 (t, each 1H, –$CH_2OCOCH_3$), 2.08 (s, 3H), 2.13 (s, 3H), 1.68 (s, 3H), and 1.61 (s, 3H).

*Acetonide of XXXIV*—The 1,2-glycol (34.9 mg) was stirred with anhydrous cupric sulfate (0.2 g) in acetone for 16 hr at room temperature. After filtration and evaporation, an acetonide (10.3 mg) was obtained; mass spectrum: *m/z* (%) 194 ($M^+$ − $H_2O$, trace), 152 (2), 139 (19), 134 (56), 119 (78), 69 (base), and 43 (77).

*Uroterpenol (XXXVI) as Acetate (11.8%)*—From the acetates of myrcene neutral metabolites, uroterpenol monoacetate was isolated in a minor yield by preparative TLC. Its mass spectrum agreed with that of an authentic sample (36). The IR (3425 and 1720 cm$^{-1}$) and $^1$H-NMR [5.38 (1H), 4.05 (2H of $CH_2OH$), and 1.67 (allylic methyl)] data support this structure; mass spectrum: *m/z* (%) 194 ($M^+$, $C_{12}H_{20}O_3$, 8), 139 (32), 134 (base), 119 (35), 105 (17), 95 (37), and 43 (84); IR (liquid film): $\nu$ 3425, 1720, 1430, 1370, 1240, and 1040 cm$^{-1}$; $^1$H-NMR: $\delta$ 5.38 (bs, 1H), 4.05 (s, 2H), 2.12 (s, 3H), 1.67 (s, 3H), and 1.15 (s, 3H).

*2-Hydroxymyrcene-1-carboxylic Acid (XXXV) as Methyl Ester*—An acidic metabolite was isolated as the methyl ester, and the mass spectrum showed the molecular ion at *m/z* 198 of $C_{11}H_{18}O_3$. Its IR spectra showed the presence of a hydroxyl group at 3450 cm$^{-1}$ and −CH(*OH*) at 3.06 ppm (d, $J$ = 6 Hz), and the isopropenyl and 3(10)-endmethylene groups remained unchanged. The hydroxyl proton signal at 60 MHz disappeared in the case of 90 MHz, and the −C*H*(OH) signal became broad. Thus, the structure of this hydroxyl ester was determined to be methyl 2-hydroxymyrcene-1-carboxylate (XXXV*a*), $[\alpha]_D$ ±0° (*c*, 1.1); mass spectrum: *m/z* (%) 198 ($M^+$, $C_{11}H_{18}O_3$, 2), 180 (2), 173 (3), 138 (13), and 69 (base); IR (liquid film): $\nu$ 3450, 1730, 1370, 1260, 1210, 1080, 1050, 982, and 900 cm$^{-1}$; $^1$H-NMR: $\delta$ 5.18 and 5.04 (s, each 1H, =$CH_2$), 5.20–5.00 (bs, 1H, C=CH), 4.60 [d, 1H, $J$ = 6 Hz, C*H*(OH)], 3.06 [d, 1H, $J$ = 6 Hz, CH(*OH*)], 3.82 (s, 3H), 2.15 (2H), 2.11 (2H), 1.70 (s, 3H, 9-$CH_3$), and 1.63 (s, 3H, 8-$CH_3$).

*3-Hydroxymyrcene-10-carboxylic Acid (XXXIII) as Methyl Ester*—The alternative hydroxyacid, 3-hydroxymyrcene-10-carboxylic acid, was estimated tentatively from its GLC–mass spectrometric spectrum as a methyl ester; mass spectrum: *m/z* (%) 198 ($M^+$, $C_{11}H_{18}O_3$, 2), 180 (18), 165 (22), 139 (26), 121 (55), 116 (92), 93 (22), 83 (39), 69 (base), 55 (74), and 41 (50).

**Metabolites of *p*-Cymene**—In *p*-cymene (XXXVII), the neutral metabolites were isolated by preparative TLC; acidic metabolites were identified by the GLC–mass spectrometric spectra.

p-*Cymen-9-ol (XXXVIII) (50%)*—Mass spectrum: *m/z* (%) 150 ($M^+$, $C_{10}H_{14}O$, 18), 120 (12), 119 (base), 117 (12), 91 (25), 77 (8), and 65 (6); IR (liquid film): $\nu$ 3370, 1520, 1040, 1020, and 819 cm$^{-1}$; $^1$H-NMR: $\delta$ 7.15 (s, 4H), 3.66 (d, 2H, $J$ = 7 Hz), 2.83 [m, 1H, C*H*($CH_3$)$_2$], 2.35 (s, 3H), and 1.27 (d, 3H, $J$ = 7 Hz). These data were coincident with those of *p*-cymen-9-ol (XL) in the literature (37).

*α-p-Tolylpropionic Acid (XXXIX) as Methyl Ester*—The spectral data agreed with those of methyl α-*p*-tolyl propionate (37); mass spectrum: *m/z* (%) 178 ($M^+$, $C_{11}H_{14}O_2$, 42), 120 (74), and 91 (base); IR (liquid film): $\nu$ 1735, 1518, 1280, 820, and 715 cm$^{-1}$; $^1$H-NMR: $\delta$ 7.15 (s, 4H), 3.65 (s, 3H), 3.44 (q, 1H, $J$ = 6 Hz, 8-CH), 2.33 (s, 3H), and 1.48 (d, 3H, $J$ = 6 Hz).

p-*Cymen-8-ol (XXVI) (28%)*—Mass spectrum: *m/z* (%) 150 ($M^+$, $C_{10}H_{14}O$, 9), 135 (base), 132 (19), 117 (17), 115 (10), 105 (4), 91 (25), 77 (6), 65 (10), and 43 (base); IR (liquid film): $\nu$ 3400, 1518, 1024, 968, 868, 820, and 725 cm$^{-1}$; $^1$H-NMR: $\delta$ 7.34 (q, 2H, $J$ = 8 Hz), 7.21 (d, 2H, $J$ = 8 Hz), 2.38 (s, 3H), and 1.58 (s, 6H). All of these spectra agreed with those of *p*-cymen-8-ol (XXVI) (19, 23).

Another four acidic metabolites were estimated tentatively on the basis of mass spectra. These compounds were not isolated because of the small amounts.

*α-Tolyl-α-hydroxylpropionic Acid (XL) as Methyl Ester*—Mass spectrum: *m/z* (%) 176 ($M^+$ − $H_2O$, base), 164 (16), 163 (10), 149 (9), 145 (26), 131 (5), 92 (6), and 91 (10).

*α-Tolylacrylic Acid (XLI) as Methyl Ester*—Mass spectrum: *m/z* (%) 176 ($M^+$, $C_{11}H_{12}O_2$, 55), 146 (12), 145 (base), 117 (12), 116 (8), 115 (27), and 91 (13).

p-*Isopropylbenzoic Acid (XLII) as Methyl Ester*—Mass spectrum: *m/z* (%) 178 ($M^+$, $C_{11}H_{14}O_2$, 38), 163 (base), 119 (65), and 91 (29).

p-*1-Hydroxyisopropylbenzoic Acid (XLIII) as Methyl Ester*—Mass spectrum: *m/z* (%) 176 ($M^+$ − $H_2O$, base), 162 (32), 145 (51), and 91 (10).

## DISCUSSION

Scheme I shows the metabolic routes of α- and β-pinenes. The main

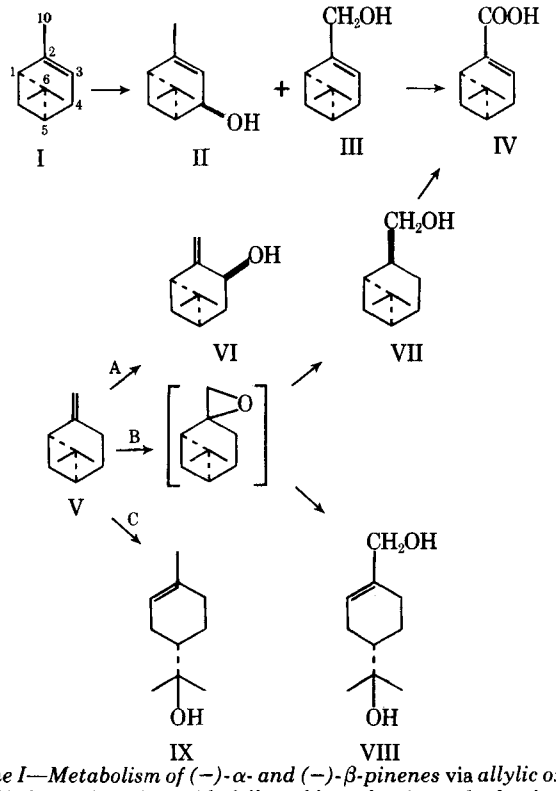

*Scheme I—Metabolism of (−)-α- and (−)-β-pinenes* via *allylic oxidation (A), formation of epoxide followed by reduction or hydration (B), and ring cleavage of the four-membered ring (C).*

urinary metabolites of α-pinene in rabbits were the verbenols. The purities and optical rotations of the verbenols are shown in Table II. In the case of (−)-α-pinene (I), the purity of verbenol by GLC of neutral metabolites was 99%. On the other hand, the purities of verbenols from (+)- and (±)-α-pinenes were 67 and 68%, respectively. This finding means that the biotransformation of (−)-α-pinene in rabbits is remarkably efficient in the preparation of (−)-*trans*-verbenol (II). Another method of the chemical preparation of (−)-*trans*-verbenol was reported by Mori (38). In addition, the relation of the signs and values of the optical rotations between the administered α-pinenes and the obtained verbenols suggests the stereoselective hydroxylation of α-pinene. As minor metabolites of α-pinene, two allylic products, myrtenol (III) and myrtenic acid (IV), were obtained.

In (−)-β-pinene (V), among three metabolic routes (A, B, and C in Scheme I), Route B is thought to be the main route judging from the yields of 10-pinanol (VII) and 1-*p*-menthene-7,8-diol (VIII) (39 and 30%, respectively). This route includes epoxide formation of the end-methylene group. Such epoxide formation also was found in the metabolism of camphene in rabbits (13), and it was confirmed by the administration of camphene epoxide to obtain camphanol (39). Myrtenic acid might be

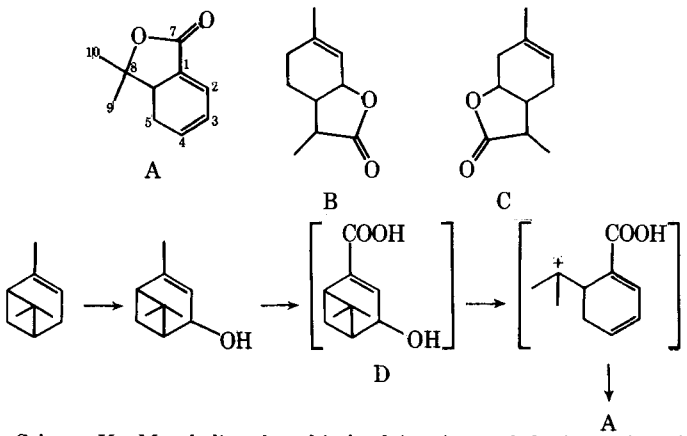

*Scheme II—Metabolites found in koala's urine and the formation of Lactone A.*

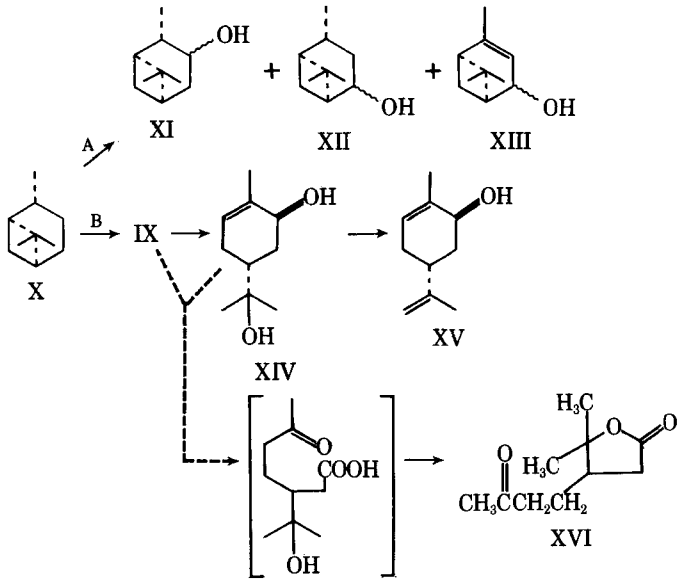

*Scheme III—Metabolism of (−)-cis-pinane* via *simple hydroxylation at secondary carbon atoms (A) and ring cleavage of the four-membered ring and hydration (B).*

derived through this route from β-pinene. The additional routes, A and C, are estimated from the corresponding metabolites. On the other hand, the koala fed a diet of *Eucalyptus punctata* containing α- and β-pinenes metabolized the lactones A, B, and C (Scheme II) (9), and later it was pointed out that A is yielded through 4-hydroxymyrtenic acid (D, Scheme II) (40). The presence of this acid (D) was suggested as a metabolite of α-pinene in rabbits[10]. In the present study, however, it was not detected even in GLC–mass spectrometry, so it is concluded that it is a species-specific metabolite of α-pinene in mammals.

In pinane (Scheme III), Route B was the main metabolic route [α-terpineol (IX) (43%)]. In the first step, it can be estimated that eradication of a hydride ion occurred. The three compounds of Route A [3-pinanol (XI), 4-pinanol (XII), and verbenol (XIII)] were clearly estimated as metabolites on the basis of the isolated oxidation products (3-pinanone, 4-pinanone, and verbenone, respectively) of the neutral portion. A lactonic compound (XVI) might be yielded as an artifact from α-terpineol

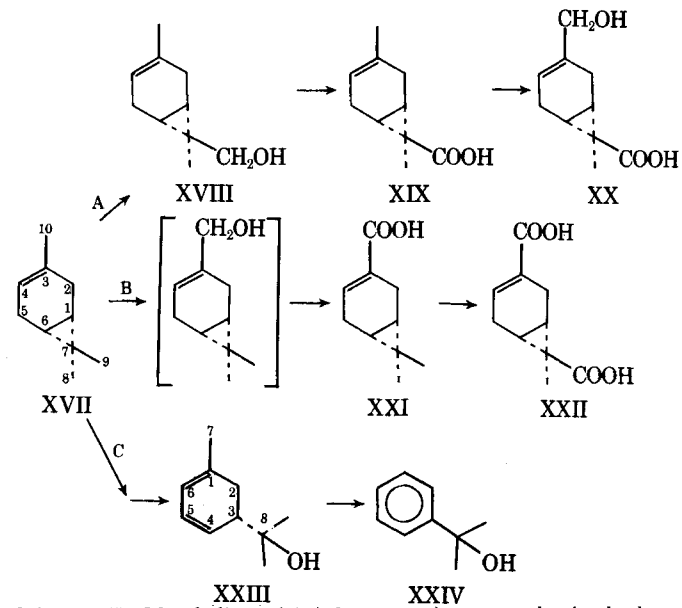

*Scheme IV—Metabolism of (+)-3-carene* via *stereoselective hydroxylation at* gem*-dimethyl followed by carboxylation (A), allylic oxidation at an allylic methyl group (B), and allylic hydroxylation at a secondary carbon atom (C).*

[10] R. Mechoulam, Hebrew University of Jerusalem, Jerusalem, Israel, personal communication.

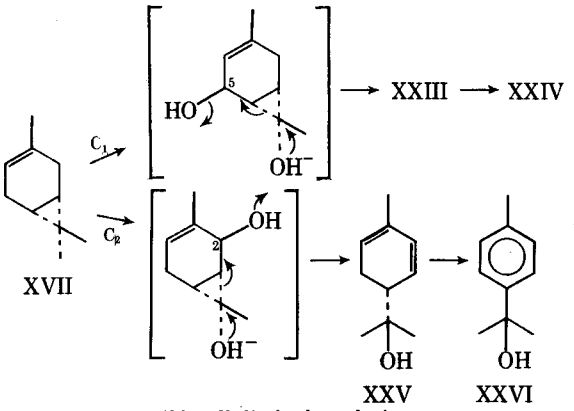


*Scheme V—Two possible allylic hydroxylation routes at secondary carbon atoms (C-2 and C-5) of 3-carene.*

(IX) or sobrerol (XIV) by Jones oxidation of a neutral portion of the metabolites.

As shown in Scheme IV, 3-carene (XVII) was stereoselectively hydroxylated and carboxylated. In this case, *m*-mentha-4,6-dien-8-ol (XXIV) was a main urinary neutral metabolite (71.8%) along with its aromatized *m*-cymen-8-ol (XXIV) (<1%). The formation of 3-caren-9-ol (XVIII) in Route A in Scheme IV is explained as allylic hydroxylation due to the cyclopropane ring. Four compounds were isolated as acidic metabolites: 3-carene-9-carboxylic acid (XIX), 3-carene-9,10-dicarboxylic acid (XXII), chamic acid (XXI), and 3-caren-10-ol-9-carboxylic acid (XX). Metabolites XVIII, XIX, XX, and XXII in Scheme IV have not been reported yet in literature.

Routes A and B show the stereoselective hydroxylation and carboxylation of the *gem*-dimethyl group. Such reactions have not been found in the chemical oxidation of 3-carene, indicating the enzymatic specificity in the metabolism. In Route C, two metabolic pathways ($C_1$ and $C_2$) can be proposed as the *endo*-cyclic allylic hydroxylation (Scheme V). It is reported that 1,3-rearrangement of the hydroxyl group in 3-caren-5-ol to *m*-mentha-4,6-dien-8-ol (XXIII) occurs easily due to the cyclopropane ring (41). Thus, Route $C_1$ in Scheme V includes 3-caren-5-ol as an intermediate. In the same manner, Route $C_2$ [formation of 3-caren-2-ol, followed by the rearrangement to a dienol (XXV) and the formation of an aromatic alcohol (XXVI)] may be postulated, but neither XXV or XXVI was found in this experiment. Consequently, Route $C_2$ is ruled out. Therefore, the position of C-5 in 3-carene is thought to be more easily hydroxylated than C-2 by enzymatic systems in the liver of a rabbit. The same example can be seen in the metabolism of 1-methylcyclohexene in rabbits (12).

In carane, the C-9 and C-10 methyl groups were metabolized by enzymes (Scheme VI). The carboxylation of the *gem*-dimethyl group is said to be stereoselective and is one kind of allylic oxidation due to the cyclopropane ring; the secondary C-10 methyl group of carane was metabolized as in the case of carboxylation of the secondary methyl of patchoulol (6). Therefore, oxidation of the C-10 methyl group of carene does not always seem to be affected by the double bond. This is the first case in which carane-9,10-dicarboxylic acid has been reported. As a

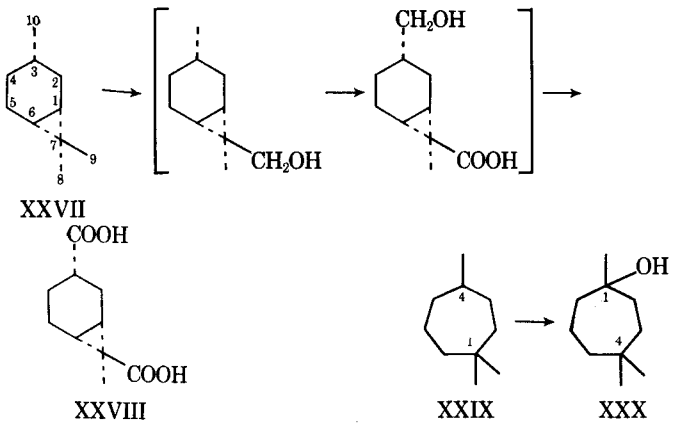


*Scheme VI—Metabolism of (−)-*cis*-carane via stereoselective gem-dimethyl and secondary methyl hydroxylation and carboxylation in 3-carane.*

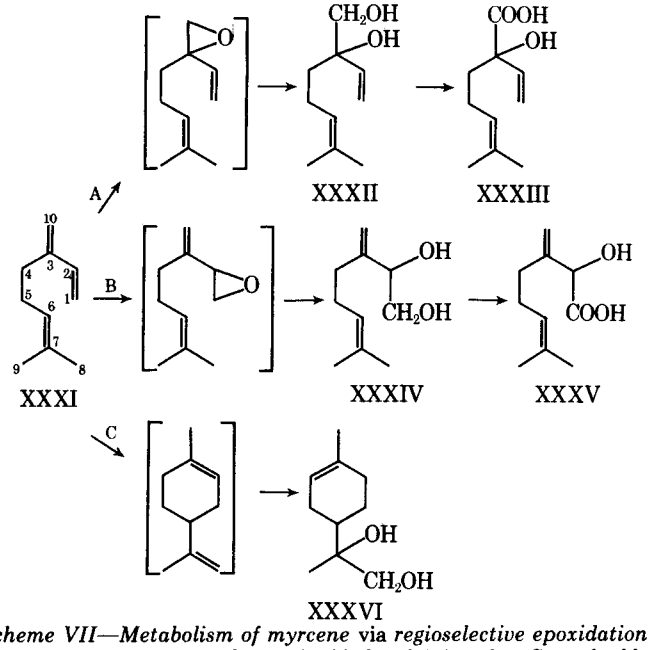


*Scheme VII—Metabolism of myrcene via regioselective epoxidation followed by hydration at C-3,10 double bond (A) and at C-1,2 double bond (B).*

neutral metabolite of carane, 1,4,4-trimethylcycloheptan-1-ol (XXX) was identified by spectral data. This alcohol can be explained as a metabolite from 1,1,4-trimethylcycloheptane (XXIX), which was reported as a main reduction product of 3-carene in some conditions (42) and whose minor presence in the administered carane was confirmed by comparison of GLC–mass spectrometry of authentic samples. The formation of this tertiary alcohol was reported in methylcyclohexane metabolism (43, 44).

Scheme VII shows the metabolism of myrcene (XXXI). Among these metabolites, two compounds had not been reported previously [myrcene-3(10)-glycol (XXXII) and 2-hydroxymyrcene-1-carboxylic acid (XXXV)], and myrcene-1,2-glycol (XXXIV) was newly obtained as a natural product. The formation of two glycols was due to the hydration of the corresponding epoxides formed as intermediates. The yield of 3(10)-glycol was higher than 1,2-glycol, indicating the facile enzymatic attack to the fixed 3(10)-double bond. The optical rotation of these glycols each showed a value of zero, meaning that there is an equal chance of attack by enzymes to the double bond from both sides. The formation of uroterpenol (XXXVI) may proceed through limonene, which was clearly derived from myrcene in the acidic conditions of rabbit stomachs.

At first, four allylic alcohols (E, F, G, and H) were expected as the neutral metabolites of myrcene. However, none of these compounds was obtained. The fact that the allylic positions (C-4, C-5, C-8, and C-9) of myrcene were not hydroxylated shows the regioselective hydroxylation by enzymes in rabbits. This metabolism of myrcene offers one type of biotransformation of $\beta$-farnesene (J), a linear sesquiterpene hydrocarbon having the same partial structure as myrcene.

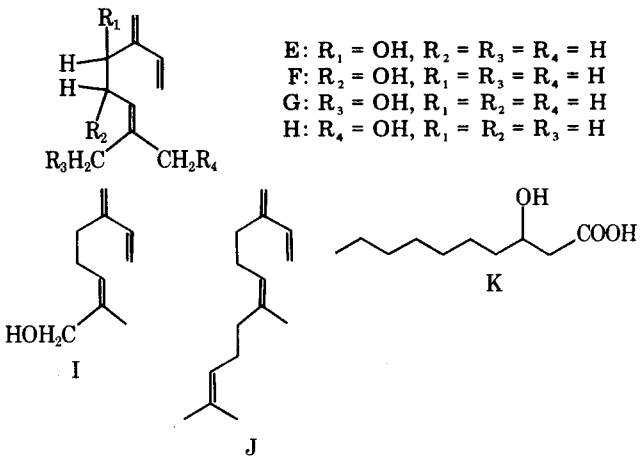

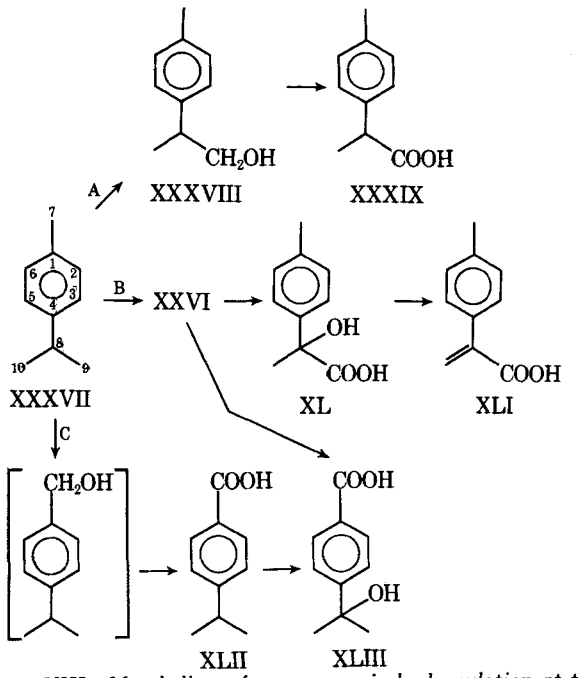


*Scheme VIII—Metabolism of* p-*cymene* via *hydroxylation at the ω position (A), at the ω-1 position (B), and at the benzyl position (C).*

Biotransformation of aromatic hydrocarbons has been studied extensively in relation to carcinogenic activity. However, the metabolism of *p*-cymene (XXXVII), which is often found in essential oils, remains to be established in mammals. As shown in Scheme VIII, seven metabolites were identified or estimated. The intraperitoneal administration of *p*-cymene gave the same metabolites as did oral administration, suggesting that all terpenoids used were biotransformed not microbiologically but through liver enzymatic systems. Cumene was metabolized in rabbits and gave 2-phenyl-2-propanol (40%), 2-phenyl-1-propanol (25%), and 2-phenylpropionic acid (25%) (45). In addition, isopropyl diphenyl was metabolized in many mammals (dog, monkey, rat, and human), and species-different metabolic routes were proposed previously (46). Those studies and the present results establish the metabolism of aromatic hydrocarbons having an aliphatic group as follows:

1. Aromatic hydrogen atoms are not replaced by hydroxyl groups.
2. In the metabolism of methyl and isopropyl groups on aromatic hydrocarbons, the isopropyl group is more easily hydroxylated or carboxylated (Routes A and B) than the benzyl methyl group (Route C), judging from their yields.

On the other hand, in the microbial transformation of *p*-cymene, the carboxylation of the benzyl methyl group and the hydroxylation of aromatic hydrogens were reported (37). Thus, the biotransformation of *p*-cymene in rabbits and microorganisms are considerably different. The metabolism of ethyl benzene was reported and a similar pathway was proposed (47).

From the point of biological activity, mammals (rabbits) and insects (bark beetles) show an interesting relationship in the metabolism of monoterpenoids. Namely, verbenol and pinocarveol also were reported as oxidation products of α- and β-pinenes, respectively, in a bark beetle, *Dendroctonus frontalis* (48). Moreover, (−)-*cis*- and (+)-*trans*-verbenols have pheromonal activity in *Ips paraconfusus* and in *Dendroctonus brevicomis*, respectively (49). In addition, myrcene was metabolized to ipsdienol (Structure F) and ipsenol (Structure I), both known as pheromones that are widely used in Scandinavia (50), in *Ips* spp. (51, 52). *p*-Cymen-8-ol (XXVI) also was found from the frass of a longhorn beetle, *Hylotrupes bajalus* (53). The high yield (50% of the dose) of *p*-cymen-8-ol following intraperitoneal administration offers a new preparation method for this pheromone.

2-Hydroxymyrcene-1-carboxylic acid (XXXV) has a structure similar to myrmicacin (Structure K) (54), so it is expected to have some biological activity.

## REFERENCES

(1) "New Natural Products and Plant Drugs with Pharmacological, Biological or Therapeutical Activity," H. Wagner and P. Wolff, Eds., Springer, Berlin, Germany, 1977, p. 137.

(2) J. S. Robertson and M. Hussain, *Biochem. J.*, **113,** 57 (1969).

(3) K. C. Leibman and E. Ortiz, *Metab. Disp.*, **1,** 543 (1973).

(4) LUU Bang and G. Ourisson, *Tetrahedron Lett.*, **1975,** 1881.

(5) E. Trifilieff, LUU Bang, and G. Ourisson, *ibid.*, **1975,** 4307.

(6) LUU Bang, G. Ourisson, and P. Teissire, *ibid.*, **1975,** 2211.

(7) R. Kodama, T. Yano, K. Furukawa, K. Noda, and H. Ide, *Xenobiotica*, **6,** 377 (1976).

(8) J. W. Regan and L. F. Bjeldane, *J. Agr. Food Chem.*, **24,** 377 (1976).

(9) I. A. Southwell, *Tetrahedron Lett.*, **1975,** 1885.

(10) T. M. Flynn and I. A. Southwell, *Aust. J. Chem.*, **32,** 2093 (1979).

(11) I. A. Southwell, T. M. Flynn, and R. Degabriele, *Xenobiotica*, **10,** 17 (1980).

(12) T. Ishida, Y. Asakawa, M. Okano, and T. Aratani, *Tetrahedron Lett.*, **1977,** 2437.

(13) T. Ishida, Y. Asakawa, T. Takemoto, and T. Aratani, *J. Pharm. Sci.*, **68,** 928 (1979).

(14) N. Ikekawa, Y. Fujimoto, M. Ishiguro, S. Suwa, Y. Hirayama, and H. Mizunuma, *Science*, **204,** 1223 (1979).

(15) J. A. A. Renwick, *Contrib. Boyce Thompson Inst.*, **23,** 355 (1967).

(16) T. Toda and K. Takahashi, *Sci. Rep. Tohoku Univ., Ser. 1*, **53,** 72 (1970).

(17) V. S. Joshi, N. P. Damodaran, and S. Dev, *Tetrahedron*, **24,** 5817 (1968).

(18) M. P. Hartshorn and A. F. A. Wallis, *J. Chem. Soc.*, **1964,** 5254.

(19) B. M. Mitzer, V. J. Mancini, S. Lemberg, and T. Theimer, *Appl. Spectrosc.*, **22,** 34 (1968).

(20) N. Nakagawa and S. Saito, *Tetrahedron Lett.*, **1967,** 1003.

(21) T. Sato, *Nippon Kagaku Zasshi*, **88,** 1005 (1967).

(22) "Spectral Atlas of Terpenes and the Related Compounds," Y. Yukawa and S. Ito, Eds., Hirokawa, Tokyo, Japan, 1973, p. 210.

(23) "Eight Peak Index of Mass Spectra", vol. 1, Mass Spectrometry Data Centre, AWRE, Aldermaston, Reading, England, 1974, pp. 762, 768.

(24) C. Nishino and H. Takayanagi, *Agr. Biol. Chem.*, **43,** 1967 (1979).

(25) "Aldrich Library of Infrared Spectra," C. J. Pouchert, Ed., Aldrich, Milwaukee, Wis., 1975, p. 364-B.

(26) "Aldrich Library of NMR Spectra," vol. 3, C. J. Pouchert, Ed., Aldrich, Milwaukee, Wis., 1974, p. 77-C.

(27) K. Gollnick, G. Shade, and G. Schroeter, *Tetrahedron*, **22,** 139 (1966).

(28) W. G. Dauben, M. Lorber, and D. S. Fullerton, *J. Org. Chem.*, **34,** 3587 (1969).

(29) W. D. P. Burns, M. S. Carson, W. Cocker, and P. V. R. Shannon, *J. Chem. Soc. (C)*, **1968,** 3073.

(30) S. P. Acharya, *Tetrahedron Lett.*, **1966,** 4117.

(31) H. Erdtman, W. E. Harvey, and J. G. Topliss, *Acta Chem. Scand.*, **10,** 1381 (1956).

(32) T. Norin, *Arkiv Kemi*, **22,** 123 (1963).

(33) M. Christl and J. D. Roberts, *J. Org. Chem.*, **37,** 3443 (1972).

(34) J. B. Stothers, "Carbon-13 NMR Spectroscopy," Academic, New York, N.Y., 1972, p. 436.

(35) R. J. Reynolds Tobacco Co., U.S. pat. 3,751,477 (Aug. 7, 1973).

(36) A. P. Wade, G. S. Wilkinson, F. M. Dean, and A. W. Price, *Biochem. J.*, **101,** 727 (1966).

(37) K. M. Madhyastha and P. K. Bhattacharyya, *Indian J. Biochem.*, **5,** 102 (1968).

(38) K. Mori, *Agr. Biol. Chem.*, **40,** 415 (1976).

(39) T. Ishida, Y. Asakawa, T. Takemoto, and T. Aratani, "23rd Symposium on the Chemistry of Terpenes, Essential Oils and Aromatics," Chemical Society of Japan, Tokyo, Japan, 1979, p. 39.

(40) N. Lander and R. Mechoulam, *J. Chem. Soc. Perkin I*, **1976,** 484.

(41) D. A. Baines and W. Coker, *ibid.*, **1975,** 2232.

(42) W. Coker, P. V. R. Shannon, and P. A. Staniland, *J. Chem. Soc. (C)*, **1966,** 41.

(43) T. H. Eliott, R. C. C. Tao, and R. T. Williams, *Biochem. J.*, **95,** 70 (1965).

(44) U. Frommer, V. Ullrich, and H. Staudinger, *Hoppe-Seylers Physiol. Chem.*, **351,** 903 (1970).

(45) S. Goenechea, K. Olek, and P. Wardenbach, *J. Chromatogr.*, **154,** 282 (1978).

(46) H. R. Sullivan, R. E. McMahon, D. G. Hoffman, and A. S. Ridolfo,

in "Mass Spectrum Drug Metabolism" (Proceedings of an International Symposium), F. Albert, Ed., 1977, p. 31.
(47) M. Kiese and W. Lenk, *Xenobiotica*, **4**, 337 (1974).
(48) J. A. A. Renwick, P. R. Hughes, and T. Y. Tanletin Dej, *J. Insect Physiol.*, **19**, 1735 (1973).
(49) J. A. A. Renwick, P. R. Hughes, and I. S. Kull, *Science*, **191**, 199 (1976).
(50) D. A. O'Sullivan, *Chem. Eng. News*, **1979**, No. 31, p. 10.
(51) R. H. Fish, L. E. Browe, D. L. Wood, and L. B. Hendry, *Tetrahedron Lett.*, **1979**, 1465.
(52) P. R. Hughes, *J. Insect Physiol.*, **20**, 1271 (1974).
(53) M. D. Higgs and D. A. Evans, *Experientia*, **34**, 46 (1978).
(54) Y. Iwanami and T. Iwadare, *Bot. Gaz.*, **140**, 1 (1979).

### ACKNOWLEDGMENTS

The authors thank Professor Y. Matsubara, Kinki University, for the pinane sample, the Yasuhara Perfumary Co. for the samples of 3-carene and carane, and Professor W. Cocker, Trinity College, for the authentic sample of 1,1,4-trimethylcycloheptane. The authors also thank Professor J. Sakurai, Tokushima-Bunri University, for the intraperitoneal injection of *p*-cymene to rabbits and Dr. S. Imai, Hiroshima University, for the measurements of 90-MHz $^1$H-NMR spectra of metabolites. They also thank Dr. V. S. Joshi, National Chemical Laboratory, Poona, India, for the $^1$H-NMR and IR spectra of (+)-*trans*-pinocarveol, Mr. I. A. Southwell, Biological and Chemical Research Institute, N.S.W., Australia, for the NMR and IR spectra of Lactone A, Dr. C. Nishio, Mitsubishi Kasei Institute of Life Sciences, for the IR and $^1$H-NMR spectra of *cis*-3-pinanone, *trans*-3-pinanone, *cis*-4-pinanone, and *trans*-4-pinanone, the R. J. Reynolds Tobacco Co., Winston-Salem, N.C., for the $^1$H-NMR spectrum of myrcene-1,2-glycol, Professor H. Miki, Osaka Institute of Technology, for the $^1$H-NMR spectrum of pinocarvone, and Professor K. Yamasaki, Hiroshima University, for the assignment of the $^{13}$C-NMR spectrum of dimethyl 3-carene-9,10-dicarboxylate.

# Quantitative TLC Determination of Epimeric Ratios of 16-Methyl 17-Ketone Oxidation Products of Dexamethasone and Related Drugs

**E. C. JUENGE ˣ and P. E. FLINN**

Received April 3, 1980, from the *National Center for Drug Analysis, Food and Drug Administration, St. Louis, MO 63101.* Accepted for publication September 22, 1980.

**Abstract** □ A TLC system sensitive enough to detect, identify, and allow quantitation of the 16-methyl $\alpha$- and $\beta$-epimers of 9-fluoro-11$\beta$-hydroxy-16-methylandrosta-1,4-diene-3,17-dione is described. These epimeric 17-ketones may be present as impurities in dexamethasone, betamethasone, or related drugs. A spectrodensitometer with a TLC scanning attachment was used, and results from densitometry compared favorably with quantitation by high-performance liquid chromatography, as was described recently. TLC was convenient in the rapid examination of drug samples for the detection and identification of epimeric 17-ketones and for the determination of the $\alpha$ to $\beta$ ratio of such epimers. Various applied photographic techniques for documenting TLC data are described.

**Keyphrases** □ TLC—detection and identification of 16$\alpha$- and 16$\beta$-methyl epimers of 9-fluoro-11$\beta$-hydroxy-16-methylandrosta-1,4-diene-3,17-dione, impurities in dexamethasone, betamethasone, and related drugs □ Dexamethasone impurities—16$\alpha$- and 16$\beta$-methyl 17-ketone oxidation products, identification and quantitative detection by TLC □ Epimers—16$\alpha$- and 16$\beta$-methyl 17-ketone oxidation products, possible impurities in dexamethasone, betamethasone, and related drugs, TLC detection and identification of $\alpha$- and $\beta$-epimers

The TLC or partition chromatography of $C_{18}$ steroid estrogens (1–3), $C_{19}$ androstanes (4–6) such as androgenic hormones, $C_{21}$ pregnanes (7–10) including cortisone, and the related oxygenated derivatives of these families is documented. The $C_{22}$ steroids such as dexamethasone and betamethasone and their $C_{20}$ oxidation products have not received such detailed study.

Interest has developed in qualitative and quantitative studies of these epimeric $C_{20}$ oxidation products by high-performance liquid chromatography (HPLC) (11) and TLC (12) because of their presence as impurities in dexamethasone (11–13) and dexamethasone sodium phosphate (I) drug samples. Inherently, the $C_{22}$ steroids and their 17-oxo derivatives possess a structural feature not exhibited by the $C_{19}$ and $C_{21}$ steroids and their oxygenated derivatives, namely, an optical center resulting from the additional methyl group at the C-16 position. These epimeric optical isomers were subjected to HPLC and TLC in this study.

## BACKGROUND

The 17-oxo derivative, *i.e.*, 9-fluoro-11$\beta$-hydroxy-16-methylandrosta-1,4-diene-3,17-dione (epimers II$\alpha$ and II$\beta$), recently was reported to be present (12) at ~2% as an impurity in drug products from five of six dexamethasone manufacturers for the Canadian market. In addition, a massive contamination (50%) by the $\alpha$- and $\beta$-epimers of this ketone (II$\alpha$ and II$\beta$) was reported (11) in a commercial sample of dexamethasone sodium phosphate (I) solution for injection. In that study (11), it was found by HPLC that this 17-keto oxidation product was actually an epimeric mixture of the 16$\alpha$- and 16$\beta$-methyl compounds and that the $\alpha$ to $\beta$ ratio could be determined approximately. Identification of the 16-methyl 17-ketone epimers (II$\alpha$ and II$\beta$) by TLC systems similar in nature to the reversed-phase HPLC system was attempted, but the TLC systems failed to separate the $\alpha$- and $\beta$-epimers; dexamethasone acetate, a related compound, consistently exhibited the same $R_f$ value as the epimers (11).

Another report (12) indicated that separation between the 16$\alpha$- and 16$\beta$-methyl epimers (II$\alpha$ and II$\beta$) can be effected by TLC ($R_f$ 0.60 and 0.59, respectively). The epimeric corticosteroids, dexamethasone and betamethasone, which differ in configuration at the C-16 optical center, were separated by paper chromatographic liquid partition (14). General techniques for photographic documentation of data collected on TLC plates were reported (15).

A method to determine the $\alpha$ to $\beta$ epimeric ratio of the impurity is important because the components of the impurity are diastereoisomeric with different physiological properties and, consequently, different effects on the patient. An overview of possible physiological effects of such contamination, including references, was given previously (11).

The aim of the present work was to develop a TLC technique that allows identification of epimeric 16-methyl 17-ketones (II$\alpha$ and II$\beta$) in samples of drugs related to dexamethasone. Furthermore, the method must determine the $\alpha$ to $\beta$ ratio of the impurity. In the first part of the

0022-3549/81/0400-0415$01.00/0
© 1981, American Pharmaceutical Association

in "Mass Spectrum Drug Metabolism" (Proceedings of an International Symposium), F. Albert, Ed., 1977, p. 31.
(47) M. Kiese and W. Lenk, *Xenobiotica*, **4**, 337 (1974).
(48) J. A. A. Renwick, P. R. Hughes, and T. Y. Tanletin Dej, *J. Insect Physiol.*, **19**, 1735 (1973).
(49) J. A. A. Renwick, P. R. Hughes, and I. S. Kull, *Science*, **191**, 199 (1976).
(50) D. A. O'Sullivan, *Chem. Eng. News*, **1979**, No. 31, p. 10.
(51) R. H. Fish, L. E. Browe, D. L. Wood, and L. B. Hendry, *Tetrahedron Lett.*, **1979**, 1465.
(52) P. R. Hughes, *J. Insect Physiol.*, **20**, 1271 (1974).
(53) M. D. Higgs and D. A. Evans, *Experientia*, **34**, 46 (1978).
(54) Y. Iwanami and T. Iwadare, *Bot. Gaz.*, **140**, 1 (1979).

### ACKNOWLEDGMENTS

The authors thank Professor Y. Matsubara, Kinki University, for the pinane sample, the Yasuhara Perfumary Co. for the samples of 3-carene and carane, and Professor W. Cocker, Trinity College, for the authentic sample of 1,1,4-trimethylcycloheptane. The authors also thank Professor J. Sakurai, Tokushima-Bunri University, for the intraperitoneal injection of *p*-cymene to rabbits and Dr. S. Imai, Hiroshima University, for the measurements of 90-MHz $^1$H-NMR spectra of metabolites. They also thank Dr. V. S. Joshi, National Chemical Laboratory, Poona, India, for the $^1$H-NMR and IR spectra of (+)-*trans*-pinocarveol, Mr. I. A. Southwell, Biological and Chemical Research Institute, N.S.W., Australia, for the NMR and IR spectra of Lactone A, Dr. C. Nishio, Mitsubishi Kasei Institute of Life Sciences, for the IR and $^1$H-NMR spectra of *cis*-3-pinanone, *trans*-3-pinanone, *cis*-4-pinanone, and *trans*-4-pinanone, the R. J. Reynolds Tobacco Co., Winston-Salem, N.C., for the $^1$H-NMR spectrum of myrcene-1,2-glycol, Professor H. Miki, Osaka Institute of Technology, for the $^1$H-NMR spectrum of pinocarvone, and Professor K. Yamasaki, Hiroshima University, for the assignment of the $^{13}$C-NMR spectrum of dimethyl 3-carene-9,10-dicarboxylate.

# Quantitative TLC Determination of Epimeric Ratios of 16-Methyl 17-Ketone Oxidation Products of Dexamethasone and Related Drugs

**E. C. JUENGE ˣ and P. E. FLINN**

Received April 3, 1980, from the *National Center for Drug Analysis, Food and Drug Administration, St. Louis, MO 63101.* Accepted for publication September 22, 1980.

**Abstract** □ A TLC system sensitive enough to detect, identify, and allow quantitation of the 16-methyl $\alpha$- and $\beta$-epimers of 9-fluoro-11$\beta$-hydroxy-16-methylandrosta-1,4-diene-3,17-dione is described. These epimeric 17-ketones may be present as impurities in dexamethasone, betamethasone, or related drugs. A spectrodensitometer with a TLC scanning attachment was used, and results from densitometry compared favorably with quantitation by high-performance liquid chromatography, as was described recently. TLC was convenient in the rapid examination of drug samples for the detection and identification of epimeric 17-ketones and for the determination of the $\alpha$ to $\beta$ ratio of such epimers. Various applied photographic techniques for documenting TLC data are described.

**Keyphrases** □ TLC—detection and identification of 16$\alpha$- and 16$\beta$-methyl epimers of 9-fluoro-11$\beta$-hydroxy-16-methylandrosta-1,4-diene-3,17-dione, impurities in dexamethasone, betamethasone, and related drugs □ Dexamethasone impurities—16$\alpha$- and 16$\beta$-methyl 17-ketone oxidation products, identification and quantitative detection by TLC □ Epimers—16$\alpha$- and 16$\beta$-methyl 17-ketone oxidation products, possible impurities in dexamethasone, betamethasone, and related drugs, TLC detection and identification of $\alpha$- and $\beta$-epimers

The TLC or partition chromatography of $C_{18}$ steroid estrogens (1–3), $C_{19}$ androstanes (4–6) such as androgenic hormones, $C_{21}$ pregnanes (7–10) including cortisone, and the related oxygenated derivatives of these families is documented. The $C_{22}$ steroids such as dexamethasone and betamethasone and their $C_{20}$ oxidation products have not received such detailed study.

Interest has developed in qualitative and quantitative studies of these epimeric $C_{20}$ oxidation products by high-performance liquid chromatography (HPLC) (11) and TLC (12) because of their presence as impurities in dexamethasone (11–13) and dexamethasone sodium phosphate (I) drug samples. Inherently, the $C_{22}$ steroids and their 17-oxo derivatives possess a structural feature not exhibited by the $C_{19}$ and $C_{21}$ steroids and their oxygenated derivatives, namely, an optical center resulting from the additional methyl group at the C-16 position. These epimeric optical isomers were subjected to HPLC and TLC in this study.

## BACKGROUND

The 17-oxo derivative, *i.e.*, 9-fluoro-11$\beta$-hydroxy-16-methylandrosta-1,4-diene-3,17-dione (epimers II$\alpha$ and II$\beta$), recently was reported to be present (12) at ~2% as an impurity in drug products from five of six dexamethasone manufacturers for the Canadian market. In addition, a massive contamination (50%) by the $\alpha$- and $\beta$-epimers of this ketone (II$\alpha$ and II$\beta$) was reported (11) in a commercial sample of dexamethasone sodium phosphate (I) solution for injection. In that study (11), it was found by HPLC that this 17-keto oxidation product was actually an epimeric mixture of the 16$\alpha$- and 16$\beta$-methyl compounds and that the $\alpha$ to $\beta$ ratio could be determined approximately. Identification of the 16-methyl 17-ketone epimers (II$\alpha$ and II$\beta$) by TLC systems similar in nature to the reversed-phase HPLC system was attempted, but the TLC systems failed to separate the $\alpha$- and $\beta$-epimers; dexamethasone acetate, a related compound, consistently exhibited the same $R_f$ value as the epimers (11).

Another report (12) indicated that separation between the 16$\alpha$- and 16$\beta$-methyl epimers (II$\alpha$ and II$\beta$) can be effected by TLC ($R_f$ 0.60 and 0.59, respectively). The epimeric corticosteroids, dexamethasone and betamethasone, which differ in configuration at the C-16 optical center, were separated by paper chromatographic liquid partition (14). General techniques for photographic documentation of data collected on TLC plates were reported (15).

A method to determine the $\alpha$ to $\beta$ epimeric ratio of the impurity is important because the components of the impurity are diastereoisomeric with different physiological properties and, consequently, different effects on the patient. An overview of possible physiological effects of such contamination, including references, was given previously (11).

The aim of the present work was to develop a TLC technique that allows identification of epimeric 16-methyl 17-ketones (II$\alpha$ and II$\beta$) in samples of drugs related to dexamethasone. Furthermore, the method must determine the $\alpha$ to $\beta$ ratio of the impurity. In the first part of the

0022-3549/81/0400-0415$01.00/0
© 1981, American Pharmaceutical Association

study, the TLC method was evaluated as a qualitative tool for detection of the epimeric 16-methyl 17-ketones in drug samples submitted to this laboratory for quality assurance studies; such a method must be convenient and flexible, including reliable procedures for documentation of results. In the second part, the suitability of the TLC method was investigated for quantitative measurement of the epimeric ketones.

## EXPERIMENTAL

**Instruments**—A spectrodensitometer[1] with a TLC scanning attachment and basic computing readout system, a UV–near-IR spectrophotometer[2], and a grating IR spectrophotometer[3] were used. Melting points were taken with a microscopic[4] melting-point stage[5]. An analytical balance[6] equipped with a printer was used to weigh samples for quantitative TLC. A UV viewing box[7] and a tracing table[8] were used for observing and photographing TLC spots under UV irradiation or by transmission of white light. A calculator–printer[9] was used for statistical calculations. A 35-mm camera with black and white, color, and slide film was used[10].

**Reagents, TLC Plates, and Pipets**—Acetone and antimony trichloride were analytical reagent grade. Chloroform was NF grade. Bratton–Marshall reagent[11] was used as received. Absolute methanol was analyzed reagent grade. TLC plates[12] were precoated with silica gel.

Dexamethasone NF, betamethasone NF, and dexamethasone phosphate USP reference standards were used. Dexamethasone phosphate disodium salt was obtained as a research sample[13]. Micropipets[14] were used in TLC.

**Preparation of 9-Fluoro-11β-hydroxy-16α-methylandrosta-1,4-diene-3,17-dione (IIα) and 9-Fluoro-11β-hydroxy-16β-methylandrosta-1,4-diene-3,17-dione (IIβ)**—These compounds were synthesized for use as analytical standards by a modification (11) of the procedure of Rausser and Oliveto (16). The epimers were recrystallized twice to provide adequate purity. The α-epimer was recrystallized from acetone and hexane (16), and the β-epimer was recrystallized from methanol. The standards were dried in a drying apparatus at 55° and 5 mm and stored in a desiccator over phosphorus pentoxide overnight. Their purities were assessed from their melting points, UV and IR spectra, and TLC chromatograms.

**TLC**—All substances in methanol were spotted at origins 15 mm from the base of the plate. The chromatograms were developed with chloroform–acetone (9:1) until the solvent front ascended 170 mm above the origins. Equilibrated plate development was achieved in a Desaga gas-flushing tank fitted with stopcocks that allowed both addition of the mobile solvents and relief of any pressure imbalance arising from solvent mixing after the tank was covered. The spotted plates were developed three times before they were scanned with the densitometer. Plates used for quantitative determinations were scored 170 mm from the origin (15 mm from the top).

**Sample Preparation and Procedure**—Qualitative TLC was performed on the synthesized α- and β-epimers (IIα and IIβ), dexamethasone, betamethasone, dexamethasone acetate, dexamethasone phosphate, and dexamethasone phosphate disodium salt as well as on the epimeric impurity (IIα and IIβ) obtained from a contaminated commercial sample of the dexamethasone phosphate disodium injection solution. The densitogram of the epimeric impurity from the drug sample was compared with a chromatogram obtained from HPLC examination of another sample of the epimeric impurity extracted from the same batch of the commercial dexamethasone phosphate disodium solution for injection. The sample of the epimeric impurity and its high-performance liquid chromatogram were provided by the authors of the HPLC study (11). This qualitative work (11) included studies on the photographic methods of documentation conducted on concocted mixtures of the synthesized epimers (IIα and IIβ) and on the natural epimeric impurity (IIα and IIβ) found in a commercial injection solution of I.

**Table I—Peak Heights of Epimeric 16-Methyl 17-Ketones in Synthetic Mixtures and Drug Impurity [a]**

| Sample | 17-Ketone, % α | 17-Ketone, % β | Peak Heights[b]: α/(α + β) | CV |
|---|---|---|---|---|
| 1 | 20 | 80 | 0.286 | 1.32[c] |
| 2 | 30 | 70 | 0.371 | 1.10 |
| 3 | 40 | 60 | 0.451 | 0.95 |
| 4 | 50 | 50 | 0.527 | 0.68 |
| 5 | 60 | 40 | 0.597 | 0.70 |
| 6 | 70 | 30 | 0.677 | 0.78 |
| 7 | Impurity | | 0.721 | 0.72 |
| 8 | 80 | 20 | 0.757 | 0.76 |

[a] Each plate was spotted once with each sample. [b] Average peak height fractions obtained from densitograms from 12 TLC plates. [c] Some plates failed to show appreciable resolution (Sample 1) because of nearness (1 cm) of the spot to the edge of the plate. Half of the plates gave resolution adequate to permit measurement.

The epimers (IIα and IIβ) were freshly synthesized for the quantitative study, and a sample of the drug impurity was freshly extracted. The prepared standard mixtures, containing various ratios of the synthesized α- and β-epimers, and a sample of the epimeric impurity extracted (11) from the commercial dexamethasone phosphate disodium injection solution were subjected to TLC. Quantitative data on the epimeric composition were collected by measuring the peak heights of the α- and β-epimers in densitograms of the standard 17-ketone mixtures and of the sample impurity.

For the quantitative study, six pairs of TLC plates were prepared. Eight spots of solutions were applied to each plate from a 1-μl pipet handled with a clamp. The spots were placed 25 mm apart, starting 10 mm from the left side of the plate. (The spots nearest the edges of the plate were used to evaluate the influence of "spot edge" proximity on densitometric measurements.) Each pair of plates was developed simultaneously in the same tank and subjected simultaneously to densitometry at a later date. In accordance with the data shown in Table I, the spots were numbered in increasing order from left to right; each spot contained either a mixture of the synthesized reference standards or the impurity from the drug sample.

Only one pair of plates was not from the same original manufacturer's packed carton. This pair and another pair were developed simultaneously three times in the same tank. Between the spotting, development, and densitometry steps, no special arrangements were made for storing the chromatographic plates other than keeping them in a closed cardboard box.

Stock solutions were prepared by individually dissolving 50.12 mg of α-epimer and 50.11 mg of β-epimer in 50.00 ml of absolute methanol. With these convenient concentrations (1.0 mg of 17-ketone/ml) and the use of volumetric pipets, mixtures of the synthetic 17-ketones with the percentages of α- and β-epimers designated in Table I were prepared. A freshly extracted sample of epimeric 17-ketones obtained from a previously described (11) sample of contaminated dexamethasone phosphate disodium was dissolved in methanol to give a concentration of ~1 mg/ml. The sample solutions were concentrated fivefold to provide concentrations within the range of those of the standard mixtures used to spot the TLC plates.

**Treatment of Plates for Identification and Photography of Chromatographic Spots**—Several methods were used to locate spots on the TLC plates. In the first method, the plates were viewed under shortwave UV irradiation, and the spots were located through fluorescence diminution of the fluorescent silica gel material. In the second method, the plates were sprayed heavily with a saturated solution of antimony trichloride in chloroform and then placed in an oven at 110° for 15 min. If the spots were not dark enough, the process was repeated. The spots also were observed by their fluorescence under longwave UV light. In a third procedure, the nonfluorescent plates were sprayed with a fluorescent material, Bratton–Marshall reagent, prepared by dissolving 200 mg of *N*-(1-naphthyl)ethylenediamine dihydrochloride in 10 ml of deionized water and adding 90 ml of methanol.

Black and white photographs of the fluorescent plates were taken at a view box under shortwave UV excitation. To photograph the colored spots obtained by treatment with antimony trichloride and heat, the plate was placed on the lighted surface of a tracing table[8] and photographed in color or black and white from above by transmitted light. The fluo-

[1] Model SD 3000, Schoeffel Instrument Corp., Westbrook, NJ 07675.
[2] Model ACTA MIV, Beckman Instruments, Fullerton, CA 92634.
[3] Model 337, Perkin-Elmer Corp., Norwalk, CT 06856.
[4] Carl Zeiss, New York, NY 10018.
[5] Kofler, Arthur H. Thomas Co., Philadelphia, PA 19105.
[6] Mettler balance model HL 52 and printer model GA 20, Mettler Instrument Corp., Hightstown, NJ 08520.
[7] Chromato-vue, model CC-20, Ultraviolet Products, San Gabriel, CA 91775.
[8] Model J-52 reader, Ionker, Gaithersburg, MD 20760.
[9] Model 9100A, Hewlett-Packard, St. Louis, MO 63144.
[10] Canon FTb 35-mm camera, Kodak Plus-X panchromatic, Kodacolor II, and Kodachrome 64 film.
[11] Certified ACS.
[12] Silica gel 60 F-254 and silica gel 60, E. Merck Laboratories, Elmsford, NY 10523.
[13] Merck Sharp and Dohme Research Laboratories, West Point, PA 19486.
[14] Drummond Scientific Co., Broomall, PA 19008.

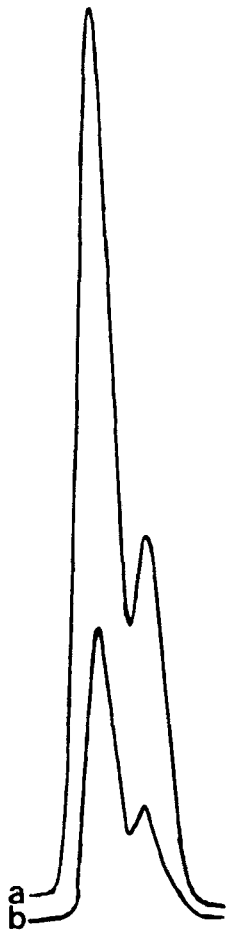


**Figure 1**—*Densitogram (a) and HPLC chromatogram (b) of drug impurity containing 16α- (left peak) and 16β-methyl (right peak) 17-ketones.*

rescence of these spots was also photographed by turning the TLC plate upside down and photographing the back (glass) side of the plate in a view box under longwave UV irradiation.

**Spectrodensitometry**—The operating conditions included a 150-w xenon lamp as the light source, an excitation wavelength of 240 nm, 2-mm band slit widths, a 3-mm plate beam width, a 10-mm plate beam length, measurement in reflectance and double-beam modes, a scanning speed of 1.27 cm/min, and a paper speed of 3.8 cm/min.

## RESULTS AND DISCUSSION

Figure 1 shows a superimposition of the densitogram of the TLC separation (curve a) and the chromatogram of the HPLC separation (curve b); both demonstrate the separation of the α- and β-epimers of the impurity from the commercial drug injection. The TLC and HPLC estimations are in good agreement, and both indicate that the α- and β-epimers (IIα and IIβ) were ~3:1, respectively. Three developments of the TLC plate appeared to give the most satisfactory chromatograms.

The UV spectra of all materials were obtained just before qualitative chromatography, and no photodecomposition was detected by this method. The epimeric mixture from the drug impurity (IIα and IIβ), the synthesized α-epimer, and the synthesized β-epimer each showed maximum absorption at 240 nm, in agreement with reported values (11).

Table II gives $R_f$ values obtained after one ($R_f$), two ($R_{2f}$), and three ($R_{3f}$) developments for densitometry. Table II includes data (under $R_{2f}$) on the use of nonfluorescent silica gel plates; these plates were sprayed with Bratton–Marshall reagent prior to viewing under shortwave UV light. Dexamethasone acetate was clearly detectable in the presence of dexamethasone or its epimeric 17-ketone oxidation products.

The system described here lends itself to the direct inspection of dexamethasone phosphate disodium drug samples and related samples for the presence of epimeric 16-methyl 17-ketones and possibly other oxidation products or impurities (Table II). To promote this objective, the TLC system retains dexamethasone 21-phosphate and dexamethasone 21-phosphate disodium at the origin, thus preventing interference with spots representing possible impurities being investigated, and distinguishes between dexamethasone 21-acetate, which is sometimes found at low levels in drug preparations of the respective parent corticosteroid (12), dexamethasone, and its 17-ketone oxidation products.

**Table II—$R_f$ Values[a] of Substances Studied**

| Substance | $R_f$[b] | $R_{2f}$[c] | $R_{3f}$[b] |
|---|---|---|---|
| 16α-Methyl 17-ketone (IIα) | 0.29 | 0.557 | 0.63 |
| 16β-Methyl 17-ketone (IIβ) | 0.26 | 0.483 | 0.58 |
| Dexamethasone | 0.005 | 0.103 | 0.12 |
| Betamethasone | 0.005 | 0.097 | 0.11 |
| Dexamethasone acetate | 0.20 | 0.40 | 0.45 |
| Dexamethasone 17-phosphate and 17-phosphate disodium | 0.00 | 0.00 | 0.00 |

[a] The adsorbent was silica gel, and the solvent was chloroform–acetone (9:1). The $R_f$ values are given for plates developed once ($f$), twice ($2f$), or three times ($3f$). [b] The $R_f$ and $R_{3f}$ data were collected from the same fluorescent silica gel plate under shortwave UV light; alternatively, the plate was treated with antimony trichloride followed by heat and observed under longwave UV light. [c] The silica gel plate was sprayed with Bratton–Marshall reagent and viewed under shortwave UV light; alternatively, the plate was treated with antimony trichloride followed by heat and observed under longwave UV light.

Furthermore, this method offers an $R_f$ of about ~0.3 for the epimeric impurity; this $R_f$ is ideal for multiple development of TLC plates because it allows maximum separation within the limit of two or three developments usually imposed by the time available to analyze one sample and by diffusion. Moreover, the Thoma (17) equation indicates that the ideal number of developments ($N_{opt}$) to obtain the maximum separation by unidimensional multiple chromatography of the two epimers with an average $R_f$ value of 0.275 ($R_f'$) is approximately three:

$$N_{opt} = \frac{-1}{\ln (1 - R_f')} = \frac{-1}{\ln 0.725} = 3.1 \qquad \text{(Eq. 1)}$$

Theoretical consideration of the steric nature of the 17-ketone also suggests that adsorption occurs on the underside or α-side of 9-fluoro-11β-hydroxy-16-methylandrosta-1,4-diene-3,17-dione (II) where steric hindrance is minimal. In these terms, IIα would be adsorbed less firmly than IIβ, which is consistent with the observed, faster migration found for the α-epimer in the present TLC study and the previous HPLC study (11).

Vertical diffusion was diminished somewhat in the unidimensional multiple chromatography procedure in a fashion similar to that observed in multiple development or programmed multiple development; with the proper developing solvent, programmed multiple development causes more rapid migration in the lower areas of the spot, and this engenders longitudinal narrowing (18–20). Under the conditions investigated, more than three developments offered no improvement in separation. No attempt was made to examine centered programmed multiple development (18, 21) to improve the densitogram resolution.

Paper chromatographic liquid partition was described for identification of the epimeric corticosteroids dexamethasone ($R_f$ 0.21) and betamethasone ($R_f$ 0.16) by a 35-cm descending development with a mobile phase of chloroform saturated with formamide on filter paper[15] impregnated with 40% formamide in methanol (14). This method seemed to offer good prospects for separation of the epimers (IIα and IIβ), which differed from one another by configuration at the C-16 optical center in the exact same manner as the corticosteroids. Unfortunately the epimers followed the solvent front in this chromatographic system. A convenient TLC method to distinguish between dexamethasone and betamethasone would be to stir the material in question with sodium bismuthate in a suitable solvent, such as aqueous acetic acid, and to analyze a portion of the solution for 16α- or 16β-methyl 17-ketone by TLC with the use of reference materials.

In the quantitative studies, location of the spots on the plates was facilitated by placing the chromatograms under shortwave UV light. The spots then were subjected to densitometry in the reflectance mode with irradiation at 240 nm. Twelve pairs of resolved peaks (α- and β-epimers) from 12 plates were obtained for each standard mixture and sample, except for Standard Mixture 1 (20% α and 80% β). This mixture was spotted close (10 mm) to the edge of the plate, and occasional drift to the edge occurred, disrupting the chromatogram. In six cases where drift to the edge did not occur, excellent results were obtained and were included in the statistical calculations.

Small differences in the time chosen for spotting, development, and densitometry appeared to make little difference in the peak ratio data obtained. In one case, 3 days elapsed between spotting and development

[15] Whatman No. 1, Whatman Inc., Clifton, NJ 07014.

**Table III—Treatment of Plates for Identification and Photography of Chromatographic Spots**

| Irradiation | Technique | Compound[a] | TLC Spot Colors on Prints: Color/Background[b] B and W Film | Color Film |
|---|---|---|---|---|
| | | Untreated Fluorescent Plate | | |
| Shortwave UV | Fluorescence extinction | Z | B/W | — |
| | | Fluorescent Plate Treated with Antimony Trichloride and Heat | | |
| White light | Transmitted and reflected light | D | B/W | YO/W |
| | | B | B/W | YO/W |
| | | $\alpha$ | B/W | YO/W |
| | | $\beta$ | B/W | YO/W |
| | | DA | B/W | P/W |
| Longwave UV | Fluorescence | D | W/B | Y/B |
| | | B | W/B | Y/B |
| | | $\alpha$ | W/B | Y/B |
| | | $\beta$ | W/B | Y/B |
| | | DA | W/B | R/B |
| | | Nonfluorescent Plate Treated with *N*-1-(Naphthyl)ethylenediamine | | |
| Shortwave UV | Fluorescence extinction | Z | B/W | — |

[a] D = dexamethasone, B = betamethasone, $\alpha$ = II$\alpha$, $\beta$ = II$\beta$, DA = dexamethasone acetate, and Z = all previously listed compounds. [b] B = black, W = white, Y = yellow, YO = yellowish orange, P = purple, and R = red.

of the plates, and 2 more days passed before densitometry was carried out; no significant difference in the results or peak ratios was observed. In fact, the plates may be stored for at least 2 months before densitometry. One plate was reexamined by densitometry 2 months later, and a comparison of data from both densitograms of this plate showed no significant difference. Another pair of plates taken from a different carton from the same manufacturer showed no difference in peak ratios when compared with the other plates.

The peak heights (represented as $\alpha$ and $\beta$ in Table I) were measured and are presented as the ratio of the $\alpha$-epimer to the sum of the $\alpha$- plus $\beta$-epimers. Under ideal conditions, if this ratio is plotted against the percent of the $\alpha$-epimer, a linear correlation should be obtained. The average ratio of each standard mixture and of the drug impurity is given in Table I. The peak heights obtained from the sample and from each standard mixture show good agreement and low coefficients of variation. A plot of the percent of the $\alpha$-epimer *versus* the ratio of the $\alpha$- and $\beta$-epimers placed all points practically on a straight line. A linear regression analysis of all 78 data from the standards gave $y = 0.770x + 0.139$, where $y$ is the ratio defined earlier and $x$ is the percent of the $\alpha$-epimer, and a correlation coefficient ($r$) of 0.99925. From the peak height ratio of the impurity from the drug sample and the plot of the standard data, it was found that the impurity was composed of 75.2% $\alpha$-epimer and 24.8% $\beta$-epimer. The peak of the $\beta$-epimer was broader and shorter than that of the $\alpha$-epimer, and the $\beta$ peak overlapped its neighboring $\alpha$ peak to a greater extent than the reverse effect. These factors give rise to the characteristics of the linear equation and the standard plot.

Stereoisomers often fail to separate chromatographically or may give incomplete resolution as was observed for the epimeric compounds in the present study. A peak ratio approach then may be desirable for quantitative studies, especially when the overlapping peaks are not symmetrical. In such an approach, the unknown sample is compared with a series of standard mixtures, each possessing a different ratio of the two contaminants. Groups of chromatograms must be examined; thus, a technique that offers simultaneous chromatographic determination is an asset. TLC provides an excellent means of collecting groups of data under similar conditions.

Operation of the spectrodensitometer was most efficient when the spots were applied 25 mm apart. By placing one spot 10 mm from the left edge and another 15 mm from the right edge, it was possible to evaluate whether the proximity of the spot to the edge of the plate influenced the analytical result. Spots placed 10 mm from the edge of the plate occasionally ran off the plate. Chromatograms not suffering from this disruption gave good results. However, only seven spots should be applied to a 20 × 20-cm plate.

The treatment of TLC plates for identification of the chromatographic spots is described in Table III. Fluorescent plates may be documented permanently by photography under shortwave UV irradiation in a view box.

Plates treated with antimony trichloride and heat gave yellow-orange spots for the epimers (II$\alpha$ and II$\beta$), dexamethasone, and betamethasone but light-purple spots for dexamethasone acetate under white light. Distinct photographs showing black or colored spots on a white background were obtained by placing the TLC plates on a tracing table and photographing the transmitted white light.

Under longwave UV light, the spots obtained by treatment with antimony trichloride and heat fluoresced. In this case, the best results were obtained by photographing the plates upside down in the UV chamber; ideally, only the longwave exciting light will penetrate the glass, and only the colored fluorescent emitted light will transmit for the photographic record. The sorbent itself on the plate does not fluoresce. When these sprayed plates were viewed under longwave UV light, the epimers (II$\alpha$ and II$\beta$), dexamethasone, and betamethasone appeared as yellow spots, whereas dexamethasone acetate appeared as a red spot.

With nonfluorescent plates, it is possible to apply a fluorescent material to the plate after development to observe the chromatogram by fluorescence diminution. This technique was effective when chromatograms of the epimers (II$\alpha$ and II$\beta$) were sprayed with Bratton–Marshall reagent, *N*-(1-naphthyl)ethylenediamine, for subsequent viewing under shortwave UV light [Tables II ($R_{2f}$) and III].

Methods for positive and permanent documentation of laboratory results are important, particularly to regulatory bodies such as the Food and Drug Administration; photographic techniques were stressed in the present TLC study. Applied photographic documentation was discussed recently (15), and the general techniques were employed in this study.

The TLC system allows simultaneous detection of some related substances of interest in drug monitoring (Tables II and III), and densitometry is convenient for determining the relative amounts of 16$\alpha$- and 16$\beta$-epimers of the 17-ketone impurity in dexamethasone-related drugs (Table I). There are distinct advantages in the use of TLC instead of HPLC for the analysis of 17-ketone oxidation products in dexamethasone phosphate disodium samples. When many samples must be examined for this contamination, a rapid qualitative technique such as TLC is ideal. The equipment is commonly available. With current techniques for multiple spotting and development, the method allows the simultaneous examination of numerous drug samples, a situation frequently encountered in drug-monitoring programs. The stability of the TLC chromatograms permits storage for reference, documentation by photography, and subsequent densitometry at the convenience of the analyst.

## REFERENCES


(1) B. P. Lisboa and E. Diczfalusy, *Acta Endocrinol.*, **40**, 60 (1962).

(2) *Ibid.*, **43**, 545 (1963).

(3) M. Barbier and S. I. Zav'yalov, *Izv. Akad. Nauk SSSR, Otd. Khim. Nauk.*, **1960**, 1309 (1960).

(4) W. G. Dyer, J. P. Gould, N. A. Maistrellis, T.-C. Peng, and P. Ofner, *Steroids*, **1**, 231 (1963).

(5) E. Change, *ibid.*, **4**, 237 (1964).

(6) B. P. Lisboa, *J. Chromatogr.*, **13**, 391 (1964).

(7) B. P. Lisboa, *Acta Endocrinol.*, **43**, 47 (1963).

(8) R. D. Bennett and E. Heftmann, *J. Chromatogr.*, **9**, 348 (1962).

(9) G. Cavina and C. Vicari, in "Thin-Layer Chromatography," G. B. Marini-Bettolo, Ed., Elsevier, Amsterdam, The Netherlands, 1964, p. 180.

(10) D. Waldi, in "Thin-Layer Chromatography," E. Stahl, Ed., Academic, New York, N.Y., 1965, p. 262.

(11) E. C. Juenge and J. F. Brower, *J. Pharm. Sci.*, **68**, 551 (1979).

(12) M. Lanouette and B. A. Lodge, *J. Chromatogr.*, **129**, 475 (1976).

(13) B. A. Lodge, H. Watanaba, and L. Watts, *Can. J. Pharm. Sci.*, **10**, 107 (1975).

(14) C. A. Johnson and S. Fowler, *J. Pharm. Pharmacol.*, **16** (Suppl.), 17T (1964).

(15) D. E. Heinz and R. K. Vitek, *J. Chromatog. Sci.*, **13**, 570 (1975).

(16) R. Rausser and E. P. Oliveto, U.S. pat. 3,010,958 (Nov. 28, 1961).

(17) J. A. Thoma, *Anal. Chem.*, **35**, 214 (1963).

(18) J. G. Kirchner, *J. Chromatog. Sci.*, **13**, 558 (1975).

(19) J. H. Jupille and J. A. Perry, *J. Chromatog. Sci.*, **13**, 163 (1975).

(20) J. A. Perry, T. H. Jupille, and L. J. Glunz, *Anal. Chem.*, **47**, 65A (1975).

(21) J. A. Perry, *J. Chromatog.*, **110**, 27 (1975).

ACKNOWLEDGMENTS

The authors appreciate the help of Clyde E. Wells and Terry W. Moore, particularly that related to photographic work, and they thank James F. Brower for providing a sample of the epimeric 17-ketone impurity and performing an additional HPLC analysis that gave the chromatogram used in Fig. 1.

# Isolation and Identification of Impurities in 4-Acetyl-2-(2′-hydroxyethyl)-5,6-bis(4-chlorophenyl)-2*H*-pyridazin-3-one, an Antihypertensive Agent

**LARRY J. POWERS ˣ, DAVID J. ECKERT *, and LANE GEHRLEIN ‡**

Received December 17, 1979, from the *T. R. Evans Research Center, Diamond Shamrock Corporation, Painesville, OH 44077.* Accepted for publication September 19, 1980. *Present address: Altex Scientific Inc., Berkeley, CA 94710. ‡Present address: Lederle Laboratories, Pearl River, NY 10965.

**Abstract** □ Three trace impurities found in 4-acetyl-2-(2′-hydroxyethyl)-5,6-bis(4-chlorophenyl)-2*H*-pyridazin-3-one (II), a novel antihypertensive agent, were isolated by a combination of low-pressure liquid chromatography and preparative TLC. These impurities were identified as the formate ester of II, a pyridazinone having a 2-methyl rather than the 2′-hydroxyethyl substituent, and a bis(pyridazinonyl)methane analog. In addition, the product of *O*-alkylation rather than of *N*-alkylation of 4-acetyl-5,6-bis(4-chlorophenyl)-2*H*-pyridazin-3-one (I) with ethylene carbonate was detected by high-performance liquid chromatography. The biological activity of these four impurities was compared to that of II.

**Keyphrases** □ 4-Acetyl-2-(2′-hydroxyethyl)-5,6-bis(4-chlorophenyl)-2*H*-pyridazin-3-one—synthesis, isolation of impurities by low-pressure liquid chromatography and preparative TLC and identification by high-pressure liquid chromatography, biological activity of impurities compared with parent compound □ High-pressure liquid chromatography—identification of impurities in 4-acetyl-2-(2′-hydroxyethyl)-5,6-bis(4-chlorophenyl)-2*H*-pyridazin-3-one, isolation of impurities by low-pressure liquid chromatography and preparative TLC □ Antihypertensive agents—4-acetyl-2-(2′-hydroxyethyl)-5,6-bis(4-chlorophenyl)-2*H*-pyridazin-3-one, isolation and identification of impurities, high-pressure liquid chromatography

The purification of a biologically active substance prior to pharmacological or toxicological evaluation is important in drug development. Such care is essential so that biological activity (including toxic effects) of trace impurities are not attributed to the molecule of interest. To ensure that trace impurities are innocuous, the biological activity of these substances can be studied independently if isolation, identification, and synthesis of the impurity can be successfully completed. The recent investigations of Reepmeyer and Kirchhoefer (1, 2) on the isolation and quantification of trace impurities in aspirin illustrate such an undertaking.

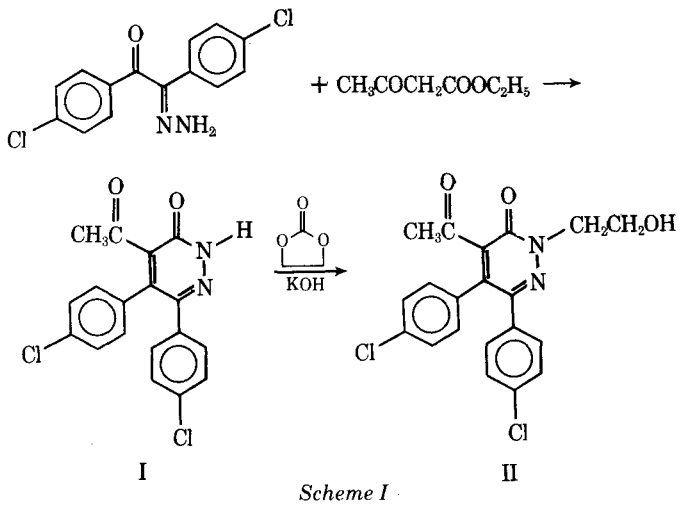


*Scheme I*

4-Acetyl-2-(2′-hydroxyethyl)-5,6-bis(4-chlorophenyl)-2*H*-pyridazin-3-one (II) is an antihypertensive agent prepared as illustrated in Scheme I. The various batches of II prepared in this manner have ~0.5% impurities after recrystallization. As part of a program (3, 4) to evaluate this compound, the major trace impurities present in the recrystallized material were isolated, identified, and synthesized. The antihypertensive activity and acute toxicity of four trace impurities were investigated.

## EXPERIMENTAL[1]

**Instruments**—Melting points were determined on a capillary melting-point apparatus[2] and are uncorrected. NMR spectra were determined on a 90-MHz Fourier transform spectrometer[3] with tetramethylsilane as the internal reference. IR spectra were obtained on a grating spectrophotometer[4] as potassium bromide disks. Electron-impact mass spectra[5] were obtained by direct-sample inlet.

**Chromatography**—A low-pressure column was filled with dry silica gel (0.032–0.063 mm), and toluene–ethyl acetate–acetonitrile (2:1:1) (Solvent 1, Fig. 1) was pumped through the column until all air bubbles were removed. Column dimensions were 91 × 2.5 cm. Compound II (4.996 g) was dissolved in dimethylformamide (27 ml). Ten milliliters of this solution was injected onto the column, and the compound was eluted with Solvent 1. Fractions of 15 ml each were collected. The remainder of II was injected onto the column after the first injection had eluted. Fractions 11–28 and 74–84 (second injection) were combined to give A (Fig. 1).

A preparative thin-layer[6] plate (20 cm × 20 cm × 1.0 mm) was cleaned by eluting with acetone and then dried. Fraction A was dissolved in chloroform and applied to the preabsorbent. The plate was then eluted with Solvent 2. Subsequent preparative layer separations are summarized in Fig. 1.

High-performance liquid chromatography[7] (HPLC) with UV detec-

[1] Elemental analyses were performed on a Perkin-Elmer model 240 carbon, hydrogen, and nitrogen analyzer by the Central Analytical Department, Diamond Shamrock Corp.

[2] Thomas–Hoover, Arthur H. Thomas Co., Philadelphia, Pa.

[3] WH-90 Fourier transform NMR spectrometer, Bruker Instruments Inc., Billerica, Mass.

[4] Model 297, Perkin-Elmer Corp., Norwalk, Conn.

[5] Varian/MAT-CH-7 mass spectrometer with SS-166 data systems, Varian Associates, Palo Alto, Calif.

[6] $SiO_2$ PLQF 1000, Quantum Industries.

[7] Model 100 solvent delivery system (Altex Scientific, Berkeley, Calif.) with a model CV-6-UHPa-N60 sample injector (Valco Instrument Co., Houston, Tex.).

0022-3549/81/0400-0419$01.00/0
© 1981, American Pharmaceutical Association

(21) J. A. Perry, *J. Chromatog.*, **110**, 27 (1975).

ACKNOWLEDGMENTS

The authors appreciate the help of Clyde E. Wells and Terry W. Moore, particularly that related to photographic work, and they thank James F. Brower for providing a sample of the epimeric 17-ketone impurity and performing an additional HPLC analysis that gave the chromatogram used in Fig. 1.

# Isolation and Identification of Impurities in 4-Acetyl-2-(2′-hydroxyethyl)-5,6-bis(4-chlorophenyl)-2*H*-pyridazin-3-one, an Antihypertensive Agent

**LARRY J. POWERS ˣ, DAVID J. ECKERT *, and LANE GEHRLEIN ‡**

Received December 17, 1979, from the *T. R. Evans Research Center, Diamond Shamrock Corporation, Painesville, OH 44077.* Accepted for publication September 19, 1980. *Present address: Altex Scientific Inc., Berkeley, CA 94710. ‡Present address: Lederle Laboratories, Pearl River, NY 10965.

**Abstract** □ Three trace impurities found in 4-acetyl-2-(2′-hydroxyethyl)-5,6-bis(4-chlorophenyl)-2*H*-pyridazin-3-one (II), a novel antihypertensive agent, were isolated by a combination of low-pressure liquid chromatography and preparative TLC. These impurities were identified as the formate ester of II, a pyridazinone having a 2-methyl rather than the 2′-hydroxyethyl substituent, and a bis(pyridazinonyl)methane analog. In addition, the product of *O*-alkylation rather than of *N*-alkylation of 4-acetyl-5,6-bis(4-chlorophenyl)-2*H*-pyridazin-3-one (I) with ethylene carbonate was detected by high-performance liquid chromatography. The biological activity of these four impurities was compared to that of II.

**Keyphrases** □ 4-Acetyl-2-(2′-hydroxyethyl)-5,6-bis(4-chlorophenyl)-2*H*-pyridazin-3-one—synthesis, isolation of impurities by low-pressure liquid chromatography and preparative TLC and identification by high-pressure liquid chromatography, biological activity of impurities compared with parent compound □ High-pressure liquid chromatography—identification of impurities in 4-acetyl-2-(2′-hydroxyethyl)-5,6-bis(4-chlorophenyl)-2*H*-pyridazin-3-one, isolation of impurities by low-pressure liquid chromatography and preparative TLC □ Antihypertensive agents—4-acetyl-2-(2′-hydroxyethyl)-5,6-bis(4-chlorophenyl)-2*H*-pyridazin-3-one, isolation and identification of impurities, high-pressure liquid chromatography

The purification of a biologically active substance prior to pharmacological or toxicological evaluation is important in drug development. Such care is essential so that biological activity (including toxic effects) of trace impurities are not attributed to the molecule of interest. To ensure that trace impurities are innocuous, the biological activity of these substances can be studied independently if isolation, identification, and synthesis of the impurity can be successfully completed. The recent investigations of Reepmeyer and Kirchhoefer (1, 2) on the isolation and quantification of trace impurities in aspirin illustrate such an undertaking.

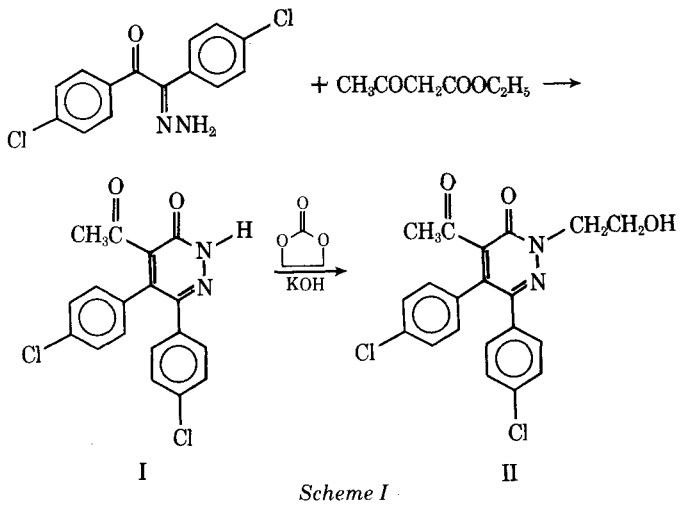


*Scheme I*

4-Acetyl-2-(2′-hydroxyethyl)-5,6-bis(4-chlorophenyl)-2*H*-pyridazin-3-one (II) is an antihypertensive agent prepared as illustrated in Scheme I. The various batches of II prepared in this manner have ~0.5% impurities after recrystallization. As part of a program (3, 4) to evaluate this compound, the major trace impurities present in the recrystallized material were isolated, identified, and synthesized. The antihypertensive activity and acute toxicity of four trace impurities were investigated.

## EXPERIMENTAL[1]

**Instruments**—Melting points were determined on a capillary melting-point apparatus[2] and are uncorrected. NMR spectra were determined on a 90-MHz Fourier transform spectrometer[3] with tetramethylsilane as the internal reference. IR spectra were obtained on a grating spectrophotometer[4] as potassium bromide disks. Electron-impact mass spectra[5] were obtained by direct-sample inlet.

**Chromatography**—A low-pressure column was filled with dry silica gel (0.032–0.063 mm), and toluene–ethyl acetate–acetonitrile (2:1:1) (Solvent 1, Fig. 1) was pumped through the column until all air bubbles were removed. Column dimensions were 91 × 2.5 cm. Compound II (4.996 g) was dissolved in dimethylformamide (27 ml). Ten milliliters of this solution was injected onto the column, and the compound was eluted with Solvent 1. Fractions of 15 ml each were collected. The remainder of II was injected onto the column after the first injection had eluted. Fractions 11–28 and 74–84 (second injection) were combined to give A (Fig. 1).

A preparative thin-layer[6] plate (20 cm × 20 cm × 1.0 mm) was cleaned by eluting with acetone and then dried. Fraction A was dissolved in chloroform and applied to the preabsorbent. The plate was then eluted with Solvent 2. Subsequent preparative layer separations are summarized in Fig. 1.

High-performance liquid chromatography[7] (HPLC) with UV detec-

[1] Elemental analyses were performed on a Perkin-Elmer model 240 carbon, hydrogen, and nitrogen analyzer by the Central Analytical Department, Diamond Shamrock Corp.

[2] Thomas–Hoover, Arthur H. Thomas Co., Philadelphia, Pa.

[3] WH-90 Fourier transform NMR spectrometer, Bruker Instruments Inc., Billerica, Mass.

[4] Model 297, Perkin-Elmer Corp., Norwalk, Conn.

[5] Varian/MAT-CH-7 mass spectrometer with SS-166 data systems, Varian Associates, Palo Alto, Calif.

[6] $SiO_2$ PLQF 1000, Quantum Industries.

[7] Model 100 solvent delivery system (Altex Scientific, Berkeley, Calif.) with a model CV-6-UHPa-N60 sample injector (Valco Instrument Co., Houston, Tex.).

0022-3549/81/0400-0419$01.00/0
© 1981, American Pharmaceutical Association

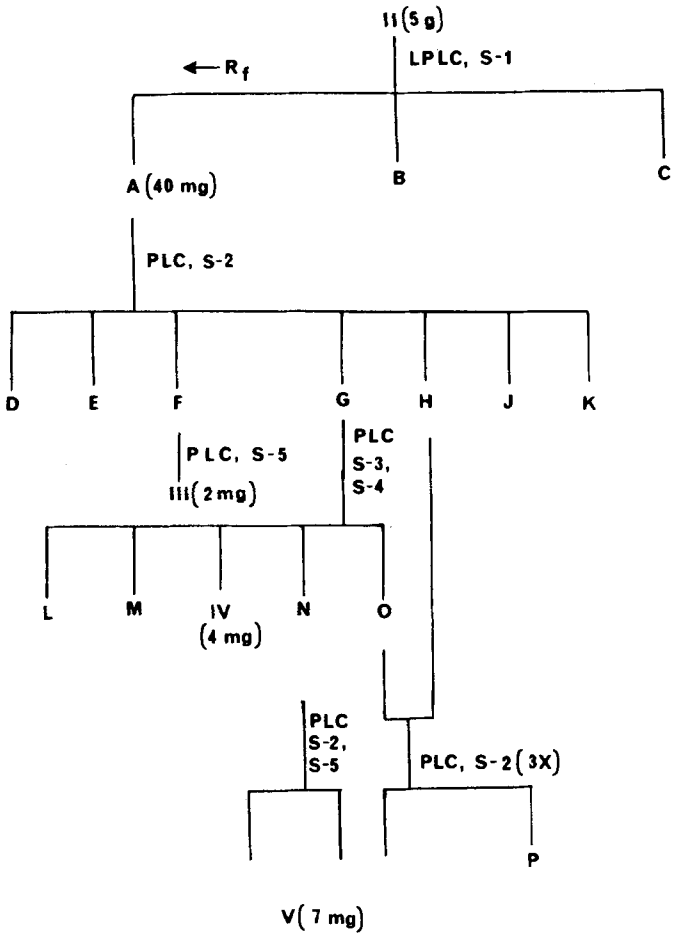


**Figure 1**—*Isolation of impurities from 5.0 g of II. All chromatography was on silica gel. Solvent systems were: Solvent 1 (S-1), toluene–ethyl acetate–acetonitrile (2:1:1); Solvent 2 (S-2), chloroform–ethyl acetate (17:3); Solvent 3 (S-3), toluene–ethyl acetate (17:3); Solvent 4 (S-4), toluene–ethyl acetate (3:1); and Solvent 5 (S-5), chloroform–ethyl acetate (9:1). Fractions of highest* $R_f$ *are at the left of the figure. PLC = preparative-layer chromatography, and LPLC = low-pressure liquid chromatography. The weights given on the chart represent the approximate weight of each fraction. The fractions indicated by letters are mixtures of components. The fractions indicated by numbers contain only one component. These numbers correspond to the compound numbers used in the text.*

tion[8] was performed on a 300 × 3.9-mm silica gel[9] column at a flow rate of 2 ml/min. The mobile phases were prepared from hexane[10], methylene chloride, and 2-propanol. The retention of the chromatographic peaks was expressed as the capacity ratio, $k$, which was calculated by:

$$k = (t_r - t_0)/t_0 \qquad \text{(Eq. 1)}$$

where $t_0$ and $t_r$ are the retention times of an unretained solute and the solute in question, respectively.

**Preparation of 4-Acetyl-5,6-bis(4-chlorophenyl)-2*H*-pyridazin-3-one (I)**—A 75.8-liter (20-gallon) reactor was charged with xylene (34.2 liters) and bis(*p*-chlorobenzil) monohydrazone (13.76 kg, 46.94 moles), and the reactor was heated with steam. When the reaction temperature had reached 60° (10 min), pyridine (4.05 kg, 51.2 moles) was added. After an additional 17 min (reaction temperature of 110°), methyl acetoacetate (2017 g in 2 liters of xylene) was added. After an additional 8 min, 2019 g of methyl acetoacetate in 2.0 liters of xylene was added. After an additional 15 min, 1921 g of methyl acetoacetate (total of 51.3 moles of methyl acetoacetate) in 1.5 liters of xylene was added.

The reaction mixture was heated at between 110 and 136° for 7 hr and 25 min, during which time 1.3 liters of the water–alcohol layer was removed by azeotropic distillation. The reaction mixture then was cooled and filtered. The residue was washed with xylene and petroleum ether and air dried overnight. The crude product was dried at 75° for 6 hr (yield 5844 g, 34.7%, mp 262–270°).

The dried crude product was slurried in methanol, filtered, and rinsed with additional methanol (total of 3 liters of methanol). The filter cake was rinsed with 3 more liters of methanol followed by petroleum ether (2 × 400 ml). The filter cake was allowed to air dry overnight.

*Anal.*—Calc. for $C_{18}H_{12}Cl_2N_2O_2$: C, 60.2; H, 3.4; N, 7.8. Found: C, 60.0; H, 3.2; N, 8.0.

The resulting product was recrystallized from methylene chloride, mp 270–272°.

*Anal.*—Found: C, 60.0; H, 3.3; N, 7.9.

**Preparation of II**—To a 1-liter round-bottom flask equipped with an agitator, thermometer, Dean–Stark trap, and condenser were added dimethylformamide (300 ml), I (200 g), potassium carbonate (0.9 g), and ethylene carbonate (61 g). The reaction mixture was heated to 95° and maintained at this temperature for 2 hr. Then the reaction mixture was cooled, and a slow addition of water (500 ml) was begun at 60°. At 16°, the reaction mixture was filtered and rinsed with 700 ml of water. After drying at 75° for 48 hr, the product gave 222 g (99.1%), mp 190–192°. This product was recrystallized from methanol, mp 191–193°.

*Anal.*—Calc. for $C_{20}H_{16}Cl_2N_2O_2$: C, 59.6; H, 4.0; N, 6.9. Found: C, 59.4; H, 4.0; N, 6.7.

**Preparation of 4-Acetyl-5,6-bis(4-chlorophenyl)-2-(2′-hydroxyethyl)-2*H*-pyridazin-3-one Formate (III)**—Compound II (10 g, 0.025 mole) was stirred at 55° in 88% formic acid (100 ml) for 3 hr. The formic acid was removed *in vacuo*, and the residual oil was dissolved in ether. After the ether solution was washed with 5% $NaHCO_3$, the solvent was removed to give a yellow foam (8.0 g); this foam was chromatographed on dry-column silica gel using ethyl acetate–cyclohexane (1:3) as the eluting solvent. The UV-absorbing band of the highest $R_f$ value was removed and extracted with ether. The ether was removed, and the residue was recrystallized from methylene chloride–cyclohexane, 38% yield, mp 99–100°.

*Anal.*—Calc. for $C_{21}H_{16}Cl_2N_2O_4$: C, 58.5; H, 3.7; N, 6.5. Found: C, 58.1; H, 3.5; N, 6.3.

**Preparation of 4-Acetyl-5,6-bis(4-chlorophenyl)-2-methyl-2*H*-pyridazin-3-one (IV)**—A mixture of I (17.95 g, 0.05 mole), methyl iodide (71.0 g, 0.5 mole), potassium carbonate (13.8 g, 0.1 mole), and dimethylformamide (50 ml) was stirred in a sealed vessel and heated to 80° for 18 hr. The cooled mixture was poured into water (250 ml), and the resulting aqueous mixture was extracted with chloroform (3 × 100 ml). The combined extracts were dried (calcium sulfate) and evaporated *in vacuo* to a brown syrup. The syrup was dissolved in 2-propanol (100 ml), and the solution was allowed to cool to room temperature. The yellow, crystalline material that separated was collected by filtration, air dried, and then dried under vacuum at 100° overnight, giving 11.7 g (63% yield), mp 119–120°.

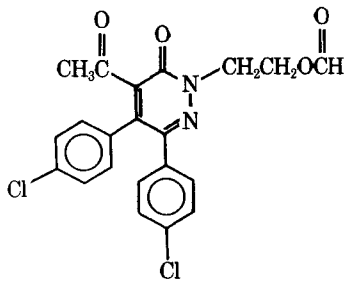


III

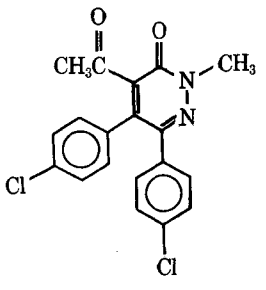


IV

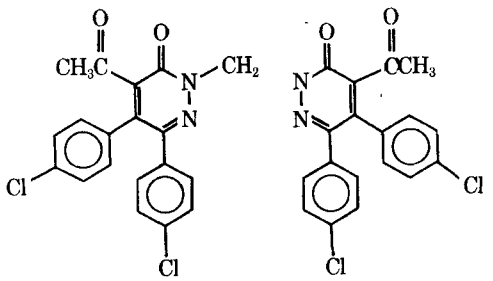


V

[8] Model 153, Altex Scientific Inc.
[9] μPorasil (10 μm), Waters Associates, Milford, Mass.
[10] HPLC grade, Fisher Scientific Co., Pittsburgh, Pa.

*Anal.*—Calc. for $C_{19}H_{14}Cl_2N_2O_2$: C, 61.1; H, 3.8; N, 7.5. Found: C, 61.1; H, 3.7; N, 7.6.

**Reaction of I with Methylene Chloride**—Compound I (10 g, 0.0279 mole) and potassium carbonate (4.0 g) were stirred at reflux in methylene chloride–dimethylformamide (250 ml, 3:2) for 24 hr. An additional 4.0 g of potassium carbonate was added, and refluxing was continued for 3 hr. The solution was filtered, and the residue was washed with water. After drying, the residue (6.9 g) was recrystallized from chloroform–acetonitrile. An additional 1.9 g of V was obtained (86% yield, mp > 260°) from the original filtrate.

*Anal.*—Calc. for $C_{37}H_{24}Cl_4N_4O_4$: C, 60.8; H, 3.3; N, 7.7. Found: C, 60.6; H, 3.1; N, 7.7.

**Preparation of 4-Acetyl-3-chloro-5,6-bis(4-chlorophenyl)pyridazine (VI)**—Compound I (15.0 g, 0.042 mole) was stirred in phosphorus oxychloride (60 ml), and triethylamine (4.5 ml) was added dropwise to the reaction mixture. When the addition was complete, the reaction mixture was heated to reflux temperature. After 2 hr, the reaction mixture was cooled and poured onto ice. The resulting precipitate was separated by filtration, and the residue was recrystallized from acetonitrile, 10.5 g (67% yield), mp 179–180°.

*Anal.*—Calc. for $C_{18}H_{11}Cl_3N_2O$: C, 57.2; H, 7.4; N, 2.9. Found: C, 56.9; H, 7.6; N, 2.8.

**Preparation of 4-Acetyl-3-(2′-hydroxyethoxy)-5,6-bis(4-chlorophenyl)pyridazine (VII)**—Compound VI (24.0 g, 0.063 mole) and ethylene glycol (250 ml) were stirred together, and dioxane (250 ml) was added to the slurry. Potassium carbonate (30 g) was added to the solution, and the mixture was heated on a steam bath (pot temperature of 90°) for 13 hr. The dark-red solution was partitioned between ether and water. After washing with water, the organic layer was dried (sodium sulfate) and concentrated. The resulting dark residue was recrystallized from hexane–ethyl acetate and then from hexane–chloroform to give an off-white solid, 68% yield, mp 153–155°.

*Anal.*—Calc. for $C_{20}H_{16}Cl_2N_2O_3$: C, 59.6; H, 4.0; N, 6.9. Found: C, 59.3; H, 3.9; N, 6.7.

**Biological Activity**—The antihypertensive activity and toxicity determination of the isolated impurities were determined[11] using a procedure reported elsewhere (3).

## RESULTS AND DISCUSSION

The particular batch of II used in the separation of impurities was 99.5% pure as determined by differential scanning calorimetry[12] analyses. The procedure outlined in Fig. 1 resulted in the isolation of three compounds. The structures of III and IV were proposed as the formate ester and the *N*-methyl derivative, respectively, based on the 90-MHz PMR spectra (Table I). These structural assignments were confirmed by comparison of the isolated compounds with compounds synthesized from II and I, respectively. The synthetic and isolated material were identical when compared in two TLC systems (Table II) and had identical PMR spectra (Table I).

The formate ester, III, probably results from formylation of II by dimethylformamide (or formic acid) during the hydroxyethylation of I. The *N*-methyl compound, IV, could be formed during synthesis of I by reaction of I with methyl acetoacetate. If this is the case, the *N*-methyl compound should also be present in I and determined by use of the methyl ester of acetoacetic acid in this reaction. It is also possible that IV is formed during hydroxyethylation of I as a result of reaction with dimethylformamide or an impurity in the dimethylformamide.

A mobile phase of hexane–methylene chloride–2-propanol (16:3:1) was used for the HPLC separation of IV and I with capacity ratios of $k = 0.6$ and 1.1, respectively. Examination of I under these conditions revealed that there was no detectable amount of IV present in I. This finding indicates that IV isolated from II did not result from the reaction of I with methyl acetoacetate. Upon heating I with dimethylformamide and powdered potassium hydroxide at 110° for 19 hr, a compound that cochromatographed with IV in the previously described HPLC system was detected. This reaction mixture was analyzed with a second mobile phase of hexane–methylene chloride–2-propanol (36:3:1). Again, resolution of IV and I was obtained with respective $k$ values of 1.4 and 3.3.

The impurity generated in I by heating with potassium hydroxide in dimethylformamide again cochromatographed with the synthetic *N*-methyl compound. This result suggests that I is methylated by interaction with dimethylformamide or some impurity in this solvent of reagent grade.

The third impurity isolated from II was V. Examination of the PMR spectrum and mass spectrum of this compound suggested a bis(pyridazinonyl)methane structure. A sample of this compound was prepared by allowing I to react with methylene chloride in dimethylformamide in the presence of potassium carbonate. No *N*-chloromethylpyridazinone was isolated from this reaction. Apparently the rate of the second displacement reaction was much faster than the initial alkylation of I with methylene chloride. A similar result was obtained using bromochloromethane in a large excess.

Compound V probably results from the reaction of I with methylene chloride during the formation of II. Methylene chloride is used in the

**Table I—90-MHz NMR Spectral Data**

| Compound | Assignment | Shift, δ[a] Isolated Sample | Shift, δ[a] Synthetic Sample |
|---|---|---|---|
| III | O‖ O—C—H | 8.063 | 8.060 |
| | Aromatic H | 7.339 | 7.336 |
| | | 7.264 | 7.265 |
| | | 7.244 | 7.241 |
| | | 7.176 | 7.175 |
| | | 7.058 | 7.058 |
| | | 7.032 | 7.033 |
| | | 6.960 | 6.960 |
| | | 6.938 | 6.936 |
| | N—$CH_2$—$CH_2$—O | 4.629 | 4.628 |
| | | 4.610 | 4.606 |
| | O‖ $CH_3$—C | 2.239 | 2.249 |
| IV | Aromatic H | 7.322 | 7.330 |
| | | 7.257 | 7.260 |
| | | 7.228 | 7.232 |
| | | 7.169 | 7.173 |
| | | 7.068 | 7.074 |
| | | 7.042 | 7.047 |
| | | 7.016 | 7.021 |
| | | 6.974 | 6.976 |
| | | 6.921 | 6.925 |
| | N—$CH_3$ | 3.909 | 3.912 |
| | $CH_3$CO | 2.243 | 2.246 |
| V | Aromatic H | 7.345 | 7.347 |
| | | 7.326 | 7.325 |
| | | 7.260 | 7.252 |
| | | 7.169 | 7.170 |
| | | 7.143 | 7.145 |
| | | 7.022 | 7.025 |
| | | 6.928 | 6.927 |
| | N—$CH_2$—N | 6.527 | 6.525 |
| | $CH_3$CO | 2.246 | 2.244 |

[a] In deuterated chloroform.

**Table II—$R_f$ Values[a] for III–V**

| Solvent[b] | III | IV | V |
|---|---|---|---|
| Solvent 3 | 0.28 | 0.39 | 0.16 |
| Solvent 2 | 0.53 | 0.68 | 0.37 |

[a] In each case, the synthetic and isolated material cochromatographed on $SiO_2$ GHLP (Analtech). [b] Solvent 3 was toluene–ethyl acetate (17:3), and Solvent 2 was chloroform–ethyl acetate (17:3).

**Table III—Biological Activity**

| Compound | SHR[a] | Estimated $LD_{50}$[b], mg/kg |
|---|---|---|
| II | ++ | >300 |
| III | ++ | >300 |
| IV | 0 | >300 |
| V | 0 | ND[c] |
| VII | + | 180 |

[a] SHR = spontaneously hypertensive rat model of hypertension. Key: ++ = active, $p < 0.05$; + = slightly active, $p > 0.05$; and 0 = inactive; $n = 5$. The procedure for this assay was reported elsewhere (3). [b] Based on the number of deaths in mice after intraperitoneal administration of 30, 100, and 300 mg/kg; $n$ = 4/dose level. [c] Not determined.

[11] Pharmakon Laboratories, Scranton, Pa., under the direction of Richard J. Matthews.

[12] Perkin-Elmer model DSC-2 equipped with a Tektronic 31 programmable calculator and a 4661 digital plotter.

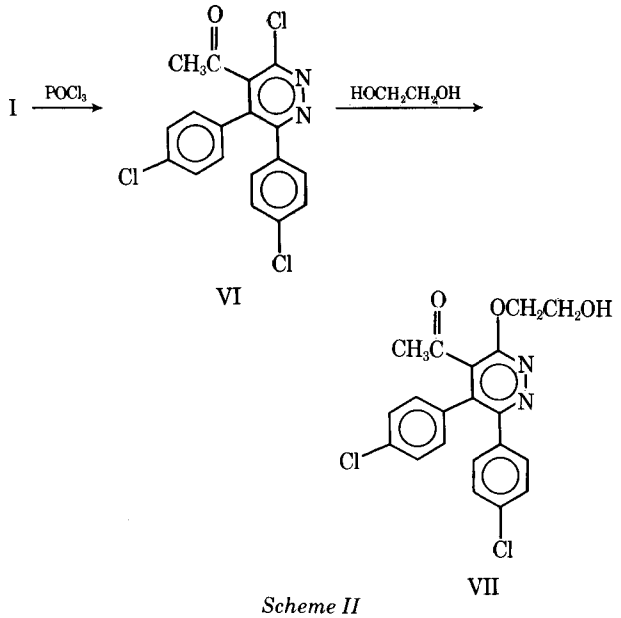

Scheme II

purification of I and probably is entrapped in the crystalline product. This solvent entrapment by the pyridazinones is observed frequently. As with III and IV, the synthetic and isolated samples of V were identical in the two TLC systems and had identical NMR and IR spectra. Of particular note was the downfield shift of the methylene protons between the two pyridazinone rings (Table I).

This initial investigation did not result in the isolation of any product of the *O*-alkylation of I by ethylene carbonate. A synthesis for the *O*-alkylated compound, VII, was developed following the route shown in Scheme II. However, this compound was not resolved from II by the chromatographic systems outlined in Fig. 1. Using an authentic sample of VII, a TLC and HPLC system was developed that separated VII from I and II. With a mobile phase of hexane–methylene chloride–2-propanol (16:3:1), the capacity factors for II and VII were 3.7 and 4.4, respectively. This system indicated that VII was present in II at a level of 0.1%. This conclusion was supported by the spiking of the II sample with synthetic VII.

The biological activities of III–V and VII were compared with that of II. As shown in Table III, both IV and V lacked antihypertensive activity and were not acutely toxic. The formate ester, III, had antihypertensive activity similar to that of II. This activity also was observed for other aliphatic and aromatic esters of II (4). Compound VII had slight, although not statistically significant, antihypertensive activity. In addition, VII appeared to be more toxic than II.

## REFERENCES


(1) J. C. Reepmeyer and R. D. Kirchhoefer, *J. Pharm. Sci.*, **68**, 1167 (1979).

(2) R. D. Kirchhoefer, J. C. Reepmeyer, and W. E. Juhl, *ibid.*, **69**, 550 (1980).

(3) R. Buchman, J. A. Scozzie, Z. S. Ariyan, R. D. Heilman, D. J. Rippin, W. J. Pyne, L. J. Powers, and R. J. Matthews, *J. Med. Chem.*, **23**, 1398 (1980).

(4) S. W. Fogt, J. A. Scozzie, R. D. Heilman, and L. J. Powers, *ibid.*, **23**, 1445 (1980).


## ACKNOWLEDGMENTS


The authors thank Russell M. Bimber and Craig E. Finch for preparation of I and II, Russell Buchman for preparation of IV, and Donna Rippin for preparation of VII.


# Comparative Bioavailability of Three Commercial Acetaminophen Tablets


**J. B. SOTIROPOULUS, T. DEUTSCH, and F. M. PLAKOGIANNIS** ˣ



Received June 4, 1979, from the *Division of Pharmaceutics, Arnold & Marie Schwartz College of Pharmacy and Health Sciences, Brooklyn, NY 11201.* Accepted for publication August 5, 1980.



**Abstract** □ Four different acetaminophen products (three tablets and one liquid) were evaluated for their *in vitro* properties and *in vivo* comparative bioavailability. The *in vivo* properties included assay, hardness, thickness, friability, weight variation, content uniformity, disintegration, and dissolution. A statistically significant variation was observed in friability, disintegration, and dissolution. The dissolution rates were determined in 0.1 *N* HCl under sink conditions, and the $T_{50\%}$ value for Brand A was 50 min while the values for Brands B and C were 1 min. The *in vivo* evaluation was completed in four subjects with a urinary excretion experiment using a crossover design. The calculated elimination half-lives were 4.12, 2.77, 3.14, and 2 hr for Brands A, B, and C and the standard, respectively. The relative bioavailabilities (with respect to solution) were 82, 87, and 92% for Brands A, B, and C, respectively. The mean amount excreted with Brand A was less than the reference at all time points, although it was not significant. Comparison of the *in vitro* and *in vivo* data for the three tablets indicated that the rate and amount of acetaminophen excreted may be related to the dissolution rate.



**Keyphrases** □ Acetaminophen—bioavailability, *in vitro* and *in vivo* properties of three commercial tablets compared □ Bioavailability—acetaminophen, *in vitro* and *in vivo* properties of three commercial tablets compared □ Tablets—acetaminophen, bioavailability, *in vitro* and *in vivo* properties of three commercial tablets compared


The popularity of acetaminophen, a nonsalicylate and analgesic/antipyretic, as an aspirin substitute has increased to the point that the drug is now available from many sources in several dosage forms in the United States. However, of the more than 30 manufacturers and distributors of acetaminophen tablets, only four companies provided bioavailability data in a recent survey (1, 2).

Mattok *et al.* (3, 4) and McGilveray *et al.* (5) studied the physiological availability of different commercial dosage forms and found no significant differences among the formulations in blood level or urinary excretion parameters. However, other investigators (6, 7) reported differences in blood and plasma levels of acetaminophen after administration of various formulations. Therefore, this study evaluated three commercially available[1] acetaminophen products (A, B, and C) and a reference solution[2] (D), utilizing urinary excretion data, and correlated these data with several physicochemical and manufacturing parameters.

[1] Brand A was acetaminophen tablets USP, lot 027791, Interstate Drug Exchange, Plainview, NY 11805; Brand B was Tylenol tablets, lot 2751, McNeil Laboratories, Fort Washington, PA 19034; and Brand C was Datril tablets, lot DA853401, MNFL, Bristol Myers Co., New York, NY 10022.

[2] Brand D was acetaminophen powder, McNeil Laboratories, Fort Washington, PA 19034.




0022-3549/81/0400-0422$01.00/0



© 1981, American Pharmaceutical Association

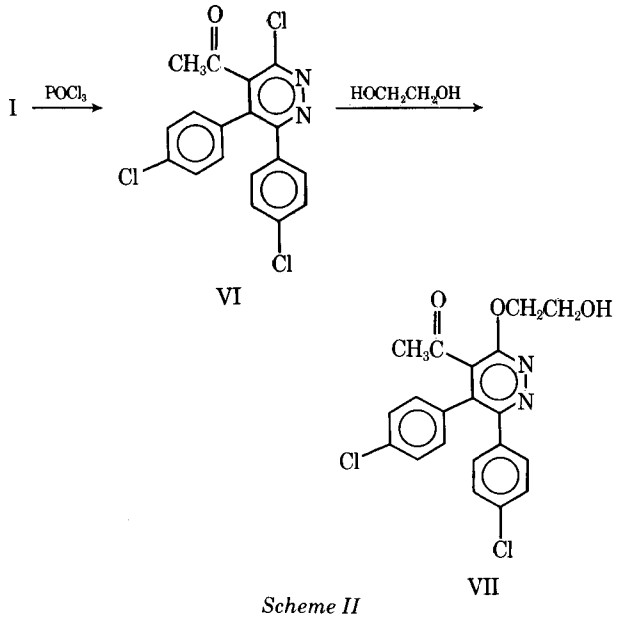

Scheme II

purification of I and probably is entrapped in the crystalline product. This solvent entrapment by the pyridazinones is observed frequently. As with III and IV, the synthetic and isolated samples of V were identical in the two TLC systems and had identical NMR and IR spectra. Of particular note was the downfield shift of the methylene protons between the two pyridazinone rings (Table I).

This initial investigation did not result in the isolation of any product of the *O*-alkylation of I by ethylene carbonate. A synthesis for the *O*-alkylated compound, VII, was developed following the route shown in Scheme II. However, this compound was not resolved from II by the chromatographic systems outlined in Fig. 1. Using an authentic sample of VII, a TLC and HPLC system was developed that separated VII from I and II. With a mobile phase of hexane–methylene chloride–2-propanol (16:3:1), the capacity factors for II and VII were 3.7 and 4.4, respectively. This system indicated that VII was present in II at a level of 0.1%. This conclusion was supported by the spiking of the II sample with synthetic VII.

The biological activities of III–V and VII were compared with that of II. As shown in Table III, both IV and V lacked antihypertensive activity and were not acutely toxic. The formate ester, III, had antihypertensive activity similar to that of II. This activity also was observed for other aliphatic and aromatic esters of II (4). Compound VII had slight, although not statistically significant, antihypertensive activity. In addition, VII appeared to be more toxic than II.

## REFERENCES


(1) J. C. Reepmeyer and R. D. Kirchhoefer, *J. Pharm. Sci.*, **68**, 1167 (1979).

(2) R. D. Kirchhoefer, J. C. Reepmeyer, and W. E. Juhl, *ibid.*, **69**, 550 (1980).

(3) R. Buchman, J. A. Scozzie, Z. S. Ariyan, R. D. Heilman, D. J. Rippin, W. J. Pyne, L. J. Powers, and R. J. Matthews, *J. Med. Chem.*, **23**, 1398 (1980).

(4) S. W. Fogt, J. A. Scozzie, R. D. Heilman, and L. J. Powers, *ibid.*, **23**, 1445 (1980).


## ACKNOWLEDGMENTS


The authors thank Russell M. Bimber and Craig E. Finch for preparation of I and II, Russell Buchman for preparation of IV, and Donna Rippin for preparation of VII.


# Comparative Bioavailability of Three Commercial Acetaminophen Tablets


**J. B. SOTIROPOULUS, T. DEUTSCH, and F. M. PLAKOGIANNIS** ˣ



Received June 4, 1979, from the *Division of Pharmaceutics, Arnold & Marie Schwartz College of Pharmacy and Health Sciences, Brooklyn, NY 11201.* Accepted for publication August 5, 1980.



**Abstract** □ Four different acetaminophen products (three tablets and one liquid) were evaluated for their *in vitro* properties and *in vivo* comparative bioavailability. The *in vivo* properties included assay, hardness, thickness, friability, weight variation, content uniformity, disintegration, and dissolution. A statistically significant variation was observed in friability, disintegration, and dissolution. The dissolution rates were determined in 0.1 *N* HCl under sink conditions, and the $T_{50\%}$ value for Brand A was 50 min while the values for Brands B and C were 1 min. The *in vivo* evaluation was completed in four subjects with a urinary excretion experiment using a crossover design. The calculated elimination half-lives were 4.12, 2.77, 3.14, and 2 hr for Brands A, B, and C and the standard, respectively. The relative bioavailabilities (with respect to solution) were 82, 87, and 92% for Brands A, B, and C, respectively. The mean amount excreted with Brand A was less than the reference at all time points, although it was not significant. Comparison of the *in vitro* and *in vivo* data for the three tablets indicated that the rate and amount of acetaminophen excreted may be related to the dissolution rate.



**Keyphrases** □ Acetaminophen—bioavailability, *in vitro* and *in vivo* properties of three commercial tablets compared □ Bioavailability—acetaminophen, *in vitro* and *in vivo* properties of three commercial tablets compared □ Tablets—acetaminophen, bioavailability, *in vitro* and *in vivo* properties of three commercial tablets compared


The popularity of acetaminophen, a nonsalicylate and analgesic/antipyretic, as an aspirin substitute has increased to the point that the drug is now available from many sources in several dosage forms in the United States. However, of the more than 30 manufacturers and distributors of acetaminophen tablets, only four companies provided bioavailability data in a recent survey (1, 2).

Mattok *et al.* (3, 4) and McGilveray *et al.* (5) studied the physiological availability of different commercial dosage forms and found no significant differences among the formulations in blood level or urinary excretion parameters. However, other investigators (6, 7) reported differences in blood and plasma levels of acetaminophen after administration of various formulations. Therefore, this study evaluated three commercially available[1] acetaminophen products (A, B, and C) and a reference solution[2] (D), utilizing urinary excretion data, and correlated these data with several physicochemical and manufacturing parameters.

[1] Brand A was acetaminophen tablets USP, lot 027791, Interstate Drug Exchange, Plainview, NY 11805; Brand B was Tylenol tablets, lot 2751, McNeil Laboratories, Fort Washington, PA 19034; and Brand C was Datril tablets, lot DA853401, MNFL, Bristol Myers Co., New York, NY 10022.

[2] Brand D was acetaminophen powder, McNeil Laboratories, Fort Washington, PA 19034.




0022-3549/81/0400-0422$01.00/0



© 1981, American Pharmaceutical Association

**Table I—Manufacturing Parameters of the Brands of Acetaminophen Tablets**

| Parameter | Brand A | Brand B | Brand C |
|---|---|---|---|
| Weight, g | | | |
| Mean | 397.60 | 434.2 | 479.1 |
| *SD* | 8.52 | 4.36 | 6.60 |
| *CV* | 2.00 | 1.00 | 1.37 |
| Hardness, kg | | | |
| Mean | 3.1 | 6.7 | 9.3 |
| *SD* | 0.43 | 0.78 | 0.82 |
| Thickness, mm | | | |
| Mean | 5.00 | 4.9 | 5.00 |
| *SD* | 0.08 | 0.03 | 0.03 |
| Friability | — | 1.93 | 1.01 |
| Content uniformity, % | | | |
| Mean | 99.36 | 102.00 | 99.00 |
| *SD* | 3.00 | 1.99 | 3.05 |

## EXPERIMENTAL

***In Vivo* Study**—Four healthy volunteers, one female and three males, 24–35 years old, were the subjects. The treatments consisted of three brands of acetaminophen tablets acquired by normal channels of drug distribution. A 650-mg dose of acetaminophen (two 325-mg tablets) was administered to each subject. The control was 650 mg of pure acetaminophen in 100 ml of water acidified with 0.1 *N* HCl in which the acetaminophen was completely dissolved.

The subjects received each of the four treatments (A–D) in a completely randomized Latin square design. A 1-week period was employed between each dosage interval to allow for complete drug elimination. Urine voids were collected predose and 0.5, 1, 1.5, 2, 3, 4, 6, 8, 10, and 12 hr postadministration. Urine samples were collected in 500-ml plastic graduated cylinders. The volume was measured and recorded, and an aliquot was frozen until it was assayed. [4]

**Spectrophotometric Determination of Acetaminophen in Urine**—The method used for the determination of acetaminophen in urine was a modified form of the spectrophotometric assay developed by Plakogiannis and Saad (8, 9) for plasma acetaminophen. To 2 ml of urine in a screw-capped, 20-ml centrifuge tube was added 4 ml of 3 *N* HCl, and the sample was diluted with distilled water to 10 ml. The tube was centrifuged at 5000 rpm for 1 hr, and the clear supernate was treated with ether (4 ml) two to three times. The *p*-aminophenol then was extracted from ether with 10 ml of 1 *N* HCl. Five milliliters of 5% vanillin in isopropanol was added to 2 ml of the acidic extract; the resulting yellow color was measured at 395 nm. Concentrations were determined from a previously constructed standard curve.

***In Vitro* Assessment of Dosage Forms**—Weight variation tests were performed on 20 tablets of each brand according to the USP XIX method (10) for determining permissible limits of weight variation. Although hardness variation is not specified for acetaminophen tablets, the ability of the tablets to withstand physical abuse was determined[3]. Their variation in thickness and their friability[4] also were determined.

Disintegration times were determined using an apparatus conforming to the USP XIX (11) specifications and six tablets of each brand. The disintegration times were determined in purified water, simulated gastric fluid[5] without enzymes (pH 1.2), and simulated intestinal fluid[6] (pH 7.5) maintained at 37 ± 1° as the immersion fluid.

Dissolution rates were determined in 0.1 *N* HCl in a basket stirrer assembly meeting the USP XIX (11) requirements and equipped with Pyrex beakers. The stirrer speed was 85 rpm. The whole assembly was immersed in a suitable water bath that kept the water constantly in motion and held the temperature at 37 ± 0.5°. At time zero, one tablet was introduced into the dissolution medium; at the same time, 5.0 ml of the dissolution medium was withdrawn and replaced with 5 ml of the appropriate fluid.

[3] Stokes–Monsanto tester, Erweka Chemical and Pharmaceutical Industry Co., New York, N.Y.

[4] Roche friabilator, Erweka Chemical and Pharmaceutical Industry Co., New York, N.Y.

[5] The simulated gastric fluid was prepared by adding 2 g of sodium chloride to 7.0 ml of hydrochloric acid and bringing the solution to 1000 ml with distilled water.

[6] The simulated intestinal fluid was made by dissolving monobasic potassium phosphate (6.8 g) in 250 ml of water. Then 190 ml of 0.2 *N* NaOH and 400 ml of water were added. The resulting solution was adjusted with 0.2 *N* NaOH to pH 7.5 ± 1 and diluted with water to 1000 ml.

**Table II—Disintegration Data [a] of the Three Brands of Acetaminophen Tablets**

| Brand | Water | Gastric Fluid | Intestinal Fluid |
|---|---|---|---|
| A | 22 | >30 | 5.1 |
| B | 0.28 | 0.33 | 3.0 |
| C | 2.9 | 1.9 | 0.28 |

[a] Each value is expressed in minutes and is the average of six tablets.

**Table III—Percentage of Drug Liberated at Different Dissolution Times [a]**

| Brand | $T_{25\%}$ | $T_{50\%}$ | $T_{75\%}$ |
|---|---|---|---|
| A | 30.0 ± 3.27 | 50 ± 0.00 | 85 ± 6.8 |
| B | 0.5 ± 0.00 | 1 ± 1.73 | 3 ± 0.00 |
| C | 0.5 ± 1.35 | 1 ± 2.70 | 3 ± 2.65 |

[a] The values are expressed in minutes and include the standard deviation.

The samples were filtered and placed in a 30-ml bottle, which was immersed in ice to slow hydrolysis. In the same manner, samples were taken every 0.5 min for 7 min for Brands B and C. For Brand A, the samples were analyzed every 5 min for up to 90 min. The reproducibility of dissolution was confirmed with three sets of tablets from each lot, and all analyses were performed in triplicate. The samples were analyzed spectrophotometrically.

**Tablet Assay**—The analysis was done according to the method of Plakogiannis and Saad (8, 9). Twenty acetaminophen tablets were weighed and pulverized, and an accurate weight of the powder sample corresponding to 200 mg of acetaminophen, based on the label claim, was transferred to a suitable container. Then 50 ml of 4 *N* HCl was added. The solution was shaken mechanically for 20 min, filtered into a 100-ml volumetric flask, and diluted to volume with 4 *N* HCl. The flask contents were mixed well, and 1 ml was transferred to a test tube. Then 5 ml of 4 *N* HCl was added, and the tube was heated for 1 hr in a water bath. The tubes were allowed to cool, and the contents were transferred quantitatively to a 50-ml volumetric flask. The amount of *p*-aminophenol was calculated from a calibration curve and multiplied by a factor of 1.385.

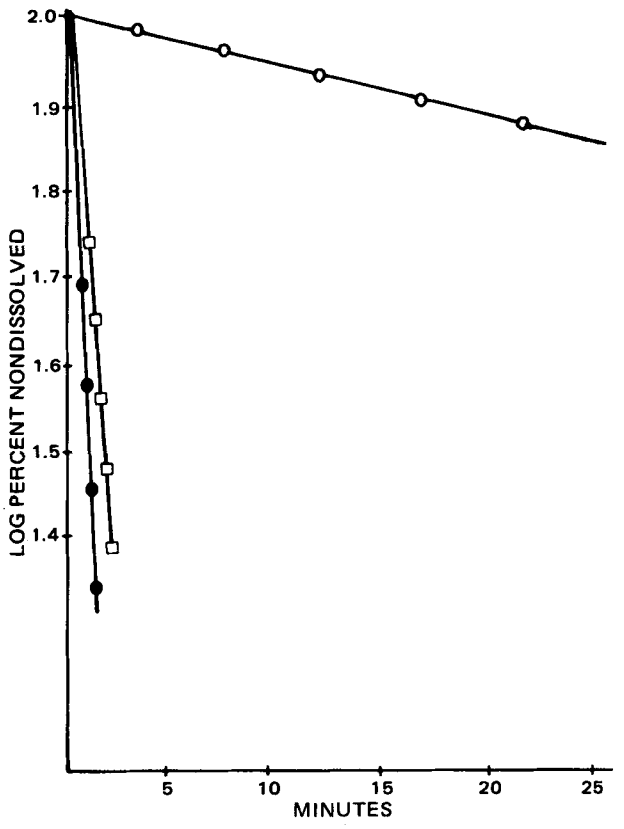


**Figure 1**—In vitro *dissolution of three formulations of acetaminophen tablets. Key:* ○, *Brand A;* ●, *Brand B; and* □, *Brand C.*

**Table IV—Cumulative Percent Urinary Excretion of Four Brands of Acetaminophen as a Function of Time [a]**

| Hours | Brand A | Brand B | Brand C | Brand D |
|---|---|---|---|---|
| 0.5 | 3.69 (1.2) | 11.24 (2.60) | 13.38 (1.33) | 17.71 (3.03) |
| 1.0 | 16.67 (3.92) | 27.76 (2.88) | 23.19 (2.67) | 28.65 (3.32) |
| 1.5 | 25.48 (6.31) | 32.25 (4.66) | 32.77 (2.96) | 39.26 (3.33) |
| 2.0 | 36.41 (7.47) | 41.42 (5.10) | 40.61 (3.32) | 48.36 (3.85) |
| 3.0 | 40.59 (6.95) | 55.26 (6.93) | 54.34 (4.65) | 62.65 (3.78) |
| 4.0 | 52.77 (4.07) | 65.80 (7.18) | 63.30 (5.30) | 72.53 (3.84) |
| 6.0 | 81.46 (5.45) | 78.13 (7.20) | 77.38 (5.15) | 85.34 (2.89) |
| 8.0 | 91.50 (4.99) | 87.30 (4.47) | 85.65 (4.27) | 92.30 (2.88) |
| 12.0 | 96.65 (1.81) | 92.85 (2.19) | 94.23 (3.31) | 97.07 (1.07) |

[a] Each value is the average percent excreted for four subjects. The values in parentheses are the relative standard deviations.

**Table V—Repeated-Measures Analysis of Variance for *In Vivo* Data (0–12 hr)**

| Source | *df* | Mean Square | *F* | Probability |
|---|---|---|---|---|
| Drug | 3 | 0.04130 | 3.08 | 0.0831 |
| Error | 9 | 0.01342 | | |
| Time | 8 | 0.52573 | 384.40[a] | 0.0000 |
| Error | 24 | 0.00137 | | |
| Drug–time interaction | 24 | 0.00062 | 0.75 | 0.7771 |
| Error | 72 | 0.00083 | | |

[a] Significance level = $p < 0.001$.

**Table VI—Repeated-Measures Analysis of Variance for *In Vivo* Data (0–4 hr)**

| Source | *df* | Mean Square | *F* | Probability |
|---|---|---|---|---|
| Drug | 3 | 0.02052 | 5.34[a] | 0.0218 |
| Error | 9 | 0.00384 | | |
| Time | 5 | 0.14788 | 112.97[b] | 0.0000 |
| Error | 15 | 0.00131 | | |
| Drug–time interaction | 15 | 0.0057 | 1.40 | 0.1911 |
| Error | 45 | 0.00040 | | |

[a] Significance level = $p < 0.05$. [b] Significance level = $p < 0.001$.

## RESULTS AND DISCUSSION

The manufacturing parameters for all three brands are given in Table I. All brands passed the weight variation test as specified in USP XIX. Furthermore, the coefficient of variation of weight was within the standards reported by Pietra and Setnikav (12). The resistance of the tablet to chipping, abrasion or breakage, transportation, and handling before use depends on its hardness. According to King (13), a hardness of 4 kg is the minimum for a satisfactory tablet, but Brand A had a hardness of <4 kg (Table I).

Although standards for uniformity in thickness have not been established by the USP, King (13) postulated that a difference in thickness of ±5% may be allowed, depending on the tablet. The average thicknesses (±*SD*) of the acetaminophen tablets were 5.026 ± 0.08, 4.90 ± 0.03, and 5.067 ± 0.03 mm for Brands A, B, and C, respectively (Table I), which fall within the limits set forth by King (13). Official limits for friability also have not been established; however, according to Gunsel and Kanig (14), a weight loss of <0.8% is considered satisfactory. Only Brand C was close to this unofficial limit (Table I). Since most of the Brand A tablets lost their edges and showed capping, their friability values were not calculated.

The disintegration tests, as specified in USP XIX (11), were performed on all of the brands. The average disintegration times were determined in water, simulated gastric fluid (without enzymes), and intestinal fluids (without enzymes) (Table II). The disintegration time of Brand A in the gastric fluid was longer than the times of the other two lots; furthermore, small tablet cores were observed in the basket after 30 min.

The dissolution behavior of the three brands is shown in Fig. 1 and Table III. Figure 1 was constructed by plotting the log concentration of undissolved drug *versus* time. This profile indicates that dissolution is associated with apparent first-order kinetics and occurs under sink conditions (15, 16). The release constants in 0.1 *N* HCl were determined

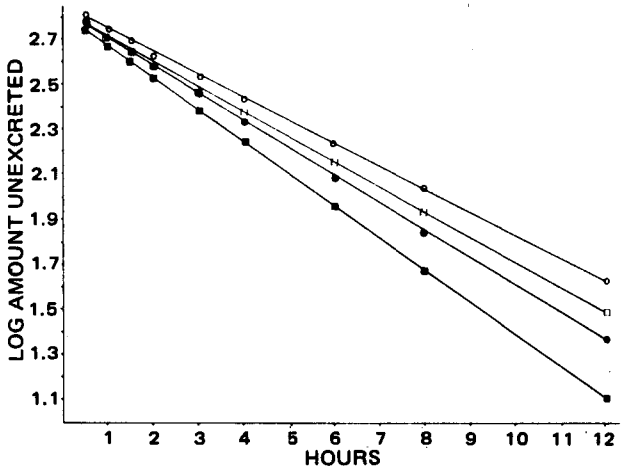


**Figure 2**—*Amount of unexcreted acetaminophen from four products. Key:* ○, *Brand A;* ●, *Brand B;* □, *Brand C; and* ■, *Brand D.*

from the slope of the lines and were 0.1, 0.74, and 0.62/min for Brands A, B, and C, respectively. Brand A tablets had the slowest dissolution rate. In fact, 90 min was required for 80% of the drug from Brand A to be released, while only 1 min was required for 99.8 and 100% of the drug to be released from Brands B and C, respectively. The slow dissolution rate of Brand A is also evident from the $T_{50\%}$ value, which was 50 min; it was only 1 min for Brands B and C. Brand A also exhibited the longest disintegration time.

Since acetaminophen is eliminated by first-order kinetics (17), some pharmacokinetic parameters were calculated by plotting the log concentration of the excreted drug *versus* time. The elimination constant ($K_e$) and the elimination half-life were calculated from the resultant slopes (Fig. 2). The mean half-lives were: Brand A, 4.12 hr with a range of 3.36–4.80 hr; Brand B, 2.77 hr with a range of 2.42–3.17 hr; Brand C, 3.12 hr with a range of 1.90–3.70 hr; and Brand D, 2.00 hr with a range of 1.51–2.86 hr. Nelson and Morioka (18) reported a mean half-life of 1.95 ± 0.23 hr, while Cummings *et al.* (17) and McGilveray *et al.* (5) reported values of 2.2 and 3.14 hr, respectively. Hence, Brand A had the longest half-life, which is consistent with its performance with respect to disintegration and dissolution; that is, the relatively short elimination half-life of acetaminophen is distorted by the long absorption half-life of Brand A.

Table IV illustrates the cumulative amount of drug excreted in the urine for each dosage form as a function of time. These data were analyzed using analysis of variance and covariance, including repeated measures. Table V shows that the calculated *F* values (0–12 hr) of 3.08 for the drug and 0.75 for the drug–time interaction were not significant ($p = 0.001$) across the elapsed time. However, the sample times showed a significant difference ($F = 384.40$). Therefore, the data at sample times from 0 to 4 hr were analyzed (Table VI). These data show that the calculated *F* values of 5.34 for the drug ($p = 0.05$) and of 112.97 for time ($p = 0.001$) were significant.

Furthermore, an analysis of variance, one for each week, was performed (one-way analysis of variance) (Table VII); there was no effect at any one of the nine times. These results indicate that absorption is dissolution rate controlled and agree with the suggestion of Levy and Yacobi (19) that urine collections be made at <3 hr to detect a meaningful difference.

Significant difference ($p = 0.05$) in drug elimination at selected times between brand interactions was observed by utilizing the Tukey procedure (Table VIII). Brand A was significantly different from Brand D at

**Table VII—One-Way Analysis of Variance for Each Week**

| Hours | $F$ | Probability[a] |
|---|---|---|
| 0.5 | 0.6561 | 0.5944 |
| 1.0 | 0.2979 | 0.8263 |
| 1.5 | 0.3271 | 0.8058 |
| 2.0 | 0.7519 | 0.5421 |
| 3.0 | 0.5732 | 0.6434 |
| 4.0 | 0.2914 | 0.8308 |
| 6.0 | 1.074 | 0.3967 |
| 8.0 | 1.147 | 0.3697 |
| 12.0 | 1.145 | 0.3707 |

[a] No significance.

**Table VIII—Significant Differences in Drug Elimination at Selected Times Using the Tukey Procedure**

| Hours | Brands A and B | Brands D and A | Brands D and C | Brands B and A | Brands B and C | Brands A and C |
|---|---|---|---|---|---|---|
| 0.5 | *[a] | *[a] | | *[a] | | *[a] |
| 1.0 | | *[a] | | | | |
| 1.5 | | *[a] | | | | |
| 2.0 | | *[a] | | | | |
| 3.0 | | | | | | |
| 4.0 | | *[a] | | | | |

[a] * = significant at the 0.05 level.

0.5, 1, 1.5, 2, and 4 hr and from Brands B and C at 0.5 hr. This result could be expected since only 0.5 min was required for 25% of Brands B and C to be dissolved whereas 30 min was required for 25% of Brand A to be dissolved.

## REFERENCES


(1) *J. Am. Pharm. Assoc.*, **NS 13,** 278 (1973).

(2) *Ibid.*, **NS 17,** 517 (1977).

(3) G. L. Mattok, I. J. McGilveray, and D. Cook, *Can. J. Pharm. Sci.*, **6,** 35 (1971).

(4) G. L. Mattok, I. J. McGilveray, and C. A. Mainville, *J. Pharm. Sci.*, **60,** 561 (1971).

(5) I. J. McGilveray, G. L. Mattok, J. R. Fooks, N. Jordan, and D. Cook, *Can. J. Pharm. Sci.*, **6,** 39 (1971).

(6) J. R. Gwilt, A. Robertson, L. Goldman, and A. W. Blanchard, *J. Pharm. Pharmacol.*, **15,** 445 (1963).

(7) L. F. Prescott, *Clin. Pharmacol. Ther.*, **10,** 383 (1969).

(8) F. M. Plakogiannis and A. M. Saad, *J. Pharm. Sci.*, **64,** 1547 (1975).

(9) *Ibid.*, **67,** 561 (1978).

(10) "The United States Pharmacopeia," 19th rev., Mack Publishing Co., Easton, Pa., 1975, p. 671.

(11) *Ibid.*, pp. 650, 651.

(12) J. Pietra and J. Setnikar, *J. Pharm. Sci.*, **59,** 530 (1970).

(13) R. E. King, in "Remington's Pharmaceutical Sciences," 15th ed., Mack Publishing Co., Easton, Pa., 1976, p. 1576.

(14) W. C. Gunsel and J. L. Kanig, in "The Theory and Practice of Industrial Pharmacy," 2nd ed., L. Lachman, H. A. Lieberman, and J. L. Kanig, Eds., Lea & Febiger, Philadelphia, Pa., 1976, p. 348.

(15) M. Gibaldi and S. Feldman, *J. Pharm. Sci.*, **56,** 1238 (1967).

(16) J. G. Wagner, *ibid.*, **58,** 1253 (1969).

(17) A. J. Cummings, M. L. King, and B. K. Martin, *Br. J. Pharmacol. Chemother.*, **29,** 150 (1967).

(18) E. Nelson and T. Morioka, *J. Pharm. Sci.*, **52,** 864 (1963).

(19) G. Levy and A. Yacobi, *J. Clin. Pharmacol.*, **15,** 525 (1975).


## ACKNOWLEDGMENTS


Presented in part at the APhA Academy of Pharmaceutical Sciences, Kansas City meeting, November 1979.

Abstracted from a thesis submitted by J. B. Sotiropoulus to the Graduate Faculty, Arnold & Marie Schwartz College of Pharmacy and Health Sciences, in partial fulfillment of the Master of Science degree requirements.


# Quantitative Structure–Activity Relationships of Purines I: Choice of Parameters and Prediction of pKa Values


**ZOHAR NEIMAN ˣ and FRANK R. QUINN**



Received August 21, 1980, from the *Laboratory of Medicinal Chemistry and Biology, Division of Cancer Treatment, National Cancer Institute, National Institutes of Health, Bethesda, MD 20205.* Accepted for publication September 22, 1980.



**Abstract** □ Linear free energy relationships were derived for several monosubstituted purines. The derived equations relate the pKa to the Hammett constants $\sigma_m$ and $\sigma_p$. A general linear free energy relationship was derived that permits calculation of the pKa of polysubstituted purines. The results suggest that correlation of biological data with standard parameters is feasible.



**Keyphrases** □ Purines—quantitative structure–activity relationships, prediction of pKa for polysubstituted purines from pKa of monosubstituted purines, linear free energy relationship equations □ Structure–activity relationships, quantitative—monosubstituted and polysubstituted purines, choice of parameters for prediction of pKa □ Models, mathematical—linear free energy relationship derived for calculation of pKa of polysubstituted purines


Purine analogs (I–XLV) comprise an important class of potential anticancer agents. Synthetic, unnatural purines can be administered exogenously and utilized by the intact animal to meet its requirements for nucleotides. These analogs then may produce disturbances that disrupt purine biosynthesis and interconversion or be incorporated directly into RNA and DNA, eventually producing cell death (1). These considerations led to the synthesis (2) and testing of thousands of purine derivatives for their anticancer properties, but only two purine analogs, mercaptopurine (6-MP) and its guanine analog (6-TG), have found general clinical use in the treatment of human cancer (3).

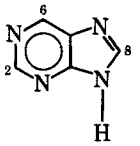


I-XLV


*0022-3549/81/0400-0425$01.00/0*


*© 1981, American Pharmaceutical Association*

**Table VII—One-Way Analysis of Variance for Each Week**

| Hours | $F$ | Probability[a] |
|---|---|---|
| 0.5 | 0.6561 | 0.5944 |
| 1.0 | 0.2979 | 0.8263 |
| 1.5 | 0.3271 | 0.8058 |
| 2.0 | 0.7519 | 0.5421 |
| 3.0 | 0.5732 | 0.6434 |
| 4.0 | 0.2914 | 0.8308 |
| 6.0 | 1.074 | 0.3967 |
| 8.0 | 1.147 | 0.3697 |
| 12.0 | 1.145 | 0.3707 |

[a] No significance.

**Table VIII—Significant Differences in Drug Elimination at Selected Times Using the Tukey Procedure**

| Hours | Brands A and B | Brands D and A | Brands D and C | Brands B and A | Brands B and C | Brands A and C |
|---|---|---|---|---|---|---|
| 0.5 | *[a] | *[a] | | *[a] | | *[a] |
| 1.0 | | *[a] | | | | |
| 1.5 | | *[a] | | | | |
| 2.0 | | *[a] | | | | |
| 3.0 | | | | | | |
| 4.0 | | *[a] | | | | |

[a] * = significant at the 0.05 level.

0.5, 1, 1.5, 2, and 4 hr and from Brands B and C at 0.5 hr. This result could be expected since only 0.5 min was required for 25% of Brands B and C to be dissolved whereas 30 min was required for 25% of Brand A to be dissolved.

## REFERENCES


(1) *J. Am. Pharm. Assoc.*, **NS 13,** 278 (1973).

(2) *Ibid.*, **NS 17,** 517 (1977).

(3) G. L. Mattok, I. J. McGilveray, and D. Cook, *Can. J. Pharm. Sci.*, **6,** 35 (1971).

(4) G. L. Mattok, I. J. McGilveray, and C. A. Mainville, *J. Pharm. Sci.*, **60,** 561 (1971).

(5) I. J. McGilveray, G. L. Mattok, J. R. Fooks, N. Jordan, and D. Cook, *Can. J. Pharm. Sci.*, **6,** 39 (1971).

(6) J. R. Gwilt, A. Robertson, L. Goldman, and A. W. Blanchard, *J. Pharm. Pharmacol.*, **15,** 445 (1963).

(7) L. F. Prescott, *Clin. Pharmacol. Ther.*, **10,** 383 (1969).

(8) F. M. Plakogiannis and A. M. Saad, *J. Pharm. Sci.*, **64,** 1547 (1975).

(9) *Ibid.*, **67,** 561 (1978).

(10) "The United States Pharmacopeia," 19th rev., Mack Publishing Co., Easton, Pa., 1975, p. 671.

(11) *Ibid.*, pp. 650, 651.

(12) J. Pietra and J. Setnikar, *J. Pharm. Sci.*, **59,** 530 (1970).

(13) R. E. King, in "Remington's Pharmaceutical Sciences," 15th ed., Mack Publishing Co., Easton, Pa., 1976, p. 1576.

(14) W. C. Gunsel and J. L. Kanig, in "The Theory and Practice of Industrial Pharmacy," 2nd ed., L. Lachman, H. A. Lieberman, and J. L. Kanig, Eds., Lea & Febiger, Philadelphia, Pa., 1976, p. 348.

(15) M. Gibaldi and S. Feldman, *J. Pharm. Sci.*, **56,** 1238 (1967).

(16) J. G. Wagner, *ibid.*, **58,** 1253 (1969).

(17) A. J. Cummings, M. L. King, and B. K. Martin, *Br. J. Pharmacol. Chemother.*, **29,** 150 (1967).

(18) E. Nelson and T. Morioka, *J. Pharm. Sci.*, **52,** 864 (1963).

(19) G. Levy and A. Yacobi, *J. Clin. Pharmacol.*, **15,** 525 (1975).


## ACKNOWLEDGMENTS


Presented in part at the APhA Academy of Pharmaceutical Sciences, Kansas City meeting, November 1979.

Abstracted from a thesis submitted by J. B. Sotiropoulus to the Graduate Faculty, Arnold & Marie Schwartz College of Pharmacy and Health Sciences, in partial fulfillment of the Master of Science degree requirements.


# Quantitative Structure–Activity Relationships of Purines I: Choice of Parameters and Prediction of pKa Values


**ZOHAR NEIMAN ˣ and FRANK R. QUINN**



Received August 21, 1980, from the *Laboratory of Medicinal Chemistry and Biology, Division of Cancer Treatment, National Cancer Institute, National Institutes of Health, Bethesda, MD 20205.* Accepted for publication September 22, 1980.



**Abstract** □ Linear free energy relationships were derived for several monosubstituted purines. The derived equations relate the pKa to the Hammett constants $\sigma_m$ and $\sigma_p$. A general linear free energy relationship was derived that permits calculation of the pKa of polysubstituted purines. The results suggest that correlation of biological data with standard parameters is feasible.



**Keyphrases** □ Purines—quantitative structure–activity relationships, prediction of pKa for polysubstituted purines from pKa of monosubstituted purines, linear free energy relationship equations □ Structure–activity relationships, quantitative—monosubstituted and polysubstituted purines, choice of parameters for prediction of pKa □ Models, mathematical—linear free energy relationship derived for calculation of pKa of polysubstituted purines


Purine analogs (I–XLV) comprise an important class of potential anticancer agents. Synthetic, unnatural purines can be administered exogenously and utilized by the intact animal to meet its requirements for nucleotides. These analogs then may produce disturbances that disrupt purine biosynthesis and interconversion or be incorporated directly into RNA and DNA, eventually producing cell death (1). These considerations led to the synthesis (2) and testing of thousands of purine derivatives for their anticancer properties, but only two purine analogs, mercaptopurine (6-MP) and its guanine analog (6-TG), have found general clinical use in the treatment of human cancer (3).

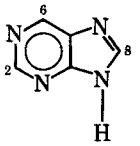


I-XLV


*0022-3549/81/0400-0425$01.00/0*


*© 1981, American Pharmaceutical Association*

**Table I—Physicochemical Parameters**

| Substituent | $\pi$ | $\sigma_m$ | $\sigma_p$ | $\mathcal{F}$ | $\mathcal{R}$ | *MR* |
|---|---|---|---|---|---|---|
| H | 0 | 0 | 0 | 0 | 0 | 0.103 |
| $CH_3$ | 0.56 | −0.07 | −0.17 | −0.04 | −0.13 | 0.565 |
| $C_6H_5$ | 1.96 | 0.06 | −0.01 | 0.08 | −0.08 | 2.536 |
| $CF_3$ | 0.88 | 0.43 | 0.54 | 0.38 | 0.19 | 0.502 |
| CN | −0.57 | 0.56 | 0.66 | 0.51 | 0.19 | 0.633 |
| $CH_2OH$ | −1.03 | 0 | 0 | 0 | 0 | 0.719 |
| CHO | −0.65 | 0.35 | 0.42 | 0.31 | 0.13 | 0.688 |
| $COO^-$ | −4.36 | −0.10 | 0 | −0.15 | 0.13 | 0.605 |
| $CO(NHCH_3)$ | −1.27 | 0.35 | 0.36 | 0.34 | 0.05 | 1.457 |
| F | 0.14 | 0.34 | 0.06 | 0.43 | −0.34 | 0.092 |
| Cl | 0.71 | 0.37 | 0.23 | 0.41 | −0.15 | 0.602 |
| $OCH_3$ | −0.02 | 0.12 | −0.27 | 0.26 | −0.51 | 0.787 |
| $OC_2H_5$ | 0.38 | 0.10 | −0.24 | 0.22 | −0.44 | 1.247 |
| $SCH_3$ | 0.61 | 0.15 | 0 | 0.20 | −0.18 | 1.382 |
| $SC_2H_5$ | 1.07 | 0.18 | 0.03 | 0.23 | −0.18 | 1.842 |
| $SO_2CH_3$ | −1.63 | 0.60 | 0.72 | 0.54 | 0.22 | 1.349 |
| $SO_3^-$ | −4.76 | 0.05 | 0.09 | 0.03 | 0.07 | — |
| $NH_2$ | −1.23 | −0.16 | −0.66 | 0.02 | −0.68 | 0.542 |
| $NHCH_3$ | −0.47 | −0.30 | −0.84 | −0.11 | −0.74 | 1.033 |
| $N(CH_3)_2$ | 0.18 | −0.15 | −0.83 | 0.10 | −0.92 | 1.555 |
| $^+N(CH_3)_3$ | −5.96 | 0.88 | 0.82 | 0.89 | 0 | — |
| NHOH | −1.34 | −0.04 | −0.34 | 0.06 | −0.40 | 0.722 |
| $NHCONH_2$ | −1.30 | −0.03 | −0.24 | 0.04 | −0.28 | 1.372 |
| $NHCOOC_2H_5$ | 0.17 | 0.07 | −0.15 | 0.14 | −0.28 | 2.118 |

## BACKGROUND

No detailed quantitative structure–activity study of the action of the purines against cancer has been published (4), perhaps due to the difficulty of establishing a suitable set of physicochemical parameters. In quantitative structure–activity relationship studies, the usual approach is to achieve correlations with parameters that were determined in conventional aromatic (5) (*e.g.*, benzoic acid) or aliphatic (6) systems. Thus, the basic set of parameters consists of hydrophobic constants (log *P* or $\pi$), electronic parameters ($\sigma_m$, $\sigma_p$, $\mathcal{F}$, $\mathcal{R}$), and volume parameters such as Taft's steric parameter ($E_s$) (6) and molar refractivity (*MR*) (4). In treating alicyclic or heterocyclic systems, it is assumed that the Hammett approach can be extended to any rigid system that prevents direct steric interactions (7).

With purine analogs, the situation with respect to hydrophobic and electronic parameters is more complex since positions 2, 6, and 8 are not equivalent and behave differently toward chemicals (2) and enzymes (8). Thus, substituents at positions 2 and 6 are attached to a six-membered, $\pi$-electron-deficient pyrimidine ring, while those at position 8 are located on a $\pi$-electron-excessive imidazole moiety (9). Theoretically, new sets of physicochemical parameters should be determined for each of the three nucleus positions of purine. This task is not impossible but is a major undertaking.

Tomasik *et al.* (10) examined the application of linear free energy relationships to nitrogen heterocyclic systems, including purines. They reported the correlation of a small set of pKa values of monosubstituted purines in terms of $\sigma_m$. The reason this parameter was selected is unknown, and the arbitrary elimination of data points was not explained. In addition, the customary statistical criteria (*e.g.*, *F* statistics) were not given. Perrin (11) reported the prediction of the pKa values of three aminopurines from a Hammett equation for pyridines.

Hammett electronic constants are determined by measuring the pKa values of the appropriately substituted benzoic acids (5). In the present study, this procedure was reversed so that correlations were derived that relate the pKa values of monosubstituted purines to a set of well-established substituent constants. General equations then were derived that permit the prediction of the pKa values of polysubstituted purines. The predicted pKa values from these equations then were compared with experimental values. The results demonstrate the feasibility of deriving quantitative structure–activity relationships for the biological activity of purines.

## EXPERIMENTAL

The parameters employed are given in Table I and were taken from the recent literature (12). The pKa values were collected from several sources (13) and are listed with the references in Table II. The *MR* values were scaled to one-tenth of the original values (14).

Reported pKa values for purines vary extensively. Thus, for adenine (6-aminopurine, XXXIII), reported values for anion formation range from 9.30 (15) to 9.96 (16). Also, some pKa values were measured in aqueous organic solvents (13), which suppress ionization and may cause the pKa values to differ by as much as 0.5 unit (17).

In this study, purines with substituents capable of (thio)lactim–(thio)lactam tautomerization were excluded. The reason was that for the prototropy: RNH—C=X ⇌ RN=C—XH (X = S,O), there are no "true" parameters for the X–H or C=X substituents, and it was felt that use of normal aromatic values for SH and OH was not justified. This ap-

**Table II—Observed and Predicted pKa Values of Monosubstituted Purines**

| Compound | Substituent at Position 2 | 6 | 8 | pKa[a] Obs. | Calc.[b] | \|ΔpKa\| | Reference[c] |
|---|---|---|---|---|---|---|---|
| I | H | H | H | 8.93 | 9.43 (1), 8.85 (3) | 0.50, 0.08 | 22 |
| | | | | 2.52 | 2.82 (2), 1.86 (4) | 0.30, 0.66 | |
| | | | | | 8.43 (5), 8.71 (7) | 0.50, 0.22 | |
| | | | | | 2.61 (6), 2.69 (8) | 0.09, 0.17 | |
| II | $CH_3$ | — | — | 9.10 | 9.65 (1), 9.04 (7) | 0.55, 0.06 | 23 |
| | | | | ND[d] | 3.19 (2), 3.05 (8) | — — | |
| III | — | $CH_3$ | — | 9.02 | 9.19 (3), 9.06 (7) | 0.16, 0.03 | 24–26 |
| | | | | 2.60 | 2.34 (4), 3.05 (8) | 0.26, 0.45 | |
| IV | — | — | $CH_3$ | 9.37 | 8.80 (5), 9.10 (7) | 0.57, 0.27 | 24–26 |
| | | | | 2.85 | 3.08 (6), 3.16 (8) | 0.23, 0.31 | |
| V | $C_6H_5$ | — | — | 9.60 | 9.25 (1), 8.73 (7) | 0.35, 0.87 | 23 |
| | | | | ND | 2.50 (2), — | — — | |
| VI | — | — | $C_6H_5$ | 8.09 | 8.12 (5), 8.37 (7) | 0.03, 0.28 | 24 |
| | | | | 2.68 | 2.63 (6), 2.71 (8) | 0.05, 0.03 | |
| VII | — | $CH_3$ | — | 7.35 | 7.75 (3), 7.60 (7) | 0.40, 0.25 | 25, 26 |
| | | | | ND | 0.31 (4), 0.44 (8) | — — | |
| VIII | — | — | $CF_3$ | 5.10 | 6.17 (5), 6.30 (7) | 1.07, 1.20 | 25, 26 |
| | | | | 1.00 | 1.09 (6), 1.19 (8) | 0.09, 0.19 | |

**Table II**—*Continued*

| Compound | Substituent at Position 2 | 6 | 8 | pKa[a] Obs. | Calc.[b] | \|ΔpKa\| | Reference[c] |
|---|---|---|---|---|---|---|---|
| IX | — | CN | — | 6.88 | 7.50 (3), 7.35 (7) | 0.62, 0.47 | 25, 26 |
| | | | | 0.30 | −0.03 (4), −0.23 (8) | 0.33, 0.53 | |
| X | — | — | $CH_2OH$ | 8.79 | 8.43 (5), 8.71 (7) | 0.36, 0.08 | 27 |
| | | | | 2.62 | 2.61 (6), 2.69 (8) | 0.01, 0.07 | |
| XI | — | CHO | — | 8.80 | 7.99 (3), 7.85 (7) | 0.81, 0.95 | 28 |
| | | | | —[e] | 0.65 (4), 0.86 (8) | — — | |
| XII | — | — | COOH | 9.37 | 8.96 (5), 9.27 (7) | 0.41, 0.10 | 29 |
| | | | | 2.91 | 2.61 (6), 2.69 (8) | 0.30, 0.22 | |
| XIII | — | $CO(NHCH_3)$ | — | 8.90 | 8.12 (3), 7.97 (7) | 0.78, 0.93 | 25, 26 |
| | | | | 1.00 | 0.83 (4), 0.86 (8) | 0.17, 0.14 | |
| XIV | F | — | — | 8.17 | 8.40 (1), 8.59 (7) | 0.23, 0.42 | 30 |
| | | | | ND | 1.02 (2), 0.91 (8) | — — | |
| XV | Cl | — | — | 8.21 | 8.30 (1), 8.27 (7) | 0.09, 0.06 | 31 |
| | | | | 0.69 | 0.86 (2), 0.75 (8) | 0.17, 0.06 | 31 |
| XVI | — | Cl | — | 7.88 | 8.38 (3), 8.24 (7) | 0.50, 0.36 | 31 |
| | | | | 0.45 | 1.20 (4), 0.76 (8) | 0.75, 0.31 | |
| XVII | — | — | Cl | 6.02 | 6.49 (5), 6.64 (7) | 0.47, 0.62 | 31 |
| | | | | 1.77 | 1.96 (6), 2.05 (8) | 0.19, 0.28 | |
| XVIII | $OCH_3$ | — | — | 9.20 | 9.07 (1), 9.23 (7) | 0.13, 0.03 | 24 |
| | | | | 2.44 | 2.18 (2), 2.06 (8) | 0.26, 0.38 | |
| XIX | — | $OCH_3$ | — | 9.16 | 9.40 (3), 9.27 (7) | 0.24, 0.11 | 24 |
| | | | | 2.21 | 2.63 (4), 2.06 (8) | 0.42, 0.15 | |
| XX | — | — | $OCH_3$ | 7.73 | 7.80 (5), 8.04 (7) | 0.07, 0.31 | 32 |
| | | | | 3.14 | 3.36 (6), 3.43 (8) | 0.22, 0.29 | |
| XXI | $OC_2H_5$ | — | — | 9.47 | 9.13 (7), 9.17 (7) | 0.34, 0.30 | 33 |
| | | | | 2.46 | 2.29 (2), 2.16 (8) | 0.17, 0.30 | |
| XXII | — | $OC_2H_5$ | — | 9.52 | 9.34 (3), 9.20 (7) | 0.18, 0.32 | 33 |
| | | | | 2.13 | 2.54 (4), 2.16 (8) | 0.41, 0.03 | |
| XXIII | $SCH_3$ | — | — | 8.91 | 8.98 (1), 8.71 (7) | 0.07, 0.20 | 24 |
| | | | | 1.91 | 2.02 (2), 1.90 (8) | 0.11, 0.01 | |
| XXIV | — | $SCH_3$ | — | 8.75 | 8.85 (3), 8.71 (7) | 0.10, 0.04 | 32, 34 |
| | | | | 1.63 | 1.86 (4), 1.90 (8) | 0.23, 0.22 | |
| XXV | — | — | $SCH_3$ | 7.67 | 7.65 (5), 7.87 (7) | 0.02, 0.20 | 24, 32 |
| | | | | 2.95 | 2.61 (6), 2.69 (8) | 0.34, 0.26 | |
| XXVI | $SC_2H_5$ | — | — | 9.19 | 8.89 (1), 8.65 (7) | 0.30, 0.54 | 35 |
| | | | | ND | 1.87 (2), 1.74 (8) | — — | |
| XXVII | — | $SC_2H_5$ | — | 8.86 | 8.79 (3), 8.65 (7) | 0.07, 0.21 | 35 |
| | | | | 1.72 | 1.77 (4), 1.75 (8) | 0.05, 0.03 | |
| XXVIII | — | — | $SC_2H_5$ | 7.72 | 7.49 (5), 7.70 (7) | 0.23, 0.02 | 35 |
| | | | | 3.04 | 2.52 (6), 2.60 (8) | 0.52, 0.44 | |
| XXIX | — | — | $SO_2CH_3$ | 4.87 | 5.28 (5), 5.35 (7) | 0.41, 0.48 | 36 |
| | | | | 0.42 | 0.59 (6), 0.69 (8) | 0.17, 0.27 | |
| XXX | — | $SO_3H$ | — | 8.56 | 8.67 (3), 8.53 (7) | 0.11, 0.03 | 37 |
| | | | | 1.13 | 1.60 (4), 2.43 (8) | 0.47, 1.30 | |
| XXXI | — | — | $SO_3H$ | 6.93 | 8.17 (5), 8.43 (7) | 1.24, 1.50 | 37 |
| | | | | 2.22 | 2.35 (6), 2.44 (8) | 0.13, 0.22 | |
| XXXII | $NH_2$ | — | — | 9.93 | 9.92 (1), 9.98 (7) | 0.01, 0.05 | 24–26 |
| | | | | 3.80 | 3.66 (2), 3.52 (8) | 0.14, 0.28 | |
| XXXIII | — | $NH_2$ | — | 9.96 | 10.19 (3), 10.07 (7) | 0.23, 0.11 | 16 |
| | | | | 4.22 | 3.75 (4), 3.52 (8) | 0.47, 0.70 | |
| XXXIV | — | — | $NH_2$ | 9.36 | 9.28 (5), 9.60 (7) | 0.08, 0.24 | 24 |
| | | | | 4.68 | 4.46 (6), 4.51 (8) | 0.22, 0.17 | |
| XXXV | $NHCH_3$ | — | — | 10.32 | 10.35 (1), 10.32 (7) | 0.03, 0.00 | 38 |
| | | | | 4.01 | 4.40 (2), 4.25 (8) | 0.39, 0.24 | |
| XXXVI | — | $NHCH_3$ | — | 9.99 | 10.56 (3), 10.44 (7) | 0.57, 0.45 | 24, 39 |
| | | | | 4.18 | 4.26 (4), 4.25 (8) | 0.08, 0.07 | |
| XXXVII | — | — | $NHCH_3$ | 9.56 | 10.01 (5), 10.39 (7) | 0.45, 0.83 | 24 |
| | | | | 4.78 | 4.96 (6), 5.01 (8) | 0.18, 0.23 | |
| XXXVIII | $N(CH_3)_2$ | — | — | 10.22 | 9.89 (1), 10.30 (7) | 0.33, 0.08 | 24 |
| | | | | 4.02 | 3.61 (2), 3.42 (8) | 0.41, 0.55 | |
| XXXIX | — | $N(CH_3)_2$ | — | 10.50 | 10.54 (3), 10.42 (7) | 0.04, 0.08 | 24, 30, 39 |
| | | | | 3.87 | 4.23 (4), 3.47 (8) | 0.36, 0.40 | |
| XL | — | — | $N(CH_3)_2$ | 9.73 | 9.22 (5), 9.55 (7) | 0.51, 0.18 | 24 |
| | | | | 4.80 | 4.93 (6), 4.98 (8) | 0.13, 0.18 | |
| XLI | — | $^+N(CH_3)_3$ | — | 6.85 | 7.18 (3), 7.02 (7) | 0.33, 0.17 | 40 |
| | | | | ND | −0.49 (4), −1.90 (8) | — — | |
| XLII | — | — | $^+N(CH_3)_3$ | 4.88 | 3.81 (5), 3.79 (7) | 1.07, 1.09 | 40 |
| | | | | ND | 0.31 (6), 0.42 (8) | — — | |
| XLIII | — | NHOH | — | 9.83 | 9.54 (3), 9.41 (7) | 0.29, 0.42 | 25, 26 |
| | | | | 3.80 | 2.83 (4), 2.89 (8) | 0.97, 0.91 | |
| XLIV | — | $NHCONH_2$ | — | 9.95 | 9.34 (3), 9.20 (7) | 0.61, 0.75 | 25, 26 |
| | | | | 2.35 | 2.54 (4), 2.84 (8) | 0.19, 0.49 | |
| XLV | — | $NHCOOC_2H_5$ | — | 9.63 | 9.15 (3), 9.02 (7) | 0.48, 0.61 | 25, 26 |
| | | | | 2.40 | 2.29 (4), 2.32 (8) | 0.11, 0.08 | |

[a] Underlined values refer to cations. [b] The equation number is in parentheses. [c] The references refer to the source of the observed values. [d] No data available. [e] Unstable in acid (*cf.*, footnote 1 in text).

proach may narrow the conclusions since many purines possess these substituents. In the case of mercaptopurine and its guanine analog, it was shown that one active form is the 6-methylthio derivative obtained by *in vivo* *S*-methylation (3). Although these methylthio compounds are incapable of thiolactam–thiolactim tautomerization, they are active themselves and were included in this study.

Aminopurines exist mainly in the $NH_2$ form rather than as the imino (NH=) tautomer (18). For this reason, use of established parameters for

**Table III—Equations Correlating pKa Values of Purines with Physicochemical Constants**

| Equation | $n$ | $r$ | $s$ | $F_{1,x}$[a] | Equation | $n$ | $r$ | $s$ | $F_{1,x}$[a] |
|---|---|---|---|---|---|---|---|---|---|
| 2-Monosubstituted purines (anions) | | | | | 8-Monosubstituted purines (cations) | | | | |
| 1. pKa = 9.43(±0.22) − 3.05(±1.10)$\sigma_m$ | 12 | 0.891 | 0.328 | 38.40 | 6. pKa = 2.61(±0.14) − 2.80(±0.32)$\sigma_p$ | 15 | 0.982 | 0.246 | 353.11 |
| 2-Monosubstituted purines (cations) | | | | | Combined equation (anions) | | | | |
| 2. pKa = 2.82(±0.27) − 5.28(±1.33)$\sigma_m$ | 8 | 0.970 | 0.308 | 94.25 | 7. pKa = 8.71(±0.17) − 1.92(±0.79)$\sigma_{p(2)}$ − 2.06(±0.54)$\sigma_{p(6)}$ − 5.59(±0.86)$\sigma_{m(8)}$ | 45 | 0.931 | 0.535 | 89.07 |
| 6-Monosubstituted purines (anions) | | | | | | | | | |
| 3. pKa = 8.85(±0.22) − 2.04(±0.47)$\sigma_p$ | 19 | 0.910 | 0.447 | 81.79 | | | | | |
| 6-Monosubstituted purines (cations) | | | | | Combined equation (cations) | | | | |
| 4. pKa = 1.86(±0.27) − 2.86(±0.65)$\sigma_p$ | 16 | 0.930 | 0.477 | 88.88 | 8. pKa = 2.69(±0.14) − 5.23(±1.48)$\sigma_{m(2)}$ − 5.21(±0.96)$\sigma_{m(6)}$ − 2.77(±0.51)$\sigma_{p(8)}$ | 37 | 0.950 | 0.414 | 100.74 |
| 8-Monosubstituted purines (anions) | | | | | | | | | |
| 5. pKa = 8.43(±0.37) − 5.26(±1.14)$\sigma_m$ | 16 | 0.935 | 0.634 | 97.68 | | | | | |

[a] $p < 0.001$.

**Table IV—Correlation Matrix for Equations 1–6** [a]

| Parameter | $\pi$ for Position | | | $\sigma_m$ for Position | | | $\sigma_p$ for Position | | | $\mathcal{F}$ for Position | | | $\mathcal{R}$ for Position | | | $MR$ for Position | | |
|---|---|---|---|---|---|---|---|---|---|---|---|---|---|---|---|---|---|---|
| | 2 | 6 | 8 | 2 | 6 | 8 | 2 | 6 | 8 | 2 | 6 | 8 | 2 | 6 | 8 | 2 | 6 | 8 |
| $\pi$ | | 1.0 | | | | | | | | | | | | | | | | |
| $\sigma_m$ | 0.22 | 0.12 | 0.08 | | 1.0 | | | | | | | | | | | | | |
| | 0.55 | 0.01 | 0.03 | | | | | | | | | | | | | | | |
| $\sigma_p$ | 0.38 | 0.09 | 0.10 | 0.75 | 0.87 | 0.80 | | 1.0 | | | | | | | | | | |
| | 0.44 | 0.00 | 0.11 | 0.82 | 0.84 | 0.78 | | | | | | | | | | | | |
| $\mathcal{F}$ | 0.07 | 0.12 | 0.05 | 0.85 | 0.93 | 0.91 | 0.36 | 0.64 | 0.53 | | 1.0 | | | | | | | |
| | 0.49 | 0.06 | 0.05 | 0.86 | 0.88 | 0.85 | 0.47 | 0.52 | 0.40 | | | | | | | | | |
| $\mathcal{R}$ | 0.38 | 0.04 | 0.07 | 0.32 | 0.49 | 0.29 | 0.82 | 0.83 | 0.73 | 0.04 | 0.23 | 0.07 | | 1.0 | | | | |
| | 0.25 | 0.04 | 0.37 | 0.50 | 0.51 | 0.36 | 0.88 | 0.88 | 0.82 | 0.15 | 0.18 | 0.06 | | | | | | |
| $MR$ | 0.43 | 0.00 | 0.06 | 0.01 | 0.03 | 0.07 | 0.00 | 0.00 | 0.01 | 0.01 | 0.10 | 0.11 | 0.00 | 0.06 | 0.01 | | 1.0 | |
| | 0.11 | 0.23 | 0.73 | 0.02 | 0.00 | 0.00 | 0.14 | 0.02 | 0.00 | 0.01 | 0.03 | 0.02 | 0.27 | 0.08 | 0.02 | | | |

[a] Underlined values refer to cations.

**Table V—Development of Equations 7 and 8**

| Intercept | $\sigma_{p(2)}$ | $\sigma_{p(6)}$ | $\sigma_{m(8)}$ | $r$ | $s$ | $F_{1,x}$ | $p$ | Equation |
|---|---|---|---|---|---|---|---|---|
| | | | | Equation 7 | | | | |
| 8.46 | −2.25 | — | — | 0.329 | 1.352 | $F_{1,44} = 5.22$ | <0.05 | *a* |
| 8.57 | — | −2.08 | — | 0.440 | 1.286 | $F_{1,44} = 10.30$ | <0.005 | *b* |
| 8.86 | — | — | −5.78 | 0.776 | 0.903 | $F_{1,44} = 65.15$ | <0.001 | *c* |
| 8.83 | — | −2.04 | −5.74 | 0.888 | 0.666 | $F_{1,43}$[a] = 36.93 | <0.001 | *d* |
| 8.71 | −1.92 | −2.06 | −5.59 | 0.931 | 0.535 | $F_{1,42}$[b] = 24.21 | <0.001 | *e* |
| | | | | Equation 8 | | | | |
| 2.60 | −5.19 | — | — | 0.388 | 1.180 | $F_{1,36} = 6.22$ | <0.025 | *a* |
| 2.76 | — | −5.32 | — | 0.614 | 1.011 | $F_{1,36} = 21.23$ | <0.001 | *b* |
| 2.50 | — | — | −2.85 | 0.625 | 1.000 | $F_{1,36} = 22.44$ | <0.001 | *c* |
| 2.67 | — | −5.18 | −2.78 | 0.865 | 0.652 | $F_{1,35}$[a] = 48.44 | <0.001 | *d* |
| 2.69 | −5.23 | −5.21 | −2.77 | 0.950 | 0.414 | $F_{1,34}$[b] = 51.25 | <0.001 | *e* |

[a] This $F$ value is obtained by comparison with Eq. *c*. [b] This $F$ value is obtained by comparison with Eq. *d*.

the amino group was justified. Purine-6-carboxaldehyde was not included in the cation equations since this compound is sensitive to acids and may decompose during pKa determination[1].

In the pKa correlations, all pKa values found in the literature were included without any attempt to eliminate "outliers," *i.e.*, to reject suspect values. The broader scope of the conclusions more than justified the somewhat lower correlation coefficients that were obtained as a consequence.

## RESULTS AND DISCUSSION

The data in Tables I and II were used to develop Eqs. 1–6 (Table III). The observed and predicted pKa values are given in Table II with the cation values being underlined. The correlation matrix for Eqs. 1–6 is given in Table IV.

The negative coefficient of the electronic terms in Eqs. 1–6 reflects the well-known relationship that electron-withdrawing groups at positions 2, 6, and 8 of purines increase the acidity. The absence of steric or hydrophobic terms indicates that ionization of these compounds is due mainly to electronic effects.

Analysis of Eq. 3 reveals that 14 of the 19 compounds undergo anion formation only at the imidazole moiety (I, II, VII, IX, XI, XVI, XIX, XXII, XXIV, XXVII, XXXIII, XXXVI, XXXIX, and XLI) and that five derivatives (XIII, XXX, and XLIII–XLV) may undergo ionization elsewhere. If the correlation is restricted to compounds that undergo anion formation exclusively at the imidazole ring, the equation improves:

$$\text{pKa} = 8.70(\pm 0.22) - 2.04(\pm 0.44)\sigma_p \qquad \text{(Eq. 3}a\text{)}$$

$$n = 14 \quad r = 0.946 \quad s = 0.385 \quad F_{1,13} = 101.26 \quad (p < 0.001)$$

Although Eq. 3*a* has better statistics, Eq. 3 is preferred because of its broader applicability.

Equations 5 and 7 have rather large standard deviations, which may reflect some uncertainties in the pKa measurements.

Because the correlations appeared to be statistically sound for the pKa values of monosubstituted purines, it seemed desirable to combine all of the data into one equation so that the pKa values of the disubstituted and trisubstituted purines could be computed. The procedure used was as follows. Monosubstituted purines were assigned the appropriate substituent constant at the substituted position only, and zeros were assigned to the other positions. With the six parameters ($\pi$, $\sigma_m$, $\sigma_p$, $\mathcal{F}$, $\mathcal{R}$, and $MR$) for the three purine positions, 18 variables are obtained. By

[1] A. Giner-Sorolla, Sloan-Kettering Institute for Cancer Research, Rye, N.Y., personal communication.

**Table VI—Observed and Predicted pKa Values of Disubstituted and Trisubstituted Purines [a]**

| Compound | Substituent at Position 2 | 6 | 8 | pKa [b] Obs. | Calc. | \|ΔpKa\| | Reference [c] |
|---|---|---|---|---|---|---|---|
| I | $CH_3$ | $CH_3$ | $CH_3$ | 9.90 | 9.78 | 0.12 | 41 |
| | | | | 4.49 [b] | 3.89 | 0.60 | |
| II | $CH_3$ | $CH_3$ | $OC_2H_5$ | 8.74 | 8.83 | 0.09 | 42 |
| | | | | 4.71 | 4.08 | 0.63 | |
| III | $CH_3$ | $NHCH_3$ | — | ND [d] | (10.76) | — | 39 |
| | | | | 5.08 | 4.62 | 0.46 | |
| IV | F | $NH_2$ | — | 9.58 | 9.95 | 0.37 | 30 |
| | | | | ND | (1.74) | — | |
| V | F | $N(CH_3)_2$ | — | 9.97 | 10.30 | 0.33 | 30 |
| | | | | ND | (1.69) | — | |
| VI | Cl | Cl | — | 7.06 | 7.79 | 0.73 | 31 |
| | | | | −1.16 | −1.18 | 0.02 | |
| VII | Cl | Cl | Cl | 3.96 | 5.72 | 1.76 | 31 |
| | | | | −3.10 | −1.81 | 1.29 | |
| VIII | $NH_2$ | — | $C_6H_5$ | 9.20 | 9.64 | 0.44 | 35 |
| | | | | 3.98 | 3.55 | 0.43 | |
| IX | $NH_2$ | $NH_2$ | — | 10.77 | 11.34 | 0.57 | 24–26, 39 |
| | | | | 5.09 | 4.36 | 0.73 | |
| X | $NH_2$ | $NH_2$ | $NH_2$ | 10.79 | 12.23 | 1.44 | 24 |
| | | | | 6.23 | 6.18 | 0.05 | |
| XI | $NH_2$ | $CF_3$ | — | 8.87 | 8.87 | 0.00 | 25, 26 |
| | | | | 1.85 | 1.28 | 0.57 | |
| XII | $NH_2$ | — | $CF_3$ | 6.14 | 7.57 | 1.43 | 36 |
| | | | | 2.59 | 2.03 | 0.56 | |
| XIII | $NH_2$ | $CF_3$ | $CF_3$ | 5.02 | 6.46 | 1.44 | 25, 26 |
| | | | | 0.30 | −0.21 | 0.51 | |
| XIV | $NH_2$ | $NH_2$ | $CF_3$ | 7.55 | 8.93 | 1.38 | 25, 26 |
| | | | | 3.68 | 2.86 | 0.82 | |
| XV | $NH_2$ | — | $SCH_3$ | 8.48 | 9.14 | 0.66 | 36 |
| | | | | 4.40 | 3.52 | 0.88 | |
| XVI | $NH_2$ | — | $SO_2CH_3$ | 5.61 | 6.62 | 1.01 | 36 |
| | | | | 2.08 | 1.53 | 0.55 | |
| XVII | $N(CH_3)_2$ | $CH_3$ | — | 10.32 | 10.65 | 0.33 | 35 |
| | | | | 4.14 | 3.83 | 0.31 | |
| XVIII | $N(CH_3)_2$ | $C_2H_5$ | — | 10.73 | 10.61 | 0.12 | 35 |
| | | | | 4.42 | 3.83 | 0.59 | |
| XIX | $N(CH_3)_2$ | $CH_3$ | $CH_3$ | 10.83 | 11.05 | 0.22 | 35 |
| | | | | 4.92 | 4.31 | 0.61 | |
| XX | $N(CH_3)_2$ | $CH_3$ | $C_2H_5$ | 11.11 | 11.05 | 0.06 | 35 |
| | | | | 5.05 | 4.25 | 0.80 | |
| XXI | $N(CH_3)_2$ | $C_2H_5$ | $CH_3$ | ND | (11.00) | — | 35 |
| | | | | 4.90 | 4.31 | 0.59 | |
| XXII | $SCH_3$ | — | $CH_3$ | 9.58 | 9.10 | 0.48 | 41 |
| | | | | 2.83 | 2.37 | 0.46 | |
| XXIII | $SCH_3$ | $C_2H_5$ | — | 9.35 | 9.02 | 0.33 | 35 |
| | | | | 2.50 | 2.27 | 0.23 | |
| XXIV | $SCH_3$ | — | $C_2H_5$ | 9.75 | 9.10 | 0.65 | 35 |
| | | | | 2.80 | 2.32 | 0.48 | |
| XXV | $SCH_3$ | $CH_3$ | $CH_3$ | 9.70 | 9.45 | 0.25 | 41, 43 |
| | | | | 3.04 | 2.74 | 0.30 | |
| XXVI | $SCH_3$ | $CH_3$ | $C_2H_5$ | 9.75 | 9.45 | 0.30 | 35 |
| | | | | 3.08 | 2.68 | 0.40 | |
| XXVII | $SCH_3$ | $C_2H_5$ | $CH_3$ | 9.52 | 9.41 | 0.11 | 35 |
| | | | | 3.05 | 2.74 | 0.31 | |
| XXVIII | $SCH_3$ | $CH_3$ | $CF_3$ | 5.67 | 6.65 | 0.98 | 43 |
| | | | | 1.25 | 0.77 | 0.48 | |
| XXIX | $SCH_3$ | — | $SCH_3$ | 7.73 | 7.87 | 0.14 | 36 |
| | | | | 2.19 | 1.90 | 0.29 | |
| XXX | $SCH_3$ | $CH_3$ | $SCH_3$ | 7.94 | 8.22 | 0.28 | 41 |
| | | | | 2.74 | 2.27 | 0.47 | |
| XXXI | $SC_2H_5$ | $CH_3$ | — | 9.43 | 9.00 | 0.43 | 35 |
| | | | | 2.67 | 2.11 | 0.56 | |
| XXXII | $SC_2H_5$ | — | $CH_3$ | 9.50 | 9.04 | 0.46 | 35 |
| | | | | 2.71 | 2.22 | 0.49 | |
| XXXIII | $SC_2H_5$ | — | $C_2H_5$ | 9.62 | 9.04 | 0.58 | 35 |
| | | | | 2.81 | 2.16 | 0.65 | |

[a] Calculated from Eqs. 7 and 8. [b] Underlined values refer to cations. [c] The references refer to the source of the observed values. [d] No data available.

employing all combinations of these parameters, it is possible to generate 262,143 equations. However, this number of equations can be reduced by generating only equations that are chemically and statistically meaningful. In this instance, only about seven equations have one to seven independent variables. In this study, a stepwise regression procedure (19) generated the desired equations having the best statistics in a minimum of computer time. Equations 7 and 8 are the best combined pKa correlations of the purines; their development is given in Table V.

Equation 7 indicates that the main contribution to the anionic pKa is from the $\sigma_m$ variable at position 8, *i.e.*, at the imidazole moiety where most anion formation occurs.

According to Eq. 8, the main contribution to the cationic pKa is from substituents at positions 2 and 6, *i.e.*, on the pyrimidine ring. This finding does not imply that cation formation necessarily takes place at the pyrimidine moiety. The purine skeleton possesses four heterocyclic nitrogen atoms, each of which is prone to protonation, and little is known about the exact site of protonation of most of these compounds. Furthermore, exocyclic groups such as NHR, SR, and OR may be protonated to some extent.

The observed and predicted pKa values for monosubstituted purines calculated from Eqs. 7 and 8 are given in Table II. It is not surprising that Eq. 7 describes the electronic effects at position 2 in terms of $\sigma_p$ while

Eq. 1 employs $\sigma_m$. Table IV shows a strong intercorrelation between $\sigma_m$ and $\sigma_p$ (arc cos 0.75 = 41°) (20). Similarly, in Eq. 8, $\sigma_m$ replaces $\sigma_p$ of Eq. 4 in the treatment of electronic effects at position 6 (arc cos 0.84 = 33°). Another interesting fact derived from the correlation matrix is considerable autocorrelation of $\pi$, especially at position 2, with $\sigma_m$ and $\sigma_p$. A similar phenomenon was observed for some benzene derivatives (21).

The pKa values of 33 disubstituted and trisubstituted purines were calculated from Eqs. 7 and 8 and compared with measured values reported in the literature (Table VI). The agreement between observed and predicted values is reasonable considering the variation in experimental methods.

Studies are in progress on the correlation of the antitumor potency and toxicity of polysubstituted purines with the structural parameters described in this paper.

## REFERENCES


(1) W. H. Cole, "Chemotherapy of Cancer," Lea & Febiger, Philadelphia, Pa., 1970, chap. 1.

(2) J. H. Lister, "Purines," Wiley–Interscience, New York, N.Y., 1971, p. 9.

(3) "The Pharmacological Basis of Therapeutics," 5th ed., L. S. Goodman and A. Gilman, Eds., Macmillan, New York, N.Y., 1975, p. 1279.

(4) C. Hansch, *Farmaco, Ed. Sci.*, **34**, 89 (1979).

(5) L. P. Hammett, *J. Am. Chem. Soc.*, **59**, 96 (1937).

(6) R. W. Taft, in "Steric Effects in Organic Chemistry," M. S. Newman, Ed., Wiley, New York, N.Y., 1956, chap. 13.

(7) O. Exner, in "Advances in Linear Free Energy Relationships," N. B. Chapman and J. Shorter, Eds., Plenum, New York, N.Y., 1972, p. 42.

(8) J. A. Montgomery, *Handb. Exp. Pharmakol.*, **38**, 76 (1974).

(9) Z. Neiman, *Experientia*, **31**, 996 (1975).

(10) P. Tomasik, R. Zalewski, and J. Chodzinski, *Chem. Zvesti*, **33**, 105 (1979).

(11) D. D. Perrin, *J. Chem. Soc.*, **1965**, 5590.

(12) C. Hansch and A. Leo, "Substituent Constants for Correlation Analysis in Chemistry and Biology," Wiley, New York, N.Y., 1979.

(13) W. H. Cole, "Chemotherapy of Cancer," Lea & Febiger, Philadelphia, Pa., 1970, chap. 13 and references cited therein.

(14) C. Silipo and C. Hansch, *Mol. Pharmacol.*, **10**, 954 (1974).

(15) M. A. Guichelaar and J. Reedijk, *Rec. Trav. Chim. Pays-Bas*, **97**, 295 (1978).

(16) S. Lewin and N. W. Tann, *J. Chem. Soc.*, **1962**, 1466.

(17) A. Albert and E. P. Serjeant, "The Determination of Ionization Constants," 2nd ed., Chapman and Hall, London, England, 1971, p. 39.

(18) W. H. Cole, "Chemotherapy of Cancer," Lea & Febiger, Philadlephia, Pa., 1970, p. 8.

(19) A. J. Barr, J. H. Goodnight, J. P. Sall, and J. T. Helwig, "Statistical Analysis System," SAS Circle, Cary, N.C., 1979.

(20) C. Hansch, A. Leo, S. H. Unger, K. H. Kim, D. Nikitani, and E. J. Lien, *J. Med. Chem.*, **16**, 1207 (1973).

(21) T. Fujita, J. Iwasa, and C. Hansch, *J. Am. Chem. Soc.*, **86**, 5157 (1964).

(22) A. Bendich, P. J. Russell, and J. J. Fox, *ibid.*, **76**, 6073 (1954).

(23) F. Bergmann, A. Kalmus, H. Unger-Waron, and H. Kwietny-Govrin, *J. Chem. Soc.*, **1963**, 3729.

(24) A. Albert and D. J. Brown, *ibid.*, **1954**, 2061.

(25) A. Giner-Sorolla and A. Bendich, *J. Am. Chem. Soc.*, **80**, 5744 (1958).

(26) *Ibid.*, **80**, 3932 (1958).

(27) A. Albert, *J. Chem. Soc.*, **1955**, 2690.

(28) A. Giner-Sorolla, I. Zimmerman, and A. Bendich, *J. Am. Chem. Soc.*, **81**, 2515 (1959).

(29) A. Albert, *J. Chem. Soc.*, **1960**, 4705.

(30) J. A. Montgomery and K. Hewson, *J. Am. Chem. Soc.*, **82**, 463 (1960).

(31) G. B. Barlin and N. B. Chapman, *J. Chem. Soc.*, **1965**, 3017.

(32) D. J. Brown and S. F. Mason, *ibid.*, **1965**, 682.

(33) G. B. Barlin, *ibid. B*, **1967**, 954.

(34) A. Albert, *ibid. C*, **1969**, 2379.

(35) R. Badger, D. J. Brown, and J. H. Lister, *ibid. Perkin Trans. I*, **1974**, 152.

(36) A. Albert, *ibid. B*, **1966**, 438 (1966).

(37) D. J. Brown and J. A. Hoskins, *Aust. J. Chem.*, **25**, 2641 (1972).

(38) D. J. Brown and N. W. Jacobsen, *J. Chem. Soc.*, **1965**, 3770.

(39) B. M. Lynch, R. K. Robins, and C. C. Cheng, *ibid.*, **1958**, 2973.

(40) G. B. Barlin and A. C. Young, *ibid. B*, **1971**, 821.

(41) D. J. Brown, R. L. Jones, A. M. Angyal, and G. W. Grigg, *ibid. Perkin Trans. I*, **1972**, 1819.

(42) D. J. Brown and R. K. Lynn, *ibid. Perkin Trans. I*, **1974**, 349.

(43) M. D. Fenn and J. H. Lister, *ibid. Perkin Trans. I*, **1975**, 485.


## ACKNOWLEDGMENTS


The authors thank Dr. A. Giner-Sorolla, Sloan-Kettering Institute for Cancer Research, Rye, N.Y., and Dr. D. J. Brown, Australian National University, Canberra, Australia, for helpful comments regarding the pKa values of purines and Dr. C. Hansch for suggestions regarding $\pi$ and its interrelations with other variables. Z. Neiman thanks the Fogarty International Center, National Institutes of Health, for a fellowship and Dr. J. S. Driscoll for his hospitality.


# Clofibrate Microcapsules II: Effect of Wall Thickness on Release Characteristics


**P. L. MADAN**



Received July 24, 1980, from the *College of Pharmacy and Allied Health Professions, St. John's University, Jamaica, NY 11439.* Accepted for publication September 25, 1980.



**Abstract** □ The effect of wall thickness on the release characteristics of clofibrate from microcapsules prepared in gelatin–sodium sulfate was investigated. The wall thickness, calculated by recovering the wall material from the microcapsules and using the relationship between two concentric spheres, was related to the surface area of the droplets being encapsulated. Thinner walled microcapsules gave faster release and showed greater deviation from zero-order kinetics but followed the square root of time plots. Microcapsules having thicker walls approximated zero-order release but deviated from the square root of time plots. A theoretical model was developed to explain the release characteristics of the microcapsules. A linear correlation was found between the wall thickness and the *in vitro* $t_{50\%}$ release time.



**Keyphrases** □ Clofibrate—microcapsules, effect of wall thickness on release characteristics □ Microcapsules—clofibrate, effect of wall thickness on release characteristics □ Hypocholesterolemic agents—clofibrate, effect of microcapsule wall thickness on release characteristics


A recent investigation (1) reported the microencapsulation of clofibrate USP, a liquid hypocholesterolemic agent. Prepared by simple coacervation in gelatin–sodium sulfate, the microcapsules were recovered as discrete




*0022-3549/81/0400-0430$01.00/0*


*© 1981, American Pharmaceutical Association*

Eq. 1 employs $\sigma_m$. Table IV shows a strong intercorrelation between $\sigma_m$ and $\sigma_p$ (arc cos 0.75 = 41°) (20). Similarly, in Eq. 8, $\sigma_m$ replaces $\sigma_p$ of Eq. 4 in the treatment of electronic effects at position 6 (arc cos 0.84 = 33°). Another interesting fact derived from the correlation matrix is considerable autocorrelation of $\pi$, especially at position 2, with $\sigma_m$ and $\sigma_p$. A similar phenomenon was observed for some benzene derivatives (21).

The pKa values of 33 disubstituted and trisubstituted purines were calculated from Eqs. 7 and 8 and compared with measured values reported in the literature (Table VI). The agreement between observed and predicted values is reasonable considering the variation in experimental methods.

Studies are in progress on the correlation of the antitumor potency and toxicity of polysubstituted purines with the structural parameters described in this paper.

## REFERENCES


(1) W. H. Cole, "Chemotherapy of Cancer," Lea & Febiger, Philadelphia, Pa., 1970, chap. 1.

(2) J. H. Lister, "Purines," Wiley–Interscience, New York, N.Y., 1971, p. 9.

(3) "The Pharmacological Basis of Therapeutics," 5th ed., L. S. Goodman and A. Gilman, Eds., Macmillan, New York, N.Y., 1975, p. 1279.

(4) C. Hansch, *Farmaco, Ed. Sci.*, **34**, 89 (1979).

(5) L. P. Hammett, *J. Am. Chem. Soc.*, **59**, 96 (1937).

(6) R. W. Taft, in "Steric Effects in Organic Chemistry," M. S. Newman, Ed., Wiley, New York, N.Y., 1956, chap. 13.

(7) O. Exner, in "Advances in Linear Free Energy Relationships," N. B. Chapman and J. Shorter, Eds., Plenum, New York, N.Y., 1972, p. 42.

(8) J. A. Montgomery, *Handb. Exp. Pharmakol.*, **38**, 76 (1974).

(9) Z. Neiman, *Experientia*, **31**, 996 (1975).

(10) P. Tomasik, R. Zalewski, and J. Chodzinski, *Chem. Zvesti*, **33**, 105 (1979).

(11) D. D. Perrin, *J. Chem. Soc.*, **1965**, 5590.

(12) C. Hansch and A. Leo, "Substituent Constants for Correlation Analysis in Chemistry and Biology," Wiley, New York, N.Y., 1979.

(13) W. H. Cole, "Chemotherapy of Cancer," Lea & Febiger, Philadelphia, Pa., 1970, chap. 13 and references cited therein.

(14) C. Silipo and C. Hansch, *Mol. Pharmacol.*, **10**, 954 (1974).

(15) M. A. Guichelaar and J. Reedijk, *Rec. Trav. Chim. Pays-Bas*, **97**, 295 (1978).

(16) S. Lewin and N. W. Tann, *J. Chem. Soc.*, **1962**, 1466.

(17) A. Albert and E. P. Serjeant, "The Determination of Ionization Constants," 2nd ed., Chapman and Hall, London, England, 1971, p. 39.

(18) W. H. Cole, "Chemotherapy of Cancer," Lea & Febiger, Philadlephia, Pa., 1970, p. 8.

(19) A. J. Barr, J. H. Goodnight, J. P. Sall, and J. T. Helwig, "Statistical Analysis System," SAS Circle, Cary, N.C., 1979.

(20) C. Hansch, A. Leo, S. H. Unger, K. H. Kim, D. Nikitani, and E. J. Lien, *J. Med. Chem.*, **16**, 1207 (1973).

(21) T. Fujita, J. Iwasa, and C. Hansch, *J. Am. Chem. Soc.*, **86**, 5157 (1964).

(22) A. Bendich, P. J. Russell, and J. J. Fox, *ibid.*, **76**, 6073 (1954).

(23) F. Bergmann, A. Kalmus, H. Unger-Waron, and H. Kwietny-Govrin, *J. Chem. Soc.*, **1963**, 3729.

(24) A. Albert and D. J. Brown, *ibid.*, **1954**, 2061.

(25) A. Giner-Sorolla and A. Bendich, *J. Am. Chem. Soc.*, **80**, 5744 (1958).

(26) *Ibid.*, **80**, 3932 (1958).

(27) A. Albert, *J. Chem. Soc.*, **1955**, 2690.

(28) A. Giner-Sorolla, I. Zimmerman, and A. Bendich, *J. Am. Chem. Soc.*, **81**, 2515 (1959).

(29) A. Albert, *J. Chem. Soc.*, **1960**, 4705.

(30) J. A. Montgomery and K. Hewson, *J. Am. Chem. Soc.*, **82**, 463 (1960).

(31) G. B. Barlin and N. B. Chapman, *J. Chem. Soc.*, **1965**, 3017.

(32) D. J. Brown and S. F. Mason, *ibid.*, **1965**, 682.

(33) G. B. Barlin, *ibid. B*, **1967**, 954.

(34) A. Albert, *ibid. C*, **1969**, 2379.

(35) R. Badger, D. J. Brown, and J. H. Lister, *ibid. Perkin Trans. I*, **1974**, 152.

(36) A. Albert, *ibid. B*, **1966**, 438 (1966).

(37) D. J. Brown and J. A. Hoskins, *Aust. J. Chem.*, **25**, 2641 (1972).

(38) D. J. Brown and N. W. Jacobsen, *J. Chem. Soc.*, **1965**, 3770.

(39) B. M. Lynch, R. K. Robins, and C. C. Cheng, *ibid.*, **1958**, 2973.

(40) G. B. Barlin and A. C. Young, *ibid. B*, **1971**, 821.

(41) D. J. Brown, R. L. Jones, A. M. Angyal, and G. W. Grigg, *ibid. Perkin Trans. I*, **1972**, 1819.

(42) D. J. Brown and R. K. Lynn, *ibid. Perkin Trans. I*, **1974**, 349.

(43) M. D. Fenn and J. H. Lister, *ibid. Perkin Trans. I*, **1975**, 485.


## ACKNOWLEDGMENTS


The authors thank Dr. A. Giner-Sorolla, Sloan-Kettering Institute for Cancer Research, Rye, N.Y., and Dr. D. J. Brown, Australian National University, Canberra, Australia, for helpful comments regarding the pKa values of purines and Dr. C. Hansch for suggestions regarding $\pi$ and its interrelations with other variables. Z. Neiman thanks the Fogarty International Center, National Institutes of Health, for a fellowship and Dr. J. S. Driscoll for his hospitality.


# Clofibrate Microcapsules II: Effect of Wall Thickness on Release Characteristics


**P. L. MADAN**



Received July 24, 1980, from the *College of Pharmacy and Allied Health Professions, St. John's University, Jamaica, NY 11439.* Accepted for publication September 25, 1980.



**Abstract** □ The effect of wall thickness on the release characteristics of clofibrate from microcapsules prepared in gelatin–sodium sulfate was investigated. The wall thickness, calculated by recovering the wall material from the microcapsules and using the relationship between two concentric spheres, was related to the surface area of the droplets being encapsulated. Thinner walled microcapsules gave faster release and showed greater deviation from zero-order kinetics but followed the square root of time plots. Microcapsules having thicker walls approximated zero-order release but deviated from the square root of time plots. A theoretical model was developed to explain the release characteristics of the microcapsules. A linear correlation was found between the wall thickness and the *in vitro* $t_{50\%}$ release time.



**Keyphrases** □ Clofibrate—microcapsules, effect of wall thickness on release characteristics □ Microcapsules—clofibrate, effect of wall thickness on release characteristics □ Hypocholesterolemic agents—clofibrate, effect of microcapsule wall thickness on release characteristics


A recent investigation (1) reported the microencapsulation of clofibrate USP, a liquid hypocholesterolemic agent. Prepared by simple coacervation in gelatin–sodium sulfate, the microcapsules were recovered as discrete




*0022-3549/81/0400-0430$01.00/0*


*© 1981, American Pharmaceutical Association*

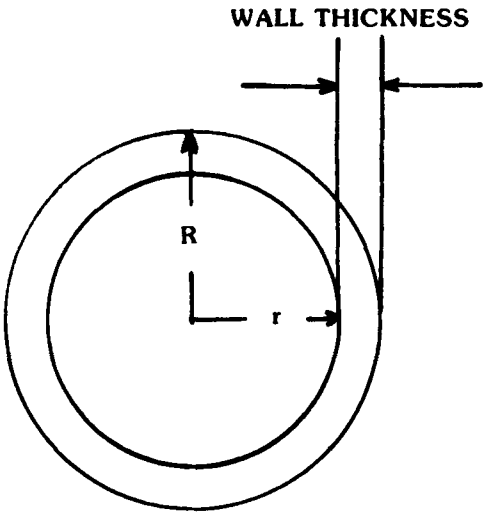


**Figure 1**—*Model of a microcapsule based on the concept of two concentric spheres.*

free-flowing particles and exhibited zero-order release at all hardening times studied. A linear correlation was found between the hardening time and the *in vitro* $t_{50\%}$ release time of the microcapsules. The microcapsules could not be hardened for longer than 8 hr without rupture, resulting in significant loss of clofibrate. Microcapsules hardened for 8 hr extended the drug release to a maximum of ~6 hr.

The effect of wall thickness on the release characteristics of clofibrate from the microcapsules is reported with a view to extending drug release from the microcapsules for longer periods.

## EXPERIMENTAL

**Materials**—All materials were similar to those reported in the earlier investigation (1).

**Microencapsulation**—The method used for the production of monodisperse spheres of clofibrate was similar to that reported previously (1). The spheres were microencapsulated by simple coacervation in gelatin–sodium sulfate and recovered as discrete free-flowing particles (1). To attain uniformity and reproducibility, all experiments were conducted under identical conditions.

**Dissolution**—Dissolution was followed by examining triplicate samples containing about 30 mg of drug using the modified flask method (1). Concentrations were determined spectrophotometrically at 226 nm.

**Wall Thickness Determination**—The wall material was recovered from the encapsulated particles by extracting clofibrate with 2-propanol (2, 3). The wall thickness of the microcapsules was then determined from the volume relationship of two concentric spheres (Fig. 1) as follows.

When uniform, smooth, spherical particles are assumed, the average wall thickness is given by:

$$\text{wall thickness} = R - r \qquad \text{(Eq. 1)}$$

where $R$ is the radius of the large sphere (microcapsule) and $r$ is the radius of the small sphere (clofibrate droplet). If $W$ is the weight of the microcapsules, $W_w$ is the weight of the wall material recovered, $d_w$ is the density of the wall material, and $d$ is the density of clofibrate, then:

$$\text{volume of } n \text{ spherical clofibrate spheres} = n\frac{4}{3}\pi r^3 \qquad \text{(Eq. 2)}$$

and the weight of $n$ spherical spheres is:

$$W - W_w = n\frac{4}{3}\pi r^3 d \qquad \text{(Eq. 3)}$$

Similarly:

$$\text{volume of } n \text{ microcapsules} = n\frac{4}{3}\pi R^3 \qquad \text{(Eq. 4)}$$

From the relationship that the volume of $n$ microcapsules equals the volume of $n$ spheres and the volume of shell enclosing $n$ spheres:

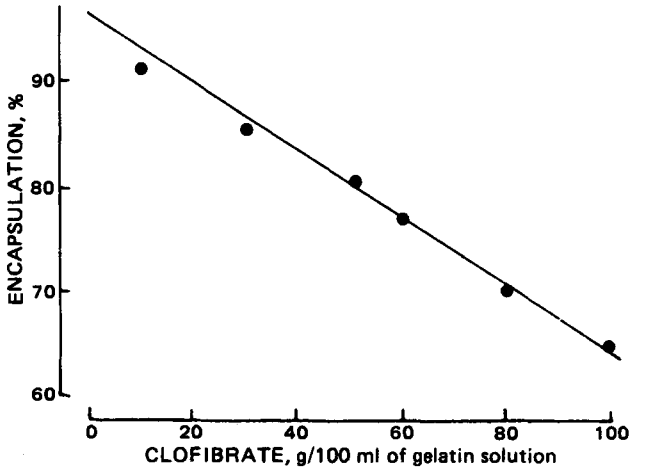


**Figure 2**—*Encapsulation efficiency of clofibrate at constant droplet size.*

shell volume enclosing $n$ spheres

$$= \left(n\frac{4}{3}\pi R^3\right) - \left(n\frac{4}{3}\pi r^3\right) = n\frac{4}{3}\pi(R^3 - r^3) \qquad \text{(Eq. 5)}$$

Therefore, the shell weight enclosing $n$ clofibrate spheres is:

$$W_w = n\frac{4}{3}\pi(R^3 - r^3)d_w \qquad \text{(Eq. 6)}$$

Dividing Eq. 6 by Eq. 3 gives:

$$\frac{W_w}{(W - W_w)} = \frac{n\frac{4}{3}\pi(R^3 - r^3)d_w}{n\frac{4}{3}\pi r^3 d} \qquad \text{(Eq. 7)}$$

which, upon rearranging, gives:

$$\frac{R^3 - r^3}{r^3} = \frac{W_w d}{(W - W_w)d_w} \qquad \text{(Eq. 8)}$$

$$\frac{R}{r} = \left[\frac{W_w d}{(W - W_w)d_w} + 1\right]^{1/3} \qquad \text{(Eq. 9)}$$

Subtracting 1 from both sides gives:

$$\frac{R - r}{r} = \left[\frac{W_w d}{(W - W_w)d_w} + 1\right]^{1/3} - 1 \qquad \text{(Eq. 10)}$$

Multiplying both sides by $r$ gives the wall thickness:

$$R - r = r\left\{\left[\frac{W_w d}{(W - W_w)d_w} + 1\right]^{1/3} - 1\right\} \qquad \text{(Eq. 11)}$$

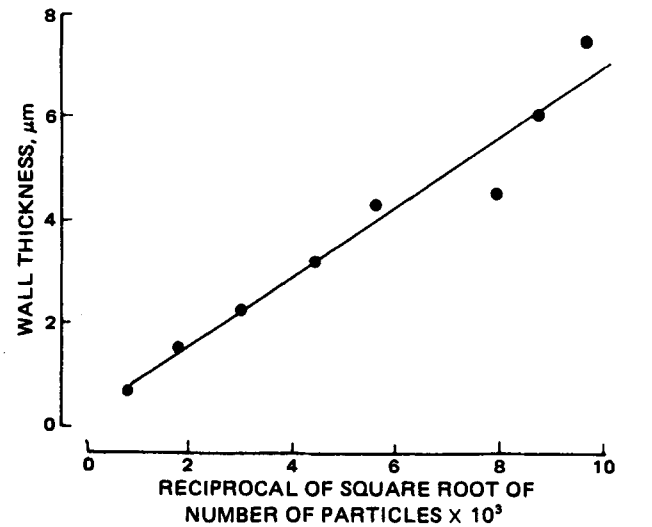


**Figure 3**—*Wall thickness as a function of the square root of the number of droplets.*

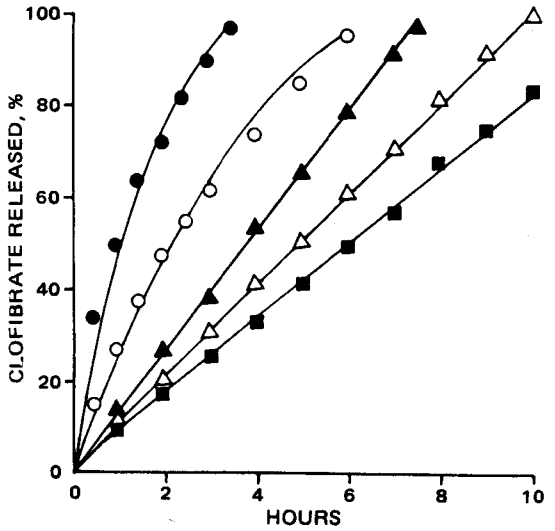


**Figure 4**—*Release of clofibrate from the microcapsules having wall thickness of 2.7 (●), 6.0 (○), 10.4 (▲), 13.5 (△), and 16.9 (■) μm.*

## RESULTS AND DISCUSSION

**Production of Monodisperse Spheres**—One method commonly used for preparing droplets of a liquid is its emulsification in another liquid in which it is immiscible. Although simple in operation, this method generally produces a heterogeneous mixture of droplets that may exhibit a large size distribution.

To maintain uniformity, the droplets being encapsulated must be monodisperse. The capillary method employed for generating clofibrate droplets produced essentially monodisperse spheres (1).

Two methods were used to study the effect of wall thickness. In the first method, the diameter of the clofibrate spheres being encapsulated was varied while the volume of clofibrate was kept constant. In the second method, the diameter of the spheres was held constant but the quantity of clofibrate encapsulated was varied.

**Microencapsulation of Clofibrate Spheres**—Encapsulation of all batches of clofibrate spheres was ascertained microscopically. The extent of clofibrate encapsulated was determined by briefly washing the dried microcapsules with 2-propanol. Unencapsulated clofibrate or partially encapsulated clofibrate spheres were dissolved by 2-propanol, leaving the encapsulated spheres intact. The percent of clofibrate encapsulated was then calculated from the original weight of clofibrate and the dried weight remaining following the brief 2-propanol wash.

The encapsulation efficiency was a function of the surface area of the core material being encapsulated. For example, at constant droplet size, the encapsulation efficiency decreased as the volume of liquid increased (Fig. 2). At constant volume, the encapsulation efficiency decreased with decreasing droplet size.

**Wall Thickness Determination**—The most direct method of determining the wall thickness of a microcapsule is by measurement using a microscope fitted with a micrometer after slicing the microcapsule with a microtome. The accuracy of such lengthy and tedious determinations is highly dependent on the precision of obtaining a section through the exact center of the microcapsule (Fig. 1). Any deviation from this center may produce a larger section of wall than exists (4). Since the microtome sections obtained are frequently at distances from the center, these readings represent an average that may exaggerate the true value. The wall thickness determined microscopically represents an average of the many determinations representative of various sections. Therefore, the volume relationship of two concentric spheres used for the calculation of wall thickness gives a better description of the average wall thickness without being time consuming and tedious.

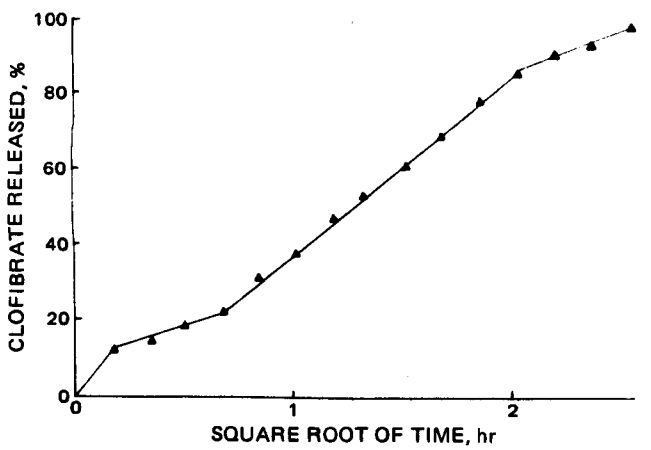


**Figure 5**—*Square root of the time plot of microcapsules having a wall thickness of 10.4 μm.*

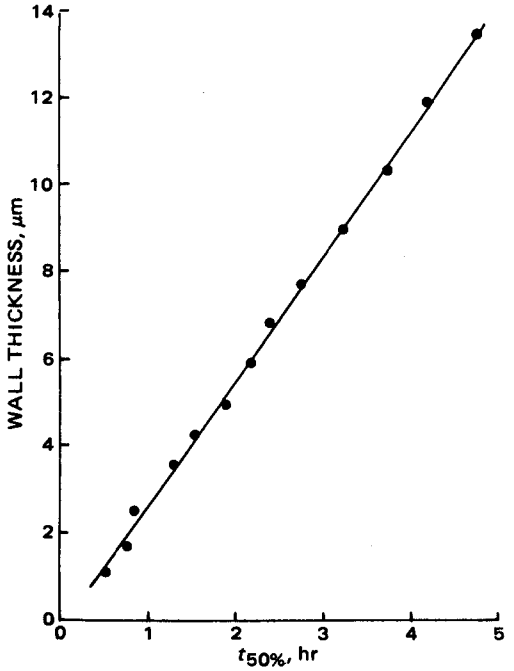


**Figure 6**—*Wall thickness of microcapsules as a function of* in vitro $t_{50\%}$ *release time.*

The wall thickness of the microcapsules also was dependent on the surface area of the core material. At a constant volume of clofibrate, smaller diameter droplets gave thinner walls than those with larger diameter. Similarly, reducing the quantity of the core material while maintaining a constant sphere diameter gave thicker walls. Although the wall thickness decreased with increasing surface area of the encapsulated droplets, a linear relationship could not be established. However, the wall thickness was inversely related to the square root of the number of droplets present when either the droplet size or the volume of clofibrate encapsulated was varied (Fig. 3). This observation seems to confirm the hypothesis that, in a coacervation system where part of the total colloid present is used in coating the core material, the coating thickness is influenced by the total number of particles present in the system (3).

**Dissolution**—The release profiles of the drug from the microcapsules were different from those observed previously (1). Microcapsules with thinner walls did not follow zero-order kinetics; as the wall thickness increased, the tendency toward zero-order release also increased (Fig. 4).

Various release mechanisms were considered, but no single mechanism could explain all of the data completely. Other investigators (5) also reported difficulty in explaining the dissolution data by any one type of treatment.

The square root of time plots characteristic of release through simple diffusion or through leaching by dissolution into the permeating fluid was linear, or nearly so, only for the thin-walled microcapsules. As the wall thickness was increased, the tendency toward linearity decreased. The release from the microcapsules having much thicker walls appeared to follow four stages (Fig. 5): (*a*) an initial large surge of release of drug, which was retained on or near the surface of the microcapsules; (*b*) slow release due to the lag time required for the dissolution medium to wet the microcapsules and to penetrate into the microcapsules; (*c*) relatively faster release for the major portion of the release profile, indicating a steady state; and (*d*) slow release toward the end, suggesting an insufficient quantity of drug remaining in the microcapsules to sustain the required concentration gradient.

The release of the drug from the microcapsules was related directly to the wall thickness (Fig. 6). Increasing the wall thickness retarded the release of the drug for longer than 12 hr from the unhardened microcapsules. Since the drug release rate from the hardened microcapsules is substantially lower than from the unhardened microcapsules (1), this procedure has potential for the development of a dosage form that may substantially reduce the frequency of administration, thus resulting in fewer missed doses.

## REFERENCES


(1) P. L. Madan, D. K. Madan, and J. C. Price, *J. Pharm. Sci.*, **65**, 1476 (1976).

(2) P. L. Madan, in "Microencapsulation: New Techniques and Application," T. Kondo, Ed., Techno Inc., Tokyo, Japan, 1979, pp. 11–34.

(3) P. L. Madan, L. A. Luzzi, and J. C. Price, *J. Pharm. Sci.*, **63**, 280 (1974).

(4) L. Si-Nang, P. F. Carlier, P. Delort, J. Gazzola, and D. Lafont, *ibid.*, **62**, 452 (1973).

(5) J. R. Nixon and S. E. Walker, *J. Pharm. Pharmacol.*, **23**, 147S (1971).


## ACKNOWLEDGMENTS


Presented at the Industrial Pharmaceutical Technology Section, APhA Academy of Pharmaceutical Sciences, Montreal meeting, 1978.


# Synthesis and Preliminary Pharmacology of an Internal Standard for Assay of Neostigmine


**H. E. WARD, Jr. *, J. J. FREEMAN *, J. W. SOWELL ‡, and J. W. KOSH *x**



Received August 5, 1980, from the **Division of Pharmacology and the* ‡*Division of Medicinal Chemistry, College of Pharmacy, University of South Carolina, Columbia, SC 29208.* Accepted for publication September 19, 1980.



**Abstract** □ The synthesis of the diethyl analog of neostigmine, its preliminary pharmacology, and its use as an internal standard for the GLC assay of neostigmine are described. Both the diethyl analog and neostigmine undergo thermal demethylation in the injection port. The column selected produced satisfactory resolution and short retention times for neostigmine and the diethyl analog. The diethyl analog apparently possesses acetylcholinesterase-inhibiting properties, as evidenced by potentiation of the contractile response to acetylcholine on the ileum. In addition, acetylcholine levels in the brain were elevated slightly. Water solutions of the diethyl analog appeared to lose biological activity with time. The diethyl analog appears to be suitable for use as an internal standard for the GLC assay of neostigmine.



**Keyphrases** □ Neostigmine—acetylcholine analog, synthesis and preliminary pharmacology of neostigmine analogs, quantification by GLC using flame-ionization detection □ GLC, flame ionization—analysis, neostigmine and analogs, synthesis, preliminary pharmacological studies in rats □ Cholinergics—neostigmine and analogs, synthesis, pharmacological activity evaluated in rat brain and smooth muscle, quantification by GLC


Neostigmine, a quaternary ammonium compound, has been measured following isolation from biological fluids by many methods, including chemical modification of the molecule followed by polarography (1), photocolorimetry (2), or spectrophotometry (3, 4). Other quaternary ammonium compounds have been isolated from biological fluids using ion-pair extraction (5–7). Neostigmine also has been analyzed using counterion complexation followed by liquid scintillation spectrometry (8), GLC (9, 10), or GLC–mass spectrometry (11).

Recent assays for neostigmine used pyridostigmine as an internal standard followed by thermal dimethylation in the injection port and GLC separation. Neostigmine and pyridostigmine are both employed clinically, and their combined therapy presents a problem with currently available assays. Since GLC is widely used with substantial economic advantages over GLC–mass spectrometry, it was necessary to synthesize an analog of neostigmine applicable to the assay of quaternary ammonium cholinesterase inhibitors.

Since neostigmine possesses cholinomimetic properties, the structural similarity of the diethyl analog suggested that it may possess similar pharmacological actions. The present study reports the synthesis of the diethyl analog of neostigmine, its use as an internal standard in the quantification of neostigmine, and preliminary pharmacological findings.

## EXPERIMENTAL

**Synthesis[1] of Diethyl Amino and Tertiary Analogs of Neostigmine**—The preparation of the diethyl analog of neostigmine required the synthesis of an intermediate, 3-[[(diethylamino)carbonyl]oxy]-*N,N*-dimethylaniline (I), which subsequently was converted to the diethyl analog, 3-[[(diethylamino)carbonyl]oxy]-*N,N,N*-trimethylbenzenaminium iodide (II).

*Synthesis of I*—Compound I was synthesized by a modified procedure of Yanagisawa (12). A solution of 3-dimethylaminophenol (10.0 g, 0.073 mole) in anhydrous tetrahydrofuran (100 ml) was added dropwise with stirring to phosgene in 12.5% benzene (192 ml) in an ice bath. After 24

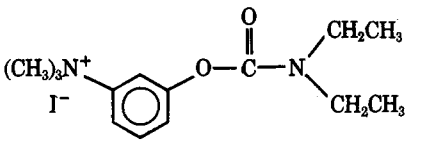


II

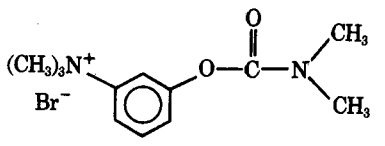


IV

[1] IR spectral data were determined on a Beckman Acculab 4 spectrophotometer using the potassium bromide technique. NMR spectra were determined on a Varian EM 360A high-resolution spectrometer with tetramethylsilane as the internal reference. Melting points were obtained using a Thomas-Hoover capillary apparatus and are uncorrected. TLC was performed using Eastman chromatogram sheets, type 6060 (silica gel); the sheets were developed in an iodine chamber. Carbon, hydrogen, nitrogen, and iodide values were obtained from analyses performed by Atlantic Microlabs, Atlanta, Ga.


*0022-3549/81/0400-0433$01.00/0*


*© 1981, American Pharmaceutical Association*

The release of the drug from the microcapsules was related directly to the wall thickness (Fig. 6). Increasing the wall thickness retarded the release of the drug for longer than 12 hr from the unhardened microcapsules. Since the drug release rate from the hardened microcapsules is substantially lower than from the unhardened microcapsules (1), this procedure has potential for the development of a dosage form that may substantially reduce the frequency of administration, thus resulting in fewer missed doses.

## REFERENCES


(1) P. L. Madan, D. K. Madan, and J. C. Price, *J. Pharm. Sci.*, **65**, 1476 (1976).

(2) P. L. Madan, in "Microencapsulation: New Techniques and Application," T. Kondo, Ed., Techno Inc., Tokyo, Japan, 1979, pp. 11–34.

(3) P. L. Madan, L. A. Luzzi, and J. C. Price, *J. Pharm. Sci.*, **63**, 280 (1974).

(4) L. Si-Nang, P. F. Carlier, P. Delort, J. Gazzola, and D. Lafont, *ibid.*, **62**, 452 (1973).

(5) J. R. Nixon and S. E. Walker, *J. Pharm. Pharmacol.*, **23**, 147S (1971).


## ACKNOWLEDGMENTS


Presented at the Industrial Pharmaceutical Technology Section, APhA Academy of Pharmaceutical Sciences, Montreal meeting, 1978.


# Synthesis and Preliminary Pharmacology of an Internal Standard for Assay of Neostigmine


**H. E. WARD, Jr. *, J. J. FREEMAN *, J. W. SOWELL ‡, and J. W. KOSH *x**



Received August 5, 1980, from the **Division of Pharmacology and the* ‡*Division of Medicinal Chemistry, College of Pharmacy, University of South Carolina, Columbia, SC 29208.* Accepted for publication September 19, 1980.



**Abstract** □ The synthesis of the diethyl analog of neostigmine, its preliminary pharmacology, and its use as an internal standard for the GLC assay of neostigmine are described. Both the diethyl analog and neostigmine undergo thermal demethylation in the injection port. The column selected produced satisfactory resolution and short retention times for neostigmine and the diethyl analog. The diethyl analog apparently possesses acetylcholinesterase-inhibiting properties, as evidenced by potentiation of the contractile response to acetylcholine on the ileum. In addition, acetylcholine levels in the brain were elevated slightly. Water solutions of the diethyl analog appeared to lose biological activity with time. The diethyl analog appears to be suitable for use as an internal standard for the GLC assay of neostigmine.



**Keyphrases** □ Neostigmine—acetylcholine analog, synthesis and preliminary pharmacology of neostigmine analogs, quantification by GLC using flame-ionization detection □ GLC, flame ionization—analysis, neostigmine and analogs, synthesis, preliminary pharmacological studies in rats □ Cholinergics—neostigmine and analogs, synthesis, pharmacological activity evaluated in rat brain and smooth muscle, quantification by GLC


Neostigmine, a quaternary ammonium compound, has been measured following isolation from biological fluids by many methods, including chemical modification of the molecule followed by polarography (1), photocolorimetry (2), or spectrophotometry (3, 4). Other quaternary ammonium compounds have been isolated from biological fluids using ion-pair extraction (5–7). Neostigmine also has been analyzed using counterion complexation followed by liquid scintillation spectrometry (8), GLC (9, 10), or GLC–mass spectrometry (11).

Recent assays for neostigmine used pyridostigmine as an internal standard followed by thermal dimethylation in the injection port and GLC separation. Neostigmine and pyridostigmine are both employed clinically, and their combined therapy presents a problem with currently available assays. Since GLC is widely used with substantial economic advantages over GLC–mass spectrometry, it was necessary to synthesize an analog of neostigmine applicable to the assay of quaternary ammonium cholinesterase inhibitors.

Since neostigmine possesses cholinomimetic properties, the structural similarity of the diethyl analog suggested that it may possess similar pharmacological actions. The present study reports the synthesis of the diethyl analog of neostigmine, its use as an internal standard in the quantification of neostigmine, and preliminary pharmacological findings.

## EXPERIMENTAL

**Synthesis[1] of Diethyl Amino and Tertiary Analogs of Neostigmine**—The preparation of the diethyl analog of neostigmine required the synthesis of an intermediate, 3-[[(diethylamino)carbonyl]oxy]-*N,N*-dimethylaniline (I), which subsequently was converted to the diethyl analog, 3-[[(diethylamino)carbonyl]oxy]-*N,N,N*-trimethylbenzenaminium iodide (II).

*Synthesis of I*—Compound I was synthesized by a modified procedure of Yanagisawa (12). A solution of 3-dimethylaminophenol (10.0 g, 0.073 mole) in anhydrous tetrahydrofuran (100 ml) was added dropwise with stirring to phosgene in 12.5% benzene (192 ml) in an ice bath. After 24

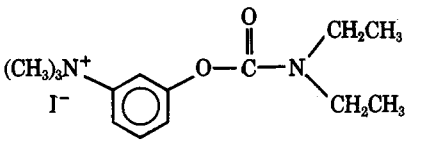


II

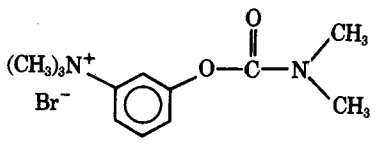


IV

[1] IR spectral data were determined on a Beckman Acculab 4 spectrophotometer using the potassium bromide technique. NMR spectra were determined on a Varian EM 360A high-resolution spectrometer with tetramethylsilane as the internal reference. Melting points were obtained using a Thomas-Hoover capillary apparatus and are uncorrected. TLC was performed using Eastman chromatogram sheets, type 6060 (silica gel); the sheets were developed in an iodine chamber. Carbon, hydrogen, nitrogen, and iodide values were obtained from analyses performed by Atlantic Microlabs, Atlanta, Ga.


*0022-3549/81/0400-0433$01.00/0*


*© 1981, American Pharmaceutical Association*

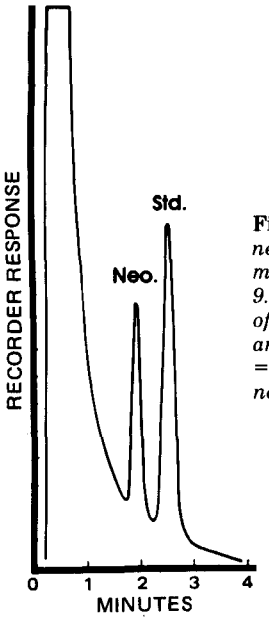


**Figure 1**—*Representative chromatogram of neostigmine with internal standard. Two microliters of chloroform solution containing 9.3 nmoles of neostigmine and 11.8 nmoles of internal standard was subjected to GLC analysis as described in* Experimental. *Neo = neostigmine, and Std. = diethyl analog of neostigmine (II, internal standard).*

hr at ambient temperature, the solvents and excess phosgene were removed *in vacuo*.

The residue was dissolved in tetrahydrofuran (100 ml) and was stirred in an ice bath as diethylamine (18.0 g, 0.25 mole) was added dropwise. After 12 hr at ambient temperature, the solvent and excess diethylamine were removed *in vacuo*. The residue was dissolved in chloroform (100 ml), extracted with 3 × 50-ml portions of 5% NaOH, and then extracted with several portions of saturated aqueous sodium chloride solution. The chloroform solution was dried over anhydrous sodium sulfate, and the remaining chloroform was removed *in vacuo* to yield 12.4 g of an oily residue. The IR spectrum was consistent with the assigned structure, and the oil was used for methiodide salt formation without further purification.

*Synthesis of Diethyl Analog (II) of Neostigmine*—A solution of I (5.0 g, 0.021 mole) in anhydrous ether (50 ml) was treated with methyl iodide (9.1 g, 0.064 mole). The methiodide salt, which precipitated over several days, was collected and dried. A portion of the crude product (4.1 g, 51.2%) was recrystallized from acetone–ethyl acetate–hexane (1:1:2) to yield a white powder. This powder was homogeneous on TLC with acetone ($R_f$ 0.28), mp 130–131°; IR (KBr): 1715, 1420, 1270, 1230, 1210, and 1150 $cm^{-1}$; NMR (deuterochloroform): $\delta$ 1.25 (t, 6H, $CH_3$ groups of diethylamino), 3.50 (q, 4H, methylene groups of diethylamino), 3.95 [s, 9H, $(CH_3)_3N$], and 7.2–7.8 (m, 4H, aromatic H) ppm.

*Anal.*—Calc. for $C_{14}H_{23}IN_2O_2$: C, 44.45; H, 6.13; I, 33.55; N, 7.41. Found: C, 44.60; H, 6.14; I, 33.38; N, 7.31.

*Synthesis of Tertiary Analog (III) of Neostigmine*—The tertiary analog, 3-[[(dimethylamino)carbonyl]oxy]-*N*,*N*-dimethylaniline (III), was synthesized according to the procedure for I, except that dimethylamine was added instead of diethylamine.

**GLC Procedures for Neostigmine (IV) and Its Analogs**—Prior to chromatographic analysis, neostigmine[2] and/or its analogs were dissolved in 25 μl of chloroform. Two microliters of the chloroform solution was injected into a gas chromatograph[3] equipped with a flame-ionization detector and a 1.2-m × 2-mm i.d. glass column packed with 5% OV-17 on diatomaceous earth[4]. Assay temperatures were: column, 210°; injection port, 300°; and detector, 250°. The carrier gas was helium at a flow rate of 40 ml/min. Flow rates for air and hydrogen were 250 and 50 ml/min, respectively.

**Animals and Drugs**—Male albino Sprague–Dawley rats, 225–325 g, were provided with a commercial diet and water *ad libitum*.

Saline solutions of acetylcholine[2] or neostigmine were prepared immediately prior to use. Saline solutions of the diethyl analog were prepared immediately and up to 1 hr prior to use.

**Measurement of Acetylcholine and Choline in Brain**—Rats were implanted with intraventricular cannulas[5] (13) following anesthetization with pentobarbital (30 mg/kg) and urethan (950 mg/kg) and allowed to recover for 1–2 days. Neostigmine or the diethyl analog was administered intraventricularly in 2 μl of saline with a microliter syringe. Histological verification of cannula placement was conducted periodically using toluidine blue. Acetylcholine and choline were determined *via* GLC using ion-pair extraction followed by chemical demethylation by the method of Kosh *et al.* (14). Fifty nanomoles of butyrylcholine was added to the brain homogenate as an internal standard. Two microliters of the final chloroform extract was injected into a gas chromatograph equipped with a flame-ionization detector.

**Measurement of Ileal Response**—After removal of the ileal tissue, 1.25-cm segments were placed in a 15-ml tissue bath containing Tyrode's solution (15) aerated with 100% oxygen and maintained at 38°. Smooth muscle activity was monitored using a physiological recorder[6]. Following a 10-min control period, acetylcholine was added to the bath (final concentration of $2.8 \times 10^{-6}$ *M*), and the response was noted. After washing with Tyrode's solution, the diethyl analog (II) was added to the bath (final concentration of $1 \times 10^{-5}$ *M*). After 2 min of exposure to II, acetylcholine was introduced into the bath, and the response was compared to the effect of acetylcholine alone.

**Table I—Effect of Diethyl Analog (II) and Neostigmine (IV) on Rat Brain Levels[a] of Acetylcholine and Choline**

| Treatment | Acetylcholine[b], nmoles/g (±*SE*) | Choline[b], nmoles/g (±*SE*) |
|---|---|---|
| Saline | 17.2 ± 0.7 | 52.7 ± 1.9 |
| II, 30 nmoles | 19.3 ± 0.5* | 53.5 ± 1.5 |
| II, 60 nmoles | 19.5 ± 0.8** | 48.9 ± 6.6 |
| IV, 30 nmoles | 26.6 ± 0.72*** | 47.2 ± 5.9 |

[a] Male albino Sprague–Dawley rats were pretreated for 1 hr with II or IV intraventricularly in saline. [b] Brain tissue was examined for acetylcholine and choline content as described in *Experimental*. * = $p < 0.02$, ** = $p < 0.05$, and *** = $p < 0.001$; $n = 4$.

**Table II—Effect of the Diethyl Analog (II) and Neostigmine (IV) on the Ileal[a] Response to Acetylcholine**

| Treatment | Contractile[b] Force, % | $n$[c] |
|---|---|---|
| Acetylcholine | 100 ± 30.1 | 10 |
| II[d] + acetylcholine | 404 ± 49.5* | 6 |
| II (1-hr-old solution) | 33.5 ± 84 | 2 |

[a] Ileal strips (1.25 cm) from rats were suspended in Tyrode's solution aerated with 100% oxygen and maintained at 38°. Acetylcholine and II were added to produce a final concentration of $2.8 \times 10^{-6}$ and $1 \times 10^{-5}$ *M*, respectively. [b] Smooth muscle contractile response to acetylcholine represents 100% (1.5 g of force). * = $p < 0.01$. [c] Number of ileal strips. [d] Compound II alone did not produce a significant response.

## RESULTS

A typical GLC profile following injection of 2 μl of a chloroform solution of neostigmine (IV) (9.3 nmoles) and an internal standard [diethyl analog of neostigmine (II), 11.8 nmoles] is seen in Fig. 1. The peak forms for both IV and II were symmetrical and resolved from the solvent peak. Complete separation was obtained between the peaks for IV (retention time of 2.0 min) and II (2.7 min). Calculation of the resolution (16) of the IV and II peaks gave a value of 1.8. Column efficiency, expressed in terms of theoretical plates per foot for IV and II, was 424 and 551, respectively. The longer retention time seen for II was predicted for the OV-17 column since II contains two more methyl groups than IV (diethyl *versus* dimethyl, respectively).

The possibility of thermal demethylation of IV in the injection port was investigated by injecting the tertiary analog (III) of neostigmine. Both compounds gave identical retention times (2 min).

The effect of IV and II on acetylcholine and choline levels in rat brain is seen in Table I. Intraventricular administration of 30 nmoles of II significantly ($p < 0.02$) increased the brain concentration of acetylcholine (19.3 *versus* 17.2 nmoles/g). Increasing the dose of II to 60 nmoles also caused a significant ($p < 0.05$) but equal increase in acetylcholine concentration (19.5 ± 0.8) over that of the control. Thirty nanomoles of IV caused a more pronounced increase in acetylcholine levels than did II (26.6 ± 0.72 *versus* 19.3 ± 0.5 nmoles/g). Neither II nor IV significantly altered the choline concentration. Treatment with IV caused a noticeable

[2] Sigma Chemical Co., St. Louis, Mo.
[3] Beckman GC-65, Fullerton, Calif.
[4] Gas Chrom Q, Applied Science Laboratories, State College, Pa.
[5] Intramedic polyethylene tubing (0.28 mm i.d.; 0.61 mm o.d.), Clay Adams, Parsippany, N.J.
[6] Physiograph DMP-4A with myograph A, Narco Bio-Systems, Houston, Tex.

anergic syndrome (ataxia, lethargy, and reduced motor activity), whereas II did not.

The effect of II on the ileal response to acetylcholine is shown in Table II. The diethyl analog alone ($1 \times 10^{-5}$ *M*) produced a nonsignificant increase in the frequency of spontaneous contractions compared to resting tension. The ileal response to $2.8 \times 10^{-6}$ *M* acetylcholine was selected as representing 100% contraction. The contractile response to acetylcholine in the presence of II was increased more than 400% ($p < 0.01$). In addition, the frequency and amplitude of the spontaneous contractions increased compared to acetylcholine alone. Freshly prepared solutions of II appeared to be more biologically active than older ones. While freshly prepared solutions of II increased the contractile force to acetylcholine (404%), solutions prepared 1 hr prior to use decreased it (33%).

## DISCUSSION

The total yield for the synthesis of II was ~60%. Most of the product was obtained over 2 days, with additional product precipitating over 2–3 weeks. The diethyl analog (II) was freely soluble in water, chloroform, methanol, and acetone and was insoluble in cyclohexanone, pentane, and hexane.

Water solutions of II appeared to turn light pink with time at room temperature, suggesting that the compound was undergoing chemical modification in solution which might alter its biological activity. This possibility was confirmed by measuring ileal contraction, blood pressure, and the elevation of brain acetylcholine by II.

In the presence of II ($1 \times 10^{-5}$ *M*), the contractile response to acetylcholine was increased over 400% (Table II). This response suggested that II possesses cholinesterase-inhibiting properties. However, at a higher concentration ($1 \times 10^{-3}$ *M*), the analog completely relaxed the ileum and abolished spontaneous rhythmicity, suggesting a more complex mechanism of action. A $1 \times 10^{-5}$ *M* solution of II after 1 hr at room temperature partially blocked (33%) the effect of acetylcholine on ileal tissue.

Experiments on blood pressure demonstrated that II administered intravenously (0.025 mg/kg) possessed hypotensive activity. The vasodepressor effects of the analog were variable and diminished with the age of the solution. For instance, the hypotensive response at 5 min was −80 mm Hg, which decreased to −30 mm at 45 min. The loss of biological activity in the smooth muscle and blood pressure preparations confirms that II undergoes rapid molecular change that causes a loss of biological activity. The exact chemical or pharmacological reasons for these observations are unknown.

At both doses (30 or 60 nmoles intraventricularly), II produced an equal increase in brain acetylcholine levels (Table I). However, the elevation of acetylcholine was not as pronounced as that obtained following 30 nmoles of IV. The lower potency of II compared to IV may be due to the loss of biological activity with time since acetylcholine levels were measured at 1 hr in brain.

Compound II proved to be satisfactory as an internal standard in the GLC determination of IV (Fig. 1). The column and temperatures used provided good resolution with symmetrical peaks, which facilitated quantification. A previous report (9) indicated that IV could thermally demethylate in the injection port. Thermal demethylation under the present experimental conditions was confirmed by injecting the tertiary analog of IV, which had a retention time identical to that of IV. Furthermore, demethylation was essentially complete since chemical demethylation (14) gave equal peak heights. Although aged solutions lose their biological potency, II can be used as an internal standard for the assay of IV since GLC sensitivity is unchanged with time.

## REFERENCES


(1) B. Novotny, *Chem. Tech. (Leipzig)*, **6,** 662 (1954).

(2) I. Solomon-Ionescu, M. Prodescu, and E. Cuciureanu, *Farmacia (Bucharest)*, **10,** 551 (1962); through *Chem. Abstr.*, **58,** 7785h (1963).

(3) R. E. Kling, *J. Assoc. Off. Anal. Chem.*, **54,** 21 (1971).

(4) *Ibid.*, **56,** 128 (1973).

(5) J. H. G. Jonkman, J. Wijsbeek, S. H. Brouwer, and R. A. DeZeeuw, *J. Pharm. Pharmacol. Suppl.*, **26,** 63P (1974).

(6) A. Kloppel, D. Post, G. Schneider, and H. Schuta, *Z. Anal. Chem.*, **252,** 279 (1970).

(7) G. Schill and B. Danielsson, *Anal. Chim. Acta*, **21,** 248 (1959).

(8) H. E. Barber, G. R. Bourne, and G. A. Buckley, *J. Pharm. Pharmacol.*, **24,** 907 (1972).

(9) K. Chan, N. E. Williams, J. D. Baty, and T. N. Clavey, *J. Chromatogr.*, **120,** 349 (1976).

(10) N. E. Williams, T. N. Calvey, and K. Chan, *Br. J. Anaesth.*, **50,** 1065 (1978).

(11) S. M. Aquilonius, S. A. Eckernas, P. Hartvig, J. Hultman, B. Lindstrom, and P. O. Osterman, *Eur. J. Clin. Pharmacol.*, **15,** 367 (1979).

(12) S. Yanagisawa, Japanese pat. 3071 (June 13, 1951); through *Chem. Abstr.*, **47,** 4908 (1953).

(13) F. deB. Verster, C. A. Robinson, C. A. Hengeveld, and E. S. Bush, *Life Sci.*, **10** (part 1), 1395 (1971).

(14) J. W. Kosh, M. B. Smith, J. W. Sowell, and J. J. Freeman, *J. Chromatogr.*, **163,** 205 (1979).

(15) F. R. Domer, "Animal Experiments in Pharmacological Analysis," Charles C Thomas, Springfield, Ill., 1971, p. 573.

(16) F. W. Rowland, "The Practice of Gas Chromatography," Hewlett-Packard, Avondale, Pa., 1973.


## ACKNOWLEDGMENTS


The authors thank Dean Julian H. Fincher of the College of Pharmacy for generous support and Mrs. Sheila B. Lilly for excellent typing assistance.

# Electrophoretic Determination of Charge on Carrier-Free $^{99m}$Tc-Labeled Complexes

**H. DONALD BURNS ˣ, DAVID T. SOWA, PAUL WORLEY, RICHARD VAUM, and LUIGI G. MARZILLI**

Received July 18, 1979, from the *Division of Nuclear Medicine and Department of Chemistry, Johns Hopkins University, Balitmore, MD 21205.* Accepted for publication August 6, 1980.

**Abstract** □ A new method for determining the charge on carrier-free $^{99m}$Tc-labeled complexes is described. This method and mixed-ligand experiments were used to determine if the charge on the technetium 99m complex of *N*-(2,6-dimethylphenylcarbamoylmethyl)iminodiacetic acid (I) is −1 and if the ligand to technetium ratio in the complex is 2:1. The preparation of an iodinated analog (II) of I and its $^{99m}$Tc-labeled complex is described, as is the biodistribution of the $^{99m}$Tc-labeled complex in mice. The syntheses of the $^{51}$Cr(III)- and $^{57}$Co(III)-labeled complexes also are described. The net biliary excretion in mice of both the $^{99m}$Tc- and $^{51}$Cr-labeled complexes of II was significantly greater than that of the $^{99m}$Tc-labeled complex of I.

**Keyphrases** □ *N*-(2,6-Dimethylphenylcarbamoylmethyl)iminodiacetic acid—complexation with technetium 99m, electrophoretic determination of charge on carrier-free $^{99m}$Tc-labeled complexes, synthesis and evaluation of net biliary excretion □ Radiopharmaceuticals—$^{99m}$Tc-labeled iminodiacetic acid derivatives, electrophoretic determination of charge on carrier-free $^{99m}$Tc-labeled complexes, synthesis, evaluation of net biliary excretion □ Complexes—technetium 99m with iminodiacetic acid derivatives, electrophoretic determination of charge on carrier-free $^{99m}$Tc-labeled complexes, evaluation of net biliary excretion

Since the first reported use of a technetium 99m-labeled compound as a diagnostic radiopharmaceutical in 1962 (1), numerous attempts have been made to design $^{99m}$Tc-labeled radiopharmaceuticals. Of the many compounds that have been labeled, a large number have one common feature: their biodistributions depend to some extent on their interaction with structurally specific receptors located in various tissues in the body (2, 3).

## BACKGROUND

In most cases, the structural requirements for receptor binding are rigid so that the structure of the compound must be controlled carefully. There has been little success in the design of $^{99m}$Tc-labeled radiopharmaceuticals of this type, in part due to the lack of a well-defined chemistry of technetium. The technetium concentration utilized in $^{99m}$Tc-labeled radiopharmaceuticals is $10^{-10}$ *M*, which is too low to permit the study of their chemistry by standard techniques (4).

To facilitate the design of $^{99m}$Tc-labeled radiopharmaceuticals, an investigation was aimed toward developing new techniques for obtaining structural information. A mixed-ligand experiment was described previously and can be used to determine ligand–technetium stoichiometry in $^{99m}$Tc-labeled complexes at concentrations as low as $10^{-13}$ *M* (4). This paper reports an extension of the previous study; the net charge on $^{99m}$Tc-labeled complexes at concentrations as low as $10^{-13}$ *M* can be determined. This approach is illustrated with work on a new hepatobiliary radiopharmaceutical, the $^{99m}$Tc-labeled complex of *N*-(2,6-dimethylphenylcarbamoylmethyl)iminodiacetic acid[1] (I).

To prepare a $^{99m}$Tc-labeled lidocaine analog, I was synthesized containing an iminodiacetic acid functional group (5). This functional group can form stable complexes with transition metals such as technetium. Harvey *et al.* (5) showed that I forms a stable complex with technetium 99m, which is excreted unchanged after intravenous injection into mice and dogs. Excretion occurs mainly *via* the hepatobiliary system with minimal urinary excretion. The extensive biliary excretion of the $^{99m}$Tc-labeled complex of I led to considerable interest in this complex as a radiopharmaceutical for the evaluation of hepatobiliary function.

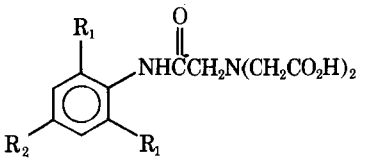


I: $R_1 = CH_3$, $R_2 = H$
II: $R_1 = CH_3$, $R_2 = I$
III: $R_1 = H$, $R_2 = CO_2H$
IV: $R_1 = H$, $R_2 = NH_2$

It was recently reported that the ratio of ligand to technetium in $^{99m}$Tc-labeled I is 2:1 and that the oxidation state of technetium is +3 (6). This finding and results of stoichiometry and charge studies led to the study of the $^{51}$Cr(III)- and $^{57}$Co(III)-labeled complexes of a similar compound, *N*-(2,6-dimethyl-4-iodophenylcarbamoylmethyl)-iminodiacetic acid (II). The iminodiacetic acid and methyliminodiacetic acid complexes of Cr(III) and Co(III) were prepared previously and shown to be mononegative bis-complexes. This paper reports the results of experiments with I that have established the ligand–technetium stoichiometry and the overall charge of the $^{99m}$Tc-labeled complexes of I–IV.

The mixed-ligand and charge determination experiments required (in addition to I) analogs of I that would complex technetium similarly but that differed in charge. Two such ligands are *N*-(*p*-carboxyphenylcarbamoylmethyl)iminodiacetic acid (III) and *N*-(*p*-aminophenylcarbamoylmethyl)iminodiacetic acid (IV). The iminodiacetic acid functional groups of these compounds form essentially identical complexes with technetium 99m as I. In addition, the arylcarboxyl group of III imparts additional negative charge to the complex at pH > 5, and the amino functional group of IV makes the $^{99m}$Tc-labeled complex more positive than that of I at pH < 5.

## EXPERIMENTAL

Compounds I and III were synthesized as reported previously (7). The amino-substituted (IV) and iodinated (II) analogs were prepared as described later. PMR spectra were obtained on a 60-MHz spectrometer[2], with chemical shifts reported relative to tetramethylsilane. IR spectra were obtained on a grating IR spectrometer[3]. Melting points[4] were determined and are uncorrected. Elemental analyses were performed for carbon, hydrogen, and nitrogen[5].

All chemicals used were at least reagent grade. Sodium [$^{99m}$Tc]pertechnetate was eluted from a molybdenum 99–technetium 99m generator[6] with normal saline at a specific concentration of 10–20 mCi/ml. [$^{51}$Cr]Chromic chloride and [$^{57}$Co]cobaltous chloride were obtained commercially in 0.5 *M* HCl[7].

***N*-(4-Aminophenylcarbamoylmethyl)iminodiacetic Acid (IV)**—A solution of *N*-(4-nitrophenylcarbamoylmethyl)iminodiacetic acid (7) (2.0 g, 0.0064 mole) in 250 ml of water was prepared, and sufficient ammonium hydroxide was added to raise the pH to 8. A catalytic amount of 10% palladium-on-charcoal was added, and the solution was hydrogenated for 16 hr at 40 psi[8]. Removal of the catalyst by filtration and evaporation to dryness *in vacuo* yielded a yellow oil, which solidified upon addition of ether and anhydrous ethanol. Recrystallization from 95%

[1] HIDA.

[2] Perkin-Elmer Hitachi R-12A.
[3] Pye-Unicam Sp-1000.
[4] Mel-Temp apparatus.
[5] Robertson Microanalytical Laboratory, Florham Park, N.J.
[6] Squibb, Minitech.
[7] New England Nuclear Corp.
[8] Parr apparatus.



*0022-3549/81/0400-0436$01.00/0*
© *1981, American Pharmaceutical Association*

ethanol yielded 1.47 g (78.3%) of the monoammonium salt of IV as white needles, mp 298° dec.; IR (mineral oil): 3200–3400 (broad, NH) and 1680–1700 (broad, C=O) $cm^{-1}$; PMR ($D_2O$): δ 3.34 (s, 4H, $NCH_2CO_2^-$), 3.55 (s, 2H, $NCH_2CON$), 6.62 (d, 2H, aromatic H), and 6.98 (d, 2H, aromatic H).

*Anal.*—Calc. for $C_{12}H_{15}N_3O_5 \cdot NH_3$: C, 48.32; H, 6.09; N, 18.78. Found: C, 48.09; H, 6.12; N, 18.48.

**N-(2,6-Dimethyl - 4 - iodophenylcarbamoylmethyl)iminodiacetic Acid (II)**—A suspension of nitrilotriacetic acid (3.87 g, 0.02 mole) in 50 ml of anhydrous pyridine was placed in a three-necked, round-bottom flask equipped with a nitrogen inlet tube, a condenser, a calcium sulfate drying tube, and a thermometer. After flushing with nitrogen, the suspension was heated at 50° for 10 min, at which time most of the nitrilotriacetic acid had dissolved. Acetic anhydride (3.09 g, 0.03 mole) was added, and the solution was heated at 100° for 60 min. After cooling to 50°, *p*-iodoxylidene (5.0 g, 0.02 mole) was added, and the solution was heated to 100° for 2 hr.

Evaporation of the pyridine *in vacuo* left a purple oil, which then was dissolved in a minimal amount of aqueous sodium hydroxide (pH 10–11). After extraction with equal portions of ether and treatment with decolorizing carbon, the almost colorless aqueous layer was acidified to pH 4, resulting in the formation of a white syrupy solid. Trituration with ethanol–ether yielded a white powder. This powder was recrystallized from 85% ethanol–water as white needles (3.5 g, 40%), mp 205° dec.; IR (mineral oil): 3300 (NH) and 1660–1710 (broad, acid and amide C=O) $cm^{-1}$; PMR (dimethyl sulfoxide-$d_6$): δ 2.14 (s, 6H, aromatic $CH_3$), 3.4 (s, 6H, $COCH_2N$), and 7.48 (s, 2H, aromatic H).

*Anal.*—Calc. for $C_{14}H_{17}IN_2O_5$: C, 40.02; H, 4.08; N, 6.67. Found: C, 40.15; H, 3.93; N, 6.66.

**Preparation of $^{99m}$Tc-Labeled Complexes of I, III, and IV**—A solution of 10 mg (0.02–0.034 mmole) of the appropriate compound (I, III, or IV) in 0.5 ml of 0.1 *N* NaOH was prepared, and the pH was adjusted to 5.0–5.5 with 0.5 *N* HCl. After addition of 0.3 ml of the generator eluate (obtained by saline elution of a 400-mCi molybdenum 99–technetium 99m generator at a specific concentration of 10–20 mCi/ml), the solution was purged with nitrogen for 5 min. Then 0.1 ml of freshly prepared stannous chloride dihydrate solution (250 μg/ml in 0.001 *N* HCl) was added. The solution was kept at room temperature for 20 min prior to use.

**Preparation of $^{99m}$Tc-Labeled Complex of I *via* Sodium Borohydride**—A solution of 10 mg (0.034 mmole) of I in 0.5 ml of 0.1 *N* NaOH was prepared, and the pH was adjusted to 5.5 with 0.5 *N* HCl. After addition of 0.3 ml of the generator eluate, the solution was purged with nitrogen for 5 min. Then 0.1 ml of freshly prepared 0.5 *N* sodium borohydride solution (18.0 mg/ml of water) was added. After 20 min at room temperature, the solution was filtered[9], and an aliquot of the filtrate was analyzed by electrophoresis.

**Mixed-Ligand Experiment**—A solution containing 5 mg (0.016 mmole) of I and 5 mg (0.016 mmole) of III in 0.5 ml of 0.1 *N* NaOH was prepared, and the pH was adjusted to 5.0–5.5 with 0.01 *N* HCl. After addition of 0.3 ml of the generator eluate, the solution was purged with nitrogen for 5 min. Then 0.1 ml of freshly prepared solution of stannous chloride dihydrate (250 μg/ml in 0.001 *N* HCl) was added. This solution was left at room temperature for 20 min prior to use.

**Preparation of Co(III)–II Complex**—To a solution of II (10 mg, 0.034 mmole) dissolved in 0.95 ml of 0.05 *M* aqueous NaOH was added 2 mg (0.005 mmole) of cobaltous chloride hexahydrate. After the salt dissolved, 0.05 ml of [$^{57}$Co]cobaltous chloride in 0.5 *M* HCl and 0.05 ml of 0.5 *M* NaOH were added simultaneously to the stirred solution from syringes. Hydrogen peroxide (1.5 ml, 30%) was added to the clear pink solution. The oxidation of Co(II) to Co(III) required 20–30 min, at which time the solution became deep purple.

The solution then was absorbed into a 15 × 0.7-cm diameter cation-exchange column[10] in the $Na^+$ form. [This column reserves any remaining unoxidized Co(II).] The column was eluted with a solution of 0.15 *M* NaCl and 0.01 *M* $NaHCO_3$. The desired product eluted with the bed volume and was identified easily by the purple color characteristic of Co(III) complexes chelated by two iminodiacetic acid moieties.

Evidently, the presence of the methylcarbamoyl group reduces the ligand field strength of the iminodiacetic acid group sufficiently to destabilize the Co(III) state relative to the Co(II) state. Consequently, if the solution was to be stored, 1 ml of 30% $H_2O_2$ was added to maintain the Co(III) oxidation state. The complex showed a band at 552 nm (ε 269). The absorptivity was determined by using a cobalt concentration determined by atomic absorption spectroscopy.

**Preparation of Cr(III)–II Complex**—Water (0.2 ml) and dimethylformamide (0.3 ml) were added to a 2-ml vial containing II (150 mg, 0.5 mmole). After the addition of sodium hydroxide (15 mg, 0.32 mmole), the mixture was stirred at ~70° until all solids were dissolved. The pH at this point was ~4.8. To this hot solution was added [$^{51}$Cr]chromic chloride (25 μl in 0.5 *M* HCl), and the solution was maintained at 70° for 15 hr. Then, the hot solution was placed on a 15 × 0.7-cm column of fine grain sand[11].

On cooling, the reaction mixture solidified and formed a pellet in the top of the sand. Elution with 95% ethanol yielded the desired product in the sixth 0.3-ml fraction. (A neutral complex was obtained in the 19th 0.3-ml fraction.) The ethanol was evaporated from the sixth fraction, and the $[Cr–(II)_2]^-$ was redissolved in saline.

**Preparation of $[Tc–(II)_2]^-$**—To a 2-ml vial containing 18 mg (0.043 mmole) of II and 0.3 ml of 0.2 *N* NaOH was added 0.2–0.4 ml of a sodium [$^{99m}$Tc]pertechnetate solution in saline. Product formation was complete within 30 min of the addition of a stannous chloride solution (0.1 ml) containing 250 μg of $SnCl_2 \cdot 2H_2O$/ml of ethanol. The final solution was filtered[12].

**Electrophoresis**—Low-voltage electrophoresis was performed on paper[13] at 300 v for 30 min or at 600 v for 15 min in a 0.01 *M* $NaHCO_3$ buffer (pH 7). Under these conditions, the [$^{99m}$Tc]pertechnetate anion migrated ~13 cm. A pertechnetate standard was utilized with all samples. High-voltage electrophoresis was performed on paper[14] using 0.01 *M* $NaHCO_3$ buffer at 3000 v at 17° for 25 min.

Silical gel[15] chromatography was performed with 7.5-cm strips and dimethylformamide–*n*-butanol (1:1 v/v) saturated with 3 *M* $NH_4OH$. The distance each complex migrated was determined by scanning the dried paper with a chromatogram scanner equipped with a 2.54-cm sodium iodide detector and a collimator, which consisted of a 0.635-cm thick sheet of lead with a 2.54-cm × 3-mm slit. The results obtained on any given electrophoragram were expressed as:

$$R_s = \frac{\text{distance migrated by complex}}{\text{distance migrated by pertechnetate ion}} \qquad \text{(Eq. 1)}$$

These $R_s$ values were essentially independent of the distance migrated by the pertechnetate ion over at least 11–15 cm.

Low-voltage electrophoresis at pH 3 was performed as described except that a mixed citrate–phosphate buffer was used in place of the bicarbonate buffer. The citrate–phosphate buffer was prepared by mixing 39.8 ml of 0.1 *M* citric acid (19.21 g/1000 ml) and 10.2 ml of 0.2 *M* dibasic sodium phosphate ($Na_2HPO_4 \cdot 7H_2O$, 53.65 g/1000 ml), followed by dilution to 1000 ml.

Chromatography was performed on silica gel[15] with acetone as the elution solvent.

Biodistributions were performed in 25–35-g ICR albino mice[16]. A solution of the complex in 0.1 ml of saline was injected into the tail vein. Six mice were used for each data point. The animals were sacrificed by ether asphyxiation 60 min postinjection. A blood sample (100 μl) was obtained immediately before death by cardiac puncture. The lungs, heart, spleen, liver, stomach, intestines, kidneys, and bladder were removed and weighed. Care was taken to prevent urine from contaminating the carcass when the bladder was removed. The organs and carcasses were counted, and the percent of the injected dose per organ and carcass was calculated by comparison to a standard prepared from 0.10 ml of the injection solution at the time of injection.

## RESULTS AND DISCUSSION

Preparation of the $^{99m}$Tc-labeled complex of I using stannous chloride reduction yielded a complex that migrated as a single discrete spot on electrophoresis with an $R_s$ of 0.68. Use of sodium borohydride instead of stannous chloride as a reducing agent for the preparation of this complex also gave a complex that migrated as a single spot with an $R_s$ of 0.68.

This result, coupled with the fact that both procedures yielded complexes with identical biodistributions in mice (Table I), indicates that tin is not incorporated into the complex. This interpretation is supported

[9] Millipore.
[10] Chelex 100, 50–100 mesh.
[11] Fisher.
[12] Millipore, 0.45 or 0.2 μm.
[13] Whatman 3 mm.
[14] Whatman No. 1.
[15] Bakerflex 113-P.
[16] Camm Research Laboratories.

**Table I—Biodistribution of Technetium 99m–$(I)_2$ Complex in Mice 60 min Postinjection**

| Sample | Percent of Dose per Organ[a] | |
|---|---|---|
| | Stannous Chloride Preparation | Sodium Borohydride Preparation |
| Blood[b] | 0.05 ± 0.02 | 0.07 ± 0.03 |
| Kidneys | 0.60 ± 0.13 | 0.57 ± 0.23 |
| Lungs | 0.08 ± 0.03 | 0.10 ± 0.07 |
| Heart | 0.02 ± 0.01 | 0.03 ± 0.01 |
| Spleen | 0.02 ± 0.01 | 0.03 ± 0.01 |
| Liver | 1.52 ± 0.96 | 1.53 ± 1.05 |
| Stomach | 0.63 ± 0.11 | 1.40 ± 0.90 |
| Intestine | 68.6 ± 4.2 | 66.7 ± 3.7 |
| Carcass | 3.44 ± 1.17 | 3.79 ± 1.10 |
| Excreted | 24.1 | 24.5 |

[a] Each point represents the mean of six mice ± 1 *SD*. [b] Per 0.1 ml.

by recent work where tin 113 was not incorporated into the complex (6).

Electrophoresis of the $^{99m}$Tc-labeled complex of III showed only one complex in solution; it migrated with an $R_s$ of 0.97. Since it was impossible to distinguish between this complex and $^{99m}$Tc-labeled pertechnetate using this electrophoretic procedure, chromatography was performed for all samples on silica gel eluted with acetone. Chromatography easily established the absence of pertechnetate in the sample since the complex remained at the origin while pertechnetate migrated with the solvent front. The finding that the $^{99m}$Tc-labeled complex of III migrated farther than the $^{99m}$Tc-labeled complex of I on electrophoresis was expected since III has an additional carboxyl group, which imparts a greater overall charge to the complex.

When the mixed-ligand experiment was performed with I and III, electrophoresis showed three complexes. One migrated with an $R_s$ of 0.68 and corresponded to the $^{99m}$Tc-labeled complex of I. A second complex migrated with an $R_s$ of 0.97, identical to that of the $^{99m}$Tc-labeled complex of III. The third complex migrated with an $R_s$ of 0.83 and represented a new, mixed-ligand complex containing one molecule of I and one molecule of III. As discussed previously (4), this result in a mixed-ligand experiment indicates that the complexes formed are bis-complexes with two molecules of ligand bound per molecule of technetium.

Electrophoresis of the $^{99m}$Tc-labeled complex of I at pH 3 showed that the complex migrated the same distance as it did at pH 7, indicating that no functional groups can be protonated over the pH 7–3 range. This finding implies that all of the iminodiacetic acid carboxyl groups are bound to technetium 99m in these complexes. This finding also permitted the determination of the net charge on the complex. From the mixed-ligand experiment, it was shown that these iminodiacetic acid ligands form bis-complexes with technetium 99m, as is illustrated in Fig. 1 for the $^{99m}$Tc-labeled complex of IV. The overall charge on this complex at pH 7 was identical to that of the $^{99m}$Tc-labeled complex of I since both were approximately the same size and both migrated the same distance when electrophoresis was performed at pH 7. When electrophoresis was performed at pH 3, the $^{99m}$Tc-labeled complex of I still migrated toward the anode with an $R_s$ of 0.68; however, the $^{99m}$Tc-labeled complex of IV migrated toward the cathode, indicating that the overall charge on the complex was positive at this pH.

Since the $^{99m}$Tc-labeled complex of IV contains only two amino groups that are protonated at pH 3, protonation can, at most, add two units of positive charge to the complex. The fact that addition of only two units

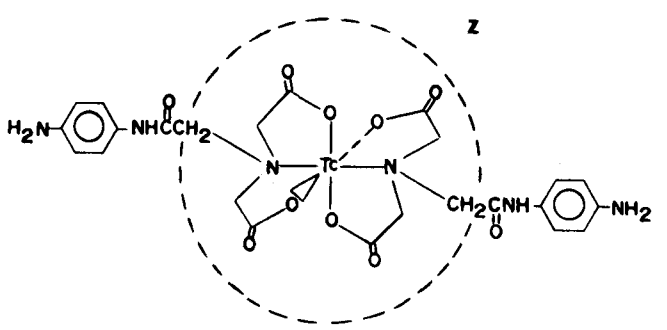


**Figure 1**—*Suggested structure of iminodiacetic acid complexes of technetium illustrating the presence of two iminodiacetic acid molecules in the complex.*

**Table II—Chromatographic and Electrophoretic Behaviors of $[M–(II)_2]^-$[a]**

| | Technetium | Cobalt | Chromium |
|---|---|---|---|
| Chromatography[b] | 0.65 | 0.58 | 0.8 |
| Low-voltage electrophoresis[c] | 8 | 8 | 7.5 |
| High-voltage electrophoresis[c] | 11.5 | 11.5 | 11.5 |

[a] M = transition metals technetium, cobalt, and chromium. [b] $R_f$ values. [c] Distance from origin in centimeters.

**Table III—Biodistribution of $^{99m}$Tc–$(II)_2$ and $^{51}$Cr–$(II)_2$ in Mice 60 min Postinjection**

| Sample | Percent of Dose per Organ[a] | |
|---|---|---|
| | $^{99m}$Tc–$(II)_2$ | $^{51}$Cr–$(II)_2$ |
| Blood[b] | 0.01 ± 0.001 | 0.07 ± 0.01 |
| Kidneys | 0.21 ± 0.12 | 1.05 ± 0.43 |
| Lungs | 0.02 ± 0.01 | 0.09 ± 0.02 |
| Heart | 0.01 ± 0.01 | 0.02 ± 0.01 |
| Spleen | 0.01 ± 0.01 | 0.02 ± 0.01 |
| Liver | 1.04 ± 0.89 | 8.2 ± 3.7 |
| Stomach | 0.05 ± 0.04 | 0.22 ± 0.08 |
| Intestine | 82.3 ± 4.5 | 80.6 ± 6.5 |
| Carcass | 0.79 ± 0.08 | 4.8 ± 1.5 |

[a] Each point represents the mean of six mice ± 1 *SD*. [b] Per 0.1 ml.

of positive charge to the $^{99m}$Tc-labeled complex of IV yielded a cationic complex indicates that, at pH 7, the negative charge on the $^{99m}$Tc-labeled complex of IV can be no more than 1. The fact that the $^{99m}$Tc-labeled complex of IV migrated toward the anode at pH 7 indicates that the negative charge can be no less than 1. These findings, taken together, establish that the net charge on this complex at pH 7 (and, thus, the net charge on the $^{99m}$Tc-labeled complex of I) is −1.

The results of chromatographic and electrophoretic experiments comparing the $^{99m}$Tc-, $^{57}$Co-, and $^{51}$Cr-labeled complexes of II are shown in Table II. The finding that each complex behaved in essentially the same manner on chromatography and electrophoresis, coupled with the previous report that Cr(III) and Co(III) formed mononegative bis-complexes with iminodiacetic acid ligands, supports our conclusion that the charge on the $^{99m}$Tc-labeled complex of I is −1. These findings also suggest that the extensive known chemistry of Cr(III) and Co(III) may be useful in predicting the types of complexes formed by Tc(III), at least for amino acid-type ligands.

The biodistributions of the $^{99m}$Tc- and $^{51}$Cr-labeled complexes of II in mice 60 min postinjection are shown in Table III. The net biliary excretion of these complexes was higher than that of the $^{99m}$Tc-labeled complex of I, with 83% of the complex excreted in the bile at 60 min compared to 67–68% for the $^{99m}$Tc-labeled complex of I. Furthermore, the distributions of the $^{99m}$Tc- and $^{51}$Cr-labeled complexes of II were essentially identical. The biodistribution of the $^{57}$Co-labeled complex of II could not be obtained since the Co(III) center was reduced too readily to Co(II).

The recent report by Loberg and Fields (6) that the oxidation state of technetium 99m in the $^{99m}$Tc-labeled complex of I is +3, coupled with the present finding that the net charge on this complex is −1, suggests that, in this case, technetium is hexacoordinate with only the iminodiacetic acid nitrogens and oxygens bound to technetium (Fig. 1).

Although the possibility for *cis*- and *trans*-isomers exists, only the *trans*-isomer probably actually forms. Iminodiacetic acid complexes of Cr(III) form only the *trans*-isomer when the iminodiacetic acid nitrogen is substituted by methyl or larger groups due to steric hindrance between the *N*-substituents in the *cis*-isomer (8).

The possibility that the technetium is in a $Tc(V)O^{3+}$ unit cannot be excluded, but the similar biodistribution of the technetium and chromium compounds and the reported (6) determination of the oxidation state as +3 make such an explanation unlikely.

Although this report demonstrates the utility of this type of experiment for determining structural information on carrier-free $^{99m}$Tc-labeled complexes, these methods can be applied to other $^{99m}$Tc-labeled radiopharmaceuticals, provided appropriate ligands can be designed and synthesized. A particularly attractive feature of this approach is that the isolation of chemically pure technetium complexes is not required. The difficulties involved in the isolation and characterization of $^{99m}$Tc-labeled complexes that are functionalized to be radiopharmaceuticals are reflected by the fact that no $^{99m}$Tc-labeled complex identical to a clinically used $^{99m}$Tc-labeled complex in solution has been characterized. Of par-

ticular note was the failure of many attempts to obtain crystalline products of I or analogs of I when they were attached to Co(III) or Cr(III), although the iminodiacetic acid and methyl iminodiacetic acid complexes are prepared and isolated easily. It is hoped that the approach outlined here for gaining information on the structure of $^{99m}$Tc-labeled radiopharmaceuticals will be useful for understanding the mechanisms of localization of currently used radiopharmaceuticals and in the design of new radiopharmaceuticals.

## REFERENCES


(1) P. V. Harper, G. Andrus, and K. Lathrup, U.S. AEC Report ARCH-18, Argonne Cancer Research Hospital, Sept. 1962, pp. 77, 78.

(2) H. D. Burns, in "The Chemistry of Radiopharmaceuticals," N. D. Heindel, H. D. Burns, T. Honda, and L. W. Brady, Eds., Masson, New York, N.Y., 1978, pp. 35–53.

(3) W. C. Eckelman, R. C. Reba, R. E. Gibson, N. J. Rzeszotarski, F. Vieras, J. K. Mazaitis, and B. Francis, *J. Nucl. Med.*, **20**, 350 (1979).

(4) L. G. Marzilli, P. Worley, and H. D. Burns, *ibid.*, **20**, 871 (1979).

(5) E. Harvey, M. D. Loberg, and M. Cooper, *ibid.*, **16**, 533 (1975).

(6) M. D. Loberg and A. T. Fields, *Int. J. Appl. Radiat. Isot.*, **29**, 167 (1978).

(7) H. D. Burns, D. T. Sowa, and L. G. Marzilli, *J. Pharm. Sci.*, **67**, 1434 (1978).

(8) J. A. Weyh and R. E. Hamm, *Inorg. Chem.*, **7**, 2431 (1968).


## ACKNOWLEDGMENTS


Supported by U.S. Public Health Service Grants GM10548 and HL17655.


# Radiolabeled Benzoylcholine Derivatives as Possible Myocardial-Imaging Agents


**ROBERT F. DANNALS, H. DONALD BURNS ˣ, LUIGI G. MARZILLI, TIMOTHY C. TRAGESER, and HENRY N. WAGNER, Jr.**



Received February 22, 1980, from the *Division of Nuclear Medicine and the Department of Chemistry, Johns Hopkins University, Baltimore, MD 21205.* Accepted for publication September 25, 1980.



**Abstract** □ Two radioiodinated analogs of benzoylcholine were investigated as possible myocardial-imaging agents. *O*-([2-$^{125}$I]Iodobenzoyl)-choline and *N*-([2-$^{125}$I]iodobenzoyl)cholamine were prepared by nucleophilic substitution of sodium [$^{125}$I]iodide for stable iodine in *O*-(*N,N*-dimethylaminoethyl)-2-iodobenzoate and *N*-(*N',N'*-dimethylaminoethyl)-2-iodobenzamide, respectively, and by methylation with methyl iodide. The *in vivo* distribution of each compound in mice was determined as a function of time. Favorable heart-to-blood and heart-to-lung ratios were obtained with *N*-([2-$^{125}$I]iodobenzoyl)cholamine.



**Keyphrases** □ Benzoylcholine, radioiodinated analogs—synthesized and evaluated as possible myocardial-imaging agents, biodistribution studies in mice □ Radionuclide imaging, myocardial—radioiodinated benzoylcholine analogs synthesized and evaluated for use as myocardial-imaging agents, mice □ Radiopharmaceuticals, iodinated—benzoylcholine analogs, synthesis and evaluation for use as myocardial-imaging agents, mice □ Biodistribution—radioiodinated benzoylcholine analogs synthesized and evaluated for use as myocardial-imaging agents, mice


The use of radiolabeled enzyme inhibitors as potential organ-imaging agents has been suggested by several investigators. Wieland *et al.* (1) studied the distribution of several radiolabeled inhibitors of the adrenal cortex enzymes, 20$\alpha$-hydroxylase, 11$\beta$-hydroxylase, and 17$\alpha$-hydroxylase. The finding that some of these inhibitors localized in the adrenal cortex suggested that radiolabeled enzyme inhibitors might be useful in the design of new diagnostic radiopharmaceuticals.

## BACKGROUND

Recently, Burns *et al.* (2) studied the distribution of a simple, positively charged inhibitor of acetylcholinesterase. Their results suggested that labeled inhibitors of acetylcholinesterase might be useful as myocardial-imaging agents due to relatively high levels of acetylcholinesterase activity in the heart of some species.

Another study demonstrated that the cholinesterases of erythrocytes and plasma were different (3). The work of several investigators (4–8) clearly established the distinguishing characteristics between acetylcholinesterase (true cholinesterase or acetylcholine hydrolase) and pseudocholinesterase (butyrylcholinesterase or acylcholine acylhydrolase). Acetylcholinesterase predominates in erythrocytes, the central nervous system, and the motor endplates of skeletal muscle. Pseudocholinesterase predominates in the liver, plasma, and many types of smooth muscle. Both enzymes occur in high concentrations in autonomic ganglia (9). In some species, the distribution of pseudocholinesterase activity (10) indicates that an appropriate radiolabeled substrate or inhibitor might be a useful imaging agent for the myocardium.

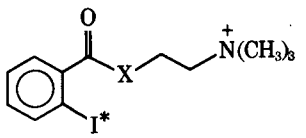


V: X = O
VI: X = NH

Many compounds are hydrolyzed by pseudocholinesterase including butyrylcholine, acetylcholine, and benzoylcholine. The fact that benzoylcholine is a substrate for butyrylcholinesterase, coupled with the observation that iodoaryl compounds are generally resistant to *in vivo* deiodination (11), prompted the investigation of two radioiodinated analogs of benzoylcholine as potential myocardial-imaging agents. This report details the syntheses and preliminary biological studies of *O*-([2-$^{125}$I]iodobenzoyl)choline (V) and *N*-([2-$^{125}$I]iodobenzoyl)cholamine (VI).

## EXPERIMENTAL[1]

***O*-(*N,N*-Dimethylaminoethyl)-2-iodobenzoate (I)**—2-Iodobenzoic acid (19.7 g, 0.077 mole), thionyl chloride (19.2 g, 0.162 mole), and a catalytic amount of dimethylformamide (50 $\mu$l) were warmed gently in a water bath. The evolution of hydrogen chloride and sulfur dioxide ceased after 60 min, and the solution was evaporated under reduced pressure to remove excess thionyl chloride. Benzene (100 ml) was added to the

[1] PMR spectra were obtained on a Varian T-60 spectrometer, with chemical shifts reported relative to tetramethylsilane or 3-(trimethylsilyl)propionic acid sodium salt as noted. IR spectra were recorded on a Pye-Unicam SP-1000 spectrometer. Melting points were determined in a Mel-Temp apparatus and are uncorrected. Elemental analyses were performed by Robertson Microanalytical Laboratory, Florham Park, N.J. Radioactive iodine was obtained from New England Nuclear Corp. as a carrier-free solution of sodium [$^{125}$I]iodide in a pH 8–10 aqueous solution (reductant free) at a specific activity of ~350 mCi/ml. The solution was diluted with normal saline to a specific activity of 10 mCi/ml.


0022-3549/81/0400-0439$01.00/0


© 1981, American Pharmaceutical Association

ticular note was the failure of many attempts to obtain crystalline products of I or analogs of I when they were attached to Co(III) or Cr(III), although the iminodiacetic acid and methyl iminodiacetic acid complexes are prepared and isolated easily. It is hoped that the approach outlined here for gaining information on the structure of $^{99m}$Tc-labeled radiopharmaceuticals will be useful for understanding the mechanisms of localization of currently used radiopharmaceuticals and in the design of new radiopharmaceuticals.

## REFERENCES


(1) P. V. Harper, G. Andrus, and K. Lathrup, U.S. AEC Report ARCH-18, Argonne Cancer Research Hospital, Sept. 1962, pp. 77, 78.

(2) H. D. Burns, in "The Chemistry of Radiopharmaceuticals," N. D. Heindel, H. D. Burns, T. Honda, and L. W. Brady, Eds., Masson, New York, N.Y., 1978, pp. 35–53.

(3) W. C. Eckelman, R. C. Reba, R. E. Gibson, N. J. Rzeszotarski, F. Vieras, J. K. Mazaitis, and B. Francis, *J. Nucl. Med.*, **20**, 350 (1979).

(4) L. G. Marzilli, P. Worley, and H. D. Burns, *ibid.*, **20**, 871 (1979).

(5) E. Harvey, M. D. Loberg, and M. Cooper, *ibid.*, **16**, 533 (1975).

(6) M. D. Loberg and A. T. Fields, *Int. J. Appl. Radiat. Isot.*, **29**, 167 (1978).

(7) H. D. Burns, D. T. Sowa, and L. G. Marzilli, *J. Pharm. Sci.*, **67**, 1434 (1978).

(8) J. A. Weyh and R. E. Hamm, *Inorg. Chem.*, **7**, 2431 (1968).


## ACKNOWLEDGMENTS


Supported by U.S. Public Health Service Grants GM10548 and HL17655.


# Radiolabeled Benzoylcholine Derivatives as Possible Myocardial-Imaging Agents


**ROBERT F. DANNALS, H. DONALD BURNS ˣ, LUIGI G. MARZILLI, TIMOTHY C. TRAGESER, and HENRY N. WAGNER, Jr.**



Received February 22, 1980, from the *Division of Nuclear Medicine and the Department of Chemistry, Johns Hopkins University, Baltimore, MD 21205.* Accepted for publication September 25, 1980.



**Abstract** □ Two radioiodinated analogs of benzoylcholine were investigated as possible myocardial-imaging agents. *O*-([2-$^{125}$I]Iodobenzoyl)-choline and *N*-([2-$^{125}$I]iodobenzoyl)cholamine were prepared by nucleophilic substitution of sodium [$^{125}$I]iodide for stable iodine in *O*-(*N,N*-dimethylaminoethyl)-2-iodobenzoate and *N*-(*N',N'*-dimethylaminoethyl)-2-iodobenzamide, respectively, and by methylation with methyl iodide. The *in vivo* distribution of each compound in mice was determined as a function of time. Favorable heart-to-blood and heart-to-lung ratios were obtained with *N*-([2-$^{125}$I]iodobenzoyl)cholamine.



**Keyphrases** □ Benzoylcholine, radioiodinated analogs—synthesized and evaluated as possible myocardial-imaging agents, biodistribution studies in mice □ Radionuclide imaging, myocardial—radioiodinated benzoylcholine analogs synthesized and evaluated for use as myocardial-imaging agents, mice □ Radiopharmaceuticals, iodinated—benzoylcholine analogs, synthesis and evaluation for use as myocardial-imaging agents, mice □ Biodistribution—radioiodinated benzoylcholine analogs synthesized and evaluated for use as myocardial-imaging agents, mice


The use of radiolabeled enzyme inhibitors as potential organ-imaging agents has been suggested by several investigators. Wieland *et al.* (1) studied the distribution of several radiolabeled inhibitors of the adrenal cortex enzymes, 20$\alpha$-hydroxylase, 11$\beta$-hydroxylase, and 17$\alpha$-hydroxylase. The finding that some of these inhibitors localized in the adrenal cortex suggested that radiolabeled enzyme inhibitors might be useful in the design of new diagnostic radiopharmaceuticals.

## BACKGROUND

Recently, Burns *et al.* (2) studied the distribution of a simple, positively charged inhibitor of acetylcholinesterase. Their results suggested that labeled inhibitors of acetylcholinesterase might be useful as myocardial-imaging agents due to relatively high levels of acetylcholinesterase activity in the heart of some species.

Another study demonstrated that the cholinesterases of erythrocytes and plasma were different (3). The work of several investigators (4–8) clearly established the distinguishing characteristics between acetylcholinesterase (true cholinesterase or acetylcholine hydrolase) and pseudocholinesterase (butyrylcholinesterase or acylcholine acylhydrolase). Acetylcholinesterase predominates in erythrocytes, the central nervous system, and the motor endplates of skeletal muscle. Pseudocholinesterase predominates in the liver, plasma, and many types of smooth muscle. Both enzymes occur in high concentrations in autonomic ganglia (9). In some species, the distribution of pseudocholinesterase activity (10) indicates that an appropriate radiolabeled substrate or inhibitor might be a useful imaging agent for the myocardium.

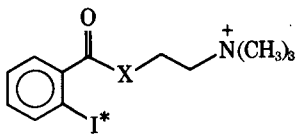


V: X = O
VI: X = NH

Many compounds are hydrolyzed by pseudocholinesterase including butyrylcholine, acetylcholine, and benzoylcholine. The fact that benzoylcholine is a substrate for butyrylcholinesterase, coupled with the observation that iodoaryl compounds are generally resistant to *in vivo* deiodination (11), prompted the investigation of two radioiodinated analogs of benzoylcholine as potential myocardial-imaging agents. This report details the syntheses and preliminary biological studies of *O*-([2-$^{125}$I]iodobenzoyl)choline (V) and *N*-([2-$^{125}$I]iodobenzoyl)cholamine (VI).

## EXPERIMENTAL[1]

***O*-(*N,N*-Dimethylaminoethyl)-2-iodobenzoate (I)**—2-Iodobenzoic acid (19.7 g, 0.077 mole), thionyl chloride (19.2 g, 0.162 mole), and a catalytic amount of dimethylformamide (50 $\mu$l) were warmed gently in a water bath. The evolution of hydrogen chloride and sulfur dioxide ceased after 60 min, and the solution was evaporated under reduced pressure to remove excess thionyl chloride. Benzene (100 ml) was added to the

[1] PMR spectra were obtained on a Varian T-60 spectrometer, with chemical shifts reported relative to tetramethylsilane or 3-(trimethylsilyl)propionic acid sodium salt as noted. IR spectra were recorded on a Pye-Unicam SP-1000 spectrometer. Melting points were determined in a Mel-Temp apparatus and are uncorrected. Elemental analyses were performed by Robertson Microanalytical Laboratory, Florham Park, N.J. Radioactive iodine was obtained from New England Nuclear Corp. as a carrier-free solution of sodium [$^{125}$I]iodide in a pH 8–10 aqueous solution (reductant free) at a specific activity of ~350 mCi/ml. The solution was diluted with normal saline to a specific activity of 10 mCi/ml.


0022-3549/81/0400-0439$01.00/0


© 1981, American Pharmaceutical Association

light-yellow oil that remained, and 2-dimethylaminoethanol (6.59 g, 0.074 mole) was added dropwise with stirring. After refluxing for 120 min, the solution was allowed to cool to room temperature.

The hydrochloride salt of the product was extracted into water (75 ml). Sodium hydroxide (5 ml, 10%) was added to the aqueous phase, which was extracted with ether (25 ml). This process was repeated five times. The ether extracts were dried (magnesium sulfate) and then concentrated under reduced pressure to yield 14.6 g (62%) of pale-yellow oil. The product was isolated as the hydrochloride salt for analysis, mp 162–163.5°; IR (mineral oil): 1725 (C=O) $cm^{-1}$; PMR [deuterium oxide, 3-(trimethylsilyl)propionic acid sodium salt]: δ 3.00 [s, 6H, $N(CH_3)_2$], 4.50–4.73 (m, 4H, $CH_2CH_2$), 6.80–7.43 (m, 2H, aromatic H-4,H-5), and 7.60–7.82 (m, 2H, aromatic H-3,H-6) ppm.

*Anal.*—Calc. for $C_{11}H_{14}INO_2 \cdot HCl$: C, 37.15; H, 4.25; N, 3.94. Found: C, 36.95; H, 4.40; N, 3.81.

***O*-(2-Iodobenzoyl)choline Iodide (II)**—Methyl iodide (7.1 g, 50 mmoles) was added to a solution of I (4.0 g, 12.5 mmoles) in chloroform (50 ml). The solution was refluxed for 60 min and then allowed to cool to room temperature. The precipitate that formed was collected by filtration, washed twice with ether, and dried *in vacuo*, yielding 5.48 g (95%) of white needles, mp 148–149°; IR (mineral oil): 1720 (C=O) $cm^{-1}$; PMR (dimethyl sulfoxide-$d_6$, tetramethylsilane): δ 3.40 [s, 9H, $^+N(CH_3)_3$], 4.05 (m, 2H, $CH_2N$), 4.80 (broad s, 2H, $COOCH_2$), 7.12–7.70 (m, 2H, aromatic H-4,H-5), and 7.80–8.13 (m, 2H, aromatic H-3,H-6) ppm.

*Anal.*—Calc. for $C_{12}H_{17}I_2NO_2$: C, 31.26; H, 3.72; N, 3.04. Found: C, 31.11; H, 3.72; N, 2.99.

***N*-(*N'*,*N'*-Dimethylaminoethyl)-2-iodobenzamide (III)**—2-Iodobenzoic acid (5.0 g, 0.02 mole), thionyl chloride (5.05 g, 0.042 mole), and a catalytic amount of dimethylformamide (50 μl) were warmed gently in a water bath. The solution was treated as was I to yield a light-yellow oil, which was added to a solution of *N*,*N*-dimethylethylenediamine (1.70 g, 0.019 mole) in 10% NaOH (50 ml). After stirring for 30 min at room temperature, the precipitate that formed was collected by filtration and recrystallized from hot ethanol–water to yield 4.27 g (70%) of white crystals, mp 113.5–115.5°; IR (mineral oil): 1640 (C=O) and 3160 (N–H) $cm^{-1}$; PMR (chloroform-*d*, tetramethylsilane): δ 2.10 [s, 6H, $N(CH_3)_2$], 2.45 (t, 2H, $CH_2N$), 3.44 (q, 2H, $CONHCH_2$), 6.73 (broad s, 1H, CONH), 6.90–7.42 (m, 3H, aromatic H), and 7.78 (d, 1H, aromatic H *ortho* to amide) ppm.

*Anal.*—Calc. for $C_{11}H_{15}IN_2O$: C, 41.53; H, 4.75; N, 8.80. Found: C, 41.54; H, 4.80; N, 8.69.

***N*-(2-Iodobenzoyl)cholamine (IV) Iodide**—Methyl iodide (1.12 g, 7.8 mmoles) was added to a solution of III (2.5 g, 7.8 mmoles) in chloroform (50 ml), and then the solution was stirred for 60 min at room temperature. The precipitate that formed was collected by filtration and recrystallized from 1-propanol to yield 2.56 g (71%) of white crystals, mp 156–157.5°; IR (mineral oil): 1650 (C=O) and 3300 (N–H) $cm^{-1}$; PMR (dimethyl sulfoxide-$d_6$, tetramethylsilane): δ 3.35 [s, 9H, $^+N(CH_3)_3$], 3.75 (broad s, 4H, $CH_2CH_2$), 7.11–7.63 (m, 3H, aromatic H), 7.93 (d, 1H, aromatic H *ortho* to amide), and 8.97 (broad s, 1H, CONH) ppm.

*Anal.*—Calc. for $C_{12}H_{18}I_2N_2O$: C, 31.33; H, 3.94; N, 6.09. Found: C, 31.46; H, 4.04; N, 6.02.

***O*-([2-$^{125}$I]Iodobenzoyl)choline (V) Chloride**—A small aliquot of an aqueous stock solution of sodium [$^{125}$I]iodide (10 mCi/ml) containing 0.1 mCi was mixed with methanol (100 μl) and evaporated to dryness in a 1-ml serum vial. Compound I (10 mg, 0.03 mmole) was added to the vial, which was sealed with a vented polytef-lined stopper. The vial was heated in an oil bath at 103° for 20 min and then was allowed to cool to room temperature. A saturated sodium metabisulfite solution (250 μl) was added to the vial, and the pH of the resulting solution was adjusted to 11 with 10% NaOH. The solution was extracted three times with chloroform (500 μl). The chloroform extracts, which contained 60% of the initial activity, were combined and dried over magnesium sulfate.

Methyl iodide (100 μl, 1.6 mmoles) was added to the solution, which was refluxed for 30 min and then cooled to room temperature. The chloroform was extracted twice with normal saline (1 ml). More than 95% of the remaining activity was found in the saline extracts, resulting in an overall radiochemical yield of 57%. The saline extracts were passed through a 1 × 3-cm column of anion-exchange resin[2] eluted with normal saline. The solution was passed through a 0.22-μm filter[3] and diluted with saline to an activity of 10 μCi/ml. The specific activity of the product was ~1.9 mCi/mmole. The radiochemical purity was verified by TLC prior to the biodistribution studies.

***N*-([2-$^{125}$I]Iodobenzoyl)cholamine (VI) Chloride**—A small aliquot (0.1 mCi) of an aqueous stock solution of sodium [$^{125}$I]iodide was prepared as described for V. Compound III (10 mg, 0.03 mmole) was added to the vial, which was sealed with a vented polytef stopper and immersed in an oil bath at 120° for 15 min. After the vial was allowed to cool to room temperature, the reaction mixture was treated as described for V. The chloroform extracts contained 48% of the initial activity, and the saline extracted >95% of the remaining activity, resulting in an overall radiochemical yield of 46%. The specific activity of the product was ~1.6 mCi/mmole. The radiochemical purity was verified by chromatographic methods prior to use in the biodistribution studies.

**TLC**[4]—The radiochemical purity of the products was verified using TLC with the following solvent systems: acetone–water (4:1), chloroform–methanol (4:1), and chloroform–methanol–30% ammonium hydroxide (10:1.5:0.1). Table I shows the $R_f$ values determined for I–IV, 2-iodobenzoic acid, sodium [$^{125}$I]iodide, and 2-iodohippuric acid.

**Biodistribution Studies**—The tissue distributions of V and VI were determined as a function of time in normal ICR mice. The mice, 30–40 g, were divided in groups of six and sacrificed under ether anesthesia at 5, 30, 60, and 120 min following the intravenous administration of 1 μCi of either compound in 0.1 ml of saline. Samples of blood, heart, lungs, kidneys, liver, spleen, and muscle were taken and counted in a scintillation well counter. Care was taken to prevent urine from contaminating the carcass when the bladder was removed. The results were expressed as the percentage of injected dose per organ and per gram of wet tissue.

Samples of urine were collected at various intervals and developed on TLC using the described solvent systems. The radiochromatograms were compared with the original samples.

## RESULTS AND DISCUSSION

Standard methods of electrophilic carrier-free iodinations (*e.g.*, lactoperoxidase or *N*-chloro-*p*-toluenesulfonamide sodium salt) are not useful for preparation of iodoaryl compounds where the aromatic ring contains deactivating groups. However, halogens bound to an aromatic ring in a position *ortho* to an electron-withdrawing group are activated with respect to nucleophilic substitution. While this method does not produce the high specific activity product produced by electrophilic iodination, it does allow for the rapid incorporation of radioactive iodine into a molecule of known structure.

Labeling of both I and III by nucleophilic isotopic exchange under high temperature conditions was achieved without significant decomposition, as confirmed by TLC. The reaction products were methylated easily with methyl iodide and extracted into saline for use in the biodistribution studies. Compound V was stable in aqueous solution for several weeks when refrigerated at 5°, and VI was stable for several months under the same conditions.

The biodistributions of V and VI were determined at 5, 30, 60, and 120 min postinjection (Tables II–V). Compound VI cleared rapidly from the blood, with only 1.7% of the injected dose remaining in circulation 5 min after injection. More than 30% of the injected dose was excreted *via* the kidneys after 5 min postinjection. Chromatography of urine samples at various intervals indicated that VI was excreted unchanged, with no evidence of amide hydrolysis or deiodination. Its accumulation in the heart was significant, 6.4% of the dose/g at 5 min postinjection. Although the activity in the heart did not remain constant, the compound cleared slowly enough that heart-to-blood ratios of >6 and heart-to-lung ratios of >2 were maintained at least 2 hr after administration (Table VI).

Unlike VI, V exhibited no significant accumulation in the heart, with heart-to-blood and heart-to-lung ratios of <1 at all times studied (Table VI). Compound V cleared slowly from the circulation, with 17.4% of the injected dose remaining after 5 min and ~3% remaining after 30 min. The clearance from the body was rapid, with only 25% of the injected dose remaining after 30 min and <10% remaining after 60 min.

Excretion of V was primarily *via* the kidneys. Chromatography of urine samples at various intervals indicated that the compound was hydrolyzed and excreted in the form of [2-$^{125}$I]iodobenzoic acid. The fate of the hydrolyzed choline could not be determined by these experiments. The observation that 2-iodobenzoic acid, which is generated by the hydrolysis of V, was excreted intact was unexpected. Substituted benzoic acids are conjugated *in vivo* with glycine to form the corresponding substituted hippuric acids prior to excretion (12). However, TLC of an authentic sample of 2-iodohippuric acid[5] in acetone–water and chloroform–methanol showed that it was excreted as 2-iodobenzoic acid.

[2] Bio-Rad AG-1X8, chloride form.
[3] Type GS, 0.22 μm, Millipore Corp.
[4] Chromatography was performed on Baker-flex silica gel IB-F (7.5 × 2.5 cm).
[5] Hippuran, Mallinckrodt Chemical Works, St. Louis, Mo.

**Table I—TLC $R_f$ Values**

| System[a] | I | II | III | IV | Sodium [$^{125}$I]Iodide | 2-Iodobenzoic Acid | 2-Iodohippuric Acid |
|---|---|---|---|---|---|---|---|
| A | 0.60 | 0.24 | 0.25 | 0.20 | 0.71 | 0.75 | 0.49 |
| B | 0.60 | 0.11 | 0.55 | 0.12 | 0.31 | 0.50 | 0.11 |
| C | 0.66 | 0.04 | 0.70 | 0.06 | 0.60 | 0.10 | 0.00 |

[a] A = acetone–water (4:1), B = chloroform–methanol (4:1), and C = chloroform–methanol–ammonium hydroxide (10:1.5:0.1).

**Table II—Biodistribution of *O*-([2-$^{125}$I]Iodobenzyl)choline in Mice**

| Organ | Mean Percent of Dose per Organ ± *SD*[a] | | | |
|---|---|---|---|---|
| | 5 min | 30 min | 60 min | 120 min |
| Blood[b] | 17.44 ± 1.97 | 3.05 ± 1.02 | 0.45 ± 0.25 | 0.18 ± 0.07 |
| Heart | 0.52 ± 0.07 | 0.08 ± 0.02 | 0.01 ± 0.01 | —[c] |
| Lungs | 1.07 ± 0.15 | 0.23 ± 0.06 | 0.03 ± 0.01 | 0.02 ± 0.01 |
| Kidneys | 14.38 ± 1.94 | 4.60 ± 2.80 | 0.34 ± 0.17 | 0.18 ± 0.24 |
| Liver | 5.64 ± 0.85 | 1.40 ± 0.36 | 0.22 ± 0.08 | 0.09 ± 0.03 |
| Spleen | 0.19 ± 0.03 | 0.07 ± 0.02 | 0.01 ± 0.01 | 0.01 ± 0.01 |
| Carcass | 41.37 ± 4.19 | 15.70 ± 4.72 | 5.52 ± 3.92 | 1.86 ± 0.72 |
| Total | 80.6 | 25.1 | 6.5 | 2.3 |

[a] Six mice studied at each time. [b] Based on 7% of the body weight. [c] Not significantly above background.

**Table III—Biodistribution of *O*-([2-$^{125}$I]Iodobenzoyl)choline in Mice**

| Organ | Mean Percent of Dose per Gram ± *SD*[a] | | | |
|---|---|---|---|---|
| | 5 min | 30 min | 60 min | 120 min |
| Blood | 6.08 ± 1.28 | 1.43 ± 0.44 | 0.19 ± 0.12 | 0.09 ± 0.03 |
| Heart | 3.36 ± 0.31 | 0.81 ± 0.29 | 0.09 ± 0.05 | —[b] |
| Lungs | 4.56 ± 0.48 | 0.99 ± 0.25 | 0.16 ± 0.06 | 0.07 ± 0.04 |
| Kidneys | 27.88 ± 3.59 | 12.36 ± 6.99 | 0.80 ± 0.51 | 0.36 ± 0.47 |
| Liver | 2.91 ± 0.47 | 0.77 ± 0.19 | 0.13 ± 0.06 | 0.05 ± 0.01 |
| Spleen | 1.69 ± 0.43 | 0.54 ± 0.20 | 0.10 ± 0.04 | 0.05 ± 0.02 |
| Muscle | 1.15 ± 0.12 | 0.40 ± 0.17 | 0.07 ± 0.06 | 0.05 ± 0.08 |

[a] Six mice studied at each time. [b] Not significantly above background.

**Table IV—Biodistribution of *N*-([2-$^{125}$I]Iodobenzoyl)cholamine in Mice**

| Organ | Mean Percent of Dose per Organ ± *SD*[a] | | | |
|---|---|---|---|---|
| | 5 min | 30 min | 60 min | 120 min |
| Blood[b] | 1.68 ± 0.23 | 0.59 ± 0.18 | 0.57 ± 0.13 | 0.23 ± 0.08 |
| Heart | 1.10 ± 0.20 | 0.71 ± 0.12 | 0.45 ± 0.09 | 0.10 ± 0.03 |
| Lungs | 0.85 ± 0.17 | 0.35 ± 0.27 | 0.17 ± 0.02 | 0.06 ± 0.02 |
| Kidneys | 7.90 ± 4.37 | 1.75 ± 0.88 | 1.12 ± 0.44 | 0.48 ± 0.49 |
| Liver | 24.43 ± 3.02 | 9.95 ± 2.79 | 6.53 ± 1.70 | 0.99 ± 0.28 |
| Spleen | 0.10 ± 0.03 | 0.08 ± 0.02 | 0.06 ± 0.01 | 0.03 ± 0.01 |
| Carcass | 30.68 ± 6.63 | 20.31 ± 4.14 | 19.16 ± 3.69 | 14.19 ± 4.36 |
| Total | 66.7 | 33.7 | 28.1 | 16.0 |

[a] Six mice studied at each time. [b] Based on 7% of the body weight.

**Table V—Biodistribution of *N*-([2-$^{125}$I]Iodobenzoyl)cholamine in Mice**

| Organ | Mean Percent of Dose per Gram ± *SD*[a] | | | |
|---|---|---|---|---|
| | 5 min | 30 min | 60 min | 120 min |
| Blood | 0.61 ± 0.12 | 0.21 ± 0.06 | 0.21 ± 0.05 | 0.08 ± 0.03 |
| Heart | 6.40 ± 1.59 | 4.64 ± 0.63 | 3.20 ± 0.75 | 0.51 ± 0.21 |
| Lungs | 2.80 ± 0.66 | 1.29 ± 0.59 | 0.69 ± 0.16 | 0.21 ± 0.09 |
| Kidneys | 14.54 ± 10.03 | 3.43 ± 1.84 | 2.26 ± 0.72 | 0.74 ± 0.75 |
| Liver | 12.95 ± 1.71 | 4.96 ± 1.23 | 3.67 ± 0.95 | 0.48 ± 0.19 |
| Spleen | 0.78 ± 0.19 | 0.66 ± 0.09 | 0.56 ± 0.14 | 0.20 ± 0.06 |
| Muscle | 0.34 ± 0.08 | 0.26 ± 0.14 | 0.21 ± 0.04 | 0.19 ± 0.07 |

[a] Six mice studied at each time.

**Table VI—Heart-to-Blood and Heart-to-Lung Ratios as a Function of Time in Mice**

| | 5 min | 30 min | 60 min | 120 min |
|---|---|---|---|---|
| V | | | | |
| Heart/blood | 0.6 | 0.6 | 0.5 | NA[a] |
| Heart/lung | 0.7 | 0.8 | 0.6 | NA |
| VI | | | | |
| Heart/blood | 10.5 | 22.1 | 15.2 | 6.4 |
| Heart/lung | 2.3 | 3.6 | 4.6 | 2.4 |

[a] Not available.

Positively charged quaternary ammonium compounds can bind to the negatively charged anionic pocket of the cholinesterase active site by a combination of coulombic and van der Waals' dispersion forces (13). Compounds V and VI were designed to interact with the enzyme as a result of these interactions. It is possible that V is a substrate for pseudocholinesterase (6) in light of the active hydrolysis of benzoylcholine by that enzyme. Enzymatic hydrolysis may account for the high blood activity found in the biodistribution studies and the urinary excretion of [2-$^{125}$I]iodobenzoic acid. On the other hand, by virtue of its amide functionality, which is more stable to hydrolysis by esterase enzymes, VI is not expected to be a substrate for either pseudocholinesterase or

acetylcholinesterase. Although VI was prepared as an inhibitor of pseudocholinesterase and may be an inhibitor of acetylcholinesterase, there is no evidence that the uptake of VI by the heart is related to binding to either enzyme. *In vitro* studies are in progress to investigate the specific mechanism responsible for the accumulation of VI in heart muscle.

The simple, rapid synthetic technique employed in the preparation of VI would easily allow the 13-hr half-life of iodine 123, which has excellent imaging characteristics, to be substituted for the stable iodine in the molecule. The apparent *in vivo* stability and the high heart-to-blood and heart-to-lung ratios obtained in mice with VI suggest that iodine 123-labeled VI may be useful for imaging the heart in humans and warrants further study as a myocardial-imaging agent.

## REFERENCES


(1) D. M. Wieland, R. D. Ice, and W. H. Beierwaltes, *J. Nucl. Med.*, **17**, 525 (1976).

(2) H. D. Burns, L. G. Marzilli, R. F. Dannals, T. E. Dannals, T. C. Trageser, P. Conti, and H. N. Wagner, Jr., *ibid.*, **21**, 875 (1980).

(3) G. A. Alles and R. C. Hawes, *J. Biol. Chem.*, **133**, 375 (1940).

(4) K.-B. Augustinsson, *Acta Physiol. Scand.*, **15** (Suppl. 52), 1 (1948).

(5) K.-B. Augustinsson, in "Handbook of Experimental Pharmacology," vol. 15, G. B. Koelle, Ed., Springer-Verlag, Berlin, Germany, 1963, pp. 89–128.

(6) B. Mendel, D. B. Mundell, and H. Rudney, *Biochem. J.*, **37**, 473 (1943).

(7) B. Mendel and H. Rudney, *ibid.*, **37**, 59 (1943).

(8) D. Nachmansohn and M. A. Rothenburg, *J. Biol. Chem.*, **158**, 653 (1945).

(9) G. B. Koelle, in "Handbook of Experimental Pharmacology," vol. 15, G. B. Koelle, Ed., Springer-Verlag, Berlin, Germany, 1963, pp. 187–298.

(10) M. G. Ord and R. H. S. Thompson, *Biochem. J.*, **46**, 346 (1950).

(11) R. E. Counsell and R. D. Ice, in "Drug Design," vol. VI, E. J. Ariens, Ed., Academic, New York, N.Y., 1975, p. 187.

(12) H. G. Gray, B. G. Humpris, W. V. Thorpe, K. White, and P. B. Wood, *Biochem. J.*, **59**, 162 (1955).

(13) A. R. Main, in "Biology of Cholinergic Function," A. M. Goldberg and I. Hanin, Eds., Raven, New York, N.Y., 1976, p. 281.


## ACKNOWLEDGMENTS


Supported in part by U.S. Public Health Service Grants GM-10548 and HL-17655.


# Effect of Macromolecules on Aqueous Solubility of Cholesterol and Hormone Drugs


**DONALD E. CADWALLADER ˣ and DEVENDRA K. MADAN**



Received August 6, 1980, from the *Department of Pharmaceutics, School of Pharmacy, University of Georgia, Athens, GA 30602.* Accepted for publication October 1, 1980.



**Abstract** □ The solubility of cholesterol and some hormone drugs in aqueous macromolecule solutions was investigated. Polyvinylpyrrolidone, dextrans, and heparin increased the solubilities of progesterone, testosterone, and diethylstilbestrol, while acacia, pectin, and carrageenans decreased their solubilities. Dextrans increased the solubilities of cholesterol and the three hormone drugs. Acacia and pectin greatly increased cholesterol solubility; however, these macromolecules significantly decreased progesterone and diethylstilbestrol solubilities and slightly decreased testosterone solubility. Heparin decreased cholesterol solubility and increased progesterone, testosterone, and diethylstilbestrol solubilities. Carrageenans significantly decreased cholesterol, progesterone, and testosterone solubilities and had little effect on diethylstilbestrol solubility. A strong bathochromic shift in the absorption spectra of progesterone and testosterone in polyvinylpyrrolidone solutions indicated an attachment between the polymer and the C=O group of the steroids.



**Keyphrases** □ Cholesterol—effect of macromolecules on aqueous solubility □ Hormone drugs—effect of macromolecules on aqueous solubility □ Solubility—cholesterol and hormone drugs, effect of macromolecules □ Macromolecules—effect on aqueous solubility of cholesterol and hormone drugs


Several macromolecular compounds have been reported to have hypercholesterolemic effects. Acacia and pectin (1–6) and dextran (6–11) have been reported to lower serum cholesterol in humans and animals. Heparin reportedly retards atherosclerosis development and minimizes the degree of hypercholesterolemia (12–14). Carrageenans have been found effective in suppressing hyperlipidemia and atherosclerosis in cholesterol-fed rabbits (15, 16). Polyvinylpyrrolidone was reported to have hypocholesterolemia activity (17).

These reports contain conflicting statements concerning the *in vivo* effect and mechanism of action of these macromolecules for lowering serum cholesterol. A previous article from this laboratory (18) reported on the interesting *in vitro* effects of carbohydrate macromolecules on the aqueous solubility of cholesterol. The large increases in the apparent solubility of cholesterol in 0.5% pectin and acacia solutions provided a possible explanation for the serum cholesterol-lowering ability of these hydrocolloids and prompted further solubility studies involving other macromolecules. This report concerns the effect of various macromolecules on the solubility behavior of cholesterol and the related hormone drugs, testosterone, progesterone, and diethylstilbestrol.

## EXPERIMENTAL

**Materials**—Diethylstilbestrol[1], progesterone[2], and testosterone[3] were recrystallized from ethanol. Cholesterol[4] was purified by recrystallization from acetic acid, and the crystals were dried at 90°. The sample was then recrystallized from 70% alcohol–water and dried in a vacuum desiccator. The melting points and IR spectra of the compounds were in good agreement with literature values. Dextrans[5], pectin (citrus)[6], acacia[1], polyvinylpyrrolidone[7], heparin sodium[2], and carrageenans[8] were used as received.

**Solubility Experiments**—A stock solution of cholesterol in benzene was prepared containing 1.0 mg of cholesterol and 10 $\mu$Ci of [26-$^{14}$C]-cholesterol[9]. Stock solutions of testosterone and progesterone were

[1] Matheson, Coleman and Bell.
[2] Sigma Chemical Co.
[3] Supplied by Schering Laboratories.
[4] Fisher Scientific.
[5] Dextran $T_{40}$ and $T_{70}$, Pharmacia Laboratories.
[6] Eastman Kodak Co.
[7] NP-K30, GAF Corp.
[8] Seakem 11 and 21, Marine Colloids.
[9] Nuclear Chicago.




0022-3549/81/0400-0442$01.00/0


© 1981, American Pharmaceutical Association

acetylcholinesterase. Although VI was prepared as an inhibitor of pseudocholinesterase and may be an inhibitor of acetylcholinesterase, there is no evidence that the uptake of VI by the heart is related to binding to either enzyme. *In vitro* studies are in progress to investigate the specific mechanism responsible for the accumulation of VI in heart muscle.

The simple, rapid synthetic technique employed in the preparation of VI would easily allow the 13-hr half-life of iodine 123, which has excellent imaging characteristics, to be substituted for the stable iodine in the molecule. The apparent *in vivo* stability and the high heart-to-blood and heart-to-lung ratios obtained in mice with VI suggest that iodine 123-labeled VI may be useful for imaging the heart in humans and warrants further study as a myocardial-imaging agent.

## REFERENCES


(1) D. M. Wieland, R. D. Ice, and W. H. Beierwaltes, *J. Nucl. Med.*, **17**, 525 (1976).

(2) H. D. Burns, L. G. Marzilli, R. F. Dannals, T. E. Dannals, T. C. Trageser, P. Conti, and H. N. Wagner, Jr., *ibid.*, **21**, 875 (1980).

(3) G. A. Alles and R. C. Hawes, *J. Biol. Chem.*, **133**, 375 (1940).

(4) K.-B. Augustinsson, *Acta Physiol. Scand.*, **15** (Suppl. 52), 1 (1948).

(5) K.-B. Augustinsson, in "Handbook of Experimental Pharmacology," vol. 15, G. B. Koelle, Ed., Springer-Verlag, Berlin, Germany, 1963, pp. 89–128.

(6) B. Mendel, D. B. Mundell, and H. Rudney, *Biochem. J.*, **37**, 473 (1943).

(7) B. Mendel and H. Rudney, *ibid.*, **37**, 59 (1943).

(8) D. Nachmansohn and M. A. Rothenburg, *J. Biol. Chem.*, **158**, 653 (1945).

(9) G. B. Koelle, in "Handbook of Experimental Pharmacology," vol. 15, G. B. Koelle, Ed., Springer-Verlag, Berlin, Germany, 1963, pp. 187–298.

(10) M. G. Ord and R. H. S. Thompson, *Biochem. J.*, **46**, 346 (1950).

(11) R. E. Counsell and R. D. Ice, in "Drug Design," vol. VI, E. J. Ariens, Ed., Academic, New York, N.Y., 1975, p. 187.

(12) H. G. Gray, B. G. Humpris, W. V. Thorpe, K. White, and P. B. Wood, *Biochem. J.*, **59**, 162 (1955).

(13) A. R. Main, in "Biology of Cholinergic Function," A. M. Goldberg and I. Hanin, Eds., Raven, New York, N.Y., 1976, p. 281.


## ACKNOWLEDGMENTS


Supported in part by U.S. Public Health Service Grants GM-10548 and HL-17655.


# Effect of Macromolecules on Aqueous Solubility of Cholesterol and Hormone Drugs


**DONALD E. CADWALLADER ˣ and DEVENDRA K. MADAN**



Received August 6, 1980, from the *Department of Pharmaceutics, School of Pharmacy, University of Georgia, Athens, GA 30602.* Accepted for publication October 1, 1980.



**Abstract** □ The solubility of cholesterol and some hormone drugs in aqueous macromolecule solutions was investigated. Polyvinylpyrrolidone, dextrans, and heparin increased the solubilities of progesterone, testosterone, and diethylstilbestrol, while acacia, pectin, and carrageenans decreased their solubilities. Dextrans increased the solubilities of cholesterol and the three hormone drugs. Acacia and pectin greatly increased cholesterol solubility; however, these macromolecules significantly decreased progesterone and diethylstilbestrol solubilities and slightly decreased testosterone solubility. Heparin decreased cholesterol solubility and increased progesterone, testosterone, and diethylstilbestrol solubilities. Carrageenans significantly decreased cholesterol, progesterone, and testosterone solubilities and had little effect on diethylstilbestrol solubility. A strong bathochromic shift in the absorption spectra of progesterone and testosterone in polyvinylpyrrolidone solutions indicated an attachment between the polymer and the C=O group of the steroids.



**Keyphrases** □ Cholesterol—effect of macromolecules on aqueous solubility □ Hormone drugs—effect of macromolecules on aqueous solubility □ Solubility—cholesterol and hormone drugs, effect of macromolecules □ Macromolecules—effect on aqueous solubility of cholesterol and hormone drugs


Several macromolecular compounds have been reported to have hypercholesterolemic effects. Acacia and pectin (1–6) and dextran (6–11) have been reported to lower serum cholesterol in humans and animals. Heparin reportedly retards atherosclerosis development and minimizes the degree of hypercholesterolemia (12–14). Carrageenans have been found effective in suppressing hyperlipidemia and atherosclerosis in cholesterol-fed rabbits (15, 16). Polyvinylpyrrolidone was reported to have hypocholesterolemia activity (17).

These reports contain conflicting statements concerning the *in vivo* effect and mechanism of action of these macromolecules for lowering serum cholesterol. A previous article from this laboratory (18) reported on the interesting *in vitro* effects of carbohydrate macromolecules on the aqueous solubility of cholesterol. The large increases in the apparent solubility of cholesterol in 0.5% pectin and acacia solutions provided a possible explanation for the serum cholesterol-lowering ability of these hydrocolloids and prompted further solubility studies involving other macromolecules. This report concerns the effect of various macromolecules on the solubility behavior of cholesterol and the related hormone drugs, testosterone, progesterone, and diethylstilbestrol.

## EXPERIMENTAL

**Materials**—Diethylstilbestrol[1], progesterone[2], and testosterone[3] were recrystallized from ethanol. Cholesterol[4] was purified by recrystallization from acetic acid, and the crystals were dried at 90°. The sample was then recrystallized from 70% alcohol–water and dried in a vacuum desiccator. The melting points and IR spectra of the compounds were in good agreement with literature values. Dextrans[5], pectin (citrus)[6], acacia[1], polyvinylpyrrolidone[7], heparin sodium[2], and carrageenans[8] were used as received.

**Solubility Experiments**—A stock solution of cholesterol in benzene was prepared containing 1.0 mg of cholesterol and 10 $\mu$Ci of [26-$^{14}$C]-cholesterol[9]. Stock solutions of testosterone and progesterone were

[1] Matheson, Coleman and Bell.
[2] Sigma Chemical Co.
[3] Supplied by Schering Laboratories.
[4] Fisher Scientific.
[5] Dextran $T_{40}$ and $T_{70}$, Pharmacia Laboratories.
[6] Eastman Kodak Co.
[7] NP-K30, GAF Corp.
[8] Seakem 11 and 21, Marine Colloids.
[9] Nuclear Chicago.




0022-3549/81/0400-0442$01.00/0


© 1981, American Pharmaceutical Association

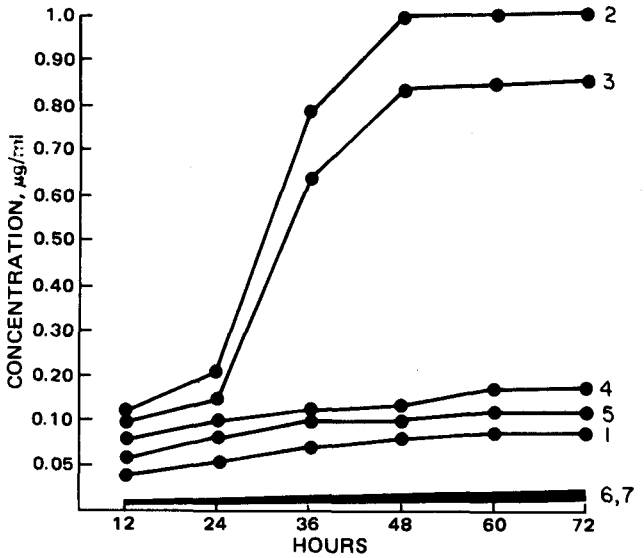


**Figure 1**—*Effect of various macromolecules on the aqueous solubility of cholesterol at 30°. Key: 1, water; 2, 0.5% pectin; 3, 0.5% acacia; 4, 10% dextran; 5, 6% dextran; 6, 1% heparin; and 7, 0.1% carrageenans.*

prepared to contain 200 mg of untagged compound and 5 μCi of labeled compound ([26-$^{14}$C]progesterone and [26-$^{14}$C]testosterone)[9] in 100 ml of benzene. A similar stock solution of diethylstilbestrol (using [*monoethyl*-1-$^{14}$C]diethylstilbestrol)[9] was prepared in methanol.

A known amount of a particular stock solution was transferred into a 125-ml iodine flask, and the solvent was evaporated under a mild nitrogen stream with constant shaking. A 50-ml volume of dissolution medium kept at 30° was added to the flask. Dissolution studies were carried out at 30 ± 0.5° using a controlled environment unit[10] to maintain the temperature. The solution was stirred at ~300 rpm using a magnetic stirrer and a 2.7 × 1-cm polytef[11]-coated spin bar. A 100-ml volume of dissolution medium in a 250-ml iodine flask was used for testosterone experiments.

For each dissolution study, the amount of compound used was in ~10-fold excess of its previously determined aqueous solubility. At predetermined intervals, samples were withdrawn from the system and filtered immediately and rapidly through a filtration assembly[12] containing a 0.45-μm filter. Because filtration adsorption losses may cause errors (19), stock solutions containing known amounts of the compounds were filtered and compared. No significant adsorption was detected with the rapid filtration technique.

**Radioactive Assay**—A 0.20-ml volume of the particle-free filtrate was pipetted into a liquid scintillation vial. To this vial was transferred 15 ml of dioxane–naphthalene scintillation cocktail (20). The scintillation vial was tightly capped and shaken for about 30 sec to ensure thorough mixing of the experimental solution and the cocktail. At the same time, a blank was prepared in the same manner except that the compound was omitted from the solution. The standard was prepared by pipetting 0.10 ml of the standard solution of the experimental compound into a scintillation vial. After the solvent (benzene or methanol) was evaporated, 0.20 ml of water and 15 ml of dioxane–naphthalene scintillation cocktail were added and the vial was shaken.

Duplicate samples along with appropriate standards and blanks were counted directly using a liquid scintillation system[13]. Sufficient time was allowed for the samples to cool to 4.0° to minimize quenching, and the samples were counted for 10 min. The solubility values were obtained from the ratio of the counts per minute of the internal standard and the sample.

**UV Absorption Studies**—Progesterone and testosterone in water both absorb a maximum of radiated energy at 249 nm. With a spectrophotometer[14], UV scans were carried out for each of these two hormones in aqueous solutions containing various concentrations of the macromolecules. Macromolecule solutions containing no hormone drugs were used as blanks in comparison cells.

[10] Hot Pack model 1278-8.
[11] Teflon.
[12] Millipore.
[13] Unilux II, Nuclear Chicago.
[14] Perkin-Elmer model 202.

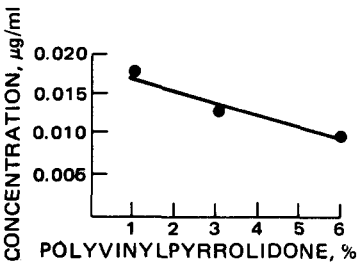


**Figure 2**—*Effect of polyvinylpyrrolidone solutions on the aqueous solubility of cholesterol after 72 hr at 30°.*

## RESULTS AND DISCUSSION

The aqueous solubilities of cholesterol, progesterone, testosterone, and diethylstilbestrol were reported previously (21). Figures 1–7 illustrate the effect of various macromolecules on the solubility behavior of these compounds. Each point on the solubility curves represents an average of at least six or eight determinations. Statistical analyses of the data with *t* and *F* tests at 95% confidence levels indicated the differences in solubilities between various test solutions to be significant.

Figure 1 illustrates the effect of various macromolecules on cholesterol. The large increases in 0.5% pectin and acacia solutions and the slight increase in dextran solutions were discussed previously (21). Heparin and both carrageenans[8] decreased the aqueous solubility (at equilibrium) of cholesterol to ~0.01 and 0.02 μg/ml, respectively. Polyvinylpyrrolidone decreased the aqueous solubility of cholesterol, and the decrease was proportional to the polyvinylpyrrolidone concentration (Fig. 2).

The solution behavior of testosterone (Figs. 3 and 4) showed that heparin and 10% dextran slightly increased the solubility; 6% dextran (both high and low molecular weights), pectin, and acacia had no significant effect; and the carrageenans decreased solubility. Testosterone solubility was significantly increased in polyvinylpyrrolidone solutions, and the increase was proportional to the polyvinylpyrrolidone concentration (Fig. 7). The equilibrium solubility of testosterone in water and macromolecule solutions, with the exception of heparin, was approached from supersaturation and not from undersaturation. The portion of the solution behavior curve that depicts the solubility decrease after the peak was reached is apparently indicative of the rate at which the less soluble hydrated form of testosterone is crystallized out of solution (22–24). Heparin appears to prevent crystallization.

Polyvinylpyrrolidone, dextran (both high and low molecular weights), and heparin significantly increased progesterone solubility (Fig. 5). Pectin, acacia, and carrageenans[8] all decreased progesterone solubility to approximately the same level.

Polyvinylpyrrolidone, dextran (10%), and heparin increased diethylstilbestrol solubility, whereas dextran (at the 6 and 2% levels) and carrageenans had no significant effect (Fig. 6). Acacia and pectin decreased the aqueous solubility.

In general, polyvinylpyrrolidone, dextran, and heparin increased the solubilities of the hormone drugs while acacia, pectin, and the carrageenans decreased their solubilities. In this study, dextran was the only macromolecule that increased the solubilities of cholesterol and the three hormone drugs.

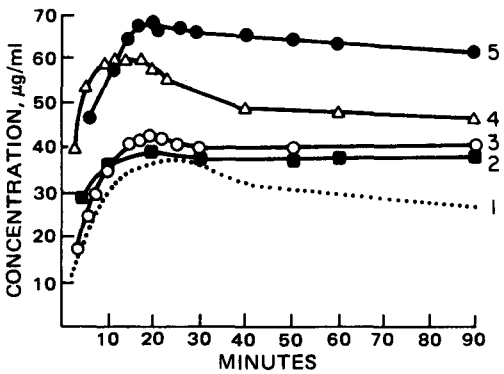


**Figure 3**—*Effect of various macromolecules on the aqueous solubility of testosterone at 30°. Key: 1, water; 2, 1% heparin; 3, 1% polyvinylpyrrolidone; 4, 3% polyvinylpyrrolidone; and 5, 6% polyvinylpyrrolidone.*

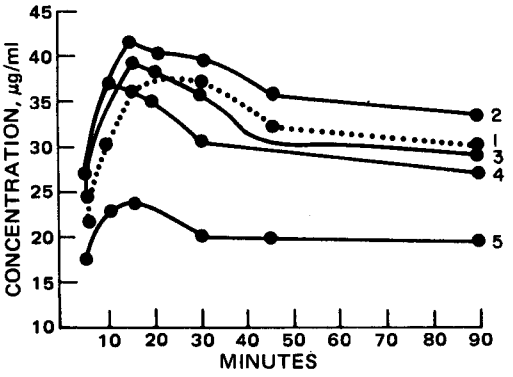


**Figure 4**—*Effect of various macromolecules on the aqueous solubility of testosterone at 30°. Key: 1, water; 2, 10% dextran; 3, 6% dextran; 4, 0.5% pectin or 0.5% acacia; and 5, 0.1% carrageenans.*

A 10% dextran solution almost doubled diethylstilbestrol and cholesterol solubilities, caused an appreciable increase in progesterone solubility, and produced a slight increase in testosterone solubility. Dextran at the 6% level increased cholesterol and progesterone solubilities; however, there was little effect on testosterone and diethylstilbestrol solubilities. Although the solubilities of cholesterol and the hormone drugs were dependent on the dextran concentration, the degree of solubility of each compound was inconsistent. For example, the solubilities of progesterone in 10, 6, or 2% dextran solution were nearly the same (17–16 μg/ml), while the solubilities for diethylstilbestrol in 10 and 6% dextran were 46.1 and 26.6 μg/ml, respectively. Solubility experiments were carried out with both high and low molecular weight dextrans[5]; in all instances, the solubility data were essentially identical for each test compound, and their curves were superimposable. The dextran solubility curves in Figs. 1 and 4–6 represent the behavior of both high and low molecular weight dextrans and indicate that the molecular weight of dextran was not a factor in these solubility phenomena. Dextran, a linear glucose polymer, forms colloidal solutions in water, and it is possible that drug molecules may be dispersed or adsorbed on the colloidal particles. Starches rich in amylose (25), cyclodextrins, and modified dextrans (26) form inclusion compounds and are capable of complexing with various drug molecules.

Acacia and pectin greatly increased cholesterol solubility; however, these carboxylic acid-type polysaccharides significantly decreased progesterone and diethylstilbestrol solubilities and slightly decreased testosterone solubility. On the other hand, heparin, a highly sulfated mucopolysaccharide, decreased cholesterol solubility and increased progesterone, testosterone, and diethylstilbestrol solubilities. Carrageenans[10]

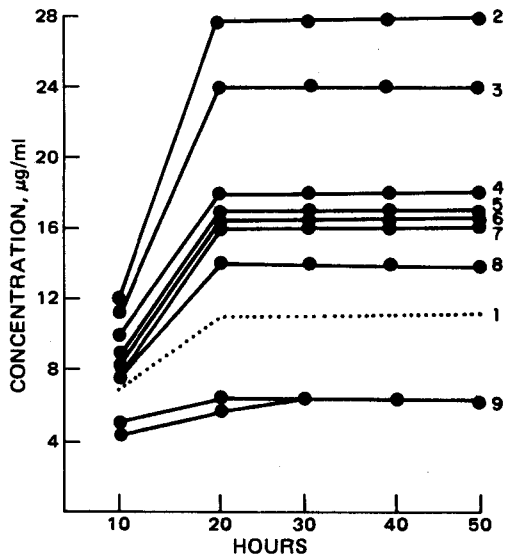


**Figure 5**—*Effect of various macromolecules on the aqueous solubility of progesterone at 30°. Key: 1, water; 2, 6% polyvinylpyrrolidone; 3, 3% polyvinylpyrrolidone; 4, 1% polyvinylpyrrolidone; 5, 10% dextran; 6, 6% dextran; 7, 2% dextran; 8, 1% heparin; and 9, 0.5% pectin, 0.5% acacia, or 0.1% carrageenans.*

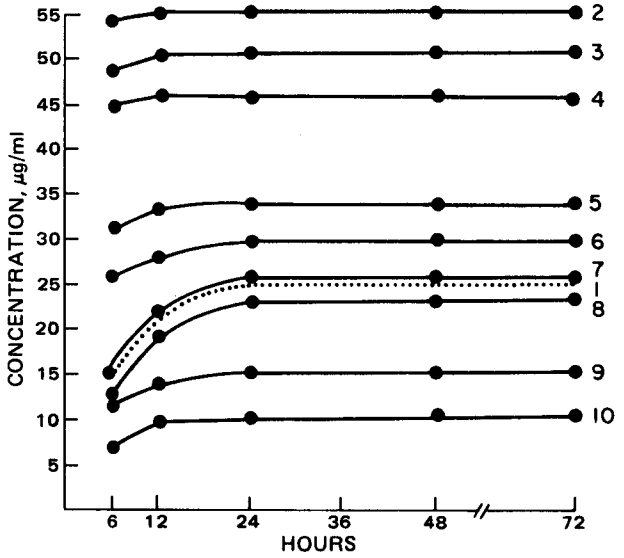


**Figure 6**—*Effect of various macromolecules on the aqueous solubility of diethylstilbestrol at 30°. Key: 1, water; 2, 6% polyvinylpyrrolidone; 3, 3% polyvinylpyrrolidone; 4, 10% dextran; 5, 1% polyvinylpyrrolidone; 6, 1% heparin; 7, 6% dextran; 8, 0.1% carrageenans; 9, 0.5% acacia; and 10, 0.5% pectin.*

(sulfated polysaccharides) at the 0.1% level significantly decreased the solubilities of cholesterol, progesterone, and testosterone and had little effect on diethylstilbestrol solubility. A pattern emerges that indicates that acid-type polysaccharides will interact and solubilize a very nonpolar, lipophilic molecule such as cholesterol and interact and reduce the solubilities of other more polar hormone compounds, whereas the opposite behavior occurs for the sulfated polysaccharides. This pattern holds for acacia, pectin, and heparin; however, the consistency appears to break down for the carrageenans, which decreased the solubility of cholesterol and other hormone compounds. This finding is not surprising since the carrageenans are strongly charged anionic polyelectrolytes of large size and can probably enter into reactions with other substances through several mechanisms involving ionic bonding, hydrogen bonding, or van der Waals forces.

Graham *et al.* (27) studied the complex formation between hydrocolloids and tranquilizers and hypotensive agents and found that the sulfated polysaccharides were the most reactive and that the carrageenans formed insoluble complexes with reserpine, chlorpromazine hydrochlo-

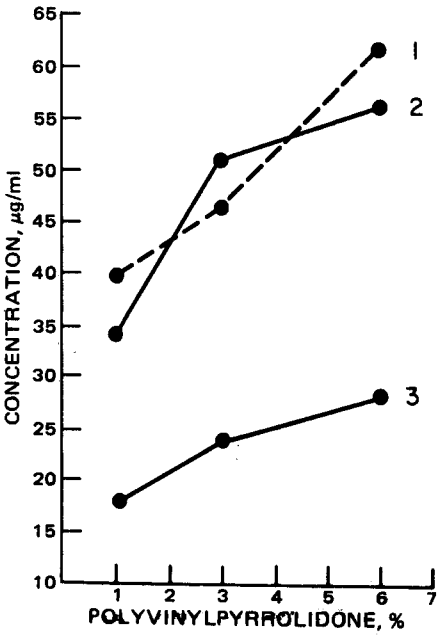


**Figure 7**—*Effect of polyvinylpyrrolidone on the aqueous solubility of testosterone (1), diethylstilbestrol (2), and progesterone (3) at equilibrium at 30°.*

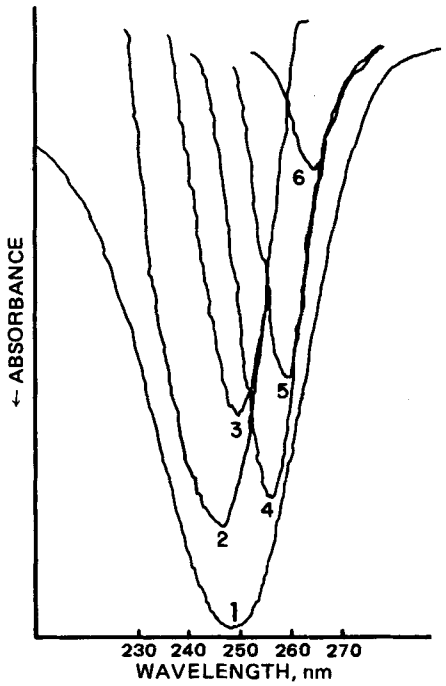


**Figure 8**—*Effect of polyvinylpyrrolidone on the absorption spectra of testosterone and progesterone. Key: 1, water; 2, 0.5%; 3, 1%; 4, 5%; 5, 10%; and 6, 20%.*

ride, and promazine hydrochloride. They reported the relative reactivities of four types of carrageenans with these drugs to be from 16 to 10 while the relative reactivities of acacia and pectin with the same drugs were 0.15 to 0.01. Pectin also formed precipitates with promazine and chlorpromazine hydrochlorides but not with reserpine; acacia did not precipitate any of these drugs (27). In the current study, the processes that bring about solubilization or decreased solubility phenomena of cholesterol and hormone drugs by various macromolecules are very difficult to describe qualitatively and quantitatively because of the complexities of both the hormone drugs and macromolecules (especially the natural hydrocolloids).

Polyvinylpyrrolidone significantly increased the testosterone, progesterone, and diethylstilbestrol solubilities (Fig. 7) and decreased cholesterol solubility (Fig. 2). Both increases and decreases in solubility were dependent on the polyvinylpyrrolidone concentration. Polyvinylpyrrolidone has the ability to complex with drugs, dyes, toxins, and other substances, and these complexes may be water soluble or water insoluble (28). Numerous investigations have been carried out on and mechanisms advanced for the binding of polyvinylpyrrolidone with drugs, preservatives, and organic ions such as dyes (29–40). Jurgensen Eide and Speiser (29, 30) reported that ionic compounds having an —OH, —$NH_2$, or —COOH group showed a higher degree of complexation than compounds without such groups and suggested that the complexing tendency was due to hydrogen bonding. Frank (26) suggested that van der Waals forces between the aromatic system of erythrosine ions and the paraffinic chain of the polyvinylpyrrolidone molecule are responsible for the binding of this dye. Higuchi and Kuramoto (31, 32) also suggested that the polyvinylpyrrolidone molecule could associate through ion dipole and van der Waals interactions. The polyvinylpyrrolidone molecule does not have an ionizable group; however, the lactam bond in the pyrrolidone ring represents a dipole that may undergo ion–dipole interaction with anions and aid in their binding by supplying the necessary attraction force to bring the two components into close contact (37).

Figures 8 and 9 show the effect of polyvinylpyrrolidone on the absorption spectra of testosterone and progesterone. As the polyvinylpyrrolidone concentration increased, the absorbance also increased. This bathochromic effect indicated an attachment between the polymer and the C=O group of the hormones. Anderson and Boyce (38) observed similar behavior in the interaction between erythrosine and polyvinylpyrrolidone, and other investigators (36, 37) attributed the bathochromic shifts observed between polyvinylpyrrolidone and erythrosine sodium dye to charge transfer or van der Waals forces, and Anderson and Boyce supported this suggestion (38). The decrease in the $\lambda_{max}$ with the low (0.5%) concentration of polyvinylpyrrolidone might indicate micellar solubilization (41).

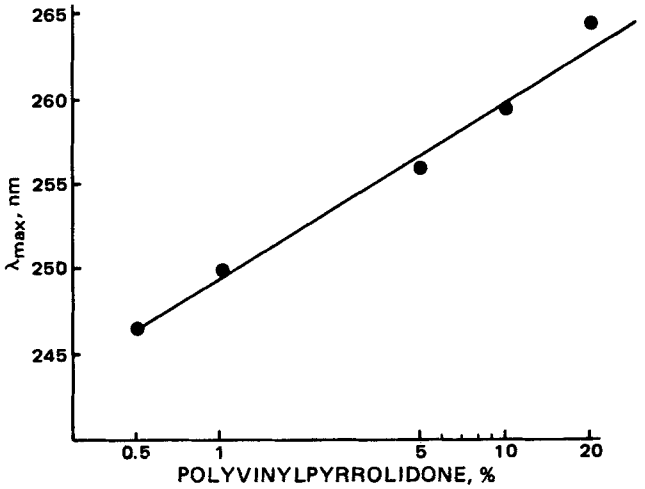


**Figure 9**—*Effect of polyvinylpyrrolidone solutions on the $\lambda_{max}$ of testosterone and progesterone.*

With the carrageenans (0.25 and 0.5%), a slight shift toward longer wavelength was observed (from 249 to 252.5 nm), indicating direct participation with the carbonyl groups of progesterone and testosterone. No change was observed in the $\lambda_{max}$ of testosterone or progesterone in aqueous solutions containing various concentrations (0.25–20%) of dextran, acacia, and pectin. That the shifts were not due to changes in pH or ionic strength of the system was confirmed by the absence of changes in the $\lambda_{max}$ after the addition of acid, base, or 0.1 *M* NaCl.

## REFERENCES

(1) A. F. Wells and B. J. Ershoff, *J. Nutr.*, **74**, 87 (1961).

(2) H. Fisher, P. Griminger, and W. Siller, *Fed. Proc. Fed. Am. Soc. Exp. Biol.*, **24**, 263 (1965).

(3) A. Keys, F. Grande, and J. T. Anderson, *Proc. Soc. Exp. Biol. Med.*, **106**, 555 (1961).

(4) R. M. Kay, P. A. Judd, and A. S. Truswell, *Am. J. Clin. Nutr.*, **31**, 562 (1978).

(5) H. Fisher, G. W. Van der Woot, W. S. McGrath, and P. Griminger, *J. Atheroscler. Res.*, **6**, 190 (1966).

(6) T. M. Lin, K. S. Kim, E. Karvinen, and A. C. Ivy, *Am. J. Physiol.*, **188**, 66 (1957).

(7) A. W. Mollison and J. B. Rennie, *Br. Med. J.*, **1**, 893 (1954).

(8) G. Wallneius, *Nord. Med.*, **57**, 283 (1957).

(9) C. T. Flotte and R. W. Buxton, *Circulation (Suppl.)*, **28**, 721 (1963). *Ibid.*, **32**, 85 (1965).

(10) D. M. Brahmankar and W. E. Connor, *Circ. Res.*, **21**, 817 (1967).

(11) J. Ditzel and J. Dyerberg, *J. Atheroscler. Res.*, **10**, 5 (1969).

(12) H. Engelberg, R. Kuhn, and M. Steiman, *Circulation*, **23**, 489 (1956).

(13) L. Horlick and G. Duff, *Arch. Pathol.*, **57**, 417, 495 (1954).

(14) G. Szag and F. Harder, *ibid.*, **56**, 36 (1953).

(15) B. Ershoff and A. F. Wells, *Proc. Soc. Exp. Biol. Med.*, **110**, 580 (1962).

(16) K. Murata, *Nature*, **191**, 189 (1961).

(17) J. C. Allen, J. H. Baxter, and H. Goodman, *J. Clin. Invest.*, **40**, 499 (1961).

(18) D. K. Madan and D. E. Cadwallader, *J. Pharm. Sci.*, **59**, 1363 (1970).

(19) R. Hahnel, *J. Steroid Biochem.*, **2**, 61 (1971).

(20) G. A. Bray, *Anal. Biochem.*, **1**, 279 (1960).

(21) D. K. Madan and D. E. Cadwallader, *J. Pharm. Sci.*, **62**, 1567 (1973).

(22) A. L. Thakker and N. A. Hall, *ibid.*, **56**, 1121 (1967).

(23) *Ibid.*, **57**, 1394 (1968).

(24) *Ibid.*, **58**, 68 (1969).

(25) E. Guth and Z. Mansour, *J. Pharm. Sci.*, **57**, 404 (1968).

(26) S. G. Frank, *ibid.*, **64**, 1585 (1975).

(27) H. Graham, Y. M. Baker, and A. N. Njoku-obi, *ibid.*, **52**, 192 (1963).

(28) "PVP—An Annotated Bibliography, 1951–1966," vol. 1, General Aniline & Film Corp., New York, N.Y., 1967, pp. 13–20.

(29) G. Jurgensen Eide and P. Speiser, *Acta Pharm. Suec.*, **4**, 185

(1967).
(30) *Ibid.*, **4**, 20 (1967).
(31) T. Higuchi and R. Kuramoto, *J. Am. Pharm. Assoc., Sci. Ed.*, **43**, 393 (1954).
(32) *Ibid.*, **43**, 398 (1954).
(33) G. M. Miyawaki, N. K. Patel, and H. B. Kostenbauder, *ibid.*, **48**, 315 (1959).
(34) D. Guttman and T. Higuchi, *ibid.*, **45**, 659 (1956).
(35) P. Molyneux and H. P. Frank, *J. Am. Chem. Soc.*, **83**, 3169 (1961).
(36) H. P. Frank, S. Barkin, and T. R. Eirich, *J. Phys. Chem.*, **61**, 1375 (1957).
(37) R. E. Phares, Jr., *J. Pharm. Sci.*, **57**, 53 (1968).
(38) J. C. Anderson and G. M. Boyce, *ibid.*, **58**, 1425 (1969).
(39) A. P. Simonelli, S. C. Mehta, and W. I. Higuchi, *ibid.*, **59**, 633 (1970).
(40) M. J. Cho, A. G. Mitchell, and M. Pernarowski, *ibid.*, **60**, 720 (1971).
(41) S. Riegelman, N. A. Allawalla, M. K. Hrenoff, and L. A. Strait, *J. Colloid Sci.*, **13**, 208 (1958).

# Analysis of Pilocarpine and Isopilocarpine in Ophthalmic Solutions by Normal-Phase High-Performance Liquid Chromatography

**DANNY L. DUNN ˣ, BRITT S. SCOTT, and EDWIN D. DORSEY**

Received June 26, 1980, from *New Product Research/Analytical Chemistry, Alcon Laboratories, Inc., Fort Worth, TX 76101.* Accepted for publication October 2, 1980.

**Abstract** □ A normal-phase high-performance liquid chromatographic separation for pilocarpine and isopilocarpine was developed which is suitable for the routine analysis of ophthalmic preparations. The method utilizes a column packed with 5-μm silica with a mobile phase of hexane–2% ammonium hydroxide in 2-propanol (70:30). Peak detection is by UV at 220 nm. It is suggested that a partition separation mechanism is involved rather than adsorption. A separation factor ($\alpha$) of 1.17 was obtained with a relative separation ($R_s$) of 2.13. Column lifetimes were typically 6–8 months with daily use. Several standard pilocarpine–isopilocarpine mixtures and five commercially available ophthalmic solutions from different manufacturers were analyzed. The method was specific for pilocarpine and isopilocarpine in the presence of each other and pilocarpic acid and is a significant improvement over the nonspecific colorimetric methods of analysis.

**Keyphrases** □ Pilocarpine—high-performance liquid chromatographic analysis in the presence of isopilocarpine, ophthalmic solutions □ Isopilocarpine—high-performance liquid chromatographic analysis in the presence of pilocarpine, ophthalmic solutions □ High-performance liquid chromatography—separation of pilocarpine and isopilocarpine, ophthalmic solutions

Pilocarpine, a widely used alkaloid, possesses several important pharmacological properties. For example, it is a miotic and lowers intraocular pressure. The major ophthalmic application of pilocarpine has been for the treatment of glaucoma. The structure of pilocarpine is well established and contains both an imidazole and a lactone.

In aqueous solution, pilocarpine (I) decomposes through two major pathways, which are both base catalyzed (Scheme I). The lactone ring can undergo hydrolysis, resulting in the formation of pilocarpic acid (II), or epimerization can occur at the $\alpha$-carbon to form isopilocarpine (III). Both pilocarpic acid and isopilocarpine are essentially pharmacologically inactive (1, 2).

## BACKGROUND

Analytical methods to measure the extent of pilocarpine degradation in ophthalmic medications have been published, but most cannot differentiate between pilocarpine and isopilocarpine. For instance, the USP method for determining pilocarpine is a colorimetric assay based on the formation of hydroxamic acid (3). Since the moiety responsible for producing color is an intact lactone ring, the assay can distinguish between pilocarpine and pilocarpic acid but not between pilocarpine and isopilocarpine (4). This flaw is serious since recent studies indicated that the primary degradation product of pilocarpine is not pilocarpic acid but its diastereomer, isopilocarpine (4).

Several techniques have been investigated to produce an analytical separation of pilocarpine and isopilocarpine. Some of the published methods include TLC (5), NMR (6–9), IR spectroscopy (10), GLC (8, 11), and polarimetry (12, 13). However, most of these separations are not suitable for development into a routine analysis. The reported TLC separation is questionable and could not be duplicated by one investigator (10); the NMR analysis requires an expensive 100-MHz instrument (10); IR analysis gives poor results when one diastereomer predominates (10), which is usually the case in ophthalmic solutions; and GLC requires derivatization prior to analysis, which makes multiple-sample runs too time consuming. Of these techniques, only polarimetry seems to have practical value. In fact, a UV–optical rotation analysis has been used successfully by this laboratory for several years[1].

The UV–optical rotation method requires elaborate sample preparation and is tedious in actual practice. An analytical procedure such as high-performance liquid chromatography (HPLC), which minimizes sample preparation and retains a high separation capability, would be highly desirable, and several HPLC separations of pilocarpine and isopilocarpine have been reported. Initially, ion-exchange columns packed with cation-exchange resins[2] were used with UV peak detection at 217 nm (4). Unfortunately, these HPLC systems gave variable peak retention times and generally produced erratic results (10, 14).

Khalil (15) reported an HPLC analysis for pilocarpine using an octa-

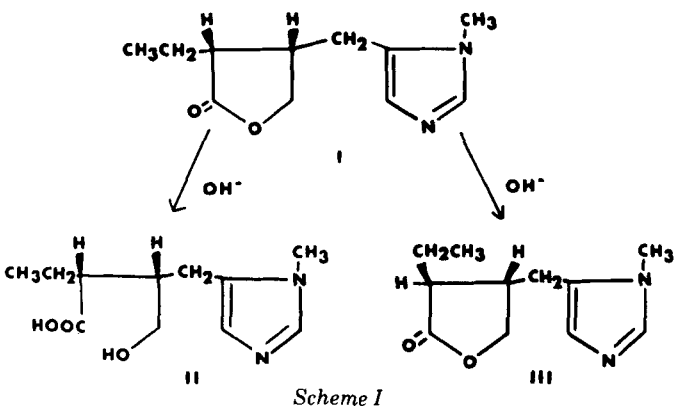


*Scheme I*

[1] See B. S. Scott, D. L. Dunn, and E. D. Dorsey, *J. Pharm. Sci.*, in press.
[2] Aminex A-7 (7–11 μm), Bio-Rad Laboratories.



*0022-3549/81/0400-0446$01.00/0*
*© 1981, American Pharmaceutical Association*

(1967).
(30) *Ibid.*, **4**, 20 (1967).
(31) T. Higuchi and R. Kuramoto, *J. Am. Pharm. Assoc., Sci. Ed.*, **43**, 393 (1954).
(32) *Ibid.*, **43**, 398 (1954).
(33) G. M. Miyawaki, N. K. Patel, and H. B. Kostenbauder, *ibid.*, **48**, 315 (1959).
(34) D. Guttman and T. Higuchi, *ibid.*, **45**, 659 (1956).
(35) P. Molyneux and H. P. Frank, *J. Am. Chem. Soc.*, **83**, 3169 (1961).
(36) H. P. Frank, S. Barkin, and T. R. Eirich, *J. Phys. Chem.*, **61**, 1375 (1957).
(37) R. E. Phares, Jr., *J. Pharm. Sci.*, **57**, 53 (1968).
(38) J. C. Anderson and G. M. Boyce, *ibid.*, **58**, 1425 (1969).
(39) A. P. Simonelli, S. C. Mehta, and W. I. Higuchi, *ibid.*, **59**, 633 (1970).
(40) M. J. Cho, A. G. Mitchell, and M. Pernarowski, *ibid.*, **60**, 720 (1971).
(41) S. Riegelman, N. A. Allawalla, M. K. Hrenoff, and L. A. Strait, *J. Colloid Sci.*, **13**, 208 (1958).

# Analysis of Pilocarpine and Isopilocarpine in Ophthalmic Solutions by Normal-Phase High-Performance Liquid Chromatography

**DANNY L. DUNN ˣ, BRITT S. SCOTT, and EDWIN D. DORSEY**

Received June 26, 1980, from *New Product Research/Analytical Chemistry, Alcon Laboratories, Inc., Fort Worth, TX 76101.* Accepted for publication October 2, 1980.

**Abstract** □ A normal-phase high-performance liquid chromatographic separation for pilocarpine and isopilocarpine was developed which is suitable for the routine analysis of ophthalmic preparations. The method utilizes a column packed with 5-μm silica with a mobile phase of hexane–2% ammonium hydroxide in 2-propanol (70:30). Peak detection is by UV at 220 nm. It is suggested that a partition separation mechanism is involved rather than adsorption. A separation factor ($\alpha$) of 1.17 was obtained with a relative separation ($R_s$) of 2.13. Column lifetimes were typically 6–8 months with daily use. Several standard pilocarpine–isopilocarpine mixtures and five commercially available ophthalmic solutions from different manufacturers were analyzed. The method was specific for pilocarpine and isopilocarpine in the presence of each other and pilocarpic acid and is a significant improvement over the nonspecific colorimetric methods of analysis.

**Keyphrases** □ Pilocarpine—high-performance liquid chromatographic analysis in the presence of isopilocarpine, ophthalmic solutions □ Isopilocarpine—high-performance liquid chromatographic analysis in the presence of pilocarpine, ophthalmic solutions □ High-performance liquid chromatography—separation of pilocarpine and isopilocarpine, ophthalmic solutions

Pilocarpine, a widely used alkaloid, possesses several important pharmacological properties. For example, it is a miotic and lowers intraocular pressure. The major ophthalmic application of pilocarpine has been for the treatment of glaucoma. The structure of pilocarpine is well established and contains both an imidazole and a lactone.

In aqueous solution, pilocarpine (I) decomposes through two major pathways, which are both base catalyzed (Scheme I). The lactone ring can undergo hydrolysis, resulting in the formation of pilocarpic acid (II), or epimerization can occur at the $\alpha$-carbon to form isopilocarpine (III). Both pilocarpic acid and isopilocarpine are essentially pharmacologically inactive (1, 2).

## BACKGROUND

Analytical methods to measure the extent of pilocarpine degradation in ophthalmic medications have been published, but most cannot differentiate between pilocarpine and isopilocarpine. For instance, the USP method for determining pilocarpine is a colorimetric assay based on the formation of hydroxamic acid (3). Since the moiety responsible for producing color is an intact lactone ring, the assay can distinguish between pilocarpine and pilocarpic acid but not between pilocarpine and isopilocarpine (4). This flaw is serious since recent studies indicated that the primary degradation product of pilocarpine is not pilocarpic acid but its diastereomer, isopilocarpine (4).

Several techniques have been investigated to produce an analytical separation of pilocarpine and isopilocarpine. Some of the published methods include TLC (5), NMR (6–9), IR spectroscopy (10), GLC (8, 11), and polarimetry (12, 13). However, most of these separations are not suitable for development into a routine analysis. The reported TLC separation is questionable and could not be duplicated by one investigator (10); the NMR analysis requires an expensive 100-MHz instrument (10); IR analysis gives poor results when one diastereomer predominates (10), which is usually the case in ophthalmic solutions; and GLC requires derivatization prior to analysis, which makes multiple-sample runs too time consuming. Of these techniques, only polarimetry seems to have practical value. In fact, a UV–optical rotation analysis has been used successfully by this laboratory for several years[1].

The UV–optical rotation method requires elaborate sample preparation and is tedious in actual practice. An analytical procedure such as high-performance liquid chromatography (HPLC), which minimizes sample preparation and retains a high separation capability, would be highly desirable, and several HPLC separations of pilocarpine and isopilocarpine have been reported. Initially, ion-exchange columns packed with cation-exchange resins[2] were used with UV peak detection at 217 nm (4). Unfortunately, these HPLC systems gave variable peak retention times and generally produced erratic results (10, 14).

Khalil (15) reported an HPLC analysis for pilocarpine using an octa-

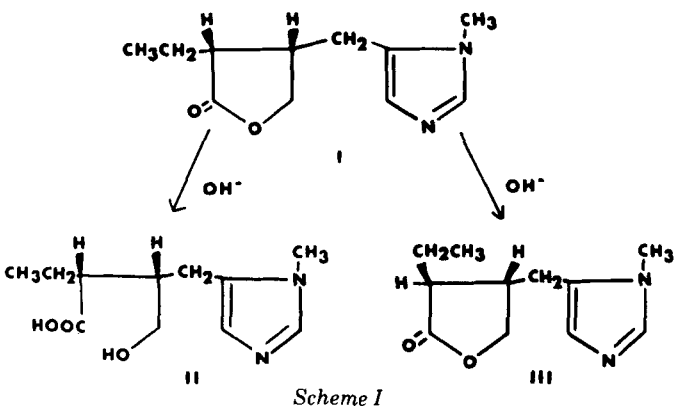


*Scheme I*

[1] See B. S. Scott, D. L. Dunn, and E. D. Dorsey, *J. Pharm. Sci.*, in press.
[2] Aminex A-7 (7–11 μm), Bio-Rad Laboratories.



*0022-3549/81/0400-0446$01.00/0*
*© 1981, American Pharmaceutical Association*

**Table I—Pilocarpine Hydrochloride Analysis of Standard Mixtures**

| Pilocarpine Hydrochloride, mg/ml | Isopilocarpine Nitrate, mg/ml | Pilocarpine Peak Height, cm | Peak Height/ Concentration, cm/mg/ml | Pilocarpine Hydrochloride Concentration Found[a], mg/ml | Recovery, % |
|---|---|---|---|---|---|
| 1.12 | 0.080 | 8.95 | 7.99 | 1.12 | 100.0 |
| 1.12 | 0.080 | 9.00 | 8.04 | 1.13 | 100.9 |
| 1.36 | 0.080 | 10.95 | 8.05 | 1.37 | 100.7 |
| 1.36 | 0.080 | 11.00 | 8.09 | 1.38 | 101.5 |
| 1.60 | 0.080 | 12.85 | 8.03 | 1.61 | 100.6 |
| 1.60 | 0.080 | 12.85 | 8.03 | 1.61 | 100.6 |
| 1.84 | 0.080 | 14.65 | 7.96 | 1.84 | 100.0 |
| 1.84 | 0.080 | 14.65 | 7.96 | 1.84 | 100.0 |
| 2.08 | 0.080 | 16.75 | 8.05 | 2.10 | 101.1 |
| 2.08 | 0.080 | 16.75 | 8.05 | 2.10 | 101.1 |

[a] A standard containing 1.60 mg of pilocarpine hydrochloride/ml was used to calculate these concentrations.

**Table II—Isopilocarpine Nitrate Analysis of Standard Mixtures**

| Pilocarpine Hydrochloride, mg/ml | Isopilocarpine Nitrate, mg/ml | Isopilocarpine Peak Height, cm | Peak Height/ Concentration, cm/mg/ml | Isopilocarpine Nitrate Concentration Found[a], mg/ml | Recovery, % |
|---|---|---|---|---|---|
| 1.61 | 0.0367 | 2.45 | 66.75 | 0.0367 | 100.0 |
| 1.61 | 0.0367 | 2.45 | 66.75 | 0.0367 | 100.0 |
| 1.61 | 0.0735 | 4.90 | 66.67 | 0.0735 | 100.0 |
| 1.61 | 0.0735 | 4.80 | 65.31 | 0.0720 | 98.0 |
| 1.61 | 0.1102 | 7.25 | 65.79 | 0.1087 | 98.6 |
| 1.61 | 0.1102 | 7.25 | 65.79 | 0.1087 | 98.6 |
| 1.61 | 0.1470 | 9.80 | 66.67 | 0.1469 | 99.9 |
| 1.61 | 0.1470 | 9.70 | 65.99 | 0.1454 | 98.9 |
| 1.61 | 0.1837 | 12.30 | 66.96 | 0.1844 | 100.4 |

[a] A standard containing 0.1102 mg of isopilocarpine nitrate/ml was used to calculate these concentrations.

decylsilane[3] and cyanopropylsilane[4] column in series. However, no separation of isopilocarpine was demonstrated, and UV peak detection was at 254 nm. Since neither pilocarpine nor isopilocarpine absorb appreciably at 254 nm, this procedure seems questionable. More recently, a system using a noncommercial octadecylsilane column[5] with refractive index detection was reported (14). With commercially available columns and UV detection at 215 nm, the separation between pilocarpine and isopilocarpine was insufficient for a good analytical procedure.

An HPLC separation for pilocarpine and isopilocarpine is discussed here; a commercially available silica column[6] with UV peak detection at 220 nm is used. This normal-phase system was satisfactory for the routine analysis of pilocarpine or isopilocarpine in ophthalmic solutions. Data are included to demonstrate that the procedure gives a linear response and is specific. The actual analysis of five ophthalmic products from different manufacturers is presented, and several methods of pilocarpine analysis are compared.

## EXPERIMENTAL

**Reagents and Solvents**—Pilocarpine hydrochloride USP and isopilocarpine nitrate[7] (reagent grade) were used without further purification. Hexane[8] was UV grade; 2-propanol[8], methanol[8], and ammonium hydroxide were reagent grade.

**Equipment**—A liquid chromatograph equipped with a high-pressure pump[9], a variable-wavelength UV detector[10], a fixed-loop injector[11], and a strip-chart recorder[12] was used with a 25-cm × 4.6-mm i.d. column packed with 5-μm silica[6]. No precolumn was used.

**Mobile Phase**—Concentrated ammonium hydroxide (10.0 ml) was diluted to 500 ml with 2-propanol. This 2% ammonium hydroxide solution (300 ml) was mixed with hexane (700 ml) and filtered through a 0.5-μm filter[13] before use.

**HPLC Analysis Conditions**—The mobile phase was pumped through the column at a flow rate of 2.0 ml/min. UV detection was at 220 nm, and the attenuation used for isopilocarpine analysis was four times more sensitive than for pilocarpine analysis. The injection size was 10 μl for pilocarpine and 20 μl for isopilocarpine. The plate count for the silica column, determined at a chart speed of 1.27 cm/min with a 1.60-mg/ml pilocarpine hydrochloride solution, was 8000 plates/m[14]. After completion of the analysis, hexane was pumped through the silica column prior to storage.

**Preparation of Standard Solutions**—The following methanol dilutions were made with a pilocarpine hydrochloride or an isopilocarpine nitrate stock solution:

1. Pilocarpine standard curve—five samples were prepared over the concentration range of 1.12–2.08 mg of pilocarpine hydrochloride/ml. Each solution also contained 0.080 mg of isopilocarpine nitrate/ml.
2. Isopilocarpine standard curve—five samples were prepared over the concentration range of 0.037–0.184 mg of isopilocarpine nitrate/ml. Each solution also contained 1.61 mg of pilocarpine hydrochloride/ml.

**Preparation of Commercially Available Ophthalmic Products**—Aliquots of each sample were pipetted accurately into separate volumetric flasks and diluted with methanol to obtain a final concentration of ~1.6 mg of pilocarpine hydrochloride/ml. The resulting solutions were injected directly into the liquid chromatograph. The concentration of pilocarpine or isopilocarpine then was determined by comparing the sample peak height with the peak height of a pilocarpine or isopilocarpine standard, respectively.

## RESULTS AND DISCUSSION

Standard solutions containing pilocarpine and isopilocarpine in the ratio of about 19:1 were prepared and analyzed (Tables I and II). This pilocarpine to isopilocarpine ratio corresponds to what would be expected from the analysis of an actual ophthalmic solution. By using the normal-phase HPLC system described under *Experimental*, pilocarpine eluted at ~16 min and isopilocarpine eluted at ~20 min.

Pilocarpine and isopilocarpine had capacity factors ($K'$) of 12.07 and 14.13, respectively[15]. These factors correspond to a separation factor ($\alpha$)

[3] μBondapak $C_{18}$ (10 μm), Waters Associates.
[4] μBondapak CN (10 μm), Waters Associates.
[5] The packing material was LiChrosorb RP-18 (10 μm), E. Merck.
[6] Si 60 Hibar (5 μm), E. Merck.
[7] Aldrich Chemical Co.
[8] Burdick & Jackson "Distilled in Glass".
[9] M-6000A, Waters Associates.
[10] Model SF 770, Schoeffel Instruments.
[11] Model 710A, Rheodyne.
[12] Omniscribe model A5111-1, Houston Instruments.
[13] Fluoropore, Millipore Corp.

[14] Theoretical plates per meter ($N$) = 16 $(T/T_w)^2(100/L)$, where $T$ is the retention time of pilocarpine, $T_w$ is the peak width of pilocarpine measured along the baseline, and $L$ is the column length in centimeters (16).
[15] An injection of carbon tetrachloride was used to determine the elution time of a nonretained sample (*i.e.*, $T_0$).

**Table III—Determination of Pilocarpine and Isopilocarpine in Various Commercial Pilocarpine Ophthalmic Solutions**

| Manufacturer | Concentration, Salt | Pilocarpine Analysis[a], % HPLC | Pilocarpine Analysis[a], % USP[b] | Pilocarpine Analysis[a], % UV–Optical Rotation[c] | Isopilocarpine Analysis[a], % HPLC | Isopilocarpine Analysis[a], % UV–Optical Rotation[c] | pH |
|---|---|---|---|---|---|---|---|
| 1 | 2%, HCl | 101, 100 | 100, 98 | 99, 98 | 0.7, 0.8 | 0.0, 0.8 | 3.75 |
| 2 | 2%, HCl | 98, 99 | 99, 99 | 97, 99 | 0.9, 1.0 | 0.0, 1.0 | 3.63 |
| 3 | 2%, $HNO_3$ | 94, 95 | 127, 128[d] | 105, 108[d] | 1.2, 1.2 | 0.0, 4.0 | 4.50 |
| 4 | 1%, HCl | 94, 96 | 95, 96 | 96, 95 | 1.4, 1.4 | 2.7, 4.4 | 4.22 |
| 5 | 2%, HCl | 102, 101 | 103, 104 | 99, 100 | 3.7, 3.6 | 3.7, 3.9 | 4.16 |

[a] Percent labeled amount of pilocarpine salt. [b] The current USP method for pilocarpine analysis is reaction with hydroxylamine to form hydroxamic acid and subsequent colorimetric analysis. [c] B. S. Scott, D. L. Dunn, and E. D. Dorsey, *J. Pharm. Sci.*, in press. [d] This sample contained polyvinyl alcohol, which caused noticeable positive interference when analyzed by the USP and UV–optical rotation methods.

of 1.17. Since $\alpha$ is $\leq 1.20$, this separation can be classified as "moderately difficult" using Snyder and Kirkland's terminology (16). This finding is not surprising since only subtle polarity differences exist between the two diastereomers. A relative separation ($R_s$) of 2.13 was calculated[16], which means a quantitative separation suitable for an analytical procedure was obtained (16). Typical chromatograms are given in Figs. 1 and 2.

The average recoveries obtained for the analysis of pilocarpine and isopilocarpine standards were 100.7 and 99.4%, respectively. These values indicate that the method is specific for each diastereomer in the presence of the other. In addition, a plot of concentration *versus* peak height gave a linear curve that intercepted the origin. A least-squares analysis of the data in Tables I and II yielded a correlation coefficient of 0.9997 and a $y$ intercept of 0.02 cm for the pilocarpine analysis. For the isopilocarpine analysis, the correlation coefficient was 0.9998 and the $y$ intercept was −0.04 cm. The use of peak areas instead of peak heights to measure response might possibly produce more accurate results. However, a suitable integrator was not available, and peak height measurements gave acceptable recoveries and standard curve statistics for a routine analysis.

A pilocarpic acid sample was prepared using a previously described method (14, 15). Pilocarpine hydrochloride was subjected to basic hydrolysis, neutralized, and injected directly into the liquid chromatograph. No peak for pilocarpic acid was observed after 60 min. Therefore, analysis of carpic acids (*i.e.*, pilocarpic acid and isopilocarpic acid) requires another technique, such as UV spectroscopy, which can determine the total imidazole present (*i.e.*, pilocarpine, isopilocarpine, pilocarpic acid, and isopilocarpic acid). After pilocarpine and isopilocarpine analysis, total carpic acids then may be found by taking the difference.

Five different manufacturers's commercially available pilocarpine ophthalmic solutions were analyzed for pilocarpine and isopilocarpine content (Table III). These solutions contained excipients usually found in ophthalmic formulations, such as benzalkonium chloride, chlorobutanol, edetate disodium, sodium acetate, citric acid, boric acid, menthol, camphor, and hydroxypropyl methylcellulose. The USP colorimetric analysis for pilocarpine was compared to the normal-phase HPLC analysis and the UV–optical rotation analysis. This latter method is based on the difference in optical rotation shown by pilocarpine and isopilocarpine, and details will be published elsewhere[1].

Excipient interference was noticed in only one sample, which contained polyvinyl alcohol (Manufacturer 3, Table III). Accurate analysis of this sample was difficult using the USP method. Less interference was noted with the UV–optical rotation method, but the HPLC analysis seemed to be completely unaffected. With this one exception, all three pilocarpine analyses gave similar results. The isopilocarpine analysis by HPLC ranged from 0.7 to 3.7% of the labeled pilocarpine concentration. In general, there appeared to be a higher isopilocarpine content in more basic solutions. This relationship was observed previously (10).

Attempts to improve the HPLC analysis by increasing resolution and decreasing the retention time were unsuccessful. Mobile phases containing other alcohols, such as methanol, ethanol, or 2-methyl-1-propanol, did not give a comparable separation. Since the silica columns used daily for this analysis had quite remarkable lifetimes (6–8 months with daily use) considering the mobile phase contained 30% 2-propanol, the separation probably is due to a partition mechanism rather than adsorption. 2-Propanol molecules theoretically could be adsorbed on the polar silica sites to form a stationary organic phase. Pilocarpine and isopilocarpine then could be partitioned differently between the mobile phase and the stationary organic phase. This process would explain why other alcohols were not as satisfactory as 2-propanol.

Silica columns containing 10-$\mu$m particles instead of 5-$\mu$m particles can be used for pilocarpine analysis but not isopilocarpine. In general, 10-$\mu$m columns operate at much lower pressures than 5-$\mu$m columns. This operation allows higher flow rates and shorter retention times. Unfortunately, a corresponding decrease in resolution also is observed.

During initial development of the analysis, UV peak detection was at 230 nm but was changed to 215 nm because of a corresponding increase in peak height of 100%. Detection was finally increased to 220 nm to reduce noise and to stabilize the baseline, causing only a 5% decrease in peak

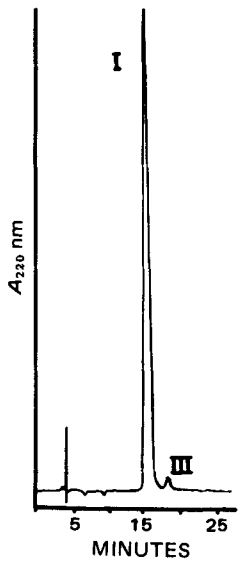


**Figure 1**—*Typical chromatogram for pilocarpine (I) analysis in a 1.60-mg/ml pilocarpine hydrochloride solution containing ~3% isopilocarpine nitrate (III).*

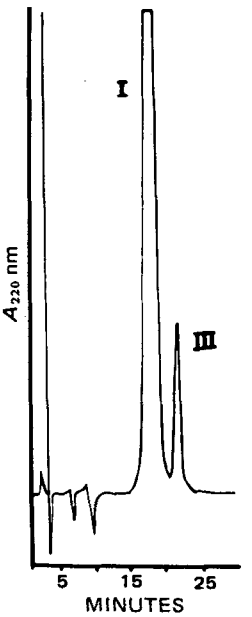


**Figure 2**—*Typical chromatogram for isopilocarpine (III) analysis in a 1.60-mg/ml pilocarpine hydrochloride (I) solution containing ~3% isopilocarpine nitrate.*

[16] $R_s = 2(T_2 - T_1)/(T_{w1} + T_{w2})$, where $T_1$ is the retention time of pilocarpine, $T_2$ is the retention time of isopilocarpine, $T_{w1}$ is the peak width of pilocarpine measured along the baseline, and $T_{w2}$ is the peak width of isopilocarpine measured along the baseline (16).

height. Since the nitrate ion absorbs at this wavelength, an injection of isopilocarpine nitrate solution gave an extra peak at ~40–50 min after injection, presumably due to ammonium nitrate elution. This peak can be avoided, if desired, by first passing the isopilocarpine nitrate sample through an ion-exchange column to replace the nitrate ion with a UV inactive ion.

## REFERENCES


(1) R. K. Hill and S. Barcza, *Tetrahedron*, **22**, 2889 (1966).

(2) R. A. Anderson and J. B. Cowle, *Br. J. Ophthalmol.*, **52**, 607 (1968).

(3) "The United States Pharmacopeia," 20th rev., United States Pharmacopeial Convention, Rockville, Md., 1980, p. 628.

(4) T. Urbanyi, A. Piedmont, E. Willis, and G. Manning, *J. Pharm. Sci.*, **65**, 257 (1976).

(5) V. Massa, F. Gal, P. Susplugas, and G. Maestre, *Trav. Soc. Pharm. Montpellier*, **30**, 267 (1970).

(6) M. A. Nunes and E. Brochmann-Hanssen, *J. Pharm. Sci.*, **63**, 716 (1974).

(7) K. Baeschlin, J. Etter, and H. Moll, *Pharm. Acta Helv.*, **44**, 301 (1969).

(8) H. Link and K. Bernauer, *Helv. Chim. Acta*, **55**, 1053 (1972).

(9) G. A. Neville, F. B. Hasan, and I. C. P. Smith, *Can. J. Chem.*, **54**, 2094 (1976).

(10) J. D. Weber, *J. Assoc. Off. Anal. Chem.*, **59**, 1409 (1976).

(11) W. F. Bayne, L.-C. Chu, and F. T. Tao, *J. Pharm. Sci.*, **65**, 1724 (1976).

(12) P.-H. Chung, T.-F. Chin, and J. L. Lach, *ibid.*, **59**, 1300 (1970).

(13) R. A. Anderson, *Can. J. Pharm. Sci.*, **2**, 25 (1967).

(14) A. Noordam, K. Waliszewski, C. Olieman, L. Maat, and H. C. Beyerman, *J. Chromatogr.*, **153**, 271 (1978).

(15) S. K. W. Khalil, *J. Pharm. Sci.*, **66**, 1625 (1977).

(16) L. R. Snyder and J. J. Kirkland, "Introduction to Modern Liquid Chromatography," Wiley, New York, N.Y., 1974, pp. 25–62.


## ACKNOWLEDGMENTS


The authors thank Karen Haggard, New Product Research/Analytical Chemistry, for technical assistance, Sam Numajiri, Medicinal Chemistry, for preparation of the pilocarpic acid samples, and Linda Brammer, New Products Research/Analytical Chemistry, for proofreading the final manuscript and giving many helpful suggestions.


# Effect of Dosing Volume on Intramuscular Absorption Rate of Aminoglycosides


**MORRIS PFEFFER** ˣ **and DONALD R. VAN HARKEN**



Received July 30, 1980, from the *Department of Drug Metabolism and Pharmacokinetics, Bristol Laboratories, Syracuse, NY 13201.* Accepted for publication September 29, 1980.



**Abstract** □ The Loo–Riegelman method was applied to serum amikacin level data after intravenous and intramuscular administration. Intramuscular amikacin absorption can be described by first-order kinetics, but the absorption rate constant decreased from 1.95 $hr^{-1}$ at a 125-mg dose to 1.00 $hr^{-1}$ at a 750-mg dose. This rate change apparently is a physical phenomenon due to differing dosing volumes at different doses and attendant changes in the surface area to volume ratio at the injection site. Amikacin absorption rates on intramuscular injection can be maximized by giving several smaller injections rather than a single larger injection. This phenomenon should be generally observed with aminoglycoside antibiotics and could be partly responsible for reported variations in absorption rate and the poor predictability of serum concentrations.



**Keyphrases** □ Aminoglycosides—effect of dosing volume on intramuscular absorption rate □ Absorption, intramuscular—aminoglycosides, dosing volume effects □ Amikacin—intramuscular absorption rates, dosing volume effects


In a review of the clinical pharmacokinetics of aminoglycoside antibiotics, Pechere and Dugal (1) referred to reports of wide intramuscular absorption rate variations within and between studies and antibiotics. They commented: "In view of the fact that rates of absorption vary widely, nomograms based on equations which make use of a universal absorption rate constant should be critically examined. This, incidentally, may be partly responsible for the poor predictability of serum aminoglycoside concentrations noted by some authors." According to Greenblatt and Koch-Weser (2), nonlinear intramuscular absorption may be fairly common because local and systemic factors that influence the absorption rate rarely remain constant while absorption is taking place.

In this study, available intravenous and intramuscular amikacin data were used to estimate intramuscular absorption kinetics of an aminoglycoside antibiotic. Since the data were derived from separate studies, mean values were used for the pharmacokinetic parameters and intramuscular serum levels. A crossover intravenous–intramuscular amikacin study at 125- and 500-mg doses was reported, but no estimates of the intramuscular absorption kinetics were made (3).

## EXPERIMENTAL

The data analyzed were drawn from three Phase I amikacin clinical investigations (Studies 1, 2, and 7). The subjects in all three studies were normal, healthy adult males ranging from 21 to 40 years and from 60 to 90 kg.

In Study 7, 7.5 mg/kg was administered intravenously as 5-, 30-, and 60-min infusions. Six subjects received both the 30- and 60-min infusions, according to a balanced crossover design, into an antecubital vein using an infusion pump[1]. Six other subjects received the 5-min infusion as a push injection into an antecubital vein.

In Studies 1 and 2, amikacin was administered into the right or left superior lateral gluteal quadrant. In Study 1, 12 subjects each received 250- and 500-mg doses; some results were previously published (4). In Study 2, three subjects each received 125-, 250-, 500-, or 750-mg doses.

Blood samples were collected for serum preparation, and serum samples were analyzed for amikacin content using a standard cup plate bioassay (5) with *Bacillus subtilis* (ATCC 6633) as the bioassay organism. The minimum quantitative sensitivity of the assay was 0.06 μg/ml. Typically, an analysis of variance of the regression slope of the standard response line (zone diameter *versus* log concentration) yielded $F(1, 3) = 240$.

Mean postinfusion intravenous data were fitted to the biexponential equation for an open, two-compartment model of drug distribution with central compartment elimination only:

$$C = A' \exp(-\alpha t') + B' \exp(-\beta t') \qquad \text{(Eq. 1)}$$

[1] Model 940, Harvard Instrument Co., South Natick, Mass.


*0022-3549/81/0400-0449$01.00/0*


*© 1981, American Pharmaceutical Association*

height. Since the nitrate ion absorbs at this wavelength, an injection of isopilocarpine nitrate solution gave an extra peak at ~40–50 min after injection, presumably due to ammonium nitrate elution. This peak can be avoided, if desired, by first passing the isopilocarpine nitrate sample through an ion-exchange column to replace the nitrate ion with a UV inactive ion.

## REFERENCES


(1) R. K. Hill and S. Barcza, *Tetrahedron*, **22**, 2889 (1966).

(2) R. A. Anderson and J. B. Cowle, *Br. J. Ophthalmol.*, **52**, 607 (1968).

(3) "The United States Pharmacopeia," 20th rev., United States Pharmacopeial Convention, Rockville, Md., 1980, p. 628.

(4) T. Urbanyi, A. Piedmont, E. Willis, and G. Manning, *J. Pharm. Sci.*, **65**, 257 (1976).

(5) V. Massa, F. Gal, P. Susplugas, and G. Maestre, *Trav. Soc. Pharm. Montpellier*, **30**, 267 (1970).

(6) M. A. Nunes and E. Brochmann-Hanssen, *J. Pharm. Sci.*, **63**, 716 (1974).

(7) K. Baeschlin, J. Etter, and H. Moll, *Pharm. Acta Helv.*, **44**, 301 (1969).

(8) H. Link and K. Bernauer, *Helv. Chim. Acta*, **55**, 1053 (1972).

(9) G. A. Neville, F. B. Hasan, and I. C. P. Smith, *Can. J. Chem.*, **54**, 2094 (1976).

(10) J. D. Weber, *J. Assoc. Off. Anal. Chem.*, **59**, 1409 (1976).

(11) W. F. Bayne, L.-C. Chu, and F. T. Tao, *J. Pharm. Sci.*, **65**, 1724 (1976).

(12) P.-H. Chung, T.-F. Chin, and J. L. Lach, *ibid.*, **59**, 1300 (1970).

(13) R. A. Anderson, *Can. J. Pharm. Sci.*, **2**, 25 (1967).

(14) A. Noordam, K. Waliszewski, C. Olieman, L. Maat, and H. C. Beyerman, *J. Chromatogr.*, **153**, 271 (1978).

(15) S. K. W. Khalil, *J. Pharm. Sci.*, **66**, 1625 (1977).

(16) L. R. Snyder and J. J. Kirkland, "Introduction to Modern Liquid Chromatography," Wiley, New York, N.Y., 1974, pp. 25–62.


## ACKNOWLEDGMENTS


The authors thank Karen Haggard, New Product Research/Analytical Chemistry, for technical assistance, Sam Numajiri, Medicinal Chemistry, for preparation of the pilocarpic acid samples, and Linda Brammer, New Products Research/Analytical Chemistry, for proofreading the final manuscript and giving many helpful suggestions.


# Effect of Dosing Volume on Intramuscular Absorption Rate of Aminoglycosides


**MORRIS PFEFFER** ˣ **and DONALD R. VAN HARKEN**



Received July 30, 1980, from the *Department of Drug Metabolism and Pharmacokinetics, Bristol Laboratories, Syracuse, NY 13201.* Accepted for publication September 29, 1980.



**Abstract** □ The Loo–Riegelman method was applied to serum amikacin level data after intravenous and intramuscular administration. Intramuscular amikacin absorption can be described by first-order kinetics, but the absorption rate constant decreased from 1.95 $hr^{-1}$ at a 125-mg dose to 1.00 $hr^{-1}$ at a 750-mg dose. This rate change apparently is a physical phenomenon due to differing dosing volumes at different doses and attendant changes in the surface area to volume ratio at the injection site. Amikacin absorption rates on intramuscular injection can be maximized by giving several smaller injections rather than a single larger injection. This phenomenon should be generally observed with aminoglycoside antibiotics and could be partly responsible for reported variations in absorption rate and the poor predictability of serum concentrations.



**Keyphrases** □ Aminoglycosides—effect of dosing volume on intramuscular absorption rate □ Absorption, intramuscular—aminoglycosides, dosing volume effects □ Amikacin—intramuscular absorption rates, dosing volume effects


In a review of the clinical pharmacokinetics of aminoglycoside antibiotics, Pechere and Dugal (1) referred to reports of wide intramuscular absorption rate variations within and between studies and antibiotics. They commented: "In view of the fact that rates of absorption vary widely, nomograms based on equations which make use of a universal absorption rate constant should be critically examined. This, incidentally, may be partly responsible for the poor predictability of serum aminoglycoside concentrations noted by some authors." According to Greenblatt and Koch-Weser (2), nonlinear intramuscular absorption may be fairly common because local and systemic factors that influence the absorption rate rarely remain constant while absorption is taking place.

In this study, available intravenous and intramuscular amikacin data were used to estimate intramuscular absorption kinetics of an aminoglycoside antibiotic. Since the data were derived from separate studies, mean values were used for the pharmacokinetic parameters and intramuscular serum levels. A crossover intravenous–intramuscular amikacin study at 125- and 500-mg doses was reported, but no estimates of the intramuscular absorption kinetics were made (3).

## EXPERIMENTAL

The data analyzed were drawn from three Phase I amikacin clinical investigations (Studies 1, 2, and 7). The subjects in all three studies were normal, healthy adult males ranging from 21 to 40 years and from 60 to 90 kg.

In Study 7, 7.5 mg/kg was administered intravenously as 5-, 30-, and 60-min infusions. Six subjects received both the 30- and 60-min infusions, according to a balanced crossover design, into an antecubital vein using an infusion pump[1]. Six other subjects received the 5-min infusion as a push injection into an antecubital vein.

In Studies 1 and 2, amikacin was administered into the right or left superior lateral gluteal quadrant. In Study 1, 12 subjects each received 250- and 500-mg doses; some results were previously published (4). In Study 2, three subjects each received 125-, 250-, 500-, or 750-mg doses.

Blood samples were collected for serum preparation, and serum samples were analyzed for amikacin content using a standard cup plate bioassay (5) with *Bacillus subtilis* (ATCC 6633) as the bioassay organism. The minimum quantitative sensitivity of the assay was 0.06 μg/ml. Typically, an analysis of variance of the regression slope of the standard response line (zone diameter *versus* log concentration) yielded $F(1, 3) = 240$.

Mean postinfusion intravenous data were fitted to the biexponential equation for an open, two-compartment model of drug distribution with central compartment elimination only:

$$C = A' \exp(-\alpha t') + B' \exp(-\beta t') \qquad \text{(Eq. 1)}$$

[1] Model 940, Harvard Instrument Co., South Natick, Mass.


*0022-3549/81/0400-0449$01.00/0*


*© 1981, American Pharmaceutical Association*

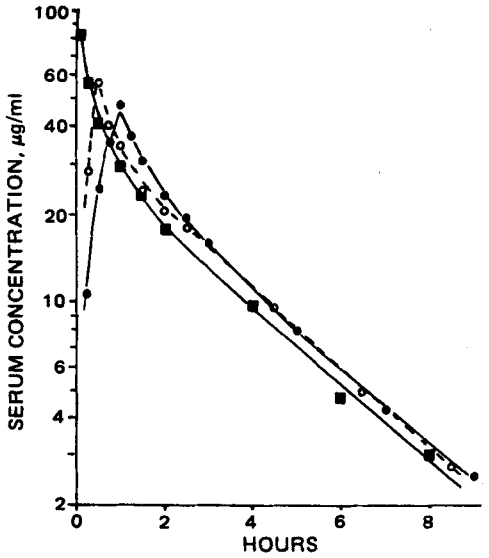


**Figure 1**—*Mean serum amikacin concentrations after intravenous infusion (Study 7). Key: ●, 60-min infusion; ○, 30-min infusion; and ■, 5-min infusion.*

where $C$ is the observed serum concentration at time $t' = t - T$, $t$ is time from the start of the infusion, and $T$ is the duration of the infusion. The fitting was performed by nonlinear regression analysis using the digital computer program NONLIN (6), which employs Hartley's modification of the Gauss–Newton method (7). Goodness of fit was measured using the sum of squares of the deviations of the fitted concentrations ($\hat{C}$) from the observed concentrations:

$$S = \sum(C - \hat{C})^2 \qquad \text{(Eq. 2)}$$

and a coefficient of determination:

$$R^2 = \frac{\sum C^2 - \frac{(\sum C)^2}{n} - S}{\sum C^2 - \frac{(\sum C)^2}{n}} \qquad \text{(Eq. 3)}$$

The coefficients $A'$ and $B'$ were corrected to their equivalent values for intravenous bolus injection, $A$ and $B$, using (8):

$$A = A'\alpha T/[1 - \exp(-\alpha T)] \qquad \text{(Eq. 4a)}$$

$$B = B'\beta T/[1 - \exp(-\beta T)] \qquad \text{(Eq. 4b)}$$

Given $A$, $\alpha$, $B$, and $\beta$, the pharmacokinetic parameters could be calculated according to standard methods (9).

The intramuscular absorption profiles, as percent of dose unabsorbed *versus* time, for amikacin were determined using the mean intramuscular serum data and the mean intravenous pharmacokinetic parameters according to the Loo–Riegelman method (10). The equation defining peripheral compartment concentrations was used without the Taylor expansion simplification. All cumulative areas under the mean intramuscular drug concentration *versus* time curves were determined using the trapezoidal rule. The values representing percent of dose unabsorbed *versus* time were analyzed by suitable transformation and least-squares linear regression analysis to determine kinetic order, lag time, and absorption rate constants.

**Table I—Pharmacokinetic Parameters from Mean Intravenous Data**

| Parameter | 60-min Infusion | 30-min Infusion | 5-min Infusion | Mean (*SD*) |
|---|---|---|---|---|
| $A^a$, μg/ml | 37.4 | 39.8 | 46.0 | 41.1 (4.4) |
| $\alpha$, $hr^{-1}$ | 1.39 | 2.78 | 1.85 | 2.01 (0.71) |
| $B^a$, μg/ml | 28.4 | 35.5 | 31.9 | 31.9 (3.6) |
| $\beta$, $hr^{-1}$ | 0.290 | 0.313 | 0.301 | 0.301 (0.012) |
| $K_{21}$, $hr^{-1}$ | 0.766 | 1.48 | 0.934 | 1.06 (0.37) |
| $K_{12}$, $hr^{-1}$ | 0.388 | 1.02 | 0.595 | 0.669 (0.325) |
| $K_{el}$, $hr^{-1}$ | 0.527 | 0.589 | 0.619 | 0.578 (0.047) |
| $V_1$, liters/kg | 0.114 | 0.100 | 0.096 | 0.103 (0.009) |
| $\int_0^\infty C_{dt}$, μg hr/ml | 125 | 128 | 131 | 128 (3) |
| $R^2$ | 0.9958 | 0.9982 | 0.9837 | |
| $S$ | 7.7574 | 4.3811 | 91.1586 | |

[a] Values of $A$ and $B$ after correction to bolus administration case.

**Table II—Results of Linear Regression Analysis on Natural Logarithm of Percent of Dose Remaining to be Absorbed *versus* Time**

| Study | Dose, mg | $K_a$, $hr^{-1}$ | $t_{1/2}$, min | $t_0$, min |
|---|---|---|---|---|
| 1 | 250 | 1.38 | 30 | 3 |
| | 500 | 1.08 | 38 | 3 |
| 2 | 125 | 1.95 | 21 | 3 |
| | 250 | 1.36 | 31 | 8 |
| | 500 | 1.00 | 42 | 4 |
| | 750 | 1.05 | 40 | 4 |

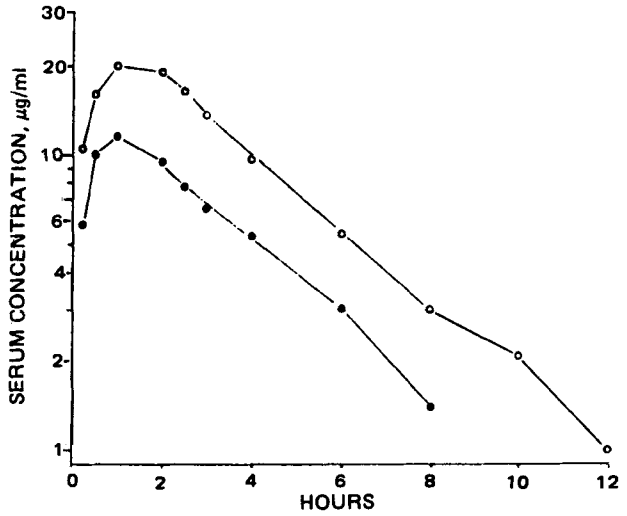


**Figure 2**—*Mean serum amikacin concentrations after intramuscular injection (Study 1). Key: ●, 250-mg dose; and ○, 500-mg dose.*

## RESULTS AND DISCUSSION

Figure 1 is a semilogarithmic plot of the mean intravenous data. The results of the pharmacokinetic analyses of these data are listed in Table I. The reason for the poorer fit to the 5-min infusion data probably was the difficulty in timing a push injection exactly. The overall mean values of $K_{21}$, $K_{12}$, and $K_{el}$ of 1.06, 0.669, and 0.578 $hr^{-1}$, respectively (Table I), were used in the Loo–Riegelman analysis.

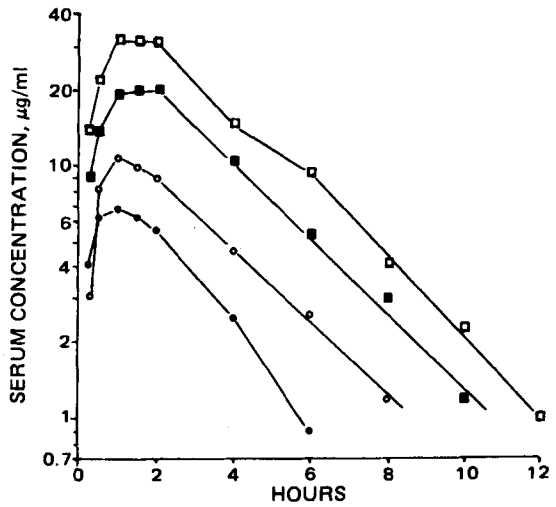


**Figure 3**—*Mean serum amikacin concentrations after intramuscular injection (Study 2). Key: ●, 125-mg dose; ○, 250-mg dose; ■, 500-mg dose; and □, 750-mg dose.*

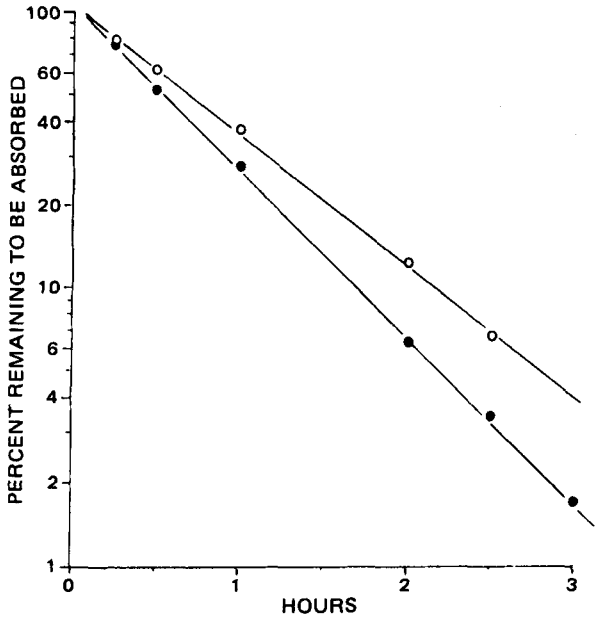


**Figure 4**—*Absorption profiles from Study 1 data. Key: ●, 250-mg dose; and ○, 500-mg dose.*

The mean intramuscular serum levels from Studies 1 and 2 are plotted semilogarithmically in Figs. 2 and 3. The calculated intramuscular absorption profiles were straight lines when plotted semilogarithmically (Figs. 4 and 5), indicating that intramuscular amikacin absorption could be a single first-order process. In all cases, the correlation coefficients from least-squares linear regression analysis of the natural logarithm of the percent remaining to be absorbed *versus* time were ≥0.9998. The absorption rate constants ($K_a$), absorption half-times ($t_{1/2} = \ln 2/K_a$), and absorption lag times ($t_0$) are listed in Table II. The overall mean $t_{1/2} \pm SD$ was 34 ± 8 min.

The values for $K_a$, 1–2 $hr^{-1}$, were sufficiently close to the values for $\alpha$ (Table II), 1.4–2.8 $hr^{-1}$, so that, on intramuscular administration, $K_a$ and $\alpha$ would effectively disappear as separate coefficients, producing a compound rate constant that could be misinterpreted as an absorption rate constant.

The value of $K_a$ decreased as the dose increased. There was a statistically significant linear regression of ln $K_a$ on ln $D$ ($D$ is dose in milligrams):

$$\ln K_a = 2.388 - 0.370 \ln D \qquad \text{(Eq. 5)}$$

$$df = 4 \quad r = 0.957 \quad p < 0.01$$

which transformed to (Fig. 6):

$$K_a = 10.9D^{-0.370} \qquad \text{(Eq. 6)}$$

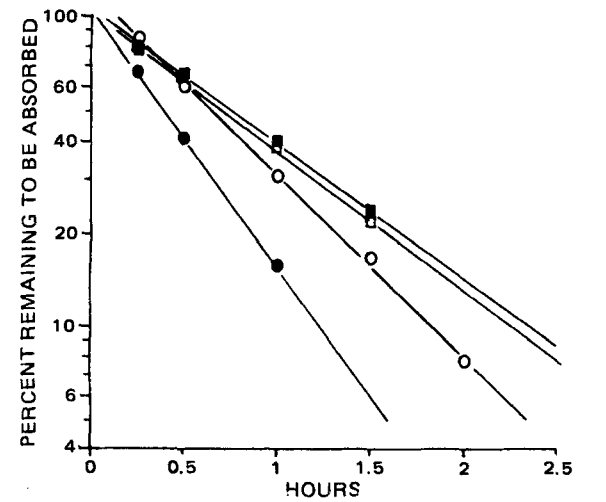


**Figure 5**—*Absorption profiles from Study 2 data. Key: ●, 125-mg dose; ○, 250-mg dose; ■, 500-mg dose; and □, 750-mg dose.*

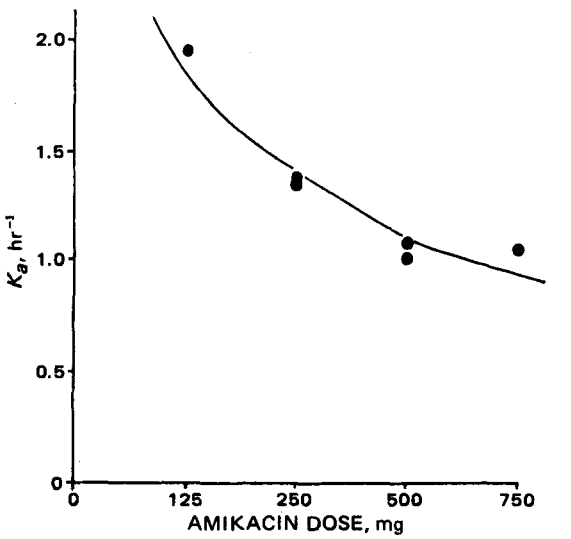


**Figure 6**—*Relationship between amikacin absorption rate constant and doses.*

According to Ballard (11), $K_a$, a first-order rate constant, is directly proportional to the dosing solution surface area to volume ratio ($SA/V_s$) when the membrane thickness and the drug's diffusion and partition coefficients are constant. If the physical distribution of injected dosing solutions is approximated as a sphere, then:

$$SA = 4\pi r^2 \qquad \text{(Eq. 7a)}$$

$$V_s = 4\pi r^3/3 \qquad \text{(Eq. 7b)}$$

where $r$ is the sphere's radius. If 1 ml = 1 $cm^3$ (Eq. 7b), then the sphere's area in square centimeters can be determined from the volumes using Eqs. 7a and 7b. A plot of $K_a$ *versus* $SA/V_s$ should be a straight line that passes through the origin.

Amikacin for intramuscular injection was supplied as a formulated 250-mg/ml solution in a buffered aqueous vehicle. Therefore, a constant concentration was injected, but $V_s$ varied with the dose. For the 125-, 250-, 500-, and 750-mg doses, the respective values of $V_s$ were 0.5, 1, 2, and 3 $cm^3$; the respective values of $SA/V_s$ were 6.09, 4.84, 3.84, and 3.35 $cm^{2/3}$. Least-squares linear regression analysis of $K_a$ *versus* $SA/V_s$ yielded a statistically significant ($df = 4$, $r = 0.968$, $p < 0.01$) straight line which passed through the origin (Fig. 7):

$$K_a = 0.294(SA/V_s) \qquad \text{(Eq. 8)}$$

Apparently, the variations in $K_a$ were a purely physical result of the variation in the dosing volume. The best strategy for maximizing absorption rates is to administer a dose as several smaller volumes rather than a single larger volume. It may be difficult to detect absorption nonlinearities on the basis of the peak serum level and time to peak serum level unless sufficiently short serum sampling intervals are used.

Differences in the intrinsic absorbability of other aminoglycosides may exist due to differences in their diffusion and partition coefficients; but

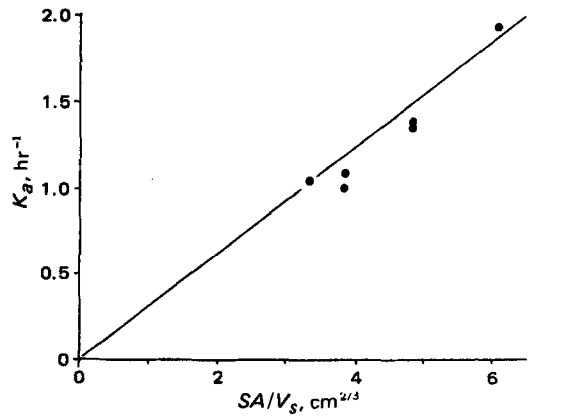


**Figure 7**—*Relationship between amikacin absorption rate constant and surface area to volume ratio.*

since they are marketed as preformulated dosing solutions, the same variations in $K_a$ with dosing volume might be expected. Part of the variations noted earlier may be due to the effects of the different recommended dosing schedules and different dosing solution volumes on the volumes administered. The question of variations in aminoglycoside absorption rates is an interesting phenomenon that warrants further investigation.

## REFERENCES


(1) J. C. Pechere and R. Dugal, *Clin. Pharmacokinet.*, **4**, 170 (1979).

(2) D. J. Greenblatt and J. Koch-Weser, *N. Engl. J. Med.*, **295**, 542 (1976).

(3) R. A. Yates, M. Mitchard, and R. Wise, *J. Antimicrob. Chemother.*, **4**, 335 (1978).

(4) B. E. Cabana and J. G. Taggart, *Antimicrob. Agents Chemother.*, **3**, 478 (1973).

(5) D. C. Grove and W. A. Randall, "Assay Methods of Antibiotics—A Laboratory Manual," Medical Encyclopedia, Inc., New York, N.Y., 1955.

(6) C. M. Metzler, "NONLIN, a Computer Program for Parameter Estimation in Nonlinear Situations," Technical Report 7292/69/7292/005, Upjohn Co., Kalamazoo, Mich., 1969.

(7) H. O. Hartley, *Technometrics*, **3**, 269 (1961).

(8) J. C. K. Loo and S. Riegelman, *J. Pharm. Sci.*, **59**, 53 (1970).

(9) M. Gibaldi and D. Perrier, "Pharmacokinetics," Dekker, New York, N.Y., 1975, pp. 73, 293.

(10) J. C. K. Loo and S. Riegelman, *J. Pharm. Sci.*, **57**, 918 (1968).

(11) B. E. Ballard, *ibid.*, **57**, 357 (1968).


## ACKNOWLEDGMENTS


The authors thank Dr. B. E. Cabana and Dr. J. G. Taggart.


# Theophylline Absorption and Disposition in Rabbits: Oral, Intravenous, and Concentration-Dependent Kinetic Studies


**ADNAN EL-YAZIGI** * **and RONALD J. SAWCHUK** ˣ



Received May 27, 1980, from the *Department of Pharmaceutics, College of Pharmacy, University of Minnesota, Minneapolis, MN 55455.* Accepted for publication October 3, 1980. *Present address: Faculty of Pharmacy, Riyad University, Riyad, Saudi Arabia.



**Abstract** □ Theophylline pharmacokinetics following oral and intravenous administration were studied, and the absolute bioavailability of five commercially available products was determined using the rabbit as an *in vivo* model. Concentration-dependent clearance studies were performed by multiple constant-rate infusion and multiple bolus dose administration of aminophylline. Theophylline pharmacokinetics following the oral adminstration of these products obeyed the one-compartment open model adequately. However, the data obtained following rapid intravenous aminophylline administration in the rabbit fit either the one-compartment model (half-life = 2.8 hr and the volume of distribution = 0.586 liter/kg) or the two-compartment model ($\beta$-phase half-life = 4.4 hr and $V_{d(\beta)}$ = 0.708 liter/kg). There were no significant product-to-product differences in the time to peak ($t_{max}$), the rate constant of absorption ($k_a$), or the percent of dose absorbed at 1 hr ($F_1$); however, differences in the absolute bioavailability ($F$), dose-normalized peak serum concentration ($C_{max(n)}$), and percent of dose absorbed at 6 hr ($F_6$) were significant. There was no evidence of concentration-dependent clearance for theophylline in the rabbit in the serum concentration range studied, but the results of the multiple constant-rate infusion study suggest that total clearance decreases at higher serum theophylline concentrations.



**Keyphrases** □ Theophylline—pharmacokinetics, oral and intravenous administration, concentration-dependent clearance □ Pharmacokinetics—theophylline, oral and intravenous administration, concentration-dependent clearance □ Bioavailability—theophylline, oral administration, aminophylline, intravenous administration


Several pharmacokinetic studies have investigated theophylline bioavailability from various dosage forms (1–5). Two studies (3, 5) determined the absolute theophylline bioavailability from oral dosage forms. However, additional research is needed to examine the intrasubject variability in theophylline elimination kinetics (6).

The present work concerned theophylline pharmacokinetics in the rabbit following intravenous and oral administration to determine the absolute bioavailability of theophylline from five commercially available dosage forms using the rabbit as an *in vivo* model and to examine the possibility of concentration-dependent clearance of this drug. Although no reports suggested dose-dependent kinetics for theophylline in the rabbit, it may be that at sufficiently high dosages the relationship between the dose and the serum concentration–time integral becomes nonlinear. Such a finding would preclude the use of traditional approaches for quantitating absolute or relative bioavailability.

## EXPERIMENTAL

**Materials and Methods**—All dosage forms studied (A[1], B[2], C[3], D[4], and E[5]) were purchased commercially. Anhydrous theophylline[6] was used as supplied. Aminophylline[7] injection, 250 mg (25 mg/ml), was used for intravenous administration.

*Animals*—Male New Zealand White rabbits, 2.4–3.9 kg, were maintained on commercial rabbit food[8] and tap water and were fasted overnight prior to each oral experiment. Water was allowed *ad libitum* during fasting and throughout the experiment. Each animal received one oral dosage form of theophylline, followed 24 hr later by an intravenous dose of aminophylline.

*Oral Administration of Drugs*—The animal was restrained, and its mouth was opened by inserting hemostatic forceps from the side into the oral cavity immediately behind the rabbit's incisors. A small animal capsule administration device, with the tablet or capsule in its slotted end, was placed over the rabbit's tongue and advanced ~4–5 cm into the pharynx. The capsule or tablet then was released by pushing the plunger rapidly and completely. This administration was followed by ~10 ml of water. After the device and forceps were removed, the rabbit's mouth and nostrils were held closed until swallowing occurred.

*Rapid Intravenous Administration of Aminophylline*—A dose of 24.33

[1] Tablets (aminophylline, 200 mg), lot 776-991, Searle, Chicago, Ill.
[2] Capsules (theophylline, 200 mg), lot 1W60531, Cooper, Wayne, N.J.
[3] Tablets (theophylline, 125 mg), lot 68308, Riker Laboratories, St. Paul, Minn.
[4] S. R. Capsules (theophylline, 2 gr), lot 6090204, Fleming, Fenton, Mo.
[5] S. R. Capsules (theophylline, 1 gr), lot 6090204, Fleming, Fenton, Mo.
[6] Anhydrous theophylline, Nutritional Biochemicals, Cleveland, Ohio.
[7] Aminophylline Injection, Searle, Chicago, Ill.
[8] Purina Laboratory Rabbit Chow, Ralston-Purina, St. Louis, Mo.




*0022-3549/81/0400-0452$01.00/0*


*© 1981, American Pharmaceutical Association*

since they are marketed as preformulated dosing solutions, the same variations in $K_a$ with dosing volume might be expected. Part of the variations noted earlier may be due to the effects of the different recommended dosing schedules and different dosing solution volumes on the volumes administered. The question of variations in aminoglycoside absorption rates is an interesting phenomenon that warrants further investigation.

## REFERENCES


(1) J. C. Pechere and R. Dugal, *Clin. Pharmacokinet.*, **4**, 170 (1979).

(2) D. J. Greenblatt and J. Koch-Weser, *N. Engl. J. Med.*, **295**, 542 (1976).

(3) R. A. Yates, M. Mitchard, and R. Wise, *J. Antimicrob. Chemother.*, **4**, 335 (1978).

(4) B. E. Cabana and J. G. Taggart, *Antimicrob. Agents Chemother.*, **3**, 478 (1973).

(5) D. C. Grove and W. A. Randall, "Assay Methods of Antibiotics—A Laboratory Manual," Medical Encyclopedia, Inc., New York, N.Y., 1955.

(6) C. M. Metzler, "NONLIN, a Computer Program for Parameter Estimation in Nonlinear Situations," Technical Report 7292/69/7292/005, Upjohn Co., Kalamazoo, Mich., 1969.

(7) H. O. Hartley, *Technometrics*, **3**, 269 (1961).

(8) J. C. K. Loo and S. Riegelman, *J. Pharm. Sci.*, **59**, 53 (1970).

(9) M. Gibaldi and D. Perrier, "Pharmacokinetics," Dekker, New York, N.Y., 1975, pp. 73, 293.

(10) J. C. K. Loo and S. Riegelman, *J. Pharm. Sci.*, **57**, 918 (1968).

(11) B. E. Ballard, *ibid.*, **57**, 357 (1968).


## ACKNOWLEDGMENTS


The authors thank Dr. B. E. Cabana and Dr. J. G. Taggart.


# Theophylline Absorption and Disposition in Rabbits: Oral, Intravenous, and Concentration-Dependent Kinetic Studies


**ADNAN EL-YAZIGI** * **and RONALD J. SAWCHUK** ˣ



Received May 27, 1980, from the *Department of Pharmaceutics, College of Pharmacy, University of Minnesota, Minneapolis, MN 55455.* Accepted for publication October 3, 1980. *Present address: Faculty of Pharmacy, Riyad University, Riyad, Saudi Arabia.



**Abstract** □ Theophylline pharmacokinetics following oral and intravenous administration were studied, and the absolute bioavailability of five commercially available products was determined using the rabbit as an *in vivo* model. Concentration-dependent clearance studies were performed by multiple constant-rate infusion and multiple bolus dose administration of aminophylline. Theophylline pharmacokinetics following the oral adminstration of these products obeyed the one-compartment open model adequately. However, the data obtained following rapid intravenous aminophylline administration in the rabbit fit either the one-compartment model (half-life = 2.8 hr and the volume of distribution = 0.586 liter/kg) or the two-compartment model ($\beta$-phase half-life = 4.4 hr and $V_{d(\beta)}$ = 0.708 liter/kg). There were no significant product-to-product differences in the time to peak ($t_{max}$), the rate constant of absorption ($k_a$), or the percent of dose absorbed at 1 hr ($F_1$); however, differences in the absolute bioavailability ($F$), dose-normalized peak serum concentration ($C_{max(n)}$), and percent of dose absorbed at 6 hr ($F_6$) were significant. There was no evidence of concentration-dependent clearance for theophylline in the rabbit in the serum concentration range studied, but the results of the multiple constant-rate infusion study suggest that total clearance decreases at higher serum theophylline concentrations.



**Keyphrases** □ Theophylline—pharmacokinetics, oral and intravenous administration, concentration-dependent clearance □ Pharmacokinetics—theophylline, oral and intravenous administration, concentration-dependent clearance □ Bioavailability—theophylline, oral administration, aminophylline, intravenous administration


Several pharmacokinetic studies have investigated theophylline bioavailability from various dosage forms (1–5). Two studies (3, 5) determined the absolute theophylline bioavailability from oral dosage forms. However, additional research is needed to examine the intrasubject variability in theophylline elimination kinetics (6).

The present work concerned theophylline pharmacokinetics in the rabbit following intravenous and oral administration to determine the absolute bioavailability of theophylline from five commercially available dosage forms using the rabbit as an *in vivo* model and to examine the possibility of concentration-dependent clearance of this drug. Although no reports suggested dose-dependent kinetics for theophylline in the rabbit, it may be that at sufficiently high dosages the relationship between the dose and the serum concentration–time integral becomes nonlinear. Such a finding would preclude the use of traditional approaches for quantitating absolute or relative bioavailability.

## EXPERIMENTAL

**Materials and Methods**—All dosage forms studied (A[1], B[2], C[3], D[4], and E[5]) were purchased commercially. Anhydrous theophylline[6] was used as supplied. Aminophylline[7] injection, 250 mg (25 mg/ml), was used for intravenous administration.

*Animals*—Male New Zealand White rabbits, 2.4–3.9 kg, were maintained on commercial rabbit food[8] and tap water and were fasted overnight prior to each oral experiment. Water was allowed *ad libitum* during fasting and throughout the experiment. Each animal received one oral dosage form of theophylline, followed 24 hr later by an intravenous dose of aminophylline.

*Oral Administration of Drugs*—The animal was restrained, and its mouth was opened by inserting hemostatic forceps from the side into the oral cavity immediately behind the rabbit's incisors. A small animal capsule administration device, with the tablet or capsule in its slotted end, was placed over the rabbit's tongue and advanced ~4–5 cm into the pharynx. The capsule or tablet then was released by pushing the plunger rapidly and completely. This administration was followed by ~10 ml of water. After the device and forceps were removed, the rabbit's mouth and nostrils were held closed until swallowing occurred.

*Rapid Intravenous Administration of Aminophylline*—A dose of 24.33

[1] Tablets (aminophylline, 200 mg), lot 776-991, Searle, Chicago, Ill.
[2] Capsules (theophylline, 200 mg), lot 1W60531, Cooper, Wayne, N.J.
[3] Tablets (theophylline, 125 mg), lot 68308, Riker Laboratories, St. Paul, Minn.
[4] S. R. Capsules (theophylline, 2 gr), lot 6090204, Fleming, Fenton, Mo.
[5] S. R. Capsules (theophylline, 1 gr), lot 6090204, Fleming, Fenton, Mo.
[6] Anhydrous theophylline, Nutritional Biochemicals, Cleveland, Ohio.
[7] Aminophylline Injection, Searle, Chicago, Ill.
[8] Purina Laboratory Rabbit Chow, Ralston-Purina, St. Louis, Mo.




*0022-3549/81/0400-0452$01.00/0*


*© 1981, American Pharmaceutical Association*

**Table I—Results of the Multiple-Rate Intravenous Infusion Experiments for the Concentration-Dependent Clearance Study**

| Experiment | Rabbit Weight, kg | Infusion Time, hr | Infusion Rate, mg/hr | $\bar{C}_{ss}$, mg/liter | $Cl_{TB}$, liter/hr/kg |
|---|---|---|---|---|---|
| P IF | 4.13 | 0–24 | 3.60 | 14.4 | 0.060 |
| P IF | 4.13 | 24–48 | 7.20 | 28.7 | 0.061 |
| P IF | 4.13 | 48–66 | 10.80 | 56.3 | 0.046 |
| Q IF | 3.21 | 0–24 | 2.59 | 7.5 | 0.108 |
| Q IF | 3.21 | 24–48 | 5.18 | 16.9 | 0.095 |
| Q IF | 3.21 | 48–72 | 7.77 | 41.7 | 0.058 |

**Table II—Pharmacokinetic Parameters for Theophylline following Intravenous Administration in the Rabbit Using the One-Compartment Open Model**

| Experiment | $k_d$, $hr^{-1}$ | $t_{1/2}$, hr | $V_d$, liter/kg | $Cl_{TB}$, liter/kg/hr |
|---|---|---|---|---|
| A1 IV | 0.322 | 2.2 | 0.666 | 0.214 |
| A2 IV | 0.303 | 2.3 | 0.544 | 0.165 |
| A3 IV[a] | 0.083 | 8.4 | 0.770 | 0.064 |
| B3 IV | 0.218 | 3.2 | 0.420 | 0.091 |
| D1 IV | 0.190 | 3.6 | 0.575 | 0.109 |
| D2 IV | 0.201 | 3.4 | 0.620 | 0.125 |
| D3 IV | 0.403 | 1.7 | 0.628 | 0.253 |
| E3 IV | 0.210 | 3.3 | 0.650 | 0.137 |
| Mean | 0.264 | 2.8 | 0.586 | 0.156 |
| *SD* | 0.080 | 0.73 | 0.085 | 0.059 |

[a] Values not included in the calculation of the mean and standard deviation.

mg of aminophylline injection USP/kg (25 mg/ml), equivalent to 15 mg of theophylline/kg, was administered through a catheter into the marginal ear vein of the rabbit over 5 min.

**Concentration-Dependent Kinetic Studies**—*Multiple-Dose Rapid Intravenous Administration*—After the cannulation of the marginal ear vein, a dose equivalent to 15 mg of theophylline/kg was administered intravenously into the catheter. A second dose, equivalent to 22.5 mg of theophylline/kg, was administered 24 hr after the first injection; a third dose, equivalent to 30 mg of theophylline/kg, was injected 24 hr after the second dose.

*Multiple-Rate Infusion*—The infusion of aminophylline was carried out using a variable-speed, syringe-type infusion pump[9] at an initial rate for the first 24 hr, at twice this rate for the second 24 hr, and at triple this rate for the rest of the experiment. The infusion rates and periods are listed in Table I.

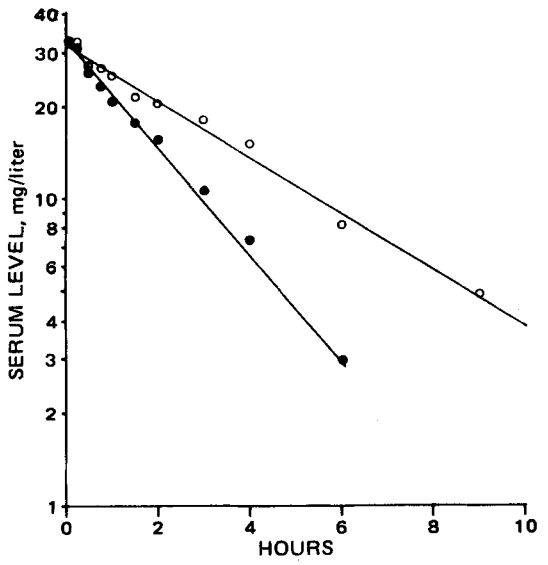


**Figure 1**—*Serum theophylline concentration–time data fitted to the one-compartment model. Key: ●, Experiment D3 IV; and ○, Experiment E3 IV.*

[9] Model 975, Harvard Apparatus Co., Millis, Mass.

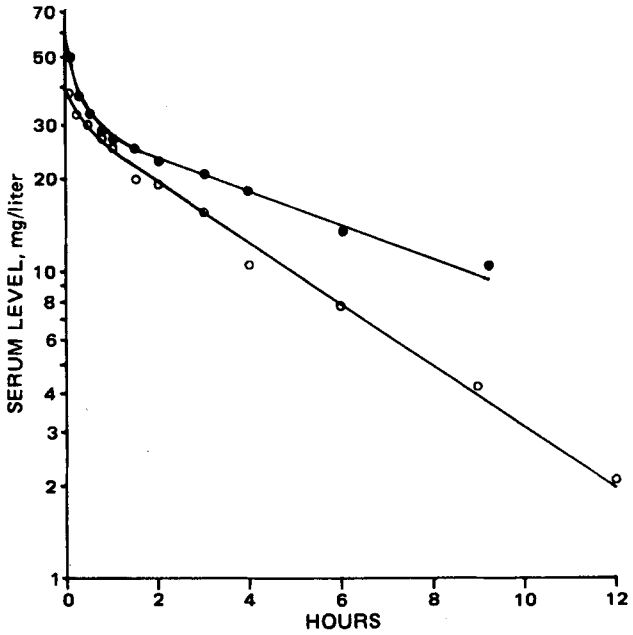


**Figure 2**—*Serum theophylline concentration–time data fitted to the two-compartment model. Key: ●, Experiment B4 IV; and ○, Experiment E1 IV.*

**Analysis of Theophylline in Serum**—A modified version of the Schack and Waxler method (7) was used for theophylline analysis in serum. Serum, 0.5 ml, was extracted with chloroform containing 5% (v/v) isopropyl alcohol after the addition of 0.2 ml of 0.1 *N* HCl. The chloroform layer then was back-extracted with 0.1 *N* NaOH, and the absorbance of this solution was read at 272 and 310 nm. The corrected absorbance of the sample was calculated as:

$$A_{sample} = (A_{272} - A_{310})_{sample} - (A_{272} - A_{310})_{blank} \quad \text{(Eq. 1)}$$

where $A$ is the absorbance and the subscript indicates the wavelength at which it was determined.

## RESULTS

Each experiment in this study is designated by a letter–number code. The letter indicates the product administered in the oral study, and the number identifies the animal used in the intravenous or oral study.

**Rapid Intravenous Administration**—The data obtained from the intravenous administration experiments were fitted to either a one- or two-compartment open model using the computer program KINA (8). The parameters obtained from the data that fitted the one-compartment model appear in Table II; those obtained using the two-compartment model are listed in Table III. Typical fits of the data can be seen in Figs. 1 and 2.

**Oral Administration**—The serum concentration–time data were

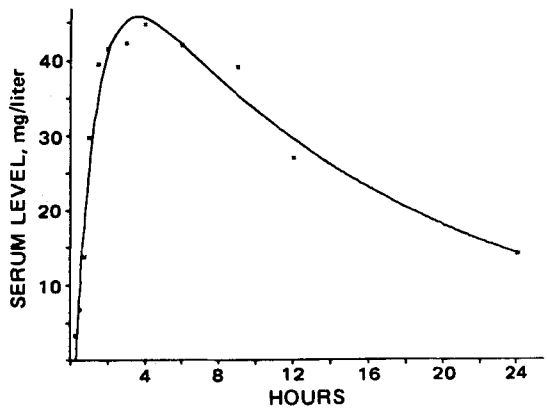


**Figure 3**—*Computer-generated plot of serum theophylline concentration–time data of Experiment A1 PO fitted to the one-compartment model with first-order absorption.*

**Table III—Pharmacokinetic Parameters for Theophylline following Intravenous Administration in the Rabbit Using the Two-Comparment Open Model**

| Experiment | $\alpha$, $hr^{-1}$ | $\beta$, $hr^{-1}$ | $t_{1/2}$, hr | $k_1$, $hr^{-1}$ | $k_2$, $hr^{-1}$ | $V_{d(\beta)}$, liter/kg | $V_c$, liter/kg | $Cl_{TB}$, liter/kg/hr |
|---|---|---|---|---|---|---|---|---|
| A4 IV | 7.18 | 0.109 | 6.4 | 3.10 | 3.99 | 0.616 | 0.343 | 0.066 |
| B2 IV[a] | 2.83 | 0.038 | 18.2 | 1.24 | 1.56 | 0.771 | 0.425 | 0.029 |
| B4 IV | 4.52 | 0.127 | 5.5 | 2.02 | 2.38 | 0.665 | 0.351 | 0.084 |
| C1 IV | 5.84 | 0.154 | 4.5 | 2.12 | 3.62 | 0.616 | 0.383 | 0.094 |
| C3 IV | 1.97 | 0.255 | 2.7 | 0.77 | 0.90 | 0.856 | 0.392 | 0.218 |
| C4 IV | 5.14 | 0.121 | 5.7 | 2.10 | 2.95 | 0.664 | 0.383 | 0.084 |
| E1 IV | 2.11 | 0.228 | 3.0 | 0.43 | 1.60 | 0.681 | 0.517 | 0.155 |
| E2 IV | 4.01 | 0.258 | 2.7 | 1.66 | 2.14 | 0.855 | 0.453 | 0.220 |
| Mean | 4.39 | 0.179 | 4.4 | 1.74 | 2.51 | 0.708 | 0.403 | 0.132 |
| *SD* | 1.90 | 0.066 | 1.6 | 0.90 | 1.09 | 0.104 | 0.061 | 0.066 |

[a] Values not included in the calculation of the mean and standard deviation.

**Table IV—Pharmacokinetic Parameters for Oral Theophylline Products**

| Parameters | Product A | B | C | D | E |
|---|---|---|---|---|---|
| Number of experiments | 4 | 4 | 4 | 3 | 3 |
| $t_{1/2}$, hr | 13.4[a] (5.1)[b] | 15.5 (5.8) | 7.3 (2.1) | 16.6 (8.5) | 15.9 (8.1) |
| $k_a$, $hr^{-1}$ | 0.447 (0.291) | 0.899 (0.638) | 0.260 (0.267) | 0.174 (0.163) | 0.993 (1.32) |
| $AUC$ $\int_{0(n)}^{\infty}$[c], kg hr/liter | 19.6 (4.8) | 19.0 (8.6) | 15.4 (3.1) | 9.2 (8.9) | 12.2 (8.3) |
| $C_{max(n)}$[d], kg/liter | 0.763 (0.170) | 0.708 (0.285) | 0.724 (0.095) | 0.205 (0.182) | 0.388 (0.120) |
| $t_{max}$, hr | 6.2 (2.3) | 7.1 (7.9) | 6.7 (2.6) | 12.3 (8.1) | 6.1 (4.3) |
| $f_1 \times 100$, % | 40.8 (14.5) | 45.7 (31.2) | 32.7 (29.3) | 28.1 (29.0) | 39.5 (30.4) |
| $f_6 \times 100$, % | 90.4 (13.0) | 81.4 (38.0) | 65.0 (28.1) | 52.9 (29.6) | 85.7 (8.00) |
| $F$, % | 68.7 (15.9) | 50.2 (22.9) | 120 (13.7) | 19.1 (10.9) | 39.0 (13.9) |
| $F_1$, % | 27.8 (12.5) | 21.1 (17.8) | 22.1 (13.5) | 6.46 (9.41) | 13.3 (5.76) |
| $F_6$, % | 61.8 (16.6) | 39.8 (32.2) | 62.1 (14.4) | 10.5 (10.7) | 33.3 (9.50) |

[a] Mean. [b] Standard deviation. [c] Normalized area under the curve ($AUC$/dose). [d] Normalized peak serum concentration ($C_{max}$/dose).

fitted to the one-compartment open model with first-order absorption and elimination using the computer program KINA. The parameters obtained are listed in Table IV. A typical fit of the data is shown in Fig. 3.

**Determination of Absolute Bioavailability ($F$)**—The absolute bioavailability ($F$) was calculated according to:

$$F = \frac{k_{d_{or}} \int_0^{\infty} C\,dt_{or} D_{iv}}{k_{d_{iv}} \int_0^{\infty} C\,dt_{iv} D_{or}} \times 100 \qquad \text{(Eq. 2)}$$

where $D$ is the dose, $\int_0^{\infty} C\,dt$ is the area under the serum concentration–time curve, and $k_d$ is the rate constant for elimination. The subscripts or and iv refer to the oral and intravenous routes. The values of $F$ are presented in Table IV.

**Determination of Cumulative Percent of Dose Absorbed at 1 ($F_1$) and 6 ($F_6$) hr**—The cumulative fraction of drug absorbed at 1 ($f_1$) and 6 ($f_6$) hr was calculated according to the Wagner–Nelson equation (9):

$$f_t = \frac{C_t + k_d \int_0^{t} C\,dt}{k_d \int_0^{\infty} C\,dt} \qquad \text{(Eq. 3)}$$

where $C_t$ is the serum theophylline concentration at time $t$.

Using the values of $f_1$ and $f_6$, the cumulative percent of dose absorbed at 1 ($F_1$) and 6 ($F_6$) hr was calculated as follows:

$$F_1 = f_1 F \qquad \text{(Eq. 4a)}$$

and:

$$F_6 = f_6 F \qquad \text{(Eq. 4b)}$$

The values of $F_1$ and $F_6$ are given in Table IV.

**Determination of Time to Peak ($t_{max}$) and Peak Serum Concentration ($C_{max}$)**—The time to peak was calculated from:

$$t_{max} = \frac{1}{k_a - k_d} \ln \frac{k_a A}{k_d B} \qquad \text{(Eq. 5)}$$

where $k_a$ is the absorption rate constant, $A$ is the preexponential coefficient for the absorption phase, and $B$ is the preexponential coefficient for the elimination phase. All four parameters ($k_a$, $k_d$, $A$, and $B$) were calculated by KINA.

The peak serum concentration was calculated by substituting the $t_{max}$ value in:

$$C_{max} = -Ae^{-k_a t_{max}} + Be^{-k_d t_{max}} \qquad \text{(Eq. 6)}$$

Values of $t_{max}$ and $C_{max}$ appear in Table IV.

**Concentration-Dependent Clearance Studies**—*Multiple-Dose Rapid Intravenous Administration*—The pharmacokinetic parameters obtained from these experiments using KINA are listed in Table V.

*Multiple-Rate Infusion*—The mean steady-state serum concentration ($\bar{C}_{ss}$) at different infusion rates ($k_0$) and the corresponding total body clearance ($Cl_{TB}$) obtained from these experiments are presented in Table I.

The total body clearance for theophylline was calculated according to:

$$Cl_{TB} = \frac{k_0}{\bar{C}_{ss}} \qquad \text{(Eq. 7)}$$

## DISCUSSION

**Rapid Intravenous Administration**—For animals whose data fitted the one-compartment model, there appeared to be a fairly rapid elimination of theophylline with a mean half-life of 2.8 hr (Table II). The mean value of the volume of distribution was 0.609 liter/kg, and the mean total body clearance was 0.144 liter/hr/kg. However, for the other eight rabbits whose data fitted the two-compartment model, the mean $\beta$-phase half-life, $t_{1/2(\beta)}$, was 4.4 hr. This value is similar to the $t_{1/2(\beta)}$ reported for humans (4.4–6.7 hr) (10, 11). A mean distribution phase rate constant ($\alpha$) of 4.2 $hr^{-1}$ was found for theophylline in this study in the rabbit (Table III). This value is close to that obtained in humans (5.8 $hr^{-1}$) (11). The volume of the central compartment was 0.30 liter/kg for humans (11). A slightly higher value (0.41 liter/kg) was found in this study for the rabbit.

**Oral Administration**—The mean values of the absolute bioavailability ($F$) for Products A, B, C, D, and E were 68.7, 50.2, 120, 19.1, and 39.7%, respectively. The analysis of variance showed that the difference in $F$ among products was significant ($p < 0.001$). The absolute bioavailability ($F$) was determined according to Eq. 2, in which it is assumed that the volume of distribution remains constant and the area–dose relationship is linear. Both assumptions appear to be valid since the volume of distribution and the total body clearance did not change as the dose was increased (Table V).

Equation 2 also considers differences occurring in the apparent half-life observed following intravenous and oral administration in the same rabbit. It is assumed that differences in clearances following intravenous

Table V—Results of the Multiple-Dose Rapid Intravenous Administration Experiments for the Concentration-Dependent Kinetic Study

| Experiment | Rabbit Weight, kg | Dose, mg/kg | $k_d$, $hr^{-1}$ | $V_d$, liter/kg | $AUC \int_0^\infty$, mg hr/liter | $Cl_{TB}$, liter/hr/kg |
|---|---|---|---|---|---|---|
| K1 | 3.44 | 15.0 | 0.185 | 0.781 | 104 | 0.144 |
| K2 | 3.44 | 22.5 | 0.172 | 0.750 | 175 | 0.129 |
| K3 | 3.44 | 30.0 | 0.187 | 0.789 | 203 | 0.148 |
| L1 | 3.48 | 15.0 | 0.166[a] | 0.714[b] | 127 | 0.118 |
| L2 | 3.48 | 22.5 | 0.247 | 0.549 | 166 | 0.136 |
| L3 | 3.48 | 30.0 | 0.258 | 0.638 | 182 | 0.164 |
| M1 | 2.87 | 15.0 | 0.199 | 0.512 | 147 | 0.102 |
| M2 | 2.87 | 22.5 | 0.205 | 0.504 | 218 | 0.103 |
| M3 | 2.87 | 30.0 | 0.200 | 0.501 | 300 | 0.100 |

[a] $\beta$. [b] $V_{d(\beta)}$.

and oral administration in the same animal are reflected by the elimination half-life of the drug and that this half-life is derived from the terminal log-linear portion of the serum concentration–time curve in experiments involving oral theophylline administration.

It was reported (12) that the rabbit presents problems as a model for drug absorption studies since fasting markedly prolongs stomach emptying. It was shown (12) that it is difficult to achieve an empty stomach in the rabbit by withholding food. Other investigators (13) suggested the use of a special solid diet to control gastric emptying rates in the rabbit. More rapid theophylline absorption might have been observed in the present study if the animals had not been fasted prior to oral dosing.

It is possible that theophylline absorption in the rabbit is sufficiently slow that the terminal portion of the serum concentration curve represents absorption, especially since gastric emptying is quite slow. This possibility may explain the discrepancy between the apparent half-lives observed following oral and intravenous administrations in the same animal. In this situation, it is incorrect to use the rate constant derived from the terminal portion of the serum concentration–time curve as $k_{d_{or}}$ in Eq. 2. If it can be assumed that the clearances are not changing:

$$F = \frac{\int_0^\infty C\,dt_{or} D_{iv}}{\int_0^\infty C\,dt_{iv} D_{or}} \qquad \text{(Eq. 8)}$$

When $F$ was calculated using Eq. 8, 69% of the values were >100%, suggesting that the assumption of constant clearance is incorrect. Only 19% of the $F$ values calculated using Eq. 2 were >100%, and all of these values occurred with Product C (Table IV).

The existence of a "flip-flop" model (14), which precludes the use of rate constants from the terminal portion of the serum concentration–time curve in Eq. 2, would be supported by a correspondence between the elimination rate constant determined from intravenous data and the rate constant associated with the rising portion of the serum concentration–time curve observed on oral theophylline administration to the same animal. However, these parameters were not similar in this study.

The calculation of the cumulative fraction of drug absorbed at various times using Eq. 3 assumes that theophylline distributes rapidly throughout its volume of distribution and is eliminated by a first-order process. Since the data from some animals receiving intravenous theophylline were fitted by the two-compartment open model, the Loo–Riegelman method (15) may be appropriate for the estimation of the absorption rate constant in these cases. However, this method requires that the model parameters for both modes of administration be similar, which was not the case in the present study. Although intravenous data are not needed in the calculation of the $f$ values using Eq. 3, translation of these parameters into cumulative percent of dose absorbed requires an estimate of $F$, as indicated in Eq. 4.

The time to peak ($t_{max}$) was calculated using Eq. 5, which includes the terms $A$ and $B$. In the traditional equation used for calculating $t_{max}$, $A$ and $B$ are assumed to be equal. The use of these terms provides better estimates of $t_{max}$ where a lag phase exists.

There was no significant difference in $t_{max}$, $k_a$, or $F_1$ among the products studied; however, product-to-product differences in the dose-normalized $C_{max}$ [$C_{max(n)}$] and $F_6$ values were significant ($p < 0.005$ and $< 0.05$, respectively).

**Concentration-Dependent Clearance Studies**—*Multiple-Dose Rapid Intravenous Administration*—As shown in Table V, changes in $k_d$, $V_d$, and total body clearance for Rabbits K and M as the dose was increased were nonexistent or very slight. The fact that there was no change in total body clearance for Rabbits K and M and only a slight increase for Rabbit L suggests that theophylline demonstrates concentration-independent clearance in the rabbit at doses up to 30 mg/kg.

*Multiple-Rate Infusion*—The results of the multiple constant-rate intravenous infusion studies indicate that the dose–*AUC* relationship in the concentration range utilized here is linear; however, at higher concentrations, this finding may not be true. This phenomenon is shown in Table I, where increasing the infusion rate to three times the initial value resulted in steady-state serum concentrations which were increased 4- and 5.6-fold, respectively. This decrease in the total body clearance at higher infusion rates may be brought about by saturable metabolism or excretion processes, a pharmacodynamic effect of the drug resulting in reduced clearance, or a change in the function of eliminating organs with time. The possibility of time-dependent elimination kinetics may be investigated by performing the experiment in order of descending infusion rates. Although no evidence for capacity-limited elimination of theophylline was observed in another study of four rabbits receiving the drug as an intravenous bolus (16), the dose administered was only 10 mg/kg.

Dose-dependent kinetics of this drug in children were demonstrated by a reduction in clearance at increasing serum theophylline concentrations during infusion at differing rates (17). These results were interpreted in terms of Michaelis–Menten kinetics and suggested the possibility of at least one saturable elimination process among the multiple parallel pathways involved. The evidence for capacity-limited pharmacokinetics of theophylline in humans recently was reviewed (18), and the problems associated with dose-dependent elimination in theophylline bioavailability studies in humans also was addressed (19).

## CONCLUSIONS

On the basis of the results of this study, it appears that the variability in the elimination kinetics of theophylline in the rabbit following intravenous administration was relatively small compared to that in humans, as evidenced by the variation in total body clearance and volume of distribution. Moreover, there were significant differences in the absolute bioavailability of the products investigated in the rabbit. Further studies in humans are needed to determine the clinical significance of such differences. In addition, theophylline did not exhibit concentration-dependent kinetics in the rabbit in the serum concentration range studied; however, at higher serum levels, total body clearance decreased substantially.

## REFERENCES


(1) J. W. Jenne, E. Wyze, F. S. Rood, and F. M. MacDonald, *Clin. Pharmacol. Ther.*, **13**, 349 (1972).

(2) H. Salem and R. H. Jackson, *Ann. Allergy*, **32**, 189 (1974).

(3) P. A. Mitenko and R. I. Ogilvie, *Clin. Pharmacol. Ther.*, **16**, 720 (1974).

(4) D. L. Spangler, D. D. Kalof, F. L. Bloom, and H. J. Wittig, *Ann. Allergy*, **40**, 6 (1978).

(5) L. Hendeles, M. Weinberger, and L. Bighley, *Am. J. Hosp. Pharm.*, **34**, 525 (1977).

(6) R. A. Upton, J. F. Thiercelin, J. R. Powell, L. Sansome, S. M. Wallace, and S. Riegelman, "Abstracts of Papers Presented at the APhA Academy of Pharmaceutical Sciences," Phoenix meeting, 1977.

(7) J. A. Schack and S. H. Waxler, *J. Pharmacol. Exp. Ther.*, **97**, 283 (1949).

(8) R. J. Hunt, Ph.D. thesis, University of Minnesota, Minneapolis, Minn., 1976, p. 21.
(9) J. G. Wagner and E. Nelson, *J. Pharm. Sci.*, **52**, 610 (1963).
(10) P. A. Mitenko and R. I. Ogilvie, *Clin. Pharmacol. Ther.*, **13**, 329 (1972).
(11) *Ibid.*, **14**, 509 (1973).
(12) W. L. Chiou, S. Riegelman, and J. R. Amberg, *Chem. Pharm. Bull.*, **17**, 2170 (1969).
(13) T. Madea, H. Takenata, Y. Yamahira, and T. Noguchi, *J. Pharm. Sci.*, **66**, 69 (1977).
(14) M. Gibaldi and D. Perrier, "Pharmacokinetics," Dekker, New York, N.Y., 1975, p. 35.
(15) J. C. K. Loo and S. Riegelman, *J. Pharm. Sci.*, **57**, 918 (1968).
(16) P. K. Ng and R. A. Locock, *Res. Commun. Pathol. Pharmacol.*, **26**, 509 (1979).
(17) M. Weinberger and E. Ginchansky, *J. Pediatr.*, **91**, 820 (1977).
(18) L. J. Lesko, *Clin. Pharmacokinet.*, **4**, 449 (1979).
(19) S. Sved, I. J. McGilveray, and D. L. Wilson, "Abstracts of Papers Presented at the APhA Academy of Pharmaceutical Sciences," Montreal meeting, 1978.

## NOTES

# Effect of Capsule Size on Permeability of Gelatin–Acacia Microcapsules toward Sodium Chloride

**IVAN JALŠENJAK * and TAMOTSU KONDO ˣ**

Received January 8, 1980, from the *Faculty of Pharmaceutical Sciences, Science University of Tokyo, Shinjuku-ku, Tokyo, Japan 162.* Accepted for publication September 9, 1980. *Present address: Faculty of Pharmacy and Biochemistry, University of Zagreb, Domagojeva 2, 41000 Zagreb, Yugoslavia.

**Abstract** □ The effect of capsule size on the permeability of gelatin–acacia microcapsules toward sodium chloride was investigated. Gelatin–acacia microcapsules containing olive oil were prepared by phase separation. The encapsulated olive oil was extracted with acetone and the acetone-loaded microcapsules dispersed in acetone were fractionated by a series of mesh screens. The core material of acetone then was replaced by water. The permeability of each capsule fraction toward sodium chloride was estimated from the change in electrical conductance with time of the mixture of microcapsule suspension and sodium chloride solution. The permeability decreased with decreasing capsule size. Structured water in and around the capsule wall may be the cause of the observed size effect.

**Keyphrases** □ Gelatin–acacia microcapsules—prepared by phase separation, capsule-size effect on permeability toward sodium chloride □ Permeability—gelatin–acacia microcapsules, evaluated for capsule-size effect □ Capsule size—effect on permeability of gelatin–acacia microcapsules □ Microcapsules, gelatin–acacia—capsule-size effect on permeability toward sodium chloride

Relatively few papers (1–4) have dealt with the permeability characteristics of microcapsules, and many uncertainties remain (5) in spite of their importance in the sustained release of encapsulated drugs and chemicals and the application of microcapsules in enzyme technology and therapy and in the removal of waste products by polymer-coated charcoal. Among the various permeability characteristics of microcapsules, the effect of capsule size seems to be the most ignored; only one paper (6) described the size effect on the permeability of ethylcellulose microcapsules toward electrolytes. This situation prompted the present study to see if capsule size affects the permeability of microcapsules made of polymers other than ethylcellulose. The observed size effect on the permeability of gelatin–acacia microcapsules toward sodium chloride is reported here.

## EXPERIMENTAL

**Preparation of Microcapsules**—The gelatin–acacia microcapsules were prepared as described earlier (7). Gelatin and acacia solutions were made by dissolving separately 5 g each of gelatin[1] (pI 5.0) and acacia[2] in 100 ml of distilled water. These solutions were allowed to hydrate for 10 min at room temperature and then for 30 min at ~47°. Coacervation was induced at 47°.

Fifty milliliters of olive oil was added in small portions to the gelatin solution with gentle stirring. The stirring rate then was increased for 15 sec. The acacia solution then was added in portions with moderate stirring to the newly formed emulsion. With this procedure, a favorable degree of emulsification and spherical mononuclear microcapsules were obtained. The system was adjusted to pH 3.5 by dropwise addition of 10% acetic acid after the addition of the acacia solution.

Coacervation was brought about by adding 170 ml of distilled water prewarmed at 47° in 3-ml portions during 20 min. The temperature was decreased to 5° at a rate of 0.3°/min. This cooling rate was found to be very important in obtaining spherical microcapsules. When the temperature reached 5°, a dilute formaldehyde solution was added to the microcapsule dispersion to make the final aldehyde concentration ~6 m*M*, and the pH was raised to 8.5 by the addition of 10% NaOH. After a 2-hr reaction time, the insolubilized microcapsules were separated by centrifugation in a low field of no higher than 100×*g* to avoid possible breakdown of the capsules.

**Fractionation of Microcapsules**—A wet mass of the microcapsules (~10 g) was transferred into 1000 ml of acetone to extract the encapsulated olive oil. The suspension was stirred vigorously by a magnetic stirrer to prevent capsule aggregation. Ten minutes later, the microcapsules were filtered and transferred into 200 ml of acetone. After this procedure was repeated four times, the acetone-loaded gelatin–acacia microcapsules dispersed in acetone were obtained.

The acetone-loaded microcapsules were fractionated in acetone by a series of mesh screens. Each capsule fraction of a given size was filtered through a coarse filter paper. The separated microcapsules of each fraction were transferred into a large volume of distilled water with vigorous stirring. In this way, acetone was replaced by water. The procedure was not repeated more than twice, because the water-containing gelatin–acacia microcapsules thus obtained were sticky to the surface of the filter paper.

**Determination of Microcapsule Size**—To determine the size of the microcapsules, a sample of each capsule fraction was placed on a hemocytometer, and the microcapsules were photographed under an optical microscope. The photographed film was projected on a large section of paper, and 500 enlarged capsule images were measured to the nearest 0.8 μm. The scale in the hemocytometer was used for calibration. Finally,

[1] Nippi Co., Tokyo, Japan.
[2] Gum acacia JP, Kokusan Chemicals, Tokyo, Japan.



0022-3549/81/0400-0456$01.00/0
© 1981, American Pharmaceutical Association

(8) R. J. Hunt, Ph.D. thesis, University of Minnesota, Minneapolis, Minn., 1976, p. 21.
(9) J. G. Wagner and E. Nelson, *J. Pharm. Sci.*, **52**, 610 (1963).
(10) P. A. Mitenko and R. I. Ogilvie, *Clin. Pharmacol. Ther.*, **13**, 329 (1972).
(11) *Ibid.*, **14**, 509 (1973).
(12) W. L. Chiou, S. Riegelman, and J. R. Amberg, *Chem. Pharm. Bull.*, **17**, 2170 (1969).
(13) T. Madea, H. Takenata, Y. Yamahira, and T. Noguchi, *J. Pharm. Sci.*, **66**, 69 (1977).
(14) M. Gibaldi and D. Perrier, "Pharmacokinetics," Dekker, New York, N.Y., 1975, p. 35.
(15) J. C. K. Loo and S. Riegelman, *J. Pharm. Sci.*, **57**, 918 (1968).
(16) P. K. Ng and R. A. Locock, *Res. Commun. Pathol. Pharmacol.*, **26**, 509 (1979).
(17) M. Weinberger and E. Ginchansky, *J. Pediatr.*, **91**, 820 (1977).
(18) L. J. Lesko, *Clin. Pharmacokinet.*, **4**, 449 (1979).
(19) S. Sved, I. J. McGilveray, and D. L. Wilson, "Abstracts of Papers Presented at the APhA Academy of Pharmaceutical Sciences," Montreal meeting, 1978.

## NOTES

# Effect of Capsule Size on Permeability of Gelatin–Acacia Microcapsules toward Sodium Chloride

**IVAN JALŠENJAK * and TAMOTSU KONDO ˣ**

Received January 8, 1980, from the *Faculty of Pharmaceutical Sciences, Science University of Tokyo, Shinjuku-ku, Tokyo, Japan 162.* Accepted for publication September 9, 1980. *Present address: Faculty of Pharmacy and Biochemistry, University of Zagreb, Domagojeva 2, 41000 Zagreb, Yugoslavia.

**Abstract** □ The effect of capsule size on the permeability of gelatin–acacia microcapsules toward sodium chloride was investigated. Gelatin–acacia microcapsules containing olive oil were prepared by phase separation. The encapsulated olive oil was extracted with acetone and the acetone-loaded microcapsules dispersed in acetone were fractionated by a series of mesh screens. The core material of acetone then was replaced by water. The permeability of each capsule fraction toward sodium chloride was estimated from the change in electrical conductance with time of the mixture of microcapsule suspension and sodium chloride solution. The permeability decreased with decreasing capsule size. Structured water in and around the capsule wall may be the cause of the observed size effect.

**Keyphrases** □ Gelatin–acacia microcapsules—prepared by phase separation, capsule-size effect on permeability toward sodium chloride □ Permeability—gelatin–acacia microcapsules, evaluated for capsule-size effect □ Capsule size—effect on permeability of gelatin–acacia microcapsules □ Microcapsules, gelatin–acacia—capsule-size effect on permeability toward sodium chloride

Relatively few papers (1–4) have dealt with the permeability characteristics of microcapsules, and many uncertainties remain (5) in spite of their importance in the sustained release of encapsulated drugs and chemicals and the application of microcapsules in enzyme technology and therapy and in the removal of waste products by polymer-coated charcoal. Among the various permeability characteristics of microcapsules, the effect of capsule size seems to be the most ignored; only one paper (6) described the size effect on the permeability of ethylcellulose microcapsules toward electrolytes. This situation prompted the present study to see if capsule size affects the permeability of microcapsules made of polymers other than ethylcellulose. The observed size effect on the permeability of gelatin–acacia microcapsules toward sodium chloride is reported here.

## EXPERIMENTAL

**Preparation of Microcapsules**—The gelatin–acacia microcapsules were prepared as described earlier (7). Gelatin and acacia solutions were made by dissolving separately 5 g each of gelatin[1] (pI 5.0) and acacia[2] in 100 ml of distilled water. These solutions were allowed to hydrate for 10 min at room temperature and then for 30 min at ~47°. Coacervation was induced at 47°.

Fifty milliliters of olive oil was added in small portions to the gelatin solution with gentle stirring. The stirring rate then was increased for 15 sec. The acacia solution then was added in portions with moderate stirring to the newly formed emulsion. With this procedure, a favorable degree of emulsification and spherical mononuclear microcapsules were obtained. The system was adjusted to pH 3.5 by dropwise addition of 10% acetic acid after the addition of the acacia solution.

Coacervation was brought about by adding 170 ml of distilled water prewarmed at 47° in 3-ml portions during 20 min. The temperature was decreased to 5° at a rate of 0.3°/min. This cooling rate was found to be very important in obtaining spherical microcapsules. When the temperature reached 5°, a dilute formaldehyde solution was added to the microcapsule dispersion to make the final aldehyde concentration ~6 m*M*, and the pH was raised to 8.5 by the addition of 10% NaOH. After a 2-hr reaction time, the insolubilized microcapsules were separated by centrifugation in a low field of no higher than 100×*g* to avoid possible breakdown of the capsules.

**Fractionation of Microcapsules**—A wet mass of the microcapsules (~10 g) was transferred into 1000 ml of acetone to extract the encapsulated olive oil. The suspension was stirred vigorously by a magnetic stirrer to prevent capsule aggregation. Ten minutes later, the microcapsules were filtered and transferred into 200 ml of acetone. After this procedure was repeated four times, the acetone-loaded gelatin–acacia microcapsules dispersed in acetone were obtained.

The acetone-loaded microcapsules were fractionated in acetone by a series of mesh screens. Each capsule fraction of a given size was filtered through a coarse filter paper. The separated microcapsules of each fraction were transferred into a large volume of distilled water with vigorous stirring. In this way, acetone was replaced by water. The procedure was not repeated more than twice, because the water-containing gelatin–acacia microcapsules thus obtained were sticky to the surface of the filter paper.

**Determination of Microcapsule Size**—To determine the size of the microcapsules, a sample of each capsule fraction was placed on a hemocytometer, and the microcapsules were photographed under an optical microscope. The photographed film was projected on a large section of paper, and 500 enlarged capsule images were measured to the nearest 0.8 μm. The scale in the hemocytometer was used for calibration. Finally,

[1] Nippi Co., Tokyo, Japan.
[2] Gum acacia JP, Kokusan Chemicals, Tokyo, Japan.



0022-3549/81/0400-0456$01.00/0
© 1981, American Pharmaceutical Association

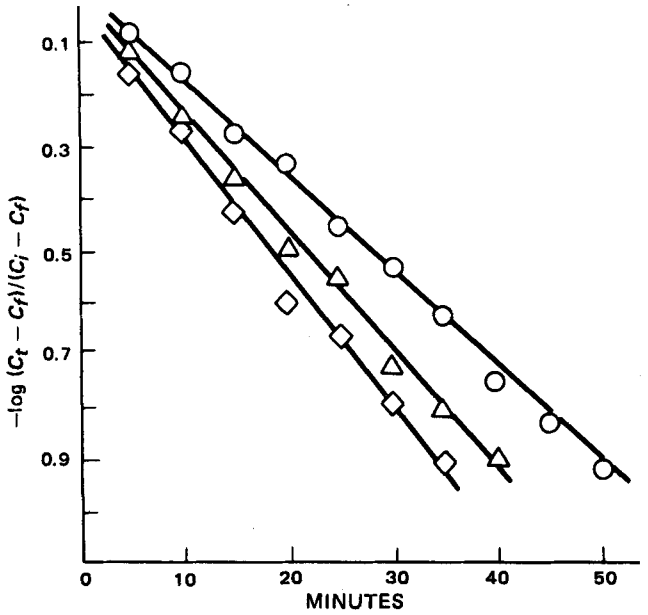


**Figure 1**—*Plot of log* $(C_t - C_f)/(C_i - C_f)$ *against time for the entry of sodium chloride into gelatin–acacia microcapsules. Key (capsule fraction):* ○, *A;* △, *B; and* ◇, *C.*

the mean diameter of the microcapsules was calculated using the measured diameters.

**Permeability Estimation**—As in previous work (2–4, 6), the permeability of the microcapsules was estimated from the change in electrical conductance with time of the microcapsule dispersion–electrolyte solution mixture. To 100 ml of 0.05 *M* NaCl solution in a conductance cell immersed in a constant-temperature bath was quickly added, with stirring, 100 ml of the microcapsule dispersion previously kept at the same temperature. The conductance reading was begun soon after mixing and was taken at suitable time intervals. The electrical conductance measurements were carried out at 10 ± 0.1°. The stirring was continued throughout the measurements.

The permeability coefficient for the electrolyte ($P$) was calculated from (3, 4, 6):

$$P = -\frac{2.303 C_f V_m}{C_i A t} \log \frac{C_t - C_f}{C_i - C_f} \qquad \text{(Eq. 1)}$$

where $C_i$, $C_t$, and $C_f$ are the initial, intermediary (at time $t$), and final concentrations of electrolyte in the dispersion medium, respectively, and $V_m$ and $A$ are the total volume and total surface area of the microcapsules, respectively. The validity of the equation can be checked by plotting log $(C_t - C_f)/(C_i - C_f)$ against time. If the plot is linear, the equation strictly holds and the permeability coefficient can be evaluated from the slope of the line.

## RESULTS AND DISCUSSION

Figure 1 shows plots of log $(C_t - C_f)/(C_i - C_f)$ against time for the entry of sodium chloride into the gelatin–acacia microcapsules of different sizes. For all fractions, the plot was a straight line 5 min after mixing the electrolyte solution and microcapsule dispersion. This finding seems to confirm the validity of the equation for the calculation of the permeability coefficient.

The permeability coefficients for sodium chloride calculated from the slope of the straight line are given in Table I. The permeability coefficient decreased with decreasing capsule size. The same trend was observed with other preparations of gelatin–acacia microcapsules, although the permeability coefficient value varied from one preparation to another.

**Table I—Mean Diameter, Total Volume, and Permeability Coefficient for Sodium Chloride of Gelatin–Acacia Microcapsules**

| Fraction | Mean Diameter, μm | Total Volume, % | Permeability Coefficient, × $10^6$ cm/sec |
|---|---|---|---|
| A | 79 | 13 | 0.95 |
| B | 115 | 12 | 1.86 |
| C | 151 | 12 | 3.12 |

In view of the highly hydrophilic nature of both gelatin and acacia, the wall of gelatin–acacia microcapsules can be assumed to be a hydrogel even after treatment with formaldehyde. Thus, sodium and chloride ions are transported through a capillary network filled with water of the microcapsule wall. Under these circumstances, the rate of ion transport is expected to depend on the wall thickness (extent of capillary network), total volume of the microcapsules (size of sink), and total surface area of the microcapsules.

The wall thickness was constant and independent of the capsule size for gelatin–acacia microcapsules obtained in one preparation (8), and the total microcapsule volume was approximately the same for all fractions (Table I). Hence, the observed size-dependent permeability should arise from the difference in the total surface area of the microcapsules. According to Fick's first law of diffusion, however, the rate of ion transport increases with increasing total surface area or decreasing capsule size. This concept is contrary to the observed capsule-size effect.

A recent paper (9) indicated that the water structure in and around the wall of polyamide microcapsules is different from that of the bulk, and this difference may be responsible for the decreasing permeability of the microcapsules toward electrolytes with decreasing capsule size. This effect occurs because the structured water in and around the capsule wall retards the movement of hydrated ions, and the amount of structured water is greater in a dispersion containing numerous microcapsules of a small size than in that containing few microcapsules of a large size, assuming that the total microcapsule volume is identical for both dispersions. This observation also may account for the size effect on the permeability of gelatin–acacia microcapsules toward sodium chloride observed in the present work.

## REFERENCES

(1) T. M. S. Chang and M. J. Poznansky, *J. Biomed. Mater. Res.*, **2**, 187 (1968).

(2) Y. Shigeri and T. Kondo, *Chem. Pharm. Bull.*, **17**, 1073 (1969).

(3) K. Takamura, M. Koishi, and T. Kondo, *Kolloid-Z. Z. Polym.*, **248**, 929 (1971).

(4) K. Takamura, M. Koishi, and T. Kondo, *J. Pharm. Sci.*, **62**, 610 (1973).

(5) T. Kondo, in "Surface and Colloid Science," vol. 10, E. Matijevic, Ed., Plenum, New York, N.Y., 1978, pp. 1–43.

(6) Y. Ohta, M. Arakawa, and T. Kondo, *Membrane*, **3**, 283 (1978).

(7) L. A. Luzzi and R. J. Gerraughty, *J. Pharm. Sci.*, **53**, 429 (1964).

(8) L. Si-Nang, P. F. Carlier, P. Delort, J. Gazzola, and D. Lafont, *ibid.*, **62**, 452 (1973).

(9) T. Ishizaka, M. Koishi, and T. Kondo, *J. Membrane Sci.*, **5**, 283 (1979).

## ACKNOWLEDGMENTS

I. Jalšenjak is grateful to the Japan Society for the Promotion of Science for financial assistance during his stay in Tokyo.

# High-Pressure Liquid Chromatographic Method with Postcolumn, In-Line Hydrolysis and Fluorometric Detection for Indomethacin in Biological Fluids

**W. F. BAYNE ˣ, T. EAST, and D. DYE**

Received June 9, 1980, from *Alza Corporation, Palo Alto, CA 94304.* Accepted for publication September 18, 1980.

**Abstract** □ A rapid and sensitive method for the analysis of indomethacin in plasma and urine was developed using high-pressure liquid chromatography, postcolumn, in-line hydrolysis of indomethacin to a fluorophore, and detection of the fluorophore with a fluorometer. The lower limit of detection was 1.5 ng/ml of plasma. The coefficient of variation at 30 ng/ml of plasma was 4.5% ($n$ = 5). The nonconjugated metabolites of indomethacin, aspirin, and salicylate were resolved from indomethacin and the internal standard, α-methylindomethacin.

**Keyphrases** □ Indomethacin—high-pressure liquid chromatographic determination using fluorometric detection, human plasma and urine □ High-pressure liquid chromatography—analysis, indomethacin, fluorometric detection following hydrolysis of indomethacin to fluorophore □ Anti-inflammatory agents—indomethacin, high-pressure liquid chromatographic determination using fluorescence detection

Indomethacin, a widely used anti-inflammatory, has been assayed in biological fluids and tissues by spectrofluorometry (1–6), radiometric methods (7, 8), GLC with electron-capture detection (9–12), GLC with selective-ion monitoring (13), high-pressure liquid chromatography (HPLC) (14–16), and TLC (17).

## BACKGROUND

The original spectrofluorometric methods (1–5) were modified recently (6) to eliminate errors in the quantification of the drug caused by its metabolites, *N*-deschlorobenzoylindomethacin, *O*-desmethylindomethacin, and *N*-deschlorobenzoyl-*O*-desmethylindomethacin (7). The 5-*O*-desmethyl metabolites were destroyed by oxidation with cupric ion, and the *N*-deschlorobenzoyl metabolite resulting from alkaline hydrolysis of indomethacin was accounted for by a differential technique (hydrolysis *versus* no hydrolysis). The method was reported to be capable of quantifying 100 ng of indomethacin in 3 ml of plasma.

Isotope dilution analyses have been developed for indomethacin, its metabolites, and their conjugates in biological fluids (7). Although capable of quantifying the parent drug and its metabolites, the method requires administration of radiolabeled drug. Its principal use is in ascertaining the metabolic fate of the drug.

A radioimmunoassay for indomethacin was reported that can determine concentrations as low as 50 ng/ml (8). The assay is highly cross-reactive to the glucuronide conjugates of indomethacin and desmethylindomethacin and is slightly cross-reactive to desmethylindomethacin.

The GLC methods include derivatization of the drug to facilitate chromatography as an integral part of the assay. Esters of the drug have been prepared successfully by alkylation with diazoalkanes (diazomethane, diazoethane, and diazopropane) (9–12), by extractive alkylation with alkyl iodides (11), by alkylation in an organic solvent with alkyl iodides in contrast to extractive alkylations (11), and by silylation with bis(trimethylsilyl)acetamide (12). Diazomethane could be employed to esterify indomethacin without the concomitant methylation of the phenolic group of 5-*O*-desmethylindomethacin (12), which, if it occurred, could render the assay nonspecific.

To eliminate the necessity for derivatization and the potential hazards with the diazoalkanes, HPLC methods recently were developed as an alternative to GLC (14–16). The UV absorbance of the drug is used as a means of detection. Detection limits of 100 ng/ml of serum were reported for two of the HPLC methods, with absorbance of the drug being measured at 200 (15) and 235 (16) nm.

An HPLC method with postcolumn, in-line, alkaline hydrolysis of indomethacin to a fluorophore and measurement of the generated fluorophore with a fluorometric detector was developed to: (*a*) increase the sensitivity above that achievable with a UV absorbance detector and (*b*) reduce the biological background relative to indomethacin in extracted samples by increasing the specificity in detection. Furthermore, since hydrolysis was performed in-line, sample preparation and workup were considerably less intensive than with conventional spectrofluorometric methods.

## EXPERIMENTAL

**Apparatus**—A liquid chromatographic system was assembled from two high-pressure reciprocating pumps[1]; a stainless steel chromatographic column (25 cm × 4 mm i.d.) packed with microparticulate material[2]; an automatic injector[3]; coiled polytef tubing (4.8 m × 0.7 cm i.d.), which served as a postcolumn, in-line reactor; a water bath[4] (64°) in which the polytef tubing was immersed; a T-fitting[5], which served to connect the reactor, one pump, and the column; and a fluorescence detector[6]. Fluorescence was quantified with an integrator-calculator[7].

Samples were chromatographed in the reversed-phase mode. An alkaline solution was introduced into the mobile phase exiting the column to hydrolyze indomethacin and the internal standard (α-methylindomethacin) to fluorophores. The fluorophores were excited at 295 nm with the detector, and fluorescence of <340 nm was excluded with a cutoff filter.

**Solutions**—The mobile phase was 76% methanol in 0.025 *M* phosphate buffer (pH 4.0), prepared from monobasic potassium phosphate and phosphoric acid. The volumetric flow rate of the mobile phase was 1.0 ml/min.

The alkaline solution introduced into the mobile phase, postcolumn, was 0.1 *N* NaOH at a flow rate of 0.1 ml/min.

β-Glucuronidase[8] (0.5 mg/ml) was dissolved in 0.5 *M* citrate buffer (pH 5) prepared from citric acid monohydrate and sodium hydroxide.

Indomethacin[9] and α-methylindomethacin[9] were weighed accurately and dissolved in methanol to prepare working solutions of 1.4 and 7 μg/ml, respectively. Methanolic solutions (5 μg/ml) of *N*-deschlorobenzoyl-*O*-desmethylindomethacin[9], *N*-deschlorobenzoylindomethacin[9], and *O*-desmethylindomethacin[9] were prepared and used to ascertain the resolution of metabolites from indomethacin and the internal standard.

**Plasma Extraction**—Extraction of plasma samples was carried out in silanized glass, 40-ml, stoppered centrifuge tubes. Citrate buffer (1 ml of a 0.5 *M* solution, pH 5.0) and ethylene dichloride (10 ml) were added to the plasma samples (1 ml). The centrifuge tubes were sealed with polytef stoppers and shaken gently with a horizontal shaker for 20 min. They then were centrifuged at 1000×*g* for 5 min, and the upper aqueous layer was aspirated. The remaining organic phase was carefully poured into a conical test tube (15 ml) and evaporated to dryness under nitrogen in a 50° water bath. The residues were dissolved in methanol (100 μl), and the solution was mixed with a vortex mixer.

**Extraction of Urine**—Urine samples were prepared for analysis in a manner similar to that described for the plasma samples. In addition, prior to extraction with ethylene dichloride, β-glucuronidase (0.3 ml of a 5000-units/ml solution) was added to the buffered urine sample to hydrolyze the glucuronide conjugate. The contents were incubated at 37° for 30 min. These hydrolytic conditions (incubation time and amount

[1] Model 6000 A solvent delivery system, Waters Associates, Milford, Mass.
[2] ODS-Hypersil, Shandon Southern.
[3] WISP automatic sample processor, Waters Associates, Milford, Mass.
[4] Model 1420 Thermomix, B. Braun.
[5] Altech, Arlington Heights, Ill.
[6] Model FS970 fluorometer, Schoeffel Instrument Corp., Westwood, N.J.
[7] Model 4100, Spectra-Physics, Santa Clara, Calif.
[8] Type B-10 (10,000 units/mg), Sigma Chemical Co., St. Louis, Mo.
[9] Merck Sharp and Dohme Research Laboratories, West Point, Pa.



0022-3549/81/0400-0458$01.00/0
© 1981, American Pharmaceutical Association

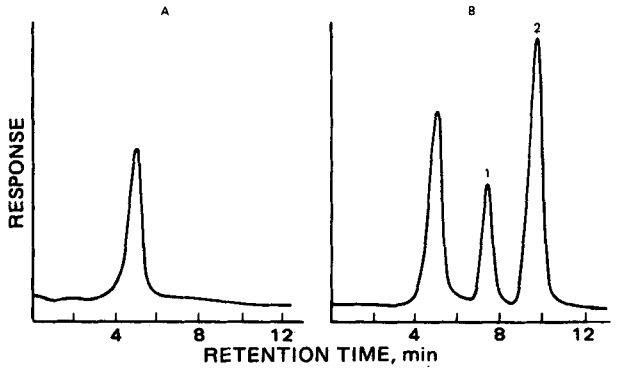


**Figure 1**—*Chromatograms from blank plasma (1 ml) (A) and from plasma (1 ml) containing 89.4 ng of indomethacin/ml (1) and 298 ng of α-methylindomethacin/ml (2) (B).*

of enzyme) produced the maximum amount of free indomethacin in urine samples from subjects previously administered the drug.

**Standard Curves**—Standard curves were generated by spiking blank plasma and urine samples (1-ml volumes) with varying amounts of indomethacin and a constant amount of internal standard. Microliter aliquots of the working solutions or a 1:10 dilution of the working solution were added to the biological samples. The internal standard concentrations in the plasma and urine samples were 0.25 and 2.5 μg/ml, respectively. The indomethacin concentration ranges in the plasma and urine samples were 0.03–3.0 and 0.3–30 μg/ml, respectively.

The samples were prepared according to the extraction procedures described. Plots of the peak area ratios (indomethacin to internal standard) against the respective indomethacin concentrations were linear. Typical standard curves for indomethacin in plasma and urine had a correlation coefficient of 0.9999.

The coefficients of variation for five replicate assays at 0.03, 0.09, 0.3, 0.9, and 3.0 μg/ml of plasma were 4.5, 1.8, 1.2, 0.6, and 0.9%, respectively. The coefficients of variation for five replicate assays at 0.3, 0.9, 3.0, 8.9, and 29.8 μg/ml of urine were 2.8, 0.9, 0.9, 1.2, and 0.8%, respectively.

A typical chromatogram for a plasma extract is presented in Fig. 1. The retention times for indomethacin and the internal standard were 7.5 and 9.5 min, respectively. Chromatograms obtained from urine extracts over the concentration range studied were similar to those obtained from the plasma extracts; only the background peak at 5 min was discernible.

## RESULTS AND DISCUSSION

The achievable detection limit for indomethacin in plasma using the method described is 1.5 ng/ml (1 ml of plasma volume). The method is as sensitive as GLC methods utilizing electron-capture detection [2 (12) and 5 (11) ng/sample] but does not require derivatization. The high sensitivity of the method is due in part to the detection specificity that results from a low biological background relative to indomethacin. The high sensitivity permits the use of biological samples of <1 ml.

The recoveries of indomethacin (400 ng/ml) and the internal standard (400 ng/ml) were >99% when the compounds were extracted from plasma using the described procedure. Helleberg (10) showed that the recovery of indomethacin was nearly quantitative (95%) when serum was buffered at pH 5.0 and extracted with ethylene dichloride. The recoveries decreased markedly when the pH was greater or less than pH 5.0

The maximum responses (peak area) for indomethacin and α-methylindomethacin were achieved by delivering 0.1 *N* NaOH at a volumetric flow rate of 0.1 ml/min, postcolumn, into the mobile phase. As the sodium hydroxide concentration or the volumetric flow rate was increased, the responses decreased. At optimal conditions, the pH of the mixed streams leaving the reactor coil was 9.0. Hvidberg *et al.* (4), in investigating hydrolytic conditions for a spectrofluorometric method, stated that the fluorescence develops slower but to a greater intensity in buffers that are less alkaline than 0.1 *N* NaOH.

The reactor coil was heated in a water bath to facilitate rapid, in-line conversion of indomethacin to the fluorophore. Under the hydrolytic conditions described, the response per mole of indomethacin was greater than that for deschlorobenzoylindomethacin, the presumed hydrolysis product. Hence, the hydrolysis product apparently is converted to a nonfluorescent species as it proceeds through the reactor coil. However, although processes secondary to the hydrolysis of indomethacin are likely to occur in the reaction coil, the method is sensitive and reproducible.

The peak shape and resolution also were improved markedly by heating the reaction coil. It is possible that the flow characteristics approached that of plug flow at the elevated temperature.

The three major nonconjugated metabolites of indomethacin, *N*-deschlorobenzoylindomethacin, *O*-desmethylindomethacin, and *O*-desmethyl-*N*-deschlorobenzoylindomethacin, all had retention times less than the retention time of indomethacin. Aspirin and salicylate also had shorter retention times. Therefore, these compounds did not constitute a source of error in indomethacin quantification.

By utilizing a solvent gradient (methanol and 0.01 *M* phosphate buffer, pH 4.0), the drug and metabolites could be resolved from each other within 15 min. Thus, with fluorometric detection, this method has the potential to quantify the metabolites in addition to indomethacin, as is the case with a recently published HPLC method using spectrophotometric detection (16).

The method has been used to analyze indomethacin in over 1000 biological samples collected for a multiple-dose bioavailability study[10]. No deterioration of column performance or of the assay as a whole was observed.

## REFERENCES

(1) L. P. J. Holt and C. F. Hawkins, *Br. Med. J.*, **1**, 1354 (1965).

(2) H. B. Hucker, A. G. Zacchei, S. V. Cox, D. A. Brodie, and N. H. R. Cantwell, *J. Pharmacol. Exp. Ther.*, **153**, 237 (1966).

(3) H. W. Emori, G. D. Champion, R. Bluestone, and H. S. Paulus, *Ann. Rheum. Dis.*, **32**, 433 (1972).

(4) E. Hvidberg, H. H. Lausen, and J. A. Jansen, *Eur. J. Clin. Pharmacol.*, **4**, 119 (1972).

(5) B. Lindquist, K. Moller, K. M. Jensen, H. Johansson, and T. Hansen, *Clin. Pharmacol. Ther.*, **15**, 247 (1974).

(6) K. C. Kwan, G. O. Breault, R. L. Davis, B. W. Lei, A. W. Czerwinski, G. W. Besselaar, and D. E. Duggan, *J. Pharmacokinet. Biopharm.*, **6**, 451 (1978).

(7) D. E. Duggan, A. F. Hogans, K. C. Kwan, and F. G. McMahon, *J. Pharmacol. Exp. Ther.*, **181**, 563 (1972).

(8) L. E. Hare, C. A. Ditzler, and D. E. Duggan, *J. Pharm. Sci.*, **66**, 486 (1977).

(9) D. G. Ferry, D. M. Ferry, P. W. Moller, and E. G. McQueen, *J. Chromatogr.*, **89**, 110 (1974).

(10) L. Helleberg, *ibid.*, **117**, 167 (1976).

(11) A. Arbin, *ibid.*, **144** (1977).

(12) B. Plazonnet and W. J. A. VandenHeuvel, *ibid.*, **142**, 587 (1977).

(13) L. Palmer, L. Bertilsson, G. Alvan, M. Orme, F. Sjöqvist, and B. Holmstedt, in "Prostaglandin Synthetase Inhibitors," H. J. Robinson and J. R. Vane, Eds., Raven, New York, N.Y., 1974, p. 91.

(14) G. G. Skellern and E. G. Salole, *J. Chromatogr.*, **114**, 483 (1975).

(15) S. J. Soldin and T. Gero, *Clin. Chem.*, **25**, 589 (1979).

(16) C. P. Terweij-Groen, S. Hoemstra, and J. C. Kraak, *J. Chromatogr. (Biomed. Appl.)*, **181**, 385 (1980).

(17) M. J. Van der Meer and H. Hundt, *ibid.*, **181**, 282 (1980).

[10] To be published.

# Quality Control of Phenylbutazone I: Analysis of Phenylbutazone and Decomposition Products in Drugs by TLC

**H. FABRE** ˣ **and B. MANDROU**

Received June 2, 1980, from the *Laboratoire de Chimie Analytique, Faculté de Pharmacie, 34060 Montpellier Cedex, France.* Accepted for publication September 30, 1980.

**Abstract** □ A modified TLC procedure for the analysis of phenylbutazone and its degradates on silica plates is reported. This method avoids phenylbutazone degradation *in situ* by chelating the iron of the silica plate, which allows rapid characterization with a fluorescence indicator. A selective and sensitive assay of phenylbutazone (0.025 μg), using a chromatographic spectrophotometer, was performed on silica plates without a fluorescence indicator. Quantitative analysis of an injectable solution is outlined.

**Keyphrases** □ Phenylbutazone—degradation products, TLC, qualitative and quantitative analyses, UV reflectometric measurements on plates □ Degradation—phenylbutazone, qualitative and quantitative analyses □ TLC—analysis, phenylbutazone and degradation products

Stability studies of phenylbutazone (I) in drugs and raw materials have been widely reported (1–7). A semiquantitative method to estimate the degradation products by TLC (1) was later modified (2) to minimize the rapid air oxidation of phenylbutazone on the silica coating, which occurs during analysis (2, 4, 8). This paper demonstrates the original causes of phenylbutazone degradation on precoated silica plates and proposes a TLC procedure to avoid this decomposition. An accurate estimation of phenylbutazone and its main degradation products can be achieved with a chromatogram spectrophotometer.

## BACKGROUND

Under normal conditions, phenylbutazone (I) is oxidized. The main decomposition products were identified, and the mechanism of their formation was proposed previously (2, 9).

In TLC, phenylbutazone degradation *in situ* on the silica plate is not always evident (1, 6, 10). Various investigators reported this decomposition (2, 8) and proposed modified procedures to delay the formation of the major oxidation products on the plate [oxyphenbutazone, 4-hydroxyphenylbutazone, II, and *N*-(2-carboxycaproyl)hydrazobenzene, III].

Oxidation on the plate, which occurs with other pyrazolones (8, 11, 12), may be important; after 2 hr of contact, decomposition may reach 100%, depending on the coating material and the solvent system. Macek (8) suggested that this reaction probably is due to the iron content of the silica.

Empiric studies suggested preparation of the coating by mixing silica with pH 6 McIlvaine buffer (citric acid–dibasic sodium phosphate) (2), bismuth nitrate (13), or acid sodium sulfite (4).

To clarify the cause of the degradation, silica plates impregnated with either 0.2 *M* $Na_2HPO_4$ or 0.1 *M* citric acid were prepared (2). In the first case, significant I degradation occurred; in the second case, no decomposition was observed even after 1 hr of contact. This test indicated that degradation on the plate was not mainly due to the acidic pH of the silica, although phenylbutazone decomposition is accelerated under acid and alkaline conditions (1, 9, 14, 15). When using pH 6 McIlvaine buffer, phosphate ions may delay the phenylbutazone autoxidation and hydrolysis, but citric acid is the major agent avoiding the degradation. As suggested previously (8), iron (present in silica) is the main degradative agent that catalyzes the oxidation of the finely divided phenylbutazone on the plate. Citric acid complexes the iron of the coating and prevents phenylbutazone from the oxidation. The use of silica plates impregnated with edetate sodium supports this hypothesis.

Precoated plates sprayed with acid sodium sulfite (4) and bismuth nitrate (13) were used. A rapid degradation on the plate was observed with quenched fluorescence in the former case; no decomposition, within the limits of sensitivity (iodine vapor detection), was evident after 1 hr of contact in the latter. Bismuth nitrate is a quenching agent, which does not allow the use of silica gel $F_{254}$ precoated plates. However, an aqueous solution cannot permeate precoated plates as easily as alcoholic solutions.

A simple and rapid analytical procedure using precoated silica plates washed with an alcoholic citric acid solution is proposed.

**Table I—$R_f$ Values (×100) of Phenylbutazone and Degradation Compounds**

| Compound | Relative to Phenylbutazone (I) | Relative to Phthalic Acid (VI) |
|---|---|---|
| I | 100 | 528 |
| II | 42 | 224 |
| III | 33 | 172 |
| IV | 29 | 152 |
| V[a] | 119 | 628 |

[a] Compound V was detected by spraying with 0.5% (w/v) dichromate in 20% (v/v) $H_2SO_4$.

## EXPERIMENTAL

**Materials and Reagents**—Glassware was rinsed with hot nitric acid. A 10-μl syringe[1] was calibrated at 0.1-μl intervals. A chromatogram spectrophotometer[2] was equipped with a chart recorder[3] and an electronic integrator[4]. Precoated silica gel $F_{254}$ glass plates[5] (0.25 mm thick) were used for qualitative determinations, and precoated silica gel G glass plates[5] (0.25 mm thick) were used for qualitative and quantitative determinations.

All solvents were distilled from a glass apparatus (the absence of iron was checked with ferrozine reagent). Citric acid, phthalic acid, and formic acid were analytical grade. Phenylbutazone and the degradation products[6] were used as received. The solutions of phenylbutazone and degradates were freshly prepared and stored in the dark in a refrigerator.

The solvent system was hexane–chloroform–ethanol–formic acid (60:30:9:1). The silica plates for qualitative and quantitative analyses were soaked in alcoholic citric acid solution (1%) for a few minutes with occasional stirring, dried at 40° for 15 min and then at 105° for 15 min, and stored in a desiccator.

**Procedure**—For qualitative analysis, the mixed standard ethanolic solution was prepared as follows: I, 10 mg/ml; II, 100 μg/ml; III, 100 μg/ml; *N*-(2-carboxy-2-hydroxycaproyl)hydrazobenzene (IV), 100 μg/ml; and azobenzene (V), 100 μg/ml.

The standard solution (5 μl) and an injectable formulation (600 mg of phenylbutazone and 30 mg of lidocaine diluted to 3 ml with vehicle) suitably diluted (5 μl) were spotted on a precoated silica gel G $F_{254}$ plate, previously washed as noted, and developed using the solvent system to a height of ~15 cm. Plates were air dried and examined at 254 nm. Detection was completed by iodine vapor visualization. Relative $R_f$ values were determined by using phthalic acid (VI) as the internal standard (2 mg/ml).

For quantitative analysis, the mixed standard ethanolic solution with I–IV (400 μg/ml of each compound) was prepared. The standard solution was diluted with ethanol two, four, five, and eight times, respectively. To an aliquot (5 ml) of each dilution, 2 ml of the internal standard solution (phthalic acid in ethanol, 2 mg/ml) was added. Two dilutions of the

[1] Hamilton, Bonaduz, Switzerland.
[2] PM QII Zeiss.
[3] B.B.C. GOERZ.
[4] Minigrator Intersmat.
[5] Merck, Darmstadt, West Germany.
[6] Courtesy of Geigy Laboratories, Basel, Switzerland.



0022-3549/81/0400-0460$01.00/0
© 1981, American Pharmaceutical Association

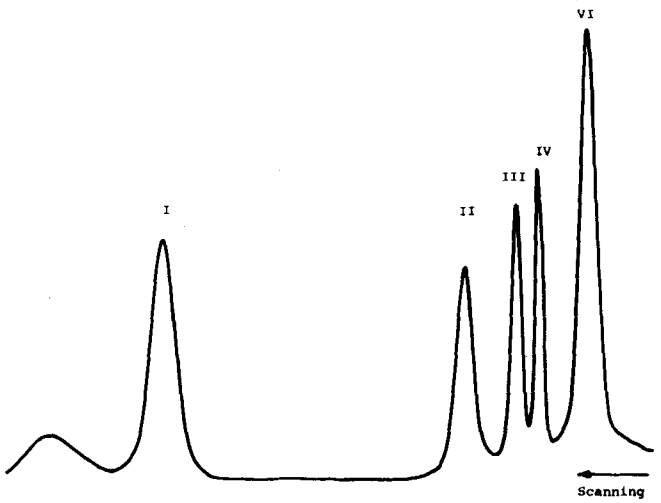


**Figure 1**—*Chromatogram on silica plate for a mixed sample (phenylbutazone and degradation products) with phthalic acid as the internal standard. Reflectometric measurement was at 237 nm, scanning speed was 30 mm/min, and chart paper speed was 20 mm/min. Key: I, 190 μg/ml; II, 150 μg/ml; III, 160 μg/ml; and IV, 330 μg/ml.*

sample, 1:1000 for the phenylbutazone assay and 1:50 for the degradates assay, were prepared. The same internal standard solution (2 ml) was added to an aliquot (5 ml) of each diluted sample.

Silica gel G plates, without fluorescence indicator, were washed as described. Mixed diluted standard solutions (4 μl) and diluted sample (4 μl) were spotted and allowed to air dry. The plates were developed, using the described solvent system, to a height of ~15 cm and allowed to air dry.

Reflectance spectrometric measurements were performed with a chromatogram spectrophotometer at 237 nm, the maximum absorbance wavelength of I. The detector head was adjusted on the center of each spot to be recorded. Each peak was scanned twice at 237 nm; the reproducibility of duplicates should be better than 2%. The calibration curve was constructed for each compound by plotting the average peak area ratio (solute to internal standard) *versus* solute concentration. From the graphs, the amount of I–IV in the sample was determined.

## RESULTS AND DISCUSSION

Table I lists the relative $R_f$ values obtained from the analysis on silica plates using a fluorescence indicator.

UV spectra of phenylbutazone and its degradates were scanned. The maximum absorbance wavelength was ~237 nm for I–IV, which allowed quantitative analysis at the same wavelength. Maximum absorbance was 320 nm for V, so its quantitation would not be performed at 237 nm. Figure 1 illustrates the chromatogram at 237 nm of a mixed sample with phthalic acid as the internal standard. The calibration curve was obtained by plotting the area ratios (solute to internal standard) *versus* concentration. The calibration curve was linear for I–IV and went through the origin. Correlation coefficients were 0.99 for I and II, 0.95 for III, and 0.97 for IV. The phenylbutazone content of the injectable solution was 553 mg. No interference was observed from lidocaine ($R_f$ 0.01 relative to phenylbutazone).

The sensitivity of the proposed procedure allowed a satisfactory assay of each degradate with a convenient dilution (1:50) of the sample. The injectable solution contained 11.7 mg of IV. The sensitivities tested were 0.05 μg for I, 0.04 μg for II and III, and 0.03 μg for IV. These levels suggest an application for pharmacokinetic studies.

The reported procedure allows the identification and quantitation of phenylbutazone and its degradates; its main use is the TLC qualitative test. It should be proposed as an available complement to the acidimetric assay specified in the pharmacopeias (16–18); because the phenylbutazone assay lacks specificity, it cannot give information about the purity of phenylbutazone.

## REFERENCES

(1) H. D. Beckstead, K. K. Kaistha, and S. J. Smith, *J. Pharm. Sci.*, **57**, 1952 (1968).

(2) D. V. C. Awang, A. Vincent, and F. Matsui, *J. Chromatogr.*, **62**, 1673 (1973).

(3) J. R. Watson, F. Matsui, R. C. Lawrence, and P. M. J. McConnel, *ibid.*, **76**, 141 (1973).

(4) O. E. Schultz and M. Mocha, *Pharm. Ztg.*, **122**, 1305 (1977).

(5) S. L. Ali and T. Strittmatter, *ibid.*, **123**, 720 (1978).

(6) F. Matsui, D. L. Robertson, P. Lafontaine, H. Kolasinski, and E. G. Lovering, *J. Pharm. Sci.*, **67**, 646 (1978).

(7) H. Bungaard, *Arch. Pharm. Chemi, Sci. Ed.*, **6**, 223 (1978).

(8) K. Macek, *J. Chromatogr.*, **33**, 332 (1968).

(9) E. Pawelczyk and R. Wachowiak, *Diss. Pharm. Pharmacol.*, **20**, 653 (1968).

(10) F. Gouezo, J. P. Roman, and B. Cristau, *Ann. Pharm. Fr.*, **26**, 303 (1968).

(11) W. Awe and H. G. Tracht, *Pharm. Ztg.*, **108**, 1365 (1963).

(12) F. Pechtold, *Arzneim.-Forsch.*, **14**, 1056 (1964).

(13) Z. Golucki and A. Kobylinska-Luczko, *Farm. Pol.*, **33**, 275 (1977).

(14) N. J. Pound, I. J. Mc Gilveray, and R. W. Sears, *J. Chromatogr.*, **89**, 23 (1974).

(15) E. Pawelczyk and R. Wachowiak, *Diss. Pharm. Pharmacol.*, **22**, 475 (1970).

(16) "Pharmacopée Française," vol. 2, 9th ed., Direction Commission Nationale Pharmacopée Ordre National des Pharmaciens, Paris, France, 1976.

(17) "The United States Pharmacopeia," 19th rev., Mack Publishing Co., Easton, Pa., 1975, p. 377.

(18) "British Pharmacopoeia, 1973," Her Majesty's Stationery Office, London, England, 1973, p. 365.

## ACKNOWLEDGMENTS

The authors thank Mr. H. Eddine for technical assistance.

# High-Performance Liquid Chromatographic Determination of Ethmozin in Plasma

**CHARLES C. WHITNEY ˣ, STEPHEN H. WEINSTEIN, and JANET C. GAYLORD**

Received February 13, 1980, from the *Stine Laboratory, E. I. du Pont de Nemours & Company, Inc., Newark, DE 19711.* Accepted for publication September 25, 1980.

**Abstract** □ A sensitive, specific high-performance liquid chromatographic procedure was developed for the determination of plasma ethmozin levels. Basic plasma samples were partitioned with methylene chloride. The organic extract was washed with water and then evaporated to dryness under reduced pressure. The residue was redissolved in 0.2 ml of the mobile phase, consisting of hexane–tetrahydrofuran–methanol–water (66:27:6.3:0.7 v/v), and then chromatographed on a microporous silica column. With a variable-wavelength UV detector set at 268 nm, 10 ng of ethmozin/ml of plasma was measured. The utility of the method for human pharmacokinetic studies was demonstrated.

**Keyphrases** □ Ethmozin—analysis, high-performance liquid chromatography, plasma □ High-performance liquid chromatography—analysis, plasma ethmozin levels □ Pharmacokinetics—plasma ethmozin levels, high-performance liquid chromatography, humans

Ethmozin, 10-(3-morpholinopropionyl)phenothiazine-2-carbamic acid ethyl ester hydrochloride, is an antiarrhythmic drug that suppresses atrial and ventricular premature depolarizations (1–4).

The reported assays for ethmozin are a nonspecific spectrophotometric method (5) and a TLC–spectrophotometry method (6). Both are unsatisfactory for pharmacokinetic studies because they lack either specificity or sensitivity.

This report describes a plasma assay for ethmozin that involves a single solvent extraction, a water wash, and an evaporation step. The assay is sufficiently sensitive to measure the compound at the 10-ng/ml level.

## EXPERIMENTAL

**Reagents**—Ethmozin[1], borate buffer[2] (0.1 *M*, pH 9), tetrahydrofuran[3], methanol[3], hexane[3], and methylene chloride[3] were used without further purification.

**Apparatus**—The liquid chromatograph[4] was fitted with a valve-loop injector[5] with a 50-μl loop, a variable-wavelength UV detector[6] set at 268 nm, an electronic filter[7], and a microporous silica column[8]. The mobile phase flow rate was ~1 ml/min.

**Mobile Phase**—A solution containing hexane–tetrahydrofuran–methanol–water (66:27:6.3:0.7 v/v) was prepared as required.

**Standard Curves**—Standard curves were prepared from extracted, ethmozin-spiked plasma samples. Solutions of ethmozin in methanol (0.25, 0.50, and 1.0 μg/ml) were used to spike plasma samples for the preparation of the extracted plasma standards. Spiked plasma samples were prepared by pipetting 0.5 ml of each ethmozin solution into 50-ml, polytef-lined[9], screw-capped glass tubes[10]. The methanolic solutions were evaporated to dryness[11], and then 5.0 ml of control plasma was added to each tube. Control plasma from whole blood drawn in heparinized, evacuated tubes[12] was used because plasma from blood banks often contained an impurity that interfered with the assay.

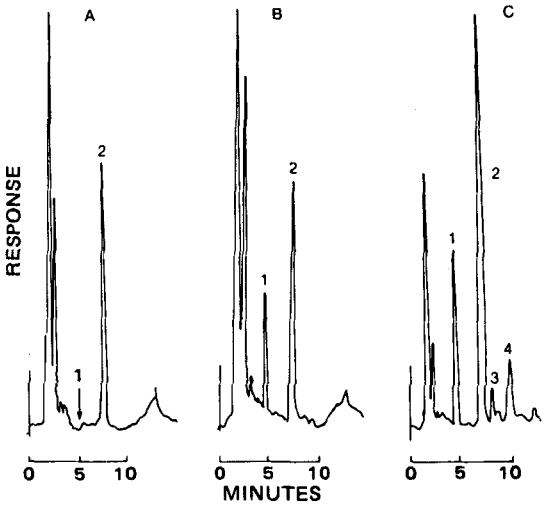


**Figure 1**—*Chromatograms of extracts from a plasma blank (A), spiked (0.10 μg/ml) plasma (B), and plasma from an individual taking ethmozin (C). Key: 1, ethmozin; 2, caffeine; and 3 and 4, ethmozin metabolites.*

The spiked plasma samples were adjusted to pH 9 using a few drops of 1 *N* NaOH and then were diluted with 5 ml of 0.1 *M* borate buffer (pH 9). Following the addition of methylene chloride (12 ml) to each tube, the tubes were capped and then shaken on a wrist-action shaker[13] for 30 min. The mixture was centrifuged for 10 min at 4000×*g*, and the aqueous phase was discarded. The organic phase was washed with 5 ml of distilled water in a clean 25-ml glass tube. The mixture was centrifuged for 5 min, and then 8.0 ml of the methylene chloride layer was evaporated to dryness in a 15-ml graduated centrifuge tube. All of the residue was dissolved in 0.2 ml of the mobile phase. Aliquots (50 μl) were injected into the column and chromatographed.

A standard curve was prepared by plotting the ethmozin peak heights from the extracted plasma samples *versus* the plasma ethmozin concentrations.

**Recovery Study**—Plasma ethmozin recoveries were determined by comparing the peak heights of the spiked plasma standards with those of the unextracted ethmozin standards (Table I) after correcting for the fact that only 8 ml of the original 12 ml of methylene chloride was analyzed.

**Quantitation**—A standard curve was constructed by plotting the ethmozin peak height of spiked plasma standards *versus* the plasma ethmozin concentration. Caffeine and several ethmozin metabolites elute near ethmozin, hindering use of an internal standard. To eliminate the need for several internal standards or an internal standard with a long retention time, external standards were used. Unextracted standards were chromatographed daily to monitor instrument performance and to calculate percent recoveries of the extracted standards.

Unknown samples were analyzed by comparing ethmozin peak heights from the plasma extracts to the extracted standard curve.

**Plasma Level Study**—Ethmozin (500 mg) was administered orally with 500 ml of water to three healthy human males, 59–75 kg, who had fasted overnight. Blood samples (15 ml) were withdrawn prior to dosing

[1] E. I. du Pont de Nemours & Co., Wilmington, Del.
[2] Fisher Scientific Co., Fair Lawn, N.J.
[3] Burdick & Jackson Laboratories, Muskegon, Mich.
[4] Model 830, E. I. du Pont de Nemours & Co., Wilmington, Del.
[5] Model SVOV-6-3, Glenco Scientific, Houston, Tex.
[6] Model 1030B, Hewlett-Packard, King of Prussia, Pa.
[7] Model 1020, Spectrum Scientific Corp., Newark, Del.
[8] Microporasil, 3.9 × 300 mm, Waters Associates, Milford, Mass.
[9] Teflon, E. I. du Pont de Nemours & Co., Wilmington, Del.
[10] Corex, Corning Glass Works, Corning, N.Y.
[11] Evapo-mix, Buchler Instruments, Fort Lee, N.J.
[12] Vacutainers, Becton–Dickinson and Co., Missonga, Ontario, Canada.
[13] Model 75, Burrell Corp., Pittsburgh, Pa.



0022-3549/81/0400-0462$01.00/0
© 1981, American Pharmaceutical Association

**Table I—Linearity of Unextracted Ethmozin Standards**

| Ethmozin[a], μg/ml | Peak Height, mm | Mean Peak Height, mm (*CV*) | Response Factor[b] |
|---|---|---|---|
| 0.5 | 19 | 19 (3.1) | 38.0 |
| | 20 | | |
| | 19 | | |
| 1.0 | 36 | 36 (0) | 36.0 |
| | 36 | | |
| | 36 | | |
| 2.0 | 69 | 71 (2.1) | 35.5 |
| | 71 | | |
| | 72 | | |
| 4.0 | 136 | 136 (1.1) | 34.0 |
| | 134 | | |
| | 137 | | |

[a] As ethmozin hydrochloride. [b] Peak height divided by concentration.

**Table II—Recovery of Ethmozin from Spiked Plasma**

| Ethmozin, μg/ml | *n* | Recovery, % (*CV*) |
|---|---|---|
| 0.025 | 11 | 100.8 (12.5) |
| 0.050 | 13 | 99.7 (7.5) |
| 0.100 | 17 | 102.8 (9.0) |
| 0.500 | 6 | 96.9 (7.0) |
| 1.000 | 6 | 91.4 (6.3) |
| 5.000 | 5 | 89.7 (2.6) |

and at specified times up to 48 hr after dosing. The blood samples were centrifuged, and the plasma was stored frozen in clean plastic tubes[14]. The samples were assayed using the procedure described for ethmozin-spiked plasma. The elimination half-lives for these individuals were determined using linear regression analysis of the terminal plasma level–time data points.

## RESULTS AND DISCUSSION

Under the described chromatographic conditions, ethmozin eluted from the column in ~5 min. However, ethmozin is similar to other phenothiazines in that it undergoes extensive metabolic transformation when given to humans[15]. There are large interindividual differences in the number and concentration of these metabolites. For this reason, a column cleanout time between samples was required and external standards were used. Representative chromatograms from blank and spiked human plasma extracts and a plasma extract from a subject given 500 mg of ethmozin are shown in Fig. 1.

A variable-wavelength detector at 268 nm was used to eliminate background contributions to the ethmozin peak at 254 nm in blank plasma extracts. The mobile phase was not used for more than 1 week because tetrahydrofuran oxidizes, reducing chromatogram quality.

The linearity of unextracted ethmozin standard response is shown in Table I. Peak heights were proportional to the standard concentrations from 0.5 to 4 μg/ml, as evidenced by the fairly constant response factors (34.0–38.0).

Recoveries of ethmozin from spiked plasma samples were nearly quantitative at plasma concentrations of 0.025–5.0 μg/ml, with average recoveries ranging from 89.7 to 102.8% and coefficients of variation ranging from 2.6 to 12.5% (Table II).

Figure 2 illustrates the plasma ethmozin concentration profile in three healthy volunteers given single oral 500-mg doses. Peak concentrations

[14] Model 2017, Falcon, Oxnard, Calif.
[15] C. C. Whitney and J. C. Gaylord, unpublished data.

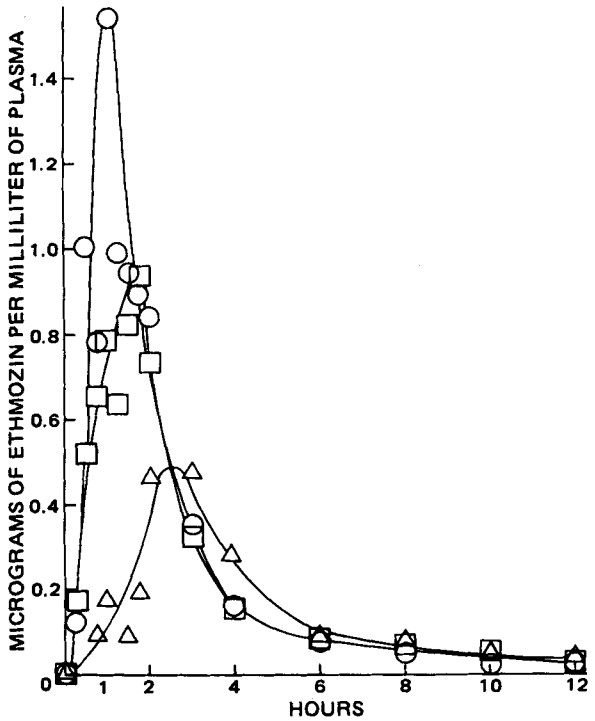


**Figure 2**—*Ethmozin profiles in three healthy adult human males following a single oral 500-mg dose.*

of 0.48–1.54 μg/ml occurred between 1 and 3 hr. The elimination half-lives were 2.8–4.3 hr.

Since ethmozin may be given concurrently with other drugs, several were examined to determine whether they would influence the ethmozin assay. No interference was observed with diazepam, hydralazine, prazosin, guanethidine, procainamide, quinidine, propranolol, chlorpromazine, fluphenazine, nicotine, caffeine, codeine, warfarin, phenytoin, cephalexin, aminopyrine, or perphenazine. Chlordiazepoxide, reserpine, trifluoperazine, and clonidine had approximately the same retention time as ethmozin.

## REFERENCES

(1) N. V. Kaverina, Z. P. Senova, Yu. I. Vikhlyaev, and O. V. Ulyanova, *Farmakol. Toksikol. (Moscow)*, **6**, 693 (1970).

(2) H. Kennedy, J. Pescarmona, V. Joyner, D. Caralis, and P. Poblete, *Circulation, Suppl. II*, **57, 58**, 177 (1978).

(3) J. Morganroth, D. W. Orth, E. L. Michelson, W. B. Dunkman, A. S. Pearlman, L. N. Horowitz, M. E. Josephson, and J. A. Kastor, *ibid.*, 103 (1978).

(4) J. Morganroth, L. N. Horowitz, A. S. Pearlman, W. B. Dunkman, M. E. Josephson, and J. A. Kastor, *Circulation, Suppl. III*, **55, 56**, 180 (1977).

(5) V. M. Avakumov, *Farmakol. Toksikol. (Moscow)*, **3**, 339 (1969).

(6) S. V. Merinova, G. A. Melenteva, A. N. Gritsenko, and I. Z. Prutkin, *Nek. Probl. Farm. Nauki. Prakt., Mater. Sezda Farm. Kaz. 1st*, 134 (1975); through *Chem. Abstr.*, **87**, 58561W (1977).

## ACKNOWLEDGMENTS

The authors thank Mr. George Juergens for excellent technical assistance.

# Effect of Chloroacetyl Derivatives of *para*-Substituted Phenylalanines on Microbial Antitumor Prescreens

**THEODORE T. OTANI ˣ and MARY R. BRILEY**

Received April 1, 1980, from the *Laboratory of Pathophysiology, National Cancer Institute, Bethesda, MD 20205.* Accepted for publication September 18, 1980.

**Abstract** □ The chloroacetyl derivatives of four representative *para*-substituted phenylalanines, *N*-chloroacetyl-*p*-chloro-DL-phenylalanine, *N*-chloroacetyl-*p*-nitro-DL-phenylalanine, $N^a$,$N^p$-di(chloroacetyl)-*p*-amino-DL-phenylalanine, and *N*-chloroacetyl-*O*-methyl-L-tyrosine, were prepared and tested for growth inhibitory activity in *Lactobacillus casei*. The inhibition with these compounds approximated that of most other inhibitory chloroacetyl amino acids reported previously. However, *N*-chloroacetyl-*p*-chloro-DL-phenylalanine, the most active of these compounds, exhibited an activity approximately that of *N*-chloroacetyl-β-hydroxy-D-norleucine B, the most active *N*-chloroacetyl derivative studied thus far. In view of this finding, the *N*-chloroacetyl derivatives of other *para*-halogenated phenylalanines were prepared and tested. The inhibitory capacity of the *N*-chloroacetyl derivatives of *p*-bromo- and *p*-iodophenylalanine was even greater than that of *p*-chlorophenylalanine, and the order of activity of these compounds increased from the chloroacetyl derivative of *p*-chloro- to that of *p*-bromo- to that of *p*-iodo-DL-phenylalanine. The activity of *N*-chloroacetyl-*p*-bromo- and *N*-chloroacetyl-*p*-iodo-DL-phenylalanine was as great as that of the ring-substituted *N*-benzoylphenylalanines, the most potent *N*-acyl derivatives observed.

**Keyphrases** □ *N*-Chloroacetyl derivatives of *para*-substituted phenylalanines—tested for growth inhibition in microbial antitumor prescreen, structure–activity relationships □ Amino acid derivatives—*N*-chloroacetyl derivatives of *para*-substituted phenylalanine, structure–activity relationships, growth inhibition in microbial antitumor prescreen □ Structure–activity relationships—*N*-chloroacetyl derivatives of *para*-substituted phenylalanines tested for growth inhibition in microbial antitumor prescreen □ Antineoplastic activity, potential—*N*-chloroacetyl derivatives of *para*-substituted phenylalanines, tested for growth inhibition in microbial antitumor prescreen, structure–activity relationships

Previous studies (1, 2) demonstrated that *N*-chloroacetyl derivatives of certain amino acids and amino acid analogs inhibited growth in a microbial antitumor prescreen where no activity was noted with the parent amino acid. In these studies, a commercially obtained *N*-chloroacetyl-L-tyrosine, even after recrystallization, showed marked inhibitory activity[1]. Whereas most of the other "active" *N*-chloroacetyl amino acids inhibited growth by 20–30% at 4.47 m*M* (2), this preparation of *N*-chloroacetyl-L-tyrosine showed essentially complete inhibition at 0.2 m*M*. Since chloroacetyl-L-phenylalanine exhibited no remarkable activity over that observed for the other inhibitory chloroacetyl amino acids, it was of interest to determine whether the *N*-chloroacetyl derivatives of other *para*-substituted phenylalanines would show the level of activity noted with *N*-chloroacetyl-L-tyrosine.

The *N*-chloroacetyl derivatives of some representative phenylalanines containing *para*-substituted electrophilic or electrophobic groups were prepared and tested for growth inhibition in a microbial antitumor prescreen. This article reports the results of that study.

## EXPERIMENTAL

**Materials**—The free amino acids were obtained from commercial sources and were recrystallized from water–ethanol before use. Purity was ascertained by elemental analysis and by paper chromatography in at least four different solvent systems (2).

**Methods**—The amino acids were chloroacetylated by the conventional Schotten–Baumann procedure (3). The products were recrystallized from ethyl acetate, and their purity was ascertained by elemental analysis, Van Slyke nitrous acid determination of primary amino nitrogen (4), melting-point determination, and, where applicable, optical rotation measurements (Table I).

Van Slyke nitrous acid determination of primary amino nitrogen (4) was made on 1-ml samples containing an equivalent of 0.250–0.300 mg of the amino nitrogen (when hydrolyzed). Melting points were determined on a melting-point block[2] and are uncorrected. Optical rotation measurements were made on a polarimeter[3] equipped with a sodium lamp, using 100-mm tubes having a 3-mm bore size and a 0.7-ml sample capacity.

**Microbial Antitumor Prescreen**—The compounds were tested for antitumor activity using a microbial antitumor prescreen described by Foley *et al.* (5). The microbial system used was *Lactobacillus casei* 7469[4] in a riboflavin-supplemented riboflavin assay system. The test compounds were dissolved in water, the solution pH was adjusted to 6 by the addition of 0.1 *N* NaOH, and then the solution was sterilized by passage through an all-glass bacterial filter.

The extent of growth was determined by turbidity measurements in a Klett–Summerson photoelectric colorimeter equipped with a red filter (660 nm) after 19 hr of growth at 37° (1). At least three duplicate determinations were made for each compound. The duplicate values in each determination agreed within ±5 Klett units. The details of the assay were described previously (1).

## RESULTS AND DISCUSSION

Table II shows the extent of inhibition caused by the *N*-chloroacetyl derivatives of *para*-substituted phenylalanines assayed in accordance with the microbial antitumor prescreening protocol (5). Initially $N^a$,$N^p$-di(chloroacetyl)-*p*-amino-DL-phenylalanine, *N*-chloroacetyl-*p*-chloro-DL-phenylalanine, *N*-chloroacetyl-*O*-methyl-L-tyrosine, and *N*-chloroacetyl-*p*-nitro-DL-phenylalanine were tested. Except for *N*-chloroacetyl-*p*-chloro-DL-phenylalanine, the compounds showed modest inhibition, which was similar to that of most of the other inhibiting chloroacetyl derivatives reported earlier (2), *i.e.*, ~20% at 4.47 m*M*. *N*-Chloroacetyl-*p*-chloro-DL-phenylalanine showed considerably more activity (42% inhibition), approaching a positive test according to the screening protocol, *i.e.*, 50% inhibition at 1 mg/ml (5).

When the inhibitory activities of these compounds were compared on an equimolar basis among themselves (Table III) and with other chloroacetyl derivatives (2), it was found that, with the exception of *N*-chloroacetyl-*p*-chloro-DL-phenylalanine, they were approximately the same as those of the other inhibitory chloroacetyl compounds (2). The activity of *N*-chloroacetyl-*p*-chloro-DL-phenylalanine was approximately that of *N*-chloroacetyl-β-hydroxy-D-norleucine B, the most potent chloroacetyl derivative studied thus far (2, 6).

Because of the striking inhibition exhibited by *N*-chloroacetyl-*p*-chloro-DL-phenylalanine, it was of interest to test the inhibitory activity of the *N*-chloroacetyl derivatives of other *para*-halogenated phenylalanines. Therefore, the *N*-chloroacetyl derivatives of *p*-bromo- and *p*-iodo-DL-phenylalanine were prepared (Table I) and tested for growth

[1] Although subsequent preliminary studies indicated that the inhibitory factor was not *N*-chloroacetyl-L-tyrosine but rather a contaminant present in the commercial product, the results obtained supplement earlier studies on chloroacetylated amino acids (2), especially in view of the relatively potent inhibitions noted with some compounds.

[2] Fisher–Johns.

[3] Rudolph model 80.

[4] American Type Culture Collection, Rockville, Md.



0022-3549/81/0400-0464$01.00/0
© 1981, American Pharmaceutical Association

**Table I—Purity Data of *N*-Chloroacetyl Derivatives of *para*-Substituted Phenylalanines**

| Compound | Melting Point | Optical Rotation[a] $[\alpha]_D^{22-24°}$ | Primary Amino Nitrogen | Empirical Formula | Analysis[b], % | Calc. | Obs. |
|---|---|---|---|---|---|---|---|
| $N^a$,$N^p$-Di(chloroacetyl)-*p*-amino-DL-phenylalanine, monohydrate | 183–185° | 0° (W) | 0.7 | $C_{13}H_{14}Cl_2N_2O_4$ | C | 45.63 | 45.62 |
| | | | | | H | 4.01 | 4.35 |
| | | | | | Cl | 20.19 | 20.48 |
| | | | | | N | 8.18 | 8.22 |
| *N*-Chloroacetyl-*p*-chloro-DL-phenylalanine | 153–155° | 0° (A) | 1.8 | $C_{11}H_{11}Cl_2NO_3$ | C | 47.85 | 47.58 |
| | | | | | H | 4.02 | 4.35 |
| | | | | | Cl | 25.68 | 25.26 |
| | | | | | N | 5.07 | 5.33 |
| *N*-Chloroacetyl-*O*-methyl-L-tyrosine | 112–113° | +59.1° (A) | 2.3 | $C_{12}H_{14}ClNO_4$ | C | 53.05 | 53.13 |
| | | | | | H | 5.19 | 5.39 |
| | | | | | Cl | 13.05 | 12.95 |
| | | | | | N | 5.16 | 5.16 |
| *N*-Chloroacetyl-*p*-nitro-DL-phenylalanine | 131° | 0° (A) | 1.8 | $C_{11}H_{11}ClN_2O_5$ | C | 46.09 | 45.99 |
| | | | | | H | 3.87 | 4.05 |
| | | | | | Cl | 12.37 | 12.31 |
| | | | | | N | 9.77 | 9.88 |
| *N*-Chloroacetyl-*p*-bromo-DL-phenylalanine | 156–157° | 0° (A) | 0 | $C_{11}H_{11}BrClNO_3$ | C | 41.21 | 41.52 |
| | | | | | H | 3.46 | 3.44 |
| | | | | | N | 4.37 | 4.37 |
| | | | | | X[c] | 22.12 | 21.90 |
| *N*-Chloroacetyl-*p*-iodo-DL-phenylalanine | 162–166° | 0° (A) | 0.8 | $C_{11}H_{11}ClINO_3$ | C | 35.94 | 36.31 |
| | | | | | H | 3.02 | 3.05 |
| | | | | | N | 3.81 | 3.65 |
| | | | | | X | 19.29 | 19.07 |

[a] Optical rotation measurements: W = in water plus 1 equivalent of sodium hydroxide, *c*, 2. A = in absolute ethanol, *c*, 2. [b] Elemental analyses were performed by the Microanalytical Laboratory, National Institute of Arthritis, Metabolism, and Digestive Diseases, National Institutes of Health, Bethesda, Md. [c] X = percent of total halide as chloride.

inhibitory activity. These compounds also showed considerable activity, some 55% at 1 mg/ml (Table II).

A comparison of activity at equimolar levels showed that both *N*-chloroacetyl-*p*-bromo-DL-phenylalanine and *N*-chloroacetyl-*p*-iodo-DL-phenylalanine inhibited the growth of the test organism to a greater degree than did *N*-chloroacetyl-*p*-chloro-DL-phenylalanine (Table III). At 4.47 m*M*, the concentration at which the activities of the various acyl derivatives were compared, these two acyl derivatives showed almost complete inhibition.

A more detailed study on the relative activities of these *p*-halogenated phenylalanines was made (Fig. 1). The activity increased in order from *N*-chloroacetyl-*p*-chloro-DL-phenylalanine, to *N*-chloroacetyl-*p*-bromo-DL-phenylalanine, to *N*-chloroacetyl-*p*-iodo-DL-phenylalanine. The $ID_{50}$ values of these compounds were 4.3, 2.5, and 1.8 μmoles/ml, respectively. The $ID_{50}$ value of *N*-chloroacetyl-*p*-fluoro-DL-phenylalanine, extrapolated from its inhibition at 4.47 μmoles/ml reported previously (2), was 14.1 μmoles/ml. Thus, the activity of the *N*-chloroacetyl-*p*-halogenated phenylalanine increases with increasing atomic size of the *para*-substituted halogen atom.

In view of the observation that *N*-benzoyl-*p*-chloro-DL-phenylalanine also showed marked inhibition (7, 8), it appears that the *p*-halogenated phenylalanine moiety of the acylated compound exerts an important effect on the final activity of the acylated amino acid. However, the nature of the acyl moiety is also likely to be important since the *N*-benzoyl derivative of *p*-chlorophenylalanine was markedly more active than the corresponding chloroacetyl derivative, the former showing complete inhibition at 4.47 μmoles/ml and the latter showing 48% inhibition at that concentration.

It is unlikely that the activity is due to the hydrolytic release of the parent amino acid, *i.e.*, *p*-chloro-DL-phenylalanine, *p*-bromo-DL-phenylalanine, or *p*-iodo-DL-phenylalanine, since these amino acids showed no appreciable activity when tested in equimolar concentration (Table III). Previous studies (2) also showed that there was no significant hydrolysis of the acylated amino acid during incubation.

The other *para*-substituted phenylalanines showed activity comparable to the active *N*-acylated amino acid analogs (2) and in no way were as inhibitory as the *para*-halogenated derivatives (Tables II and III). Hence, it is unlikely that *para*-substitution *per se* increased activity. Also, since the *p*-nitrophenylalanine derivatives did not show the same degree of activity as the *para*-halogenated phenylalanine derivatives, it is unlikely that the electronegativity of the *para*-substituted species plays a role in conferring the activity.

While the possibility that the observed activity is caused by minute quantities of highly active contaminants is not excluded, it is unlikely since all of the compounds were prepared in these laboratories using identical procedures and were purified using identical reagents for re-

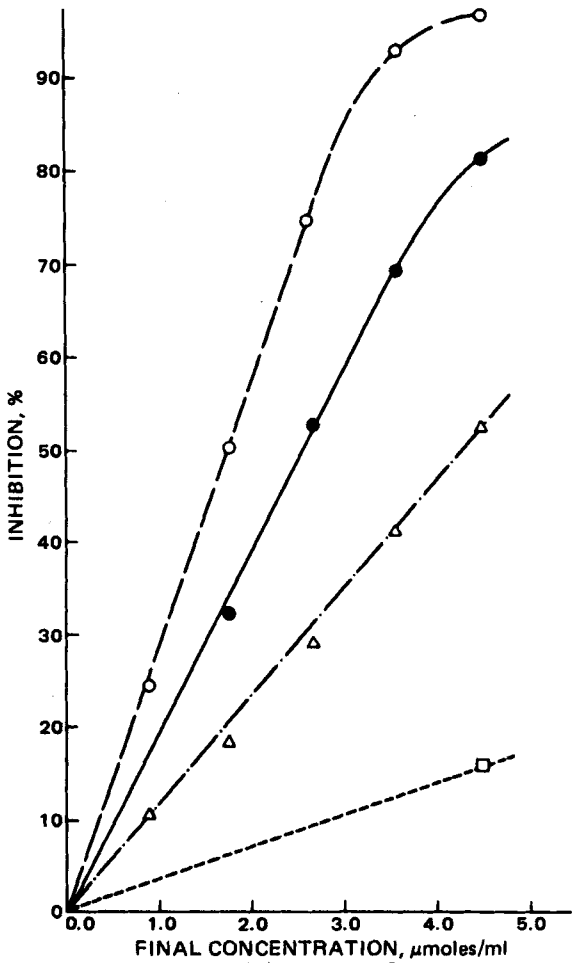


**Figure 1**—*Comparison of inhibition by* N-*chloroacetyl*-p-*halogenated phenylalanines. Key:* △, N-*chloroacetyl*-p-*chloro*-DL-*phenylalanine;* ●, N-*chloroacetyl*-p-*bromo*-DL-*phenylalanine;* ○, N-*chloroacetyl*-p-*iodo*-DL-*phenylalanine; and* □, N-*chloroacetyl*-p-*fluoro*-DL-*phenylalanine (2).*

Table II—Effect of *N*-Chloroacetyl Derivatives of *para*-Substituted Phenylalanines on the Growth of *L. casei*[a]

| Compound | Concentration Equivalent at 1 mg/ml, m*M* | Inhibition[b], % 0.1 mg/ml[c] | 0.5 mg/ml[c] | 1.0 mg/ml[c] |
|---|---|---|---|---|
| *N*-Chloroacetyl-*p*-chloro-DL-phenylalanine | 3.62 | 5 | 19 | 42 |
| *N*-Chloroacetyl-*p*-nitro-DL-phenylalanine | 3.49 | 3 | 10 | 18 |
| $N^{a}$,$N^{p}$-Di(chloroacetyl)-*p*-amino-DL-phenylalanine | 3.00 | 6 | 13 | 21 |
| *N*-Chloroacetyl-*O*-methyl-L-tyrosine | 3.68 | 4 | 11 | 20 |
| *N*-Chloroacetyl-*p*-bromo-DL-phenylalanine | 3.12 | 2 | 25 | 56 |
| *N*-Chloroacetyl-*p*-iodo-DL-phenylalanine | 2.72 | +3 | 35 | 54 |

[a] For details of assay procedure, see Refs. 1 and 2. [b] Turbidity readings of the inoculated control tubes (containing no test compounds) were 188–196. [c] Final concentration in the assay system.

crystallization. Since widely different inhibitory activities were observed, contaminants producing inhibition would have had to be present in the original compounds and retained during the preparative and purification procedures. This is clearly not the case since compounds that were not chloroacetylated did not inhibit. Therefore, it seems reasonable that the inhibitory activities are intrinsic properties of the newly synthesized compounds and are related principally to the chloroacetylation of the amino group and, secondarily, to the introduction of substituent groups into the aromatic ring of the amino acid.

**Table III—Comparison of the Effect of Equimolar Concentrations of *N*-Chloroacetyl Derivatives of *para*-Substituted Phenylalanines on the Growth of *L. casei*[a]**

| Compound | Inhibition[b], % |
|---|---|
| *N*-Chloroacetyl-*p*-chloro-DL-phenylalanine | 48 |
| *N*-Chloroacetyl-*p*-nitro-DL-phenylalanine | 19 |
| $N^{a}$,$N^{p}$-Di(chloroacetyl)-*p*-amino-DL-phenylalanine | 22 |
| *N*-Chloroacetyl-*O*-methyl-L-tyrosine | 20 |
| *N*-Chloroacetyl-DL-phenylalanine | 20 |
| *N*-Chloroacetyl-*p*-bromo-DL-phenylalanine | 86 |
| *N*-Chloroacetyl-*p*-iodo-DL-phenylalanine | 93 |
| *p*-Bromo-DL-phenylalanine[c] | +3 |
| *p*-Chloro-DL-phenylalanine[c] | 0 |
| *p*-Iodo-DL-phenylalanine[c] | 0 |

[a] Maximum growth in inoculated control tubes (containing no test compound) was 186–196 Klett units. [b] Concentration was 4.47 μmoles/ml and was the final concentration of the assay system. [c] Free amino acid.

In studies of this nature, where empirical relationships of inhibitory capabilities are sought, there is little information regarding the mechanism of action. To study the mechanism of action, more sophisticated experiments are required.

The activity of the *N*-benzoyl-*p*-bromo and *N*-benzoyl-*p*-iodophenylalanine is being studied and compared with the corresponding *N*-chloroacetyl compounds.

## REFERENCES


(1) T. T. Otani, *Cancer Chemother. Rep.*, **38**, 25 (1964).

(2) T. T. Otani and M. R. Briley, *J. Pharm. Sci.*, **67**, 520 (1978).

(3) J. P. Greenstein and M. Winitz, in "Chemistry of the Amino Acids," Wiley, New York, N.Y., 1961, p. 1267.

(4) D. D. Van Slyke, *J. Biol. Chem.*, **83**, 425 (1929).

(5) G. E. Foley, R. E. McCarthy, V. M. Binns, E. E. Snell, B. M. Guirard, G. W. Kidder, V. C. Dewey, and P. S. Thayer, *Ann. N.Y. Acad. Sci.*, **76**, 413 (1958).

(6) T. T. Otani and M. R. Briley, *J. Pharm. Sci.*, **65**, 534 (1976).

(7) *Ibid.*, **68**, 260 (1979).

(8) *Ibid.*, **68**, 1366 (1979).


## ACKNOWLEDGMENTS


The authors thank Dr. Walter C. Schneider for many helpful discussions.


# *COMMUNICATIONS*

## Nasal Absorption of Natural Contraceptive Steroids in Rats—Progesterone Absorption


**Keyphrases** □ Progesterone—nasal absorption compared with that following intravenous and intraduodenal administration, rats □ Absorption, nasal—progesterone, compared with absorption following intravenous and intraduodenal administration, rats □ Contraceptives, natural—progesterone, nasal absorption compared with that following intravenous and intraduodenal administration, rats □ TLC—identification of unchanged progesterone following nasal administration to rats, compared with intravenous and intraduodenal administration


*To the Editor:*

Contraceptive natural steroids such as progesterone and estradiol are ineffective when given orally due to extensive metabolism in the GI tract during absorption and first-pass metabolism (1, 2). Thus, highly potent and potentially harmful synthetic steroids are currently being used in oral dosage forms.

To enhance progesterone bioavailability from nonparenteral routes, the nasal route was examined. Previous studies showed that propranolol is absorbed efficiently from the nasal mucosa of rats and dogs (3, 4). Sprague–Dawley male rats, 300 g, were anesthetized with pentobarbital sodium (50 mg/kg). For each dose and for each administration route, four to six rats were used.

For nasal administration, three doses of 50, 100, and 150 μg of [4-$^{14}$C]progesterone (8 μCi) in 0.1 ml of 1% polysorbate 80–saline solution were administered to the nasal cavity of each rat by a micropipet according to the procedure described previously (3). For intravenous administration, the same doses were injected through the femoral vein. For intraduodenal administration, the abdomen was opened by a midline incision, and the 50-μg dose in 0.1 ml of 1% polysorbate 80–saline solution was injected directly through the duodenum.

After administration, 0.2 ml of blood was sampled periodically from the femoral aorta. The blood sample was




0022-3549/81/0400-0466$01.00/0


© 1981, American Pharmaceutical Association

Table II—Effect of *N*-Chloroacetyl Derivatives of *para*-Substituted Phenylalanines on the Growth of *L. casei*[a]

| Compound | Concentration Equivalent at 1 mg/ml, m*M* | Inhibition[b], % 0.1 mg/ml[c] | 0.5 mg/ml[c] | 1.0 mg/ml[c] |
|---|---|---|---|---|
| *N*-Chloroacetyl-*p*-chloro-DL-phenylalanine | 3.62 | 5 | 19 | 42 |
| *N*-Chloroacetyl-*p*-nitro-DL-phenylalanine | 3.49 | 3 | 10 | 18 |
| $N^{a}$,$N^{p}$-Di(chloroacetyl)-*p*-amino-DL-phenylalanine | 3.00 | 6 | 13 | 21 |
| *N*-Chloroacetyl-*O*-methyl-L-tyrosine | 3.68 | 4 | 11 | 20 |
| *N*-Chloroacetyl-*p*-bromo-DL-phenylalanine | 3.12 | 2 | 25 | 56 |
| *N*-Chloroacetyl-*p*-iodo-DL-phenylalanine | 2.72 | +3 | 35 | 54 |

[a] For details of assay procedure, see Refs. 1 and 2. [b] Turbidity readings of the inoculated control tubes (containing no test compounds) were 188–196. [c] Final concentration in the assay system.

crystallization. Since widely different inhibitory activities were observed, contaminants producing inhibition would have had to be present in the original compounds and retained during the preparative and purification procedures. This is clearly not the case since compounds that were not chloroacetylated did not inhibit. Therefore, it seems reasonable that the inhibitory activities are intrinsic properties of the newly synthesized compounds and are related principally to the chloroacetylation of the amino group and, secondarily, to the introduction of substituent groups into the aromatic ring of the amino acid.

**Table III—Comparison of the Effect of Equimolar Concentrations of *N*-Chloroacetyl Derivatives of *para*-Substituted Phenylalanines on the Growth of *L. casei*[a]**

| Compound | Inhibition[b], % |
|---|---|
| *N*-Chloroacetyl-*p*-chloro-DL-phenylalanine | 48 |
| *N*-Chloroacetyl-*p*-nitro-DL-phenylalanine | 19 |
| $N^{a}$,$N^{p}$-Di(chloroacetyl)-*p*-amino-DL-phenylalanine | 22 |
| *N*-Chloroacetyl-*O*-methyl-L-tyrosine | 20 |
| *N*-Chloroacetyl-DL-phenylalanine | 20 |
| *N*-Chloroacetyl-*p*-bromo-DL-phenylalanine | 86 |
| *N*-Chloroacetyl-*p*-iodo-DL-phenylalanine | 93 |
| *p*-Bromo-DL-phenylalanine[c] | +3 |
| *p*-Chloro-DL-phenylalanine[c] | 0 |
| *p*-Iodo-DL-phenylalanine[c] | 0 |

[a] Maximum growth in inoculated control tubes (containing no test compound) was 186–196 Klett units. [b] Concentration was 4.47 μmoles/ml and was the final concentration of the assay system. [c] Free amino acid.

In studies of this nature, where empirical relationships of inhibitory capabilities are sought, there is little information regarding the mechanism of action. To study the mechanism of action, more sophisticated experiments are required.

The activity of the *N*-benzoyl-*p*-bromo and *N*-benzoyl-*p*-iodophenylalanine is being studied and compared with the corresponding *N*-chloroacetyl compounds.

## REFERENCES


(1) T. T. Otani, *Cancer Chemother. Rep.*, **38**, 25 (1964).

(2) T. T. Otani and M. R. Briley, *J. Pharm. Sci.*, **67**, 520 (1978).

(3) J. P. Greenstein and M. Winitz, in "Chemistry of the Amino Acids," Wiley, New York, N.Y., 1961, p. 1267.

(4) D. D. Van Slyke, *J. Biol. Chem.*, **83**, 425 (1929).

(5) G. E. Foley, R. E. McCarthy, V. M. Binns, E. E. Snell, B. M. Guirard, G. W. Kidder, V. C. Dewey, and P. S. Thayer, *Ann. N.Y. Acad. Sci.*, **76**, 413 (1958).

(6) T. T. Otani and M. R. Briley, *J. Pharm. Sci.*, **65**, 534 (1976).

(7) *Ibid.*, **68**, 260 (1979).

(8) *Ibid.*, **68**, 1366 (1979).


## ACKNOWLEDGMENTS


The authors thank Dr. Walter C. Schneider for many helpful discussions.


# *COMMUNICATIONS*

## Nasal Absorption of Natural Contraceptive Steroids in Rats—Progesterone Absorption


**Keyphrases** □ Progesterone—nasal absorption compared with that following intravenous and intraduodenal administration, rats □ Absorption, nasal—progesterone, compared with absorption following intravenous and intraduodenal administration, rats □ Contraceptives, natural—progesterone, nasal absorption compared with that following intravenous and intraduodenal administration, rats □ TLC—identification of unchanged progesterone following nasal administration to rats, compared with intravenous and intraduodenal administration


*To the Editor:*

Contraceptive natural steroids such as progesterone and estradiol are ineffective when given orally due to extensive metabolism in the GI tract during absorption and first-pass metabolism (1, 2). Thus, highly potent and potentially harmful synthetic steroids are currently being used in oral dosage forms.

To enhance progesterone bioavailability from nonparenteral routes, the nasal route was examined. Previous studies showed that propranolol is absorbed efficiently from the nasal mucosa of rats and dogs (3, 4). Sprague–Dawley male rats, 300 g, were anesthetized with pentobarbital sodium (50 mg/kg). For each dose and for each administration route, four to six rats were used.

For nasal administration, three doses of 50, 100, and 150 μg of [4-$^{14}$C]progesterone (8 μCi) in 0.1 ml of 1% polysorbate 80–saline solution were administered to the nasal cavity of each rat by a micropipet according to the procedure described previously (3). For intravenous administration, the same doses were injected through the femoral vein. For intraduodenal administration, the abdomen was opened by a midline incision, and the 50-μg dose in 0.1 ml of 1% polysorbate 80–saline solution was injected directly through the duodenum.

After administration, 0.2 ml of blood was sampled periodically from the femoral aorta. The blood sample was




0022-3549/81/0400-0466$01.00/0


© 1981, American Pharmaceutical Association

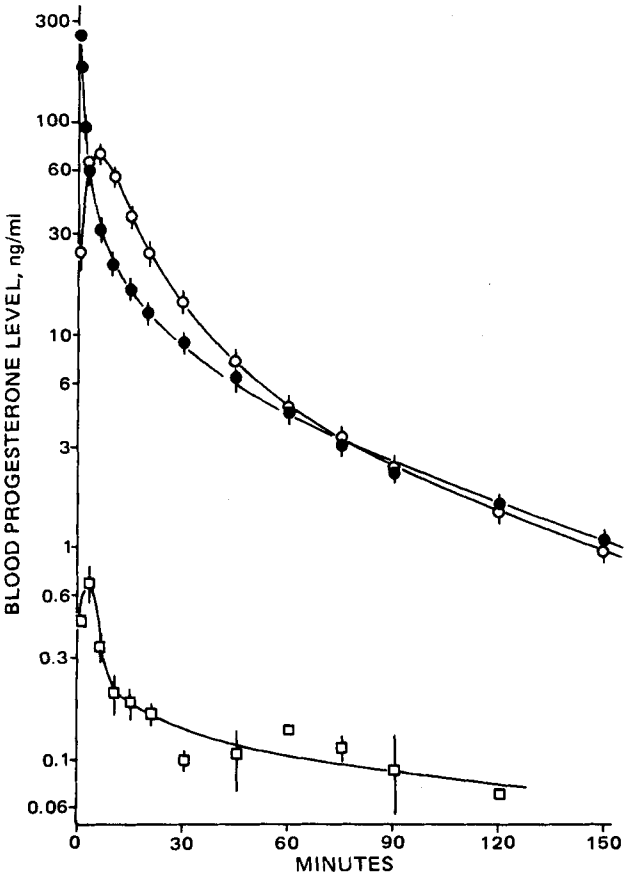


**Figure 1**—*Mean blood progesterone levels after nasal (○), intravenous (●), and intraduodenal (□) administration of 50 μg of progesterone. The lines were drawn through the points, and the vertical bars represent standard error.*

shaken with 5 ml of ether, and the ether layer was evaporated to dryness. The residue then was dissolved in 50 μl of toluene, and 40 μl was spotted on TLC plates and developed using toluene–ethanol (9:1 v/v). The spot that corresponded to unchanged progesterone then was scraped off the plate, and the powder was suspended in scintillation cocktail for a radioactivity count. The developing solvent system separated the unchanged progesterone from its metabolites.

Figure 1 shows the mean blood progesterone levels for the three administration routes at the 50-μg dose. The

**Table I—Area under the Curves after Intravenous, Nasal, and Intraduodenal Administration of Progesterone in Rats**

| Dose, μg/rat | $AUC_0^\infty$, (ng min)/ml | | | Nasal | Intraduodenal |
|---|---|---|---|---|---|
| | Intravenous | Nasal | Intraduodenal | Intravenous | Intravenous |
| 50 | 1612.2[a] ±80.8 | 1659.0 ±109.2 | 19.0 ±4.6 | 1.029 | 0.012 |
| 100 | 3520.0 ±491.0 | 3599.0 ±621.4 | — | 1.022 | — |
| 150 | 4480.2 ±466.4 | 4798.9 ±188.5 | — | 1.071 | — |

[a] Mean ± *SE* ($n$ = 4–6).

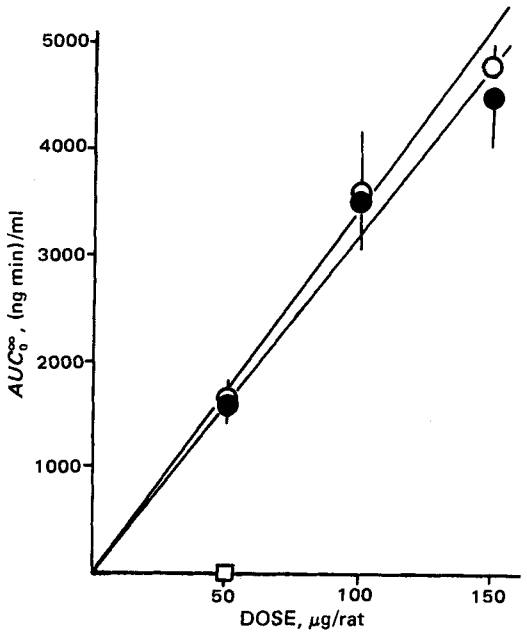


**Figure 2**—*Relationship between dose and* AUC *after nasal (○) and intravenous (●) administration of progesterone. The square (□) represents intraduodenal administration. The vertical bars represent standard error.*

blood drug levels after nasal administration increased rapidly and attained the peak level within 6 min, whereas the intraduodenal administration resulted in considerably lower blood levels.

Table I and Fig. 2 summarize the area under the blood drug level curve (*AUC*) for the three administration routes at various doses. The *AUC* was directly proportional to the dose administered nasally and intravenously. The nasal bioavailability calculated from the ratio of the *AUC* [(nasal/intravenous) × 100] was 100% at the different doses; the intraduodenal bioavailability was only 1.2% that of the intravenous bioavailability at the dose studied.

These results indicate that the natural contraceptive steroid, progesterone, is absorbed rapidly from the nasal mucosa into systemic blood without first-pass metabolism and that nasal administration of progesterone is superior to the intraduodenal route.

(1) C. Longcope and K. I. H. Williams, *J. Clin. Endocrinol. Metab.*, **38**, 602 (1974).

(2) "The Pharmacological Basis of Therapeutics," 5th ed., L. S. Goodman and A. Gilman, Eds., Macmillan, New York, N.Y., 1975, chap. 68.

(3) A. A. Hussain, S. Hirai, and R. Bawarshi, *J. Pharm. Sci.*, **68**, 1196 (1979).

(4) *Ibid.*, **69**, 1411 (1980).

*Anwar A. Hussain* ˣ
*Shinichiro Hirai*
*Rima Bawarshi*
College of Pharmacy
University of Kentucky
Lexington, KY 40506

Received September 30, 1980.
Accepted for publication January 12, 1981.

## REVIEWS

**Drug Design. Vol. IX.** Edited by E. J. ARIENS. Academic, 111 Fifth Ave., New York, NY 10003. 1980. 355 pp. 15 × 23 cm. Price $39.50.

This book is the ninth in the Drug Design series dating back to 1971. This seven-chapter volume emphasizes quantitative methods of structure–activity relationships (SAR) and drug design.

The first chapter by Ariens deals with toxicity considerations on designing candidate molecules with expected biological activity. The processes leading to toxicity are discussed with consideration of SAR. Chapter 2 covers a wide variety of subjects generally centering around physicochemical properties and their relation to biological activity. Some interesting aspects of property–activity relationships are raised, but too great a variety of subjects is covered with the sacrifice of much depth.

Chapter 3 describes recent contributions to orally active prodrugs based on physical–chemical properties. The authors, Yalkowsky and Morozowich, develop these factors systematically and present recent work from their laboratory. Chapter 4, authored by Mager, describes the MASCA model in the first of a two-part presentation. The second part will appear in Volume X. Considerable space is devoted to a development of the mathematics involved with only limited illustration of its application. The two chapters are clearly interdependent and perhaps should have appeared in the same volume.

Chapter 5, by deBlaey and Polderman, is a good description of the design of rectal and vaginal drug delivery forms. In Chapter 6, Meyer reviews interactive graphics, touching on hardware and software data banks with some applications. The last chapter, by Golender and Rozenblit, discusses the logico-structural approach to drug design. The chapter develops the analytical method in a clear and useful manner.

The book will be of particular interest to medicinal chemists engaged in drug design using theoretical methods to analyze and predict activity.

*Reviewed by* Lemont B. Kier
*Department of Pharmaceutical Chemistry*
*School of Pharmacy*
*Medical College of Virginia*
*Virginia Commonwealth University*
*Richmond, VA 23298*

**Official Methods of Analysis of the AOAC, 13th ed.** Edited by WILLIAM HORWITZ. The Association of Official Analytical Chemists, 1111 N. 19th St., Arlington, VA 22209. 1980. 1038 pp. 22 × 28 cm. 2.4 kg. Price $78.00.

This, the latest, largest, and most weighty of "Methods," received about 175 new methods and lost 83 during the current 5 years between editions. Page size was increased to maintain the book as a single volume in the interest of convenience and cost. Methods employing GLC now are more numerous than spectrophotometric methods. HPLC makes its first appearance in this edition.

"Methods of Analysis" is a compendium of quantitative and qualitative analytical methods and other procedures used by regulatory agencies in monitoring regulated industries. The methods also are specified in certain government purchase orders. "Methods" has a worldwide distribution.

These methods were tested by collaborative assays and found to satisfy the criteria set by the subcommittee having jurisdiction. In theory, the methods are precise and accurate referee methods suitable for resolving differences of opinion. In practice, the methods are a mixture of the tried and true, recent innovations, the obsolete but barely adequate, the worthless, and methods to be used only when conditions beyond the control of the analyst require them. Nonetheless, the book belongs in the library of any analyst who must do official assays; assays agricultural products; determines efficacy of disinfectants; assays pesticide formulations, foods, food additives, cosmetics, drugs, drugs in animal feeds, vitamins, and amino acids; looks for filth in foods and for microbial contaminants in raw and processed foods; or needs to develop latent fingerprints and make voice print identifications. There is something for everyone from the agricultural chemist to the budding Sherlock Holmes.

When the first edition of "Methods" was published in 1920, the editors could make the valid assumption that it would be used by trained and experienced analysts. Today, that assumption can no longer be made, and presentation of procedures should be modified accordingly. Many people in certain fields are not trained in analytical techniques. Although the editors can do nothing about this misapplication of people, they could provide tutorial material to teach basic techniques. One of the first skills to be taught should be how to select and use volumetric pipets and flasks. This gives an idea of the extent of the needs.

Of particular interest to pharmaceutical scientists are the chapters on disinfectants, flavors, food additives, metals, and other elements as residues in foods, sugars and syrups, color additives, cosmetics, drugs (five chapters), and vitamins and other nutrients.

"Methods" grows with each edition. Vigorous steps need to be taken to keep its size within reasonable limits for a one-volume book and to control its cost. The 68 pages of tables at the back of the book probably could be put on one or two pages as comments and as equations suitable for solution by the ubiquitous digital calculators. Space could be saved by presenting general procedures once and, thereafter, giving only deviations under the specific assay. More information could be placed in tables, and needless instructions could be omitted.

Equations for the wet chemistries would help the analyst understand what he or she is doing. Not everyone who uses "Methods" has a complete file of the *Journal of the Association of Official Analytical Chemists* or other sources of information. The absence of supporting theory gives "Methods" the appearance of a cookbook.

The chapter on drugs in feeds has 56 procedures for extracting a drug from feeds. In 45 of them, solids are included in the total volume of extract, thus causing possible bias.

The section on microbiological assays for antibiotics in animal feed has turbidimetric methods for the first time. The turbidimetric method is manual for chlortetracycline, and an AUTOTURB® System is used for monensin. The latter assay could be improved considerably at no cost of time or money. Also, the AUTOTURB System is not operated to give the accuracy and precision it was designed to give. Even the name of the system is incorrect.

The diffusion assays for antibiotics in feeds, being obsolete both in design and practice, contain possible inherent and easily avoidable errors. At that, the methods may be superior to those in the E.E.C. Possible significant biases in certain diffusion assays, such as those of bacitracin, hygromycin B, and monensin, are not mentioned. Collaborative assays have shown the bacitracin method to be an activity check and not a quantitative assay.

Theory and practice of microbiological assays for vitamins (Chapter 43) have progressed little since the Snell and Strong publication in 1939. Fortunately, accurate assays rarely are needed. Improvement in the quality of methods could come from someone with access to an AUTOTURB System who operates it correctly. Factors that need to be studied are: composition of media, preparation of inocula, time and temperature of incubation, dose–response line, computation of potency, and proper statistical treatment of data. Once these studies have been done, the influence of assay specificity, interferences, and details of sample preparation on accuracy and precision of assays for vitamins and amino acids could be investigated with profit. Microbiological assays, in contrast to chemical methods, have been stagnant too long.

*Reviewed by* Frederick Kavanagh
*829 N.W. 36th Street*
*Corvallis, OR 97330*

## REVIEWS

**Drug Design. Vol. IX.** Edited by E. J. ARIENS. Academic, 111 Fifth Ave., New York, NY 10003. 1980. 355 pp. 15 × 23 cm. Price $39.50.

This book is the ninth in the Drug Design series dating back to 1971. This seven-chapter volume emphasizes quantitative methods of structure–activity relationships (SAR) and drug design.

The first chapter by Ariens deals with toxicity considerations on designing candidate molecules with expected biological activity. The processes leading to toxicity are discussed with consideration of SAR. Chapter 2 covers a wide variety of subjects generally centering around physicochemical properties and their relation to biological activity. Some interesting aspects of property–activity relationships are raised, but too great a variety of subjects is covered with the sacrifice of much depth.

Chapter 3 describes recent contributions to orally active prodrugs based on physical–chemical properties. The authors, Yalkowsky and Morozowich, develop these factors systematically and present recent work from their laboratory. Chapter 4, authored by Mager, describes the MASCA model in the first of a two-part presentation. The second part will appear in Volume X. Considerable space is devoted to a development of the mathematics involved with only limited illustration of its application. The two chapters are clearly interdependent and perhaps should have appeared in the same volume.

Chapter 5, by deBlaey and Polderman, is a good description of the design of rectal and vaginal drug delivery forms. In Chapter 6, Meyer reviews interactive graphics, touching on hardware and software data banks with some applications. The last chapter, by Golender and Rozenblit, discusses the logico-structural approach to drug design. The chapter develops the analytical method in a clear and useful manner.

The book will be of particular interest to medicinal chemists engaged in drug design using theoretical methods to analyze and predict activity.

*Reviewed by* Lemont B. Kier
*Department of Pharmaceutical Chemistry*
*School of Pharmacy*
*Medical College of Virginia*
*Virginia Commonwealth University*
*Richmond, VA 23298*

**Official Methods of Analysis of the AOAC, 13th ed.** Edited by WILLIAM HORWITZ. The Association of Official Analytical Chemists, 1111 N. 19th St., Arlington, VA 22209. 1980. 1038 pp. 22 × 28 cm. 2.4 kg. Price $78.00.

This, the latest, largest, and most weighty of "Methods," received about 175 new methods and lost 83 during the current 5 years between editions. Page size was increased to maintain the book as a single volume in the interest of convenience and cost. Methods employing GLC now are more numerous than spectrophotometric methods. HPLC makes its first appearance in this edition.

"Methods of Analysis" is a compendium of quantitative and qualitative analytical methods and other procedures used by regulatory agencies in monitoring regulated industries. The methods also are specified in certain government purchase orders. "Methods" has a worldwide distribution.

These methods were tested by collaborative assays and found to satisfy the criteria set by the subcommittee having jurisdiction. In theory, the methods are precise and accurate referee methods suitable for resolving differences of opinion. In practice, the methods are a mixture of the tried and true, recent innovations, the obsolete but barely adequate, the worthless, and methods to be used only when conditions beyond the control of the analyst require them. Nonetheless, the book belongs in the library of any analyst who must do official assays; assays agricultural products; determines efficacy of disinfectants; assays pesticide formulations, foods, food additives, cosmetics, drugs, drugs in animal feeds, vitamins, and amino acids; looks for filth in foods and for microbial contaminants in raw and processed foods; or needs to develop latent fingerprints and make voice print identifications. There is something for everyone from the agricultural chemist to the budding Sherlock Holmes.

When the first edition of "Methods" was published in 1920, the editors could make the valid assumption that it would be used by trained and experienced analysts. Today, that assumption can no longer be made, and presentation of procedures should be modified accordingly. Many people in certain fields are not trained in analytical techniques. Although the editors can do nothing about this misapplication of people, they could provide tutorial material to teach basic techniques. One of the first skills to be taught should be how to select and use volumetric pipets and flasks. This gives an idea of the extent of the needs.

Of particular interest to pharmaceutical scientists are the chapters on disinfectants, flavors, food additives, metals, and other elements as residues in foods, sugars and syrups, color additives, cosmetics, drugs (five chapters), and vitamins and other nutrients.

"Methods" grows with each edition. Vigorous steps need to be taken to keep its size within reasonable limits for a one-volume book and to control its cost. The 68 pages of tables at the back of the book probably could be put on one or two pages as comments and as equations suitable for solution by the ubiquitous digital calculators. Space could be saved by presenting general procedures once and, thereafter, giving only deviations under the specific assay. More information could be placed in tables, and needless instructions could be omitted.

Equations for the wet chemistries would help the analyst understand what he or she is doing. Not everyone who uses "Methods" has a complete file of the *Journal of the Association of Official Analytical Chemists* or other sources of information. The absence of supporting theory gives "Methods" the appearance of a cookbook.

The chapter on drugs in feeds has 56 procedures for extracting a drug from feeds. In 45 of them, solids are included in the total volume of extract, thus causing possible bias.

The section on microbiological assays for antibiotics in animal feed has turbidimetric methods for the first time. The turbidimetric method is manual for chlortetracycline, and an AUTOTURB® System is used for monensin. The latter assay could be improved considerably at no cost of time or money. Also, the AUTOTURB System is not operated to give the accuracy and precision it was designed to give. Even the name of the system is incorrect.

The diffusion assays for antibiotics in feeds, being obsolete both in design and practice, contain possible inherent and easily avoidable errors. At that, the methods may be superior to those in the E.E.C. Possible significant biases in certain diffusion assays, such as those of bacitracin, hygromycin B, and monensin, are not mentioned. Collaborative assays have shown the bacitracin method to be an activity check and not a quantitative assay.

Theory and practice of microbiological assays for vitamins (Chapter 43) have progressed little since the Snell and Strong publication in 1939. Fortunately, accurate assays rarely are needed. Improvement in the quality of methods could come from someone with access to an AUTOTURB System who operates it correctly. Factors that need to be studied are: composition of media, preparation of inocula, time and temperature of incubation, dose–response line, computation of potency, and proper statistical treatment of data. Once these studies have been done, the influence of assay specificity, interferences, and details of sample preparation on accuracy and precision of assays for vitamins and amino acids could be investigated with profit. Microbiological assays, in contrast to chemical methods, have been stagnant too long.

*Reviewed by* Frederick Kavanagh
*829 N.W. 36th Street*
*Corvallis, OR 97330*

A publication of the
American Pharmaceutical Association—
the National Professional Society
of Pharmacists

# JOURNAL OF PHARMACEUTICAL SCIENCES

## INDEX TO AUTHORS
## INDEX TO SUBJECTS

VOLUME 70
JANUARY TO DECEMBER, 1981

*Published monthly under the supervision of the Board of Trustees*

MARY H. FERGUSON
*Editor*

NANCY E. BROWN
*Production Editor*

JOHN PATRICK EVANS
*Copy Editor*

MICHAEL K. HAYES
*Copy Editor*

EDWARD G. FELDMANN
*Contributing Editor*

SAMUEL W. GOLDSTEIN
*Contributing Editor*

BELLE R. BECK
*Editorial Secretary*

EDWARD G. FELDMANN
*Acting Director of Publications*

EDITORIAL ADVISORY BOARD

John Autian
Norman R. Farnsworth
William J. Jusko
Herbert A. Lieberman
David E. Mann, Jr.
Ian W. Mathison
Gerald J. Papariello
Edward G. Rippie

JOURNAL OF PHARMACEUTICAL SCIENCES

MAY 1981
VOLUME 70 NUMBER 5

*LITERATURE SURVEY*

# Fluorescence Immunoassay

**GARY C. VISOR and STEPHEN G. SCHULMAN ˣ**

Received from the *College of Pharmacy, University of Florida, Gainesville, FL 32610.*

**Keyphrases** □ Fluorescence immunoassay—overview of methods currently in use, homogeneous and heterogeneous methods compared to radioimmunoassay and chromatographic determinations □ Immunoglobulins—role in pharmaceutical analysis, fluorescence immunoassays of drug–carrier protein conjugate □ Homogeneous fluorescence immunoassays—reactant-labeled fluorescence, quenching and enhancement immunoassays, fluorescence polarization, time-resolved fluorescence immunoassays, role in pharmaceutical analysis □ Drug–carrier protein conjugate—overview of fluorescence immunoassay methods currently in use

The recent advances made in the area of immunoassays of biologically active compounds have had a significant impact on the health care community. Highly specific and sensitive immunological procedures are available that provide picomole sensitivity on a routine basis (1). In most of these assays, a radioactive label is used to monitor the competitive binding between a labeled and unlabeled ligand for receptor sites on specific antibodies (2, 3). The analysis of this competitive binding allows the construction of a standard curve representing the antibody-bound radioactivity as a function of the unlabeled ligand concentration. This approach gives the analyst the capacity to quantitate, quite specifically, the ligand (analyte) of interest as well as the ability to detect it at far lower concentrations than is possible by other chemical methods due to the extremely sensitive methods available for the detection of radioactivity.

The major limitations of radioimmunoassay result from the biological hazards of radioactivity, the difficulties associated with various licensing requirements, the safe disposal of wastes, and the expense and inconvenience incurred by the short radioactive lifetimes of the labels (4, 5).

A rather recent development in the area of immunoassays provides a major alternative to the use of radiolabels. Fluorescent probes are used in place of the radiolabels, and their spectral characteristics are monitored as a function of the immunoreactions between the ligand and the antibody. In the foreseeable future, this new immunological technique may possibly be comparable in both selectivity and sensitivity to current radioimmunoassay methods.

In this overview of fluorescence immunoassay, the methods currently in use will be evaluated and likely future developments will be discussed.

## NATURE OF IMMUNE RESPONSE AND ITS ROLE IN PHARMACEUTICAL ANALYSIS

The ability of an organism to synthesize specialized proteins (antibodies) directed against an invasive foreign material forms the basis of the immune response. Antibodies are a group of structurally related proteins known as the immunoglobulins (Ig). There are five major classes of immunoglobulins: IgG, IgM, IgA, IgD, and IgE. The predominant immunoglobulin in serum, IgG, is usually associated with the majority of antigen binding activity in the highly diluted solutions used in sensitive immunoassays (6). The IgG class has an average molecular weight of 150,000–160,000 daltons. The structure of IgG proteins is characterized by four polypeptide chains, two of which are heavy or H-chains (50,000 daltons) and two of which are light or L-chains (20,000 daltons). Each immunoglobulin molecule contains two binding sites at the terminal regions of the H-chains. These binding sites contain variable amino acid sequences and appear to be responsible for the binding specificity common to antibodies (7).

The immunoglobulins are produced by the B-lymphocytes. The process of the maturation and development of these lymphocytes into cells capable of antibody production is not understood fully (8).

The ability of a molecule to elicit an immunoresponse appears to depend on its size. Molecules with molecular weights below 10,000 daltons usually are not immunogenic. Most proteins, large polymeric carbohydrates, and lipopolysaccharides are immunogenic. The antibodies developed in response to these molecules recognize and bind to only a small section of the antigen. Antibody specificity usually involves no more than six or seven amino acid residues of a large protein-like structure (9).

0022-3549/81/0500-0469$01.00/0
© 1981, American Pharmaceutical Association

The investigations performed by Landsteiner (10) determined that an immunoresponse can be elicited from an organism to small molecules (haptens) coupled to proteins or polypeptides; antibodies to the hapten–protein conjugate, capable of recognizing part of the hapten even when it was not coupled to the carrier protein, could be generated. Drugs and their metabolites normally are not immunogenic unless they are first coupled covalently to macromolecules.

The human and bovine serum albumins and, recently, some synthetic polypeptides have been used as carriers for drugs and other small molecules. However, the population of antibodies directed toward the hapten–carrier protein conjugate is not homogeneous. Rather, some of the antibodies produced may recognize portions of the protein carrier and some recognize the hapten itself. Only those antibodies directed toward the hapten will be useful in immunoassay, and it is the heterogeneity of the isolated antibodies that makes it difficult to describe the immunoreactions quantitatively in terms of simple competitive equilibria.

To synthesize a drug–carrier protein conjugate, the drug must have at least one functional group available for attachment to the carrier reactive sites under suitable chemical conditions. The coupling of the drug to the carrier must not cause significant structural alterations or denature the carrier itself. Low molecular weight substances have commonly been conjugated to proteins through carboxyl, amino, and hydroxyl groups (11). A detailed review of the procedures and applications of various conjugation procedures was published by Beiser *et al.* (12). Selected methods and applications of pharmaceutical interest will be discussed briefly.

The selection of a conjugation procedure for the coupling of a hapten with a protein is determined by the available functional groups on the hapten, the stability and solubility of the hapten, and the mode of attachment to the protein (13). The most common sites of conjugation on a protein molecule are the amino groups of the *N*-terminal and lysine residues, the carboxyl groups of the *C*-terminal and aspartic and glutamic acid residues, the phenolic functions of tyrosine, and the secondary NH group of histidine. The sulfhydryl groups of cysteine also have been used for conjugation (13).

An example of a conjugative procedure used to couple a hapten with a carboxyl group to a protein carrier is provided by the production of the D-lysergic acid–poly(L-lysine) conjugate. The agent used to initiate the reaction was a water-soluble carbodiimide, 1-ethyl-3-(3-dimethylaminopropyl)carbodiimide hydrochloride (14, 15). The D-lysergic acid was bonded covalently by its carboxyl function to the $\epsilon$-amino group of poly(L-lysine) (mol. wt. 95,000). The resulting condensation resulted in amide bond formation to give a poly(L-lysine)–lysergamide conjugate (16).

Haptens with aromatic amino groups may be conjugated to proteins by a relatively simple diazotization procedure. The reaction involves conversion of the aromatic amine to a diazonium salt that couples to the aromatic and other side chains of a protein carrier (17, 18). Nitrous acid reacts with the aromatic amine to form the diazonium salt; at alkaline pH, the diazonium salt couples to the tyrosine, histidine, and tryptophan residues of the carrier through the azo group (19). An important pharmaceutical application of this procedure is the conjugation of chloramphenicol to bovine $\gamma$-globulin (20). In these experiments, the nitro group of the chloramphenicol was reduced to an amino group prior to conjugation.

Assuming that a suitable procedure for conjugation can be found, it should be possible to obtain specific antibodies for any biologically active compound. However, there is a certain amount of cross-reactivity of the hapten-directed antibodies with molecules of structure similar to that of the hapten. This problem is not significant in most instances, but it should be considered in any immunoassay. Another difficulty that may arise is the binding of the active compound by nonantibody proteins in the test serum, urinary, or cerebrospinal fluid solution. Again, this problem may not be significant, but the possibility of interference should be recognized.

## FLUORESCENT PROBES

The fluorogenic molecules used to label covalently the ligands (drugs) and, in some instances, the antibodies in a fluorescence immunoassay fall into the category of fluorescent probes (21, 22). Fluorescent probes are small molecules whose fluorescent properties are altered subsequent to interactions with proteins or other macromolecules (23). The proper selection of a fluorescent label and the technique employed for its conjugation to the ligand are critical to the sensitivity and selectivity obtained in an immunoassay.

In quantitative immunoassays using fluorescent labels, the fluorochrome should possess several basic chemical and spectroscopic properties. The labeled ligand should have a relatively high water solubility because immunoassays are usually carried out in the aqueous environment of biological samples (*i.e.*, serum, urine, and cerebrospinal fluid). The presence of certain potentially reactive functionalities on the fluorochrome facilitates its conjugation to the ligand. Derivatives of the fluorochromes containing reactive groups such as acid chlorides, isothiocyanates, and diazonium salts can be used for the conjugation of the label to the ligand. A major concern in labeling a ligand with a fluorescent probe is the alteration of the specificity of the ligand for its antibody. The site of conjugation should provide maximum exposure of the functional groups necessary for antibody recognition. The stability and shelflife are also important.

The spectral characteristics of greatest importance in the selection of a fluorochrome are the molar absorptivity at the selected excitation wavelength, the quantum yield of fluorescence of the labeled species, the spectral regions of absorption and emission of radiation, and the Stokes shift. Ideally, the fluorescent label should have a high molar absorptivity in the visible region of the electromagnetic spectrum, which is well removed from the excitation spectra of proteins and other endogenous interferences normally present in biological fluids. The emission wavelength should also lie well in the visible region with Stokes shift (displacement of the fluorescence maximum from the longest wavelength absorption maximum) of at least 50 nm. A high quantum yield of fluorescence in the antibody-bound or free labeled ligand is also desirable.

Due to the rather stringent requirements placed on fluorescent labels used for monitoring immunoreactions,

only a few substances have given satisfactory results. The labels most commonly used are fluorescein isothiocyanate and several rhodamine dyes (usually tetramethylrhodamine isothiocyanate). Fluorescein isothiocyanate has a relatively high quantum yield and can be conjugated to drugs and other ligands under fairly mild conditions (24). Gentamicin, as the free base, was conjugated with fluorescein isothiocyanate at alkaline pH, forming fluoresceinthiocarbamyl gentamicin. The reaction mixture was purified on a Sephadex column, with unreacted gentamicin being well separated from the fluorescein-labeled gentamicin. Polarization and quenching immunoassays (*vide infra*) were performed with the conjugate, and the results were comparable in sensitivity to bioassay and radioimmunoassay (25, 26).

Recent work in ligand labeling with fluorescent metal chelates has opened a new area of research in fluorescent probes (27). The chelates of rare earth metals have unique emission characteristics in that, upon excitation of aromatic portions of the ligand of the lanthanide complex, the energy of excitation is efficiently transferred to the lanthanide ion. This causes f–f transitions, which produce narrow, almost line-like emission bands with fairly long decay times (1 μsec–1 msec). In addition, the rare earth chelates possess large quantum yields in combination with very large Stokes shifts. The excitation region of these chelates is fairly broad and allows excellent sensitivity and selectivity, enabling the use of fairly wide bandwidths for excitation and narrow bandwidths for emission. With the proper combination of a rare earth chelate and fluorometric technique, sensitive immunoassays can be developed that avoid interferences commonly encountered in the immunoassay.

The development of new fluorescent probes for fluorescent immunoassay, having greater environmental sensitivity and larger Stokes shifts than observed in the compounds in use currently, should provide a fertile area for research.

## HOMOGENEOUS FLUORESCENCE IMMUNOASSAY

Fluorescence immunoassays can be divided into two broad classes, homogeneous and heterogeneous. The homogeneous technique differs from the heterogeneous primarily in that fluorometric quantitation of the ligand can be performed without separating the free ligand from the antibody-bound labeled ligand. The elimination of the need to separate bound and free ligands, normally present in other immunoassays (*e.g.*, radioimmunoassay) represents a major advantage of fluorescence immunoassay and provides the opportunity for a simple, fast, and reliable quantitation. This procedure can be performed because of the different microenvironments in which the free and bound ligands reside and their effects on the spectral characteristics of the label.

In the aqueous environment, the free labeled antigen experiences strong polarizing forces and perhaps hydrogen bonding forces at acidic or basic functional groups as a result of interactions with water molecules. These forces are exerted to different degrees in the ground and excited states of the labeled antigen because these states have different dipole moments. Moreover, certain functional groups on the fluorophore are free to rotate subsequent to the fluorescent transition in water. On the other hand, in the hydrophobic environment of an antibody binding site, the dielectric strength is low, and rotation of functional groups on the fluorophore is severely restricted. The solvation and restricted rotational freedom of the antibody-bound labeled antigen usually cause this species to fluoresce at shorter wavelengths than the free labeled antigen because the relative stabilization of the excited state of the latter, by strong electrostatic and electromeric interactions, is much greater than in the bound labeled antigen. In addition, the weak solvation and restricted rotational freedom of the antibody-bound probe also cause the bound probe to fluoresce more intensely than the free probe because the bound probe is somewhat shielded from internal and external conversions, which compete with fluorescence for deactivation of the excited state.

If the fluorescent emission spectrum of the bound labeled ligand is shifted sufficiently from that of the free labeled ligand, the resulting spectroscopic measurements can be used for quantitation without a separation step. In essence, a spectroscopic separation rather than a chemical separation is employed and contributes to the simplicity and speed of analysis.

Despite their speed and simplicity, homogeneous assays may not always provide the sensitivity needed in certain solutions due to the endogenous background fluoresence of the proteinaceous material present. The Rayleigh and Raman scattering caused by the high protein content in solution and the intrinsic fluorescence from certain amino acid residues are major obstacles to a sensitive assay.

The three major types of homogeneous fluorescence immunoassay are quenching and enhancement, fluorescence polarization, and reactant-labeled fluorescence immunoassay. Each technique will be discussed briefly and evaluated for its sensitivity and reliability.

**Reactant-Labeled Fluorescence Immunoassay**—An interesting variation of homogeneous immunoassay in which neither the labeled ligand *per se* nor the antibody-labeled ligand complex is fluorescent is seen in reactant-labeled fluorescence immunoassay. The technique is based on the quantitation of the fluorescent product resulting from the enzymatic cleavage of the unbound labeled ligand. The fluorescent probe labeling the ligand exists in nonfluorescent form as long as it is linked covalently to the ligand through the bond that will be cleaved by enzymatic action (usually hydrolysis). If the labeled ligand is complexed by specific antibodies prior to hydrolysis, it cannot act as a substrate for the enzyme. The complex prevents any reaction between the enzyme and labeled ligand and thereby inhibits fluorescence from excited labels (28, 29). The unavailability of the conjugated substrates (drug and label) to the enzyme is reversed by the presence of free unlabeled ligand (in the unknown solution), which then competes with the labeled conjugate for the antibody binding sites. The labeled ligand thus displaced from its antibody binding site can be cleaved by the enzyme, liberating the fluorescent form of the label. The extent of fluorescence is proportional to the free ligand or analyte concentration.

A reactant-labeled fluorescence immunoassay was applied to the analysis of gentamicin in human serum (30). Gentamicin is a widely used antibiotic but, in systemic therapy, the range between therapeutic and potentially toxic serum levels is narrow (31). Thus, a fast, reliable, and

sensitive procedure was developed based on reactant-labeled fluorescence. The assay uses umbelliferyl β-galactoside as a label for gentamicin and the enzyme β-galactosidase to obtain fluorescent products. Gentamicin is conjugated to β-galactosylumbelliferone to form a nonfluorescent substrate. Hydrolysis of the uncomplexed β-galactosylumbelliferone–gentamicin conjugate is catalyzed by the enzyme β-galactosidase to form a fluorescent product, the free 7-hydroxycoumarinate anion. However, hydrolysis is inhibited if the gentamicin conjugate is bound with specific antigentamicin antibodies since steric hindrance from the antibody prevents the enzyme from acting on the substrate. The extent of fluorescence is proportional to the gentamicin concentration, and the sensitivity is comparable to that of radioimmunoassay.

**Quenching and Enhancement Immunoassays**—Fluorescent quenching methods are based on the observed reduction in fluorescence intensity of a labeled ligand upon complexation by the antibody. The exact mechanism has not been established, but it is generally agreed that it involves alteration of the electronic structure and perhaps of the vibrational composition of the electronic states of the labeled antigen upon binding by the antibody. Alteration in the electronic distribution of the bound labeled ligand can enhance the probability of radiationless deactivation of the first excited singlet state. A possible explanation might be the vibrational coupling of the bound labeled ligand with the normal vibrational modes of the protein, a process that could enhance the rate of internal conversion to the ground state. If the extent of quenching of the bound labeled ligand is great enough, the competitive binding of unlabeled ligand for antibody binding sites can be quantitated by measuring the fluorescence of the displaced labeled ligand.

Serum gentamicin levels were studied using a quenching fluoroimmunoassay (32). With fluorescein-labeled gentamicin as the labeled conjugate, the degree of quenching of its fluorescence emission upon binding by an antibody was related to the concentration of unlabeled gentamicin present, using a standard curve.

A novel homogeneous quenching assay was developed for morphine that employs a fluorescein-labeled antigen and a quencher-labeled antibody (33). The mechanism of quenching is associated with energy transfer from the fluorescent donor (fluorescein) to the fluorescent acceptor (rhodamine) or quencher. The emission of the fluorescein-labeled antigen is quenched by the rhodamine-labeled antibody upon complexation. The effectiveness of energy transfer quenching is dependent on the overlap of the fluorescence and absorption spectra of the donor and acceptor, respectively. The efficiency of energy transfer is also dependent on the distance between the bound labeled antigen and the energy acceptor (quencher) in the antibody complex. The quenching can be prevented by competitive binding with unlabeled antigen, which forms the basis for the analysis of the latter. The sensitivity obtained for the morphine assay was in the nanomolar range, but unusually high purity requirements for antibodies and background interference, as well as the difficulty and tedium of labeling of both antigen and antibody, limit routine applications.

Fluorescent enhancement assays are similar to those of the quenching techniques in that there is a change in fluorescent intensity upon antibody binding. The difference is that there is an increase in the quantum yield of ligand fluorescence upon binding. This phenomenon was reported for the binding between fluorescein-labeled thyroxine and its antibodies (34). In this case, the proposed mechanism is a decrease in the thyroxine-induced spin-orbital coupling between the singlet and triplet states of fluorescein. This decrease is a result of the alteration of the separation between the lowest excited singlet states of fluorescein and thyroxine, induced by the low polarity of the antibody binding site (35). The sensitivity is less than that of typical radioimmunoassay procedures.

**Fluorescence Polarization**—Fluorescence polarization provides valuable information on the interactions of antigens or haptens with antibodies. The use of fluorescence polarization in the study of macromolecules was initiated by Weber in 1952 (36) and has become a major tool in structural investigations of the binding of small molecules to proteins.

The physical principle underlying fluorescence polarization immunoassay involves the selective elimination of light waves whose electric vectors do not all lie in a single plane. This is accomplished by passing the exciting light through a polarizing filter. The resulting polarized radiation selectively excites those molecules whose absorption transition moments have a significant component in the plane of the electrical vector of the exciting beam (37). As a result, molecules excited with polarized light emit radiation that is polarized in the same direction as the exciting light, to a degree that is inversely related to the amount of Brownian rotation occurring during the interval between absorption and emission of light (38). In other words, the photoselected molecules originally excited by polarized light and having fairly small volumes (*i.e.*, free labeled antigen) have a rotational relaxation time that is much shorter than their fluorescence decay time and thus become completely randomized before fluorescing. Therefore, little polarized fluorescence is displayed. However, photoselected molecules having very large volumes, such as antibody proteins and their complexes, rotate at a rate comparable to or slower than the rate at which they fluoresce. Consequently, randomization of the fluorescent transition moments does not occur in the large molecules, and substantial fluorescence polarization is observed.

Upon the binding of an antigen to an antibody, there is a reduction or a restriction in the rotational Brownian motion as well as an increase in the overall size of the fluorescent label. This result causes considerable polarization of the fluorescence along or perpendicular to the optical axis of the excitation polarizer, depending on whether the fluorescence transition moment of the molecule is oriented closer to 0 or 90° to the transition moment associated with the absorption band excited. The case where the transition moments for excitation and fluorescence are parallel (or nearly so) will be discussed first.

If a second polarizing film (emission polarizer) is placed between the fluorescing sample and the photodetector of the fluorometer with its optical axis perpendicular to that of the polarizing film between the lamp and the sample, the highly polarized fluorescence from the antibody-labeled ligand is filtered to a much greater extent than is the unpolarized fluorescence from the same concentration of

free labeled ligand excited under the same conditions. If the optical axes of both polarizers are parallel and the excitation and emission moments of the fluorophore are parallel (or nearly so), the emission polarizer passes relatively more radiation from the bound labeled ligand than from the free labeled ligand to the detector, because the polarized emission is concentrated along the optical axis of each polarizer while the unpolarized emission is dispersed over all angles to the optical axis of the emission polarizer and some, therefore, is filtered. Regardless of the orientation of the optical axis of the second polarizer with respect to the first, the fluorescence intensity registered by the detector, ideally, should be the same for unpolarized fluorescence (*i.e.*, that of the free labeled ligand). In the case of parallel absorption and fluorescence transition moments, the intensity of the polarized fluorescence (that from the bound labeled ligand) measured when the optical axes of the polarizers are parallel ($F_{\parallel}$) should be greater than when the optical axes of the polarizers are perpendicular ($F_{\perp}$). In the case of perpendicular absorption and fluorescence transition moments, $F_{\parallel} = F_{\perp}$ also for the free labeled ligand (unpolarized fluorescence) and $F_{\parallel} < F_{\perp}$ for the bound labeled ligand (polarized fluorescence).

The degree of polarization may be defined as:

$$p = \frac{F_{\parallel} - F_{\perp}}{F_{\parallel} + F_{\perp}} \qquad \text{(Eq. 1)}$$

Ideally, at any given excitation wavelength, $p$ should be a property of a pure species and be invariant with respect to concentration. For a free labeled ligand, $F_{\parallel} = F_{\perp}$ so that $p = 0$ at all excitation wavelengths. For a bound labeled ligand, it is possible to have $+1/2 > p > -1/3$, depending on the excitation wavelength. However, if a system is contrived that originally contains all antibody-bound labeled ligand and to which the free unlabeled ligand is added so that some labeled ligand is displaced, the relative increase in unpolarized fluorescence and decrease in polarized fluorescence from the solution cause a net decrease in $p$, as calculated from its operational definition in Eq. 1. If all of the labeled ligand is ultimately displaced from the antibody complex, $p$ falls to zero. The fact that, depending on the extent of binding of the labeled ligand, the degree of polarization varies between some nonzero value and zero permits the construction of a calibration curve of the degree of fluorescence polarization *versus* the concentration of unlabeled ligand and permits execution of a homogeneous immunoassay.

The use of polarized fluorescence for the quantitation of several antigen–antibody reactions was reported (39, 40). Two assays of particular interest were those applied to the measurement of serum levels of gentamicin and phenytoin (41, 42). Fluorescein-labeled ligands were used in both cases, and the polarization measurements correlated well with other instrumental and bioassay techniques.

The use of fluorescence polarization as a routine method for drug level determinations has been limited not only by the expense of the instrumentation but also by the energy losses due to the polarizing films and the background interferences that result in reduced sensitivity. In addition, the nonlinear polarization response as a function of concentration, combined with the nonlinear relationship in competitive binding between antigen and antibody, severely limits the dynamic range of the procedure (5).

## TIME-RESOLVED FLUORESCENCE IMMUNOASSAY

All of the fluorometric techniques considered so far have been based on the measurement of the intensity of fluorescence produced under "steady-state" conditions. Steady-state fluorometry is derived from the excitation of the sample with a continuous temporal output of exciting radiation. The lamps and their power supplies used in conventional fluorometers are sources of continuous radiation. After a short initial excitation of the sample, a steady state is established in which the rate of excitation of the analyte is equal to the sum of the rates of all processes deactivating the lowest excited singlet state (fluorescence, internal conversion, and intersystem crossing). When the steady state is established, the observed fluorescence intensity becomes time invariant and produces the temporally constant signal which is measured by the photodetector.

However, with the development of modern electrooptics, it has become possible to excite a potentially fluorescent sample with a thyratron-pulsed flash lamp that emits its radiation in bursts of 2–10-nsec duration with ~0.2 msec between pulses. A fluorescent sample excited with such a pulsed source does not fluoresce continuously. Rather, its fluorescence intensity, excited by a single pulse, decays exponentially until the next pulse again excites the sample. The pulsed source acts much as does a mechanical chopper in phosphorimetry. The fluorescence from the sample excited by the pulsed source can be represented, after detection, as a function of time on a fast sampling oscilloscope or on an $x$–$y$ plotter used with a multichannel pulse analyzer.

The former approach is called stroboscopic fluorometry, and the latter is called time-correlated single-photon counting. In either case, fluorescences with decay times much longer than the lamp pulse characteristics can be treated in the same way that radioactive decay curves are analyzed. A semilogarithmic plot of fluorescence intensity against time yields a straight line (or a series of overlapping lines if several fluorophores have comparable but not identical decay times) whose slope is proportional to the decay time and whose vertical axis intercept can be compared with that of a standard solution of the fluorophore for quantitative analysis. However, if the lamp pulse time and the decay time of the fluorophore are comparable, the lamp characteristics must be subtracted from the observed signal to obtain the fluorophore's decay characteristics. A computer is usually used to solve a deconvolution integral representing the composite temporal characteristics of the lamp and the fluorophore output (43–45).

The pulsed-source (time-resolved) method effects spectroscopic separation of the emissions of several fluorescing species by taking advantage of differences in their decay times rather than their fluorescence intensities. Thus, several overlapping fluorescences, such as those of free and antibody-bound ligand, can be quantitated simultaneously. Although the stroboscopic approach is useful when a single species has a decay time much longer than other species in the solution, it does not give good results when several species in solution have fairly close (within an order of magnitude) decay times. In this regard, time-correlated single-photon counting is indispensable. Time-resolved fluorometry is also extremely useful for the elimination of interferences due to Rayleigh and Raman

scatter. Since these processes occur on a time scale of $10^{-14}$–$10^{-13}$ sec, they are faster than the lamp pulse time and are not represented in the signal that reaches the detector.

Time-resolved fluorometry has not reached its full potential. Its routine use in fluorescence immunoassay is inhibited by the high cost and complexity of the instrumentation, but this situation could change in the foreseeable future.

## HETEROGENEOUS ASSAYS

Most research and development of fluorescence immunoassays have been concentrated in the area of homogeneous assay. However, a major limitation in the application of homogeneous fluoroimmunoassay to the therapeutic monitoring of drug concentrations in human serum is the presence of endogenous interferences. This limitation usually takes the form of a loss of fluorometric sensitivity due to the presence of a high background emission from endogenous proteins and other species and a small signal from the analyte. Notwithstanding the speed and simplicity of the homogeneous assays, it is occasionally desirable to circumvent the problem of background emission by physically separating the antibody–ligand complex from other species in the sample before fluorometric quantitation. This approach forms the basis of heterogeneous immunoassay.

The separation of the antibody-bound–ligand complex from free ligands and other fluorescing species present in solution can be accomplished by various methods that are already in use in radioimmunoassay. These methods are based on the chemical or immunological differences between the free ligand and the antibody–ligand complex. The charge, size, solubility, and surface configuration (immunological specificity) are among the determinants used to separate the free and bound forms (1).

Some techniques that are most commonly encountered in heterogeneous methodology are gel permeation chromatography, chemical precipitation with inorganic salts or organic solvents, and double antibody methods (46, 47). Gel permeation or filtration chromatography enables the separation of free and bound forms of the fluorescent ligand due to the differences in molecular size between the micro- and macromolecular entities (48). The chemical precipitation methods used in radioimmunoassay have not been thoroughly investigated for use in fluoroimmunoassay. The procedures are based essentially on the differential precipitation of proteins. Antibodies can be precipitated with ethanol and dioxane or salted out with ammonium sulfate. Double antibody separation techniques are highly versatile and can be applied to almost any assay system. The separation of the ligand–antibody complex results from the precipitate that forms after a second antibody is introduced. The second antibody is directed against the antibodies of the primary ligand–antibody reaction and is produced in a different species of animal than the first. A good example is the heterogeneous assay of gentamicin. After the competitive binding between gentamicin and labeled gentamicin for sites on a rabbit antibody (directed against gentamicin) comes to equilibrium, separation is achieved by precipitation of the gentamicin–rabbit antibody and labeled gentamicin–rabbit antibody complexes with goat anti-rabbit immunoglobulins.

One promising separation (heterogeneous) technique involves the use of a solid phase support to which an antibody population is either adsorbed or bonded covalently (49). The solid material may be paper disks, the walls of test tubes, glass or plastic beads, or even Sephadex or Sepharose (50, 51).

Once the antibodies are immobilized on the solid support, labeled and unlabeled ligands are introduced and allowed to compete for available binding sites on the antibody. The bound labeled fraction then is separated from the labeled ligand remaining in solution by washing. The labeled ligand complexed to the antibody then can be measured directly, without removal from the solid phase, by a fluorometer with a front-surface fluorescence attachment (52). The fluorescent label also may be removed from the solid phase by a denaturant and measured in a conventional fluorometer (4).

A variation of the solid-phase methodology may involve a solid-phase ligand that competes with free ligand and labeled antibody. The solid-phase bound, labeled antibody then may be measured after washing to remove the unbound, labeled antibody.

The ability to reduce background interference commonly encountered in fluoroimmunoassays will make heterogeneous assays more attractive in the near future. The time and effort spent in immobilizing the antigen or antibody in this system, as well as the actual separation of the labeled and unlabeled species, will ultimately be rewarded with enhanced sensitivity. Advances in the technology of the solid phases and instrumentation used for heterogeneous immunoassay are likely. Already, specialized "immunofluorometers" designed for front-surface illumination are available commercially.

## CONCLUSION

The application of fluorescence immunoassay to the detection and quantitation of biologically active compounds provides a major alternative to chromatographic and radiochemical methods of analysis. The elimination of potentially hazardous radioactive labels and the ability to measure, quite sensitively, serum levels of active agents without prior extraction and separation have propelled fluoroimmunoassay into the mainstream of modern analytical techniques. Further developments in fluorescent probes, antibody production, heterogeneous methodology, and fluorescence instrumentation will enhance the attractiveness of fluoroimmunoassay.

The development of novel fluorescent probes for use in immunoassays will be an important area of research. Probes having greater Stokes shifts, greater environmental sensitivities, and high quantum yields of fluorescence that are easily coupled to drugs may replace the limited number of probes now in routine use.

The introduction of new instrumentation and accompanying methodology will also broaden the scope of the applications and improve the sensitivity obtained in fluoroimmunoassay. A recent study reported the use of an argon-ion laser in the detection system of a high-pressure liquid chromatographic separation of free and bound fluorescent antigens (48). This technique employs gel per-

meation chromatography for the separation of fluorescein-labeled insulin, bound by specific antibodies, from the free fluorescent antigen. The detection limit is comparable to that obtained in radioimmunoassay. The laser as an excitation source will no doubt play a much greater role in fluoroimmunoassay (48).

## REFERENCES


(1) J. I. Thorell and S. M. Larson, "Radioimmunoassay and Related Techniques," Mosby, St. Louis, Mo., 1978.

(2) W. D. Odell and W. H. Daughaday, "Principles of Competitive Protein Binding Assays," Lippincott, Philadelphia, Pa., 1971.

(3) S. A. Berson and R. S. Yalow, *J. Clin. Invest.*, **38**, 1996 (1959).

(4) C. M. O'Donell and S. C. Suffin, *Anal. Chem.*, **51**, 33A (1979).

(5) E. Soini and I. Hemmila, *Clin. Chem.*, **25**, 353 (1979).

(6) C. W. Parker, in "Principles of Competitive Protein Binding Assays," W. D. Odell and W. H. Daughaday, Eds., Lippincott, Philadelphia, Pa., 1971, p. 25.

(7) G. M. Edelman and W. E. Gall, *Annu. Rev. Biochem.*, **38**, 415 (1969).

(8) "B. and T. Cells in Immune Recognition," F. Loor and G. E. Roelants, Eds., Wiley, New York, N.Y., 1977.

(9) M. Sela, *Adv. Immunol.*, **5**, 29 (1966).

(10) K. Landsteiner, "The Specificity of Seriological Reactions," Harvard University Press, Boston, Mass., 1962.

(11) V. P. Butler and S. M. Beiser, *Adv. Immunol.*, **17**, 255 (1973).

(12) S. M. Beiser, V. P. Butler, Jr., and B. F. Erlanger, in "Textbook of Immunopathology," P. A. Mecher and H. J. Muller-Eberhard, Eds., Grune and Stratton, New York, N.Y., 1976.

(13) C. W. Parker, "Radioimmunoassay of Biologically Active Compounds," Prentice-Hall, Englewood Cliffs, N.J., 1976, chap. 2.

(14) J. C. Sheehan and J. S. Hlavaka, *J. Org. Chem.*, **21**, 439 (1956).

(15) T. L. Goodfriend, L. Levin, and G. D. Fasman, *Science*, **144**, 1344 (1964).

(16) H. V. Vunakis, J. T. Farrow, H. B. Gjika, and L. Lerine, *Proc. Natl. Acad. Sci. USA*, **68**, 1483 (1971).

(17) "Methods in Immunology and Immunochemistry," vol. I, C. A. Williams and M. W. Chase, Eds., Academic, New York, N.Y., 1967.

(18) E. A. Kabat, in "Experimental Immunochemistry," 2nd ed., E. A. Kabat and M. M. Mayers, Eds., Charles C Thomas, Springfield, Ill., 1961, pp. 798–802.

(19) A. N. Howard and F. Wild, *Biochem. J.*, **65**, 651 (1957).

(20) R. N. Hamburger, *Science*, **152**, 203 (1966).

(21) Y. Kanaoka, *Angew. Chem. Int. Ed. Engl.*, **16**, 137 (1977).

(22) L. Brand and J. R. Gohlke, *Annu. Rev. Biochem.*, **41**, 843 (1972).

(23) G. M. Edelman and W. O. McClure, *Acc. Chem. Res.*, **1**, 65 (1968).

(24) W. B. Dandliker, R. Alonso, and C. Y. Meyers, *Immunochemistry*, **4**, 295 (1967).

(25) R. A. A. Watson, J. Landon, E. J. Shaw, and D. S. Smith, *Clin. Chim. Acta*, **73**, 51 (1976).

(26) E. J. Shaw, R. A. A. Watson, J. Landon, and D. S. Smith, *J. Clin. Pathol.*, **30**, 526 (1977).

(27) R. C. Leif, R. A. Thomas, T. A. Yopp, B. D. Watson, V. R. Guarino, D. H. K. Hindman, N. Lefkove, and L. M. Vallarino, *Clin. Chem.*, **23**, 1492 (1977).

(28) J. F. Burd, R. J. Cauico, M. C. Fetter, R. T. Buchler, R. D. Johnson, R. C. Boguslaski, and J. E. Christner, *Anal. Biochem.*, **77**, 56 (1977).

(29) H. R. Schroeder, P. O. Bogelhut, R. J. Cauico, R. C. Boguslaski, and R. T. Buckler, *Anal. Chem.*, **48**, 1933 (1976).

(30) J. B. Burd, R. C. Wong, J. E. Feeney, R. J. Cauico, and R. C. Boguslaski, *Clin. Chem.*, **23**, 1402 (1977).

(31) D. S. Reeves, *Br. J. Hosp. Med.*, **12**, 837 (1974).

(32) E. F. Shaw, R. A. A. Watson, W. J. Landon, and D. S. Smith, *J. Clin. Pathol.*, **30**, 526 (1977).

(33) E. F. Velman, M. Schwarzberg, and K. E. Rubenstein, *J. Biol. Chem.*, **251**, 172 (1976).

(34) D. S. Smith, *FEBS Lett.*, **77**, 25 (1977).

(35) H. R. Schroeder and F. M. Yeager, *Anal. Chem.*, **50**, 1114 (1978).

(36) G. Weber, *Biochem. J.*, **51**, 145 (1952).

(37) S. Udenfriend, "Fluorescence Assay in Biology and Medicine," vol. 1, Academic, New York, N.Y., 1962.

(38) R. F. Chen, in "Practical Fluorescence: Theory, Methods and Techniques," G. G. Guilbault, Ed., Dekker, New York, N.Y., 1973, chap. 12.

(39) W. B. Dandliker, in "Immunochemistry of Proteins," M. Z. Atassi, Ed., Plenum, New York, N.Y., 1977, p. 231.

(40) W. B. Dandliker, R. J. Kelly, J. Dandliker, J. Farquhar, and J. Leirn, *Immunochemistry*, **10**, 219 (1973).

(41) R. A. A. Watson, J. Landon, E. J. Shaw, and D. S. Smith, *Clin. Chim. Acta*, **73**, 51 (1976).

(42) A. R. McGregor, J. O. Crockall-Grenning, J. Landon, and D. S. Smith, *ibid.*, **83**, 161 (1978).

(43) L. J. Cline Love and L. M. Upton, *Anal. Chem.*, **52**, 496 (1980).

(44) L. J. Cline Love and L. A. Shaver, *ibid.*, **52**, 154 (1980).

(45) *Ibid.*, **48**, 364A (1976).

(46) L. Wide, in "Proceedings of a Symposium on Radioimmunoassay and Related Procedures in Medicine," vol. 1, International Atomic Energy Agency, Vienna, Austria, 1978, p. 143.

(47) W. M. Hunter, in "Handbook of Experimental Immunology," D. M. Weir, Ed., Blackwell Scientific Publications, London, England, 1978, p. 141.

(48) S. D. Lidofsky, T. Imasaka, and R. N. Zare, *Anal. Chem.*, **51**, 1602 (1979).

(49) R. C. Aalberse, *Clin. Chim. Acta*, **48**, 109 (1973).

(50) M. Ceska and V. Lundkurst, *Immunochemistry*, **9**, 1021 (1972).

(51) J. J. Haaijman, F. F. Bloemen, and C. M. Ham, *Ann. N.Y. Acad. Sci.*, **254**, 187 (1975).

(52) G. C. Blanchard and R. Gardner, *Clin. Chem.*, **24**, 808 (1978).

# Viscoelastic Stress/Strain Behavior of Pharmaceutical Tablets: Analysis during Unloading and Postcompression Periods

**EDWARD G. RIPPIE** ˣ **and DOUGLAS W. DANIELSON** *

Received May 15, 1980, from the *Department of Pharmaceutics, College of Pharmacy, University of Minnesota, Minneapolis, MN 55455.* Accepted for publication November 11, 1980. *Present address: Merrell National Laboratories, Cincinnati, OH 45215.

**Abstract** □ The processes of nonequilibrium generation and decay of axial and radial stresses within tablet compacts were analyzed in terms of three-dimensional linear viscoelastic theory. A rotary tablet press was instrumented to measure punch and die wall stresses during the compression and postcompression periods. Following compression, tablets were permitted to remain at the compression site within the die, and the die wall stress was followed. Microcrystalline cellulose, spray-processed lactose, and sulfacetamide are known to have different compression characteristics and were found to differ significantly in their viscoelastic parameters. Compacts assumed their final viscoelastic state prior to the time of punch separation. Theory permits separation of material behavior into dilation and distortion components. Dilation, thought to be dependent on voids, was elastic in all cases. Distortion effects could be described well by a Kelvin solid model. Results indicate that viscoelastic properties are functions of compression conditions and may be useful in adjusting compression conditions to avoid problems such as capping.

**Keyphrases** □ Viscoelastic behavior—analysis of tablets during unloading and postcompression □ Tablet formulation—analysis of viscoelastic behavior during unloading and postcompression □ Compression cycle—analysis of viscoelastic behavior during tablet formulation

The compression of powdered or granular material into a cohesive mass during the formation of a pharmaceutical tablet is a complex and irreversible dynamic process, in contrast to its apparent simplicity. Mechanically, the process consists of imposing a strain on the powder by progressively confining it to a diminishing volume, reaching approximately that of the completed tablet. The dimensional constraints imposed by the punches and die then are removed, and the compact is allowed to relax. The compacted material exerts stress against the punches and die during this process in response to the imposed strain. For this reason, useful information concerning the fundamental structure of tablets is available from compression stress/strain data, as reflected by the substantial volume of literature in the area.

In the present investigation, three-dimensional viscoelastic models of both the unloading portion of the compression event and the postcompression relaxation period were studied. They were examined for their utility in the analysis of internal structural behavior and changes that result from tablet compression. For this purpose, axial and radial stress/strain data were obtained under nonequilibrium conditions at normal operating speeds in a rotary tablet machine and were interpreted *via* these models.

## BACKGROUND

The stress/strain behavior observed in tablet compaction is a composite of effects arising from primary particle reorientation, elastic deformation, particle fracture, viscous and/or plastic flow, and the formation and breaking of interparticulate bonds. Some of these processes are time dependent and occur at various rates over the period of tablet formation. Therefore, the compact is not at stress/strain equilibrium during the compression event. Thus, the physical characteristics of the finished tablet may be expected to depend on the strain rate profile imposed by the tablet machine, the viscoelastic properties of the compact, and the resultant stresses during compaction and ejection from the die.

Arguments and evidence (1, 2) have indicated that the nature of stress release during decompression and stress unloading may be a major factor responsible for the success or failure of tablet formation. Studies of the quasistatic (2–5) and dynamic (6–8) loading characteristics of pharmaceutical compacts support the widely held view that substantial internal mass flow occurs during tableting. This flow is manifested as stress relaxation under constant (1) and changing (8–11) external strain. The strains applied during compression require the compacted material to yield or flow and to produce stresses that can result from four fundamental processes: elastic yield, viscous flow, plastic deformation, and mass acceleration. The meanings of these terms may differ somewhat in various contexts and will be defined as follows for this discussion.

Elastic yield is the instantaneous and totally reversible response to an applied load. It may be represented in linear form by a massless spring having no inertia. Viscous flow is defined, in its linear form, as Newtonian flow and is symbolized by a dashpot for which the rate of strain is directly proportional to the applied stress. Irreversible strains that result from stresses above a threshold value (elastic limit) are termed plastic deformations. The stress necessary to maintain motion, once begun in a perfectly plastic material, is independent of the strain rate. This idealized plastic behavior is analogous to a weight being slid across a level surface after static friction has been overcome. Inertial forces resulting from the movement of mass within a tablet also contribute to its stress/strain behavior during compression. However, because of the small masses and low accelerations involved, these forces are negligible and may be disregarded.

A model based on brittle fracture as the mechanism for tablet consolidation (12) has been applied to granular material subject to quasistatic stress loading and unloading. However, it is generally recognized that some plastic flow occurs at points of interparticulate contact during compression. Due to the force-concentrating effect of asperities (5), overall pressures required for this process are much lower than would produce plastic flow of the bulk material. This phenomenon generally has been termed "microsquashing" in the powder technology literature and is commonly thought to occur when particles are smaller than 1 mm. If only brittle fracture occurred during compaction, the result would be a finer powder rather than a coherent compact. However, strong compacts can be made of brittle materials even though extensive fragmentation of the primary particles is observed (13). A more general model (14), based on plastic yielding, is compatible with the consolidation pattern observed in isostatic loading. Both of these models are intended to apply only to quasistatic loading. It was demonstrated (8) that the punch to die wall pressure behavior observed during dynamic compaction in a rotary tablet press is markedly different than that observed during quasistatic loading.

In practice, loading and unloading of stresses within the tablet and its powdered precursor are accomplished in a few milliseconds. It was suggested that the resultant transient processes occur in stages during this brief period (15). A decrease in voids is most probably caused by interparticulate slippage in Stage I. Stage II is characterized by the formation



0022-3549/81/0500-0476$01.00/0
© 1981, American Pharmaceutical Association

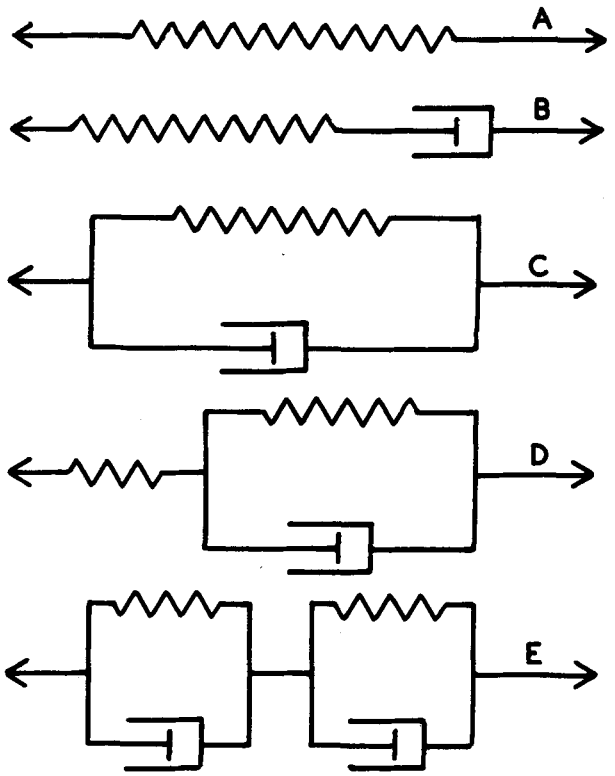


**Figure 1**—*Fundamental viscoelastic models. Key: A, elastic solid; B, Maxwell fluid; C, Kelvin solid; D, three-parameter solid; and E, four-parameter solid.*

of temporary struts, columns, and vaults protecting small voids and generally supporting the imposed load. In Stage III, this structure fails by particle fracture or plastic flow. The final condition is reached in Stage IV when the structure formed is strong enough to support the imposed load and any further reduction in volume of the compact involves the normal compressibility of the solid material. At this stage, any permanent decrease in the voids of a still porous compact can only be achieved by exceeding the crushing strength of the structure and/or by plastic deformation.

Depending on the kinetics of the various fundamental processes involved, Stage IV may not be reached until the punches are receding and stress unloading is well underway. It may be postulated that the structure responsible for the viscoelastic properties of the tablet are established during this final stage. These properties would then be the cumulative result of changes brought about during compact formation. Thus, they may be expected to be a function of the stress/strain history of the tablet and could change if the conditions of earlier stages were recreated as, for example, by recompression.

In the present studies, measurements of the viscoelastic behavior of the compact during the latter portion of the unloading phase of compaction are combined with results obtained immediately after punch separation but before ejection from the die. The viscoelastic parameters, derived from data obtained under these two sets of conditions, are useful in predicting evolutionary changes in the tablet prior to ejection. This prediction is important if the stress/strain condition of the tablet upon ejection from the die is to be calculated from information gathered earlier in the cycle.

## THEORETICAL

**Viscoelastic Constitutive Equations in One Dimension**—The time-dependent behavior of viscoelastic materials can be closely modeled by the use of combinations of discrete elastic and viscous elements (16, 17). The arrangement of the spring and dashpot elements within the models determines their characteristics and whether the material is a viscoelastic fluid or solid. For example, the coupling of a spring and dashpot in series is termed a Maxwell fluid. When the two elements are coupled in parallel, the model is a Kelvin solid. If a second spring is added in series to the Kelvin solid, the result is a standard three-parameter solid. These and other models used in this investigation are illustrated in Fig. 1. The equation of a linear elastic element, conforming to Hooke's law, is:

$$\sigma = F\epsilon \qquad \text{(Eq. 1)}$$

where $\sigma$ and $\epsilon$ are the stress and strain, respectively, and $F$ is the modulus for the spring. The viscous behavior of a Newtonian dashpot is given by:

$$\sigma = G\dot{\epsilon} \qquad \text{(Eq. 2)}$$

where $\dot{\epsilon}$ is $d\epsilon/dt$, the strain rate, and $G$ is the viscous coefficient. A tablet, left in the die after compression, exerts a residual die wall stress indefinitely, and a solid viscoelastic model, such as a Kelvin or a three-parameter solid, is needed to describe this behavior.

The constitutive equation of a Kelvin solid, where a spring and dashpot are coupled in parallel, is based on an equal strain of the two elements. Thus, the stress is distributed between them so that, from Eqs. 1 and 2:

$$\sigma = F\epsilon + G\dot{\epsilon} \qquad \text{(Eq. 3)}$$

More complicated models can be built systematically in the pattern shown in Fig. 1. The differential equations of these and other types of viscoelastic models (17) have the general form:

$$\sigma + p_1\dot{\sigma} + p_2\ddot{\sigma} + \cdots = q_0\epsilon + q_1\dot{\epsilon} + q_2\ddot{\epsilon} + \cdots \qquad \text{(Eq. 4)}$$

where $p_0 \equiv 1$. In the case of the Kelvin solid, $p_{i\neq 0} = 0$, $q_0 = F$, $q_1 = G$, and $q_{i\geq 2} = 0$. For other more complicated models, the coefficients $p_i$ and $q_i$ are various functions of the elastic and viscous constants corresponding to the constituent springs and dashpots. It is convenient to write these equations in differential operator notation:

$$P\sigma = Q\epsilon \qquad \text{(Eq. 5)}$$

where $P$ and $Q$ are defined as:

$$P = \sum p_i\, d^i/dt^i \qquad \text{(Eq. 6)}$$

$$Q = \sum q_i\, d^i/dt^i \qquad \text{(Eq. 7)}$$

and where, for a Kelvin solid:

$$P = 1 \qquad \text{(Eq. 8)}$$

$$Q = q_0 + q_1\, d/dt \qquad \text{(Eq. 9)}$$

**Three-Dimensional Viscoelastic Behavior**—The theory described thus far is adequate only when stresses and strains are in just one dimension. For the case of a tablet under compaction in a rigid die, axial

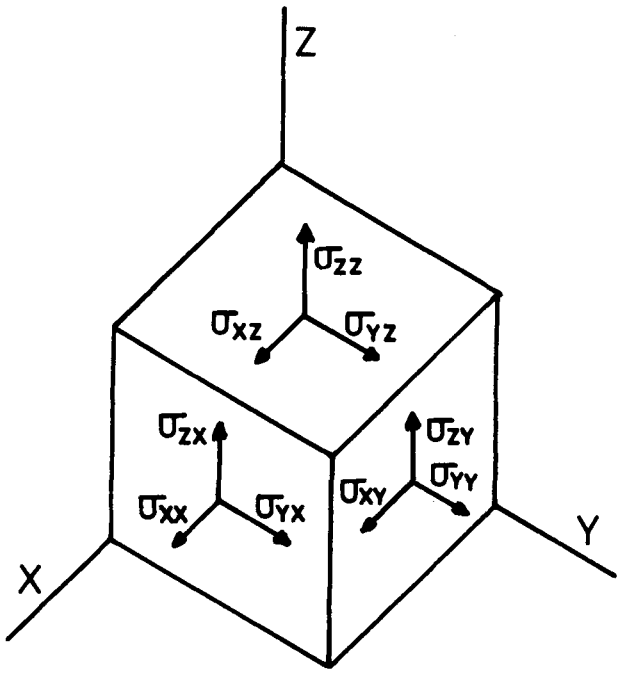


**Figure 2**—*Stress components acting on a cubical element within a stressed body.*

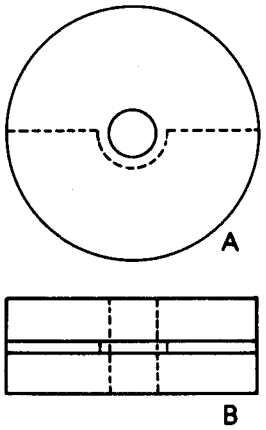


**Figure 3**—*Schematic drawing of tablet die, showing top (A) and side (B) views.*

strains are imposed by the punches and radial strains result, in part, from the lateral wedging of the particles as they are driven together. A more general expression of viscoelastic behavior than that given by Eqs. 5–7 is needed to account for processes occurring in three dimensions.

Three-dimensional viscoelastic theory can be developed from a consideration of the stresses and strains experienced by an infinitesimal cubical element within a stressed and strained solid body. Nine stress components, as illustrated in Fig. 2, comprise the stress tensor, $\hat{\sigma}$:

$$\hat{\sigma} = \begin{bmatrix} \sigma_{xx} & \sigma_{xy} & \sigma_{xz} \\ \sigma_{yx} & \sigma_{yy} & \sigma_{yz} \\ \sigma_{zx} & \sigma_{zy} & \sigma_{zz} \end{bmatrix} \quad \text{(Eq. 10)}$$

where $\sigma_{ij}$ denotes the stress in the $i$th direction on the $j$th face of the cube. Thus, where $i = j$, the stresses are normal to the surface; where $i \neq j$, shear stresses are indicated. If the cube is in moment equilibrium and not undergoing angular acceleration, $\sigma_{ij} = \sigma_{ji}$, so that there are six independent stress components under these conditions.

The stress tensor can be split into two parts, as in Eq. 11, so that the stresses leading to isostatic compression or dilation, $\hat{s}$, can be separated from those, $\hat{S}$, producing distortion of shape:

$$\hat{\sigma} = \hat{s} + \hat{S} \quad \text{(Eq. 11)}$$

where:

$$\hat{s} = \begin{bmatrix} s & 0 & 0 \\ 0 & s & 0 \\ 0 & 0 & s \end{bmatrix} \quad \text{(Eq. 12)}$$

and:

$$\hat{S} = \begin{bmatrix} S_{xx} & S_{xy} & S_{xz} \\ S_{yx} & S_{yy} & S_{yz} \\ S_{zx} & S_{zy} & S_{zz} \end{bmatrix} \quad \text{(Eq. 13)}$$

The isostatic stress components, $s$, are each taken as equal to $(\sigma_{xx} + \sigma_{yy} + \sigma_{zz})/3$. It follows from Eqs. 10–13 that $S_{xx} + S_{yy} + S_{zz} = 0$.

A similar operation may be performed on the strain tensor, $\hat{\epsilon}$, resolving it into isostatic, $\hat{e}$, and distortional, $\hat{E}$, strain tensors:

$$\begin{bmatrix} \epsilon_{xx} & \epsilon_{xy} & \epsilon_{xz} \\ \epsilon_{yx} & \epsilon_{yy} & \epsilon_{yz} \\ \epsilon_{zx} & \epsilon_{zy} & \epsilon_{zz} \end{bmatrix} = \begin{bmatrix} e & 0 & 0 \\ 0 & e & 0 \\ 0 & 0 & e \end{bmatrix} + \begin{bmatrix} E_{xx} & E_{xy} & E_{xz} \\ E_{yx} & E_{yy} & E_{yz} \\ E_{zx} & E_{zy} & E_{zz} \end{bmatrix} \quad \text{(Eq. 14)}$$

where $e = (\epsilon_{xx} + \epsilon_{yy} + \epsilon_{zz})/3$ and $E_{xx} + E_{yy} + E_{zz} = 0$.

For an isotropic viscoelastic material, $\hat{s}$ causes only volumetric changes, while only distortional changes are produced by $\hat{S}$. This behavior can be expressed by constitutive equations, analogous to Eq. 5, in which the volumetric and distortional effects are separated:

$$P''\hat{s} = Q''\hat{e} \quad \text{(Eq. 15)}$$

where:

$$P'' = \sum p_i'' \, d^i/dt^i \quad \text{(Eq. 16)}$$

$$Q'' = \sum q_i'' \, d^i/dt^i \quad \text{(Eq. 17)}$$

and:

$$P'\hat{S} = Q'\hat{E} \quad \text{(Eq. 18)}$$

where:

$$P' = \sum p_i' \, d^i/dt^i \quad \text{(Eq. 19)}$$

$$Q' = \sum q_i' \, d^i/dt^i \quad \text{(Eq. 20)}$$

The operator pairs $P''$ and $Q''$ and $P'$ and $Q'$ are totally independent of each other under these conditions. The nature of the viscoelastic material, *i.e.*, elastic solid, Kelvin solid, *etc.*, is expressed in Eqs. 15 and 18 *via* the operator pairs. For these reasons, it is possible to construct models in which the isostatic behavior is different from that proposed for distortion.

**Uniaxial Stress and Strain**—In applying three-dimensional theory to viscoelastic behavior, it is useful to consider the special case of a simple tension, $\sigma_{xx}$, applied to a three-dimensional body. The diagonal elements of $\hat{s}$ each become equal to $\sigma_{xx}/3$, and the nonzero elements of $\hat{S}$ are then $S_{xx} = 2\sigma_{xx}/3$ and $S_{yy} = S_{zz} = -\sigma_{xx}/3$. The strains resulting from these stresses appear as an elongation, $\epsilon_{xx}$, coupled with transverse contractions, $\epsilon_{yy} = \epsilon_{zz}$, which contribute to $\hat{e}$ and $\hat{E}$ so that $e = (\epsilon_{xx} + 2\epsilon_{yy})/3$, $E_{xx} = 2(\epsilon_{xx} - \epsilon_{yy})/3$, and $E_{yy} = E_{zz} = -(\epsilon_{xx} - \epsilon_{yy})/3$. Furthermore, if it is assumed that the operators $P$ and $Q$ are linear and time invarient, Eqs. 15 and 18 may be written in terms of the applied uniaxial stress:

$$(P''Q' + 2P'Q'')\sigma_{xx} = 3Q'Q''\epsilon_{xx} \quad \text{(Eq. 21)}$$

$$(P''Q' - P'Q'')\sigma_{xx} = 3Q'Q''\epsilon_{yy} = 3Q'Q''\epsilon_{zz} \quad \text{(Eq. 22)}$$

By analogous arguments applied to Eqs. 15 and 18, and with the same restrictions on $P$ and $Q$, the following equations may be derived for the case of an applied uniaxial strain, $\epsilon_{xx}$:

$$(P'Q'' + 2P''Q')\epsilon_{xx} = 3P'P''\sigma_{xx} \quad \text{(Eq. 23)}$$

$$(P'Q'' - P''Q')\epsilon_{xx} = 3P'P''\sigma_{yy} = 3P'P''\sigma_{zz} \quad \text{(Eq. 24)}$$

More detailed expositions (16, 17) of fundamental linear viscoelastic theory are available; however, the theory outlined here suffices for the present study. With the limitations and assumptions implicit in their derivation, Eqs. 21–24 can be applied, in linear combination, in modeling the process of tablet formation.

## EXPERIMENTAL

**Press Instrumentation**—Tablets were compressed using flat-faced punches on a rotary tablet machine[1]. A single station was instrumented with resistance strain gauges to monitor both die wall and punch stresses. All other stations were blank. The ejection cam was removed so that the tablet remained in the die after compaction, and its stress relaxation could be observed over an indefinitely extended period. Punch stress was measured by four strain gauges[2] attached to the lower compression roller support rod in a Poisson configuration. The gauges were activated in a direct-current Wheatstone bridge coupled[3] to the strain-gauge amplifier[4].

The die recess in the active station was enlarged to accommodate a specially made 9.525-mm laminar tablet die (Fig. 3). Mating surfaces of the three die layers were surface ground to ensure a close fit. The center layer, 1.5 mm thick, had a reduced wall thickness of 3.2 mm for half of its circumference. The upper and lower surfaces of this thin-walled segment each were ground down 5 $\mu$m to provide clearance for free radial expansion of the arch under stress. Extrusion of tablet material into this space was negligible, and only infrequent disassembly was needed for cleaning. An active strain gauge[5] was bonded to the arch and a second gauge was bonded to the lower die segment for temperature compensation. The Wheatstone bridge was completed internally, using precision wound resistors[6], within the strain-gauge amplifier to which it was hard wired[3].

Amplifier output signals were displayed on a storage oscilloscope[7], and stress measurements were made[8] from photos[9] of the traces. A typical

[1] Colton model 216, Cherry-Burrell Corp., Park Ridge, IL 60068.
[2] CEA-06-125WT-350, Micro-Measurement, Romulus, MI 48174.
[3] Cable 8434-100, Belden Corp., Chicago, IL 60644.
[4] Model 13-4312-00, Gould Inc., Cleveland, OH 44117.
[5] EA-06-031De-120, Micro-Measurement, Romulus, MI 48174.
[6] Type NS-112, Dale Electronics, Norfolk, NE 68701.
[7] Model 5103N, Tektronix, Beaverton, OR 97077.
[8] ID data tablet/digitizer, Summagraphics Corp., Fairfield, CT 06430.
[9] C5A Camera/Land Pack Back, Tektronix, Beaverton, OR 97077.

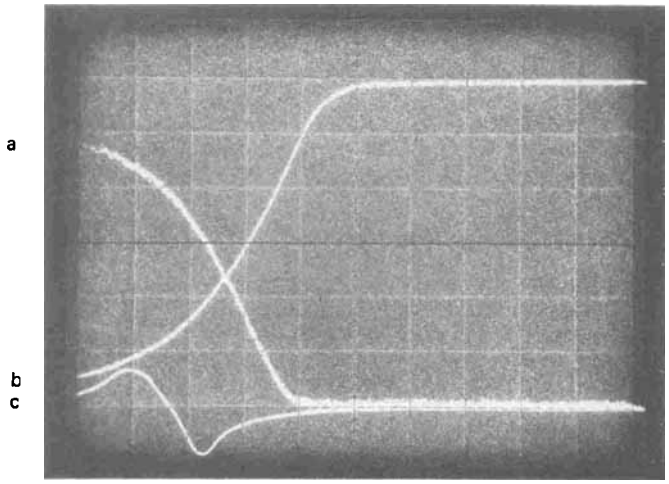


**Figure 4**—*Oscilloscope tracing of decompression and postcompression phases of sulfacetamide compression at a maximum pressure of 333 MPa at a sweep rate of 10 msec/division. Vertical deflections (division per volt) differ for the three traces: a, axial stress; b, radial stress; and c, turret rotation marker.*

example of these traces is shown in Fig. 4. When postcompression stress measurements were made over several minutes, the amplifier output signal was passed through a low-pass filter to reduce noise and to improve resolution.

**Calibration**—The instrumented die was calibrated under static conditions. A closely fitting rubber plug was placed in the die cavity, and known pressure was applied by loading weights onto a substitute upper punch in the form of a platform pedestal. A linear response was obtained, $r^2 = 0.989$, over the full range of 333 MPa.

Punch stress, as indicated by strain at the lower compression roller support rod, was calibrated against die wall stress under both static and dynamic conditions. In the latter case, the press was run at normal speed with a rubber plug in the die cavity. Oscilloscope traces of the simultaneously generated die wall and punch stresses were compared. Results obtained in this manner were indistinguishable from those observed when the turret was turned slowly by hand. Plots of die wall *versus* punch stress were linear with $r^2 \geq 0.999$.

**Punch Displacement**—It was not feasible to measure punch movement using a displacement transducer due to difficulty in mounting such a device. Instead, punch position, as a function of time, was calculated from tablet machine dimensions, turret velocity, and punch position relative to the compression rollers. The latter two quantities were computed from signals generated by a frame-mounted magnetic pickup in response to the passage of three turret-mounted permanent magnets. These were arranged so that one pulse was produced immediately prior to the compression event and two pulses after. Simultaneous punch and die stress curves for the compression of a rubber plug were symmetrical and exhibited maxima at the same time. Therefore, the punches were assumed to be centered between the compression rollers at the time corresponding to the common axis of symmetry of the stress *versus* time curves. The magnetic pickup signals were used as references for punch location, measurement of turret velocity, and triggering the oscilloscope.

The vertical displacement of the upper punch, $z$, as it passes under the compression roller (Fig. 5) is:

$$z = [(r_1 + r_2)^2 - x^2]^{1/2} \qquad \text{(Eq. 25)}$$

where $r_1$ and $r_2$ are the radii of the compression roller and the vertical curvature of the punch head rim, respectively; and $x$ and $x_2$ are the horizontal distances between the vertical center lines of the compression roller and upper punch, respectively, and the center of vertical curvature of the punch head rim. The horizontal angle, $\phi$, measured from the punch axis to the vertical centerline of the roller (Fig. 6) is a function of the turret angular velocity, $\omega$. Thus, from Eq. 25, upper punch displacement at the position of greatest penetration into the die is:

$$z = [(r_1 + r_2)^2 - (r_3 \sin \omega t - x_2)^2]^{1/2} \qquad \text{(Eq. 26)}$$

where $r_3$ is the radial distance between the turret and punch axes. Equation 26 applies when the head of the punch, except for the flat, is in contact with the compression roller. During the period when the punch

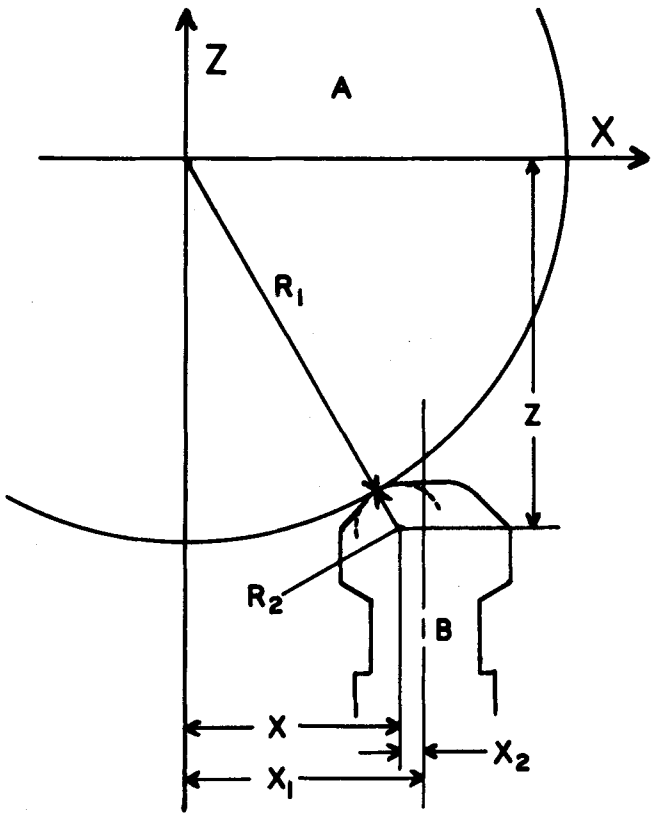


**Figure 5**—*Diagram of the geometric relationships between the compression roller (A) and punch (B) viewed from the side;* z, x, $x_1$, $x_2$, $r_1$, *and* $r_2$ *are as defined in Eqs. 25 and 26.*

head flat bears against the roller, the displacement equals $r_1$ plus $r_2$. This definition of displacement, $z$, is convenient for this study since it permits punch movements to be referred to the centers of the compression rollers.

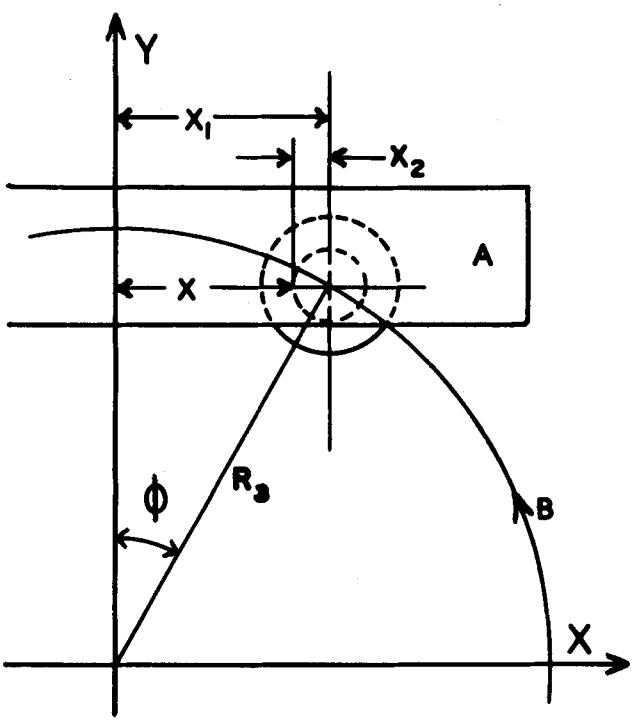


**Figure 6**—*Diagram of the geometric relationships between the compression roller (A) and the punch viewed from above. The vertical axis of the punch follows horizontal path B;* x, $x_1$, *and* $x_2$ *are as defined in Eq. 26.*

The punch displacement, $z_0$, at the instant the punches break contact with the tablet depends on the amount and the nature of the material in the die cavity. Taking into account the symmetry of compression by the upper and lower punches, the axial strain during the unloading phase is given by:

$$\epsilon_{zz} = \frac{2}{L}\{-[(r_1 + r_2)^2 - (r_3 \sin \omega t - x_2)^2]^{1/2} + |z_0|\} \quad \text{(Eq. 27)}$$

where $L$ is the tablet thickness. When the flat region of the punch head is under the compression roller, axial strain is constant and equals:

$$\epsilon_{zz} = \frac{2}{L}[-(r_1 + r_2) + |z_0|] \quad \text{(Eq. 28)}$$

**Stress Measurements**—The die wall was lubricated prior to each compression by swabbing with a 10% slurry of magnesium stearate in ethanol. A precisely weighed amount of unlubricated powder was placed in the die cavity and leveled. The weight of the material was varied to achieve different compaction pressures. Each tablet was compressed in exactly the same location in the die, extending an equal distance above and below the radial stress-sensing element. The tablets were compacted at a turret velocity of 2.759 rad/sec and were allowed to remain in the die for several minutes until equilibrium radial stress was reached. Ejected tablets were ~5.5 mm in height, depending on fill weight and the material.

Stresses were recorded over the entire compaction cycle to obtain axial and radial pressure maxima. Separate recordings were made at faster scope sweep rates to provide better time resolution of the last 20–25 msec of the compaction cycle (the entire unloading period lasted ~30 msec) and the first 50–55 msec of the postcompaction period. Photographs of the scope tracings were digitized every 0.5 msec during unloading and every millisecond during postcompression. All experimentation was done in triplicate.

**Materials**—The materials to be compressed were dried in an oven at 145° for 2.5 hr and were stored over anhydrous calcium sulfate under vacuum until used. The compounds tested, microcrystalline cellulose[10], spray-processed lactose[11], and sulfacetamide[12], were otherwise used as received and were not mixed with a lubricant or other material prior to compression.

## DATA ANALYSIS

Experimental data were analyzed using viscoelastic models which consisted of various combinations, in isostatic dilation and in distortion, of the basic models illustrated in Fig. 1. The simplest model yielding a good fit of the data was found to be elastic in dilation and Kelvin in distortion.

**Unloading Phase**—During the initial period of their withdrawal, the punches remain in contact with the tablet and, together with the die, prescribe its axial and radial strains, $\epsilon_{zz}$, $\epsilon_{xx}$, and $\epsilon_{yy}$, respectively[13]. Superimposing the individual contributions of these strains to axial stress, using Eqs. 23 and 24, yields the expression:

$$(P'Q'' + 2P''Q')\epsilon_{zz} + 2(P'Q'' - P''Q')\epsilon_{xx} = 3P'P''\sigma_{zz} \quad \text{(Eq. 29)}$$

since, by symmetry, $\epsilon_{xx} = \epsilon_{yy}$. In the same manner, the equal radial stresses, $\sigma_{xx}$ and $\sigma_{yy}$, can be obtained from Eqs. 23 and 24 in the form:

$$(P'Q'' - P''Q')\epsilon_{zz} + (2P'Q'' + P''Q')\epsilon_{xx} = 3P'P''\sigma_{xx} \quad \text{(Eq. 30)}$$

If it is assumed that the tablet is elastic in isostatic dilation and behaves as a Kelvin solid in distortion, $P'' = 1$ and $Q'' = q_0''$, while $P'$ and $Q'$ follow Eqs. 8 and 9. Substituting these expressions, together with Eq. 27, into Eqs. 29 and 30 provides equations for the axial and radial stresses during the experimentally imposed unloading conditions:

$$\sigma_{zz} = A_1 - A_2[(r_1 + r_2)^2 - (r_3 \sin \omega t - x_2)^2]^{1/2} + \frac{A_3 \omega r_3 \cos \omega t (r_3 \sin \omega t - x_2)}{[(r_1 + r_2)^2 - (r_3 \sin \omega t - x_2)^2]^{1/2}} \quad \text{(Eq. 31)}$$

where:

$$A_1 = (2/3)[(q_0'' - q_0')\epsilon_{xx} + (2q_0' + q_0'')|z_0|/L] \quad \text{(Eq. 32)}$$

$$A_2 = (2/3)(2q_0' + q_0'')/L \quad \text{(Eq. 33)}$$

$$A_3 = (4/3)q_1'/L \quad \text{(Eq. 34)}$$

and:

$$\sigma_{xx} = B_1 - B_2[(r_1 + r_2)^2 - (r_3 \sin \omega t - x_2)^2]^{1/2} - \frac{B_3 \omega r_3 \cos \omega t (r_3 \sin \omega t - x_2)}{[(r_1 + r_2)^2 - (r_3 \sin \omega t - x_2)^2]^{1/2}} \quad \text{(Eq. 35)}$$

where:

$$B_1 = (1/3)[(2q_0'' + q_0')\epsilon_{xx} + 2(q_0'' - q_0')|z_0|/L] \quad \text{(Eq. 36)}$$

$$B_2 = (2/3)(q_0'' - q_0')/L \quad \text{(Eq. 37)}$$

$$B_3 = (2/3)q_1'/L \quad \text{(Eq. 38)}$$

The macroconstants, $A_i$ and $B_i$, of Eqs. 31 and 35 were determined from experimentally measured punch and die wall stresses by regression analysis (18). Equations 32, 33, 36, and 37 can be taken pairwise in any combination to calculate the microconstants, $q_0'$ and $q_0''$. However, Eqs. 32 and 33 and Eqs. 36 and 37 are nearly parallel and were not paired for computation since the resulting calculated values of $q_0'$ and $q_0''$ were sensitive to experimental error.

The vertical punch displacement at separation from the tablet, $z_0$, was determined from the time at which punch pressure fell to zero rather than from the macroconstants. Although $z_0$ values obtained by these two methods agreed within 0.05 mm, the latter method was less direct and was not used. For the same reason, $\epsilon_{xx}$ was calculated from measurements of ejected tablets rather than from Eqs. 32 and 36. Again, however, values obtained by the two methods agreed within ~0.05 mm.

**Postcompression Phase**—Radial stress and strain were the only variables measured directly during this period. Although a progressive change in the axial strain occurred, there was no means of reliably estimating it. Axial stress, however, can be estimated in various ways; because it is small in comparison with residual radial stress, effects of error are minor. Three hypotheses were tested in which axial stress was assumed to be either equal to zero, proportional to radial stress, or an exponentially decreasing function of time. Equations based on these assumptions were fitted to experimental data and showed the axial stress to be statistically indistinguishable from zero. From Eqs. 21 and 22, radial strain can be expressed as:

$$(2P''Q' + P'Q'')\sigma_{xx} + (P''Q' - P'Q'')\sigma_{zz} = 3Q'Q''\epsilon_{xx} \quad \text{(Eq. 39)}$$

If it is assumed that the tablet is elastic in dilation and Kelvin in distortion and if $\sigma_{zz}$ is set equal to zero, Eq. 39 reduces to:

$$(q_0'' + 2q_0' + 2q_1' d/dt)\sigma_{xx} = 3q_0''(q_0' + q_1' d/dt)\epsilon_{xx} \quad \text{(Eq. 40)}$$

Integrating from time of punch separation, $t = 0$, to time $t$ gives:

$$\sigma_{xx} = [\sigma_{xx}(0) - C_1]\exp(-C_2 t) + C_1 \quad \text{(Eq. 41)}$$

where:

$$C_1 = \frac{3q_0'q_0''\epsilon_{xx}(0)}{2q_0' + q_0''} \quad \text{(Eq. 42)}$$

$$C_2 = (2q_0' + q_0'')/2q_1' \quad \text{(Eq. 43)}$$

Equation 41 was fitted by nonlinear regression (19) to experimentally measured die wall stresses; $C_1$ is the equilibrium radial stress, and $C_2$ is the first-order rate constant for radial stress relaxation.

## RESULTS AND DISCUSSION

The viscoelastic parameters of a tablet can be expected to depend heavily on the time course of compression and not solely on the chemical and physical nature of the powdered precursor. To investigate the effects of pressure, fill weights of the materials tested were adjusted to produce three pressure maxima: 125, 208, and 333 MPa. These pressures fall in the usual range for tablet compression. Test substances that differ in their compressibility were selected to provide for a sensitivity evaluation of the present method of data analysis to differences in material properties.

During the unloading period, the elastic behavior of the compacts predominated. This fact was evidenced by viscous contributions to the total distortion stress of ~1% only. Because the estimates of $q_1''$, calculated from $A_3$ and $B_3$, are of the same magnitude as the experimental error during this period, they are not reported. However, the relaxation pro-

[10] Avicel Ph 101, Food and Pharmaceutical Products Division, FMC Corp., Philadelphia, PA 19103.

[11] Fast-Flo Lactose, Foremost Dairies, Appleton, WI 54911.

[12] Ruger Chemical Co., New York, NY 07111.

[13] Subscripts refer to the reference axes of the compact, which are not necessarily labeled the same as in Eqs. 21–24.

**Table I—Viscoelastic Constants [a] for Unloading and Postcompression Phases of Tablet Compression [b]**

| Viscoelastic Constant | Macroconstants [c] | Maximum Punch Pressure, MPa | | |
|---|---|---|---|---|
| | | 125 | 208 | 333 |
| | | Microcrystalline Cellulose | | |
| $q_0'$ | $A_1B_1$ | 131 ± 6 | 169 ± 11 | 530 ± 20 |
| $q_0'$ | $A_2B_2$ | 132 ± 6 | 171 ± 11 | 529 ± 20 |
| $q_0''$ | $A_1B_1$ | 684 ± 32 | 1220 ± 82 | 2070 ± 78 |
| $q_0''$ | $A_2B_2$ | 687 ± 32 | 1220 ± 81 | 2050 ± 76 |
| $q_1'$ | $A_1B_1C_2$ | 0.844 ± 0.030 | 1.11 ± 0.05 | 3.83 ± 0.14 |
| $q_1'$ | $A_2B_2C_2$ | 0.858 ± 0.031 | 1.13 ± 0.05 | 3.79 ± 0.14 |
| | | Spray-Processed Lactose | | |
| $q_0'$ | $A_1B_1$ | 1180 ± 29 | 725 ± 13 | 1160 ± 15 |
| $q_0'$ | $A_2B_2$ | 1180 ± 29 | 727 ± 13 | 1160 ± 15 |
| $q_0''$ | $A_1B_1$ | 2120 ± 52 | 2400 ± 43 | 3000 ± 39 |
| $q_0''$ | $A_2B_2$ | 2120 ± 52 | 2410 ± 43 | 3010 ± 39 |
| $q_1'$ | $A_1B_1C_2$ | 3.79 ± 0.10 | 1.54 ± 0.06 | 2.10 ± 0.06 |
| $q_1'$ | $A_2B_2C_2$ | 3.80 ± 0.10 | 1.55 ± 0.06 | 2.11 ± 0.06 |
| | | Sulfacetamide | | |
| $q_0'$ | $A_1B_1$ | 25.7 ± 2.6 | 689 ± 21 | 28.2 ± 1.6 |
| $q_0'$ | $A_2B_2$ | 27.6 ± 2.6 | 691 ± 21 | 34.4 ± 2.0 |
| $q_0''$ | $A_1B_1$ | 986 ± 99 | 2050 ± 63 | 1730 ± 101 |
| $q_0''$ | $A_2B_2$ | 990 ± 95 | 2060 ± 63 | 1740 ± 100 |
| $q_1'$ | $A_1B_1C_2$ | 0.604 ± 0.035 | 9.19 ± 0.19 | 0.590 ± 0.022 |
| $q_1'$ | $A_2B_2C_2$ | 0.651 ± 0.036 | 9.24 ± 0.19 | 0.724 ± 0.027 |

[a] Calculated from mean macroconstants derived from triplicate compressions. [b] Units are MPa for $q_0$ and MPa sec for $q_1$. Standard errors are shown. [c] Macroconstants used in calculation of viscoelastic constants.

cesses that occur during the postcompression phase are kinetically dependent on viscous behavior and are largely controlled by it. The viscous microconstants, $q_1'$, were calculated from $C_2$ and from the values of $q_0'$ and $q_0''$ obtained during unloading (Table I).

Microcrystalline cellulose produced very strong tablets at all three pressures. These tablets exceeded the measurement range of the hardness tester[14]. All viscoelastic parameters increased with increased pressure. The elastic moduli were several times larger in dilation than in distortion, indicating that the material was more easily sheared than compressed. This latter behavior was observed for all three materials at all three pressures. In this regard, it is important to emphasize that a small elastic constant does not necessarily imply a small limiting stress at failure, and vice versa.

Tablets produced from spray-processed lactose also were very strong and exceeded the capacity of the hardness tester, except those produced at the lowest pressure. These latter tablets relaxed most slowly to their residual die wall pressures. This behavior was reflected by their relatively higher $q_1'$ value shown in Table I.

The sulfas are noted for capping and splitting, which are often experienced in making tablets from them. With sulfacetamide, all three viscoelastic parameters passed through a maximum at intermediate pressures. Tablets produced at all three pressures were moderately strong and broke in the $xz$ plane at about the same tensile stress of ~0.20–0.25 MPa. Tablets compressed at 208 MPa relaxed particularly slowly to equilibrium die wall stress. These tablets would be expected to be the most likely to cap had they been ejected at the normal time interval following compression.

The residual die wall stress at equilibrium, $C_1$, can be seen from Eq. 42 to be a function only of the elastic constants, $q_0'$ and $q_0''$, and the radial strain, $\epsilon_{xx}$. The rate constant, $C_2$, for the exponential decay of die wall stress is inversely proportional to $q_1'$, as shown by Eq. 43. At the time of ejection from the die, the value of $\sigma_{xx}$ is critical in determining if the tablet will fracture transversely (12) and exhibit capping or splitting.

Insight into tablet behavior during and after compression can be gained through viscoelastic parameters such as are examined in this study. However, the assumptions and approximations made in applying viscoelastic theory must be considered when interpreting the data. Although descriptive of fully dense materials, the theory also is able to accommodate porous materials. The mechanisms proposed for elastic yield or viscous flow in porous materials must be made in light of the influence of the voids. For example, in a porous solid, isostatic stress may cause fracture or plastic flow as the particles are forced into the pores. Under similar conditions and in the absence of fracture or flow, however, particles can elastically distort into voids. While shearing stresses can produce distortion solely through elastic deformations, they may also produce viscous flow. Distortion flow may be facilitated by voids and does not in itself reduce the void space available for the mass displacements that it produces.

This general behavior, elastic in dilation and Kelvin in distortion, was observed in the materials reported here. Although viscoelastic equations based on more complex models also correlated well with the stress/strain data, their use could not be justified because they did not significantly improve the fit between theory and experiment.

Further refinement of the theory to account for tablet anisotropy is possible but not currently feasible because of the limitations of present experimental methods. The number of viscoelastic parameters, arising from such anisotropic models, far exceeds the number of variables that can be measured simultaneously in the present apparatus. As a consequence, a set of indeterminate equations results. The models presented in this paper are being extended to a wider range of pharmaceutical solids and their mixtures.

[14] Pfizer, Pfizer Chemical Division, New York, NY 10017.

## REFERENCES


(1) S. Shlanta and G. Milosovich, *J. Pharm. Sci.*, **53**, 562 (1964).

(2) E. N. Hiestand, J. E. Wells, C. B. Peot, and J. F. Ochs, *ibid.*, **66**, 510 (1977).

(3) S. Leigh, J. E. Carless, and B. W. Burt, *ibid.*, **56**, 888 (1967).

(4) J. E. Carless and S. Leigh, *J. Pharm. Pharmacol.*, **26**, 289 (1974).

(5) M. P. Summers, R. P. Enever, and J. E. Carless, *ibid.*, **28**, 89 (1976).

(6) E. Shotton, J. J. Deer, and D. Ganderton, *ibid.*, **15**, 106 (1963).

(7) E. L. Knoechel, C. C. Sperry, H. E. Ross, and C. J. Lintner, *J. Pharm. Sci.*, **56**, 106 (1967).

(8) K. Ridgway and P. H. Rosser, *J. Pharm. Pharmacol.*, **23**, 202S (1971).

(9) S. T. David and L. L. Augsburger, *J. Pharm. Sci.*, **66**, 155 (1977).

(10) T. Higuchi, T. Shimamoto, S. P. Eriksen, and T. Yashiki, *ibid.*, **54**, 111 (1965).

(11) J. E. Rees and P. J. Rue, *J. Pharm. Pharmacol.*, **30**, 601 (1978).

(12) W. M. Long, *Powder Metall.*, **6**, 73 (1960).

(13) J. S. Hardman and B. A. Lilley, *Nature*, **228**, 353 (1970).

(14) N. P. Suh, *Int. J. Powder Metall.*, **5**, 69 (1969).

(15) D. Train, *J. Pharm. Pharmacol.*, **8**, 745 (1956).

(16) D. R. Bland, "The Theory of Linear Viscoelasticity," Pergamon, New York, N.Y., 1960, pp. 1–17.

(17) W. Flugge, "Viscoelasticity," 2nd ed., Springer-Verlag, New York,

N.Y., 1975.
(18) N. H. Nie, C. H. Hull, J. G. Jenkins, K. Steinbrenner, and D. H. Bent, "Statistical Package for the Social Sciences," 2nd ed., McGraw-Hill, St. Louis, Mo., 1975.
(19) "Statistical Package for the Social Sciences; NONLINEAR Regression Subprogram," Vogelback Computing Center, Northwestern University, Evanston, Ill., 1978.

ACKNOWLEDGMENTS

Presented in part at the Basic Pharmaceutics Section, APhA Academy of Pharmaceutical Sciences, Anaheim meeting, April 1979.

Abstracted in part from a dissertation submitted by D. W. Danielson to the University of Minnesota in partial fulfillment of the Doctor of Philosophy degree requirements.

# TLC Identification and GLC Determination of Meperidine and Its Metabolites in Biological Fluids

**S. Y. YEH ˣ and H. A. KREBS**

Received July 6, 1978, from the *National Institute on Drug Abuse, Division of Research, Addiction Research Center, Lexington, KY 40583.* Accepted for publication October 15, 1980.

**Abstract** □ Procedures were developed for TLC identification and GLC determination of meperidine and its metabolites, *i.e.*, *p*-hydroxymeperidine, normeperidine, and meperidinic and normeperidinic acids. Meperidine, *p*-hydroxymeperidine, and normeperidine were extracted with ether from biological fluids at pH 10, whereas meperidinic and normeperidinic acids and conjugated metabolites remained in the aqueous phase. The residue, upon evaporation of the extract to dryness, was derivatized with trifluoroacetic anhydride and gas chromatographed. Total (free and conjugated) meperidinic and normeperidinic acids in the aqueous phase were converted and determined as meperidine and normeperidine, respectively. A preliminary result of urinary disposition of meperidine and its metabolites in the rat is presented. The identity of these metabolites was confirmed with GLC–mass spectrometry.

**Keyphrases** □ Meperidine—and metabolites, TLC identification and GLC determination in biological fluids, rat, dog, and human □ Metabolites—meperidine, TLC identification and GLC determination in biological fluids of rat, dog, and human □ TLC—identification of meperidine and metabolites in biological fluids of rat, dog, and human □ GLC–mass spectrometry—determination of meperidine and metabolites in biological fluids of rat, dog, and human

The known major metabolites of meperidine are normeperidine and meperidinic and normeperidinic acids (1–4); *p*-hydroxymeperidine (5), meperidine *N*-oxide (6), hydroxymethoxymeperidine (7), *N*-hydroxynormeperidine (7), and *p*-hydroxynormeperidine[1] are minor metabolites (Scheme I). The hydrophilic and hydroxylated metabolites are excreted mainly in conjugated forms (1–3, 5, 7).

In earlier studies, radioisotopic and methyl orange dye methods (1–3, 8) were used to estimate meperidine and normeperidine in biological fluids. In later studies, meperidine, normeperidine, and *p*-hydroxymeperidine were estimated by GLC or GLC–mass spectrometry (9–19). Total meperidinic and normeperidinic acid were estimated as meperidine and normeperidine by methyl orange, GLC, and GLC–mass spectrometric methods after esterification (1–4, 9–20). This paper presents a simpler and more sensitive method for the determination of meperidine and its metabolites in biological fluids, primarily using GLC.

## EXPERIMENTAL

**Drugs**—Meperidine hydrochloride[2], [*N-methyl*-$^{14}$C]meperidine hydrochloride[3] (3.4 mCi/mmole), normeperidine hydrochloride[2], *p*-hydroxymeperidine[4], and lidocaine hydrochloride[5] were used. The purity of the radiolabeled meperidine, determined by TLC with three solvent systems, was at least 98%. [*N-methyl*-$^{14}$C]Meperidinic, meperidinic, and normeperidinic acids were obtained by alkaline hydrolysis of their respective esters, and their purity was found to be 98% by TLC and GLC–mass spectrometry.

Meperidine *N*-oxide was synthesized by oxidation of meperidine (100 mg) by adding 85% *m*-chloroperbenzoic acid[6] (150 mg) in dried ether (2 ml) dropwise over 5 min. After the addition was completed, the solution was left at room temperature for 2 hr. Upon removal of the solvent, the residue was suspended in 2 ml of 10% potassium carbonate solution and extracted with ethylene dichloride containing 30% isopropyl alcohol (3 × 10 ml). Crystals were obtained upon concentration of the extract to ~1 ml. After cooling, centrifugation, and aspiration of the final drops of extract, the crystals were washed with ether and dried under vacuum, yielding 99 mg.

*N*-Hydroxynormeperidine was synthesized by oxidation of normeperidine with *m*-chloroperbenzoic acid (7). The final product was contaminated with normeperidine and other by-products but was sufficient for TLC and GLC–mass spectrometric identification.

**GLC**—The chromatograph[7] was equipped with flame-ionization detectors and 182-cm × 2-mm glass columns packed with 3% Poly I-110 coated on 80–100-mesh Gas Chrom Q. The temperatures of the oven, injector, and detector were 205, 225, and 250°, respectively. The gas flow rates of nitrogen, hydrogen, and compressed dry air were 30, 30, and 400 ml/min, respectively.

**GLC–Mass Spectrometry**—Chemical-ionization mass spectral data were obtained on a gas chromatograph–mass spectrometer[8] equipped with an interactive data system[9] and a 182-cm × 2-mm glass column packed with 3% Poly I-110 coated on 80–100-mesh Gas Chrom Q. The temperatures of the injector, column, and ion source were 230, 210, and 100°, respectively. Other specifications of the mass spectrometer were described previously (21).

**TLC**—Standard TLC procedures were followed. Aliquots (50 μl) of methanolic solution containing 50 μg of meperidine or its metabolites were spotted on instant thin-layer silica gel sheets[10] and linear, precoated glass silica plates[11]. Chromatograms were developed with one of the following solvent systems: A, *n*-butanol–water–acetic acid (35:10:3); B, ethyl acetate–ammonium hydroxide (17:1); C, ethyl acetate–methanol–ammonium hydroxide (17:2:1); D, benzene–methanol–diethylamine (48:1:1); E, *n*-butanol–3% ammonium hydroxide in water (50:50) using the upper phase; and F, ethyl acetate–diethylamine (17:1).

The chromatogram of nonlabeled standards was sprayed with iodo-

[1] Unpublished observations.
[2] Sterling-Winthrop Pharmaceutical Co., Rensselaer, N.Y.
[3] Mallinckrodt Chemical Co., St. Louis, Mo.
[4] Professor C. Lindberg, Department of Organic Pharmaceutical Chemistry, University of Uppsala, Uppsala, Sweden.
[5] Astra Pharmaceutical Products, Worcester, Mass.
[6] Practical grade, Aldrich Chemical Co., Milwaukee, Wis.
[7] Model 2700, Varian Aerograph, Varian Associates, Palo Alto, Calif.
[8] Model 3300, Finnigan Corp., Sunnyvale, Calif.
[9] Model 6000, Finnigan Corp., Sunnyvale, Calif.
[10] Gelman Instrument Co., Ann Arbor, Mich.
[11] Quantum Industries, Fairfield, N.J.



0022-3549/81/0500-0482$01.00/0
© 1981, American Pharmaceutical Association

N.Y., 1975.
(18) N. H. Nie, C. H. Hull, J. G. Jenkins, K. Steinbrenner, and D. H. Bent, "Statistical Package for the Social Sciences," 2nd ed., McGraw-Hill, St. Louis, Mo., 1975.
(19) "Statistical Package for the Social Sciences; NONLINEAR Regression Subprogram," Vogelback Computing Center, Northwestern University, Evanston, Ill., 1978.

ACKNOWLEDGMENTS

Presented in part at the Basic Pharmaceutics Section, APhA Academy of Pharmaceutical Sciences, Anaheim meeting, April 1979.

Abstracted in part from a dissertation submitted by D. W. Danielson to the University of Minnesota in partial fulfillment of the Doctor of Philosophy degree requirements.

# TLC Identification and GLC Determination of Meperidine and Its Metabolites in Biological Fluids

**S. Y. YEH ˣ and H. A. KREBS**

Received July 6, 1978, from the *National Institute on Drug Abuse, Division of Research, Addiction Research Center, Lexington, KY 40583.* Accepted for publication October 15, 1980.

**Abstract** □ Procedures were developed for TLC identification and GLC determination of meperidine and its metabolites, *i.e.*, *p*-hydroxymeperidine, normeperidine, and meperidinic and normeperidinic acids. Meperidine, *p*-hydroxymeperidine, and normeperidine were extracted with ether from biological fluids at pH 10, whereas meperidinic and normeperidinic acids and conjugated metabolites remained in the aqueous phase. The residue, upon evaporation of the extract to dryness, was derivatized with trifluoroacetic anhydride and gas chromatographed. Total (free and conjugated) meperidinic and normeperidinic acids in the aqueous phase were converted and determined as meperidine and normeperidine, respectively. A preliminary result of urinary disposition of meperidine and its metabolites in the rat is presented. The identity of these metabolites was confirmed with GLC–mass spectrometry.

**Keyphrases** □ Meperidine—and metabolites, TLC identification and GLC determination in biological fluids, rat, dog, and human □ Metabolites—meperidine, TLC identification and GLC determination in biological fluids of rat, dog, and human □ TLC—identification of meperidine and metabolites in biological fluids of rat, dog, and human □ GLC–mass spectrometry—determination of meperidine and metabolites in biological fluids of rat, dog, and human

The known major metabolites of meperidine are normeperidine and meperidinic and normeperidinic acids (1–4); *p*-hydroxymeperidine (5), meperidine *N*-oxide (6), hydroxymethoxymeperidine (7), *N*-hydroxynormeperidine (7), and *p*-hydroxynormeperidine[1] are minor metabolites (Scheme I). The hydrophilic and hydroxylated metabolites are excreted mainly in conjugated forms (1–3, 5, 7).

In earlier studies, radioisotopic and methyl orange dye methods (1–3, 8) were used to estimate meperidine and normeperidine in biological fluids. In later studies, meperidine, normeperidine, and *p*-hydroxymeperidine were estimated by GLC or GLC–mass spectrometry (9–19). Total meperidinic and normeperidinic acid were estimated as meperidine and normeperidine by methyl orange, GLC, and GLC–mass spectrometric methods after esterification (1–4, 9–20). This paper presents a simpler and more sensitive method for the determination of meperidine and its metabolites in biological fluids, primarily using GLC.

## EXPERIMENTAL

**Drugs**—Meperidine hydrochloride[2], [*N-methyl*-$^{14}$C]meperidine hydrochloride[3] (3.4 mCi/mmole), normeperidine hydrochloride[2], *p*-hydroxymeperidine[4], and lidocaine hydrochloride[5] were used. The purity of the radiolabeled meperidine, determined by TLC with three solvent systems, was at least 98%. [*N-methyl*-$^{14}$C]Meperidinic, meperidinic, and normeperidinic acids were obtained by alkaline hydrolysis of their respective esters, and their purity was found to be 98% by TLC and GLC–mass spectrometry.

Meperidine *N*-oxide was synthesized by oxidation of meperidine (100 mg) by adding 85% *m*-chloroperbenzoic acid[6] (150 mg) in dried ether (2 ml) dropwise over 5 min. After the addition was completed, the solution was left at room temperature for 2 hr. Upon removal of the solvent, the residue was suspended in 2 ml of 10% potassium carbonate solution and extracted with ethylene dichloride containing 30% isopropyl alcohol (3 × 10 ml). Crystals were obtained upon concentration of the extract to ~1 ml. After cooling, centrifugation, and aspiration of the final drops of extract, the crystals were washed with ether and dried under vacuum, yielding 99 mg.

*N*-Hydroxynormeperidine was synthesized by oxidation of normeperidine with *m*-chloroperbenzoic acid (7). The final product was contaminated with normeperidine and other by-products but was sufficient for TLC and GLC–mass spectrometric identification.

**GLC**—The chromatograph[7] was equipped with flame-ionization detectors and 182-cm × 2-mm glass columns packed with 3% Poly I-110 coated on 80–100-mesh Gas Chrom Q. The temperatures of the oven, injector, and detector were 205, 225, and 250°, respectively. The gas flow rates of nitrogen, hydrogen, and compressed dry air were 30, 30, and 400 ml/min, respectively.

**GLC–Mass Spectrometry**—Chemical-ionization mass spectral data were obtained on a gas chromatograph–mass spectrometer[8] equipped with an interactive data system[9] and a 182-cm × 2-mm glass column packed with 3% Poly I-110 coated on 80–100-mesh Gas Chrom Q. The temperatures of the injector, column, and ion source were 230, 210, and 100°, respectively. Other specifications of the mass spectrometer were described previously (21).

**TLC**—Standard TLC procedures were followed. Aliquots (50 μl) of methanolic solution containing 50 μg of meperidine or its metabolites were spotted on instant thin-layer silica gel sheets[10] and linear, precoated glass silica plates[11]. Chromatograms were developed with one of the following solvent systems: A, *n*-butanol–water–acetic acid (35:10:3); B, ethyl acetate–ammonium hydroxide (17:1); C, ethyl acetate–methanol–ammonium hydroxide (17:2:1); D, benzene–methanol–diethylamine (48:1:1); E, *n*-butanol–3% ammonium hydroxide in water (50:50) using the upper phase; and F, ethyl acetate–diethylamine (17:1).

The chromatogram of nonlabeled standards was sprayed with iodo-

[1] Unpublished observations.
[2] Sterling-Winthrop Pharmaceutical Co., Rensselaer, N.Y.
[3] Mallinckrodt Chemical Co., St. Louis, Mo.
[4] Professor C. Lindberg, Department of Organic Pharmaceutical Chemistry, University of Uppsala, Uppsala, Sweden.
[5] Astra Pharmaceutical Products, Worcester, Mass.
[6] Practical grade, Aldrich Chemical Co., Milwaukee, Wis.
[7] Model 2700, Varian Aerograph, Varian Associates, Palo Alto, Calif.
[8] Model 3300, Finnigan Corp., Sunnyvale, Calif.
[9] Model 6000, Finnigan Corp., Sunnyvale, Calif.
[10] Gelman Instrument Co., Ann Arbor, Mich.
[11] Quantum Industries, Fairfield, N.J.



0022-3549/81/0500-0482$01.00/0
© 1981, American Pharmaceutical Association

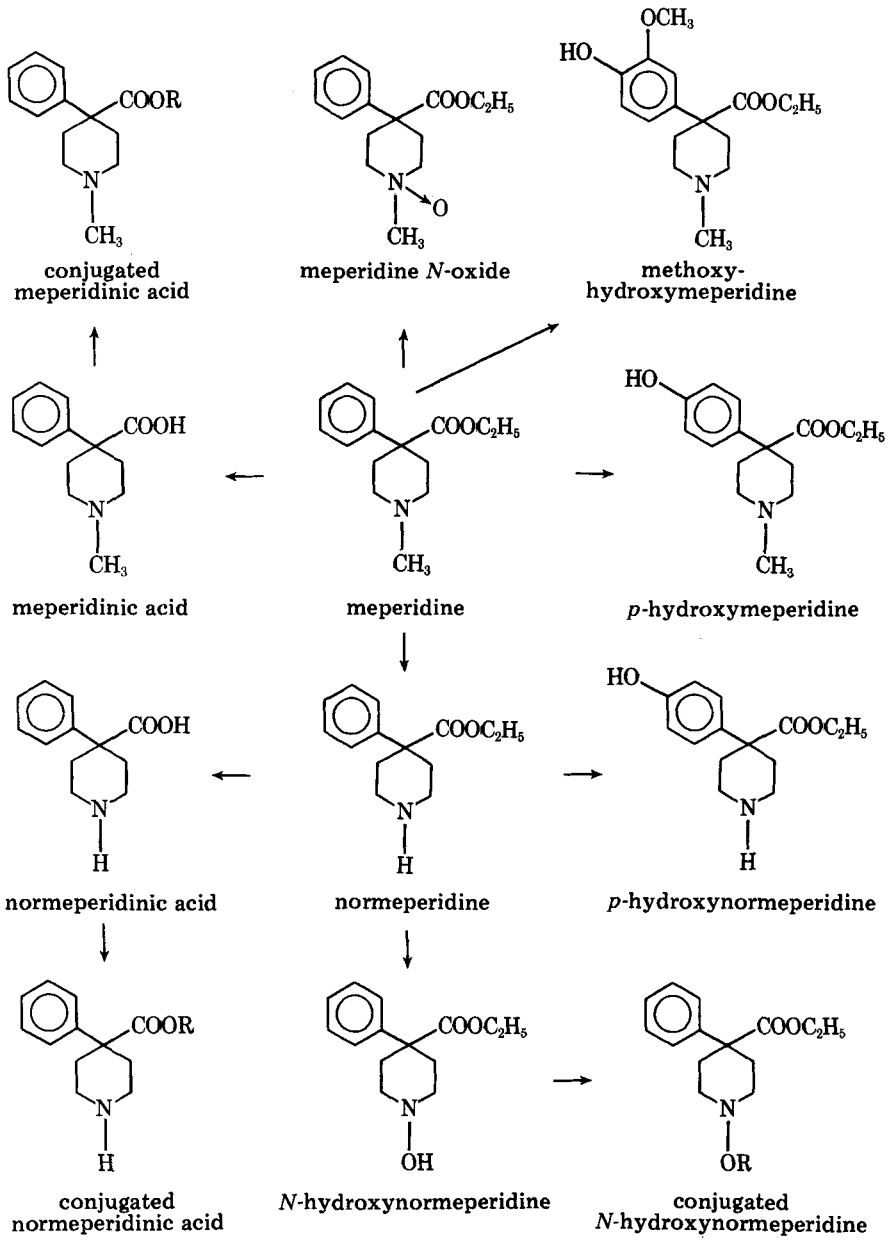


*Scheme I—Metabolic pathways of meperidine.*

platinate or ammonia–silver nitrate (for *n*-hydroxynormeperidine). The radiochromatogram of [*N-methyl*-$^{14}$C]meperidinic acid was analyzed by placing each strip (obtained by cutting the sheet into 1-cm strips) in a liquid scintillation vial, swirling with 0.5 ml of methanol, and counting with 10 ml of Bray's solution[12] in a liquid scintillation spectrometer[13].

**Determination of Meperidine, *p*-Hydroxymeperidine, and Normeperidine in Urine**—One-half to 2 ml of urine, water (to make up a total volume of 2 ml), and 0.1 ml of lidocaine hydrochloride solution (0.2 mg/ml, an internal standard) were placed in a 15-ml stoppered centrifuge tube, adjusted to pH 10 with 0.1 ml of concentrated ammonium hydroxide, and extracted twice with 5 ml of ether by shaking each time at 280 oscillations/min for 10 min and centrifuging for 5 min. The extract was transferred without the aqueous phase to an acylation tube and evaporated to dryness under a nitrogen stream at room temperature. Upon evaporation of the ethereal extract to dryness, the residue was used for TLC identification and GLC determination of free meperidine, *p*-hydroxymeperidine, and normeperidine.

The aqueous phase was used to determine total meperidinic and normeperidinic acids and conjugated *p*-hydroxymeperidine.

For GLC determination, the residue was derivatized with 0.1 ml of trifluoroacetic anhydride by heating the mixture in an ethylene glycol bath at 60° for 10 min. After evaporation of the excess derivatizing agent by a nitrogen stream at room temperature, dried ethyl acetate (50 μl) was added; 1 μl of the solution was injected into the gas chromatograph. Calibration curves at the peak height ratio (compound to internal standard) *versus* the concentration for meperidine, *p*-hydroxymeperidine, and normeperidine were linear ($r$ = 0.99) over the range of 1–200 μg/2 ml. A concentration of meperidine, *p*-hydroxymeperidine, and normeperidine as low as 150 ng/2 ml of urine could be measured.

For studying the recovery of drugs from biological fluids, lidocaine was added to the residues of the ethereal extract prior to derivatization. The recovery was calculated from a comparison of the peak height ratio of extracted drug to lidocaine to that of unextracted drug to lidocaine.

**Determination of Total Meperidinic and Normeperidinic Acids in Urine**—After extraction of meperidine, normeperidine, and free *p*-hydroxymeperidine, the aqueous phase was evaporated almost to dryness (~0.1 ml) at 55° under reduced pressure with an evaporator[14] and then evaporated to complete dryness in a freeze drier. The residue was refluxed with 3 ml of absolute alcohol containing 10% sulfuric acid at 100° for 5 hr. This method hydrolyzed conjugated *p*-hydroxymeperidine and

[12] Bray's solution consists of naphthalene (60 g), 2,5-diphenyloxazole (4 g), 1,4-bis[2-(5-phenyloxazolyl)]benzene (200 mg), methanol (100 ml), ethylene glycol (20 ml), and dioxane to make 1 liter.

[13] Mark III, Searle Analytic, Des Plaines, Ill.

[14] Evaporator-mix, Buchler Instruments, Fort Lee, N.J.

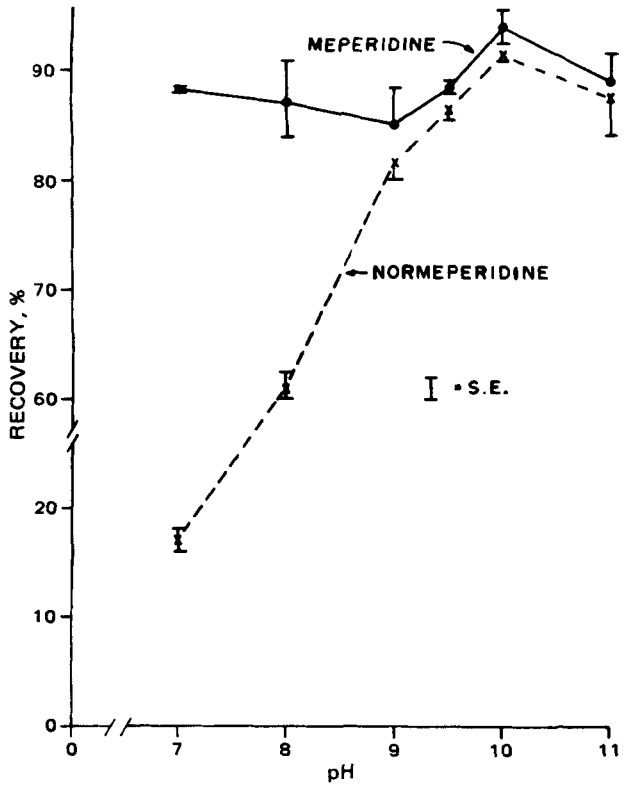


**Figure 1**—*Effect of pH on the recovery of meperidine and normeperidine. Meperidine (20 μg) and normeperidine (20 μg) from urine (2 ml) were extracted into the organic phase (6 ml of ether) by shaking for 10 min.*

meperidinic and normeperidinic acids to the free form; meperidinic and normeperidinic acids were esterified to meperidine and normeperidine, respectively.

The solution was reduced to ~0.3–0.5 ml (removal of ethanol) by evaporation at 55° under reduced pressure with an evaporator[14]. To the residue were added 1.0 ml of concentrated ammonium hydroxide (pH ~9–10) and 0.1 ml of lidocaine hydrochloride (0.2 mg/ml) solution. Then the solution was extracted with 6 ml of ether, and 5 ml of the extract was evaporated to dryness. The residue was derivatized with trifluoroacetic anhydride and determined by GLC. Calibration curves for both acids and *p*-hydroxymeperidine were linear ($r$ = 0.98–0.99) in the concentration range of 10–200 μg/2 ml. Recoveries of water-soluble metabolites were only ~30–40%.

**Determination of Meperidine and Its Metabolites in Blood and Plasma**—The procedure for urine was modified slightly for determination of meperidine and normeperidine in plasma and blood. The plasma or blood (2 ml), including the internal standard, was adjusted to pH 10 and extracted with 8 ml of ether. After removal of the aqueous phase, 6 ml of the ethereal extract was shaken with 1 ml of 1 *N* HCl for 5 min and centrifuged for 5 min. The organic phase was carefully aspirated off without removal of any aqueous phase. The acidic aqueous phase was adjusted to pH 10 with 0.5 ml of concentrated ammonium hydroxide and extracted with 6 ml of ether. After centrifugation, 5 ml of the organic phase was transferred to an acylation tube and then treated as described for the determination of meperidine and normeperidine.

**Pilot Experiment on Urinary Disposition of Meperidine in Rats**—Meperidine hydrochloride (35 mg/kg) dissolved in saline was administered intraperitoneally to Wistar male rats housed individually in air-conditioned quarters (23°) with 12-hr light–dark cycles. Food and water were given *ad libidum*. Urine was collected 24 hr prior to drug administration (control) and 0–24 and 24–48 hr after drug administration. After the pH and volume were measured, all urine was frozen until the time of drug analysis.

## RESULTS AND DISCUSSION

**Extraction and Recovery of Meperidine and Its Metabolites**—[*N-methyl*-$^{14}$C]Meperidine hydrochloride was used to study some factors influencing meperidine recovery such as pH, solvent, number of extractions, salting, shaking time, and temperature on evaporation of the solvent extract. The mean recovery of [*N-methyl*-$^{14}$C]meperidine (2 μg) from aqueous solution was constant over pH 7–10 (Fig. 1) and was ~98.56 ± 2.14% (*SE*). The recovery of meperidine from solution at pH 9.5 by extraction with ether was ~20% greater than that with benzene, chloroform, or toluene extractions. The presence or absence of 0.5 g of sodium chloride appeared to make no difference in recovery. The meperidine recovery was inversely proportional to the length of the solvent evaporation time on a slide warmer[15] set at 50°; better results were obtained when the solvent was evaporated to dryness at room temperature under a nitrogen stream. There were no significant differences in recovery with 5, 10, or 15 min of shaking with 6 ml of ether at pH 9.5.

No appreciable radioactivity was extracted in the organic phase when [*N-methyl*-$^{14}$C]meperidinic acid (1–100 μg) in aqueous solutions at pH 10 was extracted. It is likely that normeperidinic acid also would not be extracted. However, it was reported (20) that meperidinic and normeperidinic acids could be extracted at pH 9–10 with ethylene dichloride, although this finding could not be confirmed.

Use of a resin column[16] for extraction of meperidinic and normeperidinic acids, with the eluate analyzed for meperidinic and normeperidinic acids and esterification at various steps, was investigated. However, no variations saved time or gave clearer extracts than the organic solvent extraction and determination from the aqueous phase described.

The optimum pH for recovery of normeperidine from aqueous solution determined (in triplicate) with GLC was at pH 10 (Fig. 1). The recovery of normeperidine added to the control urine was 95.79 ± 3.15% (*SE*).

The recovery of *p*-hydroxymeperidine added to the control urine was 101.83 ± 3.31%.

**TLC Identification of Meperidine and Its Metabolites**—The $R_f$ values of meperidine and its metabolites developed with various solvent systems on both instant TLC sheets and silica gel plates are presented in Table I. Solvent System D appeared to be best for separation of meperidine and its metabolites on TLC silica gel plates. None of the systems using instant TLC sheets was satisfactory.

**GLC Determination of Meperidine and Its Metabolites**—Figure 2 shows the chromatogram of the extract of rat control urine with added internal standard after a single extraction and shows only a single peak of lidocaine (panel 1). The extract of control urine with added internal standard plus authentic standards showed peaks of meperidine, *p*-hydroxymeperidine, normeperidine, and lidocaine (panel 3) with retention times of 3.7, 4.1, 7.7, and 9.3 min, respectively. The retention times of these compounds varied slightly from column to column, but the sequence remained the same.

The chromatogram of the extract of the 0–24-hr rat urine extracted for free drugs showed peaks with retention times corresponding to meperidine, *p*-hydroxymeperidine, and normeperidine and an unidentified peak with a retention time of 10.3 min (panel 4). The identity of meperidine and its metabolites was confirmed further with GLC–mass

**Table I—$R_f$ Values of Meperidine and Its Metabolites**

| Compound | Solvent System A | B | C | D | E | F |
|---|---|---|---|---|---|---|
| Instant Thin-Layer Silica Gel Sheet[a] | | | | | | |
| Meperidine | 1.00 | 1.00 | 1.00 | 1.00 | 1.00 | 1.00 |
| *p*-Hydroxymeperidine | 1.00 | 1.00 | 1.00 | 1.00 | 1.00 | 1.00 |
| Meperidine *N*-oxide | 1.00 | 0.37 | 0.93 | 0.33 | 1.00 | 1.00 |
| Meperidinic acid | 1.00 | 0.00 | 0.00 | 0.29 | 1.00 | 0.22 |
| Normeperidine | 1.00 | 1.00 | 1.00 | 1.00 | 1.00 | 1.00 |
| *N*-Hydroxynormeperidine | 1.00 | 1.00 | 0.95 | 0.90 | 1.00 | 1.00 |
| Normeperidinic acid | 0.00 | NV[b] | NV | NV | NV | NV |
| Thin-Layer Silica Gel Plates[c] | | | | | | |
| Meperidine | 0.47 | 0.87 | 0.85 | 0.71 | 0.69 | 0.79 |
| *p*-Hydroxymeperidine | 0.45 | 0.55 | 0.72 | 0.17 | 0.66 | 0.40 |
| Meperidine *N*-oxide | 0.50 | 0.03 | 0.25 | 0.04 | 0.43 | 0.19 |
| Meperidinic acid | 0.37 | NV | NV | 0.00 | 0.28[d] | 0.18 |
| Normeperidine | 0.60 | 0.38 | 0.56 | 0.24 | 0.46 | 0.33 |
| *N*-Hydroxynormeperidine | 0.85 | 0.73 | 0.84 | 0.44 | 0.30 | 0.67 |
| Normeperidinic acid | 0.48[e] | NV | NV | NV | 0.20[d] | NV |

[a] Gelman Instrument Co., Ann Arbor, Mich. [b] NV = not visible. [c] Quantum Industries, Fairfield, N.J. [d] Gray spot. [e] Spot was seen overnight after spraying.

[15] Fisher Scientific Co.
[16] Amberlite XAD-2, Brinkmann Instrument Co., Westbury, N.Y.

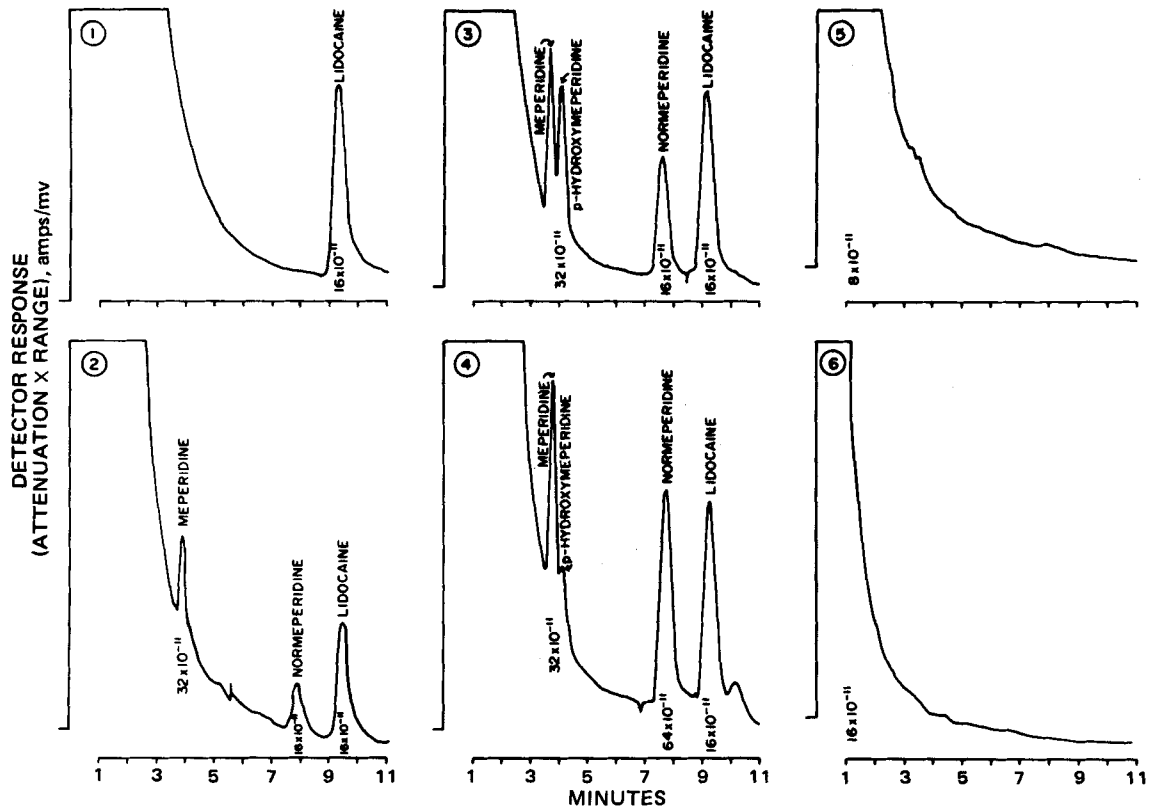


**Figure 2**—*Chromatograms of the extracts. Key: 1, control urine of rat with added lidocaine; 2, aqueous phase of the rat urine after ether extraction and sulfuric acid ethanol treatment with added lidocaine; 3, control urine of rat with added authentic standards; 4, urine of rat administered meperidine with added lidocaine; 5, control plasma of a dog; and 6, control plasma of a man.*

spectrometry. The chromatogram shown in panel 2 was obtained from the extract for determination of conjugated *p*-hydroxymeperidine and total meperidinic and normeperidinic acids. It showed peaks with retention times corresponding to meperidine and normeperidine, which were converted from free and conjugated meperidinic and normeperidinic acids, respectively. A peak of *p*-hydroxymeperidine appeared in the chromatogram of the extract of free drugs but not of the conjugated drugs, indicating that acid hydrolysis is not optimal for the determination of conjugated *p*-hydroxymeperidine.

The chromatogram of the extract obtained from normal dog plasma after one extraction showed no interfering peaks (panel 5). The chromatogram of the extract of human plasma and blood showed small peaks that interfered with the peaks of meperidine and *p*-hydroxymeperidine. The peak height of the interfering peak obtained from 2 ml of human plasma or blood corresponded to ~150 ng of meperidine. After a triple reverse extraction, the interfering substances were eliminated (panel 6).

The GLC determination of meperidine and normeperidine is similar to, but simpler than, that reported by Klotz *et al.* (12) since the extraction of derivatized normeperidine (as trifluoroacetamide) from aqueous solution is eliminated. For determination of meperidinic and normeperidinic acids, the procedure is similar to, but more sensitive than, that reported by Wainer and Stambaugh (4) by derivatization of normeperidine with trifluoroacetic anhydride.

Several GLC columns were investigated. The Poly I-110 column appeared to be more sensitive for the determination of normeperidine (as trifluoroacetamide) than 3% OV-17 and 3% SE-30 columns, although it appeared no different for the determination of meperidine.

Chlorophenylamine hydrochloride and diphenhydramine hydrochloride have been used as internal standards in the GLC analysis of meperidine. In this GLC system, they had a retention time considerably longer than lidocaine.

**GLC–Mass Spectrometric Identification of Meperidine Metabolites in Rat Urine**—The total ion current chromatogram and mass spectra of the extract (as trifluoroacetyl derivatives) of the unhydrolyzed urine of a male rat administered meperidine is shown in Fig. 3. The chromatogram showed peaks with retention times corresponding to authentic meperidine (spectrum 47), *p*-hydroxymeperidine (spectrum 56), normeperidine (spectrum 117), and lidocaine (spectrum 146). The fragmentation patterns of these peaks were identical to those of the authentic standards (Table II).

Since the peak (spectrum 56) with a retention time corresponding to that of *p*-hydroxymeperidine was small, a limited chromatogram at *m/z* 360 (M + 1 ion of trifluoroacetylated *p*-hydroxymeperidine) was recorded to confirm the existence of this mass; this technique only shows the peaks with mass equal to 360. The chromatogram showed a major peak at the retention time (spectrum 57) corresponding to that of the small peak appearing in the integrated total ion current chromatogram and a small peak (spectrum 117), due to the isotope mass of *m/z* 358, corresponding to that of normeperidine. The fragment pattern of the peak at spectrum

**Table II—GLC and Chemical-Ionization GLC–Mass Spectral Characteristics of Standard Meperidine Metabolites and Extract from Urine of a Rat Administered Meperidine Hydrochloride, 35 mg/kg**

| Sample | Derivative | GLC $R_t$, min | GLC–Mass Spectrometry $(M-F^a)^+$ | GLC–Mass Spectrometry $(M+1)^+$ | *m/z* $(M+29)^+$ | Other Prominent Ions | | Identification |
|---|---|---|---|---|---|---|---|---|
| Meperidine | — | 3.7 | — | 248 (100)[b] | 276 (88) | 202 (15) | 174 (27) | — |
| *p*-Hydroxymeperidine | Trifluoroacetyl | 4.1 | 340 (10) | 360 (100) | 388 (17) | — | — | — |
| Normeperidine | Trifluoroacetyl | 7.7 | 310 (40) | 330 (100) | 358 (50) | 256 (100) | 284 (12) | — |
| Extract of rat urine | Trifluoroacetyl | 3.7 | — | 248 (100) | 276 (73) | 202 (12) | 174 (23) | Meperidine |
| | | 4.1 | 340 (10) | 360 (100) | 388 (17) | — | — | *p*-Hydroxymeperidine |
| | | 7.7 | 310 (80) | 330 (100) | 358 (90) | 256 (100) | 284 (22) | Normeperidine |

[a] F = fluoride ion. [b] Percentage of relative intensity.

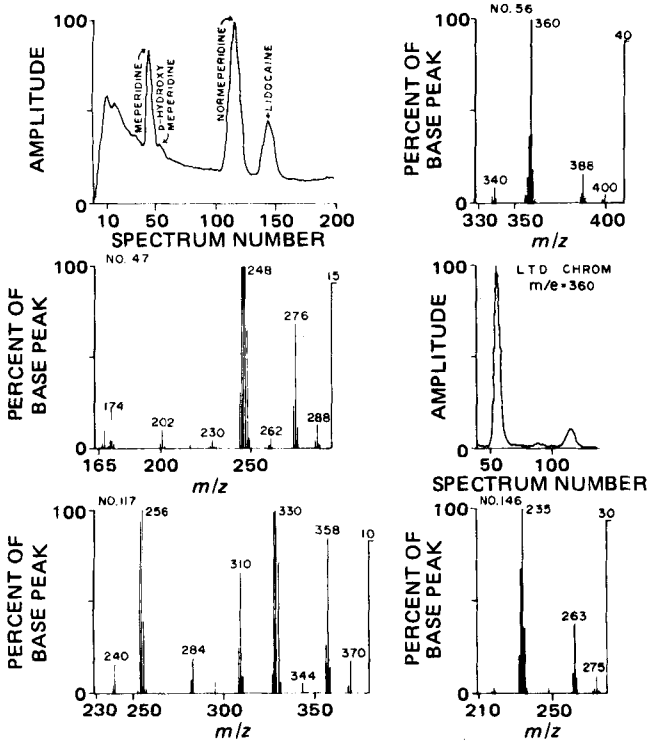


**Figure 3**—*GLC–mass spectrometric chromatogram, as trifluoroacetyl derivatives, of the 24-hr urinary extract of a rat administered meperidine. Key: upper left, integrated total ion current chromatogram; middle right; limited chromatogram at m/z 360; spectrum 47, meperidine; spectrum 56, p-hydroxymeperidine; spectrum 117, normeperidine; and spectrum 146, lidocaine (added internal standard).*

56 showed *m/z* 388 $(M + 29)^+$, 360 $(M + 1)^+$, and 340 $(M -$ fluoride ion$)^+$. The identity of *p*-hydroxymeperidine and normeperidine as metabolites thus was established and confirmed the observation of Lindberg *et al.* (5) that *p*-hydroxymeperidine is a metabolite of meperidine in the rat.

**Urinary Excretion of Meperidine and Its Metabolites in Rats**—A preliminary determination of the urinary excretion of meperidine and its metabolites in the rat indicated meperidine (6.1%), *p*-hydroxymeperidine (0.36%), total meperidinic acid (16.1%), normeperidine (24%), and total normeperidinic acid (3.9%) of administered meperidine hydrochloride (35 mg/kg). A detailed study of the urinary disposition of meperidine and its metabolites in several mammalian species will be reported in a separate paper.

## REFERENCES

(1) J. J. Burns, B. L. Berger, P. A. Lief, A. Wollack, E. M. Papper, and B. B. Brodie, *J. Pharmacol. Exp. Ther.*, **114**, 289 (1955).

(2) N. P. Plotnikoff, E. L. Way, and H. W. Elliott, *ibid.*, **117**, 414 (1956).

(3) A. M. Asatoor, D. R. London, M. D. Milne, and M. L. Simenhoff, *Br. J. Pharmacol.*, **20**, 285 (1963).

(4) I. W. Wainer and J. E. Stambaugh, *J. Pharm. Sci.*, **67**, 116 (1978).

(5) C. Lindberg, C. Bogentoft, U. Bodesson, and B. Danielsson, *J. Pharm. Pharmacol.*, **27**, 975 (1975).

(6) M. Mitchard, M. J. Kendall, and K. Chan, *ibid.*, **24**, 915 (1972).

(7) W. G. Stillwell, C. S. Myron, and J. T. Steward, *Res. Commun. Chem. Pathol. Pharmacol.*, **14**, 605 (1976).

(8) N. P. Plotnikoff, H. W. Elliott, and E. L. Way, *J. Pharmacol. Exp. Ther.*, **104**, 377 (1952).

(9) V. R. Jenkins, II, W. M. Talbert, and P. V. Dilts, Jr., *Obstet. Gynecol.*, **39**, 254 (1972).

(10) T. J. Goehl and C. Davison, *J. Pharm. Sci.*, **62**, 907 (1973).

(11) L. E. Mather and G. T. Tucker, *ibid.*, **63**, 306 (1974).

(12) U. Klotz, T. S. McHorse, G. R. Wilkinson, and S. Schender, *Clin. Pharmacol. Ther.*, **16**, 667 (1974).

(13) K. Chan, M. J. Kendall, and M. Mitchard, *J. Chromatogr.*, **89**, 168 (1974).

(14) C. Lindberg, C. Bogentoft, and B. Danielsson, *Acta Pharm. Suec.*, **11**, 201 (1974).

(15) A. P. L. Shih, K. Robinson, and W. Y. Au, *Eur. J. Clin. Pharmacol.*, **9**, 451 (1976).

(16) P. Hartvig, K. E. Karlsson, and L. Johansson, *J. Chromatogr.*, **121**, 235 (1976).

(17) J. Caldwell, L. A. Wakile, L. T. Notarianni, R. L. Smith, G. T. Correy, B. A. Lieberman, R. W. Beard, M. D. A. Finnie, and W. Snedden, *Life Sci.*, **22**, 589 (1978).

(18) C. Lindberg, K.-E. Karlsson, and P. Hartvig, *Acta Pharm. Suec.*, **15**, 327 (1978).

(19) C. Lindberg and C. Bogentoft, *ibid.*, **12**, 507 (1975).

(20) S. E. O'Donoghue-Ryan and T. P. Ryan, *Biochem. Soc. Trans.* **5**, 715 (1977).

(21) S. Y. Yeh, H. A. Krebs, and C. W. Gorodetzky, *J. Pharm. Sci.*, **68**, 133 (1979).

## ACKNOWLEDGMENTS

The authors thank Dr. C. W. Gorodetzky for interest in this project and for reviewing the manuscript.

# Electrokinetic Studies of Magnesium Hydroxide

**HANS SCHOTT**

Received June 13, 1980, from the *School of Pharmacy, Temple University, Philadelphia, PA 19140.* Accepted for publication October 5, 1980.

**Abstract** □ The electrophoretic mobility of magnesium hydroxide was studied as a function of the concentration of its potential-determining ions, namely, of the magnesium ions, and of the hydroxide ions or pH. The zero point of charge was located at ~10.8. The $\zeta$-potential of magnesium hydroxide below this pH was positive. The addition of magnesium nitrate to magnesium hydroxide suspensions increased the positive $\zeta$-potential and lowered the pH. The low solubility of magnesium hydroxide in water prevented the attainment of substantial concentrations of magnesium ions in solution. Increasing the hydroxide-ion concentration or the pH produced charge inversion. The largest negative $\zeta$-potential was attained at pH 11.5. Further increases in pH produced no significant increase in the negative value of the $\zeta$-potential.

**Keyphrases** □ Magnesium hydroxide—electrophoretic mobility in aqueous solution □ Electrophoretic mobility—magnesium hydroxide in aqueous solution □ Zero point of charge—magnesium hydroxide

Even though magnesium hydroxide suspensions are used extensively as antacids and laxatives, the information available on their electrokinetic properties is meager. Two sets of limited data, based on electro-osmosis and electrophoresis, were published in 1917 and 1934, respectively, for magnesium hydroxide that was precipitated with little



*0022-3549/81/0500-0486$01.00/0*
*© 1981, American Pharmaceutical Association*

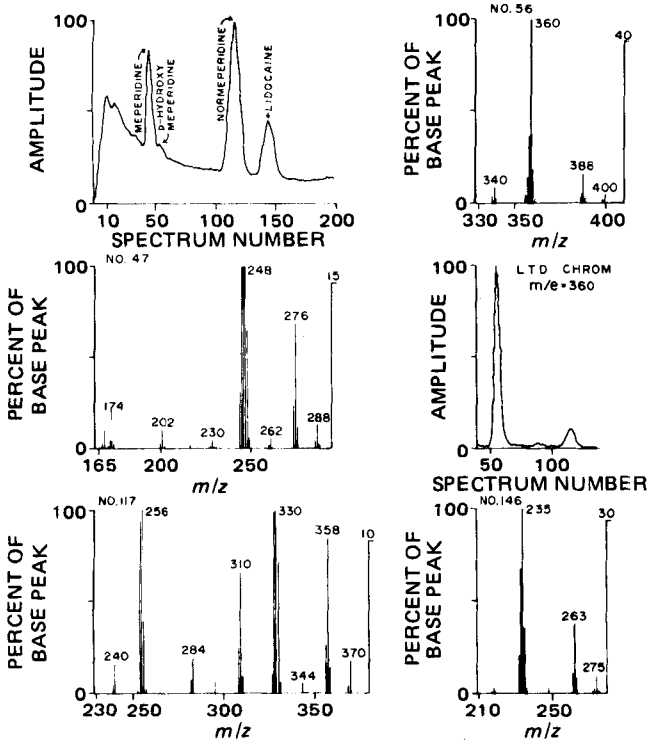


**Figure 3**—*GLC–mass spectrometric chromatogram, as trifluoroacetyl derivatives, of the 24-hr urinary extract of a rat administered meperidine. Key: upper left, integrated total ion current chromatogram; middle right; limited chromatogram at m/z 360; spectrum 47, meperidine; spectrum 56, p-hydroxymeperidine; spectrum 117, normeperidine; and spectrum 146, lidocaine (added internal standard).*

56 showed *m/z* 388 $(M + 29)^+$, 360 $(M + 1)^+$, and 340 $(M -$ fluoride ion$)^+$. The identity of *p*-hydroxymeperidine and normeperidine as metabolites thus was established and confirmed the observation of Lindberg *et al.* (5) that *p*-hydroxymeperidine is a metabolite of meperidine in the rat.

**Urinary Excretion of Meperidine and Its Metabolites in Rats**—A preliminary determination of the urinary excretion of meperidine and its metabolites in the rat indicated meperidine (6.1%), *p*-hydroxymeperidine (0.36%), total meperidinic acid (16.1%), normeperidine (24%), and total normeperidinic acid (3.9%) of administered meperidine hydrochloride (35 mg/kg). A detailed study of the urinary disposition of meperidine and its metabolites in several mammalian species will be reported in a separate paper.

## REFERENCES

(1) J. J. Burns, B. L. Berger, P. A. Lief, A. Wollack, E. M. Papper, and B. B. Brodie, *J. Pharmacol. Exp. Ther.*, **114**, 289 (1955).

(2) N. P. Plotnikoff, E. L. Way, and H. W. Elliott, *ibid.*, **117**, 414 (1956).

(3) A. M. Asatoor, D. R. London, M. D. Milne, and M. L. Simenhoff, *Br. J. Pharmacol.*, **20**, 285 (1963).

(4) I. W. Wainer and J. E. Stambaugh, *J. Pharm. Sci.*, **67**, 116 (1978).

(5) C. Lindberg, C. Bogentoft, U. Bodesson, and B. Danielsson, *J. Pharm. Pharmacol.*, **27**, 975 (1975).

(6) M. Mitchard, M. J. Kendall, and K. Chan, *ibid.*, **24**, 915 (1972).

(7) W. G. Stillwell, C. S. Myron, and J. T. Steward, *Res. Commun. Chem. Pathol. Pharmacol.*, **14**, 605 (1976).

(8) N. P. Plotnikoff, H. W. Elliott, and E. L. Way, *J. Pharmacol. Exp. Ther.*, **104**, 377 (1952).

(9) V. R. Jenkins, II, W. M. Talbert, and P. V. Dilts, Jr., *Obstet. Gynecol.*, **39**, 254 (1972).

(10) T. J. Goehl and C. Davison, *J. Pharm. Sci.*, **62**, 907 (1973).

(11) L. E. Mather and G. T. Tucker, *ibid.*, **63**, 306 (1974).

(12) U. Klotz, T. S. McHorse, G. R. Wilkinson, and S. Schender, *Clin. Pharmacol. Ther.*, **16**, 667 (1974).

(13) K. Chan, M. J. Kendall, and M. Mitchard, *J. Chromatogr.*, **89**, 168 (1974).

(14) C. Lindberg, C. Bogentoft, and B. Danielsson, *Acta Pharm. Suec.*, **11**, 201 (1974).

(15) A. P. L. Shih, K. Robinson, and W. Y. Au, *Eur. J. Clin. Pharmacol.*, **9**, 451 (1976).

(16) P. Hartvig, K. E. Karlsson, and L. Johansson, *J. Chromatogr.*, **121**, 235 (1976).

(17) J. Caldwell, L. A. Wakile, L. T. Notarianni, R. L. Smith, G. T. Correy, B. A. Lieberman, R. W. Beard, M. D. A. Finnie, and W. Snedden, *Life Sci.*, **22**, 589 (1978).

(18) C. Lindberg, K.-E. Karlsson, and P. Hartvig, *Acta Pharm. Suec.*, **15**, 327 (1978).

(19) C. Lindberg and C. Bogentoft, *ibid.*, **12**, 507 (1975).

(20) S. E. O'Donoghue-Ryan and T. P. Ryan, *Biochem. Soc. Trans.* **5**, 715 (1977).

(21) S. Y. Yeh, H. A. Krebs, and C. W. Gorodetzky, *J. Pharm. Sci.*, **68**, 133 (1979).

## ACKNOWLEDGMENTS

The authors thank Dr. C. W. Gorodetzky for interest in this project and for reviewing the manuscript.

# Electrokinetic Studies of Magnesium Hydroxide

**HANS SCHOTT**

Received June 13, 1980, from the *School of Pharmacy, Temple University, Philadelphia, PA 19140.* Accepted for publication October 5, 1980.

**Abstract** □ The electrophoretic mobility of magnesium hydroxide was studied as a function of the concentration of its potential-determining ions, namely, of the magnesium ions, and of the hydroxide ions or pH. The zero point of charge was located at ~10.8. The $\zeta$-potential of magnesium hydroxide below this pH was positive. The addition of magnesium nitrate to magnesium hydroxide suspensions increased the positive $\zeta$-potential and lowered the pH. The low solubility of magnesium hydroxide in water prevented the attainment of substantial concentrations of magnesium ions in solution. Increasing the hydroxide-ion concentration or the pH produced charge inversion. The largest negative $\zeta$-potential was attained at pH 11.5. Further increases in pH produced no significant increase in the negative value of the $\zeta$-potential.

**Keyphrases** □ Magnesium hydroxide—electrophoretic mobility in aqueous solution □ Electrophoretic mobility—magnesium hydroxide in aqueous solution □ Zero point of charge—magnesium hydroxide

Even though magnesium hydroxide suspensions are used extensively as antacids and laxatives, the information available on their electrokinetic properties is meager. Two sets of limited data, based on electro-osmosis and electrophoresis, were published in 1917 and 1934, respectively, for magnesium hydroxide that was precipitated with little



*0022-3549/81/0500-0486$01.00/0*
*© 1981, American Pharmaceutical Association*

Table I—Electrophoretic Mobility Values of Magnesium Hydroxide in Various Media

| Suspension | Electrolytes and Concentrations | Mobility ± *SEM*[a], (μm/sec)/(v/cm) | Specific Conductance, millimho/cm | pH |
|---|---|---|---|---|
| 1 | 0.0200 *M* $NaNO_3$ | 1.60 ± 0.06 | 2.43 | 9.6 |
| 2 | 0.0200 *M* $NaNO_3$[b] | 1.29 ± 0.06 | 2.23 | 9.6 |
| 3 | 0.0100 *M* $NaNO_3$[b,c] | 1.36 ± 0.07 | 1.15 | 10.2 |
| 4 | 0.00666 *M* $Na_2SO_4$ | 1.64 ± 0.05 | — | 9.5 |
| 5 | 0.0100 *M* $NaNO_3$ + 0.00333 *M* $Mg(NO_3)_2$ | 1.91 ± 0.09 | 1.89 | 9.4 |
| 6 | 0.00666 *M* $Mg(NO_3)_2$ | 2.07 ± 0.10 | 1.49 | 9.0 |
| 7 | 0.00666 *M* $Mg(NO_3)_2$[b] | 1.85 ± 0.05 | 1.49 | 9.5 |
| 8 | 0.00333 *M* $Mg(NO_3)_2$[c] | 2.75 ± 0.07 | 0.74 | 9.8 |
| 9 | 0.0195 *M* $NaNO_3$ + 0.0005 *M* NaOH | 1.36 ± 0.07 | — | 10.2 |
| 10 | 0.0180 *M* $NaNO_3$ + 0.0020 *M* NaOH | −1.62 ± 0.04 | 2.08 | 11.2 |
| 11 | 0.0150 *M* $NaNO_3$ + 0.0050 *M* NaOH | −1.95 ± 0.04 | 2.97 | 11.5 |
| 12 | 0.0100 *M* $NaNO_3$ + 0.0100 *M* NaOH | −1.96 ± 0.05 | 3.72 | 11.8 |
| 13 | 0.0200 *M* NaOH | −1.99 ± 0.04 | 5.00 | 12.2 |

[a] Average of 10 measurements ± *SEM*. [b] Contained approximately 10 times more suspended magnesium hydroxide. All other suspensions contained 0.1 g/liter of magnesium hydroxide. [c] At an initial ionic strength of 0.0100 *M*, *i.e.*, one-half of that of other suspension media.

or no subsequent purification (1, 2). The ionic strength of the suspensions apparently was not controlled.

This paper reports the electrophoretic properties of magnesium hydroxide with emphasis on the effect of potential-determining ions on its electrophoretic mobility.

## BACKGROUND

Potential-determining ions are ions whose concentration in solution determines the $\psi_0$-potential of the suspended particles, *i.e.*, the electric potential at the particle surface (3–5). For magnesium hydroxide, the potential-determining ions are the magnesium ions and hydroxide ions. Since these ions determine the potential at the particle surface rather than the $\zeta$-potential at the plane of shear within the electric double layer, they affect the colloidal properties of magnesium hydroxide suspensions more strongly than other ions, which cannot become an integral part of the particle surface.

The state of aggregation of colloidal dispersions and coarse suspensions depends on the magnitude of the electrostatic repulsion between particles that opposes the omnipresent interparticle London–van der Waals attraction. The former, in turn, depends on the $\psi_0$- and $\zeta$-potentials. Thus, the state of aggregation of suspended magnesium hydroxide is strongly pH dependent because the hydrogen-ion concentration in aqueous media varies inversely with the concentration of the potential-determining hydroxide ions.

Slightly soluble hydroxides $M^{z+}(OH)_z^-$ of polyvalent cations are amphoteric; $z$ represents the valence of the cation. The surface charge of the hydroxide particles depends on the composition of their surface layer, $[M^{z+}(OH)_n]^{z-n}$. At relatively low pH values where $z > n$, a positive charge results because, in the case of magnesium hydroxide, the ratio of the concentration of magnesium ions to that of hydroxide ions in the surface layer exceeds 1:2. Alternatively, the positive charge may be ascribed to proton adsorption on a neutral surface. At high pH values where $z < n$, a negative surface charge results.

At an intermediate pH where $z = n$, the particles have a zero net surface charge. At this pH, known as the zero point of charge or isoelectric point (3–6), the surface layer has the same 1:2 ratio of magnesium-ion concentration to hydroxide-ion concentration as the bulk of the particles. Since the surface layer is electrically neutral, the $\psi_0$- and $\zeta$-potentials of the magnesium hydroxide particles are zero.

Because an electric surface charge is absent, the suspensions are flocculated more extensively at the zero point of charge than at any other pH, as was demonstrated by maxima in the rate and volume of sedimentation and in viscosity (3–5). Hence, the tendency toward caking is smallest at the zero point of charge. Old electro-osmosis (1) and electrophoresis (2) measurements indicated a zero point of charge of ~12 for nonpurified magnesium hydroxide, while recent correlations placed the zero point of charge of pure magnesium hydroxide at 12.0 (7) and at 12.3 (8).

## EXPERIMENTAL

**Materials**—All chemicals were ACS reagent grade. The water was double distilled and free of carbon dioxide. Magnesium hydroxide was precipitated by the action of sodium hydroxide on magnesium sulfate, using a literature procedure (9) with the following two modifications. The sodium hydroxide was prepared first as a 50% solution, which was filtered to remove any traces of sodium carbonate. A slurry of the precipitated magnesium hydroxide was prepared in water, filtered, and washed extensively with water on the filter. This procedure was performed eight times.

**Methods**—The electrophoretic mobility of magnesium hydroxide suspensions was determined by microelectrophoresis using a commercial instrument[1] with an acrylic cell equipped with a cylindrical molybdenum anode and a platinum–iridium strip cathode. The cell constant and equations for calculating specific conductance of the suspension from current intensity, electrophoretic mobility from velocity of migration, and $\zeta$-potential from electrophoretic mobility were reported previously (10). The ionic strength was maintained constant at 0.0200 *M* for most measurements and at 0.0100 *M* for the others.

Most suspensions for electrophoretic measurements were prepared by diluting 0.5 ml of 2.0% (w/v) magnesium hydroxide stock suspensions with 99.5 ml of the various electrolyte solutions. The final magnesium hydroxide concentration is 10 times higher than its solubility in water.

The electrophoresis cell was filled with two aliquots from each diluted suspension, and five particles were tracked for each aliquot. All electrophoretic measurements were made within 30 min of mixing but, in the two instances tested, aging for 4 hr did not alter the results.

The pH of each diluted suspension aliquot was measured before and after the mobility determinations. The differences between the two readings were 0.2 pH unit or less.

## RESULTS

The results are presented in Table I. Negative values of the electrophoretic mobility indicate that the particles were negatively charged and migrated to the anode.

Preliminary measurements indicated that the concentration of magnesium hydroxide present in a suspension had some effect on electrophoretic mobility. Comparison of Suspensions 1 and 2 and of 6 and 7 shows that higher magnesium hydroxide concentrations resulted in lower mobilities. These decreases were about an order of magnitude greater than the increase in apparent viscosity resulting from the higher magnesium hydroxide concentration, indicating that viscosity increases did not cause the drop in mobility. Subsequent measurements were made at the constant magnesium hydroxide concentration of 0.10 g/liter.

Suspensions 1 and 4, in which the supporting electrolytes were sodium nitrate and sodium sulfate of identical ionic strengths, respectively, had the same electrophoretic mobility within experimental error. This fact indicates that there was no specific interaction between magnesium hydroxide and either anion. Specific anion effects are due exclusively to the hydroxide ion.

**Effect of Magnesium Ion**—Comparison of the electrophoretic mobility of Suspensions 1 and 5 shows that the addition of the potential-determining magnesium ions as the soluble nitrate increased the positive electrophoretic mobility or the positive $\zeta$-potential by ~20%. Evidently, this addition forced more magnesium ions into the particle surface, increasing the positive surface-charge density. However, because of the low solubility product of magnesium hydroxide ($1.6 \times 10^{-11}$), the concen-

[1] Zeta-Meter, Zeta Meter Inc., New York, N.Y.

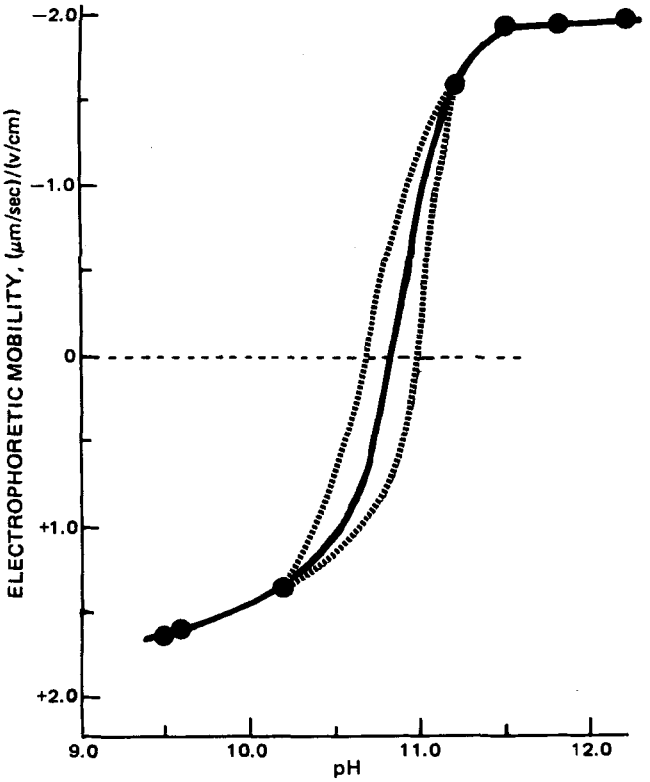


**Figure 1**—*Electrophoretic mobility of magnesium hydroxide as a function of pH. The conditions were ionic strength of 0.0200* M *and no added soluble magnesium salt.*

tration of magnesium ions in solution cannot exceed $10^{-4}$ *M*. All or most of the magnesium added as magnesium nitrate to make Suspension 5 must have precipitated as magnesium hydroxide.

Further addition of magnesium nitrate, which occurred when going from Suspension 5 to Suspension 6, produced only a minor change in electrophoretic mobility which was not statistically significant. Evidently, the incorporation of excess magnesium ions from solution into the surface layer of magnesium hydroxide particles became increasingly more difficult as their $\zeta$-potential became more positive because the increasingly greater excess of magnesium ions over hydroxide ions in the surface layer resulted in greater positive surface-charge density, which, in turn, caused increased electrostatic repulsion of the added magnesium ions and increased attraction for the hydroxide ions (5).

The replacement of sodium nitrate by equivalent amounts of magnesium nitrate caused the pH to drop from 9.6 (before such replacement, Suspension 1) to 9.4 (when half of the sodium nitrate was replaced by magnesium nitrate, No. 5) to 9.0 (when all of the sodium nitrate was replaced, Suspension 6). Similarly, Suspension 8, with one-half of the concentration of added magnesium nitrate as Suspension 6, had a pH that was 0.8 unit higher. The decreases in pH produced by the addition of magnesium nitrate were probably due to the adsorption of hydroxide ions from solution onto the surface of positively charged magnesium hydroxide particles, especially of those particles that freshly precipitated as a result of the addition of magnesium nitrate in amounts exceeding the magnesium hydroxide solubility.

An equivalent explanation for this decrease in pH is the hydrolysis of most of the added magnesium nitrate according to the equilibrium $Mg^{2+} + 2H_2O \rightleftharpoons Mg(OH)_2(s) + 2H^+$. In view of the low solubility product of magnesium hydroxide and the high pH, the bulk of the magnesium ions added as magnesium nitrate must have precipitated as magnesium hydroxide with the simultaneous formation of hydrogen ions, shifting the equilibrium forward.

**Effect of Hydroxide Ion**—While the magnesium-ion concentration cannot be raised much in the vicinity of the zero point of charge because of precipitation of magnesium hydroxide, the concentration of the hydroxide ions can be raised considerably. With an increasing concentration of added hydroxide ions and an increasing pH at a constant ionic strength of 0.0200 *M*, the electrophoretic mobility became less positive (Suspensions 1 and 9), went through zero, and, after charge inversion, became negative (Suspensions 10–13).

Comparison of the electrophoretic mobilities of Suspensions 10–13 was made by the *F* test (11). When Suspension 10 was included, the differences between the four mobility values were statistically significant. Without Suspension 10, the differences between the three mobility values of Suspensions 11–13 were not significant, despite the trend of increasingly greater negative mobility values with increasing pH. At constant ionic strength, hydroxide-ion concentrations above those corresponding to pH 11.5 did not increase the negative value of the $\zeta$-potential of magnesium hydroxide. This observation may indicate that the surface layer of the magnesium hydroxide particles consisted of a monomolecular layer of extra hydroxide ions at pH $\geq$11.5 (5).

***Zero Point of Charge***—*Direct determination of the zero point of* charge as the pH corresponding to zero mobility was unsuccessful. At pH 10.8 and an ionic strength of 0.0200 *M*, many particles did not move in the electric field, some particles moved sluggishly toward the anode, and others migrated toward the cathode.

Therefore, the zero point of charge was estimated by graphical interpolation of the electrophoretic mobility values obtained at a constant ionic strength of 0.0200 *M* in the absence of added magnesium nitrate (Suspensions 1, 4, and 9–13). These points (Fig. 1) form the familiar S-shaped curve (12). The best zero point of charge estimate, corresponding to the smoothest and most symmetric curve (solid line), is 10.8. The extreme values (dotted lines) are 10.7 and 10.9. The zero point of charge value of 10.8 is certainly accurate within a range of ±0.2.

This 10.8 value is more than one pH unit below the published zero point of charge values. The 1917 and 1934 publications (1, 2) did not indicate how extensively the magnesium hydroxide samples were purified or whether they were separated from the mother liquor, nor did they specify the ionic strength of the suspensions or whether the ionic strength was controlled.

The addition of magnesium nitrate to magnesium hydroxide suspensions, which may be considered analogous to purifying precipitated magnesium hydroxide incompletely, increased the positive value of the electrophoretic mobility and lowered the pH. However, it is doubtful that these changes could increase the zero point of charge by a full pH unit.

## DISCUSSION

There are probably two reasons why the nitrate and sulfate anions produced no specific effects on the $\zeta$-potential. First, these anions do not form complexes with magnesium ions in aqueous solution, thereby making their uptake by the magnesium hydroxide particles unlikely. By analogy with aluminum hydroxide (13, 14), the chloride and citrate anions, being better ligands, are probably chemisorbed to some extent by magnesium hydroxide, affecting its colloidal properties.

Second, magnesium nitrate and magnesium sulfate are very soluble in water as opposed to the phosphates, fluoride, and carbonate of magnesium, which range from very slightly soluble to insoluble. If the latter anions were present in magnesium hydroxide suspensions, they probably would be bound extensively to the surface layer of the particles, possibly acting as potential-determining ions, and affect their colloidal properties considerably.

The observation that mobility values depended on the solids content of the magnesium hydroxide suspensions may be due to impurities, or even to somewhat soluble magnesium hydroxo complexes (15), released from the suspended solids during electrophoresis. It is impossible to wash gelatinous precipitates such as magnesium hydroxide completely free of adsorbed ions. The product used in the present experiments was similar to that of commercial magnesium hydroxide pastes used to manufacture milk of magnesia, except that it was washed more extensively. Thus, the present data are applicable to the formulation of antacid and laxative suspensions based on magnesium hydroxide.

Precipitated magnesium hydroxide purified further by electrodialysis–electrodecantation or magnesium hydroxide prepared in the absence of anions other than hydroxide, *e.g.*, by the reaction of water with magnesium amalgam or with dialkyl magnesium compounds, could well exhibit zero point of charge values at variance with the present estimate.

## REFERENCES

(1) S. Glixelli, *Anz. Akad. Wiss. Krakow*, **1917** (A), 102; cited by L. Michaelis, "Hydrogen Ion Concentration," vol. I, Williams & Wilkins, Baltimore, Md., 1926, pp. 258–261.

(2) S. Mattson and A. J. Pugh, *Soil Sci.*, **38**, 299 (1934).

(3) P. C. Hiemenz, "Principles of Colloid and Surface Chemistry," Dekker, New York, N.Y., 1977, chap. 9.

(4) H. Schott, in "Remington's Pharmaceutical Sciences," 16th ed.,

Mack Publishing Co., Easton, Pa., 1980, chap. 20.
(5) K. J. Mysels, "Introduction to Colloid Chemistry," Wiley-Interscience, New York, N.Y., 1967, chap. 17.
(6) G. A. Parks, *Chem. Rev.*, **65**, 177 (1965).
(7) H. Schott, *J. Pharm. Sci.*, **66**, 1548 (1977).
(8) R. H. Yoon, T. Salman, and G. Donnay, *J. Colloid Interface Sci.*, **70**, 483 (1979).
(9) "U. S. Pharmacopeia," 10th rev., Lippincott, Philadelphia, Pa., 1925, p. 229.
(10) H. Schott and C. Y. Young, *J. Pharm. Sci.*, **61**, 182 (1972).
(11) W. J. Youden, "Statistical Methods for Chemists," Wiley, New York, N.Y., 1951, chap. 3.
(12) H. S. Abramson, "Electrokinetic Phenomena and their Application in Biology and Medicine," Chemical Catalog Co., New York, N.Y., 1934, chaps. 5, 7, and 8.
(13) K. F. N. K. Kwong and P. M. Huang, *Soil Sci. Soc. Am. J.*, **41**, 692 (1977).
(14) S. S. S. Rajan, K. W. Perrott, and W. M. H. Saunders, *J. Soil Sci.*, **25**, 438 (1974).
(15) L. G. Sillen, *Pure Appl. Chem.*, **17**, 55 (1968).

# Molecular Requirements of the Active Site of Cholinergic Receptors XV: Synthesis and Biological Activity of 2,3-Dehydrodeoxamuscarone and 2,3-Dehydrodeoxamuscarines

**PIERO ANGELI, LIVIO BRASILI, DARIO GIARDINÀ, and CARLO MELCHIORRE** ˣ

Received June 30, 1980, from the *Institute of Pharmaceutical Chemistry, University of Camerino, 62032 Camerino (MC), Italy.* Accepted for publication October 10, 1980.

**Abstract** □ To elucidate the molecular requirements of the active sites of cholinergic receptors, 3-methyl-4-oxo-1-(*N,N*-dimethylaminomethyl)cyclopent-2-ene methiodide (2,3-dehydrodeoxamuscarone) and *cis*- and *trans*-3-methyl-4-hydroxy-1-(*N,N*-dimethylaminomethyl)cyclopent-2-ene methiodides (*cis*- and *trans*-dehydrodeoxamuscarines) were synthesized and tested. The results, compared with those of the corresponding oxygenated compounds, seem to indicate that 2,3-dehydrodeoxamuscarines and muscarine bind at the same site while 2,3-dehydrodeoxamuscarone interacts with the site normally occupied by muscarone. Furthermore, the previously suggested hypothesis that the unpolar site might somehow incorporate that of muscarone was considered.

**Keyphrases** □ Cholinergic receptors—molecular requirements of active sites, synthesis of 2,3-dehydrodeoxamuscarone and *cis*- and *trans*-dehydrodeoxamuscarines □ Structure–activity relationships—2,3-dehydrodeoxamuscarone and *cis*- and *trans*-dehydrodeoxamuscarines, molecular requirements of cholinergic receptors, dualism of receptor active sites □ 2,3-Dehydrodeoxamuscarone and 2,3-dehydrodeoxamuscarine—synthesis and biological activity

To investigate the molecular requirements of cholinergic receptors, many compounds incorporating a cyclopentane nucleus were synthesized in the past few years (1). As a consequence of these studies, the hypothesis of Triggle and Triggle (2) concerning an accessory site of reduced polarity and low steric demand of the cholinergic receptor gained further support (3–5). In fact, most of these compounds, although lacking oxygenated functions, are fairly active on both nicotinic and muscarinic receptors. However, their specificity is generally low when compared with the corresponding oxygenated compounds (*i.e.*, muscarine).

To gain more information on the dualism of the active site of the cholinergic receptors, *cis*- and *trans*-3-methyl-4-hydroxy-1-(*N,N*-dimethylaminomethyl)cyclopent-2-ene methiodides (*cis*- and *trans*-2,3-dehydrodeoxamuscarines, I*a* and I*b*) and 3-methyl-4-oxo-1-(*N,N*-dimethylaminomethyl)cyclo-pent-2-ene methiodide (2,3-dehydrodeoxamuscarone, II) were synthesized and tested. Their pharmacological results were compared with those of 3-methyl-1-(*N,N*-dimethylaminomethyl)cyclopent-2-ene methiodide (III), because it incorporates a double bond at the same position 2 of the cyclopentyl moiety as a basic feature and is one of the most active compounds among those lacking oxygenated functions (5).

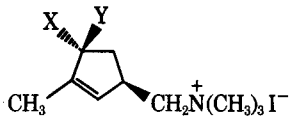


I*a*: X = H, Y = OH
I*b*: X = OH, Y = H
III: X = Y = H

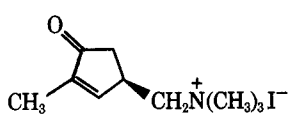


II

## EXPERIMENTAL

Melting points[1] were taken in sealed capillaries and are uncorrected. NMR spectra were recorded on a 90-MHz apparatus[2] with tetramethylsilane or 3-(trimethylsilyl)propanesulfonic acid sodium salt as the internal standard. Chromatographic separations were performed on silica gel (Kieselgel[3] 60, 0.063–0.200 mm) columns. Organic solutions were dried over anhydrous sodium sulfate.

**3-Methyl-4-oxo-1-carbomethoxycyclopent-2-ene (VI)**—Bromine (7.56 ml) in carbon tetrachloride (100 ml) was added to a vigorously stirred solution of V (21.9 g) (6) in carbon tetrachloride (100 ml) at room temperature. After the reaction started, the addition was continued with cooling at 0°. The solvent then was evaporated to give an oil, which was kept at 120° for 15 min under 50 mm pressure and then distilled, bp 130–135°/30 mm (12.7-g yield); IR[4] (liquid film): 1640 (C=C), 1710 (C=O), and 1735 (COO) $cm^{-1}$; NMR (chloroform-*d*): $\delta$ 1.70 (broad s, 3H, 3-$CH_3$), 2.60 (d, 2H, 5-$H_2$), 3.70 (s, 3H, $OCH_3$), 3.50–4.00 (m, 1H, 1-H), and 7.13 (m, 1H, 2-H) ppm.

*Anal.*—Calc. for $C_8H_{10}O_3$: C, 62.32; H, 6.54. Found: C, 62.20; H, 6.60.

***cis*- and *trans*-3-Methyl-4-hydroxy-1-carbomethoxycyclopent-2-enes (VII*a* and VII*b*)**—The overall procedure recommended by Brown and Hess (7) was followed. Thus, a solution of 0.55 *M* 9-borabicyclo[3.3.1]nonane in tetrahydrofuran[5] (36.5 ml) was added dropwise over 2 hr to a stirred and cooled (0°) solution of VI (3 g, 19.5 mmoles) in dry tetrahydrofuran (5 ml) under a dry nitrogen stream. After 4 hr at 0°,

[1] Büchi SMP-20 apparatus.
[2] Model EM-390, Varian.
[3] Merck.
[4] Perkin-Elmer 297 spectrophotometer.
[5] Aldrich.

0022-3549/81/0500-0489$01.00/0
© 1981, American Pharmaceutical Association

Mack Publishing Co., Easton, Pa., 1980, chap. 20.
(5) K. J. Mysels, "Introduction to Colloid Chemistry," Wiley-Interscience, New York, N.Y., 1967, chap. 17.
(6) G. A. Parks, *Chem. Rev.*, **65**, 177 (1965).
(7) H. Schott, *J. Pharm. Sci.*, **66**, 1548 (1977).
(8) R. H. Yoon, T. Salman, and G. Donnay, *J. Colloid Interface Sci.*, **70**, 483 (1979).
(9) "U. S. Pharmacopeia," 10th rev., Lippincott, Philadelphia, Pa., 1925, p. 229.
(10) H. Schott and C. Y. Young, *J. Pharm. Sci.*, **61**, 182 (1972).
(11) W. J. Youden, "Statistical Methods for Chemists," Wiley, New York, N.Y., 1951, chap. 3.
(12) H. S. Abramson, "Electrokinetic Phenomena and their Application in Biology and Medicine," Chemical Catalog Co., New York, N.Y., 1934, chaps. 5, 7, and 8.
(13) K. F. N. K. Kwong and P. M. Huang, *Soil Sci. Soc. Am. J.*, **41**, 692 (1977).
(14) S. S. S. Rajan, K. W. Perrott, and W. M. H. Saunders, *J. Soil Sci.*, **25**, 438 (1974).
(15) L. G. Sillen, *Pure Appl. Chem.*, **17**, 55 (1968).

# Molecular Requirements of the Active Site of Cholinergic Receptors XV: Synthesis and Biological Activity of 2,3-Dehydrodeoxamuscarone and 2,3-Dehydrodeoxamuscarines

**PIERO ANGELI, LIVIO BRASILI, DARIO GIARDINÀ, and CARLO MELCHIORRE** ˣ

Received June 30, 1980, from the *Institute of Pharmaceutical Chemistry, University of Camerino, 62032 Camerino (MC), Italy.* Accepted for publication October 10, 1980.

**Abstract** □ To elucidate the molecular requirements of the active sites of cholinergic receptors, 3-methyl-4-oxo-1-(*N,N*-dimethylaminomethyl)cyclopent-2-ene methiodide (2,3-dehydrodeoxamuscarone) and *cis*- and *trans*-3-methyl-4-hydroxy-1-(*N,N*-dimethylaminomethyl)cyclopent-2-ene methiodides (*cis*- and *trans*-dehydrodeoxamuscarines) were synthesized and tested. The results, compared with those of the corresponding oxygenated compounds, seem to indicate that 2,3-dehydrodeoxamuscarines and muscarine bind at the same site while 2,3-dehydrodeoxamuscarone interacts with the site normally occupied by muscarone. Furthermore, the previously suggested hypothesis that the unpolar site might somehow incorporate that of muscarone was considered.

**Keyphrases** □ Cholinergic receptors—molecular requirements of active sites, synthesis of 2,3-dehydrodeoxamuscarone and *cis*- and *trans*-dehydrodeoxamuscarines □ Structure–activity relationships—2,3-dehydrodeoxamuscarone and *cis*- and *trans*-dehydrodeoxamuscarines, molecular requirements of cholinergic receptors, dualism of receptor active sites □ 2,3-Dehydrodeoxamuscarone and 2,3-dehydrodeoxamuscarine—synthesis and biological activity

To investigate the molecular requirements of cholinergic receptors, many compounds incorporating a cyclopentane nucleus were synthesized in the past few years (1). As a consequence of these studies, the hypothesis of Triggle and Triggle (2) concerning an accessory site of reduced polarity and low steric demand of the cholinergic receptor gained further support (3–5). In fact, most of these compounds, although lacking oxygenated functions, are fairly active on both nicotinic and muscarinic receptors. However, their specificity is generally low when compared with the corresponding oxygenated compounds (*i.e.*, muscarine).

To gain more information on the dualism of the active site of the cholinergic receptors, *cis*- and *trans*-3-methyl-4-hydroxy-1-(*N,N*-dimethylaminomethyl)cyclopent-2-ene methiodides (*cis*- and *trans*-2,3-dehydrodeoxamuscarines, I*a* and I*b*) and 3-methyl-4-oxo-1-(*N,N*-dimethylaminomethyl)cyclo-pent-2-ene methiodide (2,3-dehydrodeoxamuscarone, II) were synthesized and tested. Their pharmacological results were compared with those of 3-methyl-1-(*N,N*-dimethylaminomethyl)cyclopent-2-ene methiodide (III), because it incorporates a double bond at the same position 2 of the cyclopentyl moiety as a basic feature and is one of the most active compounds among those lacking oxygenated functions (5).

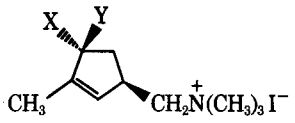


I*a*: X = H, Y = OH
I*b*: X = OH, Y = H
III: X = Y = H

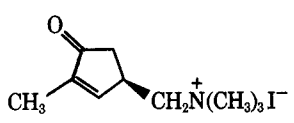


II

## EXPERIMENTAL

Melting points[1] were taken in sealed capillaries and are uncorrected. NMR spectra were recorded on a 90-MHz apparatus[2] with tetramethylsilane or 3-(trimethylsilyl)propanesulfonic acid sodium salt as the internal standard. Chromatographic separations were performed on silica gel (Kieselgel[3] 60, 0.063–0.200 mm) columns. Organic solutions were dried over anhydrous sodium sulfate.

**3-Methyl-4-oxo-1-carbomethoxycyclopent-2-ene (VI)**—Bromine (7.56 ml) in carbon tetrachloride (100 ml) was added to a vigorously stirred solution of V (21.9 g) (6) in carbon tetrachloride (100 ml) at room temperature. After the reaction started, the addition was continued with cooling at 0°. The solvent then was evaporated to give an oil, which was kept at 120° for 15 min under 50 mm pressure and then distilled, bp 130–135°/30 mm (12.7-g yield); IR[4] (liquid film): 1640 (C=C), 1710 (C=O), and 1735 (COO) $cm^{-1}$; NMR (chloroform-*d*): $\delta$ 1.70 (broad s, 3H, 3-$CH_3$), 2.60 (d, 2H, 5-$H_2$), 3.70 (s, 3H, $OCH_3$), 3.50–4.00 (m, 1H, 1-H), and 7.13 (m, 1H, 2-H) ppm.

*Anal.*—Calc. for $C_8H_{10}O_3$: C, 62.32; H, 6.54. Found: C, 62.20; H, 6.60.

***cis*- and *trans*-3-Methyl-4-hydroxy-1-carbomethoxycyclopent-2-enes (VII*a* and VII*b*)**—The overall procedure recommended by Brown and Hess (7) was followed. Thus, a solution of 0.55 *M* 9-borabicyclo[3.3.1]nonane in tetrahydrofuran[5] (36.5 ml) was added dropwise over 2 hr to a stirred and cooled (0°) solution of VI (3 g, 19.5 mmoles) in dry tetrahydrofuran (5 ml) under a dry nitrogen stream. After 4 hr at 0°,

[1] Büchi SMP-20 apparatus.
[2] Model EM-390, Varian.
[3] Merck.
[4] Perkin-Elmer 297 spectrophotometer.
[5] Aldrich.

0022-3549/81/0500-0489$01.00/0
© 1981, American Pharmaceutical Association

the solution was stirred at 25° for 2 hr. Then methanol (0.5 ml) was added, and the solvent was removed under reduced pressure. Ethanolamine (1.23 g) and *n*-pentane (100 ml) were added, and the sticky precipitate was extracted several times with *n*-pentane. Evaporation of the solvent gave an oil (1.64 g), which was purified by column chromatography using ethyl acetate–cyclohexane (1:1) as the eluting system. The first fraction was the starting material.

The second fraction was VII*a* (0.42 g); IR (chloroform): 1720 (C=O), 3460 (bonded OH), and 3580 (free OH) $cm^{-1}$; NMR (chloroform-*d*): δ 1.80 (broad s, 3H, 3-$CH_3$), 1.90–2.78 (m, 2H, 5-$H_2$), 2.78 (s, 1H, OH), 3.32 (m, 1H, 1-H), 3.65 (s, 3H, $OCH_3$), 4.38 (dd, 1H, 4-H), and 5.38 (m, 1H, 2-H) ppm.

*Anal.*—Calc. for $C_8H_{12}O_3$: C, 61.52; H, 7.75. Found: C, 61.65; H, 7.84.

The third fraction was VII*b* (0.26 g); IR (chloroform): 1730 (C=O), 3480 (bonded OH), and 3590 (free OH) $cm^{-1}$; NMR (chloroform-*d*): δ 1.78 (broad s, 3H, 3-$CH_3$), 1.80–2.70 (m, 2H, 5-$H_2$), 2.65 (s, 1H, OH), 3.30–3.80 (m, 1H, 1-H), 3.60 (s, 3H, $OCH_3$), 4.62 (t, 1H, 4-H), and 5.40 (m, 1H, 2-H) ppm.

*Anal.*—Calc. for $C_8H_{12}O_3$: C, 61.52; H, 7.75. Found: C, 61.74; H, 7.84.

***cis*-3-Methyl-4-hydroxy-1-(*N,N*-dimethylcarboxamido)cyclopent-2-ene (VIII*a*)**—*Method A*—Dimethylamine (10 ml) was added to VII*a* (or VII*b*) (0.5 g) and heated at 95–100° in a sealed tube for 48 hr. Workup of the reaction mixture gave 0.25 g of VIII*a*, which was used without further purification; IR (chloroform): 1620 (C=O), 3360 (bonded OH), and 3590 (free OH) $cm^{-1}$; NMR (chloroform-*d*): δ 1.82 (broad s, 3H, 3-$CH_3$), 1.95–2.50 (m, 2H, 5-$H_2$), 2.92 (s, 3H, $NCH_3$), 3.11 (s, 3H, $NCH_3$), 3.50–3.90 (m, 1H, 1-H), 4.25 (dd, 1H, 4-H), 4.58 (s, 1H, OH), and 5.31 (m, 1H, 2-H) ppm.

*Method B*—Ethyl chloroformate (0.62 g, 5.7 mmoles) in chloroform (10 ml) was added to a stirred and cooled solution of XV*a* (0.81 g, 5.7 mmoles) and triethylamine (0.58 g, 5.7 mmoles), followed after 5 min by 33% dimethylamine in benzene (5.6 ml). The mixture was allowed to stand at room temperature for 30 min and then was washed with 2 *N* HCl and saturated sodium bicarbonate solution and dried. Evaporation of the solvent gave 0.74 g of VIII*a*.

***cis*-3-Methyl-4-hydroxy-1-(*N,N*-dimethylaminomethyl)cyclopent-2-ene (IX*a*)**—A solution of VIII*a* (0.34 g, 2.01 mmoles) in dry tetrahydrofuran (100 ml) was added to a suspension of aluminum lithium hydride (0.15 g, 4.02 mmoles) in dry tetrahydrofuran (100 ml) with stirring and cooling. The suspension then was heated to reflux for 5 hr. After cooling, the excess aluminum lithium hydride was decomposed with ethyl acetate (50 ml) and water (5 ml). The organic layer was decanted, and the solid was washed with ethyl acetate (2 × 50 ml). Evaporation of the dried solvent gave a nearly pure oil (0.26 g), which was used without further purification; IR (chloroform): 3350 (bonded OH) and 3500 (free OH) $cm^{-1}$; NMR (chloroform-*d*): δ 1.17–1.60 (m, 1H, 5-H), 1.79 (broad s, 3H, 3-$CH_3$), 2.00–2.90 (m, 4H, 1-$CH_2$, 1-H, and 5-H), 2.26 [s, 6H, $N(CH_3)_2$], 4.19 (s, 1H, OH), 4.26 (dd, 1H, 4-H), and 5.37 (broad s, 1H, 2-H) ppm.

***cis*-2,3-Dehydrodeoxamuscarine (I*a*)**—An excess of methyl iodide (2 ml) was added to a solution of IX*a* (0.2 g) in anhydrous ether (20 ml), and the solution was left to stand overnight at room temperature. The white solid was filtered off and recrystallized (0.23 g) from anhydrous ethanol–ether, mp 153–154°; IR (mineral oil): 3350 (OH) $cm^{-1}$; NMR (water-*d*): δ 1.30–1.80 (m, 1H, 5-H), 1.76 (s, 3H, 3-$CH_3$), 2.66–3.66 (m, 4H, 1-H, 4-H, and 1-$CH_2$), 3.17 [s, 9H, $^+N(CH_3)_3$], 4.70 (4H, obscured by water), and 5.50 (broad s, 1H, 2-H) ppm.

*Anal.*—Calc. for $C_{10}H_{20}INO$: C, 40.42; H, 6.78; N, 4.71. Found: C, 40.38; H, 6.92; N, 4.64.

**3-Methyl-4-oxo-1-(*N,N*-dimethylaminomethyl)cyclopent-2-ene (X)**—A solution of chromium trioxide (1.13 g, 11.0 mmoles) in 2.5 *M* $H_2SO_4$ (10 ml) was added slowly to a stirred and cooled (0°) solution of IX*a* (1.76 g, 11.0 mmoles) in 2.5 *M* $H_2SO_4$ (5 ml). After standing at room temperature for 2 hr, the solution was made basic with 5 *N* NaOH and extracted with methylene chloride. Evaporation of the dried solvent gave X (1.0 g), which was purified by column chromatography with chloroform–petroleum ether–methanol–concentrated ammonium hydroxide (250:150:50:5) as the eluting system; IR (liquid film): 1635 (C=C) and 1705 (C=O) $cm^{-1}$; NMR (chloroform-*d*): δ 1.72 (d, 3H, 3-$CH_3$), 2.20 [s, 6H, $N(CH_3)_2$], 2.10–3.50 (m, 5H, 5-$H_2$, 1-H, and 1-$CH_2$), and 7.28 (m, 1H, 2-H) ppm.

*Anal.*—Calc. for $C_9H_{15}NO$: C, 70.55; H, 9.87; N, 9.14. Found: C, 70.41; H, 9.79; N, 9.21.

**2,3-Dehydrodeoxamuscarone (II)**—Compound II was obtained from X as a white solid following the procedure described for I*a* (from anhydrous ethanol–ether) in an 80% yield, mp 230–231°; IR (mineral oil): 1710 (CO) $cm^{-1}$; NMR (water-*d*): δ 1.79 (broad s, 3H, 3-$CH_3$), 2.58 (m, 1H, 1-H), 2.82 (m, 2H, 5-$H_2$), 3.20 [s, 9H, $^+N(CH_3)_3$], 3.52 (m, 2H, 1-$CH_2$), and 7.40 (m, 1H, 2-H) ppm.

*Anal.*—Calc. for $C_{10}H_{18}INO$: C, 40.49; H, 6.15; N, 4.74. Found: C, 40.77; H, 6.27; N, 4.88.

***trans*-3-Methyl-4-hydroxy-1-(*N,N*-dimethylaminomethyl)cyclopent-2-ene (IX*b*)**—*Method A*—Compound IX*b* was obtained starting from X (1.1 g) following the procedure described for VII and was purified by column chromatography with chloroform–petroleum ether–methanol–concentrated ammonium hydroxide (250:150:50:5) as the eluting system. The first fraction was the starting material (0.2 g). The second fraction was IX*a* (0.12 g). The third fraction was IX*b* (0.35 g); IR (chloroform): 3380 (bonded OH) and 3600 (free OH) $cm^{-1}$; NMR (chloroform-*d*): δ 1.79 (broad s, 3H, 3-$CH_3$), 1.84 (t, 2H, 5-$H_2$), 2.06–2.45 (m, 1H, 1-H), 2.21 [s, 6H, $N(CH_3)_2$], 2.86 (s, 1H, 4-OH), 2.96 (m, 2H, 1-$CH_2$), 4.59 (t, 1H, 4-H), and 5.42 (m, 1H, 2-H) ppm.

*Anal.*—Calc. for $C_9H_{17}NO$: C, 69.63; H, 11.04; N, 9.02. Found: C, 69.57; H, 10.96; N, 9.13.

*Method B*—Compound IX*b* was also synthesized starting from VIII*b* (0.09 g) by the procedure described for IX*a*; 0.059 g of nearly pure oil was obtained and was used without further purification.

***trans*-2,3-Dehydrodeoxamuscarine (I*b*)**—Compound I*b* was obtained starting from IX*b* by the procedure described for I*a* and was recrystallized from anhydrous ethanol–ether (85% yield), mp 151–152°; IR (mineral oil): 3410 (OH) $cm^{-1}$; NMR (water-*d*): δ 1.76 (s, 3H, 3-$CH_3$), 2.13 (t, 2H, 4-$H_2$), 3.13 [s, 9H, $^+N(CH_3)_3$], 2.66–3.66 (m, 3H, 1-H and 1-$CH_2$), 4.69 (t, 1H, 4-H), and 5.56 (m, 1H, 2-H) ppm.

*Anal.*—Calc. for $C_{10}H_{20}INO$: C, 40.42; H, 6.78; N, 4.71. Found: C, 40.39; H, 6.95; N, 4.75.

***cis*-3-Methyl-4-hydroxy-1-hydroxymethylcyclopent-2-ene (XI*a*)**—A solution of VII*a* (1.14 g, 7.3 mmoles) in anhydrous tetrahydrofuran (20 ml) was added to a stirred and cooled (0°) suspension of aluminum lithium hydride (0.34 g, 8.9 mmoles) in anhydrous tetrahydrofuran (20 ml). The suspension then was heated to reflux for 48 hr and worked up as described for IX*a* to give an oil, which was used without further purification (0.93 g); IR (liquid film): 3320 (OH) $cm^{-1}$; NMR (chloroform-*d*): δ 1.0–2.6 (m, 3H, 5-$H_2$ and 1-H), 1.79 (s, 3H, 3-$CH_3$), 3.3–4.5 (m, 3H, 1-$CH_2$ and 4-H), 3.26 (s, 2H, OH), and 5.50 (broad s, 1H, 2-H) ppm.

***trans*-3-Methyl-4-hydroxy-1-hydroxymethylcyclopent-2-ene (XI*b*)**—Compound XI*b* was obtained in an 85% yield starting from VII*b* by the procedure described for XI*a*; IR (liquid film): 3300 (OH) $cm^{-1}$; NMR (chloroform-*d*): δ 1.0–2.3 (m, 3H, 5-$H_2$ and 1-H), 1.86 (s, 3H, 3-$CH_3$), 3.3–4.3 (m, 3H, 1-$CH_2$ and 4-H), 3.59 (s, 2H, OH), and 5.56 (m, 1H, 2-H) ppm.

***cis*-3-Methyl-4-hydroxy-1-methyl-*p*-toluenesulfonatecyclopent-2-ene (XII*a*)**—*p*-Toluenesulfonyl chloride (1.42 g) was added portionwise to a stirred and cooled (0°) solution of XI*a* (0.97 g) in anhydrous pyridine (10 ml). The mixture was kept 4 days at room temperature and then acidified with 2 *N* HCl and extracted with methylene chloride. The organic layer was washed with a saturated sodium bicarbonate solution and then evaporated at room temperature to give a nearly pure oil (0.47 g), which was used without further purification; NMR (chloroform-*d*): δ 1.65 (broad s, 3H, 3-$CH_3$), 1.40–2.30 (m, 2H, 5-$H_2$), 2.30–3.00 (m, 1H, 1-H), 2.38 (s, 3H, aromatic $CH_3$), 3.78 (d, 2H, 1-$CH_2$), 4.12 (m, 2H, OH and 4-H), 5.12 (m, 1H, 2-H), and 7.38 (q, 4H, aromatic H) ppm. The compound has to be stored at low temperature because of its tendency to polymerize.

***trans*-3-Methyl-4-hydroxy-1-methyl-*p*-toluenesulfonatecyclopent-2-ene (XII*b*)**—Compound XII*b* was obtained starting from XI*b* (0.31 g) as described for XII*a* (0.17 g); NMR (chloroform-*d*): δ 1.65 (broad s, 3H, 3-$CH_3$), 1.40–2.10 (m, 2H, 5-$H_2$), 2.38 (s, 3H, aromatic $CH_3$), 2.92 (m, 1H, 1-H), 3.62 (s, 1H, 4-OH), 3.68 (d, 2H, 1-$CH_2$), 4.35 (t, 1H, 4-H), and 5.10 (s, 1H, 2-H) ppm. It has to be stored at low temperature.

***cis*-3-Methyl-4-hydroxycyclopent-2-ene-1-carboxylic Acid (XV*a*)**—Compound VII*a* (1.64 g) was dissolved in 2 *N* NaOH (5 ml) and heated at 70° for 10 min. After cooling, the solution was washed with chloroform, acidified with 2 *N* HCl and then extracted with chloroform to give a white solid. This solid was recrystallized (0.97 g) from benzene, mp 69–71°; IR (mineral oil): 1685 (C=O), 2460, and 3340 (OH) $cm^{-1}$; NMR (chloroform-*d*): δ 1.82 (d, 3H, 3-$CH_3$), 1.70–2.70 (m, 2H, 5-$H_2$), 3.38 (m, 1H, 1-H), 4.43 (dd, 1H, 4-H), 5.48 (broad s, 1H, 2-H), and 7.20 (s, 2H, OH) ppm.

*Anal.*—Calc. for $C_7H_{10}O_3$: C, 59.56; H, 6.43. Found: C, 59.44; H, 6.51.

The same reaction on VII*b* gave a sticky oil, which could not be re-

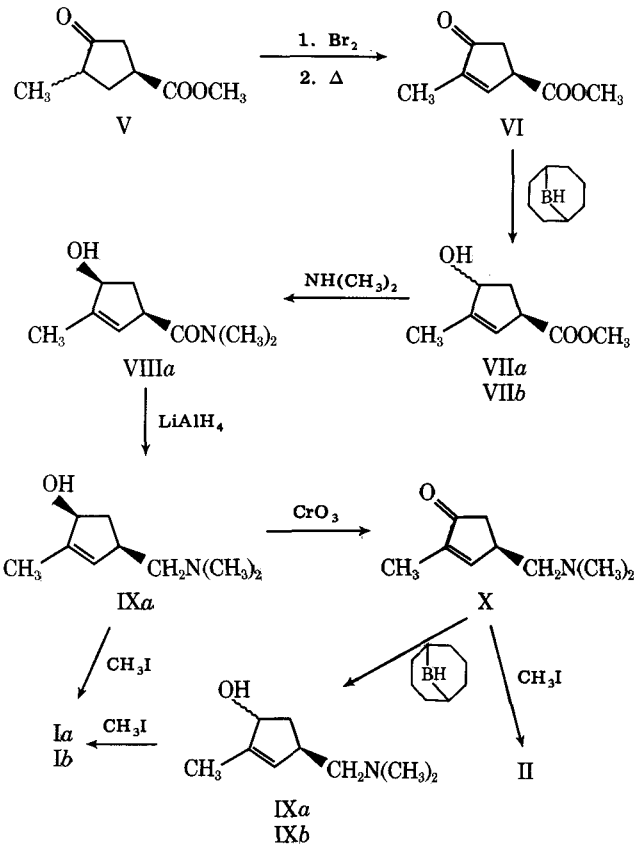

*Scheme I*

crystallized and which was possibly a mixture of the two isomeric acids.

**3-Methyl-4-oxo-1-(*N,N*-dimethylcarboxamido)cyclopent-2-ene (XIV)**—Bromine (4 ml, 78.0 mmoles) in carbon tetrachloride (50 ml) was added to a solution of XIII (6) (13 g, 77.0 mmoles) in carbon tetrachloride (100 ml) at room temperature under vigorous stirring. After the reaction started, the addition was continued with cooling at 0°. The solvent then was evaporated to give a solid, which was treated with a saturated sodium bicarbonate solution (100 ml) and extracted with chloroform. Removal of solvent gave an oil, which was distilled to give 5.23 g of XIV, bp 137–140°/0.25 mm. Much of XIV decomposed to a gummy product during the distillation; IR (liquid film): 1640 and 1700 (CO) $cm^{-1}$; NMR (chloroform-*d*): δ 1.78 (broad s, 3H, 3-$CH_3$), 2.60 (m, 2H, 5-$H_2$), 2.98 (s, 3H, $NCH_3$), 3.18 (s, 3H, $NCH_3$), 2.80–3.50 (m, 1H, 1-H), 4.00 (m, 1H, 1-H), and 7.20 (m, 1H, 2-H) ppm.

*Anal.*—Calc. for $C_9H_{13}NO_2$: C, 64.65; H, 7.84; N, 8.38. Found: C, 64.81; H, 7.70; N, 8.24.

***trans*-3-Methyl-4-hydroxy-1-(*N,N*-dimethylcarboxamido)cyclopent-2-ene (VIII*b*)**—Compound VIII*b* was obtained starting from XIV (0.83 g) by the procedure described for VII and was purified by column chromatography with chloroform–ethyl acetate–ethanol (90:5:5) as the eluting system. The first fraction was VIII*a* (0.35 g). The second fraction was VIII*b* (0.09 g); IR (chloroform): 1620 (CO), 3370 (bonded OH), and 3600 (free OH) $cm^{-1}$; NMR (chloroform-*d*): δ 1.80 (d, 3H, 3-$CH_3$), 1.60–2.80 (m, 2H, 5-$H_2$), 2.88 (s, 3H, $NCH_3$), 3.08 (s, 3H, $NCH_3$), 3.30–4.10 (m, 2H, 1-H and OH), 4.70 (t, 1H, 4-H), and 5.38 (s, 1H, 2-H) ppm.

*Anal.*—Calc. for $C_9H_{15}NO_2$: C, 63.88; H, 8.94; N, 8.28. Found: C, 64.03; H, 8.70; N, 8.41.

**Pharmacological Testing**—Testing was accomplished using guinea pig ileum and frog rectus abdominis preparations according to the protocol described previously (8).

## RESULTS AND DISCUSSION

**Chemistry**—Compounds I*a*, I*b*, and II were synthesized according to Scheme I. The introduction of the double bond in V (6) went smoothly and only at position 2, as revealed by NMR spectra. The reduction of the carbonyl group was eventually achieved with 9-borabicyclo[3.3.1]nonane (9) since other common reducing agents gave saturation of the double bond through a 1,4-addition to the enone system (7, 10). The reaction of either VII*a* or VII*b*, separated by column chromatography, with dimethylamine in a sealed tube at 80° invariably gave the *cis*-isomer (VIII*a*) through isomerization, possibly at C-1 (11, 12). The reduction of VIII*a* with aluminum lithium hydride followed by the reaction of IX*a* with methyl iodide gave I*a*. The *trans*-isomer (I*b*) was obtained through the oxidation of IX*a* to X followed by reduction with 9-borabicyclo-[3.3.1]nonane to yield IX as a *cis–trans* mixture, which was separated by column chromatography and the final reaction of IX*b* with methyl iodide. Compound II was easily obtained from X through the reaction with methyl iodide.

Scheme II shows some pathways that were explored to obtain the two isomers of I in a simpler way. In a first attempt, VII*a* and VII*b* were reduced to the corresponding alcohols (XI*a* and XI*b*) followed by reaction with *p*-toluenesulfonyl chloride to give a selective tosylation of primary hydroxyl groups. Unfortunately, both XII*a* and XII*b* are difficult to handle since they decompose quickly into dark solids showing no double bond. The hydrolysis of VII*a* and VII*b* was unsatisfactory with acids. In one case (VII*a*), 2 *N* NaOH afforded the *cis* acid (XV*a*); in the other case (VII*b*), a *cis–trans* mixture of XV was obtained. Finally, the reduction of amide XIV, obtained in poor yield from XIII (6), afforded VIII*a* and only traces of the *trans*-isomer (VIII*b*), which were separated by column chromatography.

**Identification of Compounds**—The structures of VI and XIV were established by NMR spectra, which showed a broad singlet for the methyl group at position 3 (δ 1.70 and 1.78, respectively), thus proving the double bond at position 2.

The attribution of structures to VII*a*, VII*b*, VIII*a*, and VIII*b* depended mainly on IR spectra at different dilutions, which showed a nearly constant ratio between the intensity of free and bonded hydroxy absorption for the *cis*-isomers (VII*a* and VIII*a*). The *trans*-isomers (VII*b* and VIII*b*) presented a strong variation of the same ratio upon dilution. NMR spectra confirmed this attribution since the proton at position 4 of VII*b* [δ 4.62 (t)] and VIII*b* [δ 4.70 (t)] was more deshielded than the corre-

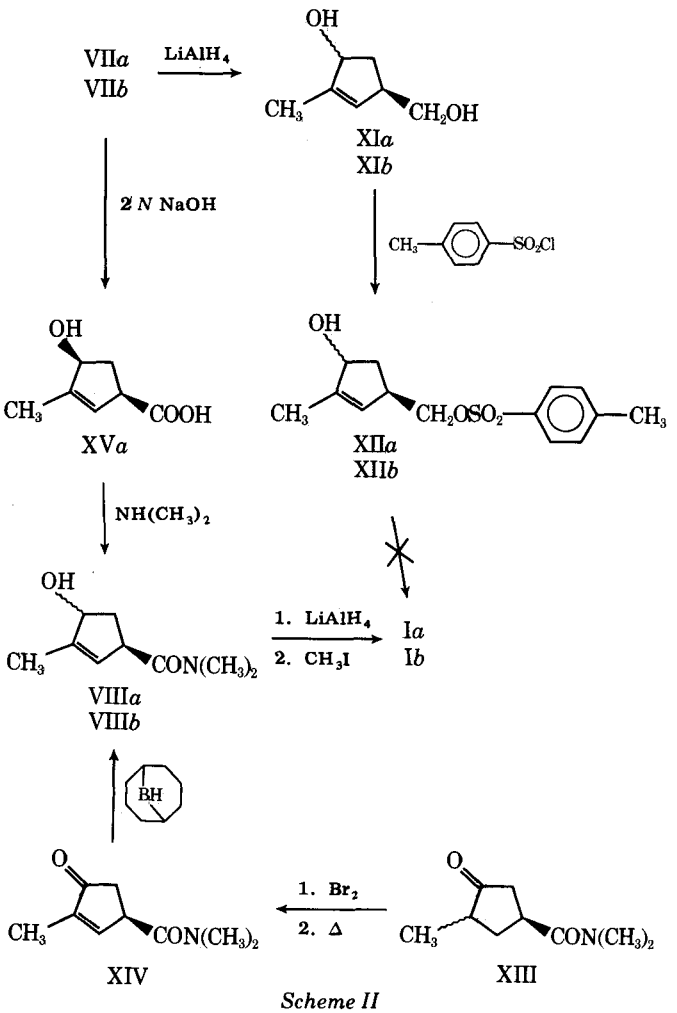

*Scheme II*

**Table I—Comparative Biological Activity on Guinea Pig Terminal Ileum and Frog Rectus Abdominis [a]**

| Compound | EPMR[b] Guinea Pig Ileum[c] | EPMR[b] Frog Rectus Abdominis[d] | $EPMR_N/EPMR_M$[e] |
|---|---|---|---|
| Ia | 1000 | 94 | 0.1 |
| Ib | 50 | >500 | >10 |
| II | 5.85 | 0.66 | 0.1 |
| III | 26.6[f] | 3.1[f] | 0.1 |

[a] The choice, performance, and evaluation of the bioassay were described in detail in Ref. 8. [b] EPMR = equipotent molar ratios between $ED_{50}$ of compound and $ED_{50}$ of acetylcholine calculated through the regression of the angular transformate of the fractional effects *versus* the log concentrations of the agonists. The statistical significance of the EPMR averages was estimated by the $t$ test at the $p \leq 0.05$ level. Experiments were repeated at least four times. The standard error of the mean $ED_{50}$ values for the compounds was <10%. [c] The $ED_{50}$ value of acetylcholine = $3.2 \times 10^{-7}$ $M$. [d] The $ED_{50}$ value of acetylcholine = $2.58 \times 10^{-5}$ $M$. [e] Ratio between frog rectus abdominis (N) and guinea pig ileum (M) EPMR values. [f] Data from Ref. 5.

sponding proton of VII*a* [δ 4.38 (dd)] and VIII*a* [δ 4.25 (dd)], owing to the anisotropic effect of the groups at position 1. In the *cis* series, the proton at position 4 appeared as a double doublet; in the *trans* series, it was a triplet. This difference allowed a safe identification of the derivatives of VII and VIII. Accordingly, XV shows a *cis* structure.

**Pharmacology**—The cholinergic activities of I*a*, I*b*, and II on guinea pig ileum and frog rectus abdominis preparations are listed in Table I together with those of III (5). Introduction of the carbonyl group in III to give II improved both muscarinic and nicotinic activities. The specificity of II, as far as muscarinic activity is concerned as revealed by the $EPMR_N/EPMR_M$ ratio, remained low; its activity was 10 times lower than that of the corresponding muscarones but nearly equivalent to that of deoxamuscarone (11). The influence of the double bond, which imposed a planar configuration to the methyl group at position 2, did not seem to be relevant in this case. The difference of activity between *cis*- and *trans*-muscarone is practically insignificant (1).

The introduction of a hydroxyl group had a totally different effect. With I*a*, there was a drop of two orders of magnitude in both muscarinic and nicotinic activities. In fact, muscarinic activity was nearly lost while nicotinic activity fell dramatically and the specificity remained low. With I*b*, there was a small drop in muscarinic activity, but the specificity was greatly increased since nicotinic activity was practically absent. Compound I*b* had a pattern of activity fairly similar to that of muscarine. Moreover, since I*b* was also less active than deoxamuscarine as a muscarinic agent, the planar configuration of the methyl group seems to be of some relevance in this case, unlike the corresponding carbonyl compound (II). Introduction of the hydrophilic hydroxyl group dramatically changed the biological profile of the molecule, giving further support to the hypothesis of Triggle and Triggle (2). The same conclusions were reached by Barlow (13) who evaluated the consequences of the introduction of a hydroxyl group in a series of alkyltrimethylammonium compounds. In any case, the hydroxyl group that drives away the molecule from the unpolar binding site has to be oriented properly to allow interaction with the polar binding site.

The similarity of the pattern of activity of II, III, muscarones, and deoxamuscarone suggests that such compounds act at the same binding site, which seems to be quite different from where I*b*, muscarine, and deoxamuscarine interact. This difference is further stressed by different stereochemical requirements of the site interacting with the methyl group. It is known that the enantiomers of muscarine show high stereospecificity toward the muscarinic receptor. Should I*b* interact with the same muscarine binding site (as was previously suggested), the prediction that the chiral effects of the two enantiomers of I*b* would manifest themselves could be made.

It also is well known that the stereospecificity of muscarone is fairly different from that of muscarine qualitatively and quantitatively. Various rationalizations have been advanced; one of these implies a different site of action for muscarone (14). The results reported herein, while adding further evidence to the hypothesis of Belleau and Puranen (14), suggest the intriguing possibility that the accessory unpolar area (2) might incorporate the site of action of muscarone (14). Work is in progress to test this hypothesis.

## REFERENCES


(1) F. Gualtieri, P. Angeli, M. Giannella, C. Melchiorre, and M. Pigini, in "Recent Advances in Receptor Chemistry," F. Gualtieri, M. Giannella, and C. Melchiorre, Eds., Elsevier/North-Holland Biomedical Press, Amsterdam, The Netherlands, 1979, pp. 267–279.

(2) D. J. Triggle and C. R. Triggle, "Chemical Pharmacology of the Synapse," Academic, London, England, 1976, chap. 3.

(3) C. Melchiorre, F. Gualtieri, M. Giannella, M. Pigini, M. L. Cingolani, G. Gamba, P. Pigini, L. Re, and L. Rossini, *Farmaco, Ed. Sci.*, **31**, 218 (1976).

(4) P. Angeli, C. Melchiorre, M. Giannella, and M. Pigini, *J. Med. Chem.*, **20**, 398 (1977).

(5) M. Giannella, M. Leonelli, and M. Pigini, *Farmaco, Ed. Sci.*, **35**, 263 (1980).

(6) F. Gualtieri, M. Giannella, C. Melchiorre, and M. Pigini, *J. Med. Chem.*, **17**, 455 (1974).

(7) H. C. Brown and M. M. Hess, *J. Org. Chem.*, **34**, 2206 (1969).

(8) F. Gualtieri, M. Giannella, C. Melchiorre, M. Pigini, M. L. Cingolani, G. Gamba, P. Pigini, and L. Rossini, *Farmaco, Ed. Sci.*, **30**, 223 (1975).

(9) S. Krishnammuty and H. C. Brown, *J. Org. Chem.*, **40**, 1865 (1975).

(10) M. R. Johnson and B. Rickborn, *ibid.*, **35**, 1041 (1970).

(11) C. Melchiorre, F. Gualtieri, M. Giannella, M. Pigini, M. L. Cingolani, G. Gamba, P. Pigini, and L. Rossini, *Farmaco, Ed. Sci.*, **30**, 287 (1975).

(12) C. Melchiorre, M. Giannella, D. Giardinà, and F. Gualtieri, *Synth. Commun.*, **5**, 95 (1975).

(13) R. B. Barlow, *J. Pharm. Pharmacol.*, **30**, 703 (1978).

(14) B. Belleau and J. Puranen, *J. Med. Chem.*, **6**, 325 (1963).


## ACKNOWLEDGMENTS


Supported in part by the Italian National Research Council, Rome, Italy.

The authors thank Professor F. Gualtieri for valuable discussions and suggestions and Mr. A. Biondi, Mr. M. Brandi, and Mr. F. Lupidi for technical assistance.

# Estimation of Protein and Drug Adsorption onto Silicone-Coated Glass Surfaces

TAKAHARU MIZUTANI

Received May 15, 1980, from the *Faculty of Pharmaceutical Sciences, Nagoya City University, Mizuho-ku, Nagoya 467, Japan.* Accepted for publication October 14, 1980.

**Abstract** □ Porous glass coated with silicone adsorbed proteins such as albumin, globulin, hemoglobin, lysozyme, and peroxidase in pH 7.2 phosphate-buffered saline in the amount of 33–53 mg of protein/g of glass (39.4 $m^2$/g of glass). These proteins were not adsorbed from distilled water (except peroxidase). The amounts of albumin adsorbed onto coated glass from several buffers at ionic strength >0.05 $\mu$ were similar to amounts adsorbed from saline, despite the difference in salts and pH. The enzymes adsorbed onto coated glass were stable for at least 1 month. Drugs such as insulin, atropine sulfate, physostigmine salicylate, and epinephrine were adsorbed onto the coated glass in the amounts of 28, 0.32, 1.53, and 0.01 mg/g of glass, respectively. The adsorption of pharmaceutical biologicals composed of proteins such as hormones and vaccines onto silicone-coated glass containers must be recognized and compensated for, particularly at low concentrations. Protein adsorption onto coated glass might be caused by hydrophobic interaction.

**Keyphrases** □ Adsorption—proteins, drugs onto silicone-coated glass □ Silicone-coated glass surfaces—adsorption of drugs and proteins □ Proteins—adsorption onto silicone-coated glass surfaces □ Glass containers—adsorption of proteins onto silicone-coated surfaces

Uncoated porous glass was developed for exclusion chromatography (1). Glass with a large surface area is useful for the accurate estimation of drugs and proteins adsorbed onto glass surfaces (2). From the maximum amount of protein adsorbed (233 mg/97 $m^2$), the amounts of protein drugs adsorbed onto a glass container with a 20-ml capacity were estimated to be >12 $\mu$g (2). After adsorption onto uncoated glass surfaces for a long time, protein activity decreased (3).

Glass surfaces are anionic, and 1 g of glass (97 $m^2$) adsorbs 5 $\mu$moles of cationic drugs, such as atropine and physostigmine, and other biological components (4). Insulin also was adsorbed onto glass surfaces from a pH 2.6 isotonic glycerin solution (2). Serum globulin was adsorbed to a greater extent than albumin; antibodies (IgG and IgM) are also well adsorbed onto glass from physiological saline (5).

Pharmaceutical glass containers generally are coated with silicone to prevent drug adsorption and inactivation during storage. Surfaces coated with silicone can repulse a water layer and thus decrease adsorption. However, silicone-coated glass has been shown to adsorb the hormone secretin, although albumin blocks secretin adsorption (6). Adsorption of albumin and cells such as platelets and leucocytes onto silicone-coated glass also was reported (7–9). The USP (10) and the JP (11) do not provide standards for silicone coating, and the properties of the glass surfaces coated with silicone are not defined. The purpose of this investigation was to estimate drug and protein adsorption onto silicone-coated glass surfaces.

## EXPERIMENTAL

**Methods**—Adsorption of proteins and other substances was studied using silicone-coated porous glass packed in columns. Silicone-coated porous glass floats on water because of the repulsion between water and silicone, making an accurate estimation of adsorption impossible. Therefore, silicone-coated glass was precipitated as follows.

The controlled porous glass[1], composed of 100-$\mu$m particles with a pore diameter of 240 Å, was suspended in a chromic acid mixture. The glass then was packed in a column and washed thoroughly with distilled water to neutrality. The beads were dried at 180° in an evaporating dish, and 1 g of the dried beads was added to 3 ml of carbon tetrachloride containing 200 mg of silicone[2] (dimethylpolysiloxane). After evaporation of carbon tetrachloride, the glass was heated at 300° for 10 min to enhance a tight coating with silicone. The surface area of the silicone-coated glass measured 39.4 $m^2$/g of glass using equipment[3] with nitrogen gas.

The porous glass coated with silicone was precipitated in 0.05 *M* phosphate (pH 7.3) by using a detergent, 0.7% sodium lauryl sulfate, and the precipitate was packed in columns (12). Precipitation was caused by the loss of repulsion between water and silicone, because the glass surfaces were coated with sulfate residues of lauryl sulfate, which were bound to silicone residues by hydrophobic bonding. After washing with ~100 column volumes of hot water, lauryl sulfate residues on the glass were completely removed. The complete removal was confirmed by passing a 0.2% $BaCl_2$ solution through the column (13). Frontal analysis was used to estimate the amount of sample adsorbed onto silicone-coated glass (14). Sample solutions were loaded at a flow rate of 1.5 ml/min/$cm^2$ at room temperature. The column size was 0.6 × 4.0 cm.

**Materials**—The proteins used were bovine serum albumin[4], egg lysozyme[5], horseradish peroxidase[5], bovine hemoglobin[5], and bovine serum globulin prepared from bovine serum by fractional precipitation with ammonium sulfate. These proteins were dissolved at a concentration of 1 mg/ml in distilled water or pH 7.2 phosphate-buffered saline composed of 0.137 *M* NaCl, 2.7 m*M* KCl, and 9.5 m*M* phosphate. Other active enzymes were alkaline phosphatase[6] from *Escherichia coli* and malate dehydrogenase[7].

The drugs used were insulin[8], atropine sulfate[9], epinephrine[10], and physostigmine salicylate[11]. Insulin was dissolved in pH 2.6 isotonic glycerin solution, and epinephrine was dissolved in saline containing 0.01 *N* HCl. Atropine and physostigmine were dissolved in pH 7.2 phosphate-buffered saline. Amino acids[12], glucose, and nucleic acid components[5] were commercial reagents. The concentrations of proteins and nucleic acid components were determined by absorbance measurements at 280 and 260 nm, respectively. The amino acid concentrations were determined by the color reaction with ninhydrin.

## RESULTS AND DISCUSSION

**Protein Adsorption**—Figure 1 shows the patterns of protein adsorption onto silicone-coated glass columns (0.6 × 4 cm, 0.5 g). In phosphate-buffered saline, proteins were well adsorbed onto the glass; the amounts of albumin, globulin, lysozyme, hemoglobin, and peroxidase adsorbed onto 1 g (39.4 $m^2$) of the glass were 42 mg (0.64 $\mu$mole), 53 mg (0.3 $\mu$mole), 38 mg (2.7 $\mu$moles), 47 mg (0.73 $\mu$mole), and 33 mg (0.83 $\mu$mole), respectively. From these values, the amount of proteins adsorbed onto silicone-coated surfaces of a glass container (50 $cm^2$ of surface area, 20-ml capacity) and a glass injector was estimated to be >7 $\mu$g. The 7-$\mu$g/20-ml concentration must have been a minimum point not significantly affected by adsorption onto silicone-coated glass surfaces.

[1] CPG-10, Electro-Nucleonics, Fairfield, N.J.
[2] KF 96, Shin-Etsu Chemicals, Tokyo, Japan.
[3] Orr surface-area pore-volume analyzer model 2100D, Micromeritics Instrument Corp., Norcross, Ga.
[4] Miles Laboratories, Elkhart, Ind.
[5] Sigma Chemical Co., St. Louis, Mo.
[6] P-L Biochemical Inc., Milwaukee, Wis.
[7] Boehringer GmbH, Mannheim, West Germany.
[8] Fluka AG, Buchs, Switzerland.
[9] Wako Pure Chemicals Ltd., Osaka, Japan.
[10] Katayama Chemicals, Osaka, Japan.
[11] E. Merck AG, Darmstadt, West Germany.
[12] Ajinomoto Co. Inc., Kawasaki, Japan.

0022-3549/81/0500-0493$01.00/0
© 1981, American Pharmaceutical Association

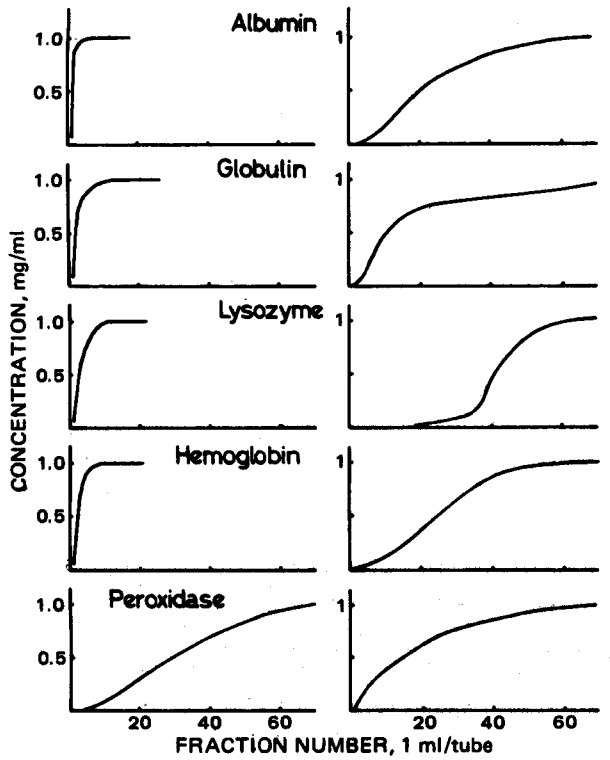


**Figure 1**—*Adsorption patterns of protein (1 mg/ml) from distilled-water medium (left) and phosphate-buffered saline (PBS) (right) on the silicone-coated porous glass column (0.6 × 4 cm, 0.5 g). Proteins are the same in both sides of the figure.*

One example of a protein solution being used at a low concentration is the purified protein derivative of tuberculin, which is used at 0.5 μg/ml in phosphate-buffered saline. Therefore, the adsorption of pharmaceutical biologicals composed of proteins such as hormones and vaccines onto silicone-coated glass must be recognized and compensated for, particularly at low concentrations and when an accurate dose of an injection is required.

The amounts adsorbed onto silicone-coated glass (83–133 mg/100 $m^2$ of glass) were similar to those (100–200 mg/100 $m^2$) of protein adsorbed onto noncoated glass in a distilled water medium. The value (133 mg/100 $m^2$) of bovine serum globulin was slightly higher than that (83 mg/100 $m^2$) for noncoated glass (5). Thus, the antibody in antiserum also is well adsorbed onto silicone-coated glass surfaces, and this adsorption must be seriously considered upon storage of purified antiserum in pharmaceutical glass containers coated with silicone.

In distilled water, the amounts of albumin, globulin, lysozyme, and hemoglobin adsorbed were 1.2, 2.7, 1.7, and 2.4 mg/g of glass, respectively. These values were lower than those in phosphate-buffered saline (Fig. 1). The discrepancy in protein affinities for the coated glass in phosphate-buffered saline and in distilled water must have been due to the ionic environment in the solution. The peroxidase from horseradish adsorbed well onto silicone-coated glass in water (62 mg/g of glass). This adsorption of peroxidase onto coated glass contrasts to that onto noncoated glass; peroxidase adsorption in distilled water onto coated glass was the strongest, but on noncoated glass, it was the weakest among the proteins examined.

This phenomenon might be explained by the difference in bonding between proteins and glass. On noncoated glass, proteins are adsorbed mainly by amine–silanol bonding and a cooperative aggregative force between silica and proteins. On coated glass, proteins must be adsorbed mainly by hydrophobic bonding between aliphatic residues on proteins and silicone residues on coated glass. This hypothesis is supported partly by the observation that some proteins adsorbed onto noncoated porous glass were eluted with several different buffers, while proteins adsorbed onto the coated glass were not unless detergents such as sodium lauryl sulfate were added to the elution buffers.

The difference in the strength of adsorption onto silicone-coated glass was examined next by using protein mixtures in phosphate-buffered saline. In the top section of Fig. 2, the absorbance at 403 nm shows the elution of peroxidase; the absorbance at 280 nm was due to total proteins (peroxidase plus albumin). The ratio of $A_{280}$ to $A_{403}$ was 0.6 at the 20th

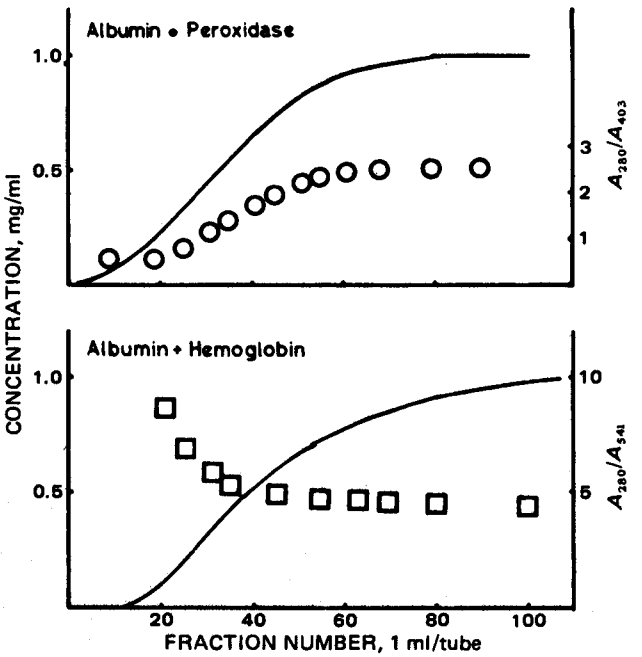


**Figure 2**—*Adsorption patterns of mixtures on silicone-coated glass columns in pH 7.2 phosphate-buffered saline. The upper profile is for a mixture of bovine serum albumin (0.5 mg/ml) and horseradish peroxidase (0.5 mg/ml); the lower profile is for a mixture of albumin (0.5 mg/ml) and hemoglobin (0.5 mg/ml). Key:* ○, *ratio of* $A_{280}$ *to* $A_{403}$; *and* □, *ratio of* $A_{280}$ *to* $A_{541}$.

tube and increased to 2.3 at the 60th tube, which is identical to that of the original mixture. This result indicates that peroxidase was adsorbed more weakly onto coated glass surfaces than was albumin.

The absorbance at 541 nm shown at the bottom of Fig. 2 represents hemoglobin. The ratio (8.6) of $A_{280}$ to $A_{541}$ at the 21st tube indicates that hemoglobin adsorption was stronger than that of albumin. Thus, various proteins have different affinities for silicone-coated glass surfaces, and the affinities of three proteins onto the coated glass are in the order of hemoglobin > albumin > peroxidase. This order parallels the aliphatic amino acid content (44% in hemoglobin, 36% in albumin, and 31% in peroxidase) and is independent of molecular weight.

These results suggest that the protein adsorption onto silicone-coated glass was caused at least partially by hydrophobic interaction. These results also suggest that prevention of adsorption of hormones or vaccines by the addition of nonactive proteins such as albumin should depend on the ratio of those drugs to the adduct and on the difference in the affinities of the proteins to the coated glass.

**Adsorption Properties of Proteins**—Figure 3 shows albumin adsorption patterns (isoelectric point 4.7) in 0.1 *M* citrate buffer at pH 3.0

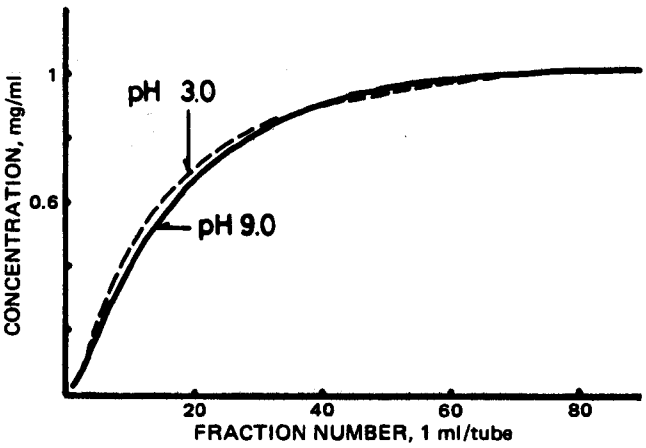


**Figure 3**—*Adsorption patterns of bovine serum albumin on the coated glass column at pH 3.0 and 9.0 with buffers of 0.1* M *sodium citrate and 0.5* M *tris(hydroxymethyl)aminomethane hydrochloride, respectively.*

**Table I—Amounts of Bovine Serum Albumin Adsorbed onto Silicone-Coated Porous Glass in Buffers**

| Buffer | Ionic Strength, $\mu$ | pH | Amount, mg/g (39.4 $m^2$ of the glass) |
|---|---|---|---|
| Distilled water | 0 | — | 1.2 |
| Phosphate-buffered saline | 0.16 | 7.2 | 42 |
| 0.1 *M* Citrate | 0.20 | 3.0 | 32 |
| 0.5 *M* Tris(hydroxymethyl)-aminomethane hydrochloride | 0.05 | 9.0 | 31 |
| 0.01 *M* Phosphate | 0.026 | 7.3 | 1.0 |
| 0.5 *M* Phosphate | 1.3 | 7.3 | 32 |
| 0.01 *M* Phosphate + 0.05 *M* NaCl | 0.076 | 7.3 | 20 |
| 0.01 *M* Phosphate + 2 *M* NaCl | 2.026 | 7.3 | 43 |
| 0.1 *M* Tris(hydroxymethyl)-aminomethane hydrochloride | 0.09 | 7.6 | 41 |
| 0.1 *M* Acetate | 0.1 | 7.0 | 19 |
| 0.5 *M* Acetate | 0.45 | 5.6 | 36 |
| 0.2 *M* Glycine | 0.01 | 8.0 | 2.4 |
| 0.5 *M* Glycine | 0.1 | 9.0 | 28 |
| 20% Sucrose | — | — | 10 |

and in 0.5 *M* tris(hydroxymethyl)aminomethane hydrochloride at pH 9.0. The albumin adsorption pattern at pH 7.2 is shown in Fig. 1. At these three pH points, the patterns were similar, indicating that pH did not affect protein adsorption onto silicone-coated glass. Thus, the adsorption is not caused by ionic bonding, even though protein adsorption onto noncoated glass is caused partially by ionic bonding (2).

Table I shows the amounts of bovine serum albumin adsorbed onto silicone-coated glass in various buffers. Albumin was well adsorbed (from 20 to 43 mg/g) onto the glass in phosphate, acetate, glycine, and tris(hydroxymethyl)aminomethane hydrochloride buffers at ionic strengths higher than 0.05 $\mu$. However, only 1–2.4 mg of albumin/g was adsorbed from buffers at ionic strengths of <0.026 $\mu$. Thus, ionic strength is an important factor for protein adsorption onto coated glass; the marginal ionic strength for albumin was ~0.02–0.05 $\mu$. Meanwhile, a small amount of albumin was adsorbed at high concentrations (20%) of nonionic substances such as sucrose. Glycine buffer prevented protein adsorption onto noncoated glass (15) but did not interfere with adsorption onto silicone-coated glass. These results also demonstrate that protein adsorption onto coated and noncoated glass is different.

The amounts of amino acids and other biological components adsorbed onto coated glass are shown in Table II. The values were low, 0.03–0.7 $\mu$mole/g (6–60 $\mu$g/g). The values for lysine, nucleic acid components, and glucose were small (0.03–0.08 $\mu$mole/g, the minimum values to be measured accurately under these conditions). Some hydrophobic amino acids such as isoleucine, methionine, and phenylalanine were adsorbed in the amounts of 0.3–0.7 $\mu$mole/g (39.4 $m^2$); these values were similar to those of proteins (0.3–2.7 $\mu$moles/g) in Fig. 1. Some amino acids were adsorbed in distilled water, even though those proteins in Fig. 1 (except peroxidase) were not adsorbed in water.

**Drug Adsorption**—The adsorption patterns of some drugs on silicone-coated glass are shown in Fig. 4. Insulin adsorbed well (71 mg/100 $m^2$) onto the glass in pH 2.6 isotonic glycerin solution; this value was

**Table II—Amounts of Biological Components Adsorbed onto Silicone-Coated Glass in pH 7.2 Phosphate-Buffered Saline**

| Sample | Amount on Silicone-Coated Glass, $\mu$mole/g | $\mu$g/g |
|---|---|---|
| Lysine | 0.04 | 7 |
| Aspartic acid | 0.39 | 52 |
| Isoleucine | 0.38 (0.16)[a] | 50 |
| Methionine | 0.24 | 36 |
| Serine | 0.76 | 80 |
| Asparagine | 0.36 | 48 |
| Tryptophan | 0.08 (0.02)[a] | 16 |
| Tyrosine | 0.16 (0.26)[a] | 29 |
| Phenylalanine | 0.36 (0.18)[a] | 59 |
| Adenosine | 0.18 | 47 |
| Cytidine | 0.04 | 9.6 |
| Guanosine | 0.07 | 20 |
| Uridine | 0.06 | 15 |
| 5′-Adenylic acid | 0.08 | 29 |
| Crude tRNA | 0.05[b] | 15 |
| Glucose | 0.03 | 5.4 |

[a] Values in a distilled water medium. [b] Value of phosphate.

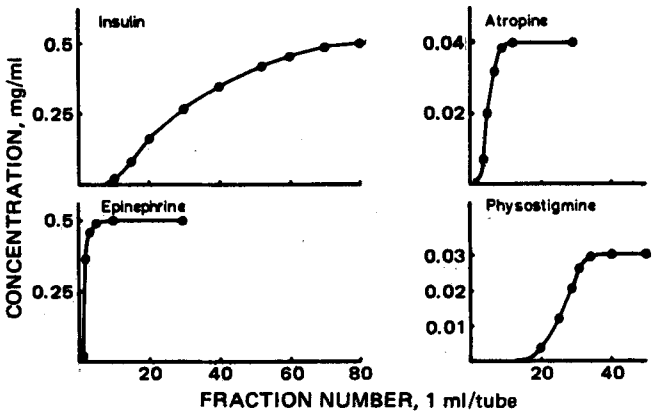


**Figure 4**—*Adsorption patterns of drugs on columns of the silicone-coated porous glass. The concentrations of insulin and epinephrine were measured by absorbance at 280 nm. Atropine and physostigmine concentrations were measured at 220 and 260 nm, respectively. The column size was 0.6 × 4 cm. Insulin was dissolved in pH 2.6 isotonic glycerin solution, epinephrine was dissolved in saline containing 0.01* N *HCl, and atropine sulfate and physostigmine salicylate were dissolved in pH 7.2 phosphate-buffered saline.*

similar to the values in Fig. 1 but was higher than the value (6.14 mg/100 $m^2$) on noncoated glass (2). In phosphate-buffered saline, the values for atropine and physostigmine were 0.81 and 3.88 mg/100 $m^2$, respectively, about five times higher than the amounts on noncoated glass in saline.

Very little epinephrine was adsorbed (<0.02 mg/100 $m^2$) onto silicone-coated glass. The amount of insulin adsorbed onto the surface of a coated glass container (50 $cm^2$, 20 ml) was 0.085 U. This value was relatively low compared to the usual dosage, although an accurate dosage should be influenced by this adsorption. The values for atropine and physostigmine adsorbed onto the surface of a coated glass container were very low (60–200 ng).

**Stability of Adsorbed Proteins**—The stability of enzymes adsorbed onto silicone-coated glass was studied using alkaline phosphatase, malate dehydrogenase, and horseradish peroxidase. After these enzymes were adsorbed onto the coated glass column, the solutions containing substrates, such as *p*-nitrophenylphosphate for phosphatase, $\beta$-nicotinamide-adenine dinucleotide in the reduced form for dehydrogenase, and guaiacol hydrogen peroxide for peroxidase, were loaded on the columns and the absorbance of the eluates was measured.

The alkaline phosphatase activities after adsorption for 1 week and 1 month were 98 and 96%, respectively, of the value obtained on the 1st day. The malate dehydrogenase activities after adsorption for 1 week and 1 month were 97 and 89%, respectively, under the same conditions. Peroxidase retained full activity after being adsorbed onto the column for 1 month. The activities of phosphatase in free and in bound forms were

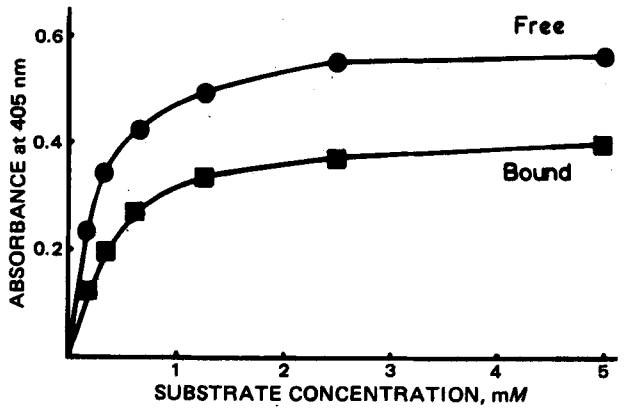


**Figure 5**—*Substrate concentration curve of alkaline phosphatase immobilized on the silicone-coated glass and in free solution. The reaction mixtures of 3 ml in 1* M *tris(hydroxymethyl)aminomethane hydrochloride (pH 8.6) contained substrate and 25 $\mu$g of free or bound enzyme on 1 ml of coated glass. The reaction was carried out at room temperature; the absorbance at 405 nm was measured after incubation for 30 sec in both cases. The substrate was* p*-nitrophenyl phosphate. Key: ●, free solution; and ■, enzyme immobilized on the glass.*

compared as a function of substrate concentration (Fig. 5). The activity of bound enzyme was determined by mixing with the substrate solution for 30 sec, using a mechanical mixer, and measuring the absorbance of the supernate after standing for 10 sec. The maximum velocity of the immobilized enzyme was slightly lower than that of the free enzyme, but the $K_m$ values were similar. These properties did not vary on adsorption for 1 week. Hence, the surfaces of silicone-coated glass may be useful as a support for the enzymes to be immobilized, but the surfaces of noncoated glass are not appropriate for this purpose (3).

With the noncoated glass in the column, the top portion of the glass turned milky white after albumin solution was applied whereas no color change was observed when coated glass was used. Albumin might have precipitated on the noncoated glass but was well adsorbed onto the coated glass. The difference in the adsorption forces between amine–silanol ionic bonding and hydrophobic interaction might have caused this difference.

**Adsorption on Synthetic Polymers**—Synthetic polymers such as polyethylene and polyethylmethacrylate are useful for pharmaceutical containers. However, polyethylene was shown to adsorb 155 mg of human serum albumin/100 $m^2$ of polyethylene surface (16). Hemoglobin also is adsorbed onto polyethylene (17). Polyethylmethacrylate and polyhydroxyethylmethacrylate adsorb plasma proteins such as hemoglobin, albumin, fibrinogen, and $\gamma$-globulin (18). Polystyrene adsorbs human serum albumin, ribonuclease, and muscle proteins (19, 20). The reported amounts of proteins adsorbed onto synthetic polymers are comparable to those adsorbed onto coated and noncoated glass, although the mechanisms of protein adsorption onto synthetic polymers and glass must be different.

Pharmaceutical preparations composed of proteins such as hormones and vaccines adsorb onto the surfaces of their containers. This adsorption is particularly significant at low protein concentrations since at least 7 $\mu$g of protein is adsorbed by the surface of a 20-ml glass container. Thus, it is important to compensate for this adsorption when dispensing low doses of such substances.

## REFERENCES


(1) W. Haller, *Nature*, **206**, 693 (1965).

(2) T. Mizutani and A. Mizutani, *J. Pharm. Sci.*, **67**, 1102 (1978).

(3) T. Mizutani, *ibid.*, **69**, 279 (1980).

(4) T. Mizutani and A. Mizutani, *Anal. Biochem.*, **83**, 216 (1977).

(5) T. Mizutani, *J. Pharm. Sci.*, **69**, 1226 (1980).

(6) J. Ogino, K. Noguchi, and K. Terato, *Chem. Pharm. Bull.*, **27**, 3160 (1979).

(7) J. L. Brash, *Ann. N.Y. Acad. Sci.*, **283**, 356 (1977).

(8) M. A. Packham, G. Evans, M. F. Glynn, and J. F. Mustard, *J. Lab. Clin. Med.*, **73**, 686 (1969).

(9) K. Shortman, N. Williams, H. Jackson, P. Russell, P. Byrt, and E. Diener, *J. Cell. Biol.*, **48**, 566 (1971).

(10) "The United States Pharmacopeia," 19th rev., Mack Publishing Co., Easton, Pa., 1975, pp. 642–647.

(11) "The Japan Pharmacopoeia," 9th ed., Hirokawa Shoten, Tokyo, Japan, 1976, pp. 665–667.

(12) T. Mizutani, *J. Chromatogr.*, **196**, 485 (1980).

(13) T. Mizutani and A. Mizutani, *J. Non-Cryst. Solids*, **27**, 437 (1978).

(14) N. I. Nakano, T. Oshio, Y. Fujimoto, and T. Amiya, *J. Pharm. Sci.*, **67**, 1005 (1978).

(15) T. Mizutani and A. Mizutani, *J. Chromatogr.*, **111**, 214 (1975).

(16) E. Brynda, M. Houska, Z. Pokorná, N. A. Cepalova, Yu. V. Moiseev, and J. Kálal, *J. Bioeng.*, **2**, 411 (1978).

(17) T. A. Horbett, P. K. Weatherby, and A. S. Hoffman, *ibid.*, **1**, 61 (1977).

(18) T. A. Horbett, P. K. Weatherby, and A. S. Hoffman, *Thromb. Res.*, **12**, 319 (1978).

(19) W. Norde and J. Lyklema, *J. Colloid Interface Sci.*, **66**, 257 (1978).

(20) S. Puszkin and E. Rubin, *Arch. Biochem. Biophys.*, **177**, 574 (1976).


## ACKNOWLEDGMENTS


The author thanks Dr. A. Otsuka and Dr. K. Danjo of Meijo University for the measurement of the silicone-coated porous glass surface area, Mr. R. Hiramatsu for an invaluable suggestion, and Dr. H. Okuyama for manuscript revision.


# Synthesis of Tetracycline Ring A Analogs


**R. E. MOSKALYK ˣ, A. L. C. MAK, L. G. CHATTEN, and R. A. LOCOCK**



Received July 29, 1980, from the *Faculty of Pharmacy and Pharmaceutical Sciences, University of Alberta, Edmonton, Alberta, Canada T6G 2N8.* Accepted for publication October 16, 1980



**Abstract** □ Studies directed at the synthesis of tetracycline ring A analogs are described. 4-Carbethoxycyclohexane-1,3-dione was converted to the ethyl urethan dispiro[1,3-dioxolane-2,2′-cyclohexane-4′,2″(1,3)-dioxolane]-1′-carbamic acid ethyl ester *via* the dispiro[1,3-dioxolane-2,2′-cyclohexane-4′,2″(1,3)-dioxolane]-1′-carboxylic acid hydrazide. An improved synthesis of another cyclohexenone from methyl vinyl ketone and ethyl nitroacetate is reported. Reaction of *N*-(3-hydroxy-1-oxo-2-cyclohexen-4-yl)benzamide with $\alpha$-chloroacetyl isocyanate afforded a 4(5*H*)-oxazolone derivative, as did the identical reaction on 5,5-dimethyl-1,3-cyclohexanedione (dimedone). This reaction provides a novel approach to these oxazolones with potential therapeutic importance. Other ring A analogs were synthesized also.



**Keyphrases** □ Tetracycline—synthesis of ring A analogs □ 4(5*H*)-Oxazolones—tetracycline ring A analogs, synthesis □ Analogs—tetracycline ring A analogs, synthesis


Following a study of the mechanism of the polarographic reduction of tetracycline compounds (1), the need arose for simpler analogs encompassing some or all structural features of ring A of the tetracyclines. A literature search, followed by some preliminary attempts at duplicating one synthetic approach, revealed that a ready access to these compounds had not been published.

Smissman *et al.* (2) attempted, without success, to prepare ring A analogs by cyclizing appropriate alicyclic molecules. Muxfeldt *et al.* (3) prepared several ring A analogs by the condensation of unsaturated oxazolones with active methylene compounds. Compound I was obtained, which could be hydrolyzed and decarboxylated to give II. Alternatively, treatment of I with Meerwein's reagent afforded III (Scheme I).

A different approach was reported (4, 5) for preparing ring A analogs, involving catalytic hydrogenation of substituted resorcinols to yield the corresponding 1,3-cyclohexanedione derivatives. All efforts at duplicating this synthesis were unsuccessful. Several reported approaches




*0022-3549/81/0500-0496$01.00/0*


*© 1981, American Pharmaceutical Association*

compared as a function of substrate concentration (Fig. 5). The activity of bound enzyme was determined by mixing with the substrate solution for 30 sec, using a mechanical mixer, and measuring the absorbance of the supernate after standing for 10 sec. The maximum velocity of the immobilized enzyme was slightly lower than that of the free enzyme, but the $K_m$ values were similar. These properties did not vary on adsorption for 1 week. Hence, the surfaces of silicone-coated glass may be useful as a support for the enzymes to be immobilized, but the surfaces of noncoated glass are not appropriate for this purpose (3).

With the noncoated glass in the column, the top portion of the glass turned milky white after albumin solution was applied whereas no color change was observed when coated glass was used. Albumin might have precipitated on the noncoated glass but was well adsorbed onto the coated glass. The difference in the adsorption forces between amine–silanol ionic bonding and hydrophobic interaction might have caused this difference.

**Adsorption on Synthetic Polymers**—Synthetic polymers such as polyethylene and polyethylmethacrylate are useful for pharmaceutical containers. However, polyethylene was shown to adsorb 155 mg of human serum albumin/100 $m^2$ of polyethylene surface (16). Hemoglobin also is adsorbed onto polyethylene (17). Polyethylmethacrylate and polyhydroxyethylmethacrylate adsorb plasma proteins such as hemoglobin, albumin, fibrinogen, and $\gamma$-globulin (18). Polystyrene adsorbs human serum albumin, ribonuclease, and muscle proteins (19, 20). The reported amounts of proteins adsorbed onto synthetic polymers are comparable to those adsorbed onto coated and noncoated glass, although the mechanisms of protein adsorption onto synthetic polymers and glass must be different.

Pharmaceutical preparations composed of proteins such as hormones and vaccines adsorb onto the surfaces of their containers. This adsorption is particularly significant at low protein concentrations since at least 7 $\mu$g of protein is adsorbed by the surface of a 20-ml glass container. Thus, it is important to compensate for this adsorption when dispensing low doses of such substances.

## REFERENCES


(1) W. Haller, *Nature*, **206**, 693 (1965).

(2) T. Mizutani and A. Mizutani, *J. Pharm. Sci.*, **67**, 1102 (1978).

(3) T. Mizutani, *ibid.*, **69**, 279 (1980).

(4) T. Mizutani and A. Mizutani, *Anal. Biochem.*, **83**, 216 (1977).

(5) T. Mizutani, *J. Pharm. Sci.*, **69**, 1226 (1980).

(6) J. Ogino, K. Noguchi, and K. Terato, *Chem. Pharm. Bull.*, **27**, 3160 (1979).

(7) J. L. Brash, *Ann. N.Y. Acad. Sci.*, **283**, 356 (1977).

(8) M. A. Packham, G. Evans, M. F. Glynn, and J. F. Mustard, *J. Lab. Clin. Med.*, **73**, 686 (1969).

(9) K. Shortman, N. Williams, H. Jackson, P. Russell, P. Byrt, and E. Diener, *J. Cell. Biol.*, **48**, 566 (1971).

(10) "The United States Pharmacopeia," 19th rev., Mack Publishing Co., Easton, Pa., 1975, pp. 642–647.

(11) "The Japan Pharmacopoeia," 9th ed., Hirokawa Shoten, Tokyo, Japan, 1976, pp. 665–667.

(12) T. Mizutani, *J. Chromatogr.*, **196**, 485 (1980).

(13) T. Mizutani and A. Mizutani, *J. Non-Cryst. Solids*, **27**, 437 (1978).

(14) N. I. Nakano, T. Oshio, Y. Fujimoto, and T. Amiya, *J. Pharm. Sci.*, **67**, 1005 (1978).

(15) T. Mizutani and A. Mizutani, *J. Chromatogr.*, **111**, 214 (1975).

(16) E. Brynda, M. Houska, Z. Pokorná, N. A. Cepalova, Yu. V. Moiseev, and J. Kálal, *J. Bioeng.*, **2**, 411 (1978).

(17) T. A. Horbett, P. K. Weatherby, and A. S. Hoffman, *ibid.*, **1**, 61 (1977).

(18) T. A. Horbett, P. K. Weatherby, and A. S. Hoffman, *Thromb. Res.*, **12**, 319 (1978).

(19) W. Norde and J. Lyklema, *J. Colloid Interface Sci.*, **66**, 257 (1978).

(20) S. Puszkin and E. Rubin, *Arch. Biochem. Biophys.*, **177**, 574 (1976).


## ACKNOWLEDGMENTS


The author thanks Dr. A. Otsuka and Dr. K. Danjo of Meijo University for the measurement of the silicone-coated porous glass surface area, Mr. R. Hiramatsu for an invaluable suggestion, and Dr. H. Okuyama for manuscript revision.


# Synthesis of Tetracycline Ring A Analogs


**R. E. MOSKALYK ˣ, A. L. C. MAK, L. G. CHATTEN, and R. A. LOCOCK**



Received July 29, 1980, from the *Faculty of Pharmacy and Pharmaceutical Sciences, University of Alberta, Edmonton, Alberta, Canada T6G 2N8.* Accepted for publication October 16, 1980



**Abstract** □ Studies directed at the synthesis of tetracycline ring A analogs are described. 4-Carbethoxycyclohexane-1,3-dione was converted to the ethyl urethan dispiro[1,3-dioxolane-2,2′-cyclohexane-4′,2″(1,3)-dioxolane]-1′-carbamic acid ethyl ester *via* the dispiro[1,3-dioxolane-2,2′-cyclohexane-4′,2″(1,3)-dioxolane]-1′-carboxylic acid hydrazide. An improved synthesis of another cyclohexenone from methyl vinyl ketone and ethyl nitroacetate is reported. Reaction of *N*-(3-hydroxy-1-oxo-2-cyclohexen-4-yl)benzamide with $\alpha$-chloroacetyl isocyanate afforded a 4(5*H*)-oxazolone derivative, as did the identical reaction on 5,5-dimethyl-1,3-cyclohexanedione (dimedone). This reaction provides a novel approach to these oxazolones with potential therapeutic importance. Other ring A analogs were synthesized also.



**Keyphrases** □ Tetracycline—synthesis of ring A analogs □ 4(5*H*)-Oxazolones—tetracycline ring A analogs, synthesis □ Analogs—tetracycline ring A analogs, synthesis


Following a study of the mechanism of the polarographic reduction of tetracycline compounds (1), the need arose for simpler analogs encompassing some or all structural features of ring A of the tetracyclines. A literature search, followed by some preliminary attempts at duplicating one synthetic approach, revealed that a ready access to these compounds had not been published.

Smissman *et al.* (2) attempted, without success, to prepare ring A analogs by cyclizing appropriate alicyclic molecules. Muxfeldt *et al.* (3) prepared several ring A analogs by the condensation of unsaturated oxazolones with active methylene compounds. Compound I was obtained, which could be hydrolyzed and decarboxylated to give II. Alternatively, treatment of I with Meerwein's reagent afforded III (Scheme I).

A different approach was reported (4, 5) for preparing ring A analogs, involving catalytic hydrogenation of substituted resorcinols to yield the corresponding 1,3-cyclohexanedione derivatives. All efforts at duplicating this synthesis were unsuccessful. Several reported approaches




*0022-3549/81/0500-0496$01.00/0*


*© 1981, American Pharmaceutical Association*

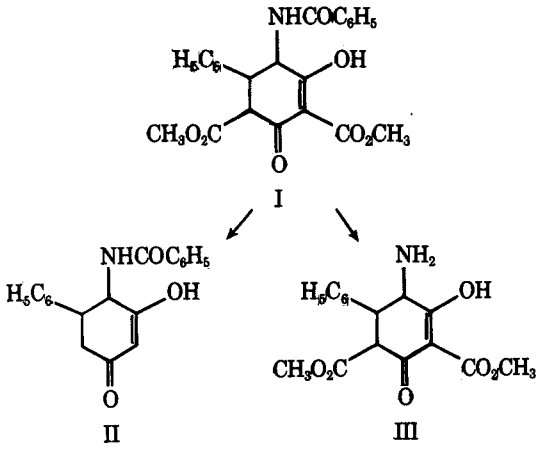

*Scheme I*

lead to two-ring compounds that include some features of the B as well as the A ring of the tetracyclines (6, 7).

This paper reports the results from studies directed at synthesizing some ring A analogs of the tetracyclines.

## RESULTS AND DISCUSSION

The initial synthetic approach to the ring A analogs started with the previously reported 4-carbethoxycyclohexane-1,3-dione (V) (8). This compound was prepared by cyclization of the keto ester (IV), using sodium hydride in anhydrous benzene to effect the cyclization. Spencer *et al.* (8) employed sodium ethoxide in ethanol as the cyclizing agent and obtained variable yields. The enol ether (VI) often was isolated as the major product, arising presumably from the further reaction of ethoxide ion on the cyclized product. An interesting feature of the NMR spectrum of V was the two overlapping triplet–quartet ethyl systems separated by $\delta$ <0.1. This observation is consistent with proton tautomerism as depicted in Scheme II.

Ketalization of V was carried out in the usual manner in ethylene glycol and benzene with a catalytic amount of *p*-toluenesulfonic acid to give VII. Crude VII was used without further purification and was treated with hydrazine hydrate to form the hydrazide derivative (VIII). The hydrazide was converted to the ethyl urethan (IX) en route to its conversion to the amine. Difficulty was encountered with the attempted hydrolysis of the urethan; invariably, the $\beta$-dicarbonyl system was destroyed under the conditions necessary to effect hydrolysis. Since an alternative entry to the amino group seemed promising, further attempts at hydrolysis of the urethan were discontinued.

In the alternative route, the amino function was introduced at C-4 by catalytic hydrogenation of the intermediate nitro compound, affording the key intermediate (XIV) (Scheme III). Ethyl nitroacetate (XI) was prepared by the method of Rodionov *et al.* (9). Addition of this active methylene compound to the activated double bond in methyl vinyl ketone (X) was accomplished in good yield using tributyl phosphine as the cat-

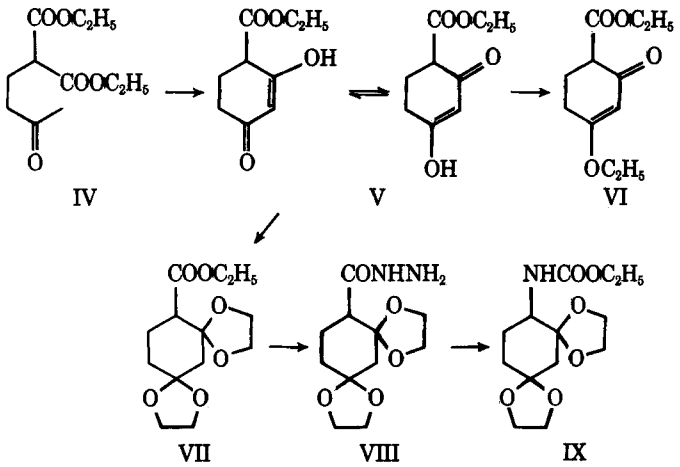

*Scheme II*

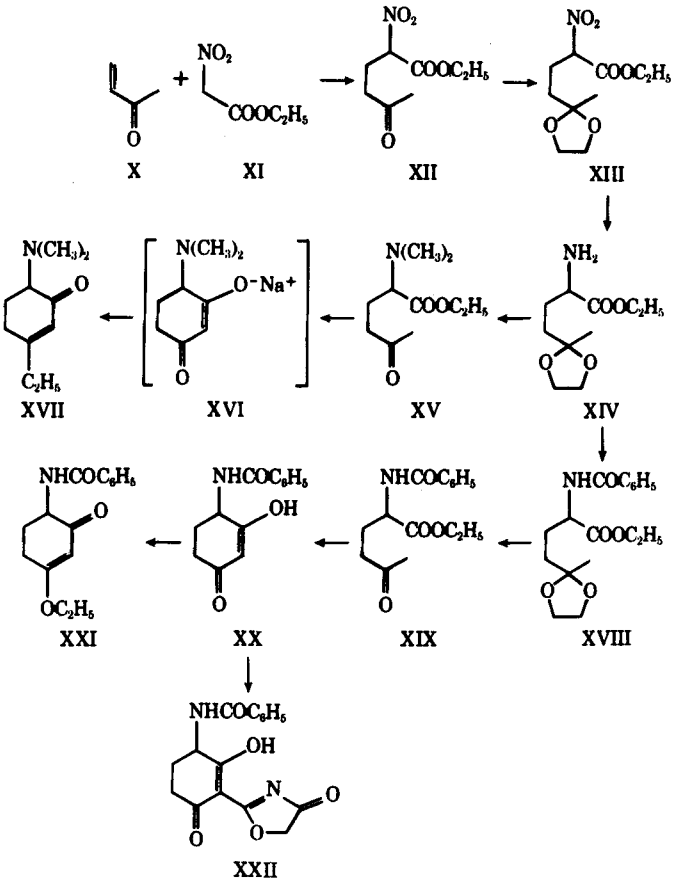

*Scheme III*

alyst. Protection of the carbonyl group by ketal formation was followed by reduction with 10% palladium-on-charcoal at 1000–1500 psi. The amine (XIV) could be reductively alkylated in excellent yield by treatment with excess formaldehyde and hydrogen at 40 psi using the same catalyst. The ketal protective group was removed in the usual manner by acid hydrolysis, and the compound was characterized as ketone XV.

When cyclization of XV was attempted with sodium hydride in anhydrous benzene, an amorphous precipitate was obtained after 10 hr of refluxing. This precipitate was the sodium salt of 3-hydroxy-4-dimethylamino-2-cyclohexen-1-one (XVI). Attempts to isolate the free acid by adding dilute hydrochloric acid, adjusting the pH to 8–9, and extracting with ether failed. At this point, the aqueous solution was made acidic (pH 2) and evaporated to dryness *in vacuo*. The resultant mass was extracted with absolute ethanol and, after workup, afforded XVII.

The problems encountered in attempting to isolate the free acid of XVI appeared to be associated with its amphoteric nature. Therefore, another approach was tried involving conversion of the basic amino moiety to a neutral species, followed by cyclization and subsequent removal of the protective group. The benzoylamino group was chosen since conditions for its hydrolysis have been well documented (10–12). The amino ketal ester (XIV) was converted to the benzoylamino derivative (XVIII) by treatment with benzoyl chloride. Acid hydrolysis at room temperature afforded XIX. Crude XIX was cyclized to XX with sodium hydride in anhydrous benzene. Compound XX had been prepared previously by another synthetic route (4).

Attempted removal of the benzoyl protective group by the procedure described by Muxfeldt *et al.* (13) gave XXI. The isolation of this *O*-alkylated product was in agreement with experiments conducted by Durckheimer (14), who employed the same reagent to effect etherification at position 1 (or 3) of some tetracyclines. Since all compounds studied by Muxfeldt *et al.* (13) contained a substituent at C-2, further attempts at removing the protective group were postponed until a substituent could be introduced at C-2.

Carboxamidation experiments with potassium cyanate failed to yield any products capable of being isolated. Since acetyl isocyanate is difficult to prepare, it was decided to try the more readily accessible $\alpha$-chloroacetyl isocyanate (15). Initial experiments with the sodium enolate of 5,5-dimethyl-1,3-cyclohexanedione (dimedone) (XXIII) (Scheme IV) gave

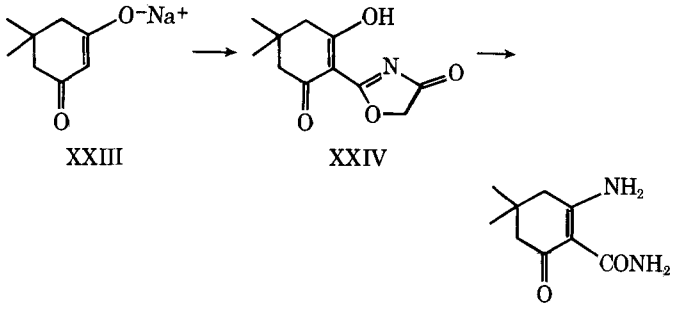


XXIII XXIV XXV

*Scheme IV*

the unexpected product XXIV. Compound XXIV exhibited UV behavior that was characteristic of enolic β-diketones. In basic solution, a bathochromic shift and a hyperchromic (16) effect were observed, which could be reverted by neutralization with acids. This compound contained the 4(5*H*)-oxazolone system, the spectral properties of which were reported previously (17). This reaction represents a novel approach to the synthesis of 4(5*H*)-oxazolones, which potentially are of therapeutic importance. Interest in this class of compounds has grown recently, particularly in the 2-amino derivatives; they have found use as tranquilizers, antidepressants, memory aids, and appetite suppressants (18). The antibiotic indolmycin contains the 4(5*H*)-oxazolone system (19).

Since the 4(5*H*)-oxazolone ring system in XXIV is strained (carbonyl absorption is at 1770 $cm^{-1}$), it was thought that it might collapse under rather mild conditions. Hence, treatment of XXIV with saturated ammonia in methanol at room temperature gave what appeared to be XXV. The high-resolution mass spectrum was consistent with this structure. The only perplexing feature preventing a conclusive structural assignment was the four-proton methylene singlet at δ 2.4 in the NMR spectrum. There was no evidence of any resolution in deuteroacetic acid, deuterochloroform, deuteropyridine, or deuterotrifluoroacetic acid. When α-chloroacetyl isocyanate was allowed to react with XX, the 4(5*H*)-oxazolone (XXII) was obtained.

## EXPERIMENTAL[1]

Melting points[2] and boiling points are uncorrected. IR spectra[3] were recorded as thin films or as potassium bromide disks. UV spectra[4] were taken as solutions in ethanol. NMR spectra[5] were taken in deuterated solvents from commercial sources with tetramethylsilane as the internal standard. Mass spectra[6] were determined using the direct-probe technique.

**Dispiro[1,3-dioxolane-2,2′-cyclohexane-4′,2″(1,3)-dioxolane]-1′-carboxylic Acid Ethyl Ester (VII)**—A stirred mixture of V (18.5 g, 0.1 mole), benzene (250 ml), ethylene glycol (100 g, 1.6 moles), and *p*-toluenesulfonic acid (0.5 g) was heated to reflux for 2 days in a round-bottom flask fitted with a Dean–Stark water separator. The benzene layer was separated, and the glycol layer was extracted with ether (3 × 40 ml). The benzene and ether extracts were combined and washed with 10% sodium carbonate followed by water. The organic layer was dried and evaporated to dryness under reduced pressure (20.3 g, 74%). An analytical sample was obtained through TLC [benzene–ethanol (9:1), silica gel]; $n_D^{24.4}$ 1.4826; IR (neat): 2980, 2790, 1730 (ester carbonyl), 1450, 1370, 1180, 1080, 1030, 950, and 825 $cm^{-1}$; NMR ($CDCl_3$): δ 1.30 (t, 3H, $J$ = 6–7 Hz, $OCH_2CH_3$), 1.5–3.1 (m, 7H, cyclohexane ring protons), and 4.0–4.4 [m, 10H, $OCH_2CH_3$ and $2(OCH_2CH_2O)$].

*Anal.*—Calc. for $C_{13}H_{20}O_6$: C, 57.34; H, 7.40. Found: C, 57.77; H, 7.46.

**Dispiro[1,3-dioxolane-2,2′-cyclohexane-4′2″(1,3)-dioxolane]-1′-carboxylic Acid Hydrazide (VIII)**—Hydrazine hydrate (40 ml, 0.6 mole) in anhydrous ethanol (20 ml) was stirred magnetically and heated to reflux. The diketal ester (VII) (27.2 g, 0.1 mole) in anhydrous ethanol (20 ml) was added dropwise over 0.5 hr. The solution was refluxed for 30 hr, the ethanol was removed at reduced pressure, and the remaining solution was evaporated to dryness *in vacuo*. The residual oil was dried in a vacuum desiccator for 2 days and then triturated with anhydrous ethanol to give 25 g of the crude product.

Recrystallization from ethanol afforded VIII, mp 115–116°; IR (KBr): 3400, 3300, 3200 (N–H), 1670 (amide carbonyl), 1510 (N–H binding), 1370, 1210, 1150, 1090, 1070, 1060, 1040, 950, 830, 800, and 740 $cm^{-1}$; NMR ($CDCl_3$): δ 1.6–2.2 (m, 6H, $3CH_2$), 2.52 [t, 1H, $J$ = 6 Hz, O=C(NHNH$_2$)C*H*], 3.68 (broad s, 2H, O=CNHN$H_2$), 3.93 [d, 8H, $J$ = 3 Hz, $2(OCH_2CH_2O)$], and 7.64 (broad s, 1H, O=CN*H*NH$_2$); mass spectrum: parent ion $m/z$ 258.1214 (53.8%) (calc. for $C_{11}H_{18}NO_3$: 258.1211), 259 (7.2), 199 (13.7), 172 (26.1), 141 (50.8), 113 (49.1), 99 (98.7), 87 (63.4), 86 (45.8), 69 (26.1), and 55 (100).

**Dispiro[1,3-dioxolane-2,2′-cyclohexane-4′,2″(1,3)-dioxolane]-1′-carbamic Acid Ethyl Ester (IX)**—The hydrazide (VIII) (2.2 g, 8.5 mmoles), dissolved in 6 *N* HCl (3 ml), 5% acetic acid (5 ml), and ether (25 ml), was chilled to 0–5° and stirred magnetically. A solution of sodium nitrite (0.6 g in 1 ml of water, 8.5 mmoles) then was added at such a rate that the temperature did not rise above 10°. After addition was complete, the ether layer was separated and the aqueous solution was extracted four times with ether. The combined extract was washed twice with a saturated sodium bicarbonate solution and twice with water, dried, and filtered. To the filtrate was added an excess of anhydrous ethanol. The ether was removed by distillation, and the resultant ethanolic solution was refluxed for 4 hr.

The ethanol was evaporated under reduced pressure, and the viscous liquid residue solidified on cooling (1.85 g, 75%). Recrystallization from chloroform afforded IX, mp 124°; IR (KBR): 3340 (N–H stretching), 2980, 2790, 1720 (urethan carbonyl), 1545, 1330, 1250, 1150, 1080, 1060, 1030, 950, and 830 $cm^{-1}$; NMR ($CDCl_3$): δ 1.26 (t, 3H, $J$ = 7 Hz, $OCH_2CH_3$), 3.7–4.3 [m, 10H, $2(OCH_2CH_2O)$ and $OCH_2CH_3$], and 4.8 [broad s, 1H, N*H*($CO_2C_2H_5$)]; mass spectrum: $m/z$ 288 (0.6%), 287 (1.5), 201 (63.9), 187 (14.1), 173 (26.4), 159 (27.2), 157 (73.3), 100 (29.2), 99 (54.1), 87 (70.7), 86 (100), 73 (33.5), 57 (31.7), and 55 (27.7).

*Anal.*—Calc. for $C_{13}H_{21}NO_6$: C, 54.34; H, 7.36; N, 4.81. Found: C, 53.99; H, 7.28; N, 4.92.

**2-Nitro-5-oxohexanoic Acid Ethyl Ester (XII)**—To a stirred solution of ethyl nitroacetate (XI) (13.3 g, 0.1 mole) and methyl vinyl ketone (X) (7 g, 0.1 mole) in tetrahydrofuran (50 ml) at room temperature was added dropwise a catalytic amount of tributyl phosphine. The heat evolved was sufficient to bring the solution to a gentle reflux. After the solution had returned to room temperature (~2 hr), methyl iodide was added to remove the phosphine. Direct distillation yielded XII (16 g, 78%), bp 134–138°/3.5 mm; $n_D^{23.2}$ 1.4473; IR (neat): 2980, 2960, 2940, 2910, 2870, 1750, 1720, 1560 (nitro stretching), 1370, 1260, 1170, 1020, and 860 $cm^{-1}$; NMR ($CDCl_3$): δ 1.28 (t, 3H, $J$ = 7 Hz, $OCH_2CH_3$), 2.14 (s, 3H, $COCH_3$), 4.25 (q, 2H, $J$ = 7 Hz, $OCH_2CH_3$), and 5.26 [t, 1H, $CH(NO_2)CO_2C_2H_5$].

*Anal.*—Calc. for $C_8H_{13}NO_5$: C, 47.28; H, 6.44; N, 6.89. Found: C, 47.23; H, 6.40; N, 6.81.

**2-Methyl-2-(α-nitrobutanoic acid)-1,3-dioxolane Ethyl Ester (XIII)**—A stirred mixture of XII (15 g, 74 mmoles) in benzene (160 ml), ethylene glycol (100 ml), and *p*-toluenesulfonic acid (0.5 g) was heated to reflux under a Dean–Stark trap for 24 hr. The mixture was extracted with ether (3 × 80 ml) and washed once with 10% sodium bicarbonate and once with water. The ether was dried, filtered, and evaporated *in vacuo*. The resulting liquid was slowly and carefully vacuum distilled to yield a pale-yellow liquid (12 g, 68%), bp 112–116°/2 mm; $n_D^{20.0}$ 1.4547; IR (neat): 2980, 2960, 2930, 2880, 1750, 1560 (nitro stretching), 1450, 1375, 1260, 1060, 1040, 950, and 860 $cm^{-1}$; NMR ($CDCl_3$): δ 1.33 (t, 6H, $J$ = 7 Hz, terminal methyl and $OCH_2CH_3$), 3.96 (s, 4H, $OCH_2CH_2O$), 4.3 (q, 2H, $OCH_2CH_3$), and 5.28 [t, 1H, $J$ = 7 Hz, $CH(NO_2)CO_2C_2H_5$]; mass spectrum ($M^+ - CH_3$): 232.0820 (14.9%) (calc. for $C_{10}H_{17}NO_6 - CH_3$: 232.0820), 99 (14.8), 87 (100), and 86 (24.3).

*Anal.*—Calc. for $C_{10}H_{17}NO_6$: C, 48.58; H, 6.93; N, 5.67. Found: C, 49.64; H, 7.10; N, 5.78.

**2-(α-Aminobutanoic acid)-2-methyl-1,3-dioxolane Ethyl Ester (XIV)**—Compound XIII (20.3 g, 85 mmoles) was mixed with 5 g of 10% palladium-on-charcoal in 95% ethanol (150 ml). Hydrogenation was carried out under 1500 psi at 50° for 10 hr. The catalyst was filtered, and the solvent was removed by evaporation. The liquid residue was dissolved in benzene, dried, and finally evaporated to give an oily liquid (17 g, 93%), which solidified on standing after a few days at room temperature. An analytic sample had a melting point of 212–214° dec.; IR (KBr): 3200, 3080, 3030 (N–H stretching), 2980, 2880, 1670, 1450, 1380, 1330, 1250, 1220, 1140, 1065, 1050, 950, and 870 $cm^{-1}$; NMR ($CDCl_3$): δ 1.0–1.5 (m, 6H, terminal methyl and $OCH_2CH_3$), 2.25 [s, 2H, $CH(NH_2)CO_2C_2H_5$], 3.90 (s, 4H, $OCH_2CH_2O$), and 4.17 (q, 2H, $J$ = 7 Hz, $OCH_2CH_3$).

*Anal.*—Calc. for $C_{10}H_{19}NO_4$: C, 55.28; H, 8.81; N, 6.44. Found: C, 55.27;

[1] Microanalyses were performed by the Microanalytical Laboratory, Chemistry Department, University of Alberta.
[2] Thomas-Hoover capillary apparatus.
[3] Unicam SP1000 or Perkin-Elmer model 267 grating IR spectrophotometer.
[4] Unicam SP1800 UV spectrophotometer.
[5] Varian A-60 or EM-360 60-MHz spectrometer.
[6] AEI MS-12 or MS-50 mass spectrometer.

H, 8.80; N, 6.32.

**2-Dimethylamino-5-oxohexanoic Acid Ethyl Ester (XV)**—Compound XIV (2.17 g, 10 mmoles) in 95% ethanol (60 ml) was hydrogenated at 40 psi over 10% palladium-on-charcoal with an excess of formaldehyde (37% solution) for 5 hr. The catalyst was filtered, and the solution was evaporated under reduced pressure. The residue was hydrolyzed with 10% HCl (12 ml) for 6 hr at room temperature. The resulting solution was made alkaline with dilute potassium hydroxide and extracted three times with hot chloroform. The combined extracts were washed once with water and dried. Evaporation under reduced pressure gave 1.5 g (75% overall yield) of the desired compound in a fairly pure state as evidenced by TLC [methanol–chloroform (1:9), silica gel]; IR (neat): 2950, 2930, 2860, 2820, 2780, 1730–1710 (strong, keto and ester carbonyl groups), 1450, 1360, 1170, 1160, and 1030 $cm^{-1}$; NMR ($CDCl_3$): $\delta$ 1.28 (t, 3H, $J$ = 7 Hz, $OCH_2CH_3$), 2.13 (s, 3H, $COCH_3$), 2.30 [s, 6H, $N(CH_3)_2$], 3.10 [t, 1H, $J$ = 7 Hz, $CHN(CH_3)_2$], and 4.15 (q, 2H, $J$ = 7 Hz, $OCH_2CH_3$).

*Anal.*—Calc. for $C_{10}H_{19}NO_3$: C, 59.68; H, 9.51. Found: C, 60.10; H, 9.66.

**3-Ethoxy-6-dimethylamino-2-cyclohexen-1-one (XVII)**—Sodium hydride (288 mg, 50% suspension in oil, 2 equivalents) in benzene (15 ml) was stirred under dry nitrogen and heated to 40°. The dimethylamino keto ester (XV) (603 mg) then was added dropwise. After addition was complete, the mixture was refluxed for 10 hr. The solid was collected by filtration and washed with benzene. It then was dissolved in water, and the solution was acidified with 2 *N* HCl. The resultant solution was evaporated to dryness *in vacuo*. The solid mass was extracted with ethanol, and the solvent was removed by evaporation.

The salt obtained was dissolved in water and made alkaline with dilute sodium bicarbonate solution. The resultant solution was extracted three times with chloroform. Evaporation of the solvent under reduced pressure gave a liquid, which was purified by TLC [chloroform–methanol (3:1), silica gel]; IR (neat): 2980, 2930, 2860, 2820, 2780 (dimethylamino stretching), 1650 (conjugated carbonyl), 1600 (double bond conjugated with carbonyl), 1375, 1235, 1200, 1170, 1035, 1020, 900, 850, 810, and 690 $cm^{-1}$; NMR ($CDCl_3$): $\delta$ 1.33 (t, 3H, $J$ = 7 Hz, $OCH_2CH_3$), 2.40 [s, 6H, $N(CH_3)_2$], 3.85 (q, 2H, $J$ = 7 Hz, $OCH_2CH_3$), and 5.28 (s, 1H, olefinic proton); mass spectrum: parent ion $m/z$ 183.1255 (3.1%) (calc. for $C_{10}H_{17}NO_2$: 183.1255), 140 (32.6), 112 (6.0), 84 (11.3), and 71 (100).

**2-($\alpha$-Benzoylaminobutanoic acid)-2-methyl-1,3-dioxolane Ethyl Ester (XVIII)**—To a stirred solution of XIV (17 g, 80 mmoles) in pyridine (20 ml) and benzene (40 ml) was added dropwise benzoyl chloride (11.5 g, 80 mmoles) in benzene (5 ml). The resulting mixture was heated to gentle reflux for 30 min and poured into 200 ml of water. The benzene layer was separated, and the aqueous solution was extracted twice with benzene. The combined benzene extracts were washed with water and with 5% sodium carbonate solution and dried (anhydrous sodium sulfate). The drying agent was removed by filtration, and the benzene was evaporated to a small volume (10 ml).

Hexane (40 ml) was stirred into the mixture, and the benzoyl derivative crystallized out on standing (13 g, 50.7%). Recrystallization from benzene and pentane gave a white solid, mp 87–88°; IR (KBr): 3340 (amide NH), 3060 (aromatic C–H), 2970, 2880, 1740 (ester C=O), 1640 (amide C=O), 1510, 1490, 1370, 1210, 1190, 1060, 950, 860, 720, and 690 $cm^{-1}$; NMR ($CDCl_3$): $\delta$ 1.30 (t, 3H, $J$ = 6.5 Hz, $OCH_2CH_3$), 3.92 (s, 4H, $OCH_2CH_2O$), 4.22 (q, 2H, $J$ = 7 Hz, $OCH_2CH_3$), 4.75 (t, 1H, $J$ = 6.5 Hz, CH), and 7.0–8.0 (m, 6H, $C_6H_5$ and NHCO).

*Anal.*—Calc. for $C_{17}H_{23}NO_5$: C, 63.53; H, 7.21; N, 4.36. Found: C, 63.35; H, 7.27; N, 4.38.

**2-Benzoylamino-5-oxohexanoic Acid Ethyl Ester (XIX)**—Compound XIX was obtained in quantitative yield from XVIII by hydrolysis in dilute hydrochloric acid at room temperature for several hours; NMR ($CDCl_3$): $\delta$ 1.27 (t, 3H, $J$ = 7 Hz, $OCH_2CH_3$), 2.12 (s, 3H, $COCH_3$), 4.20 (q, 2H, $J$ = 7 Hz, $OCH_2CH_3$), 4.76 (t, 1H, $J$ = 6.5 Hz, CH), and 7.0–8.0 (m, 6H, $C_6H_5$ and NHCO).

***N*-(3-Hydroxy-1-oxo-2-cyclohexen-4-yl)benzamide (XX)**—To a stirred mixture of sodium hydride (2.4 g, 50% suspension in oil, 50 mmoles) in dry benzene (150 ml) under nitrogen was added dropwise a solution of XIX (7 g, 25 mmoles) in benzene (20 ml). The mixture was kept at 50–60° for 1 hr and brought to a gentle reflux for 5 hr. The solvent was filtered, and the solid obtained was dissolved in water (150 ml) and acidified with dilute hydrochloric acid. The solution was filtered, and the precipitate was collected. The filtrate was extracted twice with acetonitrile, dried, and evaporated *in vacuo*. The solid obtained was combined with that obtained from filtration.

Recrystallization from acetone gave a white solid, mp 175–177° dec. [lit. (3) mp 175–177°]; IR (KBr): 3300 (amide NH), 3060 (aromatic CH), 2920, 2880, 2700–2500 (broad, associated OH), 1630–1590, 1540–1520, 1340, 1330, 1260, 1200, 920, 840, 710, and 700 $cm^{-1}$; NMR (dimethyl sulfoxide-$d_6$): $\delta$ 4.65 [t, 1H, $J$ = 7 Hz, $CH(NHCOC_6H_5)$], 5.3 [s, 1H, $CH$=C(OH)], 7.00–8.00 (m, 6H, $C_6H_5$ and NHCO), and 8.36 [m, 1H, CH=C(O*H*)]; mass spectrum: $m/z$ 231 (16.7%), 203 (98), 185 (7.6), 175 (3.5), 122 (95), 105 (100), and 77 (99); metastable ions were at 178.5, 150.9, 168.5, and 73.3.

*Anal.*—Calc. for $C_{13}H_{13}NO_3$: C, 67.53; H, 5.66; N, 6.05. Found: C, 67.58; H, 5.79; N, 5.80.

***N*-(3-Ethoxy-1-oxo-2-cyclohexen-6-yl)benzamide (XXI)**—Compound XX (378 mg, 1.6 mmoles) and *N,N,N',N'*-tetramethyl-1,8-naphthalenediamine[7] (428 mg, 2 mmoles) were stirred in anhydrous methylene chloride (10 ml) under a dry nitrogen atmosphere. To the clear solution was added triethyloxonium tetrafluoroborate (1.52 g, 8 mmoles) in methylene chloride (10 ml). After 4 hr of stirring, 20 ml of anhydrous methanol was added, and stirring was continued for 10 hr more. The solvent was evaporated *in vacuo*, and the brown oil obtained was dissolved in ethyl acetate and stirred with an aqueous solution of sodium acetate for 3 hr. The organic layer was separated, and the aqueous portion was extracted twice with ethyl acetate. The combined organic extracts were washed with brine.

Evaporation of the solvent *in vacuo* gave a viscous brown oil (165 mg, 39.8%); IR (neat): 3300 (broad), 3060, 2970, 2930, 1715, 1640 (broad, intense), 1600 (intense), 1575, 1540, 1530, 1485, 1380, 1330, 1230, 1200, 1100, 1035, 980, 920, 710, and 690 $cm^{-1}$; NMR ($CDCl_3$): $\delta$ 1.20 (t, 3H, $J$ = 7 Hz, $OCH_2CH_3$), 3.50 (q, 2H, $J$ = 7 Hz, $OCH_2CH_3$), 4.50 [m, 1H, $CH(NHCOC_6H_5)$], 5.45 [s, 1H, $CH$=C($OC_2H_5$)], and 7.00–8.00 (m, 6H, $C_6H_5$ and NHCO); mass spectrum: parent ion $m/z$ 259.1199 (2.1%) (calc. for $C_{15}H_{17}NO_3$: 259.1204), 245 (2.1), 203 (3.2), 154 (3.7), 138 (19.8), 112 (3.2), 106 (6.5), 105 (100), 98 (20.6), 97 (3.6), 84 (2.5), 77 (72.7), and 68 (34.6).

**$\alpha$-Chloroacetyl Isocyanate**—This compound was prepared by the method of Speziale and Smith (15) and was further characterized as its ethyl urethan, $ClCH_2CONHCO_2C_2H_5$, mp 127.5–128°.

*Anal.*—Calc. for $C_5H_8ClNO_3$: C, 36.27; H, 4.87; N, 8.46. Found: C, 36.18; H, 4.80; N, 8.31.

**2-(4-Benzoylamino-3-hydroxy-1-oxo-2-cyclohexen-2-yl)-4(5*H*)-oxazolone (XXII)**—Compound XX (462 mg, 2 mmoles) was stirred for 1 hr with a 2 *N* ethanolic solution of sodium ethoxide (1 ml, 2 mmoles). The ethanol was evaporated *in vacuo*, and the resulting sodium enolate of XX was dried *in vacuo* overnight. To the dried sodium enolate in acetonitrile (15 ml) under a dry nitrogen atmosphere was added $\alpha$-chloroacetyl isocyanate (480 mg, 4 mmoles) from a syringe. The mixture was stirred for 1 hr at room temperature and then refluxed for 8 hr. Water (5 ml) was added, and the mixture was acidified to pH 2 with dilute hydrochloric acid and extracted with ethyl acetate–acetonitrile (1:2). The combined extracts were washed with brine, dried (anhydrous sodium sulfate), and evaporated *in vacuo*.

After evaporation, the brown liquid residue was triturated with chloroform to give 305 mg (48.5%) of XXII; IR (KBr): 3300 (medium), 3060, 2960, 2900, 1790 (intense), 1680 (intense), 1625 (broad, intense), 1600 (strong), 1580, 1520 (broad, intense), 1440, 1400, 1350, 1305 (strong), 1205, 1100, 1060, 1045, 985, 960, 940, 860, 815, 800, 765, 715, and 680 $cm^{-1}$; NMR (dimethyl sulfoxide-$d_6$): $\delta$ 5.00 (s, 2H, $CH_2$), 7.00–8.00 (m, 6H, $C_6H_5$ and NHCO), and 8.60 (m, 1H, OH); mass spectrum: parent ion $m/z$ 314.0908 (13.1%) (calc. for $C_{16}H_{14}N_2O_5$: 314.0902), 315 (M + 1) (2.7), 209 (15.8), 194 (5.3), 193 (53.4), 181 (8.9), 167 (5.3), 161 (5.1), 154 (3.2), 151 (4.9), 149 (10.7), 126 (10.4), 125 (3.5), 123 (0.8), 122 (5.0), 106 (8.2), 105 (100), 84 (5.3), 77 (47.8), 68 (5.8), and 67 (4.5).

**2-(3-Hydroxy-5,5-dimethyl-1-oxo-2-cyclohexen-2-yl)-4(5*H*)-oxazolone (XXIV)**—A solution of dimedone sodium enolate (XXIII) (1.4 g, 10 mmoles) and $\alpha$-chloroacetyl isocyanate (2.4 g, 20 mmoles) in acetonitrile (30 ml) was refluxed for 6 hr. The solution was acidified with acetic acid (1 ml) and evaporated *in vacuo*. The residue was stirred with water (10 ml) and acidified with dilute hydrochloric acid until distinctly acidic. The acid solution was extracted with ethyl acetate (2 × 40 ml), washed with saturated sodium chloride solution (30 ml), dried, filtered, and evaporated under reduced pressure. The residue was triturated with petroleum ether to give a solid precipitate (1.6 g, 73%).

Recrystallization from acetone afforded a yellow, puff-like solid, mp 227–229°; UV: $\lambda_{max}$ (ethanol) 236 (log $\epsilon$ 3.95) and 290 (4.14) nm; $\lambda_{max}$ (ethanol–sodium hydroxide) 258 (4.04) and 308 (4.22) nm; IR (KBr): 3140, 2950, 1770, 1670, 1600, 1515, 1430, 1320, 1200, 1060, 980, 820, 750, 680, and 620 $cm^{-1}$; NMR ($CDCl_3$): $\delta$ 1.08 (s, 6H, *gem*-dimethyl groups), 2.48 (d, 4H, $J$ = 8 Hz, methylene groups), 4.85 (s, 2H, $CH_2$), and 12.5 (s, 1H,

[7] Proton-Sponge.

OH); mass spectrum: parent ion *m/z* 223.0849 (63.7%) (calc. for $C_{11}H_{13}NO_4$: 223.0843), 224 (M + 1) (9.8), 195 (6.4), 167 (33.5), 139 (7.4), 126 (45.0), 111 (100), 83 (61.8), and 67 (23.0).

**3-Amino-5,5-dimethyl-1-oxo-2-cyclohexene-2-carboxamide (XXV)**—Compound XXIV (223 mg, 1 mmole) was dissolved in 5 ml of saturated ammoniacal methanol. After standing at room temperature for 24 hr, the solvent was evaporated *in vacuo*. The residue was dissolved in acetone, from which colorless crystals appeared (115 mg, 63%), mp 188–189° dec.; UV: $\lambda_{max}$ (ethanol) 260 (log $\epsilon$ 64.6) nm; IR (KBr): 3400, 3300, 3200, 3140, 2950, 2930, 2860, 1630 (intense), 1600–1580 (broad, intense), 1470, 1390, 1385, 1380, 1370, 1330, 1280, 1080, 760, and 635 $cm^{-1}$; NMR ($CD_3COCD_3$): $\delta$ 1.04 (s, 6H, *gem*-dimethyl groups), 2.40 (s, 4H, methylene groups), 3.07 (s, 2H, $NH_2$), 6.77 (broad s, 1H, CONH), and 10.57 (broad s, 1H, CONH); mass spectrum: parent ion *m/z* 182.1049 (100%) (calc. for $C_9H_{14}N_2O_2$: 182.1054), 183 (M + 1) (10.4), 167 (8.3), 154 (17.4), 139 (6.3), 126 (32.0), 113 (13.2), 98 (17.6), 85 (93.9), 84 (71.7), 71 (8.4), 70 (27.5), 68 (26.0), 57 (10.4), 56 (17.2), and 55 (21.7).

## REFERENCES


(1) L. G. Chatten, R. E. Moskalyk, R. A. Locock, and K.-S. Huang, *J. Pharm. Sci.*, **65**, 1315 (1976).

(2) E. E. Smissman, M. Wachter, C. Barfknecht, and R. B. Gabbard, *ibid.*, **62**, 1772 (1973).

(3) H. Muxfeldt, J. Behling, G. Grethe, and W. Rogalski, *J. Am. Chem. Soc.*, **89**, 4991 (1967).

(4) K. Tomino, *Yakugaku Zasshi*, **78**, 1419 (1958).

(5) K. Tomino, *Chem. Pharm. Bull.*, **6**, 320 (1958).

(6) M. M. Shemyakin, M. N. Kolosov, Y. A. Arbusov, V. V. Onoprienko, and H. Yu-Yuan, *J. Gen. Chem. (USSR)*, **30**, 566 (1961).

(7) Y. A. Berlin, M. N. Kolosov, and M. M. Shemyakin, *ibid.*, **34**, 796 (1964).

(8) T. A. Spencer, M. D. Newton, and S. W. Baldwin, *J. Am. Chem. Soc.*, **29**, 787 (1964).

(9) V. M. Rodionov, I. V. Machinskaya, and V. M. Belikov, *Zh. Obshch. Khim.*, **18**, 917 (1948); through *Chem. Abstr.*, **43**, 127 (1949).

(10) H. Muxfeldt and W. Rogalski, *J. Am. Chem. Soc.*, **87**, 933 (1965).

(11) H. Muxfeldt, W. Rogalski, and K. Streigler, *Chem. Ber.*, **95**, 2581 (1962).

(12) H. Meerwein, G. Hinz, P. Hofmann, E. Korning, and E. Pfeil, *J. Prakt. Chem.*, **147**, 257 (1936).

(13) H. Muxfeldt, H. Dopp, J. E. Kaufman, J. Schneider, P. E. Hansen, H. Sasaki, and T. Geiser, *Angew. Chem. Int. Ed. Engl.*, **12**, 497 (1973).

(14) W. Durckheimer, *ibid.*, **14**, 721 (1975).

(15) A. J. Speziale and L. R. Smith, *Org. Syn.*, **46**, 16 (1966).

(16) R. M. Silverstein, G. C. Bassler, and T. C. Morrill, "Spectrometric Identification of Organic Compounds," 3rd ed., Wiley, New York, N.Y., 1967, p. 243.

(17) R. M. Rodehorst and T. H. Koch, *J. Am. Chem. Soc.*, **97**, 7298 (1975).

(18) R. Filler, "Advances in Heterocyclic Chemistry," vol. 21, A. R. Katritzky and A. J. Boulton, Eds., Academic, New York, N.Y., 1977, p. 175.

(19) V. Hornemann, L. H. Hurley, M. K. Speedie, and H. G. Floss, *J. Am. Chem. Soc.*, **93**, 3028 (1971).


## ACKNOWLEDGMENTS


Abstracted in part from a thesis submitted by A. L. C. Mak to the University of Alberta in partial fulfillment of the Master of Science degree requirements.

A. L. C. Mak is grateful to the Medical Research Council of Canada for financial support through a studentship.


# Determination of Platinum in Serum and Ultrafiltrate by Flameless Atomic Absorption Spectrophotometry


**DAVID A. HULL *, NASEEM MUHAMMAD *ˣ, JOHN G. LANESE *§, STEVEN D. REICH *¶, THEODORE T. FINKELSTEIN ‡‖, and SUSAN FANDRICH ‡**



Received August 7, 1980, from **Bristol Laboratories, Division of Bristol-Myers Company, Syracuse, NY 13201*, and the ‡*Department of Pharmacology, Upstate Medical Center, Syracuse, NY 13210.* Accepted for publication October 16, 1980.


§Present address: Wallace Laboratories, Cranbury, NJ 08512. ¶Present address: Department of Medicine, University of Massachusetts Medical School, Worcester, MA 01605. ‖Present address: Long Island University, Southampton College, Southampton, NY 11978.



**Abstract** □ A graphite furnace atomic absorption spectrophotometric assay, capable of accurately determining nanogram amounts of platinum in serum and ultrafiltrate, was developed. A sample serum or ultrafiltrate was acidified with nitric acid and heated to destroy the protein–platinum bond. A measured excess of ammonium 1-pyrrolidinedithiocarbamate was added, and the platinum complex was extracted into isopropylacetone. The extract was injected into the graphite furnace. The sample was dried, charred, and atomized using optimal conditions. The resulting absorbance was used to determine the platinum content.



**Keyphrases** □ Platinum—determination in serum and ultrafiltrate, flameless atomic absorption spectrophotometry □ Atomic absorption spectrophotometry, flameless—determination of platinum in serum and ultrafiltrate □ Analytical techniques—determination of platinum in serum and ultrafiltrate by flameless atomic absorption spectrophotometry


A procedure to determine platinum levels in serums and ultrafiltrates of patients receiving *cis*-diamminedichloroplatinum(II)[1] [$PtCl_2(NH_3)_2$] was investigated. Platinum levels were monitored during a course of treatment using both serum and ultrafiltrate samples.

[1] Platinol.

## BACKGROUND

Several analytical techniques to determine platinum in biological samples have been reported, such as neutron activation analysis (1), X-ray fluorescence (2), radioisotope dilution (3), flameless atomic absorption spectrophotometry (4–7), and high-performance liquid chromatography (8). Atomic absorption spectrophotometry has facilitated the determination of minute concentrations of metals in biological fluids. Flameless atomic absorption spectrophotometry was chosen for this study.

Previous procedures for platinum estimation in biological fluids using this technique involved wet-ashing with nitric acid–perchloric acid for sample preparation prior to injection into the graphite furnace. In the present study, two parameters had to be considered, the limited volume of each serum sample and ultrafiltrate and the number of samples to be assayed for platinum content. Wet-ashing was not suitable for the present study. Attempts to determine platinum levels in serum and ultrafiltrate by direct injection into the graphite furnace with no prior sample treatment were unsuccessful. The results obtained by direct injection were highly variable due to sample splatter within the graphite furnace and onto the quartz end-windows during charring.

The present report describes a technique that involves the formation




*0022-3549/81/0500-0500$01.00/0*


*© 1981, American Pharmaceutical Association*

OH); mass spectrum: parent ion *m/z* 223.0849 (63.7%) (calc. for $C_{11}H_{13}NO_4$: 223.0843), 224 (M + 1) (9.8), 195 (6.4), 167 (33.5), 139 (7.4), 126 (45.0), 111 (100), 83 (61.8), and 67 (23.0).

**3-Amino-5,5-dimethyl-1-oxo-2-cyclohexene-2-carboxamide (XXV)**—Compound XXIV (223 mg, 1 mmole) was dissolved in 5 ml of saturated ammoniacal methanol. After standing at room temperature for 24 hr, the solvent was evaporated *in vacuo*. The residue was dissolved in acetone, from which colorless crystals appeared (115 mg, 63%), mp 188–189° dec.; UV: $\lambda_{max}$ (ethanol) 260 (log $\epsilon$ 64.6) nm; IR (KBr): 3400, 3300, 3200, 3140, 2950, 2930, 2860, 1630 (intense), 1600–1580 (broad, intense), 1470, 1390, 1385, 1380, 1370, 1330, 1280, 1080, 760, and 635 $cm^{-1}$; NMR ($CD_3COCD_3$): $\delta$ 1.04 (s, 6H, *gem*-dimethyl groups), 2.40 (s, 4H, methylene groups), 3.07 (s, 2H, $NH_2$), 6.77 (broad s, 1H, CONH), and 10.57 (broad s, 1H, CONH); mass spectrum: parent ion *m/z* 182.1049 (100%) (calc. for $C_9H_{14}N_2O_2$: 182.1054), 183 (M + 1) (10.4), 167 (8.3), 154 (17.4), 139 (6.3), 126 (32.0), 113 (13.2), 98 (17.6), 85 (93.9), 84 (71.7), 71 (8.4), 70 (27.5), 68 (26.0), 57 (10.4), 56 (17.2), and 55 (21.7).

## REFERENCES


(1) L. G. Chatten, R. E. Moskalyk, R. A. Locock, and K.-S. Huang, *J. Pharm. Sci.*, **65**, 1315 (1976).

(2) E. E. Smissman, M. Wachter, C. Barfknecht, and R. B. Gabbard, *ibid.*, **62**, 1772 (1973).

(3) H. Muxfeldt, J. Behling, G. Grethe, and W. Rogalski, *J. Am. Chem. Soc.*, **89**, 4991 (1967).

(4) K. Tomino, *Yakugaku Zasshi*, **78**, 1419 (1958).

(5) K. Tomino, *Chem. Pharm. Bull.*, **6**, 320 (1958).

(6) M. M. Shemyakin, M. N. Kolosov, Y. A. Arbusov, V. V. Onoprienko, and H. Yu-Yuan, *J. Gen. Chem. (USSR)*, **30**, 566 (1961).

(7) Y. A. Berlin, M. N. Kolosov, and M. M. Shemyakin, *ibid.*, **34**, 796 (1964).

(8) T. A. Spencer, M. D. Newton, and S. W. Baldwin, *J. Am. Chem. Soc.*, **29**, 787 (1964).

(9) V. M. Rodionov, I. V. Machinskaya, and V. M. Belikov, *Zh. Obshch. Khim.*, **18**, 917 (1948); through *Chem. Abstr.*, **43**, 127 (1949).

(10) H. Muxfeldt and W. Rogalski, *J. Am. Chem. Soc.*, **87**, 933 (1965).

(11) H. Muxfeldt, W. Rogalski, and K. Streigler, *Chem. Ber.*, **95**, 2581 (1962).

(12) H. Meerwein, G. Hinz, P. Hofmann, E. Korning, and E. Pfeil, *J. Prakt. Chem.*, **147**, 257 (1936).

(13) H. Muxfeldt, H. Dopp, J. E. Kaufman, J. Schneider, P. E. Hansen, H. Sasaki, and T. Geiser, *Angew. Chem. Int. Ed. Engl.*, **12**, 497 (1973).

(14) W. Durckheimer, *ibid.*, **14**, 721 (1975).

(15) A. J. Speziale and L. R. Smith, *Org. Syn.*, **46**, 16 (1966).

(16) R. M. Silverstein, G. C. Bassler, and T. C. Morrill, "Spectrometric Identification of Organic Compounds," 3rd ed., Wiley, New York, N.Y., 1967, p. 243.

(17) R. M. Rodehorst and T. H. Koch, *J. Am. Chem. Soc.*, **97**, 7298 (1975).

(18) R. Filler, "Advances in Heterocyclic Chemistry," vol. 21, A. R. Katritzky and A. J. Boulton, Eds., Academic, New York, N.Y., 1977, p. 175.

(19) V. Hornemann, L. H. Hurley, M. K. Speedie, and H. G. Floss, *J. Am. Chem. Soc.*, **93**, 3028 (1971).


## ACKNOWLEDGMENTS


Abstracted in part from a thesis submitted by A. L. C. Mak to the University of Alberta in partial fulfillment of the Master of Science degree requirements.

A. L. C. Mak is grateful to the Medical Research Council of Canada for financial support through a studentship.


# Determination of Platinum in Serum and Ultrafiltrate by Flameless Atomic Absorption Spectrophotometry


**DAVID A. HULL *, NASEEM MUHAMMAD *ˣ, JOHN G. LANESE *§, STEVEN D. REICH *¶, THEODORE T. FINKELSTEIN ‡‖, and SUSAN FANDRICH ‡**



Received August 7, 1980, from **Bristol Laboratories, Division of Bristol-Myers Company, Syracuse, NY 13201*, and the ‡*Department of Pharmacology, Upstate Medical Center, Syracuse, NY 13210.* Accepted for publication October 16, 1980.


§Present address: Wallace Laboratories, Cranbury, NJ 08512. ¶Present address: Department of Medicine, University of Massachusetts Medical School, Worcester, MA 01605. ‖Present address: Long Island University, Southampton College, Southampton, NY 11978.



**Abstract** □ A graphite furnace atomic absorption spectrophotometric assay, capable of accurately determining nanogram amounts of platinum in serum and ultrafiltrate, was developed. A sample serum or ultrafiltrate was acidified with nitric acid and heated to destroy the protein–platinum bond. A measured excess of ammonium 1-pyrrolidinedithiocarbamate was added, and the platinum complex was extracted into isopropylacetone. The extract was injected into the graphite furnace. The sample was dried, charred, and atomized using optimal conditions. The resulting absorbance was used to determine the platinum content.



**Keyphrases** □ Platinum—determination in serum and ultrafiltrate, flameless atomic absorption spectrophotometry □ Atomic absorption spectrophotometry, flameless—determination of platinum in serum and ultrafiltrate □ Analytical techniques—determination of platinum in serum and ultrafiltrate by flameless atomic absorption spectrophotometry


A procedure to determine platinum levels in serums and ultrafiltrates of patients receiving *cis*-diamminedichloroplatinum(II)[1] [$PtCl_2(NH_3)_2$] was investigated. Platinum levels were monitored during a course of treatment using both serum and ultrafiltrate samples.

[1] Platinol.

## BACKGROUND

Several analytical techniques to determine platinum in biological samples have been reported, such as neutron activation analysis (1), X-ray fluorescence (2), radioisotope dilution (3), flameless atomic absorption spectrophotometry (4–7), and high-performance liquid chromatography (8). Atomic absorption spectrophotometry has facilitated the determination of minute concentrations of metals in biological fluids. Flameless atomic absorption spectrophotometry was chosen for this study.

Previous procedures for platinum estimation in biological fluids using this technique involved wet-ashing with nitric acid–perchloric acid for sample preparation prior to injection into the graphite furnace. In the present study, two parameters had to be considered, the limited volume of each serum sample and ultrafiltrate and the number of samples to be assayed for platinum content. Wet-ashing was not suitable for the present study. Attempts to determine platinum levels in serum and ultrafiltrate by direct injection into the graphite furnace with no prior sample treatment were unsuccessful. The results obtained by direct injection were highly variable due to sample splatter within the graphite furnace and onto the quartz end-windows during charring.

The present report describes a technique that involves the formation




*0022-3549/81/0500-0500$01.00/0*


*© 1981, American Pharmaceutical Association*

of an organic solvent-extractable platinum complex to overcome sample splatter during charring. The procedure has the sensitivity, specificity, and ease of operation required for the routine analysis of platinum in serum and ultrafiltrate.

## EXPERIMENTAL

**Reagents and Materials**—Distilled, deionized water was passed through a 0.45-μm hydrophobic filter[2]. Isopropylacetone[3], 1-pyrrolidinedithiocarbamate[4], nitric acid[3], hydrochloric acid[3], and *cis*-diamminedichloroplatinum(II)[5] were used as received.

**Instrumentation**—The atomic absorption spectrometer[6] was equipped with a graphite furnace and ramp accessory[7] and an autosampler system[8]. A platinum, hollow cathode lamp[9] was the light source. The graphite furnace was supplied with pyrolytic-coated graphite tubes. Atomization peak heights of platinum were recorded on a strip-chart recorder[10] at a chart speed of 10 mm/min and recorder current of 10 mv.

**Operating Conditions**—The optimum parameters for platinum determination in the test solutions were: drying cycle, 120° for 15 sec with a temperature ramp of 10 sec; charring cycle, 1100° for 15 sec with a temperature ramp of 15 sec; and atomization cycle, 2700° for 8 sec with no ramping. The ramp setting permitted a gradual rise in the furnace temperature during each run. The carrier gas was argon at a flow rate of 40 ml/min. Atomization peak heights were recorded at 265.9 nm, using a 3× scale expansion.

**Instrument Calibration**—When 20 μl of the platinum standard solution (1 μg/ml) is injected into the furnace, the resulting signal should not be <0.6 absorbance unit.

**Preparation of Standard Solutions**—*Platinum Stock Standard Solution—cis*-Diamminedichloroplatinum(II) (0.1541 g, 99.8% purity)[11] was weighed accurately into a 1-liter volumetric flask. Distilled, deionized water (50 ml) and 20 ml of concentrated hydrochloric acid were added, and the mixture was heated gently on a hot plate until dissolution. The solution was cooled to room temperature and diluted to volume with distilled, deionized water. Each milliliter is equivalent to 100 μg of platinum.

*Platinum Working Standard Solution*—One milliliter of the platinum stock standard solution was diluted to 100.0 ml with distilled, deionized water. Each milliliter is equivalent to 1.0 μg of platinum. This solution was prepared fresh each working day.

*Ammonium 1-Pyrrolidinedithiocarbamate Solution, 1% in Distilled, Deionized Water*—If the solution was not clear, it was filtered[12]. This solution was prepared fresh each working day.

Isopropylacetone was saturated with distilled, deionized water.

*Platinum-Free Serum and Ultrafiltrate*[13]—The ultrafiltrate was prepared by filtering serum through ultrafiltrate cones[14], which filtered out molecules of >50,000 daltons.

**Preparation of Standard Curve**—One milliliter of the platinum-free serum or ultrafiltrate was pipetted as needed into each of five 16 × 125-mm screw-capped test tubes. Then 0, 25, 50, 100, and 250 μl of the platinum working standard was added to each tube, and the solutions were allowed to stand 5 min. Then 0.5 ml of concentrated nitric acid was added to each tube and mixed well. The tubes were capped and placed in a boiling water bath for 5 min. They then were removed from the bath and cooled to room temperature. Distilled, deionized water (5 ml) was added to each tube and mixed; then 5.0 ml of 1% ammonium 1-pyrrolidinedithiocarbamate solution was added and mixed vigorously for 1 min. Then 1.0 ml of isopropylacetone saturated with distilled, deionized water was added and mixed vigorously for 2 min.

The solution was centrifuged for 3 min at 1000×*g*. With a Pasteur pipet, the isopropylacetone (upper) layer was transferred carefully to the polyethylene sample cups to avoid trapping water droplets in the transfer. The instrument was optimized and the sampler was set to 3. The instrument recorded the absorbance of the blank (zero) and each sample. The instrument was autozeroed after each blank reading. The three absorbance readings of each standard were averaged, and a working curve of absorbance *versus* concentration of platinum was plotted.

**Sample Preparation**—One milliliter of serum or ultrafiltrate was pipetted into a 16 × 125-mm screw-capped test tube. Then 0.5 ml of concentrated nitric acid was added, and sample preparation proceeded as already described. The three absorbance readings were averaged, and the concentration of platinum was obtained from the working curve. If the sample absorbance was greater than the absorbance of the highest standard, the sample was diluted with platinum-free serum or ultrafiltrate and the determination was repeated.

If there were more than six samples per run, an additional blank was placed at the end of the run and the 100-ng/ml platinum standard was rerun to observe any drift in instrument conditions.

**Table I—Absorbance Data for Standard Platinum Solutions**

| Solution | Platinum, ng/ml | Absorbance 1 | 2 | 3 | $\bar{X}$ |
|---|---|---|---|---|---|
| Serum | | | | | |
| 1 | 25 | 0.035 | 0.036 | 0.036 | 0.036 |
| 2 | 50 | 0.078 | 0.066 | 0.069 | 0.071 |
| 3 | 100 | 0.145 | 0.131 | 0.140 | 0.139 |
| 4 | 250 | 0.309 | 0.337 | 0.341 | 0.329 |
| Ultrafiltrate | | | | | |
| 1 | 25 | 0.028 | 0.033 | 0.035 | 0.033 |
| 2 | 50 | 0.063 | 0.062 | 0.064 | 0.063 |
| 3 | 100 | 0.147 | 0.134 | 0.140 | 0.140 |
| 4 | 250 | 0.333 | 0.357 | 0.344 | 0.345 |

**Table II—Recovery Data for Standard Platinum in Serum and Ultrafiltrate *versus* Standard Platinum in Water**

| Platinum Added, ng/ml | Platinum Found, ng/ml Serum | Ultrafiltrate | Recovery, %[a] Serum | Ultrafiltrate |
|---|---|---|---|---|
| 50 | 44.1 | 39.7 | 88.2 | 79.4 |
| 100 | 92.2 | 87.5 | 92.2 | 87.5 |
| 200 | 182.6 | 182.6 | 91.3 | 91.6 |

[a] Recovery values are an average of three values.

## RESULTS AND DISCUSSION

Initial work on the determination of platinum in serum used whole serum injected directly into the furnace without prior treatment. During drying, either ramped or unramped, an audible cracking or frying sound was heard; at times, a cinder of dried sample was physically ejected from the furnace. During charring, ramped or unramped, the sample crusted over. As the temperature increased to ~350°, the sample literally exploded due to improper drying and spattered the quartz end-windows with charred sample. Because of these and other problems in direct sample injection, another procedure was investigated.

Ammonium 1-pyrrolidinedithiocarbamate forms organic-soluble complexes with over 30 elements, including platinum (9). The platinum complex forms in the pH 1–14 range and is extracted quantitatively into isopropylacetone in the pH 1–10 range. By heating the sample with nitric acid to destroy the protein, the platinum–ammonium 1-pyrrolidinedithiocarbamate complex can be extracted into isopropylacetone to eliminate matrix effects from the untreated serum or ultrafiltrate. Standard curves of platinum in serum or ultrafiltrate gave a linear response over the 25–250-ng of platinum/ml range when run against platinum in distilled, deionized water, but platinum recoveries were low. This low recovery can be improved by preparing the standards in either serum or ultrafiltrate as required.

**Table III—Recovery Data for Standard Platinum in Serum and Ultrafiltrate Using Sample Matrix**

| Platinum Added, ng/ml | Platinum Found, ng/ml Serum | Ultrafiltrate | Recovery, %[a] Serum | Ultrafiltrate |
|---|---|---|---|---|
| 50 | 47.6 | 47.1 | 95.2 | 94.2 |
| 100 | 96.6 | 96.5 | 96.6 | 96.5 |
| 200 | 195.0 | 194.8 | 97.5 | 97.4 |

[a] Recovery values are an average of three values.

[2] Millipore Corp., Bedford, MA 01730.
[3] ACS grade, Fisher Scientific Co., Pittsburgh, PA 15219.
[4] White Label, Eastman Organic Chemicals, Rochester, NY 14650.
[5] Bristol Laboratories, Division of Bristol-Myers Co., Syracuse, NY 13201.
[6] Model 460, Perkin-Elmer Corp., Norwalk, CT 06856.
[7] Model HGA2200, Perkin-Elmer Corp., Norwalk, CT 06856.
[8] Model AS-1, Perkin-Elmer Corp., Norwalk, CT 06856.
[9] Intensitron 303-6501, Perkin-Elmer Corp., Norwalk, CT 06856.
[10] Model 156, Perkin-Elmer Corp., Norwalk, CT 06856.
[11] Purity was established by nonaqueous titration with perchloric acid in acetic acid.
[12] Whatman No. 30 filter paper.
[13] Supplied by Upstate Medical Center, Syracuse, NY 13210.
[14] Centriflo membrane cones, CF50A, Amicon Corp., Lexington, MA 02173.

**Table IV—Day-To-Day Variability Data**

| Day | Concentration of Platinum, ng/ml | Average Absorbance | |
|---|---|---|---|
| | | Serum | Ultrafiltrate |
| 1 | 50 | 0.081 | 0.079 |
| | 100 | 0.160 | 0.160 |
| | 250 | 0.390 | 0.389 |
| 2 | 50 | 0.073 | 0.064 |
| | 100 | 0.151 | 0.140 |
| | 250 | 0.349 | 0.324 |
| 3 | 50 | 0.075 | 0.071 |
| | 100 | 0.148 | 0.140 |
| | 250 | 0.369 | 0.352 |

Table I contains the absorbance data obtained for a typical standard curve of platinum in serum and in ultrafiltrate; the relationship of platinum to absorbance was linear in the 0–250-ng/ml range. Table II contains the recovery data for serum and ultrafiltrate with known amounts of standard platinum as compared to similarly treated pure solutions of platinum in distilled, deionized water. The recoveries ranged from 79.4 to 92.2%. This result demonstrates that a standard curve of platinum cannot be prepared from distilled, deionized water. Recoveries of platinum from serum and ultrafiltrates using the respective matrix to prepare the standard curve are shown in Table III.

The day-to-day variability data in Table IV indicate that a standard working curve must be run each time for significant results. Placement of a standard at the end of each sample run is used to monitor the drift in instrument conditions during the run. The sampler trays[8] hold 30 polyethylene cups, giving a maximum run of four standards and 24 samples. The pyrolytic-coated graphite furnaces were replaced routinely at ~200 injections. Studies were not run to determine the maximum number of injections possible with these furnaces. It was necessary to optimize the optical alignment and the furnace alignment each day before beginning a run.

## REFERENCES


(1) A. F. LeRoy, M. L. Wehling, H. L. Sponseller, W. S. Friauf, R. E. Solomon, R. L. Dedrick, C. L. Litterst, T. E. Gram, A. M. Guarino, and D. A. Becker, *Biochem. Med.*, **18**, 184 (1977).

(2) S. J. Bannister, L. A. Sternson, A. J. Repta, and G. W. James, *Clin. Chem.*, **22**, 2258 (1976).

(3) M. F. Pera and H. C. Harder, *ibid.*, **23**, 1245 (1977).

(4) J. B. Tillery and D. E. Johnson, *Environ. Health Perspect.*, **12**, 19 (1975).

(5) C. L. Litterst, T. E. Gram, R. L. Dedrick, A. F. LeRoy, and A. M. Guarino, *Cancer Res.*, **36**, 2340 (1976).

(6) A. H. Jones, *Anal. Chem.*, **48**, 1472 (1976).

(7) S. J. Bannister, Y. Chang, L. A. Sternson, and A. J. Repta, *Clin. Chem.*, **24**, 877 (1978).

(8) S. J. Bannister, L. A. Sternson, and A. J. Repta, *J. Chromatogr.*, **173**, 33 (1979).

(9) C. A. Watson, "Ammonium Pyrrolidine Dithiocarbamate," Monograph 74, Hopkin and Williams, London, England, 1965.


# Solubility and Partitioning IV: Aqueous Solubility and Octanol–Water Partition Coefficients of Liquid Nonelectrolytes


**S. C. VALVANI ˣ, S. H. YALKOWSKY, and T. J. ROSEMAN**



Received November 28, 1979, from *Pharmacy Research, The Upjohn Company, Kalamazoo, MI 49001.* Accepted for publication October 21, 1980.



**Abstract** □ The aqueous solubility and octanol–water partition coefficient of over 100 nonelectrolyte organic liquid solutes are related by the simple equation $\log S_w = -1.016 \log PC + 0.515$, where $S_w$ is the molar solubility of liquid solutes in water and $PC$ is the experimental partition coefficient of the solutes in the octanol–water system. The liquids studied represent a wide variety of organic compounds including aliphatic and aromatic hydrocarbons, alcohols, esters, ethers, aldehydes, and ketones. This finding is in agreement with that reported by Hansch and coworkers. However, these results are signficant because only the experimental values for the aqueous solubilities and octanol–water partition coefficients are included, as opposed to the calculated partition coefficients used by Hansch. This relationship is extremely useful in understanding the overall solubility and partitioning phenomenon for organic liquids and provides a basis for studying crystalline solids and gases.



**Keyphrases** □ Aqueous solubility—aliphatic and aromatic hydrocarbons, liquid nonelectrolytes, experimental values compared with calculated values □ Partitioning—octanol–water partition coefficients, experimental values compared with calculated values, aliphatic and aromatic hydrocarbons, liquid nonelectrolytes □ Hydrocarbons, aliphatic and aromatic—aqueous solubility and partition coefficients obtained experimentally compared with calculated values □ Liquid nonelectrolytes—aliphatic and aromatic hydrocarbons, aqueous solubility and partition coefficients obtained experimentally compared with calculated values


The aqueous solubility and partition coefficient of a drug are key parameters in determining its biological activity. The partition coefficient frequently is used in quantitative structure–activity studies. Its usefulness in the assessment of transport properties of drugs through biological membranes, extraction of solutes in aqueous–organic liquid systems, measurement of equilibria, and design of controlled-release drug delivery systems is well documented (1–4).

The aqueous solubility of a drug influences the dissolution rate and thus the rate and extent of absorption through biological membranes. The efficiency or biological performance of drugs from these formulations depends on the release and transfer of drug molecules to the systemic circulation. The release and transport of drugs are determined by solubility and the partition coefficient. The combined effects of aqueous solubility and the membrane–water partition coefficient on absorption were quantitatively described by Yalkowsky and coworkers (5–8).

This paper is part of a series dealing with the relationship between solubility and partitioning and deals exclusively with liquid nonelectrolyte solutes in water and octanol–water partitioning systems. In subsequent contributions, nonelectrolyte crystalline solids as well as weak acids and bases will be investigated.

There is a direct quantitative relationship between aqueous solubility and partitioning. However, due to a lack of reliable solubility and partitioning data, attempts to quantitate this relationship have met with only limited success (9).

This report demonstrates that there is a simple, nearly




*0022-3549/81/0500-0502$01.00/0*


*© 1981, American Pharmaceutical Association*

**Table IV—Day-To-Day Variability Data**

| Day | Concentration of Platinum, ng/ml | Average Absorbance | |
|---|---|---|---|
| | | Serum | Ultrafiltrate |
| 1 | 50 | 0.081 | 0.079 |
| | 100 | 0.160 | 0.160 |
| | 250 | 0.390 | 0.389 |
| 2 | 50 | 0.073 | 0.064 |
| | 100 | 0.151 | 0.140 |
| | 250 | 0.349 | 0.324 |
| 3 | 50 | 0.075 | 0.071 |
| | 100 | 0.148 | 0.140 |
| | 250 | 0.369 | 0.352 |

Table I contains the absorbance data obtained for a typical standard curve of platinum in serum and in ultrafiltrate; the relationship of platinum to absorbance was linear in the 0–250-ng/ml range. Table II contains the recovery data for serum and ultrafiltrate with known amounts of standard platinum as compared to similarly treated pure solutions of platinum in distilled, deionized water. The recoveries ranged from 79.4 to 92.2%. This result demonstrates that a standard curve of platinum cannot be prepared from distilled, deionized water. Recoveries of platinum from serum and ultrafiltrates using the respective matrix to prepare the standard curve are shown in Table III.

The day-to-day variability data in Table IV indicate that a standard working curve must be run each time for significant results. Placement of a standard at the end of each sample run is used to monitor the drift in instrument conditions during the run. The sampler trays[8] hold 30 polyethylene cups, giving a maximum run of four standards and 24 samples. The pyrolytic-coated graphite furnaces were replaced routinely at ~200 injections. Studies were not run to determine the maximum number of injections possible with these furnaces. It was necessary to optimize the optical alignment and the furnace alignment each day before beginning a run.

## REFERENCES


(1) A. F. LeRoy, M. L. Wehling, H. L. Sponseller, W. S. Friauf, R. E. Solomon, R. L. Dedrick, C. L. Litterst, T. E. Gram, A. M. Guarino, and D. A. Becker, *Biochem. Med.*, **18**, 184 (1977).

(2) S. J. Bannister, L. A. Sternson, A. J. Repta, and G. W. James, *Clin. Chem.*, **22**, 2258 (1976).

(3) M. F. Pera and H. C. Harder, *ibid.*, **23**, 1245 (1977).

(4) J. B. Tillery and D. E. Johnson, *Environ. Health Perspect.*, **12**, 19 (1975).

(5) C. L. Litterst, T. E. Gram, R. L. Dedrick, A. F. LeRoy, and A. M. Guarino, *Cancer Res.*, **36**, 2340 (1976).

(6) A. H. Jones, *Anal. Chem.*, **48**, 1472 (1976).

(7) S. J. Bannister, Y. Chang, L. A. Sternson, and A. J. Repta, *Clin. Chem.*, **24**, 877 (1978).

(8) S. J. Bannister, L. A. Sternson, and A. J. Repta, *J. Chromatogr.*, **173**, 33 (1979).

(9) C. A. Watson, "Ammonium Pyrrolidine Dithiocarbamate," Monograph 74, Hopkin and Williams, London, England, 1965.


# Solubility and Partitioning IV: Aqueous Solubility and Octanol–Water Partition Coefficients of Liquid Nonelectrolytes


**S. C. VALVANI ˣ, S. H. YALKOWSKY, and T. J. ROSEMAN**



Received November 28, 1979, from *Pharmacy Research, The Upjohn Company, Kalamazoo, MI 49001.* Accepted for publication October 21, 1980.



**Abstract** □ The aqueous solubility and octanol–water partition coefficient of over 100 nonelectrolyte organic liquid solutes are related by the simple equation $\log S_w = -1.016 \log PC + 0.515$, where $S_w$ is the molar solubility of liquid solutes in water and $PC$ is the experimental partition coefficient of the solutes in the octanol–water system. The liquids studied represent a wide variety of organic compounds including aliphatic and aromatic hydrocarbons, alcohols, esters, ethers, aldehydes, and ketones. This finding is in agreement with that reported by Hansch and coworkers. However, these results are signficant because only the experimental values for the aqueous solubilities and octanol–water partition coefficients are included, as opposed to the calculated partition coefficients used by Hansch. This relationship is extremely useful in understanding the overall solubility and partitioning phenomenon for organic liquids and provides a basis for studying crystalline solids and gases.



**Keyphrases** □ Aqueous solubility—aliphatic and aromatic hydrocarbons, liquid nonelectrolytes, experimental values compared with calculated values □ Partitioning—octanol–water partition coefficients, experimental values compared with calculated values, aliphatic and aromatic hydrocarbons, liquid nonelectrolytes □ Hydrocarbons, aliphatic and aromatic—aqueous solubility and partition coefficients obtained experimentally compared with calculated values □ Liquid nonelectrolytes—aliphatic and aromatic hydrocarbons, aqueous solubility and partition coefficients obtained experimentally compared with calculated values


The aqueous solubility and partition coefficient of a drug are key parameters in determining its biological activity. The partition coefficient frequently is used in quantitative structure–activity studies. Its usefulness in the assessment of transport properties of drugs through biological membranes, extraction of solutes in aqueous–organic liquid systems, measurement of equilibria, and design of controlled-release drug delivery systems is well documented (1–4).

The aqueous solubility of a drug influences the dissolution rate and thus the rate and extent of absorption through biological membranes. The efficiency or biological performance of drugs from these formulations depends on the release and transfer of drug molecules to the systemic circulation. The release and transport of drugs are determined by solubility and the partition coefficient. The combined effects of aqueous solubility and the membrane–water partition coefficient on absorption were quantitatively described by Yalkowsky and coworkers (5–8).

This paper is part of a series dealing with the relationship between solubility and partitioning and deals exclusively with liquid nonelectrolyte solutes in water and octanol–water partitioning systems. In subsequent contributions, nonelectrolyte crystalline solids as well as weak acids and bases will be investigated.

There is a direct quantitative relationship between aqueous solubility and partitioning. However, due to a lack of reliable solubility and partitioning data, attempts to quantitate this relationship have met with only limited success (9).

This report demonstrates that there is a simple, nearly




*0022-3549/81/0500-0502$01.00/0*


*© 1981, American Pharmaceutical Association*

quantitative relationship between aqueous solubility and the partition coefficient for nonionizable liquids and that significant deviation from this relationship is justifiable reason to question the accuracy of the data.

## EXPERIMENTAL

**Solutes**—Several nonelectrolyte solutes, which are liquids at room temperature (mp ≤ 25°) and for which aqueous solubility data (between 20 and 40°) as well as experimental partition coefficient data in octa-

**Table I—Observed Aqueous Solubility, Octanol–Water Partition Coefficient (*PC*), and Aqueous Solubility Predicted by Eq. 3 for Liquid Nonelectrolytes**

| Solute | Experimental Log *PC* | Observed Log Molar Solubility | Observed Log Solubility Average | Log Solubility Predicted by Eq. 3 | Solute | Experimental Log *PC* | Observed Log Molar Solubility | Observed Log Solubility Average | Log Solubility Predicted by Eq. 3 |
|---|---|---|---|---|---|---|---|---|---|
| Carbon tetrachloride | 2.83 | −1.99<br>−2.24<br>−2.28<br>−2.28<br>−2.30 | −2.22 | −2.36 | Methyl ethyl ketone | 0.35 | 0.58<br>0.55<br>0.52<br>0.58<br>0.55 | 0.52 | 0.16 |
| Chloroform | 1.96 | −0.95<br>−1.19<br>−1.16<br>−1.16 | −1.12 | −1.48 | | | 0.52<br>0.27<br>0.57<br>0.58 | | |
| Methylene chloride | 1.25 | −0.40<br>−0.81<br>−0.63<br>−0.81<br>−0.63 | −0.65 | −0.75 | Propyl formate | 0.83 | −0.50<br>−0.51<br>−0.54 | −0.52 | −0.33 |
| Methyl iodide | 1.69 | −1.01<br>−1.02 | −1.01 | −1.20 | Vinyl ethyl ether | 1.04 | −0.90 | −0.90 | −0.55 |
| Nitromethane | −0.34 | 0.22<br>0.19<br>0.19 | 0.20 | 0.86 | Ethyl acetate | 0.70 | −0.02<br>−0.04<br>−0.06<br>−0.08 | −0.06 | −0.19 |
| Trichloroethylene | 2.29 | −2.12 | −2.20 | −1.82 | | | −0.10<br>−0.14 | | |
| Ethylidene chloride | 1.79 | −1.26<br>−1.29 | −1.27 | −1.30 | | | −0.05<br>−0.05 | | |
| Ethylene dichloride | 1.48 | −1.04<br>−1.06<br>−1.06<br>−1.04 | −1.05 | −0.99 | | | −0.01<br>−0.08 | | |
| Ethyl bromide | 1.61 | −1.06<br>−1.08<br>−1.08 | −1.07 | −1.12 | *n*-Butyl chloride | 2.64 | −2.14<br>−2.10 | −2.12 | −2.16 |
| Ethyl chloride | 1.43 | −0.93<br>−1.05<br>−1.03<br>−1.05 | −1.02 | −0.94 | 1-Nitrobutane | 1.47 | −1.46 | −1.46 | −0.98 |
| Ethyl iodide | 2.00 | −1.59<br>−1.60 | −1.60 | −1.52 | *n*-Butyl nitrate | 2.15 | −2.19 | −2.19 | −1.67 |
| Nitroethane | 0.18 | −0.44<br>−0.22<br>−0.22 | −0.29 | 0.33 | *n*-Butyl alcohol | 0.89 | 0.01<br>−0.03<br>−0.05<br>0.00<br>−0.03<br>0.03<br>−0.01<br>0.00 | −0.01 | −0.38 |
| Acrylonitrile | −0.92 | 0.14<br>0.17<br>0.14 | 0.15 | 1.45 | | | 0.02<br>0.00<br>−0.02 | | |
| Propionitrile | 0.10 | 0.33<br>0.32 | 0.33 | 0.41 | | | −0.04<br>−0.05 | | |
| Methyl acetate | 0.18 | 0.52<br>−0.18<br>0.63<br>0.65<br>0.63 | 0.45 | 0.33 | | | 0.03<br>−0.02<br>−0.05<br>−0.03<br>0.00 | | |
| 1,3-Dichloropropane | 2.00 | −1.60<br>−1.60<br>−1.62 | −1.60 | −1.52 | | | −0.01<br>0.00<br>0.03 | | |
| Propyl bromide | 2.10 | −1.69<br>−1.73 | −1.71 | −1.62 | | | 0.08<br>0.02 | | |
| 1-Nitropropane | 0.87 | −0.80 | −0.80 | −0.37 | | | −0.02<br>−0.05 | | |
| Propyl chloride | 2.04 | −1.46 | −1.46 | −1.55 | *sec*-Butyl alcohol | 0.61 | 0.38<br>0.35 | 0.39 | −0.10 |
| Isopropyl chloride | 1.90 | −1.40 | −1.40 | −1.41 | | | 0.40<br>0.52 | | |
| Methylal | 0.00 | 0.64 | 0.64 | 0.52 | | | 0.23 | | |
| Furan | 1.34 | −0.83 | −0.83 | −0.84 | | | 0.48 | | |
| Thiophene | 1.81 | −1.45 | −1.45 | −1.33 | Isobutyl alcohol | 0.75 | 0.07<br>0.08<br>0.13 | 0.06 | −0.25 |
| 1,3-Butadiene | 1.99 | −1.86 | −1.86 | −1.51 | | | | | |
| 2-Bromobutyric acid | 1.42 | −0.40 | −0.40 | −0.92 | | | 0.04<br>0.02<br>0.01 | | |

*(continued)*

**Table I—*Continued***

| Solute | Experimental Log *PC* | Observed Log Molar Solubility | Observed Log Solubility Average | Log Solubility Predicted by Eq. 3 |
|---|---|---|---|---|
| Diethyl ether | 0.83 | −0.09 | −0.06 | −0.32 |
| | | −0.03 | | |
| | | −0.09 | | |
| | | −0.01 | | |
| | | −0.03 | | |
| | | −0.09 | | |
| | | −0.14 | | |
| | | −0.06 | | |
| | | −0.14 | | |
| | | −0.09 | | |
| | | −0.03 | | |
| | | −0.09 | | |
| | | −0.01 | | |
| | | −0.03 | | |
| 1-Butanethiol | 2.28 | −2.08 | −2.08 | −1.80 |
| Ethyl sulfide | 1.95 | −1.47 | −1.46 | −1.46 |
| | | −1.46 | | |
| 1,4-Pentadiene | 1.48 | −2.09 | −2.09 | −0.99 |
| Ethyl propionate | 1.21 | −0.77 | −0.72 | −0.72 |
| | | −0.63 | | |
| | | −0.77 | | |
| 1-Pentanol | 1.48 | −0.60 | −0.60 | −0.99 |
| | | −0.62 | | |
| | | −0.60 | | |
| | | −0.57 | | |
| | | −0.62 | | |
| | | −0.67 | | |
| | | −0.57 | | |
| | | −0.60 | | |
| | | −0.64 | | |
| | | −0.64 | | |
| | | −0.60 | | |
| | | −0.50 | | |
| | | −0.60 | | |
| | | −0.51 | | |
| 3-Pentanol | 1.21 | −0.20 | −0.23 | −0.71 |
| | | −0.23 | | |
| | | −0.27 | | |
| | | −0.28 | | |
| | | −0.22 | | |
| | | −0.21 | | |
| 3-Methyl-2-butanol | 1.28 | −0.16 | −0.21 | −0.78 |
| | | −0.20 | | |
| | | −0.24 | | |
| | | −0.26 | | |
| 2,2-Dimethyl-1-propanol | 1.34 | −0.37 | −0.42 | −0.84 |
| | | −0.40 | | |
| | | −0.43 | | |
| | | −0.44 | | |
| | | −0.44 | | |
| 2-Methyl-1-butanol | 1.29 | −0.44 | −0.48 | −0.79 |
| | | −0.47 | | |
| | | −0.49 | | |
| | | −0.53 | | |
| Isopentyl alcohol | 1.29 | −0.52 | −0.52 | −0.79 |
| | | −0.52 | | |
| *tert*-Pentyl alcohol | 0.89 | 0.20 | 0.20 | −0.39 |
| Ethyl methylal | 0.84 | −0.17 | −0.17 | −0.34 |
| *o*-Dichlorobenzene | 3.38 | −3.01 | −3.13 | −2.92 |
| | | −3.26 | | |
| *m*-Dichlorobenzene | 3.38 | −3.08 | −3.08 | −2.92 |
| Bromobenzene | 2.99 | −2.58 | −2.39 | −2.52 |
| | | −2.50 | | |
| | | −2.10 | | |
| Chlorobenzene | 2.84 | −2.35 | −2.26 | −2.37 |
| | | −2.36 | | |
| | | −2.36 | | |
| | | −2.36 | | |
| | | −1.80 | | |
| | | −2.32 | | |
| Fluorobenzene | 2.27 | −1.79 | −1.79 | −1.79 |
| | | −1.80 | | |
| | | −1.80 | | |
| Iodobenzene | 3.25 | −3.05 | −2.87 | −2.79 |
| | | −2.78 | | |
| | | −2.78 | | |
| Nitrobenzene | 1.87 | −2.19 | −2.07 | −1.38 |
| | | −2.16 | | |
| | | −2.14 | | |
| | | −2.11 | | |
| | | −2.01 | | |
| | | −1.80 | | |
| | | −2.09 | | |
| Benzene | 2.01 | −1.66 | −1.66 | −1.53 |
| | | −1.65 | | |
| | | −1.65 | | |
| | | −1.64 | | |
| | | −1.63 | | |
| | | −1.61 | | |
| | | −1.57 | | |
| | | −1.57 | | |
| | | −1.65 | | |
| | | −1.65 | | |
| | | −1.62 | | |
| | | −1.63 | | |
| | | −1.64 | | |
| | | −1.63 | | |
| | | −1.61 | | |
| | | −1.64 | | |
| | | −1.64 | | |
| | | −1.64 | | |
| | | −1.71 | | |
| | | −1.74 | | |
| | | −1.64 | | |
| | | −1.63 | | |
| | | −1.61 | | |
| | | −1.64 | | |
| | | −1.65 | | |
| | | −1.71 | | |
| | | −2.05 | | |
| Aniline | 0.93 | −0.39 | −0.15 | −0.43 |
| | | 0.10 | | |
| 1,4-Cyclohexadiene | 2.30 | −2.06 | −1.97 | −1.82 |
| | | −1.93 | | |
| | | −1.92 | | |
| Phenylhydrazine | 1.25 | 0.07 | 0.07 | −0.75 |
| Cyclohexene | 2.86 | −2.59 | −2.61 | −2.39 |
| | | −2.44 | | |
| | | −2.43 | | |
| | | −2.80 | | |
| | | −2.80 | | |
| 1,5-Hexadiene | 2.45 | −2.69 | −2.69 | −1.97 |
| Cyclohexanone | 0.81 | −0.61 | −0.33 | −0.30 |
| | | −0.05 | | |
| Cyclohexane | 3.44 | −3.18 | −3.07 | −2.98 |
| | | −2.98 | | |
| | | −2.98 | | |
| | | −3.10 | | |
| | | −3.17 | | |
| | | −3.02 | | |
| Methyl butyl ketone | 1.38 | −0.76 | −0.83 | −0.89 |
| | | −0.76 | | |
| | | −0.78 | | |
| | | −0.85 | | |
| | | −0.78 | | |
| | | −0.85 | | |
| | | −0.76 | | |
| | | −0.79 | | |
| | | −0.82 | | |
| | | −0.69 | | |
| | | −0.84 | | |
| | | −0.46 | | |
| | | −1.66 | | |
| Cyclohexanol | 1.23 | 0.07 | −0.30 | −0.73 |
| | | −0.25 | | |
| | | −0.44 | | |
| | | −0.49 | | |
| | | −0.41 | | |
| *n*-Caproic acid | 1.90 | −1.08 | −1.07 | −1.41 |
| | | −1.06 | | |
| | | −1.03 | | |
| | | −1.17 | | |
| | | −1.06 | | |
| | | −1.02 | | |

**Table I—*Continued***

| Solute | Experimental Log *PC* | Observed Log Molar Solubility | Observed Log Solubility Average | Log Solubility Predicted by Eq. 3 |
|---|---|---|---|---|
| 2,2-Dimethylbutane | 3.82 | −3.67 | −3.61 | −3.37 |
| | | −3.56 | | |
| | | −3.61 | | |
| 2,3-Dimethylbutane | 3.85 | −3.58 | −3.62 | −3.40 |
| | | −3.65 | | |
| 1-Hexanol | 2.03 | −1.24 | −1.24 | −1.55 |
| | | −1.27 | | |
| | | −1.29 | | |
| | | −1.21 | | |
| | | −1.22 | | |
| | | −1.22 | | |
| | | −1.26 | | |
| | | −1.26 | | |
| | | −1.25 | | |
| | | −1.16 | | |
| | | −1.23 | | |
| | | −1.23 | | |
| | | −1.24 | | |
| | | −1.25 | | |
| 3,3-Dimethyl-2-butanol | 1.48 | −0.59 | −0.65 | −0.99 |
| | | −0.62 | | |
| | | −0.66 | | |
| | | −0.72 | | |
| Propyl ether | 2.03 | −1.32 | −1.49 | −1.55 |
| | | −1.28 | | |
| | | −1.61 | | |
| | | −1.53 | | |
| | | −1.61 | | |
| | | −1.61 | | |
| Acetal | 0.84 | −0.37 | −0.37 | −0.34 |
| *n*-Dipropylamine | 1.70 | −0.54 | −0.54 | −1.21 |
| Triethylamine | 1.45 | −0.83 | −0.83 | −0.96 |
| Benzotrifluoride | 2.79 | −2.51 | −2.51 | −2.32 |
| Benzaldehyde | 1.48 | −1.18 | −1.37 | −0.99 |
| | | −1.21 | | |
| | | −1.40 | | |
| | | −1.21 | | |
| | | −1.49 | | |
| | | −1.48 | | |
| | | −1.43 | | |
| | | −1.21 | | |
| | | −1.51 | | |
| | | −1.51 | | |
| | | −1.57 | | |
| *o*-Chlorotoluene | 3.42 | −2.53 | −2.53 | −2.96 |
| *p*-Chlorotoluene | 3.33 | −2.53 | −2.53 | −2.87 |
| *o*-Nitrotoluene | 2.30 | −2.32 | −2.32 | −1.82 |
| *m*-Nitrotoluene | 2.43 | −2.44 | −2.44 | −1.96 |
| Toluene | 2.58 | −2.22 | −2.24 | −2.11 |
| | | −2.27 | | |
| | | −2.27 | | |
| | | −2.28 | | |
| | | −2.42 | | |
| | | −2.24 | | |
| | | −2.17 | | |
| | | −2.24 | | |
| | | −2.25 | | |
| | | −2.17 | | |
| | | −2.14 | | |
| | | −2.21 | | |
| Benzyl alcohol | 1.02 | −0.47 | −0.45 | −0.52 |
| | | −0.43 | | |
| Ethynylbenzene | 2.53 | −2.35 | −2.35 | −2.06 |
| Styrene | 2.95 | −2.54 | −2.54 | −2.48 |
| Methyl benzoate | 2.12 | −1.95 | −1.81 | −1.64 |
| | | −1.73 | | |
| | | −1.75 | | |
| Acetophenone | 1.66 | −1.33 | −1.31 | −1.17 |
| | | −1.28 | | |
| Phenethyl alcohol | 1.36 | −0.88 | −0.88 | −0.87 |
| *o*-Xylene | 2.95 | −2.72 | −2.76 | −2.48 |
| | | −2.78 | | |
| | | −2.79 | | |
| | | −2.70 | | |
| | | −2.80 | | |
| *m*-Xylene | 3.20 | −2.79 | −2.82 | −2.74 |
| | | −2.73 | | |
| | | −2.86 | | |
| | | −2.82 | | |
| | | −2.90 | | |
| *p*-Xylene | 3.15 | −2.72 | −2.77 | −2.69 |
| | | −2.73 | | |
| | | −2.83 | | |
| | | −2.76 | | |
| | | −2.83 | | |
| Ethylbenzene | 3.15 | −2.80 | −2.81 | −2.69 |
| | | −2.71 | | |
| | | −2.84 | | |
| | | −2.82 | | |
| | | −2.82 | | |
| | | −2.78 | | |
| | | −2.91 | | |
| | | −2.79 | | |
| | | −2.85 | | |
| 2-Phenylethanol | 1.36 | −0.79 | −0.74 | −0.87 |
| | | −0.70 | | |
| *o*-Methylbenzyl alcohol | 1.59 | −0.39 | −0.39 | −1.10 |
| *p*-Methylbenzyl alcohol | 1.59 | −1.20 | −1.20 | −1.10 |
| 2-Phenoxyethanol | 1.16 | −0.71 | −0.71 | −0.67 |
| | | −0.71 | | |
| Phenetole | 2.51 | −2.08 | −2.08 | −2.04 |
| Octanol | 3.15 | −2.49 | −2.39 | −2.68 |
| | | −2.42 | | |
| | | −2.39 | | |
| | | −2.35 | | |
| | | −2.35 | | |
| | | −2.34 | | |
| 2-Ethylhexylamine | 2.82 | −1.71 | −1.71 | −2.35 |
| *n*-Dibutylamine | 2.75 | −1.44 | −1.44 | −2.28 |
| Quinoline | 2.03 | −0.33 | −0.33 | −1.55 |
| Cinnamaldehyde | 1.90 | −1.97 | −1.97 | −1.42 |
| Ethyl benzoate | 2.64 | −2.08 | −2.22 | −2.17 |
| | | −2.32 | | |
| | | −2.27 | | |
| *n*-Propylbenzene | 3.63 | −3.34 | −3.14 | −3.17 |
| | | −3.30 | | |
| | | −3.00 | | |
| | | −3.00 | | |
| | | −3.08 | | |
| Cumene | 3.66 | −3.22 | −3.21 | −3.20 |
| | | −3.38 | | |
| | | −3.36 | | |
| | | −3.26 | | |
| | | −3.39 | | |
| | | −2.85 | | |
| | | −3.17 | | |
| | | −3.17 | | |
| | | −3.14 | | |
| Mesitylene | 3.42 | −3.09 | −3.24 | −2.96 |
| | | −3.40 | | |
| 3-Phenylpropanol | 1.88 | −1.38 | −1.38 | −1.39 |
| Ethyl cinnamate | 2.99 | −3.00 | −3.00 | −2.52 |
| Phenyl ether | 4.28 | −2.60 | −2.60 | −3.83 |
| 1-Dodecanol | 5.13 | −5.04 | −4.80 | −4.70 |
| | | −4.81 | | |
| | | −4.71 | | |
| | | −4.64 | | |
| Diphenylmethane | 4.14 | −4.08 | −4.07 | −3.70 |
| | | −4.06 | | |
| Tributyrin | 2.54 | −3.48 | −3.48 | −2.06 |

nol–water partition systems are available, were included. A total of 111 compounds were studied.

**Solubility**—The aqueous solubility data in the desired temperature range were obtained from a compilation of data gathered from several literature sources. All available aqueous solubility values for each compound are listed in Table I. Also shown in Table I are the average of solubility values used for statistical analysis.

**Partition Coefficients**—Although partition coefficients are reported for nearly 100 oil–water partitioning systems, almost one-quarter of the compiled data refer to the octanol–water system (10). Therefore, the octanol–water partitioning system was chosen. The experimental partition coefficients for all the compounds were obtained from Ref. 10. In cases where multiple partition coefficients were reported for a compound, the values were averaged. Only a few obvious outliers were omitted in the averaging of partition coefficients.

**Calculations and Treatment of Data**—All reported aqueous solubilities were converted to grammar (grams per liter) or molar (moles per liter) units with appropriate use of the solute molecular weight. Approximate mole fractional solubilities ($X$) were calculated from molar solubilities ($S_w$) by:

$$X = \frac{S_w}{S_w + \dfrac{1000 - (\text{mol. wt.})\, S_w}{18}} \qquad \text{(Eq. 1)}$$

This approximation assumes a density of unity and equivalent molar and partial molal volumes for all compounds, an approximation that is not strictly valid but that introduces no systematic error in the calculations.

The mole fractional partition coefficients ($PC_x$) were calculated from the reported octanol–water partition coefficients ($PC$) by:

$$PC_x = PC\frac{M_w}{M_o} \qquad \text{(Eq. 2)}$$

where $M_w$ and $M_o$ are the molarities of pure water (55.5) and pure octanol (6.35), respectively.

**Statistical Analysis**—The statistical data analysis was performed using standard statistical analysis procedures.

## RESULTS

The molar aqueous solubility ($S_w$) and the octanol–water partition coefficient ($PC$) are related by:

$$\log S_w = -1.016 \log PC + 0.515 \qquad \text{(Eq. 3)}$$
$$n = 111 \quad r = 0.931 \quad s = 0.421$$

where $n$ is the number of observations, $r$ is the correlation coefficient, and $s$ is the standard deviation.

The aqueous solubility and octanol–water partition coefficients used for Eq. 3 are presented in Table I. Figure 1 is a graphical representation of the observed and predicted solubilities based on Eq. 3.

If aqueous solubility is expressed as grams per liter ($S_g$) instead of moles per liter, the following relationship is obtained:

$$\log S_g = -0.95 \log PC + 2.40 \qquad \text{(Eq. 4)}$$
$$n = 111 \quad r = 0.916 \quad s = 0.438$$

For mole fractional units, the expression is:

$$\log X = -1.026 \log PC_x - 0.23 \qquad \text{(Eq. 5)}$$
$$n = 111 \quad r = 0.931 \quad s = 0.427$$

where $X$ is the mole fractional aqueous solubility and $PC_x$ is the octanol–water partition coefficient in mole fractional units.

## DISCUSSION

Thermodynamically, the partition coefficient is defined as an equilibrium constant relating the activity of the solute in two immiscible phases at equilibrium (11):

$$PC = \frac{\alpha_o}{\alpha_w} \qquad \text{(Eq. 6)}$$

where $\alpha_o$ and $\alpha_w$ are the activities of the solute in oil and water, respectively. An alternative form of Eq. 6 is:

$$PC = \frac{\gamma_o C_o}{\gamma_w C_w} \qquad \text{(Eq. 7)}$$

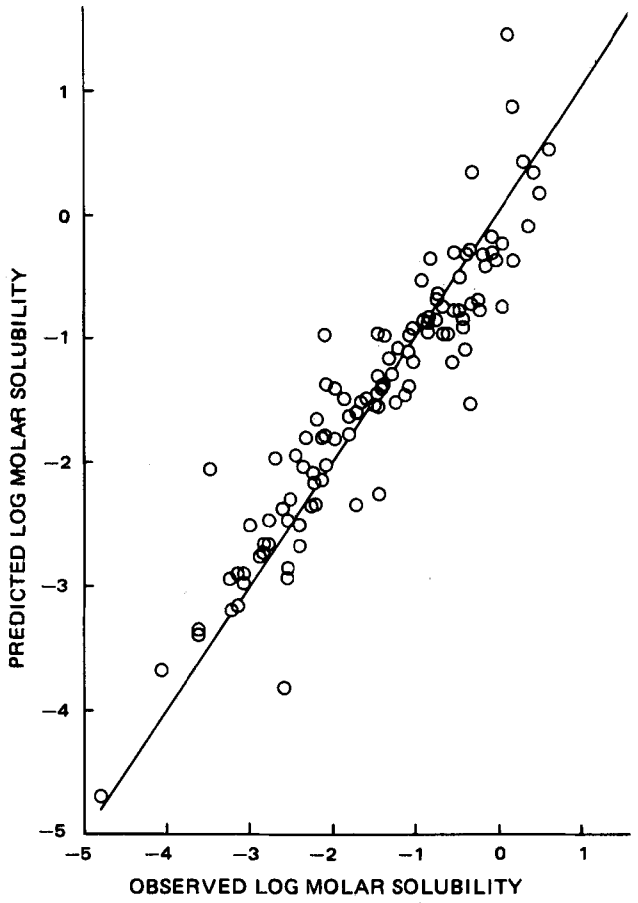


**Figure 1**—*Observed molar aqueous solubility* versus *molar solubility predicted by Eq. 3.*

where the activity is replaced by a product of the activity coefficient ($\gamma$) and the concentration ($C$) of the solute. In dilute solutions, the activity coefficients can be approximated by unity. Therefore, Eq. 7 reduces to:

$$PC = \frac{C_o}{C_w} \qquad \text{(Eq. 8)}$$

For most liquid solutes, the concentrations at saturation are equal to the solubilities in oil and water phases, respectively. Therefore:

$$PC = \frac{S_o}{S_w} \qquad \text{(Eq. 9)}$$

The logarithmic form of Eq. 9 is:

$$\log S_w = -\log PC + \log S_o \qquad \text{(Eq. 10)}$$

Although partitioning was restricted to octanol–water systems in the present study, it is applicable to most solvent systems. The major difference may be in the coefficient values of some equations.

If the solubilities of liquid solutes in octanol are comparable, the log $S_o$ term in Eq. 10 will nearly be constant. In fact, almost all liquids included in this study are completely miscible with octanol. Therefore, their solubilities in octanol are equal to their molarities in the pure state or, on a mole fractional scale, they are equal to unity.

This finding suggests that octanol behaves as a nearly ideal (in thermodynamic sense) solvent for the liquid solutes considered. The reason for this excellent solvency of octanol for organic liquids is that its polarity is in the middle of the range where most organic liquids are found. If the solubility parameter ($\delta$) is used as a measure of solvent polarity, octanol has a $\delta$ value of 10.3 (12). The lowest normally encountered $\delta$ value for pure hydrocarbons is about 7. Most nonionizable compounds have solubility parameters between 7 and 15. The exceptions are water and some polyhydroxy alcohols; ethylene glycol, glycerol, and propylene glycol have $\delta$ values greater than 15. Methanol and ethanol have $\delta$ values of 14.5 and 13, respectively.

The results obtained from this study are in excellent agreement with Eq. 10. The coefficients of log $PC$ for Eqs. 3–5 are almost identical and

very close to −1 as predicted by Eq. 10. This finding is noteworthy since the data used for these analyses cover a wide variety of organic nonelectrolyte liquids and span over five orders of magnitude. Furthermore, the aqueous solubility and partition coefficient data were taken from the work of many independent investigators who used various experimental techniques and compounds of various degrees of purity. Moreover, the aqueous solubility data cover a temperature range of 20–40°.

Along with the variation in the solubility and partition coefficients, a slight deviation in log *PC* may be attributed to the nonideal behavior of liquid solutes. The assumption of dilute solutions and activity coefficients being unity may not be completely valid. In fact, the data include several compounds with aqueous solubilities greater than 1.0 *M*. Mutual solubility and self-association of low molecular weight solutes may contribute to the deviation observed.

If the aqueous solubilities and octanol–water partition coefficients are expressed in mole fraction units and if it is assumed that the solutes are completely miscible with octanol, then log $S_o$ in Eq. 10 is expected to be zero. Examination of Eq. 5, which relates the mole fractional aqueous solubilities and partition coefficients, reveals that the intercept is indeed close to zero.

The significance of the intercept can be further explained as follows. If it is assumed that the solutes are miscible with octanol and that the average density of liquid solutes is ~1 g/ml, then the solubility of liquid solutes in octanol can be approximated with their densities. Upon substitution of the average density value in Eq. 10, an intercept value of 3.0 is expected. The intercept value obtained (2.54) from Eq. 4 is in reasonable agreement with the value expected from Eq. 10. The assumption of miscibility and the use of average density were verified in great detail by Roseman[1].

These results, although in qualitative agreement with those of Hansch *et al.* (9), differ significantly in the coefficient of log *PC*. The relationship between molal aqueous solubility and partition coefficients of several liquid nonelectrolytes was reported in their work (9):

$$\log S = -1.339 \log PC + 0.978 \qquad \text{(Eq. 11)}$$
$$n = 156 \quad r = 0.935 \quad s = 0.472$$

Almost all of the partition coefficients used in Eq. 11 were calculated from the group contribution approach. Only 22 of 156 partition coefficients reported were experimentally determined. The coefficient of log *PC* in Eq. 11 is significantly different from −1, the value expected from Eq. 10. The deviation may be attributed to a systematic error in the calculated partition coefficients for hydrocarbons[2]. The significance of the results reported in this study can be illustrated by the following:

1. Only experimentally determined partition coefficients and solubility values were used.
2. A greater number of experimentally measured partition coefficients are available now than were available in 1968.
3. More solubility values were used.
4. Since no calculated values were used, systematic errors in values for a series of compounds are not likely.

Furthermore, these results are supported by the equality of partition coefficients and solubility ratios observed by Roseman[1] for various drugs in several oil–water systems. This relationship is important in understanding the solubility and partitioning phenomena of liquids and will provide a basis for crystalline solids and gaseous compounds.

These equations can be helpful in assessing the reliability of reported values for aqueous solubility estimation. These equations were employed to verify the solubility or partition coefficients of a few compounds that showed a great difference between the calculated and observed values, and this study will be the subject of a separate report.

## REFERENCES


(1) C. Hansch and W. J. Dunn, III, *J. Pharm. Sci.*, **61**, 1 (1972).
(2) C. Hansch and J. M. Clayton, *ibid.*, **62**, 1 (1973).
(3) A. Leo, C. Hansch, and D. Elkins, *Chem. Rev.*, **71**, 525 (1971).
(4) T. J. Roseman, *J. Pharm. Sci.*, **61**, 46 (1972).
(5) G. L. Flynn and S. H. Yalkowsky, *ibid.*, **61**, 838 (1972).
(6) S. H. Yalkowsky and G. L. Flynn, *ibid.*, **62**, 218 (1973).
(7) *Ibid.*, **63**, 1276 (1974).
(8) S. H. Yalkowsky, T. G. Slunick, and G. L. Flynn, *J. Pharm. Sci.*, **63**, 691 (1974).
(9) C. Hansch, J. E. Quinlan, and G. L. Lawrence, *J. Org. Chem.*, **33**, 347 (1968).
(10) C. Hansch and A. J. Leo, "Substituent Constants for Correlation Analysis in Chemistry and Biology," Wiley, New York, N.Y., 1979.
(11) K. S. Pitzer and L. Brewer, in "Thermodynamics," G. N. Lewis and M. Randall, Eds., McGraw-Hill, New York, N.Y., 1961, pp. 242–256.
(12) J. H. Hildebrand and R. L. Scott, "The Solubility of Non-electrolytes," Reinhold, New York, N.Y., 1950.


[1] T. J. Roseman, The Upjohn Co., Kalamazoo, Mich., unpublished data.

[2] A. Leo and C. Hansch, Department of Chemistry, Pomona College, Claremont, Calif., personal communication.

# High-Performance Liquid Chromatographic Assay for Fenoprofen in Human Plasma


**R. J. BOPP ˣ, K. Z. FARID, and J. F. NASH**



Received April 8, 1980, from the *Analytical Development Department, Lilly Research Laboratories, Eli Lilly and Company, Indianapolis, IN 46285.* Accepted for publication October 15, 1980.



**Abstract** □ A high-performance liquid chromatographic method is described for the quantitation of fenoprofen, *dl*-2-(3-phenoxyphenyl)-propionic acid, in human plasma. The proteins in plasma were precipitated by the addition of hydrochloric acid. Fenoprofen and the internal standard, *dl*-2-(4-phenoxyphenyl)valeric acid, were extracted into butyl chloride and then back-extracted into sodium hydroxide. The aqueous solution was injected onto a reversed-phase alkylphenyl column, and the compounds were eluted using a mobile phase of acetonitrile–water–acetic acid (50:50:2 v/v/v). At a flow rate of 1 ml/min, the retention times of fenoprofen and the internal standard were 8 and 12 min, respectively. The absorbance was monitored at 272 nm. The method requires 1.0 ml of plasma and is sensitive to 0.5 μg/ml. This procedure has been used for routine assay of multiple samples from bioavailability and compliance studies.



**Keyphrases** □ Fenoprofen—high-performance liquid chromatographic analysis, human plasma □ High-performance liquid chromatography—assay, fenoprofen, human plasma □ Anti-inflammatory agents—fenoprofen, high-performance liquid chromatographic analysis, human plasma


The pharmacological and toxicological properties of fenoprofen [*dl*-2-(3-phenoxyphenyl)propionic acid, I] have been studied extensively and were reviewed recently (1–3). Compound I was shown to be absorbed readily after oral administration. It is extensively metabolized to I glucuronide and to *dl*-2-[3-(4-hydroxyphenoxy)phenyl]propionic acid (II) glucuronide, both of which are excreted rapidly in the urine (4, 5).


0022-3549/81/0500-0507$01.00/0


© 1981, American Pharmaceutical Association

very close to −1 as predicted by Eq. 10. This finding is noteworthy since the data used for these analyses cover a wide variety of organic nonelectrolyte liquids and span over five orders of magnitude. Furthermore, the aqueous solubility and partition coefficient data were taken from the work of many independent investigators who used various experimental techniques and compounds of various degrees of purity. Moreover, the aqueous solubility data cover a temperature range of 20–40°.

Along with the variation in the solubility and partition coefficients, a slight deviation in log *PC* may be attributed to the nonideal behavior of liquid solutes. The assumption of dilute solutions and activity coefficients being unity may not be completely valid. In fact, the data include several compounds with aqueous solubilities greater than 1.0 *M*. Mutual solubility and self-association of low molecular weight solutes may contribute to the deviation observed.

If the aqueous solubilities and octanol–water partition coefficients are expressed in mole fraction units and if it is assumed that the solutes are completely miscible with octanol, then log $S_o$ in Eq. 10 is expected to be zero. Examination of Eq. 5, which relates the mole fractional aqueous solubilities and partition coefficients, reveals that the intercept is indeed close to zero.

The significance of the intercept can be further explained as follows. If it is assumed that the solutes are miscible with octanol and that the average density of liquid solutes is ~1 g/ml, then the solubility of liquid solutes in octanol can be approximated with their densities. Upon substitution of the average density value in Eq. 10, an intercept value of 3.0 is expected. The intercept value obtained (2.54) from Eq. 4 is in reasonable agreement with the value expected from Eq. 10. The assumption of miscibility and the use of average density were verified in great detail by Roseman[1].

These results, although in qualitative agreement with those of Hansch *et al.* (9), differ significantly in the coefficient of log *PC*. The relationship between molal aqueous solubility and partition coefficients of several liquid nonelectrolytes was reported in their work (9):

$$\log S = -1.339 \log PC + 0.978 \qquad \text{(Eq. 11)}$$
$$n = 156 \quad r = 0.935 \quad s = 0.472$$

Almost all of the partition coefficients used in Eq. 11 were calculated from the group contribution approach. Only 22 of 156 partition coefficients reported were experimentally determined. The coefficient of log *PC* in Eq. 11 is significantly different from −1, the value expected from Eq. 10. The deviation may be attributed to a systematic error in the calculated partition coefficients for hydrocarbons[2]. The significance of the results reported in this study can be illustrated by the following:

1. Only experimentally determined partition coefficients and solubility values were used.
2. A greater number of experimentally measured partition coefficients are available now than were available in 1968.
3. More solubility values were used.
4. Since no calculated values were used, systematic errors in values for a series of compounds are not likely.

Furthermore, these results are supported by the equality of partition coefficients and solubility ratios observed by Roseman[1] for various drugs in several oil–water systems. This relationship is important in understanding the solubility and partitioning phenomena of liquids and will provide a basis for crystalline solids and gaseous compounds.

These equations can be helpful in assessing the reliability of reported values for aqueous solubility estimation. These equations were employed to verify the solubility or partition coefficients of a few compounds that showed a great difference between the calculated and observed values, and this study will be the subject of a separate report.

## REFERENCES


(1) C. Hansch and W. J. Dunn, III, *J. Pharm. Sci.*, **61**, 1 (1972).
(2) C. Hansch and J. M. Clayton, *ibid.*, **62**, 1 (1973).
(3) A. Leo, C. Hansch, and D. Elkins, *Chem. Rev.*, **71**, 525 (1971).
(4) T. J. Roseman, *J. Pharm. Sci.*, **61**, 46 (1972).
(5) G. L. Flynn and S. H. Yalkowsky, *ibid.*, **61**, 838 (1972).
(6) S. H. Yalkowsky and G. L. Flynn, *ibid.*, **62**, 218 (1973).
(7) *Ibid.*, **63**, 1276 (1974).
(8) S. H. Yalkowsky, T. G. Slunick, and G. L. Flynn, *J. Pharm. Sci.*, **63**, 691 (1974).
(9) C. Hansch, J. E. Quinlan, and G. L. Lawrence, *J. Org. Chem.*, **33**, 347 (1968).
(10) C. Hansch and A. J. Leo, "Substituent Constants for Correlation Analysis in Chemistry and Biology," Wiley, New York, N.Y., 1979.
(11) K. S. Pitzer and L. Brewer, in "Thermodynamics," G. N. Lewis and M. Randall, Eds., McGraw-Hill, New York, N.Y., 1961, pp. 242–256.
(12) J. H. Hildebrand and R. L. Scott, "The Solubility of Non-electrolytes," Reinhold, New York, N.Y., 1950.


[1] T. J. Roseman, The Upjohn Co., Kalamazoo, Mich., unpublished data.

[2] A. Leo and C. Hansch, Department of Chemistry, Pomona College, Claremont, Calif., personal communication.

# High-Performance Liquid Chromatographic Assay for Fenoprofen in Human Plasma


**R. J. BOPP ˣ, K. Z. FARID, and J. F. NASH**



Received April 8, 1980, from the *Analytical Development Department, Lilly Research Laboratories, Eli Lilly and Company, Indianapolis, IN 46285.* Accepted for publication October 15, 1980.



**Abstract** □ A high-performance liquid chromatographic method is described for the quantitation of fenoprofen, *dl*-2-(3-phenoxyphenyl)-propionic acid, in human plasma. The proteins in plasma were precipitated by the addition of hydrochloric acid. Fenoprofen and the internal standard, *dl*-2-(4-phenoxyphenyl)valeric acid, were extracted into butyl chloride and then back-extracted into sodium hydroxide. The aqueous solution was injected onto a reversed-phase alkylphenyl column, and the compounds were eluted using a mobile phase of acetonitrile–water–acetic acid (50:50:2 v/v/v). At a flow rate of 1 ml/min, the retention times of fenoprofen and the internal standard were 8 and 12 min, respectively. The absorbance was monitored at 272 nm. The method requires 1.0 ml of plasma and is sensitive to 0.5 μg/ml. This procedure has been used for routine assay of multiple samples from bioavailability and compliance studies.



**Keyphrases** □ Fenoprofen—high-performance liquid chromatographic analysis, human plasma □ High-performance liquid chromatography—assay, fenoprofen, human plasma □ Anti-inflammatory agents—fenoprofen, high-performance liquid chromatographic analysis, human plasma


The pharmacological and toxicological properties of fenoprofen [*dl*-2-(3-phenoxyphenyl)propionic acid, I] have been studied extensively and were reviewed recently (1–3). Compound I was shown to be absorbed readily after oral administration. It is extensively metabolized to I glucuronide and to *dl*-2-[3-(4-hydroxyphenoxy)phenyl]propionic acid (II) glucuronide, both of which are excreted rapidly in the urine (4, 5).


0022-3549/81/0500-0507$01.00/0


© 1981, American Pharmaceutical Association

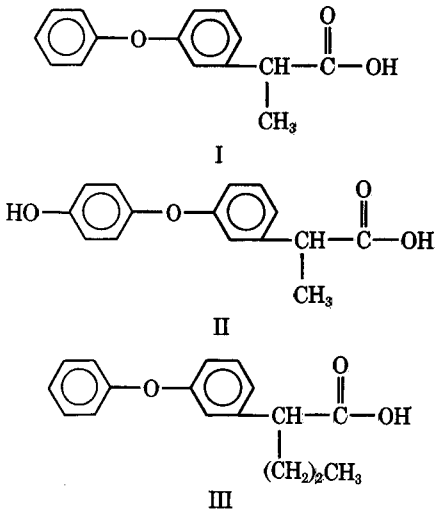

I



II



III

As I and other anti-inflammatory agents of the arylalkanoic acid family were discovered, methodology for assaying these compounds in plasma was developed (6–12). Most of the methods employ GLC of the derivatized drug. Although these methods are reported to be accurate and reproducible, they require extensive sample cleanup prior to derivatization of the extracted compounds. Liquid chromatographic methods were reported recently for the analysis of naproxen in plasma and urine (13) and of ketoprofen in biological fluids (14, 15).

This paper reports a simple, sensitive, and reproducible high-performance liquid chromatographic (HPLC) plasma assay of I that was used in bioavailability studies.

## EXPERIMENTAL

**Chemicals and Reagents**—Fenoprofen sodium [sodium *dl*-2-(3-phenoxyphenyl)propionate dihydrate], *dl*-2-[3-(4-hydroxyphenoxy)-phenyl]propionic acid (II), and *dl*-2-(4-phenoxyphenyl)valeric acid (III) as the internal standard were synthesized[1]. All organic solvents were distilled in glass[2]. Sodium hydroxide, hydrochloric acid, and acetic acid were analytical grade. Plasma was separated from fresh heparinized blood of normal human volunteers. The plasma was pooled and stored at 4° in glass containers and used within 1 month.

**Instrumentation**—The chromatograph consisted of a pump[3], an autosample injector[4] modified with a pneumatic-actuated injection valve fitted with a 50-μl sample loop[5], a microparticulate reversed-phase column[6] (30 cm × 3.9 mm), a variable-wavelength detector[7], and a potentiometric recorder[8].

The HPLC system was operated at ambient temperature with acetonitrile–distilled water–acetic acid (50:50:2 v/v/v) as the mobile phase at a flow rate of 1.0 ml/min. Prior to use, the mobile phase was degassed by refluxing for 10 min. The detector was set at 272 nm and a sensitivity of 0.02 aufs.

**Procedure**—A calibration curve was prepared by pipetting 1.0 ml of fresh human plasma into five individual centrifuge tubes followed by the addition of 0, 50, 150, 300, and 600 μl of an aqueous solution of 100 μg of I/ml. The tubes represented 0, 5, 15, 30, and 60 μg of I/ml of plasma, respectively. To each tube was added 0.5 ml of III (60 μg/ml) in 0.01 *N* NaOH.

The standards were acidified with 1 ml of 1.0 *N* HCl and vortexed, and I and III were extracted into 10 ml of butyl chloride by use of a rotating mixer[9] set at 20 rpm for 10 min. The rotating speed should be low enough so that emulsification does not occur. The organic phase was separated by centrifugation at 2000 rpm for 5 min and then transferred to another centrifuge tube containing 1.0 ml of 0.1 *N* NaOH. The phases were mixed at 40 rpm for 5 min and separated by centrifugation, and the butyl chloride was discarded. The aqueous phase (0.7 ml) was placed into an autoinjector sample vial[10], and 50 μl of the solution was injected onto the column. One milliliter of the unknown plasma samples was assayed for I in a similar manner.

The calibration curve was constructed by plotting the peak height

[1] Eli Lilly and Co., Indianapolis, Ind.
[2] Burdick & Jackson Laboratories, Muskegon, Mich.
[3] Model 6000A, Waters Associates, Milford, Mass.
[4] Model 725, Micromeritics Instrument Corp., Norcross, Ga.
[5] Model 70-10A, Rheodyne, Berkeley, Calif.
[6] μBondapak alkylphenyl, Waters Associates, Milford, Mass.
[7] Model 450, Waters Associates, Milford, Mass.
[8] Model 355, Linear Instruments Corp., Irvine, Calif.
[9] Roto-Torque, Cole Parmer, Chicago, Ill.

**Table I—Efficiency of the Extraction of Fenoprofen from Plasma**

| Fenoprofen Added, μg/ml | Peak Heights, mm (*SD*) Absolute Standards[a] | Extracted Standards[b] | Extraction Efficiency, % |
|---|---|---|---|
| 5 | 9.5 (0.0) | 8.5 (0.3)[c] | 89.5 |
| 15 | 28.8 (0.4) | 27.5 (0.0) | 95.5 |
| 30 | 57.8 (0.4) | 55.6 (0.4) | 96.2 |
| 60 | 119.0 (2.1) | 113.3 (0.5) | 95.2 |

[a] Two replicates. [b] Four replicates. [c] Corrected to reflect 75% recovery of butyl chloride.

**Table II—Reproducibility of Standard Curves of Fenoprofen in Human Plasma on 3 Successive Days[a]**

| Fenoprofen Added, μg/ml | Peak Height Ratio (*SD*) of Fenoprofen to Internal Standard | Fenoprofen (*SD*) Found, μg/ml |
|---|---|---|
| 5 | 0.401 (0.024) | 5.36 (0.48) |
| 15 | 1.063 (0.044) | 14.70 (0.11) |
| 30 | 2.131 (0.064) | 29.78 (0.85) |
| 60 | 4.286 (0.110) | 60.15 (0.39) |

[a] Linear regression equation: $y = 0.07132\ (0.00224)x + 0.02779\ (0.04308)$; $r = 0.99970\ (0.00028)$.

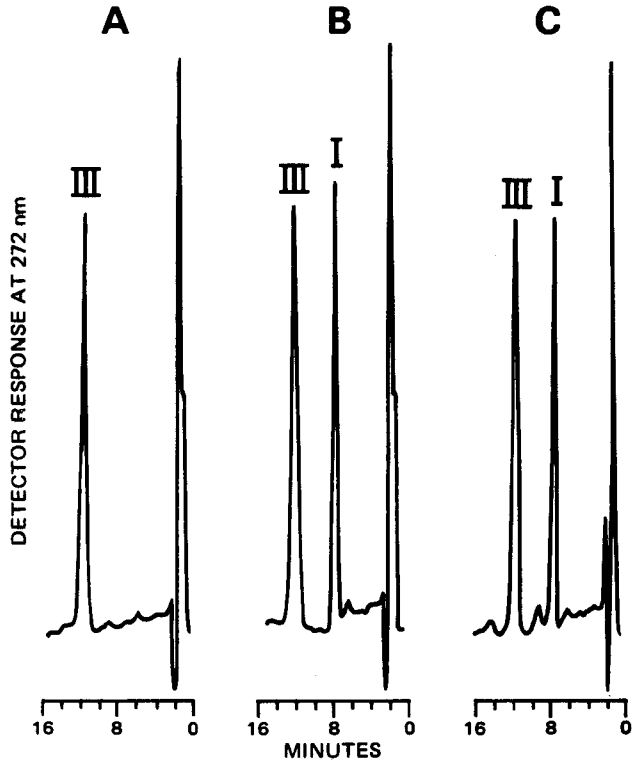


**Figure 1**—*Chromatograms of the extracts of a plasma sample at time zero spiked with 30 μg of III/ml (A), human plasma spiked with 15 μg of fenoprofen (I) and 30 μg of III/ml (B), and a plasma sample taken 0.5 hr after administration of 300 mg of I and spiked with 30 μg of III/ml (C).*

[10] Catalog models 08035-A and 41221013, Brockway Glass Co., Indianapolis, Ind.

**Table III—Precision of the HPLC Assay for Fenoprofen in Human Plasma**

| Day | *In Vivo* Pools of Fenoprofen ($n$ = 5) 1 | 2 | 3 | 4 |
|---|---|---|---|---|
| Day 1 | | | | |
| $\bar{X}$, μg/ml | 5.66 | 4.28 | 11.90 | 22.82 |
| *RSD*, % | 2.30 | 1.87 | 1.34 | 1.10 |
| Day 2 | | | | |
| $\bar{X}$, μg/ml | 4.24 | 3.28 | 10.96 | 22.38 |
| *RSD*, % | 3.54 | 3.96 | 2.65 | 1.16 |
| Day 3 | | | | |
| $\bar{X}$, μg/ml | 5.14 | 3.80 | 11.80 | 22.32 |
| *RSD*, % | 5.06 | 4.47 | 3.14 | 1.70 |
| Overall precision | | | | |
| Between-day *RSD*, % | 14.2 | 13.1 | 4.3 | 1.06 |
| Within-day *RSD*, % | 3.8 | 3.5 | 2.5 | 1.33 |
| Total *RSD*, % | 14.7 | 13.6 | 5.0 | 1.70 |

ratios of I to III *versus* the concentration of I per milliliter of plasma. The concentration of I in the unknown samples was obtained by determining the peak height ratios of the samples and reading from the calibration curve.

**Bioavailability Study (9)**—The utility of this method for determining the concentration of I in plasma was demonstrated by assaying plasma samples from three subjects administered a single 300-mg oral dose of I.

## RESULTS AND DISCUSSION

A UV spectrum of a solution of I (1 mg/ml) in the mobile phase showed the absorption maximum to be at 272 nm with shoulders at 265 and 279 nm.

Table I gives the extraction efficiency of I from plasma. The UV response (as noted by peak height) of absolute standards of 5, 15, 30, and 60 μg of I/ml were compared to the same concentrations of extracted standards from plasma. These data showed ~95% recovery of I from plasma.

The day-to-day variability of the calibration curves was determined by preparing and assaying spiked standards of 5, 15, 30, and 60 μg of I/ml of plasma on 3 successive days (Table II). The calibration curves were linear and reproducible over the concentration range of 5–60 μg/ml; the mean (*SD*) linear regression equation was $y = 0.07132\ (0.00224)x + 0.02779\ (0.04308)$, and the mean (*SD*) correlation coefficient was 0.99970 (0.00028).

The within-day and between-day variabilities of the assay were determined by utilizing plasma samples obtained during a bioavailability study. These samples were mixed into four pools on the basis of their drug concentrations. Each *in vitro* pool then was assayed in quintuplicate on 3 different days (Table III). The within-day variability was <4% *RSD* for the four pools, which ranged from 4 to 23 μg of I/ml; however, the between-day variability of the 4.28- and 5.66-μg/ml pools was larger, 13.1 and 14.2 *RSD*, respectively.

Quantitation of I in plasma samples that were assayed immediately and again after several months of storage at 4° showed that there was no significant drug loss.

Chromatograms of extracts from a plasma sample containing III at 0 hr, a plasma sample spiked with I and III, and a plasma sample taken 0.5 hr after administration of a single 300-mg dose of I plus added III are shown in Fig. 1. Compounds I and III ($R_t$ of 8 and 12 min, respectively) were well separated from endogenous interferences.

The elution time of the major metabolite, II ($R_t$ ~6 min), was sufficiently different from I so as not to interfere in the assay. Plasma samples from subjects receiving 300 mg of I contained only traces of unconjugated II.

Injection of 50 μl of 0.1 *N* NaOH containing I had no effect on the elution time or the peak height of I when compared with a 50-μl injection of I in the mobile phase. The amount of acetic acid (0.38 *M*) in the mobile phase was more than sufficient to neutralize rapidly the sodium hydroxide (0.1 *N*) in the injection solvent. The sodium hydroxide solution was used in the assay of hundreds of samples with no deleterious effect on column resolution.

The plasma concentration–time profile of I from three subjects in the bioavailability study is shown in Fig. 2. The among-subject variability

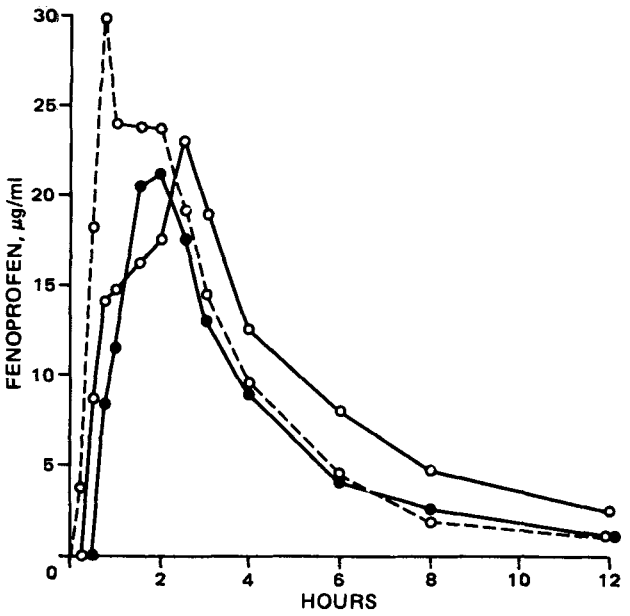


**Figure 2**—*Plasma time–concentration profiles of fenoprofen after administration of a single oral dose of 300 mg to three subjects. Key:* o—, *Subject RB;* ●, *Subject ML; and* o---, *Subject DP.*

was evident by examination of the differences in the concentration maxima and time to reach the peak blood level concentration.

Ibuprofen and benoxaprofen had identical elution times as I under the assay conditions described. Therefore, this assay cannot be used to distinguish between these drugs in clinical samples. Naproxen, with an elution time of 7.8 min, can be distinguished from I.

The described assay was used routinely during the past year to study the bioavailability of fenoprofen from dosage forms containing 50–300 mg of I. The method is simple, sensitive, and reproducible.

## REFERENCES

(1) R. N. Bogden, R. M. Pinder, T. M. Speight, and G. S. Avery, *Drugs*, **13**, 241 (1977).

(2) P. P. Evans, *Am. J. Hosp. Pharm.*, **36**, 622 (1979).

(3) R. E. Pemberton and L. J. Strand, *Dig. Dis. Sci.*, **24**, 53 (1979).

(4) J. F. Nash, L. D. Bechtol, C. A. Bunde, R. J. Bopp, K. Z. Farid, and C. T. Spradlin, *J. Pharm. Sci.*, **68**, 1087 (1979).

(5) A. Rubin, B. E. Rodda, P. Warrick, A. S. Ridolfo, and C. M. Gruber, Jr., *ibid.*, **61**, 739 (1972).

(6) J. F. Nash, R. J. Bopp, and A. Rubin, *ibid.*, **60**, 1062 (1971).

(7) D. G. Kaiser and G. J. Vangiessen, *ibid.*, **63**, 219 (1974).

(8) D. G. Kaiser, S. R. Shaw, and G. J. Vangiessen, *ibid.*, **63**, 567 (1974).

(9) J. P. Desager, M. Vanderbist, and C. Harvengt, *J. Clin. Pharmacol.*, **4**, 189 (1976).

(10) R. V. Smith, D. W. Humprey, and H. Escalona-Castillo, *J. Pharm. Sci.*, **66**, 132 (1977).

(11) R. Runkel, M. D. Chaplin, H. Sevelius, E. Ortega, and E. Segre, *Clin. Pharmacol. Ther.*, **20**, 269 (1977).

(12) D. G. Kaiser and R. S. Martin, *J. Pharm. Sci.*, **67**, 627 (1978).

(13) D. Westerlund, A. Theodorsen, and Y. Jaksch, *J. Liq. Chromatogr.*, **2**, 969 (1979).

(14) A. Bannier, J. L. Brazier, B. Ribon, and C. Quincy, *J. Pharm. Sci.*, **69**, 763 (1980).

(15) R. Ballerini, A. Cambi, P. Del Soldato, F. Melani, and A. Meli, *ibid.*, **68**, 366 (1979).

## ACKNOWLEDGMENTS

The authors thank Dr. L. D. Bechtol of the Lilly Clinic for the plasma samples of fenoprofen from the bioavailability study and Mr. P. R. Page for analysis of these samples.

# Synthesis and Antihistaminic Activity of 1-[(4-Substituted-1,2,3-thiadiazol-5-yl)arylmethyl]-4-methylpiperazines

**A. SHAFIEE** *x, **M. MOHAMADPOUR** *, **F. ABTAHI** ‡, and **A. KHOYI** ‡

Received June 18, 1979, from the *Department of Chemistry, College of Pharmacy, and the ‡Department of Experimental Medicine and Pharmacology, Faculty of Medicine, Tehran University, Tehran, Iran. Accepted for publication December 20, 1979.

**Abstract** □ Starting with readily available aryl 4-substituted-1,2,3-thiadiazol-5-yl ketones, a series of 1-[(4-substituted-1,2,3-thiadiazol-5-yl)arylmethyl]-4-methylpiperazines was synthesized and tested for antihistaminic and anticholinergic activities. Four compounds were potent antihistamines, and two of these compounds displayed moderate anticholinergic activity.

**Keyphrases** □ Antihistaminic activity—1-[(4-substituted-1,2,3-thiadiazol-5-yl)arylmethyl]-4-methylpiperazines, synthesis, IR, NMR, and mass spectral analyses □ Anticholinergic activity—1-[(4-substituted-1,2,3-thiadiazol-5-yl)arylmethyl]-4-methylpiperazines, synthesis, IR, NMR, and mass spectral analyses □ 1-[(4-Substituted-1,2,3-thiadiazol-5-yl)arylmethyl]-4-methylpiperazines—synthesis, antihistaminic and anticholinergic activity

It was reported that piperazine derivatives such as chlorcyclizine (I) and meclizine (II) have significant antihistaminic activity (1). 1,2,3-Thiadiazole derivatives of benzimidazole, benzoxazole, and benzothiazole were reported to be anthelmintics (2). Some phosphorus compounds having the 1,2,3-thiadiazole ring system showed insecticide activity (3), and 4-amino-1,2,3-thiadiazolesulfonamides exhibited antibacterial properties (4). The synthesis and antibacterial activity of 4-substituted-(1,2,3-thiadiazol-5-yl)carbamic acid esters were reported recently (5).

In a continuing effort to find a potent antihistamine with low toxicity (6), a series of 1-[(4-substituted-1,2,3-thiadiazol-5-yl)arylmethyl]-4-methylpiperazines was prepared, and efficacy was determined.

## RESULTS AND DISCUSSION

**Chemistry**—Ethyl 4-substituted-1,2,3-thiadiazole-5-carboxylates were prepared by an oxidative cyclization of methyl or methylene ketone semicarbazones with thionyl chloride (7).

Aryl 4-phenyl-1,2,3-thiadiazol-5-yl ketones (IV, R = $C_6H_5$) were prepared from the reaction of aryllithium (8) with 4-phenyl-1,2,3-thiadiazole-5-carboxylic acid (III, R = $C_6H_5$), and aryl 4-methyl-1,2,3-thiadiazol-5-yl ketones (IV, R = $CH_3$) were prepared from the Friedel–Crafts reaction of 4-methyl-1,2,3-thiadiazole-5-carboxyl chloride (V, R = $CH_3$) with aromatic hydrocarbones. Reduction of IV with sodium borohydride gave (4-substituted-1,2,3-thiadiazol-5-yl)arylcarbinol (VI). Reaction of VI with thionyl chloride in benzene at room temperature gave VII as an intermediate, which was transformed to VIII at 80°. The latter compound afforded IX through reaction with *N*-methylpiperazine. Transformation of VII (R = $CH_3$, R′ = $OCH_3$) to VIII could not be achieved under different experimental conditions. In all cases, a mixture of products was obtained. However, VII (R = $CH_3$, R′ = $OCH_3$) could be converted directly to IX (R = $CH_3$, R′ = $OCH_3$) through the reaction with *N*-methylpiperazine (Scheme I).

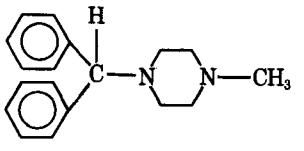

I

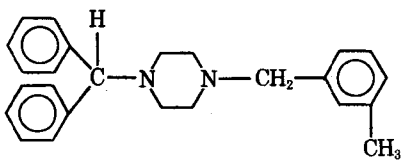

II

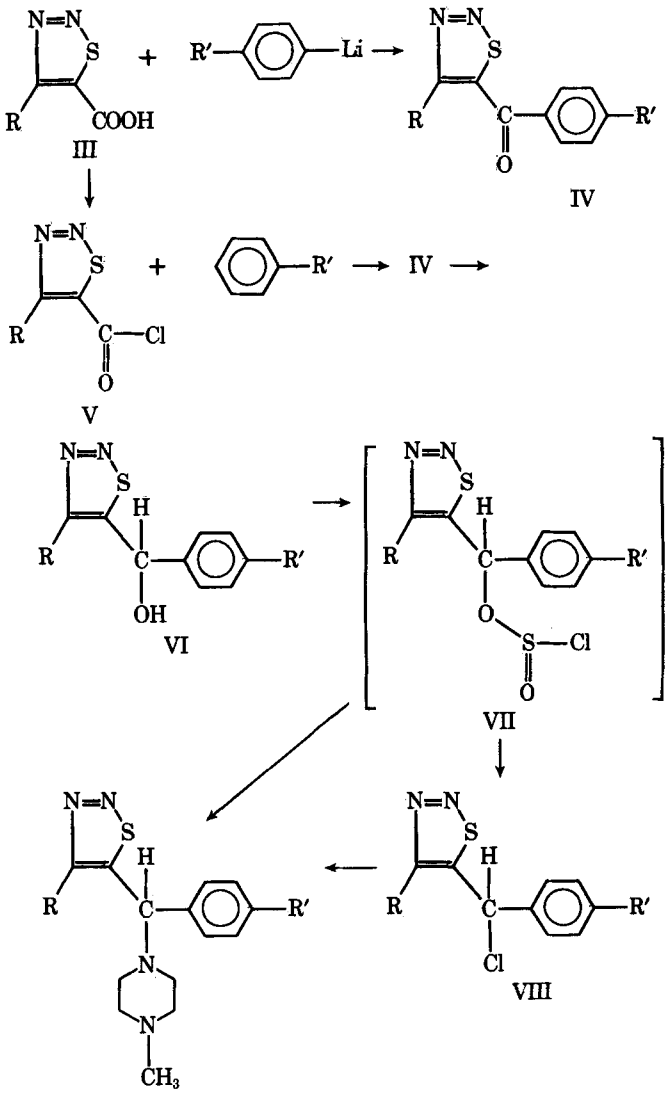

*a*: R = $CH_3$, R′ = H
*b*: R = $CH_3$, R′ = $CH_3$
*c*: R = $CH_3$, R′ = $CH_3O$
*d*: R = $CH_3$, R′ = Br
*e*: R = $CH_3$, R′ = Cl
*f*: R = $C_6H_5$, R′ = H
*g*: R = $C_6H_5$, R′ = $CH_3$
*h*: R = $C_6H_5$, R′ = Cl

*Scheme I*



0022-3549/81/0500-0510$01.00/0
© 1981, American Pharmaceutical Association

**Table I—Aryl 4-Substituted-1,2,3-thiadiazol-5-yl Ketones [a]**

| Compound | R | R′ | Yield, % | Melting Point [b] | Formula | Analysis, % | Calc. | Found |
|---|---|---|---|---|---|---|---|---|
| IV*a* | $CH_3$ | H | 70 | 180–182° [c] | $C_{10}H_8N_2OS$ | C | 58.82 | 58.66 |
| | | | | | | H | 3.92 | 3.74 |
| | | | | | | N | 13.73 | 13.64 |
| IV*b* | $CH_3$ | $CH_3$ | 87 | 170–172° [c] | $C_{11}H_{10}N_2OS$ | C | 60.55 | 60.72 |
| | | | | | | H | 4.59 | 4.75 |
| | | | | | | N | 12.84 | 12.99 |
| IV*c* | $CH_3$ | $OCH_3$ | 66 | 53–55° | $C_{11}H_{10}N_2O_2S$ | C | 56.41 | 56.60 |
| | | | | | | H | 4.27 | 4.39 |
| | | | | | | N | 11.97 | 11.81 |
| IV*d* | $CH_3$ | Br | 71 | 82–84° | $C_{10}H_7BrN_2OS$ | C | 42.40 | 42.35 |
| | | | | | | H | 2.47 | 2.65 |
| | | | | | | N | 9.89 | 9.72 |
| IV*e* | $CH_3$ | Cl | 64 | 55–57° | $C_{10}H_7ClN_2OS$ | C | 50.31 | 50.50 |
| | | | | | | H | 2.94 | 2.75 |
| | | | | | | N | 11.74 | 11.86 |
| IV*f* | $C_6H_5$ | H | 66 | 130–132° [c] | $C_{15}H_{10}N_2OS$ | C | 67.67 | 67.48 |
| | | | | | | H | 3.76 | 3.89 |
| | | | | | | N | 10.53 | 10.65 |
| IV*g* | $C_6H_5$ | $CH_3$ | 68 | 88–90° | $C_{16}H_{12}N_2OS$ | C | 68.57 | 68.71 |
| | | | | | | H | 4.29 | 4.12 |
| | | | | | | N | 10.0 | 10.15 |
| IV*h* | $C_6H_5$ | Cl | 50 | 137–139° | $C_{15}H_9ClN_2OS$ | C | 59.90 | 59.98 |
| | | | | | | H | 2.99 | 3.15 |
| | | | | | | N | 9.32 | 9.51 |

[a] IR, NMR, and mass spectra of all compounds were as expected. [b] Unless otherwise indicated, the recrystallization solvent was ether. [c] The boiling point was obtained at 4 mm Hg.

**Table II—(4-Substituted-1,2,3-thiadiazol-5-yl)arylcarbinols [a]**

| Compound | R | R′ | Yield, % | Melting Point [b] | Formula | Analysis, % | Calc. | Found |
|---|---|---|---|---|---|---|---|---|
| VI*a* | $CH_3$ | H | 90 | 94–96° | $C_{10}H_{10}N_2OS$ | C | 58.25 | 58.44 |
| | | | | | | H | 4.85 | 4.98 |
| | | | | | | N | 13.59 | 13.74 |
| VI*b* | $CH_3$ | $CH_3$ | 84 | 113–115° | $C_{11}H_{12}N_2OS$ | C | 60.00 | 59.85 |
| | | | | | | H | 5.45 | 5.63 |
| | | | | | | N | 12.73 | 12.91 |
| VI*c* | $CH_3$ | $OCH_3$ | 96 | 111–113° | $C_{11}H_{12}N_2O_2S$ | C | 55.93 | 55.98 |
| | | | | | | H | 5.08 | 5.24 |
| | | | | | | N | 11.86 | 11.98 |
| VI*d* | $CH_3$ | Br | 72 | 102–104° | $C_{10}H_9BrN_2OS$ | C | 42.11 | 42.29 |
| | | | | | | H | 3.16 | 3.28 |
| | | | | | | N | 9.82 | 9.67 |
| VI*e* | $CH_3$ | Cl | 86 | 108–110° | $C_{10}H_9ClN_2OS$ | C | 49.90 | 49.75 |
| | | | | | | H | 3.74 | 3.61 |
| | | | | | | N | 11.64 | 11.46 |
| VI*f* | $C_6H_5$ | H | 91 | 58–60° [c] | $C_{15}H_{12}N_2OS$ | C | 67.16 | 67.02 |
| | | | | | | H | 4.48 | 4.29 |
| | | | | | | N | 10.45 | 10.31 |
| VI*g* | $C_6H_5$ | $CH_3$ | 86 | 63–64° [c] | $C_{16}H_{14}N_2OS$ | C | 68.09 | 68.22 |
| | | | | | | H | 4.96 | 4.78 |
| | | | | | | N | 9.93 | 9.75 |
| VI*h* | $C_6H_5$ | Cl | 94 | 86–88° [c] | $C_{15}H_{11}ClN_2OS$ | C | 59.50 | 59.28 |
| | | | | | | H | 3.64 | 3.82 |
| | | | | | | N | 9.26 | 9.42 |

[a] IR, NMR, and mass spectra of all compounds were as expected. [b] Unless otherwise indicated, the recrystallization solvent was ether. [c] This compound was crystallized from petroleum ether.

The physical data for the intermediates IV, VI, and VIII and the final compound IX are summarized in Tables I–IV.

**Pharmacological Assay**—The compounds listed in Table IV were screened for antihistaminic and anticholinergic activities. Isolated guinea pig ileum was prepared according to the method of Magnus (9) and suspended in a 10-ml bath filled with Tyrode solution, which was aerated at 36°. The isotonic concentrations were recorded through an isotonic transducer on a polygraph[1]. The $pA_2$ values were determined by a literature method (10).

Histamine and acetylcholine were used as agonists, and promethazine was tested for comparison. The results are presented in Table V.

Compounds IX*e*–IX*h* were the most potent antihistamines. However, only IX*e* and IX*h* displayed moderate anticholinergic activity. The $LD_{50}$ value of IX*h* in mice, estimated by the moving average method (11), was 155.5 (141.2–171.4) mg/kg.

[1] Narco Biosystems.

## EXPERIMENTAL[2]

**4-Phenyl-1,2,3-thiadiazole-5-carboxylic Acid (III, R = $C_6H_5$)**—A solution of ethyl 4-phenyl-1,2,3-thiadiazole-5-carboxylate (23.4 g, 0.1 mole) and sodium hydroxide (4.4 g, 1.1 moles) in ethanol–water (150 ml) was refluxed for 2 hr. The solvent was evaporated, and the residue was crystallized from ethanol to give 15.5 g (75% yield) of III, mp 152–153°.

*Anal.*—Calc. for $C_9H_6N_2O_2S$: C, 52.43; H, 2.91; N, 13.59. Found: C, 52.61; H, 2.74; N, 13.76.

**Phenyl 4-Phenyl-1,2,3-thiadiazol-5-yl Ketone (IV*f*)**—To a solution of phenyllithium (0.1 mole) in 150 ml of dry ether (12) was added III (R = $C_6H_5$, 4.12 g, 0.02 mole) at 0°. The mixture was stirred for 36 hr at room

[2] Melting points were taken on a Kofler hot-stage microscope and are uncorrected. IR spectra were recorded using a Perkin-Elmer 267 spectrometer. Mass spectra were recorded on a Varian Mat III instrument. NMR spectra were determined with a Varian T-60A instrument.

**Table III—5-(α-Chlorobenzyl)-4-methyl-1,2,3-thiadiazoles**

| Compound | R | R′ | Yield, % | Melting Point | Formula | Analysis, % | Calc. | Found |
|---|---|---|---|---|---|---|---|---|
| VIII*a* | $CH_3$ | H | 76 | 138–140° [a] | $C_{10}H_9ClN_2S$ | C | 53.45 | 53.28 |
| | | | | | | H | 4.01 | 4.18 |
| | | | | | | N | 12.47 | 12.65 |
| VIII*b* | $CH_3$ | $CH_3$ | 60 | 144–146° [a] | $C_{11}H_{11}ClN_2S$ | C | 55.35 | 55.52 |
| | | | | | | H | 4.61 | 4.80 |
| | | | | | | N | 11.74 | 11.92 |
| VIII*d* | $CH_3$ | Br | 98 | Oil | $C_{10}H_8BrClN_2S$ | C | 39.54 | 39.72 |
| | | | | | | H | 2.64 | 2.46 |
| | | | | | | N | 9.23 | 9.05 |
| VIII*e* | $CH_3$ | Cl | 98 | 140–142° [a] | $C_{10}H_8Cl_2N_2S$ | C | 46.33 | 46.48 |
| | | | | | | H | 3.09 | 3.25 |
| | | | | | | N | 10.81 | 10.96 |
| VIII*f* | $C_6H_5$ | H | 86 | 104–106° [b] | $C_{15}H_{11}ClN_2S$ | C | 62.83 | 62.95 |
| | | | | | | H | 3.84 | 3.68 |
| | | | | | | N | 9.77 | 9.59 |
| VIII*g* | $C_6H_5$ | $CH_3$ | 94 | Oil | $C_{16}H_{13}ClN_2S$ | C | 63.89 | 63.71 |
| | | | | | | H | 4.33 | 4.18 |
| | | | | | | N | 9.32 | 9.48 |
| VIII*h* | $C_6H_5$ | Cl | 95 | 56–57° [c] | $C_{15}H_{10}Cl_2N_2S$ | C | 56.07 | 56.19 |
| | | | | | | H | 3.12 | 3.24 |
| | | | | | | N | 8.72 | 8.91 |

[a] The boiling point was obtained at 4 mm Hg. [b] This compound was crystallized from petroleum ether. [c] This compound was crystallized from ether.

**Table IV—[(4-Substituted-1,2,3-thiadiazol-5-yl)arylmethyl]-4-methylpiperazines**

| Compound | R | R′ | Yield, % | Melting Point[a] | Formula | Analysis, % | Calc. | Found |
|---|---|---|---|---|---|---|---|---|
| IX*a* | $CH_3$ | H | 62 | 217–218° | $C_{15}H_{20}N_4S$ | C | 62.50 | 62.68 |
| | | | | | | H | 6.94 | 6.99 |
| | | | | | | N | 19.44 | 19.62 |
| IX*b* | $CH_3$ | $CH_3$ | 65 | 152–155° | $C_{16}H_{22}N_4S$ | C | 63.58 | 63.74 |
| | | | | | | H | 7.28 | 7.45 |
| | | | | | | N | 18.54 | 18.72 |
| IX*c* | $CH_3$ | $OCH_3$ | 65 | 145–148° | $C_{16}H_{22}N_4OS$ | C | 60.38 | 60.19 |
| | | | | | | H | 6.92 | 6.98 |
| | | | | | | N | 17.61 | 17.43 |
| IX*d* | $CH_3$ | Br | 62 | 156–160° | $C_{15}H_{19}BrN_4S$ | C | 49.05 | 49.22 |
| | | | | | | H | 5.18 | 5.34 |
| | | | | | | N | 15.26 | 15.08 |
| IX*e* | $CH_3$ | Cl | 68 | 160–163° | $C_{15}H_{19}ClN_4S$ | C | 55.81 | 55.69 |
| | | | | | | H | 5.89 | 5.95 |
| | | | | | | N | 17.36 | 17.18 |
| IX*f* | $C_6H_5$ | H | 75 | 226–230° | $C_{20}H_{22}N_4S$ | C | 68.57 | 68.74 |
| | | | | | | H | 6.29 | 6.18 |
| | | | | | | N | 16.0 | 16.18 |
| IX*g* | $C_6H_5$ | $CH_3$ | 70 | 251–255° | $C_{21}H_{24}N_4S$ | C | 69.23 | 69.18 |
| | | | | | | H | 6.59 | 6.74 |
| | | | | | | N | 15.38 | 15.24 |
| IX*h* | $C_6H_5$ | Cl | 86 | 192–196° | $C_{20}H_{21}ClN_4S$ | C | 62.42 | 62.31 |
| | | | | | | H | 5.46 | 5.29 |
| | | | | | | N | 14.56 | 14.38 |

[a] All compounds were crystallized from absolute ethanol as the hydrochloride.

temperature under nitrogen, water was added, and the ether was evaporated. The residue was distilled to give 3.5 g (66% yield) of IV*f*, bp 130–132° (4 mm); IR (KBr): 1660 (C=O) $cm^{-1}$; mass spectrum: *m/z* (relative intensity) 266 ($M^+$, 45), 208 (45), 207 (68), 195 (41), 194 (64), 167 (43), 99 (61), 56 (100), and 44 (23).

*Anal.*—Calc. for $C_{15}H_{10}N_2OS$: C, 67.67; H, 3.76; N, 10.53. Found: C, 67.48; H, 3.89; N, 10.65.

**p-Chlorophenyl 4-Phenyl-1,2,3-thiadiazol-5-yl Ketone (IV*h*)**—To a stirring solution of *p*-chlorophenyllithium, prepared from *p*-chlorobromobenzene (9.575 g, 0.05 mole) and *n*-butyllithium (32 ml of 10% solution in hexane, 0.05 mole) according to the literature (8), was added III (R = $C_6H_5$, 2.06 g, 0.01 mole). The mixture was stirred overnight under nitrogen at room temperature. Ice water was added to the mixture, followed by extraction with ether. The ether was dried, filtered, and evaporated. The residue was purified by TLC (silica gel, chloroform–petroleum ether, 50:50) and crystallized from ether to give 10.5 g (50% yield) of IV*h*, mp 137–139°; IR (KBr): 1650 (C=O) $cm^{-1}$.

*Anal.*—Calc. for $C_{15}H_9ClN_2OS$: C, 59.90; H, 2.99; N, 9.32. Found: C, 59.98; H, 3.15; N, 9.51.

Compound IV*g* was prepared similarly.

**4-Methyl-1,2,3-thiadiazol-5-carboxyl Chloride (V, R = $CH_3$)**—A mixture of 4-methyl-1,2,3-thiadiazole-5-carboxylic acid (14.4 g, 0.1 mole) (13) and thionyl chloride (40 ml) was refluxed for 4 hr. The solvent was evaporated, and the residue was distilled to give 15.5 g (95% yield) of V (R = $CH_3$), bp 102–104° (20 mm).

*Anal.*—Calc. for $C_4H_3ClN_2OS$: C, 29.54; H, 1.85; N, 17.23. Found: C, 29.72; H, 1.98; N, 17.41.

**Phenyl 4-Methyl-1,2,3-thiadiazol-5-yl Ketone (IV*a*)**—A stirring mixture of V (R = $CH_3$, 3.25 g, 0.02 mole) and aluminum chloride (5.34 g, 0.04 mole) in 30 ml of dry benzene was refluxed for 8 hr. After cooling, the complex was decomposed with ice water and dilute hydrochloric acid. The organic layer was separated, and the mother liquor was extracted once more with benzene. The combined organic solvent was washed with a saturated aqueous sodium bicarbonate solution. The organic layer was dried, filtered, and evaporated, and the residue was distilled to give 2.9 g (71% yield) of IV*a*, bp 180–182° (4 mm); IR (KBr): 1660 (C=O) $cm^{-1}$; NMR ($CDCl_3$): 8.0–7.53 (m, 5H, aromatic) and 2.8 (s, 3H, $CH_3$) ppm; mass spectrum: *m/z* (relative intensity) 204 ($M^+$, 2), 186 (38), 105 (28), and 77 (100).

*Anal.*—Calc. for $C_{10}H_8N_2OS$: C, 58.82; H, 3.92; N, 13.73. Found: C, 58.66; H, 3.74; N, 13.64.

Compounds IV*b*–IV*e* were prepared similarly at the boiling point of the respective solvent, except IV*c* which was prepared at 100° (Table I).

**(4-Methyl-1,2,3-thiadiazol-5-yl)phenylcarbinol (VI*a*)**—To a stirring solution of IV*a* (2.04 g, 0.01 mole) in 50 ml of methanol was added

**Table V—Antihistaminic and Anticholinergic Activities of 1,2,3-Thiadiazole Derivatives**

| Compound | $pA_2$ Values: Antihistaminic Activity | $pA_2$ Values: Anticholinergic Activity |
|---|---|---|
| IX*a* | 5.37 | NT[a] |
| IX*b* | 4.59 | NT[a] |
| IX*c* | 5.02 | —[b] |
| IX*d* | 5.22 | —[b] |
| IX*e* | 6.69 | 4.94 |
| IX*f* | 6.92 | —[b] |
| IX*g* | 6.67 | —[b] |
| IX*h* | 7.72 ± 0.26 (5) | 4.6 |
| Promethazine | 10.47 | 6.9 |

[a] Not tested. [b] Inactive up to the concentration of $2 \times 10^{-5}$ *M*.

sodium borohydride (0.38 g, 0.01 mole). The mixture was stirred 30 min. Water (100 ml) was added to the mixture, which then was extracted with chloroform (3 × 100 ml). The chloroform was dried, filtered, and evaporated, and the residue was crystallized from ether to give 1.85 g (90% yield) of VI*a*, mp 94–96°; IR (KBr): 3250 (OH) $cm^{-1}$; NMR ($CDCl_3$): 7.36 (s, 5H, $C_6H_5$), 6.11 (s, 1H, HCO), 3.56 (broad s, 1H, OH), and 2.41 (s, 3H, $CH_3$) ppm; mass spectrum: *m/z* (relative intensity) 206 ($M^+$, 1), 177 (22), 107 (100), 79 (99), 77 (99), 51 (66), and 45 (65).

*Anal.*—Calc. for $C_{10}H_{10}N_2OS$: C, 58.25; H, 4.85; N, 13.59. Found: C, 58.44; H. 4.98; N, 13.74.

Compounds VI*b*–VI*h* were prepared similarly (Table II).

**5-(α-Chlorobenzyl)-4-methyl-1,2,3-thiadiazole (VIIIa)**—A solution of VI*a* (2.06 g, 0.01 mole) and thionyl chloride (4 ml) in 120 ml of dry benzene was stirred overnight. The mixture was filtered, and the solvent was evaporated. The residue was distilled to give 1.70 g (76% yield) of VIII*a*, bp 138–140° (4 mm); NMR ($CDCl_3$): 7.40 (s, 5H, $C_6H_5$), 6.25 (s, 1H, HCCl), and 2.55 (s, 3H, $CH_3$) ppm; mass spectrum: *m/z* (relative intensity) 224 ($M^+$, 2), 195 (56), 161 (56), 125 (68), and 59 (100).

*Anal.*—Calc. for $C_{10}H_9ClN_2S$: C, 53.45; H, 4.01; N, 12.47. Found: C, 53.28; H, 4.18; N, 12.65.

Compounds VIII*b*–VIII*h* were prepared similarly (Table III).

**1-[(4-Methyl-1,2,3-thiadiazol-5-yl)phenylmethyl]-4-methylpiperazine (IXa)**—A solution of VIII*a* (2.245 g, 0.01 mole) and *N*-methylpiperazine (2.0 g, 0.02 mole) in 30 ml of pyridine was refluxed under nitrogen overnight. The solvent was evaporated. Water (15 ml) was added to the residue and then extracted with ether. The ether was evaporated, and the residue was purified by TLC (chloroform–methanol, 95:5) to give 1.73 g (60% yield) of IX*a*; NMR ($CDCl_3$): 7.33 (s, 5H, $C_6H_5$), 4.7 (s, 1H, HCN), 2.56 (s, 3H, $CH_3$), 2.46 (s, 8H, $CH_2N$), and 2.3 (s, 3H, $CH_3$) ppm.

*Anal.*—Calc. for $C_{15}H_{20}N_4S$: C, 62.50; H, 6.94; N, 19.44. Found: C, 62.68; H, 6.99; N, 19.62.

This compound was crystallized as the hydrochloride (mp 217–218°) from absolute ethanol.

Compounds IX*b* and IX*d*–IX*h* were prepared similarly (Table IV).

**1-[(4-Methyl-1,2,3-thiadiazol-5-yl)-*p*-methoxyphenylmethyl]-4-methylpiperazine (IXc)**—A solution of VI*c* (2.36 g, 0.01 mole) and thionyl chloride (4 ml) in 120 ml of benzene was stirred overnight. The solvent was evaporated under reduced pressure at 0° to give VII*c* as an oil; IR (KBr): 1250 and 1180 ($SO_2$) $cm^{-1}$; NMR ($CDCl_3$): 7.14 (q, 4H, aromatic), 6.26 (s, 1H, HCOSOCl), 3.8 (s, 3H, $CH_3O$), and 2.55 (s, 3H, $CH_3$) ppm. This compound was not purified further. To the residue were added pyridine (25 ml) and *N*-methylpiperazine (2 g, 0.02 mole). The mixture was refluxed under nitrogen and treated as was IX*a* to give 2.1 g (66% yield) of IX*c*; NMR ($CDCl_3$): 7.0 (q, 4H, aromatic), 4.65 (s, 1H, HCN), 3.73 (s, 3H, $CH_3O$), 2.53 (s, 3H, $CH_3$), 2.43 (s, 8H, $CH_2N$), and 2.23 (s, 3H, $CH_2N$) ppm.

*Anal.*—Calc. for $C_{16}H_{22}N_4OS$: C, 60.38; H, 6.92; N, 17.61. Found: C, 60.19; H, 6.98; N, 17.43.

This compound was crystallized from absolute ethanol as the hydrochloride, mp 145–148°.

## REFERENCES


(1) C. O. Wilson, O. Gisvold, and R. F. Doerge, "Textbook of Organic Medicinal and Pharmaceutical Chemistry," Lippincott, Philadelphia, Pa., 1971, p. 693.

(2) L. H. Sarett and H. D. Brown, U.S. pats. 3,017,415 (1962), 3,357,884 (1967), and 3,478,046 (1969) and French pat. M 4234 (1966); through *Chem. Abstr.*, **56,** 15517c (1962); **69,** 2951j (1968); **72,** 90475x (1970); and **68,** 68990g (1968), respectively.

(3) R. L. McConnell and H. W. Coover, Jr., U.S. pat. 3,072,669; through *Chem. Abstr.*, **58,** 12574f (1963).

(4) D. L. Pain and R. Slack, *J. Chem. Soc.*, **1965,** 5166.

(5) A. Shafiee, I. Lalezari, S. Yazdani, F. M. Shahbazian, and T. Partovi, *J. Pharm. Sci.*, **65,** 304 (1976).

(6) I. Lalezari, A. Shafiee, A. Badaly, M. M. Salimi, M. A. Khoyi, F. Abtahi, and M. R. Zarrindast, *ibid.*, **64,** 1250 (1975).

(7) I. Lalezari, A. Shafiee, and S. Yazdani, *ibid.*, **63,** 628 (1974).

(8) H. Gilmar, W. Langham, and F. W. Moore, *J. Am. Chem. Soc.*, **62,** 2327 (1940).

(9) J. Magnus, *Pflugers Arch. Gesamti Physiol. Menschen Tiere*, **102,** 123 (1904).

(10) H. O. Schild, *Br. J. Pharmacol.*, **2,** 189 (1947).

(11) C. S. Weil, *Biometrics*, **8,** 243 (1952).

(12) J. C. W. Evans and C. F. H. Allen, "Organic Synthesis," coll. vol. 2, Wiley, New York, N.Y., 1955, p. 517.

(13) R. Raap and R. G. Micetich, *Can. J. Chem.*, **46,** 1057 (1968).


## ACKNOWLEDGMENTS


Supported by Grant 400-7-35/2 from the Ministry of Culture and Higher Education.

# High-Pressure Liquid Chromatographic Determination of Ibuprofen in Plasma

JUDY L. SHIMEK, N. G. S. RAO, and S. K. WAHBA KHALIL ˣ

Received July 14, 1980, from the *College of Pharmacy, North Dakota State University, Fargo, ND 58105.* Accepted for publication October 23, 1980.

**Abstract** □ A high-pressure liquid chromatographic method is presented for the determination of ibuprofen in human plasma. Ibuprofen is extracted from plasma acidified with 1.0 *M* phosphoric acid using hexane containing *p*-phenylphenol as an internal standard. A reversed-phase octadecylsilane column was used with a liquid phase of 65% methanol and 35% 0.10 *M* acetate buffer (pH 5.0). A spectrofluorometric detector with an excitation wavelength of 253 nm and a band pass filter (230–420 nm) provided a detectable peak for 1 μg of ibuprofen/ml of plasma. The effect of the pH and molarity of the mobile phase on the capacity factor was studied.

**Keyphrases** □ Ibuprofen—high-pressure liquid chromatographic determination in human plasma □ High-pressure liquid chromatography—determination of ibuprofen in human plasma □ Anti-inflammatory drugs—clinical determination of plasma levels in humans

Ibuprofen, an arylalkonic acid, is an oral, nonsteroidal anti-inflammatory drug used in the treatment of arthritis and for the relief of mild to moderate pain (1). The wide range of plasma levels encountered during therapy with ibuprofen indicates the need for clinical determination of plasma levels, which may allow maximum therapeutic effect while minimizing adverse affects. The incidence of GI bleeding with ibuprofen is reportedly lower than with aspirin; however, severe bleeding occurs, especially with patients taking anticoagulants or with hematological disorders (2). Monitoring is critical for patients requiring concomitant administration of other antiarthritic drugs with ibuprofen (3).

Several GLC procedures for the quantitative determination of ibuprofen were reported, but the majority require either derivatization or an electron-capture detector (4–7). A high-pressure liquid chromatographic (HPLC) method using UV detection quantitated ibuprofen in dog plasma (8). Recently, an HPLC method using dual UV detectors was reported for screening solid dosage forms for drugs used in the treatment of arthritis (9). Due to the greater specificity and sensitivity of fluorescence detection, a method for the determination of ibuprofen in human plasma that combines HPLC with fluorometry is described. Conditions are discussed for the extraction, separation, and detection of ibuprofen.

## EXPERIMENTAL

**Instrumentation**—The high-pressure liquid chromatograph[1] was equipped with a fluorometric detector[2] and an octadecylsilane column[3], 250 mm long × 4 mm i.d. The degassed mobile phase was pumped through the column at 1.5 ml/min (3700–3800 psi) at ambient temperature until a stable baseline was obtained. The fluorometer was set at an excitation wavelength of 253 nm, and a band pass filter with an entrance transmission of 230–420 nm was used.

**Chemicals and Reagents**—Sodium acetate, sodium phosphate, acetic acid, phosphoric acid, hexane, ethyl acetate, ether, methylene chloride, and chloroform were reagent grade. HPLC-grade methanol[4] was used. Ibuprofen was obtained courtesy of the manufacturer[5], and *p*-phenylphenol was obtained commercially[6].

**Table I—Effect of Buffer Molarity at pH 5 on the Capacity Factor of Ibuprofen and Internal Standard**

| Buffer Molarity | Capacity Factor | |
|---|---|---|
| | Ibuprofen | Internal Standard |
| 0.01 | 2.45 | 1.95 |
| 0.02 | 2.05 | 1.60 |
| 0.03 | 2.00 | 1.65 |
| 0.04 | 2.20 | 1.70 |
| 0.06 | 2.30 | 1.70 |
| 0.08 | 2.25 | 1.55 |
| 0.10 | 2.45 | 1.70 |
| 0.12 | 3.00 | 2.12 |
| 0.15 | 2.93 | 2.06 |

**Mobile Phase**—The mobile phase was prepared by adding an appropriate amount of methanol to the aqueous phase and degassing under vacuum. The aqueous phases consisted of pH 4 and 5 acetate buffers (0.01, 0.02, 0.03, 0.04, 0.06, 0.08, 0.10, 0.12, and 0.15 *M*) and acetic acid solutions (0.01, 0.02, and 0.03 *M*). The effect of various pH levels and concentrations of the aqueous portion of the mobile phase on retention times was studied.

**Stock Solutions**—A solution containing 10 mg of ibuprofen in 25 ml of methanol was prepared fresh monthly. A solution of *p*-phenylphenol was prepared by dissolving 3 mg of *p*-phenylphenol in 100 ml of methanol; it was prepared fresh monthly. A dilution of *p*-phenylphenol was prepared from 1 ml of the original *p*-phenylphenol solution, which was brought to a volume of 100 ml with methanol. The working internal

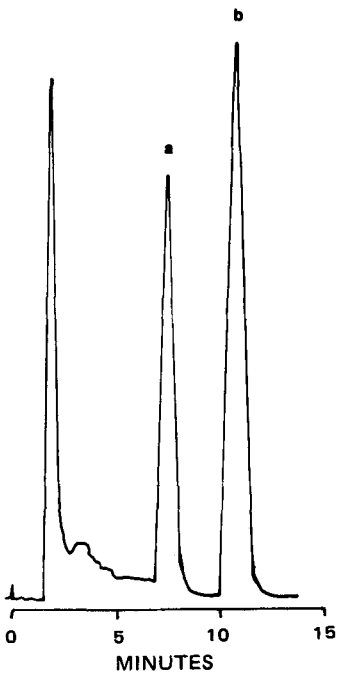


**Figure 1**—*Typical chromatogram of a plasma extract containing ibuprofen (15 μg/ml). Key: a, p-phenylphenol (internal standard); and b, ibuprofen.*

[1] Model 202 chromatograph, M600 pump, and U6K Universal injector, Waters Associates, Milford, Mass.
[2] FS970, Schoeffel, Westwood, N.J.
[3] Dupont, Wilmington, Del.
[4] Fisher Scientific Co., Fair Lawn, N.J.
[5] The Upjohn Co., Kalamazoo, Mich.
[6] Eastman Organic Chemicals, Rochester, N.Y.



0022-3549/81/0500-0514$01.00/0
© 1981, American Pharmaceutical Association

**Table II—Effect of pH on Capacity Factor of Ibuprofen and Internal Standard**

| Molarity | pH | Capacity Factor | |
|---|---|---|---|
| | | Ibuprofen | Internal Standard |
| 0.01 | 5[a] | 2.45 | 1.95 |
| | 4[a] | 4.25 | 1.65 |
| | 3.37[b] | 4.70 | 2.70 |
| 0.03 | 5[a] | 2.00 | 1.65 |
| | 4[a] | 5.15 | 1.95 |
| | 3.13[b] | 4.15 | 1.40 |

[a] Sodium acetate buffer. [b] Acetic acid.

**Table III—Nonsteroidal Antiarthritics Tested for Possible Interference**

| Drug or Metabolite | Fluorescence at Assay Conditions | Retention Time, min |
|---|---|---|
| Aspirin | Yes | Solvent front |
| Fenoprofen | Yes | 5.9 |
| Indomethacin | No | — |
| Des(chlorobenzoyl) metabolite | Yes | Solvent front |
| *O*-Desmethyl metabolite | No | — |
| Naproxen | Yes | 4.0 |
| Desmethyl metabolite | Yes | — |
| Oxyphenbutazone | No | — |
| Phenylbutazone | No | — |
| Sulindac | No | — |
| Sulfide metabolite | No | — |
| Sulfone metabolite | No | — |
| Tolmetin | No | — |
| Metabolite | No | — |

standard solution was prepared by transferring 1.7 ml of the *p*-phenylphenol dilution to a 250-ml volumetric flask and diluting to volume with hexane.

**Extraction Conditions**—The extraction of ibuprofen and the internal standard (*p*-phenylphenol) from plasma acidified at several pH levels was studied using five solvents: hexane, ethyl acetate, ether, methylene chloride, and chloroform.

**Analytical Procedure**—To 1.0 ml of heparinized plasma (in 15-ml screw-capped centrifuge tubes) were added 300 μl of 1.0 *M* phosphoric acid, 5 ml of hexane containing 2.0 ng of *p*-phenylphenol/ml as the internal standard, and an aliquot of the ibuprofen solution containing 1–40 μg (2.5–100 μl of methanolic solution). The tubes were vortexed for 10 sec and centrifuged for 5 min at 900×*g*. A 4-ml volume of the organic phase was transferred to special concentration tubes[7] and evaporated to dryness at ambient temperature under a gentle nitrogen stream. The residue was dissolved in 150 μl of methanol, and 100 μl was injected[8].

A standard curve was constructed by injecting the plasma extracts

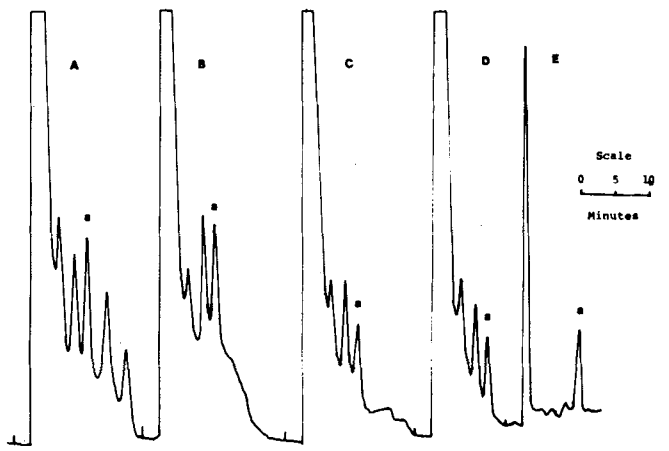


**Figure 2**—*Chromatograms of plasma extracts containing ibuprofen (5 μg/ml) (a). Key: A, methylene chloride; B, chloroform; C, ether; D, ethyl acetate; and E, hexane.*

[7] Concentratubes, Laboratory Research Co., Los Angeles, Calif.
[8] Hamilton Co., Reno, Nev.

**Table IV—Assay Accuracy (Serum Concentration in Micrograms per Milliliter)**

| Theoretical | Experimental[a] | Difference, % |
|---|---|---|
| 1.0 | 1.11 | 11.0 |
| 3.0 | 3.15 | 5.0 |
| 5.0 | 5.07 | 1.4 |
| 10.0 | 9.98 | 0.2 |
| 15.0 | 14.37 | 4.2 |
| 20.0 | 20.06 | 0.3 |
| 25.0 | 24.72 | 1.1 |
| 30.0 | 30.38 | 1.3 |
| 35.0 | 35.41 | 1.2 |
| 40.0 | 40.01 | 0.0 |

[a] Mean of five determinations.

simulating concentrations of ibuprofen from 1 to 40 μg/ml (corresponding to 0.4–16 μg of ibuprofen on the column). The chromatograms were recorded at a chart speed of 5 mm/min[9]. The peak heights were measured, and the ratios (ibuprofen to *p*-phenylphenol) were calculated and plotted *versus* ibuprofen concentrations expressed as micrograms per milliliter.

**Interferences**—The possible interferences from normal plasma constituents and other drugs that might be administered simultaneously were studied.

**Recovery**—For the recovery study, 10- and 25-μg/ml plasma standards were prepared as described under *Analytical Procedure*. After evaporation, the residue was dissolved in 150 μl of methanol containing 7.5 μg of ibuprofen. A volume of 100 μl was injected onto the column.

**Sample Preparation and Assay**—Heparinized plasma samples from patients receiving oral ibuprofen were processed in duplicate as described under *Analytical Procedure*. The amount of ibuprofen was calculated by comparison with standards prepared daily.

## RESULTS AND DISCUSSION

Increasing buffer molar concentrations first decreased and then increased the capacity factor of ibuprofen and the internal standard (Table I). The capacity factor was also affected by pH changes (Table II).

A mobile phase of 65% methanol and 35% acetate buffer (pH 5 and 0.10 *M*) gave well-resolved, sharp peaks for ibuprofen and *p*-phenylphenol with retention times of 10.9 and 7.5 min, respectively (Fig. 1). Aspirin, fenoprofen, naproxen, and other commonly used nonsteroidal antiarthritic agents (Table III) did not interfere with the analysis. The choice of the fluorometric parameters allowed a concentration of ibuprofen as low as 1 μg/ml of plasma to be quantitated.

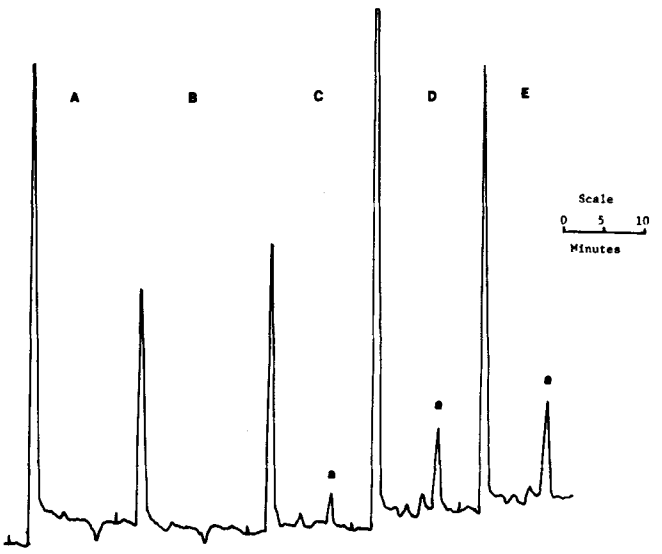


**Figure 3**—*Chromatograms of plasma extracts containing ibuprofen (5 μg/ml) (a) using hexane for extraction. Key: A, 0.1 M phosphate buffer (pH 4); B, 0.1 M phosphate buffer (pH 3); C, 0.1 M acetate buffer (pH 4); D, 2.0 M phosphoric acid; and E, 1.0 M phosphoric acid.*

[9] Model 56, Perkin-Elmer, Norwalk, Conn.

Hexane was selected for extraction of ibuprofen from plasma acidified with 1 *M* phosphoric acid. This selection was based on the highest amount of ibuprofen and/or the lowest amount of interfering fluorescent material being extracted. Ethyl acetate, ether, methylene chloride, and chloroform extracted excessive fluorescent substances from plasma (Fig. 2).

When phosphate buffers of pH 3 and 4 were used to acidify plasma, no ibuprofen was extracted. A pH 4 acetate buffer allowed extraction of only minimal amounts of ibuprofen. Phosphoric acid (1.0, 2.0, 3.0, 4.0, and 5.0 *M*) produced maximal extraction of ibuprofen; however, with 1.0 *M* phosphoric acid, minimal interfering constituents were extracted (Fig. 3). The optimum recovery of ibuprofen (74.91 ± 0.56%) from spiked plasma samples was obtained using 1.0 *M* phosphoric acid to acidify the plasma prior to extraction with hexane.

The ratio of the peak height of ibuprofen to the peak height of the internal standard was calculated. Statistical analysis indicated excellent linearity in the range of 1–40 μg of ibuprofen/ml of plasma with a correlation coefficient of 0.993, a slope of 0.0625 ± 0.0016, and an intercept of −0.11743 ± 0.0326 (Table IV).

Plasma levels of volunteers receiving one 600-mg oral dose of ibuprofen were as high as 40 μg/ml and as low as 15 μg/ml at 2 and 6 hr, respectively, after dosing.

The method reported here for the determination of ibuprofen will be a valuable tool for studying pharmacokinetic parameters and for monitoring patients, especially when they receive other nonsteroidal anti-inflammatory drugs.

## REFERENCES


(1) "Facts and Comparisons," Facts and Comparisons, Inc., St. Louis, Mo., 1980, p. 253i.

(2) *Med. Lett.*, **22**, 29 (1980).

(3) D. M. Grennan, D. G. Ferry, M. E. Ashworth, R. E. Kenney, and M. Mackinnon, *Br. J. Clin. Pharmacol.*, **8**, 497 (1979).

(4) D. J. Hoffman, *J. Pharm. Sci.*, **66**, 749 (1977).

(5) D. G. Kaiser and R. S. Martin, *ibid.*, **67**, 627 (1978).

(6) D. G. Kaiser and G. J. Vangiessen, *ibid.*, **63**, 219 (1974).

(7) K. K. Midha, J. K. Cooper, J. W. Hubbard, and I. J. McGilveray, *Can. J. Pharm. Sci.*, **12**, 29 (1977).

(8) D. Pitre and M. Grandi, *J. Chromatogr.*, **170**, 278 (1979).

(9) J. K. Baker and E. K. Fifer, *J. Pharm. Sci.*, **69**, 590 (1980).


# Chronic Dog Intestinal Loop Model for Studying Drug Absorption as Exemplified by β-Adrenoreceptor Blocking Agents, Atenolol and Propranolol


**DAVID C. TAYLOR ˣ, ROSALIND GRUNDY, and BERNARD LOVEDAY**



Received December 4, 1979, from the *Pharmaceutical and Biology I Departments, Pharmaceuticals Division, ICI Limited, Alderley Park, Macclesfield, Cheshire, England.* Accepted for publication October 8, 1980.



**Abstract** □ Chronic *in situ* loops of dog small intestine (jejunum or ileum) were used to investigate the absorption of the β-adrenoreceptor blocking agents atenolol and propranolol. Absorption measurements were made in conscious dogs by monitoring drug disappearance from solution in the loop, with correction for intestinal water absorption. The jejunum had a mean resting pH of 7.3 and a slight net secretion of water into the lumen; the ileum had a resting pH of 7.9 and a strong net absorption of water. Propranolol absorption was rapid and first order in both regions, with the ileum showing faster absorption than the jejunum due to its higher resting pH. In contrast, atenolol absorption was negligible in the jejunum and only moderate in the ileum. The data were quantitatively consistent with the pH–partition mechanism for the absorption of propranolol but not for atenolol. The model was validated for atenolol by showing that, following drug administration into jejunal and ileal loops, drug disappearance rates were similar to absorption rates calculated from systemic blood levels. This technique is useful, realistic, and relatively simple for studying intestinal drug absorption without seriously perturbing normal GI conditions.



**Keyphrases** □ Atenolol—absorption studied in chronic *in situ* ileal and jejunal loops in dogs □ Propranolol—absorption studied in chronic *in situ* ileal and jejunal loops in dogs □ Absorption—atenolol and propranolol, studied in chronic *in situ* ileal and jejunal loops in dogs □ β-Adrenoreceptor blocking agents—atenolol and propranolol, absorption studied in chronic *in situ* ileal and jejunal loops in dogs


The widespread use of *in situ* intestinal loop preparations for studying drug absorption is partly a result of the difficulty of extracting absorption rate data from blood level measurements. In addition, these techniques allow drug absorption to be measured directly at the absorption site, by monitoring the disappearance of a drug introduced into the intestinal lumen, and require much less experimental effort than blood level studies. Models using rats (1, 2) and dogs (3) have been reported.

However, physiological factors that affect *in vivo* absorption rates (*e.g.*, intestinal pH, water and ion flux, and intestinal blood flow) may themselves be affected by the surgical manipulation and anesthesia involved in preparing the animal for absorption measurements in the acute situation (4–9). In some cases, these effects may render an animal model unsuitable for particular drugs. For instance, it was found (10) that the Doluisio rat *in situ* preparation (2) was a valid model for the *in vivo* absorption of one β-adrenoreceptor blocking agent (propranolol) but not for another (practolol). This result was attributed to the effects of anesthetic and surgical shock on the animal.

A technique designed to overcome some of these problems is described in this paper. It consists of an isolated intestinal loop *in situ* in the conscious dog and is a development of the classical Thiry Vella loop technique (11). The use of this model is illustrated by investigation of the absorption characteristics of two β-adrenoreceptor blocking agents, atenolol and propranolol. This comparison is relevant because of the different extent of absorption of the two drugs in humans and because of the previous observation that the Doluisio *in situ* rat technique is not a good model for this type of compound. Attempts also were made to demonstrate the validity of the technique. Preliminary observations with this model were reported previously (12), and this paper represents an expansion and continuation of this work.

## EXPERIMENTAL

**Preparation of Intestinal Loops**—Adult male beagle dogs, 13–17 kg, were trained to sit unrestrained on a table for 1 hr or more. Thiry Vella




0022-3549/81/0500-0516$01.00/0



© 1981, American Pharmaceutical Association

Hexane was selected for extraction of ibuprofen from plasma acidified with 1 *M* phosphoric acid. This selection was based on the highest amount of ibuprofen and/or the lowest amount of interfering fluorescent material being extracted. Ethyl acetate, ether, methylene chloride, and chloroform extracted excessive fluorescent substances from plasma (Fig. 2).

When phosphate buffers of pH 3 and 4 were used to acidify plasma, no ibuprofen was extracted. A pH 4 acetate buffer allowed extraction of only minimal amounts of ibuprofen. Phosphoric acid (1.0, 2.0, 3.0, 4.0, and 5.0 *M*) produced maximal extraction of ibuprofen; however, with 1.0 *M* phosphoric acid, minimal interfering constituents were extracted (Fig. 3). The optimum recovery of ibuprofen (74.91 ± 0.56%) from spiked plasma samples was obtained using 1.0 *M* phosphoric acid to acidify the plasma prior to extraction with hexane.

The ratio of the peak height of ibuprofen to the peak height of the internal standard was calculated. Statistical analysis indicated excellent linearity in the range of 1–40 μg of ibuprofen/ml of plasma with a correlation coefficient of 0.993, a slope of 0.0625 ± 0.0016, and an intercept of −0.11743 ± 0.0326 (Table IV).

Plasma levels of volunteers receiving one 600-mg oral dose of ibuprofen were as high as 40 μg/ml and as low as 15 μg/ml at 2 and 6 hr, respectively, after dosing.

The method reported here for the determination of ibuprofen will be a valuable tool for studying pharmacokinetic parameters and for monitoring patients, especially when they receive other nonsteroidal anti-inflammatory drugs.

## REFERENCES


(1) "Facts and Comparisons," Facts and Comparisons, Inc., St. Louis, Mo., 1980, p. 253i.

(2) *Med. Lett.*, **22**, 29 (1980).

(3) D. M. Grennan, D. G. Ferry, M. E. Ashworth, R. E. Kenney, and M. Mackinnon, *Br. J. Clin. Pharmacol.*, **8**, 497 (1979).

(4) D. J. Hoffman, *J. Pharm. Sci.*, **66**, 749 (1977).

(5) D. G. Kaiser and R. S. Martin, *ibid.*, **67**, 627 (1978).

(6) D. G. Kaiser and G. J. Vangiessen, *ibid.*, **63**, 219 (1974).

(7) K. K. Midha, J. K. Cooper, J. W. Hubbard, and I. J. McGilveray, *Can. J. Pharm. Sci.*, **12**, 29 (1977).

(8) D. Pitre and M. Grandi, *J. Chromatogr.*, **170**, 278 (1979).

(9) J. K. Baker and E. K. Fifer, *J. Pharm. Sci.*, **69**, 590 (1980).


# Chronic Dog Intestinal Loop Model for Studying Drug Absorption as Exemplified by β-Adrenoreceptor Blocking Agents, Atenolol and Propranolol


**DAVID C. TAYLOR ˣ, ROSALIND GRUNDY, and BERNARD LOVEDAY**



Received December 4, 1979, from the *Pharmaceutical and Biology I Departments, Pharmaceuticals Division, ICI Limited, Alderley Park, Macclesfield, Cheshire, England.* Accepted for publication October 8, 1980.



**Abstract** □ Chronic *in situ* loops of dog small intestine (jejunum or ileum) were used to investigate the absorption of the β-adrenoreceptor blocking agents atenolol and propranolol. Absorption measurements were made in conscious dogs by monitoring drug disappearance from solution in the loop, with correction for intestinal water absorption. The jejunum had a mean resting pH of 7.3 and a slight net secretion of water into the lumen; the ileum had a resting pH of 7.9 and a strong net absorption of water. Propranolol absorption was rapid and first order in both regions, with the ileum showing faster absorption than the jejunum due to its higher resting pH. In contrast, atenolol absorption was negligible in the jejunum and only moderate in the ileum. The data were quantitatively consistent with the pH–partition mechanism for the absorption of propranolol but not for atenolol. The model was validated for atenolol by showing that, following drug administration into jejunal and ileal loops, drug disappearance rates were similar to absorption rates calculated from systemic blood levels. This technique is useful, realistic, and relatively simple for studying intestinal drug absorption without seriously perturbing normal GI conditions.



**Keyphrases** □ Atenolol—absorption studied in chronic *in situ* ileal and jejunal loops in dogs □ Propranolol—absorption studied in chronic *in situ* ileal and jejunal loops in dogs □ Absorption—atenolol and propranolol, studied in chronic *in situ* ileal and jejunal loops in dogs □ β-Adrenoreceptor blocking agents—atenolol and propranolol, absorption studied in chronic *in situ* ileal and jejunal loops in dogs


The widespread use of *in situ* intestinal loop preparations for studying drug absorption is partly a result of the difficulty of extracting absorption rate data from blood level measurements. In addition, these techniques allow drug absorption to be measured directly at the absorption site, by monitoring the disappearance of a drug introduced into the intestinal lumen, and require much less experimental effort than blood level studies. Models using rats (1, 2) and dogs (3) have been reported.

However, physiological factors that affect *in vivo* absorption rates (*e.g.*, intestinal pH, water and ion flux, and intestinal blood flow) may themselves be affected by the surgical manipulation and anesthesia involved in preparing the animal for absorption measurements in the acute situation (4–9). In some cases, these effects may render an animal model unsuitable for particular drugs. For instance, it was found (10) that the Doluisio rat *in situ* preparation (2) was a valid model for the *in vivo* absorption of one β-adrenoreceptor blocking agent (propranolol) but not for another (practolol). This result was attributed to the effects of anesthetic and surgical shock on the animal.

A technique designed to overcome some of these problems is described in this paper. It consists of an isolated intestinal loop *in situ* in the conscious dog and is a development of the classical Thiry Vella loop technique (11). The use of this model is illustrated by investigation of the absorption characteristics of two β-adrenoreceptor blocking agents, atenolol and propranolol. This comparison is relevant because of the different extent of absorption of the two drugs in humans and because of the previous observation that the Doluisio *in situ* rat technique is not a good model for this type of compound. Attempts also were made to demonstrate the validity of the technique. Preliminary observations with this model were reported previously (12), and this paper represents an expansion and continuation of this work.

## EXPERIMENTAL

**Preparation of Intestinal Loops**—Adult male beagle dogs, 13–17 kg, were trained to sit unrestrained on a table for 1 hr or more. Thiry Vella




0022-3549/81/0500-0516$01.00/0



© 1981, American Pharmaceutical Association

loops of jejunum or ileum were surgically constructed in each dog (one loop per dog), using a procedure similar to that described by Markowitz *et al.* (11). The dogs were fasted prior to surgery but allowed water *ad libitum*. Anesthesia was induced with thiopental sodium and maintained with halothane[1]–oxygen given by intubation.

A midline abdominal incision was made, and an abdominal retractor was used to expose the small intestine. The section of intestine required for loop formation was identified; it was the midjejunum or terminal ileum (25–50 cm long) and enclosed one complete vascular arch. The mesentery was divided, and each end of the loop was clamped. A second clamp was positioned at each end 2–3 cm from the first clamps. The intestine then was cut between the clamps, and the cut ends were anastomosed to reestablish the integrity of the small intestine. The cut ends of the loop were overstitched, and a small incision was made in the intestinal fold at each end of the loop. A purse-string suture was inserted around this incision, and a titanium cannula[2] (84.5 mm × 9 mm o.d.) was introduced.

The cannula was tied firmly in position and anchored with additional stitches to the flange. The suture lines and insertion of cannulas were covered with a layer of omentum. The mesentery of the small intestine was repaired, and the retractor was removed. The cannulas were exteriorized through stab incisions on the right flank of the animal. The midline incision was repaired, and the animal was allowed to recover.

Postoperatively, the dogs were deprived of food for 24 hr (water *ad libitum*), and a normal diet was introduced gradually over the next 5 days. Antibiotics[3] were administered for 3 days. A recovery period of 2–3 weeks was allowed before any experimental work with the loop was attempted. In addition, the saline washout procedure (see *Absorption Experiments in Loops*) was performed at least once a week during the working life of the loop. Except during absorption experiments, the fistulae were open to the atmosphere.

**Histological Examination of Loops**—Two dogs were killed ~6 months after construction of the loops. Postmortem examinations were carried out, and several samples of tissue from different regions of the loop and from normal intestine were excised. The tissue was fixed in 10% formaldehyde solution–saline and processed by embedding in paraffin wax, sectioning at 4 μm, and staining with hematoxylin and eosin. Transverse and longitudinal sections prepared in this way were examined microscopically.

**Absorption Experiments in Loops**—The experiments were carried out in 16 loop dogs (nine jejunal and seven ileal) over ~3 years. A strict crossover design was not possible, but the determination of absorption rates was repeated, both within and between animals, to determine the amount of biological variation in this parameter and to provide an accurate comparison of the absorption of atenolol and propranolol in both the jejunum and ileum.

The dog was allowed to sit or lie quietly and unrestrained on a table, and a balloon catheter[4] was inserted into the proximal fistula. It was secured in position by air inflation of the balloon. With a 50-ml syringe, 30 ml of 0.154 *M* NaCl (warmed to 37°) was flushed through the loop to remove excess mucus and cellular debris. A similar catheter (no extension piece) then was positioned in the distal fistula, and 30 ml of drug solution (37°) was introduced into the loop *via* the proximal catheter. The solution in the loop was sampled immediately after introduction (time zero) and at 2.5- or 5-min intervals up to 1 hr by aspirating the solution into the 50-ml syringe and withdrawing 0.5-ml samples into a 1-ml syringe *via* a three-way tap. At the end of the experiment, the loop was rinsed with 0.154 *M* NaCl.

Drug solutions contained atenolol or propranolol at 0.5 mg/ml (1.9 and 1.7 m*M*, respectively) in 0.154 *M* NaCl. $^{14}$C-Labeled polyethylene glycol 4000[5] (0.01 mg/ml) was included as a nonabsorbed marker (13). The solutions were adjusted to pH 7 by addition of 0.1 *N* HCl.

**Blood Atenolol Level Experiments**—In the blood level experiments, drug was administered either into the intestinal loop [30 ml at 3.33 mg/ml (12.7 m*M*)] or orally (as a rapidly dissolving 100-mg tablet). The blood profile of atenolol after a 40-mg/ml iv bolus was measured in seven nonloop dogs of similar age and weight and from the same colony. In both cases, blood samples (4 ml) were taken from jugular or brachial veins at frequent intervals over 8 hr and collected in sodium oxalate-treated containers.

**Analytical Techniques**—The pH values of the drug solution samples removed from the loop were measured using a pH meter fitted with a microdual electrode[6]. Measurements were made immediately after withdrawal of the final sample (~70 min after time zero).

The drug content of the intestinal loop samples was measured fluorometrically. The drug concentrations were calculated from peak heights by reference to a calibration curve. For atenolol, aliquots (50 μl) were alkalinized with 2 ml of 0.1 *N* NaOH and extracted with cyclohexane–*n*-butanol (50:50). The drug then was back-extracted from the organic layer into 0.1 *N* HCl (4 ml). The acidic layer was read on a fluorescence spectrophotometer[7] with excitation and emission wavelengths of 235 and 300 nm, respectively. Blood samples of atenolol (1 ml of whole blood) were processed in the same way. For propranolol, intestinal loop samples (100 μl) were diluted to 10 ml in distilled water and read directly on the fluorescence spectrophotometer. Excitation and emission wavelengths were 290 and 340 nm, respectively.

The effective volume of the drug solution in the loop at each time was estimated by measuring the concentration of $^{14}$C-labeled polyethylene glycol in the withdrawn samples. Aliquots (0.1 ml) of loop samples were placed in 10 ml of scintillant[8] and counted for 10 min on a scintillation counter[9]. Counting efficiencies were determined by internal standardization, using a spike of 50 μl of $^{14}$C-labeled *n*-hexadecane[5] containing 10,000 dpm.

**Intestinal Loop Calculations**—The polyethylene glycol 4000 concentration in each loop sample (expressed as disintegrations per minute per milliliter) was used to correct the measured drug concentration (milligrams of atenolol per milliliter) for changes in solution volume, occurring as a result of net water absorption or secretion in the intestinal loop, as follows. The $^{14}$C-labeled polyethylene glycol 4000 concentration ($D_0$) at time zero was divided by the value ($D_t$) at each sampling time to give $D_0/D_t$. This fraction is an index of the change in drug solution volume. The measured drug concentration ($C_t$) at each sampling time was divided by the value ($C_0$) at time zero to give the fraction $C_t/C_0$. Multiplying $C_t/C_0$ by $D_0/D_t$ gives $f_t$, which is the fraction of the initial dose remaining in the loop at any given time, corrected for changes in drug solution volume during the experiment.

The ratio $D_0/D_t$ is equivalent to $V_t/V_0$, where $V_0$ and $V_t$ are the actual volumes (in milliliters) of drug solution in the loop at time zero and time $t$; $V_0$ is not the same as the volume of drug solution introduced (30 ml) due to dilution by residual fluid in the loop. Comparison of the polyethylene glycol 4000 concentration at time zero ($D_0$) with that in the drug solution before introduction shows that $V_0$ is usually about 32 ml, but it varies from experiment to experiment.

The slopes of the plots of log $f_t$ *versus* time were obtained by linear regression using least mean squares. First-order disappearance rate constants ($k_{a(dis)}$) and half-lives ($t_{1/2}$) were calculated from the slopes. With propranolol in both the jejunum and ileum and with atenolol in the jejunum, inspection of the disappearance plots showed that any lag time prior to disappearance was short. Therefore, all time points were used to calculate the disappearance rate constant. With atenolol in the ileum, a distinct lag time was present in nearly all of the disappearance plots, and points obviously not on the first-order part of the plot were excluded from the linear regression. In both cases, the lag time was obtained from the regression equation.

**Blood Level Calculations**—Absorption rate constants ($k_{a(blood)}$) were calculated from mean blood level results using the instantaneous midpoint-input principle (14).

## RESULTS

**Conditions of Loop Dogs**—Once dogs had recovered from surgery, little special care was necessary to maintain them in good condition. The loops remained viable for up to 9 months, allowing several series of experiments to be carried out in some dogs. Postmortem examination of loop tissue, and comparison with normal intestinal tissue, showed that no gross histological changes occurred over 6 months as a result of the

[1] Fluothane, Imperial Chemical Industries Ltd., Macclesfield, Cheshire, England.

[2] One flange (18.3-mm diameter) was placed at one end, and another (~25-mm diameter) was separated from the first flange by 8.0 mm.

[3] Streptopen (Glaxovet Ltd., Greenford, England); 4 ml (1 g of penicillin G procaine and 1 g of dihydrostreptomycin) was administered by intramuscular injection once daily.

[4] A WSP 4116 two-way (18F9) (Warne Surgical Products Ltd., Andover, England) catheter was fitted with a 10-cm extension piece of 2-mm i.d. Silastic link.

[5] Radiochemical Centre, Amersham, England.

[6] Model 3550 pH meter with Cecar electrode, Beckman Instruments, Irvine, Calif.

[7] Model MPF 43, Perkin-Elmer Ltd., Beaconsfield, England.

[8] Cocktail N, Fisons Ltd., Loughborough, England.

[9] Model 524, Packard Instruments Ltd., Caversham, England, or Intertechnique SL 4000, Kontron Analytical Ltd., St. Albans, England.

**Table I—Intestinal Loop Disappearance Parameters for Atenolol [a]**

| Parameter for Jejunum | Dog 349N | 190P | 141M[b] | 514-78 | 527-78 | Mean ± *SD* |
|---|---|---|---|---|---|---|
| $k_{a(dis)}$, $min^{-1}$ | 0.0037 | 0[c] | 0[c] | 0.0017 | 0.0007 | 0.0012 ± 0.0016 |
| $t_{1/2}$, min | 187 | — | — | 408 | 990 | 529 ± 414 |
| Lag time, min | 12 | — | — | 19 | 33 | 21 ± 11 |
| *n* | 13 | 13 | 7 | 13 | 13 | — |
| *r* | 0.819 | 0.408[c] | 0.142[c] | 0.645 | 0.585 | — |
| Resting pH of loop | 7.25 | 7.21 | 7.43 | 7.34 | 7.34 | 7.31 ± 0.009 |

| Parameter for Ileum | Dog 337N[b] Exp. 1 | 337N[b] Exp. 2 | 397N[b] Exp. 1 | 397N[b] Exp. 2 | 397N[b] Exp. 3 | 397N[b] Exp. 4 | 352MN | 279MP | 206-78 | Mean ± *SD* |
|---|---|---|---|---|---|---|---|---|---|---|
| $k_{a(dis)}$, $min^{-1}$ | 0.023 | 0.025 | 0.019 | 0.018 | 0.010 | 0.021 | 0.018 | 0.012 | 0.019 | 0.018 ± 0.0048 |
| $t_{1/2}$, min | 30 | 28 | 36 | 39 | 69 | 33 | 39 | 58 | 36 | 41 ± 14 |
| Lag time, min | 11 | 15 | 9 | 6 | 13 | 7 | 2 | 11 | 20 | 10 ± 5 |
| *n* | 10 | 6 | 7 | 7 | 11 | 7 | 7 | 8 | 8 | — |
| *r* | 0.981 | 0.976 | 0.948 | 0.993 | 0.939 | 0.949 | 0.958 | 0.973 | 0.921 | — |
| Resting pH of loop | —[d] | 7.91 | 7.67 | 7.98 | 7.83 | 7.64 | 8.01 | 7.97 | 8.03 | 7.88 ± 0.15 |

[a] Initial drug concentration was 0.5 mg/ml, unless otherwise shown. [b] Initial drug concentration was 3.33 mg/ml. [c] No significant correlation ($p < 0.05$) between log $f_t$ and time (linear regression). [d] Not recorded.

isolation of the intestinal segment. The only evidence of any difference was a slight reduction in thickness of the muscularis layer of the loop, attributed to its isolation from the passage of normal gut contents.

**pH and Volume Changes in Intestinal Loops**—Drug solutions, which were adjusted to pH 7 but unbuffered, underwent changes in pH and volume during an experiment. Distinct and characteristic differences were seen between jejunal and ileal loops (Fig. 1). In the jejunum, the pH rose to ~7.5 and then declined gradually back to 7.2 at 60 min (mean ± *SD* was 7.34 ± 0.19). In contrast, the ileum showed an initial rise before the significantly higher "resting" level of 7.88 ± 0.13 was reached. The resting pH in each experiment is recorded in Tables I and II. The pH values recorded for each experiment were measured immediately after completion of the experiment (~70 min after time zero). Control experiments showed that a small increase in sample pH occurred during this time but that it was not significant ($p < 0.05$). There was no difference in the behavior of jejunal and ileal loop samples.

The drug solution volume during a 60-min experiment remained essentially constant in the jejunal loops but showed a marked and consistent decrease in ileal loops. This finding is consistent with other reports (15, 16). Considerable dog-to-dog and experiment-to-experiment variations existed in these volume changes (much more so than with intestinal pH), but the characteristic difference between the jejunum and ileum was nearly always present.

**Drug Disappearance Rates**—Disappearance profiles for atenolol and propranolol were characteristic of the drug and the type of loop. Mean plots for disappearance of both drugs in the jejunum and ileum are shown in Fig. 2, and the parameters derived from the separate experiments are listed in Tables I and II.

Rapid first-order disappearance of propranolol occurred in both jejunal and ileal loops, with no appreciable lag time before the onset of disappearance. Disappearance half-lives were 17 and 7.1 min for the jejunum and ileum, respectively. The corresponding profiles for atenolol show a slower disappearance. Disappearance in the jejunum was very slow, averaging only 7% of the initial drug concentration in 60 min. Therefore, disappearance parameters are only approximate in this case. Values of $k_{a(dis)}$ and half-life are quoted only if there was a significant linear correlation between log $f_t$ and time over 60 min; where there was no correlation, the rate constant was taken as zero. Atenolol disappearance in the ileum (half-life of 41 min) was first order and much faster than in the jejunum. It had a lag time of ~10 min.

Repeat determinations of $k_{a(dis)}$ for each drug in either the jejunum or ileum showed good reproducibility both between dogs and within the same dog. There was no indication of any progressive change in the rate constant due to loop deterioration during the working life of any dog. Individual values of $k_{a(dis)}$ for each situation varied by a factor of two or less, except for atenolol in the jejunum where the disappearance was so slow that accurate measurements were impossible.

**Combined Loop and Blood Level Experiments**—Systemic levels of atenolol were measured after administration of drug solution into jejunal or ileal loops and after oral administration (Fig. 3). Blood atenolol levels following jejunal administration were low; after ileal administration, they were similar to those resulting from oral administration of an equivalent dose. This finding indicates that the rate of drug appearance in the systemic circulation was much slower after introduction into the jejunal loop than into the ileal loop, reflecting the pattern of disappearance rates from the loops. Values of $k_{a(blood)}$ in these experiments were calculated from the blood level data in Fig. 3 using intravenous data obtained in a separate group of seven dogs. Actual blood atenolol concen-

**Table II—Intestinal Loop Disappearance Parameters for Propranolol [a]**

| Parameter for Jejunum | Dog 349N Exp. 1 | 349N Exp. 2 | 547MR | 135R Exp. 1 | 135R Exp. 2 | 862P | 900P | Mean ± *SD* |
|---|---|---|---|---|---|---|---|---|
| $k_{a(dis)}$, $min^{-1}$ | 0.048 | 0.048 | 0.026 | 0.051 | 0.028 | 0.043 | 0.065 | 0.044 ± 0.014 |
| $t_{1/2}$, min | 14 | 14 | 27 | 14 | 25 | 16 | 11 | 17 ± 6 |
| Lag time, min | +2.9 | −1.6 | +0.3 | −0.2 | −0.8 | −6.3 | −2.2 | −1.1 |
| *n* | 15 | 14 | 14 | 14 | 12 | 14 | 7 | — |
| *r* | 0.997 | 0.991 | 0.998 | 0.997 | 0.995 | 0.974 | 0.992 | — |
| Resting pH of loop | 7.50 | 7.38 | 7.46 | 7.34 | 7.67 | 7.18 | 6.92 | 7.35 ± 0.24 |

| Parameter for Ileum | Dog 377N Exp. 1 | 377N Exp. 2 | 479P | 31P | 206.78 | Mean ± *SD* |
|---|---|---|---|---|---|---|
| $k_{a(dis)}$, $min^{-1}$ | 0.12 | 0.095 | 0.067 | 0.14 | 0.096 | 0.11 ± 0.033 |
| $t_{1/2}$, min | 5.8 | 7.3 | 10.3 | 5.0 | 7.2 | 7.1 ± 2.0 |
| Lag time, min | +1.1 | +0.7 | +0.1 | +0.4 | +4.0 | +1.3 |
| *n* | 7 | 10 | 12 | 8 | 10 | — |
| *r* | 0.976 | 0.980 | 0.995 | 0.995 | 0.997 | — |
| Resting pH of loop | 7.95 | 7.95 | 7.98 | 7.89 | 7.73 | 7.90 ± 0.10 |

[a] See footnotes to Table I.

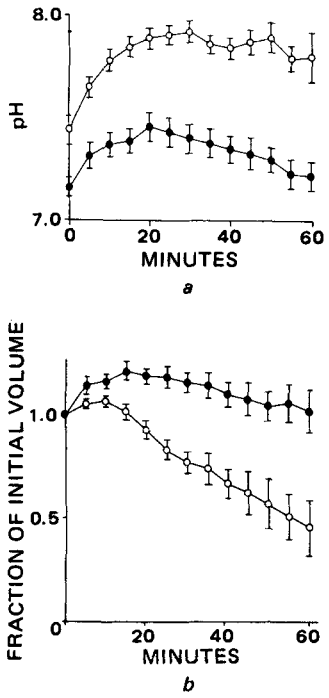


**Figure 1**—*The pH changes (a) and volume changes (b) in jejunal (●) and ileal (○) loops. Each point is the overall mean value (±SE) from all atenolol and propranolol experiments detailed in Tables I and II.*

trations used in the calculations are shown in Table III. Plots of the fraction unabsorbed (log scale) against time are shown in Fig. 4, and the derived rate constants are shown in Table IV. Values of $k_{a(\text{blood})}$ for jejunal and ileal absorption were similar to $k_{a(\text{dis})}$ values obtained from experiments in the intestinal loops. In addition, values of $k_{a(\text{blood})}$ for ileal and oral administration were almost identical.

## DISCUSSION

Apart from the preliminary article (12), there have been no previous reports in which isolated intestinal loops were used in this way for studying drug absorption in the conscious dog. A similar surgical technique was reported (3), but the animals were anesthetized and absorption was followed by blood sampling. Such an approach does not utilize the full potential of the technique for simulating intestinal conditions *in vivo*.

The histological observations, although limited, suggest that this preparation maintained the integrity of the isolated intestinal segments over the 6–9-month period during which they were used. This concept is supported by the lack of significant change in drug disappearance rates over this period and by reports from other investigators (17, 18). The intestinal loops should be normal functionally as well as histologically. Care was taken during surgery to maintain the mesenteric blood supply intact; with the lack of anesthetic and surgical stress, blood flow to the intestinal tissues during absorption experiments should be the same as in intact gut *in vivo*. Normal function in the intestinal loops was indicated by the return of peristalsis on recovery from the operation, by water absorption in the ileum, and by the strong buffering capacity of the loops toward drug solutions.

The use of buffered drug solutions was avoided so that absorption measurements could be made under intestinal conditions close to normal. Therefore, intestinal pH changed in response to the normal ion absorption and secretion processes of the loops, giving the characteristic pH profiles in the jejunum and ileum (Fig. 1).

To validate such an absorption model, it is necessary to show a correlation between lumenal drug disappearance and appearance on the serosal side of the intestinal membrane. Ideally, this approach involves collecting blood from the mesenteric veins serving the loop to allow direct measurement of drug arrival on the serosal side of the membrane. This study was attempted in other animal models (19, 20), but the techniques are invariably complex and usually necessitate the use of anesthetized animals. To avoid modification of the basic technique, the rate of drug appearance on the serosal side of the membrane was estimated by the less direct method of measuring systemic blood levels and calculating absorption rate constants ($k_{a(\text{blood})}$) for drug administered orally or into jejunal or ileal loops. These experiments were performed only with atenolol since it is largely unmetabolized after oral administration (21, 22). For this drug, there should be a quantitative balance between drug absorbed from the intestinal lumen and that appearing intact in the systemic circulation. This is not the case with propranolol, which is extensively extracted during the first pass through the liver both in humans and in dogs (23, 24).

These experiments showed that $k_{a(\text{dis})}$ and $k_{a(\text{blood})}$ not only correlate well in a relative sense (*i.e.*, ileal *versus* jejunal rates) but are quantitatively almost identical. Therefore, the atenolol disappearance measured in this model was an accurate reflection of true drug absorption into the systemic circulation. In addition, the similarity of $k_{a(\text{blood})}$ values following oral and ileal administration suggests that absorption from the intestinal loops is quantitatively similar to that in the intact small intestine and that the ileum is probably the major site of atenolol absorption in the intestinal tract.

General conclusions concerning the validity of the technique should apply to propranolol as well as to atenolol, although, in this case, the rate of disappearance from the loop corresponds to the appearance of "total" drug (*i.e.*, intact drug and metabolites) in the blood. Significant membrane storage of highly lipophilic drugs (25) destroys the direct correlation between lumenal disappearance of drug and absorption. However, the biexponential disappearance profiles characteristic of this situation were not seen in the dog intestinal loop experiments. In addition, there is some evidence (9) that membrane storage only occurs under conditions of significantly reduced intestinal blood flow (which may be present in an anesthetized *in situ* gut preparation) but not in a relatively stress-free chronic preparation such as the one described here.

Disappearance profiles for atenolol and propranolol in the intestinal loops show distinct and interesting differences between the two drugs and for each drug between jejunal and ileal loops. Both drugs are basic and have pKa values[10] close to 9.5. Therefore, they are more unionized in the ileum (pH 7.88) than in the jejunum (pH 7.34); the theoretical fractions unionized ($f_u$) are 0.02 and 0.007, respectively. Therefore, the more rapid absorption of both drugs in the ileum than in the jejunum was as expected. The fact that propranolol was absorbed more rapidly than atenolol in both loops is attributable to its much greater lipophilicity (octanol–water log $P$ values of 3.65 and 0.23 for propranolol and atenolol, respectively[10]) and, hence, its more ready partitioning between intestinal mucosa and gut contents. Quantitative comparison of $k_{a(\text{dis})}$ values from Tables I and II showed that propranolol was absorbed 37 times more rapidly than atenolol in the jejunum and six times more rapidly in the ileum. The ratios of ileal to jejunal rates were 2.5 for propranolol and 15 for atenolol.

There was an apparent overall adherence to the pH–partition principle (1, 4) since more rapid absorption occurred when a greater proportion of drug was present unionized and the more lipophilic drug was absorbed more rapidly. However, the ileal to jejunal ratios of $k_{a(\text{dis})}$ indicate a basic difference in the behavior of the two drugs. With propranolol, the observed ileal to jejunal ratio of 2.5 was almost exactly that predicted, for both drugs, from the ratio of 2.9 between $f_u$ in the two loops. For atenolol,

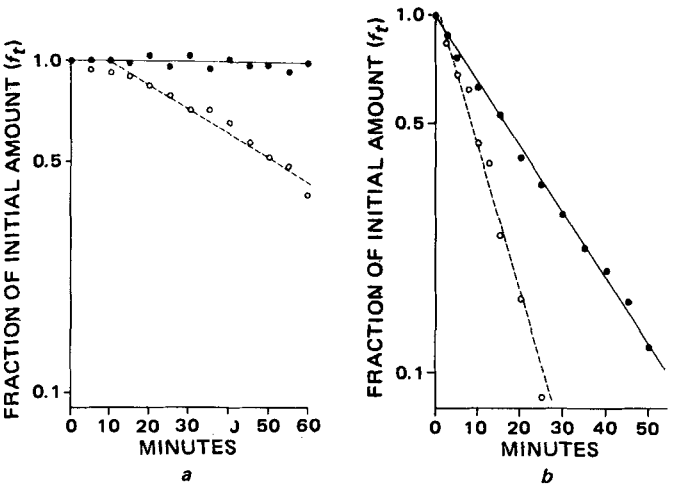


**Figure 2**—*Disappearance plots for atenolol (a) and propranolol (b) in jejunal (●) and ileal (○) loops. Each point is the mean value from experiments detailed in Tables I and II.*

[10] P. J. Taylor, ICI Ltd., Alderley Park, Cheshire, England, personal communication.

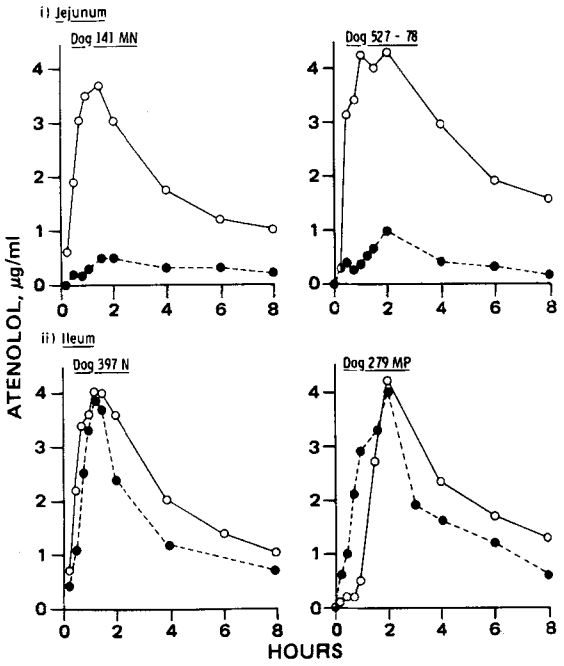


**Figure 3**—*Atenolol whole blood levels after administration of 100 mg of drug into jejunal (i) or ileal (ii) loops (●) and after oral administration (○). Results are for two dogs with jejunal loops and for two dogs with ileal loops.*

the more slowly absorbed drug, a much larger ratio of 15 was found under the same conditions. This result cannot be explained simply in terms of the difference in the resting pH between the two loops. Even if the absorption rate was controlled by a microclimate pH at the mucosal surface (4, 26) rather than by bulk phase pH, it would be expected to affect both drugs in a similar way.

A fundamental difference in the absorption mechanisms of these two drugs is, therefore, indicated. Propranolol absorption is explicable in simple pH–partition terms, whereas an alternative or additional mechanism is implied for atenolol in the ileum. It is possible that a hydrophilic molecule such as this one is subject to solvent drag or an active transport mechanism, although the current work contains no evidence for it. However, in the ileum the onset of atenolol absorption and net water absorption corresponded closely, both occurring after an initial lag time of ~10 min.

**Table III—Atenolol Systemic Blood Concentration Data Used in Calculation of $k_{a(blood)}$ [a]**

| Hours after Dose | Mean Atenolol Blood Concentration, μg/ml: Intravenous Administration[b] ($n$ = 7) | Oral Administration[c] ($n$ = 4) | Administration into Jejunal Loop ($n$ = 2) | Administration into Ileal Loop ($n$ = 2) |
|---|---|---|---|---|
| 0.08 | 13.6 | —[d] | —[d] | —[d] |
| 0.17 | 9.2 | —[d] | —[d] | —[d] |
| 0.25 | 7.9 | 0.43 | 0.15 | 0.50 |
| 0.33 | 6.7 | —[d] | —[d] | —[d] |
| 0.50 | 5.4 | 1.9 | 0.28 | 1.1 |
| 0.75 | 4.5 | 2.5 | 0.23 | 2.3 |
| 1.0 | 3.9 | 3.0 | 0.33 | 3.1 |
| 1.5 | 3.2 | 3.5 | 0.58 | 3.5 |
| 2.0 | 2.7 | 3.8 | 0.73 | 3.2 |
| 3.0 | 2.1 | —[d] | —[d] | —[d] |
| 4.0 | 1.7 | 2.2 | 0.35 | 1.4 |

[a] Dose of 100 mg. [b] Dogs without intestinal loops. $n$ = number of animals. [c] Two dogs with jejunal loops and two with ileal loops. [d] Not measured.

**Table IV—Values of $k_{a(blood)}$ for Atenolol Calculated [a] from Systemic Blood Concentrations**

| Parameter | Oral Administration[b] | Administration into Jejunal Loop[c] | Administration into Ileal Loop[c] |
|---|---|---|---|
| $k_{a(blood)}$, $min^{-1}$ | 0.015 | 0.013 | 0.014 |
| $n$ | 7 | 7 | 7 |
| $r$ | 0.993 | 0.988 | 0.998 |

[a] Reference 13. [b] Four dogs. [c] Two dogs.

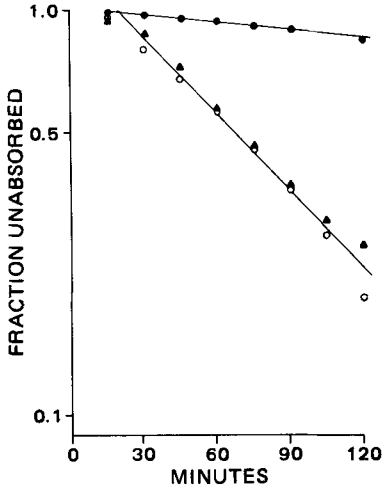


**Figure 4**—*Plots of fraction unabsorbed (log scale) against time for atenolol, calculated from whole blood levels after administration of 100 mg of atenolol orally (○) and into jejunal (●) and ileal (▲) loops. Mean results are for four dogs dosed orally and for two each with jejunal and ileal loops.*

Much has been published on the pharmacokinetics and metabolism of atenolol and propranolol, but detailed knowledge of their absorption mechanism is lacking. Thus, comparison of the dog intestinal loop data with existing data is possible only in a general sense. Propranolol is absorbed rapidly after oral administration both in dogs and humans, the systemic availability of intact drug being controlled largely by extensive extraction or metabolism at the first pass through the liver (21, 22). In contrast, atenolol is more slowly absorbed. Overall absorption is incomplete (~50%) in humans, rhesus monkeys, and rats but is markedly higher (~90%) in dogs (21, 22, 27). The extent of metabolism of this drug is small. The data obtained for atenolol and propranolol in the dog intestinal loops were consistent with this general picture.

From a clinical viewpoint, both drugs are adequately absorbed in humans, and the fact that atenolol absorption is incomplete is of no therapeutic importance (28). Mechanistically, however, the comparison is of great interest. The intestinal loop experiments suggest that there is not simply a rate difference in the absorption of the two drugs but also a difference in absorption mechanism. They also demonstrate that the animal model used is a useful, realistic, and relatively simple means of studying intestinal drug absorption without seriously perturbing normal GI conditions.

## REFERENCES

(1) L. S. Schanker, D. J. Tocco, B. B. Brodie, and C. A. M. Hogben, *J. Pharmacol. Exp. Ther.*, **123**, 81 (1958).

(2) J. T. Doluisio, N. F. Billups, L. W. Dittert, E. T. Sugita, and J. V. Swintosky, *J. Pharm. Sci.*, **58**, 1196 (1969).

(3) R. G. Sample, C. V. Rossi, and E. W. Packman, *ibid.*, **57**, 795 (1968).

(4) C. A. M. Hogben, D. J. Tocco, B. B. Brodie, and L. S. Schanker, *J. Pharmacol Exp. Ther.*, **125**, 275 (1959).

(5) W. G. Crouthamel, G. H. Tan, L. W. Dittert, and J. T. Doluisio, *J. Pharm. Sci.*, **60**, 1160 (1971).

(6) H. Ochsenfahrt and D. Winne, *Life Sci.*, **11**, 1115 (1972).

(7) S. Kojima and J. Miyake, *Chem. Pharm. Bull.*, **23**, 1274 (1975).

(8) D. Winne and J. Remischovsky, *J. Pharm. Pharmacol.*, **22**, 640 (1970).

(9) W. G. Crouthamel, L. Diamond, L. W. Dittert, and J. T. Doluisio, *J. Pharm. Sci.*, **64**, 664 (1975).

(10) D. C. Taylor and R. U. Grundy, *J. Pharm. Pharmacol. Suppl.*, **27**, 65P (1975).

(11) J. Markowitz, J. Archibald, and H. G. Downie, "Experimental Surgery," 5th ed., Williams & Wilkins, Baltimore, Md., 1964, p. 143.

(12) D. C. Taylor, R. U. Grundy, and B. E. Loveday, *J. Pharm. Pharmacol. Suppl.*, **29**, 51P (1977).

(13) D. L. Miller and H. P. Schedl, *Gastroenterology*, **58**, 40 (1970).

(14) W. L. Chiou, *J. Pharm. Sci.*, **69**, 57 (1980).

(15) J. W. L. Robinson, H. Menge, F. V. Sepulveda, and V. Mirkovitch,

*Digestion*, **15**, 188 (1977).
(16) L. A. Turnberg, *ibid.*, **9**, 357 (1973).
(17) W. H. Halliwell, D. A. Schmidt, and D. P. Hutcheston, *Am. J. Physiol.*, **196**, 74 (1976).
(18) E. Y. Berger, G. Kanzaki, M. A. Homer, and J. M. Steele, *ibid.*, **196**, 74 (1956).
(19) W. H. Barr and S. Riegelman, *J. Pharm. Sci.*, **59**, 154 (1970).
(20) R. K. Nayak and L. Z. Benet, *J. Pharmacokinet. Biopharm.*, **2**, 417 (1974).
(21) P. R. Reeves, D. G. Barnfield, S. Longshaw, D. A. D. McIntosh, and M. J. Winrow, *Xenobiotica*, **8**, 305 (1978).
(22) *Ibid.*, **8**, 313 (1978).
(23) J. W. Paterson, M. E. Connolly, C. T. Dollery, A. Hayes, and R. G. Cooper, *Eur. J. Clin. Pharmacol.*, **2**, 127 (1970).
(24) D. G. Shand, G. H. Evans, and A. S. Nies, *Life Sci.*, **10**, 1417 (1971).
(25) J. T. Doluisio, W. G. Crouthamel, G. H. Tan, J. V. Swintosky, and L. W. Dittert, *J. Pharm. Sci.*, **59**, 72 (1970).
(26) M. L. Lucas, J. A. Blair, B. T. Cooper, and W. T. Cooke, *Biochem. Soc. Trans.*, **1976**, 154.
(27) J. McAinsh, *Postgrad. Med. J., Suppl. 3*, **53**, 74 (1977).
(28) J. D. Fitzgerald, R. Ruffin, K. G. Smedstad, R. Roberts, and J. McAinsh, *Eur. J. Clin. Pharmacol.*, **13**, 81 (1978).

## ACKNOWLEDGMENTS

The authors thank Dr. J. McAinsh for permission to use the intravenous blood atenolol level data.

# Bioavailability of Orally Administered Propiram Fumarate in Humans

**C. A. KORDUBA ˣ, J. VEALS, E. RADWANSKI, S. SYMCHOWICZ, and M. CHUNG**

Received August 18, 1980, from the *Department of Drug Metabolism and Pharmacokinetics, Schering Corporation, Bloomfield, NJ 07003.* Accepted for publication October 23, 1980.

**Abstract** □ Propiram bioavailability was determined in 10 healthy volunteers after a single oral administration of 50 mg (base equivalent) of propiram fumarate in tablet or solution dosage form in a randomized crossover design. The plasma drug concentration–time curve revealed a one-compartment open model with first-order absorption kinetics. There were no statistically significant differences ($p > 0.05$) between all of the measured pharmacokinetic parameters obtained from the tablet and the solution with the exception of the absorption lag time ($t_{lag}$), where the tablet had a significantly longer $t_{lag}$. The drug given as a tablet or solution was absorbed rapidly after oral administration with an apparent absorption rate constant of 3.7 $hr^{-1}$ for both dosage forms. The $C_{max}$ value (308 ng/ml for the tablet and 342 ng/ml for the solution) was attained at ~1 hr after oral administration. The elimination half-life was 5.2 hr for the tablet and 4.4 hr for the solution, and the apparent distribution volume was 2.31 liters/kg for the tablet and 1.94 liters/kg for the solution. Total body clearance was much greater than renal clearance, indicating extensive metabolic clearance for both dosage forms. The study showed that propiram administered as the tablet was bioequivalent to the solution.

**Keyphrases** □ Propiram—bioavailability in humans, tablet *versus* solution □ Hydrolysis—fluorescence analysis, despropionylpropiram □ Bioavailability—orally administered propiram in humans □ Antispasmotics—propiram, tablet *versus* solution bioavailability in humans

Propiram fumarate, *N*-(1-methyl-2-piperidinoethyl)-*N*-2-pyridylpropionamide fumarate, was shown in clinical studies to have analgesic efficacy following oral and parenteral administration. The drug was active in dogs, cats, mice, rats, rabbits, and humans (1, 2) and displayed no physical dependency, carcinogenicity, embryo toxicity, or influence on general reproductive performance (3).

Although pharmacokinetic studies of propiram fumarate in animals (3) and humans (3, 4) have been reported, a detailed pharmacokinetic analysis of the plasma propiram concentration–time data is not available. Thus, the present study was conducted to provide comprehensive information on propiram pharmacokinetics and bioavailability in healthy volunteers after a single oral administration of propiram fumarate in a tablet or solution.

## EXPERIMENTAL

**Drug Formulation**—Two preparations containing propiram fumarate were tested, propiram fumarate tablet[1] and propiram fumarate solution[2] containing 50 mg as propiram.

**Study Protocol**—Ten healthy male adult volunteers (25–40 years of age) participated. Routine laboratory profiles including a complete blood count, urinalysis, and chemistry panel were obtained prior to the study and 48 hr after drug administration.

The study, a randomized crossover design, was composed of two segments. In the first segment, after an overnight fast, each subject received a single dose of propiram fumarate (equivalent to 50 mg of base) as a tablet or solution with 100 ml of water according to a random code. After at least a 4-day washout period, the subjects were given the other dosage form. No food was allowed until the 4th-hr blood sample was collected, after which a low-fat meal was given.

Blood samples were obtained at 0, 0.5, 0.75, 1.0, 1.5, 2.0, 2.5, 3, 4, 5, 8, 12, 16, and 24 hr. The plasma was separated by centrifugation and stored frozen until it was assayed.

Urine was collected prior to drug administration and for two intervals, 0–24 and 24–48 hr, after drug administration. The total volume of each collection was measured, and an aliquot was frozen until it was assayed.

**Assay**—A modified method of Pütter and Kroneberg (3) was used. The propionyl group was removed from propiram by acid hydrolysis, and the formed secondary amine (despropionylpropiram) showed a strong fluorescence at specific wavelengths in acidic solution.

Five milliliters of plasma, or 0.5 ml of urine sample plus 4.5 ml of water, was adjusted to pH 11 with 5 *N* NaOH and extracted with 7 ml of toluene. Six milliliters of the toluene phase then was extracted with 3 ml of 1 *N* $H_2SO_4$. An aliquot of the acidic aqueous phase (2.5 ml) then was transferred to a 3-ml serum bottle[3]. After the air was displaced with argon, the vial was closed with a stopper[4] and aluminum seal and placed in a manifold block[5] heater for 4 hr at 120°. After cooling to room temperature, the fluorescence of the formed despropionylpropiram was measured at 314 (excitation) and 380 (emission) nm in a spectrophotofluorometer[6].

[1] FMR 76228D-06, batch 8747-40, Schering Corp., Bloomfield, N.J.
[2] FMR 77571D, batch 9383-44, Schering Corp., Bloomfield, N.J.
[3] No. CA8290, 3 ml T-1, Kimble Glass, Paramus, N.J.
[4] No. 541, Teflon-lined natural rubber stopper, 13 mm, West Rubber Co., Phoenixville, Pa.
[5] Multi-Temp block heater, No. 2093, Lab-Line Instruments, Melrose Park, Ill.
[6] Aminco-Bowman, American Instruments Co., Silver Spring, Md.

0022-3549/81/0500-0521$01.00/0
© 1981, American Pharmaceutical Association

*Digestion*, **15**, 188 (1977).
(16) L. A. Turnberg, *ibid.*, **9**, 357 (1973).
(17) W. H. Halliwell, D. A. Schmidt, and D. P. Hutcheston, *Am. J. Physiol.*, **196**, 74 (1976).
(18) E. Y. Berger, G. Kanzaki, M. A. Homer, and J. M. Steele, *ibid.*, **196**, 74 (1956).
(19) W. H. Barr and S. Riegelman, *J. Pharm. Sci.*, **59**, 154 (1970).
(20) R. K. Nayak and L. Z. Benet, *J. Pharmacokinet. Biopharm.*, **2**, 417 (1974).
(21) P. R. Reeves, D. G. Barnfield, S. Longshaw, D. A. D. McIntosh, and M. J. Winrow, *Xenobiotica*, **8**, 305 (1978).
(22) *Ibid.*, **8**, 313 (1978).
(23) J. W. Paterson, M. E. Connolly, C. T. Dollery, A. Hayes, and R. G. Cooper, *Eur. J. Clin. Pharmacol.*, **2**, 127 (1970).
(24) D. G. Shand, G. H. Evans, and A. S. Nies, *Life Sci.*, **10**, 1417 (1971).
(25) J. T. Doluisio, W. G. Crouthamel, G. H. Tan, J. V. Swintosky, and L. W. Dittert, *J. Pharm. Sci.*, **59**, 72 (1970).
(26) M. L. Lucas, J. A. Blair, B. T. Cooper, and W. T. Cooke, *Biochem. Soc. Trans.*, **1976**, 154.
(27) J. McAinsh, *Postgrad. Med. J., Suppl. 3*, **53**, 74 (1977).
(28) J. D. Fitzgerald, R. Ruffin, K. G. Smedstad, R. Roberts, and J. McAinsh, *Eur. J. Clin. Pharmacol.*, **13**, 81 (1978).

## ACKNOWLEDGMENTS

The authors thank Dr. J. McAinsh for permission to use the intravenous blood atenolol level data.

# Bioavailability of Orally Administered Propiram Fumarate in Humans

**C. A. KORDUBA ˣ, J. VEALS, E. RADWANSKI, S. SYMCHOWICZ, and M. CHUNG**

Received August 18, 1980, from the *Department of Drug Metabolism and Pharmacokinetics, Schering Corporation, Bloomfield, NJ 07003.* Accepted for publication October 23, 1980.

**Abstract** □ Propiram bioavailability was determined in 10 healthy volunteers after a single oral administration of 50 mg (base equivalent) of propiram fumarate in tablet or solution dosage form in a randomized crossover design. The plasma drug concentration–time curve revealed a one-compartment open model with first-order absorption kinetics. There were no statistically significant differences ($p > 0.05$) between all of the measured pharmacokinetic parameters obtained from the tablet and the solution with the exception of the absorption lag time ($t_{lag}$), where the tablet had a significantly longer $t_{lag}$. The drug given as a tablet or solution was absorbed rapidly after oral administration with an apparent absorption rate constant of 3.7 $hr^{-1}$ for both dosage forms. The $C_{max}$ value (308 ng/ml for the tablet and 342 ng/ml for the solution) was attained at ~1 hr after oral administration. The elimination half-life was 5.2 hr for the tablet and 4.4 hr for the solution, and the apparent distribution volume was 2.31 liters/kg for the tablet and 1.94 liters/kg for the solution. Total body clearance was much greater than renal clearance, indicating extensive metabolic clearance for both dosage forms. The study showed that propiram administered as the tablet was bioequivalent to the solution.

**Keyphrases** □ Propiram—bioavailability in humans, tablet *versus* solution □ Hydrolysis—fluorescence analysis, despropionylpropiram □ Bioavailability—orally administered propiram in humans □ Antispasmotics—propiram, tablet *versus* solution bioavailability in humans

Propiram fumarate, *N*-(1-methyl-2-piperidinoethyl)-*N*-2-pyridylpropionamide fumarate, was shown in clinical studies to have analgesic efficacy following oral and parenteral administration. The drug was active in dogs, cats, mice, rats, rabbits, and humans (1, 2) and displayed no physical dependency, carcinogenicity, embryo toxicity, or influence on general reproductive performance (3).

Although pharmacokinetic studies of propiram fumarate in animals (3) and humans (3, 4) have been reported, a detailed pharmacokinetic analysis of the plasma propiram concentration–time data is not available. Thus, the present study was conducted to provide comprehensive information on propiram pharmacokinetics and bioavailability in healthy volunteers after a single oral administration of propiram fumarate in a tablet or solution.

## EXPERIMENTAL

**Drug Formulation**—Two preparations containing propiram fumarate were tested, propiram fumarate tablet[1] and propiram fumarate solution[2] containing 50 mg as propiram.

**Study Protocol**—Ten healthy male adult volunteers (25–40 years of age) participated. Routine laboratory profiles including a complete blood count, urinalysis, and chemistry panel were obtained prior to the study and 48 hr after drug administration.

The study, a randomized crossover design, was composed of two segments. In the first segment, after an overnight fast, each subject received a single dose of propiram fumarate (equivalent to 50 mg of base) as a tablet or solution with 100 ml of water according to a random code. After at least a 4-day washout period, the subjects were given the other dosage form. No food was allowed until the 4th-hr blood sample was collected, after which a low-fat meal was given.

Blood samples were obtained at 0, 0.5, 0.75, 1.0, 1.5, 2.0, 2.5, 3, 4, 5, 8, 12, 16, and 24 hr. The plasma was separated by centrifugation and stored frozen until it was assayed.

Urine was collected prior to drug administration and for two intervals, 0–24 and 24–48 hr, after drug administration. The total volume of each collection was measured, and an aliquot was frozen until it was assayed.

**Assay**—A modified method of Pütter and Kroneberg (3) was used. The propionyl group was removed from propiram by acid hydrolysis, and the formed secondary amine (despropionylpropiram) showed a strong fluorescence at specific wavelengths in acidic solution.

Five milliliters of plasma, or 0.5 ml of urine sample plus 4.5 ml of water, was adjusted to pH 11 with 5 *N* NaOH and extracted with 7 ml of toluene. Six milliliters of the toluene phase then was extracted with 3 ml of 1 *N* $H_2SO_4$. An aliquot of the acidic aqueous phase (2.5 ml) then was transferred to a 3-ml serum bottle[3]. After the air was displaced with argon, the vial was closed with a stopper[4] and aluminum seal and placed in a manifold block[5] heater for 4 hr at 120°. After cooling to room temperature, the fluorescence of the formed despropionylpropiram was measured at 314 (excitation) and 380 (emission) nm in a spectrophotofluorometer[6].

[1] FMR 76228D-06, batch 8747-40, Schering Corp., Bloomfield, N.J.
[2] FMR 77571D, batch 9383-44, Schering Corp., Bloomfield, N.J.
[3] No. CA8290, 3 ml T-1, Kimble Glass, Paramus, N.J.
[4] No. 541, Teflon-lined natural rubber stopper, 13 mm, West Rubber Co., Phoenixville, Pa.
[5] Multi-Temp block heater, No. 2093, Lab-Line Instruments, Melrose Park, Ill.
[6] Aminco-Bowman, American Instruments Co., Silver Spring, Md.

0022-3549/81/0500-0521$01.00/0
© 1981, American Pharmaceutical Association

Table I—Plasma Propiram Concentrations (Nanograms per Milliliter) after a Single Oral Administration of Propiram Fumarate Tablet or Solution (50-mg Base Equivalent) in Normal Subjects[a]

| Dosage Form | Hours after Drug Administration | | | | | | | | | | | |
|---|---|---|---|---|---|---|---|---|---|---|---|---|
| | 0.5 | 0.75 | 1 | 1.5 | 2 | 2.5 | 3 | 4 | 6 | 8 | 12 | 16 | 24 |
| Solution | 223.20 ±46.06 (65.26)[b] | 276.00 ±51.72 (56.21) | 287.20 ±36.02 (39.66) | 285.70 ±29.49 (32.64) | 237.30 ±24.50 (32.65) | 236.56 ±32.35 (41.02) | 208.00 ±21.46 (32.63) | 179.88 ±21.27 (33.44) | 171.67 ±23.53 (41.12) | 84.56 ±10.91 (38.69) | 52.80 ±13.39 (80.19) | 29.20 ±9.75 (105.65) | 17.20 ±7.40 (136.05) |
| Tablet | 94.90 ±26.92 (89.70)[b] | 187.11 ±29.99 (48.09) | 257.70 ±24.13 (29.61) | 300.70 ±27.88 (29.32) | 219.70 ±22.13 (31.85) | 189.70 ±19.02 (31.71) | 197.60 ±20.31 (32.50) | 173.40 ±16.13 (29.41) | 145.20 ±16.44 (35.81) | 114.30 ±15.93 (44.08) | 61.10 ±12.81 (66.32) | 31.70 ±8.47 (84.48) | 21.80 ±8.04 (116.61) |

[a] Data are reported as mean ± *SEM*, $n = 10$. [b] The numbers in parentheses are the coefficients of variation in percent of the mean.

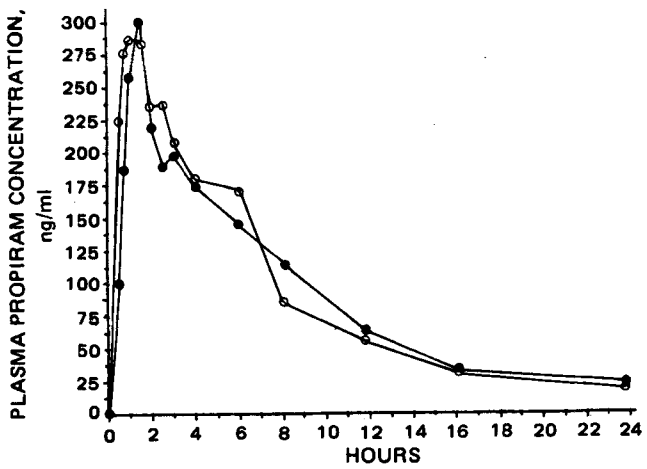


**Figure 1**—*Mean plasma propiram concentrations–time curve after a single oral administration of propiram fumarate (50-mg base equivalent) in normal subjects. Key: ●, tablet; and ⊖, solution.*

The drug concentration was determined from measured fluorescence in each sample by comparison with a calibration curve obtained with pure despropionylpropiram. The correction factor for differences in molecular weight between propiram and despropionylpropiram was applied.

Under the assay conditions, the detection limit for propiram, defined as the lowest point on the calibration curve producing a mean ± *SD* where the coefficient of variation did not exceed 10%, was 25 ng/ml. Levels below 25 ng/ml were estimated from the calibration curve.

**Data Analysis**—The plasma propiram concentration–time data from individual subjects were analyzed by CSTRIP (5) to obtain initial polyexponential parameter estimates. The computer stripping revealed that the individual data were described adequately by a biexponential equation. The coefficients and rate constants obtained then were used as preliminary estimates for further computer analysis by the nonlinear least-squares program NONLIN (6). Specific first-order rate constants for absorption ($K_a$) and elimination ($K$), as well as apparent volume of distribution ($V_d$), were obtained using the one-compartment open model with first-order absorption. The plasma concentration of drug ($C_p$) at any time ($t$) after a single dose ($D$) is described by:

$$C_p = \frac{FD}{V_d}\left(\frac{K_a}{K_a - K}\right)\left[e^{-K(t-t_{lag})} - e^{-K_a(t-t_{lag})}\right] \qquad \text{(Eq. 1)}$$

where $F$ is the fraction of dose absorbed and $t_{lag}$ is the absorption lag time (the time elapsed between dosing and the time of appearance of measurable plasma drug concentration).

The area under the plasma drug concentration–time curve from 0 to 24 hr ($AUC_{24\ hr}$) was calculated by the trapezoidal rule, and the total area ($AUC_\infty$) was estimated by $AUC_{24\ hr} + C_{p,24\ hr}/K$, where $C_{p,24\ hr}$ is the estimated plasma drug concentration at 24 hr after drug administration. The observed maximum plasma drug concentration ($C_{max}$) and the time ($T_{max}$) to reach $C_{max}$ were obtained from the individual plasma drug concentration–time data.

The total body clearance ($Cl_{TB}$) was calculated from the ratio of the administered dose to $AUC_\infty$. The renal clearance ($Cl_R$) was calculated from the ratio of the cumulative urinary excretion (0–48 hr), $\Sigma Du_{48\ hr}$ to $AUC_\infty$.

The estimated pharmacokinetic parameters of propiram for the two formulations were compared statistically *via* analyses of variance for crossover design.

## RESULTS AND DISCUSSION

The mean plasma propiram concentrations with time for the tablet and solution are given in Table I and Fig. 1. A substantial intersubject variation in the plasma propiram concentration was observed at 30 min and 12 hr for both dosage forms (in which the coefficient of variation was >50% of the mean value). Similar variation in plasma concentration at 30 min was observed by Pütter and Kroneberg (3). The large variation in propiram concentration seen at the 24-hr sampling time in the present study may have been due to levels being near detection limits of the assay.

The individual plasma drug concentration–time data were fitted best by a one-compartment open model with first-order absorption. The mean

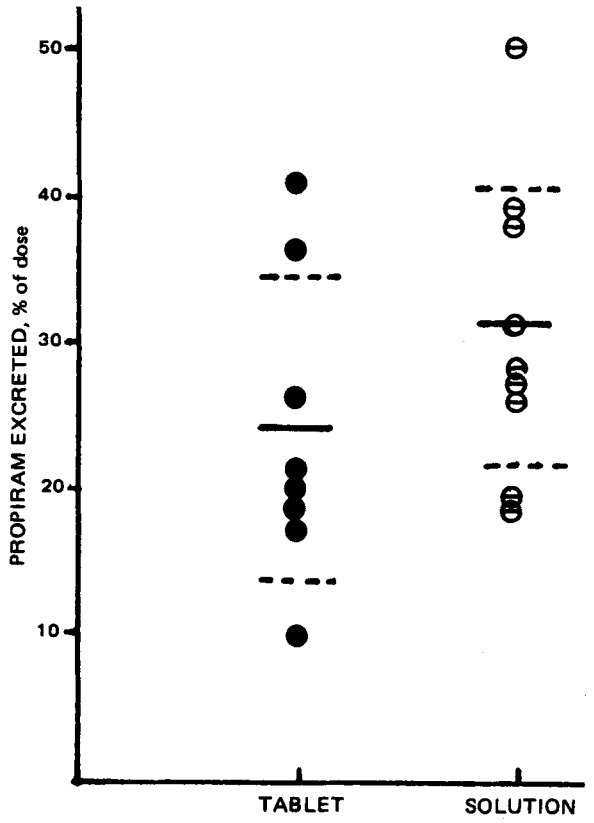


**Figure 2**—*Cumulative urinary excretion of propiram (0–48 hr) after a single oral administration of propiram fumarate (50-mg base equivalent) in normal subjects. Key:* ●, *tablet,* n = 8, *mean* ± SD = 24.3 ± 10.3; *and* ⊖, *solution,* n = 9, *mean* ± SD = 31.5 ± 10.0.

and standard errors of the estimated pharmacokinetic parameters of propiram for both dosage forms are presented in Table II. The data in Table II indicate that the drug was absorbed rapidly after administering either the tablet or solution with an apparent absorption rate constant ($K_a$) of 3.7 $hr^{-1}$; however, the $t_{lag}$ of the tablet (0.34 hr) was longer than that of the solution (0.14 hr). The differences (0.2 hr) in the $t_{lag}$ represent the disintegration–dissolution time of the tablet dosage form. Comparison of other pharmacokinetic–bioavailability parameters of the two dosage forms revealed no statistically significant differences ($p > 0.05$). This finding indicates that the dissolution rate of the propiram fumarate tablet is fast and may not be rate limiting in absorption. After oral administration, propiram was >97% absorbed (3). Thus, the fraction of dose absorbed ($F$) can be considered as unity.

The time to reach maximum plasma concentration ($T_{max}$) was 1.4 hr for the tablet and 1.2 hr for the solution. These values were in accord with literature data for the tablet (3). The maximum plasma drug concentrations ($C_{max}$) of propiram were similar with the two dosage forms: 308.3 ng/ml for the tablet and 342.3 ng/ml for the solution. The areas under the plasma drug concentration–time curves from 0 to 24 hr ($AUC_{24\ hr}$) were 2098.35 and 2150.73 (ng hr)/ml for the tablet and solution, respectively. The size of the area integral under the plasma levels *versus* time curve indicates that the same magnitude of bioavailability was obtained after either the tablet or solution dosage form.

**Table II—Pharmacokinetic Parameters of Propiram after a Single Oral Administration of Propiram Fumarate Tablet or Solution (50-mg Base Equivalent) in Normal Subjects**

| Parameter | Tablet[a] | Solution[a] |
|---|---|---|
| $C_{max}$, ng/ml | 308.30 ± 26.51 | 342.30 ± 29.33 |
| $T_{max}$, hr | 1.38 ± 0.09 | 1.20 ± 0.19 |
| $AUC_{24\ hr}$, ng·hr/ml | 2098.35 ± 269.65 | 2150.73 ± 300.25 |
| $AUC_{\infty}$, ng·hr/ml | 2219.52 ± 323.75 | 2234.70 ± 342.46 |
| $Cl_{TB}$, ml/min | 444.30 ± 58.02 | 441.31 ± 53.55 |
| $\Sigma Du_{48\ hr}$, % of dose | 24.34 ± 3.65 | 31.59[c] ± 3.34 |
| $Cl_R$, ml/min | 105.17[b] ± 22.53 | 124.77[c] ± 14.23 |
| $K_a$, $hr^{-1}$ | 3.68 ± 0.48 | 3.67 ± 0.62 |
| $K$, $hr^{-1}$ | 0.15 ± 0.02 | 0.18 ± 0.02 |
| $t_{1/2K_a}$, hr | 0.22 ± 0.03 | 0.27 ± 0.05 |
| $t_{1/2K}$, hr | 5.17 ± 0.58 | 4.35 ± 0.47 |
| $V_d$, liters/kg | 2.31 ± 0.16 | 1.94 ± 0.09 |
| $t_{lag}$, hr | 0.34[d] ± 0.05 | 0.14 ± 0.06 |

[a] Mean ± *SEM* of 10 subjects. [b] Mean of eight subjects. [c] Mean of nine subjects. [d] Statistically significant ($p < 0.05$) when the tablet was compared to the solution *via* analysis of variance.

A large distribution volume (2.3 liters/kg for the tablet and 1.9 liters/kg for the solution) indicates extensive metabolism and/or distribution. The disposition (elimination) half-life (5.17 hr for the tablet and 4.35 hr for the solution) obtained was lower than the value (~7 hr) reported by Horster *et al.* (4) using a $^{14}C$-labeled propiram fumarate tablet.

The cumulative amounts of propiram excreted in the 0–48-hr urine ($\Sigma Du_{48\ hr}$) after the tablet and solution are compared in Fig. 2. The mean $\Sigma Du_{48\ hr}$ after the tablet (24.34%) was not significantly different ($p > 0.05$) from that after the solution (31.59%), showing that approximately one-third of the administered dose was recovered in the urine as unchanged propiram. A substantial intrasubject variation in $\Sigma Du_{48\ hr}$ values, as seen in Fig. 2, may have been due to the degree of metabolism differences among the subjects.

For both the tablet and the solution, total body clearance (444 and 441 ml/min) was much greater than renal clearance (105 and 125 ml/min), indicating that metabolic clearance is a major route of the drug disposition in humans.

## REFERENCES

(1) V. F. Hoffmeister, G. Kroneberg, U. Schlichting, and W. Wuttke, *Arzneim.-Forsch.*, **24**, 600 (1974).

(2) V. B. Duhm, W. Maul, H. Medenwald, K. Patzschke, and L. A. Wegner, *ibid.*, **24**, 632 (1974).

(3) V. J. Pütter and G. Kroneberg, *ibid.*, **24**, 643 (1974).

(4) V. F. A. Horster, B. Duhm, W. Maul, H. Medenwald, K. Patzschke, and L. A. Wegner, *ibid.*, **24**, 652 (1974).

(5) A. J. Sedman and J. G. Wagner, *J. Pharm. Sci.*, **65**, 1006 (1976).

(6) C. M. Metzler, G. L. Elfring, and A. J. McEwen, "NONLIN 2 and Associated Programs," Upjohn Co., Kalamazoo, Mich., 1975.

## ACKNOWLEDGMENTS

The authors thank Dr. Richard I. H. Wang, Woods Veteran's Administration Hospital, Milwaukee, Wis., for conducting the clinical aspect of this study.

# Bioavailability of 11 Quinidine Formulations and Pharmacokinetic Variation in Humans

**I. J. McGILVERAY ˣ, K. K. MIDHA *, M. ROWE, N. BEAUDOIN, and C. CHARETTE**

Received July 3, 1980, from the *Drug Research Laboratories, Health Protection Branch, Health and Welfare Canada, Tunney's Pasture, Ottawa, Ontario, Canada K1A 0L2.* Accepted for publication October 23, 1980. *Present address: College of Pharmacy, University of Saskatchewan, Saskatoon, Saskatchewan, Canada S7N 0W0.

**Abstract** □ The bioavailabilities of eight quinidine sulfate, two gluconate, and one polygalacturonate formulations were compared, with one of the sulfate formulations as a reference (R) in a panel of 24 volunteers, according to a design comprising duplicate 6 × 6 Latin squares in two subject groups. Only one gluconate formulation (H) gave a significantly lower ($p < 0.05$) area under the curve from 0 to 30 hr ($AUC^{30}$), 90% of R, which was not as significant as $AUC^{\infty}$ (94% of R). Formulation H also gave a significantly lower peak concentration ($C_{max}$) and a longer time to peak concentration ($t_{max}$) and generally exhibited some characteristics of a sustained-release product. In addition, one product (F) gave a significantly higher $C_{max}$ while another formulation (D) gave a longer $t_{max}$. The wide range of dissolution times obtained with these products with three test conditions was not reflected in the $AUC$, $C_{max}$, or $t_{max}$ values obtained, except that Formulation H was consistently the slowest to dissolve. The terminal rate constants, expressed as $t_{1/2}$, of the 24 subjects gave an overall mean of 7.49 ± 0.77 hr and ranged from 6.24 ± 0.28 to 9.49 ± 0.90 hr in individuals. The estimated total body clearance, with the assumption that the oral bioavailability was 70%, gave an overall mean of 4.22 ± 1.05 and ranged from 2.49 ± 0.28 to 6.42 ± 0.70 ml/min/kg in individuals, demonstrating the wide range of quinidine disposition even in healthy subjects; this finding is in agreement with recently published results.

**Keyphrases** □ Quinidine—bioavailability and pharmacokinetic variations of various quinidine formulations studied in humans □ Bioavailability—quinidine formulations evaluated for variations in drug content, dissolution, absorption, and clearance characteristics in humans □ Pharmacokinetics—quinidine formulations, evaluation for variations in bioavailability, humans

The cinchona alkaloid, quinidine, is an important antiarrhythmic agent, which has been limited in use for maintenance therapy because of difficulties in defining the appropriate dosage schedule for the individual patient (1). Erratic patient response and marked variations in serum quinidine concentrations, in subjects to whom equivalent doses were administered, were observed by many investigators (2). While some variations are attributable to the disease (3–5), some contribution from bioavailability differences was suspected (2). However, few studies have tested this supposition. Other criteria suggesting that quinidine is a prime candidate for bioavailability studies were also reported (2).

One crossover study (6) noted that, while there was no significant difference in bioavailability between solution, capsule, and tablet formulations of quinidine sulfate, their bioavailabilities were all significantly lower than the bioavailability of an intramuscular injection of quinidine gluconate.

An oral solution of quinidine gluconate gave ~70% of the area under the curve ($AUC$) of an intravenous solution, with the loss attributed to a first-pass effect (7). Another study (8) compared an intramuscular lactate salt formulation and oral sulfate and gluconate formulations with an intravenous dose of lactate. The intramuscular route gave ~87%, the oral sulfate gave ~80%, and the oral gluconate gave 66% of the $AUC$ obtained for the intravenous lactate. Guentert *et al.* (9) also compared intravenous quinidine gluconate and an oral quinidine sulfate solution and found a mean oral bioavailability of 70%.

The bioavailability of chemically equivalent brands of quinidine sulfate tablets was compared; while no significant bioavailability differences were found, there were significant differences among brands in some rate parameters (10). These rate parameters were correlated with disintegration and dissolution (11) parameters.

The present study compares the bioavailabilities of available Canadian oral dose forms of quinidine having similar dosage recommendations and relates the *in vivo* results with dissolution properties.

## EXPERIMENTAL

**Drugs**—Commercial production lots consisting of eight tablet formulations of quinidine sulfate, two of quinidine gluconate, and one of quinidine polygalacturonate were obtained directly from the manufacturers. The label claim of the sulfate was 200 mg (equivalent to 165 mg of anhydrous base), that of the gluconate was 325 mg (equivalent to 203 mg of base), and that of the polygalacturonate was 275 mg (equivalent to 166 mg of base).

***In Vitro* Tests**—Samples were tested for identity and drug content by the USP procedure (12). Dissolution characteristics were determined by the USP procedure (13), by a modification of that procedure in which distilled water was used as the dissolution fluid, and by the paddle flask procedure of Poole (14) with 900 ml of glycine buffer, pH 4.0, stirred at 50 rpm.

**Human Study Protocol**—Twenty-four healthy volunteers (24–60 years old, 50.8–88.5 kg) were admitted to the study. The pretrial medical assessment included a full history and attention to cardiovascular, renal, hepatic, and GI conditions. Complete blood counts, urinalysis, and liver function tests were assessed before and between administrations. ECGs were assessed before and for 4 hr following a 100-mg test dose of quinidine sulfate before admission to the trial.

Volunteers with a history of sensitivity to any drug or who had suffered from allergy or allergic response were excluded.

The subjects were required to avoid all drugs for 3 weeks preceding and until 4 days after the study, to inform the physician of any emergency drug use required, and to report any adverse effects. Subjects were also asked to abstain from any alcoholic beverage from 24 hr before to 3 days after study completion and to fast from 10 hr before (overnight) to 4 hr after each administration. Written informed consent was obtained.

The subjects were randomly assigned into two groups (Table I). In the first study, the 12 subjects were administered six quinidine sulfate formulations (A–E and the innovator reference R-1) according to two replicate balanced 6 × 6 Latin squares. The second study was similar, with the treatments being three quinidine sulfate formulations (F, G, and the innovator R-2), two quinidine gluconate formulations (H and K), and a polygalacturonate (J). The innovator reference tablets (R-1 and R-2) were taken from the same bottle.

Each overnight-fasted volunteer received a single dose of a different quinidine formulation (165–203 mg of equivalent base) given with 50 ml of water early on each investigational day. No food or drink was taken for 4 hr postadministration with the exception of 150 ml of carbonated noncaffeine-containing beverage 1.5 hr after dosing. There was a 2-week interval between treatments. Blood samples (10 ml) were drawn by



0022-3549/81/0500-0524$01.00/0
© 1981, American Pharmaceutical Association

**Table I—Mean of the Terminal Half-Lives[a] and Mean Apparent Total Body Clearance[b] Values for All Subjects**

| | | | | | | | | | | | | |
|---|---|---|---|---|---|---|---|---|---|---|---|---|
| Group I | | | | | | | | | | | | |
| Subject | 1 | 2 | 3 | 4 | 5 | 6[c] | 7 | 8 | 9 | 10 | 11 | 12 |
| Weight, kg | 79.5 | 71.7 | 77.2 | 73.5 | 84.0 | 71.7 | 88.5 | 70.4 | 88.5 | 69.0 | 68.1 | 70.4 |
| Age, years | 24 | 27 | 25 | 37 | 36 | 60 | 34 | 35 | 27 | 28. | 28 | 37 |
| $t_{1/2}$[a], hr | 7.50 | 7.34 | 6.66 | 7.57 | 7.08 | 8.09 | 8.54 | 7.46 | 7.19 | 7.10 | 6.69 | 7.60 |
| *RSD*, % | 14.77 | 1.30 | 3.72 | 11.59 | 2.70 | 8.44 | 10.78 | 11.66 | 5.69 | 5.08 | 9.52 | 10.46 |
| *Cl*[d], ml/min | 392.7 | 331.3 | 366.7 | 350.6 | 679.6 | 455.3 | 566.4 | 249.9 | 449.6 | 440.2 | 571.4 | 433.7 |
| $Cl_{tot}$[b], ml/min/kg | 4.94 | 4.62 | 4.75 | 4.77 | 8.09 | 6.35 | 6.40 | 3.55 | 5.08 | 6.38 | 8.39 | 6.16 |
| *RSD*, % | 11.59 | 16.04 | 12.49 | 11.80 | 9.44 | 12.12 | 14.89 | 11.24 | 6.54 | 10.34 | 7.70 | 8.82 |
| $Cl_{corr}$[e], ml/min/kg | 3.46 | 3.23 | 3.33 | 3.40 | 5.66 | 4.45 | 4.48 | 2.49 | 3.56 | 4.47 | 5.87 | 4.31 |
| Group II[f] | | | | | | | | | | | | |
| Subject | 13 | 14 | 15 | 16 | 17 | 18[c] | 19 | 20 | 21 | 22 | 23[c] | 24 |
| Weight, kg | 79.5 | 77.2 | 84.0 | 81.7 | 77.2 | 50.8 | 77.2 | 68.1 | 68.1 | 86.3 | 57.7 | 77.2 |
| Age, years | 32 | 34 | 29 | 25 | 28 | 30 | 29 | 39 | 31 | 39 | 41 | 44 |
| $t_{1/2}$[a], hr | 7.11 | 6.76 | 8.60 | 8.66 | 7.79 | 7.06 | 9.49 | 7.14 | 6.67 | 8.27 | 6.24 | 7.23 |
| *RSD*, % | 5.79 | 10.25 | 9.91 | 5.30 | 10.32 | 9.12 | 9.46 | 15.43 | 7.78 | 11.29 | 4.49 | 2.77 |
| *Cl*[d], ml/min | 442.8 | 433.9 | 572.0 | 344.0 | 549.7 | 308.9 | 426.9 | 597.9 | 468.5 | 441.0 | 526.8 | 321.2 |
| $Cl_{tot}$[b], ml/min/kg | 5.57 | 5.62 | 6.81 | 4.21 | 7.12 | 6.08 | 5.53 | 8.78 | 6.88 | 5.11 | 9.13 | 4.16 |
| *RSD*, % | 10.02 | 19,58 | 9.82 | 8.24 | 9.26 | 21.71 | 7.82 | 7.21 | 8.73 | 14.18 | 11.00 | 3.34 |
| $Cl_{corr}$[e], ml/min/kg | 3.90 | 3.93 | 4.77 | 2.95 | 4.98 | 4.26 | 3.87 | 6.15 | 4.82 | 3.58 | 6.39 | 2.91 |

[a] Calculated from $0.693/\beta$, where $\beta$ = slope of 7–30 hr. [b] Apparent total body clearance = *Cl*/body weight. [c] Female subject. [d] Apparent clearance, which is dose/$AUC^{30}$. [e] Corrected apparent total body clearance = $0.7 \times Cl_{tot}$, where 0.7 is a correction factor for oral to intravenous (see Ref. 19). [f] Formulation H data were omitted.

venipuncture at 0, 0.5, 1, 2, 3, 5, 7, 24, 26, 28, and 30 hr following each administration. Plasma, separated within 2 hr, was stored at −18° until it was assayed.

**Plasma Assay**—Aliquots (1 ml) of plasma were assayed in duplicate for each time point by the double-extraction fluorescence technique of Armand and Badinand (15) using a suitable spectrofluorometer[1]. Selected samples were also assayed by a GLC procedure (16) and a novel high-performance liquid chromatographic (HPLC) procedure (17).

**Data Analyses**—For the statistical treatment, six variables were examined: (*a*) the area under the plasma concentration curve from 0 to 30 hr ($AUC^{30}$), in which values for each individual treatment were determined using the linear trapezoidal method; (*b*) the area under the plasma concentration curve extrapolated from zero to infinity ($AUC^{\infty}$) calculated for each individual treatment using:

$$AUC^{\infty} = \int_0^7 Cp\,dt + \frac{Ie^{-7\beta}}{\beta} \qquad \text{(Eq. 1)}$$

where *Cp* is the observed plasma concentration, $\int_0^7 Cp\,dt$ is determined using the trapezoidal rule, *I* is the *Cp* intercept using the linear least-squares regression of ln *Cp versus* time over 7–30 hr, and $\beta$ is the negative slope of the same regression line; (*c*) $\beta$ as defined in (*b*); (*d*) the maximum observed concentration ($C_{max}$) for each individual profile; (*e*) the time to $C_{max}$ ($t_{max}$); and (*f*) the apparent total body clearance ($Cl_{tot}$), which was calculated by:

$$Cl_{tot} = \frac{\text{apparent clearance}}{\text{body weight}} = \frac{\text{dose}}{AUC^{30} \times \text{body weight}} \qquad \text{(Eq. 2)}$$

In each study, the analysis of variance was conducted on the logarithmic transform of the raw data for the variables $AUC^{30}$, $AUC^{\infty}$, and $C_{max}$ and on the raw data for the remaining variables. The subject effect, period effect, and formulation effect were taken into account in each analysis. Comparisons between the means of the tested and reference formulations for each variable were also made with the least-significant difference test, which is basically a Student *t* test using the pooled error variance of the analysis of variance. For comparison of $\beta$ and $Cl_{tot}$ between subjects, however, paired *t* tests were applied.

Absorption rate estimates were obtained by the Wagner–Nelson (18) treatment of the mean plasma concentration values for the formulations. Corrected apparent total body clearance estimates ($Cl_{corr}$) were adjusted by multiplying by a factor of 0.7 from $Cl_{tot}$ for the difference between oral and intravenous doses (19).

## RESULTS AND DISCUSSION

The *in vitro* results are presented in Table II. The drug content ranged from 97.7 to 104.9% and was within limits. The gluconate products presented a 20% larger dose. An assay (20) also was applied to determine the amounts of dihydroquinidine in each formulation; a maximum of 6% was found, well below the 20% USP limit. Only one sulfate formulation (R, the innovator) failed the USP dissolution test, which requires that 90% be dissolved in 30 min (introduced shortly after the study was initiated). One gluconate formulation (H) was outside this limit, which is not official for this salt. Results with the other dissolution tests gave variable results for the different formulations. However, only the gluconate Formulation H gave consistently long dissolution times.

Spectrofluorometric procedures for quinidine analysis in plasma recently were criticized for lack of specificity (19, 21). However, in single-dose studies, the major interfering 3-hydroxy metabolite present with chronic dosing was not detected in the plasma (21). Although the Armand–Badinand (15) procedure may also extract a portion of the recently described *N*-oxide metabolite present in single-dose samples (19), previously reported comparisons (17) of values from the Armand–Badinand procedure with those obtained with a specific HPLC procedure indicated general agreement. While there was some divergence (up to 15%) in the later 24–30-hr samples, with HPLC values being lower, the area under the curve values were not affected markedly, although some pharmacokinetic estimates could be (9, 19). The previously reported comparison of results from the Armand–Badinand determination with those from a GLC procedure (22) tended to support this lack of interference in single-dose bioavailability studies. In that study, some steady-state samples from patients had up to 30% greater values by fluorometric analysis than by GLC analysis, while single-dose data were in excellent agreement.

Agreement was obtained between GLC and spectrofluorometric procedures in a limited comparison with plasma samples from patients maintained on quinidine (23). A reasonable correlation ($r^2 = 0.92$) was obtained in a similar comparison using more samples, although the data indicated that the fluorescent procedure gave higher values for most samples (24). Comparisons of HPLC and fluorescent procedures were described for samples from patients maintained on quinidine (25–27), with reasonable agreement being reported. However, some of these chromatographic procedures, as with fluorescent procedures, may not separate quinidine metabolites (19, 21). The spectrofluorometric method does not differentiate quinidine from the cardioactive congener dihydroquinidine. However, since this impurity was present in amounts averaging <5% in formulations and the difference of randomly selected *AUC* values generated by the fluorometric and specific HPLC procedures was of that order (17), the bioavailability assessment was not affected.

The mean plasma level results, by formulation, are given in Table III with no correction for the actual dose administered. The peak levels of ~0.5 μg/ml occurred at 2–3 hr with all formulations except the gluconate (H). The dose correction was applied in Table IV, which lists the average $AUC^{30}$ and $AUC^{\infty}$ values by formulation, and in Table V, in which the average peak concentration and time to peak are presented with estimates of the mean absorption rate parameters. In Group I, there were no significant differences between formulations in either the $AUC^{30}$ comparison (ranging from 98.1 to 107.2% of R) or $C_{max}$. Formulation D had a significantly longer $t_{max}$ than R (Table V). The overall relative standard deviation of 11.2% for $AUC^{30}$ was reasonable for this size of experiment and could detect a difference of 10%. In this group, the $AUC^{\infty}$ results were equivalent to those of $AUC^{30}$.

In Group II, Formulation H had a significantly lower $AUC^{30}$ (Table IV, 90%), a lower $C_{max}$ (Table V, 72.2%), and a longer $t_{max}$ (Table V, 2.5 hr) than R. The $AUC^{\infty}$ at 94% was not significantly lower. The only other

[1] Spectrophotofluorometer model SPF 125 (American Instrument Co., Silver Spring, MD 20910). The excitation and emission wavelengths were 361 and 448 nm, respectively, with a slit width of 2 mm for both.

**Table II—Drug Content and Dissolution Data of Quinidine Formulations**

| Formulation | Salt[a] | Label Strength, mg | Assay, % | Dose as Quinidine Base, mg | Dissolution: USP XIX[b] Percent at 30 min ± *RSD* | Dissolution: USP XIX[b] $\bar{t}_{60}$ min ± *RSD* | Dissolution: USP I[c], $\bar{t}_{60}$ min ± *RSD* | Dissolution: Paddle Flask[d], $\bar{t}_{60}$ min ± *RSD* |
|---|---|---|---|---|---|---|---|---|
| R(1 + 2) | Sulfate | 200 | 101.0 | 166.9 | 87 ± 10 | 15 ± 16 | 38 ± 19 | 14 ± 15 |
| A | Sulfate | 200 | 100.7 | 166.4 | 95 ± 3 | 13 ± 12 | 89 ± 9 | 42 ± 41 |
| B | Sulfate | 200 | 99.3 | 164.0 | 101 ± 4 | 12 ± 17 | 63 ± 32 | 55 ± 28 |
| C | Sulfate | 200 | 99.1 | 163.7 | 106 ± 4 | 3 ± 4 | 8 ± 129 | 3.6 ± 13 |
| D | Sulfate | 200 | 104.9 | 173.3 | 101 ± 4 | 7.3 ± 33 | 19 ± 5 | 24 ± 37 |
| E | Sulfate | 200 | 97.7 | 161.4 | 103 ± 4 | 3.6 ± 34 | 4.3 ± 16 | 4.2 ± 8 |
| F | Sulfate | 200 | 99.7 | 164.7 | 103 ± 3 | 10 ± 6 | 16 ± 6 | 19 ± 24 |
| G | Sulfate | 200 | 101.1 | 167.0 | 103 ± 4 | 3 ± 6 | 4.8 ± 28 | 10 ± 82 |
| H | Gluconate | 325 | 100.0 | 202.5 | 28 ± 1 | 127 ± 3 | 47[e] ± 4 | 28[e] ± 4 |
| J | Polygalacturonate | 275 | 104.8 | 168.0 | — | — | 8.5[f] ± 10 | 16 ± 61 |
| K | Gluconate | 325 | 101.1 | 204.7 | 98 ± 1 | 10 ± 22 | 14 ± 7 | 18 ± 15 |

[a] Quinidine sulfate, gluconate, and polygalacturonate contain the equivalent of 82.6, 62.3, and 60.4% anhydrous quinidine, respectively. [b] The USP XIX 4th Supplement procedure requires apparatus I with 0.1 *N* HCl as the medium. The limit is >90% in 30 min. The time, $\bar{t}_{60}$, for 60% is also given. [c] USP apparatus I rotated at 100 rpm with distilled water. [d] Not USP apparatus (see text); pH 4.0 glycine buffer used as dissolution medium. [e] Percent dissolved in 120 min. [f] Percent dissolved in 60 min.

significant difference was a $C_{max}$ of 117.6% for the sulfate formulation (F) (Table V). Again, the overall variation (*RSD* = 12.5%) for $AUC^{30}$ was reasonable for the size of the experiment. The range of mean profiles is illustrated in Fig. 1.

The different methods of calculation of $AUC^{30}$ (linear trapezoidal) and $AUC^{\infty}$ (linear, 0–7 hr; exponential, 7 hr to infinity) do not contribute to large differences in the estimate of the means (Table IV). The potential for differences between the "linear" and "exponential" trapezoidal calculation was discussed previously (28), and Guentert *et al.* (9) applied an appropriate correction to quinidine data. The mean $AUC^{30}$, adjusted for 330 mg of base for comparison with that of Guentert *et al.* (9), was 13.00 (μg hr)/ml for Group I and 12.44 (μg hr)/ml for Group II. These values were less than those of Greenblatt *et al.* (8) and other studies which used less specific procedures and were similar to the means [12.7 (μg hr)/ml] of those single-dose studies considered by Guentert *et al.* (19, 21) to have used specific procedures for measurement of plasma quinidine. The different methods in the *AUC* calculation resulted in different findings for the *AUC* comparison of Formulations H and R. Product H had a late peak (Tables III and V and Fig. 1), which contributed to slight differences in the estimates with the two methods. Thus, the $AUC^{30}$ ratio estimate for H to R had a significantly ($p < 0.05$) lower value of 90%, whereas the $AUC^{\infty}$ ratio estimate was 94% and was not significant.

From these comparisons (Tables IV and V), the quinidine sulfate formulations, A–G and R, were acceptable and interchangeable with the polygalacturonate (J) and gluconate (K) formulations.

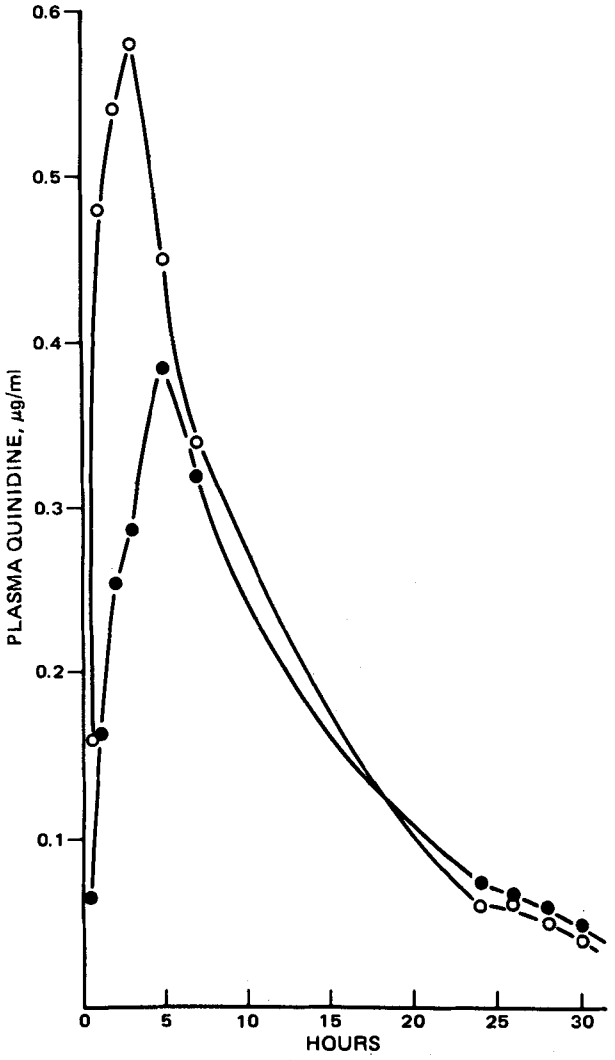


**Figure 1**—*Mean plasma quinidine concentrations for Formulations F (○) and H (●) corrected for dose.*

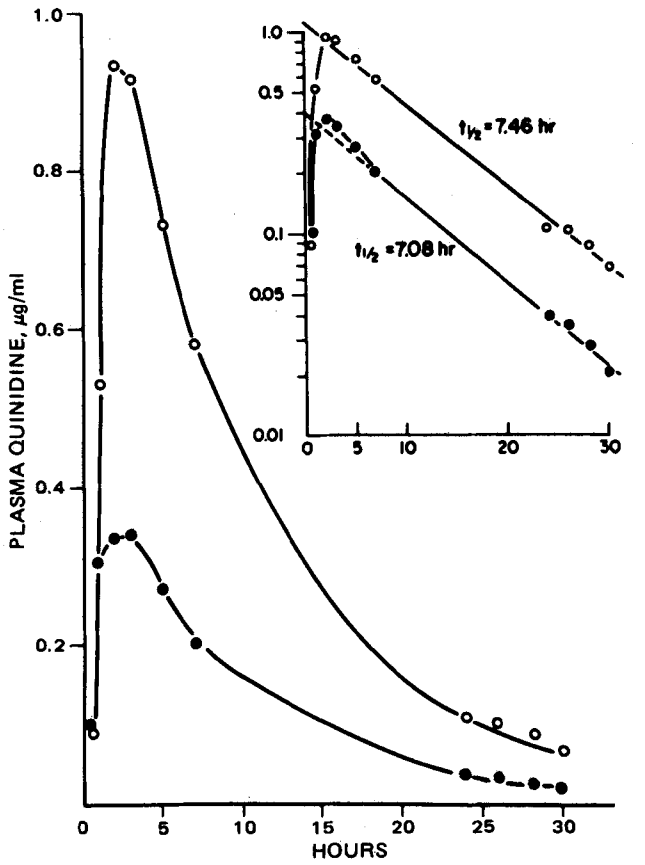


**Figure 2**—*Mean plasma quinidine concentrations for formulations (n = 6) taken by Subject 5, showing a high clearance (●), and Subject 8, showing a low clearance (○). The insert is a log plasma profile illustrating the similarity of half-lives.*

**Table III—Average Plasma Quinidine Concentrations by Formulation, Uncorrected for Quinidine Content**

| Formulation | Sample Time, hr | | | | | | | | | |
|---|---|---|---|---|---|---|---|---|---|---|
| | 0.5 | 1.0 | 2.0 | 3.0 | 5.0 | 7.0 | 24 | 26 | 28 | 30 |
| | | | | | Group I | | | | | |
| R-1 | 0.19[a] | 0.51 | 0.56 | 0.51 | 0.43 | 0.34 | 0.07 | 0.06 | 0.05 | 0.04 |
| | (104.0)[b] | (51.8) | (26.9) | (25.3) | (33.8) | (36.0) | (36.7) | (37.8) | (37.2) | (44.9) |
| A | 0.16 | 0.46 | 0.59 | 0.60 | 0.47 | 0.35 | 0.06 | 0.06 | 0.05 | 0.04 |
| | (56.6) | (33.9) | (34.4) | (47.4) | (37.7) | (37.2) | (31.8) | (32.5) | (32.8) | (33.7) |
| B | 0.19 | 0.49 | 0.61 | 0.53 | 0.45 | 0.36 | 0.07 | 0.06 | 0.05 | 0.04 |
| | (68.1) | (25.5) | (38.0) | (25.9) | (35.8) | (34.1) | (32.3) | (32.3) | (29.5) | (30.0) |
| C | 0.17 | 0.45 | 0.52 | 0.52 | 0.45 | 0.34 | 0.06 | 0.05 | 0.04 | 0.04 |
| | (73.8) | (41.0) | (31.8) | (35.0) | (31.9) | (34.7) | (39.1) | (32.7) | (33.2) | 32.2) |
| D | 0.07 | 0.36 | 0.52 | 0.58 | 0.45 | 0.37 | 0.07 | 0.06 | 0.06 | 0.04 |
| | (110.6) | (50.0) | (33.6) | (31.8) | (28.2) | (30.5) | (35.6) | (39.6) | (46.3) | (41.1) |
| E | 0.17 | 0.39 | 0.52 | 0.48 | 0.41 | 0.31 | 0.07 | 0.06 | 0.05 | 0.04 |
| | (83.8) | (34.7) | (23.3) | (25.2) | (27.4) | (29.2) | (45.7) | (46.3) | (45.0) | (39.6) |
| | | | | | Group II | | | | | |
| R-2 | 0.18 | 0.36 | 0.48 | 0.48 | 0.38 | 0.32 | 0.06 | 0.05 | 0.05 | 0.04 |
| | (94.7) | (49.9) | (21.8) | (22.7) | (26.9) | (27.3) | (32.4) | (37.5) | (38.6) | (36.0) |
| F | 0.16 | 0.48 | 0.54 | 0.58 | 0.45 | 0.34 | 0.06 | 0.06 | 0.05 | 0.04 |
| | (82.6) | (49.4) | (29.5) | (35.0) | (38.4) | (31.8) | (34.2) | (38.5) | (38.6) | (42.1) |
| G | 0.35 | 0.52 | 0.53 | 0.51 | 0.39 | 0.32 | 0.06 | 0.05 | 0.05 | 0.04 |
| | (69.1) | (49.8) | (16.5) | (28.6) | (26.0) | (31.5) | (34.7) | (36.9) | (35.5) | (40.1) |
| H | 0.08 | 0.20 | 0.31 | 0.35 | 0.47 | 0.39 | 0.09 | 0.08 | 0.07 | 0.06 |
| | (98.1) | (50.2) | (27.9) | (29.6) | (29.2) | (29.6) | (30.6) | (34.4) | (27.2) | (28.6) |
| J | 0.19 | 0.42 | 0.53 | 0.54 | 0.43 | 0.34 | 0.07 | 0.06 | 0.06 | 0.05 |
| | (73.0) | (41.7) | (27.1) | (34.3) | (33.9) | (28.8) | (36.4) | (38.8) | (43.4) | (48.6) |
| K | 0.15 | 0.52 | 0.66 | 0.62 | 0.51 | 0.40 | 0.07 | 0.07 | 0.06 | 0.05 |
| | (82.9) | (49.5) | (25.0) | (30.5) | (28.1) | (26.2) | (31.6) | (36.6) | (37.0) | (35.4) |

[a] Level in micrograms per milliliter. [b] Relative standard deviation (*RSD*) expressed in percent is in parentheses.

Formulation H, which had different absorption characteristics, also was studied by Greenblatt *et al.* (8) and Ochs *et al.* (29). In comparison with intravenous quinidine, tablet doses of a sulfate formulation and Formulation H gave $AUC^{30}$ ratios of 81 and 71%, respectively; *i.e.*, H was 88% of the oral sulfate formulation and significantly lower (8), which is in excellent agreement with the 90–94% of the present study. Covinsky *et al.* (30) found that this gluconate gave 95% of the *AUC* of a sulfate reference (not significant) with a 52% $C_{max}$ value. In a chronic dose study, Ochs *et al.* (29) found that this 10% difference in serum or plasma levels (H was lower than sulfate) was maintained. Both studies (8, 29) also noted that variability with this formulation was greater than with the oral sulfate. In the current study, although the $AUC^{30}$ of Formulation H was ~10% lower than that of the sulfate, the intersubject variations in $AUC^{30}$ for Formulation H (*RSD* = 27.4%) were no larger than those for other Group II formulations, which ranged from 22 to 30%.

The absorption half-lives ($t_{1/2,abs}$) and the estimated time for 50% to be absorbed ($A_{50}$) were calculated from the formulation mean plasma concentration *versus* time data with the Wagner–Nelson procedure (18). Although this procedure assumes a one-compartment model [which often is not appropriate for quinidine (9)] since intravenous data were not available for more complex modeling, it allows some estimate of the relative absorption rate of the formulations.

These absorption parameters (Table V) were useful for comparison with the dissolution times in Table II. However, since there were few differences between formulations in the *in vivo* results, only limited information can be derived. Formulation D, which had a longer $t_{max}$ than R, had shorter dissolution times than R in two tests. Formulation F, which had a high $C_{max}$ (118% of R) and apparently a more rapid absorption rate, had a faster dissolution than R in water but not in pH 4 glycine buffer. However, other formulations, such as C and G, gave shorter times than both F and R in those systems with no *in vivo* difference. The only consistent finding was the slow dissolution of Formulation H in all systems. Indeed, although H had dosage recommendations that were similar to the other formulations, it was designed as a slow-release product.

Since all Group I products were similar and only Formulation H in Group II was significantly different, it was possible to examine the inter- and intrasubject variations in some pharmacokinetic parameters. In Group II, with Formulation H, the estimated half-life tended to be longer and the clearance estimate higher, because of the significantly lower $AUC^{30}$. Therefore, subject comparisons were made without this formulation. Presumably, the terminal slope ($\beta$) from 7 to 30 hr is distorted by the extended absorption from this formulation (Table V).

Since several studies indicated that the pharmacokinetics of intravenous quinidine require fitting with different models in different subjects

**Table IV—Average Values (Geometric Means) of Bioavailability Parameters of Quinidine Formulations (Corrected per Dose)[a]**

| Group | Formulation | $AUC^{30}$[b], (μg hr)/ml | Relative $AUC^{30}$, % | $AUC^{30}$, 95% CI[c] | $AUC^{\infty}$[b], (μg hr)/ml | Relative $AUC^{\infty}$, % |
|---|---|---|---|---|---|---|
| I | R-1 | 6.40 | 100 | | 6.58 | 100 |
| | A | 6.63 | 103.6 | (94.5, 113.5) | 6.82 | 103.7 |
| | B | 6.86 | 107.2 | (97.8, 117.5) | 7.01 | 106.5 |
| | C | 6.49 | 101.4 | (92.5, 111.1) | 6.55 | 99.5 |
| | D | 6.47 | 101.1 | (92.3, 110.8) | 6.66 | 101.2 |
| | E | 6.28 | 98.1 | (89.5, 107.5) | 6.43 | 97.7 |
| | *RSD*[d] | 11.2% | | | | |
| II | R-2 | 6.00 | 100 | | 6.09 | 100 |
| | F | 6.60 | 109.9 | (99.2, 121.8) | 6.80 | 111.7 |
| | G | 6.18 | 102.9 | (92.9, 114.0) | 6.29 | 103.3 |
| | H | 5.40 | 90.0[e] | (81.2, 99.7) | 5.73 | 94.0 |
| | J | 6.28 | 104.6 | (94.4, 115.9) | 6.47 | 106.2 |
| | K | 6.24 | 104.0 | (93.8, 115.2) | 6.27 | 103.0 |
| | *RSD* | 12.5% | | | | |

[a] Corrected for equivalent weight of the salt by label claim and drug content in Table II. [b] Area under plasma concentration–time curve from 0 to 30 hr ($AUC^{30}$) calculated by linear trapezoidal, and area under plasma concentration–time curve from 0 to ∞ ($AUC^{\infty}$) as given in text. [c] The 95% confidence interval. [d] Overall relative standard deviation. [e] Significantly different than R ($p < 0.05$).

**Table V—Means of Parameters Reflecting Absorption Rate**

| Formulation | $C_{max}$[a], hr | $C_{max}$[a] Ratio, % | $t_{max}$[a], hr | $t_{1/2,abs}$[b], hr | $A_{50}$[c], hr |
|---|---|---|---|---|---|
| R-1 | 0.57 | 100 | 2.00 | 0.32 | 0.65 |
| A | 0.61 | 106.1 | 2.25 | 0.42 | 0.75 |
| B | 0.59 | 103.6 | 1.96 | 0.36 | 0.72 |
| C | 0.60 | 105.3 | 2.50 | 0.40 | 0.72 |
| D | 0.56 | 97.2 | 2.75[d] | 0.65 | 1.00 |
| E | 0.53 | 92.2 | 2.00 | 0.42 | 0.75 |
| R-2 | 0.51 | 100 | 2.33 | 0.60 | 0.77 |
| F | 0.60 | 117.6[d] | 1.92 | 0.32 | 0.70 |
| G | 0.56 | 108.6 | 1.72 | 0.34 | 0.42 |
| H | 0.37 | 72.2[d] | 4.75[d] | 1.50 | 1.75 |
| J | 0.51 | 100.2 | 2.00 | 0.45 | 0.68 |
| K | 0.55 | 107.2 | 2.08 | 0.38 | 0.75 |

[a] See text for symbols. [b] Wagner–Nelson estimate from mean plasma concentration by formulation absorption half-life. [c] As in footnote *b*; graphical estimate of time for 50% to be absorbed ($A_{50}$), which includes any lag time. [d] Significantly different than R ($p < 0.05$).

(8, 9) and often give poor prediction of steady-state levels (9, 31, 32), fitting of the oral curves and derivation of meaningful individual absorption rates (*e.g.*, two- and three-compartment fitting) could not be accomplished. Some data (Fig. 2) appeared to be fitted by one compartment (*e.g.*, Subject 8), while some (*e.g.*, Subject 5) obviously required two-compartment fitting. The terminal half-lives were calculated for each subject from the 7–30-hr data points (Table I) and ranged from 6.66 ± 0.24 (*SD*) to 8.54 ± 0.92 hr in Group I with a mean of 7.42 hr and from 6.24 ± 0.28 to 9.49 ± 0.90 hr in Group II with a mean of 7.49 hr. The extremes are illustrated in Fig. 3. The between-subject variation was greater than the within-subject variation, and many subjects were significantly different from each other. The terminal half-lives of Subjects 3 and 4 in Group I were significantly shorter ($p < 0.05$) than those of all other subjects. In addition, the long terminal half-lives of Subjects 6 and 7 were significantly different ($p < 0.01$) from those of the other subjects, and the terminal half-life of Subject 7 was significantly different ($p < 0.05$) from that of Subject 6. For Group II, Subject 19 was significantly longer ($p < 0.01$) than all other subjects. The values obtained were well within the extremes reported by Mason *et al.* (6) (1.16–15.75 hr) and within the range of mean values reported elsewhere (7–10).

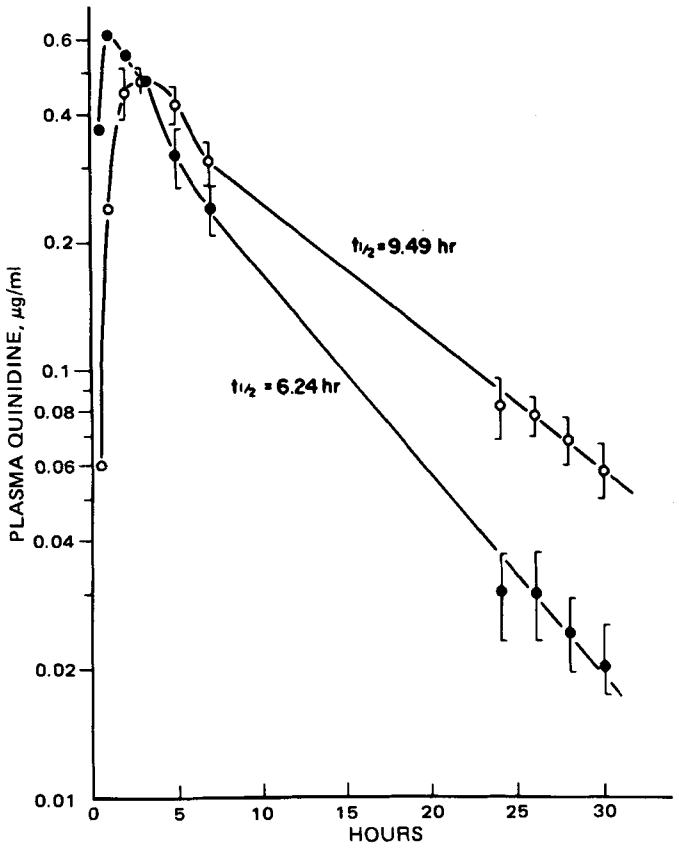


**Figure 3**—*Mean plasma quinidine concentrations* ±SD *of the volunteers with the shortest (Subject 23, ●) and the longest (Subject 19, ○) terminal half-lives* (n = 5).

The apparent total body clearance of quinidine in this study ranged from 3.55 ± 0.40 to 8.39 ± 0.65 ml/kg/min in Group I and from 4.16 ± 0.14 to 9.13 ± 1.00 ml/min/kg in Group II with means of 5.79 ± 1.44 and 6.25 ± 1.58 ml/min/kg, respectively. As expected, the intersubject variation of ~25% (*RSD*) was much greater than the intrasubject variation of 10% or less. Many subjects were significantly different when compared. For Group I, Subject 8 was significantly lower ($p < 0.05$) than all other subjects; Subjects 5 and 11, with high apparent total body clearance values, were significantly greater ($p < 0.01$) than the other subjects. The apparent total body clearance values for Subjects 20 and 23 in Group II were significantly higher ($p < 0.01$) than those of all other subjects.

Since the oral absorption of quinidine was shown (7–9) to be only 70–80% of intravenous absorption, the estimated corrected total body clearance ($Cl_{corr}$) is also given for comparison with the literature, using the factor of 0.7 as was suggested by Guentert *et al.* (19) to be the most accurate. The overall mean value for $Cl_{corr}$ was 4.22 ± 1.05 (*SD*) ml/min/kg, close to that (3.85 ± 1.09) of Greenblatt *et al.* (8) and to that (4.26 ± 1.42) of Fremstad *et al.* (33), who also used a spectrofluorometric procedure which was criticized by Guentert *et al.* (9, 19). However, the range of $Cl_{corr}$ values in this present study (Table I) overlapped those of Guentert *et al.* (mean of 4.88 ± 1.56) and also agreed with studies reported by Ueda *et al.*, who found means of 4.7 ± 1.78 (31), 4.95 ± 1.36 (34), and 4.02 ± 1.94 (5) ml/min/kg in three separate studies. Recently, Drayer *et al.* (35), who used HPLC, found a range of quinidine clearances in patients from 3.8 ± 3.9 ml/min for a "low metabolizing" group to 9.0 ± 3.6 ml/min for a group with higher levels of the 3-hydroxy metabolite. These clearances were calculated with an oral absorption factor of 0.87; the values were converted to 3.27 ± 3.36 and 7.76 ± 3.10, using the 0.7 factor of Guentert *et al.* (19) for comparison purposes, rather similar to the range of values found in this study in normal subjects (Table I).

The fluorescence procedure used to estimate plasma quinidine does not differentiate dihydroquinidine; however, this limitation is not expected to influence the clearance since Ueda *et al.* (5) found similar clearance values for this analog (4.17 ± 1.81 *versus* 4.02 ± 1.94 for quinidine) in the same subjects.

The terminal half-life obviously has some influence on clearance. However, recent studies (33, 36) support intersubject differences in protein binding capacity, possibly an α-1-acid glycoprotein or lipoprotein,

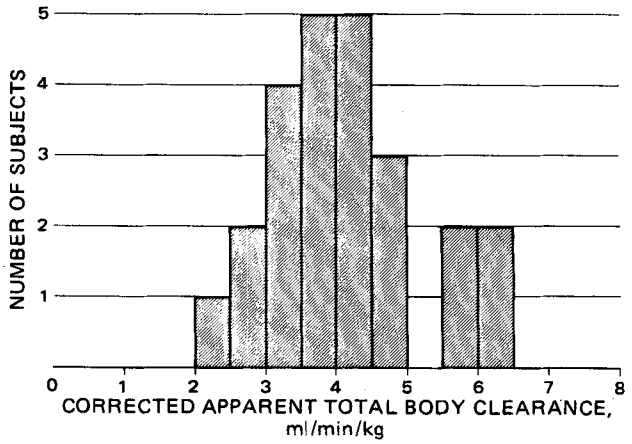


**Figure 4**—*Frequency distribution of mean corrected total body clearance* ($Cl_{corr}$) *of quinidine in the 24 subjects.*

as a major influence on clearance and volume of distribution. There was no correlation between the half-life and clearance (Table I), as shown in Fig. 2, and there were major differences in *AUC* and minor differences in $t_{1/2}$ between subjects.

Drayer *et al.* (35), who measured (3*S*)-3-hydroxyquinidine to quinidine ratios in patients, found evidence to suggest a bimodal distribution in the hydroxylating efficiency, which related reasonably well with quinidine clearance. In the present study of 24 healthy subjects, the frequency distribution of clearance (Fig. 4) appeared to be normal.

In conclusion, the bioavailabilities of eight quinidine sulfate, one gluconate, and one polygalacturonate products were found to be similar from plasma concentration estimates. The bioavailability of one gluconate product was significantly lower ($p < 0.05$) in one estimate, and its plasma concentration showed sustained-release characteristics. There was no meaningful correlation between the absorption parameters and dissolution, except that the slow-dissolving gluconate product had the lowest *AUC* and $C_{max}$ values and the longest $t_{max}$ value. The pharmacokinetics of quinidine in the 24 subjects in terms of terminal half-life (mean of 7.49 ± 0.76 hr) and total body clearance (mean of 4.22 ± 1.05 ml/min/kg) showed considerable intersubject variation (*RSD* ≃ 25%) and less intrasubject variation (*RSD* ≃ 10%).

## REFERENCES


(1) J. P. Amlie, L. Storstein, B. Olsson, D. Fremstad, and S. Jacobsen, *Eur. J. Clin. Pharmacol.*, **16,** 45 (1979).

(2) *J. Am. Pharm. Assoc.*, **NS 16,** 413 (1976).

(3) R. W. Kalmansohn and J. J. Sampson, *Circulation*, **1,** 569 (1950).

(4) S. Bellet, L. R. Roman, and A. Boza, *Am. J. Cardiol.*, **27,** 368 (1971).

(5) C. T. Ueda, B. J. Williamson, and B. S. Dzindzio, *Res. Commun. Chem. Pathol. Pharmacol.*, **14,** 215 (1976).

(6) W. D. Mason, J. O. Covinsky, J. L. Valentine, K. I. Kelly, O. H. Weddle, and B. L. Martz, *J. Pharm. Sci.*, **65,** 1325 (1976).

(7) C. T. Ueda, B. J. Williamson, and B. S. Dzindzio, *Clin. Pharmacol. Ther.*, **20,** 260 (1976).

(8) D. J. Greenblatt, H. J. Pfeifer, H. R. Ochs, K. Franke, D. S. MacLaughlin, T. W. Smith, and J. Koch-Weser, *J. Pharmacol. Exp. Ther.*, **202,** 365 (1977).

(9) T. W. Guentert, N. H. G. Holford, P. E. Coates, R. A. Upton, and S. Riegelman, *J. Pharmacokinet. Biopharm.*, **7,** 315 (1979).

(10) J. D. Strum, J. L. Colaizzi, J. M. Jaffe, P. C. Martineau, and R. I. Poust., *J. Pharm. Sci.*, **66,** 539 (1977).

(11) J. D. Strum, J. W. Ebersole, J. M. Jaffe, J. L. Colaizzi, and R. I. Poust, *ibid.*, **67,** 568 (1978).

(12) "The United States Pharmacopeia," 19th rev., Mack Publishing Co., Easton, Pa., 1975, p. 435.

(13) "The United States Pharmacopeia," 19th rev., 4th suppl., Mack Publishing Co., Easton, Pa., 1978, p. 150.

(14) J. W. Poole, *Drug Inf. Bull.*, **3,** 8 (1969).

(15) J. Armand and A. Badinand, *Ann. Biol. Clin. (Paris)*, **30,** 599 (1972).

(16) K. K. Midha and C. Charette, *J. Pharm. Sci.*, **63,** 1244 (1974).

(17) S. Sved, I. J. McGilveray, and N. Beaudoin, *J. Chromatogr.*, **145,** 437 (1978).

(18) J. G. Wagner and E. Nelson, *J. Pharm. Sci.*, **53,** 1392 (1964).

(19) T. W. Guentert, R. A. Upton, N. M. G. Holford, and S. Riegelman, *J. Pharmacokinet. Biopharm.*, **7,** 303 (1979).

(20) N. J. Pound and R. W. Sears, *Can. J. Pharm. Sci.*, **10,** 122 (1975).

(21) T. W. Guentert, P. E. Coates, R. A. Upton, D. L. Combs, and S. Riegelman, *J. Chromatogr.*, **162,** 59 (1979).

(22) K. K. Midha, I. J. McGilveray, C. Charette, and M. Rowe, *Can. J. Pharm. Sci.*, **12,** 41 (1977).

(23) J. L. Valentine, P. Driscoll, E. L. Hamburg, and E. D. Thompson, *J. Pharm. Sci.*, **65,** 96 (1976).

(24) D. H. Huffman and C. E. Hignite, *Clin. Chem.*, **22,** 810 (1976).

(25) K. A. Conrad, B. L. Molk, and C. A. Chidsey, *Circulation*, **55,** 1 (1977).

(26) W. G. Crouthamel, B. Kowarski, and P. K. Narang, *Clin. Chem.*, **23,** 2030 (1977).

(27) M. A. Peat and T. A. Jennison, *ibid.*, **24,** 2166 (1978).

(28) W. L. Chiou, *J. Pharmacokinet. Biopharm.*, **6,** 539 (1978).

(29) H. R. Ochs, D. J. Greenblatt, E. Woo, K. Franke, H. J. Pfeifer, and T. W. Smith, *Am. J. Cardiol.*, **41,** 770 (1978).

(30) J. O. Covinsky, J. Russo, K. L. Kelly, J. Cashman, E. N. Amick, and W. D. Mason, *J. Clin. Pharmacol.*, **19,** 261 (1979).

(31) C. T. Ueda, D. S. Hirschfeld, M. M. Scheinman, U. Rowland, B. J. Williamson, and B. S. Dzindzio, *Clin. Pharmacol. Ther.*, **19,** 30 (1976).

(32) W. A. Mahon, M. Mayersohn, and T. Inaba, *ibid.*, **19,** 566 (1976).

(33) D. Fremstad, O. G. Nilsen, L. Storstein, J. Amlie, and S. Jacobsen, *Eur. J. Clin. Pharmacol.*, **15,** 187 (1979).

(34) C. T. Ueda and B. S. Dzindzio, *Clin. Pharmacol. Ther.*, **23,** 158 (1978).

(35) D. E. Drayer, M. Hughes, B. Lorenzo, and M. M. Reidenberg, *ibid.*, **27,** 72 (1980).

(36) E. Woo and D. J. Greenblatt, *J. Pharm. Sci.*, **68,** 466 (1979).


## ACKNOWLEDGMENTS


Presented in part at the Basic Pharmaceutics Section, APhA Academy of Pharmaceutical Sciences, Montréal meeting, May 1978.

The authors are grateful for the assistance and collaboration of the supervising physician Dr. Allan G. Bellack. They also thank Dr. W. Tostowaryk for statistical analysis and Dr. R. D. Hossie for dissolution measurements.

# High-Pressure Liquid Chromatographic Determination of Corticosteroids in Topical Pharmaceuticals

**PATRICIA A. WILLIAMS** *x **and EDWARD R. BIEHL** ‡

Received June 16, 1980, from the *Dallas District, Food and Drug Administration, Dallas, TX 75204, and the ‡Department of Chemistry, Southern Methodist University, Dallas, TX 75275. Accepted for publication October 23, 1980.

**Abstract** □ Cortisone, hydrocortisone, prednisolone, and prednisone were separated on a reversed-phase microparticulate high-pressure liquid chromatographic (HPLC) column with a ternary mobile solvent containing tetrahydrofuran, methanol, and water. Cortisone acetate, hydrocortisone acetate, and prednisolone acetate were separated on the same reversed-phase column using acetonitrile–water. Various commercial topical formulations of these corticosteroids, except cortisone and prednisone, were prepared by both simple dilution and by extraction for analysis by the proposed HPLC procedure, by the blue tetrazolium procedure, and by the isoniazid procedure and/or phenylhydrazine method. Retention data are given for some common degradation products (C-17 ketones and C-17 carboxylic acid derivatives) and for methyl-, propyl-, and butylparabens with these mobile solvents.

**Keyphrases** □ Corticosteroids—analysis of topical pharmaceuticals, high-pressure liquid chromatography □ Steroids—analysis in topical pharmaceuticals, high-pressure liquid chromatography □ High-pressure liquid chromatography—analysis, corticosteroids in topical pharmaceuticals

High-pressure liquid chromatography (HPLC) is a powerful tool in providing a specific method of analysis for corticosteroids in pharmaceutical preparations (1–30). HPLC methods for corticosteroids in topical preparations such as creams, lotions, and ointments (5, 6, 10–14, 16, 19, 21, 22, 25–28, 30) are particularly useful because of the complex nature of the sample matrix and the potential for interference in colorimetric or UV methods.

The official blue tetrazolium (31, 32), phenylhydrazine (33), isoniazid (34), and UV methods are subject to interference from several sources (35, 36). HPLC can provide both the separation and determination steps, thereby eliminating most interference problems in other methods.

Although official methods of analysis of many corticosteroids are being changed to HPLC methods (37), all corticosteroids chosen for this study are still being determined officially by the blue tetrazolium or phenylhydrazine methods (31, 37).

The described reversed-phase HPLC procedure effectively separates the corticosteroid of interest from its most common decomposition products, closely related steroids, other common active ingredients, and product excipients. Comparisons of results of HPLC, blue tetrazolium, isoniazid, and/or phenylhydrazine methods were made for various commercial preparations. Simple dilution and extraction procedures also were compared. The corticosteroids studied were cortisone, hydrocortisone, prednisone, prednisolone, cortisone acetate, hydrocortisone acetate, and prednisolone acetate.

## EXPERIMENTAL

**Materials**—*Standards*—Cortisone acetate[1], dexamethasone[1], hydrocortisone[1], hydrocortisone acetate[1], prednisolone[1], prednisolone acetate[1], prednisone[1], cortisone[2], androst-4-ene-3,17-dione[2] (I), 11β-hydroxyandrost-4-ene-3,17-dione[2] (II), 11β-hydroxyandrosta-1,4-diene-3,17-dione[2] (III), androsta-1,4-diene-3,11,17-trione[2] (IV), 17α-hydroxy-3,11-dioxoandrost-4-ene-17-carboxylic acid[3] (V), 11β,17α-dihydroxy-3-oxoandrost-4-ene-17-carboxylic acid[3] (VI), 11β,17α-dihydroxy-3-oxoandrosta-1,4-diene-17-carboxylic acid[3] (VII), 17α-hydroxy-3,11-dioxoandrosta-1,4-diene-17-carboxylic acid[3] (VIII), and 11β,17α-dihydroxy-3-oxo-9-fluoro-16α-methylandrosta-1,4-diene-17-carboxylic acid[3] (IX) were used.

*Reagents*—ACS reagent grade or equivalent chloroform, cyclohexane, acetic acid, sodium chloride, and basic aluminum oxide powder were used.

HPLC grade or distilled-in-glass grade acetonitrile, methanol, and tetrahydrofuran (no stabilizers) were used. Tetrahydrofuran was treated to remove peroxides just before use in the mobile solvent by passing it through an aluminum oxide column containing 10 g of aluminum oxide/100 ml of tetrahydrofuran (38).

**HPLC**—The high-pressure liquid chromatograph was equipped with a 6000-psi pump, a high-pressure injector or automatic injector, a 254-nm detector[4], a 10-mv recorder[5], and an electronic digital integrator[6]. The instrument was operated at ambient temperature, and the detector sensitivity used was 0.05 aufs.

**Column**—The column[7] (25 cm × 4.6 mm) was purchased prepacked with octylsilane chemically bonded to porous microsilica particles, 5 μm in diameter. The theoretical plates ($N$) for hydrocortisone were determined to be 3467 with the formula $N = 16(V/W)^2$, where $V$ is the retention volume of the component and $W$ is the width of the base of the peak.

**Mobile Solvents**—Each mobile solvent was filtered through a micropore filter[8] just before use. Solvent A (for hydrocortisone, prednisolone, and prednisone determinations) was 25% (v/v) tetrahydrofuran and 12.5% (v/v) methanol in water. A flow rate of 1 ml/min was used at a column back-pressure of 1800 psi. The retention volume for hydrocortisone ranged from 9 to 10.5 ml. The retention volume for dexamethasone ranged from 14 to 16.5 ml. The resolution was 1.3 for prednisone–cortisone, 1.6 for cortisone–prednisolone, and 1.0 for prednisolone–hydrocortisone. Resolution ($R_s$) was determined by the formula $R_s = 2(V_2 - V_1)/(W_2 + W_1)$, where $V_2$ and $V_1$ are the retention volumes of the two components and $W_2$ and $W_1$ are the corresponding widths of the bases of the peaks.

Solvent B (for cortisone acetate, hydrocortisone acetate, and prednisolone acetate determinations) was 45% (v/v) acetonitrile in water. A flow rate of 1 ml/min was used at a column back-pressure of 800 psi. The retention volume for cortisone acetate ranged from 10 to 11 min. The resolution ($R_s$) was 0.80 for prednisolone acetate–hydrocortisone acetate and 3.0 for hydrocortisone acetate–cortisone acetate.

**Internal Standard Preparations**—*For Hydrocortisone, Prednisolone, and Prednisone Determinations*—The dexamethasone stock internal standard solution was ~150 μg of dexamethasone/ml of methanol. To prepare the dexamethasone diluted internal standard solution, the stock internal standard solution was diluted quantitatively one to five with methanol to obtain a solution with ~30 μg of dexamethasone/ml.

*For Corticosteroid Acetate Determinations*—Cortisone acetate was used for hydrocortisone acetate and prednisolone acetate determinations, and hydrocortisone acetate was used for cortisone acetate determinations.

[1] USP reference standards.

[2] Research Plus Steroids Laboratories, Denville, N.J.

[3] Prepared by Millard Maienthal, Division of Drug Chemistry, Food and Drug Administration, Washington, D.C.

[4] Model 204 liquid chromatograph with model 6000 A pump, model U6K loop injector or WISP 710A sample processor, and model 440 absorbance detector, Waters Associates, Milford, Mass.

[5] Model A-25 strip-chart recorder, Varian Instrument Division, Aerograph Products, Palo Alto, Calif.

[6] Supergrator 3, Columbia Scientific Industries, Austin, Tex.

[7] Zorbax $C_8$, DuPont Chemical Co., Wilmington, Del.

[8] Millipore type LS, 5.0-μm pore size, Millipore Corp., Bedford, Mass.



0022-3549/81/0500-0530$01.00/0
© 1981, American Pharmaceutical Association

**Table I—Comparison of HPLC Columns**

| Corticosteroid | Octadecylsilane[a] Column RRV[c] | Octadecylsilane[a] Column $R_s$ | Octylsilane[b] Column RRV[c] | Octylsilane[b] Column $R_s$ |
|---|---|---|---|---|
| Prednisone | 0.77 | 1.2 | 0.80 | 1.3 |
| Cortisone | 0.85 | 1.2 | 0.86 | 1.6 |
| Prednisolone | 0.92 | 1.1 | 0.94 | 1.0 |
| Hydrocortisone | 1.00 | | 1.00 | |
| Cortisone acetate | 2.30 | | 2.15 | |
| Prednisolone acetate | 2.33 | | 2.12 | |
| Hydrocortisone acetate | 2.60 | | 2.32 | |
| Methylparaben | 1.26 | | 1.24 | |
| Propylparaben | 4.01 | | 3.30 | |
| Butylparaben | 4.56 | | 3.52 | |

[a] Zorbax ODS (25-cm × 4.6-mm) column, DuPont Chemical Co., $N$ (hydrocortisone) = 3364 plates. [b] Zorbax $C_8$ (25-cm × 4.6-mm) column, DuPont Chemical Co., $N$ (hydrocortisone) = 3467 plates. [c] Retention volume relative to hydrocortisone, $V$ = 9–10 ml.

The stock internal standard solution was ~100 μg of internal standard/ml in methanol. To prepare the diluted internal standard solution, the stock internal standard solution was diluted quantitatively one to five with 0.5% acetic acid in methanol to obtain a solution with ~20 μg of corticosteroid acetate/ml.

**Standard Preparations**—*For Hydrocortisone, Prednisolone, and Prednisone Determinations*—Corticosteroid reference standard, about 10 mg accurately weighed, was transferred to a 100-ml volumetric flask and dissolved and diluted to volume with methanol. A 10.0-ml aliquot was transferred to a 50-ml volumetric flask, 10.0 ml of the dexamethasone stock internal standard solution was added, and the solution was diluted to volume with methanol. The final dilution contained 20 μg of corticosteroid reference standard/ml and 30 μg of dexamethasone internal standard/ml.

*For Cortisone Acetate, Hydrocortisone Acetate, and Prednisolone Acetate Determinations*—Corticosteroid acetate reference standard, about 10 mg accurately weighed, was transferred to a 100-ml volumetric flask and dissolved and diluted to volume with 0.5% acetic acid in methanol. A 10.0-ml aliquot was transferred to a 50-ml volumetric flask, 10.0 ml of the appropriate corticosteroid acetate stock internal standard solution was added, and the solution was diluted to volume with 0.5% acetic acid in methanol. The final dilution contained 20 μg of corticosteroid acetate reference standard/ml and 20 μg of corticosteroid acetate internal standard/ml.

**Sample Preparations for Hydrocortisone, Prednisolone, and Prednisone Determinations**—*Direct Dilution*—An accurately weighed quantity of product, equivalent to ~10 mg of corticosteroid, was transferred to a 150-ml beaker, and 25 ml of methanol was added. The solution was heated on a steam bath with periodic agitation until the sample material was thoroughly dispersed. The solution was cooled in an ice bath

**Table II—Retention Data of Octylsilane Microsilica Particle (5-μm) Column**

| Compound | Mobile Solvent A RRV[a] | Mobile Solvent A $K'$[b] | Mobile Solvent B RRV[c] | Mobile Solvent B $K'$[b] |
|---|---|---|---|---|
| Cortisone | 0.86 | 2.3 | 1.07 | 0.9 |
| Cortisone acetate | 2.15 | 7.1 | 2.44 | 3.4 |
| I | 0.96 | — | 2.01 | — |
| V | 0.44 | — | 0.74 | — |
| Hydrocortisone | 1.00 | 2.8 | 1.00 | 0.8 |
| Hydrocortisone acetate | 2.32 | 7.7 | 2.08 | 2.7 |
| II | 1.13 | — | 1.82 | — |
| VI | 0.63 | — | 0.78 | — |
| Prednisolone | 0.94 | 2.6 | 0.97 | 0.7 |
| Prednisolone acetate | 2.12 | 7.0 | 2.03 | 2.6 |
| III | 1.02 | — | 1.72 | — |
| VII | 0.54 | — | 0.76 | — |
| Prednisone | 0.80 | 2.0 | 1.04 | 0.9 |
| IV | 0.90 | — | 1.90 | — |
| VIII | 0.37 | — | 0.64 | — |
| Dexamethasone | 1.64 | 5.2 | 1.30 | 1.3 |
| IX | 1.59 | — | 0.87 | — |
| Methylparaben | 1.24 | — | 1.22 | — |
| Propylparaben | 3.30 | — | 2.33 | — |
| Butylparaben | 3.52 | — | 3.77 | — |

[a] Retention volume relative to hydrocortisone, $V$ = 9–10 ml. [b] $K' = (V - V_0)/V_0$, where $V_0$ = 2.4 ml. [c] Retention volume relative to hydrocortisone, $V$ = 4–5 ml.

**Table III—Replication Study with Standards**

| Mobile Solvent | Amount Injected, μg | Retention Volume, ml | Coefficient of Variation[a] Peak Height | Coefficient of Variation[a] Peak Area |
|---|---|---|---|---|
| | | Hydrocortisone | | |
| A | 0.25 | 9.35–9.49 | 1.38 | 3.19 |
| B | 0.15 | 4.34 | 1.62 | 0.89 |
| | | Dexamethasone | | |
| A | 0.375 | 15.30–15.62 | 1.34 | 2.33 |
| B | 0.225 | 5.62–5.65 | 1.61 | 3.61 |
| | | Cortisone Acetate | | |
| A | 0.53 | 20.10–20.47 | 1.30 | 1.39 |
| B | 0.30 | 10.60–10.66 | 1.14 | 1.83 |

[a] For 10 replicate injections.

until the residue solidified, and then the liquid was decanted into a 100-ml volumetric flask. The extraction was repeated with three 20-ml portions of methanol, decanting each into a volumetric flask after cooling. After the methanol solution reached room temperature, it was diluted to volume with methanol and filtered if necessary.

A 10.0-ml aliquot was transferred to a 50-ml volumetric flask, 10.0 ml of the dexamethasone stock internal standard solution was added, and the solution was diluted to volume with methanol.

*Extraction*—A 10.0-ml aliquot of the first sample dilution from the direct dilution procedure, equivalent to ~1 mg of corticosteroid, was transferred to a 125-ml separator. Then 2 ml of aqueous saturated sodium chloride solution and 25 ml of cyclohexane were added, and the separator was shaken vigorously for 1 min. After the layers separated, the lower methanol layer was drained into a 250-ml separator containing 50 ml of distilled water. The cyclohexane layer was extracted with two 2-ml portions of 80% methanol–water. These extracts were added to the solution in the 250-ml separator, and the cyclohexane layer was discarded.

The solution in the 250-ml separator was extracted with three 50-ml and one 45-ml portions of chloroform, with shaking of the separator for 2 min for each extraction. Each chloroform extract was filtered through a cotton plug into a 200-ml volumetric flask. The solution was diluted to volume with chloroform and mixed.

A 20.0-ml aliquot of the chloroform solution was transferred to a 25-ml conical flask, and the chloroform was evaporated just to dryness on a steam bath under a stream of air. Then 5.0 ml of the dexamethasone diluted internal standard solution was added to the residue in the flask.

**Sample Preparation for Cortisone Acetate, Hydrocortisone Acetate, and Prednisolone Acetate Determinations**—The method for corticosteroid alcohols was followed, except that 0.5% acetic acid in methanol was substituted for methanol in both the direct dilution and extraction procedures. Also, the appropriate corticosteroid acetate internal standard solution was used in place of the dexamethasone internal standard solution.

**HPLC Determination**—Ten microliters of each standard and sample preparation was injected onto an HPLC column that had been previously

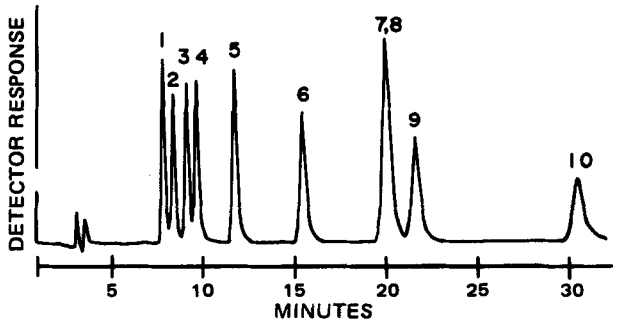


**Figure 1**—*Chromatogram of a standard mixture. The column was octylsilane bonded to microsilica (5 μm). Solvent A was 25% tetrahydrofuran–12.5% methanol in water. The flow rate was 1 ml/min, the pressure was 1800 psi, the temperature was ambient, and the detector was at 254 nm (0.05 aufs). Key: 1, prednisone; 2, cortisone; 3, prednisolone; 4, hydrocortisone; 5, methylparaben; 6, dexamethasone; 7, prednisolone acetate; 8, cortisone acetate; 9, hydrocortisone acetate; and 10, propylparaben.*

**Table IV—Linearity Study with Standards**

| Mobile Solvent | Amount Injected, μg | Coefficient of Determination ($r^2$) Peak Height | Peak Area |
|---|---|---|---|
| | Hydrocortisone | | |
| A | 0.05–0.4 | 0.9993 | 0.9977 |
| B | 0.05–0.4 | 0.9995 | 0.9999 |
| | Dexamethasone | | |
| A | 0.075–0.6 | 0.9994 | 0.9977 |
| B | 0.075–0.6 | 0.9993 | 0.9986 |
| | Cortisone Acetate | | |
| A | 0.1–0.8 | 0.9996 | 0.9934 |
| B | 0.1–0.8 | 0.9995 | 0.9993 |

**Table V—Recovery following Extraction**

| Sample[a] | HPLC | Percent of Recovered Standard Blue Tetrazolium | Isoniazid |
|---|---|---|---|
| 1 | 103.2 | 102.6 | 103.6 |
| 3 | 99.1 | 103.0 | 100.3 |
| 4 | 98.9 | 99.5 | 102.3 |
| 5 | 99.1 | 99.3 | 101.4 |
| 7 | 101.4 | 102.8 | 103.1 |
| 9 | 99.4 | 97.3 | 100.2 |
| 10 | 100.4 | 101.7 | 98.2 |
| 12*a* | 91.6 | 91.6 | 98.2 |
| 12*b* | 100.1 | 115.8 | 110.6 |
| 13*a* | 95.1 | 92.8 | 100.9 |
| 13*b* | 102.1 | 109.5 | 107.0 |
| 14 | 100.2 | 100.6 | — |
| 16 | 99.8 | 101.2 | 102.3 |
| 17 | 99.3 | 102.9 | 102.0 |
| 18 | 98.4 | 108.4 | 103.7 |
| 19 | 100.4 | 98.0 | 100.8 |
| 20 | 99.3 | 106.8 | 105.1 |
| 21 | 98.4 | 103.0 | — |
| 22 | 99.3 | 103.6 | — |
| Average | 99.24 | 102.13 | 102.48 |
| *SD* | 2.48 | 5.60 | 3.16 |
| *CV* | 2.5 | 5.48 | 3.08 |

[a] Sample numbers correspond to samples in Table VII.

equilibrated for 0.5–1 hr with the appropriate mobile solvent (Solvent A for hydrocortisone, prednisolone, and prednisone; Solvent B for cortisone acetate, hydrocortisone acetate, and prednisolone acetate). The corticosteroid peak response should be ~50% full scale at 0.05 aufs. If not, the injection volume should be adjusted.

From the chromatogram, the peak height ratios of the corticosteroid to the internal standard in the sample and standard were determined. The amount of corticosteroid in the sample is found using:

$$\frac{\text{mg of corticosteroid}}{\text{g of sample}} = \frac{\text{sample ratio}}{\text{standard ratio}} \frac{\mu\text{g of standard}}{\text{ml}} \times \frac{\text{sample dilution}}{\text{g of sample}} \frac{1\text{ mg}}{1000\ \mu\text{g}} \quad \text{(Eq. 1)}$$

For lotion samples, the value, in milligrams per gram, is multiplied by sample density to determine the value in milligrams per milliliter.

**Blue Tetrazolium Determination**—The USP (31) "Assay for Steroids" procedure was used.

**Phenylhydrazine Method**—The Silber–Porter (33) procedure was followed.

**Isoniazid Method**—The Umberger (34) procedure was followed using twice the recommended concentration of hydrochloric acid to increase sensitivity. Prednisolone, prednisolone acetate, and prednisone reactions were run in a 50° water bath[9].

## RESULTS AND DISCUSSION

**HPLC Parameters**—Two reversed-phase columns, octadecylsilane and octylsilane chemically bonded to microparticle silica (5 μm), were used. Column efficiency results (theoretical plates) were comparable, but the octylsilane column gave slightly better resolution for prednisone, cortisone, prednisolone, and hydrocortisone with Solvent A (Table I).

Attempts were made to find a mobile solvent that would separate the seven steroids with resolutions greater than 1.0. Binary mixtures of methanol–water, acetonitrile–water, and tetrahydrofuran–water and ternary mixtures of methanol–acetonitrile–water, tetrahydrofuran–acetonitrile–water, and tetrahydrofuran–methanol–water were tried. In

[9] Suggested by Sharon R. Reed and Stephen M. Walters, Food and Drug Administration, Detroit, Mich., personal communication.

**Table VI—Precision of HPLC Analysis of Samples**

| Run | Percent of Declared 0.25% Hydrocortisone Lotion[a] Methanol Dilution | Chloroform Extraction | 0.25% Hydrocortisone Acetate Lotion Methanol Dilution | Chloroform Extraction |
|---|---|---|---|---|
| 1 | 50.8 | 49.7 | 96.1 | 94.7 |
| 2 | 51.0 | 50.7 | 97.7 | 95.6 |
| 3 | 51.4 | 49.7 | 96.7 | 95.3 |
| 4 | 51.7 | 51.8 | 96.4 | 96.0 |
| 5 | 51.5 | 49.5 | 96.3 | 95.7 |
| 6 | 51.0 | 51.3 | 96.3 | 94.7 |
| Mean | 51.23 | 50.45 | 96.58 | 95.33 |
| *SD* | 0.35 | 0.96 | 0.58 | 0.54 |
| *CV* | 0.68 | 1.90 | 0.68 | 0.57 |

[a] Hydrocortisone decomposed. See Sample 8 in Table VIII.

**Table VII—Composition of Commercial Corticosteroid Samples Studied**

| Sample | Sample Type and Declared Amount of Corticosteroid | Other Active Ingredients |
|---|---|---|
| Cortisone acetate | | |
| 1 | Ophthalmic ointment, 1.5% | Neomycin sulfate, 0.5% |
| Hydrocortisone | | |
| 2 | Cream, 0.25%[a,b] | — |
| 3 | Cream, 0.25%[a,b] | Neomycin sulfate, 0.5% |
| 4 | Cream, 0.5%[a] | Diiodohydroxyquin, 1% |
| 5 | Cream, 0.5% | Diiodohydroxyquin, 1% |
| 6 | Gel, 1% | — |
| 7 | Lotion, 0.125%[a,b] | — |
| 8 | Lotion, 0.25% | — |
| 9 | Lotion, 0.25%[a,b] | — |
| 10 | Lotion, 0.25%[a] | Coal tar solution, 2%; diiodohydroxyquin, 1% |
| 11 | Lotion, 0.5%[a,b] | — |
| 12 | Lotion, 0.5%[a,b] | Benzoyl peroxide, 5.5%; chlorhydroxyquinoline, 0.25% |
| 13 | Lotion, 0.5%[a,b] | Benzoyl peroxide, 5.0%; chlorhydroxyquinoline, 0.25% |
| 14 | Ointment, 0.5% | — |
| 15 | Ointment, 0.5% | Polymyxin B sulfate, 5000 U/g; bacitracin zinc, 400 U/g; neomycin sulfate, 0.5% |
| Hydrocortisone acetate | | |
| 16 | Cream, 0.5%[a] | Polymyxin B sulfate, 10,000 U/g; neomycin sulfate, 0.5%; gramicidin, 0.25% |
| 17 | Cream, 0.5%[a,b] | Lidocaine, 3%; iodochlorhydroxyquin, 3% |
| 18 | Cream, 0.5%[a,b] | Lidocaine, 3% |
| 19 | Cream, 0.5%[a] | Chlorcyclizine hydrochloride, 2% |
| 20 | Cream, 0.5% | Salicylic acid, 2% |
| Prednisolone | | |
| 21 | Cream, 0.5%[a,c] | Aluminum chlorhydroxy allantoinate, 0.25% |
| 22 | Ophthalmic ointment, 0.5% | Chloramphenicol, 1% |
| Prednisolone acetate | | |
| 23 | Ophthalmic ointment, 0.2% | Sulfacetamide sodium, 10.0% |
| 24 | Ophthalmic ointment, 0.5%[a,b] | Sulfacetamide sodium, 10.0% |

[a] Methylparaben is present in the sample. [b] Propylparaben is present in the sample. [c] Butylparaben is present in the sample.

**Table VIII—Assay Results (Percent of Declared Value) of the Commercial Corticosteroid Samples**

| Sample | Proposed HPLC | | Blue Tetrazolium | | Other Methods | |
|---|---|---|---|---|---|---|
| | Methanol Dilution | Chloroform Extraction | Methanol Dilution | Chloroform Extraction | Methanol Dilution | Chloroform Extraction |
| 1*a*[a] | 76.2 | 75.2 | 74.6 | 76.1 | 78.3[b] | — |
| 1*b* | 55.3 | 55.5 | 55.3 | 58.5 | 56.5[b] | 57.2[b] |
| 2 | 74.6[c] | 72.4[c] | 92.8 | 85.0[c] | — | 78.4[d] |
| 3 | 95.2[c] | 92.0 | 101.4 | 96.3 | 105.3[b] | 105.3[b] |
| 4 | 77.9 | 76.9 | 80.6 | 80.7 | 101.4[b] | 89.7[b] |
| 5 | 93.2 | 93.9 | — | 96.0 | — | 107.2[b] |
| 6 | 90.2[c] | 87.3[c] | 98.7 | 96.2[c] | — | 95.9[d] |
| 7 | 83.9 | 83.2 | 91.0 | 88.8 | 99.0[b] | 99.4[b] |
| 8 | 53.0[c] | 51.8[c] | 74.2 | 59.4[c] | — | 57.1[d] |
| 9 | 55.2[c] | 54.7[c] | 86.3 | 68.2[c] | — | 55.8[d] |
| 10 | 96.6 | 95.9[c] | — | 102.3 | — | 126.7[b] |
| 11 | 94.5[c] | 92.4[c] | 100.2 | 98.2[c] | — | 93.1[d] |
| 12*a*[e] | 99.6 | 92.3 | 139.4 | 91.9 | 148.3[b] | 124.5[b] |
| 12*b* | 92.0 | 95.8 | 177.3 | 97.4 | 164.6[b] | 112.4[b] |
| 13*a*[e] | 104.7 | 88.9 | 88.1 | 86.4 | 133.3[b] | 110.0[b] |
| 13*b* | 103.3 | 105.7 | 108.4 | 116.7 | 130.4[b] | 130.7[b] |
| 14 | 88.3 | 92.2 | 92.6 | 94.5 | — | 92.7[d] |
| 15 | 101.0 | 98.3 | 109.8 | 100.4 | 99.5[b] | 100.4[b] |
| 16 | 100.0[c] | 100.1[c] | 107.4 | 102.2[c] | 97.7[b] | 103.8[b] |
| 17 | 102.6 | 100.9 | 110.1 | 108.3 | 104.7[b] | 102.7[b] |
| 18 | 100.7 | 99.7 | 279.1 | 213.1 | 103.1[b] | 103.8[b] |
| 19 | 99.7[c] | 99.5[c] | 104.2 | 104.8[c] | 103.5[b] | 105.6[b,c] |
| 20 | 108.4 | 105.3 | 182.1 | 113.3 | 112.6[b] | 109.3[b] |
| 21 | 82.7 | 81.4 | 85.9 | 88.0 | — | — |
| 22 | 106.8 | 106.4 | 110.8 | 110.4 | — | — |
| 23 | 104.8 | 102.0 | 109.9 | 108.4 | — | — |
| 24 | 96.7 | 100.6 | 96.9 | 101.2 | — | — |

[a] Results *a* and *b* are for two separate units of product. [b] Isoniazid method. [c] Result is the average of two or three replicate determinations. [d] Phenylhydrazine method. [e] Result *a* from product with benzoyl peroxide added and *b* from product without benzoyl peroxide.

the preliminary search for a suitable mobile solvent, a solvent programmer was used with the HPLC instrument[10].

The best separation of the four steroids, prednisone, cortisone, prednisolone, and hydrocortisone, was obtained using the ternary solvent of 25% tetrahydrofuran–12.5% methanol in water (Solvent A). The resolution with this ternary system was optimized (39) by combining the two binary mixtures, 30% tetrahydrofuran–water and 50% methanol–water. Although baseline separation was not achieved, each steroid could be analyzed successfully in the presence of up to 10% of the other three steroids. An experiment was performed utilizing hydrocortisone standard (20 μg/ml) with 2 μg/ml each of the other three steroids added and dexamethasone (internal standard, 30 μg/ml). The hydrocortisone in this mixture was determined to be 99.9% (area ratio) and 98.6% (peak height ratio).

The best separation of the steroid acetates, cortisone acetate, prednisolone acetate, and hydrocortisone acetate, was obtained using 30% tetrahydrofuran in water. However, the retention times were too long (~30 min) for routine analytical work. The best separation within an acceptable time was obtained with 45% acetonitrile in water (Solvent B).

Table II gives the retention data, and Figs. 1 and 2 provide typical chromatograms obtained using the octylsilane microparticle (5 μm) silica column with Solvents A and B.

**Replication Study**—A mixture of hydrocortisone, dexamethasone, and cortisone acetate reference standards in 0.5% acetic acid in methanol was used. Ten 10-μl injections were made onto the octylsilane-bonded column with the automatic injector (Table III).

In general, the coefficient of variation was more acceptable for peak height values. Therefore, peak heights were used for all sample determinations.

**Linearity Study**—Standard mixtures containing hydrocortisone, dexamethasone, and cortisone acetate in 0.5% acetic acid in methanol were injected onto the octylsilane-bonded column. A straight line was fit to the peak height and area data by linear least squares, and the coefficient of determination ($r^2$) was calculated (Table IV).

These corticosteroids give linear responses in the given concentration ranges. Peak height data appeared to be more acceptable for quantitation of these corticosteroids.

**Extraction Recovery Studies**—A known amount of reference standard (~0.5 mg) was added to a 5.0-ml aliquot of the first dilution of the sample preparation and 5 ml of methanol in a 125-ml separator. The extraction was followed beginning with "Then 2 ml of aqueous saturated sodium chloride solution. . . ."

The recovery of standard added to the sample was determined by the proposed HPLC, blue tetrazolium (31), and isoniazid (34) methods (Table V). The results show that extraction is suitable.

**Precision of HPLC Analysis of Samples**—Six replicate determinations of two commercial samples were performed by the proposed direct dilution and extraction procedures (Table VI).

**Analysis**—The results of the analysis of commercial samples (Table VII) are given in Table VIII. The HPLC results for most samples by both procedures were comparable, indicating that either is suitable. However, since continuous injections of methanolic extracts of cream, lotion, or ointment samples could plug or otherwise shorten the life of the HPLC column, the proposed extraction procedure is the sample preparation method of choice.

A 0.5% solution of acetic acid in methanol was recommended as the diluting solvent for corticosteroid acetate esters so that ester hydrolysis

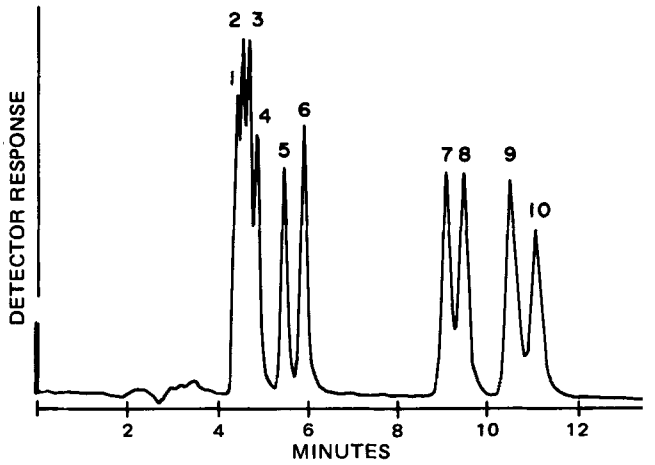


**Figure 2**—*Chromatogram of standard mixture. The column was octylsilane bonded to microsilica (5μm). Solvent B was 45% acetonitrile in water. The flow rate was 1 ml/min, the pressure was 800 psi, the temperature was ambient, and the detector was at 254 nm (0.05 aufs). Key: 1, prednisolone; 2, hydrocortisone; 3, prednisone; 4, cortisone; 5, methylparaben; 6, dexamethasone; 7, prednisolone acetate; 8, hydrocortisone acetate; 9, propylparaben; and 10, cortisone acetate.*

[10] Model 201 liquid chromatograph with two model 6000 pumps and a model 660 solvent programmer, Waters Associates, Milford, Mass.

will not occur in the sample preparation. Without acetic acid, Samples 23 and 24 had almost completely hydrolyzed within 1–2 hr. The 10% sulfacetamide sodium in these samples probably caused the rapid hydrolysis, but other corticosteroid acetate ester samples and standards also had small amounts of free corticosteroid alcohol present (<2%) after being in methanol solution overnight.

Samples 2, 7–9, 11, and 14, which were official USP hydrocortisone preparations, illustrate the need for a more specific assay such as HPLC. The official blue tetrazolium results for these samples were 5–30% higher than those from the proposed HPLC method. Chromatograms for Samples 2, 7–9 (hydrocortisone), and 21 (prednisolone) had one or more small peaks (<5% of the main peak) in addition to the main steroid peak. The retention volume for one of these small peaks in each chromatogram corresponded to that of the C-17 ketone degradation standard (Table II, Compounds I and III). Samples 2, 4, 8, and 9 also had an early eluting peak with a retention volume close to that of the C-17 carboxylic acid degradation product of hydrocortisone, which was reduced or completely removed by extraction (Table II, Compound VI).

Other active ingredients in the samples did not interfere with the proposed HPLC determination. Most of these compounds either were not detected by the 254-nm absorbance detector or were probably retained completely by the column (iodohydroxyquin and related compounds). Sulfacetamide and salicylic acid eluted mainly in the column dead volume, 2–3 ml. Chloramphenicol ($V$ = 22 ml) was detected but was well separated from prednisolone ($V$ = 9.5 ml). Samples 12 and 13 were analyzed with and without benzoyl peroxide (which was packaged in a separate vial to be added to the lotion before dispensing), because decomposition appeared to begin soon after addition of benzoyl peroxide.

The parabens were well separated from the steroids studied, except cortisone acetate. With Solvent B, the recommended solvent for acetate esters, propylparaben and cortisone acetate eluted too close for accurate quantitation of cortisone acetate. Therefore, cortisone acetate cannot be used as an internal standard for other acetate esters; another mobile solvent must be used for cortisone acetate analysis in the presence of propylparaben.

The proposed HPLC procedure is recommended to replace or at least to supplement the blue tetrazolium, phenylhydrazine, isoniazid, and UV spectrophotometric methods in the analysis of corticosteroids in topical pharmaceuticals based on the data presented in this and other (1–30) papers.

## REFERENCES


(1) W. Butte, *J. High Resolut. Chromatogr.—Chromatogr. Commun.*, **2,** 74 (1979); through *Chem. Abstr.*, **91,** 153700g (1979).

(2) V. D. Gupta, *J. Pharm. Sci.*, **68,** 908 (1979).

(3) *Ibid.*, **68,** 926 (1979).

(4) E. C. Juenge and J. F. Brower, *J. Pharm. Sci.*, **68,** 551 (1979).

(5) A. L. W. Po, W. J. Irwin, and Y. W. Yip, *J. Chromatogr.*, **176,** 399 (1979).

(6) T. Sato, Y. Saito, K. Yamaoka, and M. Nishikawa, *Yakuzaigaku*, **39,** 20 (1979); through *Chem. Abstr.*, **92,** 82314S (1980).

(7) E. Smith, *J. Assoc. Off. Anal. Chem.*, **62,** 812 (1979).

(8) M. D. Smith and D. J. Hoffman, *J. Chromatogr.*, **168,** 163 (1979).

(9) H. M. Abdou, T. M. Ast, and F. J. Cioffi, *J. Pharm. Sci.*, **67,** 1397 (1978).

(10) M. Amin and P. W. Schneider, *Analyst*, **103,** 1076 (1978).

(11) E. Von Arx and M. Faupel, *J. Chromatogr.*, **154,** 68 (1978).

(12) C. Burgess, *ibid.*, **149,** 233 (1978).

(13) G. Cavina, G. Moretti, B. Gallinella, R. Alimenti, and R. Barchiesi, *Boll. Chim. Farm.*, **117,** 534 (1978); through *Chem. Abstr.*, **90,** 76630 (1979).

(14) V. D. Gupta, *J. Pharm. Sci.*, **67,** 299 (1978).

(15) K. H. Mueller and B. Stuber, *Pharm. Acta Helv.*, **53,** 124 (1978); through *Chem. Abstr.*, **89,** 220962t (1978).

(16) Y. Tankawa, *Hokkaidoritsu Eisei Kenkyusho Ho*, **28,** 105 (1978); through *Chem. Abstr.*, **91,** 62792X (1979).

(17) L. M. Upton, E. R. Townley, and F. D. Sancilio, *J. Pharm. Sci.*, **67,** 913 (1978).

(18) J. H. M. Van Den Berg, J. Milley, N. Vonk, and R. S. Deelder, *J. Chromatogr.*, **132,** 421 (1977).

(19) G. B. Cox, C. R. Loscombe and K. Sugden, *Anal. Chim. Acta*, **92,** 345 (1977).

(20) S. Hara and S. Hayashi, *J. Chromatogr.*, **142,** 689 (1977).

(21) D. Wang, P. Chung, and J. Lai, *T'ai-wan Yao Hsueh Tsa Chih*, **28,** 11 (1977); through *Chem. Abstr.*, **88,** 110586v (1978).

(22) G. Gordon and P. R. Wood, *Analyst*, **101,** 876 (1976).

(23) J. Korpi, D. P. Wittner, B. J. Sandmann, and W. G. Haney, Jr., *J. Pharm. Sci.*, **65,** 1087 (1976).

(24) J. W. Higgins, *J. Chromatogr.*, **115,** 232 (1975).

(25) E. Gaetani and C. F. Laureri, *Farmaco, Ed. Prat.*, **29,** 110 (1974); through *Chem. Abstr.*, **81,** 41381r (1974).

(26) F. Bailey and P. N. Britain, *J. Chromatogr.*, **83,** 431 (1973).

(27) M. C. Olson, *J. Pharm. Sci.*, **62,** 2001 (1973).

(28) W. C. Landgraf and E. C. Jennings, *ibid.*, **62,** 278 (1973).

(29) J. C. Touchstone and W. Wortmann, *J. Chromatogr.*, **76,** 244 (1973).

(30) J. A. Mollica and R. F. Strusz, *J. Pharm. Sci.*, **61,** 444 (1972).

(31) "The United States Pharmacopeia," 19th rev., Mack Publishing Co., Easton, Pa., 1975, p. 622.

(32) "The National Formulary," 14th ed., Mack Publishing Co., Easton, Pa., 1975, p. 976.

(33) R. H. Silber and C. C. Porter, *J. Biol. Chem.*, **210,** 923 (1954).

(34) E. J. Umberger, *Anal. Chem.*, **27,** 768 (1955).

(35) R. E. Graham, P. A. Williams, and C. T. Kenner, *J. Pharm. Sci.*, **59,** 1152 (1970).

(36) *Ibid.*, **59,** 1472 (1970).

(37) "The United States Pharmacopeia," 20th rev., United States Pharmacopeial Convention, Rockville, Md., 1980, p. 916.

(38) "Official Methods of Analysis of the Association of Analytical Chemists," 12th ed., Association of Official Analytical Chemists, Washington, D.C., 1975, p. 471.

(39) J. G. Stewart and P. A. Williams, *J. Chromatogr.*, **198,** 489 (1980).


## ACKNOWLEDGMENTS


Supported by the Food and Drug Administration under the Science Advisors Research Associate Program.

The authors thank Millard Maienthal, Division of Drug Chemistry, Food and Drug Administration, Washington, D.C., for the preparation of the C-17 carboxylic acid derivatives of cortisone, dexamethasone, hydrocortisone, prednisolone, and prednisone, and James P. Hanus, Food and Drug Administration, Dallas, Tex,, for assistance in the HPLC instrument operation and maintenance.

# Disintegration–Dissolution Analysis of Percent Dissolved–Time Data

**ADNAN EL-YAZIGI**

Received June 2, 1980, from the *Department of Pharmaceutics, College of Pharmacy, University of Riyadh, Riyadh, Saudi Arabia.* Accepted for publication October 28, 1980.

**Abstract** □ A simple, graphical method is described for the disintegration–dissolution analysis of cumulative percent dissolved–time data. The technique is based on a biexponential equation with the assumption of first-order disintegration and dissolution according to a simple dissolution model. The dissolution data obtained for six commercial tablets and capsules adequately fit the developed equation. The described method is simple and can handle initial data points that are usually ignored by other techniques.

**Keyphrases** □ Disintegration–dissolution—analysis of percent dissolved–time data □ Dissolution model—method for analysis of percent dissolved–time data □ Pharmacokinetics—method for analysis of percent dissolved–time data

Most techniques used to interpret the percent dissolved–time data of tablets and capsules are based on semilogarithmic plots in which the early data points that precede the dissolution lag time are not considered (1–4). Kitazawa *et al.* (5, 6) utilized the initial data points and calculated the dissolution rate constants of uncoated tablets from the two straight lines obtained by plotting the dissolution data semilogarithmically against time. It was assumed that when the two lines intersect, the surface area greatly increases, causing a sudden increase in the dissolution rate. This assumption, however, is questionable since the change in the surface area is likely to be continuous. Furthermore, the early data points that most frequently form a curve above the terminal line (1) may be a function of both dissolution and disintegration. Drug release from conventional tablets or capsules usually involves two sequential time-dependent processes, disintegration (or content deaggregation for capsules) and dissolution, which occur simultaneously until disintegration is completed.

Drug release from a tablet having a rather idealized formulation was analyzed previously according to a disintegration–dissolution model; however, the mathematics involved are complicated and require computer programs, which may not be available or suitable for routine analysis of dissolution data (7, 8). This paper describes a simple graphical method for disintegration–dissolution analysis of percent dissolved–time data for commercial tablets or capsules in which all data points obtained were utilized and the dissolution and disintegration rate constants were estimated.

## THEORETICAL

When a tablet or capsule dissolves, it first disintegrates (capsule disintegration implies shell dissolution and content deaggregation) into small particles which, in turn, due to their large surface area, release the drug into the dissolution liquid. A more detailed scheme comprising an additional step in which the drug dissolves directly from the tablet surface also was reported (9); however, the amount released through this step is very small and need not be considered.

If one assumes that disintegration and dissolution are first-order processes and that $A$, $A_p$, and $A_s$ represent the amounts of drug in the dosage form, small particles, and solution, respectively, at any given time, $A \xrightarrow{k_d} A_p \xrightarrow{k_s} A_s$, the following differential equations can be written:

$$\frac{dA}{dt} = -k_d A \qquad \text{(Eq. 1)}$$

$$\frac{dA_p}{dt} = k_d A - k_s A_p \qquad \text{(Eq. 2)}$$

$$\frac{dA_s}{dt} = k_s A_p \qquad \text{(Eq. 3)}$$

where $k_d$ and $k_s$ are apparent first-order rate constants for disintegration and dissolution, respectively.

The Laplace transforms of Eqs. 1–3 are:

$$s\bar{A} - A_0 = -k_d\bar{A} \qquad \text{(Eq. 4)}$$

$$s\bar{A}_p = k_d\bar{A} - k_s\bar{A}_p \qquad \text{(Eq. 5)}$$

$$s\bar{A}_s = k_s\bar{A}_p \qquad \text{(Eq. 6)}$$

where the bar above the function and the $s$ represent the Laplace transform for the function and $A_0$ is the amount of drug in the dosage form at time zero. Rearrangement of Eq. 4, substitution for $\bar{A}$ in Eq. 5, and rearrangement yield:

$$\bar{A}_p = \frac{k_d A_0}{(s + k_d)(s + k_s)} \qquad \text{(Eq. 7)}$$

Substituting for $\bar{A}_p$ in Eq. 6 and rearranging produce:

$$\bar{A}_s = \frac{k_s k_d A_0}{s(s + k_d)(s + k_s)} \qquad \text{(Eq. 8)}$$

which, when solved using Laplace transform table (8) and rearranged, gives:

$$A_0 - A_s = \frac{k_d A_0}{k_d - k_s} e^{-k_s t} - \frac{k_s A_0}{k_d - k_s} e^{-k_d t} \qquad \text{(Eq. 9)}$$

Multiplying both sides of Eq. 9 by $100/A_0$ yields:

$$100 - f_s = \frac{100 k_d}{k_d - k_s} e^{-k_s t} - \frac{100 k_s}{k_d - k_s} e^{-k_d t} \qquad \text{(Eq. 10)}$$

where $f_s = (A_s/A_0) \times 100$ is the cumulative percent dissolved at time $t$.

If disintegration is more rapid than dissolution (*i.e.*, $k_d > k_s$), which is generally the case (7), a semilogarithmic plot of $(100 - f_s)$ *versus* time results in a biexponential curve with a terminal linear segment whose slope is equal to $-(k_s/2.303)$. The apparent first-order disintegration rate constant ($k_d$) can be estimated from the plot using the method of residuals (10).

## EXPERIMENTAL

**Materials**—Anhydrous theophylline[1], isoniazid[2], tetracycline hydrochloride[1], and ampicillin[3] were used for the preparation of standard curves as obtained. All tablet and capsule formulations tested (A[4], B[5], C[6], D[7], E[8], and F[9]) were purchased commercially.

**Dissolution Studies**—Dissolution tests were performed using a two-blade stirrer apparatus at 25 or 50 rpm. This apparatus was similar to the USP XIX apparatus, except that the basket assembly was replaced

[1] Sigma Co., St. Louis, Mo.
[2] BDH Ltd., Poole, England.
[3] The Upjohn Co., Kalamazoo, Mich.
[4] Isoniazid Tablets (50 mg), Hoffmann–La Roche, Basle, Switzerland.
[5] Theophylline Tablets (125 mg), Riker Laboratories, Northridge, Calif.
[6] Acetaminophen Tablets (500 mg), APM Co., Sult, Jordan.
[7] Ampicillin Capsules (250 mg), Wyeth Laboratories, Philadelphia, Pa.
[8] Tetracycline Hydrochloride Capsules (25 mg), Lagap SA, Lugano, Switzerland.
[9] Tetracycline Phosphate Capsules (250 mg), Bristol Italiana, Rome, Italy.

0022-3549/81/0500-0535$01.00/0
© 1981, American Pharmaceutical Association

**Table I—Apparent First-Order Rate Constants and Preexponential Coefficients for Dissolution and Disintegration**

| Formulation Code | Dosage Form | $Q_s$[a] | $k_s$, min$^{-1}$ | $Q_d$[a] | $k_d$, min$^{-1}$ |
|---|---|---|---|---|---|
| A | Tablet | 160.0 | 0.089 | 69.2 | 0.321 |
| B | Tablet | 246.4 | 0.250 | 143.0 | 0.461 |
| C | Tablet | 168.6 | 0.165 | 81.1 | 0.456 |
| D | Capsule | 127.6 | 0.0859 | 25.0 | 0.365 |
| E | Capsule | 120.3 | 0.0619 | 22.1 | 0.413 |
| F | Capsule | 259.7 | 0.103 | 166.8 | 0.203 |

[a] $Q_s$ and $Q_d$ are the preexponential coefficients for dissolution and disintegration, respectively [$Q_s = 100k_d/(k_d - k_s)$ and $Q_d = 100k_s/(k_d - k_s)$].

**Table II—Experimentally Determined Disintegration Times ($DT_{exp}$) and Values Estimated According to Eq. 11 ($DT_{calc}$)**

| Formulation | $DT_{exp}$, min ($n = 6$) | $DT_{calc}$, min | $DT_{exp}/DT_{calc}$ |
|---|---|---|---|
| A | 14.0[a] (1.47)[b] | 13.0 | 1.08 |
| B | 10.4 (0.55) | 9.02 | 1.15 |
| C | 6.77 (2.9) | 9.12 | 0.74 |
| D | 11.4 (1.09) | 11.4 | 1.0 |
| E | 9.92 (5.6) | 10.1 | 0.98 |
| F | 24.6 (2.09) | 20.5 | 1.2 |

[a] Mean. [b] Standard deviation.

by a 30-cm long glass shaft with one end attached to the motor and the other end equipped with a 7.6-cm glass blade connected in the center to the shaft. The dissolution medium, 900 ml of distilled water, was maintained at 37 ± 0.1°. The tablet or capsule was dropped directly into the vessel, and stirring and timing were initiated. At the indicated intervals (Fig. 1), 1-ml samples were withdrawn through a filtration unit[10] and analyzed spectrophotometrically at the maximum for each drug after suitable dilution.

**Disintegration Test**—Disintegration times were determined in the same apparatus used for the dissolution studies with a minor modification. This modification consisted of a slightly concave, round, 10-mesh stainless steel screen placed in the vessel horizontally and anchored on the wall so that the distance between the screen center and the vessel bottom was 1 cm. The disintegration test was carried out under the same conditions as in the dissolution studies. The distance between the blade and the screen center (2 cm) was identical to that used in the dissolution test. The disintegration time was defined as the time when the disintegrated particles passed through the screen or suspended in the dissolution fluid. The described method permits the determination of disintegration time under the same conditions as in dissolution tests, as well as observation of the disintegration process.

**Estimation of Disintegration Time from Dissolution Data**—Theoretically, as Eq. 10 indicates, the disintegration time is equal to infinity. However, since the percent remaining for disintegration after six disintegration half-lives is equal to 1.56%, which is negligible, it may be assumed that the disintegration time $DT_{calc} = 6t_{1/2d}$ or:

$$DT_{calc} = 6\left(\frac{0.693}{k_d}\right) = \frac{4.158}{k_d} \qquad \text{(Eq. 11)}$$

The values of $DT_{calc}$ calculated from Eq. 11 coincided well with those estimated from the semilogarithmic plots, where $DT_{calc}$ was taken as the time when the straight-line segment of the curve commences.

## RESULTS AND DISCUSSION

Figure 1 demonstrates the dissolution profiles obtained for the tablet and capsule formulations tested. The selection of these commercial products for evaluation of the described method was arbitrary.

The apparent first-order dissolution and disintegration rate constants ($k_s$ and $k_d$, respectively) were estimated by plotting log $(100 - f_s)$ *versus* time and the slope of the terminal linear segment is equal to $-(k_s/2.303)$. The apparent first-order disintegration rate constant was determined

[10] Millipore.

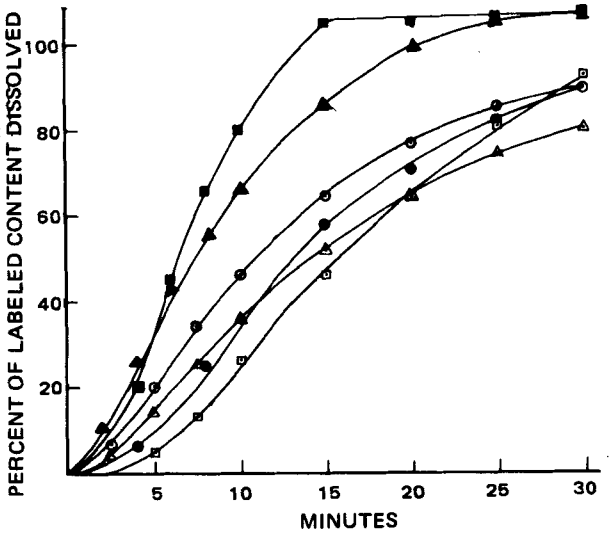


**Figure 1**—*Dissolution profiles for the formulations tested (mean of six determinations). Key: ●, A; ■, B; ▲, C; ○, D; △, E; □, F; solid symbols, tablets; and open symbols, capsules.*

by plotting the residual $(100 - f_s)$ against time semilogarithmically and the slope of the resulting straight line equal to $-(k_d/2.303)$. The values of $k_s$ and $k_d$ obtained are provided in Table I.

As demonstrated in Figs. 2 and 3, the fit was adequate; however, better fit may have been obtained if the analysis was carried out using nonlinear regression analysis. For Formulation B, dissolution was rapid and fewer data points were used.

The estimation of $k_d$ and $k_s$ also can be achieved by plotting log $(dA_s/dt)$ (rate of dissolution) *versus* time using the method of residuals given by:

$$\frac{dA_s}{dt} = \frac{k_s k_d A_0}{k_d - k_s}\left(e^{-k_s t} - e^{-k_d t}\right) \qquad \text{(Eq. 12)}$$

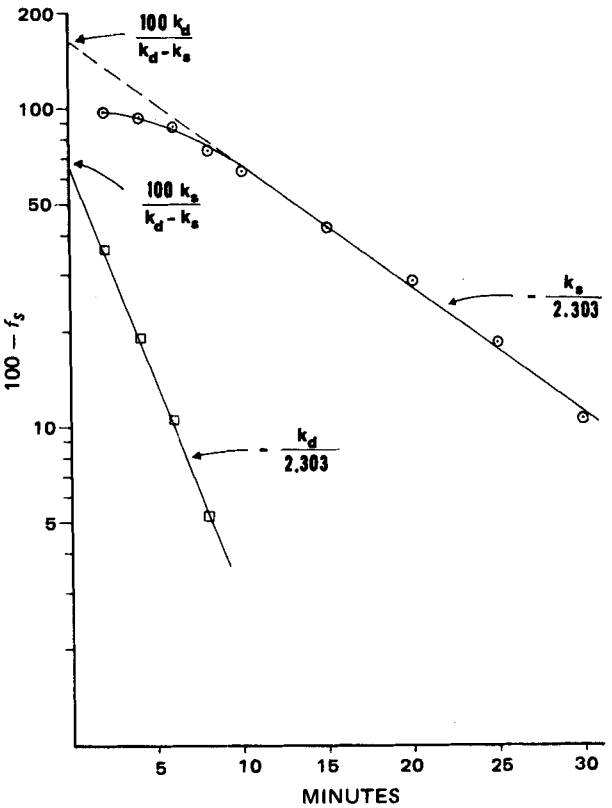


**Figure 2**—*Semilogarithmic plot of 100 minus cumulative percent dissolved (100 − $f_s$) against time for Tablet A. Key: ○, actual values; and □, residual values.*

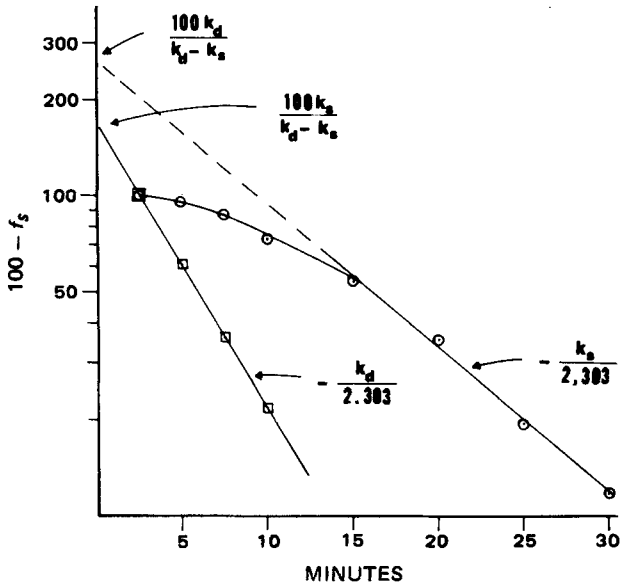


**Figure 3**—*Semilogarithmic plot of 100 minus cumulative percent dissolved (100 − $f_s$) versus time for Capsule F. Key:* ○, *actual values; and* □, *residual values.*

which can be derived by solving Eq. 7 to yield:

$$A_p = \frac{k_d A_0}{k_d - k_s}(e^{-k_s t} - e^{-k_d t}) \qquad \text{(Eq. 13)}$$

and substituting for $A_p$ in Eq. 3. To estimate $k_d$ accurately using Eq. 12, dissolution tests should be carried out automatically so that a sufficient number of early ($dA_s/dt$) points can be used in the plotting.

The values of $DT_{exp}$ were in good agreement with those of $DT_{calc}$ (Table II). These data confirm that the method proposed, in addition to its simplicity, is capable of reliably characterizing both dissolution and disintegration. In fact, if the percent dissolved–time data are well described by Eq. 10, the amount of drug in small particles at any given time ($A_p$) can be determined by employing Eq. 12, which permits the prediction of the disintegration time course. Such an approach is being investigated.

Previous models (5, 6) are in sharp disagreement with the present method, which assumes that dissolution occurs at a single rate constant throughout the dissolution test. In fact, the early data points that constitute the first dissolution phase according to previous models (5, 6) may not only represent dissolution but disintegration as well. By separating the disintegration component of these points from that of dissolution, a good estimate of the disintegration rate constant ($k_d$) may be obtained.

The described method provides a comprehensive, practical, and simple tool for the disintegration–dissolution analysis of dissolution rate data where familiar mathematics is employed. The good fit of the data obtained to the developed equation does not imply that drug dissolution and disintegration are first order in nature; it indicates that dissolution data for conventional tablets and capsules may be described by Eq. 10, in which case $k_s$ and $k_d$ can be estimated graphically.

## REFERENCES

(1) J. G. Wagner, *J. Pharm. Sci.*, **58**, 1253 (1969).
(2) M. Gibaldi and S. Feldman, *ibid.*, **56**, 1238 (1967).
(3) F. Langenbucher, *J. Pharm. Pharmacol.*, **24**, 979 (1972).
(4) A. El-Yazigi, *Int. J. Pharm.*, **5**, 89 (1980).
(5) S. Kitazawa, I. Johno, Y. Ito, S. Teramura, and J. Okada, *J. Pharm. Pharmacol.*, **27**, 765 (1975).
(6) S. Kitazawa, I. Johno, T. Minouchi, and J. Okada, *ibid.*, **29**, 453 (1977).
(7) K. G. Nelson and L. Y. Wang, *J. Pharm. Sci.*, **66**, 1758 (1977).
(8) *Ibid.*, **67**, 86 (1978).
(9) A. J. Aguiar, J. E. Zelmir, and A. W. Kinkel, *ibid.*, **56**, 1243 (1967).
(10) M. Gibaldi and D. Perrier, "Pharmacokinetics," Dekker, New York, N.Y., 1974, pp. 270, 281.

# Synthesis of Alkylaminoalkylamides of Substituted 2-Aminopyrroles as Potential Local Anesthetic and Antiarrhythmic Agents II: β-Amines

**J. WALTER SOWELL, Sr. *x, ALAN J. BLOCK ‡, MARY ELIZABETH DERRICK *§, JOHN J. FREEMAN *, JOSEPH W. KOSH *, PHILIP F. MUBARAK *§, and PAUL A. TENTHOREY ‡¶**

Received September 9, 1980, from the **College of Pharmacy, University of South Carolina, Columbia, SC 29208*, and ‡*Astra Research Laboratory, Framingham, MA 01701.* Accepted for publication October 23, 1980. §Present address: Medical University of South Carolina, Charleston, SC 29403. ¶Present address: Bristol-Myers International Division, New York, NY 10022.

**Abstract** □ The synthesis, local anesthetic and antiarrhythmic properties, and CNS toxicity of 14 2-(3-alkylaminoalkylamido)-pyrroles are described. Most of the compounds exhibited local anesthetic activity by the guinea pig wheal test, with seven showing comparable or greater activity than lidocaine. Most compounds also exhibited antiarrhythmic activity; three compounds had more potent activity than lidocaine. All compounds exhibiting antiarrhythmic activity also were toxic to the CNS. However, two of the three compounds having greater activity than lidocaine possessed more desirable therapeutic indexes.

**Keyphrases** □ 2-(3-Alkylaminoalkylamido)pyrroles—synthesis, evaluated for local anesthetic activity in guinea pigs and for antiarrhythmic activity and CNS toxicity in mice □ Anesthetic activity, potential—2-(3-alkylaminoalkylamido)pyrroles synthesized and evaluated for activity in guinea pigs, structure–activity relationships □ Antiarrhythmic activity, potential—2-(3-alkylaminoalkylamido)pyrroles synthesized and evaluated for activity in mice, structure–activity relationships □ Structure–activity relationships—2-(3-alkylaminoalkylamido)pyrroles synthesized and evaluated for anesthetic activity and antiarrhythmic activity and CNS toxicity in guinea pigs and mice

Previous publications reported the synthesis and pharmacological evaluation of several series of 2-(2-alkylaminoalkylamido)pyrroles (I*a*) as potential local anesthetic and antiarrhythmic agents (1–3). Many of these compounds possessed significant activity (1–3), but most compounds with the desired activity were also toxic to the central nervous system (CNS).

Several series of antiarrhythmic agents derived from substituted anilines were reported recently (4–6). The β-amino analog (II*b*) of tocainide (II*a*) was more potent

0022-3549/81/0500-0537$01.00/0
© 1981, American Pharmaceutical Association

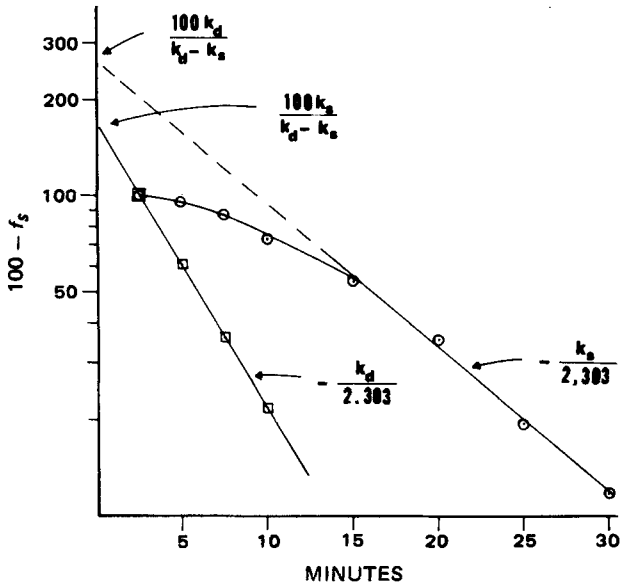


**Figure 3**—*Semilogarithmic plot of 100 minus cumulative percent dissolved (100 − $f_s$) versus time for Capsule F. Key:* ○, *actual values; and* □, *residual values.*

which can be derived by solving Eq. 7 to yield:

$$A_p = \frac{k_d A_0}{k_d - k_s}(e^{-k_s t} - e^{-k_d t}) \qquad \text{(Eq. 13)}$$

and substituting for $A_p$ in Eq. 3. To estimate $k_d$ accurately using Eq. 12, dissolution tests should be carried out automatically so that a sufficient number of early ($dA_s/dt$) points can be used in the plotting.

The values of $DT_{exp}$ were in good agreement with those of $DT_{calc}$ (Table II). These data confirm that the method proposed, in addition to its simplicity, is capable of reliably characterizing both dissolution and disintegration. In fact, if the percent dissolved–time data are well described by Eq. 10, the amount of drug in small particles at any given time ($A_p$) can be determined by employing Eq. 12, which permits the prediction of the disintegration time course. Such an approach is being investigated.

Previous models (5, 6) are in sharp disagreement with the present method, which assumes that dissolution occurs at a single rate constant throughout the dissolution test. In fact, the early data points that constitute the first dissolution phase according to previous models (5, 6) may not only represent dissolution but disintegration as well. By separating the disintegration component of these points from that of dissolution, a good estimate of the disintegration rate constant ($k_d$) may be obtained.

The described method provides a comprehensive, practical, and simple tool for the disintegration–dissolution analysis of dissolution rate data where familiar mathematics is employed. The good fit of the data obtained to the developed equation does not imply that drug dissolution and disintegration are first order in nature; it indicates that dissolution data for conventional tablets and capsules may be described by Eq. 10, in which case $k_s$ and $k_d$ can be estimated graphically.

## REFERENCES

(1) J. G. Wagner, *J. Pharm. Sci.*, **58**, 1253 (1969).
(2) M. Gibaldi and S. Feldman, *ibid.*, **56**, 1238 (1967).
(3) F. Langenbucher, *J. Pharm. Pharmacol.*, **24**, 979 (1972).
(4) A. El-Yazigi, *Int. J. Pharm.*, **5**, 89 (1980).
(5) S. Kitazawa, I. Johno, Y. Ito, S. Teramura, and J. Okada, *J. Pharm. Pharmacol.*, **27**, 765 (1975).
(6) S. Kitazawa, I. Johno, T. Minouchi, and J. Okada, *ibid.*, **29**, 453 (1977).
(7) K. G. Nelson and L. Y. Wang, *J. Pharm. Sci.*, **66**, 1758 (1977).
(8) *Ibid.*, **67**, 86 (1978).
(9) A. J. Aguiar, J. E. Zelmir, and A. W. Kinkel, *ibid.*, **56**, 1243 (1967).
(10) M. Gibaldi and D. Perrier, "Pharmacokinetics," Dekker, New York, N.Y., 1974, pp. 270, 281.

# Synthesis of Alkylaminoalkylamides of Substituted 2-Aminopyrroles as Potential Local Anesthetic and Antiarrhythmic Agents II: β-Amines

**J. WALTER SOWELL, Sr. *x, ALAN J. BLOCK ‡, MARY ELIZABETH DERRICK *§, JOHN J. FREEMAN *, JOSEPH W. KOSH *, PHILIP F. MUBARAK *§, and PAUL A. TENTHOREY ‡¶**

Received September 9, 1980, from the **College of Pharmacy, University of South Carolina, Columbia, SC 29208*, and ‡*Astra Research Laboratory, Framingham, MA 01701.* Accepted for publication October 23, 1980. §Present address: Medical University of South Carolina, Charleston, SC 29403. ¶Present address: Bristol-Myers International Division, New York, NY 10022.

**Abstract** □ The synthesis, local anesthetic and antiarrhythmic properties, and CNS toxicity of 14 2-(3-alkylaminoalkylamido)-pyrroles are described. Most of the compounds exhibited local anesthetic activity by the guinea pig wheal test, with seven showing comparable or greater activity than lidocaine. Most compounds also exhibited antiarrhythmic activity; three compounds had more potent activity than lidocaine. All compounds exhibiting antiarrhythmic activity also were toxic to the CNS. However, two of the three compounds having greater activity than lidocaine possessed more desirable therapeutic indexes.

**Keyphrases** □ 2-(3-Alkylaminoalkylamido)pyrroles—synthesis, evaluated for local anesthetic activity in guinea pigs and for antiarrhythmic activity and CNS toxicity in mice □ Anesthetic activity, potential—2-(3-alkylaminoalkylamido)pyrroles synthesized and evaluated for activity in guinea pigs, structure–activity relationships □ Antiarrhythmic activity, potential—2-(3-alkylaminoalkylamido)pyrroles synthesized and evaluated for activity in mice, structure–activity relationships □ Structure–activity relationships—2-(3-alkylaminoalkylamido)pyrroles synthesized and evaluated for anesthetic activity and antiarrhythmic activity and CNS toxicity in guinea pigs and mice

Previous publications reported the synthesis and pharmacological evaluation of several series of 2-(2-alkylaminoalkylamido)pyrroles (I*a*) as potential local anesthetic and antiarrhythmic agents (1–3). Many of these compounds possessed significant activity (1–3), but most compounds with the desired activity were also toxic to the central nervous system (CNS).

Several series of antiarrhythmic agents derived from substituted anilines were reported recently (4–6). The β-amino analog (II*b*) of tocainide (II*a*) was more potent

0022-3549/81/0500-0537$01.00/0
© 1981, American Pharmaceutical Association

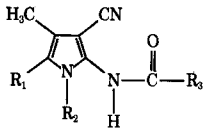

**Table I—Data for Amides of Substituted 2-Aminopyrroles**

| Compound | $R_1$ | $R_2$ | $R_3$ | Melting Point | $R_f$[a] | Recrystallization Solvent | Yield, % | Formula | Analysis, % | Calc. | Found |
|---|---|---|---|---|---|---|---|---|---|---|---|
| IIIa | $CH_3$ | $CH_3$ | $CH{=}CHCH_3$ | 174.5–175.5° | 0.46 | Methanol | 42.3 | $C_{12}H_{15}N_3O \cdot 0.625\ CH_3OH$ | C | 63.90 | 63.87 |
| | | | | | | | | | H | 7.43 | 7.54 |
| | | | | | | | | | N | 17.71 | 17.77 |
| IIIb | $CH_3$ | $CH_3$ | $CH_2CHBrCH_3$ | 134.5–135.5° | 0.50 | Benzene | 82.8 | $C_{12}H_{16}BrN_3O$ | C | 48.33 | 48.36 |
| | | | | | | | | | H | 5.41 | 5.41 |
| | | | | | | | | | Br | 26.80 | 26.76 |
| | | | | | | | | | N | 14.09 | 14.05 |
| IIIc | $CH_3$ | H | $CH_2CHBrCH_3$ | 141.5–142.5° | 0.66 | Methanol–water (4:1) | 88.6 | $C_{11}H_{14}BrN_3O$ | C | 46.49 | 46.68 |
| | | | | | | | | | H | 4.97 | 5.01 |
| | | | | | | | | | Br | 28.12 | 27.93 |
| | | | | | | | | | N | 14.79 | 14.83 |
| IIId | $CH_3$ | $CH_3$ | $CH_2CH_2Cl$ | 181.5–182.5° | 0.47 | Ethanol | 64.8 | $C_{11}H_{14}ClN_3O$ | C | 55.12 | 55.06 |
| | | | | | | | | | H | 5.89 | 5.94 |
| | | | | | | | | | Cl | 14.79 | 14.69 |
| | | | | | | | | | N | 17.53 | 17.51 |
| IIIe | $CH_3$ | H | $CH_2CH_2Cl$ | 209–210° dec. | 0.55 | Ethanol | 86.0 | $C_{10}H_{12}ClN_3O$ | C | 53.22 | 53.27 |
| | | | | | | | | | H | 5.36 | 5.39 |
| | | | | | | | | | Cl | 15.71 | 15.66 |
| | | | | | | | | | N | 18.62 | 18.62 |
| IIIf | $C_2H_5$ | H | $CH_2CH_2Cl$ | 176–176.5° | 0.54 | Ethanol | 88.0 | $C_{11}H_{14}ClN_3O$ | C | 55.11 | 55.22 |
| | | | | | | | | | H | 5.89 | 5.96 |
| | | | | | | | | | Cl | 14.79 | 14.77 |
| | | | | | | | | | N | 17.53 | 17.55 |
| IIIg | $C_6H_5$ | H | $CH_2CH_2Cl$ | 221.5–222° | 0.55 | Ethanol | 90.4 | $C_{15}H_{14}ClN_3O$ | C | 62.61 | 62.68 |
| | | | | | | | | | H | 4.90 | 4.95 |
| | | | | | | | | | Cl | 12.32 | 12.29 |
| | | | | | | | | | N | 14.60 | 14.61 |
| IIIh | $CH_2C_6H_5$ | H | $CH_2CH_2Cl$ | 157–158° | 0.54 | Ethanol | 92.8 | $C_{16}H_{16}ClN_3O$ | C | 63.68 | 63.73 |
| | | | | | | | | | H | 5.35 | 5.38 |
| | | | | | | | | | Cl | 11.75 | 11.76 |
| | | | | | | | | | N | 13.92 | 13.93 |

[a] Ethyl acetate.

and had a more favorable therapeutic ratio for CNS side-effects in animals than tocainide (6). Therefore, elongation of the intermediate chain between amide and amine functions might improve the pharmacological properties of aminoanilides related to lidocaine. The transfer of this method to a series of pyrrole analogs of lidocaine was considered a reasonable approach to enhance antiarrhythmic activity and to decrease CNS toxicity in this new class of antiarrhythmic agents.

As an extension of the 2-(2-alkylaminoalkylamido)-pyrrole (Ia) research, the synthesis and pharmacological evaluation of 14 2-(3-alkylaminoalkylamido)pyrroles (Ib) are presented. Compounds with a more acceptable therapeutic index than those previously reported are being sought.

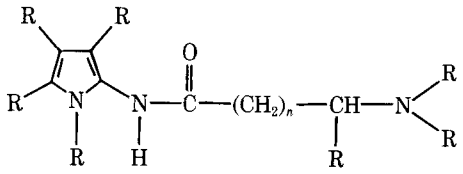

Ia: $n = 0$
Ib: $n = 1$

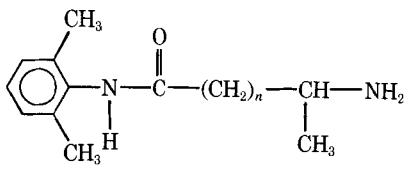

IIa: $n = 0$
IIb: $n = 1$

## RESULTS AND DISCUSSION

**Chemistry**—Acylation of various substituted 2-amino-3-cyanopyrroles (7–10) with 3-bromobutyryl chloride (11), *trans*-2-butenoyl chloride, or 3-chloropropionyl chloride in acetone, utilizing pyridine as a base, gave the requisite amide (IIIa–IIIh) precursors to the 2-(3-alkylaminoalkylamido)pyrroles (Ib) (Table I). The purity of these amides was determined by elemental analyses and TLC. IR and NMR spectra were consistent with the assigned structures.

The various substituted 2-(3-alkylaminoalkylamido)-3-cyanopyrroles (IVa–IVl) (Table II) were obtained either by Michael addition of a primary or secondary amine to the 2-butenamide (IIIa) or by nucleophilic displacement of the halogen of the β-haloamides (IIIb–IIIh) by the appropriate primary or secondary amine. For both methods, the products were obtained after refluxing (6–12 hr) the requisite amide (IIIa–IIIh) in ethanol or 2-propanol with a four- to fivefold excess of amine.

The crude products were isolated by removal of the alcohol and excess unreacted amines *in vacuo*. The residues were dissolved in 5–10% HCl and filtered, and the aqueous filtrates were made alkaline (pH 9–10) with 10% NaOH. The solid products (IVe, IVf, IVi, IVj, and IVl) were collected and purified further by recrystallization from methanol–water (4:1). The amines that oiled or gummed upon addition of alkali were extracted into chloroform, and the chloroform was removed *in vacuo* after drying. The residues were dissolved in an appropriate boiling solvent, treated with charcoal, and collected as oils or gums upon cooling.

The 2-(3-alkylaminoalkylamido)-3-carbamylpyrroles (IVm and IVn) were obtained by hydrolysis of the nitrile in IVi and IVj, respectively, in 85% phosphoric acid at 125–130° for 5 min. The free amines were precipitated by alkalinization of the cold dilute phosphoric acid solutions with 20% NaOH.

Percent yields, melting points, and purification data for the 2-(3-alkylaminoalkylamido)pyrroles (IVa–IVn) are given in Table II. These amines were characterized as their corresponding hydrochloride salts.

The 2-(3-alkylaminoalkylamido)pyrrole hydrochlorides (Va–Vf and Vh–Vn) were prepared by treating an acetone solution or suspension of the corresponding free bases with a slight excess of concentrated hydrochloric acid. In the case of IVg, the hydrochloride salt (Vg) precipi-

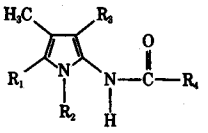

**Table II—Data for Alkylaminoalkylamides of Substituted 2-Aminopyrroles and Corresponding Hydrochloride Salts**

| Compound | $R_1$ | $R_2$ | $R_3$ | $R_4$ | Precursor | Melting Point | $R_f$ | Recrystallization Solvent[a] | Yield[b], % | Formula | Analysis, % | Calc. | Found |
|---|---|---|---|---|---|---|---|---|---|---|---|---|---|
| IV*a* | $CH_3$ | $CH_3$ | CN | $CH_2CH(CH_3)N$ | III*a* | Gum | — | Cyclohexane | — | $C_{16}H_{24}N_4O$ | | — | — |
| V*a* | Hydrochloride | | | | IV*a* | 222–223° | 0.28[c] | —[d] | 50.0 | $C_{16}H_{25}ClN_4O$ | C | 59.15 | 58.90 |
| | | | | | | | | | | | H | 7.76 | 7.75 |
| | | | | | | | | | | | Cl | 10.91 | 10.83 |
| | | | | | | | | | | | N | 17.25 | 17.16 |
| IV*b* | $CH_3$ | $CH_3$ | CN | $CH_2CH(CH_3)N$ (pyrrolidine) | III*b* | Gum | — | Cyclohexane | — | $C_{17}H_{26}N_4O$ | | — | — |
| V*b* | Hydrochloride | | | | IV*b* | 209.5–210.5° dec. | 0.53[c] | —[d] | 73.8 | $C_{17}H_{27}ClN_4O$ | C | 60.25 | 60.36 |
| | | | | | | | | | | | H | 8.04 | 8.07 |
| | | | | | | | | | | | Cl | 10.46 | 10.42 |
| | | | | | | | | | | | N | 16.53 | 16.49 |
| IV*c* | $CH_3$ | $CH_3$ | CN | $CH_2CH(CH_3)N(H)$-*n*-$C_4H_9$ | III*b* | Gum | — | Cyclohexane–benzene (6:1) | — | $C_{16}H_{26}N_4O$ | | — | — |
| V*c* | Hydrochloride | | | | IV*c* | 208.5–209.5° dec. | 0.36[c] | —[d] | 74.0 | $C_{16}H_{27}ClN_4O \cdot 0.4\ H_2O$ | C | 57.52 | 57.44 |
| | | | | | | | | | | | H | 8.39 | 8.33 |
| | | | | | | | | | | | Cl | 10.61 | 10.57 |
| | | | | | | | | | | | N | 16.77 | 16.75 |
| IV*d* | $CH_3$ | $CH_3$ | CN | $CH_2CH(CH_3)N(H)$-*iso*-$C_4H_9$ | III*a* | Gum | — | Cyclohexane | — | $C_{16}H_{26}N_4O$ | | — | — |
| V*d* | Hydrochloride | | | | IV*d* | 194–194.5° dec. | 0.06[e] | Water | 53.5 | $C_{16}H_{27}ClN_4O$ | C | 58.79 | 58.57 |
| | | | | | | | | | | | H | 8.33 | 8.38 |
| | | | | | | | | | | | Cl | 10.85 | 10.81 |
| | | | | | | | | | | | N | 17.14 | 17.08 |
| IV*e* | $CH_3$ | H | CN | $CH_2CH(CH_3)N$ (pyrrolidine) | III*c* | 168–169° | 0.47[e] | Methanol–water (4:1) | 83.3 | $C_{15}H_{22}N_4O$ | | — | — |
| V*e* | Hydrochloride | | | | IV*e* | 94.0–95.5° | 0.24[e] | —[d] | 89.2 | $C_{15}H_{23}ClN_4O \cdot 1.0\ H_2O$ | C | 54.78 | 54.80 |
| | | | | | | | | | | | H | 7.66 | 7.66 |
| | | | | | | | | | | | Cl | 10.78 | 10.80 |
| | | | | | | | | | | | N | 17.04 | 17.04 |
| IV*f* | $CH_3$ | H | CN | $CH_2CH(CH_3)N(C_2H_5)_2$ | III*c* | 156.5–158° | 0.47[e] | Methanol–water (4:1) | 32.0 | $C_{15}H_{24}N_4O$ | | — | — |
| V*f* | Hydrochloride | | | | IV*f* | 120–121° | 0.53[e] | 2-Propanol–acetone (1:10) | 72.0 | $C_{15}H_{25}ClN_4O \cdot 0.54\ H_2O$ | C | 55.84 | 55.84 |
| | | | | | | | | | | | H | 8.15 | 8.18 |
| | | | | | | | | | | | Cl | 10.99 | 11.01 |
| | | | | | | | | | | | N | 17.37 | 17.35 |
| IV*g*[f] | $CH_3$ | H | CN | $CH_2CH(CH_3)N(H)$-*n*-$C_4H_9$ | III*c* | — | — | — | — | $C_{15}H_{24}N_4O$ | | — | — |
| V*g* | Hydrochloride | | | | IV*g* | 180.5–181.5° | 0.26[e] | Water | 65.0 | $C_{15}H_{25}ClN_4O \cdot 1.83\ H_2O$ | C | 52.09 | 52.09 |
| | | | | | | | | | | | H | 7.29 | 7.40 |
| | | | | | | | | | | | Cl | 10.25 | 10.22 |
| | | | | | | | | | | | N | 16.20 | 16.21 |
| IV*h* | $CH_3$ | $CH_3$ | CN | $CH_2CH_2N(C_2H_5)_2$ | III*d* | Gum | — | Cyclohexane | — | $C_{15}H_{24}N_4O$ | | — | — |
| V*h* | Hydrochloride | | | | IV*h* | 169–171.5° dec. | 0.38[c] | —[d] | 65.0 | $C_{15}H_{25}ClN_4O$ | C | 57.59 | 57.36 |
| | | | | | | | | | | | H | 8.06 | 8.09 |
| | | | | | | | | | | | Cl | 11.33 | 11.27 |
| | | | | | | | | | | | N | 17.91 | 17.83 |
| IV*i* | $CH_3$ | H | CN | $CH_2CH_2N(C_2H_5)_2$ | III*e* | 126.5–127° | — | Methanol–water (4:1) | 93.5 | $C_{14}H_{22}N_4O$ | | — | — |
| V*i* | Hydrochloride | | | | IV*i* | 183.5–184.5° | 0.18[e] | —[d] | 94.1 | $C_{14}H_{23}ClN_4O \cdot 1.0\ H_2O$ | C | 53.07 | 53.14 |
| | | | | | | | | | | | H | 7.95 | 7.95 |
| | | | | | | | | | | | Cl | 11.19 | 11.17 |
| | | | | | | | | | | | N | 17.68 | 17.69 |
| IV*j* | $C_2H_5$ | H | CN | $CH_2CH_2N(C_2H_5)_2$ | III*f* | 122.5–123.5° | — | Methanol–water (4:1) | 84.5 | $C_{15}H_{24}N_4O$ | | — | — |
| V*j* | Hydrochloride | | | | IV*j* | 80–85° (hydrate) (151.5–152.5°) | 0.23[e] | —[d] | 88.3 | $C_{15}H_{25}ClN_4O \cdot 1.0\ H_2O$ | C | 54.45 | 54.47 |
| | | | | | | | | | | | H | 8.23 | 8.25 |
| | | | | | | | | | | | Cl | 10.72 | 10.75 |
| | | | | | | | | | | | N | 16.93 | 16.93 |
| IV*k* | $C_6H_5$ | H | CN | $CH_2CH_2N(C_2H_5)_2$ | III*g* | Oil | — | Methanol–water (1:1) | 43.3 | $C_{19}H_{24}N_4O$ | | — | — |
| V*k* | Hydrochloride | | | | IV*k* | 140.5–141.5° | 0.21[e] | Methanol–acetone (1:10) | 64.7 | $C_{19}H_{25}ClN_4O \cdot 0.1\ H_2O$ | C | 62.92 | 63.02 |
| | | | | | | | | | | | H | 7.00 | 7.08 |
| | | | | | | | | | | | Cl | 9.78 | 10.01 |
| | | | | | | | | | | | N | 15.45 | 15.22 |
| IV*l* | $CH_2C_6H_5$ | H | CN | $CH_2CH_2N(C_2H_5)_2$ | III*h* | 120–121° | — | Methanol–water (4:1) | 96.6 | $C_{20}H_{26}N_4O$ | | — | — |
| V*l* | Hydrochloride | | | | IV*l* | 168–169° | 0.21[b] | —[d] | 93.1 | $C_{20}H_{27}ClN_4O \cdot 1.0\ H_2O$ | C | 61.13 | 61.17 |
| | | | | | | | | | | | H | 7.44 | 7.45 |
| | | | | | | | | | | | Cl | 9.02 | 9.04 |
| | | | | | | | | | | | N | 14.26 | 14.28 |
| IV*m* | $CH_3$ | H | $CONH_2$ | $CH_2CH_2N(C_2H_5)_2$ | IV*i* | 145–146° | — | Methanol–water (1:2) | 71.3 | $C_{14}H_{24}N_4O_2$ | | — | — |
| V*m* | Hydrochloride | | | | IV*m* | 213–214° dec. | 0.07[b] | 2-Propanol | 83.1 | $C_{14}H_{25}ClN_4O_2$ | C | 53.07 | 52.98 |
| | | | | | | | | | | | H | 7.95 | 8.02 |
| | | | | | | | | | | | Cl | 11.19 | 11.21 |
| | | | | | | | | | | | N | 17.68 | 17.69 |
| IV*n* | $C_2H_5$ | H | $CONH_2$ | $CH_2CH_2N(C_2H_5)_2$ | IV*j* | 126–126.5° | — | Methanol–water (7:3) | 85.1 | $C_{15}H_{26}N_4O$ | | — | — |
| V*n* | Hydrochloride | | | | IV*n* | 194–195° | 0.07[b] | —[d] | 88.9 | $C_{15}H_{27}ClN_4O$ | C | 54.45 | 54.51 |
| | | | | | | | | | | | H | 8.23 | 8.26 |
| | | | | | | | | | | | Cl | 10.72 | 10.75 |
| | | | | | | | | | | | N | 16.93 | 16.94 |

[a] The oils and gums were dissolved in boiling recrystallization solvent(s), treated with activated charcoal, filtered, and collected as oils or gums after cooling. [b] Where yields were not reported for free amine, the yield for salt was based on the haloamide or crotonamide precursor. [c] Acetone. [d] Hydrochloride salt obtained was analytically pure. [e] Ethyl acetate. [f] Hydrochloride was formed during workup procedure; therefore, free base was not isolated.

tated upon addition of 5% HCl to the crude residue remaining after removal of the reaction solvent and excess *n*-butylamine *in vacuo*.

Data for the hydrochloride salts (V*a*–V*n*) are given in Table II. These compounds were characterized on the basis of elemental analyses, TLC, and IR and NMR spectral data.

The β-haloamides and final products possessing an asymmetric center were obtained as racemic mixtures in this work.

**Pharmacology**—*Local Anesthetic Activity*—Activity was observed for all compounds evaluated at a solution concentration of 0.50%. Noticeable differentiation in local anesthetic activity was observed at 0.25%. At that concentration, V*a*–V*d* were more potent than lidocaine, V*k*, V*l*, and V*n* were comparable in potency, and all remaining compounds were less potent.

Further evaluation of V*a*–V*d* at a 0.125% solution concentration demonstrated their superiority over lidocaine under these test conditions. The durations of local anesthetic activity were 1.67, 1.42, 2.67, and 1.75 times longer than that of lidocaine (Table III).

Local anesthetic data previously reported (3) and the present results strongly support the introduction of a methyl group on the pyrrole nitrogen to augment local anesthetic activity. This finding applies for the 2-(2-alkylaminoalkylamido)pyrroles (I*a*) and the 2-(3-alkylaminoalkylamido)pyrroles (I*b*). The present work shows that the I*b* compounds are substantially more potent local anesthetics than their corresponding α-amine homologs (I*a*).

*Antiarrhythmic Activity and CNS Toxicity*—Antiarrhythmic activity, measured as protection against chloroform-induced ventricular tachycardia, and acute CNS toxicity, measured as drug-induced ataxia, were determined in mice as previously described (3). The results are listed as $ED_{50}$ values, together with 95% Fieller limits and therapeutic indexes, in Table IV. All compounds tested, except V*g*, had antiarrhythmic activity; V*a*, V*c*, and V*d* were more potent than lidocaine, V*b* was equipotent, and the rest were less potent. Paralleling the findings on local anesthetic activity, the derivatives with a methyl substituent on the pyrrole nitrogen were more potent than those with a hydrogen substituent. More importantly, therapeutic indexes were also increased by the introduction of an *N*-methyl substituent. A comparison with previously published α-alkylaminoalkylamidopyrroles showed the β-derivatives to have higher potencies (except V*e*) and higher therapeutic indexes (except in hydrogen-substituted pyrroles). The extension of the intermediate chain, leading from α-amines to β-amines, again improved the therapeutic properties of a class of antiarrhythmic agents.

## EXPERIMENTAL[1]

**2-(2-Butenamido)-3-cyano-1,4,5-trimethylpyrrole (III*a*)**—A solution of 2-amino-3-cyano-1,4,5-trimethylpyrrole (22.3 g, 0.15 mole) (10) in 150 ml of acetone with pyridine (13.1 g, 0.16 mole) was prepared in a 500-ml round-bottom flask equipped with a drying tube. This solution was stirred in an ice bath for 10 min, followed by the dropwise addition of *trans*-2-butenoyl chloride (18.8 g, 0.18 mole). The solution was stirred in the ice bath for 10 min and then for another 15 min after the ice bath was removed. The reaction mixture was brought to reflux and allowed to cool to room temperature, and then the dark solution was poured over crushed ice (500 g).

After the ice had melted, the crude product was collected by filtration, suspended in distilled water, filtered, and dried. The gray product (13.8 g, 42.3%) was recrystallized twice from absolute methanol to yield light-tan crystals (homogeneous on TLC; in ethyl acetate, $R_f$ 0.46), mp 174.5–175.5° dec.; IR (KBr): 3420, 3050, 2980, 2920, 2220, 1675, 1645, 1540, 1195, 960, 935, 830, and 680 $cm^{-1}$; NMR (dimethyl sulfoxide-$d_6$): δ 1.9 (d, 3H, $CH_3$ of CO–C=C–$CH_3$), 2.00 (s, 3H, $CH_3$ at C-4), 2.09 (s, 3H, $CH_3$ at C-5), 3.33 (s, 3H, $CH_3$ at N-1), 5.8–6.3 (complex m, 1H, CH of CO–CH=C–C), 6.5–7.1 (complex m, 1H, CH of CO–C=CH–C), and 9.7–10.1 (broad s, 1H, NH of amide) ppm. Table I gives the results of the elemental analyses.

**2-(3-Bromobutyramido)-3-cyano-4,5-dimethylpyrrole (III*c*)**—The procedure for III*c* is given as a general method of synthesis of III*b*–III*h*. A solution of 2-amino-3-cyano-4,5-dimethylpyrrole (40.5 g, 0.30 mole) (7) in pyridine (26.1 g, 0.33 mole) and 300 ml of acetone was stirred in an ice bath while 3-bromobutyryl chloride (61.2 g, 0.33 mole) (11) was added dropwise. After the addition was complete, the dark-brown solution was stirred at room temperature for an additional 20 min; it then was poured over 400 g of ice. The resulting suspension was stirred until the ice had melted, and the crude product was collected by filtration.

The product was resuspended in 300 ml of distilled water, collected by filtration, and air dried. One gram of the crude amide (75.5 g, 88.6%) was recrystallized from 25 ml of methanol–water (4:1) to yield a white powder (homogeneous on TLC; in ethyl acetate, $R_f$ 0.66), mp 141.5–142.5°; IR (KBr): 3420, 3160, 3100, 3020, 2900, 2205, 1650, 1610, 1500, 1480, 1450, 1320, 1230, 1210, 1000, and 670 $cm^{-1}$; NMR (dimethyl sulfoxide-$d_6$): δ 1.70 (d, 3H, CHBrC$H_3$), 1.90 (s, 3H, $CH_3$ at C-4), 2.02 (s, 3H, $CH_3$ at C-5), 2.92 (d, 2H, $COCH_2$), 4.50 (q, 1H, C*H*BrCH$_3$), 10.52 (s, 1H, NH), and 11.17 (s, 1H, NH). Table I gives the results of the elemental analyses.

**Method A: 2-(3-Pyrrolidinobutyramido)-3-cyano-1,4,5-trimethylpyrrole Hydrochloride (V*a*)**—The procedure for the synthesis of V*a* was also used for V*d*. A suspension of III*a* (8.7 g, 0.04 mole) in 80 ml of absolute 2-propanol with pyrrolidine (11.4 g, 0.16 mole) was refluxed, with continuous stirring, for 12 hr to give a clear brown solution. The solvent and excess pyrrolidine were removed *in vacuo*, and the gummy residue was dissolved in 50 ml of warm 10% HCl. The acidic solution was filtered, 200 g of ice was added, and the product was suspended in the solution by the addition of 10% aqueous potassium hydroxide. The alkaline aqueous suspension (pH 9–10) was extracted with two 150-ml

**Table III—Local Anesthetic Activity of 2-(3-Alkylaminoalkylamido)pyrrole Hydrochlorides as Determined by the Guinea Pig Wheal Test [a]**

| Compound | Solution Concentration 0.50% | 0.25% | 0.125% |
|---|---|---|---|
| Lidocaine | 100 (36) | 100 (31) | 100 (12) |
| V*a* | 100 (36) | 110 (34) | 167 (20) |
| V*b* | 100 (36) | 112 (35) | 142 (17) |
| V*c* | 100 (36) | 116 (36) | 267 (32) |
| V*d* | 100 (36) | 116 (36) | 175 (21) |
| V*e* | 67 (24) | 52 (16) | — |
| V*f* | 61 (22) | 13 (4) | — |
| V*g* | 86 (31) | 55 (17) | — |
| V*h* | 94 (34) | 77 (24) | — |
| V*i* | 47 (17) | 29 (9) | — |
| V*j* | 89 (32) | 52 (16) | — |
| V*k* | 100 (36) | 106 (33) | — |
| V*l* | 100 (36) | 103 (32) | — |
| V*m* | 61 (22) | 58 (18) | — |
| V*n* | 100 (36) | 100 (31) | — |
| Sodium chloride | 0 (00) | — | — |

[a] Values given are percent protection; the numbers in parentheses represent the number of pinpricks failing to elicit a response (skin twitch or cry) from the wheal resulting from intradermal injection of 0.25 ml of the test compound in preshaven guinea pig backs ($n$ = 2).

**Table IV—Antiarrhythmic [a] and CNS Toxic [b] Effects in Mice**

| Compound | $ED_{50}$[c], mg/kg (95% Fieller Limits) Protection | Ataxia | Therapeutic Index |
|---|---|---|---|
| Lidocaine | 48 (44–53) | 45 (40–50) | 0.94 |
| V*a* | 9 (4–29) | 8 (5–11) | 0.89 |
| V*b* | 39 (20–60) | 107 (67–298) | 2.74 |
| V*c* | 33 (24–39) | 129 (91–282) | 3.91 |
| V*d* | 24 (15–41) | 131 (44–386)[d] | 5.46 |
| V*e* | 330 (183–900) | 125 (85–240) | 0.38 |
| V*f* | 164 (86–301) | 134 (83–202) | 0.82 |
| V*g*[e] | — | — | — |
| V*h* | 145 (74–1168) | 470 (356–737) | 3.24 |
| V*i* | 345 (220–569) | 159 (71–238) | 0.46 |
| V*j* | 159 (116–226) | 169 (101–212) | 1.06 |
| V*k* | 125 (86–153) | 78 (36–108) | 0.62 |
| V*l* | 142 (53–379)[d,f] | 253 (158–620) | 1.78 |
| V*m* | 304 (190–411) | 302 (186–400) | 0.99 |
| V*n* | 316 (261–427) | 292 (252–358) | 0.92 |

[a] Protection against chloroform-induced tachycardia. [b] Observed prior to exposure to chloroform. [c] Subcutaneous administration. [d] Approximate 95% Fieller limits. [e] Lack of water solubility prevented determination. [f] Tremor, $ED_{50}$ <20 mg/kg.

[1] All IR spectral data were determined on a Beckman Acculab-4 spectrophotometer using the potassium bromide technique. NMR spectra were determined on a Hitachi Perkin-Elmer R24 high-resolution spectrophotometer with tetramethylsilane as the internal reference. The reported melting points were obtained using a Thomas-Hoover capillary apparatus and are uncorrected. The reported analyses of carbon, hydrogen, chlorine, and nitrogen were obtained from Atlantic Microlab, Atlanta, Ga. TLC was performed using Eastman Chromatogram sheets (type 6060, silica gel); the sheets were developed in an iodine chamber.

portions of chloroform, and the organic solution then was extracted with 300 ml of saturated sodium chloride solution. The chloroform was removed *in vacuo*, and the residue was dissolved in 200 ml of boiling cyclohexane, treated with activated charcoal, and immediately filtered while hot.

After cooling to room temperature, a gummy residue was collected from the bottom of the flask by decantation. This residue was dissolved in 100 ml of acetone, 4 ml of concentrated hydrochloric acid was added, and the mixture was placed in the freezer. After 24 hr, fine gray crystals (6.5 g, 50%) were collected (homogeneous on TLC; in acetone, $R_f$ 0.28), mp 222–223° dec.; IR (KBr): 3130, 3020, 2575, 2485, 2210, 1690, 1550, 1530, 1440, 1175, 1150, 975, and 710 $cm^{-1}$; NMR (dimethyl sulfoxide-$d_6$): $\delta$ 1.39 [d, 3H, $CH_3$ of $-CO-C-C(CH_3)-N^+$], 1.6–2.0 (complex m, 4H, $\beta$-methylenes of pyrrolidino), 1.99 (s, 3H, $CH_3$ at C-4), 2.05 (s, 3H, $CH_3$ at C-5), 2.7–3.1 [complex m, CH, $\alpha$-methylenes of pyrrolidino and methylene of $CO-CH_2-C(C)-N^+$], 3.26 (s, 3H, $CH_3$ at N-1), 3.6–4.0 [complex m, 1H, methine of $-CO-C-CH(C)-N^+$], 10.5 (s, 1H, NH of amide or $^+NH$), and 11.1–11.6 (broad s, 1H, $^+NH$ or NH of amide) ppm. Table II gives the results of the elemental analysis.

**Method B: 2-(3-Pyrrolidinobutyramido)-3-cyano-4,5-dimethylpyrrole (IV*e*)**—The procedure for IV*e* is given as a general method of synthesis of IV*b*, IV*c*, and IV*e*–IV*l*. A solution of 2-(3-bromobutyramido)-3-cyano-4,5-dimethylpyrrole (III*c*) (20.0 g, 0.07 mole) in 150 ml of *n*-propanol was stirred while pyrrolidine (29.9 ml, 0.42 mole) was added. The solution was refluxed with stirring for 8 hr, and then the solvent and excess amine were removed *in vacuo*. The residue was dissolved in 300 ml of 5% HCl, and the solution was filtered. The acidic filtrate was poured over 200 g of ice and made alkaline with 10% NaOH (pH 10), and the tan precipitate was collected by filtration. The crude product was recrystallized from 280 ml of methanol–water (4:1), yielding white crystals (16.0 g, 83.3%) which were collected and dried. The crystals were suitable for hydrochloride salt formation (homogeneous on TLC; in ethyl acetate, $R_f$ 0.47), mp 168–169°. The data for the analogs are given in Table II.

**2-(3-Pyrrolidinobutyramido)-3-cyano-4,5-dimethylpyrrole Hydrochloride (V*e*)**—The procedure for V*e* is given as a general method of synthesis of V*b*, V*c*, and V*e*–V*n*. A solution of the free amine (IV*e*) (8.0 g, 0.03 mole) in 100 ml of acetone was filtered, and the filtrate was treated with 3.0 ml of concentrated hydrochloric acid. The sealed flask was placed in the freezer for 1 hr, yielding white crystals; these crystals were collected by filtration, washed with acetone, and dried. The crystals (8.3 g, 89.2%) were analytically pure (homogeneous on TLC; in ethyl acetate, $R_f$ 0.24), mp 94–95.5° dec.; IR (KBr): 3510, 3400, 3225, 3030, 2980, 2640, 2600, 2210, 1670, 1620, 1460, 1330, 1230, 1180, 1080, and 760 $cm^{-1}$; NMR (dimethyl sulfoxide-$d_6$): $\delta$ 1.40 (d, 3H, $CHCH_3$), 1.95 (s, 3H, $CH_3$ at C-4), 2.05 (s, 3H, $CH_3$ at C-5), 2.00 (broad m, 4H, $\beta$-carbons on pyrrolidine), 2.95 (d, 2H, $COCH_2$), 3.50 (m, 1H, $COCH_2CH$), 2.80–3.80 (broad m, 4H, $\alpha$-carbons on pyrrolidine), 10.80 (s, 1H, NH), and 11.35 (s, 2H, NH). Table II lists the results of the elemental analyses.

**Method C: 2-(3-Diethylaminopropionamido)-3-carbamyl-4,5-dimethylpyrrole (IV*m*)**—The procedure for IV*m* was also used for IV*n*. A solution of 2-(3-diethylaminopropionamido)-3-cyano-4,5-dimethylpyrrole (IV*i*) (13.12 g, 0.05 mole) in 85% $H_3PO_4$ (30 ml) was heated with stirring at 127–129° for 5 min. The contents of the vessel were cooled, crushed ice (200 g) was added, and the pH was adjusted to 10 by the addition of a saturated sodium hydroxide solution. The product was collected, resuspended in distilled water (300 ml), collected by filtration, and dried. The crude amine (10.0 g, 71.3%) was recrystallized from methanol–water (1:2) to yield off-white crystals (9.0 g, 90%), which were suitable for hydrochloride salt formation. [See Table II for analog and *Method B* for hydrochloride salt (V*m*) formation.]

**Pharmacology**—*Local Anesthetic Activity*—The guinea pig wheal method of Bulbring and Wajda (12) was employed in determining activity. The methodology was described previously (1–3).

*Antiarrhythmic Activity and CNS Toxicity*—A modification of the method of Lawson (13) was employed in assessing the antiarrhythmic activity and acute CNS toxicity. The methodology was described previously (3). Briefly, the mice were exposed to chloroform following subcutaneous injection of the target compounds. After respiratory arrest was evoked, a thoracotomy was performed; multilead ECGs were recorded for ~45 sec. If the ventricular rate was <520 beats per minute during this period, it was presumed that ventricular tachycardia had been prevented and the mouse was considered "protected." Symptoms of ataxia were monitored during the 20-min period between injection of the target compound and exposure to chloroform.

## REFERENCES


(1) R. W. Johnson, T. H. Keenan, J. W. Kosh, and J. W. Sowell, Sr., *J. Pharm. Sci.*, **68**, 317 (1979).

(2) *Ibid.*, **68**, 955 (1979).

(3) J. W. Sowell, Sr., A. J. Block, M. E. Derrick, J. J. Freeman, J. W. Kosh, R. J. Mattson, P. F. Mubarak, and P. A. Tenthorey, *J. Pharm. Sci.*, **70**, 135 (1981).

(4) E. W. Byrnes, P. D. McMaster, E. R. Smith, M. R. Blair, R. N. Boyes, B. R. Duce, H. S. Feldman, G. H. Kronberg, B. H. Takman, and P. A. Tenthorey, *J. Med. Chem.*, **22**, 1171 (1979).

(5) P. D. McMaster, E. W. Byrnes, H. S. Feldman, B. H. Takman, and P. A. Tenthorey, *ibid.*, **22**, 1177 (1979).

(6) P. A. Tenthorey, R. L. DiRubio, H. S. Feldman, B. H. Takman, E. W. Byrnes, and P. D. McMaster, *ibid.*, **22**, 1182 (1979).

(7) R. Gewald, *Z. Chem.*, **1**, 349 (1961).

(8) V. I. Shvedov, M. V. Mezentseva, and A. N. Grinev, *Khimiya Geterotsikl. Soedin.*, **9**, 1219 (1975); through *Chem. Abstr.*, **84**, 59299 (1976).

(9) R. W. Johnson, R. J. Mattson, and J. W. Sowell, Sr., *J. Heterocycl. Chem.*, **14**, 383 (1977).

(10) R. J. Mattson and J. W. Sowell, Sr., *Synthesis*, **1979**, 217.

(11) D. M. Hall and E. E. Turner, *J. Chem. Soc.*, **1948**, 1909.

(12) E. Bulbring and I. Wajda, *J. Pharmacol. Exp. Ther.*, **85**, 78 (1945).

(13) J. W. Lawson, *ibid.*, **160**, 22 (1968).


## ACKNOWLEDGMENTS


Adapted in part from theses submitted by M. E. Derrick and P. F. Mubarak to the University of South Carolina in partial fulfillment of the Master of Science degree requirements.

The authors from the University of South Carolina express their appreciation to Astra Pharmaceutical Products, Inc., for financial support of this research.

# Human Metabolism of 7-Substituted Theophyllines: $N^3$-Demethylation and Lack of Oxidation of Proxyphylline

E. TARRUS, I. GARCIA, and J. SEGURA ˣ

Received July 24, 1980, from the *Division of Biochemistry and Biopharmaceutics, Institute of Research, Laboratories Almirall, Cardoner, 68-74, Barcelona-24, Spain.* Accepted for publication October 17, 1980.

**Abstract** □ Proxyphylline metabolism after oral administration to humans was studied. The only metabolic process detected was $N^3$-demethylation, and 1-methyl-7-(2-hydroxypropyl)xanthine was isolated and identified. Proxyphylline was excreted in urine both as unchanged compound (12.7% of dose) and as its metabolic product (30.2% of dose). The latter substance was not found (detection limit = 1 μg/ml) in the systemic circulation. Thus, it probably does not participate in the pharmacological activity of proxyphylline *in vivo*, although it was as active as the parent drug in relaxing the guinea pig tracheal chain. Lack of metabolism to uric acid derivatives is explained by the low affinity of both substances toward the enzymes that oxidize xanthine (xanthine oxidase) and methylxanthine derivatives. The presence of the metabolite in urine interferes with some analytical methods developed for estimation of unchanged proxyphylline. Published data on the urinary excretion of this drug need reevaluation.

**Keyphrases** □ Proxyphylline—metabolism after oral administration, $N^3$-demethylation □ Pharmacokinetics—proxyphylline, diuretics, $N^3$-demethylation □ Xanthine derivatives—metabolism of proxyphylline in humans □ Diuretics—proxyphylline, metabolism after oral administration, $N^3$-demethylation

Substitution of the hydrogen atom at position 7 of the theophylline nucleus has received increased attention in the search for better tolerated and pharmacologically more selective theophylline-like compounds (1–9). The biodegradation of 7-substituted theophyllines follows three main metabolic pathways in humans: $N$-dealkylation of one or two of the alkyl groups at positions 1, 3, and 7; $C^8$-oxidation of the unchanged drug and/or its $N$-dealkylated metabolites to uric acid derivatives; and conjugative or oxidative metabolism of the $N^7$-side chain.

The chemical structure of the $N^7$-substitution dictates the relative importance of these metabolic pathways for each individual compound. The metabolism of theophyllines with small alkyl side chains such as caffeine (10–13) or with large ones such as pimefylline (14), xanthinol (15), or fenethylline (16) has been described. Little is known, however, about the biodegradation of theophyllines substituted by medium-sized hydroxy alkyl groups (17, 18), although some of them, such as etofylline, dyphylline, and proxyphylline, are widely used in treatment of respiratory tract diseases.

A study of proxyphylline [7-(2-hydroxypropyl)theophylline] metabolism was undertaken because serious discrepancies exist in the literature about the amount of unchanged proxyphylline excreted in the urine of volunteers given the drug orally (19, 20). The variability of the results seems to be unrelated to the specificity of the analytical method used and suggests the existence of metabolic products structurally similar to the parent drug. Other methylxanthines are oxidized to uric acid derivatives either by xanthine oxidase, *i.e.*, 1-methylxanthine (21–23), or by other enzymatic systems (24). In a preliminary step, the possible interaction between proxyphylline and xanthine oxidase was investigated. Nevertheless, relevant information was obtained after oral administration of the drug to volunteers. The results of these studies confirm the existence of a metabolite and indicate that the main, if not the only, metabolic process of the drug in humans is $N^3$-demethylation.

## EXPERIMENTAL

**Incubations with Xanthine Oxidase**—The determination of enzymatic activity was carried out by the method of Domingo (25), which measures the absorbance at 600 nm of the oxidized form of 2,6-dichloroindophenol. The enzymatic system contained 0.027 mg of xanthine oxidase[1]/ml, $3.5 \times 10^{-5}$ $M$ 2,6-dichloroindophenol[2], and several concentrations of xanthine[2], proxyphylline[3], and isolated proxyphylline metabolite. The incubation medium and the solutions used were prepared in a 0.05 $M$ phosphate buffer (pH 7.4) (26). Solutions of xanthine, theophylline[3], and metabolite were prepared by dissolving the drugs in a small volume of concentrated sodium hydroxide, followed by addition of the phosphate buffer and final adjustment of the pH to 7.4 with dilute hydrochloric acid. The temperature was maintained at 25 ± 1°, and the absorbance was determined with a spectrophotometer[4].

**Drug Administration to Humans**—In a preliminary qualitative assay, an oral dose of 300 mg of proxyphylline was administered to two healthy men. Proxyphylline was dissolved in water containing sucrose. No food was allowed from 9 hr before until 2 hr after drug administration. Urine was collected prior to the experiment and for the 0–8 and 8–24-hr periods. Excreted volumes were measured, and 25-ml samples were stored at −20° until analysis by TLC.

In a second quantitative assay, 300 mg of proxyphylline was administered to five healthy men (73–98 kg, mean 81.8 kg; 23–38 years, mean 30.8 years). The administration conditions and urine collection procedures were the same as in the preliminary assay. Blood samples were obtained from the cubital veins of the forearm with heparinized syringes immediately before administration and at 0.5, 1, 2, 4, 6, 8, and 12 hr. The plasma was separated after centrifugation and stored under the same conditions as urine until analysis.

To isolate enough of the proxyphylline metabolite to study its structure and properties, three gelatin capsules, each containing 750 mg of proxyphylline, were administered to six healthy men, one capsule every 12 hr. All urine excreted for 9 hr after the third dose was collected and stored at −20° until analysis.

**Isolation and Purification of Proxyphylline Metabolite**—Urine excreted by the six volunteers (2.85 liters) was chromatographed through a glass column (30 × 3.5 cm) filled with resin[5]. Excess water in the column then was removed by vacuum applied to the lower end, and the column was eluted with 900 ml of methanol. Air bubbles were removed by gentle agitation of the resin with a glass rod. The methanol eluate was evaporated to dryness *in vacuo*. The residue was washed three times with 50 ml of methanol, once with 35 ml of chloroform, and twice with 14 ml of ethanol and was dried *in vacuo* over phosphoric anhydride for 2 days. A white powder (364 mg) was obtained.

This compound was shown by TLC[6] in Solvent Systems 1 (chloroform–methanol–25% ammonia solution, 10:4:1) and 2 (chloroform–methanol–ethyl acetate–99.5% acetic acid, 78:10:10:2) to be mainly the expected proxyphylline metabolite ($R_f$ 0.42 in Solvent 1 and $R_f$ 0.23 in Solvent 2). Its purity was 84–88% as determined by comparison of its molar absorptivity with that of proxyphylline and xanthine at 270 nm (pH 7.4). The identification of its structure was carried out by spectro-

[1] Extracted from cow milk, Boehringer Mannheim, West Germany.
[2] Merck, Darmstadt, West Germany.
[3] Knoll, Ludwigshafen, West Germany.
[4] Perkin-Elmer model 550.
[5] Amberlite XAD-2, Rohm & Haas, Philadelphia, Pa.
[6] Silica gel 60 $F_{254}$, Merck, Darmstadt, West Germany.



0022-3549/81/0500-0542$01.00/0
© 1981, American Pharmaceutical Association

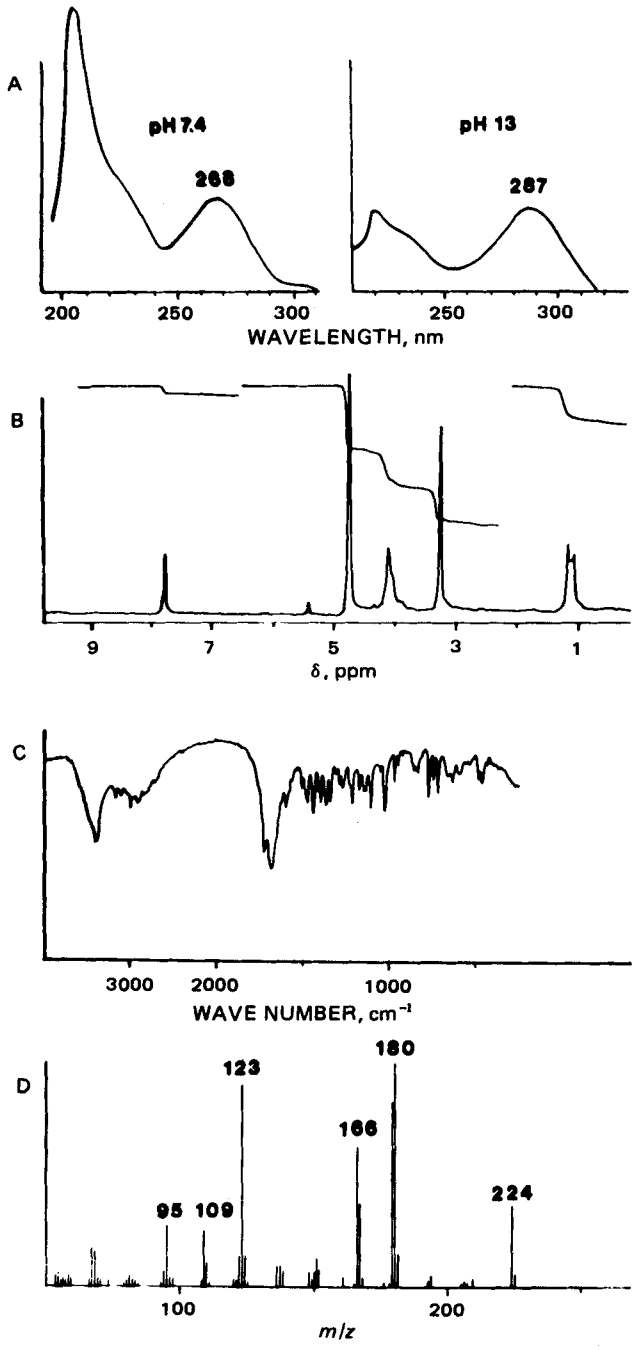


**Figure 1**—*UV (A), NMR (B), IR (C), and mass (D) spectra of the metabolic product of proxyphylline, 1-methyl-7-(2-hydroxypropyl)-xanthine, isolated from human urine.*

metric methods. Measurements of UV absorption spectra[4] were performed in methanol or aqueous solutions. The spectra in aqueous solutions were obtained at pH 13 (0.5 *N* NaOH) or pH 7.4. [The compounds were dissolved in a minimal amount of concentrated sodium hydroxide, 0.1 *M* phosphate buffer (pH 7.4) was added, and the pH was adjusted to 7.4 with dilute hydrochloric acid]. IR spectra[7] were obtained using potassium bromide pellets. NMR spectra[8] were obtained in a 0.5 *N* NaOD solution in deuterium oxide. Tetramethylsilane was used as the internal standard. Mass spectra[9] were obtained at 70 ev, and samples were introduced by direct-probe insertion.

**Pharmacological Activity of Proxyphylline and Its Purified Metabolite on Isolated Guinea Pig Tracheal Chain**—A guinea pig tracheal chain was prepared according to the method of Castillo and De Beer (27). It was immersed in a bath containing an oxygenated Kreb's solution and was subjected to an initial tension of 0.5 g. The addition of isoproterenol[10], theophylline, proxyphylline, and the purified proxyphylline metabolite to the bath allowed comparison of their relative myorelaxant effects[11]. Isoproterenol, theophylline, and proxyphylline were dissolved directly in saline (0.9% NaCl). However, to obtain a saline solution of proxyphylline metabolite, it was necessary to boil and reflux the suspension for ~15 min. The metabolite was stable under these conditions. The concentrations studied for each compound are indicated in Fig. 2.

**Quantitative Analysis of Proxyphylline and Its Metabolite in Human Plasma and Urine**—*Proxyphylline in Plasma*—Plasma samples (1 ml) were made alkaline with 0.5 *N* NaOH (0.2 ml) and were extracted for 1 hr with chloroform (6 ml). The organic phase was separated by centrifugation and evaporated under a nitrogen stream. The residue was dissolved in chloroform, applied to precoated thin-layer plates[6], and developed further with Solvent System 2. Quantification was carried out by photodensitometry[12] by measuring the diminution of background fluorescence at 525 nm (excitation at 254 nm) induced by the proxyphylline spot ($R_f$ 0.36). The calibration curves were obtained after addition of known amounts of proxyphylline to plasma samples subsequently subjected to extraction.

*Proxyphylline Metabolite in Plasma*—Plasma samples (1 ml) were added to resin[5] (0.3 g) and shaken for 5 min. The aqueous phase was separated, and the resin was eluted three times with 1 ml of methanol with vigorous shaking for 5 min. The extracts were combined and evaporated to dryness under a nitrogen stream, and the residue was dissolved in a small amount of methanol. Quantitation was carried out by TLC and photodensitometry[12] as previously described, using Solvent System 2. The addition of known amounts of purified metabolite to plasma samples showed that the extraction yield was nearly 100%. The detection limit was 1 μg/ml.

*Proxyphylline and Its Metabolite in Urine*—Samples of urine (40 μl) were applied directly onto precoated thin-layer plates, which were developed with Solvent System 1. Analysis was performed by photodensitometry[12] as previously described. The responses were compared with those obtained from known amounts of proxyphylline and its purified metabolite added to control urines. The $R_f$ value of proxyphylline in this system was 0.79.

## RESULTS AND DISCUSSION

The oral administration of caffeine (1,3,7-trimethylxanthine) to rats and humans gives rise to the excretion of the following substances: 1,3,7-trimethylxanthine (10), 1,3,7-trimethyluric acid (11), 1,3-dimethylxanthine (theophylline) (12), 1,3-dimethyluric acid (10), 1,7-dimethylxanthine (paraxanthine) (10), 1,7-dimethyluric acid (13), 1-methylxanthine (10), 1-methyluric acid (10, 13), 7-methylxanthine (10), 7-methyluric acid (13), and 3-methyluric acid (11). Thus, there are two main metabolic pathways for caffeine, *N*-demethylation and $C^8$-oxidation of the various methylxanthines to uric acid derivatives. The metabolism of theophylline and theobromine, when given orally to humans, is similar (10, 28).

The $C^8$-oxidative metabolism can be partially studied by following the reaction of each substrate with the enzyme, xanthine oxidase. It is known that caffeine (29) and other methylxanthines are not oxidized by this enzyme, whereas 1-methylxanthine is oxidized to its uric acid derivative by bovine milk (21) or by rat hepatic (22) xanthine oxidases. Recently, it was demonstrated by giving theophylline and allopurinol to humans (23) that 1-methyluric acid seems to be the only metabolite arising from direct oxidation of its substrate (1-methylxanthine) by hepatic xanthine oxidase. Therefore, the oxidative metabolism of proxyphylline and its isolated metabolite by xanthine oxidase was studied.

Bovine milk xanthine oxidase was used since this enzyme and human hepatic xanthine oxidase have a similar specificity for purine derivatives (21). Proxyphylline was incubated at concentrations of $1 \times 10^{-4}$ and $1 \times 10^{-3}$ *M*, and its metabolite was incubated at $1 \times 10^{-4}$ and $5 \times 10^{-4}$ *M*. These concentrations were equal to and were five and 10 times higher than the concentration of xanthine that saturates the system (21). Under these conditions, no reaction was observed, which may have been due to either a lack of affinity for the enzyme or a lack of intrinsic activity of the enzyme when the substrates are at the active site. The ability of proxyphylline and its metabolite to inhibit competitively the xanthine–xan-

[7] Beckman model Acculab 10.
[8] Perkin-Elmer model R-24.
[9] Hewlett-Packard model 5930A.
[10] Boehringer Ingelheim, West Germany.
[11] Transducer and recorder, Ugo Basile, Milan, Italy.
[12] Vitatron photodensitometer model TLD 100.

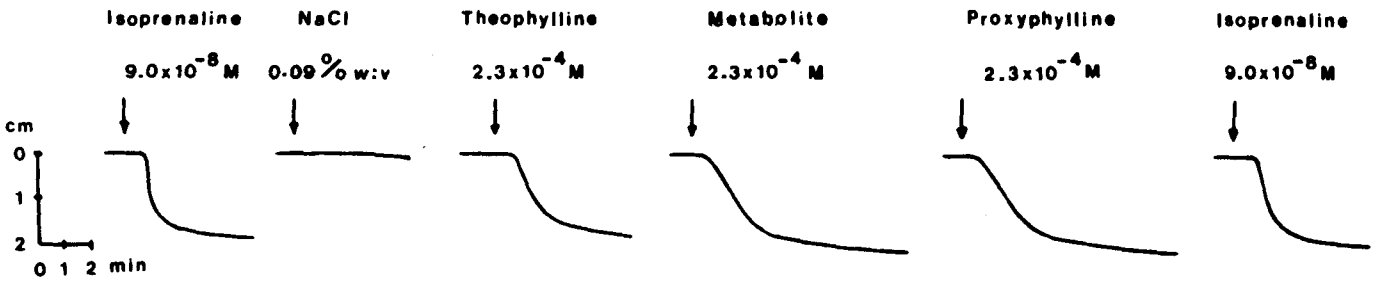


**Figure 2**—*Effects induced by isoproterenol (isoprenaline), theophylline, proxyphylline, and its metabolite on the myorelaxation of the isolated guinea pig tracheal chain. The substances were dissolved in 0.9% NaCl and were added (4 ml) to the bath (40 ml) to reach the final concentrations indicated in the figure.*

thine oxidase system was studied to distinguish between these possibilities. The xanthine concentrations in the incubation media were $2.5 \times 10^{-6}$, $5 \times 10^{-6}$, $1 \times 10^{-5}$, and $1 \times 10^{-4}$ *M*. The concentrations of proxyphylline and the metabolite were the same as previously indicated. Neither substance altered the oxidation rate of xanthine, which suggests that they have a low affinity for the enzyme, as is the case for caffeine, theophylline, and theobromine (30). Apparently the di- and trisubstitution of the xanthine nucleus prevents the interaction with xanthine oxidase (21, 30).

When 300 mg of proxyphylline was given orally to two volunteers, visual evaluation (254 nm) of thin-layer plates of urine extracts showed only two new spots compared with control urine. One spot was identified as unchanged proxyphylline. Only 28.4 mg was excreted during the first 8 hr, and 24.8 mg was excreted during the following 16 hr. The second compound had lower $R_f$ values and was excreted in higher concentrations. This metabolite was isolated from the combined urine of six volunteers given high doses of proxyphylline. Its structure was investigated by spectral methods, and it was identified as 1-methyl-7-(2-hydroxypropyl)xanthine based on the following evidence:

1. The UV absorption spectrum of the metabolite in methanol and aqueous neutral solutions (Fig. 1A) was virtually identical to that of proxyphylline and xanthine. Under these conditions, the absorbance maximum of uric acid was at 290 nm. The absorption maximum of the metabolite shifted to 287 nm in alkaline solutions (Fig. 1A), as occurs with xanthine but not with proxyphylline. The tautomerism of $N^3$-H is involved in the bathochromic shift of the xanthine spectrum (31). No tautomerism exists for $N^1$-H (31).

2. Apart from the disappearance of the singlet corresponding to a 1-methyl group, the NMR spectrum of the metabolite (Fig. 1B) was similar to that of proxyphylline: $\delta$ 1.28 (d, C–$CH_3$), 3.27 (s, N–$CH_3$), 3.46 (s, N–$CH_3$), 4.10 (m, $CH_2$–CHOH), and 8.08 (s, ≡CH) ppm. It was shown (32, 33) that the $N^1$-methyl group always appears upfield with respect to the $N^3$-methyl group. Thus, the methyl group ($\delta$ 3.25 ppm) in the spectrum of the metabolite is located at position 1.

3. The IR spectrum of the metabolite (Fig. 1C) confirmed the lack of $C^8$-oxidation since no variation was observed in the CO stretching bands when compared to proxyphylline (1650 and 1690 $cm^{-1}$).

4. The mass spectrum (Fig. 1D) confirmed the postulated structure. The molecular ion ($M^+$ at *m/z* 224) is in accordance with the formula $C_9H_{12}N_4O_3$. The $N^7$-side chain is unaltered as indicated by the fragmentation of the $\alpha$ and $\beta$ bonds (*m/z* 166, 167, 179, and 180) when compared to proxyphylline (34). All ions bearing the purine ring appeared 14 amu lower than the corresponding ions in the proxyphylline spectrum (34), thus confirming the absence of the $N^3$-methyl group.

5. The solubility of the metabolite in aqueous neutral solutions (pH 7.4) was comparable to that of xanthine but much lower than that of proxyphylline. The solubility of the metabolite increased in strong alkaline media due to the ionization of the tautomeric enolic form involving $C^2$ and $N^3$.

$N^3$-Demethylation of proxyphylline is in accord with the metabolic stability of the caffeine methyl groups (1 > 7 > 3) in humans (10). No $N^7$- or $N^1$-metabolic dealkylation of proxyphylline metabolite is subsequently produced, in accordance with the results of Cornish and Christman (10), who found that didealkylation did not occur when theophylline and theobromine were given to humans. They did not observe urinary excretion of xanthine or uric acid above the normal levels. Other $N^7$-substituted theophyllines with larger side chains are $N^7$-dealkylated to produce theophylline, *e.g.*, pimefylline {7-[2-[(3-pyridylmethyl)amino]ethyl]theophylline} (14) and fenethylline {7-[2-[($\alpha$-methylphenethyl)amino]ethyl]theophylline} (16), whereas xanthinol {7-[2-hydroxy-3-[(2-hydroxyethyl)methylamino]propyl]theophylline} and dyphylline [7-(2,3-dihydroxypropyl)theophylline] behave as proxyphylline and its metabolite since no $N^7$-dealkylation is observed (15, 17, 18). The latter four compounds carry an hydroxyl group on the $\beta$-position of the side chain that may prevent the carbinolamine formation postulated (35, 36) to be the first step of *N*-dealkylation. The complexity of the $N^7$-side chain also seems to play an important role in the $C^8$-metabolic oxidation of this class of substances. Proxyphylline and its metabolite, like other theophyllines substituted in position 7 by large groups, are not oxidized, whereas the 7-methylxanthines are excreted partially as uric acid derivatives (10, 11, 13). The enzymatic system involved, however, was not determined. Xanthine oxidase does not seem to be involved (21, 24, 30).

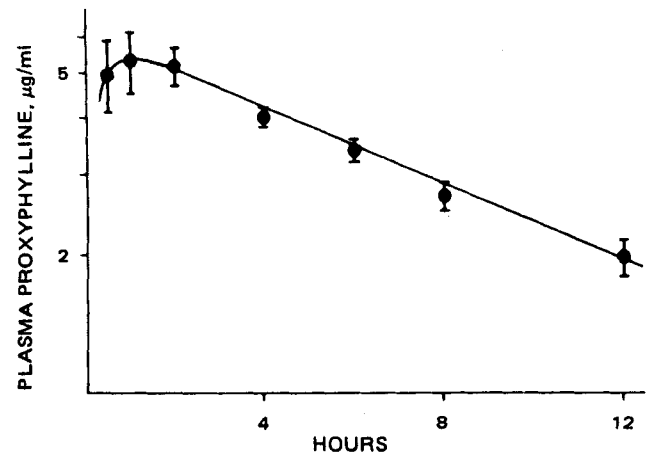


**Figure 3**—*Mean plasma concentrations of unchanged proxyphylline in five human volunteers given 300 mg of the drug by the oral route. Vertical bars are units of the standard error of the mean.*

Equimolar amounts of proxyphylline and its metabolite gave an equivalent relaxation of the isolated guinea pig tracheal chain, although these compounds were less active than theophylline and isoproterenol (Fig. 2). The metabolite was not detected (detection limit = 1 µg/ml) in the plasma samples of six volunteers given 300 mg of proxyphylline orally. The levels of the parent drug in the same samples (Fig. 3) were similar to those previously described for an equivalent dose (19, 20, 37–40). These results indicated that in spite of its $\beta$-adrenergic activity, 1-methyl-7-(2-hydroxypropyl)xanthine probably does not participate in the clinical actions of proxyphylline. Despite the lack of detection of the metabolite in the systemic circulation, it was verified as the major pathway for the renal excretion of proxyphylline in humans (Table I). The mean values of metabolite excreted in the urine were 16.9% of the dose in the 0–8-hr period and 13.3% of the dose during the following 16 hr. These values were twice those found for proxyphylline (8.5 and 4.1%, respectively).

**Table I—Cumulative Urinary Excretion of Proxyphylline and Its Metabolite** [a]

| Hours | Proxyphylline | Metabolite |
|---|---|---|
| 8 | 8.5 ± 3.0 [b] | 16.9 ± 2.9 |
| 24 | 12.6 ± 2.9 | 30.2 ± 3.6 |

[a] Oral administration of 300 mg of proxyphylline to five humans. [b] Percentage of dose (mean ± *SEM*).

The high amounts of 1-methyl-7-(2-hydroxypropyl)xanthine appearing in the urine of humans given proxyphylline and the close similarity between the chemical structure of both compounds indicate the need for specific methods to estimate the unchanged drug concentrations in those samples. Some results obtained by nonspecific spectrophotometric methods (19, 41, 42) will need reevaluation. It has been verified that the method of Driever (43), modified by Ritschel and Banarer (41) to estimate unchanged proxyphylline in urine, does estimate the unchanged drug plus its metabolite, 1-methyl-7-(2-hydroxypropyl)xanthine.

## REFERENCES


(1) A. Lespagnol, J. Vanlerenberghe, and L. Masse, *Bull. Soc. Pharm. Lille*, **2**, 18 (1948).

(2) F. E. Roth, M. M. Winbury, and W. M. Govier, *J. Pharmacol. Exp. Ther.*, **121**, 487 (1957).

(3) H. Daweke and A. Oberdorf, *Arzneim.-Forsch.*, **8**, 190 (1958).

(4) L. Fabbrini and R. Cencioni, *Farmaco, Ed. Sci.*, **17**, 660, (1962).

(5) R. Hemmer and E. Diezemann, *Arzneim.-Forsch.*, **12**, 672 (1962).

(6) R. Fischbach and R. Haas, *ibid.*, **17**, 313 (1967).

(7) G. Ciacieri and G. Attaguile, *Gazz. Med. Ital.*, **132**, 108 (1973).

(8) E. Duranti, P. Bonitazi, C. Balsamini, G. Peruzzi, and G. Lombardelli, *Farmaco, Ed. Sci.*, **34**, 284 (1979).

(9) "Martindale, The Extra Pharmacopoeia," 27th ed., R. G. Todd, Ed., Pharmaceutical Press, London, England, 1977, p. 276.

(10) H. H. Cornish and A. A. Christman, *J. Biol. Chem.*, **228**, 315 (1957).

(11) K. L. Khanna, G. S. Rao, and H. H. Cornish, *Toxicol. Appl. Pharmacol.*, **23**, 720 (1972).

(12) M. J. Arnaud, *Biochem. Med.*, **16**, 67 (1976).

(13) E. A. Johnson, *Biochem. J.*, **51**, 133 (1952).

(14) D. Pitre, U. Tiepolo, and A. Mengassini, *Farmaco, Ed. Prat.*, **29**, 486 (1974).

(15) M. Tauscher, G. Eckhardt, B. Geisel, and K. Gedner, *Arźneim.-Forsch.*, **26**, 1342 (1976).

(16) T. Ellison, L. Levy, J. W. Bolger, and R. Okun, *Eur. J. Pharmacol.*, **13**, 123 (1970).

(17) J. Zuidema and F. W. H. M. Merkus, *Curr. Med. Res. Opin.*, **6**, 14 (1979).

(18) F. W. H. M. Merkus and J. Zuidema, *Int. J. Clin. Pharmacol. Ther. Toxicol.*, **18**, 97 (1980).

(19) M. Banarer and W. A. Ritschel, *Bull. Tech. Gattefosse*, **68**, 56 (1973).

(20) G. Graffner, G. Johnson, and J. Sjögren, *Acta Pharm. Suec.*, **10**, 425 (1973).

(21) F. Bergmann and S. Dikstein, *J. Biol. Chem.*, **223**, 765, (1956).

(22) S. M. Lohmann and R. P. Miech, *J. Pharmacol. Exp. Ther.*, **196**, 213 (1976).

(23) A. H. Van Gennip, J. Grift, and E. J. Van Bree-Blom, *J. Chromatogr.*, **163**, 351 (1979).

(24) "The Pharmacological Basis of Therapeutics," 4th ed., L. S. Goodman and A. Gilman, Eds., Macmillan, London, England, 1970, p. 366.

(25) E. Domingo, Ph.D. thesis, University of Barcelona, Barcelona, Spain, 1969, p. 35.

(26) G. Gomori, in "Methods in Enzymology," vol. I, P. Colowick and N. O. Kaplan, Eds., Academic, New York, N.Y., 1955, p. 143.

(27) J. C. Castillo and E. J. De Beer, *J. Pharmacol. Exp. Ther.*, **90**, 104 (1947).

(28) T. J. Monks, J. Caldwell, and R. L. Smith, *Clin. Pharmacol. Ther.*, **26**, 513 (1979).

(29) E. J. Morgan, C. P. Stewart, and F. G. Hopkins, *Proc. R. Soc. (London) Series B*, **94**, 109 (1922).

(30) H. I. Coombs, *Biochem. J.*, **21**, 1259 (1927).

(31) F. Bergman, D. Lichtenberg, and Z. Neiman, *Jerusalem Symp. Quantum Chem. Biochem.*, **4**, 247 (1972).

(32) T. G. Alexander and M. Maienthal, *J. Pharm. Sci.*, **53**, 962 (1964).

(33) R. Ottinger, G. Boulvin, J. Reisse, and G. Chiurdogln, *Tetrahedron*, **21**, 3435 (1965).

(34) K. Kamei and A. Momose, *Chem. Pharm. Bull.*, **21**, 1228 (1973).

(35) R. E. Mc Mahon, H. W. Culp, J. C. Craig, and N. Ekwuribe, *J. Med. Chem.*, **22**, 1100 (1979).

(36) G. Huizing, J. Segura, and A. H. Beckett, *J. Pharm. Pharmacol.*, **32**, 651 (1980).

(37) M. Ervik, *Acta Pharm. Suec.*, **7**, 697 (1970).

(38) G. Graffner, G. Johnson, and J. Sjögren, *ibid.*, **11**, 125 (1974).

(39) B. A. Sims, J. G. Kelly, and R. G. Shanks, *Br. J. Clin. Pharmacol.*, **3**, 194 (1976).

(40) A. Arbin, M. Berg, and L. O. Borens, *Acta Pharm. Suec.*, **13**, 235 (1976).

(41) W. A. Ritschel and M. Banarer, *Arzneim.-Forsch.*, **23**, 1031 (1973).

(42) W. A. Ritschel and M. Banarer, *Bol. Soc. Quim. Perú*, **38**, 212 (1972).

(43) C. W. Driever, *J. Pharm. Pharmacol.*, **21**, 470 (1969).


## ACKNOWLEDGMENTS


Presented in part at the VIIth International Symposium on Medicinal Chemistry, Torremolinos, Spain, September 1980.

The authors thank Mr. J. Llupiá and Dr. D. J. Roberts for providing the pharmacological activity data, Dr. R. G. W. Spickett for reviewing the manuscript and helpful comments, and Mrs. L. Borja for valuable aid.

# Biodehalogenation and Metabolism of [$^{125}$I]-4-Iodobiphenyl

**J. E. SINSHEIMER** [x] **and Y. Y. SHUM** *

Received January 31, 1980, from the *College of Pharmacy, University of Michigan, Ann Arbor, MI 48109.* Accepted for publication October 14, 1980. *Present address: Warner-Lambert/Parke-Davis Pharmaceutical Resarch Division, Ann Arbor, MI 48106.

**Abstract** □ [$^{125}$I]-4-Iodobiphenyl has been used as a model compound to investigate the *in vivo* metabolism of iodinated aromatic compounds in the rat. Material balance studies showed that 57.6% of the injected dose was excreted *via* feces and 41.2% *via* urine. Distribution studies indicated uptake of inorganic iodide in the thyroid. In the feces, 2.2% of the dose was unmetabolized iodobiphenyl, 2.6% was 2-hydroxy-4′-iodobiphenyl, 21.9% was 4-hydroxy-4′-iodobiphenyl, and 20.9% was a polar fraction of which only 10.3% could be silylated. In urine, 1.6% of the dose was 2-hydroxy-4′-iodobiphenyl, 4.9% was 4-hydroxy-4′-iodobiphenyl, 1.9% was 2-hydroxy-4′-iodobiphenyl, 17.7% was 4-hydroxy-4′-iodobiphenyl glucuronide and sulfate conjugates, and 8.2% was inorganic iodide. About 3.0% of the dose in the urine polar fraction could be methylated.

**Keyphrases** □ 4-Iodobiphenyl—metabolism in rats, distribution studies □ Metabolism—4-iodobiphenyl and metabolites, distribution studies in rats □ Distribution—4-iodobiphenyl and metabolites, metabolism and distribution studies in rats

The increasing medicinal use of iodinated organic compounds as positive X-ray contrast media (1) as well as diagnostic, scanning, and radiopharmaceutical agents (2) prompted this study of the biodehalogenation and metabolism of iodocompounds. *In vitro* mechanisms for the biodehalogenation of some model compounds were reported previously (3). This paper describes the *in vivo* biodehalogenation and metabolism of 4-iodobiphenyl (I) as a model compound used in rats.

## EXPERIMENTAL[1]

**Chromatographic Solvent Systems**—Benzene–methanol–formic acid (90:9:1) (Solvent System 1) and benzene–methanol (85:15) (Solvent System 2) were used for TLC[2], *n*-butyl alcohol–0.5 *M* $NH_4OH$–ethanol–water (20:20:2:1) (Solvent System 3) was used for paper chromatography, and *n*-butyl alcohol–acetone–concentrated ammonium hydroxide–water (65:20:10:5) (Solvent System 4) was used for resin paper chromatography.

**[$^{125}$I]-4-Iodobiphenyl**—This compound (specific activity, 9.0 μCi/mg; radiochemical purity by reverse isotopic dilution, 99.7%) was synthesized by an exchange reaction described previously (3).

**4-Hydroxy-4′-iodobiphenyl (II)**—Compound II was prepared from 4-hydroxybiphenyl and benzoyl chloride according to a literature method (4). The product was recrystallized in chloroform, mp 202° [lit. (4) mp 199°]; IR (KBr): 3300 (OH), 1580, 1520 (aromatic H), 1470–1420 (CH), 1380, 1250 (aromatic OH), 1120, 1000, 810, and 720 (aromatic H) $cm^{-1}$; NMR (acetone-$d_6$): δ 8.57 (broad s, 1H, aromatic OH), 7.92 (d of d, 2H, $J_{ab}$ = 9.0 Hz, $J_{ac}$ = 2.6 Hz, aromatic H), and 7.07 (d of d, 2H, $J_{ab}$ = 9.0 Hz, $J_{ac}$ = 2.0 Hz, aromatic H); mass spectrum (75 ev): *m/z* (relative intensity) 298 (1.0%) $[M + 2]^+$, 297 (14.1) $[M + 1]^+$, 296 (100) $[M]^+$, 267 (1.3), 169 (7.5) $[M - I]^+$, 168 (10.6) $[M - HI]^+$, 152 (3.8) $[M - HOI]^+$, 141 (19.7), 139 (8.0), 118 (metastable), 115 (14.3), and 96.5 (metastable).

**2-Hydroxy-4′-iodobiphenyl (III)**—Compound III was synthesized from 2-hydroxybiphenyl and benzoyl chloride using the same procedure as used for the preparation of II. The product was recrystallized in pentane, mp 75° [lit. (5) mp 74°]; IR (KBr): 3470–3020 (aromatic OH), 1470, 1390 (aromatic H), 1268 (aromatic OH), 1188, 1130, 1120, 1042, 1010, 834, 814, 756, 700, 612, and 540 (aromatic H) $cm^{-1}$; NMR ($CDCl_3$): δ 5.40 (s, 1H, aromatic OH), 6.90 (d of t, 1H, $J_{ab}$ = 9.0 Hz, $J_{ac}$ = 2.0 Hz, aromatic H), 7.20 (d of d, 2H, $J_{ab}$ = 9.0 Hz, $J_{ac}$ = 2.0 Hz, aromatic H), 7.40 (t, 1H, $J_{ab}$ = 2.0 Hz, aromatic H), 7.68 (d of d, 2H, $J_{ab}$ = 9.0 Hz, $J_{ac}$ = 2.0 Hz, aromatic H), and 7.94 (d, 2H, $J_{ab}$ = 9.0 Hz, aromatic H); mass spectrum (75 ev): *m/z* (relative intensity) 297 (14%) $[M + 1]^+$, 296 (100) $[M]^+$, 170 (20) $[M - I]^+$, 169 (10), 168 (2.0), 141 (9.0), and 115 (4.0).

**Reverse Isotopic Dilution**—In a manner analogous to previously reported analyses (6), ~1 g of II or III, accurately weighed, was transferred to a 300-ml round-bottom flask and dissolved completely in a small volume of acetone. Fecal extracts or urine samples were pipetted (1.0 ml) into the flask, and sufficient methanol was added to give a homogeneous solution. Solvents were removed *in vacuo*, and the residue was recrystallized from chloroform. Three samples of ~10 mg from each recrystallization were weighed accurately and counted for radioactivity in a γ-counting system. Recrystallization was repeated until constant specific activity was obtained.

***In Vivo* Studies**—Sprague–Dawley rats, 200–250 g, were housed in separate stainless steel metabolism cages and quarantined for at least 1 day prior to use. Rat food[3] and water were supplied *ad libitum*.

[$^{125}$I]-4-Iodobiphenyl was diluted with carrier 4-iodobiphenyl (I) and dissolved in sterilized peanut oil to give a final concentration of 110 μCi/100 mg/ml for intraperitoneal injection.

Tissue distribution studies were conducted after a single intraperitoneal injection of 0.5 ml of the peanut oil solution was given to 18 female rats. Sets of three rats were killed in an ether chamber at 3, 6, 24, 48, 72, and 96 hr after injection, and major tissues were excised and weighed. Representative samples of these tissues were weighed, and their radioactivities were determined (Table I).

Pretreatment with Lugol's solution was done with two rats, which were administered orally 0.3 ml of Lugol's solution (50 mg of elemental iodine and 100 mg of potassium iodide in 100 ml of water) once per day for 2 days. Control rats were dosed with distilled water under the same schedule. On the 3rd day, 3.9 μCi of [$^{125}$I]-4-iodobiphenyl in 0.5 ml of ethanol was administered to each rat by intraperitoneal injection. Rats were kept in separate metabolic cages for 24 hr before they were killed. Thyroid glands from each rat were excised, trimmed, weighed, and counted for activity in a γ-counting system.

Balance studies were conducted on three male rats, each receiving a single intraperitoneal injection of 1.0 ml of the dosage solution. Urine and fecal samples were collected for 18 days to observe excretion patterns of the metabolites.

Three rats received a single intraperitoneal injection of 1.0 ml of the dosage solution every 4 days for a total of 3.0 ml of solution to accumulate higher quantities of metabolites. Control rats were treated in a manner corresponding to each group but were injected only with sterilized peanut oil.

Rat urine and feces were collected separately after [$^{125}$I]-4-iodobiphenyl injections. Urine samples were quantitated for radioactivity, quick frozen in an acetone–dry ice bath to prevent mold growth, and stored at −25° until analyzed for metabolites. Feces were air dried and powdered, and samples (5–10 mg) were measured daily for radioactivity by γ-counting. They also were stored at −25° until investigated further.

For identification of fecal metabolites, the total combined daily powdered feces were extracted with methanol for 48 hr in a soxhlet apparatus. The methanol extract was reduced to 50.0 ml *in vacuo*. Aliquots (100 μl) of this solution were assayed by γ-counting to estimate the percentage of extractable activity.

Volumes (0.5 ml) of the concentrated fecal methanol extract were subjected to TLC analysis in Solvent Systems 1 and 2. Unmetabolized [$^{125}$I]-4-iodobiphenyl and its hydroxylated metabolites were identified by cochromatography with nonradioactive reference compounds in these solvent systems. The main body of the fecal methanol extract was applied to preparative chromatographic plates and developed in System 1. Bands of [$^{125}$I]-4-iodobiphenyl and its hydroxylated metabolites were extracted from the plates with appropriate solvents, concentrated, and subjected

[1] Spectra were obtained on Perkin-Elmer 337 IR, Varian A-60-A NMR, and DuPont 21-490 mass spectrometers. γ-Counting was either by liquid scintillation counting on Beckman LS-200 and 150 instruments with a phosphorus 32 window at 5% accuracy or 5-min intervals or with a Searle 1185 γ-system.

[2] Brinkmann 5 × 20 × 0.025-cm silica gel 60 F-254 on glass or Eastman silica chromatogram sheet 6060 for analytical measurements and Brinkmann 20 × 20 × 0.2-cm silica gel 60 F-254 on glass for preparative separations.

[3] Ralston-Purina Co.



0022-3549/81/0500-0546$01.00/0
© 1981, American Pharmaceutical Association

to GLC–mass spectrometric analysis. Part of the GLC output was collected *via* a three-way collector into scintillation vials and quantitated by liquid scintillation counting. Only the radioactive GLC peaks were analyzed by mass spectrometry.

Assay of [$^{125}$I]-4-iodobiphenyl and its hydroxylated metabolites was accomplished by estimation of their percentage contributions in TLC patterns developed in Solvent System 1. The results were subsequently confirmed by reverse isotopic dilution in the fecal methanol extracts with corresponding reference compounds.

Acid or base hydrolysis of the fecal polar fraction was done by extracting origin band materials with methanol and reducing the extract to 1.0 ml with nitrogen. An equal volume of 8 *N* HCl or 5% NaOH was added. The mixture was refluxed for 5 hr, and the solution was extracted with ether. Both aqueous and ether solutions were examined with TLC in Solvent System 1 for products.

Enzyme hydrolysis of the fecal polar fraction was performed by taking the methanol extract of the origin band to dryness under a nitrogen stream. The residue was dissolved in 2.5 ml of pH 7.4 phosphate buffer to which 0.1 ml (10,000 Fishman units) of β-glucuronidase–arylsulfatase of snail origin[4] (*Helix pomatia*) was added before it was incubated at 37° for 72 hr. After incubation, the content was centrifuged at 1720×*g* for 30 min, and the supernate was chromatographed in Solvent System 1 for detection of hydrolyzed products.

Silylation of the fecal polar fraction was carried out by reducing the methanol extract of the origin band to complete dryness. The dried residue was reacted with 1.0 ml of *N,O*-bis(trimethylsilyl)acetamide, and the mixture was refluxed in a tightly capped vial for 30 min in a sand bath until a clear solution was observed. This solution was cooled and spotted on TLC plates to be developed in Solvent System 2. The distribution of activity on the chromatogram was reconstructed by liquid scintillation counting of silica gel fractions scraped from consecutive 0.5-cm strips. Radioactivity was extracted from the detected bands, purified, and subjected to GLC–mass spectrometric analysis.

Urine samples (50–100 μl) were assayed daily for radioactivity by γ-counting. Radioactivity distributions of unmetabolized [$^{125}$I]-4-iodobiphenyl, their hydroxylated metabolites, and the conjugates were estimated after TLC in Solvent System 1. Values for II and III and their glucuronide and sulfate conjugates were confirmed after hydrolysis by reverse isotopic dilution.

Enzymatic hydrolysis was done on 2.0-ml samples of urine, which had been dried under a gentle nitrogen stream. To the residue were added 1.0 ml of pH 7.4 phosphate buffer and 0.1 ml of β-glucuronidase–arylsulfatase[4] (*Helix pomatia*) or β-glucuronidase[4] (bovine liver). The mixture was incubated in a constant-temperature water bath at 37° for 48–72 hr with constant shaking. The hydrolysis was stopped by heating in a steam bath for 5 min, and the protein was removed by centrifugation. The supernate was spotted on TLC plates and developed in Solvent System 1.

The urinary polar fractions, which failed to be hydrolyzed by enzymes, were methylated by dimethylformamide dimethylacetal (7) and quantitated by TLC in Solvent System 2 after derivatization.

The radioactivity of inorganic iodide in the urine was estimated by paper (8) and resin paper (9) chromatography in Solvent Systems 3 and 4, respectively. These values were confirmed by lead iodide reverse isotopic dilution and methyl iodide exchange experiments (9).

## RESULTS

**Tissue Distribution**—Typical tissue radioactivities of iodine 125 for the organ examined are listed in Table I. At all times, the thyroid gland had the highest activity. After 24 hr, there was minor but consistent uptake of radioactivity by fatty tissue as compared to blood levels. Pretreatment of rats with Lugol's iodide solution daily for 2 days prior to administration of [$^{125}$I]-4-iodobiphenyl suppressed thyroid uptake by 90%. This competitive thyroid uptake experiment indicated that the thyroid activity was due to metabolically liberated inorganic iodide.

**Balance Studies**—The excretion of radioactivity in feces and urine for three rats was followed for 18 days, with an average total fecal excretion of 57.6% of the administered dose and an average total urinary excretion of 41.2%. In both cases, most radioactivity was eliminated in the first 6 days.

**Fecal Metabolites**—Methanol extraction of powdered dry feces indicated that 96.7% of feces activity could be extracted by this method. Chromatographic analysis of the concentrated feces methanol extract on TLC plates in Solvent System 1 gave rise to four radioactive bands with $R_f$ values at 0.00, 0.21, 0.38 and 0.64. They were labeled $F_A$, $F_B$, $F_C$, and $F_D$ and found to possess 20.9, 26.4, 8.4, and 2.4% of the radioactivity of the original dose, respectively. Each radioactive band was scraped off the plate, extracted, and subjected to further analysis.

A radioactive band from the condensed hexane extract of $F_D$ cochromatographed with 4-iodobiphenyl (I) at $R_f$ 0.64 (System 1) and 0.62 (System 2) and corresponded to I by GLC–mass spectrometry after separation on a 5% OV-1 column. Reverse isotopic dilution with I indicated 3.8% of the fecal methanol extract (2.2% of the injected dose) was due to unmetabolized [$^{125}$I]-4-iodobiphenyl, a value in agreement with the 2.4% found for band $F_D$.

Radioactive band $F_C$ was extracted with chloroform. When this extract was cochromatographed with 2-hydroxy-4′-iodobiphenyl (III), a radioactive spot corresponding to a UV-quenching spot was obtained at $R_f$ 0.38 in System 1 and at $R_f$ 0.50 in System 2. GLC–mass spectrometric analysis of the $F_C$ chloroform extract, similar to that described for $F_D$, resulted in a mass spectral fragmentation pattern consistent with III: *m/z* (relative intensity) 297 (16%), 296 (100), 170 (6.0), 169 (13), 168 (13), 141 (52), and 115 (42).

When reverse isotopic dilution experiments of the fecal methanol extract were done with III, only 2.6% of the injected dose activity could be identified as III. Based on the similarity of the mass spectrum of band $F_C$ to the spectra of both references II and III, band $F_C$ probably contained other hydroxylated metabolites in addition to III. The reverse isotopic dilution results compared to the TLC results indicate that the 2-hydroxy isomer (III) is about a third of band $F_C$ (Table II).

Cochromatography of an extract of radioactive band $F_B$ with 4-hydroxy-4′-iodobiphenyl (II) gave radioactive spots with $R_f$ values of 0.21 in System 1 and 0.28 in System 2, which corresponded to the reference material. GLC–mass spectrometric analysis of band $F_B$ was also consistent with that of II: *m/z* (relative intensity) 297 (15.4), 296 (100), 267 (2.3), 169 (10.8), 168 (10), 152 (3.8), 151 (3.8), 148 (5.4), 141 (20.8), 139 (18.5), and 115 (18.5). Reverse isotopic dilution experiments with II on the fecal methanol extract indicated that 21.9% of the dose activity was converted to II in the feces.

On the basis of TLC Systems 1 and 2, band $F_A$, which consistently remained at the origin, contains highly polar metabolites such as sulfates, glucuronides, and mercapturic acid derivatives.

Repeated attempts to hydrolyze band $F_A$ materials with acid, base, and β-glucuronidase–arylsulfatase enzymes failed to create new radioactive TLC bands of higher $R_f$ values in either System 1 or 2. Derivatization of $F_A$ materials finally led to the formation of a product with *N,O*-bis(trimethylsilyl)acetamide. Upon chromatography of this product, a radioactive band at $R_f$ 0.81 in System 2 was obtained, and it was estimated that about half of the original $F_A$ materials had reacted (9.8% of the injected dose). Efforts to elucidate the structure of this $F_A$ derivative by GLC–mass spectrometry were not successful.

**Urinary Metabolites**—Analysis of the urinary metabolites started with cochromatography of the urine with fecal methanol extracts in Solvent System 1. This chromatogram indicated that most of the urinary metabolite activity (~32.0% of the injected dose) lay under the origin

**Table I—Tissue Distribution of Radioactivity after Intraperitoneal Administration of [$^{125}$I]-4-Iodobiphenyl (55 μCi/0.5 ml of Injection) to Rats**

| Tissue | Radioactivity, cpm/mg | | | | | |
|---|---|---|---|---|---|---|
| | 3 hr | 6 hr | 24 hr | 48 hr | 72 hr | 96 hr |
| Thyroid | 79 | 63 | 2426[a] | 5377 | 7255 | 3025 |
| Fat | 4 | 17 | 96 | 78 | 59 | 53 |
| Pituitary | 10 | 17 | 53 | 25 | 47 | 17 |
| Adrenals | 8 | 13 | 30 | 19 | 22 | 13 |
| Kidneys | 22 | 11 | 11 | 15 | 21 | 14 |
| Ovaries | 6 | 8 | 22 | 13 | 23 | 9 |
| Intestine | 3 | 17 | 42 | 10 | 23 | 14 |
| Liver | 46 | 9 | 14 | 10 | 20 | 12 |
| Vagina | 2 | 5 | 23 | 7 | 15 | 6 |
| Uterus | 2 | 6 | 48 | 11 | 12 | 7 |
| Blood | 39 | 10 | 23 | 9 | 19 | 5 |
| Lungs | 9 | 5 | 10 | 6 | 10 | 6 |
| Brain | 3 | 4 | 4 | 4 | 3 | 3 |
| Muscle | 1 | 2 | 15 | 3 | 6 | 3 |
| Spleen | 39 | 3 | 6 | 3 | 5 | 3 |

[a] In separate experiments, in which rats were pretreated with Lugol's solution prior to administration of 3.9 μCi of [$^{125}$I]-4-iodobiphenyl, 24-hr thyroid activities were 9.7 and 21.6 cpm/mg. These values were compared to 137.4, 199.2, and 258.9 cpm/mg for nonpretreated rats at the same dose of I.

[4] Sigma Chemical Co.

**Table II—4-Iodobiphenyl and Metabolites Expressed as Percent of Dose**

| Compound | Feces | | Urine | |
|---|---|---|---|---|
| | TLC[a] | RID[b] | TLC | RID |
| 4-Iodobiphenyl (I) | 2.4[c] (1.8–2.8)[e] | 2.2 (2.11–2.26) | None detected | —[d] |
| 4-Hydroxy-4′-iodobiphenyl (II) | 26.4 (24.0–27.2) | 21.9 (21.3–22.5) | 4.9 (4.0–5.4) | — |
| Total other monohydroxy iodobiphenyls | 8.4 (7.0–9.2) | — | 1.6 (1.2–1.8) | — |
| 2-Hydroxy-4′-iodobiphenyl (III) | — | 2.6 (2.53–2.63) | — | — |
| II β-glucuronide or sulfate | None detected | — | 18.2 (16.1–19.8) | 17.7 (17.2–18.3) |
| Total other monohydroxy iodobiphenyl β-glucuronide or sulfate | None detected | — | 6.4 (5.9–7.5) | — |
| III β-glucuronide or sulfate | None detected | — | — | 1.9 (1.82–1.93) |
| Methylated urinary polar metabolites | — | — | 3.0 (1.6–4.0) | — |
| Silylated fecal polar metabolites | 10.3 (8.0–13.7) | — | — | — |
| Inorganic iodide | — | — | 7.3[f] (6.91–7.87) | 8.2[g] (8.10–8.26) |

[a] TLC values are averages of data from three rats. [b] Reverse isotopic dilution values. [c] Numerical values are expressed as percentage of administered dose. [d] Not determined. [e] Numbers in parentheses express the range of values. [f] Determined by resin paper chromatography (Ref. 9). [g] Determined by lead iodide reverse isotopic dilution method (Ref. 9).

band, representing highly polar materials. Only 4.9% of the dose activity could be accounted for in the urine as free phenolic II, and an additional 1.6% was III. No unmetabolized I could be detected in urine.

To determine if any glucuronide or sulfate conjugates were present in the urinary polar fraction, the polar fraction at the origin was extracted with methanol, dried, and hydrolyzed in buffer solution with β-glucuronidase–arylsulfatase enzyme (*Helix pomatia*). TLC of the hydrolyzed products in System 1 showed that 18.2 and 6.4% of the injected dose in the urinary polar fraction corresponded in $R_f$ to II and III, respectively. Thus, in the urine, a total of 23.1% of the dose activity could be accounted for as II and its glucuronide or sulfate conjugates. Similarly, 8.0% of the dose activity was transformed into metabolites corresponding in $R_f$ to III and its conjugates.

Confirmation of the TLC-derived quantitation of the two free phenolic metabolites was sought by two separate reverse isotopic dilution experiments using the urinary polar radioactive fraction that had been hydrolyzed enzymatically. Compounds II and III were used as the reference compounds. Based on these results, it was calculated that II accounted for 17.7% (18.2% by TLC) and III accounted for 1.9% (TLC indicated 6.4%) of the original dose. The remaining 4.5% was speculated to be due to other monohydroxy iodobiphenyls in a manner similar to the corresponding fecal metabolite band.

Differentiation between glucuronide and sulfate conjugates of the phenolic metabolites was made by independent enzyme hydrolysis of the urinary polar fraction methanolic extracts by β-glucuronidase–arylsulfatase from *Helix pomatia versus* bovine β-glucuronidase. Comparisons by TLC indicated that of the 18.2% of II released by enzyme hydrolysis, 16.1% was from sulfate conjugates while only 2.2% was due to glucuronide conjugates. Similarly, of the 6.4% released as material cochromatographing with III, 5.1% was from sulfate and only 1.3% was from glucuronide conjugates.

Treatment of the polar band left at the origin after enzyme hydrolysis with dimethylformamide dimethylacetal revealed that about half (3.1% of dose) of the activity could react. The product, when chromatographed in System 1, showed a radioactive band at $R_f$ 0.70. When chromatographed in System 2, this band appeared at $R_f$ 0.60. Due to the minute quantity that could be isolated from this radioactive band, attempted GLC–mass spectrometric analyses to characterize its structure were not successful.

The various metabolites of I found in the rat feces and urine are summarized in Table II, together with their relative percentages of the administered dose.

## DISCUSSION

While biotransformations of 4-iodobiphenyl (I) have not been reported previously, those of 4-chlorobiphenyls have been studied extensively (10–14). Results of the present study agree with the literature in that hydroxylation at the *para*-position and subsequent partial conjugation are the major metabolic pathways.

No hydroxylation at position 2′ was found for a number of animal species administered 4-chlorobiphenyl (10–14). However, the present finding of hydroxylation at this position for iodobiphenyl agrees with such transformation of biphenyl *per se* (15–18).

The presence of metabolites hydroxylated at positions 2′ and 4′ of I is consistent with the formation of 2′,3′- and of 3′,4′-arene oxide intermediates of I in the initial biotransformation of this compound. The reaction product of the urinary polar fraction after enzyme hydrolysis and subsequent reaction with dimethylformamide dimethylacetal was speculated to be a methyl derivative of a mercapturic acid metabolite of I. A mercapturic acid metabolite would be a logical arene oxide derivative, and the electron-withdrawing effect of the attached iodophenyl moiety would stabilize the arene oxide which, in turn, would allow more time for glutathione conjugation (19). The findings of West *et al.* (20), who reported isolation of *N*-acetyl-*S*-biphenyl-L-cysteine from rat urine after dosing with biphenyl, support such conjugation. Also supporting this conjugation is the work of Wood and his associates (21, 22) who were able to isolate [$^{131}$I]-4-iodophenylmercapturic acid after oral administration of [$^{131}$I]iodobenzene to rats.

The fecal polar fraction resisted hydrolysis, indicating the absence of glucuronide or sulfate metabolites, but it reacted with *N,O*-bis(trimethylsilyl)acetamide. This fraction also could contain mercapturic acid conjugates or their precursors.

Even though no deiodination was detected in metabolic studies of 4,4′-diiodobiphenyl in rabbits (23), results from the present studies indicated that a substantial amount of inorganic iodide could be found from the metabolism of I in rats. The absence of dehalogenation by rabbits also was pointed out by Block and Cornish (10) in their studies of 4-chlorobiphenyl. Thus, a species difference in dehalogenation of biphenyl compounds may be indicated.

## REFERENCES


(1) H.-J. Herms and V. Taenzer, in "Drug Design, Vol. VI," E. J. Ariens, Ed., Academic, New York, N.Y., 1975, p. 262.

(2) R. E. Counsell and R. Ice, in *ibid.*, p. 171.

(3) J. E. Sinsheimer, T. Wang, S. Röder, and Y. Y. Shum, *Biochem. Biophys. Res. Commun.*, **83**, 281 (1978).

(4) H. R. Schmidt, C. M. Savoy, and J. L. Abernethy, *J. Am. Chem. Soc.*, **66**, 491 (1944).

(5) M. Oki and H. Iwamura, *Bull. Chem. Soc. Jpn.*, **34**, 1395 (1961).

(6) L. G. Dring, R. L. Smith, and R. T. Williams, *Biochem. J.*, **116**, 425 (1970).

(7) J. P. Thenot and E. C. Horning, *Anal. Lett.*, **5**, 519 (1972).

(8) R. Grasbeck, B. A. Lamberg, and F. Bjorksten, *Acta Endocrinol.*, **34**, 113 (1960).

(9) Y. Y. Shum and J. E. Sinsheimer, *J. Pharm. Sci.*, **68**, 258 (1979).

(10) W. D. Block and H. H. Cornish, *J. Biol. Chem.*, **234**, 3301

(1959).
(11) S. Safe, O. Hutzinger, and D. Ecobichon, *Experientia*, **30**, 720 (1974).
(12) S. Safe, O. Hutzinger, and D. Jones, *J. Agric. Food Chem.*, **23**, 851 (1975).
(13) O. Hutzinger, D. M. Nash, S. Safe, A. S. W. DeFreitas, R. J. Norstrom, D. J. Wildish, and V. Zitko, *Science*, **178**, 312 (1972).
(14) S. Safe, N. Platonow, and O. Hutzinger, *J. Agric. Food Chem.*, **23**, 259 (1975).
(15) P. J. Creaven, D. V. Parke, and R. T. Williams, *Biochem. J.*, **96**, 879 (1965).
(16) R. Ammon, H. Berninger, and I. Berninger, *Qual. Plant. Mater. Veg.*, **16**, 263 (1968).
(17) H. Berninger, R. Ammon, and I. Berninger, *Arzneim.-Forsch.*, **18**, 880 (1968).
(18) P. Raig and R. Ammon, *ibid.*, **20**, 1266 (1970).
(19) D. M. Jerina, *Lloydia*, **37**, 212 (1974).
(20) H. D. West, J. R. Lawson, I. H. Miller, and G. R. Mathura, *Arch. Biochem. Biophys.*, **60**, 14 (1956).
(21) G. C. Mills and J. L. Wood, *J. Biol. Chem.*, **219**, 1 (1956).
(22) M. M. Barnes, S. P. James, and P. B. Wood, *Biochem. J.*, **71**, 680 (1959).
(23) S. Safe, D. Jones, and O. Hutzinger, *J. Chem. Soc., Perkin Trans. I*, **4**, 357 (1976).

# Optical Studies on Interaction of Biliary Contrast Agents with Native and Modified Human Serum Albumin

**K. J. FEHSKE and W. E. MÜLLER ˣ**

Received July 24, 1980, from the *Pharmakologisches Institut der Universität Mainz, D-6500 Mainz, West Germany.* Accepted for publication October 24, 1980.

**Abstract** □ The interaction of two homologous series of biliary contrast agents with native human and bovine serum albumin and with modified human serum albumin was investigated using circular dichroism and equilibrium dialysis. For most derivatives, extrinsic Cotton effects were observed for the interaction with both albumins. In some cases, these effects were strongly affected by only small changes in the chemical structure of the drugs. These large differences in extrinsic Cotton effects can be explained by definite effects of the chemical structures on the binding site selectivity of some drugs. For example, iopodate preferentially binds to the warfarin binding site of human serum albumin, while an ethyl group into the propionic acid side chain reduces the affinity for the warfarin site but strongly increases the affinity for the diazepam binding site of human serum albumin.

**Keyphrases** □ Biliary contrast agents—interaction with native and modified human serum albumin, optical studies on warfarin and diazepam binding sites of albumin □ Albumin, human serum—interaction of biliary contrast agents with native and modified albumin, optical studies of warfarin and diazepam binding sites □ Binding sites—warfarin and diazepam binding sites on human serum albumin molecule, interaction of biliary contrast agents with albumin □ Structure–activity relationships—interaction of biliary contrast agents with native and modified human serum albumin, optical studies of warfarin and diazepam binding sites

Contrast agents for the intravenous or oral visualization of the biliary tract are, in general, highly bound to albumin in the blood of humans and laboratory animals (1). Because of their strong binding to albumin, their low lipophilicity, and their low volumes of distribution, plasma protein binding of biliary contrast agents seems to be an important determinant of the pharmacokinetics of these drugs (2, 3). Furthermore, since the toxicity of the biliary contrast agents increases with increasing plasma protein binding, binding mechanisms leading to high albumin binding and high toxicity may have similarities (1, 4).

Therefore, detailed knowledge of the degree of albumin binding of the biliary contrast agents and of the binding mechanisms is of great interest. Thus, it must be determined which moieties of the contrast medium molecules are important for high binding and to which sites of the human serum albumin molecule the substances are bound. While some quantitative data on affinity constants and numbers of binding sites for two groups of homologous biliary contrast agents were published previously (5), this study describes qualitatively their interaction with human serum albumin, using optical methods and modified albumin derivatives.

## EXPERIMENTAL

**Materials**[1]—The human serum albumin[2] had an electrophoretic purity of 100%. All other chemicals were obtained from commercial suppliers.

**Preparation of Albumin Derivatives**—The modification of human serum albumin with 2-hydroxy-5-nitrobenzyl bromide (XII·Br) was reported in detail elsewhere (6). Human serum albumin was dissolved in 10 *M* urea adjusted to pH 4.4 by acetic acid, and a 1100-fold molar excess of XII·Br was added (XII–albumin). Another albumin sample was treated similarly but without the reagent and was called urea–albumin (control). Albumin modified with *o*-nitrophenylsulfenyl chloride (XIII·Cl) was prepared with a 22-fold molar excess of the reagent in 20% acetic acid (7) to yield XIII–albumin. With both reagents, the lone tryptophan residue of human serum albumin was modified completely (7).

For the preparation of tetranitromethane- (XIV) modified human serum albumin derivatives (XIV–albumin), a 4-, 15-, or 64-fold molar excess of tetranitromethane was added to human serum albumin dissolved in 0.05 *M* tromethamine buffer and adjusted to pH 8.0, resulting in the modification of 2.2, 5.1, or 7.8 tyrosine residues per albumin molecule, respectively. The modification was described in detail elsewhere (7).

The degree of tryptophan and tyrosine residue modification of the albumin derivatives was determined spectrophotometrically and by amino acid analysis (6, 7).

**Circular Dichroism Measurements**—Circular dichroism measurements were performed with a spectropolarimeter[3] calibrated with *d*-camphorsulfonic acid. All solutions were prepared in 67 m*M* phosphate buffer (pH 7.4). Results are expressed as molar ellipticities $[\theta]$ (degree square centimeter per decimole), calculated with reference to the albumin concentration, using a molecular weight of 69,000. The optical path length was 10 mm, and the albumin concentration was 30 or 13.1 $\mu M$. Difference spectra were obtained by subtracting the effect of the corresponding albumin derivative as the blank.

**Equilibrium Dialysis Experiments**—The binding of the $^{125}$I-labeled

[1] Biliary contrast agents were the gifts of Dr. U. Speck (Schering AG, Berlin), except iopanoic and iophenoxic acids, which were gifts of Dr. G. H. Mudge (Dartmouth Medical School).
[2] Behringwerke, Marburg, West Germany.
[3] Cary 61.

0022-3549/81/0500-0549$01.00/0
© 1981, American Pharmaceutical Association

(1959).
(11) S. Safe, O. Hutzinger, and D. Ecobichon, *Experientia*, **30**, 720 (1974).
(12) S. Safe, O. Hutzinger, and D. Jones, *J. Agric. Food Chem.*, **23**, 851 (1975).
(13) O. Hutzinger, D. M. Nash, S. Safe, A. S. W. DeFreitas, R. J. Norstrom, D. J. Wildish, and V. Zitko, *Science*, **178**, 312 (1972).
(14) S. Safe, N. Platonow, and O. Hutzinger, *J. Agric. Food Chem.*, **23**, 259 (1975).
(15) P. J. Creaven, D. V. Parke, and R. T. Williams, *Biochem. J.*, **96**, 879 (1965).
(16) R. Ammon, H. Berninger, and I. Berninger, *Qual. Plant. Mater. Veg.*, **16**, 263 (1968).
(17) H. Berninger, R. Ammon, and I. Berninger, *Arzneim.-Forsch.*, **18**, 880 (1968).
(18) P. Raig and R. Ammon, *ibid.*, **20**, 1266 (1970).
(19) D. M. Jerina, *Lloydia*, **37**, 212 (1974).
(20) H. D. West, J. R. Lawson, I. H. Miller, and G. R. Mathura, *Arch. Biochem. Biophys.*, **60**, 14 (1956).
(21) G. C. Mills and J. L. Wood, *J. Biol. Chem.*, **219**, 1 (1956).
(22) M. M. Barnes, S. P. James, and P. B. Wood, *Biochem. J.*, **71**, 680 (1959).
(23) S. Safe, D. Jones, and O. Hutzinger, *J. Chem. Soc., Perkin Trans. I*, **4**, 357 (1976).

# Optical Studies on Interaction of Biliary Contrast Agents with Native and Modified Human Serum Albumin

**K. J. FEHSKE and W. E. MÜLLER ˣ**

Received July 24, 1980, from the *Pharmakologisches Institut der Universität Mainz, D-6500 Mainz, West Germany.* Accepted for publication October 24, 1980.

**Abstract** □ The interaction of two homologous series of biliary contrast agents with native human and bovine serum albumin and with modified human serum albumin was investigated using circular dichroism and equilibrium dialysis. For most derivatives, extrinsic Cotton effects were observed for the interaction with both albumins. In some cases, these effects were strongly affected by only small changes in the chemical structure of the drugs. These large differences in extrinsic Cotton effects can be explained by definite effects of the chemical structures on the binding site selectivity of some drugs. For example, iopodate preferentially binds to the warfarin binding site of human serum albumin, while an ethyl group into the propionic acid side chain reduces the affinity for the warfarin site but strongly increases the affinity for the diazepam binding site of human serum albumin.

**Keyphrases** □ Biliary contrast agents—interaction with native and modified human serum albumin, optical studies on warfarin and diazepam binding sites of albumin □ Albumin, human serum—interaction of biliary contrast agents with native and modified albumin, optical studies of warfarin and diazepam binding sites □ Binding sites—warfarin and diazepam binding sites on human serum albumin molecule, interaction of biliary contrast agents with albumin □ Structure–activity relationships—interaction of biliary contrast agents with native and modified human serum albumin, optical studies of warfarin and diazepam binding sites

Contrast agents for the intravenous or oral visualization of the biliary tract are, in general, highly bound to albumin in the blood of humans and laboratory animals (1). Because of their strong binding to albumin, their low lipophilicity, and their low volumes of distribution, plasma protein binding of biliary contrast agents seems to be an important determinant of the pharmacokinetics of these drugs (2, 3). Furthermore, since the toxicity of the biliary contrast agents increases with increasing plasma protein binding, binding mechanisms leading to high albumin binding and high toxicity may have similarities (1, 4).

Therefore, detailed knowledge of the degree of albumin binding of the biliary contrast agents and of the binding mechanisms is of great interest. Thus, it must be determined which moieties of the contrast medium molecules are important for high binding and to which sites of the human serum albumin molecule the substances are bound. While some quantitative data on affinity constants and numbers of binding sites for two groups of homologous biliary contrast agents were published previously (5), this study describes qualitatively their interaction with human serum albumin, using optical methods and modified albumin derivatives.

## EXPERIMENTAL

**Materials**[1]—The human serum albumin[2] had an electrophoretic purity of 100%. All other chemicals were obtained from commercial suppliers.

**Preparation of Albumin Derivatives**—The modification of human serum albumin with 2-hydroxy-5-nitrobenzyl bromide (XII·Br) was reported in detail elsewhere (6). Human serum albumin was dissolved in 10 *M* urea adjusted to pH 4.4 by acetic acid, and a 1100-fold molar excess of XII·Br was added (XII–albumin). Another albumin sample was treated similarly but without the reagent and was called urea–albumin (control). Albumin modified with *o*-nitrophenylsulfenyl chloride (XIII·Cl) was prepared with a 22-fold molar excess of the reagent in 20% acetic acid (7) to yield XIII–albumin. With both reagents, the lone tryptophan residue of human serum albumin was modified completely (7).

For the preparation of tetranitromethane- (XIV) modified human serum albumin derivatives (XIV–albumin), a 4-, 15-, or 64-fold molar excess of tetranitromethane was added to human serum albumin dissolved in 0.05 *M* tromethamine buffer and adjusted to pH 8.0, resulting in the modification of 2.2, 5.1, or 7.8 tyrosine residues per albumin molecule, respectively. The modification was described in detail elsewhere (7).

The degree of tryptophan and tyrosine residue modification of the albumin derivatives was determined spectrophotometrically and by amino acid analysis (6, 7).

**Circular Dichroism Measurements**—Circular dichroism measurements were performed with a spectropolarimeter[3] calibrated with *d*-camphorsulfonic acid. All solutions were prepared in 67 m*M* phosphate buffer (pH 7.4). Results are expressed as molar ellipticities $[\theta]$ (degree square centimeter per decimole), calculated with reference to the albumin concentration, using a molecular weight of 69,000. The optical path length was 10 mm, and the albumin concentration was 30 or 13.1 $\mu M$. Difference spectra were obtained by subtracting the effect of the corresponding albumin derivative as the blank.

**Equilibrium Dialysis Experiments**—The binding of the $^{125}$I-labeled

[1] Biliary contrast agents were the gifts of Dr. U. Speck (Schering AG, Berlin), except iopanoic and iophenoxic acids, which were gifts of Dr. G. H. Mudge (Dartmouth Medical School).
[2] Behringwerke, Marburg, West Germany.
[3] Cary 61.

0022-3549/81/0500-0549$01.00/0
© 1981, American Pharmaceutical Association

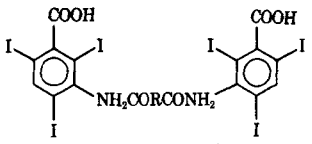


**Table I—Structural Requirements for the Generation of Extrinsic Cotton Effects: Intravenous Biliary Contrast Agents** [a]

| Compound | R | Human Serum Albumin $\lambda_{max}$, nm | Human Serum Albumin $[\theta] \times 10^{-4}$ [b] | Bovine Serum Albumin $\lambda_{max}$, nm | Bovine Serum Albumin $[\theta] \times 10^{-4}$ [b] |
|---|---|---|---|---|---|
| I (iodipamide) | $(CH_2)_4$ | 310 | +0.44 ± 0.02 | — | — |
| | | 285 | −0.70 ± 0.03 | | |
| | | 270 | −0.97 ± 0.02 | | |
| II (ioglycamide) | $CH_2OCH_2$ | 270 | −1.32 ± 0.06 | — | — |
| III | $(CH_2OCH_2)_2$ | 295 | −0.20 ± 0.03 | 260 | +1.45 ± 0.08 |
| IV (iotroxamide) | $(CH_2OCH_2)_3$ | 280 | +0.37 ± 0.06 | 315 | −0.45 ± 0.05 |
| | | | | 280 | +1.12 ± 0.07 |
| V (iodoxamide) | $CH_2—(CH_2OCH_2)_4—CH_2$ | 280 | −0.49 ± 0.05 | 290 | −0.38 ± 0.08 |
| | | | | 260 | +2.48 ± 0.12 |

[a] Extrinsic Cotton effects are given as molar ellipticities ($[\theta]$), calculated with reference to the concentration of drug bound at the wavelength of the induced circular dichroism maximum ($\lambda_{max}$). All data are difference values, using the Cotton effects of human or bovine serum albumin at the same wavelength as the blank. Albumin concentrations of 30 $\mu M$ and drug concentrations of 60 $\mu M$ were used. [b] $\bar{x} \pm s_{\bar{x}}$ = mean ± *SEM*; $n = 6$.

biliary contrast agents, [$^{14}$C]warfarin, and [$^{14}$C]diazepam to the albumin derivatives was determined by equilibrium dialysis using an albumin concentration of 36 $\mu M$ and varying concentrations of the contrast agents. All solutions were prepared with 67 m$M$ phosphate buffer (pH 7.4). The albumin solution (0.9 ml) was dialyzed for 16 hr at 25° in the dark against the buffer (0.9 ml) containing the labeled drugs. Dialysis cells (1 ml) and cellophane dialysis membranes[4] were used. The radioactivity on both sides of the membrane was determined by liquid scintillation spectrometry.

## RESULTS

**Interaction with Native Human and Bovine Serum Albumin**—The binding of most of the intravenous and oral biliary contrast agents to native human and bovine serum albumin significantly changed the circular dichroism spectra of the proteins between 250 and 350 nm (Fig. 1). Maxima and shoulders of the induced circular dichroism spectra correlated sufficiently with maxima and shoulders of the UV absorbance spectra of the ligands. Thus, the induced Cotton effects undoubtedly were extrinsic in origin and originated by binding-induced optical perturbations of electronic transitions of the contrast agent molecules.

The extrinsic Cotton effects of iodipamide (an example of the intravenous contrast agents) consisted of at least three Gaussian components (8), with a small positive band at ~310 nm, a larger negative one at 270 nm, and a shoulder at ~285 nm (Fig. 1). Increasing the length of the aliphatic bridge between both triiodobenzoic acid nuclei of the intravenous contrast agents significantly altered the induced Cotton effects (Table I). The weak band at 310 nm disappeared completely, while the strong band at ~270 nm was present in all intravenous contrast agents investigated, although great differences in the intensity and sign of this band were observed (Table I).

The intensity of the extrinsic Cotton effects depended on the concentration of the ligands, as shown for I (iodipamide) in Fig. 2, where the three extrinsic circular dichroism bands of I increased differently with increasing concentrations. The positive band at 310 nm seemed to be associated mainly with binding to the single high-affinity binding site (5) since this band increased only to about one molecule bound per molecule of human serum albumin (Fig. 2). The band at 270 nm also was generated at secondary binding sites. The induced Cotton effects at 285 nm seemed to be higher at the secondary sites than at the high-affinity binding site, as might be concluded from the shape of the curve in Fig. 2.

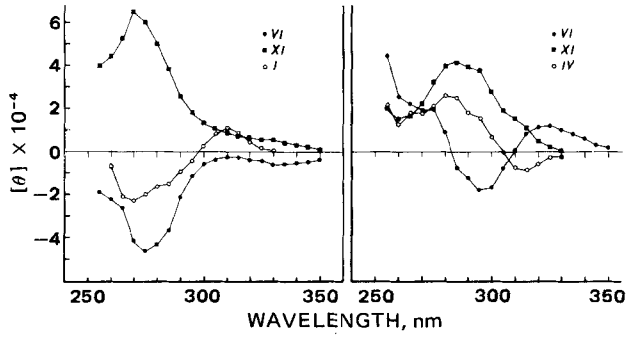


**Figure 1**—*Extrinsic Cotton effects of some biliary contrast agents (60 μM) in the presence of human (left) or bovine (right) serum albumin. The albumin concentration was 30 μM. The data are difference values, using the Cotton effects of the albumins at each wavelength as a blank. Each point represents the mean of three determinations.*

While I and II are bound to human serum albumin more strongly than III–V, I and II are bound less strongly to bovine serum albumin than the other three derivatives (5). Accordingly, only for the interaction of III–V with bovine serum albumin were induced Cotton effects found (Fig. 1 and Table I). The positions of the circular dichroism band were in agreement with those found in the interaction with human serum albumin (Table I).

As with the intravenous agents, the binding of the oral biliary contrast agents to human serum albumin induced extrinsic Cotton effects with a strong band at ~270 nm and a weak band above 300 nm (Fig. 1 and Table II). The band intensity at 270 nm differed little for the six compounds, but the sign of this band was highly dependent on the substitu-

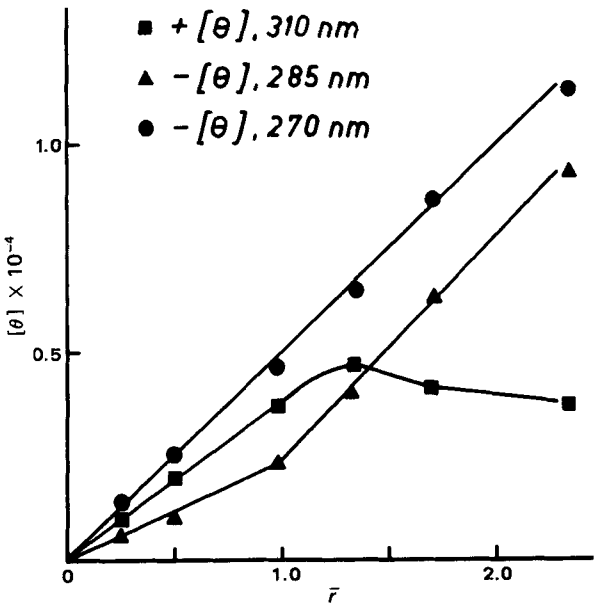


**Figure 2**—*Correlation between the concentration of I bound to human serum albumin (30 μM) and the intensity of the induced Cotton effects at three different maxima (given as molar ellipticity, [θ], calculated with reference to the albumin concentration). The concentration bound is given as r̄ (moles of I bound per mole of albumin). Each point represents the mean of six determinations.*

[4] Union Carbide.

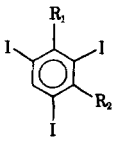

**Table II—Structural Requirements for the Generation of Extrinsic Cotton Effects: Oral Biliary Contrast Agents** [a]

| Compound | $R_1$ | $R_2$ | Human Serum Albumin $\lambda_{max}$, nm | Human Serum Albumin $[\theta] \times 10^{-4}$ [b] | Bovine Serum Albumin $\lambda_{max}$, nm | Bovine Serum Albumin $[\theta] \times 10^{-4}$ [b] |
|---|---|---|---|---|---|---|
| VI | $CH_2CH(C_2H_5)COOH$ | $N{=}CH{-}N(CH_3)_2$ | 330<br>275 | −0.13 ± 0.01<br>−1.85 ± 0.03 | 325<br>295<br>270 | +0.39 ± 0.01<br>−0.42 ± 0.06<br>+0.82 ± 0.08 |
| VII | $CH_2CH_2COOH$ | $N{=}C(CH_3){-}NHCH_3$ | 330<br>270 | +0.30 ± 0.02<br>+1.52 ± 0.12 | 305 | −0.07 ± 0.01 |
| VIII | $CH_2CH_2COOH$ | $N{=}C(CH_3){-}NH_2$ | 330<br>295<br>270* | +0.28 ± 0.01<br>−0.26 ± 0.02<br>+1.76 ± 0.16 | 300<br>260* | +0.33 ± 0.01<br>+1.19 ± 0.04 |
| IX | $CH_2CH_2COOH$ | $N{=}C(C_2H_5){-}NH_2$ | 295<br>270* | −0.60 ± 0.07<br>+1.36 ± 0.15 | 265* | +1.93 ± 0.04 |
| X | $CH_2CH(C_2H_5)COOH$ | $N{=}C(CH_3){-}NHC_2H_5$ | 270 | +1.07 ± 0.04 | 330<br>300<br>270 | +0.35 ± 0.01<br>−0.74 ± 0.00<br>+1.48 ± 0.00 |
| XI (iopodate) | $CH_2CH_2COOH$ | $N{=}CH{-}N(CH_3)_2$ | 270 | +2.43 ± 0.04 | 280 | +1.35 ± 0.03 |

[a] Extrinsic Cotton effects are given as molar ellipticities ($[\theta]$), calculated with reference to the concentration of drug bound at the wavelength of the induced circular dichroism maximum ($\lambda_{max}$) or shoulder (*). All data are difference values, using the Cotton effects of human or bovine serum albumin at the same wavelength as the blank. Albumin concentrations of 30 $\mu M$ and drug concentrations of 60 $\mu M$ were used. [b] $\bar{x} \pm s_{\bar{x}}$; $n = 6$.

ents of the triiodobenzene moiety (Table II). While this band was positive for VII and XI, the introduction of an ethyl group in the propionic acid side chain of XI made this band negative (VI in Table II). This dramatic effect was not found for the binding to bovine serum albumin since the band at 270 nm, if present, was positive for all compounds.

As found for the intravenous contrast agent I, the intensity of the extrinsic Cotton effects of the oral contrast agents depended on the ligand concentration. The induced optical activity of XI (iopodate) bound to human serum albumin increased only until the first molecule of XI was bound per albumin molecule but decreased at higher concentrations (Fig. 3). Again, the introduction of an ethyl group in XI was followed by a binding change to optically active binding sites, as shown by the increase of both bands of VI with increasing numbers of molecules bound per molecule of human serum albumin (Fig. 3).

**Optical Studies with Tryptophan- and Tyrosine-Modified Human Serum Albumin**—Previous studies labeled the specific warfarin binding site of human serum albumin by modification of the lone tryptophan residue with XII-Br or XIII-Cl (8). The highly reactive tyrosine residue is part of the indole and benzodiazepine binding site, which can be modified selectively with XIV (7). Accordingly, XII–albumin and XIV–albumin were used to investigate the significance of the warfarin and the diazepam binding sites for the interaction of the biliary contrast agents with human serum albumin. Since the tryptophan modification by XII-Br includes an unfolding of the protein in acidic urea solution, urea–albumin was used to measure the effect of the acidic unfolding on the binding of the compounds to human serum albumin.

The unfolding procedure only slightly changed the extrinsic Cotton effects of I, VI, and XI and those of iophenoxic acid and iopanoic acid, two oral biliary contrast agents that are structurally related to VI and XI (Table III). However, the tryptophan modification reduced the extrinsic Cotton effects of I and iophenoxic acid at both concentrations investigated by ~40–50%. The most striking observation was made for VI where the large negative band at 270 nm disappeared after the tryptophan modification and a small positive band appeared at ~260 nm (Fig. 4 and Table III). On the other hand, the extrinsic Cotton effects of XI and of iopanoic acid were not reduced by the tryptophan modification.

The modification of about two out of the 18 tyrosine residues of human serum albumin (XIV–albumin) had no influence on the extrinsic Cotton effects of I at 310 nm, while those at 270 nm were reduced to ~50% (Table IV). Furthermore, the extrinsic Cotton effects of iophenoxic acid were influenced only slightly by the modification of two tyrosine residues, but

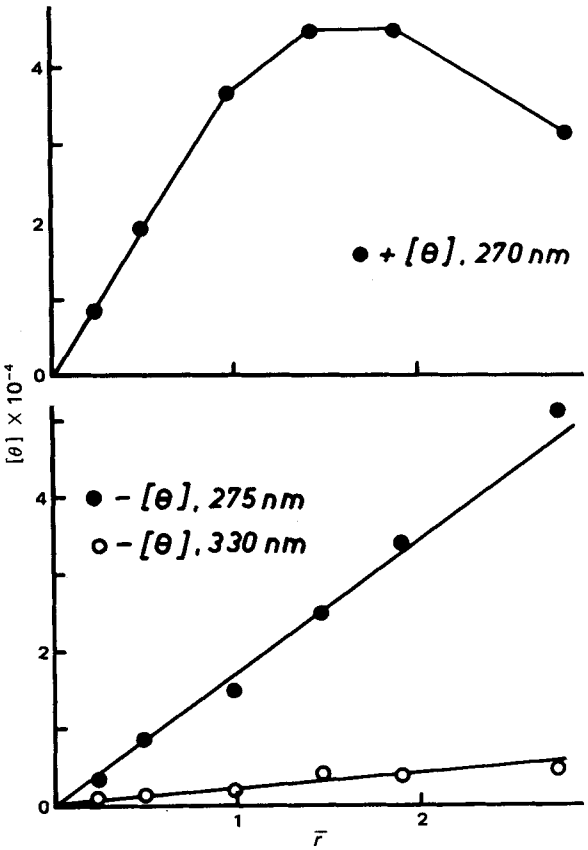


**Figure 3**—*Correlation between the concentration of XI (upper) and VI (lower) bound to human serum albumin (30 μM) and the intensity of the induced Cotton effects at different maxima (given as molar ellipticity, [θ], calculated with reference to the albumin concentration). The concentration bound is given as r̄ (moles of drug bound per mole of albumin). Each point represents the mean of six determinations.*

**Table III—Tryptophan and Tyrosine Modification of Human Serum Albumin: Influence of the Extrinsic Cotton Effects [a]**

| Drug | λ, nm | Drug/Protein, [M/M] | $[\theta] \times 10^{-3}, \bar{x} \pm s_{\bar{x}}$ Control ($n = 4$) | XIV-Albumin ($n = 4$) (%) | Urea-Albumin ($n = 3$) | XII-Albumin ($n = 6$) (%) |
|---|---|---|---|---|---|---|
| I | 310 | 1 | +8.9 ± 0.5 | +9.9 ± 0.2 (111) | +7.4 ± 0.3 | +3.8 ± 0.3 (51) |
| | 310 | 3 | +10.5 ± 0.3 | +12.0 ± 0.2 (114) | +11.3 ± 0.3 | +5.4 ± 0.3 (48) |
| | 270 | 1 | −5.7 ± 0.5 | −5.0 ± 0.6 (88) | −8.9 ± 0.8 | −6.5 ± 0.4 (73) |
| | 270 | 3 | −16.8 ± 1.1 | −8.9 ± 0.5 (53) | −17.2 ± 0.9 | −10.8 ± 0.3 (63) |
| VI | 275 | 1 | −9.6 ± 0.7 | −23.8 ± 0.4 (248) | −10.1 ± 0.4 | +4.2 ± 0.4 (−42) |
| | 275 | 3 | −34.8 ± 2.0 | −61.0 ± 0.8 (175) | −34.7 ± 1.0 | −2.7 ± 0.9 (8) |
| XI | 270 | 1 | +35.9 ± 0.8 | +1.1 ± 0.3 (3) | +35.8 ± 0.1 | +35.2 ± 0.6 (98) |
| | 270 | 3 | +41.7 ± 0.3 | −31.6 ± 0.8 (−76) | +25.3 ± 0.2 | +45.4 ± 0.6 (179) |
| Iophenoxate | 320 | 1 | −41.5 ± 0.4 | −27.6 ± 0.3 (67) | −41.8 ± 0.7 | −25.6 ± 0.3 (61) |
| | 320 | 3 | −34.9 ± 0.4 | −39.3 ± 0.6 (113) | −38.1 ± 0.8 | −27.3 ± 0.3 (72) |
| Iopanoate | 303 | 1 | −13.8 ± 0.3 | −4.1 ± 0.3 (30) | −12.5 ± 0.2 | −12.7 ± 0.3 (102) |
| | 303 | 3 | −5.6 ± 0.3 | −1.1 ± 0.3 (20) | −4.5 ± 0.4 | −9.8 ± 0.3 (218) |

[a] The molar ellipticities ($[\theta]$), calculated with reference to the albumin concentration, of various contrast agents bound to native (control) and tryptophan- (XII-albumin) and tyrosine- (XIV-albumin) modified human serum albumin, at the wavelength of their induced circular dichroism maxima (λ). Albumin concentrations of 13.1 μM were used with two different molar drug to albumin concentration ratios (D/P).

**Table IV—Binding of I (Iodipamide) and XI (Iopodate) to Tryptophan- and Tyrosine-Modified Human Serum Albumin [a]**

| | I | | | | XI | | | |
|---|---|---|---|---|---|---|---|---|
| | $n_1$ | $K_1 \times 10^{-4}$, $M^{-1}$ | $n_2$ | $K_2 \times 10^{-4}$, $M^{-1}$ | $n_1$ | $K_1 \times 10^{-4}$, $M^{-1}$ | $n_2$ | $K_2 \times 10^{-4}$, $M^{-1}$ |
| Control | 1.1 | 307 | 2.0 | 9 | 1.1 | 254 | 4.1 | 12 |
| Urea-albumin | 1.0 | 314 | 1.8 | 8 | 1.1 | 198 | 3.7 | 12 |
| XII-albumin | 0.8 | 71 | 1.8 | 6 | 1.0 | 167 | 4.0 | 6 |
| XIII-albumin | 0.8 | 61 | 2.1 | 6 | 1.2 | 313 | 3.8 | 11 |
| XIV-albumin | 0.8 | 228 | 1.9 | 6 | 0.9 | 60 | 3.9 | 13 |

[a] The binding of the two contrast agents to the human serum albumin derivatives (36 μM) was investigated by equilibrium dialysis. Curved Scatchard plots were resolved to obtain $n$ (number of binding sites) and $K$ (association constant) by a graphical method according to Pennock (9). For each individual Scatchard plot, 30–40 experiments at eight to 10 different concentrations of the drugs were performed.

those of iopanoic acid were strongly reduced at both ligand concentrations. However, the modification of only two tyrosine residues (XIV-albumin) had an interesting effect on the extrinsic Cotton effects of the structurally related compounds, VI and XI. While the negative Cotton effects of VI were increased by nearly 100% at both ligand concentrations (Fig. 4 and Table III), the positive band of XI disappeared at a molar drug to albumin ratio of one and became negative at higher drug to albumin ratios (Fig. 5 and Table III). Increasing the degree of tyrosine modification to 5.1 was followed by a reduction of the Cotton effects of VI and XI, and the Cotton effects of both contrast agents became positive again when 7.8 tyrosine residues were modified per molecule of albumin (Figs. 4 and 5).

**Equilibrium Dialysis Studies on Binding of I and XI to Native and Modified Human Serum Albumin**—As calculated from the curved Scatchard plot (Fig. 6) by the method of Pennock (9), I binds to native human serum albumin *via* one high-affinity and two low-affinity binding sites (Table IV). While the unfolding in acidic urea (urea-albumin) was nearly without effect on the binding of I, the modification of the lone tryptophan residue with XII-Cl as well as with XIII-Br strongly reduced the association constant of the high-affinity binding site for I (Fig. 6 and Table IV). The secondary binding sites remained nearly unaffected by the tryptophan modifications. The modification of about two tyrosine residues with XIV, on the other hand, had a significantly smaller effect on the high-affinity binding site of I than did the modification of the tryptophan residue. In all three modified albumin derivatives, the number of high-affinity binding sites was reduced from ~1.0 to ~0.7–0.82, possibly not an effect of the modification of a specific amino acid residue.

In contrast to I, neither tryptophan modification affected the high-affinity binding site of XI. The slightly reduced affinity found for XII-albumin also was found for urea-albumin and, therefore, may be an effect of unfolding during modification. Also in contrast to I, the tyrosine modification reduced the affinity of the high-affinity binding site up to ~25% of the value found for native albumin. Neither tryptophan nor the tyrosine modifications significantly changed the number of high-affinity

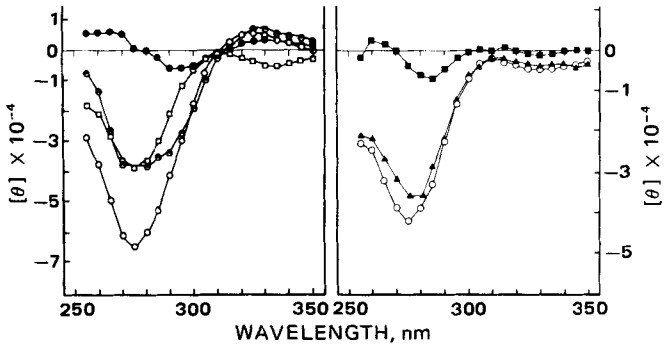


**Figure 4**—*Induced circular dichroism spectra of VI bound to human serum albumin and modified albumin derivatives (all were 13.1 μM). Intensity is given as molar ellipticity, [θ], calculated with respect to the albumin concentration. Compound VI was used at a molar drug to albumin ratio of 3. Data are difference values, using the Cotton effects of the albumin alone as a blank. Each point is the mean of three determinations. Key (left): □, native human serum albumin; ○, XIV-albumin (degree of modification 2.2); ◒, XIV-albumin (5.1); and ●, XIV-albumin (7.8). Key (right): ○, albumin; ▲, urea-albumin; and ■, XII-albumin.*

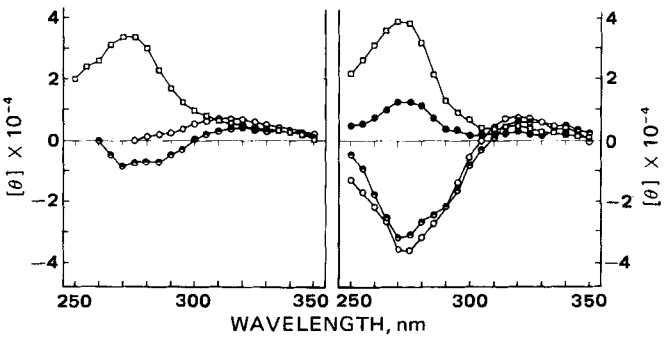


**Figure 5**—*Induced circular dichroism spectra of XI bound to human serum albumin and modified albumin derivatives (all were 13.1 μM). Intensity is given as molar ellipticity, [θ], calculated with respect to the albumin concentration. Compound XI was used at molar drug to albumin ratios of 1 (left) and 3 (right). Data are difference values, using the Cotton effects of the albumins alone as a blank. Each point is the mean of three determinations. Key: □, native human serum albumin; ○, XIV-albumin (degree of modification 2.2); ◒, XIV-albumin (5.1); and ●, XIV-albumin (7.8).*

Table V—Inhibition (Percent Displacement, $\bar{x} \pm s_{\bar{x}}$, $n = 3$) of Diazepam and Warfarin Binding to Human Serum Albumin by Biliary Contrast Agents [a]

| Displacer | Diazepam | | Warfarin | |
|---|---|---|---|---|
| | D/P 1.5 | D/P 4.5 | D/P 1.5 | D/P 4.5 |
| Iopanoic acid | 32.2 ± 1.0 | 38.2 ± 0.7 | 10.3 ± 0.6 | 46.6 ± 1.6 |
| Iophenoxic acid | 6.1 ± 0.9 | 26.9 ± 1.0 | 37.8 ± 0.6 | 78.7 ± 1.1 |
| I (iodipamide) | 1.8 ± 0.9 | 3.4 ± 1.0 | 23.1 ± 0.8 | 43.4 ± 1.5 |
| VI | 16.0 ± 1.0 | 36.2 ± 1.1 | 8.0 ± 1.4 | 29.0 ± 1.7 |
| XI (iopodate) | 7.1 ± 0.4 | 14.0 ± 0.2 | 7.0 ± 1.4 | 23.2 ± 1.0 |

[a] The inhibition of the binding of diazepam (40 $\mu M$) and of warfarin (72 $\mu M$) to human serum albumin was investigated by equilibrium dialysis, using the displacing drugs at two different molar drug to albumin concentration ratios (D/P). The data are given as percent displacement of the fraction bound under control conditions (diazepam = 84.9%; warfarin = 79.7%).

binding sites nor the properties of the secondary binding sites of XI (Table IV).

**Effect of Biliary Contrast Agents on Binding of Diazepam and Warfarin to Native Human Serum Albumin**—Only a few specific binding sites exist on the human serum albumin molecule, which mediate the high-affinity binding of most strongly albumin-bound drugs (10). Two of the most important are the warfarin and diazepam binding sites (10). To determine to which site the contrast agents are bound, displacement of the two specific ligands, warfarin and diazepam, was studied by equilibrium dialysis (Table V).

At low concentrations (drug to protein ratio of ~1), iopanoic acid preferentially bound to the diazepam site and iophenoxic acid bound to the warfarin site. At higher concentrations, both drugs seemed to bind to both binding sites.

By contrast, even at higher concentrations, I did not interfere with the diazepam binding site, as was demonstrated by its failure to displace diazepam. The high potency in displacing warfarin, however, suggests that the high-affinity binding site of I might be identical with the warfarin binding site.

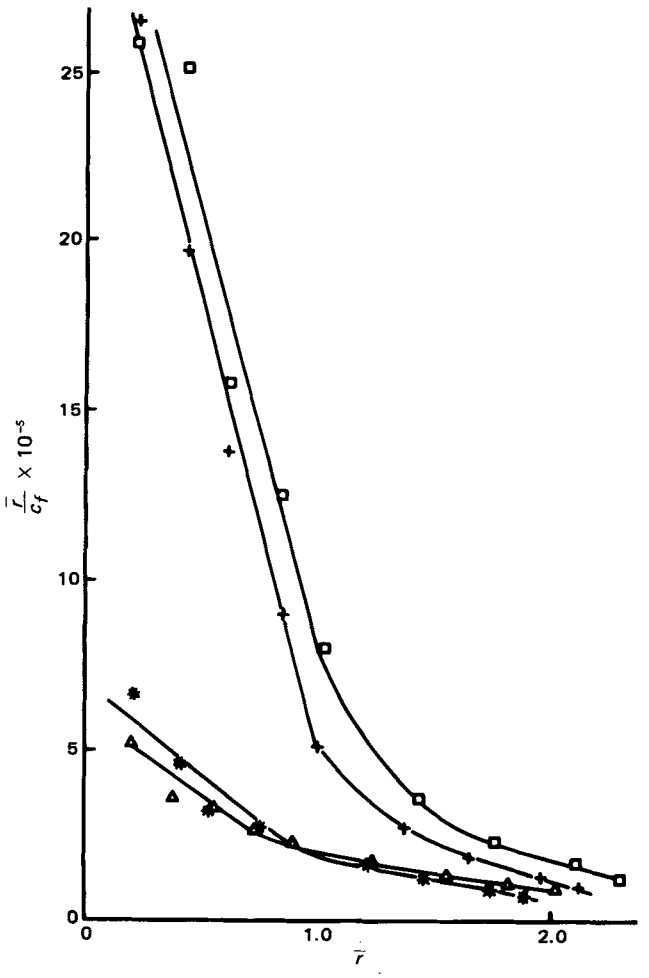


**Figure 6**—*Scatchard plot of the binding of I to human serum albumin and modified albumin derivatives. The albumin concentration was 36 μM. Each point is the mean of three or four determinations. Key: □, albumin; △, XIII-albumin; +, urea-albumin; and *, XII-albumin.*

Compounds VI and XI, which differ largely regarding their extrinsic Cotton effects in the presence of the modified albumin derivatives, seemed to bind to both sites. However, VI preferentially interacted with the diazepam site while XI had a higher affinity for the warfarin site, as suggested by their potencies in inhibiting the binding of diazepam and warfarin, respectively (Table V).

## DISCUSSION

The binding of optically inactive small organic molecules to optically active macromolecules can induce optical activity into the ligand molecule so that, within the range of the UV or visible absorption spectra of the ligands, induced Cotton effects can be observed (11, 12). Such induced circular dichroism spectra have proved to be extremely useful in gaining insight into the molecular mechanism of the interactions of drugs with serum albumins (7, 8, 11–13).

The induced circular dichroism spectra of the investigated intravenous biliary contrast agents, as far as induced optical activity was observed, had one component in common: an induced band around 270 nm whose sign and intensity varied for the compounds. This band might be due to optical perturbations of electronic transitions in the triiodobenzoic acid moieties of the compounds, the only common structure of the investigated intravenous biliary contrast agents. However, the structural parameters leading to high induced optical activity of the intravenous contrast agents are not obvious since neither the degree of albumin binding (5) nor the length or lipophilicity of the aliphatic bridge between both triiodobenzoic acid moieties seemed to be the major determinant for high induced optical activity.

In general, considering their extremely high binding to human serum albumin, the intravenous biliary contrast agents gave only weak extrinsic Cotton effects when bound to human serum albumin. This result and the failure to find any clear correlation between intensity of the extrinsic Cotton effects and their chemical structure may indicate that the complex between these compounds and human serum albumin lacks the structural specificity found for other drugs when bound to albumin (14–17).

As was found for the intravenous biliary contrast agents, all oral biliary contrast agents had a common induced circular dichroism band around 270 nm when bound to human or bovine serum albumin, possibly due to the triiodobenzene moiety of the drugs. With human serum albumin, the band intensity varied little for the oral compounds, suggesting a similar spatial relationship of their complexes with human serum albumin. For the binding of VI and XI to human serum albumin, their Cotton effects at 270 nm had opposite signs, even though the only difference in their chemical structure was the introduction of an ethyl group in position 2 of the propionic side chain (VI). This observation supports earlier findings on iophenoxic acid, indicating that the optical properties of the complexes of the oral biliary contrast agents are extremely sensitive to even small changes of the ligand chemical structure (18).

As already mentioned, the positive Cotton effects of XI seemed to be associated mainly with its high-affinity binding site, while the negative Cotton effects were induced at all binding sites of XI. Accordingly, only negative Cotton effects were observed after tyrosine modification, presumably induced at the secondary binding sites.

Previously it was shown that the lone tryptophan residue of human serum albumin is part of the warfarin binding site and can be selectively modified by XII-Br and XIII-Cl (8), while a highly reactive tyrosine residue, which can be nitrated selectively by low concentrations of XIV, is part of the indole and benzodiazepine binding site (7). Thus, the interaction of drugs with both specific binding sites of human serum albumin can be studied indirectly by displacement of the marker ligands, diazepam and warfarin, and directly by the binding of the drugs to the

modified albumin derivatives.

The results obtained with I give some evidence that the single high-affinity binding site of the intravenous biliary contrast agents (5) might be identical with the warfarin binding site of human serum albumin. This conclusion can be made from the strong displacement of bound warfarin, the large reduction of the extrinsic Cotton effects of I bound to XII–albumin at 310 nm that are associated only with binding to the high-affinity binding site, and the large reduction of the association constant of the high-affinity binding site for XII–albumin or XIII–albumin. By contrast, binding of I to the diazepam binding site may be negligible, as shown by the lack of any displacement of human serum albumin-bound diazepam and by the small effects of the tyrosine modification on the binding parameters of I.

With the oral biliary contrast agents, the specificity for one of the two sites of human serum albumin is not so pronounced. However, as revealed by their displacing potencies for diazepam and warfarin and their binding behavior for tyrosine- and tryptophan-modified albumin, VI is bound preferentially to the warfarin binding site but XI is bound to the diazepam binding site. This observation is interesting considering the small difference in the chemical structures of these contrast agents. A similar observation was made for the structurally related oral biliary contrast agents, iopanoic and iophenoxic acids, which differ only by the substitution of a phenolic hydroxyl group in iophenoxic acid and by an amino group in iopanoic acid (18). The data support earlier observations that the high-affinity binding sites of both drugs are different (18, 19); it seems that iophenoxic acid is bound preferentially to the warfarin site while iopanoic acid is bound preferentially to the diazepam binding site.

The latter results indicate that it will be difficult to find common characteristics for drugs bound specifically to the warfarin binding site and for drugs bound specifically to the indole and benzodiazepine binding site since only small changes in the chemical structure of the ligands can have pronounced effects on the binding site selectivity of the drugs.

In summary, the data clearly showed that the serum albumin binding of biliary contrast agents is quite unusual in respect to the structural parameters leading to strong binding to human and bovine serum albumin. Furthermore, small variations of the chemical structure of the contrast agents can effect large changes in the binding site selectivity. The diazepam and the warfarin binding sites of human serum albumin (two important drug binding sites of the protein) are involved in the binding of the biliary contrast agents. Since many other drugs also are bound to these sites, the biliary contrast agents must be considered as potent displacers of many drugs *in vivo*, especially with regard to their high plasma concentration *in vivo* (20, 21). However, the short plasma half-life of the intravenous biliary contrast agents or the short use of the oral biliary contrast agents makes it unlikely that such displacements are clinically important. However, evidence is accumulating that the plasma protein binding of the biliary contrast agents is extremely important for their distribution, hepatic uptake, and biliary and renal elimination (20–23). Therefore, exact knowledge about the mechanisms involved in the plasma protein binding of these drugs could be helpful for understanding the pharmacokinetics of the biliary contrast agents.

## REFERENCES


(1) P. K. Knoefel, in "Radiocontrast Agents," vol. 1, P. K. Knoefel, Ed., Pergamon, New York, N.Y., 1971, pp. 133–145.

(2) S. K. Lin, A. A. Moss, and S. Riegelman, *J. Pharm. Sci.*, **66,** 1670 (1977).

(3) S. K. Lin, A. A. Moss, R. Motson, and S. Riegelman, *ibid.*, **67,** 930 (1978).

(4) E. C. Lasser, R. S. Farr, T. Iujimagari, and W. N. Tripp, *Am. J. Roentgenol.*, **87,** 338 (1962).

(5) W. E. Müller, *Naunyn-Schmiedebergs Arch. Pharmacol.*, **302,** 227 (1978).

(6) K. J. Fehske, W. E. Müller, and U. Wollert, *Hoppe-Seylers Z. Physiol. Chem.*, **359,** 709 (1978).

(7) K. J. Fehske, W. E. Müller, and U. Wollert, *Biochim. Biophys. Acta*, **577,** 346 (1979).

(8) K. J. Fehske, W. E. Müller, U. Wollert, and L. Velden, *Mol. Pharmacol.*, **16,** 778 (1979).

(9) B. E. Pennock, *Anal. Biochem.*, **56,** 306 (1973).

(10) W. E. Müller and U. Wollert, *Pharmacology*, **19,** 59 (1979).

(11) C. F. Chignell, *Adv. Drug Res.*, **5,** 55 (1970).

(12) J. H. Perrin and P. A. Hart, *J. Pharm. Sci.*, **59,** 431 (1970).

(13) J. J. Vallner, *ibid.*, **66,** 447 (1977).

(14) W. E. Müller, *Klin. Wochenschr.*, **55,** 105 (1977).

(15) J. H. Perrin, *J. Pharm. Pharmacol.*, **25,** 208 (1973).

(16) C. F. Chignell, *Mol. Pharmacol.*, **5,** 455 (1969).

(17) T. Sjödin, N. Roosdorp, and I. Sjöholm, *Biochem. Pharmacol.*, **25,** 2131 (1976).

(18) K. J. Fehske and W. E. Müller, *Res. Commun. Chem. Pathol. Pharmacol.*, **19,** 119 (1978).

(19) G. H. Mudge, N. Desbienz, and G. R. Stibitz, *Drug. Metab. Disp.*, **6,** 432 (1978).

(20) R. N. Berk, P. M. Loeb, and B. A. Ellzey, in "Radiocontrast Agents," R. E. Miller and J. Skucas, Eds., University Park Press, Baltimore, Md., 1977, pp. 223–250.

(21) R. N. Berk and P. M. Loeb, in *ibid.*, pp. 195–221.

(22) W. E. Müller and A. Stillbauer, *Arch. Int. Pharmacodyn. Ther.*, **246,** 187 (1980).

(23) W. E. Müller and A. Stillbauer, *Pharmacology*, in press.


## ACKNOWLEDGMENTS


Supported by a grant from the Deutsche Forschungsgemeinschaft.


# Interaction of Xanthan Gum with Suspended Solids


**JOSEPH S. TEMPIO * and JOEL L. ZATZ ˣ**



Received August 18, 1980, from the *College of Pharmacy, Rutgers—the State University of New Jersey, Piscataway, NJ 08854.* Accepted for publication October 24, 1980.


*Present address: Smith Kline and French Laboratories, Philadelphia, PA 19101.



**Abstract** □ Xanthan gum was adsorbed significantly by magnesium carbonate, aluminum hydroxide, zinc oxide, and calcium carbonate, giving Langmuir-type isotherms. Saturation adsorption was higher from 0.9% NaCl than from water due to reduced mutual repulsion of polymer segments in the presence of the salt. Adsorption resulted from electrostatic attraction between positively charged particles and the negatively charged polymer. $\zeta$-Potential measurements correlated with the adsorption data but were not predictive of the flocculation state. The results indicate that flocculation of magnesium carbonate and aluminum hydroxide by xanthan gum is consistent with a bridging mechanism.



**Keyphrases** □ Xanthan gum—interaction with magnesium carbonate, aluminum hydroxide, zinc oxide, and calcium carbonate □ Adsorption—xanthan gum by suspended solids □ Flocculation—bridging mechanism, magnesium carbonate and aluminum hydroxide with xanthan gum


Xanthan gum produces flocculation of pharmaceutical suspensions (1, 2). Studies utilizing sedimentation volume, microscopy, and particle-size measurement showed that changes in interparticulate structure could be induced by the polymer (2). Flocculation was attributed to the joining of several particles by adsorbed polymer molecules, which




*0022-3549/81/0500-0554$01.00/0*


*© 1981, American Pharmaceutical Association*

modified albumin derivatives.

The results obtained with I give some evidence that the single high-affinity binding site of the intravenous biliary contrast agents (5) might be identical with the warfarin binding site of human serum albumin. This conclusion can be made from the strong displacement of bound warfarin, the large reduction of the extrinsic Cotton effects of I bound to XII–albumin at 310 nm that are associated only with binding to the high-affinity binding site, and the large reduction of the association constant of the high-affinity binding site for XII–albumin or XIII–albumin. By contrast, binding of I to the diazepam binding site may be negligible, as shown by the lack of any displacement of human serum albumin-bound diazepam and by the small effects of the tyrosine modification on the binding parameters of I.

With the oral biliary contrast agents, the specificity for one of the two sites of human serum albumin is not so pronounced. However, as revealed by their displacing potencies for diazepam and warfarin and their binding behavior for tyrosine- and tryptophan-modified albumin, VI is bound preferentially to the warfarin binding site but XI is bound to the diazepam binding site. This observation is interesting considering the small difference in the chemical structures of these contrast agents. A similar observation was made for the structurally related oral biliary contrast agents, iopanoic and iophenoxic acids, which differ only by the substitution of a phenolic hydroxyl group in iophenoxic acid and by an amino group in iopanoic acid (18). The data support earlier observations that the high-affinity binding sites of both drugs are different (18, 19); it seems that iophenoxic acid is bound preferentially to the warfarin site while iopanoic acid is bound preferentially to the diazepam binding site.

The latter results indicate that it will be difficult to find common characteristics for drugs bound specifically to the warfarin binding site and for drugs bound specifically to the indole and benzodiazepine binding site since only small changes in the chemical structure of the ligands can have pronounced effects on the binding site selectivity of the drugs.

In summary, the data clearly showed that the serum albumin binding of biliary contrast agents is quite unusual in respect to the structural parameters leading to strong binding to human and bovine serum albumin. Furthermore, small variations of the chemical structure of the contrast agents can effect large changes in the binding site selectivity. The diazepam and the warfarin binding sites of human serum albumin (two important drug binding sites of the protein) are involved in the binding of the biliary contrast agents. Since many other drugs also are bound to these sites, the biliary contrast agents must be considered as potent displacers of many drugs *in vivo*, especially with regard to their high plasma concentration *in vivo* (20, 21). However, the short plasma half-life of the intravenous biliary contrast agents or the short use of the oral biliary contrast agents makes it unlikely that such displacements are clinically important. However, evidence is accumulating that the plasma protein binding of the biliary contrast agents is extremely important for their distribution, hepatic uptake, and biliary and renal elimination (20–23). Therefore, exact knowledge about the mechanisms involved in the plasma protein binding of these drugs could be helpful for understanding the pharmacokinetics of the biliary contrast agents.

## REFERENCES


(1) P. K. Knoefel, in "Radiocontrast Agents," vol. 1, P. K. Knoefel, Ed., Pergamon, New York, N.Y., 1971, pp. 133–145.

(2) S. K. Lin, A. A. Moss, and S. Riegelman, *J. Pharm. Sci.*, **66,** 1670 (1977).

(3) S. K. Lin, A. A. Moss, R. Motson, and S. Riegelman, *ibid.*, **67,** 930 (1978).

(4) E. C. Lasser, R. S. Farr, T. Iujimagari, and W. N. Tripp, *Am. J. Roentgenol.*, **87,** 338 (1962).

(5) W. E. Müller, *Naunyn-Schmiedebergs Arch. Pharmacol.*, **302,** 227 (1978).

(6) K. J. Fehske, W. E. Müller, and U. Wollert, *Hoppe-Seylers Z. Physiol. Chem.*, **359,** 709 (1978).

(7) K. J. Fehske, W. E. Müller, and U. Wollert, *Biochim. Biophys. Acta*, **577,** 346 (1979).

(8) K. J. Fehske, W. E. Müller, U. Wollert, and L. Velden, *Mol. Pharmacol.*, **16,** 778 (1979).

(9) B. E. Pennock, *Anal. Biochem.*, **56,** 306 (1973).

(10) W. E. Müller and U. Wollert, *Pharmacology*, **19,** 59 (1979).

(11) C. F. Chignell, *Adv. Drug Res.*, **5,** 55 (1970).

(12) J. H. Perrin and P. A. Hart, *J. Pharm. Sci.*, **59,** 431 (1970).

(13) J. J. Vallner, *ibid.*, **66,** 447 (1977).

(14) W. E. Müller, *Klin. Wochenschr.*, **55,** 105 (1977).

(15) J. H. Perrin, *J. Pharm. Pharmacol.*, **25,** 208 (1973).

(16) C. F. Chignell, *Mol. Pharmacol.*, **5,** 455 (1969).

(17) T. Sjödin, N. Roosdorp, and I. Sjöholm, *Biochem. Pharmacol.*, **25,** 2131 (1976).

(18) K. J. Fehske and W. E. Müller, *Res. Commun. Chem. Pathol. Pharmacol.*, **19,** 119 (1978).

(19) G. H. Mudge, N. Desbienz, and G. R. Stibitz, *Drug. Metab. Disp.*, **6,** 432 (1978).

(20) R. N. Berk, P. M. Loeb, and B. A. Ellzey, in "Radiocontrast Agents," R. E. Miller and J. Skucas, Eds., University Park Press, Baltimore, Md., 1977, pp. 223–250.

(21) R. N. Berk and P. M. Loeb, in *ibid.*, pp. 195–221.

(22) W. E. Müller and A. Stillbauer, *Arch. Int. Pharmacodyn. Ther.*, **246,** 187 (1980).

(23) W. E. Müller and A. Stillbauer, *Pharmacology*, in press.


## ACKNOWLEDGMENTS


Supported by a grant from the Deutsche Forschungsgemeinschaft.


# Interaction of Xanthan Gum with Suspended Solids


**JOSEPH S. TEMPIO * and JOEL L. ZATZ ˣ**



Received August 18, 1980, from the *College of Pharmacy, Rutgers—the State University of New Jersey, Piscataway, NJ 08854.* Accepted for publication October 24, 1980.


*Present address: Smith Kline and French Laboratories, Philadelphia, PA 19101.



**Abstract** □ Xanthan gum was adsorbed significantly by magnesium carbonate, aluminum hydroxide, zinc oxide, and calcium carbonate, giving Langmuir-type isotherms. Saturation adsorption was higher from 0.9% NaCl than from water due to reduced mutual repulsion of polymer segments in the presence of the salt. Adsorption resulted from electrostatic attraction between positively charged particles and the negatively charged polymer. $\zeta$-Potential measurements correlated with the adsorption data but were not predictive of the flocculation state. The results indicate that flocculation of magnesium carbonate and aluminum hydroxide by xanthan gum is consistent with a bridging mechanism.



**Keyphrases** □ Xanthan gum—interaction with magnesium carbonate, aluminum hydroxide, zinc oxide, and calcium carbonate □ Adsorption—xanthan gum by suspended solids □ Flocculation—bridging mechanism, magnesium carbonate and aluminum hydroxide with xanthan gum


Xanthan gum produces flocculation of pharmaceutical suspensions (1, 2). Studies utilizing sedimentation volume, microscopy, and particle-size measurement showed that changes in interparticulate structure could be induced by the polymer (2). Flocculation was attributed to the joining of several particles by adsorbed polymer molecules, which




*0022-3549/81/0500-0554$01.00/0*


*© 1981, American Pharmaceutical Association*

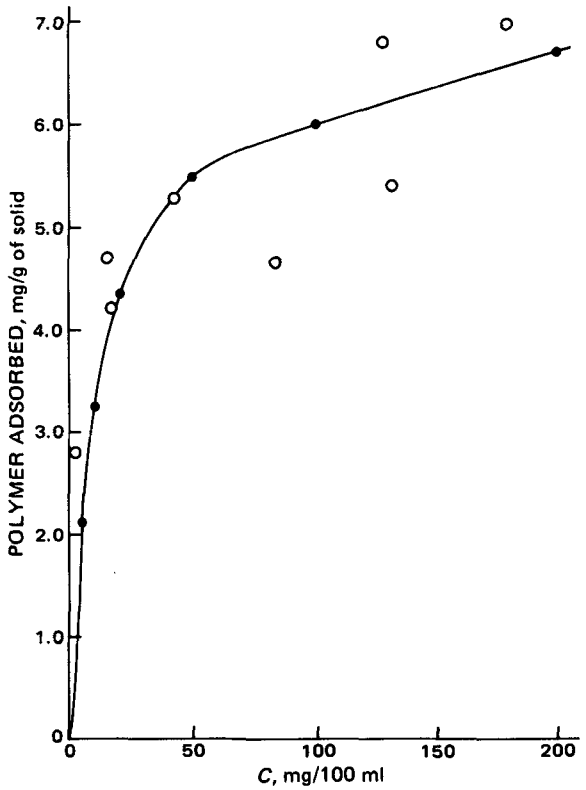


**Figure 1**—*Adsorption isotherm of xanthan gum from water onto magnesium carbonate. Key: ●, values calculated with Eq. 2; and ○, experimental values.*

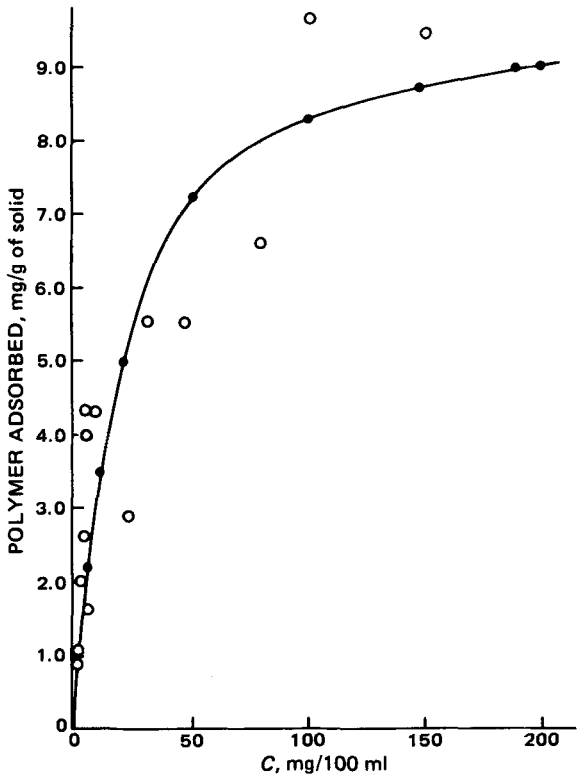


**Figure 2**—*Adsorption isotherm of xanthan gum from 0.9% NaCl onto magnesium carbonate. Key: ●, theoretical values calculated with Eq. 2; and ○, experimental values.*

are incorporated into the network of aggregated particles (1). Polymer adsorption is an essential feature of this flocculation mechanism. Microelectrophoretic measurements demonstrated that polymeric flocculants were adsorbed by suspended colloidal particles (3). In the presence of excess flocculant, the $\zeta$-potential of several materials was controlled by the surface properties of the flocculant and was independent of the nature of the material. Electrostatic attraction often is involved in adsorption (4), but both adsorption and flocculation can occur if the polymer and particle surface carry the same charge, provided that the $\zeta$-potential of the particle is not too high (5). In some systems, a given polymer functions as both flocculant and deflocculant, depending on its concentration at the particle surface (6).

This study investigated the adsorption of xanthan gum by the solids whose suspension properties were reported previously (2). Adsorption is a prerequisite for flocculation by bridging, and these data are required to decide whether bridging is the mechanism of flocculation by xanthan gum, as was suggested (1).

## EXPERIMENTAL

**Materials**—Xanthan gum, dried aluminum hydroxide gel, magnesium carbonate, calcium carbonate, and zinc oxide were the same materials used in a previous study (2). Silica[1] was 80–100 mesh. Water was distilled. All other materials were USP or reagent grade.

**Preparation of Suspensions**—The procedure used was described previously (2).

**Polymer Analysis**—Polymer samples were analyzed for the concentration of xanthan gum by the Seliwanoff reaction. This method is valid for systems where xanthan gum is the only carbohydrate present.

A 1-ml sample of polymer solution (containing 5–250 ppm of xanthan gum) was pipetted into a 10-ml screw-capped culture tube. Then 1 ml of a 4% resorcinol solution in distilled water (prepared fresh daily) was added, followed by 6 ml of concentrated sulfuric acid. The acid was added rapidly, and the tube was mixed with a vortex mixer. Heat and gas were evolved in most cases. The tubes then were placed in an ice water bath for ~5 min until cooled to near room temperature and then were allowed to stand at room temperature for 10–25 min. The concentrations were determined spectrophotometrically at 494 nm within ~1 hr of preparation (7, 8). The absorbance of the samples was read in 1-cm silica cells on a spectrophotometer[2].

Reagent and polymer blanks were run with each analysis. The Beer's law plot in water and 0.9% NaCl was linear throughout the concentration range of interest ($y = 50.8x - 0.10$ and $y = 45.9x + 0.0085$, respectively, for concentrations of 0.005–0.03%).

**Adsorption Determinations**—The amount of polymer adsorbed was determined indirectly from the difference between the initial polymer concentration and the amount found at equilibrium upon analysis of the supernate after drug addition. Kinetic studies indicated that 3–7 days was required for equilibrium.

Flasks containing the suspensions were placed in a shaker bath[3] at 25 ± 1°. Agitation was at a level sufficient to maintain the bulk of the powders in suspension in all samples. After 7 days, the samples were removed from the shakers, and 1-ml aliquots were withdrawn and diluted, if necessary, for analysis.

When the supernate was not clear, it was decanted from the settled fraction and centrifuged[4] at 2000 rpm for 20 min.

**$\zeta$-Potential**—The $\zeta$-potential of the suspensions was measured by electrophoresis[5]. All samples were diluted with distilled water prior to the measurement of the electrophoretic mobility. $\zeta$-Potentials were calculated by the Helmholtz–Smoluchowski formula (9):

$$\zeta = \frac{\nu_e 4\pi\eta}{\epsilon} \qquad \text{(Eq. 1)}$$

where $\nu_e$ is the electrophoretic mobility of the particle, $\eta$ is the viscosity, and $\epsilon$ is the dielectric constant of the suspending medium.

[1] MCB.

[2] Gilford model 222.
[3] Gyrotary model G-76, New Brunswick Scientific, New Brunswick, N.J.
[4] Damon International centrifuge model CU-5000.
[5] Zeta Meter, Inc., New York, N.Y.

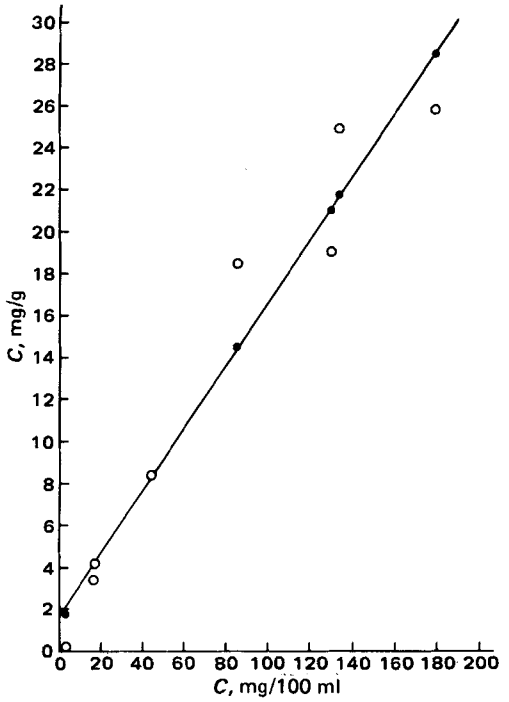


**Figure 3**—*Linearized Langmuir plot of xanthan gum from water onto magnesium carbonate. Key:* ●, *theoretical values calculated with Eq. 3; and* ○, *experimental values.*

**Surface Tension**—Surface tensions of the xanthan solutions were determined using the Wilhelmy plate method. A roughened platinum plate was employed, and double-distilled water was used as a standard.

## RESULTS AND DISCUSSION

**Surface Tensions**—At concentrations up to 0.3%, xanthan gum lowered the surface tension of water or 0.9% NaCl by no more than 3 dynes/cm. Thus, this polymer exhibited little surface activity in aqueous solution.

**Adsorption Isotherms**—Isotherms for xanthan gum adsorption by magnesium carbonate from solution in water and 0.9% NaCl are plotted in Figs. 1 and 2, respectively. The isotherms appear to be the Langmuir type, represented by:

$$Y = Y_m bC/(1 + bC) \qquad \text{(Eq. 2)}$$

where $Y$ is amount adsorbed (in milligrams per gram), $Y_m$ is the amount adsorbed at saturation of the solid surface, $C$ is the equilibrium polymer concentration, and $b$ is a constant. Taking the reciprocal and multiplying through by $C$ yield:

$$C/Y = 1/Y_m b + C/Y_m \qquad \text{(Eq. 3)}$$

This equation is recognizable as the equation of a line with a slope of $1/Y_m$ and intercept $1/Y_m b$.

The adsorption data are plotted according to Eq. 3 in Figs. 3 and 4. The curves are linear; correlation coefficients were significant at the 95% confidence level.

Figures 1–4 were typical of all isotherms. Equation 3 was used to determine the parameters of the isotherms (Tables I and II). For each solid, the saturation adsorption, $Y_m$, from the salt solution (Table II) was greater than that from water (Table I). The amount of polymer that can be accommodated at a saturated surface depends on the available surface area and the area required for each polymer unit. When polymer segments are charged, as xanthan gum is, mutual repulsion prevents close approach of the segments to each other. Polymer–polymer repulsion is reduced in the presence of 0.9% NaCl, permitting closer packing of the polymer segments at the solid–liquid interface, thereby reducing the average area occupied by each polymer unit and raising the $Y_m$ value.

Adsorption alone is insufficient to define a flocculation mechanism. The essential question is whether adsorption is extensive enough in the suspensions to make bridging possible. The adsorption isotherms represent a plot of adsorption *versus* the equilibrium polymer concentrations. The total amount of polymer in the system is the sum of the amount adsorbed and the amount remaining in solution:

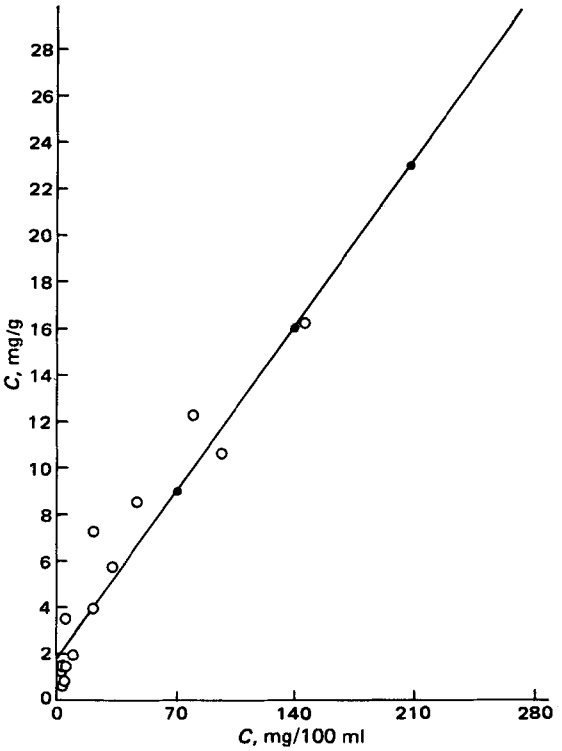


**Figure 4**—*Linearized Langmuir plot of xanthan gum from 0.9% NaCl onto magnesium carbonate. Key:* ●, *theoretical values calculated with Eq. 3; and* ○, *experimental values.*

$$\text{total polymer} = YA + VC \qquad \text{(Eq. 4)}$$

where $A$ is the amount of adsorbent present (in grams) and $V$ is the volume of liquid in contact with the adsorbent. Half-coverage at the solid–liquid interface (*i.e.*, $Y = \frac{1}{2}Y_m$) is taken to represent sufficiently extensive adsorption for bridging (10).

Previous studies on suspensions containing the same solid drugs contained 5 g of solid (except for the calcium carbonate suspension, which used 10 g of solid) and 30–200 mg of xanthan gum in 100 ml of suspension medium (2). The adsorption isotherms and Eq. 4 were used to calculate the amount of xanthan gum at half-coverage in those systems (Table III). The amount required was 23–81 mg, and these values fell within the range of xanthan gum amounts that were actually utilized. Thus, it may be concluded that adsorption is extensive enough to allow flocculation by polymer bridging.

**Table I—Adsorption of Xanthan Gum from Water at 25°**

| Substance | $Y_m$, mg/g | Intercept of Linearized Plot, g/100 ml[a] | $r$ |
|---|---|---|---|
| Magnesium carbonate | 6.67 | 1.6 | 0.972 |
| Aluminum hydroxide | 16.6 | 1.1 | 0.944 |
| Calcium carbonate | 3.59 | 4.8 | 0.961 |
| Zinc oxide | 4.55 | 2.7 | 0.964 |

[a] According to Eq. 3.

**Table II—Adsorption of Xanthan Gum from 0.9% NaCl Solution at 25°**

| Substance | $Y_m$, mg/g | Intercept of Linearized Plot, g/100 ml[a] | $r$ |
|---|---|---|---|
| Magnesium carbonate | 9.83 | 1.8 | 0.949 |
| Aluminum hydroxide | 22.6 | 1.1 | 0.972 |
| Calcium carbonate | 11.1 | 2.3 | 0.947 |
| Zinc oxide | 7.30 | 2.9 | 0.949 |

[a] According to Eq. 3.

**Table III—Total Amount of Xanthan Gum in Pharmaceutical Suspension at Half-Coverage**

| Substance | Total Xanthan Gum, mg | |
|---|---|---|
| | Water | 0.9% NaCl |
| Magnesium carbonate[a] | 27 | 43 |
| Aluminum hydroxide[a] | 60 | 81 |
| Calcium carbonate[b] | 35 | 81 |
| Zinc oxide[a] | 23 | 39 |

[a] Using 5 g + 100 ml of suspension medium. [b] Using 10 g + 100 ml of suspension medium.

**Desorption**—Several samples that had reached adsorption equilibrium were centrifuged to separate solid material from the liquid phase. Fifty milliliters of the liquid medium was replaced with medium containing no xanthan gum and then agitated for 7 days in the shaker bath. When the samples were reanalyzed, the xanthan gum concentration in solution did not exceed half its value prior to dilution. This finding indicated that the adsorbed polymer molecules were not desorbed upon dilution.

**ζ-Potential and Surface Charge**—The zero point of charge is the condition when the charge at a solid interface is zero. For solids dispersed in water, pH values may be used as an indication of the surface charge, provided that hydrogen or hydroxyl ions are potential-determining ions. This appears to be the case for oxides, hydroxides, and carbonates in aqueous systems (11–14).

A slightly soluble hydroxide like aluminum hydroxide has a positive surface charge below the pH of the zero point of charge due to the dissociation of amphoteric surface hydroxide groups and the adsorption from solution of metal–hydroxo complexes (11). The surface potential of calcium carbonate is due to the hydrolysis or adsorption of surface ions or complexes. The hydroxide ion is dominant (13). At pH below the point of zero charge, the surface potential of zinc oxide is expected to be dominated by the $Zn^{2+}$ ion and adsorption of $H^+$ and metal–hydroxo complexes (14).

The pH values for a suspension supernate were compared with reported values of the zero point of charge for the various solids (Table IV). The ζ-potential values are believed to be a more reliable indication of the surface condition. The zero point of charge for a particular sample of substance depends markedly on the history of the sample, and literature zero point of charge values for different samples of the same material vary widely (17).

Classical theory dictates that high absolute values of ζ-potential are associated with deflocculated systems. The potential energy–distance curves for such systems show a primary minimum at short distances, due to van der Waals attractive forces, and a relatively steep threshold, due to charge–charge repulsion. However, only one system studied, calcium carbonate, was deflocculated in water. Parodoxically, calcium carbonate had the lowest ζ-potential.

The measurement of ζ-potential of concentrated suspensions containing polymers by electrophoresis is complicated because dilution is required. Dilution of systems containing adsorbed materials can result in desorption, with consequent alterations in the measured potential. Since xanthan gum did not undergo desorption upon dilution, this measurement was feasible.

The addition of xanthan gum to the suspended solids caused a reduction in ζ-potential and a reversal in sign to negative values (Fig. 5). The curves resemble the adsorption isotherms in that the potentials approach limiting values. The ζ-potential curves confirm polymer adsorption and indicate that the potential is determined largely by the layer of adsorbed polymer, which is negatively charged.

In the presence of xanthan gum, aluminum hydroxide and magnesium carbonate are flocculated (2). The fact that the ζ-potential is not negligible for these systems again illustrates its limited utility in predicting flocculation behavior. ζ-Potential measurements are of value, but they must be combined with other techniques to obtain a complete view of a disperse system.

**Table IV—pH of Supernate of Suspended Solids**

| Substance | Supernatant pH | Zero Point of Charge | Reference |
|---|---|---|---|
| Magnesium carbonate | 9.2 | 8.5 | 11 |
| Aluminum hydroxide | 6.3 | 8.5 | 12 |
| Calcium carbonate | 11.1 | 10.8 | 15 |
| Zinc oxide | 7.2 | 9.0 | 16 |

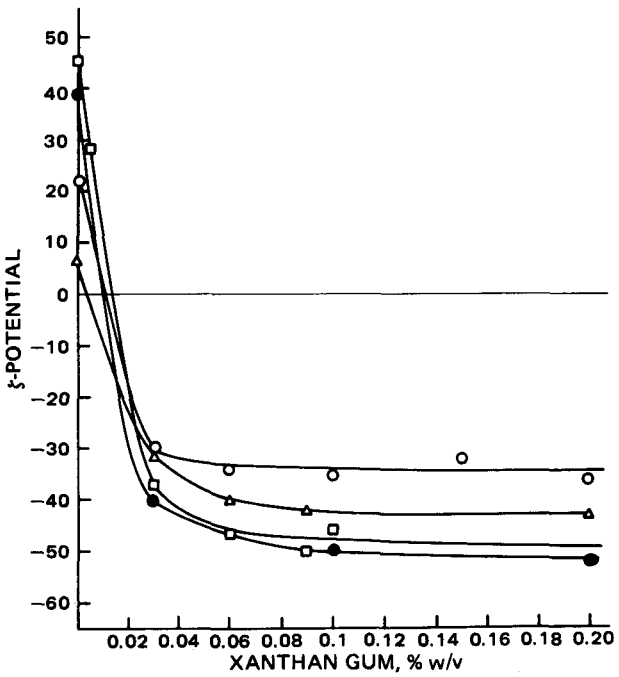


**Figure 5**—*ζ-Potential of solid drugs as a function of xanthan gum concentration. Key:* □, *aluminum hydroxide;* ●, *zinc oxide;* ○, *magnesium carbonate; and* △, *calcium carbonate.*

The adsorption mechanism of xanthan gum by the solids investigated is most likely electrostatic. The positively charged surfaces are expected to attract strongly the oppositely charged polymer molecules. Since xanthan gum has little surface activity, an adsorption mechanism based on hydrophobic interaction with the surface is not likely.

Experiments with silica provide an interesting comparison. The ζ-potential of silica in water was 55 mv. Suspensions containing 5 g of silica in 100 ml of water were deflocculated, with a sedimentation volume of 0.05. There was no change in sedimentation volume upon addition of xanthan gum. Adsorption studies revealed that xanthan gum was not adsorbed to any significant extent. In this case, the negative potential on the particles prevented polymer adsorption and precluded flocculation by bridging.

**Conclusion**—The results provide evidence for bridging as a flocculation mechanism of xanthan gum. Significant adsorption occurred on solids that underwent a change in flocculation state because of the gum. ζ-Potential measurements confirmed polymer adsorption. Previously, it was shown that salt effects on the flocculation of aluminum hydroxide, magnesium carbonate, zinc oxide, and calcium carbonate were minimal and that double-layer repulsion alteration by the electrolyte was not important in the flocculation–deflocculation behavior of these suspensions (2). The lack of correlation between the ζ-potential and the flocculation state is another indication that double-layer effects do not play a major role in controlling flocculation of these materials by xanthan gum.

## REFERENCES


(1) A. Felmeister, G. M. Kuchtyak, S. Koziol, and C. J. Felmeister, *J. Pharm. Sci.*, **62**, 2026 (1973).

(2) J. S. Tempio and J. L. Zatz, *ibid.*, **69**, 1209 (1980).

(3) H. E. Ries, Jr., *Nature*, **226**, 72 (1970).

(4) H. E. Ries, Jr., and B. L. Meyers, *Science*, **160**, 1449 (1968).

(5) J. P. Friend and J. A. Kitchener, *Chem. Eng. Sci.*, **28**, 1071 (1973).

(6) J. L. Zatz, L. Schnitzer, and P. Sarpotdar, *J. Pharm. Sci.*, **68**, 1491 (1979).

(7) "Xanthan Gum," 2nd ed., Kelco Inc., 1976.

(8) H. D. Graham, *J. Dairy Sci.*, **54**, 1622 (1971).

(9) "Zeta Meter Manual," 2nd ed., Zeta Meter, Inc., New York, N.Y., 1968.

(10) R. H. Smellie, Jr., and V. K. LaMer, *J. Colloid Sci.*, **13**, 589 (1958).

(11) H. Schott, *J. Pharm. Sci.*, **66**, 1549 (1977).

(12) J. J. Predali and J. M. Cases, *J. Colloid Interface Sci.*, **45**, 449

(1973).
(13) P. Somasundaran and G. E. Agar, *ibid.*, **24**, 433 (1967).
(14) G. A. Parks, *Chem. Rev.*, **65**, 1977 (1965).
(15) E. Herczynaska and K. Proszynska, Polish Academy of Sciences, Institute of Nuclear Research, Report No. 372/v., Warsaw, Poland, 1962.
(16) M. C. Fuerstenau, G. Geutierrez, and D. A. Elginlani, *Trans. AIME*, **24**, 319 (1968).
(17) A. K. Helmy and E. A. Ferreiro, *Z. Phys. Chem. (Leipzig)*, **257**, 881 (1976).

**ACKNOWLEDGMENTS**

The authors thank Mr. Kim Bildstein and Ms. Eve Haligowski for technical assistance. Dr. Tempio acknowledges the fellowship support extended by Johnson and Johnson.

# Synthesis and Structure–Activity Relationships of Selected Tricyclic Oxime *O*-Ethers as Potential Anticholinergic Agents

**VILAS A. PRABHU *, ROBERT G. BROWN, and JAIME N. DELGADO ˣ**

Received September 29, 1980, from the *College of Pharmacy, University of Texas at Austin, Austin, TX 78712.* Accepted for publication November 3, 1980. *Present address: College of Pharmacy, Southwestern Oklahoma State University, Weatherford, OK 73096.

**Abstract** □ Selected isomeric and nonisomeric oxime *O*-ether derivatives of thioxanthone oxime were synthesized and evaluated for anticholinergic activity. The oxime *O*-ethers were prepared *via O*-alkylation of the oximate anion with appropriate aminoaklyl halides. Separation and isolation of the structural isomers were accomplished through dry-column chromatography. The racemic α-methyl isomer was resolved *via* formation of tartrate diastereomers, which were subsequently isolated. All synthesized compounds exhibited significant antimuscarinic activity. A comparison of the antimuscarinic activities of these compounds revealed that the racemic α-methyl isomer was the most potent and that the racemic β-methyl isomer was the least potent. Structure–activity relationships among the oxime *O*-ether derivatives synthesized are discussed.

**Keyphrases** □ Anticholinergics, potential—selected tricyclic oxime *O*-ethers, synthesis, structure–activity relationships □ Structure–activity relationships—selected tricyclic oxime *O*-ethers as potential anticholinergics, synthesis □ Antimuscarinic activity—comparison of synthesized tricyclic oxime *O*-ethers □ Oxime derivatives—synthesis, comparison as potential anticholinergics

Various structurally and stereochemically different esters exhibiting anticholinergic activity were studied previously (1–4) to obtain information concerning stereospecificity of the parasympathetic postganglionic acetylcholine receptor. One report (3), dealing with α- and β-methylcholine esters of 2-cyclohexyl-2-hydroxy-2-phenylacetic acid, concluded that α-methyl substitution significantly increased antimuscarinic activity and that such an increase was independent of the configuration of the α-substituted carbon atom. Based on these findings, the report indicated that the stereochemistry of the aminoalcohol moiety was not significant in determining antimuscarinic activity.

Previous work (5, 6) demonstrated that oxime derivatives are useful model compounds for the study of structure–activity relationships. More recent studies related geometric (7, 8) and enantiomeric (8) isomerism in oxime *O*-ethers to their anticholinergic activity. These findings (8), however, were not in complete agreement with earlier reports (1–3) concerning the stereochemical significance of the aminoalcohol moiety in determining antimuscarinic potency.

The present study was a further investigation of the possible relationships between structural and stereochemical properties and antimuscarinic activity among oxime *O*-ethers. Selected isomeric and nonisomeric oxime *O*-ethers of thioxanthone oxime (Table I) were synthesized, and a preliminary pharmacological evaluation was conducted to determined their antimuscarinic activity.

## DISCUSSION

Preparation of the oxime directly from thioxanthone was attempted *via* methods described by Gomer *et al.* (6), for the synthesis of xanthoxime, and Wylie *et al.* (9), for the preparation of benzophenone oxime, but was unsuccessful. This failure can be explained by the fact that, in thioxanthone, the carbonyl carbon is considerably less electrophilic and, therefore, less susceptible to nucleophilic attack by the hydroxylamine nitrogen. Subsequently, thioxanthone oxime was prepared by a modified method of Nagrajan *et al.* (10). Accordingly, thioxanthone was converted first to the thione by refluxing it with excess phosphorus pentasulfide in xylene. The thione then was refluxed with hydroxylamine hydrochloride and potassium *t*-butoxide in anhydrous ethanol to yield the oxime in fair yields. Based on the reported mechanism (8, 11) involved in the synthesis of oximes from highly aromatic ketones, a general base-catalyzed mechanism was proposed for the synthesis of thioxanthone oxime. The oxime was quite unstable when exposed to direct sunlight, decomposing to the ketone. The major steps involved in the synthesis of the oxime and the oxime *O*-ethers are depicted in Scheme I.

The oxime *O*-ethers included in this study (Table I) were prepared *via O*-alkylation of the oximate anion with the appropriate aminoalkyl halides. The mechanism of *O*-alkylation involves a nucleophilic attack by the base-generated anionic oximate species on the aminoalkyl halide, resulting in the displacement of the halide ion (12).

The procedure of Huerta *et al.* (8) was used to prepare the α- and β-methylcholine *O*-ethers of the oxime. Accordingly, 2-chloro-*N*,*N*-

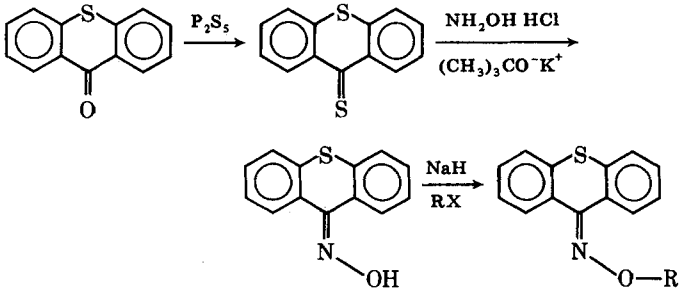


RX = aminoalkyl halide

*Scheme I*



*0022-3549/81/0500-0558$01.00/0*
*© 1981, American Pharmaceutical Association*

(1973).
(13) P. Somasundaran and G. E. Agar, *ibid.*, **24**, 433 (1967).
(14) G. A. Parks, *Chem. Rev.*, **65**, 1977 (1965).
(15) E. Herczynaska and K. Proszynska, Polish Academy of Sciences, Institute of Nuclear Research, Report No. 372/v., Warsaw, Poland, 1962.
(16) M. C. Fuerstenau, G. Geutierrez, and D. A. Elginlani, *Trans. AIME*, **24**, 319 (1968).
(17) A. K. Helmy and E. A. Ferreiro, *Z. Phys. Chem. (Leipzig)*, **257**, 881 (1976).

**ACKNOWLEDGMENTS**

The authors thank Mr. Kim Bildstein and Ms. Eve Haligowski for technical assistance. Dr. Tempio acknowledges the fellowship support extended by Johnson and Johnson.

# Synthesis and Structure–Activity Relationships of Selected Tricyclic Oxime *O*-Ethers as Potential Anticholinergic Agents

**VILAS A. PRABHU *, ROBERT G. BROWN, and JAIME N. DELGADO ˣ**

Received September 29, 1980, from the *College of Pharmacy, University of Texas at Austin, Austin, TX 78712.* Accepted for publication November 3, 1980. *Present address: College of Pharmacy, Southwestern Oklahoma State University, Weatherford, OK 73096.

**Abstract** □ Selected isomeric and nonisomeric oxime *O*-ether derivatives of thioxanthone oxime were synthesized and evaluated for anticholinergic activity. The oxime *O*-ethers were prepared *via O*-alkylation of the oximate anion with appropriate aminoaklyl halides. Separation and isolation of the structural isomers were accomplished through dry-column chromatography. The racemic α-methyl isomer was resolved *via* formation of tartrate diastereomers, which were subsequently isolated. All synthesized compounds exhibited significant antimuscarinic activity. A comparison of the antimuscarinic activities of these compounds revealed that the racemic α-methyl isomer was the most potent and that the racemic β-methyl isomer was the least potent. Structure–activity relationships among the oxime *O*-ether derivatives synthesized are discussed.

**Keyphrases** □ Anticholinergics, potential—selected tricyclic oxime *O*-ethers, synthesis, structure–activity relationships □ Structure–activity relationships—selected tricyclic oxime *O*-ethers as potential anticholinergics, synthesis □ Antimuscarinic activity—comparison of synthesized tricyclic oxime *O*-ethers □ Oxime derivatives—synthesis, comparison as potential anticholinergics

Various structurally and stereochemically different esters exhibiting anticholinergic activity were studied previously (1–4) to obtain information concerning stereospecificity of the parasympathetic postganglionic acetylcholine receptor. One report (3), dealing with α- and β-methylcholine esters of 2-cyclohexyl-2-hydroxy-2-phenylacetic acid, concluded that α-methyl substitution significantly increased antimuscarinic activity and that such an increase was independent of the configuration of the α-substituted carbon atom. Based on these findings, the report indicated that the stereochemistry of the aminoalcohol moiety was not significant in determining antimuscarinic activity.

Previous work (5, 6) demonstrated that oxime derivatives are useful model compounds for the study of structure–activity relationships. More recent studies related geometric (7, 8) and enantiomeric (8) isomerism in oxime *O*-ethers to their anticholinergic activity. These findings (8), however, were not in complete agreement with earlier reports (1–3) concerning the stereochemical significance of the aminoalcohol moiety in determining antimuscarinic potency.

The present study was a further investigation of the possible relationships between structural and stereochemical properties and antimuscarinic activity among oxime *O*-ethers. Selected isomeric and nonisomeric oxime *O*-ethers of thioxanthone oxime (Table I) were synthesized, and a preliminary pharmacological evaluation was conducted to determined their antimuscarinic activity.

## DISCUSSION

Preparation of the oxime directly from thioxanthone was attempted *via* methods described by Gomer *et al.* (6), for the synthesis of xanthoxime, and Wylie *et al.* (9), for the preparation of benzophenone oxime, but was unsuccessful. This failure can be explained by the fact that, in thioxanthone, the carbonyl carbon is considerably less electrophilic and, therefore, less susceptible to nucleophilic attack by the hydroxylamine nitrogen. Subsequently, thioxanthone oxime was prepared by a modified method of Nagrajan *et al.* (10). Accordingly, thioxanthone was converted first to the thione by refluxing it with excess phosphorus pentasulfide in xylene. The thione then was refluxed with hydroxylamine hydrochloride and potassium *t*-butoxide in anhydrous ethanol to yield the oxime in fair yields. Based on the reported mechanism (8, 11) involved in the synthesis of oximes from highly aromatic ketones, a general base-catalyzed mechanism was proposed for the synthesis of thioxanthone oxime. The oxime was quite unstable when exposed to direct sunlight, decomposing to the ketone. The major steps involved in the synthesis of the oxime and the oxime *O*-ethers are depicted in Scheme I.

The oxime *O*-ethers included in this study (Table I) were prepared *via O*-alkylation of the oximate anion with the appropriate aminoalkyl halides. The mechanism of *O*-alkylation involves a nucleophilic attack by the base-generated anionic oximate species on the aminoalkyl halide, resulting in the displacement of the halide ion (12).

The procedure of Huerta *et al.* (8) was used to prepare the α- and β-methylcholine *O*-ethers of the oxime. Accordingly, 2-chloro-*N*,*N*-

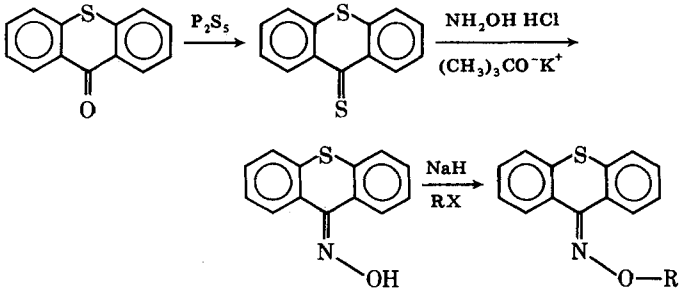


RX = aminoalkyl halide

*Scheme I*



*0022-3549/81/0500-0558$01.00/0*
*© 1981, American Pharmaceutical Association*

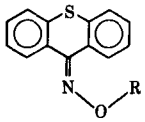

**Table I—Oxime *O*-Aminoalkyl Ethers**

| Compound[a] | Yield, % | R | NMR Data[b], ppm | | | | IR Data[c], $cm^{-1}$ | | |
|---|---|---|---|---|---|---|---|---|---|
| | | | $OCH_2$ | $NCH_2$ | $N(CH_3)_2$ | Aromatic H | C=N | C–O | N–O |
| I | 40 | $-CH_2CH_2N(CH_3)_2$ | 4.37 | 2.73 | 2.20 | 7.13–8.60 | 1640 | 1030 | 980 |
| II | 40 | 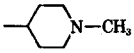 | 4.42–3.92[d] | 2.75–1.58[e] | 2.15[f] | 7.00–8.43 | 1620 | 1030 | 980 |
| III | 70 | $-CH_2CH_2CH_2N(CH_3)_2$ | 4.16 | 2.50–1.50[g] | 2.13 | 6.90–8.17 | 1640 | 1030 | 980 |
| (±)-IV | 31 | $-CH_2CHN(CH_3)_2$ <br> $CH_3$ | 4.67–4.00 | 3.25–2.83[h] | 2.33 | 7.20–8.57 | 1620 | 1040, 1030 | 980 |
| (±)-V | 15 | $-CHCH_2N(CH_3)_2$ <br> $CH_3$ | 4.83–4.42[d] | 2.83–2.40 | 2.38 | 7.17–8.30 | 1640 | 1065, 1030 | 980 |

[a] Chromatographed on silica gel dry column. [b] Chemical shifts are expressed as δ; deuterochloroform was used as the solvent in all determinations except with II where carbon tetrachloride was used. [c] Frequency of absorptions for neat samples. [d] The OCH proton. [e] The $N(CH_2)_2$ and $C(CH_2)_2$ protons. [f] The $NCH_3$ protons. [g] The $NCH_2$–$CH_2$ protons. [h] The NCH proton.

**Table II—Oxime *O*-(α-Methylcholinyl) Ether Tartrates and Methylbromides**

| Compound | Recrystallization Solvent | Melting Point | $[\alpha]_D^{25}$ | Empirical Formula | Analysis, % | |
|---|---|---|---|---|---|---|
| | | | | | Calc. | Found |
| IV-Tartrate | Ethanol | 118–120° | +8.13° | $C_{22}H_{26}N_2O_7S$ | C 57.13 | 56.98 |
| | | | | | H 5.67 | 5.71 |
| | | | | | N 6.06 | 5.98 |
| (+)-IV · $CH_3Br$ | Isopropyl alcohol–isopropyl ether | 219–220° | +16.33 | $C_{19}H_{23}BrN_2OS$ | C 56.02 | 56.20 |
| | | | | | H 5.69 | 5.80 |
| | | | | | N 6.88 | 6.81 |
| IV-Tartrate | Isopropyl alcohol–isopropyl ether | 128–130° | +18.60° | $C_{22}H_{26}N_2O_7S$ | C 57.13 | 57.17 |
| | | | | | H 5.67 | 5.80 |
| | | | | | N 6.06 | 5.79 |
| (−)-IV · $CH_3Br$ | Isopropyl alcohol | 216–218° | −16.43° | $C_{19}H_{23}BrN_2OS$ | C 56.02 | 55.73 |
| | | | | | H 5.69 | 5.85 |
| | | | | | N 6.88 | 6.58 |

dimethylpropylamine was used as the alkylating agent, resulting in the synthesis of both structural isomers (IV and V) in the same reaction mixture. The proposed mechanism (13) implicates the generation of a cyclic aziridinium-ion intermediate, followed by a nucleophilic attack by the oximate anion on the two possible nucleophilic sites of the cyclic aziridinium ion. An attack on the secondary carbon results in the formation of the α-methyl isomer (IV), and a corresponding attack on the tertiary carbon results in the β-methyl isomer (V). It was apparent from the α–β isomeric ratio that a nucleophilic attack on the secondary carbon of the aziridinium ion was favored.

An attempt to separate the structural isomers by high-vacuum distillation failed because of the high thermal decomposition of the oily mixture. Dry-column chromatography was effective for large-scale separation. This technique allowed direct application of the optimal conditions, previously determined by using TLC, to a column adsorbent of the same composition. The separation and purification of the structural isomers were monitored by TLC, and they were identified conclusively based on their NMR and IR spectra.

The NMR spectral data were particularly conclusive. In the α-methyl isomer, the α-methyl group is influenced only by the methine proton adjacent to the amino nitrogen; thus, it was represented by a doublet peak at δ 1.10. The corresponding doublet for the β-methyl group in the β-methyl isomer appeared slightly downfield at δ 1.40, indicating that the methine group influencing the β-methyl group must be adjacent to the ether oxygen. Other differences in the NMR spectra also were useful in assigning the correct structures (Table I).

Resolution of the racemic α-methyl structural isomer into its respective enantiomers was accomplished by preparing diastereomeric salts with tartaric acid, followed by repeated recrystallizations until each diastereomer exhibited a constant melting point and specific rotation. The enantiomeric free bases were liberated from the diastereomers separately by treatment with triethylamine and derivatized to their respective methyl bromide salts. These methyl bromide salts, after several recrystallizations, exhibited essentially equal but opposite specific rotations. All of the established criteria (14) for confirming the relative optical purity of enantiomers were met during resolution. Elemental analyses and optical rotation data of the diastereomers and enantiomers are summarized in Table II.

The β-methyl isomer was not resolved because preliminary pharmacological screening indicated that the α-methyl isomer was several times more potent as an antimuscarinic agent. The chemical purity and structural characterizations of the oxime *O*-ether methyl halide derivatives prepared were confirmed by elemental analyses (Table III).

## EXPERIMENTAL[1]

**Oxime**—*Thioxanthone Oxime*—A previous method (10) was adopted with modifications. Thioxanthone (212 g, 1 mole) was combined with distilled phosphorus pentasulfide (444 g, 2 moles) and refluxed in xylene (2000 ml) for 24 hr. The reaction was monitored with TLC using benzene as the developing solvent. The reaction mixture was filtered while hot, and the filtrate was washed quickly with five 100-ml portions of 2 *N* NaOH followed by five 100-ml portions of distilled water. The filtrate was evaporated under reduced pressure, and the resulting residue was recrystallized from hot absolute ethanol. The crystalline material, thioxanthione (160 g, 70%), melted at 167–168° [lit. (10) mp 168°].

Potassium *t*-butoxide (224 g, 2 moles) was added in small portions to a stirred solution of thioxanthione (160 g, 0.7 mole) in absolute ethanol (1000 ml). Hydroxylamine hydrochloride (140 g, 2 moles) was added to this stirred mixture, which then was refluxed for 8 hr. The reaction mixture was filtered while hot, and the filtrate was evaporated under reduced pressure. The resulting residue was washed several times with xylene and then recrystallized from hot benzene. The analytically pure oxime (63 g, 40%) melted at 193–194° [lit. (10) mp 192–193°]; IR (KBr

[1] Melting points were determined on a Thomas–Hoover Uni-Melt apparatus and are uncorrected. A Beckman IR-8 spectrophotometer was used to obtain IR spectra. Proton NMR spectra were obtained on JEOL C-60HL and Perkin-Elmer R-12A spectrometers with tetramethylsilane and dimethyl sulfoxide as internal standards. Optical rotation data were obtained on a Perkin-Elmer 141 polarimeter. Elemental analyses were performed by Schwarzkopf Microanalytical Laboratories, Woodside, N.Y. Pharmacological determinations were made on a Marco physiograph desk model DMP-4A.

**Table III—Quaternary Oxime *O*-Aminoalkyl Ether Methyl Halides**

| Compound | Melting Point | Empirical Formula | | Analysis, % Calc. | Found |
|---|---|---|---|---|---|
| I · $CH_3Br$ | 233–234.5° | $C_{18}H_{21}BrN_2OS$ | C | 54.96 | 55.25 |
| | | | H | 5.38 | 5.42 |
| | | | N | 7.12 | 7.18 |
| I · $CH_3I$ | 223–225° | $C_{18}H_{21}IN_2OS$ | C | 49.09 | 49.29 |
| | | | H | 4.81 | 4.90 |
| | | | N | 6.36 | 6.34 |
| II · $CH_3Br$ | 277–278° | $C_{20}H_{23}BrN_2OS$ | C | 57.28 | 56.99 |
| | | | H | 5.53 | 5.61 |
| | | | N | 6.68 | 6.72 |
| III · $CH_3Br$ | 211–212.5° | $C_{19}H_{23}BrN_2OS$ | C | 56.02 | 55.76 |
| | | | H | 5.69 | 5.90 |
| | | | N | 6.88 | 6.77 |
| (±)-IV · $CH_3Br$ | 218–219° | $C_{19}H_{23}BrN_2OS$ | C | 56.02 | 55.89 |
| | | | H | 5.69 | 5.79 |
| | | | N | 6.88 | 6.72 |
| (±)-IV · $CH_3I$ | 177–179° | $C_{19}H_{23}IN_2OS$ | C | 50.22 | 50.46 |
| | | | H | 5.10 | 5.23 |
| | | | N | 6.17 | 6.20 |
| (±)-V · $CH_3Br$ | 209–211° | $C_{19}H_{23}BrN_2OS$ | C | 56.02 | 56.07 |
| | | | H | 5.69 | 5.85 |
| | | | N | 6.88 | 6.93 |
| (±)-V · $CH_3I$ | 176–178° | $C_{19}H_{23}IN_2OS$ | C | 50.22 | 49.84 |
| | | | H | 5.10 | 4.90 |
| | | | N | 6.17 | 5.90 |

disk): 1620 (C=N) and 980 (N–O) $cm^{-1}$; NMR (dimethylsulfoxide-$d_6$): δ 7.13–8.50 (m, 8H, aromatic H) and 13.07 (s, 1H, NOH).

*Oxime O-Ethers*—Elemental analyses data and appropriate physical constants for all final compounds are summarized in Tables I–III.

**Thioxanthone Oxime *O*-(*N*-Dimethylaminoethyl) Ether (I) and Methyl Halides**—The oxime (7.95 g, 0.035 mole) was dissolved in warm absolute ethanol (100 ml) and placed in a three-necked round-bottom flask. Sodium hydride (3.28 g of a 51.6% mineral oil dispersion, 0.07 mole) was added in small portions to the stirred solution. 2-Chloro-*N*,*N*-dimethylethylamine hydrochloride (1.89 g, 0.035 mole) was dissolved in hot absolute ethanol (100 ml) and added dropwise to the reaction mixture over 30 min. The stirred mixture was refluxed for 72 hr and filtered while hot. The filtrate was evaporated under reduced pressure, and the resulting oily residue was dissolved in petroleum ether. The solution was filtered, and the solvent was evaporated under reduced pressure.

The oily product (6.27 g, 60%) was purified further *via* dry-column chromatography after proper conditions (with respect to solvent and column material) were established with silica gel TLC. A 50.8-cm strip of nylon column was packed with silica gel powder (300 g, 60–200 mesh), and the crude oily product was eluted with ethyl acetate–methanol (10:1). The elution was stopped when the solvent front reached the bottom of the column, which then was sliced into 2.54-cm sections. The contents of each section were extruded into separate beakers and extracted with absolute ethanol (25 ml). The extract in each beaker was analyzed by TLC, and the extracts containing the pure oxime *O*-ether were combined. The combined extracts were filtered, and the filtrate was evaporated under reduced pressure. The oily residue was dissolved in petroleum ether, and the mixture was filtered. Then the solvent was evaporated under reduced pressure to yield the pure oxime *O*-ether (4.37 g, 40%).

The methy bromide derivative (I · $CH_3Br$) was prepared by treating a solution of the free base in absolute ethanol with excess methyl bromide. The mixture was placed in a freezer for 24 hr, and the resulting precipitate was collected on a filter. Recrystallization from absolute ethanol yielded an analytically pure sample, mp 233–234.5°. The methyl iodide derivative was prepared similarly by treating a solution of the free base in absolute ethanol with excess methyl iodide, mp 223–225°.

**Thioxanthone Oxime *O*-[4-(1-Methylpiperidinyl)] Ether (II) and Methyl Bromide Derivative**—Sodium hydride (1.6 g of a 51.6% mineral oil dispersion, 0.034 mole) was added in small portions to a stirred solution of the oxime (3.85 g, 0.017 mole) in dimethyl sulfoxide (100 ml). 4-Chloro-1-methylpiperidine hydrochloride (2.08 g, 0.017 mole) was added to the stirred mixture in small portions. Then the mixture was refluxed for 4 hr, treated with distilled water (200 ml), and extracted with five 100-ml portions of chloroform. The combined chloroform extracts were washed twice with distilled water (100 ml) and dried over anhydrous calcium carbonate. The mixture was filtered, and the solvent was evaporated under reduced pressure. The crude oily material, on purification *via* dry-column chromatography using ethyl acetate–petroleum ether–ethanol (1:1:0.1), yielded the pure oxime *O*-ether (2.2 g, 40%). The methyl bromide derivative was prepared and recrystallized from absolute ethanol, mp 277–278°.

**Thioxanthone Oxime *O*-(*N*-Dimethylaminopropyl) Ether (III) and Methyl Bromide Derivative**—The procedure described for the synthesis of II was adopted for the synthesis of III. Sodium hydride (1.9 g of a 51.6% mineral oil dispersion, 0.04 mole) and 3-chloro-*N*,*N*-dimethylpropylamine hydrochloride (3.2 g, 0.02 mole) were added to a stirred solution of the oxime (4.54 g, 0.02 mole) in dimethyl sulfoxide, and the mixture was refluxed for 4 hr. The reaction mixture was combined with distilled water (200 ml) and extracted with five 100-ml portions of chloroform. The combined chloroform extracts were washed twice with distilled water (100 ml) and dried over anhydrous calcium carbonate. The mixture was filtered, and the solvent was evaporated under reduced pressure. The resulting crude product, on purification *via* dry-column chromatography using ethyl acetate–petroleum ether–ethanol (1:1:0.1), yielded the pure oxime *O*-ether (4.4 g, 70%). The methyl bromide derivative was prepared and recrystallized from absolute ethanol, mp 211–212.5°.

**Thioxanthone Oxime *O*-(α- and β-Methylcholinyl) Ethers (IV and V) and Methyl Halide Derivatives**—A reported method (8) was adopted. Sodium hydride (9.3 g of a 51.6% mineral oil dispersion, 0.2 mole) was added in small portions to a stirred solution of the oxime (20.30 g, 0.1 mole) in absolute ethanol. A solution of 2-chloro-*N*,*N*-dimethylpropylamine hydrochloride (15.8 g, 0.1 mole) in absolute ethanol was added dropwise to the stirred, refluxing, reaction mixture over 1 hr. The mixture was refluxed further for 12 hr, during which the reaction was monitored with TLC using ethyl acetate–petroleum ether–ethanol (1:1:0.1). The hot reaction mixture was filtered, and the filtrate was evaporated under reduced pressure. The resulting oily residue was extracted with isopropyl ether, and the combined extracts were filtered. Evaporation of the solvent under reduced pressure yielded a crude oily mixture of the α- and β-methyl structural isomers (21.88 g, 70%).

**Separation and Isolation of Structural Isomers**—The initial separation of the structural isomers was accomplished on a small scale, with silica gel TLC using ethyl acetate–petroleum ether–ethanol (1:1:0.1). One isomer had an $R_f$ value of 0.14, and the other isomer exhibited an $R_f$ value of 0.28. These TLC results were applied directly to silica gel dry-column chromatography for the large-scale separation. A 91.4-cm nylon column was packed with silica gel (1200 g, 60–200 mesh) powder, previously activated at 115° for 1 hr. The isomeric mixture (20 g) was adsorbed on a separate portion of adsorbent and added to the top of the column. The column then was eluted with a solvent mixture identical to the one used during TLC separation. Development of the column was stopped when the solvent front reached the bottom of the column. The column then was cut into 2.54-cm sections, and the adsorbent in each section was extracted with absolute ethanol into separate beakers.

The contents of each beaker were analyzed by TLC, and extracts containing a single compound with identical $R_f$ values were combined and filtered. Evaporation of the filtrates under reduced pressure yielded the pure α-methyl (9.5 g) and β-methyl (4.5 g) isomers. Based on their IR and NMR spectral data, the isomer with an $R_f$ value of 0.14 was identified as the α-methyl isomer; the isomer with an $R_f$ value of 0.28 was identified as the β-methyl isomer. The IR spectrum of the α-isomer exhibited a charcteristic C=O stretching band at 1040 $cm^{-1}$, while the β-isomer had a corresponding band at 1065 $cm^{-1}$. The NMR spectrum of the α-isomer exhibited a characteristic doublet at δ 1.10 for the α-methyl protons, while the corresponding doublet for the β-methyl protons appeared further downfield at δ 1.40 due to the greater influence of the oxygen atom. Other characteristic differences also were observed in the NMR spectra (Table I) of these structural isomers.

Methyl bromide and methyl iodide derivatives were prepared. The analytically pure methyl bromide derivative of the racemic α-methyl isomer melted at 218–219°, and the methyl iodide derivative melted at 177–179°. The analytically pure methyl bromide derivative of the racemic β-methyl isomer melted at 209–211°, and the methyl iodide derivative melted at 176–178°.

**Resolution**—The racemic α-methyl isomer (6.72 g, 0.018 mole) was dissolved in absolute ethanol (50 ml), and the solution was combined with an equimolar solution of tartaric acid (5.02 g, 0.018 mole) in absolute ethanol (50 ml). The mixture was stirred for 4 hr and allowed to stand for 24 hr. Since no precipitate formed, anhydrous ether was added to the solution, and the mixture was allowed to stand for an additional 12 hr. The resulting crystalline precipitate was collected on a filter and washed several times with anhydrous ether. The crystalline material (9.6 g, mp 110–127°) was redissolved in hot absolute ethanol (30 ml), and the solution was allowed to stand for 8 hr.

The resulting precipitate was recrystallized five times from hot absolute

ethanol to yield a crystalline product {2.0 g, mp 128–130°, $[\alpha]_D^{25}$ +18.60° (*c*, 1.5%, absolute methanol)}. The combined filtrate remaining after isolation of the pure diastereomer (mp 128–130°) was evaporated under reduced pressure. The residue (6.6 g) was dissolved in hot isopropyl alcohol (30 ml) and allowed to stand at room temperature for 12 hr. The precipitate (0.6 g, mp 128–130°) was filtered off, and anhydrous isopropyl ether was added to the filtrate. The precipitate formed; after the solution was allowed to stand for 12 hr, it was collected and recrystallized three times from isopropyl alcohol–isopropyl ether {2.5 g, mp 118–120°, $[\alpha]_D^{25}$ +8.13° (*c*, 2.5%, absolute methanol)}.

The methyl bromide derivative of (+)-IV was prepared from the lower melting diastereomer after regeneration of the free base. The diastereomer (2.5 g) was dissolved in distilled water (20 ml), and the solution was treated with excess triethylamine. The mixture was stirred for 1 hr, and anhydrous isopropyl ether (20 ml) was added. The mixture then was stirred for 30 min. The isopropyl ether layer was isolated, and the aqueous layer was extracted twice with isopropyl ether (10 ml). The isopropyl ether extracts were combined, dried over calcium carbonate, and filtered, and the solvent was evaporated under reduced pressure. The resulting oily residue was redissolved in anhydrous isopropyl ether (20 ml), and the solution was treated with excess methyl bromide. The mixture was placed in a freezer for 24 hr, and the resulting precipitate (1.2 g, mp 217–220°) was recrystallized four times from isopropyl alcohol–isopropyl ether {0.4 g, mp 219–220°, $[\alpha]_D^{25}$ +16.33° (*c*, 5%, absolute methanol)}.

The methyl bromide derivative of (−)-IV was prepared from the higher melting diastereomer after regeneration of the free base. Excess triethylamine was added to the diastereomer (2.6 g) in distilled water (20 ml). The mixture then was stirred for 1 hr, isopropyl ether was added, and the mixture was stirred for an additional 30 min. The isopropyl ether layer was isolated, and the aqueous layer was extracted twice with isopropyl ether (10 ml). The combined extracts were dried over anhydrous calcium carbonate and filtered, and the solvent was evaporated under reduced pressure. The oily residue was dissolved in anhydrous isopropyl ether, and the solution was treated with excess methyl bromide. The mixture was placed in a freezer for 24 hr, and the resulting precipitate (1.6 g, mp 206–212°) was collected and recrystallized three times from isopropyl alcohol {0.5 g, mp 216–218°, $[\alpha]_D^{25}$ −16.43° (*c*, 5%, absolute methanol)}.

Melting points, optical rotation data, and elemental analyses of the diastereomers (tartrates) and enantiomers (methyl bromide) of the α-methyl isomer (IV) are presented in Table II.

## PHARMACOLOGY

Methyl bromide derivatives of the synthesized isomeric and nonisomeric oxime *O*-ethers were evaluated for antimuscarinic (spasmolytic) activity. Various test compound concentrations were used to obtain recordable dose–response curves. The spasmogen (urecholine) concentration was $2.55 \times 10^{-4}$ mmole/90 ml for each dose increment. The atropine sulfate concentration used in all determinations was $2.00 \times 10^{-7}$ mmole/90 ml. All test solutions were freshly prepared aqueous solutions.

**Method**—The method involved measurement of the inhibition (by a spasmolytic agent) of a spasmogen-induced contraction in a smooth muscle tissue (rat ileum) (15). The apparatus consisted of a glass cylinder (100-ml capacity) with an inlet for introducing the Tyrode bathing solution (90 ml) and an outlet for drainage. The bath solution was aerated continuously. The smooth muscle tissues were uniform strips of ileum taken from an unanesthetized, recently sacrificed, albino rat. The normal contractions of the ileum (0% response) were recorded on a physiograph through a myograph transducer. The spasmogen-induced contractions were produced by successive additions of the spasmogen dose increments at regular intervals until maximum response (100%) was achieved. There were no washes between the cumulative additions of the spasmogen.

Determination of antimuscarinic activity of the test compounds was initiated with a standard spasmogen curve, as already described, followed by washings of the muscle tissue. After the muscle strip had resumed its natural, spontaneous contractions, an appropriate dose of the test compound or atropine sulfate was introduced into the bath solution. After a brief interval (1.5 min), spasmogen dose increments were added to the bath until maximum response was achieved. The muscle strip then was washed and the whole process was repeated after 5–10 min for the next determination.

The data (percent response) were plotted on a probability scale (ordinate) *versus* the log of the spasmogen dose, in micromoles per 90 ml (abscissa). The spasmogen dose necessary to elicit a 50% response ($ED_{50}$) after pretreatment with the respective test compound or atropine sulfate was determined graphically. The relative potencies of the test compounds were calculated by comparing their respective $ED_{50}$ values with those of atropine sulfate. The pharmacological data are summarized in Table IV.

**Table IV—Summary of Pharmacological Data** [a]

| Compound | Dose[b], m*M*/90 ml | $ED_{50}$[c], m*M* | Relative[d] Potency | Isomeric[e] Potency Ratio |
|---|---|---|---|---|
| I · $CH_3Br$ | $5.00 \times 10^{-6}$ | $3.23 \times 10^{-3}$ | 0.074 | — |
| II · $CH_3Br$ | $5.00 \times 10^{-6}$ | $2.26 \times 10^{-3}$ | 0.052 | — |
| III · $CH_3Br$ | $5.00 \times 10^{-6}$ | $1.46 \times 10^{-3}$ | 0.033 | — |
| (±)-IV · $CH_3Br$ | $1.00 \times 10^{-6}$ | $2.44 \times 10^{-3}$ | 0.279 | — |
| (±)-V · $CH_3Br$ | $5.00 \times 10^{-6}$ | $1.25 \times 10^{-3}$ | 0.029 | 9.62 |
| (+)-IV · $CH_3Br$ | $1.00 \times 10^{-6}$ | $2.33 \times 10^{-3}$ | — | 1.09 |
| (−)-IV · $CH_3Br$ | $1.00 \times 10^{-6}$ | $2.12 \times 10^{-3}$ | — | — |

[a] Four consecutive determinations using the same muscle strip were made for each compound. [b] Dose of spasmolytic agent. [c] Spasmogen dose necessary to elicit a 50% response after pretreatment with the spasmolytic agent. [d] Spasmolytic activity of the test compound when compared with the spasmolytic activity of atropine sulfate. [e] Comparison of spasmolytic activities of the isomers based on their respective $ED_{50}$.

**Results**—All test compounds exhibited significant antimuscarinic activity (Table IV). Among the compounds tested, (±)-IV was the most potent (1/3 as potent as atropine sulfate) and (±)-V was the least potent (1/35 as potent as atropine sulfate).

The fact that (±)-IV was at least five times more potent than the corresponding *O*-(α-methylcholinyl) ether derivative of benzophenone oxime, which was reported (16) to be 1/22 as potent as atropine sulfate, indicated that the introduction of a sulfur atom in the umbrella-like portion of the oxime *O*-ether increased its antimuscarinic activity. This observation may indicate that the flat, nonpolar area of the muscarinic receptor, with which the umbrella-like moiety is believed to interact, is fairly extensive.

Compounds I, II, and III were 1/14, 1/19, and 1/30 as potent as atropine sulfate, respectively. The data indicate that antimuscarinic activity is optimal when a two-atom *O*-alkyl chain separates the ether oxygen from the amino nitrogen.

The fact that the racemic α-methyl isomer, (±)-IV, was considerably more potent than the racemic β-methyl isomer, (±)-V, was in agreement with previous reports (2, 3, 8). Furthermore, (±)-IV was more potent than the unsubstituted *O*-cholinyl ether derivative, I. These observations, coupled with the fact (17) that, at the receptor site involved, the activity of an antagonist is determined by its ability to bind with the receptor, may explain the α-methyl group's overall positive effect on the binding of (±)-IV with the muscarinic receptor. Such a contribution could be due to the production of a preferred conformation or to binding at an additional site on the receptor. The fact that the β-methyl isomer was less active than I would lead to an opposite conclusion: that the β-methyl group makes a negative overall contribution to the binding of (±)-V with the receptor.

It may be that the relatively large potency difference between the structural isomers cannot be due merely to binding or failure to bind of the methyl group but rather to the effect of the methyl group on binding of the rest of the molecule with the receptor. Such a conclusion would be entirely consistent with earlier reports (17–19) which observed that apparently minor structural changes in a compound can produce unusually large differences in affinities for the muscarinic receptor; such differences cannot be attributed to binding or failure to bind of any one group but rather are due to marked changes in the binding ability of the rest of the molecule.

Finally, no significant enantiomeric potency ratio was observed between (+)-IV and (−)-IV, which is consistent with earlier reports (3, 8). It may be concluded that the α-methyl group contributed positively to the binding of the rest of the molecule; however, configurational changes in the α-carbon atom did not alter significantly the binding of the rest of the molecule with the muscarinic receptor. Hence, no significant potency ratio was observed between the enantiomers.

## REFERENCES

(1) E. J. Ariens, in "Advances in Drug Research," vol. 3, N. J. Harper and A. B. Simmonds, Eds., Academic, London, England, 1966, p. 260.

(2) B. W. J. Ellenbroek, R. J. F. Nivard, J. M. Van Rossum, and E. J. Ariens, *J. Pharm. Pharmacol.*, **17**, 393 (1965).

(3) R. W. Brimblecombe, D. Green, and T. D. Inch, *ibid.*, **22**, 951 (1970).

(4) R. W. Brimblecombe, D. M. Green, T. D. Inch, and P. B. J.

Thompson, *ibid.*, **23**, 745 (1971).
(5) M. M. Kochhar, R. G. Brown, and J. N. Delgado, *J. Pharm. Sci.*, **54**, 393 (1965).
(6) S. K. Gomer, E. I. Isaacson, R. G. Brown, and J. N. Delgado, *ibid.*, **57**, 1586 (1968).
(7) W. G. Haney, R. G. Brown, E. I. Isaacson, and J. N. Delgado, *ibid.*, **66**, 1602 (1977).
(8) P. L. Huerta, E. I. Isaacson, R. G. Brown, and J. N. Delgado, *ibid.*, **66**, 1120 (1977).
(9) B. B. Wylie, E. I. Isaacson, and J. N. Delgado, *ibid.*, **54**, 1373 (1965).
(10) K. Nagrajan, C. L. Kulkarni, and A. Venkateswarlu, *Indian J. Chem.*, **6**, 226 (1968).
(11) N. Campbell, S. R. McCallum, and D. J. McKenzie, *J. Chem. Soc.*, **22**, 1922 (1957).
(12) P. A. S. Smith and J. E. Robertson, *J. Am. Chem. Soc.*, **84**, 1198 (1962).
(13) E. S. Gould, "Mechanism and Structure in Organic Chemistry," Holt, Rinehart and Winston, New York, N.Y., 1959, p. 570, and references cited therein.
(14) E. L. Eliel, "Stereochemistry of Carbon Compounds," McGraw-Hill, New York, N.Y., 1962, p. 83, and references cited therein.
(15) E. J. Ariens, paper presented at the APhA Academy of Pharmaceutical Sciences, Detroit meeting, Apr. 1965.
(16) P. L. Huerta, Ph.D. dissertation, University of Texas, Austin, Tex., 1972.
(17) R. B. Barlow, *J. Pharm. Pharmacol.*, **23**, 90 (1970).
(18) R. B. Barlow, F. M. Franks, and J. D. M. Pearson, *J. Med. Chem.*, **16**, 439 (1973).
(19) F. B. Abramson, R. B. Barlow, M. G. Mustafa, and R. P. Stephenson, *Br. J. Pharmacol.*, **37**, 207 (1969).

# Transport of Prostaglandins through Silicone Rubber

**T. J. ROSEMAN ˣ, L. J. LARION, and S. S. BUTLER**

Received August 14, 1980, from *Pharmacy Research, The Upjohn Company, Kalamazoo, MI 49001.* Accepted for publication November 6, 1980.

**Abstract** □ The *in vitro* release profiles of the F-series of prostaglandins were determined from a silicone rubber matrix of constant surface area. Silicone rubber was selective toward prostaglandin transport and offers potential as a controlled-release delivery system. Drug release patterns were dependent on the lipophilicity of the prostaglandin molecule. For dinoprost (prostaglandin $F_{2\alpha}$), the following sequence was observed: methyl ester > free acid > tromethamine salt. The biologically potent carboprost methyl [(15*S*)-15-methylprostaglandin $F_{2\alpha}$ methyl ester] was released considerably faster than the methyl ester of the parent dinoprost molecule, while release of the tromethamine salts of the two prostaglandins was similar. Permeability rates of the salts were depressed substantially when compared to their respective C-1 methyl esters. Results from independent membrane transport studies supported the observed dependence of steady-state flux on the chemical structure of the prostaglandin molecule. Plots of the amount released per unit area *versus* the square root of time were linear except for the initial drug release phase, and the total amount of prostaglandin released increased as the initial loading dose was raised. The data were analyzed according to a physical model describing drug release from inert matrix systems. The observed concentration dependence was consistent with the predictions of the model.

**Keyphrases** □ Prostaglandins—transport through silicone rubber, effect of lipophilicity, *in vitro* release profiles □ Dinoprost—transport through silicone rubber □ Carboprost—transport through silicone rubber □ Controlled-release delivery—transport of prostaglandins through silicone rubber □ Dosage forms—transport of prostaglandins through silicone rubber

Prostaglandins are a class of $C_{20}$ lipid-like substances that produce a wide spectrum of biological responses (1). Their clinical application in fertility control is well recognized since they possess luteolytic and abortifacient properties, alter ovum transport, and induce menses (2). Naturally occurring dinoprost[1] (prostaglandin $F_{2\alpha}$) and dinoprostone[2] (prostaglandin $E_2$) have been tested clinically by numerous routes of administration in solution, tablet, and suppository dosage forms. The (15*S*)-15-methyl analogs also are being explored as fertility-regulating agents and are considerably more potent (3, 4).

Intrauterine administration reduces undesirable side effects associated with the systemic intravenous route since drug is delivered closer to the uterus. The vaginal route, however, allows for self-administration, and it has been used successfully to terminate pregnancy with dinoprostone suppositories given by a multiple-dosing regimen (5) and with a single carboprost methyl[3] [(15*S*)-15-methylprostaglandin $F_{2\alpha}$ methyl ester] vaginal suppository (6).

## BACKGROUND

Studies in these laboratories have been directed toward the development of a prostaglandin delivery module that can be self-administered, is reversible, and provides continuous drug release for the treatment period following a single administration. Structural modifications of polymeric materials have been made to attain satisfactory prostaglandin release rates.

Nuwayser and Williams (7) showed that the permeability rate of dinoprost in deacetylated cellulose acetate was much greater than in other cellulose derivatives; in the rabbit, Akkapeddi *et al.* (8) demonstrated the abortifacient effectiveness of dinoprost and dinoprostone when incorporated into a series of hydrophilic polymeric materials. Polyacrylamide and polyvinylpyrrolidone gels containing dinoprostone or dinoprost also were effective in fertility control in several animal systems (9–12). Silicone rubber, however, was impervious to dinoprost transport and was discounted as a possible delivery system (9). Yet Spilman and Roseman (13) showed that silicone vaginal rings impregnated with carboprost methyl were effective in producing increased uterine muscle activity, luteolysis, and abortion in the Rhesus monkey.

The delivery system design, therefore, not only depends on the delivery module but also on the chemical form of the drug molecule. The present article provides a physicochemical analysis of the transport mechanism of prostaglandins through silicone rubber. The influence of lipophilicity on release is a dominant factor in assessing the utility of silicone rubber as a delivery system. In this regard, these findings parallel an earlier study with steroids (14).

## EXPERIMENTAL

The prostaglandins[4], dinoprost, dinoprost tromethamine, dinoprost

[1] Prostin $F_2$ alpha, The Upjohn Co., Kalamazoo, MI 49001.
[2] Prostin $E_2$, The Upjohn Co., Kalamazoo, MI 49001.
[3] Prostin M/15, The Upjohn Co., Kalamazoo, MI 49001.
[4] Supplied by the Pharmaceutical Research and Development Division, The Upjohn Co., Kalamazoo, MI 49001.



0022-3549/81/0500-0562$01.00/0
© 1981, American Pharmaceutical Association

Thompson, *ibid.*, **23**, 745 (1971).
(5) M. M. Kochhar, R. G. Brown, and J. N. Delgado, *J. Pharm. Sci.*, **54**, 393 (1965).
(6) S. K. Gomer, E. I. Isaacson, R. G. Brown, and J. N. Delgado, *ibid.*, **57**, 1586 (1968).
(7) W. G. Haney, R. G. Brown, E. I. Isaacson, and J. N. Delgado, *ibid.*, **66**, 1602 (1977).
(8) P. L. Huerta, E. I. Isaacson, R. G. Brown, and J. N. Delgado, *ibid.*, **66**, 1120 (1977).
(9) B. B. Wylie, E. I. Isaacson, and J. N. Delgado, *ibid.*, **54**, 1373 (1965).
(10) K. Nagrajan, C. L. Kulkarni, and A. Venkateswarlu, *Indian J. Chem.*, **6**, 226 (1968).
(11) N. Campbell, S. R. McCallum, and D. J. McKenzie, *J. Chem. Soc.*, **22**, 1922 (1957).
(12) P. A. S. Smith and J. E. Robertson, *J. Am. Chem. Soc.*, **84**, 1198 (1962).
(13) E. S. Gould, "Mechanism and Structure in Organic Chemistry," Holt, Rinehart and Winston, New York, N.Y., 1959, p. 570, and references cited therein.
(14) E. L. Eliel, "Stereochemistry of Carbon Compounds," McGraw-Hill, New York, N.Y., 1962, p. 83, and references cited therein.
(15) E. J. Ariens, paper presented at the APhA Academy of Pharmaceutical Sciences, Detroit meeting, Apr. 1965.
(16) P. L. Huerta, Ph.D. dissertation, University of Texas, Austin, Tex., 1972.
(17) R. B. Barlow, *J. Pharm. Pharmacol.*, **23**, 90 (1970).
(18) R. B. Barlow, F. M. Franks, and J. D. M. Pearson, *J. Med. Chem.*, **16**, 439 (1973).
(19) F. B. Abramson, R. B. Barlow, M. G. Mustafa, and R. P. Stephenson, *Br. J. Pharmacol.*, **37**, 207 (1969).

# Transport of Prostaglandins through Silicone Rubber

**T. J. ROSEMAN ˣ, L. J. LARION, and S. S. BUTLER**

Received August 14, 1980, from *Pharmacy Research, The Upjohn Company, Kalamazoo, MI 49001.* Accepted for publication November 6, 1980.

**Abstract** □ The *in vitro* release profiles of the F-series of prostaglandins were determined from a silicone rubber matrix of constant surface area. Silicone rubber was selective toward prostaglandin transport and offers potential as a controlled-release delivery system. Drug release patterns were dependent on the lipophilicity of the prostaglandin molecule. For dinoprost (prostaglandin $F_{2\alpha}$), the following sequence was observed: methyl ester > free acid > tromethamine salt. The biologically potent carboprost methyl [(15*S*)-15-methylprostaglandin $F_{2\alpha}$ methyl ester] was released considerably faster than the methyl ester of the parent dinoprost molecule, while release of the tromethamine salts of the two prostaglandins was similar. Permeability rates of the salts were depressed substantially when compared to their respective C-1 methyl esters. Results from independent membrane transport studies supported the observed dependence of steady-state flux on the chemical structure of the prostaglandin molecule. Plots of the amount released per unit area *versus* the square root of time were linear except for the initial drug release phase, and the total amount of prostaglandin released increased as the initial loading dose was raised. The data were analyzed according to a physical model describing drug release from inert matrix systems. The observed concentration dependence was consistent with the predictions of the model.

**Keyphrases** □ Prostaglandins—transport through silicone rubber, effect of lipophilicity, *in vitro* release profiles □ Dinoprost—transport through silicone rubber □ Carboprost—transport through silicone rubber □ Controlled-release delivery—transport of prostaglandins through silicone rubber □ Dosage forms—transport of prostaglandins through silicone rubber

Prostaglandins are a class of $C_{20}$ lipid-like substances that produce a wide spectrum of biological responses (1). Their clinical application in fertility control is well recognized since they possess luteolytic and abortifacient properties, alter ovum transport, and induce menses (2). Naturally occurring dinoprost[1] (prostaglandin $F_{2\alpha}$) and dinoprostone[2] (prostaglandin $E_2$) have been tested clinically by numerous routes of administration in solution, tablet, and suppository dosage forms. The (15*S*)-15-methyl analogs also are being explored as fertility-regulating agents and are considerably more potent (3, 4).

Intrauterine administration reduces undesirable side effects associated with the systemic intravenous route since drug is delivered closer to the uterus. The vaginal route, however, allows for self-administration, and it has been used successfully to terminate pregnancy with dinoprostone suppositories given by a multiple-dosing regimen (5) and with a single carboprost methyl[3] [(15*S*)-15-methylprostaglandin $F_{2\alpha}$ methyl ester] vaginal suppository (6).

## BACKGROUND

Studies in these laboratories have been directed toward the development of a prostaglandin delivery module that can be self-administered, is reversible, and provides continuous drug release for the treatment period following a single administration. Structural modifications of polymeric materials have been made to attain satisfactory prostaglandin release rates.

Nuwayser and Williams (7) showed that the permeability rate of dinoprost in deacetylated cellulose acetate was much greater than in other cellulose derivatives; in the rabbit, Akkapeddi *et al.* (8) demonstrated the abortifacient effectiveness of dinoprost and dinoprostone when incorporated into a series of hydrophilic polymeric materials. Polyacrylamide and polyvinylpyrrolidone gels containing dinoprostone or dinoprost also were effective in fertility control in several animal systems (9–12). Silicone rubber, however, was impervious to dinoprost transport and was discounted as a possible delivery system (9). Yet Spilman and Roseman (13) showed that silicone vaginal rings impregnated with carboprost methyl were effective in producing increased uterine muscle activity, luteolysis, and abortion in the Rhesus monkey.

The delivery system design, therefore, not only depends on the delivery module but also on the chemical form of the drug molecule. The present article provides a physicochemical analysis of the transport mechanism of prostaglandins through silicone rubber. The influence of lipophilicity on release is a dominant factor in assessing the utility of silicone rubber as a delivery system. In this regard, these findings parallel an earlier study with steroids (14).

## EXPERIMENTAL

The prostaglandins[4], dinoprost, dinoprost tromethamine, dinoprost

[1] Prostin $F_2$ alpha, The Upjohn Co., Kalamazoo, MI 49001.
[2] Prostin $E_2$, The Upjohn Co., Kalamazoo, MI 49001.
[3] Prostin M/15, The Upjohn Co., Kalamazoo, MI 49001.
[4] Supplied by the Pharmaceutical Research and Development Division, The Upjohn Co., Kalamazoo, MI 49001.



0022-3549/81/0500-0562$01.00/0
© 1981, American Pharmaceutical Association

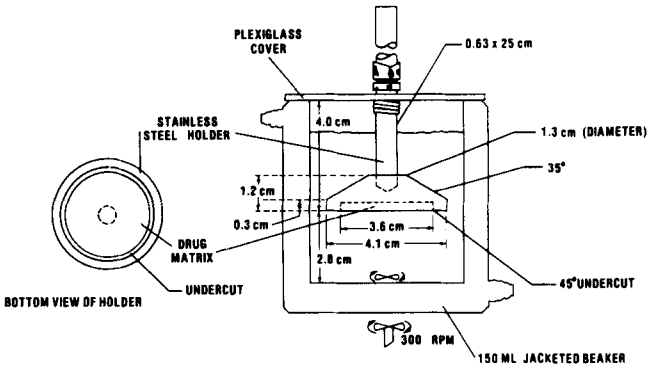


**Figure 1**—*Sketch of release apparatus and mold used to study the release of prostaglandins from silicone rubber.*

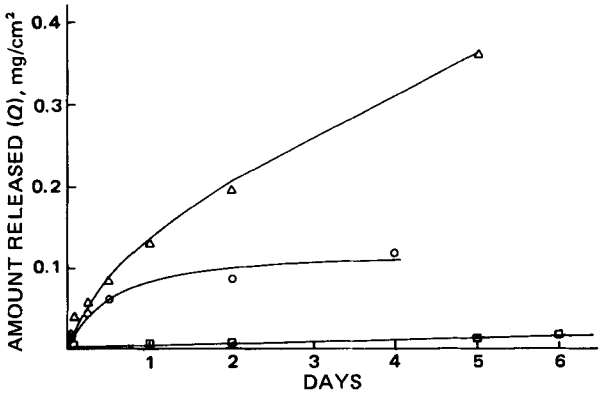


**Figure 2**—*Release profiles of dinoprost (prostaglandin $F_{2\alpha}$) from silicone rubber at a loading of 2%. Key: △, dinoprost methyl ester; ○, dinoprost free acid; and □, dinoprost tromethamine.*

methyl ester, carboprost methyl, and carboprost tromethamine, were at least 99% pure by GLC and showed a single major zone by TLC. Compression-distilled water and analytical reagent grade chemicals were used. Distilled-in-glass chloroform was used for prostaglandin extraction.

**Release Method**—The preparation of the prostaglandin matrixes and the experimental design of the release rate studies were similar to those reported previously (15). The methyl esters of dinoprost and carboprost first were triturated in a mortar to reduce their particle size. After the prostaglandins were suspended in the silicone monomer[5] and catalyzed with stannous octoate, the mix was placed into a stainless steel circular mold having an exposed surface area of 10 $cm^2$ (Fig. 1). During the curing step, an acrylic resin plate was placed over the elastomer to provide a smooth surface for the subsequent release experiments. The matrix was cured overnight at room temperature, the acrylic resin plate was removed, and the excess flashings were trimmed before release determinations were made.

Release measurements were performed in 100 ml of 0.1 *M* tromethamine buffer (pH 7.0) at 37°. Agitation of the solution was provided by a 300-rpm synchronous motor which rotated a magnetic stirrer. Samples (15–25 ml) were withdrawn through the acrylic resin cover with a syringe and needle, extracted with chloroform, and assayed. The withdrawn solution was replaced with an equal volume of buffer preequilibrated at 37°. For dinoprost tromethamine and dinoprost (free acid), the procedures were identical except that the tromethamine salt was micronized and the waxy free acid was levigated directly into the silicone phase.

The dissolution medium pH was selected to maintain sink conditions for dinoprost when used as the tromethamine salt and free acid. Since concentrations were <0.01 mg/ml and the aqueous solubility at this pH is >200 mg/ml (16), the sink condition was met. This same pH was used for the esters to maintain uniformity of dissolution and to retard any drug decomposition during the experiment. For the methyl esters, the concentrations during dissolution were <10% of their equilibrium solubility values. Stability studies with the methyl ester prostaglandins indicated that no decomposition occurred during sample preparation for dissolution. However, after about 1 week, some degradation of carboprost methyl was noted in the elution medium. When necessary, the concentrations were corrected to reflect accurately the total prostaglandin released. To avoid the potential effect of surface diffusion of drug on the release profiles, dissolution studies were performed within 1 week after device preparation.

The methyl ester samples (15–25 ml) were extracted directly with three equal volumes of chloroform and dried under vacuum with mild heat[6]. For the tromethamine salt and free acid runs, the pH of the withdrawn samples was lowered to 3 with 0.2 *M* citrate buffer (pH 3) and extracted with chloroform as outlined for the esters.

**Membrane Transport**—Fillerless silicone membranes were prepared by polymerizing the silicone monomer[7] with stannous octoate and placing the mix between metal plates separated by the appropriately sized spacers. After curing, the sheet was removed and circular membranes of the desired diameter were punched out. The membrane was soaked overnight in water and then mounted into a diffusion cell originally designed by Flynn and Smith (17), without the screen and with a 60-rpm motor. Throughout the experiment, temperature was maintained at 37°.

At time zero, a preequilibrated saturated solution containing excess prostaglandin in pH 7.0 tromethamine buffer was placed in the donor compartment, while the receptor side contained the buffer with no drug. Samples were taken as a function of time by flushing the receptor compartment with three volumes of fresh buffer. The entire sample then was extracted with chloroform (3 × 25 ml).

The diffusion coefficient of tritium-labeled carboprost methyl [(15*S*)-15-methylprostaglandin $F_{2\alpha}$-11$\beta$-[$^3$H]methyl ester] was determined using the described diffusion cell. Samples (1 ml) were withdrawn, diluted with 10 ml of scintillation fluid[8], and then counted on a liquid scintillation counter[9].

**Analytical Procedures**—GLC was employed to determine prostaglandin concentrations. The dried prostaglandin extracts were treated with 3–4 drops of dry pyridine and 0.5 ml of silylating reagent containing 1 or 3 mg of cholesteryl acetate (internal standard)/ml. For the 15-methylprostaglandin $F_{2\alpha}$ compounds, the silylating reagent was bis(trimethylsilyl)trifluoroacetamide plus 1% trimethylchlorosilane[10], and the solution was allowed to react overnight at room temperature. With the dinoprost compounds, a silylation mixture of *N,O*-bis(trimethylsilyl)-acetamide–trimethylchlorosilane[11] (4:1) was utilized; the reaction was completed in 30 min. Reference standards were prepared by direct treatment of 1 mg of prostaglandin with the appropriate silylating reagent.

After the reaction was complete, 1 μl was injected onto the glass (0.63-cm i.d. × 1.2-m length) column[12] packed with 3% UCW-98 on 80–100-mesh Gas Chrom Q[13]. The flash heater was off, and the column and detector temperatures were 260 and 270°, respectively. The helium gas flow was 60 ml/min, and air and hydrogen rates were adjusted to maximize response; the attenuation was 10 × 32. Unknown prostaglandin concentrations were determined by peak area ratios with standards injected with the samples.

Extraction of solution from a placebo run showed no interfering peaks. The efficiency of the analytical procedures was checked by analyzing samples of known concentrations. Complete prostaglandin recovery resulted from the extractions from aqueous media.

## RESULTS AND DISCUSSION

**Release Profiles of Dinoprost (Prostaglandin $F_{2\alpha}$)**—Studies on prostaglandin release from silicone rubber were initiated using the naturally occurring dinoprost as the model compound. Figure 2 illustrates the release pattern of dinoprost as a function of its chemical form at the C-1 position. Silicone rubber was almost impervious to the transport of dinoprost as the tromethamine salt, while the methyl ester was released continuously as a function of time. The release profile of dinoprost (free acid) fell in between the methyl ester and tromethamine salt. Qualitatively, the release data correlated directly with the expected degree of lipophilicity of the prostaglandin molecule in the silicone matrix phase, *i.e.*, methyl ester > free acid > tromethamine salt.

[5] Silastic 382, Dow Corning Corp., Midland, MI 48640.
[6] Büchi-Rotavapor-R, Switzerland.
[7] Fillerless Silastic 382 was supplied by the Dow Corning Corp., Midland, MI 48640.
[8] PCS, Amersham Co., Arlington Heights, IL 60005.
[9] Mark III model 6880, Searle Analytical Inc., Des Plaines, IL 60016.
[10] Regisil, Regis Chemical Co., Morton Grove, IL 60053.
[11] Pierce Chemical Co., Rockford, IL 61105.
[12] Model 402, Hewlett-Packard, Skokie, IL 60076.
[13] Applied Science Laboratories, State College, PA 16801.

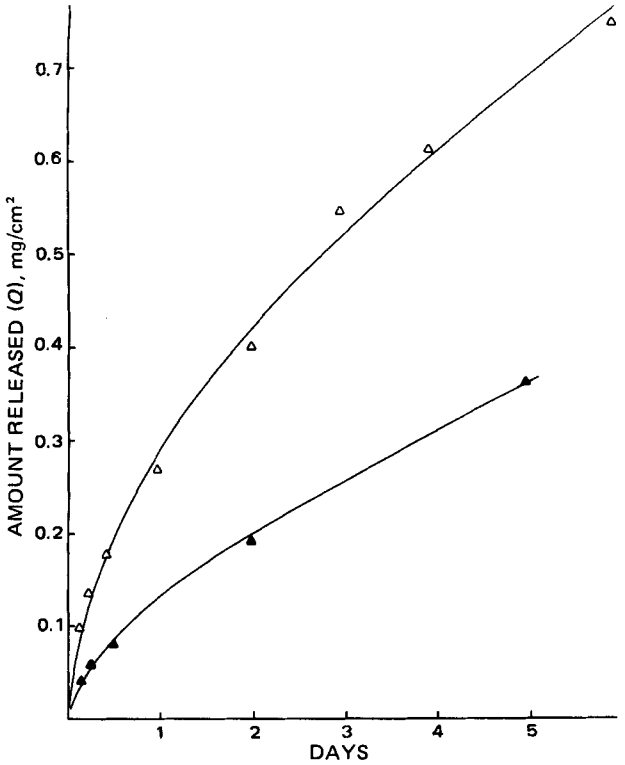


**Figure 3**—*Release profile of dinoprost methyl (prostaglandin $F_{2\alpha}$ methyl ester) from silicone rubber. Key: ▲, 2%; and △, 5%.*

Earlier work on the release of neutral steroidal compounds from silicone rubber suggested that drug transport is due mainly to diffusion through the matrix phase (18). The extremely slow release of dinoprost tromethamine supports this mechanism. At pH 7.0, dinoprost has a solubility in excess of 200 mg/ml. If transport through aqueous channels or pores is an important route for drug release, then the large aqueous solubility of the salt would provide a highly favorable driving force (concentration gradient) for the rapid diffusion of prostaglandin. The lower release rate of the salt form was probably due to a rather limited solubility in the silicone rubber phase. In contrast to the methyl ester of dinoprost, the free acid form was released for only about 2 days. The polymerization reaction for dinoprost (free acid) required a two- to threefold increase in the catalyst concentration, and it appears that the drug participated in the polymerization. If this is the case, the effective drug concentration in the matrix would be reduced and limit the availability of the prostaglandin molecule, as evidenced by the plateau region in Fig. 2. The dependence of release on the initial prostaglandin loading dose is shown in Fig. 3 for dinoprost methyl ester.

**Comparison of Permeability Rates of Dinoprost Methyl (Prostaglandin $F_{2\alpha}$ Methyl Ester) and Carboprost Methyl [(15*S*)-15-Methylprostaglandin $F_{2\alpha}$ Methyl Ester]**—The synthesis and biological activity of carboprost methyl was reported by Bundy *et al.* (19). This compound, along with other 15-methyl analogs of the A and E series of prostaglandins, was not a substrate for the enzyme, 15-hydroxyprostaglandin dehydrogenase, which rapidly inactivates the naturally occurring prostaglandins. The 15-methyl analog is 10 times more potent than dinoprost in promoting uterine activity and has been used successfully to terminate pregnancy by several administration routes (20). Silicone rings and devices containing carboprost methyl exhibit antifertility activity in the Rhesus monkey. A single intravaginal insertion of this device resulted in prolonged uterine activity, luteolysis, and termination of pregnancy (13, 15).

The *in vitro* release of this compound is presented in Fig. 4 for the 0.5–10% concentration range. Continuous drug release was observed for as long as 36 days, with the amount released at a given time increasing as the concentration was raised. This dependence is similar to the release of dinoprost methyl ester as seen in Fig. 3. However, the release rate of the 15-methyl analog was 1.4 times faster than the parent ester of dinoprost. At equal matrix concentrations, this factor reflects the ratio of the square root of the permeability constants ($P$), *i.e.*, the product of the drug solubility in the polymer ($C_s$) times the drug diffusivity in the polymer ($D_s$) (see *Theoretical Analysis*). Steady-state fluxes across a silicone

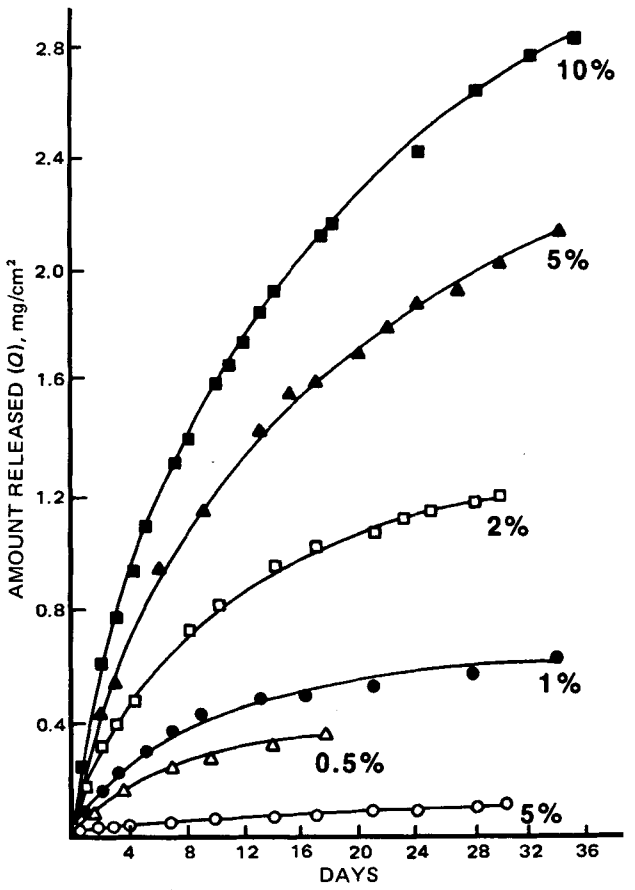


**Figure 4**—In vitro *release profiles of carboprost methyl [(15S)-15-methylprostaglandin $F_{2\alpha}$ methyl ester] from silicone rubber as a function of prostaglandin concentration in the matrix. Key:* ○, *5% tromethamine salt; and all other curves, methyl ester.*

membrane confirm the observed dependence on prostaglandin structure (Fig. 5). When the donor compartment in the diffusion cell is maintained at saturation, the following expression from Fick's law (21) is applicable:

$$\text{rate} = \left(\frac{dQ}{dt}\right)_{ss} = \frac{C_s D_s}{l} \qquad \text{(Eq. 1)}$$

where $l$ is the membrane thickness. Steady-state diffusion rates are related linearly to $C_s D_s$ and, as expected, the flux of the two prostaglandins is different at equal membrane thicknesses. Increasing the thickness decreases the transport in accord with Eq. 1. In contrast to the observed

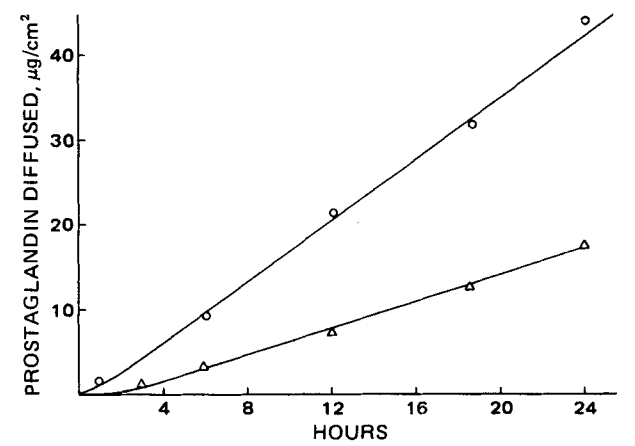


**Figure 5**—*Amount of prostaglandin diffused across a 0.047-cm thick silicone rubber membrane as a function of time. Key:* ○, *carboprost methyl [(15S)-15-methylprostaglandin $F_{2\alpha}$ methyl ester]; and* △, *dinoprost methyl (prostaglandin $F_{2\alpha}$ methyl ester).*

**Table I—Comparisons of Prostaglandin Permeability Constants [a] ($C_sD_s$) from Matrix Release and Membrane Transport Experiments**

| | Matrix Release | Membrane Transport |
|---|---|---|
| Dinoprost methyl (prostaglandin $F_{2\alpha}$ methyl ester) | $0.84^b \times 10^{-8}$ | $0.98 \times 10^{-8c}$ |
| Carboprost methyl [(15*S*)-15-methylprostaglandin $F_{2\alpha}$ methyl ester] | $1.6^b \times 10^{-8}$ | $2.1^c \times 10^{-8}$, $2.6^d \times 10^{-8}$ |

[a] Units are milligrams per centimeter per second. [b] Calculated average from the least-squares slope of $(Q/t^{1/2})$ *versus* $A^{1/2}$. [c] Calculated using a 0.097-cm thick membrane. [d] Calculated using a 0.0470-cm thick membrane.

transport of the esters, the tromethamine salts diffused at negligible rates.

**Theoretical Analysis**—The general equation for drug release from a planar silicone rubber surface is:

$$Q = \frac{-D_s h_a K A \epsilon}{D_a \tau} + \left[\left(\frac{D_s h_a K A \epsilon}{D_a \tau}\right)^2 + \frac{2AD_sC_s\epsilon t}{\tau}\right]^{1/2} \quad \text{(Eq. 2)}$$

where:

$Q$ = amount released per unit area
$t$ = time
$A$ = total concentration of drug in matrix
$D_a$ = diffusion coefficient in the dissolution medium
$D_s$ = diffusion coefficient in the matrix phase
$K$ = partition coefficient ($C_s/C_a$)
$C_a$ = solubility in the dissolution medium
$C_s$ = solubility in the matrix phase
$h_a$ = boundary diffusion layer thickness
$\epsilon$ = volume fraction
$\tau$ = tortuosity

Equation 2 was derived from a physical model which considers both diffusion through the matrix and transport away from its surface across a boundary diffusion layer[14]. For drugs that exhibit high permeability rates, the boundary diffusion layer can offer a major resistance to drug release. However, when the matrix is rate controlling, Eq. 2 reduces to:

$$Q = \left(\frac{2AD_sC_s\epsilon t}{\tau}\right)^{1/2} \quad \text{(Eq. 3)}$$

which was originally derived (22) for drug release from inert matrix systems. Plots of $Q$ *versus* $t^{1/2}$ for the prostaglandin methyl esters are shown in Figs. 6 and 7. Except for an early nonlinear period, Eq. 3 is obeyed. The curvature at early times follows predictions from Eq. 2 when the resistance of the diffusion layer plays a significant role in the total diffusion. As noted in Fig. 7, where a wide range of concentrations are presented, the curvature becomes less as the concentration in the silicone rubber phase decreases. This finding supports the applicability of Eq. 2 at early times because the depleted region in the matrix recedes less at high

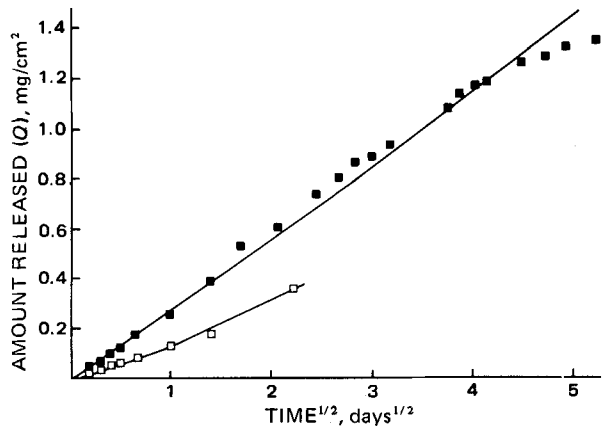


**Figure 6**—*Dependence of* Q *on* $t^{1/2}$ *for the release of dinoprost methyl (prostaglandin $F_{2\alpha}$ methyl ester) from silicone rubber at different loading doses. Key: □, 2%; and ■, 5%.*

[14] The assumptions in the derivation can be found in Ref. 18.

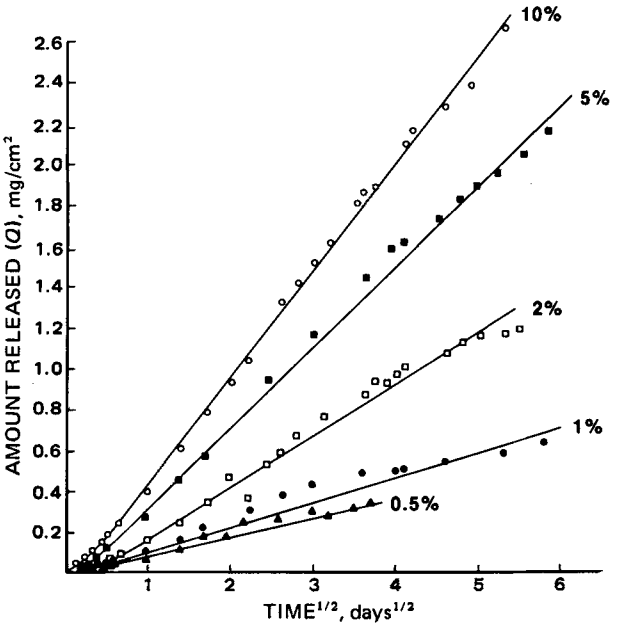


**Figure 7**—*Dependence of* Q *on* $t^{1/2}$ *for the release of carboprost methyl [(15S)-15-methylprostaglandin $F_{2\alpha}$ methyl ester] from silicone rubber at different loading doses.*

loading doses. At low matrix concentrations, drug diffusion occurs across a depleted zone of greater depth and Eq. 3 becomes operative sooner. This is evident in the 0.5% curve where $Q$ *versus* $t^{1/2}$ plots are linear even during the early release stage.

Calculated values for the permeability constants, $C_sD_s$, are given in Table I. Considering the complexities of the studies, favorable agreement between the matrix release and membrane transport data is noted. The slightly higher numbers associated with the membrane transport experiments may be a consequence of faster drug diffusion through a fillerless polymer[15]. Fillerless material was used to obtain additional information on the diffusivity of the prostaglandins since silicone rubber reinforced with diatomaceous earth or silica was reported (23, 24) to increase the lag times ($L$) and yield anomalous diffusivity values calculated from the lag time expression (25):

$$D_s = \frac{l^2}{6L} \quad \text{(Eq. 4)}$$

where $l$ is the membrane thickness and $L$ is the lag time[16]. In the present study, extrapolation of the steady-state portions of the curve in Fig. 5 yielded lag times with high standard errors of the mean, and accurate values could not be determined. However, by utilizing radiolabeled carboprost methyl, the diffusion coefficient of the prostaglandin was determined to be $0.485 \times 10^{-7}$ ($\pm 0.020 \times 10^{-7}$) $cm^2$/sec. The C-15 methyl group is not expected to alter the diffusivity of this series, and the same value can be reasonably assumed for dinoprost methyl ester. The estimated values of $C_s$ for carboprost methyl and dinoprost methyl ester are 0.48 and 0.20 $mg/cm^3$, respectively. Methylation at the C-15 position of dinoprost methyl ester, therefore, appears to make the prostaglandin ester more lipophilic, resulting in increased transport rates.

Previous studies (26) demonstrated that substitution of a less polar carbonyl group for the hydroxyl moiety at C-9 (*i.e.*, dinoprost → dinoprostone) and the addition of lipophilic ester groups at C-1 significantly increase the transport rates of prostaglandins across silicone rubber. The agreement between the permeability constants in Table I for matrix release and membrane transport suggests that membrane transport studies can be used to predict *a priori* release profiles of prostaglandins from monolithic devices according to:

$$Q = \left[2Al\left(\frac{dQ}{dt}\right)_{ss}\right]^{1/2} t^{1/2} \quad \text{(Eq. 5)}$$

[15] Filler, such as silica, is incorporated in the polymer to increase its mechanical properties.

[16] This expression applies when the major resistance to diffusion resides in the membrane. It is valid for these prostaglandins since the resistance in the membrane is at least 100 times greater than in the diffusion layer.

and:

$$\text{rate} = \left[\frac{Al}{2}\left(\frac{dQ}{dt}\right)_{ss}\right]^{1/2} t^{-1/2} \qquad \text{(Eq. 6)}$$

where $(dQ/dt)_{ss}$ is the slope of the steady-state portion of the curve from a diffusion cell experiment (Fig. 5) and the other terms are as were defined. This approach is valuable in screening compounds to assess whether release rates are consistent with their biological dosing patterns.

## REFERENCES


(1) T. O. Oesterling, W. Morozowich, and T. J. Roseman, *J. Pharm. Sci.*, **61**, 1861 (1972).

(2) "Prostaglandins and Reproduction," S. M. M. Karim, Ed., Medical and Technical Publishing Co., Lancaster, England, 1975.

(3) S. M. M. Karim and S. D. Sharma, *J. Obstet. Gynaecol. Br. Commonw.*, **79**, 737 (1972).

(4) M. Toppozada, F. Beguin, M. Bygdeman, and N. Wiqvist, *Prostaglandins*, **2**, 239 (1972).

(5) S. L. Corson and R. J. Bolognese, *J. Reprod. Med.*, **14**, 43 (1975).

(6) A. Bhaskar, V. Dimov, S. Baliga, G. Kinra, V. Hingorani, and K. R. Laumas, *Contraception*, **20**, 519 (1979).

(7) E. S. Nuwayser and D. L. Williams, in "Controlled Release of Biologically Active Agents," A. C. Tanquary and R. E. Lacey, Eds., Plenum, New York, N.Y., 1974, p. 145.

(8) M. K. Akkapeddi, B. D. Halpern, R. H. Davis, and H. Balin, in *ibid.*, p. 165.

(9) B. K. Davis and M. C. Chang, *Acta Endocrinol.*, **70**, 97 (1972).

(10) B. K. Davis, *Prostaglandins*, **7**, 393 (1974).

(11) S. K. Saksena, I. F. Lau, and M. C. Chang, *ibid.*, **7**, 507 (1974).

(12) I. F. Lau, S. K. Saksena, and M. C. Chang, *Am. J. Obstet. Gynecol.*, **120**, 837 (1974).

(13) C. H. Spilman and T. J. Roseman, *Contraception*, **11**, 409 (1975).

(14) T. J. Roseman, *J. Pharm. Sci.*, **61**, 46 (1972).

(15) C. H. Spilman, D. C. Beuving, A. D. Forbes, T. J. Roseman, and L. J. Larion, *Prostaglandins, Suppl.*, **12**, 1 (1976).

(16) T. J. Roseman and S. H. Yalkowsky, *J. Pharm. Sci.*, **62**, 1680 (1973).

(17) G. L. Flynn and E. W. Smith, *ibid.*, **60**, 1713 (1971).

(18) T. J. Roseman and W. I. Higuchi, *ibid.*, **59**, 353 (1970).

(19) G. L. Bundy, E. W. Yankee, J. R. Weeks, and W. L. Miller, *Adv. Biosci.*, **9**, 125 (1972).

(20) M. Bygdeman, J. N. Martin, N. Wiqvist, K. Green, and S. Bergström, *Prostaglandins*, **8**, 157 (1974).

(21) W. Jost, "Diffusion in Solids, Liquids and Gases," Academic, New York, N.Y., 1960.

(22) T. Higuchi, *J. Pharm. Sci.*, **52**, 1145 (1963).

(23) C. F. Most, Jr., *J. Appl. Polym. Sci.*, **14**, 1019 (1970).

(24) G. L. Flynn and T. J. Roseman, *J. Pharm. Sci.*, **60**, 1788 (1971).

(25) R. M. Barrer, *Trans. Faraday Soc.*, **35**, 628 (1939).

(26) T. J. Roseman, *J. Pharm. Sci.*, **68**, 263 (1979).


# NOTES

# Synthesis and Antibacterial and Antifungal Activities of Alkyl and Polyhalophenyl Esters of Benzo[*b*]thiophene-3-carbamic Acid


**A. SHAFIEE ˣ, M. VOSSOGHI, J. WOSSOOGHI, and S. YAZDANI**



Received June 29, 1979, from the *Department of Chemistry, College of Pharmacy, Tehran University, Tehran, Iran.* Accepted for publication December 20, 1979.



**Abstract** □ Several alkyl and polyhalophenyl esters of benzo[*b*]thiophene-3-carbamic acid were prepared and tested for antibacterial and antifungal activities. Two compounds exhibited the highest activity of growth inhibition against some bacteria and fungi.



**Keyphrases** □ Antibacterial activity—alkyl and polyhalophenyl esters of benzo[*b*]thiophene-3-carbamic acid □ Antifungal activity—alkyl and polyhalophenyl esters of benzo[*b*]thiophene-3-carbamic acid □ Benzo[*b*]thiophene-3-carbamic acid—alkyl and polyhalophenyl esters, synthesis, antibacterial and antifungal activities


Dialkylaminoalkyl esters of benzo[*b*]thiophene-2-carboxylic acid[1] reportedly are useful as hypotensive, antiviral, and antifungal agents (1). Derivatives of benzo[*b*]-thiophene-2-carboxamide were reported to have local anesthetic and analgesic activities (2). Some carbamic acids having the benzo[*b*]thiophene moiety showed pesticidal, fungicidal, and insecticidal activities (3).

In continuing studies on the chemistry and antibacterial and fungicidal activities of carbamic acid esters (4–7), alkyl and polyhalophenyl esters of benzo[*b*]thiophene-3-carbamic acid were synthesized and their efficacy was determined.

## DISCUSSION

**Chemistry**—The desired compounds were prepared according to Scheme I.

The reaction of *N*-bromosuccinimide with readily available 3-chloromethylbenzo[*b*]thiophene (I) (8) afforded II. Hydrolysis of II gave benzo[*b*]thiophene-3-carboxylic acid (III) (9). Compound III was converted to benzo[*b*]thiophene-3-carboxyhydrazide (V) by a literature method (10). The hydrazide (V) then was transformed to the carboxazide (VI) by reaction with sodium nitrite in acetic acid. Curtius rearrangement of the azide was achieved readily through heating with alcohols or with polyhalophenols in refluxing benzene. The physical data of the compounds prepared are summarized in Table I.

**Antifungal and Antibacterial Activities**—All compounds listed in Table I were tested against *Candida albicans* (28012), *Penicillium not-*

[1] Benzo[*b*]thiophene also is known as thianaphthene.




0022-3549/81/0500-0566$01.00/0



© 1981, American Pharmaceutical Association

and:

$$\text{rate} = \left[\frac{Al}{2}\left(\frac{dQ}{dt}\right)_{ss}\right]^{1/2} t^{-1/2} \qquad \text{(Eq. 6)}$$

where $(dQ/dt)_{ss}$ is the slope of the steady-state portion of the curve from a diffusion cell experiment (Fig. 5) and the other terms are as were defined. This approach is valuable in screening compounds to assess whether release rates are consistent with their biological dosing patterns.

## REFERENCES


(1) T. O. Oesterling, W. Morozowich, and T. J. Roseman, *J. Pharm. Sci.*, **61**, 1861 (1972).

(2) "Prostaglandins and Reproduction," S. M. M. Karim, Ed., Medical and Technical Publishing Co., Lancaster, England, 1975.

(3) S. M. M. Karim and S. D. Sharma, *J. Obstet. Gynaecol. Br. Commonw.*, **79**, 737 (1972).

(4) M. Toppozada, F. Beguin, M. Bygdeman, and N. Wiqvist, *Prostaglandins*, **2**, 239 (1972).

(5) S. L. Corson and R. J. Bolognese, *J. Reprod. Med.*, **14**, 43 (1975).

(6) A. Bhaskar, V. Dimov, S. Baliga, G. Kinra, V. Hingorani, and K. R. Laumas, *Contraception*, **20**, 519 (1979).

(7) E. S. Nuwayser and D. L. Williams, in "Controlled Release of Biologically Active Agents," A. C. Tanquary and R. E. Lacey, Eds., Plenum, New York, N.Y., 1974, p. 145.

(8) M. K. Akkapeddi, B. D. Halpern, R. H. Davis, and H. Balin, in *ibid.*, p. 165.

(9) B. K. Davis and M. C. Chang, *Acta Endocrinol.*, **70**, 97 (1972).

(10) B. K. Davis, *Prostaglandins*, **7**, 393 (1974).

(11) S. K. Saksena, I. F. Lau, and M. C. Chang, *ibid.*, **7**, 507 (1974).

(12) I. F. Lau, S. K. Saksena, and M. C. Chang, *Am. J. Obstet. Gynecol.*, **120**, 837 (1974).

(13) C. H. Spilman and T. J. Roseman, *Contraception*, **11**, 409 (1975).

(14) T. J. Roseman, *J. Pharm. Sci.*, **61**, 46 (1972).

(15) C. H. Spilman, D. C. Beuving, A. D. Forbes, T. J. Roseman, and L. J. Larion, *Prostaglandins, Suppl.*, **12**, 1 (1976).

(16) T. J. Roseman and S. H. Yalkowsky, *J. Pharm. Sci.*, **62**, 1680 (1973).

(17) G. L. Flynn and E. W. Smith, *ibid.*, **60**, 1713 (1971).

(18) T. J. Roseman and W. I. Higuchi, *ibid.*, **59**, 353 (1970).

(19) G. L. Bundy, E. W. Yankee, J. R. Weeks, and W. L. Miller, *Adv. Biosci.*, **9**, 125 (1972).

(20) M. Bygdeman, J. N. Martin, N. Wiqvist, K. Green, and S. Bergström, *Prostaglandins*, **8**, 157 (1974).

(21) W. Jost, "Diffusion in Solids, Liquids and Gases," Academic, New York, N.Y., 1960.

(22) T. Higuchi, *J. Pharm. Sci.*, **52**, 1145 (1963).

(23) C. F. Most, Jr., *J. Appl. Polym. Sci.*, **14**, 1019 (1970).

(24) G. L. Flynn and T. J. Roseman, *J. Pharm. Sci.*, **60**, 1788 (1971).

(25) R. M. Barrer, *Trans. Faraday Soc.*, **35**, 628 (1939).

(26) T. J. Roseman, *J. Pharm. Sci.*, **68**, 263 (1979).


# NOTES

# Synthesis and Antibacterial and Antifungal Activities of Alkyl and Polyhalophenyl Esters of Benzo[*b*]thiophene-3-carbamic Acid


**A. SHAFIEE ˣ, M. VOSSOGHI, J. WOSSOOGHI, and S. YAZDANI**



Received June 29, 1979, from the *Department of Chemistry, College of Pharmacy, Tehran University, Tehran, Iran.* Accepted for publication December 20, 1979.



**Abstract** □ Several alkyl and polyhalophenyl esters of benzo[*b*]thiophene-3-carbamic acid were prepared and tested for antibacterial and antifungal activities. Two compounds exhibited the highest activity of growth inhibition against some bacteria and fungi.



**Keyphrases** □ Antibacterial activity—alkyl and polyhalophenyl esters of benzo[*b*]thiophene-3-carbamic acid □ Antifungal activity—alkyl and polyhalophenyl esters of benzo[*b*]thiophene-3-carbamic acid □ Benzo[*b*]thiophene-3-carbamic acid—alkyl and polyhalophenyl esters, synthesis, antibacterial and antifungal activities


Dialkylaminoalkyl esters of benzo[*b*]thiophene-2-carboxylic acid[1] reportedly are useful as hypotensive, antiviral, and antifungal agents (1). Derivatives of benzo[*b*]-thiophene-2-carboxamide were reported to have local anesthetic and analgesic activities (2). Some carbamic acids having the benzo[*b*]thiophene moiety showed pesticidal, fungicidal, and insecticidal activities (3).

In continuing studies on the chemistry and antibacterial and fungicidal activities of carbamic acid esters (4–7), alkyl and polyhalophenyl esters of benzo[*b*]thiophene-3-carbamic acid were synthesized and their efficacy was determined.

## DISCUSSION

**Chemistry**—The desired compounds were prepared according to Scheme I.

The reaction of *N*-bromosuccinimide with readily available 3-chloromethylbenzo[*b*]thiophene (I) (8) afforded II. Hydrolysis of II gave benzo[*b*]thiophene-3-carboxylic acid (III) (9). Compound III was converted to benzo[*b*]thiophene-3-carboxyhydrazide (V) by a literature method (10). The hydrazide (V) then was transformed to the carboxazide (VI) by reaction with sodium nitrite in acetic acid. Curtius rearrangement of the azide was achieved readily through heating with alcohols or with polyhalophenols in refluxing benzene. The physical data of the compounds prepared are summarized in Table I.

**Antifungal and Antibacterial Activities**—All compounds listed in Table I were tested against *Candida albicans* (28012), *Penicillium not-*

[1] Benzo[*b*]thiophene also is known as thianaphthene.




0022-3549/81/0500-0566$01.00/0



© 1981, American Pharmaceutical Association

**Table I—Physical Constants of Benzo[*b*]thiophene-3-carbamic Acid Esters**

| Compound | R | Yield, % | Melting Point[a] | Formula | Analysis, % | Calc. | Found |
|---|---|---|---|---|---|---|---|
| VII*a* | $CH_3$ | 82 | 63–65° | $C_{10}H_9NO_2S$ | C | 57.97 | 57.73 |
| | | | | | H | 4.35 | 4.51 |
| | | | | | N | 6.76 | 6.95 |
| VII*b* | $C_2H_5$ | 80 | 67–70° | $C_{11}H_{11}NO_2S$ | C | 59.73 | 59.91 |
| | | | | | H | 4.98 | 4.79 |
| | | | | | N | 6.33 | 6.51 |
| VII*c* | $n$-$C_3H_7$ | 75 | 56–58° | $C_{12}H_{13}NO_2S$ | C | 61.28 | 61.09 |
| | | | | | H | 5.53 | 5.38 |
| | | | | | N | 5.96 | 6.18 |
| VII*d* | $n$-$C_4H_9$ | 80 | 70–73° | $C_{13}H_{15}NO_2S$ | C | 62.65 | 62.84 |
| | | | | | H | 6.02 | 5.89 |
| | | | | | N | 5.62 | 5.43 |
| VII*e* | $n$-$C_6H_{13}$ | 75 | 55–57° | $C_{15}H_{19}NO_2S$ | C | 64.98 | 64.79 |
| | | | | | H | 6.86 | 6.63 |
| | | | | | N | 5.05 | 4.88 |
| VII*f* | Cyclohexyl | 75 | 95–97° | $C_{15}H_{17}NO_2S$ | C | 65.45 | 65.27 |
| | | | | | H | 6.18 | 6.02 |
| | | | | | N | 5.09 | 4.93 |
| VII*g* | $C_6H_5$ | 60 | 103–105° | $C_{15}H_{11}NO_2S$ | C | 66.91 | 66.72 |
| | | | | | H | 4.09 | 4.28 |
| | | | | | N | 5.20 | 5.38 |
| VII*h* | $o$-$ClC_6H_4$ | 85 | 142–144° | $C_{15}H_{10}ClNO_2S$ | C | 59.31 | 59.50 |
| | | | | | H | 3.29 | 3.48 |
| | | | | | N | 4.61 | 4.82 |
| VII*i* | $m$-$ClC_6H_4$ | 85 | 114–116° | $C_{15}H_{10}ClNO_2S$ | C | 59.31 | 59.12 |
| | | | | | H | 3.29 | 3.46 |
| | | | | | N | 4.61 | 4.52 |
| VII*j* | $p$-$ClC_6H_4$ | 80 | 131–133° | $C_{15}H_{10}ClNO_2S$ | C | 59.31 | 59.50 |
| | | | | | H | 3.29 | 3.46 |
| | | | | | N | 4.61 | 4.48 |
| VII*k* | $p$-$BrC_6H_4$ | 65 | 138–140° | $C_{15}H_{10}BrNO_2S$ | C | 51.72 | 51.53 |
| | | | | | H | 2.87 | 2.64 |
| | | | | | N | 4.02 | 3.85 |
| VII*l* | 2,3-Dichlorophenyl | 45 | 125–127° | $C_{15}H_9Cl_2NO_2S$ | C | 53.25 | 53.44 |
| | | | | | H | 2.66 | 2.84 |
| | | | | | N | 4.14 | 4.32 |
| VII*m* | 2,4-Dichlorophenyl | 45 | 164–166° | $C_{15}H_9Cl_2NO_2S$ | C | 53.25 | 53.05 |
| | | | | | H | 2.66 | 2.84 |
| | | | | | N | 4.14 | 4.02 |
| VII*n* | 2,6-Dichlorophenyl | 45 | 152–154° | $C_{15}H_9Cl_2NO_2S$ | C | 53.25 | 53.15 |
| | | | | | H | 2.66 | 2.84 |
| | | | | | N | 4.14 | 4.32 |
| VII*o* | 2,4,5-Trichlorophenyl | 80 | 170–172° | $C_{15}H_8Cl_3NO_2S$ | C | 48.32 | 48.15 |
| | | | | | H | 2.15 | 2.02 |
| | | | | | N | 3.76 | 3.89 |
| VII*p* | 2,4,6-Trichlorophenyl | 65 | 160–162° | $C_{15}H_8Cl_3NO_2S$ | C | 48.32 | 48.51 |
| | | | | | H | 2.15 | 2.37 |
| | | | | | N | 3.76 | 3.65 |
| VII*q* | 2,4,6-Tribromophenyl | 60 | 172–174° | $C_{15}H_8Br_3NO_2S$ | C | 35.57 | 35.74 |
| | | | | | H | 1.58 | 1.79 |
| | | | | | N | 2.77 | 2.96 |
| VII*r* | Pentachlorophenyl | 62 | 160–162° | $C_{15}H_6Cl_5NO_2S$ | C | 40.77 | 40.56 |
| | | | | | H | 1.36 | 1.17 |
| | | | | | N | 3.17 | 3.39 |

[a] All compounds were crystallized from ether–petroleum ether.

*atum* (S-13), and *Aspergillus niger* (23171) *in vitro* using Sabouraud dextrose agar medium[2].

Each compound was dissolved in acetone to a concentration of 1 mg/ml. These solutions were diluted with hot culture medium to the desired concentrations and autoclaved at 120° for 2 hr. Five replicates of each concentration were prepared. The antifungal activity of all compounds tested, except VIIo and VIIr, was insignificant at a concentration of 10 μg/ml against *A. niger* and *C. albicans*, while most compounds were effective at this concentration against *P. notatum*. Griseofulvin was used as a control (Table II).

All compounds also were tested against *Bacillus subtilis* (NCTC 3610), *Staphylococcus aureus* (ATCC 6538), and *Escherichia coli* (ATCC 10536). Nitrofurantoin was used as a control. The compounds were dissolved in dimethylformamide and diluted to a 0.5% concentration. Standard paper disks with a 6-mm diameter were immersed in the solution and were placed on the inoculated assay medium surface[3].

All of the compounds tested, except VIIo and VIIr, had insignificant antibacterial activity against *S. aureus*. Compounds VII*m* and VIIo–VIIr exhibited moderate activity against *B. subtilis*. The activity of VIIo, VII*q*, and VIIr against *E. coli* was significant (Table III).

## EXPERIMENTAL[4]

**Benzo[*b*]thiophene-3-carboxylic Acid (III)**—A mixture of I (18.25 g, 0.1 mole) and *N*-bromosuccinimide (35.6 g, 0.2 mole) in 250 ml of carbon tetrachloride was irradiated with a 500-w lamp[5] while heating and stirring at reflux temperature for 4 hr. Then the reaction mixture was cooled and filtered, and the solvent was evaporated. The residue was made alkaline with 300 ml of 10% sodium carbonate solution and was heated with stirring on a steam bath for 2 hr. The mixture was cooled and extracted with 200 ml of benzene. Acidification of the aqueous sodium carbonate portion with 6 *N* HCl gave a precipitate. This precipitate was filtered and crystallized from benzene to give 4.4 g (55% yield) of III, mp 175–176° [lit. (9) mp 175–176°].

[2] These microorganisms were obtained from the Department of Parasitology, Public Health Institute, Tehran, Iran.

[3] BP (1968) antibiotic assay medium.

[4] Melting points were taken on a Kofler hot-stage microscope and are uncorrected. IR spectra were recorded using a Perkin-Elmer 267 spectrometer. NMR spectra were determined with a Varian T-60A instrument. Mass spectra were recorded on a Varian Mat III instrument.

[5] General Electric photospot lamp.

**Table II—Antifungal Activity [a] of Benzo[*b*]thiophene-3-carbamic Acid Esters**

| Compound | *A. niger* | | | *C. albicans* | | | *P. notatum* | | |
|---|---|---|---|---|---|---|---|---|---|
| | 10 μg/ml | 20 μg/ml | 50 μg/ml | 10 μg/ml | 20 μg/ml | 50 μg/ml | 10 μg/ml | 20 μg/ml | 50 μg/ml |
| VII*a* | − | − | + | − | − | + | − | + | + |
| VII*b* | − | − | + | − | − | + | − | + | + |
| VII*c* | − | − | + | − | − | + | − | − | + |
| VII*d* | − | − | + | − | − | + | − | + | + |
| VII*e* | − | − | + | − | − | + | − | − | + |
| VII*f* | − | − | + | − | − | + | + | + | + |
| VII*g* | − | − | + | − | − | + | + | + | + |
| VII*h* | − | − | + | − | − | + | − | + | + |
| VII*i* | − | − | + | − | − | − | − | − | + |
| VII*j* | − | − | + | − | − | + | + | + | + |
| VII*k* | − | − | + | − | − | − | − | − | + |
| VII*l* | − | − | + | − | − | + | − | + | + |
| VII*m* | − | − | + | − | − | + | − | + | + |
| VII*n* | − | − | + | − | − | + | + | + | + |
| VII*o* | + | + | + | + | + | + | + | + | + |
| VII*p* | − | + | + | − | + | + | + | + | + |
| VII*q* | − | + | + | − | + | + | + | + | + |
| VII*r* | + | + | + | + | + | + | + | + | + |
| Griseofulvin | − | − | + | − | − | + | − | + | + |

[a] Key: + = complete inhibition and − = no inhibition.

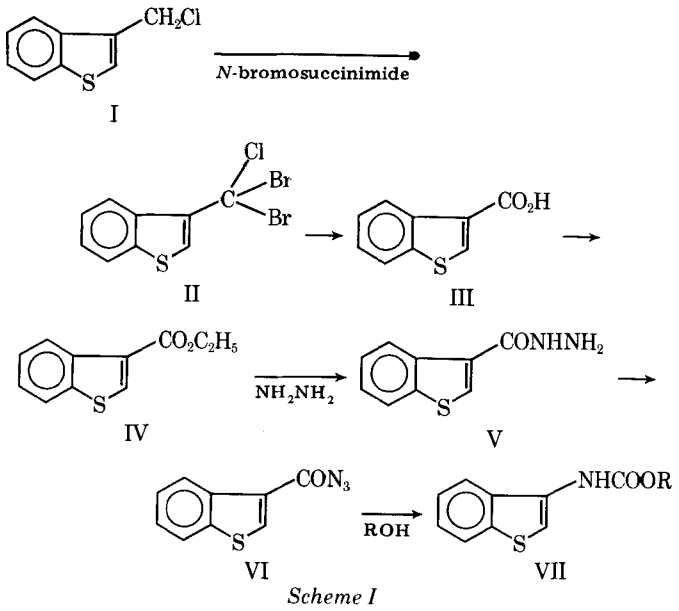


*Scheme I*

**Benzo[*b*]thiophene-3-carboxazide (VI)**—To a stirring solution of V (19.2 g, 0.1 mole) (10) in 200 ml of 50% acetic acid at 0° was added dropwise a solution of sodium nitrite (6.9 g, 0.1 mole) in 100 ml of water. The reaction mixture was stirred for an additional 30 min. The precipitate was filtered, washed with water, dried at room temperature under reduced pressure, and crystallized from ether–petroleum ether to give 4 g (76% yield) of VI, mp 103–105°; IR (KBr): 2170 (azide) $cm^{-1}$.

*Anal.*—Calc. for $C_9H_5N_3OS$: C, 53.20; H, 2.46; N, 20.69. Found: C, 53.45; H, 2.64; N, 20.85.

**Methyl Benzo[*b*]thiophene-3-carbamate (VII*a*)**—A solution of VI (2.03 g, 0.01 mole) in 20 ml of methanol was refluxed for 6 hr. The solvent was evaporated, and the residue was crystallized from ether–petroleum ether to give 1.70 g (82% yield) of VII*a*, mp 63–65°; IR (KBr): 3340 (NH) and 1700 (ester) $cm^{-1}$; NMR ($CDCl_3$): δ 8.10–7.33 (m, 5H, aromatic), 7.05 (broad s, 1H, NH), and 3.85 (s, 3H, $OCH_3$) ppm; mass spectrum: *m/z* (relative intensity) 207 ($M^+$, 100), 175 (57), 148 (39), and 121 (39).

*Anal.*—Calc. for $C_{10}H_9NO_2S$: C, 57.97; H, 4.35; N, 6.76. Found: C, 57.73; H, 4.51; N, 6.95.

Compounds VII*b*–VII*f* were prepared similarly (Table I).

**Phenyl Benzo[*b*]thiophene-3-carbamate (VII*g*)**—A solution of VI (2.03 g, 0.01 mole) and phenol (0.94 g, 0.01 mole) in 30 ml of dry benzene was refluxed for 5 hr, and the mixture then was filtered. The solvent was evaporated, and the residue was crystallized from ether–petroleum ether to give 1.61 g (60% yield) of VII*g*, mp 103–105°; IR (KBr): 3280 (NH) and 1710 (CO) $cm^{-1}$.

*Anal.*—Calc. for $C_{15}H_{11}NO_2S$: C, 66.91; H, 4.09; N, 5.20. Found: C, 66.72; H, 4.28; N, 5.38.

Compounds VII*h*–VII*r* were prepared similarly (Table I).

**Table III—Antibacterial Activity [a] of Benzo[*b*]thiophene-3-carbamic Acid Esters**

| Compound | Average Inhibition Zone Diameter, mm | | |
|---|---|---|---|
| | *E. coli* | *S. aureus* | *B. subtilis* |
| VII*a* | − | − | − |
| VII*b* | − | − | − |
| VII*c* | − | 14 | 10 |
| VII*d* | − | − | − |
| VII*e* | − | − | − |
| VII*f* | − | 12 | − |
| VII*g* | − | 8 | 12 |
| VII*h* | 12 | − | − |
| VII*i* | 8 | − | − |
| VII*j* | − | − | − |
| VII*k* | − | − | − |
| VII*l* | − | − | − |
| VII*m* | − | − | 20 |
| VII*n* | − | − | − |
| VII*o* | 22 | 17 | 15 |
| VII*p* | 11 | − | 15 |
| VII*q* | 24 | − | 20 |
| VII*r* | 30 | 24 | 20 |
| Nitrofurantoin | 25 | 25 | 25 |

[a] Key: − = inactive.

## REFERENCES


(1) W. Voegtli, U.S. pat. 2,857,383 (1958); through *Chem. Abstr.*, **53,** 6249 (1959).

(2) E. Campaigne and T. Bosin, *J. Med. Chem.*, **10,** 945 (1967).

(3) J. R. Kilsheimer and H. A. Kaufman, U.S. pat. 3,288,673 (1966); through *Chem. Abstr.*, **66,** 104900x (1967).

(4) A. Shafiee, I. Lalezari, S. Yazdani, and A. Pournorouz, *J. Pharm. Sci.*, **62,** 839 (1973).

(5) I. Lalezari, H. Golgolab, A. Shafiee, and M. Wossoughi, *ibid.*, **62,** 332 (1973).

(6) A. Shafiee, I. Lalezari, S. Yazdani, F. M. Shahbazian, and T. Partovi, *ibid.*, **65,** 304 (1976).

(7) F. Ghabgharan, H. Kooshkabadi, M. Emami, A. Rashidbaghi, and A. Shafiee, *ibid.*, **65,** 1085 (1976).

(8) F. F. Blicke and D. G. Sheets, *J. Am. Chem. Soc.*, **70,** 3768 (1948).

(9) H. J. Brabander, *J. Heterocycl. Chem.*, **10,** 127 (1973).

(10) D. F. Elliott and C. Harington, *J. Chem. Soc.*, **1949,** 1374.


## ACKNOWLEDGMENTS


Supported by a grant from the Tehran University Research Council.

# Simultaneous Determination of Tetracaine and Its Degradation Product, *p*-*n*-Butylaminobenzoic Acid, by High-Performance Liquid Chromatography

**G. N. MENON and B. J. NORRIS** ˣ

Received January 18, 1980, from the *Department of Analytical Research, Abbott Laboratories, North Chicago, IL 60064.* Accepted for publication October 14, 1980.

**Abstract** □ A high-performance liquid chromatographic method was developed for the simultaneous determination of tetracaine hydrochloride and its hydrolytic degradation product, *p*-*n*-butylaminobenzoic acid. Separation was achieved using a μBondapak $C_{18}$ column and the eluent, water–acetonitrile–methanol (60:20:20), containing 0.06% (v/v) sulfuric acid, 0.5% (w/v) sodium sulfate, and 0.02% (w/v) sodium heptanesulfonate, at a flow rate of 2 ml/min. Salicylic acid and propiophenone were used as internal standards. The UV detector response at 305 nm was linear for tetracaine hydrochloride in the 0.4–2.0-mg/ml range and for *p*-*n*-butylaminobenzoic acid in the 0.003–0.02-mg/ml range. The method is simple and precise.

**Keyphrases** □ Tetracaine—determination by high-performance liquid chromatography □ *p*-*n*-Butylaminobenzoic acid—determination by high-performance liquid chromatography □ High-performance liquid chromatography—determination of tetracaine, *p*-*n*-butylaminobenzoic acid

Tetracaine, a widely used local anesthetic, is formulated either as a 1% solution in water or in combination with other *p*-aminobenzoic esters such as procaine and benzocaine. Hydrolytic degradation of tetracaine occurs in solution, resulting in the formation of *p*-*n*-butylaminobenzoic acid and diethylaminoethanol. *p*-*n*-Butylaminobenzoic acid is only sparingly soluble in water and potentially can cause crystal deposition in tetracaine hydrochloride injection.

## BACKGROUND

To study the ideal pH range for maximum stability of tetracaine hydrochloride in water, it was necessary to determine accurately the intact drug and the extent of *p*-*n*-butylaminobenzoic acid formation at various pH values. The USP method for the tetracaine hydrochloride assay involves extraction of the drug as its free base and back-extraction into dilute acid followed by spectrophotometry (1). Although theoretically *p*-*n*-butylaminobenzoic acid can be determined in the aqueous phase after basic extraction of tetracaine, the values are likely to be high due to the greater susceptibility of tetracaine to alkaline hydrolysis during analytical manipulations.

Therefore, it was necessary to develop a simple analytical scheme to determine both the intact drug and its degradation product, preferably by a single approach. The other available methods are measurement of refractive index, GLC, and partition chromatography (2–5), none of which is ideally suited for a simultaneous assay scheme.

This paper describes a high-performance liquid chromatographic (HPLC) method for the determination of both tetracaine and *p*-*n*-butylaminobenzoic acid in tetracaine hydrochloride injection. The same chromatographic conditions also are applicable to the analyses of several other local anesthetics.

## EXPERIMENTAL

The chromatographic system was equipped with a dual-piston reciprocating pump[1], universal injector[2], and a variable-wavelength UV detector[3]. The separation was performed on a 30-cm × 4-mm i.d. column containing microparticulate (10 μm) bonded octadecylsilane material[4]. The chromatographic peaks were electronically integrated and recorded[5].

**Eluent**—The eluent was water–acetonitrile[6]–methanol[6] (60:20:20) containing 0.06% (v/v) sulfuric acid, 0.5% (w/v) sodium sulfate, and 0.02% (w/v) sodium heptanesulfonate[7] (pH 2.6).

**Internal Standard Solutions**—A 10-mg/ml salicylic acid[8] solution in methanol–water (1:1) was used as the internal standard for tetracaine, and a 10-mg/ml solution of propiophenone[8] in methanol–water (1:1) was used as the internal standard for *p*-*n*-butylaminobenzoic acid.

**Standard Preparation**—The standard solution was prepared by weighing 50 mg of tetracaine hydrochloride USP reference standard into a 50-ml volumetric flask. Five milliliters of a 0.05-mg/ml *p*-*n*-butylaminobenzoic acid reference standard[9] in methanol–water (1:1), 20.0 ml of

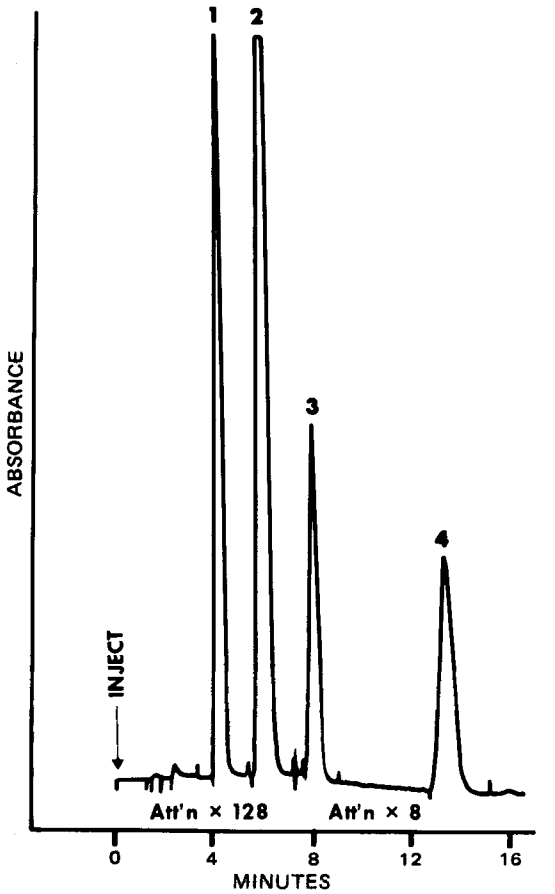


**Figure 1**—*HPLC analysis of tetracaine hydrochloride injection. Key: 1, salicylic acid; 2, tetracaine; 3, propiophenone; and 4,* p-n-*butylaminobenzoic acid.*

[1] Model 6000A, Waters Associates, Milford, MA 01757.
[2] Model U6K, Waters Associates, Milford, MA 01757.
[3] Model SF 770, Schoeffel, Westwood, NJ 07675, or model LC-55, Perkin-Elmer, Norwalk, CT 06856.
[4] μBondapak $C_{18}$, Waters Associates, Milford, MA 01757.
[5] Model 3385A automation system, Hewlett-Packard, Avondale, CA 19311.
[6] Distilled in glass, Burdick & Jackson, Muskegon, MI 49442.
[7] Eastman Organic Chemicals, Rochester, NY 14650.
[8] Aldrich Chemical Co., Milwaukee, WI 53233.
[9] Alfred Bader Chemicals, Aldrich Chemical Co., Milwaukee, WI 53233 (characterized and designated Abbott House Reference Standard).

0022-3549/81/0500-0569$01.00/0
© 1981, American Pharmaceutical Association

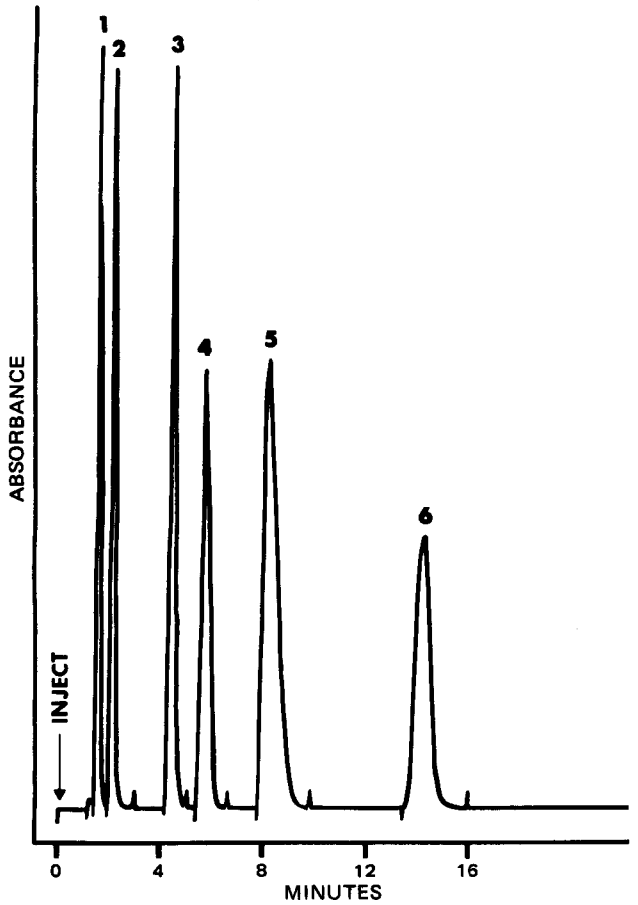


**Figure 2**—*HPLC analysis of a mixture of local anesthetics. Key: 1, procaine; 2, lidocaine; 3, benzocaine; 4, tetracaine; 5, pramoxine; and 6, butamben.*

the salicylic acid internal standard solution, and 5.0 ml of the propiophenone internal standard solution were pipetted into the flask. The solution was diluted to volume with methanol–water (1:1).

**Sample Preparation**—The sample formulation contained 1% tetracaine in a solution of sodium chloride and acetone sodium bisulfite in water. Five milliliters of the formulation, 20 ml of the salicylic acid internal standard solution, and 5 ml of the propiophenone internal standard solution were pipetted into a 50-ml volumetric flask and diluted to volume with methanol–water (1:1). For analysis of formulations with suspected crystal deposition, it is necessary to homogenize the sample prior to analysis.

**Analysis**—The following chromatographic conditions were used for the analysis: flow rate, 2 ml/min; detector wavelength, 305 nm; and injection volumes for tetracaine hydrochloride and *p-n*-butylaminobenzoic acid, 5 and 50 μl, respectively. Quantitative analysis was accomplished by comparing the peak area ratios of the standard preparations to those of the sample preparations.

## RESULTS AND DISCUSSION

At the pH of the chromatographic eluent, both tetracaine and *p-n*-butylaminobenzoic acid were ionized and formed ion-pairs with heptanesulfonate. Figure 1 shows a typical chromatogram resulting from a 50-μl injection of the sample preparation. The linearity of the detector response was established for 5-μl injections of tetracaine hydrochloride in the 0.4–2.0-mg/ml range (*y*-intercept, 0.017; correlation coefficient, 0.9997) and for 50-μl injections of *p-n*-butylaminobenzoic acid in the 0.003–0.02-mg/ml range (*y*-intercept, 0.01; correlation coefficient, 0.9999). Since the peak area ratio for tetracaine analysis obtained from a 50-μl injection fell beyond the linear working range, the assay was performed using a 5-μl injection.

The accuracy and reproducibility of the method were demonstrated by replicate analyses of a simulated formulation that contained 10.0 mg of tetracaine hydrochloride/ml and was spiked with 0.050 mg of *p-n*-butylaminobenzoic acid/ml. The data generated from these analyses show that the method is accurate and precise.

For eight replicate analyses of a 10-mg/ml tetracaine hydrochloride injection spiked with 0.050 mg of *p-n*-butylaminobenzoic acid/ml, the results were: for tetracaine hydrochloride, 10.0 ± 0.12 mg/ml (*SD*), *RSD* = ±1.2%; and for *p-n*-butylaminobenzoic acid, 0.050 ± 0.0005 mg/ml (*SD*), *RSD* = ±1.0%.

Standard addition experiments also were performed to demonstrate method accuracy. Four formulations were prepared, containing tetracaine hydrochloride at levels ranging from 4 to 20 mg/ml and *p-n*-butylaminobenzoic acid at levels ranging from 0.03 to 0.2 mg/ml. These four formulations were diluted and analyzed according to the experimental conditions; recoveries of tetracaine hydrochloride varied from 98.3 to 101.4% with an average recovery of 99.5 ± 1.4%. Recoveries of *p-n*-butylaminobenzoic acid varied from 100.6 to 104.0% with an average recovery of 102.2 ± 1.7% for the four formulations; the tetracaine hydrochloride bulk drug used to prepare the formulations for the standard addition experiments contained <0.1% of *p-n*-butylaminobenzoic acid, which resulted in slightly higher recoveries of the added degradation product.

*p-n*-Butylaminobenzoic acid has low solubility in aqueous solution, which may result in crystal deposition of the degradation product in tetracaine hydrochloride injection subjected to long-term storage. No crystallization has been observed in actual formulations. However, when simulated formulations were subjected to hydrolytic degradation at high temperature (85°), crystal deposition occurred at concentrations of >0.6 mg of *p-n*-butylaminobenzoic acid/ml in the pH 3.15–5.15 range.

Figure 2 shows a chromatogram obtained from a mixture of six common local anesthetics analyzed with the same HPLC conditions. In the absence of either sulfuric acid or sodium sulfate in the eluent, butamben and pramoxine eluted together and the peaks had certain asymmetry. Slight increases in the capacity factors for the different solutes could be obtained by decreasing the salt concentration; this finding was in agreement with published data on salt effects (6).

Ion-pair reversed-phase chromatography permits simultaneous analysis of tetracaine hydrochloride and its hydrolytic degradation product. The described system has utility in analyzing several other local anesthetics with which it may be coformulated.

## REFERENCES

(1) "The United States Pharmacopeia," 19th rev., Mack Publishing Co., Easton, Pa., 1975, p. 494.

(2) R. N. Longshaw and N. Walli, *J. Hosp. Pharm.*, **1973**, 36.

(3) N. D. Greenwood, *ibid.*, **1971**, 240.

(4) N. D. Greenwood and H. E. Nursten, *J. Chromatogr.*, **92**, 323 (1974).

(5) T. D. Doyle and J. B. Proctor, *J. Assoc. Off. Anal. Chem.*, **58**, 88 (1975).

(6) C. Horvath, W. Melander, I. Molnar, and P. Molnar, *Anal. Chem.*, **49**, 2295 (1977).

# Mass Transport Properties of Co(polyether)polyurethane Membranes I: Preparation and Characterization

**LLOYD E. MATHESON, Jr.** [x], **and WILLIAM A. HUNKE** *

Received September 4, 1979, from the *College of Pharmacy, University of Iowa, Iowa City, IA 52242.* Accepted for publication October 15, 1980. *Present address: Sterling-Winthrop Research Institute, Rensselaer, NY 12144.

**Abstract** □ A series of polyurethane copolymers containing polyethylene glycol 600, 1000, or 1540 was synthesized, purified by reprecipitation, and cast into clear, tough, flexible membranes using the solution method. The weight average molecular weight of each polymer was estimated by gel permeation chromatography. The ability of the various polymers to absorb water was measured and increased with the increasing molecular weight of the polyethylene glycol. The ability of the copolymer membranes to hold a pH gradient decreased with increasing polyethylene glycol molecular weight.

**Keyphrases** □ Model membrane systems—polyurethane copolymers, synthesis and analysis, mass transport properties □ Copolymers, polyurethane—model membrane systems, synthesis and analysis, mass transport properties □ Permeability—polyurethane copolymers, model membrane system, synthesis and analysis

Much attention has been focused on the use of polymeric materials as drug delivery (1, 2) and model membrane (3–5) systems. Most early work utilized polydimethylsiloxane which, while highly permeable to lipophilic drugs (6, 7), is only weakly permeable to hydrophilic, charged species (8). More recently, polymers known as hydrogels have been shown to control release of hydrophobic and hydrophilic agents. Variation in release rates can be controlled by changes in both monomer composition and the amount of cross-linking agent present (9–13).

## BACKGROUND

A promising approach for the development of new model membranes is to modify systematically the polymer structure to alter its diffusion characteristics. It was suggested (14) that the hydrophilic–hydrophobic character of a membrane may be controlled by the choice of suitable structural modifications. Membranes that combine the seemingly opposite properties of mechanical strength and the ability to swell in water have been prepared by simultaneous polymerization (copolymerization) of hydrophilic and hydrophobic reactants (15–17). The membranes formed from these copolymers permitted the transport of permeants at rates comparable to porous dialysis membranes but with the apparent selectivity of partitioning-type membranes (18).

Therefore, a series of copolymers composed of hydrophilic polyethylene glycol blocks and hydrophobic urethane segments was chosen for study. Since these polymers were not readily available commercially, it was necessary to synthesize them and to characterize some of their properties prior to diffusion work. These properties included the abilities of the membranes to hydrate and to maintain a pH gradient. A molecular weight distribution and weight average molecular weight of each polymer system also were determined.

## EXPERIMENTAL

**Materials**—Polystyrene standards[1] were used as received. Isopropylacetone[2] was purified by collecting the fraction boiling at 114–115° at atmospheric pressure, and methylenebis(4-phenyl isocyanate)[3] was distilled at 0.1–0.17 mm Hg. The colorless, clear fraction boiling at 147–151° was collected and stored in a freezer. 1,5-Pentanediol[2] was purified by distillation at 0.2–0.45 mm Hg, and the fraction boiling at 96–99° was collected. All distillates were stored in glass under dry nitrogen. Polyethylene glycols[4] 1540, 1000, and 600 were dried by the application of vacuum and heat for 4 hr. The flask then was flushed with dry nitrogen.

**Methods**—The average molecular weights of the polyethylene glycols were determined by end-group titration (19).

The synthetic procedures used to prepare the co(polyether)polyurethane polymers were similar to those outlined previously (16). Polyethylene glycol (0.012 mole) was dried in a 200-ml, three-necked, round-bottom flask equipped with a sealed polytef stirrer[5], a gas inlet valve, and a 200-mm West condenser fitted with a drying tube. The flask was heated to 110 ± 3°, and a suspension of 0.024 mole of methylenebis(4-phenyl isocyanate) in 25 ml of methyl sulfoxide and 25 ml of isopropylacetone was added to the polyethylene glycol with stirring. The flask was maintained at 110° for 1 hr while stirring continuously.

To the resulting clear, yellowish solution, 0.024 mole of 1,5-pentanediol and 0.016 mole of methylenebis(4-phenyl isocyanate) were added. An additional 2 hr of heating produced a viscous, yellowish solution. The polymer was isolated by pouring the solution into ~500 ml of distilled water, which produced a tough, rubbery, white precipitate. After washing with several volumes of distilled water, the polymer was dried in a heated vacuum desiccator[6] at 50°.

Individual polymer batches were blended and purified by precipitation in distilled water from a 5% (w/v) polymer solution in *N,N*-dimethylformamide. The reprecipitated polymer was washed with five 2000-ml portions of distilled water and placed in a vacuum oven for 48 hr. This procedure was carried out twice for each polymer synthesized.

The membranes were solution cast on plate glass sheets from a filtered 15% (w/v) polymer solution in *N,N*-dimethylformamide. The solution was filtered through a 0.5-μm filter[5] in a pressure filtration apparatus[7] using a 25–50-psi pressure head of dry nitrogen. The solution was spread on the glass plates with the aid of an adjustable doctor knife. The plates then were transferred quickly to an oven and dried at 50° overnight. The membrane was left on the glass plates, stored in a desiccator, and protected from light until used.

To test the effects of reprecipitating the polymer, pieces of membrane prepared from the polyethylene glycol 600 copolymer, either as originally obtained or reprecipitated (once or twice), were soaked in 30 ml of distilled water for 8 hr at 37°. An aliquot of each solution was filtered and then scanned from 240 to 350 nm.

Membranes were removed from the glass plates after hydration with 0.05 *M* phosphate buffer and were soaked for at least 20 min before use in buffer.

The thickness and diameter of both wet and dry membranes were measured by a method similar to that of Garrett and Chemburkar (20) at seven equally spaced points. The percent of water sorbed was determined by weight, and the percent swelling in thickness and diameter was determined by the difference between wet and dry measurements.

The weight average molecular weight of each synthesized polymer was estimated by gel permeation chromatography (21) using a series of gel permeation columns[8] ($10^5$, $10^4$, $10^3$, and 500 Å) with UV grade, nitrogen-blanketed tetrahydrofuran as the mobile phase.

Solutions of polystyrene (0.1–0.5%) calibration standards and polymer (0.5%) samples were prepared and chromatographed using a flow rate of 2.0 ml/min, a chart speed of 2.5 cm/min, and detector sensitivity at 0.5–1.0 aufs.

The intrinsic viscosity of the polystyrene standards in tetrahydrofuran at 25° was estimated using an empirical relationship (22), while the intrinsic viscosity of the polymer samples was measured using a capillary viscometer (23). Intrinsic viscosity was calculated as described previously (24, 25).

[1] Waters Associates, Millford, MA 01757.
[2] Aldrich Chemical Co., Milwaukee, WI 53222.
[3] Pfaltz and Bauer, Stamford, CT 06902.
[4] J. T. Baker Chemical Co., Phillipsburg, NJ 08865.
[5] Teflon.
[6] Precision Scientific Co., Chicago, IL 60647.
[7] Millipore Corp., Bedford, MA 01730.
[8] μStyragel, Waters Associates, Milford, MA 01757.

0022-3549/81/0500-0571$01.00/0
© 1981, American Pharmaceutical Association

Table I—Effect of Polyethylene Glycol Content on Various Physical Parameters of the Co(polyether)polyurethane Membranes [a]

| Polymer Membrane | Polyethylene Glycol Content, % | Water Content in Hydrated Membrane, % | Swelling in Hydrated Membrane (Diameter), % | Swelling in Hydrated Membrane (Thickness), % | Apparent Wet Density, g/cm$^3$ | Apparent Dry Density, g/cm$^3$ |
|---|---|---|---|---|---|---|
| 600 | 37 | 9 | 3 | 1 | 1.26 | 1.24 |
| 1000 | 49 | 26 | 8 | 11 | 1.22 | 1.25 |
| 1540 | 56 | 49 | 14 | 28 | 1.12 | 1.24 |

[a] Average of three membranes.

The surface and cross section of each type of dried polymer membrane were examined using a scanning electron microscope[9]. The conditions used to visualize the sample were varied to optimize the resolution, while the magnification ranged from 100 to 40,000×.

A diffusion cell similar to that described by Flynn and Smith (26) was utilized.

To determine the ability of hydrogen ion to cross the membrane, the donor side of the diffusion cell was connected by tubing[8] from its sampling ports to a two-channel tubing pump[10] and an open donor solution reservoir. The receiving side of the diffusion cell was connected similarly in a closed loop to a glass-jacketed constant-temperature reservoir. A three-hole stopper sealed the reservoir and accommodated the receiving side tubing, a nitrogen inlet, and a pH electrode.

The pH-holding experiment was initiated by thoroughly flushing the receiving side reservoir with dry nitrogen. Exactly 50 ml of preheated 0.001 *M* NaCl was introduced into the nitrogen-blanketed receiving reservoir. The pH of this solution was taken as the zero-time pH reading. The experiment was begun by injecting ~15 ml of preheated 0.001 *M* HCl into the donor side connected to a 100-ml reservoir maintained at 37°. At the specified times, the tubing pump was stopped, and the solution in the receiving side reservoir was allowed to equilibrate for 1 min before the pH reading was taken. The two-channel tubing pump was set to deliver ~18 ml/min. The exact flow rate was determined prior to an experiment by measuring the amount of solution delivered in 3 min.

## RESULTS AND DISCUSSION

Batches of a co(polyether)polyurethane after blending, but prior to casting, were purified by reprecipitation. The efficiency of the procedure in the removal of UV-absorbing impurities from the polymeric material was demonstrated easily by the drop in absorbance at 240 nm from 0.65 prior to reprecipitation to zero after the second reprecipitation. No attempt was made to identify the impurities.

The molecular weight distribution for each polymer demonstrated a large, sharp spike of high molecular weight material followed by the lower molecular weight materials. The weight average molecular weights were 71,000, 28,000, and 34,000 for the 1540, 1000, and 600 copolymers, respectively. The actual values of the average molecular weight calculated for a given polymer are probably less important than the fact that large differences in molecular weight and molecular weight distribution among the polymers were not observed.

Physical measurements were made on the membranes in both the hydrated and dry state. The water content of the swollen membranes was directly proportional to the amount of glycol in the polymer (Table I). This finding is in agreement with the idea that the polyethylene glycol molecules serve as hydrophilic blocks that allow the membrane to swell in aqueous solution (18). The hydrophobic urethane linkages have been considered to act as cross-links between the polymer chains and to anchor the hydrated glycol segments (27).

Examinations of the surfaces and cross sections of each polymer membrane by scanning electron microscopy (resolution limit ~0.05 μm) showed uniform homogeneous structures with no unusual morphology and no apparent pore structure. From these results, it can be concluded that a porous structure, if it exists, would probably be <500 Å in diameter.

The ability of the membranes to maintain a pH gradient was studied since it may be an indication of the permeability of the membranes to ions (Fig. 1). The 600 copolymer membrane successfully maintained the pH gradient throughout the experiment (~1 hr), while the apparent diffusion coefficient for the 1000 and 1540 copolymer membranes were $6.9 \times 10^{-9}$ and $7.0 \times 10^{-8}$ cm$^2$/sec, respectively. The amount of glycol in the polymer molecules and, consequently, the amount of water sorbed do influence the capacity of the membrane to hold a pH gradient.

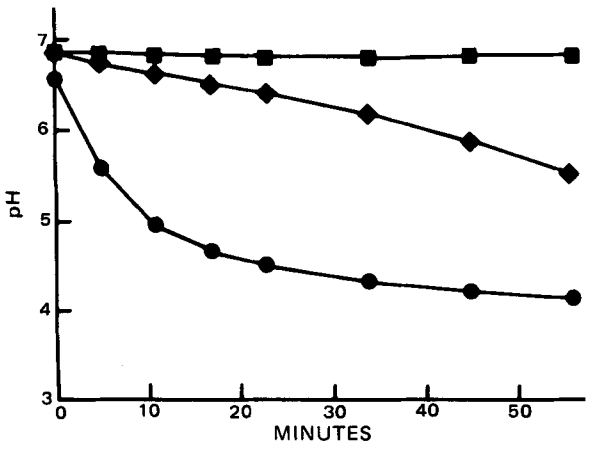


**Figure 1**—*Results of pH gradient-holding experiments for 600 copolymer (■), 1000 copolymer (♦), and 1540 copolymer (●).*

[9] Model JSM-35C, JEOL USA, Medford, MA 02155.

[10] Master-flex pump drive (5–100 rpm) with pump head No. 7016 and add-on pump head No. 7016, Cole-Parmer Instrument Co., Chicago, IL 60648.

## REFERENCES

(1) T. J. Roseman and W. I. Higuchi, *J. Pharm. Sci.*, **59,** 353 (1970).

(2) T. J. Roseman, *ibid.*, **61,** 46 (1972).

(3) V. F. Smolen and D. E. Hagman, *J. Colloid Interface Sci.*, **42,** 70 (1973).

(4) D. O. Jordan and A. E. Polack, *Aust. J. Pharm. Sci.*, **NS2,** 25 (1973).

(5) M. Z. Biber and C. T. Rhodes, *J. Pharm. Sci.*, **65,** 564 (1976).

(6) T. J. Roseman, in "Controlled Release of Biologically Active Agents," A. C. Tanquary and R. E. Lacey, Eds., Plenum, New York, N.Y., 1974, p. 99.

(7) R. E. Lacey and D. R. Cowsar, in *ibid.*, p. 117.

(8) E. R. Garrett and P. B. Chemburkar, *J. Pharm. Sci.*, **57,** 949 (1968).

(9) J. M. Anderson, T. Koinis, T. Nelson, M. Horst, and D. S. Love, in "Hydrogels for Medical and Related Applications," J. D. Andrade, Ed., Symposium Series 31, American Chemical Society, Washington, D.C., 1976, p. 167.

(10) D. R. Cowsar, O. R. Tarwater, and A. C. Tanquary, in *ibid.*, p. 180.

(11) J. Drobnik, P. Spacek, and O. Wichterle, *J. Biomed. Mater. Res.*, **8,** 45 (1974).

(12) G. M. Zentner, J. R. Cardinal, and S. W. Kim, *J. Pharm. Sci.*, **67,** 1347 (1978).

(13) *Ibid.*, **67,** 1352 (1978).

(14) R. E. Kesting, "Synthetic Polymeric Membranes," McGraw-Hill, New York, N.Y., 1971, p. 16.

(15) D. J. Lyman, B. H. Loo, and R. W. Crawford, *Biochemistry*, **3,** 985 (1964).

(16) D. J. Lyman and B. H. Loo, *J. Biomed. Mater. Res.*, **1,** 17 (1967).

(17) W. M. Muir, R. A. Gray, J. M. Courtney, and P. D. Ritchie, *ibid.*, **7,** 3 (1973).

(18) D. J. Lyman and S. W. Kim, *Biomater. Med. Devices Artif. Organs*, **1,** 431 (1973).

(19) W. R. Sorenson and T. W. Campbell, "Preparative Methods of Polymer Chemistry," Interscience, New York, N.Y., 1961, p. 134.

(20) E. R. Garrett and P. B. Chemburkar, *J. Pharm. Sci.*, **57,** 944 (1968).

(21) Z. Grubisic, P. Rempp, and H. Benoit, *J. Polym. Sci.*, **B5**, 753 (1967).
(22) E. A. Collins, J. Bares, and F. W. Billmeyer, "Experiments in Polymer Science," Wiley, New York, N.Y., 1973, p. 151.
(23) W. R. Sorenson and T. W. Campbell, "Preparative Methods of Polymer Chemistry," Interscience, New York, N.Y., 1961, p. 38.
(24) D. K. Carpenter and L. Westerman, in "Techniques and Methods of Polymer Evaluation," vol. 4, part II, P. E. Slade and L. T. Jenkins, Eds., Dekker, New York, N.Y., 1975, p. 478.
(25) R. N. Shroff, *J. Appl. Polym. Sci.*, **9**, 1547 (1965).
(26) G. L. Flynn and E. W. Smith, *J. Pharm. Sci.*, **60**, 1713 (1971).
(27) C. T. Chen, R. F. Eaton, Y. J. Chang, and A. V. Tobolsky, *J. Appl. Polym. Sci.*, **16**, 2105 (1972).

**ACKNOWLEDGMENTS**

Presented in part at the APhA Academy of Pharmaceutical Sciences, Kansas City meeting, November 1979.

Abstracted in part from a dissertation submitted by W. A. Hunke to the Graduate School, University of Iowa, in partial fulfillment of the Doctor of Philosophy degree requirements.

Supported in part by Initial Research Support for Junior Faculty of the University of Iowa and the National Institutes of Health.

The authors thank Dr. Gordon Flynn for the diffusion cell plans and Dr. Gene Shih for assistance in the scanning electron microscopic studies.

W. A. Hunke is a Fellow of the American Foundation for Pharmaceutical Education.

# Mass Fragmentographic Determination of Timolol in Human Plasma and Urine

**J. B. FOURTILLAN *x, M. A. LEFEBVRE, J. GIRAULT, and Ph. COURTOIS**

Received May 5, 1980, from the *Department of Chromatography and Mass Spectrometry Applied to Clinical Pharmacy, Faculté of Pharmacy, University of Poitiers, Poitiers, France.* Accepted for publication October 28, 1980. *Present address: Laboratoire de Pharmacie Chimique, U.E.R. de Médecine et de Pharmacie, 34, rue du Jardin des Plantes, 86034 Poitiers Cedex, France.

**Abstract** □ A mass fragmentographic procedure was developed for measuring quantities of <1.0 ng of timolol/ml of plasma or urine. The lower limit of sensitivity was 0.5 ng of timolol maleate/ml of plasma. The unchanged drug was extracted into heptane–4% isopentyl alcohol from alkalinized plasma or urine, together with propranolol hydrochloride as the internal standard. The compounds were subsequently back-extracted into 0.1 *N* HCl and then into chloroform following adjustment of the acidic phase to an alkaline pH. The chloroform layer was evaporated to dryness, and the compounds were derivatized with *N*-methyl-*N*-trimethylsilyltrifluoroacetamide–acetonitrile to form the trimethylsilyl derivatives; these derivatives were quantitated by mass fragmentography. Recovery of timolol added to normal plasma and urine was quantitative and reproducible, and no interfering substances were observed in normal biological samples. After a 20-mg oral dose of timolol maleate, plasma levels of ~3.0 ng/ml were observed at 12 hr.

**Keyphrases** □ Timolol—extraction, derivatization, mass fragmentographic determination, plasma and urine □ β-Adrenergic blocking agents—timolol, extraction, derivatization, mass fragmentographic determination, plasma and urine □ Mass fragmentography—determination, timolol, plasma and urine

Timolol maleate, (−)-1-(*tert*-butylamino)-3-[(4-morpholino-1,2,5-thiadiazol-3-yl)oxy]-2-propanol maleate, is a β-adrenergic receptor blocking agent with a high β-adrenergic inhibitor capacity. Due to the intensity of its effect, it is administered orally in small doses, varying between 10 and 20 mg, depending on the treatment needs. In addition, its high extravascular diffusion rate gives it an average apparent volume of distribution of 3.64 liters/kg. A low administered dose and a high apparent volume of distribution contribute to low plasma concentrations. For a proper pharmacokinetic study, assay techniques must be capable of measuring plasma levels as low as 0.5 ng of timolol/ml.

An electron-capture GLC determination of timolol in human plasma and urine was described by Tocco *et al.* (1). The lower limit of sensitivity was 2.0 ng/ml.

This report describes a mass fragmentographic procedure whose sensitivity threshold of 0.5 ng of timolol/ml of plasma enables plasma concentrations to be monitored for over 12 hr after oral administration of a 20-mg single dose of timolol maleate in a healthy adult.

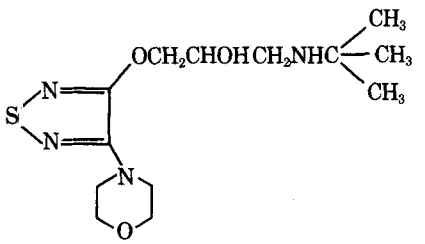

I

## EXPERIMENTAL

**Reagents**—Timolol (I) was used as the maleate salt[1], and propranolol (II) hydrochloride[2] served as the internal standard. All concentrations were expressed in terms of the base salt. Pesticide quality *n*-heptane[3], isopentyl alcohol[3], methylene chloride[4], ethyl acetate[5], and acetonitrile[6] nanograde reagent were used without further purification. Hydrochloric acid, sodium hydroxide, and double-distilled water were used in the preparation of 0.1 *N* HCl and 1.0 and 2.0 *N* NaOH. *N*-Methyl-*N*-trimethylsilyltrifluoroacetamide[7] served as the reagent for preparing the trimethylsilyl derivatives of timolol and propranolol.

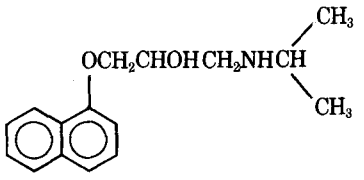

II

[1] Merck Sharp & Dohme, Chibret, Paris, France.
[2] I.C.I., Enghien Les Bains, France.
[3] Prolabo R.P., Paris, France.
[4] Merck, Interchim, Montluçon, France.
[5] Fluka A.G., Interchim, Montluçon, France.
[6] Mallinckrodt, Interchim, Montluçon, France.
[7] Pierce Chemical Co., Interchim, Montluçon, France.

0022-3549/81/0500-0573$01.00/0
© 1981, American Pharmaceutical Association

(21) Z. Grubisic, P. Rempp, and H. Benoit, *J. Polym. Sci.*, **B5**, 753 (1967).
(22) E. A. Collins, J. Bares, and F. W. Billmeyer, "Experiments in Polymer Science," Wiley, New York, N.Y., 1973, p. 151.
(23) W. R. Sorenson and T. W. Campbell, "Preparative Methods of Polymer Chemistry," Interscience, New York, N.Y., 1961, p. 38.
(24) D. K. Carpenter and L. Westerman, in "Techniques and Methods of Polymer Evaluation," vol. 4, part II, P. E. Slade and L. T. Jenkins, Eds., Dekker, New York, N.Y., 1975, p. 478.
(25) R. N. Shroff, *J. Appl. Polym. Sci.*, **9**, 1547 (1965).
(26) G. L. Flynn and E. W. Smith, *J. Pharm. Sci.*, **60**, 1713 (1971).
(27) C. T. Chen, R. F. Eaton, Y. J. Chang, and A. V. Tobolsky, *J. Appl. Polym. Sci.*, **16**, 2105 (1972).

**ACKNOWLEDGMENTS**

Presented in part at the APhA Academy of Pharmaceutical Sciences, Kansas City meeting, November 1979.

Abstracted in part from a dissertation submitted by W. A. Hunke to the Graduate School, University of Iowa, in partial fulfillment of the Doctor of Philosophy degree requirements.

Supported in part by Initial Research Support for Junior Faculty of the University of Iowa and the National Institutes of Health.

The authors thank Dr. Gordon Flynn for the diffusion cell plans and Dr. Gene Shih for assistance in the scanning electron microscopic studies.

W. A. Hunke is a Fellow of the American Foundation for Pharmaceutical Education.

# Mass Fragmentographic Determination of Timolol in Human Plasma and Urine

**J. B. FOURTILLAN *x, M. A. LEFEBVRE, J. GIRAULT, and Ph. COURTOIS**

Received May 5, 1980, from the *Department of Chromatography and Mass Spectrometry Applied to Clinical Pharmacy, Faculté of Pharmacy, University of Poitiers, Poitiers, France.* Accepted for publication October 28, 1980. *Present address: Laboratoire de Pharmacie Chimique, U.E.R. de Médecine et de Pharmacie, 34, rue du Jardin des Plantes, 86034 Poitiers Cedex, France.

**Abstract** □ A mass fragmentographic procedure was developed for measuring quantities of <1.0 ng of timolol/ml of plasma or urine. The lower limit of sensitivity was 0.5 ng of timolol maleate/ml of plasma. The unchanged drug was extracted into heptane–4% isopentyl alcohol from alkalinized plasma or urine, together with propranolol hydrochloride as the internal standard. The compounds were subsequently back-extracted into 0.1 *N* HCl and then into chloroform following adjustment of the acidic phase to an alkaline pH. The chloroform layer was evaporated to dryness, and the compounds were derivatized with *N*-methyl-*N*-trimethylsilyltrifluoroacetamide–acetonitrile to form the trimethylsilyl derivatives; these derivatives were quantitated by mass fragmentography. Recovery of timolol added to normal plasma and urine was quantitative and reproducible, and no interfering substances were observed in normal biological samples. After a 20-mg oral dose of timolol maleate, plasma levels of ~3.0 ng/ml were observed at 12 hr.

**Keyphrases** □ Timolol—extraction, derivatization, mass fragmentographic determination, plasma and urine □ β-Adrenergic blocking agents—timolol, extraction, derivatization, mass fragmentographic determination, plasma and urine □ Mass fragmentography—determination, timolol, plasma and urine

Timolol maleate, (−)-1-(*tert*-butylamino)-3-[(4-morpholino-1,2,5-thiadiazol-3-yl)oxy]-2-propanol maleate, is a β-adrenergic receptor blocking agent with a high β-adrenergic inhibitor capacity. Due to the intensity of its effect, it is administered orally in small doses, varying between 10 and 20 mg, depending on the treatment needs. In addition, its high extravascular diffusion rate gives it an average apparent volume of distribution of 3.64 liters/kg. A low administered dose and a high apparent volume of distribution contribute to low plasma concentrations. For a proper pharmacokinetic study, assay techniques must be capable of measuring plasma levels as low as 0.5 ng of timolol/ml.

An electron-capture GLC determination of timolol in human plasma and urine was described by Tocco *et al.* (1). The lower limit of sensitivity was 2.0 ng/ml.

This report describes a mass fragmentographic procedure whose sensitivity threshold of 0.5 ng of timolol/ml of plasma enables plasma concentrations to be monitored for over 12 hr after oral administration of a 20-mg single dose of timolol maleate in a healthy adult.

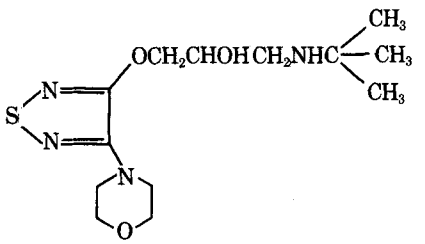

I

## EXPERIMENTAL

**Reagents**—Timolol (I) was used as the maleate salt[1], and propranolol (II) hydrochloride[2] served as the internal standard. All concentrations were expressed in terms of the base salt. Pesticide quality *n*-heptane[3], isopentyl alcohol[3], methylene chloride[4], ethyl acetate[5], and acetonitrile[6] nanograde reagent were used without further purification. Hydrochloric acid, sodium hydroxide, and double-distilled water were used in the preparation of 0.1 *N* HCl and 1.0 and 2.0 *N* NaOH. *N*-Methyl-*N*-trimethylsilyltrifluoroacetamide[7] served as the reagent for preparing the trimethylsilyl derivatives of timolol and propranolol.

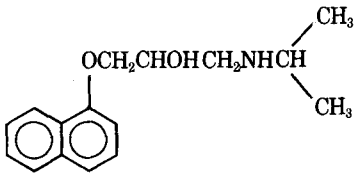

II

[1] Merck Sharp & Dohme, Chibret, Paris, France.
[2] I.C.I., Enghien Les Bains, France.
[3] Prolabo R.P., Paris, France.
[4] Merck, Interchim, Montluçon, France.
[5] Fluka A.G., Interchim, Montluçon, France.
[6] Mallinckrodt, Interchim, Montluçon, France.
[7] Pierce Chemical Co., Interchim, Montluçon, France.

0022-3549/81/0500-0573$01.00/0
© 1981, American Pharmaceutical Association

**Table I—Repeatability Assay with Timolol Maleate Plasma Samples**

| Samples with 1 ng/ml | Found, ng/ml |
|---|---|
| 1 | 0.77 |
| 2 | 0.79 |
| 3 | 0.82 |
| 4 | 0.98 |
| 5 | 1.05 |
| 6 | 1.27 |
| 7 | 0.93 |
| 8 | 1.11 |
| 9 | 0.93 |
| 10 | 0.98 |
| Mean ± *RSD* | 0.96 ± 0.15 |

**Table II—Repeatability Assay with Timolol Maleate Plasma Samples**

| Samples with 50 ng/ml | Found, ng/ml |
|---|---|
| 1 | 47.2 |
| 2 | 50.4 |
| 3 | 51.7 |
| 4 | 54.0 |
| 5 | 49.8 |
| 6 | 48.1 |
| 7 | 50.2 |
| 8 | 52.3 |
| 9 | 48.7 |
| 10 | 51.3 |
| Mean ± *RSD* | 50.4 ± 2.1 |

**Apparatus**—The samples were analyzed on a GLC–mass spectrometer equipped for mass fragmentography[8] (M.I.D.). The gas chromatograph[9] was equipped with a 20-m × 0.03-cm glass capillary column with 2% OV1[10]. The gas chromatograph was operated isothermally with oven and injection temperatures maintained at 230 and 250°, respectively. The helium carrier gas flow rate was 10 ml/min. Other operating conditions were: source temperature, 260°; separator temperature, 240°; electron-impact energy, 35 ev; and trap current, 100 μamp. The M.I.D. program[11] was used with a computer[12].

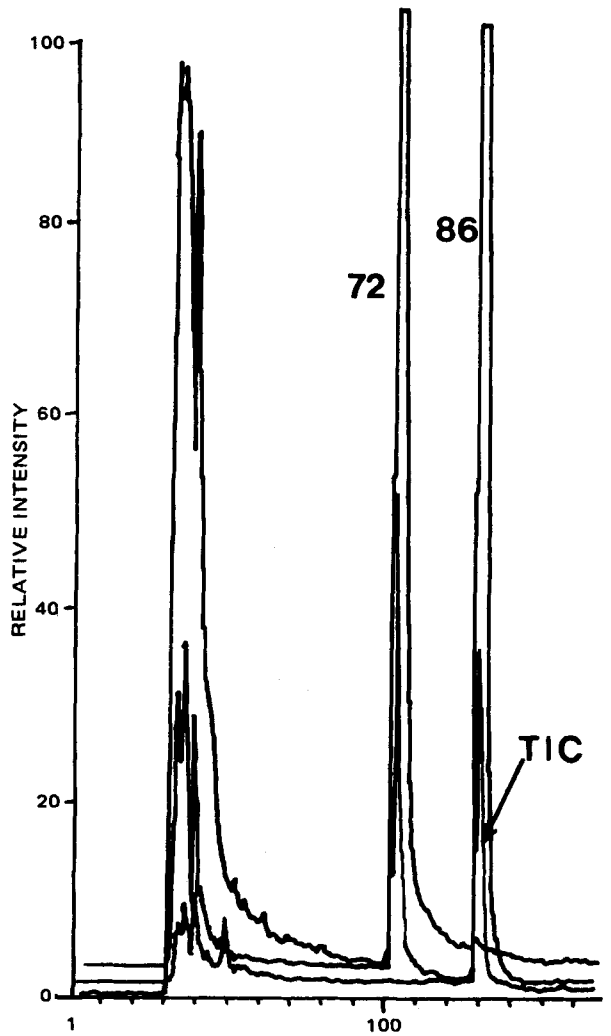


**Figure 1**—*Total ion current of a sample spiked with propranolol and timolol showing the traces of M − 72 and M − 86 fragments corresponding to the most abundant ions of trimethylsilyl derivations of propranolol and timolol.*

**Assay**—The extraction was similar to that described by Tocco *et al.* (1). In a 10-ml glass-stoppered centrifuge tube were placed 1.0 ml of plasma or 0.1 ml of urine, 50 μl of propranolol internal standard (stock solution, 1000 ng/ml of water), 0.1 ml of 1.0 *N* NaOH, and 7 ml of heptane–4% isopentyl alcohol. The mixture was shaken mechanically for 10 min and centrifuged. In a 10-ml glass-stoppered centrifuge tube were placed 1.0 ml of 0.1 *N* HCl and 6 ml of the organic phase.

After the tubes were shaken and centrifuged, the organic phase was discarded by aspiration. To the aqueous phase were added 0.2 ml of 2.0 *N* NaOH and 7.0 ml of methylene chloride. The samples were shaken for 10 min and centrifuged.The organic phase was removed carefully, and 6.0 ml was added to a 10-ml silanized glass-stoppered tube. The contents were evaporated to dryness in a 60° heating block under a nitrogen stream.

The residue was dissolved in 0.1 ml of *N*-methyl-*N*-trimethylsilyltrifluoroacetamide–acetonitrile reagent (10% in acetonitrile), and the stoppered tube was heated at 50° for 45 min. The tubes were cooled to room temperature, and then the contents were evaporated to dryness at 60° using a nitrogen stream. The residue was dissolved in 0.050 ml of ethyl acetate, and 2 μl was chromatographed.

The retention times of derivatized timolol and derivatized propranolol (internal standard) were 410 and 340 sec, respectively. GLC–mass spectrometric analysis showed that the products of silylation were the monotrimethylsilyl derivatives formed with the alcohol function of the lateral chain.

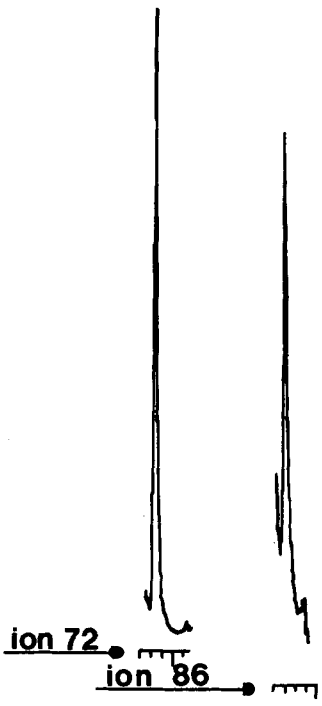


**Figure 2**—*Peaks obtained by mass fragmentography with plasma containing 50.0 ng of propranolol hydrochloride (amplification 20.0, m/z 72) and 1.0 ng of timolol maleate (amplification 150.0, m/z 86)/ml.*

[8] Model 2091 (electron impact, chemical ionization), L.K.B. Clinicon, Orsay, France.
[9] Pye Unicam Philips 204, Paris, France.
[10] Acta Co., Paris, France.
[11] Clinicon Co., Sweden.
[12] Digital PDP 11 with Tektronix 4012 and Central Printing Rank, Xerox, Paris, France.

**Table III—Plasma Timolol Maleate Levels (Nanograms per Milliliter) in Five Human Subjects after a Single 20-mg Oral Dose of Timolol Maleate**

| Hours after Single Dose | Subject 1 | 2 | 3 | 4 | 5 | Mean ± *SEM*[a] |
|---|---|---|---|---|---|---|
| 0.50 | 32.2 | 1.4 | 26.0 | 15.6 | 108.1 | 36.7 ± 18.6 |
| 1.00 | 50.1 | 37.1 | 20.4 | 67.3 | 52.8 | 45.5 ± 7.9 |
| 1.50 | 33.1 | 81.2 | 53.2 | 63.4 | 52.8 | 56.6 ± 7.9 |
| 1.75 | 19.4 | 84.2 | 22.8 | 98.4 | 69.8 | 58.9 ± 16.1 |
| 2.00 | 26.6 | 60.7 | 32.1 | 68.0 | 36.0 | 44.7 ± 8.2 |
| 3.00 | 13.0 | 103.1 | 22.4 | 59.1 | 37.7 | 47.1 ± 16.0 |
| 4.00 | 11.1 | 54.6 | 15.5 | 30.2 | 25.2 | 27.3 ± 7.6 |
| 6.00 | 5.00 | 27.3 | 8.8 | 18.7 | 17.1 | 15.4 ± 3.9 |
| 8.00 | 3.2 | 15.7 | 4.6 | 10.5 | 10.0 | 8.8 ± 5.0 |
| 12.00 | 0.8 | 7.2 | 1.4 | 3.8 | 2.7 | 3.2 ± 2.5 |

[a] $SEM = RSD/\sqrt{5}$.

The M − 72 and M − 86 fragments, which constituted the most intense fragments in the mass spectra of the trimethylsilyl derivatives of propranolol and timolol, respectively, were used for the mass fragmentographic determination of propranolol and timolol.

Two standard curves (0–10 and 10.0–100.0 ng/ml of plasma) were constructed by analysis of samples of control plasma containing known quantities of timolol and propranolol. The ratios obtained by dividing the intensities of ion 86 by ion 72 were expressed and plotted against the concentrations of timolol maleate, in nanograms per milliliter of plasma or urine. The regression line of the data corresponding to the experimental points was drawn through the origin. Concentrations of timolol maleate were determined by interpolation from the standard curves.

**Timolol in Human Plasma**—Five healthy human subjects (two women and three men) were given a single 20-mg oral dose of timolol maleate (two tablets[13] of 10 mg). Blood was collected in heparinized containers at intervals over 12 hr following the single dose. Plasma was separated by centrifugation and frozen until assayed.

## RESULTS AND DISCUSSION

Figure 1 shows a chromatogram obtained with plasma containing 50 ng of the internal standard and 50 ng of timolol (timolol maleate)/ml using total ion current detection. These peaks correspond to ions *m/z* 72 and 86 that were chosen for mass fragmentographic determination.

Blank plasma or urine samples gave no interfering peaks on the chromatogram. Metabolites of timolol with an unaltered lateral chain could interfere with the timolol peak, but their retention times are different. Two calibration curves prepared from two ranges of plasma levels (0–10.0 and 0–100 ng/ml of a same pool of plasma) indicated that intensity ratios of ions *m/z* 86 and 72 were linear when plotted against the concentrations of timolol maleate.

The lower limit of sensitivity was <0.5 ng of timolol maleate/ml of plasma or urine. Figure 2 shows the run obtained with a human plasma sample when 1.0 ng of timolol maleate was added to 1.0 ml of plasma. This concentration of timolol gave, for *m/z* 86, a peak height of ~100 mm with an amplification value equal to 150. The upper limit of linearity was at least 100 ng/ml. The coefficients of correlation were 0.9804 and 0.9948 for the low and high calibration curves, respectively.

[13] Timacor, Laboratoires Merck Sharp & Dohme, Chibret, Paris, France.

Repeatability assays were performed throughout the experiment on two pools of human plasma samples containing 1 and 50 ng/ml (Tables I and II). Timolol maleate concentrations were determined by interpolation from the corresponding standard curves. The mean concentrations (±*RSD*) were 0.96 ± 0.15 and 50.4 ± 2.1 ng of timolol maleate/ml of plasma with the low and high concentration plasma samples, respectively.

The lower limit of sensitivity for plasma levels expressed as the timolol salt is approximately five times lower than that obtained by Tocco *et al.* (1) using electron-capture GLC.

The accuracy of the technique is good since the relative standard deviation scarcely exceeded 16.0 and 4.2% of the averages obtained in the repeatability tests performed on plasma samples containing 1 (Table I) and 50 ng of timolol maleate/ml of plasma (Table II). These figures reflect an accuracy greater than that obtained with GLC analysis (1, 2).

This mass fragmentographic method is presumed to be specific for determining the intact compound in plasma and urine. The same procedure was applied to numefous urine samples in pharmacokinetic studies.

Plasma timolol levels were determined in five healthy human subjects over 12 hr following a single 20-mg oral dose of timolol maleate (Table III). Mean plasma timolol levels were near 3.2 ng/ml (Table III). The sensitivity level enables good approximate measurement of the plasma concentrations throughout pharmacokinetic studies. The terminal half-life of timolol was 2.62 ± 0.38 hr, and peak plasma levels of 82.5 ng/ml occurred at 1.55 hr after drug administration.

## REFERENCES

(1) D. J. Tocco, F. A. de Luna, and A. E. W. Duncan, *J. Pharm. Sci.*, **64**, 1879 (1975).

(2) P. Vermeij, M. El. Sherbini-Schepers, and P. A. Van Zwieten, *J. Pharm. Pharmacol.*, **30**, 53 (1978).

## ACKNOWLEDGMENTS

The authors thank Dr. Jean Espie, MSD Chibret Laboratories, for assistance.

# Synthesis of [4-$^{14}$C]Theophylline

**MICHAEL G. WILLIAMS * and ALBERT M. MATTOCKS ˣ**

Received September 19, 1980, from the *School of Pharmacy, University of North Carolina, Chapel Hill, NC 27514.* Accepted for publication November 4, 1980. *Present address: College of Pharmacy, Medical University of South Carolina, Charleston, SC 29403.

**Abstract** □ The synthesis of [4-$^{14}$C]theophylline is presented with the radiolabel introduced in the first step of the procedure. The label is carried stoichiometrically to theophylline, and yields are satisfactory. The position of the label at position 4 of the purine ring is attractive for discerning metabolic pathways of the drug.

**Keyphrases** □ Theophylline, radiolabeled—synthesis □ Radiolabeled compounds—[4-$^{14}$C]theophylline, synthesis □ Antiasthmatics—synthesis of [4-$^{14}$C]theophylline

Theophylline (3,7-dihydro-1,3-dimethyl-1*H*-purine-2,6-dione), used to alleviate symptoms of bronchial asthma, has been a popular drug for metabolic and pharmacokinetic studies (1–7). Problems inherent in determining its metabolic profile are compounded by the fact that other commonly ingested methylxanthines form metabolites in common with theophylline. In addition, some metabolites are similar to endogenous compounds.

The best method of distinguishing the metabolites of theophylline from those of its analogs or from other compounds is to insert a radiolabel in the purine ring. Theophylline synthesis has been accomplished (8–10), and a general method (8) was used (6) in [8-$^{14}$C]theophylline synthesis. This procedure calls for the insertion of the radiolabel during the last step of synthesis by adding [$^{14}$C]formic acid in excess to 1,3-dimethyl-4,5-diaminouracil. The reaction is stoichiometric with respect to the latter compound and results in yields of ~7.5% with respect to the label.

A high-yield synthetic procedure (Scheme I) was developed to introduce the carbon 14 label stoichiometrically to maintain a desired specific activity during synthesis and to avoid loss of the expensive $^{14}$C-labeled intermediate.

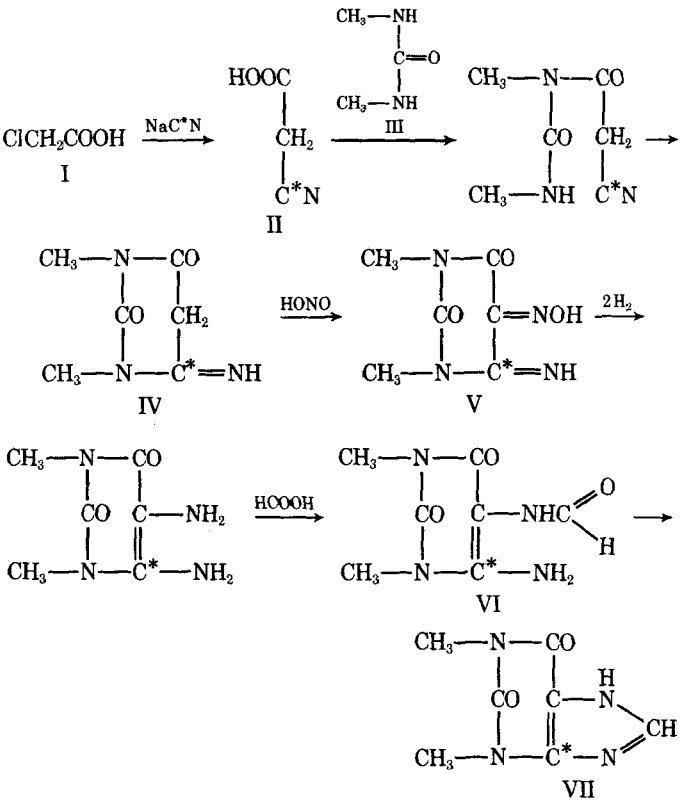


*Scheme I—Synthesis of [4-$^{14}$C]theophylline.*

## EXPERIMENTAL

**Materials**—The following reagent grade materials were used as supplied: chloroacetic acid, sodium carbonate, sodium cyanide, hydrochloric acid, ethanol, 1,3-dimethylurea, acetic anhydride, acetic acid, sodium nitrite, zinc dust, 90% formic acid, and sodium hydroxide. Sodium [$^{14}$C]cyanide[1] (54 mCi/mmole) was diluted with sodium cyanide to give a starting material with a specific activity of 0.72 mCi/mmole.

**[$^{14}$C]Cyanoacetic Acid (II) (11)**—A solution of 0.370 g of chloroacetic acid (I) in 0.6 ml of water at 50° was slowly made alkaline with 0.222 g of sodium carbonate. To the stirred solution at 0° was added dropwise 0.204 g of sodium [$^{14}$C]cyanide in 0.7 ml of ice water, keeping the temperature low. The clear solution was brought to room temperature for 30 min, heated to boiling for 5 min, cooled in an ice bath for 30 min, and slowly acidified with 0.47 ml of concentrated hydrochloric acid.

The clear solution was placed in a desiccator under vacuum until dry, and then the crystalline residue was taken up in 95% ethanol. The sodium chloride byproduct was removed by centrifugation and washed with several portions of alcohol. The combined alcoholic solutions were evaporated at 45° under reduced pressure, leaving a clear viscous concentrate of cyanoacetic acid (II) in alcohol. This material was stored in a desiccator until the last of the alcohol had evaporated and the product had crystallized.

**[4-$^{14}$C]-1,3-Dimethyl-4-amino-2,6-pyrimidinedione (IV) (12)**—To the cyanoacetic acid (II) were added 0.352 g of 1,3-dimethylurea (III), 0.82 ml of acetic anhydride, and 1 ml of acetic acid, and the mixture was heated at 60° for 3 hr. The clear solution became slightly orange. The acetic acid and excess anhydride then were removed as well as possible under reduced pressure without raising the temperature, leaving a burnt-orange viscous residue. This residue was dissolved in 8 ml of water and made alkaline by the slow addition of sodium carbonate and boiling for 2 hr. On cooling, a pale-yellow crystalline precipitate was formed. The yield was 0.375 g or 58% based on sodium cyanide.

**[4-$^{14}$C]-1,3-Dimethyl-4-amino-5-nitroso-2,6-pyrimidinedione (V) (9, 10, 13)**—The dried compound (IV) was dissolved in 8 ml of hot water, and 0.2 g of sodium nitrite was added with stirring. A mixture of 0.85 ml of acetic acid, 0.86 ml of water, and 2.6 g of ice was added in small portions with stirring. The solution turned deep red, and tiny dark-red crystals appeared. The solution was left in the refrigerator overnight to allow the complete precipitation of crystalline product. The product then was filtered out and dried in a desiccator. The yield was 0.420 g or 55% with respect to sodium cyanide.

**[4-$^{14}$C]-1,3-Dimethyl-4-amino-5-formamido-2,6-pyrimidinedione (VI) (10, 14)**—The nitrosated compound (V) was mixed with 0.36 g of zinc dust and placed in a 100-ml round-bottom flask equipped with a reflux condenser. Five milliliters of 90% formic acid was added to the mixture, and the apparatus was swirled continuously as the mixture heated spontaneously. The solution changed from oxblood to yellow over several minutes. The solution then was heated at 60° for 1.5 hr while 2 ml of acetic anhydride was added slowly. Finally, the mixture was cooled, the zinc formate was removed by filtration, and the clear yellow filtrate was dried under reduced pressure at 60°, leaving a solid residue with a yellow-white color. The residue was stored in a desiccator until completely dry.

**[4-$^{14}$C]Theophylline (VII) (10)**—Compound VI was dissolved in 4.5 ml of boiling water, and 0.36 ml of 40% NaOH was added dropwise with

[1] Sodium [$^{14}$C]cyanide, International Chemical and Nuclear Corp.



*0022-3549/81/0500-0576$01.00/0*
*© 1981, American Pharmaceutical Association*

vigorous stirring. The solution was heated for 10 min, at which time another 0.36 ml of 40% NaOH was added. Finally, 50% acetic acid was added in sufficient quantity to give a weak acid reaction. Pale-yellow crystals of theophylline precipitated on cooling. The yield was 0.370 g or 49% with respect to sodium cyanide. The crude theophylline was dissolved in a 10-fold quantity of boiling water, charcoal was added, and the hot solution was filtered. On cooling, white crystals of theophylline were formed.

## RESULTS AND DISCUSSION

A solution of [4-$^{14}$C]theophylline was prepared by dissolving 15.45 mg in sufficient deuterated dimethyl sulfoxide to make 1 ml, and an NMR[2] spectrum was taken with tetramethylsilane as an internal standard. It was identical to the spectrum of a commercial theophylline powder[3]. Furthermore, a methanolic solution of the synthesized compound was spotted on a silica gel plate and developed in chloroform–methanol (9:1) (15) along with a sample of commercial theophylline powder on the same plate. UV spectrodensitometry[4] at 274 nm showed the synthesized and commercial products to have identical $R_f$ values of 0.47; no other UV-absorbing compounds were detected. Scanning the plate with a radiochromatogram scanner[5] showed no measurable radioactivity except that associated with the theophylline peak. Two 0.02-ml samples of the radiolabeled product solution in deuterated dimethyl sulfoxide were counted by scintillation spectrometry[6], and the specific activity was calculated to be 0.69 mCi/mmole.

The introduction of a radiolabel within the purine ring of theophylline is desirable and advantageous in metabolism studies. The described synthesis gives a high yield based on the isotope and is stoichiometric as shown by the calculated and resultant specific activities of the product.

[2] Jeolco C-60HL.
[3] Sigma Chemical Co.
[4] Vis-UV-2, Farrand Optical Co.
[5] Model 7201, Packard Instrument Co.
[6] Model 3320, Packard Instrument Co.

## REFERENCES


(1) B. B. Brodie, J. Axelrod, and J. Reichenthal, *J. Biol. Chem.*, **194,** 215 (1952).

(2) H. Weinfeld and A. A. Christman, *ibid.*, **200,** 345 (1953).

(3) H. H. Cornish and A. A. Christman, *ibid.*, **228,** 315 (1956).

(4) R. D. Thompson, H. T. Nagasawa, and J. W. Jenne, *J. Lab. Clin. Med.*, **84,** 584 (1974).

(5) J. W. Jenne, H. T. Nagasawa, and R. D. Thompson, *Clin. Pharmacol. Ther.*, **19,** 375 (1976).

(6) S. M. Lohmann and R. P. Miech, *J. Pharmacol. Exp. Ther.*, **196,** 213 (1976).

(7) J. Caldwell, R. Lancaster, T. J. Monks, and R. L. Smith, *Br. J. Clin. Pharmacol.*, **4,** 637 P (1977).

(8) W. Traube, *Chem. Ber.*, **33,** 3052 (1900).

(9) F. Grinberg, *J. Appl. Chem. USSR*, **13,** 1461 (1940).

(10) B. Gepner and L. Kreps, *ibid.*, **16,** 179 (1946).

(11) A. Murray, III, and D. L. Williams, "Organic Synthesis with Isotopes, Part I, Compounds of Isotopic Carbon," Interscience, New York, N.Y., 1958, pp. 441, 442.

(12) J. H. Speer and A. L. Raymond, *J. Am. Chem. Soc.*, **75,** 114 (1953).

(13) A. Murray, III, and D. L. Williams, "Organic Synthesis with Isotopes, Part I, Compounds of Isotopic Carbon," Interscience, New York, N.Y., 1958, pp. 769–771.

(14) L. F. Fieser, "Experiments in Organic Chemistry," 2nd ed., D.C. Heath, New York, N.Y., 1941, p. 401.

(15) B. Wesley-Hadzija and A. M. Mattocks, *J. Chromatogr.*, **115,** 501 (1975).


## ACKNOWLEDGMENTS


Abstracted in part from a thesis submitted by M. G. Williams to the University of North Carolina in partial fulfillment of the Doctor of Philosophy degree requirements.

# Kinetics of Pharmacological Effects on Constant-Rate Intravenous Infusion

**Keyphrases** □ Pharmacokinetics—mathematical method for analysis of pharmacological effects on constant-rate intravenous drug infusion □ Mathematics—method for analysis of pharmacological effects on constant-rate intravenous drug infusion □ Kinetics—mathematical method for analysis of pharmacological effects on constant-rate intravenous drug infusion

*To the Editor:*

Over the last 10 years, great interest has developed in monitoring drug and metabolite concentrations in biological fluids to aid in optimizing individual patient drug therapy (1–6). Of course, such drug concentrations are only an indirect index of the ideal monitoring parameter, *i.e.*, pharmacological response. The theoretical bases for quantifying pharmacological response for reversible pharmacodynamic processes were examined thoroughly (7–10). These mathematical relationships were used to elucidate the kinetics of the pharmacological effect of tubocurarine (11–14), succinylcholine (15–17), lysergide (18–20), mercaptomerin (21), ethanol (22), warfarin (23, 24), theophylline (25), and cocaine (26). Each of these drugs elicits a pharmacological effect that can be accurately and reproducibly quantified. This report describes a method for elucidating pharmacokinetic properties following constant-rate intravenous infusion of drugs eliciting quantifiable, reversible pharmacological responses that are immediate, not delayed, effects.

The linear portion of the classic log concentration–response relationship can be described by (7):

$$E = m \log C + e \qquad \text{(Eq. 1)}$$

where $C$ is the concentration, $E$ is the response, $m$ is the slope of the linear portion of $E$ *versus* log $C$, and $e$ is the unit concentration intercept of $E$ *versus* log $C$. With the assumption of instantaneous drug distribution and first-order drug elimination, plasma drug concentration during constant-rate intravenous infusion can be described by the following function of time:

$$C = \frac{k_0}{Cl}(1 - e^{-Kt}) \qquad \text{(Eq. 2)}$$

where $k_0$ is the zero-order infusion rate, $Cl$ is the total body clearance, $K$ is the first-order elimination rate constant, and $t$ is time.

Substitution of Eq. 2 into Eq. 1 provides the relationship describing the pharmacological effect as a function of time during ongoing intravenous infusion:

$$E = m \log \frac{k_0}{Cl}(1 - e^{-Kt}) + e \qquad \text{(Eq. 3a)}$$

or:

$$E = m \log k_0 - m \log Cl + m \log (1 - e^{-Kt}) + e \qquad \text{(Eq. 3b)}$$

As infusion continues toward steady state, the term $e^{-Kt}$ approaches zero. Therefore, at steady state, Eq. 3*b* becomes:

$$E_{ss} = m \log k_0 - m \log Cl + e \qquad \text{(Eq. 4a)}$$

where $E_{ss}$ is the pharmacological effect at steady state. This relationship is most useful following conversion to the form:

$$E_{ss} = m \log k_0 - b \qquad \text{(Eq. 4b)}$$

where $b = m \log Cl - e$; $b$ is the $y$ intercept of $E_{ss}$ *versus* log $k_0$.

For a drug satisfying the prior assumptions, Eq. 4*b* indicates that a plot of the steady-state pharmacological effect *versus* the logarithm of the intravenous zero-order infusion rate is linear with a slope equal to $m$, the slope of the linear portion of the log concentration–response relationship.

Consider the time course of declining pharmacological effect. Rearrangement of Eq. 1 yields:

$$\log C = \frac{E - e}{m} \qquad \text{(Eq. 5)}$$

Postinfusion, monoexponential decline of the plasma drug concentration from the steady-state concentration ($C_{ss}$) achieved *via* constant-rate intravenous infusion is described by:

$$\log C = \log C_{ss} - \frac{Kt}{2.303} \qquad \text{(Eq. 6)}$$

Substituting for log $C$ and log $C_{ss}$ in Eq. 6 from Eq. 5 yields:

$$\frac{E - e}{m} = \frac{E_{ss} - e}{m} - \frac{Kt}{2.303} \qquad \text{(Eq. 7a)}$$

or:

$$E = E_{ss} - \frac{mK}{2.303}t \qquad \text{(Eq. 7b)}$$

Equation 7*b* indicates that a plot of postinfusion pharmacological effect *versus* time declines linearly from steady state, with the slope providing an estimate of the product of $K$ and $m$. Construction of plots of $E_{ss}$ *versus* log $k_0$ (Eq. 4*b*) and $E$ *versus* time, for effect declining from steady state (Eq. 7*b*), provides estimates of $m$ and $mK$, respectively, and thereby enables estimation of $K$. But knowing $K$, the biological half-life ($t_{1/2}$) is readily calculated from:

$$t_{1/2} = \frac{\ln 2}{K} \qquad \text{(Eq. 8)}$$

In addition to the assumptions stated in the original papers on this type of pharmacological effect model, inference of the pharmacokinetic behavior of a drug based on pharmacological effect data requires that no metabolites have measurable interfering pharmacological activity (27). If the decline of pharmacological effect is rate limited by the drug diffusion rate from the site of action, the reformation rate of an essential enzyme, or homeostatic control mechanisms, the apparent elimination rate constant calculated from the equations discussed in this paper will be representative of the rate-limiting process (11, 28).

This method was applied to data obtained from a previous study (29). In that study, 54 patients in a state of hypertensive emergency received sodium nitroprusside infusions in a dose-titration manner to achieve the desired hypotensive effect. Individual data were presented for four

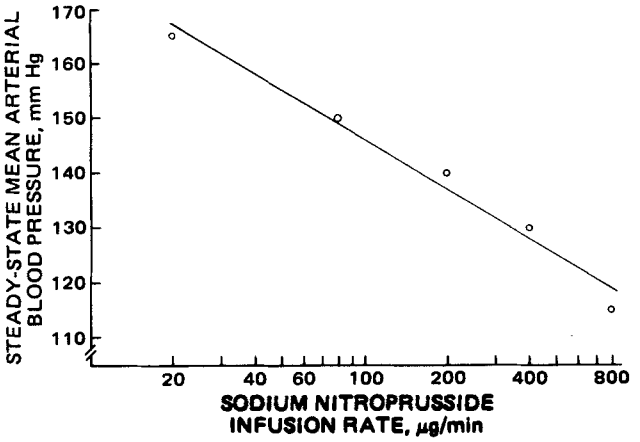


**Figure 1**—*Relationship between steady-state mean arterial blood pressure and sodium nitroprusside infusion rate in one patient with malignant hypertension. The linear regression line is shown (r = −0.99).*

representative patients. Data on one patient, a 45-year-old male with malignant hypertension, renal failure, and congestive heart failure, were presented in sufficient detail to permit the proposed analysis. In accordance with Eq. 4*b*, a linear relationship was obtained between steady-state mean arterial blood pressure and the logarithm of sodium nitroprusside infusion rate over a 40-fold range of zero-order infusion rates (Fig. 1). As shown in Fig. 2, plotting the time course of the hypotensive effect declining from steady state following discontinuation of sodium nitroprusside infusion illustrates adherence to Eq. 7*b*.

Calculation of the slopes in Figs. 1 and 2 provides direct estimates of $m$ and $mK$ of −30.1 mm Hg and 1.40 mm Hg/min, respectively. Therefore, $K$ can be estimated as 0.0465 $min^{-1}$ with a corresponding biological half-life of 14.9 min. This estimate of biological half-life is consistent with the rapidly achieved steady-state hypotensive response observed clinically. This relatively short half-life supports the prior interpretation of the mean arterial blood pressures in Fig. 1 as being reasonable approximations of steady-state values.

This analysis for sodium nitroprusside is exemplary of the potential utility of studying the pharmacokinetic properties of intravenously administered drugs eliciting a quantifiable response. Constant-rate intravenous infusion of a drug having a relatively short biological half-life will enable rapid achievement of steady state at each of the several infusion rates. Although this technique may not be applicable to all drugs, it may provide a basis for practical, exploratory analysis of pharmacological effect data for drugs such as nitroprusside, diazoxide, nitroglycerin, and trimethaphan.

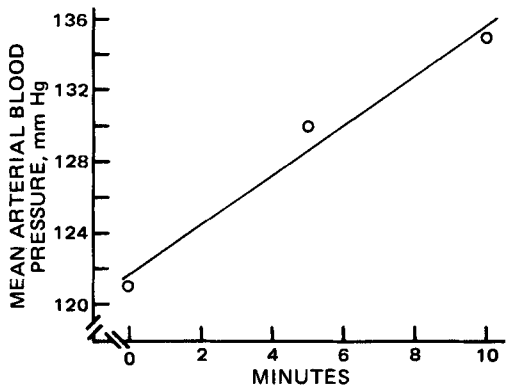


**Figure 2**—*Time course of increasing mean arterial blood pressure following discontinuation of sodium nitroprusside infusion. The linear regression line is shown (r = 0.99).*

(1) E. S. Vesell and G. T. Passananti, *Clin. Chem.*, **17**, 851 (1971).
(2) J. Koch-Weser, *N. Engl. J. Med.*, **287**, 227 (1972).
(3) "Biological Effects of Drugs In Relation to Their Plasma Concentrations," D. S. Davies and B. N. C. Pritchard, Eds., Macmillan, London, England, 1973.
(4) G. Levy, "Clinical Pharmacokinetics: A Symposium," American Pharmaceutical Association, Washington, D.C., 1974, p. 1.
(5) D. Perrier and M. Gibaldi, *J. Clin. Pharmacol.*, **14**, 415 (1974).
(6) A. Richens and S. Warrington, *Drugs*, **17**, 488 (1979).
(7) G. Levy, *Clin. Pharmacol. Ther.*, **7**, 362 (1966).
(8) J. G. Wagner, *J. Theoret. Biol.*, **20**, 173 (1968).
(9) J. G. Wagner, *J. Mond. Pharm.*, **14**, 279 (1971).
(10) E. R. Garrett, "Progress in Drug Research," vol. 21, Birkhaüser Verlag, Basel, Switzerland, 1977, p. 105.
(11) G. Levy, *J. Pharm. Sci.*, **53**, 342 (1964).
(12) G. Levy, *Br. J. Anaesth.*, **36**, 694 (1964).
(13) M. Gibaldi, G. Levy, and W. Hayton, *Anesthesiology*, **36**, 213 (1972).
(14) M. Gibaldi and G. Levy, *J. Pharm. Sci.*, **61**, 567 (1972).
(15) G. Levy, *ibid.*, **56**, 1687 (1967).
(16) G. Levy, *Anesthesiology*, **32**, 551 (1970).
(17) G. Levy, *Br. J. Anaesth.*, **42**, 979 (1970).
(18) J. G. Wagner, G. K. Aghajanian, and O. H. L. Bing, *Clin. Pharmacol. Ther.*, **9**, 635 (1968).
(19) G. Levy, *ibid.*, **10**, 134 (1969).
(20) C. M. Metzler, *ibid.*, **10**, 737 (1969).
(21) G. Levy, *J. Nucl. Med.*, **5**, 302 (1964).
(22) A. R. DiSanto and J. G. Wagner, *J. Pharm. Sci.*, **58**, 1077 (1969).
(23) R. Nagashima, R. A. O'Reilly, and G. Levy, *Clin. Pharmacol. Ther.*, **10**, 22 (1969).
(24) G. Levy, *J. Pharmacokinet. Biopharm.*, **1**, 541 (1973).
(25) G. Levy and R. Koysooko, *J. Pediatr.*, **86**, 789 (1975).
(26) M. Mayersohn and D. Perrier, *Res. Commun. Chem. Pathol. Pharmacol.*, **22**, 465 (1978).
(27) A. J. Atkinson and J. M. Strong, *J. Pharmacokinet. Biopharm.*, **5**, 95 (1977).
(28) G. Levy, *Proc. Ann. Res. Sci. Dev. Conf. Proprietary Assoc.*, **1961**, 32.
(29) I. Tuzel, R. Limjuco, and D. Kahn, *Curr. Ther. Res.*, **17**, 95 (1975).

*David M. Cocchetto*
Clinical Pharmacodynamics Section
Department of Clinical Research
Wellcome Research Laboratories
Research Triangle Park, NC 27709

Received December 8, 1980.
Accepted for publication February 19, 1981.

## Plasma Theobromine after Oral Administration of Caffeine to Dogs

**Keyphrases** □ Theobromine—caffeine metabolite, plasma levels following oral administration of caffeine to dogs □ Caffeine—metabolism in dogs, plasma theobromine levels following oral administration of caffeine to dogs □ Metabolism—of caffeine, plasma levels of metabolite theobromine following oral administration of caffeine to dogs

*To the Editor:*

Caffeine (1,3,7-trimethylxanthine), a compound in coffee, tea, and many other beverages, has been used successfully for the treatment of apnea in premature infants

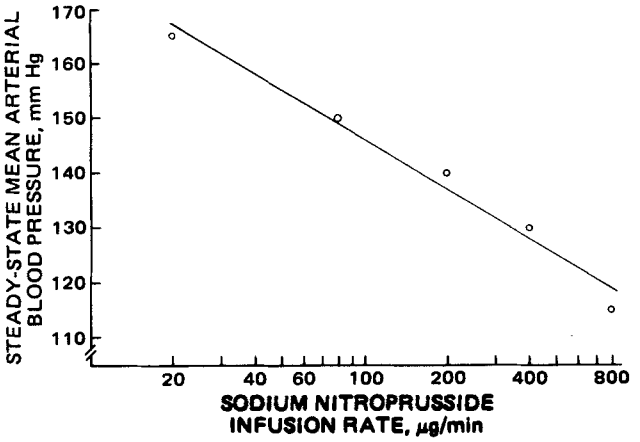


**Figure 1**—*Relationship between steady-state mean arterial blood pressure and sodium nitroprusside infusion rate in one patient with malignant hypertension. The linear regression line is shown (r = −0.99).*

representative patients. Data on one patient, a 45-year-old male with malignant hypertension, renal failure, and congestive heart failure, were presented in sufficient detail to permit the proposed analysis. In accordance with Eq. 4*b*, a linear relationship was obtained between steady-state mean arterial blood pressure and the logarithm of sodium nitroprusside infusion rate over a 40-fold range of zero-order infusion rates (Fig. 1). As shown in Fig. 2, plotting the time course of the hypotensive effect declining from steady state following discontinuation of sodium nitroprusside infusion illustrates adherence to Eq. 7*b*.

Calculation of the slopes in Figs. 1 and 2 provides direct estimates of $m$ and $mK$ of −30.1 mm Hg and 1.40 mm Hg/min, respectively. Therefore, $K$ can be estimated as 0.0465 $min^{-1}$ with a corresponding biological half-life of 14.9 min. This estimate of biological half-life is consistent with the rapidly achieved steady-state hypotensive response observed clinically. This relatively short half-life supports the prior interpretation of the mean arterial blood pressures in Fig. 1 as being reasonable approximations of steady-state values.

This analysis for sodium nitroprusside is exemplary of the potential utility of studying the pharmacokinetic properties of intravenously administered drugs eliciting a quantifiable response. Constant-rate intravenous infusion of a drug having a relatively short biological half-life will enable rapid achievement of steady state at each of the several infusion rates. Although this technique may not be applicable to all drugs, it may provide a basis for practical, exploratory analysis of pharmacological effect data for drugs such as nitroprusside, diazoxide, nitroglycerin, and trimethaphan.

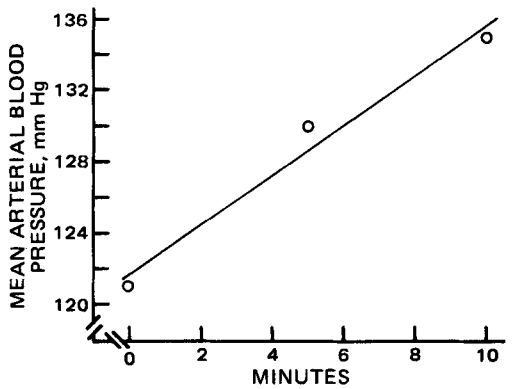


**Figure 2**—*Time course of increasing mean arterial blood pressure following discontinuation of sodium nitroprusside infusion. The linear regression line is shown (r = 0.99).*

(1) E. S. Vesell and G. T. Passananti, *Clin. Chem.*, **17**, 851 (1971).
(2) J. Koch-Weser, *N. Engl. J. Med.*, **287**, 227 (1972).
(3) "Biological Effects of Drugs In Relation to Their Plasma Concentrations," D. S. Davies and B. N. C. Pritchard, Eds., Macmillan, London, England, 1973.
(4) G. Levy, "Clinical Pharmacokinetics: A Symposium," American Pharmaceutical Association, Washington, D.C., 1974, p. 1.
(5) D. Perrier and M. Gibaldi, *J. Clin. Pharmacol.*, **14**, 415 (1974).
(6) A. Richens and S. Warrington, *Drugs*, **17**, 488 (1979).
(7) G. Levy, *Clin. Pharmacol. Ther.*, **7**, 362 (1966).
(8) J. G. Wagner, *J. Theoret. Biol.*, **20**, 173 (1968).
(9) J. G. Wagner, *J. Mond. Pharm.*, **14**, 279 (1971).
(10) E. R. Garrett, "Progress in Drug Research," vol. 21, Birkhaüser Verlag, Basel, Switzerland, 1977, p. 105.
(11) G. Levy, *J. Pharm. Sci.*, **53**, 342 (1964).
(12) G. Levy, *Br. J. Anaesth.*, **36**, 694 (1964).
(13) M. Gibaldi, G. Levy, and W. Hayton, *Anesthesiology*, **36**, 213 (1972).
(14) M. Gibaldi and G. Levy, *J. Pharm. Sci.*, **61**, 567 (1972).
(15) G. Levy, *ibid.*, **56**, 1687 (1967).
(16) G. Levy, *Anesthesiology*, **32**, 551 (1970).
(17) G. Levy, *Br. J. Anaesth.*, **42**, 979 (1970).
(18) J. G. Wagner, G. K. Aghajanian, and O. H. L. Bing, *Clin. Pharmacol. Ther.*, **9**, 635 (1968).
(19) G. Levy, *ibid.*, **10**, 134 (1969).
(20) C. M. Metzler, *ibid.*, **10**, 737 (1969).
(21) G. Levy, *J. Nucl. Med.*, **5**, 302 (1964).
(22) A. R. DiSanto and J. G. Wagner, *J. Pharm. Sci.*, **58**, 1077 (1969).
(23) R. Nagashima, R. A. O'Reilly, and G. Levy, *Clin. Pharmacol. Ther.*, **10**, 22 (1969).
(24) G. Levy, *J. Pharmacokinet. Biopharm.*, **1**, 541 (1973).
(25) G. Levy and R. Koysooko, *J. Pediatr.*, **86**, 789 (1975).
(26) M. Mayersohn and D. Perrier, *Res. Commun. Chem. Pathol. Pharmacol.*, **22**, 465 (1978).
(27) A. J. Atkinson and J. M. Strong, *J. Pharmacokinet. Biopharm.*, **5**, 95 (1977).
(28) G. Levy, *Proc. Ann. Res. Sci. Dev. Conf. Proprietary Assoc.*, **1961**, 32.
(29) I. Tuzel, R. Limjuco, and D. Kahn, *Curr. Ther. Res.*, **17**, 95 (1975).

*David M. Cocchetto*
Clinical Pharmacodynamics Section
Department of Clinical Research
Wellcome Research Laboratories
Research Triangle Park, NC 27709

Received December 8, 1980.
Accepted for publication February 19, 1981.

## Plasma Theobromine after Oral Administration of Caffeine to Dogs

**Keyphrases** □ Theobromine—caffeine metabolite, plasma levels following oral administration of caffeine to dogs □ Caffeine—metabolism in dogs, plasma theobromine levels following oral administration of caffeine to dogs □ Metabolism—of caffeine, plasma levels of metabolite theobromine following oral administration of caffeine to dogs

*To the Editor:*

Caffeine (1,3,7-trimethylxanthine), a compound in coffee, tea, and many other beverages, has been used successfully for the treatment of apnea in premature infants

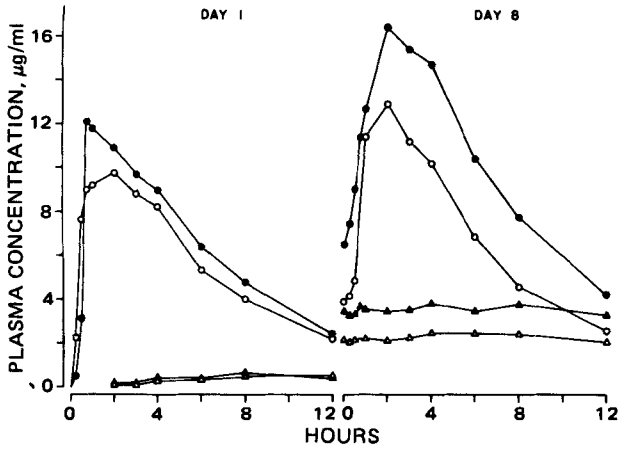


**Figure 1**—*Plasma concentrations of caffeine (●, Dog A; and ○, Dog B) and theobromine (▲, Dog A; and △, Dog B) after the morning doses on Days 1 and 8 during a 100-mg caffeine twice daily regimen.*

(1). Caffeine is absorbed efficiently following oral doses in humans and is eliminated almost entirely by biotransformation (2).

A first step in caffeine metabolism in humans is *N*-demethylation, which may occur at the 1-, 3-, or 7-position. It was suggested that the removals of the 3- and 7-methyl groups to form 1,7-dimethylxanthine and theophylline, respectively, are the major pathways, while the removal of the 1-methyl group to form theobromine is of minor importance (3). Nevertheless, 5% of an administered dose of caffeine was excreted as theobromine in rats (4). Another investigation found the same pathway in beagle dogs after single intravenous caffeine doses of 20 mg/kg (5).

In a recent study in this laboratory (6), the pharmacokinetics of caffeine were examined after single and repeated oral doses to beagle dogs. Theobromine was detected as a metabolite in plasma. Significant accumulation of this metabolite was observed after multiple caffeine doses, as described here.

Two beagle dogs (1-year-old male, Dog A, 11.4 kg, and 2-year-old female, Dog B, 11.7 kg) each received one 100-mg caffeine tablet[1] twice daily at 9:00 am and 9:00 pm for 8 days. The dogs were fasted overnight before the morning doses on Days 1 and 8, after which serial venous blood samples were collected. Plasma caffeine and theobromine were measured by high-performance liquid chromatography as previously described (6). Complete peak resolution was obtained for caffeine, theobromine, and β-hydroxyethyltheophylline (the internal standard), with retention times of 9.6, 4.0, and 6.5 min, respectively. Other xanthines did not interfere.

[1] NoDoz, Bristol-Myers, New York, N.Y.

Individual plasma caffeine and theobromine concentrations in the two dogs are summarized in Fig. 1. Caffeine was absorbed efficiently from a single oral dose, reaching the peak plasma level at 1–2 hr. The average elimination half-life calculated by nonlinear regression analysis (7) of individual data was 4.5 hr. Detectable theobromine levels appeared in the plasma at 2 hr following caffeine administration, rising slowly to 0.5–0.6 μg/ml at 8 hr. The peak time and normalized peak concentration showed excellent agreement with an earlier report (5). After repeated doses of caffeine, the drug showed some accumulation as predicted from the single-dose data. The average caffeine half-life was 3.9 hr, slightly shorter than the single-dose case. Of primary interest here, however, was the accumulation of the metabolite, theobromine. The Day 8 plasma levels, apparently at steady state, indicated a five- to six-fold increase from the single-dose data.

Results of the present study provided quantitative information on *N*-demethylation of caffeine in the dog to form theobromine. While plasma theobromine levels after a single caffeine dose were low, significant accumulation of this metabolite occurred after repeated caffeine administration. This phenomenon needs to be verified in humans. Since theobromine shares some of the common pharmacological activities of caffeine and theophylline (8), it may be necessary to recognize circulating levels of this metabolite when monitoring patients on caffeine therapy.

(1) J. V. Aranda, W. Gorman, H. Bergsteinsson, and T. Gunn, *J. Pediatr.*, **90,** 467 (1977).

(2) J. Axelrod and J. Reichenthal, *J. Pharmacol. Exp. Ther.*, **107,** 519 (1953).

(3) H. H. Cornish and A. A. Christman, *J. Biol. Chem.*, **228,** 315 (1957).

(4) K. L. Khanna, G. S. Rao, and H. H. Cornish, *Toxicol. Appl. Pharmacol.*, **23,** 720 (1972).

(5) A. Aldridge and A. H. Neims, *Drug Metab. Dispos.*, **7,** 378 (1979).

(6) F. L. S. Tse, K. H. Valia, D. W. Szeto, T. J. Raimondo, and B. Koplowitz, *J. Pharm. Sci.*, **70,** 395 (1981).

(7) C. M. Metzler, G. L. Elfring, and A. J. McEwen, *Biometrics*, **30,** 562 (1974).

(8) "The Pharmacological Basis of Therapeutics," 6th ed., A. G. Gilman, L. S. Goodman, and A. Gilman, Eds., Macmillan, New York, N.Y., 1980, pp. 592–607.

*F. L. S. Tse**x
*K. H. Valia*
College of Pharmacy
Rutgers—The State University
Piscataway, NJ 08854

Received December 15, 1980.
Accepted for publication February 19, 1981.
Supported by Biomedical Research Support Grant RR 7058-15 from the U.S. Public Health Service.

* Present address: Pharmaceutical Research & Development, Sandoz Inc., East Hanover, NJ 07936.

## REVIEWS

**Goodman and Gilman's The Pharmacological Basis of Therapeutics: 6th Ed.** Edited by ALFRED GOODMAN GILMAN, LOUIS S. GOODMAN, and ALFRED GILMAN. Macmillan, 866 Third Ave., New York, NY 10022. 1980. 1843 pp. 18 × 26 cm. Price $45.00.

This latest edition of L. S. Goodman and A. Gilman continues a time-honored tradition of serving as an accurate source of past and present knowledge upon which therapeutics is based. It differs from its predecessors, however, in the recognition that diseases are dynamic and that standard therapy is inadequate to meet the needs of a patient who, for example, has a myocardial infarction accompanied by diabetes mellitus. Much emphasis is placed on individualization of therapy, the need for compliance, and the results of noncompliance.

Principles of pharmacokinetics and biotransformation patterns appear in the early chapters and reappear in Appendix II under the heading Design and Optimization of Dosage Regimens along with pharmacokinetic data pertaining to oral availability, urinary excretion, plasma binding, and clearance of 100 widely used agents to expedite drug selection by the physician. The intervening chapters reflect those areas that have advanced rapidly in recent years—autonomic and antihypertensive agents, anti-inflammatories, autacoids, antineoplastics, and antimicrobials—and those that haven't—local anesthetics, cathartics, antianemics, salts and ions, vitamins, and oxytocics.

Looking back 4 decades at the first edition, when pharmacology was discarding the mantle of *materia medica* and computer technology was at the abacus stage, the reviewer is impressed with the amount of basic material then available, with the skill of the two authors who organized the information so logically and clearly, and with the realization that practitioners without an understanding of prodrugs, receptor configurations, pharmacokinetics, food and drug interactions, and the phenomena of tolerance and addiction could practice medicine reasonably well. In this edition, 55 contributors, some of whom are specialists in areas unheard of a few decades ago, have produced a noteworthy successor to earlier editions that will enable those who utilize therapeutic skills directly or indirectly in patient management to achieve a refinement in combating disease hitherto unequaled.

*Reviewed by* David E. Mann, Jr.
*School of Pharmacy*
*Temple University*
*Philadelphia, PA 19140*

---

**Biochemical Applications of Mass Spectrometry: First Supplementary Volume.** Edited by GEORGE R. WALLER and OTIS C. DERMER. Wiley, 605 Third Ave., New York, NY 10016. 1980. 1279 pp. 21 × 28 cm. Price $150.00.

The editors of *Biochemical Applications of Mass Spectrometry: First Supplementary Volume* are to be congratulated on a job well done. Between the covers of this book (which are separated by 4.6 cm of pages), the novice and the experienced mass spectrometrist alike can find valuable information relating to a host of mass spectrometry-related topics. A section on instrumentation (spectrometers and data systems) is followed by one on the interpretation of mass spectra. Emphasis is on the data systems found in 10 of the leading mass spectrometry laboratories around the world and on computer-based identification of unknowns. Inclusion of a general chapter discussing the interpretation of spectra might have been desirable at this point.

These two sections are followed by the major section—applications—containing approximately 30 chapters covering nearly all of the topics in which biochemists and scientists in related fields would have an interest. Although many of these chapters discuss chemical-ionization and field-desorption-based analyses, this reviewer finds it unfortunate that no chapters are dedicated specifically to these two important techniques. Chapters discussing $^{252}Cf$ plasma desorption mass spectrometry and negative-ion mass spectrometry are included. The emphasis of most of the applications chapters is on structure elucidation, but quantitation is by no means ignored and Chapter 37 covers this topic exclusively. (I must disagree with the authors of this chapter on one point: isotope effects are not always "negligible," and a labeled compound need not behave "isographically" with the analogous unlabeled compound in all chromatographic systems.)

Some of the applications chapters are descriptive, and several are highly detailed and crammed with fragmentation pathways complete with mechanisms. Chapter 25 (flavor components) should be of special value to students and teachers involved in learning about basic mass spectrometry since it contains numerous fundamental fragmentation pathways plus simple but highly illustrative spectra. This chapter also answered a question some of us home gardeners have asked for years—what is the source of the characteristic aroma produced by tomato plant leaves. The answer—2-isobutylthiazole. Chapter 34 (Volatiles Emitted by Humans) reports on some "way-out" applications of mass spectrometry, but it is short on hard data.

Classic chapters include those on fatty acids, amino acids and amino acid sequencing, steroids, hormones, flavonoids, vitamins, and carbohydrates. Newer fields covered equally well are pheromones, drug metabolism, pollutants, and clinical medicine. The value of derivatization and GLC–mass spectrometry is made abundantly clear by many of the authors, and some speak with hope about liquid chromatography–mass spectrometry. All chapters contain useful lists of recent references.

This book should be a welcome addition to the libraries of natural products, synthetic organic and drug metabolism chemists, many persons involved in biological studies where structure elucidation and quantitation are necessary for advances, and researchers working on environmental problems.

*Reviewed by* William J. A. VandenHeuvel
*Merck Sharp & Dohme Research Laboratories*
*Rahway, NJ 07065*

The first supplementary volume continues the standard of excellence established in the original compendium of biochemical mass spectrometry [*cf.*, Book Reviews, *J. Pharm. Sci.*, **62**, 516 (1973)]. Largely written by the original authors, as the subtitle indicates, the discussions and the reference, figure, and table numbering continue from the earlier review. The editors have maintained consistent styles among the 35 chapters contributed by nearly 80 authors. Section I, Instrumentation, begins with a useful discussion of newer ionization and sample handling techniques (Chapter 2). Of less interest to the nonspecialist is the discussion on Data Acquisition and Processing in the following chapter.

Section II, Interpretation of Mass Spectra, describes the latest advances and utility of metastable ions as an aid to interpretation (Chapter 5). Compound Identification by Computer Matching (Chapter 6) might be helpful to those contemplating purchasing access to the MSDC/EPA/NIH MSSS system. On the other hand, the computer programs, the basis for the discussion on automated scientific inferences (Chapter 7), may not be readily accessible.

Section III, Applications, comprising 30 chapters and over 1000 pages, more than amply fulfills the editors' objective to promote mass spectrometric research capabilities and interests in a diverse group of investigators. Building on the discussions of the original volume, the experts chosen to write the individual chapters clearly develop guidelines for the interpretation of the various classes of compounds encountered in biochemistry and organic chemistry. Both the expert and novice would benefit from these reviews in the elucidation of unknown structures. The chapters in this section are filled with structures, fragmentation patterns, and mass spectra. Each review appears to have referenced the literature through 1977, with a significant number of them containing several references from 1978 and a few references from 1979. It should be relatively easy to locate the most recent articles working from the combined reference list of both volumes and Science Citation Index.

The negative-ion review is very timely. Notable omissions from the supplementary volume is the review of positive-ion chemical-ionization and field-ionization/desorption. More recent reviews should be consulted, rather than the original volume, for a background in these areas. The original volume, still in print, should be consulted for the more fundamental interpretation of the various classes of compounds. In summary, the complementary volumes should be in every book collection in institutions where mass spectrometry is being used.

*Reviewed by* A. I. Cohen
*Squibb Institute for Medical Research*
*Princeton, NJ 08540*

## REVIEWS

**Goodman and Gilman's The Pharmacological Basis of Therapeutics: 6th Ed.** Edited by ALFRED GOODMAN GILMAN, LOUIS S. GOODMAN, and ALFRED GILMAN. Macmillan, 866 Third Ave., New York, NY 10022. 1980. 1843 pp. 18 × 26 cm. Price $45.00.

This latest edition of L. S. Goodman and A. Gilman continues a time-honored tradition of serving as an accurate source of past and present knowledge upon which therapeutics is based. It differs from its predecessors, however, in the recognition that diseases are dynamic and that standard therapy is inadequate to meet the needs of a patient who, for example, has a myocardial infarction accompanied by diabetes mellitus. Much emphasis is placed on individualization of therapy, the need for compliance, and the results of noncompliance.

Principles of pharmacokinetics and biotransformation patterns appear in the early chapters and reappear in Appendix II under the heading Design and Optimization of Dosage Regimens along with pharmacokinetic data pertaining to oral availability, urinary excretion, plasma binding, and clearance of 100 widely used agents to expedite drug selection by the physician. The intervening chapters reflect those areas that have advanced rapidly in recent years—autonomic and antihypertensive agents, anti-inflammatories, autacoids, antineoplastics, and antimicrobials—and those that haven't—local anesthetics, cathartics, antianemics, salts and ions, vitamins, and oxytocics.

Looking back 4 decades at the first edition, when pharmacology was discarding the mantle of *materia medica* and computer technology was at the abacus stage, the reviewer is impressed with the amount of basic material then available, with the skill of the two authors who organized the information so logically and clearly, and with the realization that practitioners without an understanding of prodrugs, receptor configurations, pharmacokinetics, food and drug interactions, and the phenomena of tolerance and addiction could practice medicine reasonably well. In this edition, 55 contributors, some of whom are specialists in areas unheard of a few decades ago, have produced a noteworthy successor to earlier editions that will enable those who utilize therapeutic skills directly or indirectly in patient management to achieve a refinement in combating disease hitherto unequaled.

*Reviewed by* David E. Mann, Jr.
*School of Pharmacy*
*Temple University*
*Philadelphia, PA 19140*

---

**Biochemical Applications of Mass Spectrometry: First Supplementary Volume.** Edited by GEORGE R. WALLER and OTIS C. DERMER. Wiley, 605 Third Ave., New York, NY 10016. 1980. 1279 pp. 21 × 28 cm. Price $150.00.

The editors of *Biochemical Applications of Mass Spectrometry: First Supplementary Volume* are to be congratulated on a job well done. Between the covers of this book (which are separated by 4.6 cm of pages), the novice and the experienced mass spectrometrist alike can find valuable information relating to a host of mass spectrometry-related topics. A section on instrumentation (spectrometers and data systems) is followed by one on the interpretation of mass spectra. Emphasis is on the data systems found in 10 of the leading mass spectrometry laboratories around the world and on computer-based identification of unknowns. Inclusion of a general chapter discussing the interpretation of spectra might have been desirable at this point.

These two sections are followed by the major section—applications—containing approximately 30 chapters covering nearly all of the topics in which biochemists and scientists in related fields would have an interest. Although many of these chapters discuss chemical-ionization and field-desorption-based analyses, this reviewer finds it unfortunate that no chapters are dedicated specifically to these two important techniques. Chapters discussing $^{252}Cf$ plasma desorption mass spectrometry and negative-ion mass spectrometry are included. The emphasis of most of the applications chapters is on structure elucidation, but quantitation is by no means ignored and Chapter 37 covers this topic exclusively. (I must disagree with the authors of this chapter on one point: isotope effects are not always "negligible," and a labeled compound need not behave "isographically" with the analogous unlabeled compound in all chromatographic systems.)

Some of the applications chapters are descriptive, and several are highly detailed and crammed with fragmentation pathways complete with mechanisms. Chapter 25 (flavor components) should be of special value to students and teachers involved in learning about basic mass spectrometry since it contains numerous fundamental fragmentation pathways plus simple but highly illustrative spectra. This chapter also answered a question some of us home gardeners have asked for years—what is the source of the characteristic aroma produced by tomato plant leaves. The answer—2-isobutylthiazole. Chapter 34 (Volatiles Emitted by Humans) reports on some "way-out" applications of mass spectrometry, but it is short on hard data.

Classic chapters include those on fatty acids, amino acids and amino acid sequencing, steroids, hormones, flavonoids, vitamins, and carbohydrates. Newer fields covered equally well are pheromones, drug metabolism, pollutants, and clinical medicine. The value of derivatization and GLC–mass spectrometry is made abundantly clear by many of the authors, and some speak with hope about liquid chromatography–mass spectrometry. All chapters contain useful lists of recent references.

This book should be a welcome addition to the libraries of natural products, synthetic organic and drug metabolism chemists, many persons involved in biological studies where structure elucidation and quantitation are necessary for advances, and researchers working on environmental problems.

*Reviewed by* William J. A. VandenHeuvel
*Merck Sharp & Dohme Research Laboratories*
*Rahway, NJ 07065*

The first supplementary volume continues the standard of excellence established in the original compendium of biochemical mass spectrometry [*cf.*, Book Reviews, *J. Pharm. Sci.*, **62**, 516 (1973)]. Largely written by the original authors, as the subtitle indicates, the discussions and the reference, figure, and table numbering continue from the earlier review. The editors have maintained consistent styles among the 35 chapters contributed by nearly 80 authors. Section I, Instrumentation, begins with a useful discussion of newer ionization and sample handling techniques (Chapter 2). Of less interest to the nonspecialist is the discussion on Data Acquisition and Processing in the following chapter.

Section II, Interpretation of Mass Spectra, describes the latest advances and utility of metastable ions as an aid to interpretation (Chapter 5). Compound Identification by Computer Matching (Chapter 6) might be helpful to those contemplating purchasing access to the MSDC/EPA/NIH MSSS system. On the other hand, the computer programs, the basis for the discussion on automated scientific inferences (Chapter 7), may not be readily accessible.

Section III, Applications, comprising 30 chapters and over 1000 pages, more than amply fulfills the editors' objective to promote mass spectrometric research capabilities and interests in a diverse group of investigators. Building on the discussions of the original volume, the experts chosen to write the individual chapters clearly develop guidelines for the interpretation of the various classes of compounds encountered in biochemistry and organic chemistry. Both the expert and novice would benefit from these reviews in the elucidation of unknown structures. The chapters in this section are filled with structures, fragmentation patterns, and mass spectra. Each review appears to have referenced the literature through 1977, with a significant number of them containing several references from 1978 and a few references from 1979. It should be relatively easy to locate the most recent articles working from the combined reference list of both volumes and Science Citation Index.

The negative-ion review is very timely. Notable omissions from the supplementary volume is the review of positive-ion chemical-ionization and field-ionization/desorption. More recent reviews should be consulted, rather than the original volume, for a background in these areas. The original volume, still in print, should be consulted for the more fundamental interpretation of the various classes of compounds. In summary, the complementary volumes should be in every book collection in institutions where mass spectrometry is being used.

*Reviewed by* A. I. Cohen
*Squibb Institute for Medical Research*
*Princeton, NJ 08540*

## NOTICES

*Development of Mammalian Absorptive Processes.* Ciba Foundation Symposium 70 (new series). Excerpta Medica, P.O. Box 211, 1000 AE Amsterdam, The Netherlands. 1979. 338 pp. 16 × 24 cm. Price $41.50. (Distributed in the United States by Elsevier/North-Holland, 52 Vanderbilt Ave., New York, NY 10017.)

*Blood Cells and Vessel Walls: Functional Interactions.* Ciba Foundation Symposium 71 (new series). Excerpta Medica, P.O. Box 211, 1000 AE Amsterdam, The Netherlands. 1980. 357 pp. 16 × 24 cm. Price $43.50. (Distributed in the United States by Elsevier/North-Holland, 52 Vanderbilt Ave., New York, NY 10017.)

*Extrahepatic Metabolism of Drugs and Other Foreign Compounds.* Edited by THEODORE E. GRAM. SP Medical & Scientific Books, 17520 Wexford Terrace, Jamaica, NY 11432. 1980. 601 pp. 15 × 23 cm. Price $55.00.

*Abrégé de Droit et Deontologie du Laboratoire D'Analyses de Biologie Medicale.* By MONIQUE TISSEYRE-BERRY. Masson, 120 boulevard Saint-Germain, 75280 Paris Cedex 06, France. 1980. 110 pp. 13 × 21 cm.

*Advances in Drying: Vol. 1.* Edited by ARUN S. MUJUMDAR. Hemisphere Publishing Corp., Global Bldg., 1025 Vermont Ave., N.W., Washington, DC 20005. 1980. 301 pp. 15 × 23 cm. Price $55.00.

*Drying '80: Vol. 1: Developments in Drying.* Edited by ARUN S. MUJUMDAR. Hemisphere Publishing Corp., Global Bldg., 1025 Vermont Ave., N.W., Washington, DC 20005. 1980. 518 pp. 20 × 28 cm. Price $62.00.

*Drying '80: Vol. 2: Proceedings of the Second International Symposium.* Edited by ARUN S. MUJUMDAR. Hemisphere Publishing Corp., Global Bldg., 1025 Vermont Ave., N.W. Washington, DC 20005. 1980. 532 pp. 20 × 28 cm. Price $58.00.

*A–Z of Clinical Chemistry.* By W. HOOD. Halsted Press–Wiley, 605 Third Ave., New York, NY 10016. 1980. 386 pp. 13 × 22 cm. Price $19.95.

*A Literature Survey and Design Study of Fumecupboards and Fume-Dispersal Systems.* (Occupational Hygiene Monograph No. 4.). By D. HUGHES. Science Reviews Ltd., 28 High Ash Drive, Leeds, LS 17 8RA, England. 1980. 82 pp. 14 × 21 cm.

*Anionic Surfactants: Biochemistry, Toxicology, Dermatology* (Surfactant Science Series, Vol. 10). Edited by CHRISTIAN GLOXHUBER. Dekker, 270 Madison Ave., New York, NY 10016. 1980. 456 pp. 15 × 23 cm. Price $59.75.

*The Role of Peptides in Neuronal Function.* Edited by JEFFERY L. BARKER and T. G. SMITH, Jr. Dekker, 270 Madison Ave., New York, NY 10016. 1980. 768 pp. 15 × 23 cm. Price $95.00 (20% higher outside United States and Canada).

*Neurological Clinical Pharmacology.* By MERVYN J. EADIE and JOHN H. TYRER. Adis Press, 515 Madison Ave., New York, NY 10022. 1980. 470 pp. 16 × 24 cm. Price $47.50.

*Nucleotide Analogs: Synthesis and Biological Function.* By KARL HEINZ SCHEIT. Wiley, 605 Third Ave., New York, NY 10016. 1980. 288 pp. 16 × 23 cm. Price $29.50.

*Principles and Methods of Pharmacy Management, 2nd Ed.* By HARRY A. SMITH. Lea & Febiger, 600 S. Washington Square, Philadelphia, PA 19106. 1980. 413 pp. Price $19.50.

*PAR Pseudo-Allergic Reactions: Involvement of Drugs and Chemicals, Vol. 1: Genetic Aspects and Anaphylactoid Reactions.* Edited by P. DUKOR (Basel), P. KALLÓS (Helsingborg), H. D. SCHLUMBERGER (Wuppertal), and G. B. West (Epsom, Surrey). S. Karger, Arnold-Böcklin-Strasse 25, CH-4011 Basel, Switzerland. 1980. 307 pp. 17 × 24 cm. Price $78.00.

*PAR Pseudo-Allergic Reactions: Involvement of Drugs and Chemicals, Vol. 2: Cytotoxic and Complement Mediated Reactions.* Edited by P. DUKOR (Basel), P. KALLÓS (Helsingborg), H. D. SCHLUMBERGER (Wuppertal), and G. B. WEST (Epsom, Surrey). S. Karger, P.O. Box Postfach, CH-4009 Basel, Switzerland. 1980. 143 pp. 16 × 24 cm. Price $39.00.

*Topics In Antibiotic Chemistry. Vol. 5.* Edited by P. G. SAMMES. Wiley, 605 Third Ave., New York, NY 10016. 1980. 312 pp. 15 × 23 cm. Price $87.50.

*Heterocyclic Chemistry, Vol. 1.* (A Specialist Periodical Report.) By H. SUSCHITZKY and O. METH-COHN. Royal Society of Chemistry, Distribution Centre, Blackhorse Rd., Letchworth, Herts, SG6 1HN, England. 522 pp. 13 × 21 cm. Price $194.50.

*The Pill.* By JOHN GUILLEBAUD. Oxford University Press, 200 Madison Ave., New York, NY 10016. 1980. 252 pp. 11 × 18 cm. Price $16.95 hard cover, $6.95 soft cover.

*Environmental Chemicals, Enzyme Function and Human Disease.* Ciba Foundation Symposium 76 (new series). Excerpta Medica, P.O. Box 211, 1000 AE Amsterdam, The Netherlands. 1980. 380 pp. 16 × 24 cm. Price $43.50. (Distributed in the United States by Elsevier/North-Holland, 52 Vanderbilt Ave., New York, NY 10017.)

## NEW JOURNALS

*Medicinal Research Reviews.* An International Journal. Edited by GEORGE deSTEVENS. Wiley, 605 Third Ave., New York, NY 10016. Price $45.00 (4 issues per year).

A publication of the
American Pharmaceutical Association—
the National Professional Society
of Pharmacists

# JOURNAL OF PHARMACEUTICAL SCIENCES

## INDEX TO AUTHORS
## INDEX TO SUBJECTS

VOLUME 70
JANUARY TO DECEMBER, 1981

*Published monthly under the supervision of the Board of Trustees*

MARY H. FERGUSON
*Editor*

NANCY E. BROWN
*Production Editor*

JOHN PATRICK EVANS
*Copy Editor*

MICHAEL K. HAYES
*Copy Editor*

EDWARD G. FELDMANN
*Contributing Editor*

SAMUEL W. GOLDSTEIN
*Contributing Editor*

BELLE R. BECK
*Editorial Secretary*

EDWARD G. FELDMANN
*Acting Director of Publications*

EDITORIAL ADVISORY BOARD

John Autian
Norman R. Farnsworth
William J. Jusko
Herbert A. Lieberman
David E. Mann, Jr.
Ian W. Mathison
Gerald J. Papariello
Edward G. Rippie

JOURNAL OF PHARMACEUTICAL SCIENCES

JUNE 1981
VOLUME 70 NUMBER 6

RESEARCH ARTICLES

# Derivation and Significance of Valence Molecular Connectivity

LEMONT B. KIER *x and LOWELL H. HALL ‡

Received September 8, 1980, from the *Department of Pharmaceutical Chemistry, Medical College of Virginia, Virginia Commonwealth University, Richmond, VA 23298, and the ‡Department of Chemistry, Eastern Nazarene College, Quincy, MA 02170. Accepted for publication January 7, 1981.

**Abstract** □ The physical basis for valence molecular connectivity was studied. The $\delta^v$ and $\delta$ values are cardinal numbers describing the electronic structure of atoms in their valence states. The value $\delta^v + \delta$ describes the volume of a bonding atom while the value $\delta^v - \delta$ describes the electronegativity. By using the principle of electronegativity equalization, bond electronegativity is defined as $(\delta_i^v \delta_j^v)^{-1/2}$, and the valence molecular connectivity index ($^1\chi^v$) is derived as a sum of these bond descriptions. The valence chi index is interpreted in terms of the information encoded, describing both the volume and electronic characteristics of bonds in molecules. Examples of close relationships with molecular volume and electronic properties are shown. A new way of estimating valence state electronegativity is proposed from a count of exterjacent electrons divided by the quantum number squared for at least the first three quantum levels.

**Keyphrases** □ Molecular connectivity indexes—relationship between molecular volume and electronic composition, mathematical estimation of valence state electronegativity □ Structure–activity relationships—usefulness of molecular connectivity indexes, mathematical estimation, relationship between molecular volume and electronic composition □ Electronegativity—mathematical estimation, usefulness of molecular connectivity indexes, relationship between molecular volume and electronic composition

Molecular connectivity is a method for the quantitation of molecular structure that encodes information about size, branching, cyclization, unsaturation, and heteroatom content (1). It was developed in several stages, beginning with an alkane branching index proposed by Randic (2), a treatment of unsaturation (1, 3), a development of extended bond quantitation (4), and, finally, the most useful addition for the medicinal chemist, a rational way of quantifying heteroatom content (5). The treatment of heteroatoms, introduced by Kier and Hall (1) and called valence molecular connectivity, brought molecular connectivity into the role of a structure quantitation method useful in structure–activity analyses of drug molecules. Several investigators have employed valence molecular connectivity in structure–activity relationship analyses of drugs (Table I).

The growing use of molecular connectivity has resulted in an interest in the significance of the elements of the method and the meaning of the calculated indexes. Several misconceptions have arisen as a result of incomplete understanding of molecular connectivity or of previous bias grounded in physicochemical relationships to drug action. This study explores the fundamental basis of molecular connectivity.

## DISCUSSION

**Method**—The simple molecular connectivity index arises from the assignment of numerical adjacency values to each atom other than hydrogen (the molecular skeleton) in a molecule. These values, called $\delta$ values, are cardinal numbers enumerating the presence of nonhydrogenic-bonded neighbors, irrespective of what the element is or what multiplicity of bonding is present. The assignment of $\delta$ values for acetic acid is shown in Fig. 1*a*. The molecule is dissected into bonds, each described by two $\delta$ values.

A term for each bond ($C_{ij}$) is calculated according to $C_k = (\delta_i \delta_j)_k^{-1/2}$. These terms are summed over the entire molecule to give the simple molecular connectivity index of the first order ($^1\chi$):

$$^1\chi = \Sigma(\delta_i \delta_j)_k^{-1/2} = \Sigma C_k \qquad \text{(Eq. 1)}$$

Applied to acetic acid in Fig. 1*a*, the calculated value for $^1\chi = 3(1 \times 3)^{-1/2} = 1.732$.

An inspection of the acetone molecule in Fig. 1*b* shows an assignment of $\delta$ values. This set of $\delta$ values is the same as for acetic acid. It is possible that the $^1\chi$ value of 1.732 for both of these molecules is sufficiently descriptive so that certain general properties, *e.g.*, size and shape, may be predicted from a relating equation. However, it is more than likely that the obvious difference in the structures must be encoded to relate the molecules to many properties.

To accomplish the encoding of structural differences, Kier and Hall went beyond the structural fact of adjacency and considered the count of the valence electrons participating in sigma, pi, and lone-pair orbitals on each atom, exclusive of bonds to hydrogen. This count, again a cardinal number, is the valence delta ($\delta^v$) used to calculate a valence molecular connectivity index ($^1\chi^v$). The assignment of the $\delta^v$ value to an atom is based on the number of valence electrons ($Z^v$) not involved in bonds to hydrogen. Thus, $\delta_i^v = Z_i^v - h_i$, where $h_i$ is the number of bonded hydrogens on atom $i$. The significance of suppressing hydrogen in this count

0022-3549/81/0600-0583$01.00/0
© 1981, American Pharmaceutical Association

**Table I—Use of Valence Connectivity Indexes in Structure–Activity Relationship Studies**

| Study | Molecules | Reference |
|---|---|---|
| Toxicity of anesthetics | Ethers | 14 |
| Anesthetic potency | Ethers, ketones | 15 |
| Barbiturate potency | Barbiturates | 16 |
| Partition coefficient | Hydroxyureas | 17 |
| Carminative activity | Alcohols, esters | 18 |
| Chromatographic retention | Alcohols | 19 |
| Hückel pi electron energy | Aromatic hydrocarbons | 20 |
| Taste threshold | Alcohols, carbonyls, acids, esters | 21 |
| Bitter taste | Amino acids, peptides | 22 |
| Boiling point | Alcohols, amines, halides | 23 |
| Solubilities | | 23 |
| Molar refraction | | 23 |
| General anesthetics | Mixed | 24 |
| Cytochrome conversion | Phenols | 25 |
| Sweet taste | Nitroanilines | 25 |
| Enzyme inhibition | Benzyl alcohols | 25 |
| Toxicity | Phenyl phosphates | 25 |
| Odor | Benzaldehydes, nitrobenzenes | 26 |
| Hallucinogenic activity | Phenylisopropyl amines | 27 |
| Mutagenicity | Nitrosamines | 28 |
| Serotonin antagonists | Phenalkylamines | 29 |
| Serotonin antagonists | Lysergic acid amides | 30 |
| Muscarinic antagonists | Amines | 31 |
| Antimicrobial activity | Phenyl propyl ethers | 32 |
| Chromatographic retention | Mixed | 33 |
| General anesthetics | Halocarbons | 34 |
| Hallucinogenic agents | Phenethylamines | 35 |
| Monoamine oxidase inhibitors | Hydrazines | 36 |
| Hormone class | Steroids | 37 |
| Reductase inhibitors | Benzohydroxamic acids | 38 |

will be discussed later. The calculation of $^1\chi^v$ proceeds exactly as described for the simple molecular connectivity index.

Figures 1*c* and 1*d* show the assignments of $\delta^v$ values to acetic acid and acetone, respectively. The calculated $^1\chi^v$ values are clearly different, 0.928 for acetic acid and 1.204 for acetone. Structural information is encoded in these two different values and also in the common value for the simple $^1\chi$ index. Studies have employed $^1\chi$ and $^1\chi^v$ indexes singly and in concert as structural descriptors in structure–activity relationship analyses. Since molecular information encoded in these $\chi$ values is derived from the $\delta$ values of the atoms, insight into the significance of molecular connectivity begins with analysis of the $\delta$ values.

**Significance of Delta**—Within the context of molecular connectivity, as developed by Kier and Hall, an atom in its valence state can be described by two cardinal numbers: $\delta$, the number of bonded neighbors (excluding hydrogen), and $\delta^v$, the number of valence electrons (excluding those bonding hydrogen). This dual description of atoms is revealed in the matrix shown in Fig. 2 for second quantum level atoms in their valence states. Superimposed on this same matrix are the hydrides of these atoms.

It is apparent that $\delta_i$ is a count of the nonhydrogen sigma-bond electrons contributed by atom $i$. It follows that $\delta_i^v$ is a more inclusive count of all valence electrons (not bonding to hydrogen), including those sigma electrons ($\sigma_i$) enumerated by $\delta_i$. Thus, the relationship is:

$$\delta_i^v = \delta_i + p_i + n_i = \sigma_i + p_i + n_i - h_i \qquad \text{(Eq. 2)}$$

where $p_i$ is the number of $p$ orbital electrons and $n_i$ is the number of lone-pair electrons on atom $i$. The values of $\delta^v$ and $\delta$ depend on the element represented, its valence (hybrid) state, and the number of bonded hydrogen atoms. Thus, from Fig. 2, $\delta = 2$; $\delta^v = 4$, 5, and 6 describes an $sp$ carbon, an $sp^2$ nitrogen, and an $sp^3$ oxygen, respectively. In contrast, $\delta^v$

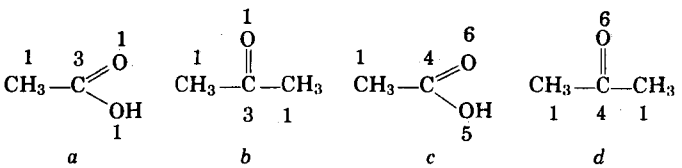


**Figure 1**—*Assignment of $\delta$ and $\delta^v$ values to heteroatom molecules. Key:* a, *acetic acid with simple $\delta$ values;* b, *acetone with simple $\delta$ values;* c, *acetic acid with valence $\delta^v$ values; and* d, *acetone with valence $\delta^v$ values.*

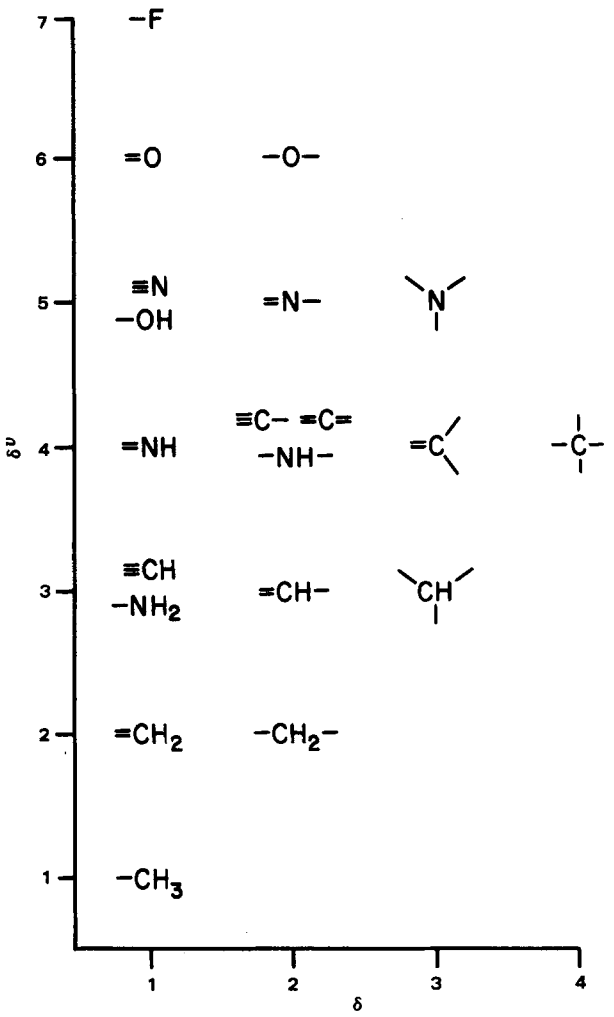


**Figure 2**—*Atoms (and hydrides) defined by $\delta$ and $\delta^v$ values.*

= 4; $\delta$ = 2, 3, and 4 describes an $sp$ carbon, an $sp^2$ carbon, and an $sp^3$ carbon, respectively.

Both $\delta^v$ and $\delta$ contribute to a description of the hybrid state of an element or hydride. With these two cardinal numbers, 20 second quantum level atom valence states and hydrides are described in the matrix in Fig. 2.

It might be anticipated that the information available from $\delta_i^v$ and $\delta_i$, when formulated into bond descriptions and ultimately summed to a molecular value, would be of considerable utility in ranking molecules according to physical property values and biological activities. A wealth of published experience confirms this expectation.

Two basically different kinds of information are encoded in the $\delta^v$ and $\delta$ values of atoms and groups shown in Fig. 2. First, since $\delta^v$ and $\delta$ count sigma, pi, and lone-pair orbitals, it is expected that the space occupied by these orbitals might be described. This orbital space defines the expanse of the atom in its valence state due to the number and kind of orbital domains of the atom. The measured or calculated volume of an atom (hence molecule) is a consequence of the number and kind of orbitals. The physicochemical manifestations of the volume (and closely related surface area) of a molecule are well known and are expected to be related to the volumes of the constituent atoms.

The second type of information expected from the $\delta^v$ and $\delta$ values of a covalently bound atom is of an electronic character. The numbers of sigma, pi, and lone-pair electrons must govern certain electronic properties that may be closely related to $\delta^v$ and $\delta$ of the atoms. When translated into bonds and molecules, this electronic information may bear a significant relationship to certain molecular properties.

**Volume Information from $\delta$ and $\delta^v$**—A number of investigators have dissected molecules into constituent fragment volumes to estimate the molecular volume. A notable contribution in this regard is the work of Bondi (6). Superimposing the Bondi atom volumes onto the $\delta^v$, $\delta$ matrix produces a pattern for direct comparison in Fig. 3.

Figure 3 reveals that the volume of the atom or hydride diminishes with

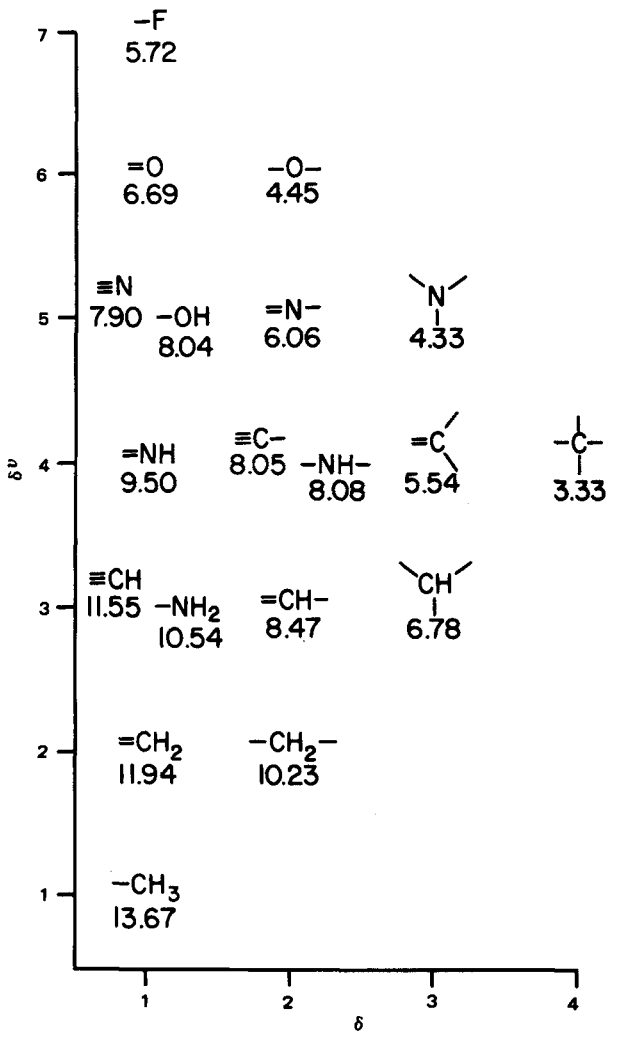


**Figure 3**—*Bondi atom and hydride volumes and $\delta^v$, $\delta$. The value for -O- is averaged from alkyl aryl ethers.*

an increasing $\delta^v$ value when holding $\delta$ constant. The volume also diminishes when $\delta$ increases for a constant $\delta^v$ value. These observations are not unexpected among cases where the number of hydrogens in the group diminishes. In cases where the fragment is a single atom in its valence state, the volume increases with an increase in the number of pi orbitals. This phenomenon occurs even though the number of valence electrons may be less. It is also apparent that the volume diminishes when the number of sigma electrons increases for a constant $\delta^v$ value.

From these observations, it is concluded that the structural features encoded by $\delta^v$ and $\delta$ act cooperatively to diminish the volume as numerical values increase. Such a relationship is revealed using regression analysis:

$$V_{\text{Bondi}} = 17.03 - 1.59(\delta^v + \delta) \qquad \text{(Eq. 3)}$$

$$r = 0.990 \quad s = 0.52 \quad n = 20 \quad F = 859$$

The calculated values are compared with the Bondi volumes in Table II. With Eq. 3, additional fragments and small molecules are predicted. The ability to predict fragment values where experimental data are lacking is an important consequence of this relationship.

So far, only second quantum level elements ($N = 2$) have been considered. A more general equation is possible, accounting for the greater distance of the valence electron orbitals from the nuclei in third quantum level atoms:

$$V_{\text{Bondi}} = 17.03 - 6.36\frac{(\delta^v + \delta)}{N^2} \qquad \text{(Eq. 4)}$$

where $N$ is the principal quantum number. For third-level atoms ($N = 3$), the equation predicts the volumes for -S- and -Cl of 11.38 cm$^3$/mole each, compared to 10.8 and 11.62 cm$^3$/mole from Bondi (6).

Bondi used the fragment values in a roughly additive way to estimate molecular volume. Empirically based correction factors were introduced to account for branching, cyclization, and other structural effects. The formalism of molecular connectivity achieves a similar result without tabulated correction factors. The $\delta$ values are used to describe bonds that are summed to give a molecular index. The molecular index ($^1\chi^v$) can correlate closely with experimental or computed volumes derived from various methods or procedures. For example, amino acid side-chain molar volumes in Table III correlate with a single-valence connectivity index, $^1\chi^v$ (7):

$$V(A)^3 = 29.46\,{}^1\chi^v + 36.30 \qquad \text{(Eq. 5)}$$

$$r = 0.989 \quad s = 3.93 \quad n = 18 \quad F = 696$$

**Table II—Delta Values of Valence-State Atoms or Hydrides and Bondi Volumes**

| Atom/Hydride | $\delta$ | $\delta^v$ | Volume, cm$^3$/mole: Bondi[a] | Volume, cm$^3$/mole: Calculated[b] |
|---|---|---|---|---|
| >C< | 4 | 4 | 3.33 | 4.31 |
| —CH< | 3 | 3 | 6.78 | 7.49 |
| >CH$_2$ | 2 | 2 | 10.23 | 10.67 |
| —CH$_3$ | 1 | 1 | 13.67 | 13.85 |
| =CH$_2$ | 1 | 2 | 11.94 | 12.26 |
| —C≡, =C= | 2 | 4 | 7.50[c] | 7.49 |
| ≡CH | 1 | 3 | 11.55 | 10.67 |
| =CH— | 2 | 3 | 8.47 | 9.08 |
| —O— | 2 | 6 | 4.45[c] | 4.31 |
| —OH | 1 | 5 | 8.04 | 7.49 |
| —NH$_2$ | 1 | 3 | 10.54 | 10.67 |
| >NH | 2 | 4 | 8.08 | 7.49 |
| >N— | 3 | 5 | 4.33 | 4.31 |
| ≡N | 1 | 5 | 7.90 | 7.49 |
| >C= | 3 | 4 | 5.54 | 5.90 |
| =O | 1 | 6 | 6.79 | 5.90 |
| =NH | 1 | 4 | 9.50 | 9.08 |
| =N— | 2 | 5 | 6.06 | 5.90 |
| CH$_4$ | 0 | 0 | 17.12 | 17.03 |
| NH$_3$ | 0 | 2 | 13.80 | 13.85 |

[a] From Ref. 6. [b] From Eq. 3. [c] Average values.

**Electronic Information from $\delta$ and $\delta^v$**—The $\delta^v$ and $\delta$ values are

**Table III—Amino Acid Side-Chain Volume and $^1\chi^v$**

| Amino Acid, R | $^1\chi^v$ | $V(A)^3$[a] | $V(A)^3$ calc. |
|---|---|---|---|
| Glycine | 0 | 36.3 | 36.3 |
| Alanine | 0.577 | 52.6 | 53.3 |
| Valine | 1.488 | 85.1 | 80.1 |
| Leucine | 1.971 | 102.0 | 94.4 |
| Isoleucine | 2.026 | 102.0 | 96.0 |
| Phenylalanine | 2.672 | 113.9 | 115.0 |
| Proline | 1.408 | 73.6 | 77.8 |
| Tryptophan | 3.417 | 135.4 | 137.0 |
| Tyrosine | 2.807 | 116.2 | 119.0 |
| Histidine | 2.079 | 91.1 | 97.6 |
| Threonine | 1.169 | 71.2 | 70.7 |
| Serine | 0.724 | 54.9 | 57.6 |
| Asparagine | 1.255 | 72.4 | 73.3 |
| Glutamine | 1.755 | 92.7 | 88.0 |
| Aspartic acid | 1.190 | 68.4 | 71.4 |
| Glutamic acid | 1.690 | 84.7 | 86.1 |
| Lysine | 2.224 | 105.1 | 101.8 |
| Arginine | 2.550 | 109.1 | 111.4 |

[a] From Ref. 7.

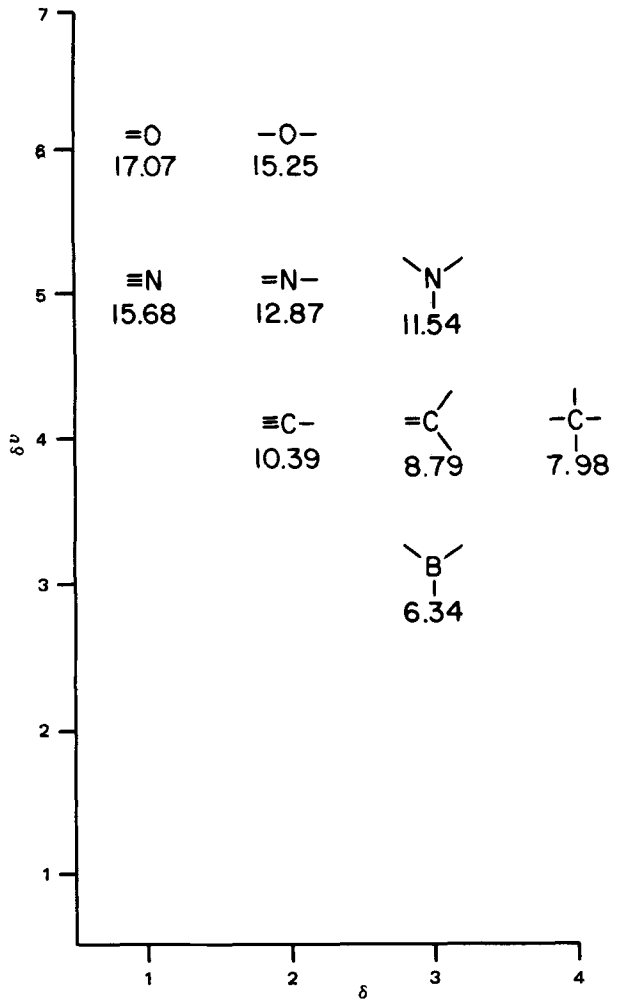


**Figure 4**—*Mulliken electronegativities and* $\delta^v$, $\delta$.

counts of electrons in sigma, pi, or lone-pair orbitals. The number and distribution of electrons certainly influence the electronic characteristics associated with atoms in the valence state. An obvious electronic property of a bonded atom in a molecule is electronegativity. Pauling (8) proposed this concept and defined it as a measure of the power of a chemically bonded atom to attract electrons to itself. Several measures of this characteristic were suggested, the most satisfactory being that of Mulliken (9). He computed electronegativity ($X_M$) as the average value of the ionization potential and the electron affinity. Expressed in electron volts, this value was computed for atoms in their bonding valence states (10). The electronegativity scale of Pauling (8) is more familiar to chemists but does not distinguish among hybrid states of the same atom, although they certainly have different electronegativities (10).

Figure 4 shows the Mulliken electronegativity values on the $\delta$, $\delta^v$ matrix for some second-row atoms. Inspection reveals some obvious trends. For constant $\delta^v = 4$, $\delta = 2$, 3, and 4 describes $sp$, $sp^2$, and $sp^3$ carbon atoms. Electronegativity diminishes in the same order. This electronic effect manifests itself in the decreasing acidity of the bonds:

$$\equiv C\text{–}H > =\overset{|}{C}\text{–}H > -\overset{|}{\underset{|}{C}}\text{–}H$$

As $\delta^v$ decreases for constant $\delta$, electronegativity decreases. The trends suggest that electronegativity is some function of $\delta^v - \delta$. For the nine second-row atom valence states in Fig. 4, the following relationship obtains:

$$X_M = 2.05(\delta^v - \delta) + 6.99 \qquad \text{(Eq. 6)}$$

$$r = 0.989 \quad s = 0.60 \quad n = 9 \quad F = 305$$

This correlation is excellent, with the standard deviation being less than the estimate of Hinze and Jaffe (10) due to uncertainties in the electron affinities. The intercept is close to the electronegativity of hydrogen (7.17 ev), which would have a $\delta^v - \delta$ value of zero.

The interpretation of Eq. 6 is clear. It states that the electronegativity of an atom in its valence state is closely related to the number of electrons in pi and lone-pair orbitals. This is apparent from the relationships:

$$\delta^v = \sigma + p + n - h \qquad \text{(Eq. 7}a\text{)}$$

$$\delta = \sigma - h \qquad \text{(Eq. 7}b\text{)}$$

$$\delta^v - \delta = p + n \qquad \text{(Eq. 7}c\text{)}$$

where $\sigma$ is the number of sigma bonding electrons other than to hydrogen. The observation that the electronegativity of a bound atom is due to the presence of pi and lone-pair orbitals leads to the conclusion that these electrons are inferior to sigma electrons on an atom in screening the core charge. This follows from the usual model that electronegativity manifests itself through sigma bonds; thus, electrons outside of these orbitals leave the core charge ($+Z^v$) less screened than when all valence electrons are sigma bonding ($Csp^3$).

The relationship can be made more general to include atoms of other rows by realizing that the nuclear attraction for valence electrons (hence, the electronegativity) must be related to their distance from the nucleus and the screening effect of intervening electrons. This distance effect may be approximated by the square of the principal quantum number, $N$ (11). The general expression relating the Mulliken electronegativities to the $\delta$ values for 19 atom valence states of the first, second, and third rows, which are prominent in forming covalent bonds, takes the form of:

$$X_m = 7.99\frac{\delta^v - \delta}{N^2} + 7.07 \qquad \text{(Eq. 8)}$$

$$r = 0.988 \quad s = 0.48 \quad n = 19 \quad F = 660$$

The $\delta^v$ value in Eq. 8 for third-row atoms is defined as $\delta^v = Z^v - h$. The usual expression $\delta^v = (Z^v - h)/(Z - Z^v)$ is not used since the use of $N^2$ corrects for the distance of the valence electrons from the nucleus and is more useful in relating the electronegativity directly to the count of exterjacent electrons, $\delta^v - \delta$. The two expressions are numerically very close.

The experimental and calculated results are shown in Table IV. The fifth column in Table IV, $(\delta^v - \delta)/N^2$, is the molecular connectivity valence state electronegativity. This value can be compared to the Pauling estimate of electronegativity by adding 2.5 to the value, although the Pauling value is for an atom irrespective of the valence state.

To conclude this section, it is stated that the number derived from $\delta_i^v - \delta_i$ for atom $i$ describes a property of a valence state atom closely approximated by the electronegativity. Also, the number derived from $\delta_i^v + \delta_i$ for atom $i$ describes a property of a valence state atom closely approximated by the van der Waals volume contribution to the molecule. Mathematically, $\delta_i^v - \delta_i$ and $\delta_i^v + \delta_i$ are orthogonal; that is, they are independent of each other. This orthogonality corresponds to the observation that the Bondi volume and the Mulliken electronegativities from Figs. 3 and 4 autocorrelate only to the extent of $r^2 = 0.21$. Orthogonal descriptors $\delta^v - \delta$ and $\delta^v + \delta$, simply derived from an inspection of atomic valence state structure and relating to electronegativity and van der Waals volume, should be of great practical use.

**Bond Formation**—The $\delta^v$ and $\delta$ values for atoms in their valence states encode information about the electronegativity of atoms. The electronegativity of atoms in bonds influences several properties including ionicity, bond dipole, partial atomic charge, and bond strength, all resulting from electronegativity equalization (12). The calculation of molecular connectivity indexes as a sum of bond indexes thus incorporates some information about electronic structure, encoded in the $\delta$ values.

The $\delta^v$ and $\delta$ values contain information about electron domains or orbitals associated with atoms. Thus, a volume characteristic is encoded in the $\delta$ values. As a result, molecular connectivity indexes contain volume information. With the structural and physical significance of $\delta^v$ and $\delta$ revealed, it is possible to derive the bond index encoding information about structure and properties. A series of concise statements develops this index.

1. The $\delta^v$ value is the number of nonhydrogenic valence electrons on an atom. The $\delta$ value is the number of $\delta^v$ electrons participating in nonhydrogenic $\sigma$ bonds from an atom.

2. The properties of electronegativity and volume encoded in $\delta_A^v$ for an atom ($A$) are considered to be contributed equally from all valence electrons or their orbitals. Thus, one electron from atom $A$ forming one $\sigma$ bond will possess the fraction $1/\delta_A^v$ of the properties encoded in $\delta_A^v$.

3. Atom $A$ brings to the bond $A$–$B$ the fraction $1/\delta_A^v$ of the properties encoded by $\delta_A^v$. Atom $B$ brings to the same bond the fraction $1/\delta_B^v$ of the properties encoded by $\delta_B^v$.

**Table IV—Delta Values of Valence State Atoms and Mulliken Electronegativities**

| Atom | Hybrid State | $\delta^v$ | $\delta$ | $\frac{\delta^v - \delta}{N^2}$ | $X_M$[a], ev | $X$ calc.[b] |
|---|---|---|---|---|---|---|
| H | s | 1 | 1 | 0 | 7.17 | 7.05 |
| B | trtrtr | 3 | 3 | 0 | 6.34 | 7.05 |
| C | didi$\pi\pi$ | 4 | 2 | 0.50 | 10.39 | 11.04 |
| | trtrtr$\pi$ | 4 | 3 | 0.25 | 8.79 | 9.05 |
| | tetetete | 4 | 4 | 0 | 7.98 | 7.05 |
| N | di$^2$di$\pi\pi$ | 5 | 1 | 1.00 | 15.68 | 15.04 |
| | tr$^2$trtr$\pi$ | 5 | 2 | 0.75 | 12.87 | 13.04 |
| | te$^2$tetete | 5 | 3 | 0.50 | 11.54 | 11.04 |
| O | tr$^2$tr$^2$tr$\pi$ | 6 | 1 | 1.25 | 17.07 | 17.04 |
| | te$^2$te$^2$tete | 6 | 2 | 1.00 | 15.25 | 15.04 |
| Si | didi$\pi\pi$ | 4 | 2 | 0.22 | 9.06 | 8.82 |
| | trtrtr$\pi$ | 4 | 3 | 0.11 | 7.90 | 7.93 |
| | tetetete | 4 | 4 | 0 | 7.30 | 7.05 |
| P | di$^2$di$\pi\pi$ | 5 | 1 | 0.44 | 11.25 | 10.60 |
| | tr$^2$trtr$\pi$ | 5 | 2 | 0.33 | 9.67 | 9.71 |
| | tetetete | 5 | 3 | 0.22 | 8.90 | 8.82 |
| S | tr$^2$tr$^2$tr$\pi$ | 6 | 1 | 0.55 | 10.88 | 11.49 |
| | te$^2$te$^2$tete | 6 | 2 | 0.44 | 10.14 | 10.60 |
| Cl | te$^2$te$^2$te$^2$te | 7 | 1 | 0.66 | 11.84 | 12.37 |

[a] From Ref. 9. [b] From Eq. 8.

4. If the property under consideration is the electronegativity, then orbitals from $A$ and $B$ contributing the fractions $1/\delta_A^v$ and $1/\delta_B^v$, respectively, will become adjusted toward an equal intermediate electronegativity, which may be ascribed to the bond. This principle of electronegativity equalization was set forth by Sanderson (12, 13), who proposed that the geometric mean of the atom electronegativities leads to the best description of the bond electronegativity.

5. From Sanderson (12, 13), $[(1/\delta_A^v)(1/\delta_B^v)]^{1/2}$ is the algorithm appropriate for two bonded atoms. This algorithm is identical to the molecular connectivity description of a bond (1) as shown in Eq. 1.

6. The volume contributed by atom $A$ to a bond $A$–$B$ is the fraction $1/\delta_A^v$ of the total. The fraction $1/\delta_B^v$ is the volume contributed from atom $B$. The bond has a "volume" due to orbital overlap that can be approximated by 2 $[(1/\delta_A^v)(1/\delta_B^v)]^{1/2}$. With a constant of 2, $[(1/\delta_A^v)(1/\delta_B^v)]^{1/2}$ reflects the relative volume of the bond $A$–$B$. This is the same expression describing the electronegativity of the $A$–$B$ bond from statement 5.

7. The orthogonal expressions $\delta_A^v - \delta_A$ and $\delta_A^v + \delta_A$ reflect the electronegativity and volume of atom $A$, respectively. What is the role of $\delta_A$ in the calculation of $^1\chi^v$? Each $\delta_A^v$ appears $\delta_A$ times in the summation of $[(1/\delta_A^v)(1/\delta_B^v)]^{1/2}$ to give $^1\chi^v$. Thus, $^1\chi^v$ can be expected to correlate with some properties related to molecular volume and electronic character.

**Hydrogen Suppression**—It has been stated that hydrogen atoms are "suppressed" in the count of valence electrons and bonding neighbors to an atom (1). Thus:

$$\delta^v = Z^v - h \qquad \text{(Eq. 9}a\text{)}$$

$$\delta = \sigma - h \qquad \text{(Eq. 9}b\text{)}$$

where $Z^v$ is the number of valence electrons, $h$ is the number of hydrogens, and $\sigma$ is the number of bonding sigma electrons. The hydrogen influence in reality is subsummed into modified $\delta^v$ and $\delta$ values reflecting the number of hydrogen atoms on the atom in question. The $\delta^v$ value in combination with the $\delta$ value thus is a description of an atom possessing volume and electronegativity characteristics associated with the hydride group, which is treated as a single atom. The $\delta^v$ and $\delta$ values accurately reflect the volume of the hydrides as seen in Table II. The $\delta^v$ and $\delta$ values for hydride groups also correctly order the group electronegativities of OH, $NH_2$, SH, and $CH_3$, based on various estimates of these values. Thus, from Eq. 8, the predicted group electronegativities are $X_M(OH) = 15.07$, $X_M(NH_2) = 11.07$, $X_M(SH) = 10.63$, and $X_M(CH_3) = 9.07$, all on the Mulliken scale.

The uniform exclusion of hydrogen makes the electronegativity and the volume of this atom a reference point. Note that in Eq. 8 relating to Mulliken electronegativity, the $y$ intercept (when $\delta^v - \delta = 0$) is the electronegativity of hydrogen. Similarly in Eq. 4 relating to the Bondi fragment volume, the $y$ intercept (when $\delta^v = \delta = 0$) for methane is the value of the $sp^3$ carbon fragment plus all four hydrogen atoms.

**Index for a Molecule**—The index for the molecule, $^1\chi^v$, is written as a summation of the bond terms:

$$^1\chi^v = \Sigma(\delta_i^v\delta_j^v)^{-1/2} \qquad \text{(Eq. 10)}$$

This is the valence molecular connectivity index of first order since it is summed over all bonds that are single-path fragments of the molecule.

Valence molecular connectivity is built on the sigma electron or interjacent electron framework of the molecule. The presence of an atom, $i$, with nonsigma valence electrons, pi, or lone-pair electrons, which can be called exterjacent electrons, results in the fraction $1/\delta_i^v$ being smaller than $1/\delta_i$. The value of $^1\chi^v$ for the molecule containing atom $i$ with exterjacent electrons reflects the total number of bonds and their adjacency, but it also reflects the diminished value, $1/\delta_i^v$, due to the presence of exterjacent electrons on atom $i$.

With the data in Table V, a series of comparisons reveals the encoded structural information in $^1\chi^v$ values. Molecule 1, butane, is the reference structure where all $\delta_i^v = \delta_i$; hence, $^1\chi^v = {}^1\chi = 1.914$. There are no exterjacent electrons so $^1\chi - {}^1\chi^v = 0$.

Molecules 2 and 3 in Table V are four-atom amines (excluding hydrogens), each with two exterjacent electrons on the nitrogen. Since the positions of the nitrogen atoms in the chains are different in each case, the fractional contributions of valence electrons forming nonhydrogenic

**Table V—Information Encoded in $^1\chi^v$ and $\delta^v$ Values for Four-Atom Chains with $\delta$ Values of $A^1$–$B^2$–$C^2$–$D^1$**

| Number | Molecule | $A$ | $B$ | $C$ | $D$ | $^1\chi^v$ | Exterjacent Electrons | $^1\chi - {}^1\chi^v$ |
|---|---|---|---|---|---|---|---|---|
| 1 | $CH_3CH_2CH_2CH_3$ | 1 | 2 | 2 | 1 | 1.914 | 0 | 0 |
| 2 | $CH_3CH_2CH_2NH_2$ | 1 | 2 | 2 | 3 | 1.615 | 2 | 0.299 |
| 3 | $CH_3CH_2NHCH_3$ | 1 | 2 | 4 | 1 | 1.561 | 2 | 0.353 |
| 4 | $CH_3CH_2CH_2OH$ | 1 | 2 | 2 | 5 | 1.523 | 4 | 0.391 |
| 5 | $CH_3CH_2$—O—$CH_3$ | 1 | 2 | 6 | 1 | 1.404 | 4 | 0.510 |
| 6 | $CH_3CH_2CH$=$CH_2$ | 1 | 2 | 3 | 2 | 1.524 | 2 | 0.390 |
| 7 | $CH_3CH$=$CHCH_3$ | 1 | 3 | 3 | 1 | 1.488 | 2 | 0.426 |
| 8 | $CH_3CH_2CH$=O | 1 | 2 | 3 | 6 | 1.351 | 6 | 0.563 |
| 9 | $CH_3CH_2C$≡CH | 1 | 2 | 4 | 3 | 1.349 | 4 | 0.565 |
| 10 | $CH_3C$≡$CCH_3$ | 1 | 4 | 4 | 1 | 1.250 | 4 | 0.664 |
| 11 | HO—$CH_2CH_2$—OH | 5 | 2 | 2 | 5 | 1.132 | 8 | 0.782 |
| 12 | $CH_3CH$=N—OH | 1 | 3 | 5 | 5 | 1.036 | 8 | 0.878 |
| 13 | O=CH—CH=O | 6 | 3 | 3 | 6 | 0.805 | 12 | 1.109 |

**Table VI—Mixotropic Series Solvents Ranked by Polarity and $^1\chi^v$**

| Solvent | $^1\chi^v$ | Dielectric Constant |
|---|---|---|
| Hexane | 2.914 | 1.89 |
| Carbon tetrachloride | 2.390 | 2.24 |
| *p*-Dioxane | 2.155 | 2.21 |
| Benzene | 2.000 | 2.30 |
| Ethyl ether | 1.992 | 4.34 |
| Ethyl acetate | 1.904 | 6.02 |
| Methyl ethyl ketone | 1.765 | 18.50 |
| Propanol | 1.523 | 20.10 |
| Acetone | 1.204 | 20.70 |
| Ethanol | 1.023 | 24.3 |
| Methanol | 0.447 | 32.80 |
| Water | 0 | 78.0 |

bonds are different. The nitrogen in Molecule 2 contributes one-third $[(1/\delta^v_N) = 1/3]$ of its nonhydrogenic valence electrons to form one sigma bond to carbon. The nitrogen in Molecule 3, contributes one-fourth $[(1/\delta^v_N) = 1/4]$ of its nonhydrogenic valence electrons to each of two sigma bonds with adjacent carbons. The indexes for bonds *B–C* and *C–D* thus are different for these cases. As a consequence, the $^1\chi^v$ indexes are different for Molecules 2 and 3, and each, in turn, is different and less than the value for Molecule 1.

Viewed in terms of valence electron structure information, it is obvious that in Molecule 2 the nitrogen bonds only once to a carbon and, therefore, participates only once as an amine group in an electronegativity equalization event (12). In Molecule 3, the nitrogen is located midchain and, therefore, participates in two bonds to carbons, with two opportunities to participate in electronegativity equalization. Clearly, electronically governed properties differ and are potentially correlated with the $^1\chi^v$ values. The formation of two sigma bonds by nitrogen in Molecule 3 leads to two electronegativity equalization events, resulting in a greater buildup of charge on the nitrogen in Molecule 3. Thus, Molecule 3 is more basic than Molecule 2. Within closely related amines, the $^1\chi - {}^1\chi^v$ difference appears to parallel this effect. It follows that $^1\chi - {}^1\chi^v$ for trimethylamine is 0.390, suggesting that it is more basic than Molecule 3. This is true in the gas phase.

The two amines, Molecules 2 and 3, have the same number and kind of atoms. They differ from the reference structure, butane, by having two exterjacent electrons on one atom. The calculated $^1\chi^v$ value reflects both the presence of the exterjacent electrons and the adjacency relationship of that atom (nitrogen) to other atoms in the molecule. The diminished value of $^1\chi^v$ for Molecule 3, relative to butane and to its positional isomeric amine, parallels structural differences that can be interpreted in electronic terms such as relative charge and basicity.

As a companion to the electronic interpretation of the information encoded by the different $^1\chi^v$ values, the volumes are expected to be different. Thus, properties governed by volume are expected to, and have been shown to, parallel the calculated $^1\chi^v$ values for a series of amines (1).

In Molecules 4 and 5 (Table V), oxygen is the atom contributing exterjacent electrons to the molecules. The same pattern of results is found as for the amines. The terminal oxygen in Molecule 4 with six valence electrons has a bonded hydrogen; hence, $\delta^v = Z^v - h = 6 - 1 = 5$. Thus, $(1/\delta^v) = 1/5$ describes the sigma electron fraction forming a hydroxyl oxygen bond to a carbon. Only one sigma bond involves the hydroxyl oxygen group. In Molecule 5, the $\delta^v$ for oxygen is 6; hence, $(1/\delta^v) = 1/6$ describes each of two sigma electrons bonding to two adjacent carbons. Electronegativity equalization and atom volume overlapping are possible through two bonds in Molecule 5 but only one in Molecule 4. The greater $^1\chi - {}^1\chi^v$ calculated for Molecule 5 reflects the consequences of this greater degree of adjacency. Note also that the $^1\chi^v$ for Molecule 4 is less than that of Molecule 2 (and 5 is less than that of 3), reflecting more exterjacent electrons on the oxygen-containing molecules. A physical manifestation mirroring this result is the lower ionization potentials of ethers relative to alcohols of the same size. A lone-pair electron is the one lost in this process.

**Table VII—Relative Benzene-Likeness of Hydrocarbons and Heterocycles**

| Molecule | $^1\chi^v$ | $^1\chi^v$/Bonds | $B^a$ |
|---|---|---|---|
| Benzene | 2.000 | 0.333 | 1.00 |
| Naphthalene | 3.405 | 0.310 | 0.93 |
| Phenanthrene | 4.815 | 0.301 | 0.90 |
| Anthracene | 4.808 | 0.300 | 0.90 |
| Pyrrole | 1.577 | 0.315 | 0.95 |
| Pyridine | 1.850 | 0.308 | 0.93 |
| Furan | 1.471 | 0.294 | 0.88 |
| Pyrazine | 1.716 | 0.286 | 0.86 |
| Imidazole | 1.427 | 0.285 | 0.86 |
| Pyrimidine | 1.699 | 0.283 | 0.85 |
| Isoxazole | 1.343 | 0.269 | 0.81 |
| Oxazole | 1.321 | 0.264 | 0.79 |
| Sydnone | 1.338 | 0.223 | 0.67 |

[a] Benzene-likeness from [$^1\chi^v$/bonds (for molecule)]/[$^1\chi^v$/bonds (for benzene)].

Molecules 6 and 7 in Table V describe a different situation. In these isomeric alkenes, there are two exterjacent electrons but they are not paired on the same atom, as with the amines; they are located on adjacent atoms. Thus, the $\delta^v$ values for Molecule 6 are different from the reference butane structure in the case of two atoms. This situation is typical of an unsaturated bond. As a consequence, of the three bond indexes calculated for each alkene molecule, two differ from the reference molecule for Molecule 6 and all three differ for Molecule 7. Thus, the $^1\chi^v$ for Molecule 7 is lower than that for Molecule 6. The lower $^1\chi^v$ value for Molecule 7 relative to Molecule 6 presages a greater availability of the pi electrons. Thus, Molecule 7 reacts faster with electrophiles and has a lower heat of hydrogenation and a lower ionization potential.

By extending this list of four-atom molecules in Table V, it can be seen that with an increasing number of exterjacent electrons, $^1\chi^v$ decreases. The series might be called an increasing "exterjacency series." There is a parallel with physical experience relating to stability, polarity as a solvent, and chemical reactivity. Table VI ranks common solvents by polarity, expressed as the dielectric constant correlating with $^1\chi^v$. The relative exterjacency, encoded in the $^1\chi^v$ value, manifests itself as a structural description in another way. For benzene, for example, the simple $\delta$ values for the ring atoms are uniformly 2. The $^1\chi$ value is 3.000. In contrast, the $\delta^v$ values are uniformly 3, leading to a $^1\chi^v$ value of 2.000. The specific exterjacency (per bond) $(^1\chi - {}^1\chi^v)/6$ is 0.333. It is now possible to rank cyclic heterocycles relative to benzene to compare their likeness to it (Table VII).

The molecular volume information encoded in $^1\chi^v$ is easy to envision. A glance down the molecules in Table V reveals that $^1\chi^v$ decreases with decreasing bond lengths. Thus, the ranking closely parallels the molecular volume.

## SUMMARY


The valence molecular connectivity index ($^1\chi^v$) is derived from a cardinal number ($\delta^v$) enumerating the valence electrons on an atom not bonding to hydrogen. The $\delta^v$ number is used $\delta$ times in calculating $^1\chi^v$, where $\delta$ is the number of sigma electrons on an atom not bonding to hydrogen. These two cardinal numbers specify the hybrid states or valence states of any atom within a quantum level.

In this study, it was shown that the atomic fragment volume approximations used in assessing molecular volume are highly correlated with the value of $\delta^v + \delta$ for an atom in its valence state. It also was shown that the valence state electronegativity estimates of Mulliken correlate well with the value of $\delta^v - \delta$ for an atom in its valence state. These two relationships are general for atoms in at least the first three quantum levels.

The $\delta^v$ value, when formulated into the $^1\chi^v$ value for a molecule, carries with it information relating to both volume and electronic character. A simple analogy is the observation that the number 12 carries information about the space occupied by a dozen freshly laid eggs and the number of embryonic heartbeats. Thus, an $sp^3$ nitrogen atom has a $\delta^v = 5$. The cardinal number, 5, counts orbitals contributing to a spatial property, volume. The number 5 concurrently counts the number of valence electrons, which govern electronic characteristics. This duality in the information encoded in the cardinal number ($\delta^v$) leads to a duality of structural information encoded in the derived $^1\chi^v$ value.

The volume information encoded in $^1\chi^v$ values has been demonstrated on numerous occasions in the form of close correlations with volume-related physical properties (39). Other studies showed that properties largely governed by electronic composition also correlate with $^1\chi^v$ indexes. Inspection of the many studies using valence connectivity indexes (Table I) show both aspects of structure relating to these indexes.

In this study, for the first time, a derivation of $^1\chi^v$ from $\delta^v$ has been shown. It is based on the assignment of fractional parts of properties ascribed to the valence electrons of a bonding atom. The fractions $1/\delta^v$

for bonding atoms contribute to the bond so that the geometric mean of the fraction products characterizes the new physical environment. Thus, a bond index is born. The bond indexes $[(1/\delta_A^v)(1/\delta_B^v)]^{1/2}$ are summed to form the molecular connectivity index, $^1\chi^v$.

## REFERENCES


(1) L. B. Kier and L. H. Hall, "Molecular Connectivity in Chemistry and Drug Research," Academic, New York, N.Y., 1976.

(2) M. Randic, *J. Am. Chem. Soc.*, **97**, 6609 (1975).

(3) W. J. Murray, L. H. Hall, and L. B. Kier, *J. Pharm. Sci.*, **64**, 1978 (1975).

(4) L. B. Kier, W. J. Murray, M. Randic, and L. H. Hall, *ibid.*, **65**, 1226 (1976).

(5) L. B. Kier and L. H. Hall, *ibid.*, **65**, 1806 (1976).

(6) A. Bondi, *J. Phys. Chem.*, **68**, 441 (1964).

(7) C. C. Bigelow, *J. Theoret. Biol.*, **16**, 187 (1967).

(8) L. Pauling, "The Nature of the Chemical Bond," 3rd ed., Cornell University Press, Ithaca, N.Y., 1960.

(9) R. S. Mulliken, *J. Chem. Phys.*, **2**, 782 (1934).

(10) J. Hinze and H. H. Jaffe, *J. Am. Chem. Soc.*, **84**, 540 (1962).

(11) C. E. Sun, *J. Chin. Chem. Soc.*, **10**, 77 (1943).

(12) R. T. Sanderson, *J. Chem Educ.*, **31**, 2 (1954).

(13) R. T. Sanderson, "Chemical Bonds and Bond Energy," Academic, New York, N.Y., 1976.

(14) T. DiPaolo, *J. Pharm. Sci.*, **67**, 564 (1978).

(15) *Ibid.*, **67**, 566 (1978).

(16) M. Bonjean and C. L. Duk, *Eur. J. Med. Chem.*, **13**, 73 (1978).

(17) G. R. Parker, *J. Pharm. Sci.*, **67**, 513 (1978).

(18) B. K. Evans, K. C. James, and D. K. Luscombe, *ibid.*, **68**, 370 (1979).

(19) J. S. Millership and A. D. Woolfson, *J. Pharm. Pharmacol.*, **30**, 483 (1978).

(20) S. P. Gupta and P. Singh, *Bull. Chem. Soc. Jpn.*, **52**, 2745 (1979).

(21) R. J. Gardner, *Tech. Q. Master Brew. Assoc. Am.*, **16**, 204 (1979).

(22) R. J. Gardner, *J. Sci. Food Agric.*, **31**, 23 (1980).

(23) L. B. Kier and L. H. Hall, *J. Pharm. Sci.*, **65**, 1806 (1976).

(24) T. DiPaolo, L. B. Kier, and L. H. Hall, *Mol. Pharmacol.*, **13**, 31 (1977).

(25) L. H. Hall and L. B. Kier, *J. Pharm. Sci.*, **66**, 642 (1977).

(26) L. B. Kier, T. DiPaolo, and L. H. Hall, *J. Theoret. Biol.*, **67**, 585 (1977).

(27) L. B. Kier and L. H. Hall, *J. Med. Chem.*, **20**, 1631 (1977).

(28) L. B. Kier, R. J. Simons, and L. H. Hall, *J. Pharm. Sci.*, **67**, 725 (1978).

(29) L. B. Kier and R. A. Glennon, *Life Sci.*, **22**, 1589 (1978).

(30) R. A. Glennon and L. B. Kier, *Eur. J. Med. Chem.*, **13**, 219 (1978).

(31) L. B. Kier and L. H. Hall, *J. Pharm. Sci.*, **67**, 1408 (1978).

(32) L. H. Hall and L. B. Kier, *ibid.*, **67**, 1743 (1978).

(33) L. B. Kier and L. H. Hall, *ibid.*, **68**, 120 (1979).

(34) T. DiPaolo, L. B. Kier, and L. H. Hall, *ibid.*, **68**, 39 (1979).

(35) R. A. Glennon, L. B. Kier, and A. T. Shulgin, *ibid.*, **68**, 906 (1979).

(36) A. J. Richard and L. B. Kier, *ibid.*, **69**, 124 (1980).

(37) D. R. Henry and J. H. Block, *Eur. J. Med. Chem.*, **15**, 133 (1980).

(38) B. Vant Riet, L. B. Kier, and H. L. Elford, *J. Pharm. Sci.*, **69**, 856 (1980).

(39) L. H. Hall and L. B. Kier, *Eur. J. Med. Chem.*, in press.


# Analysis of Drug Contamination from Parabens in Theophylline Olamine


**E. C. JUENGE ˣ, D. F. GURKA, and M. A. KREIENBAUM**



Received July 1, 1980, from the *National Center for Drug Analysis, Food and Drug Administration, 1114 Market Street, St. Louis, MO 63101.* Accepted for publication September 29, 1980.



**Abstract** □ Contaminants in a commercial enema sample of theophylline olamine were found to be derived from parabens and ethanolamine. These contaminants, whose presence was characterized by the loss of preservatives and solubilizing agent, were isolated directly from the drug sample and identified. A high-performance liquid chromatographic (HPLC) system was developed to separate completely and to measure quantitatively theophylline, the two impurities, 4-hydroxybenzoic acid and *N*-(2-hydroxyethyl)-4-hydroxybenzamide, and the remaining parabens. The material balance obtained from the results of quantitative HPLC indicated the formation of these impurities at the expense of parabens. TLC, IR, and UV spectrophotometry and NMR and mass spectrometric analyses were used for identification or for comparisons of the new compound and the known *N*-(2-hydroxyethyl)benzamide.



**Keyphrases** □ Theophylline olamine—contaminants, identification and quantitation, high-performance liquid chromatographic analysis □ Contaminants—identification and quantitation, theophylline olamine enema solutions, high-performance liquid chromatographic analysis □ Paraben preservatives—contamination in theophylline olamine enema solutions, high-performance liquid chromatographic analysis, identification and quantitation □ High-performance liquid chromatography—contamination from paraben preservatives in theophylline olamine enema solutions


During a survey of xanthine derivative drugs conducted by the National Center for Drug Analysis, assay of some enema solutions containing theophylline olamine was attempted with a high-performance liquid chromatographic (HPLC) method that had been used successfully for theophylline elixirs. The analysis showed that, in addition to theophylline and parabens, the sample contained two impurities. This paper discusses the identification and quantitation of these two substances.

## BACKGROUND

The approach followed in this laboratory study was dictated primarily by the small amounts of sample initially available. It involved, first, the original detection of the impurities 4-hydroxybenzoic acid (I) and *N*-(2-hydroxyethyl)-4-hydroxybenzamide (II) by HPLC and TLC, with characterization of their aromatic nature by UV spectrophotometry; and, second, identification by isolation of the impurities from the drug sample and direct comparison with standards by mixed melting-point determinations and IR and NMR analyses. Identities were confirmed by HPLC and TLC comparisons of the original drug solution with commercial and synthesized standards and by a wide collection of spectral data. Finally, the theophylline peak was displaced from the narrow region between the impurity peaks by adjusting the mobile phase to enable quantitative HPLC analysis.

The question of isomerism in the conventional syntheses used to prepare the amides arose because two materials whose elemental analyses were consistent for *N*-(2-hydroxyethyl)benzamide (III) showed different properties. The problem was resolved by purification that showed the materials to be identical; moreover, the mass fragmentations were consistent with the structures given for II and its structural analog, III.

This work demonstrates that parabens can interact chemically with amines used as complexing agents in the compounding of theophylline


0022-3549/81/0600-0589$01.00/0


© 1981, American Pharmaceutical Association

for bonding atoms contribute to the bond so that the geometric mean of the fraction products characterizes the new physical environment. Thus, a bond index is born. The bond indexes $[(1/\delta_A^v)(1/\delta_B^v)]^{1/2}$ are summed to form the molecular connectivity index, $^1\chi^v$.

## REFERENCES


(1) L. B. Kier and L. H. Hall, "Molecular Connectivity in Chemistry and Drug Research," Academic, New York, N.Y., 1976.

(2) M. Randic, *J. Am. Chem. Soc.*, **97**, 6609 (1975).

(3) W. J. Murray, L. H. Hall, and L. B. Kier, *J. Pharm. Sci.*, **64**, 1978 (1975).

(4) L. B. Kier, W. J. Murray, M. Randic, and L. H. Hall, *ibid.*, **65**, 1226 (1976).

(5) L. B. Kier and L. H. Hall, *ibid.*, **65**, 1806 (1976).

(6) A. Bondi, *J. Phys. Chem.*, **68**, 441 (1964).

(7) C. C. Bigelow, *J. Theoret. Biol.*, **16**, 187 (1967).

(8) L. Pauling, "The Nature of the Chemical Bond," 3rd ed., Cornell University Press, Ithaca, N.Y., 1960.

(9) R. S. Mulliken, *J. Chem. Phys.*, **2**, 782 (1934).

(10) J. Hinze and H. H. Jaffe, *J. Am. Chem. Soc.*, **84**, 540 (1962).

(11) C. E. Sun, *J. Chin. Chem. Soc.*, **10**, 77 (1943).

(12) R. T. Sanderson, *J. Chem Educ.*, **31**, 2 (1954).

(13) R. T. Sanderson, "Chemical Bonds and Bond Energy," Academic, New York, N.Y., 1976.

(14) T. DiPaolo, *J. Pharm. Sci.*, **67**, 564 (1978).

(15) *Ibid.*, **67**, 566 (1978).

(16) M. Bonjean and C. L. Duk, *Eur. J. Med. Chem.*, **13**, 73 (1978).

(17) G. R. Parker, *J. Pharm. Sci.*, **67**, 513 (1978).

(18) B. K. Evans, K. C. James, and D. K. Luscombe, *ibid.*, **68**, 370 (1979).

(19) J. S. Millership and A. D. Woolfson, *J. Pharm. Pharmacol.*, **30**, 483 (1978).

(20) S. P. Gupta and P. Singh, *Bull. Chem. Soc. Jpn.*, **52**, 2745 (1979).

(21) R. J. Gardner, *Tech. Q. Master Brew. Assoc. Am.*, **16**, 204 (1979).

(22) R. J. Gardner, *J. Sci. Food Agric.*, **31**, 23 (1980).

(23) L. B. Kier and L. H. Hall, *J. Pharm. Sci.*, **65**, 1806 (1976).

(24) T. DiPaolo, L. B. Kier, and L. H. Hall, *Mol. Pharmacol.*, **13**, 31 (1977).

(25) L. H. Hall and L. B. Kier, *J. Pharm. Sci.*, **66**, 642 (1977).

(26) L. B. Kier, T. DiPaolo, and L. H. Hall, *J. Theoret. Biol.*, **67**, 585 (1977).

(27) L. B. Kier and L. H. Hall, *J. Med. Chem.*, **20**, 1631 (1977).

(28) L. B. Kier, R. J. Simons, and L. H. Hall, *J. Pharm. Sci.*, **67**, 725 (1978).

(29) L. B. Kier and R. A. Glennon, *Life Sci.*, **22**, 1589 (1978).

(30) R. A. Glennon and L. B. Kier, *Eur. J. Med. Chem.*, **13**, 219 (1978).

(31) L. B. Kier and L. H. Hall, *J. Pharm. Sci.*, **67**, 1408 (1978).

(32) L. H. Hall and L. B. Kier, *ibid.*, **67**, 1743 (1978).

(33) L. B. Kier and L. H. Hall, *ibid.*, **68**, 120 (1979).

(34) T. DiPaolo, L. B. Kier, and L. H. Hall, *ibid.*, **68**, 39 (1979).

(35) R. A. Glennon, L. B. Kier, and A. T. Shulgin, *ibid.*, **68**, 906 (1979).

(36) A. J. Richard and L. B. Kier, *ibid.*, **69**, 124 (1980).

(37) D. R. Henry and J. H. Block, *Eur. J. Med. Chem.*, **15**, 133 (1980).

(38) B. Vant Riet, L. B. Kier, and H. L. Elford, *J. Pharm. Sci.*, **69**, 856 (1980).

(39) L. H. Hall and L. B. Kier, *Eur. J. Med. Chem.*, in press.


# Analysis of Drug Contamination from Parabens in Theophylline Olamine


**E. C. JUENGE ˣ, D. F. GURKA, and M. A. KREIENBAUM**



Received July 1, 1980, from the *National Center for Drug Analysis, Food and Drug Administration, 1114 Market Street, St. Louis, MO 63101.* Accepted for publication September 29, 1980.



**Abstract** □ Contaminants in a commercial enema sample of theophylline olamine were found to be derived from parabens and ethanolamine. These contaminants, whose presence was characterized by the loss of preservatives and solubilizing agent, were isolated directly from the drug sample and identified. A high-performance liquid chromatographic (HPLC) system was developed to separate completely and to measure quantitatively theophylline, the two impurities, 4-hydroxybenzoic acid and *N*-(2-hydroxyethyl)-4-hydroxybenzamide, and the remaining parabens. The material balance obtained from the results of quantitative HPLC indicated the formation of these impurities at the expense of parabens. TLC, IR, and UV spectrophotometry and NMR and mass spectrometric analyses were used for identification or for comparisons of the new compound and the known *N*-(2-hydroxyethyl)benzamide.



**Keyphrases** □ Theophylline olamine—contaminants, identification and quantitation, high-performance liquid chromatographic analysis □ Contaminants—identification and quantitation, theophylline olamine enema solutions, high-performance liquid chromatographic analysis □ Paraben preservatives—contamination in theophylline olamine enema solutions, high-performance liquid chromatographic analysis, identification and quantitation □ High-performance liquid chromatography—contamination from paraben preservatives in theophylline olamine enema solutions


During a survey of xanthine derivative drugs conducted by the National Center for Drug Analysis, assay of some enema solutions containing theophylline olamine was attempted with a high-performance liquid chromatographic (HPLC) method that had been used successfully for theophylline elixirs. The analysis showed that, in addition to theophylline and parabens, the sample contained two impurities. This paper discusses the identification and quantitation of these two substances.

## BACKGROUND

The approach followed in this laboratory study was dictated primarily by the small amounts of sample initially available. It involved, first, the original detection of the impurities 4-hydroxybenzoic acid (I) and *N*-(2-hydroxyethyl)-4-hydroxybenzamide (II) by HPLC and TLC, with characterization of their aromatic nature by UV spectrophotometry; and, second, identification by isolation of the impurities from the drug sample and direct comparison with standards by mixed melting-point determinations and IR and NMR analyses. Identities were confirmed by HPLC and TLC comparisons of the original drug solution with commercial and synthesized standards and by a wide collection of spectral data. Finally, the theophylline peak was displaced from the narrow region between the impurity peaks by adjusting the mobile phase to enable quantitative HPLC analysis.

The question of isomerism in the conventional syntheses used to prepare the amides arose because two materials whose elemental analyses were consistent for *N*-(2-hydroxyethyl)benzamide (III) showed different properties. The problem was resolved by purification that showed the materials to be identical; moreover, the mass fragmentations were consistent with the structures given for II and its structural analog, III.

This work demonstrates that parabens can interact chemically with amines used as complexing agents in the compounding of theophylline


0022-3549/81/0600-0589$01.00/0


© 1981, American Pharmaceutical Association

drugs. As a result, foreign substances are introduced into the drug sample, the amount of active drug in the form of the absorbable soluble amine complex is reduced, and the bactericidal and fungicidal properties of the paraben preservative are reduced because of its consumption.

## EXPERIMENTAL

**Materials**—Distilled-in-glass chloroform[1], acetone[1], methanol[1], and acetonitrile[1] and reagent grade sodium bicarbonate, hydrochloric acid, acetic acid, ethanol, silver nitrate, and magnesium sulfate were used. Deionized water was used in preparing mobile phases and in extraction. Benzene[2] was 99 mole % pure, and ether[3] was anhydrous analytical reagent grade. The reactants, primary standard benzoic acid[3], organic reagent 4-hydroxybenzoic acid[3], reagent grade methyl and propyl *p*-hydroxybenzoate[4], and purified grade ethanolamine[4], were used as received.

Theophylline monohydrate[3] (USP grade), phenol[3] (analytical reagent grade), and ferric chloride[2] (certified ACS grade) were used. The spray reagents, ninhydrin[5] [0.2% in methanol–isopropanol (30:70)] and bromcresol green[6] (0.05% in isopropanol), were used as detection agents for TLC. Base-range[7] and short-range[8] pH paper, silica gel columns[9] (2.5 cm), and TLC plates[10] were used.

**Instruments and Parameters**—Grating IR spectrophotometers[11], a UV/near-IR spectrophotometer[12], a 60-MHz NMR spectrometer[13], a high-performance liquid chromatograph[14], and a double-focusing mass spectrometer[15] interfaced to a data system[16] were employed. Melting points were taken in a capillary melting-point apparatus[17].

Direct insertion by probe was used for mass spectrometry under the following conditions: acceleration voltage, 300 v; source temperature, 200°; electron energy, 70 ev; emission current, 1 mamp; scan rate (SR 22), 4 sec/mass decade, exponential; and multiplier, 16-stage dynode at 2.6 kv ($10^6$ gain, minimum).

Instrument parameters for HPLC included a UV detector with a fixed wavelength of 254 nm and a microparticulate reversed-phase column[18] (30 cm × 3.9 mm i.d.). The mobile phase was 0.1% acetic acid in 10% acetonitrile. A flow rate of 2.0 ml/min and an automatic injector with a 20-$\mu$l loop were used. Retention times were converted to capacity factors.

**TLC**—Substances were spotted as methanol solutions. The drug sample was spotted directly on silica gel plates (5 × 7.5 cm) or was acidified toward litmus with hydrochloric acid and extracted once or twice with equal volumes of chloroform before spotting. The chromatograms were developed with a mixed solvent (equal volumes of chloroform and acetone) by the equilibrated, ascending technique in a tank lined with filter paper.

Spots were placed 1 cm from the base of the plate, and the solvent was developed just to the top of the plate. Most spots were located by short-wave UV irradiation, but ethanolamine spots were developed either by spraying the plate with ninhydrin and placing it in an oven at 100° for 3 min or by spraying with bromcresol green.

**Detection of Impurities by HPLC and TLC–UV Characterization**—The mobile phase consisted of 0.1% acetic acid in 10% acetonitrile. A sample of the drug solution diluted with 10 volumes of absolute methanol was injected directly for HPLC analysis. To remove the parabens, another sample was made acidic to litmus with 6 *N* HCl and washed three times with equal volumes of chloroform prior to HPLC analysis. These aqueous layers also were analyzed by TLC. Materials represented by the outside halves of the two peaks of the impurities were collected during elution in the HPLC of the drug sample that previously had been washed free of parabens. These eluents were examined by TLC and then by UV spectrophotometry.

An authentic theophylline monohydrate sample was dissolved in a solvent consisting of 0.1% acetic acid in 10% acetonitrile and also was examined by UV spectrophotometry for comparison.

**Extraction of Drug Sample Impurities**—*Separation of Impurities from Theophylline and Parabens and Isolation of I*—A 10-ml portion of the basic (pH 8.8) enema solution was adjusted to pH 5.0 with short-range paper by dropwise addition of 6 *N* HCl and was extracted by shaking for 5 min with 60 ml of chloroform. The extraction was repeated three times to provide complete separation of theophylline and parabens from the aqueous solution as ascertained by TLC. The aqueous solution then was extracted twice with 40-ml portions of ether and saved for subsequent isolation of II.

The combined ether extracts, containing any free I, were dried over anhydrous magnesium sulfate and filtered. To obtain the product, the ether was removed from the solution on a steam bath under nitrogen; the residue was kept on the steam bath under nitrogen for 5 min to ensure complete solvent removal. The material was recrystallized from acetonitrile, dried at 55°/3 mm for 1 hr, and examined by IR and NMR analyses and melting-point determination.

*Isolation of II*—A 50-ml portion of the drug sample was treated as already described, and the aqueous solution remaining after chloroform and ether extraction was evaporated to dryness on a steam bath under a strong nitrogen flush. The solid residue was extracted twice with 15 ml of boiling acetonitrile to remove II. The undissolved portion of the residue remained fluid during the hot extraction but solidified immediately upon cooling, permitting solvent decantation. The undissolved residue was recrystallized from absolute ethanol and identified by comparison with a synthesized sample of ethanolamine hydrochloride, whose preparation will be described.

The acetonitrile solutions were combined and filtered, and a portion of the filtrate was tested by TLC for the presence of II and residual ethanolamine. The remaining filtrate was evaporated on a steam bath under a nitrogen flush to remove the solvent, leaving a semisolid residue. Amide II was detected on TLC plates by fluorescence diminution, and ethanolamine at the origin of the chromatogram was detected by pH-sensitive bromcresol green spray or by ninhydrin spray followed by a 3–4-min exposure to 100° heat.

A 2.5-cm silica gel cartridge[9] was preconditioned by passing 40 ml of chloroform through it. The semisolid residue from the acetonitrile evaporation was dissolved in the minimum amount (~4–5 drops) of absolute methanol, transferred with a capillary tube to the top of the column, and washed onto the cartridge three times with minimum portions of chloroform.

Chloroform (100 ml) was passed through the column to remove any impurities present in the forerun, and II then was eluted with chloroform–acetone (1:1). For product isolation and identification, the first few milliliters of eluate were evaporated to dryness by warming under a flush of nitrogen. The residue was used for subsequent identification of II.

In addition to characterizing the impurities directly in the drug sample through extraction, HPLC evidence was obtained by spiking the drug sample with additional amounts of reagent grade I and synthesized II.

**Preparation of Ethanolamine Hydrochloride**—An aqueous solution of ethanolamine containing 10% molar excess of hydrochloric acid was evaporated almost to dryness by boiling and completely to dryness by azeotropic removal of water with benzene. The white crystals obtained upon cooling were recrystallized from a small amount of absolute ethanol under a nitrogen atmosphere to preclude moisture, but they were not particularly deliquescent. The crystallized material was dried at 55°/3–4 mm for 3 hr, mp 83.0–83.8°.

*Anal.*—Calc. for $C_2H_8ClNO$: C, 24.68; H, 8.27; N, 14.36. Found: C, 24.81; H, 8.35; N, 14.29.

**Synthesis of II from Methylparaben and Ethanolamine**—Methyl 4-hydroxybenzoate (15.2 g, 0.10 mole) and 6.11 g of ethanolamine (0.10 mole) were placed in a round-bottom flask fitted with a vacuum adapter to a small 15-ml receiver. The system was flushed with nitrogen, and the reaction was carried out under a nitrogen atmosphere. The flask was immersed in an oil bath at 103–107° for 10.5 hr, with the clear melt being agitated by a magnetic stirring bar. Only a few drops of liquid collected in the receiver, but a hard, sticky semisolid formed in the reaction mixture upon cooling. The solid was triturated for 10 min with 60 ml of chloroform.

This process was repeated four times, during which the semisolid became tacky and hard. The solid was triturated twice with 40 ml of dry ether, which left a granular white solid. Crystallization from a small amount of absolute ethanol gave 6.00 g (33%) of white solid (II), mp 145–151°. Recrystallization two more times and drying at 100°/5 mm for 2 hr gave a sample, mp 155.3–156.3°, suitable for analysis. IR spectral

[1] Burdick & Jackson Laboratories, Muskegon, Mich., and Taylor Chemical Co., St. Louis, MO 63144.
[2] Fisher Scientific Co., Fair Lawn, NJ 07410.
[3] Mallinckrodt Chemical Works, St. Louis, MO 63147.
[4] Sigma Chemical Co., St. Louis, MO 63118.
[5] Quantum Industries, Fairfield, NJ 07006.
[6] EM reagent, Curtin Matheson Scientific, Maryland Heights, MO 63043.
[7] Accutint indicator paper, Anachemia Chemicals, Champlain, NY 12919.
[8] Short-range Alkacid, Fisher Scientific Co., Fair Lawn, NJ 07410.
[9] Sep-Pak silica cartridge, Waters Associates, Milford, MA 01757.
[10] EM 60 F-254 silica gel plates, EM Laboratories, Elmsford, NY 10523.
[11] Models 337 and 621, Perkin-Elmer Corp., Norwalk, CT 06856.
[12] Model ACTA MIV, Beckman Instruments, Fullerton, CA 92634.
[13] Varian Instrument Division, Palo Alto, CA 94303.
[14] Model 3500B, Spectra-Physics, Santa Clara, CA 95051.
[15] MAT 311, Varian Associates, Instrument Group, Palo Alto, CA 94303.
[16] 620 L 100, Varian Associates, Instrument Group, Palo Alto, CA 94303.
[17] Thomas–Hoover, Arthur H. Thomas Co., Philadelphia, PA 19105.
[18] $\mu$Bondapak $C_{18}$, Waters Associates, Milford, MA 01757.

analysis showed prominent bands at 3370, 3240, 1610, 1570, 1510, 1320, 1290, 1240, 1185, 1080, 1065, 860, and 710 $cm^{-1}$. The product was insoluble in chloroform and ether and also could be crystallized from water, acetonitrile, and acetone. A sample also was submitted for mass spectrometric and elemental analyses.

*Anal.*—Calc. for $C_9H_{11}NO_3$: C, 59.66; H, 6.12; N, 7.72. Found: C, 59.80; H, 6.44; N, 7.52.

**Preparation of II by Reaction between I and Ethanolamine**—A very low yield of product was obtained in this procedure. A mixture of 13.8 g of I (0.10 mole) and 6.11 g of ethanolamine (0.10 mole) was heated gradually to 200° according to the procedure of Wenker (1). Vacuum distillation, after a small forerun, gave ~10 ml of a colorless liquid having a phenol odor, bp 77–79°/11 mm. This distillate had a boiling point corresponding to that of phenol but gave a negative test for phenol with 1% ferric chloride solution and with ferric chloride–urea reagent (2), and it gave a poor IR spectral match with pure phenol.

A developed TLC plate containing the material indicated the presence of ethanolamine when sprayed with bromcresol green. Approximately 4 drops of the distillate were dissolved in chloroform and placed on the top of a silica gel cartridge that had been conditioned previously with 40 ml of chloroform. When ethyl acetate was passed through the cartridge, pure phenol eluted within the first 2 ml and was identified by TLC after comparison with phenol spotted alongside the distillate ($R_f$ 0.68). When the chromatogram was sprayed with bromcresol green, no blue spot for ethanolamine appeared. The material purified by chromatography gave a deep-purple color with 1% ferric chloride solution and with ferric chloride–urea reagent, as expected for phenol. The IR spectrum also matched that of an authentic phenol sample.

A small amount of the desired product was obtained from the sticky, semisolid residue (2.3 g) left after the distillation. This residue was triturated twice with 10 ml of chloroform and once with 10 ml of anhydrous ether, leaving 2.13 g (11.8%) of light-brown granular solid. After two recrystallizations from absolute ethanol, the product melted at 155.2–156.2°. It was shown to be II by mixed melting point with the analytically pure sample of this substance prepared as already described and by comparison of the IR spectrum with that of the pure compound. TLC of the two synthesized samples and the isolated amide II showed identical $R_f$ values.

**Synthesis of III from Benzoic Acid and Ethanolamine**—Compound III was synthesized by the procedure of Wenker (1). In the present study, a reaction on a 0.1 *M* scale gave a forerun of ~1 g of sublimate upon distillation. This white solid was recrystallized twice from 95% ethanol (mp 143.5–144.5°) and dried at 55°/3 mm for 1.5 hr. Results of elemental analysis were consistent with the structure for β-hydroxyethylammonium benzoate.

*Anal.*—Calc. for $C_9H_{13}NO_3$: C, 59.00; H, 7.15; N, 7.65. Found: C, 59.12; H, 7.41; N, 7.57.

The identity of this substance was confirmed as follows. Known β-hydroxyethylammonium benzoate was obtained as a white solid, which crystallized on cooling from a hot acetone solution of equimolar amounts of benzoic acid and ethanolamine. No melting-point depression was observed from a mixture of the known and unknown materials.

Continued distillation yielded ~8 g of an oily product, which failed to give a dry crystalline product on attempted crystallization from common solvents; however, a crystalline product was obtained in two ways. First, in a crystal growth technique, a small amount of the oil was placed in an erlenmeyer flask with a small overlayer of dry ether; the flask was stoppered and stored in the freezer compartment of a refrigerator. Soft, fibrous, single needles, 3 cm long, grew out of the mass overnight, leaving at the origin only a very small amount of liquid unconverted to crystals. The product was collected quickly, washed with a small amount of dry ether, dried in air, and crushed to a white powder, $R_f$ 0.30, mp 63.5–65.8° [lit. (3) mp 66–67°].

The product (III) was dried over phosphorus pentoxide for 1 hr and then at 55°/4 mm for 1.5 hr. It then was submitted for mass spectrometric and elemental analyses.

*Anal.*—Calc. for $C_9H_{11}NO_2$: C, 65.44; H, 6.71; N, 8.48. Found: C, 65.20; H, 6.93; N, 8.31.

Some crystals were used to seed the crude distillate. On standing several hours, the distillate crystallized to a semisolid laced with needles. However, the needles were thixotropic, and the crystals became fluid and were adsorbed when collection on filter paper by filtration or by pressing on tile was attempted.

In the second purification procedure, a double silica gel cartridge (two silica gel cartridges[9] connected in tandem with an inserted small piece of glass tubing) was preconditioned with chloroform as already described. A portion of the crude distillate (119 mg) was dissolved in 0.2 ml of chloroform, applied to the top of the column, and washed into the column by two applications of a few drops of chloroform. Chloroform was used for development and elution. The first 10 ml of eluate contained only small amounts of impurities and was discarded.

The amide product (III) eluted completely in the next 70 ml. The solvent was removed from this fraction by warming under nitrogen, leaving a heavy oil. When scratched with a stirring rod, this oil formed a hard white solid, mp 63.8–64.5°. This product was free of ethanolamine, as determined by TLC and bromcresol green spray. The products isolated by the crystal growth and silica gel cartridge techniques were shown to be identical by mixed melting-point and IR analyses (3300, 3140, 1600, 1520, 1440, 1370, 1320, 1290, 1200, 1150, 1060, 1040, 870, 800, 760, and 690 $cm^{-1}$).

**Quantitative Study by HPLC**—*Mobile Phase*—Impurities II and I and theophylline were determined by HPLC, using a mobile phase of 0.5% acetic acid in 2.8% aqueous acetonitrile. Methylparaben was determined with 0.5% acetic acid in 10% aqueous acetonitrile, and propylparaben was determined with 0.5% acetic acid in 25% aqueous acetonitrile.

*Sample and Standard Solutions*—A stock solution of II (synthesized from paraben) was prepared by dissolving 22.1 mg of the recrystallized compound in 250.0 ml of methanol (88.4 μg/ml). This stock solution was diluted to 79.6, 44.2, and 26.5 μg/ml with methanol. A sample solution was prepared by diluting 5.0 ml of enema solution to 50.0 ml with methanol.

A solution of I was prepared by dissolving 60.0 mg in 200.0 ml of methanol (300 μg/ml) and was used directly. Another solution of I was prepared by dissolving 42.6 mg in 200.0 ml of methanol (213 μg/ml), and an aliquot of this solution was diluted to 102 μg/ml with methanol. A sample solution was prepared by diluting 5.0 ml of enema solution to 50.0 ml with methanol.

The stock methylparaben solution was prepared by dissolving 20.0 mg of methylparaben in 100.0 ml of methanol (200 μg/ml), and aliquots were diluted to 160, 80, 60, and 44 μg/ml with methanol. A sample solution was prepared by diluting 6.0 ml of enema solution to 50.0 ml with methanol.

The stock propylparaben solution was prepared by dissolving 20.0 mg of propylparaben in 100.0 ml of methanol (200 μg/ml). This stock solution was diluted to 128, 100, and 50 μg/ml with methanol. A sample solution was prepared by diluting 17.0 ml of enema solution to 50.0 ml with methanol.

A stock solution of theophylline was prepared by dissolving 153 mg of anhydrous theophylline in 100.0 ml of methanol (1.530 mg/ml), and aliquots were diluted to 1.150, 0.770, and 0.380 mg/ml with methanol. A sample solution was prepared by diluting 3.0 ml of enema solution to 50.0 ml with methanol.

*HPLC Method*—After the approximate concentration of each component of the sample solution was determined, standard solutions were prepared to range from ~50 to 150% of these concentrations. Each sample and standard solution was injected at least three times, and peak heights were measured manually. Each sample component was calculated by:

$$C_c = H_s/H_{std}C_sDF \qquad \text{(Eq. 1)}$$

where $C_c$ and $C_s$ are the concentrations (milligrams per milliliter) of each component of the sample solution and of the corresponding standard, respectively; $H_s$ and $H_{std}$ are the peak heights of the sample and standard solutions, respectively, such that the standard concentration is chosen to yield a standard peak height within 5% of the sample peak height; and $DF$ is the sample dilution factor.

The full-scale absorbance settings were: theophylline and I, 0.64; II and methylparaben, 0.16; and propylparaben, 0.08. The recorder chart was operated at 30.48 cm/hr.

**Ethanolamine**—Ethanolamine was determined by the official NF method (4).

## RESULTS AND DISCUSSION

The chromatogram obtained from the HPLC (0.1% acetic acid in 10% acetonitrile) determination of the diluted enema solution or the drug solution applied directly on the $C_{18}$ reversed-phase column showed a cluster of peaks reflecting capacity factors of 0.87 for II, the first impurity to elute, 1.62 for theophylline, and 2.25 for I, the second impurity to elute. The peak of the major impurity, I, was almost three times as large as that of the minor impurity, II, and the theophylline peak was the largest of the three. The parabens eluted much later than this cluster.

Acidification of the drug sample and subsequent extraction with chloroform completely removed the parabens and concentrated the im-

**Table I—$R_f$ Values for Isolated and Synthesized Compounds [a]**

| Compound | $R_f$ |
|---|---|
| Theophylline | 0.22 |
| I | 0.27 |
| II | 0.17 |
| III[b] | 0.30 |
| Methylparaben | 0.70 |
| Propylparaben | 0.74 |
| Ethanolamine | 0.00[c] |

[a] Silica gel plates and solvent system composed of equal volumes of chloroform and acetone. [b] *N*-(2-Hydroxyethyl)benzamide. [c] Developed with bromcresol green spray or ninhydrin spray followed by heating at 100° for 3 min.

purities at the expense of theophylline. The completeness of this process was reflected in chromatograms of the extracted samples by the absence of peaks for parabens and the modification of peak heights in the cluster. Relative heights of the peaks for the impurities remained essentially unaltered and suggested repeated extractions of this type as a first step in the isolation of the impurities from the drug sample. The UV spectra of selected fractions eluted during HPLC showed a $\lambda_{max}$ of 252 nm for II and a $\lambda_{max}$ of 256 nm for I, indicating the aromatic nature of the compounds. The $\lambda_{max}$ of theophylline in the mobile phase was 272 nm, which suggested that the impurities were not simple derivatives of that substance. Methylparaben itself showed an absorption at 255 nm.

TLC confirmed that two impurities were present in the drug sample. The $R_f$ values for the smaller impurity (0.17), theophylline (0.22), and the larger impurity (0.27) (Table I) indicated a reverse order of migration for the substances on 7.5-cm silica gel TLC plates compared with that on $C_{18}$ reversed-phase HPLC, as expected. The $R_f$ values from 20-cm TLC plates were essentially the same as those from 7.5-cm plates.

After the acidified drug solution was washed repeatedly with chloroform, no theophylline could be detected by TLC. The first impurity (I) was isolated by ether extraction and was obtained as a white solid after removal of the ether solvent. Two such treatments involving chloroform and ether extractions of acidified drug sample gave 8.0 and 7.4 mg of this impurity, representing 4.8 and 4.4%, respectively, relative to the weight of the therapeutic component, theophylline. After recrystallization, the isolated impurity melted at 205.5–206.0°.

*Anal.*—Calc. for $C_7H_6O_3$: C, 60.86; H, 4.38; mol. wt. 138. Found: C, 60.91; H, 4.27; mol. wt. 142.

After analysis indicated that the extracted product was I, identification was confirmed by using an authentic sample of I in IR and NMR comparisons and by mixed melting-point determination.

Because limited sample was available and the impurities were present in a very dilute state, subsequent extractions leading to identification of II, which was present in an even smaller amount, seemed difficult without a reference standard. UV analysis of the isolated HPLC eluate suggested that II could have an aromatic structure similar to that of the parabens. In the search for a reference standard, various xanthines and uric acids were examined, as were heated reaction mixtures from methylparaben with theophylline and with ethanolamine. The latter reaction provided the desired source. Initial HPLC of the crude product indicated that the major product of the reaction was identical with the minor impurity (II) in the commercial sample. TLC also supported this identity.

After I was extracted from the aqueous residue, II was isolated by evaporation of the residue to dryness and preliminary extraction with acetonitrile to remove II from the insoluble ethanolamine hydrochloride. This procedure left 175 mg of residue which, after crystallization from absolute ethanol, yielded 122 mg of ethanolamine hydrochloride, mp 83.0–83.5°. This material appeared to be a dry, not readily deliquescent material, whereas the literature described the substance as deliquescent (5) and gave two melting points, 75–77° (5) and 100° (6). Therefore, the recrystallized substance was identified further as ethanolamine hydrochloride by comparing its IR and NMR spectra with those of synthesized ethanolamine hydrochloride. A mixture of known ethanolamine hydrochloride and the unknown gave no depression in melting point.

The acetonitrile extraction removed most of the amide impurity from the ethanolamine salt, and TLC examination of the extract by fluorescence diminution showed only II and no I or theophylline. Moreover, only a small amount of ethanolamine was detectable compared with a similar examination of the residue before the acetonitrile treatment. The ethanolamine showed little or no migration from the origin (Table I) and was detected as a blue spot with bromcresol green or as a red spot with ninhydrin followed by heat. This low migration allowed purification of II on a short silica gel column.

The residue remaining after acetonitrile evaporation was applied to the column; passage of a large volume of chloroform removed traces of impurities from II, which showed little migration with this eluent. When the solvent was changed to chloroform–acetone (1:1), II eluted immediately; elution was complete within the next 7 ml without release of any ethanolamine. An additional 40 ml of the solvent failed to elute any ethanolamine, attesting to the effectiveness of the method. Solvent removal from the 7-ml fraction of mixed solvent left 9.33 mg of dry white powder, mp 154.0–156.0°. The impurity was identified as II by IR and NMR comparisons with the analytically pure, synthesized compound. A mixture of the known and unknown compounds gave no depression in melting point.

Although I and II were detected initially by HPLC and TLC, these procedures allowed identification of the impurities by direct extraction from the drug sample.

In terms of the active ingredient, ~7.7 mg of I [4.6% by weight relative to the weight (166 mg) of theophylline expected by label declaration] and ~1.9 mg or 1.1% of II were obtained by extraction of 10 ml of the drug sample. Heavy losses were expected from the multiple extractions used in purification. Refinement of the HPLC technique, which allowed quantitative analysis and reflected chemical changes that resulted in formation of the contaminant, will be described.

The impurities in the drug sample were identified directly by extraction and the use of reference standards. Confirmatory identification was obtained from HPLC by spiking drug samples with the reference standards, resulting in enlargements of the peaks representing the impurities without any new peaks.

The problems associated with the isolation and identification of II were the lack of a preparation method for it and the high solubility of such amides in water, a property shared by ethanolamine, a possible contaminant of these amides. Ethanolamine can be removed by silica gel columns, onto which the ethanolamine is tenaciously adsorbed. A method (1) was described for the preparation of the structural analog, amide III, directly from I and the amine, but a more effective approach seemed to be a reaction between an ester and the amine. Moreover, the reaction between paraben esters and ethanolamine warranted study as a source for generation of II in the drug sample. The reaction gave a product that was identical with one impurity in the drug sample and whose identity was confirmed by elemental analysis.

Reported methods for preparation of III are not without discrepancies, but they were resolved. Prepared as already described, the compound was initially a water-soluble liquid, in accordance with the description of Wenker (1), who reported that the compound could not be obtained in crystalline form. However, Fränkel and Cornelius (3) reported that the compound was a crystalline solid when prepared by the Schotten–Baumann reaction followed by hydrolysis of the dibenzoyl derivative of ethanolamine. The structure of these two products rested on the reported elemental analysis for nitrogen.

In this laboratory, a reaction was attempted between I and ethanolamine by gradually heating the mixture to 200° under the conditions used by Wenker to prepare the liquid parent compound. The reaction gave phenol primarily, which resulted from the ease of decarboxylation attributed to resonance effects of the 4-hydroxy group. However, some II was generated and was identical with the product obtained by reaction of methylparaben and ethanolamine and with the impurity contained in the drug sample. The reaction of Wenker was repeated and yielded a liquid that could not be obtained as a crystalline solid by the usual procedures but was obtained in crystalline form by a crystal growth technique under dry ether or by use of a silica gel cartridge. The melting point of these crystals was essentially the same as that previously obtained (3), indicating that this amide and that of Wenker were identical. It is unlikely that I formed first in the drug sample and then partially reacted with ethanolamine to generate II. Even when these reactants were heated gradually to 200°, as already described, phenol was formed primarily by decarboxylation.

In view of the slight differences in reports describing the synthesis of the parent amide, both II and III were analyzed by mass spectrometry. A rather general similarity of fragmentation pattern was shown by these substances (Table II). The spectra for II and III showed molecular ions at *m/z* 181 and 165, respectively, and base peaks, as expected, at *m/z* 121 and 105, respectively. The odd *m/z* ratio of the molecular ion confirmed the odd number of nitrogen atoms in the compounds. Postulated structures for some major ions are given in Table II.

The NMR spectrum of II (methanol-$d_4$ solvent) showed essentially two doublets for the *ortho* and *meta* aromatic hydrogens centered at 6.75 and 6.90 ppm, splitting each other with a coupling constant of $J = 4.2$ Hz. Both I and methylparaben also had very similar pairs of doublets for

**Table II—Postulated Structures of Some Major Ions Generated in Mass Spectrometric Fragmentation of $RCONHCH_2CH_2OH$**

| Fragment Ion | R = $HOC_6H_4$[a] | | R = $C_6H_5$[b] | |
|---|---|---|---|---|
| | m/z | Intensity[c] | m/z | Intensity[c] |
| $RCONHCH_2CH_2OH^{+\cdot}$ ($M^{+\cdot}$) | 181 | 3.28 | 165 | 2.24 |
| $RCONHCH{=}CH_2^{+\cdot}$ ($M - H_2O$) | 163 | 20.45 | 147 | 13.63 |
| $RCONHCH_2^+$ | 150 | 5.29 | 134 | 8.96 |
| $R(HO)C{=}NH_2^+$ | 138 | 12.50 | 122 | 20.01 |
| $RC{\equiv}O^+$ | 121 | 100.00 | 105 | 100.00 |
| $R^+$ | 93 | 32.19 | 77 | 66.68 |

[a] Probe heated at 125° to volatilize sample; background subtracted. [b] Probe heated at 80° to volatilize sample; background subtracted. [c] Ratio against base peak, percent.

coupling between these two types of aromatic protons. Both III and II showed similarly shaped multiplets for the methylene protons, 3.48–3.78 ppm. The aromatic regions for these compounds were quite different, and aromatic absorptions for III with complicated multiplets centered at 7.26 and 7.82 ppm were identical with those in the spectrum of *N*-(2-hydroxyethyl)thiobenzamide previously reported (7).

Other investigators (8) recently reported a chemically related contamination resulting from a reaction between ethylenediamine complexing agent and a suppository base.

The high efficiency of the reversed-phase column produced a wide range of capacity factors, which necessitated the use of three mobile phases to separate the five components of the enema solution. Resolution to baseline was achieved for the analysis of each component. Acetic acid was added to the mobile phases to reduce peak tailing.

The original conditions (10% acetonitrile, Table III) used for detection of the impurities in the drug sample placed the peak for theophylline in a narrow region between the peaks for the impurities, leading to considerable overlap and precluding quantitative determination of the impurities. Fortunately, the capacity factor of theophylline on the lipophilic column was much more sensitive to the polar nature of the mobile phase than were the impurities. In general, the capacity factors increased as the percentage of acetonitrile declined. However, from 10.0 to 2.8% acetonitrile, the differential capacity factor $k'(I)-k'(T)$ for I relative to theophylline went through an inversion (Table III) from 0.2 to −4.8, *i.e.*, the separation factor [relative retention, $\alpha = k'(I)/k'(T)$] became fractional. This general trend was reflected by collection of data with a mobile phase containing no acetonitrile (Table III). The problem was resolved by removing the theophylline peak from its location between the peaks for the impurities, allowing quantitation of the impurities by use of 2.8% acetonitrile as the mobile phase. However, since retentions for the parabens were excessively long with this mobile phase, 10 and 25% acetonitrile were used for quantitation of methyl- and propylparabens, respectively.

Before the use of peak heights to measure sample concentrations, it was determined that injection volumes were reproducible to better than 1%. Standard calibration curves for each enema component demonstrated linearity of peak heights with concentrations between 50 and 150% of the actual component concentration in the enema sample. The mean peak height for at least three injections was used in all calculations. The concentration of each component of the enema solution is listed in Table IV.

These analytical data indicate that only 96 mg of total paraben remained from a label claim of 360 mg of total paraben/100 ml of enema solution. The residual parabens along with impurities accounted for 106% of the label claim for total parabens on a molar basis, indicating that 73.3% of the parabens had chemically decomposed. Thus, the fungistatic and bacteriostatic properties of the solution were seriously lowered. In addition, 6% (0.26 mg/ml) of the label quantity of ethanolamine was converted to II, decreasing the ethanolamine concentration to 23.6% of the labeled quantity of theophylline olamine; the official limits are 22–28% of label.

**Table III—Capacity Factors in Quantitative HPLC of Enema Solution**

| Acetonitrile[a], % | Amide Impurity $k'(II)$ | Theophylline $k'(T)$ | 4-Hydroxybenzoic Acid $k'(I)$ | Methylparaben | Propylparaben |
|---|---|---|---|---|---|
| 0 | 10.4 | 33.0 | 12.1 | — | — |
| 2.8 | 3.4 | 10.0 | 5.2 | — | — |
| 10.0 | 1.0 | 2.8 | 3.0 | 12.5 | — |
| 25.0 | — | — | — | — | 16.6 |

[a] Each mobile phase contained 0.5% acetic acid.

**Table IV—HPLC Analysis of Enema Solution**

| Component | Label Claim, mg/ml | Found, mg/ml | Percent of Label Claim |
|---|---|---|---|
| Methylparaben | 3.00 | 0.67 | 22.3 |
| Propylparaben | 0.60 | 0.29 | 48.3 |
| Theophylline | 12.61 | 12.96 | 103.0 |
| Ethanolamine | 4.28 | 3.92 | 91.6 |
| I | — | 1.95 | — |
| II | — | 0.77 | — |

By salt formation with xanthine drugs, *e.g.*, theophylline and theobromine, amines such as ethanolamine and ethylenediamine effectively solubilize these drugs. However, because they are rather reactive substances, esters such as parabens are chemically vulnerable, particularly toward attack by amines. These reactions of the complexing agent may reduce the amount of drug in solution and consume the preservative. Loss of preservative may result in drug biodegradation or in a health hazard through bacterial or fungal contamination of the dosage form; such loss also may create a source of chemical contamination by generation of foreign substances. Improper treatment, such as excessive temperatures and extremely high or low pH during formulation, packaging, and storage, may increase reaction rates and lead to such paraben reactions as acylation and hydrolysis. Hydrolysis of methylparaben in basic and acidic solutions (pH 6–8) was previously studied (9). Autoclaving at pH 9 (close to the measured pH of the sample used in this study) for 30 min left only 58% of the initial methylparaben concentration. The hydrolysis rates of methylparaben at 70, 80, and 85° were greater when the solutions were basic, as were the enema solutions investigated.

In this study, relative to theophylline, 4.6% by weight of II and 11.7% of I were found in the drug sample with a corresponding 73.3% loss of parabens in the solution. The corresponding amide from salicylic acid, *N*-(2-hydroxyethyl)-3-hydroxybenzamide, was described previously (10), but to the knowledge of the authors, II is unknown and its physiological effects are unexplored.

It should be noted that paraben losses may occur by direct chemical decomposition as well as by microbial degradation or complex formation with macromolecules. Despite their phenolic moiety, structures such as paraben esters are not resistant to all microbes and, like other phenols with electron-withdrawing substituents (*e.g.*, picric acid), may give complex formation with macromolecules. These factors may result in loss of the preservative effects of parabens in drug samples. This study shows that the ester functional group of parabens also may give rise to loss of preservative action by direct chemical decomposition. Interactions similar to those between parabens and ethanolamine described here also should apply to ethylenediamine complexing agent.

## REFERENCES


(1) H. Wenker, *J. Am. Chem. Soc.*, **57**, 1079 (1935).

(2) "The United States Pharmacopeia," 19th rev., Mack Publishing Co., Easton, Pa., 1975, p. 39.

(3) S. Fränkel and M. Cornelius, *Berichte*, **51**, 1654 (1918).

(4) "The National Formulary," 14th ed., Mack Publishing Co., Easton, Pa., 1975, p. 697.

(5) "The Merck Index," 9th ed., Merck & Co., Rahway, N.J., 1976, p. 3648.

(6) "Dictionary of Organic Compounds," vol. 1, Oxford University Press, New York, N.Y., 1953, p. 91.

(7) Spectrum 42109, Maybridge Chemical Co., N. Cornwall, England, published by Sadtler Research Laboratory, Philadelphia, Pa.

(8) J. F. Brower, E. C. Juenge, D. P. Page, and M. L. Dow, *J. Pharm. Sci.*, **69**, 942 (1980).

(9) N. N. Raval and E. L. Parrott, *ibid.*, **56**, 274 (1967).

(10) G. Tilly, *Chim. Ther.*, **2**, 57 (1967); through *Chem. Abstr.*, **67**, 32432 (1967).


## ACKNOWLEDGMENTS


The authors thank J. F. Brower, National Center for Drug Analysis, for technical assistance. The authors also are indebted to R. J. Losure, R. P. Barron, and W. R. Benson, Division of Drug Chemistry, Food and Drug Administration, for mass spectral analyses and interpretations.

# Precaution on Use of Hydrochloride Salts in Pharmaceutical Formulation

**SHOZO MIYAZAKI ˣ, MIDORI OSHIBA, and TANEKAZU NADAI**

Received April 30, 1980, from the *Faculty of Pharmaceutical Sciences, Josai University, Sakado, Saitama 350-02, Japan.* Accepted for publication November 3, 1980.

**Abstract** □ Previous reports suggested that the formation of hydrochloride salts does not always enhance solubility due to the common ion effect. The extent of the common ion effect seems to be related to aqueous solubility, with slightly soluble hydrochlorides being more sensitive to the common ion, *i.e.*, chloride ion. The relationship between solubility in water and the extent of the common ion effect was examined, and a high correlation was found, suggesting that hydrochlorides possessing solubilities in water at least of the order observed for papaverine and demeclocycline hydrochlorides (~32 mg/ml at 25° and 42 mg/ml at 37°) are less soluble than the corresponding free base at gastric pH.

**Keyphrases** □ Hydrochlorides—effect on solubility, common ion effect □ Solubility—effect of hydrochlorides, common ion effect □ Common ion effect—effect of hydrochlorides on solubility □ Physicochemistry—effect of hydrochlorides on solubility, common ion effect

Salt formation is one of the first approaches used to modify drug solubility and dissolution rates. Because of simple availability and physiology, the monohydrochloride salts have been the most frequent choice of the available salts of basic drugs (1). However, previous reports (2–5) showed that hydrochloride salt formation does not necessarily enhance solubility and bioavailability. This finding is based on the common ion effect of chloride on the solubility product equilibrium of hydrochloride salts (6), which often is overlooked. Hydrochloride salts of the drugs frequently exhibit less than desirable solubility in gastric fluid because of the abundance of chloride ion.

## BACKGROUND

Unusual pH–solubility profiles containing maxima at pH 2–3 were reported previously (2) for chlortetracycline, demeclocycline, and methacycline hydrochlorides in sodium acetate–hydrochloric acid buffers. The decrease in solubility at lower pH values was attributed to the common ion effect of chloride on the solubility product equilibrium of the hydrochloride salts. The apparent dissolution rates and solubilities of these hydrochloride salts were less than those of the respective free base forms in chloride-containing media. Evidence was presented for greater bioavailability from the chlortetracycline and methacycline free bases compared to the hydrochloride salts (3). The common ion effect also influenced the solubilities and dissolution rates of the hydrochloride salts of papaverine, trihexyphenidyl, isoxsuprine, phenazopyridine, cyproheptadine, and bromhexine (4, 5).

On the other hand, tetracycline hydrochloride solubility, which increased with a pH decrease, showed a usual pH profile in chloride-containing buffers (2). Tetracycline hydrochloride exhibited a greater solubility than its free base in hydrochloric acid at pH 1.2 since the hydrochloride exhibited a low sensitivity to the chloride ion. The differences between tetracycline and the other drugs in sensitivity to the chloride ion may result because the aqueous solubility of tetracycline hydrochloride is much higher than that of the others.

The addition of a common ion often reduces the solubility of a slightly soluble electrolyte. Although the concept of solubility product equilibrium originated in inorganic chemistry, this principle can be applied to slightly soluble organic salts (7). The drugs under study are basic amino compounds and form slightly or sparingly soluble hydrochloride salts. Since the salt in solution is partially dissociated, further solubility suppression may be caused by the common ion effect. The equilibrium involved is shown in Scheme I.

From previous results, it seems that the extent of the common ion effect

$$BH^+Cl^-_{(solid)} \rightleftharpoons (BH^+)_{aq} + (Cl^-)_{aq}$$

*Scheme I*

is related to aqueous solubility, with slightly soluble salts being more sensitive to the chloride ion. In this study, an attempt was made to determine the relationship of solubilities in water and their sensitivities to the chloride ion of nine hydrochloride salts that showed unusual solution properties. The salting-out constant with sodium chloride, based on the Setschenow equation (8), was taken as the parameter of the extent of the common ion effect, *i.e.*, sensitivity to chloride ion. The Setschenow equation was found to be applicable to an amine hydrochloride (9).

## EXPERIMENTAL

The drugs studied are listed in Table I. Solubility measurements in distilled water were made at 25 and 37°. An excess of the drugs was placed into each vial containing the solvent, and the vials were equilibrated by shaking overnight. Equilibrated mixtures were filtered[1], and the filtrates were assayed spectrophotometrically.

The solubility of each drug in sodium chloride solutions also was determined as already described. Experimental salting-out constants were calculated according to the Setschenow equation (8):

$$\log S_0/S = kC \qquad \text{(Eq. 1)}$$

where $S$ and $S_0$ are the solubilities in the salt solution and in pure water, respectively; $C$ is the molar concentration of the electrolyte; and $k$ is the empirical salting-out constant.

## RESULTS

Table I summarizes the solubility data obtained for each hydrochloride salt and their experimentally determined salting-out constants with sodium chloride at 25 and 37°; the solution pH is also given. Setschenow plots for these drugs in sodium chloride at 25° are shown in Fig. 1. There appears to be a distinct relationship between the solubility in water and the salting-out constant with sodium chloride; as the solubility in water increased, the salting-out constant decreased. Thus, phenazopyridine, cyproheptadine, and bromhexine hydrochlorides, which had the smallest solubilities, were sensitive to the chloride ion to the greatest extent. The most soluble drugs, papaverine and demeclocycline hydrochlorides, were the least sensitive to the chloride ion.

Figure 2 shows the salting-out constant with sodium chloride as a function of solubility in water at 25 and 37°. A least-squares line was fitted to all points in each log–log plot. A high correlation coefficient ($r$) was obtained at both 25 ($r$ = 0.902) and 37° ($r$ = 0.946), indicating that the smaller the solubility in water, the larger the salting-out constant.

Furthermore, the data are interesting with regard to their general applicability to other slightly soluble organic hydrochlorides. For all drugs listed in Table I, much greater solubility and dissolution rates were obtained by the free bases than by hydrochloride salts in hydrochloric acid solution at pH 1.2. Perhaps this phenomenon applies to hydrochloride salts having water solubilities less than ~32 mg/ml at 25° and 42 mg/ml at 37°, which are the solubilities of papaverine and demeclocycline hydrochlorides.

## DISCUSSION

Comparison of the solubilities in water to the salting-out constant revealed an inverse relationship between these quantities. Although it would be desirable to develop this relationship further, a general statement concerning hydrochloride salt formation within the solubility range found in this study may be possible: hydrochloride salts having solubil-

[1] Millipore 0.45-μm filter.



*0022-3549/81/0600-0594$01.00/0*
*© 1981, American Pharmaceutical Association*

**Table I—Solubility in Water and Salting-Out Constant with Sodium Chloride at 25 and 37° [a]**

| Hydrochloride (Molecular Weight) | Temperature | Solubility[b], mg/ml | pH[c] | Salting-Out Constant, $k$[d] |
|---|---|---|---|---|
| Phenazopyridine (249.7) | 25° | 2.81 (4, 0.03) | 3.35 | 18.06 |
| | 37° | 4.03 (6, 0.06) | 3.28 | 11.57 |
| Cyproheptadine[e] (350.9) | 25° | 2.98 (3, 0.02) | 5.74 | 21.18 |
| | 37° | 4.56 (3, 0.05) | 5.29 | 14.80 |
| Bromhexine (412.6) | 25° | 3.85 (5, 0.05) | 4.00 | 20.00 |
| | 37° | 4.85 (9, 0.03) | 3.83 | 16.78 |
| Trihexyphenidyl (337.9) | 25° | 5.17 (5.04, 5.29) | 5.51 | 8.24 |
| | 37° | 11.34 (7, 0.37) | 5.23 | 5.66 |
| Isoxsuprine (337.9) | 25° | 8.86 (8.84, 8.88) | 5.45 | 6.32 |
| | 37° | 11.60 (5, 0.85) | 5.10 | 6.30 |
| Chlortetracycline (515.4) | 25° | 10.72 (10.67, 10.77) | 2.39 | 9.60 |
| | 37° | 11.74 (7, 0.34) | 2.28 | 6.52 |
| Methacycline (478.9) | 25° | 16.89 (3, 0.04) | 2.26 | 8.24 |
| | 37° | 19.49 (3, 0.89) | 1.94 | 6.36 |
| Papaverine (375.8) | 25° | 31.78 (4, 0.29) | 2.90 | 5.09 |
| | 37° | 41.74 (41.73, 41.75) | 3.13 | 3.60 |
| Demeclocycline[f] (519.4) | 25° | 32.55 (32.06, 33.04) | 2.11 | 3.73 |
| | 37° | 41.49 (40.64, 42.34) | 1.86 | 2.68 |

[a] As reported in Refs. 2, 4, and 5. [b] The averaged result is reported where there were more than two determinations, followed by parentheses containing the number of determinations and the standard error. For two determinations, the average is followed by parentheses containing the individual values. All data are expressed as the free base equivalent. [c] The pH of a saturated solution. [d] Estimated from the initial slope. [e] Contained 3/2 mole of water. [f] Monohydrate.

ities in water at least of the order observed for papaverine and demeclocycline hydrochlorides are less soluble than the corresponding free base at gastric pH. This finding may be useful in predicting the most soluble form of similar drugs from known or readily determined water solubility values.

Lin *et al.* (9) illustrated a similar phenomenon that decreases the dissolution rate of the salt below that of its free base form. The free base of an experimental antihypertensive exhibited a greater dissolution rate

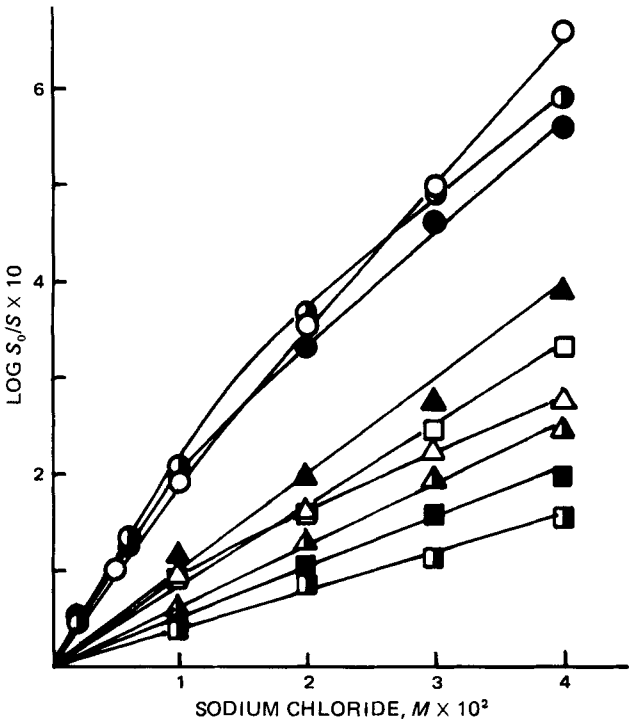


**Figure 1**—*Setschenow plots for hydrochloride salts in sodium chloride solutions at 25°. Key: ○, phenazopyridine; ◑, cyproheptadine; ●, bromhexine; △, trihexyphenidyl; ▲, isoxsuprine; ▲, chlortetracycline; □, methacycline; ■, papaverine; and ◨, demeclocycline.*

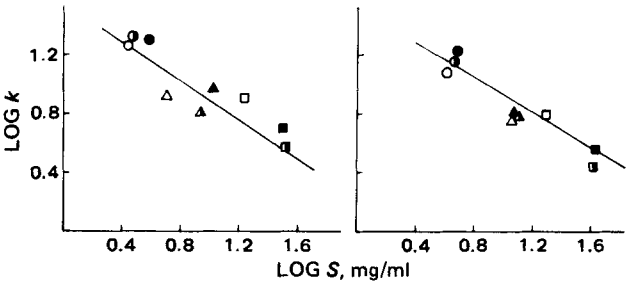


**Figure 2**—*Relationship between solubility in water and salting-out constant at 25 (left) and 37° (right). Key: see Fig. 1.*

than the monohydrochloride salt in 0.1 *N* HCl, and this finding was attributed to the common ion effect. The equilibrium solubility of the monohydrochloride at 37° was 16 mg/ml in water.

Because of the high aqueous solubility (133.7 and 164.4 mg/ml at 25 and 37°, respectively) and low sensitivity of tetracycline hydrochloride to the chloride ion ($k$ = 0.94 and 0.85, respectively), this antibiotic showed unusual solubility characteristics (2). The freely soluble hydrochlorides normally exhibit no serious problem.

Although doxycycline hydrochloride solubility in water at 25° is 50 mg/ml (10), the free base dissolved from the compressed pellet form about sixfold faster than the hydrochloride in 0.1 *N* HCl (11). Common ion equilibrium with chloride strongly reduces the dissolution rate of doxycycline hydrochloride from the pellet, while the free base is not affected. Dissolution of hydrochloride salts from crystalline powder in chloride-containing media probably represents a problem only with slightly or sparingly soluble hydrochlorides, but dissolution certainly may be a problem with the tablet dosage form when the hydrochloride is soluble.

The solubility of solids is a very useful parameter since an orally administered drug in solid dosage form must dissolve in the GI tract prior to absorption. The GI absorption of chlortetracycline and its hydrochloride was studied in rats and humans (3), and the results indicated that the free base was more efficiently absorbed than the hydrochloride from the GI tract. Similar results also were noted for methacycline and its hydrochloride. The differences between the bioavailability of the free base and the hydrochloride were attributed mainly to differences in solubility at gastric pH.

Since the absorption of basic drugs occurs chiefly from the intestine, these drugs should reach the intestine in a dissolved or readily soluble form. The solubility of the drugs in the stomach is of decisive importance for absorption since basic drugs have very low solubility in the alkaline environment of the intestine. Drug particles that do not dissolve in the stomach are emptied into the intestine and generally will be unabsorbed.

The pH of the gastric fluid usually ranges from 1 to 3; fasting tends to decrease the pH to 1.2–1.8 (12). In addition, the chloride ion is present in body fluids at a high level, which also is unfavorable for dissolution of the hydrochloride due to the common ion suppression of the solubility product equilibrium. These factors create conditions less favorable for hydrochloride dissolution in gastric fluid, thus affecting bioavailability. In such cases, selection of an alternative salt form or free base may improve dissolution and bioavailability.

Special precautions should be taken when drugs are used as hydrochloride salts in pharmaceutical formulation. Consequently, extensive and systematic preformulation studies of the physicochemical properties, including salt formation, of each new drug entity are necessary to determine the most suitable form for drug formulation by the pharmaceutical industry.

## REFERENCES

(1) S. M. Berge, L. D. Bighley, and D. C. Monkhouse, *J. Pharm. Sci.*, **66**, 1 (1977).

(2) S. Miyazaki, M. Nakano, and T. Arita, *Chem. Pharm. Bull.*, **23**, 1197 (1975).

(3) *Ibid.*, **23**, 2151 (1975).

(4) S. Miyazaki, H. Inoue, T. Nadai, T. Arita, and M. Nakano, *Chem. Pharm. Bull.*, **27**, 1441 (1979).

(5) S. Miyazaki, M. Oshiba, and T. Nadai, *Int. J. Pharm.*, **6**, 77 (1980).

(6) L. W. Dittert, T. Higuchi, and D. R. Reese, *J. Pharm. Sci.*, **53**, 1325 (1964).

(7) J. V. Swintosky, E. Rosen, R. E. Chamberlain, and J. R. Guarini, *J. Am. Pharm. Assoc., Sci. Ed.*, **45**, 34, 37 (1956).
(8) F. A. Long and W. F. McDevit, *Chem. Rev.*, **51**, 119 (1952).
(9) S.-L. Lin, L. Lachman, C. J. Swartz, and C. F. Huebner, *J. Pharm. Sci.*, **61**, 1418 (1972).
(10) J. B. Bogardus and R. K. Blackwood, Jr., *ibid.*, **68**, 188 (1979).
(11) *Ibid.*, **68**, 1183 (1979).
(12) M. Gibaldi, "Introduction to Biopharmaceutics," Lea & Febiger, Philadelphia, Pa., 1971, p. 13.

**ACKNOWLEDGMENTS**

The authors thank Dr. Takaichi Arita and Dr. Masahiro Nakano for helpful advice and Mrs. Hitomi Inoue for technical assistance.

# Urinary Excretion of Methenamine and Formaldehyde: Evaluation of 10 Methenamine Products in Humans

**RAMACHANDER GOLLAMUDI, ARTHUR B. STRAUGHN, and MARVIN C. MEYER ˣ**

Received June 30, 1980, from the *Departments of Pharmaceutics and Medicinal Chemistry, College of Pharmacy, University of Tennessee Center for the Health Sciences, Memphis, TN 38163.* Accepted for publication November 5, 1980.

**Abstract** □ The urinary excretion of both methenamine and formaldehyde was measured for 48 hr after the oral administration of 10 different methenamine products to 10 human subjects in a crossover study. The following dosage forms were evaluated: a tablet of methenamine base, a methenamine hippurate tablet, and eight products containing methenamine mandelate, including six enteric-coated tablets, a suspension, and a granule dosage form. The nonenteric-coated dosage forms were absorbed more rapidly, based on maximum excretion rates that occurred within 3 hr after dosing. The enteric-coated tablets, which were designed not to release methenamine until reaching the intestinal tract, exhibited maximum excretion rates that did not occur until 7–17 hr after dosing. There were no significant differences ($p > 0.05$) among products in terms of total excretion of free formaldehyde in the urine. However, large differences ($p < 0.05$) were noted among products for urinary recovery of total methenamine, with the amount of administered dose recovered ranging from 16 to 83%.

**Keyphrases** □ Methenamine—evaluation of 10 products, urinary excretion of formaldehyde □ Bioavailability—methenamine in 10 products, humans □ Urinary tract antibacterials—evaluation of 10 methenamine products, excretion of formaldehyde □ Antibacterials, urinary tract—evaluation of 10 methenamine products, excretion of formaldehyde

Methenamine (hexamethylenetetramine) is a urinary tract antibacterial agent. It is absorbed from the intestinal tract, circulates unchanged in blood, and is excreted in the urine. Under acidic conditions in the urine, it undergoes hydrolysis to formaldehyde. Approximately 10–30% of the drug also is believed to be converted to formaldehyde in the acidic environment of the stomach (1). Enteric-coated preparations are designed to withstand such premature hydrolysis by releasing drug only in the intestine. With such dosage forms, drug absorption may be delayed due to slow gastric emptying or may be incomplete due to failure of the product to release methenamine in the intestine.

A crossover study was undertaken to evaluate the relative bioavailability of 10 methenamine products. The urinary excretion of both methenamine and formaldehyde was determined in 10 human volunteers who received all 10 dosage forms.

## EXPERIMENTAL

**Methenamine Products**—The 10 methenamine products evaluated are summarized in Table I. Products 1–3 were included as reference products for comparison with the hippurate tablet and the six enteric-coated tablets. All products were supplied by the U.S. Food and Drug Administration, except Products 1 and 2, which were purchased from a local pharmacy.

**Table I—Methenamine Products Tested**

| Product[a] | Dosage Form | Administered Dose | Calculated Methenamine Content, g |
|---|---|---|---|
| 1 | Methenamine tablets (0.5 g) | 1 tablet | 0.500 |
| 2 | Methenamine mandelate suspension (50 mg/ml) | 20 ml | 0.480 |
| 3 | Methenamine mandelate granules (0.5 g/package) | 2 packages | 0.480 |
| 4 | Methenamine mandelate tablets (0.5 g)[b] | 2 tablets | 0.480 |
| 5 | Methenamine mandelate tablets (0.5 g)[b] | 2 tablets | 0.480 |
| 6 | Methenamine mandelate tablets (0.5 g)[b] | 2 tablets | 0.480 |
| 7 | Methenamine mandelate tablets (0.5 g)[b] | 2 tablets | 0.480 |
| 8 | Methenamine mandelate tablets (0.5 g)[b] | 2 tablets | 0.480 |
| 9 | Methenamine mandelate tablets (0.5 g)[b] | 2 tablets | 0.480 |
| 10 | Methenamine hippurate tablets (1.0 g) | 1 tablet | 0.439 |

[a] Manufacturer (lot number): 1, Eli Lilly (9SW09A); 2, Warner/Chilcott (8425105A); 3, Warner/Chilcott (9607055-B); 4, Warner/Chilcott (6479016A); 5, J.W.S. Delavau Co. (unknown); 6, Tablicaps (31931); 7, Standard Pharmacal (41870); 8, Vangard Laboratories (420924); 9, Heather Drug Co. (510059); and 10, Riker Laboratories (57729). [b] Enteric coated.

**Study Protocol**—Ten male volunteers[1], average age 26 years (range of 23–30 years), average weight 81 kg (range of 63.5–95.3 kg), and average height 179.9 cm (range of 170.1–190.5 cm) underwent a hematological and blood chemistry[2] analysis and a urinalysis to ensure inclusion of only healthy subjects. One subject was dropped after the 3rd week because of illness that was not related to the study. He was replaced by Subject 6, who received all 10 products in the order originally assigned to the dropped subject.

Each subject received one methenamine product at intervals of at least 1 week, except for Subject 6 who received doses at 4-day intervals to permit completion of the study at the same time as the other nine subjects. The administration sequence was based on a crossover matrix designed to minimize any residual or cumulative effects of the preceding dose (2).

Each methenamine product was given along with 200 ml of water after an overnight fast. Subsequent water intake was unrestricted but was

[1] Staff and students of the University of Tennessee Center for the Health Sciences. Written informed consent was obtained.
[2] SMA 12/60.



*0022-3549/81/0600-0596$01.00/0*
*© 1981, American Pharmaceutical Association*

(7) J. V. Swintosky, E. Rosen, R. E. Chamberlain, and J. R. Guarini, *J. Am. Pharm. Assoc., Sci. Ed.*, **45**, 34, 37 (1956).
(8) F. A. Long and W. F. McDevit, *Chem. Rev.*, **51**, 119 (1952).
(9) S.-L. Lin, L. Lachman, C. J. Swartz, and C. F. Huebner, *J. Pharm. Sci.*, **61**, 1418 (1972).
(10) J. B. Bogardus and R. K. Blackwood, Jr., *ibid.*, **68**, 188 (1979).
(11) *Ibid.*, **68**, 1183 (1979).
(12) M. Gibaldi, "Introduction to Biopharmaceutics," Lea & Febiger, Philadelphia, Pa., 1971, p. 13.

**ACKNOWLEDGMENTS**

The authors thank Dr. Takaichi Arita and Dr. Masahiro Nakano for helpful advice and Mrs. Hitomi Inoue for technical assistance.

# Urinary Excretion of Methenamine and Formaldehyde: Evaluation of 10 Methenamine Products in Humans

**RAMACHANDER GOLLAMUDI, ARTHUR B. STRAUGHN, and MARVIN C. MEYER ˣ**

Received June 30, 1980, from the *Departments of Pharmaceutics and Medicinal Chemistry, College of Pharmacy, University of Tennessee Center for the Health Sciences, Memphis, TN 38163.* Accepted for publication November 5, 1980.

**Abstract** □ The urinary excretion of both methenamine and formaldehyde was measured for 48 hr after the oral administration of 10 different methenamine products to 10 human subjects in a crossover study. The following dosage forms were evaluated: a tablet of methenamine base, a methenamine hippurate tablet, and eight products containing methenamine mandelate, including six enteric-coated tablets, a suspension, and a granule dosage form. The nonenteric-coated dosage forms were absorbed more rapidly, based on maximum excretion rates that occurred within 3 hr after dosing. The enteric-coated tablets, which were designed not to release methenamine until reaching the intestinal tract, exhibited maximum excretion rates that did not occur until 7–17 hr after dosing. There were no significant differences ($p > 0.05$) among products in terms of total excretion of free formaldehyde in the urine. However, large differences ($p < 0.05$) were noted among products for urinary recovery of total methenamine, with the amount of administered dose recovered ranging from 16 to 83%.

**Keyphrases** □ Methenamine—evaluation of 10 products, urinary excretion of formaldehyde □ Bioavailability—methenamine in 10 products, humans □ Urinary tract antibacterials—evaluation of 10 methenamine products, excretion of formaldehyde □ Antibacterials, urinary tract—evaluation of 10 methenamine products, excretion of formaldehyde

Methenamine (hexamethylenetetramine) is a urinary tract antibacterial agent. It is absorbed from the intestinal tract, circulates unchanged in blood, and is excreted in the urine. Under acidic conditions in the urine, it undergoes hydrolysis to formaldehyde. Approximately 10–30% of the drug also is believed to be converted to formaldehyde in the acidic environment of the stomach (1). Enteric-coated preparations are designed to withstand such premature hydrolysis by releasing drug only in the intestine. With such dosage forms, drug absorption may be delayed due to slow gastric emptying or may be incomplete due to failure of the product to release methenamine in the intestine.

A crossover study was undertaken to evaluate the relative bioavailability of 10 methenamine products. The urinary excretion of both methenamine and formaldehyde was determined in 10 human volunteers who received all 10 dosage forms.

## EXPERIMENTAL

**Methenamine Products**—The 10 methenamine products evaluated are summarized in Table I. Products 1–3 were included as reference products for comparison with the hippurate tablet and the six enteric-coated tablets. All products were supplied by the U.S. Food and Drug Administration, except Products 1 and 2, which were purchased from a local pharmacy.

**Table I—Methenamine Products Tested**

| Product[a] | Dosage Form | Administered Dose | Calculated Methenamine Content, g |
|---|---|---|---|
| 1 | Methenamine tablets (0.5 g) | 1 tablet | 0.500 |
| 2 | Methenamine mandelate suspension (50 mg/ml) | 20 ml | 0.480 |
| 3 | Methenamine mandelate granules (0.5 g/package) | 2 packages | 0.480 |
| 4 | Methenamine mandelate tablets (0.5 g)[b] | 2 tablets | 0.480 |
| 5 | Methenamine mandelate tablets (0.5 g)[b] | 2 tablets | 0.480 |
| 6 | Methenamine mandelate tablets (0.5 g)[b] | 2 tablets | 0.480 |
| 7 | Methenamine mandelate tablets (0.5 g)[b] | 2 tablets | 0.480 |
| 8 | Methenamine mandelate tablets (0.5 g)[b] | 2 tablets | 0.480 |
| 9 | Methenamine mandelate tablets (0.5 g)[b] | 2 tablets | 0.480 |
| 10 | Methenamine hippurate tablets (1.0 g) | 1 tablet | 0.439 |

[a] Manufacturer (lot number): 1, Eli Lilly (9SW09A); 2, Warner/Chilcott (8425105A); 3, Warner/Chilcott (9607055-B); 4, Warner/Chilcott (6479016A); 5, J.W.S. Delavau Co. (unknown); 6, Tablicaps (31931); 7, Standard Pharmacal (41870); 8, Vangard Laboratories (420924); 9, Heather Drug Co. (510059); and 10, Riker Laboratories (57729). [b] Enteric coated.

**Study Protocol**—Ten male volunteers[1], average age 26 years (range of 23–30 years), average weight 81 kg (range of 63.5–95.3 kg), and average height 179.9 cm (range of 170.1–190.5 cm) underwent a hematological and blood chemistry[2] analysis and a urinalysis to ensure inclusion of only healthy subjects. One subject was dropped after the 3rd week because of illness that was not related to the study. He was replaced by Subject 6, who received all 10 products in the order originally assigned to the dropped subject.

Each subject received one methenamine product at intervals of at least 1 week, except for Subject 6 who received doses at 4-day intervals to permit completion of the study at the same time as the other nine subjects. The administration sequence was based on a crossover matrix designed to minimize any residual or cumulative effects of the preceding dose (2).

Each methenamine product was given along with 200 ml of water after an overnight fast. Subsequent water intake was unrestricted but was

[1] Staff and students of the University of Tennessee Center for the Health Sciences. Written informed consent was obtained.
[2] SMA 12/60.



*0022-3549/81/0600-0596$01.00/0*
*© 1981, American Pharmaceutical Association*

Table II—Mean Free Formaldehyde Urine Concentration [a] (Micrograms per Milliliter) at Various Sampling Times

| Product | Urine Collection Time, hr | | | | | | | | |
|---|---|---|---|---|---|---|---|---|---|
| | 1 | 2 | 4 | 6 | 8 | 12 | 24 | 36 | 48 |
| 1 | 19.9 | 22.5 | 35.0 | 32.7 | 39.5 | 39.7 | 23.4 | 9.96 | 9.84 |
| | (116) | (124) | (112) | (83.4) | (75.1) | (82.6) | (72.2) | (54.7) | (116) |
| 2 | 12.7 | 25.6 | 25.6 | 34.4 | 34.5 | 39.7 | 25.8 | 9.40 | 3.18 |
| | (133) | (110) | (110) | (106) | (109) | (99.9) | (140) | (112) | (140) |
| 3 | 28.2 | 21.3 | 11.6 | 23.3 | 25.3 | 55.8 | 21.7 | 28.5 | 4.54 |
| | (81.8) | (104) | (112) | (104) | (107) | (163) | (72.7) | (273) | (116) |
| 4 | 3.48 | 1.06 | 9.55 | 23.9 | 37.4 | 28.6 | 37.3 | 6.29 | 4.97 |
| | (157) | (216) | (114) | (103) | (99.4) | (59.8) | (44.5) | (103) | (117) |
| 5 | 8.82 | 7.31 | 1.80 | 10.3 | 10.7 | 42.7 | 18.5 | 28.5 | 11.5 |
| | (267) | (186) | (115) | (228) | (140) | (180) | (199) | (160) | (118) |
| 6 | 6.42 | 5.28 | 16.0 | 40.6 | 44.3 | 42.4 | 32.9 | 10.6 | 8.16 |
| | (180) | (104) | (67.3) | (78.7) | (124) | (109) | (73.1) | (72.6) | (47.9) |
| 7 | 1.90 | 1.46 | 3.06 | 19.5 | 19.9 | 34.2 | 26.8 | 21.8 | 7.10 |
| | (119) | (181) | (138) | (112) | (111) | (93.4) | (112) | (204) | (110) |
| 8 | 1.91 | 2.22 | 13.8 | 38.5 | 38.9 | 27.3 | 42.4 | 16.3 | 5.92 |
| | (134) | (115) | (76.6) | (112) | (90.6) | (64.2) | (85.2) | (59.9) | (137) |
| 9 | 2.91 | 3.17 | 16.4 | 40.4 | 23.2 | 29.1 | 36.9 | 6.59 | 6.40 |
| | (156) | (158) | (94.6) | (145) | (71.4) | (116) | (78.4) | (121) | (96.5) |
| 10 | 17.3 | 26.3 | 23.7 | 16.6 | 36.7 | 44.2 | 12.2 | 8.67 | 7.37 |
| | (113) | (113) | (136) | (150) | (126) | (77.9) | (92.9) | (94.3) | (62.3) |

[a] Mean values of 10 subjects with percent relative standard deviation in parentheses. See Table I for product number identification.

maintained at a sufficient level to provide for adequate urine output. No food was permitted until 4 hr after drug administration.

Urine samples were obtained at 0, 1, 2, 3, 4, 6, 8, 12, 24, and 48 hr. The subjects were instructed to provide complete urine collections at each voiding. Immediately upon voiding, the urine volume and pH[3] were measured. A urine aliquot was diluted 15 times with water and stored at −18° until analysis, which was performed within 7 days. Samples voided at other times were collected similarly and stored. At the time of analysis, samples voided between sampling times were combined with the sample obtained at the next required sampling time. The samples were pooled using aliquot volumes proportional to the individual volumes of voided urine.

**Urine Analysis**—Urine formaldehyde and methenamine concentrations were determined in duplicate using a spectrophotometric method (3).

**Statistical Analysis**—Urine free formaldehyde concentrations, as well as free formaldehyde and total methenamine excretion rates and the cumulative amount and percent excreted, were subjected to an analysis of variance to determine the level of significance for differences among products, subjects, and weeks. The data were analyzed using a logarithmic transformation because of significant nonadditivity in the untransformed data. Where significant differences were found ($p < 0.05$), the Newman–Keuls *a posteriori* test was applied to identify where these differences occurred.

## RESULTS AND DISCUSSION

**Free Formaldehyde Concentrations**—The mean urine free formaldehyde concentrations at each sampling are presented in Table II. The maximum mean formaldehyde concentrations ranged from 34.2 (Product 7) to 55.8 (Product 3) μg/ml at 12 hr. Although this difference was not significant ($p > 0.05$), significant differences ($p < 0.05$) were evident at 1, 2, 4, and 24 hr. The Newman–Keuls *a posteriori* test indicated the enteric-coated formulations (Products 4–9) generally resulted in lower formaldehyde concentrations than the other products during the first 4 hr. This finding is consistent with the fact that an enteric-coated dosage form must reach the intestinal tract before drug can be released. Maximum mean free formaldehyde concentrations were attained between 6 and 12 hr with all products, except Product 8, which had a maximum mean concentration at 24 hr.

The minimum inhibitory concentration for formaldehyde in urine was reported to range from 13 (4) to 18 μg/ml (5). Mean free formaldehyde levels in this range were attained within 1–2 hr from the nonenteric-coated Products 1–3 and 10; the enteric-coated products required 4–12 hr to provide free formaldehyde concentrations in this range.

The therapeutic efficacy of a methenamine product is thought to be related to the formaldehyde concentration in the urine. Formaldehyde formation is governed mainly by the rate and extent of intestinal absorption and renal excretion of methenamine and by the volume and pH of the urine. The mean free formaldehyde concentrations exhibited high relative standard deviations, partially because fluid intake and urine pH were not controlled in these subjects. In general, the urine pH ranged from 5.5 to 6.8, and the fluctuations within and among individuals obscured any correlations between urine pH and the formaldehyde concentrations obtained with the different products.

The mean cumulative 48-hr excretion of formaldehyde from each dosage form, expressed as methenamine equivalents, ranged from 26.8 (Product 10) to 37.7 (Product 6) mg. This 29% difference among products was not significant ($p > 0.05$). Since the total amount of methenamine administered was not identical in all 10 products, the cumulative amount of formaldehyde excreted at each sampling also was calculated as a percent of the total methenamine dose. The cumulative percent of formaldehyde excreted at 48 hr (Fig. 1) ranged from 5.5 (Product 2) to 8.7% (Product 8), but this 37% difference among products also was not significant ($p > 0.05$).

**Cumulative Excretion of Total Methenamine**—Although the measurement of free formaldehyde provided useful information, the large variations in these levels precluded a meaningful evaluation of dosage form bioavailability. Thus, the excretion of total methenamine equiva-

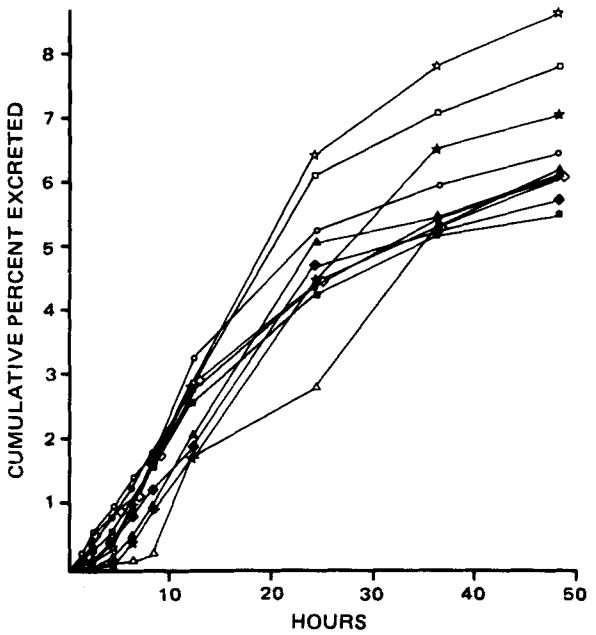


**Figure 1**—*Cumulative excretion of free formaldehyde, calculated as methenamine and expressed as a percent of the total methenamine dose. Each data point represents the mean of 10 subjects. Key: ●, Product 1; ■, Product 2; ○, Product 3; ▲, Product 4; △, Product 5; □, Product 6; ☆, Product 7; ★, Product 8; ◆, Product 9; and ◇, Product 10.*

[3] Hydrion test paper, pH range 5.5–8.0, Micro-Essential Laboratory, Brooklyn, N.Y.

**Table III—Product Ranking for Total Methenamine Excreted [a]**

| Parameter | Product Ranking (Lowest to Highest) [b] | | | | | | | | | |
|---|---|---|---|---|---|---|---|---|---|---|
| Cumulative percent of total methenamine excreted at: | | | | | | | | | | |
| 1 hr | 7 | 5 | 4 | 8 | 6 | 9 | 2 | 10 | 1 | 3 |
| 2 hr | 7 | 5 | 4 | 6 | 8 | 9 | 2 | 3 | 10 | 1 |
| 4 hr | 5 | 7 | 4 | 8 | 6 | 9 | 2 | 3 | 1 | 10 |
| 6 hr | 5 | 7 | 4 | 8 | 6 | 9 | 2 | 3 | 1 | 10 |
| 8 hr | 5 | 7 | 4 | 8 | 6 | 9 | 2 | 3 | 10 | 1 |
| 12 hr | 5 | 7 | 4 | 8 | 6 | 9 | 3 | 2 | 1 | 10 |
| 24 hr | 5 | 7 | 4 | 8 | 6 | 3 | 2 | 9 | 1 | 10 |
| 36 hr | 5 | 7 | 4 | 8 | 3 | 6 | 2 | 9 | 10 | 1 |
| 48 hr | 5 | 7 | 4 | 8 | 3 | 6 | 2 | 9 | 10 | 1 |
| Maximum excretion rate, mg/hr | 5 | 7 | 4 | 8 | 6 | 9 | 2 | 3 | 10 | 1 |
| Maximum excretion rate, % dose/hr | 5 | 7 | 4 | 8 | 6 | 9 | 2 | 3 | 1 | 10 |
| Time of maximum excretion rate, hr | 1 | 3 | 10 | 2 | 9 | 8 | 6 | 4 | 7 | 5 |

[a] All data were subjected to a ln $(X + 0.1)$ transformation because of a significant nonadditivity in the untransformed data. [b] Products ranked on the basis of the Newman–Keuls *a posteriori* test. Products underlined by a common line did not differ significantly ($p > 0.05$). See Table I for product number identification.

**Table IV—Mean [a] Maximum Excretion Rates and Time of Maximum Excretion Rate for Total Methenamine**

| Product | Maximum Rate of Total Methenamine, mg/hr | Maximum Rate of Total Methenamine, % of dose/hr | Time of Maximum Rate of Total Methenamine, hr |
|---|---|---|---|
| 1 | 57.6 (18.8) | 11.5 (18.8) | 1.59 (32.0) |
| 2 | 43.7 (22.3) | 9.12 (22.3) | 2.90 (62.1) |
| 3 | 43.4 (30.5) | 9.89 (30.5) | 1.90 (46.1) |
| 4 | 28.9 (35.7) | 6.05 (35.7) | 8.00 (20.8) |
| 5 | 4.78 (151.1) | 1.00 (150.9) | 17.1 (72.6) |
| 6 | 32.6 (31.2) | 6.81 (31.2) | 7.40 (25.6) |
| 7 | 13.4 (20.8) | 2.81 (20.7) | 12.6 (50.5) |
| 8 | 31.1 (29.0) | 6.50 (29.0) | 7.22 (26.6) |
| 9 | 37.8 (15.7) | 7.89 (15.7) | 6.81 (15.1) |
| 10 | 51.3 (13.8) | 11.7 (13.7) | 2.30 (41.3) |

[a] Mean values of 10 subjects with percent relative standard deviation in parentheses. See Table I for product number identification.

lents also was determined. The sum of the amount of methenamine excreted as free formaldehyde and as free methenamine was expressed as milligrams of total methenamine. Statistical analysis of the mean cumulative amounts of total methenamine excreted at various sampling times showed highly significant differences ($p < 0.001$) among products at all sampling times.

One hour after administration of Products 1, 3, and 10, the mean cumulative amount of total methenamine excreted was 42.2, 39.8, and 31.1 mg, respectively. These recoveries were significantly higher than those for the other products. The 17.4 mg excreted at 1 hr with Product 2 was significantly higher than the amount for the enteric-coated tablets. The lowest levels at 1 hr were found with Product 5 (0.1 mg). At 2 and 4 hr, the excretion of total methenamine was significantly higher ($p < 0.05$) for the nonenteric-coated products than for the other dosage forms. Among the enteric-coated preparations, Products 5 and 7 gave the lowest total methenamine recoveries. At subsequent collections, Product 5 resulted in cumulative total methenamine levels that were significantly lower than those for all other products. Product 7 gave significantly higher cumulative total methenamine levels than Product 5 at 4, 6, 8, and 12 hr, but the levels with this product were lower than those attained with any other product.

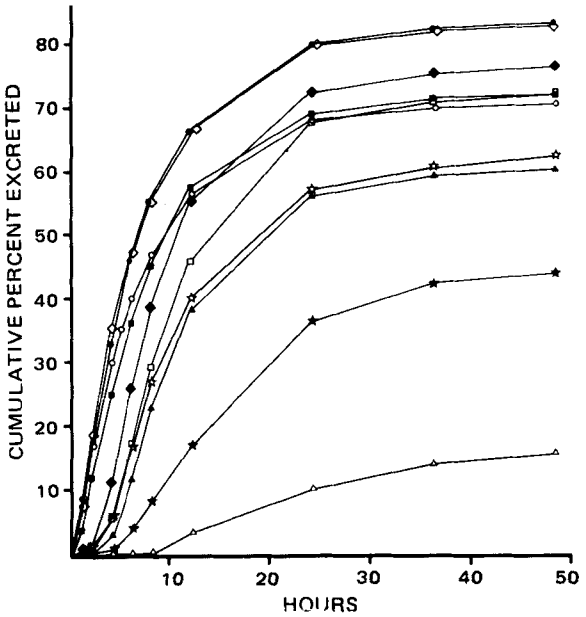


**Figure 2**—*Cumulative excretion of total methenamine, expressed as a percent of the administered dose. Each data point represents the mean of 10 subjects. Key:* ●, *Product 1;* ■, *Product 2;* ○, *Product 3;* ▲, *Product 4;* △, *Product 5;* □, *Product 6;* ☆, *Product 7;* ★, *Product 8;* ◆, *Product 9; and* ◇, *Product 10.*

The mean cumulative excretion of total methenamine, expressed as percent of administered dose at various collection times, is illustrated in Fig. 2. The results of the statistical evaluation are summarized in Table III. The percent of total methenamine excreted at 1 hr ranged from 0.03% for Products 5 and 7 to 8.4% for Product 1. At this sampling time, Products 1, 3, and 10 gave significantly higher total methenamine recoveries than did the other products. The 2-hr total methenamine values ranged from 0.06% for Product 7 to 18.6% for Product 1, with the values for Products 1, 3, and 10 being significantly higher than those for the other products.

The lowest cumulative total methenamine percentages at subsequent sampling times were with Product 5. Although the total methenamine excretion after Product 7 was significantly higher than after Product 5, it was lower than the values obtained with the other products at 4, 6, 8, 12, and 24 hr. The lowest cumulative percentage of total methenamine excreted at 48 hr was with Products 5 (16.2%) and 7 (44.2%). The total recoveries of all other products exceeded 60% at 48 hr.

**Excretion Rate of Total Methenamine**—The mean maximum excretion rates and times of the maximum excretion rate for total methenamine are summarized in Table IV. Statistically significant differences are indicated in Table III. The maximum excretion rate of total methenamine ranged from 4.8 mg/hr with Product 5 to 57.6 mg/hr with Product 1. The rates observed with Product 1 were significantly higher than those found with Products 4, 5, and 7. Product 5 exhibited significantly lower excretion rates compared to all others. The maximum excretion rate for Product 7 was higher than for Product 5 but was significantly lower than the rates for all other products.

In terms of percent of administered dose, the maximum excretion rate was highest for Product 10 (11.7%/hr) and lowest for Product 5 (1.0%/hr). The latter value was significantly lower than that observed after Product 7 (2.8%/hr). The times of the maximum excretion rate ($T_{max}$) were 1.6, 1.9, 2.3, and 2.9 hr for the nonenteric-coated Products 1, 3, 10, and 2, respectively. These times were significantly lower than those found for the other products. Products 5 and 7 yielded significantly longer $T_{max}$ values of 17.1 and 12.6 hr, respectively.

**Subject and Week Effects**—Each urinary excretion parameter also was statistically analyzed to determine the significance of differences observed among subjects and administration sequences (weeks). Since Subject 6 began the study several weeks after the other nine subjects and took the medication at 4-day intervals, the analysis of weekly differences actually related to differences that could have arisen because a dose was the first, second, third, *etc.*, dose administered.

Since there were no significant weekly differences, it may be concluded that the bioavailability of a particular dose of methenamine was not influenced by the previous administration of other dosage forms of the drug. Results of the analysis of the blank (zero time) urine samples also were monitored each week to determine if they showed any progressive increase, which would have occurred if the drug had been accumulating. No such trend was found in the blank readings. Furthermore, the statistical analysis did not indicate any significant differences among subjects in the excretion of either free formaldehyde or total methenamine.

## CONCLUSIONS

Methenamine compressed tablets, methenamine mandelate granules, and methenamine hippurate tablets showed the highest methenamine urinary recovery and were considered bioequivalent. The suspension dosage form exhibited adequate bioavailability but was less well absorbed than the other dosage forms. In general, the enteric-coated products exhibited delayed urinary excretion of methenamine, but Products 4, 6, 8, and 9 did not differ significantly from the nonenteric-coated products in most measurements. Two enteric-coated products (Products 5 and 7) were significantly less bioavailable than all other products tested. None of the 10 products differed significantly ($p > 0.05$) in urinary formaldehyde concentrations. However, the large intersubject variability precluded an accurate assessment of dosage form bioavailability using only free formaldehyde determinations.

## REFERENCES

(1) "The Pharmacological Basis of Therapeutics," L. S. Goodman and A. Gilman, Eds., Macmillan, New York, N.Y., 1970, p. 1040.

(2) E. J. Williams, *Aust. J. Sci. Res. A*, **2**, 14 (1949).

(3) R. Gollamudi, M. C. Meyer, and A. B. Straughn, *Biopharm. Drug Disp.*, **1**, 27 (1979).

(4) J. M. T. Hamilton-Miller, W. Brumfitt, and E. H. Brooker, *Invest. Urol.*, **14**, 287 (1976).

(5) H. Miller and E. Phillips, *ibid.*, **8**, 21 (1970).

## ACKNOWLEDGMENTS

Supported in part by contracts from the Tennessee Department of Public Health and U.S. Food and Drug Administration (FDA 223-74-3097).

The authors express their appreciation to Ms Irma Miller, Ms Andrea Smith, and Ms Cathy Wibking for skillful technical assistance and to Mrs. Ann McEachran for assistance in the statistical analysis.

# Effect of Antacid on Bioavailability of Theophylline from Rapid and Timed-Release Drug Products

**LEON SHARGEL ˣ, JUDY A. STEVENS, JOB E. FUCHS, and ANDREW B. C. YU ***

Received September 10, 1980, from the *College of Pharmacy and Allied Health Professions, Northeastern University, Boston, MA 02115.* Accepted for publication November 7, 1980. *Present address: Sterling-Winthrop Research Institute, Rensselaer, NY 12144.

**Abstract** □ Magnesium aluminum hydroxide suspension (an antacid) was given concurrently with either theophylline anhydrous tablets or theophylline anhydrous timed-release capsules to 13 volunteers using a four-way crossover design. Serum theophylline was measured by reversed-phase high-pressure liquid chromatography. The serum level–time curves were individually fitted to an oral absorption one-compartment open model. The pharmacokinetic parameters (mean ± *SD*) $K_A$, $K$, $AUC$, and $F/V$ for theophylline from the rapid release theophylline anhydrous tablets were 2.1 ± 1.3 $hr^{-1}$, 0.15 ± 0.06 $hr^{-1}$, 89.2 ± 30 μg hr/ml, and 0.0023 ± 0.002 kg/ml, respectively; from the anhydrous timed-release capsules, they were 0.27 ± 0.08 $hr^{-1}$, 0.20 ± 0.07 $hr^{-1}$, 79.0 ± 27 μg hr/ml, and 0.0030 ± 0.0007 kg/ml, respectively. The concurrent administration of 15 ml of antacid (magnesium aluminum hydroxide suspension) with the theophylline products did not significantly affect any of these pharmacokinetic parameters. The extent of theophylline bioavailability from all drug products was consistent and similar as shown by the $F/V$ and $AUC$ values.

**Keyphrases** □ Theophylline—effect of antacid on bioavailability, tablets and timed-release capsules □ Antacids—effects on theophylline bioavailability, tablets and timed-release capsules □ Pharmacokinetics—effect of antacid on theophylline, tablets and timed-release capsules □ Dosage forms—tablets and timed-release capsules, effect of antacid on theophylline bioavailability

Theophylline is used extensively in the treatment of various respiratory diseases (1–4). When taken in the recommended dosage, it relieves or prevents symptoms associated with asthma, bronchitis, and emphysema. The amount of relief produced is directly related to the serum drug concentration. Side effects (nausea, vomiting, headache, and restlessness) are usually associated with high blood theophylline levels (>20 μg/ml), although some individuals may experience side effects at lower levels (1–4).

Magnesium aluminum hydroxide suspension is a commonly used antacid for the symptomatic relief of hyperacidity, gastritis, and heartburn. However, antacids affect the bioavailability of various drugs (5–8). The object of this investigation was to determine the effect of concurrent antacid therapy on the rate and extent of theophylline absorption from theophylline anhydrous tablets and theophylline anhydrous timed-release capsules.

## EXPERIMENTAL

**Reagents and Chemicals**—All reagents and chemicals including theophylline anhydrous[1], sodium acetate[1], 7-(β-hydroxypropyl)theophylline[1], β-hydroxyethyltheophylline[1], 8-chlorotheophylline[1], theo-

[1] Sigma Chemical Co., St. Louis, Mo.

0022-3549/81/0600-0599$01.00/0
© 1981, American Pharmaceutical Association

In terms of percent of administered dose, the maximum excretion rate was highest for Product 10 (11.7%/hr) and lowest for Product 5 (1.0%/hr). The latter value was significantly lower than that observed after Product 7 (2.8%/hr). The times of the maximum excretion rate ($T_{max}$) were 1.6, 1.9, 2.3, and 2.9 hr for the nonenteric-coated Products 1, 3, 10, and 2, respectively. These times were significantly lower than those found for the other products. Products 5 and 7 yielded significantly longer $T_{max}$ values of 17.1 and 12.6 hr, respectively.

**Subject and Week Effects**—Each urinary excretion parameter also was statistically analyzed to determine the significance of differences observed among subjects and administration sequences (weeks). Since Subject 6 began the study several weeks after the other nine subjects and took the medication at 4-day intervals, the analysis of weekly differences actually related to differences that could have arisen because a dose was the first, second, third, *etc.*, dose administered.

Since there were no significant weekly differences, it may be concluded that the bioavailability of a particular dose of methenamine was not influenced by the previous administration of other dosage forms of the drug. Results of the analysis of the blank (zero time) urine samples also were monitored each week to determine if they showed any progressive increase, which would have occurred if the drug had been accumulating. No such trend was found in the blank readings. Furthermore, the statistical analysis did not indicate any significant differences among subjects in the excretion of either free formaldehyde or total methenamine.

## CONCLUSIONS

Methenamine compressed tablets, methenamine mandelate granules, and methenamine hippurate tablets showed the highest methenamine urinary recovery and were considered bioequivalent. The suspension dosage form exhibited adequate bioavailability but was less well absorbed than the other dosage forms. In general, the enteric-coated products exhibited delayed urinary excretion of methenamine, but Products 4, 6, 8, and 9 did not differ significantly from the nonenteric-coated products in most measurements. Two enteric-coated products (Products 5 and 7) were significantly less bioavailable than all other products tested. None of the 10 products differed significantly ($p > 0.05$) in urinary formaldehyde concentrations. However, the large intersubject variability precluded an accurate assessment of dosage form bioavailability using only free formaldehyde determinations.

## REFERENCES

(1) "The Pharmacological Basis of Therapeutics," L. S. Goodman and A. Gilman, Eds., Macmillan, New York, N.Y., 1970, p. 1040.

(2) E. J. Williams, *Aust. J. Sci. Res. A*, **2**, 14 (1949).

(3) R. Gollamudi, M. C. Meyer, and A. B. Straughn, *Biopharm. Drug Disp.*, **1**, 27 (1979).

(4) J. M. T. Hamilton-Miller, W. Brumfitt, and E. H. Brooker, *Invest. Urol.*, **14**, 287 (1976).

(5) H. Miller and E. Phillips, *ibid.*, **8**, 21 (1970).

## ACKNOWLEDGMENTS

Supported in part by contracts from the Tennessee Department of Public Health and U.S. Food and Drug Administration (FDA 223-74-3097).

The authors express their appreciation to Ms Irma Miller, Ms Andrea Smith, and Ms Cathy Wibking for skillful technical assistance and to Mrs. Ann McEachran for assistance in the statistical analysis.

# Effect of Antacid on Bioavailability of Theophylline from Rapid and Timed-Release Drug Products

**LEON SHARGEL ˣ, JUDY A. STEVENS, JOB E. FUCHS, and ANDREW B. C. YU ***

Received September 10, 1980, from the *College of Pharmacy and Allied Health Professions, Northeastern University, Boston, MA 02115.* Accepted for publication November 7, 1980. *Present address: Sterling-Winthrop Research Institute, Rensselaer, NY 12144.

**Abstract** □ Magnesium aluminum hydroxide suspension (an antacid) was given concurrently with either theophylline anhydrous tablets or theophylline anhydrous timed-release capsules to 13 volunteers using a four-way crossover design. Serum theophylline was measured by reversed-phase high-pressure liquid chromatography. The serum level–time curves were individually fitted to an oral absorption one-compartment open model. The pharmacokinetic parameters (mean ± *SD*) $K_A$, $K$, $AUC$, and $F/V$ for theophylline from the rapid release theophylline anhydrous tablets were 2.1 ± 1.3 $hr^{-1}$, 0.15 ± 0.06 $hr^{-1}$, 89.2 ± 30 μg hr/ml, and 0.0023 ± 0.002 kg/ml, respectively; from the anhydrous timed-release capsules, they were 0.27 ± 0.08 $hr^{-1}$, 0.20 ± 0.07 $hr^{-1}$, 79.0 ± 27 μg hr/ml, and 0.0030 ± 0.0007 kg/ml, respectively. The concurrent administration of 15 ml of antacid (magnesium aluminum hydroxide suspension) with the theophylline products did not significantly affect any of these pharmacokinetic parameters. The extent of theophylline bioavailability from all drug products was consistent and similar as shown by the $F/V$ and $AUC$ values.

**Keyphrases** □ Theophylline—effect of antacid on bioavailability, tablets and timed-release capsules □ Antacids—effects on theophylline bioavailability, tablets and timed-release capsules □ Pharmacokinetics—effect of antacid on theophylline, tablets and timed-release capsules □ Dosage forms—tablets and timed-release capsules, effect of antacid on theophylline bioavailability

Theophylline is used extensively in the treatment of various respiratory diseases (1–4). When taken in the recommended dosage, it relieves or prevents symptoms associated with asthma, bronchitis, and emphysema. The amount of relief produced is directly related to the serum drug concentration. Side effects (nausea, vomiting, headache, and restlessness) are usually associated with high blood theophylline levels (>20 μg/ml), although some individuals may experience side effects at lower levels (1–4).

Magnesium aluminum hydroxide suspension is a commonly used antacid for the symptomatic relief of hyperacidity, gastritis, and heartburn. However, antacids affect the bioavailability of various drugs (5–8). The object of this investigation was to determine the effect of concurrent antacid therapy on the rate and extent of theophylline absorption from theophylline anhydrous tablets and theophylline anhydrous timed-release capsules.

## EXPERIMENTAL

**Reagents and Chemicals**—All reagents and chemicals including theophylline anhydrous[1], sodium acetate[1], 7-(β-hydroxypropyl)theophylline[1], β-hydroxyethyltheophylline[1], 8-chlorotheophylline[1], theo-

[1] Sigma Chemical Co., St. Louis, Mo.

0022-3549/81/0600-0599$01.00/0
© 1981, American Pharmaceutical Association

**Table I—Patient Data and Doses of Theophylline for Each Drug Product**

| Volunteer | Age, years | Height, m | Weight, kg | Product A, mg | Product A, mg/kg | Product B, mg | Product B, mg/kg | Product C, mg | Product C, mg/kg | Product D, mg | Product D, mg/kg |
|---|---|---|---|---|---|---|---|---|---|---|---|
| 1 | 18 | 1.72 | 83.4 | 400 | 4.796 | 435 | 5.216 | 400 | 4.796 | 435 | 5.216 |
| 2 | 18 | 1.82 | 99.8 | 500 | 5.010 | 500 | 5.010 | 500 | 5.010 | 500 | 5.010 |
| 3[a] | 18 | 1.82 | 71.8 | — | — | 375 | 5.223 | 350 | 4.875 | 375 | 5.223 |
| 4 | 19 | 1.80 | 71.1 | 350 | 4.923 | 375 | 5.274 | 350 | 4.923 | 375 | 5.274 |
| 5 | 18 | 1.80 | 64.1 | 300 | 4.680 | 310 | 4.836 | 300 | 4.680 | 310 | 4.836 |
| 6 | 23 | 1.82 | 91.4 | 450 | 4.923 | 435 | 4.759 | 450 | 4.923 | 435 | 4.759 |
| 7 | 25 | 1.78 | 74.5 | 350 | 4.698 | 375 | 4.034 | 350 | 4.698 | 375 | 5.034 |
| 8 | 26 | 1.78 | 81.8 | 400 | 4.890 | 435 | 5.318 | 400 | 4.890 | 435 | 4.318 |
| 9 | 24 | 1.78 | 79.5 | 400 | 5.031 | 375 | 4.717 | 400 | 5.031 | 375 | 4.717 |
| 10 | 22 | 1.87 | 82.7 | 400 | 4.837 | 435 | 5.260 | 400 | 4.837 | 435 | 5.260 |
| 11 | 19 | 1.87 | 93.2 | 450 | 4.828 | 435 | 4.667 | 450 | 4.828 | 435 | 4.667 |
| 12 | 23 | 1.70 | 60.9 | 300 | 4.926 | 310 | 5.090 | 300 | 4.296 | 310 | 5.090 |
| 13[b] | 18 | 1.72 | 65.7 | 350 | 5.327 | — | — | — | — | — | — |
| 14 | 19 | 1.75 | 62.7 | 300 | 4.785 | 310 | 4.944 | 300 | 4.785 | 310 | 4.944 |
| Mean | 20.7 | | 77.3 | | 4.896 | | 5.027 | | 4.867 | | 5.027 |
| *SD* | 3.0 | | 12.1 | | 0.167 | | 0.227 | | 0.109 | | 0.227 |

[a] Volunteer withdrew from study after receiving Treatments B–D. [b] Volunteer withdrew from study after receiving Treatment A only.

bromine[2], caffeine[3], and acetonitrile[4] were of USP, NF, or analytical grade and were used as received. Normal serum samples[5] were obtained from healthy students. All other reagents and solvents were purchased from commercial sources and used without further purification.

**Design**—Fourteen male volunteers (18–26 years old), weighing an average of 77 kg, were judged healthy by physical examination. The volunteers refrained from all other medications, smoking, and theophylline-containing beverages such as coffee, tea, chocolate, and cola prior to and during the study. Each volunteer fasted overnight prior to and for 4 hr after receiving the theophylline formulation.

The following drug products were given to each volunteer in a four-way crossover Latin-square design with a 1-week interval between treatments: Product A, theophylline anhydrous tablets[6]; Product B, theophylline anhydrous timed-release capsules[7]; Product C, theophylline anhydrous tablets[6] with 15 ml of magnesium aluminum hydroxide suspension[8]; and Product D, theophylline anhydrous timed-release capsules[7] with 15 ml of magnesium aluminum hydroxide suspension[8].

All doses of theophylline were based on 5 mg/kg, and each drug product was given with 240 ml of water. Both serum and urine samples were obtained at zero time and periodically after medication. Serum samples were assayed for theophylline, and urine samples were tested for pH.

**Theophylline Assay**—Serum samples were assayed for theophylline concentrations by reversed-phase high-pressure liquid chromatography (HPLC) (9) with $\beta$-hydroxyethyltheophylline as the internal standard.

The high-pressure liquid chromatograph[9] was fitted with a UV (254 nm) absorbance detector and strip-chart recorder[10]. Samples were chromatographed on a reversed-phase HPLC column, 30 cm × 4 mm i.d., packed with 10-$\mu$m octadecyltrichlorosilane-coated silica beads[11]. The mobile phase was prepared by mixing 930 ml of a 10-mmole sodium acetate buffer (pH 4.0) with 70 ml of acetonitrile. The mobile phase was degassed and filtered[12] prior to use.

All determinations were performed at ambient temperature with a solvent flow rate of 2 ml/min. The detector sensitivity scale was 0.005, and the chart speed was 0.25 cm/min. Pressure was maintained at ~2200 psi. All sample injections were 10 $\mu$l.

A standard theophylline concentration curve was prepared daily by processing pooled serum samples spiked with known concentrations of theophylline concurrently with the unknown serum samples. A statistical least-squares fitting procedure was employed for calculating the standard curve by comparing the peak height ratio of theophylline to $\beta$-hydroxyethyltheophylline to the spiked serum theophylline concentrations. Assay sensitivity was ~0.5 $\mu$g/ml, which is adequate for measuring the expected serum theophylline concentrations. This HPLC procedure was validated using control human serum samples containing known concentrations of theophylline, which were unknown to the operator ($r$ 0.972).

**Table II—Effect of Antacid on Theophylline Pharmacokinetics from Rapid and Timed-Release Drug Products**

| Parameter | Product A | Product B | Product C | Product D |
|---|---|---|---|---|
| $K_A$, hr$^{-1}$ | 2.10[a] (1.31) | 0.27[b] (0.08) | 2.41 (1.77) | 0.24[b] (0.06) |
| $K$, hr$^{-1}$ | 0.15 (0.06) | 0.20 (0.07) | 0.16 (0.07) | 0.17 (0.06) |
| $F/V$, kg/ml | 0.0023 (0.0003) | 0.0030 (0.0007) | 0.0025 (0.0004) | 0.0024 (0.0005) |
| $AUC$, $\mu$g hr/ml | 89.2 (30.4) | 79.0 (27.4) | 87.3 (28.5) | 76.2 (32.5) |
| $t_{max}$[c], hr | 1.66 (0.67) | 4.45[b] (0.92) | 1.73 (0.91) | 5.04[b,d] (0.89) |
| $C_{max}$[c], $\mu$g/ml | 9.07 (1.32) | 6.18[b] (1.37) | 9.04 (1.53) | 5.24[b,d] (1.44) |

[a] Each value represents the mean for 13 volunteers with the standard deviation in parentheses. [b] $p < 0.01$ compared to Product A. [c] Obtained by calculation. [d] $p < 0.01$ compared to Product B.

## RESULTS

The patient data and doses of theophylline appear in Table I. The serum theophylline concentration–time curves obtained from each patient were fitted to an oral absorption one-compartment open model using a least-squares regression analysis program[13]. Preliminary parameter

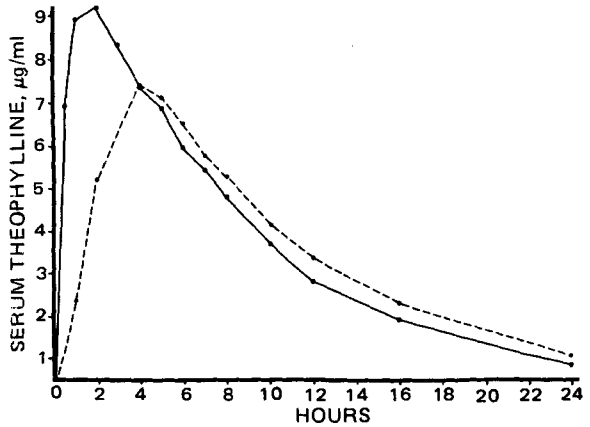


**Figure 1**—*Comparison of mean theophylline level–time curves in volunteers after receiving either Product A, theophylline anhydrous tablets (●—), or Product B, theophylline anhydrous time-release capsules (○- - -); n = 13.*

[2] Merck & Co., Rahway, N.J.
[3] Mallinckrodt, St. Louis, Mo.
[4] J. T. Baker Chemical Co., Phillipsburg, N.J.
[5] Lane Health Center, Northeastern University, Boston, Mass.
[6] Slo-Phyllin, Dooner Laboratories, Haverhill, Mass.
[7] Slo-Phyllin Gyrocaps, Dooner Laboratories, Haverhill, Mass.
[8] Maalox, William H. Rorer, Fort Washington, Pa.
[9] ALC GPC model 204, Waters Associates, Milford, Mass.
[10] Fisher Recordall Series 500, Fisher Scientific Co., Fair Lawn, N.J.
[11] $\mu$Bondapak $C_{18}$, Waters Associates, Milford, Mass.
[12] Millipore filtering system (type GS), Millipore Corp., Bedford, Mass.
[13] C. M. Metzler, The Upjohn Co., Kalamazoo, MI 49001, personal communication.

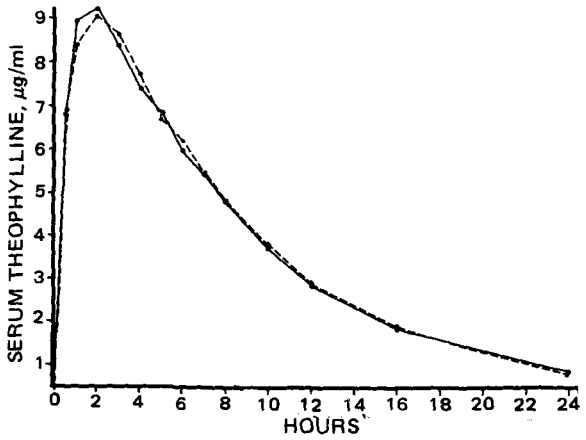


**Figure 2**—*Comparison of mean theophylline level–time curves in volunteers after receiving either Product A, theophylline anhydrous tablets (●—), or Product C, theophylline anhydrous tablets plus 15 ml of antacid (○- - -); n = 13.*

estimates were made using the Wagner–Nelson method (10). The one-compartment oral absorption model (Scheme I) is described by:

$$\xrightarrow{K_A} \boxed{V, C} \xrightarrow{K}$$

*Scheme I*

$$C = \frac{FDK_A}{(K_A - K)V}(e^{-Kt} - e^{-K_{at}}) \qquad \text{(Eq. 1)}$$

where $K_A$ is the first-order absorption rate constant, $K$ is the first-order elimination rate constant, $D$ is the dose, $C$ is the serum drug concentration, $V$ is the volume of distribution, $t$ is the time after drug adminstration, and $F$ is the fraction of drug absorbed.

The time for peak serum theophylline level ($t_{max}$) for each subject was calculated from:

$$t_{max} = \frac{\ln(K_A/K)}{K_A - K} \qquad \text{(Eq. 2)}$$

and the maximum serum theophylline level ($C_{max}$) was calculated by substitution of $t_{max}$ for $t$ in Eq. 1. Computer estimation of theophylline pharmacokinetic parameters for each patient and each drug product was obtained. Coefficients of correlation for the theophylline anhydrous tablets and the theophylline anhydrous timed-release capsules were 0.97–0.99 and 0.96–0.99, respectively, demonstrating excellent fit of the data. The $t_{max}$ is the time for peak serum theophylline concentration as calculated from $K_A$ and $K$.

The mean pharmacokinetic parameters obtained for the theophylline anhydrous tablets and theophylline anhydrous timed-release capsules are shown in Table II. As expected, the $K_A$ value (2.10 ± 1.31 $hr^{-1}$) for the theophylline bioavailability rate from the rapid release tablet was significantly larger than the $K_A$ (0.27 ± 0.08 $hr^{-1}$) for theophylline bioavailability from the timed-release capsules. Furthermore, the $t_{max}$ for rapid release theophylline anhydrous tablets (Product A) was 1.66 ± 0.67 hr, which was significantly shorter than the $t_{max}$ of 4.45 ± 0.92 hr for the theophylline anhydrous timed-release capsules (Product B). The corresponding serum theophylline level–time curves for Products A and B are shown in Fig. 1.

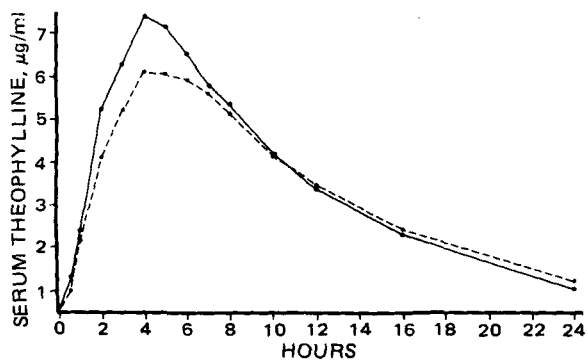


**Figure 3**—*Comparison of mean theophylline level–time curves in volunteers after receiving either Product B, theophylline anhydrous timed-release capsules (●—), or Product D, theophylline anhydrous timed-release capsules plus 15 ml of antacid (○- - -); n = 13.*

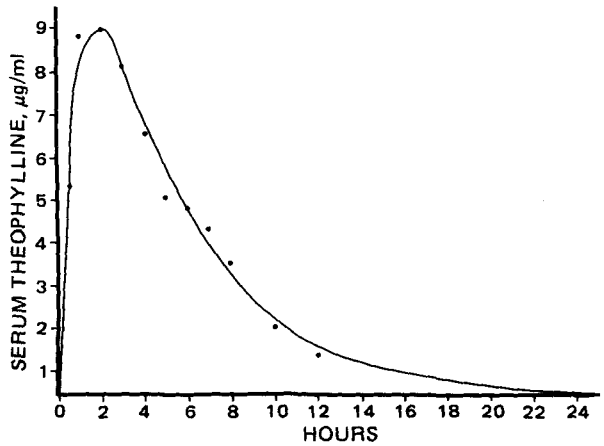


**Figure 4**—*Predicted serum theophylline level time–curve in Patient 1 after receiving Product A, theophylline anhydrous tablets. Experimental values are indicated.*

The medication of 15 ml of magnesium aluminum hydroxide suspension given concurrently with the theophylline products did not affect the $t_{max}$ for the rapid release theophylline tablets (Product C) but significantly ($p < 0.05$) increased the $t_{max}$ for the timed-release theophylline capsules (Product D) (Table II and Figs. 2 and 3). However, the apparent rate constant for absorption, $K_A$, for theophylline from the timed-release capsules was not affected by concurrent antacid administration.

The extent of theophylline bioavailability from both rapid release and timed-release forms was essentially similar as shown by the *AUC* values. Furthermore, there were no differences in the *F/V* values for both drug products, demonstrating that theophylline availability was similar and consistent. Moreover, the concurrent administration of 15 ml of magnesium aluminum hydroxide suspension with either the rapid release or timed-release theophylline drug products did not affect the *AUC* or *F/V* values (Table II).

The observed serum theophylline concentration–time curves and the theoretically calculated curves for each drug product in one patient are shown in Figs. 4–7. All curves from each patient demonstrated excellent correlation coefficients, indicating that the data were well described by the oral absorption one-compartment open model.

Urine pH was measured for each individual. No significant differences in urine pH due to antacid were apparent in the specimens collected during the entire 24 hr of sampling.

## DISCUSSION

Theophylline pharmacokinetics after an intravenous bolus have been described as a two-compartment open model with a very rapid distribution phase (3, 11–14). The results of this study confirm previous reports that the one-compartment open model may be used to describe the oral absorption of theophylline from a rapid release tablet or a timed-release capsule (3, 13, 14).

Concurrent administration of 15 ml of magnesium aluminum hy-

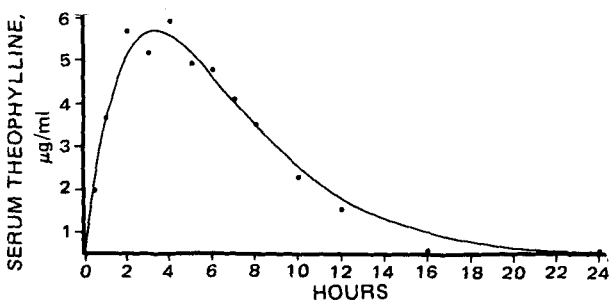


**Figure 5**—*Predicted serum theophylline level–time curve in Patient 1 after receiving Product B, theophylline anhydrous timed-release capsules. Experimental values are indicated.*

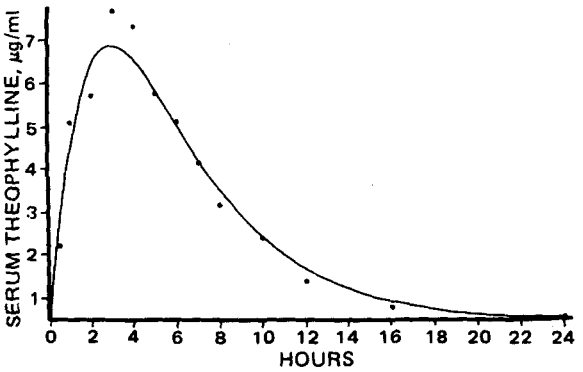


**Figure 6**—*Predicted serum theophylline level–time curve in Patient 1 after receiving Product C, theophylline anhydrous tablets plus 15 ml of antacid. Experimental values are indicated.*

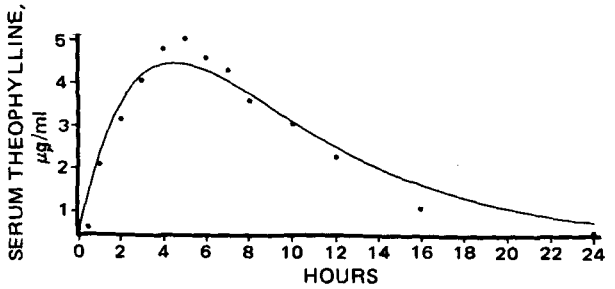


**Figure 7**—*Predicted serum theophylline level–time curve in Patient 1 after receiving Product D, theophylline anhydrous timed-release capsules plus 15 ml of antacid. Experimental values are indicated.*

droxide suspension with the rapid release theophylline anhydrous tablets did not affect theophylline bioavailability, as shown by the lack of any significant effect on the various pharmacokinetic parameters measured.

Antacid given with the theophylline anhydrous timed-release capsules increased the time for peak serum concentration, $t_{max}$, by ~13%. However, both the absorption rate constant, $K_A$, and the *AUC* for theophylline from the timed-release capsules were not affected by concurrent antacid administration. Therefore, the extent of theophylline bioavailability from the timed-release capsules was unaffected by antacid, and the theophylline bioavailability rate was affected only slightly.

A previous study (5) reported that 30 ml of magnesium aluminum hydroxide suspension significantly decreased the $K_A$ for theophylline in volunteers given a single 200-mg dose of aminophylline tablets. This decrease may have been due to the fact that theophylline was given as the ethylenediamine salt (aminophylline) and in smaller doses compared to the present study. In addition, 30 ml of antacid was given compared to the 15 ml used in this study. In both studies, the elimination rate constant, $K$, *AUC*, and $F/V$ values were in good agreement.

In conclusion, these data demonstrate that the concurrent administration of 15 ml of magnesium aluminum hydroxide suspension does not significantly affect the bioavailability of theophylline from theophylline anhydrous tablets or theophylline anhydrous timed-release capsules.

## REFERENCES

(1) L. Hendeles, M. Weinberger, and G. Johnson, *Clin. Pharmacokinet.*, **3**, 294 (1978).

(2) J. W. Kern and A. G. Lipman, *Drug Intell. Clin. Pharm.*, **11**, 144 (1977).

(3) R. J. Olgilvie, *Clin. Pharmacokinet.*, **3**, 267 (1978).

(4) M. Weinberger, *J. Pediatr. (Berlin)*, **92**, 1 (1978).

(5) L. A. Arnold, G. H. Spurbeck, W. H. Shelver, and W. M. Henderson, *Am. J. Hosp. Pharm.*, **36**, 1059 (1979).

(6) M. Gibaldi, B. Grundhofer, and G. Levy, *Clin. Pharmacol. Ther.*, **16**, 520 (1974).

(7) M. Gibaldi, B. Grundhofer, and G. Levy, *J. Pharm. Sci.*, **64**, 2003 (1975).

(8) J. A. Romankiewcz, *Primary Care*, **3**, 537 (1976).

(9) J. J. Orcutt, P. P. Kozak, Jr., S. A. Gillman, and L. H. Cummins, *Clin. Chem.*, **23**, 599 (1977).

(10) J. G. Wagner and E. Nelson, *J. Pharm. Sci.*, **53**, 1392 (1964).

(11) R. A. Floyd and J. L. Cohen, *Am. J. Hosp. Pharm.*, **34**, 402 (1976).

(12) F. A. Chrzanowski, P. J. Niebergall, P. J. Mayock, J. M. Taubin, and E. T. Sugita, *Clin. Pharmacol. Ther.* **22**, 188 (1977).

(13) F. H. Dvorchik and E. S. Vesell, *ibid.*, **23**, 617 (1978).

(14) P. A. Mitenko and R. I. Ogilve, *ibid.*, **14**, 509 (1973).

## ACKNOWLEDGMENTS

The authors thank Mr. Edward Ridolfi, Jr., for technical assistance and Mr. James M. Audibert, Dooner Laboratories, Haverhill, Mass., for advice and encouragement.

# Preparation and Antidiabetic Activity of New 3-Methyl-5-phenylpyrazolesulfonylurea Derivatives

**RAAFAT SOLIMAN** *x **and HASSAN M. FEID-ALLAH** ‡

Received January 7, 1980, from the *Department of Pharmaceutical Chemistry, Faculty of Pharmacy, and the ‡Department of Chemistry, Faculty of Science, University of Alexandria, Alexandria, Egypt. Accepted for publication September 26, 1980.

**Abstract** □ Two series of *p*-(3-methyl-5-phenylpyrazole-1)benzenesulfonylurea and *p*-(4-bromo-3-methyl-5-phenylpyrazole-1)benzenesulfonylurea derivatives were prepared for evaluation as hypoglycemic agents. Preliminary biological testing revealed that the new compounds possess potent antidiabetic activity.

**Keyphrases** □ 3-Methyl-5-phenylpyrazolesulfonylurea derivatives—preparation and evaluation for antidiabetic activity □ Structure–activity relationships—3-methyl-5-phenylpyrazolesulfonylurea derivatives and antidiabetic activity □ Antidiabetic activity—3-methyl-5-phenylpyrazolesulfonylurea derivatives synthesized and tested

Since 3,5-dimethylpyrazole and its active metabolite, 5-methylpyrazole-3-carboxylic acid, have potent hypoglycemic activity (1–5), studies have been performed on the synthesis of several new 3,5-disubstituted pyrazoles (6–8). In a continuation of previous work (8), many new substituted 3-methyl-5-phenylpyrazolesulfonylurea derivatives were prepared[1]. These compounds are analogous to, but vary in structure from, the aryl sulfonylurea derivatives.

The proposed compounds might provide valuable information concerning the structural requirements for

[1] Application for a patent was made for the compounds described in this report.



0022-3549/81/0600-0602$01.00/0
© 1981, American Pharmaceutical Association

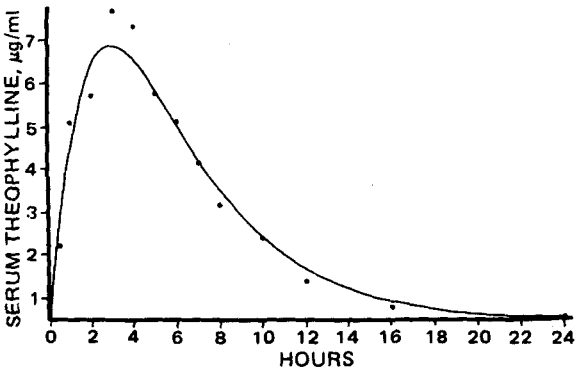


**Figure 6**—*Predicted serum theophylline level–time curve in Patient 1 after receiving Product C, theophylline anhydrous tablets plus 15 ml of antacid. Experimental values are indicated.*

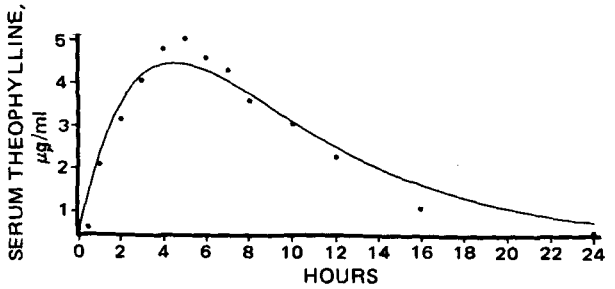


**Figure 7**—*Predicted serum theophylline level–time curve in Patient 1 after receiving Product D, theophylline anhydrous timed-release capsules plus 15 ml of antacid. Experimental values are indicated.*

droxide suspension with the rapid release theophylline anhydrous tablets did not affect theophylline bioavailability, as shown by the lack of any significant effect on the various pharmacokinetic parameters measured.

Antacid given with the theophylline anhydrous timed-release capsules increased the time for peak serum concentration, $t_{max}$, by ~13%. However, both the absorption rate constant, $K_A$, and the *AUC* for theophylline from the timed-release capsules were not affected by concurrent antacid administration. Therefore, the extent of theophylline bioavailability from the timed-release capsules was unaffected by antacid, and the theophylline bioavailability rate was affected only slightly.

A previous study (5) reported that 30 ml of magnesium aluminum hydroxide suspension significantly decreased the $K_A$ for theophylline in volunteers given a single 200-mg dose of aminophylline tablets. This decrease may have been due to the fact that theophylline was given as the ethylenediamine salt (aminophylline) and in smaller doses compared to the present study. In addition, 30 ml of antacid was given compared to the 15 ml used in this study. In both studies, the elimination rate constant, $K$, *AUC*, and $F/V$ values were in good agreement.

In conclusion, these data demonstrate that the concurrent administration of 15 ml of magnesium aluminum hydroxide suspension does not significantly affect the bioavailability of theophylline from theophylline anhydrous tablets or theophylline anhydrous timed-release capsules.

## REFERENCES

(1) L. Hendeles, M. Weinberger, and G. Johnson, *Clin. Pharmacokinet.*, **3**, 294 (1978).

(2) J. W. Kern and A. G. Lipman, *Drug Intell. Clin. Pharm.*, **11**, 144 (1977).

(3) R. J. Olgilvie, *Clin. Pharmacokinet.*, **3**, 267 (1978).

(4) M. Weinberger, *J. Pediatr. (Berlin)*, **92**, 1 (1978).

(5) L. A. Arnold, G. H. Spurbeck, W. H. Shelver, and W. M. Henderson, *Am. J. Hosp. Pharm.*, **36**, 1059 (1979).

(6) M. Gibaldi, B. Grundhofer, and G. Levy, *Clin. Pharmacol. Ther.*, **16**, 520 (1974).

(7) M. Gibaldi, B. Grundhofer, and G. Levy, *J. Pharm. Sci.*, **64**, 2003 (1975).

(8) J. A. Romankiewcz, *Primary Care*, **3**, 537 (1976).

(9) J. J. Orcutt, P. P. Kozak, Jr., S. A. Gillman, and L. H. Cummins, *Clin. Chem.*, **23**, 599 (1977).

(10) J. G. Wagner and E. Nelson, *J. Pharm. Sci.*, **53**, 1392 (1964).

(11) R. A. Floyd and J. L. Cohen, *Am. J. Hosp. Pharm.*, **34**, 402 (1976).

(12) F. A. Chrzanowski, P. J. Niebergall, P. J. Mayock, J. M. Taubin, and E. T. Sugita, *Clin. Pharmacol. Ther.* **22**, 188 (1977).

(13) F. H. Dvorchik and E. S. Vesell, *ibid.*, **23**, 617 (1978).

(14) P. A. Mitenko and R. I. Ogilve, *ibid.*, **14**, 509 (1973).

## ACKNOWLEDGMENTS

The authors thank Mr. Edward Ridolfi, Jr., for technical assistance and Mr. James M. Audibert, Dooner Laboratories, Haverhill, Mass., for advice and encouragement.

# Preparation and Antidiabetic Activity of New 3-Methyl-5-phenylpyrazolesulfonylurea Derivatives

**RAAFAT SOLIMAN** *x **and HASSAN M. FEID-ALLAH** ‡

Received January 7, 1980, from the *Department of Pharmaceutical Chemistry, Faculty of Pharmacy, and the ‡Department of Chemistry, Faculty of Science, University of Alexandria, Alexandria, Egypt. Accepted for publication September 26, 1980.

**Abstract** □ Two series of *p*-(3-methyl-5-phenylpyrazole-1)benzenesulfonylurea and *p*-(4-bromo-3-methyl-5-phenylpyrazole-1)benzenesulfonylurea derivatives were prepared for evaluation as hypoglycemic agents. Preliminary biological testing revealed that the new compounds possess potent antidiabetic activity.

**Keyphrases** □ 3-Methyl-5-phenylpyrazolesulfonylurea derivatives—preparation and evaluation for antidiabetic activity □ Structure–activity relationships—3-methyl-5-phenylpyrazolesulfonylurea derivatives and antidiabetic activity □ Antidiabetic activity—3-methyl-5-phenylpyrazolesulfonylurea derivatives synthesized and tested

Since 3,5-dimethylpyrazole and its active metabolite, 5-methylpyrazole-3-carboxylic acid, have potent hypoglycemic activity (1–5), studies have been performed on the synthesis of several new 3,5-disubstituted pyrazoles (6–8). In a continuation of previous work (8), many new substituted 3-methyl-5-phenylpyrazolesulfonylurea derivatives were prepared[1]. These compounds are analogous to, but vary in structure from, the aryl sulfonylurea derivatives.

The proposed compounds might provide valuable information concerning the structural requirements for

[1] Application for a patent was made for the compounds described in this report.



0022-3549/81/0600-0602$01.00/0
© 1981, American Pharmaceutical Association

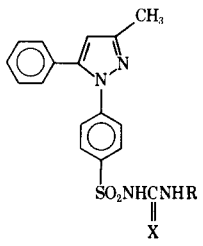

**Table I—Substituted *p*-(3-Methyl-5-phenylpyrazole-1)benzenesulfonylurea (V) and Thiourea (VI) Derivatives**

| Compound | R | X | Yield, % | Melting Point | Formula | Analysis, % | Calc. | Found |
|---|---|---|---|---|---|---|---|---|
| V*a* | $C_2H_5$ | O | 85 | 198° | $C_{19}H_{20}N_4O_3S$ | C | 59.4 | 59.8 |
| | | | | | | H | 5.2 | 5.4 |
| | | | | | | N | 14.6 | 14.8 |
| | | | | | | S | 8.3 | 8.1 |
| V*b* | $(CH_2)_2CH_3$ | O | 80 | 196° | $C_{20}H_{22}N_4O_3S$ | C | 60.3 | 60.4 |
| | | | | | | H | 5.5 | 5.3 |
| | | | | | | N | 14.1 | 14.2 |
| | | | | | | S | 8.0 | 8.3 |
| V*c* | $(CH_2)_3CH_3$ | O | 70 | 140° | $C_{21}H_{24}N_4O_3S$ | C | 61.2 | 61.3 |
| | | | | | | H | 5.8 | 5.7 |
| | | | | | | N | 13.6 | 13.7 |
| | | | | | | S | 7.8 | 7.9 |
| V*d* | $C_6H_{11}$ | O | 75 | 177° | $C_{23}H_{26}N_4O_3S$ | C | 63.0 | 63.1 |
| | | | | | | H | 5.9 | 5.6 |
| | | | | | | N | 12.8 | 12.7 |
| | | | | | | S | 7.3 | 7.2 |
| V*e* | $C_6H_5$ | O | 80 | 180° | $C_{23}H_{20}N_4O_3S$ | C | 63.9 | 64.0 |
| | | | | | | H | 4.6 | 4.4 |
| | | | | | | N | 13.0 | 13.2 |
| | | | | | | S | 7.4 | 7.6 |
| VI*a* | $C_2H_5$ | S | 80 | 187° | $C_{19}H_{20}N_4O_2S_2$ | C | 57.0 | 56.8 |
| | | | | | | H | 5.0 | 5.3 |
| | | | | | | N | 14.0 | 13.7 |
| | | | | | | S | 16.0 | 16.0 |
| VI*b* | $CH_2CH{=}CH_2$ | S | 70 | 174° | $C_{20}H_{20}N_4O_2S_2$ | C | 58.3 | 58.4 |
| | | | | | | H | 4.9 | 4.9 |
| | | | | | | N | 13.6 | 13.3 |
| | | | | | | S | 15.5 | 15.3 |
| VI*c* | $(CH_2)_3CH_3$ | S | 75 | 172° | $C_{21}H_{24}N_4O_2S_2$ | C | 58.9 | 59.2 |
| | | | | | | H | 5.6 | 5.4 |
| | | | | | | N | 13.1 | 13.3 |
| | | | | | | S | 15.0 | 15.4 |
| VI*d* | $C_6H_{11}$ | S | 70 | 186° | $C_{23}H_{26}N_4O_2S_2$ | C | 60.8 | 60.5 |
| | | | | | | H | 5.7 | 5.5 |
| | | | | | | N | 13.3 | 13.1 |
| | | | | | | S | 14.1 | 14.4 |
| VI*e* | $C_6H_5CH_2$ | S | 70 | 207° | $C_{24}H_{22}N_4O_2S_2$ | C | 62.3 | 62.4 |
| | | | | | | N | 4.8 | 4.4 |
| | | | | | | N | 12.1 | 12.0 |
| | | | | | | S | 13.9 | 13.7 |
| VI*f* | *p*-$CH_3C_6H_4$ | S | 75 | 210° | $C_{24}H_{22}N_4O_2S_2$ | C | 62.3 | 62.1 |
| | | | | | | H | 4.8 | 4.8 |
| | | | | | | N | 12.1 | 12.5 |
| | | | | | | S | 13.9 | 14.0 |

hypoglycemic activity. Therefore, two main series of *p*-(3-methyl-5-phenylpyrazole-1)benzenesulfonylurea and *p*-(4-bromo -3- methyl-5-phenylpyrazole-1)benzenesulfonylurea derivatives were synthesized. Some synthesized compounds were tested for hypoglycemic activity. Preliminary biological testing revealed that the compounds possess potent antidiabetic activity.

## DISCUSSION

The new pyrazoles are listed in Tables I and II. The antidiabetic activity of selected compounds is listed in Table III.

1-Phenylbutane-1,3-dione (1) reacts with aryl hydrazines to give a monohydrazone. On heating, this monohydrazone cyclizes to 1-aryl-3-methyl-5-phenylpyrazoles (9–12).

1-(*p*-Sulfamylphenyl)-3-methyl-5-phenylpyrazole (III) was prepared by treating *p*-sulfamylphenylhydrazine (II) with an equivalent amount of 1-phenylbutane-1,3-dione. Alkaline potassium permanganate oxidation of III afforded 1-(*p*-sulfamylphenyl)-5-phenylpyrazole-3-carboxylic acid (IV).

Bromination of III afforded 1-(*p*-sulfamylphenyl)-4-bromo-3-methyl-5-phenylpyrazole (VII). Acetylation of III with acetic anhydride afforded the monoacetyl derivative, as confirmed by microanalysis and IR and PMR spectra.

Substituted *p*-(3-methyl-5-phenylpyrazole-1)benzenesulfonylurea (V) and *p*-(4-bromo-3-methyl-5-phenylpyrazole-1)benzenesulfonylurea (VIII) derivatives were prepared by the reaction between III or VII and the appropriate isocyanate in dry acetone (13).

Substituted *p*-(3-methyl-5-phenylpyrazole-1)benzenesulfonylthiourea (VI) and *p*-(4-bromo-3-methyl-5-phenylpyrazole-1)benzenesulfonylthiourea (IX) derivatives were prepared by treatment of III or VII with the appropriate isothiocyanate.

## EXPERIMENTAL[2]

**1-(*p*-Sulfamylphenyl)-3-methyl-5-phenylpyrazole (III)**—A mixture of *p*-sulfamylphenylhydrazine (18.7 g, 0.1 mole) and 1-phenylbutan-1,3-dione (16.6 g, 0.1 mole) in ethanol (150 ml) was refluxed for

[2] Melting points were determined on a Kofler block and are uncorrected. IR spectra were determined as Nujol mulls with a Beckman IR-4210 spectrometer. PMR spectra were recorded on a Varian A-60 A spectrometer. Microanalyses were performed by the Microanalytical Unit, Faculty of Science, University of Cairo, Cairo, Egypt.

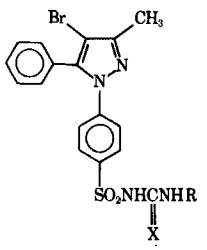

**Table II—Substituted *p*-(4-Bromo-3-methyl-5-phenylpyrazole-1)benzenesulfonylurea (VIII) and Thiourea (IX) Derivatives**

| Compound | R | X | Yield, % | Melting Point | Formula | Analysis, % | Calc. | Found |
|---|---|---|---|---|---|---|---|---|
| VIII*a* | $C_2H_5$ | O | 85 | 205° | $C_{29}H_{19}BrN_4O_3S$ | C | 49.2 | 49.3 |
| | | | | | | H | 4.1 | 4.5 |
| | | | | | | Br | 17.3 | 17.4 |
| | | | | | | N | 12.1 | 12.1 |
| | | | | | | S | 6.9 | 6.8 |
| VIII*b* | $(CH_2)_2CH_3$ | O | 70 | 180° | $C_{20}H_{21}BrN_4O_3S$ | C | 50.3 | 50.1 |
| | | | | | | H | 4.4 | 4.1 |
| | | | | | | Br | 16.8 | 16.4 |
| | | | | | | N | 11.7 | 11.6 |
| | | | | | | S | 6.7 | 6.9 |
| VIII*c* | $(CH_2)_3CH_3$ | O | 60 | 128° | $C_{21}H_{23}BrN_4O_3S$ | C | 51.3 | 51.3 |
| | | | | | | H | 4.7 | 4.8 |
| | | | | | | Br | 16.3 | 16.4 |
| | | | | | | N | 11.4 | 11.3 |
| | | | | | | S | 6.5 | 6.4 |
| VIII*d* | $C_6H_{11}$ | O | 65 | 222° | $C_{23}H_{25}BrN_4O_3S$ | C | 53.4 | 53.5 |
| | | | | | | H | 4.8 | 5.0 |
| | | | | | | Br | 15.5 | 15.7 |
| | | | | | | N | 10.8 | 10.7 |
| | | | | | | S | 6.2 | 6.1 |
| VIII*e* | $C_6H_5$ | O | 70 | 195° | $C_{23}H_{19}BrN_4O_3S$ | C | 54.0 | 54.3 |
| | | | | | | H | 3.7 | 3.5 |
| | | | | | | Br | 15.7 | 15.9 |
| | | | | | | N | 11.0 | 10.7 |
| | | | | | | S | 6.3 | 6.1 |
| IX*a* | $C_2H_5$ | S | 70 | 192° | $C_{19}H_{19}BrN_4O_2S_2$ | C | 47.6 | 47.6 |
| | | | | | | H | 4.0 | 3.8 |
| | | | | | | Br | 16.7 | 16.5 |
| | | | | | | N | 11.7 | 11.3 |
| | | | | | | S | 13.4 | 13.4 |
| IX*b* | $CH_2CH{=}CH_2$ | S | 60 | 126° | $C_{20}H_{19}BrN_4O_2S_2$ | C | 48.9 | 49.1 |
| | | | | | | H | 3.9 | 4.0 |
| | | | | | | Br | 16.3 | 16.1 |
| | | | | | | N | 11.4 | 11.3 |
| | | | | | | S | 13.0 | 13.3 |
| IX*c* | $(CH_2)_3CH_3$ | S | 70 | 164° | $C_{21}H_{23}BrN_4O_2S_2$ | C | 49.7 | 50.0 |
| | | | | | | H | 4.5 | 4.4 |
| | | | | | | Br | 15.8 | 15.7 |
| | | | | | | N | 11.0 | 11.3 |
| | | | | | | S | 12.6 | 12.3 |
| IX*d* | $C_6H_{11}$ | S | 60 | 188° | $C_{23}H_{25}BrN_4O_2S_2$ | C | 51.8 | 51.8 |
| | | | | | | H | 4.7 | 4.6 |
| | | | | | | Br | 15.0 | 14.7 |
| | | | | | | N | 10.5 | 10.4 |
| | | | | | | S | 12.0 | 12.0 |
| IX*e* | $C_6H_5CH_2$ | S | 70 | 192° | $C_{24}H_{21}BrN_4O_2S_2$ | C | 53.2 | 53.6 |
| | | | | | | H | 3.9 | 3.7 |
| | | | | | | Br | 14.8 | 14.6 |
| | | | | | | N | 10.4 | 10.4 |
| | | | | | | S | 11.8 | 11.7 |
| IX*f* | *p*-$CH_3C_6H_4$ | S | 65 | 230° | $C_{24}H_{21}BrN_4O_2S_2$ | C | 53.2 | 53.4 |
| | | | | | | H | 3.9 | 4.0 |
| | | | | | | Br | 14.8 | 14.5 |
| | | | | | | N | 10.4 | 10.0 |
| | | | | | | S | 11.8 | 11.6 |

4–6 hr on a steam bath, concentrated, and allowed to cool. The crude product was separated and recrystallized (75% yield) from ethanol, mp 198°.

*Anal.*—Calc. for $C_{16}H_{15}N_3O_2S$: C, 61.3; H, 4.8; N, 13.4; S, 10.2. Found: C, 61.4; H, 4.5; N, 13.2; S, 10.1.

**1-(*p*-Sulfamylphenyl)-5-phenylpyrazole-3-carboxylic Acid (IV)**—A stirred mixture of III (0.1 mole) and sodium hydroxide (0.15 mole) in water (100 ml) was treated with powdered potassium permanganate (30 g) over 4 hr with stirring and cooling (temperature should not exceed 20°). Stirring was continued for 2 additional hr, and the mixture was left standing overnight. The mixture then was filtered and neutralized with 2 *N* HCl. The crude product was separated and crystallized from ethanol as colorless needles (65% yield), mp 185°.

*Anal.*—Calc. for $C_{16}H_{13}N_3O_4S$: C, 56.0; H, 3.8; N, 12.2; S, 9.3. Found: C, 55.7; H, 3.6; N, 12.0; S, 9.7.

**1-(*p*-Sulfamylphenyl) -4- bromo-3-methyl-5-phenylpyrazole (VII)**—A mixture of III (0.1 mole) in chloroform (100 ml) was stirred with bromine (0.1 mole) for 1 hr. The crude product that separated during stirring was filtered and recrystallized from ethanol as colorless needles (85% yield), mp 228°.

*Anal.*—Calc. for $C_{16}H_{14}BrN_3O_2S$: C, 49.0; H, 3.6; Br, 20.4; N, 10.7; S, 8.2. Found: C, 49.2; H, 3.4; Br, 20.6; N, 10.6; S, 8.4.

**1-(*p*-Acetamidosulfonylphenyl)-3-methyl-5-phenylpyrazole**—A mixture of III (0.01 mole), sodium acetate (0.02 mole), and acetic anhydride (10 ml) was refluxed for 3 hr. After cooling, the reaction mixture was poured onto water. The acetyl derivative was recrystallized from

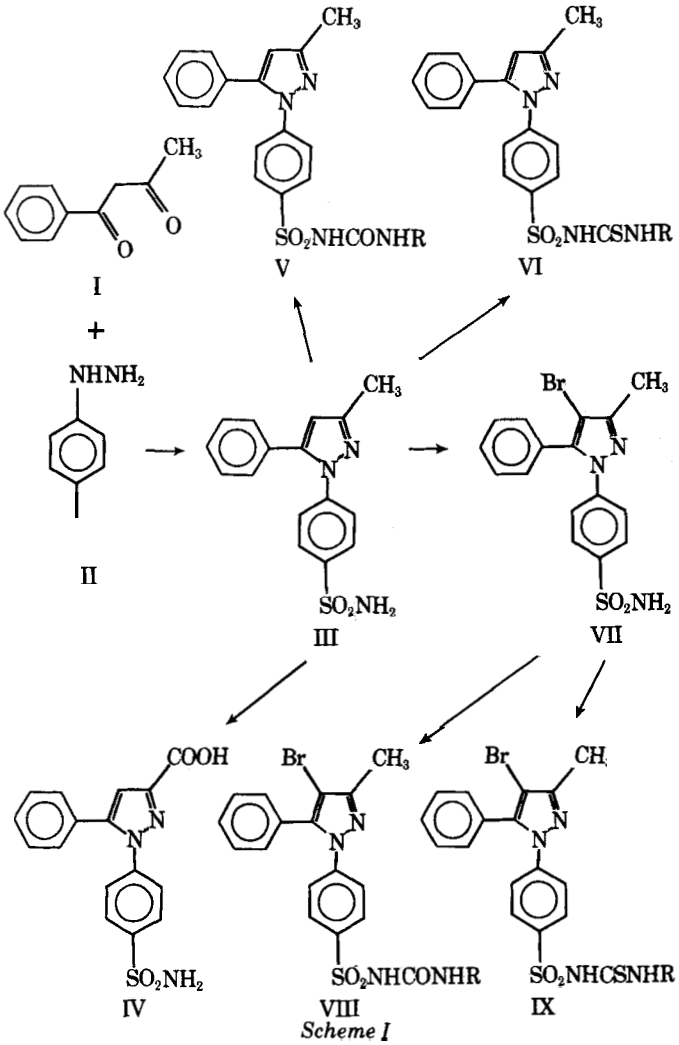

*Scheme I*

methanol as white needles (65% yield), mp 172°.

*Anal.*—Calc. for $C_{18}H_{17}N_3O_3S$: C, 60.8; H, 4.8; N, 11.8; S, 9.0. Found: C, 61.1; H, 4.7; N, 11.5; S, 9.3.

The IR spectra of this acetyl derivative revealed a secondary carbonyl amide absorption at 1710 $cm^{-1}$ in addition to the two bands of the $SO_2N$ group at 1350 and 1170 $cm^{-1}$. The PMR spectra showed three singlets at δ 6.2, 2.3, and 1.8 for C-4, acetyl, and methyl protons, respectively, in addition to the aromatic protons at δ 7.9–7.1.

**Substituted *p*-(3-Methyl-5-phenylpyrazole-1)benzenesulfonylurea (V) and *p*-(4-Bromo-3-methyl-5-phenylpyrazole-1)benzenesulfonylurea (VIII) Derivatives**—A mixture of III or VII (0.05 mole) and anhydrous potassium carbonate (0.1 mole) in dry acetone (100 ml) was stirred and refluxed for 1.5 hr. At this temperature, a solution of the appropriate isocyanate (0.075 mole) in dry acetone (20 ml) was added dropwise. After the mixture was stirred and refluxed overnight, acetone was removed under reduced pressure, and the solid residue was dissolved in water. The crude product was isolated by acidification with 2 *N* HCl and purified by recrystallization from ethanol. The IR spectra of these compounds revealed two absorption bands at 1350–1330 and 1190–1170 $cm^{-1}$, indicative of the $SO_2N$ group as well as a urea carbonyl band at 1660 $cm^{-1}$.

**Substituted *p*-(3-Methyl-5-phenylpyrazole-1)benzenesulfonylthiourea (VI) and *p*-(4-Bromo-3-methyl-5-phenylpyrazole-1)benzenesulfonylthiourea (IX) Derivatives**—A mixture of III or VII (0.05 mole) and anhydrous potassium carbonate (0.1 mole) in dry acetone (100 ml) was stirred and treated with the appropriate isothiocyanate (0.06 mole). After the mixture was stirred and refluxed for 10 hr, acetone was removed under reduced pressure. The solid mass thus obtained was dissolved in water and acidified with 2 *N* HCl. The crude product was purified by recrystallization from dilute ethanol.

The IR spectra of these compounds revealed two absorption bands at 1350–1335 and 1180–1170 $cm^{-1}$, indicative of the $SO_2N$ group, and a band at 1200–1050 $cm^{-1}$, indicative of the C=S group, with the C–N absorption (III) at 1300 $cm^{-1}$.

**1-[*p*-(2-Pyrimidinylsulfamyl)phenyl]-3-methyl-5-phenylpyrazole**—A mixture of *p*-(2-pyrimidinylsulfamyl)phenylhydrazine (0.05 mole) and 1-phenylbutane-1,3-dione (0.05 mole) in ethanol (50 ml) was refluxed for 6 hr on a steam bath, concentrated, and allowed to cool. The crude product was recrystallized from ethanol as colorless crystals (75% yield), mp 265°.

*Anal.*—Calc. for $C_{20}H_{17}N_5O_2S$: C, 61.3; H, 4.3; N, 17.9; S, 8.2. Found: C, 60.9; H, 4.5; N, 17.5; S, 8.0.

**Biological Testing Method**—Compounds IV, V*b*–V*e*, VI*c*, VIII*d*, and IX*e* were tested for hypoglycemic activity using alloxan-treated female albino mice weighing 20 g. Alloxan, 100 mg/kg, was injected into the tail vein in a 10-mg/ml saline solution. Three days later, the mice were given the test compounds orally in suspension in 1% carboxymethylcellulose solution at the rate of 10 mg/kg.

Each day, a group of six mice was used as a control, and one group of six mice was given the standard, 100 mg of phenformin/kg. Up to six groups of six mice received the test compounds. Blood samples were collected into 0.04% NaF solution at 0, 1, and 3 hr.

Glucose was determined by the microcolorimetric copper reduction technique of Haslewood and Strookman (14). Results are expressed as a percentage reduction of the plasma glucose level compared to the control value.

Statistical significance was assessed by a Student *t* test. Statistical significance was accepted where the calculated *t* value exceeded the tabulated *t* value at $p = 0.05$.

From the data presented in Table III, it is obvious that V*b*–V*d* and VIII*d* possess marked hypoglycemic activity. The potency of these compounds is more than that of phenformin, and they are much more active than the parent compound, 3,5-dimethylpyrazole.

**Table III—Antidiabetic Activity of Substituted *p*-(3-Methyl-5-phenylpyrazole-1)benzenesulfonylurea Derivatives**

| Compound | Reduction in Plasma Glucose Level, % | *p* |
|---|---|---|
| Phenformin | 10 | <0.01[a] |
| 3,5-Dimethylpyrazole | 4 | <0.05[a] |
| IV | <1 | 0.05 |
| V*b* | 20 | <0.01[a] |
| V*c* | 21 | <0.01[a] |
| V*d* | 12.5 | <0.01[a] |
| V*e* | 4 | 0.05 |
| VI*c* | 2 | 0.05 |
| VIII*d* | 15 | <0.01[a] |
| IX*e* | 2 | 0.05 |

[a] Statistically significant.

## REFERENCES


(1) J. B. Wright, W. E. Dulin, and J. H. Markillie, *J. Med. Chem.*, **7**, 102 (1964).

(2) G. C. Gerritsen and W. E. Dulin, *Diabetes*, **14**, 507 (1965).

(3) D. L. Smith, A. A. Forist, and W. E. Dulin, *J. Med. Chem.*, **8**, 350 (1965).

(4) G. C. Gerritsen and W. E. Dulin, *J. Pharmacol. Exp. Ther.*, **150**, 491 (1965).

(5) D. L. Smith, A. A. Forist, and G. C. Gerritsen, *ibid.*, **150**, 316 (1965).

(6) R. Soliman, H. Mokhtar, and E. S. El Ashry, *Pharmazie*, **33**, 184 (1978).

(7) H. Mokhtar and R. Soliman, *ibid.*, **33**, 649 (1978).

(8) R. Soliman, *J. Med. Chem.*, **22**, 321 (1979).

(9) V. Auwers and Stuhlmann, *Chem. Ber.*, **59**, 1043 (1926).

(10) G. Soliman and L. Ratib, *J. Chem. Soc.*, **1956**, 3663.

(11) *Ibid.*, **1960**, 1426.

(12) H. El Khadem, L. Ratib, and H. Mokhtar, *J. Chem. Soc. C*, **1968**, 1845.

(13) F. J. Marshall, M. V. Sigal, and M. A. Root, *J. Med. Chem.*, **6**, 60 (1963).

(14) G. A. D. Haslewood and T. A. Strookman, *Biochem. J.*, **33**, 920 (1939).


## ACKNOWLEDGMENTS


The authors thank Dr. S. A. El Sayed, Faculty of Medicine, University of Alexandria, for the biological testing.

# Preparation and Antidiabetic Activity of New Substituted 3,5-Diarylpyrazolesulfonylurea Derivatives

**RAAFAT SOLIMAN** *x, **HASSAN M. FEID-ALLAH** §, **SAMIR K. EL SADANY** §, and **HOSNY F. MOHAMED** ‡

Received August 18, 1980, from the *Department of Pharmaceutical Chemistry and the ‡Department of Pharmacology, Faculty of Pharmacy, and the §Department of Chemistry, Faculty of Science, University of Alexandria, Alexandria, Egypt. Accepted for publication September 26, 1980.

**Abstract** □ Four series of *p*-(3,5-diphenylpyrazole-1)-, *p*-[5-(*p*-chlorophenyl)-3-phenylpyrazole-1]-, *p*-[5-(*p*-chlorophenyl)-4-hydroxy-3-phenyl-2-pyrazolin-1-yl]-, and *p*-[5-(*p*-chlorophenyl)-4-hydroxy-3-phenylpyrazole-1]benzenesulfonylurea derivatives were prepared for evaluation as hypoglycemic agents. Preliminary biological testing revealed that the new compounds possess potent hypoglycemic activity.

**Keyphrases** □ 3,5-Diarylpyrazolesulfonylurea derivatives, substituted—preparation and evaluation for antidiabetic activity □ Structure–activity relationships—substituted 3,5-diarylpyrazolesulfonylurea derivatives and antidiabetic activity □ Antidiabetic activity—substituted 3,5-diarylpyrazolesulfonylurea derivatives synthesized and tested

Since several 3,5-dimethylpyrazoles possess hypoglycemic activities as great as 100 times that of tolbutamide in glucose-primed intact rats (1–5), studies have been conducted on the synthesis of new 3,5-disubstituted pyrazoles (6–9). In continuation of previous work (8, 9), many new substituted 3,5-diarylpyrazolesulfonylurea derivatives were prepared[1].

In light of the biological data reported in this paper and previously (8, 9), a possible structure–activity relationship for hypoglycemic activity may result.

Four series of *p*-(3,5-diphenylpyrazole-1)-, *p*-[5-(*p*-chlorophenyl)-3-phenylpyrazole-1]-, *p*-[5-(*p*-chlorophenyl)-4-hydroxy-3-phenyl-2-pyrazolin-1-yl]-, and *p*-[5-(*p*-chlorophenyl)-4-hydroxy -3- phenylpyrazole-1]benzenesulfonylurea derivatives were synthesized. Some compounds were tested for hypoglycemic activity. Preliminary biological testing revealed that the compounds showed potent antidiabetic activity.

## DISCUSSION

The new pyrazoles are listed in Tables I and II. The compounds listed in Table III were tested for antidiabetic activity.

1-(*p*-Sulfamylphenyl)-3,5-diphenylpyrazole (III) was prepared by treating *p*-sulfamylphenylhydrazine (I) with an equivalent amount of epoxybenzalacetophenone (II) (Scheme I). Acetylation of III with acetic anhydride afforded the monoacetyl derivative (IV*a*). Similarly, benzoylation of III with benzoyl chloride or *p*-methoxybenzoyl chloride in pyridine afforded the corresponding monobenzoyl (IV*b*) and the *p*-methoxybenzoyl (IV*c*) derivatives, respectively, as affirmed by microanalysis and IR spectra.

Condensation of I with an equivalent amount of epoxy-*p*-chlorobenzalacetophenone (VII) afforded a mixture of 1-(*p*-sulfamylphenyl)-5-(*p*-chlorophenyl)-3-phenylpyrazole (VIII) and 1-(*p*-sulfamylphenyl)-5-(*p*-chlorophenyl)-4-hydroxy-3-phenyl-2-pyrazoline (IX). Compound IX, on oxidation with bromine water, gave 1-(*p*-sulfamylphenyl)-5-(*p*-chlorophenyl)-4-hydroxy-3-phenylpyrazole (X). Benzoylation of VIII and IX afforded the corresponding benzamidosulfonyl derivatives (Scheme II).

Substituted *p*-(3,5-diphenylpyrazole-1)- (V), substituted *p*-[5-(*p*-chlorophenyl)-3-phenylpyrazole-1]- (XII), substituted *p*-[5-(*p*-chlorophenyl)-4-hydroxy-3-phenyl-2-pyrazolin-1-yl]- (XIII), and substituted *p*-[5-(*p*-chlorophenyl) -4- hydroxy-3-phenylpyrazole-1]benzenesulfonylurea (XIV) derivatives were prepared by the reaction between III, VIII, IX, or X and the appropriate isocyanate in dry acetone (10).

Substituted *p*-(3,5-diphenylpyrazole-1)- (VI), substituted *p*-[5-(*p*-chlorophenyl)-3-phenylpyrazole-1]- (XII), substituted *p*-[5-(*p*-chlorophenyl)-4-hydroxy-3-phenyl-2-pyrazolin-1-yl]- (XIII), and substituted *p*-[5-(*p*-chlorophenyl)-4-hydroxy -3- phenylpyrazole-1]benzenesulfonylthiourea (XIV) derivatives were prepared by the reaction between III, VIII, IX, or X and the appropriate isothiocyanates in dry acetone.

Substituted *p*-[5-(*p*-chlorophenyl)-4-hydroxy-3-phenylpyrazole-1]-benzenesulfonylurea and thiourea derivatives were also prepared by direct oxidation of the corresponding 2-pyrazoline derivatives (XIII*a*–XIII*f*) using bromine water.

## EXPERIMENTAL[2]

**1-(*p*-Sulfamylphenyl)-3,5-diphenylpyrazole (III)**—A mixture of *p*-sulfamylphenylhydrazine (I, 0.1 mole) and epoxybenzalacetophenone (II, 0.1 mole) in absolute ethanol (50 ml) was refluxed for 3 hr on a steam bath, concentrated, and allowed to cool. The crude product was filtered and recrystallized from ethanol as colorless prismatic needles (75% yield), mp 172°. The IR spectrum of III revealed two characteristic bands at 1365 and 1170 $cm^{-1}$, indicative of the $SO_2N$ group, and two bands at 3170 and 3350 $cm^{-1}$, indicative of the $NH_2$ group.

*Anal.*—Calc. for $C_{21}H_{17}N_3O_2S$: C, 67.2; H, 4.5; N, 11.2; S, 8.5. Found: C, 67.2; H, 4.4; N, 11.3; S, 8.4.

**1-(*p*-Acetamidosulfonylphenyl)-3,5-diphenylpyrazole (IV*a*)**—A mixture of III (0.01 mole), sodium acetate (0.02 mole), and acetic anhydride (10 ml) was refluxed for 4 hr. After cooling, the reaction mixture was diluted with water. The crude acetyl derivative was recrystallized from dilute methanol in yellow needles (65% yield), mp 98°. The IR spectrum of IV*a* revealed a secondary carbonyl amide absorption at 1720 $cm^{-1}$ and an NH band at 3090 $cm^{-1}$ in addition to the two bands of the $SO_2N$ group at 1365 and 1170 $cm^{-1}$.

*Anal.*—Calc. for $C_{23}H_{19}N_3O_3S$: C, 66.2; H, 4.6; N, 10.1; S, 7.7. Found: C, 66.0; H, 4.8; N, 10.3; S, 7.9.

**1-(*p*-Benzamidosulfonylphenyl)-3,5-diphenylpyrazole (IV*b*)**—A solution of III (0.001 mole) in pyridine (5 ml) was heated with benzoyl chloride (0.001 mole) for 20 min. The reaction mixture was left at room temperature for 6 hr and then diluted with ice-cold water. The crude product was purified by recrystallization from dilute methanol to give white needles (70% yield), mp 135°. The IR spectrum of IV*b* revealed a secondary carbonyl amide absorption at 1705 $cm^{-1}$ and an NH band at 3100 $cm^{-1}$, in addition to the two bands of the $SO_2N$ group at 1365 and 1170 $cm^{-1}$.

*Anal.*—Calc. for $C_{28}H_{21}N_3O_3S$: C, 70.1; H, 4.4; N, 8.8; S, 6.7. Found: C, 69.8; H, 4.2; N, 9.0; S, 6.7.

**1-[*p*-(*p*-Methoxybenzamido)sulfonylphenyl]-3,5-diphenylpyrazole (IV*c*)**—A solution of III (0.001 mole) in pyridine (5 ml) was heated with *p*-methoxybenzoyl chloride (0.001 mole) for 20 min. The reaction mixture then was left at room temperature for 6 hr and diluted with ice-cold water. The crude product was purified by recrystallization from dilute methanol to give white needles (70% yield), mp 225°. The IR spectrum of IV*c* revealed a secondary carbonyl amide absorption at 1700 $cm^{-1}$ and an NH band at 3090 $cm^{-1}$ in addition to the two bands of the $SO_2N$ group at 1365 and 1170 $cm^{-1}$.

[1] Application for a patent was made for compounds described in this report.

[2] Melting points were determined on a Kofler block and are uncorrected. IR spectra were determined as Nujol mulls with a Beckman IR-4210 spectrometer. PMR spectra were recorded on a Varian A-60 A spectrometer. Microanalyses were performed by the Microanalytical Unit, Faculty of Science, University of Cairo, Cairo, Egypt.



0022-3549/81/0600-0606$01.00/0
© 1981, American Pharmaceutical Association

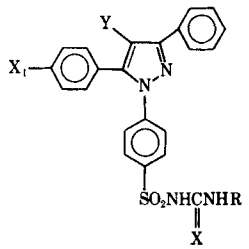


**Table I—Substituted *p*-(3,5-Diarylpyrazole-1)benzenesulfonylurea Derivatives**

| Compound | R | X | $X_1$ | Y | Yield, % | Melting Point | Formula | Analysis, % | Calc. | Found |
|---|---|---|---|---|---|---|---|---|---|---|
| V*a* | $C_2H_5$ | O | H | H | 70 | 208° | $C_{24}H_{22}N_4O_3S$ | C | 64.6 | 64.2 |
| | | | | | | | | H | 4.9 | 4.7 |
| | | | | | | | | N | 12.6 | 12.5 |
| | | | | | | | | S | 7.2 | 7.2 |
| V*b* | $CH_3(CH_2)_2$ | O | H | H | 65 | 205° | $C_{25}H_{24}N_4O_3S$ | C | 65.2 | 65.5 |
| | | | | | | | | H | 5.2 | 5.4 |
| | | | | | | | | N | 12.2 | 12.6 |
| | | | | | | | | S | 7.0 | 7.1 |
| V*c* | $CH_3(CH_2)_3$ | O | H | H | 60 | 235° | $C_{26}H_{26}N_4O_3S$ | C | 65.8 | 66.1 |
| | | | | | | | | H | 5.5 | 5.4 |
| | | | | | | | | N | 11.8 | 12.2 |
| | | | | | | | | S | 6.8 | 6.7 |
| V*d* | $C_6H_{11}$ | O | H | H | 80 | 212° | $C_{28}H_{28}N_4O_3S$ | C | 67.2 | 67.5 |
| | | | | | | | | H | 5.6 | 5.2 |
| | | | | | | | | N | 11.2 | 11.1 |
| | | | | | | | | S | 6.4 | 6.4 |
| V*e* | $C_6H_5$ | O | H | H | 70 | 220° | $C_{28}H_{22}N_4O_3S$ | C | 68.0 | 68.2 |
| | | | | | | | | H | 4.5 | 4.5 |
| | | | | | | | | N | 11.3 | 11.6 |
| | | | | | | | | S | 6.5 | 6.5 |
| VI*a* | $C_2H_5$ | S | H | H | 65 | 175° | $C_{24}H_{22}N_4O_2S_2$ | C | 62.3 | 62.1 |
| | | | | | | | | H | 4.8 | 4.8 |
| | | | | | | | | N | 12.1 | 12.5 |
| | | | | | | | | S | 13.9 | 13.7 |
| VI*b* | $CH_3(CH_2)_3$ | S | H | H | 60 | 162° | $C_{26}H_{26}N_4O_2S_2$ | C | 63.6 | 64.0 |
| | | | | | | | | H | 5.3 | 5.3 |
| | | | | | | | | N | 11.4 | 11.2 |
| | | | | | | | | S | 13.1 | 13.3 |
| VI*c* | $C_6H_{11}$ | S | H | H | 70 | 210° | $C_{28}H_{28}N_4O_2S_2$ | C | 65.1 | 64.9 |
| | | | | | | | | H | 5.4 | 5.7 |
| | | | | | | | | N | 10.8 | 10.4 |
| | | | | | | | | S | 12.4 | 12.3 |
| VI*d* | *p*-$CH_3C_6H_4$ | S | H | H | 65 | 214° | $C_{29}H_{24}N_4O_2S_2$ | C | 66.4 | 66.2 |
| | | | | | | | | H | 4.6 | 4.5 |
| | | | | | | | | N | 10.7 | 10.3 |
| | | | | | | | | S | 12.2 | 12.1 |
| VI*e* | $C_6H_5CH_2$ | S | H | H | 65 | 158° | $C_{29}H_{24}N_4O_2S_2$ | C | 66.4 | 66.4 |
| | | | | | | | | H | 4.6 | 4.8 |
| | | | | | | | | N | 10.7 | 10.6 |
| | | | | | | | | S | 12.2 | 12.6 |
| XII*a* | $C_2H_5$ | O | Cl | H | 70 | 215° | $C_{24}H_{21}ClN_4O_3S$ | C | 59.9 | 60.0 |
| | | | | | | | | H | 4.4 | 4.3 |
| | | | | | | | | Cl | 7.4 | 7.1 |
| | | | | | | | | N | 11.7 | 11.8 |
| | | | | | | | | S | 6.7 | 6.7 |
| XII*b* | $CH_3(CH_2)_2$ | O | Cl | H | 65 | 222° | $C_{25}H_{23}ClN_4O_3S$ | C | 60.7 | 61.1 |
| | | | | | | | | H | 4.7 | 4.9 |
| | | | | | | | | Cl | 7.2 | 7.0 |
| | | | | | | | | N | 11.3 | 11.0 |
| | | | | | | | | S | 6.5 | 6.3 |
| XII*c* | $CH_3(CH_2)_3$ | O | Cl | H | 60 | 205° | $C_{26}H_{25}ClN_4O_3S$ | C | 61.4 | 61.6 |
| | | | | | | | | H | 4.9 | 5.2 |
| | | | | | | | | Cl | 7.0 | 7.3 |
| XII*d* | $C_6H_{11}$ | O | Cl | H | 70 | 220° | $C_{28}H_{27}ClN_4O_3S$ | C | 62.7 | 63.0 |
| | | | | | | | | H | 5.1 | 5.0 |
| | | | | | | | | Cl | 6.6 | 7.0 |
| | | | | | | | | N | 10.5 | 10.7 |
| | | | | | | | | S | 6.0 | 5.7 |
| XII*e* | $C_6H_5$ | O | Cl | H | 65 | 223° | $C_{28}H_{21}ClN_4O_3S$ | C | 63.6 | 63.4 |
| | | | | | | | | H | 4.0 | 4.2 |
| | | | | | | | | Cl | 6.7 | 6.5 |
| | | | | | | | | N | 10.6 | 10.6 |
| | | | | | | | | S | 6.1 | 6.2 |
| XII*f* | $C_6H_{11}$ | S | Cl | H | 70 | 210° | $C_{28}H_{27}ClN_4O_2S_2$ | C | 61.0 | 61.3 |
| | | | | | | | | H | 4.9 | 4.8 |
| | | | | | | | | Cl | 6.4 | 6.2 |
| | | | | | | | | N | 10.2 | 10.4 |
| | | | | | | | | S | 11.6 | 11.9 |

(*continued*)

**Table I**—*Continued*

| Compound | R | X | $X_1$ | Y | Yield, % | Melting Point | Formula | Analysis, % Calc. | Found |
|---|---|---|---|---|---|---|---|---|---|
| XIV*a* | $C_2H_5$ | O | Cl | OH | 60 | 195° | $C_{24}H_{21}ClN_4O_4S$ | C 58.0 | 58.0 |
| | | | | | | | | H 4.2 | 4.6 |
| | | | | | | | | Cl 7.2 | 7.3 |
| | | | | | | | | N 11.2 | 11.0 |
| XIV*b* | $C_6H_5$ | O | Cl | OH | 65 | 282° | $C_{28}H_{21}ClN_4O_4S$ | C 61.7 | 62.1 |
| | | | | | | | | H 4.0 | 4.1 |
| | | | | | | | | N 10.3 | 10.2 |
| | | | | | | | | S 5.9 | 5.9 |
| XIV*c* | $C_2H_5$ | S | Cl | OH | 70 | 175° | $C_{24}H_{21}ClN_4O_3S_2$ | C 56.2 | 56.5 |
| | | | | | | | | H 4.1 | 4.3 |
| | | | | | | | | Cl 6.9 | 6.5 |
| | | | | | | | | N 10.9 | 10.8 |
| | | | | | | | | S 12.5 | 12.5 |
| XIV*d* | $C_6H_{11}$ | S | Cl | OH | 60 | 185° | $C_{28}H_{27}ClN_4O_3S_2$ | C 59.3 | 59.2 |
| | | | | | | | | H 4.8 | 5.2 |
| | | | | | | | | Cl 6.3 | 6.1 |
| | | | | | | | | N 9.9 | 10.0 |
| | | | | | | | | S 11.3 | 11.1 |

*Anal.*—Calc. for $C_{29}H_{23}N_3O_4S$: C, 68.4; H, 4.5; N, 8.3; S, 6.3. Found: C, 68.4; H, 4.2; N, 8.3; S, 6.4.

**1 - (*p* - Sulfamylphenyl)-5-(*p*-chlorophenyl)-3-phenylpyrazole (VIII)**—A mixture of *p*-sulfamylphenylhydrazine (0.1 mole) and epoxy-*p*-chlorobenzalacetophenone (0.1 mole) in absolute ethanol (50 ml) was refluxed for 3 hr on a steam bath, concentrated, and allowed to cool. The crude product was filtered and recrystallized from a mixture of benzene and ethanol to give yellow needles (60% yield), mp 275°. The IR spectrum of VIII revealed two characteristic bands at 1360 and 1150 $cm^{-1}$, indicative of the $SO_2N$ group, and two bands at 3170 and 3320 $cm^{-1}$, indicative of the $NH_2$ group.

*Anal.*—Calc. for $C_{21}H_{16}ClN_3O_2S$: C, 61.5; H, 3.9; Cl, 8.7; N, 10.3; S, 7.8. Found: C, 61.4; H, 3.5; Cl, 8.5; N, 10.1; S, 7.7.

**1-(*p*-Sulfamylphenyl)-5-(*p*-chlorophenyl)-4-hydroxy-3-phenyl-2-pyrazoline (IX)**—When the mother liquor of the previous reaction was left to evaporate slowly, the pyrazoline derivative separated out. It was recrystallized from methanol as colorless plates (40% yield), mp 225°. The IR spectrum of IX revealed a band at 3400 $cm^{-1}$, indicative of an OH group, and two bands at 3220 and 3280 $cm^{-1}$, indicative of the $NH_2$ group.

*Anal.*—Calc. for $C_{21}H_{18}ClN_3O_3S$: C, 58.9; H, 4.2; Cl, 8.3; N, 9.8; S, 7.5. Found: C, 59.2; H, 4.5; Cl, 8.1; N, 10.1; S, 7.6.

**1 - [*p*-(*p*-Methoxybenzamido)sulfonylphenyl]-5-(*p*-chlorophenyl)-3-phenylpyrazole (XI)**—A solution of VIII (0.001 mole) in pyridine (5 ml) was heated with *p*-methoxybenzoyl chloride (0.001 mole) for 20 min. The mixture was left at room temperature for 6 hr and then diluted with ice-cold water. The crude product was purified by recrystallization (50% yield) from dilute methanol, mp 242°. The IR spectrum of XI re-

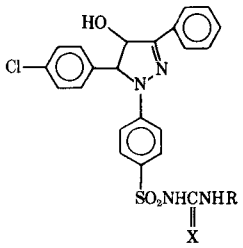


**Table II—Substituted *p*-[5-(*p*-Chlorophenyl)-4-hydroxy-3-phenyl-2-pyrazolin-1-yl]benzenesulfonylurea Derivatives**

| Compound | R | X | Yield, % | Melting Point | Formula | Analysis, % Calc. | Found |
|---|---|---|---|---|---|---|---|
| XIII*a* | $C_2H_5$ | O | 65 | 215° | $C_{24}H_{23}ClN_4O_4S$ | C 57.8 | 58.0 |
| | | | | | | H 4.6 | 4.6 |
| | | | | | | Cl 7.1 | 7.3 |
| | | | | | | N 11.2 | 11.1 |
| | | | | | | S 6.4 | 6.4 |
| XIII*b* | $C_6H_{11}$ | O | 70 | 230° | $C_{28}H_{29}ClN_4O_4S$ | C 60.8 | 60.5 |
| | | | | | | H 5.3 | 5.4 |
| | | | | | | Cl 6.4 | 6.0 |
| | | | | | | N 10.1 | 10.3 |
| | | | | | | S 5.7 | 5.8 |
| XIII*c* | $C_6H_5$ | O | 60 | 172° | $C_{28}H_{23}ClN_4O_4S$ | C 61.5 | 61.5 |
| | | | | | | H 4.2 | 4.4 |
| | | | | | | Cl 6.5 | 6.4 |
| | | | | | | N 10.2 | 10.5 |
| | | | | | | S 5.9 | 5.9 |
| XIII*d* | $C_2H_5$ | S | 65 | 195° | $C_{24}H_{23}ClN_4O_3S_2$ | C 56.0 | 55.9 |
| | | | | | | H 4.5 | 4.1 |
| | | | | | | Cl 6.9 | 6.5 |
| | | | | | | N 10.9 | 10.8 |
| | | | | | | S 12.5 | 12.5 |
| XIII*e* | $C_6H_{11}$ | S | 70 | 218° | $C_{28}H_{29}ClN_4O_3S_2$ | C 59.1 | 59.2 |
| | | | | | | H 5.1 | 5.3 |
| | | | | | | Cl 6.2 | 6.1 |
| | | | | | | N 9.9 | 9.5 |
| XIII*f* | $C_6H_5CH_2$ | S | 65 | 142° | $C_{29}H_{25}ClN_4O_3S_2$ | C 60.4 | 60.7 |
| | | | | | | H 4.3 | 4.3 |
| | | | | | | Cl 6.2 | 6.1 |
| | | | | | | N 9.7 | 10.1 |
| | | | | | | S 11.1 | 11.5 |

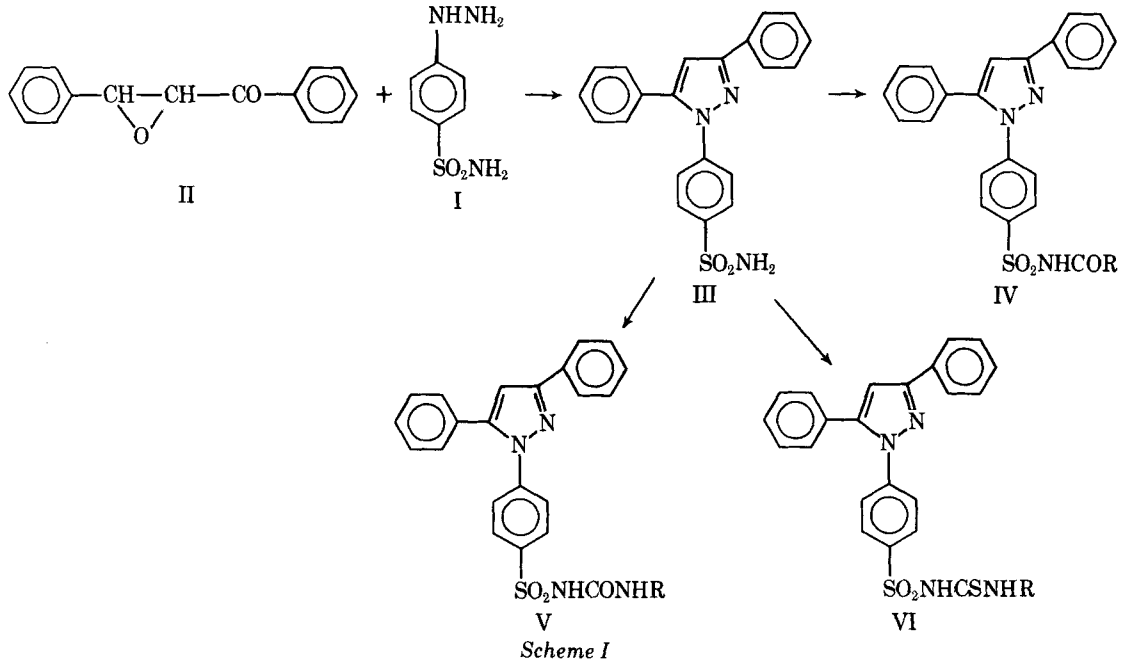


*Scheme I*

vealed a secondary carbonyl amide band at 1705 $cm^{-1}$ and an NH band at 3090 $cm^{-1}$.

*Anal.*—Calc. for $C_{29}H_{22}ClN_3O_4S$: C, 64.0; H, 4.0; Cl, 6.5; N, 7.7; S, 5.9. Found: C, 64.4; H, 4.1; Cl, 6.4; N, 7.9; S, 5.5.

**1-(*p*-Benzamidosulfonylphenyl)-5-(*p*-chlorophenyl)-4-hydroxy-3-phenyl-2-pyrazoline**—A solution of IX (0.001 mole) in pyridine (5 ml) was heated with benzoyl chloride (0.001 mole) for 20 min. The reaction mixture then was left at room temperature for 6 hr and diluted with ice-cold water. The crude product was purified by recrystallization from methanol to give white needles (75% yield), mp 162°. The IR spectrum revealed a band at 3380 $cm^{-1}$, indicative of an OH group, a secondary carbonyl amide band at 1710 $cm^{-1}$, and an NH band at 3100 $cm^{-1}$.

*Anal.*—Calc. for $C_{28}H_{22}ClN_3O_4S$: C, 63.2; H, 4.1; Cl, 6.7; N, 7.9; S, 6.0. Found: C, 63.4; H, 4.5; Cl, 6.8; N, 7.7; S, 6.0.

**1-[*p*-(*p*-Methoxybenzamido)sulfonylphenyl] -5- (*p*-chlorophenyl)-4-hydroxy-3-phenyl-2-pyrazoline**—A solution of IX (0.001 mole) in pyridine (5 ml) was heated with *p*-methoxybenzoyl chloride (0.001 mole) for 20 min. The reaction mixture then was left at room temperature for 6 hr and diluted with ice-cold water. The crude product was purified by recrystallization from ethanol to give white needles (70% yield), mp 190°. The IR spectrum revealed a band at 3350 $cm^{-1}$, indicative of an OH group, a secondary carbonyl amide band at 1715 $cm^{-1}$, and an NH band at 3100 $cm^{-1}$.

*Anal.*—Calc. for $C_{29}H_{24}ClN_3O_5S$: C, 62.0; H, 4.3; Cl, 6.3; N, 7.5; S, 5.7. Found: C, 62.2; H, 4.3; Cl, 6.1; N, 7.6; S, 5.8.

**1 - (*p* - Sulfamylphenyl)-5-(*p*-chlorophenyl)-4-hydroxy-3-phenylpyrazole (X)**—A suspension of IX (0.01 mole) in water (10 ml) was treated with 5% bromine water until a faint-yellow color developed with stirring. Stirring continued for 2 hr, and the crude pyrazole was filtered and recrystallized from methanol as colorless needles (45% yield), mp 252°. The IR spectrum of X showed a band at 3400 $cm^{-1}$, indicative of an OH group, and two bands at 3230 and 3290 $cm^{-1}$, indicative of an $NH_2$ group.

*Anal.*—Calc. for $C_{21}H_{16}ClN_3O_3S$: C, 59.2; H, 3.8; Cl, 8.3; N, 9.9; S, 7.5. Found: C, 59.1; H, 3.9; Cl, 8.1; N, 10.1; S, 7.5.

**Substituted *p*-(3,5-Diarylpyrazole-1)benzenesulfonylurea (V, XII, and XIV) Derivatives**—A mixture of III, VIII, or X (0.01 mole) and anhydrous potassium carbonate (0.02 mole) in dry acetone (25 ml) was stirred and refluxed for 1 hr. At this temperature, a solution of the appropriate isocyanate (0.015 mole) in dry acetone (5 ml) was added dropwise. After the mixture was stirred and refluxed overnight, acetone was removed under reduced pressure, and the solid residue was dissolved in water. The crude product was isolated by acidification with 2 *N* HCl and purified by recrystallization from ethanol (Table I).

**Substituted *p*-(3,5-Diarylpyrazole-1)benzenesulfonylthiorea (VI, XII, and XIV) Derivatives**—A mixture of III, VIII, or X (0.01 mole) and anhydrous potassium carbonate (0.02 mole) in dry acetone (25 ml) was stirred and treated with the appropriate isothiocyanate (0.012 mole). After the mixture was stirred and refluxed for 10 hr, acetone was removed under reduced pressure, and the solid mass was dissolved in water and acidified with 2 *N* HCl. The crude product was purified by recrystallization from dilute ethanol (Table I).

**Substituted *p*-[5-(*p*-Chlorophenyl)-4-hydroxy-3-phenyl-2-pyrazolin-1-yl]benzenesulfonylurea and Thiourea (XIIIa–XIII*f*) Derivatives**—Compounds XIII*a*–XIII*f* were prepared by the same procedures used in the preparation of substituted *p*-(3,5-diarylpyrazole-1)benzenesulfonylurea and thiourea derivatives.

Substituted *p*-[5-(*p*-chlorophenyl)-4-hydroxy-3-phenylpyrazole-1]-benzenesulfonylurea and thiourea (XIV*a*–XIV*d*) derivatives could also be prepared by bromine water oxidation of their corresponding pyrazoline derivatives (XIII*a*–XIII*f*).

The IR spectra of V*a*–V*e* showed a band at 1660–1680 $cm^{-1}$, indicative of C=O, and a band at 3110–3080 $cm^{-1}$, indicative of an NH group. Compounds VI*a*–VI*e* showed a characteristic band in the region of 1100–1140 $cm^{-1}$, indicative of a C=S group, and a band in the region of 3100–3080 $cm^{-1}$, indicative of an NH group. Compounds XII*a*–XII*e* showed a characteristic band at 1660–1640 $cm^{-1}$, indicative of a secondary carbonyl amide, in addition to the two bands of the $SO_2N$ group at 1360–1330 and 1180–1150 $cm^{-1}$. Compounds XIII*a*–XIII*c* showed two characteristic bands at 3400–3380 $cm^{-1}$, indicative of an OH group, and at 1665–1650 $cm^{-1}$, indicative of a carbonyl group. Compounds XIII*d* and XIII*e* showed a characteristic band at 1100–1220 $cm^{-1}$, indicative of a C=S group, in addition to the band of an OH group at 3450–3400 $cm^{-1}$.

The PMR spectra of VI*c* showed aromatic protons at $\delta$ 7.2–8.0, a multiplet at $\delta$ 0.5–1.9 for the cyclohexyl protons, and a singlet at $\delta$ 6.9 due to the C-4 proton.

The PMR spectra of XIII*d* showed a multiplet in the region of $\delta$ 8.1–8.8 for the aromatic protons with the two NH protons, a triplet at $\delta$ 1.1 for the $CH_3$ of the ethyl group, and a quartet at $\delta$ 3.7 for the $CH_2$ of the ethyl group. The C-4 and C-5 protons appeared as a triplet and doublet at $\delta$

**Table III—Antidiabetic Activity of Substituted 3,5-Diarylpyrazole-1-benzenesulfonylurea Derivatives**

| Compound | Reduction in Plasma Glucose Level, % | *p* |
|---|---|---|
| Phenformin | 10 | <0.01[a] |
| III | <1 | 0.05 |
| V*c* | 12 | <0.01[a] |
| V*d* | 10 | <0.01[a] |
| VI*c* | 7.5 | <0.01[a] |
| XII*c* | 3 | 0.01[a] |
| XII*f* | 2 | 0.01[a] |
| XIII*b* | 7 | <0.01[a] |
| XIV*b* | 10 | <0.01[a] |

[a] Statistically significant.

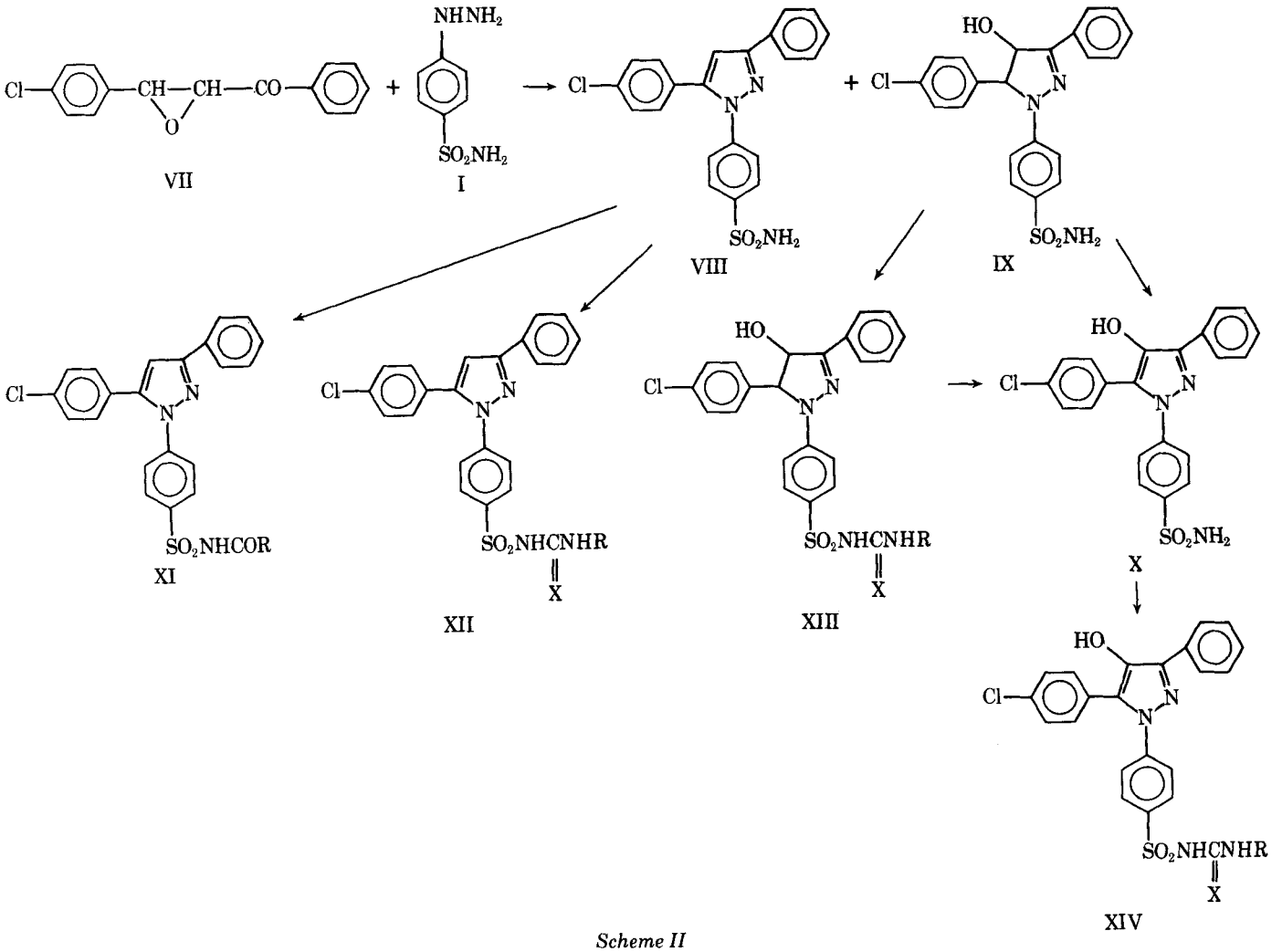

*Scheme II*

3.3 and 1.5, respectively. The signal at $\delta$ 6.5 was due to the OH group.

**Biological Testing Method**—Compounds III, Vc, Vd, VIc, XIIc, XII*f*, XIII*b*, and XIV*b* were tested for hypoglycemic activity using alloxan-treated female albino mice weighing 20 g. Alloxan, 100 mg/kg, was injected into the tail vein in a 10-mg/ml saline solution. Three days later, the mice were given the test compounds orally in suspension in 1% carboxymethylcellulose solution at the rate of 0.2 mmole/kg.

Each day, a group of four mice was used as the control, and one group of four mice was given the standard, 100 mg (0.4 mmole) of phenformin/kg. Up to six groups of four mice received the test compounds. Blood samples were collected into 0.04% NaF solution at 0, 1, and 3 hr.

Glucose was determined by the microcolorimetric copper reduction technique of Haslewood and Strookman (11). Results are expressed as a percentage reduction of plasma glucose levels compared to the control value.

Statistical significance was assessed by the Student $t$ test. Statistical significance was accepted where the calculated $t$ value exceeded the tabulated $t$ value at the $p = 0.05$ level.

## RESULTS

Compounds Vc, Vd, VIc, XIII*b*, and XIV*b* possess marked hypoglycemic activity (Table III). The potency of these compounds, however, is more than that of phenformin (0.2 mmole of test compound/kg compared to 0.4 mmole of phenformin/kg) and much more active than 3,5-dimethylpyrazole.

From the data presented previously (8, 9) and in this study, it is obvious that many 3,5-disubstituted pyrazolebenzenesulfonylurea derivatives possess marked hypoglycemic activity. Thiourea derivatives are much less active. Introduction of a bromine atom at position 4 of the pyrazole ring increases the hypoglycemic activity of the sulfonylurea derivative. The 3-methyl-5-phenylpyrazole derivatives are much more active than their corresponding 3,5-dimethylpyrazole analogs. 3,5-Diarylpyrazolesulfonylurea derivatives are quite active as antidiabetic agents. 3,5-Diphenylpyrazole derivatives are much more active than their corresponding 3-phenyl-5-(*p*-chlorophenyl)pyrazole analogs. The presence of an hydroxy group in position 4 of the pyrazole ring of benzenesulfonylurea derivatives increases hypoglycemic activity.

## REFERENCES


(1) J. B. Wright, W. E. Dulin, and J. H. Markillie, *J. Med. Chem.*, **7**, 102 (1964).

(2) G. C. Gerritsen and W. E. Dulin, *Diabetes*, **14**, 507 (1965).

(3) D. L. Smith, A. A. Forist, and W. E. Dulin, *J. Med. Chem.*, **8**, 350 (1965).

(4) G. C. Gerritsen and W. E. Dulin, *J. Pharmacol. Exp. Ther.*, **150**, 491 (1965).

(5) D. L. Smith, A. A. Forist, and G. C. Gerritsen, *ibid.*, **150**, 316 (1965).

(6) R. Soliman, H. Mokhtar, and E. S. H. El Ashry, *Pharmazie*, **33**, 184 (1978).

(7) H. Mokhtar and R. Soliman, *ibid.*, **33**, 649 (1978).

(8) R. Soliman, *J. Med. Chem.*, **22**, 321 (1979).

(9) R. Soliman and H. M. Feid-Allah, *J. Pharm. Sci.*, **70**, 602 (1981).

(10) F. J. Marshall, M. V. Sigal, and M. A. Root, *J. Med. Chem.*, **6**, 60 (1963).

(11) G. A. D. Haslewood and T. A. Strookman, *Biochem. J.*, **33**, 920 (1939).

# Carboxymethylcellulose: Effect of Degree of Polymerization and Substitution on Tablet Disintegration and Dissolution

**N. H. SHAH *, J. H. LAZARUS *, P. R. SHETH *, and C. I. JAROWSKI ˣ**

Received January 21, 1980, from the *Department of Allied Health and Industrial Sciences, College of Pharmacy and Allied Health Professions, St. John's University, Jamaica, NY 11439.* Accepted for publication November 6, 1980. *Present address: Hoffmann-La Roche Inc., Nutley, NJ 07110.

**Abstract** □ Highly polymerized grades of carboxymethylcellulose sodium serve effectively as disintegrating agents for tablets. The preferred disintegrants have a high degree of polymerization with a small number of carboxymethyl groups. Grades with a low degree of polymerization are poor disintegrating agents irrespective of their degree of substitution. The dissolution rates of sulfamethoxazole tablets correlated with the disintegration times.

**Keyphrases** □ Carboxymethylcellulose—effect of polymerization and substitution on tablet disintegration and dissolution □ Disintegrants—carboxymethylcellulose, effect of polymerization and substitution on tablet disintegration and dissolution □ Binders—carboxymethylcellulose, effect of polymerization and substitution on tablet disintegration and dissolution □ Disintegration—tablets, effect of carboxymethylcellulose polymerization and substitution □ Dissolution—tablets, effect of carboxymethylcellulose polymerization and substitution

Carboxymethylcellulose sodium is the sodium salt of the polycarboxymethyl ether of cellulose. The cellulose molecule consists of repeating cellobiose units, which are composed of two anhydroglucose units. The structures of the cellulose and carboxymethylcellulose molecules are (1):

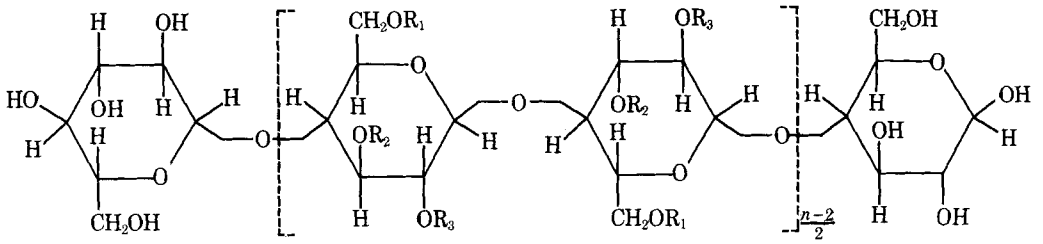

cellulose: $R_1 = R_2 = R_3 = H$
carboxymethylcellulose: degree of substitution = 1 when $R_1 = CH_2COOH$, $R_2 = R_3 = H$
degree of substitution = 3 when $R_1 = R_2 = R_3 = CH_2COOH$ ($n$ = number of anhydroglucose units or degree of polymerization)

The degree of substitution refers to the average number of carboxymethyl groups that are substituted per anhydroglucose unit. Thus, carboxymethylcellulose sodium has a degree of substitution of 0.7 when an average of seven carboxymethyl groups have been substituted per 10 anhydroglucose units; it has a degree of substitution of 1.2 when an average of 12 carboxymethyl groups have been substituted per 10 anhydroglucose units.

The average molecular weight of carboxymethylcellulose sodium is determined by the average chain length and the degree of substitution. The viscosity of carboxymethylcellulose sodium dispersions increases as the molecular weight increases and thus is used as a measure of the degree of polymerization.

The USP XX has a specification for sodium content calculated on a dry basis of not less than 6.5% and not more than 9.5% (2). The upper limit represents a degree of substitution of about 0.7. There is no specification for viscosity so the degree of polymerization can vary. As the degree of substitution decreases, the chemical structure of carboxymethylcellulose sodium approaches the chemical structure of natural cellulose.

For many years, carboxymethylcellulose sodium has been used in tablets as a binder and as a viscosity builder in aqueous solutions (1). Carboxymethylcellulose sodium with a low sodium content and a degree of substitution below 0.2 was reported to be a suitable tablet disintegrant (3). Although there are no reports on the effect of different grades of carboxymethylcellulose sodium having varying degrees of polymerization and substitution on tablet characteristics, the physicochemical properties of cellulose are altered significantly with changes in the degree of substitution and polymerization.

The present study evaluated the effect of various grades of carboxymethylcellulose sodium on the disintegration and dissolution rates of a sulfamethoxazole tablet.

## EXPERIMENTAL

**Materials**—Sulfamethoxazole[1], carboxymethylcellulose sodium[2] of various grades, pregelatinized starch[3], and magnesium stearate[4] were used.

**Equipment**—A single-punch tablet press[5], a friabilator[6], a hardness tester[7], a USP disintegration apparatus[8], a USP dissolution apparatus[9], a viscometer LVT[10], U.S. sieves numbers 14 and 20[11], and a mixer[12] were used.

[1] Research compound, Hoffmann-La Roche, Nutley, N.J.
[2] Hercules Inc., Wilmington, Del.
[3] National Starch, Bridgewater, N.J.
[4] Mallinckrodt Corp., St. Louis, Mo.
[5] Thomas Engineering Co., Hoffmann Estates, Ill.
[6] Hoffmann-La Roche, Nutley, N.J.
[7] Cherry-Burrell Corp., Cedar Rapids, Iowa.
[8] Scientific Glass Co., Bloomfield, N.J.
[9] Van-Kel Industries, Chatham, N.J.
[10] Brookfield Engineering Laboratories, Stoughton, Mass.
[11] U.S. Standard Sieves, Newark Wire Cloth Co., Newark, N.J.
[12] Hobart Manufacturing Co., Troy, N.Y.

0022-3549/81/0600-0611$01.00/0
© 1981, American Pharmaceutical Association

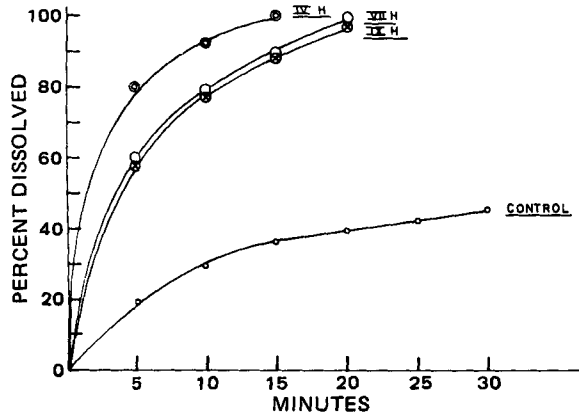


**Figure 1**—*Effect of the degree of substitution of highly polymerized carboxymethylcellulose sodium on the dissolution rate of sulfamethoxazole tablets.*

**Solubility Studies**—The solubility of the sulfamethoxazole in various solvents was determined by the method specified in USP XX (2).

**Viscosity Studies**—The viscosity of various carboxymethylcellulose sodium samples was determined in distilled water at 25° with a viscometer. The percentage concentration, spindle number, and speed recommended by the supplier were used.

**Manufacture of Tablets**—The raw materials were used as received. The formulations used in the study were as follows:

| | control formula, mg | experimental formula 1, mg | experimental formula 2, mg |
|---|---|---|---|
| sulfamethoxazole | 500 | 500 | 500 |
| pregelatinized starch | 25 | 25 | 25 |
| carboxymethylcellulose sodium | — | 15 | 25 |
| magnesium stearate | 2.5 | 2.5 | 2.5 |

The sulfamethoxazole was mixed with the pregelantinized starch and passed manually through a 20-mesh sieve. The mixture was remixed and granulated with water (240 ml of distilled water for 1000 tablets) and the granulation was placed on trays and dried overnight in an oven set at 54.4°. The dried granulation was screened manually through a 14-mesh screen. Then carboxymethylcellulose sodium was mixed with the dried granulation for 10 min. The granulation was lubricated with magnesium stearate by blending the mixture for 5 min. The tablets were compressed on a single-punch tablet press using 1.3-cm (0.5-in.) diameter flat-faced beveled-edge punches to a hardness of ~15 Strong–Cobb units.

**Assay**—The UV spectrum of sulfamethoxazole showed a maximum absorption at 265 nm. It obeyed Beer's law in 0.84 *N* HCl.

**Disintegration**—Tablet disintegration was carried out in simulated gastric and intestinal fluids at 37° using the USP XX disintegration apparatus without disks.

**Dissolution Rate**—The dissolution rate was measured by the USP XX method using the rotating basket at 100 rpm with 0.84 *N* HCl as the dissolution medium. The percentage of the drug released was determined as a function of time.

**Table I—Sulfamethoxazole Solubility in Various Solvents at 25°**

| Solvent | Solubility, mg/ml |
|---|---|
| 95% Ethanol | 30 |
| Methanol | 90 |
| 0.1 *N* NaOH | 16 |
| Water | 0.5 |
| 0.1 *N* HCl | 0.03 |
| 0.84 *N* HCl | 2.85 |

**Table II—Viscosities of Various Grades of Carboxymethylcellulose Sodium in Water at 25°**

| Degree of Substitution | Grade[a] | Concentration, % | Viscosity Range[b], cps | Actual Viscosity, cps |
|---|---|---|---|---|
| 0.4 | IVH | 1 | 400–1000 | 1080 |
| 0.4 | IVM | 2 | 300–600 | 350 |
| 0.4 | IVL | 2 | 24 maximum | 16 |
| 0.7 | VIIH | 1 | 1500–2500 | 1580 |
| 0.7 | VIIM | 2 | 300–600 | 320 |
| 0.7 | VIIL | 2 | 25–50 | 30 |
| 0.9 | IXH | 1 | 2500–4500 | 3200 |
| 0.9 | IXM | 2 | 400–800 | 360 |
| 1.2 | XIIM | 2 | 800–3100 | 850 |

[a] The first number represents the degree of substitution. Thus, IV, V, VII, IX, or XII represents the degree of substitution of 0.4, 0.5, 0.7, 0.9, or 1.2, respectively. The L, M, or H signifies low, medium, or high viscosity. [b] According to supplier.

## RESULTS AND DISCUSSION

Sulfamethoxazole was poorly soluble in distilled water as well as in 0.1 *N* HCl (Table I). Its solubility was markedly improved in 0.84 *N* HCl. As a consequence, the latter solvent was used in the dissolution studies.

The viscosities of the various grades of carboxymethylcellulose sodium are shown in Table II. In addition, the nomenclature for the various grades is explained.

All tablets manufactured met USP specifications for weight variation, content uniformity, and friability. They had a hardness range of 13–16 Strong–Cobb units. The data on the disintegration and dissolution rates of the various tablets are given in Table III and in Figs. 1–3. The results clearly show that the highly polymerized grades of carboxymethylcellulose sodium are good disintegrating agents. The disintegration properties were significantly influenced by the degree of substitution. The gums with a low degree of substitution together with a high degree of polymerization were excellent disintegrating agents. The disintegration properties of carboxymethylcellulose sodium decreased as the degree of substitution increased and the degree of polymerization decreased. Thus, carboxymethylcellulose sodium with a degree of substitution of 0.4 and a high degree of polymerization would be an excellent disintegrant. However,

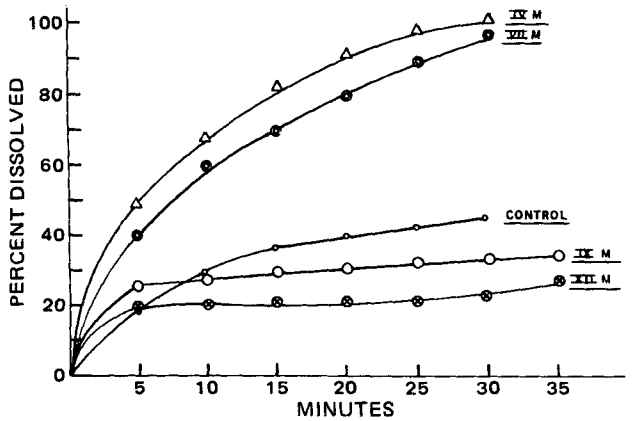


**Figure 2**—*Effect of the degree of substitution of carboxymethylcellulose sodium on the dissolution rate of sulfamethoxazole tablets.*

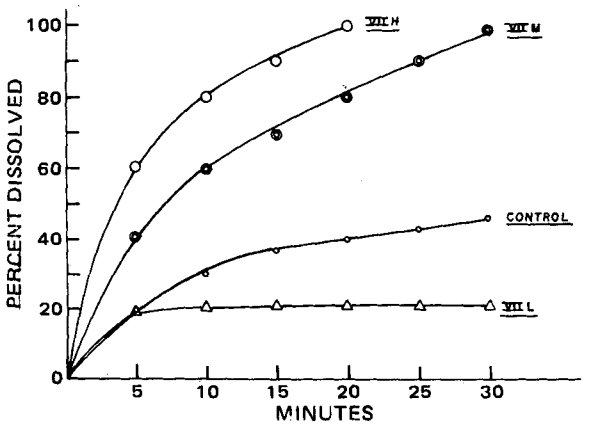


**Figure 3**—*Effect of the degree of polymerization of carboxymethylcellulose sodium on the dissolution rate of sulfamethoxazole tablets.*

Table III—Disintegration Rates of Sulfamethoxazole Tablets Containing 3% of Various Grades of Carboxymethylcellulose Sodium

| Grade | Degree of Substitution | Degree of Polymerization | Disintegration Time, sec: Simulated Gastric Fluid | Disintegration Time, sec: Simulated Intestinal Fluid |
|---|---|---|---|---|
| — | Control | — | >1800 | >1800 |
| IVH | 0.4 | High | 30 | 30 |
| IVM | 0.4 | Medium | 90 | 300 |
| IVL | 0.4 | Low | >1800 | >1800 |
| VIIH | 0.7 | High | 90 | 600 |
| VIIM | 0.7 | Medium | 100 | 900 |
| VIIL | 0.7 | Low | >1800 | >1800 |
| IXH | 0.9 | High | 100 | 900 |
| IXM | 0.9 | Medium | >1800 | >1800 |
| XIIM | 1.2 | Medium | >1800 | >1800 |

carboxymethylcellulose sodium with a degree of substitution of 1.2 and a low degree of polymerization would be a poor disintegrating agent. The results are summarized as follows:

1. The highly polymerized grades of carboxymethylcellulose sodium are good disintegrating agents. The preferred disintegrant has a high degree of polymerization together with a low degree of substitution. Type IVH is preferred over VIIH, which is preferred over IXH (Fig. 1).

2. The medium-polymerized carboxymethylcellulose sodium with a degree of substitution of 0.7 or less has moderate disintegrant properties; but as substitution increases from 0.7 to 1.2, the medium-polymerized grades of carboxymethylcellulose sodium are not as effective as tablet disintegrants. Thus, medium-viscosity carboxymethylcellulose sodium with a degree of substitution of 0.4 or 0.7 has moderate disintegrant properties. Those with a higher degree of substitution, such as 0.9 or 1.2, are poor disintegrants (Fig. 2). Highly substituted carboxymethylcellulose sodium can only be used as a disintegrant when the degree of polymerization is high.

3. With the same degree of substitution, the higher the degree of polymerization, the better are the disintegrant properties. The disintegrant efficacy improves directly with an increase in polymerization. Thus, VIIH is a better disintegrant than VIIM, which is better than VIIL (Fig. 3).

4. Carboxymethylcellulose sodium with a low degree of polymerization is a poor disintegrant irrespective of the degree of substitution. Thus, low-viscosity carboxymethylcelluloses with degree of substitution values of 0.4, 0.7, 0.9, and 1.2 are poor disintegrating agents.

5. The dissolution rate of the sulfamethoxazole tablets correlated with the disintegration times of the tablets.

6. There was no significant difference in disintegration time and in dissolution rate between the two experimental formulas.

Table IV—Minimum Viscosities for Good Disintegration Properties

| Degree of Substitution | Minimum Viscosity of 2% Aqueous Dispersion at 25° Using Propeller-Type Mixer, cps |
|---|---|
| 0.4 | >150 |
| 0.7 | >200 |
| 0.9 | >1500 |
| 1.2 | >3000 |

The minimum viscosity required for effective disintegration properties for the various grades of carboxymethylcellulose sodium is shown in Table IV. Aqueous dispersions of carboxymethylcellulose sodium with a degree of substitution of 0.4 should have a viscosity above 150 cps to have good disintegration properties. Similarly, the higher substituted carboxymethylcellulose sodium should meet the requirements for minimum viscosities to be considered a good disintegrant. Whenever a high degree of polymerization is mentioned, the viscosity will be much greater than the minimum stated in Table IV. Carboxymethylcellulose sodium with a low degree of polymerization will exhibit viscosities less than the minimum value in Table IV.

Further studies are in progress to evaluate the effect of carboxymethylcellulose sodium in solid dosage forms for: (*a*) disintegrants in tablets containing weak acids, weak bases, or neutral drugs; (*b*) comparisons with other presently available disintegrants; and (*c*) alteration of drug delivery systems through the utilization of the appropriate grade.

## REFERENCES


(1) "Cellulose Gum, Chemical & Physical Properties," Hercules Inc., Wilmington, Del.

(2) "The United States Pharmacopeia," 20th rev., United States Pharmacopeial Convention, Rockville, Md., 1980, p. 120.

(3) F. Laminet, L. Delattre, and J. P. Delaport, *Pharm. Acta Helv.*, 44, 418 (1969).


# Rotary Press Utilizing a Flexible Die Wall


**GREGORY E. AMIDON, DONALD P. SMITH, and EVERETT N. HIESTAND** ˣ



Received March 31, 1980, from *The Upjohn Company, Kalamazoo, MI 49001.* Accepted for publication November 7, 1980.



**Abstract** □ A die with a flexible wall was constructed and evaluated on a specially modified instrumented rotary tablet press. The design permits an inward deflection of the die wall by a side punch, which rolls past a side compression roll during compression–decompression. The side compression roll is instrumented to monitor the applied side compression roll forces. On decompression, return of the die wall to its original position permits release of residual die wall pressure. The decreased residual die wall pressure can decrease fracture and capping of tablets for problem formulations. The performance was tested on three experimental formulations. For these formulations, tablets made in a conventional die exhibited severe capping problems. However, most tablets compressed in the special die were superior. With proper adjustment of punch and die wall compression forces, excellent tablets could be manufactured. The merits of the special die and modified tablet machine are substantiated, although this initial design did not provide adequate die wall pressure for all formulations. Further engineering efforts could result in practical production equipment.



**Keyphrases** □ Tableting machine—tablets produced from modified tableting machine with flexible die wall compared with those compressed conventionally □ Tablets—compressed with modified tableting machine compared with those conventionally compressed □ Compressed tablets—produced from modified tableting machine with flexible die wall, compared with tablets produced conventionally


It is generally accepted that bonding in a compressed tablet is the result of establishing and maintaining sufficient true areas of contact between particles. Lamination or capping of tablets, therefore, may seem unexplained since significant portions of a laminated or capped tablet remain densely packed after compression–decompression.


0022-3549/81/0600-0613$01.00/0


© 1981, American Pharmaceutical Association

Table III—Disintegration Rates of Sulfamethoxazole Tablets Containing 3% of Various Grades of Carboxymethylcellulose Sodium

| Grade | Degree of Substitution | Degree of Polymerization | Disintegration Time, sec: Simulated Gastric Fluid | Disintegration Time, sec: Simulated Intestinal Fluid |
|---|---|---|---|---|
| — | Control | — | >1800 | >1800 |
| IVH | 0.4 | High | 30 | 30 |
| IVM | 0.4 | Medium | 90 | 300 |
| IVL | 0.4 | Low | >1800 | >1800 |
| VIIH | 0.7 | High | 90 | 600 |
| VIIM | 0.7 | Medium | 100 | 900 |
| VIIL | 0.7 | Low | >1800 | >1800 |
| IXH | 0.9 | High | 100 | 900 |
| IXM | 0.9 | Medium | >1800 | >1800 |
| XIIM | 1.2 | Medium | >1800 | >1800 |

carboxymethylcellulose sodium with a degree of substitution of 1.2 and a low degree of polymerization would be a poor disintegrating agent. The results are summarized as follows:

1. The highly polymerized grades of carboxymethylcellulose sodium are good disintegrating agents. The preferred disintegrant has a high degree of polymerization together with a low degree of substitution. Type IVH is preferred over VIIH, which is preferred over IXH (Fig. 1).

2. The medium-polymerized carboxymethylcellulose sodium with a degree of substitution of 0.7 or less has moderate disintegrant properties; but as substitution increases from 0.7 to 1.2, the medium-polymerized grades of carboxymethylcellulose sodium are not as effective as tablet disintegrants. Thus, medium-viscosity carboxymethylcellulose sodium with a degree of substitution of 0.4 or 0.7 has moderate disintegrant properties. Those with a higher degree of substitution, such as 0.9 or 1.2, are poor disintegrants (Fig. 2). Highly substituted carboxymethylcellulose sodium can only be used as a disintegrant when the degree of polymerization is high.

3. With the same degree of substitution, the higher the degree of polymerization, the better are the disintegrant properties. The disintegrant efficacy improves directly with an increase in polymerization. Thus, VIIH is a better disintegrant than VIIM, which is better than VIIL (Fig. 3).

4. Carboxymethylcellulose sodium with a low degree of polymerization is a poor disintegrant irrespective of the degree of substitution. Thus, low-viscosity carboxymethylcelluloses with degree of substitution values of 0.4, 0.7, 0.9, and 1.2 are poor disintegrating agents.

5. The dissolution rate of the sulfamethoxazole tablets correlated with the disintegration times of the tablets.

6. There was no significant difference in disintegration time and in dissolution rate between the two experimental formulas.

Table IV—Minimum Viscosities for Good Disintegration Properties

| Degree of Substitution | Minimum Viscosity of 2% Aqueous Dispersion at 25° Using Propeller-Type Mixer, cps |
|---|---|
| 0.4 | >150 |
| 0.7 | >200 |
| 0.9 | >1500 |
| 1.2 | >3000 |

The minimum viscosity required for effective disintegration properties for the various grades of carboxymethylcellulose sodium is shown in Table IV. Aqueous dispersions of carboxymethylcellulose sodium with a degree of substitution of 0.4 should have a viscosity above 150 cps to have good disintegration properties. Similarly, the higher substituted carboxymethylcellulose sodium should meet the requirements for minimum viscosities to be considered a good disintegrant. Whenever a high degree of polymerization is mentioned, the viscosity will be much greater than the minimum stated in Table IV. Carboxymethylcellulose sodium with a low degree of polymerization will exhibit viscosities less than the minimum value in Table IV.

Further studies are in progress to evaluate the effect of carboxymethylcellulose sodium in solid dosage forms for: (*a*) disintegrants in tablets containing weak acids, weak bases, or neutral drugs; (*b*) comparisons with other presently available disintegrants; and (*c*) alteration of drug delivery systems through the utilization of the appropriate grade.

## REFERENCES


(1) "Cellulose Gum, Chemical & Physical Properties," Hercules Inc., Wilmington, Del.

(2) "The United States Pharmacopeia," 20th rev., United States Pharmacopeial Convention, Rockville, Md., 1980, p. 120.

(3) F. Laminet, L. Delattre, and J. P. Delaport, *Pharm. Acta Helv.*, 44, 418 (1969).


# Rotary Press Utilizing a Flexible Die Wall


**GREGORY E. AMIDON, DONALD P. SMITH, and EVERETT N. HIESTAND** ˣ



Received March 31, 1980, from *The Upjohn Company, Kalamazoo, MI 49001.* Accepted for publication November 7, 1980.



**Abstract** □ A die with a flexible wall was constructed and evaluated on a specially modified instrumented rotary tablet press. The design permits an inward deflection of the die wall by a side punch, which rolls past a side compression roll during compression–decompression. The side compression roll is instrumented to monitor the applied side compression roll forces. On decompression, return of the die wall to its original position permits release of residual die wall pressure. The decreased residual die wall pressure can decrease fracture and capping of tablets for problem formulations. The performance was tested on three experimental formulations. For these formulations, tablets made in a conventional die exhibited severe capping problems. However, most tablets compressed in the special die were superior. With proper adjustment of punch and die wall compression forces, excellent tablets could be manufactured. The merits of the special die and modified tablet machine are substantiated, although this initial design did not provide adequate die wall pressure for all formulations. Further engineering efforts could result in practical production equipment.



**Keyphrases** □ Tableting machine—tablets produced from modified tableting machine with flexible die wall compared with those compressed conventionally □ Tablets—compressed with modified tableting machine compared with those conventionally compressed □ Compressed tablets—produced from modified tableting machine with flexible die wall, compared with tablets produced conventionally


It is generally accepted that bonding in a compressed tablet is the result of establishing and maintaining sufficient true areas of contact between particles. Lamination or capping of tablets, therefore, may seem unexplained since significant portions of a laminated or capped tablet remain densely packed after compression–decompression.


0022-3549/81/0600-0613$01.00/0


© 1981, American Pharmaceutical Association

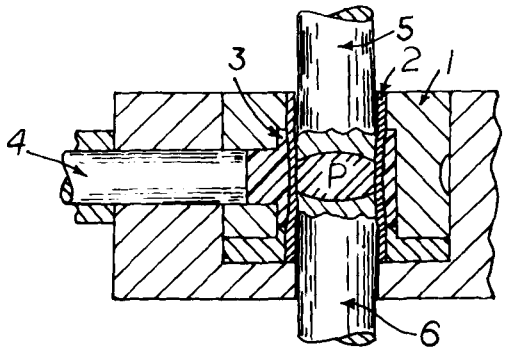


**Figure 1**—*Schematic diagram of specially designed triaxial die.*

A sufficient true area of contact apparently is established in these regions to bond ingredients together, yet the bonding is not sufficient to prevent fracture.

## BACKGROUND

Fracture is thought to be the result of inadequate plastic flow, resulting in highly stressed regions within the compact. A previous report (1) demonstrated that the die wall pressure for several materials is limited by the shear strength of the compacted material and that it changes with time (viscoelastic effects). Furthermore, it was concluded that the dynamic shear strength is exceeded over much of the compression–decompression cycle. When the shear strength is exceeded, either permanent deformation *via* plastic flow or fracture occurs.

Fracture need not occur if plastic flow occurs before stresses are high enough to cause fracture by crack propagation. Very brittle materials such as phenacetin, methenamine, and acetaminophen cannot relieve local stresses as easily as other materials by plastic deformation. Since high die wall pressure results, fracture is more likely to occur in compacts of these materials. These fractures may occur on decompression or on ejection where the die edge may concentrate stress and cause capping.

A decrease of die wall pressure (either by allowing the die wall pressure to decay with time or by relieving the pressure mechanically) should decrease the likelihood of fracture. A specially designed die was reported (2) that allowed the simultaneous release of punch and die wall pressure. The special square die, split along its diagonal, was placed in a frame holding the two halves together with a hydraulic cylinder. By fluid coupling of this hydraulic cylinder with the cylinder on the hand press that pushes the punches together, the die wall and punch pressures could be reduced simultaneously during decompression. In this manner, intact compacts of materials known to laminate on decompression or ejection (*e.g.*, phenacetin, erythromycin, methenamine, and acetaminophen) could be made.

Success with this split die led to the circular die with the flexible die wall reported in this investigation. The die was mounted into a modified rotary press. A specially designed side compression roll (3) and side punch permit pressure to be applied to the die wall, which contracts under compression. In this way, die wall pressure can be released as the die wall returns to its original shape during decompression. Three direct-compaction formulations were studied, and the capping tendencies of tablets formed in the special die were compared with those prepared in a conventional die on the same machine.

**Apparatus**—The special die is shown in cross-section in Fig. 1. The internal wall of the die, 1, is lined and defined by a sleeve, 2, made of thin steel to provide slight radial flexibility. The sleeve is surrounded by a pressure-transmitting material, 3, such as rubber, which evenly distributes pressure around the sleeve. Application of pressure through the side punch, 4, permits a slight (one thousandth or two thousandth inch) inward deflection of the steel sleeve. Proper timing of the movement of the radial punch and axial punches, 5 and 6, permit the simultaneous three-dimensional or triaxial compression of powders. Release of the side punch pressure, which is simultaneous with axial punch pressure release, permits the steel sleeve to return to its original position.

The side compression roll, 7, and mounting block are shown attached to the rotary press in Fig. 2. The side compression roll is positioned such that pressure is applied simultaneously to the upper, lower, and side punches by the upper, 8, lower, 9, and side compression roll. Appropriate measures were taken to prevent overloading of the machine parts due to the excessive stress conditions. Side compression roll pressure was

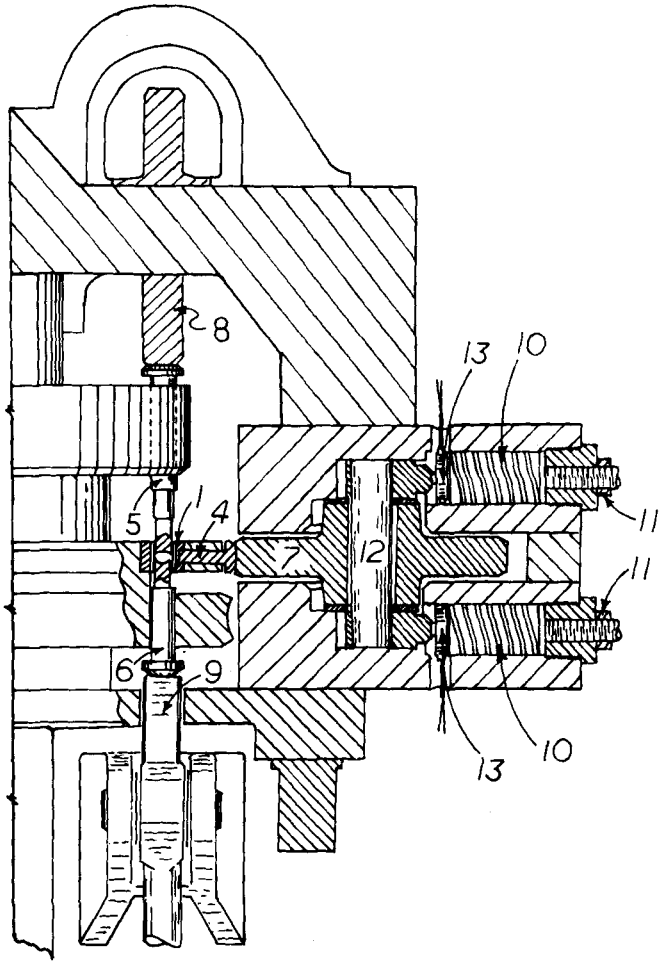


**Figure 2**—*Schematic diagram of modified rotary press showing details of the side compression roll.*

adjusted by incorporating two springs, 10, and adjusting nuts, 11, which apply pressure to each end of the side compression roll pin, 12. Strain-gauge sensors, 13, permit monitoring of the side compression force. Adjustable stops incorporated within the mounting block prevent application of excess pressure to the side punch when the die is empty.

The modified rotary press[1] is shown in Fig. 3. For the following experiments, only two of the 16 stations were used. One station consisted of a set of round 1.111-cm ($^7/_{16}$-in.) concave (0.075-cm deep cup) punches and die. On the opposite side of the table was the specially designed die. Similar round 1.106-cm ($^7/_{16}$-in.) concave punches were used in the special die. These punch diameters were reduced by 0.005 cm to allow enough clearance between the collapsed die wall and the punch during compression. The two types of tablets can be separated as they come off the machine, and direct comparisons can be made between them.

The axial punch pressure was monitored by a strain gauge attached to the lower roll support and calibrated with a known load. During operation, all three strain gauges were monitored so that the compression forces were known for both die types and the die wall–punch forces were known for the triaxial die.

**Limitations in Design**—Technical requirements placed important restrictions on the design and construction of the special die, particularly in the amount of die wall pressure that could be released by die wall flexing. Maximum flexing of the die wall on compression is desired to allow adequate die wall pressure release on decompression. However, the contraction of the die wall radius is limited by the upper and lower punches in the die. At the same time, an excessive gap between the punch and die wall is not acceptable since large weight variation due to powder slipping past the lower punch might occur.

Excessive powder between the punch and die wall also could cause sticking of the punches in the die and failure of the die wall to contract correctly. For these reasons, the punch diameters for the triaxial die were

[1] Model B2, F. J. Stokes Corp., Division of Pennwalt Corp., Philadelphia, Pa.

Table I—Composition of the Three Direct-Compression Formulations Used to Test the Modified Rotary Tablet Machine

| Formulation | Composition, % |
|---|---|
| Ascorbic acid | |
| Ascorbic acid USP | 42.9 |
| Compressible sugar NF | 46.3 |
| Microcrystalline cellulose NF | 4.2 |
| Starch USP | 2.5 |
| Orange oil NF | 2.6 |
| Magnesium stearate USP | 0.8 |
| Colloidal silicon dioxide NF | 0.7 |
| Phenacetin | |
| Phenacetin USP | 42.9 |
| Compressible sugar NF | 46.3 |
| Microcrystalline cellulose NF | 4.2 |
| Starch USP | 5.1 |
| Magnesium stearate USP | 0.8 |
| Colloidal silicon dioxide NF | 0.7 |
| Acetaminophen | |
| Acetaminophen | 41.4 |
| Lactose USP | 47.4 |
| Microcrystalline cellulose NF | 8.4 |
| Starch USP | 2.2 |
| Colloidal silicon dioxide NF | 0.12 |
| FD&C Blue No. 2 Aluminum Lake | 0.04 |
| Magnesium stearate USP | 0.44 |

reduced by 0.005 cm to permit this amount of flexing of the die wall. It was felt that this change would provide sufficient die wall radius contraction and, at the same time, minimize the amount of powder slipping past the lower punch. This limited flexibility of the special die, unlike the split die that allows complete release of the die wall pressure, is expected to release only a portion of the residual die wall pressure during decompression.

The present design requires enough side compression roll pressure to flex the steel die wall sleeve inward; therefore, the actual force applied to the compact is not equal to the side compression roll force. However, the observed values for the side compression roll force should be approximately proportional to the actual applied force in the radial direction. The efficiency of the pressure-transmitting material within the die at transferring the pressure from the side punch to the die wall and the elastic properties of the compression roll and mounting block also influence the actual pressure applied to the die wall.

Only one design, the initial effort, was used in these studies. Because the force for die wall contraction in the presence of powder in the die and of small amounts of powder between the die wall and punch could not be evaluated in advance, the choice of spring sizes and load cells for the die compression was conjecture. The experimental results indicate that the springs and load cells were somewhat undersize, which restricted the amount of die wall pressure that could be applied. Some of the experimental results may have been due to this limitation. This limitation results from the arbitrary choice of capacities and is not inherent in the application of the principle.

## EXPERIMENTAL

**Materials**—Ascorbic acid USP[2], phenacetin USP[3] (passed through a No. 64 tensile bolting cloth), and acetaminophen[4] were used as the primary ingredient in each formulation. Other excipients included microcrystalline cellulose NF[5], colloidal silicon dioxide NF[6], starch USP[7] (cornstarch passed through a No. 105 tensile bolting cloth), compressible sugar NF[8], FD&C Blue No. 2 Aluminum Lake[9], lactose USP[10] (hydrous spray process), and orange oil NF[11]. Magnesium stearate USP powder, food grade[12], was used as a lubricant.

**Methods**—Three direct-compression formulations were prepared as shown in Table I. The ascorbic acid and phenacetin formulations were similar and were prepared in the following manner. All ingredients except magnesium stearate were passed through a 20-mesh screen and blended in a V-blender for 10 min. Subsequently, a portion of this blend was passed through a 20-mesh screen with the magnesium stearate, and all powder was mixed for an additional 2 min. The acetaminophen formulation was prepared by blending, in a V-blender, a portion of a 75% acetaminophen–25% spray-dried lactose mixture with an appropriate amount of a blend of the remaining ingredients to obtain the desired percentage of acetaminophen.

These formulations were prepared to study differences in capping tendencies between conventionally compressed (uniaxially compressed) tablets and tablets compressed in the special triaxial compression die. Other properties such as disintegration and dissolution were not evaluated.

The primary means of assessing capping tendency was visual inspection of each tablet after the hardness test. Breaking strengths were obtained on at least five tablets using an electronic hardness tester[13]. Tablets classified as "capped" normally had the entire intact dome separated from the body of the tablet. Tablets that did not cap in the hardness tester were inspected and broken by hand to check for laminations. Tablets classified as "not capped" had no visible laminations. Friability[14] was determined occasionally but often did not adequately distinguish between capped and noncapped tablets when only small fracture lines were present.

The direct-compression formulations were compressed at various punch and side compression roll forces. Normal operation speed was 24.5 rpm, although one formulation was done at 31.5 rpm. Before operation of the tablet machine, sufficient material was added to fill the feed frame (50–100 g). Normal operation time was 30–60 sec at each die wall and punch pressure setting. This procedure produced ~25–50 tablets; half

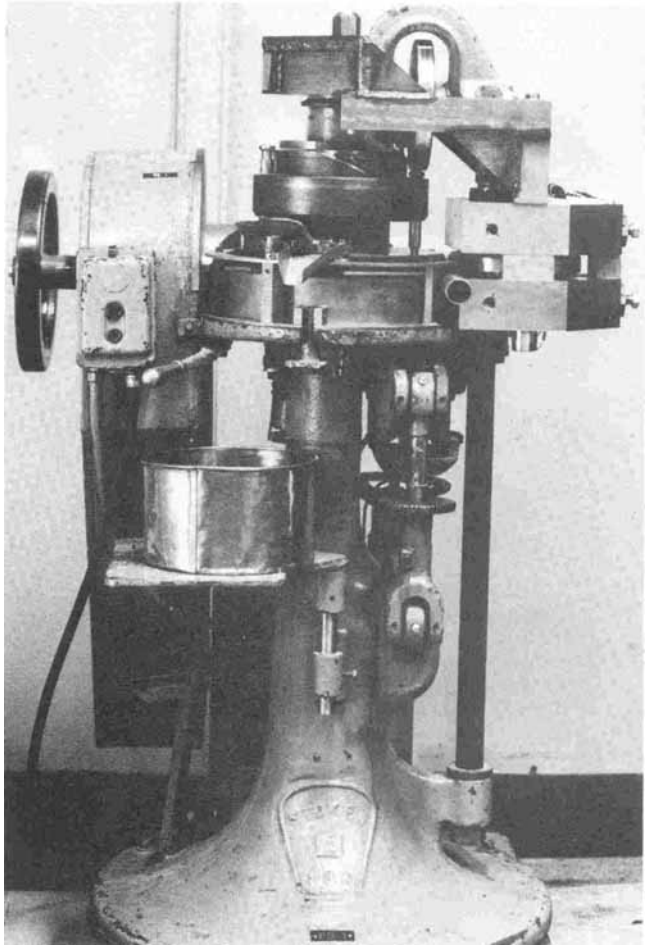

**Figure 3**—*Modified rotary tablet press with triaxial decompression capability.*

[2] Pfizer, New York, N.Y.
[3] Monsanto Co., St. Louis, Mo.
[4] Eastman Chemical Products, Kingsport, Tenn.
[5] Avicel PH-101, FMC Corp., Marcus Hook, Pa.
[6] Cabot Corp., Cab-O-Sil Division, Boston, Mass.
[7] Morrison and Watkins, West Bloomfield, Mich.
[8] DiPac, Amstar Corp., New York, N.Y.
[9] Colorcon, West Point, Pa.
[10] Foremost Foods Co., San Francisco, Calif.
[11] International Flavors and Fragrances, New York, N.Y.
[12] Mallinckrodt, Lodi, N.J.
[13] Heberlein and Co., AG, Zurich, Switzerland.
[14] Chemical and Pharmaceutical Industry Co., New York, N.Y.

**Table II—Comparison of Tablets from Uniaxial Die and Triaxial Die [a] Ascorbic Acid Formulation**

| Punch Force, kN | Side Compression Roll Force, kN | Uniaxial Die: Breaking Strength, N × $10^{-1}$ | Uniaxial Die: Percent of Tablets Capped | Uniaxial Die: Friability, % of weight lost | Triaxial Die: Breaking Strength, N × $10^{-1}$ | Triaxial Die: Percent of Tablets Capped | Triaxial Die: Friability, % of weight lost |
|---|---|---|---|---|---|---|---|
| 25.0 | 14.4 | 4.2 | 100 | — | 6.0 | 80 | — |
| 24.4 | 16.3 | 4.2 | 100 | — | 4.3 | 100 | — |
| 25.5 | 21.9 | — | — | — | 6.0 | 50 | 3.4 |
| 25.1 | 23.8 | 3.3 | 100 | — | 5.3 | 20 | 0.79 |

[a] Machine speed at 31.5 rpm.

**Table III—Comparison of Tablets from Uniaxial Die and Triaxial Die [a] Phenacetin Formulation**

| Punch Force, kN | Side Compression Roll Force, kN | Uniaxial Die: Breaking Strength, N × $10^{-1}$ | Uniaxial Die: Percent of Tablets Capped | Uniaxial Die: Friability, % of weight lost | Triaxial Die: Breaking Strength, N × $10^{-1}$ | Triaxial Die: % of Tablets Capped | Triaxial Die: Friability, % of weight lost |
|---|---|---|---|---|---|---|---|
| 13.0 | 16.1 | 4.8 | 100 | — | 4.5 | 0 | 2.8 |
| 13.2 | 19.4 | 3.3 | 100 | — | 5.0 | 0 | 2.1 |
| 12.4 | 22.7 | 3.8 | 100 | — | 5.3 | 0 | 3.8 |
| 12.0 | 26.1 | 3.6 | 100 | — | 4.8 | 0 | 1.7 |
| 18.2 | 26.3 | 6.2 | 100 | — | 6.6 | 80 | — |
| 23.2 | 16.2 | 5.5 | 100 | — | 5.0 | 100 | — |

[a] Machine speed at 24.5 rpm.

**Table IV—Comparison of Tablets from Uniaxial Die and Triaxial Die [a] Acetaminophen Formulation**

| Punch Force, kN | Side Compression Roll Force, kN | Uniaxial Die: Breaking Strength, N × $10^{-1}$ | Uniaxial Die: Percent of Tablets Capped | Uniaxial Die: Friability, % of weight lost | Triaxial Die: Breaking Strength, N × $10^{-1}$ | Triaxial Die: Percent of Tablets Capped | Triaxial Die: Friability, % of weight lost |
|---|---|---|---|---|---|---|---|
| 11.0 | 26.0 | 2.8 | 100 | — | 2.4 | 20 | — |
| 15.8 | 26.0 | 4.6 | 100 | — | 5.0 | 0 | — |
| 21.2 | 26.1 | 5.2 | 100 | — | 5.0 | 100 | — |

[a] Machine speed at 24.5 rpm.

**Table V—Comparison of Tablets from Uniaxial Die and Triaxial Die [a] Ascorbic Acid Formulation**

| Punch Force, kN | Side Compression Roll Force, kN | Uniaxial Die: Breaking Strength, N × $10^{-1}$ | Uniaxial Die: Percent of Tablets Capped | Uniaxial Die: Friability, % of weight lost | Triaxial Die: Breaking Strength, N × $10^{-1}$ | Triaxial Die: Percent of Tablets Capped | Triaxial Die: Friability, % of weight lost |
|---|---|---|---|---|---|---|---|
| 18.9 | 16.7 | 1.6 | 100 | — | 3.6 | 0 | 1.5 |
| 19.7 | 11.3 | 4.3 | 20 | — | 5.7 | 0 | — |
| 21.7 | 15.6 | 4.4 | 100 | — | 6.4 | 0 | — |
| 23.3 | 18.8 | 3.0 | 100 | 100[b] | 5.1 | 0 | 0.93 |
| 23.7 | 16.5 | 4.2 | 100 | — | 5.5 | 0 | 0.92 |
| 23.8 | 14.2 | 4.3 | 100 | — | 6.1 | 0 | — |
| 24.4 | 18.9 | 4.2 | 100 | — | 6.2 | 0 | — |
| 25.2 | 14.2 | 3.5 | 100 | 100[b] | 5.5 | 0 | 0.98 |

[a] Machine speed at 24.5 rpm. [b] Capped.

were compressed in the standard die, and the other half were compressed in the triaxial die. The triaxially compressed tablets were marked with a felt pen as they came off the press to distinguish them from the uniaxially compressed tablets. Tablet weights, breaking strengths, and capping tendencies were checked immediately after completion of the run. Punch forces were set to ensure breaking strengths between 30 and 70 N, depending on the specific formulation.

## RESULTS

The results for three test formulations are shown in Tables II–V. These formulations showed a substantial difference between the uniaxially and triaxially compressed tablets. Several other formulations showed no capping or laminations for either kind of tablet. Two test formulations (containing materials known to induce capping) were tested in which both the triaxially and the uniaxially compressed tablets capped. Even with inadequate die wall pressure relief, the triaxially compressed tablets were at least as good as the uniaxially compressed ones. With some materials, adequate die wall pressure relief made the differences very dramatic: good tablets from the triaxial die and laminated ones from the uniaxial die.

The punch and side compression roll load cell outputs were monitored throughout each experiment. The punch force was obtained by multiplying the voltage output of the strain gauge by an experimentally determined calibration constant. This punch force was the same for both the uniaxially and triaxially compressed tablets under any given set of conditions. The side compression roll force is the sum of the calculated applied forces of the upper and lower load cells and was adjusted before each run to ensure even pressure on the side compression roll.

The average breaking strength of the tablets and the percentage of tablets that had visible laminations upon breaking were recorded. Friability is reported either as the percentage of the tablets that capped in the friabilator or as the percentage of the original weight lost after 4 min. All tablets were compressed at a speed of 24.5 rpm, except for the ascorbic acid tablets (Table II) which were made at 31.5 rpm.

## DISCUSSION

The results in Tables II–V demonstrate the differences in capping tendency between the uniaxially compressed and triaxially compressed tablets. Proper adjustment of the punch and side compression roll force generally resulted in triaxially compressed tablets that were superior to those compressed in the standard die.

The results for the ascorbic acid formulation (Table II) were obtained at a relatively constant punch force (24.4–25.5 kN) while the side compression roll force was varied. The uniaxially compressed tablets capped 100% of the time. With adequate die wall compression, the triaxially compressed tablets showed substantial improvement in quality, both in breaking strength and capping tendency. At lower side compression roll forces, the triaxially compressed tablets approached the poorer quality of the uniaxially compressed ones.

Apparently, as the side compression roll force increased, greater deflection of the triaxial die wall occurred. This deflection allowed greater release of die wall pressure on decompression and better relief of accumulated stresses. At lower side compression roll forces, less die wall deflection tended to produce tablets similar to the uniaxially compressed tablets. An apparent minimum side compression roll force is probably necessary for sufficient die wall deflection and adequate die wall pressure release. This minimum side compression roll force has to overcome the resistance of the die wall sleeve to deformation as well as any frictional resistances within the system. The applied punch pressure and the physical properties of the powders in the formulation (*i.e.*, tensile strength, shear strength, brittle fracture propensity, stress relaxation rate, *etc.*) also influence the minimum side compression roll force necessary to eliminate capping.

Similar success was obtained (*i.e.*, superior tablets) in the triaxial die for the phenacetin formulation (Table III). At moderate punch forces (12.0–13.0 kN), tablets compressed triaxially were obtained that showed no capping and that had tablet breaking strengths of 45–53 N. At this compression force, a range of side compression roll forces (16.1–26.1 kN) produced acceptable tablets. Conversely, the tablets compressed in the standard die showed a severe capping tendency, with some tablets capping upon ejection from the die. All uniaxially compressed tablets showed laminations that would make them unacceptable for production purposes. At higher punch forces, adequate release of residual die wall pressure could not be attained even with the maximum available compression roll force of 26.3 kN (*i.e.*, the design limitation), and the triaxially compressed tablets began to show capping.

The acetaminophen formulation (Table IV) showed the effect of varying the punch force without altering the side compression roll force. Only compressions at three punch forces were done, but differences between the tablets from the two dies were seen. Only at the high punch force was the quality of the triaxially compressed tablets reduced to become comparable to the uniaxially compressed tablets, *i.e.*, they showed excessive capping. Higher side compression roll force may have decreased capping in the triaxial die at the highest pressure, but this machine was incapable of such high forces. However, correct adjustment of the punch and side compression roll forces produced excellent tablets from the triaxial die.

The influence of machine speed on capping tendency can be seen by comparing the results for the ascorbic acid formulation in Tables II and V. A 30% increase in the machine speed changed the properties of both tablets. Uniaxially compressed tablets were of poor quality at both speeds. Although the triaxially compressed tablets were, in general, superior to the uniaxially compressed tablets at both rotation speeds, the triaxially compressed tablets showed evidence of capping at the higher speed. At the lower speed, a wide range of punch and side compression roll forces produced excellent tablets from the triaxial die (Table V). At the higher speed, capping was not eliminated completely with this material even at the maximum available side compression roll force, due perhaps in part to the time-dependent nature of stress relaxation.

The time-dependent nature of stress relaxation is an important mechanism of stress relief at the higher speed even in the triaxial die unless the stress relief rate of the punch and die wall is matched to minimize internal stress. Apparently, the longer time that the tablet spent in the die at the slower rotation speed allowed greater stress relief due to plastic flow within the compact. The large difference in the quality of the uniaxially and triaxially compressed tablets made at the lower speed shows that mechanical release of some die wall pressure by the triaxial die improves the tablet quality. At the higher speed, the mechanical release of the die wall pressure in the triaxial die was not sufficient by itself to eliminate capping. Future machines should have increased capacity and thus be capable of applying larger die wall forces, which would permit greater latitudes in the die wall forces applied. In this way, more die wall pressure could be released when the formulation and compression characteristics warrant it.

## SUMMARY

These preliminary investigations show that the mechanical release of die wall pressure, using a specially designed die with a flexible die wall, decreases or eliminates capping in three direct-compression formulations when compared to the same formulation compressed in a standard die. Correct adjustment of the applied side compression roll force and punch pressure allows sufficient release of residual die wall pressure on decompression to prevent or diminish capping due to the excessive stress concentrations within the compact during decompression or ejection. The force required for the side compression roll and for success in eliminating capping during decompression or ejection is dependent on the physical properties of the formulation, the applied punch pressure, the viscoelastic properties of the formulation materials, and the efficiency with which the applied force from the side compression roll is transmitted to the die wall.

This preliminary report (an outgrowth of the principles developed from basic research on the physical properties of materials) demonstrates the feasibility of designing and constructing equipment for the successful manufacture of otherwise troublesome formulations. This design offers the advantages of simultaneous and more uniform release of residual die wall pressure, as well as the capability of adjusting the pressure applied to the die wall. Further engineering efforts can result in practical production equipment design and utilization.

## REFERENCES

(1) E. N. Hiestand, J. E. Wells, C. B. Peot, and J. F. Ochs, *J. Pharm. Sci.*, **66**, 510 (1977).

(2) E. N. Hiestand, Proceedings of the International Conference on Powder Technology and Pharmacy, Basel, Switzerland, June 1978, Powder Advisory Centre, London, England.

(3) D. E. McLain, R. E. Melson, and C. C. Sperry (The Upjohn Co.), U.S. pat. 4,168,137 (1979).

## ACKNOWLEDGMENTS

The authors thank Chester Sperry, Robert Melson, Donald McLain, and Harry Dankert of the Mechanical Engineering Department, The Upjohn Co., for the design and construction of the machine and special die.

# Comparison of Anticonvulsant Potencies of Cyheptamide, Carbamazepine, and Phenytoin

GARY L. JONES ˣ, ROBERT J. AMATO, GARY H. WIMBISH, and GAYLON A. PEYTON

Received September 25, 1980, from the *Department of Pharmacology, Texas College of Osteopathic Medicine, Fort Worth, TX 76107.* Accepted for publication November 11, 1980.

**Abstract** □ Carbamazepine and cyheptamide have certain stereochemical features in common with phenytoin; when superimposed, two bulky hydrophobic groups in each permit the approximate apposition of two electron donor atoms. The anticonvulsant activity of each compound was determined in mice using a standard maximal electroshock procedure, and the relative potencies are expressed in terms of the blood and brain concentrations as well as the intraperitoneal dosage. Although cyheptamide was much less potent than carbamazepine or phenytoin on the basis of intraperitoneal dosage, the difference in potency was much less when blood or brain concentrations were compared. These data should be of value for quantitative structure–activity relationship studies.

**Keyphrases** □ Carbamazepine—anticonvulsant activity, intraperitoneal dosage, blood and brain concentrations □ Cyheptamide—anticonvulsant activity, intraperitoneal dosage, blood and brain concentrations □ Phenytoin—anticonvulsant activity, intraperitoneal dosage, blood and brain concentrations □ Anticonvulsant activity—carbamazepine, cyheptamide, phenytoin, blood and brain concentrations □ Structure–activity relationships—carbamazepine, cyheptamide, and phenytoin compared for anticonvulsant activity

A stereochemical basis of anticonvulsant drug action was described (1–5) for various chemically unrelated molecules. When brought into apposition, it becomes apparent that molecules as chemically unrelated as phenytoin (I) and diazepam not only have bulky hydrophobic groups with similar orientations in space but also have electron-donating groups in similar spatial positions. By using space-filling and Dreiding stereomodels, it can be seen that carbamazepine (II) and cyheptamide (III) (10,11-dihydro-5*H*-dibenzo[*a*,*d*]cycloheptene-5-carboxamide) also bear obvious structural similarities to phenytoin. The two phenyl rings in each, when approximately superimposed, permit the reasonable apposition of a carbonyl oxygen as well as a second electron donor, the imide nitrogen in phenytoin and the amide nitrogen in carbamazepine and cyheptamide.

Although several reports (6–8) have dealt with the pharmacological properties of cyheptamide, the procedures employed do not permit direct comparison of its anticonvulsant activity with that of carbamazepine, phenytoin, and other structurally related anticonvulsants. The present investigation presents such data for comparative purposes. In a preliminary experiment, the $ED_{50}$ of cyheptamide after intraperitoneal administration was 81.0 mg/kg (based on a maximal electroshock technique). According to Krall *et al.* (9), this value would represent a potential antiepileptic worthy of further study. Therefore, the relative potencies of cyheptamide, carbamazepine, and phenytoin were determined with respect to blood and brain concentrations in addition to intraperitoneal dosage. The results should be of value in quantitative structure–activity analysis involving the particular class of compounds known to conform to the previously mentioned stereochemistry.

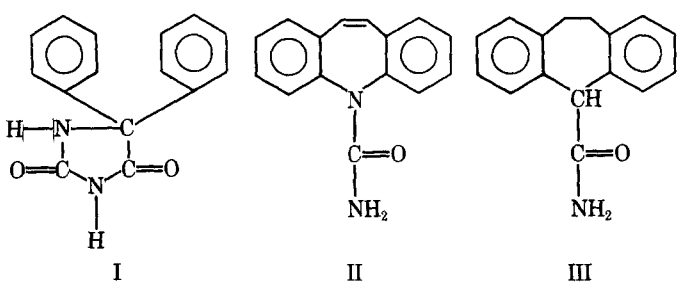

I II III

## EXPERIMENTAL

Male CF1 mice[1], 30–32 days old when received, were allowed to acclimate for several days after possible food and water deprivation during transportation. They were permitted food and water *ad libitum* except during the short time when removed from their cages for testing.

Carbamazepine[2] and phenytoin sodium[3] were suspended in 30% aqueous polyethylene glycol 400, and cyheptamide[4] was suspended in 5% gum acacia. The suspensions were sonicated for ~5 min to produce a fine suspension. The drugs were administered intraperitoneally (0.01 ml/g) to mice weighing an average of 22 g.

Each compound was assayed at the time of its peak anticonvulsant effect. A maximal electroshock (MES) test (10) was employed for the peak time determinations as well as for subsequent dose–response experiments. Briefly, this test is a measure of the ability of a drug to abolish the hindlimb extensor component of the seizure pattern induced by a 60-Hz alternating current of 50 mamp delivered for 0.2 sec *via* corneal electrodes. The animal was restrained only by hand and was released at the moment of stimulation to permit observation of the seizure throughout its entire course. Protection against the extensor component beyond a 90° angle with the trunk was required for an anticonvulsant effect to be registered. An approximate $ED_{50}$ of the drug to be tested was given to groups of five mice, and the maximal electroshock test was performed 15 min after administration and at 30-min intervals thereafter until the time of peak effect had obviously passed (indicated by fewer animals being protected than at an earlier time). All subsequent dose–response determinations were based on assays of the drug at its established peak time.

Immediately after the maximal electroshock test, 100 μl of blood was collected in 2% sodium fluoride and the animal was decapitated. The entire brain was removed and blotted on filter paper, and the specimens (including blood) were stored at −80° until they were assayed. Blood and brains from 10 mice were pooled for each dose, and at least five doses were employed for each drug.

The blood and brain concentrations for each phenytoin dose were assayed by GLC with 5-(*p*-methylphenyl)-5-phenylhydantoin as an internal standard. The blood and homogenized whole brain specimens were saturated with ammonium sulfate, acidified, and extracted with toluene. The toluene layer was separated and back-extracted with tetramethylammonium hydroxide according to the procedure of Johnson *et al.* (11). The samples were analyzed on 3% OV-17 on 80–100-mesh Supelcoport at 230° and detected by flame ionization (injector port and detector temperature 300°).

Carbamazepine was extracted from alkalinized blood and homogenized whole brain specimens by *n*-butyl chloride. The *n*-butyl chloride was

[1] From Charles River Breeding Laboratories.
[2] Geigy Pharmaceuticals.
[3] Warner-Lambert Co.
[4] Pierce Chemical Co.



0022-3549/81/0600-0618$01.00/0
© 1981, American Pharmaceutical Association

**Table I—Anti-Maximal Electroshock Potencies of Phenytoin, Carbamazepine, and Cyheptamide**

| $ED_{50}$[a] | Phenytoin | Carbamazepine | Cyheptamide |
|---|---|---|---|
| Intraperitoneal, mg/kg | 7.1 (6.5–7.8) | 9.7 (8.5–11.0) | 81.0 (52.0–127.0) |
| Blood, μg/ml | 2.2 (1.8–2.8) | 2.4 (2.2–2.7) | 5.5 (3.9–7.8) |
| Brain, μg/g | 5.3 (4.7–5.9) | 4.9 (4.1–5.7) | 8.9 (7.5–10.6) |

[a] The $ED_{50}$ values are listed with 95% confidence intervals in parenthesis. Potencies are expressed in terms of the intraperitoneal dose and blood and brain concentrations.

evaporated to dryness, and the residue was derivatized with pentafluorobenzoyl chloride to increase sensitivity by electron capture. 10-Methoxycarbamazepine was added as an internal standard. The samples were analyzed by the method described by Schwertner *et al.* (12).

Cyheptamide was extracted from blood and brain specimens in the manner described for carbamazepine. The *n*-butyl chloride was evaporated to dryness and reconstituted in 50 μl of chloroform. Carbamazepine was used as an internal standard. The analysis was performed on 3% OV-17 on 80–100-mesh Supelcoport at 250° and detected by flame ionization (injector port temperature 270° and detector temperature 300°). A typical chromatogram for cyheptamide extracted from brain tissue is depicted in Fig. 1.

The anticonvulsant data were evaluated with 95% confidence limits by the statistical method of Litchfield and Wilcoxon (13). The relative anticonvulsant potencies ($ED_{50}$) are expressed in terms of the blood and brain concentrations as well as the intraperitoneal dosage.

## RESULTS AND DISCUSSION

The comparative times of peak anticonvulsant effect of carbamazepine, cyheptamide, and phenytoin were ~30, 45, and 60 min, respectively. Although the anti-maximal electroshock potency of carbamazepine was similar to that of phenytoin, the potency of cyheptamide was considerably less (Table I and Fig. 2). The dose of cyheptamide necessary to protect 50% of the mice from tonic hindlimb extension ($ED_{50}$) was 81.0 mg/kg (95% confidence limits of 52.0–127.0), expressed as the intraperitoneal dose. The respective $ED_{50}$ values (95% confidence limits) for carbamazepine and phenytoin were 9.7 (8.5–11.0) and 7.1 (6.5–7.8) mg/kg, respectively (Table I). However, when the blood and brain concentrations of the three drugs were compared, the relative potencies were not that

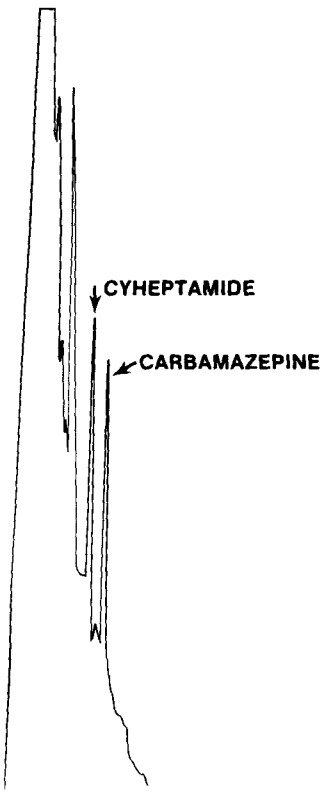


**Figure 1**—*Gas–liquid chromatogram of cyheptamide from brain extract. The internal standard was carbamazepine.*

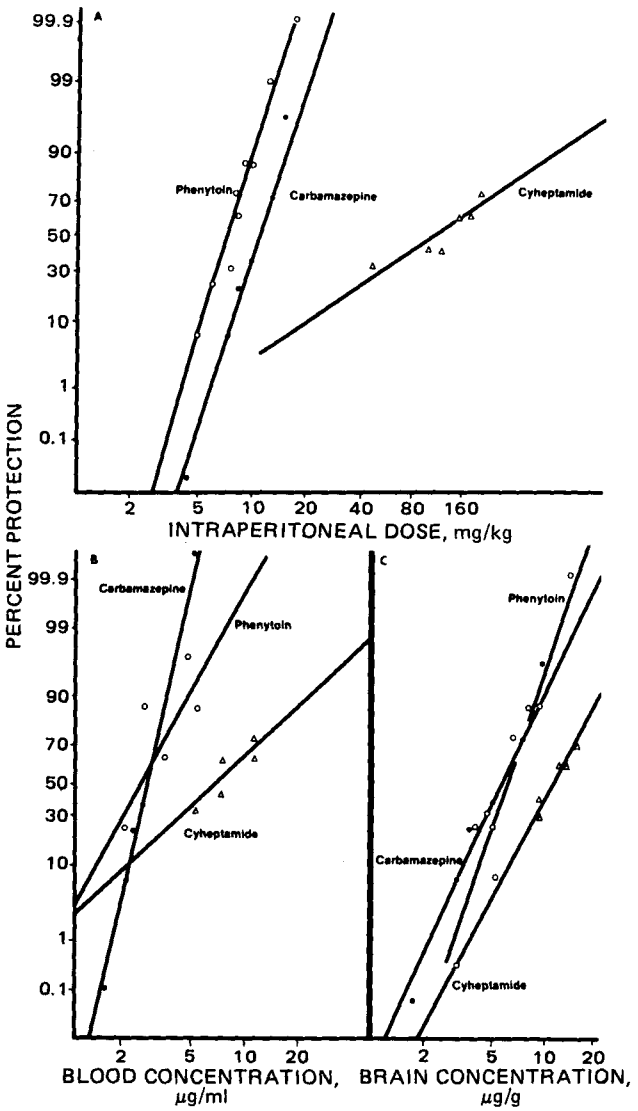


**Figure 2**—*Log dose–response curves for phenytoin, carbamazepine, and cyheptamide expressed in terms of the intraperitoneal dosage (A), blood concentration (B), and brain concentration (C).*

dissimilar. Cyheptamide again was the least potent (Table I). But the potency ratio (95% confidence limits) of cyheptamide to phenytoin, 11.4 (7.3–17.9) on a milligram per kilogram basis, was only 2.5 (1.6–3.8) when blood concentrations (micrograms per milliliter) were compared. When brain concentrations (micrograms per gram) were compared, the ratio was even less, 1.7 (1.4–2.1). In the comparison of cyheptamide to carbamazepine, the ratios were 8.3 (6.1–11.6) on a milligram per kilogram basis, 2.3 (1.7–2.9) for blood concentrations, and 1.8 (1.8–1.9) for brain concentrations. Phenytoin was only slightly more potent than carbamazepine on a milligram per kilogram basis ($p = 0.05$), but the difference was not significant based on blood or brain concentrations.

The large difference in the $ED_{50}$ (intraperitoneal) for cyheptamide might be explained by its lipophilicity. Calculations of log *P* based upon hydrophobicity constants (14) produce an estimated partition coefficient of 550[5] (log $P = 2.74$). The compound is so lipid soluble that it might not achieve the same aqueous dispersion as phenytoin or carbamazepine when given intraperitoneally; thus, absorption would be relatively less due to the smaller effective surface area to which the drug is exposed. The calculated partition coefficients[5] for phenytoin and carbamazepine were fairly similar, 170 (log $P = 2.23$) and 151 (log $P = 2.18$), respectively. This

[5] Log *P* calculations: cyheptamide, from log *P* $(C_6H_5)_2CH_2 + \frac{1}{3}\pi$(cyclohexane) + $\pi(CONH_2)$ = 4.14 + 0.84 + (−2.24) = 2.74; carbamazepine, from log *P* $(C_6H_5)_2NCONH_2 + \frac{1}{3}\pi(C_6H_5)$ = 1.53 + 0.65 = 2.18; phenytoin, from log *P* (hydantoin) + $2\pi(C_6H_5)$ = −1.69 + 3.92 = 2.23. Note that the calculated log *P* for phenytoin is slightly different than the experimental value of 2.47 (14). Only calculated values were used to maintain consistency.

result may explain their similar potencies when their $ED_{50}$ values are compared by any of the three criteria.

An alternative explanation of the potency difference, also based on relative lipophilicities, might be the parabolic dependence of potency on hydrophobicity described by Penniston *et al.* (15) and McFarland (16). Although potency among various compounds is known to increase with increasing lipophilicity, there is frequently an optimum hydrophobicity beyond which potency actually decreases. A quantitative description of this phenomenon is expressed according to (17):

$$\log \frac{1}{C} = -k(\log P)^2 + k' \log P + k'' \qquad \text{(Eq. 1)}$$

Although various explanations might account for such behavior, the following concept is popular. A certain degree of lipophilicity is necessary so that molecules may "dissolve" in and penetrate the lipid matrix of membranes. However, extremely lipophilic substances may actually take up "residence" within the lipid matrix of the membrane. Each membrane interposed along the path a drug might follow to its receptor thus lessens the probability that the drug will reach the receptor. The greatest reduction in such probability occurs at extreme values of the partition coefficient. Drugs with low partition coefficients may have difficulty entering the membrane, while those with high coefficients may not leave readily. Thus, the rather large increase in the partition coefficient of cyheptamide relative to phenytoin and carbamazepine might be responsible for its significantly lower potency. Furthermore, it might be assumed that fewer membranes are interposed between the bulk drug concentrations and the receptors when drug activity is expressed in terms of brain concentrations than when expressed as the intraperitoneal dose or blood concentration. Therefore, the smaller potency ratios observed for the brain concentrations are likely an expression of the smaller difference in probability permitted by fewer barriers separating the drug from its receptor.

The higher brain to blood concentration ratio for phenytoin (2.4) in comparison with carbamazepine (2.0) might reflect its slightly more lipophilic character, but a greater binding of carbamazepine to plasma protein also might be involved. Because cyheptamide is the most lipophilic of these compounds, its surprisingly low brain to blood ratio (1.6) is probably the result of substantial binding to plasma protein.

Previous investigations of cyheptamide produced significantly lower potency estimates than the present data indicate. The probable explanation for this difference points to the problem many investigators have when correlating anticonvulsant structure with activity, namely, the failure to apply a uniform experimental model of epilepsy. In the earliest study (6), mice were subjected to a maximal electroshock procedure in which 30 mamp of 60-Hz current was applied for 0.2 sec *via* corneal electrodes. The $ED_{50}$ value was $25 \pm 1$ mg/kg by the intraperitoneal route and $33 \pm 3.5$ mg/kg by the oral route. A later report cited an $ED_{50}$ (oral) of 38 mg/kg (7). In that study, the current was only 25 mamp (60 Hz), again delivered for 0.2 sec through corneal electrodes. The lower potency of cyheptamide determined in the present study is likely the result of the higher (50 mamp) current, as prescribed in the most thoroughly documented model of grand mal epilepsy (9, 18).

In summary, the relatively low anti-maximal electroshock potency described previously (6, 7) for cyheptamide has been verified. However, its potency is not so discrepant from that of structurally related carbamazepine and phenytoin as might be inferred from the intraperitoneal dosage. The $ED_{50}$ values expressed in terms of tissue concentrations might be of greater value in a quantitative structure–activity investigation than those values based on parenteral dosage.

## REFERENCES


(1) A. Camerman and N. Camerman, *Acta Crystallogr., Sect. B*, **27**, 2205 (1971).

(2) N. Camerman and A. Camerman, *Mol. Pharmacol.*, **7**, 406 (1971).

(3) N. Camerman and A. Camerman, *J. Am. Chem. Soc.*, **94**, 8553 (1972).

(4) A. Camerman and N. Camerman, *ibid.*, **94**, 268 (1972).

(5) A. Camerman and N. Camerman, *Proc. Natl. Acad. Sci. USA*, **74**, 1264 (1977).

(6) M. A. Davis, S. O. Winthrop, R. A. Thomas, F. Herr, M. Charest, and R. Gaudry, *J. Med. Chem.*, **7**, 88 (1964).

(7) A. B. H. Funcke, M. C. vanBeek, G. vanHell, U. I. Lavy, H. Timmerman, and P. Zandberg, *Arch. Int. Pharmacodyn. Ther.*, **187**, 174 (1970).

(8) C. J. vanEeken, R. D. R. Birtwhistle, and D. Mulder, *ibid.*, **188**, 79 (1970).

(9) R. L. Krall, J. K. Penry, B. G. White, H. J. Kupferberg, and E. A. Swinyard, *Epilepsia*, **19**, 409 (1978).

(10) E. A. Swinyard, W. C. Brown, and L. S. Goodman, *J. Pharmacol. Exp. Ther.*, **106**, 319 (1952).

(11) G. F. Johnson, W. A. Dechtiaruk, and H. M. Solomon, *Clin. Chem.*, **21**, 144 (1975).

(12) H. A. Schwertner, H. E. Hamilton, and J. E. Wallace, *ibid.*, **24**, 895 (1978).

(13) J. T. Litchfield and F. Wilcoxon, *J. Pharmacol. Exp. Ther.*, **96**, 99 (1949).

(14) C. Hansch and A. Leo, "Substituent Constants for Correlation Analysis in Chemistry and Biology," Wiley, New York, N.Y., 1979.

(15) J. T. Penniston, L. Beckett, D. L. Bentley, and C. Hansch, *Mol. Pharmacol.*, **5**, 333 (1969).

(16) J. W. McFarland, *J. Med. Chem.*, **13**, 1192 (1970).

(17) C. Hansch, A. R. Steward, S. M. Anderson, and D. Bentley, *ibid.*, **11**, 1 (1967).

(18) D. M. Woodbury, in "Experimental Models of Epilepsy—A Manual for the Laboratory Worker," D. P. Purpura, J. K. Penry, D. B. Tower, D. M. Woodbury, and R. D. Walter, Eds., Raven, New York, N.Y., 1972.


## ACKNOWLEDGMENTS


Supported in part by grants from the Epilepsy Foundation of America and the Texas College of Osteopathic Medicine.

The authors are grateful to Geigy Pharmaceuticals and Warner-Lambert Co. for their gifts of carbamazepine and phenytoin, respectively.

# Effect of Antacids on Activity of Oral Hypoglycemics

S. A. SAID ˣ and M. E. ABDULLAH

Received February 5, 1980, from the *Department of Pharmaceutics, College of Pharmacy, University of Riyad, Riyad, Saudi Arabia.* Accepted for publication November 13, 1980.

**Abstract** □ The effect of some antacids on the dissolution and hypoglycemic activity of acetohexamide, tolazamide, and tolbutamide tablets was investigated, as was the adsorption of the three drugs onto the antacids. The dissolution rates of the three drugs in the presence of magnesium oxide, aluminum hydroxide, magnesium carbonate, and calcium carbonate increased (0.5–1 hr) and then plateaued or decreased (1–3 hr). Magnesium trisilicate directly suppressed the dissolution of the three drugs. The antacids reduced the hypoglycemic activity of tolbutamide in the following order: magnesium trisilicate > magnesium oxide > aluminum hydroxide > magnesium carbonate > calcium carbonate. The same order occurred for the first three antacids with acetohexamide and tolazamide. Decreased hypoglycemic activity of the drugs may have been due to their adsorption to the coadministered antacids.

**Keyphrases** □ Antacids—effect on oral hypoglycemics, dissolution, adsorption, hypoglycemic activity □ Hypoglycemics, oral—effect of antacids, dissolution, adsorption, hypoglycemic activity □ Dissolution—effect of antacids on oral hypoglycemics, adsorption, hypoglycemic activity □ Adsorption—effect of antacids on oral hypoglycemics, dissolution, hypoglycemic activity

The effect of antacids on the dissolution and bioavailability of drugs has been studied extensively (1–7). Drug–antacid interactions may be caused by several effects. Antacids can change the absorption rate by altering the ionization state of the drug molecule (1, 2), delaying stomach emptying (3), changing the fluid pH in the body (4), and adsorbing drugs (5–7). In addition to affecting bioavailability, a chemical or strong physical interaction between the antacid and drug can have important ramifications in therapy.

Since no information is available on the effect of coadministration of antacids on the bioavailability of oral hypoglycemics, the present study investigated the influence of commonly used antacids on the dissolution and hypoglycemic activity of acetohexamide, tolazamide, and tolbutamide. The adsorption of these drugs onto some antacids also was studied.

## EXPERIMENTAL

**Materials**—Acetohexamide[1], tolazamide[2], and tolbutamide[3] tablets were used in the dissolution studies. Powdered acetohexamide[1], tolazamide[2], tolbutamide[3], magnesium trisilicate[4], magnesium carbonate[5], magnesium oxide[6], aluminum hydroxide[7], and calcium carbonate[7] were used as supplied in the adsorption and hypoglycemic activity studies.

**Dissolution Testing**—The dissolution rates of acetohexamide and tolbutamide tablets were tested according to USP XIX (6) using the USP rotating-basket dissolution apparatus[8]. Tolazamide tablets were tested similarly, but the absorbance[9] was measured at 262 nm. Tablets of the three drugs were tested for dissolution in their respective medium containing one antacid (1%).

**Measurement of Blood Glucose in Rats**—The effect of orally administered acetohexamide, tolazamide, and tolbutamide with and without antacids on blood glucose levels of adult male albino rats[10] was studied. Rats (180–250 g) were fasted 24 hr before the experiment but were allowed free access to water.

The effect of antacids on the hypoglycemic activity of tolbutamide was studied using six groups of 15 rats each. One group was given tolbutamide suspension (1%) in water containing 0.2% methylcellulose in a 200-mg/kg dose. Five other groups were given equivalent doses of tolbutamide but in the presence of 1% of the antacid.

Each group of animals was divided into five subgroups, each containing three rats. Each subgroup was kept in a separate cage and allowed free access to water. At 0.5, 1, 2, 3, 4, and 5 hr, the animals were sacrificed. A blood sample was taken from each rat and analyzed for blood glucose content (8). One group of animals was used as the control. The mean blood glucose levels of each subgroup were compared, and the differences were tested for significance by analysis of variance and a Student $t$ test.

The effect of magnesium trisilicate, magnesium oxide, and aluminum hydroxide on the blood glucose level following administration of acetohexamide and tolazamide was tested in the same manner.

**Adsorption Experiments**—The drugs were dissolved in the fluid used for dissolution testing, and 50 ml of the solution containing 2.5–40 mg of the drug was placed in 100-ml glass-stoppered conical flasks containing the antacid (1%). The drug–antacid solution was equilibrated at 37 ± 0.1° and shaken mechanically for ~24 hr to reach equilibrium. After centrifugation, the drug concentration remaining in the supernate was determined spectrophotometrically at the respective wavelength used for dissolution testing against a blank. Three replicate runs were made, and the results were averaged.

***Desorption***—The desorption of adsorbed drugs was determined at 37 ± 0.5° in the fluid used for dissolution testing as described previously (6). Three experiments were performed in each case, and the average percent desorbed was calculated.

The least significant difference procedure was used to assess the difference between two means, and the completely randomized designs–analysis of variance technique was used to evaluate the level of significance between multiple determinations (9).

## RESULTS AND DISCUSSION

Figure 1 shows the effect of the five antacids on the dissolution rates of acetohexamide, tolazamide, and tolbutamide tablets. With the exception of magnesium trisilicate, the antacids exhibited a minor increase in dissolution (0.5–1 hr) and then a plateau with a slight decrease toward the end. Magnesium trisilicate moderately decreased the dissolution rates of the three drugs. After 3 hr, the amounts of tolbutamide in solution were 82.5, 81, 66, 60, and 10% in the presence of calcium carbonate, magnesium carbonate, aluminum hydroxide, magnesium oxide, and magnesium trisilicate, respectively, as compared to 100% in the absence of these antacids. The amounts of acetohexamide, tolbutamide, and tolazamide in solution at 3 hr were 4.5, 40, and 30%, respectively, in the presence of magnesium trisilicate; at that time, complete dissolution of the three drugs was attained in the absence of antacids.

Figure 2 illustrates the effect of the tested antacids on the hypoglycemic activity of acetohexamide, tolazamide, and tolbutamide. The mean blood glucose concentration of 24-hr fasted rats was 73.25 ± 2.55 mg/100 ml and was significantly higher than all treated groups (Student $t$ test, $p < 0.05$).

The reduction in blood glucose levels was lessened in the system containing the antacid (Fig. 2). At 2 hr, the mean blood glucose level of rats taking tolbutamide alone was 2.8 mg/100 ml; it increased to 18.3, 15.3,

[1] Dimelor tablets 1843 G-27023F, Eli Lilly and Co., Basingstoke, England.
[2] Tolinase tablets, The Upjohn Co., Kalamazoo, Mich.
[3] Rastinon tablets 586A474, Hoechst, Frankfurt, West Germany.
[4] BDH, Poole, England.
[5] Mayer & Baker, Dogenham, England.
[6] Hopkin & Williams, Essex, England.
[7] Riede De Haenog, Hanover, West Germany.
[8] Erweke-Heausenstamn Kr, Offenbach/Main, West Germany.
[9] Varian Techtron, UV-VIS, model 635.
[10] Sprague-Dawley, Agouzo Strain, Egypt.

0022-3549/81/0600-0621$01.00/0
© 1981, American Pharmaceutical Association

**Table I—Blood Glucose Levels at 2 hr following a 200-mg/kg Single Oral Dose of Tolbutamide Aqueous Suspension Alone and Coadministered with Antacids**

| | Blood Glucose Level ($n$ = 3), mg/100 ml | | | | | |
|---|---|---|---|---|---|---|
| | Tolbutamide | Tolbutamide plus Magnesium Carbonate | Tolbutamide plus Magnesium Oxide | Tolbutamide plus Magnesium Trisilicate | Tolbutamide plus Aluminum Hydroxide | Tolbutamide plus Calcium Carbonate |
| Mean | 2.80 | 10.5 | 15.3 | 18.3 | 12.5 | 8.4 |
| *SD* | 1.54 | 4.32 | 0.85 | 3.27 | 2.72 | 2.59 |
| *CV*, % | 55.00 | 41.14 | 5.56 | 17.87 | 21.76 | 30.83 |

Analysis of Variance

| Source of Variation | Degrees of Freedom | Sum of Squares | Mean of Squares | $F^a$ Ratio |
|---|---|---|---|---|
| Among dosage forms | 2 | 443.22 | 221.61 | 35.69 |
| Error | 15 | 93.16 | 6.21 | |
| Total | 17 | | | |

[a] Significance at the 5% level.

**Table II—Blood Glucose Levels at 2 hr following a 200-mg/kg Single Oral Dose of Acetohexamide Suspension Alone and Coadministered with Antacids**

| | Blood Glucose Level ($n$ = 3), mg/100 ml | | |
|---|---|---|---|
| | Acetohexamide | Acetohexamide plus Magnesium Trisilicate | Acetohexamide plus Aluminum Hydroxide |
| Mean | 22.5 | 45.50 | 37.50 |
| *SD* | 8.68 | 5.19 | 4.20 |
| *CV*, % | 38.58 | 11.14 | 11.20 |

Analysis of Variance

| Source of Variation | Degrees of Freedom | Sum of Squares | Mean of Squares | $F^a$ Ratio |
|---|---|---|---|---|
| Among dosage forms | 2 | 818 | 409 | 10.24 |
| Error | 6 | 239.66 | 39.94 | |
| Total | 8 | 1057.66 | | |

[a] Significance at the 5% level.

12.5, 10.5, and 8.4 mg/100 ml in the presence of magnesium trisilicate, magnesium oxide, aluminum hydroxide, magnesium carbonate, and calcium carbonate, respectively. Analysis of variance for the results in Table I showed a highly significant difference ($p < 0.05$) in the 2-hr mean blood glucose levels among the tested dosage forms. At 2 hr, there was a significant difference (least significant difference procedure, $p < 0.05$) between the mean blood glucose when tolbutamide was administered alone and when it was administered with each tested antacid. This result indicates that a decreased absorption of tolbutamide occurred in the presence of each tested antacid.

The antacids reduced the hypoglycemic activity of acetohexamide and tolazamide in the order magnesium trisilicate > aluminum hydroxide. At 2 hr, the respective mean blood glucose levels of rats taking acetohexamide alone was 22.5 mg/100 ml, which increased to 45.5 and 37.5 mg/100 ml in the presence of magnesium trisilicate and aluminum hydroxide, respectively. At 2 hr, the mean blood glucose level of rats taking tolazamide was 6.5 mg/100 ml, which increased to 18 and 13 mg/100 ml in the presence of magnesium trisilicate and aluminum hydroxide, respectively.

Analysis of variance for the data of the 2-hr mean blood glucose levels of rats administered acetohexamide alone and with the tested antacids

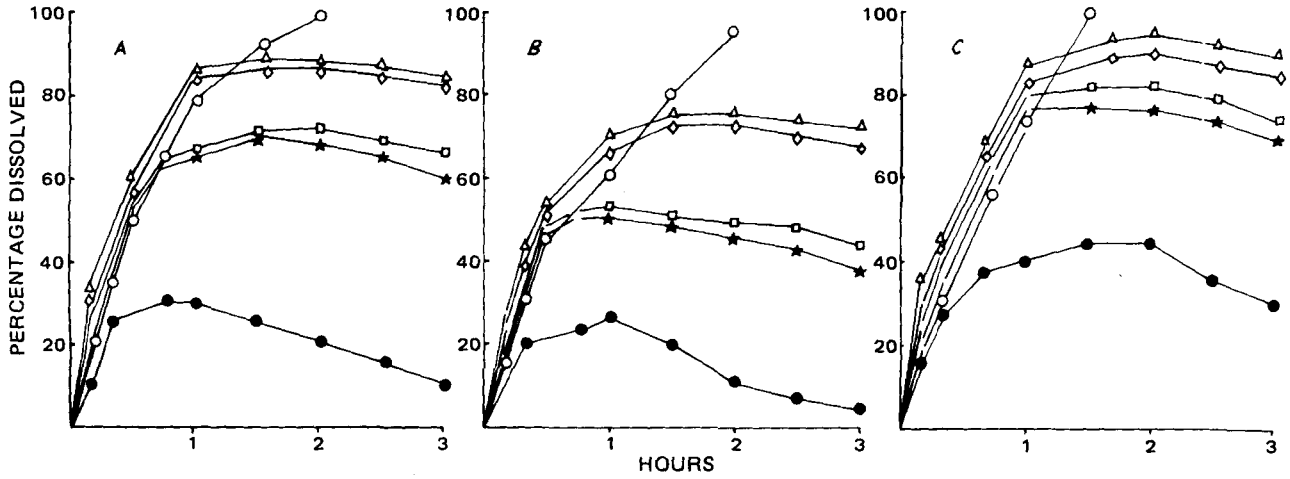


**Figure 1**—*Effect of certain antacids on the dissolution of acetohexamide (A), tolbutamide (B), and tolazamide (C). Key: ○, without antacid; and ●, ★, □, ◇, and △, in the presence of magnesium trisilicate, magnesium oxide, aluminum hydroxide, magnesium carbonate, and calcium carbonate, respectively.*

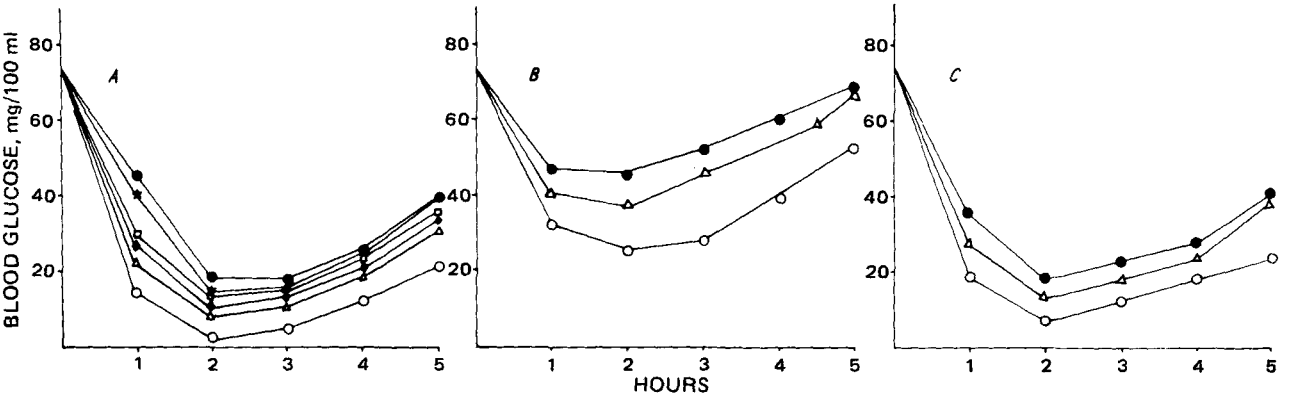


**Figure 2**—*Effect of certain antacids on the hypoglycemic activity of tolbutamide (A), acetohexamide (B), and tolazamide (C). Key: see Fig. 1.*

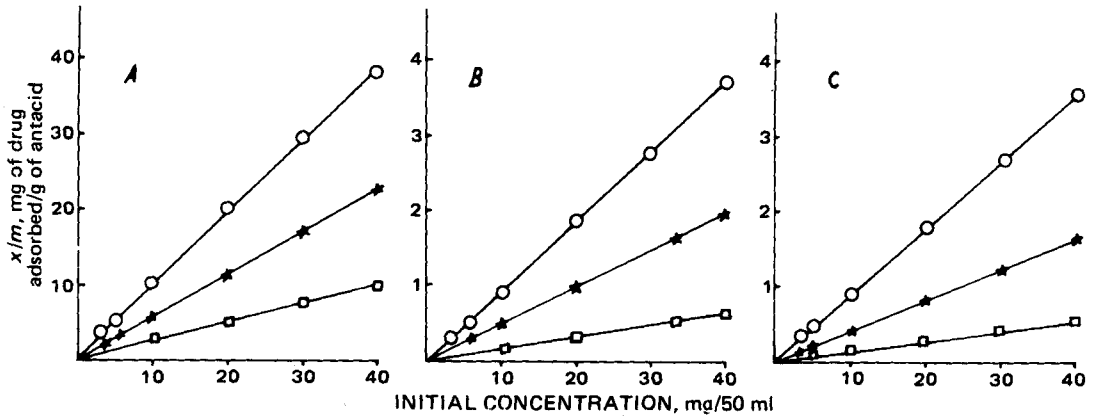


Figure 3—*Adsorption of acetohexamide (A), tolbutamide (B), and tolazamide (C) on certain antacids (1% w/v). Key:* ○, *magnesium trisilicate;* ★, *magnesium oxide; and* □, *aluminum hydroxide.*

**Table III—Blood Glucose Levels at 2 hr following a 200-mg/kg Single Oral Dose of Tolazamide Aqueous Suspension Alone and Coadministered with Antacids**

| | Blood Glucose Level ($n$ = 3), mg/100 ml | | |
|---|---|---|---|
| | Tolazamide | Tolazamide plus Magnesium Trisilicate | Tolazamide plus Aluminum Hydroxide |
| Mean | 6.50 | 18.00 | 13.00 |
| *SD* | 2.71 | 1.91 | 3.41 |
| *CV*, % | 41.69 | 10.61 | 26.23 |

Analysis of Variance

| Source of Variation | Degrees of Freedom | Sum of Squares | Mean of Squares | $F^a$ Ratio |
|---|---|---|---|---|
| Among dosage forms | 2 | 199.5 | 99.75 | 13.14 |
| Error | 6 | 45.22 | 7.59 | |
| Total | 8 | 244.72 | | |

[a] Significance at the 5% level.

**Table IV—Desorption of Tolbutamide, Tolazamide, and Acetohexamide from Antacids**

| | Mean Drug Desorbed ± *SD* ($n$ = 3), % | | |
|---|---|---|---|
| Drug | Magnesium Trisilicate | Magnesium Oxide | Aluminum Hydroxide |
| Acetohexamide | 5.17 ± 1.72 | 8.36 ± 1.12 | 10.50 ± 1.76 |
| Tolazamide | 6.50 ± 2.76 | 12.20 ± 1.45 | 13.50 ± 0.87 |
| Tolbutamide | 5.20 ± 1.42 | 8.50 ± 0.38 | 10.80 ± 0.36 |

Analysis of Variance

| Source of Variation | Degrees of Freedom | Sum of Squares | Mean of Squares | $F^a$ Ratio |
|---|---|---|---|---|
| Among dosage forms | 2 | 38.98 | 19.49 | 3.54 |
| Error | 6 | 33.02 | 5.50 | |
| Total | 8 | 71.99 | | |

[a] Significance at the 5% level.

showed that there was a significant difference ($p < 0.05$) among the tested dosage forms (Table II). There was a significant difference (least significant difference procedure, $p < 0.05$) between the mean blood glucose level when acetohexamide was administered alone and when it was administered with either magnesium trisilicate or aluminum hydroxide (Table II). Similarly, statistical comparison of the data in Table III indicated that there was a significant difference (analysis of variance, $p < 0.05$) among the tested tolazamide dosage forms as to the 2-hr mean blood glucose levels. There was also a significant difference (least significant difference procedure, $p < 0.05$) between the mean blood glucose level when tolazamide was administered alone and when it was administered with either magnesium trisilicate or aluminum hydroxide.

Figure 3 shows the plots of drug adsorption onto magnesium trisilicate (1% w/v). Preliminary experiments showed that equilibrium was attained within 6–24 hr, depending on the drug, its concentration, and the antacid. Antacid adsorption of the drugs followed the sequence magnesium trisilicate > magnesium oxide > aluminum hydroxide. These antacids adsorbed 95, 50, and 17.5% of tolbutamide, respectively. The extent of drug adsorption to antacids followed the sequence acetohexamide > tolbutamide > tolazamide. The three drugs possess varying relative polarity, and the extent of adsorption was increased with the more polar drug. This finding is concordant with the reported (10) conclusion that, for a given solvent, the more soluble solutes generally were adsorbed less strongly than the less soluble ones.

Table IV summarizes the extent of adsorption of the three drugs from the respective medium used for dissolution. These data illustrate a strong adsorption of the three drugs to magnesium trisilicate; only 5.17, 5.20, and 6.5% were desorbed from acetohexamide, tolbutamide, and tolazamide, respectively. The same sequence occurred with aluminum hydroxide and magnesium oxide. Analysis of variance of the data in Table IV showed that there was no significant difference among the tested antacids as to the extent of adsorption of the three hypoglycemics.

Statistical analysis of the data in Table IV (least significant difference procedure, $p < 0.05$) indicated that tolbutamide was adsorbed more significantly to magnesium trisilicate than to aluminum hydroxide. There appeared to be no significant differences between the extent of tolbutamide adsorption to magnesium trisilicate and magnesium oxide nor to aluminum hydroxide and magnesium oxide. Tolazamide was adsorbed more strongly to magnesium trisilicate than to the other two antacids. Acetohexamide exhibited a significantly higher adsorption to magnesium trisilicate than to aluminum hydroxide; however, no significant difference existed between the extent of its adsorption to magnesium oxide and magnesium trisilicate nor between its adsorption to aluminum hydroxide and magnesium oxide.

These results indicate that the tested antacids reduce the hypoglycemic activity of acetohexamide, tolazamide, and tolbutamide. The dissolution rates of the three oral hypoglycemics in the presence of the antacids, with the exception of magnesium trisilicate, increased (0.5–1 hr), plateaued, and then decreased. Increased dissolution in the 1st hr did not rise continually due to uptake of the dissolved drug by the antacid. Again, the earlier increased dissolution does not reflect increased hypoglycemic activity due to direct adsorption of drug by antacid decreasing the amount of free drug available for systemic absorption. Magnesium trisilicate, which showed the highest adsorption capacity for the three oral hypoglycemics, induced the paramount suppression in their hypoglycemic activity. Furthermore, the powerful adsorption of the drugs by this antacid, as indicated by minor desorption, illustrates this suppression.

From the present study, it may be concluded that the hypoglycemic activity of acetohexamide, tolazamide, and tolbutamide will be decreased considerably if these drugs are separately coadministered with the tested antacids. The extent of reduction will vary with the antacid.

## REFERENCES

(1) R. L. Lucarbotti, J. L. Colaizzi, and H. Barry, *J. Pharm. Sci.*, **61**, 903 (1972).

(2) A. Hurwitz and M. B. Sechan, *J. Pharmacol. Exp. Ther.*, **179**, 124 (1971).

(3) A. Hurwitz and D. Schozman, *Am. Rev. Respir. Dis.*, **109**, 41 (1974).

(4) M. Gibaldi, B. Grundhofer, and G. Levy, *J. Pharm. Sci.*, **64**, 2003 (1975).
(5) V. F. Naggar, S. A. Khalil, and M. W. Gouda, *ibid.*, **67**, 1029 (1978).
(6) S. A. Khalil and M. Iwuagwu, *ibid.*, **67**, 287 (1978).
(7) S. A. Khalil, *J. Pharm. Pharmacol.*, **26**, 961 (1974).
(8) P. Trinder, *Ann. Clin. Biochem.*, **6**, 24 (1969).
(9) W. G. Cochran and G. M. Cox, "Experimental Designs," Wiley, New York, N.Y., 1957, pp. 76, 95.
(10) W. A. Patrick and N. F. Eberman, *J. Phys. Chem.*, **29**, 220 (1925); through Ref. 6.

## ACKNOWLEDGMENTS

S. A. Said is on leave of absence from the Faculty of Pharmacy, Cairo University, Cairo, Egypt.

The authors thank Mr. M. Hikal, Mr. Y. Hendi, and Mr. M. Al-Helwe for technical assistance and Mr. K. Abbas for typing the manuscript.

# Stereospecific Radioimmunoassays for *d*-Pseudoephedrine in Human Plasma and Their Application to Bioequivalency Studies

**JOHN W. A. FINDLAY ˣ, JAMES T. WARREN, JOHN A. HILL, and RICHARD M. WELCH**

Received August 11, 1980, from *Wellcome Research Laboratories, Research Triangle Park, NC 27709.* Accepted for publication November 11, 1980.

**Abstract** □ Antiserum to *d*-pseudoephedrine was raised in New Zealand White rabbits in response to immunization with a conjugate of bovine serum albumin and *d*-pseudoephedrine-*N*-3-propionic acid. The hapten was prepared by reaction of methyl acrylate with *d*-pseudoephedrine, followed by ester hydrolysis. Sodium boro[$^3$H]hydride reduction of *dl*-ephedrone gave [$\alpha$-$^3$H]-*dl*-ephedrine, and a Welsh rearrangement with acetic anhydride followed by deacetylation gave [$\alpha$-$^3$H]-*dl*-pseudoephedrine, which was used as a radioligand in radioimmunoassay procedures for direct plasma analyses. Three sensitive radioimmunoassay procedures were developed, two using [$^3$H]pseudoephedrine as the radioligand and either adsorption on coated charcoal or polyethylene glycol precipitation for separation of antibody-bound from free radioligand. The third method used an [$^{125}$I]tyrosine methyl ester analog of pseudoephedrine and charcoal separation, preceded by extraction and derivatization of pseudoephedrine with methyl acrylate. All three assays could detect ≤2.5 ng of pseudoephedrine/ml. The antiserum was stereospecific, showing low cross-reactivities with *l*-pseudoephedrine and *d*- and *l*-ephedrines. *d*-Norpseudoephedrine and some other related compounds also had low cross-reactivity in these radioimmunoassay procedures. Excellent agreement was found between pseudoephedrine concentrations in human plasma determined by radioimmunoassay and by a standard GLC method. The utility of radioimmunoassay was illustrated by application of one of these procedures to an assessment of the bioequivalence of immediate- and sustained-release pseudoephedrine formulations in normal volunteers. A sustained-release preparation containing 120 mg of pseudoephedrine hydrochloride given every 12 hr was shown by *AUC* comparisons to be bioequivalent to an immediate-release tablet (containing 60 mg of pseudoephedrine hydrochloride) given every 6 hr.

**Keyphrases** □ Radioimmunoassay—*d*-pseudoephedrine, human plasma, bioequivalency studies, immediate- and sustained-release tablets □ *d*-Pseudoephedrine—radioimmunoassay, bioequivalency studies, immediate- and sustained-release tablets □ Bioequivalency studies—radioimmunoassays of *d*-pseudoephedrine in human plasma, bioequivalency studies, immediate- and sustained-release tablets □ Adrenergics—radioimmunoassays for *d*-pseudoephedrine in human plasma, bioequivalency studies, immediate- and sustained-release tablets

*d*-Pseudoephedrine was first isolated from the Chinese plant *Ma Huang* by Chou and Read (1) in 1926, and studies of its pharmacology started soon thereafter (2, 3). Although pseudoephedrine is in widespread use as a proven, clinically effective nasal decongestant (4–6), little published information is available on its disposition and pharmacokinetics in human plasma following administration of therapeutic doses. Studies have examined kinetics chiefly from the viewpoint of urinary excretion (7–9), which is liable to be influenced by alterations in urinary pH (8). Such indirect studies were necessitated by the lack of methods sufficiently sensitive to detect the relatively low circulating concentrations of pseudoephedrine in plasma following therapeutic doses.

Reported GLC procedures (7, 10, and 11) were capable of detecting only 0.3–0.5 μg of pseudoephedrine/ml. Even with nitrogen detection, Bye *et al.* (12) were able to lower the sensitivity limit only to 25 ng/ml. Kuntzman *et al.* (8) reported a procedure that involved esterification of isolated pseudoephedrine with tritiated acetic anhydride followed by separation and quantitation of the resulting radioactive product. Although capable of detecting 50 ng of pseudoephedrine/ml of plasma, this method is still relatively insensitive and time consuming. A study (13) of plasma pseudoephedrine levels relative to efficacy, using a GLC method for drug determination, was able to determine plasma concentrations up to 6 hr following a 60-mg oral dose of pseudoephedrine hydrochloride.

This report describes the development of a specific antiserum to pseudoephedrine and its application to three specific radioimmunoassay procedures for the drug. Two procedures are direct and employ a tritium-labeled radioligand; the third requires extraction and derivatization of the drug prior to assay but employs a $\gamma$-labeled radioligand. The sensitivity limits of these procedures are <2.5 ng of pseudoephedrine/ml in all cases. Their use for drug disposition studies following oral administration of both immediate- and sustained-release pseudoephedrine preparations is illustrated.

## EXPERIMENTAL

Melting points[1] are uncorrected. $^1$H-NMR spectra[2] were obtained in deuterochloroform with tetramethylsilane as the internal standard unless otherwise indicated. Low-resolution mass spectra[3] were obtained by

[1] Thomas-Hoover apparatus, Arthur H. Thomas Co., Philadelphia, Pa.
[2] Model R-24A, Perkin-Elmer Corp., Norwalk, Conn.
[3] Model MAT 731 or CH5DF, Varian Associates, Palo Alto, Calif.



0022-3549/81/0600-0624$01.00/0
© 1981, American Pharmaceutical Association

(4) M. Gibaldi, B. Grundhofer, and G. Levy, *J. Pharm. Sci.*, **64**, 2003 (1975).
(5) V. F. Naggar, S. A. Khalil, and M. W. Gouda, *ibid.*, **67**, 1029 (1978).
(6) S. A. Khalil and M. Iwuagwu, *ibid.*, **67**, 287 (1978).
(7) S. A. Khalil, *J. Pharm. Pharmacol.*, **26**, 961 (1974).
(8) P. Trinder, *Ann. Clin. Biochem.*, **6**, 24 (1969).
(9) W. G. Cochran and G. M. Cox, "Experimental Designs," Wiley, New York, N.Y., 1957, pp. 76, 95.
(10) W. A. Patrick and N. F. Eberman, *J. Phys. Chem.*, **29**, 220 (1925); through Ref. 6.

## ACKNOWLEDGMENTS

S. A. Said is on leave of absence from the Faculty of Pharmacy, Cairo University, Cairo, Egypt.

The authors thank Mr. M. Hikal, Mr. Y. Hendi, and Mr. M. Al-Helwe for technical assistance and Mr. K. Abbas for typing the manuscript.

# Stereospecific Radioimmunoassays for *d*-Pseudoephedrine in Human Plasma and Their Application to Bioequivalency Studies

**JOHN W. A. FINDLAY ˣ, JAMES T. WARREN, JOHN A. HILL, and RICHARD M. WELCH**

Received August 11, 1980, from *Wellcome Research Laboratories, Research Triangle Park, NC 27709.* Accepted for publication November 11, 1980.

**Abstract** □ Antiserum to *d*-pseudoephedrine was raised in New Zealand White rabbits in response to immunization with a conjugate of bovine serum albumin and *d*-pseudoephedrine-*N*-3-propionic acid. The hapten was prepared by reaction of methyl acrylate with *d*-pseudoephedrine, followed by ester hydrolysis. Sodium boro[$^3$H]hydride reduction of *dl*-ephedrone gave [$\alpha$-$^3$H]-*dl*-ephedrine, and a Welsh rearrangement with acetic anhydride followed by deacetylation gave [$\alpha$-$^3$H]-*dl*-pseudoephedrine, which was used as a radioligand in radioimmunoassay procedures for direct plasma analyses. Three sensitive radioimmunoassay procedures were developed, two using [$^3$H]pseudoephedrine as the radioligand and either adsorption on coated charcoal or polyethylene glycol precipitation for separation of antibody-bound from free radioligand. The third method used an [$^{125}$I]tyrosine methyl ester analog of pseudoephedrine and charcoal separation, preceded by extraction and derivatization of pseudoephedrine with methyl acrylate. All three assays could detect ≤2.5 ng of pseudoephedrine/ml. The antiserum was stereospecific, showing low cross-reactivities with *l*-pseudoephedrine and *d*- and *l*-ephedrines. *d*-Norpseudoephedrine and some other related compounds also had low cross-reactivity in these radioimmunoassay procedures. Excellent agreement was found between pseudoephedrine concentrations in human plasma determined by radioimmunoassay and by a standard GLC method. The utility of radioimmunoassay was illustrated by application of one of these procedures to an assessment of the bioequivalence of immediate- and sustained-release pseudoephedrine formulations in normal volunteers. A sustained-release preparation containing 120 mg of pseudoephedrine hydrochloride given every 12 hr was shown by *AUC* comparisons to be bioequivalent to an immediate-release tablet (containing 60 mg of pseudoephedrine hydrochloride) given every 6 hr.

**Keyphrases** □ Radioimmunoassay—*d*-pseudoephedrine, human plasma, bioequivalency studies, immediate- and sustained-release tablets □ *d*-Pseudoephedrine—radioimmunoassay, bioequivalency studies, immediate- and sustained-release tablets □ Bioequivalency studies—radioimmunoassays of *d*-pseudoephedrine in human plasma, bioequivalency studies, immediate- and sustained-release tablets □ Adrenergics—radioimmunoassays for *d*-pseudoephedrine in human plasma, bioequivalency studies, immediate- and sustained-release tablets

*d*-Pseudoephedrine was first isolated from the Chinese plant *Ma Huang* by Chou and Read (1) in 1926, and studies of its pharmacology started soon thereafter (2, 3). Although pseudoephedrine is in widespread use as a proven, clinically effective nasal decongestant (4–6), little published information is available on its disposition and pharmacokinetics in human plasma following administration of therapeutic doses. Studies have examined kinetics chiefly from the viewpoint of urinary excretion (7–9), which is liable to be influenced by alterations in urinary pH (8). Such indirect studies were necessitated by the lack of methods sufficiently sensitive to detect the relatively low circulating concentrations of pseudoephedrine in plasma following therapeutic doses.

Reported GLC procedures (7, 10, and 11) were capable of detecting only 0.3–0.5 μg of pseudoephedrine/ml. Even with nitrogen detection, Bye *et al.* (12) were able to lower the sensitivity limit only to 25 ng/ml. Kuntzman *et al.* (8) reported a procedure that involved esterification of isolated pseudoephedrine with tritiated acetic anhydride followed by separation and quantitation of the resulting radioactive product. Although capable of detecting 50 ng of pseudoephedrine/ml of plasma, this method is still relatively insensitive and time consuming. A study (13) of plasma pseudoephedrine levels relative to efficacy, using a GLC method for drug determination, was able to determine plasma concentrations up to 6 hr following a 60-mg oral dose of pseudoephedrine hydrochloride.

This report describes the development of a specific antiserum to pseudoephedrine and its application to three specific radioimmunoassay procedures for the drug. Two procedures are direct and employ a tritium-labeled radioligand; the third requires extraction and derivatization of the drug prior to assay but employs a $\gamma$-labeled radioligand. The sensitivity limits of these procedures are <2.5 ng of pseudoephedrine/ml in all cases. Their use for drug disposition studies following oral administration of both immediate- and sustained-release pseudoephedrine preparations is illustrated.

## EXPERIMENTAL

Melting points[1] are uncorrected. $^1$H-NMR spectra[2] were obtained in deuterochloroform with tetramethylsilane as the internal standard unless otherwise indicated. Low-resolution mass spectra[3] were obtained by

[1] Thomas-Hoover apparatus, Arthur H. Thomas Co., Philadelphia, Pa.
[2] Model R-24A, Perkin-Elmer Corp., Norwalk, Conn.
[3] Model MAT 731 or CH5DF, Varian Associates, Palo Alto, Calif.



0022-3549/81/0600-0624$01.00/0
© 1981, American Pharmaceutical Association

electron-ionization methods. TLC plates were precoated silica gel[4] with a layer thickness of 0.25 mm. Radiochemical purities were determined by scanning the TLC plates using a radiochromatogram scanner[5]. Bovine serum albumin (Cohn Fraction V), 1-ethyl-3-(3-dimethylaminopropyl)-carbodiimide hydrochloride, tyrosine methyl ester, and dicyclohexylcarbodiimide were purchased from a commercial supplier[6].

Radioimmunoassay grade charcoal[7] was used in the radioimmunoassay separation system. Sodium [$^{125}$I]iodide (carrier free) and sodium boro[$^{3}$H]hydride (specific activity 28 Ci/mmole) were obtained commercially[8]. Methyl acrylate[9], chloramine-T[9], Freund's complete adjuvant[10], and polyethylene glycol 6000[11] were commercial products. Quantitation of radioactivity was in liquid scintillation fluid[12]. Radioactivity was determined in a liquid scintillation counter[13] or $\gamma$-counter[14], as appropriate. Ephedrine, pseudoephedrine, and related compounds were commercially supplied[15].

**d-Pseudoephedrine-*N*-3-propionic Acid Methyl Ester (II)**—To *d*-pseudoephedrine free base (I, 1.65 g, 0.01 mole) in absolute ethanol (25 ml) containing triethylamine (1.03 g, 0.012 mole) was added methyl acrylate (1.03 g, 0.012 mole), and the sealed mixture was stirred at room temperature overnight. The volatile components were evaporated under reduced pressure, leaving an oily residue that slowly crystallized from *n*-pentane to give a colorless solid (2 g), mp 37°; NMR: $\delta$ 7.3 (s, 5H, aromatic H), 4.7 (d, 1H, $J$ = 1.5 Hz, $\alpha$-H), 3.6 (s, 3H, $COOCH_3$), 3.3 (m, 5H), 2.8 (s, 3H, N–$CH_3$), and 1.0 (s, 3H, C–$CH_3$) ppm; mass spectrum: $m/z$ 220 (M − $CH_3$), 178 (M − $CH_2COOCH_3$), and 144.

*Anal.*—Calc. for $C_{14}H_{21}NO_3$: C, 66.90; H, 8.42; N, 5.57. Found: C, 67.78; H, 8.57; N, 5.61.

**d-Pseudoephedrine-*N*-3-propionic Acid Sodium Salt (III)**—The crystalline ester II (2 g) was dissolved in warm 2 *N* NaOH (10 ml) and stirred for 2 hr. Upon cooling, the sodium salt of the acid derivative separated and was filtered. The yield was 1 g of amorphous powder, mp >200° dec.; NMR (deuterated dimethyl sulfoxide): $\delta$ 7.25 (s, 5H, aromatic H), 5.5 (s, 1H), 4.25 (d, 1H, $J$ = 1.5 Hz, $\alpha$-H), 2.5 (m, 6H), 2.2 (s, 3H, N–$CH_3$), and 0.6 (d, 3H, $J$ = 1.5 Hz, C–$CH_3$) ppm; mass spectrum: $m/z$ 282, (free acid anion$^{-1}$ · $Na^{2+}$)$^+$, 541 (L, N–$CH_3$), (anion$^{2-}$ · $Na^{3+}$)$^+$, and 800, (anion$^{3-}$ · $Na^{4+}$)$^+$.

**d-Pseudoephedrine-*N*-3-propionic Acid–Bovine Serum Albumin Amide (IV)**—The pH of a solution of the salt of acid III (0.1 g, 0.4 m*M*) and bovine serum albumin (0.1 g) in water (15 ml) was adjusted to 5.5 with dilute hydrochloric acid. 1-Ethyl-3-(3-dimethylaminopropyl)carbodiimide hydrochloride (0.1 g) was added, and the solution was stirred at room temperature for 20 hr. The immunogen was purified by ultrafiltration[16]. The solution was lyophilized, and the powdery protein residue was stored over desiccant at −80°.

**d-Pseudoephedrine-*N*-3-propionic Acid–Tyrosine Methyl Ester Amide (IV*a*)**—A solution of *d*-pseudoephedrine-*N*-3-propionic acid (0.6 g, 1.8 m*M*) and tyrosine methyl ester free base (0.35 g, 1.8 m*M*) was prepared in acetonitrile (3 ml) and dimethylformamide (1 ml). Sufficient water and dilute hydrochloric acid were added to achieve a homogeneous solution (pH 6). The solution was cooled to 0°, a solution of dicyclohexylcarbodiimide (0.49 g, 2.2 m*M*) in cold dimethylformamide (0.8 ml) was added, and the reaction mixture was stirred at 0° overnight. After filtration, the solution was added to a mixture of tetrahydrofuran (100 ml), acetic acid (15 drops), ethanol (15 ml), and triethylamine (1 ml) to destroy excess dicyclohexylcarbodiimide. Stirring was continued for 1 hr at room temperature. The solution was filtered, and the filtrate was evaporated under reduced pressure.

The residue was dissolved in chloroform (100 ml) and filtered, and the solution was extracted with 5% sodium bicarbonate (2 × 25 ml) and then with 0.1 *N* HCl (2 × 25 ml). The aqueous acid extract was made basic with excess sodium carbonate and extracted into chloroform (3 × 50 ml), and the solvent was dried with magnesium sulfate and clarified with charcoal prior to being evaporated. A methanol solution of the residue was applied to silica gel plates (0.5 mm, 20 × 20 cm) and developed in ethylene dichloride–methanol–ammonium hydroxide (100:30:4). The product band was visualized with fast blue B salt, scraped off, and eluted from the silica gel with methanol (2 × 5 ml).

The methanol solution was concentrated to 0.5 ml, and the preparative TLC purification was repeated. The amorphous residue (0.1 g), mp 162° dec., was stored over desiccant at −80°; NMR: $\delta$ 7.5 (s, 5H, aromatic H), 7.0 (q, 4H, $J$ = 1.0 Hz, aromatic H), 5.0 (d, 1H, $J$ = 1.0 Hz), 4.4 (d, 1H, $J$ = 1.5 Hz, $\alpha$-H), 3.8 (s, 3H, $COOCH_3$), 3.3–2.4 (m, 8H), 2.3 (s, 3H), and 0.7 (d, 3H, $J$ = 1.0 Hz, C–$CH_3$) ppm; mass spectrum: $m/z$ 307.1648, $C_{16}H_{23}N_2O_4$ (M − $CH_2C_6H_4OH$).

**[$^{125}$I]-*d*-Pseudoephedrine-*N*-3-propionic Acid–Tyrosine Methyl Ester Amide (V)**—Into a small test tube containing a glass bead was pipetted 70 $\mu$l of a solution of IV*a* (1.54 $\mu$g, 3.7 n*M*) in 0.5 *M* phosphate buffer, pH 7.7, followed by sodium [$^{125}$I]iodide (1 mCi, 0.56 n*M*) in 10 $\mu$l of dilute sodium hydroxide, pH 8.0. A freshly prepared solution of chloramine-T (25.2 $\mu$g, 89.6 n*M*) in 25 $\mu$l of 0.05 *M* phosphate buffer, pH 7.7, was added, and the mixture was agitated at room temperature for 1 min. A freshly prepared solution of sodium metabisulfite (341 $\mu$g, 1790 n*M*) in 100 $\mu$l of 0.05 *M* phosphate buffer, pH 7.7, was added immediately with mixing.

The mixture was set aside for 10 min at room temperature and then was applied to a silica gel plate (20 × 20 cm), which was developed in the solvent system described for IV*a*. X-ray film was exposed to the TLC plate, and the band ($R_f$ 0.6) corresponding to the main dark band on the X-ray film was scraped off, extracted with methanol (4 × 5 ml), and stored at −80° until used.

**[$\alpha$-$^{3}$H]-*dl*-Pseudoephedrine Hydrochloride (VI)**—dl-$\alpha$-*Bromopropiophenone*—Bromine (20.0 g, 0.125 mole) in methylene chloride (50 ml) was added dropwise to a stirred solution of propiophenone (13.42 g, 0.10 mole) in methylene chloride (80 ml) at 30–35°, and the mixture was heated under reflux for 60 min. Evaporation to dryness gave a pale-yellow oil, which was used in the next reaction without further purification.

dl-*Ephedrone Hydrochloride*—A solution of the crude propiophenone in ethanol (10 ml) was added dropwise under nitrogen to a stirred ice-cold solution of methylamine gas (10.0 g, 0.32 mole) in ethanol (130 ml) during 50 min, and the mixture was stirred at 0° for an additional 40 min. A mixture of 12 *N* HCl (30 ml) and ice was added to pH < 7, and the aqueous solution was extracted with ether and evaporated to dryness. The yellow solid was extracted with chloroform (4 × 50 ml), and the residual methylamine hydrochloride was discarded. Evaporation of the chloroform filtrates gave an off-white solid, which was recrystallized twice from ethanol–acetone to give 3.41 g (17.1%) of *dl*-ephedrone hydrochloride as off-white crystals, mp 176–179° [lit. (21) mp 176–177°]; NMR (dimethyl sulfoxide-$d_6$ + $D_2O$): $\delta$ 1.5 (d, 3H, C–$CH_3$), 2.7 (s, 3H, N–$CH_3$), 5.2 (q, 1H, $\alpha$-H), and 7.4–8.2 (m, 5H, aromatic H) ppm. TLC in chloroform–2-propanol–triethylamine (62:35:3) showed a single spot, $R_f$ 0.53.

*[$\alpha$-$^{3}$H]*-dl-*Ephedrine Hydrochloride*—To a stirred solution of ephedrone hydrochloride (90.1 mg, 0.45 mmole) in ethanol (12 ml) under dry argon was added dropwise a solution of sodium boro[$^{3}$H]hydride (8 Ci at 28 Ci/mmole, ~0.34 mmole) in ethanol (19 ml) during 2 min. After a further 60 min at room temperature, a solution of 12 *N* HCl (1.6 ml) in water (2.9 ml) was added dropwise. After stirring for 20 min, the colorless solution was diluted with water (90 ml) and ether (70 ml), and 1 *N* NaOH (30 ml) was added to pH > 10. The aqueous solution was extracted with ether (4 × 50 ml), and the combined ether solutions were washed with water (100 ml), evaporated to near dryness *in vacuo* at 0°, and treated with methanol (20 ml) and 12 *N* HCl (2.0 ml). Evaporation to dryness *in vacuo* yielded 89.9 mg (98.8%) of crude ephedrine as an off-white solid. TLC in chloroform–2-propanol–triethylamine (62:35:3) showed ephedrines ($R_f$ ~0.19) containing a trace of residual ephedrone ($R_f$ 0.53), and TLC in 2-butanone–2-propanol–ammonium hydroxide (6:3:1) showed mainly ephedrine ($R_f$ 0.49) containing a trace of pseudoephedrine ($R_f$ 0.82).

*[$\alpha$-$^{3}$H]*-dl-*Pseudoephedrine Hydrochloride*—A stirred mixture of crude ephedrine (89.9 mg) and acetic anhydride (3.0 ml) under dry argon was heated under reflux for 30 min. The cooled solution was evaporated to dryness *in vacuo*, water (2.0 ml) and 12 *N* HCl (0.6 ml) were added, and the mixture was distilled for 2 hr while fresh water was added continuously to the flask to replace the distillate, volume for volume. Evaporation to dryness *in vacuo* was followed by the addition of hot water (1.5 ml) and then the addition of 50% NaOH solution to the stirred ice-cold solution to pH > 13. The precipitate of [$\alpha$-$^{3}$H]-*dl*-pseudoephedrine was collected by filtration, washed with ice-cold water (1.0 ml), dissolved in methanol (10 ml), and treated with 12 *N* HCl (1.0 ml).

TLC in 2-butanone–2-propanol–ammonium hydroxide (6:3:1) showed

[4] Silica gel 60 F-254, E. Merck & Co., Darmstadt, West Germany.
[5] Berthold LB 2760, Beta Analytical Inc., Coraopolis, Pa.
[6] Sigma Chemical Co., St. Louis, Mo.
[7] Schwarz-Mann, Orangeburg, N.Y.
[8] Amersham Corp., Arlington Heights, Ill.
[9] Eastman Organic Chemicals, Rochester, N.Y.
[10] Difco Laboratories, Detroit, Mich.
[11] Fisher Scientific Co., Raleigh, N.C.
[12] Aquasol-2, New England Nuclear Corp., Boston, Mass.
[13] Model 3320 or 2650, Packard Instrument Co., Downers Grove, Ill.
[14] Model 5260 Autogamma, Packard Instrument Co., Downers Grove, Ill.
[15] Knoll Fine Chemicals, New York, N.Y.
[16] PM-10 membrane, Amicon Corp., Lexington, Mass.

almost entirely pseudoephedrine ($R_f$ 0.82), no ephedrone and no ephedrine, and a small amount of unknown material ($R_f$ 0.0). Evaporation to dryness *in vacuo* yielded 58.2 mg (64.0% from ephedrone) of crude [$^3$H]pseudoephedrine hydrochloride as an off-white solid. Two recrystallizations from 3-methyl-1-butanol–tetrahydrofuran afforded 3.8 mg of pure [$\alpha$-$^3$H]-*dl*-pseudoephedrine hydrochloride as a colorless crystalline solid. TLC in 2-butanone–2-propanol–ammonium hydroxide (6:3:1) showed almost single-spot [$^3$H]pseudoephedrine ($R_f$ 0.82) with a trace of material at the origin. Radiochromatogram scanning showed ~0.4% [$^3$H]ephedrine in otherwise radiochemically pure [$^3$H]pseudoephedrine. TLC in chloroform–2-propanol–triethylamine (62:35:3) again showed almost pure [$^3$H]pseudoephedrine ($R_f$ 0.16) with a trace of material at the origin. Radioactive chromatogram scanning showed ~2.6% of the activity in the origin material in otherwise 97.4% radiochemically pure [$^3$H]pseudoephedrine. Autoradiograms showed the same distribution pattern of radioactivity as shown by plate scanning. The specific activity was determined by scintillation counting to be 5.0 Ci/mmole.

**[$\alpha$-$^3$H]-*dl*-Pseudoephedrine-*N*-3-propionic Acid Methyl Ester (VII)**—A methanol solution of [$\alpha$-$^3$H]-*dl*-pseudoephedrine (2.82 $\mu$g, 69 $\mu$Ci, 300 $\mu$l) containing triethylamine (36.3 mg, 358 $\mu M$, 10 $\mu$l) and methyl acrylate (47.8 mg, 555 $\mu M$, 50 $\mu$l) was sealed and mixed at room temperature overnight. The solution was gently evaporated (dry nitrogen stream), and the residue was dissolved in 300 $\mu$l of methanol. A TLC radiochromatogram in ethylene dichloride–methanol–ammonium hydroxide (100:20:4) showed a single band that migrated with the unlabeled compound.

**[$\alpha$-$^3$H]-*dl*-Pseudoephedrine-*N*-3-propionitrile (VIII)**—A methanol solution of [$\alpha$-$^3$H]-*dl*-pseudoephedrine (2.82 $\mu$g, 69 $\mu$Ci, 300 $\mu$l) containing triethylamine (36.3 mg, 358 $\mu M$, 10 $\mu$l) and acrylonitrile (40.3 mg, 760 $\mu M$, 50 $\mu$l) was sealed and mixed at room temperature overnight. The solution was gently evaporated (dry nitrogen stream), and the residue was dissolved in 300 $\mu$l of methanol. A radiochromatogram in the TLC system used for VII showed a single band that migrated with the unlabeled compound.

**[$\alpha$-$^3$H]-*dl*-Pseudoephedrine-*N*-acetyl Amide (IX)**—A methanol solution of [$\alpha$-$^3$H]-*dl*-pseudoephedrine (2.82 $\mu$g, 69 $\mu$Ci, 300 $\mu$l) containing triethylamine (36.3 mg, 358 $\mu M$, 10 $\mu$l) and acetyl chloride (55.2 mg, 703 $\mu M$, 50 $\mu$l) was sealed and mixed at room temperature overnight. The solution was gently evaporated (dry nitrogen stream), and the residue was dissolved in 300 $\mu$l of methanol. A radiochromatogram in the system used for VII showed a single band that migrated with the unlabeled compound.

**Immunization Procedures**—Male New Zealand White rabbits received a primary immunization of 1 mg of bovine serum albumin–drug conjugate in 1 ml of 0.9% saline emulsified with 1 ml of Freund's complete adjuvant as two intramuscular (*vastus lateralis*) and eight subcutaneous (along each side of the dorsal column) injections of 0.2 ml each. At intervals of 2, 4, and 6 weeks following the primary immunization and at monthly intervals thereafter, booster immunizations of 0.5 mg of immunogen in 0.5 ml of saline, emulsified with 0.5 ml of Freund's complete adjuvant, were administered at multiple subcutaneous sites. Following the second and all subsequent booster immunizations, blood samples were collected from the central ear artery and the serum was separated and stored at −80°.

**Human Study**—Seventeen healthy male subjects received, for 5 days, either an immediate-release tablet[17] containing 2.5 mg of triprolidine hydrochloride and 60 mg of pseudoephedrine hydrochloride every 6 hr or a sustained-release capsule[18] containing 5 mg of triprolidine hydrochloride and 120 mg of pseudoephedrine hydrochloride every 12 hr. The study followed a double-blind crossover design so that all subjects received both treatments with a 1-week period intervening to allow for removal of residual drugs from the plasma. At each drug administration, subjects received a tablet and a capsule, one of which contained active drug and the other contained placebo materials according to the planned treatment schedule. The sustained-release preparation was administered at 8 am and 8 pm, while the immediate-release tablets were given at 8 am, 2 pm, 8 pm, and 2 am.

In each phase of the study, blood samples were collected into glass tubes[19] containing the disodium salt of ethylenediaminetetraacetic acid at 8 am, 10 am, 8 pm, and 10 pm on Days 1–4, at 8 am, 9 am, 10 am, 12 noon, 2 pm, 3 pm, 4 pm, 6 pm, 8 pm, and 10 pm on Day 5, and at 8 am and 2 pm on Day 6. Plasma was separated by centrifugation and stored at −20° until analyzed for pseudoephedrine content. The participants had not ingested any drugs for at least 1 week prior to entering the study.

**General Radioimmunoassay Procedures**—The assay buffer contained 0.05 $M$ $NaH_2PO_4$–$Na_2HPO_4$ (pH 7.4), 0.15 $M$ NaCl, 0.01 $M$ ethylenediaminetetraacetic acid disodium salt, and 1% bovine serum albumin, except where otherwise indicated. The pH of this buffer, hereafter referred to as 1% bovine serum albumin–phosphate-buffered saline, was adjusted to 7.4. For separation of antibody-bound radiolabel from free radiolabel, a bovine serum albumin-coated charcoal suspension was prepared by dissolving 0.6 g of charcoal in 100 ml of ice-cold 2% bovine serum albumin–phosphate-buffered saline. The suspension was stirred for at least 30 min at 0° prior to use.

The alternative separation system consisted of 350 g of polyethylene glycol 6000 dissolved in 1 liter of phosphate-buffered saline. For use with this system, radioligand and rabbit antibody solutions were prepared in buffer containing 0.1% bovine serum albumin (0.1% bovine serum albumin–phosphate-buffered saline); bovine serum albumin was not added to phosphate-buffered saline for any other assay applications using the polyethylene glycol 6000 immunoglobulin precipitation.

All assay points were established in duplicate, and most unknown samples were analyzed at two dilutions.

**Antiserum Titration**—*Charcoal Separation*—[$^{125}$I]-*d*-Pseudoephedrine-*N*-3-propionic acid–tyrosine methyl ester amide (100,000 dpm/assay), [$^3$H]-*dl*-pseudoephedrine-*N*-3-propionic acid methyl ester (16,000 dpm/assay), [$^3$H]-*dl*-pseudoephedrine-*N*-3-propionitrile (16,000 dpm/assay), [$^3$H]-*dl*-pseudoephedrine-*N*-acetyl amide (16,000 dpm/assay), or [$^3$H]-*dl*-pseudoephedrine (16,000 dpm/assay) in buffer (0.1 ml) was incubated with varying dilutions of rabbit antiserum in buffer (0.1 ml) and additional assay buffer (0.8 ml) at 4° overnight. Tubes containing only radiolabeled solution and buffer added to obtain the same total incubation volume served as total count tubes and background tubes.

Ice-cold 2% bovine serum albumin–charcoal suspension (0.5 ml) was added to all tubes except the total count tubes; the contents of the tubes were mixed, incubated at 4° for 5 min, and centrifuged (≥1000×$g$, 10 min). The tritium-containing supernates were decanted into scintillant (10 ml) and mixed, and the antibody-bound radioactivity was quantitated. The radioiodine-containing supernates were decanted into plastic tubes (12 × 75 cm) and capped, and their radioactivity contents were quantitated. The dilution that bound 50% of the amount bound in the presence of excess antiserum was defined as the working titer of the antiserum.

*Polyethylene Glycol Separation*—To ensure maximal precipitation of the antibody–radiolabel complex in the radioimmunoassay procedure using polyethylene glycol 6000 as an immunoglobulin precipitant, carrier immunoglobulin protein in the form of 0.1 ml of filtered (0.22 $\mu$m) pooled normal human plasma was added to the assay mixture and the amount of added buffer was reduced by 0.1 ml. After the assay mixture was incubated overnight at 4°, 1 ml of the polyethylene glycol 6000 solution was added to each assay tube (polypropylene, 12 × 55 mm) at 0° in an ice bath. The tubes were thoroughly mixed, incubated at 0° for 30 min, and centrifuged at ≥1000×$g$ for 30 min. Supernates were decanted from the immunoglobulin pellet containing antibody-bound radiolabel, the inverted tubes were allowed to drain for 15 min, and then the assay tubes were pounded on paper towels to remove the remaining supernates quantitatively. The pellets were then resolubilized in phosphate-buffered saline (0.3 ml) with mixing over 30 min. Total count tubes received 0.2 ml of phosphate-buffered saline plus 0.1 ml of labeled solution. When a homogeneous solution was achieved, scintillation fluid (2 ml) was added to the assay tubes, which were capped and mixed. These tubes were placed in specially designed scintillation vials that kept them correctly positioned for scintillation counting.

**Radioimmunoassay of Standard, Control, and Unknown Plasma Samples**—*Direct Radioimmunoassay with [$\alpha$-$^3$H]-*dl*-Pseudoephedrine Label*—A series of *d*-pseudoephedrine hydrochloride standard solutions in filtered (0.22 $\mu$m), pooled, normal human plasma (0.1 ml) ranging in concentration from 1 to 250 ng/ml (free base equivalents) was incubated as already described (for the polyethylene glycol separation) with [$\alpha$-$^3$H]-*dl*-pseudoephedrine (16,000 dpm/assay, 0.1 ml), *d*-pseudoephedrine antiserum (1:100 dilution, 0.1 ml), and assay buffer (0.7 ml). A similar series of three control solutions of *d*-pseudoephedrine added to normal human plasma varying in concentration across the range of the standard curve served as controls of assay accuracy and reproducibility. Unknown human plasma samples (0.1 ml), diluted appropriately with normal human plasma to enter the range of the assay, were also incubated with [$\alpha$-$^3$H]-*dl*-pseudoephedrine, *d*-pseudoephedrine antiserum, and assay buffer as described. Total counts and background tubes were as already described, each containing 0.1 ml of normal human plasma and a total final volume of 1 ml.

[17] Actifed, Burroughs Wellcome Co., Research Triangle Park, N.C.
[18] Actifed SA, Burroughs Wellcome Co., Research Triangle Park, N.C.
[19] Vacutainer, Becton-Dickinson and Co., Rutherford, N.J.

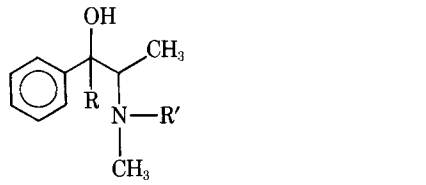

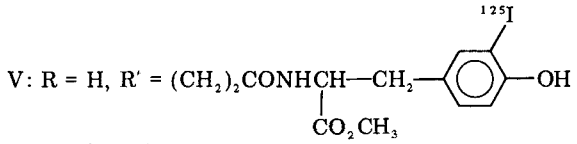

V: R = H, R′ = $(CH_2)_2CONHCH(CO_2CH_3)CH_2$–(p-$^{125}$I-phenyl)–OH

VI: R = $^3$H, R′ = H

VII: R = $^3$H, R′ = $(CH_2)_2CO_2CH_3$

VIII: R = $^3$H, R′ = $(CH_2)_2CN$

IX: R = $^3$H, R′ = $COCH_3$

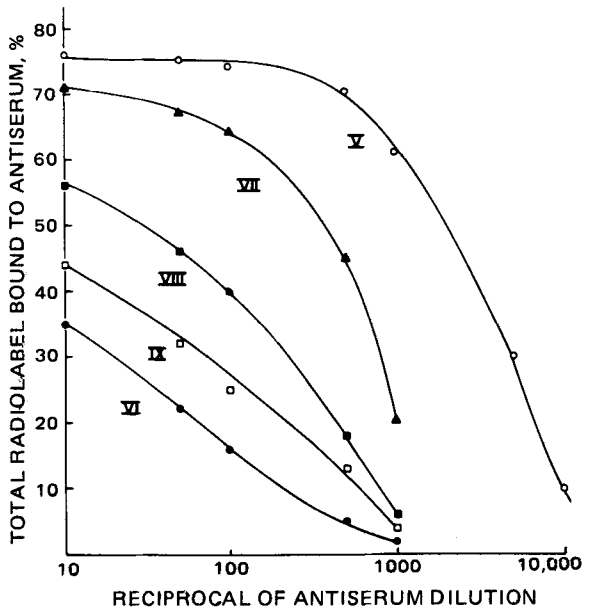


**Figure 1**—*Binding of various* d-*pseudoephedrine radioligands to increasing dilutions of* d-*pseudoephedrine antiserum.*

Separation of antibody-bound radiolabel from free radiolabel was achieved by charcoal adsorption of free radiolabel or polyethylene glycol 6000 precipitation of antibody-bound radiolabel as already described. Standard curves were expressed as % $B/B_0$ *versus* log *d*-pseudoephedrine free base concentration, where $B_0$ represents the amount (counts per minute) of [$\alpha$-$^3$H]-*dl*-pseudoephedrine bound in the absence of any unlabeled *d*-pseudoephedrine and $B$ is the amount bound at a given *d*-pseudoephedrine standard concentration (corrected for nonspecific binding).

*Indirect (Extracted and Derivatized) Assay Using [$^{125}$I]-*d*-Pseudoephedrine-*N*-3-propionic Acid–Tyrosine Methyl Ester Amide Label*—A similar series of *d*-pseudoephedrine standard solutions, control solutions, and appropriately diluted unknowns in filtered normal human plasma ranging in concentration from 0.2 to 50 ng/ml was prepared. One-milliliter aliquots of standards, controls, or unknown dilutions were pipetted into 15-ml glass centrifuge tubes with polytef-lined screw caps, followed by 2 *N* NaOH (0.5 ml, in saturated sodium sulfate). The basic plasma samples were shaken for 15 min with 7 ml of a mixture of cyclopentane–ether (1:1). After centrifugation, the lower aqueous layer was frozen in a dry ice–acetone bath and the solvent layer was decanted into a clean centrifuge tube.

The process was repeated with an additional 7 ml of solvent, and the combined extracts were evaporated under nitrogen at room temperature. The residue was taken up in methanol (2 ml) containing methyl acrylate (10 $\mu$l, 9.56 mg, 0.11 m*M*). The tubes were shaken gently overnight at room temperature, the contents were made acidic by the addition of 1 drop of a saturated solution of hydrogen chloride gas in methanol, and the tubes were shaken for 1 min. After evaporation under nitrogen at room temperature, the residues were dissolved in assay buffer (1 ml), and the tubes were shaken for 1 min.

The radioimmunoassay incubation mixture was similar to that employing the tritium label and consisted of standards, controls, or unknown plasma dilutions, after extraction and derivatization, in assay buffer (0.5 ml), [$^{125}$I]-*d*-pseudoephedrine-*N*-3-propionic acid–tyrosine methyl ester amide (100,000 dpm) in assay buffer (0.1 ml), anti-*d*-pseudoephedrine serum (1:1500 dilution) in assay buffer (0.1 ml), and assay buffer (0.3 ml). After incubation for 2 hr at 0°, free radiolabel was adsorbed onto bovine serum albumin-coated charcoal as already described; the antibody-bound radiolabel contained in the supernates was quantitated. Data were reduced to standard curves, and control and unknown dilution concentrations were determined as already described.

*Cross-Reactivity Studies*—The procedure was similar to that described for the direct radioimmunoassay. A series of standard solutions of *d*-pseudoephedrine hydrochloride (0.2–100 ng of free base equivalents/ml) and some metabolites and structurally related compounds (1–100,000 ng/ml) in normal human plasma were incubated directly, or after extraction and derivatization, with antiserum and radiolabel and processed as described. Standard curves were drawn for each compound. Cross-reactivities were expressed as the percentage ratio of the *d*-pseudoephedrine concentration required to inhibit binding of the radiolabel to antiserum by 50% ($I_{50}$) to that of each respective compound (14).

## RESULTS

**Immunogen Synthesis**—The hapten used for the immunogen preparation, *d*-pseudoephedrine-*N*-3-propionic acid (III), was prepared by aqueous base hydrolysis of the ester product of a Michael addition of methyl acrylate to *d*-pseudoephedrine (Scheme I). The product was characterized by NMR and mass spectral analyses prior to coupling to bovine serum albumin *via* a carbodiimide-mediated amide bond formation using reaction conditions similar to those described by Cheng *et al.* (15).

**Radioligand Syntheses**—*[$\alpha$-$^3$H]-*dl*-Pseudoephedrine Hydrochloride (VI)*—This compound was prepared by a modification of the methods described previously (16–19) for the unlabeled compound. Bromination of propiophenone with bromine in refluxing methylene

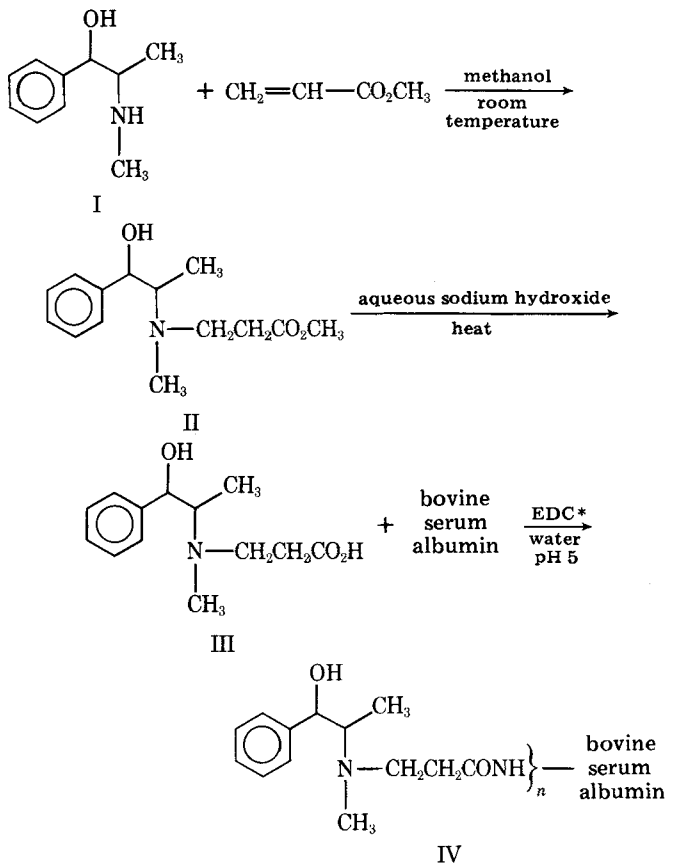


*Scheme I—Synthesis of* d-*pseudoephedrine–bovine serum albumin conjugate (*EDC = 1-ethyl-3-(3-dimethylaminopropyl)carbodiimide hydrochloride).*

**Table I—Interassay Accuracy and Precision of Pseudoephedrine Radioimmunoassay Procedures** [a]

| | | | | |
|---|---|---|---|---|
| Iodine 125–Extraction–Derivatization Method [b] | | | | |
| Concentration [c] added | 0.3 | 0.7 | 3.0 | |
| Concentration measured ± *CV*, % (*n* = 4) | 0.3 ± 3 | 0.69 ± 3 | 2.98 ± 8 | |
| Tritium–Direct–Charcoal Separation Method | | | | |
| Concentration added | 3 | 7 | 30 | 60 |
| Concentration measured ± *CV*, % (*n* = 4) | 2.8 ± 4 | 6.4 ± 2 | 27.7 ± 2 | 61.0 ± 1 |
| Tritium–Direct–Polyethylene Glycol 6000 Separation Method | | | | |
| Concentration added | 3 | 30 | 60 | |
| Concentration measured ± *CV*, % (*n* = 7) | 3.1 ± 5 | 28.3 ± 2 | 60.3 ± 1 | |

[a] Pseudoephedrine was added to blank human plasma for all recovery studies. [b] Plasma samples were carried through the entire extraction–derivatization procedures. [c] All concentration values are nanograms per milliliter.

chloride solution gave *dl*-α-bromopropiophenone, which was condensed with methylamine gas in ethanol at 0° essentially by the method of Hyde *et al.* (20) to give, after purification, *dl*-ephedrone hydrochloride. Treatment of this compound with sodium boro[$^3$H]hydride in ethanol gave a quantitative yield of predominantly the *erythro* compound, [$^3$H]-*dl*-ephedrine hydrochloride. In the Welsh procedure (18, 19), this *erythro* compound undergoes an N → O acyl migration with inversion of configuration upon reaction with refluxing acetic anhydride while the *threo* isomer undergoes the same migration with retention of configuration.

Thus, acetylation of the crude ephedrine, followed by hydrolysis in aqueous hydrochloric acid, gave the free base [$^3$H]pseudoephedrine, which was converted to VI (64% yield from ephedrine). Two recrystallizations from isoamyl alcohol–tetrahydrofuran gave pure [$^3$H]pseudoephedrine hydrochloride for use in radioimmunoassay studies. Two useful methods for determination of the enantiomeric purity of the final product were developed during the synthetic work. TLC on silica gel layers in 2-butanone–2-propanol–ammonium hydroxide (6:3:1) clearly separated ephedrine ($R_f$ 0.49) and pseudoephedrine ($R_f$ 0.82). Also, the chemical shift of the α-proton doublet in the $^1$H-NMR spectrum could be used to detect ephedrine (δ 5.24, d, $J$ = 3 Hz) in the presence of pseudoephedrine (δ 4.62, d, $J$ = 10 Hz) and vice versa. The specific radioactivity of VI was estimated to be 5 Ci/mmole.

N-*Functionalized Radioligands*—Reaction of acetyl chloride, acrylonitrile, or methyl acrylate with VI, as described under *Experimental*, gave the *N*-acetyl amide (IX), *N*-propionitrile (VIII), or *N*-propionic acid methyl ester (VII) derivatives, respectively (Fig. 1). These radioligands were used to examine the affinity of the antiserum for radioligands bearing differing components of the bridge between hapten and bovine serum albumin in the immunizing conjugate.

$^{125}$*I-Labeled Radioligand*—A radioiodine-substituted ligand (V, Fig. 1) was prepared from *d*-pseudoephedrine-*N*-3-propionic acid–tyrosine methyl ester amide by reaction with sodium [$^{125}$I]iodide and chloramine-T by the general method of Hunter and Greenwood (21). The specific radioactivity of the ligand was estimated to be 270 Ci/m*M*.

**Comparative Binding of Radioligands by Antibody**—Figure 1 compares the ability of increasing dilutions of antiserum 515-1 to bind a constant amount of tritiated radioligands under identical incubation conditions. Since the specific activities of the tritiated radioligands were the same, the figure indicates the relative affinity of the antibody for pseudoephedrine and its various side-chain analogs. As the series progressed from underivatized [$^3$H]pseudoephedrine to *N*-acetyl-[$^3$H]-pseudoephedrine to the *N*-propionitrile analog and, finally, to the *N*-propionic acid methyl ester, the immediate precursor of the hapten derivative, higher dilutions of antiserum were capable of binding similar amounts of the radioligand. Clearly, the presence of the side chain was well recognized by this antiserum. The antiserum appeared to recognize the $^{125}$I-labeled radioligand well, although affinity comparisons with the $^3$H-labeled radioligands are difficult due to the higher specific activity of the iodinated compound.

**Assay Precision and Sensitivity**—Typical mean standard curves for the three individual radioimmunoassays are shown in Fig. 2. Each mean curve was constructed from four individual standard curves. The standard deviations on the curves indicate the excellent interassay precision. Further confirmation of interassay precision is shown by the assay data (means and standard deviations) for *d*-pseudoephedrine-spiked plasma controls that varied across the range of standard curve sensitivity for the separate radioimmunoassay procedures (Table I). The coefficient

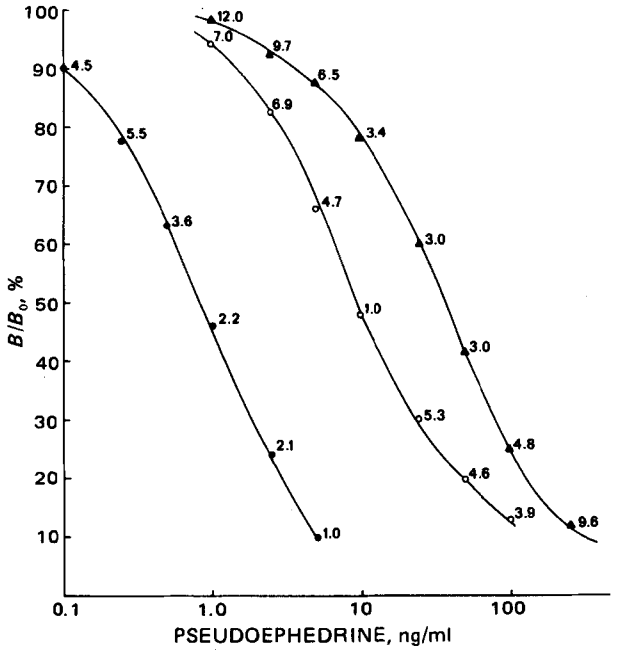


**Figure 2**—*Typical standard curves for* d*-pseudoephedrine radioimmunoassay procedures. Key:* ●, *iodine 125–derivatization–charcoal;* ○, *tritium–direct–charcoal; and* ▲, *tritium–direct–polyethylene glycol.*

of variation values did not exceed 8% for any control sample; for most samples, the coefficient of variation was <3%.

The indirect radioimmunoassay procedure, utilizing a radioiodine ligand and extraction and derivatization of *d*-pseudoephedrine prior to assay, is the most sensitive and specific technique, clearly able to detect 0.2 ng of *d*-pseudoephedrine/ml ($IC_{50}$ = 4.3 ng/ml). The direct radioimmunoassay procedure, utilizing a tritium radioligand and a bovine serum albumin-coated charcoal bound/free separation scheme, is the next most sensitive procedure with a detection limit of 1 ng of *d*-pseudoephedrine/ml ($IC_{50}$ = 10 ng/ml). However, due to the observed time-dependent tendency of the bovine serum albumin-coated charcoal to remove [$^3$H]-*dl*-pseudoephedrine from its binding sites on the antibody, the capacity of the assay (standards, controls, and unknowns) is limited.

For this reason, an alternative direct radioimmunoassay procedure using [$^3$H]-*dl*-pseudoephedrine was developed. Polyethylene glycol 6000 precipitates immunoglobulins (22) and, thus, antibody-bound radiolabel from the assay mixture. This precipitation achieves a separation of antibody-bound from free radiolabel that is relatively independent of time. The lower detection limit of this assay is 2.5 ng/ml ($IC_{50}$ = 35 ng/ml).

**Assay Specificity**—The relative specificities of the three radioimmunoassay procedures are shown in Table II. *d*-Norpseudoephedrine cross-reacted between 0.8 and 5.0%, with the indirect extraction–derivatization radioimmunoassay procedure being most specific and the direct–charcoal method being least specific. *l*-Ephedrine, the diastereomer of *d*-pseudoephedrine, was recognized by the antiserum 200–800 times less effectively than *d*-pseudoephedrine. In this case, while cross-reactivity was low in all three procedures, the direct–charcoal method was the most specific. *l*-Pseudoephedrine, the optical isomer of *d*-pseudoephedrine, had very low cross-reactivity in all assays (<0.003–0.01%).

More detailed cross-reaction studies were pursued using the polyethylene glycol 6000–direct procedure. The antibody was clearly able to distinguish the lack of a β-methyl group (*N*-methylphenylethanolamine, 0.26%), the lack of an α-hydroxy group (methamphetamine, 0.08%), oxidation of the α-hydroxy group (ephedrone, <0.003%), and hydroxylation of the aromatic ring (*p*-hydroxyephedrine, <0.003%). Endogenous phenylethanolamines, such as epinephrine, and drugs that may be coadministered with pseudoephedrine, such as triprolidine and codeine, cross-reacted <0.003%.

**Validation of Radioimmunoassays (Correlation with Standard GLC Assay)**—Final validation of the assays was achieved by comparative analysis by radioimmunoassay and GLC of human plasma samples containing *d*-pseudoephedrine (obtained from volunteers who had ingested a 60-mg tablet of *d*-pseudoephedrine hydrochloride). Figure 3 shows correlation diagrams relating plasma *d*-pseudoephedrine levels

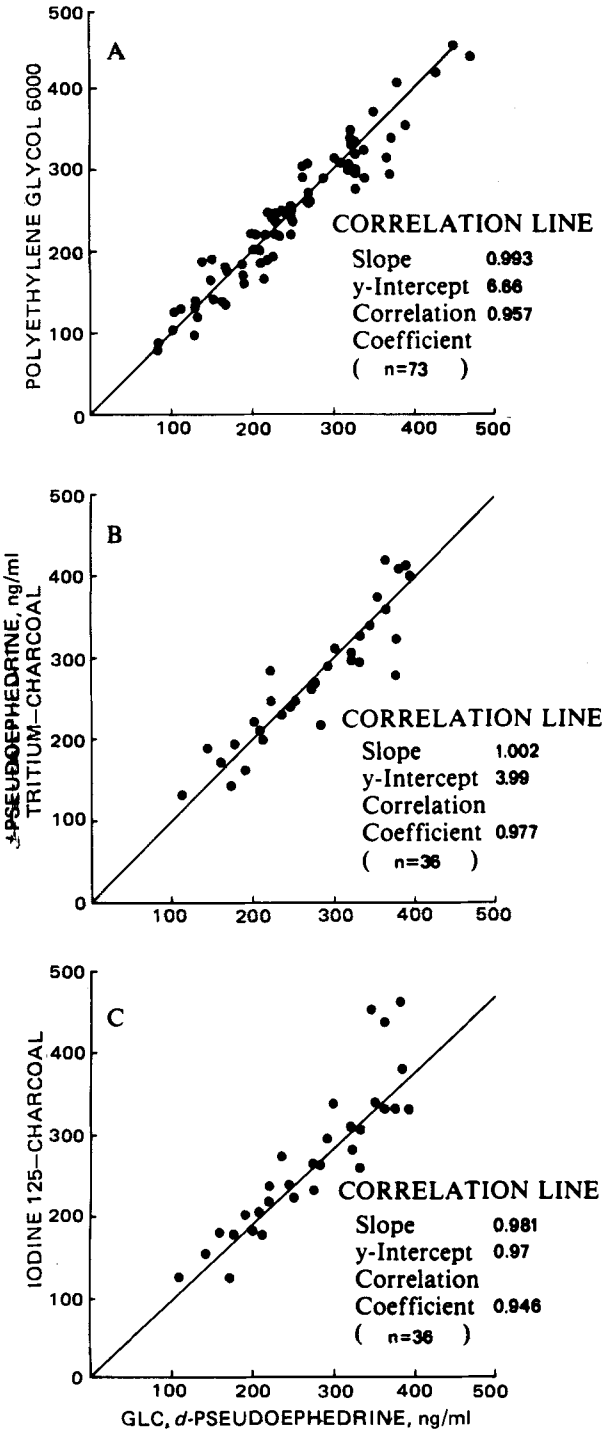


**Figure 3**—*Correlation of pseudoephedrine concentrations in human plasma samples as analyzed by a GLC procedure and tritium–direct–polyethylene glycol radioimmunoassay (A), tritium–direct–charcoal radioimmunoassay (B), or iodine 125–derivatization–charcoal radioimmunoassay (C).*

determined by a derivatization GLC procedure with electron-capture detection (10) to those determined by the three radioimmunoassays. In each case, linear regression analysis gave correlation coefficients between 0.946 and 0.977 and slopes of 0.981–1.002, indicating excellent agreement between all three radioimmunoassay procedures and the reference GLC assay.

**Disposition Studies in Humans**—For convenience and ease of operation, the direct radioimmunoassay utilizing [$^3$H]pseudoephedrine and the polyethylene glycol 6000 separation method was used in all human drug disposition studies. This assay was applied to a bioequivalence comparison of *d*-pseudoephedrine from a sustained-release preparation

**Table II—Cross-Reactivities (%) of Related Compounds in Pseudoephedrine Radioimmunoassay Procedures**

| Compound | Tritium–Direct–Charcoal | Tritium–Direct–Polyethylene Glycol 6000 | Iodine 125–Extraction–Derivatization |
|---|---|---|---|
| *d*-Pseudoephedrine | 100 | 100 | 100 |
| *d*-Norpseudoephedrine | 5.0 | 1.75 | 0.8 |
| *l*-Pseudoephedrine | 0.01 | 0.05 | <0.003 |
| *l*-Ephedrine | 0.13 | 0.44 | 0.32 |
| *l*-Norephedrine | — | 0.02 | — |
| *d*-Ephedrine | — | 0.35 | — |
| *N*-Methylphenylethanolamine | — | 0.26 | — |
| Methamphetamine | — | 0.08 | — |
| *dl*-*p*-Hydroxyephedrine | — | <0.003 | — |
| Ephedrone | — | <0.003 | — |
| Metaraminol | — | <0.003 | — |
| Methoxamine | — | <0.003 | — |
| Phenylethylamine | — | <0.003 | — |
| *l*-Phenylephrine | — | <0.003 | — |
| Epinephrine | — | <0.003 | — |
| Triprolidine | — | <0.003 | — |
| Codeine | — | <0.003 | — |

(containing 120 and 5 mg, respectively) and an immediate-release preparation (containing 2.5 and 60 mg, respectively) of *d*-pseudoephedrine hydrochloride and triprolidine hydrochloride in 17 healthy male subjects. The study extended over 126 hr in each of two separate periods, during which all subjects received both formulations (*Experimental*). Doses of sustained-release medication were administered at 12-hr intervals (8 am and 8 pm), while immediate-release tablets were given at 6-hr intervals (8 am, 2 pm, 8 pm, and 2 am) throughout the first 120 hr. Mean plasma pseudoephedrine levels in these subjects over the entire 126-hr study period as determined by the direct radioimmunoassay are shown in Fig. 4.

Steady-state concentrations were approached with both drug formulations by the 3rd day of treatment, with mean trough concentrations of 280–350 ng/ml and mean peak concentrations of 420–560 ng/ml for the two preparations. Additional blood samples were taken from 8 am to 8 pm on Day 5 to define more closely the plasma concentration–time profiles at steady state for immediate- and sustained-release preparations. The mean plasma concentration–time curves for all subjects during this period are shown in Fig. 5. The mean observed peak concentration following the first (8 am) dose of the immediate-release tablet (containing 60 mg of pseudoephedrine hydrochloride) was 565.8 ng/ml and that following the second (2 pm) dose was 554.6 ng/ml. The maximum concentration observed following administration (at 8 am) of the sustained-release preparation (which contained 120 mg of pseudoephedrine hydrochloride) was 550.6 ng/ml. Although the mean peak plasma concentrations achieved with the two formulations were not significantly different, mean plasma concentrations of pseudoephedrine were maintained for a considerably longer period with the sustained-release preparation.

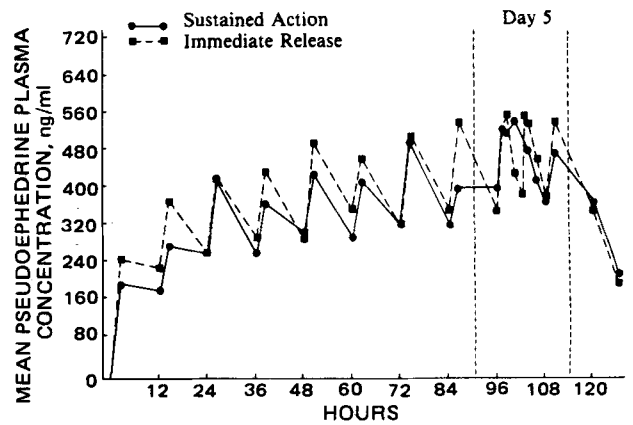


**Figure 4**—*Mean plasma pseudoephedrine concentrations over 126 hr in 17 healthy volunteers who received either a sustained-release preparation of pseudoephedrine every 12 hr or an immediate-release preparation every 6 hr for the first 5 days.*

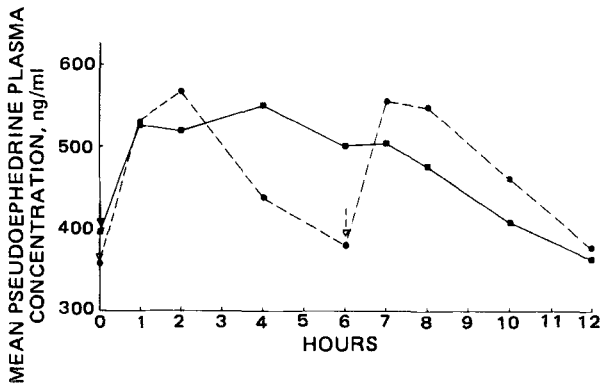


**Figure 5**—*Detailed presentation of the 8 am–8 pm period on Day 5 of the study presented in Fig. 4. Key: ■, sustained release; and ●, immediate release.*

## DISCUSSION

Previous investigations demonstrated the need for conjugation of drugs to macromolecules to render them immunogenic (23–25). In the present study, *d*-pseudoephedrine was easily derivatized *via* the nitrogen atom by reaction with methyl acrylate followed by alkaline hydrolysis to give the *N*-3-propionic acid derivative for coupling to bovine serum albumin for immunization purposes. Antiserum raised in response to this immunization procedure was used to develop three radioimmunoassay procedures. In one, a tyrosine methyl ester derivative of the original hapten, prepared by carbodiimide-mediated reaction with tyrosine methyl ester followed by iodination, provided a radioligand with the convenience of a $\gamma$-emitting radioisotope. However, since this ligand could not be displaced by *d*-pseudoephedrine at the required sensitivity level, this assay modification required prior extraction of all pseudoephedrine-containing samples and derivatization with methyl acrylate before their addition to the radioimmunoassay system.

[$\alpha$-$^3$H]-*dl*-Pseudoephedrine and unlabeled pseudoephedrine were used to demonstrate that the drug could be extracted and derivatized by this method with a mean overall recovery of >95% across the concentration range of 0.1–500 ng/ml when performed under the conditions specified under *Experimental*. This assay modification has better sensitivity and specificity than the other variations and may be useful in studies where maximal sensitivity is required, such as tissue distribution experiments. The assay variants employing [$^3$H]pseudoephedrine as the radioligand are somewhat less sensitive than the derivatization assay using the $^{125}$I-labeled radioligand and use the antiserum at a much lower titer, but these variations have the distinct advantage of providing reliable drug analyses directly on plasma, *i.e.*, without prior extraction. The assay using the polyethylene glycol 6000 method for separation of antibody-bound from free radioligand had the advantage of being less time dependent when compared to the bovine serum albumin-coated charcoal separation method. Thus, large assay runs were more reliably performed with the former system.

All three assay systems are accurate and precise (Table I), and have sensitivity limits in the range of 0.2–2.5 ng/ml for iodine 125–derivatized and tritium–polyethylene glycol methods, respectively (0.2–0.25-ng actual mass of pseudoephedrine, see *Experimental*). This sensitivity far exceeds that of the earlier GLC procedures for pseudoephedrine (7, 10, 11) and is better than that of a more recent GLC method using nitrogen detection that was capable of detecting a lower limit of 25 ng/ml (12). Acetylation of pseudoephedrine with [$^3$H]acetic anhydride provides a method capable of detecting 50 ng/ml of the drug in plasma (8). Recently, a pseudoephedrine pharmacokinetic study (26) was reported in the rat using an electron-capture GLC microtechnique capable of detecting 2 ng of drug. This method is still less sensitive and far more cumbersome than direct radioimmunoassay with the [$^3$H]pseudoephedrine radioligand described here. All three radioimmunoassay variants were validated by comparison with an accepted GLC analytical method (10), giving an excellent correlation in each case (Fig. 3).

The ability of drug antiserum to discern changes in molecular architecture is normally greatest for structural changes at sites distant from the site of attachment of the drug to the macromolecular carrier. Thus, *d*-norpseudoephedrine, which was reported to be a minor metabolite of pseudoephedrine (11) in humans, unexpectedly cross-reacted only to the extent of 0.8–5.0% (Table II). In the nor compound, a methyl group was lacking on the nitrogen atom on which the bridge to protein in the immunogen was attached. The low cross-reactivity in the derivatized assay with the $\gamma$ label is easier to understand in that norpseudoephedrine would presumably react with methyl acrylate in the derivatization step to give a bis adduct, which would then be recognized less effectively by the antiserum.

Several recent reports described the ability of antiserum to discern stereochemical differences in drug molecules. Cook *et al.* (27) described the development of stereoselective radioimmunoassay procedures for (*R*)- and (*S*)-warfarin, Gross and Soares (28) prepared antiserum to *d*-amphetamine, and Kawashima *et al.* (29) reported radioimmunoassay procedures for *l*- and racemic propranolol. The *d*-pseudoephedrine antiserum developed in the present study also possesses a high degree of stereospecificity, as shown by the very low cross-reactivities of *l*-pseudoephedrine, *d*- and *l*-ephedrines, and *l*-norephedrine. A change in the aromatic ring of the ephedrine series, such as in *dl*-*p*-hydroxyephedrine, essentially eliminates recognition by the antiserum. Changes in side-chain structure, as represented by ephedrine, *N*-methylphenylethanolamine, methamphetamine, metaraminol, methoxamine, phenylethylamine, and *l*-phenylephrine, are well recognized by the antiserum, resulting in very low cross-reactivities. A representative catecholamine, epinephrine, caused no inhibition of radioligand binding, nor did triprolidine and codeine, which may, on occasion, be coadministered with pseudoephedrine.

The pharmacokinetics of *d*-pseudoephedrine in humans have not yet been investigated in detail, although some data relating plasma levels to pharmacological effects were reported (12). A major limitation to the pursuit of such studies has been the lack of suitable analytical methodology. The applicability of the present radioimmunoassay technique to pharmacokinetic studies is shown by the data in Figs. 4 and 5. The day-to-day plasma levels in this bioequivalence study were measured easily with the direct radioimmunoassay procedure with polyethylene glycol 6000 as the separation system. As seen in Fig. 4, the assay demonstrated that steady-state plasma concentrations of pseudoephedrine were approached by Day 3 of dosing with either formulation.

The bioequivalence of the immediate- and sustained-release preparations in these subjects was demonstrated by the lack of significant difference between the mean area under their plasma concentration–time curve (*AUC*) values over the entire 126-hr period of the study [43,796 ± 2738 (*SEM*) ng/ml hr for the sustained release and 47,910 ± 3085 (*SEM*) ng/ml hr for the immediate release]. Since this *AUC* comparison was approximate due to the infrequent blood collections during Days 1–4, a similar *AUC* comparison was made for 8 am–8 pm on Day 5, when steady-state concentrations had been achieved and additional blood samples were collected. From these data (Fig. 5), *AUC* calculations again indicated bioequivalence of immediate- and sustained-release preparations [5744 ± 395 (*SEM*) ng/ml hr for the sustained release and 5674 ± 354 (*SEM*) ng/ml hr for the immediate release].

Figure 5 clearly shows that, although the observed maximum plasma concentrations following each formulation were not significantly different, the mean concentrations were maintained in the 450–550-ng/ml range for ~8 hr with the sustained-release preparation, thus avoiding the trough at 6 hr and the peak at 7–8 hr that occurred with the two-dose regimen of the immediate-release preparation. Thus, the radioimmunoassay has been used to demonstrate the rationale for this type of sustained-release preparation. Recently, studies of similar pseudoephedrine formulations have produced similar results (30, 31).

These radioimmunoassay procedures are being applied currently to detailed studies of the disposition of *d*-pseudoephedrine in animals and humans.

## REFERENCES

(1) T. Q. Chou and B. E. Read, *Proc. Soc. Exp. Biol. Med.*, **23**, 618 (1926).

(2) T. King and C. Pak, *Chinese J. Physiol.*, **1**, 445 (1927).

(3) K. K. Chen, C.-K. Wu, and E. Henriksen, *J. Pharmacol. Exp. Ther.*, **36**, 363 (1929).

(4) M. K. Benson, *Eur. J. Clin. Pharmacol.*, **3**, 182 (1971).

(5) D. W. Empey, C. Bye, M. Hodder, and D. T. D. Hughes, *Ann. Allergy*, **34**, 41 (1971).

(6) M. G. Britton, D. W. Empey, G. C. John, K. A. McDonnell, and D. T. D. Hughes, *Br. J. Clin. Pharmacol.*, **6**, 51 (1978).

(7) A. H. Beckett and B. Testa, *J. Pharm. Pharmacol.*, **25**, 382 (1973).

(8) R. G. Kuntzman, I. Tsai, L. Brand, and L. C. Mark, *Clin. Pharmacol. Ther.*, **12**, 62 (1971).

(9) A. H. Beckett and G. R. Wilkinson, *J. Pharm. Pharmacol.*, **17**,

104S (1965).
(10) L. M. Cummins and M. J. Fourier, *Anal. Lett.*, **2**, 403 (1969).
(11) E. T. Lin, D. C. Brater, and L. Z. Benet, *J. Chromatogr.*, **140**, 275 (1977).
(12) C. Bye, H. M. Hill, D. T. D. Hughes, and A. W. Peck, *Eur. J. Clin. Pharmacol.*, **8**, 47 (1975).
(13) R. P. Roth, E. J. Cantekin, D. Bluestone, R. M. Welch, and Y. W. Cho, *Ann. Otol. Rhinol. Laryngol.*, **86**, 235 (1977).
(14) G. E. Abraham, *J. Clin. Endocrinol. Metab.*, **29**, 866 (1969).
(15) L. T. Cheng, S. Y. Kim, A. Chung, and A. Castro, *FEBS Lett.*, **36**, 339 (1973).
(16) A. Eberhard, *Arch. Pharm.*, **253**, 62 (1915).
(17) *Ibid.*, **258**, 114 (1920).
(18) L. H. Welsh, *J. Am. Chem. Soc.*, **69**, 128 (1947).
(19) *Ibid.*, **71**, 3500 (1949).
(20) J. F. Hyde, E. Browning, and R. Adams, *J. Am. Chem. Soc.*, **50**, 2287 (1928).
(21) W. M. Hunter and F. C. Greenwood, *Nature*, **194**, 495 (1962).
(22) M. J. Barrett and P. S. Cohen, *Clin. Chem.*, **18**, 1339 (1972).
(23) B. F. Erlanger, *Pharmacol. Rev.*, **25**, 271 (1973).
(24) J. Landon and A. C. Moffat, *Analyst*, **101**, 225 (1976).
(25) V. P. Butler, *Pharmacol. Rev.*, **29**, 103 (1978).
(26) A. E. Till and L. Z. Benet, *Pharmacology*, **18**, 306 (1979).
(27) C. E. Cook, N. H. Ballentine, T. B. Seltzman, and C. R. Tallent, *J. Pharmacol. Exp. Ther.*, **210**, 391 (1979).
(28) S. J. Gross and J. R. Soares, in "Immunoassays for Drugs Subject to Abuse," S. J. Mule, I. Sunshine, M. Braude, and R. E. Willette, Eds., CRC Press, Cleveland, Ohio, 1974, pp. 3–11.
(29) K. Kawashima, A. Levy, and S. Spector, *J. Pharmacol. Exp. Ther.*, **196**, 517 (1976).
(30) J. Dickerson, D. Perrier, M. Mayersohn, and R. Bressler, *Eur. J. Clin. Pharmacol.*, **14**, 253 (1978).
(31) A. Yacobi, R. G. Stoll, G. C. Chao, J. E. Carter, D. M. Baaske, B. L. Kamath, A. H. Amann, and C. M. Lai, "Abstracts," vol. 9, American Pharmaceutical Association, Academy of Pharmaceutical Sciences, Washington, D.C., 1979, p. 108.

**ACKNOWLEDGMENTS**

Presented in preliminary form at the FASEB meeting, Atlantic City, April 1978 [*Fed. Proc. Fed. Am. Soc. Exp. Biol.*, **37**, 725 (1978)].

The authors thank Dr. D. Brent and his staff of the Organic Chemistry Department, Wellcome Research Laboratories, for the mass spectral data and Dr. R. Zweidinger, Research Triangle Institute, for the comparative GLC data.

# Comparative Teratogenicity of Cortisone and Phenytoin in Mice

**JOSEPH M. McDEVITT, RONALD F. GAUTIERI ˣ, and DAVID E. MANN, Jr.**

Received September 2, 1980, from the *Department of Pharmacology, School of Pharmacy, Temple University, Philadelphia, PA 19140.* Accepted for publication November 13, 1980.

**Abstract** □ Single administrations of cortisone or phenytoin to pregnant mice on Days 11–14 of gestation caused similar skeletal and dissimilar soft tissue fetal anomalies. Cortisone reduced both maternal and fetal weight, whereas phenytoin only reduced fetal weight without adversely affecting maternal weight. A correlation between fetal weight reduction and cleft palate incidence was evident for each drug. Because probit analysis of dose–response regression lines did not deviate from parallelism after drug challenge, it was concluded that cortisone and phenytoin may produce palatal anomalies in the mouse fetus by a similar mechanism.

**Keyphrases** □ Teratogenicity—effects of cortisone and phenytoin on mice □ Cortisone—teratogenic effects on mice □ Phenytoin—teratogenic effects on mice □ Antiepileptics—teratogenic effects of phenytoin on mice

The experimental use of various agents to elicit and inhibit cleft palate has been pursued vigorously in recent years to determine its cause and to prevent its occurrence in human newborns. Although cortisone is the prototypal agent employed for the induction of this anomaly in lower species (1), phenytoin is of particular interest because of the purported link between its use as an antiepileptic drug during pregnancy and the appearance of cleft palate in offspring (2, 3).

The purpose of this investigation was to compare the teratogenic effects of phenytoin with those of cortisone by means of dose–response relationships in mice and to ascertain whether the mechanism involved in cleft palate inception by cortisone and phenytoin is similar.

## EXPERIMENTAL

**Animals**—CF-1 albino mice[1] (25–35 g) were used. Females were confined in groups of 10 to aggregate cages for at least 2 weeks prior to mating. Males were placed individually in metal cages (12.5 × 15 × 10 cm) with a wire mesh front and floor[2]. Adult mice were maintained on a commercial diet[3] and tap water *ad libitum*. The breeding room was equipped with an electrical system[4], which provided 12 hr of light (7:00 am–7:00 pm) and 12 hr of darkness. Room temperature was maintained between 22 and 26°.

**Preparation of Solutions**—Saline and cortisone acetate solutions were prepared commercially[5,6]. Fresh aliquots (10 ml) of phenytoin solution were prepared as needed on the day of injection by dissolving the drug[7] in a stock solution of 70% propylene glycol[8] (in saline). Phenytoin solutions were prepared containing 10, 14, 16, or 18 mg of phenytoin/ml of vehicle in injection volumes of 0.1–0.3 ml. All injections were made with a glass syringe[9]. The bone-staining solution was prepared by dissolving 18 mg of alizarin red-S in each liter of 1% KOH in distilled water. A 50:50 mixture of 70% ethyl alcohol and 100% glycerin was used to fix and clear the specimens. Fetuses chosen for soft tissue analysis were fixed in Bouin's solution.

**Breeding Procedure and Treatment Regimen**—The breeding procedure was previously described (4). Gravid females were randomly

[1] Charles River Breeding Laboratories, Wilmington, Mass.
[2] RD-T unit, Norwich Wire Works, Norwich, N.Y.
[3] Rodent Laboratory Chow 5001, Ralston-Purina Co., St. Louis, Mo.
[4] Astronomic dial time switch with "skipper," model V-45073, International Register Co., Spring Grove, Ill.
[5] Sodium chloride injection USP (0.9%), lot B7D091A, McGraw Laboratories, Division of American Hospital Supply Corp., Irvine, Calif.
[6] Cortone, lot 0613A, Merck Sharp and Dohme, West Point, Pa.
[7] Dilantin Sodium, lot PE338, Parke-Davis Co., Detroit, Mich.
[8] Lot P-810, Amend Drug and Chemical Co., Irvington, N.J.
[9] B-D 1-ml tuberculin syringe with 1.27-cm, 26-gauge needle.

0022-3549/81/0600-0631$01.00/0
© 1981, American Pharmaceutical Association

104S (1965).
(10) L. M. Cummins and M. J. Fourier, *Anal. Lett.*, **2**, 403 (1969).
(11) E. T. Lin, D. C. Brater, and L. Z. Benet, *J. Chromatogr.*, **140**, 275 (1977).
(12) C. Bye, H. M. Hill, D. T. D. Hughes, and A. W. Peck, *Eur. J. Clin. Pharmacol.*, **8**, 47 (1975).
(13) R. P. Roth, E. J. Cantekin, D. Bluestone, R. M. Welch, and Y. W. Cho, *Ann. Otol. Rhinol. Laryngol.*, **86**, 235 (1977).
(14) G. E. Abraham, *J. Clin. Endocrinol. Metab.*, **29**, 866 (1969).
(15) L. T. Cheng, S. Y. Kim, A. Chung, and A. Castro, *FEBS Lett.*, **36**, 339 (1973).
(16) A. Eberhard, *Arch. Pharm.*, **253**, 62 (1915).
(17) *Ibid.*, **258**, 114 (1920).
(18) L. H. Welsh, *J. Am. Chem. Soc.*, **69**, 128 (1947).
(19) *Ibid.*, **71**, 3500 (1949).
(20) J. F. Hyde, E. Browning, and R. Adams, *J. Am. Chem. Soc.*, **50**, 2287 (1928).
(21) W. M. Hunter and F. C. Greenwood, *Nature*, **194**, 495 (1962).
(22) M. J. Barrett and P. S. Cohen, *Clin. Chem.*, **18**, 1339 (1972).
(23) B. F. Erlanger, *Pharmacol. Rev.*, **25**, 271 (1973).
(24) J. Landon and A. C. Moffat, *Analyst*, **101**, 225 (1976).
(25) V. P. Butler, *Pharmacol. Rev.*, **29**, 103 (1978).
(26) A. E. Till and L. Z. Benet, *Pharmacology*, **18**, 306 (1979).
(27) C. E. Cook, N. H. Ballentine, T. B. Seltzman, and C. R. Tallent, *J. Pharmacol. Exp. Ther.*, **210**, 391 (1979).
(28) S. J. Gross and J. R. Soares, in "Immunoassays for Drugs Subject to Abuse," S. J. Mule, I. Sunshine, M. Braude, and R. E. Willette, Eds., CRC Press, Cleveland, Ohio, 1974, pp. 3–11.
(29) K. Kawashima, A. Levy, and S. Spector, *J. Pharmacol. Exp. Ther.*, **196**, 517 (1976).
(30) J. Dickerson, D. Perrier, M. Mayersohn, and R. Bressler, *Eur. J. Clin. Pharmacol.*, **14**, 253 (1978).
(31) A. Yacobi, R. G. Stoll, G. C. Chao, J. E. Carter, D. M. Baaske, B. L. Kamath, A. H. Amann, and C. M. Lai, "Abstracts," vol. 9, American Pharmaceutical Association, Academy of Pharmaceutical Sciences, Washington, D.C., 1979, p. 108.

**ACKNOWLEDGMENTS**

Presented in preliminary form at the FASEB meeting, Atlantic City, April 1978 [*Fed. Proc. Fed. Am. Soc. Exp. Biol.*, **37**, 725 (1978)].

The authors thank Dr. D. Brent and his staff of the Organic Chemistry Department, Wellcome Research Laboratories, for the mass spectral data and Dr. R. Zweidinger, Research Triangle Institute, for the comparative GLC data.

# Comparative Teratogenicity of Cortisone and Phenytoin in Mice

**JOSEPH M. McDEVITT, RONALD F. GAUTIERI ˣ, and DAVID E. MANN, Jr.**

Received September 2, 1980, from the *Department of Pharmacology, School of Pharmacy, Temple University, Philadelphia, PA 19140.* Accepted for publication November 13, 1980.

**Abstract** □ Single administrations of cortisone or phenytoin to pregnant mice on Days 11–14 of gestation caused similar skeletal and dissimilar soft tissue fetal anomalies. Cortisone reduced both maternal and fetal weight, whereas phenytoin only reduced fetal weight without adversely affecting maternal weight. A correlation between fetal weight reduction and cleft palate incidence was evident for each drug. Because probit analysis of dose–response regression lines did not deviate from parallelism after drug challenge, it was concluded that cortisone and phenytoin may produce palatal anomalies in the mouse fetus by a similar mechanism.

**Keyphrases** □ Teratogenicity—effects of cortisone and phenytoin on mice □ Cortisone—teratogenic effects on mice □ Phenytoin—teratogenic effects on mice □ Antiepileptics—teratogenic effects of phenytoin on mice

The experimental use of various agents to elicit and inhibit cleft palate has been pursued vigorously in recent years to determine its cause and to prevent its occurrence in human newborns. Although cortisone is the prototypal agent employed for the induction of this anomaly in lower species (1), phenytoin is of particular interest because of the purported link between its use as an antiepileptic drug during pregnancy and the appearance of cleft palate in offspring (2, 3).

The purpose of this investigation was to compare the teratogenic effects of phenytoin with those of cortisone by means of dose–response relationships in mice and to ascertain whether the mechanism involved in cleft palate inception by cortisone and phenytoin is similar.

## EXPERIMENTAL

**Animals**—CF-1 albino mice[1] (25–35 g) were used. Females were confined in groups of 10 to aggregate cages for at least 2 weeks prior to mating. Males were placed individually in metal cages (12.5 × 15 × 10 cm) with a wire mesh front and floor[2]. Adult mice were maintained on a commercial diet[3] and tap water *ad libitum*. The breeding room was equipped with an electrical system[4], which provided 12 hr of light (7:00 am–7:00 pm) and 12 hr of darkness. Room temperature was maintained between 22 and 26°.

**Preparation of Solutions**—Saline and cortisone acetate solutions were prepared commercially[5,6]. Fresh aliquots (10 ml) of phenytoin solution were prepared as needed on the day of injection by dissolving the drug[7] in a stock solution of 70% propylene glycol[8] (in saline). Phenytoin solutions were prepared containing 10, 14, 16, or 18 mg of phenytoin/ml of vehicle in injection volumes of 0.1–0.3 ml. All injections were made with a glass syringe[9]. The bone-staining solution was prepared by dissolving 18 mg of alizarin red-S in each liter of 1% KOH in distilled water. A 50:50 mixture of 70% ethyl alcohol and 100% glycerin was used to fix and clear the specimens. Fetuses chosen for soft tissue analysis were fixed in Bouin's solution.

**Breeding Procedure and Treatment Regimen**—The breeding procedure was previously described (4). Gravid females were randomly

[1] Charles River Breeding Laboratories, Wilmington, Mass.
[2] RD-T unit, Norwich Wire Works, Norwich, N.Y.
[3] Rodent Laboratory Chow 5001, Ralston-Purina Co., St. Louis, Mo.
[4] Astronomic dial time switch with "skipper," model V-45073, International Register Co., Spring Grove, Ill.
[5] Sodium chloride injection USP (0.9%), lot B7D091A, McGraw Laboratories, Division of American Hospital Supply Corp., Irvine, Calif.
[6] Cortone, lot 0613A, Merck Sharp and Dohme, West Point, Pa.
[7] Dilantin Sodium, lot PE338, Parke-Davis Co., Detroit, Mich.
[8] Lot P-810, Amend Drug and Chemical Co., Irvington, N.J.
[9] B-D 1-ml tuberculin syringe with 1.27-cm, 26-gauge needle.

0022-3549/81/0600-0631$01.00/0
© 1981, American Pharmaceutical Association

**Table I—Treatment Regimen of Experimental Drugs**

| Group[a] | Treatment[b] on Days 11–14 (mg/kg) and Route |
|---|---|
| 1 | Untreated controls |
| 2 | Saline, intramuscular |
| 3 | Propylene glycol, subcutaneous |
| 4 | I (25), intramuscular |
| 5 | I (50), intramuscular |
| 6 | I (75), intramuscular |
| 7 | I (100), intramuscular |
| 8 | I (125), intramuscular |
| 9 | II (50), subcutaneous |
| 10 | II (70), subcutaneous |
| 11 | II (80), subcutaneous |
| 12 | II (90), subcutaneous |

[a] Eight mice per group. [b] I is cortisone acetate; II is phenytoin.

assigned to one of three control groups or one of two treatment sections: I, cortisone; and II, phenytoin, the latter being divided into five groups each (Table I). Each control group and each treatment group consisted of eight females. Of the three control groups, one received no further treatment while the other two served as vehicle controls. One group received saline solution in a fixed volume of 0.3 ml, which was administered in a manner identical to that of cortisone; the remaining control group received 0.3 ml of 70% propylene glycol solution in a manner identical to that of phenytoin.

The treatment groups received cortisone or phenytoin on Days 11–14 of gestation. The steroid was injected intramuscularly into the thigh muscles of the hindlegs, alternating between the right and left legs on successive days, in 25-, 50-, 75-, 100-, and 125-mg/kg doses per group. Phenytoin was administered subcutaneously into the ventroposterior or dorsoanterior quadrant close to the axilla, in alternate quadrants on successive days, in 10-, 30-, 50-, 70-, and 90-mg/kg doses per group. It soon became apparent that a threshold dose for phenytoin teratogenicity (cleft palate production) would be >50 mg/kg. Therefore, the two lower dosage schedules were deleted, and a group of eight mice receiving 80 mg of phenytoin/kg was substituted.

**Examination of Fetuses**—On Day 18, 1 day before term, the terminal weight was recorded for each mouse[10], which then was sacrificed by cervical dislocation. The number and position of fetuses and resorption sites (metrial glands) were ascertained and recorded. The fetuses were removed, tested for viability with a blunt probe, blotted dry, and weighed to the nearest hundredth of a gram[10]. They then were examined for gross external defects and sexed.

The specimens were prepared for macroscopic examination as follows. For skeletal examination, every second fetus was prepared according to the method of Staples and Schnell (5); the remaining fetuses were fixed and decalcified in Bouin's solution in preparation for freehand razor blade sectioning (6). The palatal shelves were observed prior to sectioning, and the urogenital organs were left intact. All specimens were examined for bone and soft tissue anomalies with a binocular dissecting microscope[11].

**Statistical Methods and Analysis**—The degree of significance of observed variations among the experimental groups was determined by the Student $t$ test (7). All $t$ values were calculated on a computer[12]. The dose–response relationships for cortisone- and phenytoin-induced cleft palate were compared by probit analysis (8).

## RESULTS AND DISCUSSION

**Maternal Effects of Drugs**—The female mice were unresponsive to intramuscular injections of saline or to initial cortisone challenges, but second and third administrations of the hormone caused lethargy that persisted for over 24 hr at the higher dosage levels. Mice injected subcutaneously with either 70% propylene glycol or phenytoin experienced excitement and discomfort. As the number of injections and dosages of the antiepileptic agent was increased, Straub tail reactions, excitement (cage circling), ataxia, and depression occurred. Ataxia and depression were most pronounced in the group receiving 90 mg of phenytoin/kg. At laparotomy, most mice that had received solutions containing the propylene glycol vehicle had inflamed injection sites, particularly in the scapular region. No deaths in gravid animals resulted from drug treatment.

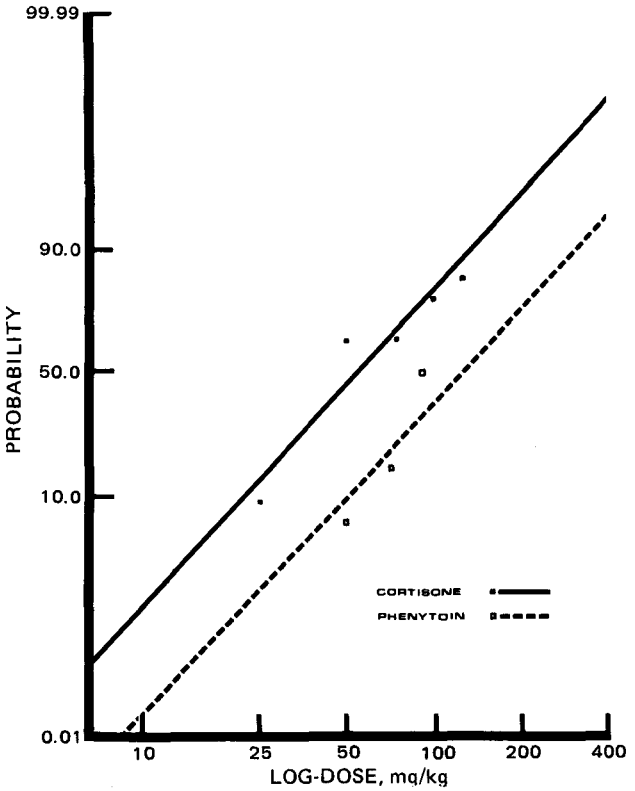


**Figure 1**—*Probit regression of the percent of cleft palate per litter on log-dose.*

Table II presents the mean values of maternal and fetal deviations of the test groups in relation to their respective saline or propylene glycol controls. Each group contained eight litters and ~100 fetuses.

**Maternal Weight**—The weight gain reflects the difference in maternal weight on Days 0 and 18 of gestation. The mean maternal weight gains among the cortisone-treated groups decreased as the dosage of the hormone was increased. Significantly lower weight gains, when compared with those in the saline group, occurred in all cortisone groups, except in the one receiving the 25-mg/kg dose. No significant differences were found when the mean maternal weight gains within the phenytoin-treated groups were compared with those of the group receiving the propylene glycol vehicle.

**Fetal Resorption**—Percent resorption is defined as the ratio of the number of resorption sites to the sum of the resorption sites and viable fetuses times 100. No significant differences were found among the control or cortisone-treated groups with respect to percent resorption. Within the phenytoin-treated groups, only mice that received 70- and 80-mg/kg doses had a significantly higher percent resorption ($p < 0.05$) than occurred in the group that received a dose of 50 mg/kg[13].

**Fetal and Sex Ratios**—No significant variations in the mean number of fetuses in either the right or left uterine horn were noted among the control or treated groups. There were no differences in the sex ratios of the phenytoin-treated and propylene glycol control groups. However, the group that received cortisone (75 mg/kg) had a significantly lower mean percentage of males when compared with the saline control.

**Mean Fetal Weight**—There were no significant differences in the mean fetal weight among the control groups. Within the cortisone-treated groups, an apparent dose-dependent reduction of this parameter occurred, with significant differences being evident with cortisone at 50, 100, and 125 mg/kg when compared with the saline control. In the phenytoin-treated group, a significant reduction in mean fetal weight was noted between the antiepileptic agent (90 mg/kg) and its propylene glycol control.

**Production of Soft Tissue and Skeletal Anomalies**—The occurrence and nature of the various soft tissue and skeletal defects representing significant deviations of the cortisone- and phenytoin-treated

[10] Torbal torsion balance model PL-800.
[11] Bausch & Lomb model ASZ30L2.
[12] Wang 2200.
[13] This intragroup comparison is not shown in Table II.

**Table II—Mean Values of Test Groups**

| Treatment Group[a] | Maternal Weight, start/gain, g | Percent Resorption | Fetal Ratio, right/left | Percent Male/Female | $\bar{X}$ Fetal Weight, g | Soft Tissue Defects[b] | Skeletal Defects[b] | Percent Soft Tissue Defects[c] | Percent Skeletal Defects[c] |
|---|---|---|---|---|---|---|---|---|---|
| 1 | 30.5/26.2 | 3.7 | 6/5 | 48.4/51.6 | 1.17 | 0.8 | 1.3 | 14.5 | 19.2 |
| 2 | 29.4/26.2 | 8.4 | 6/6 | 50.0/50.0 | 1.15 | 0.8 | 2.0 | 14.0 | 29.5 |
| 3 | 30.9/23.1 | 9.0 | 5/6 | 57.9/42.1 | 1.09 | 0.7 | 1.7 | 10.1 | 24.2 |
| 4 | 27.9/23.0 | 9.4 | 5/5 | 43.6/56.4 | 1.16 | 0.6 | 3.2 | 12.9 | 44.1 |
| 5 | 30.0/20.7[d] | 18.9 | 6/4 | 39.6/61.4 | 1.01[d] | 4.1[d] | 5.8[d] | 70.7[d] | 76.7[d] |
| 6 | 29.5/18.7[d] | 13.1 | 4/5 | 35.2/64.8[d] | 1.06 | 4.0[d] | 9.5[d] | 68.3[d] | 87.0[d] |
| 7 | 29.4/17.5[d] | 16.3 | 4/5 | 56.0/44.0 | 0.88[d] | 4.0[d] | 8.8[d] | 77.5[d] | 95.9[d] |
| 8 | 29.1/16.4[d] | 21.8 | 5/4 | 53.5/46.5 | 0.87[d] | 4.5[d] | 8.7[d] | 85.8[d] | 100.0[d] |
| 9 | 29.3/22.2 | 2.8 | 6/4 | 50.8/49.2 | 1.18 | 1.2 | 1.7 | 26.3 | 22.4 |
| 10 | 31.7/22.7 | 12.1 | 5/6 | 52.1/47.9 | 1.01 | 1.7 | 3.5 | 24.9 | 53.7[e] |
| 11 | 33.7/22.8 | 14.5 | 5/4 | 60.0/40.0 | 1.04 | 1.7 | 6.2 | 26.7 | 57.2[e] |
| 12 | 30.3/20.7 | 7.9 | 6/5 | 44.6/55.4 | 0.89[e] | 6.2[e] | 10.1[e] | 60.0[e] | 75.8[e] |

[a] Eight mice per group. [b] Mean number of defects per litter. [c] Mean percent of fetuses displaying at least one defect per litter. [d] Significance ($p < 0.05$) when compared to the saline group. [e] Significance ($p < 0.05$) when compared to the propylene glycol group.

groups from their saline and propylene glycol controls are presented in Tables III and IV, respectively.

With the exception of cleft palate, which appeared in the fetuses of both treatment groups, most soft tissue anomalies caused by single intramuscular injections of cortisone on Days 11–14 of gestation were unlike those observed after single subcutaneous administrations of phenytoin on the same days of gestation.

An inverse relationship between fetal weight and cleft palate incidence has been well documented for cortisone teratogenicity (9, 10). A similar association between reduced fetal weight and phenytoin-induced cleft palate also was reported (11). However, these are dose-dependent responses, as shown in the present study and others (11–14), which probably explain why fetal weight loss was not reported when low doses of phenytoin were used (15, 16).

An inverse relationship appeared to exist between the occurrence of a small protuberance on the forepaw and cortisone dosage, whereas a direct relationship was evident between the dosage level of the steroid and the emergence of other soft tissue anomalies, *i.e.*, cleft palate. The former situation demonstrates that the presence of one defect may be dependent on the presence or absence of another. This type of variable dependency may account for the nonlinear response observed for sternebral defects in the cortisone-treated group. The frequently appearing anomaly, crankshaft sternebrae, could positively influence the occurrence of fused sternebrae because sternebral ossification sites would be positioned closer to each other. Therefore, anomaly frequency in response to a given dose should be considered individually before conclusions concerning the teratogenic potential of a suspected agent are made.

Cryptorchidism seemed to be directly dependent on phenytoin dosage but was not related to cortisone dosage. Ovarian displacement after phenytoin treatment also appeared to be dose related. The reason why ectopic ovarian development occurred only on the left side of the fetus remains enigmatic.

In addition to the soft tissue defects listed in Table III, other soft tissue anomalies observed in the phenytoin-treated groups were curled tail, connective tissue infiltration of the cerebral hemispheres, cerebral hemorrhage, fused digit, ectrodactyly, malformed hindpaw, malformed kidney, and cleft lip. These soft tissue defects and those observed in the cortisone-treated groups, *i.e.*, curled tail, exencephaly, and fused digit, were not statistically significant when compared with the respective treatment or control groups.

Cortisone and phenytoin treatment produced fetuses with similar skeletal malformations that primarily involved the sternebral and cranial (supraoccipital) bones; this finding is in agreement with previous results (15). The following skeletal defects were observed at insignificant frequencies in their respective groups: missing sternebrae, malformed and split xiphoid processes (cortisone and phenytoin), ectopic sternebrae (cortisone, phenytoin, and untreated), and displaced sternebrae, *i.e.*, due to rotation of the sternebral ossification sites 30° off center (cortisone).

Phenytoin also interfered specifically with skeletal digit development. Delayed ossification of the digits was dose dependent (Table IV). Malformed and hypoplastic digits have been reported in human infants whose epileptic mothers were maintained on phenytoin therapy during pregnancy (17, 18).

Rugh (19) accumulated data that related organogenesis to gestational age in the mouse. Thus, from the results obtained in this and other studies that employed similar dosage schedules (12, 13, 15) of cortisone and phenytoin, it is evident that the majority of the skeletal abnormalities induced by these agents occur at sites where chondrification centers develop on Days 15–16 (supraoccipital bone, sternum, and distal phalanges). These findings indicate that the critical time for phenytoin- and cortisone-induced skeletal anomalies is several days prior to genesis of the affected tissue.

The critical periods reported for phenytoin- and cortisone-induced cleft palate are remarkably similar to those required for the production of sternebral, supraoccipital, and digital malformations. Single injections of cortisone (20) and phenytoin (12, 21) were most effective in producing cleft palate when given to mice on Day 12 of gestation, although maximum responses were obtained from multiple injections over Days 12–14. It has been determined (22) that murine palatogenesis begins on Day 14

**Table III—Significant Occurrence[a] and Nature of Soft Tissue Anomalies**

| Group[b] | Cleft Palate | Fifth-Digit Protuberance | Crypt-orchidism | Ectopic Ovary |
|---|---|---|---|---|
| 1 | — | 14.5 | — | — |
| 2 | — | 14.1 | — | — |
| 3 | — | 10.1 | — | — |
| 4 | 8.8 | 2.1[c] | 4.1 | — |
| 5 | 62.1[c,e] | 12.7 | 7.7 | — |
| 6 | 64.2[c,e] | 0.0[c,f] | 2.1 | — |
| 7 | 77.5[c,e] | 0.0[c,f] | 2.1 | — |
| 8 | 83.8[c,e] | 2.1[c] | 10.8[c] | — |
| 9 | 6.3 | 7.1 | 2.1 | 3.1 |
| 10 | 15.5 | 0.0 | 4.9 | 0.0 |
| 11 | 21.1[d] | 0.0 | 4.3 | 0.0 |
| 12 | 49.5[d,g,h] | 0.0 | 11.3[d,g] | 12.8[d,h,i] |

[a] Mean percent of defects per litter. [b] Eight mice per group. Significance ($p < 0.05$) is indicated by superscripts as compared with [c] saline and [d] propylene glycol controls and treated groups: cortisone, [e] 25 and [f] 50 mg/kg, and phenytoin, [g] 50, [h] 70, and [i] 80 mg/kg.

**Table IV—Significant Occurrence[a] and Nature of Skeletal Defects**

| Group[b] | D.O.P. | Split Supraocc. | Stern Dft. | Crank. St. | Split St. | Fused St. |
|---|---|---|---|---|---|---|
| 1 | 2.1 | — | 17.1 | 8.8 | 4.2 | 2.1 |
| 2 | 10.0 | — | 21.6 | 21.6[c] | 0.0 | 5.0 |
| 3 | 9.2 | — | 16.8 | 16.8 | 1.8 | 1.8 |
| 4 | 7.1 | 27.5[d] | 21.6 | 16.0 | 0.0 | 10.0 |
| 5 | 1.8 | 58.3[d,f] | 41.4 | 22.8 | 6.4[d,f] | 24.2[d,f] |
| 6 | 2.5 | 72.7[d,f] | 71.5[d,f] | 31.3 | 9.6 | 54.8[d,f] |
| 7 | 0.0 | 93.8[d,f,g] | 56.0[d,f] | 15.8 | 17.9[d,f] | 31.9[d,f] |
| 8 | 16.7 | 95.8[d,f,g] | 51.7[d,f] | 20.4 | 19.2[d,f] | 25.8[d,f] |
| 9 | 2.5 | 0.0 | 20.0 | 10.7 | 1.8 | 10.0 |
| 10 | 21.2 | 0.0 | 39.2[e] | 8.5 | 30.3[e,h] | 0.0 |
| 11 | 43.7[e,h] | 6.0 | 41.1 | 30.1 | 24.3[e,h] | 8.5 |
| 12 | 54.0[e,h] | 20.0[e] | 60.9[e,h,i] | 36.4[e,h,i] | 13.8[e,h,i] | 8.7 |

[a] Mean percent of defects per litter. [b] Eight mice per group. Significance ($p < 0.05$) is indicated by superscripts as compared with controls: [c] untreated, [d] saline, and [e] propylene glycol, and with treated groups: cortisone, [f] 25 and [g] 50 mg/kg, and phenytoin, [h] 50 and [i] 70 mg/kg. D.O.P. = delayed ossification of the paws; Split Supraocc. = split supraoccipital bone, Stern. Dft. = occurrence of at least one sternebral defect, Crank St. = crankshaft sternebrae, Split St. = split sternebrae, and Fused St. = fused sternebrae.

and terminates on Day 15.

Several studies linked the alteration of events common to palatogenesis and bone formation, including glycosaminoglycan (23) and collagen formation (24, 25), and the activities of enzymes (alkaline phosphatase, acid phosphatase, and β-glucuronidase) (26) and hormones (parathyroid hormone and calcitonin) (27) to the production of cortisone-induced cleft palate. Because of these relationships and the similarities that exist between cortisone- and phenytoin-induced skeletal malformations, it can be concluded that, qualitatively, the teratogenic mechanism of action of these agents in the formation of skeletal anomalies is similar.

A graphical approximation of the regression lines of the mean percent of cleft palate per litter on log-dose for cortisone- and phenytoin-treated groups appears in Fig. 1. These lines are the result of the second iteration of the method of probit analysis described by Finney (8). The original iteration was performed on lines fitted independently from the results obtained from the test groups without constraint of parallelism. The results from the second stage were employed to calculate the common slope, which was used to construct the curves in Fig. 1. Heterogenicity and parallelism were both examined by $\chi^2$ tests. Because the dose–response regression lines for cortisone- and phenytoin-induced cleft palate did not deviate from parallelism, the teratogenic mechanism of action of these agents in causing this anomaly may be similar. The relative potency of phenytoin as a cleft palate-inducing teratogen was calculated, according to the method of Finney (8), to be from 14.54 to 69.18% that of cortisone.

## REFERENCES


(1) F. C. Fraser and T. D. Fainstat, *Pediatrics*, **8**, 527 (1951).

(2) E. V. Kuenssberg and J. D. E. Knox, *Lancet*, **1**, 198 (1973).

(3) J. W. Hanson and D. W. Smith, *J. Pediatr.*, **87**, 285 (1975).

(4) R. S. Thompson and R. F. Gautieri, *J. Pharm. Sci.*, **58**, 406 (1969).

(5) R. E. Staples and V. L. Schnell, *Stain Technol.*, **39**, 61 (1964).

(6) J. G. Wilson, in "Teratology Principles and Techniques," J. G. Wilson and J. Warkany, Eds., University of Chicago Press, Chicago, Ill., 1965, p. 267.

(7) G. G. Simpson, A. Roe, and R. C. Lewontin, "Quantitative Zoology," Harcourt, Brace, New York, N.Y., 1960, pp. 176, 186.

(8) D. J. Finney, "Probit Analysis," 3rd ed., Cambridge University Press, Cambridge, England, 1971, pp. 50–80, 100–122.

(9) F. C. Fraser, in "Teratology Principles and Techniques," J. G. Wilson and J. Warkany, Eds., University of Chicago Press, Chicago, Ill., 1965, pp. 21–56.

(10) H. Loevy, *Anat. Rec.*, **145**, 117 (1963).

(11) R. B. Paulson, G. W. Paulson, and S. Jreissaty, *Arch. Neurol.*, **36**, 832 (1979).

(12) R. D. Harbison and B. A. Becker, *Teratology*, **2**, 305 (1969).

(13) F. M. Sullivan and P. R. McElhatton, *Toxicol. Appl. Pharmacol.*, **40**, 365 (1977).

(14) H. Fritz, D. Muller, and R. Hess, *Toxicology*, **6**, 323 (1976).

(15) J. J. Mitala, D. E. Mann, Jr., and R. F. Gautieri, *J. Pharm. Sci.*, **67**, 377 (1978).

(16) K. M. Massey, *J. Oral Ther. Pharmacol.*, **2**, 380 (1966).

(17) M. Barr, A. K. Poznanski, and R. D. Schmickel, *J. Pediatr.*, **84**, 254 (1974).

(18) R. M. Hill, W. M. Verniaud, M. G. Horning, L. B. McCulley, and N. F. Morgan, *Am. J. Dis. Child.*, **127**, 645 (1974).

(19) R. Rugh, "The Mouse: Its Reproduction and Development," Burgess Publishing, Minneapolis, Minn., 1970, pp. 208–295.

(20) F. G. Biddle and F. C. Fraser, *Genetics*, **84**, 743 (1976).

(21) J. E. Gibson and B. A. Becker, *Proc. Soc. Exp. Biol. Med.*, **128**, 905 (1968).

(22) G. Callas and B. E. Walker, *Anat. Rec.*, **145**, 61 (1963).

(23) R. M. Jacobs, *ibid.*, **150**, 271 (1964).

(24) R. M. Pratt and C. T. G. King, *Arch. Oral Biol.*, **16**, 1181 (1971).

(25) Y. Shapira and S. Shoshan, *ibid.*, **17**, 1699 (1972).

(26) M. E. Teaford and A. A. White, *Proc. Soc. Exp. Biol. Med.*, **117**, 541 (1964).

(27) R. E. Waterman, G. C. Palmer, S. J. Palmer, and S. M. Palmer, *Anat. Rec.*, **188**, 431 (1977).


## ACKNOWLEDGMENTS


Abstracted in part from a thesis submitted by J. M. McDevitt to Temple University in partial fulfillment of the Master of Science degree requirements.


# Oxidative Degradation of 6-Selenoguanosine in Aqueous Solutions


**A. J. REPTA ˣ and Y. A. BELTAGY ***



Received August 8, 1980, from the *Pharmaceutical Chemistry Department, School of Pharmacy, University of Kansas, Lawrence, KS 66044.* Accepted for publication November 17, 1980.


*Present address: Pharmaceutical Chemistry Department, Faculty of Pharmacy, University of Alexandria, Alexandria, Egypt.



**Abstract** □ The degradation of 6-selenoguanosine (NSC 137679)(I) in water and in various buffer systems was investigated. Drug degradation in aqueous media was monitored by high-pressure liquid chromatography. Some kinetic aspects of the degradation of I in various buffer systems at 25° also were studied spectrophotometrically. The degradation, which requires oxygen, involves autoxidation of I to the corresponding diselenide, which produces a selenide and metallic selenium in the presence of oxygen. This degradation pathway differs from that reported for the oxidation of related thio compounds.



**Keyphrases** □ 6-Selenoguanosine—oxidative degradation in aqueous solutions, kinetics □ Autoxidation, aqueous—6-selenoguanosine, selenium compounds, pharmacokinetics □ Kinetics—6-selenoguanosine, oxidative degradation in aqueous solutions, selenium compounds □ Antineoplastics—6-selenoguanosine, selenium compounds, oxidative degradation in aqueous solutions, kinetics


During a study of selenium analogs of physiologically active sulfur compounds, numerous selenium analogs were synthesized for biochemical investigation. 6-Selenopurine was synthesized (1) and found to be active as an antileukemic agent (2), but it was unstable and toxic to the host (3). Subsequently, 6-selenopurine-9-β-D-ribonucleoside was prepared, but it was even less stable than 6-selenopurine under the same conditions (3).

In a search for a more stable analog, 6-selenoguanosine (NSC 137679) (I) was synthesized (4); it was found to be an active inhibitor of several experimental tumors *in vitro* (5, 6) and *in vivo* (7, 8). Although I was reported to be more stable than preceding analogs (4, 9), it still undergoes sufficiently rapid degradation in aqueous solutions such that its formulation in a dosage form suitable for evaluation of anticancer activity presented serious problems (10).

While considerable information has been published




*0022-3549/81/0600-0634$01.00/0*


*© 1981, American Pharmaceutical Association*

and terminates on Day 15.

Several studies linked the alteration of events common to palatogenesis and bone formation, including glycosaminoglycan (23) and collagen formation (24, 25), and the activities of enzymes (alkaline phosphatase, acid phosphatase, and β-glucuronidase) (26) and hormones (parathyroid hormone and calcitonin) (27) to the production of cortisone-induced cleft palate. Because of these relationships and the similarities that exist between cortisone- and phenytoin-induced skeletal malformations, it can be concluded that, qualitatively, the teratogenic mechanism of action of these agents in the formation of skeletal anomalies is similar.

A graphical approximation of the regression lines of the mean percent of cleft palate per litter on log-dose for cortisone- and phenytoin-treated groups appears in Fig. 1. These lines are the result of the second iteration of the method of probit analysis described by Finney (8). The original iteration was performed on lines fitted independently from the results obtained from the test groups without constraint of parallelism. The results from the second stage were employed to calculate the common slope, which was used to construct the curves in Fig. 1. Heterogenicity and parallelism were both examined by $\chi^2$ tests. Because the dose–response regression lines for cortisone- and phenytoin-induced cleft palate did not deviate from parallelism, the teratogenic mechanism of action of these agents in causing this anomaly may be similar. The relative potency of phenytoin as a cleft palate-inducing teratogen was calculated, according to the method of Finney (8), to be from 14.54 to 69.18% that of cortisone.

## REFERENCES


(1) F. C. Fraser and T. D. Fainstat, *Pediatrics*, **8**, 527 (1951).

(2) E. V. Kuenssberg and J. D. E. Knox, *Lancet*, **1**, 198 (1973).

(3) J. W. Hanson and D. W. Smith, *J. Pediatr.*, **87**, 285 (1975).

(4) R. S. Thompson and R. F. Gautieri, *J. Pharm. Sci.*, **58**, 406 (1969).

(5) R. E. Staples and V. L. Schnell, *Stain Technol.*, **39**, 61 (1964).

(6) J. G. Wilson, in "Teratology Principles and Techniques," J. G. Wilson and J. Warkany, Eds., University of Chicago Press, Chicago, Ill., 1965, p. 267.

(7) G. G. Simpson, A. Roe, and R. C. Lewontin, "Quantitative Zoology," Harcourt, Brace, New York, N.Y., 1960, pp. 176, 186.

(8) D. J. Finney, "Probit Analysis," 3rd ed., Cambridge University Press, Cambridge, England, 1971, pp. 50–80, 100–122.

(9) F. C. Fraser, in "Teratology Principles and Techniques," J. G. Wilson and J. Warkany, Eds., University of Chicago Press, Chicago, Ill., 1965, pp. 21–56.

(10) H. Loevy, *Anat. Rec.*, **145**, 117 (1963).

(11) R. B. Paulson, G. W. Paulson, and S. Jreissaty, *Arch. Neurol.*, **36**, 832 (1979).

(12) R. D. Harbison and B. A. Becker, *Teratology*, **2**, 305 (1969).

(13) F. M. Sullivan and P. R. McElhatton, *Toxicol. Appl. Pharmacol.*, **40**, 365 (1977).

(14) H. Fritz, D. Muller, and R. Hess, *Toxicology*, **6**, 323 (1976).

(15) J. J. Mitala, D. E. Mann, Jr., and R. F. Gautieri, *J. Pharm. Sci.*, **67**, 377 (1978).

(16) K. M. Massey, *J. Oral Ther. Pharmacol.*, **2**, 380 (1966).

(17) M. Barr, A. K. Poznanski, and R. D. Schmickel, *J. Pediatr.*, **84**, 254 (1974).

(18) R. M. Hill, W. M. Verniaud, M. G. Horning, L. B. McCulley, and N. F. Morgan, *Am. J. Dis. Child.*, **127**, 645 (1974).

(19) R. Rugh, "The Mouse: Its Reproduction and Development," Burgess Publishing, Minneapolis, Minn., 1970, pp. 208–295.

(20) F. G. Biddle and F. C. Fraser, *Genetics*, **84**, 743 (1976).

(21) J. E. Gibson and B. A. Becker, *Proc. Soc. Exp. Biol. Med.*, **128**, 905 (1968).

(22) G. Callas and B. E. Walker, *Anat. Rec.*, **145**, 61 (1963).

(23) R. M. Jacobs, *ibid.*, **150**, 271 (1964).

(24) R. M. Pratt and C. T. G. King, *Arch. Oral Biol.*, **16**, 1181 (1971).

(25) Y. Shapira and S. Shoshan, *ibid.*, **17**, 1699 (1972).

(26) M. E. Teaford and A. A. White, *Proc. Soc. Exp. Biol. Med.*, **117**, 541 (1964).

(27) R. E. Waterman, G. C. Palmer, S. J. Palmer, and S. M. Palmer, *Anat. Rec.*, **188**, 431 (1977).


## ACKNOWLEDGMENTS


Abstracted in part from a thesis submitted by J. M. McDevitt to Temple University in partial fulfillment of the Master of Science degree requirements.


# Oxidative Degradation of 6-Selenoguanosine in Aqueous Solutions


**A. J. REPTA ˣ and Y. A. BELTAGY ***



Received August 8, 1980, from the *Pharmaceutical Chemistry Department, School of Pharmacy, University of Kansas, Lawrence, KS 66044.* Accepted for publication November 17, 1980.


*Present address: Pharmaceutical Chemistry Department, Faculty of Pharmacy, University of Alexandria, Alexandria, Egypt.



**Abstract** □ The degradation of 6-selenoguanosine (NSC 137679)(I) in water and in various buffer systems was investigated. Drug degradation in aqueous media was monitored by high-pressure liquid chromatography. Some kinetic aspects of the degradation of I in various buffer systems at 25° also were studied spectrophotometrically. The degradation, which requires oxygen, involves autoxidation of I to the corresponding diselenide, which produces a selenide and metallic selenium in the presence of oxygen. This degradation pathway differs from that reported for the oxidation of related thio compounds.



**Keyphrases** □ 6-Selenoguanosine—oxidative degradation in aqueous solutions, kinetics □ Autoxidation, aqueous—6-selenoguanosine, selenium compounds, pharmacokinetics □ Kinetics—6-selenoguanosine, oxidative degradation in aqueous solutions, selenium compounds □ Antineoplastics—6-selenoguanosine, selenium compounds, oxidative degradation in aqueous solutions, kinetics


During a study of selenium analogs of physiologically active sulfur compounds, numerous selenium analogs were synthesized for biochemical investigation. 6-Selenopurine was synthesized (1) and found to be active as an antileukemic agent (2), but it was unstable and toxic to the host (3). Subsequently, 6-selenopurine-9-β-D-ribonucleoside was prepared, but it was even less stable than 6-selenopurine under the same conditions (3).

In a search for a more stable analog, 6-selenoguanosine (NSC 137679) (I) was synthesized (4); it was found to be an active inhibitor of several experimental tumors *in vitro* (5, 6) and *in vivo* (7, 8). Although I was reported to be more stable than preceding analogs (4, 9), it still undergoes sufficiently rapid degradation in aqueous solutions such that its formulation in a dosage form suitable for evaluation of anticancer activity presented serious problems (10).

While considerable information has been published




*0022-3549/81/0600-0634$01.00/0*


*© 1981, American Pharmaceutical Association*

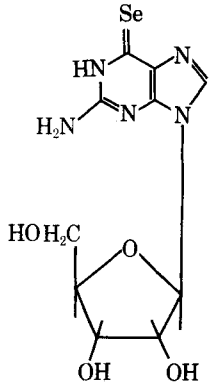

I

relative to the oxidation and other solution reactions of sulfur-containing compounds, including thiopurines and thionucleosides (11, 12), there is a lack of such information for related selenium compounds. The present work examined the nature of the degradation, including its reaction products, and investigated the factors affecting the degradation rate of I in solutions.

## RESULTS AND DISCUSSION

When I was dissolved in water (0.75 mg of I/ml of water) and air was continuously bubbled through the solution, cloudiness developed within 5 hr. The cloudy solution was filtered at 6 hr, and the solid dark-yellow residue was dissolved in methanol. When the methanolic solution was examined by high-pressure liquid chromatography (HPLC), a major peak was eluted at 21.5 ml (capacity factor $k' = 7.08$). An authentic sample of the diselenide of 6-selenoguanosine in methanol (II) also eluted at 21.5 ml. Results of the elemental analysis of the solid residue were in good agreement with those of the authentic II sample. Additionally, the UV spectra of methanolic solutions of the solid residue and authentic II also were identical. Thus, it was concluded that the cloudiness was due to II precipitation. When the filtrate of the cloudy solution at 5 hr was examined by HPLC, only a very small peak (D, Fig. 1) corresponding to II was observed; it was attributed to the fact that II is only very sparingly soluble in water (~0.1 μg/ml) and little remains in solution.

The compounds responsible for the remaining peaks in the filtrate chromatogram shown in Fig. 1 also were examined. Peak A ($k' = 1.46$) was due to I itself. Peak B ($k' = 3.92$), which was only present in small amounts, was characterized as guanosine (III) based on the fact that it coeluted with an authentic guanosine sample.

The compound responsible for peak C ($k' = 4.40$) was more difficult to characterize. In chromatograms of freshly prepared solutions of I, peak C was not observed. But on standing with exposure to molecular oxygen, peak C increased in intensity. After standing for ~10 days, the reaction appeared to reach completion; the chromatogram of the reaction mixture filtrate showed only a small peak B (corresponding to III) and a large peak C, with no remaining peak A or D. When a dilute aqueous suspension of II (0.2 mg of II/ml of water) was prepared and allowed to stand exposed to air, peak C again was formed at the expense of II. The sediment remaining after the aqueous solution of I was exposed to oxygen for 10 days was red. Separation and analysis of the solid demonstrated that it was selenium metal.

The filtrate obtained at 10 days was evaporated to dryness under reduced pressure, and the compound corresponding to peak C was isolated and recrystallized. HPLC analysis of the recrystallized solid indicated that recrystallization had not resulted in any significant compound degradation, although some contaminants, including III and selenium metal, appeared to be present in the final product. Subsequent attempts to purify the samples further resulted in some degradation, as evidenced by visual inspection and HPLC analysis. Elemental analyses of the samples obtained indicated 11–13% selenium. When the sample was treated with trimethylsilane and analyzed by chemical-ionization mass spectrometry, the parent ion ($MH^+ = 1190$) and the two major fragments (mass 635 and 555) suggested the structure of the silylated compound to be IV*a*.

While the carbon, hydrogen, and nitrogen analysis of the isolated material did not agree closely with that of IV, the discrepancy may be attributed to an inability to obtain a pure sample, even when recrystallization from various solvents was attempted. The UV spectrum of IV

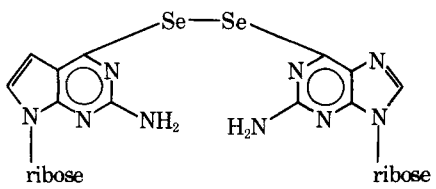

II

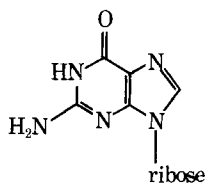

III

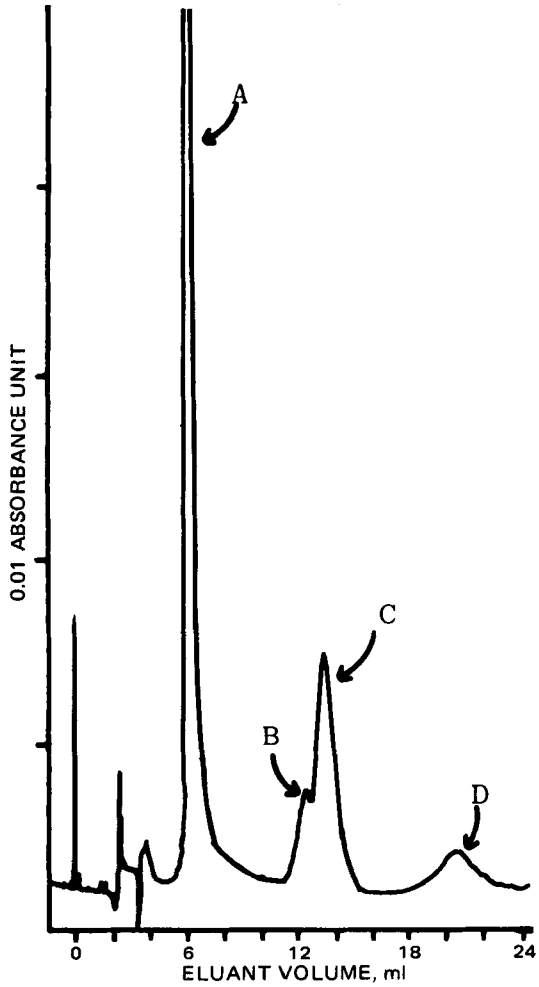


**Figure 1**—*Chromatogram (HPLC) of a solution of 6-selenoguanosine in water (pH ~4–5) after 5 hr at room temperature.*

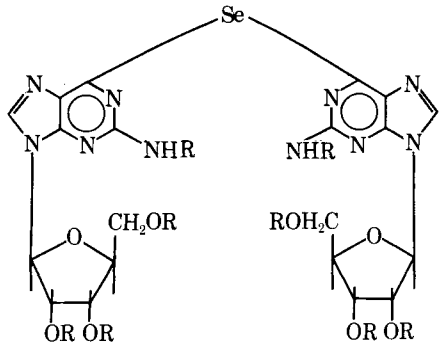

IV: R = H, bis(2-amino-9-β-D-ribofuranosyl-6-purinyl) selenide

IV*a*: R = trimethylsilyl

showed a maximum at 325 nm, indicating more conjugation in the purine ring system and the absence of the selenone group.

When I was dissolved in water that had been recently boiled and cooled (under argon or nitrogen) and the reaction mixture was kept under argon (or nitrogen), no degradation products were detected by HPLC and the solution remained clear for >6 days. Similarly, a II suspension in oxygen-free water stored under an inert gas showed no IV formation. However, when these same systems were subsequently exposed to oxygen, decomposition again was apparent within a few hours.

These data demonstrate the need for oxygen in conversion of I to II and of II to IV. These results support the following scheme:

$$2\mathrm{I} \xrightarrow{O_2} \mathrm{II} \xrightarrow{O_2} \mathrm{IV} + \mathrm{Se}$$

*Scheme I*

where the conversion of I to II involves a simple oxidation while the conversion of II to IV is a more complex transformation. While the production of IV from II appears to be a disproportionation reaction, the necessity of atmospheric oxygen precludes such a simple explanation.

Although a free radical process may be involved, available data do not provide a specific mechanistic interpretation of the conversion of the diselenide to the selenide and metallic selenium.

As already mentioned, in the degradation of I and II, traces of III were present in the solutions. It is not clear whether III occurs as a result of a minor side reaction of the decomposition of I and/or II or as a product of the slow degradation of IV. In any event, it represents only a small fraction of the products.

While II has a very low water solubility of ~1 μg/ml, both I and IV are much more soluble, with the solubility of I being ~2–3 mg/ml and that of IV being ~3.5 mg/ml.

Spectrophotometric changes observed during the described reaction also supported Scheme I. In simple aqueous solution (pH 4–5), the absorbance maximum of I was at 358 nm while in 0.1 *N* NaOH, $\lambda_{max}$ was ~330 nm. This marked change in $\lambda_{max}$ may be ascribed to tautomerization and ionization as shown in Scheme II.

Methanolic solutions of I, II, and IV yielded $\lambda_{max}$ values of 365 (log a 4.29), 318 (4.30), and 327 (4.31) nm, respectively. The chemical structures of both II and IV are related more closely to Ia than to I and thus would be expected to exhibit $\lambda_{max}$ values similar to those of Ia. When oxidation of I in water was followed spectrophotometrically at pH <7, the reaction was accompanied by a substantial time-dependent decrease in absorbance at 350–360 nm and a corresponding increase at 315–330 nm. In alkaline media of pH >10, the maximum absorbance was at 315–330 nm; little change in absorbance occurred as the reaction proceeded (as monitored by HPLC).

Similar spectral behavior has been reported and rationalized for numerous related 6-thiopurine derivatives including the corresponding disulfides and the 6-alkylmercapto compounds (12–16). In all cases, loss of the thione or selenone form resulted in a hypsochromic shift.

The initial degradation studies were carried out on solutions prepared by dissolution of I in water. The resulting solutions were in the pH 4–6 range. Subsequent efforts were directed toward determining the effects of pH on the degradation rate of I.

The rates of loss of I from aqueous buffered solution exposed to air were studied at pH 2–11 using UV spectrophotometry and/or HPLC. Over this entire pH range, the degradation rate of I appeared to be a first-order process, with linear semilog plots obtained for more than two half-lives in all cases and for up to five half-lives in most instances.

The rate data are summarized in Table I; I apparently was most stable at pH 4–5. At values of pH 7–11, there appeared to be no significant change in the rate of loss of I, which is surprising since the pKa of I was found by spectrophotometric determination to be 7.68 ± 0.05. Normally, it might be expected that the ionization involving the selenium atom would alter the rate significantly. Table I also shows that the buffers used may substantially influence the degradation rate. This finding is particularly obvious at pH 5, where acetate and citrate buffers were used and the rate in citrate was more than fourfold greater than that in acetate at concentrations of $1 \times 10^{-2}$ *M*.

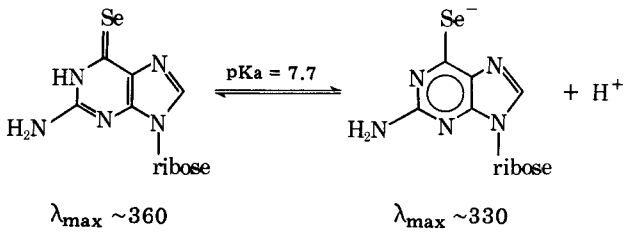


*Scheme II*

**Table I—Rate Data Obtained for the Loss of 6-Selenoguanosine [a] for Aqueous Buffered Solution at 25° and Various pH Values**

| pH | Buffer | $\lambda_{max}$, nm | $t_{1/2}$, hr | $k_{obs}$ (× $10^2$), $hr^{-1}$ |
|---|---|---|---|---|
| 11.0 | Sodium hydroxide[b,c] | 330 | 6.6 | 10.6 |
| 9.0 | 0.010 *M* borate[b] | 330 | 3.9 | 17.8 |
| 8.0 | 0.010 *M* borate[b] | 335 | 5.0 | 13.9 |
| 7.9 | 0.005 *M* phosphate | 335 | 2.5 | 27.7 |
| 7.0 | 0.005 *M* phosphate | 357 | 4.7 | 14.7 |
| 5.0 | 0.010 *M* acetate[b] | 358 | 40.8 | 1.7 |
| | | | (43.8)[c] | (1.6)[c] |
| 5.0 | 0.010 *M* citrate[b] | 358 | 10.1 | 6.9 |
| 4.0 | 0.010 *M* acetate[b] | 358 | 44.9 | 1.5 |
| | | | (49.3)[c] | (1.4)[c] |
| 2.0 | Hydrochloric acid | 360 | 27.7 | 2.5 |

[a] Initial concentration was ~$5 \times 10^{-5}$ *M*. [b] Solution contained 0.1 *M* KCl. [c] Data obtained by HPLC studies with initial concentration of I of $2 \times 10^{-4}$ *M*.

Additional absorbance studies were carried out to determine if citrate enhanced degradation or if acetate acted as a stabilizer. With both citrate and acetate buffers (pH 5), the rate of absorbance loss increased when the buffer concentrations increased, indicating that both buffer systems enhanced the rate of loss of I.

With acetate buffers, the rate enhancement due to buffer appeared to be rather small and a linear relationship appeared to exist between buffer concentration and the observed rate constant. The effect of total citrate concentration on the observed rate constant was nonlinear, exhibiting a decreasing rate dependence on citrate as the buffer concentration was increased from $1 \times 10^{-3}$ to 0.10 *M*. The precise cause for the observed asymptotic relationship is not understood but presumably involves a reversible interaction between I and citric acid (or citrate ion) to yield a species that is less stable than I itself. Studies on the effects of citrate on I degradation are continuing.

At pH 4 and 5 in acetate buffers, the rates of loss of I as determined by both spectrophotometry and HPLC appeared to accelerate at about two half-lives (60–90 hr). Whether this result was due to product catalysis or another competing side reaction was not determined. Such acceleration was not observed at other pH values or even at pH 4 and 5 when citrate buffers were used. However, in those cases, the half-lives of the reaction being monitored were much shorter and, consequently, the loss of I was largely complete in 50–60 hr.

While the oxidation of I in water is rather facile, the oxidation rates in dimethyl sulfoxide and dimethylacetamide were much faster. Within 1 hr at ambient temperature, complete conversion of I to II occurred. However, there did not appear to be any subsequent diselenide degradation in either of these organic solvents over the several days during which the solutions were monitored. Similar oxidation reactions in these solvents were reported for sulfur compounds (17).

## CONCLUSION

In a reaction analogous to the autoxidation of thiols and thionucleosides such as thioguanosine, 6-selenoguanosine (I) is oxidized in aqueous media in the presence of air to yield the corresponding diselenide. However, unlike the disulfides, which are relatively stable except in alkaline media or in the presence of potent oxidizing agents, the diselenide (II) of I undergoes a facile reaction to yield the more soluble selenide and selenium metal. Whether this is a general reaction of diselenides was not addressed in this study but may merit investigation as a simple means of preparing seleno ethers from organic selenols.

Previous reports that I was more stable than some of its analogs were based on absorption changes in aqueous solution (9). However, the comparisons made were between a solution of I in an alkaline medium (where loss of I is not accompanied by significant changes in absorption) and solutions of 6-selenopurine and related compounds at neutral pH (where loss of the parent substance is evidenced by large absorption changes). When solutions of I were studied at neutral pH values, relatively rapid and large absorbance changes were observed. Consequently, the stability of I clearly does not differ substantially from that of its closely related predecessors.

In the absence of oxygen, I was quite stable, and aqueous solutions gave no evidence of drug loss over several days. In the presence of oxygen, the minimum rates of oxidation appeared to occur at pH 4–5. Further sta-

bilization can be afforded by the incorporation of antioxidants such as ascorbic acid and dithioerythritol (10).

## EXPERIMENTAL

**Materials**—6-Selenoguanosine[1] (I) was purified by recrystallization from aqueous ascorbic acid as previously described (10). All other chemicals were analytical or chromatographic grades.

**Preparation of I Solutions for Kinetic Studies**—A stock solution of I was prepared by dissolving the drug (15–17 mg) in 100 ml of 0.1 *M* KCl. The solution obtained was filtered (0.45-μm membrane filter), and 10 ml of the clear filtrate was diluted to 100 ml with the selected buffer to yield I concentrations of $\sim 5 \times 10^{-5}$ *M*. The resulting solution was kept in a tightly closed flask and maintained at 25° in a water bath. Aliquots were withdrawn at intervals, and the UV absorption at $\lambda_{max}$ (358 nm in pH 4–5 acetate buffer, ~330 nm in more alkaline buffers, and 360 nm in acid buffers) was monitored spectrophotometrically[2].

For kinetic studies monitored by HPLC, solutions were prepared similarly, but the final concentrations of I were $\sim 2 \times 10^{-4}$ *M*. Aliquots (20 μl) were removed and analyzed by HPLC.

**pKa Determination of I**—The pKa was determined spectrophotometrically at 25° by the method of Albert and Serjeant (18). Buffers were 0.01 *M*, and calculations were based on absorbances monitored at 255, 330, and 358 nm. At all wavelengths, the value obtained was pKa = 7.68 ± 0.05.

**Chromatography**—HPLC was performed as described previously (10). Although the methodology used was unchanged, the elution volume and, consequently, the capacity factors were much smaller. These factors were observed to decrease as column use continued.

**Isolation and Characterization of Degradation Product (IV) of I in Aqueous Solution**—Compound I (300 mg) was dissolved in deionized water (400 ml). Air was continuously bubbled through the solution, and the degradation was followed chromatographically (1 ml of the reaction mixture was diluted to 10 ml with methanol and 10 μl of solution was injected) until the reaction was complete (~10 days). Water loss due to evaporation (which was accelerated by the passage of air through the solution) was compensated for by daily addition of water to a constant total volume. Such replacement of water was necessary to keep the reactants in solution.

After 10 days, the reaction mixture was filtered (0.45-μm filter), and the filtrate was evaporated to dryness under reduced pressure at ~40°. The residue was treated with absolute ethanol (30 ml, to facilitate the complete removal of water) and was again evaporated to dryness. The product was dissolved in boiling methanol (25 ml), filtered, and poured on cold ether (400 ml). The resulting liquid, containing a yellow precipitate, was kept in a refrigerator overnight. The precipitate was separated by filtration (glass filter, 4–4.5 μm), washed with cold ether (3 × 25 ml), and dried under vacuum for 24 hr to give 195 mg of IV (65% yield) as a yellow solid, which decomposed on melting at 220–222° (uncor.).

*Anal.*—Calc. for $C_{20}H_{24}N_{10}O_8Se$: C, 39.29; H, 3.96; N, 22.91; Se, 12.91. Found[3]: C, 37.77; H, 4.1; N, 21.09; Se, 11.92.

Chemical-ionization mass spectrometry[4] of the trimethylsilylated compound gave evidence of a molecular ion ($MH^+$) of 1190 and two major fragments at masses of 555 and 635, corresponding to fragmentation of the compound (IV*a*) between the selenium atom at position 6 of the purine rings. Both the parent ion and the mass 635 peaks exhibited the typical selenium cluster. These results agreed with the molecular weight of 612 for Structure IV*a*.

[1] Obtained from the National Cancer Institute.

[2] Cary model 14 or 15, Varian Instruments, Palo Alto, Calif.

[3] Analyses were performed by Schwarzkopf Microanalytical Laboratory, and by the Medicinal Chemistry Department, University of Kansas.

[4] Mass spectrometry was performed at the Pharmaceutical Chemistry Department, School of Pharmacy, University of California at San Francisco.

## REFERENCES


(1) H. G. Mautner, *J. Am. Chem. Soc.*, **78**, 5292 (1956).

(2) H. G. Mautner and J. J. Jaffer, *Cancer Res.*, **18**, 294 (1958).

(3) *Ibid.*, **20**, 381 (1960).

(4) L. B. Townsend and G. H. Milne, *J. Heterocycl. Chem.*, **7**, 753 (1970).

(5) S. H. Chu, *J. Med. Chem.*, **14**, 254 (1971).

(6) S. H. Chu and D. D. Davidson, *ibid.*, **15**, 1088 (1972).

(7) G. H. Milne and L. B. Townsend, *ibid.*, **17**, 263 (1974).

(8) A. F. Ross, K. C. Agarwal, S. H. Chu, and R. E. Parks, *J. Biochem. Pharmacol.*, **22**, 141 (1973).

(9) G. H. Milne and L. B. Townsend, *J. Heterocycl. Chem.*, **8**, 379 (1971).

(10) Y. A. Beltagy, W. Waugh, and A. J. Repta, *J. Pharm. Sci.*, **69**, 1168 (1980).

(11) I. L. Doerr, I. Wempen, D. A. Clarke, and J. J. Fox, *J. Org. Chem.*, **26**, 3401 (1961).

(12) J. J. Fox, I. Wempen, A. Hampton, and I. L. Doerr, *J. Am. Chem. Soc.*, **80**, 1669 (1958).

(13) G. B. Elion, E. Burgi, and G. H. Hitchings, *ibid.*, **74**, 411 (1952).

(14) J. A. Johnson, Jr., and H. J. Thomas, *ibid.*, **78**, 3863 (1956).

(15) G. B. Elion, I. Goodman, W. H. Lange, and G. H. Hitchings, *ibid.*, **81**, 1898 (1959).

(16) D. J. Brown and S. F. Mason, *J. Chem. Soc.*, **1959**, 682.

(17) G. Copozzi and G. Modena, in "The Chemistry of the Thiol Group, Part 2," S. Patai, Ed., Wiley, New York, N.Y., 1974, pp. 785–840.

(18) A. Albert and E. P. Serjeant," Ionization Constants of Acids and Bases," Methuen, London, England, 1962, pp. 69–77.


## ACKNOWLEDGMENTS


Supported in part by Contracts N01-CM-23217 and N01-CM-07304, Drug Development Branch, Division of Cancer Treatment, National Cancer Institute, Department of Health and Human Services.

Y. A. Beltagy gratefully acknowledges support provided by the Egyptian Ministry of Education.

The authors appreciate the efforts of Neil Castagnoli and L. T. Lang, University of California at San Francisco, in obtaining the mass spectrophotometric data.

# Effect of Adsorbed Carbonate on Surface Charge Characteristics and Physical Properties of Aluminum Hydroxide Gel

JOSEPH R. FELDKAMP *, DHIREN N. SHAH ‡, SUSAN L. MEYER ‡, JOE L. WHITE *, and STANLEY L. HEM ‡x

Received October 6, 1980, from the *Department of Agronomy and the ‡Department of Industrial and Physical Pharmacy, Purdue University, West Lafayette, IN 47907. Accepted for publication November 14, 1980.

**Abstract** □ A titration procedure was used to determine the zero point of charge of a number of chloride-containing aluminum hydroxide gels and aluminum hydroxycarbonate gels. The surface charge characteristics of aluminum hydroxide gel were determined by both hydroxyls and the surface density of specifically adsorbed carbonate anion. The wide range of zero point of charge values reported for aluminum hydroxide is thought to be due to the presence of specifically adsorbed anions such as carbonate. The effect of ionic strength on the pH of aluminum hydroxide gel is important during washing since the ease of electrolyte removal is related to surface charge. Viscosity and sedimentation characteristics are related to the relationship between the zero point of charge and bulk pH. Maximum viscosity was observed when the bulk pH was adjusted to the zero point of charge.

**Keyphrases** □ Aluminum hydroxide gel—effect of adsorbed carbonate on surface charge and physical characteristics □ Carbonate, adsorbed—effect on surface charge and physical characteristics of aluminum hydroxide gel □ Physicochemistry—effect of adsorbed carbonate on surface charge and physical characteristics of aluminum hydroxide gel

Aluminum hydroxide gels exhibit a surface charge whose sign and magnitude depend on bulk pH, specific ion adsorption, and ionic strength. When no specific adsorption of ions other than protons or hydroxyls occurs, as with chloride- or nitrate-containing aluminum hydroxide gels (1), surface charge arises by the mechanism (2) shown in Schemes I and II (which are equivalent). For clarity, only the bonds associated with the charged site are shown, even though aluminum is in sixfold coordination in each structure.

$$(Al{-}OH_2)^+ \overset{H^+}{\rightleftharpoons} Al{-}OH \overset{H^+}{\rightleftharpoons} (Al{-}O)^-$$

*Scheme I*

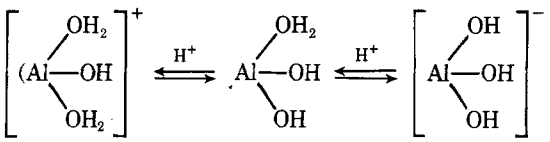

*Scheme II*

When carbonate or any other specifically adsorbed anion (1) is present as in aluminum hydroxycarbonate gel, a second mechanism (Scheme III) contributes to the surface charge. Thus, the observed surface charge of aluminum hydroxycarbonate gel depends on the surface density of each type of site.

$$Al{-}OH + CO_3^{2-} \leftrightarrows Al{-}OCO_2^- + OH^-$$

*Scheme III*

An important property of colloidal systems that possess a pH-dependent surface charge is the zero point of charge, which is the pH at which the net surface charge is zero. At this pH, the densities of the positive and negative charges arising from Schemes I–III are equal (3).

A number of anions other than carbonate affect the zero point of charge of metal oxides through specific adsorption to metal oxide surfaces. These anions include orthophosphate, pyrophosphate, tripolyphosphate, silicate, selenite, and fluoride anions (4). In each case, the specifically adsorbed anion contributes additional negative charge to the surface, thereby displacing the zero point of charge to lower pH values. The major objective of this study was to determine the effect of specifically adsorbed carbonate on the zero point of charge. Another objective was to illustrate the effect of surface charge on important physical properties such as apparent viscosity and electrolyte removal by washing.

## EXPERIMENTAL

**Materials**—Two chloride-containing aluminum hydroxide gels were prepared in an identical manner, with precautions taken to minimize the specific adsorption of carbonate. A closed, baffled reaction vessel was used as well as freshly distilled water stored in a closed container. Potassium hydroxide (1 *M*) was added with continuous stirring to 0.5 *M* $AlCl_3$ at 1 ml/min through a submerged delivery tube having a pinhole-size orifice until pH 9.5 was reached. The resulting chloride-containing aluminum hydroxide gel was allowed to stand for 24 hr and was washed with five volumes of freshly distilled water using centrifugation.

An aluminum hydroxycarbonate gel was prepared by the addition of 0.5 *M* $AlCl_3$ to a solution of 0.5 *M* $NaHCO_3$ and 0.23 *M* $Na_2CO_3$ with agitation until pH 6.6 was reached (5). The aluminum hydroxycarbonate gel was allowed to stand for 24 hr and was washed with five volumes of water using centrifugation.

Nine aluminum hydroxycarbonate gels were obtained commercially.

**Analytical Procedures**—The titration technique (6) used to measure the zero point of charge was based on the principle that changes in the ionic strength produced by the addition of an indifferent electrolyte, such as potassium chloride, will have no effect on proton adsorption or release by the gel when the gel surface charge is zero. Thus, titration curves (moles of bound or released protons *versus* pH) obtained at several ionic strengths intersect at a common point, the zero point of charge.

The zero point of charge of the laboratory chloride-containing aluminum hydroxide gels and the laboratory aluminum hydroxycarbonate gel was determined by the following procedure. Aliquots of the gel containing ~1% equivalent aluminum oxide were prepared containing the appropriate quantities of potassium chloride and hydrochloric acid or potassium hydroxide, depending on the ionic strength and pH desired. The amount of hydrochloric acid or potassium hydroxide added and the resulting pH were recorded. A blank, *i.e.*, no gel present, also was treated similarly to correct for any acid or base that did not result in the adsorption or release of protons from the surface. Curves obtained at different ionic strengths intersect at the zero point of charge. A correction was rarely needed, and a more rapid and convenient continuous titration procedure was developed for routine use.

The zero point of charge of the commercial aluminum hydroxycarbonate gels were determined by a continuous titration procedure. An aluminum hydroxycarbonate gel sample, adjusted to the desired ionic strength with potassium chloride, was titrated with either acid or base, depending on the desired direction of pH change. A blank titration was not run since experience showed that no significant correction was needed. The recorded pH values and the corresponding quantity of acid



0022-3549/81/0600-0638$01.00/0
© 1981, American Pharmaceutical Association

**Table I—Zero Point of Charge (ZPC) of Laboratory and Commercial Aluminum Hydroxide Gels**

| Sample | ZPC | Bulk pH | Apparent Surface Charge |
|---|---|---|---|
| Laboratory chloride-containing aluminum hydroxide gel 1 | 9.65 | 8.00 | + |
| | 9.65 | 8.00 | + |
| | 9.65 | 8.00 | + |
| Laboratory chloride-containing aluminum hydroxide gel 2 | 9.68 | 8.00 | + |
| Laboratory aluminum hydroxycarbonate gel | 6.65 | 7.05 | − |
| | 6.67 | 7.05 | − |
| | 6.66 | 7.05 | − |
| Commercial aluminum hydroxycarbonate gel 1 | 6.95 | 6.34 | + |
| | 6.95 | 6.34 | + |
| | 6.95 | 6.34 | + |
| Commercial aluminum hydroxycarbonate gel 2 | 6.64 | 6.38 | + |
| Commercial aluminum hydroxycarbonate gel 3 | 7.32 | 5.80 | + |
| Commercial aluminum hydroxycarbonate gel 4 | 6.30 | 6.25 | + |
| Commercial aluminum hydroxycarbonate gel 5 | 6.53 | 6.51 | ~0 |
| Commercial aluminum hydroxycarbonate gel 6 | 6.54 | 6.60 | − |
| Commercial aluminum hydroxycarbonate gel 7 | 6.68 | 6.56 | + |
| Commercial aluminum hydroxycarbonate gel 8 | 6.90 | 6.17 | + |
| Commercial aluminum hydroxycarbonate gel 9 | 6.94 | 5.63 | + |

or base added were plotted, and the intersection point of the different ionic strength curves was the zero point of charge, *i.e.*, the pH at which ionic strength has no effect.

The specific procedure was as follows:

1. A 100-ml aliquot containing ~1% equivalent aluminum oxide was transferred to a 250-ml beaker.
2. The initial pH was recorded with stirring after a stable value was achieved.
3. Sufficient 0.1 *N* KOH was added from a 10-ml buret to cause a pH change of 0.05–0.10 unit. Usually, increments of titrant ranging from 0.2 to 1.0 ml were required. When the pH was stable, the volume of titrant added and the pH were recorded.
4. Steps 1–3 were repeated but titration was performed with 0.1 *N* HCl.
5. A plot was constructed with micromoles of acid or base added on the ordinate and the resultant pH on the abscissa.
6. Steps 1–5 were repeated except that, in Step 1, 2 ml of 4 *M* KCl was added to the 100-ml volumetric flask before making the final dilution of the ~1% equivalent aluminum oxide aliquot. The data were plotted on the same graph.
7. Steps 1–5 were repeated except that, in Step 1, 10 ml of 4 *M* KCl was added to the 100-ml volumetric flask before making the final dilution of the ~1% equivalent aluminum oxide aliquot. The data were plotted on the same graph. The pH where the three curves intersected was the zero point of charge.

The equivalent aluminum oxide content was determined by the ethylenediaminetetraacetic acid titration (7).

Viscosity measurements were made on two of the commercial aluminum hydroxycarbonate gels after the gel pH was adjusted to selected values above and below the zero point of charge. The pH range of 5–9.5 was selected to avoid substantial solubilization of the aluminum hydroxycarbonate gel (8). Two hundred milliliters of a gel containing 9% equivalent aluminum oxide was adjusted to the desired pH by the addition of either 1 *N* HCl or KOH. The ionic strength of all samples was adjusted to 0.03 by adding 1 *M* KCl. The final volume of all samples was adjusted to 230 ml with distilled water. Each sample was vigorously stirred and transferred into the measuring vessel of the rotational viscometer[1] with the appropriate spindle in place. Each sample was allowed to set for 5 min before the viscosity was measured at 100 rpm.

## RESULTS AND DISCUSSION

Figure 1 illustrates the zero point of charge determination of the laboratory chloride-containing aluminum hydroxide gel 1. The value is concluded to be 9.65 because ionic strength did not affect the gel at pH 9.65. Triplicate determinations resulted in identical results (Table I), indicating the excellent precision of the individual sample adjustment method for determining the zero point of charge. The precipitation method also was very reproducible since the zero point of charge of laboratory chloride-containing aluminum hydroxide gel 2 was 9.68 (Table I). The surface charge of both gels was positive since the bulk pH was below the zero point of charge.

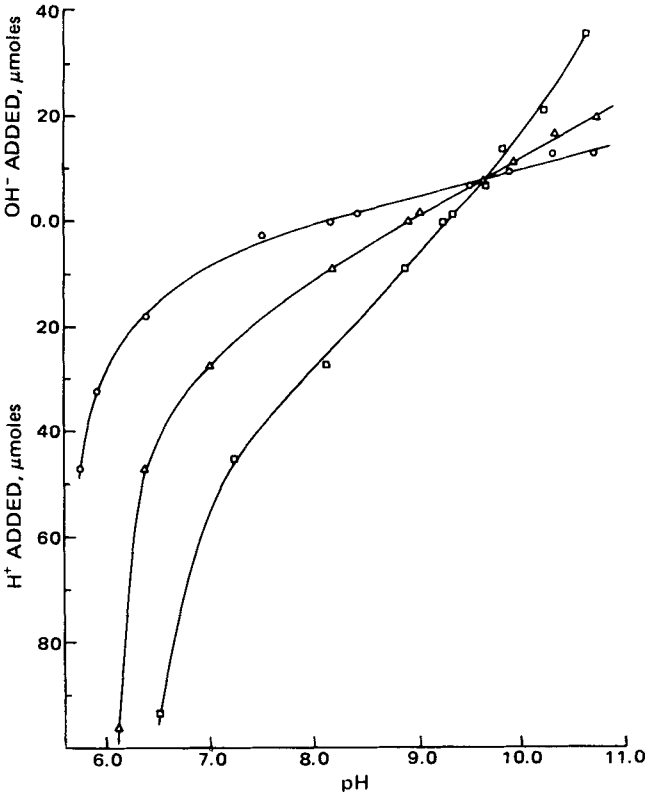


**Figure 1**—*Determination of the zero point of charge of laboratory chloride-containing aluminum hydroxide gel 1. Key:* ○, $\mu = 0.0005$; △, $\mu = 0.01$; *and* □, $\mu = 0.6$.

Specifically adsorbed carbonate had a substantial effect on the zero point of charge. The value of the laboratory aluminum hydroxycarbonate gel was 6.66 ± 0.01 based on triplicate determinations (Table I). The surface charge of this gel was negative since the bulk pH was above the zero point of charge.

The continuous titration method also measured precisely the zero point of charge; triplicate determinations on commercial aluminum hydroxycarbonate gel 1 gave identical results of 6.95 (Table I). The zero point of charge of the nine commercial aluminum hydroxycarbonate gels ranged from 6.3 to 7.3. These gels exhibited positive, neutral, and negative surface charges. The lower and more variable values obtained for the aluminum hydroxycarbonate gels in comparison to the chloride-containing aluminum hydroxide gels indicate that specifically adsorbed carbonate contributes to the surface charge characteristics as hypothesized in Scheme III.

The zero point of charge of the chloride-containing aluminum hydroxide gel was similar to values reported for highly crystalline forms of aluminum hydroxide (9), which would be expected to be largely free of specifically adsorbed carbonate. This finding suggests that chloride, like nitrate, is outside the coordination sphere of the aluminum cation and interacts by electrostatic forces (1). This observation agrees with an earlier observation that a chloride impurity in hydrous aluminum oxide does not affect the zero point of charge (9).

Thus, it appears that the wide range of zero point of charge values, *i.e.*, 3.8–10.0 (9, 10), reported for aluminum hydroxide is due to the presence of a specifically adsorbed anion such as carbonate that contributes to the surface charge characteristics (Scheme III) in addition to the contribution of surface hydroxyls (Schemes I and II). Direct adsorption of carbon dioxide from the atmosphere by aluminum hydroxide is likely to occur since carbon dioxide is known to be strongly adsorbed onto moist goethite surfaces as carbonate (11).

The effect of ionic strength on the pH of aluminum hydroxide is seen in Fig. 1. As the ionic strength increased, the pH of the aluminum hydroxide gel tended toward the zero point of charge. Conversely, lowering the ionic strength caused the pH to move away from the zero point of charge. This behavior must be considered during the washing of aluminum hydroxide gel or the final pH of the gel after washing will be un-

[1] Model RVT, Brookfield Engineering Laboratories, Stoughton, Mass.

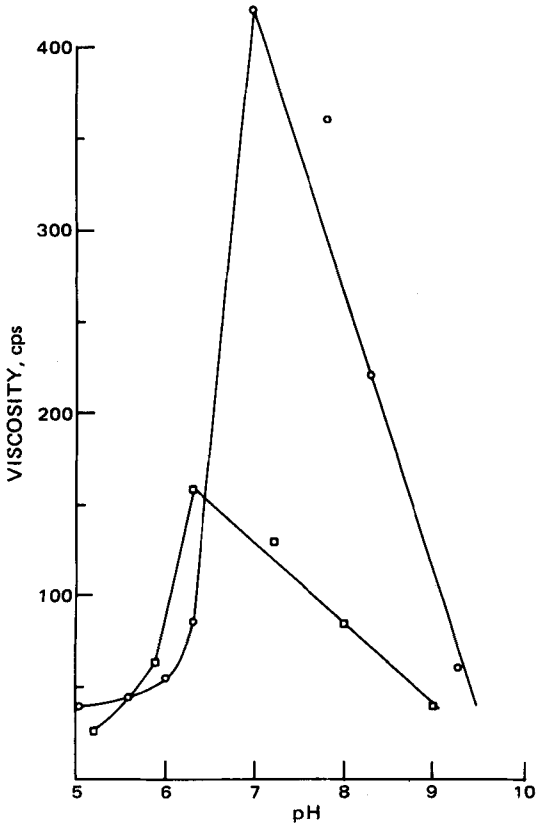


**Figure 2**—*Effect of bulk pH on apparent viscosity of commercial aluminum hydroxycarbonate gels 1 (○) and 4 (□). The zero point of charge of commercial aluminum hydroxycarbonate gels 1 and 4 are 6.95 and 6.30, respectively.*

predictable. Table I indicates that the bulk pH ranged from 5.63 to 6.60 and was as random as the zero point of charge. Figure 1 indicates that washing a gel whose pH was at the zero point of charge did not produce a pH change even though the ionic strength was reduced. Furthermore, because the gel surface is neutral when the pH is at the zero point of charge, electrolyte removal should be accomplished most readily when washing is performed under these conditions. Cations will be retained if washing occurs at pH conditions above the zero point of charge, and anions will be retained if the pH during washing is below the zero point of charge.

Physical properties of aluminum hydroxide gel such as viscosity and sedimentation characteristics are controlled largely by a sensitive interplay between the attractive and repulsive forces operating between the particles and aggregates. The coulombic repulsive force and the van der Waals attractive force are of prime importance. For molecules, van der Waals forces are weak and very short ranged, with the force being inversely proportional to the seventh power of the distance separating the molecules (12). Only in the absence of other forces and at sufficiently low temperatures do these forces manifest themselves between molecules. For particles, the situation is different. To find the magnitude of the force and the dependence on the separating distance, the assumption is often made that the individual forces operating between molecules may be summed pairwise to obtain the net force between macroscopic bodies (12). In the case of two flat slabs, where the separation distance is small compared to the thickness of either slab, the force varies inversely with the third power of the separating distance. The van der Waals force summed in this way has sufficient magnitude to be of relevance in colloidal systems. In fact, when the charge on the particle surfaces is sufficiently reduced (by adjustment of pH or ionic strength), the van der Waals forces are responsible for aggregation and associated phenomena (13). A result similar to that obtained for flat slabs also occurs for macroscopic spheres.

Another important result related to van der Waals forces is that the force between anisometric particles is a function of the relative orientations of the bodies (considering all orientations having the same center of mass separation). In particular, lath-shaped particles and needles interact most strongly when positioned end-to-end. Plates interact most strongly in an edge-to-edge orientation. For isometric particles, the same considerations apply since joining two isometric particles necessarily forms an anisometric aggregate which tends to orient itself end-on with a third particle (12).

The apparent viscosity of aluminum hydroxide gel is sensitive to the bulk pH because of particle interactions. When coulombic repulsion is sufficiently reduced by adjusting the bulk pH close to the zero point of charge or by increasing the ionic strength, the van der Waals forces cause the particles to agglomerate. Consequently, the apparent viscosity increases. The magnitude of the viscosity change depends on the aggregate structures. Figure 2 illustrates the effect of bulk pH on the apparent viscosity of commercial aluminum hydroxycarbonate gels 1 and 4. The viscosity of both aluminum hydroxycarbonate gels was at a maximum when the bulk pH was at the zero point of charge, *i.e.*, pH 6.95 and 6.30, respectively. The fact that a different maximum viscosity occurred for each aluminum hydroxycarbonate gel suggests that aluminum hydroxycarbonate gel 1 formed a more highly extended and cross-linked network of particles in comparison to aluminum hydroxycarbonate gel 4.

The apparent viscosity of aluminum hydroxycarbonate gel 1 increased eightfold as the pH increased from 5.95 to 6.95, and aluminum hydroxycarbonate gel 4 showed a sixfold increase in apparent viscosity between pH 5.30 and 6.30. A small pH change in the region of the zero point of charge produces large changes in apparent viscosity.

It is apparent from Fig. 2 that investigations of the factors affecting aggregate type will prove valuable because aluminum hydroxide gels whose apparent viscosity is not sensitive to small variations in bulk pH are more generally desirable. In addition, the pH changes that may occur when aluminum hydroxide gel is washed also may lead to changes in viscosity. Finally, the results suggest that the viscosity of aluminum hydroxide gels can be controlled by adjusting the relationship between the zero point of charge and the bulk pH to produce the desired degree of aggregation.

## REFERENCES

(1) C. J. Serna, J. L. White, and S. L. Hem, *Soil Sci. Soc. Am. J.*, **41**, 1009 (1977).

(2) T. W. Healy and L. R. White, *Adv. Colloid Interface Sci.*, **9**, 303 (1978).

(3) R. G. Gast, in "Minerals in Soil Environments," J. B. Dixon and S. B. Weed, Eds., Soil Science Society of America, Madison, Wis., 1977, pp. 27–73.

(4) F. J. Hingston, R. J. Atkinson, and J. P. Quirk, *Nature*, **215**, 1459 (1967).

(5) S. L. Hem, E. J. Russo, S. M. Bahal, and R. S. Levi, *J. Pharm. Sci.*, **59**, 317 (1970).

(6) T. F. Tadros and J. Lyklema, *J. Electroanal. Chem.*, **17**, 267 (1968).

(7) "The United States Pharmacopeia," 20th rev., United States Pharmacopeial Convention, Rockville, Md., 1980, p. 25.

(8) J. D. Hem and C. E. Robertson, Geological Survey Water-Supply Paper 1827-A, U.S. Government Printing Office, Washington, D.C., 1967, p. 147.

(9) G. A. Parks, *Chem. Rev.*, **65**, 177 (1965).

(10) H. Schott, *J. Pharm. Sci.*, **66**, 1548 (1977).

(11) J. D. Russell, E. Patterson, A. R. Fraser, and V. C. Farmer, *J. Chem. Soc., Faraday Trans.*, **71**, 1623 (1975).

(12) J. Mahanty and B. W. Ninham, "Dispersion Forces," Academic, London, England, 1976, pp. 11, 16, 21, 22.

(13) H. Van Olphen, "An Introduction to Clay Colloid Chemistry," Wiley-Interscience, New York, N.Y., 1977, p. 36.

## ACKNOWLEDGMENTS

Supported in part by William H. Rorer, Inc.

This report is Journal Paper 8120, Purdue University Agricultural Experiment Station, West Lafayette, IN 47907.

# Spectrofluorometric Determination of Acetylsalicylic Acid, Salicylamide, and Salicylic Acid as an Impurity in Pharmaceutical Preparations

**KENNETH W. STREET, Jr. *x, and GEORGE H. SCHENK**

Received September 8, 1980, from the *Department of Chemistry, Wayne State University, Detroit, MI 48202.* Accepted for publication December 2, 1980. *Present address: Department of Chemistry, Loyola University, Chicago, IL 60626.

**Abstract** □ Spectrofluorometry, either direct or in combination with a separation technique, provides a sensitive and accurate method for the determination of certain fluorescent analgesic drugs and the determination of impurities in many combination preparations. A critical examination of the UV spectra of common analgesics and related compounds indicates that the fluorescence inner filter effect should be negligible below $10^{-5}$ *M* and that selective excitation and emission wavelengths should minimize interference from other fluorescent species. Fluorometric procedures are presented for the determination of salicylamide, acetylsalicylic acid, and salicylic acid, as an impurity, in preparations containing salicylamide, acetylsalicylic acid, acetaminophen, caffeine, and phenacetin as major constituents. Inner filtering is the limiting factor only for the direct and indirect determination of salicylamide and the direct determination of acetylsalicylic acid. Results of fluorometric determinations compare favorably with other reference methods. Salicylic acid is determined in the $10^{-7}$ *M* concentration range after separation from salicylamide, acetaminophen, and caffeine.

**Keyphrases** □ Salicylic acid—analysis, spectrofluorometry, impurity in multicomponent analgesic tablets □ Salicylamide, aspirin—spectrofluorometry, as major constituent in multicomponent tablets □ Aspirin—spectrofluorometric determination of an impurity in drug combinations □ Spectrofluorometry—determination of salicylic acid, salicylamide, and acetylsalicylic acid in multicomponent analgesic tablets

Various methods for the determination of salicylamide, acetylsalicylic acid, and salicylic acid, as an impurity, are available. However, with the advent of new instrumentation, new drugs, and new drug combinations (Table I), many of these methods have become outmoded or are no longer specific. The present study developed new methods along with improvements in some older methods.

## BACKGROUND

**Methods for Acetylsalicylic Acid**—Fluorometric (8, 9) and phosphorimetric (10) methods for the determination of acetylsalicylic acid in pharmaceuticals were reported. Other fluorometric methods involve fluorophore formation by conversion to salicylic acid (11, 12). Many of these methods have never been examined for the effect of other constitcylates that interfere with the direct determination of salicylamide. Additional steps to eliminate fluoresence interference from salicylic acid are needed for the many preparations containing acetylsalicylic acid and other fluorescent salicylates. Analyses by direct UV (4, 5) and differential UV (6) spectrophotometry are both subject to interferences. One visible spectrophotometric method (7) involves a chromophore-producing reaction with ferric chloride reagent.

**Methods for Acetylsalicylic Acid**—Fluorometric (8, 9) and phosphorimetric (10) methods for the determination of acetylsalicylic acid in pharmaceuticals were reported. Other fluorometric methods involve fluorophore formation by conversion to salicyclic acid (11, 12). Many of these methods have never been examined for the effect of other constituents commonly found in recent preparations, such as other fluorescent salicylates and substances that absorb large amounts of exciting radiation. Direct UV methods for acetylsalicylic acid are based on prior separation from other components in the preparation (13–15).

**Methods for Salicylic Acid as Impurity**—The salicylic acid content in acetylsalicylic acid used for pharmaceuticals is limited to 0.3–0.75%, depending on the type of preparation relative to the acetylsalicylic acid content. The USP/NF (16) methods of analysis require separation of salicylic acid from acetylsalicylic acid *via* column chromatography after reaction with ferric chloride reagent. Other automated methods use ferric chloride reagent directly (17). Although this method works well for pure acetylsalicylic acid preparations, salicylamide also undergoes the same reaction with ferric reagents used for colorimetric determination (18). The salicylamide content of newer preparations often is as high as 40% of the total salicylate content.

Schenk *et al.* (8) proposed a direct fluorometric method for the determination of salicylic acid in acetylsalicylic acid. Unfortunately, in their solvent system, both salicylic acid and salicylamide excite and fluoresce at virtually the same wavelengths. Other methods involving chromophore-forming reactions (19) and high-pressure liquid chromatographic separations (20, 21) were proposed but never evaluated for interference by other sample constituents common in multicomponent preparations.

## EXPERIMENTAL[1]

**Solvents**—All fluorescence work was done with fluoro grade alcohol prepared by percolation through 30–40-cm columns of activated coconut charcoal[2] (40–80 mesh). After the first 50-ml portion (contaminated) was discarded, each column produced 5–10 liters of fluorescence quality alcohol.

The fluoro grade chloroform used was prepared by vigorous extraction with 0.45 *M* NaOH, two washings with small volumes of water, and filtration through chloroform-moistened filter paper.

**Organic Reagents**—The salicylamide[3] was freed from the salicylic acid impurity by recrystallization from hot concentrated chloroform solution. [Alternatively, salicylic acid could be extracted from salicylamide in chloroform by two washings with 5% sodium bicarbonate (22).]

The acetylsalicylic acid[4] was purified of an unacceptable amount of salicylic acid by two recrystallizations from hot saturated chloroform; fluorometric analysis (8) demonstrated that a third recrystallization was unnecessary.

Caffeine citrate[5] was freed from citric acid by extraction with chloroform from a nearly saturated aqueous solution at pH 8.0 (ammonia). After filtration, the evaporated chloroform gave a white powder with a UV spectrum comparable to that of Sunshine and Gerber (23).

Samples of acetaminophen[6] and phenacetin[7] were used without further purification.

**Determination of Salicylamide Alone**—To determine salicylamide in the absence of acetylsalicylic acid, salicylic acid, or buffers, a tablet, capsule, or powder (equivalent to 50–100 mg of salicylamide) was placed in a 100-ml volumetric flask, and ~50 ml of methanol was added. The sample tablet form was crushed, shaken, and diluted to volume with methanol. After insoluble materials settled, a 0.1-ml aliquot was diluted to 100 ml with methanol and filtered through medium-speed filter paper. The first 20 ml of the filtrate was discarded, and the fluorescence of the next 50 ml was measured using the instrument settings in Table II. A blank reading was subtracted from the sample fluorescence reading by running a methanol blank for each lot of filter paper. A standard curve

[1] Fluorescence measurements were taken on a Perkin-Elmer MPF-2A spectrofluorometer. Absorption spectra were taken on either a Beckman DK-2A spectrophotometer or a Cary-14 spectrophotometer; a Coleman Jr spectrophotometer was used for quantitative measurement in the visible region. GLC analysis was done on a Perkin-Elmer 3920 chromatograph (flame-ionization detector, glass column packed with 3% OV-17 on Gas Chrom Q, 100–120 mesh).

[2] Fisher, 50–200 mesh (remeshed to above specifications).

[3] Practical grade, Eastman.

[4] Reagent grade, Baker Chemical Co.

[5] USP grade, Merck.

[6] NF sample, courtesy of Wyeth Laboratories.

[7] USP grade, American Pharmaceutical Co.

0022-3549/81/0600-0641$01.00/0
© 1981, American Pharmaceutical Association

**Table I—Contents of Analgesics**

| Preparation | Unit Dosage, mg | | | | |
|---|---|---|---|---|---|
| | Salicylamide | Acetylsalicylic Acid | Acetaminophen | Caffeine | Other |
| A | 200 | — | — | — | Methapyrilene hydrochloride, 25; scopolamine aminoxide hydrobromide, 0.25 |
| B | 250 | — | — | — | Ascorbic acid, 50; ipecac and opium powder, 24; racephedrine hydrochloride, 5.0; pyrilamine maleate, 12; phenacetin, 120 |
| C | 150 | — | 150 | 100 | — |
| D | —[a] | — | —[a] | —[a] | — |
| E | 97 | 324 | — | 16 | — |
| F | 65 | 210 | 115 | 16 | — |
| G | 129.6 | 194.4 | 97 | 64.8 | — |
| H | 129.6 | 194.4 | 162 | — | Methapyrilene fumarate, 25 |

[a] Unspecified quantity.

of fluoresence *versus* concentration was prepared using 0–1.4 × $10^{-5}$ *M* salicylamide in methanol.

**Determination of Salicylamide in Acetylsalicylic Acid, Salicylic Acid, or Buffers**—The tablet(s), capsule contents, or homogeneous powder (50–100 mg of salicylamide) was weighed into a 100-ml volumetric flask, and ~75 ml of chloroform was added. After agitation for 10 min, the solution was diluted to volume with chloroform and filtered through a medium-speed filter paper. [This solution also may be used to determine acetylsalicylic acid and salicylic acid (Scheme I).] A 10-ml aliquot was transferred to a 60-ml separator, and 20 ml of chloroform and 10 ml of pH 7.0 phosphate buffer (24) were added. Then the solution was extracted.

Before the chloroform extract was filtered, a filter paper blank was run by running 100 ml of chloroform through the filter paper and measuring the chloroform fluorescence (Table II). If the blank exceeded 3% of full scale, a different lot of filter paper[8] was used. The extracted chloroform layer was filtered through chloroform-wet filter paper into a 100-ml volumetric flask. The aqueous phase was extracted twice more with 30 ml of chloroform each time, and the extracts were combined and diluted to volume with chloroform. Dilution of 0.20 ml of chloroform solution to 25 ml with chloroform was performed, and the fluorescence was measured (Table II). The chloroform-wet filter paper blank was subtracted from each reading. A standard curve was prepared from standards of 0–10 × $10^{-3}$ *M* salicylamide treated in the same manner as the samples.

**Determination of Acetylsalicylic Acid**—The tablets or capsule contents were weighed and ground. The resulting homogeneous powder (50–300 mg of acetylsalicylic acid) was weighed into a 100-ml volumetric flask. Chloroform (75 ml) was added, and the solution was agitated for 10 min and diluted to volume with chloroform. The solution was filtered through medium-speed filter paper, and a 0.1-ml aliquot was diluted to 100 ml with 1% acetic acid–chloroform. The fluorescence was measured using the settings in Table II. A blank reading was subtracted from the sample fluorescence reading by running a chloroform blank for each lot of filter paper. A standard curve of fluorescence *versus* concentration was prepared using 0–1.7 × $10^{-5}$ *M* acetylsalicylic acid in 1% acetic acid–chloroform.

**Determination of Salicylic Acid in Salicylamide (No Acetylsalicylic Acid)**—Ten tablets or the contents of 10 capsules of samples without acetylsalicylic acid were weighed and ground to homogeneity. A portion of this powder (100 mg of salicylamide) was weighed into a 100-ml volumetric flask, and 75 ml of chloroform was added. The solution was agitated for 10 min and diluted to volume with chloroform. A suitable aliquot, such as 10 ml, was filtered through medium-speed filter paper and transferred to a 60-ml separator. Another 20 ml of chloroform was added with 10 ml of pH 7.0 phosphate buffer (24), the solution was extracted, and the chloroform layer was discarded. The process was repeated three more times with 30-ml chloroform volumes, and the chloroform was discarded.

The aqueous phase was extracted with 10 ml of chloroform and 2.0 ml of 2.0 *M* HCl. The chloroform layer was filtered through chloroform-wet filter paper into a 50-ml volumetric flask. The aqueous phase was extracted with two additional 10-ml portions of chloroform and filtered, and the three extracts were combined. The solution was diluted to volume, and the fluorescence of the solution was measured (Table II).

A blank was run on the filter paper using chloroform, and the blank reading was subtracted from the sample fluorescence reading. These readings were compared to a salicylamide control in the same concentration range as the sample (7.3 × $10^{-3}$ *M*) and salicylic acid standards (3.0–9.0 × $10^{-6}$ *M*), which were extracted in the same manner.

**Determination of Salicylic Acid in Salicylamide and Acetylsalicylic Acid**—The previous procedure was followed with the following changes: (*a*) the sample size contained 45 mg of acetylsalicylic acid; (*b*) on addition of the pH 7.0 buffer, the salicylic acid was extracted into chloroform as quickly as possible with a reproducible technique; (*c*) a suitable acetylsalicylic acid control in the 2.6 × $10^{-4}$ *M* range was substituted for the salicylamide control; and (*d*) salicylic acid standards in the 0.7–7.0 × $10^{-3}$ *M* range were used.

[8] Medium speed, Whatman.

## DISCUSSION

**UV Absorption of Salicylates and Related Compounds**—The removal of a proton from salicylamide alters its UV spectrum. In alcohol, the salicylamide anion is produced by saturation of the solution with small quantities of sodium bicarbonate or sodium carbonate. In aqueous solution or in methanol, this anion has twice the molar absorptivity of molecular salicylamide, and its UV maximum shifts to 330 nm (23). In contrast, salicylic acid does not exhibit this effect in aqueous solutions (23).

The molar absorptivities and wavelengths of maximum absorption of acetylsalicylic acid and salicylic acid in chloroform and 1% acetic acid–chloroform are not significantly different (8). Thus, the lowest energy electronic transition should be approximately the same in both solvent systems.

**Fluorescence of Salicylates and Related Compounds**—For salicylates and related compounds, emission in the 330–360-nm region of the spectrum has been postulated as arising from the neutral molecule (8, 25). Emission in the 400–450-nm region of the spectrum originates from the dipolar ion formed within the lifetime of the $S_1$ state *via* either inter- or intramolecular proton transfer (8, 25–28).

For salicylamide in methanol, the 340-nm emission is weak relative to that at 420 nm. The fluorescence emissions at 410 and 420 nm are postulated as arising from the zwitterion formed *via* intramolecular transfer within the lifetime of the $S_1$ state (26, 27). In methanolic solution, the 410-nm emission arising from the 333-nm excitation, which only occurs to a small extent, can be suppressed almost completely with small amounts of acid. In methanolic solution with traces of base, the UV maximum shifts from 300 to 330 nm and the emission at 410 nm is greatly enhanced because the 330-nm UV band is twice as intense as that of the neutral species and because the quantum yield for this form of the molecule is an estimated 20 times that of the neutral molecule. It then appears that the anion is more rigid than the molecular form of salicylamide,

**Table II—Instrumental Conditions for Spectrofluorometric Determinations**

| Ingredient Determined | Wavelength, nm | | Slit Width, nm | |
|---|---|---|---|---|
| | Excitation | Emission | Excitation | Emission |
| Salicylamide | | | | |
| In methanol | 300 | 425 | 10 | 10 |
| In chloroform | 315 | 445 | 10 | 20 |
| Acetylsalicylic acid | 280 | 335 | 10 | 20 |
| Salicylic acid | 315 | 445 | 10 | 10 |

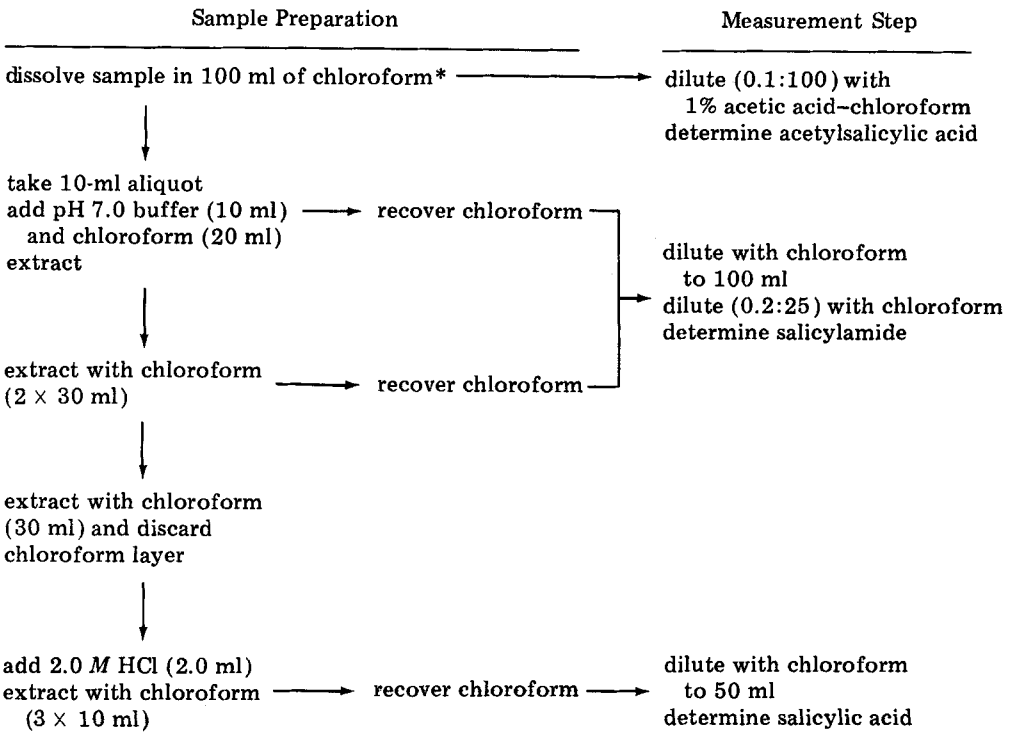


*Scheme I—Determination of salicylamide, acetylsalicylic acid, and/or salicylic acid in a multicomponent sample that may contain salicylamide, acetylsalicylic acid, acetaminophen, caffeine, and/or salicylic acid as an impurity. (* Sample must contain appropriate amounts of salicylamide and acetylsalicylic acid for subsequent determination of salicylamide, acetylsalicylic acid, and salicylic acid as an impurity.)*

possibly because the negatively charged oxygen atom can form a strong hydrogen bond to the adjacent *ortho* group. The molecular form thus will be less rigid, allowing an increase in the overall rate of internal conversion to the ground state. In addition to fluorescing in methanol, salicylamide also fluoresces weakly at 325 nm and intensely at 445 nm in chloroform.

In designing a fluorometric method for salicylamide, excitation was done at 300 nm rather than at the 310-nm excitation maximum. Excitation at 300 nm seemed to produce more reliable fluorescence emission readings since the 310-nm excitation is more sensitive to small changes in the quality of methanol. At this wavelength, good quality spectrograde methanol (which gives a low fluorescence emission blank) could be substituted for fluorescent grade solvent. Partly because pharmaceutical preparations contain basic buffers to reduce GI bleeding from aspirin, a possible fluorometric method for salicylamide in basic methanol solvent was tested. Saturation of methanol with sodium bicarbonate produced only partial (75%) conversion to the highly fluorescent anion, while saturation of methanol with sodium carbonate produced complete conversion. Other buffers such as magnesium carbonate, dihydrogen citrate, and magnesium hydroxide, which frequently are incorporated in pharmaceutical preparations, probably also could cause large variations in the 425-nm fluorescence emission. Inner filtering by acetaminophen, caffeine, and phenacetin was negligible.

The methodology was tested on several preparations with sodium carbonate-saturated methanol and 330-nm excitation. A further dilution (1:10) of the samples was required to keep the fluorescence readings on scale and the UV absorbance at the excitation wavelength low enough for negligible inner filtering. Although salicylamide was 100% converted to its anion, acetaminophen was converted only partially to its anion in this buffer. Large variations in the acetaminophen content of the sample, particularly when in combination with other buffers, may alter the percent conversion of salicylamide and/or acetaminophen to their anionic forms even in sodium carbonate-saturated methanol. (The anion of acetaminophen absorbs strongly and at longer wavelengths than the neutral molecule.) In addition, a previous study (3) reported that salicylamide decomposes in strong alkaline solution.

For excitation of samples at 300 nm in methanol, all samples must be excited under uniform conditions. The fluorescence emission readings increased in a reproducible manner with respect to the excitation time. For the most reliable readings, the sample should not be excited unless the fluorescence emission is to be read immediately.

The fluorescence of acetylsalicylic acid in chloroform and chloroform–aliphatic acid mixtures was described prviously (8). In methanol and methanol–1% acetic acid, acetylsalicylic acid does not appear to fluoresce as in the chloroform–aliphatic acid solvent systems.

A single fluorescence emission peak in both chloroform and methanol was observed for salicylic acid. For salicylic acid, intramolecular proton transfer to the excited carbonyl oxygen occurs within the lifetime of the lowest excited singlet state (25). In chloroform, low concentrations (1%) of various aliphatic acids produce an additional fluorescence emission band in the 350–400-nm region. In methanol, the fluorescence emission at 400 nm is diminished almost completely by 0.5% acetic acid when excited at 295 nm.

**Methodology**—The National Formulary specifies that salicylamide-containing tablets contain 100 ± 5.0% of the labeled content. The acetylsalicylic acid content of acetylsalicylic acid-containing capsules (NF) must be within 100 ± 7.0% of the labeled content, and tablets (USP) must contain 100 ± 5% of the labeled content. Neither the USP nor the NF have established limits of purity for salicylamide with respect to salicylic acid as an impurity, but both specify limits for purity of acetylsalicylic acid with respect to salicylic acid as an impurity (0.3% in capsules and 0.75% in tablets).

**Factors Affecting Fluorescence Assay Procedures for Salicylamide in Preparations Containing No Acetylsalicylic Acid, Salicylic Acid Impurity, or Buffers**—The salicylamide excitation band at 330 nm is extremely sensitive to solvent conditions. Thus, excitation at 330 nm was attempted in methanol, and then the specimen was reexcited after a trace of acetic acid was added. The difference between the two readings was linear in the $10^{-5}$ *M* range. Actual tablets contain ingredients that make this effect less useful for analytical purposes.

Other solvents were tested for analytical use. Although salicylamide fluoresced with greater efficiency in *n*-propanol and ethanol, *n*-propanol is not purified as easily as methanol, and ethanol is not as readily available. Chloroform was found to quench fluorescence.

Since acetaminophen, caffeine, and phenacetin also absorb in the region of salicylamide excitation, the possibility of an inner filter effect from any or all of these compounds was evaluated. At the levels normally present in pharmaceutical preparations, acetaminophen, caffeine, and phenacetin did not cause an inner filter effect in the present spectrofluorometric method.

## RESULTS

Results of spectrofluorometric determinations compared favorably with those of several reference methods when corrections were applied and the reference methodology was modified for suitable sample handling

**Table III—Determination of Salicylamide in Pharmaceuticals Containing No Acetylsalicylic Acid or Salicylic Acid Impurity**

| Preparation | Salicylamide Determined, mg: Reference Method | Salicylamide Determined, mg: Fluorescence | Percent Error |
|---|---|---|---|
| A[a] | 221 ± 9[b] | 218 ± 7[c] | −1.4 |
| B[c] | | | |
| Lot X | 239 ± 2[d,e] | 234 ± 5[d] | −2.1 |
| Lot Y | 251 ± 6[d,e] | 248.6 ± 2.3[f] | — |
| C[g] | 150.7[h,i] (152.5[h,j]) | 151.1 ± 1.0[k] | +0.3 (−0.9[j]) |
| | 146.4[b] | — | +3.2 |
| D[f] | 96.5[h,j] | 98.8 ± 0.4[k] | +2.4 |

[a] Unit dose analysis. [b] GLC using phenacetin as the internal standard. [c] Average of six determinations. [d] Average of four determinations. [e] Modification of Sunshine's salicylic acid method using Trinder's reagent (29). [f] Average of 12 determinations. [g] Aliquot representative of a unit dose taken from 10 unit doses combined and homogenized. [h] Differential UV. [i] Value corrected for error due to acetaminophen content. [j] Value not corrected for acetaminophen content. [k] Average of two determinations.

(Tables III–VI). Calibration curves were only linear to 100 mg/100 ml of salicylamide in the original sample ($7 \times 10^{-6}$ *M*) due to inner filtering; analytical results were most accurate when determined graphically with calibration standards that closely approximated the salicylamide concentration of the samples. When some of the same samples were excited at 313 nm in a filter fluorometer (mercury arc source), poor results were obtained due to the high amplification needed to measure the fluorescence emission.

**Determination of Salicylamide in Preparations Containing Acetylsalicylic Acid or Salicylic Acid Impurity**—If salicylic acid may be present, it is best to separate it from salicylamide before fluorescence analysis. Studies in this laboratory indicate that salicylamide is never completely recovered in chloroform at any pH by equal volume extractions (Fig. 1) and that better recoveries should result at a lower pH extraction than 5% sodium bicarbonate as previously reported (22). The behavior of acetylsalicylic acid and salicylic acid is similar; neither is extracted well with chloroform at pH > 5. At pH < 3, acetylsalicylic acid and salicylic acid extract significantly into chloroform. Therefore, any analytical separations must be done at pH 6–7.

The solubility of acetaminophen in chloroform is low (0.3 g/liter), and extraction into chloroform is not possible at any pH; therefore, accurate distribution ratio values, *D*, could not be determined. In contrast, caffeine is completely soluble in chloroform and is extracted so completely by chloroform over the pH range studied that accurate *D* values could not be determined for this compound either.

After three extractions, salicylamide was ~98% recovered from the aqueous phase. The salicylic acid, with ~50% of acetylsalicylic acid, remained in the aqueous phase at pH 7. After extraction with chloroform at this pH, all acetaminophen remained in the aqueous phase and all caffeine was in the chloroform with salicylamide. Solutions of molarities similar to those of the sample solutions were tested for inner filtering effects. No inner filtering by acetylsalicylic acid, acetaminophen, and caffeine was observed.

The effect of adding buffers to the pharmaceutical preparations was never critically evaluated. These compounds were assumed to be too insoluble in chloroform to alter the pH of the aqueous buffer (0.067 *M*) when equilibrated with it.

Although salicylamide has a larger molar absorptivity in chloroform than in methanol, it has a much lower quantum efficiency of fluorescence in chloroform. In spite of the former characteristic, accurate results are easily obtained in the 0–100-mg range. Self inner filtering begins at

**Table IV—Determination of Salicylamide in Pharmaceuticals Containing Acetylsalicylic Acid and Salicylic Acid as Impurity**

| Preparation | Salicylamide Determined, mg: Differential UV[a] | Salicylamide Determined, mg: Fluorescence | Percent Error[a] | Salicylamide[b], mg | Percent Error[b,c] |
|---|---|---|---|---|---|
| E | 102 | 96.7 | −5.4 | 96.1 | +0.6 |
| F | 66.8 | 62.1 | −7.0 | 64.1 | +1.1 |
| G | 134 | 130.4 | −2.7 | 129.6 | +0.6 |
| H | 134 | 128.2 | −4.3 | 127.8 | +0.3 |

[a] Differential UV uncorrected for interference due to the presence of acetylsalicylic acid and acetaminophen. [b] Differential UV corrected for the presence of acetylsalicylic acid and acetaminophen. [c] Calculated by $\%E^{a} - E_{\text{due to acetylsalicylic acid}} - \%E_{\text{due to acetaminophen}}$.

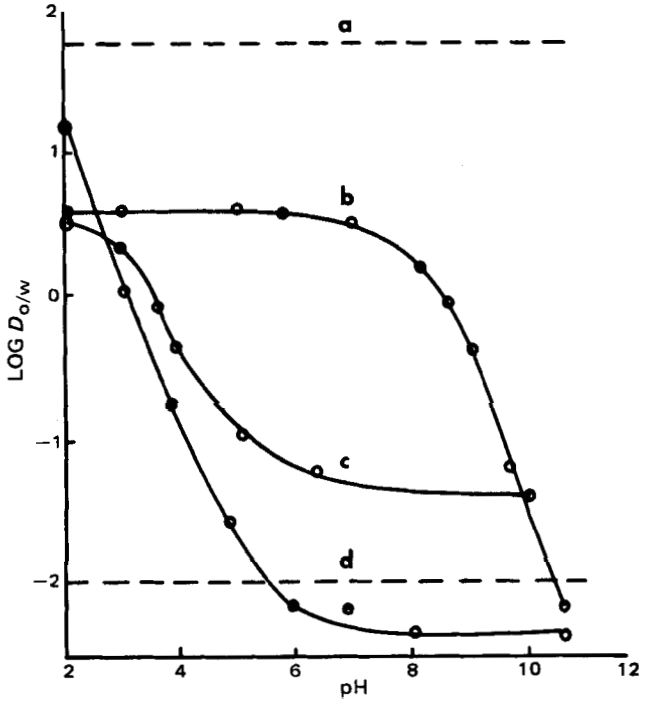


**Figure 1**—*Distribution of pharmaceuticals between chloroform and aqueous phosphate buffers. Key:* a, *caffeine;* b, *salicylamide;* c, *acetylsalicylic acid;* d, *acetaminophen; and* e, *salicylic acid.*

concentrations of >3 × $10^{-6}$ *M* salicylamide in the final solution. For accurate results, samples should be compared to extracted standards of similar salicylamide content. Comparison to extracted standards eliminates the need for extraction efficiency corrections; the extracted standards serve as controls.

**Determination of Acetylsalicylic Acid in Preparations Containing Salicylamide, Acetaminophen, and Caffeine**—Many problems associated with the fluorometric determination of acetylsalicylic acid in aspirin tablets have been solved (8), including excitation and emission wavelengths, concentration ranges, choice of a suitable solvent (level of acetic acid for enhancement of fluorescence), and elapsed time between dissolution and analysis. However, the effects of other constituents found in recent complex pain-relief preparations were never evaluated fully.

For example, caffeine has its UV maximum at the same wavelengths as acetylsalicylic acid and the acetylsalicylic acid–acetic acid complex but has approximately six times the molar absorptivity. At low caffeine to acetylsalicylic acid ratios (expressed in milligrams) in pharmaceutical preparations, caffeine was not found to inner filter. However, at ratios greater than 1:1 in preparations containing large amounts of acetylsalicylic acid, the absorbance at 280 nm was so large that inner filtering became significant. The presence of acetaminophen was never a problem at low acetaminophen to acetylsalicylic acid ratios (expressed in milligrams) but became a problem at ratios greater than 2:1 where large amounts of aspirin were being determined. Typical content ratios for these compounds in newer preparations are 0.1 < acetaminophen (milligrams)/acetylsalicylic acid (milligrams) < 1.0 and 0.0 < caffeine (milligrams)/acetylsalicylic acid (milligrams) < 0.4.

For the determination of acetylsalicylic acid in the presence of sali-

**Table V—Determination of Salicylic Acid in Pharmaceuticals Containing Salicylamide and No Acetylsalicylic Acid**

| Preparation | Salicylamide Content of Sample, mg | Determined by Fluorescence, mg | Correction for Extracted Salicylamide, mg | Salicylic Acid per Unit Dose, mg |
|---|---|---|---|---|
| A | 109 | 0.006 | −0.008 | −0.002 |
| B | | | | |
| Lot X | 164 | 0.013 | −0.011 | +0.002 |
| Lot Y | 169 | 0.013 | −0.011 | +0.002 |
| C | 92.0 | 0.004 | −0.006 | −0.002 |
| D | 84.0 | 0.004 | −0.006 | −0.002 |

Table VI—Determination of Acetylsalicylic Acid and Salicylic Acid as Impurity in Pharmaceuticals Containing Salicylamide

| Preparation | Acetylsalicylic Acid per Unit Dose, mg | | Percent Error | Salicylic Acid Determined by Fluorescence | |
|---|---|---|---|---|---|
| | Fluorescence[a] | Titration | | Salicylic Acid per Unit Dose, mg | Salicylic Acid with Respect to Acetylsalicylic Acid Content, % |
| E | 328.0 ± 0.8 | 323.4 ± 1.4 | +1.4 | 1.64 | 0.49 |
| F | 221.0 ± 3.5 | 213.3 ± 0.3 | +3.5 | 0.94 | 0.43 |
| G | 198.4 ± 0.6 | — | — | 0.46 | 0.23 |
| H | 210.2 ± 1.0 | 207.0 ± 0.5 | +1.7 | 1.15 | 0.55 |

[a] Triplicate analysis.

cylamide, several simultaneously competing effects are possible. Although salicylamide exhibits a UV minimum at 260 nm, it has a band at 270–340 nm with a molar absorptivity at 307 nm, which is approximately six times that of acetylsalicylic acid at its maximum. Hence, inner filtering of excitational radiation is possible where large amounts of acetylsalicylic acid are to be excited at 280 nm with a high weight ratio of salicylamide to acetylsalicylic acid. Since the 307-nm absorption band of salicylamide is extremely wide, inner filtering of the 335-nm acetylsalicylic acid emission also is possible. In addition, the 445-nm salicylamide emission band is broad so that a small positive interference from salicylamide emission actually is observed when measuring the acetylsalicylic acid emission at 335 nm. At smaller ratios of salicylamide to acetylsalicylic acid and small amounts of acetylsalicylic acid, the sum of these three effects is negligible. Typical content ratios in newer preparations are $0.2 \leq$ salicylamide (milligrams)/acetylsalicylic acid (milligrams) $\leq 1.3$.

Any pharmaceutical preparation containing acetaminophen and caffeine probably can be analyzed rapidly and accurately for acetylsalicylic acid content spectrofluorometrically. Any inner filtering can be avoided, at least in theory, by diluting the sample to <0.05 absorbance unit at 280 nm and using higher signal amplification. However, any positive error from salicylamide cannot be removed by dilution. At lesser content ratios, salicylamide does not contribute more than 1% positive error to the determination. Since the two emission peaks of the salicylamide–acetylsalicylic acid system are well resolved and can be read on approximately the same instrument sensitivity, multicomponent system calculations should be applicable if a large salicylamide to acetylsalicylic acid ratio is encountered.

Results of spectrofluorometric determinations compared favorably with nonaqueous titrations using chlorophenol red indicator. This indicator was not stable in the sample, and additional indicator was required as the titration proceeded; the end-point was still indistinct. In the end-point region, the kinetics of the titration became slow. The combination of these two titrimetric effects may have caused part of the overall positive error observed (Table VI). (Tablet Preparation F had the largest positive error but the lowest salicylamide to acetylsalicylic acid content ratio; the percent error due to salicylamide content was ~+0.3% for Preparations E and F and +0.6% for Preparations G and H.)

**Determination of Salicylic Acid in Salicylamide-Containing Pharmaceuticals**—Since salicylamide is separated so easily from salicylic acid, the salicylic acid content of salicylamide-containing pharmaceuticals should be negligible. Analysis of reagent grade salicylamide proved that the reagent contained significant amounts of salicylic acid; the salicylic acid content was not homogeneously distributed. Consequently, a method for the determination of salicylic acid content of salicylamide is necessary to ensure the purity of the salicylamide standard used for the direct spectrofluorometric analysis of salicylamide in methanol. This method also is applicable to pharmaceuticals containing salicylamide.

For the determination of salicylic acid in pharmaceuticals not containing acetylsalicylic acid, the only constituent of the sample solution prepared for analysis should be salicylic acid. In practice, small amounts of salicylamide appear in the final sample solution but can be compensated for by running a salicylic acid-free salicylamide control with the samples. The correction is linear from 50 to 300 mg of initial salicylamide content. Due to the reduced recovery of salicylic acid (89.4 ± 2.3%), samples should be compared to extracted standards to eliminate the need for percent recovery corrections. These standards also can serve as controls. With correction for residual salicylamide content, the detection limit for the determination of salicylic acid in samples containing 100 mg of salicylamide is ~0.05% of the total salicylamide content.

**Determination of Salicylic Acid in Pharmaceuticals Containing Salicylamide and Acetylsalicylic Acid**—One important problem in analyzing any preparation containing acetylsalicylic acid is that acetylsalicylic acid is hydrolyzed to salicylic acid in aqueous solution. At high pH, the acetylsalicylic acid is hydrolyzed immediately; in neutral and acid solution, the hydrolysis rate is slow enough that it can be compensated for accurately ($0.007 \pm 0.001_0$ mg/min and $0.001_2 \pm 0.000_3$ mg/min, respectively). In the present analyses, the hydrolysis rates were constant over the time required for the separation of acetylsalicylic acid from salicylamide, acetaminophen, and caffeine by extraction. The rates were not determined for various concentrations of acetylsalicylic acid so that the acetylsalicylic acid content of the initial sample in this method was limited to 45 ± 2 mg of acetylsalicylic acid. For best results, a previously analyzed USP grade acetylsalicylic acid control containing the same amount (within ±2 mg) of aspirin as in each sample should be processed with the samples and standards. Standards should be within the 0.01–0.1 mg of salicylic acid concentration range in the original sample. Any samples not within this range after extraction should be diluted and then remeasured.

In processing samples for salicylic acid determination, each sample must be extracted completely before the next sample is started rather than processing many samples simultaneously. (However, once in the final chloroform solution, the sample can be read within 1 hr.) This process keeps acetylsalicylic acid corrections small. The upper limit was set at 10 min for the extraction of each sample.

All of the preparations analyzed were within NF specifications with respect to the salicylic acid content.

## CONCLUSIONS

Fluorometric analysis of pharmaceutical preparations for salicylamide and acetylsalicylic acid and salicylic acid as an impurity in salicylamide-containing preparations is relatively free of interference from other associated compounds. This may not be the case with other reported methods that have never been evaluated for combination preparations. Analysis time is short, and results of determinations compare favorably with other reference methods for a wide variety of combination preparations.

## REFERENCES


(1) W. E. Lange, D. G. Floriddia, and F. J. Pruyn, *J. Pharm. Sci.*, **58,** 771 (1969).

(2) W. H. Barr and S. Riegelman, *ibid.*, **59,** 164 (1970).

(3) S. A. Veresh, F. S. Hom, and J. J. Miskel, *ibid.*, **60,** 1092 (1971).

(4) "The National Formulary," Mack Publishing Co., Easton, Pa., 1977, p. 1x. (1x references XIII ed. pp. 628, 629).

(5) "The United States Pharmacopeia," 19th rev., Mack Publishing Co., Easton, Pa., 1975, pp. 37, 38.

(6) N. Shane and M. Kowblansky, *J. Pharm. Sci.*, **57,** 1218 (1968).

(7) A. A. Vecchio, *Proanalysis*, **1,** 15 (1968); through *Chem. Abstr.*, **74,** 67762w (1971).

(8) G. H. Schenk, F. H. Boyer, C. I. Miles, and D. R. Wirz, *Anal. Chem.*, **44,** 1593 (1972).

(9) N. Shane and D. Miele, *J. Pharm. Sci.*, **59,** 397 (1970).

(10) J. D. Winefordner and M. W. Latz, *Anal. Chem.*, **35,** 1517 (1963).

(11) V. F. Cotty and H. M. Ederma, *J. Pharm. Sci.*, **55,** 837 (1966).

(12) L. Kanter and W. R. Horbaly, *ibid.*, **60,** 1898 (1971).

(13) M. Jones and R. L. Thatcher, *Anal. Chem.*, **23,** 957 (1951).

(14) R. B. Tinker and A. J. McBay, *J. Am. Pharm. Assoc., Sci. Ed.*, **43,** 315 (1954).

(15) C. A. Kelly, *J. Pharm. Sci.*, **59,** 1053 (1970).

(16) "The United States Pharmacopeia XX/The National Formulary XV," United States Pharmacopeial Convention, Rockville, Md., 1980, pp. 56–58.

(17) W. E. Juhl and R. D. Kirchhoefer, *J. Pharm. Sci.*, **69,** 544

(1980).
(18) N. Shane and R. Stillman, *ibid.*, **60,** 114 (1971).
(19) H. Bundgaard and C. Bundgaard, *J. Pharm. Pharmacol.*, **25,** 593 (1973).
(20) R. D. Kirchhoefer and W. E. Juhl, *J. Pharm. Sci.*, **69,** 548 (1980).
(21) R. D. Kirchhoefer, J. C. Reepmeyer, and W. E. Juhl, *ibid.*, **69,** 550 (1980).
(22) E. G. C. Clarke, "Isolation and Identification of Drugs," W. Clowes and Sons, London, England, 1969, p. 538.
(23) I. Sunshine and S. R. Gerber, "Spectrophotometric Analysis of Drugs," Charles C Thomas, Springfield, Ill., 1963, p. 27.
(24) R. J. Henry, D. C. Cannon, and J. W. Winkleman, "Clinical Chemistry–Principles & Technics," Harper and Row, New York, N.Y., 1974, p. 1592.
(25) A. Weller, *Z. Elektrochem.*, **60,** 1144 (1956).
(26) S. G. Schulman, P. J. Kovi, and J. F. Young, *J. Pharm. Sci.*, **62,** 1197 (1973).
(27) W. L. Paul and S. G. Schulman, *Anal. Chem.*, **45,** 415 (1973).
(28) J. F. Ireland and P. A. H. Wyatt, "Advances in Physical Organic Chemistry," vol. 12, Academic, New York, N.Y., 1976, pp. 193–195.
(29) I. Sunshine, "Methodology for Analytical Toxicology," CRC Press, Cleveland, Ohio, 1975, pp. 342, 343.

### ACKNOWLEDGMENTS

The authors thank the Wayne State University and the Wayne County Medical Examiner's Office for the use of their facilities.

# Continuous Flow Bead-Bed Dissolution Apparatus for Suppositories

**T. J. ROSEMAN ˣ, G. R. DERR, K. G. NELSON, B. L. LIEBERMAN, and S. S. BUTLER**

Received August 1, 1980, from the *Pharmacy Research Unit, The Upjohn Company, Kalamazoo, MI 49001.* Accepted for publication December 2, 1980.

**Abstract** □ A bead-bed dissolution apparatus for suppositories was evaluated by measuring the release of benzocaine from various vehicles. During dissolution, suppositories soften, deform, disintegrate, and eventually pass through a phase change from a solid to an oil. The control of the interfacial area during dissolution is a key factor in obtaining experimentally reproducible release data. The proposed suppository dissolution apparatus was designed to provide greater constancy of the exposed suppository area for dissolution. The apparatus consisted of a glass bead-bed containing the suppository. A continuous flow of liquid was passed through the bead-bed at a constant rate. Direct contact of the suppository was maintained with the dissolution medium, confining the suppository within the beads.

**Keyphrases** □ Suppositories—evaluation of a bead-bed dissolution apparatus, drug release rate □ Dissolution—bead-bed apparatus for suppositories, evaluation, drug release rate □ Drug release—suppositories, evaluation of a bead-bed dissolution apparatus

Benzocaine was selected as a model compound with both a low melting (33.5–35.5°) and a high melting (37–39°) glyceride-type suppository base. *In vitro* release of benzocaine decreased as the melting point of the suppository increased. Reproducibility of the complete release curves was acceptable. Drug release also was affected by the temperature of the dissolution media, increasing, decreasing, and increasing again at certain temperatures. This finding was related to the ability of the beads to penetrate the surface of the suppository when the suppository softened. Release profiles, however, were reproducible at the temperature studied. The proposed bead-bed dissolution apparatus should offer an improved means for measuring drug release from suppositories.

## BACKGROUND

Suppositories, administered either vaginally or rectally, are utilized as a dosage form for various drugs (1). Recent reports investigated the use of vaginally administered prostaglandins for fertility control and also emphasized certain advantages of this mode of drug therapy, *e.g.*, self-administration and single-dose therapy (2–9). This continued interest in suppositories and suppository bases (10) has led to the recognition that a dissolution test would be helpful during the initial phase of dosage form design. In addition, such a test would provide valuable information on the effect of storage time and temperature on the subsequent *in vitro* release profile.

The methods used for testing drug release rate characteristics of suppositories *in vitro* can be classified in terms of five general types (Fig. 1). The first type consists of simple placement of the suppository in a flask or beaker (11–15). The second type utilizes an existing tablet dissolution apparatus that provides a wire mesh basket for holding the sample (16–22). The third and fourth types employ a membrane; the third consists of a sample chamber separated from a reservoir by a membrane (23–33), whereas the fourth employs dialysis tubing or a natural membrane (33–46). The fifth type involves a flow system in which the sample is placed on cotton or a wire screen (47, 48).

One basic problem in testing for drug release from a suppository is that the suppository softens, deforms, melts, or disintegrates during the test, exposing a variable interfacial area to the dissolution medium. Because the release rate is dependent on the interfacial area, the variability of this factor leads to poor test reproducibility.

Membranes have been used to control the interfacial area on the principle that when the suppository softens, it would spread over the entire membrane, restricting the area exposed to the dissolution fluid. Bhavnagri and Speiser (24) designed a type three apparatus with a relatively small sample chamber. Others (39, 42) used a relatively small bag in a type four apparatus to restrict the interfacial area.

The need to control the interfacial area is important, but the intro-

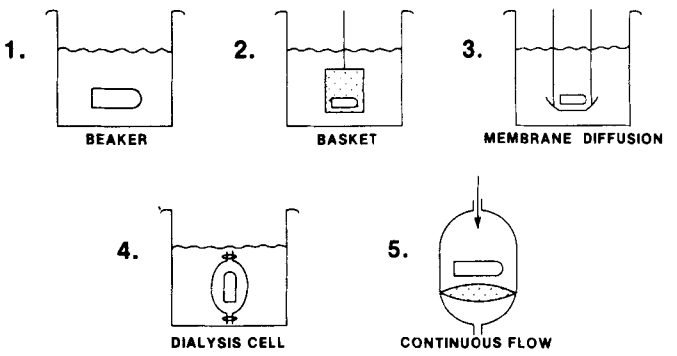


**Figure 1**—*Suppository dissolution methods.*



*0022-3549/81/0600-0646$01.00/0*
*© 1981, American Pharmaceutical Association*

(1980).
(18) N. Shane and R. Stillman, *ibid.*, **60,** 114 (1971).
(19) H. Bundgaard and C. Bundgaard, *J. Pharm. Pharmacol.*, **25,** 593 (1973).
(20) R. D. Kirchhoefer and W. E. Juhl, *J. Pharm. Sci.*, **69,** 548 (1980).
(21) R. D. Kirchhoefer, J. C. Reepmeyer, and W. E. Juhl, *ibid.*, **69,** 550 (1980).
(22) E. G. C. Clarke, "Isolation and Identification of Drugs," W. Clowes and Sons, London, England, 1969, p. 538.
(23) I. Sunshine and S. R. Gerber, "Spectrophotometric Analysis of Drugs," Charles C Thomas, Springfield, Ill., 1963, p. 27.
(24) R. J. Henry, D. C. Cannon, and J. W. Winkleman, "Clinical Chemistry–Principles & Technics," Harper and Row, New York, N.Y., 1974, p. 1592.
(25) A. Weller, *Z. Elektrochem.*, **60,** 1144 (1956).
(26) S. G. Schulman, P. J. Kovi, and J. F. Young, *J. Pharm. Sci.*, **62,** 1197 (1973).
(27) W. L. Paul and S. G. Schulman, *Anal. Chem.*, **45,** 415 (1973).
(28) J. F. Ireland and P. A. H. Wyatt, "Advances in Physical Organic Chemistry," vol. 12, Academic, New York, N.Y., 1976, pp. 193–195.
(29) I. Sunshine, "Methodology for Analytical Toxicology," CRC Press, Cleveland, Ohio, 1975, pp. 342, 343.

### ACKNOWLEDGMENTS

The authors thank the Wayne State University and the Wayne County Medical Examiner's Office for the use of their facilities.

# Continuous Flow Bead-Bed Dissolution Apparatus for Suppositories

**T. J. ROSEMAN ˣ, G. R. DERR, K. G. NELSON, B. L. LIEBERMAN, and S. S. BUTLER**

Received August 1, 1980, from the *Pharmacy Research Unit, The Upjohn Company, Kalamazoo, MI 49001.* Accepted for publication December 2, 1980.

**Abstract** □ A bead-bed dissolution apparatus for suppositories was evaluated by measuring the release of benzocaine from various vehicles. During dissolution, suppositories soften, deform, disintegrate, and eventually pass through a phase change from a solid to an oil. The control of the interfacial area during dissolution is a key factor in obtaining experimentally reproducible release data. The proposed suppository dissolution apparatus was designed to provide greater constancy of the exposed suppository area for dissolution. The apparatus consisted of a glass bead-bed containing the suppository. A continuous flow of liquid was passed through the bead-bed at a constant rate. Direct contact of the suppository was maintained with the dissolution medium, confining the suppository within the beads.

**Keyphrases** □ Suppositories—evaluation of a bead-bed dissolution apparatus, drug release rate □ Dissolution—bead-bed apparatus for suppositories, evaluation, drug release rate □ Drug release—suppositories, evaluation of a bead-bed dissolution apparatus

Benzocaine was selected as a model compound with both a low melting (33.5–35.5°) and a high melting (37–39°) glyceride-type suppository base. *In vitro* release of benzocaine decreased as the melting point of the suppository increased. Reproducibility of the complete release curves was acceptable. Drug release also was affected by the temperature of the dissolution media, increasing, decreasing, and increasing again at certain temperatures. This finding was related to the ability of the beads to penetrate the surface of the suppository when the suppository softened. Release profiles, however, were reproducible at the temperature studied. The proposed bead-bed dissolution apparatus should offer an improved means for measuring drug release from suppositories.

## BACKGROUND

Suppositories, administered either vaginally or rectally, are utilized as a dosage form for various drugs (1). Recent reports investigated the use of vaginally administered prostaglandins for fertility control and also emphasized certain advantages of this mode of drug therapy, *e.g.*, self-administration and single-dose therapy (2–9). This continued interest in suppositories and suppository bases (10) has led to the recognition that a dissolution test would be helpful during the initial phase of dosage form design. In addition, such a test would provide valuable information on the effect of storage time and temperature on the subsequent *in vitro* release profile.

The methods used for testing drug release rate characteristics of suppositories *in vitro* can be classified in terms of five general types (Fig. 1). The first type consists of simple placement of the suppository in a flask or beaker (11–15). The second type utilizes an existing tablet dissolution apparatus that provides a wire mesh basket for holding the sample (16–22). The third and fourth types employ a membrane; the third consists of a sample chamber separated from a reservoir by a membrane (23–33), whereas the fourth employs dialysis tubing or a natural membrane (33–46). The fifth type involves a flow system in which the sample is placed on cotton or a wire screen (47, 48).

One basic problem in testing for drug release from a suppository is that the suppository softens, deforms, melts, or disintegrates during the test, exposing a variable interfacial area to the dissolution medium. Because the release rate is dependent on the interfacial area, the variability of this factor leads to poor test reproducibility.

Membranes have been used to control the interfacial area on the principle that when the suppository softens, it would spread over the entire membrane, restricting the area exposed to the dissolution fluid. Bhavnagri and Speiser (24) designed a type three apparatus with a relatively small sample chamber. Others (39, 42) used a relatively small bag in a type four apparatus to restrict the interfacial area.

The need to control the interfacial area is important, but the intro-

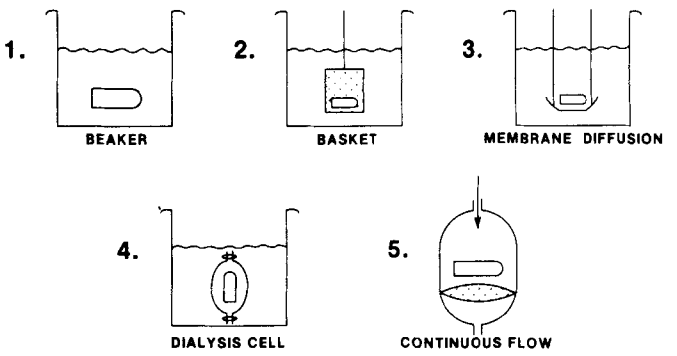


**Figure 1**—*Suppository dissolution methods.*



*0022-3549/81/0600-0646$01.00/0*
*© 1981, American Pharmaceutical Association*

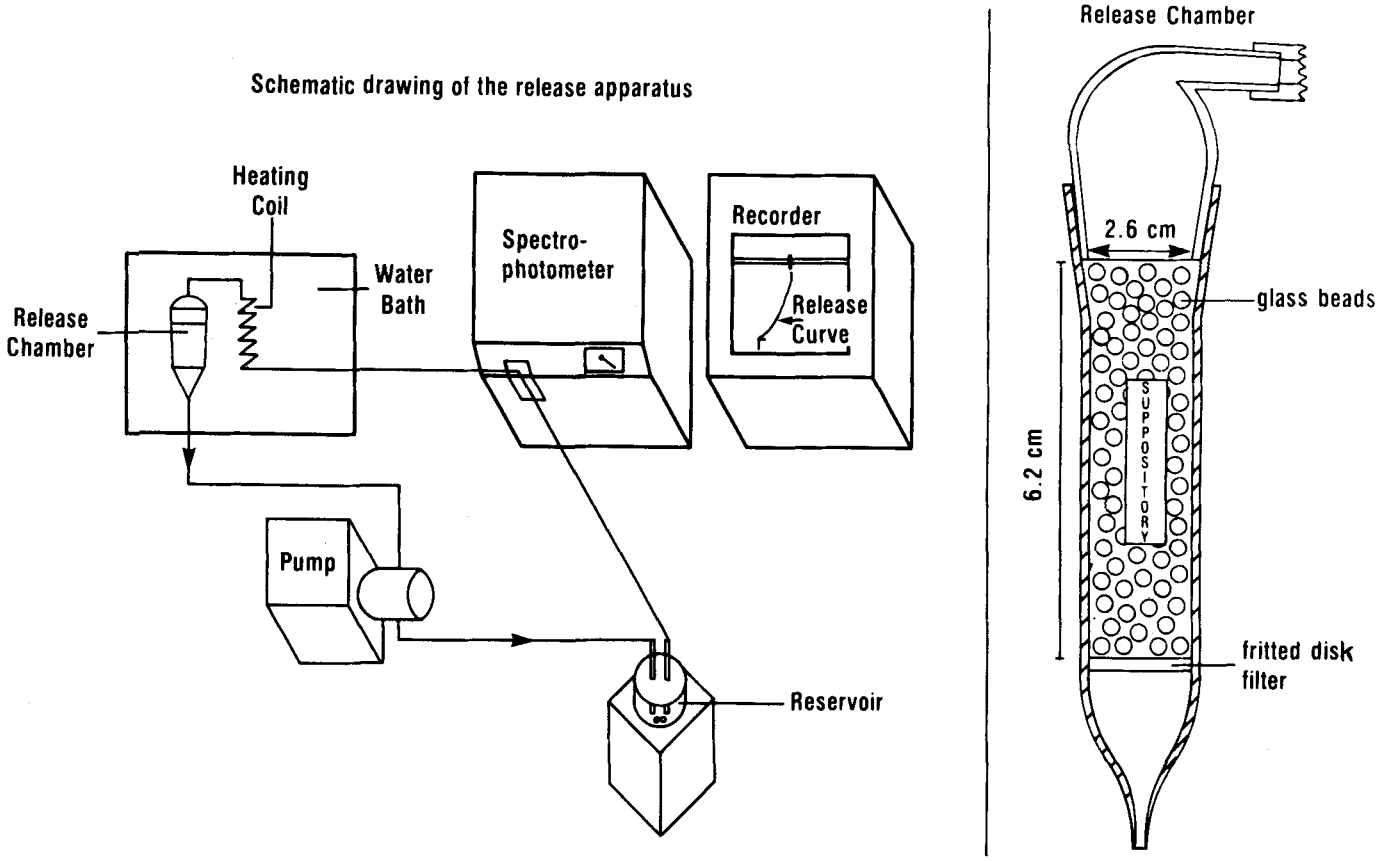


**Figure 2**—*Continuous flow bead-bed suppository dissolution apparatus.*

duction of an additional physical process, *i.e.*, membrane transport, complicates matters and may mask the real release characteristics for certain drug–suppository base combinations. Therefore, a flow-through technique was developed in which the suppository is secured in a bed of glass beads. This arrangement controls the interfacial area for most suppository bases, yet allows direct contact between the suppository and the dissolution medium.

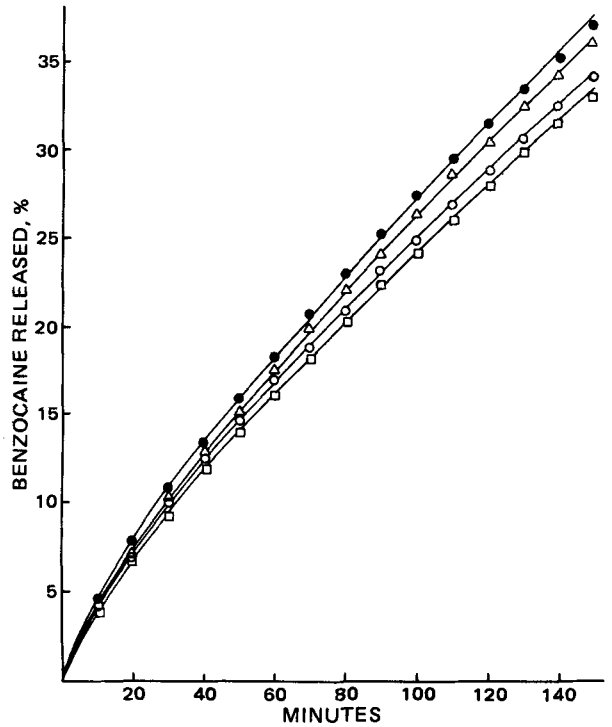


**Figure 3**—*Release of benzocaine from Base A suppositories on different days at 37° (original dissolution chamber). Key: ●, Day 1; ○, Day 2; □, Day 3; and △, Day 3.*

## EXPERIMENTAL

**Suppository Preparation**—The suppositories were prepared by first dissolving an appropriate amount of benzocaine[1] (ethyl *p*-aminobenzoate) in the melted base to yield a benzocaine concentration of 0.125% (w/w). The suppository bases, designated A[2] for the low melting (33.5–35.5°) and B[3] for the higher melting (37–39°), were melted at 5–10° above their melting points. The melt then was poured into aluminum suppository molds and allowed to cool at room temperature, and the excess base was scraped away after solidification. The molds were cooled further at room temperature (Base A) or in a refrigerator (Base B) for 30 min, and then the suppositories were ejected from the molds.

The molds consisted of tapered cavities drilled into an aluminum block. The taper permitted easy removal of the suppositories. The suppositories were 800 mg, 1.91 cm long, and 0.75 and 0.79 cm in diameter at the ends. The amount of benzocaine in each suppository was 1.0 mg.

**Design of Release Apparatus**—The release rate apparatus was designed to provide reasonable control over the interfacial area for drug dissolution (Fig. 2). A continuous eluent flow is maintained over the suppository contained in a bed of glass beads. The eluent starts in the 150-ml jacketed beaker, which is covered with an acrylic resin disk. When the pump[4] is started, water is drawn through polyethylene tubing (3 mm o.d. × 2 mm i.d.) from the 150-ml jacketed beaker to a 1-cm flowcell in the UV spectrophotometer[5]. From the spectrophotometer, the water is drawn into a preheating glass coil (glass automated analyzer coil, 1.5 cm in diameter × 16 cm in length). The glass coil is submerged in the water bath[6] to allow the water temperature to equilibrate before reaching the sample chamber, which also is submerged in the water bath. The water leaves the glass coil and enters the sample chamber from the top.

[1] Pfaltz & Bauer, Stamford, Conn.
[2] Witepsol H-15, Dynamit Nobel Chemical, Oberlar, West Germany.
[3] Witepsol E-76, Dynamit Nobel Chemical, Oberlar, West Germany.
[4] Lab pump RRP, Fluid Metering Inc., Oyster Bay, N.Y.
[5] Beckman DB with recorder, Beckman Instruments, Fullerton, Calif.
[6] Tamson PMT, Neslab Instruments, Portsmouth, N.H.

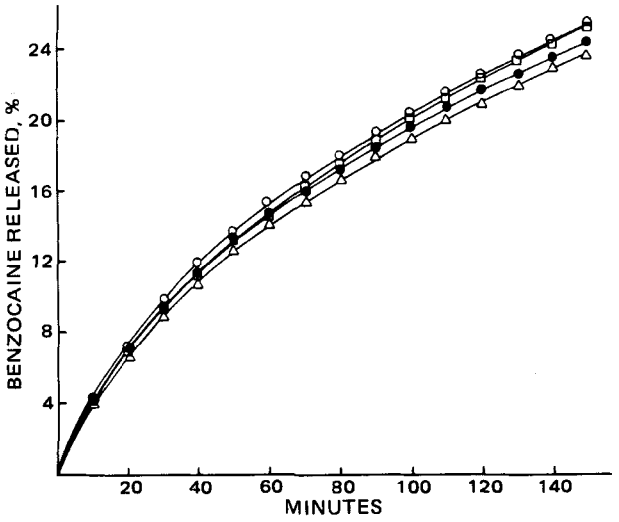


**Figure 4**—*Release of benzocaine from Base B suppositories on different days at 37° (original dissolution chamber). Key: ●, Day 1; ○, Day 1; □, Day 3; and △, Day 3.*

Originally, the chamber consisted of two 15-ml Büchner fritted disk filters connected at the top by Tygon tubing and a clamp. The present chamber consists of two sections. The bottom section is a 15-ml coarse Büchner fritted disk filter modified with a 24/40 glass joint at the top and an outlet tube narrowed to 4 mm o.d. × 2 mm i.d. The top half is a 24/40 hose-connecting joint modified with an inlet tube narrowed to 4 mm o.d. × 2 mm i.d. The water travels through the glass bead-bed (3-mm diameter, chemically resistant glass balls) and around the suppository. The dimensions of the cell containing the beads is 2.6 cm i.d. and 6.2 cm long. The original chamber was 2.3 cm i.d. and 4.6 cm long. The water leaves the test chamber, is drawn into the pump, and is pumped back into the 150-ml jacketed beaker, which is stirred by a magnetic stirrer.

**Procedure**—Before a release rate experiment was begun, a water baseline was established by adding 130 ml of deionized water to the 150-ml jacketed beaker. The water bath was adjusted to the appropriate temperature, and the system and water were allowed to equilibrate. Temperature was controlled within ±0.1°. The test chamber then was half-filled with glass beads. A weighed suppository was inserted into the center of the chamber, using a plunger assembly that allowed the operator to position the suppository reproducibly. The remainder of the chamber was filled with glass beads, and its upper section was connected. The chamber then was lowered into the water bath along with the glass coil and fixed into an upright position. The pump was started immediately in the reverse direction, allowing the water to fill the test chamber from the bottom up. As soon as the entire system was filled, the flow was reversed so that the water flowed from top to bottom in the chamber.

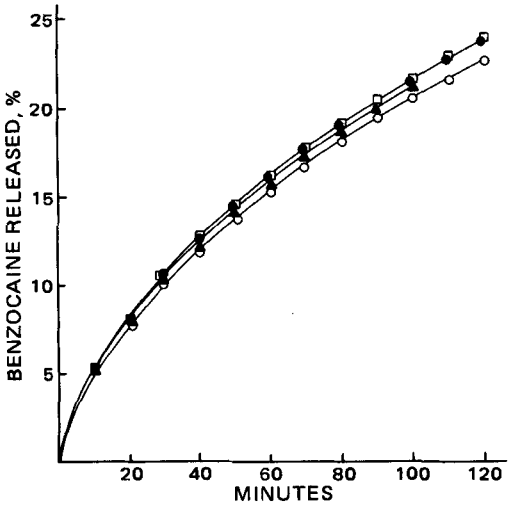


**Figure 5**—*Replicate 37° dissolution experiments for the release of benzocaine from Base B using the modified dissolution cell. Key: ○ and □, Day 1; and ▲ and ●, Day 2.*

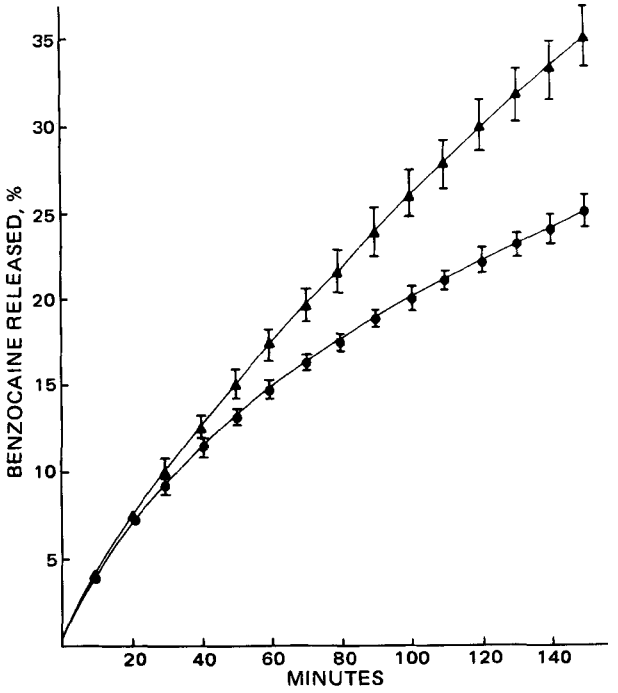


**Figure 6**—*Comparative release of benzocaine from Base A (▲) and B (●) suppositories at 37°.*

The flow rate was controlled at 30 ± 0.5 ml/min. Drug release was monitored with a UV spectrophotometer (282 nm) equipped with a recorder. The cumulative amount released with time was calculated from the recorder tracings by converting absorbance to concentration and multiplying by the volume of the dissolution medium. Before each run, the UV spectrophotometer was checked with two solutions of known benzocaine concentrations to assure that absorbance was linear with concentration.

## RESULTS AND DISCUSSION

The concept of a flow system employing a bed of beads was shown to be useful for studying dissolution rates of solids. A system for testing tablets and granules in which the sample is placed within the bed was described previously (49). Reproducible dissolution rates for drug powders were obtained (50) by mixing the powder with a diluent and placing the mixture between two layers of glass beads in a flowcell. Rippie and Huq (51) used a flowcell containing several layers of glass beads in which the bead size was reduced successively. Drug powder, introduced at the top, then migrated through the bed as dissolution occurred. These recent reports demonstrate the distinctness of this type of system opposed to the usual vessel and flow systems used for dissolution testing.

Suppository drug release is influenced by factors such as: drug–vehicle interactions; vehicle composition; crystalline form of the vehicle (polymorph); solubility, partition coefficient, and drug permeability in the vehicle; particle size of the drug (dispersed system); and drug concentration in the vehicle. Experimental parameters such as the temperature of the dissolution solvent and flow rate should influence the observed release patterns.

This report presents a preliminary evaluation of the continuous flow bead-bed concept using two types of suppository bases with benzocaine as the model compound. Benzocaine was selected because benzocaine suppositories are marketed and because it has a UV-absorbing chromophore that allows it to be easily assayed.

The two suppository bases (A and B) were mixtures of glycerides of fatty acids. They possess physicochemical properties representative of the many vehicles purchased from commercial suppliers (10) and have been studied with several different prostaglandins (3–5).

Figures 3 and 4 show the release profiles of benzocaine in duplicate from Bases A and B, respectively, on each of 2 different days, using the original dissolution chamber. Figure 5 gives the release profiles from the new chamber. These data indicate that there was no major difference between the two chambers (*i.e.*, within 10%).

The replicate runs were performed within 3 days to avoid any potential effects of a polymorphic change of the base on the drug release rate. The

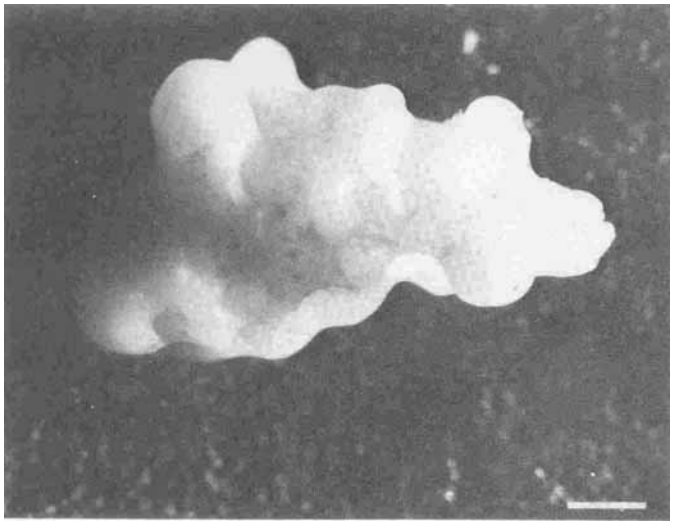

BASE A

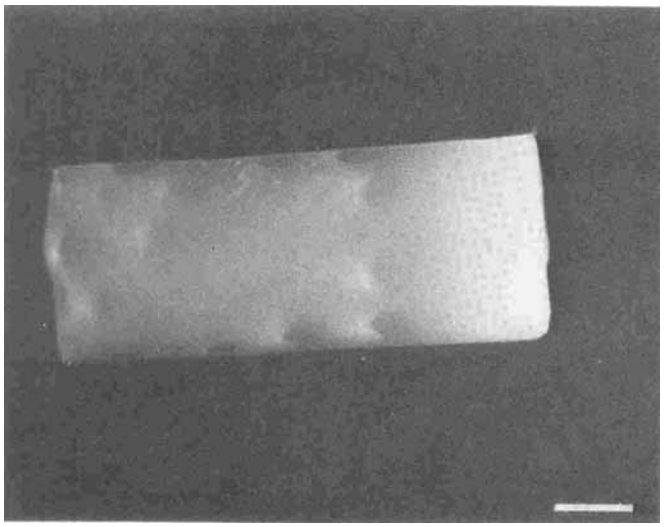

BASE B

**Figure 7**—*Photographs of suppositories after 2 hr (37°) in the bead-bed dissolution apparatus. Scale marker = 0.31 cm.*

thermal behavior of Base B (with benzocaine) was verified by differential scanning calorimetry; these scans were invariant with time[7]. The dissolution results indicate very good reproducibility of the data. Comparisons of the 15 time points on the curves from four runs gave an average relative standard deviation of 6.13% for Base A and 3.36% for Base B. Therefore, 95% of the time the complete release profile will be reproduced with a 13% variation for Base A and a 7% variation for Base B.

Release from the bases is compared in Fig. 6. The bars represent the standard deviation of the points. The percentages of benzocaine released during the first 30 min were similar, but the lower melting Base A exhibited a much faster release at later times. Figure 7 shows the physical form of the two bases after 2 hr in the bead-bed at 37°. They were allowed to solidify at room temperature before removal.

The low melting Base A softened and stayed within a confined region of the bead-bed. The higher melting Base B maintained its form, showing slight indentations from the beads. Suppositories of these types do not show complete melting at 37° but rather a softening of the suppository matrix. At temperatures well above their melting points, total liquefaction takes place. The degree to which the beads actually penetrate the suppository depends on the thermal behavior of a given suppository.

The similar early release of benzocaine from the two bases most likely results from the fact that they initially are both rigid. It requires time

[7] After ~1 month of storage at 25°, the differential scanning calorimetric curves began to change with a concomitant decrease in the release profiles. Alteration in the thermal behavior of semisynthetic bases was recently reported (52).

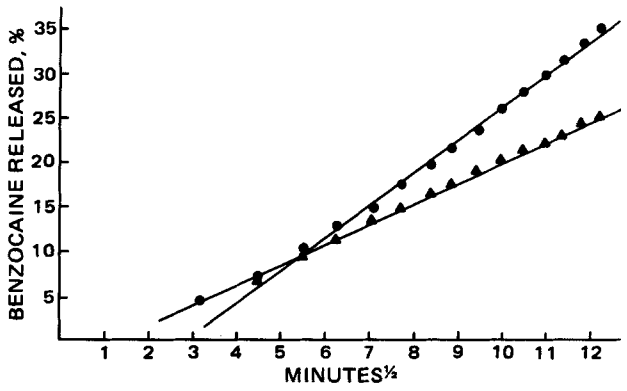


**Figure 8**—*Release of benzocaine, plotted as the square root of time, from Base A (●) and B (▲) suppositories at 37°.*

before the suppositories soften sufficiently to detect significant differences in release. Visual examination of Base A after 5 and 20 min supported this view. After this time, bead penetration restricts the area for drug release. Therefore, *in vitro* release from Base A is actually higher than observed. Plots of the percent released *versus* the square root of time were linear with correlation coefficients of 0.990 and 0.996, respectively (Fig. 8). This type of release kinetics follows the matrix-controlled release theory previously developed (53). It is particularly applicable to Base B, which maintained its shape (constant surface area) during the test period.

To investigate bead penetration further, the influence of temperature on the release of benzocaine from Base B was studied in more detail. Release curves as a function of temperature are presented in Fig. 9. The release profiles did not increase as a direct function of temperature. For example, release increased from 33 to 37°, with 39 and 40° data being comparable to the 33° run.

The fastest release profile was achieved at 45° where complete melting of the base occurred. At first, this overall temperature dependence seemed surprising. However, close examination of the physical state of the suppository in the beads provided the reason for this behavior. While the suppository was in the dissolution apparatus, it softened and eventually melted. As it softened, the beads became impressed within the suppository (Fig. 10). At 39 and 40°, the beads penetrated the surface of the suppository, thereby reducing the surface area available for drug release. Once the base melted completely (*e.g.*, 45°), release increased again due to the spreading of the oil in the bead-bed. At this temperature, oil globules were found floating at the top of the beads. Although release was temperature dependent, it was reproducible at the temperatures studied. This finding supports the continued evaluation and development of this apparatus, which is particularly well suited for suppositories that reasonably maintain their shape during the dissolution process.

In view of the influence of the beads on release at temperatures that

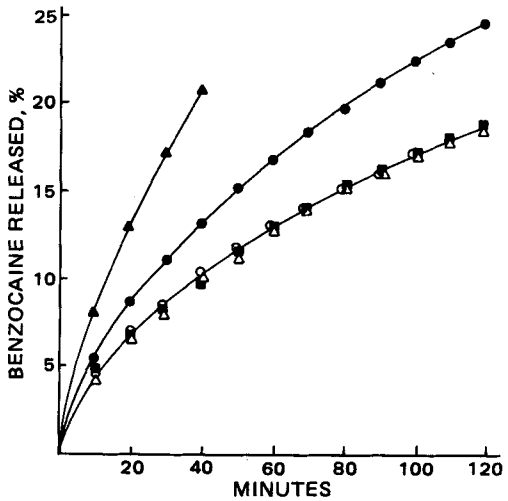


**Figure 9**—*Dependence of benzocaine release from Base B suppositories as a function of temperature. Key: ▲, 45°; ■, 40°; ○, 39°; ●, 37°; and △, 33°.*

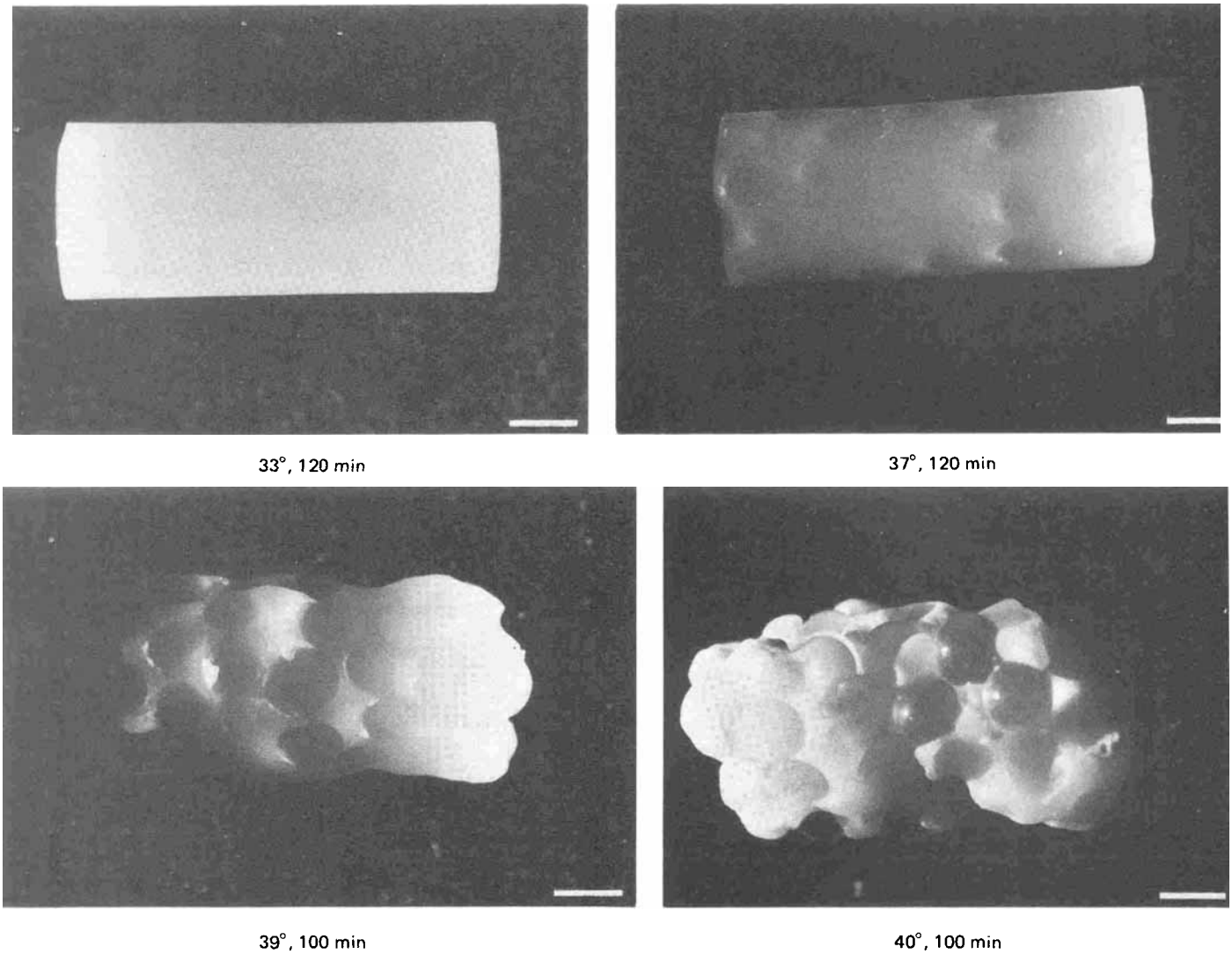


**Figure 10**—*Photographs of Base B suppositories after ~2 hr (37°) in the bead-bed dissolution apparatus. Scale marker = 0.31 cm.*

cause deformation of the base, further refinements of the bead-bed apparatus are anticipated. Consideration will be given to maintaining the beads in a stationary position, thereby eliminating the dynamics of bead penetration. This can be accomplished by using a preformed bead cavity as a mold or a porous gel instead of the beads.

## REFERENCES

(1) "Sprowl's American Pharmacy," L. W. Dittert, Ed., Lippincott, Philadelphia, Pa., 1974.

(2) T. O. Oesterling, W. Morozowich, and T. J. Roseman, *J. Pharm. Sci.*, **61**, 1861 (1972).

(3) M. Mandelin, *Prostaglandins*, **16**, 143 (1978).

(4) M. Bygdeman, J. N. Martin, A. Leader, V. Lundstrom, M. Ramadan, P. Eneroth, and K. Green, *Obstet. Gynecol.*, **48**, 221 (1976).

(5) N. H. Lauersen and K. H. Wilson, *Prostaglandins*, **10**, 1037 (1975).

(6) F. A. Kimball, G. L. Bundy, A. Robert, and J. R. Weeks, *ibid.*, **17**, 657 (1979).

(7) V. Lundstrom, M. Bygdeman, S. Fotiou, K. Green, and K. Kinoshita, *Contraception*, **16**, 167 (1977).

(8) "Obstetric and Gynaecological Uses of Prostaglandins," S. M. M. Karim, Ed., Asian Federation of Obstetrics and Gynaecology, 1st Inter-Congress, Singapore, Apr. 27–30, 1976.

(9) T. J. Roseman, G. D. Gutknecht, R. G. Stehle, and E. M. Southern, *Am. J. Obstet. Gynecol.*, **129**, 225 (1977).

(10) "The Theory and Practice of Industrial Pharmacy," L. Lachman, H. A. Lieberman, and J. L. Kanig, Eds., Lea & Febiger, Philadelphia, Pa., 1970.

(11) C. W. Whitworth and J. P. LaRocca, *J. Am. Pharm. Assoc., Sci. Ed.*, **48**, 353 (1959).

(12) A. J. M. Schoonen, F. Moolenaar, C. Haverschmidt, and T. Huizinga, *Pharm. Weekbl.*, **111**, 585 (1976).

(13) H. M. Gross and C. H. Becker, *J. Am. Pharm. Assoc., Sci. Ed.*, **42**, 96 (1953).

(14) S. N. Pagay, R. I. Poust, and J. L. Colaizzi, *J. Pharm. Sci.*, **63**, 44 (1974).

(15) P. Vaghy and P. Vaghy, *Gyogyszereszet*, **22**, 27 (1978).

(16) C. J. deBlaey and J. J. Rutten-Kingma, *Pharm. Acta Helv.*, **52**, 11 (1977).

(17) I. W. Kellaway and C. Marriott, *J. Pharm. Sci.*, **64**, 1162 (1975).

(18) V. E. Krogerus and M. Tolvi, *Acta Pharm. Suec.*, **2**, 327 (1965).

(19) E. L. Parrott, *J. Pharm. Sci.*, **64**, 878 (1975).

(20) L. Roller, *Aust. J. Hosp. Pharm.*, **7**, 97 (1977).

(21) S. E. Leucuta, L. Popa, M. Ariesan, L. Popa, R. D. Pop, M. Kory, and S. Toader, *Pharm. Acta Helv.*, **52**, 261 (1977).

(22) A. Puech, Y. Lasserre, and M. Jacob, *Trav. Soc. Pharm. Montpellier*, **37**, 165 (1977).

(23) L. Bardet and J. Cemeli, *ibid.*, **16**, 200 (1956).

(24) V. P. Bhavnagri and P. Speiser, *Pharm. Acta Helv.*, **51**, 10 (1976).

(25) M. A. Ghafoor and C. L. Huyck, *Am. J. Pharm.*, **134**, 63 (1962).

(26) A. A. Kassem, E. N. El-Din, A. A. El-Bary, and H. M. Fadel, *Pharmazie*, **30**, 472 (1975).

(27) L. Krowczynski, *Acta Pol. Pharm.*, **19**, 127 (1962).

(28) Z. Kubiak, *Gyogyszereszet*, **21**, 322 (1977).

(29) V. H. Muhlemann and R. H. Neuenschwander, *Pharm. Acta*

*Helv.*, **31**, 305 (1956).
(30) M. Kapas, E. Regdon, and G. Regdon, *Acta Pharm. Technol.*, **25**, 109 (1979).
(31) G. Regdon, A. Magyarlaki, G. Kedvessy, E. Minker, and E. Regdon, *Pharmazie*, **33**, 67 (1978).
(32) R. Voigt and G. Falk, *ibid.*, **23**, 709 (1968).
(33) G. B. Carp, D. Brossard, C. Chemtob, and J. C. Chaumeil, *Sci. Tech. Pharm.*, **7**, 159 (1978).
(34) W. H. Thomas and R. McCormack, *J. Pharm. Pharmacol.*, **23**, 490 (1971).
(35) T. Stozek, *Pol. J. Pharmacol. Pharm.*, **27**, 227 (1975).
(36) L. Turakka and V. E. Krogerus, *Farm. Aikak.*, **83**, 59 (1974).
(37) *Ibid.*, **83**, 105 (1974).
(38) J. M. Plaxco, Jr., C. B. Free, Jr., and C. R. Rowland, *J. Pharm. Sci.*, **56**, 809 (1967).
(39) J. W. Ayres, D. Lorskulsint, A. Lock, L. Kuhl, and P. A. Laskar, *ibid.*, **65**, 832 (1976).
(40) C. G. Hartman, *Ann. N.Y. Acad. Sci.*, **83**, 318 (1959).
(41) H. P. M. Kerckhoffs and T. Huizinga, *Pharm. Weekbl.*, **102**, 1187, 1255 (1967).
(42) C. F. Peterson and A. J. Guida, *J. Am. Pharm. Assoc., Sci. Ed.*, **42**, 537 (1953).
(43) H. Piasecka and Z. Zakrzewski, *Pol. J. Pharmacol. Pharm.*, **28**, 199 (1976).
(44) W. A. Ritschel and M. Banarer, *Arzneim.-Forsch.*, **23**, 1031 (1973).
(45) S. Tsuchiya, M. Hiura, and H. Matsumaru, *Chem. Pharm. Bull.*, **25**, 667 (1977).
(46) W. A. Ritschel and J. Rotmensch, *Pharm. Int.*, **3**, 4 (1974).
(47) M. R. Baichwal and T. V. Lohit, *J. Pharm. Pharmacol.*, **22**, 427 (1970).
(48) H. W. Puffer and W. J. Crowell, *J. Pharm. Sci.*, **62**, 242 (1973).
(49) U. Bogs and A. Darr, *Pharm. Praxis*, **31**, 169 (1976).
(50) F. Langenbucher and H. Rettig, *Drug Dev. Ind. Pharm.*, **3**, 241 (1977).
(51) E. G. Rippie and A. Huq, *J. Pharm. Sci.*, **68**, 938 (1979).
(52) L. J. Coben and N. G. Lordi, *ibid.*, **69**, 955 (1980).
(53) T. Higuchi, *ibid.*, **52**, 1145 (1963).

# Effect of Caffeine on Ergotamine Absorption from Rat Small Intestine

**JOHN R. ANDERSON, GERTRUDE DREHSEN, and IAN H. PITMAN ˣ**

Received July 24, 1980, from the *Victorian College of Pharmacy Ltd., Parkville, Victoria, Australia 3052.* Accepted for publication December 2, 1980.

**Abstract** □ The effect of caffeine on the absorption of ergotamine from the rat small intestine was studied. The results of a series of experiments showed that caffeine significantly enhanced absorption of ergotamine from solutions of pH 5.0 when both substances were in solution and when an intact blood supply was either absent (*in vitro* everted sac experiments) or present (*in situ* experiments). Caffeine did not appear to influence the absorption rate of ergotamine in *in situ* experiments when the solution pH was 3.0. Isosorbide dinitrate, a vasodilator, enhanced ergotamine absorption when both substances were administered simultaneously into intestinal loops *in situ*. Isosorbide dinitrate probably exerts its effect by increasing blood flow to the intestine. The results are consistent with an hypothesis that the rate-determining step in ergotamine absorption is the transport of the drug from a lipid phase (GI membrane) into an aqueous phase (blood). Caffeine is thought to exert its rate-accelerating effect by increasing the water solubility of ergotamine neutral molecules.

**Keyphrases** □ Caffeine—effect on ergotamine absorption from rat small intestine, *in vitro* and *in vivo* studies □ Ergotamine—effect of caffeine on absorption from rat small intestine, *in vitro* and *in vivo* studies □ Absorption—ergotamine, effect of caffeine on absorption from rat small intestine, *in vitro* and *in vivo* studies □ Analgesics—ergotamine, effect of caffeine on absorption from rat small intestine, *in vitro* and *in vivo* studies

Ergotamine tartrate is widely used in the treatment of migraine (1, 2). When administered parenterally, it is effective in relieving migraine pain (3, 4), but oral administration often affords no relief (5, 6). Regardless of the route, ergotamine must be administered early in an attack to be effective (7). The frequent failure of oral ergotamine therapy appears to be related to its relatively low water solubility (1:500) and the fact that its absorption from the GI tract into the systemic circulation often is slow or impaired during a migraine attack (4–9).

Simultaneous oral administration of caffeine and ergotamine results in more effective therapy than ergotamine administered alone (10–12). Recent pharmacokinetic studies in humans indicated faster and more complete absorption of ergotamine after oral administration when it is combined with caffeine (13). Zoglio *et al.* (14) conducted *in vitro* experiments to elucidate the mechanism by which caffeine enhances ergotamine absorption; caffeine increased the solubility and dissolution rates of ergotamine in 0.1 *M* HCl and in 0.1 *M* phosphate buffer (pH 6.65) and was claimed to accelerate the partitioning of ergotamine from an aqueous (pH 6.65) to an organic (chloroform) phase. These observations led to the conclusion that the solubilizing effect of caffeine on ergotamine in water is the major factor in its enhancement of oral ergotamine migraine therapy.

The present study was undertaken to determine the effect, if any, that caffeine has on ergotamine absorption across the rat small intestine when both substances are dissolved.

## EXPERIMENTAL

**Ergotamine Assay**—Ergotamine concentrations were calculated from the results of reversed-phase high-performance liquid chromatographic (HPLC) assays (15). The mobile phase was acetonitrile–1% sodium acetate/acetic acid buffer (55:45) at pH 6.5. The stationary phase was a 10/25 ODS column, and ergotamine was detected by fluorescence spectrometry ($\lambda_{ex}$ = 325 nm; $\lambda_{em}$ = 407 nm).

***In Vitro* Studies (Everted Sac Technique)**—Adult male Hooded Wistar rats, 240–280 g, were fasted in cages designed to prevent coprophagy for at least 12 hr before sacrifice. Water was allowed *ad libitum*. The rats were killed by a blow on the head. The small intestine was removed immediately, rinsed with Krebs–Henselite solution, sleeved onto a glass rod, and everted carefully. The first 15 cm, beginning with the pylorus, was discarded, and the next 8-cm segment was used in the experiments.

The segment was attached to a cannula at the proximal end, trimmed to 7 cm, and ligated at the distal end so that 6 cm of the everted intestine

0022-3549/81/0600-0651$01.00/0
© 1981, American Pharmaceutical Association

*Helv.*, **31**, 305 (1956).
(30) M. Kapas, E. Regdon, and G. Regdon, *Acta Pharm. Technol.*, **25**, 109 (1979).
(31) G. Regdon, A. Magyarlaki, G. Kedvessy, E. Minker, and E. Regdon, *Pharmazie*, **33**, 67 (1978).
(32) R. Voigt and G. Falk, *ibid.*, **23**, 709 (1968).
(33) G. B. Carp, D. Brossard, C. Chemtob, and J. C. Chaumeil, *Sci. Tech. Pharm.*, **7**, 159 (1978).
(34) W. H. Thomas and R. McCormack, *J. Pharm. Pharmacol.*, **23**, 490 (1971).
(35) T. Stozek, *Pol. J. Pharmacol. Pharm.*, **27**, 227 (1975).
(36) L. Turakka and V. E. Krogerus, *Farm. Aikak.*, **83**, 59 (1974).
(37) *Ibid.*, **83**, 105 (1974).
(38) J. M. Plaxco, Jr., C. B. Free, Jr., and C. R. Rowland, *J. Pharm. Sci.*, **56**, 809 (1967).
(39) J. W. Ayres, D. Lorskulsint, A. Lock, L. Kuhl, and P. A. Laskar, *ibid.*, **65**, 832 (1976).
(40) C. G. Hartman, *Ann. N.Y. Acad. Sci.*, **83**, 318 (1959).
(41) H. P. M. Kerckhoffs and T. Huizinga, *Pharm. Weekbl.*, **102**, 1187, 1255 (1967).
(42) C. F. Peterson and A. J. Guida, *J. Am. Pharm. Assoc., Sci. Ed.*, **42**, 537 (1953).
(43) H. Piasecka and Z. Zakrzewski, *Pol. J. Pharmacol. Pharm.*, **28**, 199 (1976).
(44) W. A. Ritschel and M. Banarer, *Arzneim.-Forsch.*, **23**, 1031 (1973).
(45) S. Tsuchiya, M. Hiura, and H. Matsumaru, *Chem. Pharm. Bull.*, **25**, 667 (1977).
(46) W. A. Ritschel and J. Rotmensch, *Pharm. Int.*, **3**, 4 (1974).
(47) M. R. Baichwal and T. V. Lohit, *J. Pharm. Pharmacol.*, **22**, 427 (1970).
(48) H. W. Puffer and W. J. Crowell, *J. Pharm. Sci.*, **62**, 242 (1973).
(49) U. Bogs and A. Darr, *Pharm. Praxis*, **31**, 169 (1976).
(50) F. Langenbucher and H. Rettig, *Drug Dev. Ind. Pharm.*, **3**, 241 (1977).
(51) E. G. Rippie and A. Huq, *J. Pharm. Sci.*, **68**, 938 (1979).
(52) L. J. Coben and N. G. Lordi, *ibid.*, **69**, 955 (1980).
(53) T. Higuchi, *ibid.*, **52**, 1145 (1963).

# Effect of Caffeine on Ergotamine Absorption from Rat Small Intestine

**JOHN R. ANDERSON, GERTRUDE DREHSEN, and IAN H. PITMAN ˣ**

Received July 24, 1980, from the *Victorian College of Pharmacy Ltd., Parkville, Victoria, Australia 3052.* Accepted for publication December 2, 1980.

**Abstract** □ The effect of caffeine on the absorption of ergotamine from the rat small intestine was studied. The results of a series of experiments showed that caffeine significantly enhanced absorption of ergotamine from solutions of pH 5.0 when both substances were in solution and when an intact blood supply was either absent (*in vitro* everted sac experiments) or present (*in situ* experiments). Caffeine did not appear to influence the absorption rate of ergotamine in *in situ* experiments when the solution pH was 3.0. Isosorbide dinitrate, a vasodilator, enhanced ergotamine absorption when both substances were administered simultaneously into intestinal loops *in situ*. Isosorbide dinitrate probably exerts its effect by increasing blood flow to the intestine. The results are consistent with an hypothesis that the rate-determining step in ergotamine absorption is the transport of the drug from a lipid phase (GI membrane) into an aqueous phase (blood). Caffeine is thought to exert its rate-accelerating effect by increasing the water solubility of ergotamine neutral molecules.

**Keyphrases** □ Caffeine—effect on ergotamine absorption from rat small intestine, *in vitro* and *in vivo* studies □ Ergotamine—effect of caffeine on absorption from rat small intestine, *in vitro* and *in vivo* studies □ Absorption—ergotamine, effect of caffeine on absorption from rat small intestine, *in vitro* and *in vivo* studies □ Analgesics—ergotamine, effect of caffeine on absorption from rat small intestine, *in vitro* and *in vivo* studies

Ergotamine tartrate is widely used in the treatment of migraine (1, 2). When administered parenterally, it is effective in relieving migraine pain (3, 4), but oral administration often affords no relief (5, 6). Regardless of the route, ergotamine must be administered early in an attack to be effective (7). The frequent failure of oral ergotamine therapy appears to be related to its relatively low water solubility (1:500) and the fact that its absorption from the GI tract into the systemic circulation often is slow or impaired during a migraine attack (4–9).

Simultaneous oral administration of caffeine and ergotamine results in more effective therapy than ergotamine administered alone (10–12). Recent pharmacokinetic studies in humans indicated faster and more complete absorption of ergotamine after oral administration when it is combined with caffeine (13). Zoglio *et al.* (14) conducted *in vitro* experiments to elucidate the mechanism by which caffeine enhances ergotamine absorption; caffeine increased the solubility and dissolution rates of ergotamine in 0.1 *M* HCl and in 0.1 *M* phosphate buffer (pH 6.65) and was claimed to accelerate the partitioning of ergotamine from an aqueous (pH 6.65) to an organic (chloroform) phase. These observations led to the conclusion that the solubilizing effect of caffeine on ergotamine in water is the major factor in its enhancement of oral ergotamine migraine therapy.

The present study was undertaken to determine the effect, if any, that caffeine has on ergotamine absorption across the rat small intestine when both substances are dissolved.

## EXPERIMENTAL

**Ergotamine Assay**—Ergotamine concentrations were calculated from the results of reversed-phase high-performance liquid chromatographic (HPLC) assays (15). The mobile phase was acetonitrile–1% sodium acetate/acetic acid buffer (55:45) at pH 6.5. The stationary phase was a 10/25 ODS column, and ergotamine was detected by fluorescence spectrometry ($\lambda_{ex}$ = 325 nm; $\lambda_{em}$ = 407 nm).

***In Vitro* Studies (Everted Sac Technique)**—Adult male Hooded Wistar rats, 240–280 g, were fasted in cages designed to prevent coprophagy for at least 12 hr before sacrifice. Water was allowed *ad libitum*. The rats were killed by a blow on the head. The small intestine was removed immediately, rinsed with Krebs–Henselite solution, sleeved onto a glass rod, and everted carefully. The first 15 cm, beginning with the pylorus, was discarded, and the next 8-cm segment was used in the experiments.

The segment was attached to a cannula at the proximal end, trimmed to 7 cm, and ligated at the distal end so that 6 cm of the everted intestine

0022-3549/81/0600-0651$01.00/0
© 1981, American Pharmaceutical Association

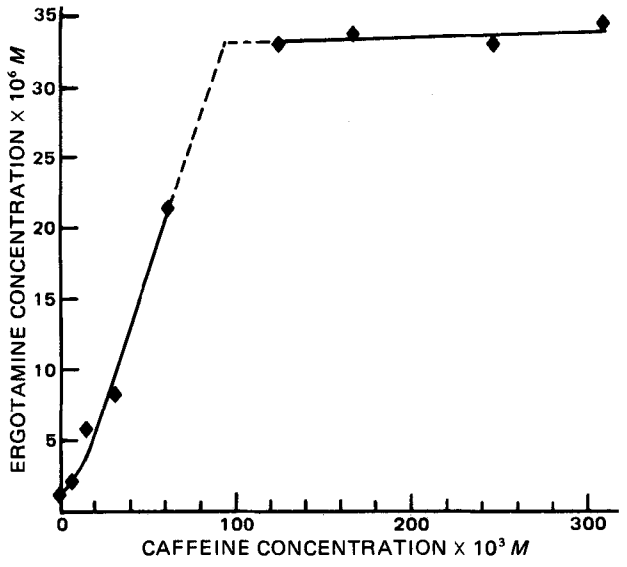


**Figure 1**—*Solubilizing effect of caffeine on ergotamine in pH 8.5 boric acid buffer. The shape of the diagram between* $[caffeine]_T = 60 \times 10^{-3}$ M *and* $120 \times 10^{-3}$ M *was not determined. The initial solid phase was ergotamine tartrate.*

was exposed to the drug solution. The intestinal sac was maintained in a vertical position during the experiment. The organ bath was filled with 60.0 ml of buffered drug solution (mucosal solution), which was maintained at 37.0 ± 0.1° and continuously gassed with 95% $O_2$–5% $CO_2$. The inner (serosal) solution consisted of 0.6 ml of buffer.

The buffer for the mucosal and serosal solutions consisted of Krebs–Henseleit solution–0.1 *M* sodium acetate (9:1), buffered to pH 5.0 with acetic acid. Quinine sulfate (0.5 mg/ml) was included to act as the internal standard in the ergotamine assay. In all experiments, the mucosal solution was the same as the serosal solution plus 0.1 mg of ergotamine tartrate/ml. In permeation experiments involving the rate of ergotamine transfer across the membrane in the presence of caffeine, 10 mg of caffeine/ml was included in the mucosal and serosal solutions.

During the experiments, 10-μl samples were withdrawn from the serosal solution at indicated times and assayed for ergotamine by the HPLC method described previously (15). The concentration of ergotamine transferred across the membrane was expressed as a percentage of the ergotamine concentration in the mucosal solution. The transfer rates were determined from the slope of a plot of log (100 − percent of ergotamine absorbed) *versus* time.

***In Situ* Studies**—Five loops of intestine (12 cm in length) were prepared in each rat according to the method described previously (16). The total volume of test solution introduced into each loop was 1.0 ml.

Two types of experiments were conducted: "time zero" studies, in which the intestine was removed from the rat immediately after the test solutions were placed in the loops, and "absorption" studies, in which the intestine remained *in situ* within the abdominal cavity of the rat for 2.5 hr before being removed.

The absorption characteristics of ergotamine tartrate were investigated in the presence of two additives, caffeine and isosorbide dinitrate. The caffeine experiments were conducted at pH 3 (0.1 *M* tartaric acid–sodium hydroxide buffer), 5 (sodium acetate–acetic acid buffer), and 6 (0.1 *M* citric acid–sodium hydroxide buffer). In the isosorbide dinitrate experiments, all test and control solutions introduced into the loops were prepared in the pH 5.0 acetate buffer, which also contained 10% dimethyl sulfoxide to solubilize the isosorbide dinitrate. The ergotamine tartrate concentration was 0.05, 0.1, or 0.2 mg/ml, the caffeine concentration was either 10 or 20 mg/ml, and the isosorbide dinitrate concentration was 2 mg/ml.

In the caffeine experiments, two loops contained an ergotamine tartrate solution at a particular concentration while another two loops contained ergotamine tartrate at the same concentration plus a particular concentration of caffeine. The remaining loop in each rat contained the appropriate buffer solution (blank loop) and served as a reference for the assay. The contents of the five loops were randomized on the basis of rows from a 5 × 5 Latin square. Five rats were used at each ergotamine tartrate and caffeine combination to complete the Latin square.

In the isosorbide dinitrate experiments, two different methods of allocating the solutions to particular loops were used. One was on the basis of a 5 × 5 Latin square, with two loops containing ergotamine tartrate solution, two loops containing ergotamine tartrate plus isosorbide dinitrate solution, and the remaining loop containing the reference solution. The second method involved placing only one type of test solution into all five loops of two rats.

At the end of each experiment, the small intestine was removed from the rat, trimmed of its mesentery and blood vessels, and rinsed in 0.9% (w/v) NaCl solution. The length of each loop was measured and recorded. The individual loops were placed in separate homogenization flasks and manually chopped as finely as possible. Five milliliters of 1.0% (w/v) tartaric acid solution was added to each flask, and the contents were homogenized for 10 min.

The homogenates were transferred quantitatively with 10 ml of absolute ethanol to centrifuge tubes. These homogenates were centrifuged at 2000×*g* for 10 min, and the supernates were decanted into 50-ml volumetric flasks. Each precipitate was resuspended and washed with three 10-ml portions of 70% ethanol and centrifuged as before, and the washings were combined with their corresponding supernates. Five milliliters of a 200-μg/ml quinine sulfate (HPLC assay internal standard) solution in 70% ethanol was added to each flask. The combined solutions were filtered through 0.80-μm membrane filters to remove solid material before they were assayed (15). Ergotamine that could not be recovered by this method was considered to have been absorbed.

A preliminary experiment was conducted to ensure that the rat intestinal secretions did not significantly alter the pH values of the test solutions during absorption. Five milliliters of the pH 5.0 acetate buffer was introduced into the rat small intestine. After 2.5 hr, the intestine was removed from the abdominal cavity, and the fluid in the lumen of the intestine was collected. The intestinal fluid was filtered through a 0.22-μm membrane filter, and the filtrate pH was measured.

**Solubility Studies**—Excess quantities of ergotamine tartrate (50 mg) were placed in 25-ml screw-capped vials together with varying, but accurately weighed, amounts of caffeine (0–480 mg) and 10 ml of pH 8.5 borate buffer (4.5 ml of 0.2 *M* boric acid and 5.5 ml of 0.05 *M* borax). The vials were placed in a constant-temperature water bath and shaken for 48 hr at 25°. Preliminary studies were conducted to determine the time required for the solutions to reach equilibrium.

The total amount of ergotamine in each equilibrated solution was determined by filtering the vial contents through a 0.22-μm membrane filter and analyzing for ergotamine concentration using the previously described HPLC method (15).

## RESULTS

**Solubility Studies**—The phase solubility diagram, obtained by saturation of caffeine solutions in pH 8.5 boric acid buffers with ergotamine tartrate, is shown in Fig. 1. The addition of 0.124 *M* caffeine increased ergotamine solubility at pH 8.5 from $1.25 \times 10^{-6}$ to $3.29 \times 10^{-5}$ *M*. Additional caffeine did not significantly alter ergotamine solubility.

***In Vitro* Studies (Everted Sac Technique)**—The absorption of ergotamine across the rat small intestine was initially studied using a modification of a reported everted sac technique (17). The volume of liquid and the concentration of quinine sulfate (internal standard) on both the serosal and mucosal sides of the everted intestine did not change appreciably during the experiment. Therefore, it was concluded that no net transfer of water or of quinine sulfate took place.

The transfer rates of ergotamine across the membrane were calculated from the slopes of plots of log (100 − percent of ergotamine absorbed) *versus* time (Fig. 2). A *t* test indicated that caffeine significantly increased the transfer rate of ergotamine from solution across the isolated rat intestine ($p < 0.001$).

***In Situ* Studies Involving Caffeine and Ergotamine**—The *in situ* technique used to measure the absorption[1] of ergotamine from the rat small intestine was based on a method developed in these laboratories by Admans *et al.* (16). It was a modification of the technique of Levine and Pelikan (18), which allows absorption of drugs from single or multiple intestinal loops to be measured.

Ergotamine solutions were introduced into four intestinal loops in an anesthetized rat, and a blank solution was introduced into a fifth loop. After 2.5 hr, the loops and their contents were homogenized separately and assayed for ergotamine. The amount of ergotamine absorbed was calculated from the difference between the amount administered and the amount remaining and was expressed as the percent absorbed.

A minor complication in calculating the amount of ergotamine remaining arose because HPLC chromatograms of ergotamine tartrate solutions that had been in the rat gut for 2.5 hr contained two more peaks than those observed for an ergotamine solution. The additional peaks

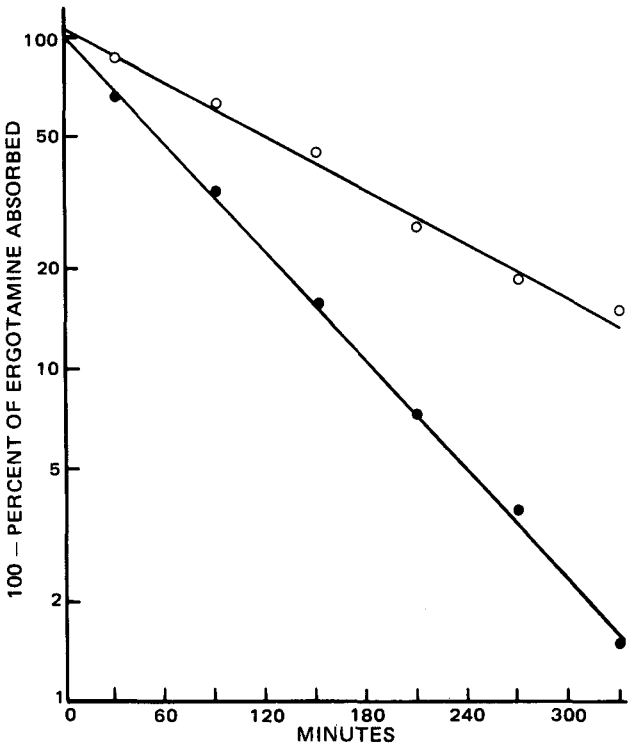


**Figure 2**—*Semilogarithmic plot against time of (100 − percent of ergotamine absorbed) in everted rat gut experiments. Key: ○, 0.1 mg of ergotamine tartrate/ml, slope = $-6.23 \times 10^{-3}$/min; and ●, 0.1 mg of ergotamine tartrate/ml plus 10 mg of caffeine/ml, slope = $-1.26 \times 10^{-2}$/min.*

had retention times of 6.5 and 7.5 min, whereas the ergotamine peak had a retention time of 9.0 min. Typical chromatograms that were measured from experiments conducted at pH 3 and 5 are shown in Fig. 3. In the experiments at pH 3.0, the metabolites or degradation product peaks were barely apparent. At pH 5.0, the metabolism was greater than at pH 3.0 but still relatively slight. When experiments at pH 6.0 were attempted, little ergotamine remained in the loops after 2.5 hr and the metabolites were significant, thereby making quantitation of absorption difficult.

Ergotaminine, an isomer of ergotamine that results from epimerization at C-8 (19), gave a peak with a retention time of 6.5 min. Thus, it was concluded that ergotaminine was one degradation product. Because fluorescence of ergotaminine is 2.5 times greater than that of ergotamine (20), it was estimated that the ratio of the amount of ergotaminine to the original amount of ergotamine after 2.5 hr at pH 5.0 was 0.03:1. Thus, conversion by metabolism of ergotamine to ergotaminine is unlikely to affect the results significantly.

The extraneous peak with a retention time of 7.5 min was twice as intense as that of ergotaminine. The nature of the compound causing this peak is uncertain, but it is likely to be *aci*-ergotamine or *aci*-ergotaminine, which is formed by the inversion of ergotamine or ergotaminine at the 2′-position (19). These compounds are more polar than ergotamine (21) and are expected to be eluted earlier with the mobile phase employed. Although the fluorescence intensity of the *aci* compounds is not known, it is unlikely that they would fluoresce much less strongly than ergotamine.

In the absence of more precise information, it was assumed that the fluorescence of the metabolites was similar to that of ergotamine. Hence, ergotamine concentrations that remained were derived by summing the areas under the peaks for ergotamine and its metabolites. This procedure should introduce a maximum error of ±10% into the results[1].

***In Situ* Studies**—*pH Value of Intestinal Contents*—The pH of the intestinal contents 2.5 hr after introduction of the pH 5.0 acetate buffer was 5.3. The pKa value of ergotamine is 6.4 (22). Therefore, at least 90%

[1] A reviewer pointed out that the above experiments do not distinguish between absorption and loss of ergotamine due to metabolism if the metabolites are themselves absorbed. This point is accepted but, in the absence of other information, the good correlations between the effect of caffeine on ergotamine absorption in *in vitro* and *in situ* experiments and the low probability that caffeine appreciably influences ergotamine metabolism are accepted as points that support the discussion in the manuscript.

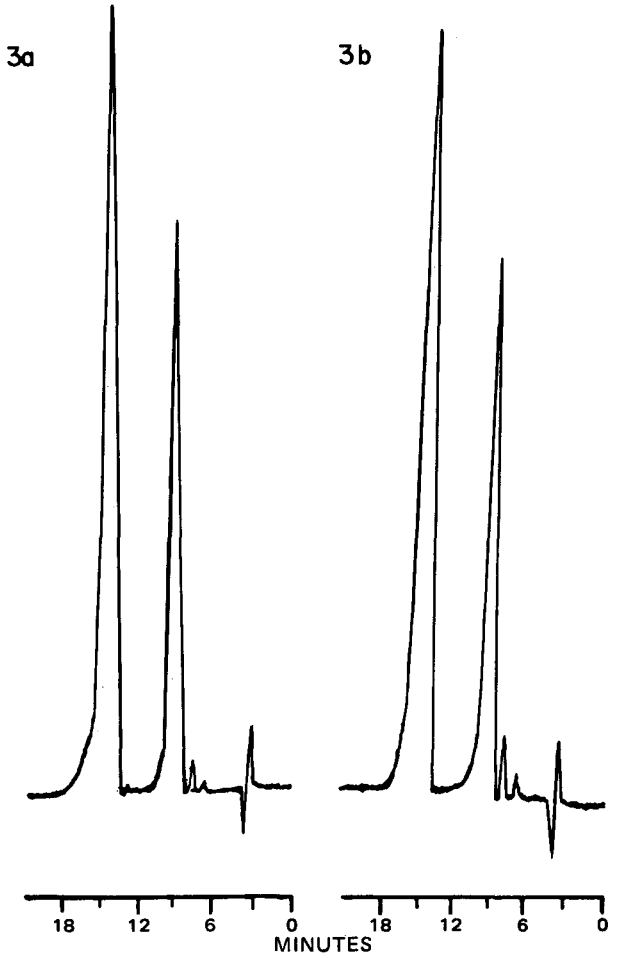


**Figure 3**—*Chromatograms of extracts from* in situ *rat intestinal homogenates. Experiments were conducted at pH 3.0 (a) and 5.0 (b). The peaks eluted after 9 and 15 min were ergotamine and quinine, respectively.*

of the ergotamine existed in the ionized form and remained in solution throughout the study. It also was found that a 0.2-mg/ml solution of ergotamine tartrate could be obtained at pH 5.3. Since the maximum concentration of ergotamine tartrate introduced into the intestinal loops was 0.2 mg/ml, all of the ergotamine in the intestinal loops, either by itself or in the presence of caffeine, probably remained in solution throughout the absorption experiments conducted at pH 5 or below.

*Significance of Blank Loop and Effect of Loop Length*—Ergotamine could disappear from a loop by either absorption into the blood or lymphatic system or by leakage into an adjoining loop. Ergotamine also could possibly be reabsorbed from the blood into the lumen of a loop. However, no ergotamine was detected in the loop containing the blank solution. Hence, it was concluded that ergotamine that had disappeared from a loop was absorbed.

An analysis of variance of the results indicated that the variation in loop length that occurred with this technique had no significant effect on the percentage of the administered amount of ergotamine absorbed from the loops ($p > 0.1$).

*Effect of Caffeine*—In the experiments designed to test the reliability of the recovery process (time zero studies), loops containing either 0.2 mg of ergotamine tartrate/ml alone or 0.2 mg of ergotamine tartrate/ml plus 20 mg of caffeine/ml were removed and assayed immediately after introduction of the test solutions into the loops. At pH 5.0, the mean recovery of ergotamine from 10 loops (five rats) was 97 ± 3%. The mean recovery of ergotamine in the presence of caffeine from 10 loops (five rats) was 98 ± 3%. At pH 3.0, the recoveries were 95 ± 6% for ergotamine tartrate solution (four loops) and 96 ± 1% for ergotamine tartrate and caffeine solution (four loops).

Analysis of variance conducted on these results indicated that caffeine had no significant effect on the recovery of ergotamine from loops at pH 3.0 ($p > 0.1$) or 5.0 ($p > 0.1$) and that the loop position (*i.e.*, distance from the pylorus) had no significant effect on the amount of ergotamine re-

**Table I—Extent of Ergotamine Absorption from *In Situ* Rat Small Intestinal Loops after 2.5 hr in the Presence and Absence of Caffeine**

| pH | Ergotamine Tartrate, mg/ml | Caffeine, mg/ml | Absorption of Ergotamine[a], % Without Caffeine | Absorption of Ergotamine[a], % With Caffeine |
|---|---|---|---|---|
| 5.0 | 0.2 | 20 | 21 (6) | 61 (6) |
| | 0.2 | 10 | 24 (9) | 49 (5) |
| | 0.1 | 10 | 25 (9) | 53 (6) |
| 3.0 | 0.2 | 10 | 47 (14) | 47 (12) |

[a] Each value is the mean of 10 loops from five rats. Standard deviation is in parentheses.

covered ($p > 0.1$). Because of the near complete recovery of ergotamine at time zero, no correction to the results obtained at 2.5 hr was necessary.

The results of the absorption studies are shown in Table I. Analysis of variance indicated that in each of three sets of experiments at pH 5.0, the presence of caffeine in the loops caused a highly significant increase in the extent of ergotamine absorption ($p < 0.001$). A $t$ test conducted on the results of the 0.2-mg/ml ergotamine tartrate experiments indicated that 20 mg of caffeine/ml had a significantly greater effect on ergotamine absorption than did 10 mg of caffeine/ml ($p < 0.001$). No significant difference was found in the percentage of ergotamine absorbed from loops containing ergotamine tartrate alone at 0.1 or 0.2 mg/ml ($p > 0.1$).

At pH 3.0, analysis of variance indicated that the presence of 20 mg of caffeine/ml in the loops had no significant effect on the extent of absorption of ergotamine ($p > 0.05$).

The position of the loop relative to the pylorus also had no significant effect on the amount of ergotamine absorbed at pH 3.0 or 5.0 ($p > 0.1$).

*Effect of Isosorbide Dinitrate*—The efficiency of the recovery process was demonstrated in the time zero experiments. The mean recovery of ergotamine from 10 loops (five rats) containing 0.2 mg of ergotamine tartrate/ml was 82 ± 5%; in the presence of 2 mg of isosorbide dinitrate/ml, it was 83 ± 5%. Analysis of variance demonstrated that neither the presence of isosorbide dinitrate nor loop position had a significant effect on ergotamine recovery ($p > 0.1$).

In the caffeine experiments, the recovery of ergotamine from loops containing 0.2 mg of ergotamine tartrate/ml alone was 97 ± 3%. The major difference between the caffeine and isosorbide dinitrate recovery experiments was the inclusion, for solubility, of 10% dimethyl sulfoxide in the pH 5.0 acetate buffer in the latter experiments. Comparison of the results using a $t$ test showed that dimethyl sulfoxide significantly affected ergotamine recovery ($p < 0.001$), but the reason for this effect is not known. The results are listed in Table II.

The ergotamine absorption figures are corrected by the factor "100/percentage of ergotamine recovered in time zero studies." This correction was necessary since the time zero studies indicated that extraction did not produce complete recovery of the ergotamine remaining in the loop. Analysis of variance indicated that isosorbide dinitrate had a significant effect on ergotamine absorption at the 5% confidence level ($0.05 > p > 0.01$) when ergotamine alone and when ergotamine plus isosorbide dinitrate were administered to the same rats. Loop position had no significant effect on absorption ($p > 0.1$).

In the second series of isosorbide dinitrate experiments, all five loops of a rat contained only one test solution. The corrected figures for the mean percentage absorption of ergotamine from loops containing ergotamine tartrate alone and from loops containing ergotamine tartrate plus isosorbide dinitrate were 19 ± 12 and 39 ± 8%, respectively. A $t$ test indicated that ergotamine absorption in rats in which all loops contained ergotamine tartrate plus isosorbide dinitrate was significantly greater than in rats in which all loops contained only ergotamine tartrate ($p < 0.001$).

The effect of isosorbide dinitrate in loops adjacent to those containing ergotamine tartrate alone was tested by comparing ergotamine absorption from the rats in the first series of experiments, where the adjacent loops contained isosorbide dinitrate, with the rats in the second series of experiments where all loops contained ergotamine tartrate only. The absorption in these two cases was 34 ± 7 and 19 ± 12%, respectively. A $t$ test indicated that isosorbide dinitrate in intestinal loops adjacent to the loops under study significantly increased ergotamine absorption, compared to similar loops in rats in which no isosorbide dinitrate was present ($0.01 > p > 0.002$).

## DISCUSSION

It was established previously that caffeine and ergotamine form one or more molecular complexes in water, but no attempt was made to calculate equilibrium constants for these reactions (14, 23).

Figure 1 shows the phase solubility diagram of ergotamine neutral molecule (E) in solutions of neutral caffeine (C). Measurements were made at pH 8 5. Caffeine was within its solubility when its concentrations were between 0 and $7 \times 10^{-2}$ $M$ (24). Solutions to which $12 \times 10^{-2}$ $M$ or more caffeine had been added were saturated with respect to caffeine. These results are consistent with ergotamine and caffeine forming 1:1 (EC) and 1:2 ($EC_2$) complexes (Schemes I and II):

$$E + C \overset{K_1}{\rightleftharpoons} EC$$

*Scheme I*

$$EC + C \overset{K_2}{\rightleftharpoons} EC_2$$

*Scheme II*

where:

$$K_1 = \frac{[EC]}{[E][C]} \qquad \text{(Eq. 1)}$$

$$K_2 = \frac{[EC_2]}{[EC][C]} \qquad \text{(Eq. 2)}$$

According to this model, the total amount of ergotamine in solution under any set of conditions, $[E]_T$, would be:

$$[E]_T = [E] + [EC] + [EC_2] \qquad \text{(Eq. 3)}$$

and the total amount of caffeine in solution, $[C]_T$, would be:

$$[C]_T = [C] + [EC] + 2[EC_2] \qquad \text{(Eq. 4)}$$

Because $[E]_T$ only varied between 1 and $34 \times 10^{-6}$ $M$ when the added caffeine concentration was varied between 0 and $6 \times 10^{-2}$ $M$, it could be assumed that $[C]_T \equiv [C]$ in all experiments performed.

On the ascending portion of the curve (*i.e.*, where the solutions were saturated with respect to ergotamine but not with respect to caffeine), [E] is the value of $[E]_T$ when [C] = 0.

Substitution of Eqs. 1 and 2 in Eq. 3 and rearrangement yield:

$$\frac{[E]_T - [E]}{[E][C]} = K_1 + K_1K_2[C] \qquad \text{(Eq. 5)}$$

Hence, if the model is compatible with the data, a plot of the left side of Eq. 5 against [C] should be linear. The value of the intercept of this line when [C] = 0 would be $K_1$, and the slope to intercept ratio would be $K_2$.

The results in Fig. 4 show that this plot is essentially linear. A least-

**Table II—Absorption of Ergotamine from the Rat Small Intestine in the Presence and Absence of Isosorbide Dinitrate at pH 5.0**

| Test Solution | Mean Percentage of Ergotamine Extracted from Loops after 2.5 hr | Mean Corrected Percentage of Ergotamine Remaining in Loops after 2.5 hr | Mean Percent Absorption of Ergotamine after 2.5 hr |
|---|---|---|---|
| Ergotamine tartrate, 0.2 mg/ml | 54.0 ± 6.0[a] | 65.9 ± 7.3[a] | 34.1[a] |
| | 66.4 ± 9.8[b] | 81.0 ± 12.0[b] | 19.0[b] |
| Ergotamine tartrate, 0.2 mg/ml, plus isosorbide dinitrate, 2 mg/ml | 48.2 ± 6.2[a] | 57.9 ± 7.5[a] | 42.1[a] |
| | 50.6 ± 9.8[b] | 61.0 ± 8.0[b] | 39.0[b] |

[a] Both solutions were administered to each rat. [b] Either ergotamine tartrate alone or ergotamine tartrate plus isosorbide dinitrate was administered to each rat.

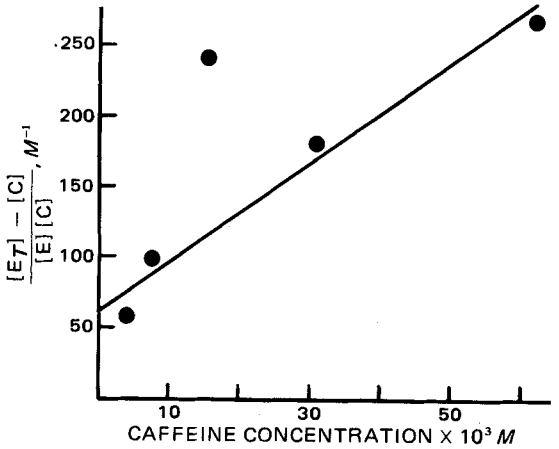


**Figure 4**—*Plot of $([E]_T - [E])/[E][C]$ against [C] for complexation of caffeine and ergotamine at pH 8.5.*

squares linear regression ($r^2 = 0.974$) of the results yielded values for $K_1$ and $K_2$ of 62 and 55 $M^{-1}$, respectively.

One test of the validity of this model comes from consideration of the results obtained in solutions saturated with caffeine (*i.e.*, when the concentration of added caffeine was greater than $12 \times 10^{-2}$ *M*). Under these conditions, a rearranged form of Eq. 5 suggests:

$$[E]_T = [E](1 + K_1[C]_S + K_1K_2[C]_S^2) \qquad \text{(Eq. 6)}$$

where $[C]_S$ is the caffeine solubility. It can be seen from Fig. 1 that, as required by Eq. 6, the value of $[E]_T$ is essentially independent of the concentration of added caffeine when the solubility of caffeine is exceeded. Solution of Eq. 6 for the solubility of caffeine yields a value of 8–9 $\times 10^{-2}$ *M*. Previous studies (24) showed that caffeine has a solubility of $1.8 \times 10^{-1}$ *M* in water but that this value was depressed by increasing the ionic strength (*e.g.*, $4.5 \times 10^{-2}$ *M* at pH > 8.5 when the ionic strength was adjusted to 3.0 *M* with sodium chloride). Hence, a value for caffeine solubility between 8 and $9 \times 10^{-2}$ *M* in a solution containing buffer salts and saturated with respect to ergotamine appears to be reasonable.

A similar analysis was made of the phase solubility diagram of ergotamine in caffeine solutions at pH 2.0 (23). Under these conditions, ergotamine is essentially completely protonated ($EH^+$), and caffeine is essentially present as a neutral molecule. The 1:1 ($ECH^+$) and 1:2 ($EC_2H^+$) complexes probably also would be essentially completely protonated (Schemes III and IV). Hence, the relevant reactions would be:

$$EH^+ + C \overset{K_3}{\rightleftharpoons} ECH^+$$

*Scheme III*

$$ECH^+ + C \overset{K_4}{\rightleftharpoons} EC_2H^+$$

*Scheme IV*

By similar reasoning to that outlined for reactions at pH 8.5, this model requires that a plot of $([E]_T - [EH^+])/([EH^+][C])$ against [C] should be linear with the intercept when [C] = 0 is equal to $K_3$ and the slope to intercept value is equal to $K_4$. A linear regression analysis of the results in Fig. 5 (which were computed from data in Ref. 23) yielded values of $K_3$ and $K_4$ of 204 and 44 $M^{-1}$, respectively. The standard deviation of the line was 0.98.

Consideration of the values of $K_1$, $K_2$, $K_3$, and $K_4$ gives some insight into the nature of the complexation reaction. Hence, the strongest complexation reaction involves caffeine and ergotamine cation ($K_3$ = 204 $M^{-1}$). The positive charge in the complex that is formed ($ECH^+$) apparently must be largely neutralized or buried since the complexation of caffeine with $ECH^+$ ($K_4$ = 44 $M^{-1}$) is a similar reaction to that of caffeine with the ergotamine neutral molecule ($K_1$ = 62 $M^{-1}$) or the neutral caffeine–ergotamine complex ($K_2$ = 55 $M^{-1}$).

***In Vitro* Absorption of Ergotamine**—The results in Fig. 2 show clearly that caffeine (10 mg/ml) significantly increased the rate at which ergotamine (initially 0.1 mg/ml) passed from the mucosal to the serosal side of the rat intestine when the pH of the contents of the former side was 5.0.

One important feature is that ergotamine was in solution on the mucosal side of the membrane. Hence, caffeine could not exert its accelerating effect on ergotamine absorption by increasing the dissolution rate of solid ergotamine. Caffeine's role in this latter process was suggested as its major role in enhancing ergotamine absorption following its administration as a solid (14).

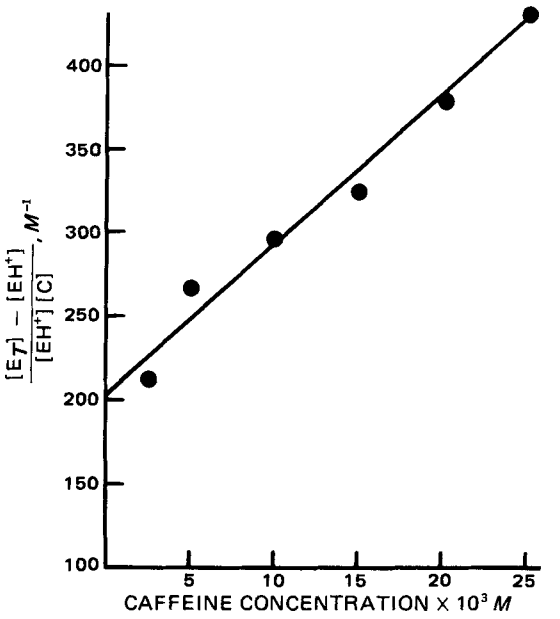


**Figure 5**—*Plot of $([E]_T - [EH^+])/[EH^+][C]$ against [C] for complexation of caffeine and ergotamine cation at pH 2.0.*

Another feature is that no blood supply was available to the intestine. Consequently, caffeine could not exert its effect by changing the blood flow rate. These results will be discussed in conjunction with the results of the *in situ* studies.

***In Situ* Absorption of Ergotamine**—The *in situ* experiments differed from the *in vitro* experiments in that an intact blood supply was present. However, as in the former experiments, ergotamine was in solution in the intestinal lumen, so the dissolution rate could not be a rate-determining factor in absorption. The results of experiments at pH 3 and 5 in both the absence and presence of caffeine are presented in Table I.

One point of interest concerns the effect, or apparent lack of effect, that varying the pH from 3 to 5 had on the absorption of the weakly basic ergotamine (pKa of conjugate acid = 6.4). Hence, although the absorption rate of ergotamine was similar at pH 3 and 5, the percent composition of the ergotamine neutral molecule in solution varied approximately 100-fold, from 0.04% at pH 3 to 3.8% at pH 5. Throughout the same pH range, the composition with respect to ergotamine cation varied from 99.96 to 96.2%.

The results in Table I also show that, at pH 3.0, the absorption rate of ergotamine (initial concentration of ergotamine tartrate 0.2 mg/ml) was the same in either the absence or the presence of caffeine (10 mg/ml). The solutions that did not contain caffeine contained 99.96% ergotamine cation and 0.04% ergotamine neutral molecule. The composition of the solutions with respect to ergotamine species are shown in Table III. Values of $K_1$, $K_2$, $K_3$, and $K_4$ for the reactions shown in Schemes I–IV, respectively, and a $K_a$ value for ergotamine of $3.98 \times 10^{-7}$ *M* were used to compute these results. Hence, while the concentration of ergotamine cation decreased from 99.96% in the absence of caffeine to 2.8%, the total concentration of ergotamine cation plus protonated complexes remained essentially constant.

The situation at pH 5.0 was quite different, because caffeine (10 or 20 mg/ml) significantly increased the absorption rate of ergotamine. The extent to which caffeine increased the absorption rate in the *in situ* experiments was similar to that in the *in vitro* experiments.

**Table III—Composition [a], as a Percentage of Total Ergotamine Species, of Solutions Containing Ergotamine (0.2 mg/ml) and Caffeine (10 mg/ml) at pH 3.0 and 5.0**

| | Concentration, % | | | | | |
|---|---|---|---|---|---|---|
| pH | $EH^+$ | $ECH^+$ | $EC_2H^+$ | E | EC | $EC_2$ |
| 3.0 | 2.8 | 29.7 | 67.6 | $1.1 \times 10^{-3}$ | $3.6 \times 10^{-3}$ | $1.0 \times 10^{-2}$ |
| 5.0 | 2.8 | 29.2 | 66.6 | $1.1 \times 10^{-1}$ | $3.5 \times 10^{-1}$ | 1.0 |

[a] Calculated as described in the text.

These results are consistent with a model for GI absorption of basic drugs described earlier (25). The appropriate model (Model A in Ref. 25) assumes that neutral molecules, but not ions, rapidly pass from the aqueous environment of the lumen into the lipoidal GI membrane and that equilibrium between these two phases is established rapidly. The slow step in overall absorption is the transport of neutral molecules from the lipoidal membrane into the aqueous blood compartment. The model for ergotamine absorption is shown schematically in Scheme V. According to this model, the rate of drug appearance in the blood is proportional to the concentration of neutral drug molecules in the membrane. Hence:

$$\text{absorption rate} = k_E[E]_m V_m + k_{EC}[EC]_m V_m + k_{EC_2}[EC_2]_m V_m \quad \text{(Eq. 7)}$$

where the terms in brackets with subscript $m$, $[\ ]_m$, refer to the concentration of the various species in the membrane and $V_m$ is the volume of the membrane. By definition:

$$P_E = \frac{[E]_m}{[E]_w} \quad \text{(Eq. 8)}$$

$$P_{EC} = \frac{[EC]_m}{[EC]_w} \quad \text{(Eq. 9)}$$

$$P_{EC_2} = \frac{[EC_2]_m}{[EC_2]_w} \quad \text{(Eq. 10)}$$

where the $P$ symbols are the intrinsic partition coefficients for the three ergotamine species between the aqueous contents of the lumen and the membrane and the terms in brackets with subscript $w$, $[\ ]_w$, refer to the concentrations of the various species in water.

Substitution of Eqs. 8–10 in Eq. 7 and expression of the various concentration terms as fractions of the total amount of ergotamine in the lumen contents and in the membrane $E_T$ yield:

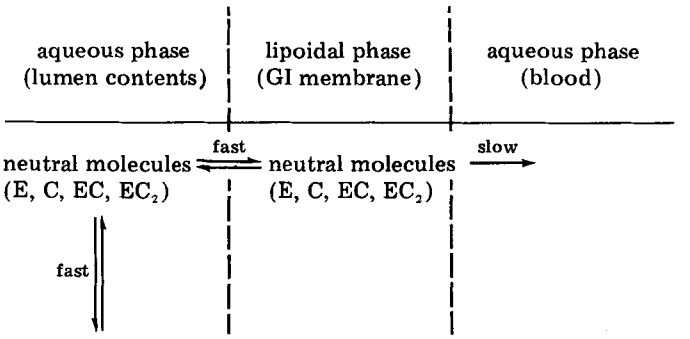


*Scheme V*

$$\text{rate of absorption} = \frac{(k_E P_E K_a + k_{EC} P_{EC} K_1 K_a [C]_w + k_{EC_2} P_{EC_2} K_1 K_2 K_a [C]_w^2) E_T}{\frac{V_w}{V_m}[K_a + 1 + K_3[C]_w + K_3 K_4 [C]_w^2 [H^+] + K_1 K_a [C]_w + K_1 K_2 K_a [C]_w^2] + K_a (P_E + P_{EC} K_1 [C]_w + P_{EC_2} K_1 K_2 [C]_w^2)} \quad \text{(Eq. 11)}$$

where $V_w$ is the volume of the aqueous lumen contents and $[C]_w$ is the concentration of caffeine in the lumen contents. If transport of a species, $i$, from the lipoidal membrane across an aqueous barrier and into the blood is the rate-determining process, then, from Fick's first law:

$$k_i = \frac{D_i A_i P_i}{h_i} \quad \text{(Eq. 12)}$$

where $D_i$ is the diffusion coefficient of the $i$ species in an aqueous barrier of surface area $A_i$ and thickness $h_i$, and $P_i$ is the partition coefficient of the species $i$ from the lipoidal membrane into the aqueous phase. This model assumes transport into a sink. If the following additional assumptions are made:

1. The values of the diffusion coefficients for the species E, EC, and $EC_2$ are equal and have the value $D$
2. The partition coefficients of the species from the lipoidal membrane into blood are the inverse of the $P$ values in Eq. 11, which were for partitioning from the aqueous lumen contents into the membrane

then substitution of the terms defined in Eq. 12 into Eq. 11 and rearrangement lead to:

$$\text{rate of absorption} = \frac{\frac{DA}{h} E_T}{\frac{V_w}{V_m} + \frac{V_w}{V_m}\frac{[H^+]}{K_a}\left\{\frac{1 + K_3[C]_w + K_3 K_4 [C]_w^2}{1 + K_1[C]_w + K_1 K_2 [C]_w^2}\right\} + P_E\left\{\frac{1 + \frac{P_{EC}}{P_E} K_1 [C]_w + \frac{P_{EC_2}}{P_E} K_1 K_2 [C]_w^2}{1 + K_1[C]_w + K_1 K_2 [C]_w^2}\right\}} \quad \text{(Eq. 13)}$$

where $A$ and $h$ are the surface area and thickness of the barrier.

When caffeine is absent, Eq. 13 reduces to:

$$\text{rate of absorption} = \frac{\frac{DA}{h} E_T}{\frac{V_w}{V_m} + \frac{V_w}{V_m}\frac{[H^+]}{K_a} + P_E} \quad \text{(Eq. 14)}$$

Hence, the model would be consistent with the data that showed that the absorption rate did not change as $[H^+]$ increased from $10^{-5}$ to $10^{-3}$ $M$ if the value of $P_E \gg (V_w/V_m)\ 2.5 \times 10^3$. This seems reasonable since $P_E$ is expected to be very large. The Merck Index (26) states that ergotamine is "freely soluble in chloroform" and "only slightly soluble in water."

The approximate doubling of the rate of ergotamine absorption in the presence of caffeine ($5.15 \times 10^{-2}$ $M$) when the pH was increased from 3 to 5 needs to be explained. The model would be consistent with this result if, in the presence of caffeine, the term in the denominator that contained $[H^+]$ and the term containing $P_E$ were of comparable value at pH 3. But if the term containing $P_E$ was much greater than the term containing $[H^+]$ at pH 5, although still being slightly less than the value of $P_E$, knowledge of the values of the equilibrium constants $K_1$, $K_2$, $K_3$, and $K_4$ indicate that the term containing $[H^+]$ would be greater in the presence of $5.15 \times 10^{-2}$ $M$ caffeine than in its absence by a factor of 2.7. The value of the term containing $P_E$ is not known precisely, but it is reasonable to expect that it would be less than $P_E$. This situation would arise if the values of the partition coefficients $P_{EC}$ and $P_{EC_2}$ were smaller than $P_E$. Although the values of these terms are not known, the phase solubility study (Fig. 1) reveals that the complexes EC and $EC_2$ have significantly higher water solubility than ergotamine. Hence, it is not unreasonable to assume that they will have a smaller tendency than ergotamine to partition into a lipoidal phase.

This model leads to the conclusion that the water-solubilizing effect of caffeine on ergotamine neutral molecules is a major factor in its accelerating effect on ergotamine absorption.

Zoglio and coworkers (14, 27, 28), in discussing the rate-accelerating effect of caffeine on the partitioning of ergotamine and related alkaloids from water to chloroform at pH 6.5, but not at pH 1.0, proposed that it did so by "preventing precipitation" of ergotamine prior to its absorption. In the present study, precipitation was not possible because solutions were not saturated with respect to ergotamine. However, the two theories are consistent in that both credit caffeine's role to the increased water solubility that it confers on the ergotamine neutral molecule.

**Effect of Isosorbide Dinitrate on Ergotamine Absorption**—Isosorbide dinitrate significantly increased the rate of ergotamine absorption. However, the nature of its effect was quite different than that of caffeine. For example, the presence of caffeine in intestinal loops adjacent to loops in the same rat that only contained ergotamine did not significantly increase the rate of ergotamine absorption. On the other hand, the presence of isosorbide dinitrate in any intestinal loop increased the rate of ergotamine absorption in other loops in the rat that did not contain isosorbide dinitrate.

Since isosorbide dinitrate is a vasodilator (29), it probably increases the rate of ergotamine absorption by increasing the rate of intestinal blood flow. This conclusion is consistent with the earlier postulate that the rate-determining step in ergotamine absorption is its rate of passage from the membrane into the blood rather than its passage into or through the membrane.

Caffeine is also a vasodilator (30); at a concentration of 2 mg/ml, it increased intestinal blood flow by 166% in anesthetized rats and increased the rate of absorption of tritiated water, urea, and antipyrine at pH 8.0 and of salicylic acid at pH 6 (31). Hence, while part of the effect that caffeine has on increasing the absorption of ergotamine at pH 5.0 may be due to its effect on the blood flow rate, this effect is thought to be minor because it does not affect absorption rates at pH 3, it does not affect absorption rates at pH 5 from adjacent loops that do not contain caffeine, and it exerts an accelerating effect on ergotamine absorption in *in vitro* experiments where no blood supply is present.

## CONCLUSION

1. Caffeine increases the rate of ergotamine absorption from the rat small intestine when the pH of the intestinal contents is 5.0 but not when it is 3.0. This effect is independent of the effect that caffeine exerts on the dissolution rate of ergotamine because, in the experiments performed, ergotamine was administered as a stable solution.

2. Although caffeine increases intestinal blood flow, this property only plays a minor role in its absorption-accelerating effects at pH 5.0. Vasodilation and increased blood flow are likely to explain the rate-accelerating effect of isosorbide dinitrate on ergotamine absorption.

3. The rate-determining step in the absorption of ergotamine appears to be transport from the intestinal membrane into the blood.

## REFERENCES


(1) J. W. Lance, "Mechanism and Management of Headache," 3rd ed., Butterworths, London, England, 1973, pp. 130–207.

(2) J. Pearce, "Migraine, Clinical Features, Mechanism and Management," Charles C Thomas, Springfield, Ill. 1969, pp. 1–36.

(3) J. Saper, *J. Am. Med. Assoc.*, **239,** 2480 (1978).

(4) G. P. Arthur, *Curr. Ther.*, **19,** 63 (1978).

(5) J. M. Bradfield, *ibid.*, **17,** 55 (1976).

(6) M. J. Eadie, *Med. J. Aust., Special Suppl.*, **2,** 26 (1972).

(7) M. Wilkinson, *Br. Med. J.*, **2,** 754 (1971).

(8) G. Selby, *Med. J. Aust., Special Suppl.*, **2,** 35 (1972).

(9) D. Orton, in "Current Concepts in Migraine Research," R. Greene, Ed., Raven, New York, N.Y., 1978, pp. 79–84.

(10) A. P. Friedman and C. Brenner, *Am. Pract.*, **2,** 467 (1948).

(11) S. G. Cohen and L. H. Creip, *N. Engl. J. Med.*, **241,** 896 (1949).

(12) C. M. Charles, *Postgrad. Med.*, **7,** 33 (1950).

(13) R. Schmidt and A. Fanchamps, *Eur. J. Clin. Pharmacol.*, **7,** 213 (1974).

(14) M. A. Zoglio, H. V. Maulding, and J. J. Windheuser, *J. Pharm. Sci.*, **58,** 222 (1969).

(15) J. R. Anderson, G. L. Blackman, and I. H. Pitman, *Aust. J. Pharm. Sci.*, **7,** 73 (1978).

(16) M. Admans, A. J. Cobcroft, B. C. Finnin, J. Nolan, and B. L. Reed, *ibid.*, **NS5,** 51 (1976).

(17) R. K. Crane and T. H. Wilson, *J. Appl. Physiol.*, **12,** 145 (1958).

(18) R. R. Levine and E. W. Pelikan, *J. Pharmacol. Exp. Ther.*, **131,** 319 (1961).

(19) B. Kreilgard and J. Kisbye, *Arch. Pharm. Chemi, Sci. Ed.*, **2,** 1 (1974).

(20) R. A. Heacock, K. R. Langille, J. D. MacNeil, and R. W. Frei, *J. Chromatogr.*, **77,** 425 (1973).

(21) H. Bethke, B. Delz, and K. Stich, *ibid.*, **123,** 193 (1976).

(22) H. V. Maulding, Jr., and M. A. Zoglio, *J. Pharm. Sci.*, **59,** 700 (1970).

(23) J. R. Anderson and I. H. Pitman, *ibid.*, **69,** 832 (1980).

(24) J. R. Anderson and I. H. Pitman, *Aust. J. Pharm. Sci.*, **8,** 117 (1979).

(25) J. G. Wagner and A. J. Sedman, *J. Pharmacokinet. Biopharm.*, **1,** 23 (1973).

(26) "The Merck Index," 9th ed., Merck & Co., Rahway, N.J., 1976.

(27) M. A. Zoglio and H. V. Maulding, *J. Pharm. Sci.*, **59,** 215 (1970).

(28) H. V. Maulding and M. A. Zoglio, *ibid.*, **59,** 384 (1970).

(29) "The Pharmacological Basis of Therapeutics," 5th ed., L. S. Goodman and A. Gilman, Eds., Macmillan, New York, N.Y., 1975, p. 727.

(30) *Ibid.*, p. 367.

(31) E. Beubler and F. Lembeck, *Naunyn-Schmiedebergs Arch. Pharmacol.*, **292,** 73 (1976).


## ACKNOWLEDGMENTS


Supported by a grant from the Nicholas Drug Research Consortium.


# Effect of Poly-2-vinylpyridine-*N*-oxide and Sucrose on Silicate-Induced Hemolysis of Erythrocytes


**DENNIS W. OSCARSON *, GEORGE E. VAN SCOYOC ‡x, and JAMES L. AHLRICHS ‡**



Received May 9, 1980, from the **Saskatchewan Institute of Pedology, University of Saskatchewan, Saskatoon, Saskatchewan, Canada S7N 0W0,* and the ‡*Department of Agronomy, Purdue University, West Lafayette, IN 47907.* Accepted for publication November 19, 1980.



**Abstract** □ The biological activity of montmorillonite, palygorskite, kaolinite, chrysotile, and silica was examined using *in vitro* hemolysis of erythrocytes. The hemolytic potency was in the order montmorillonite > silica > palygorskite > chrysotile > kaolinite. The polymer poly-2-vinylpyridine-*N*-oxide inhibited hemolysis caused by montmorillonite, palygorskite, kaolinite, and silica, but it was less effective with chrysotile. The extent of polymer binding to the silicates and red blood cells was measured by UV spectroscopy. When sucrose was substituted for the saline solution as the incubating medium, hemolysis was eliminated in all systems except chrysotile–erythrocyte, where it was enhanced. The results indicate that both hydrogen bonding and ionic interactions between silicate surfaces and the erythrocyte membrane are important in the hemolytic process.



**Keyphrases** □ Silicates—effect of poly-2-vinylpyridine-*N*-oxide on silicate-induced hemolysis □ Hemolysis—effect of poly-2-vinylpyridine-*N*-oxide, silicates □ Suspending agents—effect of poly-2-vinylpyridine-*N*-oxide on silicate-induced hemolysis


Inhaled silicate particles cause various pathological disorders (1). In addition to pulmonary tissue damage, the particles can potentially damage other body tissues because silicates such as montmorillonite, kaolinite, and palygorskite are used in many pharmaceuticals and cosmetics (primarily as fillers, stabilizers, and suspending



*© 1981, American Pharmaceutical Association*

Since isosorbide dinitrate is a vasodilator (29), it probably increases the rate of ergotamine absorption by increasing the rate of intestinal blood flow. This conclusion is consistent with the earlier postulate that the rate-determining step in ergotamine absorption is its rate of passage from the membrane into the blood rather than its passage into or through the membrane.

Caffeine is also a vasodilator (30); at a concentration of 2 mg/ml, it increased intestinal blood flow by 166% in anesthetized rats and increased the rate of absorption of tritiated water, urea, and antipyrine at pH 8.0 and of salicylic acid at pH 6 (31). Hence, while part of the effect that caffeine has on increasing the absorption of ergotamine at pH 5.0 may be due to its effect on the blood flow rate, this effect is thought to be minor because it does not affect absorption rates at pH 3, it does not affect absorption rates at pH 5 from adjacent loops that do not contain caffeine, and it exerts an accelerating effect on ergotamine absorption in *in vitro* experiments where no blood supply is present.

## CONCLUSION

1. Caffeine increases the rate of ergotamine absorption from the rat small intestine when the pH of the intestinal contents is 5.0 but not when it is 3.0. This effect is independent of the effect that caffeine exerts on the dissolution rate of ergotamine because, in the experiments performed, ergotamine was administered as a stable solution.

2. Although caffeine increases intestinal blood flow, this property only plays a minor role in its absorption-accelerating effects at pH 5.0. Vasodilation and increased blood flow are likely to explain the rate-accelerating effect of isosorbide dinitrate on ergotamine absorption.

3. The rate-determining step in the absorption of ergotamine appears to be transport from the intestinal membrane into the blood.

## REFERENCES


(1) J. W. Lance, "Mechanism and Management of Headache," 3rd ed., Butterworths, London, England, 1973, pp. 130–207.

(2) J. Pearce, "Migraine, Clinical Features, Mechanism and Management," Charles C Thomas, Springfield, Ill. 1969, pp. 1–36.

(3) J. Saper, *J. Am. Med. Assoc.*, **239,** 2480 (1978).

(4) G. P. Arthur, *Curr. Ther.*, **19,** 63 (1978).

(5) J. M. Bradfield, *ibid.*, **17,** 55 (1976).

(6) M. J. Eadie, *Med. J. Aust., Special Suppl.*, **2,** 26 (1972).

(7) M. Wilkinson, *Br. Med. J.*, **2,** 754 (1971).

(8) G. Selby, *Med. J. Aust., Special Suppl.*, **2,** 35 (1972).

(9) D. Orton, in "Current Concepts in Migraine Research," R. Greene, Ed., Raven, New York, N.Y., 1978, pp. 79–84.

(10) A. P. Friedman and C. Brenner, *Am. Pract.*, **2,** 467 (1948).

(11) S. G. Cohen and L. H. Creip, *N. Engl. J. Med.*, **241,** 896 (1949).

(12) C. M. Charles, *Postgrad. Med.*, **7,** 33 (1950).

(13) R. Schmidt and A. Fanchamps, *Eur. J. Clin. Pharmacol.*, **7,** 213 (1974).

(14) M. A. Zoglio, H. V. Maulding, and J. J. Windheuser, *J. Pharm. Sci.*, **58,** 222 (1969).

(15) J. R. Anderson, G. L. Blackman, and I. H. Pitman, *Aust. J. Pharm. Sci.*, **7,** 73 (1978).

(16) M. Admans, A. J. Cobcroft, B. C. Finnin, J. Nolan, and B. L. Reed, *ibid.*, **NS5,** 51 (1976).

(17) R. K. Crane and T. H. Wilson, *J. Appl. Physiol.*, **12,** 145 (1958).

(18) R. R. Levine and E. W. Pelikan, *J. Pharmacol. Exp. Ther.*, **131,** 319 (1961).

(19) B. Kreilgard and J. Kisbye, *Arch. Pharm. Chemi, Sci. Ed.*, **2,** 1 (1974).

(20) R. A. Heacock, K. R. Langille, J. D. MacNeil, and R. W. Frei, *J. Chromatogr.*, **77,** 425 (1973).

(21) H. Bethke, B. Delz, and K. Stich, *ibid.*, **123,** 193 (1976).

(22) H. V. Maulding, Jr., and M. A. Zoglio, *J. Pharm. Sci.*, **59,** 700 (1970).

(23) J. R. Anderson and I. H. Pitman, *ibid.*, **69,** 832 (1980).

(24) J. R. Anderson and I. H. Pitman, *Aust. J. Pharm. Sci.*, **8,** 117 (1979).

(25) J. G. Wagner and A. J. Sedman, *J. Pharmacokinet. Biopharm.*, **1,** 23 (1973).

(26) "The Merck Index," 9th ed., Merck & Co., Rahway, N.J., 1976.

(27) M. A. Zoglio and H. V. Maulding, *J. Pharm. Sci.*, **59,** 215 (1970).

(28) H. V. Maulding and M. A. Zoglio, *ibid.*, **59,** 384 (1970).

(29) "The Pharmacological Basis of Therapeutics," 5th ed., L. S. Goodman and A. Gilman, Eds., Macmillan, New York, N.Y., 1975, p. 727.

(30) *Ibid.*, p. 367.

(31) E. Beubler and F. Lembeck, *Naunyn-Schmiedebergs Arch. Pharmacol.*, **292,** 73 (1976).


## ACKNOWLEDGMENTS


Supported by a grant from the Nicholas Drug Research Consortium.


# Effect of Poly-2-vinylpyridine-*N*-oxide and Sucrose on Silicate-Induced Hemolysis of Erythrocytes


**DENNIS W. OSCARSON *, GEORGE E. VAN SCOYOC ‡x, and JAMES L. AHLRICHS ‡**



Received May 9, 1980, from the **Saskatchewan Institute of Pedology, University of Saskatchewan, Saskatoon, Saskatchewan, Canada S7N 0W0,* and the ‡*Department of Agronomy, Purdue University, West Lafayette, IN 47907.* Accepted for publication November 19, 1980.



**Abstract** □ The biological activity of montmorillonite, palygorskite, kaolinite, chrysotile, and silica was examined using *in vitro* hemolysis of erythrocytes. The hemolytic potency was in the order montmorillonite > silica > palygorskite > chrysotile > kaolinite. The polymer poly-2-vinylpyridine-*N*-oxide inhibited hemolysis caused by montmorillonite, palygorskite, kaolinite, and silica, but it was less effective with chrysotile. The extent of polymer binding to the silicates and red blood cells was measured by UV spectroscopy. When sucrose was substituted for the saline solution as the incubating medium, hemolysis was eliminated in all systems except chrysotile–erythrocyte, where it was enhanced. The results indicate that both hydrogen bonding and ionic interactions between silicate surfaces and the erythrocyte membrane are important in the hemolytic process.



**Keyphrases** □ Silicates—effect of poly-2-vinylpyridine-*N*-oxide on silicate-induced hemolysis □ Hemolysis—effect of poly-2-vinylpyridine-*N*-oxide, silicates □ Suspending agents—effect of poly-2-vinylpyridine-*N*-oxide on silicate-induced hemolysis


Inhaled silicate particles cause various pathological disorders (1). In addition to pulmonary tissue damage, the particles can potentially damage other body tissues because silicates such as montmorillonite, kaolinite, and palygorskite are used in many pharmaceuticals and cosmetics (primarily as fillers, stabilizers, and suspending



*© 1981, American Pharmaceutical Association*

agents); consequently, silicate particles are ingested in relatively large quantities or applied directly to the skin. Palygorskite (attapulgite) also has a fibrous morphology somewhat similar to chrysotile asbestos.

The effect of silicates on cellular membranes may be studied by *in vitro* hemolysis of erythrocytes. Silica (2, 3), the chrysotile variety of asbestos (4, 5), sepiolite and palygorskite (5, 6), kaolinite (7), and montmorillonite and illite (7) are known to induce *in vitro* hemolysis.

The weakly basic polymer poly-2-vinylpyridine-*N*-oxide (I) is an effective preventative against experimental silicosis (8). It also protects erythrocytes against the hemolytic action of various silica forms (9, 10) but is less effective in preventing chrysotile-induced hemolysis (5). Little is known about the effect of I on hemolysis caused by other silicates.

The purposes of this study were to determine the effect of I and sucrose on hemolysis caused by montmorillonite, kaolinite, and palygorskite and to compare these systems with the silica- and chrysotile–erythrocyte systems, which have been the most extensively studied systems. In addition, the extent of I binding to the silicates and erythrocytes was determined.

## EXPERIMENTAL

**Silicates**—Montmorillonite[1], kaolinite[1], and palygorskite[2] samples were passed through a 300-mesh sieve, and the 50-$\mu$m fraction was used for all studies. Crude chrysotile fibers were separated partially by hand and then ground[3] for 2 min. The silica[4] was a synthetic, amorphous material and was used as received. Samples of the silicates[5] were suspended in deionized water and sonicated[6] for 5 min at 80 w to assure separation and dispersion.

**Erythrocytes and Media**—Bovine blood was drawn by venipuncture directly into a sterile 60-ml polyethylene tube coated with heparin. The red blood cells were washed three times with isotonic phosphate-buffered saline solution (0.106 *M* NaCl, 0.030 *M* $Na_2HPO_4 \cdot 7H_2O$, and 0.008 *M* $KH_2PO_4$). After the final wash, a 3% (v/v) suspension of red blood cells was prepared.

Phosphate buffer (pH 7.3) was used throughout, except for the chrysotile–erythrocyte system. It was reported (10) that phosphate inhibits the hemolytic activity of chrysotile, an observation confirmed in this laboratory. The pH of the chrysotile–erythrocyte system was monitored closely, however, and remained at 7.2 ± 0.1 for the concentration of chrysotile used.

To study the effect of sucrose on silicate-induced hemolysis, 0.250 *M* sucrose (0.250 *M* sucrose is isotonic with 0.145 *M* NaCl) was substituted for the saline solution as the incubating medium.

**Hemolysis Technique**—Glass test tubes (10 × 75 ml) were used for all hemolysis studies. The silicate–red blood cell suspensions consisted of the following and were prepared in the order given: 1 ml of a silicate suspension, 3 ml of the phosphate-buffered saline solution (sodium chloride alone for the chrysotile–erythrocyte system), and 1 ml of the 3% suspension of red blood cells. For the study of the effect of I on silicate-mediated hemolysis, the polymer was added to the described mixture immediately after the silicate suspension. The total volume of the mixture was always 5 ml. A sample consisting of 4 ml of the phosphate-buffered saline solution and 1 ml of the 3% suspension of red blood cells served as a control for the possible fragility of the erythrocytes.

The test tubes were sealed[7] and gently rotated end-over-end for 1 hr at room temperature. The suspensions then were centrifuged at 1500×*g* for 5 min, and the absorbance of the supernatant solution was measured spectrophotometrically[8] at 541 nm with the control sample as the reference. The degree of hemolysis was expressed as a percentage of a totally lysed sample.

**Table I—Percentage Hemolysis Produced by the Silicates in the Presence of I**

| Silicate[a] | I Concentration, $\mu M$/ml | |
|---|---|---|
| | 0.2 | 1.0 |
| Montmorillonite | 23 ± 2[b] | ND[c] |
| Palygorskite | 20 ± 3 | 3 ± 2 |
| Kaolinite | 50 ± 2 | 20 ± 5 |
| Silica | 7 ± 4 | ND |
| Chrysotile | 50 ± 1 | 42 ± 4 |

[a] The $HC_{50}$ concentrations of the silicates were used (see text). [b] Mean ± *SD*, % ($n = 4$). [c] No detectable hemolysis.

**Binding of I**—The UV spectrum of I gives a $\lambda_{max}$ equal to 260 nm in water (11); therefore, the extent of polymer binding to the silicates and erythrocytes can be measured conveniently.

Twenty milligrams of a silicate or 10 ml of a 6% suspension of red blood cells and 1 mg of I were added to 20 ml of the phosphate-buffered saline solution in 100-ml volumetric flasks. The flasks then were brought to volume with deionized water (phosphate-buffered saline solution was used for the erythrocyte–I mixture). After 5 min of periodic shaking, a sample was removed from the flasks, placed in polypropylene centrifuge tubes, and centrifuged at 40,000×*g* for 10 min. A sample of the supernate was transferred to a quartz cell, and the absorbance was measured[9] at 260 nm.

The following formula was used to calculate the percentage of 1 mg of I bound to 20 mg of the silicate or 10 ml of a 6% suspension of red blood cells:

$$\% \text{ bound} = [A_p - (A_s - A_m)/A_p] \times 100 \qquad \text{(Eq. 1)}$$

where $A_p$ is the absorbance of a 0.001% (w/v) solution of I, $A_s$ is the absorbance of the supernate after centrifugation of a mixture of 0.001% I and a 0.02% (w/v) silicate or 0.6% (v/v) erythrocyte suspension, and $A_m$ is the absorbance of the supernate after centrifugation of a 0.02% silicate or 0.6% erythrocyte suspension.

## RESULTS AND DISCUSSION

To facilitate meaningful comparisons between the silicates, the concentration of the silicate that caused 50% hemolysis when incubated with 1 ml of a 3% suspension of erythrocytes was determined. This concentration[10] (in milligrams of silicate per milliliter of silicate–erythrocyte-buffer suspension) was as follows for the five silicates examined: montmorillonite, 0.006; silica, 0.03; palygorskite, 0.06; chrysotile, 0.1; and kaolinite, 0.6. The use of the $HC_{50}$ concentration partially compensated for physical as well as chemical differences in the untreated silicates. There appeared to be a correlation between the specific surface area of the silicates [montmorillonite > silica ≥ palygorskite > kaolinite ≥ chrysotile (12–14)] and their hemolytic activity.

It was confirmed that I is very effective in inhibiting hemolysis caused by silica, but it was much less effective with chrysotile (Table I). The polymer also decreased hemolysis produced by montmorillonite, palygorskite, and kaolinite, although its effect was somewhat less than on silica-induced hemolysis (Table I).

Two hypotheses concerning the mechanism of interaction between silica and the erythrocyte membrane have been proposed: (*a*) hydrogen bonding (9) of the silanol groups on the silica surface with the phosphate ester linkages of phospholipids and the amide groups of proteins, and (*b*) ionic interaction (15) between dissociated silanol groups on the silica surface and positively charged species on the erythrocyte membrane surface.

Compound I is a strong hydrogen bonding material; therefore, its effectiveness in preventing silica-induced hemolysis suggests that hydrogen bonding is the predominant mode of interaction between silica and the erythrocyte membrane during hemolysis. The polymer apparently bonds to the silanol groups on the silica surface and thus prevents these groups from contacting the red blood cell membrane.

Because I also inhibits hemolysis caused by montmorillonite, paly-

[1] Montmorillonite (Upton, Wyo.), kaolinite (Bath, S.C.), and chrysotile (Quebec) samples were obtained from the Wards Natural Science Establishment, Rochester, N.Y.

[2] The palygorskite (Attapulgus, Ga.) sample was obtained from the C.M.S. Clay Minerals Repository, Department of Geology, University of Missouri, Columbia, Mo.

[3] Janke-Kunkel mechanical grinder.

[4] Cab-O-Sil, Cabot Corp.

[5] Montmorillonite, kaolinite, palygorskite, chrysotile, and silica will be referred to as silicates.

[6] Model W185, Branson Sonic Power Co.

[7] Parafilm, American Can Co., Greenwich, Conn.

[8] Bausch & Lomb model 20 spectrophotometer.

[9] Beckman model Acta CII spectrophotometer.

[10] Hereafter referred to as the $HC_{50}$ concentration.

**Table II—Amount of I Bound to the Silicates and to Erythrocytes**

| Material | I Bound[a], % |
|---|---|
| Montmorillonite | 100 |
| Palygorskite | 97 ± 2[b] |
| Kaolinite | 48 ± 3 |
| Silica | 96 ± 1 |
| Chrysotile | 37 ± 4 |
| Erythrocytes | 4 ± 1 |

[a] One milligram of I was added to 20 mg of the silicates or 10 ml of a 6% suspension of erythrocytes in a total volume of 100 ml. [b] Mean ± *SD*, % ($n$ = 4).

gorskite, and kaolinite (Table I), a hydrogen bonding mechanism probably is at least partially involved in these systems. The three silicates, montmorillonite, palygorskite, and kaolinite, have many surface hydroxyl groups bound to the cations (predominantly silicon, aluminum, and magnesium exposed at crystal edges) (16, 17); these hydroxyl groups could function as hydrogen donors. Furthermore, montmorillonite has a high cation-exchange capacity (12), and the water of hydration of the exchangeable cations also can function as hydrogen donors (18).

Chrysotile, on the other hand, is a fibrous, tubular magnesium silicate with the silica sheets on the inner side and the magnesium hydroxide sheets exposed at the surface. Since the pK of chrysotile is close to 11 (19), it has a positive surface charge at physiological pH values. Compound I is relatively ineffective in preventing chrysotile-induced hemolysis (Table I), while many anionic species such as phosphate and ethylenediaminetetraacetic acid are effective inhibitors (10, 20). This fact suggests that little hydrogen bonding is involved in the chrysotile–erythrocyte system. An ionic interaction between chrysotile and the red blood cell membrane has been proposed (21).

The effect of I on silicate-induced hemolysis previously has not been clearly interpretable; it could affect the surface of the silicate, the erythrocyte membrane, or both. The data in Table II clearly show that erythrocytes bind very little of the polymer while it is readily bound to montmorillonite, palygorskite, and silica and to a lesser extent to kaolinite and chrysotile. Therefore, I probably exerts its protective action by blocking the lytic sites on the surfaces of the silicates.

When sucrose was substituted for the saline solution as the incubating medium, no hemolysis was observed when the $HC_{50}$ concentrations of montmorillonite, palygorskite, kaolinite, and silica were incubated with erythrocytes. The sucrose molecule has many potential hydrogen-accepting sites, so it can form preemptive hydrogen bonds with the hydrogen-donating surface groups of montmorillonite, palygorskite, kaolinite, and silica. Consequently, these hydrogen-donating groups cannot contact the erythrocyte membrane and hemolysis cannot occur.

In contrast, erythrocytes incubated in sucrose underwent increased lysis (65% ± 4, $n$ = 4) when the $HC_{50}$ concentration of chrysotile was used. If the chrysotile–erythrocyte interaction is predominantly ionic, the interaction would be enhanced in a medium of relatively low dielectric constant such as sucrose, and this reaction is what was observed.

A recent report indicated a correlation between hyperplastic changes in isolated hamster trachea segments and *in vitro* hemolysis of erythrocytes by chrysotile asbestos and montmorillonite (22). Elucidation of the mechanism by which various silicate minerals interact with the erythrocyte membrane *in vitro* may lead to a better understanding of silicate–membrane interactions *in vivo*.

## REFERENCES


(1) M. Timar, G. Kendrey, and Z. Juhasz, *Med. Lav.*, **57**, 1 (1966).

(2) J. D. Harley and J. Margolis, *Nature*, **189**, 1010 (1961).

(3) P. Charache, C. M. MacLeod, and P. White, *J. Gen. Physiol.*, **45**, 1117 (1962).

(4) G. C. Secchi and A. Rezzonico, *Med. Lav.*, **59**, 1 (1968).

(5) R. J. Schnitzer and F. L. Pundsack, *Environ. Res.*, **3**, 1 (1970).

(6) H. Hayaski, K. Koshi, and H. Sakabe, *Proc. Int. Clay Conf., Tokyo*, **1**, 903 (1969).

(7) S. Manyai, J. Kabai, J. Kis, E. Suveges, and M. Timar, *Med. Lav.*, **60**, 331 (1969).

(8) J. R. Ruttner and R. F. Mauerhofer, *Med. Exp.*, **8**, 55 (1963).

(9) T. Nash, A. C. Allison, and J. S. Harington, *Nature*, **210**, 259 (1966).

(10) G. Macnab and J. S. Harington, *ibid.*, **214**, 522 (1967).

(11) P. F. Holt and E. T. Nasrallah, *ibid.*, **211**, 878 (1966).

(12) R. E. Grim, "Clay Mineralogy," McGraw-Hill, New York, N.Y., 1953, pp. 129, 311.

(13) L. Baksanyi, O. Liardon, and E. Kovats, *Adv. Colloid Interface Sci.*, **6**, 95 (1976).

(14) J. S. Harington, A. C. Allison, and D. V. Badami, *Adv. Pharmacol. Chemother.*, **12**, 291 (1975).

(15) J. Depasse and J. Warlus, *J. Colloid Interface Sci.*, **56**, 618 (1976).

(16) C. J. Serna, G. E. Van Scoyoc, and J. L. Ahlrichs, *Am. Miner.*, **62**, 784 (1977).

(17) H. van Olphen, "An Introduction to Clay Colloid Chemistry," 2nd ed., Wiley, New York, N.Y., 1977, p. 191.

(18) B. K. G. Theng, "Formation and Properties of Clay–Polymer Complexes," Elsevier, New York, N.Y., 1979, pp. 65–94.

(19) S. Speil and J. P. Leineweber, *Environ. Res.*, **2**, 166 (1969).

(20) R. J. Schnitzer, G. Bunescu, and V. Baden, *Ann. N.Y. Acad. Sci.*, **172**, 759 (1971).

(21) W. G. Light and E. T. Wei, *Environ. Res.*, **13**, 135 (1977).

(22) B. T. Mossman, C. D. Woodworth, B. J. Bradley, M. W. Chates, and J. E. Craighead, The Clay Minerals Society 29th Annual Clay Minerals Conference, Waco, Tex., Abstract p. 71, 1980.


## ACKNOWLEDGMENTS


This report is Journal Paper 7794, Purdue University Agricultural Experiment Station, West Lafayette, IN 47907.

# Acute Hemodynamic Effects and Blood Pool Kinetics of Polystyrene Microspheres following Intravenous Administration

JOHN D. SLACK *§, MOTOKO KANKE ‡, GUY H. SIMMONS *, and PATRICK P. DeLUCA ‡x

Received June 23, 1980, from the *Colleges of *Medicine and ‡Pharmacy, University of Kentucky, and the §Cardiology Section, Veterans Administration Medical Center, University of Kentucky, Lexington, KY 40506. Accepted for publication October 29, 1980.

**Abstract** □ The acute hemodynamic effect of intravenous administration of polystyrene microspheres was investigated and correlated with their distribution pattern and kinetics. Microspheres of three diameters (3.4, 7.4, and 11.6 μm) were administered. The 7.4- and 11.6-μm diameter microspheres were filtered by the pulmonary capillary network following intravenous administration, the majority during the first pass. There was no significant hemodynamic effect following administration of the 7.4- and 11.6-μm diameter microspheres in doses as high as $3.0 \times 10^9$ and $6.1 \times 10^8$, respectively (total cross-sectional area of $1.3 \times 10^{11}$ and $6.4 \times 10^{10}$ $\mu m^2$, respectively). Intravenous administration of 3.4-μm diameter microspheres produced significant dose-dependent systemic hypotension and depression of myocardial performance at dosages as low as $1.0 \times 10^{10}$ (cross-sectional area of $9.1 \times 10^{10}$ $\mu m^2$). These differences in acute hemodynamic effect from the 7.4- and 11.6-μm diameter microspheres may be due to the differences in distribution kinetics and fate of the 3.4-μm diameter microspheres, which readily pass through the lungs to the systemic circulation, with late disposition primarily in the liver and spleen. Although elimination of the smaller spheres from the blood during the first 6–8 min was rapid, *i.e.*, $t_{1/2} = 1.62$ and 1.72 min from the venous and arterial blood circulation, respectively, levels of $10^3$ spheres/g of blood were present in the circulation for >1 hr. These findings must be considered in the planning of intravenous administration of microspheres as a drug delivery system to target organs.

**Keyphrases** □ Microspheres, polystyrene—acute hemodynamic effects and blood pool kinetics following intravenous administration to dogs, drug delivery system to target organs □ Drug delivery system—polystyrene microspheres, acute hemodynamic effects and blood pool kinetics following intravenous administration, dogs □ Kinetics—polystyrene microspheres, distribution and clearance in dogs following intravenous administration, drug delivery system □ Radionuclide imaging agents, potential—$^{141}$Ce-labeled polystyrene microspheres, acute hemodynamic effects and blood pool kinetics evaluated in dogs following intravenous administration

Systemic toxicity of pharmaceutical agents, particularly those used in the chemotherapy of malignancy, has prompted a search for alternative drug delivery methods. Ideally, these methods should be safe, comfortable, and convenient to the patient. To date, attempts at local therapy with surgical implants or chronic catheter placement have achieved only limited success. Intravascular administration of radioactive microspheres has been utilized safely in animals and humans for many years to assess blood flow patterns (1). Detailed investigation regarding their distribution patterns (2, 3), hemodynamic effects (4–6), and induced pathological changes (7, 8) has begun only recently, stimulated by evidence that pharmaceutical agents may be incorporated into subvisible particulates for intravenous administration, with subsequent local release after the particle lodges in the microcirculation (9–11).

While some deaths were recorded in previous studies on microsphere size, distribution time, and distribution pattern in beagle dogs (2, 4, 8), there was little evidence of tissue damage that could be attributed to the microspheres in specific organs. Due to the lack of significant clinical changes, the present study was undertaken to assess the influence of particle size on the hemodynamic changes associated with the intravenous administration of relatively large aggregate-weight bolus injections of microspheres.

## EXPERIMENTAL

**Administration of Microspheres**—Polystyrene divinylbenzene microspheres labeled with cerium 141 were obtained as a suspension in physiological saline from a commercial supplier[1]. The specific activity was ~50 mCi/g; ~500 μCi was administered to each dog. The number of radioactive spheres was calculated from:

$$\text{number of spheres/mg} = \frac{1.55 \times 10^9}{D^3} \qquad \text{(Eq. 1)}$$

where $D$ is the mean sphere diameter in microns. The nonradioactive spheres[2] were obtained as a 10% suspension in saline. The actual size and number of the microspheres were determined microscopically[3] and with an electronic particle counter[4], respectively. The appropriate dose of microspheres was drawn into a syringe, and an accurate radioactivity count was determined by a radioisotope calibrator[5]. The microspheres then were injected intravenously using a three-way stopcock. After thorough flushing of the syringe and stopcock with saline, the syringe was analyzed to exclude significant retention of the microspheres. Immediately prior to dosage administration, the vial of microspheres was placed in an ultrasonic bath for 15 min to ensure dispersion of the spheres. A surfactant, polysorbate 80, was not used in the preparation of the microspheres due to its adverse hemodynamic effect (12).

**Preparation of Animals**—Female beagle dogs, 13.0–15.0 kg, were randomly assigned to receive 3.4, 7.4, or 11.6-μm diameter microspheres. Following endotrachael intubation, anesthesia was maintained with a mixture of 1–2.5% halothane (depending on the blood pressure response and desired level of anesthesia) and oxygen delivered by a mechanical respirator. A left thoracotomy was performed, and a micromanometer-tipped catheter[6] was inserted into the left ventricle to measure systolic pressure. The rate of change of the left ventricular pressure ($dp/dt$) was derived electronically. A pair of ultrasonic piezoelectron crystals was implanted in the left ventricular subendocardial wall to measure regional myocardial wall motion and, by inference, left ventricular volume.

Micromanometer-tipped catheters[7] were inserted into the pulmonary artery and descending aorta to measure pulmonary artery pressure. A thermistor-tipped catheter[8] also was placed in the pulmonary artery to enable serial thermodilution cardiac output determinations. Catheters were positioned in the right atrium and descending aorta to allow ease in blood sampling from the venous and arterial circulation, respectively. The surface ECG was monitored continuously. The micromanometer-tipped catheters were referenced to zero and calibrated with a mercury manometer before insertion. Correction for micromanometer transducer drift was performed by superimposing electronically derived mean

[1] Nuclear Products Division, 3M Co., St. Paul, Minn.
[2] Dow Diagnostics, Indianapolis, Ind.
[3] Zetopan universal research microscope, Reichert, Austria.
[4] Coulter Counter model TAII, Coulter Electronics, Hialeah, Fla.
[5] Model CRC-6A, E. R. Squibb & Sons, Princeton, N.J.
[6] Konigsberg Co., Pasadena, Calif.
[7] Millar Co., Houston, Tex.
[8] 4F pediatric thermodilution catheter 702216, Edwards Laboratory, Santa Ana, Calif.



0022-3549/81/0600-0660$01.00/0
© 1981, American Pharmaceutical Association

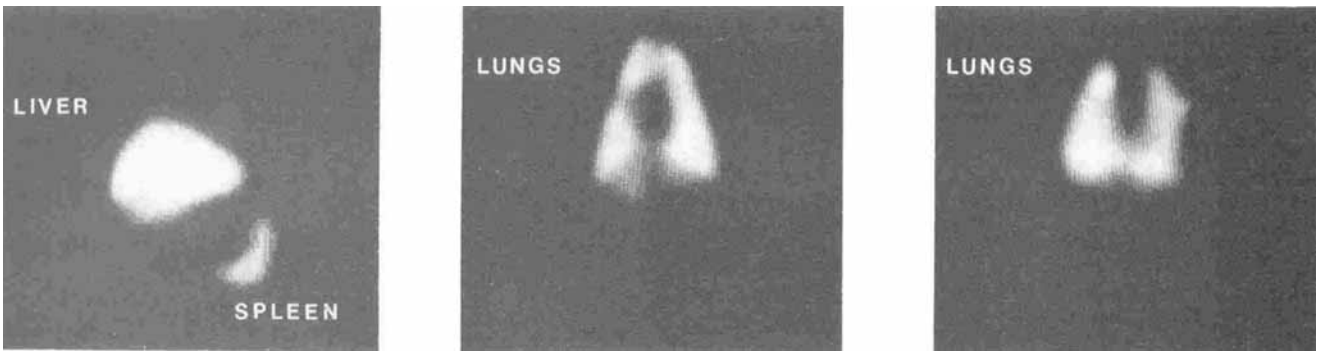


**Figure 1**—*Distribution of $^{141}$Ce-labeled microspheres as determined by external nuclear imaging 3.5 hr following intravenous administration. The larger microspheres (7.4 μm in Dog 6 and 11.6 μm in Dog 4) were localized in the lungs, whereas the smaller (3.4 μm in Dog 1) microspheres distributed to the liver and spleen.*

pressure against that of a fluid-filled catheter system connected to a pressure transducer[9] positioned at midchest level.

**Hemodynamic Protocol**—Following the surgical instrumentation, each animal was monitored for 30 min to ensure hemodynamic stability. Continuous direct measurements of the surface ECG, pulmonary artery pressure, systemic artery pressure, left ventricular pressure, rate of change of left ventricular pressure ($dp/dt$), and left ventricular segmental wall motion were recorded on magnetic tape[10]. Data were printed at predetermined intervals[11]. Serial duplicate cardiac output determinations were recorded at 20-min intervals[12]. Maximum values of $+dp/dt$ and $-dp/dt$ were determined from electronic differentiation of the left ventricular pressure waveform.

The systolic shortening fraction, which is a measure of the left ventricular regional wall motion, was calculated with ultrasonic segment-length measurement *via* the piezoelectron crystals implanted in the left ventricular subendocardium using the following expression: (end diastolic length − end systolic length)/end diastolic length. All animals were stable throughout the 30-min control period. A control animal was monitored for 3 hr following a placebo injection of physiological saline; this animal remained stable.

Following the 30-min control period, a measured number of $^{141}$Ce-labeled microspheres of a given size (Table I) was administered as a bolus injection into the right atrium. Two dogs received the 3.4-μm diameter size, two received the 7.4-μm diameter size, and two received the 11.6-μm diameter size microspheres. Hemodynamic measurements and venous and arterial blood samples were taken every 2 min for 40 min, every 5 min for 20 min, and then every 10 min for the next 2 hr.

At the conclusion of the 3-hr monitoring period, a second bolus injection of nonradioactive microspheres of the same diameter (Table I) was administered slowly (~8 ml/min) to assess possible hemodynamic effects of larger doses. Then 3.5 hr after administration of the radioactive microspheres, each animal was sacrificed and sent for nuclear scanning. Two additional dogs were instrumented similarly for additional dosing with nonradioactive 3.4-μm diameter microspheres to complete the dose–response curve.

**Scanning of Dogs**—With a digital computer[13] attached to a scintillation camera[14], distribution of the radioactive microspheres was assessed by whole body scanning.

**Blood Level of Spheres**—Blood samples removed during the 3-hr study were analyzed for radioactivity using a well-type γ-counter[15]. Application of the appropriate calibration equation yielded results in microspheres per gram of blood.

## RESULTS

**Nuclear Scanning**—Consistent with previous results, the radioactivity was confined principally to the lungs (>90%) in animals administered $^{141}$Ce-labeled 7.4- and 11.6-μm diameter microspheres. The animals given 3.4-μm diameter microspheres had little activity (~12%) remaining in the lungs 3.5 hr following administration, the majority (~83%) of the radioactive particles having accumulated in the liver and spleen (Fig. 1). Table II summarizes the results of external analysis of these organs and demonstrates the clear tendency of the microspheres to distribute in a size-dependent organ-specific pattern.

**Table I—Dosing Information**

| Dog | Microsphere Size, μm | Number | CSA[a], μm² | Weight, mg |
|---|---|---|---|---|
| Control | — | — | — | — |
| Control-NR[b] | 3.4 | $1.41 \times 10^{11}$ | $1.28 \times 10^{12}$ | 3525 |
| 1 | 3.4 | $6.25 \times 10^{8}$ | $5.68 \times 10^{9}$ | 15.6 |
| 2 | 3.4 | $8.62 \times 10^{8}$ | $7.83 \times 10^{9}$ | 21.6 |
| 2NR | 3.4 | $9.45 \times 10^{9}$ | $8.58 \times 10^{10}$ | 236 |
| 3 | 11.6 | $1.09 \times 10^{7}$ | $1.15 \times 10^{9}$ | 10.9 |
| 3NR | 11.6 | $2.02 \times 10^{8}$ | $2.14 \times 10^{10}$ | 202 |
| 4 | 11.6 | $2.13 \times 10^{7}$ | $2.25 \times 10^{9}$ | 21.3 |
| 4NR | 11.6 | $6.06 \times 10^{8}$ | $6.40 \times 10^{10}$ | 606 |
| 5 | 7.4 | $4.26 \times 10^{7}$ | $1.83 \times 10^{9}$ | 11.2 |
| 5NR | 7.4 | $1.50 \times 10^{9}$ | $6.45 \times 10^{10}$ | 394 |
| 6 | 7.4 | $5.52 \times 10^{7}$ | $2.37 \times 10^{9}$ | 14.5 |
| 6NR | 7.4 | $3.00 \times 10^{9}$ | $1.29 \times 10^{11}$ | 789 |
| 7NR | 3.4 | $1.00 \times 10^{9}$ | $9.08 \times 10^{9}$ | 25.0 |
| 7LNR[c] | 3.4 | $1.00 \times 10^{10}$ | $9.08 \times 10^{10}$ | 250 |
| 8NR | 3.4 | $9.55 \times 10^{10}$ | $8.67 \times 10^{11}$ | 2388 |

[a] CSA = cross-sectional area. [b] NR = dose of nonradioactive spheres. [c] LNR = large dose of nonradioactive spheres.

**Blood Pool Kinetics**—Serial measurements of circulating microsphere levels from venous and arterial sites drawn following intravenous administration of $^{141}$Ce-labeled microspheres are shown graphically by blood level profiles in Fig. 2. The elimination rate of the initial stage following intravenous administration is summarized in Table III. The elimination rate constant was determined by the least-squares method using first-order kinetics. These data, along with the ratios of venous and arterial blood levels presented in Table IV, demonstrate that few of the 7.4- and 11.6-μm spheres reached the arterial circulation; 98% of the 7.4- and 11.6-μm spheres were eliminated from the circulating blood pool in the first 2 min. For the 3.4-μm spheres, 10–12 min was required before 98% was eliminated. Within 10 min, the concentrations of the 11.6, 7.4, and 3.4-μm spheres in venous circulation were <10, ~10, and ~$10^3$–$10^4$ spheres/g of blood, respectively. Therefore, a ratio of 0.81 for venous to arterial circulation for the 3.4-μm spheres indicates that the smaller spheres passed readily from the venous to arterial circulation, with high arterial levels present virtually immediately after administration. The

**Table II—Microsphere Distribution in Specific Organs 3.5 hr after Intravenous Administration Determined by External Imaging**

| Size, μm | Lungs, % | Liver, % | Spleen, % | Total in the Three Organs, % |
|---|---|---|---|---|
| 3.4 | 12 | 73 | 10 | 95 |
| 7.4 | 92 | (~2%)[a] | | 94 |
| 11.6 | 93 | —[b] | —[b] | 93 |

[a] Combined level of activity in liver and spleen was ~2%. [b] Negligible level in liver and spleen.

[9] Bentley Trantec mode 800, Irvine, Calif.
[10] Honeywell Co., Denver, Colo.
[11] Brush recorder 200, Gould Co., Cleveland, Ohio.
[12] Model 9520 Cardiac Output Computer, Edwards Laboratories, Santa Ana, Calif.
[13] PDP-11/15, Digital Equipment Corp., Maynard, Mass.
[14] Pho/gamma LFOV, Searle Radiographics, Des Plaines, Ill.
[15] Spectroscaler, Picker Nuclear Corp., Northford, Conn.

**Table III—Elimination of Microspheres from Blood at Initial Stage following Intravenous Administration [a]**

| Sphere Size, μm | Elimination Rate, $min^{-1}$ | | $t^{1/2}$, min | |
|---|---|---|---|---|
| | Venous Blood | Arterial Blood | Venous Blood | Arterial Blood |
| 3.4 | −0.426 ± 0.078 | −0.403 ± 0.053 | 1.62 | 1.72 |
| 7.4 | −0.810 ± 0.168 | −0.776 ± 0.140[b] | 0.86 | 0.89 |
| 11.6 | −1.33 ± 0.320 | — | 0.52 | — |

[a] Average of two dogs in each size. [b] Essentially all 11.6-μm spheres and >95% of the 7.4-μm spheres were removed from the systemic circulation during the first pass. Therefore, this elimination rate is for a relatively small number of spheres that reached the arterial circulation.

blood level profiles show that the venous and arterial levels of 3.4-μm spheres remained essentially the same over ~3 hr, suggesting that these spheres recirculate rather freely. Even after 2 hr, the level in the circulation was $10^2$–$10^3$/g of blood.

**Hemodynamic Data**—The 7.4- and 11.6-μm diameter microspheres were not associated with significant hemodynamic changes in the dosage ranges administered. The 3.4-μm diameter microspheres, administered at a similar total cross-sectional area dosage, induced significant dose-dependent deterioration in some of the hemodynamic parameters monitored (Fig. 3). These changes are illustrated more clearly in Fig. 4, which depicts a slow continuous recording of the first 7 min following intravenous administration of $1.41 \times 10^{11}$ 3.4-μm diameter microspheres. A profound drop in the systemic blood pressure, with associated deterioration in $-dp/dt$, $+dp/dt$, and systolic segment shortening, occurred within several minutes of microsphere administration. A later secondary elevation in pulmonary artery pressure also occurred, probably due to a neurohumoral reflex response to the severe systemic hypotension.

These acute changes are most consistent with peripheral vascular collapse, not unlike those seen in anaphylactic shock. That direct myocardial depression occurs, but is not the predominant cause of shock, is evidenced by the lack of elevation in left ventricular end diastolic pressure and the reduction in end diastolic segment length. Only after a period of profound hypotension was there evidence of depressed myocardial function, *i.e.*, decreased $+dp/dt$ and decreased systolic segment shortening. Sustained ventricular tachycardia developed late following administration of 3.4-μm diameter microspheres in one animal. Cardiac output also was well maintained initially, dropping only after sustained hypotension, with its deleterious effect on the myocardium, had been present. Progressive increases in dosage of these 3.4-μm diameter microspheres resulted in progressive worsening of the severity (Fig. 5) and duration of the systemic hypotension.

## DISCUSSION

Intravascular injection of particulate matter has been performed to image organs and assess blood flow characteristics. Early investigators utilized distribution kinetics of different size microspheres to assess the physical dimensions and biological characteristics of the microcirculation of various organs (1). As early as 1961, it was reported that the majority of microspheres less than 4.0 μm in diameter injected into the femoral vein passed through the pulmonary capillary network, whereas only a relatively small portion of similarly injected microspheres of >8.0 μm diameter passed into the systemic circulation (13). Previous work in our laboratories amplifies these points and, along with the present results, demonstrates that localization of the 7.4- and 11.6-μm diameter microspheres in the lungs, presumably by mechanical filtration, occurs in the first 2 min. This rapid localization suggests passive filtration and is consistent with ultrastructure studies of the pulmonary capillary network (14, 15) and the results of other investigators working with similarly sized microspheres (13, 16). The localization in the lungs appears to be complete for the 11.6-μm spheres, but there is evidence of gradual clearance and relocation in the liver and spleen of the 7.6-μm spheres.

Because of the recirculation characteristics of the microspheres of <4.0-μm diameter, their use was generally abandoned since they were of little value in organ imaging or assessing blood flow patterns. Of considerable interest is the recent documentation (2, 8) that, following intravenous administration, the 3.4-μm diameter microspheres pass through the pulmonary circulation and distribute in a pattern consistent with reticuloendothelial system uptake. This localization of the 3.4-μm diameter microspheres in the liver and spleen requires considerably more time than localization of the larger (≥7.4-μm diameter) microspheres in the lungs, suggesting a biologically active process, *e.g.*, phagocytosis (17) rather than passive filtration. The prolonged time course required for the 3.4-μm diameter microsphere clearance from the circulating blood pool correlates well with the duration of their acute hemodynamic effects (*vide supra*) and suggests some association with blood cells, a gradual release from the lungs, or a combination of the two.

Allen *et al.* (18) suggested that pulmonary hypertension is the most sensitive sign of hemodynamic deterioration following intravenous injection of microspheres larger than 13.5-μm in diameter. These authors also demonstrated a dose–response curve that correlated the increase in pulmonary artery pressure with increasing dosage and increasing sizes of administered microspheres (5). As expected from their dose–response curve, no significant pulmonary artery pressure rise was observed following intravenous administration of 7.4- and 11.6-μm diameter microspheres. While these particles are smaller than those that Allen utilized, they are nearly completely filtered by the pulmonary capillary network during the first pass through the pulmonary circulation.

The number of 3.4-μm diameter microspheres required to produce serious hemodynamic compromise is much smaller than would be predicted using the formula suggested by Allen *et al.* (5). This result appears due to the demonstrated ability of these small microspheres to pass through the pulmonary vascular network. Indeed, the period of hemodynamic compromise coincides with the time during which the 3.4-μm

**Table IV—Ratio of Microsphere Levels in Venous and Arterial Blood (VBC/AVC) Samples following Intravenous Administration**

| Minutes | VBC/AVC | | |
|---|---|---|---|
| | 3.4 μm | 7.4 μm | 11.6 μm |
| 2 | 0.81 | 6.4 | 85 |
| 4 | 0.69 | 3.1[a] | 18[a] |
| 10 | 0.81[b] | —[c] | —[c] |
| 20 | 1.0 | — | — |
| 30 | 1.1 | — | — |

[a] Approximate venous concentration is <50 spheres/g of blood. [b] Venous concentration is $10^3$–$10^4$ spheres/g of blood. [c] Venous concentration is <10 spheres/g of blood.

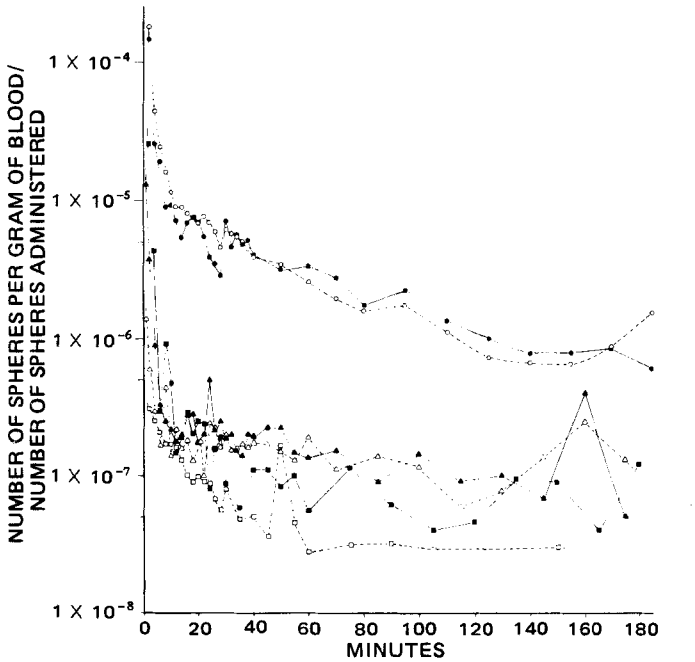


**Figure 2**—*Level of $^{141}Ce$-labeled microspheres in venous and arterial samples following intravenous administration in beagle dogs. Key: ●, 3.4 μm, venous; ○, 3.4 μm, arterial; ▲, 7.4 μm, venous; △, 7.4 μm, arterial; ■, 11.6 μm, venous; and □, 11.6 μm, arterial.*

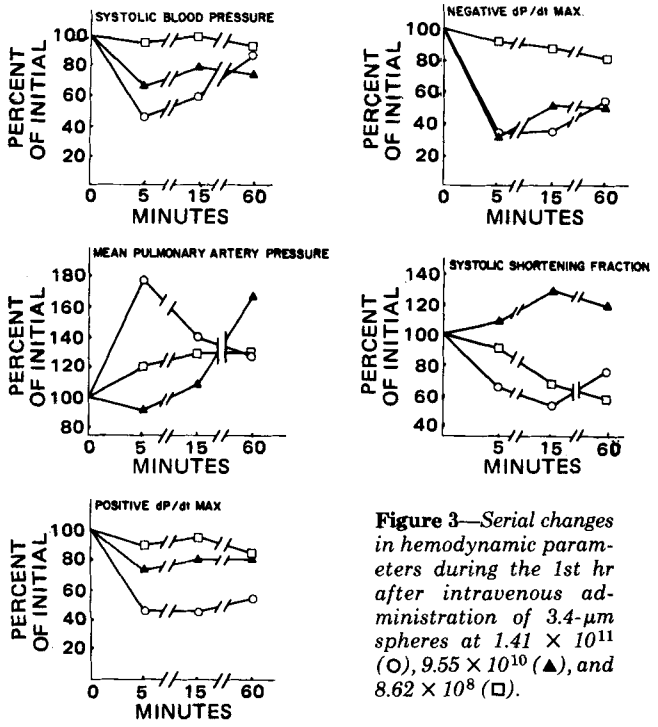


**Figure 3**—*Serial changes in hemodynamic parameters during the 1st hr after intravenous administration of 3.4-μm spheres at 1.41 × $10^{11}$ (○), 9.55 × $10^{10}$ (▲), and 8.62 × $10^{8}$ (□).*

diameter microspheres are numerous in the circulating blood pool (Figs. 2–4).

At present, the cause of the observed acute hemodynamic deterioration is unknown. Because of its similarity to anaphylaxis, a possible explanation would be the liberation of vasoactive amines as the microspheres pass through the pulmonary and peripheral vascular networks (19, 20). Alternatively, the hypotension could reflect a neurogenic reflex caused by high levels of the microspheres entering the central nervous system (21, 22). The former appears more likely based on the sequence of hemodynamic changes and the platelet clumping that occurred only around the 3.4-μm diameter microspheres upon histological examination (8, 23). The possibility that toxic monomers leaching from the smaller microspheres could promote vasomotor instability and initiate anaphylaxis was considered and discarded when injection of 20 ml of supernate from the sphere suspension into a dog caused no change in blood pressure over 0.5 hr. Furthermore, *in vitro* analyses of the supernate included UV spectra devoid of any peaks characteristic of monomer and a clean TLC analysis of a chloroform extract. The amount of residue left after drying the chloroform extract was too small to quantitate or to obtain an IR spectrum.

Incorporation of pharmacotherapeutic agents into microspheres for intravascular administration appears feasible from a technological standpoint and may have the advantages of achieving locally high drug concentrations in the target organ. Larger size (7.4- and 11.6-μm diameter) microspheres lodge in the pulmonary capillary network whereas 3.4-μm diameter microspheres appear to be taken up by the reticuloendothelial system. These differences in distribution fate following intravenous administration may be of significance in planning future chemotherapy of disease of the lungs and reticuloendothelial system.

## CONCLUSION

This study demonstrates that intravenous administration of particulate matter may be associated with significant acute hemodynamic deterioration in the experimental animal and reveals that very small microspheres (3.4-μm diameter) have a different distribution fate and time course than larger microspheres (≥7.4-μm diameter). Since the difference in distribution is associated with a more severe, acute hemodynamic effect than would be expected based on size and number alone, the limitation of particulate material for target organ drug administration may be the ability to incorporate a therapeutic dose in a finite number of particles

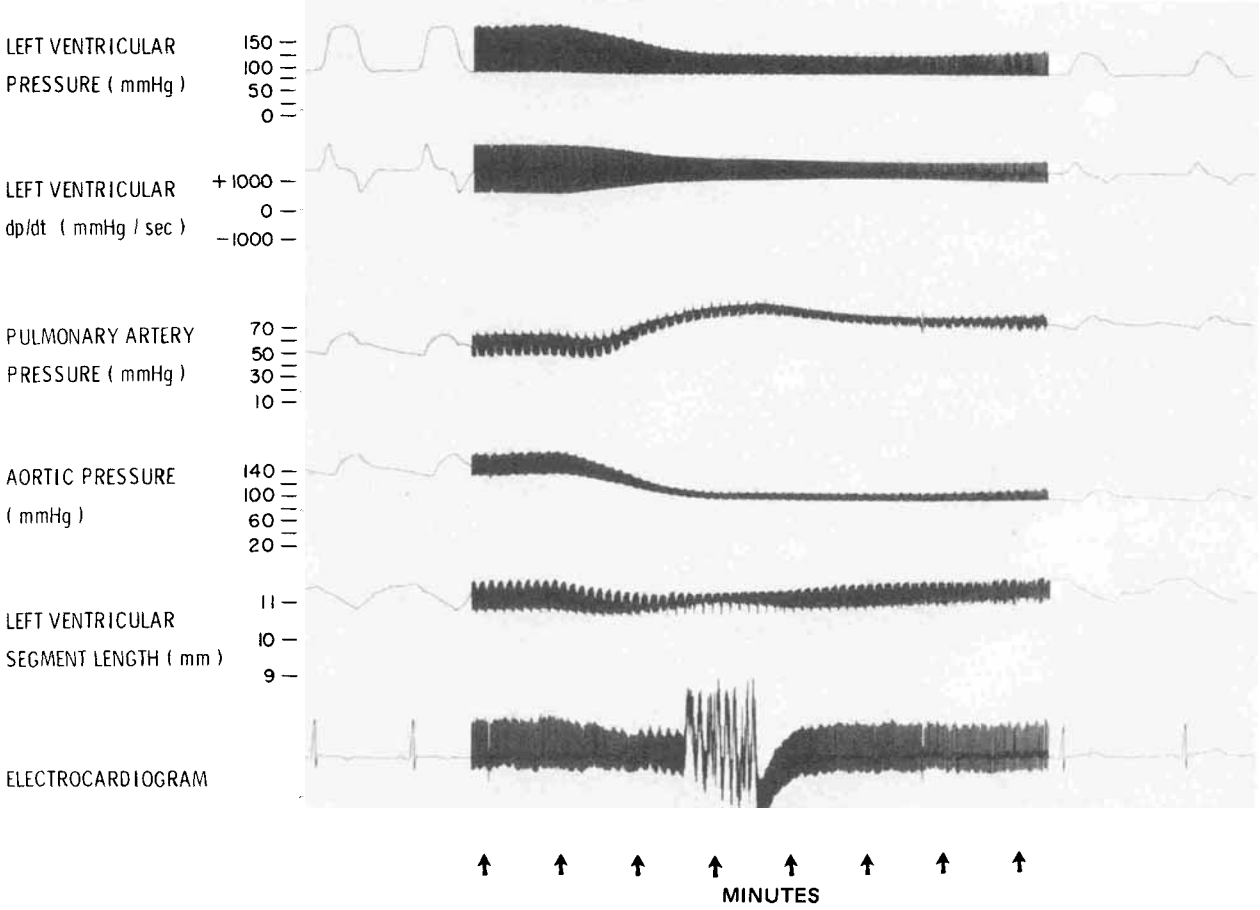


**Figure 4**—*Continuous display of the hemodynamic changes in the first 7 min following intravenous administration of 1.41 × $10^{11}$ microspheres of 3.4-μm size (area = 1.28 × $10^{12}$ μm² and weight = 3525 mg). A short lead and exit strip at chart speed of 25 mm/sec are provided to allow appreciation of individual waveforms.*

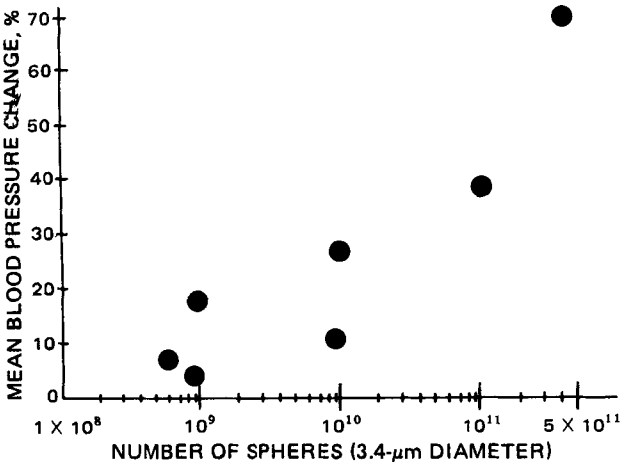


**Figure 5**—*Acute effect of intravenously administered 3.4-μm spheres on mean blood pressure as a function of concentration (r = 0.82).*

determined by their hemodynamic effect. Nevertheless, bolus intravenous injections of ~1 g of microspheres were administered to beagle dogs (13–15 kg) without serious consequences.

Therefore, the potential exists to incorporate sufficient amounts of drug into the microsphere during manufacture to provide therapeutic dosages. The influences of particle composition, surface charge, dissolution rate, and antigenicity will need to be determined. Furthermore, the acute hemodynamic effect evidenced following administration of the 3.4-μm diameter microspheres was consistently brief and reversible in the smaller dosage range. This finding suggests that a different dosage pattern, *i.e.*, smaller, more frequent administrations rather than a large bolus injection, or slower administration could avoid the risks of hemodynamic effects, thereby delivering a selected chemotherapeutic agent in relatively high local tissue concentrations to the target organ with safety.

Finally, both histological and hemodynamic studies of the long-term effects of repeated intravascular injections of microspheres must be performed to exclude the possibility of irreversible tissue damage with chronic administration.

## REFERENCES

(1) M. A. Heymann, B. D. Payne, J. I. E. Hoffman, and A. M. Rudolph, *Prog. Cardiovasc. Dis.*, **20,** 55 (1977).

(2) H. G. Schroeder, G. H. Simmons, and P. P. DeLuca, *J. Pharm. Sci.*, **67,** 504 (1978).

(3) J. Kreuter, U. Tauber, and I. Volker, *ibid.*, **68,** 1443 (1979).

(4) H. G. Schroeder, B. A. Bivins, G. P. Sherman, and P. P. DeLuca, *ibid.*, **67,** 508 (1978).

(5) D. R. Allen, J. M. Ferens, F. W. Cheney, and W. B. Nelp, *J. Nucl. Med.*, **19,** 1204 (1978).

(6) M. A. Davis and R. A. Taube, *ibid.*, **19,** 1209 (1978).

(7) J. Szymendera, O. Mioduszewska, I. Lieinska, A. Czarnomska, and B. Lucka, *ibid.*, **18,** 478 (1977).

(8) M. Kanke, G. H. Simmons, D. M. Weiss, B. A. Bivins, and P. P. DeLuca, *J. Pharm. Sci.*, **69,** 755 (1980).

(9) P. A. Kramer, *ibid.*, **63,** 1646 (1974).

(10) J. D. Scheu, G. J. Sperandio, S. M. Shaw, R. R. Landolt, and G. E. Peck, *ibid.*, **66,** 172 (1977).

(11) K. Widder, G. Flouret, and A. Senyei, *ibid.*, **68,** 79 (1979).

(12) R. W. Millard, H. Baig, and S. F. Vatner, *Am. J. Physiol.*, **232,** H331 (1977).

(13) G. C. Ring, A. S. Blum, T. Kurbator, W. G. Mass, and W. Smith, *ibid.*, **200,** 1191 (1961).

(14) D. B. Gordon, J. Flasher, and D. R. Drury, *ibid.*, **173,** 275 (1953).

(15) S. S. Sobin, M. Intagietta, W. G. Frasher, and H. M. Tremer, *Angiology*, **17,** 24 (1966).

(16) R. E. Madden, A. Paparo, and M. Schwartz, *Arch. Surg.*, **96,** 130 (1968).

(17) B. Holma, *Acta Med. Scand. Suppl.*, **473,** 1 (1967).

(18) D. R. Allen, W. B. Nelp, F. Cheney, and D. E. Hartnett, *J. Nucl. Med.*, **15,** 567 (1974).

(19) J. R. Nelson and J. R. Smith, *Am. Heart J.*, **58,** 916 (1959).

(20) D. Thomas, M. Stein, G. Tanabe, V. Rege, and S. Wessler, *Am. J. Physiol.*, **206,** 1207 (1964).

(21) D. J. Warren and J. G. Ledingham, *Cardiovasc. Res.*, **8,** 570 (1974).

(22) R. K. McEvoy, R. A. Harder, and W. A. Dale, *Surg. Gynecol. Obstet.*, **106,** 271 (1958).

(23) D. P. Thomas, V. Gurewich, and T. P. Ashford, *N. Engl. J. Med.*, **274,** 953 (1966).

## ACKNOWLEDGMENTS

Presented in part at the Basic Pharmaceutics Section, APhA Academy of Pharmaceutical Sciences, Anaheim meeting, April 1979.

Supported in part by Food and Drug Administration Contract 223-77-3018 and the Veterans Administration.

The authors acknowledge the Nuclear Medicine Department, College of Medicine, University of Kentucky, for providing the equipment for γ-imaging.

J. D. Slack was a National Heart, Lung, and Blood Institute Fellow in Cardiovascular Disease when this work was performed.

# High-Performance Liquid Chromatographic Analysis of Captopril in Plasma

**B. JARROTT ˣ, A. ANDERSON, R. HOOPER, and W. J. LOUIS**

Received September 18, 1980, from the *Clinical Pharmacology and Therapeutics Unit, Department of Medicine, University of Melbourne, Austin Hospital, Heidelberg 3084, Victoria, Australia.* Accepted for publication November 17, 1980.

**Abstract** □ A sensitive assay is described for quantitating plasma captopril levels. Captopril is an orally active inhibitor of angiotensin-converting enzyme. Blood from patients taking this drug was collected into tubes containing edetate and ascorbic acid, and the plasma was separated by centrifugation. After addition of an internal standard, the plasma was deproteinized and the supernate was adjusted to pH 6.5. *N*-(1-Pyrene)-maleimide was added to derivatize captopril and an internal standard to fluorescent adducts. These derivatives then were extracted into ethyl acetate–benzene (1:1) and separated from other derivatized thiols by high-performance liquid chromatography. The sensitivity of the assay was 150 pmoles/ml. Preliminary pharmacokinetics were obtained in patients taking captopril chronically for essential hypertension. After administration of 100 mg of captopril to patients who had fasted overnight, the plasma levels rose rapidly; peak levels were obtained at ~37 min. Thereafter, the plasma levels declined rapidly, and the terminal half-life was ~40 min. In these patients, the time course of the plasma levels did not reflect changes in blood pressure, so there appeared to be no direct relationship between plasma levels of the parent compound and blood pressure changes.

**Keyphrases** □ High-performance liquid chromatography—analysis of captopril in plasma □ Captopril—analysis using high-performance liquid chromatography □ Antihypertensives—high-performance liquid chromatographic method for captopril

Captopril (D-3-mercapto-2-methylpropanoyl-L-proline, I) is a potent and selective inhibitor of angiotensin-converting enzyme (kininase II) (1). Oral captopril administration lowers blood pressure in laboratory animals with experimental hypertension (2, 3) and in hypertensive humans (4, 5). Since the reductions in blood pressure apparently are related to the inhibition of angiotensin-converting enzyme (5), captopril appears to be the prototype of a new class of antihypertensive drug.

The disposition of captopril has been reported only in normotensive subjects taking an oral formulation of $^{35}S$-labeled captopril (6). The present paper reports the development of a sensitive high-performance liquid chromatographic (HPLC) assay for quantitating captopril in plasma and its application to a preliminary study of captopril pharmacokinetics in patients undergoing a clinical trial for the management of essential hypertension.

## EXPERIMENTAL

**Instrumentation**—Assays were carried out using a constant-flow, high-performance liquid chromatograph[1]. It consisted of a solvent delivery system[2], a universal injector[3], a radial compression module[4] with a reversed-phase permanently bonded octadecylsilane cartridge[5] (10 cm long × 8 mm i.d.), and a spectrophotofluorometer[6] equipped with a 20-μl flow-through quartz cell and a 150-w xenon arc lamp with excitation and emission monochromators set at 340 and 390 nm, respectively.

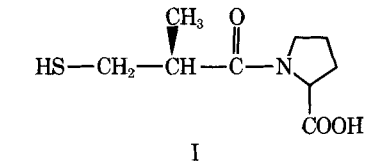

I

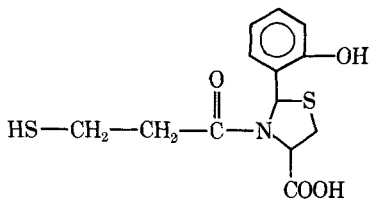

II

**Reagents**—Captopril[7] and an internal standard[8] [(4*R*)-2-(2-hydroxyphenyl)-3-(3-mercaptopropionyl)-4-thiazolidinecarboxylic acid, II] were used. The derivating reagent was *N*-(1-pyrene)maleimide[9]. Ethyl acetate and benzene[10] were analytical reagent grade, and methanol[1] was liquid chromatographic grade. All other reagents were the highest grade purity.

**Standard Solutions**—Standard solutions of captopril (1 m*M*) and II (1 m*M*) were prepared by dissolving pure drug in an aqueous solution of edetate disodium (1 m*M*) previously bubbled with nitrogen. These solutions were stored at 4° and were stable for at least 7 days. The *N*-(1-pyrene)maleimide derivatizing reagent (2 m*M*) was prepared by dissolving the powder in acetone and was stored at 4° for at least 14 days.

**Patient Sampling Procedure**—Four patients who had been taking captopril (100 mg, three times a day) for essential hypertension were studied. After an overnight fast, 100 mg of captopril was given; the patients then continued to fast for 4 hr. Immediately prior to dosing and at 0.25, 0.5, 0.75, 1.0, 1.5, 2, 3, and 4 hr, a 5-ml blood sample was taken from an indwelling catheter in a forearm vein and added to a heparinized tube containing 50 μl of a solution of edetate disodium (0.1 *M*) and ascorbic acid (0.1 *M*). After mixing, the samples were centrifuged immediately at 2000×*g* for 10 min to separate the plasma.

**Extraction Procedure**—The internal standard (10 nmoles) was added to 1.0 ml of plasma in a polypropylene tube (9.5 × 2 cm), and then 200 μl of perchloric acid (2 *M*) was added. After centrifugation at 2000×*g* for 10 min, 0.5 ml of the supernate was removed and its pH was adjusted to 6.5 with tribasic potassium phosphate (1 *M*). The derivatizing reagent was added (50 nmoles), and the solution was left at room temperature for 15 min. The solution then was extracted with 3 ml of ethyl acetate–benzene (1:1) by vortex mixing for 30 sec. Following centrifugation to separate the phases, the upper layer was transferred to a clean glass-stoppered conical tube and evaporated to dryness under nitrogen. The residue was dissolved in 100 μl of methanol and was either subjected immediately to liquid chromatography or stored overnight at 4°.

**Chromatography**—Ten-microliter injection volumes were used. The mobile phase was methanol–potassium phosphate buffer (5 m*M*, pH 6.5) (52:48), and the flow rate was maintained at 2 ml/min at a back pressure of ~1000 psi.

**Quantitation**—Since captopril is known to oxidize spontaneously into disulfides, ascorbic acid and edetate were added to the blood immediately upon sampling. Preliminary experiments demonstrated that this procedure prevented any loss of captopril when it was added to control blood and analyzed as already described.

[1] Waters Associates, Chippendale, Australia, 2008.
[2] Model 6000A, Waters Associates.
[3] Model U6K, Waters Associates.
[4] Model RCM-100, Waters Associates.
[5] PAK A cartridge, Waters Associates.
[6] Farrand Optical Co., New York, N.Y.
[7] E. R. Squibb & Sons Pty. Ltd., Melbourne, Australia.
[8] Santen Pharmaceuticals, Osaka, Japan.
[9] Polysciences.
[10] Merck, Darmstadt, West Germany.

0022-3549/81/0600-0665$01.00/0
© 1981, American Pharmaceutical Association

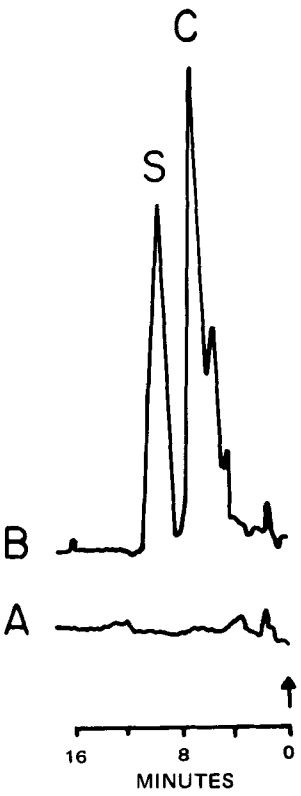


**Figure 1**—*Elution of fluorescent material from HPLC column after derivatization and extraction of control plasma (A) and plasma from a patient who had taken 100 mg of captopril 1 hr previously (B). Key: C, captopril (I); and S, internal standard (II).*

A calibration curve was constructed by adding varying amounts of captopril and a constant amount of internal standard to 1 ml of control plasma and analyzing the samples as already described. To assess linearity, the peak height ratio of captopril to the internal standard was plotted against the added captopril.

Recoveries of sulfhydryl compounds were calculated by first adding the same amount of each compound to plasma and then deproteinizating, derivatizing, extracting, evaporating, and reconstituting in methanol. The methanol extract then was injected, and the peak height was calculated. The same amount of sulfhydryl compound in phosphate buffer was derivatized and directly injected, and the peak height was measured. The percent recovery was calculated by dividing the peak height after solvent extraction by the peak height without solvent extraction and multiplying by 100.

**Pharmacokinetic Analysis**—Plasma captopril level–time data were fitted to a polyexponential equation using the nonlinear least-squares regression analysis computer program AUTOAN 2 (7). The estimated parameters were obtained assuming first-order absorption and elimination.

## RESULTS AND DISCUSSION

Captopril disposition in humans (6) and laboratory animals (8) has only been studied using a single dose of radiolabeled captopril. Thus, a sensitive and specific assay is needed for measuring blood levels of captopril in patients so that its pharmacokinetics can be defined for developing an optimal dosage regimen.

Since captopril has no prominent absorption properties in the UV or visible spectrum, methods were examined for derivatizing captopril through its thiol group to yield a suitable fluorophore. A suitable reagent

**Table I—Summary of Captopril Pharmacokinetics in Patients** [a]

| Patient | $T_{max}$, hr | $C_{max}$, nmoles/ml | $AUC$, nmoles hr/ml | $T_{1/2}$, hr |
|---|---|---|---|---|
| 1 | 0.75 | 18.5 | 18.66 | 0.92 |
| 2 | 0.67 | 20.8 | 20.12 | 0.52 |
| 3 | 0.58 | 18.3 | 17.34 | 0.70 |
| 4 | 0.50 | 9.9 | 10.99 | 0.52 |
| Mean | 0.63 | 16.9 | 16.77 | 0.66 |
| *SE* | 0.05 | 2.4 | 2.01 | 0.09 |

[a] $T_{max}$ = time when maximum plasma concentration, $C_{max}$, is reached. $AUC$ = area under curve, and $T_{1/2}$ = elimination half-life.

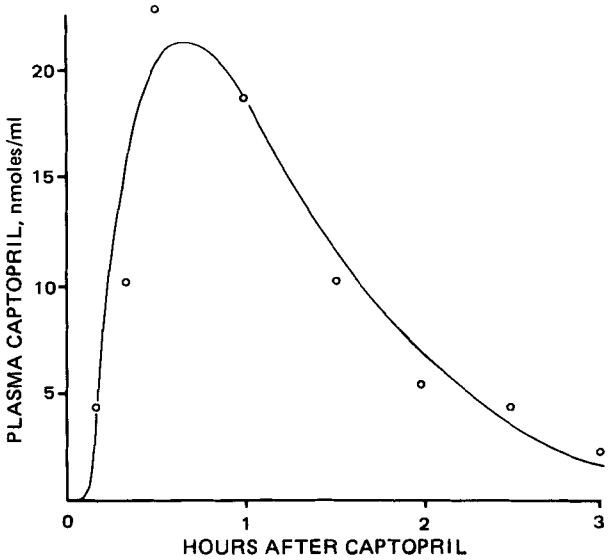


**Figure 2**—*Time–plasma concentration curve for captopril after oral administration of 100 mg to a hypertensive patient.*

was *N*-(1-pyrene)maleimide since this reagent did not fluoresce in aqueous solution but formed fluorescent adducts, under mild conditions, with thiol compounds or proteins containing such groups (9, 10). While this reagent has been used for fluorescence polarization studies of high molecular weight proteins, in the present study it formed a fluorescent adduct with captopril. However, other low molecular weight thiols such as cysteine, *N*-acetylcysteine, and glutathione also formed fluorescent derivatives that were indistinguishable from each other by their excitation and emission spectra.

Since glutathione and cysteine are present in the blood, it was apparent that an HPLC technique would be necessary to separate these derivatized thiols. Since such an assay could be improved by the incorporation of an internal standard, another thiol angiotensin-converting enzyme inhibitor (II) was included in initial studies to define the HPLC conditions for separation of the fluorescent adducts of glutathione, cysteine, captopril, and II. The conditions given under *Experimental* achieved satisfactory separations with retention times of 2.4, 3.2, 5.6, and 7.6 min, respectively. Further specificity was obtained by examining various solvents to extract the fluorescent adducts differentially after derivatization. The most suitable solvent was an equal mixture of ethyl acetate and benzene (3 ml), and the percent recovery of the succinimide derivatives at pH 6.5 was as follows: cysteine, 3%; glutathione, <1%; captopril, 68%; and II, 91%.

Figure 1 illustrates a typical chromatogram obtained after extraction of drug-free plasma (curve A) and of plasma from a patient who had taken captopril 1 hr earlier (curve B). The peak at 5.6 min represents captopril, and the peak at 7.6 min was the internal standard (II). The minor peak on the shoulder of the captopril peak was always seen when captopril was derivatized and chromatographed on the radial compression column. However, it was not seen in earlier studies when a $C_{18}$ reversed-phase column was used, presumably due to the lower efficiency of this column. Since the former column has a higher number of plates (~5000) than the latter column (~2000 plates) and, therefore, achieves a higher resolution, this minor component could be an isomer of captopril.

The threshold of captopril detection in plasma corresponding to a peak height approximately three times that of baseline noise was 150 pmoles/ml. A calibration curve for the peak height ratio of captopril to the internal standard was linear over the concentration range of 150–10,000 pmoles/ml. The within-run precision of the assay (coefficient of variation) at a concentration of 1.5 nmoles/ml was 8.1% ($n$ = 4), and the between-run precision was 9.0% ($n$ = 6).

Because of recent reports of toxicity, including neutropenia (11) and proteinuria (12), permission has not been given for single-dose pharmacokinetic studies in normotensive subjects. A limited study of captopril kinetics in patients taking this drug chronically for essential hypertension was made. Patients fasted overnight, and a predose blood sample was taken; no captopril could be detected in any predose blood sample. After the administration of a standard dose of 100 mg of captopril, absorption was very rapid in all patients; the average time for achieving peak plasma concentrations of captopril was 37 min (Table I). In two patients, the appearance rate of captopril in the blood was so rapid that it did not appear to be following a first-order process. Further experiments with

sampling at closer time intervals are needed to confirm these observations. The data for all patients could be described approximately by the sum of two exponentials, and the mean elimination half-life was ~40 min. The plasma concentration–time profile for one subject is shown in Fig. 2.

The pharmacokinetics of captopril in the four patients taking the drug chronically indicate that changes in plasma captopril concentrations do not reflect blood pressure changes. In all patients, captopril was undetected in their plasma 3–4 hr after dosing, yet blood pressure had not risen at this time. Blood levels of captopril metabolites, such as the disulfide, possibly may be a more useful index of the hemodynamics of this drug.

In conclusion, it was demonstrated that plasma captopril can be assayed with high sensitivity and specificity by first derivatizing this thiol compound to a fluorophore using *N*-(1-pyrene)maleimide and then separating the fluorescent adducts by HPLC. This procedure can also be used for assaying another thiol angiotensin-converting enzyme inhibitor, II, using captopril as the internal standard. This derivatization procedure should be suitable for assaying the mucolytic drug *N*-acetylcysteine after modification of the HPLC conditions to retard its elution.

## REFERENCES


(1) D. W. Cushman, H. S. Cheung, E. F. Sabo, and M. A. Ondetti, *Prog. Cardiovasc. Dis.*, **21**, 176 (1978).

(2) B. Rubin, M. J. Antonaccio, and Z. P. Horovitz, *ibid.*, **21**, 183 (1978).

(3) R. J. Laffan, M. E. Goldberg, J. P. High, T. R. Schaeffer, M. H. Waugh, and B. Rubin, *J. Pharmacol. Exp. Ther.*, **204**, 281 (1978).

(4) A. Jenkins and D. N. McKinstry, *Med. J. Aust., Suppl. 2*, **2**, xxxii (1979).

(5) H. Gavras, H. R. Brunner, G. A. Turini, G. R. Kershaw, C. P. Tifft, S. Cuttelod, I. Gavras, R. A. Vukovich, and D. N. McKinstry, *N. Engl. J. Med.*, **298**, 991 (1978).

(6) K. J. Kripalani, D. N. McKinstry, S. N. Singhvi, D. A. Willard, R. A. Vukovich, and B. H. Migdalof, *Clin. Pharmacol. Ther.*, **27**, 636 (1980).

(7) J. G. Wagner, "Fundamentals of Clinical Pharmacokinetics," Drug Intelligence Publications, Hamilton, Ill., 1975, p. 437.

(8) A. F. Heald and C. E. Ita, *Pharmacologist*, **19**, 129 (1977).

(9) J. K. Weltman, R. P. Szaro, A. R. Frackelton, R. M. Dowben, J. R. Bunting, and R. E. Cathou, *J. Biol. Chem.*, **248**, 3173 (1973).

(10) C. W. Wu, L. R. Yarbrough, and F. Y. H. Wu, *Biochemistry*, **15**, 2863 (1976).

(11) J. Staessen, R. Fagard, P. Lijnen, and A. Amery, *Lancet*, **1**, 926 (1980).

(12) *Lancet*, **2**, 129 (1980).


## ACKNOWLEDGMENTS


Supported by a grant from the National Heart Foundation of Australia.


# Pharmacokinetics of [$^{14}$C]Bretylium Tosylate in Rats


**BURDE L. KAMATH ˣ, HERMAN F. STAMPFLI, CHII-MING LAI, and AVRAHAM YACOBI**



Received August 29, 1980, from the *Pharmaceutical Development Department, Research & Development, American Critical Care, McGaw Park, IL 60085.* Accepted for publication November 20, 1980.



**Abstract** □ The pharmacokinetics of bretylium tosylate were investigated in eight male Charles River rats. Each animal received an intravenous dose (10 mg/kg) of [$^{14}$C]bretylium tosylate. Serial blood samples, urine, and feces were collected for up to 72 hr. Bretylium concentrations in plasma and amounts excreted in urine and feces were determined by scintillation counting. On the average, 88 and 95% of the dose were recovered in urine and feces in 24 and 72 hr, respectively. Urinary recovery accounted for 65.6% of the dose while 29.7% was excreted in the feces. Bretylium concentrations in plasma declined triexponentially and were fitted to a three-compartment open model. Bretylium has a very high apparent volume of distribution (15 liters/kg), and its $\beta$ half-life averaged 5.5 hr. Mean values of the apparent volume of the central compartment, plasma clearance, renal clearance, and excretion rate constants of bretylium in rats were 1 liter/kg, 1.93 liters/hr/kg, 1.27 liters/hr/kg, and 1.24 $hr^{-1}$, respectively. The results indicate that: (*a*) bretylium is strongly bound to the tissues and is eliminated by active urinary secretion and by biliary excretion in rats, and (*b*) there are strong similarities between the pharmacokinetics of bretylium in humans and rats and that this animal model might be suitable for interaction studies with other drugs.



**Keyphrases** □ Bretylium tosylate—pharmacokinetics, rats, compared with human studies □ Pharmacokinetics—bretylium tosylate, rats, compared with human studies □ Antiarrhythmic agents—bretylium tosylate, pharmacokinetics studied in rats, compared with human studies


Bretylium is a quaternary ammonium compound [(*o*-bromobenzyl)ethyldimethylamine] used clinically as the tosylate salt in the treatment of arrhythmias. Bretylium tosylate suppresses ventricular fibrillation in patients within minutes following intravenous administration (1). Suppression of ventricular tachycardia and other ventricular arrhythmias develops more slowly, usually 20–120 min following parenteral administration (2).

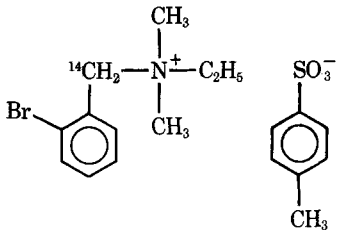


[$^{14}$C]bretylium tosylate

## BACKGROUND

In humans, bretylium is eliminated intact mainly through the renal route (3, 4). No metabolites have been identified following administration of bretylium tosylate in humans and rats (3). The biological half-life of bretylium in normal subjects was 5.5 hr (3). Romhilt *et al.* (2) reported a half-life of 9.75 hr (range 4.2–16.9) in eight patients with cardiac disease. More recently, Adir *et al.* (4) reported a half-life of 8.1 hr for a normal subject and of 16.0 and 31.5 hr for two patients with renal impairment. In the normal subject, the renal clearance of bretylium was 1 liter/min, indicating extensive active secretion, and the urinary excretion of unchanged drug accounted for 80% of the dose (4).

A previous study in the rat (3) demonstrated that 63% of the intramuscular dose (5 mg/kg) was excreted unchanged in the urine and that 31% was excreted in the feces. Most radioactivity was excreted within 24 hr. An average of 16% of the intravenous dose (2.5 mg/kg) in four rats was excreted in the bile within 5 hr.

This investigation studied the pharmacokinetics of distribution and elimination of bretylium in the rat following an intranveous dose of ra-


0022-3549/81/0600-0667$01.00/0


© 1981, American Pharmaceutical Association

sampling at closer time intervals are needed to confirm these observations. The data for all patients could be described approximately by the sum of two exponentials, and the mean elimination half-life was ~40 min. The plasma concentration–time profile for one subject is shown in Fig. 2.

The pharmacokinetics of captopril in the four patients taking the drug chronically indicate that changes in plasma captopril concentrations do not reflect blood pressure changes. In all patients, captopril was undetected in their plasma 3–4 hr after dosing, yet blood pressure had not risen at this time. Blood levels of captopril metabolites, such as the disulfide, possibly may be a more useful index of the hemodynamics of this drug.

In conclusion, it was demonstrated that plasma captopril can be assayed with high sensitivity and specificity by first derivatizing this thiol compound to a fluorophore using *N*-(1-pyrene)maleimide and then separating the fluorescent adducts by HPLC. This procedure can also be used for assaying another thiol angiotensin-converting enzyme inhibitor, II, using captopril as the internal standard. This derivatization procedure should be suitable for assaying the mucolytic drug *N*-acetylcysteine after modification of the HPLC conditions to retard its elution.

## REFERENCES


(1) D. W. Cushman, H. S. Cheung, E. F. Sabo, and M. A. Ondetti, *Prog. Cardiovasc. Dis.*, **21**, 176 (1978).

(2) B. Rubin, M. J. Antonaccio, and Z. P. Horovitz, *ibid.*, **21**, 183 (1978).

(3) R. J. Laffan, M. E. Goldberg, J. P. High, T. R. Schaeffer, M. H. Waugh, and B. Rubin, *J. Pharmacol. Exp. Ther.*, **204**, 281 (1978).

(4) A. Jenkins and D. N. McKinstry, *Med. J. Aust., Suppl. 2*, **2**, xxxii (1979).

(5) H. Gavras, H. R. Brunner, G. A. Turini, G. R. Kershaw, C. P. Tifft, S. Cuttelod, I. Gavras, R. A. Vukovich, and D. N. McKinstry, *N. Engl. J. Med.*, **298**, 991 (1978).

(6) K. J. Kripalani, D. N. McKinstry, S. N. Singhvi, D. A. Willard, R. A. Vukovich, and B. H. Migdalof, *Clin. Pharmacol. Ther.*, **27**, 636 (1980).

(7) J. G. Wagner, "Fundamentals of Clinical Pharmacokinetics," Drug Intelligence Publications, Hamilton, Ill., 1975, p. 437.

(8) A. F. Heald and C. E. Ita, *Pharmacologist*, **19**, 129 (1977).

(9) J. K. Weltman, R. P. Szaro, A. R. Frackelton, R. M. Dowben, J. R. Bunting, and R. E. Cathou, *J. Biol. Chem.*, **248**, 3173 (1973).

(10) C. W. Wu, L. R. Yarbrough, and F. Y. H. Wu, *Biochemistry*, **15**, 2863 (1976).

(11) J. Staessen, R. Fagard, P. Lijnen, and A. Amery, *Lancet*, **1**, 926 (1980).

(12) *Lancet*, **2**, 129 (1980).


## ACKNOWLEDGMENTS


Supported by a grant from the National Heart Foundation of Australia.


# Pharmacokinetics of [$^{14}$C]Bretylium Tosylate in Rats


**BURDE L. KAMATH ˣ, HERMAN F. STAMPFLI, CHII-MING LAI, and AVRAHAM YACOBI**



Received August 29, 1980, from the *Pharmaceutical Development Department, Research & Development, American Critical Care, McGaw Park, IL 60085.* Accepted for publication November 20, 1980.



**Abstract** □ The pharmacokinetics of bretylium tosylate were investigated in eight male Charles River rats. Each animal received an intravenous dose (10 mg/kg) of [$^{14}$C]bretylium tosylate. Serial blood samples, urine, and feces were collected for up to 72 hr. Bretylium concentrations in plasma and amounts excreted in urine and feces were determined by scintillation counting. On the average, 88 and 95% of the dose were recovered in urine and feces in 24 and 72 hr, respectively. Urinary recovery accounted for 65.6% of the dose while 29.7% was excreted in the feces. Bretylium concentrations in plasma declined triexponentially and were fitted to a three-compartment open model. Bretylium has a very high apparent volume of distribution (15 liters/kg), and its $\beta$ half-life averaged 5.5 hr. Mean values of the apparent volume of the central compartment, plasma clearance, renal clearance, and excretion rate constants of bretylium in rats were 1 liter/kg, 1.93 liters/hr/kg, 1.27 liters/hr/kg, and 1.24 $hr^{-1}$, respectively. The results indicate that: (*a*) bretylium is strongly bound to the tissues and is eliminated by active urinary secretion and by biliary excretion in rats, and (*b*) there are strong similarities between the pharmacokinetics of bretylium in humans and rats and that this animal model might be suitable for interaction studies with other drugs.



**Keyphrases** □ Bretylium tosylate—pharmacokinetics, rats, compared with human studies □ Pharmacokinetics—bretylium tosylate, rats, compared with human studies □ Antiarrhythmic agents—bretylium tosylate, pharmacokinetics studied in rats, compared with human studies


Bretylium is a quaternary ammonium compound [(*o*-bromobenzyl)ethyldimethylamine] used clinically as the tosylate salt in the treatment of arrhythmias. Bretylium tosylate suppresses ventricular fibrillation in patients within minutes following intravenous administration (1). Suppression of ventricular tachycardia and other ventricular arrhythmias develops more slowly, usually 20–120 min following parenteral administration (2).

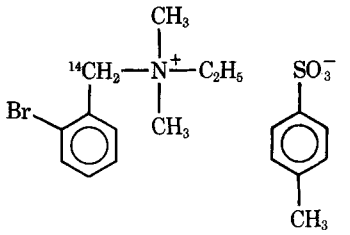


[$^{14}$C]bretylium tosylate

## BACKGROUND

In humans, bretylium is eliminated intact mainly through the renal route (3, 4). No metabolites have been identified following administration of bretylium tosylate in humans and rats (3). The biological half-life of bretylium in normal subjects was 5.5 hr (3). Romhilt *et al.* (2) reported a half-life of 9.75 hr (range 4.2–16.9) in eight patients with cardiac disease. More recently, Adir *et al.* (4) reported a half-life of 8.1 hr for a normal subject and of 16.0 and 31.5 hr for two patients with renal impairment. In the normal subject, the renal clearance of bretylium was 1 liter/min, indicating extensive active secretion, and the urinary excretion of unchanged drug accounted for 80% of the dose (4).

A previous study in the rat (3) demonstrated that 63% of the intramuscular dose (5 mg/kg) was excreted unchanged in the urine and that 31% was excreted in the feces. Most radioactivity was excreted within 24 hr. An average of 16% of the intravenous dose (2.5 mg/kg) in four rats was excreted in the bile within 5 hr.

This investigation studied the pharmacokinetics of distribution and elimination of bretylium in the rat following an intranveous dose of ra-


0022-3549/81/0600-0667$01.00/0


© 1981, American Pharmaceutical Association

**Table I—Percent of Dose of Radioactivity Recovered in Urine and Feces following Intravenous Administration of [$^{14}$C]-Bretylium Tosylate (10 mg/kg) in Eight Rats**

| Sample | Dose Recovered, % Mean | CV |
|---|---|---|
| Urine | | |
| 0–24 hr | 62.8 | 7.90 |
| 0–72 hr | 65.6 | 6.43 |
| Feces | | |
| 0–24 hr | 25.7 | 9.73 |
| 0–48 hr | 29.7 | 9.70 |
| Total | 95.3 | 5.49 |

diolabeled bretylium and examined the suitability of the rat model for further *in vivo* investigation of the drug.

## EXPERIMENTAL

Bretylium tosylate (labeled at benzyl carbon with carbon 14, specific activity 27.3 μCi/mg) was obtained commercially[1]. The radioactive drug was diluted with the cold drug[2] to a final specific activity of 3.242 μCi/mg.

Eight male Charles River CD[3] rats, 390–460 g, were kept in individual metabolism cages during the study. One day before the drug administration, a cannula was inserted surgically into the jugular vein of each rat under light ether anesthesia to allow intravenous dosing and systemic blood sampling. The preparation of the cannulas and the surgical procedure were described previously (5). At time zero, a 10-mg/kg dose of [$^{14}$C]bretylium tosylate in solution was given intravenously through the jugular vein cannula after an overnight fast. The cannula was flushed with 0.5 ml of heparinized saline.

Food was withheld for 3 hr after drug administration, but water was freely available at all times. Serial blood samples (0.4 ml) were drawn at 0 (just before drug administration), 0.25, 0.5, 0.75, 1, 1.5, 2, 3, 4, 6, 8, and 10 hr following dosing and were placed in heparinized microcentrifuge tubes; the plasma was separated immediately. The blood volume withdrawn from the rat was replaced with an equal volume of heparinized saline. Urine and feces were collected for 72 and 48 hr, respectively.

The total radioactivity in plasma was determined by counting an aliquot of the plasma or urine in a liquid scintillation counter[4]. The total radioactivity in the feces was measured after homogenization and combustion of an aliquot of the homogenate by a sample oxidizer[5].

Plasma concentration *versus* time data of each rat were fitted to a three-compartment open model (6), with elimination from the central compartment, using the NLIN procedure available in SAS[6] package (7). Marquardt's iterative method was used with a convergence criterion of $10^{-4}$. Each observation was weighted by the reciprocal of its square to estimate the $\beta$-phase parameters, $B$ and $\beta$, which were used to estimate $P$, $\pi$, $A$, and $\alpha$ without weighing. Derived constants and parameters then were calculated from the estimated parameters using standard equations (6).

## RESULTS AND DISCUSSION

Table I summarizes the recovery of bretylium measured as radioactivity in urine and feces following intravenous administration of [$^{14}$C]-bretylium tosylate to eight rats. On the average, >95% of the dose was recovered in urine and feces in 72 hr. Urinary recovery was 65.6% of the dose, and the recovery in the feces was 29.7%. These values are in good agreement with the previously reported data for rats (3). An average of 88% of the dose was excreted within the first 24 hr. In humans, however, the urinary excretion of unchanged drug in 3 days accounted for 80–90% of the dose (3).

The method used in this study to fit the plasma concentration data to the exponential curve represented by the three-compartment open model was modified slightly. Because of wide and prolonged distribution of the drug, the $\beta$ phase (4 hr after drug administration) consisted of only three or four data points. It was found that simultaneous determination of all six least-squares parameters may lead to a bias in the characterization

[1] New England Nuclear, Boston, Mass.
[2] American Critical Care, McGaw Park, Ill.
[3] Charles River Breeding Laboratories, Wilmington, Mass.
[4] Model 2425, Packard Instrument Co., Downers Grove, Ill.
[5] Model B306, Packard Instrument Co., Downers Grove, Ill.
[6] Statistical Analysis System, SAS Institute, Raleigh, N.C.

**Table II—Pharmacokinetic Parameters of Bretylium in Rats: Plasma Concentration *versus* Time following Intravenous Administration Fitted to Three-Compartment Open Model**

| Parameter | Mean | SD | CV |
|---|---|---|---|
| Model Parameters and Rate Constants[a] | | | |
| $P$, μg/ml | 4.85 | 0.925 | 19.1 |
| $\pi$, hr$^{-1}$ | 6.77 | 2.48 | 36.6 |
| $A$, μg/ml | 0.742 | 0.645 | 86.9 |
| $\alpha$, hr$^{-1}$ | 1.28 | 0.603 | 47.3 |
| $B$, μg/ml | 0.231 | 0.033 | 14.2 |
| $\beta$, hr$^{-1}$ | 0.131 | 0.024 | 18.2 |
| Derived Parameters and Constants[b] | | | |
| $t_{1/2}$, hr | 5.45 | 1.01 | 18.6 |
| $AUC$, (μg hr)/ml | 3.07 | 0.264 | 8.59 |
| $V_c$, liters/kg | 1.05 | 0.242 | 23.1 |
| $V_{d,\beta}$, liters/kg | 15.1 | 2.71 | 17.9 |
| $Cl_p$, liters/hr/kg | 1.93 | 0.166 | 8.62 |
| $Cl_r$, liters/hr/kg | 1.27 | 0.170 | 13.4 |
| $k_{12}$, hr$^{-1}$ | 1.84 | 0.949 | 51.6 |
| $k_{21}$, hr$^{-1}$ | 2.18 | 1.54 | 70.6 |
| $k_{13}$, hr$^{-1}$ | 1.97 | 0.484 | 24.5 |
| $k_{31}$, hr$^{-1}$ | 0.288 | 0.038 | 16.1 |
| $k_{10}$, hr$^{-1}$ | 1.89 | 0.305 | 23.6 |
| $k_{ex}$, hr$^{-1}$ | 1.24 | 0.210 | 16.9 |

[a] $n$ = 8. [b] See text for definitions.

of the pharmacokinetic parameters of bretylium. This problem could be overcome by first fitting only the points in the $\beta$ phase to the monoexponential equation and by weighing each observation by the reciprocal of its square. The influence of the $\alpha$ phase thus was minimized, and the best possible estimates of the $\beta$-phase parameters, $B$ and $\beta$, were obtained. By using these two predetermined parameters, all data points, including those in the $\beta$ phase, were simultaneously fitted again to the triexponential equation. This time no weighting factor was used. Through this procedure, the nonlinear least-squares estimates of $P$, $\pi$, $A$, and $\alpha$ were found, describing the distribution phase.

The mean values of the pharmacokinetic parameters estimated by this procedure, as well as the derived parameters calculated from the estimated parameters, are presented in Table II. The standard deviation and coefficient of variation of each parameter also are listed. A representative semilogarithmic plot of the plasma concentration *versus* time data from an individual rat is shown in Fig. 1.

In rats, bretylium is distributed rapidly in the body into two peripheral

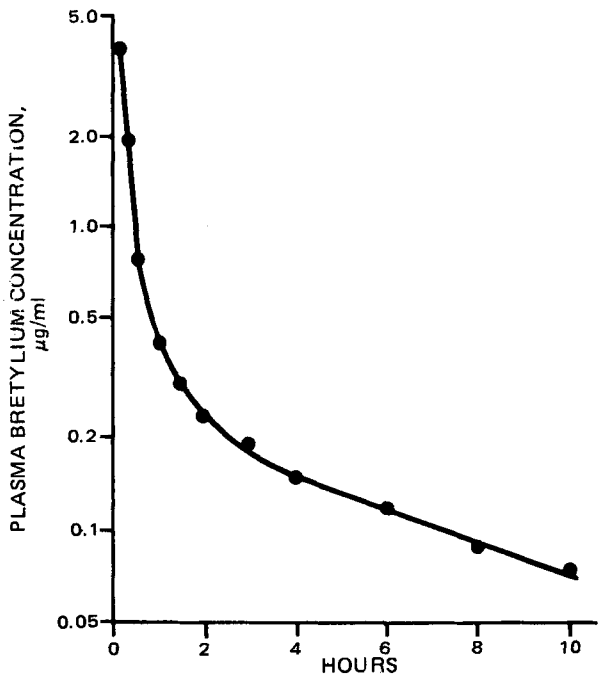


**Figure 1**—*Representative semilogarithmic plot of concentration of bretylium in plasma* versus *time following intravenous administration of bretylium tosylate (10 mg/kg) to a rat. The curve represents the data fitted to the three-compartment open model.*

compartments. The apparent equilibrium between the compartments was achieved within 3 hr. The apparent volume of the central compartment ($V_c$) was 1 liter/kg. The distribution half-life of the shallow and deep compartments (Compartments 2 and 3) were 6.14 and 32.5 min, respectively. In the postdistribution phase, the plasma levels declined with a terminal half-life of 5.45 hr (range 4.0–7.4). The plasma clearance ($Cl_p$) and the apparent volume of distribution ($V_{d,\beta}$) averaged 1.93 liters/hr/kg and 15 liters/kg, respectively. This unusually high apparent volume of distribution and the significant drop in plasma levels from 3–4 μg/ml at 6 min after injection to <200 ng/ml within 3 hr indicated extensive tissue uptake of bretylium in rats. Similar binding characteristics of bretylium were demonstrated in humans (8).

The intercompartmental distribution rate constants ($k_{12}$ and $k_{21}$) between the central compartment and Compartment 2 in the same rat were close to each other and ranged from 0.8 to 5.1 $hr^{-1}$ between rats. However, the transfer rate constant ($k_{31}$) from the third compartment to the central compartment was considerably smaller (mean 0.288 $hr^{-1}$) than either $k_{13}$ (the intercompartmental rate constant in the opposite direction, 1.97 $hr^{-1}$) or the elimination rate constant ($k_{10}$, 1.89 $hr^{-1}$). This finding suggests that tissue binding in Compartment 3 (the deep compartment) is rate limiting in the elimination of bretylium from the body.

The excretion rate constant ($k_{ex}$) and the renal clearance ($Cl_r$) of bretylium in rats were 1.24 $hr^{-1}$ and 1.27 liters/hr/kg, respectively. This renal clearance corresponds to 21 ml/min/kg and represents 66% of the total body clearance; it is about three times greater than the glomerular filtration rate of 6.64–8 ml/min/kg reported for normal rats (9, 10). It also indicates that active secretion is the major mechanism of urinary excretion of bretylium in rats. A similar mechanism of active secretion of bretylium in urine also was demonstrated for humans (4).

The major portion of the nonrenal excretion of bretylium probably occurs through the bile, as indicated by the recovery of ~30% of the dose in feces in 48 hr. If excretion in the bile is rapid immediately after dosing, there is a possibility of enterohepatic cycling. The extent of biliary excretion of bretylium has not been investigated in humans. However, on the basis of urinary excretion data, a much smaller quantity is expected to be eliminated *via* the biliary route.

In summary, these results indicate that bretylium is extensively distributed in rats, bound to the tissues, and excreted mainly unchanged in the urine, mostly by active secretion, similar to the findings in humans. Biliary excretion is the second major route of elimination of bretylium in rats. The data also show striking similarity in the pharmacokinetics of distribution and elimination of bretylium in humans and rats. This similarity might allow the use of the animal model for further *in vivo* investigations, including efficacy and drug–drug interaction studies in the rat.

## REFERENCES


(1) G. Sanna and R. Arcidiacono, *Am. J. Cardiol.*, **32**, 982 (1973).

(2) D. W. Romhilt, S. S. Bloomfield, and R. J. Lipicky, *Circulation*, **45**, 800 (1972).

(3) R. Kuntzman, I. Tsai, R. Chang, and A. H. Conney, *Clin. Pharmacol. Ther.*, **11**, 829 (1970).

(4) J. Adir, P. K. Narang, J. Josselson, and J. H. Sadler, *N. Engl. J. Med.*, **300**, 1390 (1979).

(5) P. G. Harms and S. R. Ojeda, *J. Appl. Phys.*, **36**, 391 (1974).

(6) M. Gibaldi and D. Perrier, in "Pharmacokinetics, vol. 1, Drugs and the Pharmaceutical Sciences," J. Swarbrick, Ed., Dekker, New York, N.Y., 1975.

(7) A. J. Barr, J. H. Goodnight, and J. P. Sall, "SAS User's Guide," SAS Institute, Raleigh, N.C., 1979.

(8) J. L. Anderson, E. Patterson, J. G. Wagner, J. R. Stewart, H. L. Behm, and B. R. Lucchesi, "Abstract of Papers presented at the 29th Annual Session of American College of Cardiology," Houston, Tex., Mar. 1980.

(9) W. E. Yarger, H. S. Aynedjian, and N. Bank, *J. Clin. Invest.*, **51**, 625 (1972).

(10) E. M. Renkin and J. P. Gilmore, in "Handbook of Physiology, Section 8: Renal Physiology," J. Orloff, R. W. Berliner, and S. R. Geiger, Eds., American Physiological Society, Washington, D.C., 1973, pp. 185–248.


# High-Performance Liquid Chromatographic Measurement of Cloprednol in Human Plasma


**C. LEE ˣ, B. AMOS, and S. B. MATIN**



Received October 6, 1980, from the *Department of Analytical and Metabolic Chemistry, Syntex Research, Palo Alto, CA 94304.* Accepted for publication December 2, 1980.



**Abstract** □ A rapid and specific high-performance liquid chromatographic method for the quantitative determination of cloprednol in human plasma is described. Samples were extracted using methylene chloride–ether (40:60) and then purified further by solvent and pH partitioning techniques. Cloprednol was analyzed using normal-phase chromatography and UV detection at 254 nm. The final recovery after losses during the cleanup procedure for cloprednol from human plasma was 80.8%. The lowest concentration that could be measured with confidence was 8 ng/ml.



**Keyphrases** □ Cloprednol—high-performance liquid chromatographic analysis, human plasma □ High-performance liquid chromatography—analysis, cloprednol in human plasma □ Anti-inflammatory agents—cloprednol, high-performance liquid chromatographic analysis, human plasma


Cloprednol (6-chloro-11β,17α,21-trihydroxypregna-1,4,6-triene-3,20-dione, I) is a fast-acting corticoid used in the treatment of collagen and allergic diseases (1).

Recently published analytical techniques for the quantitative determination of 17-hydroxycorticoids in

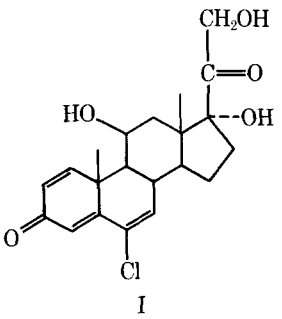


I

plasma include radioimmunoassays (2–5), competitive protein binding (6–8), GLC–mass spectrometry (9, 10), and high-performance liquid chromatography (HPLC) (11–15). The specificity in radioimmunoassays and competitive protein binding methods remains questionable due to the cross-reactivity by structurally similar compounds (16, 17). The GLC–mass spectrometric technique is specific but


0022-3549/81/0600-0669$01.00/0


© 1981, American Pharmaceutical Association

compartments. The apparent equilibrium between the compartments was achieved within 3 hr. The apparent volume of the central compartment ($V_c$) was 1 liter/kg. The distribution half-life of the shallow and deep compartments (Compartments 2 and 3) were 6.14 and 32.5 min, respectively. In the postdistribution phase, the plasma levels declined with a terminal half-life of 5.45 hr (range 4.0–7.4). The plasma clearance ($Cl_p$) and the apparent volume of distribution ($V_{d,\beta}$) averaged 1.93 liters/hr/kg and 15 liters/kg, respectively. This unusually high apparent volume of distribution and the significant drop in plasma levels from 3–4 μg/ml at 6 min after injection to <200 ng/ml within 3 hr indicated extensive tissue uptake of bretylium in rats. Similar binding characteristics of bretylium were demonstrated in humans (8).

The intercompartmental distribution rate constants ($k_{12}$ and $k_{21}$) between the central compartment and Compartment 2 in the same rat were close to each other and ranged from 0.8 to 5.1 $hr^{-1}$ between rats. However, the transfer rate constant ($k_{31}$) from the third compartment to the central compartment was considerably smaller (mean 0.288 $hr^{-1}$) than either $k_{13}$ (the intercompartmental rate constant in the opposite direction, 1.97 $hr^{-1}$) or the elimination rate constant ($k_{10}$, 1.89 $hr^{-1}$). This finding suggests that tissue binding in Compartment 3 (the deep compartment) is rate limiting in the elimination of bretylium from the body.

The excretion rate constant ($k_{ex}$) and the renal clearance ($Cl_r$) of bretylium in rats were 1.24 $hr^{-1}$ and 1.27 liters/hr/kg, respectively. This renal clearance corresponds to 21 ml/min/kg and represents 66% of the total body clearance; it is about three times greater than the glomerular filtration rate of 6.64–8 ml/min/kg reported for normal rats (9, 10). It also indicates that active secretion is the major mechanism of urinary excretion of bretylium in rats. A similar mechanism of active secretion of bretylium in urine also was demonstrated for humans (4).

The major portion of the nonrenal excretion of bretylium probably occurs through the bile, as indicated by the recovery of ~30% of the dose in feces in 48 hr. If excretion in the bile is rapid immediately after dosing, there is a possibility of enterohepatic cycling. The extent of biliary excretion of bretylium has not been investigated in humans. However, on the basis of urinary excretion data, a much smaller quantity is expected to be eliminated *via* the biliary route.

In summary, these results indicate that bretylium is extensively distributed in rats, bound to the tissues, and excreted mainly unchanged in the urine, mostly by active secretion, similar to the findings in humans. Biliary excretion is the second major route of elimination of bretylium in rats. The data also show striking similarity in the pharmacokinetics of distribution and elimination of bretylium in humans and rats. This similarity might allow the use of the animal model for further *in vivo* investigations, including efficacy and drug–drug interaction studies in the rat.

## REFERENCES


(1) G. Sanna and R. Arcidiacono, *Am. J. Cardiol.*, **32**, 982 (1973).

(2) D. W. Romhilt, S. S. Bloomfield, and R. J. Lipicky, *Circulation*, **45**, 800 (1972).

(3) R. Kuntzman, I. Tsai, R. Chang, and A. H. Conney, *Clin. Pharmacol. Ther.*, **11**, 829 (1970).

(4) J. Adir, P. K. Narang, J. Josselson, and J. H. Sadler, *N. Engl. J. Med.*, **300**, 1390 (1979).

(5) P. G. Harms and S. R. Ojeda, *J. Appl. Phys.*, **36**, 391 (1974).

(6) M. Gibaldi and D. Perrier, in "Pharmacokinetics, vol. 1, Drugs and the Pharmaceutical Sciences," J. Swarbrick, Ed., Dekker, New York, N.Y., 1975.

(7) A. J. Barr, J. H. Goodnight, and J. P. Sall, "SAS User's Guide," SAS Institute, Raleigh, N.C., 1979.

(8) J. L. Anderson, E. Patterson, J. G. Wagner, J. R. Stewart, H. L. Behm, and B. R. Lucchesi, "Abstract of Papers presented at the 29th Annual Session of American College of Cardiology," Houston, Tex., Mar. 1980.

(9) W. E. Yarger, H. S. Aynedjian, and N. Bank, *J. Clin. Invest.*, **51**, 625 (1972).

(10) E. M. Renkin and J. P. Gilmore, in "Handbook of Physiology, Section 8: Renal Physiology," J. Orloff, R. W. Berliner, and S. R. Geiger, Eds., American Physiological Society, Washington, D.C., 1973, pp. 185–248.


# High-Performance Liquid Chromatographic Measurement of Cloprednol in Human Plasma


**C. LEE ˣ, B. AMOS, and S. B. MATIN**



Received October 6, 1980, from the *Department of Analytical and Metabolic Chemistry, Syntex Research, Palo Alto, CA 94304.* Accepted for publication December 2, 1980.



**Abstract** □ A rapid and specific high-performance liquid chromatographic method for the quantitative determination of cloprednol in human plasma is described. Samples were extracted using methylene chloride–ether (40:60) and then purified further by solvent and pH partitioning techniques. Cloprednol was analyzed using normal-phase chromatography and UV detection at 254 nm. The final recovery after losses during the cleanup procedure for cloprednol from human plasma was 80.8%. The lowest concentration that could be measured with confidence was 8 ng/ml.



**Keyphrases** □ Cloprednol—high-performance liquid chromatographic analysis, human plasma □ High-performance liquid chromatography—analysis, cloprednol in human plasma □ Anti-inflammatory agents—cloprednol, high-performance liquid chromatographic analysis, human plasma


Cloprednol (6-chloro-11β,17α,21-trihydroxypregna-1,4,6-triene-3,20-dione, I) is a fast-acting corticoid used in the treatment of collagen and allergic diseases (1).

Recently published analytical techniques for the quantitative determination of 17-hydroxycorticoids in

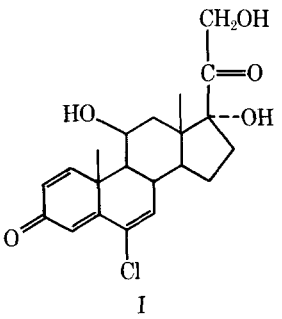


I

plasma include radioimmunoassays (2–5), competitive protein binding (6–8), GLC–mass spectrometry (9, 10), and high-performance liquid chromatography (HPLC) (11–15). The specificity in radioimmunoassays and competitive protein binding methods remains questionable due to the cross-reactivity by structurally similar compounds (16, 17). The GLC–mass spectrometric technique is specific but


0022-3549/81/0600-0669$01.00/0


© 1981, American Pharmaceutical Association

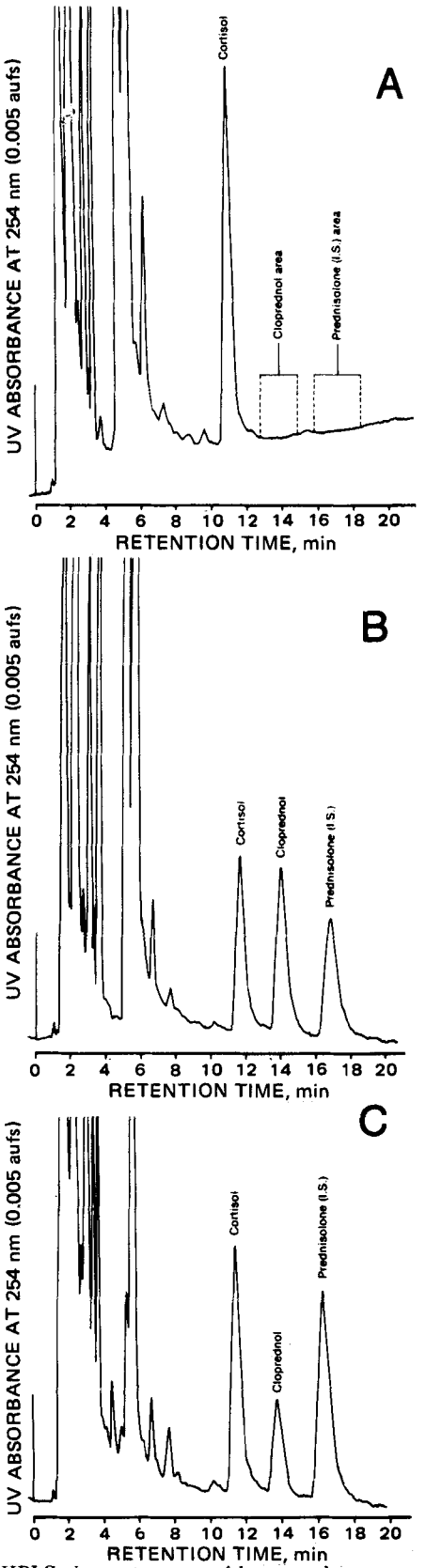


**Figure 1**—*HPLC chromatograms of human plasma assayed as described. Key: A, chromatogram from 3 ml of blank human plasma; B, chromatogram from 3 ml of human plasma spiked with 300 ng of cloprednol (100 ng/ml) and 200 ng of prednisolone (66.7 ng/ml) as the internal standard; and C, chromatogram of extracted human plasma sample (1 ml) 4 hr after an oral dose of 12.5 mg of cloprednol was diluted with blank human plasma to 3 ml and 200 ng of prednisolone (66.7 ng/ml) as an internal standard was added.*

**Table I—Extraction Efficiency of [$^3$H]Cloprednol from 3.0 ml of Human Plasma**

| Extraction Step | Percent of Spiked [$^3$H]Cloprednol |
|---|---|
| Methylene chloride–ether extraction | 88.7 |
| Methanol–water layer | 83.4 |
| Methylene chloride–ether after washing (overall extraction) | 80.4 |

requires extensive sample cleanup and time-consuming derivatization (9, 10).

A simple, sensitive, and specific HPLC method for the measurement of cloprednol in human plasma without derivatization is described here. By utilizing normal-phase chromatography, it was possible chromatographically to resolve structurally related endogenous corticoids like cortisol and drugs like prednisone. This method was applied to determine plasma concentrations in humans after the oral administration of 12.5 mg of cloprednol.

## EXPERIMENTAL

**Reagents and Materials**—Cloprednol[1], [$^3$H]cloprednol[1], prednisolone[2], and a complete oxidizer cocktail[3] were used as received. Distilled-in-glass grade[4] methanol, hexane, and methylene chloride and absolute ethanol[5] were used. All other chemicals and reagents were reagent grade and were used as received.

**Apparatus**—Analyses were performed on a high-performance liquid chromatograph[6] at ambient temperature. The chromatograph was equipped with a fixed-wavelength (254 nm) spectrophotometer[7]. A commercial 4.6-mm × 25-cm prepacked normal-phase column[8] with a precolumn[9] (2 mm × 7.1 cm) was used. Samples were introduced onto the column through a septumless injector[10] with a 100-μl syringe.

A liquid scintillation spectrometer[11] was used for [$^3$H]cloprednol counting.

**Chromatographic Conditions**—The mobile phase was methylene chloride–ethanol–acetic acid (96:4:0.01) with the flow rate adjusted to 2.0 ml/min (1300 psi) at 0.005 aufs. The solvent mixture was degassed by stirring under vacuum before use. Prednisolone was the internal standard.

**Extraction**—Sample aliquots, 0.1–3 ml, were diluted with blank plasma to 3 ml. A 200-μl spiking solution of prednisolone, used as the internal standard [equivalent to 1 ng/μl of methanol–water (1:9)], was added. Additional water was added to bring the total volume to 3.5 ml. The mixture was extracted with 10 ml of 40% methylene chloride in ether by shaking on a reciprocal shaker for 10 min. After centrifugation, the organic layer was transferred to another tube and evaporated to dryness under nitrogen at 37°.

To the dry residue was added 2 ml of methanol containing 10% water. After the tubes were vortexed, the methanol–water layer was washed three times with hexane (3 ml). The hexane washings were discarded, and the remaining methanol–water layer was dried at 37° under nitrogen. The dry residue was reconstituted in 10 ml of 40% methylene chloride in ether, and the organic layer was washed with 2 ml of 0.1 *N* HCl.

After centrifugation, the acidic layer was pipetted out, and the organic layer was washed with 3 ml of 0.1 *N* NaOH. After centrifugation, the organic layer was transferred to a 15-ml conical centrifuge tube and evaporated to dryness under nitrogen at 37°. The residue was redissolved in 100 μl of methylene chloride by vigorous vortexing, and 50–75 μl was injected for quantitation.

**Extraction Efficiency**—To drug-free pooled plasma (3 ml) were

[1] Synthesized and supplied by Syntex Research, Palo Alto, Calif.
[2] Sigma Chemical Co., St. Louis, Mo.
[3] Oxifluor-$H_2O$, New England Nuclear, Boston, Mass.
[4] Burdick & Jackson Laboratories, Muskegon, Mich.
[5] Gold Shield, Terre Haute, Ind.
[6] Model 6000A, Waters Associates, Milford, Mass.
[7] Model 440, Waters Associates, Milford, Mass.
[8] LiChrosorb Si 60 5 μm, Altex, Berkeley, Calif.
[9] HC Pellisol, Whatman, Clifton, N.J.
[10] Model U6K, Waters Associates, Milford, Mass.
[11] Model 3330, Packard Instrument Co., Chicago, Ill.

**Table II—Four Calibration Curves of Cloprednol Extracted from 3.0 ml of Pooled Human Plasma**

| Amount of Cloprednol Spiked, ng | Peak Height Ratio of Cloprednol to Internal Standard | | | | | |
|---|---|---|---|---|---|---|
| | 1 | 2 | 3 | 4 | Average | *CV*, % |
| 25 | 0.11 | 0.11 | 0.12 | 0.11 | 0.11 | 4.44 |
| 50 | 0.24 | 0.21 | 0.25 | 0.24 | 0.24 | 7.37 |
| 100 | 0.43 | 0.49 | 0.49 | 0.43 | 0.46 | 7.53 |
| 200 | 0.98 | 0.99 | 0.95 | 0.89 | 0.95 | 4.72 |
| 300 | 1.38 | 1.42 | 1.37 | 1.34 | 1.38 | 2.40 |
| Slope | 0.0047 | 0.0048 | 0.0045 | 0.0045 | 0.0045 | |
| *y* intercept | −0.0051 | −0.0091 | +0.0228 | 0.0013 | 0.0027 | |
| Linear regression (*r*) | 0.9983 | 0.9991 | 0.9995 | 0.9997 | 0.9997 | |

added a known amount of [$^3$H]cloprednol and 100 ng of cloprednol. The spiked pooled plasma sample was processed through the entire procedure. At each extraction step, an aliquot of the organic layer was taken; the amount of radioactivity extracted was determined by counting the aliquot in 10 ml of scintillation fluid[3].

## RESULTS AND DISCUSSION

Cloprednol, a compound structurally similar to prednisolone, is a synthetic derivative of glycosteroids. It has an anti-inflammatory therapeutic potency twice that of prednisone and prednisolone on a milligram per kilogram basis (1).

The method described permits the analysis of underivatized cloprednol, thus making analysis simple and rapid. Cloprednol has three UV absorption peaks at 228, 256, and 299 nm with $E_{max}$ values of 11,200, 10,400, and 10,400, respectively. In this method, cloprednol was analyzed at 254 nm because of the commercial availability of the filter for the UV detector.

Under the described chromatographic conditions, the retention times of cloprednol and prednisolone (internal standard) were 14 and 17 min, respectively. Blank plasma samples not spiked with cloprednol or internal standard were processed through the entire procedure. The chromatogram shown in Fig. 1A clearly indicates that there was no interference from endogenous substances at the retention times of cloprednol and the internal standard. The chromatogram of an extracted human plasma sample spiked with 300 ng of cloprednol and 200 ng of the internal standard is shown in Fig. 1B.

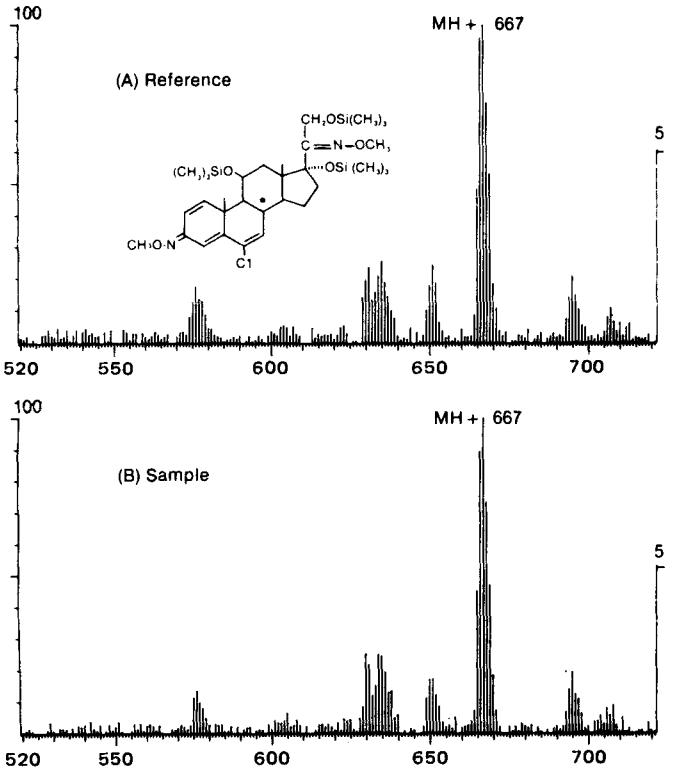


**Figure 2**—*Methane chemical-ionization mass spectra of methoxyimino trimethylsilyl derivative of cloprednol reference standard (A) and plasma extract (B).*

Plasma samples were extracted utilizing methylene chloride–ether (40:60). The extraction efficiency of cloprednol from 3.0 ml of human plasma was 88.7%. The extracts were purified further by solvent and pH partitioning techniques. Hexane was used to remove lipophilic substances, and acid–base washes were used to remove interference by endogenous substances.

The recovery of [$^3$H]cloprednol at each step during extraction was determined (Table I). The final recovery after losses during the cleanup procedure was 80.8%.

Linearity was established by preparing four calibration curves. The coefficients of variation (intraassay) at concentrations of 25, 50, 100, 200, and 300 ng/3.0 ml of plasma were 4.44, 7.37, 7.53, 4.72, and 2.40%, respectively (Table II). The calibration curve, as constructed by plotting the peak height ratio of cloprednol to the internal standard *versus* the amount of cloprednol spiked, was linear ($y$ = 0.9997) over the range (25–300 ng/3 ml) studied.

The specificity of the method was confirmed by chemical-ionization mass spectral studies. The HPLC-eluted peak of cloprednol from a dosed plasma sample was collected and derivatized as reported previously (18). The mass spectrum obtained from the cloprednol standard and that from the substance eluted in the chromatographic peak were identical (Figs. 2A and 2B). Based on this information, the peak was identified as cloprednol.

To show the applicability of the described method, a plasma sample obtained 4 hr after oral administration of cloprednol (12.5 mg) was processed. The chromatogram of the extracted sample is shown in Fig. 1C.

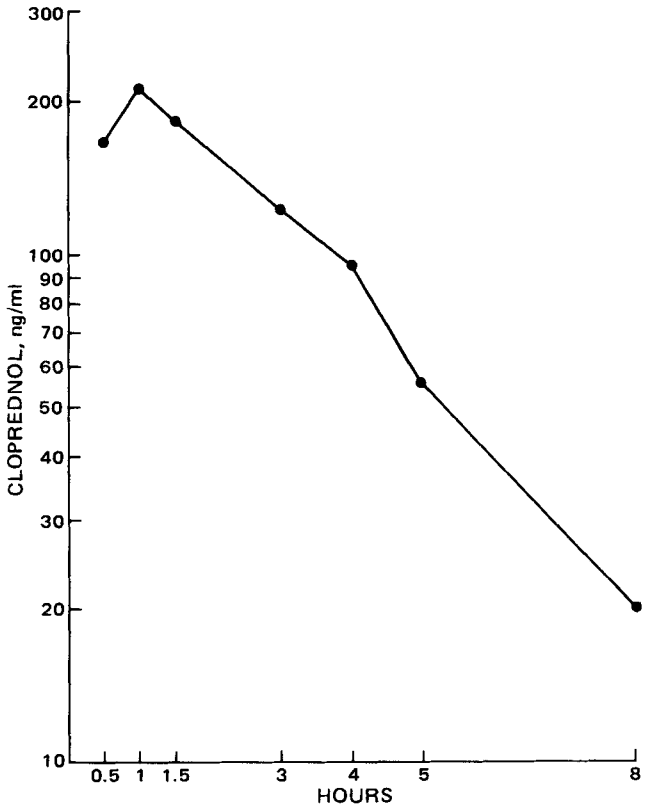


**Figure 3**—*Plasma cloprednol level–time profile of a human volunteer given a 12.5-mg oral dose.*

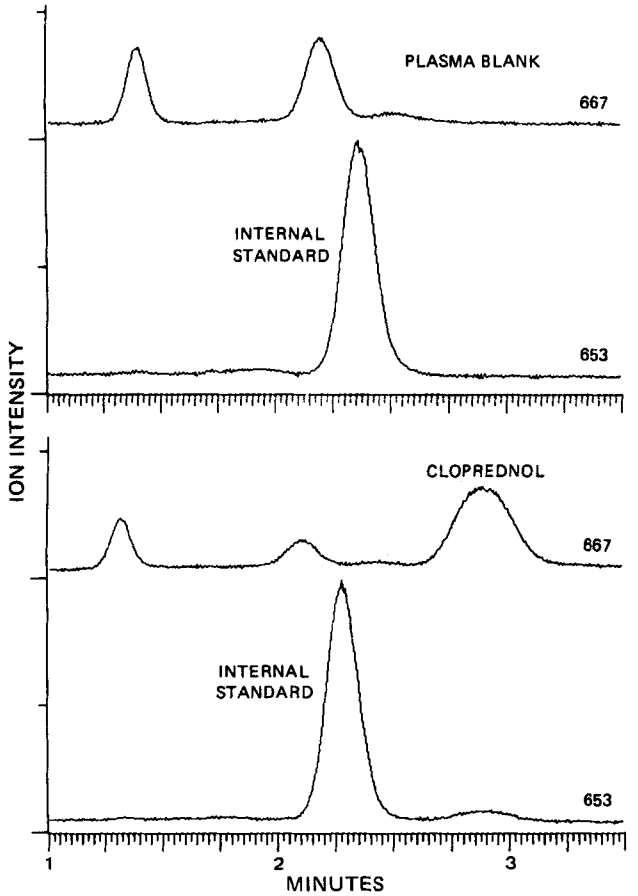


**Figure 4**—*Selected ion chromatograms of blank plasma (3 ml) spiked with the internal standard (top) and a plasma sample obtained 90 min after the administration of a 12.5-mg oral dose of cloprednol (bottom).*

The developed method also established a plasma level–time profile of a normal human volunteer following an oral dose of 12.5 mg of cloprednol (Fig. 3).

To validate the present HPLC method, plasma specimens were assayed by both HPLC and GLC–mass spectrometric[12] methods. To analyze the plasma samples by chemical-ionization mass spectrometry, the samples were extracted with ether and the extracts were cleaned by using miniature adsorption columns. A structural analog was used as an internal standard. The corticoids were converted to their methoxyimino trimethylsilyl derivatives to render them stable to analysis by GLC–mass spectrometry. A typical ion chromatogram obtained using GLC–mass spectrometry is shown in Fig. 4.

Numerous plasma samples from volunteers dosed with cloprednol were analyzed by both procedures. The excellent correlation between the two methods is indicated by the slope of 1.04 obtained from the scatter diagram shown in Fig. 5.

[12] Unpublished data.

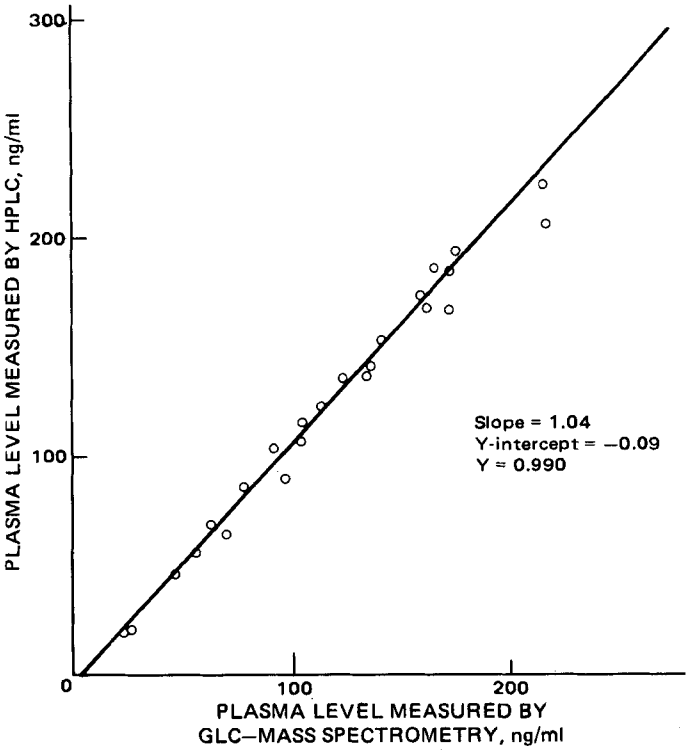


**Figure 5**—*Correlation between HPLC and GLC–mass spectrometric methods for plasma cloprednol analysis.*

## REFERENCES

(1) E. Ortega, C. Rodriquez, L. J. Strand, S. Bessler, and E. Segre, *J. Clin. Pharm.*, **16**, 122 (1976).

(2) W. A. Colburn and R. H. Buller, *Steroids*, **21**, 833 (1973).

(3) W. A. Colburn, *J. Clin. Endocrinol. Metab.*, **41**, 868 (1975).

(4) J. Chakraborty, J. English, V. Marks, M. C. Dumasia, and D. J. Chapman, *Br. J. Clin. Pharmacol.*, **3**, 903 (1976).

(5) E. Rolleri, M. Zannino, S. Orlandini, and R. Malvano, *Clin. Chim. Acta*, **66**, 319 (1976).

(6) D. H. Sandberg, C. Z. Bacallao, and W. W. Cleveland, *Biochem. Med.*, **4**, 383 (1970).

(7) A. K. Turner, C. J. Carroll, J. L. Pinkus, D. Charles, and S. C. Chattoraj, *Clin. Chem.*, **19**, 731 (1973).

(8) G. C. Cashmore, J. D. Few, and C. H. Fowles, *Ann. Clin. Biochem.*, **13**, 371 (1976).

(9) I. Bjorkhem, R. Blomstrand, O. Lantto, A. Lof, and L. Svensson, *Clin. Chim. Acta*, **56**, 241 (1974).

(10) J. P. Thenot and E. C. Horning, *Anal. Lett.*, **5**, 21 (1972).

(11) F. K. Trefz, D. J. Byrd, and W. Kochen, *J. Chromatogr.*, **107**, 181 (1975).

(12) J. C. K. Loo, A. G. Butterfield, J. Moffatt, and N. Jordan, *ibid.*, **143**, 275 (1977).

(13) J. C. K. Loo and N. Jordan, *ibid.*, **143**, 314 (1977).

(14) G. E. Reardon, A. M. Caldarella, and E. Canalis, *Clin. Chem.*, **25**, 122 (1979).

(15) J. Q. Rose and W. J. Jusko, *J. Chromatogr.*, **162**, 273 (1979).

(16) S. W. Schalm, W. H. J. Summerskill, and V. L. W. Go, *Mayo Clin. Proc.*, **51**, 761 (1976).

(17) A. V. Tembo, M. R. Hallmark, E. Sakmar, H. G. Bachmann, D. J. Weidler, and J. G. Wagner, *J. Pharmacokinet. Biopharm.*, **5**, 257 (1977).

(18) S. B. Matin and B. Amos, *J. Pharm. Sci.*, **67**, 923 (1978).

# Statistical Simulation Study of New Proposed Uniformity Requirement for Bioequivalency Studies

JOHN D. HAYNES

Received February 19, 1980, from the *Medical Research Division, Lederle Laboratories, American Cyanamid Company, Pearl River, NY 10965.* Accepted for publication November 19, 1980.

**Abstract** □ The results of a statistical simulation study of the FDA-proposed 75/75 requirement for some bioequivalency studies are presented. The study used test drug products with the same true average bioavailability as the corresponding reference drug products but with various degrees of uniformity as measured by the coefficient of variation. The performance of the 75/75 requirement indicated that the probability of the test product passing was greater if both products had identical small coefficients of variation than if both had identical large coefficients of variation. Moreover, a test product compared to a reference product with equal variability had less probability of acceptance than an equally variable test product for another drug for which the reference product had less variability. Both results indicate that the 75/75 requirement should be withdrawn. An alternative uniformly most powerful, unbiased test, the Pitman–Morgan $F$ test, is presented.

**Keyphrases** □ Bioequivalency studies—statistical simulation of the proposed 75/75 requirement □ Uniformity—statistical simulation of the proposed 75/75 requirement □ Bioavailability—statistical simulation of the proposed 75/75 requirement

The proposed rules for bioequivalency studies of tricyclic antidepressants (1), carbonic anhydrase inhibitors (2), probenecid (3), phenothiazine (4), and quinidine (5) all have a requirement dealing with the blood level results for individual subjects in addition to the usual requirement dealing with the average rate and extent of bioavailability. The new requirement essentially is that the relative bioavailability of the test product (compared to the study results for the clinically proven reference product for each subject) must be ≥75% for 75% of the subjects (or 70% for 70% of the subjects in Ref. 4).

The performance of this new 75/75 specification was found in the present study to have very undesirable characteristics for test and reference products that have equal true averages. Examination of bioequivalency studies of six hypothetical drugs indicated that the performance of the 75/75 specification sometimes can be irrelevant and inverse in practice. A different test is proposed here, consisting of the ratio of standard deviations with an adjustment for correlation.

## BACKGROUND

Until recently, the only required proof of bioequivalence of two drug products has consisted of showing that any differences in the calculated averages for rate and/or extent of bioavailability were medically and/or statistically insignificant. The study must have a number of subjects sufficient to ensure a large probability, commonly 0.80, of detecting a true difference that would be large enough to be clinically important.

The proposed rules (1–5) for bioequivalency studies of five drug types have an additional requirement on the relative bioavailability for the subjects. This requirement pertains to both the average and the range, the latter being a characteristic mentioned only recently in such guidelines. Specifically, the relative bioavailability of the test product must be ≥75% for at least 75% of the subjects (or 70/70 in Ref. 4).

This specification is similar in some respects to the content uniformity specifications on individual capsules and tablets in Ref. 6, which require almost all assay values to fall within 15% of the stated potency. Among the differences, one is very important; in place of the fixed stated potency (usually the labeled amount), the 75/75 specification requires the use of an estimate of the reference drug product potency (*e.g.*, the area under the serum drug level curve) in each subject.

While other specifications deal with the average test product results, this proposed specification places a requirement on the range, uniformity, or homogeneity of individual results. (For some drugs, but not all, this requirement may be reasonable.) There are two obvious ways to compare the test product and the reference product in this respect; one is the 75/75 approach and the other is the ratio of the standard deviations for the two products. Both methods were examined in the present study.

The performance characteristics of the 75/75 specification in the special case in which the true averages are practically equal (as they are for most well-formulated products) were examined. This study examined the success of the 75/75 specification in the detection of poor and superior uniformity of blood drug levels following administration of the test product. Its performance was considered in studies involving six hypothetical drugs with some important parameter, such as the area under the serum curve, for the test products and reference products with various intersubject coefficients of variation (Table I). In all studies, the design was a two-way crossover. The intrasubject coefficients of variation in Table I were taken as 30%, a value often obtained from the error mean square of the crossover analysis of variance, and in Table II were taken as 20%, also a common value.

## EXPERIMENTAL

**Studies with Drug D1**—Both drug products, *i.e.*, reference product and test product, have a true intersubject coefficient of variation of 60% (a common value in bioavailability studies), and the true averages are equal. Since both products are tested in the same subjects, there is usually a degree of correlation; *i.e.*, for a given subject, if the area under the serum drug curve on the reference product is above its 24-subject average, then on the test product the subject's area under the serum drug curve also is likely to be above its average.

The computerized, stochastic simulation procedure described in the *Appendix* was used to generate 1000 studies of 24 subjects (*i.e.*, 24,000 subjects) with a true correlation of 0.00 to serve as a baseline. Of these studies, 140 met the 75/75 criterion. The same procedure was followed for a range of correlation coefficients, $\rho = 0.30$–$0.90$ (Table I). The proportion increased toward 1.00 (the fair, just value for these two products) as rho increased.

**Studies with Drug D2**—Both of the products have an intersubject coefficient of variation of 40% (also a common value in bioavailability studies), and the true averages are equal. Table I shows that the proportion of D2 studies meeting the 75/75 criterion at any given $\rho$ value was notably greater than the corresponding one for Drug D1. Although for both drugs the test products are just as good as the corresponding reference product in this respect, Drug D1 test product is at a disadvantage simply because the intersubject coefficient of variation is large (although equal) for both products. The probability of accepting the test product is greater for D2 than for D1, although both test products really are equally acceptable as substitutes for their respective reference products.

**Studies with Drug D3**—The intersubject coefficient of variation is 60% for the test product and 40% for the reference product, and the true averages are equal. The proportions in Table I are intermediate to those for D1 and D2 at any given $\rho$ value except 0.80 and 0.90, where it is less than the D1 proportion. By comparing the results obtained with D1 and D3, it is seen that, according to the 75/75 specification, a test product with a range of $AUC$ values that is 50% greater than the range of the reference product $AUC$ values (D3: 60% for test product and 40% for reference product) usually has a greater chance of being declared bioequivalent, in this respect at least, than does a test product with the same range as the reference product (D1: 60% test product and 60% reference product).

**Other Drugs**—The determination of how many subjects should

0022-3549/81/0600-0673$01.00/0
© 1981, American Pharmaceutical Association

**Table I—Partial Description of Simulated Studies with Three Hypothetical Drugs**

| Drug | Intersubject $CV$, % Test Product | Intersubject $CV$, % Reference Product | Proportion of 1000 Studies (Intrasubject $CV$ = 30%, 24 Subjects in Each) Meeting 75/75 Criterion[a] $\rho$ = 0.00 | $\rho$ = 0.30 | $\rho$ = 0.40 | $\rho$ = 0.50 | $\rho$ = 0.60 | $\rho$ = 0.70 | $\rho$ = 0.80 | $\rho$ = 0.90 |
|---|---|---|---|---|---|---|---|---|---|---|
| D1 | 60 | 60 | 0.15 | 0.19 | 0.22 | 0.26 | 0.30 | 0.35 | 0.43 | 0.52 |
| D2 | 40 | 40 | 0.72 | 0.78 | 0.79 | 0.81 | 0.84 | 0.86 | 0.88 | 0.90 |
| D3 | 60 | 40 | 0.29 | 0.32 | 0.34 | 0.36 | 0.38 | 0.39 | 0.41 | 0.43 |

[a] Rho ($\rho$) is the true correlation coefficient; the *Appendix* contains the assumptions and an outline of the method of calculating the proportions.

**Table II—Partial Description of Simulated Studies with Three Different Hypothetical Drugs**

| Drug | Intersubject $CV$[a], % Test Product | Intersubject $CV$[a], % Reference Product | Proportion of 1000 Studies (Intrasubject $CV$ = 20%, 12 Subjects in Each) Meeting 75/75 Criterion $\rho$ = 0.00 | $\rho$ = 0.30 | $\rho$ = 0.40 | $\rho$ = 0.50 | $\rho$ = 0.60 | $\rho$ = 0.70 | $\rho$ = 0.80 | $\rho$ = 0.90 |
|---|---|---|---|---|---|---|---|---|---|---|
| D4 | 60 | 60 | 0.24 | 0.29 | 0.32 | 0.35 | 0.40 | 0.47 | 0.54 | 0.66 |
| D5 | 40 | 40 | 0.55 | 0.63 | 0.66 | 0.69 | 0.73 | 0.79 | 0.82 | 0.88 |
| D6 | 60 | 40 | 0.38 | 0.44 | 0.45 | 0.47 | 0.51 | 0.53 | 0.56 | 0.59 |

[a] The values in these two columns are the same as for Drugs D1–D3.

participate in a bioequivalency study was made with the conventional equation involving Type I and II error rates, intrasubject coefficient of variation, and the size of the difference, *e.g.*, in average area under the curve, which is considered clinically important, often 20%. When a study is being planned, generally the variation of only the reference product is known. Therefore, that is what is used in the equation.

Table II shows the results of the simulation procedure for drugs with a smaller intrasubject coefficient of variation of 20%. The statistical power of detection of differences in average blood level *AUC* values in the studies is substantially the same for each of the three drugs and the same as that for the first three drugs.

**Studies with Drug D5**—The D5 proportions have been brought slightly closer to those for D4 than for D1 and D3, but the conclusions are unchanged. The probability of accepting the test product is greater for D5 than for D4, although both test products really are equally acceptable as substitutes for their respective reference products.

**Studies with Drug D6**—The D6 proportions also have been reduced but exceed the D4 proportions for $\rho$ of $\leq 0.80$. The picture is less unreasonable than for D3 but still is not reasonable. The conclusion given relating to D3 must be changed slightly for Drug D6; a test product with a range of *AUC* values that is 50% greater than the range of the reference product *AUC* values usually has a greater chance of being declared bioequivalent, in this respect at least, than does a test product with the same range as the reference product.

**Independent Confirmation**—The logic of the calculation procedure and the numerical results reported in Tables I and II were checked using the distribution theory provided by Marsaglia (7). The numbers agreed exactly to two decimals or were only 1, 2, or 3 low in the second decimal place.

**Results in "Equal Means" Situations**—For test products that give blood levels just as uniform as those obtained with the corresponding reference products (*e.g.*, D1 and D2), the probability of meeting the 75/75 specification is inversely proportional to the intersubject coefficient of variation for the reference product. Thus, the specification is unfair to those particular test products that must be compared to reference products with large intersubject coefficients of variation.

For test products giving blood levels that differ significantly in uniformity from those obtained with the corresponding reference products (*e.g.*, D3), the 75/75 specification is irregular; the inferior test product, that for D3, is either more likely or just as likely to be accepted as the equivalent test product, that for D1.

## DISCUSSION

**Generalization**—The present study dealt with cases where the true means for the two products were equal, as they are for most well-formulated products. When the true means were unequal, the performance characteristics of the 75/75 specification were not investigated here; in those cases, the performance of the 75/75 requirement involves the differences in averages as well as ranges. The findings here are pertinent also in cases where the true means are almost equal. The lack of a broader generalization does not preclude a conclusion about the 75/75 specification. The results indicate that in some common situations, *i.e.*, where the means for the test and reference products are practically equal, the 75/75 requirement is unfair to some particular test products and is irregular in its disposition of test products of various qualities in other studies. Therefore, the 75/75 requirement should be dropped.

The performance (*i.e.*, the probability of accepting the test product) of the 75/75 specification when the test and reference products were truly practically identical (with only random variation operating) depended on the magnitude of the variation, an irrelevant factor. The performance was the inverse of what it should be when the test product's variability is large; with a given, fixed degree of variation for a test product, the smaller the reference product's variation (*i.e.*, the more divergent the two products), the greater the probability of acceptance of the test product.

**Pitman–Morgan *F* Specification Procedure**—A procedure for comparing the uniformity, range, or standard deviation of blood levels of the test product to the uniformity of those of the reference product is the use of intersubject standard deviations for the two products. However, since the standard deviations are determined in the same subjects (*i.e.*, in a crossover study), the usual Fisher $F$ ratio of variances must be adjusted. This adjusted $F$, which is one form used to represent the Pitman–Morgan results, was shown (8) to be a uniformly most powerful, unbiased test.

Let:

$$F = (s_2/s_1)^2 \qquad \text{(Eq. 1)}$$

where the standard deviations $s_1$ and $s_2$ are for the reference product and test product, respectively. (If $F$ is <1.00, no further calculations are necessary because the uniformity of blood levels of the test product is estimated to be as good as that of the reference product or better.)

Then:

$$\text{adjusted } F = [(F-1)^2(n-2)]/[4F(1-R^2)] \qquad \text{(Eq. 2)}$$

where $R$ is the correlation coefficient for the pairs of values for each subject. If this correlation is zero or negative, then the unadjusted $F$ test is appropriate with $N-1$ and $N-1$ degrees of freedom. The adjusted $F$ has the same distribution as the tabulated $F$ with 1 and $N-2$ degrees of freedom. The 0.05 probability level seems appropriate.

The results of one study[1] serve to illustrate the use of these equations for the area under the serum drug concentration–time curve for 18 subjects. The standard deviation of the area was 129.8 for the reference product and 156.3 for the test product. The intersubject correlation coefficient between the area values was 0.90. The Fisher $F$ ratio was 1.45, leading to a Pitman–Morgan $F$ value of 2.94 as calculated from $[(1.45-1)^2(18-2)]/[4(1.45)(1.0-0.90^2)]$. This value has 1 and 16 degrees of freedom and the associated probability is 0.11. It was concluded that the two standard deviations do not differ significantly.

The same Monte Carlo simulation data used for Drugs D1–D6 were used for the Pitman–Morgan $F$ test with the critical $F$ at the 0.05 probability level. The proportions of acceptable studies were as follows: D1 and D2, 0.992 at all $\rho$ values; D4 and D5, 0.986 at all $\rho$ values; D3 ($N$ = 24), 0.743–0.749; and D6 ($N$ = 12), 0.869–0.874. These results are reasonable.

**Statistical Power**—If the true (population) correlation coefficient were 0.80 (chosen here because it is tabulated in Ref. 9), if the Pitman–

[1] Unpublished data.

Morgan $F$ test result in a study would be declared significant at the unilateral probability level of 0.01, if the study used 18 subjects, and if the power of detection of a difference in test and reference product standard deviations were set at 0.80, then the statistically detectable ratio would be (by rough extrapolation of the data in Ref. 9) >2 or 3. In other words, a test product standard deviation that is truly more than double or triple that of the reference product is likely to be detected in a study under these conditions. Any increase in sample size to improve the detection of differences in the standard deviations is believed to be unwarranted since, in view of other sources of inherent variation known in posology but not considered further here and in view of the desirability of minimizing the use of human subjects in bioequivalency studies, the power seems ample.

## APPENDIX

It was assumed that the test product values and the reference product values followed a bivariate normal distribution with both means equal to 100, with certain chosen standard deviations and with correlation coefficients (Table I) modified to allow for the intrasubject variability which, among other things, reduces the estimated value of $\rho$ (10).

The assumption that all actual bioequivalency data follow the bivariate normal distribution may be questioned; therefore, it is noted that very large intersubject coefficients of variation for *AUC*, *e.g.*, 150%, are symptomatic of drug products with either a very skewed distribution or some outliers. In such cases, the mean and standard deviation are not sufficient to describe the bivariate nonnormal distribution. However, if differences in only means are tested, the analysis of variance has been found to be a very robust procedure that is practically undisturbed by such things. Remedies after the fact include transformation of the data (*e.g.*, logarithmic) or identification of assignable causes for outliers; remedies *a priori* consist of controlling factors that have been found to cause aberrant results for the particular drug. In cases where the log transformation is used, the 75/75 rule also must be transformed. The performance of that transformed rule would be investigated differently than here, but intuitively the deficiencies of the rule would be substantially the same. The findings in the present study are appropriate for bioavailability parameters that are normally distributed.

The Monte Carlo simulation proceeded according to a FORTRAN program[2], which used a multivariate normal random deviate generator subroutine, GGNRM[3], and a local subroutine, CALC, which applied the 75/75 rule to each of the 1000 studies in turn. The main program then tallied up the number of studies that "passed." One run was made to obtain each cell in Tables I and II. The Pitman–Morgan $F$ (9) was calculated for the identical sets of data.

## REFERENCES


(1) *Fed. Regist.*, **43**, 6968 (1978).
(2) *Ibid.*, **45**, 11853 (1980).
(3) *Ibid.*, **45**, 48160 (1980).
(4) *Ibid.*, **45**, 56832 (1980).
(5) *Ibid.*, **45**, 72200 (1980).
(6) "The United States Pharmacopeia," 20th rev., United States Pharmacopeial Convention, Rockville, Md., 1980, p. 955.
(7) G. Marsaglia, *J. Am. Stat. Assoc.*, **60**, 193 (1965).
(8) M. G. Kendall and A. Stewart, "The Advanced Theory of Statistics," 3rd ed., vol. 2, Hafner, New York, N.Y., 1973, p. 531.
(9) W. A. Morgan, *Biometrika*, **31**, 13 (1939). E. J. G. Pitman, *ibid.*, **31**, 9 (1939).
(10) K. A. Brownlee, "Statistical Theory and Methodology in Science and Engineering," 1st ed., Wiley, New York, N.Y., 1960, p. 366.


## ACKNOWLEDGMENTS


The author thanks R. Ganesan, S. Heft, R. Kohberger, J. Johnson, A. Weiss, and N. Bauman for helpful comments and Dr. Daniel Weiner for helpful comments and discussion. He also thanks T. Hoffman for the application of Marsaglia's work which provided a different viewpoint.


[2] Available from the author.
[3] International Mathematical and Statistical Libraries, Houston, Tex.

# Assignment of Conformation and Configuration to Potassium Permanganate Oxidation Products of Quinidine


**YEHUDA YANUKA, SHIMONA YOSSELSON-SUPERSTINE *, ARTOUL GERYES, and EDWARD SUPERSTINE *x**



Received August 8, 1980, from the *Department of Pharmacy, School of Pharmacy, Faculty of Medicine, Hebrew University–Hadassah Medical Center, Jerusalem, Israel.* Accepted for publication December 2, 1980. *Present address: College of Pharmacy, University of Utah, Salt Lake City, UT 84112.



**Abstract** □ Two epimeric aldehydes [(*R*)- and (*S*)-quinidinals] and the corresponding acids [(*R*)- and (*S*)-norhydroquinidinoic acids] were prepared by the oxidation of quinidine. The $\pi$–$\pi$ interactions of the carbonyl group and the aromatic moiety, as reflected in the NMR spectra, were compared with those of quinidine. NMR spectroscopic analyses made it possible to assign both the stable conformation and their configuration at C-3 to these molecules. The free hydroxyl group at C-9 must be present for the chemical shift values to be concentration dependent. These findings provide more information on association in the parent molecules.



**Keyphrases** □ Quinidine—oxidation products prepared, conformation and configuration assigned, NMR analyses □ Oxidation products—quinidine, conformation and configuration assigned to oxidation products, NMR analyses □ NMR spectroscopy—analyses, quinidine and oxidation products, conformation and configuration assigned


Previous work showed that the NMR spectra of quinidine (I) and hydroquinidine (1) differ significantly. The unique features encountered in the I molecule were attributed to $\pi$–$\pi$ interactions. If changes in these $\pi$–$\pi$ interactions are reflected in the NMR spectra of new compounds compared to the parent substances, it must be determined whether there is any correlation between the NMR data obtained and the biological activity of the compound. The antiarrhythmic activity of I and quinine differ greatly because of differences in configuration at C-8 and C-9. Comparison of the NMR data of I and quinine may provide information on the origin of these differences. Intraatomic distances in the molecules play an important role in their respective biological activities. NMR analyses may be valuable in assessing such differences and thus evaluating their possible therapeutic potential.

NMR analysis was used in the present work to measure the extent of $\pi$–$\pi$ interaction by changing the intensity of


0022-3549/81/0600-0675$01.00/0


© 1981, American Pharmaceutical Association

Morgan $F$ test result in a study would be declared significant at the unilateral probability level of 0.01, if the study used 18 subjects, and if the power of detection of a difference in test and reference product standard deviations were set at 0.80, then the statistically detectable ratio would be (by rough extrapolation of the data in Ref. 9) >2 or 3. In other words, a test product standard deviation that is truly more than double or triple that of the reference product is likely to be detected in a study under these conditions. Any increase in sample size to improve the detection of differences in the standard deviations is believed to be unwarranted since, in view of other sources of inherent variation known in posology but not considered further here and in view of the desirability of minimizing the use of human subjects in bioequivalency studies, the power seems ample.

## APPENDIX

It was assumed that the test product values and the reference product values followed a bivariate normal distribution with both means equal to 100, with certain chosen standard deviations and with correlation coefficients (Table I) modified to allow for the intrasubject variability which, among other things, reduces the estimated value of $\rho$ (10).

The assumption that all actual bioequivalency data follow the bivariate normal distribution may be questioned; therefore, it is noted that very large intersubject coefficients of variation for *AUC*, *e.g.*, 150%, are symptomatic of drug products with either a very skewed distribution or some outliers. In such cases, the mean and standard deviation are not sufficient to describe the bivariate nonnormal distribution. However, if differences in only means are tested, the analysis of variance has been found to be a very robust procedure that is practically undisturbed by such things. Remedies after the fact include transformation of the data (*e.g.*, logarithmic) or identification of assignable causes for outliers; remedies *a priori* consist of controlling factors that have been found to cause aberrant results for the particular drug. In cases where the log transformation is used, the 75/75 rule also must be transformed. The performance of that transformed rule would be investigated differently than here, but intuitively the deficiencies of the rule would be substantially the same. The findings in the present study are appropriate for bioavailability parameters that are normally distributed.

The Monte Carlo simulation proceeded according to a FORTRAN program[2], which used a multivariate normal random deviate generator subroutine, GGNRM[3], and a local subroutine, CALC, which applied the 75/75 rule to each of the 1000 studies in turn. The main program then tallied up the number of studies that "passed." One run was made to obtain each cell in Tables I and II. The Pitman–Morgan $F$ (9) was calculated for the identical sets of data.

## REFERENCES


(1) *Fed. Regist.*, **43**, 6968 (1978).
(2) *Ibid.*, **45**, 11853 (1980).
(3) *Ibid.*, **45**, 48160 (1980).
(4) *Ibid.*, **45**, 56832 (1980).
(5) *Ibid.*, **45**, 72200 (1980).
(6) "The United States Pharmacopeia," 20th rev., United States Pharmacopeial Convention, Rockville, Md., 1980, p. 955.
(7) G. Marsaglia, *J. Am. Stat. Assoc.*, **60**, 193 (1965).
(8) M. G. Kendall and A. Stewart, "The Advanced Theory of Statistics," 3rd ed., vol. 2, Hafner, New York, N.Y., 1973, p. 531.
(9) W. A. Morgan, *Biometrika*, **31**, 13 (1939). E. J. G. Pitman, *ibid.*, **31**, 9 (1939).
(10) K. A. Brownlee, "Statistical Theory and Methodology in Science and Engineering," 1st ed., Wiley, New York, N.Y., 1960, p. 366.


## ACKNOWLEDGMENTS


The author thanks R. Ganesan, S. Heft, R. Kohberger, J. Johnson, A. Weiss, and N. Bauman for helpful comments and Dr. Daniel Weiner for helpful comments and discussion. He also thanks T. Hoffman for the application of Marsaglia's work which provided a different viewpoint.


[2] Available from the author.
[3] International Mathematical and Statistical Libraries, Houston, Tex.

# Assignment of Conformation and Configuration to Potassium Permanganate Oxidation Products of Quinidine


**YEHUDA YANUKA, SHIMONA YOSSELSON-SUPERSTINE *, ARTOUL GERYES, and EDWARD SUPERSTINE *x**



Received August 8, 1980, from the *Department of Pharmacy, School of Pharmacy, Faculty of Medicine, Hebrew University–Hadassah Medical Center, Jerusalem, Israel.* Accepted for publication December 2, 1980. *Present address: College of Pharmacy, University of Utah, Salt Lake City, UT 84112.



**Abstract** □ Two epimeric aldehydes [(*R*)- and (*S*)-quinidinals] and the corresponding acids [(*R*)- and (*S*)-norhydroquinidinoic acids] were prepared by the oxidation of quinidine. The $\pi$–$\pi$ interactions of the carbonyl group and the aromatic moiety, as reflected in the NMR spectra, were compared with those of quinidine. NMR spectroscopic analyses made it possible to assign both the stable conformation and their configuration at C-3 to these molecules. The free hydroxyl group at C-9 must be present for the chemical shift values to be concentration dependent. These findings provide more information on association in the parent molecules.



**Keyphrases** □ Quinidine—oxidation products prepared, conformation and configuration assigned, NMR analyses □ Oxidation products—quinidine, conformation and configuration assigned to oxidation products, NMR analyses □ NMR spectroscopy—analyses, quinidine and oxidation products, conformation and configuration assigned


Previous work showed that the NMR spectra of quinidine (I) and hydroquinidine (1) differ significantly. The unique features encountered in the I molecule were attributed to $\pi$–$\pi$ interactions. If changes in these $\pi$–$\pi$ interactions are reflected in the NMR spectra of new compounds compared to the parent substances, it must be determined whether there is any correlation between the NMR data obtained and the biological activity of the compound. The antiarrhythmic activity of I and quinine differ greatly because of differences in configuration at C-8 and C-9. Comparison of the NMR data of I and quinine may provide information on the origin of these differences. Intraatomic distances in the molecules play an important role in their respective biological activities. NMR analyses may be valuable in assessing such differences and thus evaluating their possible therapeutic potential.

NMR analysis was used in the present work to measure the extent of $\pi$–$\pi$ interaction by changing the intensity of


0022-3549/81/0600-0675$01.00/0


© 1981, American Pharmaceutical Association

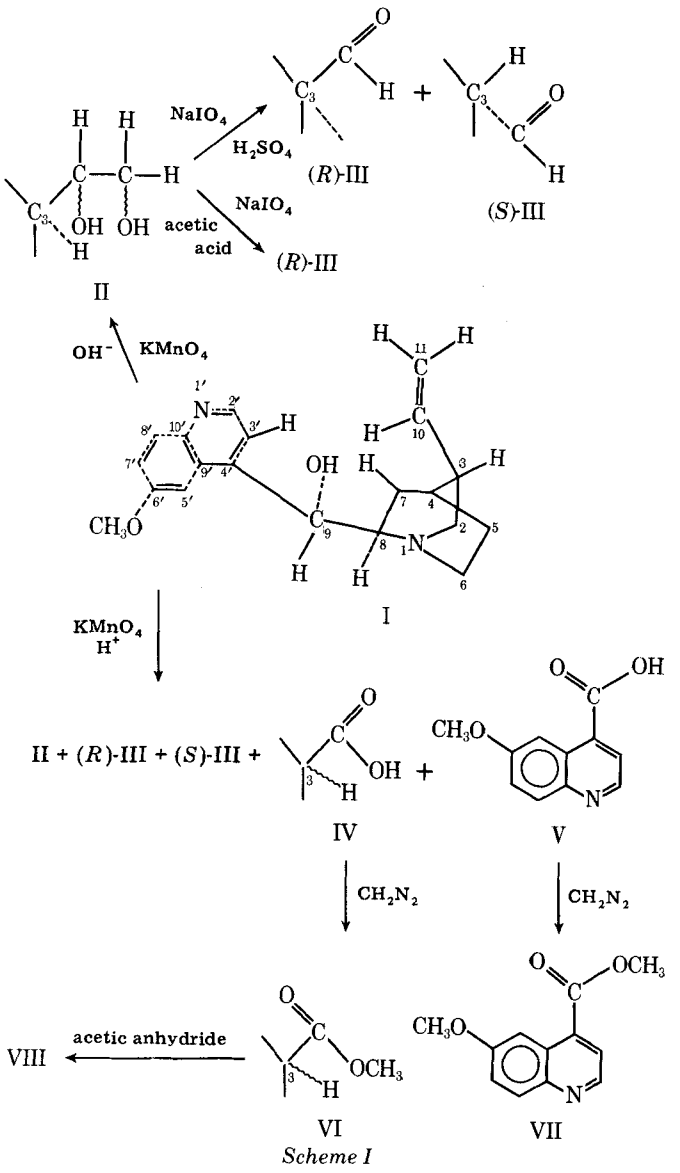


*Scheme I*

the $\pi$ system in the side chain at C-3. For this purpose, quinidinal[1] (III, a C-10 aldehydic derivative of I) and the corresponding acid norhydroquinidinoic acid (quitenidene, IV) were prepared by potassium permanganate oxidation of the vinylic group of I. Although preparation of III from I by the ozonization route was reported previously (2), the alternative method utilizing potassium permanganate was selected. With the latter method, it was possible to obtain the diol (II), the epimeric aldehydes (*R*)- and (*S*)-III, the corresponding acid (IV), and a fragmentation product (V) in one step (Scheme I). NMR analyses and TLC of the isolated products made it possible to study the characteristics and nature of the new compounds and the details of the experimental conditions.

## EXPERIMENTAL

NMR spectra were obtained at 300 MHz using an analytical NMR spectrometer[2] equipped with an automatic recorder. Tetramethylsilane in deuterochloroform was the internal standard. IR spectra were measured in potassium bromide disks on a grating IR spectrophotometer[3]. Mass spectra were recorded on a mass spectrometer[4] provided with an electric-impact and field-desorption ion source. Pure I was obtained from commercial quinidine sulfate USP[5]. TLC and preparative TLC were carried out on aluminum oxide GF 254[6] plates.

**Table I—Chemical Shift Values[a] of the Protons of (*R*)-III and (*S*)-III in 1:1 Ratio at Various Concentrations (Milligrams per 0.5 ml) and of Pure (*R*)-III**

| Proton | Concentration of (*R*)-III and (*S*)-III | | | (*R*)-III |
|---|---|---|---|---|
| | 8 mg | 15 mg | 23 mg | |
| O ‖ C–H | 9.87 (s)<br>9.78 (s) | 9.86 (s)<br>9.78 (s) | 9.85 (s)<br>9.76 (s) | 9.83 (s) |
| H-2′ | 8.66 (t)<br>(*J* = 4 Hz) | 8.63 (t)<br>(*J* = 4 Hz) | 8.58 (t)<br>(*J* = 4 Hz) | 8.58 (d)<br>(*J* = 4 Hz) |
| H-8′ | 7.97 (d)<br>(*J* = 9 Hz) | 7.95 (d)<br>(*J* = 9 Hz) | 7.93 (d)<br>(*J* = 9 Hz) | 7.98 (d)<br>(*J* = 9 Hz) |
| H-3′ | 7.54 (d)<br>(*J* = 4 Hz)<br>7.47 (d)<br>(*J* = 4 Hz) | 7.53 (d)<br>(*J* = 4 Hz)<br>7.47 (d)<br>(*J* = 4 Hz) | 7.49 (d)<br>(*J* = 4 Hz)<br>7.43 (d)<br>(*J* = 4 Hz) | 7.44 (d)<br>(*J* = 4 Hz) |
| H-7′ | —[b] | —[b] | —[b] | —[b] |
| H-5′ | 7.18 (s)<br>7.13 (d)<br>(*J* = 2 Hz) | 7.18 (s)<br>7.13 (d)<br>(*J* = 2 Hz) | 7.15 (d)<br>(*J* = 2 Hz) | —[b] |
| H–C-9–OH | 5.75 (s)<br>5.62 (d)<br>(*J* = 4 Hz) | 5.72 (s)<br>5.59 (d)<br>(*J* = 5 Hz) | 5.72 (s)<br>5.59 (d)<br>(*J* = 5 Hz) | 5.59 (d)<br>(*J* = 4 Hz) |
| $CH_3O$ | 3.91 (s)<br>3.85 (s) | 3.90 (s)<br>3.84 (s) | 3.90 (s)<br>3.84 (s) | 3.92 (s) |

[a] In parts per million. [b] Increasing overlap with the hydrogen of chloroform with concentration.

**Oxidation of I by Potassium Permanganate and Dilute Sulfuric Acid**—Quinidine (I) (1 g), as the sulfate salt, was dissolved in 20 ml of dilute sulfuric acid (2 *N*), and two equivalents of potassium permanganate (0.95 g) in aqueous solution was added. The reaction mixture was stirred for 2 hr at room temperature. Sodium bisulfite in a 10% aqueous solution was added dropwise until the precipitated manganese dioxide was dissolved. TLC revealed a mixture of polar and nonpolar products. Separation of these products was accomplished by extraction and chromatography.

**Isolation of II and III**—The clear solution obtained after the addition of sodium bisulfite was transferred to a separator and made alkaline by the addition of sodium carbonate. The mixture was extracted completely with chloroform containing 10% methanol. After evaporation of the solvents, TLC revealed the presence of hydroquinidine, a small amount of unchanged I, and two new compounds, a diol (II) appearing as two isomers and the aldehyde (III).

The mixture was chromatographed on aluminum oxide plates. The fluorescing material was viewed under UV light and divided into three fractions. The upper strip was scraped and dispersed in 20 ml of 0.1 *N* $H_2SO_4$. Sodium bicarbonate (240 mg) was added, the mixture was transferred to a separator, and I and hydroquinidine were extracted with chloroform. The middle strip containing III was treated in the same manner but was extracted with chloroform containing 10% methanol. Its melting point was nonspecific; $R_f$ 0.20 (ethyl acetate–ethanol, 9:1); IR: 1720 (CO) $cm^{-1}$; mass spectrum: *m/z* 326. The chemical shifts of III, which consisted of two epimers (*R*)-III and (*S*)-III at various concentrations, are summarized in Table I.

The lower strip, containing a 1:1 mixture of the diastereomeric diols (II), was scraped; the powder obtained was extracted directly with chloroform containing 20% methanol. The two diastereomers were separated by repeated preparative TLC on aluminum oxide plates. The more polar diol, $R_f$ 0.13 (ethanol), yielded crystals from acetone and was sparingly soluble in chloroform. When attempting to determine its melting point, the crystals began to discolor at ~200°, becoming brown (similar to the caramelization of sugar) and forming a solid lump, which eventually liquified at 225–227°. The less polar diol, $R_f$ 0.36 (ethanol), was much more soluble in acetone and chloroform and could not be induced to crystallize. Upon the addition of ether to an acetone solution of the less polar diol, an amorphous material settled out. The melting

[1] The authors suggest the name norhydroquinidinal (III) instead of quinidinal.
[2] Bruker W. H. 300.
[3] Perkin-Elmer 457.
[4] Varian Mat CHS DF.
[5] Sigma Chemical Co., St. Louis, Mo.
[6] Stahl, Merck.

**Table II—Chemical Shift Values [a] of the Protons of VII at Two Different Concentrations (Milligrams per 0.5 ml)**

| Proton | Concentration of VII | |
|---|---|---|
| | 11 mg | 7 mg |
| H-3′ | 8.87 (d) ($J$ = 4 Hz) | 8.86 (d) ($J$ = 4 Hz) |
| H-5′ | 8.25 (d) ($J$ = 3 Hz) | 8.25 (d) ($J$ = 3 Hz) |
| H-8′ | 8.08 (d) ($J$ = 9 Hz) | 8.08 (d) ($J$ = 9 Hz) |
| H-2′ | 7.94 (d) ($J$ = 4 Hz) | 7.94 (d) ($J$ = 4 Hz) |
| H-7′ | 7.44 (q) ($J_m$ = 3 Hz) ($J_0$ = 10 Hz) | 7.44 (q) ($J_m$ = 3 Hz) ($J_0$ = 10 Hz) |
| $CH_3O$–C-6′ | 4.04 (s) | 4.04 (s) |
| $CH_3O$–C(=O)– | 3.98 (s) | 3.99 (s) |

[a] In parts per million.

point of this amorphous material was nonspecific; at ~200°, it became brown and finally turned into a viscous liquid.

**Isolation of VI and VII**—The alkaline solution was made acidic by the addition of acetic acid. The mixture was extracted with chloroform–isopropyl alcohol (3:1). After evaporation of the solvents, the residue was treated with diazomethane, and the methyl esters of IV and V (VI and VII, respectively) were separated by preparative TLC. The mixture was chromatographed on aluminum oxide plates. The fluorescing material was viewed under UV light and divided into two fractions. The upper strip was scraped, and the powder obtained was extracted directly with chloroform containing 10% methanol. It contained the methyl ester of quininic acid (VII), $R_f$ 0.80 (ethyl acetate), mp 80–81°; IR: 1715 (CO) $cm^{-1}$. Table II lists the NMR data.

The lower strip was treated as was the upper strip and was found to contain the methyl ester of norhydroquinidinoic acid (VI), $R_f$ 0.14 (ethyl acetate) and $R_f$ 0.70 (ethyl acetate–ethanol, 1:1). Recrystallization from methanol gave crystals, mp 140–141°. However, there was a softening of the material at 137°, suggesting that VI consisted of two diastereomers, (*R*)-VI and (*S*)-VI. The IR spectrum showed 1725 (CO) $cm^{-1}$ with a shoulder at 1740 (CO) $cm^{-1}$, implying the existence of another diastereomer. The chemical shifts at various concentrations are summarized in Table III.

**Methyl Ester of 9-Acetyl Norhydroquinidinoic Acid (VIII)**—Pure VI (60 mg) was dissolved in 1 ml of pyridine and 1 ml of acetic anhydride, and this mixture was allowed to stand overnight for ~24 hr at room temperature. The solvents were removed with an air stream, and the solid residue was dissolved in 30 ml of chloroform. The chloroform solution was transferred to a separator, washed with 20 ml of water, and filtered without delay through anhydrous sodium sulfate since the acetylated product was prone to hydrolysis, $R_f$ 0.5 (ethyl acetate); IR: 1726, 1736, and 1746 (CO) $cm^{-1}$. The NMR data are included in Table III.

**Oxidation of I by Potassium Permanganate under Basic Conditions**—Five grams of I was dissolved in 30 ml of tetrahydrofuran. To this solution was added 40 ml of aqueous 1 *N* KOH followed by two equivalents of potassium permanganate (4.75 g) in aqueous solution. The reaction mixture was stirred magnetically for 7 days at room temperature and then was transferred in its entirety to a separator and extracted with chloroform containing 20% methanol until complete extraction was achieved. Upon removal of the solvents, a substance was readily crystallized. It proved to be a mixture of two diastereoisomers (II), which were identical to those obtained by oxidation of I under acidic conditions.

**Oxidation of II by Sodium Periodate**—*Method A: Dilute Aqueous Strong Acid*—One gram of II was dissolved in 20 ml of 1 *N* $H_2SO_4$. A 10.7% aqueous sodium periodate solution (6.5 ml) was added to the acidic solution of II, and this mixture was stirred at room temperature overnight. The solution was then transferred to a separator, made alkaline with sodium carbonate, and extracted thoroughly with chloroform containing 20% methanol. After evaporation of the solvents, an amorphous material was obtained that would not crystallize. This material was identical in all respects to the amorphous mixture of (*R*)-III and (*S*)-III obtained under acidic conditions.

*Method B: Dilute Aqueous Weak Acid*—One gram of II was dissolved in 1 ml of acetic acid and diluted with 20 ml of water. The sodium periodate was added, and the reaction mixture was stirred overnight. Once again the solution was made alkaline and extracted as for Method A. After evaporation of the solvents, a crystalline material was obtained and recrystallized from acetone, mp 205°, $R_f$ 0.20 (ethyl acetate–ethanol, 9:1). NMR analysis revealed only the natural epimer (*R*)-III (Table I).

**Epimerization of (*R*)-III**—Attempts to purify (*R*)-III by chromatography on aluminum oxide plates brought about complete epimerization, and NMR analysis showed that the final product contained a 1:1 mixture of (*R*)-III and (*S*)-III. On the other hand, NMR analysis of a freshly prepared sample of pure (*R*)-III in deuterated chloroform showed only pure (*R*)-III. After 24 hr, the same sample showed small amounts of the epimeric aldehyde (*S*)-III; after a 7-day standing period, the sample showed equal amounts of (*R*)-III and (*S*)-III.

## RESULTS AND DISCUSSION

**Assignment of Conformation and Configuration to Oxidation Products of I**—The data summarized in Table I show clearly that the chemical shift values of (*R*)-III and (*S*)-III in a mixture depend not only on the concentration of the mixture but also on the relative amounts of these epimers in the mixture. Therefore, to assign the configuration at C-3 in these molecules, NMR analysis was carried out on a mixture containing (*R*)-III and (*S*)-III in a 2:1 ratio.

*NMR Analysis of (R)-III*—The aldehydic proton resonated as a singlet at δ 9.85 ppm. The H-2′ proton appeared as a broad singlet at δ 8.54 ppm, H-3′ appeared as a doublet at δ 7.45 ppm ($J$ = 4 Hz), and H-8′ appeared as a doublet at δ 7.90 ppm ($J$ = 9 Hz). The H-5′ and H-7′ protons resonated between δ 7.28 and 7.25 ppm. The H–C-9–OH proton appeared as a doublet at δ 5.60 ppm ($J$ = 3.0 Hz). The methoxy protons absorbed at δ 3.87 ppm.

*NMR Analysis of (S)-III*—The aldehydic proton resonated as a singlet at δ 9.76 ppm, at a higher field compared to the crystalline aldehyde. The H-2′ proton appeared as a broad singlet at δ 8.54 ppm. The H-3′ proton resonated at δ 7.50 ppm ($J$ = 4 Hz), at a lower field compared to the crystalline aldehyde; H-8′ appeared at δ 7.90 ppm ($J$ = 10 Hz), the same as in the crystalline aldehyde. Both H-5′ and H-7′ appeared separately; the former proton shifted to a higher field at δ 7.11 ppm and the latter proton absorbed at almost the same frequency compared to (*R*)-III. The proton alpha to the hydroxyl group at C-9 (H–C-9–OH) appeared as a slightly broadened singlet at δ 5.71 ppm, at a lower field than (*R*)-III. The peak of the methoxy protons appeared at δ 3.81 ppm, at a slightly higher field than (*R*)-III.

While some protons were less shielded in (*R*)-III compared to those of (*S*)-III, other protons in (*R*)-III experienced more shielding than the same protons of (*S*)-III. In addition, the aldehydic protons in both epimers appeared as singlets while the coupling constants between the aldehydic proton and the proton alpha to the carbonyl group generally ranged between 1 and 3 Hz and in some cases reached a value of 6 Hz (3, 4). This finding indicates that a single rotamer prevails in the aldehydic groups with a dihedral angle of ~90° between the aldehydic proton and the proton alpha to the carbonyl group at C-3.

In a previous work based on NMR analyses (1), we assumed a stable

**Table III—Chemical Shift Values [a] of the Protons of VI at Various Concentrations (Milligrams per 0.5 ml) and of VIII**

| Proton | Concentration of VI | | | VIII, 10 and 35 mg |
|---|---|---|---|---|
| | 14 mg | 36 mg | 50 mg | |
| H-2′ | 8.67 (d) ($J$ = 4 Hz) | 8.56 (d) ($J$ = 4 Hz) | 8.51 (d) ($J$ = 4 Hz) | 8.72 (d) ($J$ = 4 Hz) |
| H-3′ | 7.51 (d) ($J$ = 4 Hz) | 7.46 (d) ($J$ = 4 Hz) | 7.44 (d) ($J$ = 4 Hz) | 7.34 (d) ($J$ = 4 Hz) |
| H-8′ | 8.00 (d) ($J$ = 9 Hz) | 7.94 (d) ($J$ = 9 Hz) | 7.87 (d) ($J$ = 9 Hz) | 8.01 (d)[b] ($J$ = 9 Hz)<br>7.96 (d)[c] ($J$ = 9 Hz) |
| H–C-9–$OCH_3$ | — | — | — | 6.61 (d) ($J$ = 4 Hz) |
| H–C-9–OH | 5.62 (d) ($J$ = 5 Hz) | 5.55 (d) ($J$ = 5 Hz) | 5.56 (d) ($J$ = 5 Hz) | —<br>4.00 (s)[b] |
| $CH_3O$–C-6′ | 3.92 (s) | 3.85 (s) | 3.82 (s) | 3.88 (s)[c] |
| $CH_3O$–C(=O)–C-10 | 3.75 (s) | 3.72 (s) | 3.70 (s) | 3.77 (s) |
| $CH_3$–C(=O)–O–C-9 | — | — | — | 2.14 (s)[b]<br>2.01 (s)[c] |

[a] In parts per million. [b] (*R*)-VIII. [c] (*S*)-VIII.

*Table IV*—**Chemical Shift Values [a] of the Protons of Hydroquinidine, VI, I, and (*R*)-III (~15 mg/0.5 ml)**

| Compound | H-2′ | H-3′ | H-8′ |
|---|---|---|---|
| Hydroquinidine | 8.63 (d) ($J$ = 4 Hz) | 7.52 (d) ($J$ = 4 Hz) | 7.95 (d) ($J$ = 9 Hz) |
| VI | 8.66 (d) ($J$ = 4 Hz) | 7.51 (d) ($J$ = 4 Hz) | 8.00 (d) ($J$ = 9 Hz) |
| I | 8.59 (d) ($J$ = 4 Hz) | 7.49 (d) ($J$ = 4 Hz) | 7.94 (d) ($J$ = 9 Hz) |
| (*R*)-III | 8.58 (d) ($J$ = 4 Hz) | 7.42 (d) ($J$ = 4 Hz) | 7.93 (d) ($J$ = 9 Hz) |

[a] In parts per million.

preferred conformation for I. On the basis of the data presented for the two aldehydes, we concluded that the molecules of each epimer exist as a stable rotamer and the structure of the rotamers depends mainly on steric and $\pi$–$\pi$ interactions in the molecule. As a result of this latter interaction, the coplanar H–C=O group in (*R*)-III is in close proximity to the nitrogen-containing aromatic ring, and this involves rotation about the C-4′–C-9–C-8 bonds, making the dihedral angle between the protons of C-9 and C-8 <90°. In (*S*)-III, the steric interaction of the proton at C-3 and the nitrogen-containing aromatic ring causes rotation in the opposite direction, bringing about a change in the dihedral angle between the protons of C-9 and C-8 from <90° to ~90°. At the same time, the H–C=O group is positioned at a greater distance from the nitrogen-containing aromatic ring as compared to (*R*)-III.

The ups and downs of the chemical shifts of some of the protons could be explained on the basis of the proposed assumption. In (*R*)-III, the close proximity of the H–C=O group to the nitrogen-containing aromatic ring places H-3′ within the positive zone of the carbonyl cone and H-2′ near its border. Consequently, H-3′ shifts to a higher field, and H-2′ appears as a broad singlet. For the same reason, the aldehydic proton in (*R*)-III is under the deshielding influence of the aromatic ring and absorbs at a lower field compared to the aldehydic proton of (*S*)-III. In (*S*)-III the nitrogen atom of the quinuclidine ring is in closer proximity to H-5′ than in (*R*)-III and, consequently, H-5′ experiences a shielding effect [due to a long-range shielding by the nitrogen atom (5, 6)].

Whereas the oxidation of I under basic conditions was relatively slow, the oxidation under acidic conditions was much faster and more complex. Its value was in the ability to: (*a*) prepare, in one reaction, carbonyl-containing compounds other than the aldehydes [(*R*)-III and (*S*)-III]; (*b*) study, with the help of NMR analyses of these additional carbonyl-containing compounds, the intensity of the $\pi$–$\pi$ interaction when the side-chain $\pi$ system varied from vinyl to aldehydic carbonyl to ester carbonyl; (*c*) explore, at the same time, their influence on the chemical shifts of some important protons in the molecule; and (*d*) determine whether they were concentration dependent.

The NMR data of (*R*)-III and (*S*)-III made it possible to assign the configuration at C-3. As the carbonyl group departed from the aromatic ring, certain apparent changes took place. The intensity of these changes depended on the mutual $\pi$–$\pi$ interactions between the aromatic ring and the side-chain $\pi$ systems. In Table IV, three $\pi$ systems (aldehyde, methoxycarbonyl, and vinyl) are compared; differences in intensity were measured by the chemical shifts experienced by H-2′, H-3′, and H-8′. For comparative purposes, hydroquinidine was also introduced. Since H-2′ is at a greater distance from the side-chain $\pi$ systems, H-3′ is more sensitive to both the intensity of the $\pi$ systems and the stable conformation of the molecule. As can be seen in Table IV, the shielding of H-3′ increased in the following order: (*R*)-III > VI ≈ I. With regard to H-2′, the order of shielding was as follows: (*R*)-III = I > VI.

These differences may be explained on the basis of different orientations of the carbonyl group of the aldehyde and methoxy functions. Since the methoxy group in VI is more bulky than the proton in the aldehydic group, rotation about C-10 takes place and makes the distance between the carbonyl group and H-3′ of the aromatic ring greater and thus lowers the shielding effect. Consequently, VI resembles hydroquinidine while (*R*)-III is closer to I with respect to the shielding effects on H-2′ and H-3′. Therefore, it is concluded that the aldehydic and vinylic groups are more appropriate for assignment of the C-3 configuration than the methoxy group, which brings about steric disturbances.

**Origin of $\pi$–$\pi$ Interaction**—The nitrogen-containing ring is relatively more $\pi$ deficient due to the electronegative character of the nitrogen atom. This $\pi$-deficiency is reflected in the chemical shifts of the protons in the two rings of the quinoline structure. The protons of the nitrogen-containing ring generally are deshielded to a greater extent than the protons of the sister ring. The $\pi$–$\pi$ interactions may be visualized as a donor–acceptor system. Thus, the $\pi$-deficient aromatic ring is the acceptor while the side-chain $\pi$ system is the donor.

**Epimerization at C-3**—Oxidation of II under weakly acidic conditions for a short time (as in Method B) yields pure natural (*R*)-III. Under more acidic conditions (as in Method A), rapid epimerization at C-3 takes place, mainly due to the tertiary nature of the carbon at C-3. In addition, the ease of epimerization suggests that, in the natural configuration (*R*)-III, the aldehydic derivative III is under steric strain and that this strain is partially relieved in the process of epimerization. An equilibrium is reached between the two epimers. The 1:1 ratio obtained at equilibrium suggests that the energy content of (*R*)-III and (*S*)-III is approximately equal. In (*R*)-III, the energy gained by the $\pi$–$\pi$ interaction is partially offset by the steric interaction developed in the vicinity of C-8–C-9. In (*S*)-III, the release of steric strain in the vicinity of C-8–C-9 is counteracted by a decrease in the $\pi$–$\pi$ interaction. Complete epimerization was also found when (*R*)-III was subjected to chromatography or dissolved in chloroform. Therefore, the enhanced sensitivity is due not only to the tertiary character of C-3 but also to the energy content of the molecule.

**Concentration Dependence of Chemical Shifts**—The concentration dependence of the chemical shifts of I and hydroquinidine were observed previously (1). It was suggested that this concentration dependence is a result of molecular association. In the present study, the same phenomenon was observed in III and IV (Tables I and III). Since the natural epimer (*R*)-III was only sparingly soluble in deuterochloroform, a mixture of (*R*)-III and (*S*)-III, which was much more soluble, was used. Compound IV was almost insoluble in deuterochloroform; therefore, the NMR analysis of its methyl ester (VI) was made. Quininic acid (V) was converted to its methyl ester (VII), which was much more soluble. Practically, no concentration dependence was observed in this compound (Table II).

These observations clearly imply that changes in the chemical shifts at different concentrations occur only when the quinuclidine moiety is connected to the quinoline moiety through the carbon atom at C-9 to which a hydroxyl group is attached. Thus, the previous suggestion that molecular association is initiated by hydrogen bonding of the hydroxyl groups has additional support. Aside from its importance in understanding the origin of the association in the molecules, the NMR data of the fragmentation derivative (VII) reveal some interesting features. Theoretically, the carbonyl group of the methoxycarbonyl moiety may be directed toward either H-5′ or H-3′ if there is no inhibition of resonance in the molecule as a whole. On the other hand, the inhibition of resonance could cause rotation about the C-4′–C-9 bond and bring about a departure of the bulky methoxy group from either H-3′ or H-5′. The NMR data of VII unambiguously show that the carbonyl group is positioned near H-5′ and that the methoxy group is in the vicinity of H-3′. The model of this molecule reveals that reversing the positions of the carbonyl group and the methoxy is associated with intensified steric strain. On the basis of this assumption, the NMR data may be rationalized. Furthermore, the concentration-independence of its chemical shifts implies that the molecule has one, and only one, stable rotamer.

When the hydroxyl group was replaced by acetoxy in VI, it was found that there was no concentration dependence in the acetyl derivative (VIII) (Table III). This result was in full agreement with previous findings (1) suggesting the absence of molecular association in the acetyl derivative of I. As expected, the presence of the acetoxy group caused a paramagnetic shift of H-2′ and a diamagnetic shift of H-3′. Another consequence of the concentration independence of this molecule was clearly shown in its NMR spectrum, namely, the presence of a second epimer (*S*)-VIII in addition to (*R*)-VIII. Since the oxidation of I under acidic conditions yielded two epimers, (*R*)-III and (*S*)-III in a 1:1 ratio, one might expect that the acids of the same oxidation reaction would also consist of two epimers (*R*)-IV and (*S*)-IV in a 1:1 ratio. The NMR data showed that this was not the case; rather, the ratio of the two epimers was ~3:1 in favor of the natural configuration. This observation suggests that I is mainly oxidized directly to an acidic product without the mediation of an aldehyde. The presence of (*S*)-IV was due to slow oxidation of the epimeric aldehydes (*R*)-III and (*S*)-III. The presence of this second epimer was not revealed in the NMR spectrum of VI but only in that of the acetylated product (VIII); this result is a consequence of the lack of molecular association.

## REFERENCES

(1) Y. Yanuka, S. Yosselson-Superstine, and E. Superstine, *J. Pharm. Sci.*, **68**, 1400 (1979).

(2) L. Seekles, *Rec. Trav. Chim.*, **42**, 69 (1923).
(3) G. J. Karbatsos and H. Hsi, *J. Am. Chem. Soc.*, **87**, 2864 (1965).
(4) L. M. Jackman and S. Sternhell "Applications of Nuclear Magnetic Resonance Spectroscopy in Organic Chemistry," 2nd ed., Pergamon, Oxford, England, 1972, p. 284.
(5) *Ibid.*, p. 81.
(6) S. Yamaguchi, S. Okuda, and N. Nakayawa, *Chem. Pharm. Bull.*, **11**, 1465 (1963).

# Impact of Stable Conformation of Cinchona Alkaloids on Protonation Site

**YEHUDA YANUKA, SHIMONA YOSSELSON-SUPERSTINE *, ARTOUL GERYES, and EDWARD SUPERSTINE *x**

Received August 8, 1980, from the *Department of Pharmacy, School of Pharmacy, Faculty of Medicine, Hebrew University–Hadassah Medical Center, Jerusalem, Israel.* Accepted for publication December 2, 1980. *Present address: College of Pharmacy, University of Utah, Salt Lake City, UT 84112.

**Abstract** □ NMR analyses of quinidine and other cinchona alkaloids and their monoprotonated salts in deuterium oxide and in deuterochloroform revealed that the molecules assume new conformations in polar and nonpolar media, affecting the protonation site and hydrophilic–lipophilic characteristics. The ion-pair feature of the salts is lost and the molecules assume a neutral feature when they are transferred from an aqueous to a lipoid phase. Hydrophobic bonds between the molecules and their environment and within the molecule itself may affect the binding of cinchona alkaloids to membranes in biological fluids.

**Keyphrases** □ Quinidine—impact of stable conformation on protonation site, effect of polar and nonpolar solvents on conformation, NMR analyses □ Alkaloids, cinchona—impact of stable conformation on protonation site, effect of polar and nonpolar solvents on conformation, NMR analyses □ Conformation—impact on protonation site of quinidine and other cinchona alkaloids, effect of polar and nonpolar solvents, NMR analyses □ NMR spectroscopy—analyses of quinidine and other cinchona alkaloids, impact of stable conformation on protonation site, polar and nonpolar solvents

The protonation site on the quinidine molecule (I) might have an important bearing on its disposition, protein binding, and activity in the body. When the nitrogen of the quinuclidine ring of I is uncharged at pH 10, the number of receptor areas in albumin increases from one to three, possibly because the polar effect of the positively charged nitrogen is lost (1). At pH 7.4, however, the quinuclidine ring apparently does not play a great part in the binding of I to albumin, as was demonstrated in the competitive inhibitory effects of related quinoline compounds on the binding of I to albumin (2). It was postulated (3) that the cardiac action of I may result from special orientation of the molecule at interfaces, with binding of the quinoline ring to membrane lipoprotein and with the charged quinuclidine ring in the aqueous phase affecting ion movement across the cardiac cell (Fig. 1).

Any factors that may change the protonation site in I, such as the polarity of the surrounding medium and the dependence of conformation on this polarity, might affect the binding of I to plasma or cell or enzyme protein and, hence, its distribution, activity, and metabolism. This study explored the dependence of hydrophilic–lipophilic and structural properties of the salts of I and other cinchona alkaloids on solvent polarity. NMR analyses of the alkaloids and their salts were utilized.

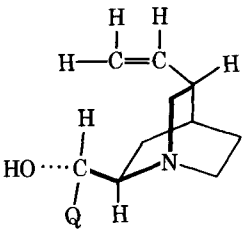

I

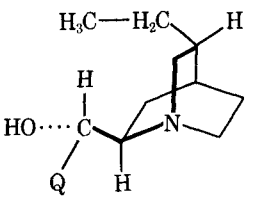

III

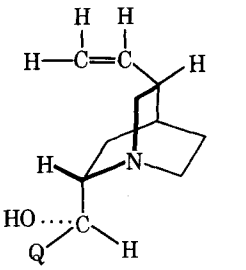

V

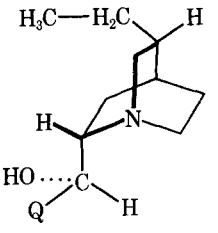

VII

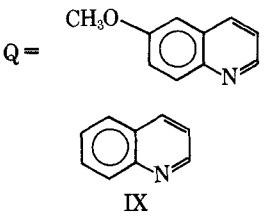

IX

## EXPERIMENTAL

NMR spectra were obtained at 300 MHz using an analytical NMR spectrometer[1] equipped with an automatic recorder. Tetramethylsilane in deuterochloroform and 2,2,3,3-tetradeutero-3-(trimethylsilyl)propionic acid sodium[2] and tetrahydrofuran in deuterium oxide were the internal standards. Pure quinidine (I), quinidine monohydrochloride (II), hydroquinidine (III), and hydroquinidine monohydrochloride (IV) were obtained from commercially available quinidine sulfate USP[3]. Pure quinine (V), quinine monohydrochloride (VI), hydroquinine (VII), and hydroquinine monohydrochloride (VIII) were obtained from commercially available quinine sulfate USP[4]. Hydrogenation of I and V was

[1] Bruker W.H. 300.
[2] Merck AG, Darmstadt, West Germany.
[3] Sigma Chemical Co., St. Louis, Mo.
[4] New York Quinine and Chemical Works, New York, N.Y.

0022-3549/81/0600-0679$01.00/0
© 1981, American Pharmaceutical Association

(2) L. Seekles, *Rec. Trav. Chim.*, **42**, 69 (1923).
(3) G. J. Karbatsos and H. Hsi, *J. Am. Chem. Soc.*, **87**, 2864 (1965).
(4) L. M. Jackman and S. Sternhell "Applications of Nuclear Magnetic Resonance Spectroscopy in Organic Chemistry," 2nd ed., Pergamon, Oxford, England, 1972, p. 284.
(5) *Ibid.*, p. 81.
(6) S. Yamaguchi, S. Okuda, and N. Nakayawa, *Chem. Pharm. Bull.*, **11**, 1465 (1963).

# Impact of Stable Conformation of Cinchona Alkaloids on Protonation Site

**YEHUDA YANUKA, SHIMONA YOSSELSON-SUPERSTINE *, ARTOUL GERYES, and EDWARD SUPERSTINE *x**

Received August 8, 1980, from the *Department of Pharmacy, School of Pharmacy, Faculty of Medicine, Hebrew University–Hadassah Medical Center, Jerusalem, Israel.* Accepted for publication December 2, 1980. *Present address: College of Pharmacy, University of Utah, Salt Lake City, UT 84112.

**Abstract** □ NMR analyses of quinidine and other cinchona alkaloids and their monoprotonated salts in deuterium oxide and in deuterochloroform revealed that the molecules assume new conformations in polar and nonpolar media, affecting the protonation site and hydrophilic–lipophilic characteristics. The ion-pair feature of the salts is lost and the molecules assume a neutral feature when they are transferred from an aqueous to a lipoid phase. Hydrophobic bonds between the molecules and their environment and within the molecule itself may affect the binding of cinchona alkaloids to membranes in biological fluids.

**Keyphrases** □ Quinidine—impact of stable conformation on protonation site, effect of polar and nonpolar solvents on conformation, NMR analyses □ Alkaloids, cinchona—impact of stable conformation on protonation site, effect of polar and nonpolar solvents on conformation, NMR analyses □ Conformation—impact on protonation site of quinidine and other cinchona alkaloids, effect of polar and nonpolar solvents, NMR analyses □ NMR spectroscopy—analyses of quinidine and other cinchona alkaloids, impact of stable conformation on protonation site, polar and nonpolar solvents

The protonation site on the quinidine molecule (I) might have an important bearing on its disposition, protein binding, and activity in the body. When the nitrogen of the quinuclidine ring of I is uncharged at pH 10, the number of receptor areas in albumin increases from one to three, possibly because the polar effect of the positively charged nitrogen is lost (1). At pH 7.4, however, the quinuclidine ring apparently does not play a great part in the binding of I to albumin, as was demonstrated in the competitive inhibitory effects of related quinoline compounds on the binding of I to albumin (2). It was postulated (3) that the cardiac action of I may result from special orientation of the molecule at interfaces, with binding of the quinoline ring to membrane lipoprotein and with the charged quinuclidine ring in the aqueous phase affecting ion movement across the cardiac cell (Fig. 1).

Any factors that may change the protonation site in I, such as the polarity of the surrounding medium and the dependence of conformation on this polarity, might affect the binding of I to plasma or cell or enzyme protein and, hence, its distribution, activity, and metabolism. This study explored the dependence of hydrophilic–lipophilic and structural properties of the salts of I and other cinchona alkaloids on solvent polarity. NMR analyses of the alkaloids and their salts were utilized.

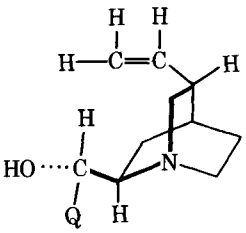

I

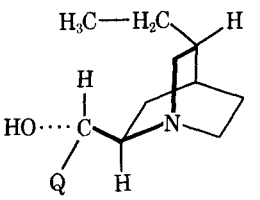

III

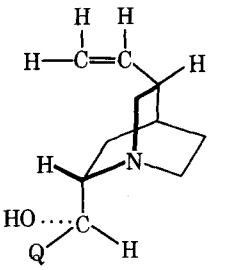

V

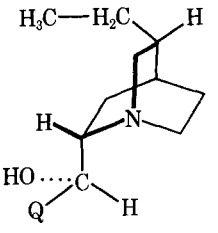

VII

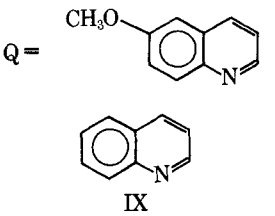

IX

## EXPERIMENTAL

NMR spectra were obtained at 300 MHz using an analytical NMR spectrometer[1] equipped with an automatic recorder. Tetramethylsilane in deuterochloroform and 2,2,3,3-tetradeutero-3-(trimethylsilyl)propionic acid sodium[2] and tetrahydrofuran in deuterium oxide were the internal standards. Pure quinidine (I), quinidine monohydrochloride (II), hydroquinidine (III), and hydroquinidine monohydrochloride (IV) were obtained from commercially available quinidine sulfate USP[3]. Pure quinine (V), quinine monohydrochloride (VI), hydroquinine (VII), and hydroquinine monohydrochloride (VIII) were obtained from commercially available quinine sulfate USP[4]. Hydrogenation of I and V was

[1] Bruker W.H. 300.
[2] Merck AG, Darmstadt, West Germany.
[3] Sigma Chemical Co., St. Louis, Mo.
[4] New York Quinine and Chemical Works, New York, N.Y.

0022-3549/81/0600-0679$01.00/0
© 1981, American Pharmaceutical Association

**Table I—Chemical Shift Values [a] of the Protons of I, III, V, and VII (20 ± 1 mg/0.5 ml)**

| Proton | I | III | V | VII |
|---|---|---|---|---|
| H-2′ | 8.58 (d) ($J$ = 4 Hz) | 8.57 (d) ($J$ = 4 Hz) | 8.48 (d) ($J$ = 4 Hz) | 8.45 (d) ($J$ = 4 Hz) |
| H-8′ | 7.93 (d) ($J$ = 9 Hz) | 7.91 (d) ($J$ = 9 Hz) | 7.89 (d) ($J$ = 9 Hz) | 7.84 (d) ($J$ = 9 Hz) |
| H-3′ | 7.51 (d) ($J$ = 4 Hz) | 7.53 (d) ($J$ = 5 Hz) | 7.47 (d) ($J$ = 4 Hz) | 7.41 (d) ($J$ = 4 Hz) |
| H-7′ | 7.28 (q) ($J_m$ = 3 Hz) ($J_o$ = 9 Hz) | 7.25 (q) ($J_m$ = 2 Hz) ($J_o$ = 9 Hz) | 7.26 (q) ($J_m$ = 3 Hz) ($J_o$ = 9 Hz) | 7.20 (q) ($J_m$ = 2 Hz) ($J_o$ = 9 Hz) |
| H-5′ | 7.16 (d) ($J$ = 2 Hz) | 7.11 (broad s) | 7.21 (d) ($J$ = 2 Hz) | 7.14 (broad s) |
| H-10 | 6.03 (m) | — | 5.71 (m) | — |
| H–C-9–OH | 5.61 (d) ($J$ = 4 Hz) | 5.83 (d) ($J$ = 4 Hz) | 5.53 (d) ($J$ = 4 Hz) | 5.48 (d) ($J$ = 3 Hz) |
| H-11 | 5.07 (broad s) | — | 4.95 (d) ($J$ = 16 Hz) | — |
| H-11 | 5.02 (broad s) | — | 4.90 (d) ($J$ = 10 Hz) | — |
| $CH_3O$ | 3.83 (s) | 3.77 (s) | 3.86 (s) | 3.78 (s) |

[a] s = singlet, d = doublet, m = multiplet, and q = quartet. Values are expressed in parts per million.

conducted in a pressure reaction apparatus[5]. Pure quinoline (IX) and quinoline hydrochloride (X) were obtained from commercially available quinoline[6]. TLC and preparative TLC were carried out on aluminum oxide GF 254[7] plates.

For NMR spectra measurements of the salts in deuterium oxide, an internal standard such as tetrahydrofuran (the chemical shifts of which were determined relative to 2,2,3,3-tetradeutero-3-(trimethylsilyl)propionic acid sodium) had to be used since the NMR spectra of the samples containing 2,2,3,3-tetradeutero-3-(trimethylsilyl)propionic acid sodium did not completely match the spectra without an internal standard. These discrepancies may originate from a proton transfer from the nitrogen to the carboxylate group of 2,2,3,3-tetradeutero-3-(trimethylsilyl)propionic acid sodium or from its influence on the mode of association of the cinchona salts. Since tetrahydrofuran was not completely without effect on association between molecules, except in the spectra of X, the absolute chemical shift values were eventually determined by matching the spectra in the presence and absence of the two different internal standards. This technique was possible because most chemical shifts, especially those on the margins, coincided.

**Purification of Commercial I and V**—Purification was carried out according to a procedure described previously (4). Table I lists the NMR data.

**Reduction of I to III**—Compound I (1 g) was dissolved in ethanol (50 ml) in a suitable vessel. Palladium-on-carbon (5%, 0.1 g) was added, and the hydrogenation was allowed to proceed for 1.5 hr at room temperature in the pressure reaction apparatus. The catalyst was removed by filtration through very retentive filter paper, the ethanol was evaporated, and III was readily crystallized. Table I lists the NMR measurements. Compound III was purified by preparative TLC (4).

**Reduction of V to VII**—Hydrogenation and purification were conducted as already described. Table I lists the NMR data.

**Purification of IX**—Purification was carried out according to a known procedure (5).

**Preparation of Hydrochloride Salts**—Each free base (I, III, V, VII, and IX) was dissolved in an accurate amount of dilute aqueous solution of hydrochloric acid. Water was removed under reduced pressure or allowed to evaporate spontaneously, and the residue of each salt was dried to constant weight.

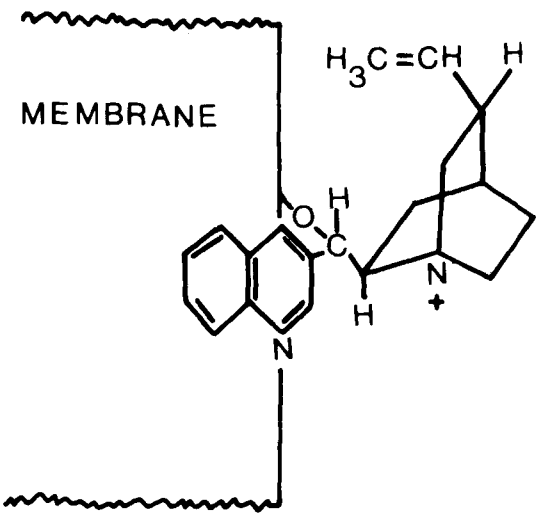


**Figure 1**—*Quinidine membrane binding hypothesis (3).*

[5] Parr Instrument Co., Moline, Ill.
[6] Hopkin and Williams, Ltd.
[7] Stahl, Merck.

## RESULTS

Comparison of the NMR data of I and II in deuterochloroform revealed that the aromatic protons of the pyridine ring in II moved to a lower field. The deviation of H-2′ was 0.01 ppm, and that of H-3′ was 0.15 ppm. This result is to be expected in protonated pyridine (6). In contrast, the protons of the benzene ring in II experienced a shielding effect and shifted upfield: H-8′ to 0.25 ppm, H-5′ to 0.37 ppm, and H-7′ to 0.38 ppm. In X (Table II), all aromatic protons absorbed at a lower field under the influence of the protonated nitrogen. These differences are attributable partly to the methoxy group at C-6′.

An outstanding deshielding effect on the proton H–C-9–OH, which appeared as a singlet, was observed in II when it moved 0.89 ppm downfield. This shift is in agreement with the reported value for a proton that is alpha to protonated nitrogen or for vinylogous hydrogen. It probably applies also to a proton alpha to a positively charged carbon (or to vinylogous hydrogen) such as C-2′ and C-4′ in the quinoline cation.

These deviations observed in the chemical shifts may be rationalized if the protonation site is assumed to be on the quinoline nitrogen and not on the quinuclidine nitrogen, which has a much higher pKa value. Had the protonation taken place on the quinuclidine nitrogen, the proton H–C-9–OH would have been deshielded to a lesser extent (0.35 ppm).

NMR data of II in deuterochloroform and in deuterium oxide showed that the proton H–C-9–OH, appearing as a singlet, shifted downfield only by 0.42 ppm in the latter, indicating that this proton could not be at a position alpha to protonated nitrogen. Other evidence was provided when the chemical shift values of the aromatic protons of the salts in the different solvents were compared. In deuterium oxide, the H-2′ and H-3′ protons and some protons of the benzene moiety resonated at lower fields (Table II). These observations imply that the protonation site is on the quinuclidine nitrogen in deuterium oxide.

Table II also shows that in II in deuterium oxide, as compared to the free base in deuterochloroform, the methoxy protons and all aromatic protons, except H-8′, experienced a paramagnetic effect.

NMR analyses of III, V, and VII and their salts (IV, VI, and VIII) in the two different solvents (Table II) demonstrated the same trend in chemical shifts, although they varied in their intensity. This finding indicated that the protonation site in these molecules is the same as that observed in I, *i.e.*, on the quinoline nitrogen in the nonpolar solvent and on the quinuclidine nitrogen in the polar solvent.

## DISCUSSION

Theoretically, protonation on the quinoline nitrogen should cause a paramagnetic effect on all aromatic protons, as was observed in X. In II in deuterochloroform, the diamagnetic effect observed on the benzene ring protons was attributed to the methoxy group at C-6′. The electron-releasing ability of this group, the capability of the molecule to pass to another conformation, and the concomitant bonding of a proton to the quinoline nitrogen in the neutral molecule increase the probability of protonation on this nitrogen. In VI in deuterochloroform, the paramagnetic effect on the pyridine protons was more pronounced than in II whereas the diamagnetic effect on the benzene protons was reduced (Table II). This result is expected when the conformations and pKa values of the two molecules are compared.

Protonation on the quinoline nitrogen causes the molecules to assume a new stable conformation in which the steric requirements for protonation on the quinuclidine nitrogen are more severe since it is now less exposed. This change is reflected in the change in the dihedral angle between the C-8 and C-9 protons. In the salts, this angle approaches 90° and is caused by rotation about the C-8–C-9 bond. The arrangement of the protons alpha to the quinuclidine nitrogen with respect to the aro-

**Table II—Differences between the Chemical Shift Values [a] of the Salts (II, IV, VI, VIII, and X) and the Free Bases (I, III, V, VII, and IX) (20 ± 1 mg/0.5 ml)**

| Proton | II − I | | IV − III | | VI − V | | VIII − VII | | X − IX | |
|---|---|---|---|---|---|---|---|---|---|---|
| | $CDCl_3$ | $D_2O$ | $CDCl_3$ | $D_2O$ | $CDCl_3$ | $D_2O$ | $CDCl_3$ | $D_2O$ | $CDCl_3$ | $D_2O$ |
| H-2′ | +0.01 | +0.12 | +0.07 | +0.15 | +0.19 | +0.25 | +0.16 | +0.29 | +0.30 | +0.10 |
| H-3′ | +0.15 | +0.26 | +0.26 | +0.33 | +0.30 | +0.43 | +0.42 | +0.43 | +0.67 | +0.66 |
| H-5′ | −0.37 | +0.09 | −0.31 | +0.22 | −0.34 | +0.07 | −0.20 | +0.11 | +0.42 | +0.23 |
| H-7′ | −0.38 | +0.13 | −0.28 | +0.26 | −0.27 | +0.19 | −0.17 | +0.16 | +0.33 | +0.26 |
| H-8′ | −0.25 | −0.09 | −0.12 | +0.03 | −0.11 | −0.05 | +0.02 | — | +0.59 | −0.01 |
| H-10 | −0.02 | — | — | — | −0.18 | −0.10 | — | — | — | — |
| H–C-9–OH | +0.89 | +0.42 | +1.10 | +0.16 | +0.90 | +0.50 | +0.92 | +0.62 | — | — |
| H-11 | +0.15 | +0.22 | — | — | +0.08 | —[b] | — | — | — | — |
| H-11 | +0.15 | +0.21 | — | — | +0.08 | —[b] | — | — | — | — |
| $CH_3O$ | −0.33 | +0.16 | +0.16 | +0.22 | −0.23 | +0.07 | −0.14 | +0.22 | — | — |
| H-4 | — | — | — | — | — | — | — | — | +0.82 | +0.82 |
| H-6 | — | — | — | — | — | — | — | — | +0.35 | +0.32 |

[a] + = downfield shift, and − = upfield shift. [b] Overlap with water. Values are expressed in parts per million.

matic rings is greatly dependent on the dihedral angle; therefore, their chemical shifts in the salts will differ from those in the free bases. The extent of these differences helps to establish the nature of the new rotamers. Four of the five protons alpha to the quinuclidine nitrogen in II in deuterochloroform moved ~0.33 ppm downfield in comparison to the same protons in the free base as a result of being closer to the pyridine ring. Proton H-8 in II was ~1 ppm downfield in comparison to its chemical shift in I as a result of facing the pyridine ring instead of the benzene ring. In V, the proton alpha to the quinuclidine nitrogen that was the most deshielded was one of the C-6 protons (Table III) since the new conformation placed it closer to the pyridine ring.

Supporting evidence for differences in conformation was provided by the analysis of the chemical shifts of vinylic and the methoxy protons in deuterochloroform. In II, the methylene protons at C-11 appeared at a field lower than that of their counterparts in the free base, and the chemical shift of the methine proton at C-10 was practically unchanged. In VI, the reverse behavior was observed when compared to its free base. This finding suggests that, in I, the vinylic moiety is arranged as in A and, in V, it is arranged as in B (Fig. 2). The protons of the methoxy group in the salts (II, VI, and VII) resonated at a higher field than in the free bases. Protonation on the quinoline nitrogen should have caused a deshielding effect on these protons. The fact that a diamagnetic effect was observed instead implies that the conformation of the molecules had changed greatly; *i.e.*, a rotation of 180° around the C-4′–C-9 bond had occurred. In this new conformation, the protons of the methoxy groups are within the shielding zone of the vinyl and ethyl cone, the nonpolar hydrophobic moieties are on one side of the molecule, and the two nitrogens are on the opposite side. In IV, the protons of the methoxy group experienced the expected paramagnetic effect since the suggested rotation did not take place because of severe steric requirements of the ethyl group at C-3.

NMR analysis of II in deuterium oxide revealed that the protonation site was on the quinuclidine nitrogen, as expected in such a polar solvent, since the positive charge on this nitrogen is stabilized by solvation. It further showed that the molecule assumed a new conformation. This change was best reflected in the pronounced paramagnetic effect on the methoxy, vinylic, and some aromatic protons in this solvent *versus* deuterochloroform.

Changes in conformation also were reflected in the NMR data of II in deuterium oxide and of the free base in deuterochloroform. The paramagnetic effect observed on almost all protons of II in deuterium oxide could be rationalized if strong hydrogen bondings between the solvent and polar groups in the molecule took place. These enhanced hydrogen bondings are a result of the lipophilic nature of the cinchona alkaloids and the high free energy content of these molecules in aqueous solution. The hydrogen bonding between the methoxy group and the solvent nullifies the electron-releasing ability of this group; consequently, the aromatic protons in the benzene ring do not move to higher field. Hydrogen bonding between the pyridine nitrogen and the solvent caused the observed shift in the protons of this group. To account for the pronounced shift of H-8′ to a higher field in the salt in deuterium oxide, the anisotropy of the quinoline nitrogen lone pair has to be invoked. This effect is present in the free base in the nonpolar solvent and is eliminated in the salt in deuterium oxide as a result of hydrogen bonding (solvation). Since neutral moieties are involved in hydrogen bonding (7, 8), only the anisotropic effect of the nitrogen lone pair on the neighboring protons

**Table III—Chemical Shift Values [a] of the Protons Alpha to the Quinuclidine Nitrogen of I and V (20 ± 1 mg/0.5 ml)**

| Proton | I | Proton | V |
|---|---|---|---|
| H-8 | 3.47 (q) (1H) | H-6 | 3.49 (m) (1H) |
| H-2 | 3.07 (m) (1H) | H-6 + H-8 | 3.06 (q) (2H) |
| H-2 + H-6 | 2.93 (q) (2H) | H-2 | 2.65 (m) (2H) |
| H-6 | 2.80 (m) (1H) | | |

[a] m = multiplet, and q = quartet. Values are expressed in parts per million.

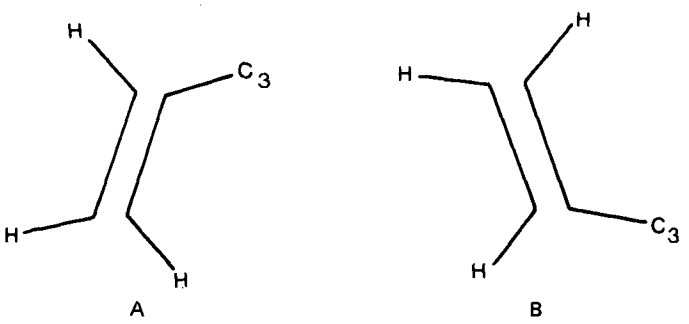


**Figure 2**—*Arrangement of the vinylic moiety in I and V.*

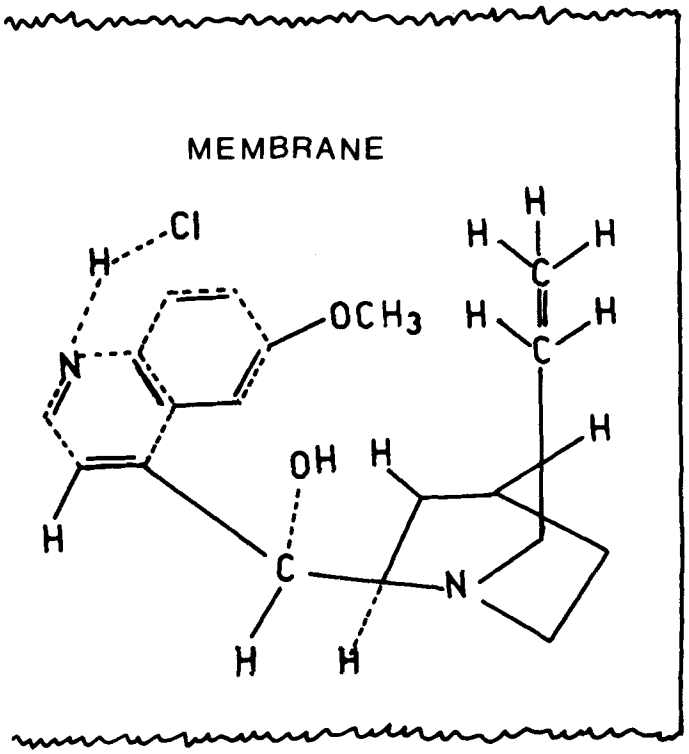


**Figure 3**—*Penetration of the monohydrochloride salt of I (II) through a membrane.*

comes into play. In the ion-pair counterpart, such as may exist in the protonated molecule, additional effects appear.

## CONCLUSION

On the basis of NMR analyses of the salts of some cinchona alkaloids, it was concluded that the protonation site on these molecules varies with their spatial orientation and the nature of the solvent. In the process of changing the conformation, when moving from a polar to nonpolar solvent, the basicity of the quinuclidine nitrogen is reduced as the quinuclidine and quinoline moieties get closer to each other. The proton is transferred from the quinuclidine nitrogen to the quinoline nitrogen, the ion-pair feature, which enhances hydrophilic capacity, is lost, and the molecule assumes a neutral feature with stronger hydrophobic bonds. As a result of this process, the hydrophilic–lipophilic properties of the molecule change in favor of a more lipophilic character.

These findings may have an important bearing on the passage of I and its congeners from an aqueous to a lipoid phase. Thus, the molecule not only is adsorbed to a membrane, as suggested in Fig. 1, but also penetrates the membrane (Fig. 3). Given the opportunity, the solute will forsake the aqueous solution for the organic environment.

The variation in conformation found in the studied cinchona alkaloids and their salts may contribute to their differences in biological activity.

## REFERENCES


(1) H. L. Conn and R. J. Luchi, *J. Clin. Invest.*, **39**, 978 (1960).

(2) *Ibid.*, **40**, 509 (1961).

(3) R. J. Luchi, H. L. Conn, and J. Helwig, *Am. J. Cardiol.*, **10**, 252 (1962).

(4) Y. Yanuka, S. Y. Superstine, and E. Superstine, *J. Pharm. Sci.*, **68**, 1400 (1979).

(5) D. D. Perrin, W. L. F. Armarego, and D. R. Perrin, "Purification of Laboratory Chemicals," 1st ed., Pergamon, Oxford, England, 1966.

(6) V. M. S. Gil and J. N. Murrell, *Trans. Faraday Soc.*, **60**, 248 (1964).

(7) R. J. Chuck and E. W. Randall, *J. Chem. Soc. B*, **1967**, 261.

(8) P. K. Bhattacharyya, *J. Pharm. Sci.*, **69**, 180 (1980).


## ACKNOWLEDGMENTS


The authors are indebted to Mrs. Evelyne Segall for assistance in NMR measurements.


# NOTES

# Biological and Phytochemical Investigation of Plants XVI: *Strumpfia maritima* (Rubiaceae)


**C. C. HSU *, R. H. DOBBERSTEIN *§, A. S. BINGEL *, H. H. S. FONG *, N. R. FARNSWORTH *x, and J. F. MORTON ‡**



Received May 15, 1980, from the **Department of Pharmacognosy and Pharmacology, College of Pharmacy, University of Illinois at the Medical Center, Chicago, IL 60612*, and the ‡*Morton Collectanea, University of Miami, Coral Gables, FL 33124.* Accepted for publication November 5, 1980. §Present address: Stevia Company, Arlington Heights, IL 60005.



**Abstract** □ An aqueous extract of the flowering tops of *Strumpfia maritima* exhibited antifertility activity in female rats. The extract also contained the flavonol glycoside narcissin. This article represents the first reported isolation of this flavonoid from the Rubiaceae, as well as the first reported phytochemical and pharmacological investigation of the genus *Strumpfia*.



**Keyphrases** □ *Strumpfia maritima*—biological and phytochemical investigation, isolation of narcissin ■ Narcissin—isolation from *Strumpfia maritima* (Rubiaceae) □ Antifertility activity—narcissin, flavonoid isolation from *Strumpfia maritima*


*Strumpfia maritima* Jacq. (Rubiaceae) is a low, maritime shrub found in southern Florida (1), the Bahamas (2), Venezuela (3), and Curacao[1]. The plant has a folkloric use as a mosquito repellent (2) and contraceptive[1]. *In vivo* testing of aqueous methanol extracts showed that the roots were devoid of antimalarial activity (4). This paper describes a preliminary screening of extracts of *S. maritima* for antifertility activity, as well as the isolation of narcissin from one of these extracts.

## RESULTS AND DISCUSSION

The powdered, defatted flowering tops of *S. maritima* were extracted with methanol. A phytochemical screening of this extract for alkaloids, saponins, sterols, cardenolides or bufadienolides, flavonoids, tannins or polyphenols, anthraquinones, and cyanogenic glycosides (5) revealed the presence of sterols, tannins and/or polyphenols, and flavonoid glycosides.

A methanolic extract was concentrated to dryness and partitioned between chloroform and water. Preliminary antifertility experiments showed that the aqueous extract administered daily (100 mg/kg ip) to rats significantly decreased the number of implantation sites relative to the number of corpora lutea of pregnancy ($p = 0.023$). No such decrease was seen in control rats treated simultaneously with the vehicle, 10% polysorbate 20. Furthermore, no such effect was seen in rats treated with either the petroleum ether or chloroform extracts, tested simultaneously with the 10% polysorbate 20 vehicle and sterol diluent control groups, respectively. These results are listed in Table I.

To isolate the biologically active compound(s) from the aqueous extract, the fraction was extracted with water-saturated 1-butanol, and the resulting organic extract was chromatographed over polyamide. Elution with distilled water and water–methanol afforded a yellow, microcrystalline flavonoid glycoside as a major component.

The UV spectrum of the isolate using standard shift reagents (7) indicated the presence of free 5-, 7-, and 4′-hydroxyl functions on the flavonoid nucleus. Hydrolysis of the glycoside with dilute acid (7) yielded isorhamnetin (melting point, mixed melting point, and UV, IR, PMR, and mass spectra were identical to the authentic compound) and two sugars. The sugars, present in equal proportions, were identified as glucose and rhamnose by TLC (8). A comparison of the UV spectra for the isolate and its aglycone in the presence of shift reagents indicated that the sugars were attached at position 3 of the aglycone. The PMR spectrum of the isolate as the trimethylsilyl ether showed signals for the rhamnosyl C-1 proton at 4.25 ppm and for the rhamnosyl methyl protons as a broad peak at 0.85 ppm, indicating that the rhamnoglucoside contains a rutinosyl rather than a neohesperidosyl moiety (7). Finally, the isolate

[1] Data collected by J. F. Morton.




*0022-3549/81/0600-0682$01.00/0*


*© 1981, American Pharmaceutical Association*

comes into play. In the ion-pair counterpart, such as may exist in the protonated molecule, additional effects appear.

## CONCLUSION

On the basis of NMR analyses of the salts of some cinchona alkaloids, it was concluded that the protonation site on these molecules varies with their spatial orientation and the nature of the solvent. In the process of changing the conformation, when moving from a polar to nonpolar solvent, the basicity of the quinuclidine nitrogen is reduced as the quinuclidine and quinoline moieties get closer to each other. The proton is transferred from the quinuclidine nitrogen to the quinoline nitrogen, the ion-pair feature, which enhances hydrophilic capacity, is lost, and the molecule assumes a neutral feature with stronger hydrophobic bonds. As a result of this process, the hydrophilic–lipophilic properties of the molecule change in favor of a more lipophilic character.

These findings may have an important bearing on the passage of I and its congeners from an aqueous to a lipoid phase. Thus, the molecule not only is adsorbed to a membrane, as suggested in Fig. 1, but also penetrates the membrane (Fig. 3). Given the opportunity, the solute will forsake the aqueous solution for the organic environment.

The variation in conformation found in the studied cinchona alkaloids and their salts may contribute to their differences in biological activity.

## REFERENCES


(1) H. L. Conn and R. J. Luchi, *J. Clin. Invest.*, **39**, 978 (1960).

(2) *Ibid.*, **40**, 509 (1961).

(3) R. J. Luchi, H. L. Conn, and J. Helwig, *Am. J. Cardiol.*, **10**, 252 (1962).

(4) Y. Yanuka, S. Y. Superstine, and E. Superstine, *J. Pharm. Sci.*, **68**, 1400 (1979).

(5) D. D. Perrin, W. L. F. Armarego, and D. R. Perrin, "Purification of Laboratory Chemicals," 1st ed., Pergamon, Oxford, England, 1966.

(6) V. M. S. Gil and J. N. Murrell, *Trans. Faraday Soc.*, **60**, 248 (1964).

(7) R. J. Chuck and E. W. Randall, *J. Chem. Soc. B*, **1967**, 261.

(8) P. K. Bhattacharyya, *J. Pharm. Sci.*, **69**, 180 (1980).


## ACKNOWLEDGMENTS


The authors are indebted to Mrs. Evelyne Segall for assistance in NMR measurements.


# NOTES

# Biological and Phytochemical Investigation of Plants XVI: *Strumpfia maritima* (Rubiaceae)


**C. C. HSU *, R. H. DOBBERSTEIN *§, A. S. BINGEL *, H. H. S. FONG *, N. R. FARNSWORTH *x, and J. F. MORTON ‡**



Received May 15, 1980, from the **Department of Pharmacognosy and Pharmacology, College of Pharmacy, University of Illinois at the Medical Center, Chicago, IL 60612*, and the ‡*Morton Collectanea, University of Miami, Coral Gables, FL 33124.* Accepted for publication November 5, 1980. §Present address: Stevia Company, Arlington Heights, IL 60005.



**Abstract** □ An aqueous extract of the flowering tops of *Strumpfia maritima* exhibited antifertility activity in female rats. The extract also contained the flavonol glycoside narcissin. This article represents the first reported isolation of this flavonoid from the Rubiaceae, as well as the first reported phytochemical and pharmacological investigation of the genus *Strumpfia*.



**Keyphrases** □ *Strumpfia maritima*—biological and phytochemical investigation, isolation of narcissin ■ Narcissin—isolation from *Strumpfia maritima* (Rubiaceae) □ Antifertility activity—narcissin, flavonoid isolation from *Strumpfia maritima*


*Strumpfia maritima* Jacq. (Rubiaceae) is a low, maritime shrub found in southern Florida (1), the Bahamas (2), Venezuela (3), and Curacao[1]. The plant has a folkloric use as a mosquito repellent (2) and contraceptive[1]. *In vivo* testing of aqueous methanol extracts showed that the roots were devoid of antimalarial activity (4). This paper describes a preliminary screening of extracts of *S. maritima* for antifertility activity, as well as the isolation of narcissin from one of these extracts.

## RESULTS AND DISCUSSION

The powdered, defatted flowering tops of *S. maritima* were extracted with methanol. A phytochemical screening of this extract for alkaloids, saponins, sterols, cardenolides or bufadienolides, flavonoids, tannins or polyphenols, anthraquinones, and cyanogenic glycosides (5) revealed the presence of sterols, tannins and/or polyphenols, and flavonoid glycosides.

A methanolic extract was concentrated to dryness and partitioned between chloroform and water. Preliminary antifertility experiments showed that the aqueous extract administered daily (100 mg/kg ip) to rats significantly decreased the number of implantation sites relative to the number of corpora lutea of pregnancy ($p = 0.023$). No such decrease was seen in control rats treated simultaneously with the vehicle, 10% polysorbate 20. Furthermore, no such effect was seen in rats treated with either the petroleum ether or chloroform extracts, tested simultaneously with the 10% polysorbate 20 vehicle and sterol diluent control groups, respectively. These results are listed in Table I.

To isolate the biologically active compound(s) from the aqueous extract, the fraction was extracted with water-saturated 1-butanol, and the resulting organic extract was chromatographed over polyamide. Elution with distilled water and water–methanol afforded a yellow, microcrystalline flavonoid glycoside as a major component.

The UV spectrum of the isolate using standard shift reagents (7) indicated the presence of free 5-, 7-, and 4′-hydroxyl functions on the flavonoid nucleus. Hydrolysis of the glycoside with dilute acid (7) yielded isorhamnetin (melting point, mixed melting point, and UV, IR, PMR, and mass spectra were identical to the authentic compound) and two sugars. The sugars, present in equal proportions, were identified as glucose and rhamnose by TLC (8). A comparison of the UV spectra for the isolate and its aglycone in the presence of shift reagents indicated that the sugars were attached at position 3 of the aglycone. The PMR spectrum of the isolate as the trimethylsilyl ether showed signals for the rhamnosyl C-1 proton at 4.25 ppm and for the rhamnosyl methyl protons as a broad peak at 0.85 ppm, indicating that the rhamnoglucoside contains a rutinosyl rather than a neohesperidosyl moiety (7). Finally, the isolate

[1] Data collected by J. F. Morton.




*0022-3549/81/0600-0682$01.00/0*


*© 1981, American Pharmaceutical Association*

Table I—Antifertility Effects of *Strumpfia maritima* Extracts [a]

| Number of Rats | Treatment | Number of Corpora Lutea (CL) ± *SD* | *p* of CL *versus* LF | Number of Live Fetuses (LF) ± *SD* | *p* of CL *versus* IS [b] | Number of Implantation Sites (IS) ± *SD* |
|---|---|---|---|---|---|---|
| 6 | Sterol diluent [c], 1 ml/kg ip | 14.50 ± 1.64 | 0.008 | 12.00 ± 0.89 | NS [d] | 13.33 ± 1.21 |
| 5 [e] | Chloroform extract, 100 mg/kg ip | 14.80 ± 2.95 | NS | 11.60 ± 1.52 | — | — |
| 6 | 10% Polysorbate 20, 1 ml/kg ip | 13.50 ± 0.55 | 0.032 | 10.33 ± 3.08 | NS | 12.00 ± 2.45 |
| 6 | Petroleum ether extract, 100 mg/kg ip | 13.17 ± 1.72 | 0.014 | 10.50 ± 1.38 | NS | 12.17 ± 1.83 |
| 6 | 10% Polysorbate 20, 1 ml/kg ip | 13.17 ± 1.17 | NS | 11.67 ± 2.42 | — | 12.00 ± 2.00 |
| 6 | Aqueous extract, 100 mg/kg ip | 13.33 ± 4.32 | 0.025 | 7.17 ± 3.76 | 0.023 | 7.50 ± 3.15 |

[a] Portions of these data were presented at the 17th annual meeting of the American Society of Pharmacognosy, Cable, Wis., July 1976 (Abstract 34). [b] A significant difference in this column means that the difference between the number of corpora lutea and the number of live fetuses could not be accounted for by the presence of dead, degenerating products of conception. [c] Sterol diluent consisted of 9 mg of benzyl alcohol, 4 mg of polysorbate 80, 5 mg of carboxymethylcellulose sodium, and 9 mg of sodium chloride/ml of distilled water (6). [d] Not significant. [e] The sixth rat was not pregnant at autopsy, presumably due to a failure to mate.

was found to be identical in all respects (TLC, melting point, mixed melting point, and UV, IR, and PMR spectra) to authentic narcissin.

The paucity of narcissin isolated did not permit testing for antifertility activity. Attempts are underway to obtain additional narcissin for biological evaluation. This work represents the first reported phytochemical and pharmacological investigation of *Strumpfia*, as well as the first isolation of narcissin from the Rubiaceae.

## EXPERIMENTAL[2]

**Extraction and Chromatography**—Dried, powdered flowering tops of *S. maritima*[3] (5 kg) were defatted by continuous extraction with petroleum ether, air dried, and extracted continuously with methanol. The methanolic extract was concentrated *in vacuo* to a thick syrup (1.1 kg), which was partitioned between water (2.5 liters) and chloroform (6 × 2 liters). After drying (sodium sulfate), the chloroform extract was evaporated *in vacuo* to give a residue (171.2 g). The water extract was lyophilized to yield 333 g of a light powder. Aliquots of the petroleum ether, chloroform, and aqueous extracts were screened for antifertility activity.

A portion of the lyophilized aqueous extract (133.2 g) was redissolved in water (2 liters) and extracted with water-saturated 1-butanol (5 × 2 liters). Evaporation of the butanol extract *in vacuo* gave 22 g of a brown gum, which was dissolved in distilled water (200 ml) and applied to the top of a polyamide column[4] (550 g).

**Isolation and Identification of Narcissin**—Elution was initiated with distilled water (5.4 liters), followed by water–methanol at ratios of 24:1 (1.4 liters), 47:3 (1 liter), 23:2 (3.2 liters), 21:4 (1.8 liters), 7:3 (2 liters), and 1:1 (10.8 liters). After elution with 5.7 liters of water–methanol (1:1), a 500-ml fraction was obtained, which gave a yellow residue on drying *in vacuo*. Crystallization and recrystallization from warm methanol afforded 184 mg of yellow microcrystals, mp 179–180° dec., which gave a positive flavonoid test (7); TLC on cellulose[5] gave an $R_f$ of 0.45 with 5% aqueous acetic acid; UV: $\lambda_{max}$ (methanol) 356 (log $\epsilon$ 4.18), 300 (sh), 265 (sh), and 253 (4.26) nm; IR: $\nu_{max}$ 3330 (br), 2920, 1660, and 1605 $cm^{-1}$; PMR (trimethylsilyl ether[6] in carbon tetrachloride): $\delta$ 0.85 (broad, 3H, rhamnosyl $CH_3$), 3.2–4.0 (m, 10H, sugar H), 3.87 (s, 3H, C-3′ methoxyl), 4.23 (broad s, 1H, rhamnosyl H-1), 5.90 (m, 1H, glucosyl H-1), 6.10 (d, 1H, $J$ = 2 Hz, H-6), 6.46 (d, 1H, $J$ = 2 Hz, H-8), 6.86 (d, 1H, $J$ = 8 Hz, H-5′), 7.41 (d, 1H, $J$ = 2 Hz, H-2′), and 7.42 (dd, 1H, $J$ = 2 and 8 Hz, H-6′).

Narcissin (20 mg) was hydrolyzed by mixing with 6% HCl (50 ml) and heating on a steam bath for 45 min. After cooling, the precipitated aglycone was filtered, and the filtrate was extracted three times with ether. The combined precipitate and ether extracts were recrystallized twice from ethanol. The aqueous filtrate was lyophilized and subjected to cellulose TLC in three solvent systems: ethyl acetate–pyridine–water (2:1:2), butanol–acetic acid–water (3:1:1), and pyridine–ethyl acetate–acetic acid–water (36:36:7:21) (8). Sugars were detected with *p*-anisidine phthalate spray reagent (8).

**Antifertility Screening**—Eight-week-old virgin female Sprague–Dawley rats were housed in environmentally controlled quarters, which provided 14 hr of light (5 am to 7 pm) per 24-hr period. After the animals had 1 week to acclimate to the environment, daily vaginal smears were initiated to provide information concerning their estrous cycles. On the 12th day of taking smears, intraperitoneal injections were begun and continued daily throughout the experiment. Groups of six rats were each administered 100 mg/kg of one of the extracts (the chloroform extract suspended in sterol diluent or the petroleum ether or aqueous extract suspended in 10% polysorbate 20). Control groups, six rats each, were treated simultaneously with the respective vehicle at 1 ml/kg.

On the 12th day of dosing, proven breeded males were placed in cages of the individually housed females. The day on which sperm were found in the smear or on which a plug was found in the vagina was defined as Day 1 of pregnancy. Rats were autopsied on Day 20 of pregnancy. The number of implantation sites in the uterus, equaling the number of live plus degenerating fetuses, was counted and compared with the number of corpora lutea of pregnancy found in the ovaries.

[2] Melting points were determined using a Kofler hot-stage instrument and are uncorrected. UV and IR spectra were recorded using a Beckman model DB-G grating spectrophotometer and a Beckman model IR-18A spectrophotometer with polystyrene calibration at 1601 $cm^{-1}$, respectively. PMR spectra were recorded at 60 MHz on a Varian T-60A instrument with a Nicolet model TT-7 Fourier attachment, using tetramethylsilane as the internal standard. Mass spectral data were obtained on a Hitachi Perkin-Elmer model RMU-6D spectrophotometer.

[3] The flowering tops of *S. maritima* Jacq. were collected (July 1971) in Curacao and identified by J. F. Morton. A voucher specimen was deposited at the Morton Collectanea, University of Miami, Coral Gables, Fla.

[4] MN-polyamide SC-6, Macherey Nagel and Co., Düren, West Germany.

[5] Precoated aluminum-backed cellulose TLC plates, E. Merck, Darmstadt, West Germany.

[6] Narcissin was trimethylsilylated (7) using Sil-Prep, Applied Science Division, Milton Roy Co. Laboratory Group, State College, Pa.

## REFERENCES


(1) A. W. Chapman, "Flora of the Southern United States," 3rd ed., American Book Co., New York, N.Y., 1897, p. 196.

(2) S. von Reis Altschul, "Drugs and Foods from Little-Known Plants. Notes in Harvard University Herbaria," Harvard University Press, Cambridge, Mass., 1973, p. 286.

(3) L. Aristeguieta, *Soc. Cienc. Nat. La Salle*, **10**, 205 (1950); through *Biol. Abstr.*, **26**, 12923 (1952).

(4) C. F. Spencer, F. R. Koniuszy, E. F. Rogers, J. Shavel, Jr., N. R. Easton, E. A. Kaczka, F. A. Kuehl, Jr., R. F. Phillips, A. Walti, K. Folkers, C. Malanga, and A. O. Seeler, *Lloydia*, **10**, 145 (1947).

(5) H. H. S. Fong, M. Tin-Wa, N. R. Farnsworth, and R. H. Dobberstein, "Phytochemical Screening Methods," College of Pharmacy, University of Illinois at the Medical Center, Chicago, Ill., 1975, pp. 30–34, 41, 42, 44, 45, 52, 53, 59, 60, 62, 63, 65, 69, 70.

(6) E. G. Worthley and C. D. Schott, *Lloydia*, **29**, 123 (1966).

(7) T. J. Maybry, K. R. Markham, and M. B. Thomas, "The Systematic Identification of Flavonoids," Springer-Verlag, New York, N.Y., 1970, pp. 35–39, 255, 269.

(8) B. A. Lewis and F. Smith, in "Thin Layer Chromatography—A Laboratory Handbook," 2nd ed., E. Stahl, Ed., Springer-Verlag, New York, N.Y., 1969, pp. 814, 815, 833, 834, 857.


## ACKNOWLEDGMENTS


The authors thank Professor H. Wagner, Institut für pharmazeutische Arzneimittellehre der Universität Munchen, Munich, West Germany, and Dr. Jacque Kagan, Department of Chemistry, University of Illinois at Chicago Circle, Chicago, Ill., for providing reference samples of isorhamnetin and narcissin, respectively. The authors also thank Ms. C. Willey for technical assistance.


For the previous paper in this series, see E. B. Thompson, G. H. Aynilian, R. H. Dobberstein, G. A. Cordell, H. H. S. Fong, and N. R. Farnsworth, *J. Natl. Prod.*, **42**, 120 (1979).

# Prolongation of Effect of Asparaginase by Implantation in Polyacrylamide in Rats

**PETER EDMAN and INGVAR SJÖHOLM** ˣ

Received May 15, 1980, from the *Department of Pharmaceutical Biochemistry, Biomedical Center, University of Uppsala, S-751 23 Uppsala, Sweden.* Accepted for publication October 23, 1980.

**Abstract** □ L-Asparaginase was immobilized in spherical polyacrylamide microparticles, which were inserted in polyacrylamide gel for implantation in rats. Intraperitoneal implantation of this gel depressed systemic L-asparagine for the same duration as was achieved with microparticles, *i.e.*, 8–10 days. The duration of the effect was prolonged up to about 25 days when the gel with the enzyme was implanted subcutaneously on the back of the rat. In both cases, a collagenous capsule formed around the gel, eventually preventing contact with the circulation. The effect of a second implantation was of the same magnitude as the first one.

**Keyphrases** □ L-Asparagine—polyacrylamide microparticles, prolongation of effect by implantation of immobilized enzyme, rats □ Polyacrylamide—microparticles containing L-asparaginase, prolongation of effect by implantation, rats □ Microparticles—L-asparaginase-containing polyacrylamide microparticles, prolongation of effect by implantation of immobilized enzyme, rats

L-Asparaginase has been used to control and depress the growth of L-asparagine-dependent tumors (1–3), and its administration in immobilized form offers some advantages (4). L-Asparaginase was immobilized in polyacrylamide microspheres (mean diameter of about 0.3 μm) in such a way that the enzymatic properties were retained. When these microspheres (1000 IU of L-asparaginase/kg) were administered in a single dose intraperitoneally, the effect on the serum L-asparagine level was prolonged from 4 to 14 days when compared with the effect of soluble enzyme. Moreover, the acrylic microspheres were cleared readily from the abdominal cavity and circulation by the reticuloendothelial system (5).

The enzyme is still active in the microparticles after the endocytosis but cannot control the systemic L-asparagine level. The duration of the effect thus is directly dependent on the time the particles stay in contact with the systemic circulation. In the present paper, data show that L-asparaginase given in polyacrylamide implants can depress L-asparagine for up to about 25 days.

## EXPERIMENTAL

**Materials**—L-Asparaginase[1] (EC 3.5.1.1) was isolated from *Escherichia coli* (ATCC 9637 and ATCC 11303). Polyacrylamide microparticles with L-asparaginase were prepared as described previously (4, 6).

**Polyacrylamide Gel Preparation for Implantation**—Microparticles of polyacrylamide containing L-asparaginase (20 and 100 IU) were suspended in 0.7 ml of monomeric acrylamide (T − C = 16–25[2]) in a cylinder with a height of 0.7 cm and a radius of 0.6 cm. A catalyst system of *N,N,N′,N′*-tetramethylethylenediamine (50 μl) and 50 μl of ammonium peroxydisulfate (500 mg/ml of water) then was added to the monomer suspension. The polymerization started immediately and was completed in 10 min. The gel tablet was washed with physiological saline for 7 days to free it from any remaining catalysts.

Determination of L-asparagine was done according to Cooney *et al.* (8).

L-Asparaginase was determined according to Yellin and Wriston (9) as described previously (4).

**Animals**—Sprague–Dawley male rats were used.

## RESULTS AND DISCUSSION

**L-Asparaginase Implanted Intraperitoneally**—Figure 1 shows the changes in the serum L-asparagine concentration in rats given single doses (20 IU) of L-asparaginase in soluble and immobilized forms. The enzyme was immobilized in polyacrylamide microspheres (T − C = 8–25), which subsequently were inserted in polyacrylamide gel (T − C = 16–25). The gel was prepared in the form of a cylinder with a height of 0.7 cm and a radius of 0.6 cm. The gel tablet was implanted in the abdominal cavity of a 110-g male rat.

The serum L-asparagine level was measured intermittently in the rats as well as in an untreated control taken from the same litter. The soluble enzyme had a short effect on the L-asparagine level, which was essentially normalized after 2 days (Fig. 1). When the enzyme was given in the polyacrylamide gel, L-asparagine immediately dropped to a level corresponding to ~25–30% of the initial value. After 8 days, the L-asparagine level was normalized.

The effect seen after intraperitoneal implantation of the gel was comparable to the effect obtained after intraperitoneal injection of L-asparaginase in microparticles (4). However, the dose in the implant corresponded to 182 IU/kg, while there were 1000 IU/kg in the microparticles.

On the 31st day, the abdominal cavity was opened. The gel was surrounded by a nonvascularized tough ligamentous capsule. No capillaries had penetrated the polyacrylamide implant, and the gel could be removed easily from the capsule. A significant amount of L-asparaginase activity still remained in the implant.

**L-Asparaginase Implanted Subcutaneously**—For subcutaneous administration, polyacrylamide gels (T − C = 16–25) were prepared containing 100 IU of L-asparaginase in microparticles (T − C = 8–25). The cylinders formed were about the same size as those used for intraperitoneal implantation. The gel implants (dose of ~700 IU/kg) were placed subcutaneously in the scapular line in two male rats weighing 147 g. The L-asparagine level was followed and compared to that in an untreated rat (Fig. 2).

A significant depression of the L-asparagine level was seen for at least 25 days, and the level was normalized on the 31st day. On the 61st day when the rats weighed 350 g, the implants were removed and a new gel tablet containing 100 IU of L-asparaginase (~300 IU/kg) was implanted in the other side of the back in the scapular line. The effect of this second implantation lasted for about 19 days (Fig. 2). In these cases also, the systemic effect of L-asparaginase was interrupted by encapsulation.

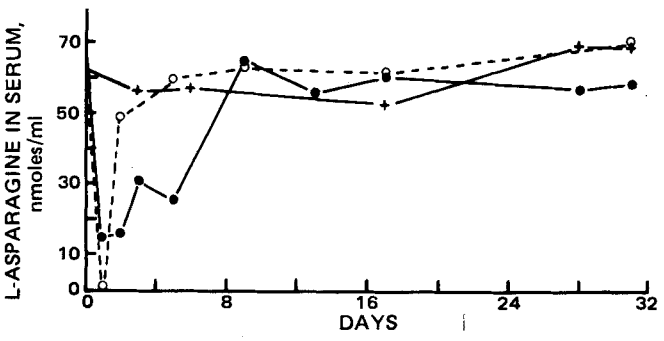


**Figure 1**—*L-Asparagine concentration in serum (nanomoles per milliliter) after intraperitoneal implantation of 20 IU of L-asparaginase (182 IU/kg) in rats (●) or after injection of the same amount in soluble form (○). The normal L-asparagine concentration (+) was obtained from an untreated rat taken from the same litter.*

[1] Crasnitin, Bayer (Sverige) AB, Stockholm, Sweden

[2] The nomenclature follows the suggestion made by Hjertén (7).



*0022-3549/81/0600-0684$01.00/0*
*© 1981, American Pharmaceutical Association*

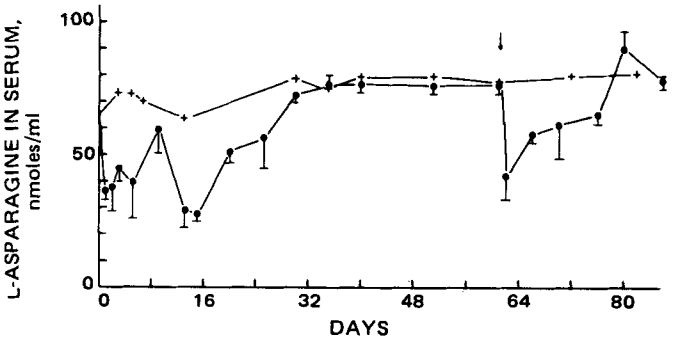


**Figure 2**—*L-Asparagine concentration in serum after subcutaneous implantation of 100 IU of L-asparaginase (700 IU/kg) in rats (●). The arrow shows the time when the implant was removed and a new gel tablet containing 100 IU of L-asparaginase (300 IU/kg) was inserted. Each point represents samples drawn from two rats and shows the mean and the range. The normal L-asparagine level (+) was obtained from an untreated rat from the same litter.*

The decrease of the serum L-asparagine concentration was of the same magnitude after the second implantation as that found initially, in spite of the lower dosage of L-asparaginase. This finding indicates that no significant amounts of antibodies were produced in the rats during the first 60 days of exposure to the implants. This conclusion is in accordance with earlier findings that proteins immobilized in highly cross-linked polyacrylamide are stably bound in the gel (6). Thus, it is feasible to assume that not enough of the immunogenic enzyme leaks out of the gel to activate the immune system.

By subcutaneous administration of L-asparaginase in implants of polyacrylamide, the effect can be substantially prolonged compared to the duration obtained by administration of soluble enzyme or by enzyme immobilized in microspheres. Although duration of the systemic effect *in vivo* was not limited by denaturation, the formation of a collagenous capsule around the implant effectively prevented the contact between the enzyme and the circulating L-asparagine. The encapsulation is a normal reaction to the presence of a foreign body. The same effects were detected after implantation of other acrylic polymers in rats (10, 11).

Updike *et al.* (12) also increased the duration of L-asparaginase by immobilizing the enzyme in resealed red blood cell ghosts. Undetected or very low levels of circulating L-asparagine lasted twice as long after the intravenous injection in monkeys of ghost-entrapped enzyme than after injection of the same amount of free enzyme. In this case, the duration of the enzymatic effect was limited by the survival of the red blood cell ghosts in the circulation.

Chang *et al.* (13) also showed that L-asparaginase entrapped in semipermeable microcapsules (~80 μm in diameter) can deamidate L-asparagine *in vitro*. When given intraperitoneally in mice, the entrapped enzyme (3.5 IU) was more efficient than native enzyme and cured 50% of the treated mice bearing an L-asparagine-dependent lymphoma cell line, 6C3HED (14).

The L-asparaginase implants thus were able to depress the systemic L-asparagine level significantly for prolonged periods. However, as is evident from the figures, the concentration of L-asparagine never reached zero. Therefore, it is not possible to predict whether the decreased level would influence the proliferation of L-asparagine-dependent tumors. Such tests may be performed with the 6C3HED cell line growing in mice.

## REFERENCES

(1) J. G. Kidd, *Recent Results Cancer Res.*, **33**, 3 (1970).

(2) J. P. Whitecar, Jr., G. P. Bodey, J. E. Harris, and E. J. Freireich, *N. Engl. J. Med.*, **282**, 732 (1970).

(3) D. Killander, A. Dohlwitz, L. Engstedt, S. Franzén, G. Gahrton, B. Gullbring, G. Holm, A. Holmberg, S. Höglund, A. Killander, D. Lockner, H. Mellstedt, P. Y. Moe, J. Palmblad, P. Reizenstein, K. O. Skårberg, B. Swedberg, A.-M. Udén, B. Wadman, L. Wide, and L. Åhström, *Cancer*, **37**, 220 (1976).

(4) P. Edman and I. Sjöholm, *J. Pharmacol. Exp. Ther.*, **211**, 663 (1979).

(5) I. Sjöholm and P. Edman, *ibid.*, **211**, 656 (1979).

(6) B. Ekman and I. Sjöholm, *J. Pharm. Sci.*, **67**, 693 (1978).

(7) S. Hjertén, *Arch. Biochem. Biophys. Suppl.*, **1**, 147 (1962).

(8) D. A. Cooney, R. L. Capizzi, and R. E. Handschumacher, *Cancer Res.*, **30**, 929 (1970).

(9) T. O. Yellin and J. C. Wriston, Jr., *Biochemistry*, **5**, 1605 (1966).

(10) M. Barvič, K. Kliment, and M. Zavadil, *J. Biomed. Mater. Res.*, **1**, 313 (1967).

(11) L. Šprincl, J. Kopeček, and D. Lím, *ibid.*, **4**, 447 (1971).

(12) S. J. Updike, R. T. Wakamiya, and E. N. Lightfoot, Jr., *Science*, **193**, 681 (1976).

(13) T. M. S. Chang, A. Pont, L. J. Johnson, and N. Malave, *Trans. Am. Soc. Intern. Organs*, **14**, 163 (1968).

(14) T. M. S. Chang, *Nature*, **229**, 117 (1971).

## ACKNOWLEDGMENTS

Supported by the Swedish Board for Technical Development and the I.F. Foundation for Pharmaceutical Research.

The authors thank Bayer (Sverige) AB for supplying L-asparaginase and Miss Siv Larsson for valuable technical assistance.

This paper is Number 3 in a series on Acrylic Microspheres *In Vivo*.

# Fluorometric Determination of All-*trans* Retinol in Rat Serum

**SU-CHEN WU, A. C. CAPOMACCHIA ˣ, and J. C. PRICE**

Received May 21, 1980, from the *Department of Pharmaceutics, School of Pharmacy, University of Georgia, Athens, GA 30602.* Accepted for publication October 23, 1980.

**Abstract** □ A rapid, specific, and sensitive fluorometric assay for retinol in rat serum is reported. Serum retinol is extracted into cyclohexane after dilution of the serum sample with aqueous acetonitrile. Sample volumes as small as 0.2 ml can be used with a limiting detectable concentration of $2.5 \times 10^{-8}$ *M* for retinol.

**Keyphrases** □ Vitamin A—fluorometric determination in rat serum □ Retinol, all-*trans*—fluorometric determination in rat serum □ Fluorometry—determination of all-*trans* retinol in rat serum

Vitamin A (all-*trans* retinol) is well known for its importance in general growth, the growth and differentiation of epithelial tissues, visual function, and reproduction (1–4). A number of retinoids prevent or inhibit the growth of epithelial tumors (5–9). As early as 1926, it had been noticed that vitamin A deficiency leads to carcinomas in

0022-3549/81/0600-0685$01.00/0
© 1981, American Pharmaceutical Association

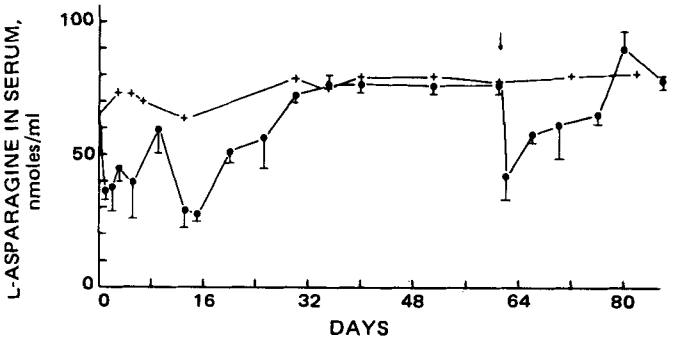


**Figure 2**—*L-Asparagine concentration in serum after subcutaneous implantation of 100 IU of L-asparaginase (700 IU/kg) in rats (●). The arrow shows the time when the implant was removed and a new gel tablet containing 100 IU of L-asparaginase (300 IU/kg) was inserted. Each point represents samples drawn from two rats and shows the mean and the range. The normal L-asparagine level (+) was obtained from an untreated rat from the same litter.*

The decrease of the serum L-asparagine concentration was of the same magnitude after the second implantation as that found initially, in spite of the lower dosage of L-asparaginase. This finding indicates that no significant amounts of antibodies were produced in the rats during the first 60 days of exposure to the implants. This conclusion is in accordance with earlier findings that proteins immobilized in highly cross-linked polyacrylamide are stably bound in the gel (6). Thus, it is feasible to assume that not enough of the immunogenic enzyme leaks out of the gel to activate the immune system.

By subcutaneous administration of L-asparaginase in implants of polyacrylamide, the effect can be substantially prolonged compared to the duration obtained by administration of soluble enzyme or by enzyme immobilized in microspheres. Although duration of the systemic effect *in vivo* was not limited by denaturation, the formation of a collagenous capsule around the implant effectively prevented the contact between the enzyme and the circulating L-asparagine. The encapsulation is a normal reaction to the presence of a foreign body. The same effects were detected after implantation of other acrylic polymers in rats (10, 11).

Updike *et al.* (12) also increased the duration of L-asparaginase by immobilizing the enzyme in resealed red blood cell ghosts. Undetected or very low levels of circulating L-asparagine lasted twice as long after the intravenous injection in monkeys of ghost-entrapped enzyme than after injection of the same amount of free enzyme. In this case, the duration of the enzymatic effect was limited by the survival of the red blood cell ghosts in the circulation.

Chang *et al.* (13) also showed that L-asparaginase entrapped in semipermeable microcapsules (~80 μm in diameter) can deamidate L-asparagine *in vitro*. When given intraperitoneally in mice, the entrapped enzyme (3.5 IU) was more efficient than native enzyme and cured 50% of the treated mice bearing an L-asparagine-dependent lymphoma cell line, 6C3HED (14).

The L-asparaginase implants thus were able to depress the systemic L-asparagine level significantly for prolonged periods. However, as is evident from the figures, the concentration of L-asparagine never reached zero. Therefore, it is not possible to predict whether the decreased level would influence the proliferation of L-asparagine-dependent tumors. Such tests may be performed with the 6C3HED cell line growing in mice.

## REFERENCES

(1) J. G. Kidd, *Recent Results Cancer Res.*, **33**, 3 (1970).

(2) J. P. Whitecar, Jr., G. P. Bodey, J. E. Harris, and E. J. Freireich, *N. Engl. J. Med.*, **282**, 732 (1970).

(3) D. Killander, A. Dohlwitz, L. Engstedt, S. Franzén, G. Gahrton, B. Gullbring, G. Holm, A. Holmberg, S. Höglund, A. Killander, D. Lockner, H. Mellstedt, P. Y. Moe, J. Palmblad, P. Reizenstein, K. O. Skårberg, B. Swedberg, A.-M. Udén, B. Wadman, L. Wide, and L. Åhström, *Cancer*, **37**, 220 (1976).

(4) P. Edman and I. Sjöholm, *J. Pharmacol. Exp. Ther.*, **211**, 663 (1979).

(5) I. Sjöholm and P. Edman, *ibid.*, **211**, 656 (1979).

(6) B. Ekman and I. Sjöholm, *J. Pharm. Sci.*, **67**, 693 (1978).

(7) S. Hjertén, *Arch. Biochem. Biophys. Suppl.*, **1**, 147 (1962).

(8) D. A. Cooney, R. L. Capizzi, and R. E. Handschumacher, *Cancer Res.*, **30**, 929 (1970).

(9) T. O. Yellin and J. C. Wriston, Jr., *Biochemistry*, **5**, 1605 (1966).

(10) M. Barvič, K. Kliment, and M. Zavadil, *J. Biomed. Mater. Res.*, **1**, 313 (1967).

(11) L. Šprincl, J. Kopeček, and D. Lím, *ibid.*, **4**, 447 (1971).

(12) S. J. Updike, R. T. Wakamiya, and E. N. Lightfoot, Jr., *Science*, **193**, 681 (1976).

(13) T. M. S. Chang, A. Pont, L. J. Johnson, and N. Malave, *Trans. Am. Soc. Intern. Organs*, **14**, 163 (1968).

(14) T. M. S. Chang, *Nature*, **229**, 117 (1971).

## ACKNOWLEDGMENTS

Supported by the Swedish Board for Technical Development and the I.F. Foundation for Pharmaceutical Research.

The authors thank Bayer (Sverige) AB for supplying L-asparaginase and Miss Siv Larsson for valuable technical assistance.

This paper is Number 3 in a series on Acrylic Microspheres *In Vivo*.

# Fluorometric Determination of All-*trans* Retinol in Rat Serum

**SU-CHEN WU, A. C. CAPOMACCHIA ˣ, and J. C. PRICE**

Received May 21, 1980, from the *Department of Pharmaceutics, School of Pharmacy, University of Georgia, Athens, GA 30602.* Accepted for publication October 23, 1980.

**Abstract** □ A rapid, specific, and sensitive fluorometric assay for retinol in rat serum is reported. Serum retinol is extracted into cyclohexane after dilution of the serum sample with aqueous acetonitrile. Sample volumes as small as 0.2 ml can be used with a limiting detectable concentration of $2.5 \times 10^{-8}$ *M* for retinol.

**Keyphrases** □ Vitamin A—fluorometric determination in rat serum □ Retinol, all-*trans*—fluorometric determination in rat serum □ Fluorometry—determination of all-*trans* retinol in rat serum

Vitamin A (all-*trans* retinol) is well known for its importance in general growth, the growth and differentiation of epithelial tissues, visual function, and reproduction (1–4). A number of retinoids prevent or inhibit the growth of epithelial tumors (5–9). As early as 1926, it had been noticed that vitamin A deficiency leads to carcinomas in

0022-3549/81/0600-0685$01.00/0
© 1981, American Pharmaceutical Association

the stomach of rats (10) and later to hyperkeratosis of the skin and to metaplastic changes in epithelia of the GI, respiratory, and urogenital tract (11–14).

In the late 1960's, several scientists showed that the induction of benign and malignant epithelial tumors in animals could be retarded or even prevented by systemically applied retinol or retinol palmitate (5, 6). The use of these compounds for cancer chemoprevention was reviewed previously (15, 16). These nutritional surveys and cancer prevention studies required a method for measuring micromolar to nanomolar amounts of retinol in small volumes of serum, a method whereby numerous analyses could be performed without undue analytical time. For these reasons, there is an intense search for exact, sensitive, and simple methods for determining retinol in biological material.

The innate sensitivity and speed of fluorescence measurements as an analytical technique have been demonstrated (17–26). However, current methodology is still not as sensitive as some recently reported high-pressure liquid chromatographic (HPLC) procedures (27–31). The present paper reports an improved fluorometric assay for retinol in rat serum that is more sensitive than reported methods and compares favorably with HPLC procedures.

## EXPERIMENTAL

**Apparatus**—All fluorescence measurements were made with a fluorescence spectrophotometer[1] equipped with an $x$–$y$ recorder. Quartz cells of a 1-cm light path were used. Daily variation in instrumental response was corrected with a dilute quinine bisulfate standard solution ($5 \times 10^{-5}$ $M$ in 0.1 $N$ $H_2SO_4$).

Since organic solvents were found to extract fluorescent substances from plastic caps, tubes, and bottles (25), a glass apparatus was used during all analytical manipulations. Glass culture tubes[2] were used to collect serum samples and extract retinol from serum.

A high-speed centrifuge[3] was used for centrifugation, and a vibrating mixer[4] was used for mixing and extraction.

**Reagents and Solutions**—Retinol[5] (all-*trans*, crystalline, synthetic Type X) and retinyl acetate[5] (all-*trans*, crystalline, synthetic Type I) were used as received. Solid samples were stored at −10° under nitrogen and protected from light. All solvents were the highest grade commercially available; they were checked for fluorescent impurities before use. A buffer solution ($\mu$ = 0.15, pH 7.4) was prepared from analytical grade monobasic sodium phosphate[6], dibasic sodium phosphate, and distilled, deionized water.

**Standard Solutions**—Sufficient retinyl acetate was weighed into a 10-ml amber volumetric flask and dissolved in 10 ml of acetonitrile to yield a standard stock solution (~$1 \times 10^{-3}$ $M$). Serial dilutions of this solution yielded working standard solutions with concentrations ranging from $1 \times 10^{-4}$ to $1 \times 10^{-6}$ $M$. All solutions were stored at −10° and protected from light. The purity of the solutions was checked by comparing their absorption spectra with their corrected fluorescence excitation spectra. Retinyl acetate was used as a standard because it has long been accepted as a standard for retinol determination by fluorometric analysis. The reported quantum efficiencies for each compound are identical, and the stability of retinol acetate solutions is much better (32–34). All experimental manipulations were conducted under yellow light and in amber glassware.

**Solvent Pair Selections**—A water-miscible–water-immiscible solvent pair was selected based on the following criteria.

1. The fluorescence of retinyl acetate in 14 nonpolar and nine polar solvents was examined.

2. The nonpolar solvents were used to extract blank rat serum to detect extractable, fluorescent serum components. The nonpolar solvents were carbon tetrachloride, chloroform, methyl chloride, methylene chloride, ethylene dichloride, tetrachloroethylene, $n$-pentane, $n$-hexane, $n$-heptane, cyclohexane, ethyl acetate, octanol, benzene, and toluene. The polar solvents were dimethyl sulfoxide, acetonitrile, dimethylformamide, formamide, ethylene glycol, water, methanol, ethanol, and dioxane.

3. Various ratios of polar solvent to water-diluted serum were examined with regard to decreasing the quantity of endogenous serum components extracted into the nonpolar solvent. For these comparisons, the serum was spiked with retinoid, diluted with water, and then diluted further with the polar solvent. The resulting aqueous solution was extracted with the nonpolar solvent.

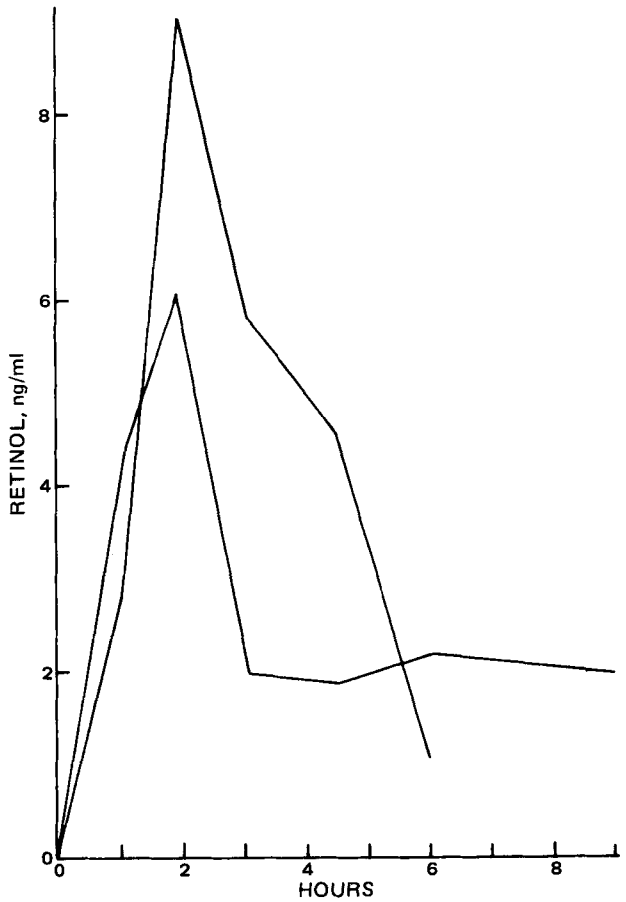


**Figure 1**—*Serum retinol blood profiles obtained from two rats after a single oral dose of 10 mg of retinyl acetate/kg. All points were corrected for blank fluorescence.*

**Serum**—Male and female rats[7] (300–400 g) were fasted for 19 hr before sacrifice. After the animal was anesthetized with ether, the rib cage was cut open to expose the heart. Total exsanguination from the left ventricle was accomplished with a 10-ml disposable plastic syringe. Approximately 10 ml of blood was obtained from each rat. The serum was obtained after centrifugation at 2500 rpm for 10 min in a glass culture tube.

The native fluorescence of the serum extracts was examined by mixing 0.2 ml of serum with 0.2 ml of phosphate buffer. To this mixture was added 2 ml of acetonitrile. After mixing, 2 ml of cyclohexane was added and shaken by a vibrating mixer for 30 sec. After this mixture was centrifuged at 2500 rpm for 5 min, the cyclohexane layer was removed for direct fluorometric measurement. The fluorescence intensity of each sample was measured at the excitation maximum of 327 nm and the emission maximum of 480 nm. This procedure was repeated with 15 different rat serum samples without drug. The average fluorescence intensity measured from these 15 blank serum samples was used as the blank.

Buffer and serum samples (0.2 ml) spiked with varying concentrations of retinyl acetate were extracted in the same manner as the blank serum extracts. Second extractions of the spiked samples were performed by adding 2 ml of cyclohexane to the aqueous mixture from which the first

[1] Model MPF-44A, Perkin-Elmer, Norwalk, CT 06856.
[2] Type 9825, 16 × 100 mm, Pyrex, Corning Glass Works, Corning, N.Y.
[3] Vari-HI Speed Centricone, Precision Scientific Co., Subsidiary of GCA Corp., Chicago, Ill.
[4] Super-Mixer, Lab-Line Instruments, Melrose Park, Ill.
[5] Sigma Chemical Co., St. Louis, MO 63178.
[6] J. T. Baker Chemical Co., Phillipsburg, NJ 08865.
[7] Sprague–Dawley strain, Hiram Davis Co., Stockbridge, Ga.

**Table I—Comparison of Fluorescence Excitation Intensity as a Function of Different Acetonitrile–Aqueous Serum Sample Ratios of Retinyl Acetate Extracted by 2 ml of Cyclohexane from Spiked Rat Serum**

| Rat Serum (ml)–Water (ml) + Acetonitrile (ml) | Net Relative Fluorescence Excitation Intensity of Cyclohexane Layer ($\lambda_{ex}$ 327; $\lambda_{em}$ 480), arbitrary units | Acetonitrile–Aqueous Serum Sample |
|---|---|---|
| 0.2:0.2 + 0 | 54.0 | 0 |
| 0.2:0 + 0.2 | 54.0 | 1:1 |
| 0.2:0 + 2 | 57.3 | 1:0.09 |
| 0.2:0 + 1 | 54.0 | 1:0.17 |
| 0.2:0.2 + 2 | 62.3 | 1:0.17[a] |
| 0.4:0.2 + 2 | 61.4 | 1:0.23 |
| 0.6:0.2 + 2 | 60.3 | 1:0.29 |
| 0.8:0.2 + 2 | 57.0 | 1:0.33 |

[a] Optimum solution conditions.

cyclohexane layer had been removed. Since the fluorescence intensity of the second sample extract was the same as that of the blank, the fluorescence intensity of each sample recorded was from the first extract.

*In vivo* experiments were performed using three sets of four rats each, administered a 2-, 4-, or 10-mg/kg dose of retinyl acetate by stomach intubation. Each dose was prepared by dissolving an appropriate quantity of drug in ethanol. Before drug administration, each rat was fasted for 19 hr. The blood was withdrawn from the heart 2 hr postadministration.

Two more rats with body weights of 390 g were given 10 mg/kg of retinyl acetate orally. Blood samples of each rat were withdrawn from the tail at 0, 1, 2, 3, 4.5, 6, and 9 hr. All samples were centrifuged, and the serum was removed and kept frozen until assayed (Fig. 1).

## RESULTS AND DISCUSSION

Cyclohexane–acetonitrile was the best solvent pair when acetonitrile was added to the water-diluted serum samples (1:1) so that the final ratio of acetonitrile to aqueous sample was 1:0.17. The validity of using these proportions was checked (Table I). Methanol and ethanol also can be used as the water-miscible component as reported previously (22, 25, 35). However, they did not decrease the cyclohexane extraction of endogenous fluorescent substances in the serum as well as did acetonitrile. The other water-miscible solvents did not demonstrate this effect, the mechanism of which is not known. However, it appears to be a specific solvation effect, dependent on the solvent concentration as well as on the water concentration in the final solution (Table I). Simple dilution of the serum sample with water, with no acetonitrile added, resulted in a lower fluorescence intensity than under optimum conditions. Dilution with acetonitrile produced the same result. Sample fluorescence was maximized only after dilution with both acetonitrile and water in the given proportions.

Standard curves were constructed at six concentration points for retinol in (*a*) cyclohexane, (*b*) cyclohexane-extracted phosphate buffer, and (*c*) cyclohexane-extracted serum. Curves *a–c* were linear from $2.5 \times 10^{-8}$ to $1.0 \times 10^{-4}$ *M*. For *a* and *b*, each point was the mean of three determinations; for *c*, each point was the mean of 15 determinations. The correlation coefficients were 0.9998, 0.9997, and 0.9995 for *a–c*, respectively.

The extraction efficiencies of retinyl acetate from buffer solution and serum were 97.1 ± 1.2 and 91.4 ± 2.9%, respectively (mean ± *SD*). The results clearly show that a standard curve of this agent in cyclohexane-extracted buffer should not be used for extracted serum samples without a correction factor. Therefore, fluorometric procedures that do not include a correction factor will consistently report lower concentration values than are really present (22–26).

The procedure reported in this study is at least 10-fold more sensitive than current fluorometric procedures (22–26). However, sample volume and precision are essentially the same with both fluorometric and HPLC procedures now in use (22–26, 28–31). The method is applicable to bioavailability and pharmacokinetic studies, as demonstrated by the data in Fig. 1 and Table II.

**Table II—Rat Serum Concentrations of Retinol Obtained 2 hr after a Single Oral Dose of Retinyl Acetate**

| Dose, mg/kg | Number of Rats and Total Samples | Serum Concentration $\times 10^7$ *M* (mean ± *SD*) |
|---|---|---|
| 2 | 4 and 16 | 4.1 ± 0.9 |
| 4 | 4 and 16 | 7.6 ± 1.1 |
| 10 | 4 and 20 | 7.3 ± 1.0 |

The mean serum retinol concentration in 12 rats (52 samples) 2 hr after a single oral dose of retinyl acetate is shown in Table II. The data indicate a nonlinear correlation between dose and serum concentration. A 4-mg/kg dose produced a serum concentration nearly equal to that of the 10-mg/kg dose. An analysis of variance on the mean serum concentrations in Table II, using a Student procedure, showed that if the mean values differed by $1.82 \times 10^{-7}$ or more, then they were different ($p \leq 0.05$). Therefore, since oral doses of 4 and 10 mg/kg produced the same serum retinol concentration, a dose-dependent saturation of some part of the absorption or metabolic network may be occurring.

## REFERENCES


(1) G. A. Pitt, in "Carotenoids," O. Isler, Ed., B. Verlag, Basel, Switzerland, 1971, p. 717.

(2) T. Moore, in "The Vitamins," vol. 1, 2nd ed., Academic, New York, N.Y., 1967, p. 245.

(3) D. McLaren, in *ibid.*, p. 267.

(4) G. Wald, *Angew. Chem.*, **80,** 857 (1968).

(5) E. W. Chu and R. A. Malmgren, *Cancer Res.*, **25,** 884 (1965).

(6) U. Staffiotti, R. Montesano, A. R. Sellakumar, and S. A. Borg, *Cancer*, **20,** 857 (1967).

(7) W. Bollag, *Experientia*, **27,** 90 (1971).

(8) W. Bollag, *Cancer Chemother. Rep.*, **55,** 53 (1971).

(9) W. Bollag, *Experientia*, **30,** 1198 (1974).

(10) Y. Fujimaki, *J. Cancer Res.*, **10,** 469 (1926).

(11) S. Mori, *Bull. Johns Hopkins Hosp.*, **33,** 357 (1922).

(12) S. B. Wolbach and P. R. Howe, *J. Exp. Med.*, **42,** 753 (1925).

(13) S. B. Wolbach and P. R. Howe, *Arch. Pathol.*, **5,** 239 (1928).

(14) T. Moore, "Vitamin A," Elsevier, Amsterdam, The Netherlands, 1957.

(15) M. B. Sporn, N. M. Dunlop, D. L. Newton, and L. M. Smith, *Fed. Proc. Fed. Am. Soc. Exp. Biol.*, **35,** 1332 (1976).

(16) W. Bollag, *Int. Z. Vitaminforsch.*, **40,** 299 (1970).

(17) P. S. Brown, W. P. Blum, and M. H. Stern, *Nature*, **184,** 1377 (1959).

(18) M. Kofler and S. H. Rubin, *Vitam. Horm.*, **18,** 315 (1960).

(19) H. Popper, *Physiol. Rev.*, **24,** 205 (1944).

(20) D. H. Blankenhorn and H. Braunstein, *J. Clin. Invest.*, **37,** 160 (1958).

(21) O. A. Bessey, O. H. Lowry, M. J. Brock, and J. A. Lopez, *J. Biol. Chem.*, **166,** 177 (1946).

(22) J. Kahan, *Scand. J. Clin Lab. Invest.*, **18,** 679 (1966).

(23) B. D. Drujan, R. Castillon, and E. Guerrero, *Anal. Biochem.*, **23,** 44 (1968).

(24) R. J. Selvaraj and T. P. Sushella, *Clin. Chim. Acta*, **27,** 165 (1970).

(25) J. N. Thompson, P. Erdody, R. Brien, and T. K. Merray, *Biochem. Med.*, **5,** 67 (1971).

(26) S. Futterman, D. Swanson, and R. E. Kalina, *Invest. Ophthalmol.*, **14,** 125 (1974).

(27) A. M. McCormick, J. L. Napoli, and H. F. Deluca, *Anal. Biochem.*, **86,** 25 (1978).

(28) C. V. Puglisi, J. Arthur, and F. De Silva, *J. Chromatogr.*, **152,** 421 (1978).

(29) C. A. Frolik, T. E. Tavela, G. L. Peck, and M. B. Sporn, *Anal. Biochem.*, **86,** 743 (1978).

(30) C. A. Frolik, T. E. Tavela, and M. B. Sporn, *J. Lipid Res.*, **19,** 32 (1978).

(31) A. B. Roberts, M. D. Nichols, C. A. Frolik, D. L. Newton, and M. B. Sporn, *Cancer Res.*, **38,** 3327 (1978).

(32) A. J. Thomson, *J. Chem. Phys.*, **51,** 4106 (1969).

(33) J. Kahan, *Acta Chem. Scand.*, **21,** 2515 (1967).

(34) *Ibid.*, **22,** 1358 (1968).

(35) E. G. Bligh and W. J. Dyer, *Can. J. Biochem. Physiol.*, **37,** 911 (1959).


## ACKNOWLEDGMENTS


Adapted in part from a thesis submitted by S.-C. Wu to the University of Georgia in partial fulfillment of the Master of Science degree requirements.

Supported in part by National Cancer Institute Contract N01 CP 85 663.

# High-Performance Liquid Chromatographic Determination of Propranolol and 4-Hydroxypropranolol in Plasma

**M. T. ROSSEEL** ˣ **and M. G. BOGAERT**

Received July 24, 1980, from the *J. F. & C. Heymans Institute of Pharmacology, University of Ghent, De Pintelaan, 135, B-9000 Gent, Belgium.* Accepted for publication November 7, 1980.

**Abstract** □ A high-performance liquid chromatographic method for the simultaneous determination of propranolol and 4-hydroxypropranolol in plasma is presented. The method involves plasma extraction at basic pH with ethyl acetate, two brief back-extractions, chromatography on a reversed-phase column, and fluorescence detection. The within-run coefficients of variation were 3.0–7.1% for propranolol and 5.8–8.3% for 4-hydroxypropranolol. The day-to-day variations were 4.6 and 8.2% for propranolol and 4-hydroxypropranolol, respectively. The method can detect 1 ng of each compound/ml of plasma.

**Keyphrases** □ High-performance liquid chromatography—propranolol and 4-hydroxypropranolol, human plasma □ Propranolol—analysis, high-performance liquid chromatography, human plasma □ 4-Hydroxypropranolol—analysis, high-performance liquid chromatography, human plasma □ β-Adrenergic antagonists—propranolol and 4-hydroxypropranolol, high-performance liquid chromatography, human plasma

Propranolol, a β-adrenergic antagonist, is used to treat angina pectoris, cardiac arrhythmias, and hypertension. 4-Hydroxypropranolol, a metabolite of propranolol in humans and animals (1), is equipotent with propranolol as a β-adrenergic antagonist (2) and is present in human plasma after acute and chronic treatment with propranolol (3–7).

Several methods for the simultaneous determination of both substances have been proposed, including mass fragmentography (3), direct fluorometry (4), and reversed-phase high-pressure liquid chromatography (HPLC) with fluorescence detection (5), but none of these methods is entirely satisfactory. In other methods, the standard curve for 4-hydroxypropranolol was not linear (8) and no internal standard was used (9).

This paper describes a specific and sensitive HPLC method for the simultaneous determination of propranolol and 4-hydroxypropranolol in plasma. The procedure has been used for the analysis of plasma samples of patients taking propranolol.

## EXPERIMENTAL

**Chemicals and Reagents**—1-Heptanesulfonic acid[1] in acetic acid was used. Propranolol, 4-hydroxypropranolol, and 4-methylpropranolol were supplied as the hydrochloride salts[2]. Methanol was Lichrosolv quality[3], and all other reagents were analytical grade.

**Instrumental Conditions**—The microprocessor-controlled high-performance liquid chromatograph[4] was equipped with a fluorescence detector[5]. The fluorometer was set at an excitation wavelength of 290 nm, with an emission cutoff filter allowing 90% transmission at 340 nm.

Chromatography was done on a reversed-phase column 250 mm long × 4.6 mm i.d.[6]. The helium degassed mobile phase was pumped through the column at a flow rate of 1.5 ml/min, which required pressures of 600–1000 psi, depending on column age. The column temperature was 40°. Samples were injected using an automatic injector[7] equipped with a 10-μl loop. Quantitation was done by peak area measurement[8].

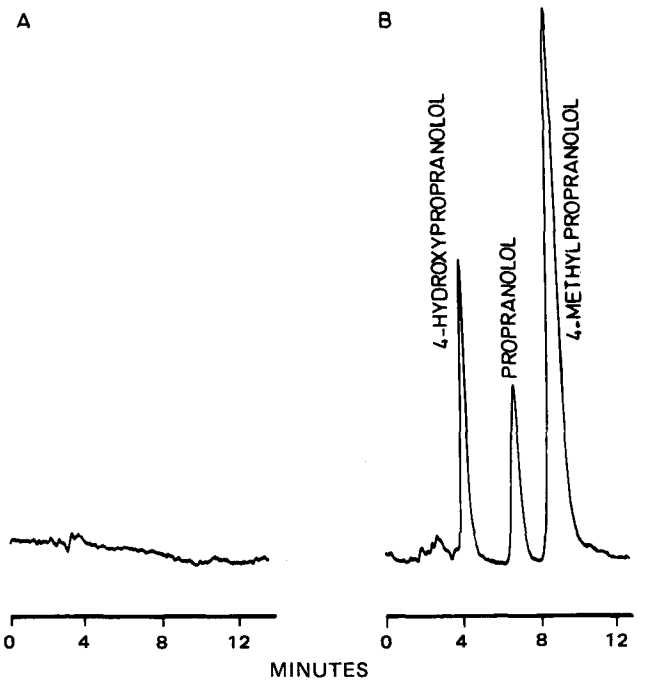


**Figure 1**—*(A) High-performance liquid chromatogram of the extract of 1 ml of blank plasma. (B) Chromatogram of an extract of 1 ml of blank plasma spiked with 20 ng of 4-hydroxypropranolol, 50 ng of propranolol, and 60 ng of the internal standard 4-methylpropranolol.*

**Mobile Phase**—1-Heptanesulfonic acid in acetic acid (25.0 ml) was mixed with 1000 ml of distilled water (Solvent A), and 25.0 ml of the same acid solution was mixed with 1000 ml of methanol (Solvent B). The mobile phase was Solvent A–Solvent B (34:66, v/v).

**Assay Standards**—Standard solutions of propranolol and of 4-hydroxypropranolol (10 mg/100 ml each, calculated as the base) were prepared in methanol and stored at −20°. For each assay, 100-fold aqueous dilutions of the standard solutions were made. The internal standard was 10 μg of 4-methylpropranolol/ml of methanol and was stored at −20°.

**Extractions**—To 1 ml of the spiked plasma or the unknown sample in a 10-ml glass-stoppered centrifuge tube, 20 mg of sodium hydrogen sulfite (20% in distilled water), 6 μl of the internal standard solution, 50 μl of 0.05 *M* triethylamine, and 500 μl of 2.5 *N* NaOH were added successively. The mixture was extracted with 4 ml of ethyl acetate by shaking horizontally for 10 min.

After centrifugation for 10 min at 6000 rpm, the organic phase was transferred with a Pasteur pipet to a 6-ml glass-stoppered conical tube. To the ethyl acetate layer, 100 μl of 0.2 *N* $H_2SO_4$ was added and the solution was mixed with a vortex mixer for 30 sec. After centrifugation the ethyl acetate layer was discarded and 100 μl of 2.5 *N* NaOH was added.

The basic solution was extracted immediately with 1 ml of ethyl acetate by mixing with a vortex mixer for 30 sec and centrifuging. The supernate was transferred with a Pasteur pipet to another 6-ml glass-stoppered conical tube, and the organic phase was removed under a gentle nitrogen stream at room temperature to near dryness. The residue was dissolved in 15 μl of the mobile phase and stored at −20° until analysis, *i.e.*, within a few hours.

[1] Reagent B-7, Waters Associates, Milford, Mass.
[2] Imperial Chemical Industries, Macclesfield, England.
[3] Merck, Darmstadt, West Germany.
[4] Spectra-Physics SP-8000, Eindhoven, The Netherlands.
[5] F.S. 970, Schoeffel Instruments Corp., West Germany.
[6] Lichrosorb 10RP8, Chrompack, Merksem, Belgium.
[7] Spectra-Physics *SP-8000*, Eindhoven, The Netherlands.
[8] Spectra-Physics SP-8000 data system, Eindhoven, The Netherlands.



*0022-3549/81/0600-0688$01.00/0*
*© 1981, American Pharmaceutical Association*

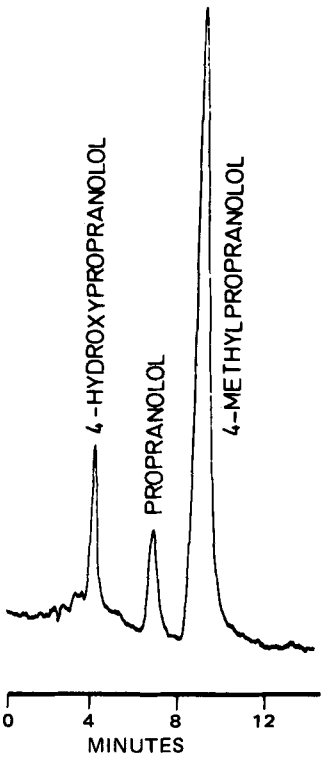


**Figure 2**—*High-performance liquid chromatogram of an extract of 1 ml of plasma of a patient receiving propranolol. To 1 ml of plasma, 60 ng of methylpropranolol was added as the internal standard.*

**Quantitation**—Human plasma samples spiked with increasing concentrations of propranolol (5–300 ng/ml) and 4-hydroxypropranolol (1–100 ng/ml) were carried through the whole procedure. Peak area ratios of propranolol or 4-hydroxypropranolol to the internal standard were plotted *versus* their concentrations, and an unweighted least-squares linear regression analysis was performed. Unknown drug concentrations were estimated from the calibration curve.

## RESULTS AND DISCUSSION

Blank plasma extracts yielded no interfering peaks from endogenous plasma components (Fig. 1A). Propranolol, 4-hydroxypropranolol, and 4-methylpropranolol were separated and eluted in ~12 min (Fig. 1B). Sensitivity limits were 1 ng/ml for each compound when the entire 1-ml plasma extract was injected. The detector response was linear for plasma propranolol concentrations of at least 5–300 ng/ml and plasma 4-hydroxypropranolol concentrations of at least 1–100 ng/ml. Typical calibration curve data are listed in Table I. Over 3 weeks, the slopes of the calibration curves demonstrated little change ($CV$ = 4.8 and 5.6% for propranolol and 4-hydroxypropranolol, respectively, $n$ = 13). The results of accuracy and precision, both within run and day to day, are shown in Table II. 4-Hydroxypropranolol is stable in plasma, if frozen, for at least 3 weeks (Table II). This stability also was reported by others (6).

Uncorrected recovery, as assessed by comparing peak areas of extracted standards with those of unextracted compounds, was 75 ± 6% ($n$ = 5) for 4-hydroxypropranolol and 80 ± 5% ($n$ = 5) for propranolol.

Figure 2 illustrates a chromatogram of the plasma extract from a patient receiving 40 mg of propranolol four times a day. The blood sample was taken 10 hr after the last dose.

There was no interference of the commonly used cardiac drugs quinidine, lidocaine, procainamide, and disopyramide added *in vitro*. *N*-Desisopropylpropranolol, another reported metabolite of propranolol (10), eluted just before propranolol, but no measurable amounts were found in the plasma of patients treated with propranolol.

**Table I—Calibration Curve Data ($y = c + mx$)**

| Compound | Range, ng/ml | Slope ($m$) | Intercept ($c$) | $r$ |
|---|---|---|---|---|
| Propranolol | 5–300 | 0.0098 | 0.0031 | 0.9990 |
| 4-Hydroxy-propranolol | 1–100 | 0.0127 | 0.0006 | 0.9992 |

**Table II—Accuracy and Within-Run and Day-to-Day Precision for Propranolol and 4-Hydroxypropranolol**

| Compound | Level, ng/ml | Mean Assay, % | $CV$, % |
|---|---|---|---|
| | Within Run ($n$ = 5) | | |
| Propranolol | 10 | 106.3 | 7.1 |
| | 50 | 99.6 | 3.0 |
| | 100 | 100.6 | 5.1 |
| 4-Hydroxypro-pranolol | 5 | 98.2 | 8.3 |
| | 20 | 101.9 | 5.8 |
| | 40 | 97.4 | 6.4 |
| | Day to Day ($n$ = 10)[a] | | |
| Propranolol | 50 | 103.7 | 4.6 |
| 4-Hydroxypro-pranolol | 15 | 98.5 | 8.2 |

[a] Pooled plasma standards, analyzed over 3 weeks.

The brief cleanup steps before chromatography, involving successive back-extractions into acid and ethyl acetate at basic pH, resulted in cleaner chromatograms than those previously reported (4, 5, 8). These cleanup steps were necessary particularly to obtain the assay sensitivity of 1 ng/ml for 4-hydroxypropranolol. In comparison to other HPLC methods for propranolol and 4-hydroxypropranolol (5, 8, 9), the described HPLC method is more sensitive, specific, and precise, particularly for the 4-hydroxypropranolol determination.

## REFERENCES

(1) P. A. Bond, *Nature*, **213**, 721 (1967).

(2) J. D. Fitzgerald and S. R. O'Donnell, *Br. J. Pharmacol.*, **43**, 222 (1971).

(3) T. Walle, J. Morrison, K. Walle, and E. Conradi, *J. Chromatogr.*, **114**, 351 (1975).

(4) P. S. Rao, L. C. Quesada, and H. S. Mueller, *Clin. Chim. Acta*, **88**, 355 (1978).

(5) D. W. Schneck, J. F. Pritchard, and A. H. Hayes, *Res. Commun. Chem. Pathol. Pharmacol.*, **24**, 3 (1979).

(6) T. W. Walle, E. C. Conradi, U. K. Walle, T. C. Fagan, and T. E. Gaffney, *Clin. Pharmacol. Ther.*, **27**, 22 (1980).

(7) L. Wong, R. L. Nation, W. L. Chiou, and P. K. Mehta, *Br. J. Clin. Pharmacol.*, **8**, 163 (1979).

(8) R. L. Nation, G. W. Peng, and W. L. Chiou, *J. Chromatogr.*, **145**, 429 (1978).

(9) W. D. Mason, E. N. Amick, and O. H. Weddle, *Anal. Lett.*, **10**, 515 (1977).

(10) D. A. Saelens, T. Walle, and P. J. Privitera, *J. Chromatogr.*, **123**, 185 (1976).

## ACKNOWLEDGMENTS

Supported by Grant 3.9001.79 from the National Fund for Medical Research, Belgium.

# Spectrophotometric Determination of Dimenhydrinate with Reinecke Salt

**A. KAR ˣ and G. I. ANIUHA**

Received August 9, 1979, from the *Department of Pharmaceutical Chemistry, Faculty of Pharmaceutical Sciences, University of Nigeria, Nsukka, Nigeria.* Accepted for publication November 13, 1980.

**Abstract** □ A convenient spectrophotometric method was developed for the determination of dimenhydrinate in bulk drug and dosage forms and in 1:1 combinations with aspirin, acetaminophen, meprobamate, phenylephrine, and tolbutamide. The method consisted of reacting dimenhydrinate with reinecke salt in an acidic medium at 27 ± 2°. The purple precipitate was filtered and dissolved in acetone, and the maximum color absorption attained in 15 min was measured at 540 nm. Evidence is provided to establish the optimal experimental parameters. The stoichiometric balance of the precipitate was determined. Reasonably ideal adherence of the color absorption pattern to the Beer–Lambert law permitted microdetermination of dimenhydrinate in pure form, commercial formulations, laboratory-made combinations, and recovery experiments with good accuracy and repeatability. No interference was observed with any of the drugs or tablet adjuvants.

**Keyphrases** □ Dimenhydrinate—spectrophotometric determination with reinecke salt □ Spectrophotometry—determination of dimenhydrinate with reinecke salt □ Reinecke salt—determination of dimenhydrinate, spectrophotometry

Dimenhydrinate is assayed by official methods (1–3) by estimating diphenhydramine and 8-chlorotheophylline individually. It also has been determined in pharmaceuticals by gas-phase chromatography (4), an argentometrical method (5), UV absorption (6), complexation with phosphomolybdic acid followed by reduction with ascorbic acid in acetone to molybdenum blue (7), and a silicotungstic acid method followed by gravimetry (7).

The present study investigated reinecke salt as a useful precipitant (8) for the spectrophotometric estimation of dimenhydrinate in pure forms, dosage formulations, and laboratory-made combinations. The study investigated color stability, effect of temperature on the colored precipitate, influence of pH on absorbance of the precipitate in acetone solution, determination of the stoichiometric balance, establishment of an absorbance–wavelength relationship, and recovery with various combinations. Adherence to Beer's law was found within a range of 200–1000 μg/ml.

## EXPERIMENTAL

**Instruments and Materials**—A single-beam spectrophotometer[1], a pH meter[2] fitted with a sealed calomel electrode, a shielded glass electrode, and a suitable thermostated[3] water bath were used.

Pharmaceutical grade dimenhydrinate, aspirin, acetaminophen, meprobamate, phenylephrine, and tolbutamide were employed as the working standards.

The commercial preparation analyzed was dimenhydrinate tablets[4]. For drug combinations, aspirin, acetaminophen, meprobamate, phenylephrine, and tolbutamide were mixed with dimenhydrinate in a 1:1 ratio.

The following reagents were used: ammonium nitrate solution[5] (10% w/v). Saturated reinecke salt solution[6] ($3 \times 10^{-3}$ *M*), ammonium thiocyanate[6] (0.01 *M*), ferric ammonium sulfate solution indicator[5], hydrochloric acid[5] (0.1 and 0.01 *M*), methylene blue solution indicator[6], silver nitrate solution[5] (0.01 *M*), and sodium hydroxide solution[6] (0.1 and 0.01 *M*, 20% w/v).

For the standard solution, dimenhydrinate (0.5 g) was dissolved in 100 ml of methanol[6] (analytical reagent).

**Sample Preparation**—An equivalent weight of a single-powdered tablet from a composite of 20 tablets was placed in a 50-ml volumetric flask and dissolved in 20 ml of methanol; then 0.5 ml of concentrated hydrochloric acid was added. The mixture was allowed to stand for 20 min with intermittent shaking. It was filtered through filter paper[7] into a dry 50-ml volumetric flask and brought to volume by rinsing with methanol.

**Procedure**—Twenty milliliters of the standard (or of the appropriately prepared sample) solution was transferred to a 100-ml volumetric flask. To it was added 0.5 ml of hydrochloric acid followed by 50 ml of saturated reinecke salt solution. The contents were shaken vigorously for 5 min. The precipitate was filtered through a sintered-glass crucible ($G_4$) and washed with 10 ml of chilled 0.02% (w/v) aqueous solution of reinecke salt. Then the precipitate was dried in a vacuum desiccator, dissolved in acetone, and transferred quantitatively to a 50-ml volumetric flask. It was brought to volume with acetone (stock). Appropriate dilutions were made, and the solution was transferred into a cell. Absorbance was determined at 540 nm *versus* a blank prepared from 20 ml of methanol and treated identically.

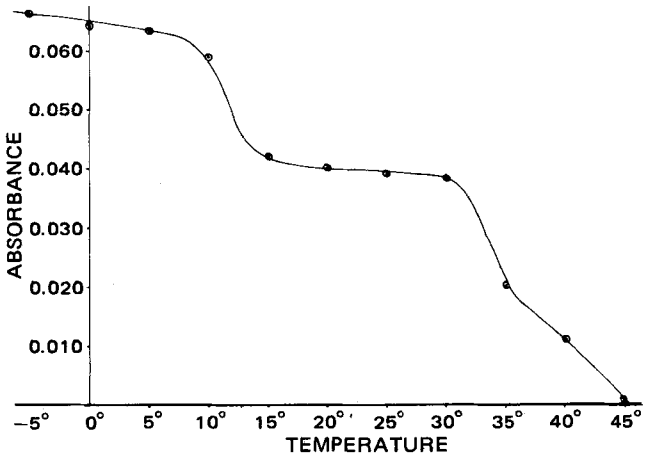


**Figure 1**—*Plot showing the absorbance* versus *temperature of dimenhydrinate with reinecke salt at 540 nm between −5 and +45°.*

## RESULTS AND DISCUSSION

Dimenhydrinate purity was ascertained by BP methods (1) and found to be 97.5 ± 0.5%. The absorbances of the colored precipitate were measured at various wavelengths ranging from 400 to 650 nm. The maximum absorbance was at 540 nm. The stability of the dimenhydrinate–reinecke salt precipitate determined at 27 ± 2° was >2 hr.

The effect of temperature on the formation of the colored precipitate was investigated using a constant-temperature water bath ranging from −5 to +5°; a $1.5 \times 10^{-3}$ *M* methanolic solution of dimenhydrinate and a $1.5 \times 10^{-3}$ *M* aqueous solution of reinecke salt (Fig. 1) were employed. Figure 1 shows two near-plateau regions, one from −5 to 7.5° and the other from 15 to 30°. The experiments were carried out at room temperature (27 ± 2°).

[1] Spectronic 20, Bausch & Lomb.
[2] H. Jurgen & Co., Bremen, West Germany.
[3] Gallenkamp.
[4] Contained 50 mg of dimenhydrinate.
[5] B.D.H. Chemicals, Poole, England.
[6] E. Merck, Darmstadt, West Germany.
[7] Whatman No. 1.



0022-3549/81/0600-0690$01.00/0
© 1981, American Pharmaceutical Association

**Table I—Average Percentage of Dimenhydrinate in Laboratory-Made Mixtures and in Commercial Samples by Proposed Method and BP Method**

| Mixture (M) (1:1) | Proposed Method Mean, %[a] | ±SD | BP Method Mean, %[a] | ±SD |
|---|---|---|---|---|
| Dimenhydrinate + aspirin ($M_1$) | 99.32 | 0.82 | 98.48 | 1.06 |
| Dimenhydrinate + acetaminophen ($M_2$) | 99.76 | 0.36 | 98.93 | 0.31 |
| Dimenhydrinate + meprobamate ($M_3$) | 98.88 | 0.39 | 98.70 | 0.65 |
| Dimenhydrinate + phenylephrine ($M_4$) | 99.76 | 0.37 | 98.82 | 0.08 |
| Dimenhydrinate + tolbutamide ($M_5$) | 99.32 | 0.31 | 99.71 | 0.19 |
| Commercial tablet[b] $T_1$ | 101.86 | 0.64 | 101.16 | 0.80 |
| Commercial tablet[b] $T_2$ | 100.53 | 0.47 | 100.44 | 0.48 |

[a] Average of four determinations. [b] Each tablet contained 50 mg of dimenhydrinate.

The effect of pH (1.60–11.20) on the absorbance of the colored precipitate (in acetone) was studied. Hydrochloric acid was used to vary the pH from 4.10 to 1.60, and dilute ammonia solution was used to vary it from 4.10 to 11.20. However, absorbance was not affected within a pH range of 2.85–8.30.

The stoichiometric balance was determined by Job's method of continuous variation (9) and a slope-ratio method (10). In Job's method, the maximum absorbance was obtained when $V_1/(V_1 + V_2) = 0.33$, which indicated the formation of the dimenhydrinate–reinecke salt precipitate in a 1:2 molar ratio. In the slope-ratio method, the $slope_1$ and $slope_2$ values were 0.0027586 and 0.0014210 $ml^{-1}$, respectively. Hence, $slope_1/slope_2$ for the precipitate was nearly equal to 2, thereby suggesting a 1:2 molar ratio.

Reinecke salt had a solubility in water of 1 in 52. Therefore, 50 ml of a saturated aqueous solution of reinecke salt was added to a 20-ml aliquot of a methanolic solution of dimenhydrinate to establish the 1:2 molar ratio requirement for maximum precipitation of dimenhydrinate.

**Table II—Recovery Experiments by Proposed Method**

| Mixture or Tablet | Quantity of Dimenhydrinate Added, g | Corresponding Concentration of Dilution Measured, g % | Mean, %[a] | ±SD |
|---|---|---|---|---|
| $M_1$ | 0.600 | 0.096 | 99.36 | 0.40 |
| $M_2$ | 0.025 | 0.075 | 99.12 | 0.66 |
| $M_3$ | 0.020 | 0.072 | 99.01 | 0.76 |
| $M_4$ | 0.055 | 0.093 | 99.36 | 0.12 |
| $M_5$ | 0.035 | 0.081 | 98.69 | 0.52 |
| $T_1$ | 0.005 | 0.033 | 99.93 | 1.17 |
| $T_2$ | 0.010 | 0.036 | 99.41 | 0.64 |

[a] Average for four determinations.

After the optimal experimental conditions for the maximal precipitation of dimenhydrinate–reinecke salt were established, the Beer's plot was obtained by employing the stock solution of the dimenhydrinate–reinecke salt precipitate in acetone. It obeyed Beer's law in the concentration range of 200–1000 μg/ml. With the least-squares method, the calibration curve from the data obtained can be described by the following regression equation: $A = 0.0045 + 1.905C$, where the regression coefficient is 0.999.

Five laboratory-made mixtures and two commercial tablet samples containing dimenhydrinate were subjected to analysis by the proposed method and the BP method (1) (Table I).

The activity of phenylephrine was checked directly with the reagent under identical experimental conditions and was found not to react.

To justify the repeatability of the proposed method, known amounts of pure dimenhydrinate were added to preanalyzed samples of mixtures and dosage forms and reassayed by the proposed method (Table II).

The presence of either pure drugs, *i.e.*, aspirin, acetaminophen, meprobamate, phenylephrine, and tolbutamide, or tablet adjuncts like starch, lactose, talc, and magnesium stearate in the quantities used caused no detectable interference in the proposed method. The analyses of two commercial products and the efficient percentage recoveries and significant reproducibility obtained suggest the feasibility of utilizing the proposed method for the quantitation of dimenhydrinate.

## REFERENCES


(1) "British Pharmacopoeia 1973," Her Majesty's Stationery Office, London, England, 1973, p. 167.

(2) "The United States Pharmacopeia," 18th rev., Mack Publishing Co., Easton, Pa., 1970, p. 203.

(3) "Specifications for the Quality Control of Pharmaceutical Preparations," 2nd ed., World Health Organization, Geneva, Switzerland, 1967, p. 180.

(4) R. Mestres and J. L. Berges, *Trav. Soc. Pharm. Montpellier*, **31**, 335 (1971).

(5) H. de Almeida Costa, *Rev. Brasil Farm.*, **45**, 161 (1964).

(6) C. B. Quentin and H. W. Sievert, *J. Lab. Clin. Med.*, **46**, 628 (1955).

(7) N. M. Sanghavi and M. G. Pai, *East. Pharm.*, **19**, 119 (1976).

(8) K. A. Connors, "A Textbook of Pharmaceutical Analysis," Wiley-Interscience New York, N.Y., 1975, p. 432.

(9) P. Job., *Ann. Chim.*, **9**, 113 (1929).

(10) A. E. Harvey and D. E. Manning, *J. Am. Chem. Soc.*, **16**, 4488 (1950).


## ACKNOWLEDGMENTS


The authors thank Professor P. Iwe. Akubue, Dean, Faculty of Pharmaceutical Sciences, for interest and encouragement and M/S Searle (India) Ltd., Bombay, for the reference sample of dimenhydrinate.


# Characteristics of Equilibrium Reaction of Zolazepam


**WEN-HAI HONG * and DALE H. SZULCZEWSKI ‡x**



Received September 18, 1980, from **Analytical Research and ‡Product Development, Warner-Lambert Pharmaceutical Research Division, Warner-Lambert Company, Morris Plains, NJ 07950.* Accepted for publication November 17, 1980.



**Abstract** □ The equilibrium reaction of zolazepam, a pyrazolodiazepinone, was studied and analyzed using the approach used previously for other pyrazolodiazepinone derivatives. The intrinsic ring closure equilibrium constant for this reaction was ~100 times larger than that observed for pyrazolodiazepinones studied previously. This study illustrates that the diazepinone ring can dominate in equilibrium mixtures formed at pH values far below the pKa of the corresponding open form.



**Keyphrases** □ Zolazepam—analysis of equilibrium reaction □ Structure–activity relationships—equilibrium reaction of zolazepam □ Pyrazolodiazepinones—equilibrium reaction of zolazepam □ Equilibrium—analysis of zolazepam in reaction


The characteristics of the equilibrium reaction of certain pyrazolodiazepinones were reported previously (1). This study was an extension of that work and concerned the equilibrium behavior of zolazepam, 4-(*o*-fluorophen-


*0022-3549/81/0600-0691$01.00/0*


*© 1981, American Pharmaceutical Association*

**Table I—Average Percentage of Dimenhydrinate in Laboratory-Made Mixtures and in Commercial Samples by Proposed Method and BP Method**

| Mixture (M) (1:1) | Proposed Method Mean, %[a] | ±SD | BP Method Mean, %[a] | ±SD |
|---|---|---|---|---|
| Dimenhydrinate + aspirin ($M_1$) | 99.32 | 0.82 | 98.48 | 1.06 |
| Dimenhydrinate + acetaminophen ($M_2$) | 99.76 | 0.36 | 98.93 | 0.31 |
| Dimenhydrinate + meprobamate ($M_3$) | 98.88 | 0.39 | 98.70 | 0.65 |
| Dimenhydrinate + phenylephrine ($M_4$) | 99.76 | 0.37 | 98.82 | 0.08 |
| Dimenhydrinate + tolbutamide ($M_5$) | 99.32 | 0.31 | 99.71 | 0.19 |
| Commercial tablet[b] $T_1$ | 101.86 | 0.64 | 101.16 | 0.80 |
| Commercial tablet[b] $T_2$ | 100.53 | 0.47 | 100.44 | 0.48 |

[a] Average of four determinations. [b] Each tablet contained 50 mg of dimenhydrinate.

The effect of pH (1.60–11.20) on the absorbance of the colored precipitate (in acetone) was studied. Hydrochloric acid was used to vary the pH from 4.10 to 1.60, and dilute ammonia solution was used to vary it from 4.10 to 11.20. However, absorbance was not affected within a pH range of 2.85–8.30.

The stoichiometric balance was determined by Job's method of continuous variation (9) and a slope-ratio method (10). In Job's method, the maximum absorbance was obtained when $V_1/(V_1 + V_2) = 0.33$, which indicated the formation of the dimenhydrinate–reinecke salt precipitate in a 1:2 molar ratio. In the slope-ratio method, the $slope_1$ and $slope_2$ values were 0.0027586 and 0.0014210 $ml^{-1}$, respectively. Hence, $slope_1/slope_2$ for the precipitate was nearly equal to 2, thereby suggesting a 1:2 molar ratio.

Reinecke salt had a solubility in water of 1 in 52. Therefore, 50 ml of a saturated aqueous solution of reinecke salt was added to a 20-ml aliquot of a methanolic solution of dimenhydrinate to establish the 1:2 molar ratio requirement for maximum precipitation of dimenhydrinate.

**Table II—Recovery Experiments by Proposed Method**

| Mixture or Tablet | Quantity of Dimenhydrinate Added, g | Corresponding Concentration of Dilution Measured, g % | Mean, %[a] | ±SD |
|---|---|---|---|---|
| $M_1$ | 0.600 | 0.096 | 99.36 | 0.40 |
| $M_2$ | 0.025 | 0.075 | 99.12 | 0.66 |
| $M_3$ | 0.020 | 0.072 | 99.01 | 0.76 |
| $M_4$ | 0.055 | 0.093 | 99.36 | 0.12 |
| $M_5$ | 0.035 | 0.081 | 98.69 | 0.52 |
| $T_1$ | 0.005 | 0.033 | 99.93 | 1.17 |
| $T_2$ | 0.010 | 0.036 | 99.41 | 0.64 |

[a] Average for four determinations.

After the optimal experimental conditions for the maximal precipitation of dimenhydrinate–reinecke salt were established, the Beer's plot was obtained by employing the stock solution of the dimenhydrinate–reinecke salt precipitate in acetone. It obeyed Beer's law in the concentration range of 200–1000 μg/ml. With the least-squares method, the calibration curve from the data obtained can be described by the following regression equation: $A = 0.0045 + 1.905C$, where the regression coefficient is 0.999.

Five laboratory-made mixtures and two commercial tablet samples containing dimenhydrinate were subjected to analysis by the proposed method and the BP method (1) (Table I).

The activity of phenylephrine was checked directly with the reagent under identical experimental conditions and was found not to react.

To justify the repeatability of the proposed method, known amounts of pure dimenhydrinate were added to preanalyzed samples of mixtures and dosage forms and reassayed by the proposed method (Table II).

The presence of either pure drugs, *i.e.*, aspirin, acetaminophen, meprobamate, phenylephrine, and tolbutamide, or tablet adjuncts like starch, lactose, talc, and magnesium stearate in the quantities used caused no detectable interference in the proposed method. The analyses of two commercial products and the efficient percentage recoveries and significant reproducibility obtained suggest the feasibility of utilizing the proposed method for the quantitation of dimenhydrinate.

## REFERENCES


(1) "British Pharmacopoeia 1973," Her Majesty's Stationery Office, London, England, 1973, p. 167.

(2) "The United States Pharmacopeia," 18th rev., Mack Publishing Co., Easton, Pa., 1970, p. 203.

(3) "Specifications for the Quality Control of Pharmaceutical Preparations," 2nd ed., World Health Organization, Geneva, Switzerland, 1967, p. 180.

(4) R. Mestres and J. L. Berges, *Trav. Soc. Pharm. Montpellier*, **31**, 335 (1971).

(5) H. de Almeida Costa, *Rev. Brasil Farm.*, **45**, 161 (1964).

(6) C. B. Quentin and H. W. Sievert, *J. Lab. Clin. Med.*, **46**, 628 (1955).

(7) N. M. Sanghavi and M. G. Pai, *East. Pharm.*, **19**, 119 (1976).

(8) K. A. Connors, "A Textbook of Pharmaceutical Analysis," Wiley-Interscience New York, N.Y., 1975, p. 432.

(9) P. Job., *Ann. Chim.*, **9**, 113 (1929).

(10) A. E. Harvey and D. E. Manning, *J. Am. Chem. Soc.*, **16**, 4488 (1950).


## ACKNOWLEDGMENTS


The authors thank Professor P. Iwe. Akubue, Dean, Faculty of Pharmaceutical Sciences, for interest and encouragement and M/S Searle (India) Ltd., Bombay, for the reference sample of dimenhydrinate.


# Characteristics of Equilibrium Reaction of Zolazepam


**WEN-HAI HONG * and DALE H. SZULCZEWSKI ‡x**



Received September 18, 1980, from **Analytical Research and ‡Product Development, Warner-Lambert Pharmaceutical Research Division, Warner-Lambert Company, Morris Plains, NJ 07950.* Accepted for publication November 17, 1980.



**Abstract** □ The equilibrium reaction of zolazepam, a pyrazolodiazepinone, was studied and analyzed using the approach used previously for other pyrazolodiazepinone derivatives. The intrinsic ring closure equilibrium constant for this reaction was ~100 times larger than that observed for pyrazolodiazepinones studied previously. This study illustrates that the diazepinone ring can dominate in equilibrium mixtures formed at pH values far below the pKa of the corresponding open form.



**Keyphrases** □ Zolazepam—analysis of equilibrium reaction □ Structure–activity relationships—equilibrium reaction of zolazepam □ Pyrazolodiazepinones—equilibrium reaction of zolazepam □ Equilibrium—analysis of zolazepam in reaction


The characteristics of the equilibrium reaction of certain pyrazolodiazepinones were reported previously (1). This study was an extension of that work and concerned the equilibrium behavior of zolazepam, 4-(*o*-fluorophen-


*0022-3549/81/0600-0691$01.00/0*


*© 1981, American Pharmaceutical Association*

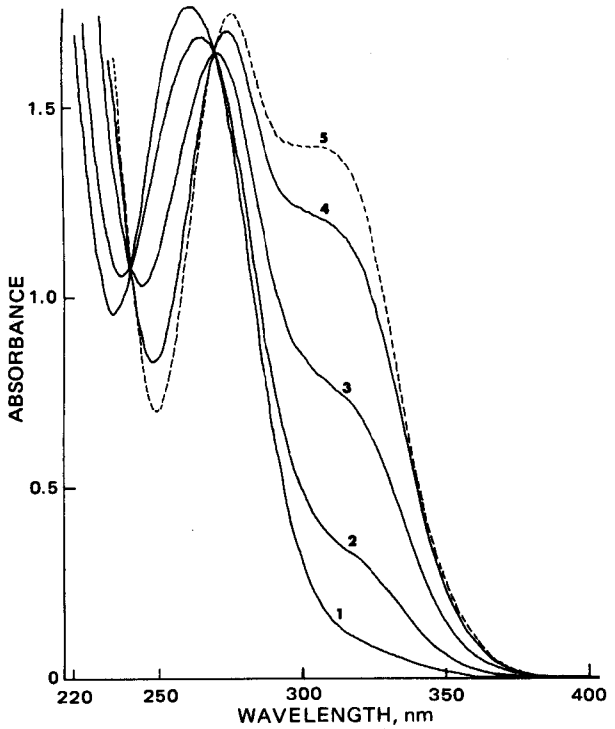


**Figure 1**—*Sequential spectra obtained for the equilibration of II at pH 3.70, 27°. Spectra 1, 2, 3, and 4 were obtained after 1, 7, 24, and 265 hr, respectively. Spectrum 4 corresponds to complete equilibration. Spectrum 5 is what would be obtained if conversion of II to I were complete.*

yl) - 6,8 - dihydro-1,3,8-trimethylpyrazolo[3,4-*e*][1,4]diazepine-7(1*H*)-one hydrochloride (I). While the nature of the reaction that occurred here was similar to that described previously, quantitative aspects differed.

## EXPERIMENTAL

**Reagents**—All chemicals used for the 0.1 and 0.05 *M* citrate and phosphate buffers of known pH values were reagent grade and were used without further purification. The hydrochloric acid solutions were prepared from prestandardized volumetric solutions[1]. The solvents, including hydrochloric acid solutions and buffers of varying pH used for kinetic studies, were adjusted to an ionic strength of 0.3 with potassium chloride. 5-(*N*-Methylaminoacetamido)-1,3-dimethyl-4-*o*-fluorobenzoylpyrazole sulfate (IIc) was used as received[2].

**Instrumentation**—The pH measurements were made using direct reading, digital pH meters[3]. UV spectra were obtained using a recording UV spectrophotometer[4].

**Equilibrium Studies**—Approximately 0.05 mEq of IIc was weighed accurately and transferred quantitatively to a 25-ml volumetric flask, using 1 ml of water to dissolve the compound. The reaction was initiated by diluting to volume with thermally equilibrated (27°) buffer with an ionic strength of 0.3 (potassium chloride). After mixing, the volumetric flasks were placed immediately in a constant-temperature water bath (27°). At appropriate intervals, 2-ml aliquots were removed, diluted to 25 ml with 0.1 *N* HCl, and mixed.

The UV spectra of the resulting solutions were obtained immediately following their preparation over 400–230 nm, using 1-cm silica cells and 0.1 *N* HCl as a blank. Samples were removed, and their spectra were obtained until redundancy was reached. The fraction of total II at equilibrium, $f_{II_T}$, was calculated by the formula: $(0.85A_i - A_{310})/0.781A_i$, where $A_i$ and $A_{310}$ are the absorbances at 271 (isosbestic point) and 310 nm, respectively. In this formula, $0.85A_i$ represents the theoretical absorbance at 310 nm for complete conversion from II to I, and $0.781A_i$ represents the expected absorbancy difference at 310 nm for complete conversion of II to I.

[1] Acculute, Anachemia Chemicals Ltd.
[2] Dr. H. Dewald, Chemistry Department, Parke-Davis/Warner-Lambert Co.
[3] Orion model 701.
[4] Cary model 11 or 14.

## RESULTS AND DISCUSSION

Typical sequential UV spectra obtained during equilibration are shown in Fig. 1. The starting material was the open form of I, 5-(*N*-methylaminoacetamido)-1,3-dimethyl-4-*o*-fluorobenzoylpyrazole (II). When II was the reactant, the spectra changed irrespective of the solution pH. When I was the starting material, changes in spectra with time were seen only at pH values of ≤6.0. As seen in Fig. 1, the spectrum of II changed to a spectrum closely resembling the spectrum of I. Isosbestic points at 240 and 271 nm were clear and sharp. At a given pH, the same redundant spectrum was produced irrespective of whether I or II was the starting material. The terminal spectra produced at pH values of ≤6.0 corresponded to the spectrum expected for mixtures of I and II containing up to 18% of II and 82% of I. The quantitative composition of equilibrium mixtures formed at various pH values is given in Table I.

The fraction of the open form ($f_{II_T}$) present at equilibrium for these systems is given by (1):

$$f_{II_T} = \frac{K_a^{IIb} + a_{H^+}}{K_a^{IIb} + a_{H^+} + K_a^{IIb}K^{*\prime}(K_a^{Ib} + a_{H^+})} = \frac{(II_T)}{(I_T) + (II_T)} \quad \text{(Eq. 1)}$$

where $I_T = (Ia) + (Ib)$, $II_T = (IIa) + (IIb)$, and:

$$K_a^{Ib} = \frac{(Ia)(H^+)}{(Ib)} \quad \text{(Eq. 2)}$$

$$K_a^{IIb} = \frac{(IIa)(H^+)}{(IIb)} \quad \text{(Eq. 3)}$$

In Eq. 1, $f_{II_T}$, $K_a^{IIb}$, and $K_a^{Ib}$ are experimentally determined known quantities (Tables I and II). Equation 1 can be rearranged so that the intrinsic ring closure constant $K^{*\prime}$ is in terms of these known quantities:

$$K^{*\prime} = \frac{(K_a^{IIb} + a_{H^+})(1 - f_{II_T})}{K_a^{IIb}(K_a^{Ib} + a_{H^+})f_{II_T}} = \frac{(Ib)}{(IIa)(H^+)} \quad \text{(Eq. 4)}$$

The value of $K^{*\prime}$ for this system was determined using Eq. 4 together with the values of $f_{II_T}$ given in Table I. The resulting values of $K^{*\prime}$ are given in Table III. As seen, the intrinsic ring closure constant for this system was ~100 times greater than it was for the ripazepam system studied previously (1).

When the values of $K^{*\prime}$, $K_a^{Ib}$, and $K_a^{IIb}$ given in Tables II and III are substituted in Eq. 1 and the values of $f_{II_T}$ are generated, the solid line shown in Fig. 2 is obtained. The calculated values correlate well with those determined by spectroscopic analysis of the equilibrium mixtures.

**Table I—Composition of Equilibrium Mixtures of I and II in Terms of $f_{II_T}$**

| pH | $f_{II_T}$[a] |
|---|---|
| 3.70 | 0.18 |
| 4.26 | 0.15 |
| 4.83 | 0.09 |
| 5.35 | 0.04 |
| 6.04 | 0.01 |

[a] These values were determined by analysis of the redundant, terminal UV spectrum obtained when equilibration was complete.

**Table II—Dissociation Constants**

| Compound | pKa | $K_a$, *M* |
|---|---|---|
| Ib[a] | 4.69 | $2.04 \times 10^{-5}$ |
| IIb[b] | 7.52 | $3.02 \times 10^{-8}$ |

[a] Determined spectrophotometrically. [b] Determined titrimetrically.

**Table III—Calculation of $K^{*\prime}$ Using Eq. 4**

| pH | $K^{*\prime}$, $M^{-1}$ |
|---|---|
| 3.70 | $1.70 \times 10^8$ |
| 4.26 | $1.48 \times 10^8$ |
| 4.83 | $1.13 \times 10^8$ |
| 5.35 | $1.14 \times 10^8$ |
| 6.04 | $1.45 \times 10^8$ |
| Average | $1.38 \times 10^8$ |

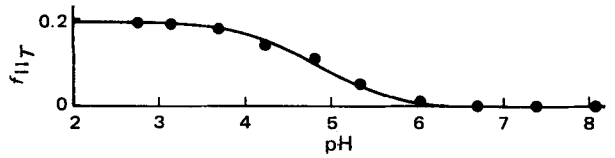


**Figure 2**—*Plot of* $f_{II_T}$ versus *pH*.

As indicated previously, at pH values below the pKa values of open and closed forms, Eq. 1 reaches a limit:

$$\lim f_{II_T}^{a\,H^+\to\infty} = \frac{1}{1 + K^{*\prime}K_a^{IIb}} \qquad \text{(Eq. 5)}$$

As seen from Eq. 5, the maximum concentration of the open form (II) that can exist in these systems depends not only on the pKa of the open form ($K_a^{IIb}$) but also on the value of the ring closure constant ($K^{*\prime}$). If, as is the case here, the value of $K^{*\prime}$ is very large ($1.38 \times 10^8\ M^{-1}$), then the maximum concentration of the open form at equilibrium is small irrespective of the solution's pH. The ring form then dominates. This situation is best understood by considering the reaction shown in Scheme I. An increase in hydrogen-ion activity serves not only to convert II to its unreactive protonated form but also to promote dehydration.

The marked increase in the value of the ring closure constant observed here may be attributed to a methyl group in position 4 of the diazepinone ring (1). Also important is the electronic distribution around the imino carbon atom (position 8). Zolazepam is a stronger base than ripazepam by a factor of 10 (1). This finding suggests that electron withdrawal from this carbon is less here than in the previous system. Attack by water would be hindered, and the ring form would be stabilized.

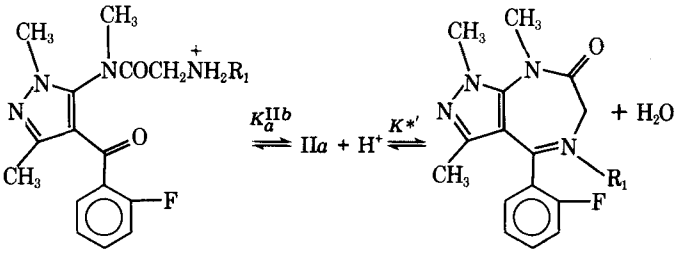


IIa: $R_1$ absent, no charge
IIb: $R_1$ = H, charge +1
IIc: IIa · $H_2SO_4$

Ia: $R_1$ absent, no charge
Ib: $R_1$ = H, charge +1

*Scheme I*

## REFERENCES

(1) W. H. Hong, C. Johnston, and D. H. Szulczewski, *J. Pharm. Sci.*, **66**, 1703 (1977).

## ACKNOWLEDGMENTS

The authors thank Dr. Kulier and Dr. DeWald for synthesizing the compounds, Mrs. D. Ayres for typing the manuscript, and Mr. F. C. Ninger for encouragement and support.

# Improved Assay for Mixtures of Citrate and Citric Acid in Systemic Alkalizer Solutions

**HENRY S. I. TAN ˣ, DIANNE M. McKIBBEN, and ARTHUR C. GLASSER**

Received May 30, 1980, from the *College of Pharmacy, University of Cincinnati–Medical Center, Cincinnati, OH 45267.* Accepted for publication November 4, 1980.

**Abstract** □ A modification of the USP method for the assay of systemic alkalizer solutions containing mixtures of citrate and citric acid is presented; it involves two titrations and ion-exchange chromatography. A diluted sample is titrated with 0.02 *N* NaOH to find the free citric acid content. The eluate from cation-exchange chromatography of an equal volume of diluted sample is titrated with 0.02 *N* NaOH to assay for total citric acid. Subtracting the results of the first titration from the second provides the citrate content. Synthetic mixtures of potassium citrate–citric acid, potassium citrate–sodium citrate–citric acid, and sodium citrate–citric acid were prepared and assayed. The method was applied to commercially available preparations. The proposed method eliminates some significant errors of the compendial method, and the accuracy and reproducibility are equal or better than those obtained with the compendial method. Theoretically, the result obtained by the compendial method does not necessarily give the citrate content.

**Keyphrases** □ Citrate–citric acid mixtures—improved assay of systemic alkalizer solutions □ Citric acid–citrate mixtures—improved assay of systemic alkalizer solutions □ Alkalizer—improved assay of citrate–citric acid mixtures

The compendial method for the assay of mixtures of citrate and citric acid solutions is a combination of an electrometric and visual titration (1). Direct application of this compendial method for the assay of citrate and citric acid to recently available commercial systemic alkalizer solutions such as potassium citrate–citric acid oral solution (I), potassium citrate–sodium citrate–citric acid oral solution (II), and sodium citrate–citric acid oral solution (III) is not practical since the preparations are generally colored and are assayed in undiluted form. Moreover, the titrants used are 1 *N* in strength. Since these difficulties allow for many sources of error, a more appropriate assay is desired for the quality control of these commercial preparations.

Alkali salts of organic acids have been analyzed by passing an aqueous solution of the salt through an ion-exchange column followed by titration of the eluate with a base (2, 3). The ion-exchange principle is included in the analysis of commercial systemic alkalizer solutions containing mixtures of citrate and citric acid. The method is simple, and the reproducibility and accuracy are equal or better than those obtained with the USP method.

## EXPERIMENTAL

**Reagents and Chemicals**—Citric acid monohydrate[1], potassium citrate monohydrate[1], sodium citrate dihydrate[1], a sulfonated polystyrene copolymer strong cation-exchange resin in the hydrogen form[2] (medium porosity), a 0.02 *N* NaOH volumetric solution obtained by quantitative dilution of 1 *N* NaOH (4), and phenolphthalein indicator solution were used. All other chemicals were reagent grade and were used without purification.

[1] Fisher Scientific Co., Fair Lawn, N.J.
[2] Rexyn 101 (H), Fisher Scientific Co., Fair Lawn, N.J.

0022-3549/81/0600-0693$01.00/0
© 1981, American Pharmaceutical Association

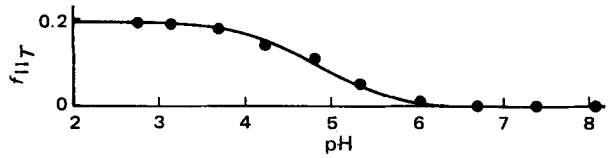


**Figure 2**—*Plot of* $f_{II_T}$ versus *pH*.

As indicated previously, at pH values below the pKa values of open and closed forms, Eq. 1 reaches a limit:

$$\lim f_{II_T}^{a\,H^+\to\infty} = \frac{1}{1 + K^{*\prime}K_a^{IIb}} \qquad \text{(Eq. 5)}$$

As seen from Eq. 5, the maximum concentration of the open form (II) that can exist in these systems depends not only on the pKa of the open form ($K_a^{IIb}$) but also on the value of the ring closure constant ($K^{*\prime}$). If, as is the case here, the value of $K^{*\prime}$ is very large ($1.38 \times 10^8\ M^{-1}$), then the maximum concentration of the open form at equilibrium is small irrespective of the solution's pH. The ring form then dominates. This situation is best understood by considering the reaction shown in Scheme I. An increase in hydrogen-ion activity serves not only to convert II to its unreactive protonated form but also to promote dehydration.

The marked increase in the value of the ring closure constant observed here may be attributed to a methyl group in position 4 of the diazepinone ring (1). Also important is the electronic distribution around the imino carbon atom (position 8). Zolazepam is a stronger base than ripazepam by a factor of 10 (1). This finding suggests that electron withdrawal from this carbon is less here than in the previous system. Attack by water would be hindered, and the ring form would be stabilized.

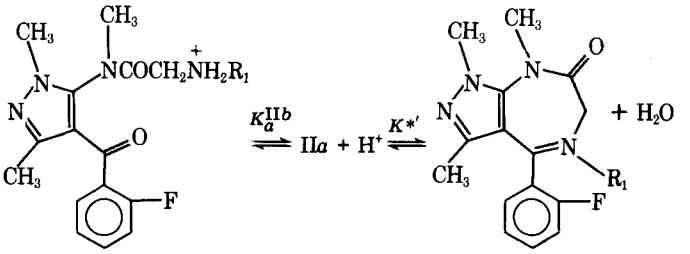


IIa: $R_1$ absent, no charge
IIb: $R_1$ = H, charge +1
IIc: IIa · $H_2SO_4$

Ia: $R_1$ absent, no charge
Ib: $R_1$ = H, charge +1

*Scheme I*

## REFERENCES

(1) W. H. Hong, C. Johnston, and D. H. Szulczewski, *J. Pharm. Sci.*, **66**, 1703 (1977).

## ACKNOWLEDGMENTS

The authors thank Dr. Kulier and Dr. DeWald for synthesizing the compounds, Mrs. D. Ayres for typing the manuscript, and Mr. F. C. Ninger for encouragement and support.

# Improved Assay for Mixtures of Citrate and Citric Acid in Systemic Alkalizer Solutions

**HENRY S. I. TAN ˣ, DIANNE M. McKIBBEN, and ARTHUR C. GLASSER**

Received May 30, 1980, from the *College of Pharmacy, University of Cincinnati–Medical Center, Cincinnati, OH 45267.* Accepted for publication November 4, 1980.

**Abstract** □ A modification of the USP method for the assay of systemic alkalizer solutions containing mixtures of citrate and citric acid is presented; it involves two titrations and ion-exchange chromatography. A diluted sample is titrated with 0.02 *N* NaOH to find the free citric acid content. The eluate from cation-exchange chromatography of an equal volume of diluted sample is titrated with 0.02 *N* NaOH to assay for total citric acid. Subtracting the results of the first titration from the second provides the citrate content. Synthetic mixtures of potassium citrate–citric acid, potassium citrate–sodium citrate–citric acid, and sodium citrate–citric acid were prepared and assayed. The method was applied to commercially available preparations. The proposed method eliminates some significant errors of the compendial method, and the accuracy and reproducibility are equal or better than those obtained with the compendial method. Theoretically, the result obtained by the compendial method does not necessarily give the citrate content.

**Keyphrases** □ Citrate–citric acid mixtures—improved assay of systemic alkalizer solutions □ Citric acid–citrate mixtures—improved assay of systemic alkalizer solutions □ Alkalizer—improved assay of citrate–citric acid mixtures

The compendial method for the assay of mixtures of citrate and citric acid solutions is a combination of an electrometric and visual titration (1). Direct application of this compendial method for the assay of citrate and citric acid to recently available commercial systemic alkalizer solutions such as potassium citrate–citric acid oral solution (I), potassium citrate–sodium citrate–citric acid oral solution (II), and sodium citrate–citric acid oral solution (III) is not practical since the preparations are generally colored and are assayed in undiluted form. Moreover, the titrants used are 1 *N* in strength. Since these difficulties allow for many sources of error, a more appropriate assay is desired for the quality control of these commercial preparations.

Alkali salts of organic acids have been analyzed by passing an aqueous solution of the salt through an ion-exchange column followed by titration of the eluate with a base (2, 3). The ion-exchange principle is included in the analysis of commercial systemic alkalizer solutions containing mixtures of citrate and citric acid. The method is simple, and the reproducibility and accuracy are equal or better than those obtained with the USP method.

## EXPERIMENTAL

**Reagents and Chemicals**—Citric acid monohydrate[1], potassium citrate monohydrate[1], sodium citrate dihydrate[1], a sulfonated polystyrene copolymer strong cation-exchange resin in the hydrogen form[2] (medium porosity), a 0.02 *N* NaOH volumetric solution obtained by quantitative dilution of 1 *N* NaOH (4), and phenolphthalein indicator solution were used. All other chemicals were reagent grade and were used without purification.

[1] Fisher Scientific Co., Fair Lawn, N.J.
[2] Rexyn 101 (H), Fisher Scientific Co., Fair Lawn, N.J.

0022-3549/81/0600-0693$01.00/0
© 1981, American Pharmaceutical Association

**Table I—Recovery Data from Synthetic Mixtures of I–III**

| Sample | Amount Analyzed[a], mg/ml | | Amount Found[b], mg/ml | | | | Recovery ± *SD*, % | | | |
|---|---|---|---|---|---|---|---|---|---|---|
| | | | Proposed Method | | USP XX Method | | Proposed Method | | USP XX Method | |
| | A | B | A | B | A | B | A | B | A | B |
| I | 220.2 | 67.3 | 220.4 | 67.5 | 220.6 | 67.2 | 100.1 ±0.9 | 100.3 ±0.3 | 100.2 ±0.6 | 99.9 ±0.2 |
| II | 128.9[c] | 66.0 | 125.6[c] | 66.5 | 127.5[c] | 67.7 | 97.4 ±0.7 | 100.7 ±0.2 | 98.9 ±0.6 | 102.6 ±0.2 |
| III | 100.2 | 62.4 | 99.7 | 63.2 | 97.9 | 62.2 | 99.5 ±0.7 | 101.2 ±0.4 | 97.7 ±0.8 | 99.7 ±0.5 |

[a] A = potassium citrate monohydrate or sodium citrate dihydrate; B = citric acid monohydrate. [b] Average of three determinations. [c] Milliequivalents of total citrate per milliliter.

**Table II—Recovery Data from Commercial Preparations of I–III**

| Sample | Label Claim[a], mg/ml | | Amount Found[b], mg/ml | | | | Label Claim ± *SD*, % | | | |
|---|---|---|---|---|---|---|---|---|---|---|
| | | | Proposed Method | | USP XX Method | | Proposed Method | | USP XX Method | |
| | A | B | A | B | A | B | A | B | A | B |
| I[c] | 220.0 | 66.8 | 207.2 | 92.9 | 210.9 | 93.1 | 94.2 ±0.4 | 139.0 ±0.2 | 95.8 ±0.4 | 139.4 ±1.0 |
| II[c] | 128.4[d] | 66.8 | 124.8[d] | 68.3 | 123.7[d] | 67.2 | 97.2 ±0.4 | 102.2 ±0.1 | 96.3 ±0.6 | 100.7 ±0.4 |
| III[c] | 100.0 | 60.1 | 98.6 | 64.2 | 102.1 | 64.7 | 98.6 ±0.9 | 106.8 ±0.0 | 102.1 ±0.3 | 107.6 ±0.8 |

[a] A = potassium citrate monohydrate or sodium citrate dihydrate; B = citric acid monohydrate. [b] Average of three determinations. [c] Sample colors: I, wine red; II, green; and III, bright yellow. [d] Milliequivalents of total citrate per milliliter.

**Cation-Exchange Column**—Ten grams of cation-exchange resin was hydrated by mixing with 50 ml of glass-distilled water in a 100-ml beaker. The resin was allowed to settle, and the excess water was decanted until a slurry of resin remained in the beaker. The slurry was poured into a 15-mm i.d. × 300-mm long glass column, provided with a fritted disk and polytef stopcock, and the resin beads were allowed to settle into a homogeneous bed. Approximately 100 ml of glass-distilled water was used to wash the resin bed. The stopcock was closed when the water level was 1–2 mm above the resin bed.

**Assay for I and II**—A 15.0-ml aliquot of sample was transferred to a 250-ml volumetric flask and diluted to volume with distilled water.

*Free Citric Acid*—Five milliliters of the diluted sample was pipetted into a 250-ml erlenmeyer flask, and 25 ml of distilled water and 5 drops of phenolphthalein were added. The contents of the flask were swirled and titrated with 0.02 *N* NaOH. The quantity, in milligrams per milliliter, of citric acid monohydrate in the original sample was found using the formula $233.50 \times A$, where $A$ is the number of milliequivalents of sodium hydroxide[3] consumed in the titration.

*Total Citric Acid*—Five milliliters of the diluted sample was added carefully to the top of the resin bed in the column. A 250-ml erlenmeyer flask was placed below the column, and the stopcock was opened until the sample entered the resin bed. The sample was eluted with 60 ml of distilled water at a flow rate of ≃5 ml/min, and ~65 ml of eluate was collected. Then 5 drops of phenolphthalein was added to the eluate, and the contents were swirled and titrated with 0.02 *N* NaOH.

*Calculation of Citrate Content*—The quantity in the original sample, in milligrams per milliliter, of potassium citrate monohydrate in I was calculated using the formula $360.46 \times (B - A)$, or the quantity of total citrate ($C_6H_5O_7$) in II was calculated using the formula $210.10 \times (B - A)$, where $A$ is as defined previously and $B$ is the number of milliequivalents of sodium hydroxide[3] consumed in the titration of the cation-exchange column eluate.

**Assay for III**—Ten milliliters of the sample was transferred to a 100-ml volumetric flask and diluted to volume with distilled water. The directions given for the assay for I and II, beginning with *Free Citric Acid*, were followed with the exception of the calculation formulas. The quantity in the original sample, in milligrams per milliliter, of citric acid monohydrate was calculated using the formula $140.10 \times A$, and the quantity of sodium citrate dihydrate was calculated using the formula $196.07 \times (B - A)$, where $A$ and $B$ are as defined previously[4].

[3] Milliequivalents of sodium hydroxide equal milliliters of sodium hydroxide consumed in the titration × normality of sodium hydroxide. Constant equals equivalent weight × dilution factor. Dilution factor = (250 ml/5 ml) (1 ml/15 ml). Equivalent weight for citric acid monohydrate is 70.05; for potassium citrate monohydrate, it is 108.14; and for $C_6H_5O_7$, it is 63.03.

[4] Dilution factor = (100 ml/5 ml) (1 ml/10 ml). Constant equals equivalent weight times dilution factor. Equivalent weight of sodium citrate dihydrate is 98.04.

## RESULTS AND DISCUSSION

In the assay of citrate, the sample solution was passed through a strong cation-exchange resin. In the process, the cations such as potassium and sodium ions of the citrate were replaced by protons from the resin, resulting in an eluate containing citric acid. Since the sample also contained free citric acid, the titration of the eluate with base gave the total citric acid concentration. The free citric acid of the sample was titrated directly with base. When equal volumes of samples were used for the determination of free citric acid and of total citric acid, the difference in titrant consumption was equivalent to the quantity of citric acid derived from citrate. Studies indicated that citrate did not interfere in the direct titration of free citric acid with 0.02 *N* NaOH. Quantitative results also were obtained when pure potassium or sodium citrate solutions were passed through the column and the eluate was titrated with base.

Recovery data for synthetic mixtures containing mixtures of potassium and/or sodium citrate and citric acid are shown in Table I. The accuracy and precision were identical to those obtained by the compendial method. The proposed method was applied to the assay of commercial systemic alkalizer solutions (Table II). The compendial assay of these commercial preparations is usually subject to greater variations between individual samples, particularly in determining the end-point of the citric acid titration with base. The commercial preparations are generally colored and are analyzed in undiluted form. For example, one commercial product is a wine-red solution. As the wine-red solution is titrated with base to the phenolphthalein end-point, the color change to pink (or red) at the equivalence point is difficult to observe and a sharp end-point cannot be obtained. Since a 1 *N* NaOH titrant is used, each drop (~0.05 ml) of titrant from the equivalence point is equivalent to 3.5 mg of citric acid monohydrate. The coloring agent present in other commercial products also masks the color change at the equivalence point. This problem accounts for the relatively larger standard deviations for the compendial results as compared to those obtained by the proposed method (Table II). No problems were encountered in the titrations following the proposed method since a sharp end-point was obtained in each case.

The compendial assay for the citrate content in the mixture involves an electrometric titration to a predetermined pH of 1.55. Since the product of this titration is citric acid, the pH at the equivalence point is simply the pH of a solution of the total citric acid, which includes citric acid formed from citrate plus free citric acid already in the sample. Theoretically, the compendial method does not necessarily give the actual citrate content. A preparation containing the correct quantity of citrate but an incorrect amount of citric acid (as stated on a label claim) would give a wrong citrate content when the titration is conducted to a predetermined pH. Titration gives a true indication of the citrate content only when the quantity of free citric acid is correct. An electrometric titration to a predetermined pH is useful if the species analyzed is the only one that determines the end-point pH. The proposed method eliminates this

problem because the citrate assay and subsequent calculation directly reflect the citrate content, regardless of the original free citric acid concentration.

Approximate calculation of the pH at the equivalence point of the compendial citrate titration showed that the value differed markedly from the stated pH of 1.55. The calculated value of 1.81 was obtained when the preparation was assumed to contain the labeled quantities of citrate and citric acid, using a $K_{a_1}$ value of $7.45 \times 10^{-4}$ and a $K_{a_2}$ value of $1.73 \times 10^{-5}$ at 25° for citric acid (5) and assuming that the third dissociation was negligible. Applying the same approximate calculation to compute the pH at the equivalence point of a similar electrometric titration of citrate in anticoagulant citrate–dextrose solution gave a value of 2.07. This value was relatively close to the stated pH of 1.98 ± 0.02 (6).

Since commercial systemic alkalizer solutions contain additives such as preservatives, flavoring, and coloring agents, the assay of a solution placebo is recommended. The placebo should be subjected to the same analytical steps as the sample, and necessary corrections should be made for titrant consumption, if any, by the placebo. In contrast, the compendium directs the use of water as a blank in the electrometric titration of citrate and no blank runs for the titration of citric acid.

## REFERENCES


(1) "The United States Pharmacopeia," 20th rev., United States Pharmacopeial Convention, Rockville, Md., 1980, pp. 644, 729.

(2) M. L. Richardson, *Anal. Chim. Acta*, **24**, 46 (1961).

(3) S. M. Blaug, *J. Am. Pharm. Assoc., Sci. Ed.*, **45**, 274 (1956).

(4) "The United States Pharmacopeia," 20th rev., United States Pharmacopeial Convention, Rockville, Md., 1980, p. 1113.

(5) "CRC Handbook of Chemistry and Physics," 60th ed., CRC Press, Boca Raton, Fla., 1979, p. D-168.

(6) "The United States Pharmacopeia," 20th rev., United States Pharmacopeial Convention, Rockville, Md., 1980, p. 49.


## ACKNOWLEDGMENTS


Presented at the Pharmaceutical Analysis and Control Section, APhA Academy of Pharmaceutical Sciences, Washington, D.C. meeting, April 1980.


# Effect of Elevated Blood Glucose Levels on Hepatic Microsomal Enzyme System in Rats


**MARTIN B. SIDEMAN**



Received August 21, 1980, from the *Division of Pharmacotherapeutics, Arnold & Marie Schwartz College of Pharmacy and Health Sciences, Long Island University, Brooklyn, NY 11201.* Accepted for publication November 11, 1980.



**Abstract** □ Elevated blood glucose levels attained by *ad libitum* drinking of 20% glucose solution inhibited *in vivo* *O*-dealkylation associated with the hepatic microsomal enzyme system. Significant inhibition of biotransformation was demonstrated after 1 day, with the maximum occurring at 3 days. Inhibition was followed by a tendency to return to normal activity. Serum levels of substrate and product were determined by liquid chromatographic techniques using 55% acetonitrile and 45% 0.1 *M* acetic acid as the mobile phase.



**Keyphrases** □ Glucose levels, blood—effect of elevation on hepatic microsomal enzyme system, rats □ Microsomal enzyme system—effect of elevated blood glucose levels, rats □ Enzyme systems—effect of elevated blood glucose levels on hepatic microsomal enzymes, rats □ Biotransformation—effect of elevated blood glucose levels on hepatic microsomal enzyme system, rats


The following reactions (1) are catalyzed by the mixed-function oxidase enzymes of the hepatic microsomal system: *N*- and *O*-dealkylation, aromatic ring side-chain hydroxylation, sulfoxide formation, *N*-oxidation, *N*-hydroxylation, deamination of primary and secondary amines, and replacement of a sulfur by an oxygen atom. Previous investigators showed that elevated blood glucose levels have inhibitory effects on several of the biotransformations mentioned in addition to depressing the cytochrome P-450 levels of the system. Hartshorn *et al.* (2) demonstrated, by *in vitro* microsomal studies in rats, the inhibition of *N*-demethylation of ethylmorphine and aniline hydroxylase as well as depression of the cytochrome P-450 content. *In vitro* microsomal studies in mice (3) showed the inhibition of hexobarbital biotransformation, primarily oxidation of the side chain at C-5, and the *N*-dealkylation of benzphetamine in addition to cytochrome P-450 depression. Strother *et al.* (4), using the *in vivo* technique of increased sleep time, also showed that elevated blood glucose levels delayed the biotransformation of various barbiturates in mice.

This investigation established, by direct measurements in blood using liquid chromatography, that elevated blood glucose levels inhibit *O*-dealkylation associated with the hepatic microsomal system.

## EXPERIMENTAL

**Animals**—Adult male Sprague–Dawley rats, 180–200 g, were individually housed in temperature-, light-, humidity-, and air-controlled quarters. Commercial laboratory chow and drinking liquid, either water or 20% glucose solution, were given *ad libitum*.

**Liquid Chromatography**—A liquid chromatographic system containing a $C_{18}$ column and an absorbance detector fixed at 254 nm was used isocratically[1]. The mobile phase consisted of 55% acetonitrile (HPLC grade) and 45% of 0.1 *M* acetic acid. Prior to use, the mobile phase was passed through a solvent-clarification apparatus to remove gases and particulates which might affect the column. Solvent delivery was at a rate of 1 ml/min. Recordings were made at a chart speed of 0.5 cm/min.

**Reagents**—Five liters of 20% glucose solution was prepared at one time and stored in the refrigerator until needed. Methanol (HPLC grade) was used as a solvent for the internal standard and as a protein precipitant.

Indomethacin[2] (I) [1-(*p*-chlorobenzoyl)-5-methoxy-2-methylindole-3-acetic acid] was used as a substrate for biotransformation and as a reference standard.

*O*-Desmethylindomethacin[3] (II) was used as a reference standard for the biotransformation product. Compound II is a major product of the

[1] The liquid chromatographic system (Waters Associates, Milford, Mass.) was composed of a solvent delivery system (M 6000 A), a stainless steel μBondapak $C_{18}$ column, an absorbance detector (M 440), and an omniscribe recorder (Houston Instruments).

[2] Lot L-590,226-00125A, generously supplied by Merck Sharp & Dohme Research Laboratories, Rahway, N.J.

[3] Lot L-594-957-00R10, generously supplied by Merck Sharp & Dohme Research Laboratories, Rahway, N.J.


0022-3549/81/0600-0695$01.00/0


© 1981, American Pharmaceutical Association

problem because the citrate assay and subsequent calculation directly reflect the citrate content, regardless of the original free citric acid concentration.

Approximate calculation of the pH at the equivalence point of the compendial citrate titration showed that the value differed markedly from the stated pH of 1.55. The calculated value of 1.81 was obtained when the preparation was assumed to contain the labeled quantities of citrate and citric acid, using a $K_{a_1}$ value of $7.45 \times 10^{-4}$ and a $K_{a_2}$ value of $1.73 \times 10^{-5}$ at 25° for citric acid (5) and assuming that the third dissociation was negligible. Applying the same approximate calculation to compute the pH at the equivalence point of a similar electrometric titration of citrate in anticoagulant citrate–dextrose solution gave a value of 2.07. This value was relatively close to the stated pH of 1.98 ± 0.02 (6).

Since commercial systemic alkalizer solutions contain additives such as preservatives, flavoring, and coloring agents, the assay of a solution placebo is recommended. The placebo should be subjected to the same analytical steps as the sample, and necessary corrections should be made for titrant consumption, if any, by the placebo. In contrast, the compendium directs the use of water as a blank in the electrometric titration of citrate and no blank runs for the titration of citric acid.

## REFERENCES


(1) "The United States Pharmacopeia," 20th rev., United States Pharmacopeial Convention, Rockville, Md., 1980, pp. 644, 729.

(2) M. L. Richardson, *Anal. Chim. Acta*, **24**, 46 (1961).

(3) S. M. Blaug, *J. Am. Pharm. Assoc., Sci. Ed.*, **45**, 274 (1956).

(4) "The United States Pharmacopeia," 20th rev., United States Pharmacopeial Convention, Rockville, Md., 1980, p. 1113.

(5) "CRC Handbook of Chemistry and Physics," 60th ed., CRC Press, Boca Raton, Fla., 1979, p. D-168.

(6) "The United States Pharmacopeia," 20th rev., United States Pharmacopeial Convention, Rockville, Md., 1980, p. 49.


## ACKNOWLEDGMENTS


Presented at the Pharmaceutical Analysis and Control Section, APhA Academy of Pharmaceutical Sciences, Washington, D.C. meeting, April 1980.


# Effect of Elevated Blood Glucose Levels on Hepatic Microsomal Enzyme System in Rats


**MARTIN B. SIDEMAN**



Received August 21, 1980, from the *Division of Pharmacotherapeutics, Arnold & Marie Schwartz College of Pharmacy and Health Sciences, Long Island University, Brooklyn, NY 11201.* Accepted for publication November 11, 1980.



**Abstract** □ Elevated blood glucose levels attained by *ad libitum* drinking of 20% glucose solution inhibited *in vivo* *O*-dealkylation associated with the hepatic microsomal enzyme system. Significant inhibition of biotransformation was demonstrated after 1 day, with the maximum occurring at 3 days. Inhibition was followed by a tendency to return to normal activity. Serum levels of substrate and product were determined by liquid chromatographic techniques using 55% acetonitrile and 45% 0.1 *M* acetic acid as the mobile phase.



**Keyphrases** □ Glucose levels, blood—effect of elevation on hepatic microsomal enzyme system, rats □ Microsomal enzyme system—effect of elevated blood glucose levels, rats □ Enzyme systems—effect of elevated blood glucose levels on hepatic microsomal enzymes, rats □ Biotransformation—effect of elevated blood glucose levels on hepatic microsomal enzyme system, rats


The following reactions (1) are catalyzed by the mixed-function oxidase enzymes of the hepatic microsomal system: *N*- and *O*-dealkylation, aromatic ring side-chain hydroxylation, sulfoxide formation, *N*-oxidation, *N*-hydroxylation, deamination of primary and secondary amines, and replacement of a sulfur by an oxygen atom. Previous investigators showed that elevated blood glucose levels have inhibitory effects on several of the biotransformations mentioned in addition to depressing the cytochrome P-450 levels of the system. Hartshorn *et al.* (2) demonstrated, by *in vitro* microsomal studies in rats, the inhibition of *N*-demethylation of ethylmorphine and aniline hydroxylase as well as depression of the cytochrome P-450 content. *In vitro* microsomal studies in mice (3) showed the inhibition of hexobarbital biotransformation, primarily oxidation of the side chain at C-5, and the *N*-dealkylation of benzphetamine in addition to cytochrome P-450 depression. Strother *et al.* (4), using the *in vivo* technique of increased sleep time, also showed that elevated blood glucose levels delayed the biotransformation of various barbiturates in mice.

This investigation established, by direct measurements in blood using liquid chromatography, that elevated blood glucose levels inhibit *O*-dealkylation associated with the hepatic microsomal system.

## EXPERIMENTAL

**Animals**—Adult male Sprague–Dawley rats, 180–200 g, were individually housed in temperature-, light-, humidity-, and air-controlled quarters. Commercial laboratory chow and drinking liquid, either water or 20% glucose solution, were given *ad libitum*.

**Liquid Chromatography**—A liquid chromatographic system containing a $C_{18}$ column and an absorbance detector fixed at 254 nm was used isocratically[1]. The mobile phase consisted of 55% acetonitrile (HPLC grade) and 45% of 0.1 *M* acetic acid. Prior to use, the mobile phase was passed through a solvent-clarification apparatus to remove gases and particulates which might affect the column. Solvent delivery was at a rate of 1 ml/min. Recordings were made at a chart speed of 0.5 cm/min.

**Reagents**—Five liters of 20% glucose solution was prepared at one time and stored in the refrigerator until needed. Methanol (HPLC grade) was used as a solvent for the internal standard and as a protein precipitant.

Indomethacin[2] (I) [1-(*p*-chlorobenzoyl)-5-methoxy-2-methylindole-3-acetic acid] was used as a substrate for biotransformation and as a reference standard.

*O*-Desmethylindomethacin[3] (II) was used as a reference standard for the biotransformation product. Compound II is a major product of the

[1] The liquid chromatographic system (Waters Associates, Milford, Mass.) was composed of a solvent delivery system (M 6000 A), a stainless steel μBondapak $C_{18}$ column, an absorbance detector (M 440), and an omniscribe recorder (Houston Instruments).

[2] Lot L-590,226-00125A, generously supplied by Merck Sharp & Dohme Research Laboratories, Rahway, N.J.

[3] Lot L-594-957-00R10, generously supplied by Merck Sharp & Dohme Research Laboratories, Rahway, N.J.


0022-3549/81/0600-0695$01.00/0


© 1981, American Pharmaceutical Association

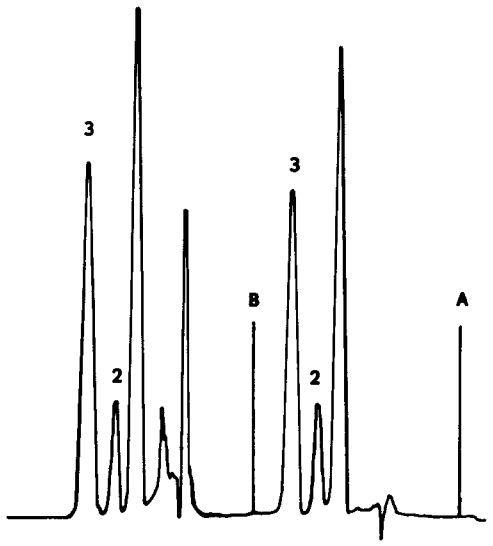


**Figure 1**—*Chromatogram of indomethacin, desmethylindomethacin, and the internal standard. Key: A, 0.5 ml of water used as the aqueous medium; B, 0.5 ml of serum used as the aqueous medium; 1, desmethylindomethacin; 2, internal standard; and 3, indomethacin.*

biotransformation of I in humans (5) and in various laboratory animals (6).

1-(*p*-Fluorobenzoyl)-5-methoxy-2-methylindole-3-acetic acid[4] (III) was used as the internal standard for chromatography.

***In Vivo* Biotransformation**—The animals drank the 20% glucose solution for varying times (1, 3, 5, 7, and 10 days). Each experimental group consisted of six rats chosen at random from the pool. The control group contained eight rats. To reduce the workload on the day of sacrifice, each group was divided in half, with the second half starting 1 day later. All groups in each half were sacrificed the same day. Controls were started at the same time as the 10-day experimental group. The glucose solutions were replaced daily to avoid bacterial growth and contamination. On the morning of the day of sacrifice, all animals were tested for glucose in their urine.

Following the urine test, the animals were weighed and injected with a saline solution of I (10 mg/kg ip) solubilized by titrating to pH 7.6–8.0. The animals then were returned to their cages and sacrificed by decapitation 30 min later. The blood was collected, allowed to clot, and centrifuged; the serum was stored at from −10 to −20° until analyzed. During collection, an aliquot of whole blood was removed and tested for glucose with glucose reagent strips[5] and a reflectance colorimeter[6].

A preliminary study of blood I and II levels *versus* time showed an increase in concentration of both to a maximum at 15 min. The succeeding fall in concentration was measurable to at least 2 hr. The 0.5-hr point was chosen because of relatively high I and II concentrations. It was also assumed that little if any I was removed from the injection site and that the blood levels were the result of cellular uptake, biotransformation, and excretion on the maximum levels, in short, normal metabolic pathways.

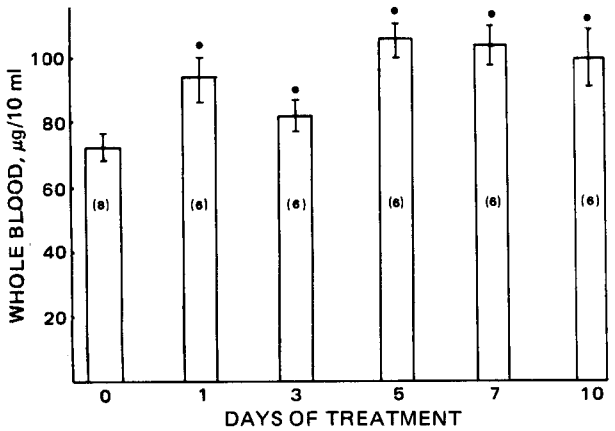


**Figure 2**—*Serum glucose levels. Key: ●, significant differences from control, p < 0.05, as determined by the Student t test.*

[4] Lot 620-370-00203, generously supplied by Merck Sharp & Dohme Research Laboratories, Rahway, N.J.

[5] Dextrostix, Ames Division of Miles Laboratories, Elkhart, Ind.

[6] Eyetone, Ames Division of Miles Laboratories, Elkhart, Ind.

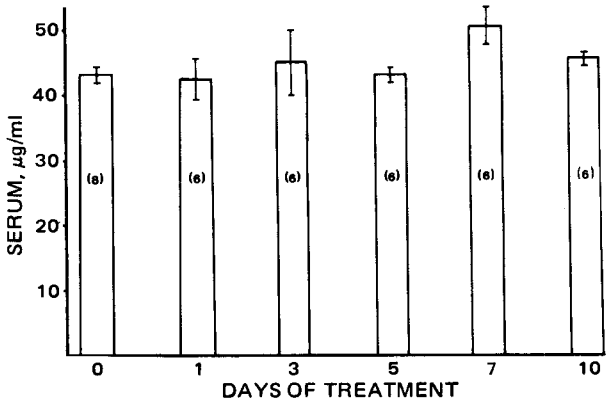


**Figure 3**—*Serum indomethacin levels.*

**Analysis**—To analyze the serum for I and II properly, substances that would interfere with the proper function of the column, principally protein, had to be removed. Methanol was added to the serum to precipitate the protein. Furthermore, methanol increased the solubility of the compounds under investigation and reduced the number of transfers needed to put them on the column. Four volumes of methanol served adequately.

The procedure used 0.5 ml of serum and 2 ml of methanol containing a fixed concentration of III. The mixture was agitated on a vortex mixer to ensure complete mixing and was centrifuged for 10 min, and the supernate was filtered to remove any particulate material. A 10-μl aliquot was placed on the column, and the peak areas were determined from standard curves.

Standard curves were prepared by plotting the ratio of the peak area produced by I or II divided by the peak produced by III *versus* the standard concentration. Recovery experiments showed that there was no loss of the three compounds if the 0.5-ml portion was methanol, water, or serum. Thus, no corrections for recovery had to be made. Figure 1 shows chromatograms of substrate, product, and internal standard added to either water or serum from a rat receiving no injections, the differences being the substances present in serum that do not interfere with the compounds under investigation. A complete chromatogram required 7 min.

All data are reported as the group mean ± *SE*. Significance to $p < 0.05$ was determined by the Student *t* test.

## RESULTS AND DISCUSSION

All animals showed good growth patterns with no significant difference in body weight. The average weight at sacrifice ranged from 263 ± 6 to 278 ± 5 g; the control group was not one of the extremes. Whole blood

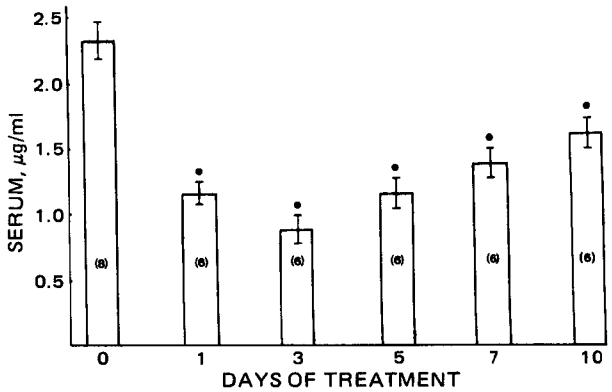


**Figure 4**—*Serum desmethylindomethacin levels. Key: ●, significant differences from control, p < 0.05, as determined by the Student t test.*

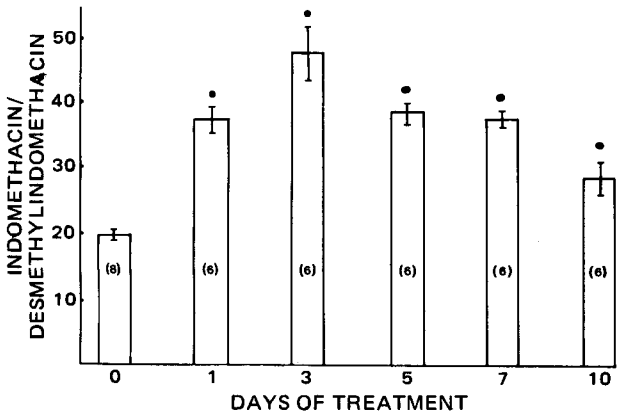


**Figure 5**—*Ratio of indomethacin divided by desmethylindomethacin. Key: ●, significant differences from control, p < 0.05, as determined by the Student t test.*

glucose levels (Fig. 2) were significantly elevated after 1 day and remained so. Although their blood levels were higher than those of the controls, none of the experimental animals had glucose in their urine on the day of sacrifice.

Figures 3 and 4 represent the serum levels of I and II, respectively. There were no significant differences in the substrate during the experiment. However, there were significant differences in the product level from Day 1 on. The maximum inhibition occurred at Day 3, followed by a tendency toward control levels as time progressed.

Elevated blood glucose levels obtained by oral administration of the 20% glucose solution rapidly led to inhibition of the hepatic microsomal mixed-function oxidase, which catalyzed *O*-dealkylation within 1 day. Although serum insulin levels were not measured, it can be projected from the urine levels at sacrifice and from the data presented by Hartshorn *et al.* (2) that the results were not due to hypoinsulinemia. Inversion of the inhibition after the maximum level at Day 3 confirmed earlier findings (7) that inhibition is short lived and returns to normal even though glucose administration is prolonged.

Since there were no significant differences in the blood substrate levels, the biotransformation inhibition could only be accounted for by the glucose affecting enzymatic activity. Kinetic studies (3) indicated that glucose caused mixed inhibition (competitive and noncompetitive) and altered the enzyme at the active site and at an allosteric site. The inversion of inhibition may have been caused by induction of new enzyme as well as displacement of old enzyme, freeing more active sites. Figure 5 shows the ratio of substrate to product, representing the biotransformation of I to II under the influence of glucose and time.

## REFERENCES

(1) "The Pharmacological Basis of Therapeutics," 5th ed., L. S. Goodman and A. Gilman, Eds., Macmillan, New York, N.Y., 1975, p. 13.

(2) R. D. Hartshorn, L. M. Demers, L. G. Sultatos, E. S. Vesell, C. M. Lang, and H. C. Hughes, Jr., *Pharmacology*, **18**, 103 (1979).

(3) M. A. Peters and A. Strother, *J. Pharmacol. Exp. Ther.*, **180**, 151 (1972).

(4) A. Strother, J. K. Throckmorton, and C. Herzer, *ibid.*, **179**, 490 (1970).

(5) D. E. Duggan, A. F. Hogans, K. C. Kwan, and F. G. McMahon, *ibid.*, **181**, 563 (1972).

(6) H. B. Hucker, A. G. Zacchei, S. V. Cox, D. A. Brodie, and N. H. R. Cantwell, *ibid.*, **153**, 237 (1966).

(7) A. Strother, *Fed. Proc. Fed. Am. Soc. Exp. Biol.*, **38**, 366 (1979).

# Simultaneous Determination of Hydroxyzine Hydrochloride and Benzyl Alcohol in Injection Solutions by High-Performance Liquid Chromatography

**G. N. MENON and B. J. NORRIS** ˣ

Received January 18, 1980, from the *Department of Analytical Research, Abbott Laboratories, North Chicago, IL 60064.* Accepted for publication November 19, 1980.

**Abstract** □ A stability-indicating, high-performance liquid chromatographic method was developed for the simultaneous determination of hydroxyzine hydrochloride and benzyl alcohol in injection solutions. Separation was achieved using a μBondapak $C_{18}$ column and the eluent [60% water, 25% acetonitrile, and 15% methanol containing 0.06% (v/v) sulfuric acid, 0.5% (w/v) sodium sulfate, and 0.02% (w/v) heptanesulfonic acid sodium salt] at a flow rate of 2 ml/min. Isobutyrophenone and *p*-nitroacetophenone were used as internal standards. The UV detector response at 257 nm was linear for hydroxyzine hydrochloride in the 3–10-mg/ml range and for benzyl alcohol in the 0.54–1.8-mg/ml range under analysis conditions. The method is accurate, simple, and precise.

**Keyphrases** □ High-performance liquid chromatography—simultaneous determination of hydroxyzine hydrochloride and benzyl alcohol, injection solutions □ Analysis, simultaneous—high-performance liquid chromatographic method for hydroxyzine hydrochloride–benzyl alcohol injection solutions □ Injection solutions—high-performance liquid chromatographic method for simultaneous determination of hydroxyzine hydrochloride and benzyl alcohol

Hydroxyzine hydrochloride is usually formulated with benzyl alcohol as a preservative (bacteriostatic) in injection solutions. Depending on conditions such as pH, light exposure, and temperature, photolysis occurs in solution, resulting in the formation of *p*-chlorobenzophenone, *p*-chlorobenzaldehyde, *p*-chlorobenzoic acid, and 1-[2-(2-hydroxyethyl)ethyl]piperazine dihydrochloride (1, 2). The compendial assay for hydroxyzine hydrochloride injection, based on titration of the free base with perchloric acid, is not indicative of drug stability in solution (3). From an analytical standpoint, a simple, rapid, and precise method is desirable for the simultaneous determination of both the drug substance and the preservative in the formulation.

This paper describes the development of a high-performance liquid chromatographic (HPLC) method for hydroxyzine hydrochloride and benzyl alcohol in an injectable formulation. The method is stability indicating of both ingredients in solution.

## EXPERIMENTAL

**Instrumentation**—The chromatographic system was equipped with a dual-piston reciprocating pump[1], a universal injector[2], and a vari-

[1] Model 6000A, Waters Associates, Milford, Mass.
[2] Model U6K, Waters Associates, Milford, Mass.

0022-3549/81/0600-0697$01.00/0
© 1981, American Pharmaceutical Association

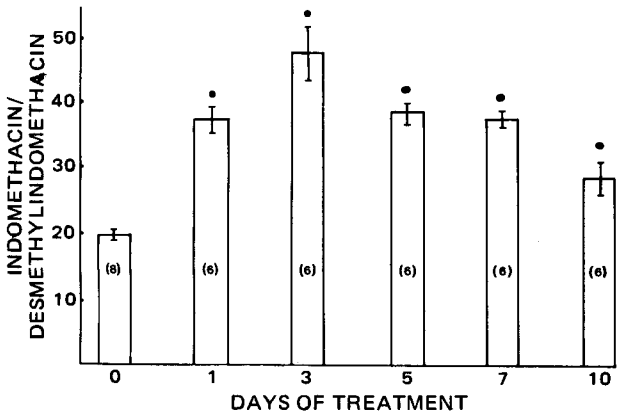


**Figure 5**—*Ratio of indomethacin divided by desmethylindomethacin. Key: ●, significant differences from control, p < 0.05, as determined by the Student t test.*

glucose levels (Fig. 2) were significantly elevated after 1 day and remained so. Although their blood levels were higher than those of the controls, none of the experimental animals had glucose in their urine on the day of sacrifice.

Figures 3 and 4 represent the serum levels of I and II, respectively. There were no significant differences in the substrate during the experiment. However, there were significant differences in the product level from Day 1 on. The maximum inhibition occurred at Day 3, followed by a tendency toward control levels as time progressed.

Elevated blood glucose levels obtained by oral administration of the 20% glucose solution rapidly led to inhibition of the hepatic microsomal mixed-function oxidase, which catalyzed *O*-dealkylation within 1 day. Although serum insulin levels were not measured, it can be projected from the urine levels at sacrifice and from the data presented by Hartshorn *et al.* (2) that the results were not due to hypoinsulinemia. Inversion of the inhibition after the maximum level at Day 3 confirmed earlier findings (7) that inhibition is short lived and returns to normal even though glucose administration is prolonged.

Since there were no significant differences in the blood substrate levels, the biotransformation inhibition could only be accounted for by the glucose affecting enzymatic activity. Kinetic studies (3) indicated that glucose caused mixed inhibition (competitive and noncompetitive) and altered the enzyme at the active site and at an allosteric site. The inversion of inhibition may have been caused by induction of new enzyme as well as displacement of old enzyme, freeing more active sites. Figure 5 shows the ratio of substrate to product, representing the biotransformation of I to II under the influence of glucose and time.

## REFERENCES

(1) "The Pharmacological Basis of Therapeutics," 5th ed., L. S. Goodman and A. Gilman, Eds., Macmillan, New York, N.Y., 1975, p. 13.

(2) R. D. Hartshorn, L. M. Demers, L. G. Sultatos, E. S. Vesell, C. M. Lang, and H. C. Hughes, Jr., *Pharmacology*, **18**, 103 (1979).

(3) M. A. Peters and A. Strother, *J. Pharmacol. Exp. Ther.*, **180**, 151 (1972).

(4) A. Strother, J. K. Throckmorton, and C. Herzer, *ibid.*, **179**, 490 (1970).

(5) D. E. Duggan, A. F. Hogans, K. C. Kwan, and F. G. McMahon, *ibid.*, **181**, 563 (1972).

(6) H. B. Hucker, A. G. Zacchei, S. V. Cox, D. A. Brodie, and N. H. R. Cantwell, *ibid.*, **153**, 237 (1966).

(7) A. Strother, *Fed. Proc. Fed. Am. Soc. Exp. Biol.*, **38**, 366 (1979).

# Simultaneous Determination of Hydroxyzine Hydrochloride and Benzyl Alcohol in Injection Solutions by High-Performance Liquid Chromatography

**G. N. MENON and B. J. NORRIS** ˣ

Received January 18, 1980, from the *Department of Analytical Research, Abbott Laboratories, North Chicago, IL 60064.* Accepted for publication November 19, 1980.

**Abstract** □ A stability-indicating, high-performance liquid chromatographic method was developed for the simultaneous determination of hydroxyzine hydrochloride and benzyl alcohol in injection solutions. Separation was achieved using a μBondapak $C_{18}$ column and the eluent [60% water, 25% acetonitrile, and 15% methanol containing 0.06% (v/v) sulfuric acid, 0.5% (w/v) sodium sulfate, and 0.02% (w/v) heptanesulfonic acid sodium salt] at a flow rate of 2 ml/min. Isobutyrophenone and *p*-nitroacetophenone were used as internal standards. The UV detector response at 257 nm was linear for hydroxyzine hydrochloride in the 3–10-mg/ml range and for benzyl alcohol in the 0.54–1.8-mg/ml range under analysis conditions. The method is accurate, simple, and precise.

**Keyphrases** □ High-performance liquid chromatography—simultaneous determination of hydroxyzine hydrochloride and benzyl alcohol, injection solutions □ Analysis, simultaneous—high-performance liquid chromatographic method for hydroxyzine hydrochloride–benzyl alcohol injection solutions □ Injection solutions—high-performance liquid chromatographic method for simultaneous determination of hydroxyzine hydrochloride and benzyl alcohol

Hydroxyzine hydrochloride is usually formulated with benzyl alcohol as a preservative (bacteriostatic) in injection solutions. Depending on conditions such as pH, light exposure, and temperature, photolysis occurs in solution, resulting in the formation of *p*-chlorobenzophenone, *p*-chlorobenzaldehyde, *p*-chlorobenzoic acid, and 1-[2-(2-hydroxyethyl)ethyl]piperazine dihydrochloride (1, 2). The compendial assay for hydroxyzine hydrochloride injection, based on titration of the free base with perchloric acid, is not indicative of drug stability in solution (3). From an analytical standpoint, a simple, rapid, and precise method is desirable for the simultaneous determination of both the drug substance and the preservative in the formulation.

This paper describes the development of a high-performance liquid chromatographic (HPLC) method for hydroxyzine hydrochloride and benzyl alcohol in an injectable formulation. The method is stability indicating of both ingredients in solution.

## EXPERIMENTAL

**Instrumentation**—The chromatographic system was equipped with a dual-piston reciprocating pump[1], a universal injector[2], and a vari-

[1] Model 6000A, Waters Associates, Milford, Mass.
[2] Model U6K, Waters Associates, Milford, Mass.

0022-3549/81/0600-0697$01.00/0
© 1981, American Pharmaceutical Association

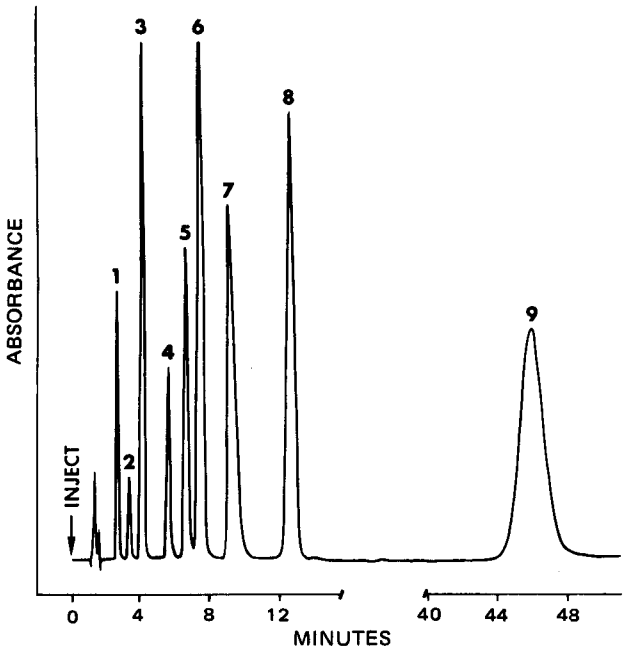


**Figure 1**—*Synthetic mixture of formulation ingredients, potential degradation products, and internal standards for quantitation. Key: 1, benzyl alcohol (0.81 mg/ml); 2, benzoic acid (0.093 mg/ml); 3, benzaldehyde (0.041 mg/ml); 4,* p-*nitroacetophenone (0.024 mg/ml); 5,* p-*chlorobenzoic acid (0.19 mg/ml); 6,* p-*chlorobenzaldehyde (0.073 mg/ml); 7, hydroxyzine hydrochloride (5.0 mg/ml); 8, isobutyrophenone (0.269 mg/ml); and 9,* p-*chlorobenzophenone (0.18 mg/ml).*

able-wavelength UV detector[3]. The separation was performed on a 30-cm × 4-mm i.d. column containing microparticulate (10-μm) bonded octadecylsilane material[4]. The chromatographic peaks were electronically integrated and recorded[5].

**Eluent**—The eluent was 60% water, 25% acetonitrile[6], and 15% methanol[6] containing 0.06% (v/v) sulfuric acid, 0.5% (w/v) sodium sulfate, and 0.02% (w/v) heptanesulfonic acid sodium salt[7]. The eluent pH was 2.6.

**Internal Standard Solution**—A methanolic solution of 0.2 mg of *p*-nitroacetophenone[8]/ml and 2.5 mg of isobutyrophenone[8]/ml was used as the internal standard solution.

**Standard Preparation**—The standard solution for analysis was prepared by dissolving 250 mg of hydroxyzine hydrochloride NF reference standard in 5 ml of water. Five milliliters of a 9-mg/ml methanolic solution of benzyl alcohol NF reference standard and 5.0 ml of the internal standard solution were pipetted into the hydroxyzine hydrochloride reference standard solution; this mixture was diluted to 50 ml with methanol.

**Sample Preparation**—The method was developed utilizing a formulation of 50 mg of hydroxyzine hydrochloride/ml containing 9 mg of benzyl alcohol/ml. The analysis sample was prepared by mixing 5.0 ml of formulation and 5.0 ml of internal standard solution and diluting the mixture to 50 ml with methanol.

**Analysis**—The following chromatographic conditions were used: flow rate, 2 ml/min; detector wavelength, 257 nm; absorbance, 0.2 aufs; and injection volume, 10 μl. Duplicate analyses were performed for both the standard and sample preparations.

## RESULTS AND DISCUSSION

A chromatographic method that is stability indicating of hydroxyzine hydrochloride was outlined previously (4); the chromatography was performed on a Bondapak phenyl/corasil column using a 5:3 mixture of 0.25% $(NH_4)_2CO_3$–acetonitrile as the eluent. A similar system using a 45:55 mixture of 0.01 *M* phosphate buffer (pH 7.8)–acetonitrile as the eluent and a μBondapak $C_{18}$ column also was used successfully to monitor hydroxyzine hydrochloride stability[9]. In both methods, a high proportion of acetonitrile is needed to elute the drug substance as the free base. Benzyl alcohol, another component in the formulation, could not be analyzed with hydroxyzine hydrochloride in either chromatographic system; it could not be retained on either column due to the high acetonitrile concentration in the eluent.

**Table I—Statistical Data Resulting from Simultaneous Analyses of Hydroxyzine Hydrochloride and Benzyl Alcohol in Hydroxyzine Hydrochloride Injection** [a]

| Parameter | Hydroxyzine Hydrochloride | Benzyl Alcohol |
|---|---|---|
| Number of analyses | 7 | 7 |
| Milligrams per milliliter (mean) | 48.7 | 8.47 |
| *SD*, mg/ml | ±0.44 | ±0.09 |
| *RSD*, % | ±0.9 | ±1.0 |

[a] Abbott Laboratories, North Chicago, Ill.; stored at 25° for 2 years.

The ion-pair reversed-phase chromatography used in this method allowed benzyl alcohol and hydroxyzine hydrochloride to be determined simultaneously. The acidity of the eluent was adjusted to a pH at which hydroxyzine hydrochloride and heptanesulfonic acid sodium salt are ionized, resulting in ion-pair formation. The ionic strength of the eluent was increased by the addition of sodium sulfate, which generally decreases the retention of compounds being chromatographed *via* the ion-pairing mechanism (5). Although the proportion of organic solvent in the eluent is high, the polarity of organic solvent was increased by using a mixture of methanol and acetonitrile. Therefore, benzyl alcohol was retained on the $C_{18}$ column; it was unaffected by the addition of heptanesulfonic acid sodium salt and sodium sulfate to the eluent, as it did not form an ion-pair.

This analysis is stability indicating of both hydroxyzine hydrochloride and benzyl alcohol (Fig. 1). A synthetic mixture of benzyl alcohol, hydroxyzine hydrochloride, several potential degradation products (benzoic acid[8], benzaldehyde[8], *p*-chlorobenzoic acid[8], *p*-chlorobenzaldehyde[8], and *p*-chlorobenzophenone[8]), and the internal standards used for quantitation, *p*-nitroacetophenone and isobutyrophenone, were separated under analytical conditions.

The detector wavelength of 257 nm was selected for maximum response for both hydroxyzine hydrochloride and benzyl alcohol. The linearity of the detector response under analytical conditions was established for hydroxyzine hydrochloride in the 3–10-mg/ml range (*y* intercept, −0.001; *r*, 0.9999) and for benzyl alcohol in the 0.54–1.8-mg/ml range (*y* intercept, 0.003; *r*, 0.9999). Since the resulting standard curves for both hydroxyzine hydrochloride and benzyl alcohol were linear and passed through the origin, sample analysis could be performed *versus* a single standard preparation.

Experiments were performed to demonstrate the accuracy of the method. Six solution mixtures were prepared ranging from 60 to 200% of the theoretical concentrations of the two components. Recoveries of benzyl alcohol varied from 99.4 to 103.0% with an average recovery of 101.0 ± 1.35%; recoveries of hydroxyzine hydrochloride varied from 99.8 to 100.7% with an average recovery of 100.2 ± 0.34%.

The reproducibility of the method was demonstrated by replicate analyses of hydroxyzine hydrochloride and benzyl alcohol in a commercial product which had been stored at 25° for 2 years. The statistical data are presented in Table I.

## REFERENCES

(1) J. Pawlaczyk, *Poznan. Tow. Przyj. Nauk, Wydz. Lek., Pr. Kom. Farm.*, **5**, 117 (1966).

(2) J. Pawlaczyk, *Ann. Pharm. (Poznan)*, **7**, 127 (1969).

(3) "The National Formulary," 14th ed., Mack Publishing Co., Easton, Pa., 1975, p. 340

(4) J. Tsau and N. DeAngelis, in "Analytical Profiles of Drug Substances," vol. 7, K. Florey, Ed., Academic, New York, N.Y., 1978, p. 319.

(5) C. Horvath, W. Melander, I. Molnar, and P. Molnar, *Anal. Chem.*, **49**, 2295 (1977).

[3] Model LC-55, Perkin-Elmer, Norwalk, Conn., or model SF 770 Spectroflow, Schoeffel, Westwood, N.J.

[4] μBondapak $C_{18}$, Waters Associates, Milford, Mass.

[5] Autolab System I (Spectra-Physics, Santa Clara, Calif.) with model 023 strip-chart recorder (Perkin-Elmer, Norwalk, Conn.) or model 3385A Automation System (Hewlett-Packard, Avondale, Pa.).

[6] Distilled in glass, Burdick & Jackson, Muskegon, Mich.

[7] Eastman Organic Chemicals, Rochester, N.Y.

[8] Aldrich, Milwaukee, Wis.

[9] L. Marchant, Abbott Laboratories, North Chicago, Ill., unpublished data.

# Synthesis and Vasodepressor Screen of a Series of 2-(2-Alkylaminoalkylamido)-3-carbamyl-4-methyl-5-benzylpyrroles

**L. D. WANG *, J. W. SOWELL, Sr. *, J. J. FREEMAN ‡, and J. W. KOSH ‡x**

Received September 15, 1980, from the **Division of Medicinal Chemistry and the* ‡*Division of Pharmacology, College of Pharmacy, University of South Carolina, Columbia, SC 29208.* Accepted for publication November 19, 1980.

**Abstract** □ A series of 2-(2-alkylaminoalkylamido)-3-carbamyl-4-methyl-5-benzylpyrroles was synthesized and screened for vasoactivity. The compounds were administered intraperitoneally as a suspension to approximate the oral route of administration and intravenously when solubilization could be affected with suitable solvents. The most active compound following intravenous or intraperitoneal administration lowered blood pressure 73 and 35.5 mm Hg at doses of 4 mg/kg iv and 100 mg/kg ip, respectively. It also exhibited the longest duration of vasodepressor activity (25 min). Several other compounds exhibited vasodepressor activity following intraperitoneal administration. Several hydrochloride salts appeared to be more potent vasoactive agents than the corresponding bases.

**Keyphrases** □ Lidocaine analogs—synthesis, analysis of vasoactivity, intraperitoneal and intravenous administration □ Vasoactive agents—synthesis, analysis, intraperitoneal and intravenous administration, lidocaine analogs □ Synthesis and analysis—vasoactive agents, lidocaine analogs, intraperitoneal and intravenous administration □ Administration routes—effect on vasoactivity, lidocaine analogs, vasoactive agents

Several series of 2-aminopyrrole analogs of lidocaine recently were investigated as local anesthetic and antiarrhythmic agents (1–3). From one series, the hydrochloride salt of the benzylcarbamyl analog [2-(diethylaminoacetamide)-3-carbamyl-4-methyl-5-benzylpyrrole, I] was found to possess potent hypotensive activity following intravenous administration at doses of 2–4 mg/kg (4, 5). Compound I was more active than lidocaine with respect to antiarrhythmic activity, local anesthetic activity, and rectal temperature and respiratory depression.

Since I exerted its potent hypotensive property following intravenous administration, its structure was utilized as a basis for designing and synthesizing amine analogs that would have hypotensive activity following oral administration. Intraperitoneal administration was chosen to simulate oral activity since the drugs must cross biological membranes prior to exerting a hypotensive action.

The present article reports the synthesis and vasoactivity of a series of 2-(alkylaminoalkylamido)-3-carbamyl-4-methyl-5-benzylpyrroles (II) following intraperitoneal and intravenous administration.

## EXPERIMENTAL

**Chemistry**[1]—*2-[(*N*-Ethyl-*N*-2-hydroxyethyl)amino]acetamido-3-carbamyl-4-methyl-5-benzylpyrrole (IIa)*—The procedure given for the synthesis of IIa is representative of that used for IIb–IIh. A suspension of 2-chloroacetamido-3-carbamyl-4-methyl-5-benzylpyrrole (7.0 g, 0.023 mole) (1) in absolute ethanol (160 ml) and 2-(ethylamino)ethanol (10.2

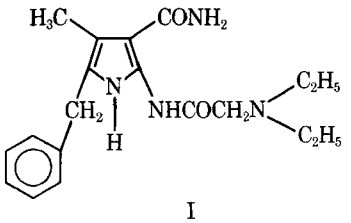

I

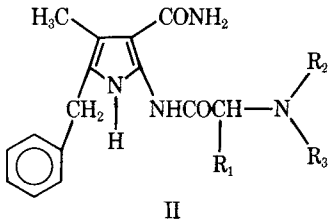

II

g, 0.115 mole) was refluxed with stirring for 8 hr. The ethanol was removed *in vacuo* to yield an orange solid. The residue was suspended in water (350 ml), and the insoluble product was collected by filtration and dried.

The crude product (6.0 g, 73.1%) was recrystallized from ethanol–water (7:3) to yield off-white crystals, mp 182.5–183.5°; IR (KBr): 3480, 3315, 3180, 2960, 1660, 1630, 1570, 1380, and 720 $cm^{-1}$; NMR (dimethyl sulfoxide-$d_6$): δ 0.97 (t, 3H, $CH_3$ of ethyl), 2.07 (s, 3H, $CH_3$ at $C_4$), 2.40–2.70 (m, 4H, α methylenes of amino radical), 3.13 (s, 2H, $-COCH_2-$), 3.25 (s, 1H, $-CH_2OH$), 3.45 (q, 2H, methylene of $-CH_2OH$), 3.80 (s, 2H, benzylic methylene), 6.57 (s, 2H, $-CONH_2$), 7.07 (s, 5H, aromatic H), 10.60 (2, 1H, NH), and 11.54 (s, 1H, NH) ppm (Table I).

*2-[(*N*-2-Hydroxyethyl-*N*-ethyl)amino]acetamido-3-carbamyl-4-methyl-5-benzylpyrrole Hydrochloride (IIIa)*—The procedure given for the synthesis of IIIa is representative of that used for IIIb and IIIc and IIIe–IIIh. A stirred suspension of IIa (1.20 g, 0.0033 mole) in acetone (25 ml) was treated with 0.4 ml of concentrated hydrochloric acid. The resulting suspension was stirred for 30 min at ambient temperature, and the white precipitate was collected by filtration, washed with acetone (25 ml), and dried. The hydrochloride salt (1.1 g, 83.0%) was homogeneous on TLC, mp 175–177° dec.; IR (KBr): broad absorption between 3400 and 2600 (with absorptions at 3400, 3320, 3120, and 3000), 1680, 1640, 1610, 1550, 1480, 1380, and 960 $cm^{-1}$ (Table I).

**Solution Preparation**—Compounds I, IIa–IIh, and IIIa–IIIh were prepared for intraperitoneal administration by suspending 50 mg/ml in 0.9% saline containing 0.5% polysorbate 80[2] and 0.5% acacia. Compound I was solubilized in 0.9% saline by adjusting the pH to 2.2 with 2 *N* HCl prior to intravenous injection. A solution of IIId (3.6 mg/ml) was prepared by adding 20 mg of IId to 5 ml of 20% dimethyl sulfoxide in saline and 0.5 ml of 10% sorbitol in saline, followed by adjustment of the pH to 2.0 with hydrochloric acid. Solubilization was effected after slight warming of the resulting solution. A solution of IIIh (4.0 mg/ml) was prepared using 20% dimethyl sulfoxide in saline.

**Blood Pressure Determination**—Male Sprague–Dawley (Spd: Sprague–Dawley, DS) rats, 300–400 g, were administered pentobarbital sodium (30 mg/kg) and urethan (950 mg/kg) intraperitoneally prior to surgery for blood pressure determination. After anesthetization, the animal was positioned on its back and the trachea, carotid artery, and jugular vein were exposed. The jugular vein was cannulated with polyethylene tubing[3]. The trachea was cannulated with a tracheal tube[4] as necessary and connected to a respirator[5] with 100% oxygen at 50 psi. The respirator was adjusted to deliver a respiratory rate of 60/min at an inspiratory pressure of 12–15 cm $H_2O$.

The carotid artery was cannulated with polyethylene tubing[3] containing 100 units of heparin/ml. Blood pressure was monitored *via* a pressure transducer[6], channel amplifier[7], and recorder[8]. Test compounds

[1] Melting points were determined on a Thomas-Hoover apparatus (capillary method) and are uncorrected. NMR spectra were determined on a Varian EM360A NMR spectrometer with tetramethylsilane as an internal standard. IR spectra were determined on a Beckman Acculab 4 spectrophotometer using the potassium bromide technique. Elemental analyses were performed by Atlantic Microlabs, Atlanta, Ga.

[2] Tween 80, ICI Americas, Wilmington, Del.
[3] PE-50 (0.58 mm i.d. × 0.97 mm o.d.), Clay Adams, Parsippany, N.J.
[4] 1.5. mm i.d. × 3.0 mm o.d., Foregger Co., Smithtown, N.J.
[5] Mark 7, Bird Corp., Palm Springs, Calif.
[6] Type P-1000B, Narco Bio-Systems, Houston, Tex.
[7] Type 7070, Narco Bio-Systems, Houston, Tex.
[8] Physiograph DMP-4A, Narco Bio-Systems, Houston, Tex.

0022-3549/81/0600-0699$01.00/0
© 1981, American Pharmaceutical Association

**Table I—Structural and Analytical Data for 2-(2-Alkylaminoalkylamido)-3-carbamyl-4-methyl-5-benzylpyrroles**

| Compound | $R_1$ | $R_2$ | $R_3$ | Recrystallization Yield, % | Recrystallization Solvent | Melting Point | Formula | Analysis, % | Calc. | Found |
|---|---|---|---|---|---|---|---|---|---|---|
| II*a* | H | $C_2H_5$ | $CH_2CH_2OH$ | 73.1 | Ethanol–water (7:3) | 182.5–183.5° | $C_{19}H_{26}N_4O_3$ | C | 63.66 | 63.59 |
| | | | | | | | | H | 7.31 | 7.35 |
| | | | | | | | | N | 15.63 | 15.58 |
| III*a* | Hydrochloride | | | 83.0 | —[a] | 175–177° dec. | $C_{19}H_{27}ClN_4O_3$ | | | |
| II*b* | H | H | $n$-$C_4H_9$ | 92.7 | Toluene | 213.0–214.5° | $C_{19}H_{26}N_4O_2$ | C | 66.64 | 66.53 |
| | | | | | | | | H | 7.65 | 7.70 |
| | | | | | | | | N | 16.36 | 16.32 |
| III*b* | Hydrochloride | | | 87.3 | Water | 228.5–229.5° | $C_{19}H_{27}ClN_4O_2$ | | | |
| II*c* | H | H | $CH_2C_6H_5$ | 84.0 | Ethanol | 179.5–181.0° | $C_{22}H_{24}N_4O_2 \cdot 0.56H_2O$ | C | 68.35 | 68.35 |
| | | | | | | | | H | 6.55 | 6.55 |
| | | | | | | | | N | 14.49 | 14.47 |
| III*c* | Hydrochloride | | | 94.5 | —[a] | 230–232° dec. | $C_{22}H_{25}ClN_4O_2$ | | | |
| II*d*[b] | $CH_3$ | $CH_3$ | $CH_2C_6H_5$ | 70.9 | Methanol | 155–157° | $C_{24}H_{28}N_4O_2$ | C | 71.26 | 71.04 |
| | | | | | | | | H | 6.98 | 7.00 |
| | | | | | | | | N | 13.85 | 13.80 |
| III*d*[c] | Hydrochloride | | | — | — | — | $C_{24}H_{29}ClN_4O_2$ | | | |
| II*e*[b] | $CH_3$ | $C_2H_5$ | $C_2H_5$ | 63.4 | Ethanol–water (3:1) | 167.0–169.0° | $C_{20}H_{28}N_4O_2$ | C | 67.39 | 67.26 |
| | | | | | | | | H | 7.92 | 7.94 |
| | | | | | | | | N | 15.72 | 15.68 |
| III*e* | Hydrochloride | | | 86.3 | —[a] | 204–205° dec. | $C_{20}H_{29}ClN_4O_2$ | | | |
| II*f* | H | $-CH_2CH_2CH_2CH_2-$ | | 92.6 | Ethanol | 243.5–244.5° dec. | $C_{19}H_{24}N_4O_2$ | C | 67.03 | 67.01 |
| | | | | | | | | H | 7.11 | 7.15 |
| | | | | | | | | N | 16.46 | 16.41 |
| III*f* | Hydrochloride | | | 88.9 | Ethanol | 233–234° | $C_{19}H_{25}ClN_4O_2$ | | | |
| II*g* | H | $-CH_2CH_2-O-CH_2CH_2-$ | | 98.2 | Toluene | 258.5–260.0° | $C_{19}H_{24}N_4O_3$ | C | 64.02 | 64.00 |
| | | | | | | | | H | 6.79 | 6.79 |
| | | | | | | | | N | 15.72 | 15.72 |
| III*g* | Hydrochloride | | | 87.3 | —[a] | 266.0–268° dec. | $C_{19}H_{25}ClN_4O_3$ | | | |
| II*h* | H | $-CH_2CH_2-N(CH_3)-CH_2CH_2-$ | | 92.0 | Ethanol | 249.0–251.0° | $C_{20}H_{27}N_5O_2$ | C | 65.01 | 64.88 |
| | | | | | | | | H | 7.37 | 7.42 |
| | | | | | | | | N | 18.95 | 18.88 |
| III*h* | Dihydrochloride | | | 87.3 | —[a] | 246–247.5° dec. | $C_{20}H_{29}Cl_2N_5O_2$ | | | |

[a] Homogeneous on TLC. [b] Racemic. [c] Salt prepared by the addition of concentrated hydrochloric acid to an equimolar amount of the free base (II*d*) suspended in water.

**Table II—Blood Pressure Response[a] to Intraperitoneally Administered 2-(2-Alkylaminoalkylamido)-3-carbamyl-4-methyl-5-benzylpyrroles**

| Compound[b] | Dose, mg/kg | Blood Pressure Response: Onset[c], min | Maximum Change, mm Hg | Average Change, mm Hg | Duration[d], min | Average Duration, min |
|---|---|---|---|---|---|---|
| I | 60 | 0 | 0 | | 0 | |
| II*a* | 100 | 5 | −15 | −7.5 | 25 | 12.5 |
| | | 0 | 0 | | 0 | |
| III*a* | 100 | 0 | 0 | −2.5 | 0 | 7.5 |
| | | 5 | −5 | | 15 | |
| II*b* | 100 | 0 | 0 | | 0 | |
| | | 0 | 0 | | 0 | |
| III*b* | 100 | 5 | +17 | +16 | 21 | 21.5 |
| | | 5 | +15 | | 22 | |
| II*c* | 100 | 0 | 0 | | 0 | |
| | | 0 | 0 | | 0 | |
| III*c* | 100 | 0 | 0 | | 0 | |
| | | 0 | 0 | | 0 | |
| II*d* | 100 | 5 | −32 | −31 | 25 | 25 |
| | | 5 | −30 | | 25 | |
| III*d* | 100 | 5 | −29 | −35.5 | 25 | 25 |
| | | 5 | −40 | | 25 | |
| II*e* | 100 | 5 | +12 | +6 | 25 | 12.5 |
| | | 0 | 0 | | 0 | |
| III*e* | 100 | 5 | −36 | −22 | 20 | 15 |
| | | 5 | −8 | | 10 | |
| II*f* | 100 | 5 | −20 | −6 | 25 | 17.5 |
| | | 5 | +8 | | 10 | |
| III*f* | 100 | 5 | +13 | +10.5 | 25 | 17.5 |
| | | 17 | +8 | | 10 | |
| II*g* | 100 | 5 | −53 | −21.6 | 25 | 21.7 |
| | | 5 | +10 | | 15 | |
| | | 5 | −22 | | 25 | |
| III*g* | 100 | 5 | +40 | +13.5 | 21 | 18.5 |
| | | 5 | −13 | | 16 | |
| II*h* | 100 | 0 | 0 | −5 | 0 | 3.5 |
| | | 23 | −10 | | 7 | |
| III*h* | 100 | 0 | 0 | −12.5 | 0 | 12.5 |
| | | 5 | −25 | | 25 | |
| Hydrazaline | 5 | 5 | −40 | −75 | 25 | 25 |
| | | 5 | −75 | | 25 | |
| | | 5 | −110 | | 25 | |

[a] $n = 2$ or 3. [b] Compound I refers to the benzylcarbamyl analog of lidocaine previously reported (4) and examined (5). Compound II refers to the free base and III refers to the hydrochloride salt of the amine analogs of the benzylcarbamyl derivative. [c] Blood pressure analysis was started 5 min after the intraperitoneal administration of the compound to avoid vehicle artifacts. [d] Duration was defined as the time required for the blood pressure to return to within 95% of the predrug value.

**Table III—Blood Pressure Response to Intravenously Administered 2-(2-Alkylaminoalkylamido)-3-carbamyl-4-methyl-5-benzylpyrroles**

| Compound | Dose, mg/kg | Blood Pressure Response[a] Average Change, mm Hg | Average Duration[b], min | n |
|---|---|---|---|---|
| Ic | 4 | −54.3 | 7.5 | 5 |
| III*d* | 4 | −73 | 30.0 | 3 |
| III*h* | 4 | −43.5 | 2.25 | 2 |

[a] Blood pressure recording was started immediately after the intravenous administration of the compound. [b] Duration was defined as the time required for the blood pressure to return within 95% of the predrug value. [c] Compound I is the benzylcarbamyl analog of lidocaine previously reported (4) and examined (5).

and the vehicle control were administered either intravenously through the jugular cannula or intraperitoneally. Saline (0.1 ml) was used to flush the cannula following each injection of the test compound or vehicle control solution.

Since the average vehicular vasodepressor response lasted 3–4 min following intraperitoneal administration, the maximal response and duration were recorded for each compound between 5 and 30 min. The blood pressure duration response was defined as the time required for the blood pressure to return to within 95% of the predrug value. Data collection of blood pressure activity for the intravenous studies began with the injection of the compound and lasted for 30 min.

## RESULTS

The blood pressure effects of the derivatives of the benzylcarbamyl analog of lidocaine following intraperitoneal administration (60 or 100 mg/kg) appear in Table II. Compounds II*a*–II*h* represent the free base forms, and III*a*–III*h* represent the corresponding hydrochloride salt forms. The most potent agents exhibiting vasodepressor activity were II*d* and III*d*. Compound II*d* lowered the blood pressure an average of 31 mm Hg with a duration of 25 min. Compound III*d* was slightly more active, depressing the blood pressure 35.5 mm Hg with a similar duration (25 min). Other compounds exhibiting vasodepressor activity were III*e* and II*g*, lowering the blood pressure 22 and 21.6 mm Hg with a duration of 15 and 21.7 min, respectively. For comparison, hydralazine, 5 mg/kg, lowered blood pressure 75 mm Hg with a duration of 25 min.

Two compounds (III*b* and III*f*) appeared to exhibit a vasopressor effect, elevating the blood pressure 16 and 10.5 mm Hg with durations of action of 21.5 and 17.5 min, respectively. The remaining compounds in Table II were inactive with respect to vasoactivity or produced inconsistent blood pressure effects.

One of the more potent vasodepressor compounds (III*d*) and one of the more variable compounds (III*h*) from Table II were administered intravenously (Table III) to compare hypotensive activity as a function of administration route. Both III*d* and III*h* exhibited a greater vasodepressor activity when administered intravenously. Compound III*d* was the most active, lowering blood pressure 73 mm Hg with a duration of 30 min.

## DISCUSSION

The present series of amine derivatives of the benzylcarbamyl analog of lidocaine was synthesized to obtain vasodepressor activity following intraperitoneal administration. The derivatives exhibited variable blood pressure effects (Table II). The vasodepressor response obtained following intraperitoneal administration indicates that the compounds can cross biological membranes prior to exerting a hypotensive action. Although the amine derivatives exerted vasodepressor activity, the most active (II*d* and III*d*) appeared to be only one-fortieth as active as hydralazine administered under similar experimental conditions. Comparison of Tables II and III indicates that intravenous administration of III*d* and III*h* produced a greater vasodepressor response than intraperitoneal administration. The decreased activity may be explained by reduced solubility, decreased absorption, or increased metabolism.

The lack of solubility of the compounds as one explanation was supported by the fact that among the active compounds (compounds *d*, *e*, and *h*) the salt was more active than the base in producing vasodepression. The compounds may not have been absorbed well into the blood following intraperitoneal administration since they were not very soluble in common solvents. An alternative explanation may be that the compounds were metabolized at an increased rate following intraperitoneal administration due to first-pass phenomena (6).

In the original series of 2-aminopyrrole analogs of lidocaine (1, 2), the benzylcarbamyl analog was the most potent vasodepressor agent (4). This fact established the structural requirements of the carbamyl function at position 3 and the benzyl group at position 5 of the pyrrole ring for maximal vasodepressor activity. Comparison of the compounds from a structure–activity relationship in the present series indicates that the secondary amines were devoid of vasodepressor activity. The most potent vasodepressors (compounds *d* and *e*) were substituted alpha to the tertiary amino functional group. From the limited data available, it appears that a benzyl substitution on the amino group enhances vasodepressor activity.

The activity of II*d* and III*d* represents an improvement over the parent compound (I), which does not appear to exert hypotensive activity following intraperitoneal administration. Additional structural modifications will be necessary to improve hypotensive activity following intraperitoneal (or oral) administration.

## REFERENCES

(1) R. W. Johnson, T. H. Keenan, J. W. Kosh, and J. W. Sowell, Sr., *J. Pharm. Sci.*, **68**, 955 (1979).

(2) *Ibid.*, **68**, 317 (1979).

(3) J. W. Sowell, Sr., A. J. Block, M. E. Derrick, J. J. Freeman, J. W. Kosh, R. J. Mattson, P. F. Mubarak, and P. A. Tenthorey, *J. Pharm. Sci.*, **70**, 135 (1981).

(4) T. H. Keenan, J. J. Freeman, J. W. Sowell, Sr., and J. W. Kosh, *Pharmacology*, **19**, 36 (1979).

(5) Y. L. Chiang, Master of Science thesis, University of South Carolina, Columbia, S.C., 1979, p. 19.

(6) G. Lukas, S. D. Brindle, and P. Greengard, *J. Pharmacol. Exp. Ther.*, **178**, 562 (1971).

## ACKNOWLEDGMENTS

Supported in part by Dean Julian H. Fincher of the College of Pharmacy and by University Research and Productive Scholarship Grants 11010-E122 and 11010-E121 awarded to J. W. Kosh and J. W. Sowell, respectively, from the University of South Carolina.

The authors are grateful for the technical assistance of Robert Friedman and Rusty Boland and for the excellent typing assistance of Mrs. Sheila B. Lilly.

# Simple High-Performance Liquid Chromatographic Assay for Norethindrone–Mestranol in Combination Tablets

GLORIA M. SUNDARESAN, THOMAS J. GOEHL ˣ, and VADLAMANI K. PRASAD

Received August 21, 1980, from the *Biopharmaceutics Laboratory Branch, Division of Biopharmaceutics, Food and Drug Administration, Washington, DC 20204.* Accepted for publication November 19, 1980.

**Abstract** □ A simple, sensitive, and specific high-performance liquid chromatographic procedure was developed to assay norethindrone–mestranol combination tablets. The method involves a chloroform extraction of a single pulverized tablet. After centrifugation, an aliquot of the supernate was injected into a modular high-performance liquid chromatograph. The effluent from the silica column was monitored serially with a fixed-wavelength UV detector (254 nm) for norethindrone quantitation and a fluorescence detector (230 nm for excitation and 280-nm cutoff filter for emission) for mestranol quantitation. Progesterone was used as an internal standard. The method was employed successfully in content uniformity studies of several brands of commercially available tablets.

**Keyphrases** □ High-performance liquid chromatography—norethindrone–mestranol tablets, content uniformity studies □ Contraceptives—norethindrone–mestranol tablets, high-performance liquid chromatography, content uniformity studies □ Hormones, synthetic—norethindrone–mestranol tablets, high-performance liquid chromatography, content uniformity studies □ Norethindrone–mestranol combinations—high-performance liquid chromatography, content uniformity studies

Two widely used synthetic hormonal contraceptive steroids are norethindrone and mestranol, and various methods have been reported for their assay. Norethindrone was determined by spectrophotometry (1–3), fluorometry (4, 5), and GLC (3, 6). Mestranol also was determined by spectrophotometry (7), fluorometry (8), and GLC (9, 10). Simultaneous analysis of norethindrone and mestranol in combination tablets was achieved by GLC (11), quantitative TLC (12), and high-pressure liquid chromatography (13). The official compendial method (14) for the combination tablets is an automated method utilizing a spectrophotometer and a fluorometer to quantitate norethindrone and mestranol, respectively.

Each published chromatographic method has certain disadvantages. The TLC method requires scanning the plates at two different wavelengths with intervening spraying. The GLC method results in chromatograms with the undesirable characteristic of widely divergent peak heights for the two steroid components. A similar peak height disparity is observed with the reported high-pressure liquid chromatographic method, and the sample preparation technique sometimes results in the solubilization of excipients that interfere in the chromatography.

The present study reports a rapid high-performance liquid chromatographic (HPLC) method for the simultaneous analysis of norethindrone and mestranol in combination tablets using peak height determinations.

## EXPERIMENTAL

**Apparatus**—The modular high-performance liquid chromatograph consisted of a constant flow pump[1], an automated injector[2], a fixed-wavelength UV detector[3] (254 nm), a fluorescence detector[4] (excitation, 230 nm; emission, 280-nm cutoff filter), and a strip-chart recorder[5] (0.5 cm/min). Stainless steel columns[6] (4.6 mm i.d. × 250 mm), packed with fully porous, irregularly shaped 5-μm silica, were obtained commercially. Sample filtration was achieved by employing a syringe-type 25-mm filter holder[7] and 0.5-μm filters[8]. [An oversized filter (47 mm) was used so that it could be wrapped around the holder to improve the seal.]

**Chromatographic Conditions**—The mobile phase was ethylene dichloride–butanol–water (97.5:2.4:0.1). A flow rate of 1.3 ml/min was established (1500 psig), and the column was conditioned initially for 16 hr.

**Reagents and Materials**—Mestranol[9], norethindrone[9], and progesterone[10] were obtained commercially. Solvents were all HPLC grade[11]. Individual stock solutions of mestranol, norethindrone, and progesterone were prepared by dissolving 10, 100, and 400 mg, respectively, in 10 ml of chloroform.

**Glassware Preparation**—All glassware including pipets and syringes were silanized by immersion into a solution of 5% trimethylchlorosilane in toluene for at least 1 hr. Then the glassware was rinsed with toluene, methanol, water, methanol, and chloroform.

**Assay**—A single tablet was crushed to a fine powder in a folded sheet of weighing paper. The powder was transferred into a 15-ml test tube, and 4 ml of chloroform was added. Then 30 μl of the progesterone internal standard solution was added with a 50-μl syringe[12]. The sample was vortexed for ~30 sec, followed by 5–10 min of standing, and then was vortexed again for 1 min. The samples then were centrifuged and filtered through a 0.5-μm filter. The filtrate was transferred to a silanized vial for subsequent loading into the automated injector, which was programmed to inject 2 μl.

The amounts of mestranol and norethindrone in the tablets were determined from standard curves prepared by plotting peak height ratios (mestranol–progesterone or norethindrone–progesterone) *versus* the concentrations of the direct standards. These direct standards were prepared by spiking, into chloroform, both mestranol and norethindrone and then bringing each to a final volume of 4 ml. The amounts of mestranol and norethindrone spiked were 0 and 0, 30 μg and 0.5 mg, 50 μg and 1.0 mg, 100 μg and 2 mg, 150 μg and 2.5 mg, and 500 μg and 7.5 mg, respectively. In some cases, an additional standard (60 μg of mestranol, 10 mg of norethindrone) was included. To each standard was added 30 μl of the internal standard solution.

**Recovery**—Five tablets were ground together to a fine powder. Four aliquots, corresponding to the weight of a single tablet, were placed into individual test tubes. Standard mestranol and norethindrone were added to two of these test tubes. The amounts of the standards added were one-half of the tablet strength of each component. All samples then were assayed. This study was conducted on seven different products[13].

**Precision**—Fifteen tablets of Product F were ground to a fine powder; then 10 aliquots, equivalent to the weight of one tablet, were transferred to 10 test tubes. All samples then were assayed.

**Content Uniformity**—Seven drug products were assayed for content uniformity.

[1] Model M6000A, Waters Associates, Milford, Mass.
[2] Model WISP 710A, Waters Associates, Milford, Mass.
[3] Model 440, Waters Associates, Milford, Mass.
[4] Model FS970, Schoeffel Instruments, Westwood, N.J.
[5] Model 9176, Varian Instruments, Palo Alto, Calif.
[6] Prepacked HI-EFF Micropart column with Lichrosorb Si60 (5 μm) silica, Applied Science Laboratories, State College, Pa.
[7] Swinnex-25, Millipore Corp., Bedford, Mass.
[8] FHUP-047-00, Millipore Corp., Bedford, Mass.
[9] Reference standard, United States Pharmacopeial Convention, Rockville, Md.
[10] Lot 87C-0082, Sigma Chemical Co., St. Louis, Mo.
[11] Burdick & Jackson Laboratories, Muskegon, Mich.
[12] Hamilton Co., Reno, Nev.
[13] Product A, Norinyl 1 + 50; Product B, Norinyl 1 + 80; and Product C, Norinyl 2/100 (Syntex, Humacao, Puerto Rico). Product D, Ortho-Novum 1/50; Product E, Ortho-Novum 1/80; Product F, Ortho-Novum 2/100; and Product G, Ortho-Novum 10/60 (Ortho Pharmaceutical Corp., Raritan, N.J.).



*0022-3549/81/0600-0702$01.00/0*
*© 1981, American Pharmaceutical Association*

**Table I—Recovery Data for Seven Commercial Tablets**

| Product | Assay Results[a] Tablet: Norethindrone, mg | Tablet: Mestranol, μg | Tablet plus Standard[b]: Norethindrone, mg | Tablet plus Standard[b]: Mestranol, μg | Percent Recovery: Norethindrone | Percent Recovery: Mestranol |
|---|---|---|---|---|---|---|
| A 1/50 | 0.99 | 50.0 | 1.46 | 75.9 | 96.0 | 104.0 |
| B 1/80 | 0.95 | 79.0 | 1.48 | 118.6 | 106.0 | 99.0 |
| C 2/100 | 1.91 | 97.4 | 2.90 | 149.0 | 98.5 | 103.0 |
| D 1/50 | 0.99 | 50.0 | 1.46 | 75.9 | 94.0 | 103.7 |
| E 1/80 | 0.95 | 78.8 | 2.44 | 119.0 | 98.0 | 100.5 |
| F 2/100 | 1.90 | 97.3 | 2.90 | 149.0 | 98.0 | 101.4 |
| G 10/60 | 9.63 | 56.3 | 14.65 | 86.2 | 100.4 | 100.0 |

[a] $n = 2$. [b] Added one-half of tablet strength of each component to the tablets.

**Table II—Content Uniformity of Seven Commercial Tablets**

| Product | Mean (*CV*, %): Norethindrone, mg | Mean (*CV*, %): Mestranol, μg | Range: Norethindrone, mg | Range: Mestranol, μg |
|---|---|---|---|---|
| A 1/50 | 1.02 (1.2) | 50.0 (2.5) | 0.99–1.03 | 47.4–51.8 |
| B 1/80 | 1.01 (2.4) | 77.2 (2.8) | 0.97–1.04 | 72.9–80.9 |
| C 2/100 | 1.85 (1.4) | 95.5 (1.8) | 1.80–1.88 | 92.6–97.2 |
| D 1/50 | 0.96 (2.0) | 49.2 (2.2) | 0.94–0.99 | 47.0–50.1 |
| E 1/80 | 0.94 (2.6) | 78.6 (2.2) | 0.92–1.00 | 74.6–80.1 |
| F 2/100 | 1.96 (2.0) | 99.1 (1.8) | 1.91–2.02 | 97.6–101.8 |
| G 10/60 | 9.56 (0.9) | 56.3 (1.0) | 9.42–9.65 | 55.1–57.0 |

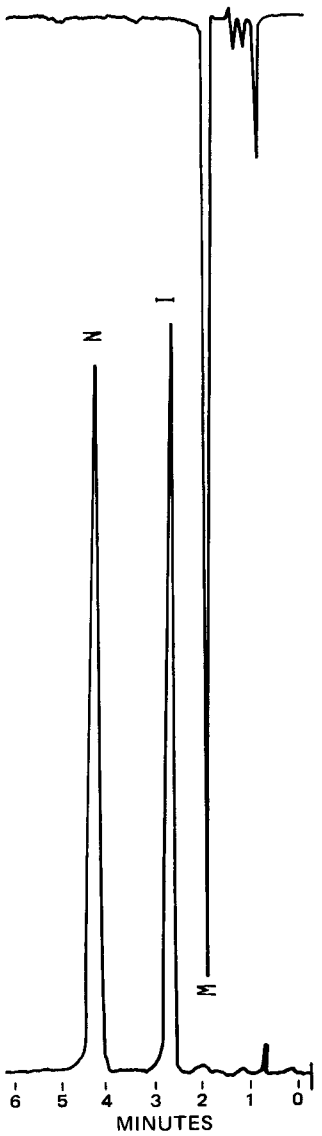


**Figure 1**—*Chromatogram obtained from HPLC assay of Product F. Column effluent was monitored for mestranol (M) using a fluorescence detector (1.0 μA range sensitivity) and for internal standard (I) and norethindrone (N) using an absorbance detector (0.05 aufs).*

## RESULTS AND DISCUSSION

The simultaneous analysis of combination drug products that contain widely different amounts of active components presents unique problems. All of the components of the drug product must be extracted quantitatively, and the detection techniques must give adequate sensitivity for even the lowest level component.

In norethindrone–mestranol tablets, the components are present in ratios from 12:1 to 160:1. Since the solubilities of both components were high in chloroform, this solvent was used for the extraction. The key to resolving the problem of adequate sensitivity for mestranol, the low level component, was the observation that estrogens possess native fluorescence (15) whereas norethindrone does not fluoresce (4). Thus, it seemed plausible to develop an HPLC method that employed a fluorescence detector and an absorbance detector to monitor the column effluent. Initial studies showed that excellent resolution of the tablet components could be obtained using a microparticulate silica column.

A chromatogram obtained in the analysis of Product F is shown in Fig. 1. By using two detectors, it was possible to optimize the response for each steroid component. The retention times for mestranol, progesterone (the internal standard), and norethindrone were 4.0, 5.6, and 8.8 min, respectively.

Initial studies indicated that drug adsorption onto the glassware was occurring. To overcome this problem, all glassware was silanized before use.

A standard linear calibration curve was obtained for direct standard solutions equivalent to 30–100 μg of mestranol/tablet and 0.5–10 mg of norethindrone/tablet. These ranges span those found in all commercially available tablets. The recovery studies were performed on spiked samples of seven drug products. The results (Table I) show excellent recovery in all cases. No interferences from any tablet excipient were observed in the resulting chromatograms. Precision was determined by multiple analyses of aliquots of a Product F composite. The means and coefficients of variation for the assay of mestranol and norethindrone were 101 μg ± 1.8% and 1.94 mg ± 2.0%, respectively. These results demonstrate excellent assay precision. An additional estimate of the precision was obtained by the evaluation of multiple direct standard curves. The values for the slopes were 0.0140 ± 1.6% (coefficient of variation) for mestranol and 0.5543 ± 1.25% for norethindrone.

The USP XX specified that coated tablets and tablets containing 50 mg or less of active ingredient must pass a content uniformity test. The newly developed HPLC assay was used in content uniformity studies of the same seven products examined in the recovery studies. The results established that the batches of the seven formulations met the compendial requirements (Table II). The methodology will be modified and used in planned dissolution studies.

## REFERENCES

(1) J. Y. P. Wu, *J. Assoc. Off. Anal. Chem.*, **57**, 747 (1974).
(2) *Ibid.*, **58**, 75 (1975).
(3) A. P. Shroff and J. Grodsky, *J. Pharm. Sci.*, **56**, 460 (1967).
(4) T. James, *ibid.*, **59**, 1648 (1970).
(5) *Ibid.*, **61**, 1306 (1972).
(6) O. D. Boughton, R. Bryant, W. J. Ludwig, and D. L. Timma, *J. Pharm. Sci.*, **55**, 951 (1966).
(7) J. Y. P. Wu, *J. Assoc. Off. Anal. Chem.*, **54**, 617 (1971).
(8) M. P. Short and C. T. Rhodes, *Can. J. Pharm. Sci.*, **8**, 26 (1973).
(9) A. P. Shroff and R. E. Huettemann, *J. Pharm. Sci.*, **57**, 882 (1968).
(10) B. A. Lodge, *Can. J. Pharm. Sci.*, **5**, 74 (1970).
(11) G. Moretti, G. Cavina, G. Chiapetta, I. Fattori, M. Petrella, and V. Pompi, *Boll. Chim. Farm.*, **116**, 463 (1977).
(12) A. P. Shroff and C. J. Shaw, *J. Chromatogr. Sci.*, **10**, 509 (1972).
(13) P. Helboe and M. Thomsen, *Arch. Pharm. Chemi Sci. Ed.*, **6**, 57 (1978).
(14) "The United States Pharmacopeia," 20th rev., United States Pharmacopeial Convention, Rockville, Md., 1980, p. 557.
(15) D. Duggan, R. Bowman, B. Brodie, and S. Udenfriend, *Arch. Biochem. Biophys.*, **68**, 1 (1957).


# Optical Crystallographic Properties of Drugs of Abuse: Commonly Used Amine Street Drugs


**EDWARD A. JULIAN *x and ELMER M. PLEIN ‡**



Received July 1, 1980, from the **School of Pharmacy, University of Wyoming, Laramie, WY 82071*, and the ‡*School of Pharmacy, University of Washington, Seattle, WA 98195.* Accepted for publication November 21, 1980.



**Abstract** □ The optical crystallographic properties of the diliturate derivatives of amine drugs found in illicit street drug preparations known as "white crosses," "mini-bennies," or "whites" were determined. The crystallographic properties, especially the crystal morphology, extinction angles, and indexes of refraction, identify the drug substances found in the white cross suite. These data can be used with UV and IR spectroscopic and chromatographic evaluations for drug identification.



**Keyphrases** □ Drugs of abuse—substance identification by optical crystallographic properties of diliturate derivatives of amine drugs □ Optical crystallography—substance identification of diliturate derivatives of amine drugs □ Amphetamines—drugs of abuse, identification of drug substance by optical crystallographic properties


Optical chemical crystallography is a physical method for rapid drug identification (1–3). Microchemical properties of amine drug salts have been determined with various reagents (4), but few studies (5, 6) concentrated on the optical crystallographic properties.

The present study reports the optical crystallographic data and constants for the diliturate derivatives of amine drugs found in illicit street drug preparations entitled "white crosses" or "mini-bennies." These preparations are so termed because of the physical shape of the small, white, cross-scored tablets purported to contain 2–8 mg of *d*-methamphetamine (7, 8). However, other drugs have been freely substituted for dextroamphetamine in these street preparations since the 1970 Drug Enforcement Administration Controlled Substances Act made the amphetamines difficult to procure for the street market (8).

## EXPERIMENTAL

**Materials**—The drugs used to prepare the diliturate derivatives were obtained from pharmaceutical manufacturers and chemical supply

**Table I—Optical Properties of Drug Diliturates**

| Derivative[a] (Optic Sign) | System[b] | Optical Orientation | Refractive Indexes | | | 2V by Nomogram[c] Method | Elongation | Habit | Extinction Angle |
|---|---|---|---|---|---|---|---|---|---|
| | | | $\alpha$ | $\beta$ | $\gamma$ | | | | |
| *dl*-Amphetamine (−) | O | Obtuse | 1.470 | 1.645 | 1.698 | 53° | (±) | Acicular | Parallel |
| Dextroamphetamine (−) | O | Obtuse | 1.471 | 1.653 | 1.704 | 52° | (±) | Tabular | Parallel |
| *dl*-Chlorpheniramine (−) | M | Inclined obtuse | 1.512 | 1.682 | 1.732 | 52° | (±) | Lamellar | 15° |
| Diphenhydramine (−) | M | Inclined acute | 1.582 | 1.608 | 1.624 | 75° | (+) | Tabular | 42° |
| *l*-Ephedrine (−) | O | Optic normal | 1.544 | 1.619 | 1.655 | 66° | (−) | Lamellar | Parallel |
| *dl*-Ephedrine (−) | T | Inclined optic axis | 1.537 | 1.662 | 1.731 | 67° | (±) | Tabular | 38° |
| Mephentermine (−) | M | Inclined optic normal | 1.488 | 1.659 | 1.688 | 40° | (−) | Acicular | 27° |
| *dl*-Methamphetamine (−) | M | Inclined obtuse | 1.482 | 1.654 | 1.656 | 8° | (−) | Acicular | 24° |
| *d*-Methamphetamine (−) | M | Acute | 1.545 | 1.648 | 1.705 | 70° | (±) | Tabular | 33° |
| Methapyrilene (−) | M | Inclined obtuse | 1.548 | 1.689 | 1.723 | 48° | (±) | Lamellar | 33° |
| Papaverine (−) | T | Inclined optic normal | 1.493 | 1.742 | 1.785 | 41° | (+) | Prismatic | 27° |
| Phentermine (−) | O | Obtuse | 1.495 | 1.665 | 1.688 | 36° | (−) | Acicular | Parallel |
| Phenylephrine (−) | T | Inclined obtuse | 1.520 | 1.664 | 1.752 | 70° | (±) | Prismatic | 42° |
| *dl*-Phenylpropanolamine (lath) (−) | O | Obtuse | 1.461 | 1.678 | 1.708 | 36° | (−) | Lath | Parallel |
| *dl*-Phenylpropanolamine (lam) (−) | O | Obtuse | 1.471 | 1.663 | 1.685 | 34° | (−) | Lamellar | Parallel |
| Propoxyphene (−) | M | Inclined obtuse | 1.495 | 1.618 | 1.658 | 55° | (±) | Acicular | 15° |
| Pseudoephedrine (−) | O | Optic normal | 1.520 | 1.622 | 1.640 | 36° | (+) | Prismatic | Parallel |
| Diliturie acid (−) | M | Inclined obtuse | 1.388 | 1.684 | >1.785 | 50° est. | (−) | Tabular | 9° |


[a] The authors acknowledge supplies of *dl*-chlorpheniramine (Chlortrimeton, Schering), mephentermine (Wyamine, Wyeth), methapyrilene (Histadyl, Lilly), phentermine (Ionamine, Penwalt), propoxyphene (Darvon, Lilly), and pseudoephedrine (Sudafed, Burroughs Wellcome) and express their appreciation to the manufacturers who supplied the amine salts.

[b] O = orthorhombic, M = monoclinic, and T = triclinic. [c] Determined by the method of Hartshorne and Stuart (11).




*0022-3549/81/0600-0704$01.00/0*


*© 1981, American Pharmaceutical Association*

## REFERENCES

(1) J. Y. P. Wu, *J. Assoc. Off. Anal. Chem.*, **57**, 747 (1974).
(2) *Ibid.*, **58**, 75 (1975).
(3) A. P. Shroff and J. Grodsky, *J. Pharm. Sci.*, **56**, 460 (1967).
(4) T. James, *ibid.*, **59**, 1648 (1970).
(5) *Ibid.*, **61**, 1306 (1972).
(6) O. D. Boughton, R. Bryant, W. J. Ludwig, and D. L. Timma, *J. Pharm. Sci.*, **55**, 951 (1966).
(7) J. Y. P. Wu, *J. Assoc. Off. Anal. Chem.*, **54**, 617 (1971).
(8) M. P. Short and C. T. Rhodes, *Can. J. Pharm. Sci.*, **8**, 26 (1973).
(9) A. P. Shroff and R. E. Huettemann, *J. Pharm. Sci.*, **57**, 882 (1968).
(10) B. A. Lodge, *Can. J. Pharm. Sci.*, **5**, 74 (1970).
(11) G. Moretti, G. Cavina, G. Chiapetta, I. Fattori, M. Petrella, and V. Pompi, *Boll. Chim. Farm.*, **116**, 463 (1977).
(12) A. P. Shroff and C. J. Shaw, *J. Chromatogr. Sci.*, **10**, 509 (1972).
(13) P. Helboe and M. Thomsen, *Arch. Pharm. Chemi Sci. Ed.*, **6**, 57 (1978).
(14) "The United States Pharmacopeia," 20th rev., United States Pharmacopeial Convention, Rockville, Md., 1980, p. 557.
(15) D. Duggan, R. Bowman, B. Brodie, and S. Udenfriend, *Arch. Biochem. Biophys.*, **68**, 1 (1957).


# Optical Crystallographic Properties of Drugs of Abuse: Commonly Used Amine Street Drugs


**EDWARD A. JULIAN *x and ELMER M. PLEIN ‡**



Received July 1, 1980, from the **School of Pharmacy, University of Wyoming, Laramie, WY 82071*, and the ‡*School of Pharmacy, University of Washington, Seattle, WA 98195.* Accepted for publication November 21, 1980.



**Abstract** □ The optical crystallographic properties of the diliturate derivatives of amine drugs found in illicit street drug preparations known as "white crosses," "mini-bennies," or "whites" were determined. The crystallographic properties, especially the crystal morphology, extinction angles, and indexes of refraction, identify the drug substances found in the white cross suite. These data can be used with UV and IR spectroscopic and chromatographic evaluations for drug identification.



**Keyphrases** □ Drugs of abuse—substance identification by optical crystallographic properties of diliturate derivatives of amine drugs □ Optical crystallography—substance identification of diliturate derivatives of amine drugs □ Amphetamines—drugs of abuse, identification of drug substance by optical crystallographic properties


Optical chemical crystallography is a physical method for rapid drug identification (1–3). Microchemical properties of amine drug salts have been determined with various reagents (4), but few studies (5, 6) concentrated on the optical crystallographic properties.

The present study reports the optical crystallographic data and constants for the diliturate derivatives of amine drugs found in illicit street drug preparations entitled "white crosses" or "mini-bennies." These preparations are so termed because of the physical shape of the small, white, cross-scored tablets purported to contain 2–8 mg of *d*-methamphetamine (7, 8). However, other drugs have been freely substituted for dextroamphetamine in these street preparations since the 1970 Drug Enforcement Administration Controlled Substances Act made the amphetamines difficult to procure for the street market (8).

## EXPERIMENTAL

**Materials**—The drugs used to prepare the diliturate derivatives were obtained from pharmaceutical manufacturers and chemical supply

**Table I—Optical Properties of Drug Diliturates**

| Derivative[a] (Optic Sign) | System[b] | Optical Orientation | Refractive Indexes | | | 2V by Nomogram[c] Method | Elongation | Habit | Extinction Angle |
|---|---|---|---|---|---|---|---|---|---|
| | | | $\alpha$ | $\beta$ | $\gamma$ | | | | |
| *dl*-Amphetamine (−) | O | Obtuse | 1.470 | 1.645 | 1.698 | 53° | (±) | Acicular | Parallel |
| Dextroamphetamine (−) | O | Obtuse | 1.471 | 1.653 | 1.704 | 52° | (±) | Tabular | Parallel |
| *dl*-Chlorpheniramine (−) | M | Inclined obtuse | 1.512 | 1.682 | 1.732 | 52° | (±) | Lamellar | 15° |
| Diphenhydramine (−) | M | Inclined acute | 1.582 | 1.608 | 1.624 | 75° | (+) | Tabular | 42° |
| *l*-Ephedrine (−) | O | Optic normal | 1.544 | 1.619 | 1.655 | 66° | (−) | Lamellar | Parallel |
| *dl*-Ephedrine (−) | T | Inclined optic axis | 1.537 | 1.662 | 1.731 | 67° | (±) | Tabular | 38° |
| Mephentermine (−) | M | Inclined optic normal | 1.488 | 1.659 | 1.688 | 40° | (−) | Acicular | 27° |
| *dl*-Methamphetamine (−) | M | Inclined obtuse | 1.482 | 1.654 | 1.656 | 8° | (−) | Acicular | 24° |
| *d*-Methamphetamine (−) | M | Acute | 1.545 | 1.648 | 1.705 | 70° | (±) | Tabular | 33° |
| Methapyrilene (−) | M | Inclined obtuse | 1.548 | 1.689 | 1.723 | 48° | (±) | Lamellar | 33° |
| Papaverine (−) | T | Inclined optic normal | 1.493 | 1.742 | 1.785 | 41° | (+) | Prismatic | 27° |
| Phentermine (−) | O | Obtuse | 1.495 | 1.665 | 1.688 | 36° | (−) | Acicular | Parallel |
| Phenylephrine (−) | T | Inclined obtuse | 1.520 | 1.664 | 1.752 | 70° | (±) | Prismatic | 42° |
| *dl*-Phenylpropanolamine (lath) (−) | O | Obtuse | 1.461 | 1.678 | 1.708 | 36° | (−) | Lath | Parallel |
| *dl*-Phenylpropanolamine (lam) (−) | O | Obtuse | 1.471 | 1.663 | 1.685 | 34° | (−) | Lamellar | Parallel |
| Propoxyphene (−) | M | Inclined obtuse | 1.495 | 1.618 | 1.658 | 55° | (±) | Acicular | 15° |
| Pseudoephedrine (−) | O | Optic normal | 1.520 | 1.622 | 1.640 | 36° | (+) | Prismatic | Parallel |
| Diliturie acid (−) | M | Inclined obtuse | 1.388 | 1.684 | >1.785 | 50° est. | (−) | Tabular | 9° |


[a] The authors acknowledge supplies of *dl*-chlorpheniramine (Chlortrimeton, Schering), mephentermine (Wyamine, Wyeth), methapyrilene (Histadyl, Lilly), phentermine (Ionamine, Penwalt), propoxyphene (Darvon, Lilly), and pseudoephedrine (Sudafed, Burroughs Wellcome) and express their appreciation to the manufacturers who supplied the amine salts.

[b] O = orthorhombic, M = monoclinic, and T = triclinic. [c] Determined by the method of Hartshorne and Stuart (11).




*0022-3549/81/0600-0704$01.00/0*


*© 1981, American Pharmaceutical Association*

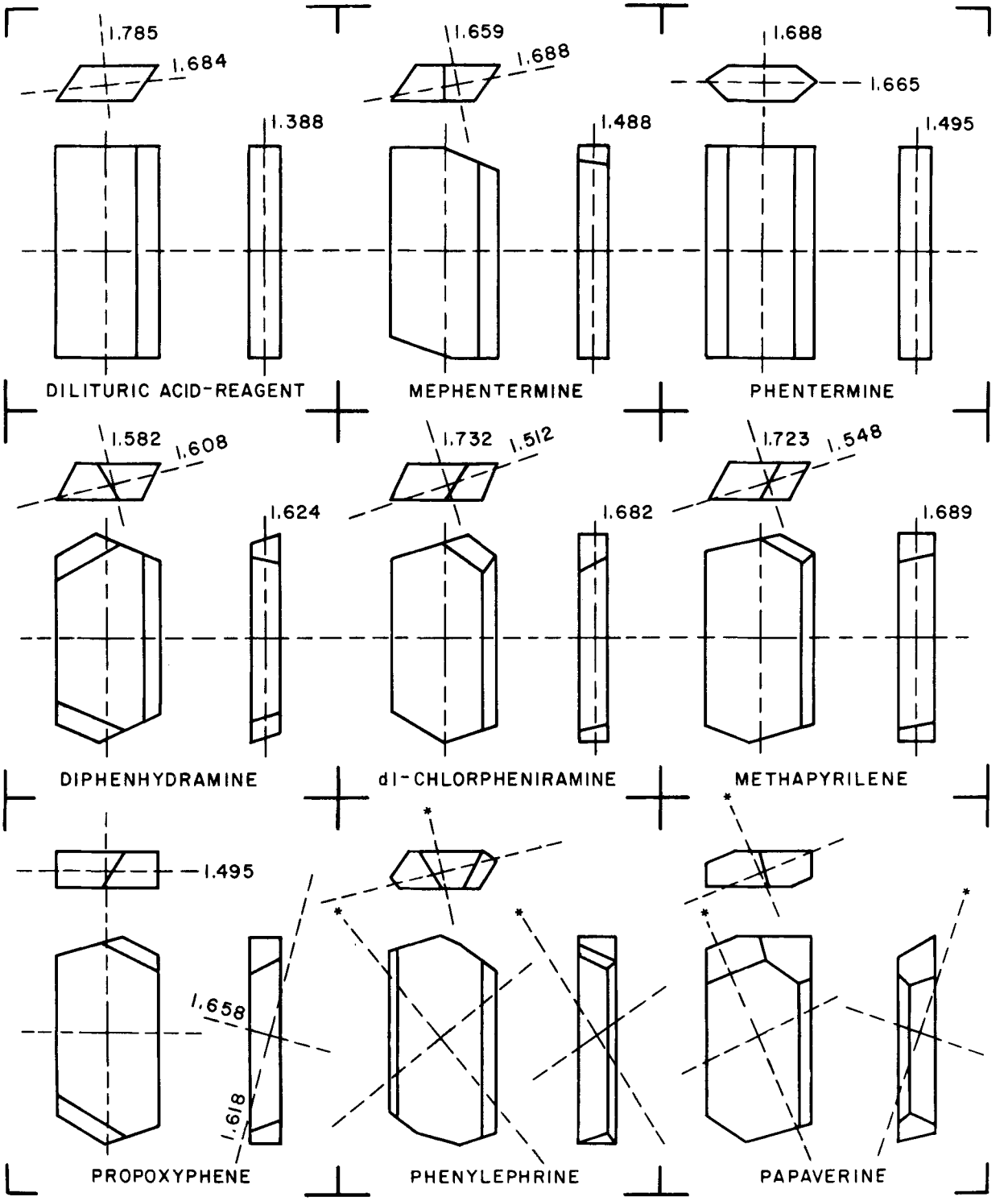


**Figure 1**—*Drawings of amine dilituratates: white cross suite.*

houses. The index of refraction standards[1,2] and the dilituric acid[3] (5-nitrobarbituric acid) used to prepare the crystalline derivatives also were purchased commercially.

**Methods**—The method utilized to prepare dilituric acid derivatives of the amine salts was that of Plein and Dewey (9). Briefly, 100 mg of the amine salt was dissolved in a minimum of water, and 10 ml of a hot, 1% aqueous solution of dilituric acid was added. The dilituratates of the amines crystallized out upon cooling in most cases, and the crystalline derivatives were recrystallized from water one to several times until compounds with sharp melting points were obtained. The purity of the salts was established by determination of percent nitrogen. All compounds analyzed for nitrogen were within 0.3% of the calculated theoretical values.

The optical data for the dilituratates of the white cross amines were determined using literature methods (9–11). The highest index of refraction liquid standard in the authors' sets of liquids was 1.785, so no value above this figure is reported. Crushed specimens were necessary to obtain some refractive indexes.

In this study, the $2V$ values were determined by a nomogram method (11). Briefly, the nomogram was utilized as a base upon which the three known refractive indexes were used to determine the fourth variable $V$ ($V = \cos^2 \theta$).

[1] R. P. Cargille Co., Cedar Grove, N.J.
[2] Series $n$ = 1.400–1.785 in increments of $n$ = 0.002 at 25°.
[3] EK-2502, Eastman Kodak Co., Rochester, N.Y.

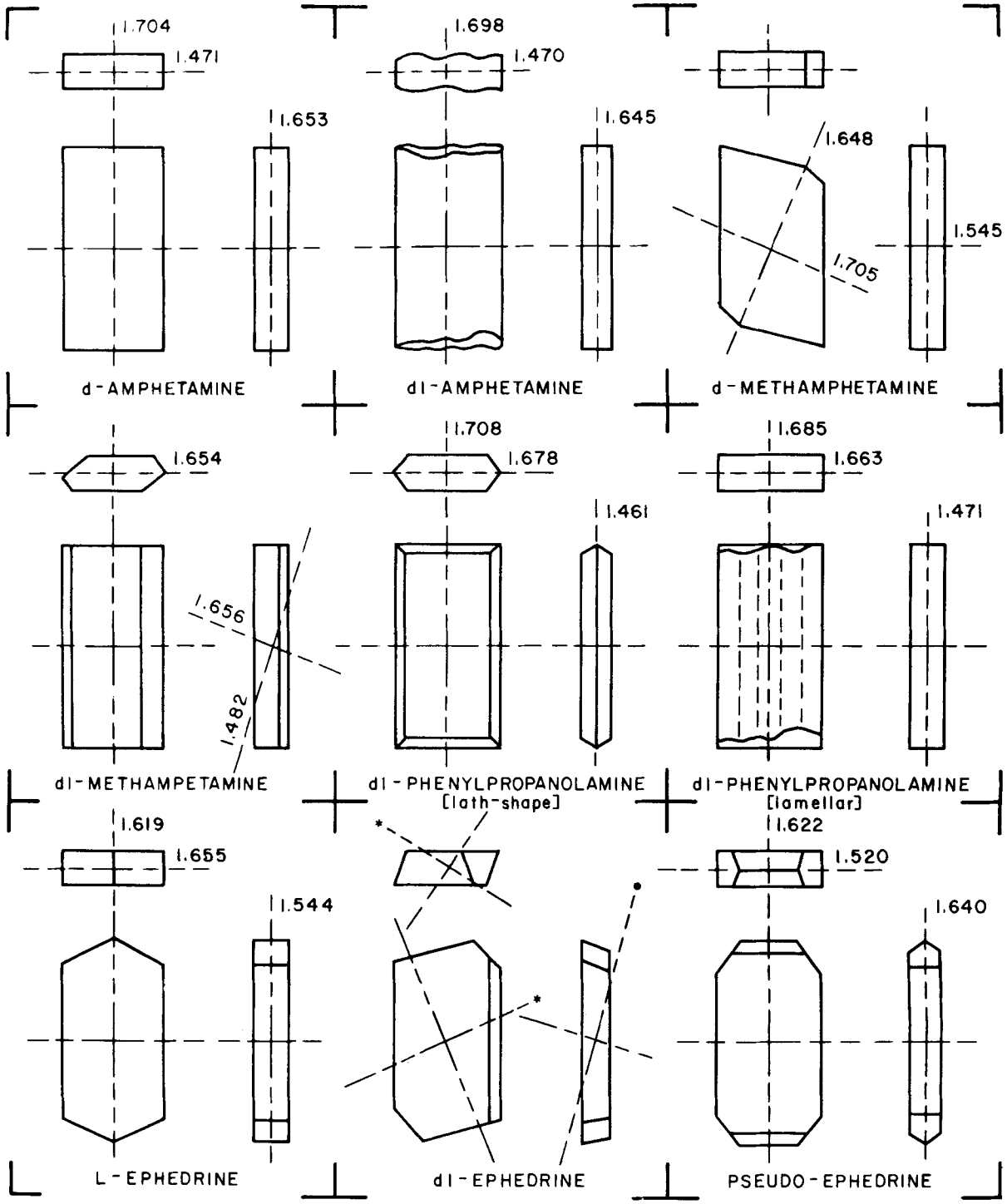


**Figure 2**—*Drawings of more amine dilituratesː white cross suite.*

## RESULTS AND DISCUSSION

The crystallographic properties of the amine dilituratesare reported in Table I and are shown in Figs. 1 and 2. Many of the crystal derivatives are so flattened that they tend to assume a common orientation when immersed in the index oils on the microscope slide. The apparent properties of habit, optical orientation, and extinction angle of each crystalline derivative as observed on the most frequently occurring orientation are listed in Table I. The optical orientations designated as acute, obtuse, and optic normal indicate that a "centered" interference figure was observed upon an uncrushed crystal in its most frequently occurring orientation. The descriptive term "inclined" denotes that centered figures were not observed on the usual orientation of the crystal; therefore, one or both refractive indexes of the front face of the crystal would be variable.

Additional optical crystallographic properties reported in Table I are the three refractive indexes, crystal system, optic sign, elongation, and optic axial angle ($2V$). The $2V$ value is an optical parameter that can distinguish between two or more similar crystals, *e.g.*, *dl*-chlorpheniramine ($2V = 52°$) and diphenhydramine ($2V = 75°$).

Figures 1 and 2 present orthographic projection drawings of the crystals showing the front, side, and top views. These drawings supplement the data appearing in Table I and the text, and they facilitate the identification of the crystalline derivatives. Dashed lines represent the vibration directions, and refractive indexes are recorded for crystals that show consistent indexes in these directions. An asterisk indicates the higher index value on views in which consistent refractive indexes could not be obtained. Crystal angles measured microscopically are shown in the corners of the diagrams.

Additional discussion of properties of the reagent and derivatives will

facilitate identification by optical crystallographic methods. Dilituric acid rarely crystallized out of the reaction solution in the concentration utilized; however, dilituric acid crystals appeared as small square- to rectangular-shaped tablets with a low $\alpha$ index ($n$ = 1.388), running parallel to the crystal length and showing a low extinction angle (9°) on the top face.

Dextroamphetamine crystallized out as thin rectangular platelets that showed bright first- to second-order polarization colors under crossed nicols as compared to its *dl*-isomer, which was observed as poorly formed acicular prisms showing a high birefringence. *d*-Methamphetamine appeared as large, well-formed, lamellar platelets twinned on 001, showing bright polarization colors and a front face extinction angle of 33°. Its *dl*-isomer occurred as bundles of elongated rods with a notably small $2V$ = 8°. Both isomers are monoclinic crystals as compared to the two amphetamine isomers which show orthorhombic symmetry.

Derivatives of *l*-ephedrine, racephedrine, *dl*-chlorpheniramine, methapyrilene, and diphenhydramine crystallized out as six-sided platelets. The two ephedrine isomers crystallized out as large hexagonal platelets. *l*-Ephedrine showed orthorhombic symmetry, while racephedrine crystallized out as a large, yellow, triclinic platelet with a 38° extinction angle on the front face. *dl*-Chlorpheniramine had a crystal size smaller than the ephedrines and also showed monoclinic symmetry with an extinction angle of 15° on the top face. Methapyrilene and diphenhydramine appeared as monoclinic crystals with extinction angles of 33 and 42°, respectively, on the top face. However, diphenhydramine occurred as stellate rosettes, and the crystals showed a large $2V$ = 75°; methapyrilene appeared as a diamond-shaped crystal with a moderate $2V$ = 48°.

Propoxyphene dilituate occurred as long, acicular, monoclinic crystals that crystallized out in stellate rosettes. The side face of this crystal showed a 15° extinction angle. The mephentermine derivative was a long, acicular, monoclinic crystal with an extinction angle of 27° appearing on the top face; the phentermine dilituate, which was of the same crystal habit, showed orthorhombic symmetry.

Pseudoephedrine, phenylephrine, and papaverine dilituates crystallized out as prisms. Derivatives of both pseudoephedrine and phenylephrine were elongated in form but were distinguished easily from each other since pseudoephedrine had an orthorhombic symmetry and a low $2V$ = 36° while phenylephrine appeared as a triclinic crystal with a $2V$ = 70° and a front face extinction angle of 42°. The papaverine dilituate was observed as an almost equant triclinic prism with multifaceted sides.

## REFERENCES


(1) W. C. McCrone, *Am. Lab.*, **7**, 11 (Apr. 1975).

(2) R. E. Stevens, *Microchem. J.*, **13**, 42 (1968).

(3) E. A. Julian and E. M. Plein, *J. Am. Pharm. Assoc., Sci. Ed.*, **48**, 207 (1959).

(4) J. E. Koles, in "Progress in Chemical Toxicology," vol. 5, A. Stolman, Ed., Academic, New York, N.Y., 1974, pp. 293–368.

(5) E. M. Plein, *J. Am. Pharm. Assoc., Sci. Ed.*, **38**, 535 (1949).

(6) E. A. Julian and E. M. Plein, *J. Pharm. Sci.*, **54**, 648 (1965).

(7) J. P. Morgan and D. Kagan, *J. Psychedelic Drugs*, **10**, 303 (1978).

(8) D. C. Perry, *Pharmchem. Newsl.*, **6**(3), 1 (1977).

(9) E. M. Plein and B. T. Dewey, *Ind. Eng. Chem., Anal. Ed.*, **15**, 534 (1943).

(10) E. M. Chamot and C. W. Mason, "Handbook of Chemical Microscopy," vol. I, 3rd ed., Wiley, New York, N.Y., 1958.

(11) N. H. Hartshorne and A. Stuart, "Crystals and the Polarising Microscope," 4th ed., Edward Arnold, London, England, 1970.


# High-Pressure Liquid Chromatographic Analysis of Phenylpropanolamine in Human Plasma following Derivatization with *O*-Phthalaldehyde


**WILLIAM D. MASON ˣ and EDWIN N. AMICK ***



Received August 12, 1980, from the *Pharmacokinetics Laboratory, Schools of Pharmacy and Medicine, University of Missouri–Kansas City, Kansas City, MO 64108.* Accepted for publication December 2, 1980. *Present address: Kansas City Analytical Services, Kansas City, MO 64127.



**Abstract** □ A high-pressure liquid chromatographic analysis of phenylpropanolamine in human plasma following extraction, back-extraction, and *O*-phthalaldehyde derivatization is presented. Using fluorescence detection, the method was sufficiently sensitive to quantitate as little as 5 ng of drug/ml of plasma; the coefficient of variation below 100 ng/ml ranged between 5.7 and 2.8%. Plasma concentration data following a single 25-mg dose of phenylpropanolamine hydrochloride in 12 healthy volunteers demonstrate the application of the analytical method.



**Keyphrases** □ High-pressure liquid chromatography—phenylpropanolamine analysis in human plasma, *O*-phthalaldehyde derivatization □ Phenylpropanolamine—high-pressure liquid chromatographic analysis in human plasma, *O*-phthalaldehyde derivatization □ Derivatization—*O*-phthalaldehyde, high-pressure liquid chromatographic analysis in human plasma


There is great interest in measuring plasma phenylpropanolamine concentrations following single therapeutic doses (25 mg of phenylpropanolamine hydrochloride) of this sympathomimetic agent. GLC following formation of a heptafluorobutyryl derivative (1) was used previously (2, 3) to study phenylpropanolamine pharmacokinetics and was adequate when doses of 60 mg or more were administered or when plasma concentrations were >40 ng/ml and 2 ml of plasma was available for each determination. TLC following acetylation with tritiated acetic anhydride (4) suffers from a high coefficient of variation and nonlinearity.

After preliminary studies of GLC and liquid chromatography with absorbance detection were found to have inadequate specificity and sensitivity, the present method was developed. Previous investigators (5–7) showed that *O*-phthalaldehyde, in the presence of 2-mercaptoethanol, reacts with primary amines to form highly fluorescent products, 1-alkylthio-2-alkyl-substituted isoindoles (8). Replacing 2-mercaptoethanol with ethanethiol was reported to provide a more stable product (9), but the latter is difficult to work with due to its unpleasant odor.

A procedure for extraction of phenylpropanolamine and an internal standard from plasma, derivatization with *O*-phthalaldehyde, separation by high-pressure liquid chromatography (HPLC), and detection by fluorescence


*0022-3549/81/0600-0707$01.00/0*


*© 1981, American Pharmaceutical Association*

facilitate identification by optical crystallographic methods. Dilituric acid rarely crystallized out of the reaction solution in the concentration utilized; however, dilituric acid crystals appeared as small square- to rectangular-shaped tablets with a low $\alpha$ index ($n$ = 1.388), running parallel to the crystal length and showing a low extinction angle (9°) on the top face.

Dextroamphetamine crystallized out as thin rectangular platelets that showed bright first- to second-order polarization colors under crossed nicols as compared to its *dl*-isomer, which was observed as poorly formed acicular prisms showing a high birefringence. *d*-Methamphetamine appeared as large, well-formed, lamellar platelets twinned on 001, showing bright polarization colors and a front face extinction angle of 33°. Its *dl*-isomer occurred as bundles of elongated rods with a notably small $2V$ = 8°. Both isomers are monoclinic crystals as compared to the two amphetamine isomers which show orthorhombic symmetry.

Derivatives of *l*-ephedrine, racephedrine, *dl*-chlorpheniramine, methapyrilene, and diphenhydramine crystallized out as six-sided platelets. The two ephedrine isomers crystallized out as large hexagonal platelets. *l*-Ephedrine showed orthorhombic symmetry, while racephedrine crystallized out as a large, yellow, triclinic platelet with a 38° extinction angle on the front face. *dl*-Chlorpheniramine had a crystal size smaller than the ephedrines and also showed monoclinic symmetry with an extinction angle of 15° on the top face. Methapyrilene and diphenhydramine appeared as monoclinic crystals with extinction angles of 33 and 42°, respectively, on the top face. However, diphenhydramine occurred as stellate rosettes, and the crystals showed a large $2V$ = 75°; methapyrilene appeared as a diamond-shaped crystal with a moderate $2V$ = 48°.

Propoxyphene dilituate occurred as long, acicular, monoclinic crystals that crystallized out in stellate rosettes. The side face of this crystal showed a 15° extinction angle. The mephentermine derivative was a long, acicular, monoclinic crystal with an extinction angle of 27° appearing on the top face; the phentermine dilituate, which was of the same crystal habit, showed orthorhombic symmetry.

Pseudoephedrine, phenylephrine, and papaverine dilituates crystallized out as prisms. Derivatives of both pseudoephedrine and phenylephrine were elongated in form but were distinguished easily from each other since pseudoephedrine had an orthorhombic symmetry and a low $2V$ = 36° while phenylephrine appeared as a triclinic crystal with a $2V$ = 70° and a front face extinction angle of 42°. The papaverine dilituate was observed as an almost equant triclinic prism with multifaceted sides.

## REFERENCES


(1) W. C. McCrone, *Am. Lab.*, **7**, 11 (Apr. 1975).

(2) R. E. Stevens, *Microchem. J.*, **13**, 42 (1968).

(3) E. A. Julian and E. M. Plein, *J. Am. Pharm. Assoc., Sci. Ed.*, **48**, 207 (1959).

(4) J. E. Koles, in "Progress in Chemical Toxicology," vol. 5, A. Stolman, Ed., Academic, New York, N.Y., 1974, pp. 293–368.

(5) E. M. Plein, *J. Am. Pharm. Assoc., Sci. Ed.*, **38**, 535 (1949).

(6) E. A. Julian and E. M. Plein, *J. Pharm. Sci.*, **54**, 648 (1965).

(7) J. P. Morgan and D. Kagan, *J. Psychedelic Drugs*, **10**, 303 (1978).

(8) D. C. Perry, *Pharmchem. Newsl.*, **6**(3), 1 (1977).

(9) E. M. Plein and B. T. Dewey, *Ind. Eng. Chem., Anal. Ed.*, **15**, 534 (1943).

(10) E. M. Chamot and C. W. Mason, "Handbook of Chemical Microscopy," vol. I, 3rd ed., Wiley, New York, N.Y., 1958.

(11) N. H. Hartshorne and A. Stuart, "Crystals and the Polarising Microscope," 4th ed., Edward Arnold, London, England, 1970.


# High-Pressure Liquid Chromatographic Analysis of Phenylpropanolamine in Human Plasma following Derivatization with *O*-Phthalaldehyde


**WILLIAM D. MASON ˣ and EDWIN N. AMICK ***



Received August 12, 1980, from the *Pharmacokinetics Laboratory, Schools of Pharmacy and Medicine, University of Missouri–Kansas City, Kansas City, MO 64108.* Accepted for publication December 2, 1980. *Present address: Kansas City Analytical Services, Kansas City, MO 64127.



**Abstract** □ A high-pressure liquid chromatographic analysis of phenylpropanolamine in human plasma following extraction, back-extraction, and *O*-phthalaldehyde derivatization is presented. Using fluorescence detection, the method was sufficiently sensitive to quantitate as little as 5 ng of drug/ml of plasma; the coefficient of variation below 100 ng/ml ranged between 5.7 and 2.8%. Plasma concentration data following a single 25-mg dose of phenylpropanolamine hydrochloride in 12 healthy volunteers demonstrate the application of the analytical method.



**Keyphrases** □ High-pressure liquid chromatography—phenylpropanolamine analysis in human plasma, *O*-phthalaldehyde derivatization □ Phenylpropanolamine—high-pressure liquid chromatographic analysis in human plasma, *O*-phthalaldehyde derivatization □ Derivatization—*O*-phthalaldehyde, high-pressure liquid chromatographic analysis in human plasma


There is great interest in measuring plasma phenylpropanolamine concentrations following single therapeutic doses (25 mg of phenylpropanolamine hydrochloride) of this sympathomimetic agent. GLC following formation of a heptafluorobutyryl derivative (1) was used previously (2, 3) to study phenylpropanolamine pharmacokinetics and was adequate when doses of 60 mg or more were administered or when plasma concentrations were >40 ng/ml and 2 ml of plasma was available for each determination. TLC following acetylation with tritiated acetic anhydride (4) suffers from a high coefficient of variation and nonlinearity.

After preliminary studies of GLC and liquid chromatography with absorbance detection were found to have inadequate specificity and sensitivity, the present method was developed. Previous investigators (5–7) showed that *O*-phthalaldehyde, in the presence of 2-mercaptoethanol, reacts with primary amines to form highly fluorescent products, 1-alkylthio-2-alkyl-substituted isoindoles (8). Replacing 2-mercaptoethanol with ethanethiol was reported to provide a more stable product (9), but the latter is difficult to work with due to its unpleasant odor.

A procedure for extraction of phenylpropanolamine and an internal standard from plasma, derivatization with *O*-phthalaldehyde, separation by high-pressure liquid chromatography (HPLC), and detection by fluorescence


*0022-3549/81/0600-0707$01.00/0*


*© 1981, American Pharmaceutical Association*

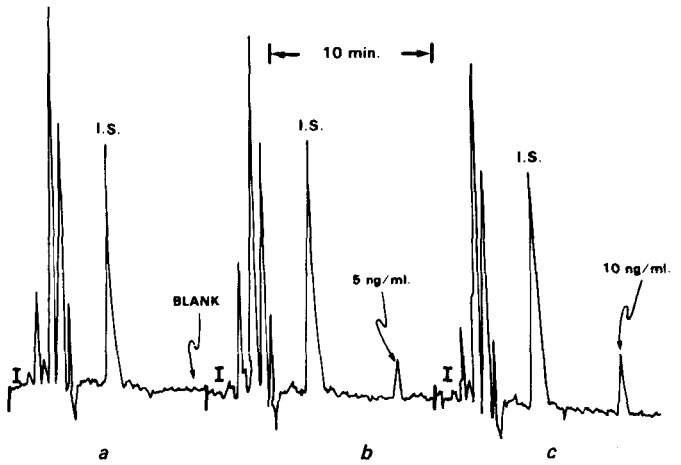


**Figure 1**—*HPLC tracings for plasma. Key:* a, *blank plasma;* b, *5 ng of phenylpropanolamine added to 1 ml of plasma; and* c, *10 ng of phenylpropanolamine added to 1 ml of plasma.*

is presented in this report. The procedure can differentiate plasma with as little as 1 ng/ml from a blank and can quantitate plasma concentrations above 5 ng/ml with accuracy and precision suitable for pharmacokinetic studies.

## EXPERIMENTAL

**Materials**—UV grade butyl chloride[1], 1-butanol[1], methanol[1], and acetonitrile[1] were employed without further preparation. Reagent grade ammonium acetate[2], boric acid[3], and ACS grade acetic acid[3] also were used as received. A derivatization solution was prepared by dissolving 50 mg of crystalline *O*-phthalaldehyde[4] in 2 ml of methanol, adding 0.2 ml of 2-mercaptoethanol[5], and diluting to 100 ml with 0.4 *M* borate buffer (pH 10.5). Phenylpropanolamine hydrochloride[6] and viloxazine hydrochloride[7] [2-(2-ethoxyphenoxymethyl)tetrahydro-1,4-oxazine hydrochloride, ICI-58,834] were used as received.

**Apparatus**—The HPLC system consisted of a pump[8], an injector[9], a 5-μm ODS column[10], and a fluorescence detector[11]. Excitation was at 230 nm (sensitivity, photomultiplier tube voltage setting, at 380 and time constant of 2.0 sec), and no filters were employed between the flowcell and photomultiplier tube. The window of the photomultiplier served as a 280-nm cutoff filter. The detection range was set at 0.2 with the recorder[12] input set to provide tracings corresponding to 0.2 and 0.02 and a chart speed of 0.5 cm/min.

**Plasma Extraction**—One milliliter of plasma, 0.1 ml of 0.1 *N* NaOH, and 8.0 ml of extraction solution (10% v/v 1-butanol in butyl chloride with 0.60 μg of viloxazine/ml as the internal standard) were placed in a 15-ml centrifuge tube. This mixture was vortexed for 60 sec and centrifuged for 5 min, and the organic layer (upper) was transferred to a second 15-ml centrifuge tube containing 300 μl of 1% acetic acid.

Back-extraction was effected by vortexing for 60 sec, and the layers were separated by centrifugation. The organic layer (upper) was discarded by aspiration, leaving the aqueous layer for derivatization. This acetic acid back-extract was stable for several days.

**Derivatization**—A 50-μl syringe was used to transfer 40 μl of a 1% acetic acid back-extract into a 4.0-ml glass tube to which 20 μl of the *O*-phthalaldehyde reagent then was added, and the solution was vortexed for 10 sec. The reaction was allowed to proceed exactly 60 sec, and then 200 μl of 1% acetic acid was added. The solution was vortexed, and 100 μl was injected immediately into the HPLC system.

**Chromatography**—A mobile phase was prepared by dissolving 10.4 g of ammonium acetate in 2400 ml of water and adding 8.0 ml of acetic acid and sufficient acetonitrile to obtain a 40% solution by volume (pH 5.6). With a flow rate of 1.8 ml/min in the HPLC system, a pressure of 2000 psig resulted. The retention times of viloxazine and the phenylpropanolamine derivative were 5.8 and 8.2 min, respectively.

**Clinical Study**—As part of a bioavailability study, 12 normal healthy subjects received single 25-mg doses of phenylpropanolamine hydrochloride in solution following an overnight fast. Blood samples were collected at 0, 0.5, 1, 1.5, 2, 3, 4, 6, 8, 12, and 24 hr in heparin-containing vacuum containers[13]. The plasma was separated immediately by centrifugation and frozen within 20 min. All samples were maintained frozen at −10° until assayed.

**Table I—Precision and Accuracy of Phenylpropanolamine Analysis**

| Actual Concentration[a], ng/ml | Number of Samples | Mean Concentration, ng/ml | *SD* | *CV*, % |
|---|---|---|---|---|
| 17.3 | 12 | 17.2 | 0.98 | 5.7 |
| 20.0 | 12 | 20.1 | 1.13 | 5.7 |
| 40.0 | 10 | 38.8 | 1.72 | 4.4 |
| 50.0 | 20 | 49.8 | 2.13 | 4.3 |
| 80.6 | 12 | 80.3 | 2.22 | 2.8 |
| 100 | 20 | 101 | 3.20 | 3.2 |
| 150 | 10 | 148 | 6.33 | 4.3 |
| 200 | 24 | 201 | 7.68 | 3.8 |

## RESULTS AND DISCUSSION

Figure 1 presents chromatograms for plasma containing 0, 5, and 10 ng of phenylpropanolamine/ml. Analysis of predose plasma samples from 22 human subjects and several batches of pooled human plasma presented no chromatographic peaks that interfered with the internal standard or phenylpropanolamine derivative. A previous report (10) suggested that no significant metabolism of phenylpropanolamine occurs, so *in vivo* interference by metabolites probably was not a problem. The ratio of the peak height of the phenylpropanolamine derivative to the viloxazine peak height varied linearly with the plasma phenylpropanolamine concentration range studied (*i.e.*, <200 ng/ml). A typical standard curve (20 points between 5 and 200 ng/ml), with the peak height ratio as the abscissa and plasma phenylpropanolamine as the ordinate, had a slope of 27.94 ng/ml and an intercept of −0.32 ng/ml with a correlation coefficient of 0.9976.

Table I demonstrates the precision and accuracy of the method following a single therapeutic dose. These data were collected over several weeks and thus demonstrate reproducibility. The lowest tabulated standard was 17.3 ng/ml; however, the method can be employed for concentrations of 5 ng/ml with slightly less precision (*i.e.*, coefficient of variation of 8%).

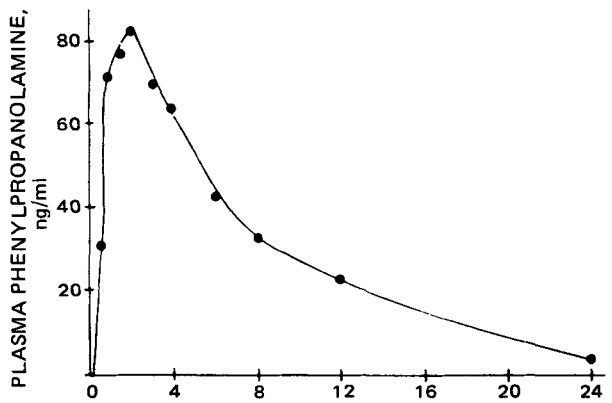


**Figure 2**—*Mean plasma phenylpropanolamine for 12 subjects following a single 25-mg dose of phenylpropanolamine hydrochloride in solution.*

[1] Burdick & Jackson, Muskegon, Mich.
[2] J. T. Baker, Phillipsburg, N.J.
[3] Mallinckrodt, St. Louis, Mo.
[4] Fluoropa, Durrum Chemical Corp., Palo Alto, Calif.
[5] Eastman Kodak Co., Rochester, N.Y.
[6] Kindly supplied by A. H. Robins Co., Richmond, Va.
[7] Kindly supplied by ICI Americas Inc., Wilmington, Del.
[8] Model 6000A, Waters Associates, Milford, Mass.; model 110A, Altex Scientific, Berkeley, Calif.
[9] Model U6K, Waters Associates, Milford, Mass.; L.D.C. Rheodyne 7125, Rheodyne Inc., Cotati, Calif.
[10] Laboratory Data Control, Riviera Beach, Fla.
[11] Schoeffel S.F.970, Kratos, Westwood, N.J.
[12] Omniscribe, Houston Instruments, Austin, Tex.
[13] Vacutainers.

Figure 2 presents the mean plasma concentration–time data for the 12 subjects who received 25 mg of phenylpropanolamine hydrochloride. The concentrations were within the quantitative range of the described method. The samples were assayed in duplicate with 2 weeks between duplicate determinations of each sample. The precision of these assays is indicated by the mean coefficient of variation of 3.0% for duplicates. A repeated analysis of 24 samples after 6 months at −10° revealed no significant differences, thus indicating sample stability.

The general approach presented in this report produced very clean chromatograms and thus should be considered for other primary amines.

## REFERENCES


(1) L. M. Cummins and M. J. Fourier, *Anal. Lett.*, **2**, 403 (1969).

(2) J. Dickerson, D. Perrier, M. Mayersohn, and R. Bressler, *Eur. J. Clin. Pharmacol.*, **14**, 253 (1978).

(3) A. Yacobi, R. G. Stoll, G. C. Chao, J. E. Carter, D. M. Baaske, B. L. Kamath, A. H. Amann, and C. M. Lai, *J. Pharm. Sci.*, **69**, 1077 (1980).

(4) R. G. Kuntzman, I. Tsai, L. Brand, and L. C. Mark, *Clin. Pharmacol. Ther.*, **12**, 62 (1971).

(5) M. Roth, *Anal. Chem.*, **43**, 880 (1971).

(6) M. Roth, *J. Chromatogr.*, **83**, 353 (1973).

(7) J. R. Benson and P. E. Hare, *Proc. Natl. Acad. Sci., USA*, **72**, 619 (1975).

(8) S. S. Simons and D. F. Johnson, *J. Am. Chem. Soc.*, **98**, 7098 (1977).

(9) S. S. Simons and D. F. Johnson, *Anal. Biochem.*, **82**, 250 (1977).

(10) J. E. Sinsheimer, I. G. During, and R. T. Williams, *Biochem. J.*, **136**, 763 (1973).


# COMMUNICATIONS

## Drug–Disintegrant Interactions: Binding of Oxymorphone Derivatives


**Keyphrases** □ Drug-disintegrant interactions—binding of oxymorphone derivatives to disintegrating agents, dissolution testing, Freundlich adsorption isotherm □ Disintegrating agents—carboxymethylcellulose sodium, sodium starch glycolate, povidone, and modified cornstarch, binding to oxymorphone derivatives compared □ Oxymorphone derivatives—binding to disintegrating agents compared, Freundlich adsorption isotherm □ Freundlich adsorption isotherm—binding of oxymorphone derivatives to disintegrating agents compared, dissolution testing □ Analgesics, narcotic—oxymorphone, binding to disintegrating agents compared, dissolution testing


*To the Editor:*

Since the USP first established a disintegration standard in 1948, the search for good disintegrating agents for tablet formulations has intensified. Starch had been used as the primary tablet disintegrant and, in most cases, was relatively effective. However, recognition of the importance of bioavailability and compendial dissolution test requirements spurred the search for new disintegrants. An ideal disintegrant would improve both disintegration and dissolution and be effective in small amounts.

The search has produced several new disintegrating agents, most notably internally cross-linked carboxymethylcellulose sodium[1], sodium starch glycolate[2], cross-linked polyvinyl pyrrolidone[3] (povidone), and modified cornstarch[4].

During the development of a tablet formulation with a rapid disintegration/dissolution rate profile for a synthetic narcotic agonist–antagonist analgesic with the general structure of oxymorphone (I), extensive binding was noted between I and cross-linked carboxymethylcellulose sodium, and lower recovery resulted during dissolution testing. However, the binding to sodium starch glycolate was substantially less extensive, and no binding was detected for carboxymethylcellulose sodium, cornstarch, and modified cornstarch.

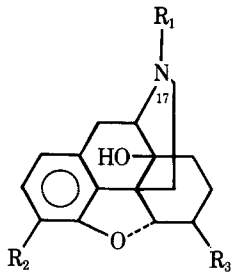


I

The binding of I to cross-linked carboxymethylcellulose sodium and sodium starch glycolate followed the Freundlich adsorption isotherm as shown in Fig. 1. The binding was sensitive to variation in solution pH (Fig. 2). Maximum binding was achieved for both cross-linked carboxy-

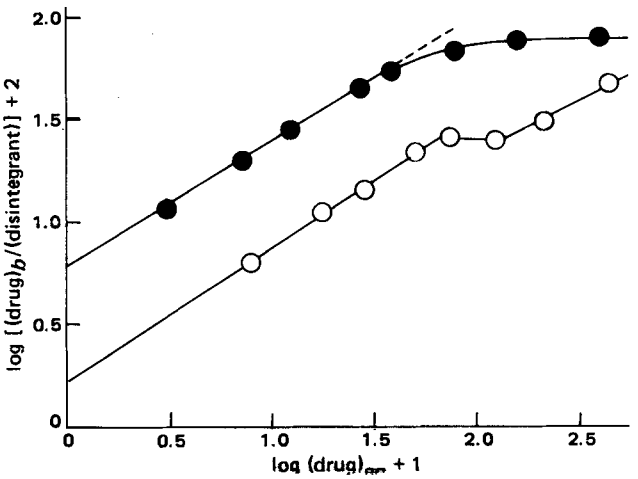


**Figure 1**—*Freundlich adsorption isotherm for the interaction of oxymorphone derivative (I) with cross-linked carboxymethylcellulose sodium (●) and sodium starch glycolate (○) in distilled water at room temperature.*

[1] Ac-Di-Sol, FMC Corp., Philadelphia, PA 19103.
[2] Explotab, E. Mendell Co., Carmel, NY 10512.
[3] PVP-XL, GAF Co., New York, NY 10020.
[4] StaRx 1500, Staley & Co., Decatur, IL 62525.


0022-3549/81/0600-0709$01.00/0


© 1981, American Pharmaceutical Association

Figure 2 presents the mean plasma concentration–time data for the 12 subjects who received 25 mg of phenylpropanolamine hydrochloride. The concentrations were within the quantitative range of the described method. The samples were assayed in duplicate with 2 weeks between duplicate determinations of each sample. The precision of these assays is indicated by the mean coefficient of variation of 3.0% for duplicates. A repeated analysis of 24 samples after 6 months at −10° revealed no significant differences, thus indicating sample stability.

The general approach presented in this report produced very clean chromatograms and thus should be considered for other primary amines.

## REFERENCES


(1) L. M. Cummins and M. J. Fourier, *Anal. Lett.*, **2**, 403 (1969).

(2) J. Dickerson, D. Perrier, M. Mayersohn, and R. Bressler, *Eur. J. Clin. Pharmacol.*, **14**, 253 (1978).

(3) A. Yacobi, R. G. Stoll, G. C. Chao, J. E. Carter, D. M. Baaske, B. L. Kamath, A. H. Amann, and C. M. Lai, *J. Pharm. Sci.*, **69**, 1077 (1980).

(4) R. G. Kuntzman, I. Tsai, L. Brand, and L. C. Mark, *Clin. Pharmacol. Ther.*, **12**, 62 (1971).

(5) M. Roth, *Anal. Chem.*, **43**, 880 (1971).

(6) M. Roth, *J. Chromatogr.*, **83**, 353 (1973).

(7) J. R. Benson and P. E. Hare, *Proc. Natl. Acad. Sci., USA*, **72**, 619 (1975).

(8) S. S. Simons and D. F. Johnson, *J. Am. Chem. Soc.*, **98**, 7098 (1977).

(9) S. S. Simons and D. F. Johnson, *Anal. Biochem.*, **82**, 250 (1977).

(10) J. E. Sinsheimer, I. G. During, and R. T. Williams, *Biochem. J.*, **136**, 763 (1973).


# COMMUNICATIONS

## Drug–Disintegrant Interactions: Binding of Oxymorphone Derivatives


**Keyphrases** □ Drug-disintegrant interactions—binding of oxymorphone derivatives to disintegrating agents, dissolution testing, Freundlich adsorption isotherm □ Disintegrating agents—carboxymethylcellulose sodium, sodium starch glycolate, povidone, and modified cornstarch, binding to oxymorphone derivatives compared □ Oxymorphone derivatives—binding to disintegrating agents compared, Freundlich adsorption isotherm □ Freundlich adsorption isotherm—binding of oxymorphone derivatives to disintegrating agents compared, dissolution testing □ Analgesics, narcotic—oxymorphone, binding to disintegrating agents compared, dissolution testing


*To the Editor:*

Since the USP first established a disintegration standard in 1948, the search for good disintegrating agents for tablet formulations has intensified. Starch had been used as the primary tablet disintegrant and, in most cases, was relatively effective. However, recognition of the importance of bioavailability and compendial dissolution test requirements spurred the search for new disintegrants. An ideal disintegrant would improve both disintegration and dissolution and be effective in small amounts.

The search has produced several new disintegrating agents, most notably internally cross-linked carboxymethylcellulose sodium[1], sodium starch glycolate[2], cross-linked polyvinyl pyrrolidone[3] (povidone), and modified cornstarch[4].

During the development of a tablet formulation with a rapid disintegration/dissolution rate profile for a synthetic narcotic agonist–antagonist analgesic with the general structure of oxymorphone (I), extensive binding was noted between I and cross-linked carboxymethylcellulose sodium, and lower recovery resulted during dissolution testing. However, the binding to sodium starch glycolate was substantially less extensive, and no binding was detected for carboxymethylcellulose sodium, cornstarch, and modified cornstarch.

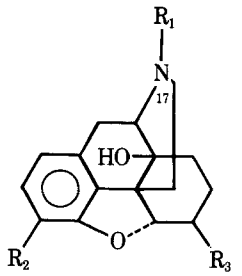


I

The binding of I to cross-linked carboxymethylcellulose sodium and sodium starch glycolate followed the Freundlich adsorption isotherm as shown in Fig. 1. The binding was sensitive to variation in solution pH (Fig. 2). Maximum binding was achieved for both cross-linked carboxy-

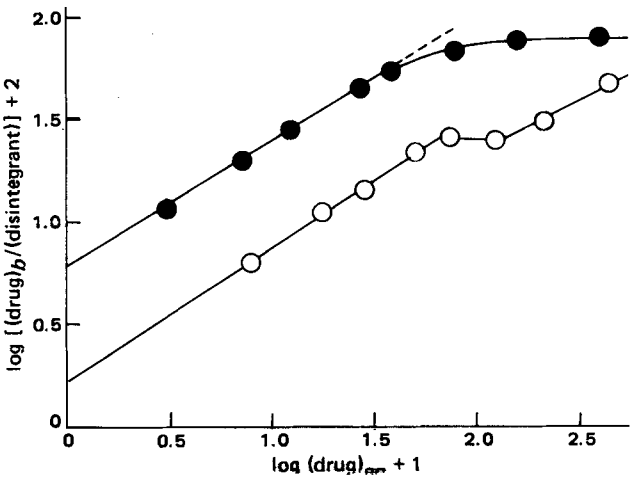


**Figure 1**—*Freundlich adsorption isotherm for the interaction of oxymorphone derivative (I) with cross-linked carboxymethylcellulose sodium (●) and sodium starch glycolate (○) in distilled water at room temperature.*

[1] Ac-Di-Sol, FMC Corp., Philadelphia, PA 19103.
[2] Explotab, E. Mendell Co., Carmel, NY 10512.
[3] PVP-XL, GAF Co., New York, NY 10020.
[4] StaRx 1500, Staley & Co., Decatur, IL 62525.


0022-3549/81/0600-0709$01.00/0


© 1981, American Pharmaceutical Association

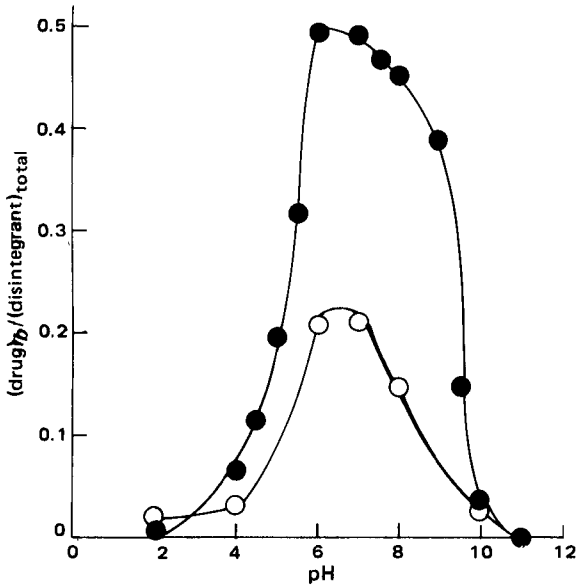


**Figure 2**—*Effect of solution pH on the interaction of oxymorphone derivative (I) with cross-linked carboxymethylcellulose sodium (●) and sodium starch glycolate (○).*

methylcellulose sodium and sodium starch glycolate at pH 6–7. However, the interaction of I with cross-linked carboxymethylcellulose sodium was twice that with sodium starch glycolate.

The interaction was believed to depend on the tertiary amine group at position 17 of I. Adsorption studies were extended to examine the interaction of cross-linked carboxymethylcellulose sodium with four derivatives of I, where substituents $R_1$, $R_2$, and $R_3$ varied and pKa values ranged from 7.9 to 8.7. Results indicated that the binding of I derivatives with cross-linked carboxymethylcellulose sodium can be described by the Freundlich adsorption isotherm as expressed by:

$$\log \frac{(\text{drug})_b}{(\text{disintegrant})} = \log k + \frac{1}{n} \log (\text{drug})_{eq} \qquad \text{(Eq. 1)}$$

where $n$ and $k$ are Freundlich adsorption constants that can be estimated from the slope and intercept of the linear portion of $\log[(\text{drug})_b/(\text{disintegrant})]$ *versus* $\log(\text{drug})_{eq}$ plots (Fig. 1); $(\text{drug})_{eq}$ is the equilibrium drug concentration in solution. Results obtained for the four I derivatives show $n$ values of 1.43–1.75 and $k$ values of 0.219–0.243. The data suggest that the structural variation of functional group $R_1$ at the tertiary amine group at position 17 of I does not greatly affect the Freundlich adsorption isotherm. All four I derivatives interacted with cross-linked carboxymethylcellulose sodium in a similar manner and to a significant extent.

The biological significance of these interactions is not known.

*Y. W. Chien* ˣ
*P. Van Nostrand*
*A. R. Hurwitz*
*E. G. Shami*
Pharmaceutical R&D Department
Endo Laboratories
DuPont Company
Garden City, NY 11530

Received January 19, 1981.
Accepted for publication March 23, 1981.

# X-Ray Crystal Structure Analysis of 14-Hydroxycaryophyllene Oxide, a New Metabolite of (−)-Caryophyllene, in Rabbits

**Keyphrases** □ Caryophyllene—X-ray crystal structure analysis of 14-hydroxycaryophyllene in rabbits □ Metabolites—of caryophyllene by X-ray crystal structure analysis, 14-hydroxycaryophyllene □ Terpenoids—caryophyllene, new metabolite, X-ray crystal structure analysis of 14-hydroxycarophyllene

*To the Editor:*

The metabolic studies of diet or crude drugs containing potentially toxic terpenoids may have significant implications for human toxicology. (−)-Caryophyllene (I), a sesquiterpene hydrocarbon having a *gem*-dimethyl group on the four-membered ring, often is found in crude drugs. For toxicological evaluation, I, $[\alpha]_D$ −10.6° (*c*, 5.64 in chloroform) (12 g), was administered to six male rabbits by a previously described method (1). The neutral metabolites (2.37 g) obtained from urine were chromatographed directly on silica gel to give crude alcohols, followed by acetylation with acetic anhydride in pyridine. The crude acetates also were chromatographed on silica gel impregnated with 5% silver nitrate to yield a pure acetate (II) (48% for total acetates).

Compound II, mp 71.5–72.5°, $[\alpha]_D$ −36.5° (*c*, 2.74 in chloroform), $C_{17}H_{26}O_3$ ($M^+$, 278), showed the presence of an acetoxymethyl group [1730 and 1240 $cm^{-1}$; δ 2.08 (s, 3H)[1] and 3.85 (s, 2H)] and an exocyclic methylene group [895 $cm^{-1}$; δ 4.90 and 5.03 (each bs, 1H)]. The PMR spectrum also contained the signals of one proton [δ 2.80 (m)] and one tertiary methyl group [δ 1.22 (s)] on carbons bearing an ether oxygen. This spectral evidence indicated that one of the *gem*-dimethyl groups on the four-membered ring might be hydroxylated. This assumption was supported further by the $^{13}C$-NMR spectrum of II, which showed the presence of two $CH_3$ groups (δ 17.0 and 17.2 ppm), five $CH_2$ groups (27.6, 28.8, 29.9, 30.3, and 34.8 ppm), two CH groups (45.8 and 48.1 ppm), a trisubstituted oxirane ring [59.4 (s) and 63.5 (d)], a tetrasubstituted $sp^3$ carbon (36.7), an exomethylene group [113.5 (t) and 151.4 (s) ppm], and an acetoxymethyl group [20.8 (q), 71.6 (t), and 170.9 (s) ppm].

Hydrolysis of II regenerated an alcohol, $[\alpha]_D$ −25.4° (*c*, 1.66 in chloroform); $C_{15}H_{24}O_2$ ($M^+$, 236); δ 1.07 and 1.25

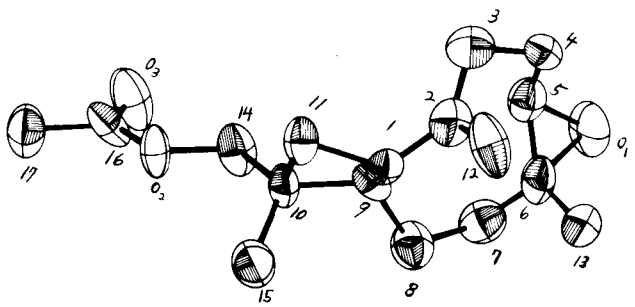


**Figure 1**—*X-ray structure of 14-acetoxycaryophyllene oxide (II).*

[1] s = singlet, bs = broad singlet, d = doublet, t = triplet, q = quartet, and m = multiplet.



*0022-3549/81/0600-0710$01.00/0*
*© 1981, American Pharmaceutical Association*

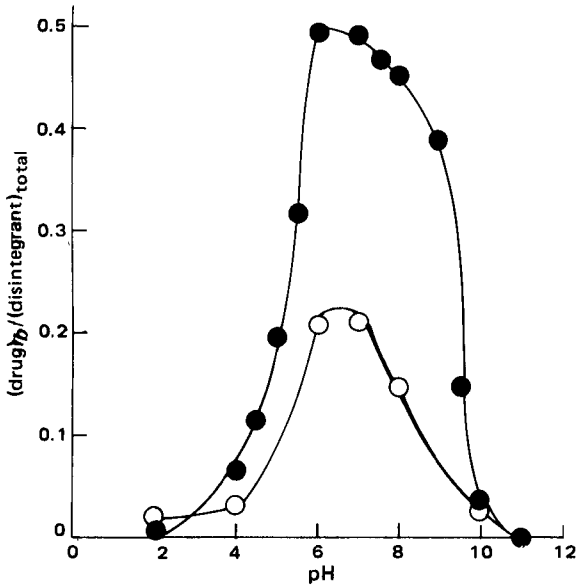


**Figure 2**—*Effect of solution pH on the interaction of oxymorphone derivative (I) with cross-linked carboxymethylcellulose sodium (●) and sodium starch glycolate (○).*

methylcellulose sodium and sodium starch glycolate at pH 6–7. However, the interaction of I with cross-linked carboxymethylcellulose sodium was twice that with sodium starch glycolate.

The interaction was believed to depend on the tertiary amine group at position 17 of I. Adsorption studies were extended to examine the interaction of cross-linked carboxymethylcellulose sodium with four derivatives of I, where substituents $R_1$, $R_2$, and $R_3$ varied and pKa values ranged from 7.9 to 8.7. Results indicated that the binding of I derivatives with cross-linked carboxymethylcellulose sodium can be described by the Freundlich adsorption isotherm as expressed by:

$$\log \frac{(\text{drug})_b}{(\text{disintegrant})} = \log k + \frac{1}{n} \log (\text{drug})_{eq} \qquad \text{(Eq. 1)}$$

where $n$ and $k$ are Freundlich adsorption constants that can be estimated from the slope and intercept of the linear portion of $\log[(\text{drug})_b/(\text{disintegrant})]$ *versus* $\log(\text{drug})_{eq}$ plots (Fig. 1); $(\text{drug})_{eq}$ is the equilibrium drug concentration in solution. Results obtained for the four I derivatives show $n$ values of 1.43–1.75 and $k$ values of 0.219–0.243. The data suggest that the structural variation of functional group $R_1$ at the tertiary amine group at position 17 of I does not greatly affect the Freundlich adsorption isotherm. All four I derivatives interacted with cross-linked carboxymethylcellulose sodium in a similar manner and to a significant extent.

The biological significance of these interactions is not known.

*Y. W. Chien* ˣ
*P. Van Nostrand*
*A. R. Hurwitz*
*E. G. Shami*
Pharmaceutical R&D Department
Endo Laboratories
DuPont Company
Garden City, NY 11530

Received January 19, 1981.
Accepted for publication March 23, 1981.

# X-Ray Crystal Structure Analysis of 14-Hydroxycaryophyllene Oxide, a New Metabolite of (−)-Caryophyllene, in Rabbits

**Keyphrases** □ Caryophyllene—X-ray crystal structure analysis of 14-hydroxycaryophyllene in rabbits □ Metabolites—of caryophyllene by X-ray crystal structure analysis, 14-hydroxycaryophyllene □ Terpenoids—caryophyllene, new metabolite, X-ray crystal structure analysis of 14-hydroxycarophyllene

*To the Editor:*

The metabolic studies of diet or crude drugs containing potentially toxic terpenoids may have significant implications for human toxicology. (−)-Caryophyllene (I), a sesquiterpene hydrocarbon having a *gem*-dimethyl group on the four-membered ring, often is found in crude drugs. For toxicological evaluation, I, $[\alpha]_D$ −10.6° (*c*, 5.64 in chloroform) (12 g), was administered to six male rabbits by a previously described method (1). The neutral metabolites (2.37 g) obtained from urine were chromatographed directly on silica gel to give crude alcohols, followed by acetylation with acetic anhydride in pyridine. The crude acetates also were chromatographed on silica gel impregnated with 5% silver nitrate to yield a pure acetate (II) (48% for total acetates).

Compound II, mp 71.5–72.5°, $[\alpha]_D$ −36.5° (*c*, 2.74 in chloroform), $C_{17}H_{26}O_3$ ($M^+$, 278), showed the presence of an acetoxymethyl group [1730 and 1240 $cm^{-1}$; δ 2.08 (s, 3H)[1] and 3.85 (s, 2H)] and an exocyclic methylene group [895 $cm^{-1}$; δ 4.90 and 5.03 (each bs, 1H)]. The PMR spectrum also contained the signals of one proton [δ 2.80 (m)] and one tertiary methyl group [δ 1.22 (s)] on carbons bearing an ether oxygen. This spectral evidence indicated that one of the *gem*-dimethyl groups on the four-membered ring might be hydroxylated. This assumption was supported further by the $^{13}C$-NMR spectrum of II, which showed the presence of two $CH_3$ groups (δ 17.0 and 17.2 ppm), five $CH_2$ groups (27.6, 28.8, 29.9, 30.3, and 34.8 ppm), two CH groups (45.8 and 48.1 ppm), a trisubstituted oxirane ring [59.4 (s) and 63.5 (d)], a tetrasubstituted $sp^3$ carbon (36.7), an exomethylene group [113.5 (t) and 151.4 (s) ppm], and an acetoxymethyl group [20.8 (q), 71.6 (t), and 170.9 (s) ppm].

Hydrolysis of II regenerated an alcohol, $[\alpha]_D$ −25.4° (*c*, 1.66 in chloroform); $C_{15}H_{24}O_2$ ($M^+$, 236); δ 1.07 and 1.25

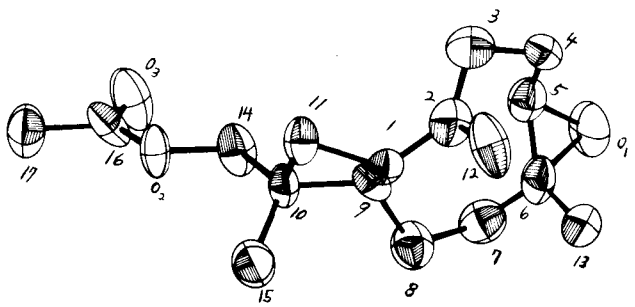


**Figure 1**—*X-ray structure of 14-acetoxycaryophyllene oxide (II).*

[1] s = singlet, bs = broad singlet, d = doublet, t = triplet, q = quartet, and m = multiplet.



*0022-3549/81/0600-0710$01.00/0*
*© 1981, American Pharmaceutical Association*

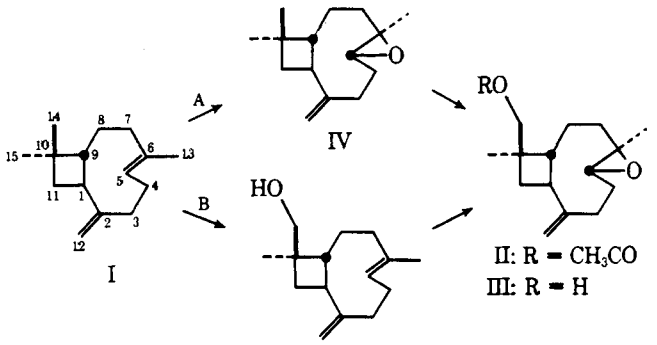


*Scheme I*

(each s, 3H), 2.92 (m, 1H, O–C–H), 3.55 (bs, 2H, $CH_2OH$), and 4.87 and 5.00 (each bs, 1H); 3450 $cm^{-1}$ (OH). These results showed that the metabolic product and its acetate were represented best as III and II, respectively. The absolute configuration of the metabolized methyl group on a four-membered ring of I was established by X-ray study of II: [a = 9.624(4) Å, b = 8.599(4) Å, c = 10.214(4) Å, $\beta$ = 105.47(3)°, space group $P2_1$, Dc = 1.13 g/$cm^3$, and z = 2]. The diffraction intensities were collected in the $\omega$-scan mode, using graphite monochromated MoK$\alpha$ radiation on a diffractomer[2], and corrected for Lorenz polarization and background effects. The structure was resolved by direct methods using a Multan program (2) and was refined by full matrix least-squares calculations. The final R value was 0.092 for 1008 reflections. The relative stereostructure of II is shown in Fig. 1.

Two metabolic pathways may be present in the biotransformation of I (Scheme I). In this connection, (−)-caryophyllene oxide (IV), $[\alpha]_D$ −35.2° (*c*, 2.19 in chloroform), also was administered to rabbits by the method already described. After being acetylated, II was obtained as the major product from the neutral metabolites. Thus, route A was confirmed. Although the presence of route B remains to be clarified, route A may be more favorable than B since IV was found in some essential oils (3–5). According to biotransformation, the hydroxylation of the *gem*-dimethyl group on the three-, four-, five-, and six-membered rings was established for 3-carene (6, 7) and carane (7); caryophyllene; camphor (8) and fenchone (9); and retinoic acid (10), respectively. The stereoselective hydroxylation of *gem*-dimethyl on the four-membered ring in mammals was not reported previously.

(1) T. Ishida, Y. Asakawa, T. Takemoto, and T. Aratani, *J. Pharm. Sci.*, **68**, 928 (1979).

(2) G. Germain, P. Main, and M. M. Woolfson, *Acta Crystallogr.*, **B26**, 274 (1970).

(3) A. S. Gupta and S. Dev, *Tetrahedron*, **27**, 635 (1971).

(4) B. M. Lawrence, J. W. Hogg, S. J. Terhune, J. K. Morton, and L. S. Gill, *Phytochemistry*, **11**, 2636 (1972).

(5) R. K. Thappa, V. N. Vashisht, J. Singh, and R. K. Sharma, *Curr. Sci.*, **1970**, 182.

(6) T. Ishida, Y. Asakawa, M. Okano, and T. Aratani, *Tetrahedron Lett.*, **1977**, 2437.

(7) T. Ishida, Y. Asakawa, T. Takemoto, and T. Aratani, *J. Pharm. Sci.*, **70**, 406 (1981).

(8) Y. Asahina and M. Ishidate, *Ber. Dtsch. Chem. Ges.*, **68B**, 947 (1935).

(9) M. Miyazawa, H. Kameoka, K. Morinaga, K. Negoro, and N. Mura, "The Abstracts of 24th Symposium on the Chemistry of Terpenes, Essential Oils and Aromatics," Chemical Society of Japan, Tokyo, Japan, 1980, p. 62 (in Japanese).

(10) R. Hanni, F. Bigler, W. Meister, and G. Fungert, *Helv. Chim. Acta*, **59**, 2221 (1976).

[2] Syntex R3.

*Y. Asakawa*
*Z. Taira*
*T. Takemoto*
Institute of Pharmacognosy
Tokushima Bunri University
Tokushima 770, Japan
*T. Ishida* ˣ
Hiroshima Institute of Technology
Itsukaichi
Hiroshima 738, Japan
*M. Kido*
*Y. Ichikawa*
Laboratories of Natural Products Chemistry
Otsuka Pharmaceutical Co. Ltd.
Kawauchi-cho
Tokushima 771-01, Japan

Received January 12, 1981.
Accepted for publication February 19, 1981.

## Relationship between Flow Rates of Granular Powders through Stationary and Moving Orifices

**Keyphrases** □ Powders, granular—relationship between flow rates of granular powders through stationary and moving orifices □ Flow rates—of powder granulations, prediction of dynamic flow rate from static flow measurements □ Models, mathematical—prediction of dynamic flow rates of powder granulations from static flow measurements

*To the Editor:*

Since the compressed tablet is the most common dosage form manufactured, the ability to predict scale-up properties of tablet formulations for high-speed processing is needed. To manufacture tablets on a rotary tablet machine, flow of granular material through a stationary orifice (*i.e.*, efflux tube on the granulation hopper) followed by flow into moving orifices (*i.e.*, tablet dies) is required. Since little data have been reported (1, 2) that characterize the latter process of dynamic flow, data from static flow measurements have been used to predict dynamic flow properties of solids. Takieddin *et al.* (3) reported that dynamic flow rates were not predicted successfully from measurements of solid flow through a stationary orifice (static flow), noting that an apparatus suitable for the study of dynamic flow was not available.

An apparatus was constructed to study the dynamic flow of granular materials (4, 5). Although the instrument does not provide an exact duplication of events that occur within the feed frame of a tablet machine, it provides a reasonable means to obtain dynamic flow data. A slight modification of the apparatus also provides a means to study static flow rates.

Dynamic flow measurements of a lactose–cornstarch wet granulation (6) were reported (7). Six measurements were obtained for each combination of granulation mesh cut (20–40, 40–60, and 60–80), orifice size [3/16 (0.48), 1/4 (0.63), 5/16 (0.8), 3/8 (0.95), and 1/2 (1.3) in. (cm)], and five die ve-

0022-3549/81/0600-0711$01.00/0
© 1981, American Pharmaceutical Association

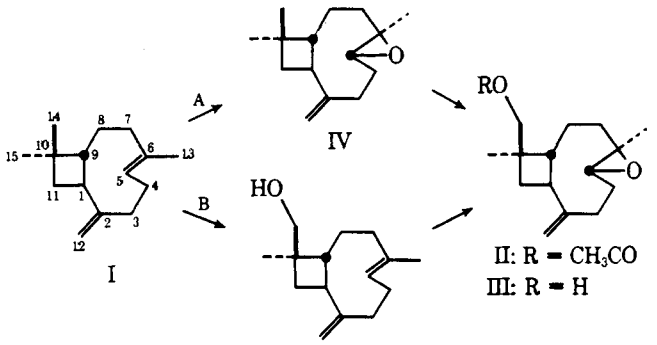


*Scheme I*

(each s, 3H), 2.92 (m, 1H, O–C–H), 3.55 (bs, 2H, $CH_2OH$), and 4.87 and 5.00 (each bs, 1H); 3450 $cm^{-1}$ (OH). These results showed that the metabolic product and its acetate were represented best as III and II, respectively. The absolute configuration of the metabolized methyl group on a four-membered ring of I was established by X-ray study of II: [a = 9.624(4) Å, b = 8.599(4) Å, c = 10.214(4) Å, $\beta$ = 105.47(3)°, space group $P2_1$, Dc = 1.13 g/$cm^3$, and z = 2]. The diffraction intensities were collected in the $\omega$-scan mode, using graphite monochromated MoK$\alpha$ radiation on a diffractomer[2], and corrected for Lorenz polarization and background effects. The structure was resolved by direct methods using a Multan program (2) and was refined by full matrix least-squares calculations. The final R value was 0.092 for 1008 reflections. The relative stereostructure of II is shown in Fig. 1.

Two metabolic pathways may be present in the biotransformation of I (Scheme I). In this connection, (−)-caryophyllene oxide (IV), $[\alpha]_D$ −35.2° (*c*, 2.19 in chloroform), also was administered to rabbits by the method already described. After being acetylated, II was obtained as the major product from the neutral metabolites. Thus, route A was confirmed. Although the presence of route B remains to be clarified, route A may be more favorable than B since IV was found in some essential oils (3–5). According to biotransformation, the hydroxylation of the *gem*-dimethyl group on the three-, four-, five-, and six-membered rings was established for 3-carene (6, 7) and carane (7); caryophyllene; camphor (8) and fenchone (9); and retinoic acid (10), respectively. The stereoselective hydroxylation of *gem*-dimethyl on the four-membered ring in mammals was not reported previously.

(1) T. Ishida, Y. Asakawa, T. Takemoto, and T. Aratani, *J. Pharm. Sci.*, **68**, 928 (1979).

(2) G. Germain, P. Main, and M. M. Woolfson, *Acta Crystallogr.*, **B26**, 274 (1970).

(3) A. S. Gupta and S. Dev, *Tetrahedron*, **27**, 635 (1971).

(4) B. M. Lawrence, J. W. Hogg, S. J. Terhune, J. K. Morton, and L. S. Gill, *Phytochemistry*, **11**, 2636 (1972).

(5) R. K. Thappa, V. N. Vashisht, J. Singh, and R. K. Sharma, *Curr. Sci.*, **1970**, 182.

(6) T. Ishida, Y. Asakawa, M. Okano, and T. Aratani, *Tetrahedron Lett.*, **1977**, 2437.

(7) T. Ishida, Y. Asakawa, T. Takemoto, and T. Aratani, *J. Pharm. Sci.*, **70**, 406 (1981).

(8) Y. Asahina and M. Ishidate, *Ber. Dtsch. Chem. Ges.*, **68B**, 947 (1935).

(9) M. Miyazawa, H. Kameoka, K. Morinaga, K. Negoro, and N. Mura, "The Abstracts of 24th Symposium on the Chemistry of Terpenes, Essential Oils and Aromatics," Chemical Society of Japan, Tokyo, Japan, 1980, p. 62 (in Japanese).

(10) R. Hanni, F. Bigler, W. Meister, and G. Fungert, *Helv. Chim. Acta*, **59**, 2221 (1976).

[2] Syntex R3.

*Y. Asakawa*
*Z. Taira*
*T. Takemoto*
Institute of Pharmacognosy
Tokushima Bunri University
Tokushima 770, Japan
*T. Ishida* ˣ
Hiroshima Institute of Technology
Itsukaichi
Hiroshima 738, Japan
*M. Kido*
*Y. Ichikawa*
Laboratories of Natural Products Chemistry
Otsuka Pharmaceutical Co. Ltd.
Kawauchi-cho
Tokushima 771-01, Japan

Received January 12, 1981.
Accepted for publication February 19, 1981.

## Relationship between Flow Rates of Granular Powders through Stationary and Moving Orifices

**Keyphrases** □ Powders, granular—relationship between flow rates of granular powders through stationary and moving orifices □ Flow rates—of powder granulations, prediction of dynamic flow rate from static flow measurements □ Models, mathematical—prediction of dynamic flow rates of powder granulations from static flow measurements

*To the Editor:*

Since the compressed tablet is the most common dosage form manufactured, the ability to predict scale-up properties of tablet formulations for high-speed processing is needed. To manufacture tablets on a rotary tablet machine, flow of granular material through a stationary orifice (*i.e.*, efflux tube on the granulation hopper) followed by flow into moving orifices (*i.e.*, tablet dies) is required. Since little data have been reported (1, 2) that characterize the latter process of dynamic flow, data from static flow measurements have been used to predict dynamic flow properties of solids. Takieddin *et al.* (3) reported that dynamic flow rates were not predicted successfully from measurements of solid flow through a stationary orifice (static flow), noting that an apparatus suitable for the study of dynamic flow was not available.

An apparatus was constructed to study the dynamic flow of granular materials (4, 5). Although the instrument does not provide an exact duplication of events that occur within the feed frame of a tablet machine, it provides a reasonable means to obtain dynamic flow data. A slight modification of the apparatus also provides a means to study static flow rates.

Dynamic flow measurements of a lactose–cornstarch wet granulation (6) were reported (7). Six measurements were obtained for each combination of granulation mesh cut (20–40, 40–60, and 60–80), orifice size [3/16 (0.48), 1/4 (0.63), 5/16 (0.8), 3/8 (0.95), and 1/2 (1.3) in. (cm)], and five die ve-

0022-3549/81/0600-0711$01.00/0
© 1981, American Pharmaceutical Association

Table I—Static and Dynamic Flow Rates for Three Granulation Mesh Cuts

| Mesh Cut[a] of USP Sieves | Average Particle Diameter[b], cm | Orifice Diameter, in. (cm) | Static Flow Rate ($W_s$), g/sec | Dynamic Flow Rate ($W_2$)[c], g/sec |
|---|---|---|---|---|
| 20–40 | 0.0630 | 3/16 (0.48) | 0.74 | 0.53 |
| | | 1/4 (0.63) | 1.71 | 1.24 |
| | | 5/16 (0.8) | 3.11 | 2.74 |
| | | 3/8 (0.95) | 5.65 | 4.75 |
| | | 1/2 (1.3) | 12.7 | 12.4 |
| 40–60 | 0.0335 | 3/16 (0.48) | 1.13 | 0.88 |
| | | 1/4 (0.63) | 2.43 | 1.99 |
| | | 5/16 (0.8) | 4.25 | 3.97 |
| | | 3/8 (0.95) | 7.44 | 7.02 |
| | | 1/2 (1.3) | 15.5 | 17.1 |
| 60–80 | 0.0214 | 3/16 (0.48) | 1.31 | 1.07 |
| | | 1/4 (0.63) | 2.73 | 2.34 |
| | | 5/16 (0.8) | 4.45 | 4.48 |
| | | 3/8 (0.95) | 8.19 | 7.84 |
| | | 1/2 (1.3) | 14.7 | 18.3 |

[a] Particle density measurements (5) for the three mesh cuts are: 20–40, $\rho$ = 1.45 g/ml; 40–60, $\rho$ = 1.49 g/ml; and 60–80, $\rho$ = 1.52 g/ml. [b] Average particle diameter is defined as the arithmetic mean of the sieve openings for each pair of USP sieves; this value is an approximation (12). [c] Values of dynamic flow rates reported by Carstensen and Laughlin (7) were incorrect.

locities (between 3 and 12.5 cm/sec); average dynamic flow rates ($W_2$), as defined by Carstensen and Laughlin (7), are listed in Table I. For static flow measurements, the movable slide of the apparatus was stationary; an aluminum tube (2.54 cm i.d.) centered above the die held the granular material. Measurement of static flow rates was made with the same three granulation mesh cuts and the same five orifice sizes as used during dynamic flow studies. Five measurements with each combination of orifice and particle size were made; mean data are reported as static flow rates ($W_s$) in Table I. An apparent difference is noted between pairs of values for each set of experimental conditions; the dynamic flow rate is smaller in most cases.

Equations developed for modeling static flow often are based on the Brown–Richards equation (8) and are written in the following form:

$$W_s = f(d)P^{n(d)} \qquad \text{(Eq. 1)}$$

where $f$ and $n$ denote "function of" and $n$ is generally 2.5, a constant. However, $n$ also has been shown to be a function of particle diameter $d$ (9, 10).

Ahmad and Pilpel (9) studied the static flow properties of six different materials. Their mathematical model was based on the Brown–Richards equation and contained a bulk density term and a particle-shape factor term. They reported (9) that one equation could predict the static flow of all six materials with an overall accuracy of ~±7%.

Danish and Parrott (10) studied the static flow properties of a crystalline solid and a granular material and derived separate equations to describe the static flow rate of each material. The Brown–Richards equation was the basis for the derivations; a true density term was included but no particle-shape factor term. They reported a 10% variation between experimental and calculated values for each of the two models.

The Brown–Richards equation can be used to describe static flow for situations where: (*a*) the flow rate decreases as the particle size is increased, (*b*) the orifice size is at least six times greater than the particle size, (*c*) the granulation height is at least two times greater than the orifice diameter, and (*d*) the ratio of orifice diameter to granulation hopper diameter is <0.5. Therefore, it should be possible to write an equation in the form of Eq. 1 that can describe the static flow data shown in Table I. Such an equation, which describes static flow as a function of orifice size ($P$), particle diameter ($d$), acceleration due to gravity ($g$), and particle density[1] ($\rho$), has been derived; measurements of static flow through the largest orifice were excluded since they failed to meet the fourth criterion for applicability of the Brown–Richards equation. The derivation approach suggested by Danish and Parrott (10) was used (5) and resulted in:

$$W_s = \frac{\pi\rho\sqrt{g}}{4}\left(\frac{P}{1.65 + 2.34d}\right)^{\left(\frac{1}{0.24-0.038\ln d}\right)} \qquad \text{(Eq. 2)}$$

The flow rates predicted with Eq. 2 were larger than the experimentally measured values in eight of 12 cases; the average of the differences between calculated and experimental values (expressed as a percent of experimental data) for static flow was +3.5%.

Dynamic flow rate is not a function of orifice velocity (5). This fact can be concluded from study of Fig. 3 and Eq. 7 in Ref. 7; values for $W_2$ are calculated from the intercept of each line. Thus, each dynamic flow rate is related to the orifice size and particle diameter but is independent of the orifice velocity. These relationships suggest that dynamic flow also can be expressed in the form of the Brown–Richards equation. Measurements of dynamic flow through the largest orifice were excluded since they apparently failed to meet the first criteria for applicability of the Brown–Richards equation. Previous work indicated that, for dynamic flow, if the exponent $n$ is a constant, it should have a value of 2.9–3.4. Dynamic flow data, collected using the four smallest orifice sizes, were used to derive:

$$W_2 = \frac{\pi\rho\sqrt{g}}{4}\left(\frac{P + 0.0009d^{-1.25}}{2.11 + 0.12\ln d}\right)^{3.33} \qquad \text{(Eq. 3)}$$

The flow rates predicted with Eq. 3 were larger than experimentally measured values in eight of 12 cases. The average of the differences between calculated and experimental values (expressed as a percent of experimental data) for dynamic flow rates was +1.4%.

[1] Brown and Richards (11) reported that it is inappropriate to relate static flow rate to bulk density of the solid material, because bulk density is a combined measurement of the true or particle density and the packing characteristics of the material. They noted that $W_s$ is a function of the voidage at the orifice; this voidage is related to the true density of a crystalline material or to the particle density of a granular material. Since the particle densities of the three granulation mesh cuts are different, it seemed most appropriate to include particle density as the parameter in the equations.

A second equation for prediction of dynamic flow rates was developed, similar in form to Eq. 2 for static flow:

$$W_2 = \frac{\pi\rho\sqrt{g}}{4}\left(\frac{P}{1.52 + 4.12d}\right)^{(2.79+6.68d)} \quad \text{(Eq. 4)}$$

Again, measurements of dynamic flow through the largest orifice were excluded. Now, the exponent $n$ is a function of the particle diameter. The flow rates predicted with Eq. 4 were larger than experimentally measured values in five of 12 cases. The average of the differences between calculated and experimental values (expressed as a percent of experimental data) for dynamic flow rates was −0.4%.

In Eqs. 2–4, which are based on the Brown–Richards equation, the static and dynamic flow rates are expressed in terms of orifice diameter, particle diameter, and particle density. If static and dynamic flow rates are not dependent on any dimensions of the apparatus except the orifice size, it should be possible to combine the relationships. Then dynamic flow rate can be expressed as a function of static flow. If Eqs. 2 and 3 are combined, dynamic flow rates can be predicted using:

$$W_2 = \frac{\pi\rho\sqrt{g}}{4}\left[\left(\frac{1.65 + 2.34d}{2.11 + 0.12\ln d}\right)\left(\frac{4W_s}{\pi\rho\sqrt{g}}\right)^{(0.24-0.038\ln d)} + \left(\frac{0.0009d^{-1.25}}{2.11 + 0.12\ln d}\right)\right]^{3.33} \quad \text{(Eq. 5)}$$

If the predicting power of Eq. 5 is good:

1. There should be the same number of positive and negative differences between calculated and experimental values (+5 and −7).
2. The average of the differences (expressed as a percent of experimental data) should be close to zero (−1.2%).
3. The arithmetic mean of the absolute value of these differences should be small (6.0%).

Thus, Eq. 5 appears to be appropriate for predicting dynamic flow rates for the granular material studied.

When Eqs. 2 and 4 are combined, another algebraic expression is obtained that describes dynamic flow rate as a function of static flow:

$$W_2 = \frac{\pi\rho\sqrt{g}}{4}\left(\frac{1.65 + 2.34d}{1.52 + 4.12d}\right)^{(2.79+6.68d)} \times \left(\frac{4W_s}{\pi\rho\sqrt{g}}\right)^{(0.67+1.60d-0.11\ln d-0.25d\ln d)} \quad \text{(Eq. 6)}$$

If the predicting power of Eq. 6 is good:

1. There should be the same number of positive and negative differences between calculated and experimental values (+0 and −12).
2. The average of the differences (expressed as a percent of experimental data) should be close to zero (−6.2%).
3. The arithmetic mean of the absolute value of these differences should be small (6.2%).

Thus, Eq. 6 appears to have fair predicting power for dynamic flow rates of the granular materials studied, although it is somewhat less accurate than Eq. 5. The limited amount of data precludes selection of the more appropriate general form for an equation to predict dynamic flow rates from static flow data.

The form of Eqs. 2–4 for static and dynamic flow is comparable to equations reported by other investigators (9, 10). While Eqs. 5 and 6 are more cumbersome, they also are of a similar form; the orifice diameter ($P$) was written implicitly as a function of the static flow rate ($W_s$). An important observation of Eqs. 5 and 6 is that dynamic flow is not first order in static flow ($W_s$) if the exponents on the $(4W_s/\pi\rho\sqrt{g})$ term are different than unity. In Eq. 5, the exponent $[(0.24 - 0.038\ln d)\ (3.33)]$ is greater than unity for all $d$ values of <0.21 cm. Similarly, for Eq. 6, the exponent $(0.67 + 1.60d - 0.11\ln d - 0.25d\ln d)$ has a value greater than 1 for all particles sizes ($d$) of <598 cm. Therefore, for particle sizes commonly found in tablet formulations, both equations predict that the dynamic flow is not first order in static flow. In addition, the dynamic flow is nonlinear with respect to both preexponential terms, which are related indirectly (*i.e.*, through particle density) or directly to the particle diameter.

The direct applicability of Eqs. 5 and 6 to other granulations and dynamic flow systems is questionable. However, the form of the equations explains why the dynamic flow rates are not easily predicted from static flow data. The relationships also suggest that static and dynamic flow rates are dependent on many of the same measurable parameters; these parameters should be considered in the development of other mathematical models for dynamic flow rates.


(1) J. Oakley, *J. Inst. Met.*, **87**, 26 (1958).
(2) J. A. Hersey, *Rheol. Acta*, **4**, 235 (1965).
(3) M. Takieddin, F. Puisieux, J. R. Didry, P. Touré, and D. Duchêne, presented at the First International Conference on Pharmaceutical Technology, Paris, France, 1977.
(4) S. M. Laughlin, L. VanCampen, M. Takieddin, D. Duchêne, F. Puisieux, and J. T. Carstensen, *Int. J. Pharm.*, **3**, 33 (1979).
(5) S. M. Laughlin, M.S. thesis, School of Pharmacy, University of Wisconsin, Madison, Wis., 1979.
(6) J. T. Carstensen, "Pharmaceutics of Solids and Solid Dosage Forms," Wiley–Interscience, New York, N.Y., 1977, p. 210.
(7) J. T. Carstensen and S. M. Laughlin, *Powder Technol.*, **23**, 79 (1979).
(8) R. L. Brown and J. C. Richards, *Trans. Inst. Chem. Eng.*, **38**, 243 (1960).
(9) M. Ahmad and N. Pilpel, *Rheol. Acta*, **8**, 448 (1969).
(10) F. Q. Danish and E. L. Parrott, *J. Pharm. Sci.*, **60**, 548 (1971).
(11) R. L. Brown and J. C. Richards, *Trans. Inst. Chem. Eng.*, **37**, 108 (1959).
(12) D. Brooke, *J. Pharm. Sci.*, **64**, 1409 (1975).



*Sharon M. Laughlin* ˣ
*Jens T. Carstensen*
School of Pharmacy
University of Wisconsin
Madison, WI 53706



Received January 28, 1980.
Accepted for publication March 9, 1981.


## Mesophase Formation during *In Vitro* Cholesterol Gallstone Dissolution: A Specific Effect of Ursodeoxycholic Acid


**Keyphrases** □ Cholesterol—gallstones, mesophase formation during *in vitro* gallstone dissolution □ Gallstones, cholesterol—effect of bile acid on gallstone dissolution *in vitro* □ Ursodeoxycholic acid—effect on cholesterol gallstone dissolution *in vitro*, compared with chenodeoxycholic acid □ Dissolution—cholesterol gallstones, effect of bile acid


*To the Editor:*

Ursodeoxycholate (I), the 7β-epimer of chenodeoxycholate (II), has been shown to be equal or superior to II when used as oral medication for the dissolution of cho-



© 1981, American Pharmaceutical Association

A second equation for prediction of dynamic flow rates was developed, similar in form to Eq. 2 for static flow:

$$W_2 = \frac{\pi\rho\sqrt{g}}{4}\left(\frac{P}{1.52 + 4.12d}\right)^{(2.79+6.68d)} \quad \text{(Eq. 4)}$$

Again, measurements of dynamic flow through the largest orifice were excluded. Now, the exponent $n$ is a function of the particle diameter. The flow rates predicted with Eq. 4 were larger than experimentally measured values in five of 12 cases. The average of the differences between calculated and experimental values (expressed as a percent of experimental data) for dynamic flow rates was −0.4%.

In Eqs. 2–4, which are based on the Brown–Richards equation, the static and dynamic flow rates are expressed in terms of orifice diameter, particle diameter, and particle density. If static and dynamic flow rates are not dependent on any dimensions of the apparatus except the orifice size, it should be possible to combine the relationships. Then dynamic flow rate can be expressed as a function of static flow. If Eqs. 2 and 3 are combined, dynamic flow rates can be predicted using:

$$W_2 = \frac{\pi\rho\sqrt{g}}{4}\left[\left(\frac{1.65 + 2.34d}{2.11 + 0.12\ln d}\right)\left(\frac{4W_s}{\pi\rho\sqrt{g}}\right)^{(0.24-0.038\ln d)} + \left(\frac{0.0009d^{-1.25}}{2.11 + 0.12\ln d}\right)\right]^{3.33} \quad \text{(Eq. 5)}$$

If the predicting power of Eq. 5 is good:

1. There should be the same number of positive and negative differences between calculated and experimental values (+5 and −7).
2. The average of the differences (expressed as a percent of experimental data) should be close to zero (−1.2%).
3. The arithmetic mean of the absolute value of these differences should be small (6.0%).

Thus, Eq. 5 appears to be appropriate for predicting dynamic flow rates for the granular material studied.

When Eqs. 2 and 4 are combined, another algebraic expression is obtained that describes dynamic flow rate as a function of static flow:

$$W_2 = \frac{\pi\rho\sqrt{g}}{4}\left(\frac{1.65 + 2.34d}{1.52 + 4.12d}\right)^{(2.79+6.68d)} \times \left(\frac{4W_s}{\pi\rho\sqrt{g}}\right)^{(0.67+1.60d-0.11\ln d-0.25d\ln d)} \quad \text{(Eq. 6)}$$

If the predicting power of Eq. 6 is good:

1. There should be the same number of positive and negative differences between calculated and experimental values (+0 and −12).
2. The average of the differences (expressed as a percent of experimental data) should be close to zero (−6.2%).
3. The arithmetic mean of the absolute value of these differences should be small (6.2%).

Thus, Eq. 6 appears to have fair predicting power for dynamic flow rates of the granular materials studied, although it is somewhat less accurate than Eq. 5. The limited amount of data precludes selection of the more appropriate general form for an equation to predict dynamic flow rates from static flow data.

The form of Eqs. 2–4 for static and dynamic flow is comparable to equations reported by other investigators (9, 10). While Eqs. 5 and 6 are more cumbersome, they also are of a similar form; the orifice diameter ($P$) was written implicitly as a function of the static flow rate ($W_s$). An important observation of Eqs. 5 and 6 is that dynamic flow is not first order in static flow ($W_s$) if the exponents on the $(4W_s/\pi\rho\sqrt{g})$ term are different than unity. In Eq. 5, the exponent $[(0.24 - 0.038\ln d)\ (3.33)]$ is greater than unity for all $d$ values of <0.21 cm. Similarly, for Eq. 6, the exponent $(0.67 + 1.60d - 0.11\ln d - 0.25d\ln d)$ has a value greater than 1 for all particles sizes ($d$) of <598 cm. Therefore, for particle sizes commonly found in tablet formulations, both equations predict that the dynamic flow is not first order in static flow. In addition, the dynamic flow is nonlinear with respect to both preexponential terms, which are related indirectly (*i.e.*, through particle density) or directly to the particle diameter.

The direct applicability of Eqs. 5 and 6 to other granulations and dynamic flow systems is questionable. However, the form of the equations explains why the dynamic flow rates are not easily predicted from static flow data. The relationships also suggest that static and dynamic flow rates are dependent on many of the same measurable parameters; these parameters should be considered in the development of other mathematical models for dynamic flow rates.


(1) J. Oakley, *J. Inst. Met.*, **87**, 26 (1958).
(2) J. A. Hersey, *Rheol. Acta*, **4**, 235 (1965).
(3) M. Takieddin, F. Puisieux, J. R. Didry, P. Touré, and D. Duchêne, presented at the First International Conference on Pharmaceutical Technology, Paris, France, 1977.
(4) S. M. Laughlin, L. VanCampen, M. Takieddin, D. Duchêne, F. Puisieux, and J. T. Carstensen, *Int. J. Pharm.*, **3**, 33 (1979).
(5) S. M. Laughlin, M.S. thesis, School of Pharmacy, University of Wisconsin, Madison, Wis., 1979.
(6) J. T. Carstensen, "Pharmaceutics of Solids and Solid Dosage Forms," Wiley–Interscience, New York, N.Y., 1977, p. 210.
(7) J. T. Carstensen and S. M. Laughlin, *Powder Technol.*, **23**, 79 (1979).
(8) R. L. Brown and J. C. Richards, *Trans. Inst. Chem. Eng.*, **38**, 243 (1960).
(9) M. Ahmad and N. Pilpel, *Rheol. Acta*, **8**, 448 (1969).
(10) F. Q. Danish and E. L. Parrott, *J. Pharm. Sci.*, **60**, 548 (1971).
(11) R. L. Brown and J. C. Richards, *Trans. Inst. Chem. Eng.*, **37**, 108 (1959).
(12) D. Brooke, *J. Pharm. Sci.*, **64**, 1409 (1975).



*Sharon M. Laughlin* ˣ
*Jens T. Carstensen*
School of Pharmacy
University of Wisconsin
Madison, WI 53706



Received January 28, 1980.
Accepted for publication March 9, 1981.


## Mesophase Formation during *In Vitro* Cholesterol Gallstone Dissolution: A Specific Effect of Ursodeoxycholic Acid


**Keyphrases** □ Cholesterol—gallstones, mesophase formation during *in vitro* gallstone dissolution □ Gallstones, cholesterol—effect of bile acid on gallstone dissolution *in vitro* □ Ursodeoxycholic acid—effect on cholesterol gallstone dissolution *in vitro*, compared with chenodeoxycholic acid □ Dissolution—cholesterol gallstones, effect of bile acid


*To the Editor:*

Ursodeoxycholate (I), the 7β-epimer of chenodeoxycholate (II), has been shown to be equal or superior to II when used as oral medication for the dissolution of cho-



© 1981, American Pharmaceutical Association

lesterol gallstones (1–4). The clinical efficacy of I is curious since *in vitro* it is a relatively poor solubilizer of cholesterol, either alone or as mixed bile acid–lecithin micelles (5–8).

The contradiction between the poor solubilization of cholesterol monohydrate by I *in vitro* and yet its successful use for the dissolution of human gallstones *in vivo* led us to investigate the dissolution behavior of cholesterol monohydrate in media containing I conjugates (9, 10). The data showed that initial dissolution rates of cholesterol monohydrate in powder and pellet forms were always lower in lecithin–ursodeoxycholylglycine (III) solutions than in the corresponding lecithin–chenodeoxycholylglycine (IV) solutions. This finding is in agreement with previous investigations (5–8). However, in these experiments, cholesterol release into the lecithin–III-containing medium continued far beyond the apparent equilibrium solubility in the isotropic phase by formation of a turbid, liquid crystalline phase (mesophase).

These experiments were extended to determine whether such mesophase formation might occur during the *in vitro* dissolution of cholesterol gallstones.

Gallstones were obtained at surgery from two patients. The first group of stones (Fig. 1A) was removed from the gallbladder of a patient 40 years old, and the second group (Fig. 1B) was obtained from a patient 85 years old with a typical history of recurrent biliary colic. All stones were washed and kept moist in water until the dissolution studies were begun. Preoperative oral cholecystograms revealed radiolucent stones, and chemical analyses of both groups of stones showed the cholesterol contents to be close to 100%.

A single stone was placed in a test tube containing either 2 or 2.5 ml of solution. The tubes were shaken at 37°, and samples were taken at suitable time intervals. Cholesterol was assayed enzymatically[1], and an organic phosphate assay (11) was employed for lecithin.

Figure 1A shows the dissolution behavior of two stones, removed from the same patient, in lecithin–III medium. The dotted line shows the apparent equilibrium solubility of cholesterol monohydrate from pellet studies[2] in the corresponding medium. The arrows in Fig. 1 show the beginning of turbidity in the media. Microscope observations under cross-polarized light of a sample of the turbid medium revealed liquid crystals. In one experiment, the entire solution was replaced by 2.0 ml of fresh medium on the 10th day, and mesophase formation was observed to continue perhaps even at a higher rate. In these experiments, the total amount of cholesterol released far exceeded the thermodynamic micellar saturation value for cholesterol monohydrate.

Figure 1B shows data for the dissolution behavior of cholesterol gallstones from another patient; the difference in behavior for stone dissolution in III and IV solutions is clearly illustrated. For IV, the initial micellar dissolution rate was relatively rapid and the curves leveled off close to the apparent solubility value for cholesterol monohydrate[2]. In contrast, the stone dissolution in III initially proceeded much more slowly (as in Fig. 1A), and the dissolution curve did not level off at the apparent solubility

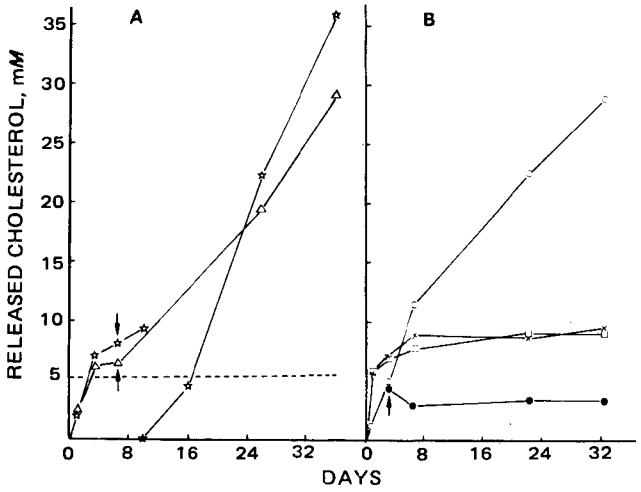


**Figure 1**—*Effect of bile acid type on cholesterol gallstone dissolution in 32 mM lecithin, 0.1 M NaCl, and 0.01 M phosphate buffer at pH 7.4 and 37°. Key: △, 126-mg stone in 2 ml of solution containing 87 mM III; ☆, 172-mg stone in 2 ml of solution containing 87 mM III (old medium was replaced by fresh medium on the 10th day); ○, 873-mg stone in 2.5 ml of solution containing 87 mM III; ×, 891-mg stone in 2.5 ml of solution containing 87 mM IV; □, 910-mg stone in 2.5 ml of solution containing 87 mM IV; and ●, 873-mg stone in 2.5 ml of solution containing 87 mM III (after centrifugation of the supernate).*

but proceeded to much higher values. In III solution, the beginning of turbidity was observed after about 3 days (see arrows), but cholesterol released from the stone continued far beyond the apparent solubility value. As in Fig. 1A, the polarizing microscope examination of the mesophase (which separates to the top of the isotropic solution after centrifugation) showed liquid crystal properties. Solid circles in Fig. 1B show the supernatant (isotropic phase) cholesterol levels after centrifugation (8000×*g* for 10 min).

Table I shows that the lecithin levels in the experiments involving IV remained relatively constant with and without centrifugation. In the experiments with III, the lecithin levels in the supernate (isotropic phase) obtained after centrifugation decreased greatly with time. Calculations based on the lecithin data in Table I and the cholesterol data in Fig. 1B showed that the separated phase(s) possessed an average cholesterol to lecithin ratio of 1:1 to 3:1. In addition, the cholesterol level obtained for the supernate (isotropic phase) after centrifugation was somewhat lower than the value corresponding to the dotted line in Fig. 1A. This finding is consistent with observed lecithin depletion from the media during mesophase formation.

Other gallstones, which are under investigation in these

**Table I—Data Showing Lecithin Concentration (Millimolar) Changes during *In Vitro*[a] Cholesterol Gallstone Dissolution in Solutions Containing III**

| Days | Lecithin–IV | | Lecithin–IV | | Lecithin–III | |
|---|---|---|---|---|---|---|
| | Before[b] | After | Before | After | Before | After |
| 0 | 32.0 | 32.0 | 32.0 | 32.0 | 32.0 | 32.0 |
| 3.1 | 33.3 | 33.2 | 28.3 | 29.8 | 25.2 | 22.0 |
| 7.0 | 32.6 | 29.4 | 27.6 | 30.6 | 25.0 | 12.6 |
| 22.5 | 32.8 | 29.8 | 27.0 | 27.4 | 25.2 | 11.8 |
| 32.7 | 31.0 | 31.5 | 28.1 | 31.0 | 25.2 | 12.0 |

[a] Changes in cholesterol concentration are shown in Fig. 1. The initial concentration of lecithin was 32 m*M*; the concentrations of IV and III were 87 m*M*. [b] The concentration of lecithin before centrifugation denotes lecithin in both the mesomorphic and isotropic phases; after centrifugation, the lecithin concentration refers to the isotropic phase because the mesophase has risen to the top of the tube.

[1] Bio-Dynamics, Indianapolis, Ind.
[2] Manuscript in preparation.

laboratories, also show that the cholesterol release in media containing III and lecithin may follow the pattern described in Scheme I.

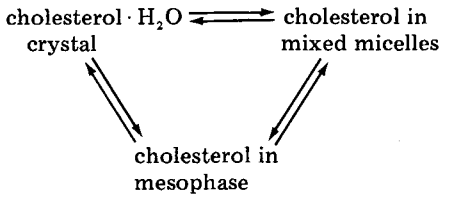


*Scheme I*

The process effectively represents a substantial mass transfer rate of cholesterol from the gallstone into the medium. Although this process is significantly slower than the micellar dissolution rate of a cholesterol gallstone in a lecithin–IV solution, after some time (several days in these experiments) the extent of dissolution and disintegration by this process may be greater.

These studies imply that the phase equilibria in III–lecithin–cholesterol–water differ from that in IV–lecithin–cholesterol–water. Conjugates of ursodeoxycholic acid apparently have a much weaker tendency to disperse mixed lecithin–cholesterol bilayers than those of chenodeoxycholic acid. The data do not answer directly the question of whether mesophase formation may occur during gallstone dissolution induced by ursodeoxycholate in humans since biliary bile acids become only moderately enriched in ursodeoxycholic acid (60–70%) during continuous ursodeoxycholate administration; therefore, further studies are needed. Mesophase formation during gallstone induction does occur in the cholesterol-fed prairie dog (12) whose bile contains predominantly cholate conjugates, and mesophases were reported to occur in some samples of human bile (13, 14).

(1) G. D. Bell, *J. R. College Physicians London*, **13,** 47 (1979).

(2) E. Roda, A. Roda, C. Sama, D. Festi, G. Mazzella, R. Aldini, and L. Barbara, *Dig. Dis. Sci.*, **24,** 123 (1979).

(3) M. Ponz deLeon, N. Carulli, P. Loria, R. Iori, and F. Zironi, *Gastroenterology*, **78,** 214 (1980).

(4) Tokyo Cooperative Gallstone Study Group, *ibid.*, **78,** 542 (1980).

(5) J. C. Montet, M. O. Reynier, A. M. Montet, and A. Gerolami, *Biochim. Biophys. Acta*, **575,** 289 (1979).

(6) H. Igimi, N. Tamesue, Y. Ikejiri, and H. Shimura, *Life Sci.*, **21,** 1373 (1977).

(7) M. C. Carey and G. Ka, in "Biological Effects of Bile Acids," G. Paumgartner, A. Stiehl, and W. Gerok, Eds., MTP Press Ltd., Lanchester, England, 1979, pp. 299–308.

(8) M. C. Carey, N. A. Mazer, and G. B. Benedek, *Gastroenterology*, **72,** 1036 (1977).

(9) C. C. Su, O. I. Corrigan, W. I. Higuchi, K. H. Kwan, and A. F. Hofmann, "Abstracts of the APhA Academy of Pharmaceutical Sciences," vol. 10, Apr. 1980, p. 91.

(10) O. I. Corrigan, C. C. Su, W. I. Higuchi, and A. F. Hofmann, *J. Pharm. Sci.*, **69,** 869 (1980).

(11) R. S. Sandhu, *Clin. Chem.*, **22,** 1973 (1976).

(12) R. T. Holzbach, C. Corbusier, M. Marsh, and H. K. Naito, *J. Lab. Clin. Med.*, **87,** 987 (1976).

(13) R. T. Holzbach and M. Marsh, *Mol. Cryst. Lig. Cryst.*, **28,** 217 (1975).

(14) R. T. Holzbach and C. Corbusier, *Biochim. Biophys. Acta*, **528,** 436 (1978).

*C. C. Su*
*J. Y. Park*
*W. I. Higuchi* ˣ
College of Pharmacy
University of Michigan
Ann Arbor, MI 48109

*M. H. Alkan*
Ankara Universitesi
Eczacilik Fakultesi
Farmasotik Teknoloji Kursusu
Tandogan/Ankara, Turkey

*O. I. Corrigan*
School of Pharmacy
Faculty of Science
Trinity College
Dublin 4, Ireland

*A. F. Hofmann*
Division of Gastroenterology
University of California
San Diego, CA 92103

*R. G. Danzinger*
St. Boniface General Hospital
Winnipeg, Manitoba, Canada

Received July 24, 1980.
Accepted for publication October 21, 1980.
Supported by National Institutes of Health Grants AM16694 and AM21506.

# BOOKS

## REVIEWS

**Pharmaceutical Calculations, 7th Ed.** By MITCHELL J. STOKLOSA and HOWARD C. ANSEL. Lea & Febiger, 600 Washington Square, Philadelphia, PA 19106. 385 pp. 15 × 23 cm. Price $15.00.

The seventh edition is in the same format as earlier ones but contains an expanded chapter on dosage calculations and additional chapters on interpreting the prescription and calculations involving parenteral admixtures. The material from the "Chemical Problems" chapter in the 6th edition is found in the appendix of the new edition. Many new practice problems have been added to appropriate chapters.

The addition of a new chapter, "Interpretation of the Prescription or Medication Order," is very good. The interpretation presented is aimed specifically at helping the student solve problems presented in the prescription, medication order, or formula and does not duplicate information given in other chapters, as one might expect. The subject matter is presented in a direct manner with enough examples to be easily understood.

Additions to the "Calculation of Doses" chapter include an expansion of the surface area method with the two DuBois and DuBois nomograms for finding body surface areas for children and adults. This is a considerable improvement over the 6th edition which contained a table of body weights and surface areas. Unfortunately, the reference to the use of this method (Harry Shirkey) uses the West nomogram, which gives results different from that of DuBois. Perhaps an expanded discussion could cover this point in the next edition.

The inclusion of calculations involving lean body mass, loading dose, maintenance dose, and the use of creatinine clearance rate is an excellent choice of subject to update the book. The explanations and examples are all clear and precise except for the calculation and use of creatinine

laboratories, also show that the cholesterol release in media containing III and lecithin may follow the pattern described in Scheme I.

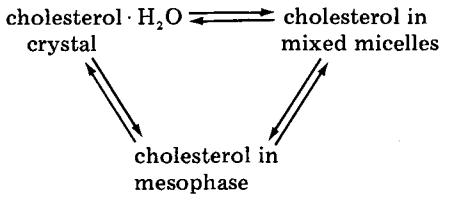


*Scheme I*

The process effectively represents a substantial mass transfer rate of cholesterol from the gallstone into the medium. Although this process is significantly slower than the micellar dissolution rate of a cholesterol gallstone in a lecithin–IV solution, after some time (several days in these experiments) the extent of dissolution and disintegration by this process may be greater.

These studies imply that the phase equilibria in III–lecithin–cholesterol–water differ from that in IV–lecithin–cholesterol–water. Conjugates of ursodeoxycholic acid apparently have a much weaker tendency to disperse mixed lecithin–cholesterol bilayers than those of chenodeoxycholic acid. The data do not answer directly the question of whether mesophase formation may occur during gallstone dissolution induced by ursodeoxycholate in humans since biliary bile acids become only moderately enriched in ursodeoxycholic acid (60–70%) during continuous ursodeoxycholate administration; therefore, further studies are needed. Mesophase formation during gallstone induction does occur in the cholesterol-fed prairie dog (12) whose bile contains predominantly cholate conjugates, and mesophases were reported to occur in some samples of human bile (13, 14).

(1) G. D. Bell, *J. R. College Physicians London*, **13,** 47 (1979).

(2) E. Roda, A. Roda, C. Sama, D. Festi, G. Mazzella, R. Aldini, and L. Barbara, *Dig. Dis. Sci.*, **24,** 123 (1979).

(3) M. Ponz deLeon, N. Carulli, P. Loria, R. Iori, and F. Zironi, *Gastroenterology*, **78,** 214 (1980).

(4) Tokyo Cooperative Gallstone Study Group, *ibid.*, **78,** 542 (1980).

(5) J. C. Montet, M. O. Reynier, A. M. Montet, and A. Gerolami, *Biochim. Biophys. Acta*, **575,** 289 (1979).

(6) H. Igimi, N. Tamesue, Y. Ikejiri, and H. Shimura, *Life Sci.*, **21,** 1373 (1977).

(7) M. C. Carey and G. Ka, in "Biological Effects of Bile Acids," G. Paumgartner, A. Stiehl, and W. Gerok, Eds., MTP Press Ltd., Lanchester, England, 1979, pp. 299–308.

(8) M. C. Carey, N. A. Mazer, and G. B. Benedek, *Gastroenterology*, **72,** 1036 (1977).

(9) C. C. Su, O. I. Corrigan, W. I. Higuchi, K. H. Kwan, and A. F. Hofmann, "Abstracts of the APhA Academy of Pharmaceutical Sciences," vol. 10, Apr. 1980, p. 91.

(10) O. I. Corrigan, C. C. Su, W. I. Higuchi, and A. F. Hofmann, *J. Pharm. Sci.*, **69,** 869 (1980).

(11) R. S. Sandhu, *Clin. Chem.*, **22,** 1973 (1976).

(12) R. T. Holzbach, C. Corbusier, M. Marsh, and H. K. Naito, *J. Lab. Clin. Med.*, **87,** 987 (1976).

(13) R. T. Holzbach and M. Marsh, *Mol. Cryst. Lig. Cryst.*, **28,** 217 (1975).

(14) R. T. Holzbach and C. Corbusier, *Biochim. Biophys. Acta*, **528,** 436 (1978).

*C. C. Su*
*J. Y. Park*
*W. I. Higuchi* ˣ
College of Pharmacy
University of Michigan
Ann Arbor, MI 48109

*M. H. Alkan*
Ankara Universitesi
Eczacilik Fakultesi
Farmasotik Teknoloji Kursusu
Tandogan/Ankara, Turkey

*O. I. Corrigan*
School of Pharmacy
Faculty of Science
Trinity College
Dublin 4, Ireland

*A. F. Hofmann*
Division of Gastroenterology
University of California
San Diego, CA 92103

*R. G. Danzinger*
St. Boniface General Hospital
Winnipeg, Manitoba, Canada

Received July 24, 1980.
Accepted for publication October 21, 1980.
Supported by National Institutes of Health Grants AM16694 and AM21506.

# BOOKS

## REVIEWS

**Pharmaceutical Calculations, 7th Ed.** By MITCHELL J. STOKLOSA and HOWARD C. ANSEL. Lea & Febiger, 600 Washington Square, Philadelphia, PA 19106. 385 pp. 15 × 23 cm. Price $15.00.

The seventh edition is in the same format as earlier ones but contains an expanded chapter on dosage calculations and additional chapters on interpreting the prescription and calculations involving parenteral admixtures. The material from the "Chemical Problems" chapter in the 6th edition is found in the appendix of the new edition. Many new practice problems have been added to appropriate chapters.

The addition of a new chapter, "Interpretation of the Prescription or Medication Order," is very good. The interpretation presented is aimed specifically at helping the student solve problems presented in the prescription, medication order, or formula and does not duplicate information given in other chapters, as one might expect. The subject matter is presented in a direct manner with enough examples to be easily understood.

Additions to the "Calculation of Doses" chapter include an expansion of the surface area method with the two DuBois and DuBois nomograms for finding body surface areas for children and adults. This is a considerable improvement over the 6th edition which contained a table of body weights and surface areas. Unfortunately, the reference to the use of this method (Harry Shirkey) uses the West nomogram, which gives results different from that of DuBois. Perhaps an expanded discussion could cover this point in the next edition.

The inclusion of calculations involving lean body mass, loading dose, maintenance dose, and the use of creatinine clearance rate is an excellent choice of subject to update the book. The explanations and examples are all clear and precise except for the calculation and use of creatinine

clearance rate for females, which is hampered somewhat by insufficient practice problems of this type at the end of the chapter.

"Some Calculations Involving Parenteral Admixtures" is another new chapter. The material covers the application of the milliequivalent and millimole concepts to the use of additive solutions in parenteral therapy. The use of various solutions obtained from ampuls or vials and the constituting of total parenteral nutrition or hyperalimentation fluids are included, as are computations of the flow rates of intravenous solutions.

"Pharmaceutical Calculations" has been a standard text for many years. Its clear but concise explanations, numerous examples, and various practice problems have made it so. The new materials are good additions to an already excellent book.

*Reviewed by* Noel O. Nuessle
*School of Pharmacy*
*University of Missouri—Kansas City*
*Kansas City, MO 64110*

---

**Sustained Release Medications.** Edited by J. C. JOHNSON. Noyes Data Corp., Mill Rd. at Grand Ave., Park Ridge, NJ 07655. 1980. 412 pp. 15 × 23 cm. Price $54.00.

In the foreword, the editor gives an excellent and precise description of the information contained in the book. The information is based on U.S. patents issued since January 1974 in the field of sustained-release medications. The editor indicates that the book is a data-based publication, providing information retrieved and made available from the U.S. patent literature. Thus, it serves a double purpose in that it supplies detailed technical information and can be used as a guide to the patent literature in this field. By indicating all the significant information and eliminating legal jargon and juristic phraseology, this book represents an advanced, commercially oriented review of recent developments in the field of sustained-release medications. The book is composed of 14 chapters; it contains 263 patents covering 204 processes.

The first chapter deals with patents describing the preparation of excipients used in the manufacture of these medications. Included are controlled-release tableting media (talc, ethylcellulose, methyl stearate mixtures, hydrated hydroxyalkylcellulose plus aliphatic alcohol, and salts of polymeric carboxylates), polymer gels (chelated hydrogels and water-insoluble hydrophilic copolymers), enteric-coating materials (cellulose ether compositions, partial esters of acrylate-unsaturated anhydride copolymers, and water-soluble coating resins), and polyesters (polymers with oxyacycloalkane units, polymers with alkoxy or oxacycloalkane substituents, bioabsorbable polyglycolic acid polyester condensates, and bioerodable partial esters of polycarboxylic acids).

Patented processes involved in the preparation and coating of microcapsules is covered in Chapter 2. Chapter 3 includes processes for preparing capsules as well as tablet cores and tablet coatings. Patents dealing with films and webs are discussed in Chapter 4. The fifth chapter describes 10 processes utilized in the design of diffusion devices containing medications soluble to some extent in the polymeric material. Chapter 6 includes 16 processes involved in the preparation of osmotic devices that use polymeric materials permeable to water and body fluids but not permeable to the drug.

The next four chapters describe devices such as implants, ocular inserts, intravaginal and intrauterine inserts, and devices for use in the GI tract. These devices utilize bioerodable polymers selected so that the device and the medication are absorbed by the body. Chapters 11–13 deal with various sustained-release medications such as heart and circulatory drugs, antispasmodics, antibiotics, aspirin, and analgesics and GI tract drugs. The final chapter describes veterinary preparations.

The book is a must for individuals interested in sustained-release technology. It is well written and would be a great timesaver and a source of many excellent ideas.

*Reviewed by* Farid Sadik
*College of Pharmacy*
*University of South Carolina*
*Columbia, SC 29208*

9307

## NOTICES

*Synthetic Peptides, Vol. 5.* By GEORGE R. PETTIT. Elsevier Scientific Publishing Co., 52 Vanderbilt Ave., New York, NY 10017. 1980. 404 pp. 14 × 22 cm. Price $109.75.

*Annual Reports in Medicinal Chemistry, Vol. 15.* HANS-JÜRGEN HESS, Editor in Chief. Academic, 111 Fifth Ave., New York, NY 10003. 1980. 346 pp. 17 × 25 cm.

*Progress in Drug Metabolism, Vol. 4.* Edited by J. W. BRIDGES and L. F. CHASSEAUD. Wiley, 605 Third Ave., New York, NY 10016. 1980. 335 pp. 15 × 23 cm. Price $72.00.

*Bioenergetics and Thermodynamics: Model Systems.* By A. BRAIBANTI. D. Reidel Publishing Co., 160 Old Derby St., Hingham, MA 02043. 1980. 471 pp. 16 × 24 cm. Price $58.00.

*Manuel de Préparation en Pharmacie d'Officine.* By MICHEL BARANCOURT. Masson, 14 E. 60th St., New York, NY 10022. 1980. 550 pp. 16 × 24 cm. (Also available from Masson, 120 Boulevard Saint-Germain, 75280 Paris Cedex 06, France.)

*Handbook for Prescribing Medications During Pregnancy.* Edited by RICHARD L. BERKOWITZ, DONALD R. COUSTAN, and TARA K. MOCHIZUKI. Little, Brown, 34 Beacon St., Boston, MA 02106. 1981. 257 pp. 11 × 20 cm. Price $11.95.

*Solids Handling.* Edited by KENNETH MCNAUGHTON and the staff of chemical engineering. McGraw-Hill, 1221 Avenue of the Americas, New York, NY 10020. 1981. 263 pp. 21 × 28 cm. Price $29.50.

*Abrégé de Matière Médicale (Pharmacognosie), Tome I.* By M. PARIS and M. HURABIELLE. Masson, 14 E. 60th St., New York, NY 10022. 1981. 339 pp. 13 × 21 cm. (Also available from Masson, 120 Boulevard Saint-Germain, 75280 Paris Cedex 06, France.)

*Abrégé de Pharmacie Galénique, 3rd ed.* By A. LE HIR. Masson, 14 E. 60th St., New York, NY 10022. 1981. 354 pp. 13 × 21 cm. (Also available from Masson, 120 Boulevard Saint-Germain, 75280 Paris Cedex 06, France.)

*The Safety of Medicines: Evaluation and Prediction.* By PETER I. FOLB. Springer–Verlag New York, 44 Hartz Way, Secaucus, NJ 07094. 1980. 103 pp. 12 × 21 cm. Price $12.90.

*Abrégé de Pharmacologie: Générale et Moléculaire, 2nd ed.* By JACQUES WEPIERRE. Masson, 14 E. 60th St., New York, NY 10022. 1981. 203 pp. 13 × 21 cm. (Also available from Masson, 120 Boulevard Saint-Germain, 75280 Paris Cedex 06, France.)

*Progress in Pharmacology, Vol. 3, No. 2. Presynaptic Mechanisms/ Vasodilator Drugs.* Edited by P. A. van SWIETEN and E. SCHÖNBAUM. (Proceedings of a symposium organized by the Dutch Pharmacological Society in Amsterdam, The Netherlands, 1979.) Gustav Fischer Verlag, D-7000 Stuttgart 72, Postfach 720 143, West Germany. 1980. 146 pp. 16 × 24 cm. Price DM 78.00.

*The Analysis of Dietary Fiber in Food.* Edited by W. P. T. JAMES and OLOF THEANDER. Dekker, 270 Madison Ave., New York, NY 10016. 1981. 276 pp. 15 × 23 cm. Price $35.00 (20% higher outside the United States and Canada).

*The Biochemistry of Psychiatric Disturbances.* Edited by G. CURZON. Wiley, 605 Third Ave., New York, NY 10016. 1980. 144 pp. 15 × 23 cm.

*Clinically Important Adverse Drug Interactions, Vol. 1: Cardiovascular and Respiratory Disease Therapy.* Edited by J. C. PETRIE. Elsevier/North-Holland, 52 Vanderbilt Ave., New York, NY 10017. 1980. 243 pp. 16 × 24 cm. Price $48.25. (Available from Elsevier, P.O. Box 1527, Amsterdam, The Netherlands.)

*Introduction to Bioinstrumentation. With Biological, Environmental, and Medical Applications* (A Volume of Contemporary Instrumentation and Analysis). By CLIFFORD D. FERRIS. Humane Press, Crescent Manor, P.O. Box 2148, Clifton, NJ 07015. 1978. 330 pp. 15 × 23 cm. Price $29.50 hardcover and $14.50 softcover.

*Metal Carcinogenesis Testing: Principles and In Vitro Methods.* By MAX COSTA. Humane Press, Crescent Manor, P.O. Box 2148, Clifton, NJ 07015. 1980. 163 pp. 15 × 23 cm. Price $29.50 ($39.50 outside North America).

clearance rate for females, which is hampered somewhat by insufficient practice problems of this type at the end of the chapter.

"Some Calculations Involving Parenteral Admixtures" is another new chapter. The material covers the application of the milliequivalent and millimole concepts to the use of additive solutions in parenteral therapy. The use of various solutions obtained from ampuls or vials and the constituting of total parenteral nutrition or hyperalimentation fluids are included, as are computations of the flow rates of intravenous solutions.

"Pharmaceutical Calculations" has been a standard text for many years. Its clear but concise explanations, numerous examples, and various practice problems have made it so. The new materials are good additions to an already excellent book.

*Reviewed by* Noel O. Nuessle
*School of Pharmacy*
*University of Missouri—Kansas City*
*Kansas City, MO 64110*

---

**Sustained Release Medications.** Edited by J. C. JOHNSON. Noyes Data Corp., Mill Rd. at Grand Ave., Park Ridge, NJ 07655. 1980. 412 pp. 15 × 23 cm. Price $54.00.

In the foreword, the editor gives an excellent and precise description of the information contained in the book. The information is based on U.S. patents issued since January 1974 in the field of sustained-release medications. The editor indicates that the book is a data-based publication, providing information retrieved and made available from the U.S. patent literature. Thus, it serves a double purpose in that it supplies detailed technical information and can be used as a guide to the patent literature in this field. By indicating all the significant information and eliminating legal jargon and juristic phraseology, this book represents an advanced, commercially oriented review of recent developments in the field of sustained-release medications. The book is composed of 14 chapters; it contains 263 patents covering 204 processes.

The first chapter deals with patents describing the preparation of excipients used in the manufacture of these medications. Included are controlled-release tableting media (talc, ethylcellulose, methyl stearate mixtures, hydrated hydroxyalkylcellulose plus aliphatic alcohol, and salts of polymeric carboxylates), polymer gels (chelated hydrogels and water-insoluble hydrophilic copolymers), enteric-coating materials (cellulose ether compositions, partial esters of acrylate-unsaturated anhydride copolymers, and water-soluble coating resins), and polyesters (polymers with oxyacycloalkane units, polymers with alkoxy or oxacycloalkane substituents, bioabsorbable polyglycolic acid polyester condensates, and bioerodable partial esters of polycarboxylic acids).

Patented processes involved in the preparation and coating of microcapsules is covered in Chapter 2. Chapter 3 includes processes for preparing capsules as well as tablet cores and tablet coatings. Patents dealing with films and webs are discussed in Chapter 4. The fifth chapter describes 10 processes utilized in the design of diffusion devices containing medications soluble to some extent in the polymeric material. Chapter 6 includes 16 processes involved in the preparation of osmotic devices that use polymeric materials permeable to water and body fluids but not permeable to the drug.

The next four chapters describe devices such as implants, ocular inserts, intravaginal and intrauterine inserts, and devices for use in the GI tract. These devices utilize bioerodable polymers selected so that the device and the medication are absorbed by the body. Chapters 11–13 deal with various sustained-release medications such as heart and circulatory drugs, antispasmodics, antibiotics, aspirin, and analgesics and GI tract drugs. The final chapter describes veterinary preparations.

The book is a must for individuals interested in sustained-release technology. It is well written and would be a great timesaver and a source of many excellent ideas.

*Reviewed by* Farid Sadik
*College of Pharmacy*
*University of South Carolina*
*Columbia, SC 29208*

9307

## NOTICES

*Synthetic Peptides, Vol. 5.* By GEORGE R. PETTIT. Elsevier Scientific Publishing Co., 52 Vanderbilt Ave., New York, NY 10017. 1980. 404 pp. 14 × 22 cm. Price $109.75.

*Annual Reports in Medicinal Chemistry, Vol. 15.* HANS-JÜRGEN HESS, Editor in Chief. Academic, 111 Fifth Ave., New York, NY 10003. 1980. 346 pp. 17 × 25 cm.

*Progress in Drug Metabolism, Vol. 4.* Edited by J. W. BRIDGES and L. F. CHASSEAUD. Wiley, 605 Third Ave., New York, NY 10016. 1980. 335 pp. 15 × 23 cm. Price $72.00.

*Bioenergetics and Thermodynamics: Model Systems.* By A. BRAIBANTI. D. Reidel Publishing Co., 160 Old Derby St., Hingham, MA 02043. 1980. 471 pp. 16 × 24 cm. Price $58.00.

*Manuel de Préparation en Pharmacie d'Officine.* By MICHEL BARANCOURT. Masson, 14 E. 60th St., New York, NY 10022. 1980. 550 pp. 16 × 24 cm. (Also available from Masson, 120 Boulevard Saint-Germain, 75280 Paris Cedex 06, France.)

*Handbook for Prescribing Medications During Pregnancy.* Edited by RICHARD L. BERKOWITZ, DONALD R. COUSTAN, and TARA K. MOCHIZUKI. Little, Brown, 34 Beacon St., Boston, MA 02106. 1981. 257 pp. 11 × 20 cm. Price $11.95.

*Solids Handling.* Edited by KENNETH MCNAUGHTON and the staff of chemical engineering. McGraw-Hill, 1221 Avenue of the Americas, New York, NY 10020. 1981. 263 pp. 21 × 28 cm. Price $29.50.

*Abrégé de Matière Médicale (Pharmacognosie), Tome I.* By M. PARIS and M. HURABIELLE. Masson, 14 E. 60th St., New York, NY 10022. 1981. 339 pp. 13 × 21 cm. (Also available from Masson, 120 Boulevard Saint-Germain, 75280 Paris Cedex 06, France.)

*Abrégé de Pharmacie Galénique, 3rd ed.* By A. LE HIR. Masson, 14 E. 60th St., New York, NY 10022. 1981. 354 pp. 13 × 21 cm. (Also available from Masson, 120 Boulevard Saint-Germain, 75280 Paris Cedex 06, France.)

*The Safety of Medicines: Evaluation and Prediction.* By PETER I. FOLB. Springer–Verlag New York, 44 Hartz Way, Secaucus, NJ 07094. 1980. 103 pp. 12 × 21 cm. Price $12.90.

*Abrégé de Pharmacologie: Générale et Moléculaire, 2nd ed.* By JACQUES WEPIERRE. Masson, 14 E. 60th St., New York, NY 10022. 1981. 203 pp. 13 × 21 cm. (Also available from Masson, 120 Boulevard Saint-Germain, 75280 Paris Cedex 06, France.)

*Progress in Pharmacology, Vol. 3, No. 2. Presynaptic Mechanisms/ Vasodilator Drugs.* Edited by P. A. van SWIETEN and E. SCHÖNBAUM. (Proceedings of a symposium organized by the Dutch Pharmacological Society in Amsterdam, The Netherlands, 1979.) Gustav Fischer Verlag, D-7000 Stuttgart 72, Postfach 720 143, West Germany. 1980. 146 pp. 16 × 24 cm. Price DM 78.00.

*The Analysis of Dietary Fiber in Food.* Edited by W. P. T. JAMES and OLOF THEANDER. Dekker, 270 Madison Ave., New York, NY 10016. 1981. 276 pp. 15 × 23 cm. Price $35.00 (20% higher outside the United States and Canada).

*The Biochemistry of Psychiatric Disturbances.* Edited by G. CURZON. Wiley, 605 Third Ave., New York, NY 10016. 1980. 144 pp. 15 × 23 cm.

*Clinically Important Adverse Drug Interactions, Vol. 1: Cardiovascular and Respiratory Disease Therapy.* Edited by J. C. PETRIE. Elsevier/North-Holland, 52 Vanderbilt Ave., New York, NY 10017. 1980. 243 pp. 16 × 24 cm. Price $48.25. (Available from Elsevier, P.O. Box 1527, Amsterdam, The Netherlands.)

*Introduction to Bioinstrumentation. With Biological, Environmental, and Medical Applications* (A Volume of Contemporary Instrumentation and Analysis). By CLIFFORD D. FERRIS. Humane Press, Crescent Manor, P.O. Box 2148, Clifton, NJ 07015. 1978. 330 pp. 15 × 23 cm. Price $29.50 hardcover and $14.50 softcover.

*Metal Carcinogenesis Testing: Principles and In Vitro Methods.* By MAX COSTA. Humane Press, Crescent Manor, P.O. Box 2148, Clifton, NJ 07015. 1980. 163 pp. 15 × 23 cm. Price $29.50 ($39.50 outside North America).

clearance rate for females, which is hampered somewhat by insufficient practice problems of this type at the end of the chapter.

"Some Calculations Involving Parenteral Admixtures" is another new chapter. The material covers the application of the milliequivalent and millimole concepts to the use of additive solutions in parenteral therapy. The use of various solutions obtained from ampuls or vials and the constituting of total parenteral nutrition or hyperalimentation fluids are included, as are computations of the flow rates of intravenous solutions.

"Pharmaceutical Calculations" has been a standard text for many years. Its clear but concise explanations, numerous examples, and various practice problems have made it so. The new materials are good additions to an already excellent book.

*Reviewed by* Noel O. Nuessle
*School of Pharmacy*
*University of Missouri—Kansas City*
*Kansas City, MO 64110*

---

**Sustained Release Medications.** Edited by J. C. JOHNSON. Noyes Data Corp., Mill Rd. at Grand Ave., Park Ridge, NJ 07655. 1980. 412 pp. 15 × 23 cm. Price $54.00.

In the foreword, the editor gives an excellent and precise description of the information contained in the book. The information is based on U.S. patents issued since January 1974 in the field of sustained-release medications. The editor indicates that the book is a data-based publication, providing information retrieved and made available from the U.S. patent literature. Thus, it serves a double purpose in that it supplies detailed technical information and can be used as a guide to the patent literature in this field. By indicating all the significant information and eliminating legal jargon and juristic phraseology, this book represents an advanced, commercially oriented review of recent developments in the field of sustained-release medications. The book is composed of 14 chapters; it contains 263 patents covering 204 processes.

The first chapter deals with patents describing the preparation of excipients used in the manufacture of these medications. Included are controlled-release tableting media (talc, ethylcellulose, methyl stearate mixtures, hydrated hydroxyalkylcellulose plus aliphatic alcohol, and salts of polymeric carboxylates), polymer gels (chelated hydrogels and water-insoluble hydrophilic copolymers), enteric-coating materials (cellulose ether compositions, partial esters of acrylate-unsaturated anhydride copolymers, and water-soluble coating resins), and polyesters (polymers with oxyacycloalkane units, polymers with alkoxy or oxacycloalkane substituents, bioabsorbable polyglycolic acid polyester condensates, and bioerodable partial esters of polycarboxylic acids).

Patented processes involved in the preparation and coating of microcapsules is covered in Chapter 2. Chapter 3 includes processes for preparing capsules as well as tablet cores and tablet coatings. Patents dealing with films and webs are discussed in Chapter 4. The fifth chapter describes 10 processes utilized in the design of diffusion devices containing medications soluble to some extent in the polymeric material. Chapter 6 includes 16 processes involved in the preparation of osmotic devices that use polymeric materials permeable to water and body fluids but not permeable to the drug.

The next four chapters describe devices such as implants, ocular inserts, intravaginal and intrauterine inserts, and devices for use in the GI tract. These devices utilize bioerodable polymers selected so that the device and the medication are absorbed by the body. Chapters 11–13 deal with various sustained-release medications such as heart and circulatory drugs, antispasmodics, antibiotics, aspirin, and analgesics and GI tract drugs. The final chapter describes veterinary preparations.

The book is a must for individuals interested in sustained-release technology. It is well written and would be a great timesaver and a source of many excellent ideas.

*Reviewed by* Farid Sadik
*College of Pharmacy*
*University of South Carolina*
*Columbia, SC 29208*

9307

## NOTICES

*Synthetic Peptides, Vol. 5.* By GEORGE R. PETTIT. Elsevier Scientific Publishing Co., 52 Vanderbilt Ave., New York, NY 10017. 1980. 404 pp. 14 × 22 cm. Price $109.75.

*Annual Reports in Medicinal Chemistry, Vol. 15.* HANS-JÜRGEN HESS, Editor in Chief. Academic, 111 Fifth Ave., New York, NY 10003. 1980. 346 pp. 17 × 25 cm.

*Progress in Drug Metabolism, Vol. 4.* Edited by J. W. BRIDGES and L. F. CHASSEAUD. Wiley, 605 Third Ave., New York, NY 10016. 1980. 335 pp. 15 × 23 cm. Price $72.00.

*Bioenergetics and Thermodynamics: Model Systems.* By A. BRAIBANTI. D. Reidel Publishing Co., 160 Old Derby St., Hingham, MA 02043. 1980. 471 pp. 16 × 24 cm. Price $58.00.

*Manuel de Préparation en Pharmacie d'Officine.* By MICHEL BARANCOURT. Masson, 14 E. 60th St., New York, NY 10022. 1980. 550 pp. 16 × 24 cm. (Also available from Masson, 120 Boulevard Saint-Germain, 75280 Paris Cedex 06, France.)

*Handbook for Prescribing Medications During Pregnancy.* Edited by RICHARD L. BERKOWITZ, DONALD R. COUSTAN, and TARA K. MOCHIZUKI. Little, Brown, 34 Beacon St., Boston, MA 02106. 1981. 257 pp. 11 × 20 cm. Price $11.95.

*Solids Handling.* Edited by KENNETH MCNAUGHTON and the staff of chemical engineering. McGraw-Hill, 1221 Avenue of the Americas, New York, NY 10020. 1981. 263 pp. 21 × 28 cm. Price $29.50.

*Abrégé de Matière Médicale (Pharmacognosie), Tome I.* By M. PARIS and M. HURABIELLE. Masson, 14 E. 60th St., New York, NY 10022. 1981. 339 pp. 13 × 21 cm. (Also available from Masson, 120 Boulevard Saint-Germain, 75280 Paris Cedex 06, France.)

*Abrégé de Pharmacie Galénique, 3rd ed.* By A. LE HIR. Masson, 14 E. 60th St., New York, NY 10022. 1981. 354 pp. 13 × 21 cm. (Also available from Masson, 120 Boulevard Saint-Germain, 75280 Paris Cedex 06, France.)

*The Safety of Medicines: Evaluation and Prediction.* By PETER I. FOLB. Springer–Verlag New York, 44 Hartz Way, Secaucus, NJ 07094. 1980. 103 pp. 12 × 21 cm. Price $12.90.

*Abrégé de Pharmacologie: Générale et Moléculaire, 2nd ed.* By JACQUES WEPIERRE. Masson, 14 E. 60th St., New York, NY 10022. 1981. 203 pp. 13 × 21 cm. (Also available from Masson, 120 Boulevard Saint-Germain, 75280 Paris Cedex 06, France.)

*Progress in Pharmacology, Vol. 3, No. 2. Presynaptic Mechanisms/ Vasodilator Drugs.* Edited by P. A. van SWIETEN and E. SCHÖNBAUM. (Proceedings of a symposium organized by the Dutch Pharmacological Society in Amsterdam, The Netherlands, 1979.) Gustav Fischer Verlag, D-7000 Stuttgart 72, Postfach 720 143, West Germany. 1980. 146 pp. 16 × 24 cm. Price DM 78.00.

*The Analysis of Dietary Fiber in Food.* Edited by W. P. T. JAMES and OLOF THEANDER. Dekker, 270 Madison Ave., New York, NY 10016. 1981. 276 pp. 15 × 23 cm. Price $35.00 (20% higher outside the United States and Canada).

*The Biochemistry of Psychiatric Disturbances.* Edited by G. CURZON. Wiley, 605 Third Ave., New York, NY 10016. 1980. 144 pp. 15 × 23 cm.

*Clinically Important Adverse Drug Interactions, Vol. 1: Cardiovascular and Respiratory Disease Therapy.* Edited by J. C. PETRIE. Elsevier/North-Holland, 52 Vanderbilt Ave., New York, NY 10017. 1980. 243 pp. 16 × 24 cm. Price $48.25. (Available from Elsevier, P.O. Box 1527, Amsterdam, The Netherlands.)

*Introduction to Bioinstrumentation. With Biological, Environmental, and Medical Applications* (A Volume of Contemporary Instrumentation and Analysis). By CLIFFORD D. FERRIS. Humane Press, Crescent Manor, P.O. Box 2148, Clifton, NJ 07015. 1978. 330 pp. 15 × 23 cm. Price $29.50 hardcover and $14.50 softcover.

*Metal Carcinogenesis Testing: Principles and In Vitro Methods.* By MAX COSTA. Humane Press, Crescent Manor, P.O. Box 2148, Clifton, NJ 07015. 1980. 163 pp. 15 × 23 cm. Price $29.50 ($39.50 outside North America).

A publication of the
American Pharmaceutical Association—
the National Professional Society
of Pharmacists

# JOURNAL OF PHARMACEUTICAL SCIENCES

## INDEX TO AUTHORS
## INDEX TO SUBJECTS

VOLUME 70
JANUARY TO DECEMBER, 1981

*Published monthly under the supervision of the Board of Trustees*

MARY H. FERGUSON
*Editor*

NANCY E. BROWN
*Production Editor*

JOHN PATRICK EVANS
*Copy Editor*

MICHAEL K. HAYES
*Copy Editor*

EDWARD G. FELDMANN
*Contributing Editor*

SAMUEL W. GOLDSTEIN
*Contributing Editor*

BELLE R. BECK
*Editorial Secretary*

EDWARD G. FELDMANN
*Acting Director of Publications*

EDITORIAL ADVISORY BOARD

John Autian
Norman R. Farnsworth
William J. Jusko
Herbert A. Lieberman
David E. Mann, Jr.
Ian W. Mathison
Gerald J. Papariello
Edward G. Rippie

JOURNAL OF PHARMACEUTICAL SCIENCES

JULY 1981
VOLUME 70 NUMBER 7

RESEARCH ARTICLES

# Dissolution Rate Behavior of Solid Cholesterol Preparations in Bile Acid Solutions

KENNETH M. FELD and WILLIAM I. HIGUCHI ˣ

Received April 28, 1980, from the *College of Pharmacy, University of Michigan, Ann Arbor, MI 48109.* Accepted for publication January 6, 1981.

**Abstract** □ Recent work in these laboratories showed that different preparations of cholesterol monohydrate and anhydrous cholesterol had different dissolution rates under the same conditions. A method was developed by which both the thermodynamic contribution ($C_s$) and the interfacial kinetic contribution ($P$) to dissolution could be determined from experimental data. The rotating-disk dissolution method was used with the Levich theory to assess the data. Dissolution rates were determined in solutions partially saturated with cholesterol. Dynamic solubilities were determined by plotting dissolution rates ($J/A$) *versus* bulk concentration ($C_b$) and extrapolating to zero $J/A$. By using a best-fit analysis, it was possible to determine solubility as well as the interfacial transport constant independently. When this method was used to study differences in dissolution behavior of different solid preparations of cholesterol, the differences could be accounted for primarily by variations in the interfacial transport constant rather than by solubility variations.

**Keyphrases** □ Cholesterol—dissolution rate behavior in bile acid solutions, comparison of solid preparations □ Dissolution—cholesterol, comparison of solid preparations in bile acid solutions □ Bile acids—cholesterol dissolution, comparison of solid preparations □ Gallstones—cholesterol dissolution, comparison of solid preparations in bile acid solutions

Most dissolution rate experiments have been interpreted satisfactorily by diffusion–convection models (1). However, recent studies (2, 3) of the dissolution rate behavior of cholesterol in bile acid solutions showed that interfacial resistance is often the dominant factor to mass transfer.

Preliminary studies in these laboratories showed that different preparations of solid cholesterol result in large variations in dissolution rate behavior. A method was needed to determine both the thermodynamic contribution and the kinetic contribution to dissolution from experimental data for different solid preparations.

The rotating-disk method was used with the accompanying Levich theory (4) to analyze results since it is well suited for quantifying the contributions of the diffusion–convection mass transfer resistance and the contributions of the interfacial barrier and/or solubilization kinetics in the diffusion layer to the overall kinetics. The purpose of this paper was to demonstrate how dissolution rate data can be analyzed when interfacial kinetics and the thermodynamic driving force for various solid phases of a substance vary simultaneously. The method was applied to the problem of cholesterol dissolution in bile acid solutions.

## THEORETICAL

According to the Nernst diffusion layer theory, the total resistance for the transfer of a solute into the solution immediately adjacent to the solid surface and then into the bulk solution is given by $h/D$, a diffusion term. Both convection and diffusion are expected to be important in most dissolution situations. Therefore, for the rotating-disk method, the effective diffusion resistance ($h/D$) may be equated to an appropriate function that considers both processes. Thus, when both diffusion and convection are important, the mass flux as given by Levich (4) is:

$$J = 0.62AD^{2/3}\nu^{-1/6}\omega^{1/2}(C_s - C_b) \qquad \text{(Eq. 1)}$$

where:

$A$ = apparent surface area of the pellet
$D$ = diffusion coefficient
$\nu$ = kinematic viscosity
$\omega$ = angular velocity of rotation
$C_s$ = saturation solubility
$C_b$ = bulk concentration

The effective diffusion layer thickness is given as:

$$h = 1.612D^{1/3}\nu^{1/6}\omega^{-1/2} \qquad \text{(Eq. 2)}$$

For the region of dissolution in which both diffusion and a first-order interfacial resistance are important, the flux as given by Levich (4) is:

$$J = \frac{A(C_s - C_b)}{1.612D^{-2/3}\nu^{1/6}\omega^{-1/2} + 1/P} \qquad \text{(Eq. 3)}$$

where $P$ is the permeability coefficient (interfacial transport constant).

In the case of pure bulk transport, the observed dissolution rate should be essentially equal to the calculated flux (Eq. 1). However, if the observed reaction rate is much lower than the calculated diffusion–convection flux, it may be concluded that dissolution is taking place in the interfacially controlled region, *i.e.*, $1/P$ has become rather large (Eq. 3).

0022-3549/81/0700-0717$01.00/0
© 1981, American Pharmaceutical Association

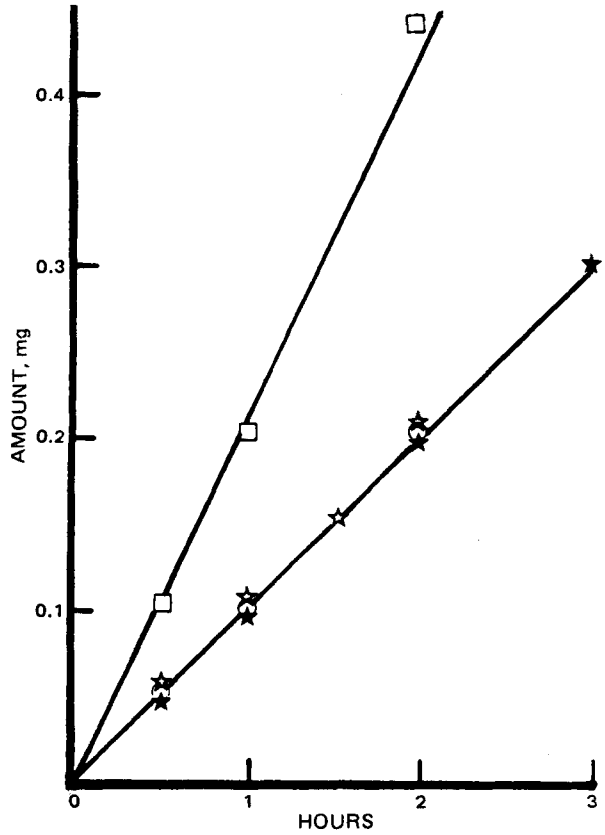


**Figure 1**—*Effect of pH on the dissolution rate of cholesterol in 5% sodium cholate solutions (pH was adjusted by addition of sodium hydroxide). Key:* □, *pH 7.1;* ★, *pH 7.4;* ○, *pH 8.02; and* ☆, *pH 11.08.*

## EXPERIMENTAL

**Solutions**—Sodium cholate test solutions were prepared by titrating equivalent amounts of cholic acid[1] with sodium hydroxide. The solution pH then was adjusted to 8.0. While this value was not the physiological pH, it was at a region where $J/A$ would experience minimum variability because of pH variations (Fig. 1). The solutions were allowed to equilibrate for at least 1 day before use.

**Materials**—Commercial cholesterol[2] was recrystallized three times from 95% ethanol. Radioactive cholesterol monohydrate was prepared by mixing [4-$^{14}$C]cholesterol[3] with a known amount of the recrystallized cholesterol at 60° (specific activity of ~10 μCi/g). The solutions then were allowed to stand undisturbed for 48 hr at room temperature. The cholesterol crystals were filtered and dried overnight *in vacuo*. The cholesterol monohydrate crystals were stored in the dark in a desiccator saturated with water vapor at room temperature.

**Preparation of Solid Phases**—Cholesterol samples that gave different dissolution rates under the same conditions were obtained. Two preparations of cholesterol monohydrate were obtained. One sample (I) was prepared by mixing 5 g of recrystallized cholesterol and 50 μCi of [4-$^{14}$C]cholesterol with 400 ml of 95% ethanol at 60°. Another sample (II) was prepared by mixing 10 g of recrystallized cholesterol and 100 μCi of [4-$^{14}$C]cholesterol with 400 ml of 95% ethanol at 60°. During the crystallization of I and II, the crystallization rates were significantly different. Crystals were first noticed ~12–15 and ~3–4 hr after dissolution[4] in I and II, respectively.

In addition, two nonhydrated forms of cholesterol were obtained by pretreatment of I. One sample (III) was prepared by melting a small amount of I at 160° for 5 min. Another preparation (IV) was obtained by heating I at 100° for 24 hr.

To check the hydrated nature of the two monohydrates and the nonhydrated nature of the melt and the heated sample, weight loss experiments were conducted on each solid form. For all of these preparations, ~1 g of the cholesterol was weighed into a vial and then heated at 100° for 15 min. After heating, the samples were reweighed. This process was repeated until the weight of the vial plus the cholesterol was constant. Any weight loss during this process was attributed to the loss of the solvation molecule (water).

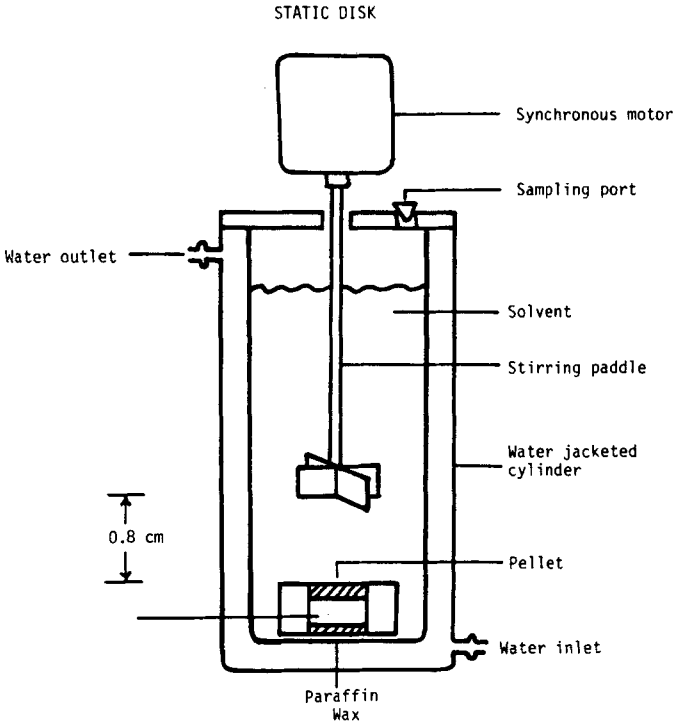


**Figure 2**—*Diagrammatic representation of the static-disk dissolution apparatus.*

For the two monohydrate samples, the loss in weight corresponded to 1.0 ± 0.3 mole of water for each mole of cholesterol. However, for the melt and the heated sample, no weight loss was detected after further heating. This finding demonstrates the monohydrate nature of the two hydrated forms and the anhydrous nature of the two heated preparations.

In addition to weight loss determination, it also was important to check for decomposition products. TLC plates were prepared and placed into tanks with chloroform–acetone (90:10) as the solvent (5). For all solid preparations, one spot with an $R_f$ value of 0.62 was found.

**Equilibrium Solubility Determination**—The solubility of each cholesterol monohydrate sample was determined by adding an excess of radiolabeled cholesterol monohydrate to a few milliliters of solvent. The tube containing the slurry then was shaken by a wrist-action shaker in a water bath maintained at 37°. Samples were taken periodically, 10 ml of scintillation fluid was added to the sample, and the amount of cholesterol dissolved was calculated from the radioactivity determined in a liquid scintillation counter[5]. When the amount of dissolved cholesterol reached a constant level, this limiting value was used to calculate the equilibrium solubility (2).

**Diffusion Coefficient Determination**—The diffusion coefficient was determined in a small-volume diaphragm cell at 37°. The apparatus and the procedure were described previously (6). The apparatus consisted of two well-stirred reservoirs separated by a silver filter membrane. Both reservoirs contained 3.4 ml of the solvent medium, and each was stirred at 150 rpm with a magnetic bar in the bottom chamber and a paddle in the upper chamber. At the end of the run, the concentration in each reservoir was determined.

**Method**—For the initial portion of this investigation, the static-disk dissolution apparatus was employed (Fig. 2). Approximately 200 mg of the various solid preparations was compressed[6] into pellets [compression load of 1362 kg (3000 lb)] with a diameter of 1.27 cm. The pellets then were placed into the dissolution setup. Exactly 10 ml of the sodium cholate solution was added, and the system was stirred with a 150-rpm stirrer[7].

[1] Weddell, London, England.
[2] J. T. Baker Chemical Co., Phillipsburg, N.J.
[3] New England Nuclear Corp., Boston, Mass.
[4] In later discussions, I will be referred to as normal cholesterol and II will be referred to as rapid cholesterol.
[5] Beckman Instruments, Irvine, Calif.
[6] Model B laboratory press, Fred Carver Inc., Summit, N.J.
[7] Model CA stirring motor, Hurst Manufacturing Co., Princeton, Ind.

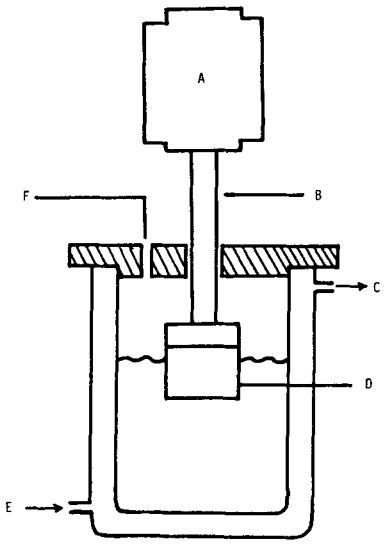


**Figure 3**—*Diagrammatic representation of the rotating-disk dissolution apparatus. Key: A, constant-speed motor; B, rotating shaft; C, water outlet; D, disk with pellet; E, water inlet; and F, sample port.*

Samples were taken at different times, and the amount dissolved was measured in a liquid scintillation counter.

For the more detailed analysis, the rotating-disk apparatus was used (Fig. 3). This apparatus consisted of three main parts: the outside water-jacketed beaker, the removable disk, and the controlled-rotating device[8]. Deviation of the experimental results from theory was assessed using benzoic acid as a model solute since benzoic acid dissolution is diffusion–convection controlled (6).

Fifty milliliters of solvent was pipetted into the water-jacketed beaker maintained at 37° for each dissolution run. The rotating disk containing the pellet then was centered at ~1 cm below the solvent level so that the distances from the disk wall to the inner surface of the beaker exceeded 0.5 cm. Samples were taken at appropriate times and assayed for the amount dissolved. All experiments were concluded early enough so that sink conditions were always maintained. Rotation speeds varied between 20 and 450 rpm. Partially saturated solutions of 5% sodium cholate and 0.1 *M* phosphate buffer at pH 8.0 were prepared by adding nonradioactive

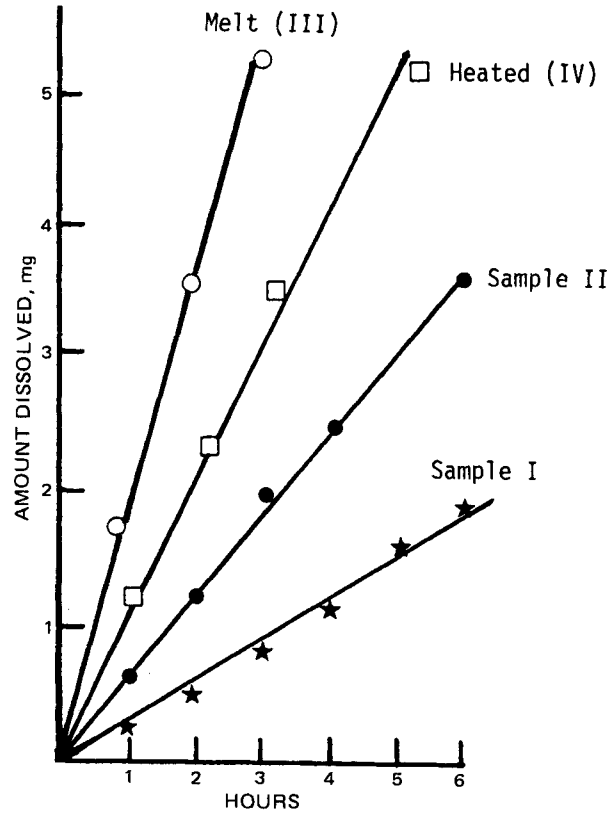


**Figure 4**—*Effect of the solid preparation on the dissolution rate in 5% sodium cholate and 0.1* M *phosphate buffer at pH 8.00 in the static-disk dissolution apparatus.*

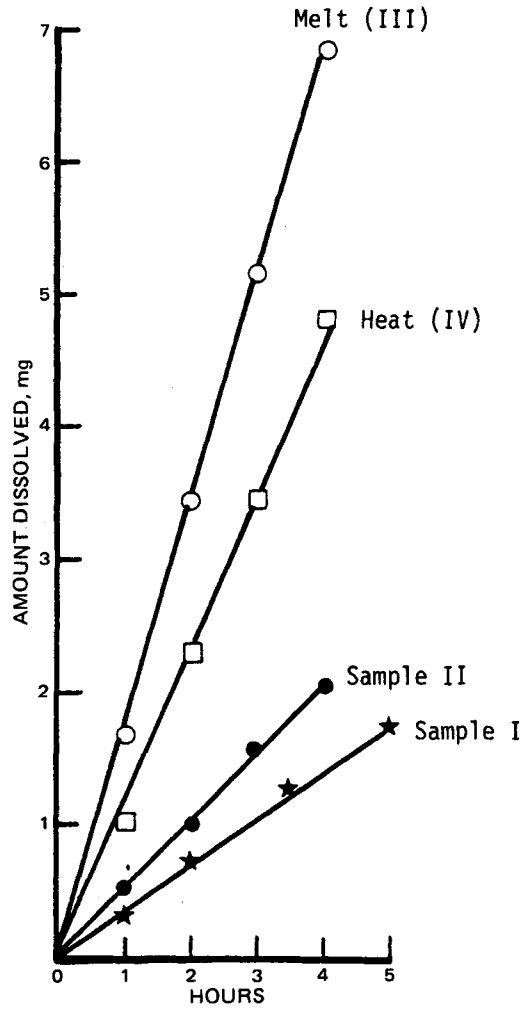


**Figure 5**—*Effect of the solid preparation on the dissolution rate in 5% sodium cholate and 0.1* M *phosphate buffer at pH 8.00 in the rotating-disk apparatus.*

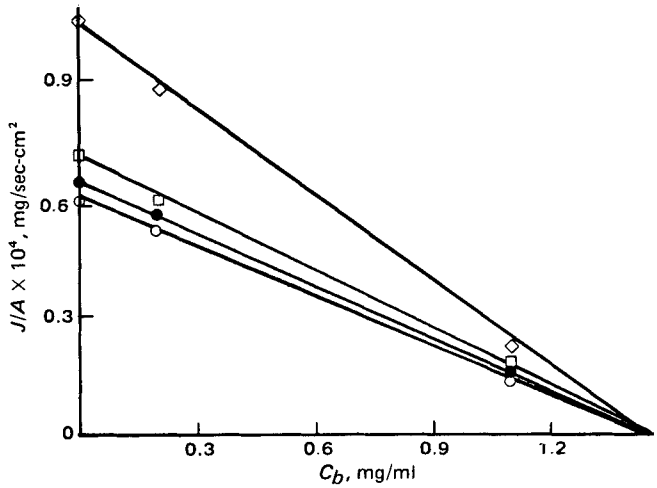


**Figure 6**—*Dissolution rate* versus *bulk concentration for the normal (I) pellets in 5% sodium cholate and 0.1* M *phosphate buffer at pH 8.00. Key: ○, 20 rpm; ●, 50 rpm; □, 150 rpm; and ◇, 450 rpm. Each J/A value is an average of two experiments. Since the typical variations are ±5–~10% for these results, which are too small to be seen, only the average values are presented here and in Figs. 7–13.*

[8] Servodyne laboratory stirrer, Cole-Parmer Instrument Co., Chicago, Ill.

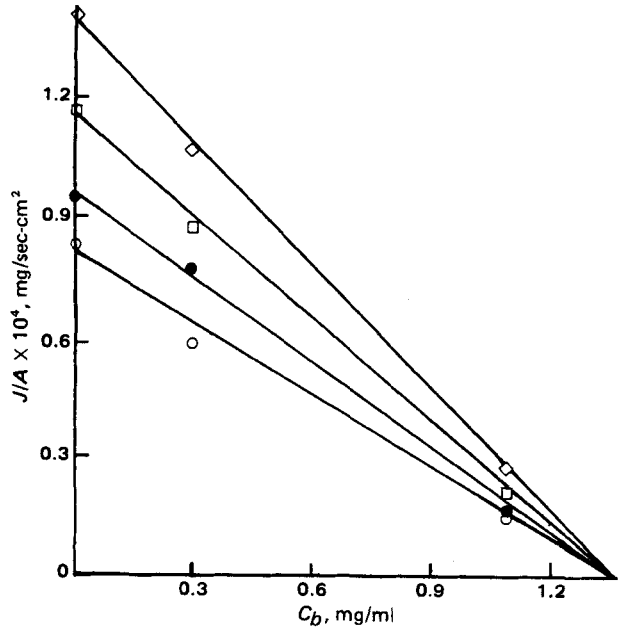


**Figure 7**—*Dissolution rate* versus *bulk concentration for the rapid (II) pellets in 5% sodium cholate and 0.1* M *phosphate buffer at pH 8.00. Key:* ○, *20 rpm;* ●, *50 rpm;* □, *150 rpm; and* ◇, *450 rpm.*

cholesterol to the solutions and allowing the cholesterol to dissolve completely. Bulk concentrations of cholesterol varied from 0 to ~1.0 mg/ml.

## RESULTS AND DISCUSSION

As already stated, different solid preparations of cholesterol give different dissolution rates under the same conditions. These differences may be caused by variations in $P$ and/or $C_s$ (Eq. 3) between the different preparations. By varying $C_b$ (bulk concentration) and $\omega$ (rotational speed), it was possible to determine $C_s$ and $P$ values for all solid preparations.

Since cholesterol dissolution is essentially surface controlled, $1/P$ is much larger than $1.612D^{-2/3}\nu^{1/6}\omega^{-1/2}$ (Eq. 3). Therefore, the actual value of $D$ is not required for the present analysis. However, as an independent check, $D$ was determined and compared to the value obtained in the later analysis.

**Dissolution Results of Benzoic Acid**—The results of benzoic acid dissolution were the same as those previously reported (6). Benzoic acid dissolution was linear at all rotation speeds. When these dissolution rates

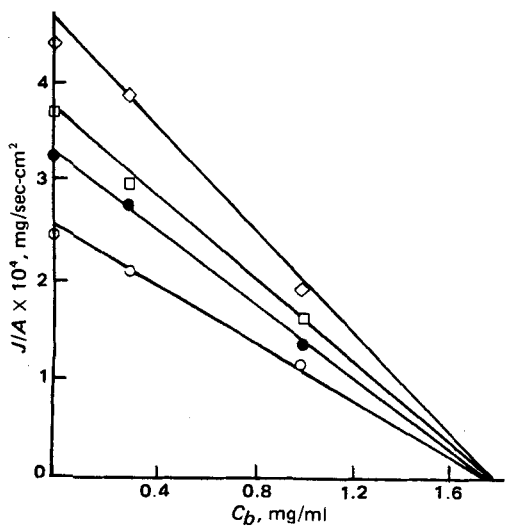


**Figure 8**—*Dissolution rate* versus *bulk concentration for the melt (III) pellets in 5% sodium cholate and 0.1* M *phosphate buffer at pH 8.00. Key:* ○, *20 rpm;* ●, *50 rpm;* □, *150 rpm; and* ◇, *450 rpm.*

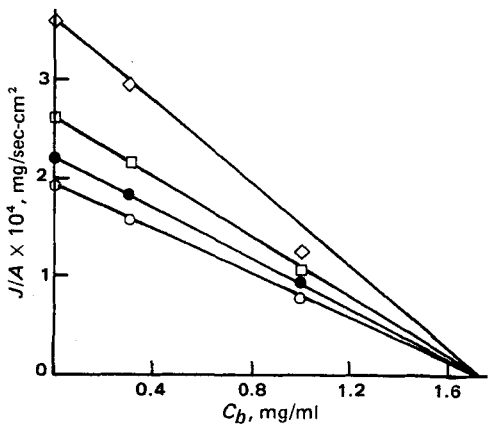


**Figure 9**—*Dissolution rate* versus *bulk concentration for the pellets (IV) prepared from I heated at 100° for 24 hr in 5% sodium cholate and 0.1* M *phosphate buffer at pH 8.00. Key:* ○, *20 rpm;* ●, *50 rpm;* □, *150 rpm; and* ◇, *450 rpm.*

were plotted *versus* the square root of the rotation speed, a linear relationship was obtained. This relationship was compared to the dissolution rates predicted by the Levich theory (4) (Eq. 1). The experimental dissolution rates were 15% lower than those predicted by the Levich theory. This discrepancy is consistent with the views of Gregory and Riddiford (7) regarding the performance of rotating-disk geometrics of the type used in the present study.

**Dissolution of Cholesterol Solid Preparations Using Static-Disk Setup**—Measurement of dissolution rates of the cholesterol solid phases showed significant differences (Fig. 4 and Table I). Sample II gave a dissolution rate that was ~70% higher than that of I. The heated preparation gave a dissolution rate ~3.6 times as great as did I, while the melt gave an increase in the dissolution rate by a factor of 5. The results of several pellets of each preparation were reproducible to ±10%. Because the differences in dissolution rates were significant, it was necessary to determine whether these differences were due to variations in $C_s$ (solubility) or $P$ (interfacial transport constant).

**Dissolution of Cholesterol Solid Preparations in Rotating-Disk Setup**—For each solid preparation, initial dissolution rates in the rotating-disk apparatus were obtained in the same manner as for the static-disk experiments. Figure 5 shows the results of some typical experiments for the various solid preparations in solutions of 5% sodium cholate and 0.1 $M$ phosphate buffer at pH 8.0 with bulk cholesterol concentrations equal to zero. As was found with the static disk, these results were reproducible to ±10%. Plots such as these were prepared under all conditions to obtain the initial dissolution rates.

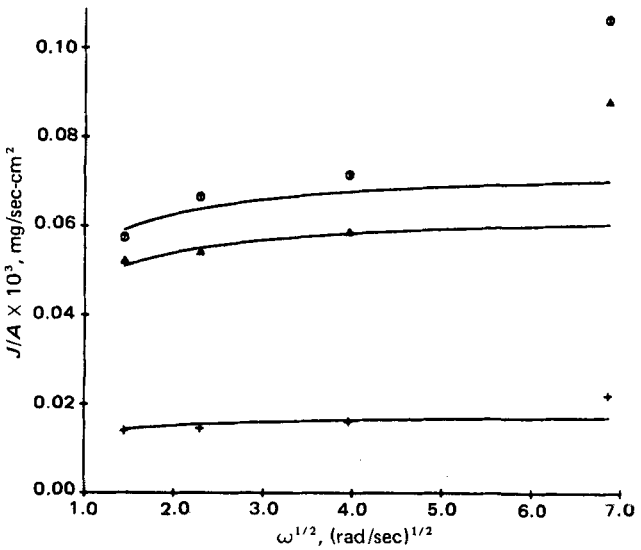


**Figure 10**—*Best-fit analysis of the normal pellets (I) in 5% sodium cholate and 0.1* M *phosphate buffer at pH 8.00. Key* ($C_b$ *in milligrams per milliliter):* ○, *0.0 mg/ml;* ▲, *0.2 mg/ml; and* +, *1.1 mg/ml.*

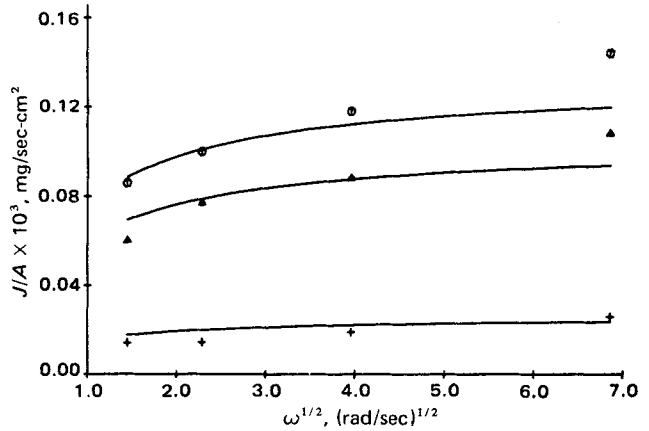


**Figure 1**—*Best-fit analysis of the rapid pellets (II) in 5% sodium cholate and 0.1* M *phosphate buffer at pH 8.00. Key* ($C_b$ *in milligrams per milliliter):* ○, *0.0 mg/ml;* ▲, *0.3 mg/ml; and* +, *1.1 mg/ml.*

To determine the dynamic solubility ($C_s$), initial dissolution rates were determined and then plotted against $C_b$ (bulk concentration). Figures 6–9 show the results of experiments carried out in 5% sodium cholate and 0.1 *M* phosphate buffer solutions at pH 8.0. The extrapolations of these data to zero $J/A$ gave the dynamic solubilities.

As was predicted, Figs. 6–9 show a linear decrease in the cholesterol monohydrate dissolution rate as saturation was approached. This finding indicates that dissolution kinetics are proportional to the change in concentration ($\Delta C$) over the entire saturation range. The dynamic solubilities for both cholesterol monohydrate samples were found by extrapolation to be ~1.40 mg/ml (Figs. 6 and 7). The $C_s$ value for the two anhydrous preparations was ~1.75 mg/ml (Figs. 8 and 9).

To look at the data in a more meaningful way, plots of $J/A$ *versus* $\omega^{1/2}$ were prepared. Figures 10–13 clearly show the important involvement of the interfacial barrier. If the interfacial barrier was not significant (*i.e.*, diffusion-controlled case), a plot of $J/A$ *versus* $\omega^{1/2}$ would give a straight line through the origin. If the interfacial barrier is significant in dissolution, a slope of <1 and a deviation from linearity should be obtained.

From a least-squares best-fit analysis, using Eq. 3 with a 15% correction, it was possible to obtain values for $C_s$, $P$, and $D$, where $P$ is the interfacial transport constant and $D$ is the diffusivity. The calculated dissolution rates using the best-fit values from Eq. 3 were compared to the experimental dissolution rates (Figs. 10–13). A good fit between experiment and theory is seen. The points at 450 rpm ($\omega^{1/2} = 6.86$) were not weighted in this analysis.

Tables II–V summarize the results of the partial saturation, the least-squares analyses, and the solubility determined by the slurry method (2). The tables show good agreement among the $C_s$ values obtained by all three methods for both I and II and nearly equivalent $C_s$ values between the samples. However, the interfacial transport constant ($P$) differed by a factor of 1.90 between the samples. Therefore, the differences in the dissolution rates between I and II can be accounted for primarily by a difference in their $P$ values.

The $C_s$ value from the partial saturation experiments for the melt-prepared and heat-prepared pellets was ~1.75 mg/ml. This value is ~20% greater than the $C_s$ value obtained from either monohydrate sample. Again, the big difference was seen in the interfacial transport constant ($P$). The $P_{IV}$:$P_I$ ratio was 3.99, while the $P_{III}$:$P_I$ ratio was 6.53. As was the case with I and II, the difference in the dissolution behavior between the anhydrous preparations can be accounted for primarily by a difference in $P$. The variations in the dissolution rates between the hydrated preparations and the nonhydrated preparations can be attributed to small changes in $C_s$ and large changes in $P$.

Experimental determination of $D$ (diffusivity) agreed well with the

**Table I—Dissolution Rates of I–IV in 5% Sodium Cholate and 0.1 *M* Phosphate Buffer at pH 8.00**

| Sample | $J/A \times 10^4$, mg/sec-cm² |
|---|---|
| I | 0.73 |
| II | 1.24 |
| III | 3.60 |
| IV | 2.64 |

**Table II—Summary of Partial Saturation Experiments and Best-Fit Analysis for Normal Cholesterol (I) Pellets in 5% Sodium Cholate and 0.1 *M* Phosphate Buffer at pH 8.00**

| $C_s$ from Slurry, mg/ml | $C_s$ from Extrapolation of Partial Saturation Data, mg/ml | Revolutions per Minute | Best-Fit Analysis $C_s$, mg/ml | $P \times 10^4$, cm/sec | $D \times 10^6$, cm²/sec |
|---|---|---|---|---|---|
| 1.34 | 1.45 | 20 | 1.45 | 0.51 | 1.25 |
| | 1.45 | 50 | | | |
| | 1.45 | 150 | | | |
| | 1.42 | 450 | | | |

**Table III—Summary of Partial Saturation Experiments and Best-Fit Analysis for II in 5% Sodium Cholate and 0.1 *M* Phosphate Buffer at pH 8.00**

| $C_s$ from Slurry, mg/ml | $C_s$ from Extrapolation of Partial Saturation Data, mg/ml | Revolutions per Minute | Best-Fit Analysis $C_s$, mg/ml | $P \times 10^4$, cm/sec | $D \times 10^6$, cm²/sec |
|---|---|---|---|---|---|
| 1.33 | 1.38 | 20 | 1.37 | 0.96 | 1.15 |
| | 1.36 | 50 | | | |
| | 1.37 | 150 | | | |
| | 1.37 | 450 | | | |

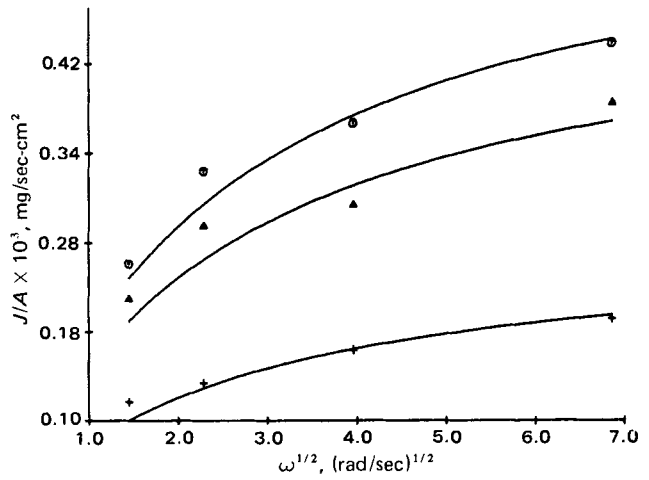


**Figure 2**—*Best-fit analysis of the melt pellets (III) in 5% sodium cholate and 0.1* M *phosphate buffer at pH 8.00. Key* ($C_b$ *in milligrams per milliliter):* ○, *0.0 mg/ml;* ▲, *0.3 mg/ml; and* +, *1.0 mg/ml.*

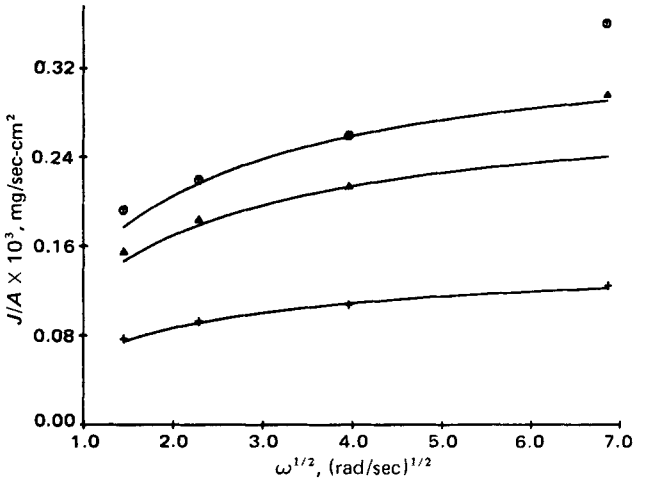


**Figure 3**—*Best-fit analysis of the pellets (IV) prepared from I heated at 100° for 24 hr in 5% sodium cholate and 0.1* M *phosphate buffer at pH 8.00. Key* ($C_b$ *in milligrams per milliliter):* ○, *0.0 mg/ml;* ▲, *0.3 mg/ml; and* +, *1.0 mg/ml.*

**Table IV—Summary of Partial Saturation Experiments and Best-Fit Analysis for III in 5% Sodium Cholate and 0.1 *M* Phosphate Buffer at pH 8.00**

| $C_s$ from Extrapolation of Partial Saturation Data, mg/ml | Revolutions per Minute | Best-Fit Analysis $C_s$, mg/ml | $P \times 10^4$, cm/sec | $D \times 10^6$, cm²/sec |
|---|---|---|---|---|
| 1.76 | 20 | 1.79 | 3.32 | 1.26 |
| 1.72 | 50 | | | |
| 1.76 | 150 | | | |
| 1.74 | 450 | | | |

**Table V—Summary of Partial Saturation Experiments and Best-Fit Analysis for IV Prepared from I Heated at 100° for 24 hr in 5% Sodium Cholate and 0.1 *M* Phosphate Buffer at pH 8.00**

| $C_s$ from Extrapolation of Partial Saturation Data, mg/ml | Revolutions per Minute | Best-Fit Analysis $C_s$, mg/ml | $P \times 10^4$, cm/sec | $D \times 10^6$, cm²/sec |
|---|---|---|---|---|
| 1.74 | 20 | 1.73 | 2.03 | 1.26 |
| 1.74 | 50 | | | |
| 1.74 | 150 | | | |
| 1.73 | 450 | | | |

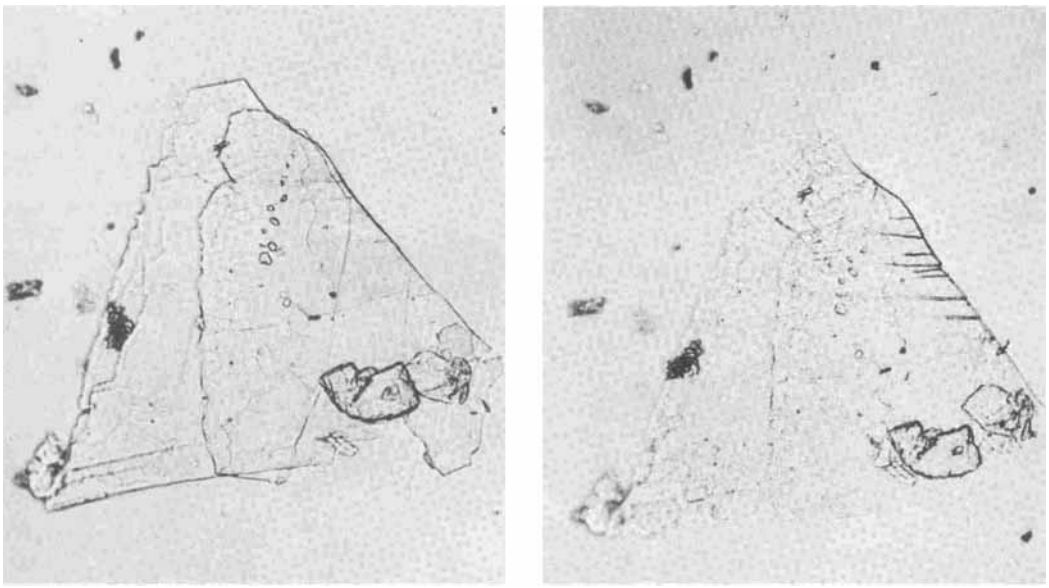

**Figure 14**—*Photographs of cholesterol monohydrate crystals (180×) in 5% sodium cholate and 0.1* M *phosphate buffer at pH 8.00. Left:* T = *0 hr. Right:* T = *2 hr.*

values of $D$ determined from the best-fit analysis. From the small-volume diaphragm cell, $D$ was determined to be $1.52 \times 10^{-6}$ cm²/sec; from the best-fit analysis, $D$ was $\sim 1.25 \times 10^{-6}$ cm²/sec.

As already stated, the data at 450 rpm ($\omega^{1/2} = 6.86$) was not weighted in the best-fit analysis. The points at 450 rpm deviate substantially from the theoretical curve (Figs. 10–13). A possible explanation for this deviation can be found in the single-crystal experiments performed previously (8). Individual cholesterol crystals were mounted in a cell containing the bile acid solution, and the cell then was placed into a 37° chamber. Microscopic examination of the crystal under static conditions showed that surface etching occurred. Within 2 hr, a definite saw-tooth pattern developed along the edge of the crystal (Fig. 14). At 450 rpm in the rotating-disk experiments, the effective surface area might possibly have increased or some shearing of the peaks along the crystal surface may have occurred. This phenomenon, along with the normal micellar dissolution, could result in a positive deviation in the apparent dissolution rate from that expected from the theory.

These findings are consistent with those of Shefter and Higuchi (9). They showed that the dissolution behavior of hydrated and nonsolvated forms of cholesterol was indeed different. The initial dissolution rate was shown to be three times greater for the nonsolvated cholesterol as for the hydrated form at 25°. They also showed that the maximum concentration reached with the nonsolvated form was 1.4 times as great as the solubility of the hydrate at 25°.

**Implications in Cholesterol Gallstone Research**—Higuchi *et al.* (2, 3) proposed that cholesterol monohydrate pellets may be employed as a model for cholesterol gallstones in *in vitro* dissolution rate experiments. Borgren and Larsson (10) examined biliary calculi from humans immediately after removal. In all cases, the cholesterol present was cholesterol monohydrate. These investigators also showed that the monohydrate can lose water to give the anhydrous form. Other investigators (11, 12) found both forms of cholesterol in gallstones, but their studies were conducted on stones that had been removed several years earlier. The authors suggested that the anhydrous cholesterol was formed from the monohydrate and that cholesterol monohydrate was formed *in vivo*.

The present investigation demonstrated that large variations in results among studies may occur if the solid phase of cholesterol is not prepared in the same manner from study to study. There was approximately a fivefold difference between the highest (melt preparation) and lowest (I) rates observed. Even two preparations of the monohydrate (I and II) may show differences in pellet dissolution rates as great as 80%. Thus, the potential for problems should be recognized and the proper cautions exercised when comparing data from different studies (especially from different laboratories).

A rather subtle but important situation concerns the study of dissolution rate accelerators. The large difference in the dissolution rates between the melt (or the anhydrous preparation) and I was due mainly to the difference in $P$ values rather than to a difference in solubility ($C_s$). Thus, for example, the $P$ value for the anhydrous cholesterol pellet prepared by heating I was approximately four times larger than that for I itself. Thus, for the same hydrodynamic (convective–diffusion) situation, the anhydrous pellet can be up to four times less sensitive than a pellet of I to agents that may influence the interfacial kinetics.

From their studies, Tao *et al.* (13) concluded that convective diffusion rather than interfacial kinetics is the major determinant of the dissolution rate and that greatly accelerating the dissolution of cholesterol gallstones could be difficult. These investigators, however, prepared their cholesterol by evaporating a cholesterol–benzene solution to dryness and, consequently, their material was anhydrous cholesterol[9]. This procedure, at least in part, may account for their experimental results being closer to convective diffusion control than those results obtained by Higuchi *et al.* (2, 3).

## REFERENCES


(1) K. G. Nelson and A. C. Shah, *J. Pharm. Sci.*, **64**, 610 (1975).

(2) W. I. Higuchi, S. Prakongpan, and F. Young, *ibid.*, **62**, 945 (1973).

(3) W. I. Higuchi, S. Prakongpan, V. Surpuriya, and F. Young, *Science*, **178**, 633 (1972).

(4) V. A. Levich, "Physicochemical Hydrodynamics," Prentice-Hall, Englewood Cliffs, N.J., 1962.


[9] Dr. Cussler, Department of Chemical Engineering, Carnegie-Mellon University, Pittsburgh, Pa., personal communication.

(5) A. M. Kamel, N. D. Weiner, and A. Felmeister, *J. Colloid Interface Sci.*, **35**, 163 (1971).
(6) S. Prakongpan, Ph.D. thesis, University of Michigan, Ann Arbor, Mich., 1974.
(7) D. P. Gregory and A. C. Riddiford, *J. Chem. Soc.*, **1956**, 3756.
(8) O. I. Corrigan, C. C. Su, W. I. Higuchi, and A. F. Hofmann, *J. Pharm. Sci.*, **69**, 869 (1980).
(9) E. Shefter and T. Higuchi, *ibid.*, **52**, 781 (1963).
(10) H. Borgren and R. Larsson, *Biochim. Biophys. Acta*, **75**, 65 (1963).
(11) D. J. Sutor and S. E. Wooley, *Gut*, **10**, 681 (1969).
(12) *Ibid.*, **12**, 55 (1971).
(13) J. C. Tao, E. L. Cussler, and D. F. Evans, *Proc. Natl. Acad. Sci. USA*, **71**, 3917 (1974).

ACKNOWLEDGMENTS

Supported by Grant AM 16694 from the National Institute of Arthritis, Metabolism, and Digestive Diseases.

# Variability in Dissolution Rates of Cholesterol Pellets in Bile Acid Solutions

**KENNETH M. FELD and WILLIAM I. HIGUCHI ˣ**

Received April 28, 1980, from the *College of Pharmacy, University of Michigan, Ann Arbor, MI 48109.* Accepted for publication January 6, 1981.

**Abstract** □ Large variations in dissolution rate behavior of cholesterol monohydrate pellets may result from small changes in experimental procedures. For example, when cholesterol monohydrate pellets were stored overnight prior to a dissolution run, the initial dissolution rates varied by more than a factor of 2. It is well known that cholesterol monohydrate is converted to anhydrous cholesterol; cholesterol may be unstable toward light, heat, and other radiation in the presence of air, leading to its decomposition. To determine the cause of the variable dissolution rates, experiments were conducted with pellets "aged" under various conditions. The data show that the probable cause of the variations is the pellet surface conversion of the monohydrate to anhydrous cholesterol, which may take place during pellet storage. The combined effects of temperature and humidity seem to be important. A uniform experimental procedure is needed if investigators hope to reproduce results within their own laboratories as well as reproduce the findings of others.

**Keyphrases** □ Cholesterol—dissolution rate behavior in bile acid solutions □ Dissolution—rate behavior of cholesterol in bile acid solutions □ Gallstones—cholesterol, dissolution rate behavior in bile acid solutions

Cholesterol monohydrate has been used as a model substance in gallstone dissolution research (1). In earlier work in this laboratory, it was noticed that small changes in the experimental procedure resulted in significant variations in the dissolution rate behavior of cholesterol pellets. In some experiments when the pellet was stored overnight at 35° prior to a dissolution run, the initial dissolution rate was two to three times greater than the dissolution rate of freshly made pellets. Since it is desirable to limit the variations to ~10–15% in many mechanistic studies on cholesterol dissolution kinetics (1–4), the cause of dissolution rate variability was investigated.

## EXPERIMENTAL

Initially, the static-disk dissolution method was used, while the more quantitative rotating-disk dissolution method was used in the later analysis. The experimental procedures were described previously (5). All dissolution rate experiments were run at 37° in 5% sodium cholate and 0.1 *M* phosphate buffer at pH 8.00.

Pellets of radiolabeled cholesterol were prepared as described previously (5). Pellets placed in the dissolution cell without solvent for varying times at ambient (room) humidity or humidity of <100% at 35° will be referred to as aged pellets. The pellets kept at 100% humidity at ambient temperature for 24 hr will be referred to as normal pellets. This latter treatment was shown to give the same dissolution rate as that of freshly made pellets.

One hundred percent humidity containers were prepared by adding water to a desiccator until it completely filled the area under the plate. The other constant-humidity chambers were prepared by making saturated aqueous solutions (6) of 80% sodium bromide and of 40% calcium chloride which then were placed in an oven at 35°.

## RESULTS AND DISCUSSION

**Static-Disk Apparatus**—When small changes in the normal experimental procedure were introduced, significant differences in dissolution behavior resulted (Fig. 1 and Table I). Figure 2 shows the effects of exposing the pellets to ambient humidity at 35° for varying periods (aging). The normally treated pellet and the pellet aged for 1 hr gave the same dissolution rate as well as the same dissolution pattern (linear). However, aging the pellet for 12 or 24 hr markedly increased the initial dissolution rate (Table II). After a few hours of dissolution, these pellets showed a definite curvature in their dissolution profiles.

Figure 3 shows the effects of varying the humidity as well as varying

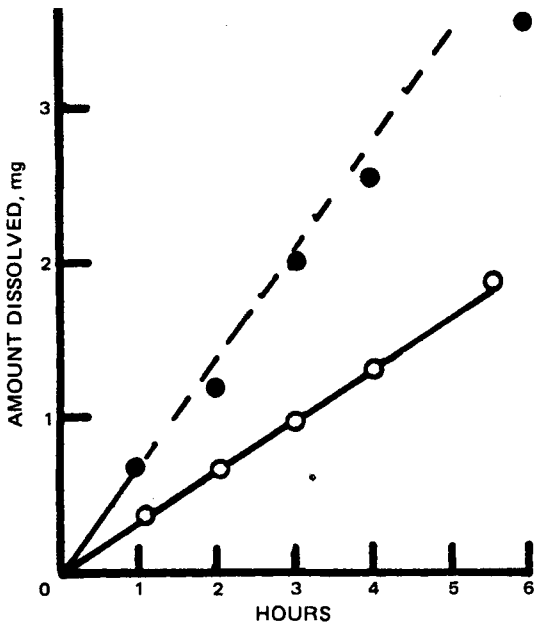


**Figure 1**—*Effect of pellet handling on the dissolution of cholesterol pellets at 150 rpm in 5% sodium cholate and 0.1* M *phosphate buffer at pH 8.00. Key:* ○, *normally prepared pellets; and* ●, *aged pellets.*

0022-3549/81/0700-0723$01.00/0
© 1981, American Pharmaceutical Association

(5) A. M. Kamel, N. D. Weiner, and A. Felmeister, *J. Colloid Interface Sci.*, **35**, 163 (1971).
(6) S. Prakongpan, Ph.D. thesis, University of Michigan, Ann Arbor, Mich., 1974.
(7) D. P. Gregory and A. C. Riddiford, *J. Chem. Soc.*, **1956**, 3756.
(8) O. I. Corrigan, C. C. Su, W. I. Higuchi, and A. F. Hofmann, *J. Pharm. Sci.*, **69**, 869 (1980).
(9) E. Shefter and T. Higuchi, *ibid.*, **52**, 781 (1963).
(10) H. Borgren and R. Larsson, *Biochim. Biophys. Acta*, **75**, 65 (1963).
(11) D. J. Sutor and S. E. Wooley, *Gut*, **10**, 681 (1969).
(12) *Ibid.*, **12**, 55 (1971).
(13) J. C. Tao, E. L. Cussler, and D. F. Evans, *Proc. Natl. Acad. Sci. USA*, **71**, 3917 (1974).

ACKNOWLEDGMENTS

Supported by Grant AM 16694 from the National Institute of Arthritis, Metabolism, and Digestive Diseases.

# Variability in Dissolution Rates of Cholesterol Pellets in Bile Acid Solutions

**KENNETH M. FELD and WILLIAM I. HIGUCHI ˣ**

Received April 28, 1980, from the *College of Pharmacy, University of Michigan, Ann Arbor, MI 48109.* Accepted for publication January 6, 1981.

**Abstract** □ Large variations in dissolution rate behavior of cholesterol monohydrate pellets may result from small changes in experimental procedures. For example, when cholesterol monohydrate pellets were stored overnight prior to a dissolution run, the initial dissolution rates varied by more than a factor of 2. It is well known that cholesterol monohydrate is converted to anhydrous cholesterol; cholesterol may be unstable toward light, heat, and other radiation in the presence of air, leading to its decomposition. To determine the cause of the variable dissolution rates, experiments were conducted with pellets "aged" under various conditions. The data show that the probable cause of the variations is the pellet surface conversion of the monohydrate to anhydrous cholesterol, which may take place during pellet storage. The combined effects of temperature and humidity seem to be important. A uniform experimental procedure is needed if investigators hope to reproduce results within their own laboratories as well as reproduce the findings of others.

**Keyphrases** □ Cholesterol—dissolution rate behavior in bile acid solutions □ Dissolution—rate behavior of cholesterol in bile acid solutions □ Gallstones—cholesterol, dissolution rate behavior in bile acid solutions

Cholesterol monohydrate has been used as a model substance in gallstone dissolution research (1). In earlier work in this laboratory, it was noticed that small changes in the experimental procedure resulted in significant variations in the dissolution rate behavior of cholesterol pellets. In some experiments when the pellet was stored overnight at 35° prior to a dissolution run, the initial dissolution rate was two to three times greater than the dissolution rate of freshly made pellets. Since it is desirable to limit the variations to ~10–15% in many mechanistic studies on cholesterol dissolution kinetics (1–4), the cause of dissolution rate variability was investigated.

## EXPERIMENTAL

Initially, the static-disk dissolution method was used, while the more quantitative rotating-disk dissolution method was used in the later analysis. The experimental procedures were described previously (5). All dissolution rate experiments were run at 37° in 5% sodium cholate and 0.1 *M* phosphate buffer at pH 8.00.

Pellets of radiolabeled cholesterol were prepared as described previously (5). Pellets placed in the dissolution cell without solvent for varying times at ambient (room) humidity or humidity of <100% at 35° will be referred to as aged pellets. The pellets kept at 100% humidity at ambient temperature for 24 hr will be referred to as normal pellets. This latter treatment was shown to give the same dissolution rate as that of freshly made pellets.

One hundred percent humidity containers were prepared by adding water to a desiccator until it completely filled the area under the plate. The other constant-humidity chambers were prepared by making saturated aqueous solutions (6) of 80% sodium bromide and of 40% calcium chloride which then were placed in an oven at 35°.

## RESULTS AND DISCUSSION

**Static-Disk Apparatus**—When small changes in the normal experimental procedure were introduced, significant differences in dissolution behavior resulted (Fig. 1 and Table I). Figure 2 shows the effects of exposing the pellets to ambient humidity at 35° for varying periods (aging). The normally treated pellet and the pellet aged for 1 hr gave the same dissolution rate as well as the same dissolution pattern (linear). However, aging the pellet for 12 or 24 hr markedly increased the initial dissolution rate (Table II). After a few hours of dissolution, these pellets showed a definite curvature in their dissolution profiles.

Figure 3 shows the effects of varying the humidity as well as varying

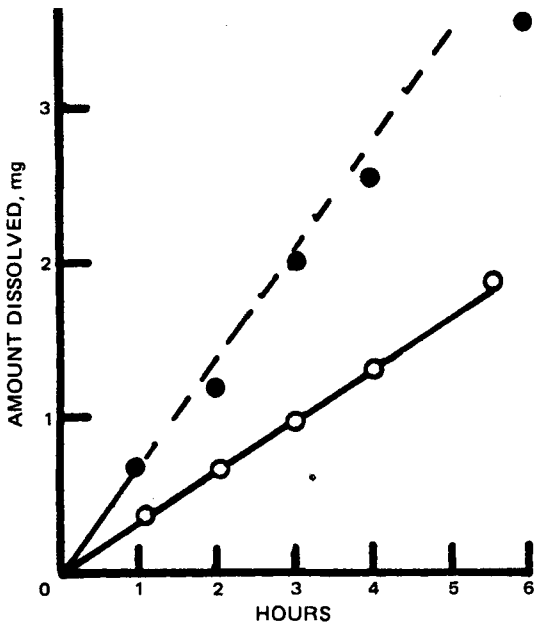


**Figure 1**—*Effect of pellet handling on the dissolution of cholesterol pellets at 150 rpm in 5% sodium cholate and 0.1* M *phosphate buffer at pH 8.00. Key:* ○, *normally prepared pellets; and* ●, *aged pellets.*

0022-3549/81/0700-0723$01.00/0
© 1981, American Pharmaceutical Association

**Table I—Dissolution Rates of Cholesterol Pellets as a Function of Treatment in 5% Sodium Cholate and 0.1 *M* Phosphate Buffer at pH 8.00** [a]

| Prerun Humidity, % | Prerun Temperature | $J/A \times 10^4$, mg/sec-cm$^2$ |
|---|---|---|
| 100 | Ambient | 0.73 |
| Ambient | 35° | 1.40 |

[a] The prerun time in the setup was 24 hr, and there was no subsequent treatment.

**Table II—Dissolution Rates of Cholesterol Pellets as a Function of Treatment in 5% Sodium Cholate and 0.1 *M* Phosphate Buffer at pH 8.00** [a]

| Prerun Time in Setup, hr | Prerun Humidity, % | Prerun Temperature | $J/A \times 10^4$, mg/sec-cm$^2$ |
|---|---|---|---|
| 24 | 100 | Ambient | 0.73 |
| 1 | Ambient | 35° | 0.73 |
| 12 | Ambient | 35° | 1.40 |
| 24 | Ambient | 35° | 1.40 |

[a] There was no subsequent treatment.

the exposure time. All pellets exposed to <100% humidity at 35° for 12 or 24 hr had an initial dissolution rate greater than that of the normally treated pellet. Table III summarizes the dissolution rates as a function of time and humidity.

At this point, it was felt that these results could be due to either dehydration of cholesterol monohydrate or to chemical decomposition (oxidation) of cholesterol. Bergstrom and Wintersteiner (7) showed that cholesterol in colloidal aqueous dispersions is attacked easily by oxygen. Weiner and coworkers (8–10) showed that monomolecular films also undergo autoxidation under different conditions. Dauben and Payot (11) showed that $^{14}C$-labeled cholesterol is unstable when stored in the presence of air. They found that the decomposition required both radiation and oxygen since unlabeled cholesterol was stable in air when stored under the same conditions and labeled material was stable when stored *in vacuo*. Thus, several factors are involved: oxygen concentration, wavelength of light, storage temperature, and surface area of the cholesterol sample. Cholesterol monohydrate is known to be converted to anhydrous cholesterol (12), although this conversion generally occurs at elevated temperatures (80–100°).

To determine the effects of temperature, humidity, and light on cholesterol dissolution, a series of experiments was run in the static-disk apparatus. By varying temperature and humidity and running the experiments in the presence and absence of room light, the contribution of each variable to the change in dissolution behavior was assessed. The effects of the variables at 100% humidity were relatively small, if any (Table IV). However, at ambient humidity, the effects on the dissolution rate of raising the temperature to 35° were large (dissolution rates varied

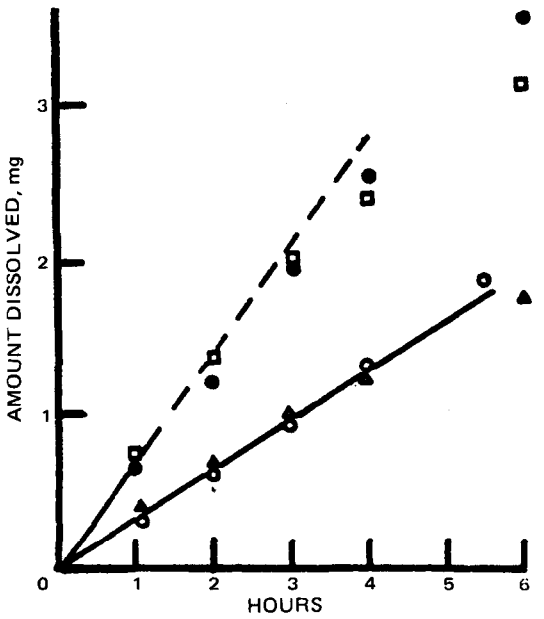


**Figure 2**—*Effect of pellet handling on the dissolution of cholesterol pellets at 150 rpm in 5% sodium cholate and 0.1* M *phosphate buffer at pH 8.00. Key:* ○, *normally prepared pellets;* ▲, *aged pellets for 1 hr;* □, *aged pellets for 12 hr; and* ●, *aged pellets for 24 hr.*

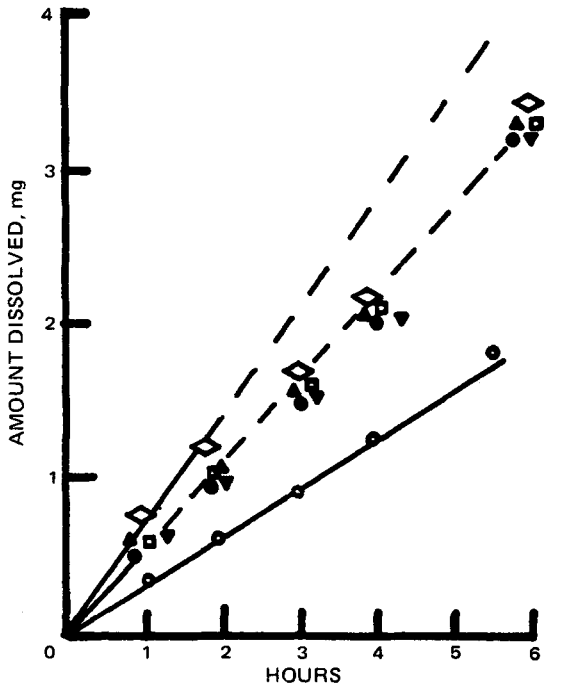


**Figure 3**—*Effect of pellet handling on the dissolution of cholesterol pellets at 150 rpm in 5% sodium cholate and 0.1* M *phosphate buffer at pH 8.00. Key:* ○, *normally treated pellets;* □, *aged pellets for 12 hr at 40% humidity;* ▲, *aged pellets for 24 hr at 40% humidity;* ▼, *aged pellets for 12 hr at 80% humidity;* ●, *aged pellets for 24 hr at 80% humidity; and* ◇, *aged pellets for 24 hr at 0% humidity. All pellets were aged at 35°.*

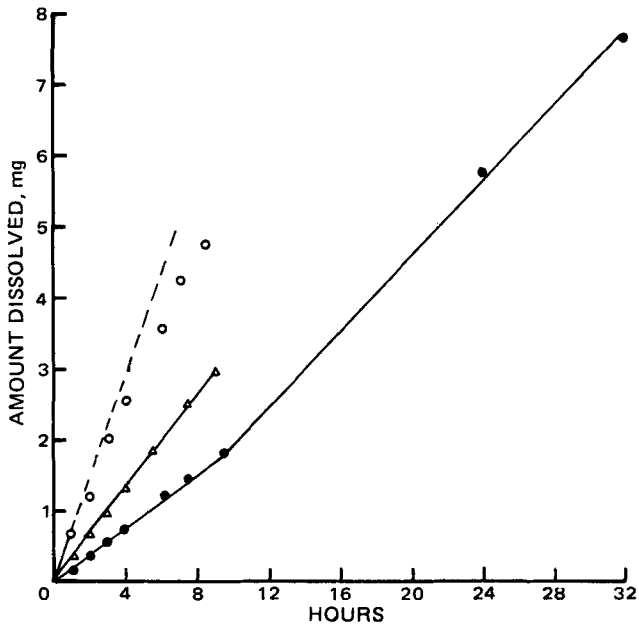


**Figure 4**—*Effect of pellet treatment on the dissolution rate of cholesterol in 5% sodium cholate and 0.1* M *phosphate buffer at pH 8.00. Key:* △, *normal pellet;* ○, *aged pellet (ambient humidity at 35° for 24 hr); and* ●, *soaked pellet. (Pellets were aged, followed by soaking in double-distilled water at 37° for 24 hr.)*

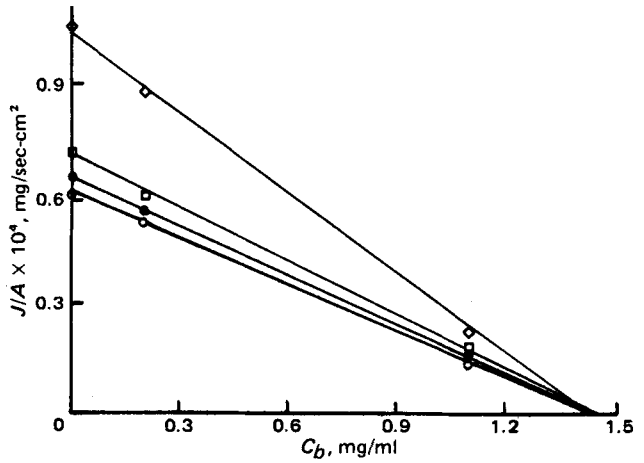


**Figure 5**—*Dissolution rate* versus *bulk concentration for normal pellets in 5% sodium cholate and 0.1* M *phosphate buffer at pH 8.00. Key:* ○, *20 rpm;* ●, *50 rpm;* □, *150 rpm; and* ◇, *450 rpm. Each* J/A *value is an average of two experiments. Since the typical variations are ±5–~10% for these results, which are too small to be seen, only the average values are presented here and in Figs. 6–10.*

by approximately two times). Therefore, the combined effect of humidity and temperature appeared to be the primary cause for the aging effect.

Because it was felt that pellet aging might lead to cholesterol decomposition, samples of bile acid–cholesterol solutions were spotted onto TLC plates. These samples were obtained during the first 30 min of actual dissolution experiments; if decomposition products were causing the large rate of dissolution, it would be possible to determine this by TLC. The plates then were placed into a tank with acetic acid–carbon tetrachloride–isopropyl ether–isoamylacetate–*n*-propanol–benzene (5:20:30:40:10:10) as the solvent (13). Good separation of the bile acids and cholesterol was obtained. For both normal and aged pellet samples, one spot for cholesterol was found ($R_f$ 0.71). To confirm that the samples obtained for TLC were from differently dissolving pellets, another sample was drawn from each dissolution cell and counted on a liquid scintillation counter[1]. The radioactivities for the aged and normal pellets were 2346.2 and 1235.2 cpm, respectively. It can be concluded that the differences in pellet behavior were not due to cholesterol decomposition during aging.

To check the dehydration hypothesis, aged pellets then were soaked in double-distilled water at 37° for 24 hr. Figure 4 shows the comparison of normal pellets, aged pellets, and aged pellets followed by soaking. Soaking an aged pellet lowered the dissolution rate, but this decrease was much greater than expected and will be discussed later.

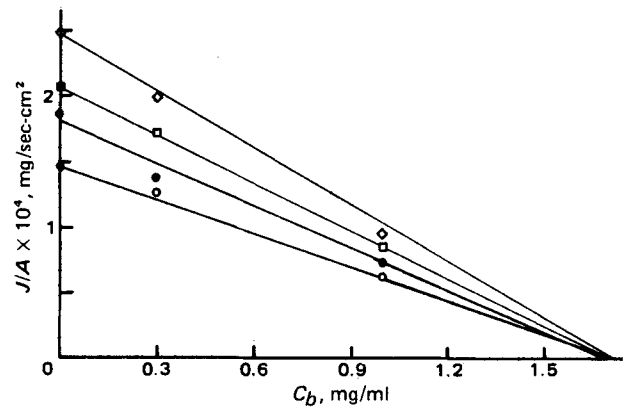


**Figure 6**—*Dissolution rate* versus *bulk concentration for aged pellets in 5% sodium cholate and 0.1* M *phosphate buffer at pH 8.00. Key:* ○, *20 rpm;* ●, *50 rpm;* □, *150 rpm; and* ◇, *450 rpm.*

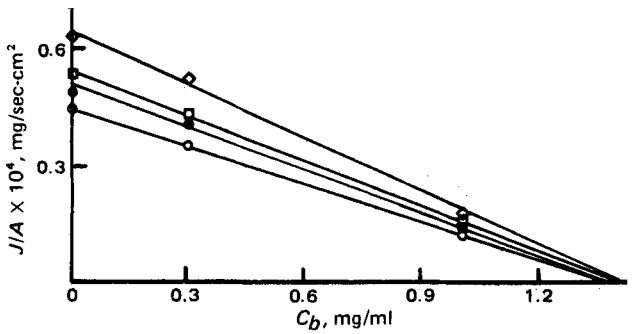


**Figure 7**—*Dissolution rate* versus *bulk concentration for soaked pellets in 5% sodium cholate, and 0.1* M *phosphate buffer at pH 8.00. Key:* ○, *20 rpm;* ●, *50 rpm;* □, *150 rpm; and* ◇, *450 rpm.*

**Table III—Dissolution Rates of Cholesterol Pellets as a Function of Treatment in 5% Sodium Cholate and 0.1 *M* Phosphate Buffer at pH 8.00 [a]**

| Prerun Time in Setup, hr | Prerun Humidity, % | Prerun Temperature | $J/A \times 10^4$, mg/sec-cm² |
|---|---|---|---|
| 24 | 100 | Ambient | 0.73 |
| 12 | 40 | 35° | 1.20 |
| 24 | 40 | 35° | 1.20 |
| 12 | 80 | 35° | 1.20 |
| 24 | 80 | 35° | 1.20 |
| 24 | 0 | 35° | 1.39 |

[a] There was no subsequent treatment.

**Table IV—Dissolution Rates of Cholesterol as a Function of Humidity, Light, and Temperature [a]**

| Number of Experiments | Humidity, % | Light | Temperature | Prerun Time in Setup, hr | $J/A \times 10^4$, mg/sec-cm² |
|---|---|---|---|---|---|
| 2 | 100 | None | Ambient | 0 | 0.71 |
| 3 | 100 | None | Ambient | 24 | 0.69–0.73 |
| 3 | 100 | None | 35° | 24 | 0.79–0.86 |
| 2 | 100 | Present | Ambient | 24 | 0.78 |
| 3 | 100 | Present | 35° | 24 | 0.86–0.91 |
| 2 | Ambient | None | Ambient | 24 | 0.78 |
| 2 | Ambient | None | 35° | 24 | 1.40 |
| 2 | Ambient | Present | Ambient | 24 | 0.86 |
| 1 | Ambient | Present | 35° | 24 | 1.40 |

[a] Ambient = room conditions.

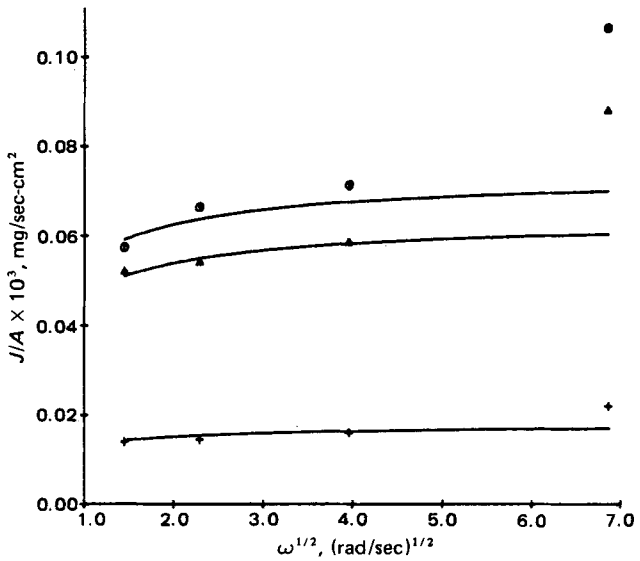


**Figure 8**—*Best-fit analysis of the normal pellets in 5% sodium cholate and 0.1* M *phosphate buffer at pH 8.00. Key (*$C_b$ *in milligrams per milliliter):* ○, *0.0;* ▲, *0.2; and* +, *1.1.*

[1] Beckman Instruments, Irvine, Calif.

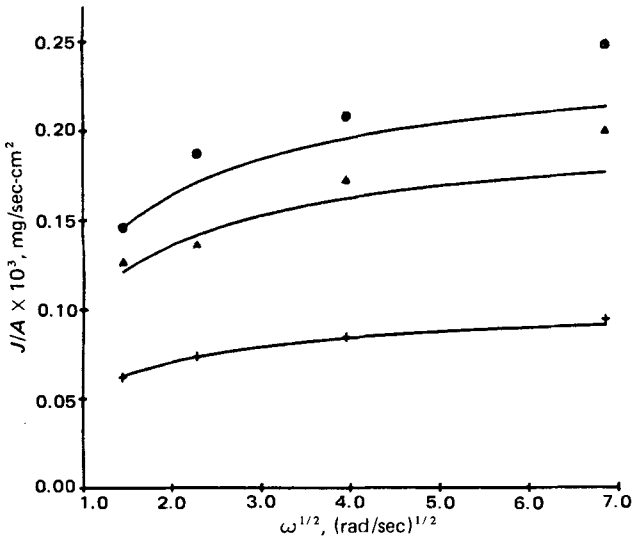


**Figure 9**—*Best-fit analysis of the aged pellets in 5% sodium cholate and 0.1* M *phosphate buffer at pH 8.00. Key ($C_b$ in milligrams per milliliter): ●, 0.0; ▲, 0.3; and +, 1.0.*

**Rotating-Disk Method**—Since minor procedural changes resulted in significant differences in the dissolution behavior of cholesterol pellets, an in-depth study was undertaken to determine if these differences were due to changes in solubility and/or interfacial transport. It was hoped that a better understanding of the changes would be gained. The pellets chosen for study were those shown in Fig. 4. As already seen, major differences were present in the dissolution rates.

To determine the dynamic solubility, initial dissolution rates were determined (5) and plotted against bulk concentration. Figures 5–7 show the results of the experiments carried out in 5% sodium cholate and 0.1 *M* phosphate buffer at pH 8.00. By extrapolating to a dissolution rate ($J/A$) of zero, it was possible to obtain the dynamic solubility. Figures 5–7 show a linear decrease in the dissolution rate as partial saturation is increased. This decrease indicates that the dissolution kinetics are proportional to the change in concentration ($\Delta C$) over the entire saturation range. From these figures, it can be seen that the solubility for the normal and soaked pellets was ~1.40 mg/ml while that for the aged pellet was ~1.73 mg/ml. The solubility obtained for the aged pellet was the same as that previously obtained (5) for the anhydrous pellets, which indicates that dissolution from the aged pellet occurs from the same phase as from the anhydrous pellets.

To look at the data in a slightly different way, plots of ($J/A$) *versus* the square root rotational speed ($\omega^{1/2}$) were prepared. Figures 8–10 show

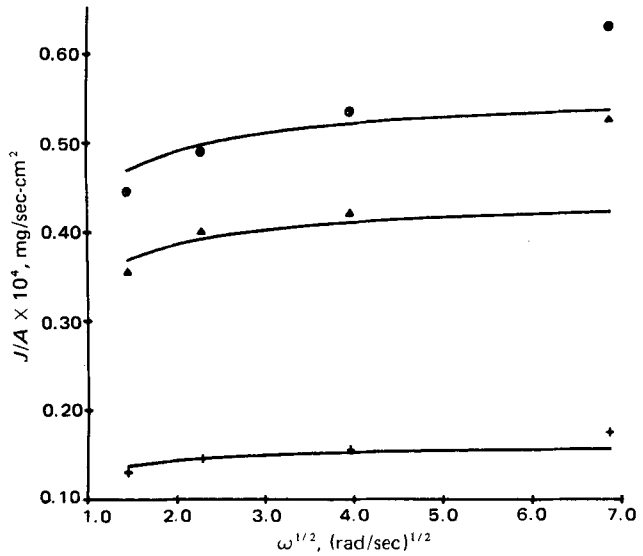


**Figure 10**—*Best-fit analysis of the soaked pellets in 5% sodium cholate and 0.1* M *phosphate buffer at pH 8.00. Key ($C_b$ in milligrams per milliliter): ●, 0.0; ▲, 0.3; and +, 1.0.*

**Table V—Summary of Partial Saturation Experiments and Best-Fit Analysis for Normal Cholesterol Pellets in 5% Sodium Cholate and 0.1 *M* Phosphate Buffer at pH 8.00**

| $C_s$[a], mg/ml | Revolutions per Minute | Best-Fit Analysis: $C_s$, mg/ml | $P \times 10^4$, cm/sec | $D \times 10^6$, cm²/sec |
|---|---|---|---|---|
| 1.45 | 20 | 1.45 | 0.51 | 1.25 |
| 1.45 | 50 | | | |
| 1.45 | 150 | | | |
| 1.42 | 450 | | | |

[a] From extrapolation of partial saturation data.

clearly the important involvement of the interfacial barrier in dissolution. If the interfacial barrier was not significant in dissolution, a plot of $J/A$ *versus* $\omega^{1/2}$ would give a straight line through the origin.

Based on a best-fit analysis using the equation previously reported (5), $J = A(C_s - C_b)/[1.612D^{-2/3}\nu^{1/6}\omega^{-1/2} + 1/P]$, it was possible to obtain values for $C_s$, $P$, and $D$, where $P$ is the interfacial transport constant and $D$ is the diffusivity. The calculated dissolution rates using the best-fit values were compared to the experimental dissolution rates; there was a good fit between experiment and theory (Figs. 8–10). The points at 450 rpm ($\omega^{1/2} = 6.86$) were not weighted in this analysis (5).

Tables V–VII summarize the results of the partial saturation experiments and the best-fit analysis. The $P_{aged}$:$P_{normal}$ ratio was ~2.71, while the $P_{soaked}$:$P_{normal}$ ratio was ~0.78. Therefore, the differences in the dissolution rates can be accounted for primarily by significant changes in $P$.

Figure 11 shows a plot of the amount of cholesterol dissolved *versus* time for the normal and aged pellets at 150 rpm using the rotating-disk apparatus. The pattern of dissolution from the normal pellet was linear while that from the aged pellet showed a definite curvature after 1 hr (Figs. 2 and 4). The fact that the normal pellet showed a linear dissolution pattern indicates that dissolution occurs from a single phase (monohydrate). The curved dissolution pattern indicates that more than one phase probably takes part in the dissolution.

Because the solubilities for the aged and anhydrous pellets (5) are

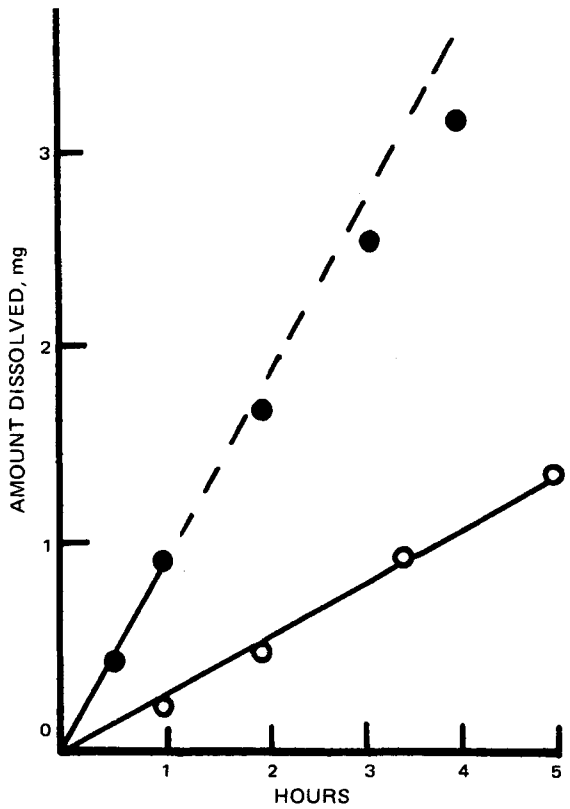


**Figure 11**—*Effect of pellet handling on the dissolution rate behavior at 150 rpm in the rotating-disk apparatus in 5% sodium cholate and 0.1* M *phosphate buffer at pH 8.00. Key: ●, aged pellet; and ○, normal pellet.*

Table VI—Summary of Partial Saturation Experiments and Best-Fit Analysis for Aged Pellets in 5% Sodium Cholate and 0.1 *M* Phosphate Buffer at pH 8.00

| $C_s$[a], mg/ml | Revolutions per Minute | Best-Fit Analysis: $C_s$, mg/ml | $P \times 10^4$, cm/sec | $D \times 10^6$, cm²/sec |
|---|---|---|---|---|
| 1.73 | 20 | 1.75 | 1.39 | 1.26 |
| 1.73 | 50 | | | |
| 1.72 | 150 | | | |
| 1.73 | 450 | | | |

[a] From extrapolation of partial saturation data.

Table VII—Summary of Partial Saturation Experiments and Best-Fit Analysis for Soaked Pellets in 5% Sodium Cholate and 0.1 *M* Phosphate Buffer at pH 8.00

| $C_s$[a], mg/ml | Revolutions per Minute | Best-Fit Analysis: $C_s$, mg/ml | $P \times 10^4$, cm/sec | $D \times 10^6$, cm²/sec |
|---|---|---|---|---|
| 1.40 | 20 | 1.41 | 0.39 | 1.26 |
| 1.40 | 50 | | | |
| 1.42 | 150 | | | |
| 1.42 | 450 | | | |

[a] From extrapolation of partial saturation data.

similar, leaving the pellet at 35° and ambient humidity for 24 hr may effectively dehydrate the outer surface layer, thereby making the pellet anhydrous. After initial dissolution removes the outer layer, dissolution again is controlled by the more slowly dissolving monohydrate layers.

Another possible explanation for this dissolution pattern is that pellet dehydration is not just a phenomenon of the outer surface layer but that the internal portions of the pellet also dehydrate. When the pellet contacts the dissolution medium, the more rapidly dissolving anhydrous material is removed from the surface. Dissolution from the internal portions of the pellet now is controlled by both anhydrous cholesterol and cholesterol monohydrate. The deeper the dissolution goes into the pellet, the less anhydrous material is present. As the curvature becomes greater, more cholesterol monohydrate probably is exposed; thus, dissolution slows and begins to approach the dissolution rate of a normal pellet.

As shown in Fig. 4, pellets exposed to ambient humidity for 24 hr at 35° and then soaked in double-distilled water at 37° for 24 hr showed linear dissolution, which indicates that soaking of an aged pellet effectively rehydrates the pellet. This rehydration is seen in the fact that the solubilities for the soaked and normal pellets are similar. However, the reformation of the monohydrate is probably not to the original state, perhaps because of precipitation of cholesterol onto the pellet surface. The newly formed crystals might be another polymorph of cholesterol monohydrate or they might be more perfect crystals (fewer defects) with fewer effective sites available for dissolution. The lower dissolution rate seen for the soaked pellet can be accounted for by either explanation. If dissolution of the soaked pellet is studied for a long period (~24 hr), a second linear portion is seen in the dissolution profile. Its slope is closer to that of the normal pellet.

## CONCLUSION

From this analysis, the need for a uniform experimental procedure can be seen. If investigators hope to reproduce results within their own laboratories as well as reproduce other investigators' findings, standard experimental procedures must be defined and used.

## REFERENCES


(1) S. Prakongpan, Ph.D. thesis, University of Michigan, Ann Arbor, Mich., 1974.

(2) K. H. Kwan, W. I. Higuchi, A. M. Molokhia, and A. F. Hofmann, *J. Pharm. Sci.*, **66**, 1094 (1977).

(3) *Ibid.*, **66**, 1105 (1977).

(4) D. C. Patel, Ph.D. thesis, University of Michigan, Ann Arbor, Mich., 1979.

(5) K. M. Feld and W. I. Higuchi, *J. Pharm. Sci.*, **70**, 717 (1981).

(6) "The Merck Index," 9th ed., Merck & Co., Rahway, N.J., 1976, p. MISC-71.

(7) S. Bergstrom and O. Wintersteiner, *J. Biol. Chem.*, **145**, 309 (1942).

(8) N. D. Weiner, P. Noomnont, and A. Felmeister, *J. Lipid Res.*, **13**, 253 (1972).

(9) A. M. Kamel, A. Felmeister, and N. D. Weiner, *ibid.*, **12**, 155 (1971).

(10) A. M. Kamel, N. D. Weiner, and A. Felmeister, *J. Colloid Interface Sci.*, **35**, 163 (1971).

(11) W. G. Dauben and P. H. Payot, *J. Am. Chem. Soc.*, **78**, 5657 (1956).

(12) G. L. Flynn, Y. Shah, S. Prakongpan, K. H. Kwan, W. I. Higuchi, and A. F. Hofmann, *J. Pharm. Sci.*, **68**, 1090 (1979).

(13) A. F. Hofmann, *J. Lipid Res.*, **3**, 127 (1962).


## ACKNOWLEDGMENTS


Supported by Grant AM 16694 from the National Institute of Arthritis, Metabolism, and Digestive Diseases.


# High-Pressure Liquid Chromatographic Analysis of Sennosides A and B Purgative Drugs


**OLUSEGUN OLUWOLE KOMOLAFE**



Received January 21, 1980, from the *Pharmaceutical Analysis Unit, Department of Pharmaceutical Chemistry, University of Ife, Ile-Ife, Nigeria.* Accepted for publication September 10, 1980.



**Abstract** □ Procedures are described for the analysis of the main anthraquinone glycosides of senna powder, senna fruit tablets, and sennoside tablets by high-pressure liquid chromatography (HPLC). In one HPLC analysis, TLC was used to separate the glycosides prior to elution on a strong anion-exchange column with 0.1 *M* ammonium nitrate solution (pH 9.0) as the mobile phase. In another HPLC analysis, separation was effected using a weak anion-exchange column with 0.1 *M* ammonium nitrate solution (pH 5.7) as the mobile phase.



**Keyphrases** □ Sennosides A and B—high-pressure liquid chromatographic analysis, separation of isomers from crude drug and pharmaceutical preparations □ Anthraquinone glycosides—high-pressure liquid chromatographic assay, separation of isomeric sennosides A and B from crude drug and pharmaceutical preparations □ High-pressure liquid chromatography—analysis, anthraquinone glycosides, separation of isomeric sennosides A and B from crude drug and pharmaceutical preparations □ Cathartics—anthraquinone glycosides, isomeric sennosides A and B, high-pressure liquid chromatographic analysis


The pods and leaves of senna as well as the pharmaceutical preparations containing sennosides A and B are widely used in medicine because of their laxative properties. An accurate, simple, and easy method is needed for estimation of sennosides A and B individually.

The most commonly used approach involves removal



© 1981, American Pharmaceutical Association

Table VI—Summary of Partial Saturation Experiments and Best-Fit Analysis for Aged Pellets in 5% Sodium Cholate and 0.1 *M* Phosphate Buffer at pH 8.00

| $C_s$[a], mg/ml | Revolutions per Minute | Best-Fit Analysis: $C_s$, mg/ml | $P \times 10^4$, cm/sec | $D \times 10^6$, cm²/sec |
|---|---|---|---|---|
| 1.73 | 20 | 1.75 | 1.39 | 1.26 |
| 1.73 | 50 | | | |
| 1.72 | 150 | | | |
| 1.73 | 450 | | | |

[a] From extrapolation of partial saturation data.

Table VII—Summary of Partial Saturation Experiments and Best-Fit Analysis for Soaked Pellets in 5% Sodium Cholate and 0.1 *M* Phosphate Buffer at pH 8.00

| $C_s$[a], mg/ml | Revolutions per Minute | Best-Fit Analysis: $C_s$, mg/ml | $P \times 10^4$, cm/sec | $D \times 10^6$, cm²/sec |
|---|---|---|---|---|
| 1.40 | 20 | 1.41 | 0.39 | 1.26 |
| 1.40 | 50 | | | |
| 1.42 | 150 | | | |
| 1.42 | 450 | | | |

[a] From extrapolation of partial saturation data.

similar, leaving the pellet at 35° and ambient humidity for 24 hr may effectively dehydrate the outer surface layer, thereby making the pellet anhydrous. After initial dissolution removes the outer layer, dissolution again is controlled by the more slowly dissolving monohydrate layers.

Another possible explanation for this dissolution pattern is that pellet dehydration is not just a phenomenon of the outer surface layer but that the internal portions of the pellet also dehydrate. When the pellet contacts the dissolution medium, the more rapidly dissolving anhydrous material is removed from the surface. Dissolution from the internal portions of the pellet now is controlled by both anhydrous cholesterol and cholesterol monohydrate. The deeper the dissolution goes into the pellet, the less anhydrous material is present. As the curvature becomes greater, more cholesterol monohydrate probably is exposed; thus, dissolution slows and begins to approach the dissolution rate of a normal pellet.

As shown in Fig. 4, pellets exposed to ambient humidity for 24 hr at 35° and then soaked in double-distilled water at 37° for 24 hr showed linear dissolution, which indicates that soaking of an aged pellet effectively rehydrates the pellet. This rehydration is seen in the fact that the solubilities for the soaked and normal pellets are similar. However, the reformation of the monohydrate is probably not to the original state, perhaps because of precipitation of cholesterol onto the pellet surface. The newly formed crystals might be another polymorph of cholesterol monohydrate or they might be more perfect crystals (fewer defects) with fewer effective sites available for dissolution. The lower dissolution rate seen for the soaked pellet can be accounted for by either explanation. If dissolution of the soaked pellet is studied for a long period (~24 hr), a second linear portion is seen in the dissolution profile. Its slope is closer to that of the normal pellet.

## CONCLUSION

From this analysis, the need for a uniform experimental procedure can be seen. If investigators hope to reproduce results within their own laboratories as well as reproduce other investigators' findings, standard experimental procedures must be defined and used.

## REFERENCES


(1) S. Prakongpan, Ph.D. thesis, University of Michigan, Ann Arbor, Mich., 1974.

(2) K. H. Kwan, W. I. Higuchi, A. M. Molokhia, and A. F. Hofmann, *J. Pharm. Sci.*, **66**, 1094 (1977).

(3) *Ibid.*, **66**, 1105 (1977).

(4) D. C. Patel, Ph.D. thesis, University of Michigan, Ann Arbor, Mich., 1979.

(5) K. M. Feld and W. I. Higuchi, *J. Pharm. Sci.*, **70**, 717 (1981).

(6) "The Merck Index," 9th ed., Merck & Co., Rahway, N.J., 1976, p. MISC-71.

(7) S. Bergstrom and O. Wintersteiner, *J. Biol. Chem.*, **145**, 309 (1942).

(8) N. D. Weiner, P. Noomnont, and A. Felmeister, *J. Lipid Res.*, **13**, 253 (1972).

(9) A. M. Kamel, A. Felmeister, and N. D. Weiner, *ibid.*, **12**, 155 (1971).

(10) A. M. Kamel, N. D. Weiner, and A. Felmeister, *J. Colloid Interface Sci.*, **35**, 163 (1971).

(11) W. G. Dauben and P. H. Payot, *J. Am. Chem. Soc.*, **78**, 5657 (1956).

(12) G. L. Flynn, Y. Shah, S. Prakongpan, K. H. Kwan, W. I. Higuchi, and A. F. Hofmann, *J. Pharm. Sci.*, **68**, 1090 (1979).

(13) A. F. Hofmann, *J. Lipid Res.*, **3**, 127 (1962).


## ACKNOWLEDGMENTS


Supported by Grant AM 16694 from the National Institute of Arthritis, Metabolism, and Digestive Diseases.


# High-Pressure Liquid Chromatographic Analysis of Sennosides A and B Purgative Drugs


**OLUSEGUN OLUWOLE KOMOLAFE**



Received January 21, 1980, from the *Pharmaceutical Analysis Unit, Department of Pharmaceutical Chemistry, University of Ife, Ile-Ife, Nigeria.* Accepted for publication September 10, 1980.



**Abstract** □ Procedures are described for the analysis of the main anthraquinone glycosides of senna powder, senna fruit tablets, and sennoside tablets by high-pressure liquid chromatography (HPLC). In one HPLC analysis, TLC was used to separate the glycosides prior to elution on a strong anion-exchange column with 0.1 *M* ammonium nitrate solution (pH 9.0) as the mobile phase. In another HPLC analysis, separation was effected using a weak anion-exchange column with 0.1 *M* ammonium nitrate solution (pH 5.7) as the mobile phase.



**Keyphrases** □ Sennosides A and B—high-pressure liquid chromatographic analysis, separation of isomers from crude drug and pharmaceutical preparations □ Anthraquinone glycosides—high-pressure liquid chromatographic assay, separation of isomeric sennosides A and B from crude drug and pharmaceutical preparations □ High-pressure liquid chromatography—analysis, anthraquinone glycosides, separation of isomeric sennosides A and B from crude drug and pharmaceutical preparations □ Cathartics—anthraquinone glycosides, isomeric sennosides A and B, high-pressure liquid chromatographic analysis


The pods and leaves of senna as well as the pharmaceutical preparations containing sennosides A and B are widely used in medicine because of their laxative properties. An accurate, simple, and easy method is needed for estimation of sennosides A and B individually.

The most commonly used approach involves removal



© 1981, American Pharmaceutical Association

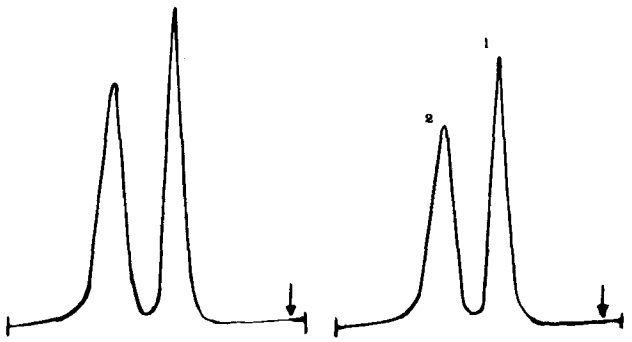

**Figure 1**—*Chromatogram of sennosides A (2) and B (1). The column was 600 × 2 mm i.d. (DuPont), strong anion exchange (30–40 μm). The mobile phase was ammonium nitrate solution (0.1 M, pH 9.0). UV detection was at 254 nm.*

of free aglycones by partitioning into an organic layer, hydrolysis and oxidation of the glycosides into aglycones and sugars, formation of colored derivatives by the action of aqueous alkali on the liberated aglycones, and absorption spectrophotometry (1–6). This procedure is not specific since it does not distinguish between the isomeric sennosides A and B but gives only a total sennoside content. Moreover, the procedure is ineffective since bianthrones such as the sennosides are not oxidized completely to anthraquinones (7, 8). The presence of several bianthrones in senna, rhubarb, cascara, and frangula suggested the need for a new assay.

The low concentrations of highly labile glycosides in their pharmacologically active forms in purgative drugs make liquid chromatography at ambient temperatures an attractive choice. Application of high-pressure liquid chromatography (HPLC) to the detection and separation of free and combined anthraquinone compounds has been reported (9–14), but HPLC has not been extended to the quantitation of anthraquinone glycosides in drugs and pharmaceutical preparations. This work attempted such a quantitation.

## EXPERIMENTAL

**Materials**—The authentic glycosides used were sennosides A and B. The drugs analyzed include powdered senna pods, senna fruit tablets[1] (each tablet contained sennosides A and B equivalent to 7.5 mg of sennoside B per tablet), and sennoside tablets[2] (each tablet contained 12 mg of sennosides A and B as calcium salts).

The HPLC eluates were monitored by UV detection at 254 nm. The strong anion-exchange columns used were 600 × 2 mm i.d., 30–40-μm particle size[3], and 125 × 4 mm i.d., 10-μm particle size[4]. The weak anion-exchange column was 600 × 2 mm i.d., 30–40-μm particle size[5]. An electronic integrator[6] was used for peak area measurement.

Silica gel was used for TLC. Precoated plastic sheets of silica gel (0.25 mm) containing a fluorescent indicator for UV detection at 254 nm also were used.

*n*-Propanol, ethyl acetate, ammonium hydroxide, nitric acid, and ethanol were analytical reagent grade. Aqueous reagents were prepared in deionized water, and all glassware was scrupulously cleaned.

**TLC**—The reference solution was prepared by dissolving sennoside A (~2 mg, accurately weighed) in the TLC mobile phase (1 ml) with gentle warming to effect complete dissolution. A reference solution of sennoside B was prepared similarly.

The test solution of senna powder, senna fruit tablets, or sennoside tablets was prepared by putting the powdered drug (~0.4 g of senna powder or senna fruit tablet powder or 0.2 g of sennoside tablet powder, accurately weighed) in a round-bottom flask and adding 5 ml of ethanol–water (50:50 v/v). The flask was weighed with its contents, a reflux condenser was attached, and the flask was heated in a boiling water bath for 15 min. Then the flask was cooled and adjusted to the original weight with ethanol (50% in water), and the contents were transferred to a centrifuge tube and centrifuged. The clear supernate was used for TLC spotting.

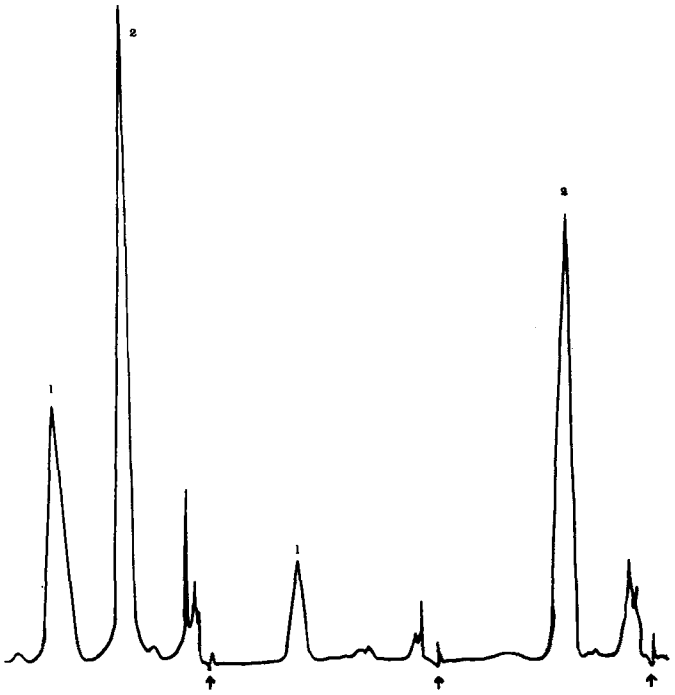

**Figure 2**—*Chromatogram of sennosides A (2) and B (1). The column was 125 × 4 mm i.d. (Partisil), strong anion exchange (10 μm). The mobile phase was ammonium nitrate solution (0.1 M, pH 7.5) and 15% ethanol. UV detection was at 254 nm.*

Aliquots (10 μl) of each standard and test solution were applied to the same chromatoplate, allowed to dry, and developed over a path of ~10 cm using *n*-propanol–ethyl acetate–water (40:40:30 v/v/v) as the developing solvent. The solvent was allowed to evaporate at room temperature, and the chromatoplate was examined under UV light to determine the spots corresponding to those of the standards.

**HPLC of TLC Spots**—Ten TLC spots from each authentic sennoside

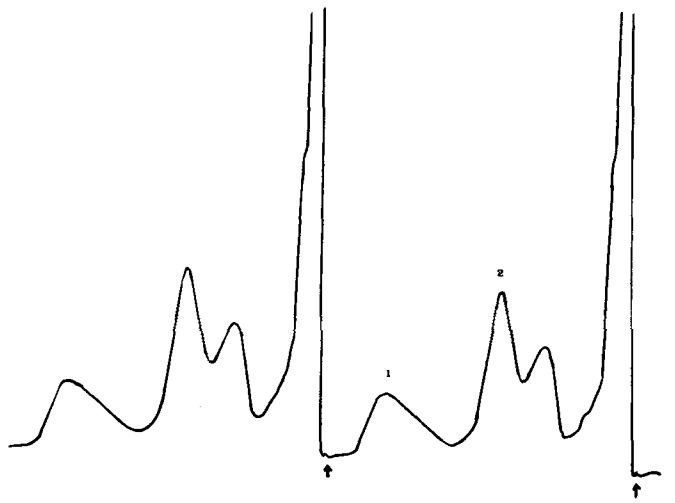

**Figure 3**—*Chromatogram of the aqueous extract of senna. The column was 600 × 2 mm i.d. (AL Pellionex), weak anion exchange (30–40 μm). The mobile phase was ammonium nitrate solution (0.1 M, pH 5.7). UV detection was at 254 nm. Key: 1, sennoside B; and 2, sennoside A.*

[1] Senokot tablets, Reckitt and Collman.
[2] Pursennid tablets, Sandoz Products Ltd.
[3] Zipax.
[4] Partisil.
[5] AL Pellionex.
[6] Minigrator.

**Table I—Sennosides A and B Content [a] of Purgative Drugs as Determined by HPLC**

| Sample | Sennoside A Content, mg (SAX[b]) | Sennoside B Content, mg SAX[b] | Sennoside B Content, mg WAX[c] | Label (Colorimetric Assay) |
|---|---|---|---|---|
| Senna (per gram) | 14.2 | 13.9 | 14.3 | 28.6 |
| Senna fruit tablets (per tablet) | 3.5 | 3.3 | 3.62 | 7.5 |
| Sennoside tablets (per tablet) | 5.9 | 5.8 | 6.05 | 12.0 |

[a] Mean of three determinations. [b] SAX = strong anion-exchange column (30–40 μm) with 0.1 *M* ammonium nitrate solution (pH 9.0) as the mobile phase. [c] WAX = weak anion-exchange column (30–40 μm) with 0.1 *M* ammonium nitrate solution (pH 5.7) as the mobile phase.

spot were extracted with the HPLC mobile phase (1 ml), and a 10-μl portion was injected into the chromatograph and eluted under the following conditions. Column 1 was Zipax, strong anion exchange (30–40 μm), with a mobile phase of 0.1 *M* ammonium nitrate solution (pH 9.0). Column 2 was Partisil, strong anion exchange (10 μm), with a mobile phase of 0.1 *M* ammonium nitrate solution (pH 7.5) and 15% ethanol. The flow rate was 1 ml/min. UV detection was at 254 nm, and attenuation was set at ×16.

Ten TLC spots of the crude senna drug corresponding to sennoside A were extracted with the HPLC mobile phase (1 ml) and eluted under the same experimental conditions as for the authentic sennosides.

Similarly, 10 TLC spots corresponding to sennoside B in the crude senna drug were extracted with the HPLC mobile phase (1 ml) and eluted under the same experimental conditions as for the authentic sennosides. The sennosides A and B content of senna fruit tablets and sennoside tablets also was determined using the same experimental procedure and conditions as outlined for crude senna drug.

**Direct HPLC Analysis**—Sennosides A and B were dissolved in 0.1 *M* ammonium nitrate (pH 5.7) containing a trace of ammonia solution to give a concentration of ~1 mg/ml each. Aliquots (10 μl) were injected into the chromatograph under the following conditions. The column was AL Pellionex weak anion exchange (30–40 μm), with a mobile phase of 0.1 *M* ammonium nitrate (pH 5.7) at a flow rate of 1 ml/min. UV detection was at 254 nm, and attenuation was set at ×16.

Senna pods or senna fruit tablets (~0.5 g of each drug powder, accurately weighed) was placed in a round-bottom flask with deionized water (10 ml). After the flask was weighed with its contents, it was refluxed in a boiling water bath for 15 min, cooled, and adjusted to the original weight with deionized water. The aqueous extract was centrifuged, and portions of the clear supernate (10 μl) were chromatographed or were mixed with the authentic sennoside solutions and then chromatographed. The same elution conditions were used as for the standard solutions.

In the assay of sennoside tablets, one tablet was ground to a fine powder and then triturated with the mobile phase (5 ml). The suspension obtained was centrifuged and 10-μl portions of the clear supernate were chromatographed or were mixed with the authentic sennoside solutions and then chromatographed under the same conditions used for the standard solutions.

## RESULTS AND DISCUSSION

Preliminary investigations showed that the use of different solvents for extraction did not affect the yield or form of the sennosides. This finding is in agreement with the observation of previous workers (15, 16) who found that hot water or water containing up to 70% methanol, ethanol, or acetone effects extraction of most glycosidal contents in a drug–percolate ratio of 1:6. Comparison of the high-pressure liquid chromatograms of the drug extracts containing authentic sennosides with those that did not confirmed the presence of the sennosides in the drugs.

Variations of the HPLC elution parameters (pH and ionic strength)

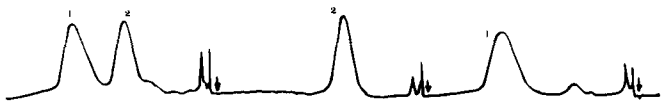

**Figure 4**—*Chromatogram of sennosides A (2) and B (1). The column was 600 × 2 mm i.d. (AL Pellionex), weak anion exchange (30–40 μm). The mobile phase was ammonium nitrate solution (0.1* M, *pH 5.7). UV detection was at 254 nm.*

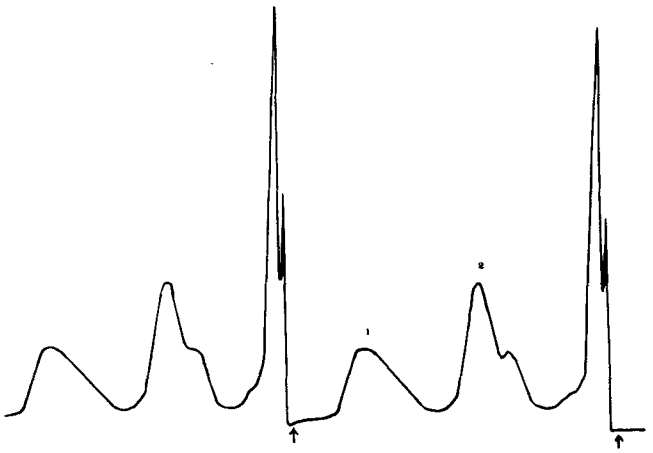

**Figure 5**—*Chromatogram of the ammonium nitrate extract of sennoside tablets. The column was 600 × 2 mm i.d. (AL Pellionex), weak anion exchange (30–40 μm). The mobile phase was ammonium nitrate solution (0.1* M, *pH 5.7). UV detection was at 254 nm. Key: 1, sennoside B; and 2, sennoside A.*

showed that the optimum conditions for the elutions of sennosides A and B in the two strong anion exchangers included 0.1 *M* ammonium nitrate (pH 9.0) in the larger particle chromedium and 0.1 *M* ammonium nitrate (pH 5.7) containing 15% ethanol in the 10-μm chromedium. At the optimum operational conditions, pure sennosides A and B had symmetrical peaks with good peak width and retention times, and they were well separated from each other. However, the resolution obtained on the larger particle chromedium was better than that obtained on the smaller particle chromedium (Figs. 1 and 2). Ethanol had to be added to the ammonium nitrate mobile phase to obtain elution of the glycosides on the 10-μm ion exchanger within a reasonable time. Alcohol molecules probably block the active adsorption sites on the chromedium, resulting in faster elution of the glycoside molecules.

The chromatogram obtained for senna fruit tablets was similar to that for senna pods on both the strong and weak anion-exchange columns (Fig. 3). This result was expected since senna fruit tablets are made from powdered senna pods. It was anticipated that the 10-μm strong anion exchange chromedium would produce better resolution than the larger particle chromedium (30–40 μm) and that the resolution might free the sennosides from unwanted matter. However, both strong anion-exchange systems, at the optimum elution conditions, did not achieve this end, making direct quantitation of the sennosides A and B content of the drug extracts impossible. However, elutions on the strong anion-exchange column (30–40 μm) with ammonium nitrate (pH 9.0) as the mobile phase gave improved separation of peaks with a decrease in the ionic strength of the mobile phase. The chromatogram of a 0.02 *M* ammonium nitrate solution showed that sennoside A was completely separated from all other peaks, although the retention time was very long (48 min) and the peak width was broad (3 cm). Therefore, direct HPLC quantitation of sennoside A in the crude purgative drug and pharmaceutical preparations might be possible using solvent programming.

TLC of pure sennoside A showed a major spot of $R_f$ 0.31 and a minor spot of $R_f$ 0.51 due to an impurity. TLC of pure sennoside B showed a major spot of $R_f$ 0.16 and two minor spots of $R_f$ 0.34 and 0.048 due to impurities (6, 8). Sennosides A and B in the drug samples were well separated by TLC. The results of the assay based on HPLC of the TLC spots are shown in Table I.

In the direct HPLC elutions of the aqueous extracts of senna pods, senna fruit tablets, and sennoside tablets using the weak anion-exchange column, only sennoside B was well separated from all other components of the drug constituents. Thus, it was possible to estimate only the sennoside B content of the drug by comparison of the peak area with that of authentic sennoside B solution of known concentration (Table I and Figs. 3–5).

The ion-exchange chromatographic separation of the sennosides from the other drug constituents is based on the presence of a carboxylic acid functional group on the sennoside molecules. Since sennosides A and B have the same functional groups and the same molecular configuration, the separation of one from the other on the ion-exchange column must include some other phenomenon (*e.g.*, hydrogen bonding, polar interaction, adsorption, or van der Waals forces) in addition to the reversible exchange of ions between the solute and the electrolyte gel.

## REFERENCES

(1) W. Kausmall and B. Becker, *Helv. Chim. Acta*, **30**, 58 (1947).

(2) B. V. Christensen and I. A. Abdel-Latif, *J. Am. Pharm. Assoc., Sci. Ed.*, **38**, 487, 589, 652 (1949).

(3) J. W. Fairbairn and I. Michaels, *J. Pharm. Pharmacol.*, **2**, 807 (1950).

(4) Joint Com. Pharm. Soc. Anal. Chem., *Analyst*, **90**, 582 (1965).

(5) J. Lemli and J. Cuveele, *Pharm. Acta Helv.*, **43**, 689 (1968).

(6) "European Pharmacopoeia," vol. 1, Council of Europe, Strasbourg, France, 1969, p. 358.

(7) H. Auterhoff and R. Sachdev, *Dtsch. Apoth.-Ztg.*, **102**, 921 (1962).

(8) J. Lemli, *J. Pharm. Pharmacol.*, **17**, 227 (1965).

(9) J. J. Kirkland, "Modern Practice of Liquid Chromatography," Wiley, New York, N.Y., 1971, p. 409.

(10) C. R. McIlwrick and R. P. Labadie, *Pharm. Weekbl.*, **107**, 535 (1972).

(11) P. R. Brown, "High Pressure Liquid Chromatography," Academic, New York, N.Y., 1973, pp. 58, 181.

(12) P. P. Rai, T. D. Turner, and S. A. Matlin, *J. Chromatogr.*, **110**, 401 (1975).

(13) V. Castaguola, G. Pentiinari, and G. A. De Vries, *Boll. Chim. Farm.*, **115**, 376 (1976).

(14) F. 'Erni, R. W. Frei, and W. Lindner, *J. Chromatogr.*, **125**, 265 (1976).

(15) "British Pharmacopoeia, 1973," Her Majesty's Stationery Office, London, England, 1973, p. 418.

(16) J. W. Fairbairn and I. Michaels, *J. Pharm. Pharmacol.*, **11**, 813 (1950).



## ACKNOWLEDGMENTS

Supported by a grant from the University of Ife, Ile-Ife, Nigeria.

The author thanks Dr. W. D. Williams, University of Strathclyde, Glasgow, Scotland, for assistance.


# Dosage Form Design for Improvement of Bioavailability of Levodopa IV: Possible Causes of Low Bioavailability of Oral Levodopa in Dogs


**KUNIHIRO SASAHARA ˣ, TAKASHI NITANAI, TAEKO HABARA, TOSHIMASA KOJIMA, YUKINORI KAWAHARA, TADASHI MORIOKA, and EIICHI NAKAJIMA**



Received April 11, 1980, from the *Product Development Laboratories, Sankyo Company, Ltd., 1-2-58, Hiromachi, Shinagawa, Tokyo, Japan.* Accepted for publication September 30, 1980.



**Abstract** □ Several potential mechanisms for reduced levodopa bioavailability following oral administration to dogs and humans were investigated by studying the influence of the administration route on plasma levodopa levels after intravenous, hepatoportal, and duodenal administrations to dogs. The observed average areas under the plasma concentration–time curves (*AUC*) of levodopa following hepatoportal injection and intravenous injection were virtually identical; but following duodenal administration a decrease in the *AUC* of levodopa was observed with a concomitant increase in the *AUC* of total dopamine. The possible involvement of intestinal microorganisms in levodopa metabolism was explored in dogs that had been administered a combination of paromomycin and kanamycin to reduce intestinal microflora. Similar patterns of plasma level profiles and urinary excretion were observed between control and treated dogs. As measured by the release of [$^{14}$C]carbon dioxide from [$^{14}$C]levodopa, the distribution of levodopa decarboxylase enzyme activity in various parts of the intestine was studied in homogenates prepared from isolated intestinal segments of the duodenum and upper, middle, and lower parts of the jejunum and ileum. The jejunum showed the highest decarboxylase activity followed by the ileum and duodenum. These data indicate that the reduced bioavailability of orally administered levodopa occurs as a result of metabolism by levodopa decarboxylase enzyme in the gut wall.



**Keyphrases** □ Levodopa—bioavailability, effect of administration route, metabolism, intestinal microorganisms, levodopa decarboxylase □ Bioavailability—levodopa, effect of administration route □ Antiparkinsonian agents—levodopa, effect of administration route on bioavailability


Previous studies (1, 2) reported that, based on the measurement of levodopa and its metabolites recovered in the urine, the total amount absorbed, including levodopa metabolites, was 80–90% of the administered dose. However, the measurements of plasma levodopa concentrations after intravenous and oral administrations indicated that 20–40% of the administered dose reached the fluids of distribution intact.

The present study with levodopa was carried out in dogs to elucidate the mechanisms responsible for the low bioavailability of orally administered levodopa.

## EXPERIMENTAL

**Influence of Administration Route on Plasma Levodopa Levels and Its Metabolites in Dogs**—Nine healthy male beagle dogs, 10.5–13.2 kg, were fasted for ~16 hr and divided into three groups. They were anesthetized with 25 mg of pentobarbital sodium/kg iv. The first group was administered 20-mg doses of levodopa[1] into their brachial vein over 30 sec. After the dogs in the second group were fixed on their backs, a laparotomy was performed and levodopa solution[1] was administered directly into the hepatoportal veins over 30 sec. A laparotomy was performed in the third group, a 20-cm segment of the duodenum was ligated, and levodopa solution was administered into the ligated loop.

Blood samples were withdrawn from each animal with a heparinized syringe from the femoral or brachial vein at the time intervals indicated in Fig. 1. The blood specimens obtained were processed as described previously (1, 3). The third group was killed by exsanguination immediately after the last blood sample was collected, and the ligated duodenal loops were removed to determine residual levodopa and its metabolites in the duodenal loops where levodopa was administered. The contents of the duodenal loops were washed with saline and then three times with 0.04 *N* $HClO_4$ solution. The irrigating solutions were assayed for residual levodopa and its metabolites.

**Influence of GI Microorganisms on Oral Levodopa Absorption**—Two healthy male mongrel dogs, 6.0 and 11.8 kg, were orally administered a single capsule containing 110 mg of paromomycin and 100 mg of kanamycin. Two control dogs also were used. The dogs were anesthetized with intravenous injection of 25 mg of pentobarbital sodium/kg. After anesthetization, a laparotomy was performed and a series of intestinal loops were made by ligating segments of the stomach, duodenum, and jejunum. The contents of each segment were suspended in saline solution and diluted with 0.1% phosphate buffer (pH 7.2). The

[1] Dopaston Injection, Sankyo Co., Tokyo, Japan.




*0022-3549/81/0700-0730$01.00/0*



© *1981, American Pharmaceutical Association*

## REFERENCES

(1) W. Kausmall and B. Becker, *Helv. Chim. Acta*, **30**, 58 (1947).

(2) B. V. Christensen and I. A. Abdel-Latif, *J. Am. Pharm. Assoc., Sci. Ed.*, **38**, 487, 589, 652 (1949).

(3) J. W. Fairbairn and I. Michaels, *J. Pharm. Pharmacol.*, **2**, 807 (1950).

(4) Joint Com. Pharm. Soc. Anal. Chem., *Analyst*, **90**, 582 (1965).

(5) J. Lemli and J. Cuveele, *Pharm. Acta Helv.*, **43**, 689 (1968).

(6) "European Pharmacopoeia," vol. 1, Council of Europe, Strasbourg, France, 1969, p. 358.

(7) H. Auterhoff and R. Sachdev, *Dtsch. Apoth.-Ztg.*, **102**, 921 (1962).

(8) J. Lemli, *J. Pharm. Pharmacol.*, **17**, 227 (1965).

(9) J. J. Kirkland, "Modern Practice of Liquid Chromatography," Wiley, New York, N.Y., 1971, p. 409.

(10) C. R. McIlwrick and R. P. Labadie, *Pharm. Weekbl.*, **107**, 535 (1972).

(11) P. R. Brown, "High Pressure Liquid Chromatography," Academic, New York, N.Y., 1973, pp. 58, 181.

(12) P. P. Rai, T. D. Turner, and S. A. Matlin, *J. Chromatogr.*, **110**, 401 (1975).

(13) V. Castaguola, G. Pentiinari, and G. A. De Vries, *Boll. Chim. Farm.*, **115**, 376 (1976).

(14) F. 'Erni, R. W. Frei, and W. Lindner, *J. Chromatogr.*, **125**, 265 (1976).

(15) "British Pharmacopoeia, 1973," Her Majesty's Stationery Office, London, England, 1973, p. 418.

(16) J. W. Fairbairn and I. Michaels, *J. Pharm. Pharmacol.*, **11**, 813 (1950).



## ACKNOWLEDGMENTS

Supported by a grant from the University of Ife, Ile-Ife, Nigeria.

The author thanks Dr. W. D. Williams, University of Strathclyde, Glasgow, Scotland, for assistance.


# Dosage Form Design for Improvement of Bioavailability of Levodopa IV: Possible Causes of Low Bioavailability of Oral Levodopa in Dogs


**KUNIHIRO SASAHARA ˣ, TAKASHI NITANAI, TAEKO HABARA, TOSHIMASA KOJIMA, YUKINORI KAWAHARA, TADASHI MORIOKA, and EIICHI NAKAJIMA**



Received April 11, 1980, from the *Product Development Laboratories, Sankyo Company, Ltd., 1-2-58, Hiromachi, Shinagawa, Tokyo, Japan.* Accepted for publication September 30, 1980.



**Abstract** □ Several potential mechanisms for reduced levodopa bioavailability following oral administration to dogs and humans were investigated by studying the influence of the administration route on plasma levodopa levels after intravenous, hepatoportal, and duodenal administrations to dogs. The observed average areas under the plasma concentration–time curves (*AUC*) of levodopa following hepatoportal injection and intravenous injection were virtually identical; but following duodenal administration a decrease in the *AUC* of levodopa was observed with a concomitant increase in the *AUC* of total dopamine. The possible involvement of intestinal microorganisms in levodopa metabolism was explored in dogs that had been administered a combination of paromomycin and kanamycin to reduce intestinal microflora. Similar patterns of plasma level profiles and urinary excretion were observed between control and treated dogs. As measured by the release of [$^{14}$C]carbon dioxide from [$^{14}$C]levodopa, the distribution of levodopa decarboxylase enzyme activity in various parts of the intestine was studied in homogenates prepared from isolated intestinal segments of the duodenum and upper, middle, and lower parts of the jejunum and ileum. The jejunum showed the highest decarboxylase activity followed by the ileum and duodenum. These data indicate that the reduced bioavailability of orally administered levodopa occurs as a result of metabolism by levodopa decarboxylase enzyme in the gut wall.



**Keyphrases** □ Levodopa—bioavailability, effect of administration route, metabolism, intestinal microorganisms, levodopa decarboxylase □ Bioavailability—levodopa, effect of administration route □ Antiparkinsonian agents—levodopa, effect of administration route on bioavailability


Previous studies (1, 2) reported that, based on the measurement of levodopa and its metabolites recovered in the urine, the total amount absorbed, including levodopa metabolites, was 80–90% of the administered dose. However, the measurements of plasma levodopa concentrations after intravenous and oral administrations indicated that 20–40% of the administered dose reached the fluids of distribution intact.

The present study with levodopa was carried out in dogs to elucidate the mechanisms responsible for the low bioavailability of orally administered levodopa.

## EXPERIMENTAL

**Influence of Administration Route on Plasma Levodopa Levels and Its Metabolites in Dogs**—Nine healthy male beagle dogs, 10.5–13.2 kg, were fasted for ~16 hr and divided into three groups. They were anesthetized with 25 mg of pentobarbital sodium/kg iv. The first group was administered 20-mg doses of levodopa[1] into their brachial vein over 30 sec. After the dogs in the second group were fixed on their backs, a laparotomy was performed and levodopa solution[1] was administered directly into the hepatoportal veins over 30 sec. A laparotomy was performed in the third group, a 20-cm segment of the duodenum was ligated, and levodopa solution was administered into the ligated loop.

Blood samples were withdrawn from each animal with a heparinized syringe from the femoral or brachial vein at the time intervals indicated in Fig. 1. The blood specimens obtained were processed as described previously (1, 3). The third group was killed by exsanguination immediately after the last blood sample was collected, and the ligated duodenal loops were removed to determine residual levodopa and its metabolites in the duodenal loops where levodopa was administered. The contents of the duodenal loops were washed with saline and then three times with 0.04 *N* $HClO_4$ solution. The irrigating solutions were assayed for residual levodopa and its metabolites.

**Influence of GI Microorganisms on Oral Levodopa Absorption**—Two healthy male mongrel dogs, 6.0 and 11.8 kg, were orally administered a single capsule containing 110 mg of paromomycin and 100 mg of kanamycin. Two control dogs also were used. The dogs were anesthetized with intravenous injection of 25 mg of pentobarbital sodium/kg. After anesthetization, a laparotomy was performed and a series of intestinal loops were made by ligating segments of the stomach, duodenum, and jejunum. The contents of each segment were suspended in saline solution and diluted with 0.1% phosphate buffer (pH 7.2). The

[1] Dopaston Injection, Sankyo Co., Tokyo, Japan.




*0022-3549/81/0700-0730$01.00/0*



© *1981, American Pharmaceutical Association*

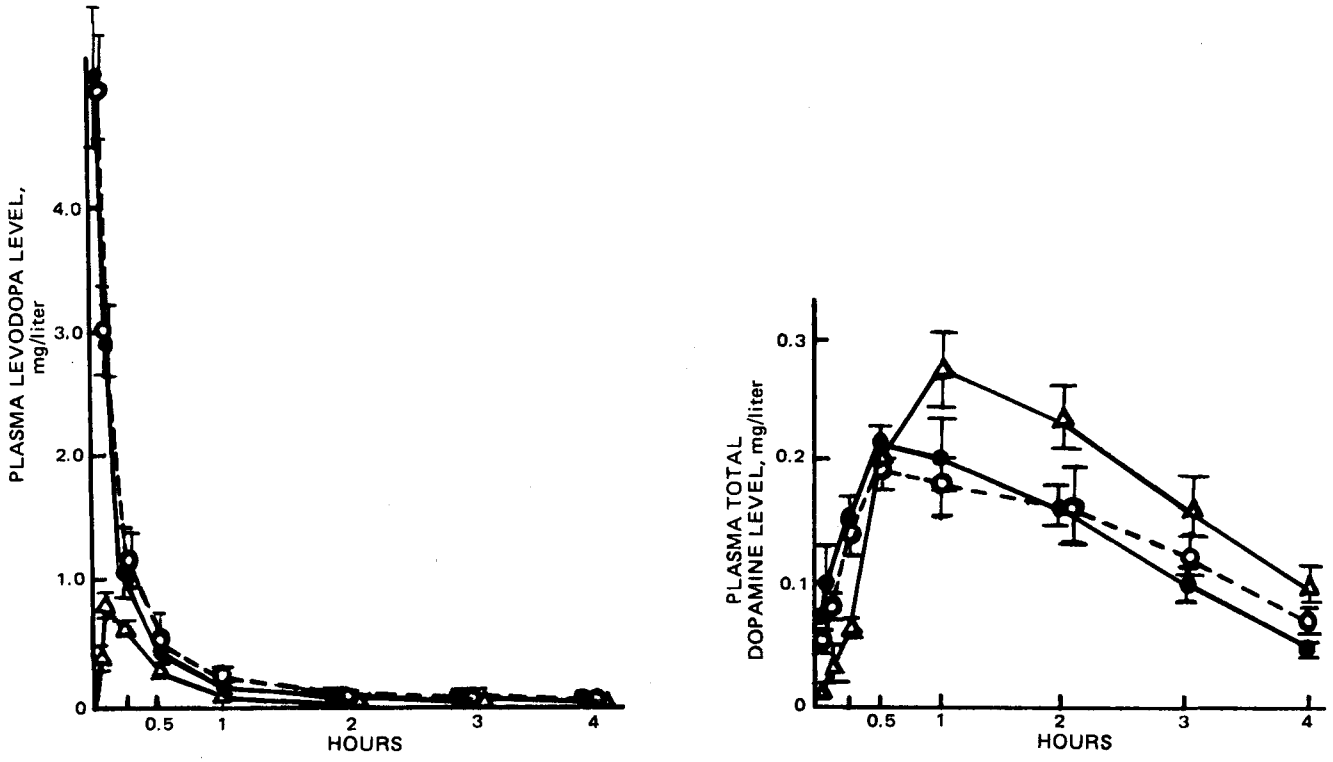


**Figure 1**—*Average plasma levels of levodopa (±SE) and total dopamine (±SE) following intravenous (●), hepatoportal (○), and duodenal (△) administrations of single 20-mg doses of levodopa to three dogs.*

diluted solution was smeared on the selective medium and cultured according to the conditions listed in Table I. After cultivation, the numbers of colonies were counted.

Following this initial study, six healthy male beagle dogs, 10.1–12.5 kg, were fasted for ~16 hr; levodopa in capsule form[2] was administered orally at a dose of 100 mg/dog with 10 ml of warm water. After 1 week, the same dogs were administered a single dose of the antibiotics as before, and levodopa in capsule form[2] was administered as previously described. Emesis was prevented by keeping the dogs' mouths closed by hand. Blood samples were obtained with a heparinized syringe at the intervals indicated in Fig. 2. The urine also was collected before and over 48 hr. The blood and urine samples were processed as previously described (1, 3).

**Distribution of Levodopa Decarboxylase Enzyme Activity in Intestinal Tract of Dogs**—Three healthy male mongrel dogs, 13.0–15.0 kg, were fasted for ~16 hr, anesthetized with 25 mg of pentobarbital sodium/kg iv, and then killed by exsanguination. Their abdomens were opened immediately, and sections of the duodenum and upper, middle, and lower parts of the jejunum and ileum were removed. The contents in each section were removed by washing three times with saline.

An homogenate of each section of the intestinal tract was prepared in 0.05 *M* phosphate buffer (pH 6.8) cooled to 0°. The volume was adjusted to reflect the final wet tissue concentration of 100 mg/ml. Then 0.2–0.5 ml of each homogenate was added to the reaction mixture consisting of 0.2 ml of 0.2 *M* phosphate buffer (pH 6.8), 0.05 ml of 0.5% (w/v) pyridoxal phosphate solution, 0.1 ml of 8.1% levodopa solution [1 g of levodopa dissolved with 0.2% (w/v) sodium bicarbonate and 0.5% (w/v) polyvinyl acetate] and $^{14}$C-labeled DL-levodopa (0.05 $\mu$Ci/410 nmoles) and then incubated for 30 min at 37°. At 30 min after incubation, the reaction was stopped by adding 0.2 ml of 30% (w/v) $HClO_4$ solution into the reaction mixture.

The [$^{14}$C]carbon dioxide evolved from decarboxylation of [$^{14}$C]levodopa by levodopa decarboxylase in the homogenate was trapped completely in filter paper impregnated with benzethonium chloride solution[3]. The filter paper was immersed in a toluene scintillation mixture of 8 g of 2,5-diphenyloxazole and 0.2 g of 1,4-bis[2-(4-methyl-5-phenyloxazoly)]-benzene dissolved in 1000 ml of toluene. The trapped radioactivity was measured by the standard procedure.

**Assay of Levodopa and Its Metabolites in Plasma and Urine**—The assay of levodopa and its metabolites in plasma and urine was carried out as previously reported (3).

**Assay of Levodopa and Its Metabolites at Administration**—Residual levodopa and its metabolites were determined in the same manner as urine.

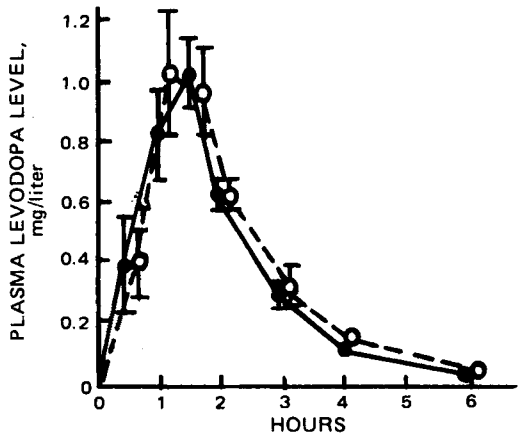


**Figure 2**—*Average plasma levodopa levels following oral administration of 100-mg doses of levodopa to six dogs treated with antibiotics (○) and to six control dogs without antibiotics (●) in a crossover fashion.*

## RESULTS

**Influence of Administration Route on Plasma Levels of Levodopa and Its Metabolites in Dogs**—The average plasma levels of levodopa and total dopamine, one of the main metabolites of levodopa, are shown in Fig. 1 following intravenous, hepatoportal, and intraduodenal administrations to dogs. Visual inspection of average plasma levodopa level curves following intravenous and hepatoportal administrations indicates that their overall disposition profiles appear similar. However, the average plasma levodopa level curves following duodenal administration were lower than observed following intravenous or hepatoportal administra-

[2] Levodopa in capsule form was prepared in the same prescription as Dopaston capsules, Sankyo Co., Tokyo, Japan.

[3] This benzethonium chloride solution was prepared from a 10-fold dilution of Hyamine, Sankyo Co., Tokyo, Japan.

**Table I—Selective Medium and Cultivation Conditions**

| Bacteria | Medium | Cultivation Conditions |
|---|---|---|
| *Enterobacteriaceae* | MacConkey agar | 37°/24 hr |
| *Streptococcus* | Endo agar | 37°/48 hr |
| *Staphylococcus* | Mannitol salt agar | 37°/48 hr |
| *Lactobacillus* | LBS agar | 37°/72 hr |

tion. On the other hand, the average plasma total dopamine levels following duodenal administration were higher than following other routes.

The average *AUC* of levodopa and total dopamine and the average ratio of the *AUC* of total dopamine to the *AUC* of levodopa are summarized in Table II. The *AUC* plots of levodopa following intravenous and hepatoportal administrations were approximately identical, but the *AUC* of levodopa following duodenal administration was significantly different from that after the other forms of administration ($p < 0.05$, $t$-test); for the *AUC* of total dopamine, the situation was inverse. The higher ratio of the *AUC* of total dopamine to the *AUC* of levodopa following duodenal administration lends evidence for the postulation that this organ is involved in levodopa metabolism. In contrast, the hepatoportal ratio did not differ significantly from that observed after intravenous administration. In addition, the residual amounts of levodopa and the total of all its metabolites at 4 hr after administration in the duodenal site were <1%. Since only insignificant levels of levodopa and its metabolites were observed, levodopa was absorbed almost completely from the duodenum.

**Influence of GI Microorganisms on Oral Levodopa Absorption**—The aerobic bacterial counts in each part of the GI tract, including the stomach, duodenum, and jejunum, in dogs treated with a single dose of paromomycin and kanamycin in contrast to control dogs are compared in Table III. The treatment led to a decrease in the number of aerobic organisms in the gut tested.

The average plasma levodopa levels following oral administration to antibiotic-treated dogs and to control dogs in crossover fashion are shown in Fig. 2. Visual inspection of average plasma levodopa level curves following oral administration to those dogs indicates that their overall disposition profiles were essentially identical. Table IV summarizes the average urinary excretion of levodopa and its metabolites after oral administration of levodopa to those dogs.

These results show that there was no difference between the dogs with and without antibiotics. Unfortunately, the results are ambiguous since the observed reduction in intestinal bacterial flora may not have been sufficient to affect levodopa metabolism, and only the reduction in aerobic organisms in the stomach, duodenum, and jejunum was observed[4]. However, the flora in these areas are thought to be predominantly aerobic.

**Distribution of Levodopa Decarboxylase Enzyme Activity in Intestinal Tract of Dogs**—Figure 3 shows the distribution of levodopa decarboxylase activity responsible for levodopa metabolism in the different parts of the intestinal tract of dogs. The jejunum showed the highest decarboxylase activity, as measured by the release of [$^{14}$C]carbon dioxide from labeled levodopa, followed by the ileum and then the duodenum.

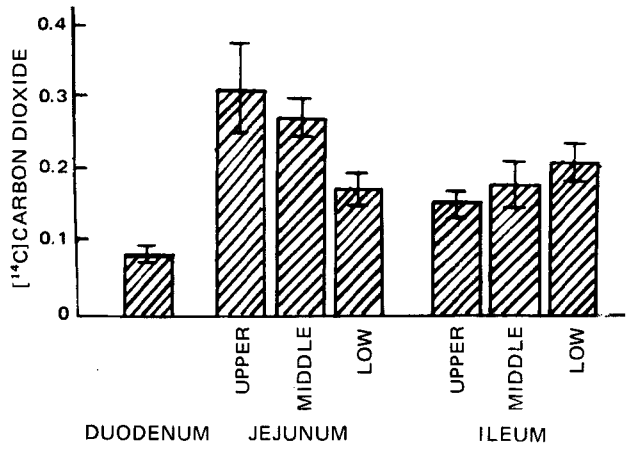


**Figure 3**—*Average distribution of levodopa decarboxylase activity in the different parts of the intestinal tract of dogs.*

[4] The duodenum will be shown to be the major absorption site in the next paper of this series.

**Table II—Average *AUC* of Levodopa and Total Dopamine and Ratio of *AUC* of Total Dopamine to Levodopa following Intravenous, Hepatoportal, and Duodenum Administrations to Dogs [a]**

| Route | *AUC* of Levodopa, (mg hr)/liter | *AUC* of Total Dopamine, (mg hr)/liter | Ratio of *AUC* of Total Dopamine to Levodopa |
|---|---|---|---|
| Intravenous | 1.70 ± 0.09[b] | 0.56 ± 0.14 | 0.34 ± 0.02 |
| Hepatoportal | 1.85 ± 0.10 | 0.57 ± 0.03 | 0.31 ± 0.01 |
| Duodenum | 0.65 ± 0.06 | 0.78 ± 0.07 | 1.20 ± 0.10 |

[a] The *AUC* from 0 to 4 hr was calculated using the trapezoidal rule. [b] Average ± *SE*.

## DISCUSSION

It was previously reported (1, 2) that the dose-dependent bioavailability of levodopa after oral administration to dogs and parkinsonian patients was probably due to metabolism during levodopa absorption. The plasma level profiles of levodopa and total dopamine were compared subsequent to intravenous, hepatoportal, and duodenal administrations to dogs. Analysis of the residual levels of levodopa and its metabolites in the duodenal loop indicated virtually complete levodopa absorption. However, plasma levodopa levels following duodenal administration were lower and plasma total dopamine levels were higher than those found after administration by other routes, leading to the highest ratio of the *AUC* of total dopamine to levodopa following duodenal administration. At the same time, the plasma level profiles of levodopa and total dopamine, the *AUC* of levodopa and total dopamine, and the ratio of the *AUC* of total dopamine to levodopa following the hepatoportal vein administration and intravenous administration were virtually identical.

These observations indicate that the first-pass metabolism of levodopa probably involves intestinal wall metabolism and, to a small extent, liver metabolism. This result is consistent with the conclusion reported previously (4, 5). Utilizing the isolated perfused rat liver technique, Mearrick *et al.* (4) reported that the major site of levodopa metabolism was the small intestine. Cotler *et al.* (5) administered [$^{14}$C]levodopa to dogs *via* hepatoportal, intravenous, and oral administrations on three separate occasions in crossover fashion. Comparisons of plasma levodopa level profiles *via* these administration routes led to the result that the physiologically impaired bioavailability of orally administered levodopa occurs virtually exclusively in the GI tract.

These results suggest the importance of levodopa metabolism in the intestine or the mucosal wall.

In addition, a similar degree of absorption and metabolism of levodopa was observed between control dogs and dogs whose numbers of intestinal bacteria decreased by treatment with antibiotics. Unfortunately, the results are not conclusive. Bakke (6) reported that levodopa was me-

**Table III—Comparison of Microflora between Dogs with and without Antibiotics**

| Group | Dog | Body Weight, kg | Segment of GI Tract | log (Number of Bacteria/Gram of Contents in GI Tract) |
|---|---|---|---|---|
| Control | 515 | 6.0 | Stomach | 7.0 |
| | | | Duodenum | 7.2 |
| | | | Jejunum | 6.8 |
| | 518 | 9.3 | Stomach | 6.6 |
| | | | Duodenum | 7.6 |
| | | | Jejunum | 7.3 |
| Treated | 114 | 8.6 | Stomach | 3.9 |
| | | | Duodenum | 3.2 |
| | | | Jejunum | 3.6 |
| | 51 | 11.8 | Stomach | 4.0 |
| | | | Duodenum | 3.7 |
| | | | Jejunum | 3.7 |

Table IV—Average Urinary Excretion of Levodopa and Its Metabolite after Oral Administration of Levodopa to Sterilized Dogs and Control Dogs

| Dogs | Total Levodopa[a] | Total Dopamine[b] | Total 3,4-Dihydroxyphenylacetic Acid[c] | Total Homovanillic Acid[d] | Total[e] |
|---|---|---|---|---|---|
| Control | 0.47 ± 0.07[f] | 8.9 ± 1.2 | 9.3 ± 1.4 | 30.4 ± 2.3 | 49.1 ± 2.4 |
| Sterilized | 0.47 ± 0.07 | 9.5 ± 1.6 | 10.1 ± 1.3 | 30.7 ± 2.5 | 50.7 ± 2.7 |

[a] Total levodopa = unconjugated levodopa + conjugated levodopa. [b] Total dopamine = unconjugated dopamine + conjugated dopamine. [c] Total 3,4-dihydroxyphenylacetic acid = unconjugated 3,4-dihydroxyphenylacetic acid + conjugated 3,4-dihydroxyphenylacetic acid. [d] Total homovanillic acid = unconjugated homovanillic acid + conjugated homovanillic acid. [e] Sum of total levodopa, total dopamine, total 3,4-dihydroxyphenylacetic acid, and total homovanillic acid. [f] Percent of dose excreted in 0–48-hr urine (average ± *SE*).

tabolized by intestinal microorganisms *in vitro* to *m*-hydroxyphenylacetic acid, 4-methylcatechol, and 4-methylguaiacol. Furthermore, levodopa was reported to be metabolized by intestinal microorganisms to *m*-hydroxyphenylacetic acid *in vivo* in conventional rats but not in germ-free rats (7–9). However, the small amount of metabolites formed by intestinal microorganisms reported by Bakke (6) and the fast absorption of levodopa from dogs observed in an *in situ* experiment[5] support the hypothesis that bacterial metabolism of levodopa may be insignificant.

The levodopa decarboxylase enzyme was widely distributed in the dog intestinal tract, with the greatest activity in the jejunum and the least activity in the duodenum. Taubin and Landsberg (10) suggested that catechol *O*-methyltransferase also played an important role in levodopa metabolism in the rat intestine. Administration of the levodopa inhibitor or benzerazide [*N*-*dl*-seryl-*N*-(1,2,3-trihydroxybenzyl)hydrazine], which cannot inhibit catechol *O*-methyltransferase, increased plasma levodopa levels (11–14). This finding implies that catechol *O*-methyltransferase plays a far less important role in intestinal metabolism of levodopa than levodopa decarboxylase.

The data presented here indicate that the reduced bioavailability of orally administered levodopa is due to metabolism of levodopa by levodopa decarboxylase in the intestine, with the greatest activity in the jejunum and the least activity in the duodenum.

## REFERENCES


(1) K. Sasahara, T. Nitanai, T. Habara, T. Morioka, and E. Nakajima, *J. Pharm. Sci.*, **69**, 261 (1980).

(2) *Ibid.*, **69**, 1374 (1980).

(3) K. Sasahara, T. Nitanai, T. Habara, A. Ninomiya, T. Morioka, and E. Nakajima, *Ann. Rep. Sankyo Res. Lab.*, **30**, 65 (1978).

(4) P. T. Mearrick, G. G. Graham, and D. N. Wade, *J. Pharmacokinet. Biopharm.*, **3**, 13 (1975).

(5) S. Cotler, A. Holazo, H. G. Boxenbaum, and S. A. Kaplan, *J. Pharm. Sci.*, **65**, 824 (1976).

(6) O. M. Bakke, *Acta Pharmacol. Toxicol.*, **29**, 106 (1971).

(7) O. Borud, T. Midtvelt, and L. R. Gjessing, *ibid.*, **30**, 185 (1971).

(8) B. R. Goldin, M. A. Peppercorn, and P. Goldman, *J. Pharmacol. Exp. Ther.*, **186**, 160 (1971).

(9) P. Goldman, M. A. Peppercorn, and B. P. Goldin, *Am. J. Clin. Nutr.*, **27**, 1368 (1974).

(10) H. L. Taubin and L. Landsberg, *Clin. Res.*, **20**, 872 (1972).

(11) A. Pletscher and G. Bartholini, *Clin. Res. Ther.*, **12**, 344 (1971).

(12) W. Birkimayer and E. Neumayer, *Z. Neurol.*, **202**, 257 (1972).

(13) A. Barbeau, L. Gillo-Joffray, and H. Mars, *Clin. Res. Ther.*, **12**, 353 (1972).

(14) E. M. Miller and L. Wiener, *Neurology*, **5**, 482 (1972).


[5] Part V of this series, to be published.

## ACKNOWLEDGMENTS


Presented in part at the Pharmaceutical Section, Pharmaceutical Society of Japan, Tokyo meeting, April 1977.

The authors thank Dr. T. Higuchi for valuable discussions, Dr. H. Negoro, Dr. S. Akagi, and Dr. T. Miki for the promotion of the research project, Dr. S. Riegelman for constructive comments on the manuscript, and Mrs. S. Tsutsumi for typing the manuscript.


# Computational Problems of Compartment Models with Michaelis–Menten-Type Elimination


**CARL M. METZLER *x and D. D. M. TONG ‡**



Received April 8, 1980, from **PR&D Biostatistics, The Upjohn Company, Kalamazoo, MI 49001*, and ‡*Western Michigan University, Kalamazoo, MI 49008.* Accepted for publication December 2, 1980.



**Abstract** □ The Michaelis–Menten equation has been applied successfully in the study of enzyme kinetics. It usually is used to estimate $v_{max}$ and $k_m$ from observations of the initial rate of reaction, $v$, at various substrate concentrations, $C_s$. A variation of this expression recently was used in pharmacokinetics, where it was assumed that the elimination rate of drug from some compartment is $VC(t)/[K + C(t)]$, where $C(t)$ is the drug concentration. The meaning of $V$ and $K$ in this context is not clear. Attempts were made to estimate $V$, $K$, and other model parameters by fitting the model to observed drug concentrations at sampling times after dosing. This paper discusses the ill-conditioning of the estimation of parameters of a differential equation that includes the so-called Michaelis–Menten output. The solution of the equation is bound by the solutions to two first-order differential equations. Parameter values in an infinite region of the parameter space are shown to have solutions also lying within these two bounds. Simulations show that a minor change in the data (observations) or in the initial estimate of the parameters may cause a large change in the final estimates. In many cases, estimation and comparison of parameter values are meaningless.



**Keyphrases** □ Models, mathematical—compartment models with Michaelis–Menten-type elimination, computational problems, parameter estimation □ Michaelis–Menten equation—computational problems of compartment models, parameter estimation □ Compartment models—computational problems of models with Michaelis–Menten-type elimination, parameter estimation □ Pharmacokinetics—analysis, computational problems of compartment models with Michaelis–Menten-type elimination, parameter estimation


Linear compartment models have been used successfully in pharmacokinetics for the past 40 years. Like all mathematical models, they are an abstraction from the real biological system to a mathematical system and thus are



© 1981, American Pharmaceutical Association

Table IV—Average Urinary Excretion of Levodopa and Its Metabolite after Oral Administration of Levodopa to Sterilized Dogs and Control Dogs

| Dogs | Total Levodopa[a] | Total Dopamine[b] | Total 3,4-Dihydroxyphenylacetic Acid[c] | Total Homovanillic Acid[d] | Total[e] |
|---|---|---|---|---|---|
| Control | 0.47 ± 0.07[f] | 8.9 ± 1.2 | 9.3 ± 1.4 | 30.4 ± 2.3 | 49.1 ± 2.4 |
| Sterilized | 0.47 ± 0.07 | 9.5 ± 1.6 | 10.1 ± 1.3 | 30.7 ± 2.5 | 50.7 ± 2.7 |

[a] Total levodopa = unconjugated levodopa + conjugated levodopa. [b] Total dopamine = unconjugated dopamine + conjugated dopamine. [c] Total 3,4-dihydroxyphenylacetic acid = unconjugated 3,4-dihydroxyphenylacetic acid + conjugated 3,4-dihydroxyphenylacetic acid. [d] Total homovanillic acid = unconjugated homovanillic acid + conjugated homovanillic acid. [e] Sum of total levodopa, total dopamine, total 3,4-dihydroxyphenylacetic acid, and total homovanillic acid. [f] Percent of dose excreted in 0–48-hr urine (average ± *SE*).

tabolized by intestinal microorganisms *in vitro* to *m*-hydroxyphenylacetic acid, 4-methylcatechol, and 4-methylguaiacol. Furthermore, levodopa was reported to be metabolized by intestinal microorganisms to *m*-hydroxyphenylacetic acid *in vivo* in conventional rats but not in germ-free rats (7–9). However, the small amount of metabolites formed by intestinal microorganisms reported by Bakke (6) and the fast absorption of levodopa from dogs observed in an *in situ* experiment[5] support the hypothesis that bacterial metabolism of levodopa may be insignificant.

The levodopa decarboxylase enzyme was widely distributed in the dog intestinal tract, with the greatest activity in the jejunum and the least activity in the duodenum. Taubin and Landsberg (10) suggested that catechol *O*-methyltransferase also played an important role in levodopa metabolism in the rat intestine. Administration of the levodopa inhibitor or benzerazide [*N*-*dl*-seryl-*N*-(1,2,3-trihydroxybenzyl)hydrazine], which cannot inhibit catechol *O*-methyltransferase, increased plasma levodopa levels (11–14). This finding implies that catechol *O*-methyltransferase plays a far less important role in intestinal metabolism of levodopa than levodopa decarboxylase.

The data presented here indicate that the reduced bioavailability of orally administered levodopa is due to metabolism of levodopa by levodopa decarboxylase in the intestine, with the greatest activity in the jejunum and the least activity in the duodenum.

## REFERENCES


(1) K. Sasahara, T. Nitanai, T. Habara, T. Morioka, and E. Nakajima, *J. Pharm. Sci.*, **69**, 261 (1980).

(2) *Ibid.*, **69**, 1374 (1980).

(3) K. Sasahara, T. Nitanai, T. Habara, A. Ninomiya, T. Morioka, and E. Nakajima, *Ann. Rep. Sankyo Res. Lab.*, **30**, 65 (1978).

(4) P. T. Mearrick, G. G. Graham, and D. N. Wade, *J. Pharmacokinet. Biopharm.*, **3**, 13 (1975).

(5) S. Cotler, A. Holazo, H. G. Boxenbaum, and S. A. Kaplan, *J. Pharm. Sci.*, **65**, 824 (1976).

(6) O. M. Bakke, *Acta Pharmacol. Toxicol.*, **29**, 106 (1971).

(7) O. Borud, T. Midtvelt, and L. R. Gjessing, *ibid.*, **30**, 185 (1971).

(8) B. R. Goldin, M. A. Peppercorn, and P. Goldman, *J. Pharmacol. Exp. Ther.*, **186**, 160 (1971).

(9) P. Goldman, M. A. Peppercorn, and B. P. Goldin, *Am. J. Clin. Nutr.*, **27**, 1368 (1974).

(10) H. L. Taubin and L. Landsberg, *Clin. Res.*, **20**, 872 (1972).

(11) A. Pletscher and G. Bartholini, *Clin. Res. Ther.*, **12**, 344 (1971).

(12) W. Birkimayer and E. Neumayer, *Z. Neurol.*, **202**, 257 (1972).

(13) A. Barbeau, L. Gillo-Joffray, and H. Mars, *Clin. Res. Ther.*, **12**, 353 (1972).

(14) E. M. Miller and L. Wiener, *Neurology*, **5**, 482 (1972).


[5] Part V of this series, to be published.

## ACKNOWLEDGMENTS


Presented in part at the Pharmaceutical Section, Pharmaceutical Society of Japan, Tokyo meeting, April 1977.

The authors thank Dr. T. Higuchi for valuable discussions, Dr. H. Negoro, Dr. S. Akagi, and Dr. T. Miki for the promotion of the research project, Dr. S. Riegelman for constructive comments on the manuscript, and Mrs. S. Tsutsumi for typing the manuscript.


# Computational Problems of Compartment Models with Michaelis–Menten-Type Elimination


**CARL M. METZLER *x and D. D. M. TONG ‡**



Received April 8, 1980, from **PR&D Biostatistics, The Upjohn Company, Kalamazoo, MI 49001*, and ‡*Western Michigan University, Kalamazoo, MI 49008.* Accepted for publication December 2, 1980.



**Abstract** □ The Michaelis–Menten equation has been applied successfully in the study of enzyme kinetics. It usually is used to estimate $v_{max}$ and $k_m$ from observations of the initial rate of reaction, $v$, at various substrate concentrations, $C_s$. A variation of this expression recently was used in pharmacokinetics, where it was assumed that the elimination rate of drug from some compartment is $VC(t)/[K + C(t)]$, where $C(t)$ is the drug concentration. The meaning of $V$ and $K$ in this context is not clear. Attempts were made to estimate $V$, $K$, and other model parameters by fitting the model to observed drug concentrations at sampling times after dosing. This paper discusses the ill-conditioning of the estimation of parameters of a differential equation that includes the so-called Michaelis–Menten output. The solution of the equation is bound by the solutions to two first-order differential equations. Parameter values in an infinite region of the parameter space are shown to have solutions also lying within these two bounds. Simulations show that a minor change in the data (observations) or in the initial estimate of the parameters may cause a large change in the final estimates. In many cases, estimation and comparison of parameter values are meaningless.



**Keyphrases** □ Models, mathematical—compartment models with Michaelis–Menten-type elimination, computational problems, parameter estimation □ Michaelis–Menten equation—computational problems of compartment models, parameter estimation □ Compartment models—computational problems of models with Michaelis–Menten-type elimination, parameter estimation □ Pharmacokinetics—analysis, computational problems of compartment models with Michaelis–Menten-type elimination, parameter estimation


Linear compartment models have been used successfully in pharmacokinetics for the past 40 years. Like all mathematical models, they are an abstraction from the real biological system to a mathematical system and thus are



© 1981, American Pharmaceutical Association

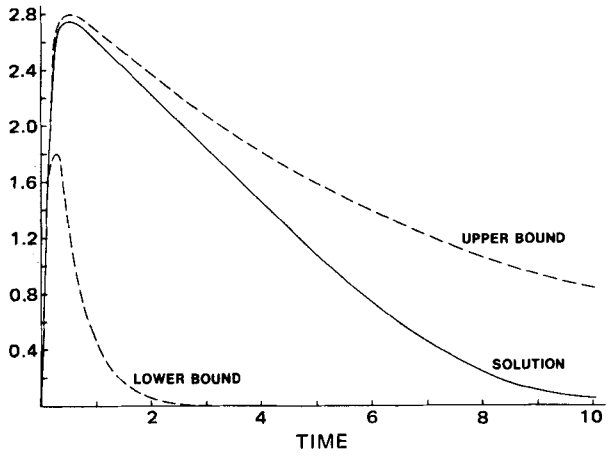


**Figure 1**—*Solution and bounds for Michaelis–Menten elimination model with* D = 3, $K_A$ = 8, V = 0.418, *and* K = 0.182.

approximations. Nevertheless, their successful use indicates that they are a good approximation with many drugs. For other drugs, they are not a good approximation, and attempts have been made to find nonlinear compartment models that are better.

## THEORETICAL

One class of nonlinear models assumes that elimination of drug from the system, rather than being a first-order process, is a Michaelis–Menten process. The well-known Michaelis–Menten equation has been used widely and successfully in enzyme kinetic studies despite difficulties in the theoretical derivation (1, 2). The Michaelis–Menten equation:

$$v = v_{max}C_s/(k_m + C_s) \qquad \text{(Eq. 1)}$$

is used to estimate $v_{max}$ and $k_m$ from observations of the initial reaction rate, $v$, at various substrate concentrations, $C_s$. It was adapted to pharmacokinetic models by assuming that the elimination rate from a compartment has a form similar to the right side of Eq. 1. Thus, if $C(t)$ is the drug concentration in a compartment, then the rate of change of $C(t)$ is:

$$\frac{dC(t)}{dt} = f(t, \theta) - VC(t)/[K + C(t)] \qquad \text{(Eq. 2)}$$

where $f(t, \theta)$ is a function determined by the input into the compartment. In the usual pharmacokinetic application of Eq. 2, attempts are made to estimate $V$ and $K$ along with the other model parameters, $\theta$, by fitting the model to observed drug concentrations at $n$ sampling times after dosing. Although Michaelis–Menten-type elimination models had been used previously, a detailed description and analysis of the simplest model incorporating Michaelis–Menten-type elimination—the one-compartment model with bolus intravenous input—were published in 1973 (3). For that model, $f(t, \theta)$ of Eq. 2 is zero; the model is expressed as:

$$\frac{dC(t)}{dt} = -VC(t)/[K + C(t)] \qquad \text{(Eq. 3)}$$

As Wagner (3) pointed out, for this model there is no solution that expresses $C(t)$ as an explicit function of $t$; thus, the solution is an implicit function. For more complex models, *i.e.*, a one-compartment model with first-order input, for which $f(t, \theta)$ in Eq. 2 is an exponential function, a solution in closed form does not exist.

It is possible, however, to fit these models to observed data by numerically integrating Eq. 2 to obtain points $[t, C(t)]$ predicted by the model. Many recent pharmacokinetic studies obtained parameter estimates by combining a nonlinear regression algorithm with numerical integration. Numerical integration requires more computation than fitting data to the solutions of the differential equations and can be expensive in terms of computer time. When combined with nonlinear regression algorithms that require many evaluations of the solution, the expense of fitting models in this way can be prohibitive. Furthermore, these methods may be unsatisfactory in terms of convergence and final fit.

These problems motivated a search for an approximate solution to Eq. 2 that might make estimation of the parameters with this model easier. During this search, mathematical properties of compartment models with Michaelis–Menten-type elimination were derived. The implications of these properties for computation and parameter estimation will be discussed. Finally, the results of computer simulation reveal the statistical properties of the parameter estimates obtained by fitting the two simplest Michaelis–Menten-type models to data.

## RESULTS

**Mathematical Development**—Tong and Metzler (4) derived the mathematical properties of solutions to Eq. 2. The mathematical details are given elsewhere (4), and only the two most important results for parameter estimation will be discussed here. The conditions on the model of Eq. 2 are that $f(t, \theta)$ be nonnegative and bounded, with $C(0) = 0$; *i.e.*, there must exist two positive constants, $C_0$ and $s$, such that:

$$0 \leq f(t, \theta) \leq C_0 \exp(-st) \qquad \text{for } t \geq 0 \qquad \text{(Eq. 4)}$$

Given these mild restrictions, the function $F(t, A)$ is a lower bound for $C(t)$ with $A = V/K$ and an upper bound for $C(t)$ with $A = V/(K + B)$, where $B$ is the maximum of $C(t)$, and was defined as (4):

$$F(t, A) = \exp(-At) \int_0^t f(\tau) \exp(A\tau)\, d\tau$$

$$= \begin{cases} \dfrac{C_0}{A - s}[\exp(-st) - \exp(-At)] & A \neq s \\ C_0 t \exp(-At) & A = s \end{cases} \qquad \text{(Eq. 5)}$$

With the assumed restrictions, Eq. 2 includes many compartment models with Michaelis–Menten-type elimination from one compartment. Equation 5 shows that the time–concentration curves of these models are bounded by functions of the same form as the model equations for a one-compartment model with first-order input and first-order output (5). This is in agreement with the statement by Wagner (3) and others (5) that, for the simplest model, the solution to Eq. 2 approaches the linear solution as the concentration increases. The distance between the bounds given by Eq. 5 depends on $V$, $K$, and the maximum of $C(t)$. As an example, the one-compartment model with first-order input (absorption rate = $K_A$) and Michaelis–Menten-type elimination will be considered. For this model, $f(t, \theta)$ is given by:

$$f(t, K_A, D) = K_a D \exp(-K_a t) \qquad \text{(Eq. 6)}$$

where $D$ is a dilution factor, roughly equal to the dose divided by a volume of distribution. By Eq. 5, the lower and upper bounds of the solution are:

$$\frac{K_A D}{K_A - V/K}[\exp(-Vt/K) - \exp(-K_A t)]$$

$$\frac{K_A D}{K_A - Q}[\exp(-Qt) - \exp(-K_A t)]$$

where $Q$ is the only solution of the equation:

$$Q + \frac{K_A D}{K}\left(\frac{Q}{K_A}\right)^{K_A/(K_A - Q)} - \frac{V}{K} = 0 \qquad \text{(Eq. 7)}$$

The bounds for the case in which $D = 3$, $K_A = 8$, $V = 0.418$, and $K = 0.182$ are shown in Fig. 1. For this case, the bounds are not restrictive. For the case in which $D = 3$, $K_A = 8$, $V = 1$, and $K = 2$, the bounds are shown in Fig. 2; for this case, the solution is bound rather closely by functions that are solutions to the linear compartment model. For larger $V$ and $K$ values, the bounds are so close together that the bounds and the solution appear as one line when plotted.

The other result of Tong and Metzler (4) is illustrated in Fig. 3. If $(K_0, V_0)$ is a point in the $(K, V)$ parameter space, then there is an infinite, open-ended wedge such that for any other $(K, V)$ in this wedge, the solution to Eq. 2 with parameters $V$ and $K$ lies within the bounds of the solution to Eq. 2 with parameters $V_0$ and $K_0$. Also, there is a line through $(K_0, V_0)$ within this wedge, such that any $(K, V)$ on this line determines a solution to Eq. 2 that is nearly identical to the solution of Eq. 2 with the parameters $(K_0, V_0)$. In other words, there is an infinite set of $(K, V)$ values that all generate the same time–concentration curve (to a finite accuracy). This observation will be illustrated further.

The parameters of Eq. 1 often are estimated by applying one of several linearizing transformations to the equation (1, 2). The parameters also may be estimated directly (and more correctly) from Eq. 1 by using a nonlinear estimation technique. In any case, the estimation of $v_{max}$ and $k_m$ will suffer from a high correlation of the estimates since the param-

**Table I—Specifications of Models and Simulations**

| Case | Model (Input) | Parameters | Parameter Values | Error Structure | $n$ | $N$ |
|---|---|---|---|---|---|---|
| 1 | Bolus intravenous | $C_0$, $V$, $K$ | 2.0, 0.22, 0.11 | Additive | 11 | 200 |
| 2 | Bolus intravenous | $C_0$, $V$, $K$ | 2.0, 0.22, 0.11 | Proportional | 11 | 200 |
| 3 | First order | $K_a$, $V$, $K$ | 1.5, 2.0, 5.0 | Additive | 11 | 200 |
| 4 | First order | $K_A$, $V$, $K$ | 1.5, 2.0, 5.0 | Proportional | 11 | 200 |
| 5 | First order | $K_A$, $V$, $K$, $D$ | 1.5, 2.0, 5.0, 10.0 | Additive | 11 | 200 |
| 6 | First order | $K_A$, $V$, $K$, $D$ | 1.5, 2.0, 5.0, 10.0 | Proportional | 11 | 200 |
| 7 | First order (three functions) | $K_A$, $V$, $K$, $D_1$, $D_2$, $D_3$ | 1.5, 2.0, 5.0, 10.0, 20.0, 40.0 | Proportional | 33 | 100 |
| 8 | First order | $K_A$, $V$, $K$, $D$ | 1.5, 2.0, 5.0, 10.0 | Proportional | 33 | 100 |
| 9 | First order | $K_A$, $V$, $K$, $D$ | 1.5, 2.0, 5.0, 40.0 | Proportional | 33 | 100 |

eters appear in a ratio in the equation and a change in the estimate of $v_{max}$ may be compensated for by a change in $k_m$. This problem is accentuated when, as in Eq. 2, the ratio of parameters does not appear in the function itself but rather in the derivative of the function being fit.

Previous work (4) showed that, for most ($K$, $V$) values, the solution to Eq. 2 is bounded by a function of two exponentials; in the previous example, these functions have one less parameter than the solution. (Approximately, $K_E$ is replaced by $V/K$.) Thus, if the data can be fit to Eq. 5, trying to fit the data to Eq. 2 by nonlinear regression methods will result in a situation analogous to singularity in the case of linear regression.

The result expressed in Fig. 3 implies that if ($V$, $K$) are estimated by least-squares techniques, the sum of squares surface will have a long valley with steep sides but little change along the floor. This situation results in difficult estimation problems (6). If an estimation algorithm can find a minimum along this narrow valley, the estimates of $V$ and $K$ will be highly correlated since they can move together along the valley floor without much change in the sum of squared residuals.

Thus, there are at least two sources of computational difficulties in fitting Eq. 2 to data:

1. Since there is no closed form solution, numerical integration must be used to obtain predicted values of $C(t)$ for a given model and $t$.
2. Parameter estimation is hampered by a high correlation between estimates of $V$ and $K$.

To understand the implications of the second difficulty, Monte Carlo simulations were performed.

**Computer Simulation**—The statistical properties of parameter estimates of nonlinear models are known only asymptotically, and it generally is not known how well these asymptotic properties approximate the results for small samples. Thus, Monte Carlo simulations were needed to determine the statistical characteristics of the estimates for a given model and experiment (7, 8). In view of the mathematical properties derived for Michaelis–Menten-type elimination models, a simulation study of the statistical properties for some simple models seemed necessary.

One shortcoming of simulation studies is that only a small part of the problem can be simulated. For this report, some representative cases (Table I) were chosen with the hope that they would yield insight into the general problem. All models were one-compartment ones with either bolus input or first-order absorption and Michaelis–Menten-type elimination. Two types of error structure were considered: (*a*) additive error in which each simulated "observation" was the model-predicted value plus a normal random number from the distribution $N(0, 0.09)$, and (*b*) proportional error in which each observation was the model-predicted value plus the product of the model value and an $N(0, 0.0025)$ random variable.

The proportional error structure is equivalent to a 5% error. This error structure violates one assumption of least-squares estimation, and either a transformation should be done or variable weights should be used. The usual least-squares estimation was carried out, however, in the belief that it reflects common practice where no error analysis is done and the error structure is not known.

The model values were obtained by numerically integrating either Eq. 3 or Eqs. 2 and 6 with the parameter values given in Table I. Each data set had $n$ observations. The values of $t$ were 0, 0.5, 1, 1.5, 2, 3, 4, 5, 6, 7, and 10 for the intravenous bolus model and 0.25, 0.5, 1, 1.5, 2, 3, 4, 6, 9, 12, and 18 for the first-order input models. Each model was simulated $N$ times; that is, $N$ sets of observations were generated; for each set of $n$ observations, the parameters were estimated by the computer program NONLIN (9), a nonlinear regression program. This program also estimated the standard deviation for each estimate and the correlation matrix of the estimates.

Table II summarizes the simulation results of Case 5 (Table I). Similar tables were prepared for all cases in Table I; for space reasons, only this table is presented in full. However, the conclusions and discussion are based on all of the tables[1].

In Table II, the first column identifies the parameters used to generate the $N = 200$ sets of observations, the standard deviations of the estimates, the largest eigenvalue ($E1$) of the estimated correlation matrix, and the correlations of the estimates. The second column gives either the values of the parameters or, in parentheses, the sample values of the 200 estimates. Thus, column 2 of the row labeled $s(V)$ contains the standard deviation of the 200 estimates of $V$; column 2 of the row labeled $C13$ contains the correlation of the 200 pairs of estimates of the first and third parameters ($K_A$ and $V$). The remaining columns of Table II give the sample statistics of the 200 estimates: minimum, maximum, 10th and 90th percentiles, mean, and median. Thus, in the row labeled $s(V)$, the first column gives the standard deviation of the 200 estimates of $V$; the following columns give the sample value followed by the statistics of the 200 estimates of $s(V)$ computed by the estimation algorithm from each

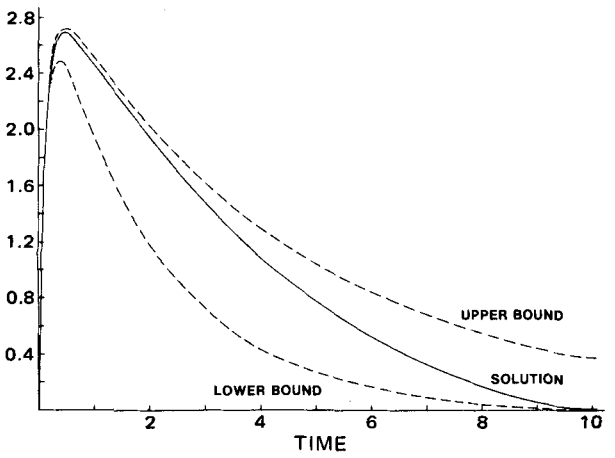


**Figure 2**—*Solution and bounds for Michaelis–Menten elimination model with* D = 3, $K_A$ = 8, V = 1, *and* K = 2.

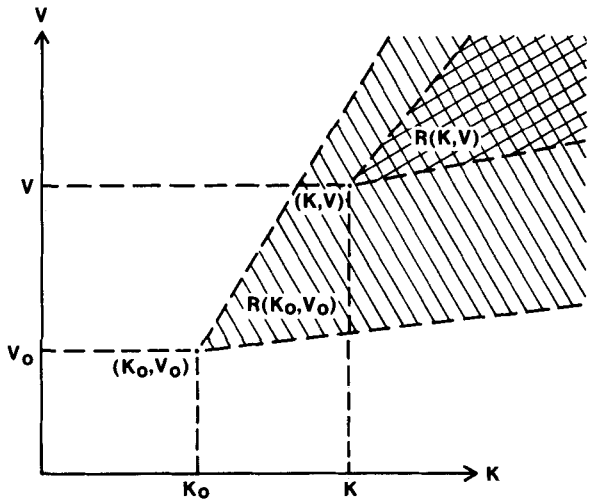


**Figure 3**—*Relation of solutions in the* V–K *parameter space.*

[1] Copies of the full set of tables may be obtained from the authors.

**Table II—Summary of Simulation of Case 5, Table I**

| Parameter | Parameter or Sample Value | Sample Statistics | | | | | |
|---|---|---|---|---|---|---|---|
| | | Minimum | $P_{10}$ | Mean | Median | $P_{90}$ | Maximum |
| $K_A$ | 1.50 | 0.88 | 1.24 | 1.48 | 1.48 | 1.74 | 2.33 |
| $V$ | 2.00 | 0.84 | 1.18 | 52.69 | 2.30 | 18.67 | 1561.0 |
| $K$ | 5.00 | 0.59 | 1.51 | 215.74 | 6.17 | 89.67 | 5875.0 |
| $D$ | 10.00 | 8.30 | 9.33 | 10.18 | 10.09 | 11.10 | 13.66 |
| $s(K_A)$ | (0.205) | 0.065 | 0.118 | 0.183 | 0.177 | 0.252 | 0.329 |
| $s(V)$ | (201.62) | 0.098 | 0.296 | 3596.0 | 1.254 | 113.87 | ∞ |
| $s(K)$ | (803.12) | 0.380 | 1.211 | 14,596.0 | 5.427 | 556.14 | ∞ |
| $s(D)$ | (0.738) | 0.170 | 0.334 | 0.691 | 0.598 | 1.144 | 3.565 |
| $E1$ | — | 3.088 | 3.328 | 3.506 | 3.518 | 3.677 | 3.860 |
| $C12$ | (−0.762) | −0.921 | −0.841 | −0.776 | −0.776 | −0.712 | −0.599 |
| $C13$ | (−0.715) | −0.920 | −0.821 | −0.718 | −0.727 | −0.610 | −0.480 |
| $C14$ | (−0.908) | −0.992 | −0.960 | −0.914 | −0.920 | −0.866 | −0.765 |
| $C23$ | (0.992) | 0.940 | 0.971 | 0.988 | 0.993 | 1.000 | 1.000 |
| $C24$ | (0.826) | 0.763 | 0.809 | 0.841 | 0.840 | 0.877 | 0.944 |
| $C34$ | (0.767) | 0.556 | 0.679 | 0.771 | 0.778 | 0.860 | 0.943 |

data set.

Table II displays a number of points important to understanding the deficiency of Michaelis–Menten-type models for pharmacokinetic analysis. The distributions of the $V$ and $K$ estimates are skewed strongly to the right with some very large estimates. This skewness inflates the means so that they are ~25–45 times larger than the parameter values used to generate the data. The medians also are shifted to the right, particularly the median of the $K$ estimates.

It may be thought that when extreme values are estimated for $V$ or $K$, the plots of the fitted curves indicate that something is wrong. However, Fig. 4 shows that very extreme values ($V$ = 1561 and $K$ = 5165) generate curves that are not much different from those generated when $V$ = 2 and $K$ = 5. Certainly, they could not be distinguished if each were represented by 11 observations containing 5% or more noise.

Table II also shows the high correlation between estimates of $V$ and $K$; for these 200 estimates, the correlation (Spearman) is 0.992. The estimate of the correlation computed by NONLIN for each data set indicates this finding; the mean estimated correlation is 0.988, the median is 0.993, and the minimum of the 200 is 0.940. The eigenvalues of the estimated correlation matrix sum to the number of parameters estimated (in this case, four) and the size of the largest eigenvalue ($E1$) indicate the dimensionality of the parameter estimation space. The average of the largest eigenvalue is ~3.5, indicating that some of the remaining three eigenvalues are close to zero. Thus, the dimensionality of the parameter space is less than four, a condition of singularity. Figure 5 is a plot of the estimates of $V$ and $K$. The top 10% was censored so that the other estimates can be shown in a reasonable scale. The estimates all lie close to a straight line.

Because the distributions of the $V$ and $K$ estimates are extremely skewed, the standard deviations are quite large [$s(V)$ = 201.6 and $s(K)$ = 803.1]. However, the 90th percentile indicates that, of the standard deviation estimates made with each data set, 90% of the $s(V)$ estimates are <114 and 90% of the $s(K)$ estimates are <557.

The main points made by Table II are:

1. Estimates of $V$ and $K$ are highly skewed to the right, with many of the estimates being many times larger than the true parameter values.
2. Estimates of $V$ and $K$ are very highly correlated so that the estimate of one almost determines the estimate of the other.
3. Estimates of $V$ and $K$ have very high variances, although the estimated variances as computed by NONLIN from individual data sets underestimate the variability.

Although not shown in Table II, the correlations of estimates of $V$ and $K$ with their respective standard deviation estimates also are high. For these 200 data sets, the correlation between estimates of $V$ and $s(V)$ is 0.977; the correlation between estimates of $K$ and $s(K)$ is 0.980.

Thus, the estimated variances of the $V$ and $K$ estimates, as computed by a nonlinear regression program, do not give a true picture of the uncertainty in the estimates.

As a related point, Table II shows that the linear parameters, $K_A$ and $D$, are estimated well in that the distributions of their estimates are symmetric with small bias and small standard deviations. The correlation of their estimates, while smaller than that of the $V$ and $K$ estimates, is still large (−0.762 for this set of 200 estimates).

The tables of the simulations of the other cases show similar results. Proportional error with a standard deviation of 5% gives much the same result as a constant error with a standard deviation of 0.05. For Cases 3 and 4 (Table I), it was assumed that $D$ = 10 was known; only three parameters were estimated. This procedure improved the estimation, but the distributions still were skewed to the right for Case 3, with means of 2.58 and 8.04 for $V$ and $K$, respectively, and 90th percentiles of 3.80 and 14.02. The correlation of the $V$ and $K$ estimates was 0.993.

Estimation was best for the simple model (Cases 1 and 2 of Table I). However, even for these cases, the distributions were skewed to the right with some very extreme values, and the correlations were high (0.934 for Case 1 and 0.974 for Case 2).

For all of these simulations, the initial estimates for the iterative nonlinear regression program were the true values of the parameters used to generate the data. A limited amount of simulation with other starting values indicated that, for a particular data set, the initial values affected the final estimates but, averaged over 200 simulations, initial estimates within 30% of the true values did not make much difference. Initial estimates that differ by more than 30% often converge to values far removed from the true parameters.

A Michaelis–Menten-type model may be well approximated by a linear model for a single drug exposure, but observations at more than one dose level will expose the nonlinearity of the system. Thus, an attempt to evaluate the effect of simultaneous fitting of observations at three dose levels was made (Case 7, Table I). For Case 7, it was assumed that $V$ and

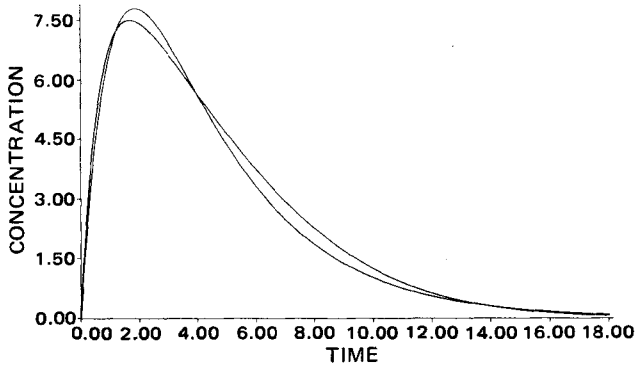


**Figure 4**—*Curves of the Michaelis–Menten elimination model for the* (V, K) *values (1561, 5165) and (2, 5).*

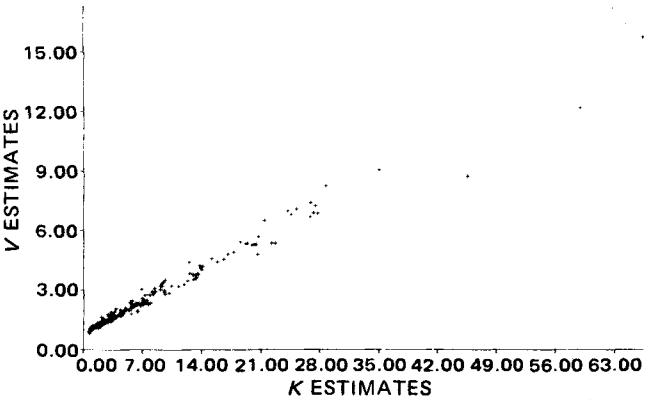


**Figure 5**—*Distribution of* K *and* V *estimates,* N = *180.*

**Table III—Summary of Parameter Estimates for Simultaneous Fitting, Case 7**

| Parameter | Parameter or Sample Value | Sample Statistics | | | | | |
|---|---|---|---|---|---|---|---|
| | | Minimum | $P_{10}$ | Mean | Median | $P_{90}$ | Maximum |
| $V$ | 2.00 | 1.68 | 1.81 | 2.00 | 2.00 | 2.18 | 2.39 |
| $K$ | 5.00 | 3.47 | 4.01 | 4.99 | 4.96 | 5.90 | 6.62 |
| $s(V)$ | (0.138) | 0.076 | 0.098 | 0.135 | 0.130 | 0.183 | 0.217 |
| $s(K)$ | (0.712) | 0.627 | 0.822 | 1.141 | 1.120 | 1.540 | 1.966 |

$K$ remained the same when $D$ = 10, 20, and 40. Data were simulated for three experiments ($D$ = 10, 20, and 40); these three observed curves, with a total of $n$ = 33 observations, were fit simultaneously to one set of $K_A$, $V$, and $K$ values and three $D$ values. This procedure gave much better parameter estimation. The distributions of the $V$ and $K$ estimates were symmetric about the true values with no extreme estimates. The results for $V$ and $K$ are shown in Table III. The correlation of the $V$ and $K$ estimates was reduced to 0.767.

When comparing Table III with Table II, it must be noted that the data sets of Table III had 33 observations while those of Table II had only 11. The improvement in estimation of $V$ and $K$ was not due only to the larger sample sizes. To confirm this fact, Cases 8 and 9 (Table I) also had 33 observations per data set but, in these cases, the observations consisted of three replications at each sampling time used in Cases 3–6. Although the variability was reduced markedly and there were no extreme estimates, the distributions were still skewed to the right and the correlations were still very high (0.991 for Case 8 and 0.983 for Case 9).

## DISCUSSION

The mathematical development and computer simulation indicate that it is not possible to estimate $V$ and $K$ of a Michaelis–Menten-type pharmacokinetic model with any precision from a single-dose experiment. Furthermore, the asymptotic theory standard deviations, as computed by a nonlinear regression program, are misleading in that they underestimate the uncertainty in the estimates. [Although the NONLIN program (9) was used in this study, this result would be true for any computer program that estimates the variance–covariance matrix of the estimates from the matrix of partial derivatives.] This observation may explain why in many studies the estimate of between-subject variability is so much larger than the estimate of within-subject variability of the estimates (10). It may be an artifact of estimation rather than a characteristic of the drug. These difficulties in estimating Michaelis–Menten parameters also make the comparison of algorithms for estimation less meaningful, as in Ref. 11.

In many situations, estimating $V$ and $K$ for the purpose of comparing values between studies (*i.e.*, in different disease states) is useless if the estimates are made from observations after only one dose of drug. However, the simulations indicate that if estimations can be made with observations obtained after two or more dose levels, then the estimations are much improved. To do this, it must be assumed that the biological system, like the computer system, can generate data with the same values of $K_A$, $V$, and $K$ at different doses and different times. It is not certain that this assumption is valid.

Although the Michaelis–Menten-type models are not useful for estimation of $V$ and $K$ with observations from only one dose, they may have other value. They may be useful to show that a system is better described by a nonlinear pharmacokinetic model than by a linear model, for describing data, and for prediction.

The size of these simulations ($N$ = 200 for most of them), while much larger than most computer simulations reported in the pharmaceutical sciences literature, is about minimum for validity. These simulations cover only a few points in the entire space of these models. Future research extending these simulations would be useful in evaluating these models. In particular, the errors assigned in these simulations were relatively small for pharmacokinetic data. Larger (and more realistic) errors could only make estimation more difficult. Development of other nonlinear models that avoid these computational problems also would be useful.

## REFERENCES


(1) C. Marmasse, "Enzyme Kinetics," Gordon and Breach, New York, N.Y., 1977.

(2) K. J. Laidler and P. S. Bunting, "The Chemical Kinetics of Enzyme Action," 2nd ed., Clarendon, Oxford, England, 1973.

(3) J. G. Wagner, *J. Pharmacokinet. Biopharm.*, **1**, 103 (1973).

(4) D. D. M. Tong and C. M. Metzler, *Math. Biosci.*, **48**, 293 (1980).

(5) M. Gibaldi and D. Perrier, "Pharmacokinetics," Dekker, New York, N.Y., 1975.

(6) G. E. P. Box and W. G. Hunter, *Technometrics*, **4**, 301 (1962).

(7) J. M. Chambers and J. E. Ertel, in "1975 Proceedings of the ASA Statistical Computing Section," American Statistical Association, Washington, D.C., 1976, p. 151.

(8) Y. Bard, "Nonlinear Parameter Estimation," Academic, New York, N.Y., 1974, chap. 7.

(9) C. M. Metzler, G. L. Elfring, and A. J. McEwen, *Biometrics*, **30**, 562 (1974).

(10) E. Martin, T. N. Tozer, L. B. Sheiner, and S. Riegelman, *J. Pharmacokinet. Biopharm.*, **5**, 579 (1977).

(11) K. C. Yeh and K. C. Kwan, *J. Pharm. Sci.*, **68**, 1120 (1979).


## ACKNOWLEDGMENTS


Presented in part at the Basic Pharmaceutics Section, APhA Academy of Pharmaceutical Sciences, Kansas City meeting, November 1979.

The authors thank Frank Schellenberg for programming the simulations and Professor L. Benet for suggesting the simulation of simultaneous fits to several dose levels.

# Sorption Properties of Cross-Linked Insoluble Polyvinylpyrrolidone

**K. H. FRÖMMING *x, W. DITTER ‡, and D. HORN ‡**

Received June 10, 1980, from the **Institut für Pharmazie, Freie Universität Berlin, Königin-Luise-Str. 2f4, 1000 Berlin 33, West Germany*, and the ‡*Hauptlaboratorium, BASF Aktiengesellschaft, 6700 Ludwigshafen/Rhein, West Germany.* Accepted for publication December 2, 1980.

**Abstract** □ The interaction of 32 drugs of diverse chemical structure with cross-linked insoluble polyvinylpyrrolidone (crospovidone) was studied. By using a polymer to drug ratio of 10:1, the sorbed amount for 20 compounds was found to be <5%. After a 10-fold decrease of the polymer concentration, the sorbed amount of eight other compounds fell to or below the 5% level. Only tannic acid and hexylresorcinol exhibited a significantly stronger sorption tendency. The interaction appeared to be controlled by phenolic groups in the active ingredient. The binding can be quantified by an interaction constant, $K_s$, whose definition is based on a bulk phase model of interaction *via* independent binding sites. The exceptionally strong binding of hexylresorcinol, however, apparently was caused by cooperative interaction of the hexyl groups in the bound state. Desorption studies revealed that the binding was fully reversible in all cases. Therefore, the presence of cross-linked polyvinylpyrrolidone as a disintegrant in pharmaceutical preparations is not expected to interfere with GI drug absorption.

**Keyphrases** □ Polyvinylpyrrolidone—interaction with 32 pharmaceuticals of diverse chemical structure, sorption and desorption studies □ Sorption—interactions of 32 pharmaceuticals of diverse chemical structure with cross-linked insoluble polyvinylpyrrolidone □ Binding—interactions of 32 pharmaceuticals of diverse chemical structure with cross-linked insoluble polyvinylpyrrolidone, sorption and desorption studies

*N*-Vinylpyrrolidone can be polymerized to yield polyvinylpyrrolidone, a readily soluble polymer, or can be transformed into a cross-linked insoluble polyvinylpyrrolidone (crospovidone, I) by proliferous polymerization (1–3).

Compound I exhibits an exceptionally high swelling pressure (4), which apparently is connected with the increased hydration capacity of the polymer (5, 6). For that reason, I is particularly useful as a disintegrating agent in pharmaceutical formulations.

## BACKGROUND

Because of its disintegrating effect, I may enhance the release rate of drug from tablet formulations. With griseofulvin tablets containing a large amount of polyethylene glycol, I enhanced drug release at a significantly higher rate than when I was not present (7).

The same advantageous effect was observed in similar formulations with other drugs (8). The release of penicillins and cephalosporins from capsules was promoted by I (9). The dissolution rate of kavaine was increased after sorption onto I as a carrier (10).

Because of the dipolar character and the porous structure of I, specific interactions with solutes cannot be predicted. Only in a single case has a relatively strong binding of tannic acid and related compounds been reported (2). Other compounds such as acetaminophen, benzocaine, metamizole, and salicylamide exhibited no stronger interaction with I than with corn starch, carboxymethyl starch, and microcrystalline cellulose (11).

The present study investigated the possible interactions of I with numerous drugs of diverse chemical structure. Some compounds chosen were known for their binding tendency with polyvinylpyrrolidone (12). The experimental results are explained on the basis of models of noncooperative and cooperative interaction.

## EXPERIMENTAL

**Materials**—The following were obtained from commercial sources: acetaminophen[1], allopurinol[2], benzocaine[3], benzoic acid[4], *p-tert*-butylphenol[5], caffeine[6], chloramphenicol[2], cinnarizine[6], diphenhydramine[6], ethaverine[6], hexylresorcinol[7], *p*-hydroxybenzoic acid[7], isoniazid[6], menadione[4], methaqualone[4], nitrofurantoin[7], papaverine hydrochloride[4], phenazone[4] (antipyrine), procaine hydrochloride[4], promethazine hydrochloride[6], propylparaben[2], pyridoxine hydrochloride[4], reserpine[7], resorcinol[4], riboflavin[4], salicylic acid[4], sodium salicylate[4], sulfadiazine[6], sulfamidopyrine[6], tannic acid[4], tetracaine hydrochloride[3], and theophylline[6].

All materials were the highest available grade and were used without further purification.

The specific surface area of cross-linked polyvinylpyrrolidone[8] (I) was determined by nitrogen adsorption, according to the Brunauer, Emmett, and Teller method[9] (13), after the samples were dried carefully.

**Sorption Experiments**—For the easily soluble substances, 1000 mg was dissolved in 1000 ml of 0.01 *N* HCl, water, or artificial intestinal fluid (USP XIX) unless otherwise noted. Where the solubility was insufficient, the suspension was filtered after vibrational stirring for 0.5 hr. The filtrate was diluted until 200 ml contained 100 mg of solute. For even less soluble samples, saturated solutions at 25° were used.

The sorption experiments were performed in a thermostatted bath at 37 ± 0.5°. Compound I was added in amounts of 1000 or 100 mg/200 ml of solution, and the suspension was maintained under steady vibrational stirring at 150 rpm for 0.5 hr. Then the suspensions were filtered or centrifuged at 37°. The amount of unbound drug was determined spectrophotometrically, with the absorbance values of the polymer-free solutions of the drugs (which had gone through the same cycle of pretreatment) as a reference.

Determination of the residual drug concentrations was performed using appropriate calibration curves measured at the following characteristic wavelengths: acetaminophen, 243 nm; allopurinol, 251 nm; benzocaine, 226 nm; benzoic acid, 230 nm; *p-tert*-butylphenol, 274.5 nm; caffeine, 273 nm; chloramphenicol, 278 nm; cinnarizine, 253 nm; diphenhydramine, 258 nm; ethaverine, 252 nm; hexylresorcinol, 279 nm; *p*-hydroxybenzoic acid, 255 nm; isoniazid, 266 nm; menadione, 261 nm; methaqualone, 233.5 nm; nitrofurantoin, 366 nm; papaverine, 251 nm; phenazone, 239 nm; procaine hydrochloride, 290 nm; promethazine hydrochloride, 250 nm; propylparaben, 255 nm; pyridoxine hydrochloride, 290.5 nm; reserpine, 267 nm; resorcinol, 273 nm; riboflavin, 267 nm; salicylic acid, 237 nm; sodium salicylate, 236.5 nm; sulfadiazine, 243 nm; sulfamidopyrine, 258 nm; tannic acid, 275 nm; tetracaine hydrochloride, 228 nm; and theophylline, 271.5 nm.

**Desorption Experiments**—Drug-loaded samples of I were prepared by centrifuging the respective suspensions following sorption. After the sediments were isolated, the desorption of bound drug was studied at 25° by vigorously shaking the 1000-mg samples three or more times with 50 or 100 ml of the respective solvent for 15 min. The degree of desorption was determined by spectrophotometric analysis of the combined supernates after centrifuging the suspensions.

## RESULTS

Under the described experimental conditions, several drugs essentially did not interact with I: allopurinol[10], chloramphenicol, cinnarizine[10], caffeine, diphenhydramine hydrochloride, ethaverine hydrochloride,

[1] Fluka, Neu-Ulm, West Germany.
[2] EGA Chemie, Steinheim, West Germany.
[3] Sigma Chemie, München, West Germany.
[4] Merck AG, Darmstadt, West Germany.
[5] BASF AG, Ludwigshafen, West Germany.
[6] Synochem, Hamburg, West Germany.
[7] Serva, Heidelberg, West Germany.
[8] Kollidon CL, BASF AG, Ludwigshafen, West Germany.
[9] Areameter, Ströhlein, Düsseldorf, West Germany.
[10] Investigated in saturated solution.



*0022-3549/81/0700-0738$01.00/0*
© *1981, American Pharmaceutical Association*

**Table I—Sorption Data of Compounds with a Moderate Binding Tendency to I [a]**

| Compound | Weighing-in Drug, g/200 ml | Sorbed Amount of Drug, % | | | | Binding Constant, $K_s$, $M^{-1}$ | | | |
|---|---|---|---|---|---|---|---|---|---|
| | | 0.01 *N* HCl | | Water | | 0.01 *N* HCl | | Water | |
| | | 1000 ml of I ($\varphi$ = 0.005) | 100 mg of I ($\varphi$ = 0.0005) | 1000 mg of I ($\varphi$ = 0.005) | 100 mg of I ($\varphi$ = 0.0005) | $\varphi$ = 0.005 | $\varphi$ = 0.0005 | $\varphi$ = 0.005 | $\varphi$ = 0.0005 |
| Acetaminophen (mol. wt. 151) | 0.1 | 8.1 | 1.4 | 7.3 | 0.3 | 2.0 | 3.2 | 1.6 | 0.7 |
| Benzocaine (mol. wt. 165) | 0.1 | 7.7 | 0.8 | 7.6 | 1.2 | 1.9 | 1.8 | 1.8 | 2.7 |
| Benzoic acid (mol. wt. 122) | 0.1 | 11.3 | 1.4 | 9.4 | 0.7 | 2.9 | 3.2 | 2.3 | 1.6 |
| Propylparaben (mol. wt. 180) | 0.035 | 23.4 | 3.1 | 21.8 | 5.3 | 6.8 | 7.2 | 6.2 | 12.6 |
| Resorcinol (mol. wt. 110) | 0.1 | 31.7 | 3.5 | 32.2 | 5.0 | 10.7 | 8.4 | 10.9 | 12.3 |
| Salicylic acid (mol. wt. 138) | 0.1 | 18.0 | 1.8 | 14.7 | 1.1 | 4.9 | 3.9 | 4.1 | 2.5 |
| Sodium salicylate (mol. wt 160) | 0.1 | 22.6 | 2.8 | 0.5 | 0.1 | 6.5 | 6.4 | 0.1 | 0.2 |
| Sulfadiazine (mol. wt. 250) | 0.02 | 7.2 | 0.9 | 4.9 | ~0 | 1.7 | 2.0 | 1.1 | ~0 |

[a] The molar concentrations of I are expressed in moles of monomer segments per unit volume.

**Table II—Sorption Data of Compounds Exhibiting Strong Binding to I**

| Compound | Weighing-in Drug, g/200 ml | Sorbed Amount of Drug, % | | | | Binding Constant, $K_s$, $M^{-1}$ | | | |
|---|---|---|---|---|---|---|---|---|---|
| | | 0.01 *N* HCl | | Water | | 0.01 *N* HCl | | Water | |
| | | 1000 mg of I ($\varphi$ = 0.005) | 100 mg of I ($\varphi$ = 0.0005) | 1000 mg of I ($\varphi$ = 0.005) | 100 mg of I ($\varphi$ = 0.0005) | $\varphi$ = 0.005 | $\varphi$ = 0.0005 | $\varphi$ = 0.005 | $\varphi$ = 0.0005 |
| *p-tert*-Butylphenol (mol. wt. 150) | 0.06 | 21.5 | 10.2 | 21.6 | 12.2 | 6 | 25 | 6 | 31 |
| Hexylresorcinol (mol. wt. 194) | 0.06 | 96.5 | 76.8 | 96.3 | 71.3 | (617)[a] | (777)[a] | (582)[a] | (616)[a] |
| *p*-Hydroxy-benzoic acid (mol. wt. 138) | 0.1 | 44.1 | 6.9 | 39.0 | 5.0 | 18 | 17 | 14 | 12 |
| Tannic acid (mol. wt. 1548) | 0.1 | 94.4 | 27.9 | 90.1 | 34.6 | (375)[a] | (86)[a] | (200)[a] | (118)[a] |

[a] The numbers in parentheses are formal values according to Eq. 8; for details, see text.

isoniazid, menadione[10], methaqualone[10], nitrofurantoin[10], papaverine hydrochloride[10], phenazone, procaine hydrochloride, promethazine hydrochloride, pyridoxine hydrochloride, reserpine[10], riboflavin[10], sulfamidopyrine, tetracaine hydrochloride, and theophylline. In all cases, the amount of material bound onto I dispersed in 0.01 *N* HCl or water was <5%.

Table I lists all materials that exhibited a degree of sorption higher than 5% at high I concentrations (*i.e.*, 1000 mg/per 100 mg of drug). Decreasing the I concentrations by a factor of 10, however, decreased the amount bound (5% level and lower) in all cases.

The compounds listed in Table II were bound by I significantly even at low polymer concentrations. The strong binding of tannic acid in aqueous suspensions of I was reported previously (2).

The results of the binding studies of selected systems with artificial intestinal fluid are shown in Table III.

Except for tannic acid, hexylresorcinol displayed the strongest binding irrespective of the suspension medium pH (Tables II and III).

As to the desorption studies, characteristic results of a few selected compounds are shown in Table IV.

To determine whether the thermodynamics of the sorption process is influenced by surface phenomena, sorption studies were performed with two types of I, which differed by a factor of five in specific surface area. Typical data are shown in Fig. 1, where $[A_0]/[A]$, the ratio of the weighing-in concentration and the unbound amount of the drug, is plotted *versus* the polymer to drug ratio.

The close similarity of the sorption behavior of both I samples indicates that sorption thermodynamics is dominated by bulk phase properties of the polymer and that any possible influence of the extent of the specific surface area of the material can be neglected. Hence, the sorption data can be treated according to the mass law of chemical equilibrium of bulk phases. When considering only the polymer compartment, it may be assumed that binding of the drug, $A$, occurs on independent free binding sites, $F$, of the polymer. Then the sorption constant $K_s$ is defined as:

$$K_s = \frac{[FA]}{[A]([F_0] - [FA])} \qquad \text{(Eq. 1)}$$

The mass balance equation then is written as $[F_0] = [F] + [FA]$, where $[F_0]$ denotes the total concentration of binding sites, $[F]$ is the concentration of free bindings sites, and $[FA]$ is the concentration of occupied binding sites and is identical with the bound amount of drug.

**Table III—Data of Sorption Studies in Artificial Intestinal Fluid (USP XIX)**

| Compound | Weighing-in Drug, g/200 ml | Sorbed Amount of Drug, % | |
|---|---|---|---|
| | | 1000 mg of I ($\varphi$ = 0.005) | 100 mg of I ($\varphi$ = 0.0005) |
| Acetaminophen (mol. wt. 151) | 0.1 | 7.9 | 0.1 |
| Benzocaine (mol. wt. 165) | 0.1 | 9.4 | 0.2 |
| Benzoic acid (mol. wt. 122) | 0.1 | 1.1 | 1.0 |
| *p-tert*-Butylphenol (mol. wt. 150) | At saturation | 21.3 | 8.9 |
| Hexylresorcinol (mol. wt. 194) | At saturation | 96.7 | 73.2 |
| *p*-Hydroxybenzoic acid (mol. wt. 138) | 0.1 | 1.2 | 0.4 |
| Promethazine hydrochloride (mol. wt. 321.5) | 0.1 | 4.5 | 2.6 |
| Propylparaben (mol. wt. 180) | At saturation | 26.8 | 3.7 |
| Resorcinol (mol. wt. 110) | 0.1 | 32.5 | 5.4 |
| Salicylic acid (mol. wt. 138) | 0.1 | 2.4 | 0.6 |
| Sulfadiazine (mol. wt. 250) | At saturation | 1.7 | 0.2 |
| Tannic acid (mol. wt. 1548) | 0.1 | 90.2 | 30.0 |

**Table IV—Desorption of Various Drugs from I in 0.1 *N* HCl at 25°: Comparison of Experimental Data with Theoretical Values**

| Compound | Sorption of Drug, mg | | | Remaining Sorbed Amount after $n$ Desorption Steps, mg | | | | | | | | | | | | | |
|---|---|---|---|---|---|---|---|---|---|---|---|---|---|---|---|---|---|
| | | | | | $n = 1, m_{s,1}$ | | $n = 2, m_{s,2}$ | | $n = 3, m_{s,3}$ | | $n = 4, m_{s,4}$ | | $n = 6, m_{s,6}$ | | $n = 10, m_{s,10}$ | |
| | $m_0$[a] | $10^2\varphi$ | $m_{s,0}$[b] | $10^2\varphi$ | Exp. | Theor. | Exp. | Theor. | Exp. | Theor. | Exp. | Theor. | Exp. | Theor. | Exp. | Theor. |
| Benzoic acid (0.25 g/liter) | 25 | 2.25 | 9.25 | 1.13 | 1.7 | 2.1 | ~0 | 0.5 | ~0 | 0.1 | — | — | — | — | — | — |
| Hexylresorcinol (0.25 g/liter) | 25 | 1.4 | 23.9 | 0.72 | 21.5 | 22.0 | 19.1 | 20.2 | 16.8 | 18.6 | 14.7 | 17.1 | 11.0 | 14.4 | 5.8 | 10.3 |
| Resorcinol (0.25 g/liter) | 25 | 1.3 | 19.1 | 0.65 | 11.9 | 11.9 | 7.3 | 7.5 | 4.3 | 4.7 | 2.4 | 2.9 | 0.4 | 1.1 | — | — |
| Salicylic acid (0.25 g/liter) | 25 | 2.0 | 13.1 | 1.0 | 3.7 | 4.7 | 0.1 | 1.7 | ~0 | 0.6 | — | — | — | — | — | — |
| Tannic acid (0.1 g/liter) | 10 | 0.1 | 9.7 | 0.05 | 9.6[c] | 9.2 | 9.5[c] | 8.7 | 9.5[c] | 8.2 | 9.4[c] | 7.8 | — | — | — | — |

[a] Amount of drug prior to sorption. [b] Initially sorbed amount of drug. [c] Experimental values too high; for further details, see text.

An alternative view of the system, based on the mass distribution of drug between the liquid and the (swollen) solid phase, is obtained by introducing the Nernst coefficient, $k$, of mass distribution of $A$:

$$k = \frac{[A]_s}{[A]} \qquad \text{(Eq. 2)}$$

where $[A]_s$ and $[A]$ denote the drug concentrations in the polymer and liquid phase, respectively.

With the assumption that $[A]$ is equilibrated with the portion of $[A]_s$ that remains unbound within the polymer phase, then:

$$k = \frac{[A] + [FA]}{[A]} \qquad \text{(Eq. 3)}$$

After introducing the phase ratio $\varphi = V_s/V_L$, in which $V_s$ and $V_L$ represent the volumes of the polymer[11] and liquid phase, respectively, the mass balance equation for the drug becomes:

$$[A_0] = [A] + \varphi[A] + \varphi[FA] \qquad \text{(Eq. 4)}$$

or, when rearranged, it becomes:

$$[FA] = \frac{1}{\varphi}([A_0] - [A]) - [A] \qquad \text{(Eq. 5)}$$

Substituting Eq. 5 into Eq. 3 gives:

$$\frac{[A_0]}{[A]} = 1 + k\varphi \qquad \text{(Eq. 6)}$$

As shown in Fig. 1, the experimental data are described by this equation, which supports the introduced model of binding. From the slope of the straight lines, the Nernst coefficient of interaction for both I samples is evaluated to be 84 and 79.

The coupling of $k$ with $K_s$ is performed by introducing Eqs. 5 and 6 into Eq. 1 to give:

$$K_s = \frac{k - 1}{[F_0] - [A](k - 1)} \qquad \text{(Eq. 7)}$$

or:

$$k = 1 + \frac{[F_0]K_s}{1 + [A]K_s} \qquad \text{(Eq. 8)}$$

This equation is closely related to an equation derived by Luck (14) to describe the Nernst partition equilibrium in certain textile dyeing processes.

From Eq. 8, it follows that for small values of the interaction constant $K_s$, the Nernst coefficient $k$ becomes independent of $[A]$ (Fig. 2). This condition holds for all compounds in Table I and those that were listed as not interacting with I. Therefore, the polymer to drug interaction may be characterized either by $k$ or $K_s$. However, to evaluate $K_s$ from experimental data according to Eqs. 6 and 7, a reasonable assumption has to be made concerning the value of $[F_0]$. If it is assumed that each monomeric subunit of the polymer may serve as a binding site, $[F_0]$ becomes equal to ~9 $M$. All $K_s$ values in Tables I–III were obtained using this assumption.

Because of the sensitive dependence of $K_s$ on experimental errors of the sorption data, the $K_s$ values in Table I obtained with $\varphi = 0.005$ and 0.0005 are in satisfactory agreement, with the exception of the propylparaben–water system; the reason for this discrepancy is unknown. In general, however, the results support the notion that sorption occurs according to a reversible equilibrium process in interacting systems.

For sodium salicylate, pronounced differences in $K_s$ were found in the

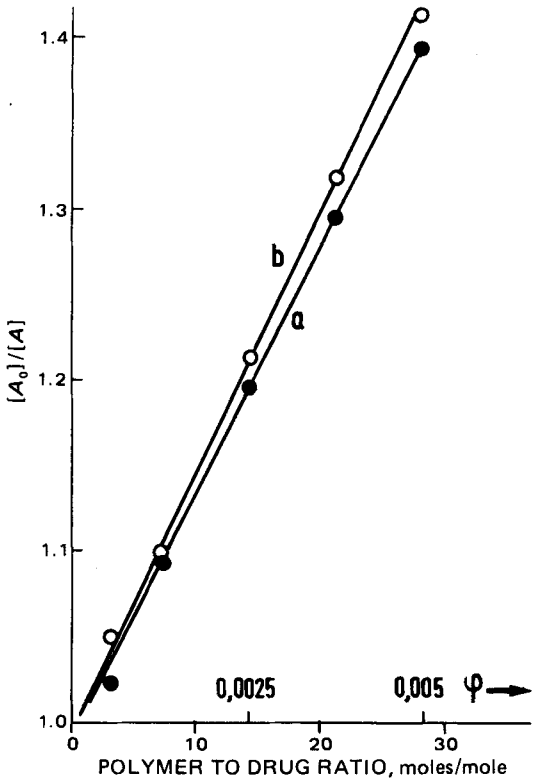


**Figure 1**—*Binding of propylparaben by I of different specific surface areas at 37°. The weighing-in concentration of the drug was 57 mg/200 ml. The specific surface areas of the I samples according to the Brunauer, Emmett, and Teller method were 5.42 (a) and 0.98 $m^2/g$ (b). The marking of the abscissa is defined by $\varphi = V_s/V_L$, where $V_s$ is the volume of the solid phase and $V_L$ is the volume of the liquid phase. Molar concentrations of the polymer refer to the molecular weight of the monomeric subunit.*

[11] For convenience, the volume of I in the dry state is considered.

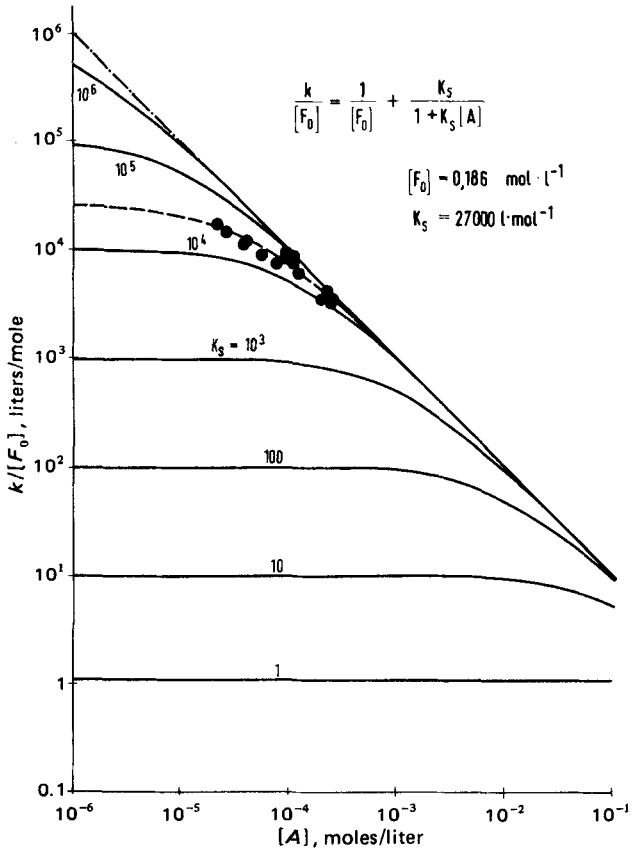


**Figure 2**—*Dependence of the Nernst coefficient on the equilibrium concentration of the interacting drug, [A], for various values of the binding constant, $K_s$. Key: —, theoretical curves according to Eq. 8; and ●– –, experimental values of tannic acid–I.*

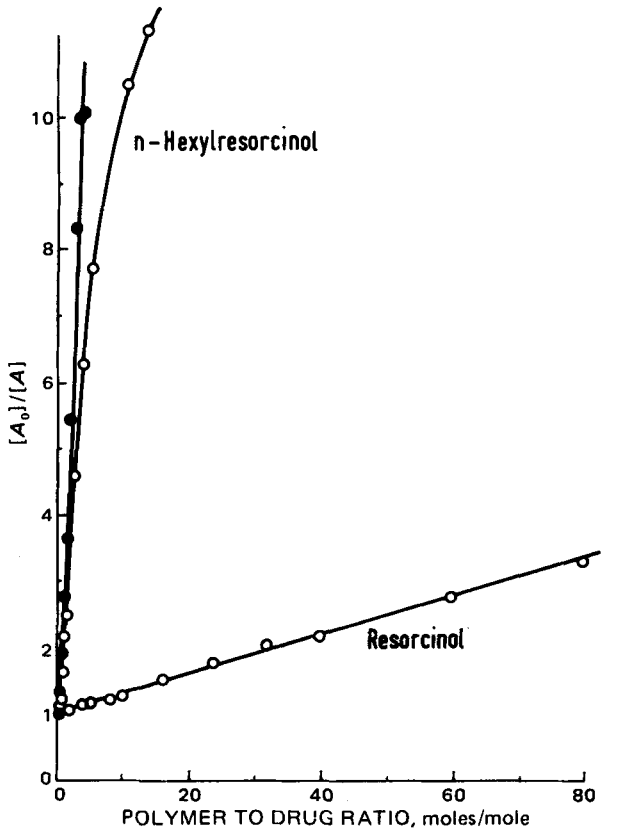


**Figure 3**—*Binding of resorcinol and of hexylresorcinol by I in 0.01* N *HCl at 37°. The weighing-in concentrations of the drug, [$A_0$], were 250 (○) and 500 (●) mg/liter.*

acidic system (0.01 *N* HCl) as compared to plain water; similar sorption experiments with salicylic acid did not show comparable differences. This difference can be explained by the fact that, at the end of the sorption experiments, pH values above 6.0 were observed in the former case while pH values always remained at ~3.1 in the latter case.

The $K_s$ values of the strongly interacting compounds are summarized in Table II. The exceptionally high $K_s$ values of tannic acid and hexylresorcinol deserve close scrutiny. In both cases, the Nernst coefficient is no longer independent of [*A*], although for different reasons.

The experimental results of a detailed investigation of the Nernst partition of the tannic acid–I system is shown in Fig. 2, where $\log(k/[F_0])$ is plotted against the logarithm of [*A*]. The experimental data are compared with theoretical curves as obtained from Eq. 8 for various $K_s$ values. For small $K_s$ values, where $[A]K_s \ll 1$ holds true, the Nernst coefficient $k$ becomes independent of [*A*]. This condition is satisfied by all compounds in Table I and by some compounds in Tables II and III.

The experimental data for tannic acid, however, closely approach the limiting straight line of slope −1 where $[A]K_s \gg 1$ and $\log k \sim \log[F_0] - \log[A]$. The concentration of effective binding sites, $[F_0]$, of the tannic acid interaction with I is, according to Eq. 8, 0.186 *M*. For the binding constant, $K_s$, a value of the order of $2.7 \times 10^4\ M^{-1}$ is estimated. These exceptional figures underline the special role tannic acid plays in the interaction behavior with I. Apparently, this interaction is related to the comparatively high molecular weight of tannic acid (mol. wt. ~1550) and its multifunctional chemical structure. In contrast to other compounds in this study, a single molecule of tannic acid covers many individual binding sites simultaneously, leading to extraordinarily strong binding.

Hexylresorcinol, on the other hand, is another example of a peculiar interaction mechanism with I. The experimental results of a detailed investigation of this system are shown in Fig. 3. With resorcinol, the plotting of $[A_0]/[A]$ *versus* $\varphi$ yields a perfect straight line; with hexylresorcinol, the situation is apparently changed. The steep slope of the curve indicates an extremely strong interaction. On the other hand, the marked deviation from linearity of the curve suggests that the introduced model of interaction no longer applies. However, the experimental results are readily explained in terms of a model of cooperative binding. A relevant plot of the data according to a theory of cooperative interaction (15) is shown in Fig. 4.

As depicted in Fig. 4, the hexylresorcinol data fit the concept of cooperative binding. Therefore, the $K_s$ values of hexylresorcinol in Table II, which were evaluated according to the model of noncooperative competitive binding, are valid only to a first approximation for the stated polymer to drug ratio. Of course, the extremely strong tendency of interaction, as documented in Figs. 3 and 4, is reflected nevertheless in the magnitude of the $K_s$ values.

The cooperative binding plot (Fig. 4) allows the maximum number of bound hexylresorcinol molecules per vinylpyrrolidone segment in the polymer to be determined. With increasing weighing-in concentrations of the drug, the binding curves approach a limiting straight line, which can be extrapolated to the polymer to drug ratio axis. The intercept yields $1/g$, where $g$ is the number of binding sites per polymer segment. An intercept value of 2 (Fig. 4) indicates that each hexylresorcinol molecule is bound by two vinylpyrrolidone residues.

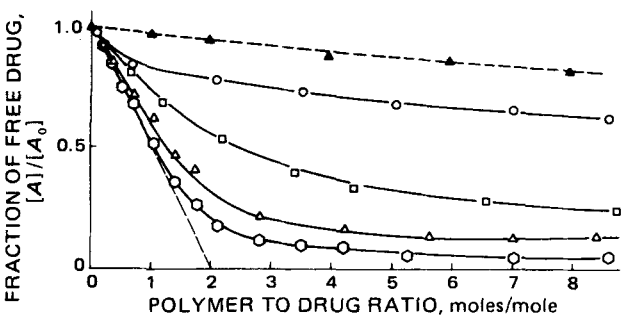


**Figure 4**—*Cooperative binding curves of hexylresorcinol–I in 0.01* N *HCl at 37°. For comparison, relevant data of the noncooperatively bound resorcinol are included. The polymer to drug ratio is expressed in moles of monomer segments per mole of drug. Key: —, hexylresorcinol at 25 (○), 80 (□), 250 (△), and 500 (○) mg/liter; and ---, resorcinol at 250 (▲) mg/liter.*

Finally, in the case of butylphenol, deviations from the expected constancy of the $K_s$ values with changing $\varphi$ are observed. There is no obvious explanation for this discrepancy. Perhaps a possible micellization reaction of the compound interferes with the polymer interaction in this case.

The results of the desorption studies also can be treated according to the introduced model of interaction. If the desorption experiment is started with an adsorbed concentration of drug of $[A]_{s,0}$, after the first desorption step the partition equilibrium can be described according to Eq. 2 as:

$$k = \frac{[A]_{s,1}}{[A]} = \frac{m_{s,1}/V_s}{m/V_L} \qquad \text{(Eq. 9)}$$

in which $m_{s,1}$ denotes the amount of the compound remaining in the polymer phase after the first desorption step and $m$ denotes the appropriate amount of desorbed material. Hence, the mass balance reads:

$$m_{s,0} = m + m_{s,1} \qquad \text{(Eq. 10)}$$

where $m_{s,0}$ represents the initially sorbed amount. From Eq. 9, it follows that:

$$k = \frac{1}{\varphi} \frac{m_{s,1}}{m_{s,0} - m_{s,1}} \qquad \text{(Eq. 11)}$$

which can be rearranged to yield for $n$ desorption steps:

$$m_{s,0} = \left(1 + \frac{1}{k\varphi}\right)^n m_{s,n} \qquad \text{(Eq. 12)}$$

The fraction, $\gamma_s$, of the initially sorbed amount $m_{s,0}$ remaining bound after $n$ desorption steps is $\gamma_s = m_{s,n}/m_{s,0}$:

$$\gamma_s = \left(1 + \frac{1}{k\varphi}\right)^{-n} \qquad \text{(Eq. 13)}$$

Experimental results of desorption studies with several substances with a pronounced sorption tendency are listed in Table IV. They are compared with theoretical values determined with Eq. 12 by considering the appropriate $k$ values as obtained from sorption studies. With 15-min equilibration times for each desorption step, generally the experimental and theoretical values are in satisfactory agreement, indicating that the molecules are reversibly bound even in cases of substantial interaction.

Again, hexylresorcinol and tannic acid play an exceptional role. With hexylresorcinol, the desorption process proceeds even faster than predicted theoretically due to the underlying cooperative mechanism of interaction, which is not accounted for in the derivation of Eq. 12. On the other hand, the discrepancies with tannic acid are explained partly by Fig. 2. As the desorption proceeds, the value of the Nernst coefficient increases, slowing down the efficiency of the stepwise desorption process. The theoretical values of Table IV, however, are based on the assumption of a constant value of $k$. The experimental verification of the degree of desorption is hampered further by the fact that tannic acid adheres to the surface of analytical glassware, disturbing a correct determination of the minute amounts desorbed in each single step.

## DISCUSSION

Thirty-two compounds of diverse chemical structure were studied with regard to their sorption tendencies toward I. Even with rather extreme polymer to drug ratios of 10:1 (never met in practice), the sorbed amount was <5% with 20 pharmaceuticals. None of the pharmaceuticals within this class carried phenolic functional groups.

Under the same experimental conditions, eight compounds showed sorption values between 5 and 33%. By decreasing the polymer concentration 10 times whereby a polymer to drug ratio of 1:1 was established, the sorbed amount fell to or below the 5% level in cases of readily soluble drugs. All compounds of this class were characterized by a simple aromatic structure, five of which (propylparaben, sodium salicylate, acetaminophen, resorcinol, and salicylic acid) carried hydroxyl groups.

Significant differences in binding between the water and 0.01 *N* HCl system were observed only with sodium salicylate; this result is explained readily by the change in pH.

In artificial intestinal fluid, the binding tendency of several pharmaceuticals (benzoic acid, *p*-hydroxybenzoic acid, and sulfadiazine) appeared to be less pronounced as compared to the sorption behavior in an acidic environment. No significant differences were found in this respect with benzocaine, *p-tert*-butylphenol, propylparaben, acetaminophen, and resorcinol. The same is true for hexylresorcinol and tannic acid, which exhibited the strongest binding tendency irrespective of the medium pH.

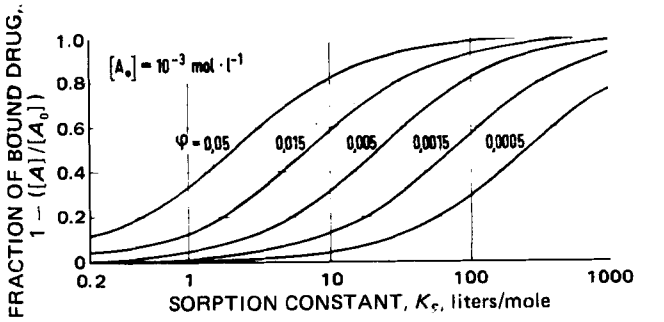


**Figure 5**—*Fraction of drug bound to I as a function of the binding constant,* $K_s$, *for various values of* $\varphi$.

As shown earlier, the degree of polymer to drug interaction is expressed by the value of the binding constant, $K_s$. Not unexpectedly, the results of binding studies with soluble polyvinylpyrrolidone (12) point out close similarities with the present findings. Higuchi and Kuramoto (16) found no complexing between soluble polyvinylpyrrolidone and citric acid, benzylpenicillin, cortisone, procaine hydrochloride, caffeine, and theophylline (16). The latter three compounds were investigated in the present study and were found to be noninteracting with I.

The affinity of other pharmaceuticals toward soluble polyvinylpyrrolidone decreased in the following order: sulfathiazole > *m*-hydroxybenzoic acid > *p*-hydroxybenzoic acid > *p*-aminobenzoic acid > salicylic acid > phenobarbital > benzoic acid > sodium salicylate > mandelic acid > chloramphenicol. These results again are in close agreement with the findings obtained with I.

Particularly interesting is the similarity of experimental results obtained with soluble polyvinylpyrrolidone and I with hexylresorcinol. Polli and Frost (17) reported particularly strong binding between polyvinylpyrrolidone and this resorcinol derivative. However, this conspicuous molecular interaction was explained vaguely as a possible change of the spatial orientation of the polymer during the interaction. The analysis of the experimental data presented here, which is also valid for the interaction of hexylresorcinol with soluble polyvinylpyrrolidone[12], clearly indicates the significance of a cooperative interaction mechanism in the sorption process (Fig. 4).

In the case of hexylresorcinol, binding to the polymer probably occurs not independently to single binding sites but preferably to the nearest neighbor binding sites, thereby inducing an aggregation of bound ligands. This peculiar mechanism of interaction (15) presumably is caused by hydrophobic interaction of the hexyl residues of nearest-neighbor ligands. In that way, the driving force of interaction, which is assumed to be dominated by hydrophilic hydrogen bonding in the case of resorcinol, is enhanced greatly.

Evidence for both hydrophilic and hydrophobic effects on the binding of benzene derivatives to polyvinylpyrrolidone also was found by Molyneux and Frank (18). In contrast to hexylresorcinol, however, the noncooperative character of interaction was basically not altered, and the interaction constants were only gradually changed. Usually, the strength of interaction increases with increasing numbers of polar functional groups and with the extent of the hydrophobic part of the molecules. The distinct complexing tendency of tannic acid with polyvinylpyrrolidone is readily explained in these terms.

The relevance of hydrogen bonding for the interaction with I is suggested by the well-known fact that phenolic compounds in general may form precipitates with soluble polyvinylpyrrolidone (19). Further evidence is offered by the observation that esterification of *p*-hydroxybenzoic acid leads to a decrease in binding strength with polyvinylpyrrolidone (20).

Of practical importance is the extent to which pharmaceuticals with a measurable binding tendency are released from the bound state during GI passage. This process may be considered as a series of desorption steps since, during the passage, intestinal absorption of the released drug takes place continuously. The release process generally relates only to the small fraction of drug staying in the bound state. The bound fraction, $\gamma_s$, can be estimated by means of Fig. 5, where $\gamma_s$ is plotted as a function of the interaction constant, $K_s$, for various solid to liquid ratios, $\varphi$. It follows that for the majority of pharmaceuticals investigated in the present study within wide limits of the polymer to drug ratio, the sorbed amount lies well below the 10% level.

[12] D. Horn and W. Ditter, to be published.

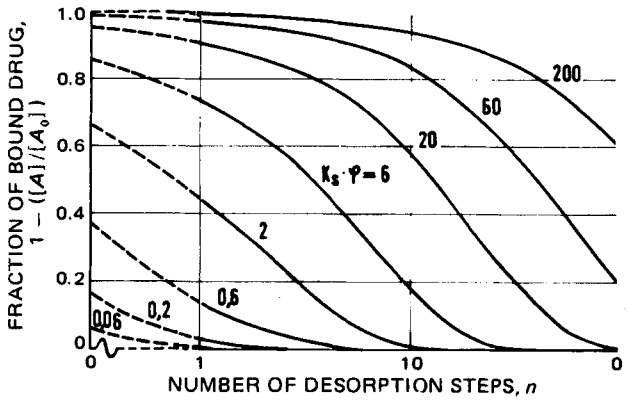


**Figure 6**—*Decrease of the initially sorbed amount of the drug as a function of the number of desorption steps,* n, *for various values of* $K_s\varphi$.

Finally, theoretical desorption curves are shown in Fig. 6 and were calculated according to Eq. 13. The graph depicts the decrease of the initially sorbed amount of the drug as a function of the number of desorption steps for increasing values of $K_s\varphi$. With regard to $K_s$ values on the order of 2–10 $M^{-1}$, indicating moderate binding (Table I) even when considering high values of $\varphi$ (*i.e.*, $\varphi = 0.02$), it follows from Fig. 6 that only a few desorption steps are necessary for complete release of the bound compound from the polymer.

Presumably, with the exception of tannic acid and closely related compounds, the presence of the disintegrant should not interfere with GI absorption of the pharmaceutical.

## REFERENCES

(1) J. W. Breitenbach, *IUPAC Int. Symp. Macromol. Chem., 1969*, p. 529.

(2) K. Seelert, *Acta Pharm. Technol.*, **21**, 211 (1975).

(3) H. F. Kauffmann and J. W. Breitenbach, *Angew. Makromol. Chem.*, **45**, 167 (1975).

(4) P. H. List and U. A. Muazzam, *Pharm. Ind.*, **41**, 459 (1979).

(5) R. Hüttenrauch and I. Keiner, *Pharmazie*, **28**, 137 (1973).

(6) S. S. Kornblum and S. B. Stoopak, *J. Pharm. Sci.*, **62**, 43 (1973).

(7) S. S. Kornblum and S. B. Stoopak, German Offen. 2,549,740 (1977); through *Chem. Abstr.*, **87**, 58,527 (1977).

(8) A. H. Bronnsack, *Pharm. Ind.*, **38**, 1181 (1976).

(9) Beecham Group Ltd., Japan Kokai 7824,014 (1978); through *Chem. Abstr.*, **89**, 48,917 (1978).

(10) B. C. Lippold and R. Lütschg, *Pharm. Ind.*, **40**, 541 (1978).

(11) S. Lang, "Abstract Jahreskongress der Arbeitsgemeinschaft für Pharmazeutische Verfahrenstechnik (APV)," 1978, S. 61.

(12) S. Keipert, J. Becker, H.-H. Schultze, and R. Voigt, *Pharmazie*, **28**, 145 (1973).

(13) R. Haul and G. Dümbgen, *Chem. Ing. Tech.*, **32**, 349 (1960).

(14) W. A. P. Luck, *Kolloid Z. Z. Polym.*, **223**, 110 (1968).

(15) G. Schwarz, *Eur. J. Biochem.*, **12**, 442 (1970).

(16) T. Higuchi and R. Kuramoto, *J. Am. Pharm. Assoc., Sci. Ed.*, **43**, 393, 398 (1954).

(17) G. P. Polli and B. M. Frost, *J. Pharm. Sci.*, **58**, 1543 (1969).

(18) P. Molyneux and H. P. Frank, *J. Am. Chem. Soc.*, **83**, 3169 (1961).

(19) D. Guttman and T. Higuchi, *J. Am. Pharm. Assoc., Sci. Ed.*, **45**, 659 (1956).

(20) E. G. Jürgensen and P. Speiser, *Acta Pharm. Suec.*, **4**, 185, 201 (1967).

## ACKNOWLEDGMENTS

The authors thank Dr. K. Seelert and Dr. S. Lang for valuable discussions and Mrs. Renate Rose and Mr. Helmut Sankowski for technical assistance.

# Improved Delivery through Biological Membranes VIII: Design, Synthesis, and *In Vivo* Testing of True Prodrugs of Aspirin

**THORSTEINN LOFTSSON *, JAMES J. KAMINSKI ‡, and NICHOLAS BODOR §x**

Received August 25, 1980, from the **Department of Pharmaceutical Chemistry, School of Pharmacy, University of Kansas, Lawrence, KS 66045*, the ‡*Inter$_x$ Research Corporation, Lawrence, KS 66044*, and the §*Department of Medicinal Chemistry, College of Pharmacy, J. Hillis Miller Health Center, University of Florida, Gainesville, FL 32610.* Accepted for publication October 16, 1980.

**Abstract** □ Novel activated ester-type prodrugs of aspirin were designed and synthesized. The methylthiomethyl, methylsulfinylmethyl, and methylsulfonylmethyl esters of aspirin (acetylsalicylic acid) were cleaved *in vitro* in plasma to form aspirin rather than the corresponding salicylates. *In vivo* studies using dogs indicated that at least one aspirin derivative, methylsulfinylmethyl-2-acetoxybenzoate, is a true aspirin prodrug since aspirin was detected in the blood after prodrug administration.

**Keyphrases** □ Aspirin—activated ester-type prodrugs of aspirin synthesized and evaluated for analgesia, *in vivo* and *in vitro* studies □ Prodrugs, aspirin—activated ester-type prodrugs synthesized and evaluated for analgesic activity, *in vitro* and *in vivo* studies □ Analgesic activity—activated ester-type prodrugs of aspirin, synthesized and evaluated for analgesia, *in vitro* and *in vivo* studies

The GI side effects of aspirin (acetylsalicylic acid, I) are well known and documented (1). These side effects are associated with the free carboxylic group; thus, transient derivatives (prodrugs) and various formulations of I were prepared and tested in which the free carboxyl group was derivatized or bound. The results obtained were unsatisfactory due to the specific properties of I. The *o*-acetyloxyl group is rather labile. Extensive studies of the chemical hydrolysis (2–8) and *in vivo* hydrolysis (9) demonstrated the facile conversion of I to salicylic acid (II). Although II is also a potent anti-inflammatory agent, it was shown (10) that I is a far more potent analgesic and, thus, delivery to the bloodstream in the intact form is desirable. To achieve this, the carboxyl-protecting function must be cleaved

0022-3549/81/0700-0743$01.00/0
© 1981, American Pharmaceutical Association

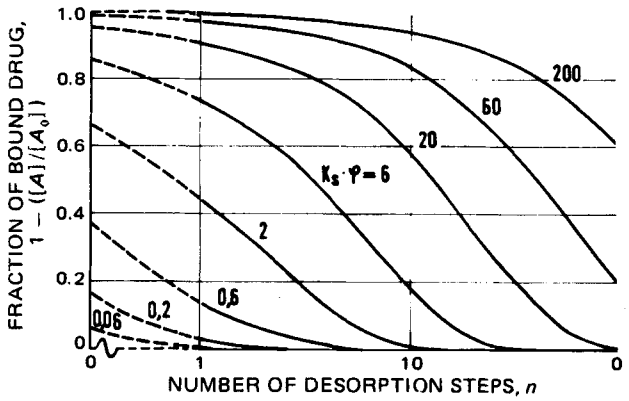


**Figure 6**—*Decrease of the initially sorbed amount of the drug as a function of the number of desorption steps,* n, *for various values of* $K_s\varphi$.

Finally, theoretical desorption curves are shown in Fig. 6 and were calculated according to Eq. 13. The graph depicts the decrease of the initially sorbed amount of the drug as a function of the number of desorption steps for increasing values of $K_s\varphi$. With regard to $K_s$ values on the order of 2–10 $M^{-1}$, indicating moderate binding (Table I) even when considering high values of $\varphi$ (*i.e.*, $\varphi = 0.02$), it follows from Fig. 6 that only a few desorption steps are necessary for complete release of the bound compound from the polymer.

Presumably, with the exception of tannic acid and closely related compounds, the presence of the disintegrant should not interfere with GI absorption of the pharmaceutical.

## REFERENCES

(1) J. W. Breitenbach, *IUPAC Int. Symp. Macromol. Chem., 1969*, p. 529.

(2) K. Seelert, *Acta Pharm. Technol.*, **21**, 211 (1975).

(3) H. F. Kauffmann and J. W. Breitenbach, *Angew. Makromol. Chem.*, **45**, 167 (1975).

(4) P. H. List and U. A. Muazzam, *Pharm. Ind.*, **41**, 459 (1979).

(5) R. Hüttenrauch and I. Keiner, *Pharmazie*, **28**, 137 (1973).

(6) S. S. Kornblum and S. B. Stoopak, *J. Pharm. Sci.*, **62**, 43 (1973).

(7) S. S. Kornblum and S. B. Stoopak, German Offen. 2,549,740 (1977); through *Chem. Abstr.*, **87**, 58,527 (1977).

(8) A. H. Bronnsack, *Pharm. Ind.*, **38**, 1181 (1976).

(9) Beecham Group Ltd., Japan Kokai 7824,014 (1978); through *Chem. Abstr.*, **89**, 48,917 (1978).

(10) B. C. Lippold and R. Lütschg, *Pharm. Ind.*, **40**, 541 (1978).

(11) S. Lang, "Abstract Jahreskongress der Arbeitsgemeinschaft für Pharmazeutische Verfahrenstechnik (APV)," 1978, S. 61.

(12) S. Keipert, J. Becker, H.-H. Schultze, and R. Voigt, *Pharmazie*, **28**, 145 (1973).

(13) R. Haul and G. Dümbgen, *Chem. Ing. Tech.*, **32**, 349 (1960).

(14) W. A. P. Luck, *Kolloid Z. Z. Polym.*, **223**, 110 (1968).

(15) G. Schwarz, *Eur. J. Biochem.*, **12**, 442 (1970).

(16) T. Higuchi and R. Kuramoto, *J. Am. Pharm. Assoc., Sci. Ed.*, **43**, 393, 398 (1954).

(17) G. P. Polli and B. M. Frost, *J. Pharm. Sci.*, **58**, 1543 (1969).

(18) P. Molyneux and H. P. Frank, *J. Am. Chem. Soc.*, **83**, 3169 (1961).

(19) D. Guttman and T. Higuchi, *J. Am. Pharm. Assoc., Sci. Ed.*, **45**, 659 (1956).

(20) E. G. Jürgensen and P. Speiser, *Acta Pharm. Suec.*, **4**, 185, 201 (1967).

## ACKNOWLEDGMENTS

The authors thank Dr. K. Seelert and Dr. S. Lang for valuable discussions and Mrs. Renate Rose and Mr. Helmut Sankowski for technical assistance.

# Improved Delivery through Biological Membranes VIII: Design, Synthesis, and *In Vivo* Testing of True Prodrugs of Aspirin

**THORSTEINN LOFTSSON *, JAMES J. KAMINSKI ‡, and NICHOLAS BODOR §x**

Received August 25, 1980, from the **Department of Pharmaceutical Chemistry, School of Pharmacy, University of Kansas, Lawrence, KS 66045*, the ‡*Inter$_x$ Research Corporation, Lawrence, KS 66044*, and the §*Department of Medicinal Chemistry, College of Pharmacy, J. Hillis Miller Health Center, University of Florida, Gainesville, FL 32610.* Accepted for publication October 16, 1980.

**Abstract** □ Novel activated ester-type prodrugs of aspirin were designed and synthesized. The methylthiomethyl, methylsulfinylmethyl, and methylsulfonylmethyl esters of aspirin (acetylsalicylic acid) were cleaved *in vitro* in plasma to form aspirin rather than the corresponding salicylates. *In vivo* studies using dogs indicated that at least one aspirin derivative, methylsulfinylmethyl-2-acetoxybenzoate, is a true aspirin prodrug since aspirin was detected in the blood after prodrug administration.

**Keyphrases** □ Aspirin—activated ester-type prodrugs of aspirin synthesized and evaluated for analgesia, *in vivo* and *in vitro* studies □ Prodrugs, aspirin—activated ester-type prodrugs synthesized and evaluated for analgesic activity, *in vitro* and *in vivo* studies □ Analgesic activity—activated ester-type prodrugs of aspirin, synthesized and evaluated for analgesia, *in vitro* and *in vivo* studies

The GI side effects of aspirin (acetylsalicylic acid, I) are well known and documented (1). These side effects are associated with the free carboxylic group; thus, transient derivatives (prodrugs) and various formulations of I were prepared and tested in which the free carboxyl group was derivatized or bound. The results obtained were unsatisfactory due to the specific properties of I. The *o*-acetyloxyl group is rather labile. Extensive studies of the chemical hydrolysis (2–8) and *in vivo* hydrolysis (9) demonstrated the facile conversion of I to salicylic acid (II). Although II is also a potent anti-inflammatory agent, it was shown (10) that I is a far more potent analgesic and, thus, delivery to the bloodstream in the intact form is desirable. To achieve this, the carboxyl-protecting function must be cleaved

0022-3549/81/0700-0743$01.00/0
© 1981, American Pharmaceutical Association

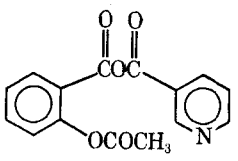

III

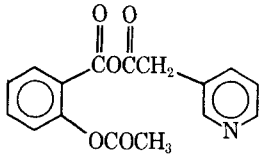

IV

prior to the labile *o*-acetyl one, which is difficult since the prodrug must at the same time be stable enough in the neat form and in formulation.

## BACKGROUND

An early recommendation for an aspirin prodrug with decreased gastric irritation was aspirin anhydride (11). However, its low solubility in water, slow dissolution rate, and immunogenicity (12, 13) prevented further development. Attempts to increase the solubility were made by preparing mixed anhydrides[1] such as the pyridine-containing derivatives III and IV. However, these mixed anhydrides cannot be synthesized in a 100% pure form since some disproportionation always occurs and aspirin anhydride is formed as an impurity, even when using the clean acyl chloride–thallium carboxylate reaction (14). Mixed anhydrides probably also have immunogenic–allergenic properties similar to aspirin anhydride. A phosphoric acid mixed anhydride[2] (V) was considered, but all attempts at preparation failed, even when the stable ester (VI) was used, due to facile intramolecular reactions leading to the stable cyclic salicylphosphate (VII).

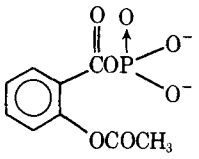

V

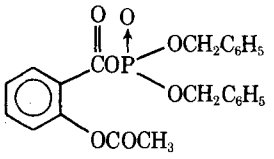

VI

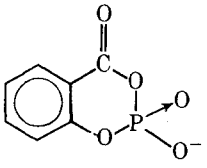

VII

Stable acyloxyalkyl derivatives of I such as the pivalyloxymethyl[1], benzoyloxymethyl, and analogous esters were synthesized, but they also showed low aqueous solubility and dissolution rates. More recently, the 4-acetamidophenyl ester (IX) (15, 16) and the triglycerides (X) (17, 18) were prepared.

Although decreased GI irritation is claimed with both IX and X, there is no proof that these derivatives are true prodrugs of I and not of salicylic acid. Recent work (18) on X showed only the blood salicylate levels and the pharmacological testing involved only anti-inflammatory studies, but X still was indicated (without any proof) to be an aspirin prodrug.

Some aspirin salts, such as lysine acetylsalicylate (XI), were reported (19) to produce three times less GI bleeding than I.

Other intended aspirin prodrugs include the 1′-ethoxyethyl ester (20), *N*-hydroxyethyl nicotinamide ester (21), and salicylamide ester (22). The patent literature also includes various derivatives but without much specific information.

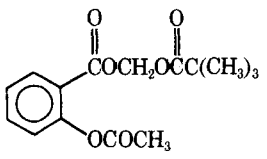

VIII

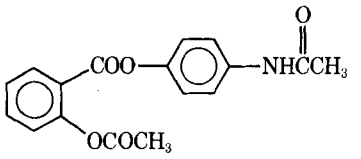

IX

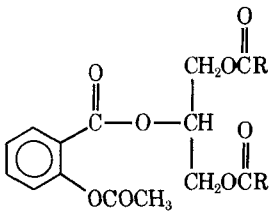

X: R = $(CH_2)_nCH_3$

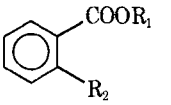

XI: $R_1 = CH_2SCH_3$, $R_2 = H$
XII: $R_1 = CH_2SOCH_3$, $R_2 = H$
XIII: $R_1 = CH_2SO_2CH_3$, $R_2 = H$
XIV: $R_1 = CH_2SCH_3$, $R_2 = OH$
XV: $R_1 = CH_2SOCH_3$, $R_2 = OH$
XVI: $R_1 = CH_2SO_2CH_3$, $R_2 = OH$
XVII: $R_1 = CH_2SCH_3$, $R_2 = OCOCH_3$
XVIII: $R_1 = CH_2SOCH_3$, $R_2 = OCOCH_3$
XIX: $R_1 = CH_2SO_2CH_3$, $R_2 = OCOCH_3$

None of the chemical derivatives of aspirin was reported to form aspirin in the body after oral or intravenous administration.

The present study reports novel derivatives of aspirin, at least one of which resulted in aspirin *in vivo*. These new prodrugs are activated esters that undergo further activation *in vivo*. The overall result is delivery of aspirin (I) rather than of salicylic acid.

Protective groups capable of being removed under mild conditions are of great value in peptide synthesis. Methylthiomethyl and β-ethylthiomethyl esters are used as protective groups for carboxylic acids for this purpose (23, 24). They are somewhat stable under normal conditions but can be made more labile by conversion into a sulfonium salt or by oxidation to the sulfone, which then is cleaved readily under neutral or mild alkaline conditions at room temperature to regenerate the acid. Therefore, similar groups might be suitable as temporary transport moieties for aspirin and other carboxylic acids.

Sulindac, a new anti-inflammatory agent containing a sulfinyl group, undergoes reversible reduction–oxidation biotransformation to the sulfide and an irreversible oxidation to the sulfone in several animal species including humans (25). The methylthiomethyl ester thus should be susceptible to enzymatic oxidation and subsequent cleavage in the body. Benzoic acid was used first as a model compound, and the corresponding methylthiomethyl (XI), methylsulfinylmethyl (XII), and methylsulfonylmethyl (XIII) esters were synthesized. Analogous derivatives of salicylic acid (XIV–XVI) and of aspirin (XVII–XIX) then were prepared.

Detailed studies as to the physicochemical properties and chemical and enzymic hydrolysis rates were carried out on XI–XIX. The results, including the complex hydrolysis characteristics of XVII–XIX, will be reported in separate papers. This report describes the enzymic hydrolysis studies on XIV–XIX; the data also show that at least one aspirin derivative is an effective true prodrug of I, resulting in aspirin *in vivo*.

## EXPERIMENTAL

**Methylthiomethyl Benzoate (XI)**—The compound was prepared by reacting benzoic acid with chloromethyl methyl sulfide in the presence of triethylamine as described earlier (23). The obtained ester was distilled under reduced pressure, bp 93–95°/0.3 mm [lit. (23) bp 106–108°/2 mm]; mol. wt. 182.24; IR (neat): 3060, 2920, 1710, 1595, 1450, 1330, 1310, 1250, 1100, 1070, 1025, 930, 750, and 710 $cm^{-1}$; NMR ($CDCl_3$): δ 7.2–8.2 (m, 5H), 5.4 (s, 2H), and 2.3 (s, 3H) ppm; mass spectrum (70 ev): *m/z* (relative intensity) 182 (9), 105 (100), and 77 (41).

**Methylsulfinylmethyl Benzoate (XII)**—To a chloroform solution containing 0.91 g (0.005 mole) of XI was added, in portions over 15 min with stirring, 1.0 g (0.005 mole) of *m*-chloroperbenzoic acid (85% solution). The resultant solution was stirred at room temperature overnight, washed twice with saturated aqueous sodium bicarbonate solution, and dried over anhydrous sodium sulfate. The reaction mixture was filtered, and the filtrate was evaporated under reduced pressure to afford a pale-yellow liquid, which crystallized on standing several hours at room temperature. Trituration of the residue in petroleum ether (bp 30–60°) gave 0.7 g (0.0035 mole) of the desired product (70% yield) as a white solid, mp 43–45°; IR (neat, melt): 3060, 3000, 2920, 1710, 1590, 1445, 1310, 1240, 1100, 1050, 800, and 710 $cm^{-1}$; NMR ($CDCl_3$): δ 7.3–8.3 (m, 5H), 5.2 (*AB*, 2H), and 2.7 (s, 3H) ppm; mass spectrum (70 ev): *m/z* (relative intensity) 168 (2), 135 (4), 105 (100), and 77 (42).

*Anal.*—Calc. for $C_9H_{10}O_3S$: C, 54.52; H, 5.08; S, 16.18. Found: C, 54.22; H, 5.22; S, 16.40.

**Methylsulfonylmethyl Benzoate (XIII)**—Use of the method described for XII, but with 2 equivalents of *m*-chloroperbenzoic acid, afforded the desired product, mp 116–118°; IR (KBr): 3060, 3000, 2920, 1730, 1590, 1545, 1420, 1300, 1250, 1095, 950, 800, and 720 $cm^{-1}$; NMR

[1] N. Bodor, unpublished work.

[2] N. Bodor, unpublished work. The pivalyloxymethyl ester (VIII) is a solid which has a low melting point (36–38°) and which is soluble to the extent of 25% in oil. The solution did not show any decomposition for 2 years at room temperature.

($CDCl_3$): δ 7.3–8.4 (m, 5H), 5.3 (s, 2H), and 3.0 (s, 3H) ppm; mass spectrum (70 ev): *m/z* (relative intensity) 184 (4), 135 (2), 105 (100), and 77 (36).

*Anal.*—Calc. for $C_9H_{10}O_4S$: C, 50.45; H, 4.71; S, 14.97. Found: C, 50.61; H, 5.00; S, 15.18.

**Methylthiomethyl 2-Hydroxybenzoate (XIV)**—To an acetonitrile solution containing 13.8 g (0.1 mole) of salicylic acid and 10.1 g (0.1 mole) of triethylamine at 0° was added dropwise, with stirring, 9.6 g (0.1 mole) of chloromethyl methyl sulfide. The solution was heated under reflux for 24 hr. The solvent was then removed under reduced pressure, and the residue was suspended in benzene. The formed triethylamine hydrochloride was removed by filtration, and the filtrate was washed twice with saturated aqueous sodium bicarbonate solution, dried over anhydrous sodium sulfate, and filtered. Removal of benzene by evaporation under reduced pressure afforded a liquid. Vacuum distillation gave 15.8 g (0.08 mole) of the desired product (80% yield) as a clear, colorless liquid, bp 107–109°/0.8 mm; IR (neat): 3200, 2920, 1670, 1600, 1580, 1480, 1415, 1350, 1280, 1200, 1170, 1140, 1080, 920, 840, 760, and 700 $cm^{-1}$; NMR ($CDCl_3$): δ 10.5 (broad s, 1H), 6.6–8.0 (m, 4H), 5.4 (s, 2H), and 2.3 (s, 3H) ppm; mass spectrum (70 ev): *m/z* (relative intensity) 198 (7), 121 (15), and 61 (100).

*Anal.*—Calc. for $C_9H_{10}O_3S$: C, 54.52; H, 5.08; S, 16.18. Found: C, 54.70; H, 5.26; S, 16.01.

**Methylsulfinylmethyl 2-Hydroxybenzoate (XV)**—Substitution of an equivalent quantity of XIV for the benzoic acid methylthiomethyl ester (XI) used for the synthesis of XII and repetition of the described procedure afforded the desired product, mp 110–112° (ethanol); IR (KBr): 3200, 3000, 1680, 1600, 1580, 1480, 1345, 1280, 1130, 1090, 940, and 770 $cm^{-1}$; NMR ($CDCl_3$): δ 10.2 (s, 1H), 6.7–8.1 (m, 4H), 5.3 (*AB*, 2H), and 2.8 (s, 3H) ppm; mass spectrum (70 ev): *m/z* (relative intensity) 214 (1), 121 (100), 93 (13), and 65 (10).

*Anal.*—Calc. for $C_9H_{10}O_4S \cdot 1/2H_2O$: C, 48.42; H, 4.97; S, 14.36. Found: C, 48.14; H, 4.51; S, 14.94.

**Methylsulfonymethyl 2-Hydroxybenzoate (XVI)**—By using the method described for the preparation of XIII, the ester XIV was transformed into the desired product in an 85% yield, mp 124–126° (ethanol); IR (KBr): 3200, 3000, 1680, 1600, 1580, 1480, 1420, 1345, 1320, 1280, 1240, 1190, 1130, 1090, 940, 770, and 710 $cm^{-1}$; NMR ($CDCl_3$): δ 10.0 (s, 1H), 6.8–8.1 (m, 4H), 5.3 (s, 2H), and 3.1 (s, 3H) ppm; mass spectrum (70 ev): *m/z* (relative intensity) 230 (10), 121 (100), 93 (10), and 65 (12).

*Anal.*—Calc. for $C_9H_{10}O_5S$: C, 46.95; H, 4.38; S, 13.93. Found: C, 47.14; H, 4.52; S, 14.52.

**Methylthiomethyl 2-Acetoxybenzoate (XVII)**—Substitution of an equivalent quantity of aspirin for the salicylic acid used in the preparation of XIV and repetition of that described procedure afforded the desired product, bp 148–150°/1 mm; IR (neat): 3060, 2920, 1755, 1715, 1600, 1480, 1450, 1365, 1280, 1200, 1060, 920, 750, and 705 $cm^{-1}$; NMR ($CDCl_3$): δ 6.9–8.2 (m, 4H), 5.3 (s, 2H), 2.3 (s, 3H), and 2.2 (s, 3H) ppm; mass spectrum (70 ev): *m/z* (relative intensity) 240 (2), 198 (10), 163 (9), 121 (41), and 61 (100).

*Anal.*—Calc. for $C_{11}H_{12}O_4S$: C, 54.98; H, 5.04; S, 13.35. Found: C, 55.17; H, 5.15; S, 13.69.

**Methylsulfinylmethyl 2-Acetoxybenzoate (XVIII)**—The method described for the synthesis of XV was used, starting with 7.2 g (0.03 mole) of the methylthiomethyl ester, XVII. Recrystallization from tetrahydrofuran of the crude product resulted in pure XVIII in an 80% yield (6.1 g), mp 118–122°; IR (KBr): 3000, 1750, 1720, 1600, 1480, 1370, 1300, 1180, 1080, 920, 830, 755, and 705 $cm^{-1}$; NMR ($CDCl_3$): δ 7.0–8.2 (m, 4H), 5.2 (*AB*, 2H), 2.6 (s, 3H), and 2.4 (s, 3H) ppm; mass spectrum (70 ev): *m/z* (relative intensity) 214 (2), 163 (23), 121 (100), 93 (7), 92 (7), and 65 (7).

*Anal.*—Calc. for $C_{11}H_{12}O_5S \cdot 1/2H_2O$: C, 49.80; H, 4.94; S, 12.09. Found: C, 49.49; H, 4.59; S, 12.69.

**Methylsulfonylmethyl 2-Acetoxybenzoate (XIX)**—To a stirred chloroform solution of 7.2 g (0.03 mole) of methylthiomethyl 2-acetoxybenzoate (XVII) at 0° was added 12.0 g (0.06 mole) of *m*-chloroperbenzoic acid. The reaction mixture was worked up as for XVI as a white crystalline product, mp 151–153°; IR (KBr): 3010, 1750, 1725, 1600, 1480, 1300, 1245, 1185, 1120, 1090, 1000, 920, 760, and 710 $cm^{-1}$; NMR ($CDCl_3$): δ 7.0–8.2 (m, 4H), 5.3 (s, 2H), 3.0 (s, 3H), and 2.4 (s, 3H) ppm; mass spectrum (70 ev): *m/z* (relative intensity) 272 (<1), 230 (21), 163 (11), 121 (100), 93 (10), 92 (10), and 65 (11).

*Anal.*—Calc. for $C_{11}H_{12}O_6S$: C, 48.52, H, 4.44; S, 11.78. Found: C, 48.48; H, 4.43; S, 11.76.

***In Vivo* Studies**—Four purebred female beagle dogs, 1.5 years old, were used to determine the blood levels of various metabolites after oral and intravenous administration of aspirin (I) and the three aspirin derivatives (XVII–XIX). For oral administration, the compounds were dissolved in polyethylene glycol 400 and placed in gelatin capsules. Dimethyl sulfoxide solutions were used for the intravenous dosing. The doses were adjusted so that the dogs received equimolar doses of aspirin and the aspirin derivatives, both intravenously and orally. Each experiment was repeated at least once. Each dog was allowed to rest for a minimum of 1 week before it was used again.

Blood (2 ml) was withdrawn from each dog and acidified immediately by mixing with 2 ml of chilled 10% aqueous potassium bisulfate and 1 drop of potassium fluoride (~25 mg) in a 15-ml centrifuge tube. This process lowers the sample pH to ~1 and quenches enzymatic ester hydrolysis. Ether (7.0 ml) was added to each tube, and the samples were mixed on a mechanical shaker for 30 min and then centrifuged. A 5.0-ml portion of the supernate was removed and evaporated to dryness, and the residue was dissolved in 1.0 ml of acetonitrile. This solution then was analyzed by high-pressure liquid chromatography (HPLC). The recoveries (±*SE*) of aspirin (I) and salicylic acid (II) from whole blood were 97.8 ± 3.2 and 98.3 ± 2.7%, respectively. Aspirin hydrolysis during the entire workup was 5.4 ± 0.5% (*SE*).

**Enzymatic Hydrolytic Cleavage of XIV–XIX and Aspirin in Human Plasma**—The plasma[3] was stored in a refrigerator and used within 1 week from the date it was collected. A portion of 100 μl of a standard solution of the compound in acetonitrile was added to 10 ml of plasma at 37°. The plasma samples were extracted according to a literature method (26). Thus, 0.50-ml samples of plasma were withdrawn from the test medium, placed in 15-ml stoppered centrifuge tubes, and acidified with 0.50 ml of 10% potassium bisulfate and 1 drop of potassium fluoride (~25 mg). Chloroform (3 ml) was added to each tube and mixed on a mechanical shaker for 15 min.

The resulting emulsions were centrifuged, and 2.0 ml of the chloroform solution was recovered. These extracts were evaporated to dryness under continuous nitrogen flow, and the residue was dissolved in 0.50 ml of methanol. The methanolic solution was analyzed by HPLC. Plasma samples were also analyzed separately by injecting 5–10 μl of plasma directly into the chromatograph. Both methods gave the same results. In the plasma studies, the substrate concentration was kept low ($<10^{-3}$ *M*), and the rate constants were calculated as first order by following the disappearance of the compound with time.

**Analytical Methods**—An HPLC method was developed for studies of the complex degradation of 2-acetoxybenzoates because hydrolysis of XVII–XIX can lead to at least three possible hydrolytic products for each compound. The chromatographic analysis was performed on a component system[4]. A 30-cm × 3.9-mm i.d. column[5], operated at ambient temperature, was used for all separations. The mobile phase used for the separation of methylthiomethyl 2-acetoxybenzoate (XVII) and its degradation products consisted of acetonitrile–acetic acid/sodium acetate–water (450:10:540). The pH was adjusted to 3.86 with 25% aqueous NaOH. At a flow rate of 2.0 ml/min, the retention times of XVII, XIV, aspirin (I), and salicylic acid (II) were 6.2, 9.2, 2.2, and 2.0 min, respectively.

The mobile phase used for separation of methylsulfinylmethyl (XVIII) and methylsulfonylmethyl (XIX) 2-acetoxybenzoates and their degradation products consisted of acetonitrile–methanol–acetic acid/sodium acetate–water (140:115:5:740). The pH was adjusted to 3.86 with 25% aqueous NaOH. At a flow rate of 2.0 ml/min, the retention times of XVIII, XIX, XV, XVI, I, and II were 6.9, 9.5, 7.1, 10.1, 5.2 and 3.6 min, respectively. For the separation of the benzoate derivatives, 70% methanol in water was used as the mobile phase. The plot of the peak heights *versus* the various amounts of each derivative studied was linear in the concentration range studied. In the reaction mixture, the concentration of the compounds was determined by comparison of the peak heights for the compounds to the corresponding standard curves. When the biological extracts or fluids were analyzed, the column was protected by a 5-cm × 2-mm i.d. precolumn packed with CO:Pell ODS[6].

## RESULTS AND DISCUSSION

The prodrugs of aspirin (XVII–XIX) and those of salicylic acid (XIV–XVI) were well-defined, stable compounds and are easy to synthesize. As expected, the melting point of the compounds increases in the

[3] The human plasma was obtained from the Community Blood Center of Greater Kansas City and contained ~80% plasma diluted with anticoagulant citrate phosphate dextrose solution USP.

[4] Waters Associates model 600-A solvent delivery system, model U-6K injector, and model 440 dual-channel detector operated at 280 nm.

[5] Waters Associates μBondpak $C_{18}$.

[6] Whatman.

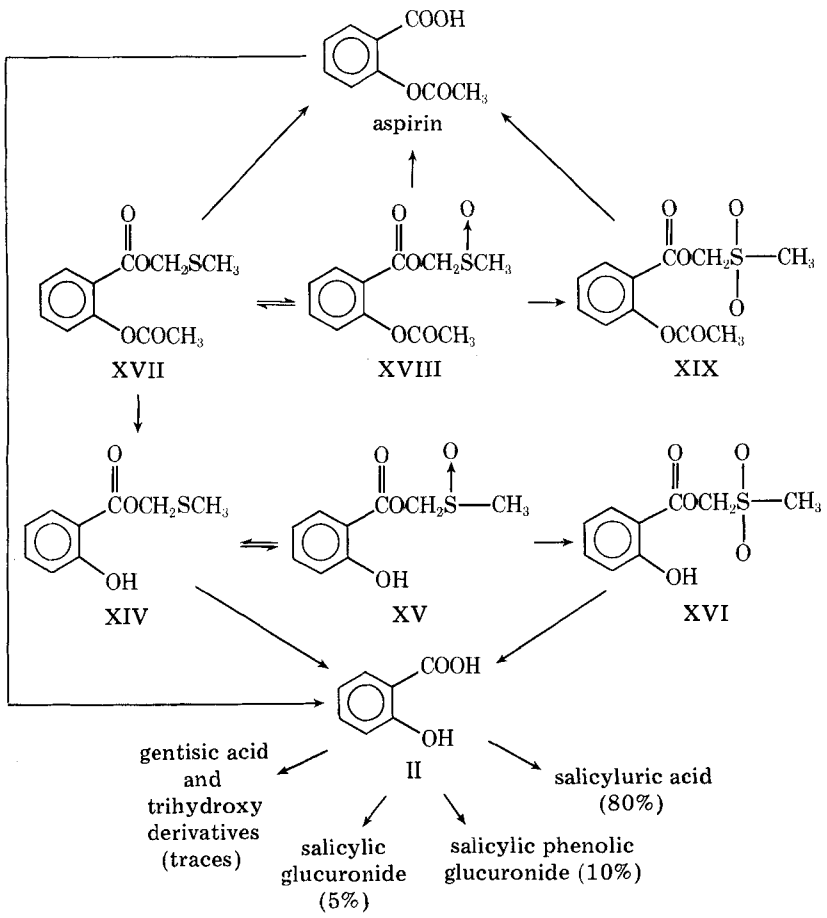


*Scheme I—Possible metabolic routes of methylthiomethyl (XVII), methylsulfinylmethyl (XVIII), and methylsulfonylmethyl (XIX) 2-acetoxybenzoates (based on Refs. 25, 27, and 28 and results obtained in this work).*

order of level of oxidation stage. Thus, while the methylthiomethyl derivative XVII is a liquid, XVIII has a melting point of 120° and XIX melts at 153°. The solubilities follow the reverse order since XVII is freely soluble in acetonitrile, methanol, and polyethylene glycol 400 (0.1 g/ml) while XIX is only sparingly soluble in methanol and acetonitrile and almost insoluble in polyethylene glycol.

Detailed physicochemical studies of the new esters, XII–XIX, were carried out after it was shown that enzymic cleavage of the aspirin prodrugs XVII–XIX results in significant amounts of aspirin.

The possible routes for the complex interconversion–metabolism of the prodrugs are shown in Scheme I. Thus, XVII, XVIII, and XIX theoretically could cleave to provide aspirin or the corresponding salicylates (XIV, XV, and XVI, respectively). Everything would finally result in salicylic acid, which undergoes the usual metabolism (25, 27, 28).

Alternatively, the thiomethyl ester(s) could undergo reversible oxidation to the sulfinyl and then to the corresponding sulfonyl esters.

Aspirin is hydrolyzed rapidly at 37° in human whole blood and plasma, with an average half-life of ~30 min and 1 hr, respectively (29). In the human body, aspirin is hydrolyzed even faster, with a half-life of 13–20 min (9) to form salicylic acid, which then is conjugated in part with glycine and glucuronic acid to form various acyl and phenolic conjugates (30). Several other minor metabolites also are formed. Free salicylic acid and its metabolites are eliminated from the body by renal excretion. For any derivative to be called a true aspirin prodrug, it has to be hydrolyzed enzymatically or nonenzymatically within the body to form aspirin. The rate of conversion must ensure buildup of the drug to a level capable of eliciting a pharmacological effect. Aspirin is much more active as an analgesic agent than salicylic acid, and aspirin formation in the body could be important for the analgesic activity of the compound (18).

Human plasma was used to determine the hydrolysis routes and rates of the compounds of main interest (XVII–XIX), as compared to the salicylates (XIV–XVI) and aspirin.

The hydrolysis rates in plasma of the 2-acetoxybenzoate esters (XVII–XIX) measured by following the disappearance of the compound with time and that of aspirin are listed in Table I. All three aryl esters have much shorter half-lives than that obtained for aspirin (~2 hr). Rowland *et al.* (9) studied aspirin hydrolysis in 90% volume fresh human blood and plasma at 37° and found the average half-life to be ~30 min in whole blood and slightly over 1 hr in plasma. In the present experiment,

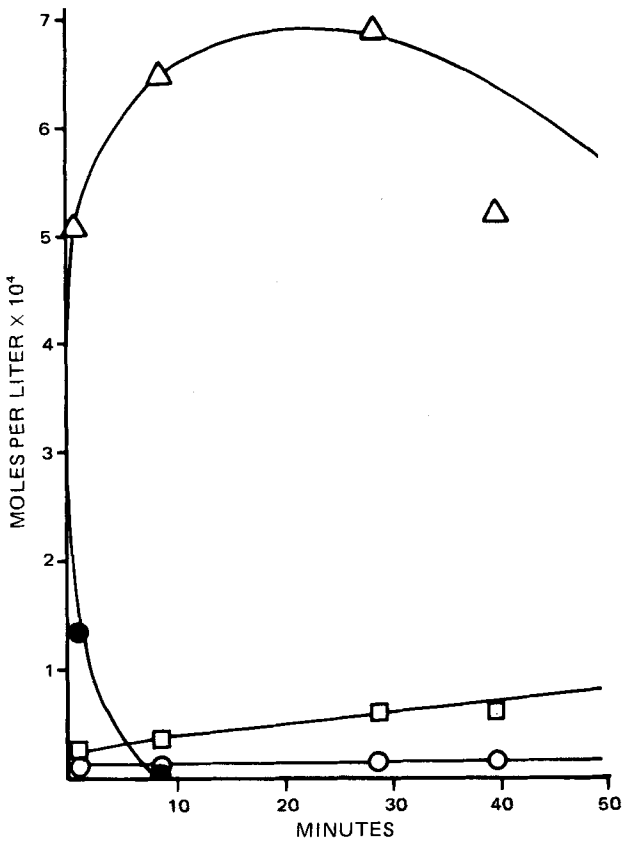


**Figure 1**—*Concentration–time profile for the hydrolytic cleavage of the aspirin derivative XVII (●) in human plasma* in vitro *at 37° and its hydrolytic products, the salicylate ester XIV (△), aspirin (□), and salicylic acid (○).*

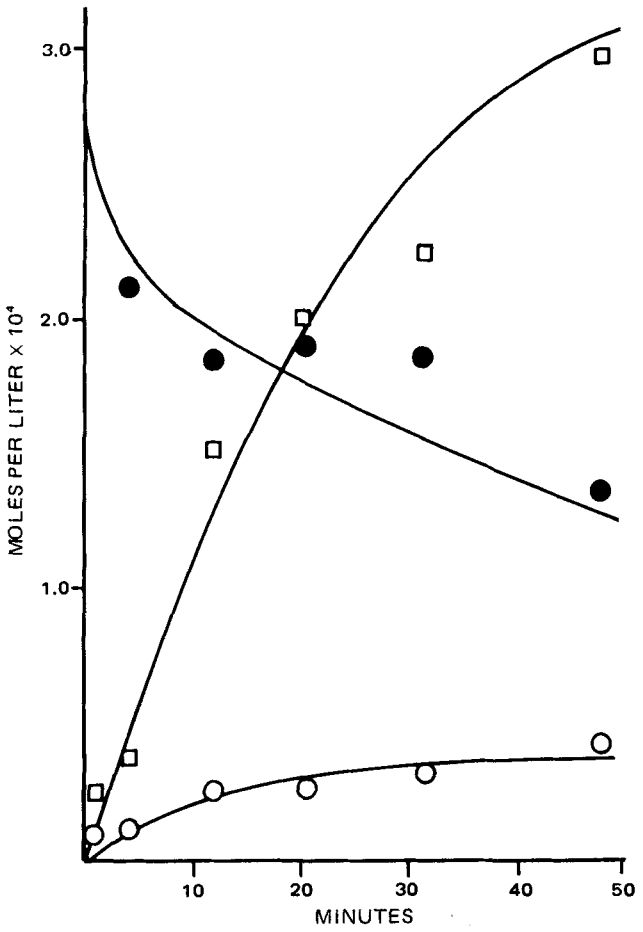


**Figure 2**—*Concentration–time profile for the hydrolytic cleavage of the ester XVIII (●) in human plasma* in vitro *at 37°. Aspirin (□) and salicylic acid (○) were forming.*

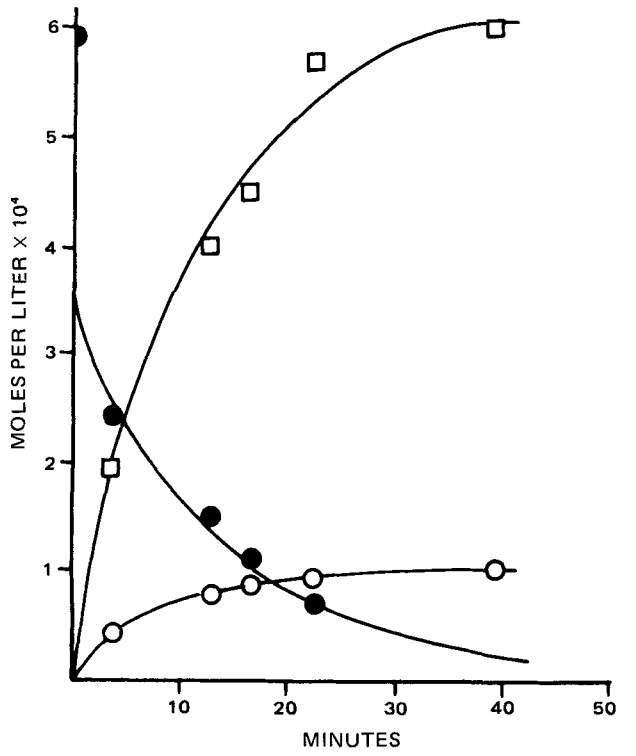


**Figure 3**—*Concentration–time profile for the hydrolysis of the aspirin derivative XIX (●) in human plasma* in vitro *at 37°. Aspirin (□) and salicylic acid (○) were the hydrolysis products.*

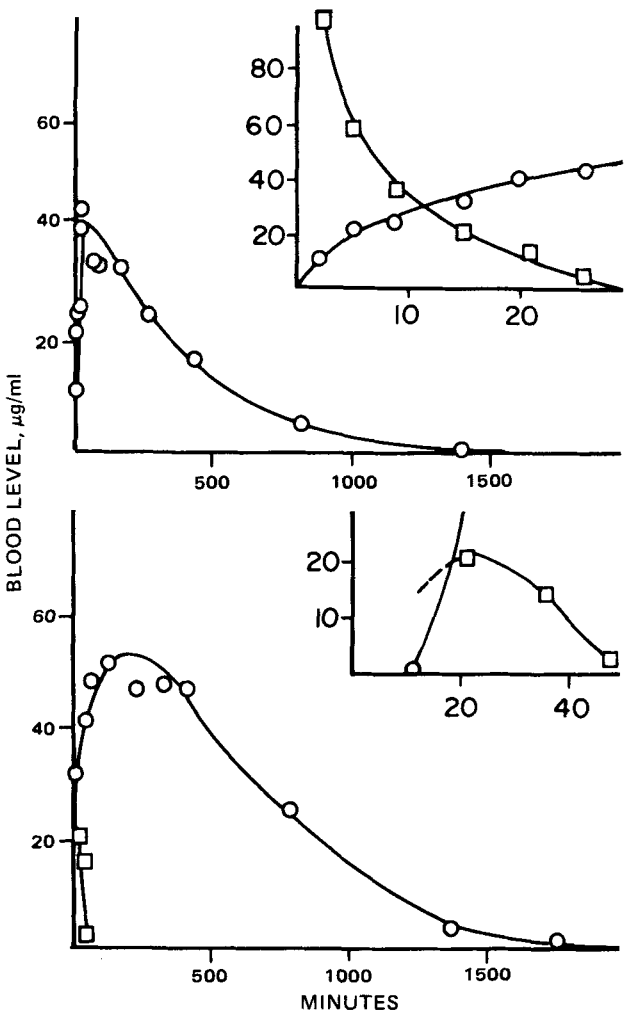


**Figure 4**—*Blood levels of aspirin (□) and salicylic acid (○) following an intravenous dose of 250 mg of aspirin (I) to an 8.4-kg dog (top) and an oral dose of 397 mg of I to an 11.6-kg dog (bottom).*

80% volume plasma was used under different conditions and the aspirin half-life was somewhat longer. A wide variation in hydrolysis rates of aspirin was seen in plasma from different individuals (31). The hydrolysis rates of the 2-hydroxybenzoates (XIV–XVI) are compared to that of methyl salicylate (XX) in Table II. The ester, XX, was selected as a model

**Table I—Hydrolysis of Methylthiomethyl (XVII), *Methylsulfinylmethyl (XVIII), and Methylsulfonylmethyl* (XIX) 2-Acetoxybenzoates and Aspirin (I) in Two Batches of Human Plasma at 37.0°**

| Compound | $k_{obs}$[a], $min^{-1}$ | | | $t_{1/2}$, min |
|---|---|---|---|---|
| | Batch I | Batch II | Average | |
| XVII | 0.45 | 0.73 | 0.59 | 1.2 |
| XVIII | $5.2 \times 10^{-2}$ | $4.8 \times 10^{-2}$ | $5.0 \times 10^{-2}$ | 14 |
| XIX | $6.6 \times 10^{-2}$ | $8.1 \times 10^{-2}$ | $7.4 \times 10^{-2}$ | 9.4 |
| I | — | $6.0 \times 10^{-3}$ | $6.0 \times 10^{-3}$ | $1.2 \times 10^{2}$ |

[a] Based on disappearance of starting compound.

**Table II—Hydrolysis Rates of the Salicylate Esters XIV, XV, and XVI and Methyl Salicylate (XX) in Human Plasma at 37°**

| Compound | $k_{obs}$, $min^{-1}$ | $t_{1/2}$, min | $k/k_m$[a] |
|---|---|---|---|
| XX | $1.4 \times 10^{-3}$ | $5.0 \times 10^{2}$ | 1.0 |
| XIV | $8.8 \times 10^{-2}$ | 79 | 6.3 |
| XV | $4.5 \times 10^{-2}$ | 15 | 32 |
| XVI | $9.4 \times 10^{-2}$ | 7.4 | 67 |

[a] Represents the relative hydrolysis rates of XIV, XV, and XVI compared to XX.

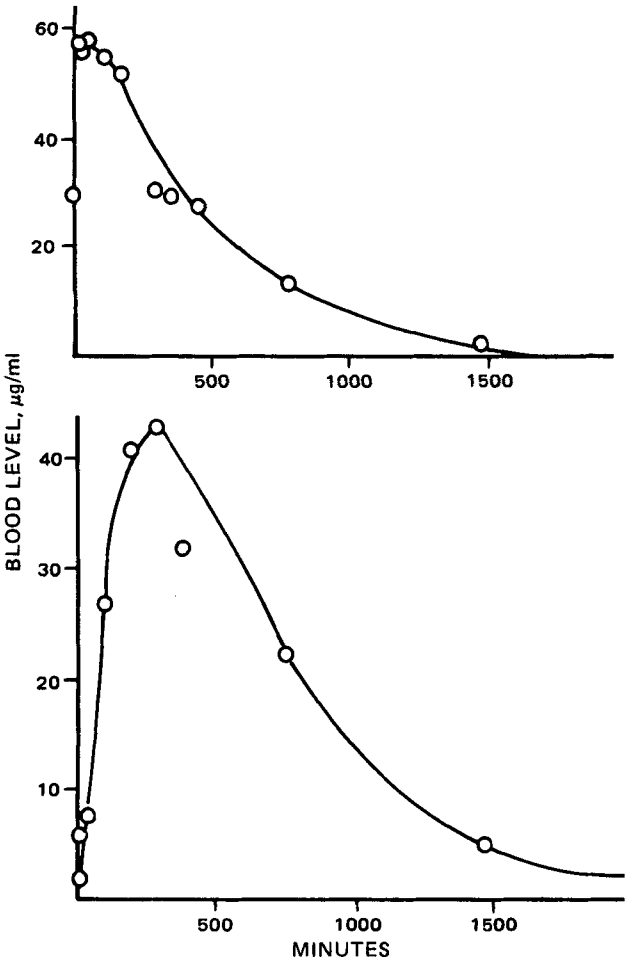


**Figure 5**—*Blood levels of salicylic acid (○) after administration of an intravenous dose of 302 mg of methylthiomethyl 2-acetoxybenzoate (XVII) to an 8.6-kg dog (top) and an oral dose of 570 mg of XVII to an 8.4-kg dog (bottom).*

for a salicylate. The $k_{obs}$ values were determined following the disappearance of the starting materials.

All sulfur-containing "activated" esters (XIV–XVI) are hydrolyzed faster in plasma than the methyl 2-hydroxybenzoate (XX). Thus, the methylsulfonylmethyl ester (XVI) is hydrolyzed 67 times faster than the methyl ester.

The disappearance of the aspirin prodrugs and appearance of aspirin, salicylic acid, and the corresponding salicylates are shown in Figs. 1–3. The prodrugs XVIII and XIX result in significant aspirin concentrations, while XVII cleaves according to both pathways, one leading to the salicylate (XIV) and the other to aspirin. These results imply that XVIII and XIX are promising true prodrugs of aspirin since no formation of the salicylates XV and XVI, respectively, was observed, and the main hydrolysis product was aspirin. The delivery characteristics of XVII–XIX thus were determined *in vivo* using beagle dogs.

After oral administration of XVII, XVIII, XIX, or aspirin equivalent to 50 mg of aspirin/kg and intravenous administration of XVII, XVIII, XIX, or aspirin equivalent to 25 mg of aspirin/kg to dogs, the appearance in the blood of the compound and its possible metabolites was followed as a function of time. With XIX, only 8 mg/kg was administered intravenously to the dog because of its low solubility in the vehicle dimethyl sulfoxide. The appearance and disappearance of salicylic acid in the blood were fitted to an exponential equation $C_p = Ne^{-k_a t} + Le^{-\alpha t} + Me^{-\beta t}$ (32, 33). The blood aspirin concentration after oral and intravenous administration of aspirin also was fit to the exponential equation, where $k_a$ was set equal to infinity after intravenous administration (34). The disappearance of XVIII in the blood after intravenous administration was fit to a simple first-order equation. The results are shown in Figs. 4–7.

The methylthiomethyl (XVII) and methylsulfonylmethyl (XIX) 2-acetoxybenzoates were metabolized rapidly in the body, resulting in peak blood salicylic acid levels within the first 10 min after an intravenous dose (Figs. 5 and 7). The first samples were withdrawn at 2 min after the intravenous injection. No aspirin, starting 2-acetoxybenzoate, or the possible intermediate 2-hydroxybenzoate esters was detected in these samples. After oral administration of XVII and XIX, only salicylic acid was detected. Methylsulfinylmethyl 2-acetoxybenzoate (XVIII) was metabolized more slowly, with a peak blood salicylic acid level at 30 min after an intravenous dose (Fig. 6), which is about the same time as obtained after intravenous aspirin (Fig. 5). Within 3–5 min after the intravenous administration, the aspirin formation rate was equal to the disappearance rate of XVII. However, after 7 min, no XVIII or aspirin was detected in the blood. After oral administration of XVIII, only salicylic acid was detected with a peak blood level at 300 min (Fig. 5).

All aspirin derivatives (XVII–XIX) apparently are metabolized mainly to salicylic acid.

Aspirin is hydrolyzed rapidly in the body to form salicylic acid. After intravenous aspirin, the plasma aspirin concentration *versus* time curve can be described by the biexponential equation $C_p = Ae^{-\alpha t} + Be^{-\beta t}$ (34). The half-life of the first exponent ($\alpha$) is 2–5 min and that of $\beta$ is 13–19 min. Therefore, aspirin disappears rapidly as it is formed from its prodrugs XVII–XIX and never reaches high blood levels. Salicylic acid was shown to be the only direct metabolite of aspirin (32). For the methylsulfinylmethyl 2-acetoxybenzoate (XVIII) to give such high aspirin levels in the body (Fig. 6), comparable to those obtained after an oral dose of aspirin (Fig. 4), a considerable fraction of the dose must be metabolized to form aspirin. Thus, at least XVIII is a true aspirin prodrug.

The analgesic efficacy of aspirin in the dog and the correlation between such analgesia and the plasma levels of aspirin and its primary metabolite, salicylic acid, were studied (35). It was concluded that the onset and duration of aspirin analgesia after oral and intravenous administration cannot be correlated with plasma aspirin levels and that, during analgesia, aspirin can only be detected in extremely low concentrations because of its rapid hydrolysis to salicylic acid. Therefore, although XVIII is the only

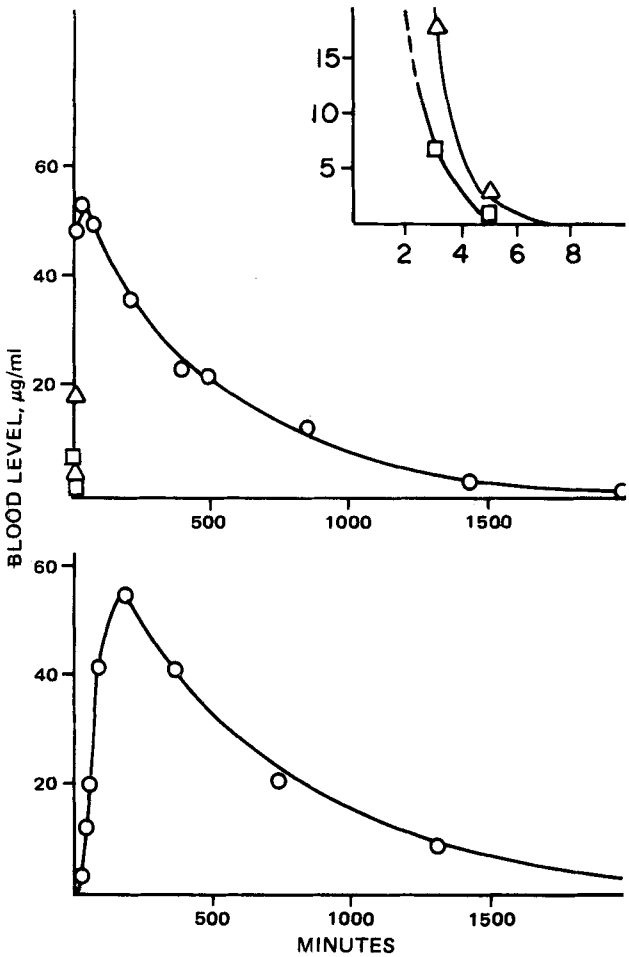


**Figure 6**—*Blood levels of methylsulfinylmethyl 2-acetoxybenzoate (XVIII) (△), aspirin (□), and salicylic acid (○) after administration of an intravenous dose of 370 mg of XVIII to a 9.2-kg dog (top) and an oral dose of 620 mg of XVIII to a 9.0-kg dog (bottom).*

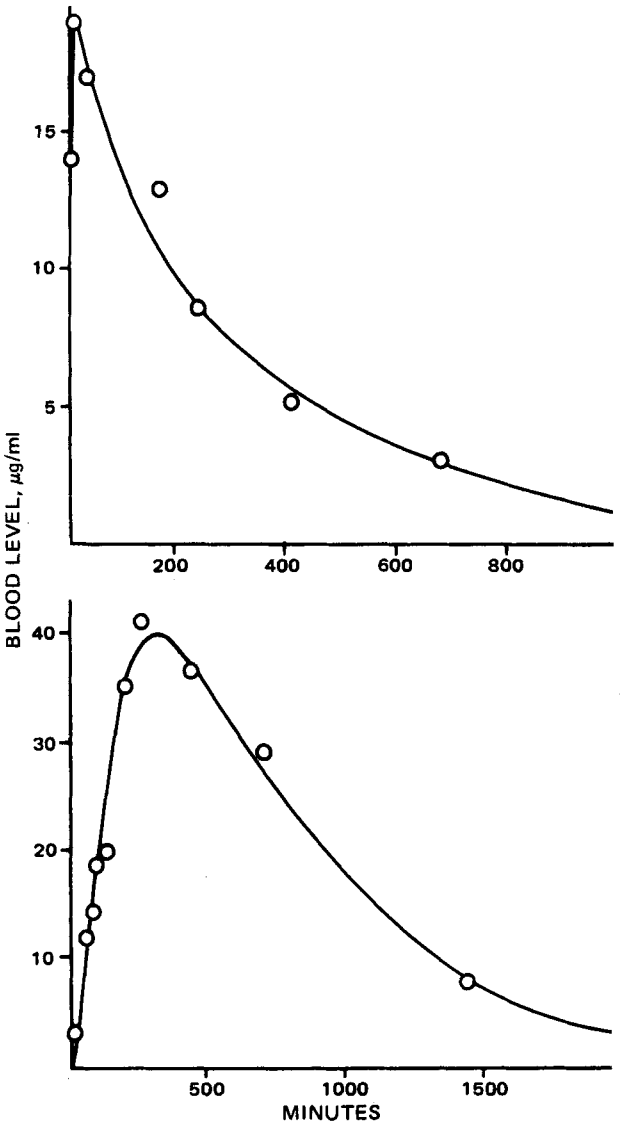


**Figure 7**—*Blood levels of salicylic acid (○) after administration of an intravenous dose of 115 mg of methylsulfonylmethyl 2-acetoxybenzoate (XIX) to a 9.2-kg dog (top) and an oral dose of 750 mg of XIX to a 9.2-kg dog (bottom).*

one of the three aspirin derivatives that gives detectable blood levels of aspirin in the dog, this finding does not necessarily mean that XVII and XIX are not useful prodrugs. This is particularly true since aspirin is metabolized about three times faster in dogs than in humans. Based on the human plasma cleavage data, XVII results mainly in the salicylate XIV. On the other hand, the methylsulfonylmethyl ester (XIX) has solubility problems. Thus, at least the methylsulfinylmethyl ester XVIII is a promising aspirin prodrug.

Similar prodrugs should be useful for improved delivery of a wide variety of acidic drugs, including the various known anti-inflammatory agents.

## REFERENCES

(1) K. D. Rainsford, *Agents Actions*, **7**, 573 (1977).
(2) L. J. Edwards, *Trans. Faraday Soc.*, **46**, 723 (1950).
(3) *Ibid.*, **48**, 696 (1952).
(4) E. R. Garrett, *J. Am. Chem. Soc.*, **79**, 3401 (1957).
(5) M. L. Bender, *Chem. Rev.*, **60**, 53 (1960).
(6) A. R. Fersht and A. J. Kirby, *J. Am. Chem. Soc.*, **89**, 4853, 4857 (1967).
(7) *Ibid.*, **90**, 5818 (1968).
(8) J. St. Pierre and W. P. Jencks, *J. Am. Chem. Soc.*, **90**, 3817 (1968).
(9) M. Rowland, S. Riegelman, P. A. Harris, and S. D. Sholkoff, *J. Pharm. Sci.*, **61**, 379 (1972).
(10) L. Lasagna, *Am. J. Med. Sci.*, **242**, 620 (1961).
(11) E. R. Garrett, *J. Am. Pharm. Assoc., Sci. Ed.*, **48**, 676 (1959).
(12) G. Levy and B. A. Gragliardi, *J. Pharm. Sci.*, **52**, 730 (1963).
(13) P. H. N. Wood, E. A. Harvey-Smith, and A. St. J. Dixon, *Br. Med. J.*, **1**, 669 (1962).
(14) E. C. Taylor, G. W. McLay, and A. McKillop, *J. Am. Chem. Soc.*, **90**, 2422 (1968).
(15) D. N. Croft, J. H. P. Cuddigan, and C. Sweetland, *Br. Med. J.*, **3**, 545 (1972).
(16) J. E. Murphy, *J. Int. Med. Res.*, **1**, 65 (1972).
(17) R. Kumar and J. D. Billimoria, *J. Pharm. Pharmacol.*, **30**, 754 (1978).
(18) G. Y. Paris, D. L. Garmaise, D. G. Cimon, L. Swett, G. W. Carter, and P. Young, *J. Med. Chem.*, **22**, 683 (1979).
(19) E. Aron, B. Delbarre, and J. C. Besnard, *Therapie*, **31**, 247 (1976).
(20) A. Hussain, M. Yamasaki, and J. Truelove, *J. Pharm. Sci.*, **63**, 627 (1974).
(21) H. Cousse, S. Casadio, and G. Mouzin, *Trav. Soc. Pharm. Montpellier*, **38**, 71 (1978).
(22) A. F. Davis and G. J. A. Dixon, British pat. 1,518,622 (1978).
(23) T. L. Ho and C. M. Wong, *J. Chem. Soc. Chem. Commun.*, **1973**, 224.
(24) P. M. Hardy, H. N. Rydon, and R. C. Thompson, *Tetrahedron Lett.*, **1968**, 2525.
(25) D. E. Duggan, K. F. Hooke, R. M. Noll, H. B. Hucker, and C. G. Van Arman, *Biochem. Pharmacol.*, **27**, 2311 (1978).
(26) L. J. Walter, D. F. Biggs, and R. T. Coutts, *J. Pharm. Sci.*, **63**, 1754 (1974).
(27) "The Pharmacological Basis of Therapeutics," L. S. Goodman and A. Gilman, Eds., Macmillan, New York, N.Y., 1970, p. 324.
(28) G. Levy, *Drug Metab. Rev.*, **9**, 3 (1979).
(29) P. A. Harris and S. Riegelman, *J. Pharm. Sci.*, **56**, 713 (1967).
(30) C. Davison, *Ann. N.Y. Acad. Sci.*, **179**, 249 (1971).
(31) A. M. Morgen and E. B. Truitt, *J. Pharm. Sci.*, **54**, 1640 (1965).
(32) M. Gibaldi and D. Perrier, "Pharmacokinetics," Marcel Dekker, New York, N.Y., 1975.
(33) J. G. Wagner, "Fundamentals of Clinical Pharmacokinetics," Drug Intelligence, Hamilton, Ill., 1975.
(34) M. Rowland and S. Riegelman, *J. Pharm. Sci.*, **57**, 1313 (1968).
(35) K. O'Dea, J. Pütter, and F. Hoffmeister, *Arzneim.-Forsch.*, **25**, 8011 (1975).

## ACKNOWLEDGMENTS

Supported by INTER$_x$ Research Corp.

The authors thank Mr. Larry Caldwell for help in the *in vivo* studies and Dr. T. Higuchi for helpful discussions.

For Part VII in this series, see N. Bodor, J. Zupan, and S. Selk, *Int. J. Pharm.*, **7**, 63 (1980).

# Improved Delivery through Biological Membranes IX: Kinetics and Mechanism of Hydrolysis of Methylsulfinylmethyl 2-Acetoxybenzoate and Related Aspirin Prodrugs

**THORSTEINN LOFTSSON * and NICHOLAS BODOR ‡x**

Received August 25, 1980, from the **Department of Pharmaceutical Chemistry, School of Pharmacy, University of Kansas, Lawrence, KS 66045*, and the ‡*Department of Medicinal Chemistry, College of Pharmacy, J. Hillis Miller Health Center, University of Florida, Gainesville, FL 32610.* Accepted for publication November 24, 1980.

**Abstract** □ The complex kinetics and mechanism of the hydrolysis of the methylthiomethyl, methylsulfinylmethyl, and methylsulfonylmethyl 2-acetoxybenzoates, novel aspirin prodrugs, were studied. The pH profiles for the related salicylates and benzoates also were determined. Based on the activation parameters, isotope effects, and other data, it was established that the methylthiomethyl esters hydrolyze *via* a unimolecular alkyl–oxygen cleavage. The methylsulfinylmethyl and methylsulfonylmethyl 2-acetoxybenzoates undergo neutral hydrolysis of esters at pH > 4 to form aspirin, while water acts as a general base; but at lower pH, a different mechanism takes place and the *o*-acetyl group cleaves first, releasing the corresponding salicylates.

**Keyphrases** □ Methylsulfinylmethyl 2-acetoxybenzoate—kinetics and mechanism of hydrolysis □ Prodrugs, aspirin—methylsulfinylmethyl 2-acetoxybenzoate, kinetics and mechanism of hydrolysis □ Hydrolysis—kinetics and mechanism established for methylsulfinylmethyl 2-acetoxybenzoate and other related aspirin prodrugs

The results of the *in vitro* enzymic cleavage studies and the *in vivo* blood level data (1) indicate that the novel aspirin derivatives of the methylsulfinylmethyl and related ester type are promising, true aspirin prodrugs. These observations warranted a detailed study of the complex kinetics and mechanism of the chemical hydrolysis of these esters. Theoretically, the new prodrugs can hydrolyze in two steps *via* two routes (Scheme I).

Thus, the pH profiles for the hydrolysis of III–V and VI–VIII were determined and compared to that of aspirin and simple related benzoates [methylthiomethyl benzoate (IX), methylsulfinylmethyl benzoate (X), and methylsulfonylmethyl benzoate (XI)]. The various activated esters (methylthiomethyl, methylsulfinylmethyl, and methylsulfonylmethyl) and the *o*-phenolacetates may have different mechanisms of hydrolysis at the various pH values. The influence of ionic strength, dielectric constant, activation parameters, and solvent isotope effects also was studied to elucidate the mechanism of the hydrolysis and to explain the shapes of the pH profiles.

Comparison of the chemical and the enzymic hydrolysis revealed interesting differences.

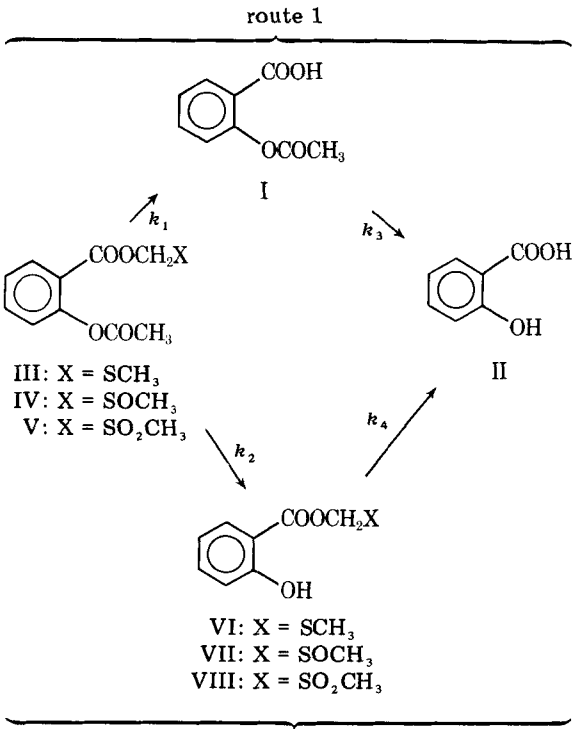


*Scheme I*

## EXPERIMENTAL

**Instrumentation**—The high-pressure liquid chromatographic (HPLC) method (1) was used for the determination of aspirin (I), salicylic acid (II), the aspirin derivatives (III–V), and the salicylates (VI–VIII), except at pH > 9.55. At these pH values, the hydrolytic rate constants were determined directly spectrophotometrically at 349 nm using a spectrophotometer[1] equipped with a thermostated cell compartment maintained at 50.8° by a circulating water bath.

The phenolic pKa values of VI–VIII were determined[1] spectrophotometrically at room temperature. Four ovens were used in the determination of the activation parameters. A research pH meter[2] was equipped with a combination glass electrode standardized at the temperature at which the kinetic data were obtained.

**Materials**—All buffer solutions for kinetic studies were prepared from deionized water that was boiled for 5 min to liberate the dissolved gases and cooled under nitrogen. Sufficient water was added to weighed amounts of various buffer salts to yield a solution of the desired molarity and ionic strength. The buffer solutions were thermostated at 50.8° where the pH and volumes were adjusted. All buffer solutions were stored under nitrogen in a refrigerator and used within 1 week. Where the buffer capacity was questionable, the pH was checked following each kinetic run. All chemicals used were analytical grade.

**Determination of Hydrolytic Rate Constants**—For the determination of the hydrolysis rate constants of aspirin (I), its derivatives (III–V), and related compounds (VI–XI), 50 μl of a concentrated acetonitrile solution of each ester was added separately to 10 ml of buffer, previously equilibrated to the desired temperature in a water bath, and mixed thoroughly to give an initial concentration of $5 \times 10^{-4}$ mole/liter. All reactions were run under pseudo-first-order conditions. Aliquots (100 μl) were injected into the column at various intervals, and the pseudo-first-order rate constants were determined from the disappearance of the compound by linear regression of natural logarithm of the peak height *versus* time plots. The half-life, correlation coefficient, and standard error

[1] Cary 219.

[2] Orion model 701.



*0022-3549/81/0700-0750$01.00/0*
*© 1981, American Pharmaceutical Association*

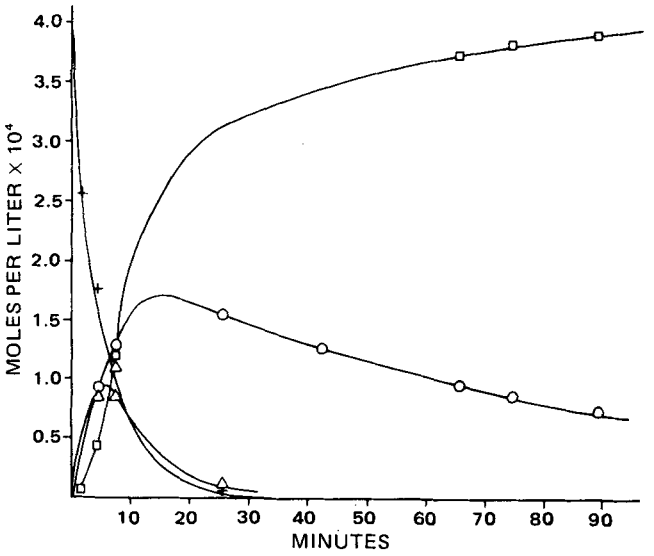


**Figure 1**—*Kinetics of hydrolysis of methylthiomethyl 2-acetoxybenzoate (III) (+) in 0.01* M *carbonate buffer (pH 9.55) at 50.8° and 0.1* M *ionic strength to form methylthiomethyl 2-hydroxybenzoate (VI) (△), aspirin (I) (○), and salicylic acid (II) (□).*

of the rate constant were calculated for each run (2).

At lower pH values, where hydrolysis was slow, the reaction mixture was introduced into ampuls of 1 or 2 ml, sealed under nitrogen, and immersed in a thermostated bath. Individual ampuls were withdrawn at various times, and the concentrations were determined using HPLC. At higher pH values, where the disappearance of absorbance at 349 nm was followed, 20 μl of a concentrated solution of the reactant in acetonitrile was added to 3 ml of buffer in a 1-cm quartz cell previously equilibrated to 50.8° in the cell compartment of the spectrophotometer. The cell was closed and shaken to ensure mixing. The pseudo-first-order rate constant was determined by linear regression of $\ln(A_t - A_\infty)$ *versus* time, where $A_\infty$ is the absorbance at 349 nm after 10 half-lives and $A_t$ is the absorbance at time $t$.

**Determination of Phenolic pKa Values of VI–VIII**—The pKa values for the 2-hydroxybenzoates (VI–VIII) were determined spectrophotometrically at room temperature (23°). Five tris(hydroxymethyl)-aminomethane and three carbonate buffers of ionic strength 0.1 *M* (using sodium chloride) were prepared at 23° in the pH 8.38–10.14 range. The UV absorption of the undissociated and dissociated forms was determined in 0.1 *N* HCl and 0.01 *M* $Na_2CO_3$ solutions. A solution (100 μl) of the compound in acetonitrile was added to 3.00 ml of buffer at time zero. Due to the rapid hydrolysis of the ester(s), the decrease in absorbance at 23° was followed at a given wavelength for a short time, and the absorbance at time zero was found by extrapolation. The pKa values were calculated using $pKa = pH - \log(a_{obs} - a_{HA})/(a_{A^-} - a_{obs})$, where $a_{obs}$ is the absorbance of the solution tested, $a_{HA}$ is absorbance of the unionized species, and $a_{A^-}$ is the absorbance of the ionized species. The pKa of methylthiomethyl 2-hydroxybenzoate (VI) was 9.60 ± 0.01; it was 9.00 ± 0.2 and 8.91 ± 0.02 for methylsulfinylmethyl 2-hydroxybenzoate (VII) and methylsulfonylmethyl 2-hydroxybenzoate (VIII), respectively.

**Determination of Activation Parameters for III and VI–VIII Hydrolysis**—The change in the reaction rates with temperature for the hydrolysis of VI–VIII in 0.1 *N* HCl (pH 1.1) and of III in unbuffered aqueous solution (pH 5) was studied. The ionic strength was maintained at 0.1 *M* with sodium chloride. Because of the slow reaction, the activation parameters for the hydrolysis of VII and VIII were determined using solutions of the compounds sealed in ampuls and stored at constant temperature for various intervals in four ovens maintained at 35.8, 44.0, 61.0, and 102.8°, respectively. The activation parameters for III and VI hydrolysis were determined by measuring the pseudo-first-order rate constants at 50–30°.

**Influence of Ionic Strength and Dielectric Constant**—The effect of the solvent ionic strength (0.05–0.5 *M* NaCl) on III hydrolysis in unbuffered aqueous solutions was studied at 50.8°. The effect of the solvent dielectric constant on the reaction rate also was investigated at 50.8° in an aqueous solution containing up to 30% dioxane. The dielectric constant of each water–dioxane mixture was calculated at 50.8° (3). The pseudo-first-order rate constants were determined using HPLC to follow the disappearance of III as a function of time.

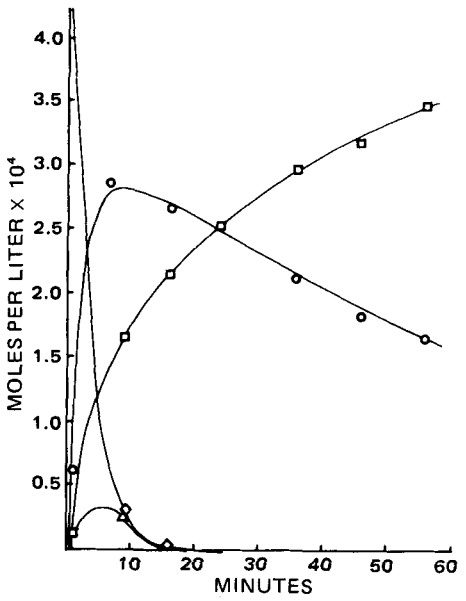


**Figure 2**—*Kinetics of hydrolysis of methylsulfinylmethyl 2-acetoxybenzoate (IV) in 0.01* M *carbonate buffer (pH 9.55) at 50.8° and 0.1* M *ionic strength to form methylsulfinylmethyl-2-hydroxybenzoate (VII) (△), aspirin (○), and salicylic acid (□).*

**Solvent Isotope Effect**—The deuterium solvent isotope effects on the hydrolysis rate of III, VII, and VIII were measured at 50.8° and ionic strength 0.1 *M*. The pseudo-first-order rate constants were determined as described. The hydrolysis rate constants for VII and VIII were determined in 0.1 *N* DCl solution in deuterium oxide (pD 0.9).

## RESULTS AND DISCUSSION

The hydrolysis rate constants were all first order for the 2-acetoxybenzoates (III–V). The pseudo-first-order rate constants ($k_{obs}$) for the three 2-acetoxybenzoates were determined by HPLC following the disappearance of the compound as a function of time at pH 1.13, 2.64, 4.00, 7.96, and 9.55 at four buffer concentrations at 50.8 ± 0.2° and ionic strength 0.1 *M*. The kinetics of the disappearance of III and the formation of the various hydrolysis products (I, II, and VI) are exemplified in Fig. 1 (pH 9.55 at 50.8°). Under the same conditions, IV gave only traces of the salicylate (VII) (Fig. 2) while the most reactive V hydrolyzed only to aspirin (Fig. 3).

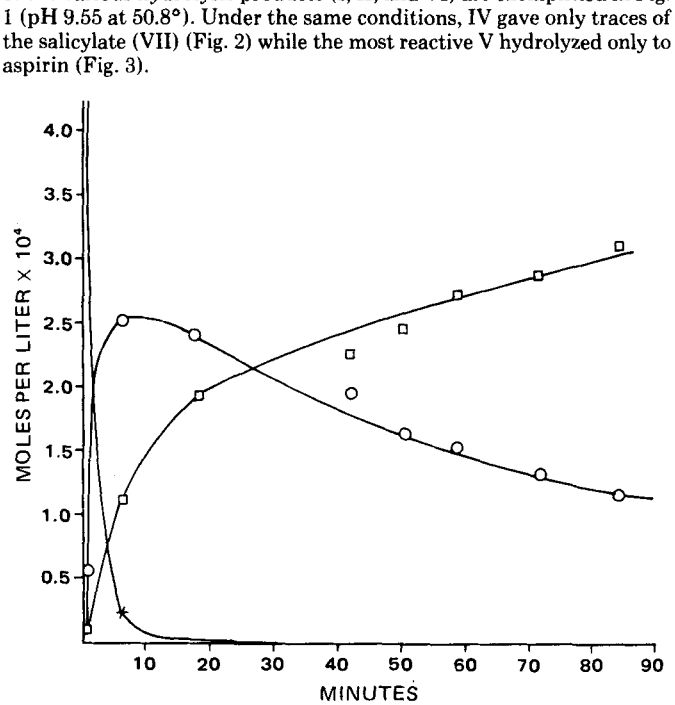


**Figure 3**—*Kinetics of hydrolysis of methylsulfonylmethyl 2-acetoxybenzoate (V) (+) in 0.01* M *carbonate buffer (pH 9.55) at 50.8° and 0.1* M *ionic strength to form aspirin (○) and salicylic acid (□).*

**Table I—Pseudo-First-Order Hydrolytic Rate Constants at Zero Buffer Concentration ($k_0$) for the Disappearance of Methylthiomethyl (III), Methylsulfinylmethyl (IV), and Methylsulfonylmethyl (V) 2-Acetoxybenzoates at 50.8 ± 0.2° and 0.1 *M* Ionic Strength**

| Buffer | pH | III | | IV | | V | |
|---|---|---|---|---|---|---|---|
| | | $k_0$, $min^{-1}$ | $t_{1/2}$, min | $k_0$, $min^{-1}$ | $t_{1/2}$, hr | $k_0$, $min^{-1}$ | $t_{1/2}$, hr |
| 0.100 *N* HCl | 1.13 | $8.26 \times 10^{-2}$ | 8.39 | $1.15 \times 10^{-3}$ | 10.0 | $0.90 \times 10^{-4}$ | 11.7 |
| Monochloroacetate | 2.64 | $5.68 \times 10^{-2}$ | 12.2 | $5.56 \times 10^{-5}$ | 208 | $5.15 \times 10^{-5}$ | 224 |
| Succinate | 4.00 | $6.10 \times 10^{-2}$ | 11.4 | $2.60 \times 10^{-5}$ | 444 | $1.95 \times 10^{-5}$ | 592 |
| Tris(hydroxymethyl)aminomethane | 7.96 | $6.39 \times 10^{-2}$ | 10.8 | $9.30 \times 10^{-3}$ | 1.24 | $1.27 \times 10^{-2}$ | 0.91 |
| Carbonate | 9.55 | 0.17 | 4.1 | 0.32 | 0.04 | 0.48 | 0.02 |

**Table II—Acid-Catalyzed, Base-Catalyzed, and Spontaneous Hydrolytic Rate Constants for Methylthiomethyl (III), Methylsulfinylmethyl (IV), and Methylsulfonylmethyl (V) 2-Acetoxybenzoates [a]**

| Rate Constant [b] | III | IV | V |
|---|---|---|---|
| $k_H$ | $2.97 \times 10^{-1}$ | $1.48 \times 10^{-2}$ | $1.42 \times 10^{-2}$ |
| $k_{H_2O}$ | $6.06 \times 10^{-2}$ | $2.35 \times 10^{-5}$ | $1.86 \times 10^{-5}$ |
| $k_{OH}$ | $5.61 \times 10^{2}$ | $1.75 \times 10^{3}$ | $2.50 \times 10^{3}$ |

[a] Conditions of 50.8 ± 0.2° and ionic strength 0.1 *M* (sodium chloride). [b] $k_H$ is the specific acid hydrolytic rate constant in liters per mole minute, $k_{H_2O}$ is the spontaneous hydrolytic rate constant in $minutes^{-1}$, and $k_{OH}$ is the specific base hydrolytic rate constant in liters per mole minute.

The $k_{obs}$ values were plotted against the buffer concentration, and the rate constants at zero buffer concentration ($k_0$) were obtained by linear regression (Table I). Only the carbonate buffer had any effect on the hydroxide-ion-catalyzed hydrolysis of III (slope = 2.50 ± 0.30) and IV (slope = 2.00 ± 0.01), but it had little effect on V hydrolysis. Tris(hydroxymethyl)aminomethane catalyzed the hydrolysis of IV (slope = 0.201 ± 0.007) and V (slope = 0.264 ± 0.009) but showed a very small effect on III (slope = 7.8 ± 0.4 × $10^{-2}$). Succinate buffer had a significant effect on the hydrolysis of V (slope = 3.15 ± 0.49 × $10^{-4}$) but little or no effect on the hydrolysis of the other two 2-acetoxybenzoate esters. The monochloroacetate buffer had a much smaller effect. The main degradation products at each pH were identified by HPLC to be the compounds according to Scheme I. At pH 4.00, 7.96, and 9.55, the main hydrolysis product was aspirin, which hydrolyzed further to salicylic acid (route 1, Scheme I); at pH 1.13, IV and V hydrolyzed to form only the corresponding 2-hydroxybenzoate esters (VII and VIII) (route 2), which are stable at low pH; no aspirin was formed. Compound III hydrolyzed mainly through route 1 at all pH values studied. The pH profiles for III–V, together with aspirin (I), are shown in Fig. 4. The curves for III–V can be described as a simple ester hydrolysis by:

$$k_0 = k_H a_{H^+} + k_{H_2O} + k_{OH} a_{OH^-} \qquad \text{(Eq. 1)}$$

where $k_{H_2O}$ is the rate constant for spontaneous water hydrolysis and $k_H$ and $k_{OH}$ are the rate constants for catalysis of the hydrolysis by hydronium and hydroxide ions, respectively.

The $k_H$, $k_{H_2O}$, and $k_{OH}$ values in Table II were calculated from the pseudo-first-order rate constants given in Table I using pKw = 13.26 at 50° (4). At pH 7.96, $k_1$ (Scheme I) was calculated by measuring the appearance of aspirin (Table III). In the hydrolysis of IV and V, tris(hydroxymethyl)aminomethane mainly affected $k_2$ but had little effect on $k_1$. At 0.04 *M* tris(hydroxymethyl)aminomethane concentration, ~50% of the hydrolysis went through route 1; but at zero buffer concentration, this route increased to ~90%. About 90% of the hydrolysis of III occurred *via* route 1 at all buffer concentrations; thus, its hydrolysis was catalyzed only very slightly by this buffer.

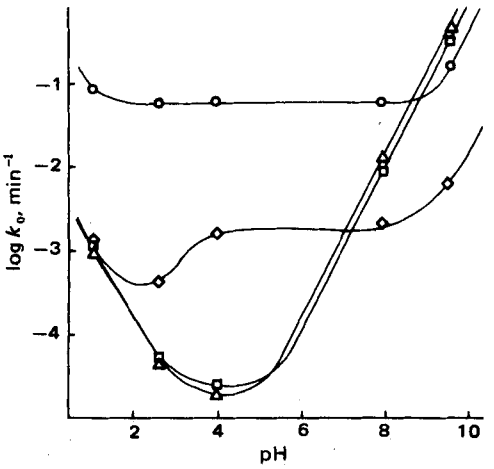


**Figure 4**—*Experimentally determined pH–rate profiles for hydrolysis of the methylthiomethyl (III) (○), methylsulfinylmethyl (IV) (□), and methylsulfonylmethyl (V) (△) 2-acetoxybenzoates at 50.8 ± 0.2° and 0.1 M ionic strength. The smooth curves from pH 0.5 to 10 were calculated using Eq. 1 and the constants given in Table II. The experimentally determined pH profile of aspirin (I) (◇) was included for comparison. The curve was calculated using Eq. 5.*

Hydrolysis of the possible intermediate salicylates (VI–VIII) also was studied. All the pseudo-first-order rate constants ($k_{obs}$) for the hydrolysis of the 2-hydroxybenzoates (VI–VIII) were determined at pH 1.13, 2.02, 2.64, 4.00, 5.97, 6.86, 7.96, 8.82, 9.55, 10.90, and 11.86 at four buffer concentrations at 50.8 ± 0.2° and ionic strength 0.1 *M*. The rate constants at zero buffer concentration ($k_0$) were obtained by extrapolation (Table IV).

Of the seven buffers, only the two trimethamine buffers had any significant effect on the hydrolysis rate. In the case of VI, this catalyzing effect was rather small at pH 7.96, and no effect was observed at pH 8.82. At pH 7.96, the slopes were 1.50 ± 0.06, 1.01 ± 0.08, and 2.23 ± 0.39 for VI, VII, and VIII, respectively. The pH rate profiles (Fig. 5) were fitted by computer to:

$$k_0 = f_{acid} k_{H_2O} + f_{base} k'_{H_2O} \qquad \text{(Eq. 2)}$$

where $k_{H_2O}$ and $k'_{H_2O}$ are the rate constants for the spontaneous water hydrolysis of the undissociated and dissociated reactant, respectively,

**Table III—Pseudo-First-Order Hydrolytic Rate Constants of Methylthiomethyl (III), Methylsulfinylmethyl (IV), and Methylsulfonylmethyl (V) 2-Acetoxybenzoates in Tris(hydroxymethyl)aminomethane Buffers at pH 7.96, 50.8 ± 0.1°, and 0.1 *M* Ionic Strength**

| Buffer, *M* | III | | | IV | | | V | | |
|---|---|---|---|---|---|---|---|---|---|
| | $k'$ [a], $min^{-1}$ | $k_1$, $min^{-1}$ | Route 1 [b], % | $k'$ [a], $min^{-1}$ | $k_1$, $min^{-1}$ | Route 1 [b], % | $k'$ [a], $min^{-1}$ | $k_1$, $min^{-1}$ | Route 1 [b], % |
| 0.01 | $6.57 \times 10^{-2}$ | $6.2 \times 10^{-2}$ | 94 | $1.12 \times 10^{-2}$ | $8.1 \times 10^{-3}$ | 72 | $1.54 \times 10^{-2}$ | $1.2 \times 10^{-2}$ | 78 |
| 0.02 | $6.65 \times 10^{-2}$ | $6.1 \times 10^{-2}$ | 92 | $1.35 \times 10^{-2}$ | $8.0 \times 10^{-3}$ | 59 | $1.77 \times 10^{-2}$ | $1.2 \times 10^{-2}$ | 68 |
| 0.03 | $6.74 \times 10^{-2}$ | $5.4 \times 10^{-2}$ | 80 | $1.53 \times 10^{-2}$ | $8.1 \times 10^{-3}$ | 53 | $2.07 \times 10^{-2}$ | $1.4 \times 10^{-2}$ | 68 |
| 0.04 | $6.80 \times 10^{-2}$ | $6.3 \times 10^{-2}$ | 93 | $1.73 \times 10^{-2}$ | $8.2 \times 10^{-3}$ | 47 | $2.32 \times 10^{-2}$ | $1.3 \times 10^{-2}$ | 56 |
| Zero | $6.50 \times 10^{-2}$ | $6.1 \times 10^{-2}$ | 94 | $9.30 \times 10^{-3}$ | $8.0 \times 10^{-3}$ | 86 | $1.27 \times 10^{-2}$ | $1.2 \times 10^{-2}$ | 94 |
| Slope | $7.8 \times 10^{-2}$ | $4 \times 10^{-2}$ | | 0.20 | $4 \times 10^{-3}$ | | 0.26 | $5 \times 10^{-2}$ | |
| *r* | 0.997 | | | 0.999 | | | 0.999 | | |

[a] $k' = k_1 + k_2$ (Scheme I). [b] Percent *via* route 1 = $(k_1/k') \times 100$.

**Table IV—Pseudo-First-Order Hydrolytic Rate Constants at Zero Buffer Concentration ($k_0$) for Methylthiomethyl (VI), Methylsulfinylmethyl (VII), and Methylsulfonylmethyl (VIII) 2-Hydroxybenzoates at 50.8 ± 0.2° and 0.1 *M* Ionic Strength (Sodium Chloride), Obtained by Following the Disappearance of the Compound**

| Buffer | pH | VI | | VII | | VIII | |
|---|---|---|---|---|---|---|---|
| | | $k_0$, min$^{-1}$ | $t_{1/2}$, min | $k_0$, min$^{-1}$ | $t_{1/2}$, min | $k_0$, min$^{-1}$ | $t_{1/2}$, min |
| 0.10 *N* NaOH | 11.86 | 0.108 | 6.42 | 0.510 | 1.36 | 0.632 | 1.10 |
| 0.01 *N* NaOH | 10.90 | 0.158 | 8.77 | 0.523 | 1.30 | 0.512 | 1.35 |
| Carbonate | 9.55 | — | — | 0.4 | 1.7 | 0.6 | 1.2 |
| Tris(hydroxymethyl)aminomethane | 8.82 | 0.307 | 2.27 | 0.148 | 4.68 | 0.202 | 3.67 |
| Tris(hydroxymethyl)aminomethane | 7.96 | 0.334 | 2.08 | $4.54 \times 10^{-2}$ | 15.3 | $6.26 \times 10^{-2}$ | 11.1 |
| Phosphate | 6.86 | — | — | $5.87 \times 10^{-3}$ | $1.18 \times 10^{2}$ | $1.09 \times 10^{-2}$ | 63.6 |
| Succinate | 5.97 | — | — | $6.94 \times 10^{-4}$ | $9.99 \times 10^{2}$ | $1.47 \times 10^{-3}$ | $4.72 \times 10^{2}$ |
| Succinate | 4.00 | 0.26 | 2.7 | $2.95 \times 10^{-5}$ | $2.35 \times 10^{4}$ | $4.12 \times 10^{-5}$ | $1.68 \times 10^{4}$ |
| Monochloroacetate | 2.64 | 0.329 | 2.11 | — | — | — | — |
| 0.01 *N* HCl | 2.02 | 0.324 | 2.14 | $2.20 \times 10^{-5}$ | $3.15 \times 10^{4}$ | $3.40 \times 10^{-5}$ | $2.04 \times 10^{4}$ |
| 0.100 *N* HCl | 1.13 | 0.349 | 1.99 | $2.26 \times 10^{-5}$ | $3.07 \times 10^{4}$ | $3.42 \times 10^{-5}$ | $2.03 \times 10^{4}$ |

and $f_{acid}$ and $f_{base}$ are the fractions of the total reactant in acidic and basic form:

$$f_{acid} = \frac{a_{H^+}}{a_{H^+} + k_a} \quad \text{(Eq. 3)}$$

$$f_{base} = \frac{k_a}{a_{H^+} + k_a} \quad \text{(Eq. 4)}$$

where $k_a$ is the dissociation constant of the phenol group estimated from the pH hydrolytic rate profiles. By using the computer fitting, the pKa, $k_{H_2O}$, and $k'_{H_2O}$ values for VI–VIII were obtained (Table V).

The pKa values obtained from the pH–rate profiles at 50.8° were in reasonable agreement with the values obtained spectrophotometrically at 23° and pH 9.60, 9.00, and 8.91, respectively. The pKa values for phenols and the $pKa_2$ values for salicylic acid decrease somewhat with increasing temperature in this temperature range (5, 6).

To complete the hydrolytic sequence, the hydrolytic rate constants for aspirin were determined by HPLC at pH 1.13, 2.64, 4.00, 7.96, and 9.55 at 50.8 ± 0.2° and ionic strength 0.1 *M* (Table VI). Only the carbonate buffer significantly influenced the hydrolysis rate (slope = 0.34 ± 0.04). According to Edwards (7, 8), $k_0$ for aspirin hydrolysis may be expressed by:

$$k_0 = \frac{a_{H^+}}{a_{H^+} + k_a}(k_H a_{H^+} + k_{H_2O}) + \frac{k_a}{a_{H^+} + k_a}(k'_{H_2O} + k'_{OH} a_{OH^-}) \quad \text{(Eq. 5)}$$

where $k_a$ is the dissociation constant of aspirin and $k_H$, $k_{H_2O}$, $k'_{H_2O}$, and $k'_{OH}$ are the rate constants for the acid-catalyzed, spontaneous, and base-catalyzed hydrolysis of aspirin in acidic and basic forms, respectively. The $k_H$, $k_{H_2O}$, and $k'_{H_2O}$ values were calculated from the pseudo-first-order rate constants at pH 1.13, 2.64, and 4.00 using pKa = 3.5 and applying the method of determinants (9). The value of $k_{OH}$ was obtained at pH 9.55. The value obtained for $k_H$ was $1.32 \times 10^{-2}$ liter/mole/min; for $k_{H_2O}$, it was $1.92 \times 10^{-4}$ min$^{-1}$; for $k'_{H_2O}$, it was $2.11 \times 10^{-3}$ min$^{-1}$; and for $k'_{OH}$, it was 32.25 liters/mole/min. All of these values agree with the literature values (10).

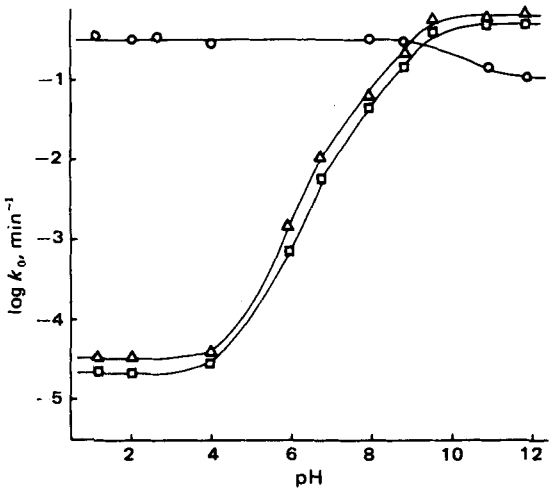


**Figure 5**—*The pH–rate profile for hydrolysis of methylthiomethyl 2-hydroxybenzoate (VI) (○), methylsulfinylmethyl 2-hydroxybenzoate (VII) (□), and methylsulfonylmethyl 2-hydroxybenzoate (VIII) (△) at 50.8 ± 0.2° and 0.1* M *ionic strength. The curves were calculated using Eqs. 1–4 based on the experimental data.*

To determine the hydrolysis mechanism of the various species (since the pH profile implies differences in the mechanism), additional investigations were conducted. Thus, the pseudo-first-order rate constants ($k_{obs}$) for the hydrolysis of IX–XI were determined by HPLC in 0.05 *M* buffers at pH 2.6, 4.0, 6.8, 7.9, and 9.2 at 25.5° (Table VII). The methylthiomethyl benzoate (IX) has a wide pH-independent region from pH 2.5 to 7, where $k_{obs}$ was ~$7.7 \times 10^{-4}$ min$^{-1}$. The methylsulfinylmethyl (X) and methylsulfonylmethyl (XI) benzoates hydrolyzed at much slower rates, the pseudo-first-order rate constants at pH 4.0 being only $1.6 \times 10^{-5}$ and $1.1 \times 10^{-5}$ min$^{-1}$, respectively. Next, the change in the reaction rates with temperature for the hydrolysis of the three 2-hydroxybenzoate derivatives (VI–VIII) in dilute hydrochloric acid and of the methylthiomethyl 2-acetoxybenzoate (III) in unbuffered aqueous solution was studied by following the disappearance of the compound (Tables VIII and IX).

The relatively high enthalpies ($\Delta H^{\ddagger}$) and small negative entropies ($\Delta S^{\ddagger}$) of activation of III and VI are typical for unimolecular ester hydrolysis following cleavage of the alkyl–oxygen bond (11). The values for VII and VIII fall into the range of neutral ester hydrolysis by general base catalysis (11) (Table X).

The effect of ionic strength on the spontaneous water hydrolysis of the

**Table V—Rate Constants and pKa Values of the Salicylate Esters**

| Compound | pKa[a] | pKa[b] | $k_{H_2O}$, min$^{-1}$ | $k'_{H_2O}$, min$^{-1}$ |
|---|---|---|---|---|
| VI | 10.2 | 9.60 × 0.01 | 0.330 | 0.105 |
| VII | 8.85 | 9.00 × 0.02 | $2.23 \times 10^{-5}$ | 0.156 |
| VIII | 8.70 | 8.91 × 0.02 | $3.41 \times 10^{-5}$ | 0.570 |

[a] Obtained from the hydrolysis rate profiles at 50.8 ± 0.2°. [b] Experimental values obtained at 23°.

**Table VI—Pseudo-First-Order Hydrolytic Rate Constants at Zero Buffer Concentration ($k_0$) for Aspirin (I) at 50.8 ± 0.2° and 0.1 *M* Ionic Strength**

| Buffer | pH | $k_0$, min$^{-1}$ | $t_{1/2}$, hr |
|---|---|---|---|
| 0.100 *N* HCl | 1.13 | $1.17 \times 10^{-3}$ | 9.87 |
| Monochloroacetate | 2.64 | $4.51 \times 10^{-4}$ | 25.6 |
| Succinate | 4.00 | $1.64 \times 10^{-3}$ | 7.00 |
| Tris(hydroxymethyl)aminomethane | 7.96 | $2.14 \times 10^{-3}$ | 5.40 |
| Carbonate | 9.55 | $6.47 \times 10^{-3}$ | 1.97 |

**Table VII—Pseudo-First-Order Rate Constants for Hydrolysis of Methylthiomethyl (IX), Methylsulfinylmethyl (X), and Methylsulfonylmethyl (XI) Benzoates in 0.5 *M* Buffers at 25.5 ± 0.1°**

| Buffer | pH | $k_{obs}$, min$^{-1}$ | | |
|---|---|---|---|---|
| | | IX | X | XI |
| Borate | 9.20 | $1.3 \times 10^{-3}$ | $4.1 \times 10^{-3}$ | $5.9 \times 10^{-3}$ |
| Phosphate | 7.93 | $1.3 \times 10^{-3}$ | $1.9 \times 10^{-4}$ | $2.9 \times 10^{-4}$ |
| Phosphate | 6.81 | $8.1 \times 10^{-4}$ | $3.2 \times 10^{-5}$ | $4.5 \times 10^{-5}$ |
| Acetate | 4.00 | $7.6 \times 10^{-4}$ | $1.6 \times 10^{-5}$ | $1.1 \times 10^{-5}$ |
| Monochloroacetate | 2.60 | $7.7 \times 10^{-4}$ | $1.6 \times 10^{-5}$ | $1.1 \times 10^{-5}$ |

**Table VIII—Observed Pseudo-First-Order Rate Constants for Hydrolysis of Methylthiomethyl (VI), Methylsulfinylmethyl (VII), and Methylsulfonylmethyl (VIII) 2-Hydroxybenzoates in 0.1 *N* HCl**

| Temperature | VI, $k_{obs}$, $min^{-1}$ | Temperature | $k_{obs}$, $min^{-1}$ | |
|---|---|---|---|---|
| | | | VII | VIII |
| 29.88° | $3.15 \pm 0.001 \times 10^{-2}$ | 35.8° | $5.51 \pm 0.24 \times 10^{-6}$ | $1.25 \pm 0.07 \times 10^{-5}$ |
| 35.68° | $6.93 \pm 0.05 \times 10^{-2}$ | 44.0° | $1.36 \pm 0.04 \times 10^{-5}$ | $2.03 \pm 0.30 \times 10^{-5}$ |
| 42.88° | $0.156 \pm 0.002$ | 61.0° | $5.64 \pm 0.14 \times 10^{-5}$ | $7.16 \pm 0.27 \times 10^{-5}$ |
| 50.78° | $0.325 \pm 0.005$ | 102.8° | $8.04 \pm 0.83 \times 10^{-4}$ | $6.13 \pm 0.11 \times 10^{-4}$ |

aspirin derivative III was investigated at 50.8 ± 0.1°. The small positive slope (0.202 ± 0.009) of the log $k_{obs}$ *versus* $\sqrt{I}$ plot indicates increased stability of the transition state with increasing ionic strength, or decreased stability of the reactant state, or both.

The effect of the solvent dielectric constant ($\epsilon$) on the rate constant of the spontaneous water hydrolysis of III to form aspirin also was studied using water–dioxane mixtures at 50.8°. The dielectric constant of each mixture at this temperature was calculated (3), and the measured $k_{obs}$ values were plotted *versus* $1/\epsilon$. The decrease in the solvent dielectric constant resulted in a decrease in the rate constant, which implies that the transition state is more polar than the reactant(s) (Table XI).

The deuterium solvent isotope effects on the hydrolysis rates of methylthiomethyl 2-acetoxybenzoate (III), methylsulfinylmethyl 2-hydroxybenzoate (VII), and methylsulfonylmethyl 2-hydroxybenzoate (VIII) were measured at 50.8° and 0.1 *M* ionic strength. The hydrolysis rate constant ($k_{D_2O}$) for III to form aspirin in unbuffered deuterium oxide solution was $5.06 \times 10^{-2}$ $min^{-1}$ compared to $6.06 \times 10^{-2}$ $min^{-1}$ in water, which results in an isotope effect ($k_{H_2O}/k_{D_2O}$) of 1.20. The hydrolysis rate constants for VII and VIII were measured in 0.1 *N* DCl solution in deuterium oxide (pD 0.9) and found to be $1.10 \times 10^{-5}$ and $1.68 \times 10^{-5}$ $min^{-1}$ compared to $2.23 \times 10^{-5}$ and $3.41 \times 10^{-5}$ $min^{-1}$ in water, respectively. The two 2-hydroxybenzoates showed the same solvent isotope effects, $k_{H_2O}/k_{D_2O} = 2.03$.

**Table IX—Observed Pseudo-First-Order Rate Constants ($k_{obs}$) for Hydrolysis of Methylthiomethyl 2-Acetoxybenzoate (III), Obtained by Following the Disappearance of III as a Function of Time in Aqueous Solution at 0.1 *M* Ionic Strength (Sodium Chloride) and Various Temperatures**

| Temperature | $k_{obs}$, $min^{-1}$ |
|---|---|
| 50.78° | $5.68 \pm 0.01 \times 10^{-2}$ |
| 44.48° | $3.11 \pm 0.03 \times 10^{-2}$ |
| 37.07° | $1.38 \pm 0.01 \times 10^{-2}$ |
| 29.20° | $5.06 \pm 0.04 \times 10^{-3}$ |

**Table X—Enthalpies and Entropies of Activation for the Hydrolysis of Methylthiomethyl and Related Esters**

| Compound | $E_a$, kcal/mole | $\Delta H^{\ddagger}$, kcal/mole | $\Delta S^{\ddagger}$, e.u. | $r$ |
|---|---|---|---|---|
| III | 21.8 ± 0.7 | 21.2 ± 0.7 | −7.1 | 0.999 |
| VI | 21.7 ± 0.9 | 21.1 ± 0.9 | −4.0 | 0.998 |
| VII | 16.2 ± 0.8 | 15.6 ± 0.8 | −40.1 | 0.998 |
| VIII | 13.5 ± 0.4 | 12.9 ± 0.4 | −48.1 | 0.999 |

**Table XI—Observed Pseudo-First-Order Rate Constants ($k_{obs}$) for Hydrolysis of Methylthiomethyl 2-Acetoxybenzoate (III) in Various Water–Dioxane Mixtures at 50.8 ± 0.1°**

| Dioxane, % | $k_{obs}$, $min^{-1}$ | ln $k_{obs}$ | $\epsilon$[a] | $1/\epsilon$ |
|---|---|---|---|---|
| 0 | $5.11 \pm 0.02 \times 10^{-2}$ | −2.98 | 69.60 | $1.44 \times 10^{-2}$ |
| 10 | $2.35 \pm 0.04 \times 10^{-2}$ | −3.75 | 61.43 | $1.63 \times 10^{-2}$ |
| 20 | $9.05 \pm 0.10 \times 10^{-3}$ | −4.71 | 53.30 | $1.88 \times 10^{-2}$ |
| 30 | $3.64 \pm 0.10 \times 10^{-3}$ | −5.62 | 45.27 | $2.21 \times 10^{-2}$ |

[a] The dielectric constant ($\epsilon$) of each mixture was calculated at 50.8° according to Ref. 3.

**Table XII—Relative Rates of Hydrolysis of Methylthiomethyl Benzoate (IX), Methylthiomethyl 2-Acetoxybenzoate (III), and Methylthiomethyl 2-Hydroxybenzoate (VI) at pH 4.00 at the Plateau and 25.5° [a]**

| Compound | $k_{obs}$, $min^{-1}$ | Relative Rate | pKa[b] |
|---|---|---|---|
| IX | $7.6 \times 10^{-4}$ | 1.0 | 4.2 |
| III | $3.45 \times 10^{-3}$ | 4.5 | 3.5 |
| VI | $1.90 \times 10^{-2}$ | 25 | 3.0 |

[a] The rate constant for IX was not extrapolated to zero buffer concentration. [b] The pKa of the carboxylic acid.

The pH–rate profiles of III and VI demonstrate large plateaus where the hydrolysis rates were pH independent. For III (Fig. 4), this plateau extended from about pH 2 to 8, with aspirin as the main hydrolytic product. Methylthiomethyl 2-hydroxybenzoate (VI) (Fig. 5) had an even wider plateau, showing no acid- or base-catalyzed regions on the pH profile from pH 1 to 12. The small decrease in the rate at ~pH 10 can be explained by the ionization of the 2-hydroxy group. Similar pH-independent hydrolysis behavior was shown by methylthiomethyl benzoate (IX) (Table VII).

The pH–rate profiles of VII and VIII show two plateaus with a large increase in the rate around the pKa of the 2-hydroxy group (Fig. 5). On the other hand, the pH–rate profiles for methylsulfinylmethyl (IV) and methylsulfonylmethyl (V) 2-acetoxybenzoates do not have these large plateaus but are V-shaped with a minimum at pH 4 (Fig. 4). The hydrolysis pathways, however, are changing with pH.

According to Fife (12), a plateau of the pH-independent rate, as for III, VI, and IX, could be due to: (*a*) attack of both hydronium ions and hydroxide ions, (*b*) water attack on the substrate, or (*c*) spontaneous, uncatalyzed decomposition of the substrate. The first possibility seems to be highly unlikely; if it occurred, the reaction would have a very large negative entropy of activation. Thus, the other two possibilities are left.

The pH–rate profiles for hydrolysis of both III and VI were obtained by following the disappearance of the compounds with time at various pH values. The main hydrolysis product of III in the plateau region is aspirin, which is hydrolyzed further to salicylic acid. Compounds III and VI have enthalpies of activation ($\Delta H^{\ddagger}$) of 21.2 and 21.1 kcal/mole and entropies of activation ($\Delta S^{\ddagger}$) of −7.12 and −4.04 e.u., respectively, in the pH-independent plateau region. These high enthalpies and low entropies of activation are characteristic for unimolecular reactions, which can be regarded as $S_N1$ reactions, where the leaving group is the carboxylate anion (11, 13) (Scheme II).

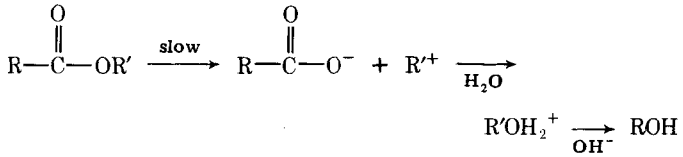


*Scheme II*

The enhanced solvation due to the charge separation in the transition state compared to the ground state results in a small negative entropy of activation but still is favorable compared to a bimolecular reaction involving water as a reactant ($S_N2$ reaction). Salomaa (14) studied the kinetics of uncatalyzed hydrolysis of some aliphatic acylals ($RCOOCHROCH_3$) in aqueous solutions and got similar values for the entropy of activation to those obtained in the present study. The hydrolysis rate of methylthiomethyl 2-acetoxybenzoate is highly dependent on the nature of the solvent, being ~14 times greater in water than in a 30% dioxane–water mixture, suggesting considerable charge development in the transition state. Change in ionic strength has a similar effect. Compound III is hydrolyzed with about the same rate in deuterium oxide as in water ($k_{D_2O}/k_{H_2O} = 1.2$). This small solvent isotope effect also is found in the hydrolysis of neutral ester molecules cleaved by alkyl–oxygen fission ($B_{AL}1$) (11, 13). The mechanism can be written as shown in Scheme III.

This mechanism would be facilitated by the fact that the carbonium ion formed is resonance stabilized by the neighboring sulfur group. In Table XII, the relative rates on the plateau for IX, III, and VI were listed at 25.5°. The increase in rate can be explained by the decreasing pKa or increased leaving group ability of the corresponding acid. The decrease

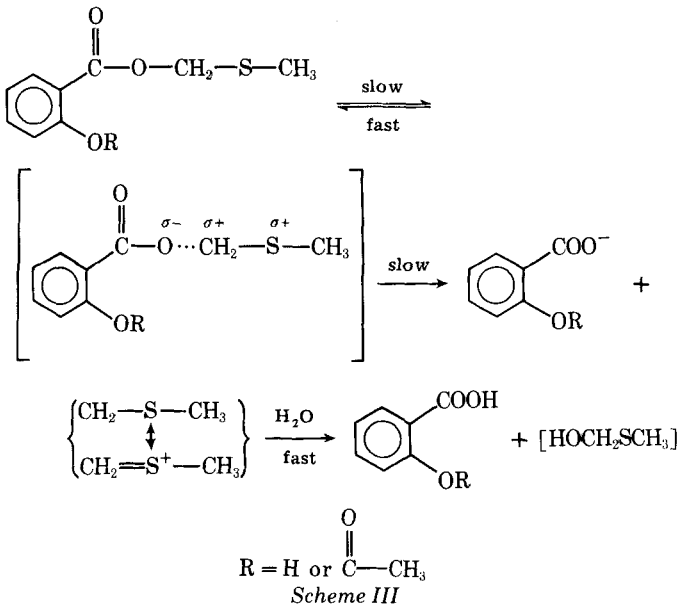

*Scheme III*

in the hydrolysis rate of VI at pH ~10 can be attributed to ionization of the 2-hydroxy group (pKa ~9.6 at 23°).

In the case of methylsulfinylmethyl (VII) and methylsulfonylmethyl (VIII) 2-hydroxybenzoates, the large negative entropy values and low enthalpies of activation are typical for neutral hydrolysis of esters, where water acts as a general base to assist the addition of a second water molecule to the ester carbonyl group (Scheme IV). The hydrolysis of both compounds show deuterium solvent isotope effect ($k_{H_2O}/k_{D_2O}$) of 2.03, which also is consistent with this mechanism. The significant rate increase at higher pH values can be explained by an intermolecular catalyzed attack by the ionized phenol group (Scheme V), as suggested by Bender *et al.* (15) in the case of *p*-nitrophenyl salicylate.

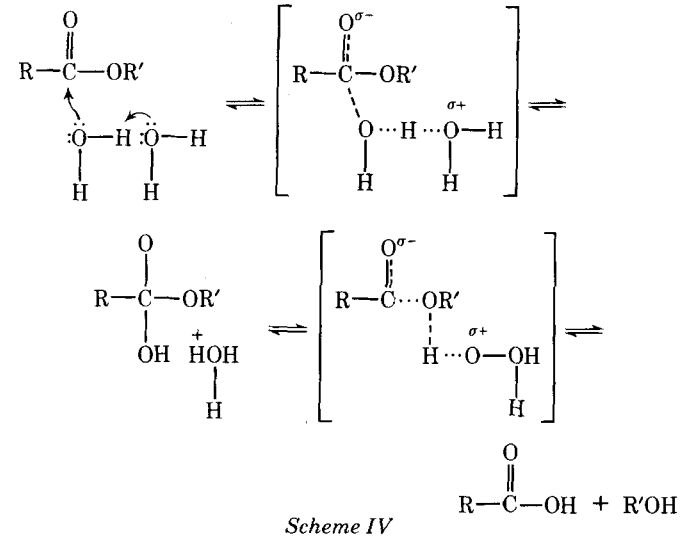

*Scheme IV*

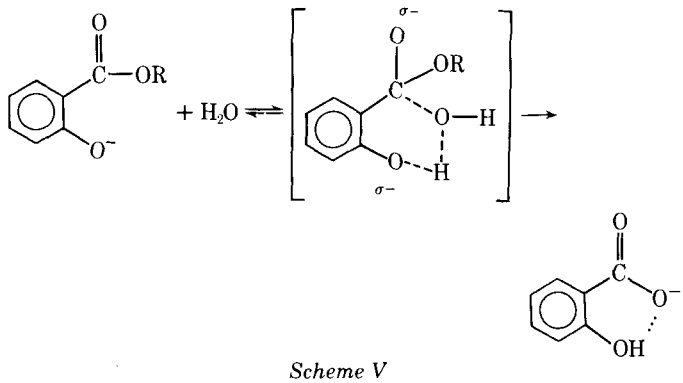

*Scheme V*

The pH profiles for the aspirin derivatives IV and V (Fig. 4) show the common V-shape at a minimum of pH 4. The hydrolysis pathways, however, change with the pH. Thus, aspirin (I) is the main product at pH > 4, but the relatively stable 2-hydroxybenzoates (VII and VIII) form at lower pH values.

While the methylthiomethyl ester (III) of aspirin at pH 7.96 hydrolyzes almost exclusively (>90%) to aspirin, the same compound in human plasma clearly hydrolyzes *via* both routes; on the other hand, IV apparently goes to aspirin in plasma but follows this route to a significantly smaller proportion in chemical hydrolysis.

As expected, the enzymic hydrolysis is significantly faster in all cases. However, the overall picture underlines the fact that, due to binding, mechanistic, and other differences, the chemical cleavage studies of esters will not necessarily predict the relative rates, possible selectivity, product ratio, *etc.*, obtained in enzymatic conditions.

## REFERENCES


(1) T. Loftsson, J. J. Kaminski, and N. Bodor, *J. Pharm. Sci.*, **70,** 743 (1981).

(2) J. G. Wagner, "Fundamentals of Clinical Pharmacokinetics," Drug Intelligence, Hamilton, Ill., 1975, p. 285.

(3) B. B. Owen and H. D. Harris, "The Physical Chemistry of Electrolytic Solutions," Reinhold, New York, N.Y., 1958, p. 162.

(4) A. N. Martin, J. Swarbrick, and A. Cammarata, "Physical Pharmacy," 2nd ed., Lea & Febiger, Philadelphia, Pa., 1969, p. 196.

(5) P. D. Bolton and L. G. Hepler, *Q. Rev.*, **25,** 521 (1971).

(6) G. Kortüm, W. Vogel, and K. Andrussow, "Dissociation Constants of Organic Acids in Aqueous Solutions," Butterworths, London, England, 1961, p. 373.

(7) L. J. Edwards, *Trans. Faraday Soc.*, **46,** 723 (1950).

(8) *Ibid.*, **48,** 696 (1952).

(9) G. Stephenson, "Mathematical Methods for Science Students," 2nd ed., Longman, London, England, 1973, p. 276.

(10) E. R. Garrett, *J. Am. Chem. Soc.*, **79,** 3401 (1957).

(11) E. K. Euranto, in "The Chemistry of Carboxylic Acids and Esters," S. Patai, Ed., Interscience, London, England, 1969, chap. 11.

(12) T. H. Fife, *J. Am. Chem. Soc.*, **87,** 271 (1965).

(13) A. J. Kirby, in "Comprehensive Chemical Kinetics, Ester Formation and Ester Hydrolysis," vol. 10, C. H. Bamford and C. F. H. Tipper, Eds., Elsevier, Amsterdam, The Netherlands, 1972, chap. 2.

(14) P. Salomaa, *Acta Chem. Scand.*, **19,** 1263 (1965).

(15) M. L. Bender, F. J. Kezdy, and B. Zerner, *J. Am. Chem. Soc.*, **85,** 3015 (1963).

# Improved Delivery through Biological Membranes X: Percutaneous Absorption and Metabolism of Methylsulfinylmethyl 2-Acetoxybenzoate and Related Aspirin Prodrugs

**THORSTEINN LOFTSSON * and NICHOLAS BODOR ‡x**

Received August 25, 1980, from the *Department of Pharmaceutical Chemistry, School of Pharmacy, University of Kansas, Lawrence, KS 66045, and the ‡Department of Medicinal Chemistry, College of Pharmacy, J. Hillis Miller Health Center, University of Florida, Gainesville, FL 32610. Accepted for publication January 21, 1981.

**Abstract** □ Oxidative–reductive interconversion of the methylthiomethyl ester of aspirin and the corresponding sulfoxide and sulfone derivatives can be detected in rat liver homogenate, in addition to the extremely facile hydrolysis of these esters. The methylthiomethyl and methylsulfinylmethyl 2-acetoxybenzoates penetrate freshly excised hairless mice skin rather easily with the simultaneous hydrolysis of the two ester functions. Contrary to *in vivo* observations in dogs, where significant amounts of aspirin formed, the prodrugs cleave to salicylic acid and/or salicylate esters rather than aspirin.

**Keyphrases** □ Methylsulfinylmethyl 2-acetoxybenzoate—percutaneous absorption and metabolism, aspirin prodrugs □ Aspirin prodrugs—percutaneous absorption and metabolism □ Prodrugs—methylsulfinylmethyl 2-acetoxybenzoate and related aspirin agents, percutaneous absorption and metabolism

In the preceding papers of this series, novel prodrugs of aspirin (I) were described, together with the corresponding salicylic acid (II) derivatives as summarized by III–VIII. Although significant differences in the chemical and plasma hydrolyses of the double esters III–V were observed, *in vivo* studies clearly indicated that at least IV cleaves to aspirin; III and V might do so, but aspirin could not be detected in the dogs in these cases.

## BACKGROUND

In addition to the direct hydrolysis of the ester functions, oxidative interconversion of the sulfur-containing alkyl groups also is possible, which might alter the expected hydrolytic behavior. Thus, similarly to the case of sulindac (1), these esters can be expected to participate in the *in vivo* redox system shown in Scheme I. Other sulfides and sulfoxides undergo similar transformations (2), which most likely occur in the liver. Thus, one objective of the present studies was to determine whether the oxidized forms, IV and V, can be detected if III is incubated with liver homogenate.

The possible topical use of the aspirin prodrugs, III–V, or the salicylic acid derivatives, VI–VIII, also is of interest. The primary use of salicylic acid in topical medication, aside from its antiseptic and germicidal uses, has been as a keratolytic and anti-inflammatory agent. Keratolytic drugs act to damage the cornified layer of the skin, which is then sloughed off to whatever depth the agent has acted. The traditional keratolytic agent has been salicylic acid in concentrations up to 6% in various creams and ointments (3).

Steroids commonly are applied topically to alleviate inflammatory

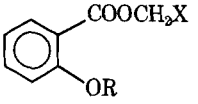

III: R = $CH_3CO$, X = $CH_3S$–
IV: R = $CH_3CO$, X = $CH_3SO$–
V: R = $CH_3CO$, X = $CH_3SO_2$–
VI: R = OH, X = $CH_3S$–
VII: R = OH, X = $CH_3SO$–
VIII: R = OH, X = $CH_3SO_2$–

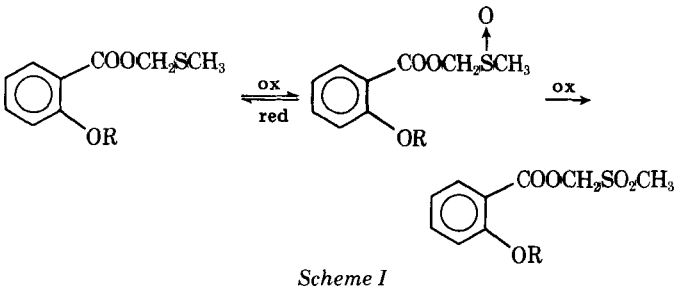

*Scheme I*

states such as some allergic skin conditions, but only one nonsteroidal anti-inflammatory agent, bufexamac, is marketed as a topical cream (4). In a recent study (5), the anti-inflammatory effects of several steroidal and nonsteroidal drugs were tested topically on guinea pig skins in which UV dermatitis was induced. Salicylic acid was just as good an anti-inflammatory agent as bufexamac, and aspirin was even more active and, in some cases, was superior to hydrocortisone (6).

In the present study, the apparent permeability of the potential prodrugs of aspirin, III and IV, through excised hairless mice skin was studied and compared to aspirin. Since the skin, as all other portals of entry into the body, possesses metabolic activity (7), simultaneous metabolism–absorption processes were considered.

## EXPERIMENTAL

**Metabolism Studies in Rat Liver Homogenate**—The liver homogenate was prepared following the method of Schneider (8). Two male Sprague–Dawley rats were killed by decapitation, and the livers were removed and chilled on an ice-cold glass plate. After cooling, the livers were weighed (total weight 28.4 g) and homogenized with a polytef pestle homogenizer in a glass mortar in 113.6 ml of 0.25 *M* sucrose (total volume 142 ml). The homogenate was centrifuged for 10 min at 600×*g*, and the supernate was decanted and centrifuged for 20 min at 24,000×*g*. The supernate, which was then 120 ml, was decanted and used undiluted for the oxidation–cleavage studies.

The supernate was stored in an ice bath and used within 5 hr after the killing of the animals. A 10-μl sample of a standard solution of the compound in acetonitrile was added to 3.0 ml of the supernate ($<10^{-3}$ *M*). Samples of 0.50 ml were removed, mixed with 0.50 ml of acetonitrile, and centrifuged for 20 min. The supernate was analyzed by high-pressure liquid chromatography (HPLC) as described previously (9).

**Permeability–Metabolism Studies Using Hairless Mice Skin**—Full-thickness dorsal skin of 12–14-week-old female hairless mice[1] was used. The mice were sacrificed by snapping of the spinal cord at the neck, and the whole dorsal skin then was removed. Adhering fat and other visceral debris were removed carefully from the undersurface. The excised skin was stretched gently over the lower opening of the plexiglass lid of a diffusion cell and secured with a rubber gasket, and excess skin was trimmed away.

The diffusion cells were manufactured[2] from plexiglass and consisted of a lower chamber (45 ml) with a side arm to allow sampling of the receptor phase, a lid, and a rubber gasket. A plastic-coated magnetic bar provided efficient mixing. The opening in the lid left exposed an 8.04-$cm^2$ area on the epidermis side through which penetration was measured. The

[1] Obtained from Jackson Laboratories, Bar Harbor, ME 04609.
[2] Kercso Engineering Consultants, Palo Alto, Calif.



*0022-3549/81/0700-0756$01.00/0*
*© 1981, American Pharmaceutical Association*

**Table I—Permeability Coefficient and Lag Times for Apparent Permeability of Aspirin (I) and Methylthiomethyl (III) and Methylsulfinylmethyl (IV) 2-Acetoxybenzoates through Excised Hairless Mice Skin at 31°**

| Compound Applied | Compound Detected in Receptor Phase[a] | Permeability Coefficient, cm/hr | Lag Time, hr |
|---|---|---|---|
| Aspirin | I | $4.9 \pm 1.0 \times 10^{-3}$ | 0.82 |
| | II | $1.4 \pm 0.1 \times 10^{-2}$ | 0.72 |
| | Total | $1.9 \pm 0.2 \times 10^{-2}$ | 0.77 |
| III | II | $4.0 \pm 0.5 \times 10^{-2}$ | 0.70 |
| IV | VII | $9.6 \pm 4.0 \times 10^{-3}$ | 1.18 |
| | II | $1.2 \pm 0.6 \times 10^{-2}$ | 0.33 |
| | Total | $2.2 \pm 1.0 \times 10^{-2}$ | 0.87 |

[a] The compounds detected in the receptor phase were aspirin (I), salicylic acid (II), and methylsulfinylmethyl 2-hydroxybenzoate (VII).

receptor was filled with pH 5.4 isotonic sodium acetate–boric acid buffer (60 mg and 1.84 g, respectively, in 100 ml of deionized water). As a preserving agent, 0.1% formaldehyde was added. All air bubbles were removed carefully from the dermal surface of the skin by tipping the cell.

A solution of the test compound was made in acetonitrile containing 10% polyethylene glycol 400. Then 200 μl of this solution was applied to the skin; and the acetonitrile was evaporated by blowing air on the surface, leaving a 2 *M* solution of the compound in polyethylene glycol 400 spread evenly on the skin. Each cell then was placed on a magnetic stirrer in a 31° incubator in which a high constant humidity was maintained. Samples of 1 ml were removed from the receptor phase *via* the side arm and replaced with fresh buffer. The samples were analyzed by HPLC.

## RESULTS AND DISCUSSION

The rat liver homogenate metabolism studies revealed that the various ester-type prodrugs of aspirin (III–V) and the corresponding salicylates (VI–VIII) were metabolized extremely fast. The disappearance rates of III and IV were 2.5 and 0.8 $min^{-1}$, corresponding to half-lives of 0.3 and 0.9 min, respectively. These values reflect significantly faster metabolism in the liver than in plasma. [The corresponding half-lives in human plasma at 37° were 1.2 (III) and 14 (IV) min, respectively.] The analysis of the liver homogenate mixtures indicated that III was hydrolyzed mainly to VI and then to salicylic acid. The main product from IV also was salicylic acid. However, despite the fast hydrolysis rates, small fractions of both IV and V could be detected after incubation of the homogenate with III. In the same way, small fractions of VII could be detected after incubation with VI, and small fractions of V could be detected after incubation of the homogenate with IV. This finding clearly indicates that some oxidative interconversion of the species occurs.

The skin permeability studies also indicated extensive metabolism of III and IV. This result is not surprising; although the stratum corneum is the main diffusion barrier (10), the conventional drug permeation mathematical models (11–13) had to be modified to account for simultaneous metabolism–permeation when prodrugs were used (14, 15). The whole skin, particularly the epidermis, contains many highly active enzyme systems (7), and some esterase activity has been found in the stratum corneum of pig skin (16).

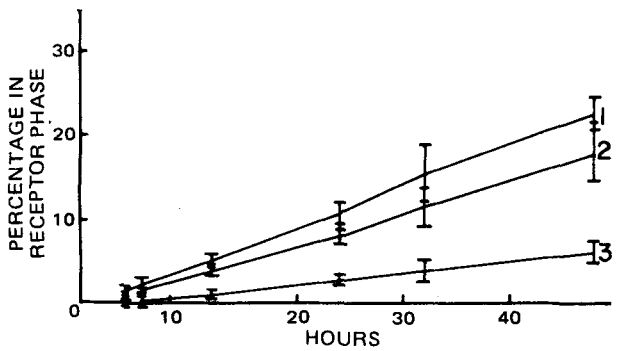


**Figure 1**—*Permeability of aspirin (I) through hairless mice skin as percentage of aspirin applied. Key: 1, total appearance in the receptor phase; 2, salicylic acid (II); and 3, aspirin.*

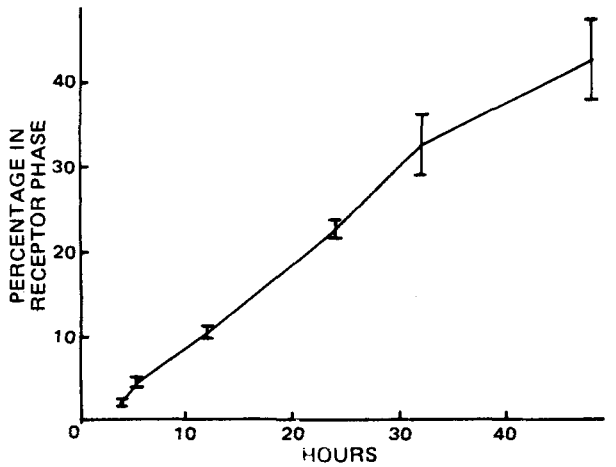


**Figure 2**—*Permeability of methylthiomethyl 2-acetoxybenzoate (III) through hairless mice skin as percentage of dose applied and appearance as salicylic acid (II) in the receptor phase.*

The main enzyme systems of interest in this study were the esterases, which can attack both the aromatic carboxyl esters and the acetyl ester in aspirin and its derivatives, and oxygenases, which could possibly oxidize the sulfur in the thiomethyl and sulfoxide derivatives.

The methylsulfonylmethyl 2-acetoxybenzoate (V) had low solubility in polyethylene glycol 400 and tended to precipitate after application to the skin. Therefore, it showed little permeability in the initial experiment and was not studied further. The obtained permeation profiles for I, III, and IV in terms of percentage in the receptor phase of the total amount applied to the skin as a function of time are displayed in Figs. 1–3. Permeability coefficients were calculated from the slopes of the amounts diffused *versus* time profile according to Eq. 1 in the time interval 5.5–24 hr:

$$P = \frac{V(dc/dt)}{AC_d} \qquad \text{(Eq. 1)}$$

where $P$ is the permeability coefficient, $V$ is the volume of the receptor phase, $A$ is the surface area of the exposed skin, and $C_d$ is the concentration of the solute in the donor phase.

The lag times were estimated graphically; they were quite sensitive to small differences in slopes, and slight experimental variability in slopes produced marked variability.

Each experiment was repeated five times, and the results given represent average values. The error bars in Figs. 1–3 represent the standard error of the mean. The permeability coefficients and lag times are listed in Table I.

The observed hydrolysis rate constant for aspirin in the receptor phase (pH 5.44) was measured separately at 31.0° and found to be $3.74 \pm 0.06 \times 10^{-4}$ $min^{-1}$ or a half-life of 31 hr. These results indicate that when aspirin is applied to the skin, ~30% penetrates the skin unmetabolized,

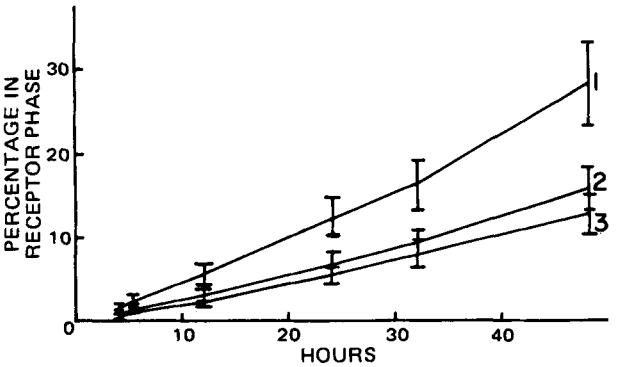


**Figure 3**—*Permeability of methylsulfinylmethyl 2-acetoxybenzoate (IV) through hairless mice skin as percentage methylsulfinylmethyl 2-hydroxybenzoate (VII) (curve 2), salicylic acid (curve 3), and total appearance (curve 1) in the receptor phase relative to the total amount applied to the skin.*

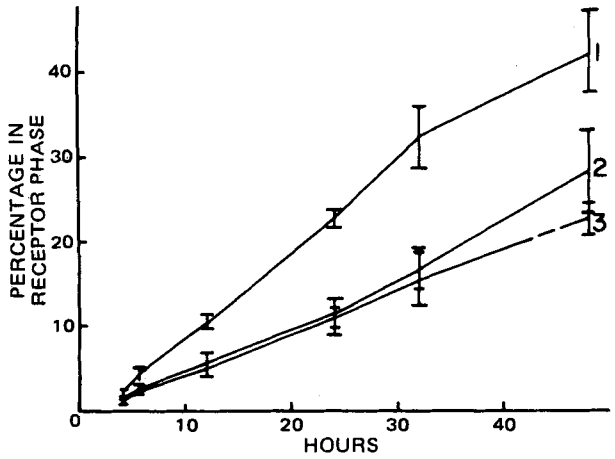


**Figure 4**—*Comparative permeability of aspirin (curve 3), methylthiomethyl 2-acetoxybenzoate (III) (curve 1), and methylsulfinylmethyl 2-acetoxybenzoate (IV) (curve 2) through hairless mice skin.*

while the major part, ~70% of the dose penetrating the skin, is hydrolyzed in the skin to salicylic acid during absorption (Fig. 1).

The hydrolysis half-life of the methylthiomethyl derivative (III) to aspirin was ~10 min and that of VI to salicylic acid, at 30° and pH 5.4, was ~9 min. If any significant amounts of aspirin are formed during passage through the skin or if III penetrates the skin without being metabolized, aspirin would be detected in the receptor phase. On the other hand, only salicylic acid was found when III was applied to the skin, which means that III is metabolized in the skin to VI or salicylic acid or both (Fig. 2).

The hydrolysis half-life of the methylsulfinylmethyl derivative (IV) to aspirin was ~10 days and that of VII to salicylic acid, at 30° and pH 5.4, was ~6 days. Thus, very little hydrolysis should occur in the receptor phase and almost all metabolites of IV detected in the receptor phase must be formed in the enzymatic cleavage in the skin. No aspirin was detected in the receptor phase after application of IV to the skin; only large amounts of VII and salicylic acid were found (Fig. 3). These results indicate that ~57% of IV penetrating the skin is metabolized to VII and that ~43% of IV is metabolized to salicylic acid.

The comparative cumulative penetration profiles for aspirin, III, and IV are shown in Fig. 4. The methylthiomethyl derivative (III) of aspirin is absorbed at a rate about two times faster than that of aspirin, while the methylsulfinylmethyl derivative (IV) is absorbed at the same rate as aspirin within experimental error.

It is clear that significant metabolism of all salicylic acid derivatives, including aspirin and its prodrugs, occur in the fresh mouse skin. The various ester functions hydrolyze with different rates and in a different order than what was shown to be their chemical hydrolysis or enzymatic cleavage in plasma or after the intravenous *in vivo* administration. The amounts penetrating the skin, however, are significant. It is possible to achieve therapeutic levels either as keratolytic or anti-inflammatory or analgesic agents. Further *in vivo* studies should be performed to answer these questions.

## REFERENCES

(1) D. E. Duggan, K. F. Hooke, R. M. Noll, H. B. Hucker, and C. G. Van Arman, *Biochem. Pharmacol.*, **27**, 2311 (1978).

(2) J. R. DeBaun and J. J. Menn, *Science*, **191**, 187 (1976).

(3) H. P. Baden, in "Recent Advances in Dermatopharmacology," P. Frost, E. C. Gomez, and N. Zaias, Eds., Spectrum New York, N.Y., 1977, p. 2.9.

(4) J. R. Vane, *J. Allergy Clin. Immunol.*, **58**, 691 (1976).

(5) E. Aron, B. Delbarre, and J. C. Besnard, *Therapie*, **31**, 247 (1976).

(6) E. G. Weirich, J. K. Longauer, and A. K. Kirkwood, *Dermatologica*, **152**, 87 (1976).

(7) A. Rannatier, P. Jenner, B. Testa, and J. C. Etter, *Drug Metab. Rev.*, **8**, 319 (1978).

(8) W. C. Schneider, *J. Biol. Chem.*, **176**, 259 (1948).

(9) T. Loftsson and N. Bodor, *J. Pharm. Sci.*, **70**, 750 (1981).

(10) M. Katz and B. J. Poulsen, in "Handbook of Experimental Pharmacology," B. B. Brodie and J. Gillett, Eds., Springer-Verlag, Berlin, Germany, 1971, chap. 7.

(11) T. Higuchi, *J. Soc. Cosmet. Chem.*, **11**, 85 (1960).

(12) R. J. Scheuplein, I. H. Blank, G. J. Brauner, and D. J. MacFarlane, *J. Invest. Dermatol.*, **52**, 63 (1969).

(13) T. Nakagawa, M. Takehara, and H. Oishi, *Chem. Pharm. Bull.*, **24**, 1774 (1976).

(14) J. L. Fox, C. D. Yu, W. I. Higuchi, and N. F. H. Ho, *Int. J. Pharm. Sci.*, **2**, 41 (1979).

(15) J. Albery and J. Hadraft, *J. Pharm. Pharmacol.*, **31**, 129 (1979).

(16) W. Meyer and N. Neurand, *Lab. Animals*, **10**, 237 (1976).

# Aluminum Chlorohydrate I: Structure Studies

**DIRK L. TEAGARDEN *, JOHN F. KOZLOWSKI ‡, JOE L. WHITE §, and STANLEY L. HEM *x**

Received October 3, 1980, from the **Department of Industrial and Physical Pharmacy, the* ‡*Department of Medicinal Chemistry and Pharmacognosy, and the* §*Department of Agronomy, Purdue University, West Lafayette, IN 47907.* Accepted for publication December 8, 1980.

**Abstract** □ X-ray diffraction and IR and $^{27}$Al-NMR spectroscopy indicate that aluminum chlorohydrate is composed of a central aluminum in a tetrahedral configuration surrounded by 12 aluminum atoms in octahedral configuration. The complex, $Al_{13}O_4(OH)_{24}(H_2O)_{12}^{7+}$, is essentially spherical, with the +7 charge equally distributed on the surface. Seven chloride ions are associated with the complex as counterions. This structure is consistent with both the method of synthesis and the proposed mechanisms of antiperspirant activity.

**Keyphrases** □ Aluminum chlorohydrate—structure proposed by X-ray diffraction and IR and $^{27}$Al-NMR spectroscopy □ X-ray diffraction—aluminum chlorohydrate, structure proposed □ Spectroscopy, IR—aluminum chlorohydrate, structure proposed □ $^{27}$Al-NMR spectroscopy—aluminum chlorohydrate, structure proposed □ Antiperspirant activity—aluminum chlorohydrate, structure proposed based on X-ray diffraction and IR and $^{27}$Al-NMR spectroscopic studies

Aluminum chlorohydrate, a basic aluminum complex, is widely used for its antiperspirant activity, for sealing porous strata in oil drilling operations, and to control the viscosity of kaolinite clays. It is known as aluminum chlorohydrate, aluminum hydroxychloride, basic aluminum chloride, or chlorhydrol. The empirical formula, $Al_2(OH)_5Cl{\cdot}2H_2O$, is known (1), but the structure has not been characterized. The chemistry of partially hydrolyzed



*0022-3549/81/0700-0758$01.00/0*
*© 1981, American Pharmaceutical Association*

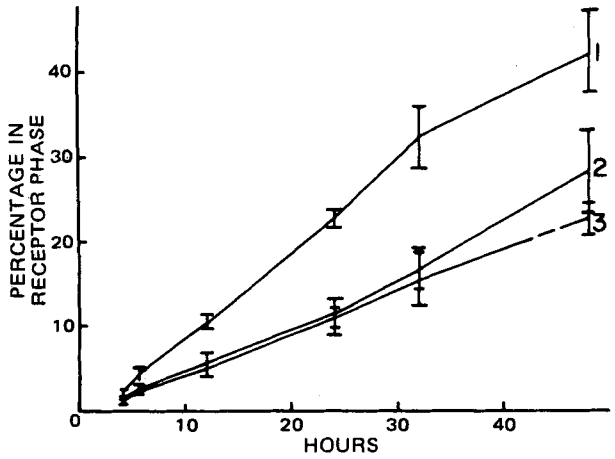


**Figure 4**—*Comparative permeability of aspirin (curve 3), methylthiomethyl 2-acetoxybenzoate (III) (curve 1), and methylsulfinylmethyl 2-acetoxybenzoate (IV) (curve 2) through hairless mice skin.*

while the major part, ~70% of the dose penetrating the skin, is hydrolyzed in the skin to salicylic acid during absorption (Fig. 1).

The hydrolysis half-life of the methylthiomethyl derivative (III) to aspirin was ~10 min and that of VI to salicylic acid, at 30° and pH 5.4, was ~9 min. If any significant amounts of aspirin are formed during passage through the skin or if III penetrates the skin without being metabolized, aspirin would be detected in the receptor phase. On the other hand, only salicylic acid was found when III was applied to the skin, which means that III is metabolized in the skin to VI or salicylic acid or both (Fig. 2).

The hydrolysis half-life of the methylsulfinylmethyl derivative (IV) to aspirin was ~10 days and that of VII to salicylic acid, at 30° and pH 5.4, was ~6 days. Thus, very little hydrolysis should occur in the receptor phase and almost all metabolites of IV detected in the receptor phase must be formed in the enzymatic cleavage in the skin. No aspirin was detected in the receptor phase after application of IV to the skin; only large amounts of VII and salicylic acid were found (Fig. 3). These results indicate that ~57% of IV penetrating the skin is metabolized to VII and that ~43% of IV is metabolized to salicylic acid.

The comparative cumulative penetration profiles for aspirin, III, and IV are shown in Fig. 4. The methylthiomethyl derivative (III) of aspirin is absorbed at a rate about two times faster than that of aspirin, while the methylsulfinylmethyl derivative (IV) is absorbed at the same rate as aspirin within experimental error.

It is clear that significant metabolism of all salicylic acid derivatives, including aspirin and its prodrugs, occur in the fresh mouse skin. The various ester functions hydrolyze with different rates and in a different order than what was shown to be their chemical hydrolysis or enzymatic cleavage in plasma or after the intravenous *in vivo* administration. The amounts penetrating the skin, however, are significant. It is possible to achieve therapeutic levels either as keratolytic or anti-inflammatory or analgesic agents. Further *in vivo* studies should be performed to answer these questions.

## REFERENCES

(1) D. E. Duggan, K. F. Hooke, R. M. Noll, H. B. Hucker, and C. G. Van Arman, *Biochem. Pharmacol.*, **27**, 2311 (1978).

(2) J. R. DeBaun and J. J. Menn, *Science*, **191**, 187 (1976).

(3) H. P. Baden, in "Recent Advances in Dermatopharmacology," P. Frost, E. C. Gomez, and N. Zaias, Eds., Spectrum New York, N.Y., 1977, p. 2.9.

(4) J. R. Vane, *J. Allergy Clin. Immunol.*, **58**, 691 (1976).

(5) E. Aron, B. Delbarre, and J. C. Besnard, *Therapie*, **31**, 247 (1976).

(6) E. G. Weirich, J. K. Longauer, and A. K. Kirkwood, *Dermatologica*, **152**, 87 (1976).

(7) A. Rannatier, P. Jenner, B. Testa, and J. C. Etter, *Drug Metab. Rev.*, **8**, 319 (1978).

(8) W. C. Schneider, *J. Biol. Chem.*, **176**, 259 (1948).

(9) T. Loftsson and N. Bodor, *J. Pharm. Sci.*, **70**, 750 (1981).

(10) M. Katz and B. J. Poulsen, in "Handbook of Experimental Pharmacology," B. B. Brodie and J. Gillett, Eds., Springer-Verlag, Berlin, Germany, 1971, chap. 7.

(11) T. Higuchi, *J. Soc. Cosmet. Chem.*, **11**, 85 (1960).

(12) R. J. Scheuplein, I. H. Blank, G. J. Brauner, and D. J. MacFarlane, *J. Invest. Dermatol.*, **52**, 63 (1969).

(13) T. Nakagawa, M. Takehara, and H. Oishi, *Chem. Pharm. Bull.*, **24**, 1774 (1976).

(14) J. L. Fox, C. D. Yu, W. I. Higuchi, and N. F. H. Ho, *Int. J. Pharm. Sci.*, **2**, 41 (1979).

(15) J. Albery and J. Hadraft, *J. Pharm. Pharmacol.*, **31**, 129 (1979).

(16) W. Meyer and N. Neurand, *Lab. Animals*, **10**, 237 (1976).

# Aluminum Chlorohydrate I: Structure Studies

**DIRK L. TEAGARDEN *, JOHN F. KOZLOWSKI ‡, JOE L. WHITE §, and STANLEY L. HEM *x**

Received October 3, 1980, from the **Department of Industrial and Physical Pharmacy, the* ‡*Department of Medicinal Chemistry and Pharmacognosy, and the* §*Department of Agronomy, Purdue University, West Lafayette, IN 47907.* Accepted for publication December 8, 1980.

**Abstract** □ X-ray diffraction and IR and $^{27}$Al-NMR spectroscopy indicate that aluminum chlorohydrate is composed of a central aluminum in a tetrahedral configuration surrounded by 12 aluminum atoms in octahedral configuration. The complex, $Al_{13}O_4(OH)_{24}(H_2O)_{12}^{7+}$, is essentially spherical, with the +7 charge equally distributed on the surface. Seven chloride ions are associated with the complex as counterions. This structure is consistent with both the method of synthesis and the proposed mechanisms of antiperspirant activity.

**Keyphrases** □ Aluminum chlorohydrate—structure proposed by X-ray diffraction and IR and $^{27}$Al-NMR spectroscopy □ X-ray diffraction—aluminum chlorohydrate, structure proposed □ Spectroscopy, IR—aluminum chlorohydrate, structure proposed □ $^{27}$Al-NMR spectroscopy—aluminum chlorohydrate, structure proposed □ Antiperspirant activity—aluminum chlorohydrate, structure proposed based on X-ray diffraction and IR and $^{27}$Al-NMR spectroscopic studies

Aluminum chlorohydrate, a basic aluminum complex, is widely used for its antiperspirant activity, for sealing porous strata in oil drilling operations, and to control the viscosity of kaolinite clays. It is known as aluminum chlorohydrate, aluminum hydroxychloride, basic aluminum chloride, or chlorhydrol. The empirical formula, $Al_2(OH)_5Cl{\cdot}2H_2O$, is known (1), but the structure has not been characterized. The chemistry of partially hydrolyzed



*0022-3549/81/0700-0758$01.00/0*
*© 1981, American Pharmaceutical Association*

aluminum solutions has been studied extensively, and various aluminum species have been proposed. At high degrees of hydrolysis, which is suggested by the hydroxyl to aluminum ratio of 2.5 in the empirical formula, the proposed aluminum species include: $Al_6(OH)_{12}(H_2O)_{12}^{6+}$ (2), $Al_8(OH)_{20}^{4+}$ (3, 4), $Al_{13}O_4(OH)_{24}(H_2O)_{12}^{7+}$ (5–10), $Al_{14}(OH)_{34}^{8+}$ (11, 12), $Al_{10}(OH)_{22}(H_2O)_{16}^{8+}$ to $Al_{54}(OH)_{144}(H_2O)_{38}^{18+}$ (13), $Al_6(OH)_{16}(H_2O)_{4-5}^{2+}$ (14), $Al_6(OH)_{15}O^{1+}$ (14), and $Al_{20}$–$Al_{200}$ (15).

This study investigated the structure of aluminum chlorohydrate using X-ray diffraction and IR and $^{27}$Al-NMR spectroscopy.

## EXPERIMENTAL

**X-Ray Diffraction**—Commercial aluminum chlorohydrate[1] solutions [50% (w/w)] were air dried, and a powder was prepared by trituration in an agate mortar and pestle. Randomly oriented powder samples were prepared in McCreery mounts. Diffractograms were recorded[2] from 4 to 60° 2$\theta$ under the following conditions: Cu$K_\alpha$ radiation, 30 kv, 28 mamp, 1000 cps, and 2°/min.

The molecular dimension of aluminum chlorohydrate was determined by examining the increase in the interlayer spacing of montmorillonite as a result of intercalation of aluminum chlorohydrate. Approximately 50 ml of a 0.69% suspension of sodium-saturated montmorillonite was centrifuged at 5000 rpm for 5 min. The supernate was discarded, and the clay was resuspended in 50 ml of a 25% (w/w) aluminum chlorohydrate solution. The suspension was centrifuged as described, and the clay was resuspended in a second portion of aluminum chlorohydrate solution.

The process was repeated a total of four times to ensure complete saturation of the clay by aluminum chlorohydrate. The aluminum chlorohydrate-saturated montmorillonite was washed four times with double-distilled water by following the described procedure and then was air dried and stored in a vacuum desiccator. X-ray diffractograms were recorded while using special precautions to avoid the adsorption of water by the clay (16).

**IR Spectroscopy**—Air-dried aluminum chlorohydrate was incorporated into potassium bromide pellets, and the IR spectrum was recorded[3].

**NMR Spectroscopy**—Aluminum chlorohydrate solutions were diluted with deuterium oxide to produce solutions that were 1 *M* in aluminum. The $^{27}$Al-NMR spectrum was obtained at 20.723 MHz and 18.7 kg[4]. Potassium aluminum sulfate (0.1 *M*) in acidified deuterium oxide at pH 1 was the reference. The chemical shift of tetrahedral aluminum in aluminate, $Al(OH)_4^-$, was determined from a solution of aluminum chloride titrated with sodium deuteroxide to the soluble region above pH 10.

## RESULTS AND DISCUSSION

An X-ray diffractogram of aluminum chlorohydrate characteristic of all of the commercial samples is shown in Fig. 1. A broad peak occurred in the range of 4–10° 2$\theta$, indicating a *d*-spacing of 11.8 Å. The X-ray diffractogram indicated a poorly ordered material. The line broadening at 11.8 Å suggested a crystallite dimension that is normal to the reflecting planes *hkl* of ~50 Å. No well-crystallized forms of aluminum hydroxide such as gibbsite or bayerite were seen.

To estimate the size of the aluminum chlorohydrate complex, montmorillonite was used as a molecular caliper (17, 18). The X-ray diffractograms indicated that the interlayer spacing of montmorillonite increased by 8.9 Å as a result of aluminum chlorohydrate intercalation. Thus, the minimum dimension of aluminum chlorohydrate is believed to be 8.9 Å.

The proposed structures of highly hydrolyzed aluminum species were examined to determine if any species has a dimension of ~8.9 Å. The $Al_{13}O_4(OH)_{24}(H_2O)_{12}^{7+}$ complex is essentially spherical and is closest in size, 9 Å (6), to the experimentally determined size of aluminum chlorohydrate.

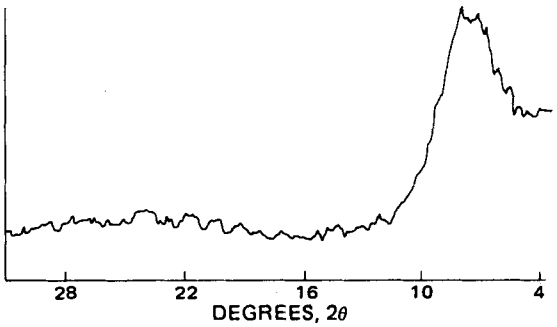


**Figure 1**—*X-ray diffractogram of aluminum chlorohydrate.*

The empirical formula for aluminum chlorohydrate, $Al_2(OH)_5Cl{\cdot}2H_2O$ (1), gives an aluminum to chloride ratio of 2:1, an aluminum to water ratio of 1:1, and an hydroxyl to aluminum ratio of 2.5:1 and compares well to the formula for the $Al_{13}O_4(OH)_{24}(H_2O)_{12}^{7+}$ complex if seven chloride anions are assumed to be present to neutralize the charge of the complex. The aluminum to chloride ratio of the proposed complex is 13:7 or ~2:1, and its aluminum to water ratio is 13:12 or approximately equal to the 1:1 ratio of the empirical formula. Its hydroxyl to aluminum ratio is 24:13. However, the four oxygen atoms in the proposed complex would appear as eight hydroxyl anions by the techniques commonly used to establish the stoichiometry of aluminum compounds (19). Therefore, the hydroxyl to aluminum ratio of the proposed complex would appear to be 32:13 or ~2.5:1, as for the empirical formula.

The excellent fit of the stoichiometry of the $Al_{13}O_4(OH)_{24}(H_2O)_{12}^{7+}$ complex to the empirical formula for commercial aluminum chlorohydrate further supports the hypothesis that the $Al_{13}O_4(OH)_{24}(H_2O)_{12}^{7+}$ complex is the structure of aluminum chlorohydrate. The small differences between the generally accepted empirical formula and the hypothesized structure may be due to the minor presence of other aluminum species in aluminum chlorohydrate and to the relatively nonspecific methods used for establishing the empirical formula.

The structure of the $Al_{13}O_4(OH)_{24}(H_2O)_{12}^{+7}$ complex is shown in Fig. 2. This structure is unusual since it contains a central aluminum atom

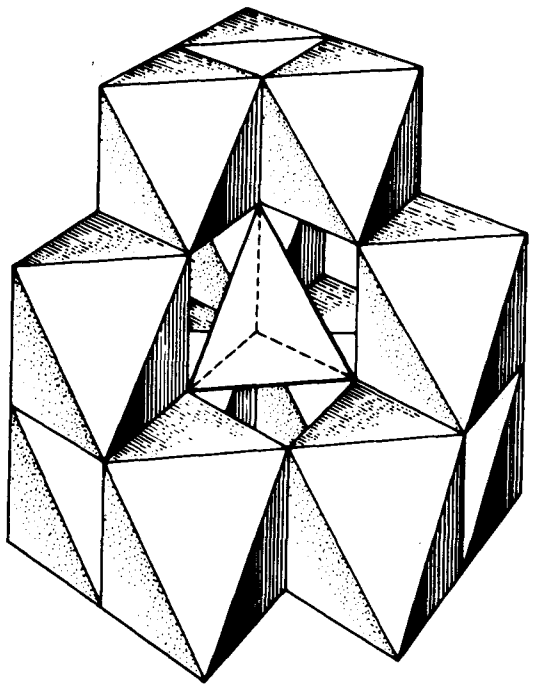

**Figure 2**—*Structure of the $Al_{13}O_4(OH)_{24}(H_2O)_{12}^{7+}$ complex showing the tetrahedral aluminum surrounded by 12 aluminums in octahedral configuration. (Reproduced, with permission, from Ref. 8.)*

[1] Lot 8473, Wicken Products, Huguenot, N.Y.; Chlorhydrol, lots 6178 and 5880, Reheis Chemical Co., Berkeley Heights, N.J.; Astringen, lot 4445, Robinson Wagner, Mamaroneck, N.Y.; lot 6138, Delmar, Elk Grove Village, N.Y.; and lot 735, Summit Research Laboratories, Somerset, N.J. All commercial samples gave similar X-ray diffractograms and IR and $^{27}$Al-NMR spectra. All data in this report were obtained using lot 8473, Wicken Products, Huguenot, N.Y.

[2] Siemens AG Kristalloflex 4 generator, type F diffractometer, Karlsruhe, West Germany.

[3] Model 180, Perkin-Elmer Corp., Norwalk, Conn.

[4] FT-80, Varian Associates, Palo Alto, Calif.

in a tetrahedral environment surrounded by 12 aluminum atoms in octahedral environments. Aluminum in a tetrahedral environment is characterized by aluminate, $Al(OH)_4^-$, which only exists at high pH conditions. Aluminum in octahedral configuration occurs at neutral and acidic pH conditions and is the configuration of aluminum in aluminum hydroxide. Thus, aluminum chlorohydrate was examined by IR and $^{27}Al$-NMR spectroscopy to determine if aluminum was present in both octahedral and tetrahedral environments.

IR spectra have been published for aluminum chlorohydrate, aluminum hydroxide chloride, aluminum hydroxide, and hydrolyzed alumina (20–24). Based on these reports, the 3700–3400-$cm^{-1}$ region should show hydroxyl-stretching vibrations for ionic or surface hydroxyl anions. The hydroxyl-stretching vibrations of aluminum in octahedral configuration, $Al(H_2O)_6^{3+}$, should occur between 3100 and 2500 $cm^{-1}$. The region of 1200–800 $cm^{-1}$ should show absorption bands for the deformation of Al–O–H or Al–OH–Al. Absorption bands for the rocking of coordinated water and the vibrations of $AlO_6$ octahedra should occur below 800 $cm^{-1}$. IR absorption bands for aluminum in tetrahedral configuration were assigned as follows based on the IR spectrum of aluminate, $Al(OH)_4^-$: 725 $cm^{-1}$, $AlO_4$ antisymmetric stretching; 625 $cm^{-1}$, $AlO_4$ symmetric stretching; and 325 $cm^{-1}$, $AlO_4$ antisymmetric bending (25). The 800-$cm^{-1}$ band in synthetic trioctahedral analogs of kaolinite was assigned as Al–O tetrahedral vibrations (26).

Figure 3 shows the hydroxyl-stretching region of the IR spectrum of aluminum chlorohydrate. Riesgraf and May (20) assigned the 3400-$cm^{-1}$ band to the stretching of hydroxyl anions bound to aluminum. Bands between 3000 and 2500 $cm^{-1}$ were attributed to antisymmetric and symmetric stretching of water coordinated to aluminum. No changes were observed in this region of the IR spectrum during aging, as was observed for aluminum hydroxide (22, 23).

Figure 4 shows the IR spectrum of aluminum chlorohydrate for the 1200–300-$cm^{-1}$ region. The 1080-$cm^{-1}$ band was assigned as Al–O–H bending of bridge hydroxyl anions, and the 970-$cm^{-1}$ band was assigned as Al–OH deformation bending of Al–OH and $Al–OH_2$ (20). The bands at 780 and 640 $cm^{-1}$ were observed previously but not assigned (20). Based on the assignments of aluminum in a tetrahedral environment (25, 26), the bands at 780, 640, and 345 $cm^{-1}$ (Fig. 4) can be assigned as an $AlO_4$ antisymmetric stretch frequency, an $AlO_4$ symmetric stretch frequency, and an $AlO_4$ antisymmetric bending frequency, respectively. Both the $AlO_4$ antisymmetric stretching and $AlO_4$ symmetric stretching bands occurred at higher frequencies than were observed in aluminate, $Al(OH)_4^-$. This finding indicates that a slightly longer Al–O bond is present in the tetrahedral aluminum of aluminum chlorohydrate in comparison to aluminate. Thus, the IR spectrum of aluminum chlorohydrate clearly shows the presence of aluminum in both octahedral and tetrahedral configurations and suggests that the tetrahedral aluminum interacts with the octahedral aluminum atoms.

$^{27}Al$-NMR spectroscopy has been used to investigate aluminum complexes in solution (9, 25, 27–36). The $^{27}Al$-NMR spectrum of aluminum chlorohydrate at pH 4.8 (Fig. 5) consisted of three distinct signals: a sharp peak at 63.5 ppm and two broad peaks at ~1.7 and −0.4 ppm. The relative chemical shift differences were referenced to an external standard of $Al(H_2O)_6^{3+}$ at pH 1. The peak at 63.5 ppm is indicative of an Al–O bond

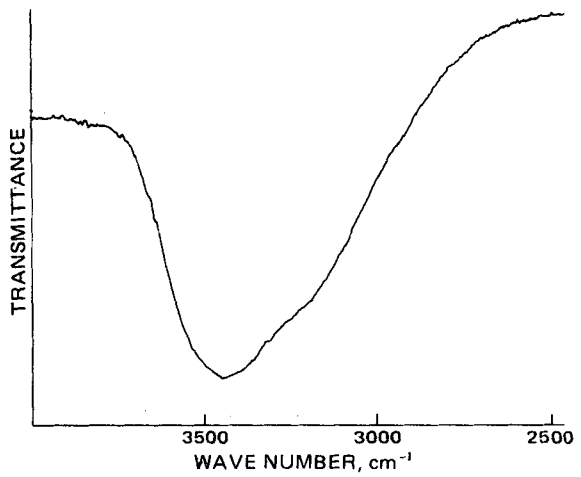


**Figure 3**—*IR spectrum of aluminum chlorohydrate in the 4000–2000-$cm^{-1}$ region.*

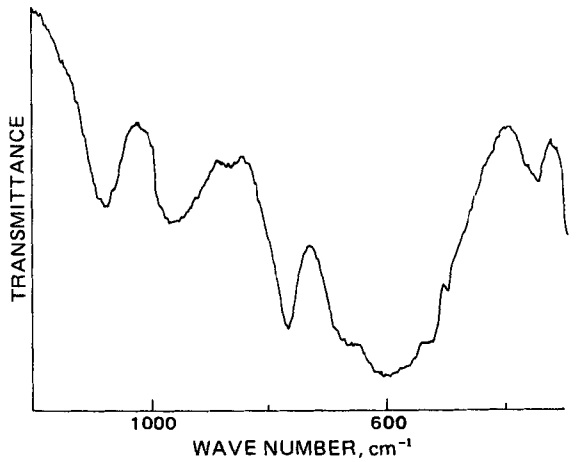


**Figure 4**—*IR spectrum of aluminum chlorohydrate in the 1200–200-$cm^{-1}$ region.*

in an $AlO_4$ tetrahedral configuration (9). The peak width of <40 Hz observed for this complex at pH 4.8 suggests that the tetrahedral aluminum is not in equilibrium with the aqueous environment since no line broadening was observed. Consequently, the tetrahedral $AlO_4$ group is thought to be bonded to other aluminum atoms. The broad resonances, *i.e.*, 150 and 400 Hz at −0.4 and 1.7 ppm, respectively, suggest the presence of aluminum atoms in octahedral environments, which are in rapid equilibrium with the aqueous solution.

The evidence is strong that aluminum chlorohydrate has a structure consisting of a central aluminum atom in a tetrahedral environment surrounded by 12 aluminum atoms in octahedral environments. Usually, tetrahedral aluminum is found only at high pH (pH >10), but the pH of aluminum chlorohydrate solutions is ~4.5. The question arises as to how this symmetrical complex forms with a tetrahedral aluminum in the center. The major synthetic procedure for preparing aluminum chlorohydrate involves the reaction of 5 moles of metallic aluminum with 1 mole of aluminum chloride (37). The pH of the reaction begins near 3 and ends near 4.5. Since the pH never rises above 4.5, it would be difficult for

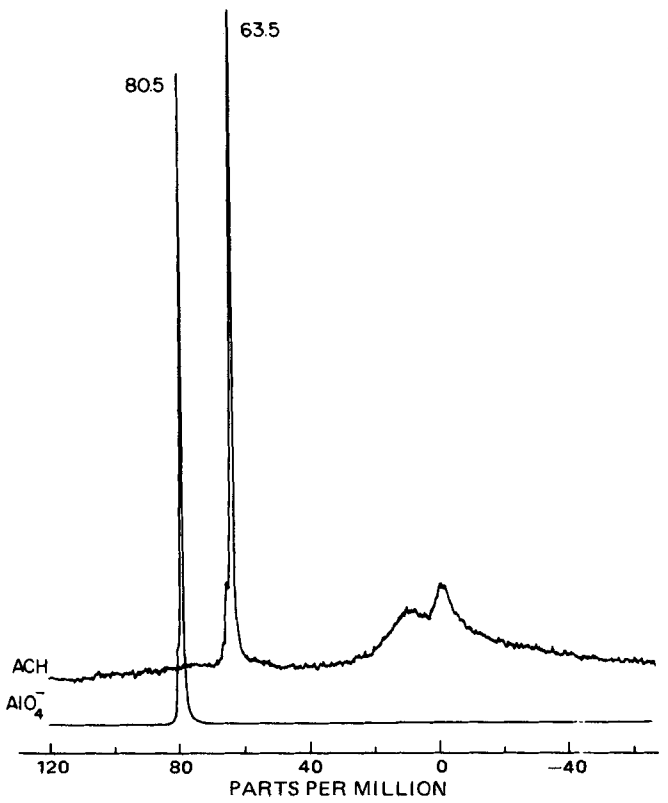


**Figure 5**—*$^{27}Al$-NMR spectrum of aluminum chlorohydrate (ACH) and sodium aluminate ($AlO_4^-$).*

a tetrahedral aluminum to form in solution. However, regions of high pH may occur during the reaction even though the bulk solution is at a much lower pH.

The main reactions that occur are the oxidation of metallic aluminum to aluminum ion ($Al^{3+}$) and the reduction of protons to produce hydrogen gas. These reactions occur only at the surface of metallic aluminum. The protons arise from water dissociation. Since the protons are quickly converted to hydrogen gas, a high hydroxyl concentration may be present at the aluminum surface, resulting in a pH gradient between the surface and the bulk. Therefore, aluminum can exist in a tetrahedral state in the system even though the apparent pH is 3–4.5.

As a cluster of tetrahedral aluminum diffuse away from the metallic aluminum surface, the pH gradient causes the tetrahedral configuration to convert to the octahedral configuration. However, the tetrahedral aluminum in the middle of the cluster is protected from the aqueous pH, and the $Al_{13}O_4(OH)_{24}(H_2O)_{12}^{7+}$ complex forms with a tetrahedral aluminum in the center and surrounded by 12 aluminum atoms in octahedral configuration. Seven chloride anions are associated with the complex as counterions to produce a neutral complex.

The structure of $Al_{13}O_4(OH)_{24}(H_2O)_{12}Cl_7$ is consistent with the current understanding of antiperspirant activity. Antiperspirant activity has been elicited primarily by the topical application of multivalent metals in ionic form (38). The exact mechanism of antiperspirant activity is controversial; several theories exist. However, most studies indicate that optimum activity is achieved when the metal is presented to the skin in ionic form. Regardless of whether the metal is acting directly as an antiperspirant and/or indirectly as a deodorant, a charged species is necessary. The $Al_{13}O_4(OH)_{24}(H_2O)_{12}^{7+}$ complex is small and compact with the charge well distributed. Therefore, its effective charge to radius ratio is high, and it will act as a highly charged form of aluminum. In addition, the pH of aluminum chlorohydrate solutions is ~4.5, which corresponds to the acid mantle of the skin. The hydroxyl groups present in the complex are responsible for the higher pH in comparison to aluminum chloride solutions. Therefore, little skin irritation is observed, and minimal clothing damage due to acid hydrolysis occurs.

## REFERENCES


(1) "The Merck Index," 9th ed., Merck & Co., Rahway, N.J., 1976, p. 47.

(2) J. L. Bersillon, D. W. Brown, F. Fiessinger, and J. Hem, *J. Res. U.S. Geol. Surv.*, **6,** 325 (1975).

(3) E. Matijevic, K. G. Mathai, R. H. Ottewill, and M. Kerker, *J. Phys. Chem.*, **65,** 826 (1961).

(4) P. Hayden and A. Rubin, *National Technical Information Service*, **PB-241,** 318 (1973).

(5) G. Johansson, G. Lundgren, L. G. Sillen, and R. Soderquist, *Acta Chem. Scand.*, **14,** 769 (1960).

(6) W. V. Rausch and H. D. Bale, *J. Chem. Phys.*, **40,** 3391 (1964).

(7) J. Aveston, *J. Chem. Soc.*, **1965,** 4438.

(8) R. Mesmer and C. Baes, "The Hydrolysis of Cations," Wiley, New York, N.Y., 1976, chap. 6.

(9) J. Akitt, N. Greenwood, B. Khandelwal, and G. Lester, *J. Chem. Soc. Dalton Trans.*, **1972,** 604.

(10) D. N. Waters and M. S. Henty, *ibid.*, **1977,** 243.

(11) R. E. Mesmer and C. F. Baes, *Inorg. Chem.*, **10,** 2290 (1971).

(12) D. D. MacDonald, P. Butler, and D. Owen, *J. Phys. Chem.*, **77,** 2474 (1973).

(13) P. H. Hsu and T. F. Bates, *Soil Sci. Soc. Am. Proc.*, **28,** 763 (1964).

(14) G. W. Brindley and R. E. Sempels, *Clay Miner.*, **12,** 229 (1977).

(15) J. D. Hem and C. E. Roberson, *U.S. Geol. Surv. Water-Supply Pap.*, **1967,** 1827-A.

(16) L. S. Porubcan, C. J. Serna, J. L. White, and S. L. Hem, *J. Pharm. Sci.*, **67,** 1081 (1978).

(17) R. Green-Kelley, *Trans. Faraday Soc.*, **51,** 412 (1955).

(18) G. W. Brindley and R. W. Hoffmann, *Clays Clay Miner.*, **9,** 546 (1960).

(19) P. H. Hsu and T. F. Bates, *Min. Mag.*, **33,** 749 (1964).

(20) D. A. Riesgraf and M. L. May, *Appl. Spectrosc.*, **32,** 362 (1978).

(21) J. J. Fripiat, F. Van Cauwelaert, and H. Bowmans, *J. Phys. Chem.*, **69,** 2458 (1965).

(22) S. L. Nail, J. L. White, and S. L. Hem, *J. Pharm. Sci.*, **65,** 231 (1976).

(23) H. Elderfield and J. D. Hem, *Min. Mag.*, **39,** 89 (1973).

(24) A. J. Leonard, F. Van Cauwelaert, and S. S. Fripiat, *J. Phys. Chem.*, **71,** 695 (1967).

(25) R. J. Moolenaar, J. C. Evans, and L. D. McKeever, *ibid.*, **74,** 3629 (1970).

(26) C. J. Serna, J. L. White, and B. D. Velde, *Min. Mag.*, **43,** 141 (1979).

(27) J. W. Akitt, N. N. Greenwood, and G. D. Lester, *J. Chem. Soc. A*, **1969,** 803.

(28) J. Akitt, N. N. Greenwood, and G. D. Lester, *Chem. Commun.*, **1969,** 988.

(29) J. W. Akitt, N. N. Greenwood, and G. D. Lester, *J. Chem. Soc. A*, **1971,** 2450.

(30) E. N. Dicarlo and H. E. Swift, *J. Phys. Chem.*, **68,** 551 (1964).

(31) J. F. Hon, *Mol. Phys.*, **15,** 57 (1968).

(32) R. G. Kidd and D. R. Truax, *J. Am. Chem. Soc.*, **90,** 6867 (1968).

(33) D. E. O'Reilly, *J. Chem. Phys.*, **32,** 1007 (1960).

(34) C. P. Poole, Jr., H. E. Swift, and J. F. Itzel, Jr., *ibid.*, **42,** 2576 (1965).

(35) H. E. Swift and J. F. Itzel, Jr., *Inorg. Chem.*, **5,** 2048 (1966).

(36) H. E. Swift, C. P. Poole, Jr., and J. F. Itzel, Jr., *J. Phys. Chem.*, **68,** 2509 (1964).

(37) W. Huehn and W. Haufe, U.S. pat. 2,196,016 (Apr. 2, 1940).

(38) L. Kennon, *J. Pharm. Sci.*, **54,** 813 (1965).


## ACKNOWLEDGMENTS


This report is Journal Paper 8254, Purdue University Agricultural Experiment Station, West Lafayette, IN 47907.

# Aluminum Chlorohydrate II: Physicochemical Properties

**DIRK L. TEAGARDEN *, JOHN F. RADAVICH §, JOE L. WHITE ‡, and STANLEY L. HEM *x**

Received October 3, 1980, from the **Department of Industrial and Physical Pharmacy, the* ‡*Department of Agronomy, and the* §*School of Materials Engineering, Purdue University, West Lafayette, IN 47907.* Accepted for publication December 8, 1980.

**Abstract** □ Determination of the chloride content of aluminum chlorohydrate by a chloride-selective electrode indicated that $\gamma_{Cl^-} \rightarrow 1$. IR analysis demonstrated that chloride was exchanged readily by nitrate and that the IR bands of the anion were not perturbed significantly. Thus, chloride is believed to act as a counterion. A high positive charge is predicted based on the critical coagulation concentration of aluminum chlorohydrate and the stability of aluminum chlorohydrate to attack by protons, as demonstrated by pH-stat titration. Potentiometric titration with sodium hydroxide showed adsorption of hydroxyl anions initially, but a higher pH than expected was observed at the end-point. This behavior is consistent with the $Al_{13}O_4(OH)_{24}(H_2O)_{12}^{7+}$ complex, which would adsorb hydroxyl anions initially and in which the central tetrahedral aluminum is shielded from the added hydroxyl anions. The reaction rate with ferron (8-hydroxy-7-iodo-5-quinolinesulfonic acid) suggests that the major species in aluminum chlorohydrate is a large aluminum polycation. A platey morphology for lyophilized, air-dried, and spray-dried aluminum chlorohydrate was observed by scanning electron microscopy. The platey appearance is consistent with the structure of $Al_{13}O_4(OH)_{24}(H_2O)_{12}^{7+}$ since the spherical nature and high uneven charge of the complex make stacking difficult.

**Keyphrases** □ Aluminum chlorohydrate—physicochemical properties determined by IR spectroscopy and pH-stat and potentiometric titrations □ Spectroscopy, IR—analysis, aluminum chlorohydrate, physicochemical properties determined □ Potentiometric titration—aluminum chlorohydrate, physicochemical properties determined, IR spectroscopy and pH-stat titration □ Critical coagulation concentration—aluminum chlorohydrate, physicochemical properties determined using IR spectroscopy and pH-stat and potentiometric titrations

X-ray diffraction and IR and $^{27}$Al-NMR spectroscopy recently showed that aluminum chlorohydrate is composed of a central aluminum in tetrahedral configuration surrounded by 12 aluminum atoms, each in an octahedral configuration (1). The complex, $Al_{13}O_4(OH)_{24}(H_2O)_{12}^{7+}$, is essentially spherical with the +7 charge equally distributed on the surface. Seven chloride ions are believed to be associated with the complex as counterions. The objectives of this study were to examine the physicochemical properties of aluminum chlorohydrate and to determine if these properties are related to the recently proposed structure.

## EXPERIMENTAL

Aluminum chlorohydrate was obtained commercially as a 50% (w/w) solution[1].

Aluminum was quantified by a chelatometric titration procedure (2). The chloride content was determined by both the modified Volhard technique (3) and a chloride-selective electrode[2]. The aluminum chlorohydrate solutions were diluted with potassium nitrate solutions prior to measurement by the chloride-selective electrode to produce a solution having $1 \times 10^{-2}$–$1 \times 10^{-4}$ *M* chloride and an ionic strength of ~0.1. The chloride concentration of aluminum chlorohydrate solutions that had been hydrolyzed by nitric acid also was determined by the modified Volhard method and by the chloride-selective electrode. Hydrolysis was accomplished by adding the quantity of nitric acid indicated in Table I and heating to 70° for 1 hr.

Chloride in aluminum chlorohydrate was replaced by nitrate; after air drying, the IR spectrum was determined in potassium bromide pellets. One hundred milliliters of 0.308 *M* silver nitrate was placed in a 400-ml beaker, and 90 ml of a diluted aluminum chlorohydrate solution (0.308 *M* in chloride) was added slowly. Silver chloride precipitated throughout the addition. The mixture was stirred for 15 min and centrifuged at 2500 rpm for 10 min. The precipitate was discarded, and the supernate was prepared for IR spectroscopy[3].

**Table I—Chloride Content of Aluminum Chlorohydrate Determined by Volhard Method and Chloride-Selective Electrode**

| Nitrate Added, *M* | Volhard Method, *M* | Chloride-Selective Electrode, *M* |
|---|---|---|
| Potassium nitrate | | |
| $9.0 \times 10^{-2}$ | $2.3 \times 10^{-3}$ | $2.3 \times 10^{-3}$ |
| $9.9 \times 10^{-2}$ | $2.3 \times 10^{-4}$ | $2.3 \times 10^{-4}$ |
| Nitric acid | | |
| $9.0 \times 10^{-2}$ | $2.3 \times 10^{-3}$ | $2.1 \times 10^{-3}$ |
| $9.9 \times 10^{-2}$ | $2.3 \times 10^{-4}$ | $2.3 \times 10^{-4}$ |

The charge of the aluminum chlorohydrate complex was determined by the method of Matijevic *et al.* (4), except that 0.69% sodium montmorillonite was used as the lyophobic colloid rather than silver iodide. Potassium chloride, calcium chloride, aluminum nitrate, and thorium nitrate were used to prepare a standard curve of the valence of the coagulating cation *versus* the ratio of the critical coagulation concentration of the cation to the critical coagulation concentration of potassium.

The potentiometric titration curve of aluminum chlorohydrate or aluminum chloride with sodium hydroxide was determined with an automated titrator[4]. The aluminum chloride solution was brought to a ratio of 2.5 (hydroxyl to aluminum) with sodium hydroxide before the recorder was activated so that both aluminum samples were titrated from a hydroxyl to aluminum ratio of 2.5 to 3.0.

The rate and extent of acid neutralization by aluminum chlorohydrate was determined at pH 1, 2, and 3 at 25° with an automated titrator[4].

The distribution of aluminum in aluminum chlorohydrate (*i.e.*, monomers, small polycations, and large polycations) was determined by

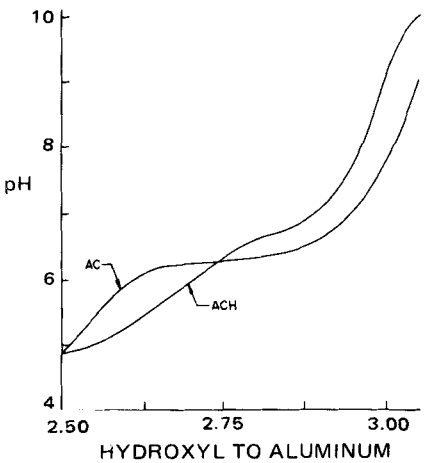


**Figure 1**—*Potentiometric titration of aluminum chlorohydrate (ACH) or aluminum chloride (AC) with sodium hydroxide.*

[1] Lot 8473, Wicken Products, Huguenot, N.Y.
[2] Model 94-17A, Orion Research, Cambridge, Mass.
[3] Model 180, Perkin-Elmer Corp., Norwalk, Conn.
[4] PHM 26, TTT 11, ABU 12 (2.5 ml), TTA 3, SBR 2, Radiometer, Copenhagen, Denmark.



*0022-3549/81/0700-0762$01.00/0*
*© 1981, American Pharmaceutical Association*

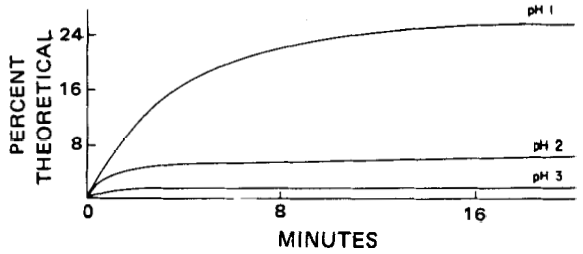


**Figure 2**—*A pH-stat titrigram of aluminum chlorohydrate at pH 1, 2, and 3.*

the ferron (8-hydroxy-7-iodo-5-quinolinesulfonic acid) test (5).

**Scanning electron photomicrographs[5] of aluminum chlorohydrate** were taken following air drying, spray drying, or lyophilization.

## RESULTS AND DISCUSSION

Table I compares the chloride content of aluminum chlorohydrate solutions as determined by the Volhard titration and the chloride-selective electrode. The results by both methods were virtually identical. In addition, the chloride content was the same for intact and hydrolyzed aluminum chlorohydrate. Thus, the chloride activity coefficient of aluminum chlorohydrate must be close to 1, indicating that the chloride ion acts as a counterion. This finding is in contrast to the activity of chloride in chloride-containing aluminum hydroxide gel. The fact that the chloride content of chloride-containing aluminum hydroxide gel, as determined by a chloride-selective electrode, was less than that determined by the Volhard titration was attributed to the binding of the chloride ion to the aluminum hydroxy complex (6).

The degree of interaction of the anion with the $Al_{13}O_4(OH)_{24}(H_2O)_{12}^{7+}$ complex could be studied by IR spectroscopy if the anion was IR active. Thus, aluminum chlorohydrate was treated with silver nitrate to attempt to replace the IR inactive chloride with IR active nitrate. Nitrate anion was chosen because it is the same approximate size and charge as chloride, and it is symmetrical so that any perturbations due to interaction with the aluminum complex would cause a shift in the IR spectrum. The IR spectrum was not affected by the replacement of chloride by nitrate except for the appearance of bands at 1380 and 830 $cm^{-1}$. Both bands correspond to the bands for nitrate in sodium nitrate, indicating that the anion in aluminum chlorohydrate is readily exchangeable. Furthermore, the IR bands of sodium nitrate at 1358 and 836 $cm^{-1}$ show little interaction of the anion with the $Al_{13}O_4(OH)_{24}(H_2O)_{12}^{7+}$ complex (7). Thus, the activity of the chloride ion and the IR spectrum of aluminum nitrohydrate indicate that the anion is not part of the aluminum complex but rather functions as a counterion. This behavior is consistent with the structure of the $Al_{13}O_4(OH)_{24}(H_2O)_{12}^{7+}$ complex.

Table II shows that the critical coagulation concentration of aluminum chlorohydrate was less than thorium. The regression equation for the known cations (charge = 0.12 $CCC/CCC_{K+}$ + 0.97)[6] had a $R^2$ value of 0.990 and predicted a valence of 5.6 for aluminum chlorohydrate. This valence is the average of all species present in the aluminum chlorohydrate solution. In addition, the valence of highly charged cations may be greater than that determined by the critical coagulation concentration method because interionic distances increase rapidly with dilution (8). Therefore, the valence of aluminum chlorohydrate as determined by the critical coagulation concentration method is consistent with the high charge of the $Al_{13}O_4(OH)_{24}(H_2O)_{12}^{7+}$ complex.

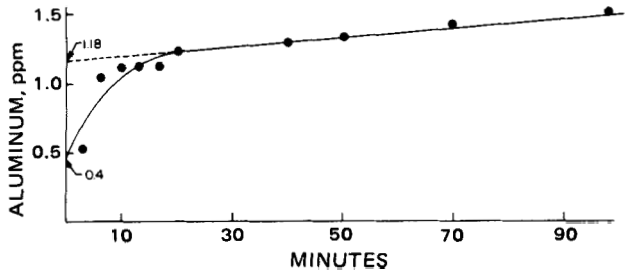


**Figure 3**—*Rate of reaction of a solution of aluminum chlorohydrate containing 9.87 ppm of aluminum with ferron.*

[5] Super III A, International Scientific Products, Mountain View, Calif.

[6] $CCC/CCC_{K+}$ is the ratio of the critical coagulation concentration of the cation to the critical coagulation concentration of potassium.

**Table II—Critical Coagulation Concentration (CCC) of Aluminum Chlorohydrate in Comparison to Known Cations**

| Ion | Charge | CCC, $N$ | $CCC/CCC_{K+}$ |
|---|---|---|---|
| Potassium | 1 | $6.25 \times 10^{-3}$ | 1.00 |
| Calcium | 2 | $8.73 \times 10^{-4}$ | 7.16 |
| Aluminum | 3 | $3.5 \times 10^{-4}$ | 17.85 |
| Thorium | 4 | $2.5 \times 10^{-4}$ | 25.00 |
| Aluminum chlorohydrate | Unknown | $1.62 \times 10^{-4}$ | 38.58 |

The titrigrams of aluminum chloride (following the addition of sodium hydroxide to produce a hydroxyl to aluminum ratio of 2.5) and of aluminum chlorohydrate are shown in Fig. 1. The pH of the aluminum chlorohydrate solution did not increase as rapidly as the aluminum chloride solution, indicating that the added hydroxyl concentration was being adsorbed by the aluminum chlorohydrate. The evenly distributed positive charge of the $Al_{13}O_4(OH)_{24}(H_2O)_{12}^{7+}$ complex would be expected to adsorb hydroxyl anions. Furthermore, the pH at the end-point (hydroxyl to aluminum ratio of 3) was higher for aluminum chlorohydrate. This finding suggests that more hydroxyl anions are in solution in the aluminum chlorohydrate solution, possibly because the tetrahedral aluminum in the center of the $Al_{13}O_4(OH)_{24}(H_2O)_{12}^{7+}$ complex is inaccessible to the added hydroxyl anions.

The reactivity of aluminum chlorohydrate to proton attack was investigated by pH-stat titration. Hydroxyl anions are released into solution if aluminum chlorohydrate breaks up under proton attack. As can be seen in Fig. 2, aluminum chlorohydrate is very stable to proton attack. Even at pH 1, only ~25% of the total hydroxyl anions in aluminum chlorohydrate were neutralized. The fact that protons do not readily attack the complex further indicates that aluminum chlorohydrate is positively charged. In addition, the charge is predicted to be high and evenly distributed to shield the hydroxyl anions of the complex from proton attack.

Based on the reaction rate with ferron, the distribution of aluminum species in aluminum chlorohydrate can be classified as 4% monomeric aluminum, 8% small polycations, and 88% large polycations (Fig. 3). The fact that the major species in aluminum chlorohydrate reacts slowly with ferron also is consistent with the structure of the $Al_{13}O_4(OH)_{24}(H_2O)_{12}^{7+}$ complex.

The morphology of aluminum chlorohydrate that had been air dried,

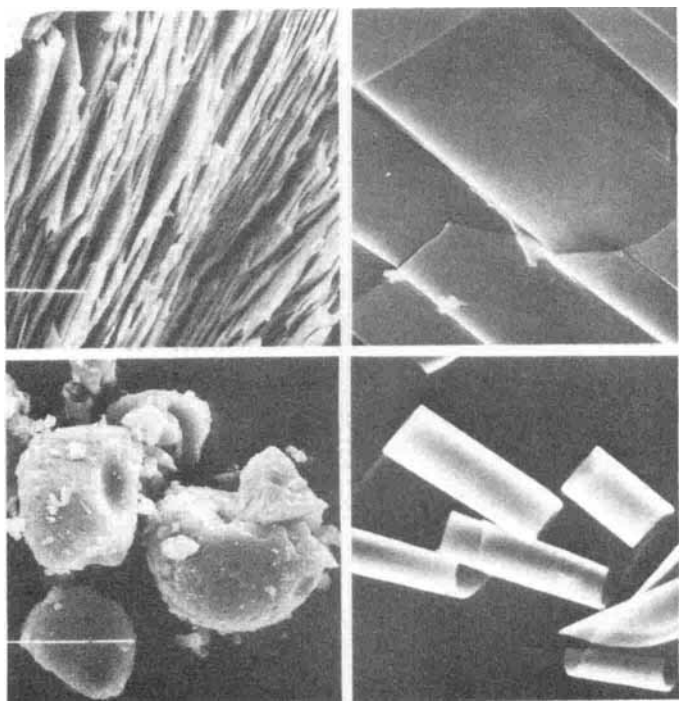

**Figure 4**—*Scanning electron photomicrographs of aluminum chlorohydrate. Key: upper left, lyophilized, 700×, line of 50 μm; upper right, lyophilized, 5000×; lower left, spray dried, 2000×, line of 5 μm; and lower right, air dried, 10,000×.*

lyophilized, or spray dried was examined by scanning electron microscopy (Fig. 4). All samples showed a platey structure, although it was most evident in the lyophilized sample. The spray-dried sample showed spherical particles that are inherent to spray drying. However, the spheres were made up of thin plates. The air-dried samples formed scroll-like sheets due to the more rapid rate of water loss from the top surface during drying. Johansson (9), in proposing the $Al_{13}O_4(OH)_{24}(H_2O)_{12}^{7+}$ complex, noted the formation of plate-like crystals during the study of a basic aluminum sulfate that was built up from the same kind of aluminum–oxygen complexes. It is suggested that the high uneven charge on the spherical units minimize contact with adjacent units so that a planar configuration provides the most favorable spatial and electrostatic arrangement.

## REFERENCES


(1) D. L. Teagarden, J. F. Kozlowski, J. L. White, and S. L. Hem, *J. Pharm. Sci.*, **70**, 758 (1981).

(2) "The United States Pharmacopeia," 20th rev., United States Pharmacopeial Convention, Rockville, Md., 1980, p. 456.

(3) I. M. Kolthoff, "Quantitative Analysis," 4th ed., Macmillan, London, England, 1969, p. 799.

(4) E. Matijevic, K. G. Mathai, R. H. Ottewill, and M. Kerker, *J. Phys. Chem.*, **65**, 826 (1961).

(5) R. W. Smith, in "Advances in Chemistry," vol. 106, R. F. Gould, Ed., American Chemical Society, Washington, D.C., 1971, p. 250.

(6) S. L. Nail, J. L. White, and S. L. Hem, *J. Pharm. Sci.*, **65**, 1188 (1976).

(7) C. J. Serna, J. L. White, and S. L. Hem, *Soil Sci. Soc. Am. J.*, **41**, 1009 (1977).

(8) E. Matijevic, D. Broadhurst, and M. Kerker, *J. Phys. Chem.*, **63**, 1552 (1959).

(9) G. Johansson, *Acta Chem. Scand.*, **14**, 771 (1960).


## ACKNOWLEDGMENTS


This report is Journal Paper 8255, Purdue University Agricultural Experiment Station, West Lafayette, IN 47907.


# Automated Dissolution Testing of Combination Drug Product Using High-Pressure Liquid Chromatography


**DALE ERIC WURSTER ˣ, WILLIAM A. WARGIN, and MARTIN DeBERARDINIS, Jr.**



Received July 24, 1980, from the *School of Pharmacy, University of North Carolina, Chapel Hill, NC 27514.* Accepted for publication December 8, 1980.



**Abstract** □ An automated high-pressure liquid chromatographic (HPLC) system compatible with any standard tablet dissolution apparatus was developed. This system allowed the individual drug concentrations within a product to be determined simultaneously, even when the drugs had similar structures and UV spectra. This automated system permitted unattended sampling and concentration determination at predetermined time intervals. The dissolution medium was pumped continuously through a fixed-volume, microprocessor-controlled injector and returned to the USP rotating-basket dissolution apparatus. No corrections for the changing dissolution medium volume were necessary since each injection onto a reversed-phase HPLC column consumed just 10 μl of medium. Dissolution tests were performed on three brands of trisulfapyrimidines tablets. Sample injections were made automatically at 5.1-min intervals for ~2 hr. Dissolution profiles were determined for each drug in each product. Statistically significant differences were found in the mean concentration–time values between drugs within a drug product and between drug products.



**Keyphrases** □ High-pressure liquid chromatography—with automated dissolution testing of a combination drug product □ Dissolution—automated high-pressure liquid chromatography, combination drug product □ Combination drugs—dissolution testing using automated high-pressure liquid chromatography □ Trisulfapyrimidines—combination drug product, dissolution testing using automated high-pressure liquid chromatography


Automated procedures for dissolution testing of pharmaceuticals have been of interest since such procedures are labor saving and increase analytical reproducibility. These automated procedures usually involve pumping the dissolution medium directly through a flowcell mounted in a UV spectrophotometer (1–6). An inherent problem with such an arrangement is the lack of drug specificity. If two or more drugs in a drug product have similar UV spectra, this procedure is useless.

In view of the number of combination products on the market, an automated technique is needed that allows each drug in a product to be quantitated individually during a dissolution run.

## BACKGROUND

High-pressure liquid chromatography (HPLC) is a versatile analytical technique that combines the specificity of chromatography with the sensitivity of refractive index, UV, fluorescence, or electrochemical detection. Optimal retention times for the separation of active ingredients and dosage form excipients may be obtained by appropriately varying the mobile phase composition, pH, and/or flow rate. Changing the chromatographic temperature and utilization of gradient elution also are viable options. Other than filtration, aqueous samples require no special preparation prior to injection onto a reversed-phase HPLC column.

While various components of an HPLC system have been used to automate drug analysis procedures (3, 7) during dissolution, the actual chromatographic process has been included only in a manual (8) or semiautomated (7) procedure.

This report describes a totally automated HPLC method that has been used successfully to characterize the dissolution profile of each drug entity in a trisulfapyrimidines USP tablet. Completely unattended dissolution analysis is possible using this technique.

## EXPERIMENTAL

A USP rotating-basket dissolution apparatus, a dissolution stirrer drive[1], and a water bath[2] were used. The basket was rotated at 150 rpm, and the temperature of the dissolution medium (0.1 *N* HCl) was 37.0 ± 0.1°. A pump[3] circulated the dissolution medium through a fixed-volume (10-μl loop) microprocessor[4]-controlled injector[5] and returned the me-

[1] Model 53, Hanson Research Corp., Northridge, CA 91234.

[2] Precision Scientific, Chicago, Ill.

[3] Milton Roy Mini-Pump, Laboratory Data Control, Riviera Beach, FL 33404.

[4] Model 740 Control Module, Micromeritics, Norcross, GA 30093. (Depending on the interfacing procedure, the Micromeritics model 753 ternary solvent mixer may also be required.)

[5] Model 735 with model 725 automatic injector valve, Micromeritics, Norcross, GA 30093.




*0022-3549/81/0700-0764$01.00/0*


*© 1981, American Pharmaceutical Association*

lyophilized, or spray dried was examined by scanning electron microscopy (Fig. 4). All samples showed a platey structure, although it was most evident in the lyophilized sample. The spray-dried sample showed spherical particles that are inherent to spray drying. However, the spheres were made up of thin plates. The air-dried samples formed scroll-like sheets due to the more rapid rate of water loss from the top surface during drying. Johansson (9), in proposing the $Al_{13}O_4(OH)_{24}(H_2O)_{12}^{7+}$ complex, noted the formation of plate-like crystals during the study of a basic aluminum sulfate that was built up from the same kind of aluminum–oxygen complexes. It is suggested that the high uneven charge on the spherical units minimize contact with adjacent units so that a planar configuration provides the most favorable spatial and electrostatic arrangement.

## REFERENCES


(1) D. L. Teagarden, J. F. Kozlowski, J. L. White, and S. L. Hem, *J. Pharm. Sci.*, **70**, 758 (1981).

(2) "The United States Pharmacopeia," 20th rev., United States Pharmacopeial Convention, Rockville, Md., 1980, p. 456.

(3) I. M. Kolthoff, "Quantitative Analysis," 4th ed., Macmillan, London, England, 1969, p. 799.

(4) E. Matijevic, K. G. Mathai, R. H. Ottewill, and M. Kerker, *J. Phys. Chem.*, **65**, 826 (1961).

(5) R. W. Smith, in "Advances in Chemistry," vol. 106, R. F. Gould, Ed., American Chemical Society, Washington, D.C., 1971, p. 250.

(6) S. L. Nail, J. L. White, and S. L. Hem, *J. Pharm. Sci.*, **65**, 1188 (1976).

(7) C. J. Serna, J. L. White, and S. L. Hem, *Soil Sci. Soc. Am. J.*, **41**, 1009 (1977).

(8) E. Matijevic, D. Broadhurst, and M. Kerker, *J. Phys. Chem.*, **63**, 1552 (1959).

(9) G. Johansson, *Acta Chem. Scand.*, **14**, 771 (1960).


## ACKNOWLEDGMENTS


This report is Journal Paper 8255, Purdue University Agricultural Experiment Station, West Lafayette, IN 47907.


# Automated Dissolution Testing of Combination Drug Product Using High-Pressure Liquid Chromatography


**DALE ERIC WURSTER ˣ, WILLIAM A. WARGIN, and MARTIN DeBERARDINIS, Jr.**



Received July 24, 1980, from the *School of Pharmacy, University of North Carolina, Chapel Hill, NC 27514.* Accepted for publication December 8, 1980.



**Abstract** □ An automated high-pressure liquid chromatographic (HPLC) system compatible with any standard tablet dissolution apparatus was developed. This system allowed the individual drug concentrations within a product to be determined simultaneously, even when the drugs had similar structures and UV spectra. This automated system permitted unattended sampling and concentration determination at predetermined time intervals. The dissolution medium was pumped continuously through a fixed-volume, microprocessor-controlled injector and returned to the USP rotating-basket dissolution apparatus. No corrections for the changing dissolution medium volume were necessary since each injection onto a reversed-phase HPLC column consumed just 10 μl of medium. Dissolution tests were performed on three brands of trisulfapyrimidines tablets. Sample injections were made automatically at 5.1-min intervals for ~2 hr. Dissolution profiles were determined for each drug in each product. Statistically significant differences were found in the mean concentration–time values between drugs within a drug product and between drug products.



**Keyphrases** □ High-pressure liquid chromatography—with automated dissolution testing of a combination drug product □ Dissolution—automated high-pressure liquid chromatography, combination drug product □ Combination drugs—dissolution testing using automated high-pressure liquid chromatography □ Trisulfapyrimidines—combination drug product, dissolution testing using automated high-pressure liquid chromatography


Automated procedures for dissolution testing of pharmaceuticals have been of interest since such procedures are labor saving and increase analytical reproducibility. These automated procedures usually involve pumping the dissolution medium directly through a flowcell mounted in a UV spectrophotometer (1–6). An inherent problem with such an arrangement is the lack of drug specificity. If two or more drugs in a drug product have similar UV spectra, this procedure is useless.

In view of the number of combination products on the market, an automated technique is needed that allows each drug in a product to be quantitated individually during a dissolution run.

## BACKGROUND

High-pressure liquid chromatography (HPLC) is a versatile analytical technique that combines the specificity of chromatography with the sensitivity of refractive index, UV, fluorescence, or electrochemical detection. Optimal retention times for the separation of active ingredients and dosage form excipients may be obtained by appropriately varying the mobile phase composition, pH, and/or flow rate. Changing the chromatographic temperature and utilization of gradient elution also are viable options. Other than filtration, aqueous samples require no special preparation prior to injection onto a reversed-phase HPLC column.

While various components of an HPLC system have been used to automate drug analysis procedures (3, 7) during dissolution, the actual chromatographic process has been included only in a manual (8) or semiautomated (7) procedure.

This report describes a totally automated HPLC method that has been used successfully to characterize the dissolution profile of each drug entity in a trisulfapyrimidines USP tablet. Completely unattended dissolution analysis is possible using this technique.

## EXPERIMENTAL

A USP rotating-basket dissolution apparatus, a dissolution stirrer drive[1], and a water bath[2] were used. The basket was rotated at 150 rpm, and the temperature of the dissolution medium (0.1 *N* HCl) was 37.0 ± 0.1°. A pump[3] circulated the dissolution medium through a fixed-volume (10-μl loop) microprocessor[4]-controlled injector[5] and returned the me-

[1] Model 53, Hanson Research Corp., Northridge, CA 91234.

[2] Precision Scientific, Chicago, Ill.

[3] Milton Roy Mini-Pump, Laboratory Data Control, Riviera Beach, FL 33404.

[4] Model 740 Control Module, Micromeritics, Norcross, GA 30093. (Depending on the interfacing procedure, the Micromeritics model 753 ternary solvent mixer may also be required.)

[5] Model 735 with model 725 automatic injector valve, Micromeritics, Norcross, GA 30093.




*0022-3549/81/0700-0764$01.00/0*


*© 1981, American Pharmaceutical Association*

**Table I—Parameter Estimates for Individual Dissolution Runs**

| Manufacturer[a] | Drug | Rate of Appearance of Drug in Solution ($K$), $min^{-1}$ | | | | | | | | Asymptote of Drug Concentration ($C_{max}$), mg/900 ml | | | | | | | |
|---|---|---|---|---|---|---|---|---|---|---|---|---|---|---|---|---|---|
| | | Run 1 | Run 2 | Run 3 | Run 4 | Run 5 | Run 6 | Mean | SD | Run 1 | Run 2 | Run 3 | Run 4 | Run 5 | Run 6 | Mean | SD |
| A | I | 0.061 | 0.070 | 0.063 | 0.057 | 0.064 | 0.062 | 0.063 | 0.004 | 141.6 | 151.7 | 151.2 | 146.9 | 152.3 | 158.4 | 150.3 | 5.6 |
| | II | 0.109 | 0.108 | 0.111 | 0.091 | 0.100 | 0.112 | 0.105 | 0.008 | 161.9 | 160.9 | 161.9 | 156.4 | 163.0 | 165.9 | 161.7 | 3.1 |
| | III | 0.181 | 0.143 | 0.164 | 0.130 | 0.147 | 0.150 | 0.152 | 0.018 | 164.0 | 164.6 | 163.4 | 156.2 | 162.9 | 167.3 | 163.1 | 3.7 |
| B | I | 0.038 | 0.042 | 0.042 | 0.045 | 0.056 | 0.052 | 0.046 | 0.007 | 158.3 | 158.1 | 152.3 | 147.6 | 150.6 | 161.9 | 154.8 | 5.4 |
| | II | 0.067 | 0.062 | 0.065 | 0.067 | 0.080 | 0.076 | 0.070 | 0.007 | 171.2 | 165.0 | 168.0 | 165.7 | 166.3 | 177.0 | 168.9 | 4.5 |
| | III | 0.083 | 0.079 | 0.081 | 0.081 | 0.099 | 0.090 | 0.085 | 0.008 | 173.3 | 158.1 | 165.7 | 166.3 | 167.3 | 175.6 | 167.8 | 6.2 |
| C | I | 0.036 | 0.031 | 0.033 | 0.042 | 0.046 | 0.052 | 0.040 | 0.008 | 169.5 | 138.2 | 137.6 | 135.0 | 135.1 | 152.0 | 144.6 | 13.8 |
| | II | 0.067 | 0.044 | 0.048 | 0.062 | 0.064 | 0.075 | 0.060 | 0.012 | 163.5 | 164.7 | 166.8 | 164.5 | 159.6 | 167.8 | 164.5 | 2.9 |
| | III | 0.095 | 0.061 | 0.064 | 0.090 | 0.091 | 0.090 | 0.082 | 0.015 | 161.1 | 162.1 | 166.1 | 163.1 | 156.7 | 167.7 | 162.8 | 3.9 |

[a] Manufacturers, trade names, lot numbers, and expiration dates are as follows: A, Eli Lilly & Co., Neotrizine, 3FV36A, September 1, 1974; B, E. R. Squibb & Sons, Terfonyl, 8L238, July 1, 1983; and C, Wyeth Laboratories, Sulfose, 1790577, January 1984.

dium to the dissolution flask. All dissolution medium was filtered through a 2-μm low-pressure solvent filter as it entered the external circulation system. Only 1.05 ml of dissolution medium was external to the bulk (900 ml) at any given moment, and the circulation rate was 2.25 ml/min. The time required for a sample of bulk dissolution medium to reach the injector loop was determined experimentally to be 0.3 min.

Another pump[6] delivered the mobile phase (180 ml of acetonitrile[7]–820 ml of 0.05 *M* sodium acetate[8] buffer, pH adjusted to 5.7 with acetic acid) through the injector and onto a 25-cm long × 4-mm i.d. reversed-phase[9] column at a flow rate of 1.50 ml/min. The chromatographic analysis was conducted at room temperature. The absorbance of the column effluent was measured[10] at 254 nm. Peak areas were integrated[11] automatically, and a recorder[12] was used to display chromatographic peaks (Scheme I).

Dissolution testing of three brands (six runs each) of trisulfapyrimidines tablets USP (500 mg) was performed according to USP XX guidelines to demonstrate the utility of the system. Each tablet consisted of 167 mg each of sulfadiazine (I), sulfamerazine (II), and sulfamethazine (III). Sample injections were made automatically at 5.1-min intervals for ~2 hr. Dissolution profiles were determined for each drug in each drug product. Six dissolution runs at 100 rpm also were performed on one formulation to assess the impact of the basket rotation rate on the dissolution profile. The dissolution medium and mobile phase (one batch each) were prepared in sufficient quantity for all runs.

A standard curve for each drug was constructed by making four solutions ranging from 0.045 to 0.185 mg/ml. Each standard solution was placed in the resin flask of the dissolution apparatus, and the apparatus was assembled in the same manner as if a dissolution test were to be conducted. When the standard solution reached 37°, solution circulation through the injector loop and basket rotation were initiated. Injections were controlled by the microprocessor, and the same injector loop was used as in the actual dissolution runs.

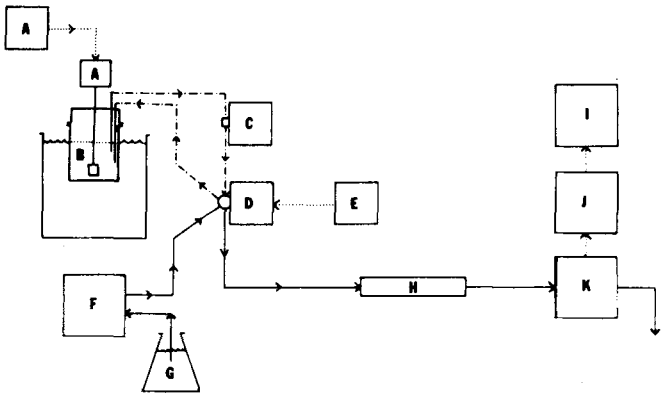


*Scheme I—Schematic diagram of the analytical system. Key: A, motor and control unit for basket rotation; B, USP dissolution flask and basket; C, dissolution medium recirculation pump; D, sample injector; E, microprocessor for injector control; F, mobile phase delivery pump; G, mobile phase container; H, reversed-phase HPLC column; I, strip-chart recorder; J, peak integrator; K, UV detector; —, mobile phase; - - -, dissolution medium; and ···, electrical signal.*

[6] Model 750 solvent delivery system, Micromeritics, Norcross, GA 30093.
[7] HPLC grade, Fisher Scientific Co., Fair Lawn, NJ 07410.
[8] Certified ACS, Fisher Scientific Co., Fair Lawn, NJ 07410.
[9] RP-18, 10-μm particle size, E. Merck, Darmstadt, West Germany.
[10] Model 790 UV detector, Micromeritics, Norcross, GA 30093.
[11] CDS-111, Varian Instruments, Sunnyvale, CA 94086.
[12] Fisher Recordall, Houston Instruments, Austin, Tex.

The standard curves were linear and exhibited coefficients of determination ($r^2$) of 0.998 for I and II and 0.997 for III. This excellent linearity allows single-point calibrations before each dissolution run to guard against changing detector response and column behavior. The coefficients of variation at each concentration were <2.0% for I and II and <2.7% for III.

## RESULTS AND DISCUSSION

Content uniformity tests were performed on each formulation according to USP XX guidelines (9). All products passed the specifications of 95.0–105.0% of the labeled amount of total sulfapyrimidines, with each drug providing not less than 31.5% nor greater than 35.0% of the total.

Figure 1 illustrates the typical chromatographic output of one dissolution run. The peaks (in the order shown) represent the amounts of I, II, and III present at a specific time. Machine integration (*Experimental*) yielded the area of each peak. Drug concentrations were determined from these integrated peak areas.

The dissolution data for each drug present in each run were fitted to:

$$C = C_{max}(1 - e^{-Kt}) \qquad \text{(Eq. 1)}$$

where $C$ is the experimentally determined sulfa drug concentration at time $t$, $C_{max}$ is the asymptote of the dissolution profile, and $K$ is the rate constant for the appearance of drug in solution, as opposed to a rate constant for dissolution, since it includes the process of disintegration.

A nonlinear least-squares regression analysis program[13] was used for fits. All coefficients of determination ($r^2$) fell in the 0.972–0.998 range, with most ≥0.990. Parameter estimates ($K$ and $C_{max}$) appear in Table I. The rate constant $K$ should be characteristic for a given drug in a particular formulation when evaluated by a specific dissolution testing procedure. The estimated rate constants presented in Table I indicate that this is the case.

Concentration values at 30.0 and 60.0 min were generated from the parameter estimates for each drug within each run (Table II). These times were chosen based on guidelines proposed by the Food and Drug Administration (10), which suggested that 50% (83.5 mg/900 ml) and 80%

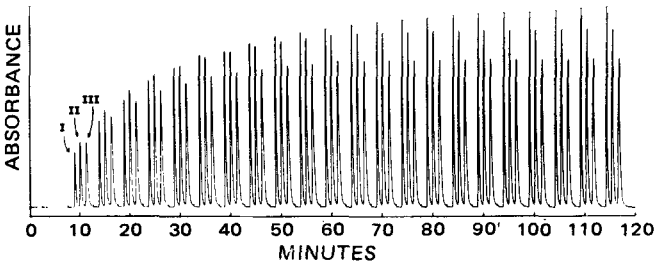


**Figure 1**—*Typical chromatographic output of one dissolution run. The time axis represents the summation of the dissolution time and the chromatographic time. The molar absorptivities of the three compounds are not equal in the present experimental conditions.*

[13] PROC NLIN, Statistical Analysis System, Raleigh, NC 27605.

**Table II—Drug Concentrations at 30 and 60 min Obtained with Parameters in Table I**

| Manufacturer | Drug | Concentration at 30 min, mg/900 ml | | | | | | | | Concentration at 60 min, mg/900 ml | | | | | | | |
|---|---|---|---|---|---|---|---|---|---|---|---|---|---|---|---|---|---|
| | | Run 1 | Run 2 | Run 3 | Run 4 | Run 5 | Run 6 | Mean | *SD* | Run 1 | Run 2 | Run 3 | Run 4 | Run 5 | Run 6 | Mean | *SD* |
| A | I | 118.8 | 132.8 | 128.3 | 120.2 | 129.8 | 133.6 | 127.2 | 6.3 | 137.9 | 149.4 | 147.8 | 142.0 | 149.0 | 154.5 | 146.8 | 5.9 |
| | II | 155.7 | 154.7 | 156.2 | 146.2 | 154.9 | 160.1 | 154.6 | 5.1 | 161.6 | 160.7 | 161.7 | 155.7 | 162.6 | 165.7 | 161.3 | 3.2 |
| | III | 163.2 | 162.3 | 162.2 | 153.1 | 160.9 | 165.5 | 161.2 | 4.2 | 164.0 | 164.6 | 163.4 | 156.2 | 162.8 | 167.3 | 163.0 | 3.7 |
| B | I | 106.9 | 112.8 | 109.6 | 109.7 | 122.5 | 127.9 | 114.9 | 9.3 | 141.6 | 145.1 | 140.3 | 137.9 | 145.4 | 154.7 | 144.2 | 5.9 |
| | II | 148.1 | 139.6 | 144.1 | 143.2 | 151.4 | 159.0 | 147.6 | 6.9 | 168.1 | 161.1 | 164.6 | 162.6 | 165.0 | 175.1 | 166.1 | 5.0 |
| | III | 159.0 | 143.1 | 151.0 | 151.9 | 158.7 | 163.6 | 154.5 | 7.4 | 172.1 | 156.7 | 164.4 | 165.1 | 166.8 | 174.8 | 166.6 | 6.4 |
| C | I | 111.1 | 84.0 | 86.3 | 96.9 | 101.1 | 119.8 | 99.9 | 13.9 | 149.4 | 117.0 | 118.4 | 124.2 | 126.6 | 145.2 | 130.2 | 13.8 |
| | II | 141.8 | 121.2 | 127.2 | 138.6 | 136.4 | 149.9 | 135.8 | 10.3 | 160.6 | 153.2 | 157.4 | 160.4 | 156.3 | 165.9 | 159.0 | 4.4 |
| | III | 151.9 | 135.8 | 141.7 | 152.2 | 146.5 | 156.5 | 147.4 | 7.6 | 160.6 | 157.8 | 162.5 | 162.3 | 156.0 | 167.0 | 161.0 | 3.9 |

**Table III—Results of Multiple Comparison Test for 30- and 60-min Mean Drug Concentrations [a]**

| Drug | Product Ranking, Highest to Lowest | | | | | |
|---|---|---|---|---|---|---|
| | 30-min Concentrations | | | 60-min Concentrations | | |
| I | A | B | C | A | B | C |
| II | A | B | C | B | A | C |
| III | A | B | C | B | A | C |

[a] Products underlined by a common line did not differ significantly ($p > 0.05$).

**Table IV—Dissolution Test Results of Formulation A at 100 and 150 rpm [a]**

| Parameter | Drug | 100 rpm | | 150 rpm | |
|---|---|---|---|---|---|
| | | Mean | *SD* | Mean | *SD* |
| $K$, min$^{-1}$ | I* | 0.045 | 0.004 | 0.063 | 0.004 |
| | II* | 0.072 | 0.004 | 0.105 | 0.008 |
| | III* | 0.105 | 0.004 | 0.152 | 0.018 |
| $C_{max}$, mg/900 ml | I | 146.9 | 5.0 | 150.3 | 5.6 |
| | II | 162.5 | 2.3 | 161.7 | 3.1 |
| | III | 163.1 | 2.4 | 163.1 | 3.7 |
| 30-min concentration, mg/900 ml | I* | 108.2 | 8.0 | 127.2 | 6.3 |
| | II* | 143.7 | 3.0 | 154.6 | 4.6 |
| | III** | 156.1 | 2.7 | 161.2 | 4.2 |
| 60-min concentration, mg/900 ml | I** | 136.6 | 6.9 | 146.8 | 5.9 |
| | II | 160.3 | 2.4 | 161.3 | 3.2 |
| | III | 162.8 | 2.4 | 163.0 | 3.7 |

[a] Results were analyzed for significance using an unpaired $t$ test ($\alpha = 0.05$); * = significant difference ($p < 0.001$), and ** = significant difference ($p < 0.05$).

(133.6 mg/900 ml) of the drug should be in solution after 30 and 60 min, respectively.

An analysis of variance[14] was performed on both the 30- and 60-min data for each drug entity to detect significant differences between formulations. When a significant difference was found, Tukey's critical difference ($\alpha = 0.05$) was used to identify the mean values responsible (Table III).

Ranking the formulations with respect to the amount of drug in solution at 30 and 60 min showed that Formulation C consistently exhibited lower levels. In all but one case, these levels were significantly lower than the formulation with the number one ranking and often were significantly lower than the second-ranked formulation. The predicted values of $C_{max}$ for Formulation C were not significantly different from those of Formulations A and B.

Figures 2–4 illustrate the product performances. In these figures, all of the concentration–time data for each drug entity within each drug product were fitted simultaneously to Eq. 1. The mean concentration points and standard deviations are superimposed on the fitted curves.

A comparison of the dissolution performance of Formulation A at basket rotation rates of 100 and 150 rpm is presented in Table IV. It has long been recognized that the dissolution rate of a drug may be greatly influenced by the degree of agitation present in the dissolution flask. Carstensen *et al.* (11) stated that rotation speeds of <150 rpm in USP Apparatus I may result in solution nonhomogeneity. For this reason, a basket rotation rate of 150 rpm was chosen for most determinations in this study.

[14] PROC ANOVA, Statistical Analysis System, Raleigh, NC 27605.

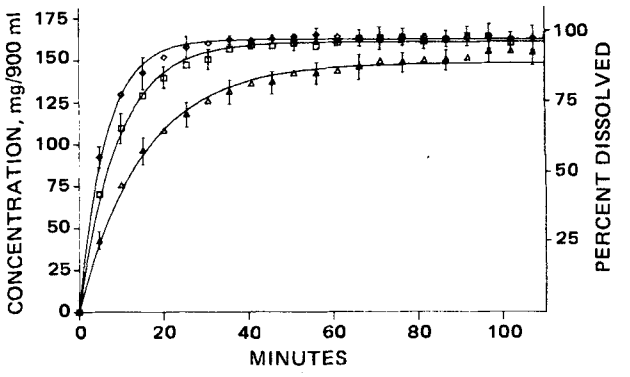


**Figure 2**—*Concentrations of drugs in solution* versus *time for Formulation A (average of six runs, basket rotation rate of 150 rpm). Standard deviations are superimposed on the plots. Key:* △, *I;* □, *II; and* ◇, *III.*

Figures 2 and 5 provide a visual comparison of the performance of Formulation A with basket rotation rates of 150 and 100 rpm, respectively. Although the rate constant for drug appearance in solution significantly increased with an increase in the basket rotation rate (Table IV), the predicted maximum concentration of drug in solution ($C_{max}$) was independent of the rotation rate.

As expected, it is possible for each active ingredient to have a unique dissolution rate (Tables I–III). Significant differences in the dissolved amounts were found between active drug entities and between manufacturers' formulations at both 30 and 60 min. Such differences necessitate the simultaneous determination of the dissolution profiles of each active component in a drug product. The typical automated dissolution apparatus, lacking the chromatographic procedure, can seldom accomplish such an analysis.

Although the system described was used with USP Apparatus I, USP Apparatus II or III can be employed equally well as long as the intake and outlet for the circulated dissolution medium are in the positions recommended by the USP. Since each injection consumes only 10 μl of dissolution medium, there is no need for volume replacement nor calculational compensation for decreasing dissolution medium volume. The 0.3 min required for a sample of bulk dissolution medium to reach the injector

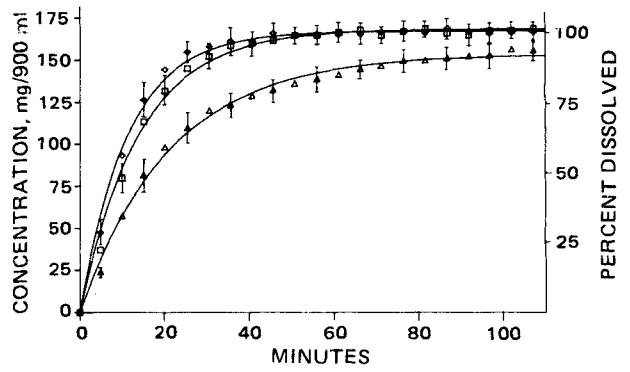


**Figure 3**—*Concentrations of drugs in solution* versus *time for Formulation B (average of six runs, basket rotation rate of 150 rpm). Standard deviations are superimposed on the plots. Key:* △, *I;* □, *II; and* ◇, *III.*

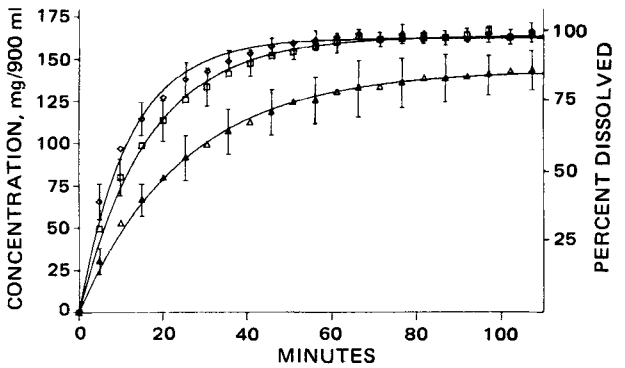


**Figure 4**—*Concentrations of drugs in solution* versus *time for Formulation C (average of six runs, basket rotation rate of 150 rpm). Standard deviations are superimposed on the plots. Key:* △, *I;* □, *II; and* ◇, *III.*

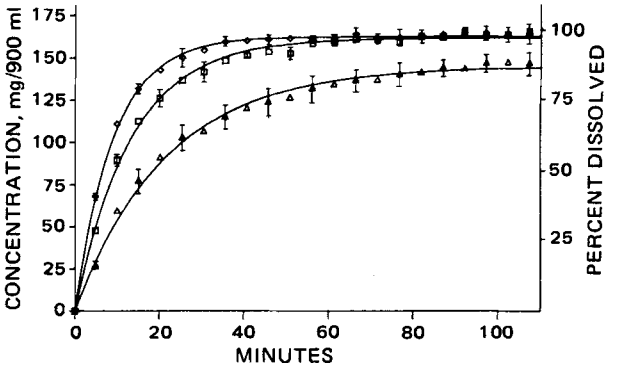


**Figure 5**—*Concentrations of drugs in solution* versus *time for Formulation A (average of six runs, basket rotation rate of 100 rpm). Standard deviations are superimposed on the plots. Key:* △, *I;* □, *II; and* ◇, *III.*

loop, while accounted for in the calculations, is actually insignificant if the dissolution time is in excess of 10 min. This rapid exchange of dissolution medium is accomplished with a relatively slow flow rate, and this slow flow rate is advantageous since it does not provide dissolution medium agitation in excess of that provided by the rotating basket. The 2-μm low-pressure solvent filter at the inlet port prevented particulate matter from scoring the injection valve and also prevented solid particulate buildup at the head of the column.

This system exhibits great flexibility for adaptation to the problems encountered with a particular product. Various drug and excipient entities can be accommodated by variations in the injection programming, the mobile phase composition, and pH and by gradient elution. Gradient elution is especially feasible in this system because it can be controlled by the same microprocessor that controls sample injections. No system is completely universal, however, and there are undoubtedly compound combinations for which adequate separations cannot be made with retention times short enough to allow injections at the intervals required by compendial specifications. The authors believe this latter case is relatively rare.

The HPLC system used in the present study is of the component or modular type. Substitution of a fluorescence, electrochemical, or refractive index detector in place of the UV detector would be a simple matter. The fluorescence detector could be especially useful for compounds present in very low concentrations. Additionally, the microprocessor can be programmed to change detector sensitivity during the chromatographic procedure, thereby furthering the ability to accommodate a drug product with widely varying concentrations of active ingredients.

After initial debugging, no reliability problems were encountered, and completely unattended dissolution testing was accomplished. Unattended testing is the ultimate aim of automation, and no method can be considered to be truly automated without this capability.

If the amount of drug dissolved from a dosage form need only be measured at widely spaced time intervals or at the end of the dissolution test, this system would be adaptable to monitoring six dissolution flasks. Such monitoring could be accomplished by the use of a multichannel pump and a switching valve to direct the flow from the appropriate dissolution flask to the injector loop. This switching valve would also have to permit return flow from the injector loop to the flask being sampled. If measurements were to be made on the contents of each dissolution flask at specific times (such as 30 and 60 min), initiation of the dissolution processes in the six flasks would need to be staggered.

The types of systems described readily lend themselves to computer interfacing. Such interfacing would mean that the operator's only contact with the dissolution test would be lowering the basket into the dissolution medium and collecting the completed dissolution profiles.

## REFERENCES

(1) W. F. Beyer and E. W. Smith, *J. Pharm. Sci.*, **60,** 1556 (1971).

(2) J. E. Tingstad and S. Riegelman, *ibid.*, **59,** 692 (1970).

(3) J. S. Kent, P. P. Wong, and G. P. Hedge, *ibid.*, **66,** 1665 (1977).

(4) F. J. Cioffi, H. M. Abdou, and A. T. Warren, *ibid.*, **65,** 1234 (1976).

(5) C. Cakiryildiz, P. J. Mehta, W. Rahmen, and D. Schoenleber, *ibid.*, **64,** 1692 (1975).

(6) J. B. Johnson, P. G. Kennedy, and S. H. Rubin, *ibid.*, **63,** 1931 (1974).

(7) H. M. Abdou, T. M. Ast, and F. J. Cioffi, *ibid.*, **67,** 1397 (1978).

(8) J. M. Huen, R. W. Frei, W. Sauti, and J. P. Thevenin, *J. Chromatogr.*, **149,** 359 (1978).

(9) "The United States Pharmacopeia," 20th rev., United States Pharmacopeial Convention, Rockville, Md., 1980.

(10) *Fed. Regist.*, **44,** 60320 (1979).

(11) J. T. Carstensen, R. Kothari, V. K. Prasad, and J. Sheridan, *J. Pharm. Sci.*, **69,** 290 (1980).

## ACKNOWLEDGMENTS

The authors thank Mr. Michael Fogarty, Micromeritics Instrument Corp., for the loan of the injector and microprocessor. The authors also acknowledge Dr. M. Robert Blum and Dr. Sam Liao, Burroughs Wellcome Co., for the use of their Tektronix 4662 data plotter.

# Intestinal Absorption Mechanism of Amphoteric β-Lactam Antibiotics I: Comparative Absorption and Evidence for Saturable Transport of Amino-β-lactam Antibiotics by *In Situ* Rat Small Intestine

**AKIRA TSUJI *x, EMI NAKASHIMA *, IZUMI KAGAMI *, and TSUKINAKA YAMANA ‡**

Received August 13, 1980, from the **Faculty of Pharmaceutical Sciences and the* ‡*Hospital Pharmacy, Kanazawa University, Takara-machi, Kanazawa 920, Japan.* Accepted for publication December 11, 1980.

**Abstract** □ The disappearance of various β-lactam antibiotics from *in situ* rat small intestinal loops was studied at pH 7.4. For monobasic penicillins, despite the wide variety of apparent partition coefficients in isobutyl alcohol–water, the disappearance from the jejunal loops was almost 30% (±5% *SD*). On the other hand, the disappearance of amphoteric derivatives of penicillins and cephalosporins having very low lipid solubility varied widely between 12 and 80%. The peak blood levels after intraduodenal administration to the rats correlated well with the extent of disappearance of amphoteric penicillins from the intestinal loops. Absorption studies utilizing *in situ* intestinal loops were performed at variable dose ranges to yield a clear dose-dependent disappearance. It is suggested that certain carrier-mediated transport systems underlie the absorption mechanisms of amphoteric β-lactam antibiotics.

**Keyphrases** □ Aminopenicillins—intestinal absorption mechanism proposed, compared with monobasic penicillins, *in situ* rat intestinal loops □ Aminocephalosporins—intestinal absorption mechanism proposed, compared with monobasic penicillins, *in situ* rat intestinal loops □ Absorption, intestinal—mechanism proposed for saturable transport of amphoteric amino-β-lactam antibiotics, *in situ* rat intestinal loops □ Antibiotics, amino-β-lactam—compared with monobasic penicillins, intestinal absorption mechanism proposed, *in situ* rat intestinal loops

Aminopenicillins, such as ampicillin, amoxicillin, and cyclacillin, and aminocephalosporins, such as cephalexin and cephradine, are acid stable and are absorbed after oral administration (1, 2). Much interest has been focused on the mechanism of the GI absorption of these antibiotics.

## BACKGROUND

Many studies on the GI absorption of β-lactam antibiotics and their amino derivatives have been conducted to assess animal models (3, 4) or to compare their bioavailability (1, 5–7) rather than to elucidate the absorption mechanism. Recently, Tsuji *et al.* (8) reported that the GI absorption rates of monobasic penicillins in rats deviated significantly from the pH-partition hypothesis, and they explained this deviation on the basis of passive transport of the undissociated molecule through both the aqueous diffusion layer barrier adjacent to the GI membrane surface and the lipid barrier of the GI membrane. With the two-compartment diffusion mechanism, the structure–absorption rate relationship of this series of penicillins and cephalosporins, such as cephalothin and cefazolin, was established (9).

However, the GI absorption of aminopenicillins and aminocephalosporins cannot be predicted from this mechanism whereby the antibiotics are absorbed from the GI tract by passive diffusion of the unionized species. Amino-β-lactam antibiotics must have a zwitterionic structure to be ionized completely and to exhibit very low lipid solubility under GI conditions. Possible mechanisms were proposed for the membrane permeability of amphoteric penicillins and cephalosporins (10–21), but the mechanism by which amino-β-lactam antibiotics are absorbed is not clearly understood.

The present investigation was undertaken to determine the difference in absorption characteristics between monobasic and amphoteric β-lactam antibiotics. The comparative absorption of aminopenicillins, including ampicillin, amoxicillin, cyclacillin, and epicillin, and of three aminocephalosporins, cephalexin, cephradine, and cefadroxil, was studied in rats by the *in situ* GI loop method. Several monobasic penicillins also were included for comparison. The *in vitro* physicochemical properties, including comparative aqueous stabilities, solubilities, and dissolution rates, of the amphoteric β-lactam antibiotics (22, 23) as well as preliminary observations on the intestinal absorption were reported previously (15, 16, 21).

## EXPERIMENTAL

**Materials**—Ampicillin anhydrate[1] (1015 μg/mg), amoxicillin trihydrate[2] (850 μg/mg), cyclacillin anhydrate[1] (983 μg/mg), epicillin anhydrate[3] (pure powder), cephalexin monohydrate[4] (925 μg/mg), cephradine monohydrate[3] (952 μg/mg), and cefadroxil monohydrate[5] (947 μg/mg) were used as supplied. The monobasic penicillins were the same as those employed previously (8). The standard solution of the penicilloic acids of ampicillin, amoxicillin, and epicillin was prepared according to a reported procedure (24).

All other chemicals were reagent grade and were utilized without further purification, except for imidazole which was purified by double recrystallization from benzene followed by thorough washing with ether.

**Animals**—Male albino Wistar rats, 200 ± 25 g, were fasted for 20 hr prior to the experiment, but water was given freely. The rats were anesthetized with urethan (1.5 g/kg ip) ~1 hr prior to surgery.

***In Situ* Experiments on Absorption from Rat GI Loops**—*Disappearance from Small Intestinal Loops*—A midline incision was made to expose the small intestine, and the bile duct was ligated. The intestinal lumen was washed gently with 50 ml of pH 7.4 isotonic phosphate buffer[6] (25). Six milliliters of air was introduced to expel residual buffer and then was gently removed. In this experiment, two loops (each 5 cm long) were prepared by double ligation. The first loop was made 2 cm from the pylorus, and 1 cm of intestine separated the consecutive loop in the duodenum. For the study in the jejunum, the consecutive loops were prepared 15 cm from the pylorus. A dose of antibiotic was dissolved in pH 7.4 isotonic phosphate buffer, and 1 ml was injected into each intestinal loop. All studies lasted 1 hr.

At the end of the experiment, the remaining antibiotic solution was collected and the intestine was washed thoroughly with isotonic buffer. The solutions were combined to make up the desired volume. The samples were analyzed after filtration with a 0.45-μm membrane filter[7] to remove solid materials.

*Disappearance from Ligated Areas of Stomach, Small Intestine, and Large Intestine*—The rat alimentary tract was divided into four portions to locate the specific area for the absorption of amino-β-lactam antibiotics as follows: stomach, upper small intestine (20-cm length below the pylorus), lower small intestine (20-cm length above the ileum), and large intestine (10-cm length below the cecum). These regions were separated by ligation, and 2 mg of cyclacillin or cefadroxil in 1 ml was injected into each region. The drug was dissolved in pH 2.0 isotonic citrate buffer (25) or saline for the experiments in the stomach or intestinal regions, respectively. After 1 hr, the ligated GI segments were removed. Three rats were used. Other experimental procedures were the same as already described.

*Blood Level and Tissue Accumulation after Stomach and Intraduo-*

[1] Takeda Chemical Industries, Osaka, Japan.
[2] Fujisawa Pharmaceutical Co., Osaka, Japan.
[3] Sankyo Co., Tokyo, Japan.
[4] Shionogi Co., Osaka, Japan.
[5] Bristol Myers Co., Tokyo, Japan.
[6] The pH was measured with a PHM26 pH-meter, Radiometer, Copenhagen, Denmark.
[7] Sartorius-Membranefilter GmbH, Göttingen, West Germany.



*0022-3549/81/0700-0768$01.00/0*
*© 1981, American Pharmaceutical Association*

**Table I—Values for pKa, Apparent Partition Coefficient in Isobutyl Alcohol–Water at pH 7.4, and Disappearance from Rat Intestinal Loops 1 hr after Administration of Various β-Lactam Antibiotics**

| Antibiotic | Dissociation Constant | | Partition Coefficient in Isobutyl Alcohol–Water | Dose, mg/ml | Disappearance from *In Situ* Jejunal Loop, % ± *SD* | |
|---|---|---|---|---|---|---|
| | $pK_1$ | $pK_2$ | | | Upper | Lower |
| Penicillin V | 2.79[a] | — | 1.10[a] | 5 | 26.9 ± 4.0 (3)[b] | 27.4 ± 1.8 (3) |
| Phenethicillin | 2.80[a] | — | 1.55[a] | 5 | 37.9 ± 4.0 (3) | 33.8 ± 1.0 (3) |
| Propicillin | 2.76[a] | — | 3.02[a] | 5 | 30.9 ± 5.5 (4) | 32.5 ± 0.6 (3) |
| Oxacillin | 2.73[a] | — | 1.78[a] | 5 | 27.2 ± 3.0 (5) | 17.9 ± 1.7 (3) |
| Cloxacillin | 2.78[a] | — | 2.40[a] | 5 | 22.1 ± 1.4 (4) | 21.3 ± 1.5 (4) |
| Dicloxacillin | 2.76[a] | — | 4.07[a] | 5 | 28.9 ± 3.7 (4) | 29.9 ± 1.2 (3) |
| Floxacillin | 2.76[a] | — | 2.57[a] | 5 | 27.0 ± 0.8 (3) | 28.1 ± 2.4 (3) |
| Ampicillin | 2.67[a] | 6.95[a] | 0.373 | 2 | 12.9 ± 5.5 (4) | 11.8 ± 2.6 (4) |
| Amoxicillin | 2.67[a] | 7.11[a] | 0.130 | 2 | 19.7 ± 1.4 (4) | 17.0 ± 2.9 (5) |
| Cyclacillin | 2.64[a] | 7.18[a] | 0.866 | 2 | 79.5 ± 3.4 (4) | 79.7 ± 12.1 (5) |
| Epicillin | 2.77[c] | 7.17[c] | 0.438 | 2 | 21.2 ± 6.9 (4) | 20.8 ± 4.9 (5) |
| Cefadroxil | 2.70[d] | 7.22[d] | 0.0813 | 2 | 66.2 ± 9.1 (4) | 70.8 ± 3.2 (4) |
| Cephalexin | 2.67[e] | 6.96[e] | 0.193 | 2 | 40.2 ± 13.6 (4) | 36.9 ± 12.4 (4) |
| Cephradine | 2.63[e] | 7.35[e] | 0.268 | 2 | 55.4 ± 6.5 (3) | 52.0 ± 12.5 (3) |

[a] Data at 37° and $\mu = 0.5$ from Refs. 22 and 30. [b] The experimental number is given in parentheses. [c] Data at 35° and $\mu = 0.5$ from Ref. 22. [d] Unpublished results at 37° and $\mu = 0.5$ from this laboratory. [e] Data at 37° and $\mu = 0.5$ from Ref. 23.

*denal Administration*—Antibiotic solutions of ampicillin, amoxicillin, epicillin, and cyclacillin, prepared by dissolution in 1 ml of saline, were given to rats at a dose of 10 mg/kg. A stomach tube was employed for administration into the stomach in rats whose pylorus was ligated. For intraduodenal administration, the drug solution was injected into the proximal duodenum in rats whose pylorus was ligated.

To determine the amount of antibiotic absorbed, blood was taken from the jugular vein at appropriate time intervals and assayed by a microbiological method and/or fluorometry after being hemolyzed with an equivalent volume of distilled water.

The accumulation in the small intestinal tissue during the *in situ* absorption experiments was examined for cyclacillin. After the 1-hr experiments, part of the whole intestine was isolated, tearing off the mesentery, and the serosal surface then was blotted with filter paper. The intestine was cut into small slices and homogenized in a polytef homogenizer with saline to give a 10% (w/v, wet weight) homogenate. An aliquot of the homogenates then was analyzed.

**Analysis of Loop Samples**—The residual antibiotic and degradation product, the penicilloic acid, were assayed simultaneously by fluorometric determination for ampicillin and amoxicillin (26, 27) and also for epicillin. The fluorescence intensity was measured[8] with reference to that of quinine sulfate prepared with 0.1 *N* $H_2SO_4$. The assay for ampicillin was applied to epicillin, but the emission and excitation wavelengths were changed to 440 and 330 nm, respectively.

Aqueous mixtures of epicillin and its penicilloic acid in three proportions were analyzed, and the average recoveries were 106 ± 3 (*SD*)% for the intact drug and 103 ± 6% for the penicilloic acid. For cyclacillin, a spectrophotometric assay method (28) using imidazole mercuric chloride reagent was employed after acylation of the amino group with acetic anhydrate at pH 9.0. The compositions of the reagents were as described for ampicillin (28, 29). This method was employed only when the sample was diluted more than 25 times with the saline and in the concentration range of 15–80 μg/ml to prevent the influence of mucus and secretion products. The accuracy of this procedure was within 2% ($n = 5$).

High-performance liquid chromatography (HPLC) was utilized[9] for the determination of cephalexin, cephradine, cefadroxil, cyclacillin (only <10 μg/ml), and several monobasic penicillins. For the amino-β-lactam antibiotics, the carrier was 3–7% acetonitrile–0.01 *M* ammonium acetate, and the column was octadecylsilane chemically bonded on totally porous silica gel prepacked into a 4.0 × 300-mm[10] or a 4.6 × 250-mm[11] stainless steel column. For cyclacillin, the carrier was 0.1 *M* phosphate buffer of pH 4.0–4.2, and the column was strong cation-exchange resin[12] packed into a 4.6 × 500-mm stainless steel column. For the monobasic penicillins, the carrier was 0.02 *M* $KH_2PO_4$ and the column was anion-exchange resin[13] prepacked into a 2.1 × 500-mm stainless steel column. The detector was a UV spectrophotometer[14] set at 210 and 254 nm for the penicillins and cephalosporins, respectively.

An aliquot (50–100 μl) of the appropriately diluted solution was injected *via* a variable loop injector on flow, and the peak heights were measured. The calibration curves for the peak heights against the antibiotic concentration were satisfactorily linear and were prepared daily. The accuracy of the HPLC analysis from many trials was within 3%.

**Analysis of Blood Samples**—Fluorometric procedures (26, 27) were utilized for ampicillin and amoxicillin. Cyclacillin, epicillin, and amoxicillin were assayed by the microbiological paper disk diffusion method employing *Sartina lutea*[15] in the usual manner. Calculation of the penicillin concentration was made from the respective calibration curves prepared using pooled blood from control rats. The accuracies of the two analytical methods, *i.e.*, fluorometry and microbiological assay, were within 5%. The analytical data obtained by the methods agreed with each other within the limits of experimental error when a sample of amoxicillin was tested.

**Analysis of Cyclacillin from Tissue Homogenates**—The microbiological assay was employed, and the calibration curve was prepared using pooled 10% gut homogenates from control rats.

**Determination of Apparent Partition Coefficients**—For the study on the distribution of amphoteric β-lactam antibiotics in isobutyl alcohol–water, the aqueous phase was prepared to give a constant $Na^+$ concentration of 0.1 *M* using phosphate buffer for the reasons described previously (30). This buffer component was determined so as to maintain a constant ionic strength of 0.15 and a pH of 7.4. A $1 \times 10^{-3}$ *M* antibiotic solution was prepared with this solution. To minimize the volume exchange due to mutual miscibility, the aqueous and organic phases were saturated previously with each solvent.

Exactly 3–10 ml of each solution was transferred to a glass-stoppered flask and shaken for 2 hr to achieve complete equilibrium at 37 ± 0.1°. The two phases separated on standing for 1 hr, and the aqueous phase was centrifuged at 3000 rpm for 10 min. If necessary, after appropriate dilution with distilled water, the concentration in the aqueous phase was determined by HPLC. The apparent partition coefficient was calculated according to the equation described previously (30).

## RESULTS AND DISCUSSION

The pKa values and apparent partition coefficients of the β-lactam antibiotics at pH 7.4 in isobutyl alcohol–water are summarized in Table I.

**Disappearance of Various β-Lactam Antibiotics from *In Situ* Intestinal Loops**—Values for the percentage disappearance of various penicillins and cephalosporins during 1 hr are shown in Table I.

Despite the fact that the seven monobasic penicillins grouped by phenoxy and isoxazole derivatives exhibit a wide variety of apparent partition coefficients in isobutyl alcohol–water, their disappearance from both the upper and lower jejunums was almost 30% (±5% *SD*). Previous data concerning the rat *in situ* intestinal recirculating method demonstrated (9) that the intestinal absorption of ionized monobasic β-lactam

[8] Model FP-4 fluorescence spectrophotometer, Japan Spectroscopic Co., Tokyo, Japan.
[9] Model FLC A-700, Japan Spectroscopic Co., Tokyo, Japan.
[10] μBondapak $C_{18}$, Waters Associates, Milford, Mass.
[11] Silica gel, SC-02, Japan Spectroscopic Co., Tokyo, Japan.
[12] Zipax SCX, DuPont Instruments, Wilmington, Del.
[13] Zipax AAX, DuPont Instruments, Wilmington, Del.
[14] Model UVIDEC-100, Japan Spectroscopic Co., Tokyo, Japan.
[15] IFO 12708, Institute for Fermentation, Osaka, Japan. The strain was derived from ATCC 9341.

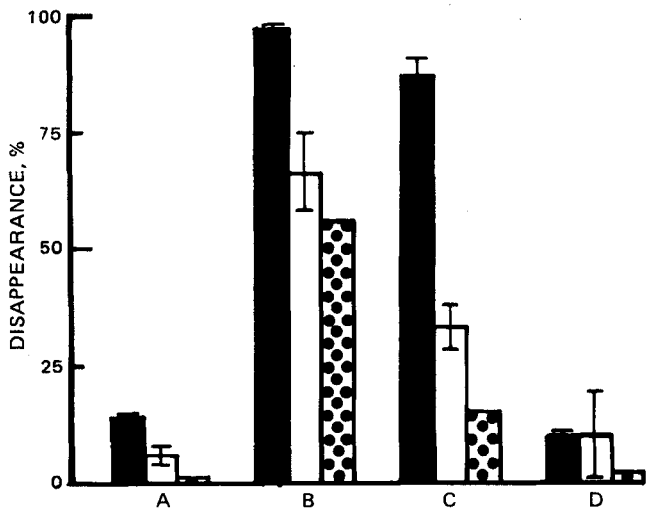


**Figure 1**—*Absorption of cyclacillin and cefadroxil from loops in the digestive tracts of rats. Key: closed columns, cyclacillin; open columns, cefadroxil; dotted columns, cephalexin; A, stomach; B, upper small intestine (20 cm below the pylorus); C, lower small intestine (20 cm above the ileocecum); and D, large intestine (10 cm below the cecum). The data for cephalexin are redrawn from Ref. 31.*

antibiotics followed apparent first-order kinetics with competing apparent first-order degradation to their β-lactam opening products. Between pH 6.5 and 9, absorption and the accompanying degradation were almost insensitive to changes in the intestinal lumen pH and initial drug concentration and to the lipophilicity of the molecules (9). The present results are consistent with those findings, suggesting that the disappearance of monobasic penicillins from the rat intestinal loops was entirely attributable to both absorption and degradation.

On the other hand, the percentage disappearance of amphoteric derivatives having rather low lipophilicity varied widely, between 12 and 80% during 1 hr at a 2-mg/ml dose (Table I). The degradation products (penicilloic acids) from aminopenicillins were determined at the end of the absorption experiment to be 1.6, 1.7, and 1.8% for ampicillin, amoxicillin, and epicillin, respectively. No detectable degradation products were observed with cyclacillin at this dose. The *in vitro* degradation of cephalexin, cephradine, and cefadroxil in the intestinal washings with isotonic phosphate buffer during 1 hr was 4.0, 4.7, and 2.1%, respectively. These findings of slight degradation of amophoteric β-lactam antibiotics strongly indicate that the high percentage disappearances of cyclacillin (80%), cephalexin (40%), cephradine (50%), and cefadroxil (70%) essentially were attributed to intestinal membrane transport resulting in accumulation by the gut tissue and/or transference into the vascular system.

These results suggest that some specialized transport mechanism may contribute to the absorption of zwitterionic antibiotics accompanying the simple diffusion transport (9) responsible in the absorption of ionized species of monobasic β-lactam antibiotics.

**Absorption and Tissue Accumulation of Cyclacillin and Cefadroxil from Different Areas of Rat Alimentary Tract and Comparative Blood Levels after Intraduodenal Administration of Aminopenicillins**—Figure 1 compares the percentage disappearances of cyclacillin and cefadroxil during 1 hr from four areas of the rat GI tract after injection into the ligated loop. The highest disappearance occurred from the small intestine, with almost all of the cyclacillin and 33–66% of the cefadroxil doses disappearing from the lumen. However, only ~10% of each dose disappeared from the stomach and large intestine. In a similar absorption study on cephalexin (redrawn in Fig. 1), Maekawa *et al.* (31) demonstrated that the total disappearance during 1 hr from the stomach, upper small intestine, lower small intestine, and large intestine of rats was 1.0, 56.2, 15.6, and 2.4%, respectively. These data are comparable with the present results for cyclacillin and cefadroxil. The accumulation of cyclacillin in the intestine was negligible (3%) during the *in situ* absorption experimental period.

Figure 2 shows the mean blood concentrations after intraduodenal administrations of aminopenicillins at a dose of 10 mg/kg. The peak blood concentrations for ampicillin, amoxicillin, and epicillin appeared after 1 hr, but cyclacillin was observed in the bloodstream within 0.5 hr after administration. The rank order of blood levels after intraduodenal administration was: cyclacillin > amoxicillin > epicillin ≥ ampicillin. The blood concentration of cyclacillin was far higher than the concentrations of the other penicillins ($p < 0.01$).

Ampicillin demonstrated a significantly lower blood level than amoxicillin ($p < 0.05$). The peak serum concentration after a single oral dose with sufficient water in humans was in the order (5, 6): cyclacillin > amoxicillin > ampicillin > epicillin, which is almost identical with that in rats. When the aminopenicillins were administered into the rat stomach, they were not detectable in the serum by microbiological assay, indicating that the aminopenicillins were scarcely absorbable from the stomach. The *in vitro* degradation of ampicillin, amoxicillin, epicillin, and cyclacillin after 1 hr at pH 2 and 35° was evaluated from the data of the degradation kinetics (22, 32) to be 5.8, 4.7, 2.9, and 7.2%, respectively. The disappearance of cyclacillin from the stomach (Fig. 1) thus may be due to its acid degradation. The present results support the claim of Lode (33) that absorption of ampicillin and cephalexin in humans occurred in the small intestine and not the stomach.

On this basis, the rat represents a suitable experimental animal for elucidation of the absorption mechanism of amino-β-lactam antibiotics in humans. Previous observations (31, 33) and the present results suggest that there is a specific area in the alimentary tract of mammals for the absorption of amino-β-lactam antibiotics. On the other hand, monobasic and lipophilic penicillins can be absorbed from both the stomach and small intestine below pH 6 (8, 9). The difference in permeability between amphoteric derivatives and monobasic ones may be attributed to a difference in the membrane transport mechanism. The latter types of β-lactam antibiotics may be absorbed by lipid membrane transport of the undissociated species through the barrier of the aqueous diffusion layer adjacent to the membrane surface (8, 9). The amino-β-lactam antibiotics, having very low lipid solubility (Table I) and being completely ionized in all alimentary tract areas, are unlikely to be absorbed by this mechanism.

**Effect of Dose on Absorption by *In Situ* Intestinal Loops**—To examine the mechanism responsible for absorption of amino-β-lactam antibiotics *in vivo*, the effect of the dose concentration on the percentage disappearance from the small intestinal lumen was investigated. If the percentage disappearance remains unaffected by the initial dose con-

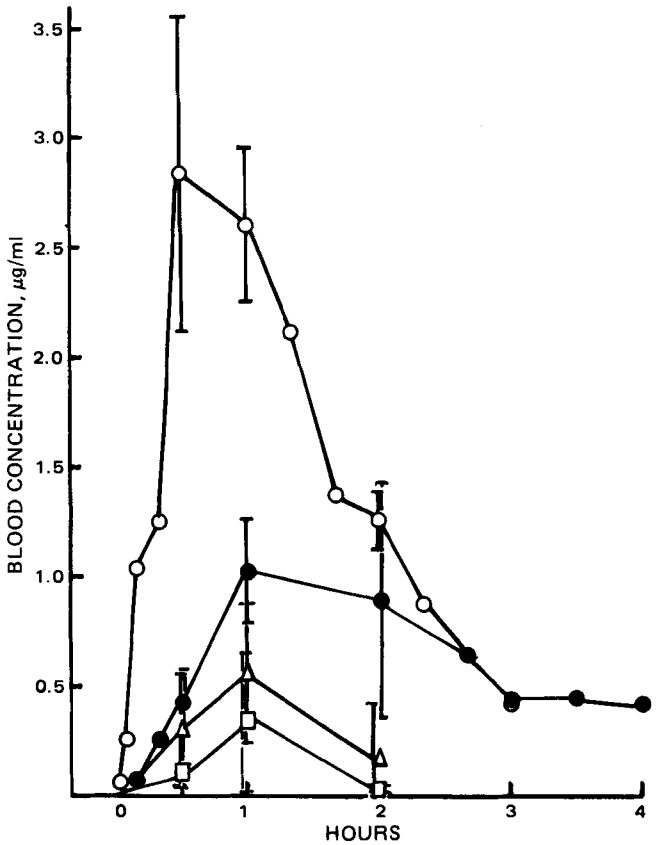


**Figure 2**—*Time courses of whole blood concentrations of aminopenicillins in rats after a 10-mg/kg dose in the duodenum. The mean levels and standard deviations (bars) for three animals are shown for 0.5, 1.0, and 2.0 hr. Key: □, ampicillin; ●, amoxicillin; ○, cyclacillin; and △, epicillin.*

**Table II—Disappearance and Degradation Products of Aminopenicillins from Rat Intestinal Loops 1 hr after Administration**

| Antibiotic | Intestinal Area | 20 μg/ml | | 2 mg/ml | | 5 mg/ml | | 20 mg/ml, |
|---|---|---|---|---|---|---|---|---|
| | | Disappearance, % ± *SD* | Product, % ± *SD* | Disappearance, % ± *SD* | Product, % ± *SD* | Disappearance, % ± *SD* | Product, % ± *SD* | Disappearance, % ± *SD* |
| Ampicillin | 1[a] | 9.0 ± 3.2 (3)[b] | 6.1 ± 0.5 (3) | 7.3 ± 1.3 (3) | 4.6 ± 2.5 (3) | — | — | — |
| | 2[c] | 5.8 ± 4.7 (3) | 4.3 ± 0.5 (3) | 9.2 ± 6.0 (3) | 2.2 ± 0.8 (3) | — | — | — |
| | 3[d] | 10.9 ± 3.5 (4) | 2.9 ± 1.0 (4) | 11.2 ± 5.2 (4) | 1.7 ± 0.9 (4) | — | — | — |
| | 4[e] | 8.4 ± 6.2 (4) | 2.8 ± 1.1 (4) | 10.4 ± 2.8 (4) | 1.4 ± 1.3 (4) | — | — | — |
| Amoxicillin | 1 | 28.6 ± 3.1 (4) | 8.5 ± 4.2 (4) | 12.1 ± 0.8 (3) | 3.9 ± 2.8 (3) | — | — | — |
| | 2 | 18.3 ± 2.1 (5) | 4.7 ± 2.0 (5) | 12.9 ± 1.9 (4) | 1.4 ± 1.1 (4) | — | — | — |
| | 3 | 21.7 ± 6.3 (5) | 0.8 ± 0.8 (5) | 18.8 ± 1.2 (4) | 2.3 ± 1.0 (5) | — | — | — |
| | 4 | 19.6 ± 6.6 (3) | 0.5 ± 0.9 (3) | 16.6 ± 2.7 (5) | 1.0 ± 0.9 (5) | — | — | — |
| Cyclacillin | 1 | — | — | 79.5 ± 8.0 (6) | — | 42.0 ± 9.8 (4) | — | 18.9 ± 5.3 (5) |
| | 2 | — | — | 78.9 ± 7.5 (5) | — | 48.9 ± 5.3 (4) | — | 16.9 ± 3.5 (4) |
| | 3 | — | — | 79.5 ± 3.4 (4) | — | 53.0 ± 13.2 (4) | 1.8 | 20.2 ± 5.6 (5) |
| | 4 | — | — | 79.7 ± 12.1 (5) | — | 47.7 ± 4.7 (4) | 1.8 | 17.8 ± 6.2 (5) |
| Epicillin | 1 | 29.9 ± 14.3 (4) | 3.5 ± 3.1 (4) | 22.1 ± 5.0 (4) | 2.6 ± 1.5 (4) | — | — | — |
| | 2 | 14.0 ± 9.4 (5) | 9.6 ± 6.2 (5) | 15.6 ± 3.2 (5) | 2.4 ± 1.5 (5) | — | — | — |
| | 3 | 20.3 ± 8.9 (5) | 1.6 ± 1.7 (5) | 19.1 ± 7.3 (8) | 1.8 ± 1.8 (4) | — | — | — |
| | 4 | 24.7 ± 12.3 (5) | 4.3 ± 5.2 (5) | 18.8 ± 9.7 (8) | 1.8 ± 1.0 (4) | — | — | — |

[a] Upper duodenum, 2 cm from the pylorus. [b] The experimental number is given in parentheses. [c] Lower duodenum, with 1-cm separation from 1. [d] Upper jejunum, 15 cm from the pylorus. [e] Lower jejunum, with 1-cm separation from 3.

centration, then the apparent first-order absorption might proceed as observed previously (8, 9) for monobasic β-lactam antibiotics. However, if this value is affected, the contribution of some specialized mechanism would be strongly suggested.

Tables II and III show the percentages of total disappearance after 1 hr in the four small intestinal segments of each 5-cm loop and at various dose concentrations. The degradation products (penicilloic acids) remaining in the lumen also were determined for ampicillin, amoxicillin, and epicillin by fluorometric assay and for cyclacillin by HPLC. Small amounts of the degradation products of these four antibiotics were found (Tables II and III).

The percentage disappearance of amoxicillin, cyclacillin, cephalexin, cephradine, and cefadroxil depended remarkably on the initial dose concentrations. These dose dependencies revealed by their general pattern that the percentage disappearance at a low dose was extremely large while that at a high dose was markedly reduced. A similar phenomenon also was observed for epicillin, although the difference between the percentage disappearance at 20 μg/ml and that at 2 mg/ml was not statistically significant. Unfortunately, with our experimental system, it was difficult to detect saturation phenomena in the disappearance of ampicillin. However, after modification of our study, Shindo *et al.* (19) successfully demonstrated evidence for saturable absorption of ampicillin using an 8-cm long rat intestinal loop *in situ*. They found that the absorption of [$^{14}$C]ampicillin, labeled at the phenylglycyl moiety, showed an apparent tendency for saturation at a dose above 3 mg/loop, and the transference into the blood was marked in the upper and middle intestine. Absorption from limited parts also was observed with amoxicillin, cephalexin, and cefadroxil (Tables II and III), while cyclacillin and cephradine were absorbed from almost all parts of the intestine to the same extent.

Such remarkable dose-dependent absorption and the existence of specific areas of absorption suggest that the absorption of amino-β-lactam antibiotics may follow the same forms of specialized and saturable transport mechanisms since the competing degradation of β-lactam in the lumen solution is presumed to be small compared to the net absorption based on the facts discussed elsewhere.

Some investigators (10, 11, 13), using isolated rat gut, indicated the presence of an active transport mechanism of cephalexin and cyclacillin. Other studies (12, 14), however, showed by a similar *in vitro* technique that the β-lactam antibiotics, including cyclacillin (12), cephalexin (12), amoxicillin (14), and ampicillin (12, 14), were not transported by an active transport mechanism. Miyazaki *et al.* (14) demonstrated that, in both *in situ* and *in vitro* studies using rat small intestinal segments, the greater binding of amoxicillin than of ampicillin to the mucosa provided a possible explanation for the difference in body fluid concentration of these two drugs.

A recent report (20) indicated that cephradine, but not cephalexin and amoxicillin, was actively transported across the everted rat intestine. More recent findings clearly revealed that the absorption of amoxicillin (15, 17), cyclacillin (16, 17), cephalexin (21), and cephradine (21) from rat small intestinal perfusion solution was saturable. Kimura *et al.* (17) concluded that amoxicillin may be transported by a facilitated diffusion mechanism and that cyclacillin may be transported in part by active transport.

The present observations showing saturable absorption as a common phenomenon indicate that the same types of carrier-mediated transport mechanisms in the rat GI tract may underlie the absorption of amino-β-lactam antibiotics. Such a carrier system may be localized only in the small intestinal area and not in the stomach since no absorption was found in the latter part of the alimentary tract. Based on the present data for cyclacillin and cefadroxil and previous data (31, 33) for cephalexin, it is concluded that such a system is likely to make a small contribution in the large intestine.

Therefore, it is conceivable that carrier-mediated absorption is a common mechanism for the intestinal absorption of amino-β-lactam antibiotics, which are known to be effective *via* the oral route. The ki-

**Table III—Disappearance of Aminocephalosporins from Rat Intestinal Loops 1 hr after Administration**

| Antibiotic | Intestinal Area | Disappearance of Administered Dose, % ± *SD* | | | Statistical Significance of Difference | |
|---|---|---|---|---|---|---|
| | | 2 mg/ml | 10 mg/ml | 20 mg/ml | $(p)^a$ | $(p)^b$ |
| Cefadroxil | 1[c] | 34.1 ± 5.9 (5)[d] | — | 29.4 ± 6.2 (4) | — | NS |
| | 2[e] | 64.6 ± 7.4 (5) | — | 35.1 ± 5.7 (4) | — | <0.001 |
| | 3[f] | 66.2 ± 9.1 (4) | — | 31.6 ± 5.7 (3) | — | <0.01 |
| | 4[g] | 70.8 ± 3.2 (4) | — | 36.8 ± 3.4 (3) | — | <0.001 |
| Cephalexin | 1 | 25.5 ± 5.4 (4) | — | 22.2 ± 3.7 (3) | — | NS |
| | 2 | 21.3 ± 6.4 (4) | — | 28.9 ± 2.3 (3) | — | NS |
| | 3 | 40.2 ± 13.6 (4) | — | 24.7 ± 2.3 (3) | — | NS |
| | 4 | 36.9 ± 12.4 (4) | — | 21.5 ± 2.0 (4) | — | <0.05 |
| Cephradine | 1 | 47.7 ± 0.5 (3) | 21.2 ± 4.4 (4) | 17.0 ± 7.1 (3) | <0.01 | <0.01 |
| | 2 | 51.4 ± 9.4 (4) | 29.2 ± 9.7 (3) | 17.3 ± 2.3 (3) | <0.05 | <0.01 |
| | 3 | 55.4 ± 6.5 (3) | 26.8 ± 1.4 (3) | 24.1 ± 10.3 (3) | <0.01 | <0.02 |
| | 4 | 52.0 ± 12.5 (3) | 28.3 ± 1.6 (3) | 22.3 ± 7.8 (3) | <0.05 | <0.05 |

[a] Two-sample *t* test; disappearances of a 2- and 10-mg/ml dose. [b] Two-sample *t* test; disappearances of a 2- and 20-mg/ml dose. [c] Upper duodenum, 2 cm from the pylorus. [d] The experimental number is given in parentheses. [e] Lower duodenum, with 1-cm separation from 1. [f] Upper jejunum, 15 cm from the pylorus. [g] Lower jejunum, with 1-cm separation from 3.

netics of the proposed carrier-mediated transport of amphoteric β-lactam antibiotics will be presented in subsequent papers.

## REFERENCES


(1) G. N. Rolinson and R. Sutherland, *Adv. Pharmacol. Chemother.*, **11**, 187 (1973), and references cited therein.

(2) C. H. Nightingale, D. S. Greene, and R. Quintiliani, *J. Pharm. Sci.*, **64**, 1899 (1975).

(3) J. W. Poole, *ibid.*, **59**, 1255 (1970).

(4) D. Perrier and M. Gibaldi, *ibid.*, **62**, 1486 (1973).

(5) A. Philipson, L. D. Sabath, and B. Rosner, *Antimicrob. Agents Chemother.*, **8**, 311 (1975).

(6) G. H. Warren, *Chemotherapy*, **22**, 154 (1976).

(7) E. A. P. Croydon and R. Sutherland, *Antimicrob. Agents Chemother.*, **1970**, 427 (1971).

(8) A. Tsuji, E. Miyamoto, N. Hashimoto, and T. Yamana, *J. Pharm. Sci.*, **67**, 1705 (1978).

(9) A. Tsuji, E. Miyamoto, O. Kubo, and T. Yamana, *ibid.*, **68**, 812 (1979).

(10) J. F. Quay and L. Foster, *Physiologist*, **13**, 287 (1970).

(11) J. F. Quay, *ibid.*, **15**, 241 (1972).

(12) S. C. Penzotti, Jr., and J. W. Poole, *J. Pharm. Sci.*, **63**, 1803 (1974).

(13) C. Dixon and L. W. Mizen, *J. Physiol.*, **269**, 549 (1977).

(14) K. Miyazaki, O. Ogino, M. Nakano, and T. Arita, *Chem. Pharm. Bull.*, **25**, 246 (1977).

(15) A. Tsuji, E. Nakashima, I. Kagami, N. Honjo, and T. Yamana, *J. Pharm. Pharmacol.*, **29**, 707 (1977).

(16) A. Tsuji, E. Nakashima, I. Kagami, T. Asano, R. Nakashima, and T. Yamana, *ibid.*, **30**, 508 (1978).

(17) T. Kimura, H. Endo, M. Yoshikawa, S. Muranishi, and H. Sezaki, *J. Pharm. Dyn.*, **1**, 262 (1978).

(18) J. L. DeYoung, H. G. H. Tan, H. E. Huber, and M. A. Zoglio, *J. Pharm. Sci.*, **67**, 320 (1978).

(19) H. Shindo, K. Fukuda, K. Kawai, and K. Tanaka, *J. Pharm. Dyn.*, **1**, 310 (1978).

(20) K. Umeniwa, O. Ogino, K. Miyazaki, and T. Arita, *Chem. Pharm. Bull.*, **27**, 2177 (1979).

(21) A. Tsuji, E. Nakashima, T. Asano, R. Nakashima, and T. Yamana, *J. Pharm. Pharmacol.*, **31**, 718 (1979).

(22) A. Tsuji, E. Nakashima, S. Hamano, and T. Yamana, *J. Pharm. Sci.*, **67**, 1059 (1978).

(23) A. Tsuji, E. Nakashima, and T. Yamana, *ibid.*, **68**, 308 (1979).

(24) M. A. Schwartz and A. J. Delduce, *ibid.*, **58**, 1137 (1969).

(25) T. Koizumi, T. Arita, and K. Kakemi, *Chem. Pharm. Bull.*, **12**, 413 (1964).

(26) K. Miyazaki, O. Ogino, and T. Arita, *ibid.*, **22**, 1910 (1974).

(27) K. Miyazaki, O. Ogino, H. Sato, M. Nakano, and T. Arita, *ibid.*, **25**, 253 (1977).

(28) H. Bundgaard and K. Ilver, *J. Pharm. Pharmacol.*, **24**, 790 (1972).

(29) H. Bundgaard, *ibid.*, **26**, 385 (1974).

(30) A. Tsuji, O. Kubo, E. Miyamoto, and T. Yamana, *J. Pharm. Sci.*, **66**, 1675 (1977).

(31) H. Maekawa, Y. Takagishi, K. Iwamoto, Y. Doi, T. Gura, M. Ito, K. Kitamura, and H. Fujimoto, *Jpn. J. Antibiot.*, **30**, 631 (1977).

(32) T. Yamana, A. Tsuji, and Y. Mizukami, *Chem. Pharm. Bull.*, **22**, 1186 (1974).

(33) H. Lode, *Chemother., Proc. Int. Congr. Chemother., 9th, 1975*, **4**, 199 (1976); through *Chem. Abstr.*, **86**, 165045g (1977).


## ACKNOWLEDGMENTS


The authors are grateful to Bristol Myers Co., Fujisawa Pharmaceutical Co., Takeda Chemical Industries, and Shionogi Co. for supplying materials. Thanks also are due to Dr. Etsuko Miyamoto for helpful discussions and Miss Naoko Honjo, Miss Ryoko Nakashima, Miss Junko Komura, Mr. Osamu Kubo, and Mr. Seiya Kagatani for technical assistance.


# Intestinal Absorption Mechanism of Amphoteric β-Lactam Antibiotics II: Michaelis–Menten Kinetics of Cyclacillin Absorption and Its Pharmacokinetic Analysis in Rats


**AKIRA TSUJI *x, EMI NAKASHIMA *, IZUMI KAGAMI *, and TSUKINAKA YAMANA ‡**



Received August 13, 1980, from the **Faculty of Pharmaceutical Sciences and the ‡Hospital Pharmacy, Kanazawa University, Takara-machi, Kanazawa 920, Japan.* Accepted for publication December 11, 1980.



**Abstract** □ The absorption of cyclacillin at pH 7.0 by the rat small intestine was investigated using *in situ* perfusion. At the lowest dose of 95 μg/ml, the antibiotic disappearance was rapid and followed first-order kinetics, with the disappearance being 85% at 100 min. At the intermediate concentrations of 770 and 1200 μg/ml, the disappearance after 100 min was 69 and 54%, respectively, and semilogarithmic plots clearly showed convex curvatures. At the highest concentration of 30 mg/ml, cyclacillin disappeared slowly from the perfusate, in an apparent first-order fashion. The disappearence was 26% after 100 min of perfusion and was similar in extent at 5.2 mg/ml. This concentration–time profile was satisfactorily fitted to the simultaneous Michaelis–Menten and first-order kinetic equations. The area under the blood concentration *versus* time curve (*AUC*) after a single intraduodenal dose of cyclacillin was almost consistent with the *AUC* after the equivalent intravenous dose (10 mg/kg). Additional evidence from a pharmacokinetic analysis of steady-state blood concentrations after constant infusion of cyclacillin through the portal vein and the small intestinal lumen indicated that cyclacillin absorption by the rat intestinal tissue at relatively low concentrations (<1 mg/ml) followed solely Michaelis–Menten kinetics. Cyclacillin may be transported by certain types of carrier-mediated mechanisms.



**Keyphrases** □ Cyclacillin—intestinal absorption kinetics *in situ*, blood levels in rats after intravenous, intraportal, and intraduodenal administration □ Absorption kinetics—rat intestinal loops, blood cyclacillin levels after intravenous, intraportal, and intraduodenal administration □ Kinetics, absorption—blood cyclacillin levels after intravenous, intraportal, and intraduodenal administration, *in situ* rat intestinal loops □ Antibiotics, amino-β-lactam—cyclacillin, *in situ* intestinal absorption kinetics, blood levels after intravenous, intraportal, and intraduodenal administration to rats □ Pharmacokinetics—cyclacillin, intestinal absorption *in situ*, blood levels after intravenous, intraportal, and intraduodenal administration to rats


Previous *in situ* absorption studies (1–4) utilizing rat intestinal loops showed that the percentage disappearance of amino-β-lactam antibiotics, such as amoxicillin, cyclacillin, cephalexin, cephradine, and cefadroxil, was extremely large at a low dose but was markedly reduced at a high dose. Accumulated results from the past 10 years




0022-3549/81/0700-0772$01.00/0


© 1981, American Pharmaceutical Association

netics of the proposed carrier-mediated transport of amphoteric β-lactam antibiotics will be presented in subsequent papers.

## REFERENCES


(1) G. N. Rolinson and R. Sutherland, *Adv. Pharmacol. Chemother.*, **11**, 187 (1973), and references cited therein.

(2) C. H. Nightingale, D. S. Greene, and R. Quintiliani, *J. Pharm. Sci.*, **64**, 1899 (1975).

(3) J. W. Poole, *ibid.*, **59**, 1255 (1970).

(4) D. Perrier and M. Gibaldi, *ibid.*, **62**, 1486 (1973).

(5) A. Philipson, L. D. Sabath, and B. Rosner, *Antimicrob. Agents Chemother.*, **8**, 311 (1975).

(6) G. H. Warren, *Chemotherapy*, **22**, 154 (1976).

(7) E. A. P. Croydon and R. Sutherland, *Antimicrob. Agents Chemother.*, **1970**, 427 (1971).

(8) A. Tsuji, E. Miyamoto, N. Hashimoto, and T. Yamana, *J. Pharm. Sci.*, **67**, 1705 (1978).

(9) A. Tsuji, E. Miyamoto, O. Kubo, and T. Yamana, *ibid.*, **68**, 812 (1979).

(10) J. F. Quay and L. Foster, *Physiologist*, **13**, 287 (1970).

(11) J. F. Quay, *ibid.*, **15**, 241 (1972).

(12) S. C. Penzotti, Jr., and J. W. Poole, *J. Pharm. Sci.*, **63**, 1803 (1974).

(13) C. Dixon and L. W. Mizen, *J. Physiol.*, **269**, 549 (1977).

(14) K. Miyazaki, O. Ogino, M. Nakano, and T. Arita, *Chem. Pharm. Bull.*, **25**, 246 (1977).

(15) A. Tsuji, E. Nakashima, I. Kagami, N. Honjo, and T. Yamana, *J. Pharm. Pharmacol.*, **29**, 707 (1977).

(16) A. Tsuji, E. Nakashima, I. Kagami, T. Asano, R. Nakashima, and T. Yamana, *ibid.*, **30**, 508 (1978).

(17) T. Kimura, H. Endo, M. Yoshikawa, S. Muranishi, and H. Sezaki, *J. Pharm. Dyn.*, **1**, 262 (1978).

(18) J. L. DeYoung, H. G. H. Tan, H. E. Huber, and M. A. Zoglio, *J. Pharm. Sci.*, **67**, 320 (1978).

(19) H. Shindo, K. Fukuda, K. Kawai, and K. Tanaka, *J. Pharm. Dyn.*, **1**, 310 (1978).

(20) K. Umeniwa, O. Ogino, K. Miyazaki, and T. Arita, *Chem. Pharm. Bull.*, **27**, 2177 (1979).

(21) A. Tsuji, E. Nakashima, T. Asano, R. Nakashima, and T. Yamana, *J. Pharm. Pharmacol.*, **31**, 718 (1979).

(22) A. Tsuji, E. Nakashima, S. Hamano, and T. Yamana, *J. Pharm. Sci.*, **67**, 1059 (1978).

(23) A. Tsuji, E. Nakashima, and T. Yamana, *ibid.*, **68**, 308 (1979).

(24) M. A. Schwartz and A. J. Delduce, *ibid.*, **58**, 1137 (1969).

(25) T. Koizumi, T. Arita, and K. Kakemi, *Chem. Pharm. Bull.*, **12**, 413 (1964).

(26) K. Miyazaki, O. Ogino, and T. Arita, *ibid.*, **22**, 1910 (1974).

(27) K. Miyazaki, O. Ogino, H. Sato, M. Nakano, and T. Arita, *ibid.*, **25**, 253 (1977).

(28) H. Bundgaard and K. Ilver, *J. Pharm. Pharmacol.*, **24**, 790 (1972).

(29) H. Bundgaard, *ibid.*, **26**, 385 (1974).

(30) A. Tsuji, O. Kubo, E. Miyamoto, and T. Yamana, *J. Pharm. Sci.*, **66**, 1675 (1977).

(31) H. Maekawa, Y. Takagishi, K. Iwamoto, Y. Doi, T. Gura, M. Ito, K. Kitamura, and H. Fujimoto, *Jpn. J. Antibiot.*, **30**, 631 (1977).

(32) T. Yamana, A. Tsuji, and Y. Mizukami, *Chem. Pharm. Bull.*, **22**, 1186 (1974).

(33) H. Lode, *Chemother., Proc. Int. Congr. Chemother., 9th, 1975*, **4**, 199 (1976); through *Chem. Abstr.*, **86**, 165045g (1977).


## ACKNOWLEDGMENTS


The authors are grateful to Bristol Myers Co., Fujisawa Pharmaceutical Co., Takeda Chemical Industries, and Shionogi Co. for supplying materials. Thanks also are due to Dr. Etsuko Miyamoto for helpful discussions and Miss Naoko Honjo, Miss Ryoko Nakashima, Miss Junko Komura, Mr. Osamu Kubo, and Mr. Seiya Kagatani for technical assistance.


# Intestinal Absorption Mechanism of Amphoteric β-Lactam Antibiotics II: Michaelis–Menten Kinetics of Cyclacillin Absorption and Its Pharmacokinetic Analysis in Rats


**AKIRA TSUJI *x, EMI NAKASHIMA *, IZUMI KAGAMI *, and TSUKINAKA YAMANA ‡**



Received August 13, 1980, from the **Faculty of Pharmaceutical Sciences and the ‡Hospital Pharmacy, Kanazawa University, Takara-machi, Kanazawa 920, Japan.* Accepted for publication December 11, 1980.



**Abstract** □ The absorption of cyclacillin at pH 7.0 by the rat small intestine was investigated using *in situ* perfusion. At the lowest dose of 95 μg/ml, the antibiotic disappearance was rapid and followed first-order kinetics, with the disappearance being 85% at 100 min. At the intermediate concentrations of 770 and 1200 μg/ml, the disappearance after 100 min was 69 and 54%, respectively, and semilogarithmic plots clearly showed convex curvatures. At the highest concentration of 30 mg/ml, cyclacillin disappeared slowly from the perfusate, in an apparent first-order fashion. The disappearence was 26% after 100 min of perfusion and was similar in extent at 5.2 mg/ml. This concentration–time profile was satisfactorily fitted to the simultaneous Michaelis–Menten and first-order kinetic equations. The area under the blood concentration *versus* time curve (*AUC*) after a single intraduodenal dose of cyclacillin was almost consistent with the *AUC* after the equivalent intravenous dose (10 mg/kg). Additional evidence from a pharmacokinetic analysis of steady-state blood concentrations after constant infusion of cyclacillin through the portal vein and the small intestinal lumen indicated that cyclacillin absorption by the rat intestinal tissue at relatively low concentrations (<1 mg/ml) followed solely Michaelis–Menten kinetics. Cyclacillin may be transported by certain types of carrier-mediated mechanisms.



**Keyphrases** □ Cyclacillin—intestinal absorption kinetics *in situ*, blood levels in rats after intravenous, intraportal, and intraduodenal administration □ Absorption kinetics—rat intestinal loops, blood cyclacillin levels after intravenous, intraportal, and intraduodenal administration □ Kinetics, absorption—blood cyclacillin levels after intravenous, intraportal, and intraduodenal administration, *in situ* rat intestinal loops □ Antibiotics, amino-β-lactam—cyclacillin, *in situ* intestinal absorption kinetics, blood levels after intravenous, intraportal, and intraduodenal administration to rats □ Pharmacokinetics—cyclacillin, intestinal absorption *in situ*, blood levels after intravenous, intraportal, and intraduodenal administration to rats


Previous *in situ* absorption studies (1–4) utilizing rat intestinal loops showed that the percentage disappearance of amino-β-lactam antibiotics, such as amoxicillin, cyclacillin, cephalexin, cephradine, and cefadroxil, was extremely large at a low dose but was markedly reduced at a high dose. Accumulated results from the past 10 years




0022-3549/81/0700-0772$01.00/0


© 1981, American Pharmaceutical Association

(1–13) suggest that the GI absorption of amino-β-lactam antibiotics does not obey the so-called lipid theory but that certain carrier-mediated mechanisms underlie their absorption.

Among these classes of β-lactam antibiotics, cyclacillin revealed a remarkable dose-dependent disappearance from the rat gut lumen (2, 4). Recently, the presence of one or more carrier systems was proposed for the active transport of cyclacillin in the rat intestinal mucosa (8, 10). However, when various cyclacillin doses were administered orally to mice (14), rats (15), dogs (16), and humans (17), the peak blood levels were almost parallel to the dose. The question now arises as to whether the dose-dependent disappearance from the intestinal lumen solution is due to absorption into the bloodstream, to gut wall accumulation, or to both absorption and degradation in the gut lumen and at the mucosal surface.

The present study on cyclacillin absorption by the rat intestine was undertaken to elucidate: (*a*) the kinetics of disappearance from the recirculating intestinal perfusion solution, (*b*) the ratio of the area under the blood concentration–time curve (*AUC*) after the intraduodenal administration to that after an intravenous dose, and (*c*) the relationship between steady-state blood levels after constant infusion into the portal vein and those after single intestinal perfusion of cyclacillin at various doses.

## EXPERIMENTAL

**Materials**—Cyclacillin anhydrate (983 μg/mg) was used as received[1]. All other reagents and solvents were the best grade available.

**Animals**—Male albino Wistar rats weighing 220 ± 4 g and 214 ± 20 g were used in the measurement of *AUC* and the other experiments, respectively. They were fasted for 20 hr prior to the experiment, but water was given freely. The rats were anesthetized with urethan (1.5 g/kg ip) ~1 hr prior to surgery.

***In Situ* Recirculating Perfusion Method**—The procedure employed was essentially the same as that described previously (2). The bile duct was ligated in all recirculating perfusion experiments. The intestine was cannulated with a glass cannula at the pylorus and jejunum ends for ~30 cm and prewashed with 100 ml of pH 7.0 isotonic phosphate buffer. After washing with 20 ml of the pH 7.0 isotonic buffer containing cyclacillin, 6 ml of this antibiotic solution was recirculated continuously to produce a final volume of ~9 ml. The pH of the lumen solution was maintained at pH 7.0 by means of a pH-stat[2]. Samples withdrawn periodically from the perfusate were filtered to remove solid materials, diluted if necessary, and analyzed as described under *Analysis*. The total sampling volume was within 6% of the perfusion solution.

**Determination of *AUC* after Intravenous or Intraduodenal Administration**—A 30-cm intestinal loop was prepared by ligation between the pylorus and jejunum. Cyclacillin solution was prepared with physiological saline, and 10-mg/kg doses were given intravenously through the femoral vein (0.5 ml) or intraduodenally (1 ml). Aliquots (0.2 ml) of blood samples taken periodically from the jugular vein were assayed by the microbiological method after being hemolyzed with an equivalent volume of distilled water. The total weight of sampled blood was within 0.7% of the rat body weight.

**Tissue Accumulation after Intraduodenal Administration**—After completion of 1- or 5-hr experiments for *AUC* determination, the intestinal area of the 30-cm intestinal loop was isolated, tearing off the mesentery, and the serosal surface then was blotted with filter paper. The intestine was cut into small slices and homogenized in a polytef homogenizer with saline to give 10% (w/v, wet weight) homogenate. An aliquot of the homogenates then was analyzed.

**Constant Intraportal Infusion**—To obtain a steady-state blood level after constant infusion into the portal vein, antibiotic solutions of 5, 10, 15, and 20 mg/ml prepared with saline were infused at 0.003 ml/min into rats whose bile duct had been cannulated with a polyethylene tube to exclude bile. Aliquots (0.2 ml) of blood samples withdrawn periodically during 7-hr experiments were analyzed after being hemolyzed.

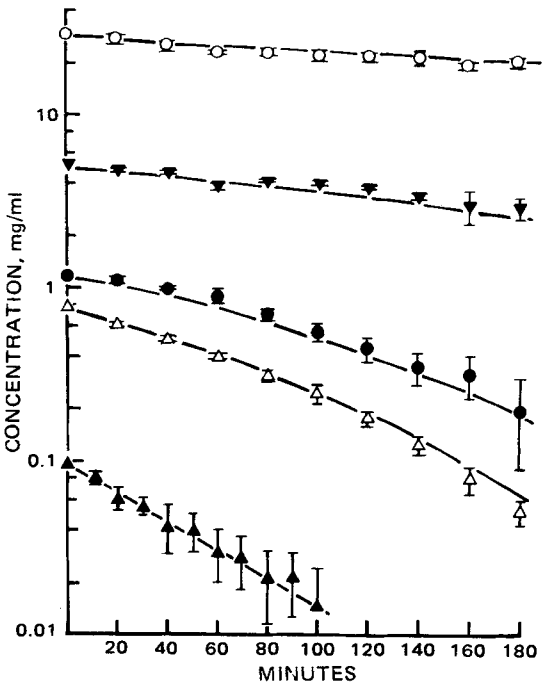


**Figure 1**—*Time courses for cyclacillin disappearance from isotonic phosphate buffer perfused through the rat small intestine as a function of dose. The points represent the mean concentration, and the vertical bars represent the standard deviations from three or six experiments. The curves are model-predicted concentrations based on nonlinear least-squares fitting of data to Eq. 1. Key: ▲, 95 μg/ml; △, 770 μg/ml; ●, 1200 μg/ml; ▼, 5200 μg/ml; and ○, 30 mg/ml.*

**Appearance in Blood after *In Situ* Single Intestinal Perfusion**—The rats were treated similarly as in the *in situ* recirculating perfusion experiments, but the bile duct was cannulated with a polyethylene tube to exclude bile. Cyclacillin solutions (0.1, 0.2, 0.5, and 1.0 mg/ml, prepared with pH 7.4 isotonic phosphate buffer) were perfused from the pylorus end at a flow rate of 2 ml/min and collected at the jejunum end. Aliquots (0.2 ml) of blood samples taken periodically during 7-hr absorption experiments were analyzed after being hemolyzed. The total weight of sampled blood was within 1% of the rat body weight.

**Analysis**—The residual cyclacillin in the recirculating perfusion solution was determined by both high-performance liquid chromatographic (HPLC) and microbiological assays.

The liquid chromatograph[3] was equipped with a UV detector[4] set at 210 nm. A strong cation-exchange resin[5] packed into a 4.6 × 500-mm stainless steel column was used as the stationary phase. The mobile phase was aqueous 0.1 *M* $KH_2PO_4$ adjusted to pH 4.0–4.2 with sodium hydroxide solution. Samples were eluted at a flow rate of 2 ml/min. The recirculating solution (10–50 μl) was withdrawn at suitable time intervals, injected *via* a variable-loop injector on flow after appropriate dilution, if necessary, and filtrated with a 0.45-μm filter[6]. The peak heights were measured, and the concentrations were calculated from calibration curves obtained daily.

The recirculating intestinal perfusion solution, intestinal tissue homogenates, and hemolyzed blood samples were analyzed by the microbiological paper disk method employing *Sartina lutea*[7]. For the latter two samples, standards were established by using fresh pooled 10% gut homogenates and fresh pooled blood, both from control rats.

The accuracies of the two analytical methods were as described previously (4).

[1] Takeda Chemical Industries, Osaka, Japan.
[2] A pH-stat titrator assembly consisting of a TTT2 titrator and ABU12b autoburet, Radiometer, Denmark.
[3] Model FLC-A700, Japan Spectroscopic Co., Tokyo, Japan.
[4] Model UVIDEC-100, Japan Spectroscopic Co., Tokyo, Japan.
[5] Zipax SCX, DuPont Instruments, Wilmington, Del.
[6] Sartorius-Membranefilter GmbH, Göttingen, West Germany.
[7] IFO 12708, Institute for Fermentation, Osaka, Japan. The strain was derived from ATCC 9341.

Table I—Percentage of Residual Antibiotic in the Lumen Solution Perfused through the Rat Small Intestine[a] at Various Doses as a Function of Time

| Minutes | Initial Concentration of Cyclacillin, μg/ml | | | | |
|---|---|---|---|---|---|
| | 95 | 770 | 1200 | 5200 | 30000 |
| 0 | 100.0 | 100.0 | 100.0 | 100.0 | 100.0 |
| 10 | 84.3 ± 7.7 | — | — | — | — |
| 20 | 64.0 ± 10.2 | 78.6 ± 1.4 | 92.4 ± 4.8 | 92.5 ± 1.5 | 93.2 ± 6.4 |
| 30 | 57.7 ± 7.5 | — | — | — | — |
| 40 | 44.4 ± 13.9 | 65.0 ± 2.9 | 82.2 ± 2.1 | 89.6 ± 2.4 | 85.8 ± 7.1 |
| 50 | 41.7 ± 10.4 | — | — | — | — |
| 60 | 31.2 ± 11.3 | 52.3 ± 3.9 | 74.7 ± 6.8 | 76.4 ± 6.3 | 78.6 ± 1.0 |
| 70 | 28.9 ± 10.0 | — | — | — | — |
| 80 | 22.0 ± 9.8 | 41.6 ± 4.7 | 58.0 ± 4.5 | 80.5 ± 1.3 | 78.3 ± 4.4 |
| 90 | 22.1 ± 8.8 | — | — | — | — |
| 100 | 15.2 ± 9.9 | 31.2 ± 3.7 | 45.8 ± 6.1 | 76.4 ± 2.0 | 73.9 ± 6.1 |
| 120 | — | 22.6 ± 2.1 | 37.0 ± 6.0 | 72.9 ± 1.8 | 72.9 ± 4.7 |
| 140 | — | 15.7 ± 1.9 | 28.6 ± 5.9 | 64.7 ± 3.1 | 71.2 ± 7.8 |
| 160 | — | 10.0 ± 1.8 | 25.3 ± 7.2 | 56.3 ± 12.2 | 63.4 ± 3.4 |
| 180 | — | 6.4 ± 1.0 | 15.8 ± 8.5 | 54.2 ± 7.4 | 65.4 ± 5.1 |

[a] $n = 3$ for all doses except the 95-μg/ml dose ($n = 6$).

## RESULTS AND DISCUSSION

**Concentration–Time Profile for *In Situ* Disappearance from Recirculating Perfusate**—Semilogarithmic plots of the disappearance of cyclacillin from the rat small intestinal lumen at pH 7.0 are given in Fig. 1. The analytical results determined by both HPLC and biological assay for samples of initial concentrations of 95, 1200, and 5200 μg/ml were in good agreement. The percentages of residual antibiotic at various doses as a function of time are summarized in Table I.

At the lowest concentration (95 μg/ml), cyclacillin disappearance was rapid and followed apparent first-order kinetics, with the disappearance being 85% at 100 min. At the intermediate concentrations of 770 and 1200 μg/ml, the disappearance after 100 min was 69 and 54%, respectively, and the semilogarithmic plots clearly showed convex curvatures. At the highest concentration (30 mg/ml), cyclacillin disappeared slowly from the perfusate in an apparent first-order fashion. The disappearance was 26% after 100 min of perfusion and was similar in extent at 5200 μg/ml. This concentration–time profile, showing a dramatic decrease in the disappearance rate with an increase in the initial cyclacillin concentration, indicates that the disappearance rate of this antibiotic from the rat intestinal perfusate can be described in the mixed kinetic terms of Michaelis–Menten and first order:

$$\frac{dC}{dt} = -\frac{V_{max}C}{K_m + C} - (k_1 + k_2)C \qquad \text{(Eq. 1)}$$

where $C$ is the cyclacillin concentration remaining in the perfusate at time $t$, $V_{max}$ is the maximum rate of disappearance, $K_m$ is the Michaelis–Menten constant, and $k_1$ and $k_2$ are the first-order rate constants of absorption and degradation, respectively, as defined previously (3).

Iterative nonlinear least-squares analysis of the data in Fig. 1 to be fitted to Eq. 1, using a NONLIN computer program (18), provided the following parameters[8,9]: $V_{max}$ = 502 ± 31 μg/ml/hr or 1.47 ± 0.09 m$M$ hr$^{-1}$, $K_m$ = 420 ± 27 μg/ml or 1.23 ± 0.08 m$M$, and $k_1 + k_2$ = 0.111 ± 0.014 hr$^{-1}$. During the fitting procedure, the concentration was weighted by the reciprocal of its square.

There were negligible concentrations of the penicilloic acid of cyclacillin on HPLC during the absorption experiments, which was consistent with previous observations using the *in situ* intestinal loop method (2, 4). The *in vitro* first-order degradation rate constant of this antibiotic was determined as 0.014 hr$^{-1}$ in the intestinal washing perfusate at 37°, indicating cumulative products of only 3% penicilloic acid from the initial dose after a 2-hr experiment. Subtraction of the first-order degradation rate constant ($k_2$) of 0.014 hr$^{-1}$ from the best fitting first-order rate constant of 0.111 hr$^{-1}$ yielded 0.097 hr$^{-1}$ as the net first-order absorption rate constant ($k_1$). This value was very close to values of other amino-β-lactam antibiotics, amoxicillin ($k_1$ = 0.062 hr$^{-1}$) (2) and cephradine ($k_1$ = 0.082 hr$^{-1}$) (3), as well as to the average first-order absorption rate constant for monobasic penicillins (0.076 hr$^{-1}$) (19) determined in similar experiments.

The solid lines in Fig. 1 were generated using Eq. 1 with the NONLIN-fitted parameters, indicating that Eq. 1 gives an excellent description of the experimental data for the cyclacillin disappearance from the rat *in situ* intestinal perfusate.

**Pharmacokinetic Evidence for Saturable Absorption by Blood Concentration Analysis**—In the disappearance of cyclacillin from the intestinal perfusate by Michaelis–Menten kinetics, it is important to distinguish between net transport across the GI tract into the bloodstream and competitive enzymatic degradation in the lumen and/or at the mucosal surface.

The contribution of each kinetic term in Eq. 1 to the total disappearance was calculated as a function of constant antibiotic concentration. At concentrations of >5 mg/ml, the first-order kinetic term, $k_1 + k_2$, may play the major role in the disappearance; with those of <1.0 mg/ml, the total disappearance is expected to be virtually due to Michaelis–Menten kinetics.

AUC *after Intraduodenal Dose Compared with Intravenous Dose*—Figure 2 shows the mean blood concentration–time profiles of cyclacillin

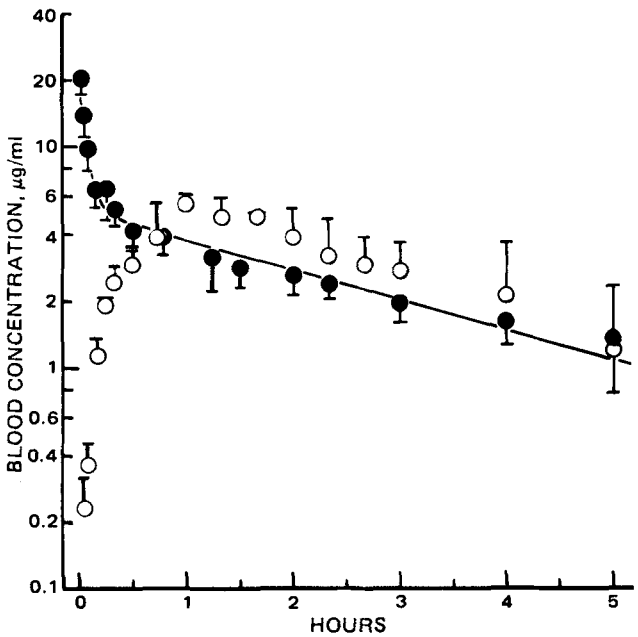


**Figure 2**—*Mean blood concentration of cyclacillin (10 mg/kg) following intravenous (●) or intraduodenal (○) administration in rats. The vertical bars represent the standard deviations from three experiments. The curve is the nonlinear least-squares line for the two-compartment open model.*

[8] Previously, we employed only the Michaelis–Menten kinetic term for the data fitting and reported $V_{max}$ = 842 ± 28 μg/ml/hr or 2.47 ± 0.08 m$M$ hr$^{-1}$ and $K_m$ = 654 ± 40 μg/ml or 1.91 ± 0.12 m$M$ (2). Additional experiments were conducted at the highest concentration of 30 mg/ml. Incorporation of a first-order kinetic term gave the best fit to all data of both the previous (2) and present studies.

[9] The computer analysis was performed with a FACOM M-160 digital computer at the Data Processing Center, Kanazawa University.

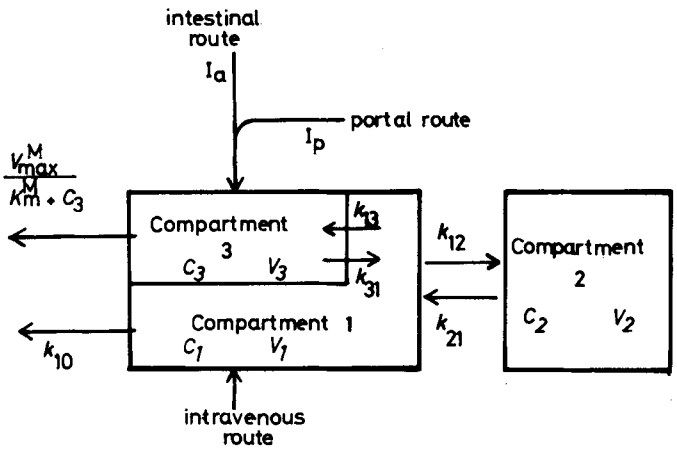


*Scheme I—Pharmacokinetic model for evaluation of the absorption rate of the drug.*

(10 mg/kg) after intravenous and intraduodenal administrations in rats whose intestine had been ligated 30 cm from the pylorus to prevent possible loss of the antibiotic into the feces. The results are summarized in Table II.

The blood concentration ($C_1$) following intravenous bolus injection declined biexponentially in accordance with:

$$C_1 = Ae^{-\alpha t} + Be^{-\beta t} \qquad \text{(Eq. 2)}$$

The data were fitted to a two-compartment open model. The values of $A$, $B$, $\alpha$, and $\beta$ were estimated to be 23.3 ± 2.4 μg/ml, 5.29 ± 0.29 μg/ml, 18.7 ± 2.2 $hr^{-1}$, and 0.326 ± 0.031 $hr^{-1}$, respectively, using the NONLIN computer program (18), where the blood concentration was weighted as its reciprocal[9]. The solid line in Fig. 2 represents the best fit of the data.

Evaluation of the data from the intraduodenal dose of cyclacillin revealed that the terminal phase of the blood level–time profile represented a function of the $\beta$ rate constant.

Both *AUC* values from the different administration routes were calculated according to the trapezoidal rule from time 0 to 5 hr, where pseudodistribution–equilibrium of cyclacillin might be attained. To each value was added the *AUC* value from 5 hr to time infinity, which was calculated using the terminal $\beta$ rate constant. The total blood areas after intravenous and intraduodenal dosing were 18.48 ± 2.28 and 18.46 ± 2.83 μg hr/ml, respectively, and thus were the same within the limits of experimental error.

These results indicate that cyclacillin was absorbed completely by the ligated intestine following intraduodenal administration and that there was no appreciable first-pass metabolism and degradation of cyclacillin in the intestine during absorption of the 10-mg/kg dose. In an absorption experiment after 1 hr, the dose of cyclacillin remaining in the intestinal lumen was determined to be 6.5%, and the accumulation in the tissue was 8.0%; the total absorption was 85.5% after 1 hr. After 5 hr, the percentages of the residual cyclacillin in the intestinal lumen and the accumulation in the tissue were 0.7 and 2.3%, respectively, indicating almost complete cyclacillin absorption in 5 hr.

*Absorption Kinetic Analysis of Steady-State Blood Concentration during Intraportal Vein Infusion and Single Intraduodenal Perfusion*—Although no significant first-pass effect was observed for cyclacillin at an intraduodenal dose of 10 mg/kg, Kind *et al.* (20) reported that penicillins were subject to significant inactivation by the isolated rat liver. Excretion of penicilloic acid after oral administration of cyclacillin in humans was reported to be 15–19% for a 0.250–1-g dose (16). Therefore, the possible consequences of metabolism in the gut or liver must be considered since such processes sometimes are saturable.

With the pharmacokinetic treatment of Gibaldi and Feldman (21), a three-compartment open model may be adequate for considering the saturable first-pass effect after intraduodenal or intraportal administration (Scheme I). The present model consists of a central compartment being sampled (Compartment 1), a rapid equilibrium hepatoportal system (Compartment 3), which is included in the central compartment, and a slow equilibrium peripheral compartment (Compartment 2). The model is based on observations of apparent biexponential pharmacokinetics following an intravenous bolus dose as described earlier. Compartment 3 includes drug metabolism in the liver during the first passage of the drug into the circulation after hepatic route administration. In this model, $C$ is the drug concentration in a given compartment and $V$ is the com-

**Table II—Mean Blood Concentrations (Micrograms per Milliliter) following Intraduodenal and Intravenous Administration of Cyclacillin (10 mg/kg) in Rats with a Ligated Intestine ($n$ = 3–4)**

| Route | Minutes | | | | | | | | | | | | | | | | | |
|---|---|---|---|---|---|---|---|---|---|---|---|---|---|---|---|---|---|---|
| | 1.5 | 3 | 5 | 10 | 15 | 20 | 30 | 45 | 60 | 75 | 80 | 90 | 100 | 120 | 140 | 160 | 180 | 240 | 300 |
| Intraduodenal | — | 0.23 ± 0.09 | 0.36 ± 0.10 | 1.10 ± 0.25 | 1.88 ± 0.19 | 2.43 ± 0.42 | 2.94 ± 0.47 | 3.91 ± 1.66 | 5.60 ± 0.47 | — | 4.82 ± 1.03 | — | 4.79 ± 0.21 | 3.91 ± 1.31 | 3.19 ± 1.50 | 2.95 ± 0.95 | 2.70 ± 1.01 | 2.12 ± 1.51 | 1.17 ± 1.15 |
| Intravenous | 20.5 ± 3.4 | 13.8 ± 2.9 | 9.76 ± 2.1 | 6.35 ± 1.12 | 6.50 ± 1.95 | 5.22 ± 0.86 | 4.17 ± 0.72 | 3.84 ± 0.57 | — | 3.11 ± 0.95 | — | 2.85 ± 0.61 | — | 2.62 ± 0.52 | 2.39 ± 0.36 | — | 1.96 ± 0.38 | 1.60 ± 0.34 | 1.36 ± 0.59 |

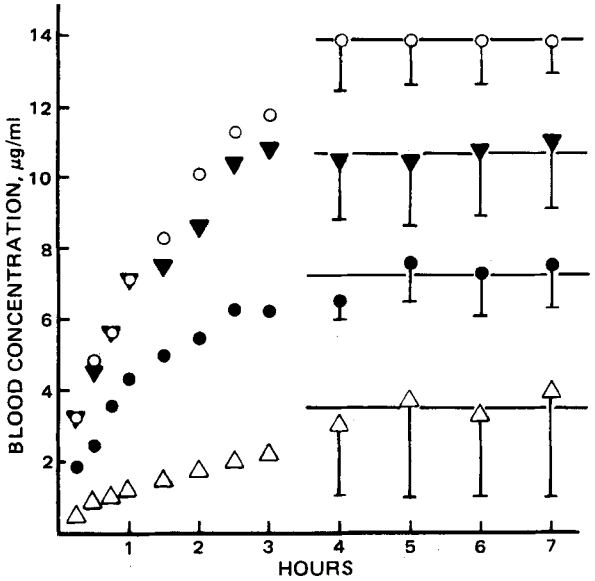


**Figure 3**—*Mean blood concentration of cyclacillin administered by constant portal vein infusion at a rate of 15.3 (△), 30.5 (●), 45.8 (▼), or 61.0 (○) μg/min. The vertical bars represent the standard deviations from three experiments.*

partment volume, $k_{10}$ represents the first-order rate constant for renal elimination, and $V^M_{max}$ and $K^M_m$ represent the maximal rate and Michaelis constant for hepatic metabolism, respectively.

From this model, the rates of drug amount in each compartment are given by:

$$V_1\frac{dC_1}{dt} = -(k_{12}+k_{13}+k_{10})V_1C_1 + k_{21}V_2C_2 + k_{31}V_3C_3 \quad \text{(Eq. 3)}$$

$$V_2\frac{dC_2}{dt} = k_{12}V_1C_1 - k_{21}V_2C_2 \quad \text{(Eq. 4)}$$

$$V_3\frac{dC_3}{dt} = k_{13}V_1C_1 - k_{31}V_3C_3 - \frac{V^M_{max}C_3}{K^M_m + C_3} + \text{input} \quad \text{(Eq. 5)}$$

$$\text{input} = I_p \text{ or } I_a \quad \text{(Eq. 6)}$$

where $I_a$ represents the absorption rate by the intestine and $I_p$ is the infusion rate through the portal vein.

At the steady state of drug distribution and elimination during a constant intestinal perfusion or constant portal vein infusion, Eqs. 7–9

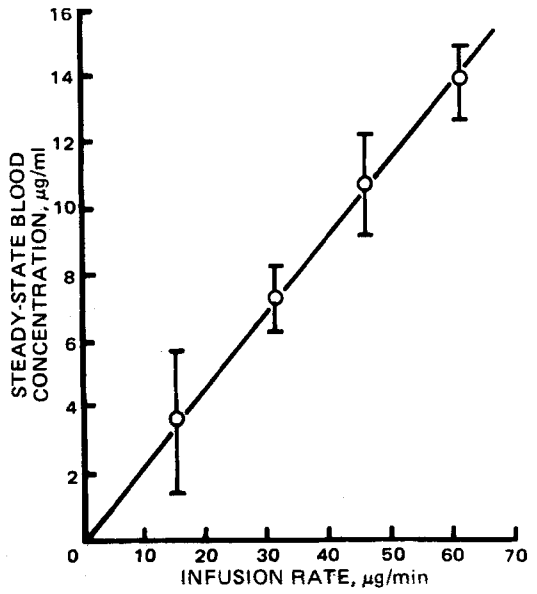


**Figure 4**—*Linear relationship between the steady-state blood concentration and portal vein infusion rate.*

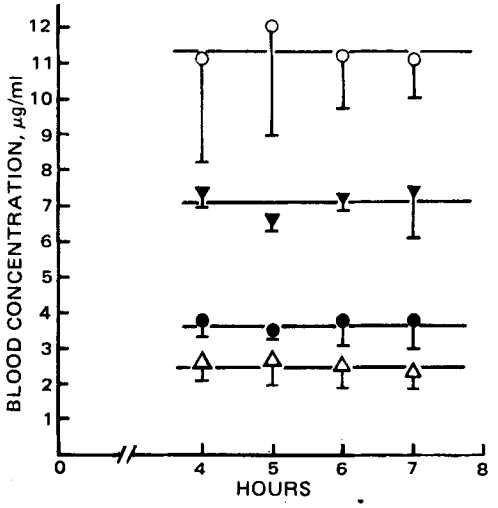


**Figure 5**—*Mean blood concentration of cyclacillin following single perfusion through the rat intestine at various drug concentrations. Key: △, 0.1 mg/ml; ●, 0.2 mg/ml; ▼, 0.5 mg/ml; and ○, 1.0 mg/ml. The vertical bars represent the standard deviation from three experiments.*

can be obtained by putting zero on the left side of Eqs. 3–6 and replacing $C_i$ by $C_i^{ss}$ (steady-state concentration) on the right sides of the equations:

$$-(k_{12}+k_{13}+k_{10})V_1C_1^{ss} + k_{21}V_2C_2^{ss} + k_{31}V_3C_3^{ss} = 0 \quad \text{(Eq. 7)}$$

$$k_{12}V_1C_1^{ss} - k_{21}V_2C_2^{ss} = 0 \quad \text{(Eq. 8)}$$

$$k_{13}V_1C_1^{ss} - k_{31}V_3C_3^{ss} - \frac{V^M_{max}C_3^{ss}}{K^M_m + C_3^{ss}} + \text{input} = 0 \quad \text{(Eq. 9)}$$

Rearrangement of Eqs. 7–9 gives:

$$\text{input} = k_{10}V_1C_1^{ss} + \frac{V^M_{max}C_3^{ss}}{K^M_m + C_3^{ss}} \quad \text{(Eq. 10)}$$

Combination of Eqs. 7 and 8 yields:

$$C_3^{ss} = \frac{(k_{13}+k_{10})V_1}{k_{31}V_3}C_1^{ss} \quad \text{(Eq. 11)}$$

where $C_3^{ss}$ is proportional to $C_1^{ss}$. If the proportionality constant is $K$, then $C_3^{ss}$ equals $KC_1^{ss}$.

When a steady-state blood concentration, $[C_1^{ss}]_{I_a}$, is achieved after constant intestinal perfusion of drug, the absorption rate, $I_a$, can be expressed as:

$$I_a = \left(k_{10}V_1 + \frac{V^M_{max}KV_3}{K^M_m + K[C_1^{ss}]_{I_a}}\right)[C_1^{ss}]_{I_a} \quad \text{(Eq. 12)}$$

Similarly, the portal vein infusion rate can be described as:

$$I_p = \left(k_{10}V_1 + \frac{V^M_{max}KV_3}{K^M_m + K[C_1^{ss}]_{I_p}}\right)[C_1^{ss}]_{I_p} \quad \text{(Eq. 13)}$$

From Eqs. 12 and 13, it can be seen that $I_a$ should be equal to $I_p$ when the steady-state levels of $[C_1^{ss}]_{I_a}$ and $[C_1^{ss}]_{I_p}$ are the same. This relationship predicts that the constant rate of intestinal absorption, $I_a$, can be determined without knowledge of any pharmacokinetic parameters such as the elimination rates from the liver and kidneys and the distribution volumes of the compartments.

As shown in Fig. 3, the steady-state blood cyclacillin concentrations during a constant rate of infusion through the portal vein in rats were 3.57 ± 2.18, 7.29 ± 1.01, 10.7 ± 1.5, and 13.9 ± 1.0 μg/ml (mean ± *SD*) between 4 and 7 hr at infusion rates of 15.3, 30.5, 45.8, and 61.0 μg/min, respectively. Plots of $[C_1^{ss}]_{I_p}$ *versus* the infusion rate, $I_p$, are given in Fig. 4. These plots apparently are linear, yielding the following regression equation:

$$I_p = 4.33[C_1^{ss}]_{I_p} \quad \text{(Eq. 14)}$$

The clearances of cyclacillin by both the renal and hepatic routes in rats appear to be linear within the range of experimental blood levels.

Figure 5 shows the blood concentration–time profiles of cyclacillin during a constant single perfusion of cyclacillin solution of $C_0$ (micrograms per milliliter) at a rate of 2 ml/min through the rat small intestine. A steady state was attained after 4 hr. The average steady-state blood levels, $[C_1^{ss}]_{I_a}$, between 4 and 7 hr were 2.50 ± 0.52, 3.67 ± 0.47, 7.11 ± 0.71, and 11.37 ± 2.09 μg/ml for intestinal cyclacillin concentrations of 0.1, 0.2, 0.5, and 1.0 mg/ml, respectively. The absorption rates, $I_a$, were calculated

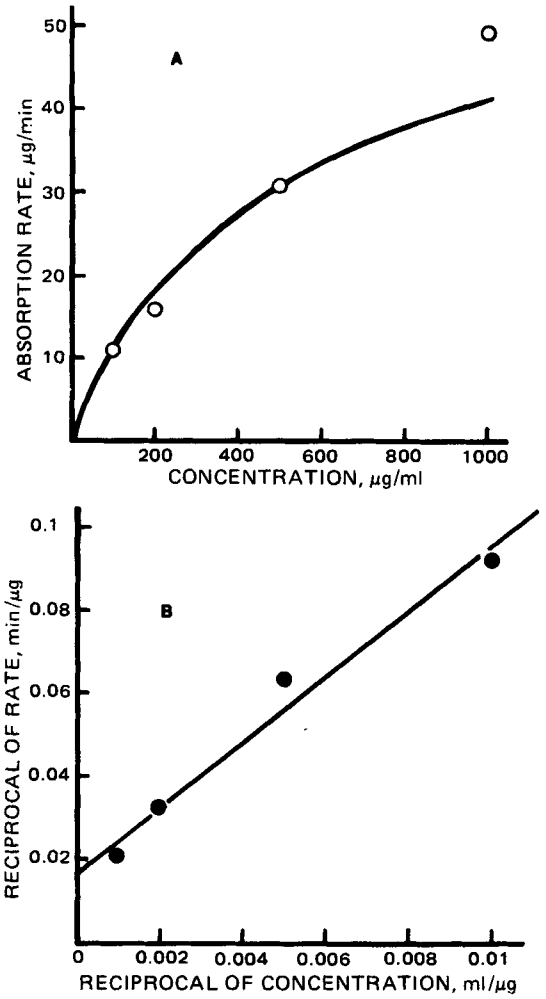


**Figure 6**—*A: Effect of drug concentration on the absorption rate of cyclacillin after rat intestinal single perfusion. B: Lineweaver–Burk plot of cyclacillin transport rate across the* in situ *rat intestinal wall to the bloodstream. The results are expressed as the means of three experiments;* $V'_{max}$ *= 3640 μg/hr and* $K_m$ *= 479 μg/ml.*

from Eq. 13 by substitution of $[C_1^{ss}]_{I_p}$ by $[C_1^{ss}]_{I_a}$ and are plotted *versus* $C_0$ in Fig. 6A. The relationship between the cyclacillin concentration perfused through the intestine, $C_0$, and the corresponding absorption rate $I_a$, demonstrated no proportionality but tended to be saturable. This finding is consistent with the fact that the disappearance of cyclacillin from the intestinal lumen in the *in situ* recirculating perfusion method followed Michaelis–Menten kinetics. If it is assumed that the net absorption of cyclacillin across the intestinal membrane is subject to a capacity-limited process at relatively low concentrations (<1.0 mg/ml), the steady-state absorption rate can be described solely by the Michaelis–Menten equation as follows:

$$I_a = \frac{V'_{max} C_0}{K_m + C_0} \qquad \text{(Eq. 15)}$$

where $V'_{max}$ is the maximal rate (micrograms per hour). A Lineweaver–Burk plot of the reciprocal of the absorption rate ($1/I_a$) *versus* the reciprocal of the cyclacillin concentration ($1/C_0$) is shown in Fig. 6B. Using the least-squares method for the plot, the calculated values of $V'_{max}$ and $K_m$ were 3640 μg/hr and 479 μg/ml, respectively, which are comparable to the values evaluated from the kinetics of disappearance from the recirculating perfusate at the same perfusion rate of 2 ml/min ($V'_{max}$ = 4520 ± 280 μg/hr[10] and $K_m$ = 420 ± 27 μg/ml).

[10] This value was estimated by multiplying $V_{max}$ by the intestinal recirculating perfusion volume of 9 ml.

## CONCLUSION

The criticism has been made that GI absorption studies of drugs based on the rate or extent of disappearance from the lumen solution utilizing proper experimental techniques *in vivo* may not necessarily reflect the net absorption into the bloodstream due to such factors as drug metabolism in the intestinal lumen and at the mocusal surface. Previous studies (2, 4) demonstrated that cyclacillin exhibited a strongly dose-dependent disappearance from rat intestinal loops, suggesting some specialized transport system. However, this finding does not exclude possible enzymatic metabolism during the absorption experiments.

The present study provided conclusive evidence that the disappearance of cyclacillin from the intestinal lumen followed simultaneous Michaelis–Menten and first-order kinetics and that cyclacillin absorption into the bloodstream was rapid and complete by comparison of both *AUC* values after intravenous and intraduodenal administration. At the dose used (10 mg/kg), the observed Michaelis–Menten kinetic term is expected to play a major role in the total disappearance from the GI lumen. Additional evidence from a pharmacokinetic analysis of the steady-state blood concentrations after constant infusion of cyclacillin into the portal vein and through the small intestinal lumen indicated that the uptake of cyclacillin by the rat intestinal tissue at relatively low concentrations of <1 mg/ml followed solely Michaelis–Menten kinetics. These results suggest that cyclacillin may be transported in the rat intestine by certain carrier systems and moved into the bloodstream without significant loss of antibiotic activity.

## REFERENCES

(1) A. Tsuji, E. Nakashima, I. Kagami, N. Honjo, and T. Yamana, *J. Pharm. Pharmacol.*, **29,** 707 (1977).

(2) A. Tsuji, E. Nakashima, I. Kagami, T. Asano, R. Nakashima, and T. Yamana, *ibid.*, **30,** 508 (1978).

(3) A. Tsuji, E. Nakashima, T. Asano, R. Nakashima, and T. Yamana, *ibid.*, **31,** 718 (1979).

(4) A. Tsuji, E. Nakashima, I. Kagami, and T. Yamana, *J. Pharm. Sci.*, **70,** 768 (1981).

(5) J. F. Quay and L. Foster, *Physiologist*, **13,** 287 (1970).

(6) J. F. Quay, *ibid.*, **15,** 241 (1972).

(7) K. Miyazaki, O. Ogino, M. Nakano, and T. Arita, *Chem. Pharm. Bull.*, **25,** 246 (1977).

(8) C. Dixon and L. W. Mizen, *J. Physiol.*, **269,** 549 (1977).

(9) M. Yasuhara, Y. Miyoshi, A. Yuasa, T. Kimura, S. Muranishi, and H. Sezaki, *Chem. Pharm. Bull.*, **25,** 675 (1977).

(10) T. Kimura, H. Endo, M. Yoshikawa, S. Muranishi, and H. Sezaki, *J. Pharm. Dyn.*, **1,** 262 (1978).

(11) J. L. DeYoung, H. G. G. Tan, H. E. Huber, and M. A. Zoglio, *J. Pharm. Sci.*, **67,** 320 (1978).

(12) H. Shindo, K. Fukuda, K. Kawai, and K. Tanaka, *J. Pharm. Dyn.*, **1,** 310 (1978).

(13) K. Umeniwa, O. Ogino, K. Miyazaki, and T. Arita, *Chem. Pharm. Bull.*, **27,** 2177 (1979).

(14) H. Freiesleben and K. Sack, *Chemotherapy (Basel)*, **22,** 75 (1976).

(15) G. H. Warren, *ibid.*, **22,** 154 (1976).

(16) S. B. Roseman, L. S. Weber, G. Owen, and G. H. Warren, *Antimicrob. Agents Chemother.-1967*, **1968,** 590.

(17) C. G. Hertz, *ibid.*, **4,** 361 (1973).

(18) C. M. Metzler, "NONLIN, A Computer Program for Parameter Estimation in Nonlinear Situations," Technical Report 729/69/7297/005, Upjohn Co., Kalamazoo, Mich.

(19) A. Tsuji, E. Miyamoto, O. Kubo, and T. Yamana, *J. Pharm. Sci.*, **68,** 812 (1979).

(20) A. C. Kind, H. N. Beaty, L. F. Fenster, and W. M. M. Kirby, *J. Lab. Clin. Med.*, **71,** 728 (1968).

(21) M. Gibaldi and S. Feldman, *J. Pharm. Sci.*, **58,** 1477 (1969).

## ACKNOWLEDGMENTS

The authors thank Miss Junko Komura and Mr. Hidemi Minami for assistance and Takeda Chemical Industries for supplying the cyclacillin.

# Xilobam: Analysis, Determination of Decomposition Products, and Assessment of Stability

C. A. JANICKI ˣ, W. D. WALKLING, R. H. ERLICH *, and C. A. BAINBRIDGE

Received September 8, 1980, from *Pharmaceutical Development, McNeil Pharmaceuticals, Spring House, PA 19477.* Accepted for publication December 10, 1980. *Present address: Bristol Laboratories, Syracuse, NY 13201.

**Abstract** □ A stability-indicating UV assay was developed for xilobam, a member of a new class of CNS agents. The method was specific, precise, and accurate. TLC and high-pressure liquid chromatography were used to support method specificity. Xilobam is sensitive to heat, moisture, and basic conditions. The degradation products were identified as *N*-methylpyrrolidone, 2,6-dimethylaniline, and *N*,*N*′-bis(2,6-dimethylphenyl)urea. At high temperatures, the incorporation of molecular sieves into glass bottles of xilobam tablets was effective in preventing decomposition caused by moisture or volatile decomposition products.

**Keyphrases** □ Xilobam—analysis, determination of decomposition products, stability assessment □ CNS agents—xilobam, analysis, determination of decomposition products, stability assessment □ Decomposition products—xilobam, analysis, stability assessment □ Muscle relaxants—xilobam, analysis, determination of decomposition products, stability assessment

Xilobam, *N*-(2,6-dimethylphenyl)-*N*′-(1-methyl-2-pyrrolidinylidene)urea, a new class of central nervous system agents, is being evaluated clinically as a skeletal muscle relaxant (1, 2). Xilobam is a sparingly soluble base with a spectrophotometrically determined pKa of 6.1. A stability-indicating assay was required to evaluate drug safety supplies and clinical dosage forms. To develop the method, it was necessary to know the various degradation products of xilobam. The isolation and identification of these degradation products and the development of a rapid spectrophotometric assay for xilobam are described. Preliminary stability data and the identification of degradation products are given for a tablet dosage form.

## EXPERIMENTAL

**Apparatus**—UV spectra were obtained using 1-cm cells on a double-beam spectrophotometer[1]. TLC plates (5 × 20 cm) were silica gel[2]. The liquid chromatograph[3] was equipped with a UV detector (254 nm), a 6000-psi pump, and a loop injector. The column was 25 cm × 2 mm i.d. stainless steel, slurry-packed with a reversed-phase $C_{18}$ packing[4]. The mobile phase was 0.1% ammonium carbonate–acetonitrile (60:40) with a 1.0-ml/min flow rate.

**Chemicals**—Solvents were analytical reagent grade. Reference standards of the degradation products were obtained[5]. The acetonitrile[6] was distilled-in-glass quality. The molecular sieves were type 4A pellets[7] (a synthesized sodium alumino silicate).

**Xilobam Degradation**—Xilobam was dissolved or mixed separately in 1 *N* HCl, 1 *N* NaOH, and water at a concentration of 10 mg/ml. The samples were heated at 80 ± 2° for 24 hr.

The tablet degradation products were extracted with methanol, chromatographed on TLC plates, isolated, and identified by IR and NMR spectroscopy and mass spectrometry.

**Intermediate Identification**—A 12.5-mg/ml solution of xilobam in methanol was prepared. Aliquots (4 ml) of the solution were diluted separately to 50 ml with pH 4.0 and 7.0 citrate–phosphate buffers. The solutions were equilibrated with 50 ml of toluene at 80° for 4 hr. The toluene layers were separated and washed with 0.1 *N* HCl to remove residual xilobam and any 2,6-dimethylaniline.

The toluene layers were dried over magnesium sulfate and then analyzed by TLC and UV and IR spectroscopy. *m*-Chloroaniline was added to the toluene layers in excess, and the mixtures were allowed to stand for 2 days. The precipitate was filtered, dried, and assayed by electron-impact mass spectrometry. A control of 2,6-dimethylphenyl isocyanate in toluene was run simultaneously.

**TLC**—Xilobam was dissolved in methanol, and the degradation compounds were dissolved in methanol or methanol–chloroform (1:1). The TLC chambers were 2-liter, wide-mouth Mason jars fitted with standard lids. The developing solvent was 0.2 *M* sodium acetate buffer (adjusted to pH 4.7)–methanol–chloroform–ethyl acetate (2.5:17.5:53:27). Each plate was developed until the solvent front was ~2.5 cm from the top of the plate. The plates were air dried and viewed under short wavelength UV light or stained with iodine vapor.

**Stability-Indicating Assay**—A sample equivalent to 100 mg of xilobam was transferred to a 120-ml screw-capped bottle to which were added exactly 50 ml of chloroform and 25 ml of 0.1 *N* NaOH. The bottle was shaken mechanically for 30 min and centrifuged, and the aqueous layer was aspirated and discarded. The chloroform layer was transferred to a clean container. A 15-ml aliquot of the chloroform layer was pipetted to a 100-ml volumetric flask, diluted to volume with chloroform, and mixed.

A 5-ml aliquot of the diluted chloroform solution was pipetted into a 60-ml screw-capped bottle containing exactly 8 ml of cyclohexane. A 50-ml aliquot of 0.1 *N* HCl was pipetted into the bottle, and the bottle was capped, shaken mechanically for 30 min, and centrifuged. The acid layer was decanted to a clean container.

A 6-ml aliquot of the acid layer was pipetted into a 25-ml volumetric flask, diluted to volume with 0.1 *N* NaOH, and mixed. The UV absorbance of the sodium hydroxide solution was recorded in 1-cm cells *versus* a solvent blank of 0.1 *N* NaOH.

A 100-mg sample of xilobam reference standard was treated as were the test samples, and its spectrum was recorded at the same time as the test samples.

The calculation was:

$$\text{percent of label amount} = \frac{A_\mu C_s}{A_s C_\mu} \times 100 \qquad \text{(Eq. 1)}$$

where $A_\mu$ and $A_s$ are the absorbance of the sample and standard, respectively, at the maximum near 245 nm and $C_\mu$ and $C_s$ are the concentrations in milligrams per milliliter of the sample and standard, respectively. The molar absorptivity at the maximum is ~23,500. A minimum occurs at 225 nm with a molar absorptivity of ~9100.

**Specificity Study**—All possible degradation products (Table I) were taken through the UV assay at a molar concentration equivalent to 100 mg of xilobam. The various tablet excipients that might be present also were assayed.

**Precision, Accuracy, and Recovery**—A stock solution of xilobam (25.27 mg/ml in methanol) was prepared. A 5-ml aliquot was added to a 120-ml screw-capped bottle, evaporated to dryness under a nitrogen stream, and assayed.

While the test samples were being assayed, a 4-ml aliquot of the stock solution was diluted to the same final concentration and solvent composition as the test samples. To assess recovery, the absorbances of these solutions were recorded and compared to the test sample absorbances.

In addition, samples of 20 tablets, each containing 200 mg of xilobam, were ground to a fine powder. Triplicate samples were weighed and assayed, and the mean and standard deviation were calculated.

**High-Pressure Liquid Chromatography (HPLC) Analysis**—

[1] Beckman Acta V.
[2] GF, Analtech, Newark, Del.
[3] Waters Associates, Milford, Mass.
[4] LiChrosorb RP-18, MCB Manufacturing Chemists.
[5] Chemical Research Department, McNeil Pharmaceuticals.
[6] Burdick & Jackson Laboratories, Muskegon, Mich.
[7] Linde, Union Carbide Corp., South Plainfield, N.J.



0022-3549/81/0700-0778$01.00/0
© 1981, American Pharmaceutical Association

Table I—TLC $R_f$ Values and HPLC Retention Times for Xilobam and Degradation Products

| Compound | TLC, $R_f$ | HPLC Retention Times, min |
|---|---|---|
| Xilobam | 0.61 | 2.1 |
| 1-Methyl-2-iminopyrrolidine fluoroborate | 0.0 | — |
| *N,N'*-Bis(2,6-dimethylphenyl)urea | 0.34 | 1.2 |
| 2,6-Dimethylaniline | 0.77 | 3.3 |
| *N*-Methylpyrrolidone | 0.55 | — |
| *N*-(2,6-Dimethylphenyl)methyl carbamate[a] | 0.74 | 2.6 |
| *N*-(2,6-Dimethylphenyl)ethyl carbamate[a] | 0.75 | 2.6 |

[a] The carbamates are not degradation products but result from reaction of 2,6-dimethylphenyl isocyanate with methanol and ethanol, respectively.

Table II—Results of Precision and Accuracy Study

| Analyst | Percent of Label Amount | |
|---|---|---|
| | Solution | Tablets |
| 1 | 96.8, 96.5 | 96.1, 95.5 |
| | 95.3, 95.4 | 95.6 |
| 2 | 98.7, 99.4 | 99.2, 99.1 |
| | 99.3 | 98.9 |
| 3 | 98.1, 98.0 | 97.6, 97.6 |
| | 97.6 | 97.5 |
| Mean | 97.5 | 97.5 |
| *SD* | 1.48 | 1.46 |

Table III—Recovery Data for Xilobam through the Assay

| Analyst | Absorbance at Maximum near 245 nm | |
|---|---|---|
| | Through Assay | Diluted Directly |
| 1 | 0.715 | 0.700 |
| | 0.713 | 0.704 |
| | 0.704 | 0.709 |
| | 0.705 | 0.709 |
| 2 | 0.709 | 0.712 |
| | 0.714 | 0.707 |
| | 0.713 | 0.709 |
| 3 | 0.712 | 0.695 |
| | 0.711 | 0.700 |
| | 0.708 | 0.703 |
| Mean | 0.710 | 0.705 |
| *SD* | 0.004 | 0.005 |

Liquid samples were diluted with methanol to a concentration of ~1 mg of xilobam/ml. A 5-ml aliquot was pipetted into a 10-ml volumetric flask, 4 ml of the internal standard solution was added, and methanol was added to volume. A 10-μl sample was injected into the chromatograph.

The internal standard was *N*-(3-chlorophenyl)-*N'*-(1-methyl-2-pyrrolidylidene)urea at a concentration of 2 mg/ml. Standard curves were obtained by plotting the peak height ratio *versus* concentration.

**pH Stability Profile**—A stock solution of xilobam (5 mg/ml in methanol) was prepared, and 4 ml was diluted to 0.1 mg/ml with buffers of varying pH. Potassium chloride–hydrochloric acid solutions were used for pH 1.0, citrate–phosphate buffers were used for pH 2.2–7.0, and glycine–sodium hydroxide buffers were used for pH 9.0–11.0. The solutions were stored at 60, 70, and 80° and were assayed for xilobam by the UV method.

## RESULTS AND DISCUSSION

**Solution Degradation Product Identification**—The acidic, basic, and aqueous hydrolysis solutions were assayed by HPLC, and assay values of 90, 0, and 0% of xilobam were obtained, respectively. By HPLC, the acidic solution gave a very large peak, which corresponded to 2,6-dimethylaniline, and two minor peaks close to the solvent peak. Sufficient solution was collected by semipreparative HPLC of the major peak, evaporated to dryness, and recrystallized; the residue was determined to be 2,6-dimethylaniline by its IR spectrum.

The basic and aqueous solutions both contained a precipitate. The precipitates were identified as *N,N'*-bis(2,6-dimethylphenyl)urea by IR and mass spectrometric analyses. The solution was chromatographed by HPLC, and the major peak was collected and purified as described. The material was identified as 2,6-dimethylaniline by IR spectrophotometry.

**Intermediate Identification**—The intermediate in xilobam decomposition was postulated to be 2,6-dimethylphenyl isocyanate. To prove this assumption, the intermediate was trapped by partitioning into toluene while xilobam was decomposed in the pH 4.0 and 7.0 solutions. The pH values represented hydrogen-ion concentrations on either side of the pKa of xilobam, which was determined spectrophotometrically to be 6.1. If different decomposition pathways occurred, it was anticipated that the different intermediates would be isolated.

The UV and IR spectra of the dried toluene layer were identical to those of 2,6-dimethylphenyl isocyanate treated similarly. TLC of the toluene layers, including the control, gave one spot each with an $R_f$ value of ~0.75, corresponding to the carbamate, formed by the *in situ* reaction with the alcohol in the mobile phase. Table I lists the $R_f$ values of the various degradation products separated from xilobam. The 2,6-dimethylphenyl isocyanate readily forms a methyl carbamate when treated with methanol. To test definitely for the isocyanate, 3-chloroaniline was added to the toluene layer. The precipitate was identified as 2,6-dimethylphenyl-3-chlorophenylurea. This compound could be formed only if the isocyanate was present in the toluene layer.

**UV Assay Specificity**—To verify assay specificity, each degradation product listed in Table I was assayed. There was no interference from any degradation product. Assay of the common tablet excipients also showed no UV interference.

**Precision, Accuracy, and Recovery**—Three analysts, to whom the stock solution concentration was unknown, assayed the solutions (Table II). The data show that the method is precise, since the standard deviation was ±1.48, and accurate, since the mean value was 97.5% of the theoretical value. A precision study also was conducted on a composite sample obtained by grinding 20 tablets. The mean from nine assays was 97.5% of the label amount with a standard deviation of 1.46.

The efficiency of the extraction was demonstrated by assaying portions of the stock solution and comparing the resulting absorbances to other portions simultaneously diluted to the same final concentration and solvent composition. The data are compared in Table III and indicate complete xilobam extraction.

**Drug Substance Stability**—Crystalline xilobam was stable for up to 3 months at 40, 60, and 40° at 80% relative humidity (RH) when stored in tight containers. Xilobam decomposed completely and rapidly at 80°. The major degradation product was identified as *N,N'*-bis(2,6-dimethylphenyl)urea.

**pH Stability Profile**—Decomposition of xilobam in solution followed first-order decomposition. The rate constants in reciprocal hours determined at 25, 60, 70, and 80° are given in Table IV. Higher pH values led to greater instability. The most stable pH range was 1–4. The calculated time in days for 10% decomposition at 25° is given in Table V.

**Dosage Form Stability**—Since xilobam hydrolyzes easily in aqueous solution, a tablet with minimum exposure to water was developed and

Table V—Estimated Time for 10% Decomposition at Room Temperature for Xilobam Solutions

| pH | Days |
|---|---|
| 2.2 | 16.1 |
| 7.0 | 8.7 |
| 11.0 | 7.2 |

Table IV—Decomposition Rate Constants of Xilobam[a]

| Temperature | pH | | | | | | | |
|---|---|---|---|---|---|---|---|---|
| | 1.0 | 2.2 | 3.0 | 4.0 | 6.0 | 7.0 | 9.0 | 11.0 |
| 80° | 0.123 | 0.140 | 0.161 | 0.239 | 1.17 | 1.32 | 1.32 | 1.37 |
| 70° | — | 0.0551 | 0.0670 | 0.0938 | 0.346 | 0.415 | 0.427 | 0.445 |
| 60° | 0.0148 | 0.0181 | 0.0204 | 0.0259 | 0.0980 | 0.101 | 0.109 | 0.110 |
| 25° (calculated) | — | 0.00027 | 0.00029 | 0.00027 | 0.00057 | 0.00050 | 0.00063 | 0.00060 |

[a] Values are in reciprocal hours.

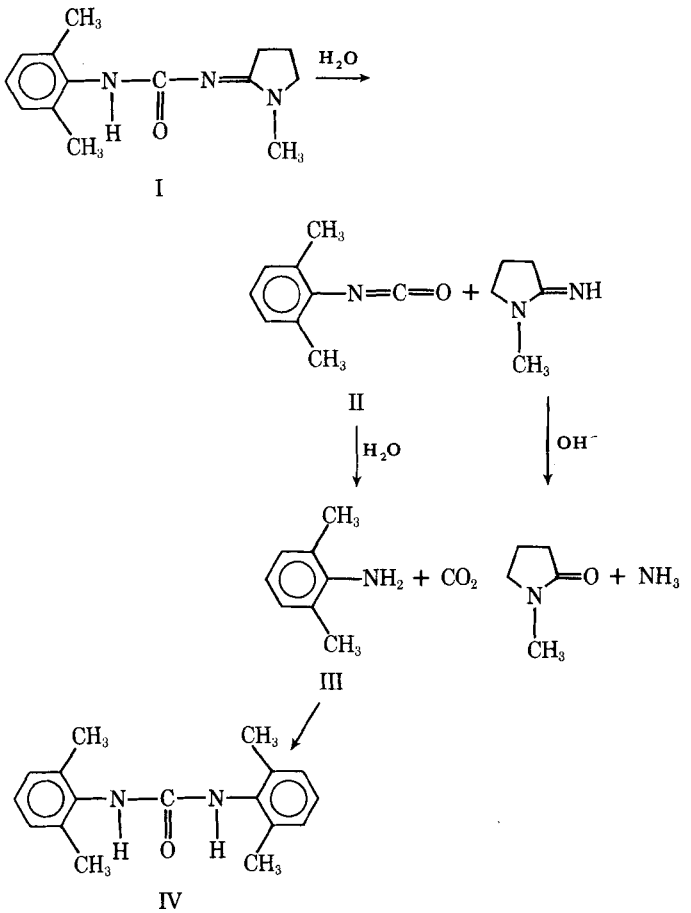

*Scheme I—Proposed decomposition pathway for xilobam.*

placed on stability. The tablets were stable at room temperature and 40° but decomposed at 40° and 80% RH and at 60° and decomposed rapidly at 80°. An odor of ammonia was noted from the decomposed samples. Tablets then were stored at 70° for 2 days in containers with and without closures. The tablets stored without closures were white and assayed satisfactorily. Tablets stored with closures were badly discolored, and

**Table VI—Xilobam Tablet Stability**

| | Percent of Label Amount (200 mg/tablet) | | | | |
|---|---|---|---|---|---|
| Days | 25° | 40° | 60° | 80° | With Molecular Sieves (80°) |
| Initial | 98.7 | 98.7 | 98.7 | 98.7 | 98.7 |
| 19 | — | — | — | — | 96.1 |
| 39 | 98.4 | 97.9 | 24.5 | 5.4 | — |
| 109 | 98.1 | 96.2 | — | — | 77.4 |

the assays showed extensive degradation. The experiment was repeated, and the headspace was analyzed by GLC–mass spectrometry. The mass spectroscopic data showed the presence of ammonia.

Molecular sieves that absorb both water and ammonia vapors were added to bottles of xilobam tablets. The tablets in amber glass bottles with standard closures were stored at 80° for 109 days. Tablets stored with molecular sieves were much more stable at 80° (Table VI). Without molecular sieves, complete degradation was observed.

The tablets that were degraded extensively were ground, extracted with methanol, and chromatographed by TLC. The separated spots were scraped from the plates; sufficient quantities were obtained to run IR, NMR, and mass spectrometric spectra. The degradation products were *N*-methylpyrrolidone, 2,6-dimethylaniline, and *N,N'*-bis(2,6-dimethylphenyl)urea. The proposed degradation pathway is given in Scheme I.

Xilobam tablets were studied for up to 2 years at 25° (room temperature) and 40° in amber glass containers. No differences were observed at these conditions for tablets stored without molecular sieves compared to those stored with molecular sieves. However, at higher temperatures, the tablets with molecular sieves were much more stable than those without them.

## REFERENCES


(1) J. F. Gardocki, W. E. Hageman, and T. P. Pruss, *Arch. Int. Pharmacodyn. Ther.*, **223**, 326 (1978).

(2) C. R. Rasmussen, J. F. Gardocki, J. N. Plampin, B. L. Twardzik, B. E. Reynolds, A. J. Molinari, N. Schwartz, W. W. Bennetts, B. E. Price, and J. Marakowski, *J. Med. Chem.*, **21**, 1044 (1978).


## ACKNOWLEDGMENTS


The authors thank J. Korpi, E. L. Kelly, H. R. Almond, R. K. Gilpin, C. Y. Ko, J. S. Ranweiler, and F. A. Chrzanowski for technical assistance.


# Studies on Drug Metabolism by Use of Isotopes XXVI: Determination of Urinary Metabolites of Rutin in Humans


**SHIGEO BABA *x, TAKASHI FURUTA *, MASANOBU HORIE *, and HISASHI NAKAGAWA ‡**



Received June 12, 1980, from the **Tokyo College of Pharmacy, 1432-1 Horinouchi, Hachioji, Tokyo 192-03, Japan*, and the ‡*Central Research Laboratory, Funai Pharmaceutical Industry, 3-11 Shodaitajika, Hirakata, Osaka, 573, Japan.* Accepted for publication December 15, 1980.



**Abstract** □ Determination of urinary metabolites of orally administered rutin and rutin-2′,5′,6′-$d_3$ in humans was carried out by TLC and GLC–mass spectrometry. In human urine, 3-hydroxyphenylacetic acid, 3-methoxy-4-hydroxyphenylacetic acid, 3,4-dihydroxyphenylacetic acid, 3,4-dihydroxytoluene, and β-*m*-hydroxyphenylhydracrylic acid were identified as rutin metabolites. Unchanged rutin and quercetin were not present in the urine.



**Keyphrases** □ Rutin—GLC–mass spectrometric analysis, urinary metabolites in humans □ GLC–mass spectrometry—analysis, urinary metabolites of rutin in humans □ Metabolites, urinary—of rutin, GLC–mass spectrometric analysis, humans


Rutin, a flavonol glycoside, has been used to treat disease states characterized by capillary bleeding associated with increased capillary fragility.

The metabolic fate of rutin has been studied extensively in animals (1–4), but there have been only a few studies in humans. Some investigators (5, 6) reported that unchanged




*0022-3549/81/0700-0780$01.00/0*


*© 1981, American Pharmaceutical Association*

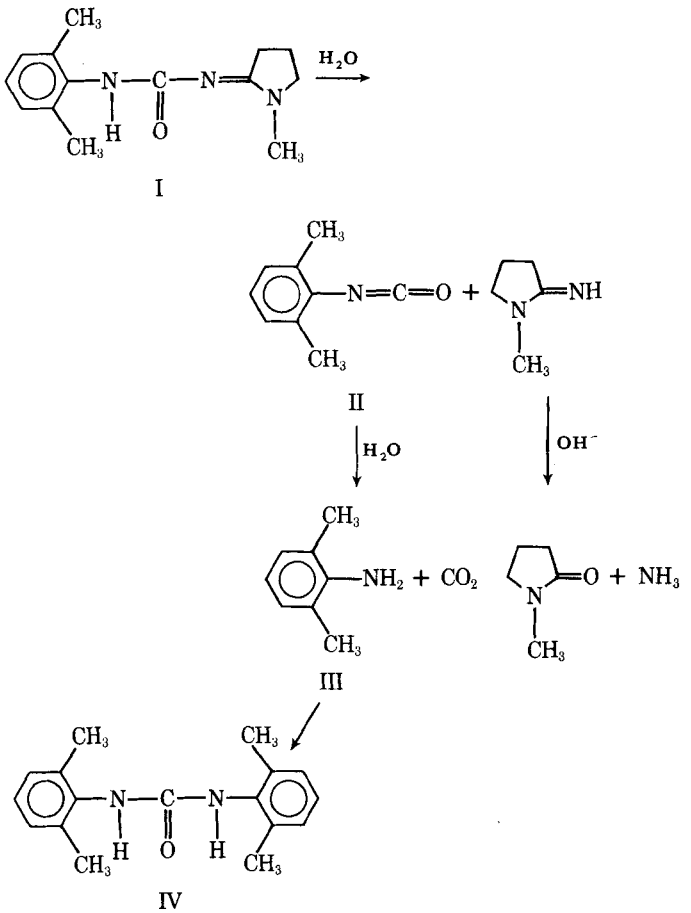

*Scheme I—Proposed decomposition pathway for xilobam.*

placed on stability. The tablets were stable at room temperature and 40° but decomposed at 40° and 80% RH and at 60° and decomposed rapidly at 80°. An odor of ammonia was noted from the decomposed samples. Tablets then were stored at 70° for 2 days in containers with and without closures. The tablets stored without closures were white and assayed satisfactorily. Tablets stored with closures were badly discolored, and

**Table VI—Xilobam Tablet Stability**

| | Percent of Label Amount (200 mg/tablet) | | | | |
|---|---|---|---|---|---|
| Days | 25° | 40° | 60° | 80° | With Molecular Sieves (80°) |
| Initial | 98.7 | 98.7 | 98.7 | 98.7 | 98.7 |
| 19 | — | — | — | — | 96.1 |
| 39 | 98.4 | 97.9 | 24.5 | 5.4 | — |
| 109 | 98.1 | 96.2 | — | — | 77.4 |

the assays showed extensive degradation. The experiment was repeated, and the headspace was analyzed by GLC–mass spectrometry. The mass spectroscopic data showed the presence of ammonia.

Molecular sieves that absorb both water and ammonia vapors were added to bottles of xilobam tablets. The tablets in amber glass bottles with standard closures were stored at 80° for 109 days. Tablets stored with molecular sieves were much more stable at 80° (Table VI). Without molecular sieves, complete degradation was observed.

The tablets that were degraded extensively were ground, extracted with methanol, and chromatographed by TLC. The separated spots were scraped from the plates; sufficient quantities were obtained to run IR, NMR, and mass spectrometric spectra. The degradation products were *N*-methylpyrrolidone, 2,6-dimethylaniline, and *N,N'*-bis(2,6-dimethylphenyl)urea. The proposed degradation pathway is given in Scheme I.

Xilobam tablets were studied for up to 2 years at 25° (room temperature) and 40° in amber glass containers. No differences were observed at these conditions for tablets stored without molecular sieves compared to those stored with molecular sieves. However, at higher temperatures, the tablets with molecular sieves were much more stable than those without them.

## REFERENCES


(1) J. F. Gardocki, W. E. Hageman, and T. P. Pruss, *Arch. Int. Pharmacodyn. Ther.*, **223**, 326 (1978).

(2) C. R. Rasmussen, J. F. Gardocki, J. N. Plampin, B. L. Twardzik, B. E. Reynolds, A. J. Molinari, N. Schwartz, W. W. Bennetts, B. E. Price, and J. Marakowski, *J. Med. Chem.*, **21**, 1044 (1978).


## ACKNOWLEDGMENTS


The authors thank J. Korpi, E. L. Kelly, H. R. Almond, R. K. Gilpin, C. Y. Ko, J. S. Ranweiler, and F. A. Chrzanowski for technical assistance.


# Studies on Drug Metabolism by Use of Isotopes XXVI: Determination of Urinary Metabolites of Rutin in Humans


**SHIGEO BABA *x, TAKASHI FURUTA *, MASANOBU HORIE *, and HISASHI NAKAGAWA ‡**



Received June 12, 1980, from the **Tokyo College of Pharmacy, 1432-1 Horinouchi, Hachioji, Tokyo 192-03, Japan*, and the ‡*Central Research Laboratory, Funai Pharmaceutical Industry, 3-11 Shodaitajika, Hirakata, Osaka, 573, Japan.* Accepted for publication December 15, 1980.



**Abstract** □ Determination of urinary metabolites of orally administered rutin and rutin-2′,5′,6′-$d_3$ in humans was carried out by TLC and GLC–mass spectrometry. In human urine, 3-hydroxyphenylacetic acid, 3-methoxy-4-hydroxyphenylacetic acid, 3,4-dihydroxyphenylacetic acid, 3,4-dihydroxytoluene, and β-*m*-hydroxyphenylhydracrylic acid were identified as rutin metabolites. Unchanged rutin and quercetin were not present in the urine.



**Keyphrases** □ Rutin—GLC–mass spectrometric analysis, urinary metabolites in humans □ GLC–mass spectrometry—analysis, urinary metabolites of rutin in humans □ Metabolites, urinary—of rutin, GLC–mass spectrometric analysis, humans


Rutin, a flavonol glycoside, has been used to treat disease states characterized by capillary bleeding associated with increased capillary fragility.

The metabolic fate of rutin has been studied extensively in animals (1–4), but there have been only a few studies in humans. Some investigators (5, 6) reported that unchanged




*0022-3549/81/0700-0780$01.00/0*


*© 1981, American Pharmaceutical Association*

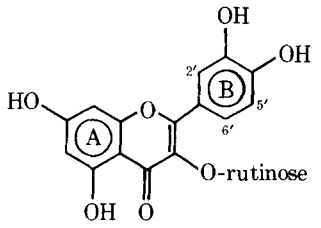


rutin

rutin and its metabolites were not present in human urine after oral administration. However, Booth *et al.* (7) identified 3-hydroxyphenylacetic acid (I), 3-methoxy-4-hydroxyphenylacetic acid (II), and 3,4-dihydroxyphenylacetic acid (III) as the urinary metabolites of rutin. The fundamental problem involved with using the method of Booth *et al.* (7) is that these compounds are excreted in the ordinary urine (8–13). Thus, an accurate determination of I–III derived from administered rutin is not possible.

A radioactive isotope tracer method is useful for metabolic studies. However, this method is inferior to a stable isotope tracer method in the structural elucidation of metabolites and in the safety in administration to humans.

This report identifies the urinary metabolites of rutin-2′,5′,6′-$d_3$ (rutin-*d*) (14) by GLC–mass spectrometry.

## EXPERIMENTAL

**Rutin and Authentic Compounds**—Rutin[1] was purified by column chromatography using cross-linked dextran gel[2] with methanol and then was recrystallized from methanol–water (1:1). Quercetin[1], 3-hydroxyphenylacetic acid[1] (I), 3-methoxy-4-hydroxyphenylacetic acid[1] (II), 3,4-dihydroxyphenylacetic acid[1] (III), 3,4-dihydroxytoluene[3] (IV), 3-(3,4-dihydroxyphenyl)propionic acid[4], and α-*p*-hydroxyphenyllactic acid[5] were obtained commercially.

β-*m*-Hydroxyphenylhydracrylic acid (V) was synthesized from β-*m*-benzyloxyphenylhydracrylic acid (mp 95°) by reductive debenzylation under hydrogen gas on 5% palladium-on-charcoal and then was recrystallized from ethyl acetate, mp 158° dec. [lit. (15) mp 159°].

*Anal.*—Calc. for $C_9H_{10}O_4$: C, 59.34; H, 5.53. Found: C, 59.38; H, 5.43.

Rutin-*d* was prepared by hydrogen exchange according to the procedure of Hiraoka *et al.* (14). PMR spectra showed the isotopic ratio of $d_1$-, $d_2$-, and $d_3$-forms in deuterium-labeled rutin prepared in these laboratories was approximately 1:6:3.

**GLC–Mass Spectrometry**—A GLC–mass spectrometer[6] and a data processing system[7] connected to a minicomputer[8] were used. The GLC system employed a 2-m × 3-mm i.d. glass column packed with 2% OV-105 on 60–80-mesh Chromosorb W; it was packed with 1.5% OV-1 on 80–100-mesh Shimalite for quercetin analysis. The column, flash heater, and separator temperatures were 160, 180, and 280°, respectively, and the helium flow rate was 20 ml/min. The mass spectrometer employed an ionization-source temperature of 310° and ionization energy of 20 ev.

One minute following injection of the sample, automatic magnet scanning was initiated, covering an *m/z* range of 50–500 every 8 sec. All scanning data were stored in the data processing system. Mass chromatograms were obtained on a digital plotter for selected mass numbers.

**Drug Administration**—Two of four healthy male volunteers received 10 mg of rutin-*d*/kg po, and the other two subjects received 50 mg of nonlabeled rutin/kg po. The test subjects were not allowed fruit and vegetables for 4 days prior to and 2 days after drug administration.

[1] Nakarai Chemicals Ltd., Kyoto, Japan.
[2] Sephadex LH-20, Pharmacia Fine Chemicals, Uppsala, Sweden.
[3] Wako Pure Chemical Industies, Tokyo, Japan.
[4] Aldrich Chemical Co., Milwaukee, Wis.
[5] Tokyo Chemical Industry, Tokyo, Japan.
[6] LKB-9000, Shimadzu Seisakusho Ltd., Kyoto, Japan.
[7] GCMSPAC-300, Shimadzu Seisakusho Ltd., Kyoto, Japan.
[8] OKITAC-4300, Oki Electric Industry Co., Tokyo, Japan.

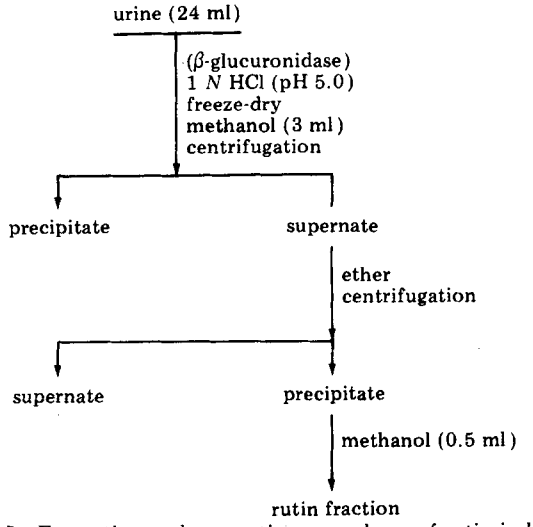


*Scheme I—Extraction and separation procedures of rutin in human urine prior to and after oral administration of rutin for TLC analysis.*

**TLC Analysis of Rutin**—Urine collections were made at 0–24 hr prior to and at 0–48 hr after administration of nonlabeled rutin. The fractionation procedure of urine samples for TLC[9] is shown in Scheme I. Conjugated metabolites were hydrolyzed by incubation with β-glucuronidase[10] (30,000 units/24 ml of urine) at 37° for 24 hr. Each ether layer thus fractionated was concentrated to dryness under reduced pressure and then was dissolved in 5 ml of methanol. An aliquot (0.1 ml) of this solution was subjected to TLC. The solvent system was *n*-butyl alcohol–acetic acid–water (4:1:2). The spots were visualized by aluminum chloride (16); rutin had an $R_f$ value of 0.45.

**Identification of Metabolites by GLC–Mass Spectrometry**—Urine was collected for 24 hr prior to and after administration of rutin-*d*. The fractionation procedure of urine samples is shown in Scheme II. The ether layer was concentrated to dryness under reduced pressure. The residue was dissolved in dry pyridine (0.1 ml) and trimethylsilylated with *N,O*-bis(trimethylsilyl)acetamide (0.05 ml) and then was subjected to the GLC–mass spectrometric computer system.

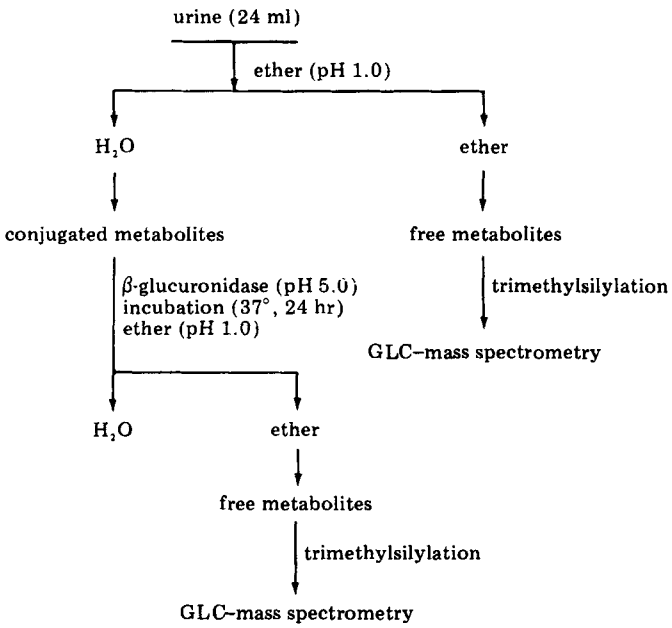


*Scheme II—Extraction and separation procedures of metabolites in human urine prior to and after oral administration of rutin-d for GLC–mass spectrometric analysis.*

[9] Merck.
[10] Type H-1, Sigma Chemical Co.

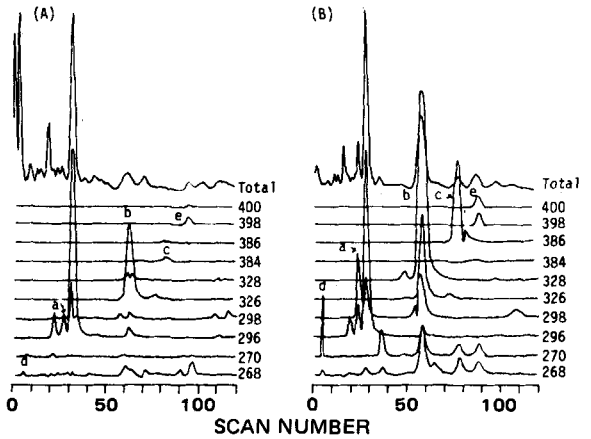


**Figure 1**—*Mass chromatograms of trimethylsilylated metabolites in human urine without β-glucuronidase hydrolysis prior to (A) and after (B) oral administration of rutin-*d. *Key: a, I [$M^+$: 296; $(M + 2)^+$: 298]; b, II [$M^+$: 326; $(M + 2)^+$: 328]; c, III [$M^+$: 384; $(M + 2)^+$: 386]; d, IV [$M^+$: 268; $(M + 2)^+$: 270]; and e, V [$M^+$: 398; $(M + 2)^+$: 400].*

## RESULTS AND DISCUSSION

**TLC Analysis of Rutin**—The rutin analysis was not performed successfully by GLC under the various conditions tested with methyl and cyanoethyl silicone phase columns. The urine samples collected prior to and after rutin administration were subjected to TLC after the extraction and separation procedures shown in Scheme I. The TLC results revealed that rutin was not detected in the urine with or without β-glucuronidase treatment. To another urine sample collected prior to rutin administration was added rutin in an amount to give a concentration of 20 μg/ml, and this sample also was subjected to TLC. In this case, rutin was detected. Therefore, excretion of rutin into the urine after rutin administration is negligible or, at least, <20 μg/ml. These findings suggest that orally administered rutin might be metabolized completely.

**Determination of Metabolites by GLC–Mass Spectrometry**—The isotopic ratio of $d_1$-, $d_2$-, and $d_3$-forms in deuterium-labeled rutin (rutin-*d*) was 1:6:3. Particular attention was paid to the $d_2$-form to determine rutin metabolites by GLC–mass spectrometry. The masses of the molecular ions of the deuterated and nondeuterated trimethylsilylated derivatives of the metabolites derived from rutin are shown in Fig. 1.

The urine samples collected prior to and after administration of rutin-*d* were subjected to trimethylsilylation with *N,O*-bis(trimethylsilyl)-acetamide and analyzed by the GLC–mass spectrometric computer system. Mass chromatograms were obtained by monitoring the molecular ions of the $d_0$- ($M^+$) and $d_2$- [$(M + 2)^+$] forms of the trimethylsilylated derivatives of possible metabolites derived from rutin. A metabolite was identified by examining the presence of duplicate peaks at the same retention time in the mass chromatogram.

Typical mass chromatograms obtained from the urine without β-glucuronidase hydrolysis are shown in Figs. 1A (prior to) and 1B (after rutin-*d* administration). The ratio of peak intensities [$(M + 2)^+$:$M^+$] shown in Fig. 1A was practically the same as that estimated from the natural abundance. On the other hand, in peaks a, b, c, and d shown in Fig. 1B, the ratios of the peak intensities [$(M + 2)^+$:$M^+$] became larger than those shown in Fig. 1A, indicating the increment of the peak intensity in the respective $(M + 2)^+$ peaks. In addition, the comparison of the peak intensity ratios of $M^+$ and $(M + 2)^+$ in the mass chromatogram peak e (Figs. 1A and 1B) indicated a clear increment of the $(M + 2)^+$ peak in Fig. 1B. These findings make it clear that orally administered rutin-*d* was metabolized to five metabolites, which also were present in the urine as endogenous metabolites.

The mass spectra corresponding to the mass chromatogram peaks a, b, and c were the trimethylsilylated derivatives of 3-hydroxyphenylacetic acid (I), 3-methoxy-4-hydroxyphenylacetic acid (II), and 3,4-dihydroxyphenylacetic acid (III), respectively. Identification was made by comparing the mass spectra and the GLC retention times of the respective mass chromatogram peaks with those of the trimethylsilylated authentic compounds.

In the mass spectrum of the mass chromatogram peak d, the ion at *m/z* 268 appeared to be the molecular ion corresponding to the trimethylsilylated derivative of 3,4-dihydroxytoluene (IV) because it was 116 mass units [$COOSi(CH_3)_3 - H$] lower than the molecular ion of the trimethylsilylated derivative of III (*m/z* 384). The GLC retention time and mass spectrum of trimethylsilylated authentic IV confirmed the structure of Metabolite d as IV. The *m/z* values of the molecular ion and fragment ion in the mass spectrum of peak d after rutin-*d* administration were 2 mass units higher than those in the mass spectrum prior to rutin-*d* administration and thus were in mass spectra a, b, and c. These findings clearly indicated that these metabolites were derived from rutin-*d*.

In the mass spectrum of the mass chromatogram peak e after rutin-*d* administration, peak intensities at *m/z* 269, 282, and 400 were larger than those estimated from the natural abundance. The metabolite, although excreted in only a small amount, should originate from rutin-*d*. This metabolite was assigned as β-*m*-hydroxyphenylhydracrylic acid (V) and was identified by comparing the GLC retention time and mass spectrum of the trimethylsilylated authentic compound. The optical rotation and the absolute configuration of this metabolite could not be determined.

These five metabolites identified in urine without β-glucuronidase hydrolysis also were found in the urine treated with β-glucuronidase.

Recently, much attention has been directed toward organic acids in human urine by the GLC–mass spectrometric computer system called "metabolic profiling" (9–13, 17). Rutin was metabolized to give four phenolic acids in human urine. The observation showed that flavonoids in plants as a diet also must be metabolized to give these types of phenolic acids in the urine.

Other possible metabolites derived from rutin-*d*, such as 3,4-dihydroxyphenylpropionic acid, α-*p*- or α-*m*-hydroxyphenyllactic acid, and β-*p*-hydroxyphenylhydracrylic acid, were excluded by the mass spectra in one investigation (18). Quercetin, an aglycone of rutin, was not found in urine. It was impossible to follow the metabolic change occurring in the A ring on which no deuterium atoms are labeled.

In this study, five metabolites (I–V) derived from orally administered rutin-*d* were differentiated from these compounds endogenously present and were successfully identified by the mass chromatographic method. These metabolites occur in urine *via* the reduction of the double bond of the γ-pyron ring (I–V) and the dehydroxylation at the 4′-position of the B ring (I and V). A study concerning the reduction in this metabolism is now in progress.

## REFERENCES

(1) O. Tamemasa, R. Goto, and S. Ogura, *Pharmacometrics*, **12**, 193 (1976).

(2) A. Barrow and L. A. Griffiths, *Xenobiotica*, **4**, 743 (1974).

(3) O. Takacs, S. Benko, L. Varga, A. Antal, and M. Gabor, *Angiologica*, **9**, 175 (1972).

(4) L. A. Griffiths and A. Barrow, *Biochem. J.*, **130**, 1161 (1972).

(5) W. L. Porter, D. F. Dicket, and J. F. Couch, *Arch. Biochem.*, **21**, 273 (1949).

(6) W. G. Clark and E. M. MacKay, *J. Am. Med. Assoc.*, **143**, 1411 (1950).

(7) A. N. Booth, C. W. Murray, F. DeEds, and F. T. Jones, *J. Biol. Chem.*, **223**, 251 (1956).

(8) M. D. Armstrong, K. N. F. Shaw, and P. E. Wall, *ibid.*, **218**, 293 (1956).

(9) S. C. Gates, M. J. Smisko, C. L. Ashendel, N. D. Young, J. F. Holland, and C. C. Sweeley, *Anal. Chem.*, **50**, 433 (1978).

(10) S. C. Gates and C. C. Sweeley, *Clin. Chem.*, **24**, 1663 (1978).

(11) S. C. Gates, N. Dendramis, and C. C. Sweeley, *ibid.*, **24**, 1674 (1978).

(12) S. C. Gates, C. C. Sweeley, W. Krivit, D. DeWitt, and B. E. Blaisdell, *ibid.*, **24**, 1680 (1978).

(13) J. A. Thompson and S. P. Markey, *Anal. Chem.*, **47**, 1313 (1975).

(14) K. Hiraoka, T. Miyamoto, S. Baba, and T. Furuta, *J. Labelled Compd. Radiopharm.*, in press.

(15) M. D. Armstrong and K. N. F. Shaw, *J. Biol. Chem.*, **225**, 269 (1957).

(16) A. Sturm, Jr., and H. W. Scheja, *J. Chromatogr.*, **16**, 194 (1964).

(17) E. Jellum, *ibid.*, **143**, 427 (1977).

(18) S. K. Wadman, C. Van Der Heiden, D. Ketting, J. P. Kamerling, and J. F. G. Vliegenthart, *Clin. Chim. Acta*, **47**, 307 (1973).

# Simultaneous High-Performance Liquid Chromatographic Determination of Theophylline, Ephedrine Hydrochloride, and Phenobarbital in Tablets

**HENRY S. I. TAN ˣ, PRAKONGSIRI C. BOONCONG, and SHARON L. FINE ***

Received June 13, 1980, from the *College of Pharmacy, University of Cincinnati–Medical Center, Cincinnati, OH 45267.* Accepted for publication December 8, 1980. *Present address: George Washington University Hospital, Washington, DC 20037.

**Abstract** □ A rapid reversed-phase high-performance liquid chromatographic (HPLC) method was developed for the simultaneous assay of theophylline, ephedrine hydrochloride, and phenobarbital in a tablet matrix. A methanolic extract of the powdered sample containing salicylamide as the internal standard was injected into the chromatograph. The HPLC system used methanol–0.007 *M* monobasic potassium phosphate (37:63, pH 2.3) as the mobile phase. Detection was at 254 nm, and quantitation was based on the drug–internal standard peak area ratio. This ratio was linear over a concentration range of 20.9–83.5 μg of theophylline, 4–15.9 μg of ephedrine hydrochloride, and 1.3–5.1 μg of phenobarbital. Overall recoveries (±*SD*) from three synthetic tablets were: theophylline, 99.8 ± 1.3%; ephedrine hydrochloride, 100.2 ± 0.6%; and phenobarbital, 99.4 ± 0.7%. The method was compared to the compendial method and also was applied to the assay of commercial tablets containing these three active ingredients. The proposed method is applicable to the assay of individual tablets.

**Keyphrases** □ High-performance liquid chromatography—simultaneous assay of theophylline, ephedrine hydrochloride, and phenobarbital □ Sedatives—simultaneous high-performance liquid chromatographic assay of theophylline, ephedrine hydrochloride, and phenobarbital □ Bronchodilators—simultaneous high-performance liquid chromatographic assay of theophylline, ephedrine hydrochloride, and phenobarbital

Tablets containing a mixture of theophylline, ephedrine hydrochloride, and phenobarbital are used as bronchodilators and sedatives. This dosage form was official in NF XIV and then was admitted to USP XX. No changes were made in the assay upon admission to USP XX, except that ephedrine sulfate instead of the hydrochloride now is used as the standard (1).

## BACKGROUND

The compendial method is laborious and time consuming (~10 hr), involving the passage of the sample solution through two liquid chromatographic columns followed by partial or complete evaporation of the several liquid fractions obtained. The method also involves solvent extraction of one of the eluates, resulting in separation of the mixture into three fractions, each containing a single drug. The fractions are measured by UV spectroscopy.

Lach *et al.* (2) analyzed these tablets by UV spectroscopy, but a separate tablet sample was required for the assay of each drug. Measurement was made after each drug was isolated from the tablet matrix by a different solvent extraction.

GLC methods for the analysis of mixtures of these three drugs in tablets or suspensions were previously reported (3, 4). In these reports, ephedrine generally was assayed separately, and the phenobarbital and theophylline were chromatographed directly after solvent extraction. Ephedrine was converted to benzaldehyde prior to chromatography by treating a second sample with periodate (3). The suspensions were assayed by separating the sample into two fractions, one containing ephedrine and the other containing theophylline and phenobarbital, which then were gas chromatographed (4).

Quantitative determinations of single entities of theophylline or phenobarbital in various dosage forms and biological samples based on reversed-phase high-performance liquid chromatography (HPLC) were published previously and reviewed (5, 6). Some reversed-phase HPLC assays for ephedrine hydrochloride also were reported (7, 8).

This paper presents the simultaneous assay of theophylline, ephedrine hydrochloride, and phenobarbital in tablet mixtures by reversed-phase HPLC with salicylamide as the internal standard. The HPLC method is simple and rapid and is also more accurate and reproducible than the compendial method.

## EXPERIMENTAL

**Apparatus**—The high-performance liquid chromatograph[1] was equipped with a constant-flow pump[2], a valve-type injector[3], a fixed-wavelength (254-nm) UV detector[4], and a strip-chart recorder[5].

**Reagents and Materials**—*l*-Ephedrine hydrochloride[6], theophylline[7], salicylamide[7], phenobarbital[8], 0.007 *M* $KH_2PO_4$ in water (adjusted to pH 2.3 with 85% aqueous phosphoric acid), and methanol[9] were used. Other chemicals used were analytical grade.

**Chromatographic Conditions**—A 25-cm × 4.5-mm i.d. 10-μm Partisil ODS II ITP column[10] was used at ambient temperature. The mobile phase was methanol–0.007 *M* $KH_2PO_4$ (pH 2.3, 37:63). This solution was filtered through a 5-μm membrane filter[11], degassed, and then pumped through the HPLC system at a rate of 1.2 ml/min. The detector was attenuated to 2.0 aufs for theophylline and salicylamide and to 0.05 aufs for ephedrine hydrochloride and phenobarbital.

**Internal Standard Solution**—The internal standard was salicylamide prepared as a 12-mg/ml solution in methanol.

**Preparation and Assay of Standard Solution**—Approximately 260 mg of theophylline, 50 mg of ephedrine hydrochloride, and 16 mg of phenobarbital were weighed accurately into a 100-ml volumetric flask. After ~25 ml of methanol was added, the mixture was placed in an ultrasonic bath for 5 min and the resulting solution was diluted to volume with methanol. Twenty milliliters of this solution was pipetted into a 25-ml volumetric flask. After addition of 1.0 ml of the internal standard solution, the solution was diluted to the mark with methanol and filtered through a 5-μm membrane filter[11]. By using a 25-μl syringe[12], three 20-μl portions of the filtrate were chromatographed under the described HPLC conditions and the average drug–salicylamide peak area ratio was determined.

**Assay of Theophylline, Ephedrine Hydrochloride, and Phenobarbital Tablets**—Twenty tablets were weighed and finely powdered. A portion of the powder equivalent to 8 mg of phenobarbital was weighed accurately and transferred to a 50-ml volumetric flask. Approximately 20 ml of methanol was added, and the mixture was placed in an ultrasonic bath for 5 min and then diluted to volume with methanol. Twenty milliliters of this mixture was pipetted into a 25-ml volumetric flask and treated as already described.

## RESULTS AND DISCUSSION

A study of theophylline, ephedrine hydrochloride, and phenobarbital tablets from 13 manufacturers revealed that 45% of the tablet lots were not chemically equivalent, indicating a need for improvement in manufacturing and quality control (2). An assay for quality control use, par-

[1] Model ALC/GPC 244, Waters Associates, Milford, Mass.
[2] Model 6000A, Waters Associates, Milford, Mass.
[3] Model U6K, Waters Associates, Milford, Mass.
[4] Model 400, Waters Associates, Milford, Mass.
[5] Omniscribe Series A-5000, Houston Instruments, Austin, Tex.
[6] Sigma Chemical Co., St. Louis, Mo.
[7] Eastman Kodak Co., Rochester, N.Y.
[8] USP grade, Merck & Co., Rahway, N.J.
[9] HPLC grade, Fisher Scientific Co., Fair Lawn, N.J.
[10] Jones Chromatography Inc., Columbus, Ohio.
[11] Mitex type LS, Millipore Corp., Bedford, Mass.
[12] Series B-110, Precision Sampling Corp., Baton Rouge, La.

0022-3549/81/0700-0783$01.00/0
© 1981, American Pharmaceutical Association

**Table I—Recovery Data from Synthetic Tablets**

| Tablet Component | Amount Weighed, mg/tablet | Amount Found[a], mg/tablet | | Average Recovery, % | |
|---|---|---|---|---|---|
| | | HPLC Method | USP XX Method | HPLC Method | USP XX Method |
| A Theophylline | 129.3 | 129.4, 129.6 | 129.2, 130.2 | 100.2 | 100.3 |
| Ephedrine hydrochloride | 24.1 | 24.0, 24.1 | 26.2, 26.3 | 99.8 | 108.5 |
| Phenobarbital | 8.1 | 8.1, 8.1 | 8.6, 8.7 | 100.0 | 106.8 |
| B Theophylline | 130.1 | 131.0, 131.3 | 131.7, 132.7 | 100.8 | 101.6 |
| Ephedrine hydrochloride | 24.1 | 24.0, 24.2 | 25.4, 26.5 | 100.0 | 107.7 |
| Phenobarbital | 8.1 | 8.0, 8.1 | 8.9, 9.1 | 99.4 | 111.1 |
| C Theophylline | 121.3 | 119.1, 119.3 | 121.4, 122.4 | 98.3 | 100.5 |
| Ephedrine hydrochloride | 23.0 | 23.2, 23.2 | 24.6, 24.7 | 100.9 | 107.2 |
| Phenobarbital | 7.6 | 7.5, 7.5 | 8.2, 8.2 | 98.7 | 107.9 |

[a] Values of duplicate assays.

**Table II—Recovery Data from Commercial Tablets[a]**

| Tablet Component | Amount Found[b], mg/tablet | | Label Claim, % | |
|---|---|---|---|---|
| | HPLC Method | USP XX Method | HPLC Method | USP XX Method |
| A Theophylline | 115.8, 116.3 | 118.4, 120.5 | 89.3 | 91.9 |
| Ephedrine hydrochloride | 24.2, 24.2 | 25.3, 25.8 | 100.8 | 106.5 |
| Phenobarbital | 7.8, 7.9 | 8.8, 8.9 | 98.2 | 110.7 |
| B Theophylline | 119.9, 121.5 | 118.5, 118.5 | 92.9 | 91.2 |
| Ephedrine hydrochloride | 24.1, 24.2 | 25.1, 25.4 | 100.6 | 105.2 |
| Phenobarbital | 8.3, 8.3 | 8.5, 8.5 | 103.8 | 106.3 |
| C Theophylline | 118.5, 119.2 | — | 91.5 | — |
| Ephedrine hydrochloride | 24.0, 24.1 | — | 100.2 | — |
| Phenobarbital | 8.3, 8.3 | — | 103.8 | — |

[a] Label claim per tablet: theophylline, 130 mg; ephedrine hydrochloride, 24 mg; and phenobarbital, 8 mg. [b] Values of duplicate assays.

ticularly for content uniformity and dissolution tests, should be simple, convenient, rapid, and accurate.

Theophylline, ephedrine hydrochloride, and phenobarbital vary greatly in acidity and polarity. In addition, the polar, strongly basic amine ephedrine has low molar absorptivity at its wavelengths of maximum absorption of 252, 257, and 263 nm. In the mobile phases that gave good symmetrical peaks for weakly acidic theophylline and phenobarbital and good separation between the three drugs at various pH values, ephedrine showed small, broad, and unsymmetrical peaks. However, the mobile phase of methanol–0.007 $M$ $KH_2PO_4$ (pH 2.3, 37:63) produced a sharp and symmetrical ephedrine peak.

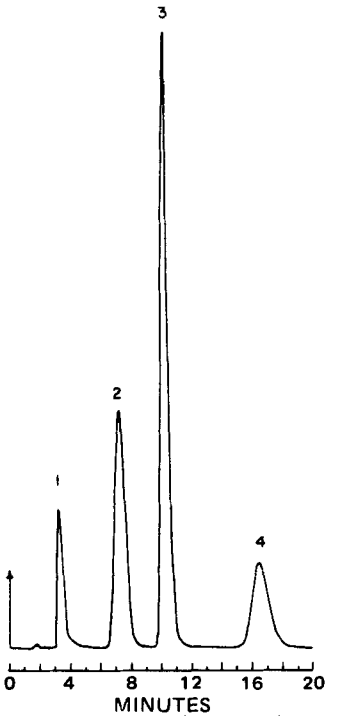


**Figure 1**—*Chromatogram of a mixture of ephedrine hydrochloride (1), theophylline (2), salicylamide (3), and phenobarbital (4) in methanol at 2.0 aufs.*

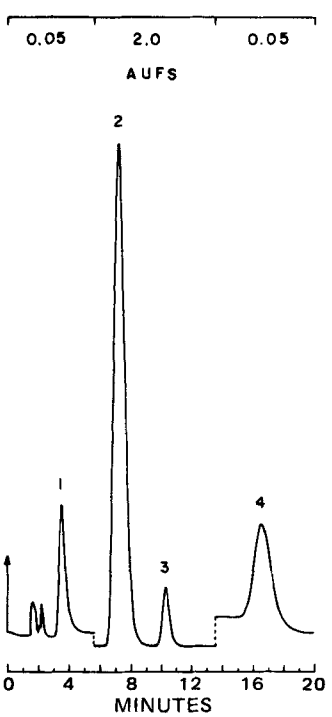


**Figure 2**—*Chromatogram of a commercial tablet. Key: 1, ephedrine hydrochloride; 2, theophylline; 3, salicylamide (internal standard); and 4, phenobarbital.*

The proposed HPLC method simultaneously assays the three drugs; the tablet sample is dissolved in methanol, and this solution is injected into the chromatograph in the presence of salicylamide as the internal standard. The peaks of the four compounds were well resolved (Fig. 1), although it was necessary to change the attenuation of the detector during the run due to the relatively lower ephedrine hydrochloride and phenobarbital concentrations. Under the experimental conditions, the retention times were: ephedrine hydrochloride, ~3.3 min; theophylline, ~7.5 min; salicylamide, ~10.5 min; and phenobarbital, ~17 min. The average height equivalent to a theoretical plate ($\pm SD$) of the column ranged from 1.47 ± 0.05 mm for ephedrine hydrochloride, to 0.80 ± 0.03 mm for theophylline, to 0.34 ± 0.02 mm for phenobarbital ($n$ = 10).

Quantitation was based on the drug–internal standard peak area ratio. With these ratios, the linearity between the detector response at 254 nm and amount of drug injected was established for the three drugs. Linearity was obtained between 20.9 and 83.5 μg of theophylline, 4 and 15.9 μg of ephedrine hydrochloride, and 1.3 and 5.1 μg of phenobarbital. The working amount was 41.6 μg of theophylline, 7.7 μg of ephedrine hydrochloride, and 2.6 μg of phenobarbital. The regression equations ($\pm SD$, $n$ = 3) for the drug–internal standard peak area ratio ($A$) and amount of drug injected ($B$, expressed in milligrams) were $A = (221.29 \pm 2.09)B + (0.90 \pm 0.11)$ for theophylline, $A = (5.24 \pm 0.13)B + (0.003 \pm 0.001)$ for ephedrine hydrochloride, and $A = (29.29 \pm 0.54)B - (0.000 \pm 0.002)$ for phenobarbital. The correlation coefficients ($\pm SD$, $n$ = 3) were 0.9987 ± 0.0009, 0.9997 ± 0.0004, and 0.9997 ± 0.0001 for theophylline, ephedrine hydrochloride, and phenobarbital, respectively.

A tablet mixture containing the same amounts of theophylline, ephedrine hydrochloride, and phenobarbital as in the commercial tablet was prepared. When the tablet placebo[13] was subjected to the assay, a small peak appeared on the chromatogram (retention time of ~2 min), which could be attributed to one or more ingredients in the placebo. No peaks were observed in the region of the peaks of salicylamide and the three active ingredients. The recovery data from the synthetic tablets are presented in Table I. The overall recoveries ($\pm SD$) from three synthetic tablet mixtures were 99.8 ± 1.3% for theophylline, 100.2 ± 0.6% for ephedrine hydrochloride, and 99.4 ± 0.7% for phenobarbital.

For comparison, the synthetic tablets also were analyzed by the compendial method. Except for theophylline, the recoveries for ephedrine hydrochloride and phenobarbital were consistently higher (Table I). The compendial overall recoveries ($\pm SD$, $n$ = 3) were 100.8 ± 0.7%, 107.8 ±

[13] The composition of the tablet placebo was: cornstarch, 52.66%; confectioners sugar, 38.89%; dextrose, 6.78%; sodium bisulfite, 0.15%; and magnesium stearate, 1.52%.

0.7%, and 108.6 ± 2.2% for theophylline, ephedrine hydrochloride, and phenobarbital, respectively.

The HPLC method was applied to the assay of commercial tablets (Table II). Again, the compendial results for ephedrine hydrochloride and phenobarbital were higher than those obtained by the proposed HPLC method. By coincidence, the theophylline content in the three commercial tablet samples investigated was low; the values were around the minimum limit of the compendial potency requirement range of 90.0–110.0% of the label claim. Figure 2 shows a typical chromatogram of the assay solution from commercial tablets.

The HPLC method is more accurate and precise and considerably less time consuming than the compendial method. The wide detector response range between theophylline and phenobarbital was due to the large difference in concentration and posed no problems. The change in the detector attenuation during the chromatographic run did not affect the results. The wide variation in polarity, which necessitated the prior separation of ephedrine in the GLC methods (4, 5), presented no problems under the proposed experimental conditions. The method also is applicable to the assay of individual tablets since the procedure is based on the quantities of drugs present in one tablet.

## REFERENCES


(1) "The United States Pharmacopeia," 20th rev., United States Pharmacopeial Convention, Rockville, Md., 1980, p. 784.

(2) J. L. Lach, T.-F. Chin, and E. L. Parrott, *Am. J. Hosp. Pharm.*, **29**, 1043 (1972).

(3) M. Elefant, L. Chafetz, and J. M. Talmage, *J. Pharm. Sci.*, **56**, 1181 (1967).

(4) H. W. Schultz and C. Paveenbampen, *ibid.*, **62**, 1995 (1973).

(5) J. L. Cohen, in "Analytical Profiles of Drug Substances," vol. 4, K. Florey, Ed., Academic, New York, N.Y., 1975, p. 466.

(6) M. K. Chao, K. S. Albert, and S. A. Fusari, in *ibid.*, vol. 7, 1978, p. 359.

(7) F. Bailey and P. N. Brittain, *J. Chromatog.*, **83**, 431 (1973).

(8) V. D. Gupta and O. H. Shek, *Am. J. Hosp. Pharm.*, **33**, 1086 (1976).


## ACKNOWLEDGMENTS


Presented at the Pharmaceutical Analysis and Control Section, APhA Academy of Pharmaceutical Sciences, St. Louis meeting, April 1981.


# Immunological Studies of Poisonous Anacardiaceae: Production of Tolerance in Guinea Pigs Using 3-*n*-Pentadecylcatechol-"Modified" Autologous Blood Cells


**EDNA S. WATSON ˣ, JAMES C. MURPHY, PHILIP W. WIRTH, MAHMOUD A. ElSOHLY, and PAUL SKIERKOWSKI**



Received July 7, 1980, from the *Research Institute of Pharmaceutical Sciences, School of Pharmacy, University of Mississippi, University, MS 38677.* Accepted for publication December 15, 1980.



**Abstract** □ The development of contact sensitivity to poison ivy urushiol in guinea pigs was prevented by intravenous injection of 3-*n*-pentadecylcatechol (I) coupled to autologous blood cells. Hartley, linebred, guinea pigs were treated with pentadecylcatechol-"modified" blood cells or sham-treated blood cells 2 weeks prior to attempted topical sensitization with I. Skin testing of all guinea pigs with 3-, 1-, and 0.3-μg doses of I applied in 5 μl of acetone to abdominal skin sites was begun 2 weeks after attempted sensitization and repeated at 2- or 4-week intervals thereafter for 6 months or until study termination. Profound tolerance to I was observed at all skin testing intervals in the group receiving haptenated red cells and did not weaken substantially with time. Contact sensitivity to I in control animals, however, waned with time; the study was terminated at 6 months because of the low sensitivity level of the control animals at that period. Complete or partial tolerance was induced in ~80% of the treated animals. The immune tolerance obtained by the single injection of pentadecylcatechol-associated red blood cells was of long duration and urushiol specific. This treatment also conferred tolerance to three unsaturated congeners of I. The allergenic potencies of the pentadecylcatechols declined with increasing saturation of the alkyl side chain. Binding studies using tritiated pentadecylcatechol showed that 81% of the activity incorporated into the red cell was membrane associated and that 19% was cell sap associated.



**Keyphrases** □ Urushiol—production of tolerance using 3-*n*-pentadecylcatechol with autologous blood cells, guinea pigs □ Poison ivy—production of tolerance to urushiol using 3-*n*-pentadecylcatechol with autologous blood cells, guinea pigs □ 3-*n*-Pentadecylcatechol—production of tolerance to urushiol, guinea pigs □ Immunology—production of tolerance to urushiol using 3-*n*-pentadecylcatechol, guinea pigs


Poison ivy (*Toxicodendron radicans*), poison oak (*T. diversilobum* and *T. quercifolium*), and poison sumac (*T. vernix*) are the main causes of contact dermatitis in the United States. One or more of these species is present in almost every state in the continental United States. These plants are so prevalent and insidious that ~80% of the U.S. population is allergic to them and 50% are clinically sensitive, *i.e.*, react to 2 μg of urushiol or less (1).

## BACKGROUND

The dermatitogenic principles contained in the resin of these plants are a group of chemically related catechols, commonly referred to as urushiols, differing mainly in the length and degree of unsaturation of the 3-*n*-alk(en)yl side chain. Poison ivy urushiol was shown to be mainly (>95%) a mixture of 3-*n*-pentadec(en)ylcatechols with zero, one, two, or three double bonds in the $C_{15}$ side chain (2–7). Poison oak urushiol, however, consists mainly (>98%) of the $C_{17}$ homologs (2, 3, 6). A small percentage of the $C_{15}$ congeners was found in poison oak urushiol, and a small percentage of the $C_{17}$ homologs was found in poison ivy components (2, 3, 6). The analysis and identification of poison sumac urushiol are incomplete.

Contact of these catechols with the skin of susceptible individuals results in sensitization to all urushiols of the plant family Anacardiaceae (8–10). Once sensitivity is developed, it is difficult, if not impossible, to eliminate. Hyposensitization by administration of plant extracts is not regularly obtained. It requires large doses and months or years to be produced, and sensitivity is rapidly regained upon cessation of treatment (10, 11). The albino guinea pig is the animal of choice for studying sensitivity to these allergens (12). Tolerance to poison ivy was reported to be produced in guinea pigs by subcutaneous injection of pentadecylcatechol (I) in mineral oil or by oral administration of large doses of I prior to attempted sensitization (13). However, since urushiols and I itself are potent primary irritants and skin sensitizers, their use for producing tolerance in nonsensitive humans is heavily compromised.

Recently, a series of ring-substituted derivatives of I was studied for potential use in the production of immune tolerance to contact sensitivity in guinea pigs (14, 15). Some 6-substituted derivatives were reported to


*0022-3549/81/0700-0785$01.00/0*


*© 1981, American Pharmaceutical Association*

0.7%, and 108.6 ± 2.2% for theophylline, ephedrine hydrochloride, and phenobarbital, respectively.

The HPLC method was applied to the assay of commercial tablets (Table II). Again, the compendial results for ephedrine hydrochloride and phenobarbital were higher than those obtained by the proposed HPLC method. By coincidence, the theophylline content in the three commercial tablet samples investigated was low; the values were around the minimum limit of the compendial potency requirement range of 90.0–110.0% of the label claim. Figure 2 shows a typical chromatogram of the assay solution from commercial tablets.

The HPLC method is more accurate and precise and considerably less time consuming than the compendial method. The wide detector response range between theophylline and phenobarbital was due to the large difference in concentration and posed no problems. The change in the detector attenuation during the chromatographic run did not affect the results. The wide variation in polarity, which necessitated the prior separation of ephedrine in the GLC methods (4, 5), presented no problems under the proposed experimental conditions. The method also is applicable to the assay of individual tablets since the procedure is based on the quantities of drugs present in one tablet.

## REFERENCES


(1) "The United States Pharmacopeia," 20th rev., United States Pharmacopeial Convention, Rockville, Md., 1980, p. 784.

(2) J. L. Lach, T.-F. Chin, and E. L. Parrott, *Am. J. Hosp. Pharm.*, **29**, 1043 (1972).

(3) M. Elefant, L. Chafetz, and J. M. Talmage, *J. Pharm. Sci.*, **56**, 1181 (1967).

(4) H. W. Schultz and C. Paveenbampen, *ibid.*, **62**, 1995 (1973).

(5) J. L. Cohen, in "Analytical Profiles of Drug Substances," vol. 4, K. Florey, Ed., Academic, New York, N.Y., 1975, p. 466.

(6) M. K. Chao, K. S. Albert, and S. A. Fusari, in *ibid.*, vol. 7, 1978, p. 359.

(7) F. Bailey and P. N. Brittain, *J. Chromatog.*, **83**, 431 (1973).

(8) V. D. Gupta and O. H. Shek, *Am. J. Hosp. Pharm.*, **33**, 1086 (1976).


## ACKNOWLEDGMENTS


Presented at the Pharmaceutical Analysis and Control Section, APhA Academy of Pharmaceutical Sciences, St. Louis meeting, April 1981.


# Immunological Studies of Poisonous Anacardiaceae: Production of Tolerance in Guinea Pigs Using 3-*n*-Pentadecylcatechol-"Modified" Autologous Blood Cells


**EDNA S. WATSON ˣ, JAMES C. MURPHY, PHILIP W. WIRTH, MAHMOUD A. ElSOHLY, and PAUL SKIERKOWSKI**



Received July 7, 1980, from the *Research Institute of Pharmaceutical Sciences, School of Pharmacy, University of Mississippi, University, MS 38677.* Accepted for publication December 15, 1980.



**Abstract** □ The development of contact sensitivity to poison ivy urushiol in guinea pigs was prevented by intravenous injection of 3-*n*-pentadecylcatechol (I) coupled to autologous blood cells. Hartley, linebred, guinea pigs were treated with pentadecylcatechol-"modified" blood cells or sham-treated blood cells 2 weeks prior to attempted topical sensitization with I. Skin testing of all guinea pigs with 3-, 1-, and 0.3-μg doses of I applied in 5 μl of acetone to abdominal skin sites was begun 2 weeks after attempted sensitization and repeated at 2- or 4-week intervals thereafter for 6 months or until study termination. Profound tolerance to I was observed at all skin testing intervals in the group receiving haptenated red cells and did not weaken substantially with time. Contact sensitivity to I in control animals, however, waned with time; the study was terminated at 6 months because of the low sensitivity level of the control animals at that period. Complete or partial tolerance was induced in ~80% of the treated animals. The immune tolerance obtained by the single injection of pentadecylcatechol-associated red blood cells was of long duration and urushiol specific. This treatment also conferred tolerance to three unsaturated congeners of I. The allergenic potencies of the pentadecylcatechols declined with increasing saturation of the alkyl side chain. Binding studies using tritiated pentadecylcatechol showed that 81% of the activity incorporated into the red cell was membrane associated and that 19% was cell sap associated.



**Keyphrases** □ Urushiol—production of tolerance using 3-*n*-pentadecylcatechol with autologous blood cells, guinea pigs □ Poison ivy—production of tolerance to urushiol using 3-*n*-pentadecylcatechol with autologous blood cells, guinea pigs □ 3-*n*-Pentadecylcatechol—production of tolerance to urushiol, guinea pigs □ Immunology—production of tolerance to urushiol using 3-*n*-pentadecylcatechol, guinea pigs


Poison ivy (*Toxicodendron radicans*), poison oak (*T. diversilobum* and *T. quercifolium*), and poison sumac (*T. vernix*) are the main causes of contact dermatitis in the United States. One or more of these species is present in almost every state in the continental United States. These plants are so prevalent and insidious that ~80% of the U.S. population is allergic to them and 50% are clinically sensitive, *i.e.*, react to 2 μg of urushiol or less (1).

## BACKGROUND

The dermatitogenic principles contained in the resin of these plants are a group of chemically related catechols, commonly referred to as urushiols, differing mainly in the length and degree of unsaturation of the 3-*n*-alk(en)yl side chain. Poison ivy urushiol was shown to be mainly (>95%) a mixture of 3-*n*-pentadec(en)ylcatechols with zero, one, two, or three double bonds in the $C_{15}$ side chain (2–7). Poison oak urushiol, however, consists mainly (>98%) of the $C_{17}$ homologs (2, 3, 6). A small percentage of the $C_{15}$ congeners was found in poison oak urushiol, and a small percentage of the $C_{17}$ homologs was found in poison ivy components (2, 3, 6). The analysis and identification of poison sumac urushiol are incomplete.

Contact of these catechols with the skin of susceptible individuals results in sensitization to all urushiols of the plant family Anacardiaceae (8–10). Once sensitivity is developed, it is difficult, if not impossible, to eliminate. Hyposensitization by administration of plant extracts is not regularly obtained. It requires large doses and months or years to be produced, and sensitivity is rapidly regained upon cessation of treatment (10, 11). The albino guinea pig is the animal of choice for studying sensitivity to these allergens (12). Tolerance to poison ivy was reported to be produced in guinea pigs by subcutaneous injection of pentadecylcatechol (I) in mineral oil or by oral administration of large doses of I prior to attempted sensitization (13). However, since urushiols and I itself are potent primary irritants and skin sensitizers, their use for producing tolerance in nonsensitive humans is heavily compromised.

Recently, a series of ring-substituted derivatives of I was studied for potential use in the production of immune tolerance to contact sensitivity in guinea pigs (14, 15). Some 6-substituted derivatives were reported to


*0022-3549/81/0700-0785$01.00/0*


*© 1981, American Pharmaceutical Association*

**Table I—Evaluation of Skin Test Responses Using Draize Scoring System [a]**

| Response | Value |
|---|---|
| No erythema | 0 |
| Erythema and eschar formation | |
| Very slight erythema (barely perceptible) | 1 |
| Well-defined erythema | 2 |
| Moderate to severe erythema | 3 |
| Severe erythema (beet redness) to slight eschar formation (injury in depth) | 4 |
| No edema | 0 |
| Very slight edema (barely perceptible) | 1 |
| Slight edema (edges of area well defined by definite raising) | 2 |
| Moderate edema (area raised ~1 mm) | 3 |
| Severe edema (raised ~1 mm and extending beyond area of exposure) | 4 |

[a] Maximum summed erythema and edema scores = 8.

produce tolerance to I and to have low sensitizing and skin irritation potential (14).

Recent studies showed that sensitization to contact sensitizers by the cutaneous route requires presentation of the contact allergen to the immune system by Langerhans cells present in the skin (16). When initial exposure is oral or parenteral by routes other than topical, immune tolerance to the sensitizer usually develops (14, 17, 18).

The discovery that intravenous injection of some skin sensitizers or closely related chemicals would prevent subsequent sensitization to the sensitizer suggested that the resulting tolerance may be mediated by coupling of the hapten with some blood components (19). Subsequent studies showed that membrane-coupled antigen (haptenated spleen, red, lymph node, thymic, or peritoneal exudate cells) is the tolerogenic form (20, 21).

The present report describes the induction of tolerance to poison ivy urushiol by intravenous injection of pentadecylcatechol-associated autologous red blood cells 2 weeks prior to attempted contact sensitization with I. Tolerance to the mono-, di-, and triolefinic congeners of I also was produced by this treatment. Tolerance induced by pentadecylcatechol-associated red cells was specific for poison ivy urushiol and not due to a general lack of immunocompetence of the tolerized animals. Radioisotopic studies using tritiated pentadecylcatechol as tracer showed that the majority of cell-bound pentadecylcatechol (81%) was associated with the red cell membrane and that the remainder was associated with the soluble cell sap.

## EXPERIMENTAL

**Animals**—Female, Camm-Hartley[1], line-bred guinea pigs, 450–500 g, were used. Guinea pig food[2] and water supplemented with ascorbic acid were provided *ad libitum*.

**Preparation of Pentadecylcatechol**—Poison ivy urushiol purified as in a previous study (3) was reduced by catalytic hydrogenation, and the resulting pentadecylcatechol was purified by passage over a dry silica gel 60 (2) column with chloroform as the eluting solvent. Fractions were collected and tested for I using 1% alcoholic ferric chloride. Fractions containing I were combined, and the solvent was evaporated. The resulting residue was chromatographed on a MN-polyamide SC 6[3] column (particle size <0.07 mm) with 90% ethanol–water as the eluting solvent. Fractions containing I were combined. The solvent was evaporated, and the residue was crystallized from hexane to give colorless needle crystals of I, mp 58–59°. The identity of I was determined by GLC and GC–mass spectrometry.

**Preparation of Poison Ivy Urushiol Congeners**—The mono-, di-, and triolefinic components of poison ivy urushiol were isolated from purified poison ivy extract by converting the urushiol to its acetate derivative with acetic anhydride and pyridine. Urushiol acetate was passed over a silica gel G column impregnated with 5% $AgNO_3$, using 1% methanol in chloroform as the solvent system. The polarity of the eluting solvent was increased gradually to 4% methanol in chloroform; fractions containing the mono-, di-, or triolefinic congener acetates were pooled based on their TLC similarities in silver nitrate-impregnated silica gel plates. Each olefinic acetate was converted to the corresponding allergenically active congener by hydrolysis with sodium carbonate in dioxane–water solution (4:1). The reaction mixture was neutralized, and the free catechols were ether extracted. The identity and purity of the olefinic congeners were determined by GLC and GC–mass spectral analysis of the trimethylsilyl derivatives (22).

**Table II—Method for Calculation of Degree of Delayed-Type Hypersensitivity**

| | Erythema and Edema Scores | | | | | |
|---|---|---|---|---|---|---|
| | 24 hr | | 48 hr | | 72 hr | |
| Animal | Erythema | Edema | Erythema | Edema | Erythema | Edema |
| Group A | | | | | | |
| 01 | 0 | 0 | 2 | 1 | 2 | 0 |
| 02 | 1 | 0 | 3 | 2 | 3 | 1 |
| 03 | 0 | 0 | 0 | 0 | 0 | 0 |
| 04 | 2 | 2 | 4 | 4 | 4 | 3 |
| Average (number of responders = 3) | 1.0 | 0.6 | 3 | 2.3 | 3 | 1.3 |
| Erythema and edema sum | 1.6 | | 5.3 | | 4.3 | |
| *Degree of delayed-type hypersensitivity = 4.4* | | | | | | |

**Tritiated Pentadecylcatechol**—Fifty milligrams of I containing 50 μg of the triolefinic congener, 3-*n*-pentadeca-8,11,14-trienylcatechol, was tritium reduced[4]. The specific activity was 10.6 mCi/mg.

**Pentadecylcatechol Solutions**—Solutions used for red cell modification consisted of 2 mg of I/ml of propylene glycol. Sensitizing solutions of I were prepared in acetone at a concentration of 1 mg/0.15 ml. All skin test solutions were prepared in acetone to contain 3, 1, or 0.3 μg of I/5 μl, except for the olefinic congeners which were prepared in acetone at 3 μg/5 μl. All solutions were analyzed for purity prior to use.

**Preparation and Injection of Pentadecylcatechol-"Modified" and Sham-Treated Red Blood Cells**—Guinea pigs were anesthetized with ether, and a 3-ml blood sample was withdrawn from each animal by cardiac puncture into heparinized syringes. To remove serum proteins, the blood cells were washed three successive times with 10-ml volumes of normal saline followed by 600×*g* centrifugation. The washed, packed red cells were resuspended in 40 ml of normal saline. Propylene glycol (0.5 ml) was added to the control cell suspensions, and 1 mg of I in 0.5 ml of propylene glycol was added to the I-treated cell suspensions.

The cell suspensions were mixed by inversion and incubated 1 hr at 37°. Cells were removed from suspension by centrifugation and washed three times with normal saline to remove unbound I. After washing, the hapten-modified or sham-treated red cells were resuspended to 3 ml with saline and injected into the marginal ear vein of the animal of cell origin. Guinea pigs were anesthetized intramuscularly with 50 mg of ketamine[5]/kg and 0.5 mg of chlorpromazine[6]/kg prior to injection.

**Sensitization**—Sensitization of all animals to I was attempted 2 weeks after haptenated or sham-treated red cell injection by topical application of 1 mg of I to the dorsal neck skin of ~5 $cm^2$. Animals were sensitized to dinitrochlorobenzene[7] by applying 2 μl of a 50% acetone solution of dinitrochlorobenzene to the dorsal surface of the left ear.

**Skin Testing**—Hair was removed from the abdominal skin with small animal clippers[8]. Test sites, ~1.5 × 1.5 cm, were delineated with a felt-tip pen[9], and 5 μl of a test solution or vehicle was dropped from a syringe[10] onto the skin within the sites. Sites not visibly healed from previous testing were not used for retesting. The test sites were observed and scored for presence and intensity of erythema and edema at 24, 48, and 72 hr after testing, using the scoring system of Draize *et al.* (23) (Table I). To compare the intensity of the inflammation of the responding sites of treated and control animals, the degree of delayed-type hypersensitivity for each group to the individual test doses was calculated. The erythema scores of the responding animals in each group were summed and divided by the number of animals in the group responding at 24, 48, and 72 hr. The edema scores of each group were averaged similarly. The averaged erythema and edema scores were added to obtain a 24-, 48-, and 72-hr value. The final degree of delayed-type hypersensitivity for each group was obtained by averaging the 24-, 48-, and 72-hr summed values as in Table II. The score of 8 is the maximal degree of delayed-type hy-

[1] Camm Institute, Wayne, N.J.
[2] Ralston-Purina, St. Louis, Mo.
[3] Brinkmann Instruments, Westbury, N.Y.
[4] New England Nuclear, Boston, Mass.
[5] Ketaset, Bristol Myers Co., Syracuse, N.Y.
[6] Thorazine, Smith Kline & French Laboratories, Philadelphia, Pa.
[7] Aldrich, Milwaukee, Wis.
[8] Angra clippers, John Oster Manufacturing Co., Milwaukee, Wis.
[9] Markette, Crestwood, Wilkes-Barre, Pa.
[10] Hamilton.

persensitivity attainable. To skin test for dinitrochlorobenzene sensitivity, a drop of 0.5% dinitrochlorobenzene in olive oil was inuncted into the flank with a glass rod; the sites were observed for presence of erythema at 24 hr after testing.

**Data Analysis**—Differences in the number of experimental and control animals presenting erythema responses to pentadecylcatechol were analyzed using $\chi^2$ statistics. The data for each test period were arranged in a 2 × 2, treatment by response, contingency table. A null hypothesis of equal proportionality was tested using one degree of freedom.

## RESULTS AND DISCUSSION

Red blood cells were either pentadecylcatechol modified or sham treated *in vitro* as described and injected intravenously into the guinea pig of cell origin 2 weeks prior to attempted sensitization with I. Groups of animals given haptenated or sham-treated red cells received identical treatment throughout the study. Pentadecylcatechol-modified red cell-induced tolerance was duplicated in five separate experiments, using a total of 55 treated and 40 control animals, with similar results. Data from two of these experiments were selected for this paper.

**Induction of Tolerance to I with Pentadecylcatechol-Modified Red Cells**—Twenty-four naive guinea pigs were injected with autologous pentadecylcatechol-modified red cells, and a similar control group was given autologous sham-treated red cells intravenously. Sensitization of both groups to I was attempted 2 weeks after treatment. A third group of 10 guinea pigs (negative controls) was not pretreated or sensitized. Two weeks after attempted sensitization and at 2- or 4-week intervals thereafter until the conclusion of the study, all animals were skin tested simultaneously with 3, 1, and 0.3 μg of I and with acetone. Test sites not visibly healed were not used. Since no erythema or edema was observed on any acetone test site, the vehicle control data were omitted.

To represent the skin test responses of each group concisely, the percentage of the animals in each group presenting erythema on one or more of the three observation periods (24, 48, and 72 hr) to the three test doses is shown in Table III. Injection of hapten–red cell conjugates 2 weeks prior to attempted sensitization to I produced a high level of tolerance to skin test doses of I that persisted for 20 weeks. The frequency of reactivity of the control group to the 3 μg of I ranged from 70 to 100% throughout the study, while the percentage responding in the haptenated red cell-treated group ranged from 21 to 33%. The reactivity of the control group to 1 μg of I ranged from 63 to 83%, whereas 0–17% of the group treated with haptenated red cells were sensitive to this test dose. None of the treated animals ever reacted to 0.3 μg of I at any time during the study, while the sensitivity of the control group to this dose ranged from 4 to 46%. Tolerance to I did not appear to wane with time but was partially broken by the second attempt at sensitization after the 20th week. However, the sensitivity of the controls tended to decrease slowly after the 8-week test period and was not strengthened by the second sensitizing dose.

The sensitivity of the pentadecylcatechol-modified red cell-treated animals ranged from complete tolerance to moderate sensitivity, whereas the control group responses were moderate to extreme. The tolerance of seven of the treated animals was complete in that they never responded to any test dose of I during the entire study. Six of the treated animals responded only once during the study, and these responses were +1 erythema to 3 μg of I. Four treated animals responded on two skin test periods to 3 μg of I; these responses were mainly +1 erythema, but an occasional +2 erythema was observed. Two additional treated animals responded to 3 μg of I on four or five of the nine test periods; most of these responses were +2 erythema with rarely a +1 edema. The remaining five treated animals (20%) were not perceivably tolerant and responded to 3 μg of I on nearly every occasion. These animals also responded occasionally to 1 μg of I.

Overall, the data indicate that 80% of the treated group was tolerant to I from the 20 weeks following attempted sensitization to I. Testing of 10 naive guinea pigs with the three test solutions resulted in primary irritancy responses in two out of the 10 animals to 3 μg of I. Since this dose was found by others to be irritating in ~50% of naive animals tested, the occasional responses to this dose in the treated animals may represent false positive responses. Only two animals in the control group failed to respond to doses of <3 μg.

To compare the differences in sensitivity of the treated and control animals, the degree of delayed-type hypersensitivity for each group was calculated (Table IV). The sensitivity of the responding animals in the control group gradually declined after the 6-week test and was not increased by a second sensitizing dose at Week 20. The sensitivity of the responding animals in the treated group, on the other hand, gradually increased until the 14th week, and a second attempt at sensitization did not increase their sensitivity.

Statistical analysis of the data showed that at the 3-μg test level, significant differences existed between the treated and control groups

**Table III—Occurrence of Erythema to 3-, 1-, and 0.3-μg Test Doses of Pentadecylcatechol in Pentadecylcatechol-Modified Red Cell-Treated and Sham-Treated Guinea Pigs**

| Treatment | Weeks[a] | Percent of Group with Definite Erythema Response to Test Doses of Pentadecylcatechol | | |
|---|---|---|---|---|
| | | 3 μg | 1 μg | 0.3 μg |
| Hapten-modified red cell | 2 | 33 | 0 | 0 |
| Control | 2 | 96 | 63 | 38 |
| Hapten-modified red cell | 4 | 33 | 0 | 0 |
| Control | 4 | 100 | 79 | 38 |
| Hapten-modified red cell | 6 | 21 | 4 | 0 |
| Control | 6 | 92 | 71 | 29 |
| Hapten-modified red cell | 8 | 21 | 8 | 0 |
| Control | 8 | 92 | 71 | 17 |
| Hapten-modified red cell | 10 | 29 | 8 | 0 |
| Control | 10 | 88 | 67 | 33 |
| Hapten-modified red cell | 14 | 33 | 17 | 4 |
| Control | 14 | 92 | 71 | 46 |
| Hapten-modified red cell | 16 | 26 | 13 | 0 |
| Control | 16 | 88 | 83 | 42 |
| Hapten-modified red cell | 20 | 26 | 9 | 0 |
| Control | 20 | 70 | 43 | 4 |
| Hapten-modified red cell | 24[b] | 52 | 22 | 0 |
| Control | 24[b] | 95 | 43 | 10 |

[a] Weeks after attempted sensitization to pentadecylcatechol. [b] A second sensitizing dose of pentadecylcatechol was given to both groups after the 20-week test period.

**Table IV—Average Degree of Delayed-Type Hypersensitivity to Pentadecylcatechol-Modified or Sham-Treated Red Cells 2 Weeks prior to Attempted Sensitization to Pentadecylcatechol**

| Treatment | Weeks[a] | Average Degree of Delayed-Type Hypersensitivity to Test Doses of Pentadecylcatechol | | |
|---|---|---|---|---|
| | | 3 μg | 1 μg | 0.3 μg |
| Hapten-modified red cell | 2 | 0.8 (8/24)[b] | 0.0 (0/24) | 0.0 (0/24) |
| Control | 2 | 3.4 (23/24) | 2.0 (15/24) | 0.8 (9/24) |
| Hapten-modified red cell | 4 | 0.9 (8/24) | 0.0 (0/24) | 0.0 (0/24) |
| Control | 4 | 3.5 (24/24) | 2.1 (19/24) | 0.8 (9/24) |
| Hapten-modified red cell | 6 | 1.1 (5/24) | 0.3 (1/24) | 0.0 (0/24) |
| Control | 6 | 3.8 (22/24) | 2.1 (17/24) | 0.3 (7/24) |
| Hapten-modified red cell | 8 | 1.6 (5/24) | 0.5 (2/24) | 0.0 (0/24) |
| Control | 8 | 2.8 (22/24) | 1.8 (17/24) | 0.9 (4/24) |
| Hapten-modified red cell | 10 | 1.4 (7/24) | 0.5 (2/24) | 0.0 (0/24) |
| Control | 10 | 2.2 (21/24) | 1.5 (16/24) | 0.7 (8/24) |
| Hapten-modified red cell | 14 | 1.7 (8/24) | 1.1 (4/24) | 0.0 (0/24) |
| Control | 14 | 2.5 (22/24) | 1.2 (17/24) | 0.8 (11/24) |
| Hapten-modified red cell | 16 | 1.7 (6/23) | 1.0 (3/23) | 0.0 (0/23) |
| Control | 16 | 1.7 (21/24) | 1.3 (20/24) | 0.6 (10/24) |
| Hapten-modified red cell | 20[c] | 1.3 (6/23) | 1.2 (2/23) | 0.0 (0/23) |
| Control | 20[c] | 2.1 (16/23) | 0.8 (10/23) | 0.7 (1/23) |
| Hapten-modified red cell | 24 | 1.4 (12/23) | 1.3 (5/23) | 0.0 (0/23) |
| Control | 24 | 1.7 (20/21) | 0.6 (9/21) | 0.7 (2/21) |

[a] Weeks after attempted sensitization to pentadecylcatechol. [b] Number of responders per number tested in parentheses. [c] A second sensitizing dose was applied after this test.

**Table V—Occurrence of Erythema Reactions to Pentadecylcatechol (I) and Its Olefinic Congeners in Pentadecylcatechol-Modified Red Cell-Treated and Sham-Treated Control Animals**

| Treatment | Weeks[a] | Percent of Group with Definite Erythema Response to Test Doses of I or Its Olefinic Congeners | | | | | |
|---|---|---|---|---|---|---|---|
| | | I | | | Monoolefin, | Diolefin, | Triolefin, |
| | | 3 μg | 1 μg | 0.3 μg | 3 μg | 3 μg | 3 μg |
| Pentadecylcatechol-modified red cell | 2 | 23[b] | 15 | 0 | NT[c] | NT | NT |
| Control | 2 | 88 | 25 | 0 | NT | NT | NT |
| Pentadecylcatechol-modified red cell | 4 | 15[b] | 0 | 0 | NT | NT | NT |
| Control | 4 | 75 | 38 | 0 | NT | NT | NT |
| Pentadecylcatechol-modified red cell | 6 | 15[b] | NT | NT | 15[d] | 15[d] | 15[d] |
| Control | 6 | 100 | NT | NT | 100 | 100 | 100 |
| Pentadecylcatechol-modified red cell | 8 | 18[b] | NT | NT | 18[b] | 18[b] | 36[b] |
| Control | 8 | 88 | NT | NT | 88 | 100 | 100 |

[a] Weeks after attempted sensitization with pentadecylcatechol. [b] $p < 0.01$. [c] Not tested. [d] $p < 0.001$.

**Table VI—Degree of Delayed-Type Hypersensitivity of Pentadecylcatechol-Modified (E) or Sham-Treated Control (C) Groups of Guinea Pigs to Pentadecylcatechol (I) and Its Olefinic Congeners**

| Treatment | Weeks[a] | Skin Test Substances | | | | | |
|---|---|---|---|---|---|---|---|
| | | I | | | Monoolefin, | Diolefin, | Triolefin, |
| | | 3 μg | 1 μg | 0.3 μg | 3 μg | 3 μg | 3 μg |
| E | 2 | 1.5 | 0.3 | 0 | NT[b] | NT | NT |
| C | 2 | 1.7 | 1.0 | 0 | NT | NT | NT |
| E | 4 | 1.0 | 0.0 | 0 | NT | NT | NT |
| C | 4 | 1.0 | 0.8 | 0 | NT | NT | NT |
| E | 6 | 0.8 | NT | NT | 2.2 | 1.8 | 2.8 |
| C | 6 | 1.1 | NT | NT | 1.7 | 2.0 | 2.8 |
| E | 8 | 1.0 | NT | NT | 1.2 | 1.1 | 3.1 |
| C | 8 | 1.6 | NT | NT | 1.2 | 1.9 | 3.1 |

[a] Weeks after attempted sensitization. [b] Not tested.

throughout the entire 24 weeks. At the 1-μg dose level, significant differences were observed over the first 14 weeks. Loss of significance at the 20 and 24th weeks to the 1-μg test level apparently resulted from a loss of sensitivity in the control group rather than from a loss of tolerance in the experimental group. At the 0.3-μg dose level, the differences in tolerant and control groups were not consistently significant due to the paucity of responses in the control group.

To show that tolerance to I was caused by haptenated red cell treatment and not by lack of immunocompetence, all treated animals were given sensitizing doses of dinitrochlorobenzene after the initial skin test with I. The control guinea pigs were not given sensitizing doses and served as negative dinitrochlorobenzene controls. None of the control group responded to dinitrochlorobenzene whereas all of the treated tolerant animals developed sensitivity to it. Therefore, tolerance induced by pentadecylcatechol-modified red cell injection was immunologically specific.

**Specificity of Pentadecylcatechol-Induced Sensitivity and Pentadecylcatechol-Modified Red Cell-Induced Tolerance**—A group of 11 guinea pigs was given tolerizing injections of haptenated red cells, and a control group of eight was given sham-treated red cells. Sensitization of both groups to I was attempted 2 weeks later. Both groups were skin tested with 3-, 1-, and 0.3-μg doses of I and with vehicle at 2 and 4 weeks after attempted sensitization. At 6 and 8 weeks after attempted sensitization, each group was tested with 3 μg each of I and its mono-, di-, and triolefinic congeners. The frequency of erythema responses of these animals to the skin test doses are shown in Table V. Animals were scored as reactive if erythema was observed at least once during the 72-hr observation period after test substance application.

The degree of delayed-type hypersensitivity of treated and control groups to I and its congeners was calculated as previously described and is shown in Table VI. All control animals developed sensitivity to I and its three congeners, but the skin reactions to the different congeners were not of equal severity. The degree of delayed-type hypersensitivity produced by triolefin was two to three times that produced by I. The degree of delayed-type hypersensitivity decreased with increased saturation of the side chain. The order of allergenic potency was triolefin > diolefin > monoolefin > I. The haptenated red cell-treated pigs were highly tolerant to I and its congeners throughout the 8 weeks of study. The differences in sensitivity of the treated and control groups were highly significant ($p < 0.01$ or $<0.001$) at the 3-μg level of I and its congeners throughout the 8 weeks. Differences were not significant at the 1- and 0.3-μg doses of I because of lack of a high degree of sensitivity of control animals. Over 80% of the treated animals in this experiment were tolerant, which confirms the results of the previous study. Again, two animals in the treated group (15%) did not develop tolerance.

**Table VII—Determination of Radioactivity Associated with Intact Tritiated Pentadecylcatechol Red Cell Conjugates, Red Cell Membrane Ghosts, and Red Cell Sap[a]**

| | Tritium, μCi | | Percent of Total Activity | | Percent of Incorporated Activity | |
|---|---|---|---|---|---|---|
| Unincorporated (incubation supernate) | 3.29 | | 47.0 | | | |
| First wash (supernate) | 0.28 | | 4.0 | | | |
| Second wash (supernate) | 0.15 | | 2.5 | | | |
| Third wash (supernate) | 0.09 | | 1.9 | | | |
| Total unincorporated | | 3.81 | | 55.4 | | |
| Incorporated | | | | | | |
| Lysate of whole cells | 0.24 | | 3.4 | | 12.7 | |
| Wash of ghosts | 0.12 | | 1.7 | | 6.3 | |
| Total cell sap | | 0.36 | | 5.1 | | 19.0 |
| Red cell ghost | | 1.53 | | 21.95 | | 80.9 |
| Total recovered activity | | 5.70 | | 82.45 | | 99.9 |

[a] Total activity added to suspension was 7 μCi.

**Determination of Membrane-Associated Pentadecylcatechol**—Tritium-labeled pentadecylcatechol red cell conjugates were prepared to determine the percentage of I that became bound to the red cell and the localization of I (membrane associated or cell sap associated). Cell suspensions were incubated with 1 mg of I (7 μCi of tritiated pentadecylcatechol). After removal of the incubation supernate (unincorporated activity) followed by three successive washes, aliquots of the conjugates were used to determine the radioactivity incorporated into the intact cells or they were lysed with hypotonic solution, and the activity associated with the red cell membrane ghosts and cell sap was determined.

The determinations were made on four separate cell suspensions with essentially the same results. The results of a typical assay are shown in Table VII. Twenty-seven percent of the activity (equivalent to 270 μg of I) became associated with the red cell. Fifty-five percent of the activity was in the incubation mixture, and the remaining 17.5% was believed to have been retained in the incubation vessel. Approximately 81% of the red cell-incorporated activity (equivalent to 219 μg of I) was associated

with the red cell membrane. The remaining 19% was associated with the red cell sap and represented ~51 μg of I.

It was reported that membrane-associated urushiol or I (red blood cell or lymphocyte membrane associated) will induce blastogenesis of peripheral blood lymphocytes *in vitro* (24). Urushiol was shown to be highly soluble in, but not covalently bound to, the cell membrane since the urushiol was not removed from the membrane with aqueous washes but was removable with dimethyl sulfoxide. Haptenated membranes were shown to induce contact sensitivity to picryl chloride *in vitro* when administered subcutaneously (25), while intravenous administration of the haptenated membranes induced specific immunological tolerance. Thus, the administration route of the membrane-associated hapten appears to be important in determining whether contact sensitivity or tolerance will result.

Since haptenated membranes can induce hapten-specific tolerance as well as contact sensitivity, it is unlikely that the haptenated membrane is the tolerogen and sensitizer. The membrane probably serves as a physiological vehicle that carries the lipophilic substance until the immune system intercepts the hapten. Whether contact sensitivity or tolerance results probably depends on the prevalence of the interceptor cell type (macrophage, Langerhans cell, T-lymphocyte, B-lymphocyte) that initially reacts with the hapten. The route of hapten administration likely would favor a higher incidence of interaction of the hapten with one of these cell types.

## REFERENCES


(1) W. L. Epstein, *Cutis*, **13**, 544 (1974).

(2) S. Billets, J. C. Craig, M. D. Corbett, and J. F. Vickery, *Phytochemistry*, **15**, 533 (1976).

(3) M. D. Corbett and S. Billets, *J. Pharm. Sci.*, **64**, 1715 (1975).

(4) W. F. Symes and C. R. Dawson, *J. Am. Chem. Soc.*, **76**, 2959 (1954).

(5) S. V. Sunthankar and C. R. Dawson, *ibid.*, **76**, 5070 (1954).

(6) K. H. Markiewitz and C. R. Dawson, *J. Org. Chem.*, **30**, 1610 (1965).

(7) M. Gross, H. Baer, and H. M. Fales, *Phytochemistry*, **14**, 2263 (1975).

(8) R. A. Johnson, H. Baer, C. A. Kirkpatrick, C. R. Dawson, and R. G. Khurana, *J. Allergy Clin. Immunol.*, **49**, 27 (1972).

(9) H. Keil, D. Wasserman, and C. R. Dawson, *Science*, **102**, 279 (1954).

(10) A. M. Kligman, *Arch. Dermatol.*, **78**, 47 (1958).

(11) W. L. Epstein, H. Baer, C. R. Dawson, and R. G. Khurana, *ibid.*, **109**, 356 (1974).

(12) H. Baer and M. Hooton, in "Animal Models in Dermatology," H. I. Maibach, Ed., Churchill Livingstone, New York, N.Y., 1975, pp. 53–55.

(13) R. T. Bowser and H. Baer, *J. Immunol.*, **91**, 791 (1963).

(14) H. Baer, M. L. Hooton, C. R. Dawson, and D. I. Lerner, *J. Invest. Dermatol.*, **69**, 215 (1977).

(15) D. Lerner, *Diss. Abstr. Int. B*, **37**(7), 3419 (1977).

(16) U. Forsiem, L. Klareskog, U. M. Tjernlund, and P. A. Peterson, *Acta Derm. Venereol. Suppl.*, **79**, 37 (1978).

(17) M. W. Chase, *Proc. Soc. Exp. Biol. Med.*, **61**, 257 (1946).

(18) I. Silberberg-Sinakin and R. L. Baer, *Prog. Allergy*, **24**, 268 (1978).

(19) J. R. Battisto and J. Miller, *Proc. Soc. Exp. Biol. Med.*, **111**, 111 (1962).

(20) J. R. Battisto and B. R. Bloom, *Nature (London)*, **212**, 156 (1966).

(21) H. N. Claman, S. D. Miller, and J. W. Moorehead, *Cold Spring Harbor Symp. Quant. Biol.*, **41**, 105 (1977).

(22) J. C. Craig, C. W. Waller, S. Billets, and M. A. ElSohly, *J. Pharm. Sci.*, **67**, 483 (1978).

(23) H. H. Draize, G. Woodward, and H. D. Calvery, *J. Pharmacol. Exp. Ther.*, **82**, 377 (1944).

(24) V. S. Byers, W. L. Epstein, N. Castagnoli, and H. Baer, *J. Clin. Invest.*, **64**, 1437 (1979).

(25) M. I. Greene, S. M. Sugimoto, and B. Benacerraf, *J. Immunol.*, **120**, 1604 (1978).


## ACKNOWLEDGMENTS


The authors thank Ms. Mary Rungeling for technical assistance in preparation of this manuscript.


# Laser Raman Investigation of Pharmaceutical Solids: Griseofulvin and Its Solvates


**BARBARA A. BOLTON and PARAS N. PRASAD** ˣ



Received July 24, 1980, from the *Department of Chemistry, State University of New York at Buffalo, Buffalo, NY 14214.* Accepted for publication December 16, 1980.



**Abstract** □ Laser Raman spectroscopy is convenient for characterizing griseofulvin solvates and investigating solute–solvent interactions and desolvation. The spectra of both lattice and intramolecular vibrations were monitored. A new solvate of griseofulvin with bromoform was characterized by Raman spectroscopy. A temperature-dependence study of the solvates of griseofulvin with chloroform, bromoform, and benzene revealed no phase transformation or chemical change. In the benzene solvate, only weak Van der Waals interactions existed between the solute and solvent. However, in solvates with chloroform and bromoform, a weak hydrogen bonding existed between the proton of the solvent and the C=O group of the benzofuran ring in griseofulvin. Examination of desolvation in these solvates revealed that the crystal did not go through any intermediate structure during desolvation. As the solvent molecule escaped, the lattice reverted to the structure of unsolvated griseofulvin.



**Keyphrases** □ Griseofulvin—unsolvated and solvate forms, laser Raman spectroscopy, physicochemical stability, desolvation □ Spectroscopy, laser Raman—investigation of griseofulvin and its solvates, physicochemical stability, desolvation □ Pharmaceutical solids, polymorphic—griseofulvin and its solvates, investigation using laser Raman spectroscopy, physicochemical stability, desolvation □ Antifungal agents—griseofulvin and its solvates, investigation with laser Raman spectroscopy, physicochemical stability, desolvation


Many drugs in the solid state exhibit polymorphism, in which the same compound exists in several crystalline modifications at the same temperature (1, 2). Interest in polymorphism stems from the fact that different crystalline modifications of the same drug have different physical and, in some cases, chemical properties that may be a serious consideration in the manufacture of the dosage form (1, 2). For example, differences in the solubility of polymorphic forms can cause serious bioavailability problems.


*0022-3549/81/0700-0789$01.00/0*


*© 1981, American Pharmaceutical Association*

with the red cell membrane. The remaining 19% was associated with the red cell sap and represented ~51 μg of I.

It was reported that membrane-associated urushiol or I (red blood cell or lymphocyte membrane associated) will induce blastogenesis of peripheral blood lymphocytes *in vitro* (24). Urushiol was shown to be highly soluble in, but not covalently bound to, the cell membrane since the urushiol was not removed from the membrane with aqueous washes but was removable with dimethyl sulfoxide. Haptenated membranes were shown to induce contact sensitivity to picryl chloride *in vitro* when administered subcutaneously (25), while intravenous administration of the haptenated membranes induced specific immunological tolerance. Thus, the administration route of the membrane-associated hapten appears to be important in determining whether contact sensitivity or tolerance will result.

Since haptenated membranes can induce hapten-specific tolerance as well as contact sensitivity, it is unlikely that the haptenated membrane is the tolerogen and sensitizer. The membrane probably serves as a physiological vehicle that carries the lipophilic substance until the immune system intercepts the hapten. Whether contact sensitivity or tolerance results probably depends on the prevalence of the interceptor cell type (macrophage, Langerhans cell, T-lymphocyte, B-lymphocyte) that initially reacts with the hapten. The route of hapten administration likely would favor a higher incidence of interaction of the hapten with one of these cell types.

## REFERENCES


(1) W. L. Epstein, *Cutis*, **13**, 544 (1974).

(2) S. Billets, J. C. Craig, M. D. Corbett, and J. F. Vickery, *Phytochemistry*, **15**, 533 (1976).

(3) M. D. Corbett and S. Billets, *J. Pharm. Sci.*, **64**, 1715 (1975).

(4) W. F. Symes and C. R. Dawson, *J. Am. Chem. Soc.*, **76**, 2959 (1954).

(5) S. V. Sunthankar and C. R. Dawson, *ibid.*, **76**, 5070 (1954).

(6) K. H. Markiewitz and C. R. Dawson, *J. Org. Chem.*, **30**, 1610 (1965).

(7) M. Gross, H. Baer, and H. M. Fales, *Phytochemistry*, **14**, 2263 (1975).

(8) R. A. Johnson, H. Baer, C. A. Kirkpatrick, C. R. Dawson, and R. G. Khurana, *J. Allergy Clin. Immunol.*, **49**, 27 (1972).

(9) H. Keil, D. Wasserman, and C. R. Dawson, *Science*, **102**, 279 (1954).

(10) A. M. Kligman, *Arch. Dermatol.*, **78**, 47 (1958).

(11) W. L. Epstein, H. Baer, C. R. Dawson, and R. G. Khurana, *ibid.*, **109**, 356 (1974).

(12) H. Baer and M. Hooton, in "Animal Models in Dermatology," H. I. Maibach, Ed., Churchill Livingstone, New York, N.Y., 1975, pp. 53–55.

(13) R. T. Bowser and H. Baer, *J. Immunol.*, **91**, 791 (1963).

(14) H. Baer, M. L. Hooton, C. R. Dawson, and D. I. Lerner, *J. Invest. Dermatol.*, **69**, 215 (1977).

(15) D. Lerner, *Diss. Abstr. Int. B*, **37**(7), 3419 (1977).

(16) U. Forsiem, L. Klareskog, U. M. Tjernlund, and P. A. Peterson, *Acta Derm. Venereol. Suppl.*, **79**, 37 (1978).

(17) M. W. Chase, *Proc. Soc. Exp. Biol. Med.*, **61**, 257 (1946).

(18) I. Silberberg-Sinakin and R. L. Baer, *Prog. Allergy*, **24**, 268 (1978).

(19) J. R. Battisto and J. Miller, *Proc. Soc. Exp. Biol. Med.*, **111**, 111 (1962).

(20) J. R. Battisto and B. R. Bloom, *Nature (London)*, **212**, 156 (1966).

(21) H. N. Claman, S. D. Miller, and J. W. Moorehead, *Cold Spring Harbor Symp. Quant. Biol.*, **41**, 105 (1977).

(22) J. C. Craig, C. W. Waller, S. Billets, and M. A. ElSohly, *J. Pharm. Sci.*, **67**, 483 (1978).

(23) H. H. Draize, G. Woodward, and H. D. Calvery, *J. Pharmacol. Exp. Ther.*, **82**, 377 (1944).

(24) V. S. Byers, W. L. Epstein, N. Castagnoli, and H. Baer, *J. Clin. Invest.*, **64**, 1437 (1979).

(25) M. I. Greene, S. M. Sugimoto, and B. Benacerraf, *J. Immunol.*, **120**, 1604 (1978).


## ACKNOWLEDGMENTS


The authors thank Ms. Mary Rungeling for technical assistance in preparation of this manuscript.


# Laser Raman Investigation of Pharmaceutical Solids: Griseofulvin and Its Solvates


**BARBARA A. BOLTON and PARAS N. PRASAD** ˣ



Received July 24, 1980, from the *Department of Chemistry, State University of New York at Buffalo, Buffalo, NY 14214.* Accepted for publication December 16, 1980.



**Abstract** □ Laser Raman spectroscopy is convenient for characterizing griseofulvin solvates and investigating solute–solvent interactions and desolvation. The spectra of both lattice and intramolecular vibrations were monitored. A new solvate of griseofulvin with bromoform was characterized by Raman spectroscopy. A temperature-dependence study of the solvates of griseofulvin with chloroform, bromoform, and benzene revealed no phase transformation or chemical change. In the benzene solvate, only weak Van der Waals interactions existed between the solute and solvent. However, in solvates with chloroform and bromoform, a weak hydrogen bonding existed between the proton of the solvent and the C=O group of the benzofuran ring in griseofulvin. Examination of desolvation in these solvates revealed that the crystal did not go through any intermediate structure during desolvation. As the solvent molecule escaped, the lattice reverted to the structure of unsolvated griseofulvin.



**Keyphrases** □ Griseofulvin—unsolvated and solvate forms, laser Raman spectroscopy, physicochemical stability, desolvation □ Spectroscopy, laser Raman—investigation of griseofulvin and its solvates, physicochemical stability, desolvation □ Pharmaceutical solids, polymorphic—griseofulvin and its solvates, investigation using laser Raman spectroscopy, physicochemical stability, desolvation □ Antifungal agents—griseofulvin and its solvates, investigation with laser Raman spectroscopy, physicochemical stability, desolvation


Many drugs in the solid state exhibit polymorphism, in which the same compound exists in several crystalline modifications at the same temperature (1, 2). Interest in polymorphism stems from the fact that different crystalline modifications of the same drug have different physical and, in some cases, chemical properties that may be a serious consideration in the manufacture of the dosage form (1, 2). For example, differences in the solubility of polymorphic forms can cause serious bioavailability problems.


*0022-3549/81/0700-0789$01.00/0*


*© 1981, American Pharmaceutical Association*

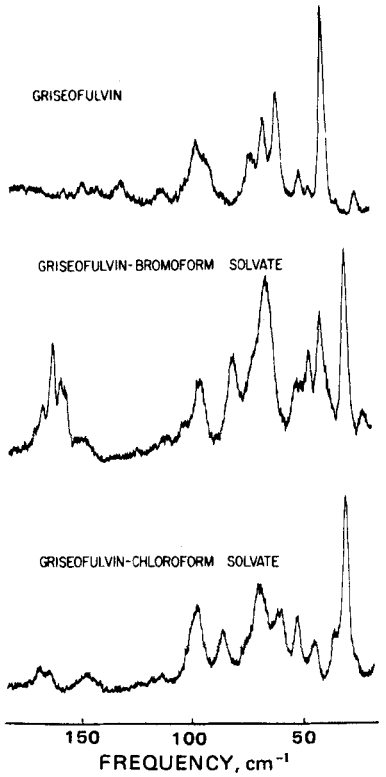


**Figure 1**—*Raman spectra of the lattice vibrations of the unsolvated griseofulvin and the griseofulvin solvates with chloroform and bromoform at 135°K.*

## BACKGROUND

The present study examined polymorphism exhibited by griseofulvin, which is used in the treatment of fungus infection (3). This compound in the solid state exists in the unsolvated form, and its solvates with chloroform (4, 5) and benzene (6) have been studied by various techniques. Reducing the particle size of griseofulvin enhances its GI tract absorption (3, 4). Particle-size reduction can be obtained by desolvating the solvates of griseofulvin. Thus, study of the stability of the solvates, the solute–solvent interaction, and the desolvation process is of great importance.

Normally, the methods used to characterize polymorphs are X-ray diffraction, optical and electron microscopy, thermal methods (differential thermal analysis, differential scanning calorimetry, and thermal gravimetric analysis), and IR spectroscopy of the internal vibrations (1, 2). Recently, Raman spectroscopy of lattice vibrations was introduced to study the polymorphism of pharmaceutical solids (7). The lattice vibrations (also called phonons) correspond to librations and translations of the entire molecule in the lattice. These vibrations are of low frequency (10–150 $cm^{-1}$) and are easily observed in the Raman spectra. The lattice vibrations are characteristic of the crystal structure and interactions. Thus, the Raman spectra of the lattice vibrations can be used to characterize the solid states of a drug and to study the stabilities of various crystalline modifications (8–10).

The Raman spectra of intramolecular vibrations also can be obtained in the same experimental arrangement. Intramolecular vibrations can be used to study both the specific nature of the solute–solvent interaction and the chemical stability of the various forms. The present study was based on the principle that a physical transformation in the solid state shows a dominant effect on the phonon spectra but only a small effect on intramolecular vibrations. On the other hand, a chemical change leads to a large change in both the phonon spectra and the spectra of intramolecular vibrations.

Laser Raman spectroscopy was used for the following investigations on griseofulvin: (*a*) the characterization and identification of unsolvated griseofulvin and its various solvates, (*b*) the physical and chemical stability of these solvates with changes of external conditions such as temperature, (*c*) the effect of chemical perturbation (*e.g.*, change of a substituent group) on the crystal structure, (*d*) the nature of solute–solvent interactions in a solvate, and (*e*) the process of solvate desolvation.

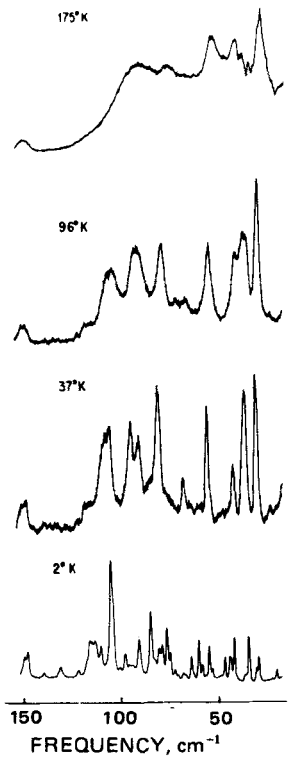


**Figure 2**—*Lattice vibration Raman spectra of the benzene solvate at several temperatures.*

## EXPERIMENTAL

The griseofulvin[1] solvates were grown from benzene (protonated and deuterated), chloroform (protonated and deuterated), and bromoform[2]. The chloroform and bromoform solvates were readily formed by slow solvent evaporation and were air stable for days. To obtain the benzene solvates, between 0.06 and 0.08 g of griseofulvin was added to 5 ml (±5%) of benzene. While the 5-ml volume was maintained, the solution was heated to boiling (~75°). When all of the griseofulvin was dissolved, the solution was transferred to a warmed beaker and checked for any visible matter. This hot solution was cooled rapidly in an ice bath to 10–15°. When this temperature was maintained for 24 hr, only the benzene solvate of griseofulvin was formed. This solvate was stable in air for only a few hours.

Raman spectra were obtained using a double monochromator[3] and the 5145-Å line of a coherent radiation argon-ion laser. Most samples were studied below room temperature because of the improved spectral resolution. Spectra were taken with the sample in liquid nitrogen or by cooling the sample with a flow of nitrogen vapor that provided an effective bath of ~125°K or higher. To obtain spectra below the liquid nitrogen temperature, crystals were cooled in a cryostat[4] using a flow of helium vapor. The spectra of the benzene solvates were taken at 2°K. To obtain this temperature, a vacuum was pulled on liquid helium, forming a superfluid state. The temperature was measured with a chromel-constantan thermocouple referenced at an ice bath. Direct-current detection was used. The band positions were measured relative to the laser line and were accurate to ±1.0 $cm^{-1}$.

## RESULTS AND DISCUSSION

The following discussion emphasizes the aspects rather than the specific system investigated.

**Characterization of Various Solvates**—Raman spectra of the phonon region provide unambiguous characterization of the various crystalline modifications of a given substance. For this purpose, the observed phonon spectral patterns were used. The spectral pattern is defined by the number of peaks observed and their frequencies and relative intensities. Although relative intensities may show some variations de-

[1] McNeil Laboratories.
[2] Aldrich Chemical Co.
[3] Spex model 14018.
[4] 10 DT Janis Research Supervaritemp.

pendent on crystal orientation, use of a polycrystalline or powdered sample helps minimize this problem and provides reproducible spectral patterns that can identify and distinguish between various polymorphs. On the other hand, the internal vibration region (which also can be investigated using IR techniques) generally shows only small shifts in frequencies and only in selected regions.

The results of phonon spectral studies to characterize griseofulvin and its chloroform and benzene solvates were reported previously (7); the present study investigated other solvates. Griseofulvin also was reported to form a solvate with dioxane (6); however, the phonon spectra obtained on crystals grown from dioxane solution were identical to those of unsolvated griseofulvin. Thus, no evidence of solvate formation with dioxane was found.

An attempt was made to form a solvate with bromoform. As shown in Fig. 1, the Raman phonon spectra of the samples obtained from chloroform and bromoform solutions clearly are different from those of the unsolvated griseofulvin. Again, the low temperature (135°K) spectra provided improved resolution of peaks (Fig. 1) and assisted in the comparison. Thus, the crystalline modification obtained from bromoform was different from that of the unsolvated griseofulvin. The presence of the solvent (bromoform) internal vibration in the internal vibration region also confirmed the formation of a solvate between bromoform and griseofulvin. This solvate was never reported previously.

**Temperature Study of Crystalline Forms**—The phonon spectra of griseofulvin and its solvates were studied from room temperature down to liquid helium temperature (2°K). As the temperature was lowered, more structures became resolved due to the reduced linewidth of the peaks, and the phonon frequencies shifted to higher values. Figure 2 shows the spectra at several temperatures for the benzene solvate in the 10–150-$cm^{-1}$ spectral region. In this region the benzene solvate showed nine resolved peaks at 96°K and 33 resolved peaks at 2°K. On the other hand, 12 peaks were observed for the chloroform solvates at 136°K, but only 31 peaks were observed for the same solvate at liquid helium temperature.

Except for the increased number of peaks due to improved resolution, the number of spectral features of each crystalline form remained the same as the temperature was varied; *i.e.*, there was no spectra discontinuity. This result clearly indicates absence of any structural phase transitions or any chemical change for either griseofulvin or any of the solvates studied. A phase transition or a chemical change will clearly reveal itself by a change in the spectral pattern of the phonon region (9, 10).

The reduction in linewidths of the peaks and the shift of frequencies with temperature are general phenomena that arise primarily from the anharmonicity of the lattice (11, 12). The temperature dependence of the phonon frequencies is derived mainly from thermal expansion of the lattice which, in turn, is a consequence of lattice anharmonicity (11). The observed effect clearly indicates a considerable degree of lattice anharmonicity for these crystals. The linewidths of the peaks reflect the contribution from disorders in the lattice as well as from anharmonic phonon–phonon interactions (12). The line broadening derived from disorder can be assumed to be temperature independent, but the broadening due to anharmonic phonon–phonon interactions is highly temperature dependent. Thus, a temperature-dependence study of the linewidth can be used to investigate the presence of disorder in the lattice (12). For griseofulvin and its solvates, the linewidths were highly dependent on temperature. At 2°K, the lines were narrow, indicating highly-ordered lattices.

**Chemical Perturbation of Crystal Structure**—It often becomes necessary to improve a drug by changing a substituent group in the molecular structure. However, since bioavailability is dependent on the crystal structure of the compound, it is helpful to know how the parent compound's crystal structure is affected by chemical substitution. A previous investigation on organic solids suggested that Raman spectroscopy can provide useful information in this area (13, 14). If a small chemical perturbation (changing only a small substituent group in the parent structure) yields a crystal structure that is identical (in space group) to the parent crystal structure, the phonon spectral pattern bears a close correspondence with that of the parent material.

For griseofulvin, this criterion was used to obtain information regarding the crystal structure of the new bromoform solvate. The bromoform solvate can be visualized as being derived from the chloroform solvate by chemical substitution of the chloroform. The phonon spectra of these two solvates at 135°K are compared in Fig. 1. Except for the shifts in phonon frequencies, there appeared to be close correspondence between the phonon peaks in the spectra of the two solvates, suggesting that they have the same crystal structures. The phonon frequencies in the bromoform solvate were lower than those for the chloroform solvate. This shift to lower frequencies was perhaps a result of a larger unit cell required by a larger solvent molecule (bromoform compared to chloroform).

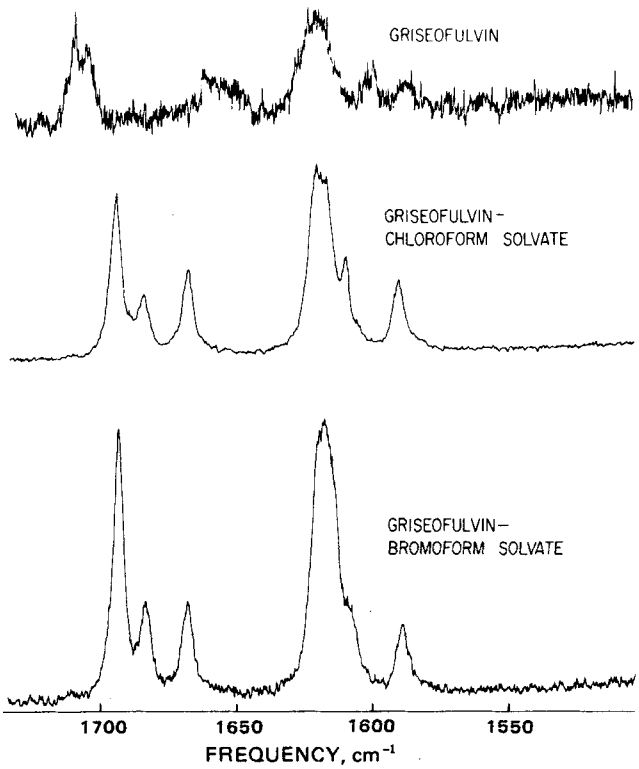


**Figure 3**—*Raman spectra of the chloroform and bromoform solvates obtained for the 1550–1800-$cm^{-1}$ spectral region.*

**Solute–Solvent Interactions**—To investigate the interaction between the griseofulvin molecule and the solvents involved in solvate formation, a comparative study of the internal vibrational frequencies of various functional groups of the drug and the solvent molecule was needed in the solvate as well as in the pure states.

The internal vibrational spectra of the benzene solvate appeared to be essentially a superposition of the spectra of pure griseofulvin and benzene. The frequency shifts of the vibrations of both components were <3 $cm^{-1}$. The solvate spectra contained no additional bands other than those observed for the pure components. Since these shifts were small, the interaction between griseofulvin and benzene was weak and of a Van der Waals type. A manifestation of this weak interaction was the loss of benzene when the griseofulvin–benzene solvate was exposed to the atmosphere. After 24 hr, an unsealed sample exhibited a spectrum identical to that of the unsolvated griseofulvin.

In the 200–1550-$cm^{-1}$ region, the chloroform and bromoform solvates exhibited a behavior similar to that of the benzene solvate. The spectra were essentially a superposition of those of the pure components. Two spectral regions showed changes: 1550–1800 and 2800–3200 $cm^{-1}$. Figure 3 shows that the 1703.5- and 1708.5-$cm^{-1}$ bands of pure griseofulvin shifted to 1684.0 and 1694.5 $cm^{-1}$ in the chloroform solvate. A similar observation was noted for the bromoform solvate where a slightly larger shift occurred. These vibrational frequencies correspond to the C=O stretching modes of the benzofuran ring of griseofulvin.

Table I shows the analysis of the C–H stretching region (2800–3200 $cm^{-1}$) of the bromoform solvate and the chloroform (deuterated and protonated) solvates. Except for the transitions at 2998 $cm^{-1}$, there was a 1:1 correlation between the three solvates. The pure chloroform-*h* solvent transition at 3011.0 $cm^{-1}$ shifted by 13 $cm^{-1}$ to 2998.0 $cm^{-1}$ in the solvate. Pure bromoform solvent transition at 3023.0 $cm^{-1}$ shifted by 24 $cm^{-1}$ to 2999.5 $cm^{-1}$. In both cases, there was a shift of the C–H stretching mode of the solvent in the solvate.

These results indicate a specific interaction between the C–H group of the solvents and the C=O group of griseofulvin and, possibly, a weak hydrogen bonding between H– –O. This result is consistent with the X-ray diffraction work of Cheng and Shefter (15) who also found a short H– –O distance.

This additional interaction tends to make these solvates more stable than the benzene solvate. When exposed to air for several days, the

**Table I—Analysis of the C–H Stretching Region (2800–3200 $cm^{-1}$) of the Bromoform Solvate and Chloroform (Deuterated and Protonated) Solvates [a]**

| Griseofulvin–Chloroform-*d* | | Griseofulvin–Chloroform-*h* | | Griseofulvin–Bromoform | |
|---|---|---|---|---|---|
| Frequency | Intensity | Frequency | Intensity | Frequency | Intensity |
| 2899.5 | m | 2899.5 | m | 2894.0 | w |
| 2912.5 | vw | 2914.0 | vw | 2911.5 | w |
| 2940.5 | w-Br | 2941.5 | w | 2938.5 | w-Br |
| 2949.0 | w | 2950.0 | w | 2944.5 | vw |
| 2960.0 | w | 2959.0 | w | 2955.5 | w-Br |
| 2973.0 | w | 2974.0 | w | 2970.5 | vw |
| 2987.5 | m | 2988.0 | m | 2986.5 | w-Br |
| | | 2998.0 | vw | 2999.5 | w |
| 3012.0 | w-m | 3012.5 | w-m | 3010.0 | w |
| 3025.5 | w | 3025.5 | s | 3025.5 | s |
| 3033.0 | w | 3033.5 | w-m | | |
| 3074.0 | w | 3075.0 | w-Br | 3076.5 | vw-Br |

[a] The following abbreviations are used: s = strong, m = medium, w = weak, vw = very weak, and Br = broad.

griseofulvin–chloroform or bromoform solvate showed no degradation.

**Desolvation**—As a crystalline solvate undergoes desolvation, the solvent molecule makes an exit due to an external perturbation (*e.g.*, rise in temperature) and the lattice can suffer several consequences. Three possibilities define the modes of desolvation:

1. The lattice still exists in the same crystalline form even in the absence of the solvent molecule.
2. Desolvation produces an intermediate structure, which eventually reverts to that of the unsolvated griseofulvin.
3. As the solvent molecule escapes, the lattice immediately (or in an extremely short period) reverts to the structure of the unsolvated griseofulvin.

Phonon spectra were used to investigate desolvation in the chloroform and benzene solvates. A crystal of the stable, deuterated chloroform solvate was washed with ethanol, air dried, and ground to a powder. A small sample of this crystal was heated uniformly with a flow of warm nitrogen vapor at 60°. After each 15-min interval, the sample was removed and cooled to 135°K, and a spectrum of the phonon region was obtained. After 1 hr, the phonon spectra (Fig. 4) appeared to be the superimposed spectra of the chloroform solvate and unsolvated griseofulvin. Additional solvate heating showed that only unsolvated griseofulvin was present. As the solvent diffused out, the solvate lattice collapsed. Since the crystal structure returned to that of unsolvated griseofulvin, the structures of these solvates were not stable without the solvent.

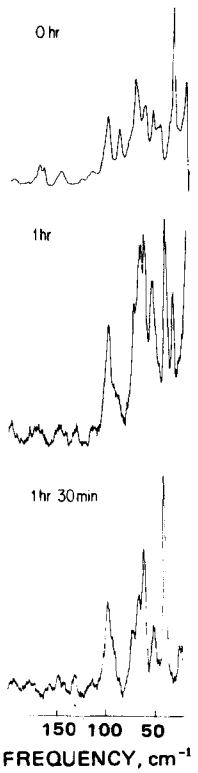


**Figure 4**—*Raman spectra of the lattice vibrations of the deuterated chloroform solvate obtained as a function of the desolvation process.*

Sekiguchi *et al.* (6) studied the desolvation mechanism of the benzene solvate by periodically measuring X-ray powder diffraction patterns. They observed a peak that was not present in the benzene solvate spectrum or in the pure griseofulvin spectrum and concluded that an intermediate structure was formed during desolvation. The benzene solvate desolvation was monitored by placing a single crystal in a focused laser beam, which allowed the monitoring of the phase boundary by periodically obtaining the phonon spectra. As Fig. 4 shows, the desolvation exhibited the appearance of an unsolvated griseofulvin peak (59 $cm^{-1}$), which grew in intensity upon further desolvation. No new peak was observed during desolvation. While the data show no intermediate structure, additional work with single-crystal X-ray crystallography may be necessary to establish unequivocally the presence or absence of an intermediate structure during desolvation.

Laser Raman spectroscopy has a number of advantages and disadvantages. It is convenient and versatile for investigating pharmaceutical solids, and spectra of both lattice vibrations and intramolecular vibrations in the same arrangement can be obtained. The spectra of lattice vibrations provide valuable information on crystalline interactions and can be used to characterize crystalline modifications, the effect of various perturbations on crystal structures, and the desolvation process. The study of intramolecular vibrations is used to study both the specific nature of the solute–solvent interaction and the chemical stability of the various forms.

From an experimental point of view, Raman spectroscopy offers several advantages over other techniques used to study drugs:

1. No special sample preparation is required, so the grinding required for X-ray powder diffraction or the pressing for IR absorption is eliminated.
2. Because the incident laser radiation can be focused into a very small spot, extremely small amounts of material can be used.
3. Raman spectra of lattice vibrations can be obtained easily in a short time.
4. The internal vibration region is examined easily in the same experiment.
5. The temperature of the sample can be controlled accurately during the experiment, allowing thermal studies of the various forms.
6. The use of a coherent, tunable, and monochromatic dye laser permits tuning of the exciting radiation to some electronic transitions. This resonance Raman technique permits work with very low laser light levels and highly colored materials.

On the other hand, Raman spectroscopy has some disadvantages. The Raman effect is highly inefficient and, thus, is more suitable for the study of concentrated species than for a small amount of impurity. In general, only relative intensities of various Raman peaks are measured, and even then the relative intensities do not easily provide quantitative information on the concentrations of various species. Moreover, with colored samples, the excitation wavelength of the laser and the power levels must be chosen carefully so that the sample does not undergo thermal or photochemical decomposition.

In view of these limitations, Raman spectroscopy cannot be used as a substitute for all other techniques. However, when used with discretion, it can be a powerful technique for the investigation of pharmaceutical solids.

## REFERENCES


(1) J. Haleblian and W. McCrone, *J. Pharm. Sci.*, **58**, 911 (1969).

(2) J. Haleblian, *ibid.*, **64**, 1269 (1975).

(3) H. Blank, *Am. J. Med.*, **39**, 831 (1965).

(4) K. Sekiguchi, K. Ito, E. Owada, and K. Ueno, *Chem. Pharm. Bull.*, **12**, 1192 (1964).

(5) K. Sekiguchi, I. Horikoshi, and I. Himuro, *ibid.*, **16**, 2495 (1968).

(6) K. Sekiguchi, K. Shirotani, M. Kanice, H. Furukawa, and M. Iwatsuru, *ibid.*, **24**, 1621 (1976).

(7) J. C. Bellows, F. P. Chen, and P. N. Prasad, *Drug Dev. Ind. Pharm.*, **3**, 451 (1977).

(8) D. E. Resetarits, K. C. Cheng, B. A. Bolton, P. N. Prasad, E. Shefter, and T. R. Bates, *Int. J. Pharm.*, **2**, 113 (1979).

(9) B. A. Bolton and P. N. Prasad, *Chem. Phys.*, **35**, 331 (1978).

(10) P. S. Friedman, R. Kopelman, and P. N. Prasad, *Chem. Phys. Lett.*, **24**, 15 (1974).

(11) J. C. Bellows and P. N. Prasad, *J. Chem. Phys.*, **70**, 1864

(1979).
(12) P. N. Prasad and R. V. Smith, *ibid.*, **71**, 4646 (1979).
(13) P. N. Prasad and E. D. Stevens, *ibid.*, **66**, 862 (1977).
(14) J. C. Bellows, E. D. Stevens, and P. N. Prasad, *Acta Crystallogr. Sect. B*, **34**, 3256 (1978).
(15) K. C. Cheng and E. Shefter, *Int. J. Pharm.*, **2**, 81 (1979).

ACKNOWLEDGMENTS

Supported in part by Air Force Office of Scientific Research Grant AFOSR-80-0287 and in part by National Institutes of Health Grant 1R01GM2735701.

P. N. Prasad was an Alfred P. Sloan Fellow.

# High-Performance Liquid Chromatographic Analysis of Clorazepate Dipotassium and Monopotassium in Solid Dosage Forms

**L. ELROD, Jr., D. M. SHADA, and V. E. TAYLOR ˣ**

Received October 14, 1980, from the *Analytical Research Department, Abbott Laboratories, North Chicago, IL 60064.* Accepted for publication December 16, 1980.

**Abstract** □ Methodology for the quantitative determination of clorazepate dipotassium and monopotassium in solid dosage forms was developed. Clorazepate was resolved from its degradation products, making the analysis specific and stability indicating. Analytical separation was performed on a octadecylsilylated silica column. Clorazepate was extracted from the dosage forms with 0.04% NaOH and chromatographed with aqueous 0.005 *M* tetra-*n*-butylammonium ion (pH 7.5)–acetonitrile (70:30) as the eluent. The analysis was completed in ~20 min with a precision of <2.4% *RSD*.

**Keyphrases** □ High-performance liquid chromatography—analysis of clorazepate dipotassium and monopotassium in solid dosage forms □ Clorazepate, dipotassium and monopotassium—high-performance liquid chromatographic analysis, solid dosage forms □ Tranquilizers—clorazepate dipotassium and monopotassium, high-performance liquid chromatographic analysis, solid dosage forms

In the past, clorazepate (I) primarily was determined chromatographically as its primary degradation product and major metabolite nordiazepam (II). Clorazepate decarboxylates to give nordiazepam; in aqueous systems (pH 2–11), the transformation is unimolecular with respect to clorazepate. Nordiazepam can undergo further metabolic transformations to oxazepam and the glucuronide in urine (1).

GLC has been used extensively (2–6) for the analysis of clorazepate as nordiazepam in biological fluids. Similarly, nordiazepam has been determined in plasma and urine by high-performance liquid chromatography (HPLC) in both reversed-phase (7–11) and normal-phase (12, 13) chromatographic modes.

Recently, a reversed-phase HPLC system for the qualitative identification of clorazepate in oral dosage forms was reported (14). With aqueous phosphate buffer (pH 8) and methanol (1:2 and 3:4) as the eluent, clorazepate was chromatographed intact on an octadecylsilylated column both with and without tetra-*n*-butylammonium ion (0.005 *M*) as an ion-pairing counterion. This paper reports the quantitation of clorazepate in its dosage forms by a similar procedure used in these laboratories for several years. The procedure has been applied to eight formulations of clorazepate (monopotassium and dipotassium), both capsules and tablets, and is specific and stability indicating.

## EXPERIMENTAL

**Reagents and Chemicals**—Acetonitrile[1], tetra-*n*-butylammonium hydroxide[2], phosphoric acid[3], and sodium hydroxide[4] were used as received. 2,6-Dimethylaniline[5] was converted to the hydrochloride by acidification of a hexane[4] solution of the amine (10% v/v) with concentrated hydrochloric acid[6]. The precipitated amine salt was filtered, washed with hexane, and dried for use as the internal standard. Distilled water was used for all aqueous reagent and mobile phase preparations.

**Apparatus**—The liquid chromatograph consisted of a pump[7], a loop-type injector[8], a variable-wavelength UV detector[9], and a recorder/data handling system[10] for quantitative work. The 30-cm × 4-mm i.d. column contained an octadecylsilylated silica material[11].

**Mobile Phase**—A 0.005 *M* aqueous solution of tetra-*n*-butylammonium ion was prepared from 5.0 ml of tetra-*n*-butylammonium hydroxide in 1 liter of water, and the pH was adjusted[12] to 7.5 with phosphoric acid. The mobile phase was prepared by diluting 300 ml of acetonitrile to 1 liter with 0.005 *M* tetra-*n*-butylammonium-ion solution. The eluent was filtered[13] through a 0.45-μm membrane filter[14], stirred magnetically, and degassed under vacuum.

**Chromatographic Conditions**—The temperature was ambient, and the flow rate was ~1.8 ml/min. The detector sensitivity was set at 0.2 au (230 nm). The injector loop size was 20 μl, and the chart speed was 0.2 cm/min.

**Sample Solvent**—Sodium hydroxide (0.04% w/v) was filtered[13] through a 0.45-μm membrane filter[14].

**Internal Standard**—2,6-Dimethylaniline hydrochloride (30 mg) was dissolved in, and diluted to 100.0 ml with, the sample solvent.

**Reference Standard**—A solution containing 50–60 μg of clorazepate reference standard[15]/ml was prepared by dissolving it in, and diluting appropriately with, the sample solvent. An ultrasonic water bath[16] was employed to aid dissolution. A 5.0-ml portion of this solution and 2.0 ml of the internal standard solution were diluted to 10.0 ml with the sample

[1] Distilled-in-glass, Burdick & Jackson Laboratories, Muskegon, Mich.
[2] Titration grade, 1.0 *M* in methanol, Southwestern Analytical Chemicals, Austin, Tex.
[3] Reagent grade (85%), J. T. Baker Chemical Co., Phillipsburg, N.J.
[4] AR grade, Mallinckrodt, Paris, Ky.
[5] Eastman Organic Chemicals, Rochester, N.Y.
[6] Baker analyzed, J. T. Baker Chemical Co., Phillipsburg, N.J.
[7] Model M6000A, Waters Associates, Milford, Mass.
[8] Model 7120, Rheodyne, Berkeley, Calif.
[9] Model 450, Waters Associates, Milford, Mass.
[10] Model 3385A, Hewlett-Packard Corp., Rolling Meadows, Ill.
[11] μBondapak $C_{18}$, Waters Associates, Milford, Mass.
[12] Model 10 pH meter, Corning Scientific, Medfield, Mass.
[13] Millipore Corp., Bedford, Mass.
[14] Flotronics Division, Selas Corp., Huntingdon Valley, Pa.
[15] Clorazepate dipotassium (lot 72-307-CA) or clorazepate monopotassium (lot 64-922-AL), House Reference Standards, Abbott Laboratories, North Chicago, Ill.
[16] Bransonic 32, Branson Cleaning Equipment Co., Shelton, Conn.

0022-3549/81/0700-0793$01.00/0
© 1981, American Pharmaceutical Association

(1979).
(12) P. N. Prasad and R. V. Smith, *ibid.*, **71**, 4646 (1979).
(13) P. N. Prasad and E. D. Stevens, *ibid.*, **66**, 862 (1977).
(14) J. C. Bellows, E. D. Stevens, and P. N. Prasad, *Acta Crystallogr. Sect. B*, **34**, 3256 (1978).
(15) K. C. Cheng and E. Shefter, *Int. J. Pharm.*, **2**, 81 (1979).

ACKNOWLEDGMENTS

Supported in part by Air Force Office of Scientific Research Grant AFOSR-80-0287 and in part by National Institutes of Health Grant 1R01GM2735701.

P. N. Prasad was an Alfred P. Sloan Fellow.

# High-Performance Liquid Chromatographic Analysis of Clorazepate Dipotassium and Monopotassium in Solid Dosage Forms

**L. ELROD, Jr., D. M. SHADA, and V. E. TAYLOR ˣ**

Received October 14, 1980, from the *Analytical Research Department, Abbott Laboratories, North Chicago, IL 60064.* Accepted for publication December 16, 1980.

**Abstract** □ Methodology for the quantitative determination of clorazepate dipotassium and monopotassium in solid dosage forms was developed. Clorazepate was resolved from its degradation products, making the analysis specific and stability indicating. Analytical separation was performed on a octadecylsilylated silica column. Clorazepate was extracted from the dosage forms with 0.04% NaOH and chromatographed with aqueous 0.005 *M* tetra-*n*-butylammonium ion (pH 7.5)–acetonitrile (70:30) as the eluent. The analysis was completed in ~20 min with a precision of <2.4% *RSD*.

**Keyphrases** □ High-performance liquid chromatography—analysis of clorazepate dipotassium and monopotassium in solid dosage forms □ Clorazepate, dipotassium and monopotassium—high-performance liquid chromatographic analysis, solid dosage forms □ Tranquilizers—clorazepate dipotassium and monopotassium, high-performance liquid chromatographic analysis, solid dosage forms

In the past, clorazepate (I) primarily was determined chromatographically as its primary degradation product and major metabolite nordiazepam (II). Clorazepate decarboxylates to give nordiazepam; in aqueous systems (pH 2–11), the transformation is unimolecular with respect to clorazepate. Nordiazepam can undergo further metabolic transformations to oxazepam and the glucuronide in urine (1).

GLC has been used extensively (2–6) for the analysis of clorazepate as nordiazepam in biological fluids. Similarly, nordiazepam has been determined in plasma and urine by high-performance liquid chromatography (HPLC) in both reversed-phase (7–11) and normal-phase (12, 13) chromatographic modes.

Recently, a reversed-phase HPLC system for the qualitative identification of clorazepate in oral dosage forms was reported (14). With aqueous phosphate buffer (pH 8) and methanol (1:2 and 3:4) as the eluent, clorazepate was chromatographed intact on an octadecylsilylated column both with and without tetra-*n*-butylammonium ion (0.005 *M*) as an ion-pairing counterion. This paper reports the quantitation of clorazepate in its dosage forms by a similar procedure used in these laboratories for several years. The procedure has been applied to eight formulations of clorazepate (monopotassium and dipotassium), both capsules and tablets, and is specific and stability indicating.

## EXPERIMENTAL

**Reagents and Chemicals**—Acetonitrile[1], tetra-*n*-butylammonium hydroxide[2], phosphoric acid[3], and sodium hydroxide[4] were used as received. 2,6-Dimethylaniline[5] was converted to the hydrochloride by acidification of a hexane[4] solution of the amine (10% v/v) with concentrated hydrochloric acid[6]. The precipitated amine salt was filtered, washed with hexane, and dried for use as the internal standard. Distilled water was used for all aqueous reagent and mobile phase preparations.

**Apparatus**—The liquid chromatograph consisted of a pump[7], a loop-type injector[8], a variable-wavelength UV detector[9], and a recorder/data handling system[10] for quantitative work. The 30-cm × 4-mm i.d. column contained an octadecylsilylated silica material[11].

**Mobile Phase**—A 0.005 *M* aqueous solution of tetra-*n*-butylammonium ion was prepared from 5.0 ml of tetra-*n*-butylammonium hydroxide in 1 liter of water, and the pH was adjusted[12] to 7.5 with phosphoric acid. The mobile phase was prepared by diluting 300 ml of acetonitrile to 1 liter with 0.005 *M* tetra-*n*-butylammonium-ion solution. The eluent was filtered[13] through a 0.45-μm membrane filter[14], stirred magnetically, and degassed under vacuum.

**Chromatographic Conditions**—The temperature was ambient, and the flow rate was ~1.8 ml/min. The detector sensitivity was set at 0.2 au (230 nm). The injector loop size was 20 μl, and the chart speed was 0.2 cm/min.

**Sample Solvent**—Sodium hydroxide (0.04% w/v) was filtered[13] through a 0.45-μm membrane filter[14].

**Internal Standard**—2,6-Dimethylaniline hydrochloride (30 mg) was dissolved in, and diluted to 100.0 ml with, the sample solvent.

**Reference Standard**—A solution containing 50–60 μg of clorazepate reference standard[15]/ml was prepared by dissolving it in, and diluting appropriately with, the sample solvent. An ultrasonic water bath[16] was employed to aid dissolution. A 5.0-ml portion of this solution and 2.0 ml of the internal standard solution were diluted to 10.0 ml with the sample

[1] Distilled-in-glass, Burdick & Jackson Laboratories, Muskegon, Mich.
[2] Titration grade, 1.0 *M* in methanol, Southwestern Analytical Chemicals, Austin, Tex.
[3] Reagent grade (85%), J. T. Baker Chemical Co., Phillipsburg, N.J.
[4] AR grade, Mallinckrodt, Paris, Ky.
[5] Eastman Organic Chemicals, Rochester, N.Y.
[6] Baker analyzed, J. T. Baker Chemical Co., Phillipsburg, N.J.
[7] Model M6000A, Waters Associates, Milford, Mass.
[8] Model 7120, Rheodyne, Berkeley, Calif.
[9] Model 450, Waters Associates, Milford, Mass.
[10] Model 3385A, Hewlett-Packard Corp., Rolling Meadows, Ill.
[11] μBondapak $C_{18}$, Waters Associates, Milford, Mass.
[12] Model 10 pH meter, Corning Scientific, Medfield, Mass.
[13] Millipore Corp., Bedford, Mass.
[14] Flotronics Division, Selas Corp., Huntingdon Valley, Pa.
[15] Clorazepate dipotassium (lot 72-307-CA) or clorazepate monopotassium (lot 64-922-AL), House Reference Standards, Abbott Laboratories, North Chicago, Ill.
[16] Bransonic 32, Branson Cleaning Equipment Co., Shelton, Conn.

0022-3549/81/0700-0793$01.00/0
© 1981, American Pharmaceutical Association

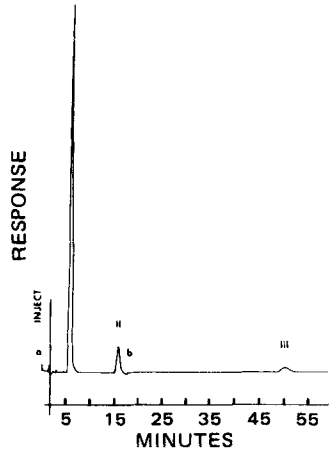


**Figure 1**—*Chromatogram of a mixture of 49.8 μg of clorazepate (I)/ml, 2.25 μg of nordiazepam (II)/ml, and 2.16 μg of 2-amino-5-chlorobenzophenone (III)/ml (a at 2.0 ml/min and b at 3.0 ml/min).*

solvent, giving 25–30 μg of clorazepate/ml and 60 μg of internal standard/ml in the final solution.

**Sample Preparation**—Sample preparations were similar for all dosage forms but varied slightly between capsule and tablet formulations.

**Clorazepate Capsules**—The average capsule fill weight was determined by weighing 20 filled capsules, emptying the contents as completely as possible, and reweighing the emptied shells.

Four capsules then were weighed, the contents were transferred to a 250-ml volumetric flask, and the emptied shells were reweighed to obtain the sample weight. Approximately 200 ml of the sample solvent was added, and the flask was placed in an ultrasonic bath[16] for 5 min. The sample was diluted to volume with the sample solvent and mixed. A portion of the sample then was filtered[17] through a 0.4–0.5-μm membrane filter[18] and diluted according to dose strength with the sample solvent as follows: 3.0–3.75 mg, no dilution; 6.5–7.5 mg, 25.0 ml to 50.0 ml; and 13–15 mg, 25.0 ml to 100.0 ml. A 5.0-ml portion of the last solution and 2.0 ml of the internal standard solution were diluted with the sample solvent to 10.0 ml.

**Clorazepate Tablets**—The number of tablets equivalent to 112.5 mg (for 11.25- and 22.5-mg tablets) or 75 mg (for 3.75-, 7.5-, and 15.0-mg tablets) of clorazepate dipotassium were placed in a 500-ml tall form beaker, and 200.0 ml of the sample solvent was added. The sample then was homogenized[19] at ~6000 rpm for 3.0 min. A portion of the blended solution was filtered[17] through a 0.4–0.5-μm membrane filter[18] and diluted according to dose strength with the sample solvent as follows: 11.25 and 22.5 mg, 5.0 ml to 50.0 ml; and 3.75, 7.5, and 15.0 mg, 15.0 ml to 100.0 ml. A 5.0-ml portion of the last solution and 2.0 ml of the internal standard solution were diluted with the sample solvent to 10.0 ml.

**Analysis and Calculation**—Twenty microliters of both the standard and sample preparations were injected. Normal run time was ~20 min since nordiazepam sometimes can be observed at 14–16 min. Multiple standard preparations were analyzed, and their response ($R_s$) was averaged for calculation purposes:

$$R_s = \left(\frac{A_2}{A_1}\right)_{std}(C) \qquad \text{(Eq. 1)}$$

where $A_1$ is the peak area of clorazepate, $A_2$ is the peak area of the internal standard, and $C$ is the concentration of clorazepate in the standard

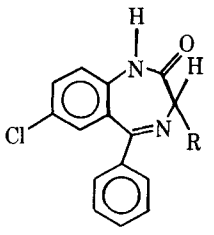


I: R = COOK (monopotassium)
I·KOH: R = COOK·KOH (dipotassium)
II: R = H

[17] Swinnex 25, Millipore Corp., Bedford, Mass.
[18] A 25-mm polycarbonate membrane, Nuclepore Corp., Pleasanton, Calif.
[19] Polytron homogenizer, Brinkmann Instruments, Westbury, N.Y.

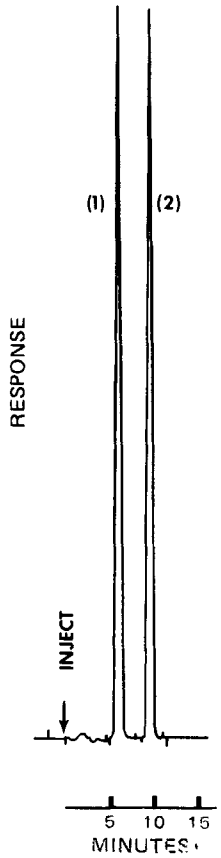


**Figure 2**—*Typical chromatogram of a sample preparation. Key: 1, clorazepate and 2, internal standard.*

(milligrams per milliliter).

For capsules:

$$\frac{\text{mg of clorazepate}}{\text{capsule}} = \left(\frac{A_1}{A_2}\right)_{spl} \times R_s \times 500 \times DF \times \frac{W_1}{W_2} \qquad \text{(Eq. 2)}$$

where $DF$ is the appropriate dilution factor from the procedure and $W_1$ and $W_2$ are the average capsule fill weight and individual sample weight, respectively, in milligrams.

For tablets:

$$\frac{\text{mg of clorazepate}}{\text{tablet}} = \left(\frac{A_1}{A_2}\right)_{spl} \times R_s \times 400 \times \frac{DF}{N} \qquad \text{(Eq. 3)}$$

where $N$ is the number of tablets used in the sample preparation.

## RESULTS AND DISCUSSION

Clorazepate (I) decarboxylates readily to give nordiazepam (II) as the primary degradation product. Further acidic hydrolysis produces 2-amino-5-chlorobenzophenone (III). Other minor degradation products have been observed but at such low levels as to not be of concern in this assay.

HPLC provided the technique by which clorazepate could be separated from its degradation products for quantitation. With an octadecylsilylated stationary phase and methanol–water mixtures, poor peak shapes and retention were obtained for clorazepate. However, clorazepate chromatographed well when an eluent containing aqueous tetra-*n*-butylammonium ion (pH 7.5) and acetonitrile was employed. The use of tetra-*n*-butylammonium ion in the HPLC of weakly acidic species was previously reviewed (15, 16).

Figure 1 shows a chromatogram of clorazepate, nordiazepam, and 2-amino-5-chlorobenzophenone mixture under chromatographic conditions similar to those described here. Clorazepate was resolved from its degradation products, making the assay both specific and stability indicating.

The sample solvent (0.04% NaOH) was chosen to improve the stability of the clorazepate solutions during the time required to perform the analysis. At the pH of this solvent (~11.3), clorazepate was stable for at least 3–4 hr, after which time a gradual decline in the assay value was observed. Samples for analysis were prepared and analyzed within a few hours.

**Table I—Clorazepate Analysis in Dosage Forms**

| Formulation | Dose, mg | Standard Addition Recovery, %[a] | Precision mg ± *SD* | Precision *RSD*, % |
|---|---|---|---|---|
| Clorazepate monopotassium capsules | 3.25 | | 3.38 ± 0.05 | 1.52 |
| | 6.25 | 97.9–100.2 | 6.49 ± 0.07 | 1.09 |
| | 13.0 | | 12.82 ± 0.18 | 1.42 |
| Clorazepate dipotassium capsules | | | | |
| A | 3.0 | 97.9–101.5 | 2.95 ± 0.07 | 2.36 |
| B | 3.75 | | | |
| | 7.5 | 96.3–100.5 | 7.56 ± 0.12 | 1.64 |
| | 15.0 | | 14.78 ± 0.25 | 1.71 |
| C | 3.75 | | | |
| | 7.5 | 98.8–102.1 | 7.19 ± 0.09 | 1.32 |
| | 15.0 | | | |
| D | 7.5 | 98.9–101.0 | 7.49 ± 0.09 | 1.18 |
| E | 7.5 | 100.7–101.2 | 7.30 ± 0.11 | 1.50 |
| Clorazepate dipotassium tablets | 11.25 | 99.7–100.4 | 10.98 ± 0.09 | 0.84 |
| | 22.5 | | 22.01 ± 0.27 | 1.25 |
| | 3.75 | | 3.68 ± 0.02 | 0.51 |
| | 7.5 | 98.7–102.1 | 7.67 ± 0.05 | 0.68 |
| | 15.0 | | 15.06 ± 0.18 | 1.21 |

[a] Clorazepate reference standard.

All samples analyzed in this work were routine research and quality assurance samples from in-house sources. A typical chromatogram for the analysis of a formulation is presented in Fig. 2. Nordiazepam sometimes was observed as a very small peak at ~14–16 min, in which case the total analysis time was ~20 min. The long retention time of nordiazepam prevented its quantitation under these conditions at the normally low levels (<1%) encountered in the formulations. 2-Amino-5-chlorobenzophenone and other related impurities were present at such low levels as not to be observed at all.

Figure 3 is a chromatogram of a sample that had been intentionally degraded at elevated temperature. The intact clorazepate assay was 15.5%. A large peak also was observed for nordiazepam, indicating that this procedure detects decomposition and is stability indicating.

**Linearity**—A plot of the ratio of the clorazepate peak area to the internal standard peak area *versus* the clorazepate concentration in the solution was linear to at least 0.3 mg/ml and passed essentially through the origin ($r > 0.999$). The analytical concentration of clorazepate was 0.025–0.030 mg/ml.

**Recovery**—A known amount of clorazepate was added to the various formulations to check the recovery of standard additions. Additions at 50, 100, and 150% of label claim were added to at least one dose strength within each formulation. Weighed amounts of clorazepate standard were added to either placebo formulations or previously assayed dosages containing the active ingredient. The preparations then were analyzed as described (Table I). Recoveries ranged from 96.3 to 102.1%.

**Precision**—Analytical precision for clorazepate was determined by replicate analysis of 10 individual sample preparations on two separate days (Table I). Different analysts also were involved in some cases. The relative standard deviations ranged from ±0.51 to ±2.36%.

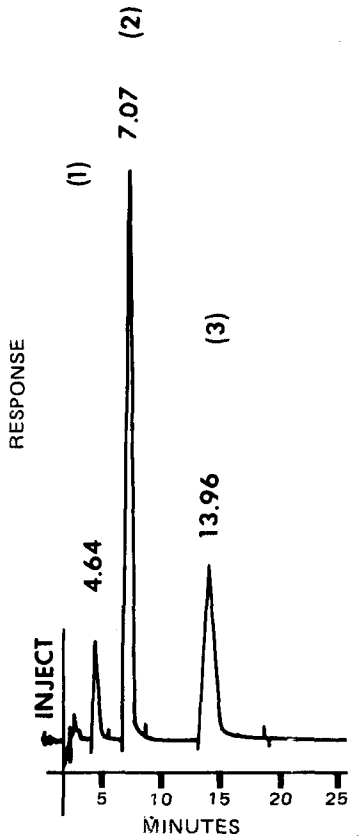


**Figure 3**—*Chromatogram for the analysis of a sample artificially degraded under accelerated conditions. Key: 1, clorazepate; 2, internal standard; and 3, nordiazepam.*

## REFERENCES


(1) J. A. Raihle and V. E. Papendick, "Analytical Profiles of Drug Substances," vol. 4, K. Florey, Ed. Academic, New York, N.Y. 1975, pp. 91–112.

(2) D. M. Hailey, *J. Chromatogr.*, **98,** 527 (1974).

(3) C. W. Abruzzo, T. Macasieb, R. Weinfeld, J. A. Rider, and S. A. Kaplan, *J. Pharmacokinet. Biopharm.*, **5,** 377 (1977).

(4) A. H. C. Chun, P. J. Carrigan, D. J. Hoffman, R. P. Kershner, and J. D. Stuart, *Clin. Pharmacol. Ther.*, **22,** 329 (1977).

(5) P. J. Carrigan, G. C. Chao, W. M. Barker, D. J. Hoffman, and A. H. C. Chun, *J. Clin. Pharmacol.*, **17,** 18 (1977).

(6) M. A. Brooks, M. R. Hackman, R. E. Weinfeld, and T. Macasieb, *J. Chromatogr.*, **135,** 123 (1977).

(7) R. R. Brodie, L. F. Chasseaud, and T. Taylor, *ibid.*, **150,** 361 (1978).

(8) G. G. Skellern, J. Meier, B. I. Knight, and B. Whiting, *Br. J. Clin. Pharmacol.*, **5,** 483 (1978).

(9) N. Strojny, C. V. Puglisi, and J. A. F. DeSilva, *Anal. Lett.*, **B11,** 135 (1978).

(10) P. M. Kabra, G. L. Stevens, and L. J. Marton, *J. Chromatogr.*, **150,** 355 (1978).

(11) K. Hartzer and R. Barchet, *ibid.*, **132,** 83 (1977).

(12) R. J. Perchalski and B. J. Wilder, *Anal. Chem.*, **50,** 554 (1978).

(13) A. Bugge, *J. Chromatogr.*, **128,** 111 (1976).

(14) C. R. Clark and F. T. Noggle, Jr., *ibid.*, **188,** 426 (1980).

(15) R. Gloor and E. L. Johnson, *J. Chromatogr. Sci.*, **5,** 413 (1977).

(16) E. Tomlinson, T. M. Jefferies, and C. M. Riley, *J. Chromatogr.*, **159,** 315 (1978).


## ACKNOWLEDGMENTS


The authors thank Dr. J. F. Bauer, Mr. J. P. Boller, and Mr. J. R. Fornnarino for assistance in the validation of this methodology.

# Dissolution Profiles and Specifications for Dihydroergotoxine Sublingual Tablets Using a New *In Vitro* Method

JOHN P. HUNT, VINOD P. SHAH, VADLAMANI K. PRASAD ˣ, DONALD J. SCHUIRMANN, and BERNARD E. CABANA

Received February 28, 1980, from the *Biopharmaceutics Laboratory, Food and Drug Administration, Washington, DC 20204.* Accepted for publication December 29, 1980.

**Abstract** □ A dissolution method (paddle method) for determining the dissolution rate profile for 0.5- and 1.0-mg dihydroergotoxine methanesulfonate sublingual tablets was developed. A fluorometric method was used for measuring drug concentration in the dissolution medium, distilled water. It was essential to filter the dissolution sample to avoid interference from undissolved excipients. When different kinds of filters were used with the dissolution samples and standards, different degrees of apparent drug binding to the filter occurred. The dissolution rate profiles for several different products were compared to the innovator's product. The *in vitro* method and data obtained were used to propose dissolution specifications for these sublingual products.

**Keyphrases** □ Dihydroergotoxine—*in vitro* dissolution method for sublingual tablets, dissolution profiles □ Dissolution—dihydroergotoxine sublingual tablets, *in vitro* method □ Psychotherapeutic agents—dihydroergotoxine, *in vitro* dissolution method for sublingual tablets

Dihydroergotoxine is a psychotherapeutic agent used in the treatment of mood depression, confusion, and unsociability in elderly patients. Dihydroergotoxine sublingual tablets contain equal amounts of the mesylate forms of the dihydrogenated ergot alkaloids dihydroergocristine, dihydroergocornine, and dihydroergokryptine (*i.e.*, sum total of dihydro-α-ergokryptine and dihydro-β-ergokryptine) (1).

This drug is not in the official compendia, but the number of applications received by the Food and Drug Administration (FDA) for marketing approval for these products[1] has increased. Since there is no published method for *in vivo* bioavailability determination of dihydroergotoxine, firms seeking FDA approval were required to meet an *in vitro* dissolution specification as an interim minimum (2). This paper describes the development of a discriminatory *in vitro* dissolution method.

## EXPERIMENTAL

**Apparatus**—A dissolution apparatus described in USP XX Method II was used to establish dissolution specifications. The apparatus was equipped with a transparent constant-temperature water bath, which held six dissolution assemblies so that six dissolution tests could be run simultaneously. The water bath was connected to a free-standing water bath pump[2]. Each stirring shaft[3] of each dissolution assembly and its attached paddle[4] were positioned so that the bottom edge of the paddle was 4.5 ± 0.2 cm from the lowest inner surface of the dissolution vessel[5]. The dissolution profile of dihydroergotoxine tablets was determined in 500 ml of distilled water at 37° and 50 rpm. A volume of 500 ml of dissolution medium was selected due to the size of the dosage strengths tested (0.5 and 1.0 mg) and the assay sensitivity limit.

**Sampling**—A sampling system was designed with a proportioning pump[6] so that filtered dissolution test specimens from six dissolution assemblies could be collected simultaneously. The pumping system had an on-line filter adapter[7], which contained a disposable filter (glass fiber[8], polytef[9], cellulose[10], or nylon[11]) for each dissolution assembly. Filters were replaced for each dissolution test.

Dissolution specimens (2–3 ml) were collected at each time, and an equivalent volume of dissolution medium was replaced immediately. Collected specimens were allowed to equilibrate to room temperature (25°) in a water bath before being read directly in a spectrophotofluorometer[12]. Prior to reading the filtered standard solutions and collected dissolution specimens, the spectrophotofluorometer was set for an emission intensity reading of 100 for a 1.0-μg/ml unfiltered standard solution.

Standard curves were linear over a concentration range of 0.05–4.0 μg/ml for both filtered and unfiltered standard solutions. A typical equation for an unfiltered standard curve was $y = 97.9x + 1.64$ ($r = 0.9980$); for a filtered standard curve using glass-fiber filters, it was $y = 91.3x + 0.450$ ($r = 0.9993$).

**Table I—Influence of Filter Composition on Dihydroergotoxine Binding [a]**

| | Polytef | Glass Fiber | Cellulose | Nylon |
|---|---|---|---|---|
| $N$[b] | 22 | 55 | 20 | 6 |
| Mean percent unbound | 93.2 | 92.2 | 74.0 | 44.3 |
| Range | 85–98.5 | 84–100 | 58–93.5 | 25–70 |
| $SD$ | 4.0 | 4.3 | 10.1 | 15.7 |
| $SE$ | 0.9 | 0.6 | 2.3 | 6.41 |
| $CV$[c] | 4.3 | 4.6 | 13.6 | 35.5 |

[a] Percent of apparent drug filter binding was determined using an aqueous 1.0-μg of dihydroergotoxine/ml standard solution. The standard's filtered fluorescence reading for each filter was compared to the standard's unfiltered fluorescence reading of 100. Binding = 100 − observed reading. [b] Number of filters tested. [c] Coefficient of variation.

## RESULTS AND DISCUSSION

Spectrophotofluorometric scans demonstrated that an aqueous solution of dihydroergotoxine methanesulfonate[13] (with the assumption that all three drug moieties have the same dissolution characteristics) had maximum excitation and emission wavelengths of 283 and 353 nm, respectively.

Initial studies revealed that dihydroergotoxine standard solutions gave lower relative emission intensity readings when filtered with cellulose filters than when read as unfiltered solutions. Further investigations were conducted using standard solutions to determine the effects other filters had on fluorescence readings. Study results indicated an apparent drug filter binding effect, which was dependent on the type of filter used (Table I). For cellulose and nylon filters, there appeared to be significant binding (~25 and 55%, respectively). For polytef and glass-fiber filters, slight binding seemed possible when the small assay variability (coefficient of variation of 4.3 and 4.6%, respectively) and the differences between unfiltered and filtered fluorescence readings for those filters (~7 and 8%, respectively) were considered.

Sublingual tablets, 0.5 and 1.0 mg, from several manufacturers were

[1] FDA files.
[2] GCA/Precision Scientific, Chicago, Ill.
[3] Part 65-700-001, Hanson Research Corp., Northridge, Calif.
[4] Part 65-700-300, Hanson Research Corp., Northridge, Calif.
[5] Part 33710-S1, Owens Illinois, Vineland, NJ.
[6] Technicon Instrument Corp., Chauncey, N.Y.
[7] Part SX0001300, Millipore Corp., Bedford, Mass.
[8] Part 61628, Gelman Instrument Co., Ann Arbor, Mich.
[9] Teflon, Part LCWP01300, Millipore Corp., Bedford, Mass.
[10] Part SCWP01300, Millipore Corp., Bedford, Mass.
[11] Part NCWP01300, Millipore Corp., Bedford, Mass.
[12] Perkin-Elmer model 204A spectrophotofluorometer with 1.0-cm quartz cells.
[13] Riker Laboratories, Northridge, Calif.



0022-3549/81/0700-0796$01.00/0
© 1981, American Pharmaceutical Association

**Table II—Dissolution Rates (Mean ± *SD*) of 0.5-mg Dihydroergotoxine Tablets in 500 ml of Distilled Water at 37° Using Rotating-Paddle Method**

| Minutes | Product[a] S1 | S2 | S3 | S4 | M1 | M2 | P | R | B1 |
|---|---|---|---|---|---|---|---|---|---|
| 2 | 4.6[b] ± 1.3 | 8.1 ± 2.6 | 9.7 ± 3.2 | 12.5 ± 4.8 | 2.3 ± 1.5 | 13.5 ± 5.8 | 3.0 ± 2.0 | 39.8 ± 9.4 | 4.2[b] ± 2.0 |
| 5 | 12.3 ± 4.4 | 28.6 ± 5.0 | 30.1 ± 2.9 | 40.1 ± 9.2 | 14.1 ± 5.8 | 43.6 ± 15.3 | 14.4 ± 4.0 | 76.3 ± 7.0 | 20.7 ± 4.6 |
| 10 | 34.1 ± 5.1 | 52.9 ± 6.9 | 61.7 ± 7.4 | 72.8 ± 13.0 | 31.0 ± 6.3 | 68.1 ± 16.3 | 38.5 ± 8.7 | 81.2 ± 10.4 | 54.6 ± 9.2 |
| 15 | 55.0 ± 7.4 | 75.6 ± 4.1 | 84.3 ± 7.7 | 90.2 ± 8.0 | 49.5 ± 13.5 | 83.6 ± 6.0 | 50.8 ± 11.3 | 87.6 ± 4.1 | 74.6 ± 5.2 |
| 20 | 73.0 ± 7.2 | 83.3 ± 7.1 | 91.1 ± 8.1 | 97.5 ± 5.2 | 61.8 ± 12.4 | 90.0 ± 6.0 | 56.3 ± 10.5 | 82.8 ± 9.3 | 80.6 ± 6.2 |
| 30 | 97.7 ± 7.0 | 90.4 ± 4.9 | 89.9 ± 7.6 | 99.4 ± 4.1 | 77.7 ± 7.1 | 94.0 ± 6.3 | 59.9 ± 11.0 | 84.9 ± 5.0 | 84.3 ± 7.2 |
| 60 | 102.8 ± 5.7 | 89.1 ± 3.2 | 92.8 ± 6.0 | 101.0 ± 5.8 | 91.1 ± 5.8 | 94.4 ± 4.1 | 76.1 ± 9.8 | 86.5 ± 7.5 | 81.4 ± 4.2 |
| ∞[c] | 98.5 ± 6.8 | 91.0 ± 5.2 | 91.9 ± 6.2 | 98.9 ± 4.4 | 98.2 ± 3.7 | 98.6 ± 7.8 | 76.2 ± 14.9 | 89.1 ± 8.5 | 86.9 ± 7.5 |

[a] S1 (lot 720X5534), S2 (lot 752X6194), S3 (lot 751X6194), and S4 (lot 717X5654) represent four lots of the innovator Sandoz Pharmaceuticals; M1 (lot 3MMJ075) and M2 (lot 3MF0082) were from Mead Johnson; P (lot A61447) was from Premo Pharmaceutical Laboratories; R (lot 57295) was from Riker Laboratories; and B1 (lot 026093) was from Bolar. Twelve tablets of each product were used except that six tablets of M1 and M2 were tested. [b] Mean of six tablets. [c] See Footnote 14.

**Table III—Dissolution Rates (Mean ± *SD*) of 1.0-mg Dihydroergotoxine Tablets in 500 ml of Distilled Water at 37° Using Rotating-Paddle Method**

| Minutes | Product[a] S5 | S6 | S7 | S8 | B2 | M3 | M4 |
|---|---|---|---|---|---|---|---|
| 2 | 8.6 ± 0.7 | 8.3 ± 0.8 | 7.9 ± 2.1 | 11.1 ± 1.4 | 19.9 ± 2.2 | 5.2 ± 1.7 | 18.6 ± 6.1 |
| 5 | 23.9 ± 1.3 | 25.2 ± 2.0 | 22.9 ± 2.2 | 31.3 ± 2.6 | 45.6 ± 2.0 | 17.1 ± 2.5 | 48.7 ± 9.9 |
| 10 | 50.7 ± 1.9 | 51.5 ± 3.2 | 46.1 ± 2.0 | 55.8 ± 2.6 | 57.2 ± 3.0 | 32.0 ± 4.4 | 79.9 ± 6.2 |
| 15 | 66.0 ± 2.1 | 76.3 ± 2.5 | 66.0 ± 3.9 | 83.3 ± 6.4 | 64.9[b] ± 3.4 | 42.6 ± 4.9 | 103.0 ± 7.4 |
| 20 | 84.9 ± 2.7 | 88.7 ± 3.7 | 76.5 ± 2.7 | 96.8 ± 4.0 | 64.6 ± 2.9 | 49.2 ± 3.3 | 107.0 ± 2.3 |
| 30 | 95.8 ± 3.1 | 91.0 ± 3.4 | 89.5 ± 3.1 | 98.9 ± 3.9 | 69.0[b] ± 5.8 | 58.4 ± 6.9 | 112.0 ± 4.7 |
| 60 | 98.6 ± 2.8 | 92.3 ± 2.1 | 93.5 ± 3.4 | 100.0 ± 3.6 | 62.9 ± 6.4 | 97.4 ± 4.5 | 106.0 ± 2.1 |
| ∞[c] | 102.0 ± 1.5 | 94.7 ± 1.7 | 95.0 ± 3.9 | 98.3 ± 2.6 | 64.1 ± 7.7 | 106.0 ± 9.6 | 110.0 ± 8.8 |

[a] S5 (lot 040X6375), S6 (lot 039Y6389), S7 (lot 035X6265), and S8 (lot 038Y6389) represent four lots of the innovator Sandoz Pharmaceuticals; B2 (lot 116581) was from Bolar; and M3 (lot 3MMJ082) and M4 (lot 3MF0081) were from Mead Johnson. Six tablets of each product were used except that 12 tablets of S7 were tested. [b] Mean of 12 tablets. [c] See Footnote 14.

tested. Glass-fiber filters were used because of their low apparent drug binding effect. Dissolution profiles from 2 min to infinity[14] were determined. For each dissolution run, at least six tablets were tested and a filtered standard curve was prepared.

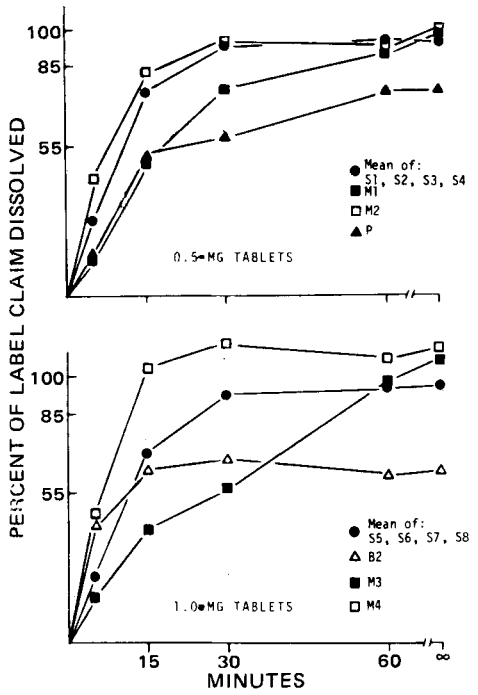


**Figure 1**—*Dissolution profiles for 0.5- and 1.0-mg dihydroergotoxine mesylate tablets in distilled water at 37° by the 50-rpm paddle method. The data points represent a mean of 48 tablets representing four batches for 0.5-mg tablets and a mean of 30 tablets representing four batches for 1.0-mg tablets for Product S. For all other brands, the values represent a mean of six or 12 tablet determinations.*

[14] Infinity dissolution was determined after stirring the dissolution medium for an additional 30 min at 200 rpm following 60 min of specimen collection.

**Table IV—*p* Values for the Significance Tests Associated with Analysis of Variance of Percent Dihydroergotoxine Dissolved**

| Effect | 0.5-mg Tablet 15 min | 0.5-mg Tablet 30 min | 1.0-mg Tablet 15 min | 1.0-mg Tablet 30 min |
|---|---|---|---|---|
| Brands | 0.602 | 0.020 | 0.989 | 0.469 |
| Lots within brands | 0.001 | 0.086 | 0.005 | 0.001 |

The dissolution test results for 0.5- (Table II) and 1.0- (Table III) mg tablets demonstrated that there were brand-to-brand and lot-to-lot dissolution differences (Fig. 1). To establish differences between brands and between lots within a brand, analyses of variance were carried out on the percent of drug dissolved for 0.5- and 1.0-mg tablets at 15 and 30 min using the NESTED procedure previously described (3). The $p$ values for the associated significance tests are summarized in Table IV. There were significant differences ($p \leq 0.005$) between lots within brands for 0.5-mg tablets at 15 min and for 1-mg tablets at 15 and 30 min. In addition, there were significant differences among brands for 0.5-mg tablets at 15 min ($p = 0.02$).

The differences observed under these test conditions were attributed to drug product manufacturing differences, excipients, and other tablet

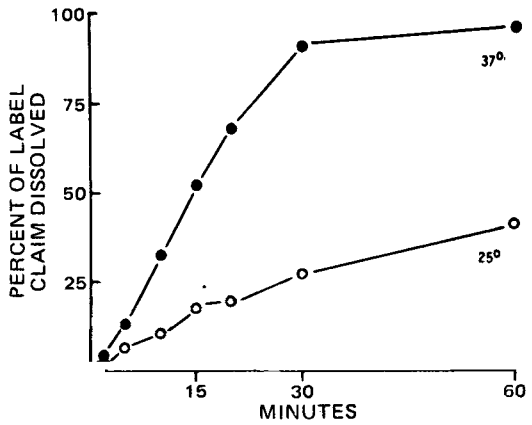


**Figure 2**—*Effect of temperature on the dissolution rate of innovator's product (S1; lot 720X5534) of 0.5-mg sublingual tablets. Dissolution values represent the average of two tablets.*

Table V—Dissolution Rates of 0.5- and 1.0-mg Dihydroergotoxine Tablets in 500 ml of Distilled Water at 25° Using Rotating-Paddle Method

| Minutes | 0.5 mg | | | | | 1.0 mg, |
|---|---|---|---|---|---|---|
| | Product M2[a] | Product P | Product B1 | Product R | Product S1 | Product M4 |
| 2 | 2.5, 5.5[b] | 0.0, 2.0 | 2.0, 0.6 | 27.3, 38.8 | 0.6, 3.0 | 8.7, 8.3 |
| 5 | 11.0, 13.0 | 4.0, 7.5 | 9.5, 5.8 | 66.8, 67.8 | 6.3, 6.0 | 20.2, 20.3 |
| 10 | 23.5, 25.5 | 16.0, 13.5 | 22.0, 23.3 | 75.3, 84.8 | 8.3, 10.6 | 37.2, 39.8 |
| 15 | 29.5, 39.0 | 22.0, 37.5 | 30.5, 37.8 | 79.8, 87.8 | 16.3, 16.0 | 48.7, 60.8 |
| 20 | 45.5, 56.0 | 33.5, 57.0 | 50.5, 59.8 | 85.3, 82.8 | 19.3, 16.5 | 73.2, 73.3 |
| 30 | 74.5, 81.2 | 41.5, 54.5 | 71.5, 70.3 | 75.8, 87.8 | 27.3, 23.0 | 94.2, 97.8 |
| 60 | 89.0, 90.5 | 61.0, 55.5 | 75.0, 75.3 | 82.8, 84.3 | 34.8, 42.0 | 106, 101 |

[a] Letter represents manufacturer, and number represents a different production lot. Refer to Tables II and III for explanation of symbols. [b] Values for two tablets.

variations. Other studies, under slightly modified test conditions, also helped to establish that dissolution differences may be due to formulation differences. Two brands, P and B2, failed to achieve total dissolution (Fig. 1). With both preparations, insoluble material in the dissolution medium and a film on the stirring shafts and paddles indicated the possibility of an insoluble complex formation. Total dissolution could be achieved only by further dilution to 900 ml of medium.

The extent of dissolution as a function of temperature was not clear cut and predictable because of the differences in formulations (Table V). For example, Products M2, P, B1, and M4 initially dissolved slowly at 25°; however, after 60 min, the extent of dissolution was comparable to that at 37°. On the other hand, temperature had no influence on Product R (the dissolution profiles at 25 and 37° were identical). However, the rate and extent of dissolution of Product S1 were decreased significantly at 25° when compared to the results obtained at 37° (Fig. 2).

Based on the *in vitro* dissolution results, the FDA implemented a dissolution specification for 0.5- and 1.0-mg sublingual tablets using the paddle method (4) where the dissolution medium is 500 ml of distilled water at 37°. The paddle height is 4.5 cm, and the stirring speed is 50 rpm. The dissolution specimens are filtered with either glass or polytef filters prior to drug content analysis.

*In vivo* bioavailability data for *in vitro–in vivo* correlations are lacking. Therefore, based on the *in vitro* performance of eight batches representing 0.5- and 1.0-mg tablets of the innovator product[15], a dissolution specification was set. For tablets to be considered acceptable, they must dissolve not less than 55% in 15 min and not less than 85% in 30 min for a mean of 12 tablets. However, no tablet should fall below 45 and 75% at those respective times.

The described *in vitro* dissolution method and its specifications should help ensure both product-to-product and lot-to-lot uniformity and consistency for dihydroergotoxine sublingual tablet dosage forms.

## REFERENCES


(1) V. Hartman, M. Rodiger, W. Ableidinger, and H. Bethke, *J. Pharm. Sci.*, **67**, 98 (1978).

(2) *Fed. Regist.*, **42** (5), 1624 (Jan. 7, 1977).

(3) "SAS User's Guide, 1979 Edition," SAS Institute, Raleigh, N.C., 1979, p. 313.

(4) "The United States Pharmacopeia," 20th rev., United States Pharmacopeial Convention, Rockville, Md., 1980, p. 959.


[15] Sandoz.

# NOTES

# Loss of Nitroglycerin from Solutions to Intravenous Plastic Containers: A Theoretical Treatment


**A. WASEEM MALICK ˣ, ANTON H. AMANN, DAVID M. BAASKE, and ROGER G. STOLL**



Received June 3, 1980, from *American Critical Care, McGaw Park, IL 60085.* Accepted for publication September 10, 1980.



**Abstract** □ The physical instability of nitroglycerin solutions in plastic containers has been reported extensively. A systematic study of potency loss in plastic infusion bags was reported recently. This paper presents a theoretical treatment of the data and a proposed model consisting of adsorption onto the surface followed by partitioning into the plastic.



**Keyphrases** □ Nitroglycerin—loss from solution to plastic intravenous containers, a theoretical treatment □ Plastic containers—loss of nitroglycerin from intravenous plastic containers, a theoretical treatment □ Adsorption, potential—nitroglycerin loss from solution in plastic intravenous containers, a theoretical treatment


Numerous studies (1–10) have reported stability problems associated with nitroglycerin solutions in plastic containers meant for intravenous infusions. Adsorption of the drug by plastic containers and infusion sets was suggested as the cause. Yuen *et al.* (8) studied the loss of nitroglycerin from aqueous solutions in immersed strips of plastic. Based on equilibrium and kinetic studies, these workers proposed an adsorption–absorption mechanism in which adsorption plays a minor role. Although their report provided some insight into the phenomenon, it did not deal with the system as a whole, *i.e.*, nitroglycerin solutions contained in intravenous bags.

The loss of nitroglycerin from solutions stored in commercial plastic intravenous bags was reported recently (10). Immediate significant losses were followed by a gradual decrease in concentration. No chemical degradation was observed. In this report, a theoretical treatment of the data and a proposed model are presented.

## EXPERIMENTAL

The applicability of the proposed model was tested using recently reported data of nitroglycerin compatibility with intravenous admixture aids (10). In brief, the procedures for obtaining the kinetic data entailed: (*a*) the addition by syringe of an aqueous nitroglycerin preparation to




*0022-3549/81/0700-0798$01.00/0*


*© 1981, American Pharmaceutical Association*

Table V—Dissolution Rates of 0.5- and 1.0-mg Dihydroergotoxine Tablets in 500 ml of Distilled Water at 25° Using Rotating-Paddle Method

| Minutes | 0.5 mg | | | | | 1.0 mg, |
|---|---|---|---|---|---|---|
| | Product M2[a] | Product P | Product B1 | Product R | Product S1 | Product M4 |
| 2 | 2.5, 5.5[b] | 0.0, 2.0 | 2.0, 0.6 | 27.3, 38.8 | 0.6, 3.0 | 8.7, 8.3 |
| 5 | 11.0, 13.0 | 4.0, 7.5 | 9.5, 5.8 | 66.8, 67.8 | 6.3, 6.0 | 20.2, 20.3 |
| 10 | 23.5, 25.5 | 16.0, 13.5 | 22.0, 23.3 | 75.3, 84.8 | 8.3, 10.6 | 37.2, 39.8 |
| 15 | 29.5, 39.0 | 22.0, 37.5 | 30.5, 37.8 | 79.8, 87.8 | 16.3, 16.0 | 48.7, 60.8 |
| 20 | 45.5, 56.0 | 33.5, 57.0 | 50.5, 59.8 | 85.3, 82.8 | 19.3, 16.5 | 73.2, 73.3 |
| 30 | 74.5, 81.2 | 41.5, 54.5 | 71.5, 70.3 | 75.8, 87.8 | 27.3, 23.0 | 94.2, 97.8 |
| 60 | 89.0, 90.5 | 61.0, 55.5 | 75.0, 75.3 | 82.8, 84.3 | 34.8, 42.0 | 106, 101 |

[a] Letter represents manufacturer, and number represents a different production lot. Refer to Tables II and III for explanation of symbols. [b] Values for two tablets.

variations. Other studies, under slightly modified test conditions, also helped to establish that dissolution differences may be due to formulation differences. Two brands, P and B2, failed to achieve total dissolution (Fig. 1). With both preparations, insoluble material in the dissolution medium and a film on the stirring shafts and paddles indicated the possibility of an insoluble complex formation. Total dissolution could be achieved only by further dilution to 900 ml of medium.

The extent of dissolution as a function of temperature was not clear cut and predictable because of the differences in formulations (Table V). For example, Products M2, P, B1, and M4 initially dissolved slowly at 25°; however, after 60 min, the extent of dissolution was comparable to that at 37°. On the other hand, temperature had no influence on Product R (the dissolution profiles at 25 and 37° were identical). However, the rate and extent of dissolution of Product S1 were decreased significantly at 25° when compared to the results obtained at 37° (Fig. 2).

Based on the *in vitro* dissolution results, the FDA implemented a dissolution specification for 0.5- and 1.0-mg sublingual tablets using the paddle method (4) where the dissolution medium is 500 ml of distilled water at 37°. The paddle height is 4.5 cm, and the stirring speed is 50 rpm. The dissolution specimens are filtered with either glass or polytef filters prior to drug content analysis.

*In vivo* bioavailability data for *in vitro–in vivo* correlations are lacking. Therefore, based on the *in vitro* performance of eight batches representing 0.5- and 1.0-mg tablets of the innovator product[15], a dissolution specification was set. For tablets to be considered acceptable, they must dissolve not less than 55% in 15 min and not less than 85% in 30 min for a mean of 12 tablets. However, no tablet should fall below 45 and 75% at those respective times.

The described *in vitro* dissolution method and its specifications should help ensure both product-to-product and lot-to-lot uniformity and consistency for dihydroergotoxine sublingual tablet dosage forms.

## REFERENCES


(1) V. Hartman, M. Rodiger, W. Ableidinger, and H. Bethke, *J. Pharm. Sci.*, **67**, 98 (1978).

(2) *Fed. Regist.*, **42** (5), 1624 (Jan. 7, 1977).

(3) "SAS User's Guide, 1979 Edition," SAS Institute, Raleigh, N.C., 1979, p. 313.

(4) "The United States Pharmacopeia," 20th rev., United States Pharmacopeial Convention, Rockville, Md., 1980, p. 959.


[15] Sandoz.

# NOTES

# Loss of Nitroglycerin from Solutions to Intravenous Plastic Containers: A Theoretical Treatment


**A. WASEEM MALICK ˣ, ANTON H. AMANN, DAVID M. BAASKE, and ROGER G. STOLL**



Received June 3, 1980, from *American Critical Care, McGaw Park, IL 60085.* Accepted for publication September 10, 1980.



**Abstract** □ The physical instability of nitroglycerin solutions in plastic containers has been reported extensively. A systematic study of potency loss in plastic infusion bags was reported recently. This paper presents a theoretical treatment of the data and a proposed model consisting of adsorption onto the surface followed by partitioning into the plastic.



**Keyphrases** □ Nitroglycerin—loss from solution to plastic intravenous containers, a theoretical treatment □ Plastic containers—loss of nitroglycerin from intravenous plastic containers, a theoretical treatment □ Adsorption, potential—nitroglycerin loss from solution in plastic intravenous containers, a theoretical treatment


Numerous studies (1–10) have reported stability problems associated with nitroglycerin solutions in plastic containers meant for intravenous infusions. Adsorption of the drug by plastic containers and infusion sets was suggested as the cause. Yuen *et al.* (8) studied the loss of nitroglycerin from aqueous solutions in immersed strips of plastic. Based on equilibrium and kinetic studies, these workers proposed an adsorption–absorption mechanism in which adsorption plays a minor role. Although their report provided some insight into the phenomenon, it did not deal with the system as a whole, *i.e.*, nitroglycerin solutions contained in intravenous bags.

The loss of nitroglycerin from solutions stored in commercial plastic intravenous bags was reported recently (10). Immediate significant losses were followed by a gradual decrease in concentration. No chemical degradation was observed. In this report, a theoretical treatment of the data and a proposed model are presented.

## EXPERIMENTAL

The applicability of the proposed model was tested using recently reported data of nitroglycerin compatibility with intravenous admixture aids (10). In brief, the procedures for obtaining the kinetic data entailed: (*a*) the addition by syringe of an aqueous nitroglycerin preparation to




*0022-3549/81/0700-0798$01.00/0*


*© 1981, American Pharmaceutical Association*

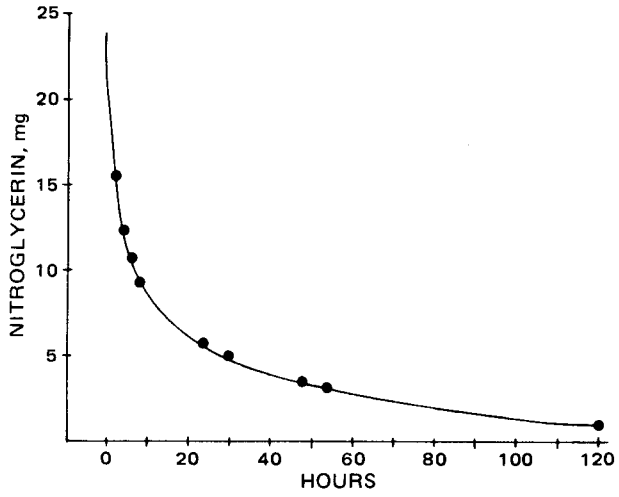


**Figure 1**—*Amount of nitroglycerin in a plastic bag as a function of time. The symbols (●) are experimental points. The solid line is the theoretically computed curve according to Eq. 10.*

a 100-ml polyvinyl chloride[1] plastic bag to yield a final nominal concentration of 50 μg/ml, and (*b*) mixing the solution and sampling at given intervals for potency determination by high-performance liquid chromatography (HPLC). Nitroglycerin potency assays were performed according to the method of Baaske *et al.* (10). Figure 1 summarizes the results.

## THEORETICAL

The loss of nitroglycerin from solution in plastic bags can be described by two processes: rapid adsorption of nitroglycerin by the surface of the plastic bag, followed by dissolution of nitroglycerin into the plastic. This loss can be represented diagramatically as in Scheme I.

$$\text{nitroglycerin in aqueous solution} \underset{k_2}{\overset{k_1}{\rightleftarrows}} \text{adsorbed nitroglycerin on plastic surface} \xrightarrow{k_3} \text{nitroglycerin dissolved in plastic matrix}$$

*Scheme I*

The process may be considered to be dependent on the following factors: (*a*) the amount of nitroglycerin in solution, (*b*) the ratio of nitroglycerin solution volume to the area of the plastic surface in contact with the solution, (*c*) the rate at which fresh nitroglycerin molecules from the solution are adsorbed at the plastic surface following the sorption of nitroglycerin by the plastic matrix, and (*d*) the solubility of nitroglycerin in the plastic matrix and the partition coefficient of nitroglycerin between plastic and the aqueous phase.

Scheme I can be expressed in terms of the instantaneous amounts of nitroglycerin in solution ($A$), nitroglycerin adsorbed to the plastic surface ($B$), and nitroglycerin dissolved in the plastic matrix ($C$) (Scheme II).

$$A \underset{k_2}{\overset{k_1}{\rightleftarrows}} B \xrightarrow{k_3} C$$

*Scheme II*

The differential equations describing the rate of change of $A$, $B$, and $C$ are:

$$\frac{dA}{dt} = -k_1A + k_2B \qquad \text{(Eq. 1)}$$

$$\frac{dB}{dt} = k_1A - k_2B - k_3B \qquad \text{(Eq. 2)}$$

$$\frac{dC}{dt} = k_3B \qquad \text{(Eq. 3)}$$

Experimental data show a rapid initial drop of nitroglycerin in solution followed by a relatively slower rate of loss. This finding suggests that the rate of nitroglycerin adsorption to the surface is much greater than the rate of sorption by the plastic matrix. The adsorbed layer of nitroglycerin onto the plastic surface can be pictured as a few molecules thick at most.

[1] Viaflex container, Travenol Laboratories, Morton Grove, IL 60053.

The molecules of the adsorbed layer of nitroglycerin that are removed by sorption into the plastic are expected to be replaced rapidly by fresh molecules from the solution. Since nitroglycerin is being adsorbed continually at the surface and removed by dissolution into the matrix, $B$ should approach steady state:

$$\frac{dB}{dt} = 0 = k_1A - k_2B - k_3B \qquad \text{(Eq. 4)}$$

By introducing the steady-state approximation and the initial conditions (at $t = 0$, $A = A_0$, $B = 0$, and $C = 0$), the following solution for $A$ is obtained:

$$A = \alpha e^{-[k_1k_3/(k_2+k_3)]t} + \beta e^{-(k_2+k_3)t} - \alpha e^{-k_1t} - \beta e^{-k_1t} + A_0e^{-k_1t} \qquad \text{(Eq. 5)}$$

where $\alpha$ and $\beta$ are constants.

A comparison of the processes controlled by $k_2$ and $k_3$ in the scheme suggests that the magnitude of $k_2$ is smaller than $k_3$. The loss of nitroglycerin from the adsorbed layer to the relatively polar aqueous phase is described by $k_2$, whereas $k_3$ describes the sorption of the adsorbed nitroglycerin molecules by the nonpolar plastic matrix. Since the affinity of nitroglycerin is expected to be much greater for the nonpolar plastic matrix than the aqueous phase, it is expected that $k_3 \gg k_2$.

Following this assumption, Eq. 5 reduces to:

$$A = \beta e^{-k_3t} + (A_0 - \beta)e^{-k_1t} \qquad \text{(Eq. 6)}$$

where:

$$\beta = \frac{A_0}{\frac{k_3^2}{k_1k_2} + \frac{k_1^2}{k_2} - \frac{2k_3}{k_2}} \qquad \text{(Eq. 7)}$$

and $k_1$ is a function of the amount of drug in solution, the surface area available for adsorption, and the formulation differences between solutions and plastic matrixes, and $k_3$ is a function of the volume of the plastic matrix and the solubility of nitroglycerin in the plastic matrix.

The $k_3/k_2$ ratio describes the overall partitioning behavior of nitroglycerin between the plastic and the aqueous phase. The relationship of the true partition coefficient ($PC$) and $k_3/k_2$ can be described by:

$$\frac{k_3}{k_2} = aPC \qquad \text{(Eq. 8)}$$

where $a$ is a proportionality constant related to, among other factors, the mass of the plastic, the volume of aqueous nitroglycerin solution, and the formulation differences between the solution and the plastic bag.

Similarly, the $k_1/k_2$ ratio can be related to the affinity constant ($k_{Lang}$) in a Langmuir type of adsorption (11):

$$\frac{k_1}{k_2} = \rho k_{Lang} \qquad \text{(Eq. 9)}$$

where $\rho$ is a proportionality constant that is also related to the surface area of the plastic, the volume of the aqueous nitroglycerin solution, and the formulation differences between the solution and the plastic bag.

Langmuir adsorption treatment cannot be applied rigorously to this model since an equilibrium situation between the adsorbate (nitroglycerin) and the adsorbent (plastic) does not exist during the experiment. The adsorbed molecules, instead of reaching an equilibrium with the nonadsorbed molecules in the aqueous solution, are removed continually from the surface by the plastic matrix.

## RESULTS AND DISCUSSION

Figure 1 shows a plot (at room temperature) of the amount of nitroglycerin remaining in the plastic bag as a function of time. As predicted by the model, a biexponential loss of nitroglycerin with time is seen. The rate constants for adsorption ($k_1$) and sorption by the plastic matrix ($k_3$), together with the constants $\beta$ and $A_0 - \beta$, were obtained by using a back-projection (stripping) technique (12). Figure 1 shows the actual data points and the curve obtained by theoretical computation. The solid theoretical curve was generated by using the equation derived for the proposed model (Eq. 6) and substituting the values of the constants obtained from the experimental data. The final form of the equation is:

$$A = 8.957e^{-0.028t} + 14.943e^{-0.235t} \qquad \text{(Eq. 10)}$$

The experimental data points show an excellent fit with the solid theoretical line. Thus, the proposed model describing (*a*) the loss of nitroglycerin from the solution in the plastic bags as a rapid adsorption to the

plastic surface, (*b*) followed by sorption of nitroglycerin to the plastic matrix by dissolution is in good agreement with the actual data. The model presented here should be useful for future investigations.

## REFERENCES


(1) W. G. Crouthamel, B. Dorsch, and R. Shangraw, *N. Engl. J. Med.*, **299**, 262 (1978).

(2) P. A. Cossum, M. S. Roberts, A. J. Galbraith, and G. W. Boyd, *Lancet*, **2**, 349 (1978).

(3) H. L. Fung, *Am. J. Hosp. Pharm.*, **35**, 528 (1978).

(4) J. K. Sturek, T. D. Sokoloski, W. T. Winsley, and P. E. Stach, *ibid.*, **35**, 537 (1978).

(5) D. J. Ludwig and C. T. Ueda, *ibid.*, **35**, 541 (1978).

(6) J. C. Boylan, R. L. Robison, and P. M. Terrill, *ibid.*, **35**, 1031 (1978).

(7) B. L. McNiff, E. F. McNiff, and H. L. Fung, *ibid.*, **36**, 173 (1979).

(8) P. H. Yuen, S. L. Denman, T. D. Sokoloski, and A. M. Burkman, *J. Pharm. Sci.*, **68**, 1163 (1979).

(9) J. K. Ingram and J. D. Miller, *Anesthesiology*, **51**, S132 (1979).

(10) D. M. Baaske, A. H. Amann, D. W. Wagenknecht, M. Mooers, J. E. Carter, H. J. Hoyt, and R. G. Stoll, *Am. J. Hosp. Pharm.*, **37**, 201 (1980).

(11) "Remington's Pharmaceutical Sciences," 15th ed., Mack Publishing Co., Easton, Pa., 1975, p. 294.

(12) J. G. Wagner, "Fundamentals of Clinical Pharmacokinetics," Drug Intelligence Publications, Hamilton, Ill., 1975.


# High-Performance Liquid Chromatographic Determination of Verapamil in Plasma by Fluorescence Detection


**ERIC WATSON * and PATRICIA A. KAPUR ˣ**



Received September 5, 1980, from the *Department of Anesthesiology, School of Medicine, Center for the Health Sciences, University of California, Los Angeles, CA 90024.* Accepted for publication October 17, 1980. *Present address: School of Pharmacy, University of Southern California, Los Angeles, CA 90033.



**Abstract** □ A rapid and highly sensitive method is reported for the quantitative determination of verapamil in plasma. Verapamil and its internal standard are extracted from alkalinized plasma with heptane and then back-extracted into dilute sulfuric acid. An aliquot is injected directly into a high-performance liquid chromatograph, separated by reversed-phase chromatography, and quantified by a fluorescence detector. The procedure is suitable for the routine determination of verapamil in plasma in concentrations as low as 1 ng/ml.



**Keyphrases** □ Verapamil—high-performance liquid chromatography, fluorescence detection, canine plasma □ High-performance liquid chromatography—verapamil, canine plasma, fluorescence detection □ Antiarrhythmic agents—high-performance liquid chromatography, verapamil, canine plasma, fluorescence detection


Verapamil, 5-[(3,4-dimethoxyphenethyl)methylamino]-2-(3,4-dimethoxyphenyl)-2-isopropylvaleronitrile (I), has been used for several years in Europe as an effective antiarrhythmic drug and is now undergoing clinical evaluation in the United States. Studies are underway in this laboratory to show the efficacy of verapamil in suppressing halothane–epinephrine arrhythmias (1).

Several analytical procedures have been reported for determining verapamil in plasma, including spectrophotometry (2), GLC with mass fragmentography (3), GLC (4), and high-performance liquid chromatography (HPLC) (5). None of these methods was considered completely satisfactory for reasons of simplicity, speed, and the ability to determine metabolites quantitatively. Therefore, an HPLC procedure was developed, and its application for the determination of verapamil in canine plasma following intravenous injection is reported here.

## EXPERIMENTAL

**Chemicals and Reagents**—Verapamil[1] (I) and its internal standard, 4-[(3,4-dimethoxyphenethyl)methylamino] -2- (3,4-dimethoxyphenyl)-2-isopropylbutyronitrile[2] (II), were obtained as hydrochloride salts. Glass-distilled heptane[3] and HPLC grade acetonitrile[4] were used. Sodium hydroxide (2 *N*), sulfuric acid (0.2 *N*), and pH 3.0 phosphate buffer (1 *M*) were prepared with deionized water.

**HPLC**—A liquid chromatograph[5] was used with a fluorescence detector[6]. The column[7] was $C_{18}$ reversed phase, and the eluting solvent was 45% acetonitrile–55% pH 3.0 potassium phosphate (0.1 *M*). The solvent was degassed prior to use by applying a vacuum. The flow rate was set at 1 ml/min. The detector settings were 203 nm for excitation with a 320-nm emission filter.

**Procedure**—To 0.5 ml of plasma were added 50 ng of II, 0.25 ml of 2 *N* NaOH, and 3 ml of heptane. The mixture was shaken mechanically for 15 min and then centrifuged. The organic layer was transferred to a 5-ml conical tube, and 50 μl of 0.2 *N* $H_2SO_4$ was added. The contents were mixed in a vortex mixer for 1 min and centrifuged, and a 10-μl sample was injected into the chromatograph.

## RESULTS AND DISCUSSION

Standard curves were prepared routinely from spiked plasma samples containing 40, 100, and 250 ng of verapamil/ml. Peak height ratios were plotted as a function of the verapamil concentration added and were linear within this range. Intercepts usually passed through the origin. The lower limit of sensitivity of the assay was ~1 ng/ml, and this level was completely adequate for analyzing the samples in this study. Assay reproducibility and precision were evaluated by the repeated analyses of spiked plasma samples containing 100 ng of verapamil/ml. The coefficient of variation at this level was 4.6% ($n$ = 12). The slopes of the standard curves from water or biological fluids were similar, indicating insignificant

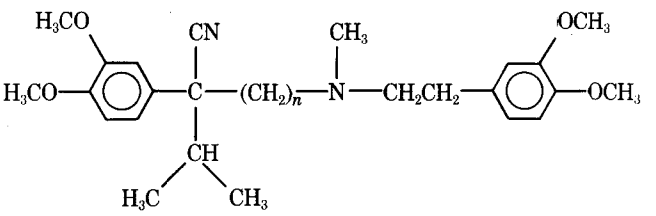


I: $n$ = 3
II: $n$ = 2

[1] Knoll Pharmaceuticals, Whippany, N.J.
[2] D517, Knoll AG, Ludwigshafen, West Germany.
[3] Mallinckrodt Chemical Co., St. Louis, Mo.
[4] MCB, Cincinnati, Ohio.
[5] Model 330, Altex, Berkeley, Calif.
[6] Model 970, Schoeffel Instruments, Westwood, N.J.
[7] Ultrasphere ODS, Altex, Berkeley, Calif.




*0022-3549/81/0700-0800$01.00/0*


*© 1981, American Pharmaceutical Association*

plastic surface, (*b*) followed by sorption of nitroglycerin to the plastic matrix by dissolution is in good agreement with the actual data. The model presented here should be useful for future investigations.

## REFERENCES


(1) W. G. Crouthamel, B. Dorsch, and R. Shangraw, *N. Engl. J. Med.*, **299**, 262 (1978).

(2) P. A. Cossum, M. S. Roberts, A. J. Galbraith, and G. W. Boyd, *Lancet*, **2**, 349 (1978).

(3) H. L. Fung, *Am. J. Hosp. Pharm.*, **35**, 528 (1978).

(4) J. K. Sturek, T. D. Sokoloski, W. T. Winsley, and P. E. Stach, *ibid.*, **35**, 537 (1978).

(5) D. J. Ludwig and C. T. Ueda, *ibid.*, **35**, 541 (1978).

(6) J. C. Boylan, R. L. Robison, and P. M. Terrill, *ibid.*, **35**, 1031 (1978).

(7) B. L. McNiff, E. F. McNiff, and H. L. Fung, *ibid.*, **36**, 173 (1979).

(8) P. H. Yuen, S. L. Denman, T. D. Sokoloski, and A. M. Burkman, *J. Pharm. Sci.*, **68**, 1163 (1979).

(9) J. K. Ingram and J. D. Miller, *Anesthesiology*, **51**, S132 (1979).

(10) D. M. Baaske, A. H. Amann, D. W. Wagenknecht, M. Mooers, J. E. Carter, H. J. Hoyt, and R. G. Stoll, *Am. J. Hosp. Pharm.*, **37**, 201 (1980).

(11) "Remington's Pharmaceutical Sciences," 15th ed., Mack Publishing Co., Easton, Pa., 1975, p. 294.

(12) J. G. Wagner, "Fundamentals of Clinical Pharmacokinetics," Drug Intelligence Publications, Hamilton, Ill., 1975.


# High-Performance Liquid Chromatographic Determination of Verapamil in Plasma by Fluorescence Detection


**ERIC WATSON * and PATRICIA A. KAPUR ˣ**



Received September 5, 1980, from the *Department of Anesthesiology, School of Medicine, Center for the Health Sciences, University of California, Los Angeles, CA 90024.* Accepted for publication October 17, 1980. *Present address: School of Pharmacy, University of Southern California, Los Angeles, CA 90033.



**Abstract** □ A rapid and highly sensitive method is reported for the quantitative determination of verapamil in plasma. Verapamil and its internal standard are extracted from alkalinized plasma with heptane and then back-extracted into dilute sulfuric acid. An aliquot is injected directly into a high-performance liquid chromatograph, separated by reversed-phase chromatography, and quantified by a fluorescence detector. The procedure is suitable for the routine determination of verapamil in plasma in concentrations as low as 1 ng/ml.



**Keyphrases** □ Verapamil—high-performance liquid chromatography, fluorescence detection, canine plasma □ High-performance liquid chromatography—verapamil, canine plasma, fluorescence detection □ Antiarrhythmic agents—high-performance liquid chromatography, verapamil, canine plasma, fluorescence detection


Verapamil, 5-[(3,4-dimethoxyphenethyl)methylamino]-2-(3,4-dimethoxyphenyl)-2-isopropylvaleronitrile (I), has been used for several years in Europe as an effective antiarrhythmic drug and is now undergoing clinical evaluation in the United States. Studies are underway in this laboratory to show the efficacy of verapamil in suppressing halothane–epinephrine arrhythmias (1).

Several analytical procedures have been reported for determining verapamil in plasma, including spectrophotometry (2), GLC with mass fragmentography (3), GLC (4), and high-performance liquid chromatography (HPLC) (5). None of these methods was considered completely satisfactory for reasons of simplicity, speed, and the ability to determine metabolites quantitatively. Therefore, an HPLC procedure was developed, and its application for the determination of verapamil in canine plasma following intravenous injection is reported here.

## EXPERIMENTAL

**Chemicals and Reagents**—Verapamil[1] (I) and its internal standard, 4-[(3,4-dimethoxyphenethyl)methylamino] -2- (3,4-dimethoxyphenyl)-2-isopropylbutyronitrile[2] (II), were obtained as hydrochloride salts. Glass-distilled heptane[3] and HPLC grade acetonitrile[4] were used. Sodium hydroxide (2 *N*), sulfuric acid (0.2 *N*), and pH 3.0 phosphate buffer (1 *M*) were prepared with deionized water.

**HPLC**—A liquid chromatograph[5] was used with a fluorescence detector[6]. The column[7] was $C_{18}$ reversed phase, and the eluting solvent was 45% acetonitrile–55% pH 3.0 potassium phosphate (0.1 *M*). The solvent was degassed prior to use by applying a vacuum. The flow rate was set at 1 ml/min. The detector settings were 203 nm for excitation with a 320-nm emission filter.

**Procedure**—To 0.5 ml of plasma were added 50 ng of II, 0.25 ml of 2 *N* NaOH, and 3 ml of heptane. The mixture was shaken mechanically for 15 min and then centrifuged. The organic layer was transferred to a 5-ml conical tube, and 50 μl of 0.2 *N* $H_2SO_4$ was added. The contents were mixed in a vortex mixer for 1 min and centrifuged, and a 10-μl sample was injected into the chromatograph.

## RESULTS AND DISCUSSION

Standard curves were prepared routinely from spiked plasma samples containing 40, 100, and 250 ng of verapamil/ml. Peak height ratios were plotted as a function of the verapamil concentration added and were linear within this range. Intercepts usually passed through the origin. The lower limit of sensitivity of the assay was ~1 ng/ml, and this level was completely adequate for analyzing the samples in this study. Assay reproducibility and precision were evaluated by the repeated analyses of spiked plasma samples containing 100 ng of verapamil/ml. The coefficient of variation at this level was 4.6% ($n$ = 12). The slopes of the standard curves from water or biological fluids were similar, indicating insignificant

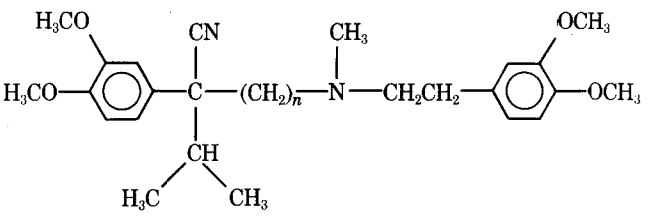


I: $n$ = 3
II: $n$ = 2

[1] Knoll Pharmaceuticals, Whippany, N.J.
[2] D517, Knoll AG, Ludwigshafen, West Germany.
[3] Mallinckrodt Chemical Co., St. Louis, Mo.
[4] MCB, Cincinnati, Ohio.
[5] Model 330, Altex, Berkeley, Calif.
[6] Model 970, Schoeffel Instruments, Westwood, N.J.
[7] Ultrasphere ODS, Altex, Berkeley, Calif.




*0022-3549/81/0700-0800$01.00/0*


*© 1981, American Pharmaceutical Association*

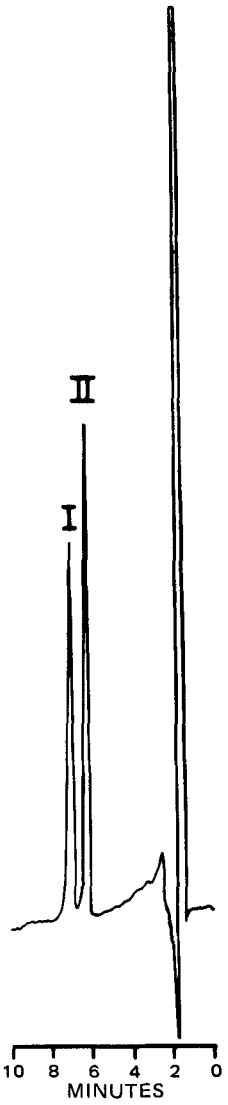


**Figure 1**—*Chromatogram of the extract of a 0.5-ml plasma sample taken 8 min after the intravenous injection of 0.2 mg of verapamil/kg. Key: I, verapamil; and II, internal standard.*

differences in the extractability of the compounds from aqueous solutions of different compositions.

A chromatogram of an extracted plasma sample from a dog that had received 0.2 mg of verapamil/kg iv 8 min previously is shown in Fig. 1. The verapamil concentration was 95 ng/ml.

Figure 2 shows a semilog plot of the concentration–time curve obtained after intravenous injection of 0.1 mg of verapamil/kg in a dog. The levels declined exponentially as fitted by the regression analysis program AUTOAN to a three-compartment open model according to:

$$C_x = Ae^{-\alpha t} + Be^{-\beta t} + Pe^{-\pi t} \qquad \text{(Eq. 1)}$$

where $C_x$ is the plasma verapamil concentration; $A$, $B$, and $P$ are the coefficients of the three compartments; and $\alpha$, $\beta$, and $\pi$ are the decay constants from these compartments. The terminal half-lives were 0.25, 6.5, and 129 hr, respectively. However, although the data from this experiment were compatible with a three-compartment model, it is not possible to state that three compartments exist for verapamil. Additional experiments of longer duration are required to reach statistically valid conclusions. The half-lives of the initial distribution phase ($t_{1/2\alpha}$, 0.25 hr) and for the apparent terminal phase ($t_{1/2\beta}$, 6.5 hr) were in agreement with previously reported values (6, 7).

The retention times of verapamil and II were 7 and 6 min, respectively. No endogenous compounds were present in plasma with the same elution times and fluorescence spectra.

A high first-pass effect was reported for patients receiving oral verapamil (6). In the study reported here, verapamil was administered intravenously only; therefore, the presence of substantial amounts of metabolic products would not be expected. Throughout the study, no evidence of metabolic products was observed. Since these products would be more polar, their elution times would be expected to be less than the elution time of verapamil. Therefore, the use of heptane as the extracting solvent is extremely advantageous since there are no major peaks eluting prior to verapamil that may possibly obscure the presence of metabolic products. While authentic metabolites have not been tested in this chromatographic system, it is reasonable to expect that they would elute ahead of verapamil.

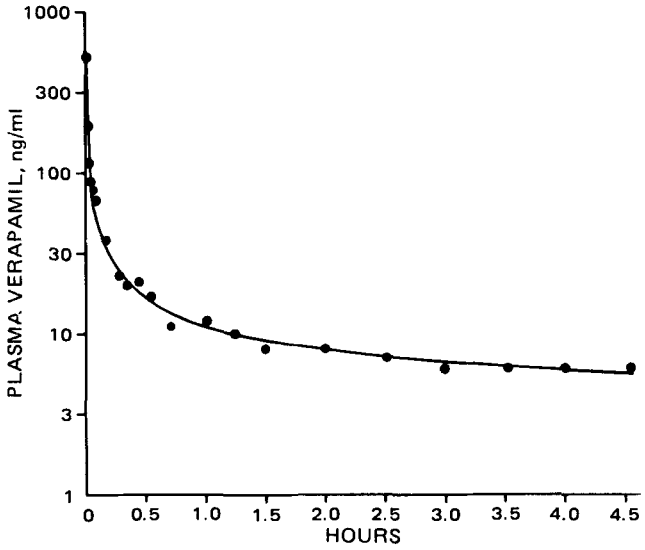


**Figure 2**—*Change in plasma verapamil concentration with time after the intravenous injection of 0.1 mg/kg at time zero.*

Other studies are being planned to evaluate the pharmacokinetics of verapamil and the individual metabolic products following oral administration. A discrepancy exists between the duration of the electrophysiological and hemodynamic effects of verapamil and its concentration in plasma. The possibility that this discrepancy may be related to the concentration of metabolites has been proposed (8), and the method described here may be of value in resolving this problem.

The ultimate objectives in undertaking pharmacokinetic metabolic and disposition studies are to predict disposition in individual patients and to optimize doses and schedules rapidly. The development of a highly sensitive and specific analytical procedure for measuring verapamil in plasma should enable more detailed and longer term clinical disposition studies than have been reported previously.

## REFERENCES

(1) P. A. Kapur and W. E. Flacke, *Anesthesiology*, in press.

(2) R. G. McAllister and S. M. Howell, *J. Pharm. Sci.*, **65,** 431 (1976).

(3) B. Spiegelhalder and M. Eichelbaum, *Arzneim.-Forsch.*, **27,** 94 (1977).

(4) R. G. McAllister, T. G. Tan, and D. W. A. Bourne, *J. Pharm. Sci.*, **68,** 574 (1979).

(5) S. R. Harapat and R. E. Kates, *J. Chromatogr.*, **170,** 385 (1979).

(6) M. Schomerus, B. Spiegelhalder, B. Stieren, and M. Eichelbaum, *Cardiovasc. Res.*, **10,** 605 (1976).

(7) Y. Koike, K. Shimamura, I. Shudo, and H. Saito, *Res. Commun. Chem. Pathol. Pharmacol.*, **24,** 37 (1979).

(8) B. N. Singh, G. Ellrodt, and C. T. Peter, *Drugs*, **15,** 169 (1978).

## ACKNOWLEDGMENTS

The authors thank Mr. Harry Graham of Knoll Pharmaceuticals, Whippany, N.J., for supplying verapamil and its internal standard.

# Parabolic Equation Relating Free and Total Drug Concentrations in Cases of Nonlinear Plasma Protein Binding

**HARRIET L. BEHM** * **and JOHN G. WAGNER** ˣ

Received September 10, 1980, from the *College of Pharmacy and the Upjohn Center for Clinical Pharmacology, University of Michigan, Ann Arbor, MI 48109.* Accepted for publication December 10, 1980. *Present address: Pharmaceutical R & D, Squibb Institute for Medical Research, New Brunswick, NJ 08903.

**Abstract** □ In many cases of nonlinear drug–protein binding, investigators have fitted data to the classical Langmuir model with two classes of binding sites involving four parameters. For human serum albumin binding of tolmetin and salicylate, a simple two-parameter parabolic equation relating free to total concentrations fitted the binding data better. Thus, the free fraction corresponding to the serum or plasma drug concentration in the blood sample taken from a subject can be estimated directly from the parabolic model. This is not the case when the Langmuir model is used to describe nonlinear binding data since the positive root of a cubic equation must be obtained to estimate the free from the total concentration. The direct relationship between free and total drug concentrations would be useful in many clinical situations.

**Keyphrases** □ Drug–protein binding—Langmuir and parabolic models compared, parameter estimation, equilibrium dialysis of salicylic acid and tolmetin with human serum albumin □ Equilibrium dialysis—drug–protein binding, Langmuir and parabolic models compared for free drug concentration estimation □ Models, mathematical—Langmuir and parabolic models compared for free drug concentration estimation, equilibrium dialysis

When equilibrium dialysis is used to measure nonlinear drug–protein binding, the free fraction of drug obtained from the equilibrium concentrations in the buffer and plasma compartments of the dialysis apparatus is always less than that in the original plasma or serum sample. The free fraction corresponding to the initial total drug concentration must be estimated from a function describing the binding over a range of equilibrium drug concentrations. If only one serum or plasma sample containing drug is available, one cannot calculate the correct free and bound drug concentrations in the original plasma or serum sample (1).

## BACKGROUND

Free fractions corresponding to the initial plasma or serum total drug concentrations can be estimated by solving a quadratic ($k = 1$) or cubic ($k = 2$) equation (1) when nonlinear drug–protein binding data, obtained using equilibrium dialysis, are fitted to the classical Langmuir model (2):

$$C_b = \sum_{i=1}^{k} \frac{n_i C_p C_f}{Kd_i + C_f} \qquad \text{(Eq. 1)}$$

where $C_b$ is the protein-bound drug concentration at equilibrium, $C_p$ is the protein concentration, $C_f$ is the free (unbound) drug concentration at equilibrium, $Kd_i$ is the dissociation constant for the $i$th class of binding sites, $n_i$ is the number of identical independent binding sites in a class, and $k$ is the number of classes. The disadvantage of this technique is that the free drug concentration corresponding to a total drug concentration cannot be estimated directly.

With tolmetin–human serum albumin ($k = 2$ or 3) (3) or salicylate–human serum albumin ($k = 2$) (4) binding data from equilibrium dialysis experiments, it was found empirically that a plot of the free fraction *versus* total equilibrium drug concentration was linear:

$$\frac{C_f}{C_t} = a + bC_t \qquad \text{(Eq. 2)}$$

where $C_t$ is the total drug concentration and $a$ and $b$ are the intercept and slope of the straight line, respectively. The constant $a$ is dimensionless, while $b$ has dimensions of $\mu M^{-1}$. This equation can be rearranged to give a simple parabolic relationship that passes through the origin and predicts zero drug bound at zero total drug concentration:

$$C_f = aC_t + bC_t^2 \qquad \text{(Eq. 3)}$$

In many cases, the binding data were fitted much better to Eq. 3 than to the classical Langmuir model (Eq. 1 with $k = 2$). This parabolic relationship is useful in many clinical situations since $C_f$ can be estimated directly for a given $C_t$ value. The concentration range was 0–1200 $\mu M$ for tolmetin and 0–2400 $\mu M$ for salicylic acid, and the parameters of Eq. 3 (Tables I and II) are valid only in these ranges.

## EXPERIMENTAL

All drug–protein binding assays were performed using equilibrium dialysis as described previously (5). Equilibration was attained when samples were placed in an oscillating water bath (at 37°) for 18 hr. Drug concentrations were estimated by methods published previously (2). The unlabeled[1] and [$^{14}$C]salicylic acid[2] were obtained commercially. Human serum albumin[3] solution (25%) was diluted with water to 4% and used in the binding studies with various buffers, while fatty acid-free human serum albumin[4] was used for the binding studies at various temperatures. The program NONLIN (6) was used for fitting the binding data to Eq. 1 ($k = 2$) or 3.

## RESULTS

The estimated parameters and their coefficients of variation for the two models (Eqs. 1 and 3) for salicylic acid–human serum albumin binding data are shown in Table I; coefficients of variation were obtained as indicated. For the Langmuir model, the estimated parameters, $P(i)$, in terms of previously defined constants were $P(1) = n_1C_p$, $P(2) = Kd_1$, $P(3) = n_2C_p$, and $P(4) = Kd_2$. Here, $n_1C_p$ and $n_2C_p$ are the binding capacities at 4% human serum albumin. With salicylic acid, fits to the parabolic relationship were much better than to the Langmuir model with two classes of binding sites ($k = 2$), as reflected by the much smaller coefficients of variation for the parabolic model than for the Langmuir model. However, fits to both models were excellent. Measures of fit[5], corr and $r^2$, for fitting of data to the parabolic model ranged from both being 0.997 to both being 1.00. The corr and $r^2$ values ranged from 0.998 and 0.999, respectively, in 0.05 $M$ $KH_2PO_4$ buffer to 0.995 and 0.996, respectively, in triethanolamine buffer when data were fitted to the Langmuir model with $k = 2$.

The estimated parameters and their coefficients of variation for the two models (Eqs. 1 and 3) for the tolmetin–human serum albumin binding data are shown in Table II. The computer fitting of data obtained using imidazole buffer provided no standard deviations for two of the estimated parameters. Again, fits to the parabolic model (as reflected by the lower coefficients of variation) were better than to the Langmuir model but were not as dramatically different as the fits with the salicylic acid data. However, fits to both models were extremely good. Measures of fit, corr and $r^2$, for the parabolic model fitting ranged from 0.992 and

[1] Mallinckrodt.
[2] Prepared by California Bionuclear Corp.
[3] Michigan State Department of Health.
[4] Sigma Chemical Co.
[5] Corr is the correlation coefficient for the regression of expected *versus* observed concentrations, and $r^2$ is the coefficient of determination.



*0022-3549/81/0700-0802$01.00/0*
*© 1981, American Pharmaceutical Association*

**Table I—Estimated Parameters and Their Coefficients of Variation for Salicylic Acid**

| Buffer | Langmuir Model | | | | Parabolic Model | |
|---|---|---|---|---|---|---|
| | $n_1C_p$, $\mu M$ | $Kd_1$, $\mu M$ | $n_2C_p$, $\mu M$ | $Kd_2$, $\mu M$ | $a$ | $b$, $\mu M^{-1}$ |
| Tromethanine | 1247[a] | 372 | 2,276 | 5,509 | 0.233 | $8.98 \times 10^{-5}$ |
| | (200)[b] | (137) | (911) | (1578) | (2.2) | (3.7) |
| 0.1 *M* $KH_2PO_4$ | 549 | 177 | 2,493 | 2,256 | 0.215 | $1.05 \times 10^{-4}$ |
| | (67.0) | (50.2) | (42.8) | (110) | (3.2) | (4.2) |
| 0.05 *M* $KH_2PO_4$ | 753 | 281 | 1,879 | 1,546 | 0.192 | $1.05 \times 10^{-4}$ |
| | (194) | (106) | (27.3) | (195) | (2.2) | (2.4) |
| "House"[c] | 1054 | 244 | 5,452 | 9,580 | 0.175 | $1.07 \times 10^{-4}$ |
| | (30.6) | (28.5) | (187) | (253) | (3.3) | (3.3) |
| 0.05 *M* $KH_2PO_4$ | 1086 | 308 | 16,610 | 40,925 | 0.218 | $1.03 \times 10^{-4}$ |
| + 0.05 *M* NaCl | (16.0) | (15.1) | (726) | (766) | (2.6) | (3.4) |
| Imidazole | 890 | 297 | — | — | 0.244 | $1.04 \times 10^{-4}$ |
| | (4.6) | (9.7) | | | (2.7) | (4.0) |
| Triethanolamine | 684 | 308 | 2,744 | 3,615 | 0.271 | $9.43 \times 10^{-5}$ |
| | (134) | (86.6) | (152) | (321) | (3.0) | (5.5) |
| 0.1 *M* $NaH_2PO_4$ | 541 | 180 | 4,779 | 3,859 | 0.222 | $7.78 \times 10^{-5}$ |
| | (61.7) | (48.9) | (83.3) | (130) | (3.3) | (5.5) |

[a] Estimated parameter. [b] Coefficient of variation (%) = (standard deviation of estimate/estimate) × 100. [c] Consists of 0.093 *M* phosphate (0.696 g of dibasic potassium phosphate, 0.138 g of dibasic sodium phosphate monohydrate, and 2.25 g of sodium chloride and brought to volume of 500 ml with water).

**Table II—Estimated Parameters and Their Coefficients of Variation for Tolmetin**

| Buffer | Langmuir Model | | | | Parabolic Model | |
|---|---|---|---|---|---|---|
| | $n_1C_p$, $\mu M$ | $Kd_1$, $\mu M$ | $n_2C_p$, $\mu M$ | $Kd_2$, $\mu M$ | $a$ | $b$, $\mu M^{-1}$ |
| Tromethamine | 301[a] | 10.2 | 1077 | 59.8 | $1.27 \times 10^{-2}$ | $7.09 \times 10^{-5}$ |
| | (291)[b] | (195) | (62.2) | (140) | (22.7) | (5.2) |
| 0.1 *M* $KH_2PO_4$ | 140 | 3.94 | 1903 | 132 | $2.19 \times 10^{-2}$ | $6.96 \times 10^{-5}$ |
| | (60.1) | (75.6) | (12.7) | (36.0) | (16.4) | (6.5) |
| 0.05 *M* $KH_2PO_4$ | 132 | 4.12 | 2083 | 163 | $2.82 \times 10^{-2}$ | $6.97 \times 10^{-5}$ |
| | (29.3) | (37.9) | (7.8) | (10.9) | (7.7) | (3.9) |
| "House"[c] | 156 | 14.2 | 2109 | 216 | $4.75 \times 10^{-2}$ | $6.87 \times 10^{-5}$ |
| | (162) | (142) | (24.1) | (77.6) | (9.3) | (7.8) |
| 0.05 *M* $KH_2PO_4$ | 435 | 16.1 | 2082 | 300 | $2.85 \times 10^{-2}$ | $7.06 \times 10^{-5}$ |
| + 0.05 *M* NaCl | (62.8) | (53.3) | (60.0) | (134) | (7.1) | (3.6) |
| Imidazole | 330 | 8.89 | 1816 | 232 | $1.50 \times 10^{-2}$ | $9.52 \times 10^{-5}$ |
| | (13.9) | (14.6) | (10.3) | (25.0) | (8.5) | (1.9) |
| Triethanolamine | 212 | 5.79 | 1650 | 142 | $1.64 \times 10^{-2}$ | $8.91 \times 10^{-5}$ |
| | (22.5) | (25.5) | (5.8) | (19.5) | (10.8) | (2.7) |
| 0.1 *M* $NaH_2PO_4$ | 332 | 4.74 | 1536 | 127 | $1.8 \times 10^{-3}$ | $8.19 \times 10^{-5}$ |
| | (21.1) | (24.4) | (10.4) | (33.4) | (109) | (3.4) |

[a] Estimated parameter. [b] Coefficient of variation (%) = (standard deviation of estimate/estimate) × 100. [c] See footnote to Table I.

0.990, respectively, in 0.1 *M* $KH_2PO_4$ to both being 0.999 in imidazole. The corr and $r^2$ values for fittings to the Langmuir model ranged from 0.993 and 0.992, respectively, in tromethamine to 0.999 and 1.00, respectively, in imidazole.

The binding of salicylic acid to two types of albumin was investigated at six temperatures, from 4 to 58 or 59°, with the higher temperature being different for the two types of albumin. These data were computer fitted to Eq. 3. With the salicylic acid–human serum albumin binding data, parameter $b$ of Eq. 3 remained constant with a change in temperature when the highest temperature was excluded. The means and standard deviations of $b$ were 1.06 (0.026) and 0.895 (0.047) for 4% albumin and 4% fatty acid-free albumin, respectively. The parameter $a$ increased with an increase in temperature, and plots of $a$ *versus* temperature exhibited convex curvature (not shown).

To compare estimated parameters obtained by the Langmuir and parabolic models, the models were manipulated to obtain limiting values for the ratios of bound to free drug concentrations as the total or free drug concentration approached zero (infinite dilution). The Langmuir model can be manipulated to obtain the limiting relationship (7):

$$\frac{C_b}{C_f} = \frac{P(1)}{P(2)} + \frac{P(3)}{P(4)} \qquad \text{(Eq. 4)}$$

For the parabolic model, the limiting relationship is:

$$\frac{C_b}{C_f} = \frac{1 - a}{a} \qquad \text{(Eq. 5)}$$

The limiting values of $C_b/C_f$ obtained from Eqs. 4 and 5 for the Langmuir and parabolic models, respectively, and for the binding of salicylic acid to human serum albumin using eight buffers are listed in Table III. The limiting values for the Langmuir and parabolic models were comparable in each case. Limiting values for the tolmetin–human serum albumin binding data (not shown) also were similar.

**Table III—Limiting Values of Ratio of Bound to Free Drug Concentrations for Salicylic Acid**

| Buffer | Langmuir Prediction[a] | Parabolic Prediction[b] |
|---|---|---|
| Tromethamine | 3.77 | 3.29 |
| 0.1 *M* $KH_2PO_4$ | 4.21 | 3.65 |
| 0.05 *M* $KH_2PO_4$ | 3.90 | 4.21 |
| "House"[c] | 4.89 | 4.71 |
| 0.05 *M* $KH_2PO_4$ + 0.05 *M* NaCl | 3.93 | 3.59 |
| Imidazole | 3.46 | 3.10 |
| Triethanolamine | 2.98 | 2.69 |
| 0.1 *M* $NaH_2PO_4$ | 4.24 | 3.50 |

[a] See Eq. 4. [b] See Eq. 5. [c] See footnote to Table I.

## DISCUSSION

Many factors can cause variability in drug–protein binding from subject to subject or patient to patient. Variables include age (8, 9), drug therapy (10, 11), prolonged bedrest (12), cigarette smoking (13), and disease (14, 15). Circadian fluctuations in drug–protein binding also can occur (16). Because of the individual differences in drug–protein binding, the binding characteristics for each subject or patient undergoing pharmacokinetic evaluation should be determined rather than using pooled plasma or serum (17).

## REFERENCES

(1) H. L. Behm and J. G. Wagner, *Res. Commun. Chem. Pathol. Pharmacol.*, **26**, 145 (1979).

(2) M. C. Meyer and D. E. Guttman, *J. Pharm. Sci.*, **57**, 895 (1968).

(3) M. L. Selley, B. W. Madsen, and J. Thomas, *Clin. Pharmacol. Ther.*, **24**, 694 (1978).
(4) S. W. Boobis and C. F. Chignell, *Biochem. Pharmacol.*, **28**, 751 (1979).
(5) I. T. Ağabeyoğlu, R. F. Bergstrom, W. R. Gillespie, J. G. Wagner, and D. R. Kay, *Eur. J. Clin. Pharmacol.*, **16**, 399 (1979).
(6) C. M. Metzler, "NONLIN, A Computer Program for Parameter Estimation in Nonlinear Situations," Technical Report 7296/69/7292/005, Upjohn Co., Kalamazoo, Mich., 1969.
(7) H. L. Behm, Ph.D. dissertation, University of Michigan, Ann Arbor, Mich., 1980, p. 109.
(8) L. E. Mather, G. T. Tucker, A. E. Pflung, M. J. Lindop, and G. Wilkinson, *Clin. Pharmacol. Ther.*, **17**, 21 (1975).
(9) C. F. Chignell, E. S. Vesell, D. K. Starkweather, and C. M. Berlin, *ibid.*, **12**, 897 (1971).
(10) E. M. Sellers and J. Koch-Weser, *ibid.*, **11**, 524 (1970).
(11) A. H. Anton, *J. Pharmacol. Exp. Ther.*, **129**, 282 (1960).
(12) L. O. Plantin, S. Ahlinder, R. Norberg, and G. Birke, *Acta Med. Scand.*, **189**, 309 (1971).
(13) L. G. Dales, G. D. Friedman, A. S. Siegelaub, and C. C. Seltzer, *J. Chronic Dis.*, **27**, 293 (1974).
(14) W. Jusko, in "The Effect of Disease States on Drug Pharmacokinetics," American Pharmaceutical Association, Washington, D.C., 1976, p. 99.
(15) G. Levy, in *ibid.*, p. 137.
(16) A. Angeli, R. Frajria, R. DePaoli, D. Fonzo, and F. Ceresa, *Clin. Pharmacol. Ther.*, **23**, 47 (1978).
(17) P. H. Hinderling and E. R. Garrett, *J. Pharmacokinet. Biopharm.*, **4**, 199 (1976).

### ACKNOWLEDGMENTS

Supported in part by McNeil Laboratories and in part by a Lilly Endowment Fellowship in Pharmacy. McNeil Laboratories kindly supplied both unlabeled tolmetin and [$^{14}$C]tolmetin.

# High-Pressure Liquid Chromatographic Assay of Theophylline, Ephedrine Hydrochloride, and Phenobarbital Tablets

**TSUN-MING CHEN ˣ and LESTER CHAFETZ**

Received October 6, 1980, from the *Analytical Research Laboratories, Warner-Lambert Pharmaceutical Research, Morris Plains, NJ 07950.* Accepted for publication December 1, 1980.

**Abstract** □ An innovative high-pressure liquid chromatographic method is described in which theophylline, ephedrine hydrochloride (measured as benzaldehyde), and phenobarbital are determined simultaneously with butabarbital as the internal standard. Chromatographic conditions were selected to afford a pH sufficient for rapid oxidation of ephedrine and relatively high UV absorbance for the barbiturates and a detection wavelength near the maximum for benzaldehyde and the barbiturates and the minimum for theophylline. Chromatograms show peaks from iodate, theophylline, phenobarbital, butabarbital, and benzaldehyde, in order of increasing retention time, all within the dynamic range of a conventional recorder. Procedures are provided for the assay of conventional and sustained-action tablet formulations.

**Keyphrases** □ High-pressure liquid chromatography—simultaneous determination of theophylline, ephedrine hydrochloride, and phenobarbital, conventional and sustained-action tablet formulations □ Theophylline—simultaneous determination with ephedrine hydrochloride and phenobarbital by high-pressure liquid chromatography, conventional and sustained-action tablet formulations □ Ephedrine hydrochloride—simultaneous determination with theophylline and phenobarbital by high-pressure liquid chromatography, conventional and sustained-action tablet formulations □ Phenobarbital—simultaneous determination with theophylline and ephedrine hydrochloride by high-pressure liquid chromatography, conventional and sustained-action tablet formulations

The theophylline, ephedrine hydrochloride, and phenobarbital tablet is recognized in USP XX (1), which provides a laborious assay in which the drug components are separated by chromatography on two partition columns and solvent extraction and then determined by UV spectrometry. Elefant *et al.* (2) described a GLC assay for this formulation, and Schultz and Paveenbampen (3) reported one for a similar suspension dosage form. Both methods require derivative formation, and neither has proved satisfactory in speed and convenience.

High-pressure liquid chromatography (HPLC) affords easy separation of the three active components of the formulations; however, the enormous differences in their relative amounts and in their UV absorption maxima and absorptivities make their simultaneous determination by HPLC with UV detection a challenging analytical problem. This report describes an innovative solution to this problem, affording peaks within one dynamic range span of a recorder.

## BACKGROUND

Conventional tablets, the USP formulation, declare 130 mg of hydrous theophylline, 24 mg of ephedrine hydrochloride, and 8 mg of phenobarbital; similar proportions are in sustained-action tablets. Hydrous theophylline shows a UV maximum at ~271 nm with an absorptivity (liters per gram centimeter) of ~48. Its UV spectrum is not affected greatly by pH. In acidic solution, ephedrine and phenobarbital have weak UV spectra due to their benzene ring structure, with maxima at ~256 nm and absorptivities of ~1.

Penner[1] developed a normal-phase HPLC method using detection at 254 nm and an attenuation change between elution of the phenobarbital and theophylline peaks to keep the latter on the recorder scale. Suraski and DiPede[2] developed this method further, using a separate injection of greater dilution to keep the theophylline peak within the recorder dynamic range. They suggested that use of a computing integrator could allow for one injection of all three drug components. In this method, ephedrine and phenobarbital are determined simultaneously and theophylline is determined separately, using the same chromatographic system. It is also possible to determine phenobarbital and theophylline together and ephedrine separately. The UV maximum of phenobarbital can be shifted to ~240 nm with an absorptivity of ~43 by raising the pH to 9–11, where the predominant UV chromophore is the monoanion of the ureide ring; however, a high pH is incompatible with HPLC column

[1] M. H. Penner, Warner-Lambert Research, Morris Plains, N.J., Aug. 1974, personal communication.
[2] H. Suraski and J. DiPede, Warner-Lambert Canada, Scarborough, Ontario, Canada, Mar. 1976, personal communication.



*0022-3549/81/0700-0804$01.00/0*
*© 1981, American Pharmaceutical Association*

(3) M. L. Selley, B. W. Madsen, and J. Thomas, *Clin. Pharmacol. Ther.*, **24**, 694 (1978).
(4) S. W. Boobis and C. F. Chignell, *Biochem. Pharmacol.*, **28**, 751 (1979).
(5) I. T. Ağabeyoğlu, R. F. Bergstrom, W. R. Gillespie, J. G. Wagner, and D. R. Kay, *Eur. J. Clin. Pharmacol.*, **16**, 399 (1979).
(6) C. M. Metzler, "NONLIN, A Computer Program for Parameter Estimation in Nonlinear Situations," Technical Report 7296/69/7292/005, Upjohn Co., Kalamazoo, Mich., 1969.
(7) H. L. Behm, Ph.D. dissertation, University of Michigan, Ann Arbor, Mich., 1980, p. 109.
(8) L. E. Mather, G. T. Tucker, A. E. Pflung, M. J. Lindop, and G. Wilkinson, *Clin. Pharmacol. Ther.*, **17**, 21 (1975).
(9) C. F. Chignell, E. S. Vesell, D. K. Starkweather, and C. M. Berlin, *ibid.*, **12**, 897 (1971).
(10) E. M. Sellers and J. Koch-Weser, *ibid.*, **11**, 524 (1970).
(11) A. H. Anton, *J. Pharmacol. Exp. Ther.*, **129**, 282 (1960).
(12) L. O. Plantin, S. Ahlinder, R. Norberg, and G. Birke, *Acta Med. Scand.*, **189**, 309 (1971).
(13) L. G. Dales, G. D. Friedman, A. S. Siegelaub, and C. C. Seltzer, *J. Chronic Dis.*, **27**, 293 (1974).
(14) W. Jusko, in "The Effect of Disease States on Drug Pharmacokinetics," American Pharmaceutical Association, Washington, D.C., 1976, p. 99.
(15) G. Levy, in *ibid.*, p. 137.
(16) A. Angeli, R. Frajria, R. DePaoli, D. Fonzo, and F. Ceresa, *Clin. Pharmacol. Ther.*, **23**, 47 (1978).
(17) P. H. Hinderling and E. R. Garrett, *J. Pharmacokinet. Biopharm.*, **4**, 199 (1976).

### ACKNOWLEDGMENTS

Supported in part by McNeil Laboratories and in part by a Lilly Endowment Fellowship in Pharmacy. McNeil Laboratories kindly supplied both unlabeled tolmetin and [$^{14}$C]tolmetin.

# High-Pressure Liquid Chromatographic Assay of Theophylline, Ephedrine Hydrochloride, and Phenobarbital Tablets

**TSUN-MING CHEN ˣ and LESTER CHAFETZ**

Received October 6, 1980, from the *Analytical Research Laboratories, Warner-Lambert Pharmaceutical Research, Morris Plains, NJ 07950.* Accepted for publication December 1, 1980.

**Abstract** □ An innovative high-pressure liquid chromatographic method is described in which theophylline, ephedrine hydrochloride (measured as benzaldehyde), and phenobarbital are determined simultaneously with butabarbital as the internal standard. Chromatographic conditions were selected to afford a pH sufficient for rapid oxidation of ephedrine and relatively high UV absorbance for the barbiturates and a detection wavelength near the maximum for benzaldehyde and the barbiturates and the minimum for theophylline. Chromatograms show peaks from iodate, theophylline, phenobarbital, butabarbital, and benzaldehyde, in order of increasing retention time, all within the dynamic range of a conventional recorder. Procedures are provided for the assay of conventional and sustained-action tablet formulations.

**Keyphrases** □ High-pressure liquid chromatography—simultaneous determination of theophylline, ephedrine hydrochloride, and phenobarbital, conventional and sustained-action tablet formulations □ Theophylline—simultaneous determination with ephedrine hydrochloride and phenobarbital by high-pressure liquid chromatography, conventional and sustained-action tablet formulations □ Ephedrine hydrochloride—simultaneous determination with theophylline and phenobarbital by high-pressure liquid chromatography, conventional and sustained-action tablet formulations □ Phenobarbital—simultaneous determination with theophylline and ephedrine hydrochloride by high-pressure liquid chromatography, conventional and sustained-action tablet formulations

The theophylline, ephedrine hydrochloride, and phenobarbital tablet is recognized in USP XX (1), which provides a laborious assay in which the drug components are separated by chromatography on two partition columns and solvent extraction and then determined by UV spectrometry. Elefant *et al.* (2) described a GLC assay for this formulation, and Schultz and Paveenbampen (3) reported one for a similar suspension dosage form. Both methods require derivative formation, and neither has proved satisfactory in speed and convenience.

High-pressure liquid chromatography (HPLC) affords easy separation of the three active components of the formulations; however, the enormous differences in their relative amounts and in their UV absorption maxima and absorptivities make their simultaneous determination by HPLC with UV detection a challenging analytical problem. This report describes an innovative solution to this problem, affording peaks within one dynamic range span of a recorder.

## BACKGROUND

Conventional tablets, the USP formulation, declare 130 mg of hydrous theophylline, 24 mg of ephedrine hydrochloride, and 8 mg of phenobarbital; similar proportions are in sustained-action tablets. Hydrous theophylline shows a UV maximum at ~271 nm with an absorptivity (liters per gram centimeter) of ~48. Its UV spectrum is not affected greatly by pH. In acidic solution, ephedrine and phenobarbital have weak UV spectra due to their benzene ring structure, with maxima at ~256 nm and absorptivities of ~1.

Penner[1] developed a normal-phase HPLC method using detection at 254 nm and an attenuation change between elution of the phenobarbital and theophylline peaks to keep the latter on the recorder scale. Suraski and DiPede[2] developed this method further, using a separate injection of greater dilution to keep the theophylline peak within the recorder dynamic range. They suggested that use of a computing integrator could allow for one injection of all three drug components. In this method, ephedrine and phenobarbital are determined simultaneously and theophylline is determined separately, using the same chromatographic system. It is also possible to determine phenobarbital and theophylline together and ephedrine separately. The UV maximum of phenobarbital can be shifted to ~240 nm with an absorptivity of ~43 by raising the pH to 9–11, where the predominant UV chromophore is the monoanion of the ureide ring; however, a high pH is incompatible with HPLC column

[1] M. H. Penner, Warner-Lambert Research, Morris Plains, N.J., Aug. 1974, personal communication.
[2] H. Suraski and J. DiPede, Warner-Lambert Canada, Scarborough, Ontario, Canada, Mar. 1976, personal communication.



*0022-3549/81/0700-0804$01.00/0*
*© 1981, American Pharmaceutical Association*

stability. The UV spectrum of ephedrine is not affected significantly by changes in pH.

One solution to the problems of simultaneous determination of all three drugs in conventional and sustained-action tablets is described here. A reversed-phase HPLC method was developed with butabarbital as the internal standard. The internal standard solution contains periodate, which oxidizes ephedrine to benzaldehyde without affecting theophylline or the barbiturates. UV detection is at 241 nm, at the maximum for the barbiturates and benzaldehyde and near the absorption minimum for theophylline, thus minimizing the concentration difference. All three drug components and the internal standard are on scale so the method can be employed using peak responses from a recorded chromatogram as well as from computerized data reduction systems.

## EXPERIMENTAL

**Apparatus**—The HPLC instrument included a solvent delivery system[3], a microparticulate reversed-phase column of octadecylsilane bonded on silica[4], and a UV detector[5] set at 241 nm. An automatic sampler[6] and a computing integrator[7] were used.

**Mobile Phase**—Acetonitrile (240 ml) was mixed with pH 7.8, 0.01 *M* phosphate buffer (760 ml).

**Internal Standard**—Butabarbital sodium (25 mg) was dissolved in 1.7% (w/v) dibasic potassium phosphate solution (50 ml). Then 40 ml of this solution was mixed with 10 ml of 1% (w/v) sodium metaperiodate solution.

**Standard Preparation**—*Tablets*—About 120 mg of theophylline USP reference standard, 8 mg of phenobarbital USP reference standard, and 25 mg of ephedrine sulfate USP reference standard were weighed accurately and transferred to a 200-ml volumetric flask. The standards were dissolved in 10 ml of methanol and ~100 ml of chloroform and diluted to the mark with chloroform. Then 15.0 ml of this solution was pipetted into a 50-ml volumetric flask and diluted to volume with chloroform.

*Sustained-Action Tablets*—About 204 mg of theophylline USP reference standard, 25 mg of phenobarbital USP reference standard, and 53 mg of ephedrine sulfate USP reference standard were weighed accurately into a 200-ml volumetric flask. This mixture was dissolved in 10 ml of methanol and ~100 ml of chloroform and diluted to volume with chloroform. Then 20.0 ml of this solution was pipetted into a 100-ml volumetric flask and diluted to volume with chloroform.

**Assay Preparation**—*Tablets*—Not less than 20 tablets were weighed and finely powdered. A portion of the powdered tablets equivalent to about one average tablet weight was weighed accurately, transferred to a 200-ml volumetric flask, and shaken mechanically for 20 min with 10 ml of methanol and 100 ml of chloroform. Chloroform was added to the mark, the solution was mixed and filtered, and exactly 15.0 ml of the filtrate was diluted to 50 ml in a volumetric flask with chloroform.

*Sustained-Action Tablets*—Not less than 20 tablets were weighed and finely powdered. An amount of powder equivalent to about one average tablet weight was weighed accurately, transferred to a 200-ml volumetric flask, and shaken mechanically for 20 min with 10 ml of methanol and 100 ml of chloroform. Chloroform was added to the mark, and the solution was mixed and filtered. Then 20.0 ml of the filtrate was pipetted into a 100-ml volumetric flask and diluted to volume with chloroform.

*Procedure*—The assay preparation (10.0 ml) and standard preparation (10.0 ml) were pipetted into 25-ml glass-stoppered conical flasks and evaporated to dryness in a warm water bath with the aid of a stream of air. The residues were dissolved in 4.0 ml of the internal standard solution, and the flasks were stoppered and mixed. Then they were permitted to stand at room temperature for 30 min. Then 1.0 ml of 1% (v/v) aqueous propylene glycol solution was added to each flask, and the flasks were stoppered and mixed.

**System Suitability**—*Resolution*—A flow rate of 1.0 ml/min for the mobile phase was set, and the system was allowed to equilibrate until a stable baseline was obtained on the recorder. Then 10 μl of the standard preparation solution was injected into the chromatograph at 0.24-aufs detection sensitivity when the recorder was used or at a suitable attenuation when a computing integrator was used. (An attenuation setting of 16 was used for the instrument employed in these studies[7].)

In order of increasing elution time, the five peaks are iodate (from the reagent), theophylline, phenobarbital, butabarbital, and benzaldehyde (from ephedrine). They should be completely resolved, with resolution factors between each pair of neighboring peaks of not less than 1.5. The resolution factor, $R$, is calculated from $2(tr_y - tr_x)/(W_y + W_x)$, where $tr_y$ and $tr_x$ are the retention times for neighboring peaks $x$ and $y$, the latter having the longer retention time, and $W_x$ and $W_y$ are the peak widths at the baseline for the respective peaks.

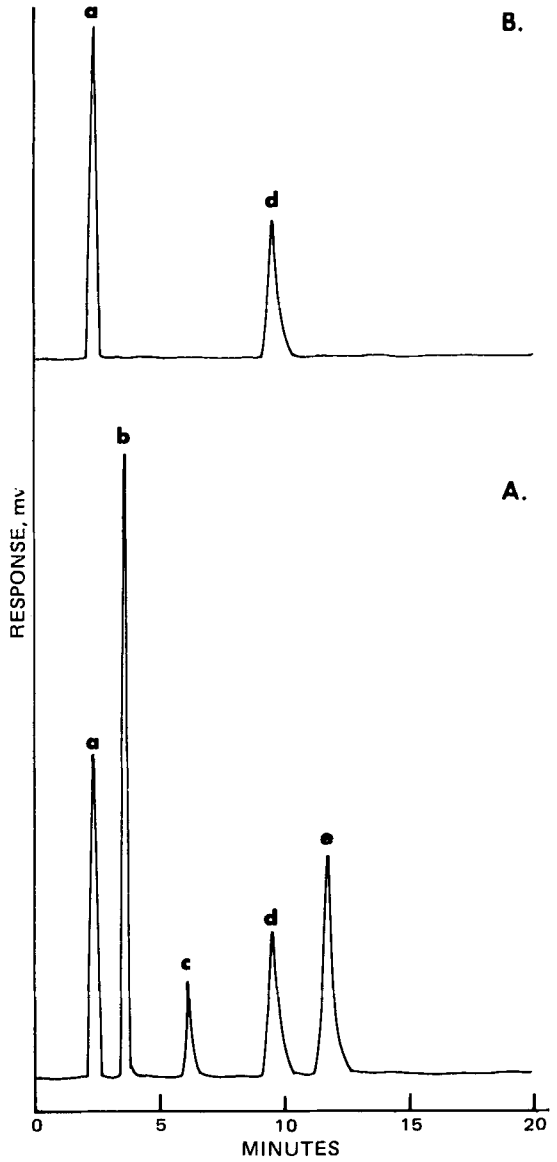


**Figure 1**—*Chromatograms of internal standard (B) and standard preparation (A). Key: a, iodate; b, theophylline; c, phenobarbital; d, butabarbital; and e, ephedrine as benzaldehyde.*

*Linearity*—Solutions at concentration levels of about 80, 90, 100, 110, and 120% of the appropriate standard preparation were prepared. Then each solution (10 μl) was injected into the liquid chromatograph. The concentrations of each active component were plotted against the respective ratios of its peak response to that of the internal standard. A straight line should be obtained in each instance.

*Assay*—Alternately 10 μl of the solutions from the standard preparation and the assay preparation was injected by means of a fixed-volume loop, and the peak responses were determined. The ratios of the peak responses were determined for theophylline, ephedrine hydrochloride as benzaldehyde, and phenobarbital to the internal standard in the chromatograms from the standard preparation and the assay preparation. The amount of each active ingredient, in milligrams per tablet, was calculated from $FC(R_U/R_S)(T/S)$, where $C$ is the exact concentration, in milligrams per milliliter, of the assayed component in the standard preparation; $R_U$ and $R_S$ are the response ratios for each to the internal standard for the chromatograms from the assay preparation and the

[3] Waters Associates model 6000A.
[4] μBondapak ODS (30 cm × 4 mm), Waters Associates.
[5] Perkin-Elmer model LC-55.
[6] Perkin-Elmer model LC-420.
[7] Spectra-Physics model SP4100.

**Table I—Dilution Factors [a]**

| Drug | Conventional Tablets | Sustained-Action Tablets |
|---|---|---|
| Theophylline | 733.3 | 1000 |
| Ephedrine hydrochloride | 627.3 | 941 |
| Phenobarbital | 667 | 1000 |

[a] The theophylline factor includes 1.100, the ratio of the molecular weights of hydrous and anhydrous theophylline. The ephedrine hydrochloride factor includes 0.941, the ratio of the equivalent weights of the hydrochloride and sulfate salts.

standard preparation, respectively; $T$ and $S$ are the weights, in milligrams, of the average tablet and of the portion of the tablet taken for assay, respectively; and $F$ represents the factors from dilutions (Table I).

## RESULTS AND DISCUSSION

Figure 1 shows typical chromatograms for a conventional tablet formulation and a placebo mixture in which a reagent peak appears at ~2.3 min due to iodate, at ~3.5 min due to theophylline, at ~6.0 min due to phenobarbital, and at ~9.4 min due to butabarbital; benzaldehyde, from ephedrine, has a retention time of ~11.7 min. The chromatograms show no interference from the excipients and the oxidation products of propylene glycol, formaldehyde, and acetaldehyde.

**Table II—Precision and Recovery Data**

| Trial | Percent Recovery: Theophylline | Ephedrine Hydrochloride | Phenobarbital |
|---|---|---|---|
| | Conventional Tablets | | |
| 1 | 98.4 | 99.2 | 97.8 |
| 2 | 99.4 | 97.6 | 100.8 |
| 3 | 98.1 | 98.0 | 96.6 |
| 4 | 98.7 | 100.1 | 99.6 |
| 5 | 100.3 | 99.2 | 100.0 |
| 6 | 98.4 | 97.5 | 96.3 |
| Mean | 98.9 | 98.6 | 98.5 |
| *RSD*, % | 0.83 | 1.07 | 1.91 |
| | Sustained-Action Tablets | | |
| 1 | 98.6 | 98.3 | 98.1 |
| 2 | 101.4 | 100.7 | 100.3 |
| 3 | 99.3 | 100.0 | 99.7 |
| 4 | 100.7 | 100.0 | 99.7 |
| 5 | 100.0 | 101.4 | 100.3 |
| 6 | 100.0 | 99.3 | 99.7 |
| Mean | 100.0 | 100.0 | 99.6 |
| *RSD*, % | 0.99 | 1.08 | 0.81 |

**Table III—Recovery Data at 80 and 120% Label Claim**

| Drug | Percent Found: 80 | 120 |
|---|---|---|
| | Conventional Tablets | |
| Theophylline | 82.2, 81.9 | 117.8, 119.5 |
| Ephedrine hydrochloride | 82.4, 82.6 | 120.3, 123.1 |
| Phenobarbital | 79.7, 79.0 | 121.4, 118.8 |
| | Sustained-Action Tablets | |
| Theophylline | 80.7, 80.7 | 117.9, 118.8 |
| Ephedrine hydrochloride | 79.4, 79.4 | 118.4, 118.6 |
| Phenobarbital | 79.1, 79.7 | 119.5, 120.3 |

The determination of ephedrine as benzaldehyde after periodate oxidation was shown to be stability indicating by Chafetz (4). Omission of periodate from the system had no effect on the retention times or response of theophylline, phenobarbital, or butabarbital. Ephedrine was moved to a retention time of ~20 min; however, its response was decreased by a factor of >200. Ephedrine can be visualized only by changing the detector to ~260 nm and using an increased concentration or lower attenuation.

The UV detection of phenobarbital and butabarbital at 241 nm is due to the monoanion form of the ureide ring, the unionized form having little absorbance in the near UV; hence, the incorporation of pH 7.8 buffer in the mobile phase. This mobile phase provides sufficient alkalinity to be in the $pKa_1$ range for the barbiturates and for a rapid reaction rate of periodate with ephedrine. (The apparent pH of the mobile phase is 8.3.)

Precision and recovery data for conventional and sustained-action theophylline, ephedrine hydrochloride, and phenobarbital tablets are shown in Tables II and III. Calculation of resolution factors between adjacent peaks provides values greater than 5. Peak response ratios *versus* concentrations for each component to the internal standard were rectilinear. Recovery was determined by adding known amounts of the drugs to the excipients, which included starch, lactose, stearic acid, and polyethylene glycol 6000 for conventional tablets and starch USP, lactose USP, stearic acid powder, polyethylene glycol 6000, guar gum, methylcellulose USP, sugar powder, ethylcellulose NF, magnesium stearate USP, carnauba wax, D&C Red No. 30 lake, and D&C Yellow No. 10 lake for sustained-action tablets.

## REFERENCES


(1) "The United States Pharmacopeia," 20th rev., United States Pharmacopeial Convention, Rockville, Md., 1980, p. 784.

(2) M. Elefant, L. Chafetz, and J. M. Talmage, *J. Pharm. Sci.*, **56**, 1181 (1967).

(3) H. W. Schultz and C. Paveenbampen, *ibid.*, **62**, 1995 (1973).

(4) L. Chafetz, *ibid.*, **60**, 291 (1971).


# Catecholamine Analogs as Potential Antitumor Agents II


**AI JENG LIN and JOHN S. DRISCOLL ˣ**



Received September 3, 1980, from the *Drug Design and Chemistry Section, Laboratory of Medicinal Chemistry and Biology, Developmental Therapeutics Program, National Cancer Institute, National Institutes of Health, Bethesda, MD 20205.* Accepted for publication December 2, 1980.



**Abstract** □ Polyhydroxybenzylamine derivatives related to dopamine were synthesized and shown to have activity against murine P-388 lymphocytic leukemia. The 3,4,5-trihydroxy- and 2,3-dihydroxybenzylamine hydroiodides were active, as were several other catechol derivatives capable of *o*-quinone formation.



**Keyphrases** □ Catecholamine analogs—polyhydroxybenzylamine hydroiodides synthesized and evaluated for antitumor activity, mice □ Structure–activity relationships—catecholamine analogs synthesized and tested for antitumor activity, mice □ Antitumor activity—catecholamine analogs synthesized and evaluated for antitumor activity, mice


Phenalkylamines (1–4) and pyridine derivatives (5) possessing vicinal hydroxyl groups have antitumor activity against *in vivo* murine tumor models and related *in vitro* systems. A previous investigation (4) explored structure–




*0022-3549/81/0700-0806$01.00/0*


*© 1981, American Pharmaceutical Association*

**Table I—Dilution Factors [a]**

| Drug | Conventional Tablets | Sustained-Action Tablets |
|---|---|---|
| Theophylline | 733.3 | 1000 |
| Ephedrine hydrochloride | 627.3 | 941 |
| Phenobarbital | 667 | 1000 |

[a] The theophylline factor includes 1.100, the ratio of the molecular weights of hydrous and anhydrous theophylline. The ephedrine hydrochloride factor includes 0.941, the ratio of the equivalent weights of the hydrochloride and sulfate salts.

standard preparation, respectively; $T$ and $S$ are the weights, in milligrams, of the average tablet and of the portion of the tablet taken for assay, respectively; and $F$ represents the factors from dilutions (Table I).

## RESULTS AND DISCUSSION

Figure 1 shows typical chromatograms for a conventional tablet formulation and a placebo mixture in which a reagent peak appears at ~2.3 min due to iodate, at ~3.5 min due to theophylline, at ~6.0 min due to phenobarbital, and at ~9.4 min due to butabarbital; benzaldehyde, from ephedrine, has a retention time of ~11.7 min. The chromatograms show no interference from the excipients and the oxidation products of propylene glycol, formaldehyde, and acetaldehyde.

**Table II—Precision and Recovery Data**

| Trial | Percent Recovery: Theophylline | Ephedrine Hydrochloride | Phenobarbital |
|---|---|---|---|
| | Conventional Tablets | | |
| 1 | 98.4 | 99.2 | 97.8 |
| 2 | 99.4 | 97.6 | 100.8 |
| 3 | 98.1 | 98.0 | 96.6 |
| 4 | 98.7 | 100.1 | 99.6 |
| 5 | 100.3 | 99.2 | 100.0 |
| 6 | 98.4 | 97.5 | 96.3 |
| Mean | 98.9 | 98.6 | 98.5 |
| *RSD*, % | 0.83 | 1.07 | 1.91 |
| | Sustained-Action Tablets | | |
| 1 | 98.6 | 98.3 | 98.1 |
| 2 | 101.4 | 100.7 | 100.3 |
| 3 | 99.3 | 100.0 | 99.7 |
| 4 | 100.7 | 100.0 | 99.7 |
| 5 | 100.0 | 101.4 | 100.3 |
| 6 | 100.0 | 99.3 | 99.7 |
| Mean | 100.0 | 100.0 | 99.6 |
| *RSD*, % | 0.99 | 1.08 | 0.81 |

**Table III—Recovery Data at 80 and 120% Label Claim**

| Drug | Percent Found: 80 | 120 |
|---|---|---|
| | Conventional Tablets | |
| Theophylline | 82.2, 81.9 | 117.8, 119.5 |
| Ephedrine hydrochloride | 82.4, 82.6 | 120.3, 123.1 |
| Phenobarbital | 79.7, 79.0 | 121.4, 118.8 |
| | Sustained-Action Tablets | |
| Theophylline | 80.7, 80.7 | 117.9, 118.8 |
| Ephedrine hydrochloride | 79.4, 79.4 | 118.4, 118.6 |
| Phenobarbital | 79.1, 79.7 | 119.5, 120.3 |

The determination of ephedrine as benzaldehyde after periodate oxidation was shown to be stability indicating by Chafetz (4). Omission of periodate from the system had no effect on the retention times or response of theophylline, phenobarbital, or butabarbital. Ephedrine was moved to a retention time of ~20 min; however, its response was decreased by a factor of >200. Ephedrine can be visualized only by changing the detector to ~260 nm and using an increased concentration or lower attenuation.

The UV detection of phenobarbital and butabarbital at 241 nm is due to the monoanion form of the ureide ring, the unionized form having little absorbance in the near UV; hence, the incorporation of pH 7.8 buffer in the mobile phase. This mobile phase provides sufficient alkalinity to be in the $pKa_1$ range for the barbiturates and for a rapid reaction rate of periodate with ephedrine. (The apparent pH of the mobile phase is 8.3.)

Precision and recovery data for conventional and sustained-action theophylline, ephedrine hydrochloride, and phenobarbital tablets are shown in Tables II and III. Calculation of resolution factors between adjacent peaks provides values greater than 5. Peak response ratios *versus* concentrations for each component to the internal standard were rectilinear. Recovery was determined by adding known amounts of the drugs to the excipients, which included starch, lactose, stearic acid, and polyethylene glycol 6000 for conventional tablets and starch USP, lactose USP, stearic acid powder, polyethylene glycol 6000, guar gum, methylcellulose USP, sugar powder, ethylcellulose NF, magnesium stearate USP, carnauba wax, D&C Red No. 30 lake, and D&C Yellow No. 10 lake for sustained-action tablets.

## REFERENCES


(1) "The United States Pharmacopeia," 20th rev., United States Pharmacopeial Convention, Rockville, Md., 1980, p. 784.

(2) M. Elefant, L. Chafetz, and J. M. Talmage, *J. Pharm. Sci.*, **56**, 1181 (1967).

(3) H. W. Schultz and C. Paveenbampen, *ibid.*, **62**, 1995 (1973).

(4) L. Chafetz, *ibid.*, **60**, 291 (1971).


# Catecholamine Analogs as Potential Antitumor Agents II


**AI JENG LIN and JOHN S. DRISCOLL ˣ**



Received September 3, 1980, from the *Drug Design and Chemistry Section, Laboratory of Medicinal Chemistry and Biology, Developmental Therapeutics Program, National Cancer Institute, National Institutes of Health, Bethesda, MD 20205.* Accepted for publication December 2, 1980.



**Abstract** □ Polyhydroxybenzylamine derivatives related to dopamine were synthesized and shown to have activity against murine P-388 lymphocytic leukemia. The 3,4,5-trihydroxy- and 2,3-dihydroxybenzylamine hydroiodides were active, as were several other catechol derivatives capable of *o*-quinone formation.



**Keyphrases** □ Catecholamine analogs—polyhydroxybenzylamine hydroiodides synthesized and evaluated for antitumor activity, mice □ Structure–activity relationships—catecholamine analogs synthesized and tested for antitumor activity, mice □ Antitumor activity—catecholamine analogs synthesized and evaluated for antitumor activity, mice


Phenalkylamines (1–4) and pyridine derivatives (5) possessing vicinal hydroxyl groups have antitumor activity against *in vivo* murine tumor models and related *in vitro* systems. A previous investigation (4) explored structure–




*0022-3549/81/0700-0806$01.00/0*


*© 1981, American Pharmaceutical Association*

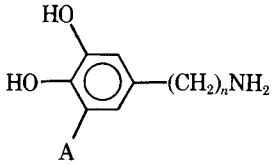

I: A = H, $n$ = 1
II: A = H, $n$ = 2
III: A = OH, $n$ = 2

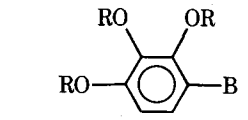

VI: B = $CH_2NH_2$, R = $CH_3$
VII: B = $CH_2\overset{+}{N}H_3I^-$, R = H
VIII: B = $COCH_3$, R = H
IX: B = $COC_9H_{19}$, R = H

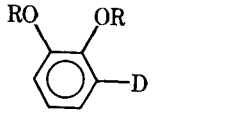

X: D = $CH_2NH_2$, R = $CH_3$
XI: D = $CH_2\overset{+}{N}H_3I^-$, R = H
XII: D = COOH, R = H

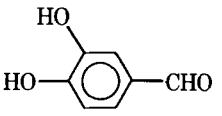

XIII

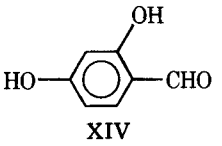

XIV

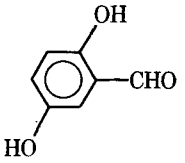

XV

activity studies among catecholamine analogs, with emphasis on the P-388 leukemia activity of phenethylamine and benzylamine compounds. In that study, the benzylamine analog (I) of dopamine (II) was active against P-388 leukemia. The trihydroxy compound, 5-hydroxydopamine (III), also was active. The current study extended this work to additional benzylamine derivatives including two trihydroxy analogs.

## RESULTS AND DISCUSSION

3,4,5-Trimethoxybenzylamine (IV) was prepared by two routes to determine the advantages of catalytic *versus* chemical reduction as synthetic procedures in the benzylamine series (Scheme I). Reduction of the amide with sodium acetoxyborohydride (6) produced IV in a 50% yield. Catalytic reduction of the nitrile in chloroform by the method of Secrist and Logue (7) gave a somewhat better yield of IV (75%) and is the method of choice. Cleavage of the methoxyl groups with hydroiodic acid (8) yielded the target compound 3,4,5-trihydroxybenzylamine as the hydroiodide (V). Several isomeric di- and trihydroxybenzylamines were prepared previously as either free bases or hydrochloride salts (9). The synthesis of 2,3,4-trihydroxybenzylamine hydroiodide (VII) was accomplished by the borohydride method, while 2,3-dihydroxybenzylamine hydroiodide (XI) was prepared in good yield by catalytic reduction of the nitrile followed by hydroiodic acid treatment.

The antitumor results are shown in Table I. The compounds (I–III) on which the present study is based were previously shown to be active against P-388 leukemia (4). The target compounds, V and XI, were determined to be active, but VII gave T/C values[1] of only 123 and 121%. The corresponding acetophenone (VIII), however, was active, and the activity of 3,4-dihydroxybenzaldehyde (XIII) was confirmed.

The generalized structure–activity relationships described previously for the catecholamines (4) continue to apply in the benzylamine series. Positioning of vicinal hydroxyl groups in the benzylamine series such that oxidation to *ortho*-derivatives might occur provides active materials (I, V, VIII, XI, and XIII). Dihydroxy compounds that cannot be oxidized to a quinoid form (XIV) or can be oxidized only to a *p*-quinone (XV) are inactive. As noted previously (4), dihydroxybenzoic acid (XII) analogs are not active. The addition of an apparent excess of lipophilic character converts an active compound (VIII) to an inactive one (IX).

2,3,4-Trihydroxybenzylamine (VII) was expected to be active against P-388 leukemia but was not. Two good P-388 dose–response experiments employing five doses each (range 600–50 mg/kg) gave values that approached but did not exceed a T/C value of 125%. Compound VII showed more toxicity than the other analogs, with the doses at 600, 400, and 200 mg/kg being toxic in each experiment.

[1] Percent T/C = (treated survival to control survival) × 100%.

**Table I—P-388 Lymphocytic Leukemia Antitumor Activity [a]**

| Compound | Optimum Dose, mg/kg/day | T/C, % | T − C, g |
|---|---|---|---|
| I | 700 | 158 | −2.9 |
| II | 600 | 168 | −1.7 |
| III | 400 | 168 | −3.6 |
| V | 600 | 157 | −3.4 |
| VII | 50 | 123 | −0.5 |
| VIII | 400 | 137 | −2.1 |
| IX | 200 | 105 | −2.6 |
| XI | 600 | 149 | −1.9 |
| XII | 100 | 104 | +0.5 |
| XIII | 400 | 138 | −0.5 |
| XIV | 100 | 102 | −0.6 |
| XV | 100 | 114 | −1.4 |

[a] See *Experimental* for conditions and definitions.

## EXPERIMENTAL[2]

**3,4,5-Trimethoxybenzylamine (IV)**—*Method A*—3,4,5-Trimethoxybenzamide (3.6 g, 18 mmoles) and sodium borohydride (3.1 g, 82 mmoles) were suspended in 40 ml of dried *p*-dioxane. To the suspension was added acetic acid (4.8 g, 80 mmoles) in 20 ml of dried *p*-dioxane over 20 min at 10°. The resulting mixture was refluxed for 3 hr. After cooling, water was added to decompose the excess borohydride, and the mixture was evaporated to dryness under reduced pressure. The residue was stirred in 100 ml of chloroform and filtered, and the filtrate was saturated with hydrogen chloride gas. A white hydrochloride was produced after evaporation, and it was dissolved in a minimum amount of water and extracted once with ethyl acetate.

The aqueous layer was made basic with 10% NaOH and saturated with sodium chloride. The mixture was extracted twice with ether. The ether extracts were combined, dried over sodium sulfate, and evaporated to dryness to give 1.8 g (50%) of an oil. The NMR spectrum indicated that IV was pure; NMR (deuterochloroform): 1.68 (s, 2H, $NH_2$), 3.9 (m, 11H, $CH_3$ and $CH_2$), and 6.65 (s, 2H, aromatic). This product was used without further purification for the next step.

*Method B*—3,4,5-Trimethoxybenzonitrile (7.5 g, 39 mmoles) was dissolved in 250 ml of absolute ethanol and 10 ml of chloroform and was

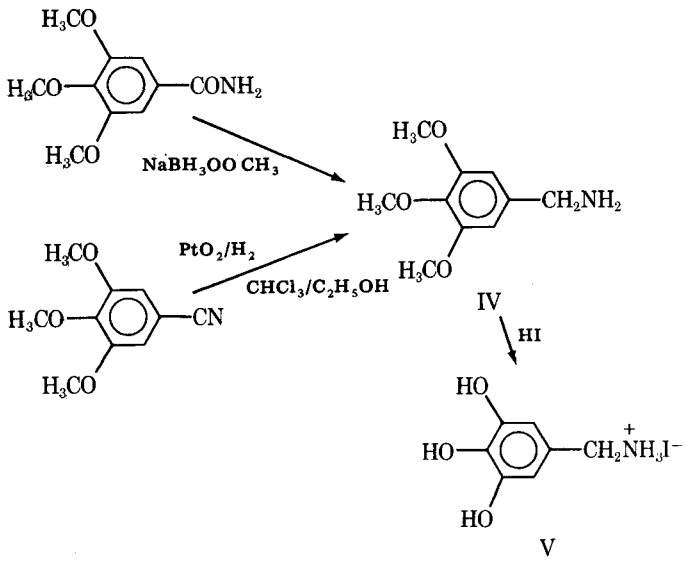


*Scheme I*

[2] All melting points are uncorrected and were recorded on a Thomas–Hoover capillary apparatus. Elemental analyses were performed by Galbraith Laboratories, Knoxville, Tenn. NMR data are delta values relative to tetramethylsilane in deuterochloroform or 3-(trimethylsilyl)propionic acid sodium salt in deuterium oxide. Starting materials and compounds not described under *Experimental* were obtained from Aldrich Chemical Co.

hydrogenated over platinum oxide (0.5 g) at 45 psi for 5 hr. The catalyst was filtered, and the filtrate was evaporated to dryness under reduced pressure to give a white powder. The hydrochloride salt thus obtained was dissolved in 30 ml of water and extracted twice with ether. The aqueous layer was made basic with 10% NaOH, saturated with sodium chloride, and extracted three times with ether. The ether extracts were combined, dried over sodium sulfate, and evaporated to dryness to give 5.6 g (75%) of pale-yellow oil with an NMR spectrum identical to that described for the product from Method A.

**3,4,5-Trihydroxybenzylamine Hydroiodide (V)**—To a magnetically stirred solution of IV (7.5 g, 38 mmoles) in 47% hydroiodic acid (75 ml, 470 mmoles) under nitrogen was added, by syringe, 43.5 ml (460 mmoles) of acetic anhydride through a septum. The reaction mixture was refluxed for 4 hr and evaporated to dryness *in vacuo*. Ethanol (100 ml) was added to the residue, and the solvent was evaporated again to yield a pale-yellow powder (5.0 g, 46%). Recrystallization from ethanol plus ether gave fine crystals, mp 196–198° dec.; NMR (deuterium oxide): 4.00 (s, 2H, $CH_2$) and 6.55 (s, 2H, aromatic).

*Anal.*—Calc. for $C_7H_9NO_3$·HI: C, 29.68; H, 3.53; N, 4.96. Found: C, 29.66; H, 3.52; N, 4.81.

**2,3,4-Trimethoxybenzylamine (VI)**—Compound VI was prepared as an oil in a 73% yield on a 5-g scale from the amide, using borohydride reduction as described for IV. It was used without further purification; NMR (deuterochloroform): 1.95 (s, 2H, $NH_2$), 3.70 (s, 2H, $CH_2$), 3.79–3.83 (m, 9H, $CH_3$), 6.50 (d, 1H, $J$ = 4.5 Hz, aromatic), and 6.85 (d, 1H, $J$ = 4.5 Hz, aromatic).

**2,3,4-Trihydroxybenzylamine Hydroiodide (VII)**—Compound VII, mp 178–181° dec., was prepared on a 7-g scale (89%) from VI by the procedure used for V; NMR (deuterium oxide): 4.15 (s, 2H, $CH_2$), 6.50 (d, 1H, $J$ = 4.5 Hz, aromatic), and 6.81 (d, 1H, $J$ = 4.5 Hz, aromatic).

*Anal.*—Calc. for $C_7H_9NO_3$·HI: C, 29.68; H, 3.53; N, 4.96. Found: C, 29.81; H, 3.70; N, 4.87.

**2,3-Dimethoxybenzylamine (X)**—2,3-Dimethoxybenzonitrile (3.29 g, 20 mmoles) was dissolved in 200 ml of absolute ethanol, and 10 ml of chloroform and 0.5 g of platinum oxide were added to this solution. The mixture was hydrogenated for 3 hr at 40 psi, the catalyst was filtered, and the solvent was evaporated. Then the residue was dissolved in a minimum amount of water and made basic with 10% NaOH. The mixture was saturated with sodium chloride and extracted three times with ether. The ether extracts were combined, dried over sodium sulfate, and evaporated to dryness to give 2.9 g (90%) of a yellow oil. The oil was used without further purification; NMR (deuterochloroform): 2.25 (s, 2H, $NH_2$), 3.8 (m, 8H, $CH_2$ and $CH_3$), and 6.81 (m, 3H, aromatic).

**2,3-Dihydroxybenzylamine Hydroiodide (XI)**—Compound XI, mp 157–158° dec., was prepared from X on a 5-g scale (60%) by the procedure used for V; NMR (deuterium oxide): 4.20 (s, 2H, $CH_2$) and 6.95 (m, 3H, aromatic).

*Anal.*—Calc. for $C_7H_9NO_2$·HI: C, 31.46; H, 3.75; N, 5.24. Found: C, 31.59; H, 3.96; N, 5.26.

**Antitumor Testing**—Antitumor activity was determined as percent T/C values, with T/C ≥ 125% defined as statistically significant (Table I). Dose–response studies were carried out for each compound according to published National Cancer Institute protocols (10). Six mice per dose were inoculated intraperitoneally with $10^6$ P-388 leukemia cells on Day 0. Control (untreated) mice usually died on about Day 11. Mice receiving drug were treated on Days 1–9 with intraperitoneal doses of the compound under investigation. Physiological saline (0.9%) was the vehicle. The mice (average weight 20 g) were weighed on Day 5; the weight difference between treated and control mice (T − C) was an indication of dose toxicity. Weight losses greater than 4 g were considered excessive.

## REFERENCES


(1) J. S. Driscoll, N. R. Melnick, F. R. Quinn, R. Ing, B. J. Abbott, G. Congleton, and L. Dudeck, *Cancer Treat. Rep.*, **62**, 45 (1978).

(2) M. M. Wick, *J. Invest. Dermatol.*, **71**, 163 (1978).

(3) M. M. Wick, *Cancer Treat. Rep.*, **63**, 991 (1979).

(4) J. S. Driscoll, *J. Pharm. Sci.*, **68**, 1519 (1979).

(5) D. R. Hwang and J. S. Driscoll, *ibid.*, **68**, 816 (1979).

(6) N. Umino, T. Iwakuma, and N. Itoh, *Tetrahedron Lett.*, **1976**, 763.

(7) J. A. Secrist and M. W. Logue, *J. Org. Chem.*, **37**, 335 (1972).

(8) J. L. Neumeyer, M. McCarthy, S. P. Battista, F. J. Rosenberg, and D. G. Teigler, *J. Med. Chem.*, **16**, 1228 (1973).

(9) W. J. Hickinbottom and R. F. Garwood, in "The Chemistry of Carbon Compounds," vol. IIIB, E. H. Rodd, Ed., Elsevier, New York, N.Y., 1956, p. 732.

(10) R. I. Geran, N. H. Greenberg, M. M. MacDonald, A. M. Schumacher, and B. J. Abbott, *Cancer Chemother. Rep., Part 3*, **3**(2), 1 (1972).


# Aluminum Chlorohydrate III: Conversion to Aluminum Hydroxide


**DIRK L. TEAGARDEN *, JOE L. WHITE ‡, and STANLEY L. HEM *x**



Received October 3, 1980, from the **Department of Industrial and Physical Pharmacy and the* ‡*Department of Agronomy, Purdue University, West Lafayette, IN 47907.* Accepted for publication December 8, 1980.



**Abstract** □ Bayerite, an aluminum hydroxide polymorph, readily forms when the hydroxyl to aluminum ratio of aluminum chlorohydrate is raised to 3 by titration with sodium hydroxide. Dilution of aluminum chlorohydrate solutions with water leads to the formation of gibbsite, another aluminum hydroxide polymorph. The mechanism of conversion in each instance is related to the structure of the $Al_{13}O_4(OH)_{24}(H_2O)_{12}^{7+}$ complex.



**Keyphrases** □ Aluminum chlorohydrate—conversion to aluminum hydroxide □ Aluminum hydroxide—conversion from aluminum chlorohydrate □ Antiperspirant activity—conversion of aluminum chlorohydrate to aluminum hydroxide


Aluminum chlorohydrate recently was shown (1) to be the $Al_{13}O_4(OH)_{24}(H_2O)_{12}^{7+}$ (I) complex described by Johansson *et al.* (2). This structure is unusual in that it is composed of a central aluminum atom in tetrahedral configuration surrounded by 12 octahedral aluminum atoms. The charge is neutralized by chloride ions. In contrast, aluminum hydroxide is composed exclusively of aluminum in octahedral configuration. The basic unit of aluminum hydroxide is a six-member ring composed of aluminum in octahedral configuration formed by a dehydration–deprotonation reaction (3). The relationship between aluminum chlorohydrate and aluminum hydroxide was demonstrated by examining the effect of neutralizing aluminum chlorohydrate by the addition of sodium hydroxide and the effect of diluting with water.

## EXPERIMENTAL

Aluminum chlorohydrate was obtained commercially as a 50% (w/w) solution[1]. The effect of increasing the hydroxyl to aluminum ratio of aluminum chlorohydrate to 3 was studied by adding 500 ml of 0.394 *N* NaOH at a rate[2] of 10 ml/min to 500 ml of an aluminum chlorohydrate

[1] Lot 8473, Wicken Products, Huguenot, N.Y.

[2] Buchler Polystaltic Pump, Buchler Co., Fort Lee, N.J.




*0022-3549/81/0700-0808$01.00/0*


*© 1981, American Pharmaceutical Association*

hydrogenated over platinum oxide (0.5 g) at 45 psi for 5 hr. The catalyst was filtered, and the filtrate was evaporated to dryness under reduced pressure to give a white powder. The hydrochloride salt thus obtained was dissolved in 30 ml of water and extracted twice with ether. The aqueous layer was made basic with 10% NaOH, saturated with sodium chloride, and extracted three times with ether. The ether extracts were combined, dried over sodium sulfate, and evaporated to dryness to give 5.6 g (75%) of pale-yellow oil with an NMR spectrum identical to that described for the product from Method A.

**3,4,5-Trihydroxybenzylamine Hydroiodide (V)**—To a magnetically stirred solution of IV (7.5 g, 38 mmoles) in 47% hydroiodic acid (75 ml, 470 mmoles) under nitrogen was added, by syringe, 43.5 ml (460 mmoles) of acetic anhydride through a septum. The reaction mixture was refluxed for 4 hr and evaporated to dryness *in vacuo*. Ethanol (100 ml) was added to the residue, and the solvent was evaporated again to yield a pale-yellow powder (5.0 g, 46%). Recrystallization from ethanol plus ether gave fine crystals, mp 196–198° dec.; NMR (deuterium oxide): 4.00 (s, 2H, $CH_2$) and 6.55 (s, 2H, aromatic).

*Anal.*—Calc. for $C_7H_9NO_3$·HI: C, 29.68; H, 3.53; N, 4.96. Found: C, 29.66; H, 3.52; N, 4.81.

**2,3,4-Trimethoxybenzylamine (VI)**—Compound VI was prepared as an oil in a 73% yield on a 5-g scale from the amide, using borohydride reduction as described for IV. It was used without further purification; NMR (deuterochloroform): 1.95 (s, 2H, $NH_2$), 3.70 (s, 2H, $CH_2$), 3.79–3.83 (m, 9H, $CH_3$), 6.50 (d, 1H, $J$ = 4.5 Hz, aromatic), and 6.85 (d, 1H, $J$ = 4.5 Hz, aromatic).

**2,3,4-Trihydroxybenzylamine Hydroiodide (VII)**—Compound VII, mp 178–181° dec., was prepared on a 7-g scale (89%) from VI by the procedure used for V; NMR (deuterium oxide): 4.15 (s, 2H, $CH_2$), 6.50 (d, 1H, $J$ = 4.5 Hz, aromatic), and 6.81 (d, 1H, $J$ = 4.5 Hz, aromatic).

*Anal.*—Calc. for $C_7H_9NO_3$·HI: C, 29.68; H, 3.53; N, 4.96. Found: C, 29.81; H, 3.70; N, 4.87.

**2,3-Dimethoxybenzylamine (X)**—2,3-Dimethoxybenzonitrile (3.29 g, 20 mmoles) was dissolved in 200 ml of absolute ethanol, and 10 ml of chloroform and 0.5 g of platinum oxide were added to this solution. The mixture was hydrogenated for 3 hr at 40 psi, the catalyst was filtered, and the solvent was evaporated. Then the residue was dissolved in a minimum amount of water and made basic with 10% NaOH. The mixture was saturated with sodium chloride and extracted three times with ether. The ether extracts were combined, dried over sodium sulfate, and evaporated to dryness to give 2.9 g (90%) of a yellow oil. The oil was used without further purification; NMR (deuterochloroform): 2.25 (s, 2H, $NH_2$), 3.8 (m, 8H, $CH_2$ and $CH_3$), and 6.81 (m, 3H, aromatic).

**2,3-Dihydroxybenzylamine Hydroiodide (XI)**—Compound XI, mp 157–158° dec., was prepared from X on a 5-g scale (60%) by the procedure used for V; NMR (deuterium oxide): 4.20 (s, 2H, $CH_2$) and 6.95 (m, 3H, aromatic).

*Anal.*—Calc. for $C_7H_9NO_2$·HI: C, 31.46; H, 3.75; N, 5.24. Found: C, 31.59; H, 3.96; N, 5.26.

**Antitumor Testing**—Antitumor activity was determined as percent T/C values, with T/C ≥ 125% defined as statistically significant (Table I). Dose–response studies were carried out for each compound according to published National Cancer Institute protocols (10). Six mice per dose were inoculated intraperitoneally with $10^6$ P-388 leukemia cells on Day 0. Control (untreated) mice usually died on about Day 11. Mice receiving drug were treated on Days 1–9 with intraperitoneal doses of the compound under investigation. Physiological saline (0.9%) was the vehicle. The mice (average weight 20 g) were weighed on Day 5; the weight difference between treated and control mice (T − C) was an indication of dose toxicity. Weight losses greater than 4 g were considered excessive.

## REFERENCES


(1) J. S. Driscoll, N. R. Melnick, F. R. Quinn, R. Ing, B. J. Abbott, G. Congleton, and L. Dudeck, *Cancer Treat. Rep.*, **62**, 45 (1978).

(2) M. M. Wick, *J. Invest. Dermatol.*, **71**, 163 (1978).

(3) M. M. Wick, *Cancer Treat. Rep.*, **63**, 991 (1979).

(4) J. S. Driscoll, *J. Pharm. Sci.*, **68**, 1519 (1979).

(5) D. R. Hwang and J. S. Driscoll, *ibid.*, **68**, 816 (1979).

(6) N. Umino, T. Iwakuma, and N. Itoh, *Tetrahedron Lett.*, **1976**, 763.

(7) J. A. Secrist and M. W. Logue, *J. Org. Chem.*, **37**, 335 (1972).

(8) J. L. Neumeyer, M. McCarthy, S. P. Battista, F. J. Rosenberg, and D. G. Teigler, *J. Med. Chem.*, **16**, 1228 (1973).

(9) W. J. Hickinbottom and R. F. Garwood, in "The Chemistry of Carbon Compounds," vol. IIIB, E. H. Rodd, Ed., Elsevier, New York, N.Y., 1956, p. 732.

(10) R. I. Geran, N. H. Greenberg, M. M. MacDonald, A. M. Schumacher, and B. J. Abbott, *Cancer Chemother. Rep., Part 3*, **3**(2), 1 (1972).


# Aluminum Chlorohydrate III: Conversion to Aluminum Hydroxide


**DIRK L. TEAGARDEN *, JOE L. WHITE ‡, and STANLEY L. HEM *x**



Received October 3, 1980, from the **Department of Industrial and Physical Pharmacy and the* ‡*Department of Agronomy, Purdue University, West Lafayette, IN 47907.* Accepted for publication December 8, 1980.



**Abstract** □ Bayerite, an aluminum hydroxide polymorph, readily forms when the hydroxyl to aluminum ratio of aluminum chlorohydrate is raised to 3 by titration with sodium hydroxide. Dilution of aluminum chlorohydrate solutions with water leads to the formation of gibbsite, another aluminum hydroxide polymorph. The mechanism of conversion in each instance is related to the structure of the $Al_{13}O_4(OH)_{24}(H_2O)_{12}^{7+}$ complex.



**Keyphrases** □ Aluminum chlorohydrate—conversion to aluminum hydroxide □ Aluminum hydroxide—conversion from aluminum chlorohydrate □ Antiperspirant activity—conversion of aluminum chlorohydrate to aluminum hydroxide


Aluminum chlorohydrate recently was shown (1) to be the $Al_{13}O_4(OH)_{24}(H_2O)_{12}^{7+}$ (I) complex described by Johansson *et al.* (2). This structure is unusual in that it is composed of a central aluminum atom in tetrahedral configuration surrounded by 12 octahedral aluminum atoms. The charge is neutralized by chloride ions. In contrast, aluminum hydroxide is composed exclusively of aluminum in octahedral configuration. The basic unit of aluminum hydroxide is a six-member ring composed of aluminum in octahedral configuration formed by a dehydration–deprotonation reaction (3). The relationship between aluminum chlorohydrate and aluminum hydroxide was demonstrated by examining the effect of neutralizing aluminum chlorohydrate by the addition of sodium hydroxide and the effect of diluting with water.

## EXPERIMENTAL

Aluminum chlorohydrate was obtained commercially as a 50% (w/w) solution[1]. The effect of increasing the hydroxyl to aluminum ratio of aluminum chlorohydrate to 3 was studied by adding 500 ml of 0.394 *N* NaOH at a rate[2] of 10 ml/min to 500 ml of an aluminum chlorohydrate

[1] Lot 8473, Wicken Products, Huguenot, N.Y.

[2] Buchler Polystaltic Pump, Buchler Co., Fort Lee, N.J.




*0022-3549/81/0700-0808$01.00/0*


*© 1981, American Pharmaceutical Association*

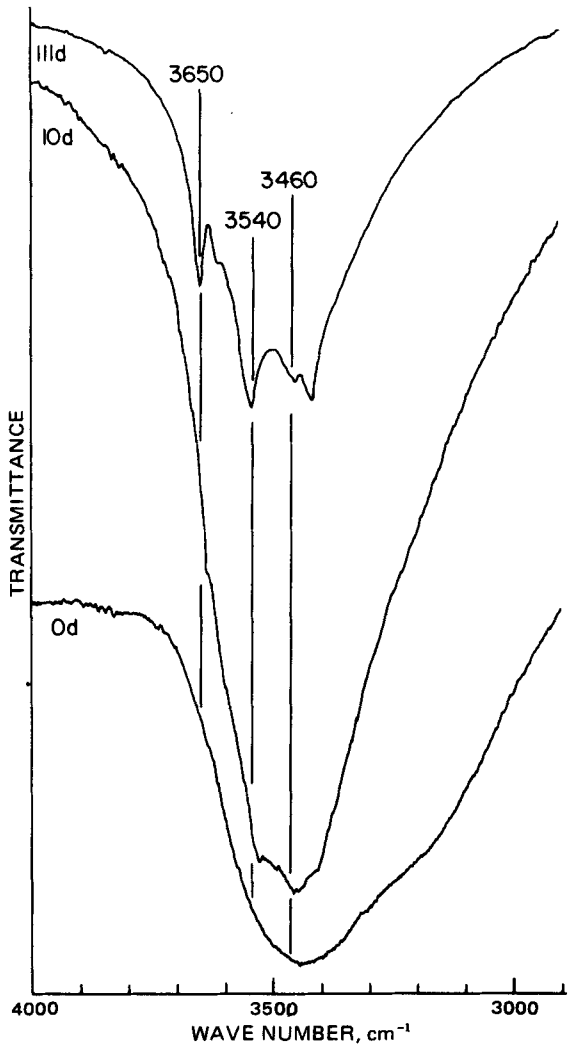


**Figure 1**—*Change in hydroxyl-stretching frequency region of IR spectrum following neutralization of aluminum chlorohydrate. Key: bottom curve, initial; middle curve, after 10 days at 25°; and top curve, after 111 days at 25°.*

solution, which was 0.788 *M* in aluminum. Upon completion of the titration, stirring was continued for 10 min; the solid phase that formed was washed with distilled water. After air drying, the solid phase was examined by X-ray diffraction[3] and IR spectroscopy[4].

The effect of dilution with deionized water was studied by adding enough distilled water to the commercial 50% (w/w) aluminum chlorohydrate solution (6.2 *M* in aluminum) to produce solutions ranging from $1.39 \times 10^{-3}$ to 2.5 *M* in aluminum. The solutions were aged at 25° in plastic bottles. Turbidity was monitored by measuring the absorbance at 400 nm. The white precipitate that formed in some solutions was collected by filtration through a 100-Å filter[5]. The solid phase was washed with distilled water and lyophilized. A sample of the filtrate also was lyophilized. Both lyophilized samples were examined by IR spectroscopy as potassium bromide pellets.

## RESULTS AND DISCUSSION

The relationship between aluminum chlorohydrate and aluminum hydroxide was investigated by titrating an aluminum chlorohydrate solution with sodium hydroxide until the hydroxyl to aluminum ratio was 3. Figure 1 shows the hydroxyl-stretching region of the IR spectrum before and after titration. After 10 days, this region was much sharper, and indications of distinct absorption bands had developed. After 111 days,

[3] Siemens A. G. Kristalloflex 4 generator, type F diffractometer, Karlsruhe, West Germany.
[4] Model 180, Perkin-Elmer Corp., Norwalk, Conn.
[5] Filter VFWP 047-00, Millipore Corp., Bedford, Mass.

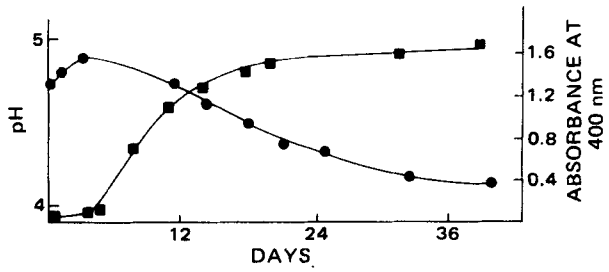


**Figure 2**—*Change in pH (●) and turbidity (■) following dilution of aluminum chlorohydrate to $2.5 \times 10^{-2}$ M in aluminum during aging at 25°.*

sharp bands occurred at 3650, 3540, and 3460 $cm^{-1}$. These hydroxyl-stretching bands correspond to the hydroxyl-stretching vibrations of bayerite (4). The X-ray diffractogram of the 111-day sample had sharp peaks at 4.72, 4.35, 3.20, 2.22, and 1.72 Å. The position of these peaks also correspond to those of bayerite (4).

The conversion of aluminum chlorohydrate to bayerite can be rationalized based on the structure of the I complex. The added hydroxyl

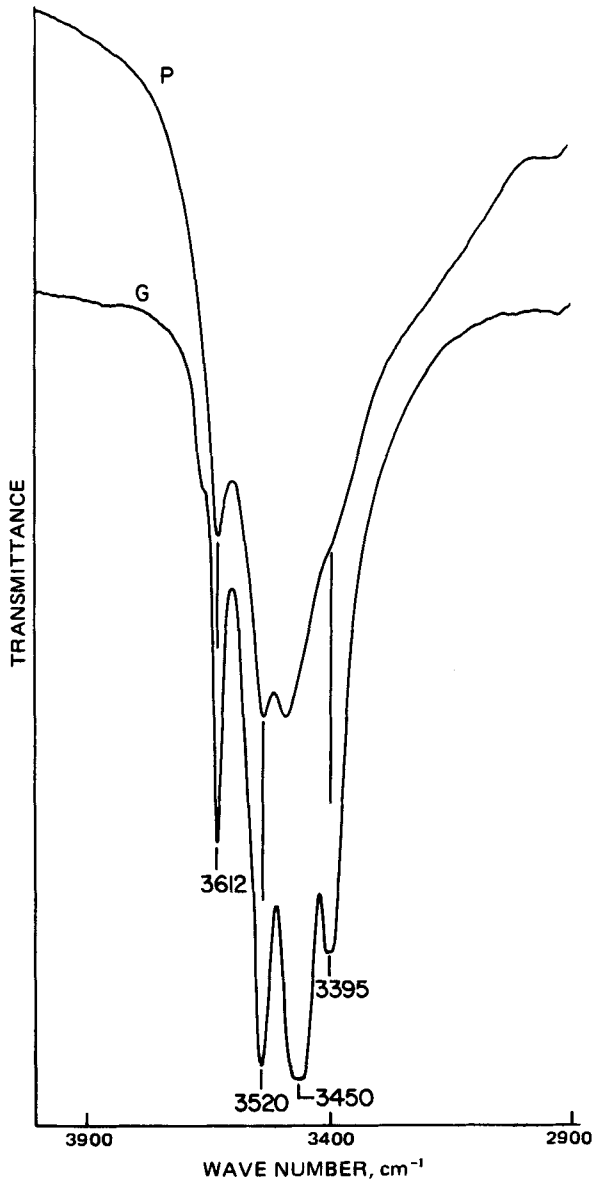


**Figure 3**—*Hydroxyl-stretching frequency region of IR spectrum of solid phase that formed following dilution of aluminum chlorohydrate to $2.5 \times 10^{-2}$ M in aluminum (P) compared to natural gibbsite (G).*

anions are strongly attracted to the highly charged aluminum polynuclear cation. As the charge is neutralized, the complex disassociates and aluminum hydroxide forms. Because the solution pH was raised to 8 by the addition of sodium hydroxide, bayerite, the aluminum hydroxide polymorph that forms under basic conditions, was produced.

Aluminum chlorohydrate also is unstable if it is diluted with water (5, 6). Figure 2 shows that when aluminum chlorohydrate was diluted to $2.5 \times 10^{-2}$ *M* in aluminum, the pH first increased and then decreased. Earlier reports only noted a decrease in pH following dilution. However, the initial increase in pH is important and is consistent with the recently proposed structure of aluminum chlorohydrate (1). The central tetrahedral aluminum in the I complex is surrounded by 12 aluminum atoms in octahedral configuration. In dilute aqueous solution, the highly charged aluminum polycations are widely separated, and the stabilizing effect of the chloride counterions and other aluminum chlorohydrate complexes is reduced. As the I complex disassociates, the tetrahedral aluminum is exposed to the aqueous environment. Since the octahedral configuration is the stable form of aluminum below pH 8 (7–10), the tetrahedral aluminum converts to an octahedral configuration. Exposure of the four negatively charged oxygens, which form the outer shell of the aluminum tetrahedral, to the aqueous environment results in the attraction of protons and water to complete the octahedral configuration. The adsorption of protons is reflected in the initial increase in pH. However, the overall trend is a decrease in pH, which is consistent with the formation of octahedral aluminum into aluminum hydroxy polymers by the deprotonation–dehydroxylation mechanism (3).

The stability of aluminum chlorohydrate is concentration dependent since very little change in pH was observed unless the solution was <0.1 *M* in aluminum. At high concentration, the positively charged I spherical complexes are tightly packed and surrounded by stabilizing chloride counterions. Thus, aluminum chlorohydrate complex is self-stabilizing at high concentration.

Turbidity measurements of the diluted aluminum chlorohydrate solutions also showed that the stability of the complex was concentration dependent. Turbidity was not observed during this study unless the concentration was ~0.1 *M* or lower in terms of aluminum. Figure 2 also shows the development of turbidity following dilution to $2.5 \times 10^{-2}$ *M* in aluminum.

The insoluble degradation product resulting from the dilution of aluminum chlorohydrate was collected by filtration and examined by IR spectroscopy. The hydroxyl-stretching bands coincide with the hydroxyl-stretching bands of gibbsite (Fig. 3). The IR spectrum of the lyophilized filtrate was identical to the reference spectrum for aluminum chlorohydrate (11). Thus, it is believed that the I complex disassociates in dilute solution. The tetrahedral aluminum converts to an octahedral configuration due to the pH, and the octahedral aluminum species form aluminum hydroxide by deprotonation–dehydration. Gibbsite is the end-product of dilution since it is the stable polymorph of aluminum hydroxide in the acidic region. Therefore, the conversion of aluminum chlorohydrate to aluminum hydroxide upon complete neutralization or following dilution with water is consistent with the structure of the I complex that was proposed recently to be aluminum chlorohydrate.

## REFERENCES


(1) D. L. Teagarden, J. F. Kozlowski, J. L. White, and S. L. Hem, *J. Pharm. Sci.*, **70**, 758 (1981).

(2) G. Johansson, G. Lundgren, L. G. Sillen, and R. Soderquist, *Acta Chem. Scand.*, **14**, 769 (1960).

(3) S. L. Nail, J. L. White, and S. L. Hem, *J. Pharm. Sci.*, **65**, 1188 (1976).

(4) *Ibid.*, **64**, 1166 (1975).

(5) T. Govett and A. M. Rubino, *Am. Perfum. Essent. Oil Rev.*, **66**, 21 (1955).

(6) J. J. Margres, A. M. Rubino, and E. S. Bretschneider, *Cosmet. Perfum.*, **90**, 36 (1975).

(7) R. J. Moolenaar, J. C. Evans, and L. D. McKeever, *J. Phys. Chem.*, **74**, 3629 (1970).

(8) E. D. O'Reilly, *J. Chem. Phys.*, **32**, 1007 (1960).

(9) H. Haraguchi and S. Fujiwara, *J. Phys. Chem.*, **73**, 3467 (1969).

(10) E. R. Lippencott, J. A. Psellos, and M. C. Tobin, *J. Chem. Phys.*, **20**, 536 (1952).

(11) D. A. Risegraf and M. L. May, *Appl. Spectrosc.*, **32**, 362 (1978).


## ACKNOWLEDGMENTS


This report is Journal Paper 8256, Purdue University Agricultural Experiment Station, West Lafayette, IN 47907.


# Modified Colorimetric Method for Plasma Prednisolone


**A. N. NARURKAR and C. I. JAROWSKI** ˣ



Received October 27, 1980, from the *College of Pharmacy and Allied Health Professions, St. John's University, Jamaica, NY 11439.* Accepted for publication January 30, 1981.



**Abstract** □ A simple, precise, rapid, and sensitive colorimetric method was adapted for the quantitative analysis of prednisolone in dog plasma. A paper chromatographic procedure was modified by the use of thin-layer plates coated with microcrystalline cellulose. Heparinized blood samples were separated from the cellular elements and extracted with methylene chloride. After washing with acid and alkali, the extract was evaporated to dryness. The residue was dissolved in methanol and streaked on the TLC plate. After development, the band that was detected by UV light was scraped off and extracted with methanol. The methanol extract was treated with the Porter–Silber reagent (phenylhydrazine). Absorbance was measured at 410 nm. Replicate assays indicated a mean recovery of 97.5% and a coefficient of variation of 5.13%.



**Keyphrases** □ Prednisolone—modified method for colorimetric determination in dog plasma □ Colorimetry—modified method for determination of plasma prednisolone □ Glucocorticoids—prednisolone, colorimetric determination in plasma


The various methods used for the determination of prednisolone in plasma all have one or more shortcomings. Jenkins and Sampson (1) used a paper chromatographic procedure for the isolation of prednisolone after preliminary extraction with methylene chloride. Their procedure was modified by replacing the paper chromatographic procedure with thin-layer plates coated with microcrystalline cellulose. Microcrystalline cellulose was tried after preliminary screening revealed that inefficient separation occurred on the silica gel-coated plates recommended in the USP XX procedure (2).

The modified procedure decreased the time required for separation and also increased assay sensitivity. As a consequence, a simple, direct, and rapid analytical method for prednisolone in plasma was developed independently.

## EXPERIMENTAL

**Materials**—Anhydrous prednisolone USP[1], methanol[2] (HPLC grade),

[1] Merck & Co., Rahway, N.J.
[2] Fisher Scientific Co., Fair Lawn, N.J.




*0022-3549/81/0700-0810$01.00/0*


*© 1981, American Pharmaceutical Association*

anions are strongly attracted to the highly charged aluminum polynuclear cation. As the charge is neutralized, the complex disassociates and aluminum hydroxide forms. Because the solution pH was raised to 8 by the addition of sodium hydroxide, bayerite, the aluminum hydroxide polymorph that forms under basic conditions, was produced.

Aluminum chlorohydrate also is unstable if it is diluted with water (5, 6). Figure 2 shows that when aluminum chlorohydrate was diluted to $2.5 \times 10^{-2}$ *M* in aluminum, the pH first increased and then decreased. Earlier reports only noted a decrease in pH following dilution. However, the initial increase in pH is important and is consistent with the recently proposed structure of aluminum chlorohydrate (1). The central tetrahedral aluminum in the I complex is surrounded by 12 aluminum atoms in octahedral configuration. In dilute aqueous solution, the highly charged aluminum polycations are widely separated, and the stabilizing effect of the chloride counterions and other aluminum chlorohydrate complexes is reduced. As the I complex disassociates, the tetrahedral aluminum is exposed to the aqueous environment. Since the octahedral configuration is the stable form of aluminum below pH 8 (7–10), the tetrahedral aluminum converts to an octahedral configuration. Exposure of the four negatively charged oxygens, which form the outer shell of the aluminum tetrahedral, to the aqueous environment results in the attraction of protons and water to complete the octahedral configuration. The adsorption of protons is reflected in the initial increase in pH. However, the overall trend is a decrease in pH, which is consistent with the formation of octahedral aluminum into aluminum hydroxy polymers by the deprotonation–dehydroxylation mechanism (3).

The stability of aluminum chlorohydrate is concentration dependent since very little change in pH was observed unless the solution was <0.1 *M* in aluminum. At high concentration, the positively charged I spherical complexes are tightly packed and surrounded by stabilizing chloride counterions. Thus, aluminum chlorohydrate complex is self-stabilizing at high concentration.

Turbidity measurements of the diluted aluminum chlorohydrate solutions also showed that the stability of the complex was concentration dependent. Turbidity was not observed during this study unless the concentration was ~0.1 *M* or lower in terms of aluminum. Figure 2 also shows the development of turbidity following dilution to $2.5 \times 10^{-2}$ *M* in aluminum.

The insoluble degradation product resulting from the dilution of aluminum chlorohydrate was collected by filtration and examined by IR spectroscopy. The hydroxyl-stretching bands coincide with the hydroxyl-stretching bands of gibbsite (Fig. 3). The IR spectrum of the lyophilized filtrate was identical to the reference spectrum for aluminum chlorohydrate (11). Thus, it is believed that the I complex disassociates in dilute solution. The tetrahedral aluminum converts to an octahedral configuration due to the pH, and the octahedral aluminum species form aluminum hydroxide by deprotonation–dehydration. Gibbsite is the end-product of dilution since it is the stable polymorph of aluminum hydroxide in the acidic region. Therefore, the conversion of aluminum chlorohydrate to aluminum hydroxide upon complete neutralization or following dilution with water is consistent with the structure of the I complex that was proposed recently to be aluminum chlorohydrate.

## REFERENCES


(1) D. L. Teagarden, J. F. Kozlowski, J. L. White, and S. L. Hem, *J. Pharm. Sci.*, **70**, 758 (1981).

(2) G. Johansson, G. Lundgren, L. G. Sillen, and R. Soderquist, *Acta Chem. Scand.*, **14**, 769 (1960).

(3) S. L. Nail, J. L. White, and S. L. Hem, *J. Pharm. Sci.*, **65**, 1188 (1976).

(4) *Ibid.*, **64**, 1166 (1975).

(5) T. Govett and A. M. Rubino, *Am. Perfum. Essent. Oil Rev.*, **66**, 21 (1955).

(6) J. J. Margres, A. M. Rubino, and E. S. Bretschneider, *Cosmet. Perfum.*, **90**, 36 (1975).

(7) R. J. Moolenaar, J. C. Evans, and L. D. McKeever, *J. Phys. Chem.*, **74**, 3629 (1970).

(8) E. D. O'Reilly, *J. Chem. Phys.*, **32**, 1007 (1960).

(9) H. Haraguchi and S. Fujiwara, *J. Phys. Chem.*, **73**, 3467 (1969).

(10) E. R. Lippencott, J. A. Psellos, and M. C. Tobin, *J. Chem. Phys.*, **20**, 536 (1952).

(11) D. A. Risegraf and M. L. May, *Appl. Spectrosc.*, **32**, 362 (1978).


## ACKNOWLEDGMENTS


This report is Journal Paper 8256, Purdue University Agricultural Experiment Station, West Lafayette, IN 47907.


# Modified Colorimetric Method for Plasma Prednisolone


**A. N. NARURKAR and C. I. JAROWSKI** ˣ



Received October 27, 1980, from the *College of Pharmacy and Allied Health Professions, St. John's University, Jamaica, NY 11439.* Accepted for publication January 30, 1981.



**Abstract** □ A simple, precise, rapid, and sensitive colorimetric method was adapted for the quantitative analysis of prednisolone in dog plasma. A paper chromatographic procedure was modified by the use of thin-layer plates coated with microcrystalline cellulose. Heparinized blood samples were separated from the cellular elements and extracted with methylene chloride. After washing with acid and alkali, the extract was evaporated to dryness. The residue was dissolved in methanol and streaked on the TLC plate. After development, the band that was detected by UV light was scraped off and extracted with methanol. The methanol extract was treated with the Porter–Silber reagent (phenylhydrazine). Absorbance was measured at 410 nm. Replicate assays indicated a mean recovery of 97.5% and a coefficient of variation of 5.13%.



**Keyphrases** □ Prednisolone—modified method for colorimetric determination in dog plasma □ Colorimetry—modified method for determination of plasma prednisolone □ Glucocorticoids—prednisolone, colorimetric determination in plasma


The various methods used for the determination of prednisolone in plasma all have one or more shortcomings. Jenkins and Sampson (1) used a paper chromatographic procedure for the isolation of prednisolone after preliminary extraction with methylene chloride. Their procedure was modified by replacing the paper chromatographic procedure with thin-layer plates coated with microcrystalline cellulose. Microcrystalline cellulose was tried after preliminary screening revealed that inefficient separation occurred on the silica gel-coated plates recommended in the USP XX procedure (2).

The modified procedure decreased the time required for separation and also increased assay sensitivity. As a consequence, a simple, direct, and rapid analytical method for prednisolone in plasma was developed independently.

## EXPERIMENTAL

**Materials**—Anhydrous prednisolone USP[1], methanol[2] (HPLC grade),

[1] Merck & Co., Rahway, N.J.
[2] Fisher Scientific Co., Fair Lawn, N.J.




*0022-3549/81/0700-0810$01.00/0*


*© 1981, American Pharmaceutical Association*

toluene[3], methylene chloride[4], sodium hydroxide pellets[2] (analytical reagent grade), acetic acid[2], nitrogen[4], sulfuric acid[2] (analytical reagent grade), and phenylhydrazine hydrochloride[5] were obtained commercially.

**Equipment**—A spectrophotometer[6], a centrifuge[7], an analytical balance[8], a multiple developing tank[9], TLC glass plates[10] precoated with Avicel F (250-$\mu$m thickness), a micropipet[11], a camera with photo-UV system[12], a minerlight lamp, a multiband UV detector[13] (254/366 nm), and a water bath[14] were used.

**Preparation of Prednisolone Standard Solution in Methanol**—A stock solution of prednisolone was prepared by dissolving 100 mg of anhydrous prednisolone USP in 1000 ml of methanol. The stock solution then was diluted serially with methanol to give standard solutions containing 0.5, 1.0, 5.0, 10.0, 20.0, 25.0, and 50.0 $\mu$g of prednisolone/ml.

**Preparation of Reagents**—Dilute sulfuric acid solution (1.63:1) was prepared by adding 190 ml of water to 310 ml of concentrated sulfuric acid. Phenylhydrazine hydrochloride solution (Porter–Silber reagent) was prepared by dissolving 65 mg of phenylhydrazine hydrochloride in 100 ml of the dilute sulfuric acid (3).

**Quantitative Color Reaction for Prednisolone**—Eight milliliters of the phenylhydrazine reagent solution was added to a prednisolone sample in 1 ml of methanol (*i.e.*, various standard solutions of prednisolone in methanol), and the solution was heated to 60 ± 1° for 20 min. The resultant yellow solution was cooled to 25° in a running cold water bath. The methanol–phenylhydrazine–sulfuric acid blank was treated similarly. With a 5-cm cell, the absorbance of the standard solution was measured against a methanol–sulfuric acid–phenylhydrazine reagent blank at 410 nm. Spectrophotometric readings usually were taken within 5 min after color formation. The standard curve then was constructed by plotting the absorbance values *versus* the corresponding prednisolone concentrations.

**Preparation of Plasma Samples**—Blood samples collected from fasted beagle dogs were placed in heparinized tubes and centrifuged at 2300 rpm for 15 min to harvest the clear plasma.

**Preparation of Plasma Standards**—A series of standards was prepared by spiking 4 ml of clear plasma samples with 5.0, 10.0, 15.0, and 20.0 $\mu$g of prednisolone.

**Extraction**—Four milliliters of the plasma standard was extracted with 25 ml of methylene chloride, and the extract was washed with 2 ml of 0.1 *N* NaOH followed by 2 ml of 0.1 *N* acetic acid and then with 2 ml of distilled water. The extract was evaporated to dryness and redissolved in 200 $\mu$l of methanol by agitating on a vortex mixer.

**TLC**—Glass plates (20 × 20 cm) precoated with microcrystalline cellulose to a thickness of 250 $\mu$m were used. The solvent system was toluene–methanol–distilled water (84.8:14.6:0.6).

The chromatographic plate was divided into three equal sections. The left section was used for spotting the prednisolone standard solution in methanol, the right section was used for spotting prednisolone solution extracted from plasma, and the center section was used for the plasma blank. The solutions were applied as streaks 2.5 cm from the bottom of the plate. The solution was dried during application with the aid of a nitrogen stream.

With the described solvent system, the chromatogram was developed in a multiple development tank, previously equilibrated and lined with absorbent paper. The solvent then was allowed to move until it reached 15 cm above the baseline. The plate was removed, dried at room temperature, and visualized under shortwave UV light. The prednisolone standard band and the corresponding bands in the spiked plasma samples and the blank solutions were marked. The $R_f$ value for prednisolone was 0.3. The bands corresponding to this $R_f$ value were removed by scraping the microcrystalline cellulose onto a glazed weighing paper, and the scrapings were pulverized and transferred to 25-ml centrifuge tubes. Methanol (10 ml) was added, and the samples were agitated on a vortex mixer for 5 min and centrifuged at 2300 rpm for 5 min.

The clear methanol layers were decanted, and the residue was treated similarly with 5 ml of methanol three times. The pooled methanolic extracts then were evaporated to a 1-ml volume. These methanolic extracts of prednisolone from plasma were analyzed according to the method described previously. The standard curve of prednisolone in plasma then was constructed by plotting the absorbance values *versus* various prednisolone concentrations.

**Table I—Estimation of Prednisolone (20 $\mu$g/4 ml) in Plasma [a]**

| Sample Replicate Number | Estimated, $\mu$g/4 ml | Recovery, % |
|---|---|---|
| 1 | 19.25 | 96.25 |
| 2 | 19.50 | 97.50 |
| 3 | 20.25 | 101.25 |
| 4 | 21.00 | 105.00 |
| 5 | 18.25 | 91.25 |
| 6 | 18.75 | 93.75 |
| Mean | | 97.50 |

[a] Coefficient of variation = (standard deviation × 100)/mean = (1 × 100)/19.50 = 5.13%.

## RESULTS AND DISCUSSION

**Variation of Absorbance with Prednisolone in Methanolic Phenylhydrazine Acid Solution**—With 0.5–50 $\mu$g of prednisolone, the absorbance varied linearly with the amount of prednisolone. Under the experimental conditions, the Porter–Silber colorimetric method was sensitive to 1 $\mu$g of prednisolone. The regression equation obtained was $y = 0.023x + 0.0062$, and the correlation coefficient was 0.9998.

**Standard Curve of Prednisolone in Plasma**—Plots of absorbance *versus* 5–20 $\mu$g of prednisolone/4 ml of plasma were linear, passing through the origin with a slope of 0.023. The extraction caused a prednisolone loss of ~10%. The regression equation obtained was $y = 0.023x + 0.0068$, and the correlation coefficient was 0.9997.

**Method Accuracy and Precision**—Table I lists the results obtained from the analysis of a number of spiked plasma samples (20 $\mu$g/4 ml). These data reflect the accuracy and precision of the method. The mean recovery and the coefficient of variation were 97.5 and 5.13%, respectively.

In summary, TLC separation of microgram quantities of prednisolone extracted from dog plasma were assayed efficiently by a simple colorimetric procedure. This procedure should be considered when more sophisticated equipment or procedures are not available.

## REFERENCES


(1) J. A. Jenkins and P. A. Sampson, *Br. Med. J.*, **2**, 205 (1967).

(2) "The United States Pharmacopeia," 20th rev., United States Pharmacopeial Convention, Rockville, Md., 1980, p. 650.

(3) C. C. Porter and R. H. Silber, *J. Biol. Chem.*, **185**, 201 (1950).


[3] Burdick & Jackson Laboratories, Muskegon, Mich.
[4] Matheson Coleman & Bell, Norwood, Ohio.
[5] Lot 702A, Eastman Kodak Co., Rochester, N.Y.
[6] Model 240, Gilford Instrument Laboratories, Oberlin, Ohio.
[7] Model UV, International Equipment Co., Needham Heights, Mass.
[8] Model 33, Mettler Instrument Corp., Hightstown, N.J.
[9] Desega, Heidelberg, West Germany.
[10] Analtech, Newark, DE 19711.
[11] Drummond Scientific Co.
[12] Polaroid Corp., Cambridge, Mass.
[13] Model UVSL-58, Ultra-Violet Products, San Gabriel, Calif.
[14] Lab-Line Instruments, Melrose Park, Ill.

# Identification of 2-Chlorothioxanthen-9-one in Gastric Aspirate in a Case of Chlorprothixene Poisoning

**JON ELLING PETTERSEN** *§x, **GERD TEIEN** ‡, and **GUNNAR ARNFINN ULSAKER** ‡

Received November 10, 1980, from the *Institute of Clinical Biochemistry, University of Oslo, Rikshospitalet, Oslo, Norway, and the ‡National Centre for Medicinal Products Control, Oslo, Norway. Accepted for publication December 2, 1980. §Present address: Department of Clinical Chemistry, Institute of Medical Biology, University of Tromsø, N-9001 Tromsø, Norway.

**Abstract** □ In gastric aspirate from a case of severe chlorprothixene poisoning, large amounts (~30% of the chlorprothixene) of a previously unrecognized compound were found and identified tentatively as 2-chlorothioxanthen-9-one by combined GLC–low-resolution mass spectrometry and high-resolution mass spectrometry. The identity of the unknown compound was verified after synthesis of 2-chlorothioxanthen-9-one by two procedures. Only negligible amounts of 2-chlorothioxanthen-9-one were formed when chlorprothixene, dissolved in acids, bases, chloroform–isopropanol, methanol, or gastric fluid, was stored in the dark. However, large amounts of the drug were converted to 2-chlorothioxanthen-9-one upon exposure to UV light. Moreover, considerable quantities of unidentified degradation products were formed when chlorprothixene was exposed to lamp light as well as to UV light. Therefore, samples from cases of acute drug poisoning should be protected from light until analysis.

**Keyphrases** □ Chlorprothixene—degradation product identification, GLC–mass spectrometry, gastric aspirate □ GLC–mass spectrometry—analysis, chlorprothixene and degradation product, gastric aspirate □ Thioxanthene derivatives—chlorprothixene and degradation product, GLC–mass spectrometric analysis, gastric aspirate □ Tranquilizers—chlorprothixene, GLC–mass spectrometric analysis, gastric aspirate, degradation product

In our hospital, gastric lavage is performed routinely in all patients with suspected intoxication, and it is useful to analyze gastric aspirate (and unknown tablets) by combined GLC–mass spectrometry for the primary detection of the intoxicants in cases of acute drug poisoning (1). An advantage of using gastric aspirate samples is that nonmetabolized drugs may be demonstrated. This task is much simpler than identifying drug metabolites, which may be found in the urine, for example.

Seven thioxanthene derivatives have been described in humans after chlorprothixene ingestion. They all are probably true metabolites of the drug and not postmortem degradation products (2, 3). In the present work, an additional thioxanthene derivative, 2-chorothioxanthen-9-one, was identified in the gastric aspirate from a case of severe chlorprothixene poisoning.

## EXPERIMENTAL

Chlorprothixene[1] [3-(2-chloro-9*H*-thioxanthen-9-ylidene)-*N*,*N*-dimethyl-1-propanamine, I] was purchased. 2-Chlorothioxanthen-9-one was synthesized by a convenient new method—*viz.*, oxidation of chlorprothixene by potassium permanganate in benzene using 1,4,7,10,13,16-hexaoxacyclooctadecane (18-crown-6) as a catalyst. The structure also was verified by a patented two-step synthesis (4). In the first step, 2-carboxy-4′-chlorophenylsulfide was made from 4-chlorothiophenol and 2-iodobenzoic acid. In the second step, the ring system was formed by dehydration in hot concentrated sulfuric acid.

Gastric aspirate was obtained from a case of severe chlorprothixene poisoning. The pH was adjusted to 9.5 prior to extraction of the neutral and basic compounds with chloroform–isopropanol (95:5 v/v). The extract was received by this laboratory for analysis after ~3 months. It was not possible to obtain reliable data on the storage conditions.

[1] Truxal, H. Lundbeck & Co. A/S, Copenhagen, Denmark.

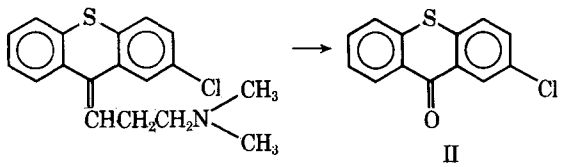


I II

*Scheme I—Structural formulas of chlorprothixene (I) and its degradation product, 2-chlorothioxanthen-9-one (II).*

Combined GLC–low-resolution mass spectrometry was performed using a gas chromatograph[2], a molecular separator of the glass frit type, and a single-focusing low-resolution mass spectrometer[3] operated with an ionizing energy of 70 ev. The gas chromatograph was equipped with a silanized glass column (2.5 m × 2 mm i.d.) packed with 3% QF-1 on Supelcoport, 80–100 mesh. The column was maintained isothermally at 210°, and helium was used as the carrier gas with a flow rate of 30 ml/min. The instrument was connected on-line to a computer system[4].

High-resolution mass spectrometry was performed with a double-focusing instrument[5] (source temperature, 220°; ionizing energy, 70 ev; ionization current, 100 μamps). The samples were introduced by the heated direct-insertion probe. Peak-matching measurements using heptacosafluorotributylamine as a standard were performed with a resolving power of 1:15,000.

## RESULTS AND DISCUSSION

GLC of the neutral and basic compounds in gastric aspirate from a case of severe chlorprothixene poisoning showed, in addition to chlorprothixene, a large peak (30% of the chlorprothixene peak area) with a relative retention volume of 0.55 compared to chlorprothixene.

The mass spectrum of the unknown compound (Fig. 1) showed prominent peaks in the high mass range and almost no fragment ions in the lower mass range, thus indicating a stable molecular structure, probably a ring structure. The peaks at *m/z* 246/248 and 218/220 indicated a chlorine atom in the compound. The direct formation of the ion at *m/z* 218 from the ion at *m/z* 246 and of the ion at *m/z* 220 from that at *m/z* 248 was shown by metastable peaks at 193.2 and 195.2, respectively.

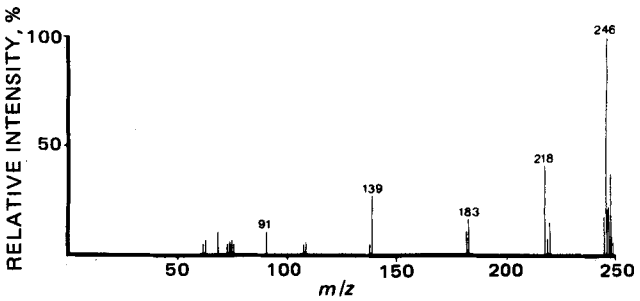


**Figure 1**—*Low-resolution mass spectrum of a previously unrecognized compound in gastric aspirate from a case of severe chlorprothixene poisoning. This mass spectrum was identical to that of authentic 2-chlorothioxanthen-9-one (not shown).*

[2] Varian 1440, Varian MAT, Bremen, West Germany.
[3] Varian CH 7, Varian MAT, Bremen, West Germany.
[4] Spectro System 100 MS, Varian MAT, Bremen, West Germany.
[5] MS 902, AEI, Manchester, England.



0022-3549/81/0700-0812$01.00/0
© 1981, American Pharmaceutical Association

Table I—Formation of 2-Chlorothioxanthen-9-one (II) from Chlorprothixene (I) under Various Conditions

| Exposure to Light | Solvent | Temperature | Days | Amount of II Formed[a], % |
|---|---|---|---|---|
| Darkness | 2 *M* HCl | 80° | 9 | ND |
| | 2 *M* KOH | 80° | 9 | ND |
| | 1 *M* NaOH | 22° | 18 | ND |
| | 5 *M* NaOH | 22° | 18 | 0.2 |
| | Gastric fluid, simulated[b] | 80° | 1 | ND |
| | Gastric fluid I (pH 2.4)[c] | 37° | 31 | 0.6 |
| | Gastric fluid II (pH 1.5)[c] | 37° | 38 | 1.5 |
| | Gastric fluid III (pH 6.5)[c] | 37° | 31 | 0.6 |
| | Chloroform–isopropanol (95:5 v/v) | 4° | 32 | ND |
| | Chloroform–isopropanol (95:5 v/v) | 4° | 580 | 0.5 |
| | Chloroform–isopropanol (95:5 v/v) | 22° | 32 | ND |
| | Chloroform–isopropanol (95:5 v/v) | 22° | 580 | 3.5 |
| Lamp light | Methanol | 22° | 34 | ND[d] |
| | Chloroform–isopropanol (95:5 v/v) | 22° | 34 | ND[d] |
| UV light (254 nm) + lamp light | Methanol | 22° | 4 + 16 | 32[d] |
| | Chloroform–isopropanol (95:5 v/v) | 22° | 4 + 16 | 31[d] |

[a] The formation of II was measured by GLC; see *Experimental*. ND = not detectable (<0.2%). [b] Prepared according to the USP method (5). [c] Obtained by gastric aspiration in three healthy adults. [d] Considerable quantities (5–40%) of degradation products of I other than II.

Exact mass measurements in a high-resolution mass spectrometer showed that the empirical formula of the ion at *m/z* 246 was $C_{13}H_7ClOS$ (theoretical mass, 245.9906; observed mass, 245.9906). Similarly, the ions at *m/z* 218 and 183 were shown to be $C_{12}H_7ClS$ (theoretical mass, 217.9957; observed mass, 217.9959) and $C_{12}H_7S$ (theoretical mass, 183.0268; observed mass, 183.0264), respectively.

From these data, the unknown compound was identified tentatively as 2-chlorothioxanthen-9-one (II). This compound was synthesized by two methods. The synthetic compounds cochromatographed with the unknown in GLC, and their mass spectra were identical. Thus, the identity of the unknown compound was established as II.

Table I shows the formation of II from chlorprothixene (I) under various storage conditions. Only negligible amounts were formed when the drug was stored in the dark or in lamp light. However, when I was treated with UV light for 4 days followed by storage in lamp light for 16 days, ~30% of I was converted to II. Moreover, considerable quantities of unidentified degradation products of I were formed when I was exposed to lamp light and UV light. These findings are in accordance with unpublished data (6). Therefore, samples from cases of acute drug poisoning should be stored in the dark.

## REFERENCES


(1) E. Saltvedt, E. Wiik-Larsen, B. Skuterud, J. E. Pettersen, P. K. M. Lunde, and E. Enger, *Tidsskr. Nor. Laegeforen.*, **97**, 227 (1977).

(2) H. Christensen, *Acta Pharmacol. Toxicol.*, **34**, 16 (1974).

(3) J. Raaflaub, *Arzneim.-Forsch.*, **17**, 1393 (1967).

(4) U.S. pat. 2,951,082 (1960).

(5) "The United States Pharmacopeia," 20th rev., United States Pharmacopeial Convention, Rockville, Md., 1980, p. 1105.

(6) B. C. Rudy and B. Z. Senkowski, in "Analytical Profiles of Drug Substances", vol. 2, K. Florey, Ed., Academic, New York, N.Y., 1973, p. 77.


# GLC Analysis of Phenylalkyl Primary Amines Using Nitrogen Detector


**J. I. JAVAID** ˣ **and J. M. DAVIS**



Received August 21, 1980, from the *Illinois State Psychiatric Institute, 1601 West Taylor Street, Chicago, IL 60612.* Accepted for publication December 2, 1980.



**Abstract** □ A comprehensive method for the analysis of several phenylalkyl primary amines of biological interest was developed. The amines were derivatized with perfluoro acid anhydrides or carbon disulfide in ethyl acetate, and the respective acyl derivatives or isothiocyanate derivatives were analyzed by GLC using nitrogen-specific detection. The described procedure was used to measure the amphetamine concentrations in rat serum, brain, and liver after intraperitoneal injection (5 mg/kg).



**Keyphrases** □ Phenylalkyl primary amines—GLC analysis using nitrogen detection, rat serum, brain, and liver □ Amphetamines—phenylalkyl primary amines, GLC analysis using nitrogen detection, rat serum, brain, and liver □ GLC—nitrogen detection, analysis, phenylalkyl primary amines in rat serum, brain, and liver


The use of nitrogen–phosphorus detection in GLC has many applications in biomedicine for the trace analyses of nitrogen-containing compounds. The nitrogen–phosphorus detector is generally 10–100 times more sensitive than the flame-ionization detector and has very little response to organic compounds that do not contain phosphorus or nitrogen atoms. Thus, therapeutic levels of many drugs containing a secondary or tertiary nitrogen, *e.g.*, anticonvulsants (1, 2), analgesics (3), tricyclic antidepressants (4–6), antipsychotics (7, 8), and drugs of abuse (9–11), can be measured. However, this approach has not yet been exploited for the analysis of primary amines. The use of GLC with nitrogen detection was suggested for the identification of amphetamine in forensic toxicology (9).

In this report, a comprehensive method for the analysis of several phenylalkyl primary amines is described. The amines were derivatized with acid anhydrides or carbon disulfide, and the *N*-acyl and isothiocyanate derivatives were analyzed by GLC with nitrogen detection.

## EXPERIMENTAL

**Materials**—All of the phenylalkyl primary amines were obtained


0022-3549/81/0700-0813$01.00/0


© 1981, American Pharmaceutical Association

Table I—Formation of 2-Chlorothioxanthen-9-one (II) from Chlorprothixene (I) under Various Conditions

| Exposure to Light | Solvent | Temperature | Days | Amount of II Formed[a], % |
|---|---|---|---|---|
| Darkness | 2 *M* HCl | 80° | 9 | ND |
| | 2 *M* KOH | 80° | 9 | ND |
| | 1 *M* NaOH | 22° | 18 | ND |
| | 5 *M* NaOH | 22° | 18 | 0.2 |
| | Gastric fluid, simulated[b] | 80° | 1 | ND |
| | Gastric fluid I (pH 2.4)[c] | 37° | 31 | 0.6 |
| | Gastric fluid II (pH 1.5)[c] | 37° | 38 | 1.5 |
| | Gastric fluid III (pH 6.5)[c] | 37° | 31 | 0.6 |
| | Chloroform–isopropanol (95:5 v/v) | 4° | 32 | ND |
| | Chloroform–isopropanol (95:5 v/v) | 4° | 580 | 0.5 |
| | Chloroform–isopropanol (95:5 v/v) | 22° | 32 | ND |
| | Chloroform–isopropanol (95:5 v/v) | 22° | 580 | 3.5 |
| Lamp light | Methanol | 22° | 34 | ND[d] |
| | Chloroform–isopropanol (95:5 v/v) | 22° | 34 | ND[d] |
| UV light (254 nm) + lamp light | Methanol | 22° | 4 + 16 | 32[d] |
| | Chloroform–isopropanol (95:5 v/v) | 22° | 4 + 16 | 31[d] |

[a] The formation of II was measured by GLC; see *Experimental*. ND = not detectable (<0.2%). [b] Prepared according to the USP method (5). [c] Obtained by gastric aspiration in three healthy adults. [d] Considerable quantities (5–40%) of degradation products of I other than II.

Exact mass measurements in a high-resolution mass spectrometer showed that the empirical formula of the ion at *m/z* 246 was $C_{13}H_7ClOS$ (theoretical mass, 245.9906; observed mass, 245.9906). Similarly, the ions at *m/z* 218 and 183 were shown to be $C_{12}H_7ClS$ (theoretical mass, 217.9957; observed mass, 217.9959) and $C_{12}H_7S$ (theoretical mass, 183.0268; observed mass, 183.0264), respectively.

From these data, the unknown compound was identified tentatively as 2-chlorothioxanthen-9-one (II). This compound was synthesized by two methods. The synthetic compounds cochromatographed with the unknown in GLC, and their mass spectra were identical. Thus, the identity of the unknown compound was established as II.

Table I shows the formation of II from chlorprothixene (I) under various storage conditions. Only negligible amounts were formed when the drug was stored in the dark or in lamp light. However, when I was treated with UV light for 4 days followed by storage in lamp light for 16 days, ~30% of I was converted to II. Moreover, considerable quantities of unidentified degradation products of I were formed when I was exposed to lamp light and UV light. These findings are in accordance with unpublished data (6). Therefore, samples from cases of acute drug poisoning should be stored in the dark.

## REFERENCES


(1) E. Saltvedt, E. Wiik-Larsen, B. Skuterud, J. E. Pettersen, P. K. M. Lunde, and E. Enger, *Tidsskr. Nor. Laegeforen.*, **97**, 227 (1977).

(2) H. Christensen, *Acta Pharmacol. Toxicol.*, **34**, 16 (1974).

(3) J. Raaflaub, *Arzneim.-Forsch.*, **17**, 1393 (1967).

(4) U.S. pat. 2,951,082 (1960).

(5) "The United States Pharmacopeia," 20th rev., United States Pharmacopeial Convention, Rockville, Md., 1980, p. 1105.

(6) B. C. Rudy and B. Z. Senkowski, in "Analytical Profiles of Drug Substances", vol. 2, K. Florey, Ed., Academic, New York, N.Y., 1973, p. 77.


# GLC Analysis of Phenylalkyl Primary Amines Using Nitrogen Detector


**J. I. JAVAID** ˣ **and J. M. DAVIS**



Received August 21, 1980, from the *Illinois State Psychiatric Institute, 1601 West Taylor Street, Chicago, IL 60612.* Accepted for publication December 2, 1980.



**Abstract** □ A comprehensive method for the analysis of several phenylalkyl primary amines of biological interest was developed. The amines were derivatized with perfluoro acid anhydrides or carbon disulfide in ethyl acetate, and the respective acyl derivatives or isothiocyanate derivatives were analyzed by GLC using nitrogen-specific detection. The described procedure was used to measure the amphetamine concentrations in rat serum, brain, and liver after intraperitoneal injection (5 mg/kg).



**Keyphrases** □ Phenylalkyl primary amines—GLC analysis using nitrogen detection, rat serum, brain, and liver □ Amphetamines—phenylalkyl primary amines, GLC analysis using nitrogen detection, rat serum, brain, and liver □ GLC—nitrogen detection, analysis, phenylalkyl primary amines in rat serum, brain, and liver


The use of nitrogen–phosphorus detection in GLC has many applications in biomedicine for the trace analyses of nitrogen-containing compounds. The nitrogen–phosphorus detector is generally 10–100 times more sensitive than the flame-ionization detector and has very little response to organic compounds that do not contain phosphorus or nitrogen atoms. Thus, therapeutic levels of many drugs containing a secondary or tertiary nitrogen, *e.g.*, anticonvulsants (1, 2), analgesics (3), tricyclic antidepressants (4–6), antipsychotics (7, 8), and drugs of abuse (9–11), can be measured. However, this approach has not yet been exploited for the analysis of primary amines. The use of GLC with nitrogen detection was suggested for the identification of amphetamine in forensic toxicology (9).

In this report, a comprehensive method for the analysis of several phenylalkyl primary amines is described. The amines were derivatized with acid anhydrides or carbon disulfide, and the *N*-acyl and isothiocyanate derivatives were analyzed by GLC with nitrogen detection.

## EXPERIMENTAL

**Materials**—All of the phenylalkyl primary amines were obtained


0022-3549/81/0700-0813$01.00/0


© 1981, American Pharmaceutical Association

commercially[1]. Glass-distilled[2] methanol, ethyl acetate, and hexane were used. Trifluoroacetic anhydride, pentafluoropropionic anhydride, and heptafluorobutyric anhydride were used as received[3]. Carbon disulfide and acetic anhydride were analytical grade.

The gas chromatograph[4] was equipped with a dual nitrogen–phosphorus detector. The instrument was set according to the instruction manual provided by the manufacturer, except that the offset current applied to the alkali metal bead was adjusted to give a recorder deflection of 20% of the full scale at a range of 1 and an attenuation of 32. The voltage input can be increased further to improve sensitivity to a point when the detector response to baseline noise ratio is optimum.

The 0.9-m coiled glass (2-mm i.d.) column was packed with 3% OV-17 on 80–100-mesh WHP Supelcoport. The gas flow rates were as follows: hydrogen, 3 ml/min; air, 50 ml/min; and helium (carrier gas), 30 ml/min. Oven temperature of 130° isothermal and injection port and detector temperatures of 200 and 300°, respectively, were used when trifluoroacetic anhydride was the derivatizing reagent.

**Procedures**—The stock solutions of standard reference compounds were made in methanol to give 1-mg (as free base) concentrations. The salts were extracted from 1 ml of 1 *N* NaOH solutions with 0.5 ml of hexane or ethyl acetate. Primary amines without derivatization eluted as broad peaks because of the polar amino group. Several derivatizing reagents were tried to find optimum conditions. Amphetamine, β-phenethylamine, and tyramine were used as prototype amines for determining these conditions. These primary amines, when underivatized, eluted immediately as broad peaks from 3% OV-17 at 130°.

**Derivatization with Carbon Disulfide**—Isothiocyanate derivatives were prepared according to a previously published method (12). Extracted solutions of amphetamine, phenethylamine, and tyramine were transferred to a reaction vial, and 0.5 ml of carbon disulfide was added. The mixture was shaken for 15 min, dried under nitrogen, redissolved in ethyl acetate, and injected into the chromatograph. Under these conditions, the derivatized amphetamine and phenethylamine eluted as symmetrical peaks with retention times of ~4.6 and 4.8 min, respectively, relative to the injection time.

**Derivatization with Acid Anhydrides**—To the amine solutions in the reaction vial was added 0.5 ml of the acid anhydride, and the mixture was shaken and left at room temperature for 1 hr. Then, the vials were either dried under nitrogen and redissolved in hexane for chromatographic analysis or washed with water and ammonium hydroxide as follows. For this purpose, the reaction was carried out in glass centrifuge tubes. After the reaction, 1 ml of distilled water was added carefully with constant mixing, the tubes were shaken for ~30 sec, and the water was discarded. Then 1 ml of 2 *N* $NH_4OH$ was added, the tubes were shaken for 5 min, and the hexane layer was separated and injected into the chromatograph.

**Amphetamine Levels in Biological Tissues**—The applicability of the method to biological fluids was determined by measuring amphetamine levels in rat serum, brain, and liver after amphetamine administration. The rats were injected intraperitoneally with amphetamine sulfate (5 mg/kg) and sacrificed 30 min later. Blood was collected, and the serum was separated by centrifugation. The brain and liver were removed and homogenized in 0.4 *N* HCl (1:10 w/v). The homogenate was centrifuged, and the amphetamine concentration was measured in the acidic layer after extraction.

To 1 ml of the serum and the brain and liver acid extracts was added 500 ng of benzylamine as the internal standard. The pH was adjusted to 10 by the addition of 0.1 ml of 5 *N* NaOH, and the mixture was extracted with 1 ml of ethyl acetate. Trifluoroacetic anhydride (0.5 ml) was added directly to this extract, and the mixture was left at room temperature for 1 hr. Then it was dried under a nitrogen stream, redissolved in 1 ml of hexane, and injected into the chromatograph.

## RESULTS AND DISCUSSION

Without derivatization, the phenylalkyl primary amines were eluted from the 3% OV-17 column at low temperatures as broad tailing peaks. However, after derivatization, the peaks were symmetrical. Figure 1 shows a representative chromatogram of six amines when analyzed after derivatization with trifluoroacetic anhydride. Since the GLC separation of free amines generally results in peak tailing due to spurious adsorption onto the column, several approaches were used for derivatization of the

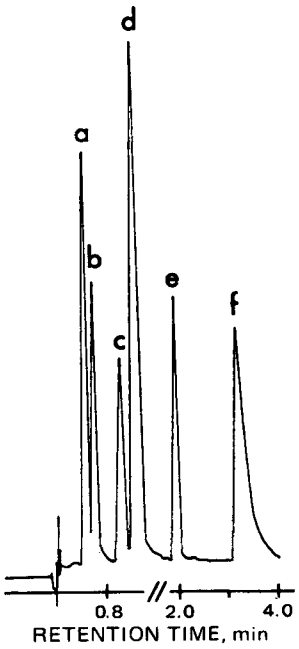


**Figure 1**—*Representative chromatogram showing the separation of six phenylalkyl primary amines as their trifluoroacyl derivatives. Key: a, α-phenethylamine; b, benzylamine; c, amphetamine; d, β-phenethylamine; e, p-methylamphetamine; and f, tyramine.*

amino groups (13, 14). The isothiocyanate derivatives of phenethylamine and amphetamine resulted in symmetrical peaks, whereas that of tyramine was not eluted. This result was probably due to the presence of the underivatized hydroxyl group in tyramine because Narasimhachari and Vouros (12) were able to analyze the isothiocyanate derivative of tyramine after silylation.

Acyl derivatives of amines, because of their ease of preparation, have been used successfully for GLC analysis. In this study, the trifluoroacetyl and heptafluorobutyryl derivatives of phenylalkyl primary amines were evaluated for GLC analysis with nitrogen detection. The best results were obtained when these amines were derivatized with trifluoroacetic anhydride. All of the primary amines, including tyramine, eluted as sym-

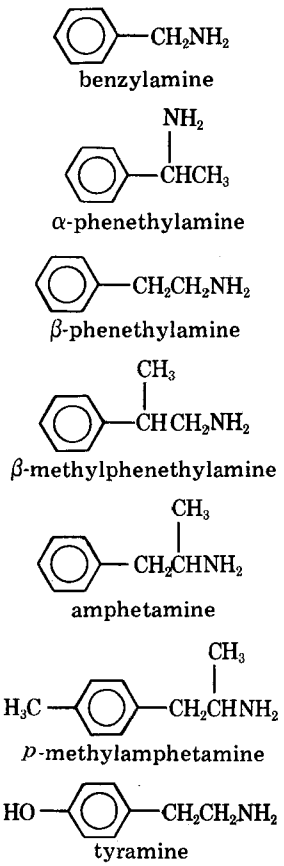


[1] Sigma Chemicals, St. Louis, MO 63178.
[2] Burdick & Jackson Laboratories, Muskegon, MI 49442.
[3] Regis Chemical Co., Morton Grove, IL 60053.
[4] Model 5730-A, Hewlett-Packard, Avondale, PA 19311.

Table I—Retention Times and Detector Response for Trifluoroacetyl and Isothiocyanate Derivatives of Phenylalkyl Primary Amines

| Amine | Nanomoles Injected | Retention Time, min | | Detector Response | |
|---|---|---|---|---|---|
| | | Trifluoroacetyl Derivative | Isothiocyanate Derivative | Trifluoroacetyl Derivative | Isothiocyanate Derivative |
| α-Phenethylamine | 0.165 | 0.80 | 2.56 | 96 | 34 |
| Benzylamine | 0.187 | 0.96 | 2.56 | 32 | 17 |
| Amphetamine | 0.148 | 1.44 | 4.64 | 212 | 31 |
| β-Phenethylamine | 0.165 | 1.60 | 4.80 | 88 | 60 |
| Tyramine | 0.146 | 4.16 | No peak | 40 | — |

metrical peaks under the described conditions. Unlike the isothiocyanate derivative, a second reaction was not needed to derivatize the phenolic hydroxyl group in tyramine. The stereoisomers of trifluoroacetyl derivatives of primary amines did not separate under the described conditions since *d*- and *l*-amphetamines eluted with the same retention times, as did the *d*- and *l*-α-phenethylamines.

The nitrogen detector response to the trifluoroacetyl derivatives was generally better than that to the corresponding isothiocyanate derivatives. Table I gives the comparison of trifluoroacetyl and isothiocyanate derivatives of some primary amines and also shows that the nitrogen detector response varied with different compounds and was not related to the amount of nitrogen present in the compound. For example, on a mole per mole basis, amphetamine has less nitrogen than benzylamine, but amphetamine as the trifluoroacetyl derivative had a 6.5 times better response than did benzylamine. This differential response probably depends on the formation of cyanide radicals after pyrolysis. Although the exact mechanism of the nitrogen detector response is not known, it was suggested (15) that the organic molecules containing nitrogen are pyrolyzed to form cyano radicals, which then remove an electron from the atomized alkali metal bead. These cyanide ions then can combine at the collector to form hydrogen cyanide, thus generating an output signal. Hence, the differential response of nitrogen-containing compounds may be due to their characteristics for producing cyanide radicals after pyrolysis.

The linearity of the nitrogen detector response was determined by derivatizing various concentrations of amphetamine (0.5–2.0 μg/ml), phenethylamine (0.5–2.0 μg/ml), and tyramine (1–10 μg/ml) in duplicate and injecting into the chromatograph. There was a linear response with all three primary amines. The regression equations by the least-squares method were: amphetamine, $y = 16.8x + 0$, $r = 0.990$; phenethylamine, $y = 27.8x - 3.25$, $r = 0.997$; and tyramine, $y = 5.76x + 1.5$, $r = 0.988$.

The excess derivatizing reagent was removed either by drying under nitrogen or by washing as described. When washing was used, the average coefficient of variation for amphetamine analysis of duplicate samples over the 0.5–2.0-μg/ml range was 4.1%, compared to an average coefficient of variation of 14.1% when the reacted samples were dried under nitrogen. However, the hydroxylated phenylalkyl primary amine (tyramine) peak disappeared if the reaction mixture was washed to remove excess trifluoroacetic anhydride. This finding suggests that *N*-acyl derivatives are more stable than *O*-acyl derivatives. This fact could be used to improve the chromatogram and reduce the analysis time by reducing the number of peaks if only a quantitation of nonhydroxylated primary amines in biological fluids is needed. The variability in the analysis of duplicate samples due to the loss during drying could be minimized by using the internal standard method.

Table II—Amphetamine Concentrations in Different Rat Tissues 30 min after Intraperitoneal Injection (5 mg/kg) [a]

| Tissue [b] | Amphetamine, ng/ml or g | *SEM* |
|---|---|---|
| Serum | 512 | ±81 |
| Brain | 4484 | ±885 |
| Liver | 5267 | ±299 |

[a] For details, see the procedures. [b] Three rats.

The amphetamine concentrations in rat serum, brain, and liver were determined (Table II). Thus, the method can be used to determine the phenylalkyl primary amines in biological fluids. However, the extraction procedure, specificity, and sensitivity of each compound must be established experimentally for each tissue.

## REFERENCES


(1) J. H. Goudie and D. Burnett, *Clin. Chim. Acta*, **43,** 423 (1973).

(2) D. D. Breimer and J. M. Van Rossum, *J. Chromatogr.*, **88,** 235 (1974).

(3) S. P. James and R. H. Waring, *ibid.*, **78,** 417 (1973).

(4) T. B. Cooper, D. Allen, and G. M. Simpson, *Psychopharmacol. Commun.*, **1,** 445 (1975).

(5) *Ibid.*, **2,** 105 (1976).

(6) D. N. Bailey and P. I. Jatlow, *Clin. Chem.*, **22,** 1697 (1976).

(7) H. Dekirmenjian, J. I. Javaid, B. Duslak, and J. M. Davis, *J. Chromatogr.*, **160,** 291 (1978).

(8) J. I. Javaid, H. Dekirmenjian, U. Liskevych, and J. M. Davis, *J. Chromatogr. Sci.*, **17,** 666 (1979).

(9) M. Reidman, *Naturwissenschaften*, **59,** 306 (1972).

(10) P. I. Jatlow and D. N. Bailey, *Clin. Chem.*, **21,** 1918 (1975).

(11) D. N. Bailey and J. J. Guba, *ibid.*, **26,** 437 (1980).

(12) N. Narasimhachari and P. Vouros, *Anal. Biochem.*, **45,** 154 (1972).

(13) J. Drozd, *J. Chromatogr.*, **113,** 303 (1975).

(14) K. Blau and G. King, "Handbook of Derivatives for Chromatography," Heydon, Philadelphia, Pa., 1978, pp. 104–151.

(15) B. Kolb and J. Bischoff, *J. Chromatogr. Sci.*, **12,** 625 (1974).


## ACKNOWLEDGMENTS


Supported in part by the Foundations' Fund for Research in Psychiatry No. 77-610.

The authors thank Ms. Evelyn Kingston for excellent technical assistance.

# Behavioral and Neurochemical Interactions of Dextroamphetamine and Methylphenidate in Rats

**T. G. REIGLE *x, W. L. ISAAC ‡, and W. ISAAC ‡**

Received November 10, 1980, from the *Department of Pharmacology, School of Pharmacy, and the ‡Department of Psychology, University of Georgia, Athens, GA 30602. Accepted for publication December 4, 1980.

**Abstract** □ The effects of dextroamphetamine and methylphenidate on locomotor activity and brain levels of norepinephrine and dopamine were compared in male Sprague–Dawley rats. Both drugs produced a dose-related increase in locomotor activity during the hour immediately following intraperitoneal administration. However, combined administration of the drugs elicited only the effect of dextroamphetamine. Brain levels of norepinephrine and dopamine also increased 1 hr after dextroamphetamine dosing. Methylphenidate did not exhibit these effects and antagonized the neurochemical changes produced by dextroamphetamine. Although both drugs are considered to exert their effects by indirect activation of brain catecholamine systems, differences in their mechanism of action appear to result in a lack of additive or antagonistic effects when dextroamphetamine and methylphenidate are coadministered. These findings may have clinical significance with respect to the use of such agents in minimal brain dysfunction.

**Keyphrases** □ Stimulants—dextroamphetamine and methylphenidate, effects on behavior and neurochemistry, rats □ Dextroamphetamine—effects on behavior and neurochemistry, rats, coadministration with methylphenidate □ Methylphenidate—effects on behavior and neurochemistry, rats, coadministration with dextroamphetamine □ CNS agents—dextroamphetamine and methylphenidate, effects on behavior and neurochemistry, rats

Both dextroamphetamine and methylphenidate have been employed successfully in the treatment of hyperkinesis or minimal brain dysfunction (1, 2). In experimental animals, these drugs exhibit the characteristic actions of central nervous system (CNS) stimulants by producing dose-dependent increases in locomotor activity and stereotyped behaviors (3, 4). Both the clinical and behavioral stimulant actions of these agents have been attributed to activation of brain catecholamine systems (5, 6). However, the mechanisms by which these drugs enhance brain catecholamine activity apparently are different.

## BACKGROUND

Reserpine, which depletes catecholamines by interfering with presynaptic granular storage, antagonizes the stimulant effects of methylphenidate but not those of dextroamphetamine (7). α-Methyl-*p*-tyrosine, an inhibitor of catecholamine synthesis, antagonizes the effects of dextroamphetamine but leaves the actions of methylphenidate relatively intact (8). These findings led to the proposal that methylphenidate facilitates the impulse-mediated release of catecholamines from reserpine-sensitive granular storage pools whereas dextroamphetamine acts primarily by increasing the release of a reserpine-resistant pool of newly synthesized cytoplasmic amines. Other investigators (9, 10) suggested that methylphenidate acts by blocking the presynaptic uptake of catecholamines released by nerve activity and that dextroamphetamine acts primarily by enhancing catecholamine release in the absence of neuronal stimulation.

Since both drugs are individually effective in ameliorating hyperkinetic symptoms, produce similar behavioral effects in animals, and indirectly activate brain catecholamine systems by different mechanisms, it was felt that coadministration of these agents might potentiate their separate effects and have possible clinical significance. This hypothesis was tested by evaluating the effects of moderate doses of dextroamphetamine and methylphenidate, individually and in combination, on the locomotor activity and brain catecholamine content of rats. The dose levels of both drugs were shown to have submaximal effects (3, 11, 12) and, thus, permitted the appearance of behavioral or neurochemical changes in either direction upon combination.

## EXPERIMENTAL

**Animals**—Sprague–Dawley male albino rats[1] were 20 days old when received and were adapted to the laboratory and daily handling for 7 days. For an additional 15 days, they were adapted to the apparatus and handling and injection procedures (13). Food and water were available at all times, and a 12-hr light–dark cycle was maintained.

**Apparatus**—The rats were housed in clear plastic mouse-breeding cages (45 × 24 × 25 cm) with a hardware cloth cover during activity measurements. Each plastic container was housed in a separate sound-treated cubicle, open at one end; it was 85 × 56 × 56 cm and individually lighted with a 20-w fluorescent bulb mounted 29 cm above the floor of the activity chamber. Twelve such cubicles were housed in a sound-treated room.

A single IR light beam bisected the length of each plastic container ~2 cm above the floor and fell upon a photocell. An IR filter covered the photocell, making it insensitive to ambient illumination. When the subjects broke the beam in their chambers, counts were recorded on individual counters in a separate room.

**Procedure**—Two dose levels of methylphenidate hydrochloride (1.6 and 3.2 mg/kg) and dextroamphetamine sulfate (0.4 and 0.8 mg/kg) and a combination of dextroamphetamine sulfate (0.4 mg/kg) and of methylphenidate hydrochloride (1.6 mg/kg) were studied. Placebo injections of the drug vehicle (bacteriostatic water) were included to give a total of six experimental conditions. All injections were administered intraperitoneally in an equal volume (1 ml/kg) 5–10 min before the subjects were placed in the activity measurement apparatus. When placed in the cubicle, all equipment was turned on and 5 min was allowed for adaptation. Activity measures were obtained for the next 60 min. Activity scores were transformed by a $\sqrt{x+1}$ transformation, as recommended for frequency scores (14).

Six separate orders of daily drug administrations were utilized, producing a 6 × 6 Latin square with two subjects within each order. All subjects were run through their orders three times. The first replication was for adaptation to the drug injections, and only scores from the last two replications were compared and evaluated by analysis of variance and Duncan's multiple range test (14).

Age-matched rats subjected to adaptation and handling procedures identical to those already described (13) were used for brain catecholamine analysis. Groups of animals (eight to 10 rats/group) received the same drug treatments utilized in the locomotor activity study and were sacrificed 30 min after intraperitoneal injection. Whole brains were removed rapidly, rinsed with tap water, and homogenized[2] in 12 ml of cold 0.4 *N* $HClO_4$. Homogenates were centrifuged at 30,000×*g* for 30 min, and the supernate was frozen immediately and stored for 1–2 days prior to chemical assay. Norepinephrine and dopamine were assayed by the fluorometric methods of Anton and Sayre (15) and Carlsson and Waldeck (16), respectively. Catecholamine concentrations were expressed as nanograms per gram of brain (wet weight) and were compared across treatments by analysis of variance and Duncan's multiple range test (14).

## RESULTS AND DISCUSSION

The locomotor activity data are presented in Fig. 1. Analysis of variance revealed that the difference between replications was not significant [$F(1,11) = 3.94$, $p > 0.05$], nor was the interaction between drug conditions and replications [$F(5,55) = 1.25$, $p > 0.05$]. The activity levels observed under the drug conditions, however, did differ significantly

[1] Southern Animal Farms, Prattville, Ala.
[2] Brinkmann Polytron homogenizer PT10-35.



0022-3549/81/0700-0816$01.00/0
© 1981, American Pharmaceutical Association

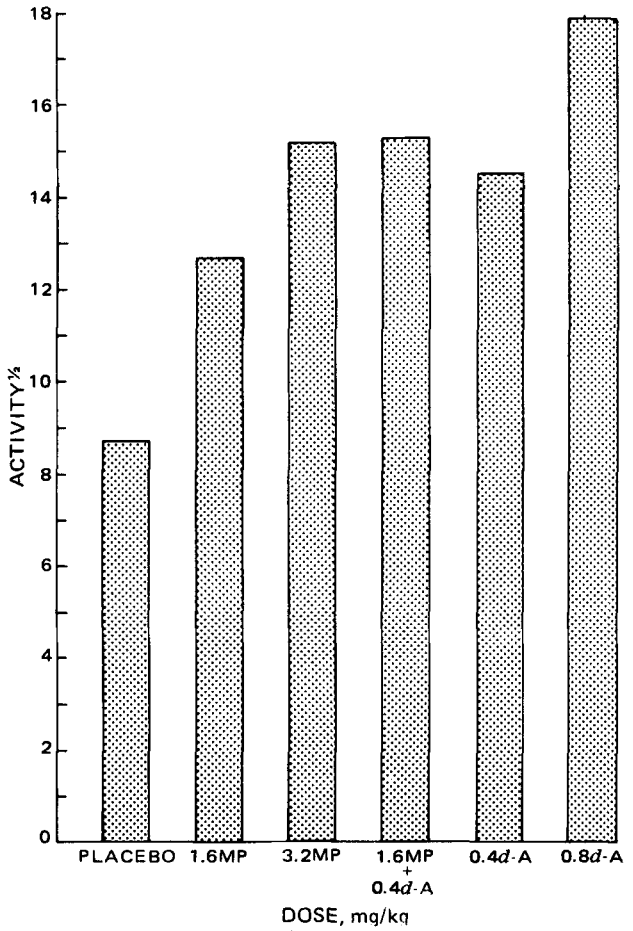


**Figure 1**—*Effects of dextroamphetamine (d-A), methylphenidate (MP), and their combination on square root-transformed locomotor activity scores in the rat.*

[$F(5,55) = 55.82$, $p < 0.01$]. Further analysis of the differences among drug treatments using the multiple range test ($\alpha = 0.01$) indicated that the placebo condition produced the lowest amount of locomotor activity and that the low dose of methylphenidate produced a significant increase. Administration of 0.4 mg of dextroamphetamine/kg, 3.2 mg of methylphenidate/kg, and the combined dose of 0.4 mg of dextroamphetamine/kg and 1.6 mg of methylphenidate/kg produced increases in locomotor activity that were significantly greater than the lower dose of methylphenidate, but the effects of these treatments did not differ significantly among themselves. The highest dose of dextroamphetamine produced a higher level of activity than the other drug conditions.

Thus, both drugs produced dose-related increases in locomotor activity and, as demonstrated previously (3), dextroamphetamine was more potent than methylphenidate. However, the drug combination was no more effective than dextroamphetamine alone. Intermediate dose levels of both drugs (3) were chosen so that changes in activity in either direction, as a consequence of the drug combination, could be detected. Since the higher dose of dextroamphetamine produced a greater increase in activity than the other treatments, the effects of the dextroamphetamine–methylphenidate combination were not limited by an activity ceiling. Also, since both the placebo and low dose of methylphenidate produced less activity than the drug combination, the results were not limited in the opposite direction. With these doses, methylphenidate neither enhanced nor suppressed the effects of dextroamphetamine on locomotor activity.

The effects of the various drug treatments on brain catecholamine levels are presented in Table I. Analysis of variance revealed significant differences among treatments on the brain levels of both norepinephrine [$F(5,51) = 5.14$, $p < 0.01$] and dopamine [$F(5,46) = 12.53$, $p < 0.01$]. Further analysis of these differences (Duncan's multiple range test; $\alpha = 0.05$) indicated that both doses of dextroamphetamine produced significant increases in brain dopamine, although the effects of these treatments were not different from each other. Brain dopamine levels following either methylphenidate or the dextroamphetamine–methylphenidate combination were not significantly different from those observed in the placebo-treated animals. Similar findings were obtained with respect to brain norepinephrine. The increase produced by 0.8 mg of dextroamphetamine/kg did not quite achieve statistical significance ($0.05 < p < 0.10$). However, the 0.4-mg/kg dose significantly increased brain norepinephrine, and the effects of the two amphetamine doses did not differ from each other. Once again, the effects of all other treatments were not significantly different from those of the placebo.

**Table I—Effects of Dextroamphetamine, Methylphenidate, and Their Combination on Rat Brain Catecholamines**

| Treatment (Dose, mg/kg) | Dopamine | | Norepinephrine | |
|---|---|---|---|---|
| | Nanograms per Gram[a] | Percent Placebo | Nanograms per Gram[a] | Percent Placebo |
| Placebo | 760 ± 14 | — | 287 ± 10 | — |
| Dextroamphetamine (0.4) | 894 ± 23[b] | 118[b] | 325 ± 12[c] | 113[c] |
| Dextroamphetamine (0.8) | 924 ± 29[b] | 122[b] | 320 ± 12[d] | 111[d] |
| Methylphenidate (1.6) | 771 ± 13 | 101 | 287 ± 10 | 100 |
| Methylphenidate (3.2) | 788 ± 24 | 104 | 257 ± 13 | 90 |
| Dextroamphetamine (0.4) + methylphenidate (1.6) | 769 ± 19 | 101 | 272 ± 13 | 95 |

[a] Data expressed as mean ± *SEM* of eight to 10 animals/group. [b] $p < 0.01$ *versus* placebo. [c] $p < 0.05$ *versus* placebo. [d] $p < 0.10$ *versus* placebo.

Thus, with respect to these neurochemical measures, not only were the effects of dextroamphetamine not enhanced by methylphenidate, they were significantly antagonized. The effects of amphetamine on brain catecholamine systems are complex. However, in agreement with the present findings, most previous reports indicated that low amphetamine doses capable of increasing locomotor activity produced increases in brain norepinephrine and dopamine while higher doses tended to cause a depletion (11, 12). In contrast, doses of methylphenidate that produced comparable increases in locomotor activity had no effect on brain catecholamines, indicating a difference in the mechanism of action of these two drugs. The doses of amphetamine employed could increase brain catecholamine levels by stimulating synthesis, inhibiting metabolism, or decreasing neuronal firing. The ability of amphetamine to inhibit monoamine oxidase has been demonstrated *in vitro*; however, rather large concentrations were required, and enzyme inhibition was difficult to observe following *in vivo* drug administration (17). Impulse flow in catecholamine neurons is inhibited by amphetamine (18), but this action also is produced by several other drugs, including methylphenidate, that have no appreciable effect on brain catecholamine levels (8).

Thus, the most plausible explanation for increases in brain catecholamines following amphetamine appears to be synthesis enhancement. The increased release elicited by amphetamine of newly synthesized catecholamines from nongranular cytoplasmic pools could reduce end-product inhibition of cytoplasmic tyrosine hydroxylase in presynaptic neurons (19). This would result in the increased formation and, hence, elevated levels of brain catecholamines observed in the present study. The greater release produced by larger amphetamine doses could exceed the synthetic capacity of the affected neurons, resulting in the net catecholamine depletion observed previously (11, 12).

The observed antagonism of amphetamine-induced increases in brain catecholamines by methylphenidate could be explained similarly. By facilitating the efflux of catecholamines from granular storage, methylphenidate would provide a source of replacement for the amines released from cytoplasmic pools by amphetamine such that synthesis could not be activated by a reduced catecholamine level in the cytoplasmic compartment. Behaviorally, this would not prevent stimulant effects due to the release of newly synthesized catecholamines by amphetamine but could prevent an additive action by methylphenidate since the amines displaced from the granules might replenish the cytoplasmic pool rather than act as a source for the activation of postsynaptic events.

Although amphetamine and methylphenidate individually exert behavioral stimulant effects and enhance the activity of brain catecholamine systems, differences in their mechanism of action can prevent additive or potentiating effects when these drugs are coadministered. These findings suggest that a therapeutic advantage may not be gained by combining amphetamine and methylphenidate in the treatment of hyperkinetic disorders.

## REFERENCES

(1) J. M. Krager and D. J. Safer, *N. Engl. J. Med.*, **291**, 1118 (1974).

(2) G. Weiss and L. Hechtman, *Science*, **205**, 1348 (1979).
(3) W. M. Kallman and W. Isaac, *Psychopharmacology*, **40**, 313 (1975).
(4) R. Pechnick, D. S. Janowsky, and L. Judd, *ibid.*, **65**, 311 (1979).
(5) P. H. Wender, *J. Nerv. Ment. Dis.*, **155**, 55 (1972).
(6) S. H. Snyder and J. L. Meyerhoff, *Ann. N.Y. Acad. Sci.*, **205**, 310 (1973).
(7) J. Scheel-Kruger, *Eur. J. Pharmacol.*, **14**, 47 (1971).
(8) C. Braestrup, *J. Pharm. Pharmacol.*, **29**, 463 (1977).
(9) S. B. Ross, *ibid.*, **30**, 253 (1978).
(10) P. Hunt, J. P. Raynaud, M. Leven, and U. Schacht, *Biochem. Pharmacol.*, **28**, 2011 (1979).
(11) C. B. Smith, *J. Pharmacol. Exp. Ther.*, **147**, 96 (1965).
(12) B. E. Leonard and S. A. Shallice, *Br. J. Pharmacol.*, **41**, 198 (1971).
(13) W. L. Isaac and W. Isaac, *Pharmacol. Biochem. Behav.*, **6**, 235 (1977).
(14) A. L. Edwards, "Experimental Design in Psychological Research," Holt, Rinehart and Winston, New York, N.Y., 1972.
(15) A. H. Anton and D. F. Sayre, *J. Pharmacol. Exp. Ther.*, **138**, 360 (1962).
(16) A. Carlsson and B. Waldeck, *Acta Physiol. Scand.*, **44**, 293 (1958).
(17) J. C. Holmes and C. O. Rutledge, *Biochem. Pharmacol.*, **25**, 447 (1976).
(18) B. S. Bunney, J. R. Walters, R. H. Roth, and G. K. Aghajanian, *J. Pharmacol. Exp. Ther.*, **185**, 561 (1973).
(19) J. C. Waymire, R. Bjur, and N. Weiner, *Anal. Biochem.*, **43**, 588 (1971).

# Plasma Protein Binding of Zomepirac Sodium

**PATRICK J. O'NEILL**

Received July 14, 1980, from the *Department of Drug Metabolism, McNeil Pharmaceutical, Spring House, PA 19477.* Accepted for publication December 19, 1980.

**Abstract** □ The plasma protein binding of zomepirac, a new nonnarcotic analgesic, was studied using equilibrium dialysis. Experiments were performed using human plasma and plasma from mice, rats, and rhesus monkeys, all species of pharmacological or toxicological interest. At concentrations approximating those achieved *in vivo*, the binding was fairly constant at 98–99% in all species except the rhesus monkey, where binding was decreased from 98 to ~96% at higher concentrations (>50 μg/ml). Zomepirac (10 μg/ml) did not appear to displace or to be displaced by warfarin (10 μg/ml) in human plasma. However, salicylate (5–200 μg/ml) caused a concentration-dependent decrease in zomepirac (10 μg/ml) binding. Zomepirac did not affect salicylate binding.

**Keyphrases** □ Zomepirac sodium—plasma protein binding studies in plasma from humans, rats, mice, and rhesus monkeys, interaction studies with warfarin and salicylic acid □ Plasma protein binding—zomepirac sodium in plasma from humans, rats, mice, and rhesus monkeys □ Warfarin—interaction studies with zomepirac sodium, effect on plasma protein binding □ Salicylic acid—interaction studies with zomepirac sodium, effect on plasma protein binding □ Analgesics, nonnarcotic—zomepirac sodium, plasma protein binding studies in humans, rats, mice, and rhesus monkeys, interaction studies with warfarin and salicylic acid

Plasma protein binding of drugs is an important factor in drug disposition (1–3). This report describes the interaction of zomepirac sodium, a new nonnarcotic analgesic agent (4–6), with plasma proteins from several species. Some preliminary binding interaction studies in human plasma are also reported.

## EXPERIMENTAL

**Materials**—Zomepirac sodium [sodium 5-(4-chlorobenzoyl)-1,4-dimethyl-1*H*-pyrrole-2-acetate dihydrate] was labeled with carbon 14 at a specific activity of 10.18 μCi/mg[1]. The drug was 96–98% radiochemically pure by TLC at the time of use. [$^{14}$C]Salicylic acid[2] and [$^{14}$C]warfarin[2] were used at specific activities of 421 and 164 μCi/mg, respectively. Both drugs were 99% radiochemically pure by TLC.

Heparinized plasma was harvested from blood collected from Wistar rats[3], CD-1 Swiss mice[3], and rhesus monkeys[4]. Citrated human plasma was purchased locally. Sorensen's buffer (0.067 *M* phosphate, pH 7.4) was prepared by dissolving 1.72 g of monobasic potassium phosphate and 7.70 g of dibasic sodium phosphate in 1 liter of distilled water.

**Methods**—Binding experiments were performed on an equilibrium dialysis system[5]. Regenerated cellulose dialysis membranes (mol. wt. cutoff of 5000) were prepared by three rinses in distilled water and three rinses in buffer. The membranes were placed between two-piece polytef dialysis cells (1-ml volume per side) mounted in a spring-loaded rack, and each half-cell was filled. One side of the cell was filled with plasma, and the other side was filled with the drug in buffer.

The cells were rotated at 12 rpm for 2 hr at room temperature, and then the half-cells were emptied and assayed for total carbon 14 as a measure of zomepirac. These dialysis conditions were selected since preliminary experiments in the absence of plasma (*i.e.*, zomepirac dialyzed against buffer) showed that equilibrium was reached in 2 hr and that plasma binding was not different at room temperature or 37°. Furthermore, TLC analysis of selected samples showed that no degradation of zomepirac occurred under these conditions.

**Interaction Studies**—[$^{14}$C]Zomepirac was dialyzed against undiluted rat, mouse, monkey, and human plasma at concentrations ranging from 0.1 to 250 μg/ml, depending on the species. These concentrations were in the ranges of those observed after pharmacological doses of zomepirac sodium (7–10).

To assess the potential for displacement of zomepirac by other agents, experiments were performed with warfarin[6] and salicylic acid[7] using human plasma. The [$^{14}$C]zomepirac concentration was 10 μg/ml. Warfarin was tested at 10 μg/ml, and salicylic acid was tested from 5 to 200 μg/ml. When the effect of zomepirac on the binding of these agents was evaluated, a tracer of [$^{14}$C]warfarin (~10,000 dpm/ml, 0.03 μg/ml) or salicylate (~10,000 dpm/ml, 0.01 μg/ml) was added, and nonradioactive zomepirac was used.

**Sample Analysis**—Total radioactivity was determined by adding aliquots of both plasma and buffer solutions (after dialysis) to 10 ml of scintillation cocktail[8]. Samples were counted in a refrigerated liquid scintillation spectrometer and were corrected for quenching using the external standard method.

Selected samples were analyzed for drug decomposition during dialysis. Zomepirac was assayed by applying aliquots of the postdialysis plasma and buffer samples to silica gel TLC plates[9] developed in chloroform–methanol–acetic acid (94:5:1 v/v/v). Analysis was by either segmentation and liquid scintillation counting or radioscan. No decomposition was observed.

[1] McNeil Pharmaceutical, Spring House, Pa.
[2] Amersham Corp., Des Plaines, Ill.
[3] Charles River, Wilmington, Mass.
[4] Primate Imports, Port Washington, N.Y.
[5] Dianorm, Diachema Ag., Ruschlikon, Switzerland.
[6] Endo Laboratories, Garden City, N.Y.
[7] J. T. Baker Chemical Co., Phillipsburg, N.J.
[8] Biofluor, New England Nuclear, Boston, Mass.
[9] GF 254 (250 μm), Analtech, Newark, Del.



0022-3549/81/0700-0818$01.00/0
© 1981, American Pharmaceutical Association

(2) G. Weiss and L. Hechtman, *Science*, **205**, 1348 (1979).
(3) W. M. Kallman and W. Isaac, *Psychopharmacology*, **40**, 313 (1975).
(4) R. Pechnick, D. S. Janowsky, and L. Judd, *ibid.*, **65**, 311 (1979).
(5) P. H. Wender, *J. Nerv. Ment. Dis.*, **155**, 55 (1972).
(6) S. H. Snyder and J. L. Meyerhoff, *Ann. N.Y. Acad. Sci.*, **205**, 310 (1973).
(7) J. Scheel-Kruger, *Eur. J. Pharmacol.*, **14**, 47 (1971).
(8) C. Braestrup, *J. Pharm. Pharmacol.*, **29**, 463 (1977).
(9) S. B. Ross, *ibid.*, **30**, 253 (1978).
(10) P. Hunt, J. P. Raynaud, M. Leven, and U. Schacht, *Biochem. Pharmacol.*, **28**, 2011 (1979).
(11) C. B. Smith, *J. Pharmacol. Exp. Ther.*, **147**, 96 (1965).
(12) B. E. Leonard and S. A. Shallice, *Br. J. Pharmacol.*, **41**, 198 (1971).
(13) W. L. Isaac and W. Isaac, *Pharmacol. Biochem. Behav.*, **6**, 235 (1977).
(14) A. L. Edwards, "Experimental Design in Psychological Research," Holt, Rinehart and Winston, New York, N.Y., 1972.
(15) A. H. Anton and D. F. Sayre, *J. Pharmacol. Exp. Ther.*, **138**, 360 (1962).
(16) A. Carlsson and B. Waldeck, *Acta Physiol. Scand.*, **44**, 293 (1958).
(17) J. C. Holmes and C. O. Rutledge, *Biochem. Pharmacol.*, **25**, 447 (1976).
(18) B. S. Bunney, J. R. Walters, R. H. Roth, and G. K. Aghajanian, *J. Pharmacol. Exp. Ther.*, **185**, 561 (1973).
(19) J. C. Waymire, R. Bjur, and N. Weiner, *Anal. Biochem.*, **43**, 588 (1971).

# Plasma Protein Binding of Zomepirac Sodium

**PATRICK J. O'NEILL**

Received July 14, 1980, from the *Department of Drug Metabolism, McNeil Pharmaceutical, Spring House, PA 19477.* Accepted for publication December 19, 1980.

**Abstract** □ The plasma protein binding of zomepirac, a new nonnarcotic analgesic, was studied using equilibrium dialysis. Experiments were performed using human plasma and plasma from mice, rats, and rhesus monkeys, all species of pharmacological or toxicological interest. At concentrations approximating those achieved *in vivo*, the binding was fairly constant at 98–99% in all species except the rhesus monkey, where binding was decreased from 98 to ~96% at higher concentrations (>50 μg/ml). Zomepirac (10 μg/ml) did not appear to displace or to be displaced by warfarin (10 μg/ml) in human plasma. However, salicylate (5–200 μg/ml) caused a concentration-dependent decrease in zomepirac (10 μg/ml) binding. Zomepirac did not affect salicylate binding.

**Keyphrases** □ Zomepirac sodium—plasma protein binding studies in plasma from humans, rats, mice, and rhesus monkeys, interaction studies with warfarin and salicylic acid □ Plasma protein binding—zomepirac sodium in plasma from humans, rats, mice, and rhesus monkeys □ Warfarin—interaction studies with zomepirac sodium, effect on plasma protein binding □ Salicylic acid—interaction studies with zomepirac sodium, effect on plasma protein binding □ Analgesics, nonnarcotic—zomepirac sodium, plasma protein binding studies in humans, rats, mice, and rhesus monkeys, interaction studies with warfarin and salicylic acid

Plasma protein binding of drugs is an important factor in drug disposition (1–3). This report describes the interaction of zomepirac sodium, a new nonnarcotic analgesic agent (4–6), with plasma proteins from several species. Some preliminary binding interaction studies in human plasma are also reported.

## EXPERIMENTAL

**Materials**—Zomepirac sodium [sodium 5-(4-chlorobenzoyl)-1,4-dimethyl-1*H*-pyrrole-2-acetate dihydrate] was labeled with carbon 14 at a specific activity of 10.18 μCi/mg[1]. The drug was 96–98% radiochemically pure by TLC at the time of use. [$^{14}$C]Salicylic acid[2] and [$^{14}$C]warfarin[2] were used at specific activities of 421 and 164 μCi/mg, respectively. Both drugs were 99% radiochemically pure by TLC.

Heparinized plasma was harvested from blood collected from Wistar rats[3], CD-1 Swiss mice[3], and rhesus monkeys[4]. Citrated human plasma was purchased locally. Sorensen's buffer (0.067 *M* phosphate, pH 7.4) was prepared by dissolving 1.72 g of monobasic potassium phosphate and 7.70 g of dibasic sodium phosphate in 1 liter of distilled water.

**Methods**—Binding experiments were performed on an equilibrium dialysis system[5]. Regenerated cellulose dialysis membranes (mol. wt. cutoff of 5000) were prepared by three rinses in distilled water and three rinses in buffer. The membranes were placed between two-piece polytef dialysis cells (1-ml volume per side) mounted in a spring-loaded rack, and each half-cell was filled. One side of the cell was filled with plasma, and the other side was filled with the drug in buffer.

The cells were rotated at 12 rpm for 2 hr at room temperature, and then the half-cells were emptied and assayed for total carbon 14 as a measure of zomepirac. These dialysis conditions were selected since preliminary experiments in the absence of plasma (*i.e.*, zomepirac dialyzed against buffer) showed that equilibrium was reached in 2 hr and that plasma binding was not different at room temperature or 37°. Furthermore, TLC analysis of selected samples showed that no degradation of zomepirac occurred under these conditions.

**Interaction Studies**—[$^{14}$C]Zomepirac was dialyzed against undiluted rat, mouse, monkey, and human plasma at concentrations ranging from 0.1 to 250 μg/ml, depending on the species. These concentrations were in the ranges of those observed after pharmacological doses of zomepirac sodium (7–10).

To assess the potential for displacement of zomepirac by other agents, experiments were performed with warfarin[6] and salicylic acid[7] using human plasma. The [$^{14}$C]zomepirac concentration was 10 μg/ml. Warfarin was tested at 10 μg/ml, and salicylic acid was tested from 5 to 200 μg/ml. When the effect of zomepirac on the binding of these agents was evaluated, a tracer of [$^{14}$C]warfarin (~10,000 dpm/ml, 0.03 μg/ml) or salicylate (~10,000 dpm/ml, 0.01 μg/ml) was added, and nonradioactive zomepirac was used.

**Sample Analysis**—Total radioactivity was determined by adding aliquots of both plasma and buffer solutions (after dialysis) to 10 ml of scintillation cocktail[8]. Samples were counted in a refrigerated liquid scintillation spectrometer and were corrected for quenching using the external standard method.

Selected samples were analyzed for drug decomposition during dialysis. Zomepirac was assayed by applying aliquots of the postdialysis plasma and buffer samples to silica gel TLC plates[9] developed in chloroform–methanol–acetic acid (94:5:1 v/v/v). Analysis was by either segmentation and liquid scintillation counting or radioscan. No decomposition was observed.

[1] McNeil Pharmaceutical, Spring House, Pa.
[2] Amersham Corp., Des Plaines, Ill.
[3] Charles River, Wilmington, Mass.
[4] Primate Imports, Port Washington, N.Y.
[5] Dianorm, Diachema Ag., Ruschlikon, Switzerland.
[6] Endo Laboratories, Garden City, N.Y.
[7] J. T. Baker Chemical Co., Phillipsburg, N.J.
[8] Biofluor, New England Nuclear, Boston, Mass.
[9] GF 254 (250 μm), Analtech, Newark, Del.



0022-3549/81/0700-0818$01.00/0
© 1981, American Pharmaceutical Association

**Table I—Zomepirac Binding to Plasma Proteins of Various Species**

| Species | Zomepirac Concentration[a], μg/ml | | | | | | | | |
|---|---|---|---|---|---|---|---|---|---|
| | 250 | 125 | 50 | 20 | 10 | 5 | 1 | 0.5 | 0.1 |
| Human | —[b] | — | — | — | 98.6 ± 0.3 | 98.6 ± 0.03 | 98.9 ± 0.1 | 98.4 ± 0.1 | 98.5 ± 0.2 |
| Rat | — | — | — | 97.7 ± 0.1 | 97.9 ± 0.1 | 98.9 ± 0.4 | 98.0 ± 0.3 | 98.1 ± 0.3 | 98.6 ± 0.5 |
| Mouse | — | — | — | — | 98.5 ± 0.6 | 98.1 ± 0.6 | 98.0 ± 0.2 | 99.1 ± 0.1 | 97.4 ± 0.4 |
| Monkey | 96.3 ± 0.4 | 96.4 ± 0.2 | 97.1 ± 0.4 | 98.4 ± 0.2 | 98.8 ± 0.5 | 98.9 ± 0.1 | 98.4 ± 0.1 | 99.1 ± 0.2 | 97.6 ± 0.8 |

[a] Values represent the starting concentration. Values represent mean percent bound ± *SD* of four to 10 determinations. [b] Not tested.

**Table II—Protein Binding Interactions of Zomepirac with Warfarin and Salicylate**

| Zomepirac | | Warfarin | |
|---|---|---|---|
| Concentration, μg/ml | Percent Bound[a] | Concentration, μg/ml | Percent Bound[a] |
| 0 | — | 10 | 98.3 ± 0.6 |
| 10 | 98.3 ± 0.1 | 10 | 98.5 ± 0.8 |
| **Zomepirac** | | **Salicylate** | |
| Concentration, μg/ml | Percent Bound[a] | Concentration, μg/ml | Percent Bound[a] |
| 0 | — | 5 | 94.5 ± 0.2 |
| 0 | — | 25 | 93.7 ± 0.3 |
| 0 | — | 100 | 85.4 ± 0.6 |
| 10 | 98.1 ± 0.3 | 5 | 94.5 ± 0.4 |
| 10 | 97.3 ± 0.3 | 25 | 93.1 ± 0.4 |
| 10 | 95.9 ± 0.7 | 100 | 83.7 ± 0.5 |
| 10 | 92.8 ± 0.6 | 200 | — |

[a] Mean ± *SD* of five determinations.

Salicylic acid was assayed by pooling plasma or buffer samples (~2 ml), adjusting to pH 1–2 with 0.5 ml of 6 *N* $H_2SO_4$, and extracting with 10 ml of ether. After shaking for 15 min and centrifuging for 5 min, an aliquot of the ether layer was counted for carbon 14 and the remainder was evaporated to dryness under nitrogen. More than 95% of the radioactivity was extracted. The residue was dissolved in a small amount of methanol and spotted on a TLC plate. The plate was developed in toluene–dioxane–acetic acid (90:24:4 v/v/v) and analyzed as described earlier. No salicylic acid degradation was observed.

Warfarin samples were pooled as described for salicylate and extracted with 10 ml of ethylene dichloride (15 min of shaking and 10 min of centrifugation). An aliquot of the organic layer was counted for carbon 14, and the remainder was evaporated to near dryness. Approximately 80% of the radioactivity was extracted. The extract was spotted on a TLC plate, and the plate was developed in toluene–ethyl formate–formic acid (5:4:1 v/v/v). Only 59% of the radioactivity in the dialysate corresponded to [$^{14}$C]warfarin, while essentially all of the carbon 14 in the plasma was unchanged warfarin. Therefore, the buffer was corrected for the presence of degradation products prior to calculating the extent of binding.

Percent bound values were calculated as follows:

$$\text{percent bound} = \frac{C_{b+f} - C_f}{C_{b+f}} \times 100 \qquad \text{(Eq. 1)}$$

where $C_{b+f}$ is the drug concentration on the plasma side of the membrane (bound plus free drug) and $C_f$ is the drug concentration on the buffer side (free drug).

## RESULTS AND DISCUSSION

Results of experiments evaluating the relationship between zomepirac concentration and extent of binding are shown in Table I. The mean percent bound to human plasma was essentially constant from 0.1 to 10 μg/ml, ranging from 98.4 to 98.9%. Similar findings were observed in the other species, although binding to monkey plasma was reduced slightly with higher zomepirac concentrations (≥50 μg/ml).

The results of the binding interaction studies in human plasma are shown in Table II. Warfarin (10 μg/ml) had no effect on zomepirac (10 μg/ml) binding, even though both drugs were tested at high concentrations relative to the those achieved after therapeutic doses of the drug (10, 11). Similarly, zomepirac did not alter warfarin binding. The effect of salicylic acid on zomepirac plasma binding is shown in Table II. At all concentrations tested, salicylate caused a statistically significant reduction in zomepirac binding, thus resulting in higher free drug concentrations. At 200 μg of salicylate/ml, this effect would result in a change in free fraction from 0.014 to 0.072, a fivefold increase. Zomepirac had no effect on salicylate binding.

Thus, similar to other acidic compounds (12, 13), zomepirac was highly bound to plasma proteins. Based on these preliminary studies, *in vivo* interactions of zomepirac and warfarin resulting from protein binding effects apparently are unlikely. While the potential for interactions with salicylate (*i.e.*, aspirin) exists, the *in vivo* importance cannot be predicted (14). Furthermore, these studies do not rule out drug interactions due to metabolic effects, additive pharmacological effects, or effects of drug metabolites.

## REFERENCES


(1) W. J. Jusko and M. Gretch, *Drug Metab. Rev.*, **5**, 43 (1976).

(2) J. W. Bridges and A. G. E. Wilson, in "Progress in Drug Metabolism," vol. 1, J. W. Bridges and L. F. Chasseaud, Eds., Wiley, New York, N.Y., 1976, p. 193.

(3) J. J. Vallner, *J. Pharm. Sci.*, **66**, 447 (1977).

(4) S. A. Cooper and D. Sullivan, *Clin. Pharmacol. Ther.*, **23**, 101 (1978).

(5) S. A. Cooper and S. Gottlieb, *ibid.*, **21**, 101 (1977).

(6) J. F. Stambaugh, *Clin. Res.*, **26**, 594A (1978).

(7) J. M. Grindel, P. J. O'Neill, K. A. Yorgey, M. H. Schwartz, L. A. McKown, B. H. Migdalof, and W. N. Wu, *Drug Metab.*, **8**, 343 (1980).

(8) K. A. Yorgey, L. A. McKown, and P. J. O'Neill, *Pharmacologist*, **22**, 225 (1980).

(9) P. J. O'Neill, K. A. Yorgey, B. H. Migdalof, and R. Z. Gussin, *J. Pharmacol. Exp. Ther.*, **209**, 366 (1979).

(10) R. K. Nayak, K. T. Ng, S. Gottlieb, and J. Plostnieks, *Clin. Pharmacol. Ther.*, **27**, 395 (1980).

(11) A. Yacobi, J. A. Udall, and G. Levy, *ibid.*, **19**, 552 (1976).

(12) J. B. Whitlam, M. J. Crooks, K. F. Brown, and P. V. Pedersen, *Biochem. Pharmacol.*, **28**, 675 (1979).

(13) D. H. Chatfield, J. N. Green, J. C. Kao, M. E. Tarrant, and T. J. Woodage, *ibid.*, **27**, 887 (1978).

(14) M. Gibaldi, G. Levy, and P. J. McNamara, *Clin. Pharmacol. Ther.*, **24**, 1 (1978).


## ACKNOWLEDGMENTS


The author thanks L. E. Weaner for synthesizing the $^{14}$C-labeled zomepirac sodium and P. S. Zappacosta for technical assistance.

# High-Pressure Liquid Chromatographic Determination of Methscopolamine Nitrate, Phenylpropanolamine Hydrochloride, Pyrilamine Maleate, and Pheniramine Maleate in Tablets

D. R. HEIDEMANN

Received August 8, 1980, from the *Analytical Research Department, Dorsey Laboratories (Division of Sandoz, Inc.), Lincoln, NE 68501.* Accepted for publication December 18, 1980.

**Abstract** □ Methscopolamine nitrate, phenylpropanolamine hydrochloride, pyrilamine maleate, and pheniramine maleate were determined in a multilayer film-sealed tablet with an enteric-coated core by reversed-phase high-pressure liquid chromatography without interference from active components and/or matrix decomposition.

**Keyphrases** □ Methscopolamine nitrate—high-pressure liquid chromatographic analysis, tablets □ Phenylpropanolamine hydrochloride—high-pressure liquid chromatographic analysis, tablets □ Pyrilamine maleate—high-pressure liquid chromatographic analysis, tablets □ Pheniramine maleate—high-pressure liquid chromatographic analysis, tablets □ High-pressure liquid chromatography—simultaneous determination of methscopolamine nitrate, phenylpropanolamine hydrochloride, pyrilamine maleate, and pheniramine maleate in tablets

Phenylpropanolamine, pyrilamine, pheniramine, and tropane alkaloids are active components employed in cold preparations. Simultaneous analysis of these compounds is complicated by the low concentration of tropane alkaloids in relationship to the other three amines and by the weak UV absorbance of the tropane alkaloid molecule.

## BACKGROUND

Various spectrophotometric methods have been employed for the analysis of phenylpropanolamine, pheniramine, and pyrilamine; however, extensive sample cleanup and separation are involved prior to the UV finishes (1, 2). Colorimetric methods and other indirect UV methods employed for the determination of methscopolamine and other tropane alkaloids are tedious and nonspecific (3–5).

Various stability-indicating high-pressure liquid chromatographic (HPLC) and GLC methods were reported for the determination of products containing one or more tropane alkaloids (6–12). The problem of simultaneously determining scopolamine and atropine with a preponderant concentration of phenylpropanolamine and chlorpheniramine was addressed by Santoro *et al.* (13) using GLC. However, this method also involved tedious sample preparation prior to injection.

The procedure described in the present study for the simultaneous determination of methscopolamine nitrate, phenylpropanolamine hydrochloride, pyrilamine maleate, and pheniramine maleate is rapid and stability indicating.

## EXPERIMENTAL

**Reagents**—Phenylpropanolamine hydrochloride[1], pyrilamine maleate[2], pheniramine maleate[3], methscopolamine nitrate[4], tropic acid[5], and acetonitrile[6] were used as obtained. Ethylenediamine sulfate was prepared by precipitating the salt from an aqueous solution of ethylenediamine[5] and sulfuric acid with methanol. All other chemicals were reagent grade and were used without further purification.

**Apparatus**—A constant-flow high-pressure liquid chromatograph[7] was used in conjunction with a variable-wavelength detector[8]. Effluents were monitored at 216.5 nm. Peak areas were determined using an electronic digital integrator[9]. The stainless steel column (25 cm × 4.6 mm i.d.) was obtained prepacked with 10-μm reversed-phase material[10]. An automatic injection system was used to introduce the sample onto the column inlet[11].

The mobile phase was $2.85 \times 10^{-3}$ *M* ethylenediamine sulfate buffer adjusted to pH 7.44 ± 0.02 with 1 *M* ammonium hydroxide–acetonitrile (1:1 v/v). The mobile phase was prepared fresh daily, and the flow rate was 3.8 ml/min.

**Sample**—The formulation investigated was a film-sealed tablet with an outer layer and an enteric-coated core[12]. The samples were assayed initially and after extended storage at elevated temperatures.

Ten tablets were crushed between paper and transferred to a 500-ml volumetric flask. Then 250 ml of 0.05 *N* hydrochloric acid in 50% alcohol was added. The preparation was heated for 15 min on a steam bath and shaken automatically for 2 hr. The sample was diluted to volume with water and filtered through glass microfiber[13]. The standard was prepared

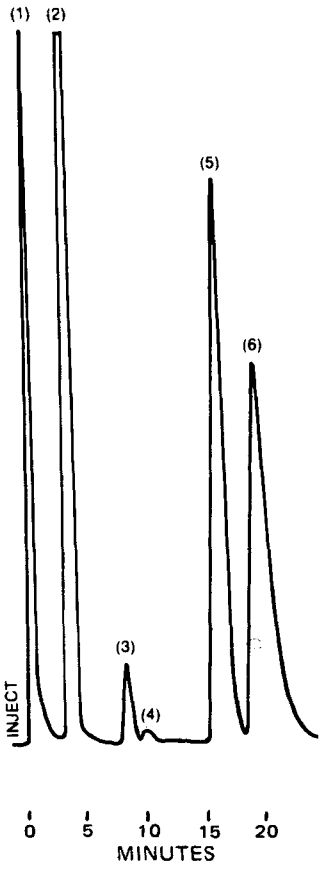


**Figure 1**—*Representative chromatogram of a tablet. Key: 1, excipients; 2, phenylpropanolamine; 3, methscopolamine; 4, excipient; 5, pyrilamine; and 6, pheniramine.*

[1] R. W. Greeff & Co., Dolton, IL 60419.
[2] Sandoz Ltd., Basel, Switzerland.
[3] Delamar, Elk Grove Village, IL 60007.
[4] Henley & Co., Lake Bluff, IL 60044.
[5] Aldrich Chemical Co., Milwaukee, WI 53233.
[6] HPLC grade, Fisher Scientific Co., St. Louis, MO 63132.
[7] Model 6000A, Waters Associates, Milford, MA 01757.
[8] Model 450, Waters Associates, Milford, MA 01757.
[9] Model 730, Waters Associates, Milford, MA 01757.
[10] Partisil-10-ODS, Whatman, Clifton, NJ 07014.
[11] Model 710A, Waters Associates, Milford, MA 01757.
[12] Dorsey Laboratories, Lincoln, NE 68501.
[13] GF/A, Whatman, Clifton, NJ 07014.



0022-3549/81/0700-0820$01.00/0
© 1981, American Pharmaceutical Association

**Table I—Recovery of Active Ingredients**

| Active Ingredient | Label, mg/tablet | Assay, mg/tablet | $CV^a$ |
|---|---|---|---|
| Phenylpropanolamine hydrochloride | 50 | 49.9 | 0.57 |
| Methscopolamine nitrate | 4 | 3.95 | 1.35 |
| Pyrilamine maleate | 25 | 24.8 | 1.14 |
| Pheniramine maleate | 25 | 25.4 | 0.63 |

[a] Standard deviation from the mean of 10 determinations divided by the mean expressed as a percent.

simultaneously in the same manner. The resulting theoretical concentrations of active components in the preparation were 1.0 mg of phenylpropanolamine hydrochloride, 0.5 mg of pyrilamine maleate, 0.5 mg of pheniramine maleate, and 0.08 mg of methscopolamine nitrate.

**Assay**—Thirty microliters of standard and sample preparations was injected into the chromatograph, and the peak areas were determined. The quantity of active components was determined by comparing the peak area of the sample to the respective peak area of the standard of known concentration.

## RESULTS AND DISCUSSION

The recovery and coefficient of variation for each active component are shown in Table I. The standard demonstrated linearity for the four active ingredients over a region of ±20% of the theoretical product content. The addition of a sample blank to the standard resulted in less than a ±1% effect for all active components. Figure 1 represents a typical chromatogram.

Tropane alkaloids are subject to degradation by both hydrolysis and dehydration. The degradation pathway of methscopolamine is shown in Scheme I (6–8). Tropic acid, methscopine, and aposcopolamine were resolved from all peaks. Tropic acid eluted at the void volume, and aposcopolamine eluted after methscopolamine (Fig. 2). Methscopine has little UV absorbance at this wavelength and concentration and was not detected. Figure 3 represents a sample spiked with tropic acid and aposcopolamine bromide.

The degradation pathway of phenylpropanolamine is not established. However, stability-indicating spectrophotometric methods such as

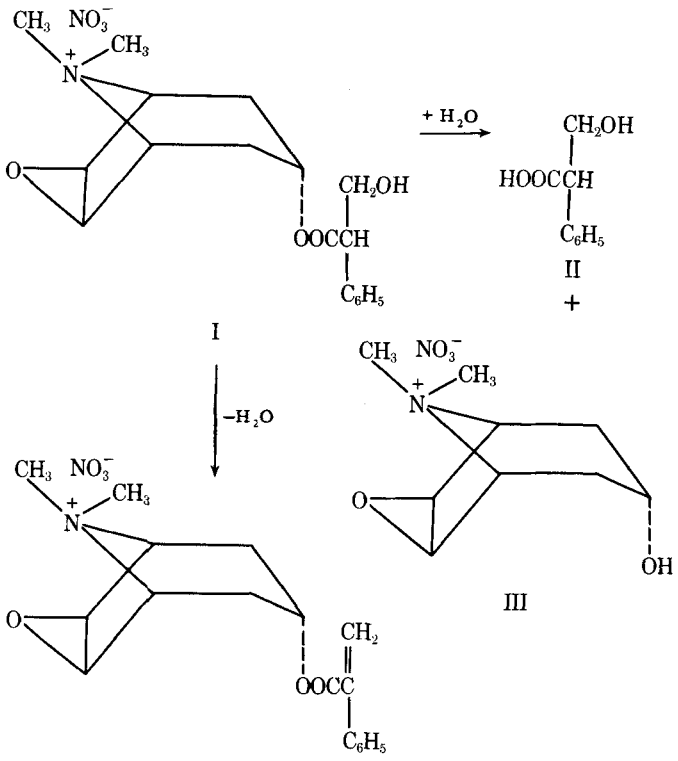


*Scheme I—Degradation pathway of methscopolamine nitrate (I) to tropic acid (II), methscopine nitrate (III), and aposcopolamine methylnitrate (IV).*

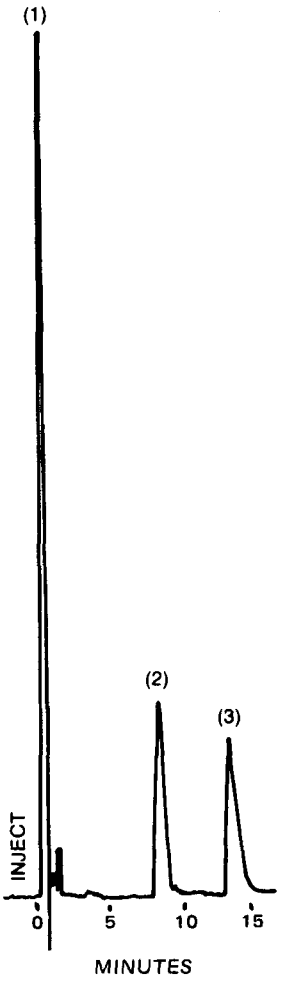


**Figure 2**—*Chromatogram of methscopolamine and its UV-active degradation products. Key: 1, tropic acid; 2, methscopolamine; and 3, aposcopolamine.*

periodate oxidation of phenylpropanolamine to benzaldehyde followed by extraction into hexane (1) indicate that the molecule is subject to decomposition in pharmaceutical preparations with time at normal and

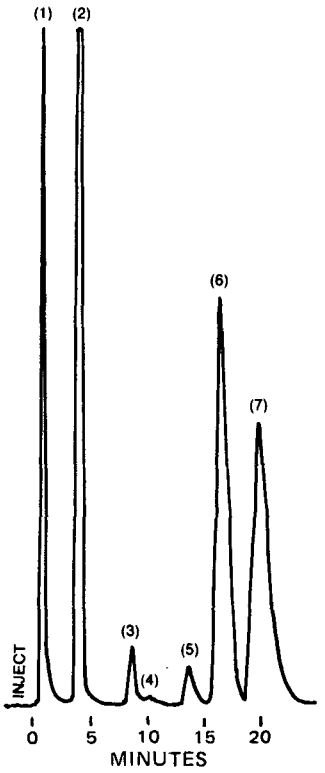


**Figure 3**—*Representative chromatogram of sample spiked with tropic acid and aposcopolamine bromide. Key: 1, tropic acid and excipients; 2, phenylpropanolamine; 3, methscopolamine; 4, excipient; 5, aposcopolamine; 6, pyrilamine; and 7, pheniramine.*

elevated temperatures. While the degradation products of phenylpropanolamine cannot be quantified by this method, a significant decrease in phenylpropanolamine was observed in stressed samples. Assay results for fresh and stressed samples by periodate oxidation correlated well with this assay, thus supporting the stability-indicating properties of this assay for phenylpropanolamine.

The recovery of the antihistamines, pyrilamine maleate[5] and pheniramine maleate, from a tablet matrix containing resinous material became increasingly difficult as the tablet was subjected to stress. Consequently, the acidic–alcoholic sample solution was exposed to heat to free the remaining antihistamines from the matrix.

In general, the chromatograms of stressed samples showed a decrease in phenylpropanolamine and methscopolamine but no loss in the pheniramine or pyrilamine content. There was no indication that excipients or degradation products interfered with the four peaks.

Careful control of buffer pH was necessary to obtain adequate separation of the pyrilamine and pheniramine peaks. The monitoring wavelength of 216.5 nm was selected as the optimum response *versus* baseline noise for the four species. At this wavelength, trace amounts of $\alpha$-aminopropiophenone, a precursor and possible trace contaminant in phenylpropanolamine, do not absorb to a significant amount.

## REFERENCES


(1) L. Chafetz, *J. Pharm. Sci.*, **60**, 291 (1971).

(2) D. J. Smith, *J. Assoc. Off. Anal. Chem.*, **49**, 536 (1966).

(3) C. Gomaa and A. Taha, *J. Pharm. Sci.*, **64**, 1398 (1975).

(4) S. A. Koch, J. Levine, and N. Zenker, *ibid.*, **54**, 1047 (1965).

(5) G. Schill, *Acta Pharm. Suec.*, **2**, 13 (1965).

(6) P. A. Hartman, *J. Assoc. Off. Anal. Chem.*, **62**, 1099 (1979).

(7) J. J. Windheuser, J. L. Sutter, and A. Sarrif, *J. Pharm. Sci.*, **61**, 1311 (1972).

(8) U. Lund and S. H. Hansen, *J. Chromatogr.*, **161**, 371 (1978).

(9) N. D. Brown and H. K. Sleeman, *ibid.*, **150**, 225 (1978).

(10) W. J. Griffen, H. P. Brand, and J. G. Dave, *J. Pharm. Sci.*, **64**, 1821 (1975).

(11) J. C. Gfeller, J. M. Huen, and J. P. Thevenin, *J. Chromatogr.*, **166**, 133 (1978).

(12) M. J. Walters, *J. Assoc. Off. Anal. Chem.*, **61**, 1428 (1978).

(13) R. Santoro, P. P. Progner, E. A. Ambush, and D. E. Guttman, *J. Pharm. Sci.*, **62**, 1346 (1973).


## ACKNOWLEDGMENTS


The author thanks Dorsey Laboratories and Dr. Eugene Brockemeyer, Director of Pharmaceutical Research and Quality Assurance, for support, and Murial V. Moffitt for technical assistance.


# Antiparasitic Structure–Activity Relationships of Congocidine Derivatives


**MEIR BIALER *[x], JOSEPH EL-ON [‡], BORIS YAGEN [§], and RAPHAEL MECHOULAM [§]**



Received October 23, 1980, from the **Department of Pharmacy, School of Pharmacy, the* [‡]*Department of Parasitology, Hadassah Medical School, and the* [§]*Department of Natural Products, School of Pharmacy, Hebrew University of Jerusalem, Jerusalem, Israel.* Accepted for publication December 17, 1980.



**Abstract** □ Several congocidine analogs were synthesized and tested for *in vivo* activity against *Trypanosoma congolense* and *in vitro* activity against amastigotes of *Leishmania tropica*. The tripyrrole derivative, β-{[*N*-methyl-4-[*N*-methyl-4-(guanidinoacetamido)pyrrole -2- carboxamido]pyrrole-2-carboxamido]pyrrole-2-carboxamido}butyroamidine dihydrochloride, was less toxic and more active than congocidine. The guanidinoacetyl moiety appears to be a structural requirement for antiparasitic activity in the congocidine series.



**Keyphrases** □ Congocidine derivatives—tri- and monopyrrole analogs, synthesized and evaluated for antiparasitic activity in mice, *in vivo* and *in vitro* studies □ Structure–activity relationships—tripyrrole derivatives of congocidine synthesized and evaluated for antiparasitic activity in mice, *in vivo* and *in vitro* studies □ Antiparasitic activity—tripyrrole derivatives of congocidine synthesized and evaluated for activity in mice, *in vitro* and *in vivo* studies


Congocidine (I) and distamycin A (II) are basic oligopeptide antiviral antibiotics isolated from the medium of *Streptomyces* sp. (1–3). The structure of congocidine was established by a series of degradations and a total synthesis (4, 5) and was shown to be identical to that of netropsin, which was isolated from a medium of *Streptomyces netropsis* (6, 7).

## BACKGROUND

Congocidine (I) and distamycin A (II) are the major components of a group of pyrrole amidine antiviral antibiotics. Unlike distamycin A and in addition to its antiviral and antibacterial activities (8, 9), congocidine also shows antiparasitic activity against *Trypanosoma congolense* (the source of its name) and other parasites (1, 2, 7). Little information is available on the structural requirements for the antiparasitic activity of congocidine. The only reported study (10) demonstrated that replacement of the *N*-methylpyrrole ring in congocidine by thiophene, pyridine, or benzene led to the loss of its trypanocidal activity.

Several studies on the distamycin series showed that when distamycin A (a tripeptide) was converted to its tetra- or pentapeptide analogs, the antiviral and antibacterial activities against some viruses and bacteria increased (11–14). At the same time, cytotoxicity was somewhat reduced, indicating that the biological and cytotoxic activities were separable.

A similar observation was made in the congocidine series. Several tripyrrole derivatives of congocidine were less cytotoxic and more active than the parent drug in three tests against Herpes simplex virus (15). The present study evaluated the antiparasitic activity of different tri- and monopyrrole derivatives of congocidine to establish some structural requirements in the congocidine molecule. Congocidine and its derivatives were tested against *Leishmania tropica*[1] *in vitro* in mouse peritoneal exudate cells and against *T. congolense*[2] *in vivo*.

## EXPERIMENTAL

**Chemistry**—The syntheses of the compounds were described previously (15, 16).

**Parasitology**[3]—*Animals*—Male mice of the inbred strains $C_3H$ and

[1] The *L. tropica* LRC-L137 strain was obtained from the strain collection of the World Health Organization's International Reference Center for Leishmaniasis (WHO-LRC) at the Department of Protozoology, Hadassah Medical School, Jerusalem, Israel.

[2] The *T. congolense* TREU 1183 strain was kindly supplied by Professor Curtis L. Patton, Department of Epidemiology and Public Health, Yale University, New Haven, Conn.

[3] Some of the parasitological work was presented at the annual meeting of the Israeli Society of Protozoologists (April 1980) and will appear as the following abstracts: J. El-On, C. L. Greenblat, D. T. Spira, R. Mechoulam, and M. Bialer, "The Effect of Congocidine Derivatives on *Leishmania tropica* and *Trypanosoma congolense*," in *J. Protozoology Supplement* (1981).




*0022-3549/81/0700-0822$01.00/0*


*© 1981, American Pharmaceutical Association*

elevated temperatures. While the degradation products of phenylpropanolamine cannot be quantified by this method, a significant decrease in phenylpropanolamine was observed in stressed samples. Assay results for fresh and stressed samples by periodate oxidation correlated well with this assay, thus supporting the stability-indicating properties of this assay for phenylpropanolamine.

The recovery of the antihistamines, pyrilamine maleate[5] and pheniramine maleate, from a tablet matrix containing resinous material became increasingly difficult as the tablet was subjected to stress. Consequently, the acidic–alcoholic sample solution was exposed to heat to free the remaining antihistamines from the matrix.

In general, the chromatograms of stressed samples showed a decrease in phenylpropanolamine and methscopolamine but no loss in the pheniramine or pyrilamine content. There was no indication that excipients or degradation products interfered with the four peaks.

Careful control of buffer pH was necessary to obtain adequate separation of the pyrilamine and pheniramine peaks. The monitoring wavelength of 216.5 nm was selected as the optimum response *versus* baseline noise for the four species. At this wavelength, trace amounts of $\alpha$-aminopropiophenone, a precursor and possible trace contaminant in phenylpropanolamine, do not absorb to a significant amount.

## REFERENCES


(1) L. Chafetz, *J. Pharm. Sci.*, **60**, 291 (1971).

(2) D. J. Smith, *J. Assoc. Off. Anal. Chem.*, **49**, 536 (1966).

(3) C. Gomaa and A. Taha, *J. Pharm. Sci.*, **64**, 1398 (1975).

(4) S. A. Koch, J. Levine, and N. Zenker, *ibid.*, **54**, 1047 (1965).

(5) G. Schill, *Acta Pharm. Suec.*, **2**, 13 (1965).

(6) P. A. Hartman, *J. Assoc. Off. Anal. Chem.*, **62**, 1099 (1979).

(7) J. J. Windheuser, J. L. Sutter, and A. Sarrif, *J. Pharm. Sci.*, **61**, 1311 (1972).

(8) U. Lund and S. H. Hansen, *J. Chromatogr.*, **161**, 371 (1978).

(9) N. D. Brown and H. K. Sleeman, *ibid.*, **150**, 225 (1978).

(10) W. J. Griffen, H. P. Brand, and J. G. Dave, *J. Pharm. Sci.*, **64**, 1821 (1975).

(11) J. C. Gfeller, J. M. Huen, and J. P. Thevenin, *J. Chromatogr.*, **166**, 133 (1978).

(12) M. J. Walters, *J. Assoc. Off. Anal. Chem.*, **61**, 1428 (1978).

(13) R. Santoro, P. P. Progner, E. A. Ambush, and D. E. Guttman, *J. Pharm. Sci.*, **62**, 1346 (1973).


## ACKNOWLEDGMENTS


The author thanks Dorsey Laboratories and Dr. Eugene Brockemeyer, Director of Pharmaceutical Research and Quality Assurance, for support, and Murial V. Moffitt for technical assistance.


# Antiparasitic Structure–Activity Relationships of Congocidine Derivatives


**MEIR BIALER *[x], JOSEPH EL-ON [‡], BORIS YAGEN [§], and RAPHAEL MECHOULAM [§]**



Received October 23, 1980, from the **Department of Pharmacy, School of Pharmacy, the* [‡]*Department of Parasitology, Hadassah Medical School, and the* [§]*Department of Natural Products, School of Pharmacy, Hebrew University of Jerusalem, Jerusalem, Israel.* Accepted for publication December 17, 1980.



**Abstract** □ Several congocidine analogs were synthesized and tested for *in vivo* activity against *Trypanosoma congolense* and *in vitro* activity against amastigotes of *Leishmania tropica*. The tripyrrole derivative, β-{[*N*-methyl-4-[*N*-methyl-4-(guanidinoacetamido)pyrrole -2- carboxamido]pyrrole-2-carboxamido]pyrrole-2-carboxamido}butyroamidine dihydrochloride, was less toxic and more active than congocidine. The guanidinoacetyl moiety appears to be a structural requirement for antiparasitic activity in the congocidine series.



**Keyphrases** □ Congocidine derivatives—tri- and monopyrrole analogs, synthesized and evaluated for antiparasitic activity in mice, *in vivo* and *in vitro* studies □ Structure–activity relationships—tripyrrole derivatives of congocidine synthesized and evaluated for antiparasitic activity in mice, *in vivo* and *in vitro* studies □ Antiparasitic activity—tripyrrole derivatives of congocidine synthesized and evaluated for activity in mice, *in vitro* and *in vivo* studies


Congocidine (I) and distamycin A (II) are basic oligopeptide antiviral antibiotics isolated from the medium of *Streptomyces* sp. (1–3). The structure of congocidine was established by a series of degradations and a total synthesis (4, 5) and was shown to be identical to that of netropsin, which was isolated from a medium of *Streptomyces netropsis* (6, 7).

## BACKGROUND

Congocidine (I) and distamycin A (II) are the major components of a group of pyrrole amidine antiviral antibiotics. Unlike distamycin A and in addition to its antiviral and antibacterial activities (8, 9), congocidine also shows antiparasitic activity against *Trypanosoma congolense* (the source of its name) and other parasites (1, 2, 7). Little information is available on the structural requirements for the antiparasitic activity of congocidine. The only reported study (10) demonstrated that replacement of the *N*-methylpyrrole ring in congocidine by thiophene, pyridine, or benzene led to the loss of its trypanocidal activity.

Several studies on the distamycin series showed that when distamycin A (a tripeptide) was converted to its tetra- or pentapeptide analogs, the antiviral and antibacterial activities against some viruses and bacteria increased (11–14). At the same time, cytotoxicity was somewhat reduced, indicating that the biological and cytotoxic activities were separable.

A similar observation was made in the congocidine series. Several tripyrrole derivatives of congocidine were less cytotoxic and more active than the parent drug in three tests against Herpes simplex virus (15). The present study evaluated the antiparasitic activity of different tri- and monopyrrole derivatives of congocidine to establish some structural requirements in the congocidine molecule. Congocidine and its derivatives were tested against *Leishmania tropica*[1] *in vitro* in mouse peritoneal exudate cells and against *T. congolense*[2] *in vivo*.

## EXPERIMENTAL

**Chemistry**—The syntheses of the compounds were described previously (15, 16).

**Parasitology**[3]—*Animals*—Male mice of the inbred strains $C_3H$ and

[1] The *L. tropica* LRC-L137 strain was obtained from the strain collection of the World Health Organization's International Reference Center for Leishmaniasis (WHO-LRC) at the Department of Protozoology, Hadassah Medical School, Jerusalem, Israel.

[2] The *T. congolense* TREU 1183 strain was kindly supplied by Professor Curtis L. Patton, Department of Epidemiology and Public Health, Yale University, New Haven, Conn.

[3] Some of the parasitological work was presented at the annual meeting of the Israeli Society of Protozoologists (April 1980) and will appear as the following abstracts: J. El-On, C. L. Greenblat, D. T. Spira, R. Mechoulam, and M. Bialer, "The Effect of Congocidine Derivatives on *Leishmania tropica* and *Trypanosoma congolense*," in *J. Protozoology Supplement* (1981).




*0022-3549/81/0700-0822$01.00/0*


*© 1981, American Pharmaceutical Association*

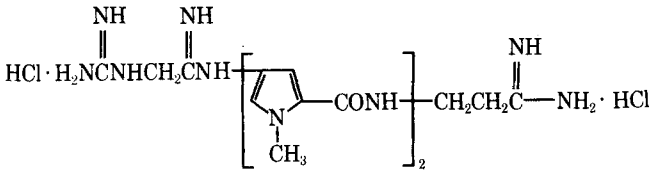

I

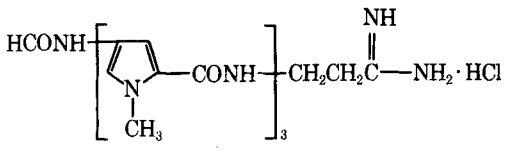

II

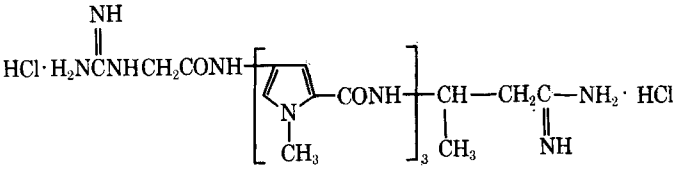

III

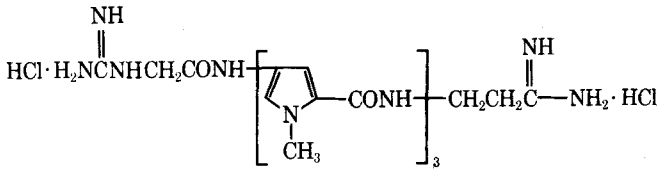

IV

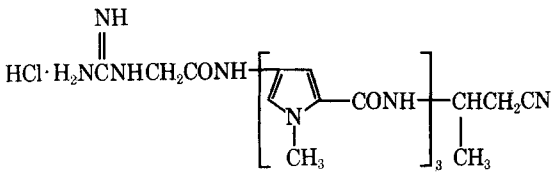

V

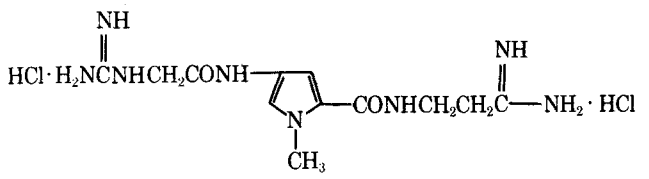

VI

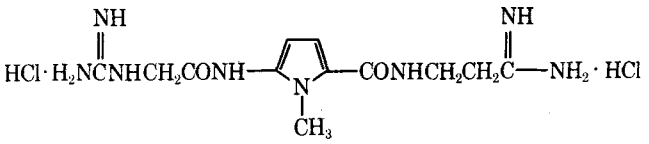

VII

Balb/c (25–35 g, 8–12 weeks old) were used. The $C_3H$ mice were the source of peritoneal exudate cells, while the Balb/c mice were used for *in vivo* studies of *T. congolense*.

*Cutaneous Leishmaniasis*—Mice peritoneal exudate cells were prepared from thioglycolate-stimulated mice as described by Handman *et al.* (17). The cells were cultivated in 24-well microplates at 37° and were infected 2 hr after cultivation with promastigotes prepared from a stabilate held at liquid nitrogen. The drug was introduced 24 hr after the transformation into intracellular amastigotes. The development of the parasites was checked daily, and the parasite survival index was determined. This index is the mean number of intracellular parasites multiplied by the percent of infection, as compared with the untreated infected control.

*Trypanosomiasis*—Balb/c mice were inoculated intraperitoneally with $5 \times 10^5$ trypanosomes. Drug treatment was begun 2–3 days after infection

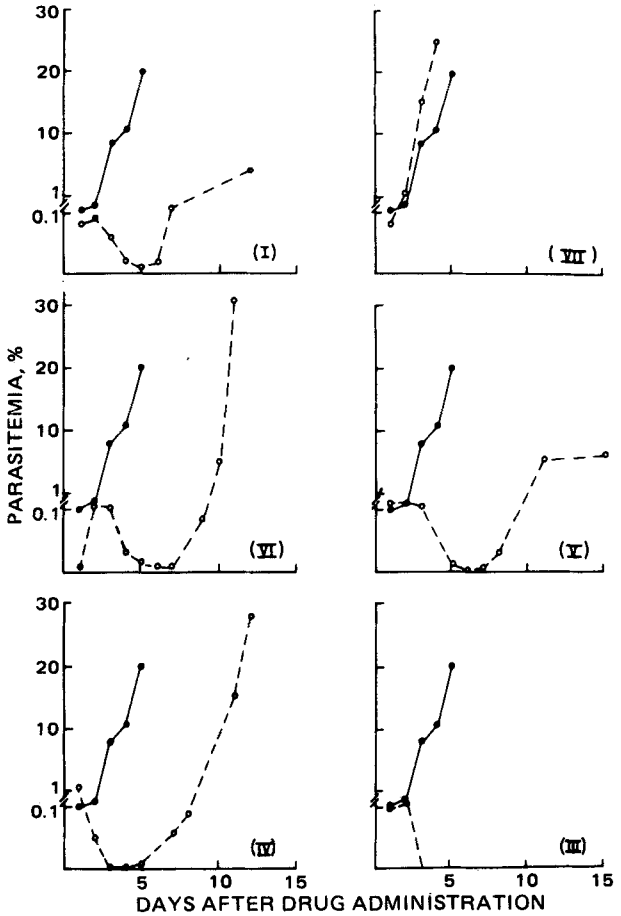


**Figure 1**—*Effect of congocidine derivatives on the growth of* T. congolense *in Balb/c mice. Day 1 is the 1st day of drug administration (40 mg/kg). The full-line (●) drawing indicates the results in mice receiving no drug.*

when parasites were detected in the blood. The parasites were counted daily in blood smears prepared from the mouse tail.

## RESULTS

The tripyrrole analog of congocidine (III) showed the greatest growth inhibition of *T. congolense* in mice. Two injections (40 mg/kg ip) given

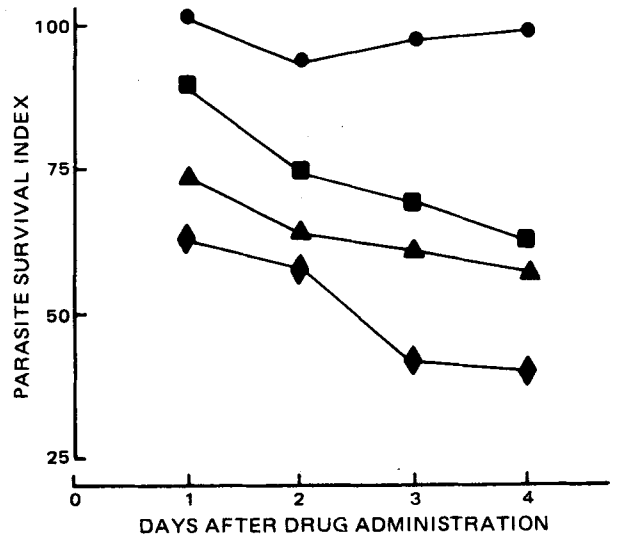


**Figure 2**—*Effect of distamycin A and congocidine derivatives on the growth of* L. tropica *amastigotes in peritoneal exudate cells from $C_3H$ mice at 37°. Key: ●, 10 μg of I/ml; ▲, 100 μg of II/ml; ♦, 10 μg of III/ml; and ■, 25 μg of IV/ml.*

on the 5th and 6th days of infection (when the parasitemia was >0.01%) were trypanocidal to such an extent that no parasites were detected over 90 days. The mice were tested every 15 days (Fig. 1). The other drugs, including the parent drugs (I and II), were less effective; they lowered parasitemias significantly but did not eliminate the parasites totally. Mice administered congocidine (I) or IV (40 mg/kg) three or more times died either from high parasitemia or from the toxic effect of the drug. Compound II was less toxic but also less effective against the parasite as compared with I. Six doses of II (40 mg/kg) did not affect the growth of the parasites, while five doses of 80 mg/kg inhibited the growth only partially.

*In vitro* studies indicated that III was also the most effective compound against *L. tropica* amastigotes in $C_3H$ mouse mononuclear phagocytes (Fig. 2). In cultures treated with 10 μg of III/ml, the parasite survival index indicated 50% survival on the 2nd day and 20% by the 4th day. Compounds IV (25 μg/ml) and II (100 μg/ml) also reduced growth but were not as effective as III. Cytotoxicity to host cells was observed at 25, 50, 50, and 200 μg/ml of I, III, IV, and II, respectively.

The doses used were the minimal effective nontoxic ones. Thus, no inhibitory effects on the growth of *L. tropica* were seen when II and IV were given in a concentration of <100 and 25 μg/ml, respectively. The monopyrrole analog of congocidine (VI) had the same effect against *T. congolense* as the parent drug. Its position isomer (VII) was completely inactive.

## DISCUSSION

In two antiparasitic tests, the tripyrrole derivative of congocidine (III) was more potent and less toxic than congocidine and more potent than its analog (IV). Although less toxic than congocidine, IV demonstrated the same inhibitory activity as the parent drug in the two systems tested. These results showed that there are considerable structural requirements in the congocidine series for their antiparasitic activity.

It was reported previously (15) that the tripeptide (IV) is more active in some antiviral tests than the dipeptide congocidine (I). However, this modification alone did not improve the antiparasitic activity, although it improved the therapeutic index. Surprisingly, the addition of a methyl group to the β-aminopropionamidine moiety in IV, leading to III, increased the antiparasitic activity and further improved the therapeutic index. The fact that distamycin A was totally inactive in the two antiparasitic tests demonstrated that the guanidinoacetyl moiety in the congocidine molecule cannot be replaced by a formamido moiety, contrary to observations in the antiviral field.

## REFERENCES


(1) C. Cosar, L. Ninet, S. Pinnert-Sindico, and J. Preudhomme, *C. R. Hebd. Seances Acad. Sci.*, **234**, 1498 (1952).

(2) C. Depois and L. Ninet, *Int. Microbiol. (Rome)*, **162**, 241 (1953).

(3) F. Arcamone, S. Penco, P. G. Orezzi, V. Nicollela, and A. Pirelli, *Nature (London)*, **203**, 1064 (1964).

(4) M. Julia and N. Preau Joseph, *C. R. Hebd. Seances Acad. Sci.*, **243**, 961 (1956).

(5) *Ibid.*, **257**, 1115 (1963).

(6) A. C. Finaly, F. A. Hochstein, B. A. Sobin, and F. X. Murphy, *J. Am. Chem. Soc.*, **73**, 341 (1951).

(7) S. Nakamura, J. Yonehara, and H. Umezawa, *J. Antibiot. (Ser. A)*, **1964**, 220.

(8) F. E. Hahn, in "Antibiotics," vol. 3, J. W. Concoran and F. E. Hahn, Eds., Springer-Verlag, New York, N.Y., 1975, p. 79.

(9) C. Zimmer, *Prog. Nucl. Acid Res. Mol. Biol.* **15**, 285 (1975).

(10) D. H. Jones and K. R. H. Wooldridge, *J. Chem. Soc. C*, **1968**, 550.

(11) F. Arcamone, V. Nicolella, S. Penco, and S. Redaelli, *Gazz. Chim. Ital.*, **94**, 632 (1969).

(12) P. Chandra, A. Gotz, A. Wacker, M. A. Vereni, A. M. Casazza, F. Fioretti, F. Arcamone, and M. Ghione, *FEBS Lett.*, **16**, 249 (1971).

(13) P. Chandra, F. Zuinno, A. Gotz, A. Wacker, D. Gericke, A. DiMarco, A. M. Casazza, and M. Guiliani, *ibid.*, **21**, 154 (1972).

(14) H. Thrum, I. Haupt, G. Bradler, C. Zimmer, and K. E. Reinert, *Antimicrob. Antineoplastic Chemother.*, **I/2**, 819 (1972).

(15) M. Bialer, B. Yagen, R. Mechoulam, and Y. Becker, *J. Med. Chem.*, **23**, 1144 (1980).

(16) M. Bialer, B. Yagen, R. Mechoulam, and Y. Becker, *J. Pharm. Sci.*, **69**, 1334 (1980).

(17) E. Handman, R. Ceredig, and G. F. Mitchell, *Aust. J. Exp. Biol. Med. Sci.*, **57**, 9 (1979).


## ACKNOWLEDGMENTS


The authors thank Mrs. R. Pardess for technical assistance.


# High-Performance Liquid Chromatographic Analysis of Carbenicillin and Its Degradation Products


**PHILIP A. TWOMEY**



Received November 19, 1980, from the *Penicillin Recovery Department, Pfizer Inc., Groton, CT 06340.* Accepted for publication December 22, 1980.



**Abstract** □ An ion-pair reversed-phase high-performance liquid chromatographic system is used to separate carbenicillin from carbenicillin penicilloic acid, carbenicillin penilloic acid, penicillin G, penicillin G penicilloic acid, and penicillin G penilloic acid. Conditions are provided for resolution of the carbenicillin diastereomer pair and for elution as a single peak, facilitating quantitation.



**Keyphrases** □ Carbenicillin—degradation products, high-performance liquid chromatographic analysis, mobile phase modifications □ High-performance liquid chromatography—analysis, carbenicillin, resolution of diastereomer pair or single-peak elution by mobile phase modifications □ Antibiotics—carbenicillin, high-performance liquid chromatographic analysis, mobile phase modifications □ Degradation—carbenicillin, high-performance liquid chromatographic analysis


Carbenicillin, a broad-spectrum semisynthetic penicillin-type antibiotic, is important because of its antipseudomonal and antiproteus effect. Most classical analytical methods available for penicillin purity or potency determinations are applicable to carbenicillin; the iodometric and hydroxylamine methods and the microbiological agar diffusion assay are the most widely used. The latter method is the one specified by the Antibiotic Regulations of the Food and Drug Administration (1). Carbenicillin monosodium monohydrate is used as a reference standard for this assay (2).

## BACKGROUND

Recent literature (3–6) indicated that high-performance liquid chromatography (HPLC), especially reversed-phase or ion-pair reversed-phase HPLC on microparticulate (≤10 μm) bonded packing materials, is amenable to the analysis of penicillins. In many penicillin analyses,




*0022-3549/81/0700-0824$01.00/0*


*© 1981, American Pharmaceutical Association*

on the 5th and 6th days of infection (when the parasitemia was >0.01%) were trypanocidal to such an extent that no parasites were detected over 90 days. The mice were tested every 15 days (Fig. 1). The other drugs, including the parent drugs (I and II), were less effective; they lowered parasitemias significantly but did not eliminate the parasites totally. Mice administered congocidine (I) or IV (40 mg/kg) three or more times died either from high parasitemia or from the toxic effect of the drug. Compound II was less toxic but also less effective against the parasite as compared with I. Six doses of II (40 mg/kg) did not affect the growth of the parasites, while five doses of 80 mg/kg inhibited the growth only partially.

*In vitro* studies indicated that III was also the most effective compound against *L. tropica* amastigotes in $C_3H$ mouse mononuclear phagocytes (Fig. 2). In cultures treated with 10 μg of III/ml, the parasite survival index indicated 50% survival on the 2nd day and 20% by the 4th day. Compounds IV (25 μg/ml) and II (100 μg/ml) also reduced growth but were not as effective as III. Cytotoxicity to host cells was observed at 25, 50, 50, and 200 μg/ml of I, III, IV, and II, respectively.

The doses used were the minimal effective nontoxic ones. Thus, no inhibitory effects on the growth of *L. tropica* were seen when II and IV were given in a concentration of <100 and 25 μg/ml, respectively. The monopyrrole analog of congocidine (VI) had the same effect against *T. congolense* as the parent drug. Its position isomer (VII) was completely inactive.

## DISCUSSION

In two antiparasitic tests, the tripyrrole derivative of congocidine (III) was more potent and less toxic than congocidine and more potent than its analog (IV). Although less toxic than congocidine, IV demonstrated the same inhibitory activity as the parent drug in the two systems tested. These results showed that there are considerable structural requirements in the congocidine series for their antiparasitic activity.

It was reported previously (15) that the tripeptide (IV) is more active in some antiviral tests than the dipeptide congocidine (I). However, this modification alone did not improve the antiparasitic activity, although it improved the therapeutic index. Surprisingly, the addition of a methyl group to the β-aminopropionamidine moiety in IV, leading to III, increased the antiparasitic activity and further improved the therapeutic index. The fact that distamycin A was totally inactive in the two antiparasitic tests demonstrated that the guanidinoacetyl moiety in the congocidine molecule cannot be replaced by a formamido moiety, contrary to observations in the antiviral field.

## REFERENCES


(1) C. Cosar, L. Ninet, S. Pinnert-Sindico, and J. Preudhomme, *C. R. Hebd. Seances Acad. Sci.*, **234**, 1498 (1952).

(2) C. Depois and L. Ninet, *Int. Microbiol. (Rome)*, **162**, 241 (1953).

(3) F. Arcamone, S. Penco, P. G. Orezzi, V. Nicollela, and A. Pirelli, *Nature (London)*, **203**, 1064 (1964).

(4) M. Julia and N. Preau Joseph, *C. R. Hebd. Seances Acad. Sci.*, **243**, 961 (1956).

(5) *Ibid.*, **257**, 1115 (1963).

(6) A. C. Finaly, F. A. Hochstein, B. A. Sobin, and F. X. Murphy, *J. Am. Chem. Soc.*, **73**, 341 (1951).

(7) S. Nakamura, J. Yonehara, and H. Umezawa, *J. Antibiot. (Ser. A)*, **1964**, 220.

(8) F. E. Hahn, in "Antibiotics," vol. 3, J. W. Concoran and F. E. Hahn, Eds., Springer-Verlag, New York, N.Y., 1975, p. 79.

(9) C. Zimmer, *Prog. Nucl. Acid Res. Mol. Biol.* **15**, 285 (1975).

(10) D. H. Jones and K. R. H. Wooldridge, *J. Chem. Soc. C*, **1968**, 550.

(11) F. Arcamone, V. Nicolella, S. Penco, and S. Redaelli, *Gazz. Chim. Ital.*, **94**, 632 (1969).

(12) P. Chandra, A. Gotz, A. Wacker, M. A. Vereni, A. M. Casazza, F. Fioretti, F. Arcamone, and M. Ghione, *FEBS Lett.*, **16**, 249 (1971).

(13) P. Chandra, F. Zuinno, A. Gotz, A. Wacker, D. Gericke, A. DiMarco, A. M. Casazza, and M. Guiliani, *ibid.*, **21**, 154 (1972).

(14) H. Thrum, I. Haupt, G. Bradler, C. Zimmer, and K. E. Reinert, *Antimicrob. Antineoplastic Chemother.*, **I/2**, 819 (1972).

(15) M. Bialer, B. Yagen, R. Mechoulam, and Y. Becker, *J. Med. Chem.*, **23**, 1144 (1980).

(16) M. Bialer, B. Yagen, R. Mechoulam, and Y. Becker, *J. Pharm. Sci.*, **69**, 1334 (1980).

(17) E. Handman, R. Ceredig, and G. F. Mitchell, *Aust. J. Exp. Biol. Med. Sci.*, **57**, 9 (1979).


## ACKNOWLEDGMENTS


The authors thank Mrs. R. Pardess for technical assistance.


# High-Performance Liquid Chromatographic Analysis of Carbenicillin and Its Degradation Products


**PHILIP A. TWOMEY**



Received November 19, 1980, from the *Penicillin Recovery Department, Pfizer Inc., Groton, CT 06340.* Accepted for publication December 22, 1980.



**Abstract** □ An ion-pair reversed-phase high-performance liquid chromatographic system is used to separate carbenicillin from carbenicillin penicilloic acid, carbenicillin penilloic acid, penicillin G, penicillin G penicilloic acid, and penicillin G penilloic acid. Conditions are provided for resolution of the carbenicillin diastereomer pair and for elution as a single peak, facilitating quantitation.



**Keyphrases** □ Carbenicillin—degradation products, high-performance liquid chromatographic analysis, mobile phase modifications □ High-performance liquid chromatography—analysis, carbenicillin, resolution of diastereomer pair or single-peak elution by mobile phase modifications □ Antibiotics—carbenicillin, high-performance liquid chromatographic analysis, mobile phase modifications □ Degradation—carbenicillin, high-performance liquid chromatographic analysis


Carbenicillin, a broad-spectrum semisynthetic penicillin-type antibiotic, is important because of its antipseudomonal and antiproteus effect. Most classical analytical methods available for penicillin purity or potency determinations are applicable to carbenicillin; the iodometric and hydroxylamine methods and the microbiological agar diffusion assay are the most widely used. The latter method is the one specified by the Antibiotic Regulations of the Food and Drug Administration (1). Carbenicillin monosodium monohydrate is used as a reference standard for this assay (2).

## BACKGROUND

Recent literature (3–6) indicated that high-performance liquid chromatography (HPLC), especially reversed-phase or ion-pair reversed-phase HPLC on microparticulate (≤10 μm) bonded packing materials, is amenable to the analysis of penicillins. In many penicillin analyses,




*0022-3549/81/0700-0824$01.00/0*


*© 1981, American Pharmaceutical Association*

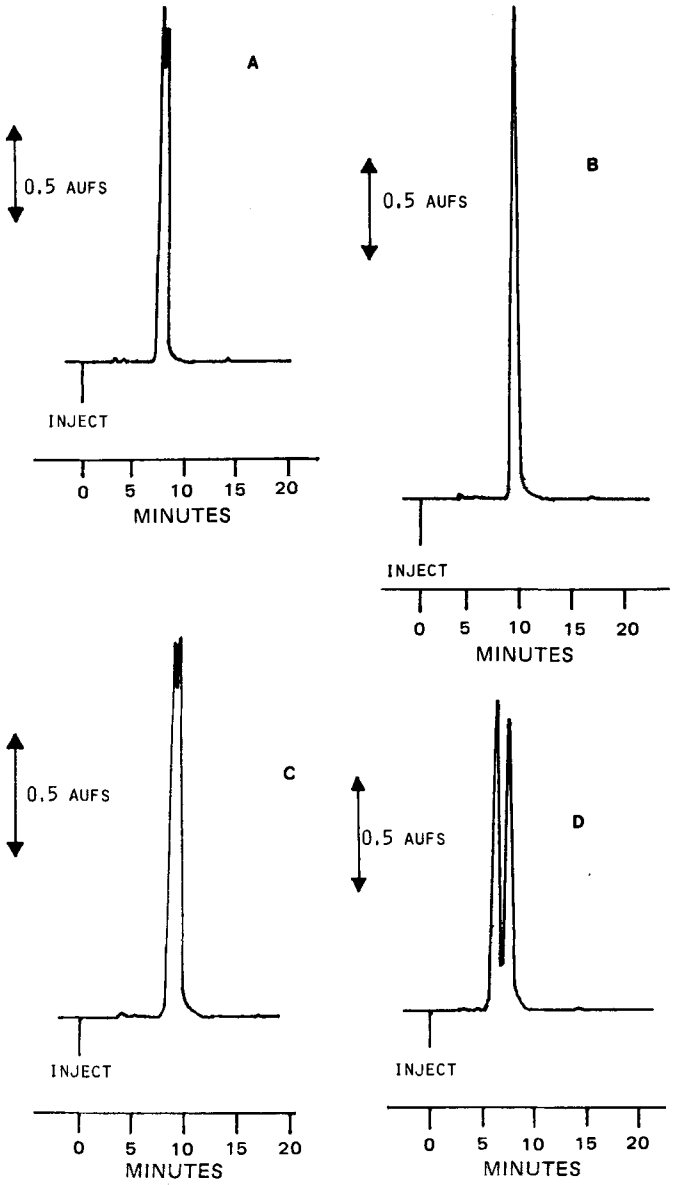


**Figure 1**—*Chromatograms of carbenicillin (0.850 mg/ml) with a mobile phase of 37% methanol at 1.2 ml/min and the detector wavelength at 220 nm. Key (pH of mobile phase): A, 3.00; B, 3.35; C, 3.70; and D, 4.35.*

HPLC procedures are the methods of choice because of demonstrated precision, accuracy, speed, and ability to provide ancillary information relative to the nature and identity of purity-depressing substances such as reaction by-products or natural degradation products present in the sample. In addition, the analyses often can be accomplished when the drug is part of a complex mixture such as a biological fluid or blend formulation.

Carbenicillin is a somewhat unique semisynthetic penicillin in that the normal synthesis routes produce a diastereomer mixture. This mixture complicates quantitative analysis by HPLC since reversed-phase microparticulate column packings generally are selected for their ability to separate the components of a mixture. Thus, the same criterion used to select HPLC as an analytical method for carbenicillin can negate its quantitation since the carbenicillin diastereomers tend to elute as two peaks, except when the chromatographic conditions are closely controlled. This tendency is especially true when methanolic mobile phases and high efficiency columns are used.

This report describes the mobile phase modifications used with a 5-$\mu$m octadecylsilyl-bonded silica-based column to provide either separation of the carbenicillin diastereomers or elution as one peak, depending on the desires of the analyst. In addition, separation of carbenicillin from some of its possible degradation products is demonstrated.

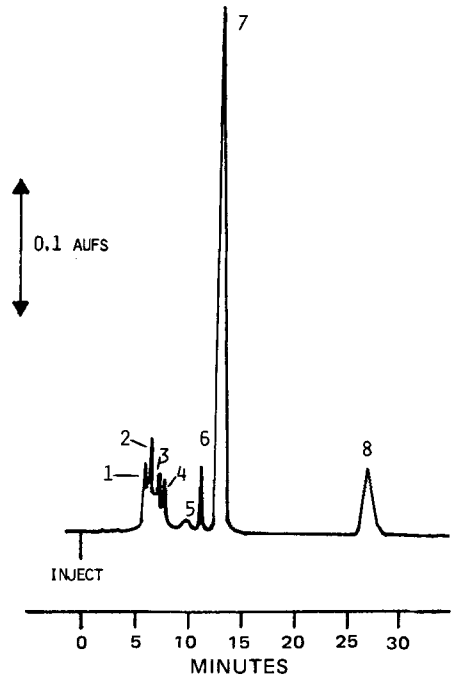


**Figure 2**—*Chromatograms of carbenicillin (1.944 mg/ml) spiked with 5–8% degradation products. The mobile phase was 35% methanol (pH 3.35) at 1.3 ml/min, and the detector was at 254 nm. Key: 1, carbenicillin penilloic acid; 2, carbenicillin penicilloic acid; 3, penicillin G penilloic acid epimer; 4, penicillin G penilloic acid epimer; 5, penicillin G penicilloic acid epimer; 6, penicillin G penicilloic acid epimer; 7, carbenicillin; and 8, penicillin G.*

## EXPERIMENTAL

**Apparatus**—The liquid chromatograph system consisted of a constant-flow pump[1], a fixed-volume loop injection valve[2], a 150 × 4.6-mm i.d. column packed in this laboratory by the method of Broquaire (7) with 5-$\mu$m Spherisorb ODS[3], a variable-wavelength UV detector[4], an electronic integrator[5], and a potentiometric recorder[6].

**Reagents**—Distilled water and distilled-in-glass methanol[7] were used. Production lots[8] of carbenicillin and penicillin G were used in the preparation of the degradation products by published methods (8). The remaining chemicals were reagent grade.

**Mobile Phase**—The mobile phases consisted of 35 or 37% methanol with the balance being 0.05 *M* $KH_2PO_4$ (v/v). Tetrabutylammonium bromide[9] (0.1%, w/v) was added as the ion-pair reagent. The pH was adjusted with 10% $H_3PO_4$, and the solution was degassed (laboratory vacuum) for 5 min prior to the initial use. Flow rates between 1.0 and 1.5 ml/min were employed.

**Carbenicillin Solutions**—A laboratory working standard of carbenicillin monosodium monohydrate dissolved in 0.02 *M* phosphate buffer (pH 7.0) was used for the liquid chromatographic work.

## RESULTS AND DISCUSSION

The HPLC resolution of the carbenicillin diastereomer pair and the subsequent quantitation problem were discussed previously (6). Diastereomers of other penicillins and cephalosporins were separated by HPLC (9), and the relationship of the mobile phase composition and pH on the degree of resolution was shown. The HPLC resolution of the carbenicillin diastereomers with a reversed-phase system and a micropar-

[1] Model II G, Laboratory Data Control, Riviera Beach, Fla.
[2] Model 210, Altex Scientific, Berkeley, Calif.
[3] Phase Separations Ltd., Hauppauge, N.Y.
[4] Spectromonitor III, Laboratory Data Control, Riviera Beach, Fla.
[5] Model E-1A, Shimadzu Scientific Instruments, Columbia, Md.
[6] Model A-25, Varian, Palo Alto, Calif.
[7] Burdick & Jackson Laboratories, Muskegon, Mich.
[8] Pfizer, Groton, Conn.
[9] Aldrich Chemical Co., Milwaukee, Wis.

ticulate column[10] first was observed in this laboratory in 1974[11], but the mobile phase pH effects were not understood fully at that time.

It was determined in the present study that the carbenicillin diastereomers can be either resolved or eluted as a single peak, depending on the mobile phase pH (Figs. 1A–1D). The conditions used to produce the chromatogram of Fig. 1B are more conducive to quantitation, either by manual or electronic methods. For example, Yamaoka *et al.* (6) were required to use a gravimetric method (cutting and weighing the HPLC recorder tracing) to obtain quantitative results.

Carbenicillin degrades *via* hydrolytic or decarboxylative routes. Penicillin G, which results from the carbenicillin side-chain decarboxylation, was present at a low level in the working standard of carbenicillin monosodium monohydrate, as evidenced by the peak near 17 min in Fig. 1B. Some carbenicillin samples were found to contain penicillin G sodium in amounts between 3.5 and 4.9% (10). The working standard also contained other process-related substances at low levels which eluted between 3 and 7 min.

To demonstrate assay noninterference, carbenicillin and penicillin G degradation products were synthesized by the methods reported previously (8), with one anomaly; the yield of penicillin G penicilloic acid as its monosodium salt monohydrate was significantly less than was reported, and this substance crystallized only with great difficulty. In addition, the conditions stated for the preparation of carbenicillin penicilloic acid apparently provide a mixture of epimers in an approximate 60:40 ratio, as evidenced by HPLC. Only one epimer crystallized.

The carbenicillin degradation products were essentially pure by HPLC[12]. The physical data obtained[13] were consistent with those reported (8, 11). A synthetically prepared mixture of carbenicillin, carbenicillin penicilloic acid, carbenicillin penilloic acid, penicillin G, penicillin G penicilloic acid, and penicillin G penilloic acid was subjected to chromatographic analysis. The chromatogram of Fig. 2 shows that carbenicillin was separated adequately from the degradation products used and that the carbenicillin peak could be quantitated easily.

A detector linearity study for carbenicillin concentrations, as its monosodium salt monohydrate, between 0.25 and 4.05 mg/ml in pH 7.0 phosphate buffer, showed an origin-oriented linear response at 254 nm. The calibration curve at 254 nm was characterized with a regression coefficient of 0.9998.

Reproducibility was demonstrated with 10 replicate analyses of the same solution (1.634 mg/ml) at 15-min intervals. The carbenicillin peaks were quantitated electronically by area, and the relative standard deviation was 0.79%.

Dissolving the carbenicillin working standard in the mobile phase adjusted to pH 7.0 caused a slow but steady degradation of carbenicillin. However, solutions of carbenicillin in 0.02 *M* phosphate buffer (pH 7.0) were stable for at least 5 hr.

This HPLC procedure is readily adaptable to the determination of penicillin G in carbenicillin samples and, with appropriate mobile phase modifications, has utility for the analysis of other penicillins.

[10] Micropak CH, 30 cm × 2.1 mm i.d., Varian, Palo Alto, Calif.

[11] Unpublished results.

[12] Penicillin G penicilloic and penilloic acids, and carbenicillin penicilloic acid to a lesser extent, tended to epimerize at the conditions (pH 3.35) used.

[13] Specific rotation, elemental analysis, IR spectra, equivalent weight, iodine titration, and Karl Fischer water determination.

## REFERENCES


(1) "Code of Federal Regulations," title 21, 1980, chap. 1.

(2) "The United States Pharmacopeia," 20th rev., United States Pharmacopeial Convention, Rockville, Md., 1980, p. 117.

(3) E. R. White, M. A. Carroll, and J. E. Zarembo, *J. Antibiot.*, **30,** 811 (1977).

(4) F. Nachtmann, *Chromatographia*, **12,** 380 (1979).

(5) M. LeBelle, K. Graham, and W. L. Wilson, *J. Pharm. Sci.*, **68,** 555 (1979).

(6) K. Yamaoka, S. Narita, T. Nakagawa, and T. Uno, *J. Chromatogr.*, **168,** 187 (1979).

(7) M. Broquaire, *ibid.*, **170,** 43 (1979).

(8) A. C. Munro, M. G. Chainey, and S. R. Woroniecki, *J. Pharm. Sci.*, **67,** 1197 (1978).

(9) F. Salto, *J. Chromatogr.*, **161,** 379 (1978).

(10) J. Birner, *J. Pharm. Sci.*, **63,** 603 (1974).

(11) L. Juhlin, S. Ahlstedt, L. Andal, B. Ekström, P. O. Svärd, and L. Wide, *Int. Arch. Allergy Appl. Immunol.*, **54,** 19 (1977).

# Enzymatic Assays for 2,4-Diamino-5-methyl-6-[(3,4,5-trimethoxyanilino)methyl]quinazoline, a Promising New "Nonclassical" Antifolate

**J. J. HEUSNER * and J. J. McCORMACK *‡x**

Received November 19, 1979, from the **Vermont Regional Cancer Center and Pharmacology Department, College of Medicine, University of Vermont, Burlington, VT 05405,* and the ‡*Laboratory of Medicinal Chemistry and Biology, Division of Cancer Treatment, National Cancer Institute, National Institutes of Health, Bethesda, MD 20205.* Accepted for publication January 7, 1981. (Inquiries should be directed to the University of Vermont.)

**Abstract** □ 2,4-Diamino-5-methyl-6-[(3,4,5-trimethoxyanilino)-methyl]quinazoline (I) is a promising new "nonclassical" antifolate. Inhibition of dihydrofolate reductase from bacterial (*Lactobacillus casei*) and mammalian (beef liver) sources was employed to develop useful enzymatic assays for this compound. A linear relationship was obtained by plotting the I concentration *versus* $1/V$. The resultant standard curves maintained linearity particularly well between the 30 and 70% control range, with a correlation coefficient of 0.99 for both enzyme systems. The two enzyme systems are characterized by differences in sensitivity, stability, and day-to-day variation. The $ID_{50}$ for the beef liver reductase system was $1.6 \times 10^{-9}$ *M* (±0.3); for the *L. casei* system, it was $1.35 \times 10^{-8}$ *M* (±0.2). The apparent advantage for the beef liver enzyme was offset somewhat by its relative instability and its higher day-to-day variability. Studies in mice demonstrated that these assays are suitable for pharmacokinetic studies *in vivo*. Such studies indicated that I has a serum $t_{1/2}$ of 45 min in mice; a similar serum $t_{1/2}$ (50 min) was estimated in studies with $^{14}C$-labeled I in position 6.

**Keyphrases** □ 2,4-Diamino-5-methyl-6-[(3,4,5-trimethoxyanilino)-methyl]quinazoline—two enzyme assays using beef liver reductase and *Lactobacillus casei* □ Enzymatic analyses—2,4-diamino-5-methyl-6-[(3,4,5-trimethoxyanilino)methyl]quinazoline using beef liver reductase and *Lactobacillus casei* □ Antifolates—2,4-diamino-5-methyl-6-[(3,4,5-trimethoxyanilino)methyl]quinazoline enzymatic analyses using beef liver reductase and *Lactobacillus casei*

2, 4-Diamino-5-methyl-6-[(3, 4, 5-trimethoxyanilino)-methyl]quinazoline (I) is a potent inhibitor of dihydrofolate reductase [5,6,7,8-tetrahydrofolate:$NADP^+$ oxidoreductase (EC 1.5.1.3)]. Compound I was originally synthesized by Elslager and colleagues as part of an effort to develop quinazoline antifolates with useful antiprotozoal activity (1). Interest in possible antineoplastic applications of I was stimulated when the agent was reported (2) to be a potent inhibitor of the enzyme from several sources, including the L-1210 murine leukemia line.

In comparison to methotrexate, I offers several qualities that may prove advantageous clinically. Since it is a much more lipophilic derivative than is methotrexate, it may penetrate the central nervous system (CNS) more readily and thus be more effective than methotrexate against CNS neoplasms.

Bertino (3) commented upon the increased uptake of I into neoplastic cells compared to methotrexate, and he and his colleagues (4) reported also that I is effective against a wider range of transplantable murine tumors than is methotrexate. Methotrexate, a weak dicarboxylic acid (pKa 4.7), can be metabolized to a 7-hydroxy metabolite, which may contribute to its nephrotoxicity (5). High-dose methotrexate therapy is associated with significant clinical nephrotoxicity in patients, despite vigorous hydration and alkalinization of the urine (6). It is possible that I may offer an advantage as a substitute for methotrexate in high-dose antifolate regimens.

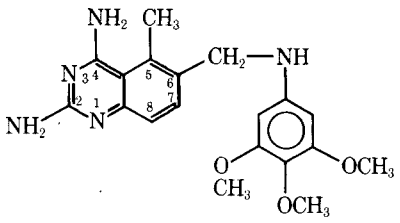

I

Studies are underway to determine the pharmacokinetic and pharmacodynamic properties of I relative to those of methotrexate. This article reports two enzymatic assays for this "nonclassical" antifolate.

## EXPERIMENTAL

Beef liver dihydrofolate reductase is available commercially[1] in 5-unit vials. The enzyme was prepared just prior to use by diluting 3 μl of the commercial suspension in 2 ml of chilled 0.1 *M* phosphate buffer at pH 7.0. *Lactobacillus casei* dihydrofolate reductase was obtained[2] in 20-unit vials. This stock enzyme solution was prepared by dissolving 1 mg of powder in 4 ml of 0.1 *M* phosphate buffer at pH 7.0.

The assay system employed was a slight modification of that described by Burchall and Hitchings (7), involving measurement of the decrease in absorbance at 340 nm, catalyzed by dihydrofolate in a 1-ml system. The system was composed of NADPH[3] ($1 \times 10^{-4}$ *M*), 2-mercaptoethanol ($1 \times 10^{-2}$ *M*), and dihydrofolate [$6.6 \times 10^{-5}$ *M*, prepared according to Futterman (8)] in 0.1 *M* phosphate buffer at pH 7.0. The quantity of enzyme solution used for each assay was sufficient to produce an absorbance decrease of 0.17 unit for the beef liver and of 0.2 unit for the *L. casei* systems over a 10.5-min assay period. The enzyme assays were performed[4] at a chamber temperature of 37°. A reference blank containing buffer, enzyme, and 2-mercaptoethanol was employed during each run.

Compound I was dissolved in dimethyl sulfoxide at $1.1 \times 10^{-3}$ *M* and then serially diluted in 0.1 *M* phosphate buffer at pH 7.0 to give a suitable range of concentrations. After a 5-min preincubation at 37°, first NADPH and then dihydrofolate (as a 1:3 dilution in 0.1 *M* phosphate buffer at pH 7.0) were added to the cells to initiate the enzymatic reaction. Controls without inhibitor were run with each assay. A NADPH control (reaction mixture minus dihydrofolate) was run daily to assess absorbance changes due to NADPH oxidation. This value was subtracted from each value determined to give a more accurate control and inhibitor value. Absorbance changes were measured every 90 sec for 10.5 min, and $ID_{50}$ values were obtained by a least-squares regression analysis of the lines determined by plotting the enzyme activity *versus* the inhibitor concentration.

Compound I was formulated for intravenous administration to mice by solubilizing 10 mg in 0.4 ml of propylene glycol with stirring. After solubilization, the addition of 0.6 ml of normal saline produced a solution suitable for injection. Injections were made into the tail vein of female

[1] Sigma Chemical Co., St. Louis, MO 63178.
[2] New England Enzyme Center (Tufts University, School of Medicine), Boston, MA 02153.
[3] P. L. Biochemicals, Milwaukee, WI 53205.
[4] Beckman 25 kinetic spectrophotometric system, Beckman Instruments, Irvine, CA 92634.

0022-3549/81/0700-0827$01.00/0
© 1981, American Pharmaceutical Association

**Table I—Levels of I in Mouse Serum after Intravenous Administration**

| Minutes | Concentration, $M \times 10^{-6}$ | |
|---|---|---|
| | Enzymatic Assay[a] | Isotopic Assay[b] |
| 15 | 20.7 (±0.3) | 2.3 (±0.1) |
| 30 | 16.5 (±0.5) | 1.8 (±0.1) |
| 60 | 9.5 (±1.3) | 1.25 (±0.1) |
| 90 | 6.1 (±1.3) | 0.73 (±0.06) |
| 120 | 4.3 (±1.1) | 0.59 (±0.07) |
| 180 | 1.7 (±0.2) | — |

[a] *L. casei* enzyme; I was administered at 10 mg/kg. Estimated serum elimination $t_{1/2}$ was 45 min. Data are from six separate experiments (one mouse for each time point). Figures in parentheses are the standard errors of the mean. [b] Data from four experiments; I was administered at 1 mg/kg. Estimated serum elimination $t_{1/2}$ was 50 min.

mice (Swiss-Webster, 20–22 g), and blood samples were collected by retro-orbital puncture. Compound I labeled in position 6 with carbon 14 (specific activity of 21 μCi/mg) was used[5]. For the isotopic studies, 10 μl of serum was placed in 10 ml of scintillation fluid[6] and radioactivity was measured by liquid scintillation spectrometry[7].

## RESULTS AND DISCUSSION

In anticipation of pharmacokinetic studies of I, two assay procedures were developed based on the inhibitory activity of I on dihydrofolate reductase from bacterial and mammalian sources. A linear relationship was obtained by plotting the I concentration *versus* $1/V$[8]. This linearity held well for I concentrations producing 30–70% inhibition of dihydrofolate reductase. The correlation coefficient for such lines was 0.99 for both enzyme systems. The standard curves obtained by linear or semilog plots of the I concentration *versus* the percent control are suitable for pharmacokinetic studies.

By using this enzymatic approach to drug assay, studies in mice indicated a serum elimination half-time of ~45 min (Table I). Sigel and colleagues[9], using a different assay, found a similar serum elimination half-time for I in the dog. A small amount of $^{14}$C-labeled I was obtained for exploratory pharmacokinetic studies in our laboratories. As shown in Table I, the elimination profile determined by the isotopic method was similar to that observed with the enzymatic method. The I levels were lower in the isotopic studies because a lower dose of I was employed (1 mg/kg).

Both enzyme assays are advantageous in that they are highly sensitive with a lower limit of sensitivity of $5 \times 10^{-10}$ *M* for the beef system and of $5 \times 10^{-9}$ *M* for the *L. casei* system (Table II). The sensitivity of both assays can be increased by lowering the amount of dihydrofolate present and/or reducing the amount of enzyme used per assay.

The two enzyme systems differ in sensitivity, stability, and accuracy. The $ID_{50}$ was $1.6 \times 10^{-9}$ *M* (±0.3) for the beef system and $1.35 \times 10^{-8}$ *M* (±0.2) for the *L. casei* system. Under the experimental conditions employed, the beef liver enzyme was about one order of magnitude more sensitive to I than was the bacterial enzyme; however, the instability of the beef preparation was reported previously (9). On the other hand, the *L. casei* enzyme was considerably more stable and easier to work with. For example, the beef enzyme began to lose activity after several hours in solution, while the bacterial enzyme solution was essentially stable throughout the day. In addition, the latter solution may be refrozen with a large measure of its activity retained upon subsequent thawing.

A disadvantage of both enzyme assays is relatively high day-to-day variability: 20% for the beef liver assay and 15% for the *L. casei* assay. Other investigators (10, 11) automated the methotrexate enzymatic assay to improve these figures. In our studies, a standard curve was generated daily. Another disadvantage of both enzyme assays is the relatively narrow range of linearity of the concentration–inhibition curve (30–70% control values have the highest reliability). However, reasonable estimates of required dilutions can be made, which will reduce assay time.

**Table II—Relationship between Inhibition of Dihydrofolate Reductase and I Concentration**

| Concentration, $M \times 10^{-9}$ | Percent Control[a] | |
|---|---|---|
| | *L. casei* | Beef Liver |
| 44 | 28 (±1.0) | — |
| 33 | 33.5 (±1.0) | — |
| 22 | 41.3 (±1.7) | — |
| 16.5 | 46.7 (±2.3) | — |
| 11 | 53.7 (±2.3) | — |
| 8.8 | 58.3 (±3.7) | — |
| 6.6 | 63 (±5.0) | — |
| 5.5 | 67.3 (±4.3) | 27.7 (±1.7) |
| 4.4 | 70.7 (±5.3) | 32 (±2.0) |
| 3.3 | 75.5 (±5.5) | 37 (±3.0) |
| 2.2 | 83.3 (±6.7) | 44.3 (±3.3) |
| 1.1 | — | 57 (±5.0) |
| 0.88 | — | 61.3 (±5.7) |
| 0.66 | — | 66.7 (±6.0) |
| 0.55 | — | 70 (±7.0) |

[a] Each value is the mean of three separate determinations of the standard curve. Figures in parentheses are the standard errors of the mean.

The described methods for determining I levels are sensitive, relatively specific, and accurate. These enzyme assays employ common laboratory equipment and readily available reagents and should prove applicable in various preclinical and clinical research situations. Measuring levels of I in biological material will be of added importance in preclinical and clinical studies in view of observations by Duch *et al.* (12) that I and related compounds can produce substantial concentration-dependent inhibition of histamine metabolism and consequent elevation of histamine levels in experimental animals.

## REFERENCES


(1) E. F. Elslager and J. Davoll, in "Lectures in Heterocyclic Chemistry," vol. II, R. N. Castle and L. B. Townsend, Eds., Hetero Corp., Orem, Utah, 1974, p. S-97.

(2) J. J. McCormack, in "Chemistry and Biology of Pteridines," W. Pfleiderer, Ed., W. deGruyter, New York, N.Y., 1976, p. 125.

(3) J. R. Bertino, *Cancer Res.*, **39,** 293 (1979).

(4) J. R. Bertino, W. L. Sawicki, B. A. Moroson, A. R. Cashmore, and E. F. Elslager, *Biochem. Pharmacol.*, **28,** 1983 (1979).

(5) S. A. Jacobs, R. G. Stoller, B. A. Chabner, and D. G. Johns, *J. Clin. Invest.*, **57,** 534 (1976).

(6) S. W. Pitman and E. Frei, III, *Cancer Treat. Rep.*, **61,** 695 (1977).

(7) J. J. Burchall and G. H. Hitchings, *Mol. Pharmacol.*, **1,** 126 (1965).

(8) S. Futterman, *J. Biol. Chem.*, **228,** 1031 (1957).

(9) R. J. Brooks, *Clin. Chem.*, **24,** 518 (1978).

(10) P. R. Fenley and R. J. Williams, *ibid.*, **23,** 2139 (1977).

(11) J. P. Persign, *J. Clin. Chem. Clin. Biochem.*, **17,** 235 (1979).

(12) D. S. Duch, M. P. Edelstein, and C. A. Nichol, *Mol. Pharmacol.*, **18,** 100 (1980).


## ACKNOWLEDGMENTS


Supported in part by grants from the Vermont Division, American Cancer Society, from the National Cancer Institute (CA22435 and CA24543), and by an Intergovernmental Personnel Transfer Award.

Compound I (NSA 249008) was obtained from the Drug Synthesis and Chemistry Branch, Division of Cancer Treatment, National Cancer Institute.

The authors are indebted to Mrs. Linda Mathews for technical assistance.


[5] Obtained from Dr. Robert Engle, Pharmaceutical Resources Branch, National Cancer Institute, Silver Spring, Md.

[6] Filtron-X, National Diagnostics, Somerville, NJ 08876.

[7] Beckman LS 7000 liquid scintillation system, Beckman Instruments, Irvine, CA 92713.

[8] Where $1/V$ = $V$ control/$V$ inhibitor = (absorbance change control/absorbance change inhibited).

[9] Dr. Carl Sigel, Wellcome Research Laboratories, Research Triangle Park, NC 27709, personal communication.

# Immunological Studies of Poisonous Anacardiaceae: Effect of Vehicle on Absorption of 3-*n*-Pentadecylcatechol and Its Diacetate Ester Derivative after Oral Feeding in Rats

PAUL SKIERKOWSKI *x, MAHMOUD A. ElSOHLY ‡, ERNEST C. HARLAND ‡, BARBARA S. KING ‡, JAMES C. MURPHY ‡, and E. S. WATSON ‡

Received September 15, 1980, from the *Department of Pharmaceutics and the ‡Research Institute of Pharmaceutical Sciences, School of Pharmacy, University of Mississippi, University, MS 38677. Accepted for publication December 22, 1980.

**Abstract** □ Tritium-labeled 3-*n*-pentadecylcatechol and its diacetate ester were fed to Sprague–Dawley rats. Both compounds were dissolved in ethanol and in corn oil vehicles and administered by gavage. The rats were placed in metabolic cages, and the urine and feces were collected. The radioactivity excreted in the urine and feces was determined by liquid scintillation counting, and the percentage of the administered dose was utilized as a measure of absorption. While there was no difference between the absorption of either compound, absorption was affected by the vehicle. Approximately 30% of the administered radioactivity appeared in the urine when ethanol was the vehicle, but about half that amount (14%) was excreted in the urine when the compounds were dissolved in corn oil. A subsequent bile cannulation study showed that the balance of the radioactivity found in the feces was not a result of biliary excretion. The majority of the activity recovered from urine and feces was eliminated within 48 hr after dosing. These data indicate that oil is a poor vehicle for GI absorption of urushiol components.

**Keyphrases** □ Absorption, GI—3-*n*-pentadecylcatechol and its diacetate derivative, effect of vehicle, rats □ 3-*n*-Pentadecylcatechol—poison ivy component, effect of vehicle on GI absorption, rats □ Urushiol—poison ivy component of 3-*n*-pentadecylcatechol, effect of vehicle on GI absorption, rats □ Poison ivy—3-*n*-pentadecylcatechol component of urushiol, effect of vehicle on GI absorption, rats

Three poisonous species of the family Anacardiaceae [*viz.*, *Toxicodendron radicans* (poison ivy), *T. diversilobum* (poison oak), and *T. vernix* (poison sumac)] are collectively responsible for most allergic contact dermatitis in the United States. Because of the ubiquity of these plants, ~80% of the U.S. population exhibit some allergic response to them, and 50% of the population is clinically allergic (sensitivity to 2 μg of urushiol or less) (1).

## BACKGROUND

The allergenic constituents of these species commonly are referred to as urushiols and consist of dihydric phenols with either a 15- or 17-carbon side chain in the third ring position, which may or may not contain 1–3 double bonds (2, 3). The administration of plant extracts to desensitize humans has been practiced clinically since the 1920's. Urushiols are insoluble in water and usually are dissolved in corn, olive, or almond oil (4). Urushiols are extreme irritants, and injection or oral administration of these substances to sensitive humans in doses sufficient to produce prophylaxis requires extreme care (5, 6).

Toxicity can be eliminated by methylation of the ring hydroxyl groups (7, 8). Experiments in this laboratory showed that esterification of the urushiol hydroxyl groups markedly reduced their toxicity. However, these ester derivatives desensitize sensitive guinea pigs and produce immunological tolerance in naive guinea pigs when administered orally or intravenously (8).

The toxicities of the free *versus* esterified urushiols were compared in this laboratory. In mice, the $LD_{50}$ of free poison oak urushiol *via* the intraperitoneal route was 73.75 mg/kg while that of the esterified urushiol was 324.70 mg/kg. Oral doses of the free urushiol in corn oil required to produce lethality were >600 mg/kg, while oral doses of 1600 mg/kg of the esterified urushiol in corn oil produced no lethality. From these studies, it appeared that corn oil prevented urushiol absorption and protected mice from its toxic effects. This study was undertaken to determine the effect of the vehicle on the absorption of the urushiol component, 3-*n*-pentadecylcatechol (I), and its diacetate derivative (II) after oral administration to rats.

## EXPERIMENTAL

**3-*n*-Pentadecylcatechol (I)**—Poison ivy urushiol was isolated by ethanolic extraction of fresh leaves, berries, and green stems of *T. radicans*[1] using a reported extraction procedure (2). The urushiol extract was partially purified (60% pure) as previously described (3). Aliquots of the purified urushiol oil were reduced to I by catalytic hydrogenation, using 5% palladium-on-carbon, and the mixture containing I was purified further by passage over a dry silica gel 60 column with chloroform as the eluting solvent.

The eluting fractions were tested for I using 1% ethanolic ferric chloride; fractions containing I were combined, and the solvent was evaporated *in vacuo*. The residue containing I was purified further by passage over a polyamide column[2] with 90% ethanol in water as the eluting solvent. Fractions containing I were combined, and the solvent was evaporated. Further purification of I was accomplished by repeated crystallization of the residue in hexane. Colorless needle crystals of I resulted, mp 58–59°. The identity of I was confirmed by GLC and GLC–mass spectral analysis using previously described procedures (2, 9).

**Pentadecylcatechol Acetate (II)**—Crystalline I was dissolved in acetic anhydride and pyridine and was stirred at room temperature overnight. The reaction mixture then was poured over crushed ice and extracted with chloroform. The chloroform extract was washed successively with chilled dilute sulfuric acid, water, saturated sodium bicarbonate, and again with water. The chloroform solution was dried (sodium sulfate), and the solvent was evaporated, yielding II. GLC–mass spectral analysis showed quantitative conversion to the diacetate derivative.

**3-*n*-Pentadeca-8,11,14-trienylcatechol (Triolefinic Congener)**—The triolefinic congener of I was isolated from purified poison ivy urushiol extract. Urushiol (>60% pure) was converted to its diacetate derivative with acetic anhydride and pyridine. The urushiol acetate was passed over a dry silica gel[3] column impregnated with silver nitrate with 1% methanol in chloroform as the eluting solvent. The polarity of the eluting solvent was increased gradually to 4% methanol in chloroform, and fractions containing the mono-, di-, or triolefinic congener acetates were pooled separately based on their TLC similarities on silver nitrate-impregnated silica gel plates. The solvent was evaporated from the pool containing the triolefinic congener acetate, and the allergenically active triolefinic congener was regenerated by basic hydrolysis using 10% sodium carbonate in dioxane–water (4:1). The reaction mixture then was acidified, and the free congener was determined by GLC and GLC–mass spectral analysis of the trimethylsilyl derivative (9).

**Radiolabeled Material**—Fifty milligrams of I containing 50 μg of the triolefinic congener was tritium reduced[4]. The specific activity was 10.6 mCi/mg of I.

[1] *T. radicans* (L.) Kuntze (Anacardiaceae) was collected near the University of Mississippi campus in Oxford, Miss., by M. A. ElSohly in 1975. The plant samples were authenticated by Dr. M. W. Quimby. Voucher species are stored in the drug plant herbarium at the School of Pharmacy, University of Mississippi, University, MS 38677.

[2] MN-polyamide SC, <0.07-mm particle size, Brinkmann Instruments, Westbury, N.Y.

[3] Silica gel 60, 70–230 mesh, MCB Manufacturing Chemicals, Cincinnati, Ohio.

[4] New England Nuclear, Boston, Mass.

0022-3549/81/0700-0829$01.00/0
© 1981, American Pharmaceutical Association

Table I—Cumulative Percentage of Orally Administered Tritiated Pentadecylcatechol (I) or Its Diacetate Derivative (II) Excreted in Urine

| Hours Postdose | Tritiated I in Ethanol | Tritiated I in Oil | Tritiated II in Ethanol | Tritiated II in Oil |
|---|---|---|---|---|
| 6 | 7.35 ± 2.84 | 4.41 ± 1.13 | 8.27 ± 3.57 | 3.63 ± 2.21 |
| 24 | 21.53 ± 5.65 | 11.49 ± 1.32 | 24.41 ± 2.06 | 11.90 ± 3.57 |
| 48 | 25.02 ± 7.04 | 13.07 ± 0.90 | 28.40 ± 1.66 | 13.17 ± 3.84 |
| 72 | 25.82 ± 7.33 | 13.55 ± 0.91 | 29.92 ± 1.87 | 13.71 ± 3.97 |
| 96 | 26.55 ± 7.71 | 13.97 ± 0.99 | 30.74 ± 1.94 | 14.11 ± 4.09 |
| 120 | 28.33 ± 7.37 | 14.22 ± 1.02 | 31.50 ± 1.84 | 14.40 ± 4.16 |

To prepare the labeled acetate derivative, the tritium-labeled I was converted to the acetate derivative using the procedure described earlier. Labeled materials were purified by preparative silica gel TLC to a purity of >90% prior to use.

**Ethanol and Corn Oil Solutions of I and II**—Aliquots of tritiated I or tritiated II in benzene were evaporated to dryness, and unlabeled I and II crystals were added as carrier. Ethanol and corn oil were the vehicles used to prepare solutions containing 2 mg of I/ml or the equivalent of 2 mg of I as the acetate per milliliter. Specific activities of prepared solutions were determined by liquid scintillation counting using internal standardization.

**Animals**—Female Sprague–Dawley rats, 250–300 g, were obtained from an in-house breeding colony. They were fasted 12 hr prior to intragastric administration of the radiolabeled solutions.

**Urine and Fecal Excretion**—Four animals each were administered 1-mg po doses of tritiated I or tritiated II in either corn oil or ethanol. After dosing, animals were housed in individual metabolism cages, and urine and feces were collected at 6, 24, 48, 72, 96, and 120 hr. The urine volumes were measured, and aliquots were mixed with 15 ml of scintillation cocktail[5]. After drying in a desiccator, the feces were weighed, frozen in liquid nitrogen, pulverized, and uniformly mixed. Aliquots of 80–120 mg were weighed accurately and then combusted in a sample oxidizer[6]; the resulting tritiated water was incorporated into 15 ml of liquid scintillation cocktail[7].

All samples were dark-adapted overnight and then counted for 10 min or 1% ($2\sigma$) error in a liquid scintillation counter[8]. Absolute activity was calculated by the use of an external standard channel ratio quench correction curve. The radioactivity in both urine and feces was expressed as the percentage of the activity of the dose excreted for the sampling period and the cumulative percent of dose amounts. Average excretion values for each collection interval then were calculated for each group.

**Biliary Excretion**—When results of the oral dosing study indicated that most of the administered dose was excreted in the feces, another study was conducted to see if this result was due to biliary excretion of the labeled material or to a lack of absorption of the compound from the GI tract.

The bile ducts of four rats were cannulated. Animals were dosed orally with a freshly prepared solution containing the equivalent of 1 mg of I in the form of tritiated II in ethanol. The bile was collected, and the volume was measured at 6, 12, 24, and 30 hr. Aliquots of bile were mixed with scintillation cocktail[5] and measured for radioactivity.

## RESULTS AND DISCUSSION

**Urine and Fecal Excretion**—Tritium-labeled I and II were dissolved in corn oil and in ethanol, and the percentage of the orally administered radioactivity appearing in the urine was taken as a measure of absorption in rats. The radioactivity appearing in the urine at 6, 24, 48, 72, 96, and 120 hr after oral dosing was determined and expressed as the cumulative percent excreted (Table I). Approximately 30% of the administered radioactivity appeared within 120 hr in the urine of rats dosed with the ethanol solutions. Only half that amount (14%) of the activity was excreted in the urine when these compounds were given in oil. In this study, the absorption patterns of the two compounds were similar in both vehicles. Seventy-five percent or more of the total activity excreted in the urine appeared within the first 24 hr regardless of the vehicle or compound. The rapid absorption of I also was noted by Godfrey *et al.* (10) from an orally administered glycerol–95% ethanol solution.

Table II—Cumulative Percentage of Orally Administered Tritiated Pentadecylcatechol (I) or Its Diacetate Derivative (II) Excreted in Feces

| Hours Postdose | Tritiated I in Ethanol | Tritiated I in Oil | Tritiated II in Ethanol | Tritiated II in Oil |
|---|---|---|---|---|
| 24 | 35.04 ± 8.94 | 61.31 ± 4.22 | 36.26 ± 8.08 | 74.65 ± 12.71 |
| 48 | 49.94 ± 1.74 | 69.42 ± 4.10 | 52.04 ± 5.10 | 79.33 ± 11.48 |
| 72 | 51.99 ± 2.18 | 70.45 ± 4.06 | 54.91 ± 5.73 | 81.51 ± 10.62 |
| 96 | 52.73 ± 2.41 | 70.83 ± 4.09 | 55.55 ± 5.75 | 81.78 ± 10.53 |
| 120 | 52.98 ± 2.46 | 71.03 ± 4.12 | 55.90 ± 5.77 | 81.91 ± 10.50 |

The radioactivity excreted in the feces at 24, 48, 72, 96, and 120 hr after oral dosing is expressed as cumulative percent excreted (Table II). The majority of the administered radioactivity of both compounds was eliminated in the feces. There was a greater percentage of tritiated I and II excreted in the feces of rats dosed with oil solution (71 and 82%, respectively) than in the feces of rats receiving the ethanol solution, apparently due to reduced absorption of these compounds from corn oil. As with the urinary excretion patterns, most of the activity eliminated in the feces (≥64%) appeared within the first 24 hr after dosing, and the bulk of the remaining material appeared during the second 24-hr period. The total recovery of the administered radioactivity within 120 hr ranged from 81 to 96%.

**Biliary Excretion**—Studies by Godfrey *et al.* (10) showed a persistence of I in the bile, liver, spleen, appendix, and body fluids, which was taken as evidence for enterohepatic circulation of I and its metabolites. Since the majority of administered radioactivity in the present study was eliminated in the feces within the first 24–48 hr, it was of interest to determine if some activity recovered in the feces might have been due to absorption followed by excretion into the feces. Thus, the bile ducts of rats were cannulated, and the animals were dosed with tritiated II in ethanol. The bile was collected at 6, 12, 24, and 30 hr, until negligible amounts of activity appeared in the bile.

Approximately 2% of the administered activity appeared in the bile every 6 hr for the first 24 hr for a cumulative total of 8.85%. After 30 hr, negligible amounts were observed in the bile. Since 8.85% of the administered radioactivity was excreted in the bile within the first 24 hr, it can be assumed from the previous experiment that a maximum of 15% of the activity appearing in the feces (64% of the administered doses) represents biliary-excreted activity.

The results of the present study indicate that oils are poor vehicles for administering urushiols or their water-insoluble derivatives. The investigation of other vehicles to improve the absorption of these compounds is in progress. Additional studies also are being conducted to determine the urinary and biliary metabolites of these compounds. Optimal absorption may significantly alter the cost of prophylaxis since less drug will be required to obtain therapeutic tissue levels. In addition, decreasing the amount of material eliminated in the feces might significantly reduce the toxic side effects, particularly perianal dermatitis.

## REFERENCES


(1) W. L. Epstein, *Cutis*, **13**, 544 (1974).

(2) M. D. Corbett and S. Billets, *J. Pharm. Sci.*, **64**, 1715 (1975).

(3) S. Billets, J. C. Craig, M. D. Corbett, and J. F. Vickery, *Phytochemistry*, **15**, 533 (1976).

(4) "Facts and Comparisons," Facts and Comparison, Inc., St. Louis, Mo., 1978, p. 565.

(5) F. A. Stevens, *J. Am. Med. Assoc.*, **127**, 912 (1945).

(6) A. M. Kligman, *Arch. Dermatol.*, **78**, 47 (1958).

(7) H. Baer, R. C. Watkins, A. P. Kurtz, J. S. Byck, and C. R. Dawson, *J. Immunol.*, **99**, 365 (1967).

(8) E. S. Watson, J. C. Murphy, P. W. Wirth, C. W. Waller, and M. A. ElSohly, *J. Invest. Dermatol.*, in press.

(9) J. C. Craig, C. W. Waller, S. Billets, and M. A. ElSohly, *J. Pharm. Sci.*, **67**, 483 (1978).

(10) H. P. Godfrey, H. Baer, and R. C. Watkins, *J. Immunol.*, **106**, 91 (1971).


## ACKNOWLEDGMENTS


The authors thank Ms. Mary Rungeling for technical assistance with the manuscript.


[5] Ready-Solv HP, Beckman Instruments, Fullerton, Calif.
[6] Packard Tri-Carb model B306, Packard Instruments, Downers Grove, Ill.
[7] Monophase 40, Packard Instruments, Downers Grove, Ill.
[8] Beckman LS-100C, Beckman Instruments, Fullerton, Calif.

# Approximation in Point–Area Deconvolution Algorithm as Mathematical Basis of Empirical Instantaneous Midpoint–Input Deconvolution Method

**Keyphrases** □ Point–area deconvolution algorithm—compared with instantaneous midpoint–input deconvolution method, drug absorption, calculation for *in vivo* drug input functions □ Drug absorption—point–area deconvolution algorithm compared with instantaneous midpoint–input deconvolution method □ Pharmacokinetics—point–area deconvolution algorithm compared with instantaneous midpoint–input deconvolution method, calculation for *in vivo* drug input functions

*To the Editor:*

Recently, Chiou (1) presented an empirically based deconvolution method for the determination of *in vivo* drug absorption, without reference to the point–area deconvolution algorithm (2). However, this empirical algorithm is equivalent to the point–area method when the analytical integration of the characteristic response is approximated by a rectangular function. Such an approximation to a defined integral can result in an unstable algorithm.

In the present communication, the relationship between the empirical method of Chiou (1) and the point–area deconvolution method (2) is derived, and the instability of the former method is demonstrated.

Define the plasma drug concentration–time function, $G(t)$, obtained after a unit drug impulse input (*e.g.*, intravenous bolus or oral solution) as the characteristic response of the body. Assume the body acts as a time-invariant linear system to drug input. Under the latter assumption, the plasma drug concentration–time function, $R(t)$, obtained after some arbitrary drug input, $In(t)$, into the body is defined by the convolution of the input function and the characteristic response. Thus, given $R(t)$ and $G(t)$, the input function, $In(t)$, can be defined by deconvolution of:

$$R(t) = \int_0^t In(t-\tau)G(t)\,d\tau \qquad \text{(Eq. 1)}$$

However, if $R(t)$ is sampled only at a set of time points $p_i (i \in 0, 1, 2, \ldots, p_0 = 0, p_{i+1} > p_i, p_i \geq 0)$, the analytical function $R(t)$ is not defined. The deconvolution of $R(p_i)$ and $G(t)$ to obtain $In(t)$ is an ill-defined problem since the convolution of a number of input functions with $G(t)$ will generate the observed responses, $R(p_i)$. Consequently, deconvolution must be based on some logical algorithm that assumes some functional form for either $R(t)$ or the input function (2–5). In particular, a staircase input function can always be derived such that the convolution of this function with $G(t)$ generates the observed responses, $R(p_i)$. The latter is the point–area deconvolution method (2).

For a staircase input function into a time-invariant linear system, the responses, $R(p_i)$, are given by:

$$R(p_i) = \sum_{j=1}^{i}\left[K_j \int_{p_i-p_j}^{p_i-p_{j-1}} G(t)\,dt\right] \qquad i \in 0, 1, 2, \ldots \qquad \text{(Eq. 2)}$$

where $R(p_0) = 0$, $K_0 = 0$, and $K_i$ $(i \in 1, 2, \ldots)$ is the magnitude of a step of duration $(p_i - p_{i-1})$ in the staircase input function. The cumulative input in any interval, $(p_i - p_{i-1})$, is $K_i(p_i - p_{i-1})$, which is given by Eq. 2 as:

$$K_i(p_i - p_{i-1}) = \frac{\left[R(p_i) - \sum_{j=1}^{i-1}\left(K_j \int_{p_i-p_j}^{p_i-p_{j-1}} G(t)\,dt\right)\right](p_i - p_{i-1})}{\int_0^{p_i-p_{i-1}} G(t)\,dt} \qquad \text{(Eq. 3)}$$

If the integrals of $G(t)$ are approximated by rectangular functions centered about the midpoint of the integration interval, then:

$$\int_{p_i-p_j}^{p_i-p_{j-1}} G(t)\,dt \simeq (p_j - p_{j-1})G\left(p_i - \frac{p_j}{2} - \frac{p_{j-1}}{2}\right) \qquad \text{(Eq. 4)}$$

Using the approximations of Eq. 4 in Eq. 3 gives:

$$K_i(p_i - p_{i-1}) = \frac{R(p_i) - \sum_{j=1}^{i-1} K_j(p_j - p_{j-1})G\left(p_i - \frac{p_j}{2} - \frac{p_{j-1}}{2}\right)}{G\left(\frac{p_i - p_{i-1}}{2}\right)} \qquad \text{(Eq. 5)}$$

Substituting $f_j = K_j(p_j - p_{j-1})$ into Eq. 5 gives:

$$f_j = \frac{R(p_i) - \sum_{j=1}^{i-1} f_i G\left(p_i - \frac{p_j}{2} - \frac{p_{j-1}}{2}\right)}{G\left(\frac{p_i - p_{i-1}}{2}\right)} \qquad \text{(Eq. 6)}$$

where $f_i (i \in 1, 2, \ldots)$ is the fraction of the dose absorbed in the time interval $(p_i - p_{i-1})$, and $\Sigma_{j=1}^{i} f_j$ is the cumulative drug input at time point $p_i$.

The deconvolution algorithm specified by Eq. 6 is equivalent to the empirical algorithm specified by Chiou (1) and is simply an approximation to the point–area method (2). The point–area deconvolution method is a correction and rationalization of a convolution method described by Resigno and Segre (6). In the latter algorithm, the integrals of $G(t)$ are approximated by rectangular functions centered about the midpoint of integration. Consequently, the new algorithm of Chiou (instantaneous midpoint–input method) is a restatement of a previously known algorithm.

Provided the approximations specified by Eq. 4 are reasonable, Eqs. 3 and 6 should give essentially similar results when applied to the determination of *in vivo* drug

**Table I—Comparison of the Theoretical and Calculated Cumulative Drug Input for a Zero-Order Lidocaine Infusion**

| Hours | $R(t)$, μg/ml | Cumulative Drug Input, mg: Theoretical | Cumulative Drug Input, mg: Calculated by Instantaneous Midpoint–Input Method |
|---|---|---|---|
| 0.5 | 0.8314 | 55.8 | 69.54 (24.62)[a] |
| 1.0 | 1.1884 | 111.6 | 132.22 (18.48) |
| 1.5 | 1.4720 | 167.4 | 192.74 (15.14) |
| 2.0 | 1.7037 | 223.2 | 252.58 (13.16) |
| 2.5 | 1.8929 | 279.0 | 312.21 (11.90) |

[a] Number in parentheses is the percent deviation from the theoretical value.

0022-3549/81/0700-0831$01.00/0
© 1981, American Pharmaceutical Association

input. This is true for the examples involving exponential drug input functions cited by Chiou (Tables I–IV in Ref. 1). Since the point–area method defines a staircase input function, the method gives exact results for zero-order absorption rates. Consequently, the examples cited by Chiou for zero-order absorption (Tables VI and VII in Ref. 1) simply reflect the degree of accuracy of the approximations, specified by Eq. 4, for the particular characteristic responses used in the examples. When the approximations of Eq. 4 are invalid, the instantaneous midpoint–input method gives erroneous cumulative drug input functions. As an example, consider the plasma concentrations (micrograms per milliliter) of lidocaine after a 1-mg iv bolus as the characteristic response, where $G(t) = 0.0276e^{-0.123t} + 0.0084e^{-0.00673t}$ and the units of $t$ are minutes.

Apply the instantaneous midpoint–input deconvolution method to the plasma drug concentrations that would result from a 1.86-mg/min constant intravenous infusion of lidocaine. The results of applying this method are given in Table I. This example illustrates the large errors that can result by approximating integrals by rectangular functions. The point–area method gives exact results for this example (Table I).

In conclusion, the instantaneous midpoint–input method is an approximation of the point–area method. The use of approximations in the latter method can result in large errors in the cumulative drug input functions, and such unnecessary approximations should be avoided.


(1) W. L. Chiou, *J. Pharm. Sci.*, **69**, 57 (1980).

(2) D. P. Vaughan and M. Dennis, *J. Pharm. Sci.*, **67**, 663 (1978).

(3) D. P. Vaughan and M. Dennis, *J. Pharmacokinet. Biopharm.*, **8**, 83 (1980).

(4) D. Cutler, *ibid.*, **6**, 243 (1978).

(5) P. V. Pederson, *J. Pharm. Sci.*, **69**, 298 (1980).

(6) A. Rescigno and G. Segre, "Drug and Tracer Kinetics," Blaisdell, New York, N.Y., 1966, pp. 189–195.



*D. P. Vaughan*

School of Pharmacy
Sunderland Polytechnic
Sunderland, Tyne and Wear
United Kingdom



Received November 10, 1980.
Accepted for publication December 3, 1980.


## Stability of Nitroglycerin Ointment


**Keyphrases** □ Nitroglycerin—stability of ointment at elevated temperatures □ Vasodilators—stability of nitroglycerin ointment at elevated temperatures □ Stability—nitroglycerin ointment at elevated temperatures


*To the Editor:*

Topical nitroglycerin therapy offers a longer duration of action than sublingual administration and thus is popular as a prophylactic treatment for angina pectoris (1, 2). Previous studies indicated that the potency of nitroglycerin tablets may be affected by the environment in which the tablets are stored (3, 4). It also was demonstrated that nitroglycerin in solutions for intravenous use interacts with plastic infusion bags and intravenous giving sets (5, 6), resulting in decreased availability of nitroglycerin. Since we are unaware of any report on the stability of nitroglycerin ointment during storage, we evaluated the stability of nitroglycerin ointment capsules stored at elevated temperatures for extended periods.

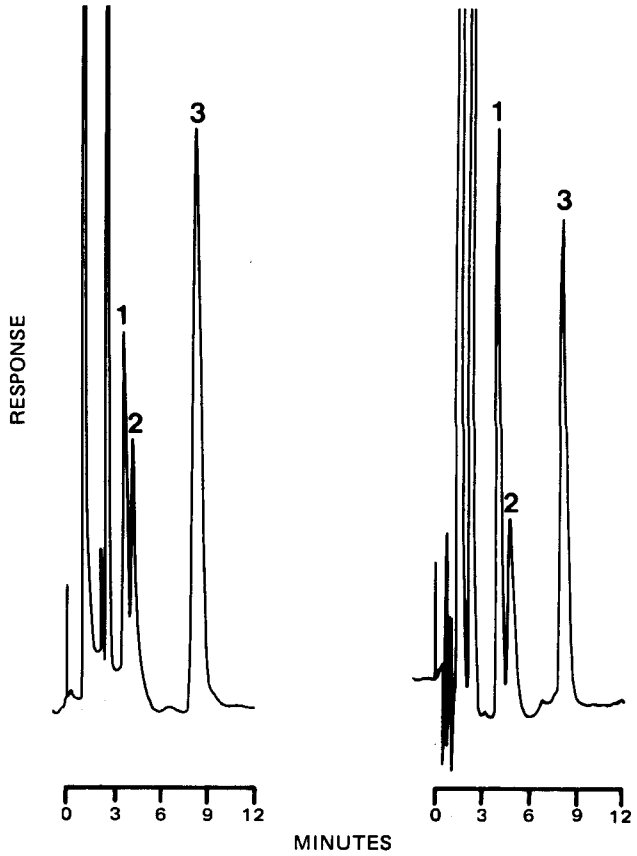


**Figure 1**—*(Left) Chromatogram of an aqueous solution of nitroglycerin and the two dinitroglycerins. Key: 1, 1,3-dinitroglycerin; 2, 1,2-dinitroglycerin; and 3, nitroglycerin. (Right) Chromatogram of an octanol extract of nitroglycerin ointment. Key: 1, unknown interfering peak; 2, unknown interfering peak; and 3, nitroglycerin.*

Capsules from unopened bottles of nitroglycerin (3% w/w) ointment capsules[1] were stored on individual glass dishes in an oven at 37 ± 1° and in the original glass bottle at room temperature (20–24°) in the dark. Capsules were removed from storage after 5, 10, and 18 weeks and were assayed for nitroglycerin content as follows. Each capsule was cut open, the ointment was removed completely, and its weight was recorded. The nitroglycerin then was extracted from the ointment by vortexing with 5 ml of octanol for 10 min and centrifuging at 3000 rpm for 10 min. This method achieved >96% extraction of nitroglycerin.

The extract then was diluted with methanol before assay using kinetic (7) and high-performance liquid chromatographic (HPLC) methods (8). Standard curves for the two methods were constructed by adding known amounts of nitroglycerin, standardized by the method of Dean and Baun (9), to octanol, which then was diluted in methanol to give appropriate concentrations for analysis. In four determinations of six different nitroglycerin concentra-

[1] Nitrolate, Roche Products, Sydney, Australia.




0022-3549/81/0700-0832$01.00/0


© 1981, American Pharmaceutical Association

input. This is true for the examples involving exponential drug input functions cited by Chiou (Tables I–IV in Ref. 1). Since the point–area method defines a staircase input function, the method gives exact results for zero-order absorption rates. Consequently, the examples cited by Chiou for zero-order absorption (Tables VI and VII in Ref. 1) simply reflect the degree of accuracy of the approximations, specified by Eq. 4, for the particular characteristic responses used in the examples. When the approximations of Eq. 4 are invalid, the instantaneous midpoint–input method gives erroneous cumulative drug input functions. As an example, consider the plasma concentrations (micrograms per milliliter) of lidocaine after a 1-mg iv bolus as the characteristic response, where $G(t) = 0.0276e^{-0.123t} + 0.0084e^{-0.00673t}$ and the units of $t$ are minutes.

Apply the instantaneous midpoint–input deconvolution method to the plasma drug concentrations that would result from a 1.86-mg/min constant intravenous infusion of lidocaine. The results of applying this method are given in Table I. This example illustrates the large errors that can result by approximating integrals by rectangular functions. The point–area method gives exact results for this example (Table I).

In conclusion, the instantaneous midpoint–input method is an approximation of the point–area method. The use of approximations in the latter method can result in large errors in the cumulative drug input functions, and such unnecessary approximations should be avoided.


(1) W. L. Chiou, *J. Pharm. Sci.*, **69**, 57 (1980).

(2) D. P. Vaughan and M. Dennis, *J. Pharm. Sci.*, **67**, 663 (1978).

(3) D. P. Vaughan and M. Dennis, *J. Pharmacokinet. Biopharm.*, **8**, 83 (1980).

(4) D. Cutler, *ibid.*, **6**, 243 (1978).

(5) P. V. Pederson, *J. Pharm. Sci.*, **69**, 298 (1980).

(6) A. Rescigno and G. Segre, "Drug and Tracer Kinetics," Blaisdell, New York, N.Y., 1966, pp. 189–195.



*D. P. Vaughan*

School of Pharmacy
Sunderland Polytechnic
Sunderland, Tyne and Wear
United Kingdom



Received November 10, 1980.
Accepted for publication December 3, 1980.


## Stability of Nitroglycerin Ointment


**Keyphrases** □ Nitroglycerin—stability of ointment at elevated temperatures □ Vasodilators—stability of nitroglycerin ointment at elevated temperatures □ Stability—nitroglycerin ointment at elevated temperatures


*To the Editor:*

Topical nitroglycerin therapy offers a longer duration of action than sublingual administration and thus is popular as a prophylactic treatment for angina pectoris (1, 2). Previous studies indicated that the potency of nitroglycerin tablets may be affected by the environment in which the tablets are stored (3, 4). It also was demonstrated that nitroglycerin in solutions for intravenous use interacts with plastic infusion bags and intravenous giving sets (5, 6), resulting in decreased availability of nitroglycerin. Since we are unaware of any report on the stability of nitroglycerin ointment during storage, we evaluated the stability of nitroglycerin ointment capsules stored at elevated temperatures for extended periods.

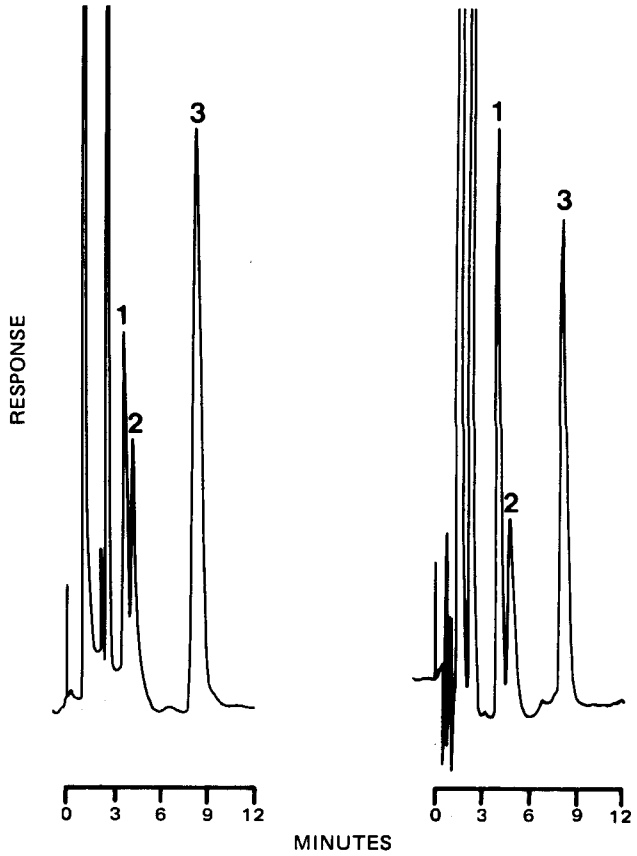


**Figure 1**—*(Left) Chromatogram of an aqueous solution of nitroglycerin and the two dinitroglycerins. Key: 1, 1,3-dinitroglycerin; 2, 1,2-dinitroglycerin; and 3, nitroglycerin. (Right) Chromatogram of an octanol extract of nitroglycerin ointment. Key: 1, unknown interfering peak; 2, unknown interfering peak; and 3, nitroglycerin.*

Capsules from unopened bottles of nitroglycerin (3% w/w) ointment capsules[1] were stored on individual glass dishes in an oven at 37 ± 1° and in the original glass bottle at room temperature (20–24°) in the dark. Capsules were removed from storage after 5, 10, and 18 weeks and were assayed for nitroglycerin content as follows. Each capsule was cut open, the ointment was removed completely, and its weight was recorded. The nitroglycerin then was extracted from the ointment by vortexing with 5 ml of octanol for 10 min and centrifuging at 3000 rpm for 10 min. This method achieved >96% extraction of nitroglycerin.

The extract then was diluted with methanol before assay using kinetic (7) and high-performance liquid chromatographic (HPLC) methods (8). Standard curves for the two methods were constructed by adding known amounts of nitroglycerin, standardized by the method of Dean and Baun (9), to octanol, which then was diluted in methanol to give appropriate concentrations for analysis. In four determinations of six different nitroglycerin concentra-

[1] Nitrolate, Roche Products, Sydney, Australia.




0022-3549/81/0700-0832$01.00/0


© 1981, American Pharmaceutical Association

**Table I—Percentage of Nitroglycerin in Ointment Capsules Stored at 37° for 18 Weeks**

| Weeks | Percent Content (Mean ± *SE*, $n = 5$) Kinetic Assay | HPLC Assay |
|---|---|---|
| 0 | 3.24 ± 0.06 | 3.19 ± 0.11 |
| 5 | 3.18 ± 0.10 | 3.23 ± 0.08 |
| 10 | 3.17 ± 0.12 | 3.20 ± 0.10 |
| 18 | 3.22 ± 0.05 | 3.19 ± 0.09 |

tions, the correlation coefficient of results obtained by the two methods was 0.988.

Unfortunately, the HPLC method and the other previously reported high-pressure liquid chromatographic method (10) were not specific for glyceryl dinitrates due to the presence of unknown interfering peaks from the ointment extract (Fig. 1). No reduction in size of the interfering peaks was achieved by using other organic solvents (hexane, ether, and methanol) to extract the ointment. The relative height of these peaks did not change over time. It was established by TLC separation (11) prior to HPLC analysis that the amount of glyceryl dinitrates present in the ointment was negligible. Triacetin, which is used as a solvent for nitroglycerin in some preparations, cochromatographed with glyceryl 1,2-dinitrate using the method of Crouthamel and Dorsch (8).

No loss of nitroglycerin was found after storage of individual capsules for 18 weeks at 37° (Table I). The amount of the dinitrates present in the ointment was negligible throughout the study.

The good stability of nitroglycerin in the ointment formulation tested is consistent with a high affinity of nitroglycerin for the lipophilic ointment base and a low affinity for the gelatin capsule in which the ointment is presented. In contrast, the availability of nitroglycerin from aqueous solutions infused from plastic infusion bags through giving sets is reduced due to the high affinity of nitroglycerin for the plastic (12).


(1) M. E. Davidov and W. J. Mroczek, *Angiology*, **27**, 205 (1976).

(2) J. O. Parker, R. J. Augustine, J. P. Burton, R. O. West, and P. W. Armstrong, *Am. J. Cardiol.*, **38**, 162 (1976).

(3) D. Banes, *J. Pharm. Sci.*, **57**, 893 (1968).

(4) B. A. Edelman, A. M. Contractor, and R. F. Shangraw, *J. Am. Pharm. Assoc.*, **NS11**, 30 (1971).

(5) M. S. Roberts, P. A. Cossum, A. J. Galbraith, and G. W. Boyd, *J. Pharm. Pharmacol.*, **32**, 237 (1980).

(6) P. A. Cossum, A. J. Galbraith, M. S. Roberts, and G. W. Boyd, *Lancet*, **2**, 349 (1978).

(7) S. K. Yap, C. T. Rhodes, and H. L. Fung, *Am. J. Hosp. Pharm.*, **32**, 1039 (1975).

(8) W. G. Crouthamel and B. Dorsch, *J. Pharm. Sci.*, **68**, 237 (1979).

(9) T. W. Dean and D. C. Baun, *Am. J. Hosp. Pharm.*, **32**, 1036 (1975).

(10) D. M. Baaske, J. E. Carter, and A. H. Amann, *J. Pharm. Sci.*, **68**, 481 (1979).

(11) M. C. Crew and F. J. Dicarlo, *J. Chromatogr.*, **35**, 506 (1968).

(12) P. Yuen, S. Denman, T. D. Sokoloski, and A. M. Burkman, *J. Pharm. Sci.*, **68**, 1163 (1979).



*Paul A. Cossum*
*Michael S. Roberts* ˣ
School of Pharmacy
University of Tasmania
G.P.O. Box 252C, Hobart
Tasmania, Australia



Received September 24, 1980.
Accepted for publication April 16, 1981.


## Comparison of Plasma and Urine Analyses for Thiazides in Bioavailability/Bioequivalence Study


**Keyphrases** □ Thiazides—plasma *versus* urine analysis in bioavailability/bioequivalence study □ Bioavailability—thiazides, plasma *versus* urine analysis □ Bioequivalence—thiazides, plasma *versus* urine analysis □ Diuretics—thiazides, plasma *versus* urine analysis in bioavailability/bioequivalence study


*To the Editor:*

Thiazides are widely used as diuretics in the treatment of hypertension. In the recent proposal (1) for bioavailability/bioequivalence requirements, the thiazides were identified as having potential bioequivalence problems. To ensure bioequivalence of thiazide products, both *in vitro* dissolution and *in vivo* bioavailability requirements were proposed. The *in vivo* requirements call for bioavailability studies in humans and comparison of blood level and/or urinary excretion profiles of the drug with a standard reference product. It is generally assumed that blood (or plasma or serum) level measurements give a better assessment of bioavailability and bioequivalence than urinary measurements because of complicated pharmacokinetic considerations such as drug metabolism and urine collection problems.

It is sometimes argued that the presence of drug in the blood is not a real estimate of the drug availability at the site of action but only an estimate of drug bioavailability. It is preferable to determine the amount of drug at the site of action or to measure therapeutic effect, but these two procedures are generally not feasible. Thiazide diuretics are weak carbonic anhydrase inhibitors that enhance the renal excretion of sodium and chloride ions and an accompanying volume of water, thereby causing diuresis. This therapeutic effect is due to inhibition of ion reabsorption in the distal tubule. Thiazides are primarily excreted unchanged in urine by active secretion in the proximal tubule (2). Thus, from a pharmacological and a therapeutic viewpoint, measurement of the urinary excretion of the drug appears to be a logical choice in lieu of measurement in blood for the assessment of bioavailability of a diuretic dosage form.

Previous work on chlorothiazide and hydrochlorothiazide suggested that urinary level measurements give adequate information for bioavailability/bioequivalence assessment (3, 4). Figure 1 shows the amount of drug eliminated in the urine ($AE$) and the area under the curve ($AUC$) in the same subjects for various thiazides. For hydrochlorothiazide, ~34% of the administered drug was recovered in 0–12-hr urine samples at all dose levels (100, 50, and 25 mg), thus suggesting a dose–response relationship. As expected, the amount of drug in urine decreased with a decrease in hydrochlorothiazide administration, but the $AUC$ did not correspond and correlate with the $AE$ values (Subjects 2 and 3, Fig. 1A). Earlier data (5) for hydrochlorothiazide showed no relationship between the $AUC$ and $AE$ (Fig. 1B), between the $AUC$ and product bioavailability, or between $C_{max}$ and dose administered or bioavailability.

A preliminary study using chlorothiazide products showed that, although approximately the same amount of drug was excreted in 48 hr from subjects administered 250-


0022-3549/81/0700-0833$01.00/0


© 1981, American Pharmaceutical Association

**Table I—Percentage of Nitroglycerin in Ointment Capsules Stored at 37° for 18 Weeks**

| Weeks | Percent Content (Mean ± *SE*, $n = 5$) Kinetic Assay | HPLC Assay |
|---|---|---|
| 0 | 3.24 ± 0.06 | 3.19 ± 0.11 |
| 5 | 3.18 ± 0.10 | 3.23 ± 0.08 |
| 10 | 3.17 ± 0.12 | 3.20 ± 0.10 |
| 18 | 3.22 ± 0.05 | 3.19 ± 0.09 |

tions, the correlation coefficient of results obtained by the two methods was 0.988.

Unfortunately, the HPLC method and the other previously reported high-pressure liquid chromatographic method (10) were not specific for glyceryl dinitrates due to the presence of unknown interfering peaks from the ointment extract (Fig. 1). No reduction in size of the interfering peaks was achieved by using other organic solvents (hexane, ether, and methanol) to extract the ointment. The relative height of these peaks did not change over time. It was established by TLC separation (11) prior to HPLC analysis that the amount of glyceryl dinitrates present in the ointment was negligible. Triacetin, which is used as a solvent for nitroglycerin in some preparations, cochromatographed with glyceryl 1,2-dinitrate using the method of Crouthamel and Dorsch (8).

No loss of nitroglycerin was found after storage of individual capsules for 18 weeks at 37° (Table I). The amount of the dinitrates present in the ointment was negligible throughout the study.

The good stability of nitroglycerin in the ointment formulation tested is consistent with a high affinity of nitroglycerin for the lipophilic ointment base and a low affinity for the gelatin capsule in which the ointment is presented. In contrast, the availability of nitroglycerin from aqueous solutions infused from plastic infusion bags through giving sets is reduced due to the high affinity of nitroglycerin for the plastic (12).


(1) M. E. Davidov and W. J. Mroczek, *Angiology*, **27**, 205 (1976).

(2) J. O. Parker, R. J. Augustine, J. P. Burton, R. O. West, and P. W. Armstrong, *Am. J. Cardiol.*, **38**, 162 (1976).

(3) D. Banes, *J. Pharm. Sci.*, **57**, 893 (1968).

(4) B. A. Edelman, A. M. Contractor, and R. F. Shangraw, *J. Am. Pharm. Assoc.*, **NS11**, 30 (1971).

(5) M. S. Roberts, P. A. Cossum, A. J. Galbraith, and G. W. Boyd, *J. Pharm. Pharmacol.*, **32**, 237 (1980).

(6) P. A. Cossum, A. J. Galbraith, M. S. Roberts, and G. W. Boyd, *Lancet*, **2**, 349 (1978).

(7) S. K. Yap, C. T. Rhodes, and H. L. Fung, *Am. J. Hosp. Pharm.*, **32**, 1039 (1975).

(8) W. G. Crouthamel and B. Dorsch, *J. Pharm. Sci.*, **68**, 237 (1979).

(9) T. W. Dean and D. C. Baun, *Am. J. Hosp. Pharm.*, **32**, 1036 (1975).

(10) D. M. Baaske, J. E. Carter, and A. H. Amann, *J. Pharm. Sci.*, **68**, 481 (1979).

(11) M. C. Crew and F. J. Dicarlo, *J. Chromatogr.*, **35**, 506 (1968).

(12) P. Yuen, S. Denman, T. D. Sokoloski, and A. M. Burkman, *J. Pharm. Sci.*, **68**, 1163 (1979).



*Paul A. Cossum*
*Michael S. Roberts* ˣ
School of Pharmacy
University of Tasmania
G.P.O. Box 252C, Hobart
Tasmania, Australia



Received September 24, 1980.
Accepted for publication April 16, 1981.


## Comparison of Plasma and Urine Analyses for Thiazides in Bioavailability/Bioequivalence Study


**Keyphrases** □ Thiazides—plasma *versus* urine analysis in bioavailability/bioequivalence study □ Bioavailability—thiazides, plasma *versus* urine analysis □ Bioequivalence—thiazides, plasma *versus* urine analysis □ Diuretics—thiazides, plasma *versus* urine analysis in bioavailability/bioequivalence study


*To the Editor:*

Thiazides are widely used as diuretics in the treatment of hypertension. In the recent proposal (1) for bioavailability/bioequivalence requirements, the thiazides were identified as having potential bioequivalence problems. To ensure bioequivalence of thiazide products, both *in vitro* dissolution and *in vivo* bioavailability requirements were proposed. The *in vivo* requirements call for bioavailability studies in humans and comparison of blood level and/or urinary excretion profiles of the drug with a standard reference product. It is generally assumed that blood (or plasma or serum) level measurements give a better assessment of bioavailability and bioequivalence than urinary measurements because of complicated pharmacokinetic considerations such as drug metabolism and urine collection problems.

It is sometimes argued that the presence of drug in the blood is not a real estimate of the drug availability at the site of action but only an estimate of drug bioavailability. It is preferable to determine the amount of drug at the site of action or to measure therapeutic effect, but these two procedures are generally not feasible. Thiazide diuretics are weak carbonic anhydrase inhibitors that enhance the renal excretion of sodium and chloride ions and an accompanying volume of water, thereby causing diuresis. This therapeutic effect is due to inhibition of ion reabsorption in the distal tubule. Thiazides are primarily excreted unchanged in urine by active secretion in the proximal tubule (2). Thus, from a pharmacological and a therapeutic viewpoint, measurement of the urinary excretion of the drug appears to be a logical choice in lieu of measurement in blood for the assessment of bioavailability of a diuretic dosage form.

Previous work on chlorothiazide and hydrochlorothiazide suggested that urinary level measurements give adequate information for bioavailability/bioequivalence assessment (3, 4). Figure 1 shows the amount of drug eliminated in the urine ($AE$) and the area under the curve ($AUC$) in the same subjects for various thiazides. For hydrochlorothiazide, ~34% of the administered drug was recovered in 0–12-hr urine samples at all dose levels (100, 50, and 25 mg), thus suggesting a dose–response relationship. As expected, the amount of drug in urine decreased with a decrease in hydrochlorothiazide administration, but the $AUC$ did not correspond and correlate with the $AE$ values (Subjects 2 and 3, Fig. 1A). Earlier data (5) for hydrochlorothiazide showed no relationship between the $AUC$ and $AE$ (Fig. 1B), between the $AUC$ and product bioavailability, or between $C_{max}$ and dose administered or bioavailability.

A preliminary study using chlorothiazide products showed that, although approximately the same amount of drug was excreted in 48 hr from subjects administered 250-


0022-3549/81/0700-0833$01.00/0


© 1981, American Pharmaceutical Association

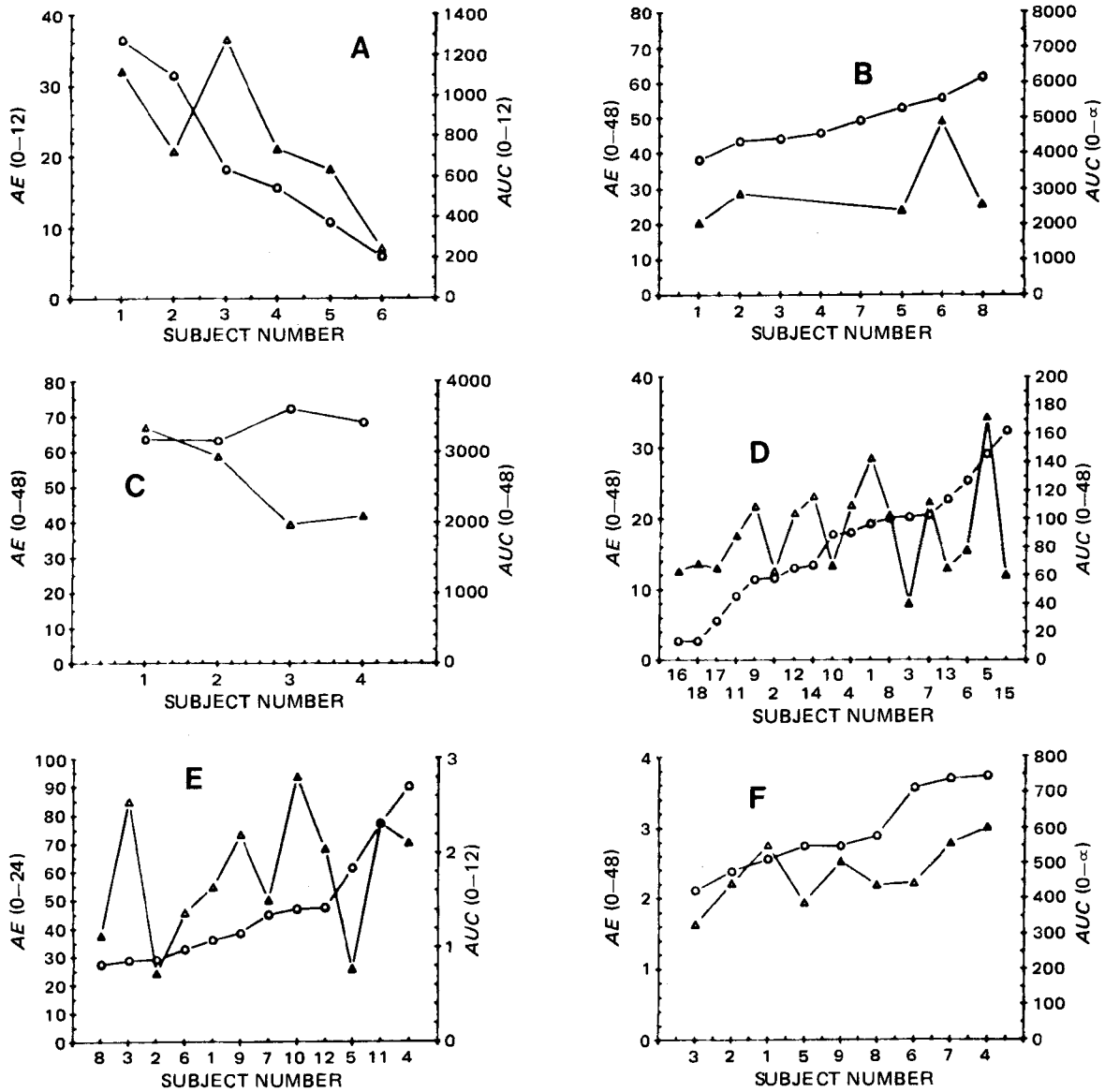


**Figure 1**—*Comparison of* AUC (△) *and* AE (○) *values for thiazides in the same subjects. Key: A, hydrochlorothiazide—Subjects 1 and 2 received a 100-mg dose, Subjects 3 and 4 received a 50-mg dose, and Subjects 5 and 6 received a 25-mg dose; B, hydrochlorothiazide—all subjects received a 75-mg dose; C, chlorothiazide—Subjects 1 and 2 received a 250-mg dose and Subjects 3 and 4 received a 500-mg dose; D, polythiazide—all subjects received a 1-mg dose; E, hydroflumethiazide—all subjects received a 100-mg dose; and F, bendroflumethiazide—all subjects received a 10-mg dose.*

and 500-mg doses, there was an approximate twofold difference in *AUC* (3), thus suggesting a lack of correlation between *AE* and *AUC* values (Fig. 1C).

Previous bioavailability studies involving plasma levels and urinary excretion measurements on polythiazide [Fig. 1D (6)], hydroflumethiazide [Fig. 1E (7)], and bendroflumethiazide [Fig. 1F (8)] were analyzed to determine the correlation between *AE* and *AUC* values. (The *AUC* values were calculated using the trapezoidal rule from the data provided.) Analysis of the data for the same panel of subjects shows wide variation in the *AUC* with nearly the same *AE*, suggesting a lack of correlation.

The lack of correlation observed between the plasma *AUC* and *AE* values is puzzling. One explanation may be the possible interaction of the thiazide with red blood cells. All thiazides have a sulfonamide group, and compounds with such groups have been shown to interact and bind with red blood cells (9). One hydrochlorothiazide study (10) also postulated an interaction between red blood cells and hydrochlorothiazide. The equilibrium drug concentration in plasma, which is most frequently measured for *AUC* determinations, is directly influenced by the interaction between the thiazide and red blood cells.

The reported plasma *AUC* measurements are more variable than the *AE* measurements, making it difficult to assess the amount of drug absorbed. On the other hand, the results of urinary excretion show comparatively less variation, making it easier for estimation of bioavailability/bioequivalence for thiazides. Thus, comparison of *AUC* and *AE* results indicate that urinary measurement from carefully planned and executed bioavailability studies are adequate to establish bioequivalence of thiazide diuretics.

(1) *Fed. Regist.*, Jan. 7, 1977.

(2) "The Pharmacological Basis of Therapeutics," L. S. Goodman and A. Gilman, Eds., Macmillan, New York, N.Y., 1975
(3) V. P. Shah, V. K. Prasad, B. E. Cabana, and P. Sojka, *Curr. Ther. Res.*, **24**, 366 (1978).
(4) V. P. Shah, J. Lee, V. K. Prasad, J. Hunt, and B. E. Cabana, "Abstracts, 27th Academy of Pharmaceutical Sciences National Meeting," Kansas City, Mo., 1979.
(5) B. Beermann, M. Groschinsky-Grind, and B. Lindstrom, *Eur. J. Clin. Pharmacol.*, **11**, 203 (1977).
(6) D. C. Hobbs and T. M. Towmey, *Clin. Pharmacol. Ther.*, **23**, 241 (1978).
(7) G. J. Yakatan, R. B. Smith, E. L. Frome, and J. T. Doluisio, *J. Clin. Pharmacol.*, **17**, 37 (1977).
(8) B. Beermann, M. Groschinsky-Grind, and B. Lindstrom, *Clin. Pharmacol. Ther.*, **22**, 385 (1977).
(9) T. H. Maren, *Physiol. Rev.*, **47**, 595 (1967).
(10) E. Redalieu, V. V. Tipnis, and W. E. Wagner, Jr., *J. Pharm. Sci.*, **67**, 726 (1978).

*Vinod P. Shah* ˣ
*John P. Hunt*
*Vadlamani K. Prasad*
*Bernard E. Cabana*
Biopharmaceutics Laboratory Branch
Food and Drug Administration
Washington, DC 20204

Received July 28, 1980.
Accepted for publication March 20, 1981.

## Technique for Preparing Appendage-Free Skin (Scar) on Hairless Mouse

**Keyphrases** □ Scar tissue—technique for preparing appendage-free skin on the hairless mouse □ Burns—examination of scar tissue, technique for preparing appendage-free skin on the hairless mouse □ Skin—technique for preparing appendage-free skin on the hairless mouse, examination of scar tissue

*To the Editor:*

Scar formation is, minimally, a reconstruction of skin that has undergone total destruction of its epidermal elements through disease or physical trauma (1). Since epidermal elements such as hair follicles often penetrate deeply into and beyond the dermal structure, significant repair of dermal and subdermal damage also is associated with the appearance and function of the scarred surface. When cells of epidermal origin are obliterated within the surface, including those deep within the follicular invaginations, the epidermis of a small wound is repaired by lateral migration of cells from its periphery. Based on histological examination of actual injuries, an epidermal structure is formed, which, as a minimally functional renewed surface, is without normal skin lines and is devoid of pilosebaceous and eccrine appendages. It has a flattened interface with the dermis. The dermis is repaired by fibroblasts that appear in large numbers in the wound. Depending on the nature and extent of the damage, the scar may be raised or depressed and is usually schlerotic (hard) due to the synthesis of new collagen.

An appendage-free structure such as scar tissue should be useful for sorting out transfollicular and transepidermal contributions to percutaneous absorption by studying it side by side with normal skin. To do this study with the least possible complications, experimental wounds need to be developed that result in scarring but that also represent minimal damage and restructuring of the dermal matrix.

Many researchers have developed methods to produce experimental wounds in laboratory animals. These procedures include excision of surface tissues (2–7), branding (8–10), severe chemical burning (11), thermal burning (12), and X-ray and UV irradiation (13, 14). The major emphasis of these investigations has been to study the healing process; the end result, the scarred surface, has been of only incidental concern. Where scar tissue has been purposefully studied histologically and otherwise, tissue samples normally have been of etiological rather than of experimental origin (15, 16). Therefore, we attempted to develop a simple reliable technique to produce scars with minimal dermal involvement in small laboratory animals for the purpose of studying the physicochemical (barrier) properties of scar tissue itself.

Male hairless mice[1], 60–80 days old, were anesthetized with methoxyflurane[2], and their dorsal surfaces were scalded using a previously reported technique (17). Essentially, the dorsal surface of an animal was immersed for 30 sec in water maintained at 60°. These conditions were chosen because they produce a borderline full-thickness burn on hairless mouse skin (17) and are routinely used to separate epidermis from dermis in preparing epidermal membranes for mass transfer studies (18). At the outset, the conditions appeared to be at or near the threshold to accomplish the stated goal.

The scalded mice were placed on a table with the burned surfaces exposed. An area was marked on the traumatized dorsal surface roughly approximating 6–8 $cm^2$ of the body surface area. With the blade of a spatula, the epidermis was scraped off the surface. Occasionally, the epidermal layer was separated as a single piece, but it usually came off in fragments. The blade was moved back and forth on the exposed skin several times, exposing the outlines of superficial blood vessels. The skin was uniformly erythematous. The animals then were returned to individual

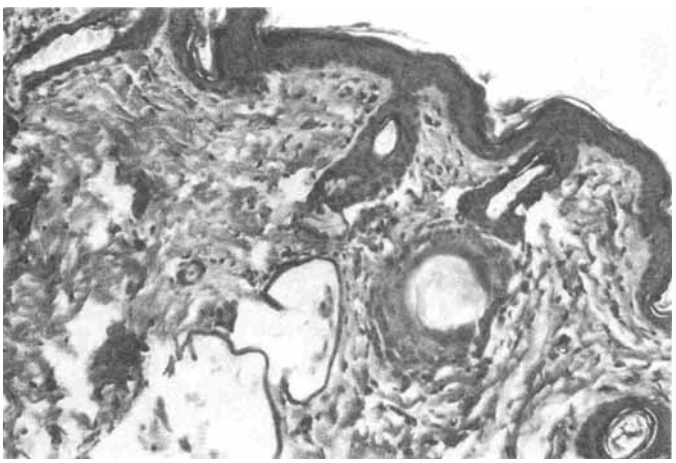

**Figure 1**—*Histological appearance of the hairless mouse normal skin.*

[1] SKH-hr$^{-1}$ strain, Skin Cancer Hospital, Philadelphia, Pa.
[2] Metofane, Pitman-Moore, Washington Crossing, N.J.

0022-3549/81/0700-0835$01.00/0
© 1981, American Pharmaceutical Association

(2) "The Pharmacological Basis of Therapeutics," L. S. Goodman and A. Gilman, Eds., Macmillan, New York, N.Y., 1975
(3) V. P. Shah, V. K. Prasad, B. E. Cabana, and P. Sojka, *Curr. Ther. Res.*, **24**, 366 (1978).
(4) V. P. Shah, J. Lee, V. K. Prasad, J. Hunt, and B. E. Cabana, "Abstracts, 27th Academy of Pharmaceutical Sciences National Meeting," Kansas City, Mo., 1979.
(5) B. Beermann, M. Groschinsky-Grind, and B. Lindstrom, *Eur. J. Clin. Pharmacol.*, **11**, 203 (1977).
(6) D. C. Hobbs and T. M. Towmey, *Clin. Pharmacol. Ther.*, **23**, 241 (1978).
(7) G. J. Yakatan, R. B. Smith, E. L. Frome, and J. T. Doluisio, *J. Clin. Pharmacol.*, **17**, 37 (1977).
(8) B. Beermann, M. Groschinsky-Grind, and B. Lindstrom, *Clin. Pharmacol. Ther.*, **22**, 385 (1977).
(9) T. H. Maren, *Physiol. Rev.*, **47**, 595 (1967).
(10) E. Redalieu, V. V. Tipnis, and W. E. Wagner, Jr., *J. Pharm. Sci.*, **67**, 726 (1978).

*Vinod P. Shah* ˣ
*John P. Hunt*
*Vadlamani K. Prasad*
*Bernard E. Cabana*
Biopharmaceutics Laboratory Branch
Food and Drug Administration
Washington, DC 20204

Received July 28, 1980.
Accepted for publication March 20, 1981.

## Technique for Preparing Appendage-Free Skin (Scar) on Hairless Mouse

**Keyphrases** □ Scar tissue—technique for preparing appendage-free skin on the hairless mouse □ Burns—examination of scar tissue, technique for preparing appendage-free skin on the hairless mouse □ Skin—technique for preparing appendage-free skin on the hairless mouse, examination of scar tissue

*To the Editor:*

Scar formation is, minimally, a reconstruction of skin that has undergone total destruction of its epidermal elements through disease or physical trauma (1). Since epidermal elements such as hair follicles often penetrate deeply into and beyond the dermal structure, significant repair of dermal and subdermal damage also is associated with the appearance and function of the scarred surface. When cells of epidermal origin are obliterated within the surface, including those deep within the follicular invaginations, the epidermis of a small wound is repaired by lateral migration of cells from its periphery. Based on histological examination of actual injuries, an epidermal structure is formed, which, as a minimally functional renewed surface, is without normal skin lines and is devoid of pilosebaceous and eccrine appendages. It has a flattened interface with the dermis. The dermis is repaired by fibroblasts that appear in large numbers in the wound. Depending on the nature and extent of the damage, the scar may be raised or depressed and is usually schlerotic (hard) due to the synthesis of new collagen.

An appendage-free structure such as scar tissue should be useful for sorting out transfollicular and transepidermal contributions to percutaneous absorption by studying it side by side with normal skin. To do this study with the least possible complications, experimental wounds need to be developed that result in scarring but that also represent minimal damage and restructuring of the dermal matrix.

Many researchers have developed methods to produce experimental wounds in laboratory animals. These procedures include excision of surface tissues (2–7), branding (8–10), severe chemical burning (11), thermal burning (12), and X-ray and UV irradiation (13, 14). The major emphasis of these investigations has been to study the healing process; the end result, the scarred surface, has been of only incidental concern. Where scar tissue has been purposefully studied histologically and otherwise, tissue samples normally have been of etiological rather than of experimental origin (15, 16). Therefore, we attempted to develop a simple reliable technique to produce scars with minimal dermal involvement in small laboratory animals for the purpose of studying the physicochemical (barrier) properties of scar tissue itself.

Male hairless mice[1], 60–80 days old, were anesthetized with methoxyflurane[2], and their dorsal surfaces were scalded using a previously reported technique (17). Essentially, the dorsal surface of an animal was immersed for 30 sec in water maintained at 60°. These conditions were chosen because they produce a borderline full-thickness burn on hairless mouse skin (17) and are routinely used to separate epidermis from dermis in preparing epidermal membranes for mass transfer studies (18). At the outset, the conditions appeared to be at or near the threshold to accomplish the stated goal.

The scalded mice were placed on a table with the burned surfaces exposed. An area was marked on the traumatized dorsal surface roughly approximating 6–8 $cm^2$ of the body surface area. With the blade of a spatula, the epidermis was scraped off the surface. Occasionally, the epidermal layer was separated as a single piece, but it usually came off in fragments. The blade was moved back and forth on the exposed skin several times, exposing the outlines of superficial blood vessels. The skin was uniformly erythematous. The animals then were returned to individual

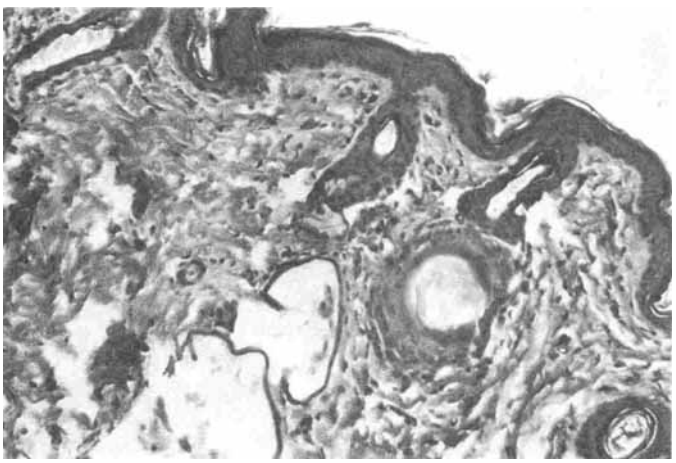

**Figure 1**—*Histological appearance of the hairless mouse normal skin.*

[1] SKH-hr$^{-1}$ strain, Skin Cancer Hospital, Philadelphia, Pa.
[2] Metofane, Pitman-Moore, Washington Crossing, N.J.

0022-3549/81/0700-0835$01.00/0
© 1981, American Pharmaceutical Association

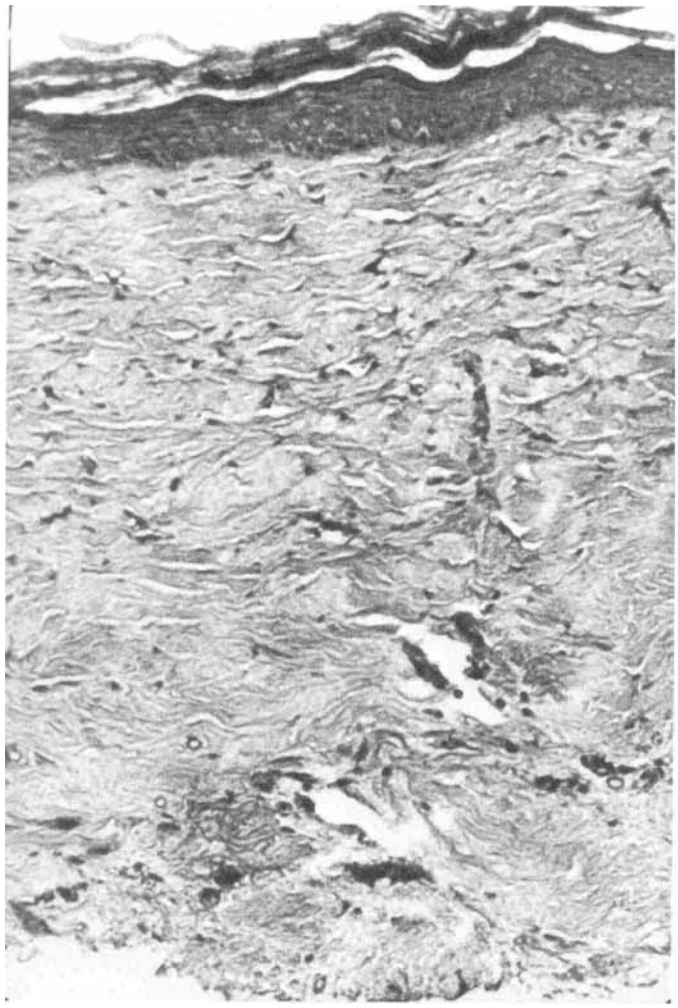

**Figure 2**—*Histological appearance of scar tissue obtained ~3 months postburn.*

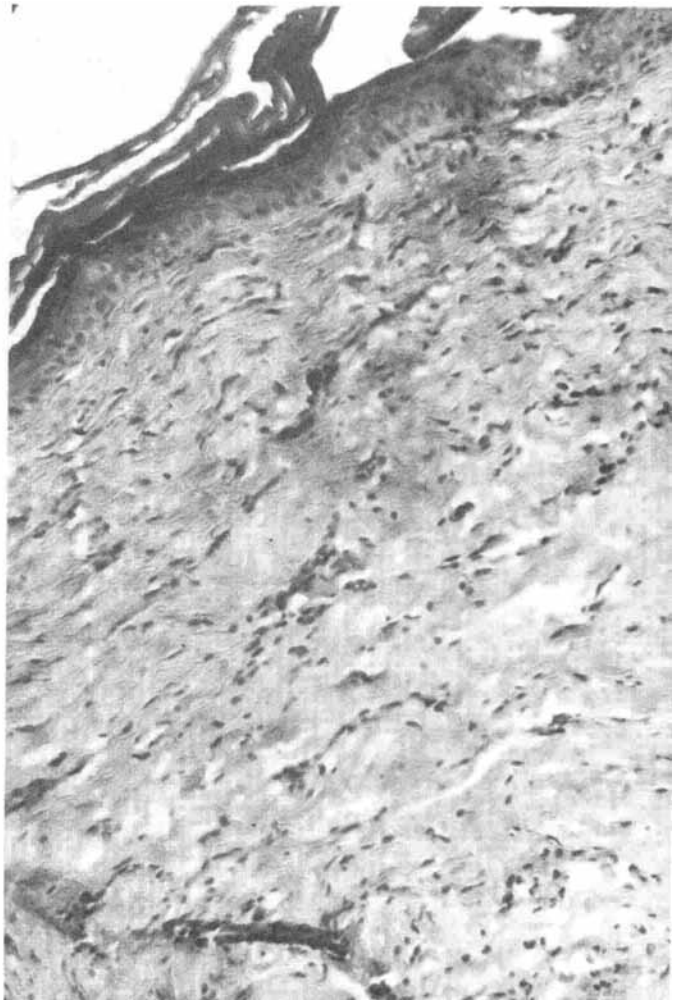

**Figure 3**—*Histological appearance of scar tissue obtained ~4 months postburn.*

cages and were supplied food and water *ad libitum*.

The traumatized animals were examined daily. A clearly defined wound was evident on the 1st day after inflicting the burn. In 1 week, a thick eschar covered the affected area. This eschar desiccated gradually and finally sloughed by about the 4th week postburn. The newly exposed surface appeared smooth and pinkish and refracted light in a manner typical of scarred surface. The scarred area was substantially contracted relative to the initial area from which the epidermis was removed. The wounds appeared to heal inward from thin margins, a process typical of full-thickness wound reepithelialization.

For purposes of histological examination, mice were sacrificed by spinal cord dislocation. Small scar biopsies were taken, and microscopic slides were prepared using standard hematoxylin and eosin staining techniques. Figure 1 represents the normal skin of the hairless mouse, and Figs. 2 and 3 represent the scar tissues obtained ~3 and 4 months, respectively, after inflicting the wound. The normal skin has a distinct epidermis and dermis containing loosely arranged connective tissue and numerous cystic pilosebaceous glands extending through the epidermis. The epidermal–dermal junction is convoluted. This normal slide can be contrasted to the 3-month-old burn scar (Fig. 2), which evidences a somewhat thickened epidermis and a more compact dermis (greater cellulosity and deposited collagen). The absence of the cystic pilosebaceous glands is notable, as is the flatness of the epidermal–dermal interface. Both features are typical of a scarred surface. The 4-month-old scar (Fig. 3) is less cellular with compact dermal collagen, a more developed stratum corneum, and a thinner viable epidermis, all features normally associated with a mature scar.

In separate experiments, attempts were made to produce scarring on the Swiss mouse and the rat. A similar procedure was employed with one minor variation. Before burning the skin for 30 sec at 60°, the anesthetized animal's dorsal surfaces were scalded briefly (60°) for ~ 5 sec, and all hair was plucked by hand. However, in these animals, the surface healed without scarring and with only a slight decrease in the density of hair. The necrotizing conditions apparently were not sufficient to destroy epidermal cells seated deeply on the follicular islands upon burning of these pellaged species. Rather, their more prominent, more deeply anchored hair follicles provided for survival of cells capable of regenerating a normal-appearing integument.

The methodology described produces the desired result in the hairless mouse[1]. A scar tissue is obtained that is being used to study permeation and other properties of skin devoid of its usual appendages. These studies should

reveal the impact of scar formation on the bioavailability of drugs and irritants applied topically over the scarred surface.

(1) T. B. Fritzpatrick and D. P. Johnson, in "Dermatology in General Medicine," T. B. Fritzgerald *et al.* Eds., McGraw-Hill, New York, N.Y., 1971, p. 20.

(2) M. Abercrombie, M. H. Flint, and D. W. James, *J. Embryol. Exp. Morphol.*, **2,** 264 (1954).

(3) T. S. Argyris, *Arch. Pathol.*, **61,** 31 (1956).

(4) A. M. Cuthbertson, *Surg. Gynecol Obstet.*, **108,** 421 (1959).

(5) T. Gillman, T. Penn, D. Bronks, and M. Roux, *Br. J. Surg.*, **43,** 141 (1955).

(6) C. Breedis, *Cancer Res.*, **14,** 575 (1954).

(7) H. C. Grillo, G. T. Watts, and J. Gross, *Am. Surg.*, **148,** 145 (1958).

(8) L. Dann, A. Glucksmann, and K. Tansley, *Br. J. Exp. Pathol.*, **22,** 1 (1941).

(9) W. W. Washburn, *J. Invest. Dermatol.*, **23,** 97 (1954).

(10) B. E. Zawacki and R. J. Jones, *Br. Plast. Surg.*, **20,** 347 (1967).

(11) G. H. Bishop, *Am. J. Anat.*, **76,** 153 (1945).

(12) J. Moserova, E. Behounkova, and Z. Konickova, *Acta Chir. Plast.*, **18,** 135 (1976).

(13) H. B. Chase and W. Montagna, *Proc. Soc. Exp. Biol. Med.*, **76,** 35 (1951).

(14) D. Tarin and C. B. Croft, *J. Anat.*, **106,** 79 (1970).

(15) T. Moriguchi and D. Fujimoto, *J. Invest. Dermatol.*, **72,** 143 (1979).

(16) M. L. Biryukov, T. N. Belyakov, and G. I. Dmitriev, *Acta Chir. Plast.*, **21,** 86 (1979).

(17) C. R. Bèhl, G. L. Flynn, T. Kurihara, O. Gatmaitan, W. I. Higuchi, N. F. H. Ho, and C. L. Pierson, *J. Invest. Dermatol.*, **75,** 340 (1980).

(18) G. L. Flynn, H. H. Durrheim, and W. I. Higuchi, *J. Pharm. Sci.*, **70,** 52 (1981).

*Charanjit Rai Behl* *
*Ann Wittkowsky*
*Michael Barrett*
*Carl L. Pierson*
*Gordon L. Flynn* ˣ
College of Pharmacy
University of Michigan
Ann Arbor, MI 48109

Received December 22, 1980.

Accepted for publication March 16, 1981.

Supported in part by National Institutes of Health Grant GM 24611.

A. Wittkowsky was a summer undergraduate researcher, and M. Barrett was a National Science Foundation summer trainee, NSF-G-SP1-7926914.

* Present address: Pharmacy Research, Roche Laboratories, Hoffmann–La Roche Inc., Nutley, NJ 07110.

# BOOKS

## REVIEWS

**Controlled Release of Bioactive Materials.** Edited by RICHARD BAKER. Academic, 111 Fifth Ave., New York, NY 10003. 1980. 473 pp. 15 × 23 cm. Price $34.50.

This book constitutes a collection of 27 papers delivered at the sixth International Symposium on Controlled-Release Materials in New Orleans in 1979. The first 12 papers deal with various aspects of controlled drug delivery systems.

In the first paper, Heller and Baker review the theory and practice of controlled drug delivery from biodegradable polymers. The mechanisms of drug release from these polymers are discussed in depth, and several illustrative examples are presented. Applications of biodegradable polymers are discussed further in the ensuing two papers by Pitt *et al.* and Petersen *et al.*

In the fourth paper, Theeuwes and Echenhoff present the applications of osmotic drug delivery systems. The design and experimental performance of two osmotic devices are described. The generic osmotic pump (Alzet) is designed to deliver the contents of 170 μl at the rate of either 1 μl/hr over a 1-week period or 0.5 μl/hr over 2 weeks. The other device is the elementary osmotic pump, which is generally fabricated in the shape of a tablet, with a single-delivery orifice. A paper by Chandrasekaran and Shaw is concerned with controlled, transdermal drug delivery.

Other papers of pharmaceutical interest deal with polymers that include poly(lactic acid) and the hydrogels. Rhine and coworkers present a new approach to achieve zero-order release kinetics from diffusion-controlled polymer matrix systems. The theoretical basis for these kinetics is presented as is a comparison of kinetics from matrix devices of other geometries.

The second half of the book is concerned essentially with topics not directly related to drug delivery systems. Controlled-release systems containing insecticides, molluscicides, and plant growth regulators are discussed and described. Implantable systems for the delivery of insect growth regulators to livestock are evaluated by Jaffe and coworkers. The basic technology used to design several of these systems is very similar to drug-containing devices.

This book is a collection of high quality research papers, prepared by scientists in widely different fields. As such, the book is highly recommended for both academic and industrial pharmaceutical scientists, chemists, biologists, and chemical engineers who have an interest in controlled-release technology.

*Reviewed by* James W. McGinity
*College of Pharmacy*
*University of Texas at Austin*
*Austin, TX 78712*

---

**British National Formulary 1981: Number 1.** The Pharmaceutical Press, 1 Lambert St., London, SE1 7JN, England. 1981. 387 pp. 12 × 23 cm. Price £3.80

*The British National Formulary* is designed for use by doctors, pharmacists, and nurses in the National Health Service in the United Kingdom. Unlike earlier editions that were published every 2 or 3 years and contained only those drugs and preparations having the confidence of the Joint Formulary Committee, the 1981 edition is an outgrowth of the Committee's response to requests for a wider coverage of drugs available in the United Kingdom and more detailed guidance in prescribing and dispensing.

This new edition provides more descriptive information to assist the prescriber in selecting the appropriate treatment for a particular patient. A double-column format was followed to accommodate the increased volume of information and to allow the book to "still fit into the doctor's pocket."

The BNF begins with sections on Guidance on Prescribing and Emergency Treatment on Poisoning. The main text consists of classified notes divided into 15 chapters: Gastro-intestinal System; Cardiovascular System; Respiratory System; Central Nervous System; Infections; Endocrine System; Obstetrics and Gynaecology; Malignant Disease and Immunosuppression; Nutrition and Blood; Musculoskeletal and Joint Diseases; Eye; Ear, Nose, and Oropharynx; Skin; Immunological Products and Vaccines; and Anaesthesia. Each chapter begins with appropriate notes for prescribers to facilitate selection of suitable treatment followed by detailed monographs of the relevant drugs and preparations (indications, contraindications, cautions, side-effects, doses, dosage forms, routes of administration, and relative prices). Drugs appear under their pharmacopoeial titles or British Approved Names and are listed alpha-

reveal the impact of scar formation on the bioavailability of drugs and irritants applied topically over the scarred surface.

(1) T. B. Fritzpatrick and D. P. Johnson, in "Dermatology in General Medicine," T. B. Fritzgerald *et al.* Eds., McGraw-Hill, New York, N.Y., 1971, p. 20.

(2) M. Abercrombie, M. H. Flint, and D. W. James, *J. Embryol. Exp. Morphol.*, **2,** 264 (1954).

(3) T. S. Argyris, *Arch. Pathol.*, **61,** 31 (1956).

(4) A. M. Cuthbertson, *Surg. Gynecol Obstet.*, **108,** 421 (1959).

(5) T. Gillman, T. Penn, D. Bronks, and M. Roux, *Br. J. Surg.*, **43,** 141 (1955).

(6) C. Breedis, *Cancer Res.*, **14,** 575 (1954).

(7) H. C. Grillo, G. T. Watts, and J. Gross, *Am. Surg.*, **148,** 145 (1958).

(8) L. Dann, A. Glucksmann, and K. Tansley, *Br. J. Exp. Pathol.*, **22,** 1 (1941).

(9) W. W. Washburn, *J. Invest. Dermatol.*, **23,** 97 (1954).

(10) B. E. Zawacki and R. J. Jones, *Br. Plast. Surg.*, **20,** 347 (1967).

(11) G. H. Bishop, *Am. J. Anat.*, **76,** 153 (1945).

(12) J. Moserova, E. Behounkova, and Z. Konickova, *Acta Chir. Plast.*, **18,** 135 (1976).

(13) H. B. Chase and W. Montagna, *Proc. Soc. Exp. Biol. Med.*, **76,** 35 (1951).

(14) D. Tarin and C. B. Croft, *J. Anat.*, **106,** 79 (1970).

(15) T. Moriguchi and D. Fujimoto, *J. Invest. Dermatol.*, **72,** 143 (1979).

(16) M. L. Biryukov, T. N. Belyakov, and G. I. Dmitriev, *Acta Chir. Plast.*, **21,** 86 (1979).

(17) C. R. Bèhl, G. L. Flynn, T. Kurihara, O. Gatmaitan, W. I. Higuchi, N. F. H. Ho, and C. L. Pierson, *J. Invest. Dermatol.*, **75,** 340 (1980).

(18) G. L. Flynn, H. H. Durrheim, and W. I. Higuchi, *J. Pharm. Sci.*, **70,** 52 (1981).

*Charanjit Rai Behl* *
*Ann Wittkowsky*
*Michael Barrett*
*Carl L. Pierson*
*Gordon L. Flynn* ˣ
College of Pharmacy
University of Michigan
Ann Arbor, MI 48109

Received December 22, 1980.

Accepted for publication March 16, 1981.

Supported in part by National Institutes of Health Grant GM 24611.

A. Wittkowsky was a summer undergraduate researcher, and M. Barrett was a National Science Foundation summer trainee, NSF-G-SP1-7926914.

* Present address: Pharmacy Research, Roche Laboratories, Hoffmann–La Roche Inc., Nutley, NJ 07110.

# BOOKS

## REVIEWS

**Controlled Release of Bioactive Materials.** Edited by RICHARD BAKER. Academic, 111 Fifth Ave., New York, NY 10003. 1980. 473 pp. 15 × 23 cm. Price $34.50.

This book constitutes a collection of 27 papers delivered at the sixth International Symposium on Controlled-Release Materials in New Orleans in 1979. The first 12 papers deal with various aspects of controlled drug delivery systems.

In the first paper, Heller and Baker review the theory and practice of controlled drug delivery from biodegradable polymers. The mechanisms of drug release from these polymers are discussed in depth, and several illustrative examples are presented. Applications of biodegradable polymers are discussed further in the ensuing two papers by Pitt *et al.* and Petersen *et al.*

In the fourth paper, Theeuwes and Echenhoff present the applications of osmotic drug delivery systems. The design and experimental performance of two osmotic devices are described. The generic osmotic pump (Alzet) is designed to deliver the contents of 170 μl at the rate of either 1 μl/hr over a 1-week period or 0.5 μl/hr over 2 weeks. The other device is the elementary osmotic pump, which is generally fabricated in the shape of a tablet, with a single-delivery orifice. A paper by Chandrasekaran and Shaw is concerned with controlled, transdermal drug delivery.

Other papers of pharmaceutical interest deal with polymers that include poly(lactic acid) and the hydrogels. Rhine and coworkers present a new approach to achieve zero-order release kinetics from diffusion-controlled polymer matrix systems. The theoretical basis for these kinetics is presented as is a comparison of kinetics from matrix devices of other geometries.

The second half of the book is concerned essentially with topics not directly related to drug delivery systems. Controlled-release systems containing insecticides, molluscicides, and plant growth regulators are discussed and described. Implantable systems for the delivery of insect growth regulators to livestock are evaluated by Jaffe and coworkers. The basic technology used to design several of these systems is very similar to drug-containing devices.

This book is a collection of high quality research papers, prepared by scientists in widely different fields. As such, the book is highly recommended for both academic and industrial pharmaceutical scientists, chemists, biologists, and chemical engineers who have an interest in controlled-release technology.

*Reviewed by* James W. McGinity
*College of Pharmacy*
*University of Texas at Austin*
*Austin, TX 78712*

---

**British National Formulary 1981: Number 1.** The Pharmaceutical Press, 1 Lambert St., London, SE1 7JN, England. 1981. 387 pp. 12 × 23 cm. Price £3.80

*The British National Formulary* is designed for use by doctors, pharmacists, and nurses in the National Health Service in the United Kingdom. Unlike earlier editions that were published every 2 or 3 years and contained only those drugs and preparations having the confidence of the Joint Formulary Committee, the 1981 edition is an outgrowth of the Committee's response to requests for a wider coverage of drugs available in the United Kingdom and more detailed guidance in prescribing and dispensing.

This new edition provides more descriptive information to assist the prescriber in selecting the appropriate treatment for a particular patient. A double-column format was followed to accommodate the increased volume of information and to allow the book to "still fit into the doctor's pocket."

The BNF begins with sections on Guidance on Prescribing and Emergency Treatment on Poisoning. The main text consists of classified notes divided into 15 chapters: Gastro-intestinal System; Cardiovascular System; Respiratory System; Central Nervous System; Infections; Endocrine System; Obstetrics and Gynaecology; Malignant Disease and Immunosuppression; Nutrition and Blood; Musculoskeletal and Joint Diseases; Eye; Ear, Nose, and Oropharynx; Skin; Immunological Products and Vaccines; and Anaesthesia. Each chapter begins with appropriate notes for prescribers to facilitate selection of suitable treatment followed by detailed monographs of the relevant drugs and preparations (indications, contraindications, cautions, side-effects, doses, dosage forms, routes of administration, and relative prices). Drugs appear under their pharmacopoeial titles or British Approved Names and are listed alpha-

reveal the impact of scar formation on the bioavailability of drugs and irritants applied topically over the scarred surface.

(1) T. B. Fritzpatrick and D. P. Johnson, in "Dermatology in General Medicine," T. B. Fritzgerald *et al.* Eds., McGraw-Hill, New York, N.Y., 1971, p. 20.

(2) M. Abercrombie, M. H. Flint, and D. W. James, *J. Embryol. Exp. Morphol.*, **2,** 264 (1954).

(3) T. S. Argyris, *Arch. Pathol.*, **61,** 31 (1956).

(4) A. M. Cuthbertson, *Surg. Gynecol Obstet.*, **108,** 421 (1959).

(5) T. Gillman, T. Penn, D. Bronks, and M. Roux, *Br. J. Surg.*, **43,** 141 (1955).

(6) C. Breedis, *Cancer Res.*, **14,** 575 (1954).

(7) H. C. Grillo, G. T. Watts, and J. Gross, *Am. Surg.*, **148,** 145 (1958).

(8) L. Dann, A. Glucksmann, and K. Tansley, *Br. J. Exp. Pathol.*, **22,** 1 (1941).

(9) W. W. Washburn, *J. Invest. Dermatol.*, **23,** 97 (1954).

(10) B. E. Zawacki and R. J. Jones, *Br. Plast. Surg.*, **20,** 347 (1967).

(11) G. H. Bishop, *Am. J. Anat.*, **76,** 153 (1945).

(12) J. Moserova, E. Behounkova, and Z. Konickova, *Acta Chir. Plast.*, **18,** 135 (1976).

(13) H. B. Chase and W. Montagna, *Proc. Soc. Exp. Biol. Med.*, **76,** 35 (1951).

(14) D. Tarin and C. B. Croft, *J. Anat.*, **106,** 79 (1970).

(15) T. Moriguchi and D. Fujimoto, *J. Invest. Dermatol.*, **72,** 143 (1979).

(16) M. L. Biryukov, T. N. Belyakov, and G. I. Dmitriev, *Acta Chir. Plast.*, **21,** 86 (1979).

(17) C. R. Bèhl, G. L. Flynn, T. Kurihara, O. Gatmaitan, W. I. Higuchi, N. F. H. Ho, and C. L. Pierson, *J. Invest. Dermatol.*, **75,** 340 (1980).

(18) G. L. Flynn, H. H. Durrheim, and W. I. Higuchi, *J. Pharm. Sci.*, **70,** 52 (1981).

*Charanjit Rai Behl* *
*Ann Wittkowsky*
*Michael Barrett*
*Carl L. Pierson*
*Gordon L. Flynn* ˣ
College of Pharmacy
University of Michigan
Ann Arbor, MI 48109

Received December 22, 1980.

Accepted for publication March 16, 1981.

Supported in part by National Institutes of Health Grant GM 24611.

A. Wittkowsky was a summer undergraduate researcher, and M. Barrett was a National Science Foundation summer trainee, NSF-G-SP1-7926914.

* Present address: Pharmacy Research, Roche Laboratories, Hoffmann–La Roche Inc., Nutley, NJ 07110.

# BOOKS

## REVIEWS

**Controlled Release of Bioactive Materials.** Edited by RICHARD BAKER. Academic, 111 Fifth Ave., New York, NY 10003. 1980. 473 pp. 15 × 23 cm. Price $34.50.

This book constitutes a collection of 27 papers delivered at the sixth International Symposium on Controlled-Release Materials in New Orleans in 1979. The first 12 papers deal with various aspects of controlled drug delivery systems.

In the first paper, Heller and Baker review the theory and practice of controlled drug delivery from biodegradable polymers. The mechanisms of drug release from these polymers are discussed in depth, and several illustrative examples are presented. Applications of biodegradable polymers are discussed further in the ensuing two papers by Pitt *et al.* and Petersen *et al.*

In the fourth paper, Theeuwes and Echenhoff present the applications of osmotic drug delivery systems. The design and experimental performance of two osmotic devices are described. The generic osmotic pump (Alzet) is designed to deliver the contents of 170 μl at the rate of either 1 μl/hr over a 1-week period or 0.5 μl/hr over 2 weeks. The other device is the elementary osmotic pump, which is generally fabricated in the shape of a tablet, with a single-delivery orifice. A paper by Chandrasekaran and Shaw is concerned with controlled, transdermal drug delivery.

Other papers of pharmaceutical interest deal with polymers that include poly(lactic acid) and the hydrogels. Rhine and coworkers present a new approach to achieve zero-order release kinetics from diffusion-controlled polymer matrix systems. The theoretical basis for these kinetics is presented as is a comparison of kinetics from matrix devices of other geometries.

The second half of the book is concerned essentially with topics not directly related to drug delivery systems. Controlled-release systems containing insecticides, molluscicides, and plant growth regulators are discussed and described. Implantable systems for the delivery of insect growth regulators to livestock are evaluated by Jaffe and coworkers. The basic technology used to design several of these systems is very similar to drug-containing devices.

This book is a collection of high quality research papers, prepared by scientists in widely different fields. As such, the book is highly recommended for both academic and industrial pharmaceutical scientists, chemists, biologists, and chemical engineers who have an interest in controlled-release technology.

*Reviewed by* James W. McGinity
*College of Pharmacy*
*University of Texas at Austin*
*Austin, TX 78712*

---

**British National Formulary 1981: Number 1.** The Pharmaceutical Press, 1 Lambert St., London, SE1 7JN, England. 1981. 387 pp. 12 × 23 cm. Price £3.80

*The British National Formulary* is designed for use by doctors, pharmacists, and nurses in the National Health Service in the United Kingdom. Unlike earlier editions that were published every 2 or 3 years and contained only those drugs and preparations having the confidence of the Joint Formulary Committee, the 1981 edition is an outgrowth of the Committee's response to requests for a wider coverage of drugs available in the United Kingdom and more detailed guidance in prescribing and dispensing.

This new edition provides more descriptive information to assist the prescriber in selecting the appropriate treatment for a particular patient. A double-column format was followed to accommodate the increased volume of information and to allow the book to "still fit into the doctor's pocket."

The BNF begins with sections on Guidance on Prescribing and Emergency Treatment on Poisoning. The main text consists of classified notes divided into 15 chapters: Gastro-intestinal System; Cardiovascular System; Respiratory System; Central Nervous System; Infections; Endocrine System; Obstetrics and Gynaecology; Malignant Disease and Immunosuppression; Nutrition and Blood; Musculoskeletal and Joint Diseases; Eye; Ear, Nose, and Oropharynx; Skin; Immunological Products and Vaccines; and Anaesthesia. Each chapter begins with appropriate notes for prescribers to facilitate selection of suitable treatment followed by detailed monographs of the relevant drugs and preparations (indications, contraindications, cautions, side-effects, doses, dosage forms, routes of administration, and relative prices). Drugs appear under their pharmacopoeial titles or British Approved Names and are listed alpha-

betically unless there is a drug of choice, which then is listed first. Preparations are listed immediately following the drug that is their main ingredient.

Appendixes 1–3 contain pertinent information on drug interactions, intravenous additives, and borderline substances. A small formulary section also is included for dispensing those preparations commonly prepared extemporaneously, as are a dental formulary, an index of manufacturers, and an extensive subject index.

The BNF is a pocket book for easy referral, and thus cannot contain all the information necessary for prescribing and dispensing, but should be supplemented by manufacturer's data sheets and specialized texts as needed.

Future editions will be published twice a year to maintain current information on the drugs and preparations.

*Staff Review*

---

**The Use of Alternatives in Drug Research.** Edited by ANDREW N. ROWAN and CARL J. STRATMANN. University Park Press, 233 E. Redwood St., Baltimore, MD 21202. 1980. 190 pp. 15 × 23 cm. Price $24.50.

The advent of the National Toxicology Program has caused a rethinking of the procedures available for economical toxicological assessment of the thousands of chemicals to which people are exposed and the means whereby such exposure can be limited or prevented. This volume follows the pathway of chemical evaluation by *in vitro* systems designed to reduce, but not eliminate, the use of animals in pharmacological and toxicological research. As the various contributors state, there comes a time when only the whole animal will provide the final answer.

Hansch's contribution points out a logical manner in which modern drug modifications can be carried out *in vitro* utilizing computer techniques that allow rational changes in basic molecules to increase potency and decrease possible side effects, utilizing partition coefficients and binding to receptor sites. Many contributors point out that *in vitro* use of bacteria and cultured cells and tissues can indicate binding sites that cannot be determined by *in vivo* studies. Thus, the techniques that have been used to develop treatments for polio, mumps, and measles now can be used to screen antiviral chemicals to determine their antiviral potency and the maximum concentrations at which no toxic effects are caused to tissue culture cells.

Macrophages can be grown in culture, and *in vitro* studies of cellular immunity can be undertaken prior to whole animal testing. Micropharmacokinetics of various agents can be undertaken with this system. Protozoan diseases now can be studied with culture systems, and the various diseases afflicting humans and animals, such as trypanosomiasis, leishmaniasis, trichomoniasis, and amoebiasis, in either vector or vertebrate forms, can be evaluated for chemical susceptibility.

Pharmacologists have utilized both tissue slices and cell-free systems to study chemical biotransformations, enabling the evaluation of metabolic processes prior to introduction into whole animals, but the conjugation processes are not usually included in such studies and overall excretion may result in damage to such organs as the kidneys. However, tissue perfusion can eliminate this drawback partially. The mechanisms whereby both inorganic and organic chemicals exert their toxic effects on cell membranes and constituents can be studied with such models as amoeba proteus and isolated rat hepatocytes. Immunological preparations have been prepared by *in vitro* methods, but numerous biologicals have caused disease in humans because they contained live viruses; either the viruses were not killed during processing or they were not susceptible to the antiviral agent used. Thus, whole animal testing must be conducted.

By far, the greatest application of *in vitro* tests is the microbiological assessment of mutagenic and possible carcinogenic potentials of chemicals. Such methods are discussed by Rosenkrantz *et al.*, who point out the various modifications of microbial assays, the activation by S-9 fractions from various tissues, and the pitfalls encountered. However, such tests coupled with various cultured animal and human cell lines greatly assist in showing cell transformations and their possible link to the mutagenic and carcinogenic processes.

Of all *in vivo* tests used for the determination of skin and eye irritation, the Draize test has had the greatest application and has caused the most emotional impact. This eye test does not differentiate intermediate irritants and has a great degree of subjectivity. Recently, a cytotoxicity test was proposed based on the *in vitro* effects of irritants on I-929 mouse embryo cells. The results obtained compare favorably with eye irritation obtained in the Draize test. However, more work must be done to establish it as the method of choice.

In general, this symposium volume should indicate to pharmacologists and toxicologists that *in vitro* procedures should be applied to drug development and chemical evaluation during preliminary research. The succinct nature of the material presented and the extensive bibliography recommend this volume, and it should be in the library of all researchers and students in these fields.

*Reviewed by* Thomas J. Haley
*National Center for Toxicological Research*
*Jefferson, AR 72079*

---

## NOTICES

*Scientific Considerations in Monitoring and Evaluating Toxicological Research.* Edited by EDWARD J. GRALLA. Hemisphere Publishing Corp., 1025 Vermont Ave., N.W., Washington, DC 20005. 1981. 221 pp. 15 × 23 cm. Price $24.50.

*Advances In Chromatography, Vol. 19.* Edited by J. CALVIN GIDDINGS, ELI GRUSHKA, JACK CAZES, and PHYLLIS R. BROWN. Dekker, 270 Madison Ave., New York, NY 10016. 1981. 312 pp. 15 × 23 cm. Price $39.75 (20% higher outside the United States and Canada).

*Recent Developments in Chromatography and Electrophoresis, 10.* Edited by ALBERTO FRIGERIO and MALCOLM McCAMISH. (Analytical Chemistry Symposia Series, Vol. 3.) Elsevier/North-Holland, 52 Vanderbilt Ave., New York, NY 10017. 1980. 342 pp. 16 × 24 cm. Price $68.25.

*High-Performance Liquid Chromatography: Advances and Perspectives, Vol. 1.* Edited by CSABA HORVATH. Academic, 111 Fifth Ave., New York, NY 10003. 1980. 330 pp. 15 × 23 cm. Price $35.00.

*High-Performance Liquid Chromatography: Advances and Perspectives, Vol. 2.* Edited by CSABA HORVATH. Academic, 111 Fifth Ave., New York, NY 10003. 1980. 341 pp. 15 × 23 cm. Price $39.50.

*Further Studies in the Assessment of Toxic Actions. Archives of Toxicology, Supplement 4.* (Proceedings of the European Society of Toxicology meeting in Dresden, 1979.) Edited by P. L. CHAMBERS and W. KLINGER. Springer–Verlag New York, 44 Hartz Way, Secaucus, NJ 07094. 1980. 507 pp. 16 × 24 cm.

*IARC Monographs on the Evaluation of the Carcinogenic Risk of Chemicals to Humans. Supplement 2. Long-Term and Short-Term Screening Assays for Carcinogens: A Critical Appraisal.* International Agency for Research on Cancer. World Health Organization, 1211 Geneva 27, Switzerland. 1980. 426 pp. 17 × 24 cm. Price U.S. $25.00 (Sw.fr. 40.00).

*IARC Monographs on the Evaluation of the Carcinogenic Risk of Chemicals to Humans. Vol. 23: Some Metals and Metallic Compounds.* International Agency for Research on Cancer. World Health Organization, 1211 Geneva 27, Switzerland. 1980. 438 pp. 16 × 24 cm. Price U.S. $30.00 (Sw.fr. 50.00).

betically unless there is a drug of choice, which then is listed first. Preparations are listed immediately following the drug that is their main ingredient.

Appendixes 1–3 contain pertinent information on drug interactions, intravenous additives, and borderline substances. A small formulary section also is included for dispensing those preparations commonly prepared extemporaneously, as are a dental formulary, an index of manufacturers, and an extensive subject index.

The BNF is a pocket book for easy referral, and thus cannot contain all the information necessary for prescribing and dispensing, but should be supplemented by manufacturer's data sheets and specialized texts as needed.

Future editions will be published twice a year to maintain current information on the drugs and preparations.

*Staff Review*

---

**The Use of Alternatives in Drug Research.** Edited by ANDREW N. ROWAN and CARL J. STRATMANN. University Park Press, 233 E. Redwood St., Baltimore, MD 21202. 1980. 190 pp. 15 × 23 cm. Price $24.50.

The advent of the National Toxicology Program has caused a rethinking of the procedures available for economical toxicological assessment of the thousands of chemicals to which people are exposed and the means whereby such exposure can be limited or prevented. This volume follows the pathway of chemical evaluation by *in vitro* systems designed to reduce, but not eliminate, the use of animals in pharmacological and toxicological research. As the various contributors state, there comes a time when only the whole animal will provide the final answer.

Hansch's contribution points out a logical manner in which modern drug modifications can be carried out *in vitro* utilizing computer techniques that allow rational changes in basic molecules to increase potency and decrease possible side effects, utilizing partition coefficients and binding to receptor sites. Many contributors point out that *in vitro* use of bacteria and cultured cells and tissues can indicate binding sites that cannot be determined by *in vivo* studies. Thus, the techniques that have been used to develop treatments for polio, mumps, and measles now can be used to screen antiviral chemicals to determine their antiviral potency and the maximum concentrations at which no toxic effects are caused to tissue culture cells.

Macrophages can be grown in culture, and *in vitro* studies of cellular immunity can be undertaken prior to whole animal testing. Micropharmacokinetics of various agents can be undertaken with this system. Protozoan diseases now can be studied with culture systems, and the various diseases afflicting humans and animals, such as trypanosomiasis, leishmaniasis, trichomoniasis, and amoebiasis, in either vector or vertebrate forms, can be evaluated for chemical susceptibility.

Pharmacologists have utilized both tissue slices and cell-free systems to study chemical biotransformations, enabling the evaluation of metabolic processes prior to introduction into whole animals, but the conjugation processes are not usually included in such studies and overall excretion may result in damage to such organs as the kidneys. However, tissue perfusion can eliminate this drawback partially. The mechanisms whereby both inorganic and organic chemicals exert their toxic effects on cell membranes and constituents can be studied with such models as amoeba proteus and isolated rat hepatocytes. Immunological preparations have been prepared by *in vitro* methods, but numerous biologicals have caused disease in humans because they contained live viruses; either the viruses were not killed during processing or they were not susceptible to the antiviral agent used. Thus, whole animal testing must be conducted.

By far, the greatest application of *in vitro* tests is the microbiological assessment of mutagenic and possible carcinogenic potentials of chemicals. Such methods are discussed by Rosenkrantz *et al.*, who point out the various modifications of microbial assays, the activation by S-9 fractions from various tissues, and the pitfalls encountered. However, such tests coupled with various cultured animal and human cell lines greatly assist in showing cell transformations and their possible link to the mutagenic and carcinogenic processes.

Of all *in vivo* tests used for the determination of skin and eye irritation, the Draize test has had the greatest application and has caused the most emotional impact. This eye test does not differentiate intermediate irritants and has a great degree of subjectivity. Recently, a cytotoxicity test was proposed based on the *in vitro* effects of irritants on I-929 mouse embryo cells. The results obtained compare favorably with eye irritation obtained in the Draize test. However, more work must be done to establish it as the method of choice.

In general, this symposium volume should indicate to pharmacologists and toxicologists that *in vitro* procedures should be applied to drug development and chemical evaluation during preliminary research. The succinct nature of the material presented and the extensive bibliography recommend this volume, and it should be in the library of all researchers and students in these fields.

*Reviewed by* Thomas J. Haley
*National Center for Toxicological Research*
*Jefferson, AR 72079*

---

## NOTICES

*Scientific Considerations in Monitoring and Evaluating Toxicological Research.* Edited by EDWARD J. GRALLA. Hemisphere Publishing Corp., 1025 Vermont Ave., N.W., Washington, DC 20005. 1981. 221 pp. 15 × 23 cm. Price $24.50.

*Advances In Chromatography, Vol. 19.* Edited by J. CALVIN GIDDINGS, ELI GRUSHKA, JACK CAZES, and PHYLLIS R. BROWN. Dekker, 270 Madison Ave., New York, NY 10016. 1981. 312 pp. 15 × 23 cm. Price $39.75 (20% higher outside the United States and Canada).

*Recent Developments in Chromatography and Electrophoresis, 10.* Edited by ALBERTO FRIGERIO and MALCOLM McCAMISH. (Analytical Chemistry Symposia Series, Vol. 3.) Elsevier/North-Holland, 52 Vanderbilt Ave., New York, NY 10017. 1980. 342 pp. 16 × 24 cm. Price $68.25.

*High-Performance Liquid Chromatography: Advances and Perspectives, Vol. 1.* Edited by CSABA HORVATH. Academic, 111 Fifth Ave., New York, NY 10003. 1980. 330 pp. 15 × 23 cm. Price $35.00.

*High-Performance Liquid Chromatography: Advances and Perspectives, Vol. 2.* Edited by CSABA HORVATH. Academic, 111 Fifth Ave., New York, NY 10003. 1980. 341 pp. 15 × 23 cm. Price $39.50.

*Further Studies in the Assessment of Toxic Actions. Archives of Toxicology, Supplement 4.* (Proceedings of the European Society of Toxicology meeting in Dresden, 1979.) Edited by P. L. CHAMBERS and W. KLINGER. Springer–Verlag New York, 44 Hartz Way, Secaucus, NJ 07094. 1980. 507 pp. 16 × 24 cm.

*IARC Monographs on the Evaluation of the Carcinogenic Risk of Chemicals to Humans. Supplement 2. Long-Term and Short-Term Screening Assays for Carcinogens: A Critical Appraisal.* International Agency for Research on Cancer. World Health Organization, 1211 Geneva 27, Switzerland. 1980. 426 pp. 17 × 24 cm. Price U.S. $25.00 (Sw.fr. 40.00).

*IARC Monographs on the Evaluation of the Carcinogenic Risk of Chemicals to Humans. Vol. 23: Some Metals and Metallic Compounds.* International Agency for Research on Cancer. World Health Organization, 1211 Geneva 27, Switzerland. 1980. 438 pp. 16 × 24 cm. Price U.S. $30.00 (Sw.fr. 50.00).

betically unless there is a drug of choice, which then is listed first. Preparations are listed immediately following the drug that is their main ingredient.

Appendixes 1–3 contain pertinent information on drug interactions, intravenous additives, and borderline substances. A small formulary section also is included for dispensing those preparations commonly prepared extemporaneously, as are a dental formulary, an index of manufacturers, and an extensive subject index.

The BNF is a pocket book for easy referral, and thus cannot contain all the information necessary for prescribing and dispensing, but should be supplemented by manufacturer's data sheets and specialized texts as needed.

Future editions will be published twice a year to maintain current information on the drugs and preparations.

*Staff Review*

---

**The Use of Alternatives in Drug Research.** Edited by ANDREW N. ROWAN and CARL J. STRATMANN. University Park Press, 233 E. Redwood St., Baltimore, MD 21202. 1980. 190 pp. 15 × 23 cm. Price $24.50.

The advent of the National Toxicology Program has caused a rethinking of the procedures available for economical toxicological assessment of the thousands of chemicals to which people are exposed and the means whereby such exposure can be limited or prevented. This volume follows the pathway of chemical evaluation by *in vitro* systems designed to reduce, but not eliminate, the use of animals in pharmacological and toxicological research. As the various contributors state, there comes a time when only the whole animal will provide the final answer.

Hansch's contribution points out a logical manner in which modern drug modifications can be carried out *in vitro* utilizing computer techniques that allow rational changes in basic molecules to increase potency and decrease possible side effects, utilizing partition coefficients and binding to receptor sites. Many contributors point out that *in vitro* use of bacteria and cultured cells and tissues can indicate binding sites that cannot be determined by *in vivo* studies. Thus, the techniques that have been used to develop treatments for polio, mumps, and measles now can be used to screen antiviral chemicals to determine their antiviral potency and the maximum concentrations at which no toxic effects are caused to tissue culture cells.

Macrophages can be grown in culture, and *in vitro* studies of cellular immunity can be undertaken prior to whole animal testing. Micropharmacokinetics of various agents can be undertaken with this system. Protozoan diseases now can be studied with culture systems, and the various diseases afflicting humans and animals, such as trypanosomiasis, leishmaniasis, trichomoniasis, and amoebiasis, in either vector or vertebrate forms, can be evaluated for chemical susceptibility.

Pharmacologists have utilized both tissue slices and cell-free systems to study chemical biotransformations, enabling the evaluation of metabolic processes prior to introduction into whole animals, but the conjugation processes are not usually included in such studies and overall excretion may result in damage to such organs as the kidneys. However, tissue perfusion can eliminate this drawback partially. The mechanisms whereby both inorganic and organic chemicals exert their toxic effects on cell membranes and constituents can be studied with such models as amoeba proteus and isolated rat hepatocytes. Immunological preparations have been prepared by *in vitro* methods, but numerous biologicals have caused disease in humans because they contained live viruses; either the viruses were not killed during processing or they were not susceptible to the antiviral agent used. Thus, whole animal testing must be conducted.

By far, the greatest application of *in vitro* tests is the microbiological assessment of mutagenic and possible carcinogenic potentials of chemicals. Such methods are discussed by Rosenkrantz *et al.*, who point out the various modifications of microbial assays, the activation by S-9 fractions from various tissues, and the pitfalls encountered. However, such tests coupled with various cultured animal and human cell lines greatly assist in showing cell transformations and their possible link to the mutagenic and carcinogenic processes.

Of all *in vivo* tests used for the determination of skin and eye irritation, the Draize test has had the greatest application and has caused the most emotional impact. This eye test does not differentiate intermediate irritants and has a great degree of subjectivity. Recently, a cytotoxicity test was proposed based on the *in vitro* effects of irritants on I-929 mouse embryo cells. The results obtained compare favorably with eye irritation obtained in the Draize test. However, more work must be done to establish it as the method of choice.

In general, this symposium volume should indicate to pharmacologists and toxicologists that *in vitro* procedures should be applied to drug development and chemical evaluation during preliminary research. The succinct nature of the material presented and the extensive bibliography recommend this volume, and it should be in the library of all researchers and students in these fields.

*Reviewed by* Thomas J. Haley
*National Center for Toxicological Research*
*Jefferson, AR 72079*

---

## NOTICES

*Scientific Considerations in Monitoring and Evaluating Toxicological Research.* Edited by EDWARD J. GRALLA. Hemisphere Publishing Corp., 1025 Vermont Ave., N.W., Washington, DC 20005. 1981. 221 pp. 15 × 23 cm. Price $24.50.

*Advances In Chromatography, Vol. 19.* Edited by J. CALVIN GIDDINGS, ELI GRUSHKA, JACK CAZES, and PHYLLIS R. BROWN. Dekker, 270 Madison Ave., New York, NY 10016. 1981. 312 pp. 15 × 23 cm. Price $39.75 (20% higher outside the United States and Canada).

*Recent Developments in Chromatography and Electrophoresis, 10.* Edited by ALBERTO FRIGERIO and MALCOLM McCAMISH. (Analytical Chemistry Symposia Series, Vol. 3.) Elsevier/North-Holland, 52 Vanderbilt Ave., New York, NY 10017. 1980. 342 pp. 16 × 24 cm. Price $68.25.

*High-Performance Liquid Chromatography: Advances and Perspectives, Vol. 1.* Edited by CSABA HORVATH. Academic, 111 Fifth Ave., New York, NY 10003. 1980. 330 pp. 15 × 23 cm. Price $35.00.

*High-Performance Liquid Chromatography: Advances and Perspectives, Vol. 2.* Edited by CSABA HORVATH. Academic, 111 Fifth Ave., New York, NY 10003. 1980. 341 pp. 15 × 23 cm. Price $39.50.

*Further Studies in the Assessment of Toxic Actions. Archives of Toxicology, Supplement 4.* (Proceedings of the European Society of Toxicology meeting in Dresden, 1979.) Edited by P. L. CHAMBERS and W. KLINGER. Springer–Verlag New York, 44 Hartz Way, Secaucus, NJ 07094. 1980. 507 pp. 16 × 24 cm.

*IARC Monographs on the Evaluation of the Carcinogenic Risk of Chemicals to Humans. Supplement 2. Long-Term and Short-Term Screening Assays for Carcinogens: A Critical Appraisal.* International Agency for Research on Cancer. World Health Organization, 1211 Geneva 27, Switzerland. 1980. 426 pp. 17 × 24 cm. Price U.S. $25.00 (Sw.fr. 40.00).

*IARC Monographs on the Evaluation of the Carcinogenic Risk of Chemicals to Humans. Vol. 23: Some Metals and Metallic Compounds.* International Agency for Research on Cancer. World Health Organization, 1211 Geneva 27, Switzerland. 1980. 438 pp. 16 × 24 cm. Price U.S. $30.00 (Sw.fr. 50.00).

A publication of the
American Pharmaceutical Association—
the National Professional Society
of Pharmacists

# JOURNAL OF PHARMACEUTICAL SCIENCES

## INDEX TO AUTHORS
## INDEX TO SUBJECTS

VOLUME 70
JANUARY TO DECEMBER, 1981

*Published monthly under the supervision of the Board of Trustees*

MARY H. FERGUSON
*Editor*

NANCY E. BROWN
*Production Editor*

JOHN PATRICK EVANS
*Copy Editor*

MICHAEL K. HAYES
*Copy Editor*

EDWARD G. FELDMANN
*Contributing Editor*

SAMUEL W. GOLDSTEIN
*Contributing Editor*

BELLE R. BECK
*Editorial Secretary*

EDWARD G. FELDMANN
*Acting Director of Publications*

EDITORIAL ADVISORY BOARD

John Autian
Norman R. Farnsworth
William J. Jusko
Herbert A. Lieberman
David E. Mann, Jr.
Ian W. Mathison
Gerald J. Papariello
Edward G. Rippie

JOURNAL OF PHARMACEUTICAL SCIENCES

AUGUST 1981
VOLUME 70 NUMBER 8

*LITERATURE SURVEY*

# Structure–Activity Relationships of Phenethylamine Hallucinogens

**DAVID E. NICHOLS**

Received from the *Department of Medicinal Chemistry and Pharmacognosy, School of Pharmacy and Pharmacal Sciences, Purdue University, West Lafayette, IN 47907.*

**Keyphrases** □ Phenethylamines—structure–activity relationships, compared with other hallucinogens, animal, human, and *in vitro* studies reviewed, literature survey □ Structure–activity relationships—phenethylamines, compared with other hallucinogens, animal, human, and *in vitro* studies reviewed, literature survey □ Hallucinogens—phenethylamines, structure–activity relationships, compared with other hallucinogens, animal, human, and *in vitro* studies reviewed, literature survey

The phenethylamine hallucinogens are simple 2-phenylethylamine derivatives of the general formula I, the majority of which are substituted with methoxy and alkyl or halogen groups. Where R is a methyl group, the compounds have been referred to as hallucinogenic "amphetamines." Although not strictly correct, this nomenclature is used throughout this discussion.

Although these drugs are not widely abused at present, several were prevalent on the illicit drug market during the 1960's. The more common ones were 1-(2,5-dimethoxy-4-methylphenyl)-2-aminopropane ("STP," II) (1), 1-(3,4-methylenedioxyphenyl)-2-aminopropane (III) (2), and 1-(4-methoxyphenyl)-2-aminopropane (IV) (3). The latter two were responsible for several deaths. Their popularity was due to their relatively high potency, coupled with the economic attractiveness of starting materials such as anisaldehyde, piperonal, and methylhydroquinone. With the exception of lysergide (LSD), the "classical" hallucinogens psilocin or psilocybin and mescaline were seldom available (4). Thus, the amphetamines served as convenient substitutes.

Structure–activity studies have been carried out with several classes of hallucinogens. However, lysergamides, related to lysergide and the most potent series, have received only limited attention, chiefly due to the molecular complexity of lysergic acid and the problems inherent in modification of such a structure. The simple tryptamines have been investigated somewhat more extensively, but few novel compounds have emerged. In addition, many of the indoles necessary as starting materials are tedious to synthesize. Therefore, the tryptamines have probably not received the attention they deserve.

In contrast, the phenethylamines have been studied extensively. The commercial availability or ease of synthesis of numerous substituted benzaldehydes has led to the synthesis and evaluation of literally hundreds of analogs. Because the mechanism of action for phenethylamine hallucinogens appears to be identical or similar to that for lysergide and the tryptamines (5–10), studies with phenethylamines could be used to infer information about the action and binding features of indoles.

This class of agents was reviewed by Nieforth (11) in 1971 as "psychotomimetic" phenethylamines. It is not the intent of this author to delve into the significance and comparisons of such terms as psychotomimetic, hallucinogenic, and psychedelic. The controversy over appropriate terminology has been considered in the literature. Within this discussion, the terms hallucinogenic and psychotomimetic are used interchangeably. Psychedelic is another term that has been used to describe this class of compounds.

A word of caution about biological data is in order. Activity is discussed for several animal and *in vitro* models, as well as for humans, where available. However, the use of *in vitro* and animal data can be misleading. For example, compounds have been compared in rats for their ability to disrupt a conditioned avoidance response. In clinical terms, this approach is meaningless. In rabbits, many compounds have been compared for their ability to elicit hyperthermia.

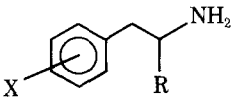


I: R = H or $CH_3$, X = OR, alkyl, halogen
II: R = $CH_3$, X = 2,5-$(OCH_3)_2$-4-$CH_3$
III: R = $CH_3$, X = 3,4-$OCH_2O$
IV: R = $CH_3$, X = 4-$OCH_3$

0022-3549/81/0800-0839$01.00/0
© 1981, American Pharmaceutical Association

Again, these data have little clinical relevance. In general, however, such tests have been correlated with potency of the compounds in humans. Many of the animal tests were found to allow predictions, albeit approximate, of human potency. Thus, in cases where animal data are cited, some effective central component of action is indicated. Nevertheless, the reader should be aware that only those compounds that were assayed in humans can be truly categorized as hallucinogenic.

There is a good deal of flexibility in interpretation even in this situation, and much of this should be attributed to the multiplicity of actions possessed by the phenethylamines. These simple structures have direct actions on serotonin receptors, both as agonists (12–14) and as antagonists (15), are capable of releasing serotonin (16), norepinephrine, and dopamine (17), have direct actions at dopamine receptors, or can be metabolized to species that further influence qualitative mechanisms of action (18), all depending on the particular structure studied. The effect on monoamine oxidase for most structures also is unknown. These and other factors combine to varying degrees for each agent. Hence, a particular compound could be said to possess a unique profile of action all its own. That is, each substitution pattern could be expected to present a slightly different qualitative pattern of clinical activity that will be revealed only by tests in humans. Therefore, when one speaks of hallucinogenic activity, it is uncertain just exactly what is meant. Most often, in humans at least, the term refers to a subjective similarity to a standard agent such as lysergide or mescaline. In this light, one can see how inadequate any animal testing will be. Fortunately, Shulgin and his coworkers provided a wealth of quantitative human data for correlation and analysis.

Although elucidation of subtle qualitative structure–activity relationships must await more structured and well-designed clinical assays, legal strictures and public sentiment presently oppose such research. One is forced to rely largely on animal assays. Ignoring the work that has used animals and *in vitro* models leaves a serious gap in an understanding of structure–activity relationships. Such studies should be considered, but with the caveats discussed always in mind.

This paper briefly, but critically, reviews the advances made in understanding the structure–activity relationships of phenethylamine hallucinogens. It is hoped that a clearer picture will emerge of the probable requirements for receptor binding and some of the essential conformational and stereochemical features. Where possible, these requirements are related to human clinical activity.

Comprehensive reviews of hallucinogens were presented by Brawley and Duffield (6) and subsequently by Shulgin (19–21). Jacobs and Trulson (22) also recently presented a brief review of the mechanism of action for hallucinogens. However, none of these reports dealt in sufficient depth with the structure–activity requirements for the most widely studied class of hallucinogens, the phenethylamines. The excellent and comprehensive reviews by Shulgin come closest to this goal but tend to focus on active compounds and a description of structure–activity relationships as they apply to human clinical studies. These reviews understandably omit several studies where activity in animal models has not been confirmed by human testing.

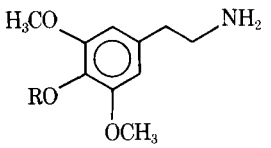


V: R = $CH_3$
VI: R = $CH_2CH_3$

The present discussion attempts to pull together findings from many approaches, both *in vivo* and *in vitro*. The treatment begins with aromatic substitution patterns and proceeds to brief highlighting of what is known about the molecular mechanism of action. It is hoped that the reader will gain a better understanding of the structural features necessary for activity and, where possible, insight into the possible reasons for their importance.

## AROMATIC SUBSTITUENTS

**Orientation**—It has been concluded that a 2,4,5-trisubstitution pattern yields optimally active compounds (19, 23). Although this statement generally remains true, some interesting exceptions exist. For example, replacement of the 4-methoxy group in mescaline (V) with an ethoxy group gives escaline (VI), which is about six times more active than mescaline (24).

Within the 3,4,5-trisubstituted series, replacement of the 4-methoxy with a bromine, alkyl, or alkylthio group leads to compounds with high activity (24). Acute dosages in humans were reported to be in the 10–20-mg range (21). In an *in vitro* assay, several 3,4,5-trisubstituted compounds showed potency comparable to similarly substituted 2,4,5-substitution patterns (25). This point is important. Attention has been called to the possibility of quinone generation from 2,5-dimethoxy-substituted compounds as an explanation for their high potency (19, 21, 23, 26). Although di-*O*-demethylation and consequent oxidation to quinones were observed in liver microsomes, no such reactions were detected *in vivo* (27). However, the potential neurotoxicity of such reactive metabolites (28), even if produced only in miniscule amounts, should give cause for concern in the unlikely event that these drugs might be used on a chronic high dosage basis.

In general, the most active compounds studied to date possess 4,5-disubstitution with a methoxy group at either the 2-position (2,4,5-substitution) or the 3-position (3,4,5-substitution). However, 2,4,6-trimethoxyamphetamine possesses about 10 times the activity of mescaline in humans (21). Since little work has been reported with 2,4,6-substituted compounds, it is impossible to assess whether further substituent modification will give more potent compounds in this series.

**Nature of Substituents**—In any substitution series, the 4-substituent has been of unique importance. Although it probably contributes a general lipophilic effect that favors more effective central nervous system (CNS) penetration (29), it also may serve in at least two other specific roles. First, the most active compounds possess *para*-substituents that are resistant to oxidative metabolism. Increasing potency generally parallels increasing stability of this group. Second, a recent *in vitro* quantitative study indicated that serotonin receptors may possess a specific hydrophobic site that accommodates the *para*-substituent,

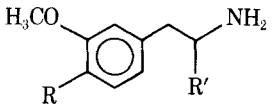

VII: R = $OCH_3$, R′ = H
VIII: R = $OCH_2CH_3$, R′ = H
IX: R = $CH_3$, R′ = H
X: R = Br, R′ = $CH_3$

providing it is <5–6 Å in length (30). These conclusions were supported by studies of molecular connectivity (31). Green *et al.* (32) also proposed a specific hydrophobic site approximately at this region of the serotonin receptor.

The unique importance of the *para*-substituent can be best illustrated with several examples. Anderson *et al.* (33, 34) evaluated a series of isomeric 2,4,5-trisubstituted dimethoxymethylamphetamines. Substantial activity in the rabbit hyperthermia model was observed only when the substituents were in the 2,5-dimethoxy-4-methyl configuration. A similar finding occurred for a series of 2,4,5-substituted dimethoxymethylthioamphetamines. Significant activity occurred only with the 2,5-dimethoxy-4-methylthio orientation (35).

The *para*-substituent is even more critical for compounds lacking an *o*-methoxy group. For example, 3,4-dimethoxyamphetamine (VII) may be orally active in humans but only at acute doses of >1 g (36). However, simple replacement of the 4-methoxy in VII with an ethoxy group gives VIII, leading to some retention of central activity. In humans, VIII possessed mood-elevating properties in the 0.1–0.2-g range (36). In an assay in mice, 3-methoxy-4-methylamphetamine (IX) was just as potent and long lasting as 2,5-dimethoxy-4-methylamphetamine (II) (37). In a series of bromomethoxyamphetamines, the 3-methoxy-4-bromo group (X), but not the isomeric 3-bromo-4-methoxy group, elicited a mescaline-like effect in rats (38). Thus, for hallucinogen-like activity in rodent models, the *o*-methoxy group may not be required. However, it was found that IX, despite its reported activity in mice, is totally inactive in humans at doses 10-fold greater than the threshold for II (36).

An interesting variation in activity is encountered where the *para*-substituent is an alkylthio group. It was speculated initially that the metabolic lability of sulfur might provide interesting biological properties, in contrast to more oxidation-resistant groups (39). Clinical studies of the first compound in this series, 1-(2,5-dimethoxy-4-methylthiophenyl)-2-aminopropane (XI), proved it to be highly active (26). Its duration of action was reduced somewhat from that observed with more metabolically stable compounds. However, this drug appears to produce a unique enhancement of intellectual function while lacking other features of the hallucinogens such as severe visual sensory distortion. Shulgin and his colleagues (21, 40) described this "aleph" effect and expanded on this lead. Alkylthio-substituted compounds in both the 2,4,5- and 3,4,5-series have been examined for activity. Several

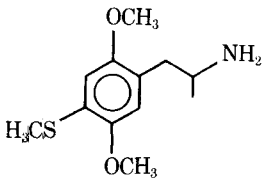

XI

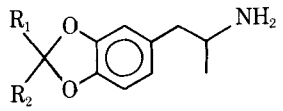

XII: $R_1 = R_2 = H$
XIII: $R_1 = H$, $R_2 = CH_3$
XIV: $R_1 = R_2 = CH_3$

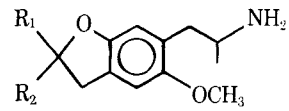

XV: $R_1 = R_2 = H$
XVI: $R_1 = H$, $R_2 = CH_3$
XVII: $R_1 = R_2 = CH_3$

are quite potent and retain the specific intellectual-enhancing properties of XI. The more interesting of these compounds contain the alkylthio group in an orientation *para* to the side chain.

Replacement of a 2-, 3-, or 5-methoxy with a larger alkoxy, methyl, or halogen usually resulted in inactive compounds (34, 41, 42), although some activity was retained in a few cases. Within the 2,5-dimethoxy series, replacement of one methoxy with a hydroxy group increased *in vitro* serotonin receptor affinity (43, 44). Substitution at the 5-position with hydroxy had a greater enhancing effect on affinity than at the 2-position.

**Steric Effects**—Recent studies are beginning to answer questions about the bulk properties of the aromatic ring substituents. Although there may be a hydrophobic region on the receptor that accommodates the *para*-substituent, bulky hydrocarbon groups are not tolerated, as illustrated by the series of 2,5-dimethoxy-4-alkyl-substituted amphetamines. Activity can be ordered in the following sequence for the 4-alkyl group: propyl > ethyl > methyl and also propyl > isopropyl > *tert*-butyl (45–47). The clinical activity of the *p*-isopropyl and *p*-*tert*-butyl homologs has not been established, and potencies are based on animal studies (46, 48). However, the *tert*-butyl homolog was inactive in humans at acute dosages up to 10 mg, far above the effective amount for a *p*-methyl group (20).

It has been proposed that the receptor that interacts with hallucinogens can be modeled as a planar surface which can tolerate little, if any, steric bulk projecting from the binding face of the hallucinogen molecule (49, 50). Nonbonded interactions between the 4-alkyl and an adjacent methoxy group certainly play a role in the allowed conformational states of the alkyl group. One can envision the type of steric profile presented to the receptor by an isopropyl or *tert*-butyl group. In the latter case, it would be impossible to rotate the *tert*-butyl group to remove bulk completely from one face of the molecule. With an isopropyl group, this would not be so severe.

Evidence to support the idea of a deleterious effect of bulky substituents comes from studies on two series of homologs. Structures XII, XIII, XV, and XVI were shown to possess clinical activity (36, 51). Compound XIV has not been tested in humans, but was inactive in animal models (52). The *gem*-dimethyl compound (XVII) is inactive in humans (20). This pattern of activity is in agreement with the suggestion that one face of the molecule must remain unhindered. This explanation may apply to the inactivity of the ethylenedioxy (XVIII*a*) and trimethylenedioxy (XVIII*b*) compounds (53).

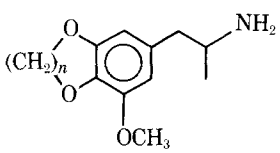

XVIII*a*: $n = 2$
XVIII*b*: $n = 3$

In addition to interactions between substituents and the receptor, interaction between the substituents themselves probably plays an important role in determining activity. X-ray crystallographic studies established that the 4-methoxy group of mescaline is twisted nearly perpendicular to the ring plane (54). It is unlikely that a more bulky group such as ethoxy can rotate from a perpendicular conformation. In view of the substantial potency, not only of escaline (VI) but of its 4-isopropoxy homolog, isoproscaline (36), it seems doubtful that the 4-oxygen plays any crucial role with respect to resonance overlap of its $n$ electrons with the $\pi$ system of the aromatic ring. This concept is reinforced by the fact that the 4-substituent can be replaced by alkyl or halogen with an increase in activity.

On the other hand, twisting of the 2- or 5-methoxy functions seems to abolish activity. Such twisting has been invoked to explain the inactivity of certain 2,3-dimethoxy-substituted compounds (55) since a 2,3-methylenedioxy group usually gives active compounds (23). One may speculate that the 2- and 5- or the 3- and 5-methoxy groups, depending on the substitution pattern, must lie coplanar with the aromatic ring. One obvious effect of this arrangement is to maximize overlap between the oxygen $n$ electrons and the ring $\pi$ system. However, this explanation seems weakened by the observation that 2,3,5- and 2,3,6-trimethoxyamphetamines are clinically active as hallucinogens (19). The picture here is not very clear, and one wonders to what extent qualitative differences in mechanism of action may be responsible.

Snyder and Richelson (56) suggested that intramolecular hydrogen bonding between the $o$-methoxy and side-chain amino groups could be important for activity. However, no evidence for such hydrogen bonding has been obtained from X-ray crystallographic studies (57, 58).

Although theoretical (59) and experimental gas-phase (60) studies indicated a noncoplanarity when two methoxy groups are adjacent, NMR solution studies found such methoxy groups to be equivalent (61). Furthermore, the high activity of the dihydrobenzofuran derivative (XV) suggests that the orientation of the 5-methoxy group is not critical if it remains coplanar with the ring. Steric effects seem to indicate that a 5-methoxy group should be directed away from the 4-alkyl group. In XV, the alkoxy function is directed toward the 4-alkyl group.

## SIDE-CHAIN MODIFICATION

**$N$-Substitution**—It has been demonstrated with several compounds that $N$-alkylation abolishes or dramatically attenuates *in vivo* activity (26, 47, 62–64) and *in vitro* receptor affinity (65). Only in the case of 3,4-methylenedioxy ring substitution has $N$-alkylation afforded active compounds, the $N$-methyl (XIX) and $N$-ethyl (XX) analogs. These analogs retain potency comparable to the primary amine (III), although qualitative aspects of the intoxication are altered (66). In III, the ($R$)-enantiomer possesses activity; upon $N$-methylation, the isomer with the ($S$)-configuration has proven to be active.

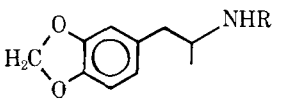


XIX: R = $CH_3$
XX: R = $CH_2CH_3$

These results have been interpreted to mean that the actions of ($R$)-III and $N$-methyl-($S$)-III are mediated by different mechanisms. This idea is reinforced by the finding that there is no cross-tolerance between III and XIX (62). This result is not too surprising since III was shown to possess both a lysergide-like and an amphetamine-like component of action (67–70). Thus, it was speculated that III exerts its effects by direct action on serotonin receptors, similar to explanations for the action of ($R$)-II. By contrast, $N$-methyl-($S$)-III was suggested to work by release of endogenous transmitter (62). Unfortunately, studies of III and its derivatives are complicated by its multiplicity of actions on various monoaminergic systems.

Although it has been concluded that $N$-methylation generally destroys activity, this conclusion may be premature since few $N$-methylated amphetamines have been examined. Cheng *et al.* (17) studied a series of substituted amphetamines and found that substitution patterns other than 2,5-dimethoxy have a significant indirect component of action. If the arguments relating to III are valid, many of these derivatives may retain or possess enhanced activity upon methylation. Furthermore, as with amphetamine, the ($S$)-isomer is expected to be the more potent releaser and thus possess activity.

Further extension of the $N$-alkyl group to higher homologs generally abolishes activity (66). $N,N$-Dialkylation does not give active compounds, even with the 3,4-methylenedioxy substitution (36).

In an analogy to the opiate antagonists, DeSantis and Nieforth (71) prepared the $N$-propyl, $N$-cyclopropylmethyl, and $N$-allyl derivatives of mescaline. In mice, the propyl and allyl derivatives produced a slight antagonism of mescaline-induced disruption of swimming behavior.

One other active substitution on nitrogen is the $N$-hydroxy group. $N$-Hydroxylation of III gives a compound possessing clinical activity (66). Coutts and Malicky (72) evaluated several congeners of II. One, the $N$-hydroxy derivative (XXI), elicited behavioral effects in rats but at about six times the dosage required for II.

**Side-Chain Alkylation**—The addition of a methyl group to the $\alpha$-side-chain position dramatically enhances the *in vivo* activity of 2,4,5-trisubstituted compounds. For example, 2,4,5-trimethoxy-$\beta$-phenethylamine is inactive (73), but addition of an $\alpha$-methyl group gives the corresponding amphetamine, which is 17 times more potent than mescaline (23). This potency increase also is observed in compounds with a hydrophobic *para*-substituent such as methyl or bromine but is less dramatic. 2,5-Dimethoxy-4-methylphenethylamine is clinically active at doses of ~15–20 mg (74); addition of an $\alpha$-methyl group to give II increases potency about fourfold.

The potency increase with $\alpha$-methylation is very small in 3,4,5-substituted compounds. Addition of an $\alpha$-methyl group to mescaline gives 3,4,5-trimethoxyamphetamine, a compound only about twice as active as mescaline (23). This slight increase is maintained in this series where the 4-substituent is a hydrophobic group. This finding probably reflects an effect on metabolism since addition of the $\alpha$-methyl group has little effect on *in vitro* receptor affinity in either series (30, 65). Thus, it is tempting to speculate

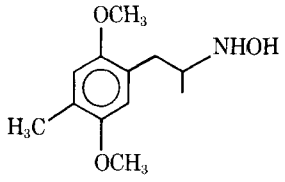

XXI

that 2,4,5-substituted compounds are more susceptible to amine oxidation than are 3,4,5-substituted analogs. However, Clark *et al.* (75) reported that 2,4,5-trimethoxyphenethylamine is deaminated less extensively than mescaline by a soluble rabbit liver amine oxidase preparation. In any case, with either substitution pattern, the simple addition of the $\alpha$-methyl group increases hydrophobicity and at least facilitates passive diffusion into the CNS.

Extension of the $\alpha$-methyl group to ethyl or higher homologs abolishes activity (76). This result was observed in 3,4,5-trimethoxy compounds and in several 2,5-dimethoxy-4-substituted analogs (77). The addition of an $\alpha$-ethyl group, while abolishing hallucinogenic action, leads to potential antidepressant compounds (77–80). At present, there is no explanation as to why this occurs.

*In vitro*, the $\alpha$-ethyl group shows mixed agonist–antagonist action at the serotonin receptor whereas the $\alpha$-methyl group is a pure agonist (81). The conformational properties, as determined by solution NMR studies, for $\alpha$-methyl and $\alpha$-ethyl compounds do not differ significantly (82). Their dynamic behavior appears comparable, and it is difficult to ascribe the difference in action to a conformational effect. Theoretical calculations using empirical potential functions likewise have failed to reveal a conformational explanation for the difference (83). Some undefined steric effect seems the most plausible answer.

Dialkyl substitution on the $\alpha$-carbon also destroys activity. This effect is evident as a loss of *in vitro* activity and a lack of behavioral effect in cats for XXII (84). Surprisingly, linking these two methyl groups in the form of a cyclopropyl ring (XXIII) restores some activity. The original report suggested that this result might be due to enhanced distribution into lipid for the cyclopropyl group but not the *gem*-dimethyl group. More recently, the difference in activity was attributed to the lack of conformational flexibility for the dimethyl compound and its inability to assume the active conformation (85). These conclusions were supported by theoretical calculations and carbon 13 spin-lattice relaxation times from solution NMR studies. The data support the idea that the active conformation is one where the side chain must be in an antiperiplanar arrangement with the aromatic ring.

On the other hand, adding a second $\alpha$-methyl group to III to give the $\alpha,\alpha$-dimethylphenethylamine led to an active compound (36). Again, the 3,4-methylenedioxy substitution presents an anomalous case. This analog can be

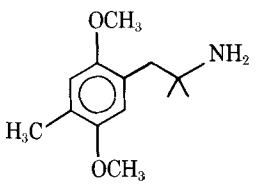

XXII

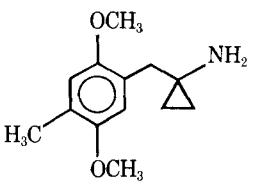

XXIII

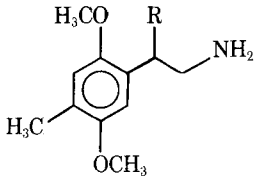

XXIV: R = H
XXV: R = $CH_3$

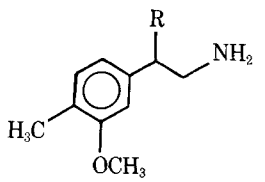

XXVI: R = H
XXVII: R = $CH_3$

viewed as a substituted phentermine derivative, and its activity also may prove to be due to the release of endogenous neurotransmitter.

The addition of a $\beta$-methyl group to the side chain dramatically attenuates *in vivo* activity in animals (47). This effect also was observed for $\beta$-hydroxy or $\beta$-keto analogs in an *in vitro* receptor affinity assay (55). In the latter instance, the beta substituent was most deleterious when an *o*-methoxy group also was present. This may be due to an unfavorable steric interaction between the beta and *ortho*-substituents. However, in the ear-scratch response in mice (48) for XXIV–XXVII, only XXV retained any activity, and it was very weak (86). This finding again emphasizes the importance of the $\alpha$-methyl and *o*-methoxy groups for optimal activity.

The $\alpha,\beta$- or $\beta,\beta$-dimethyl side-chain substitution abolishes hallucinogen-like activity in animal models (47). None of these substitutions has been tested yet in humans.

There are two reports of phenylalanine analogs of hallucinogens. The 2,5-dimethoxy-4-methyl analog (XXVIII*a*) and the mescaline congener [3-(3,4,5-trimethoxyphenyl)alanine (XXVIII*b*)] were examined for activity, although neither is expected to be a substrate for brain decarboxylases according to Ferrini and Glasser (87). Neither of these substituted phenylalanines showed biological activity (88–90).

**Stereochemistry**—It has been known for several years that in the substituted hallucinogenic amphetamines, the (*R*)-enantiomer is the most active (91–93). Although the (*S*)-enantiomers generally have not been studied at high dosage levels, the (*R*)-enantiomer subjectively and quantitatively reproduces the effect of twice its weight of racemate in humans. Both *in vitro* and animal models demonstrate stereoselectivity, with about a four- to 10-fold difference in potency between the (*R*)- and (*S*)-enantiomers (94–98). The classical approach to this observation has related the (*R*)-configuration of the amphetamines, shown in binding orientation A, to the (*R*)-configuration at C-5 of lysergide. With this view, the methyl group of the amphetamines corresponds to the C-4 methylene group of lysergide. However, the relatively small effect (30, 96) on receptor affinity in $\alpha$-methyl compounds with the (*R*)-configuration, as compared with the $\alpha$-unsubstituted phenethylamines, seems inconsistent with any interaction of the $\alpha$-methyl group with the receptor.

A newer hypothesis from these laboratories related this stereoselectivity to binding orientation B, where the

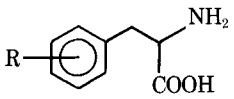

XXVIII*a*: R = 2,5-$(OCH_3)_2$-4-$CH_3$
XXVIII*b*: R = 3,4,5-$(OCH_3)_3$

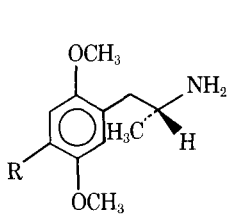

binding orientation A

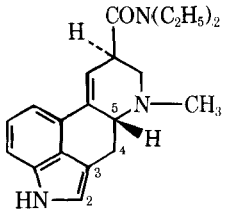

lysergide

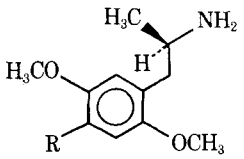

binding orientation B

$\alpha$-methyl group is allowed to project away from the binding surface (49, 50). With either hypothesis, it was assumed that the receptor binds to the alpha face of the lysergide molecule since this surface presents the most unhindered access to the N-6 unshared electrons (58, 98). The phenethylamines were assumed to bind in a conformation where the side chain is relatively coplanar with the aromatic ring in an extended, or antiperiplanar, arrangement. This arrangement would give the closest similarity to lysergide. In conformation B, the $\alpha$-methyl group is directed away from the binding surface. In this view, $\alpha$-methylation has little effect on receptor binding when the configuration is *R*. In contrast, and consistent with experimental findings (14, 96), the methyl group of the (*S*)-enantiomer has a deleterious effect on affinity.

Of the two isomers of the 2-phenylcyclopropylamine analog of II, the (1*R*,2*S*)-enantiomer (XXIX*a*) is more active (99). The (1*S*,2*R*)-isomer (XXIX*b*) showed no activity at any dose tested. If the argument is valid that the steric bulk of the C-3 methylene must project away from the receptor, then activity for the (1*R*,2*S*)-isomer is only consistent with a binding conformation for flexible analogs similar to that shown for XXIX*a*. If strict structural congruences can be invoked, this hypothesis would correlate the 5-methoxy group of the phenethylamines with the 5-hydroxy group of serotonin. This is borne out by the greater enhancement of *in vitro* receptor affinity when the 5-methoxy group of the phenethylamines is replaced by hydroxy than when the 2-methoxy group is replaced by hydroxy (43).

Problems arise in considering stereochemistry for other substituted amphetamines. As discussed in the section on *N*-substitution, methylation of III reverses the stereoselectivity of activity and it is the (*S*)-enantiomer of *N*-methyl-III that is active. However, this latter derivative may possess different mechanisms of action (62).

Both the (*R*)- and (*S*)-enantiomers of 3,4-dimethoxyamphetamine were required to elicit a mescaline-like behavioral profile in rats (100). Furthermore, coadministration of the (*R*)-enantiomer of 3,4-dimethoxyamphetamine with (*S*)-amphetamine gave a response identical to that obtained with racemic 3,4-dimethoxyamphetamine. Cheng *et al.* (17) demonstrated that this compound possessed an indirect releasing component of action in an *in vitro* smooth muscle assay. Therefore, it is possible that the *in vivo* effects of racemic 3,4-dimethoxyamphetamine also may be partially ascribed to the releasing effects of the (*S*)-enantiomer.

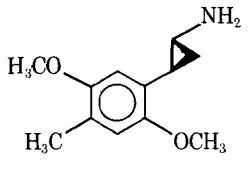

XXIX*a*
(1*R*,2*S*)

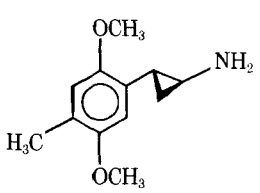

XXIX*b*
(1*S*,2*R*)

Although many additional studies are needed to elucidate such mechanisms definitively, the following conclusions would be generally consistent with previous work (17, 94, 96). For compounds possessing 2,5-dimethoxy substituents, the (*R*)-enantiomer has stereoselective *in vivo* activity. This action is correlated with *in vitro* direct agonist effects at serotonin receptors. For any other substitution patterns, a possible indirect component of action, such as a releaser of serotonin or catecholamines, must be considered. In this latter case, the (*S*)-enantiomer may contribute a significant component to *in vivo* activity. One may speculate that *N*-methylation allows retention of activity with these substitutions (62). For the 3,4,5-trisubstitution pattern of mescaline itself, *in vivo* activity appears to correlate with a direct effect at the serotonin receptor (30, 55).

**Rigid Analogs**—Several rigid analogs of phenethylamine hallucinogens have been evaluated to elucidate the binding conformation of the side chain. To date, none has been particularly revealing, although some interesting findings have emerged. The simplest rigid analogs are the substituted 2-phenylcyclopropylamines. The 3,4,5-trimethoxy compounds (XXX and XXXI) first were prepared as mescaline analogs (101). Inactivity for the *cis*-isomer (XXXI) seems to establish conclusively the side-chain binding conformation as *trans* in the flexible phenethylamines. As discussed previously, the 2,5-dimethoxy-4-methyl-substituted analog (XXXIX) has been resolved into its enantiomers. Activity only for the (1*R*,2*S*)-enantiomer has provided evidence of the binding conformation for the (*R*)-enantiomer of the amphetamines.

Recently, Law and Borne (102) reported the synthesis and preliminary pharmacology for the substituted *exo*- and *endo*-2-azabicyclo[2.2.2]octanes (XXXII and XXXIII, respectively). Examination of spontaneous activity in mice indicated that the *endo*-isomer (XXXIII) was about two times more active than the *exo*-isomer. This finding provides further evidence for an antiperiplanar side-chain conformation as important for activity.

Additional studies of the side-chain conformation and stereochemistry have been carried out utilizing rigid analogs. In particular, 2-amino-1,2,3,4-tetrahydronaphthalenes (2-aminotetralins) have received attention. Kang and Green (103) pointed out the possibility that these compounds could be compared to lysergide. The unsub-

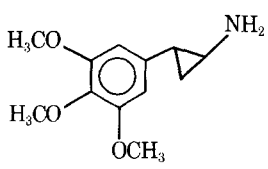

XXX

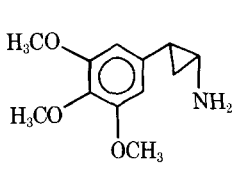

XXXI

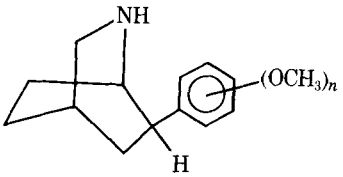

XXXII

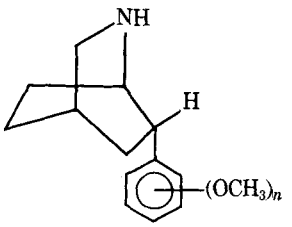

XXXIII

$n$ = 2 (3,4-substituted)
$n$ = 3 (3,4,5-substituted)

stituted parent (XXXIV), as the racemate, shows some similarity to the hallucinogens in rat models (104). The (*S*)-(−)-enantiomer seems to possess biological activity (105). This stereochemistry is inverted from that observed for lysergide. This observation was used in arguments presented earlier against orientation A as the active binding orientation for the phenethylamines (49).

Green *et al.* (106) also examined a series of methoxy- and hydroxy-substituted 2-aminotetralins. They reported that XXXV possessed electroencephalographic effects in rats that were similar to those evoked by mescaline.

In a series more closely approximating active hallucinogens, the dimethoxymethyl-substituted compounds (XXXVI–XXXVIII) were examined. Although *in vivo* activity was indicated for the aminoindan (XXXVIII) at high doses (107), other studies proved that XXXVIII was much less active than the tetralin (XXXVII) both *in vivo* (108) and *in vitro* (109). Neither compound produced a mescaline-like response in the conditioned avoidance response in rats. The dimethoxy compound (XXXVI) possessed a sedative effect in mice (104). Although none of the tetralins had clearcut hallucinogen-like action in any animal models, XXXVII produces hyperthermia in rabbits and evokes a rage response in cats (49).

Violland *et al.* (110) also examined several methoxy-substituted 2-aminotetralins as analogs of hallucinogens. In mice and dogs, these compounds possessed pharmacological activity characterized by ataxia, sedation and, in some cases, analgesia. *N*-Alkylated derivatives of 2-amino-2,3-dihydrophenalene also were prepared. Although possessing pharmacology similar to the aminotetralins, they were much more potent. Again, no clinical studies have been carried out with any of the aminotetralins or phenalenes, and there is no evidence to suggest that they possess hallucinogenic action in humans.

Numerous other investigators have explored the 2-aminotetralins as congeners of lysergic acid, with particular reference to identification of the oxytocic pharmacophore of the ergot alkaloids. Such studies are not reviewed here.

Additional rigid analogs have been prepared where the phenethylamine side chain is incorporated into a heterocyclic ring (XXXIX–XLII). Compound XXXIX could be viewed as possessing the structural features of both mescaline and methylphenidate (111), although it possessed no mescaline-like action in animal models. The morpholino

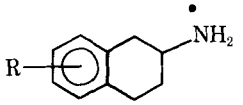

XXXIV: R = H
XXXV: R = 7-OH

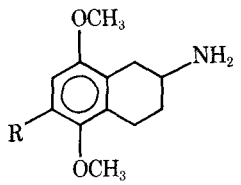

XXXVI: R = H
XXXVII: R = $CH_3$

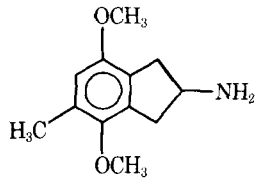

XXXVIII

analog (XL) was reported to possess more mescaline-like tendency in animals than XLI or XLII (112). It is unknown whether any of these compounds possess hallucinogenic action in humans. However, none had appreciable potency in animal models.

## EFFECTS OF DISTRIBUTION AND METABOLISM

The ability of the compounds to penetrate the CNS is a requisite for activity. As pointed out by Vogel and Evans (113), when one considers the actual levels of drug detected in the brain rather than the systemically administered dose, dramatic differences in structure–activity relationships may appear. That is, some compounds that appear to possess little activity upon peripheral adminstration are highly potent if actually administered into the CNS. For compounds with a more favorable distribution, only small doses may be needed to achieve the same brain levels. These distribution differences are independent of actual efficacy at the receptor(s). Vogel and Evans (113) argued further that structure–activity relationships should be based on minimal effective brain levels rather than on dosage measures that reflect a quantity necessary for peripheral administration. Although this approach has merit, most investigators probably will not carry out the additional studies required to establish minimal effective brain level values.

The importance of passive partitioning was noted in a study where 1-octanol–water partition coefficients were measured and correlated with human clinical activity (29). As expected, the regression obtained was parabolic, with an optimum log $P$ value of 3.14. Although $R^2$ for the regression was only 0.62, there was large variability in the human data. Furthermore, the study included numerous compounds that undoubtedly possess several components of action, as is the case for III. Coincidentally, the optimum log $P$ value from this study was nearly identical, within statistical limits, to the optimum determined in an *in vitro*

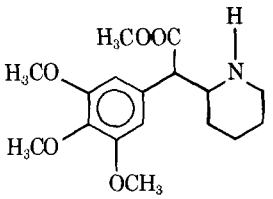

XXXIX

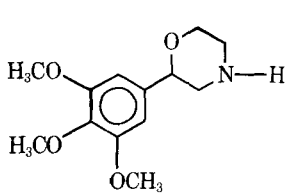

XL

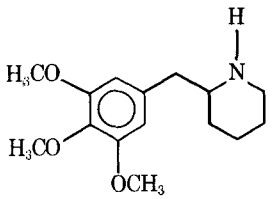

XLI

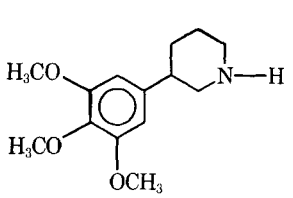

XLII

assay (30). In the latter study, this value reflected, in part, a specific hydrophobic interaction with the receptor.

The CNS distribution of [$^3$H]mescaline and the isomeric 2,3,4-trimethoxyphenethylamine was studied using autoradiography (114). The latter compound is inactive and gave weak and homogeneous labeling in the brain. By contrast, mescaline was selectively accumulated in the hippocampus and amygdala. The findings of this study are in agreement with similar results obtained for the distribution of $^3$H-labeled II (115). However, the 2,3,4-trimethoxy isomer also is metabolized more rapidly than mescaline (116). Mitoma (117) compared 2,4,5-trimethoxyamphetamine with the isomeric 2,3,4-substitution. The latter is inactive clinically while 2,4,5-trimethoxyamphetamine is 17–20 times more active than mescaline. Surprisingly, the brain levels of the inactive 2,3,4-isomer were higher than those attained with the active 2,4,5-substitution pattern in rats.

No studies of differential brain distribution for enantiomers of active amphetamines have been published. However, the (*S*)-(+)-enantiomer of II is metabolized more rapidly than the (*R*)-(−)-isomer when the drug is administered as the racemate (118, 119).

Some distinction should be made between metabolic processes that essentially "detoxify" the hallucinogenic phenethylamines and those that may be involved in the mechanism of action, *i.e.*, may be responsible for generating active species. For a discussion of the former processes, the review by Castagnoli (120) is excellent. The latter type of metabolism is of major interest here. Also of interest are processes that metabolize compounds possessing high *in vitro* potency but that lack whole animal or clinical activity.

It was once believed that phenethylamines, particularly mescaline, might be active due to the formation of a metabolite (121). A recent study (122) indicated that this is not the case, at least for mescaline. Zweig and Castagnoli (27, 123) also suggested that di-*O*-demethylation of II may generate an active metabolite that contributes to activity. The inability to generate significant amounts of these metabolites, coupled with the high observed *in vitro* activity for II, argues against this possibility. Furthermore, Ho *et al.* (124, 125) showed that II is oxidized primarily at the methyl group in the *para* position, leading to the *p*-hydroxymethyl and *p*-carboxy species. Weinkam *et al.* (126) confirmed that the *p*-hydroxymethyl derivative is the major metabolite in rabbit liver microsome preparations. Thus, if *O*-demethylation does occur, it is very minor. Unfortunately, no definitive experiments have been carried out that would settle the issue. It is this reviewer's opinion, however, that this process is not important in the intoxication mechanism. This seems to be the only instance where controversy presently exists regarding the role of an active metabolite in the activity of the phenethylamines.

There are examples to suggest that some compounds possessing high affinity for *in vitro* receptors may lack *in vivo* activity due to rapid metabolic inactivation. Such effects must be considered when developing receptor structure–activity relationships. Lack of *in vivo* or clinical activity may camouflage the fact that a particular compound actually possesses high intrinsic activity at a receptor site.

Charalampous *et al.* (127) showed that the half-life of mescaline in humans is ~6 hr. By contrast, the inactive 3,4-dimethoxyphenethylamine is metabolized extensively, with a half-life of <1 hr (128). This result is consistent with the other findings (75) that phenethylamines with more than three methoxy groups are not deaminated *in vivo*.

As was mentioned under *Aromatic Substituents*, functions in the *para* position that are resistant to metabolism give more potent compounds. Since deamination is a minor metabolic pathway in humans, increased resistance of the aromatic ring and its substituents to metabolism will certainly affect activity. The most obvious result will be an increased biological half-life and consequent duration of action.

In 3,4-dimethoxyamphetamine, the 4-methoxy group is about 15 times more extensively *O*-demethylated than the 3-methoxy group (129). Likewise, in 2,4,5-trimethoxyamphetamine, *O*-demethylation at the 4-position is about twice that at the 5-position and nearly three times that of the 2-methoxy group (130). With a *p*-alkyl, Ho *et al.* (125) found that the *p*-methyl group of II is oxidized progressively to the carboxy group. Tansey *et al.* (131) studied the metabolism of the *p*-ethyl homolog of II and reported that the benzylic carbon of the *p*-ethyl group was hydroxylated but much more slowly than the methyl of II. Finally, with a halogen in the *para* position, such as in the bromine homolog of II, no organic bromide was detectable in the urine following administration to humans (132). The stability of the *p*-halogen group, either as bromine or iodine, led to investigation of the utility of these compounds as brain-imaging radiopharmaceuticals (133).

## ACTION AT MOLECULAR LEVEL

Little is known of the mechanism of receptor interaction for hallucinogenic phenethylamines. However, circumstantial evidence indicates that one event that occurs may be electron donation to the receptor to form a charge transfer complex. This initially was suggested by Karreman *et al.* (134) in 1959, based on extended Hückel molecular orbital calculations for lysergide. Subsequent quantum chemical studies by several groups led to development of correlations between activity and energy of the highest occupied molecular orbital (135, 136).

Experimentally, the possible requirement for a high energy aromatic system was indicated by correlations between activity and: (*a*) the degree of native fluorescence (137), (*b*) the excitation wavelength and molar absorptivity (138), and (*c*) the strength of the charge transfer complex between substituted phenethylamines and 1,4-dinitrobenzene (139). Furthermore, Domelsmith and Houk (140) observed good correlation between human activity and experimentally measured energy of the first aromatic ionization potential in the gas phase. Ionization potentials are well correlated with the highest occupied molecular orbital.

Dipaolo *et al.* (141) carried out model interaction calculations for phenethylamines using 3-methylindole as the interacting species. Using CNDO calculations, they reported a correlation between human activity and interaction energy. However, this study only included interactions between the aromatic ring of the phenethylamines and the six-membered ring of indole.

Green *et al.* (142), using a more rigorous theoretical approach, calculated several electronic parameters for tryptamines. High frontier electron density at the 4- and 5-positions of the tryptamines appears to be well correlated with activity. Assuming that tryptamines and phenethylamines possess a similar mechanism of action implies that charge transfer complexation may be a possible receptor interaction for hallucinogens in general.

The biological activities for XII–XVII were discussed under *Steric Effects*. Decreased activity (or inactivity) of compounds with steric bulk protruding toward both faces of the molecule also is consistent with the formation of an electron donor–acceptor complex as a component of the molecular mechanism of action. Charton (143) pointed out the importance of such effects in model systems where bulky groups were attached to the donor molecule.

However, Glennon *et al.* (44) recently suggested that, depending on the aromatic substitution pattern, phenethylamines may orient differently upon binding to the receptor. That is, depending on the particular substituents possessed by the phenethylamine, it may bind in either binding orientation A or binding orientation B. If so, interpretation of structure–activity relationships at the molecular level may be very difficult.

Although all of the hallucinogens possess a basic nitrogen atom, there is little apparent dependence on basicity. Whereas lysergide or substituted phenylcyclopropylamines have pKa values of ~8–8.3, the phenethylamines or substituted amphetamines have higher pKa values, at ~9.4–9.8. Weinstein *et al.* (144) suggested that the amine undergoes deprotonation upon binding and that quantum chemical calculations of the bound species are carried out more properly when the amino is considered to be nonprotonated. Although this concept has not been verified experimentally, lower pKa values would facilitate deprotonation. Of course, one should also be aware that less basic amines also are less highly ionized at physiological pH. This fact normally will lead to brain levels that are higher than for a more basic amine.

At present, little else in the way of a molecular mechanism of action can be safely concluded. This situation is certainly not unique to the hallucinogens. Nevertheless, the multiplicity of pharmacological actions and the subjective nature of the effects they produce make studies difficult at the molecular level. Experiments aimed at defining these receptor interactions must be carefully designed and cautiously interpreted.

## CONCLUSIONS

The preceding sections dealt with various aspects of the nature and conformation of aromatic ring substituents and the side chain in the hallucinogenic phenethylamines. Although these empirical structure–activity relationships can be described, there is at present no clear rationale for many of them. Certainly the mechanisms at the receptor level are unknown. The multiplicity of actions these compounds have on monoaminergic systems have made their study very difficult. Furthermore, structure–activity relationships that define these multiple actions have not been approached.

Some may question whether it is realistic to expect any structural congruence between phenethylamines and tryptamines to emerge. However, this hypothesis has been the guiding principle of much of the recent work with phenethylamines. If a clear structural–functional relationship between the phenethylamines and the tryptamines could be identified, one would have the molecular pharmacology equivalent of a series of simultaneous equations. Reactive and functional sites in the two series could be studied in parallel. Quantum chemical comparisons would be most interesting. It may be justified to speculate that such findings would lead to important insights into fundamental receptor activation mechanisms.

The reality is that we are still some distance from such a unified theory. Nevertheless, significant progress has been made in the past 10 years in defining the importance to activity of various structural and physicochemical parameters within the phenethylamines. It is perhaps unfortunate that research interest in this fascinating class of compounds is limited to so few laboratories.

## REFERENCES


(1) S. H. Snyder, L. Faillace, and L. Hollister, *Science*, **158**, 669 (1967).

(2) P. N. Thiessen and D. A. Cook, *Clin. Toxicol.*, **6**, 45 (1973).

(3) G. Cimbura, *Can. Med. Assoc. J.*, **110**, 1263 (1974).

(4) F. E. Cheek, S. Newell, and M. Joffe, *Science*, **167**, 1276 (1970).

(5) A. Hofmann, in "Drugs Affecting the Central Nervous System," A. Burger, Ed., Dekker, New York, N.Y., 1968, pp. 169–235.

(6) P. Brawley and J. C. Duffield, *Pharmacol. Rev.*, **24**, 31 (1972).

(7) H. B. Wolbach, H. Isbell, and E. J. Miner, *Psychopharmacologia*, **3**, 1 (1962).

(8) J. C. Winter, *J. Pharmacol. Exp. Ther.*, **178**, 625 (1971).

(9) D. C. Dyer and D. W. Gant, *ibid.*, **184**, 366 (1973).

(10) B. Kovacic and E. F. Domino, *ibid.*, **197**, 495 (1976).

(11) K. A. Nieforth, *J. Pharm. Sci.*, **60**, 655 (1971).

(12) N. E. Anden, H. Corrodi, K. Fuxe, and T. L. Meek, *Eur. J. Pharmacol.*, **25**, 176 (1974).

(13) G. K. Aghajanian and H. J. Haigler, *Psychopharmacol. Commun.*, **1**, 619 (1975).

(14) D. C. Dyer, D. E. Nichols, D. B. Rusterholz, and C. F. Barfknecht, *Life Sci.*, **13**, 885 (1973).

(15) D. C. Dyer, *Res. Commun. Chem. Path. Pharmacol.*, **14**, 449 (1976).

(16) L. F. Tseng, *Naunyn-Schmiedebergs, Arch. Pharmacol.*, **304**, 101 (1978).

(17) H. C. Cheng, J. P. Long, D. E. Nichols, and C. F. Barfknecht, *J. Pharmacol. Exp. Ther.*, **188**, 114 (1974).

(18) G. M. Marquardt, V. DiStefano, and L. Ling, in "Psychopharmacology of Hallucinogens," R. C. Stillman and R. E. Willette, Eds., Pergamon, New York, N.Y., 1978, p. 84.

(19) A. T. Shulgin, in "Psychopharmacological Agents," vol. IV, M. Gordon, Ed., Academic, New York, N.Y., 1976, p. 59.

(20) A. T. Shulgin, in "Handbook of Psychopharmacology," vol. 11, L. L. Iversen, S. D. Iversen, and S. H. Snyder, Eds., Plenum, New York, N.Y., 1978, p. 243.

(21) A. T. Shulgin, in "Burger's Medicinal Chemistry 4th Edition," part III, M. E. Wolff, Ed., Wiley–Interscience, New York, N.Y., 1980, p. 1109.

(22) B. L. Jacobs and M. E. Trulson, *Am. Sci.*, **67**, 396 (1979).

(23) A. T. Shulgin, T. Sargent, and C. Naranjo, *Nature*, **221**, 537 (1969).

(24) U. Braun, G. Braun, P. Jacob, III, D. E. Nichols, and A. T. Shulgin, *NIDA Res. Monogr.*, **22**, 27 (1978).

(25) D. E. Nichols and D. C. Dyer, *J. Med. Chem.*, **20**, 299 (1977).

(26) A. T. Shulgin and D. E. Nichols, in "Psychopharmacology of Hallucinogens," R. C. Stillman and R. E. Willette, Eds., Pergamon, New York, N.Y., 1978, p. 74.

(27) J. S. Zweig and N. Castagnoli, Jr., *Psychopharmacol. Commun.*, **1**, 359 (1975).

(28) L. L. Butcher, *J. Neural Trans.*, **37**, 189 (1975).

(29) C. F. Barfknecht, D. E. Nichols, and W. J. Dunn, III, *J. Med. Chem.*, **18,** 208 (1975).
(30) D. E. Nichols, A. T. Shulgin, and D. C. Dyer, *Life Sci.*, **21,** 569 (1977).
(31) L. B. Kier and R. A. Glennon, *ibid.*, **22,** 1589 (1978).
(32) J. P. Green, C. L. Johnson, H. Weinstein, S. Kang, and D. Chow, in "Psychopharmacology of Hallucinogens," R. C. Stillman and R. E. Willette, Eds., Pergamon, New York, N.Y., 1978, p. 28.
(33) G. Anderson, III, P. Kollman, P. Jacob, III, A. T. Shulgin, and N. Castagnoli, Jr., 173rd National Meeting of the American Chemical Society, New Orleans, La., 1977, MEDI 0082.
(34) G. M. Anderson, III, N. Castagnoli, Jr., and P. A. Kollman, *NIDA Res. Monogr.*, **22,** 199 (1978).
(35) P. Jacob, III, G. Anderson, III, C. K. Meshul, A. T. Shulgin, and N. Castagnoli, Jr., *J. Med. Chem.*, **20,** 1235 (1977).
(36) A. T. Shulgin, Lafayette, Calif., 1980, personal communication.
(37) B. T. Ho, W. M. McIsaac, R. An, L. W. Tansey, K. E. Walker, L. F. Englert, Jr., and M. B. Noel, *J. Med. Chem.*, **13,** 26 (1970).
(38) C. F. Barfknecht and D. E. Nichols, *ibid.*, **14,** 370 (1971).
(39) D. E. Nichols and A. T. Shulgin, *J. Pharm. Sci.*, **65,** 1554 (1976).
(40) P. Jacob, III, and A. T. Shulgin, 2nd Chemical Congress of the North American Continent, American Chemical Society, San Francisco, Calif., 1980, MEDI 110.
(41) S. Sepúlveda, R. Valenzuela, and B. K. Cassels, *J. Med. Chem.*, **15,** 413 (1972).
(42) A. T. Shulgin, *ibid.*, **11,** 186 (1968).
(43) L. B. Kier and R. A. Glennon, *NIDA Res. Monogr. Ser.*, **22,** 159 (1978).
(44) R. A. Glennon, S. M. Liebowitz, D. Leming-Doot, and J. A. Rosecrans, *J. Med. Chem.*, **23,** 990 (1980).
(45) A. T. Shulgin and D. C. Dyer, *ibid.*, **18,** 1201 (1975).
(46) R. D. Morin, F. Benington, S. R. Mitchell, J. M. Beaton, R. J. Bradley, and J. R. Smythies, *Experientia*, **31,** 93 (1975).
(47) F. A. B. Aldous, B. C. Barrass, K. Brewster, D. A. Buxton, D. M. Green, R. M. Pinder, P. Rich, M. Skeels, and K. J. Tutt, *J. Med. Chem.*, **17,** 1100 (1974).
(48) A. S. Kulkarni, *Biol. Psychiatry*, **6,** 177 (1973). [In this reference, activity was reported for the *p*-isopropyl homolog. In fact, it was the *p*-*n*-propyl. (See Ref. 45.)]
(49) D. E. Nichols, H. J. R. Weintraub, W. R. Pfister, and G. K. W. Yim, *NIDA Res. Monogr. Ser.*, **22,** 70 (1978).
(50) D. E. Nichols, W. R. Pfister, and G. K. W. Yim, *Life Sci.*, **22,** 2165 (1978).
(51) M. Trampota, Prague, Czechoslovakia, 1980, personal communication.
(52) D. E. Nichols and L. J. Kostuba, *J. Med. Chem.*, **22,** 1264 (1979).
(53) A. T. Shulgin, *Experientia*, **20,** 366 (1964).
(54) S. R. Ernst and F. W. Cagle, Jr., *Acta Crystallogr.*, **B29,** 1543 (1973).
(55) R. A. Glennon, S. M. Liebowitz, and G. M. Anderson, III, *J. Med. Chem.*, **23,** 294 (1980).
(56) S. H. Snyder and E. Richelson, *Proc. Natl. Acad. Sci., USA*, **60,** 206 (1968).
(57) A. S. Horn, M. L. Post, O. Kennard, and L. Riva di Sanseverino, *J. Pharm. Pharmacol.*, **27,** 13 (1975).
(58) R. W. Baker, C. Chothia, and P. Pauling, *Mol. Pharmacol.*, **9,** 23 (1973).
(59) G. M. Anderson, III, P. A. Kollman, L. N. Domelsmith, and K. N. Houk, *J. Am. Chem. Soc.*, **101,** 2344 (1979).
(60) L. N. Domelsmith, L. L. Munchausen, and K. N. Houk, *ibid.*, **99,** 4311 (1977).
(61) A. Makriyannis and J. J. Knittel, *Tetrahedron Lett.*, **1979,** 2753.
(62) G. M. Anderson, III, G. Braun, U. Braun, D. E. Nichols, and A. T. Shulgin, *NIDA Res. Monogr. Ser.*, **22,** 8 (1978).
(63) R. G. Browne, R. T. Harris, and B. T. Ho, *Psychopharmacologia*, **39,** 43 (1974).
(64) B. T. Ho, L. W. Tansey, R. L. Balster, R. An, W. M. McIsaac, and R. T. Harris, *J. Med. Chem.*, **13,** 134 (1970).
(65) R. A. Glennon, S. M. Liebowitz, and E. C. Mack, *ibid.*, **21,** 822 (1978).
(66) U. Braun, A. T. Shulgin, and G. Braun, *J. Pharm. Sci.*, **69,** 192 (1980).
(67) W. R. Martin, *NIDA Res. Monogr. Ser.*, **22,** 60 (1978).
(68) W. R. Martin, D. B. Vaupel, M. Nozaki, and L. D. Bright, *Drug Alcohol Depend.*, **3,** 113 (1978).
(69) M. Nozaki, D. B. Vaupel, and W. R. Martin, *Eur. J. Pharmacol.*, **46,** 339 (1977).
(70) D. B. Vaupel, M. Nozaki, W. R. Martin, L. D. Bright, and E. C. Morton, *Life Sci.*, **24,** 2427 (1979).
(71) F. DeSantis, Jr., and K. A. Nieforth, *J. Pharm. Sci.*, **65,** 1479 (1976).
(72) R. T. Coutts and J. L. Malicky, *Can. J. Chem.*, **51,** 1402 (1973).
(73) A. Dittrich, *Psychopharmacologia*, **21,** 229 (1971).
(74) A. T. Shulgin and M. F. Carter, *Psychopharmacol. Commun.*, **1,** 93 (1975).
(75) L. C. Clark, F. Benington, and R. D. Morin, *J. Med. Chem.*, **8,** 353 (1965).
(76) A. T. Shulgin, *Experientia*, **19,** 127 (1963).
(77) R. T. Standridge, H. G. Howell, J. A. Gylys, R. A. Partyka, and A. T. Shulgin, *J. Med. Chem.*, **19,** 1400 (1976).
(78) H. A. Tilson, J. H. Chamberlain, and J. A. Gylys, *Psychopharmacology*, **51,** 169 (1977).
(79) H. A. Tilson, J. H. Chamberlain, and J. A. Gylys, *Pharmacol. Biochem. Behav.*, **6,** 627 (1977).
(80) R. J. Coppola, *J. Am. Osteopathic Assoc.*, **73,** 406/133 (1974).
(81) D. C. Dyer, *Res. Commun. Chem. Pathol. Pharmacol.*, **14,** 449 (1976).
(82) A. Makriyannis and J. Knittel, *NIDA Res. Monogr. Ser.*, **22,** 464 (1978).
(83) H. J. R. Weintraub and D. E. Nichols, *Int. J. Quant. Chem.*, **QBS 5,** 321 (1978).
(84) C. F. Barfknecht, J. F. Caputo, M. B. Tobin, D. C. Dyer, R. T. Standridge, H. G. Howell, W. R. Goodwin, R. A. Partyka, J. A. Gylys, and R. L. Cavanagh, *NIDA Res. Monogr. Ser.*, **22,** 16 (1978).
(85) H. J. R. Weintraub, D. E. Nichols, A. Makriyannis, and S. W. Fesik, *J. Med. Chem.*, **23,** 339 (1980).
(86) D. E. Nichols, Purdue University, West Lafayette, Ind., unpublished results.
(87) R. Ferrini and A. Glasser, *Biochem. Pharmacol.*, **13,** 798 (1964).
(88) T. R. Coutts and J. L. Malicky, *Can. J. Chem.*, **52,** 390 (1974).
(89) R. M. Acheson, D. P. Dearnley, A. O. Plunkett, and V. C. Porter, *J. Chem. Soc.*, **1963,** 2085.
(90) J. R. Smythies and E. A. Sykes, in "Amines Schizophrenia," Pap. Symposium, Atlantic City, N.J. 1965, pp. 5–18; through *Chem. Abstr.*, **68,** 37785q (1968).
(91) A. T. Shulgin, *J. Pharm. Pharmacol.*, **25,** 271 (1973).
(92) S. H. Snyder, S. Unger, R. Blatchley, and C. F. Barfknecht, *Arch. Gen. Psychiatry*, **31,** 103 (1974).
(93) J. M. Beaton, F. Benington, R. J. Bradley, K. U. Kuhlemeier, and R. D. Morin, *Br. J. Pharmacol.*, **57,** 547 (1976).
(94) D. C. Dyer, D. E. Nichols, D. B. Rusterholz, and C. F. Barfknecht, *Life Sci.*, **13,** 885 (1973).
(95) G. M. Marquardt, V. DiStefano, and L. L. Ling, *Toxicol. Appl. Pharmacol.*, **45,** 675 (1978).
(96) R. A. Glennon, *Life Sci.*, **24,** 1487 (1979).
(97) R. A. Harris, D. Snell, and H. H. Loh, *Pharmacol. Biochem. Behav.*, **7,** 307 (1977).
(98) K. Bailey and A. A. Grey, *Can. J. Chem.*, **50,** 3876 (1972).
(99) D. E. Nichols, R. Woodard, B. A. Hathaway, M. T. Lowy, and G. K. W. Yim, *J. Med. Chem.*, **22,** 458 (1979).
(100) C. F. Barfknecht and D. E. Nichols, *ibid.*, **15,** 109 (1972).
(101) P. D. Cooper and G. C. Walters, *Nature*, **238,** 96 (1972).
(102) S.-J. Law and R. F. Borne, *Eur. J. Med. Chem.*, **15,** 229 (1980).
(103) S. Kang and J. P. Green, *Proc. Natl. Acad. Sci., USA*, **67,** 62 (1970).
(104) C. F. Barfknecht, D. E. Nichols, D. B. Rusterholz, J. P. Long, J. A. Engelbrecht, J. M. Beaton, R. J. Bradley, and D. C. Dyer, *J. Med. Chem.*, **16,** 804 (1973).
(105) D. E. Nichols, W. R. Pfister, G. K. W. Yim, and R. J. Cosgrove, *Brain Res. Bull.*, **2,** 169 (1977).
(106) J. P. Green, K. Dressler, and N. Khazan, *Life Sci., Part I*, **12,** 475 (1973).
(107) R. T. Coutts and J. L. Malicky, *Can. J. Chem.*, **52,** 381 (1974).
(108) D. E. Nichols, C. F. Barfknecht, J. P. Long, R. T. Standridge, H. G. Howell, R. A. Partyka, and D. C. Dyer, *J. Med. Chem.*, **17,** 161 (1974).
(109) H. C. Cheng, J. P. Long, D. E. Nichols, C. F. Barfknecht, and D.

B. Rusterholz, *Arch. Int. Pharmacodyn. Ther.*, **208,** 264 (1974).

(110) R. Violland, N. Violland-Duperret, H. Pacheco, G. Trouiller, and A. LeBlanc, *Bull. Chim. Ther.*, **1971,** 196.

(111) R. J. Wolters, A. J. Bei, and N. S. Tanner, *J. Pharm. Sci.*, **64,** 2013 (1975).

(112) *Ibid.*, **63,** 1379 (1974).

(113) W. H. Vogel and B. D. Evans, *Life Sci.*, **20,** 1629 (1977).

(114) H. Korr and N. Seiler, *Psychopharmacology*, **46,** 53 (1976).

(115) J. E. Idänpään-Heikkilä and W. M. McIsaac, *Biochem. Pharmacol.*, **19,** 935 (1970).

(116) N. Seiler and L. Demisch, *ibid.*, **23,** 273 (1974).

(117) C. Mitoma, *Proc. Soc. Exp. Biol. Med.*, **134,** 1162 (1970).

(118) N. P. McGraw, P. S. Callery, and N. Castagnoli, Jr., *J. Med. Chem.*, **20,** 185 (1977).

(119) S. B. Matin, P. S. Callery, J. S. Zweig, A. O'Brien, R. Rapoport, and N. Castagnoli, Jr., *ibid.*, **17,** 877 (1974).

(120) N. Castagnoli, Jr., in "Handbook of Psychopharmacology," vol. 11, L. L. Iversen, S. D. Iversen, and S. H. Snyder, Eds., Plenum, New York, N.Y., 1978.

(121) A. H. Friedhoff and M. Goldstein, *Ann. N.Y. Acad. Sci.*, **96,** 5 (1962).

(122) R. G. Browne and B. T. Ho, *Pharmacol. Biochem. Behav.*, **3,** 109 (1975).

(123) J. S. Zweig and N. Castagnoli, Jr., *J. Med. Chem.*, **20,** 414 (1977).

(124) B. T. Ho, V. Estevez, L. W. Tansey, L. F. Englert, P. J. Creaven, and W. M. McIsaac, *Brain Res.*, **29,** 166 (1971).

(125) B. T. Ho, V. Estevez, L. W. Tansey, L. F. Englert, P. J. Creaven, and W. M. McIsaac, *J. Med. Chem.*, **14,** 158 (1972).

(126) R. J. Weinkam, J. Gal, P. Callery, and N. Castagnoli, Jr., *Anal. Chem.*, **48,** 203 (1976).

(127) K. D. Charalampous, A. Orengo, K. E. Walker, and V. J. Kinross-Wright, *J. Pharmacol. Exp. Ther.*, **145,** 242 (1964).

(128) A. J. Friedhoff and J. W. Schweitzer, *Am. J. Psychiatry*, **124,** 1249 (1968).

(129) T. W. Sargent, D. M. Israelstam, A. T. Shulgin, S. A. Landaw, and N. N. Finley, *Biochem. Biophys. Res. Commun.*, **29,** 126 (1967).

(130) T. Sargent, A. T. Shulgin, and N. Kusubov, *Psychopharmacol. Commun.*, **2,** 199 (1976).

(131) L. W. Tansey, V. S. Esteves, and B. T. Ho, *Proc. West. Pharmacol. Soc.*, **18,** 132 (1975).

(132) T. Sargent, D. A. Kalbhen, A. T. Shulgin, G. Brown, H. Stauffer, and N. Kusubov, *Neuropharmacology*, **14,** 165 (1975).

(133) T. Sargent, III, G. Braun, U. Braun, T. F. Budinger, and A. T. Shulgin, *Commun. Psychopharmacol.*, **2,** 1 (1978), and references cited therein.

(134) G. Karreman, I. Isenberg, and A. Szent-Gyorgi, *Science*, **130,** 1191 (1959).

(135) S. Kang and J. P. Green, *Nature*, **226,** 645 (1970).

(136) S. H. Snyder and C. R. Merril, *Proc. Natl. Acad. Sci., USA*, **54,** 258 (1965).

(137) F. Antun, J. R. Smythies, F. Benington, R. D. Morin, C. F. Barfknecht, and D. E. Nichols, *Experientia*, **27,** 62 (1971).

(138) K. Bailey and D. Verner, *J. Pharm. Sci.*, **61,** 480 (1972).

(139) M.-T. Sung and J. A. Parker, *Proc. Natl. Acad. Sci., USA*, **69,** 1346 (1972).

(140) L. N. Domelsmith and K. N. Houk, *NIDA Res. Monogr. Ser.*, **22,** 423 (1978).

(141) T. Dipaolo, L. H. Hall, and L. B. Kier, *J. Theoret. Biol.*, **71,** 295 (1978).

(142) J. P. Green, C. L. Johnson, H. Weinstein, S. Kang, and D. Chou, in "Psychopharmacology of Hallucinogens," R. C. Stillman and R. E. Willette, Eds., Pergamon, New York, N.Y., 1978, p. 28.

(143) M. Charton, *J. Org. Chem.*, **21,** 2991 (1966).

(144) H. Weinstein, D. Chou, C. L. Johnson, S. Kang, and J. P. Green, *Mol. Pharmacol.*, **12,** 738 (1976).

## ACKNOWLEDGMENTS

The author is most appreciative of research support provided over the last few years in the form of U.S. Public Health Service Grants DA-01916 and DA-02189 from the National Institute on Drug Abuse.

A warm thanks is extended to Dr. Alexander T. Shulgin for reading early drafts of the manuscript and providing many helpful comments, as well as for providing several relevant but previously unpublished values for biological activity.

# N-Hydroxymethyl Derivatives of Nitrogen Heterocycles as Possible Prodrugs I: N-Hydroxymethylation of Uracils

PADAM C. BANSAL *, IAN H. PITMAN ‡x, JOSIAH N. S. TAM *, MATHIAS MERTES *, and JAMES J. KAMINSKI *

Received October 21, 1980, from the *School of Pharmacy, University of Kansas, Lawrence, KS 66045, and the ‡Victorian College of Pharmacy Ltd., 381 Royal Parade, Parkville, Victoria, Australia. Accepted for publication January 7, 1981.

**Abstract** □ Solid samples of 1,3-dihydroxymethyluracil, 3-hydroxymethyl-1-methyluracil, and 1-hydroxymethyl-3-methyluracil were prepared, and their structures were confirmed by spectroscopic analysis. The thermodynamics and kinetics of the formation of N-hydroxymethylated uracils in aqueous formaldehyde solutions also were studied. The equilibrium constants for formation of N-1-hydroxymethyl derivatives were approximately twice those for formation of N-3-hydroxymethyl derivatives, and they were formed more rapidly throughout the pH 3–8 range. Substituents at C-5 of uracil had little effect on the thermodynamics of N-hydroxymethylation. The potential usefulness of N-hydroxymethyl compounds as prodrugs is discussed.

**Keyphrases** □ Uracil—N-hydroxymethyl derivatives synthesized, structures confirmed by NMR and elemental analyses, potential prodrugs □ N-Hydroxymethyl derivatives—of uracil, synthesis, structures confirmed by NMR and elemental analyses, potential prodrugs □ Prodrugs, potential—N-hydroxymethyl derivatives of uracil synthesized, structures confirmed by NMR and elemental analyses

The reversible reactions of formaldehyde with amines (1–7), amides (8, 9), and imides (10–15) in aqueous solution to form the corresponding N-hydroxymethyl derivatives have been studied extensively, and numerous rate and equilibrium constants have been reported. An N-hydroxymethylation reaction is represented in Scheme I. Reactions of this type are important in biological systems (16–19) and, because they can alter hydrogen-bonding possibilities in a molecule, they have been employed (20–22) to modify the secondary structure of nucleic acids in solutions. This paper is concerned with the kinetics and thermodynamics of N-hydroxymethylation of uracil (I) and several substituted uracils.

## BACKGROUND

Uracil is not a drug, but its structure is representative of many molecules that are drugs. It is a heterocyclic molecule that contains both an amide and an imide group. Molecules that contain these groups frequently are very insoluble in water and organic solvents because of large crystal lattice energies due to intermolecular hydrogen bonds. There are two acidic protons in uracil, each of which can form a hydrogen bond with a carbonyl group in another molecule. Evidence that such bonds contribute to the stability of uracil crystals comes from comparison of the melting point and the solubility of uracil with those of N-alkyl uracils (Table I). The melting point of uracil is decreased and the solubility is increased when the N-1 and/or N-3 protons are replaced by a methyl group. IR and X-ray structure studies of uracil support the conclusion that, in the uracil crystals, molecules are linked by intermolecular hydrogen bonds (23–25).

The replacement of the N–H proton by a methyl group is not normally an allowable substitution in drug molecules, because it is a permanent change and can significantly change the pharmacological properties of the drugs. A better approach toward reducing the extent of intermolecular hydrogen bonds in a molecule like uracil would be the synthesis of transient chemical derivatives, *i.e.*, prodrugs. In prodrug molecules, the N–H protons could be replaced by groups such as the hydroxymethyl, which would be removed rapidly in water.

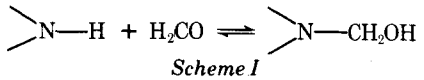

*Scheme I*

When the prodrug reverts to the parent drug, formaldehyde is released. Formaldehyde toxicity does not appear to be of great concern since pivampicillin and methenamine, which are marketed as safe drugs, also release formaldehyde in the body upon administration (26–29). However, formaldehyde toxicity may depend on the frequency of dose and the duration that the drug has to be taken.

This approach should be applicable to other heterocyclic drug molecules that are poorly soluble in water and other solvents by virtue of intermolecular hydrogen bonds in their crystalline phase. The application of some of these concepts to drug molecules recently was reported (30, 31).

## RESULTS AND DISCUSSION

**Structure of Hydroxymethyl Derivatives of Uracil (I), 3-Methyluracil (III), and 1-Methyluracil (V)**—Elemental analysis of the crystalline compound that precipitated from uracil solution in aqueous formaldehyde was consistent with the composition of 1 equivalent of uracil and 2 equivalents of formaldehyde. Evidence that the compound had Structure II rather than Structure VIII came from IR analysis (potassium bromide disks) and NMR spectra. The IR spectrum exhibited a strong peak at 1720 $cm^{-1}$, indicating the molecule contained at least one carbonyl group. The two doublets at 7.70 and 5.72 ppm in the NMR spectrum of the compound in dimethyl sulfoxide-$d_6$ (Table II), which were assigned (32) to the C-6 and C-5 protons, are much closer in chemical shift to those of the same protons of 1,3-dimethyluracil (VII, a model for Structure II, 7.68 and 5.67 ppm in dimethyl sulfoxide-$d_6$) than they are to those of 2,4-dimethoxypyrimidine (IX, a model for Structure VIII, 8.31 and 6.53 ppm).

Assignment of the other signals in the NMR spectrum of 1,3-dihydroxymethyluracil (II) was achieved by comparison with the spectra of 1-hydroxymethyl-3-methyluracil (IV) and 3-hydroxymethyl-1-methyluracil (VI) in dimethyl sulfoxide-$d_6$. The latter compounds were prepared from III and V.

Features of the NMR spectrum of a 50-mg/ml solution of IV in dimethyl sulfoxide-$d_6$ are described in Table II. The broad singlet at 6.62 ppm disappeared when water was added to the solution and can be assigned to the OH proton. The broad singlet at 5.10 ppm enclosed an area that was double that of the OH proton, and it sharpened when either deuterium oxide or trifluoroacetic acid was added (to increase exchange

**Table I—Solubility and Melting Point of Uracil and N-Alkylated Uracils**

| Compound | Melting Point | Solubility in Water, mg/ml |
|---|---|---|
| I | 340° | 3 |
| III | 180° | 200 |
| V | 232° | 20 |
| VII | 123° | 500 |



0022-3549/81/0800-0850$01.00/0
© 1981, American Pharmaceutical Association

**Table II—NMR Data for Uracil and Substituted Uracils in Aprotic Solvents**

| Compound | Solvent[a] | Concentration, mg/ml | Chemical Shifts, ppm[b] C-6 H | C-5 H | N-1 $CH_2$ | OH | N-3 $CH_2$ | OH |
|---|---|---|---|---|---|---|---|---|
| I | A | 50 | 7.65 d | 5.56 d | — | — | — | — |
| II | A | 50 | 7.70 d | 5.72 d | 5.13 bs | 6.72 bs | 5.25 d | 6.20 t |
| III | A | 50 | 7.40 d | 5.57 d | — | — | — | — |
| IV | A | 50 | 7.65 d | 5.70 d | 5.10 bs | 6.62 bs | — | — |
| | A | 10 | 7.72 d | 5.76 d | 5.13 d | 6.66 dt | — | — |
| | B | 50 | 7.30 d | 5.76 d | 5.20 bs | 4.70 bs | — | — |
| | B | 25 | 7.26 d | 5.76 d | 5.20 bs | 4.36 dt | — | — |
| | B | 12.5 | 7.26 d | 5.76 d | 5.20 d | 4.08 t | — | — |
| | B | 6.25 | 7.24 d | 5.75 d | 5.18 d | 3.87 t | — | — |
| VI | A | 50 | 7.63 d | 5.62 d | — | — | 5.20 d | 6.13 t |
| | A | 10 | 7.63 d | 5.62 d | — | — | 5.20 d | 6.13 t |
| | B | 50 | 7.20 d | 5.78 d | — | — | 5.50 d | 4.12 t |
| | B | 12.5 | 7.20 d | 5.78 d | — | — | 5.50 d | 4.12 t |

[a] Solvent A was dimethyl sulfoxide-$d_6$, and Solvent B was deuterochloroform. [b] Symbols are: d, doublet; bs, broad singlet; t, triplet; and dt, diffuse triplet.

rates) or when the OH proton was irradiated. These results indicate that the signal at 5.10 ppm can be assigned to the N-1 $CH_2O$ protons in IV and that, in this relatively concentrated solution, they are only weakly coupled to the OH proton.

The multiplicity of the signals at 6.62 and 5.10 ppm was different in less concentrated solutions. When the concentration of IV in dimethyl sulfoxide-$d_6$ was 10 mg/ml, the OH proton was a diffuse triplet at 6.66 ppm and the N-1 $CH_2O$ protons were a doublet centered at 5.13 ppm. Similar changes in multiplicity with change in concentration were observed for spectra in deuterochloroform (Table II). These results suggest that the OH proton is more strongly coupled to the N-1 $CH_2O$ protons in dilute rather than in concentrated solutions. The OH proton probably participates in intermolecular hydrogen-bonding reactions with other IV molecules in concentrated solutions.

The spectra of VI solutions in dimethyl sulfoxide-$d_6$ are described in Table II. One difference between VI and IV is that its spectra in dimethyl sulfoxide-$d_6$ and in deuterochloroform were insensitive to concentration changes between 50 and 6.25 mg/ml. The OH resonance was a triplet centered at 6.12 ppm and was strongly coupled with the N-3 $CH_2O$ protons that appeared as a sharp doublet centered at 5.26 ppm. The N-3 $CH_2OH$ proton appears to have a much smaller tendency than the N-1 $CH_2OH$ proton to participate in intermolecular hydrogen bond formation.

Comparison of the NMR spectral characteristics of II with those of IV and VI enabled the following peak assignments to be made: C-6 H, 7.70 ppm; N-1 $CH_2OH$, 6.72 ppm; N-3 $CH_2OH$, 6.20 ppm; C-5 H, 5.72 ppm; N-3 $CH_2OH$, 5.25 ppm; and N-1 $CH_2OH$, 5.13 ppm.

**Thermodynamics and Kinetics of *N*-Hydroxymethylation of III and V in Water**—The addition of 2.5 *M* formaldehyde to solutions of III or V (pH 4–10) produced changes in UV and NMR spectra that were complete within 4 hr at pH 4 and in <30 min at pH >7. The resulting spectra did not change during 7 days at 25°. UV spectral characteristics of reactants and products are in Table III, and NMR data (in deuterium oxide) are in Table IV.

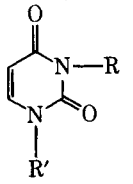

I: R = R′ = H
II: R = R′ = $CH_2OH$
III: R = $CH_3$, R′ = H
IV: R = $CH_3$, R′ = $CH_2OH$
V: R = H, R′ = $CH_3$
VI: R = $CH_2OH$, R′ = $CH_3$
VII: R = R′ = $CH_3$

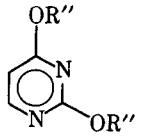

VIII: R″ = $CH_2OH$
IX: R″ = $CH_3$

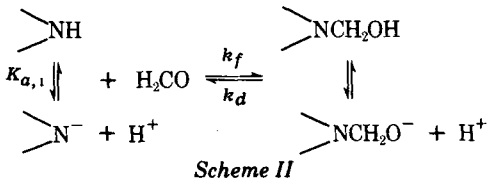

*Scheme II*

Confirmation that the products were IV and VI, respectively, came from the fact that the final solutions had identical spectra to solutions of authentic material in the same solvents.

Rate and equilibrium constants were calculated from UV changes. A pseudo-first-order rate constant, $k_{obs}$, was calculated from plots of log $(A - A_\infty)$ *versus* time for reactions in solutions containing excess formaldehyde. Values of $k_{obs}$ were related linearly to the initial formaldehyde concentration, $[H_2CO]_0$, and the line had a positive intercept on the $y$ axis when $[H_2CO]_0 = 0$. Thus, it was concluded that $k_{obs}$ values were related to values of $[H_2CO]_0$:

$$k_{obs} = k_f[H_2CO]_0 + k_d \qquad \text{(Eq. 1)}$$

where $k_f$ and $k_d$ are the second- and first-order rate constants, respectively, for the reaction depicted in Scheme II. Values of $k_f$ and $k_d$ calculated from plots of $k_{obs}$ against $[H_2CO]_0$ are in Table V.

The pH dependence of $k_f$ and $k_d$ is consistent with the conclusion that the rate-determining step in the forward reaction involves the uracil anion and formaldehyde and that for the reverse reaction involves the anion of the *N*-hydroxymethyl derivative. The mechanism proposed for the reverse reaction is identical to the one that was suggested (31, 32) to account for the decomposition of *N*-hydroxymethyl derivatives of other amides and imides.

According to the model, the rate law for the rate-determining step in the reactions would be:

$$k_{obs} = \frac{k_f' K_a^u}{K_a^u + [H^+]}[H_2CO]_0 + \frac{k_d' K_a^{HU}}{K_a^{HU} + [H^+]} \qquad \text{(Eq. 2)}$$

where $K_a^u$ and $K_a^{HU}$ are the acid dissociation constants of the uracil and the *N*-hydroxymethyl derivative (*i.e.*, to yield $>NCH_2O^-$), respectively, and $k_f'$ and $k_d'$ are the rate constants for reactions of the anionic species. The values of $K_a^u$ for III and V are $1 \times 10^{-10}$ and $2 \times 10^{-10}$, respectively (33). The $K_a^{HU}$ values are not known, but they are expected to be larger than the $K_a^u$ values because the negative charge would be localized on the oxygen atoms in the *N*-hydroxymethyl anions whereas it would be delocalized in the uracil anions. Hence, under the experimental conditions, both $K_a^{HU}$ and $K_a^u$ are less than $[H^+]$ and can be neglected from the de-

**Table III—UV Spectral Characteristics of Aqueous Solutions of Uracil Derivatives**

| Compound | Solvent | $\lambda_{max}$, nm | $\epsilon_{max}$ |
|---|---|---|---|
| V | Buffer, pH 7 | 265.5 | 9900 |
| | Buffer, pH 7, + 2.5 *M* $H_2CO$ | 268.5 | 9300 |
| III | Buffer, pH 7, | 257.5 | 7800 |
| | Buffer, pH 7, + 2.5 *M* $H_2CO$ | 258 | 8900 |
| I | Buffer, pH 7 | 257.5 | 8200 |
| | Buffer, pH 7, + 2.5 *M* $H_2CO$ | 261 | 8400 |
| VII | Buffer, pH 7 | 265 | 9200 |
| | Buffer, pH 7, + 2.5 *M* $H_2CO$ | 265 | 9200 |

**Table IV—NMR Data for Uracil and Substituted Uracils in Deuterium Oxide**

| Compound | Solvent[a] | Chemical Shifts, ppm[b] C-6 H | C-5 H | N-1 $CH_2OD$ | N-3 $CH_2OD$ |
|---|---|---|---|---|---|
| I | A | 7.55 d | 5.83 d | — | — |
| | B | 7.68 d | 5.88 d | 5.23 s | 5.33 s |
| III | A | 7.50 d | 5.86 d | — | — |
| | B | 7.68 d | 5.89 d | 5.24 s | — |
| V | A | 7.63 d | 5.80 d | — | — |
| | B | 7.57 d | 5.82 d | — | 5.39 d |

[a] Solvent A was deuterium oxide, and Solvent B was 2.5 *M* $H_2CO$ in deuterium oxide. [b] Symbols are: d, doublet; and s, singlet.

nominators in Eq. 2, which becomes:

$$k_{obs} = \frac{k_f' K_a^u}{[H^+]}[H_2CO]_0 + \frac{k_d' K_a^{HU}}{[H^+]} \quad \text{(Eq. 3)}$$

By definition:

$$k_f' = \frac{k_f[H^+]}{K_a^u} \quad \text{(Eq. 4)}$$

$$k_d' = \frac{k_d[H^+]}{K_a^{HU}} \quad \text{(Eq. 5)}$$

Confirmation that the model is consistent with the data comes from the fact that values of $k_f[H^+]/K_a^u$ (*i.e.*, $k_f'$) and $k_d[H^+]$ (*i.e.*, $k_d' K_a^{HU}$) were essentially constant between pH 3 and 6.

The anion of III is a stronger base than that of V, and it reacts ~40 times more rapidly with formaldehyde. Both properties are likely to arise because the anion of V is stabilized by delocalization of its electrons among the adjacent oxygen atoms.

Equilibrium constants for the *N*-hydroxymethylation reactions of III and V were calculated both from values of the quotient $k_f/k_r$ and from the slopes of plots of $(A_0 - A)/[H_2CO]_0$ *versus* $A$, where $A_0$ is the initial absorbance of uracil solution and formaldehyde and $A$ is the absorbance of a similar solution in which hydroxymethylation has reached equilibrium. Values of the equilibrium constants for III and V are in Table VI.

The results indicate that the magnitude of the equilibrium constant for formation of the >N-1 $CH_2OH$ derivative is double that for formation of the >N-3 $CH_2OH$ derivative. Thus, IV is formed more rapidly and to a greater extent than VI.

No *N*-hydroxymethylation of III and V was observed to occur at pH values two or more units above their pKa values.

**Thermodynamics of Uracil *N*-Hydroxymethylation**—Addition of 2.5 *M* $H_2CO$ to uracil solutions in water (or deuterium oxide) caused the UV and NMR spectra to change to those produced by equimolar solutions of II. Relevant data are shown in Tables III and IV.

Knowledge of the reactions of III and V in aqueous formaldehyde, together with the knowledge that II also is formed, leads to the conclusion that the relevant reactions of uracil are those shown in Scheme III. The magnitudes of the equilibrium constants in Scheme III were evaluated both from changes in UV absorbance and from phase solubility diagrams. All experiments were carried out at pH 3–7, a range in which the reactants and products were not appreciably ionized.

The absorbance of an equilibrated solution of uracil in aqueous formaldehyde, $A$, can be related to the initial absorbance of the solution, $A_0$:

$$\frac{A}{A_0} = \frac{1 + K_1[H_2CO]_0\epsilon_1 + K_2[H_2CO]_0\epsilon_2 + K_1K_4[H_2CO]^2\epsilon_3}{1 + K_2[H_2CO]_0 + K_2[H_2CO]_0 + K_1K_4[H_2CO]^2} \quad \text{(Eq. 6)}$$

where $\epsilon_1$ is the ratio of molar extinction coefficients for 1-hydroxymethyluracil and uracil, $\epsilon_2$ is the ratio for 3-hydroxymethyluracil and uracil, and $\epsilon_3$ is the ratio for II and uracil. An iterative procedure that utilized Eq. 6 and experimental data yielded values of $K_1 + K_2$ and $K_1K_4$.

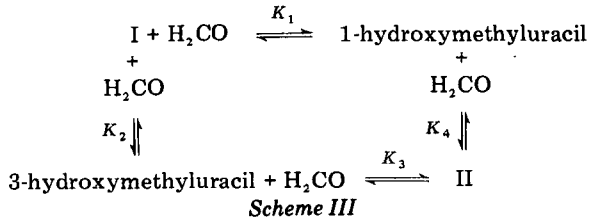


*Scheme III*

By definition:

$$K_1/K_2 = K_3/K_4 \quad \text{(Eq. 7a)}$$

The value of $K_1/K_2$ was evaluated using Eq. 7a on the basis that the value of $K_3/K_4$ would be the same as that for the ratio of equilibrium constants for *N*-hydroxymethylation of III and for V. In other words:

$$\frac{K_1}{K_2} = 2.26 \quad \text{(Eq. 7b)}$$

When this assumption had been made, values of $K_1$, $K_2$, $K_3$, and $K_4$ were computed from the values of $K_1 + K_2$, $K_1K_4$, and $K_3/K_4$ (Table VI).

The second method of calculating equilibrium constants was based on phase solubility analysis. Experiments involved measuring the total amount of uracil that dissolved $[I]_T$ in solutions containing different amounts of formaldehyde. The solubility of uracil in solutions that did not contain formaldehyde was $[I]_0$. Equilibrium constants were calculated by:

$$\frac{[I]_T - [I]_0}{[I]_0([I]_T - [I]_0 - [H_2CO]_0/2)} = \frac{4K_1K_4([I]_T - [I]_0 - [H_2CO]_0/2)}{\{(K_1 + K_2)[I]_0 - 1\}^2} + \frac{2(K_1 + K_2)}{(K_1 + K_2)[I]_0 - 1} \quad \text{(Eq. 8)}$$

Figure 1 shows a plot of $[I]_T$ *versus* $[H_2CO]_0$. The plot is an Ap type (34) of phase solubility diagram, which indicates a 1:1 interaction of ligand (formaldehyde) with the substrate (I). Figure 2 shows a linear plot of $([I]_T - [I]_0)/\{[I]_0([I]_T - [I]_0 - [H_2CO]_0/2)\}$ *versus* $([I]_T - [I]_0 - [H_2CO]_0/2)$. Values of $K_1K_4$ and $(K_1 + K_2)$ were calculated from the slope of this plot and the intercept at $[H_2CO]_0 = 0$, respectively. The magnitudes of the individual equilibrium constants were calculated by utilizing the relationship $K_3/K_4 = K_1/K_2$ and making the approximation that $K_3/K_4 = 2.26$ (Table VI).

The similarity between $K$ values calculated from both UV spectrophotometric methods and phase solubility studies adds support to the validity of the model.

Lewin (11) studied the interaction of uracil with aqueous formaldehyde by measuring changes that occur in pH when formaldehyde is added to partially neutralized uracil solutions. The pH changes occur because each *N*-hydroxymethylation reaction removes one acidic hydrogen atom from the uracil molecule. Lewin (11) interpreted his results as indicating that only IV was formed to any appreciable extent. The appropriate equilibrium constant was evaluated using:

$$\text{antilog } \Delta pH = 1 + K_2[H_2CO]_0 \quad \text{(Eq. 9)}$$

The model used in the present study requires that:

$$\text{antilog } \Delta pH = \frac{1 + (K_1 + K_2)[H_2CO]_0 + K_1K_4[H_2CO]_0^2}{1 + 0.32K_2[H_2CO]_0 + 0.63K_1[H_2CO]_0} \quad \text{(Eq. 10)}$$

where 0.63 is the ratio of acid dissociation constants for 3-hydroxymethyluracil and uracil and 0.32 is the ratio for 1-hydroxymethyluracil and uracil. These ratios were evaluated by assuming that the pKa values

**Table V—Rate Constants for *N*-Hydroxymethylation of III and V at 25°**

| Compound | pH | $10^4 k_{obs}$[a], $min^{-1}$ | $10^2 k_f$, $M^{-1}\,min^{-1}$ | $10^{-5} k_f'$, $M^{-1}\,min^{-1}$ | $10^2 k_d$, $min^{-1}$ | $10^6 k_d' K_a^{HU}$, $min^{-1}\,M$ |
|---|---|---|---|---|---|---|
| III | 3.06 | 219 | 1.46 | 1.27 | 0.73 | 6.36 |
| | 4.01 | 1,760 | 12.8 | 1.25 | 6.82 | 6.66 |
| | 5.04 | 20,000 | 128 | 1.17 | 74 | 6.75 |
| V | 4.05 | 116 | 0.75 | 0.033 | 0.47 | 0.42 |
| | 5.01 | 1,220 | 6.92 | 0.034 | 5.97 | 0.55 |
| | 6.02 | 12,000 | 68.4 | 0.033 | 54.9 | 0.52 |

[a] Values of $k_{obs}$ were calculated at $[H_2CO]_0 = 1$ *M*.

Table VI—Equilibrium Constants for *N*-Hydroxymethylation of Uracil and Uracil Derivatives at 25° and $\mu$ = 0.1 *M*

| Compound | pH Range | Method | $K, M^{-1}$ | $K_1, M^{-1}$ | $K_2, M^{-1}$ | $K_3, M^{-1}$ | $K_4, M^{-1}$ |
|---|---|---|---|---|---|---|---|
| V | 4–7 | UV | 1.5 | | | | |
| | 4–6 | Kinetic | 1.3 | | | | |
| III | 4–7 | UV | 3.4 | | | | |
| | 4–6 | Kinetic | 2.2 | | | | |
| I | 5–7 | Phase solubility | | 5.2 | 2.3 | 2.2 | 1.2 |
| | 5–7 | UV | | 5.3 | 2.3 | 4.0 | 1.8 |
| 5-Methyluracil | 4–6 | UV | | 3.1 | 1.4 | 5.8 | 2.5 |
| 5-Fluorouracil | 4 | UV | | 4.2 | 1.9 | 4.4 | 1.9 |
| 5-Chlorouracil | 4 | UV | | 4.1 | 1.8 | 6.4 | 2.8 |
| 5-Bromouracil | 4 | UV | | 4.8 | 2.1 | 5.5 | 2.4 |
| 5-Iodouracil | 4 | UV | | 4.2 | 1.9 | 6.7 | 2.9 |

of the *N*-hydroxymethyluracil derivatives were equal to those of the respective *N*-methyluracils.

If $[H_2CO]_0$ is in excess and the values $K_1 = K_2 = K_3 = K_4 = L$, Eq. 10 reduces to:

$$\text{antilog } \Delta pH = \frac{(1 + L[H_2CO]_0)^2}{1 + 0.95L[H_2CO]_0} \simeq 1 + L[H_2CO]_0 \quad \text{(Eq. 11)}$$

Hence, Lewin's method was not sensitive enough to distinguish between the various *N*-hydroxymethyl derivatives of uracil.

Inspection of the *K* values in Table VI reveals that *N*-hydroxymethylation of N-1 of uracil is the most favored reaction whether or not an *N*-hydroxymethyl group is present on N-3.

The strength of the *N*-hydroxymethylation reactions is greater than would be immediately concluded from the magnitude of the constants in Table VI. Formaldehyde exists in water as an equilibrium mixture of anhydrous and hydrated formaldehyde. The equilibrium constant for the hydration reaction (35) is 41 $M^{-1}$ at 25°. Hence, if the concentration of water is taken to be 55.5 *M*, the equilibrium constants for reaction of the uracils with anhydrous formaldehyde are the values in Table VI multiplied by the factor of 2277, which takes into account the relative concentration of anhydrous formaldehyde. Consequently, *N*-hydroxymethylation is a strong reaction as are the addition reactions of other amines to formaldehyde (36).

**Thermodynamics of *N*-Hydroxymethylation of 5-Substituted Uracils**—UV spectrophotometric measurements, identical to those described in the previous section, were used to calculate the *K* values for *N*-hydroxymethylation of the 5-substituted uracils (Table VI).

Although there is about a 200-fold difference in the acidity of the N–H functions of these compounds (pKa 7.7–9.9), the affinity of formaldehyde for 5-substituted uracils is essentially independent of their acidities, and substitution at the 5-position does not influence the magnitude of equilibrium constants in a systematic way. These results are consistent with reports that the equilibrium constants for the addition to formaldehyde of simple primary amines (1) are not much larger than those for addition of urea and amides (8), although the difference in the pKa of amine and amide groups is large.

**Melting Point, Solubility, and Dissolution Rate of II**—Comparison of uracil (I) and II indicated that II had a lower melting point (101° compared to 340°), higher water solubility (500 mg/ml compared to 2.8 mg/ml)[1], and higher water dissolution rate ($82 \times 10^{-5}$ *M*/min compared to 1.6 *M*/min)[1]. This behavior was predicted on the basis that *N*-hydroxymethylation changes intermolecular hydrogen-bonding possibilities in the solid phase. It supports the contention that such derivatives are potentially useful prodrugs.

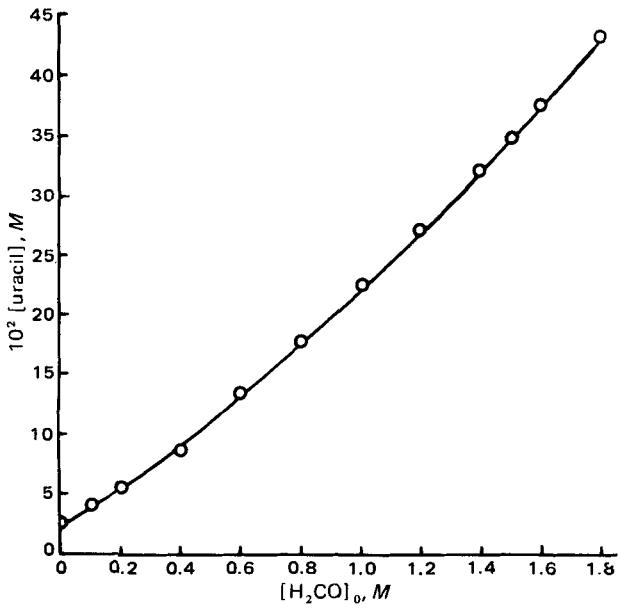


**Figure 1**—*Phase solubility diagram of uracil in aqueous formaldehyde at 25°, 0.1 M I.*

## EXPERIMENTAL

Uracil[2], 5-fluorouracil[2], 5-bromouracil[2], 5-iodouracil[2], 5-methyluracil[2], 1-methyluracil[3], and 3-methyluracil[3] were used without further purification. 5-Chlorouracil[4] was recrystallized from aqueous ethanol. Formaldehyde (37% aqueous solution) was used without further purification, and its concentration was calculated using the USP method (38). Formaldehyde used in the NMR studies was obtained by dissolving paraformaldehyde in deuterium oxide. Buffer solutions at $\mu$ = 0.1 *M* were prepared as described previously (39).

Tetramethylsilane or sodium 4,4-dimethyl-4-silapentanesulfonate was used as the reference in NMR spectral measurements.

**Preparation of *N*-Hydroxymethyl Derivatives**—*1,3-Dihydroxymethyluracil (II)*—Uracil (I) (4.75 g) was dissolved in 10 ml of 37% (w/w) formaldehyde (pH adjusted to 7 with sodium hydroxide) at 25°. Refrigeration of this solution resulted in a white crystalline precipitate which, following recrystallization from acetonitrile and drying over calcium chloride, melted at 101° (melting point of uracil was 338°). The mass spectrum (*m/z* 172) and elemental analysis of the solid were consistent with the conclusion that the compound was II.

*Anal.*—Calc. for $C_6H_8N_2O_4$: C, 41.84; H, 4.65; N, 16.28. Found: C, 41.62; H, 4.63; N, 16.38.

*3-Hydroxymethyl-1-methyluracil (VI)*—1-Methyluracil (V) (600 mg) was dissolved in 1 ml of 37% formaldehyde. Refrigeration of this solution resulted in a white crystalline precipitate which, on drying over calcium

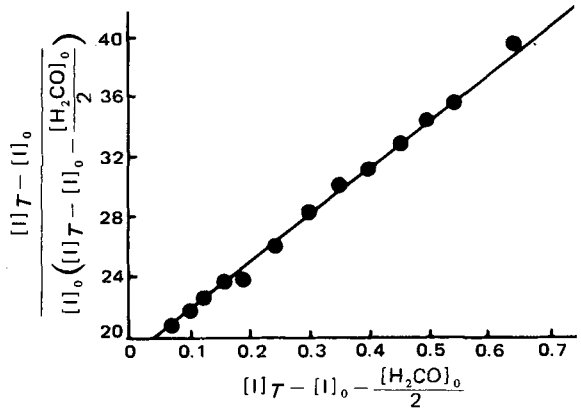


**Figure 2**—*Plot of* $([I]_T - [I]_0)/[I]_0([I]_T - [I]_0 - [H_2CO]_0/2)$ *versus* $[I]_T - [I]_0 - ([H_2CO]_0/2)$ *for the reaction of uracil and formaldehyde at 25°, 0.1 M I.*

[1] The methods of calculating these values were identical to those described in Ref. 37.

[2] Sigma Chemical Co.

[3] Cyclo Chemical Co.

[4] K & K Laboratories.

chloride, melted at 110° (melting point of V was 232°). The mass spectrum (*m/z* 156) and elemental analysis of the solid were consistent with the conclusion that the compound was VI.

*Anal.*—Calc. for $C_6H_8N_2O_3$: C, 46.15; H, 5.13; N, 17.95. Found: C, 46.28; H, 5.10; N, 18.15.

*1-Hydroxymethyl-3-methyluracil (IV)*—3-Methyluracil (III) (1 g) was dissolved in 1 ml of 37% formaldehyde. The crystals of IV were obtained as described for II and VI and, on drying over calcium chloride, melted at 92° (melting point of III was 178°). The mass spectrum (*m/z* 156) and elemental analysis of the solid were consistent with the conclusion that the compound was VI.

*Anal.*—Calc. for $C_6H_8N_2O_3$: C, 46.15; H, 5.13; N, 17.95. Found: C, 46.04; H, 5.22; N, 17.77.

**Kinetic Measurements**—The rates of formation of hydroxymethyl derivatives of III and V were monitored spectrophotometrically by following the change in UV absorbance that occurred when 0.1 ml of a 0.003 *M* solution of III or V was added to a 1-cm stoppered UV cell containing 3 ml of formaldehyde solution in buffer equilibrated at 25° and $\mu = 0.1$ *M*. The rates of the forward and reverse reactions and the equilibrium constants were determined as already described. All kinetic runs were conducted under pseudo-first-order conditions in which formaldehyde was used in large excess.

**Determination of Equilibrium Constants by Spectrophotometry**—Solutions of uracil and 5-substituted uracils (0.0001 *M*) were prepared in buffered formaldehyde solutions. The solutions were equilibrated in a thermostated bath at 25°. The UV absorbance of equilibrated solutions at a fixed wavelength was recorded at several pH values (pH 4–7), and equilibrium constants were calculated as described.

**Phase Solubility Studies**—Uracil (500 mg) was weighed in a series of 25-ml polyseal-lined screw-capped vials to which was added exactly 5 ml of formaldehyde of increasing concentrations (0–2 *M*) in buffer ($\mu = 0.1$ *M*). The vials were sealed, placed in a constant-temperature water bath at 25.00 ± 0.02°, and agitated with a rotating-action shaker until equilibrium was achieved (usually within 5 days). The total amount of uracil in solution in each vial was determined spectrophotometrically at $\lambda_{max}$ 257 nm by diluting aliquots of filtered equilibrated solutions in the buffer.

## REFERENCES


(1) R. G. Kallen and W. P. Jencks, *J. Biol. Chem.*, **241**, 5864 (1966).

(2) D. French and J. T. Edsall, *Adv. Protein Chem.*, **2**, 277 (1945).

(3) C. J. Martin and M. A. Marini, *J. Biol. Chem.*, **242**, 5736 (1967).

(4) P. Dunlap, M. Marini, H. M. Fales, E. Sokoloski, and C. J. Martin, *Bioorg. Chem.*, **2**, 235 (1973).

(5) M. Levy and D. E. Silberman, *J. Biol. Chem.*, **118**, 723 (1937).

(6) S. Lewin and D. A. Humphany, *J. Chem. Soc. B*, **1966**, 210.

(7) *Ibid.*, **1967**, 562.

(8) J. Ugelstand and J. Dejonge, *Recueil*, **76**, 919 (1957).

(9) M. Imoto and M. Kobayashi, *Bull. Chem. Soc. Jpn.*, **36**, 1505 (1963).

(10) S. Lewin, *J. Chem. Soc.*, **1962**, 1462.

(11) *Ibid.*, **1964**, 792.

(12) S. Lewin and M. A. Barnes, *J. Chem. Soc. B*, **1966**, 478.

(13) S. Lewin, *Experientia*, **20**, 666 (1964).

(14) N. N. Aylward, *J. Chem. Soc. B*, **1966**, 627.

(15) E. J. Eyring and J. Ofengard, *Biochemistry*, **6**, 2500 (1967).

(16) S. J. Benkovic, P. A. Benkovic, and D. R. Comfort, *J. Am. Chem. Soc.*, **91**, 5270 (1969).

(17) S. J. Benkovic, P. A. Benkovic, and R. Chrzanowski, *ibid.*, **92**, 523 (1970).

(18) G. P. Tuszynski and R. G. Kallen, *ibid.*, **97**, 2860 (1975).

(19) R. G. Kallen, in "Methods in Enzymology," vol. 18, N. O. Kapalan and S. Colowick, Eds., Academic, New York, N.Y., 1971, p. 705.

(20) L. Grossman, S. S. Levine, and W. S. Allison, *J. Mol. Biol.*, **3**, 47 (1961).

(21) M. L. Fenwick, *Biochem. J.*, **197**, 851 (1968).

(22) P. H. Vonhippel and K. Wong, *J. Mol. Biol.*, **61**, 587 (1971).

(23) D. C. Rather and M. Sundaralingam, *Acta Crystallogr.*, **B26**, 546 (1970).

(24) S. Furberg and L. H. Jensen, *J. Am. Chem. Soc.*, **90**, 470 (1968).

(25) M. J. E. Hewlins, *J. Chem. Soc., Perkin Trans.*, **II**, 275 (1972).

(26) "The United States Pharmacopeia," 19th rev., Mack Publishing Co., Easton, Pa., 1975, p. 651.

(27) W. Von Daehne, E. Frederiksen, E. Gunderson, F. Lund, P. March, H. J. Peterson, K. Rohalt, L. Tybring, and W. O. Godtfredsen, *J. Med. Chem.*, **13**, 607 (1970).

(28) W. Von Daehne, W. O. Godtfredsen, K. Rohalt, and L. Tybring, *Antimicrob. Agents Chemother.*, **1970**, 431.

(29) J. C. K. Loo, E. L. Feltz, H. Wallick, and K. C. Kwan, *Clin. Pharmacol. Ther.*, **16**, 35 (1974).

(30) M. Johansen and H. Bundgaard, *Arch. Pharm. Chem. Sci. Ed.*, **7**, 175 (1979).

(31) H. Bundgaard and M. Johansen, *Int. J. Pharm.*, **5**, 67 (1980).

(32) "High Resolution NMR Spectra Catalogue," vol. 2, Varian Associates, Palo Alto, Calif., 1963.

(33) J. J. Christensen, J. R. Rytting, and R. M. Izatt, *J. Chem. Soc. B*, **1970**, 1643.

(34) T. Higuchi and K. A. Connors, "Advances in Analytical Chemistry and Instrumentation," vol. 4, Wiley–Interscience, New York, N.Y., 1965, p. 136.

(35) K. Moedsitzer and J. R. Van Wazer, *J. Phys. Chem.*, **70**, 2025 (1966).

(36) E. G. Sander and W. P. Jencks, *J. Am. Chem. Soc.*, **90**, 6154 (1968).

(37) P. C. Bansal and I. H. Pitman, *J. Pharm. Sci.*, in press.

(38) "The United States Pharmacopeia," 18th rev., Mack Publishing Co., Easton, Pa., 1970, p. 843.

(39) I. H. Pitman, Ph.D. thesis, Australian National University, Canberra, Australia, 1966.


## ACKNOWLEDGMENTS


Adapted in part from a thesis submitted by P. C. Bansal to the University of Kansas in partial fulfillment of the Doctor of Philosophy degree requirements.

Supported in part by a grant from Inter$_x$ Corp., Lawrence, KS 66044.

# *N*-Hydroxymethyl Derivatives of Nitrogen Heterocycles as Possible Prodrugs II: Possible Prodrugs of Allopurinol, Glutethimide, and Phenobarbital

**PADAM C. BANSAL *, IAN H. PITMAN ‡x, and TAKERU HIGUCHI ***

Received October 21, 1980, from the **School of Pharmacy, University of Kansas, Lawrence, KS 66045*, and the ‡*Victorian College of Pharmacy Ltd., 381 Royal Parade, Parkville, Victoria, Australia.* Accepted for publication January 7, 1981.

**Abstract** □ Solid samples of 1-hydroxymethyl- and 1,5-dihydroxymethylallopurinol, 1-hydroxymethylglutethimide, and 1-hydroxymethylphenobarbital were prepared, and equilibrium constants for their formation from formaldehyde and allopurinol, glutethimide, or phenobarbital were calculated. The *N*-hydroxymethyl derivatives had higher water solubilities and faster dissolution rates than the parent drugs, and they appear to be potentially useful as prodrugs.

**Keyphrases** □ Allopurinol—*N*-hydroxymethyl derivative synthesized, structure confirmed by NMR and elemental analyses, potential prodrug □ Glutethimide—*N*-hydroxymethyl derivative synthesized, structure confirmed by NMR and elemental analyses, potential prodrug □ Phenobarbital—*N*-hydroxymethyl derivative synthesized, structure confirmed by NMR and elemental analyses, potential prodrug □ Prodrugs, potential—*N*-hydroxymethyl derivatives of allopurinol, glutethimide, and phenobarbital synthesized, structures confirmed by NMR and elemental analyses

The potential usefulness of *N*-hydroxymethyl derivatives of heterocyclic amides and imides as prodrugs was discussed in a previous paper (1). This work was consistent with studies on the *N*-hydroxymethyl derivatives of hydantoins (2) and other amides and imides (3).

The present paper is concerned with the synthesis and properties of *N*-hydroxymethyl derivatives of allopurinol (I), glutethimide (II), and phenobarbital (III). These drugs have low water solubility and dissolve slowly. Hence, it is likely that their bioavailability and delivery (4) would be improved if appropriate prodrug forms could be developed.

## RESULTS AND DISCUSSION

The interaction of formaldehyde with allopurinol (I), glutethimide (II), and phenobarbital (III) at 25° was studied by analyzing phase solubility diagrams (Figs. 1–3). These diagrams were constructed by plotting the total substrate concentration in solution $[S]_T$ *versus* the added formaldehyde concentration $[H_2CO]_T$. At least one solid phase was present in all solutions.

***N*-Hydroxymethylation of I**—Analysis, using arguments set out by Higuchi and Connors (5) of the double Bs-type phase solubility diagram for I (Fig. 1), led to the conclusion that the reactions shown in Scheme I took place. The A–E portion of the diagram is consistent with the formation of 1-hydroxymethylallopurinol (1-hydroxymethyl-4,5-dihydropyrazolo[3,4-*d*]pyrimidin-4-one, I*a*), and the E–I portion is consistent with the formation of 1,5-dihydroxymethylallopurinol {1,5-bis(hydroxymethyl)-4,5-dihydropyrazolo[3,4-*d*]pyrimidin-4-one, I*b*}. The B–C portion is believed to be caused by saturation of the solution with respect to I*a*.

Confirmation of these postulates comes from elemental analysis and NMR spectra (in dimethyl sulfoxide-$d_6$) of the solid phase at point E and in the portion H–I (Table I), from calculation of the stoichiometry of the reactions using portions B–D and F–G, and from equilibrium constants calculated from the slopes of the lines AB ($K_{Ia}$) and EF ($K_{Ib}$).

The NMR peak at 5.63 ppm in the spectrum of the solid isolated at point E and those at 5.40 and 5.63 ppm in the spectrum of the solid isolated in the portion H–I had similar chemical shifts to the N–$CH_2$–O protons in the *N*-hydroxymethyluracils (1). The stoichiometry of the solid isolated at point E calculated from the phase solubility diagram was 1 part of I to 1.03 parts of formaldehyde, and that of the compound isolated in the region H–I was 1 part of I to 2.06 parts of formaldehyde. The elemental analyses of the compounds were as expected for I*a* and I*b*.

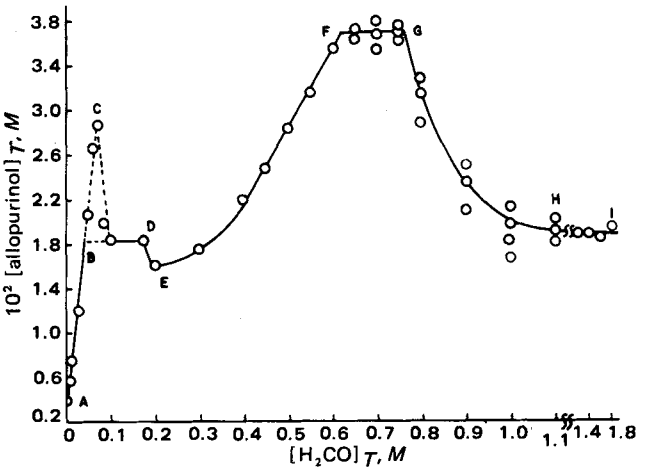


**Figure 1**—*Plot of I solubility as a function of formaldehyde concentration in aqueous buffer at pH 4.9, μ = 0.1* M, *and 25°.*

The equilibrium constants calculated from the phase solubility diagram were 120 $M^{-1}$ for formation of I*a* ($K_{Ia}$) and 4 $M^{-1}$ for the formation of I*b* ($K_{Ib}$). This value of $K_{Ia}$ is similar to values reported (6) for the addition of secondary amines to formaldehyde (40–800 $M^{-1}$). The value of $K_{Ib}$ is similar to that calculated for the addition of amino and imino groups in uracils to formaldehyde (1).

***N*-Hydroxymethylation of II**—The Bs-type phase solubility diagram in Fig. 2 was analyzed similarly to the one for *N*-hydroxymethylation of I. Elemental analysis and NMR spectral data (Table I) of the solid phase obtained at point D (from deuterium oxide solutions) indicated that it was 1-hydroxymethylglutethimide (1-hydroxymethyl-3-phenyl-2,6-piperidinedione, II*a*). Confirmation of the reactions shown in Scheme II was obtained from the facts that the phase solubility diagram indicated that the stoichiometry of the complex was 1 equivalent of II to 1.02 equivalents of formaldehyde and that the equilibrium constant for its formation, $K_{IIa}$, was 3.4 $M^{-1}$.

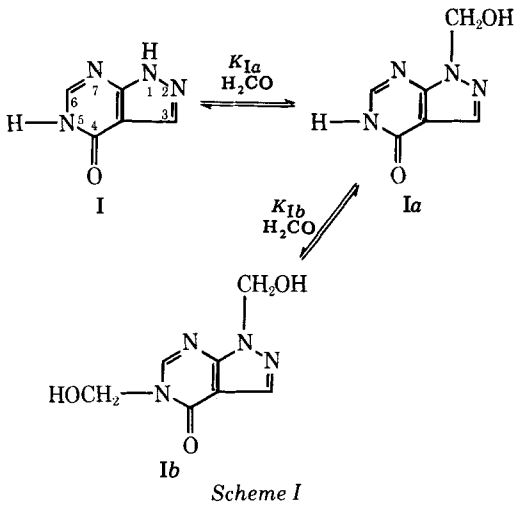


*Scheme I*

0022-3549/81/0800-0855$01.00/0
© 1981, American Pharmaceutical Association

**Table I—NMR and Elemental Analysis Data for *N*-Hydroxymethyl Compounds**

| Compound | Chemical Shifts[a], ppm | Analysis, % | Calc. | Found |
|---|---|---|---|---|
| Ia[b] | 5.63 bs | C | 43.34 | 43.02 |
| | | H | 3.61 | 3.70 |
| | | N | 33.71 | 33.32 |
| Ib[b] | 5.63 bs, 5.40 bs | C | 42.83 | 42.70 |
| | | H | 4.08 | 4.01 |
| | | N | 28.55 | 28.09 |
| IIa[c] | 5.40 d | C | 67.94 | 67.57 |
| | | H | 6.87 | 6.62 |
| | | N | 5.66 | 5.41 |
| IIIa[b] | 5.30 bs | C | 59.49 | 59.46 |
| | | H | 5.34 | 5.34 |
| | | N | 10.68 | 10.94 |

[a] Chemical shifts of protons not present in the parent compound. The area under the peak integrated for two protons, and bs and d represent broad singlet and doublet, respectively. [b] Spectra measured in dimethyl sulfoxide-$d_6$. [c] Spectrum measured in deuterochloroform.

**Table II—Amounts of Substrate and Ligand Used in Phase Solubility Studies**

| Substrate | Ligand | Total Volume, ml | Equilibrium Time, days |
|---|---|---|---|
| I, 0.1 g | Formaldehyde, 0–2 *M* | 5 | 15 |
| II, 0.4 g | Formaldehyde, 0–2 *M* | 5 | 10 |
| III, 0.4 g | Formaldehyde, 0–2 *M* | 20 | 10 |

**Table III—Melting Points, Solubilities, and Initial Dissolution Rates[a] of Drugs and Their Prodrugs**

| Compound | Melting Point | Solubility[b], *M* | Initial Dissolution Rate, *M*/min × $10^5$ |
|---|---|---|---|
| I | 360° | 0.004 | 0.2 |
| Ib | 350° | 0.019 | 1.2 |
| II | 85° | 0.005 | 1.3 |
| IIa | 82° | 0.022 | 2.2 |
| III | 178° | 0.004 | 0.9 |
| IIIa | 99° | 0.025 | 2.8 |

[a] Dissolution rates were obtained in pH 7 buffer at 25° and $\mu$ = 0.1 *M*. [b] Solubilities were obtained from phase solubility diagrams (Figs. 1–3).

Formaldehyde concentrations of >2 *M* caused the total amount of II in solution to increase, resulting in the separation of an oil (Table II). The reactions occurring in this region of the phase solubility diagram were not investigated further, but they probably are caused by addition of the >N–$CH_2OH$ group to additional formaldehyde molecules to form polymers such as >N–$[CH_2O]_n$–. There is evidence (7) that formaldehyde polymerizes in concentrated aqueous solutions.

***N*-Hydroxymethylation of III**—The complex Bs-type phase solubility diagram for this system is shown in Fig. 3.

Based on the *N*-hydroxymethylation of uracil (1) and II, the reactions shown in Scheme III were expected. However, only one compound was

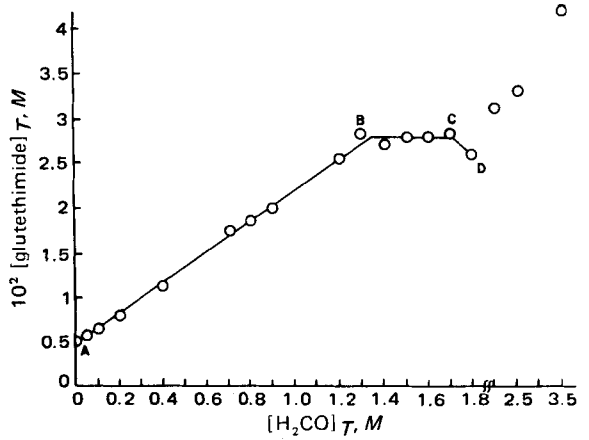


**Figure 2**—*Plot of II solubility as a function of formaldehyde concentration in aqueous buffer at pH 5.1, $\mu$ = 0.1 M, and 25°.*

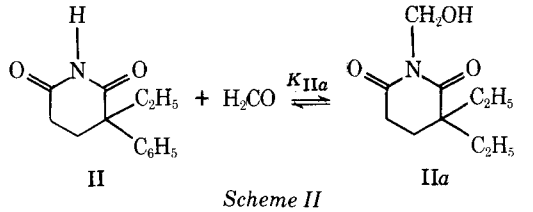

*Scheme II*

isolated from the system. The solid phase at point D had an elemental analysis and NMR spectrum consistent with it being 1-hydroxymethylphenobarbital (IIIa). Analysis of the portion B–C of the phase solubility diagram indicated that the compound had the required stoichiometric composition. Isolation of 1,3-dihydroxymethylphenobarbital was complicated by the fact that a viscous oil phase again separated out at formaldehyde concentrations of >1.6 *M*.

The shape and slope of the portion A–B of the phase solubility diagram would be a function of the equilibrium constants $K_{IIIa}$ and $K_{IIIb}$. At low formaldehyde concentrations, the curve would have a limiting slope that would be related directly (5) to $K_{IIIa}$. The $K_{IIIa}$ value was estimated to be 9 $M^{-1}$. Hence, equilibrium data are consistent with the proposed reaction scheme.

**Aqueous Solubility and Dissolution Rates**—Aqueous solubilities and relative dissolution rates in water of I, Ib, II, IIa, III, and IIIa are listed in Table III. The solubilities were obtained from the phase solubility diagrams (5), and dissolution rates were calculated as described under *Experimental*.

As expected (1), the change in intermolecular hydrogen-bonding possibilities in the solid state produced by *N*-hydroxymethylation of amines or imides increased the water solubilities of I–III. The increase in water solubility was reflected by an increase in the dissolution rate as required by the Noyes–Whitney model for dissolution (8, 9).

The *N*-hydroxymethyl derivatives were converted rapidly to the parent

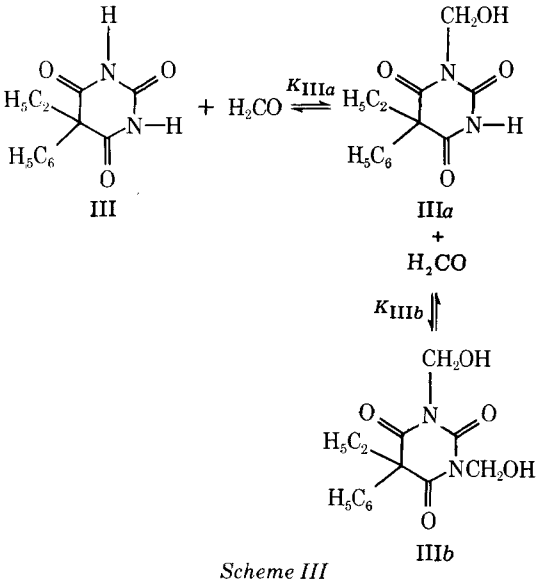

*Scheme III*

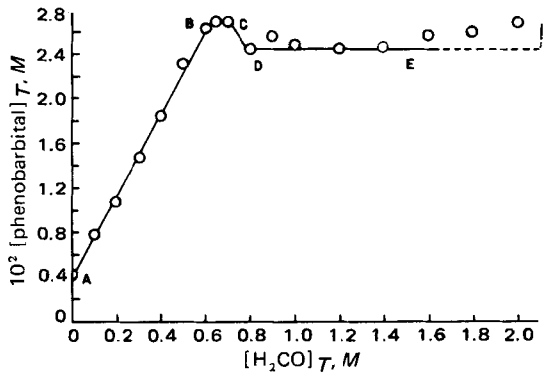


**Figure 3**—*Plot of III solubility as a function of formaldehyde concentration in aqueous buffer at pH 4.9, $\mu$ = 0.1 M, and 25°.*

drug. This result was indicated by the fact that the solid phase in a suspension of the *N*-hydroxymethyl derivatives (500 mg in 25 ml of pH 7 buffer) that had been shaken for 10 min had the same melting point and NMR spectrum in dimethyl sulfoxide as the parent drug. UV spectra of dilute solutions of the *N*-hydroxymethyl derivatives in pH 7 buffer were superimposable on those of the parent drug after the solutions had been shaken for 10 min.

All of these observations support the contention that *N*-hydroxymethyl derivatives of poorly soluble amides, imides, and amines are potentially useful prodrugs.

## EXPERIMENTAL

**Chemicals and Equipment**—Allopurinol[1] (I), phenobarbital[1] (III), and glutethimide[2] (II) were used without further purification, as was formaldehyde[3] (37% aqueous solution).

Solutions containing formaldehyde were prepared fresh by appropriate dilution of the 37% formaldehyde solution. The succinic acid–sodium borate buffers (pH 3.69–6.9, $\mu$ = 0.1 *M*) and monobasic potassium phosphate–sodium borate buffers (pH 6.3–9.25, $\mu$ = 0.1 *M*) were prepared by the method described by Pitman (10). Sodium chloride was used to adjust the ionic strength ($\mu$ = 0.1 *M*).

3-(Trimethylsilyl)propanesulfonic acid was used as an internal reference in the NMR measurements.

**Phase Solubility**—A fixed quantity of substrate, in excess of its aqueous solubility, was weighed in a series of 25-ml polyseal-lined screw-capped vials to which were added fixed volumes of formaldehyde solutions of increasing concentration in the buffer (Table II). Vials were sealed, placed in a constant-temperature water bath at 25.0 ± 0.2°, and agitated with a rotating-action shaker until equilibrium was achieved. Aliquots of the supernatant liquid were removed using a pipet (whose tip had been wrapped with glass wool) or solutions were filtered using a sintered-glass funnel of medium porosity and analyzed spectrophotometrically.

**Isolation of *N*-Hydroxymethyl Derivatives**—*1,5-Dihydroxymethylallopurinol (Ib)*—One gram of allopurinol was dissolved in 50 ml of 2 *M* formaldehyde at pH 7. Agitation of this solution for 24 hr resulted in a white crystalline precipitate. The elemental analysis (Table I) and NMR spectrum of the solid (dried over calcium chloride) were consistent with the conclusion that the compound was *Ib*.

*1-Hydroxymethylallopurinol (Ia)*—Compound I*a* was isolated in a similar manner to I*b*, except 0.2 *M* formaldehyde was used in this case. The elemental analysis (Table I) and NMR spectrum of the dry solid were consistent with it being I*a*.

*1-Hydroxymethylglutethimide (IIa)*—Compound II*a* was prepared by agitating 1 g of glutethimide in 100 ml of 1.5 *M* formaldehyde in a pH 7 buffer for 24 hr. The NMR spectrum and elemental analysis of the resultant solid (dried over calcium chloride) were consistent with it being II*a* (Table I). However, at high concentrations of formaldehyde (10 *M*), a viscous oil was isolated. This oil was believed to be II*a* and the corresponding diformyl compound, which would be formed by a dimer of formaldehyde.

*1-Hydroxymethylphenobarbital (IIIa)*—Compound III*a* was prepared by agitating 1 g of phenobarbital in 20 ml of 1 *M* formaldehyde in a pH 5 buffer for 24 hr. The resultant white crystalline precipitate melted at 99° when drying over calcium chloride. The elemental analysis (Table I) and NMR spectrum of the solid were consistent with it being III*a* (Table I). However, at high concentrations of formaldehyde (10 *M*), a viscous oil was isolated.

**Dissolution Rate**—All dissolution studies were performed according to the USP dissolution test (11).

The solid whose dissolution rate was to be measured was reduced to a uniform particle size by sifting it through a 40-mesh sieve and collecting it in a 60-mesh sieve. Approximately 250 mg of this material then was compressed into a tablet in an evacuable potassium bromide die at 10,000 psi for 30 sec using a laboratory press. The dissolution medium (500 ml, pH 7 buffer solution) was placed in a 1-liter beaker immersed in a constant-temperature bath at 25°. One tablet was placed in a basket, and the basket was rotated at 100 rpm. The samples (5 ml) were withdrawn at appropriate times and analyzed spectrophotometrically.

[1] Sigma Chemical Co.
[2] Ciba-Geigy Co.
[3] J. T. Baker Chemical Co.

## REFERENCES


(1) P. C. Bansal, I. H. Pitman, J. N. S. Tam, M. Mertes, and J. J. Kaminski, *J. Pharm. Sci.*, **70**, 850 (1981).

(2) H. Bundgaard and M. Johansen, *Int. J. Pharm.*, **5**, 67 (1980).

(3) M. Johansen and H. Bundgaard, *Arch. Pharm. Chemi. Sci. Ed.*, **7**, 175 (1979).

(4) V. J. Stella, *Aust. J. Pharm. Sci.*, **NS 2**, 57 (1973).

(5) T. Higuchi and K. A. Connors, in "Advances in Analytical Chemistry and Instrumentation," C. N. Reilly, Ed., Interscience, New York, N.Y., 1965, pp. 132–212.

(6) R. G. Kallen and W. P. Jencks, *J. Biol. Chem.*, **241**, 5864 (1966).

(7) J. F. Walker, "Formaldehyde," 3rd ed., Reinhold, New York, N.Y., 1964, p. 53.

(8) A. A. Noyes and W. R. Whitney, *J. Am. Chem. Soc.*, **19**, 930 (1897).

(9) W. Nernst and E. Brunner, *Z. Phys. Chem.*, **47**, 56 (1904).

(10) I. H. Pitman, Ph.D. thesis, Australian National University, Canberra, Australia, 1966.

(11) "The United States Pharmacopeia," 18th rev., Mack Publishing Co., Easton, Pa., 1970.


## ACKNOWLEDGMENTS


Adapted in part from a thesis submitted by P. C. Bansal to the University of Kansas in partial fulfillment of the Doctor of Philosophy degree requirements.

Supported in part by a grant from the Inter$_x$ Corp., Lawrence, KS 66044.

# Determination of Oxfendazole in Cow Milk by Reversed-Phase High-Performance Liquid Chromatography

**I. W. TSINA** ˣ **and S. B. MATIN**

Received August 18, 1980, from the *Department of Analytical and Metabolic Chemistry, Syntex Research, Palo Alto, CA 94304.*
Accepted for publication January 6, 1981.

**Abstract** □ A specific and sensitive high-performance liquid chromatographic method for the analysis of oxfendazole in cow milk is described. Oxfendazole was extracted from milk using a mixture of acetone and chloroform under alkaline conditions. The solvents were evaporated, and the oily residue was purified by hexane–acetonitrile partition and acid–base extraction. The residue obtained after cleanup was redissolved in methanol for chromatographic analysis. Chromatography was performed on a reversed-phase column with acetonitrile–water as the mobile phase. As low as 0.005 μg of oxfendazole/g can be measured by this method using 50 g of milk. The method was applied to measure oxfendazole in the milk of a cow given an oral 5-mg/kg dose.

**Keyphrases** □ Oxfendazole—high-performance liquid chromatographic analysis of cow milk □ High-performance liquid chromatography—analysis of oxfendazole in cow milk □ Anthelmintics—oxfendazole, high-performance liquid chromatographic analysis in cow milk

Oxfendazole, [5-(phenylsulfinyl)-1*H*-benzimidazol-2-yl]carbamate (I), is a new orally effective anthelmintic agent for the control of GI and lung parasites in cattle and sheep (1). The use of oxfendazole as an anthelmintic in dairy cattle may result in its presence in milk at low levels. To protect the general public from exposure to drug residue in milk, a government guideline for the safe use of animal drugs requires a sensitive analytical method for drug level monitoring in marketed milk (2).

## BACKGROUND

Oxfendazole belongs to the benzimidazole class of anthelmintics. The analysis of benzimidazole compounds in animal tissues and biological fluids by colorimetric (3), fluorometric (3–5), high-performance liquid chromatographic (HPLC) (6, 7), and radioimmunoassay (8) methods has been described. The colorimetric and fluorometric methods lack the specificity and sensitivity needed for assay from milk. HPLC and radioimmunoassay are intended for use in plasma, utilizing minimum sample cleanup. Because of the high fat content of raw milk, these methods are not applicable to the analysis of trace drug levels in milk.

An HPLC method for the analysis of benzimidazole compound in animal tissues and milk based on ion-exchange chromatography also was reported (9). The sensitivity achieved was 0.05 μg/g in cow milk and 0.1 μg/g in cattle tissues. To ascertain the safe use of oxfendazole in food-producing animals, an analytical method capable of measuring the drug level at 0.005 μg/g in milk is required.

This paper describes an analytical method using HPLC and UV detection. The nanogram per gram level of measurement was achieved by a highly efficient extraction and cleanup procedure. The method was used to establish the depletion profile of oxfendazole in milk of a dairy cow following a single oral dose of 5 mg of oxfendazole/kg.

## EXPERIMENTAL

**Reagents and Chemicals**—All solvents were distilled-in-glass grade[1]. Other reagents and chemicals were reagent grade. Phosphate saline buffer (pH 8) was 0.05 *M*, containing 9 g of sodium chloride in 1 liter of buffer. Oxfendazole and the internal standard, [5-(4-methylsulfinylphenoxy)-1*H*-benzimidazol-2-yl]carbamate (II), were obtained in-house[2].

**Apparatus**—Analyses were performed on a high-performance liquid chromatograph[3] equipped with a UV detector set at 254 nm and a 10-mv recorder. A 4-mm × 30-cm reversed-phase column[4] coupled with a precolumn[5] was used for chromatographic separation.

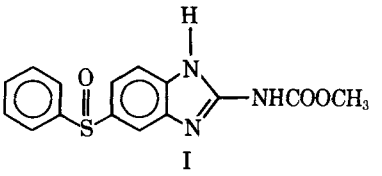


I

**Chromatographic Conditions**—The mobile phase was 24.5% acetonitrile in water at a flow rate of 2 ml/min. The columns were operated at ambient temperature, and column pressure was maintained between 1000 and 2000 psi.

**Extraction**—Raw milk (50 g) was weighed into a 250-ml polypropylene bottle, and a solution of internal standard (1 ml of a 1-μg/ml solution in 0.1 *N* HCl) was added. The bottle contents were swirled, and 150 ml of acetone was added. The bottle was capped and mechanically shaken for 10 min.

After centrifugation, the acetone extract was poured into a 500-ml separator. Then 10 ml of pH 8 phosphate buffer and 300 ml of chloroform were added to the acetone extract. The mixture was shaken for 10 min, and the layers were allowed to separate over 10 min. The lower organic layer was drained into a 500-ml erlenmeyer flask containing 80 g of granular anhydrous sodium sulfate, and the flask was stoppered and shaken briefly. The mixture was filtered through a 80-mm i.d. polypropylene powder funnel fitted with a glass wool plug.

The filtrate was collected into a 1-liter round-bottom evaporation flask. The erlenmeyer flask was rinsed with 50 ml of chloroform–acetone (2:1), and the rinse solvent was filtered through the same funnel and combined with the first extract in the 1-liter flask. The organic extract was evaporated to an oily residue, using a vacuum rotary evaporator with the water bath set at 37°. The residue obtained was transferred to a 125-ml separator with the aid of 50 ml of hexane and 50 ml of acetonitrile, and the separator was capped and shaken for 5 min. The separated acetonitrile layer then was drained into another separator and washed twice with 25 ml of hexane.

The final acetonitrile extract was drained into a 250-ml round-bottom flask and evaporated to a residue on a rotary evaporator. The residue obtained was transferred quantitatively to a 125-ml separator with the aid of 50 ml of ethyl acetate. The ethyl acetate was extracted with 0.2 *N* HCl (3 × 10 ml). The acid was combined in another 125-ml separator and washed with hexane (2 × 10 ml). All ethyl acetate and hexane layers were discarded. Then 6 ml of 1 *N* NaOH was added to the acid extract, and the solution pH was adjusted to 8 by the addition of 300 mg of sodium bicarbonate.

The basic solution was extracted with ethyl acetate (2 × 25 ml). The ethyl acetate extract was dried over a bed of anhydrous sodium sulfate (5 g) and evaporated to a residue. The residue was redissolved in 10 ml of ethyl acetate and filtered through a 0.5-μm filter[6] into a 15-ml conical test tube. The filtrate was evaporated to dryness and redissolved in 200

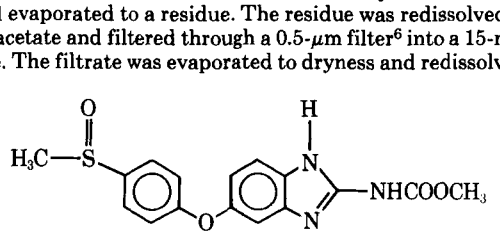


II

[1] Burdick & Jackson Laboratories, Muskegon, Mich.
[2] Syntex Research, Palo Alto, Calif.
[3] Model ALC/GPC-204, Waters Associates, Milford, Mass.
[4] μBondapak $C_{18}$, Waters Associates, Milford, Mass.
[5] Co-Pell ODS guard column, Whatman, Clifton, N.J.
[6] Fluoropore filter FHLP 1300, Millipore Corp., Bedford, Mass.



*0022-3549/81/0800-0858$01.00/0*
© *1981, American Pharmaceutical Association*

**Table I—Percent of Radioactivity Present at Each Step of Extraction**

| Extraction Step | Recovery[a], % |
|---|---|
| Acetone extract | 93.21 |
| Chloroform–acetone (2:1) extract | 92.12 |
| Aqueous layer | 1.27 |
| Hexane | 1.02 |
| Ethyl acetate after 0.2 *N* HCl extraction | 4.84 |
| Hexane wash of 0.2 *N* HCl | NM[b] |
| Base after ethyl acetate extraction | 0.57 |
| Final extract for HPLC | 79.23[c] |
| HPLC assay (μg/g) | 0.01 |

[a] From raw milk spiked with 0.01 μg of [$^{14}$C]oxfendazole/g. [b] Not measurable. [c] About 6% of the radioactivity was not accounted for, probably due to adsorption onto glassware.

μl of methanol. An aliquot (25 μl) was injected onto the chromatograph for analysis.

**Extraction Efficiency and Total Recovery**—A known amount of $^{14}$C-labeled oxfendazole was spiked into drug-free raw milk. Extraction efficiency and total recovery of oxfendazole were established by monitoring the radioactivity present in every fraction at each step.

**Calibration Curve Preparation**—Oxfendazole levels in unknown samples were determined with a calibration curve prepared in the following manner. Known amounts of oxfendazole and the internal standard were spiked into drug-free raw milk in the range of 0.005–0.05 μg of oxfendazole/g and 0.02 μg of the internal standard/g. The samples were processed as described and subjected to HPLC analysis. The calibration curve was constructed by plotting the ratio of the chromatographic peak heights of oxfendazole and the internal standard *versus* micrograms of oxfendazole spiked per gram.

Spiking solutions of oxfendazole, 0.25, 0.5, 1, 1.5, 1, and 2.5 μg/ml, were prepared by diluting the stock solution of oxfendazole with 0.1 *N* HCl. Oxfendazole stock solution was prepared by dissolving 10 mg of oxfendazole in 100 ml of methanol–0.1 *N* HCl (1:1). The internal standard spiking solution (1 μg/ml in 0.1 *N* HCl) was prepared by the dilution of a stock internal standard solution of 50 μg/ml with 0.1 *N* HCl. One milliliter of each oxfendazole spiking solution was added to 50 g of raw milk to yield spiking levels of 0.005, 0.01, 0.02, 0.03, 0.04, and 0.05 μg of oxfendazole/g. One milliliter of the spiking internal standard solution then was added to the raw milk (50 g) already fortified with oxfendazole to obtain 0.02 μg of the internal standard/g.

**Analysis of Milk Samples Containing Oxfendazole Levels of >0.05 μg/g**—Milk samples containing oxfendazole levels higher than the calibration curve range were diluted with appropriate amounts of blank milk obtained from an untreated animal. The samples after dilution were treated in the same manner as described under *Extraction*. A dilution factor then was included in the final calculation against the calibration curve.

**Table II—Statistical Parameters of Milk Calibration Curves**

| Curve Number | Correlation Coefficient | Linear Regression Intercept, μg/g | Linear Regression Slope[a] |
|---|---|---|---|
| I | 0.9995 | 0.0003 | 51.16 |
| II | 0.9997 | 0.0004 | 49.17 |
| III | 0.9993 | 0.0007 | 49.84 |
| IV | 0.9998 | 0.0002 | 50.06 |

[a] The mean was 50.06 ± 0.83 (*SD*).

## RESULTS AND DISCUSSION

Oxfendazole, a benzimidazole carbamate, was chromatographed using a reversed-phase microparticulate column and a mobile phase of 24.5% acetonitrile in water. Baseline resolution of oxfendazole and its structural analog used as an internal standard was achieved. The UV spectrum of oxfendazole in methanol indicated that its $\lambda_{max}$ was at 228 nm with a molar extinction coefficient of 45,565. Due to the ready availability of a 254-nm fixed-wavelength UV detector, detection at 254 nm was preferred. The molar extinction coefficient at 254 nm was 11,025 and was adequate for the sensitivity requirement of this assay.

Oxfendazole extraction from milk using various solvents was investigated. The extraction of milk directly with ethyl acetate caused an unbreakable emulsion. Emulsion formation also was observed when chloroform was used. To eliminate this problem, acetone was added to milk to precipitate the milk protein and also to act as an extracting solvent. The acetone extract then was partitioned with chloroform to remove water. The organic layer obtained was cleaned up further *via* hexane–acetonitrile partitioning and acid–base extraction. Until the acetone–chloroform extraction step, ~92% of the spiked [$^{14}$C]oxfendazole was extracted. The overall recovery of [$^{14}$C]oxfendazole spiked in milk that went through the entire extraction procedure was 79%. A step-by-step account of loss and recovery throughout the assay is summarized in Table I.

The chromatograms of control milk and milk spiked with oxfendazole

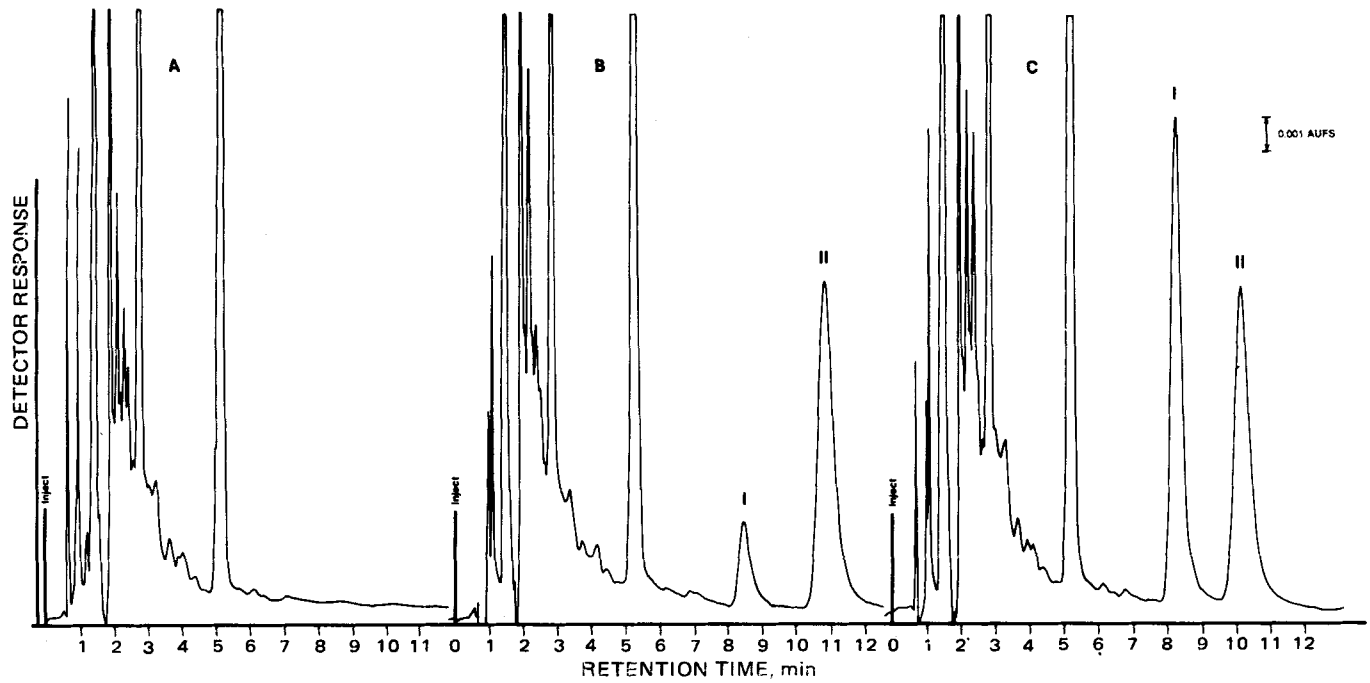


**Figure 1**—*A, high-performance liquid chromatogram obtained from the analysis of control milk processed through the procedure; B, control milk spiked with 0.005 μg of oxfendazole/g and 0.02 μg of internal standard/g; and C, control milk spiked with 0.03 μg of oxfendazole/g and 0.02 μg of internal standard/g. Chromatographic conditions were: mobile phase, 24.5% acetonitrile in water; flow rate, 2 ml/min; temperature, ambient; and detection, 254 nm at 0.01 aufs. Key: I, oxfendazole; and II, internal standard.*

Table III—Analysis of Oxfendazole Level in Spiked Cow Milk

| Oxfendazole Spiked, μg/g | Oxfendazole Found, μg/g | Mean | Ratio of Assayed to Spiked Milk |
|---|---|---|---|
| 0.005 | 0.0051 | 0.0051 | 1.02 |
| | 0.0050 | | |
| | 0.0052 | | |
| | 0.0052 | | |
| 0.01 | 0.010 | 0.0105 | 1.05 |
| | 0.010 | | |
| | 0.011 | | |
| | 0.011 | | |
| 0.02 | 0.021 | 0.0205 | 1.03 |
| | 0.020 | | |
| | 0.021 | | |
| | 0.020 | | |
| 0.03 | 0.030 | 0.030 | 1.00 |
| | 0.030 | | |
| | 0.030 | | |
| | 0.030 | | |
| 0.04 | 0.040 | 0.0405 | 1.01 |
| | 0.040 | | |
| | 0.042 | | |
| | 0.040 | | |
| 0.05 | 0.052 | 0.0503 | 1.01 |
| | 0.049 | | |
| | 0.050 | | |
| | 0.050 | | |

and the internal standard are shown in Fig. 1. The chromatogram obtained from the analysis of drug-free milk showed no interference peak at the retention time of oxfendazole and the internal standard. Chromatograms from milk spiked with 0.005 or 0.03 μg of oxfendazole/g along with 0.02 μg of the internal standard/g indicated adequate peak response for both compounds at these concentrations.

The calibration curve obtained from the analysis of blank milk spiked with oxfendazole in the 0.005–0.05-μg/g concentration range was linear. The statistical parameters showing linear regression fits of four calibration curves are given in Table II. Table III summarizes the data obtained from the repeat analysis of milk samples spiked with oxfendazole.

Coefficient of variance (standard deviation per mean) was calculated to assess assay variability. The coefficients of variance for the analysis at 0.005, 0.01, 0.02, 0.03, 0.04, and 0.05 μg/g ($n = 4$) were 1.95, 4.84, 2.94, 0.66, 1.98, and 1.99%, respectively.

Oxfendazole levels in the milk of a cow following the administration of 5 mg of oxfendazole/kg were determined by the described method. The cow was milked at 0 (predose), 4, 8, 12, and 24 hr after dose on the 1st day. For the next 6 days, milking was carried out every 12 hr. The oxfendazole levels in milk 4, 8, 12, 24, 36, 48, 60, and 72 hr following dose administration were 0.097, 0.212, 0.334, 0.460, 0.325, 0.173, 0.058, and 0.009 μg/g, respectively. Oxfendazole was not detected beyond 72 hr after dose.

## REFERENCES


(1) E. A. Averkin, C. C. Beard, C. A. Dvorak, J. A. Edwards, J. H. Fried, J. G. Kilian, and R. A. Schiltz, *J. Med. Chem.*, **18**, 1164 (1975).

(2) M. K. Perez, *J. Toxicol. Environ. Health*, **3**, 837 (1977).

(3) H. L. Pease and J. A. Gardiner, *J. Agric. Food Chem.*, **17**, 267 (1969).

(4) H. L. Pease and R. F. Holt, *J. Assoc. Off. Anal. Chem.*, **54**, 1399 (1971).

(5) "Food Additives Analytical Manual," rev. ed., Food and Drug Administration, Washington, D.C., 1973, Sec.121.260.

(6) K. B. Alton, J. E. Patrick, and J. L. McGuire, *J. Pharm. Sci.*, **68**, 880 (1979).

(7) J. A. Bogan and S. Marriner, *ibid.*, **69**, 422 (1980).

(8) C. Nerenberg, R. A. Runkel, and S. B. Matin, *ibid.*, **67**, 1553 (1978).

(9) J. J. Kirland, *J. Agric. Food Chem.*, **21**, 171 (1973).


## ACKNOWLEDGMENTS


Presented in part at the APhA Academy of Pharmaceutical Sciences, Washington, D.C. meeting, April 1980.

The authors thank Dr. Colin Beard and Dr. Charles Dvorak for the synthesis of the internal standard. The authors are indebted to Marian Fass for technical assistance, and thanks also are extended to Leigh Ann Wolfe for typing the manuscript.


# GLC Determination of Itanoxone in Biological Fluids


**HENRI COUSSE ˣ, JEAN-PAUL RIBET, and JEAN-CLAUDE VEZIN**



Received August 11, 1980, from the *P. Fabre S.A. Research Center, 17 Avenue Jean Moulin, 81106 Castres, France.* Accepted for publication January 6, 1981.



**Abstract** □ A sensitive and reliable method for the quantitative determination of itanoxone, 4-[4′-(2-chlorophenyl)phenyl]-4-oxo-2-methylenebutanoic acid, in biological fluids is described. A quantitative ethyl acetate extraction of the plasma samples is followed by reduction and methylation of itanoxone. Quantification is achieved by GLC using electron-capture detection and an internal standard. The minimum concentration of itanoxone detected in plasma is 0.1 μg/ml. Recovery of the titrated compound added to human plasma averaged 100.9 ± 2.92% (*RSD*).



**Keyphrases** □ Itanoxone—GLC determination in biological fluids □ GLC determination, electron-capture detection—analysis, itanoxone, biological fluids □ 4-[4′-(2-Chlorophenyl)phenyl]-4-oxo-2-methylenebutanoic acid—itanoxone, GLC determination in biological fluids


Itanoxone (1), 4-[4′-(2-chlorophenyl)phenyl]-4-oxo-2-methylenebutanoic acid (I), is used in the treatment of metabolic disorders (2–10). The impurities likely to be found in this raw material were studied (11), as was a purification process (12). The present study perfected a sensitive and reliable method for studying the absorption, metabolism, and excretion of I in animals and humans at relatively low doses.

TLC methods were described for the determination of I in pharmaceutical formulations[1] (13). Quantitation was achieved using the UV-absorbing properties of I. The method described in this paper used GLC followed by electron-capture detection for the determination of small quantities of I in biological fluids and pharmaceutical formulations.

## EXPERIMENTAL

**Reagents and Materials**—Itanoxone[2] (I) and internal standard (II) were obtained by a Friedel–Crafts reaction between itaconic anhydride and the corresponding aromatic derivative (14). The standard solutions

[1] A. Boucherle, University of Grenoble, Grenoble, France, expert report.

[2] F 1379.




*0022-3549/81/0800-0860$01.00/0*



*© 1981, American Pharmaceutical Association*

Table III—Analysis of Oxfendazole Level in Spiked Cow Milk

| Oxfendazole Spiked, μg/g | Oxfendazole Found, μg/g | Mean | Ratio of Assayed to Spiked Milk |
|---|---|---|---|
| 0.005 | 0.0051 | 0.0051 | 1.02 |
| | 0.0050 | | |
| | 0.0052 | | |
| | 0.0052 | | |
| 0.01 | 0.010 | 0.0105 | 1.05 |
| | 0.010 | | |
| | 0.011 | | |
| | 0.011 | | |
| 0.02 | 0.021 | 0.0205 | 1.03 |
| | 0.020 | | |
| | 0.021 | | |
| | 0.020 | | |
| 0.03 | 0.030 | 0.030 | 1.00 |
| | 0.030 | | |
| | 0.030 | | |
| | 0.030 | | |
| 0.04 | 0.040 | 0.0405 | 1.01 |
| | 0.040 | | |
| | 0.042 | | |
| | 0.040 | | |
| 0.05 | 0.052 | 0.0503 | 1.01 |
| | 0.049 | | |
| | 0.050 | | |
| | 0.050 | | |

and the internal standard are shown in Fig. 1. The chromatogram obtained from the analysis of drug-free milk showed no interference peak at the retention time of oxfendazole and the internal standard. Chromatograms from milk spiked with 0.005 or 0.03 μg of oxfendazole/g along with 0.02 μg of the internal standard/g indicated adequate peak response for both compounds at these concentrations.

The calibration curve obtained from the analysis of blank milk spiked with oxfendazole in the 0.005–0.05-μg/g concentration range was linear. The statistical parameters showing linear regression fits of four calibration curves are given in Table II. Table III summarizes the data obtained from the repeat analysis of milk samples spiked with oxfendazole.

Coefficient of variance (standard deviation per mean) was calculated to assess assay variability. The coefficients of variance for the analysis at 0.005, 0.01, 0.02, 0.03, 0.04, and 0.05 μg/g ($n = 4$) were 1.95, 4.84, 2.94, 0.66, 1.98, and 1.99%, respectively.

Oxfendazole levels in the milk of a cow following the administration of 5 mg of oxfendazole/kg were determined by the described method. The cow was milked at 0 (predose), 4, 8, 12, and 24 hr after dose on the 1st day. For the next 6 days, milking was carried out every 12 hr. The oxfendazole levels in milk 4, 8, 12, 24, 36, 48, 60, and 72 hr following dose administration were 0.097, 0.212, 0.334, 0.460, 0.325, 0.173, 0.058, and 0.009 μg/g, respectively. Oxfendazole was not detected beyond 72 hr after dose.

## REFERENCES


(1) E. A. Averkin, C. C. Beard, C. A. Dvorak, J. A. Edwards, J. H. Fried, J. G. Kilian, and R. A. Schiltz, *J. Med. Chem.*, **18**, 1164 (1975).

(2) M. K. Perez, *J. Toxicol. Environ. Health*, **3**, 837 (1977).

(3) H. L. Pease and J. A. Gardiner, *J. Agric. Food Chem.*, **17**, 267 (1969).

(4) H. L. Pease and R. F. Holt, *J. Assoc. Off. Anal. Chem.*, **54**, 1399 (1971).

(5) "Food Additives Analytical Manual," rev. ed., Food and Drug Administration, Washington, D.C., 1973, Sec.121.260.

(6) K. B. Alton, J. E. Patrick, and J. L. McGuire, *J. Pharm. Sci.*, **68**, 880 (1979).

(7) J. A. Bogan and S. Marriner, *ibid.*, **69**, 422 (1980).

(8) C. Nerenberg, R. A. Runkel, and S. B. Matin, *ibid.*, **67**, 1553 (1978).

(9) J. J. Kirland, *J. Agric. Food Chem.*, **21**, 171 (1973).


## ACKNOWLEDGMENTS


Presented in part at the APhA Academy of Pharmaceutical Sciences, Washington, D.C. meeting, April 1980.

The authors thank Dr. Colin Beard and Dr. Charles Dvorak for the synthesis of the internal standard. The authors are indebted to Marian Fass for technical assistance, and thanks also are extended to Leigh Ann Wolfe for typing the manuscript.


# GLC Determination of Itanoxone in Biological Fluids


**HENRI COUSSE ˣ, JEAN-PAUL RIBET, and JEAN-CLAUDE VEZIN**



Received August 11, 1980, from the *P. Fabre S.A. Research Center, 17 Avenue Jean Moulin, 81106 Castres, France.* Accepted for publication January 6, 1981.



**Abstract** □ A sensitive and reliable method for the quantitative determination of itanoxone, 4-[4′-(2-chlorophenyl)phenyl]-4-oxo-2-methylenebutanoic acid, in biological fluids is described. A quantitative ethyl acetate extraction of the plasma samples is followed by reduction and methylation of itanoxone. Quantification is achieved by GLC using electron-capture detection and an internal standard. The minimum concentration of itanoxone detected in plasma is 0.1 μg/ml. Recovery of the titrated compound added to human plasma averaged 100.9 ± 2.92% (*RSD*).



**Keyphrases** □ Itanoxone—GLC determination in biological fluids □ GLC determination, electron-capture detection—analysis, itanoxone, biological fluids □ 4-[4′-(2-Chlorophenyl)phenyl]-4-oxo-2-methylenebutanoic acid—itanoxone, GLC determination in biological fluids


Itanoxone (1), 4-[4′-(2-chlorophenyl)phenyl]-4-oxo-2-methylenebutanoic acid (I), is used in the treatment of metabolic disorders (2–10). The impurities likely to be found in this raw material were studied (11), as was a purification process (12). The present study perfected a sensitive and reliable method for studying the absorption, metabolism, and excretion of I in animals and humans at relatively low doses.

TLC methods were described for the determination of I in pharmaceutical formulations[1] (13). Quantitation was achieved using the UV-absorbing properties of I. The method described in this paper used GLC followed by electron-capture detection for the determination of small quantities of I in biological fluids and pharmaceutical formulations.

## EXPERIMENTAL

**Reagents and Materials**—Itanoxone[2] (I) and internal standard (II) were obtained by a Friedel–Crafts reaction between itaconic anhydride and the corresponding aromatic derivative (14). The standard solutions

[1] A. Boucherle, University of Grenoble, Grenoble, France, expert report.

[2] F 1379.




*0022-3549/81/0800-0860$01.00/0*



*© 1981, American Pharmaceutical Association*

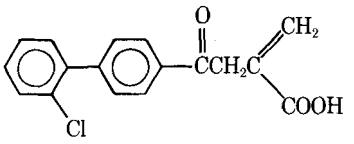

I

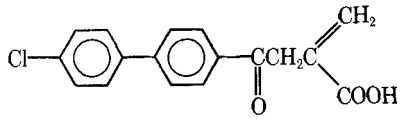

II

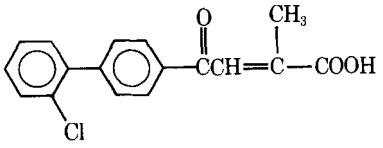

III

of the products to be analyzed were stored in glass containers at 5°. All solvents were analytical reagent grade, and the reducing catalyst was 10% palladium-on-charcoal[3].

Diazomethane (15, 16), used as the methylating agent, was obtained from *N*-methyl-*N*-nitroso-*p*-toluenesulfonamide[4] as follows. A 250-ml distilling flask was fitted with a condenser for distillation and with a funnel. The condenser was connected to two 50-ml receiver tubes immersed in ice water. Ether (10 ml) was placed in the first receiver, and 35 ml of ether was placed in the second. The outlet tube passed above the surface of the acetic acid solution in an erlenmeyer flask.

In the distilling flask was introduced 5 ml of 60% (w/w) potassium hydroxide aqueous solution, and then 5 ml of 2-ethoxyethanol and 3 ml of ether were added. In the dropping funnel was placed 20 ml of 10% (w/w) *N*-methyl-*N*-nitroso-*p*-toluenesulfonamide in ether. The flask was heated in a water bath at 70°, and the ethereal solution was transferred gently into the flask at a regular rate during 15–20 min. The diazomethane that formed was driven off by ether and collected in the two receivers.

This semimicromethod does not present any serious danger of explosion or toxicity if handled carefully under a well-ventilated hood. To avoid accidental exposure to diazomethane, work was performed in a saturated acetic acid atmosphere under a hood. The ethereal solution of diazomethane should be kept in hermetically stoppered glass tubes and stored at 5° for up to 1 week.

In compliance with these safety rules, the diazomethane solution can be titrated at 0° with an excess of accurately titrated benzoic acid solution. The benzoic acid must be in excess as evidenced by the complete decolorization of the diazomethane solution. The unreacted benzoic acid is determined using 0.2 *N* alcoholic potassium hydroxide in the presence of phenolphthalein. Any diazomethane accidentally given off is neutralized immediately by acetic acid into atoxic methyl acetate.

**Instrumentation**—A gas chromatograph[5] was fitted with a nickel 63 electron-capture detector, an integrator[6], and a recorder[7]. A densitometer[8] and a reciprocating shaker[9] also were used.

**TLC**—The products obtained by synthesis or contained in pharmaceutical formulations were evaluated on thin layers (250 μm) of silica gel 60 $F_{254}$[3], ascendingly developed with methanol–chloroform (15:85) in a saturated atmosphere (13). Each sample was taken up in 0.1% (w/w) ethanol, and 5-μl aliquots were spotted. After development to within 10 cm of the solvent front, the plates were dried and the spots were visualized by irradiation of the plates under a UV lamp (254 nm). Under these conditions, I, II, III, and IV had $R_f$ values of 0.42, 0.35, 0.29, and 0.47, respectively.

This technique also was used to analyze IV by fluorescence inhibition (13). Quantitative determination was carried out by comparison with a range of standards chromatographed under the same conditions as the samples. Aliquots equivalent to 1.5, 3.5, 7.5, and 12.5 μg of IV standard ethanolic solution likewise were spotted on the plate. A calibration curve

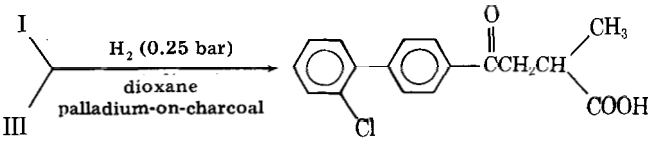

IV

*Scheme I*

was obtained by plotting the percentage of fluorescence inhibition *versus* known concentrations of IV in ethanol. Values for unknown concentrations of IV in samples were calculated from the standard curve.

**GLC Conditions**—Analyses were performed using a glass column, 1.1 m × 2 mm i.d., packed with 3% OV-225 (phenylcyanopropyl) on Chromosorb W.A.W. (80–100 mesh). The column was conditioned for 24 hr at 260° with a nitrogen flow of 10 ml/min. Gases (nitrogen, compressed air, and hydrogen) used for chromatography were purified with filters containing 4-Å molecular sieves. The detector and injector temperatures were 290 and 250°, respectively. The column was maintained isothermally at 230°. Nitrogen was the carrier gas. The flow rates for nitrogen, hydrogen, and compressed air were maintained at 50, 20, and 400 ml/min, respectively. The pulse interval for the electron-capture detector was 20 μsec. Because of the elevated temperature of the injector, high temperature septa[10] were used.

**Assay**—Itanoxone is a polar molecule that cannot be analyzed directly by GLC with specific columns generally used for organic acids. Compounds I and II were determined by GLC after two derivatizations, including reduction of the ethylenic bond followed by esterification of the acid group (17). Reduction was used to obtain a single compound from I and its isomer (III) which might form during extraction and chromatography at high temperature (Scheme I). Reduction also avoids the formation of a cyclopropane derivative (VI) by the addition of diazomethane to the ethylenic bond (Scheme II). Quantitation by TLC has been used at this step for I in pharmaceutical formulations and synthesis products.

Chromatography at low concentrations, such as those found in blood and urine, required an electron-capture detector for good sensitivity. By derivatizing the acid group, polarity was decreased and volatility was increased, thus providing increased sensitivity with a shorter analysis time. Methyl esters were formed quantitatively and rapidly with the diazomethane reagent.

**Sample Preparation**—Blood samples were collected routinely in heparinized tubes, and plasma was separated by centrifugation. Exactly 1 ml of plasma was pipetted into a 25-ml glass-stoppered extraction tube.

Plasma samples (1 ml) were spiked with 0.5 ml of the internal standard solution (10 μg). Then 1 ml of the buffer solution[11] (pH 2.2) and 10 ml of ethyl acetate were added. The preparation was shaken vigorously for 1–2 hr, and the layers were separated by centrifugation for 10 min at 3000 rpm. Ethyl acetate was transferred quantitatively to another 25-ml extraction tube and was evaporated to dryness with a gentle nitrogen stream. The residue then was dissolved in 2 ml of dioxane, and the reduction of I was performed as follows.

To the 2 ml of dioxane solution of the residue were added 0.1 ml of acetic acid in dioxane (10% w/w) and 2 mg of palladium-on-charcoal (10%). Then the solution was mixed with a magnetic stirrer; each cen-

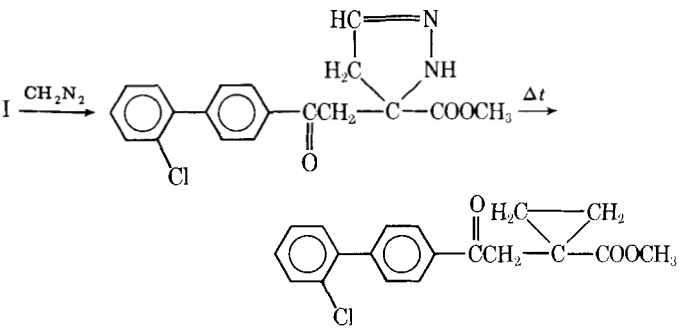

VI

*Scheme II*

[3] E. Merck, Darmstadt, West Germany.
[4] *N*-Methyl-*N*-tosyl nitrosamide, E. Merck, Darmstadt, West Germany.
[5] Girdel 3000, Giravions Dorand, Suresnes, France.
[6] Icap 50, L.T.T., Suresnes, France.
[7] Servotrace type PE, Sefram, Paris, France.
[8] Joyce Loebl Chromoscan.
[9] New Brunswick Scientific, Edison, N.J.

[10] Chromseptum red, Chrompack, Middelburg, The Netherlands.
[11] Consisted of sodium citrate–hydrochloric acid, E. Merck, Darmstadt, West Germany.

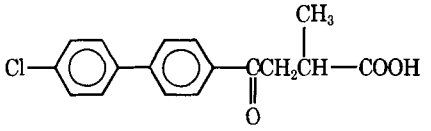

V

trifuge tube was stoppered and purged with nitrogen, and hydrogen was passed through it. Hydrogenation was conducted for 1 hr at 0.25 bar. After centrifugation for 10 min at 3000 rpm, the residue was extracted with 2 ml of dioxane and centrifuged. Dioxane fractions were collected in 10-ml conical glass vials, and the solvent was removed under reduced pressure (15 mm) at 60°. The residue then was dissolved in an ethereal solution of diazomethane until nitrogen bubbles disappeared. This mixture was allowed to react completely at room temperature for 1 hr. After evaporation[12], the residue was dissolved in 2 ml of hexane. Volumes of 1 μl were injected into the gas chromatograph.

**Calculations**—An integrator was employed for measurement of retention times and peak areas. Values for unknown concentrations of I in plasma were calculated from the internal standard (II) introduced before treatment.

## RESULTS AND DISCUSSION

The TLC method was used for the quantitative determination of the reduced compound. TLC does not require expensive instrumentation, and the time required to determine the concentration of itanoxone (I) in pharmaceutical formulations varies according to the number of samples, *i.e.*, ~4 hr for six samples. Under these conditions, the minimal detectable amount is 0.5 mg/ml. A linear relationship between fluorescence inhibition and concentration is obtained for IV over the 0–15-mg/ml range. Quantification from a standard curve was adequate. To increase precision, the results are expressed on the basis of an average of three spots; reproducibility is limited to ±1%.

GLC has an advantage over previously reported methods because of its great sensitivity for I. The samples were esterified for GLC measurements. Under the assay conditions, IV and V methyl esters had retention times of 4 and 6 min, respectively (Fig. 1). The lower limit of detection sensitivity of I in human plasma extracts is 0.1 μg/ml. This value is based on a sample signal equivalent to 10% of the full-scale response. A linear relationship between detector response and concentration was obtained for I over the 0–20-μg/ml range.

Compound I was isomerized to III during GLC. The high working temperatures favor isomerization. The olefin was reduced to IV to avoid differentiation of the two isomers I and III and the side reaction with diazomethane to form a cyclopropane derivative. A series of samples containing known amounts of I was prepared to determine optimal reaction times for the formation of IV.

The results indicated that reduction of I was completed within 60 min, using palladium-on-charcoal in dioxane media (Fig. 2). Figure 3 illustrates a chromatogram of placebo human plasma extracts.

Reduction with platinum oxide as a catalyst gave small amounts of the

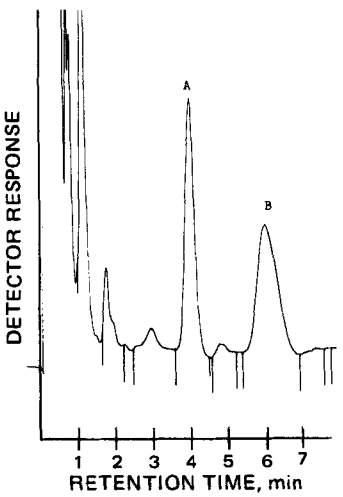


**Figure 1**—*Gas–liquid chromatogram (electron-capture detector) of human plasma extracts. Key: A, I reduced and esterified; and B, II reduced and esterified.*

[12] Rotavapor M, type HB 140, Buchi S. A., Flawil, Switzerland.

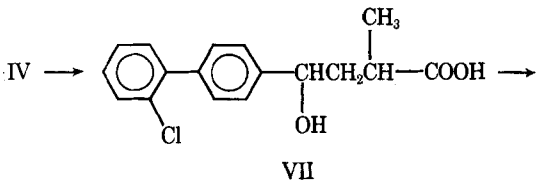

VII

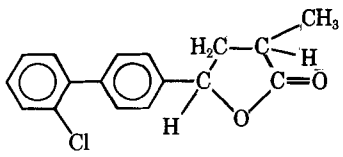

VIII

*Scheme III*

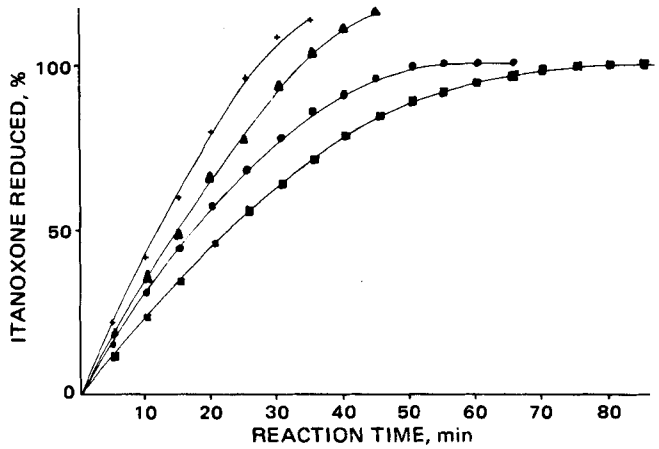


**Figure 2**—*Effect of reaction time and reducing medium on formation of saturated compound. Key: ●, palladium-on-charcoal in dioxane media; ▲, platinum oxide in dioxane–acetic acid; ■, palladium on aluminum oxide in dimethylformamide; and +, platinum oxide in dimethyl formamide–acetic acid media. Beyond 100% reduction, the ketonic group is reduced to a secondary alcohol.*

side-products VII and VIII. Reduction of the ketonic group occurred mainly with other catalysts such as platinum oxide, with a relative excess of catalyst and/or a high hydrogen pressure (Scheme III). Acetic acid was necessary, and up to 30% (w/w) water did not interfere with reduction.

The derivatives were stable for at least 3 weeks. The choice of II as the internal standard in the estimation of I was based on similar physicochemical characteristics. Compound II, the chemical isomer of I, was added prior to extraction. Partition coefficients of I and II were log $P$ = 7.65 and 7.77, respectively, indicating equal extraction of both compounds.

For recovery experiments, known amounts of I and II in ethyl acetate were evaporated to dryness in glass-stoppered extraction tubes, and plasma was added. The samples were mixed thoroughly and extracted. The materials were derivatized and analyzed by GLC.

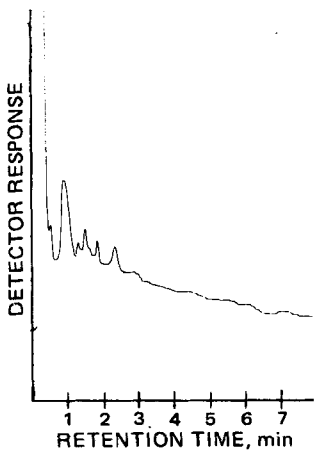


**Figure 3**—*Gas–liquid chromatogram (electron-capture detector) of placebo human plasma extracts.*

**Table I—Accuracy and Reproducibility of GLC Analysis of I Added to Human Plasma**

| Added, μg/ml | Mean Recovered Amount (Range) | Recovery, %[a] |
|---|---|---|
| 0.1 | 0.101 (0.097–0.103) | 101 |
| 0.5 | 0.49 (0.480–0.51) | 98 |
| 1 | 1.03 (0.95–1.31) | 103 |
| 5 | 4.81 (4.74–5.33) | 96.2 |
| 10 | 10.35 (9.84–10.72) | 103.5 |
| 15 | 15.50 (14.68–15.96) | 104 |

[a] Mean ± *SD* = 100.95 ± 2.92; number of analyses = 4.

The results (Table I) show the accuracy and reproducibility of the GLC analysis of I in clinical samples. The response factor was calculated using the ratio of peak areas for similar concentrations of I and II (1.22 ± 0.12). The method has been used in laboratories to determine the amount of I in rat blood compared with radioisotopic methods (18, 19). It also has been used for the determination of I in plasma and urine of humans and in pharmacokinetic studies (18).

Recently, a simple and fast high-performance liquid chromatographic method (20) was developed in which derivatization was not necessary. However, the sensitivity was not as good as that using GLC electron-capture detection.

## REFERENCES


(1) *Chron. Org. Mond. Santé*, **33** (3), list 41-8 (1975).

(2) *Drugs of the Future*, **5**(5), 246 (1980).

(3) H. Cousse, G. Mouzin, J. P. Rieu, and A. Delhon (to P. Fabre S.A.), French pat. 2,300,551 (1975).

(4) A. Bizzi, M. T. Tacconi, E. Veneroni, and M. Cini, "7ème Congrès International de Pharmacologie," Paris, France, 1978.

(5) A. Delhon, J. P. Tarayre, H. Lauressergues, and S. Casadio, in "International Conference on Atherosclerosis," Milan, Italy, Nov. 1975.

(6) J. Lubetzki and A. Mose, in *ibid.*

(7) F. Mazoyer (to P. Fabre S.A.), U.S. pat. appl. 105,420 (1979).

(8) P. Drouin, J. Demange, D. Lambert, J. P. Sauvanet, and G. Debry, in "International Conference on Atherosclerosis," Milan, Italy, May 1980.

(9) J. Rouffy, B. Chanu, R. Bakir, J. Goy-Loeper, C. Rouffy, and C. Sava, in *ibid.*

(10) A. Delhon, S. Villa, C. Palmier, M. Livio, B. Maynadier, H. Lauressergues, and G. de Gaetano, in *ibid.*

(11) J. P. Rieu, G. Mouzin, H. Cousse, and A. Boucherle, *J. Pharm. Sci.*, **69**, 49 (1980).

(12) H. Cousse, P. Hascoet, G. Mouzin, and J. P. Rieu, French pat. 7,924,582 (1979).

(13) H. Cousse, G. Mouzin, J. P. Ribet, and J. C. Vezin, *J. Pharm. Sci.*, in press.

(14) H. Cousse, G. Mouzin, and J. P. Rieu (to P. Fabre S.A.), French pat. 2,265,409 (1974) and U.S. pat. 4,058,558 (1977).

(15) H. M. Fales, T. M. Jaouni, and J. F. Babashak, *Anal. Chem.*, **45**, 2302 (1973).

(16) D. P. Schwartz and R. S. Bright, *Anal. Biochem.*, **61**, 271 (1974).

(17) D. R. Knapp, "Handbook of Analytical Derivatization Reactions," Wiley, New York, N.Y., 1979.

(18) M. C. Bret, thesis, Montpellier University, Montpellier, France, Oct. 1980.

(19) J. L. Chanal, C. Bret, and R. Marignan, in "International Conference on Atherosclerosis," Milan, Italy, 1977.

(20) J. H. Miller, A. Donath, and P. Poitou, in *ibid.*, May 1980.


## ACKNOWLEDGMENTS


The authors thank Mr. Gerard Amalric for technical assistance and Miss Eliane Kriner for help in translation.


# Synthesis, Structure, and Features of Anilinium Anilinomethanesulfonates


**MIGUEL G. NEUMANN and ROBERT A. M. C. DE GROOTE** ˣ



Received September 11, 1980, from the *Instituto de Física e Química de São Carlos, USP, C.P. 369, 13560 São Carlos, SP, Brazil.* Accepted for publication January 6, 1981.



**Abstract** □ Two series of anilinomethanesulfonate derivatives, the anilinium and *p*-toluidinium anilinomethanesulfonates, were synthesized. They present interesting spectroscopic features and can be used as characteristic derivatives of the parent compounds. These series allow the easy study of the N–H stretching frequencies of the secondary amine whereas difficulties are encountered with the parent compounds due to the occurrence of O–H stretching bands in the same frequency range. All three compounds present a common fragmentation pattern in mass spectral analysis. Through these analyses, the salt structure of the anilinium anilinomethanesulfonates is demonstrated in opposition to a sulfonamide structure, giving further support to the salt structure of other series previously reported.



**Keyphrases** □ Anilinomethanesulfonates, derivatives—synthesis and structure elucidation by elemental, IR, and mass spectral analyses □ Mass spectrometry—analysis, anilinomethanesulfonate derivatives, synthesis and structure elucidation □ IR spectroscopy—analysis, anilinomethanesulfonate derivatives, synthesis and structure elucidation


Methanesulfonation of the amine groups of pharmacologically active drugs is used to increase their solubility (1) and to control their hydrolysis in biological media (2). Some common examples are *p*-phenetidinomethanesulfonate[1], dihydroergotamine[2], and dipyrone[3]. On the other hand, some researchers have studied aminomethanesulfonic compounds as potential antiviral (3) or carcinogenic agents (4, 5) since their structures are analogous to the carboxylic amino acids. As part of research into the properties of aminomethanesulfonates, the kinetics of formation of substituted anilinomethanesulfonates were studied recently (6). The inherent difficulties of analyzing IR spectra of substituted aromatic aminomethanesulfonates with regard to the O–H stretching bands also were discussed (7).

Little work has been reported concerning the analysis of the anilinomethanesulfonates, their chemical structure, and the different products that form, depending on the synthetic method. To find appropriate methods of analysis and identification of these products, a new series of derivatives was prepared by the reaction of equimolar

[1] Nevralteine.
[2] Diergotan, dihydergot, ergotex.
[3] Conmel, novalgin, sulpyrin.


0022-3549/81/0800-0863$01.00/0


© 1981, American Pharmaceutical Association

**Table I—Accuracy and Reproducibility of GLC Analysis of I Added to Human Plasma**

| Added, μg/ml | Mean Recovered Amount (Range) | Recovery, %[a] |
|---|---|---|
| 0.1 | 0.101 (0.097–0.103) | 101 |
| 0.5 | 0.49 (0.480–0.51) | 98 |
| 1 | 1.03 (0.95–1.31) | 103 |
| 5 | 4.81 (4.74–5.33) | 96.2 |
| 10 | 10.35 (9.84–10.72) | 103.5 |
| 15 | 15.50 (14.68–15.96) | 104 |

[a] Mean ± *SD* = 100.95 ± 2.92; number of analyses = 4.

The results (Table I) show the accuracy and reproducibility of the GLC analysis of I in clinical samples. The response factor was calculated using the ratio of peak areas for similar concentrations of I and II (1.22 ± 0.12). The method has been used in laboratories to determine the amount of I in rat blood compared with radioisotopic methods (18, 19). It also has been used for the determination of I in plasma and urine of humans and in pharmacokinetic studies (18).

Recently, a simple and fast high-performance liquid chromatographic method (20) was developed in which derivatization was not necessary. However, the sensitivity was not as good as that using GLC electron-capture detection.

## REFERENCES


(1) *Chron. Org. Mond. Santé*, **33** (3), list 41-8 (1975).

(2) *Drugs of the Future*, **5**(5), 246 (1980).

(3) H. Cousse, G. Mouzin, J. P. Rieu, and A. Delhon (to P. Fabre S.A.), French pat. 2,300,551 (1975).

(4) A. Bizzi, M. T. Tacconi, E. Veneroni, and M. Cini, "7ème Congrès International de Pharmacologie," Paris, France, 1978.

(5) A. Delhon, J. P. Tarayre, H. Lauressergues, and S. Casadio, in "International Conference on Atherosclerosis," Milan, Italy, Nov. 1975.

(6) J. Lubetzki and A. Mose, in *ibid.*

(7) F. Mazoyer (to P. Fabre S.A.), U.S. pat. appl. 105,420 (1979).

(8) P. Drouin, J. Demange, D. Lambert, J. P. Sauvanet, and G. Debry, in "International Conference on Atherosclerosis," Milan, Italy, May 1980.

(9) J. Rouffy, B. Chanu, R. Bakir, J. Goy-Loeper, C. Rouffy, and C. Sava, in *ibid.*

(10) A. Delhon, S. Villa, C. Palmier, M. Livio, B. Maynadier, H. Lauressergues, and G. de Gaetano, in *ibid.*

(11) J. P. Rieu, G. Mouzin, H. Cousse, and A. Boucherle, *J. Pharm. Sci.*, **69**, 49 (1980).

(12) H. Cousse, P. Hascoet, G. Mouzin, and J. P. Rieu, French pat. 7,924,582 (1979).

(13) H. Cousse, G. Mouzin, J. P. Ribet, and J. C. Vezin, *J. Pharm. Sci.*, in press.

(14) H. Cousse, G. Mouzin, and J. P. Rieu (to P. Fabre S.A.), French pat. 2,265,409 (1974) and U.S. pat. 4,058,558 (1977).

(15) H. M. Fales, T. M. Jaouni, and J. F. Babashak, *Anal. Chem.*, **45**, 2302 (1973).

(16) D. P. Schwartz and R. S. Bright, *Anal. Biochem.*, **61**, 271 (1974).

(17) D. R. Knapp, "Handbook of Analytical Derivatization Reactions," Wiley, New York, N.Y., 1979.

(18) M. C. Bret, thesis, Montpellier University, Montpellier, France, Oct. 1980.

(19) J. L. Chanal, C. Bret, and R. Marignan, in "International Conference on Atherosclerosis," Milan, Italy, 1977.

(20) J. H. Miller, A. Donath, and P. Poitou, in *ibid.*, May 1980.


## ACKNOWLEDGMENTS


The authors thank Mr. Gerard Amalric for technical assistance and Miss Eliane Kriner for help in translation.


# Synthesis, Structure, and Features of Anilinium Anilinomethanesulfonates


**MIGUEL G. NEUMANN and ROBERT A. M. C. DE GROOTE** ˣ



Received September 11, 1980, from the *Instituto de Física e Química de São Carlos, USP, C.P. 369, 13560 São Carlos, SP, Brazil.* Accepted for publication January 6, 1981.



**Abstract** □ Two series of anilinomethanesulfonate derivatives, the anilinium and *p*-toluidinium anilinomethanesulfonates, were synthesized. They present interesting spectroscopic features and can be used as characteristic derivatives of the parent compounds. These series allow the easy study of the N–H stretching frequencies of the secondary amine whereas difficulties are encountered with the parent compounds due to the occurrence of O–H stretching bands in the same frequency range. All three compounds present a common fragmentation pattern in mass spectral analysis. Through these analyses, the salt structure of the anilinium anilinomethanesulfonates is demonstrated in opposition to a sulfonamide structure, giving further support to the salt structure of other series previously reported.



**Keyphrases** □ Anilinomethanesulfonates, derivatives—synthesis and structure elucidation by elemental, IR, and mass spectral analyses □ Mass spectrometry—analysis, anilinomethanesulfonate derivatives, synthesis and structure elucidation □ IR spectroscopy—analysis, anilinomethanesulfonate derivatives, synthesis and structure elucidation


Methanesulfonation of the amine groups of pharmacologically active drugs is used to increase their solubility (1) and to control their hydrolysis in biological media (2). Some common examples are *p*-phenetidinomethanesulfonate[1], dihydroergotamine[2], and dipyrone[3]. On the other hand, some researchers have studied aminomethanesulfonic compounds as potential antiviral (3) or carcinogenic agents (4, 5) since their structures are analogous to the carboxylic amino acids. As part of research into the properties of aminomethanesulfonates, the kinetics of formation of substituted anilinomethanesulfonates were studied recently (6). The inherent difficulties of analyzing IR spectra of substituted aromatic aminomethanesulfonates with regard to the O–H stretching bands also were discussed (7).

Little work has been reported concerning the analysis of the anilinomethanesulfonates, their chemical structure, and the different products that form, depending on the synthetic method. To find appropriate methods of analysis and identification of these products, a new series of derivatives was prepared by the reaction of equimolar

[1] Nevralteine.
[2] Diergotan, dihydergot, ergotex.
[3] Conmel, novalgin, sulpyrin.


0022-3549/81/0800-0863$01.00/0


© 1981, American Pharmaceutical Association

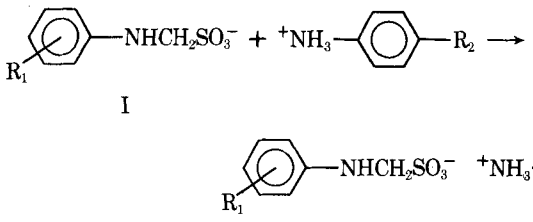

I

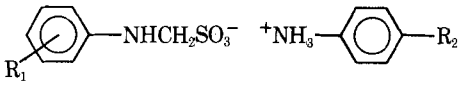

IIa: $R_2$ = H
IIb: $R_2$ = $CH_3$

*Scheme I*

amounts of the anilinomethanesulfonate (I) with anilinium or *p*-toluidinium chloride in water at room temperature to form the anilinium or *p*-toluidinium anilinomethanesulfonates (II) (Scheme I).

## EXPERIMENTAL

**Anilinomethanesulfonate Sodium Salts**—All anilinomethanesulfonates were synthesized from the corresponding anilines and sodium hydroxymethanesulfonate and were purified by previously described methods (6).

**Anilinium and *p*-Toluidinium Anilinomethanesulfonates**—These compounds were prepared by mixing equimolar amounts of the parent anilinomethanesulfonate with anilinium or *p*-toluidinium chloride at room temperature in a minimal amount of water under strong agitation. After precipitation, which was almost instantaneous, the compound was filtered, washed with cold ethanol and ether, and dried under vacuum at room temperature.

Recrystallization was performed using 50% ethanol–water. Special care was required because the anilinium compounds may be affected by light.

Elemental analysis values for all compounds were within 0.5% of those calculated from the theoretical structure of II.

The melting points for the anilinium- and *p*-toluidinium-substituted anilinomethanesulfonates, respectively, were: R = H, 118–120 and 123–124°; R = *m*-Cl, 119–120 and 123–124°; R = *p*-Cl, 129–134 and 139–142°; R = *p*-$CH_3$, 122–124 and 131°; and R = *p*-$OCH_3$, 121–123 and 134–136°. All compounds melted with decomposition.

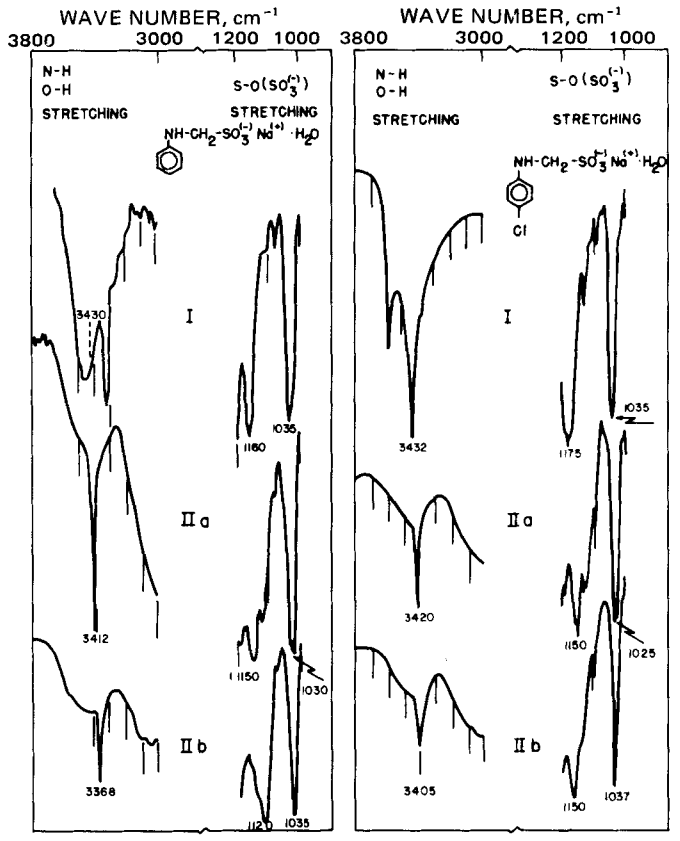


**Figure 1**—*IR spectra of sodium anilinomethanesulfonate (I), anilinium anilinomethanesulfonate (IIa), and* p*-toluidinium anilinomethanesulfonate (IIb) and its* p*-chloro-substituted derivatives.*

**Instrumentation**—IR spectra were measured on a high-resolution double-beam spectrophotometer[4]. All spectra were taken from solid pellets with 0.5% of the product in potassium bromide.

Mass spectra were taken at various temperatures with a quadrapole spectrometric system[5].

## RESULTS AND DISCUSSION

The classic synthesis of substituted anilinomethanesulfonates (I) involves the reaction of equimolar amounts of the substituted aniline hydroxymethanesulfonate in a suitable solvent (6) (Scheme II).

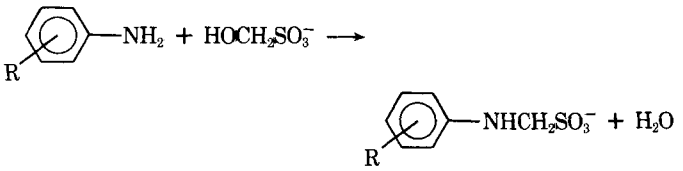

*Scheme II*

Another common method for aliphatic and, in particular, C-substituted compounds is based on the addition of sulfur dioxide to the corresponding Schiff base dissolved or suspended with enough water to form the hydrogen sulfate ion ($HSO_3^-$). Depending on the aldehyde and the amine, three products (III–V or a mixture of them) might be formed when using the Schiff base method (8) (Scheme III).

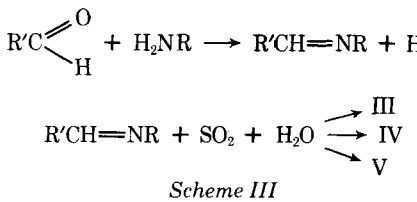

*Scheme III*

Structure III is obtained with aromatic amines, IV is obtained with aliphatic amines, and V is obtained when either the starting amine is very bulky (steric hindrance) or the aromatic aldehyde is substituted with strong withdrawing groups. In both cases for V, hydrolysis of the Schiff base is faster than the reaction with the bisulfite reagent. Considering the experimental procedure, it might be assumed that the proportion in which III and IV are formed is a function of the difference of the pKa values between aliphatic and aromatic amines.

This method cannot be used for formaldehyde derivatives (R′ = H) since a mixture of bis(phenylamino)methane and resinous material is formed (9).

**IR Spectral Analysis**—The anilinium salt structure of V was confirmed by its IR spectra. The characteristic derivatives, IIa and IIb, present very characteristic N–H and S–O ($SO_3^-$) stretching bands (10). The N–H stretching frequencies for these compounds were presented elsewhere (7). If the structure of V is sulfonamide-like, as was suggested (11), the N–H stretching frequency for the *sec*-amine group and for the sulfonamide group should be different. Therefore, two narrow stretching bands around 3400 $cm^{-1}$ should be expected for a IIIa (R′ = H) structure.

As can be seen from Fig. 1, only one sharp N–H stretching band appeared at this frequency range, well separated from the characteristic N–H ($NH_3^+$) broad band at 3200–2600 $cm^{-1}$. However, the sulfonamide S–O ($SO_2$) stretching bands appear around 1335 (asymmetric) and 1175 (symmetric) $cm^{-1}$. The main absorptions in this region for I, IIa, and IIb

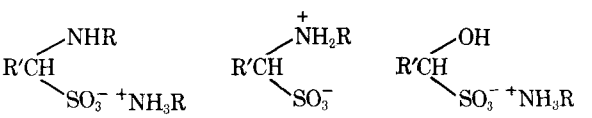

III: R′ = aryl  IV: R′ = alkyl  V: R′ = $C_6H_4NO_2$, R = alkyl, aryl; R′ = alkyl, aryl, R = *tert*-butyl

[4] Perkin-Elmer model 180.
[5] Finnigan model 1015.

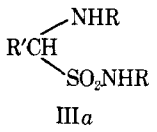

IIIa

were at 1175 (asymmetric) and 1050 (symmetric) $cm^{-1}$, which are typical of sulfonic acid salts.

**Mass Spectral Analysis**—The mass spectra of the sodium anilinomethanesulfonates (I) and their anilinium (IIa) and *p*-toluidinium (IIb) derivatives (Tables I–III) are consistent with the fragmentation pattern shown in Scheme IV. This pattern provides additional support for the anilinium salts *versus* the sulfonamide structure for two reasons: (*a*) the fragments found in the mass spectra of the anilinium (IIa) and *p*-toluidinium (IIb) derivatives were similar to those found in the mass spectra of the parent anilinomethanesulfonates; and (*b*) no fragments corresponding to the mass of the sulfonamides were apparent.

Some characteristics of these mass spectra should be mentioned.

1. The similarity of the mass spectra of I and II together with the lack of the parent peak, as would be expected for any salt (12), justifies a common fragmentation pattern for all three types of compounds.

2. The abundance of the Schiff base peaks (A and B), the cationic aniline peaks (E), and the characteristic $SO_2$ and SO peaks suggest successive or alternative fragmentations through C–S and N–C cleavages, followed by hydrogen losses.

3. The substituted phenyl fragments (C) may rearrange to other structures in accordance with the patterns for substituted aromatic compounds (13), as in the case of *p*-toluidinomethanesulfonate where peaks corresponding to the tropylium and cyclopentadienyl cations appear with 100 and 34% frequency, respectively.

4. For the halogen-substituted compounds, important fragments arise from the cleavage of the halogen atom from the aromatic ring, followed by decomposition of the latter. This pattern can be seen in Table II for the anilinium *p*-bromoanilinomethanesulfonate, for which the base peak corresponds to the cyclopentadienyl cation.

5. For the methoxy-substituted compounds, important fragments are found corresponding to $CH_3$–O cleavage, typical of aromatic ethers (14). That is, the base peak for the *p*-methoxyanilinomethanesulfonate is the $O\text{-}C_6H_5\text{-}N{=}CH_2$ fragment.

The mass spectra of the characteristic derivatives taken at tempera-

**Table I—Mass Spectra of the Substituted Sodium Anilinomethanesulfonates**

| Fragment | Substituent | | | | | | |
|---|---|---|---|---|---|---|---|
| | H | *p*-$CH_3$ | *p*-$CH_3O$[a] | *o*-Cl | *m*-Cl | *p*-Cl | *p*-Br |
| A | 11 | 17 | 2 | 95 | 35 | 48 | 69 |
| B | 2 | 1 | 1 | 1 | 4 | 3 | 1 |
| C | 100 | 100 | 5 | 40 | 55 | 50 | 38 |
| D | 57 | 50 | 90 | 100 | 100 | 100 | 100 |
| $SO_2$ | 25 | 30 | 22 | 58 | 28 | 21 | 38 |
| SO | 11 | 10 | 10 | 15 | 6 | 5 | 14 |

[a] The base peak corresponds to the *m/z* 120 fragment.

**Table II—Mass Spectra of Substituted Anilinium Anilinomethanesulfonates**

| Fragment | Substituent | | | | | | |
|---|---|---|---|---|---|---|---|
| | H | *p*-$CH_3$ | *p*-$CH_3O$ | *o*-Cl | *m*-Cl | *p*-Cl | *p*-Br[a] |
| A | 28 | 7 | 65 | 5 | 10 | 15 | 7 |
| B | 100[b] | (100)[c] | 87 | 100 | 100 | 100 | 49 |
| C | 23 | 58 | 1 | 2 | 3 | 10 | 3 |
| D | 4 | 56 | 75 | 5 | 4 | 18 | 7 |
| E | 100[b] | 69 | 100 | 58 | 17 | 23 | 36 |
| $SO_2$ | 25 | 40 | 41 | 51 | 13 | 10 | 37 |
| SO | 14 | 10 | 11 | 16 | 2 | 2 | 15 |

[a] Base peak corresponds to the cyclopentadienyl fragment (*m/z* 56). [b] Fragments B and E are indistinguishable. [c] Corresponds to (M − 1).

**Table III—Mass Spectra of Substituted *p*-Toluidinium Anilinomethanesulfonates**

| Fragment | Substituent | | | | | | |
|---|---|---|---|---|---|---|---|
| | H | *p*-$CH_3$ | *p*-$CH_3O$[a] | *o*-Cl | *m*-Cl | *p*-Cl | *p*-Br |
| A | 100 | 7 | 5 | 4 | 11 | 21 | 26 |
| B | 69 | 100[b] | 52 | 100 | 100 | 67 | 25 |
| C | 15 | 64 | 90[c] | 2 | 16 | 34 | 14 |
| D | 9 | 61 | 45 | 5 | 27 | 60 | 38 |
| E | 78 | 100[b] | 90[c] | 58 | 80 | (100)[d] | (100)[d] |
| $SO_2$ | 20 | 4 | 50 | 67 | 61 | 49 | 42 |

[a] Base peak corresponds to ($C_6H_5{}^+NH{=}CH_2$). [b] Fragments B and E are indistinguishable. [c] Fragments C and E are indistinguishable. [d] Corresponds to (M − 1).

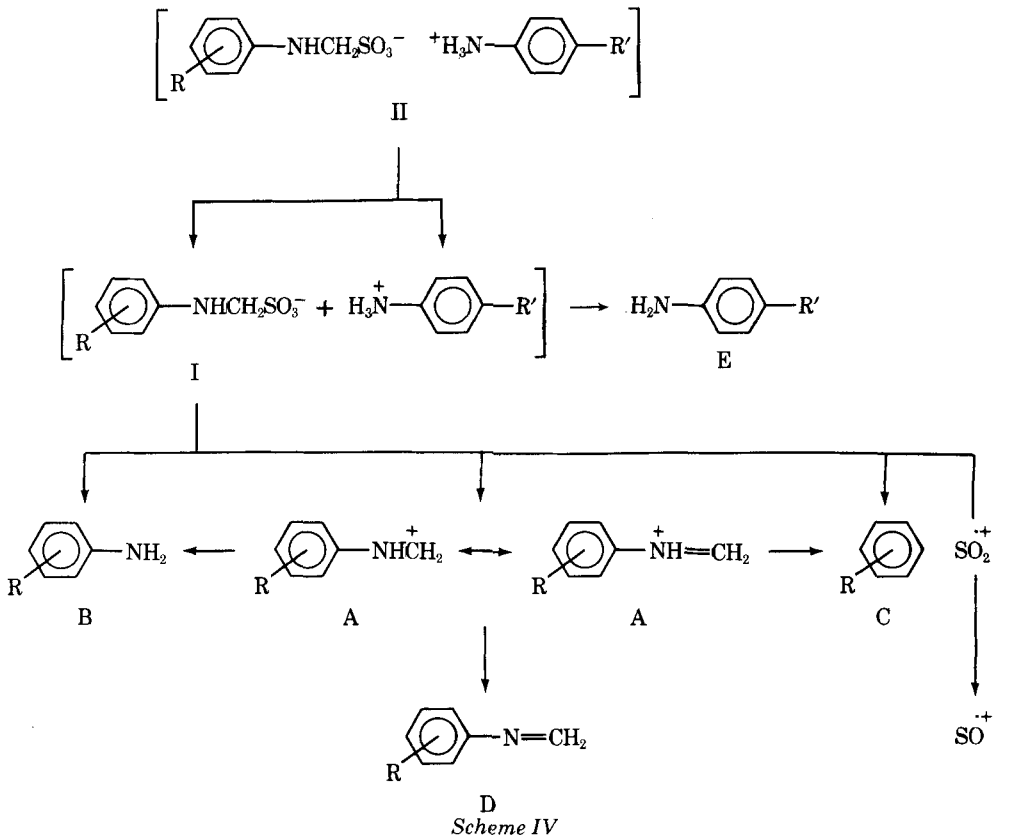


*Scheme IV*

**Table IV—Additional Fragments Originating from Polymer Formation**

| Compound | Fragment A′ Relative Intensity | Fragment A′ *m/z* | Fragment G Relative Intensity | Fragment G *m/z* | Fragment F Relative Intensity | Fragment F *m/z* | Fragment E Relative Intensity | Fragment E *m/z* | Sample Temperature | Melting Point |
|---|---|---|---|---|---|---|---|---|---|---|
| II*a* | 29 | 106 | 41 | 207 | G | | G | | 130° | 120° |
| *p*-$CH_3$·II*a* | 100 | 106 | 11 | 207 | 15 | 221 | 8 | 236 | 170° | 122° |
| *m*-$^{35}$Cl·II*a* | 20 | 106 | 30 | 207 | 19 | 242 | 4 | 276 | 130° | 119° |
| II*b* | 26 | 121 | 11 | 207 | 48 | 221 | 41 | 236 | 120° | 124° |
| *p*-$CH_3O$·II*b* | 15 | 126 | 15 | 236 | 20 | 252 | 18 | 268 | 150° | 134° |

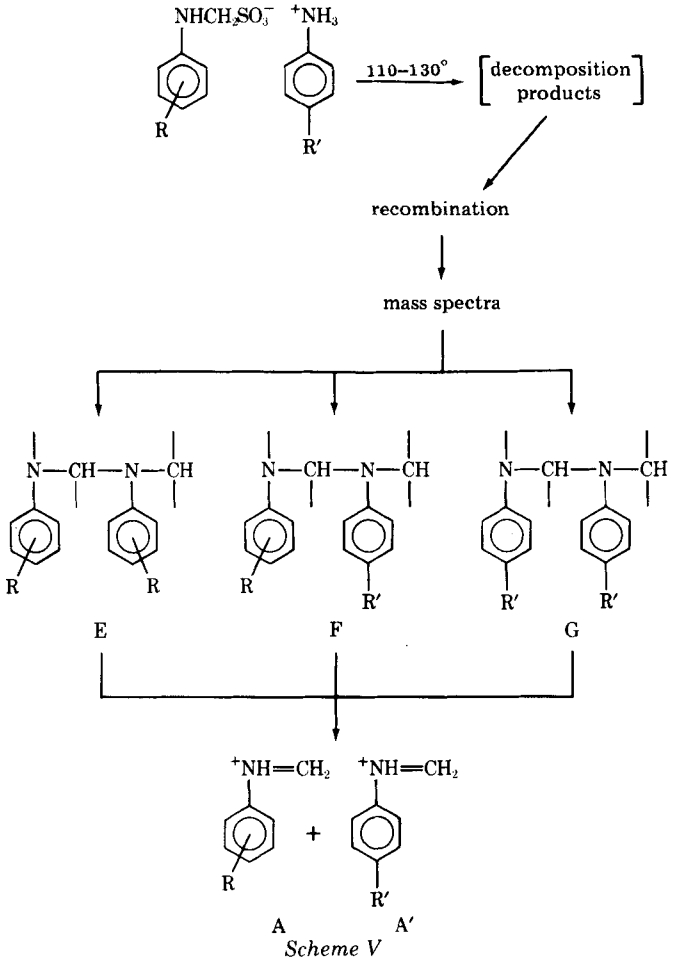


*Scheme V*

tures near their melting points (110–130°) showed significant amounts of higher molecular weight fragments. These fragments arise from dimers formed by recombination of the decomposition products of the initial compounds. The corresponding data are shown in Table IV, and the probable products are shown in Scheme V.

## CONCLUSIONS

The formation of the characteristic anilinium and *p*-toluidinium derivatives from the parent anilinomethanesulfonates displaces the water molecule of crystallization of the latter, as may be seen from elemental and IR analyses. This displacement is due to the exchange of sodium by the anilinium or *p*-toluidinium counterion. These derivatives are studied more easily than the parent compounds by mass spectra due to their lower melting points. Thus, the mass spectra must be monitored at low temperatures since polymerization occurs in the melting range of these derivatives, leading to the detection of dimer fractions and unexpected Schiff bases. This polymerization did not occur in the ionization chamber since there was no significant difference in the relative intensity of the dimer fragments when the initial compounds were monitored at different temperatures above the melting points.

The experimental method used in the present study together with the elemental, IR, and mass spectral analyses demonstrate the salt structure of V and furnishes new arguments for the salt structure of these compounds as opposed to the sulfonamide structure suggested previously (11).

The easy synthesis, low melting point, and unambiguous IR spectra suggest that these compounds can be used advantageously as characteristic derivatives for anilinomethanesulfonates.

Preliminary data[6] obtained by X-ray crystallography show that the distance between O–N ($SO_3^-H_3N^+$) is ~2.8 Å, which indicates that no covalent bonds are present in the characteristic derivatives II*a* and II*b*.

## REFERENCES


(1) W. Longeman and G. P. Miori, *Arzneim.-Forsch.*, **5,** 213 (1955).

(2) K. Ikeda, K. Miyata, T. Iwata, F. Kawata, and K. Kurome, *Chem. Pharm. Bull.*, **18,** 440 (1970). K. Ikeda, Y. Kurona, and T. Tukamoto, *ibid.*, **20,** 863 (1972).

(3) R. L. Thompson, *J. Immunol.*, **55,** 345 (1947).

(4) D. M. Greenberg and M. P. Schulman, *Science*, **106,** 271 (1947).

(5) "Evaluation of Anilinomethanesulfonates NSC 276433 to 276436," National Cancer Institute, 1977 (samples provided by Instituto de Física e Química de São Carlos, USP).

(6) M. G. Neumann and R. A. M. C. De Groote, *J. Pharm. Sci.*, **67,** 1283 (1978).

(7) R. A. M. C. De Groote, *Spectrochim. Acta*, **36A,** 137 (1980).

(8) J. F. Walker, "Formaldehyde," Reinhold, New York, N.Y., 1944, p. 204.

(9) D. R. Clark and P. Miles, *J. Chem. Res.*, **M,** 1949 (1978).

(10) C. J. Pouchert, "The Aldrich Library of Infrared Spectroscopy," Aldrich Chemical Co., Milwaukee, Wis., 1975.

(11) L. Neelakantan and W. Hartung, *J. Org. Chem.*, **29,** 1943 (1959).

(12) K. Biemann, "Mass Spectrometry, Organic Chemical Applications," McGraw Hill, New York, N.Y., 1962.

(13) P. N. Rylander, S. Meyerson, and M. Grubb, *J. Am. Chem. Soc.*, **79,** 842 (1957).

(14) J. M. Wilson, *Experimentia*, **34,** 403 (1960).


## ACKNOWLEDGMENTS


Supported by the Convênio FINEP, B 76/80/150, and by the Fundação de Amparo à Pesquisa do Estado de São Paulo through Grants 78/369 and 78/885.


[6] J. R. Lechat, Instituto de Física e Química de São Carlos, USP, São Carlos, Brazil, personal communication.

# Urinary Excretion of Meperidine and Its Metabolites

S. Y. YEH [x], H. A. KREBS [*], and A. CHANGCHIT [‡]

Received November 3, 1980, from the *National Institute on Drug Abuse, Division of Research, Addiction Research Center, Lexington, KY 40583.* Accepted for publication January 6, 1981. *Present address: Analytical Chemistry Branch, Environmental Protection Agency, Research Triangle Park, NC 27711. ‡Graduate Center for Toxicology, University of Kentucky, Lexington, KY 40506.

**Abstract** □ The urine of male and female mice, rats, guinea pigs, rabbits, cats, and dogs, given meperidine hydrochloride, 20–40 mg/kg ip, was analyzed by GLC for meperidine, normeperidine, *p*-hydroxymeperidine, and total (free and conjugated) meperidinic and normeperidinic acids. More than 90% of the excreted drugs was found in the 24-hr urine. Meperidine was observed in the urine of mice, rats, guinea pigs, and cats, but only a trace amount was observed in the urine of rabbits and dogs. Normeperidine, *p*-hydroxymeperidine (except in the mice), and total meperidinic and normeperidinic acids were observed in all species. All of the species studied have the capacity to *N*-demethylate meperidine to normeperidine and to hydrolyze meperidine and normeperidine to their respective acids. The male has a higher *N*-demethylating activity than the female with the exception of mice. Ester hydrolysis is a major metabolic pathway for meperidine metabolism.

**Keyphrases** □ Meperidine—metabolism, urinary excretion in mice, rats, guinea pigs, rabbits, cats, and dogs □ Metabolites—of meperidine, urinary excretion in mice, rats, guinea pigs, rabbits, cats, and dogs □ Metabolism—of meperidine in mice, rats, guinea pigs, rabbits, cats, and dogs □ Excretion, urinary—meperidine and its metabolites in mice, rats, guinea pigs, rabbits, cats, and dogs □ Analgesics—meperidine and its metabolites, urinary excretion in mice, rats, guinea pigs, rabbits, cats, and dogs

Urinary disposition of meperidine and its metabolite, normeperidine, has been determined in humans (1–9) and monkeys (10), but little information is available for other laboratory species. In two rats, 50% of the injected *N*-$^{14}$C-labeled meperidine could be accounted for in the urine as radioactive material within 24 hr after subcutaneous administration (11). After administration of meperidine (125 mg/kg sc or 25 mg/kg iv) to rats, 3.7% of the dose was accounted for in the 24-hr urine as meperidine, 17% as normeperidine, and 11% as meperidinic acid (11). The major metabolites of meperidine are normeperidine and free and conjugated meperidinic and normeperidinic acids. Small amounts of other metabolites have been identified, including meperidine *N*-oxide (12), *p*-hydroxymeperidine (13), *N*-hydroxynormeperidine (14), and *p*-hydroxynormeperidine[1]. The known metabolic pathways of meperidine are shown in Scheme I.

The analgesic effect of meperidine appears to differ among species, a phenomenon that may be due to differences in meperidine metabolism. Meperidine induces analgesia in mice (15–18), rats (19, 20), guinea pigs (21), cats (22), and humans (23) but not in dogs (24, 25). The present study was undertaken to investigate the differences in meperidine metabolism among species.

## EXPERIMENTAL

**Chemicals**—Meperidine hydrochloride[2], normeperidine hydrochloride[2], *p*-hydroxymeperidine[3], and lidocaine hydrochloride[4] were used as received. Meperidinic and normeperidinic acids were obtained by alkaline hydrolysis of their respective esters. Other chemicals and solvents were analytical grade.

**Animals**—Animals were housed in air-conditioned quarters (23°) with 12-hr light and dark cycles. Food and water were given *ad libitum*. A dose of meperidine hydrochloride dissolved in 0.9% NaCl was administered intraperitonally to 28 male and 21 female Swiss Webster [Lai: Cox (Wi)] mice[5], five male and five female Wistar [Lai: Cox (XW)] rats[5], five male and four female Hartley albino guinea pigs[6], two male and two female New Zealand rabbits[6], two male and two female cats, and one male and one female beagle dogs. These animals were chosen because they are commonly used in biological research.

After drug administration, all animals except the mice were caged individually in stainless steel metabolic cages. The mice were housed in groups of seven to 10 animals per cage. The mice, rats, guinea pigs, and

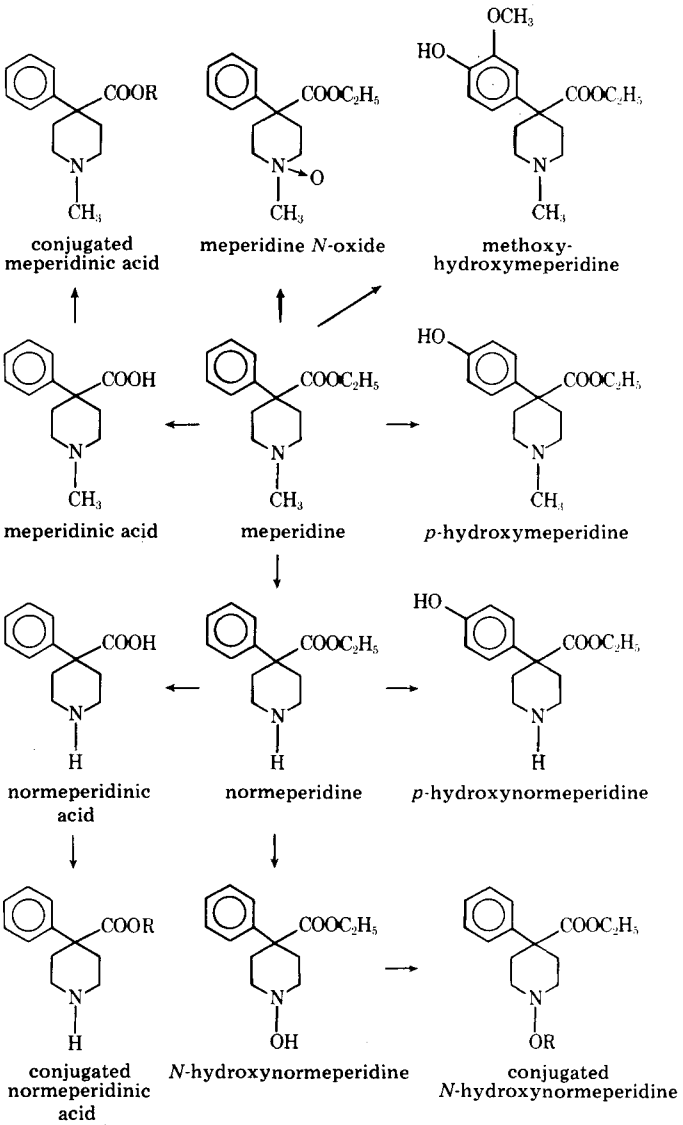


*Scheme I—Metabolic pathways of meperidine.*

[1] S. Y. Yeh, unpublished data.
[2] Sterling-Winthrop Co., Rensselaer, N.Y.
[3] Obtained from Professor C. Lindberg, Biomedical Center, University of Uppsala, Uppsala, Sweden.
[4] Astra Pharmaceutical Products, Worcester, Mass.
[5] Laboratory Supplies, Indianapolis, Ind.
[6] Williams Farm, Fern Creek, Ky.

0022-3549/81/0800-0867$01.00/0
© 1981, American Pharmaceutical Association

**Table I—Meperidine and Its Metabolites Found in Urine after Intraperitoneal Administration of Meperidine**

| Species and Sex ($n$) | Meperidine Hydrochloride, mg/kg | Collection Period, hr | Urinary pH | Mean[a], Equivalent Administered Dose, % | | | | | | |
|---|---|---|---|---|---|---|---|---|---|---|
| | | | | Meperidine | Normeperidine | $p$-Hydroxymeperidine | Total Meperidinic Acid | Total Normeperidinic Acid | Total Drug Excreted 24 hr | Total Drug Excreted 48 hr |
| Mice | | | | | | | | | | |
| Male (3)[b] | 40 | 0–24 | 7–8 | 5.17[c] ±0.23 | 13.24[c] ±1.87 | —[d] | 29.99 ±5.66 | 0.78[c] ±0.32 | 49.18 | 61.38 |
| | | 24–28 | 7.5–8 | 0.60 ±0.14 | 1.81 ±0.52 | — | 9.79 | — | | |
| Female (3)[e] | 40 | 0–24 | 7 | 3.42 ±0.46 | 20.51 ±2.80 | — | 33.67[f] 37.32 | 2.81[f] 3.30 | 62.28 | 70 |
| | | 24–48 | 7 | 0.63 ±0.15 | 2.56 ±0.76 | — | 4.29 | — | | |
| Rats | | | | | | | | | | |
| Male (5) | 35 | 0–24 | 8–9 | 5.95[c] ±1.56 | 23.13[c] ±3.85 | 0.36 ±0.10 | 16.07 ±3.82 | 4.10[c] ±0.65 | 49.25 | 53.18 |
| | | 24–48 | 8.5–9 | 0.13 ±0.03 | 1.57 ±0.24 | 0.38 ±0.08 | 2.08 ±0.53 | 0.15 ±0.08 | | |
| Female (5) | 35 | 0–24 | 6.5–9.5 | 15.25 ±4.40 | 12.53 ±1.68 | 0.00 | 12.34 ±5.33 | 12.06 ±1.42 | 52.18 | 56.52 |
| | | 24–48 | 8–9 | 0.45 ±0.11 | 2.08 ±0.37 | 0.11 ±0.07 | 1.35 ±0.73 | 0.46 ±0.05 | | |
| Guinea pigs | | | | | | | | | | |
| Male (2) | 70 | 0–24 | 7.0–8.5 | 0.89 | 7.78 | 1.06 | 16.40 | 1.12 | 26.19 | 27.49 |
| | | | | 1.45 | 14.47 | 0.00 | 20.38 | 1.50 | 37.78 | 42.60 |
| | | 24–48 | 7–9 | 0.54 | 0.23 | 1.22 | 0.53 | 0.00 | | |
| | | | | 1.14 | 2.67 | 0.00 | 0.83 | 0.18 | | |
| Male (3) | 35 | 0–24 | 6.5–8.5 | 1.40 ±0.59 | 10.09[c] ±2.06 | 3.84 ±1.95 | 16.21 ±5.75 | 1.25 ±0.71 | 28.86 | 29.91 |
| | | 24–48 | 8–9 | 0.12 ±0.07 | 0.56 ±0.33 | 0.78 ±0.41 | 0.36 ±0.31 | 0.01 ±0.01 | | |
| Guinea pigs, female (4) | 35 | 0–24 | 7–8.5 | 2.19 ±0.14 | 4.45 ±0.66 | 0.45 ±0.15 | 40.55 ±8.14 | 3.37 ±0.49 | 50.56 | 55.02 |
| | | 24–48 | 7–9 | 0.61 ±0.11 | 1.65 ±0.66 | 0.21 ±0.11 | 1.64 ±0.34 | 0.56 ±0.12 | | |
| Rabbits | | | | | | | | | | |
| Male (1) | 35 | 0–24 | 7 | 0.32 | 2.17 | 0.26 | 18.22 | 21.45 | 42.21 | 53.42 |
| | | 24–48 | 8.5 | 0.12 | 2.16 | 0.19 | 3.69 | 5.24 | | |
| Male (1) | 35 | 0–72 | 8.0 | 0.06 | 2.65 | 0.13 | 6.34 | 14.39 | 23.44 | 23.96 |
| | | 72–96 | 8.5 | 0.01 | 0.17 | 0.00 | 0.19 | 0.15 | | |
| Female (2) | 35 | 0–24 | 7.5–9 | 0.02 | 0.20 | 0.00 | 0.30 | 0.53 | 1.05 | 15.58 |
| | | | | 0.04 | 0.36 | | 1.80 | 3.00 | 4.84 | 34.63 |
| | | 24–72 | 8–9 | 0.05 | 0.71 | 0.14 | 4.27 | 5.45 | | |
| | | | | 0.09 | 8.47 | 0.32 | 12.78 | 12.07 | | |
| Cats | | | | | | | | | | |
| Male (2) | 20 | 0–24 | 6.5–7 | 3.13 | 3.13 | 2.23 | 46.56 | 0.90 | 53.72 | 60.1 |
| | | | | 13.62 | 7.57 | 2.74 | 55.76 | 2.21 | 79.16 | 91.1 |
| | | 24–48 | 6.5 | 0.19 | 1.40 | — | 4.79 | 0.00 | | |
| | | | | 0.20 | 3.37 | — | 8.26 | 1.08 | | |
| Female (2) | 20 | 0–24 | 7 | 6.04 | 3.91 | 2.33 | 52.74 | 0.26 | 62.95 | 91.7 |
| | | | | 9.52 | 4.04 | 3.20 | 58.46 | 1.78 | 73.80 | 102.8 |
| | | 24–48 | 6.5 | 0.89 | 2.47 | 0.45 | 25.17 | 0.21 | | |
| | | | | 1.37 | 5.41 | 0.48 | 22.00 | 0.24 | | |
| Dogs | | | | | | | | | | |
| Male (1) | 20 | 0–24 | 7 | 0.15 | 1.77 | 0.35 | 73.91 | 1.48 | 75.54 | 84.70 |
| | | 24–48 | 7 | 0.00 | 0.47 | — | 6.92 | 0.00 | | |
| Female (1) | 20 | 0–24 | 7.5 | 0.20 | 2.06 | 0.32 | 69.08 | 1.18 | 72.32 | 80.85 |
| | | 24–48 | 7 | 0.00 | 1.18 | 0.19 | 7.15 | 0.00 | | |

[a] Measures of variance where shown are ± $SE$. [b] Twenty-eight male mice were divided into three groups of 10, 10, and eight. [c] Significantly different from the females at $p < 0.05$ level. [d] Dashes indicate amounts below detectable limits. [e] Twenty-one female mice were divided into three groups of seven each. [f] The urine of the third group was insufficient for determination.

rabbits were deprived of food for 24 hr following drug administration, but water was given *ad libitum*. Urine was collected 24 hr prior to drug administration (control) and 0–24 and 24–48 hr after drug administration. After the pH and volume were measured, all urine was frozen until drug analysis.

**Determination of Meperidine and Its Metabolites**—Meperidine, $p$-hydroxymeperidine, normeperidine, and meperidinic and normeperidinic acids were determined with a GLC procedure previously described (26). With lidocaine as the internal standard, free drugs were extracted with ether from the urine adjusted to pH 10. Upon evaporation of the extract to dryness, the residues were derivatized with trifluoroacetic anhydride. After removal of the excess derivatizing agent, the residue was dissolved in 50 μl of ethyl acetate (dried over calcium hydride), and 1 μl was injected into a gas–liquid chromatograph equipped with a Poly I-110 (1.8 m × 2 mm) column and flame-ionization detector.

Total (free and conjugated) meperidinic and normeperidinic acids were determined as meperidine and normeperidine, respectively, after the sample was treated with ethanol–sulfuric acid. Meperidine and its metabolites were extracted from the urine as the free base but were converted to the percent equivalent of administered dose.

## RESULTS AND DISCUSSION

Urinary excretion of meperidine and its metabolites in mice, rats, guinea pigs, rabbits, cats, and dogs is presented in Table I. The amount of meperidine (Fig. 1) observed in the urine of mice, rats, guinea pigs, and cats was significantly higher than that in the urine of rabbits and dogs. The amount of meperidine in the urine of mice, rats, guinea pigs, and cats was comparable to that of humans (1–9) and monkeys (10). This observation appears to correlate well with meperidine analgesia reported between species. Normeperidine, $p$-hydroxymeperidine (except in the mice), and total meperidinic and normeperidinic acids were observed in all species studied; these metabolites also were reported in humans (7, 13).

Urinary pH affects excretion of meperidine and its metabolites in humans (6, 7). Urine acidification increases the excretion of meperidine

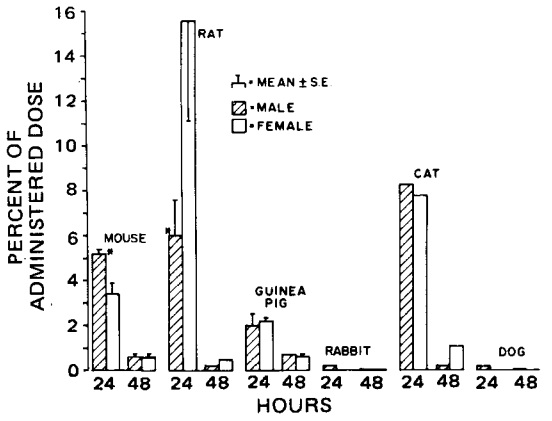


**Figure 1**—*Urinary excretion of meperidine in the mouse, rat, guinea pig, rabbit, cat, and dog after intraperitoneal administration of meperidine. The asterisk (*) indicates significantly different from the female at* $p < 0.05$ *level.*

and normeperidine, whereas very little of these compounds is excreted in alkaline urine. The recovery of meperidine and its metabolite, normeperidine, from 10 patients whose urinary pH was maintained at 4.8–5.25 varied between 10 and 50 and 2 and 20%, respectively, of the administered dose. However, 1% of the administered dose was excreted in subjects whose urinary pH was maintained at >7.0. In the present study, the urinary pH of animals was not controlled. The physiological urinary pH of dogs and rabbits appeared in the same range as the other species studied. Therefore, the small amount of meperidine and normeperidine found in the dog and rabbit urine appears to be a metabolic effect and not due to urinary pH.

The results indicate that all species studied have the capacity to *N*-demethylate meperidine to normeperidine (Fig. 2) and to hydrolyze meperidine and normeperidine to their respective acids (Figs. 3 and 4). With the exception of mice, meperidine excretion tended to be less in males than in females, and normeperidine and the sum of normeperidine and normeperidinic acids excretion tended to be greater. These data are consistent with the male having a higher *N*-demethylating activity than the female, with the exception of mice (27, 28). The present data on *in vivo* meperidine metabolism between male and female rats also correlate well with those obtained in *in vitro* studies (29).

The higher amount of normeperidine in the urine of mice, rats, and guinea pigs than in the urine of rabbits, cats, and dogs may reflect the further metabolism of normeperidine in the latter species.

Although conjugated *N*-hydroxynormeperidine was identified in the urine of rats and guinea pigs (14), *N*-hydroxynormeperidine was not determined in the present study because the pure standard was not available. Under the conditions for the determination of conjugated meperidinic and normeperidinic acids, *N*-hydroxynormeperidine probably was converted to normeperidine and measured as such or it decomposed.

The amount of meperidinic acid excreted in the urine of both sexes of the mouse, rat, guinea pig, cat, rabbit, and dog did not appear to be significantly different, suggesting that the esterase activity in both sexes may be equal. The ratios of meperidine to normeperidine excreted in 48

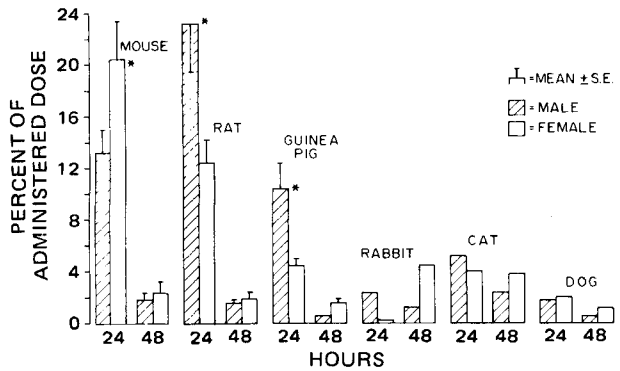


**Figure 2**—*Urinary excretion of normeperidine in the mouse, rat, guinea pig, rabbit, cat, and dog after intraperitoneal administration of meperidine. The asterisk (*) indicates significantly different from the female at* $p < 0.05$ *level.*

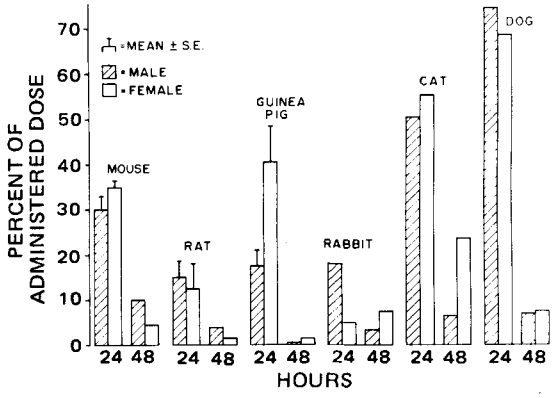


**Figure 3**—*Urinary excretion of total meperidinic acid in the mouse, rat, guinea pig, rabbit, cat, and dog after intraperitoneal administration of meperidine.*

hr in both sexes were less than one, whereas the ratios of total meperidinic acid to total normeperidinic acid ranged from 10 to 65. These data suggest that meperidine may be metabolized more extensively than its metabolite, normeperidine. The normeperidinic acid ought to be derived from normeperidine since meperidinic acid does not undergo *N*-demethylation to normeperidinic acid (4). Similarly, it was observed that morphine was metabolized more extensively than normorphine in dogs (30).

*p*-Hydroxymeperidine, a metabolite with mild analgesic effects, was observed in the urine of all species studied except mice (Table I). Free *p*-hydroxymeperidine varied among species and between sexes and accounted for 0.1–4% of the administered dose (Fig. 5). Conjugated *p*-hydroxymeperidine was not determined because the procedure is not optimal for its determination.

In one study in male guinea pigs, the dose of meperidine in one group of animals was twice that in the other. The urinary excretion profile between the two groups did not appear different.

The dogs and cats excreted 80–100% of the administered dose as total drug in the 48-hr urine; the other species excreted 16–60% of the dose. From 80 to 90% of the excreted drug was found in the 24-hr urine. This finding confirms the observation of Way *et al.* (3) that after meperidine administration to rats three times daily for several days, virtually no drug could be recovered from the animals 24 hr later. The amount unaccounted for could be due to *N*-hydroxy- and *p*-hydroxynormeperidine and metabolites excreted in the feces. Significant amounts of radioactivity have been found in the large intestine and feces of rats administered *N*-$^{14}$C-labeled meperidine (11). Gastric and biliary excretion of meperidine in humans also was observed (31).

Meperidine induces analgesia in mice (15–18), rats (19, 20), guinea pigs (21), cats[7] (22), and humans (23), and some intact meperidine was observed in the urine of these species. In the dog, a large dose (which produces toxic effects) is needed to induce mild analgesic effects (24, 25). Very little meperidine was observed in the dog urine. Meperidine could be substituted for morphine in the morphine-dependent monkey[8] and humans (23) but not in dogs (24, 25).

The small amount of meperidine and normeperidine observed in the

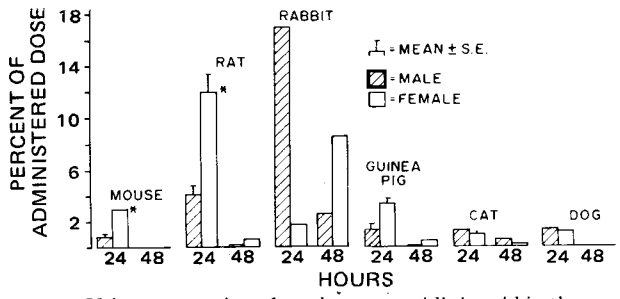


**Figure 4**—*Urinary excretion of total normeperidinic acid in the mouse, rat, guinea pig, rabbit, cat, and dog after intraperitoneal administration of meperidine. The asterisk (*) indicates significantly different from the male at* $p < 0.05$ *level.*

[7] R. G. Babington, T. L. Waldron, and P. W. Wedeking, reported to the Committee on Problems of Drug Dependence, 1968, p. 5570.

[8] G. Deneau, D. McCarthy, and M. H. Seevers, reported to the Committee on Drug Addiction and Narcotics, 1959, p. 2057.

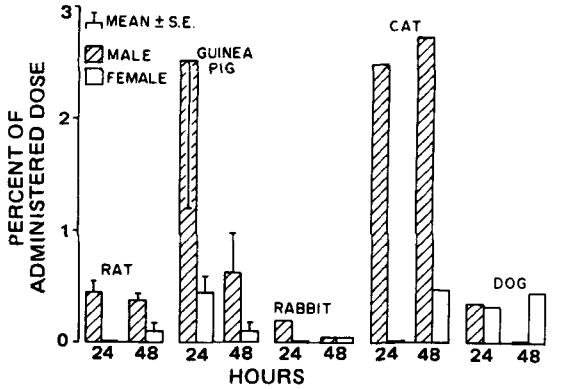


**Figure 5**—*Urinary excretion of* p*-hydroxymeperidine in the rat, guinea pig, rabbit, cat, and dog after intraperitoneal administration of meperidine.*

urine of rabbits and dogs is consistent with the mild analgesic effects of the drug in dogs. This finding suggests that these two species metabolize meperidine faster than other species, which is supported by the work of Peters *et al.* (10) on the hypothermic effect and urinary excretion of meperidine among strains of monkeys and the plasma half-life of meperidine in dogs, humans, and monkeys. These researchers reported that the median analgesic dose of meperidine in the squirrel monkey (8.0 mg/kg) was ~2.3 times that in the rhesus monkey (3.5 mg/kg) (10). Rhesus monkeys excreted substantially higher fractions of the dose as meperidine than did squirrel monkeys. On the other hand, squirrel monkeys excreted a threefold higher fraction of the dose as normeperidine than did the rhesus monkeys. This result indicates that the squirrel monkey metabolizes meperidine faster than the rhesus monkey. The plasma half-lives of meperidine in humans and monkeys are 3.0 and 1.8 hr, respectively[9] (32–34), significantly longer than the plasma half-life (0.5 hr) in the dog (4, 35).

Among the metabolites, normeperidine and *p*-hydroxymeperidine were reported to have analgesic effects with low potency (15, 16, 19), whereas meperidinic and normeperidinic acids had no analgesic effects (4). The potency ratio between meperidine and normeperidine in mice was 1:0.7 (15, 16), whereas the ratio between meperidine, normeperidine, and *p*-hydroxymeperidine in rats on a molar basis was 1:0.33:0.07 (19). If the amount of meperidine and normeperidine excreted in the urine reflects the relative amount of meperidine and normeperidine present in the body and brain, it is possible that normeperidine plays a role in the analgesic effect of meperidine because of its relatively high analgesic potency and high percentage excretion. The relationship between meperidine analgesia and the brain concentration of meperidine and normeperidine in different species administered varying doses of the drug by different routes requires further study.

In summary, after intraperitoneal administration of 20–40 mg of meperidine hydrochloride/kg to mice, rats, guinea pigs, cats, and dogs, >90% of the excreted drugs was found in the 24-hr urine. The amounts of meperidine observed in the urine of mice, rats, guinea pigs, and cats were significantly higher than those observed in the rabbits and dogs. This observation appears to correlate well with the meperidine analgesia reported in these species. Normeperidine, *p*-hydroxymeperidine (except in the mice), and total meperidinic and normeperidinic acids were observed in all species. All species studied have the capacity to *N*-demethylate meperidine to normeperidine and to hydrolyze meperidine and normeperidine to their respective acids. The male has a higher *N*-demethylating activity than the female, with the exception of mice. Ester hydrolysis is a major metabolic pathway for metabolism of meperidine.

[9] G. A. Deneau and K. Nakai, National Research Council–National Academy of Sciences Report to the Committee on Drug Addiction and Narcotics, 1961, p. 2460.

## REFERENCES

(1) R. A. Lehman and T. Aitken, *J. Lab. Clin. Med.*, **28,** 787 (1943).

(2) F. W. Oberst, *J. Pharmacol. Exp. Ther.*, **79,** 10 (1943).

(3) E. L. Way, A. I. Gimble, W. P. McKelway, H. Ross, C.-Y. Sung, and H. Ellsworth, *ibid.*, **96,** 477 (1949).

(4) J. J. Burns, B. L. Berger, P. A. Lief, A. Wollack, E. M. Papper, and B. B. Brodie, *ibid.*, **114,** 289 (1955).

(5) N. P. Plotnikoff, E. L. Way, and H. W. Elliott, *ibid.*, **117,** 414 (1956).

(6) A. M. Asatoor, D. R. London, M. D. Milne, and M. L. Simenhoff, *Br. J. Pharmacol. Chem. Ther.*, **20,** 285 (1963).

(7) K. Chan, M. J. Kendal, W. D. E. Wells, and M. Mitchard, *J. Pharm. Pharmacol.*, **27,** 235 (1975).

(8) J. E. Stambaugh and L. W. Wainer, *J. Clin. Pharmacol.*, **15,** 269 (1975).

(9) L. W. Wainer and J. E. Stambaugh, *J. Pharm. Sci.*, **67,** 116 (1978).

(10) J. H. Peters, G. R. Gordon, and S. A. Ferguson, *Toxicol. Appl. Pharmacol.*, **32,** 290 (1975).

(11) N. P. Plotnikoff, H. W. Elliott, and E. L. Way, *J. Pharmacol. Exp. Ther.*, **104,** 377 (1952).

(12) M. Mitchard, M. J. Kendall, and K. Chan, *J. Pharm. Pharmacol.*, **24,** 915 (1972).

(13) C. Lindberg and C. Bogentoft, *Acta Pharm. Suec.*, **12,** 507 (1975).

(14) W. G. Stillwell, C. S. Myran, and J. T. Steward, *Res. Commun. Chem. Pathol. Pharmacol.*, **27,** 975 (1975).

(15) A. D. MacDonald, G. Woolfe, F. Bergel, A. L. Morrison, and H. Rinderkneight, *Br. J. Pharmacol.*, **1,** 4 (1946).

(16) J. W. Miller and H. H. Anderson, *J. Pharmacol. Exp. Ther.*, **112,** 191 (1954).

(17) S. T. Christian, C. W. Gorodetzky, and D. V. Lewis, *Biochem. Pharmacol.*, **20,** 1167 (1971).

(18) R. H. K. Foster and A. J. Carman, *J. Pharmacol. Exp. Ther.*, **91,** 195 (1947).

(19) B. E. Dahlstrom, L. K. Paalzow, C. Lindberg, and C. Bogentoft, *Drug Metab. Dispos.*, **7,** 108 (1979).

(20) S. Y. Yeh, B.-L. Chang, H. A. Krebs, and C. W. Gorodetzky, *J. Pharmacol. Exp. Ther.*, **209,** 125 (1979).

(21) D. Teiger, *ibid.*, **197,** 311 (1976).

(22) D. Dubuisson, *Pain*, **4,** 161 (1977).

(23) C. K. Himmelsbach, *J. Pharmacol. Exp. Ther.*, **75,** 64 (1942).

(24) R. L. Carter and A. Wikler, *Fed. Proc. Fed. Am. Soc. Exp. Biol.*, **14,** 325 (1955).

(25) W. R. Martin, P. E. Gilbert, J. A. Thompson, and C. A. Jessee, *Drug Alcohol Depend.*, **3,** 23 (1979).

(26) S. Y. Yeh and H. A. Krebs, *J. Pharm. Sci.*, **70,** 482 (1981).

(27) S. Y. Yeh and L. A. Woods, *Proc. Soc. Exp. Biol. Med.*, **136,** 782 (1971).

(28) S. Y. Yeh and L. A. Woods, *J. Pharmacol. Exp. Ther.*, **169,** 168 (1969).

(29) J. Axelrod, *ibid.*, **117,** 322 (1956).

(30) S. Y. Yeh, R. L. McQuinn, H. A. Krebs, and C. W. Gorodetzky, *J. Pharm. Sci.*, **67,** 878 (1978).

(31) R. Dunkerley, R. Johnson, S. Schenken, and G. R. Wilkinson, *Clin. Pharmacol. Ther.*, **20,** 546 (1976).

(32) U. Klotz, T. S. McHorse, G. R. Wilkinson, and S. Schender, *ibid.*, **16,** 667 (1975).

(33) A. P. L. Shih, K. Robinson, and W. Y. W. Au, *Eur. J. Clin. Pharmacol.*, **9,** 451 (1976).

(34) J. Caldwell, L. A. Wakile, L. T. Notarianni, R. L. Smith, G. T. Correy, B. A. Lieberman, R. W. Beard, M. D. A. Finnie, and W. Snedden, *Life Sci.*, **22,** 589 (1978).

(35) T. J. Goehl and C. Davison, *J. Pharm. Sci.*, **62,** 907 (1973).

## ACKNOWLEDGMENTS

The authors thank Dr. C. W. Gorodetzky for interest in this project and for reviewing the manuscript.

A preliminary report of a part of these experiments appeared in *Fed. Proc. Fed. Am. Soc. Exp. Biol.*, **39,** 994 (1980).

# GLC–Mass Fragmentographic Determination of Saccharin in Biological Fluids

C. PANTAROTTO ˣ, M. SALMONA, R. FANELLI, M. BIANCHI, and K. SZCZAWINSKA

Received April 30, 1980, from the *Instituto di Ricerche Farmacologiche "Mario Negri," Via Eritrea, 62–20157 Milan, Italy.* Accepted for publication January 7, 1981.

**Abstract** □ A specific and sensitive method is described for the determination of saccharin in biological fluids. The compound is extracted as its methyl derivative following a salt–solvent pair procedure and assayed by GLC with either flame-ionization or mass fragmentographic detection using ethylated or trideuteromethylated saccharin, respectively, as the internal standard for quantitation. Detector response was linear over concentrations of 50 ng/ml–10 μg/ml with multiple-ion detection mass fragmentography and from 2 μg/ml up to milligram levels with flame-ionization detection. Interference from endogenous substrates was never observed. Plasma kinetics and urinary elimination of saccharin in healthy human volunteers given the sweetener orally, acutely (50 mg/60 kg of body weight) or for 5 days (130 mg/60 kg of body weight/day divided over the three main meals), also are reported.

**Keyphrases** □ Saccharin—GLC–mass fragmentographic determination in human biological fluids, plasma kinetics and urinary excretion □ GLC—determination of saccharin in human biological fluids, plasma kinetics and urinary excretion □ Mass fragmentography—determination of saccharin in human biological fluids, plasma kinetics and urinary excretion □ Sweeteners, artificial—saccharin, GLC and mass fragmentographic determination of saccharin in biological fluids, humans

Saccharin, 1,2-benzisothiazol-3(2*H*)-one 1,1-dioxide (I), is an artificial sweetener used in soft drinks, slimming diets, and diabetic foods. Recent toxicological studies (1) with this compound showed a higher incidence of bladder cancer in male rats fed during two-generation studies with a diet containing 5% I. Kinetic and distribution studies may be useful for investigating the causes of toxicity induced by exogenous compounds. However, the assay methods described in the literature for I determination are not suitable for studies in humans because of poor sensitivity or the use of labeled substrates (2, 3). Therefore, a specific and sensitive GLC–mass fragmentographic procedure was developed for the measurement of nanogram concentrations of I in biological fluids.

## EXPERIMENTAL

**Chemicals**—Saccharin[1] (I) was used as the dihydrated sodium salt. Methyl iodide[2], ethyl iodide[2], trideuteromethyl iodide[3], and tetrahexylammonium hydrogen sulfate[4] also were used. All solvents were analytical reagent grade.

**GLC**—The chromatograph[5] was equipped with a flame-ionization detector[6]. The column was a glass tube, 2 m × 4 mm i.d., packed with 100–120-mesh Gas Chrom Q coated with 3% OV-17[7]. All newly prepared columns were conditioned at 280° for 1 hr without carrier gas flow and then for 24 hr with a carrier gas flow rate of 15 ml/min. During analysis, nitrogen was used as the carrier gas at a flow rate of 30 ml/min. Air and hydrogen flow rates were adjusted to give maximum detector response. The operating conditions were: column oven temperature, 210°; injection port heater temperature, 250°; and flame-ionization detector temperature, 250°.

[1] Lot X 17PS4632, Sherwin-Williams Co., Cleveland, Ohio.
[2] Merck, Darmstadt, West Germany.
[3] CEA, Gif-sur-Yvette, France.
[4] Hässle, Göteborg, Sweden.
[5] Carlo Erba Fractovap model G1.
[6] Carlo Erba model 20.
[7] Applied Science Laboratories, State College, Pa.

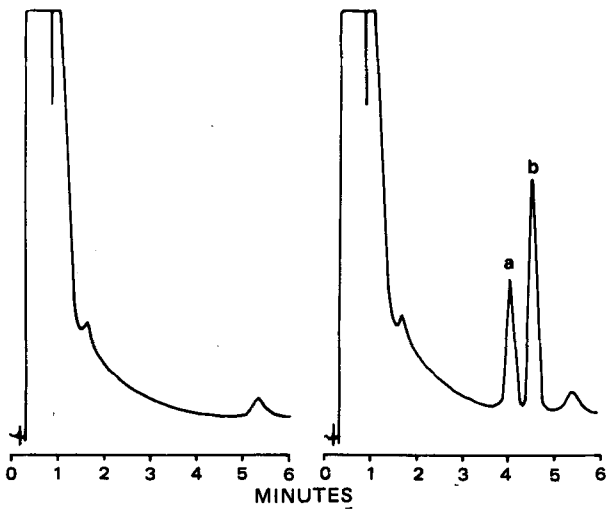


**Figure 1**—*Chromatograms obtained from control urine (left) and urine of a volunteer after I intake (right). Key: peak a, methylated I; and peak b, ethylated I (internal standard).*

**Mass Spectrometry**—Mass spectra were recorded on an instrument coupled with a gas chromatograph[8] and used under the following conditions: energy of the ionization beam, 70 ev; ion source temperature, 290°; accelerating voltage, 3.5 kv; and trap current, 60 μamp. Mass fragmentography was carried out at 70 ev by focusing the mass spectrometer[9] on the ions at *m/z* 197 and 133 for methylated I and at *m/z* 200 and 136, characteristic of the spectrum of trideuteromethylated I. In both

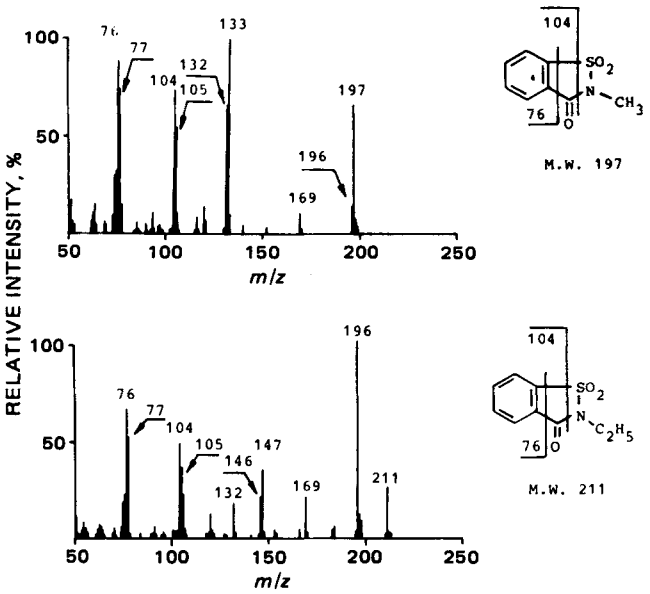


**Figure 2**—*Mass spectra of methylated I (top) and ethylated I (bottom).*

[8] LKB model 9000.
[9] LKB model 2091-B equipped with a computer system (model 2130) for data acquisition and calculation.

0022-3549/81/0800-0871$01.00/0
© 1981, American Pharmaceutical Association

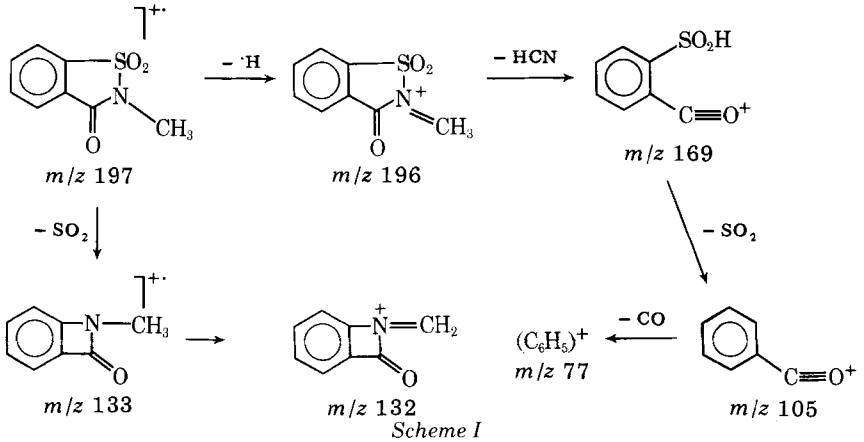


*Scheme I*

cases, the GLC conditions were as described, except that helium was the carrier gas.

**Extraction and Derivative Formation**—To 1 ml of plasma or urine, either 20 μg of ethylated I or 500 ng of trideuteromethylated I as the internal standard was added, depending on the expected concentration range and the type of detector used (flame ionization or mass fragmentography). The samples were deproteinized by the addition of 100 μl of trichloroacetic acid and then centrifuged at 4000×*g* for 20 min. The supernates were transferred to hermetically sealable glass tubes bearing a polytef disk in the inner part of the cap and were extracted with 5 ml of 0.5 *M* methyl iodide–methylene chloride solution after the addition of 70 μl of 10 *N* NaOH and 50 μl of 0.1 *M* tetrahexylammonium hydrogen sulfate solution in 0.1 *N* NaOH. Extraction was carried out for 2 hr by shaking at 60° in subdued light.

The organic phase (4 ml) was transferred to conical glass tubes and evaporated to dryness under a gentle nitrogen stream in a water bath at 35°. The residue was resuspended in 50 μl of methylene chloride, and the tetrahexylammonium salt was precipitated by the addition of 2 ml of *n*-hexane. The tubes were capped and centrifuged for 5 min at 4000×*g*. The supernatant fraction (1.8 ml) was transferred to conical glass tubes and evaporated to dryness under a nitrogen stream at 35°. The residue was dissolved in 50 μl of methylene chloride, and a 1–5-μl aliquot of this solution was injected for either GLC or mass fragmentographic analysis. Addition of I to drug-free plasma and urine samples at concentrations

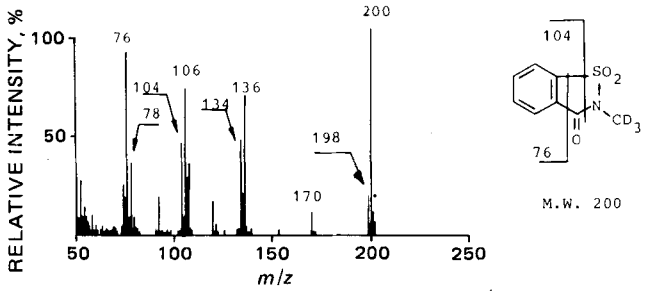


**Figure 3**—*Mass spectrum of trideuteromethylated I.*

**Table I—Precision of I Assay Method in Human Plasma and Urine**

| Parameter | Concentration of I in Plasma[a] 0.05 μg/ml | 0.5 μg/ml | 5 μg/ml | Concentration of I in Urine[b] 5 μg/ml | 50 μg/ml | 500 μg/ml |
|---|---|---|---|---|---|---|
| $\bar{X}$ | 0.0487 | 0.498 | 5.08 | 4.87 | 51.5 | 517.2 |
| *SD* | 0.0045 | 0.014 | 0.23 | 0.22 | 1.9 | 11.1 |
| *CV*, % | 9.2 | 2.8 | 4.5 | 4.5 | 3.7 | 2.2 |
| *n* | 4 | 4 | 4 | 4 | 4 | 4 |

[a] Determination by multiple-ion detection mass fragmentography. [b] Determination by flame-ionization detection GLC.

**Table II—Plasma I Kinetic Parameters Determined in Four Healthy Volunteers Given a Single Oral Dose of 50 mg/60 kg of Body Weight**

| Parameter[a] | $\bar{X} \pm SE$ |
|---|---|
| $K_a$, $min^{-1}$ | 0.045 ± 0.008 |
| $t_{1/2}$, min | 121 ± 16 |
| *AUC*, μg/ml hr | 5.02 ± 1.17 |
| Peak value, μg/ml | 1.95 ± 0.47 |
| Time of peak concentration, min | 30–60 |

[a] $K_a$ = rate constant of absorption, $t_{1/2}$ = half-life, and *AUC* = area under the curve.

ranging from nanograms to micrograms resulted in overall recoveries of 51 ± 4 and 58 ± 3%, respectively.

**Preparation of Ethylated I and Trideuteromethylated I**—Ethylated I and trideuteromethylated I were prepared according to the described salt–solvent pair procedure by extracting I from water with either 0.5 *M* ethyl iodide or 0.5 *M* trideuteromethyl iodide–methylene chloride solutions.

**Studies in Humans**—In the single-dose experiment, four healthy male volunteers ingested a 0.1% solution of I in water (50 mg/60 kg of body weight) after an overnight fast. Venous blood samples were withdrawn 0, 5, 10, 20, 30, 45, 60, 90, 120, 180, and 240 min after I intake. Urine

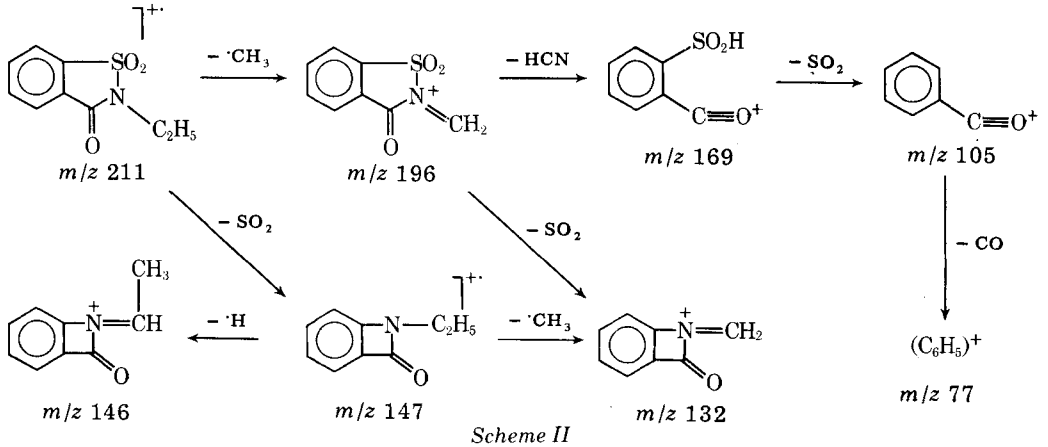


*Scheme II*

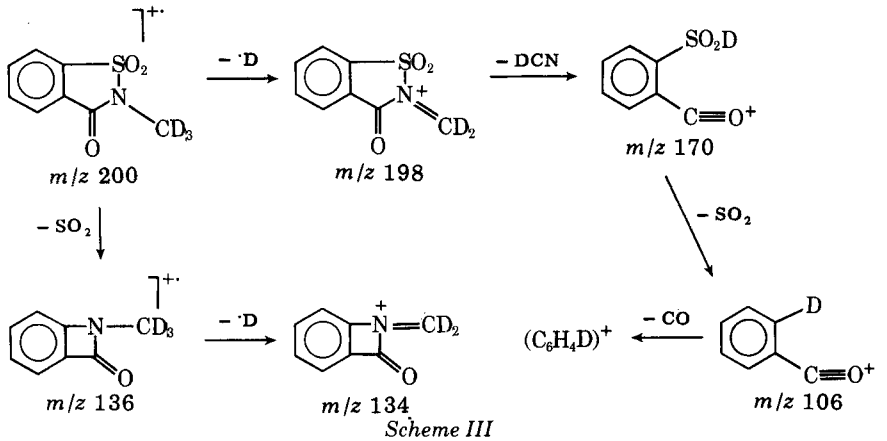


*Scheme III*

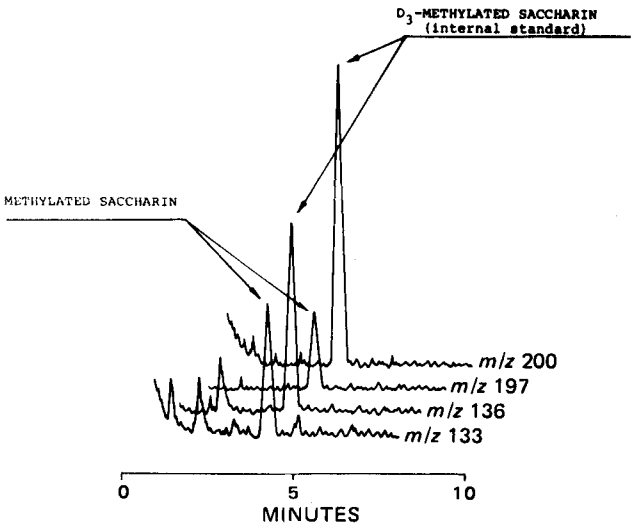


**Figure 4**—*Mass fragmentogram of a plasma extract from a human volunteer after I intake.*

samples were collected at selected intervals up to 24 hr.

In the repeated-dose experiment, another four healthy male volunteers were given I orally at a dose of 130 mg/60 kg of body weight/day for 5 days. These subjects were free to divide the amount of I into three doses daily to be taken between 7 am and 8 pm with meals. On Day 5, plasma and urine samples were collected at regular intervals over 24 hr.

**Data Analysis**—Plasma kinetic parameters of I were determined by the method of residuals (4), and the values of the area under the curve (*AUC*) were determined by the trapezoidal rule (5).

## RESULTS AND DISCUSSION

Figure 1 shows typical chromatograms obtained from the urine extracts of human volunteers before and after intake of saccharin (I). Peak a corresponds to methylated I, and peak b corresponds to an ethylated I structural analog chosen as the internal standard.

**Table III—Plasma Levels of I in Four Human Volunteers Given 130 mg/60 kg of Body Weight Orally for 5 Days**

| Hour | I Concentration, μg/ml |
|---|---|
| 0800 | ND[a] |
| 1000 | 0.35 ± 0.12 |
| 1200 | 0.13 ± 0.07 |
| 1400 | 0.28 ± 0.05 |
| 1800 | 0.07[b] |
| 2000 | 0.23 ± 0.07 |
| 2200 | ND |
| 2400 | ND |
| *AUC*, μg/ml hr | 2.24 ± 0.39 |

[a] Not detectable (<0.05 μg/ml). [b] Only one value available.

**Table IV—Urinary I Excretion by Four Healthy Volunteers Given a Single Oral Dose of 50 mg/60 kg of Body Weight**

| Time Interval | I Concentration | |
|---|---|---|
| | Milligrams | Percent of Dose |
| 1000–1200 | 15.06 ± 2.58 | 25.6 ± 4.7 |
| 1200–1400 | 10.08 ± 3.49 | 17.1 ± 6.3 |
| 1400–1600 | 9.62 ± 2.97 | 16.0 ± 4.9 |
| 1600–1800 | 4.32 ± 0.83[a] | 7.4 ± 1.7[a] |
| 1800–2000 | 3.55 ± 1.36 | 6.1 ± 2.4 |
| 2000–2400 | 2.76 ± 0.63 | 4.7 ± 1.2 |
| 2400–1000 | 2.80 ± 0.37 | 4.8 ± 0.7 |
| Excretion, 24 hr | 47.14 ± 1.62 | 79.9 ± 4.3 |

[a] Only three values available.

The chemical identity of these peaks was verified by combined GLC–mass spectrometry, and the resulting mass spectra are shown in Fig. 2. The mass spectrum of methylated I showed a prominent molecular ion at *m/z* 197; other intense fragments were present at *m/z* 133 (base peak), 132, 105, 104, 77, and 76, which arose as proposed in Scheme I. The mass spectrum of ethylated I was also consistent with the proposed structure, a molecular ion being present at *m/z* 211 and other intense fragments as shown in Scheme II.

For I determinations at nanogram concentrations, a mass fragmentographic procedure with trideuteromethylated I as the internal standard was used. Trideuteromethylated I has similar physicochemical properties to methylated I, resulting in an identical retention time. The use of such an internal standard reduces column adsorption losses and, consequently, increases the sensitivity.

Figure 3 shows the mass spectrum of trideuteromethylated I. For this compound, the assigned chemical structure was confirmed by the characteristic pattern of fragmentation (Scheme III), which was similar to that of methylated I. Therefore, stable isotope dilution mass fragmen-

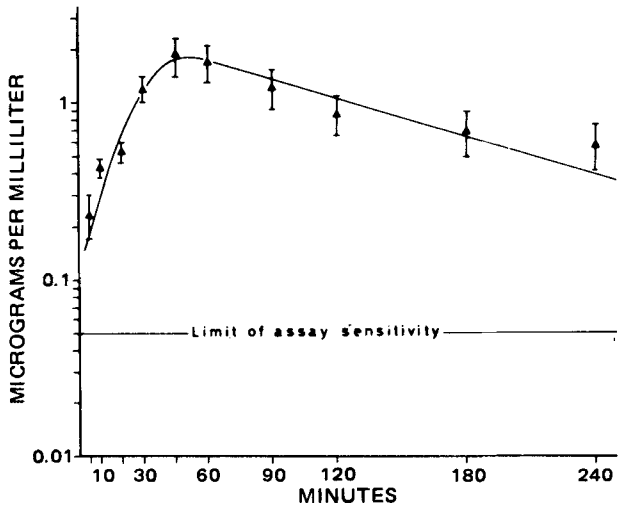


**Figure 5**—*Plasma I kinetics in four healthy volunteers given a single oral dose of 50 mg/60 kg of body weight.*

Table V—Urinary I Excretion by Four Human Volunteers Given 130 mg/60 kg po for 5 Days

| Time Interval | I Concentration, mg |
|---|---|
| 2000–0800 | 13.13 ± 2.30 |
| 0800–1200 | 20.03 ± 1.68 |
| 1200–1600 | 37.44 ± 7.31 |
| 1600–2000 | 29.06 ± 9.31 |
| Excretion, 24 hr | 89.03 ± 15.01 |
| Percent of administered dose | 80.35 ± 14.08 |

tography was carried out by focusing the instrument on the molecular ions of methylated I and trideuteromethylated I occurring at $m/z$ 197 and 200, respectively, and on the fragment ions at $m/z$ 133 and 136, which arise from the loss of sulfurous anhydride from the molecular ions. Figure 4 shows a typical mass fragmentogram obtained from a human plasma extract after I intake.

During both GLC with flame-ionization detection and mass fragmentography, no interference due to endogenous substrates was observed. Good linearity in detector response also was found over a concentration range of 50 ng/ml–10 μg/ml with multiple-ion detection mass fragmentography and from 2 μg/ml up to milligram levels for GLC with flame-ionization detection. The precision (percentage coefficients of variation) was calculated from the standard deviation/mean × 100. Assays were made in quadruplicate at six concentrations of I, thus covering the range expected in *in vivo* experiments. The results summarized in Table I refer to determinations from human plasma and urine.

The validity of this method for *in vivo* determinations was tested by studying the plasma kinetics and urinary elimination of I in healthy volunteers after single (50 mg/60 kg of body weight) or repeated (130 mg/60 kg of body weight/day for 5 days divided over the three main meals) oral doses.

Figure 5 shows plasma I kinetics in human volunteers after acute administration. The compound was absorbed rapidly through the GI tract, reaching peak plasma values between 30 and 60 min. Elimination of I followed a monoexponential decay pattern with a calculated half-life of 121 ± 16 min at the times considered (Table II).

Table III reports the plasma I levels determined in the volunteers given repeated oral doses. Concentrations were higher close to the time of I intake, *i.e.*, breakfast, lunch, and dinner. The *AUC* was about half that after a single dose of 50 mg/60 kg of body weight, although the daily dose was almost 2.5 times larger. However, these differences probably arose from differences in absorption since I was taken with food and not in a fasting condition and since the total daily dose was divided *ad libitum*, an experimental condition that may be considered closer to the real situation.

Urinary I excretion by human volunteers given a single oral dose is reported in Table IV. Compound I was eliminated within a few hours of administration, with ~60% of the dose being excreted unchanged by 6 hr, and reached 79.9% at 24 hr. Excretion of I after repeated administration is shown in Table V. Following this schedule of treatment, the 24-hr excretion again amounted to ~80% of the daily dose. These data are in good agreement with previous reports indicating that I is excreted in the urine rapidly and almost completely in humans and laboratory animals (6, 7). This observation is consistent with the relatively short plasma half-life of I, which is poorly metabolized.

## REFERENCES


(1) D. L. Arnold, C. A. Moodie, H. C. Grice, S. M. Charbonneau, B. Stavric, and I. C. Munro, "Toxicology Forum, The Eppley Institute for Research in Cancer," Omaha, Neb., May 10, 1977.

(2) L. M. Ball, A. G. Renwick, and R. T. Williams, *Xenobiotica*, **7**, 189 (1977).

(3) E. M. Ratchik and V. Viswanathan, *J. Pharm. Sci.*, **64**, 133 (1975).

(4) M. Mayersohn and M. Gibaldi, *Am. J. Pharm. Educ.*, **35**, 19 (1971).

(5) J. G. Wagner, "Biopharmaceutics and Relevant Pharmacokinetics," Drug Intelligence Publications, Hamilton, Ill., 1971.

(6) J. L. Byard, E. W. McChesney, L. Goldberg, and F. Coulston, *Food Cosmet. Toxicol.*, **12**, 175 (1974).

(7) E. J. Lethco and W. C. Wallace, *Toxicology*, **3**, 287 (1975).


# Size Exclusion Chromatography of Liposomes on Different Gel Media


**GUSTAF JEDERSTRÖM ˣ and GRAHAM RUSSELL**



Received July 24, 1980, from the *Pharmaceutical Research Department, Pharmacia AB, Box 181, S-751 25 Uppsala 1, Sweden.* Accepted for publication January 7, 1981.



**Abstract** □ Uncharged and negatively and positively charged liposomes of egg lecithin were prepared by sonication and chromatographed on three different gel media. The column effluent was investigated by turbidimetric measurements. The operational parameters were selected to obtain baseline separation of the liposomes. Liposome peaks were fractionated and identified by their $K_{av}$ (distribution coefficient) values. Baseline separation into two fractions was obtained with cross-linked dextran gel, and three fractions were obtained with cross-linked agarose gel.



**Keyphrases** □ Liposomes—synthesized and fractionated using size exclusion chromatography on different gel media □ Size exclusion chromatography—of liposomes on different gel media □ Fractionation—size exclusion chromatography of liposomes on different gel media □ Chromatography, size exclusion—liposomes, synthesized and fractionated on cross-linked agarose and cross-linked dextran gels


Parenteral and oral dosage forms with increased drug selectivity are achieved by linking drugs to carriers. Such forms are of pharmaceutical importance, and several concepts using liposomes have been suggested (1, 2). Liposomes are formed when phospholipids are allowed to swell in aqueous media. When suitably dispersed, the liposomes consist of a series of concentric lipid bilayers, which alternate with aqueous compartments. The bilayers and aqueous compartments can entrap lipid-soluble and water-soluble substances, respectively.

Size exclusion chromatography[1] (3) commonly is used to separate liposome-entrapped substances from nonentrapped material (4–6), but there has been little evaluation of different gel media for their ability to separate liposomes of different sizes. Huang (7) described the separation of vesicles of homogeneous size by using size exclusion chromatography on a gel with 4% agarose. Chen and

[1] Gel filtration traditionally is used to describe separation according to size on soft permeation media in aqueous solution (3). However, the term size exclusion chromatography is now recommended by the International Union of Pure and Applied Chemistry.




0022-3549/81/0800-0874$01.00/0



© 1981, American Pharmaceutical Association

Table V—Urinary I Excretion by Four Human Volunteers Given 130 mg/60 kg po for 5 Days

| Time Interval | I Concentration, mg |
|---|---|
| 2000–0800 | 13.13 ± 2.30 |
| 0800–1200 | 20.03 ± 1.68 |
| 1200–1600 | 37.44 ± 7.31 |
| 1600–2000 | 29.06 ± 9.31 |
| Excretion, 24 hr | 89.03 ± 15.01 |
| Percent of administered dose | 80.35 ± 14.08 |

tography was carried out by focusing the instrument on the molecular ions of methylated I and trideuteromethylated I occurring at $m/z$ 197 and 200, respectively, and on the fragment ions at $m/z$ 133 and 136, which arise from the loss of sulfurous anhydride from the molecular ions. Figure 4 shows a typical mass fragmentogram obtained from a human plasma extract after I intake.

During both GLC with flame-ionization detection and mass fragmentography, no interference due to endogenous substrates was observed. Good linearity in detector response also was found over a concentration range of 50 ng/ml–10 μg/ml with multiple-ion detection mass fragmentography and from 2 μg/ml up to milligram levels for GLC with flame-ionization detection. The precision (percentage coefficients of variation) was calculated from the standard deviation/mean × 100. Assays were made in quadruplicate at six concentrations of I, thus covering the range expected in *in vivo* experiments. The results summarized in Table I refer to determinations from human plasma and urine.

The validity of this method for *in vivo* determinations was tested by studying the plasma kinetics and urinary elimination of I in healthy volunteers after single (50 mg/60 kg of body weight) or repeated (130 mg/60 kg of body weight/day for 5 days divided over the three main meals) oral doses.

Figure 5 shows plasma I kinetics in human volunteers after acute administration. The compound was absorbed rapidly through the GI tract, reaching peak plasma values between 30 and 60 min. Elimination of I followed a monoexponential decay pattern with a calculated half-life of 121 ± 16 min at the times considered (Table II).

Table III reports the plasma I levels determined in the volunteers given repeated oral doses. Concentrations were higher close to the time of I intake, *i.e.*, breakfast, lunch, and dinner. The *AUC* was about half that after a single dose of 50 mg/60 kg of body weight, although the daily dose was almost 2.5 times larger. However, these differences probably arose from differences in absorption since I was taken with food and not in a fasting condition and since the total daily dose was divided *ad libitum*, an experimental condition that may be considered closer to the real situation.

Urinary I excretion by human volunteers given a single oral dose is reported in Table IV. Compound I was eliminated within a few hours of administration, with ~60% of the dose being excreted unchanged by 6 hr, and reached 79.9% at 24 hr. Excretion of I after repeated administration is shown in Table V. Following this schedule of treatment, the 24-hr excretion again amounted to ~80% of the daily dose. These data are in good agreement with previous reports indicating that I is excreted in the urine rapidly and almost completely in humans and laboratory animals (6, 7). This observation is consistent with the relatively short plasma half-life of I, which is poorly metabolized.

## REFERENCES


(1) D. L. Arnold, C. A. Moodie, H. C. Grice, S. M. Charbonneau, B. Stavric, and I. C. Munro, "Toxicology Forum, The Eppley Institute for Research in Cancer," Omaha, Neb., May 10, 1977.

(2) L. M. Ball, A. G. Renwick, and R. T. Williams, *Xenobiotica*, **7**, 189 (1977).

(3) E. M. Ratchik and V. Viswanathan, *J. Pharm. Sci.*, **64**, 133 (1975).

(4) M. Mayersohn and M. Gibaldi, *Am. J. Pharm. Educ.*, **35**, 19 (1971).

(5) J. G. Wagner, "Biopharmaceutics and Relevant Pharmacokinetics," Drug Intelligence Publications, Hamilton, Ill., 1971.

(6) J. L. Byard, E. W. McChesney, L. Goldberg, and F. Coulston, *Food Cosmet. Toxicol.*, **12**, 175 (1974).

(7) E. J. Lethco and W. C. Wallace, *Toxicology*, **3**, 287 (1975).


# Size Exclusion Chromatography of Liposomes on Different Gel Media


**GUSTAF JEDERSTRÖM ˣ and GRAHAM RUSSELL**



Received July 24, 1980, from the *Pharmaceutical Research Department, Pharmacia AB, Box 181, S-751 25 Uppsala 1, Sweden.* Accepted for publication January 7, 1981.



**Abstract** □ Uncharged and negatively and positively charged liposomes of egg lecithin were prepared by sonication and chromatographed on three different gel media. The column effluent was investigated by turbidimetric measurements. The operational parameters were selected to obtain baseline separation of the liposomes. Liposome peaks were fractionated and identified by their $K_{av}$ (distribution coefficient) values. Baseline separation into two fractions was obtained with cross-linked dextran gel, and three fractions were obtained with cross-linked agarose gel.



**Keyphrases** □ Liposomes—synthesized and fractionated using size exclusion chromatography on different gel media □ Size exclusion chromatography—of liposomes on different gel media □ Fractionation—size exclusion chromatography of liposomes on different gel media □ Chromatography, size exclusion—liposomes, synthesized and fractionated on cross-linked agarose and cross-linked dextran gels


Parenteral and oral dosage forms with increased drug selectivity are achieved by linking drugs to carriers. Such forms are of pharmaceutical importance, and several concepts using liposomes have been suggested (1, 2). Liposomes are formed when phospholipids are allowed to swell in aqueous media. When suitably dispersed, the liposomes consist of a series of concentric lipid bilayers, which alternate with aqueous compartments. The bilayers and aqueous compartments can entrap lipid-soluble and water-soluble substances, respectively.

Size exclusion chromatography[1] (3) commonly is used to separate liposome-entrapped substances from nonentrapped material (4–6), but there has been little evaluation of different gel media for their ability to separate liposomes of different sizes. Huang (7) described the separation of vesicles of homogeneous size by using size exclusion chromatography on a gel with 4% agarose. Chen and

[1] Gel filtration traditionally is used to describe separation according to size on soft permeation media in aqueous solution (3). However, the term size exclusion chromatography is now recommended by the International Union of Pure and Applied Chemistry.




0022-3549/81/0800-0874$01.00/0



© 1981, American Pharmaceutical Association

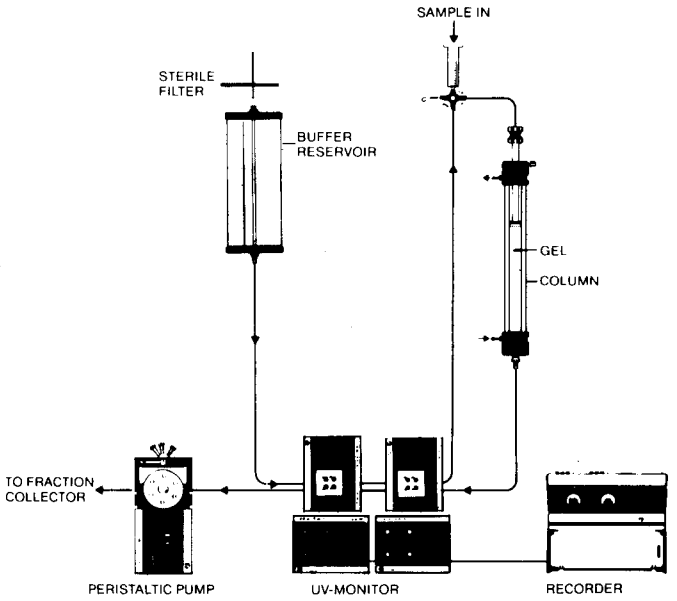


**Figure 1**—*Equipment for size exclusion chromatography.*

Schullery (8) suggested the separation of multilamellar vesicles from small unilamellar vesicles and sonication degradation products using 2% agarose gel.

This study investigated the ability of three different gels to separate liposomes into different fractions. Uncharged and negatively and positively charged liposomes were studied.

## EXPERIMENTAL

**Materials**—The uncharged liposomes were composed of egg lecithin[2]–cholesterol[3], 41:12 μmoles (33:4.64 mg). The negatively charged liposomes were composed of egg lecithin–cholesterol–phosphatidic acid[4]–dicetyl phosphate[5], 41:12:(mol. wt. unknown):6 μmoles (33:4.46:10:3.24 mg). The positively charged liposomes were composed of egg lecithin–cholesterol–stearylamine[6], 41:12:6 μmoles (33:4.46:1.6 mg).

The buffer was 3 m*M* sodium phosphate[5] (pH 7.3), containing 0.9% NaCl; it was sterilized at 121° for 25 min. Two cross-linked gels of 2[7] and 6%[8] agarose and cross-linked dextran gel[9] were used. To determine the fractionating range ($V_0 \rightarrow V_t$) of the gel bed in one separate run, a test solution was prepared from *Serratia marcescens* (ATCC 14756), which was chemically sterilized with pyrocarbonic acid diethyl ester ($V_0$), and sodium azide was dissolved in the buffer ($V_t$). Thirty microorganisms and 1 mg of sodium azide/1 ml of buffer were used.

**Preparation of Liposomal Dispersions**—Positively and negatively charged and uncharged liposomes were prepared aseptically according to a reported method (9). All glassware in contact with the preparations was sterilized by dry heat. Lipids and amphiphiles were dissolved in 5–8 ml of chloroform[10] in a 50-ml flask. The air in the flask was replaced by nitrogen or argon gas filtered through a 0.2-μm membrane filter. The organic solvent was removed in a rotary evaporator[11] at 25°, and evaporation was continued for 30 min. A thin, uniform film was visible on the wall of the flask.

Nitrogen was flushed into the flask, and 0.1–0.2 ml of the buffer solution was added immediately. Disruption of the lipid film was made by gently shaking the flask manually. A milky dispersion resulted after rotation of the flask with 1.8–1.9 ml of buffer and a few sterile glass beads.

The dispersion was stored at 4° for 12–24 hr. Before further treatment, the dispersions were inspected for microbial contamination. Only sterile dispersions were used for further investigation.

**Sonication**—The probes and glassware in contact with the product were sterilized by heat at 160° for 2 hr. Samples were sonicated[12] under nitrogen flush at 0–2°. Liposomal dispersions were transferred from a milky dispersion into a colloidal state when the sonication time exceeded 3 min at an amplitude of 8 μm. A homogeneous colloidal state, *i.e.*, a clear solution, was obtained when sonication was continued for 6 min at 8 μm followed by 2 min at 4 μm. The solution was inspected visually in polarized light immediately after preparation and, for some of the dispersions, after a month. Visually, the colloidal state was unchanged.

**Centrifugation**—All sonicated samples were centrifuged[13] at 2000 rpm for 10 min to remove titanium particles and unidentified fragments. The supernates were collected for evaluation.

**Absorption Spectra**—The absorption of the liposome components, individually and admixed, and of sonicated liposomes was measured between 600 and 200 nm with a recording double-beam spectrophotometer[14]. The concentration of all samples was identical to the concentration used in the liposomes. For components insoluble in water, chloroform was used as the solvent and reference. For liposome dispersions, the buffer was used as the external phase and as a reference.

**Size Exclusion Chromatography**—Two cross-linked agarose (2 and 6%) gels and a cross-linked dextran gel were used. These gel media have an effective fractionation range for globular proteins with a molecular weight between $2 \times 10^4$ and $3 \times 10^7$ daltons, which was of the same order as the liposomes under investigation. All material that would come in contact with the liposomes was sterilized. The gels were autoclaved at 121° for 25 min and then packed into the columns[15] and eluted with the buffer.

Effluent absorption was measured continuously with two UV monitors[16] coupled in series. The first monitor measured UV absorption at 254 or 280 nm. The second monitor was equipped with a high transmittance filter[17], which transmitted the mercury line 546 nm. The 254–280- and 546-nm readings were used to distinguish liposomes of different sizes on an empirical basis. For optimal detector performance, buffer was flushed continuously through the reference cells before entering the column. The effluent was collected in fractions of 0.8–1.2 ml using a fraction collector[18]. The equipment for size exclusion chromatography and the coupling for optimal detector performance are shown in Fig. 1.

The elution characteristics of each gel were determined by eluting 1 ml of the test solution through the column at 20 ± 1°. Flow rates (Table I) were kept constant and were adjusted with a peristaltic pump[19] or hydrostatic pressure. Figure 2 shows the elution profile of the test solution. The void volume ($V_0$), the total volume ($V_t$), and the operational volume ($V_t - V_0$) for each gel were determined as indicated in Fig. 2. The column parameters are presented in Table I.

The distribution coefficients[20] ($K_{av}$) were calculated from the elution

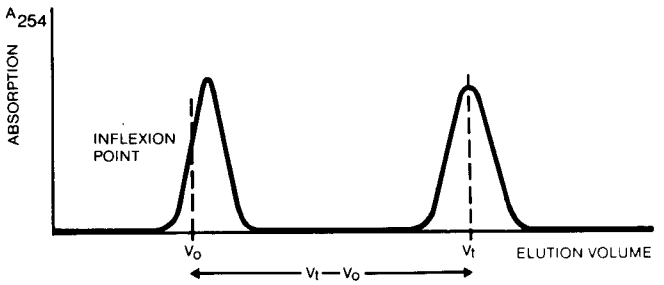


**Figure 2**—*Absorption profile for the test solution (*Serratia marcescens *and sodium azide).*

[2] Grade 1, Lipid Products, South Nutfield, England.
[3] BDH Biochemicals, Poole, England.
[4] Grade 1, Lipid Products, South Nutfield, England.
[5] Sigma Chemical Co., St. Louis, Mo.
[6] Fluka AG, Buchs, Switzerland.
[7] Sepharose C1-2B, Pharmacia Fine Chemicals, Uppsala, Sweden.
[8] Sepharose C1-6B, Pharmacia Fine Chemicals, Uppsala, Sweden.
[9] Sephacryl S-200, prepared by covalently cross-linking allyldextran with *N,N'*-methylenebis(acrylamide), Pharmacia Fine Chemicals, Uppsala, Sweden.
[10] Merck AG, Darmstadt, West Germany.
[11] Rotavapor-R, Büchi, Switzerland.
[12] Ultrasonic disintegrator, 150 w, amplitude 0–10 μm with 19-mm titanium probe, M.S.E., London, England.
[13] Multex, M.S.E., London, England.
[14] Hitachi Perkin-Elmer model 124.
[15] K16/20 and K16/70, Pharmacia Fine Chemicals, Uppsala, Sweden.
[16] Single-path monitor with recorder REC-2, Pharmacia Fine Chemicals, Uppsala, Sweden.
[17] Wratten No. 16.
[18] Stålprodukter, Uppsala, Sweden.
[19] P-3, Pharmacia Fine Chemicals, Uppsala, Sweden.
[20] The $K_{av}$ value represents the fraction of the total pore volume of the bed that is available for penetration of a given solute species; $V_t$ represents the total liquid volume of the gel bed according to the definition given. In the literature, both $K_d$ and $K_{av}$ are used to signify the fractional pore volume available and, alternatively, the fraction of the gel volume available.

**Table I—Operational Parameters Used in Size Exclusion Chromatography**

| Gel Medium | Column Dimension, Internal Diameter × Height, cm | Gel Bed Height, cm | Bed Volume, ml | Flow Rate, ml/min | Void Volume ($V_0$), ml | Total Liquid Volume ($V_t$), ml | Operational Volume ($V_t - V_0$), ml |
|---|---|---|---|---|---|---|---|
| Cross-linked 2% agarose | 1.6 × 70 | 63.2 | 127.0 | 0.12 | 38.4 | 124.2 | 85.8 |
| Cross-linked 6% agarose | 1.09 × 25 | 23.5 | 21.9 | 0.34 | 7.9 | 23.3 | 15.4 |
| Cross-linked 6% agarose | 1.6 × 20 | 14.2 | 28.5 | 1.22[a] | 8.1 | 27.2 | 19.0 |
| Cross-linked dextran | 1.6 × 20 | 14.2 | 28.5 | 0.99[a] | 9.4 | 26.6 | 17.2 |

[a] Flow regulated by hydrostatic pressure measured by volume–time measurements.

volume of the peaks of fractionated liposomes ($V_e$), the void volume, and the total liquid volume to yield $K_{av} = (V_e - V_0)/(V_t - V_0)$ (10). Newly packed columns or columns cleaned with a buffer solution of high ionic strength were eluted with three samples of liposomes and then washed with a volume of buffer equal to double the operational volume of the respective column before any test sample was applied. Thus, reproducible $K_{av}$ values for the fractions were obtained. The liposomes were stored at 4–8° and kept at 20° for 2 hr before size exclusion chromatography. Size exclusion chromatography was performed within 24 hr after liposome preparation. Sample volumes were 1–2 ml.

## RESULTS AND DISCUSSION

The liposomal components, when measured individually or admixed, displayed relatively low absorption in the 600–200-nm range. However, a low maximum or measurable absorbance was observed at 254 nm. The absorbance for lecithin was 0.4. The other components had much less absorbance at this wavelength. When the components were mixed, the absorbance at 254 nm decreased to 0.24. No explanation for this observation can be offered.

The absorption of liposome dispersions gradually increased from 600

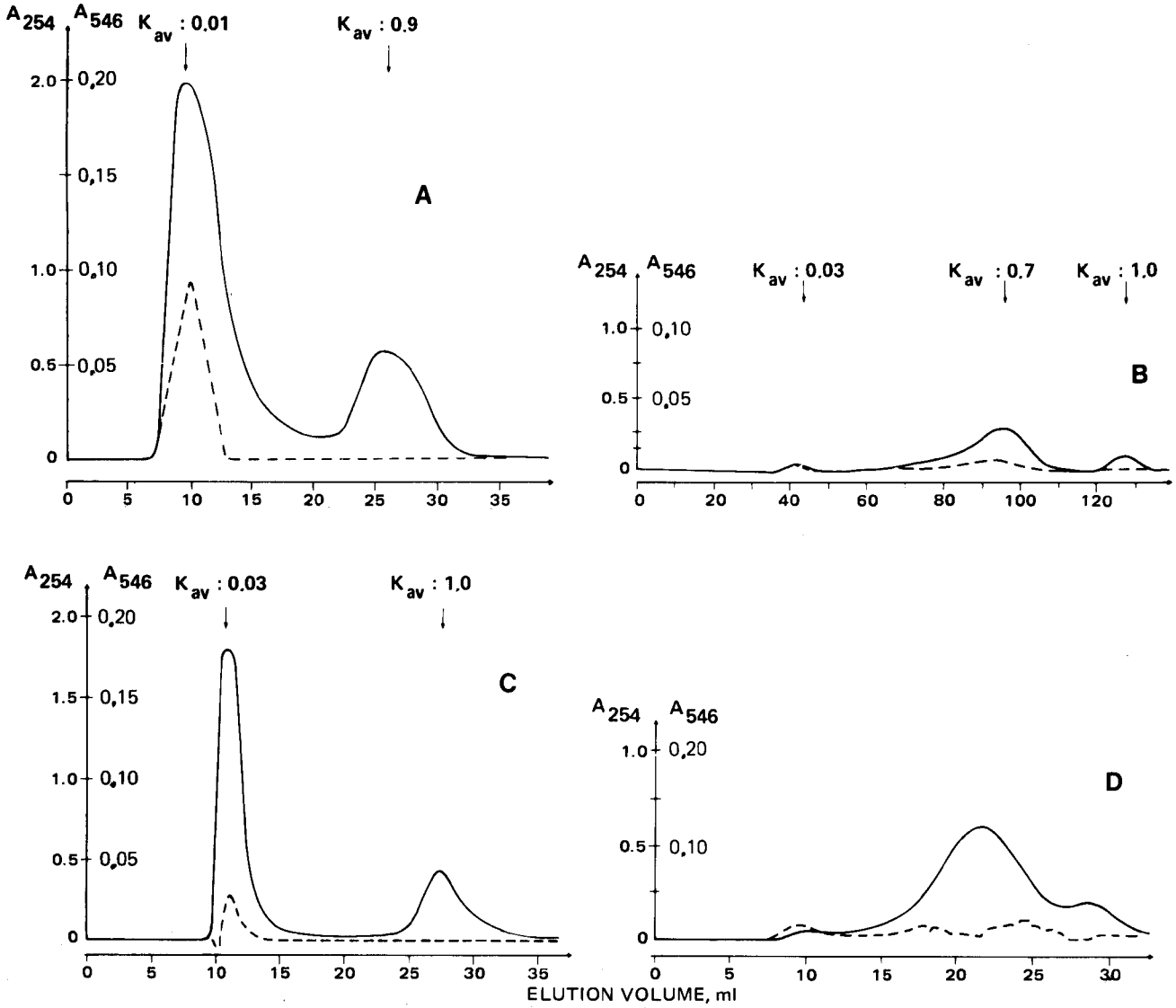


**Figure 3**—*Size exclusion chromatography of uncharged liposomes on different gel media. The eluent was phosphate buffer–saline (pH 7.3), and the temperature was 20°. Key: —, absorption profile at 254 nm, 0–2.0; and - - -, absorption profile at 546 nm, 0–0.2. A: Cross-linked 6% agarose—operational volume, 19.0 ml; sample volume, 1.5 ml; bed diameter, 1.6 cm; bed volume, 28.5 ml; and flow rate, 1.2 ml/min. B: Cross-linked 2% agarose—operational volume, 85.8 ml; sample volume, 1.5 ml; bed diameter, 1.6 cm; bed volume, 127.0 ml; and flow rate, 0.1 ml/min. C: Cross-linked dextran—operational volume, 17.2 ml; sample volume, 1.0 ml; bed diameter, 1.6 cm; bed volume, 28.5 ml; and flow rate, 1.0 ml/min. D: Cross-linked 2% agarose—operational volume, 26.3 ml; elution profile of uncharged liposomes; sample volume, 1.5 ml; and flow rate, 0.2 ml/min.*

**Table II—Size Exclusion Chromatography of Liposomes on Different Gel Media: Population of Separated Liposomes in Percent of Total Peak Area at Different $K_{av}$ Values [a]**

| Gel Medium and Operational Volume ($V_t - V_0$), ml | Absorption, nm | Uncharged | | | Negatively Charged | | | Positively Charged | | |
|---|---|---|---|---|---|---|---|---|---|---|
| | | $K_{av1}$ | $K_{av2}$ | $K_{av3}$ | $K_{av1}$ | $K_{av2}$ | $K_{av3}$ | $K_{av1}$ | $K_{av2}$ | $K_{av3}$ |
| Cross-linked 2% agarose, 85.8 | | 4 | 83 | 13 | 21 | 51 | 28 | 6 | 81 | 13 |
| | 280 | (0.03) | (0.7) | (1.0) | (0.02) | (0.5) | (1.0) | (0.02) | (0.7) | (1.0) |
| | 546 | (0.03) | (0.6) | (—) | (0.02) | (0.5) | (—) | (0.02) | (0.6) | (—) |
| Cross-linked 6% agarose, 15.4 | | 80 | 20 | — | 81 | 19 | — | 81 | 19 | — |
| | 280 | (0.02) | (1.0) | (—) | (0.02) | (1.0) | (—) | (0.04) | (1.0) | (—) |
| | 546 | (0.01) | (—) | (—) | (—) | (—) | (—) | (—) | (—) | (—) |
| Cross-linked 6% agarose, 19.0 | | 71 | 29 | — | 71 | 29 | — | 78 | 22 | — |
| | 280 | (0.01) | (0.9) | (—) | (0.01) | (0.9) | (—) | (0.0) | (0.9) | (—) |
| | 546 | (0.05) | (—) | (—) | (0.05) | (—) | (—) | (0.03) | (—) | (—) |
| Cross-linked dextran, 17.2 | | 72 | 28 | — | 75 | 25 | — | 72 | 28 | — |
| | 280 | (0.03) | (1.0) | (—) | (0.05) | (1.1) | (—) | (0.06) | (1.1) | (—) |
| | 546 | (0.07) | (—) | (—) | (0.07) | (—) | (—) | (0.1) | (—) | (—) |

[a] Different sizes of liposomes were separated and identified by $K_{av}$ values; $K_{av}$ given in parentheses.

to 200 nm. At 254 nm, the uncharged liposomes showed the lowest absorption of ~1.0. All charged liposomes had absorption of >2.0 at 254 nm. The measured absorption of liposomes was due to the light scattered by the particles and was not influenced by their individual components.

The two UV monitors for measuring the eluted peak profiles (Fig. 1) were used as turbidimeters since a decreased transmission was recorded.

Liposome fractions were separated by size, and these fractions were identified by their $K_{av}$ values. Fraction percentages were obtained by weighing the peaks of the liposome absorption profile at 280 nm (Table II).

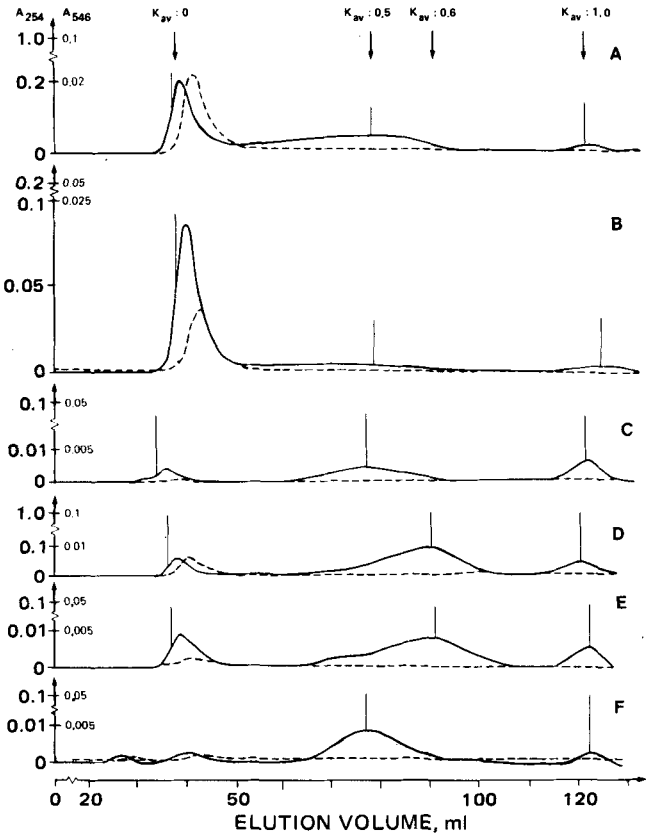


**Figure 4**—*Rechromatography of peak maxima of liposomes on cross-linked 2% agarose: operational volume, 88 ml; bed diameter, 1.6 cm; bed volume, 127 ml; flow rate, 0.19 ml/min; eluent, phosphate buffer–saline (pH 7.3), and temperature, 20°. Key: —, absorption profile at 254 nm; and - - -, absorption profile at 546 nm. A: Size exclusion chromatography of negatively charged liposomes (sample volume, 1.0 ml). B and C: Rechromatography of Peaks 1 (for B, sample volume was 2.0 ml) and 2 (for C, sample volume was 2.0 ml) from separated top fractions of negatively charged liposomes in A. D: Size exclusion chromatography of positively charged liposomes (sample volume, 1.0 ml). E and F: Rechromatography of Peaks 1 (for E, sample volume was 2.0 ml) and 2 (for F, sample volume was 2.0 ml) from separated top fractions of positively charged liposomes in D.*

Two fractions of uncharged, positively charged, and negatively charged liposomes were separated on cross-linked 6% agarose and cross-linked dextran. The largest fraction was eluted in the void volume ($K_{av}$ 0.05), and the other fraction was eluted in the total volume ($K_{av}$ 1.00). On cross-linked 2% agarose, uncharged and negatively and positively charged liposomes were separated into three fractions. The separation properties of different gel media for uncharged liposomes are shown in Fig. 3. Of cross-linked 6% agarose and cross-linked dextran, baseline separation for all liposomes could be obtained only with cross-linked dextran (Fig. 3C). Baseline separation into three different fractions was obtained for all liposomes with cross-linked 2% agarose with an operational volume of 80 ml (Fig. 3B). As the operational volume of the column was reduced (Fig. 3D), the peaks became incompletely separated.

In additional experiments with negatively and positively charged liposomes, fractions from the maxima of the first and second peaks (Fig. 4) were rechromatographed separately on the same gel (cross-linked 2% agarose). The first peak ($K_{av}$ 0.0) was eluted at the same position, but additional smaller peaks were obtained at $K_{av}$ 0.5–0.6 and 1.0. The second peak ($K_{av}$ 0.5–0.6) also emerged at the same position but with small peaks at $K_{av}$ 0.0 and 1.0. Similar results were observed for uncharged liposomes. The position of the peaks indicates that the separation properties of the gel were unchanged. The appearance of extra peaks may be due to a number of factors such as incomplete separation of liposomes, deformation of the liposomes when penetrating the gel pores, or a natural transfer of liposomes into an equilibrium state of different sizes. This observation indicates that size exclusion chromatography of liposome-entrapped material might lead to a loss of some entrapped material.

Chen and Schullery (8) also found three peaks when egg lecithin vesicles were separated on soft 2% agarose gel. The content of these peaks was found to be nonhomogeneous unless the liposomes were in rapid equilibrium. However, these investigators did not obtain a baseline separation. The assumption from the present study that the fractions obtained are homogeneous is supported by Huang (7), who concluded that a homogeneous fraction of vesicles is obtained on rechromatography on soft 4% agarose gel provided no equilibrium between fractions occurs.

Gregoriadis (11) suggested that the need for liposomes to persist in the blood for some time favors the small unilamellar version, indicating that the separation of liposomes into different sizes may be of great importance.

In conclusion, the experiments showed that macroporous agarose gels can be used to separate liposomes into well-defined fractions. These fractions will be investigated further by small-angle X-ray-scattering techniques.

## REFERENCES

(1) G. Gregoriadis, *Nature*, **265**, 407 (1977).

(2) A. Trouet, *Eur. J. Cancer*, **14**, 105 (1978).

(3) J. Porath and P. Flodin, *Nature*, **183**, 1657 (1959).

(4) G. Gregoriadis, "Drug Carriers in Biology and Medicine," Academic, New York, N.Y., 1979, pp. 286, 341.

(5) R. L. Juliano and D. Stamp, *Biochem. Pharmacol.*, **27**, 21

(1977).
(6) D. Papahadjopoulos, G. Poste, W. J. Vail, and J. Biedler, *Cancer Res.*, **36**, 2988 (1976).
(7) C.-H. Huang, *Biochemistry*, **1**, 344 (1969).
(8) C.-Y. Chen and S. Schullery, *J. Biochem. Biophys. Methods*, **1**, 189 (1979).
(9) G. Gregoriadis, in "Methods in Enzymology," vol. 44, K. Mosbach, Ed., Academic, New York, N.Y., 1976, pp. 218, 227.
(10) T. C. Laurent and J. Killander, *J. Chromatogr.*, **14**, 317 (1964).
(11) G. Gregoriadis, *Nature*, **283**, 814 (1980).

**ACKNOWLEDGMENTS**

The authors thank Ms. E. Jacobsson for skillful assistance and Dr. J. Brewer, Dr. K. Granath, and Dr. L. Hagel for valuable comments and advice.

# High-Performance Liquid Chromatographic Determination of Components of Bleomycin Preparations

**A. ASZALOS ˣ, J. CRAWFORD, P. VOLLMER, N. KANTOR, and T. ALEXANDER**

Received September 8, 1980, from the *National Center for Antibiotics Analysis, Food and Drug Administration, Washington, DC 20204.* Accepted for publication January 6, 1981.

**Abstract** □ A fast and sensitive method was developed for the quantitative determination of at least 10 components of pharmaceutical bleomycin sulfate preparations. The method is based on the reversed-phase high-performance liquid chromatographic (HPLC) separation of the components on a μBondapak $C_{18}$ column with a mobile phase having a linear gradient of 10–40% methanol in aqueous 0.005 *M* 1-pentanesulfonic acid at pH 4.3. With this assay, the average standard deviations for components $A_2$ and $B_2$ are 0.92 and 0.87, respectively, for a 7.5–22.5 × $10^{-3}$-mg sample. Regulatory agencies presently use the official Code of Federal Regulations (CFR) method, which is based on CM-Sephadex column chromatography. It was demonstrated that this CFR method does not separate the bleomycin $A_2$ component from some other minor bleomycin components. After elution from the CM-Sephadex column, the "$A_2$ component" was separated into five components by the HPLC method. Bleomycin $A_2$ is stable under these HPLC conditions.

**Keyphrases** □ High-performance liquid chromatography—reversed phase, bleomycin assay, separation of bleomycin components □ Bleomycin—high-performance liquid chromatographic determination, separation of components □ Antineoplastics—bleomycin, high-performance liquid chromatographic analysis

Bleomycins (I) are a family of glycopeptide antibiotics obtained from the fermentation broth of *Streptomyces verticillus* (1). Bleomycins are effective against various human neoplasms, particularly against squamous cell carcinoma, sarcoma, and malignant lymphoma (2–4). Preparations used in the treatment of these neoplasms contain several bleomycins. The main components are bleomycins $A_2$ and $B_2$. Some minor components such as bleomycin acid, demethylbleomycin-$A_2$, and bleomycin $B_4$ also are present. Among these minor components, bleomycin $B_4$ is the most toxic (5).

The Code of Federal Regulations (CFR) (6) requires that bleomycin preparations for therapeutic use meet the following composition specifications: bleomycin $A_2$, not less than 60% and not more than 70%; bleomycin $B_2$, not less than 25% and not more than 32%; bleomycin $B_4$, not more than 1%; and bleomycins $A_2$ and $B_2$ combined, not less than 90% of the total bleomycins. The present established method is based on a lengthy CM-Sephadex column chromatographic procedure, essentially that described by Fujii *et al.* (7).

Reported high-performance liquid chromatographic (HPLC) methods were unsuitable for routine quantitative analysis. With one method (8), baseline resolution was incomplete; another method (9) was not designed for quantitative purposes; and a third method (10), which could be used to determine bleomycins $A_2$ and $B_2$, did not

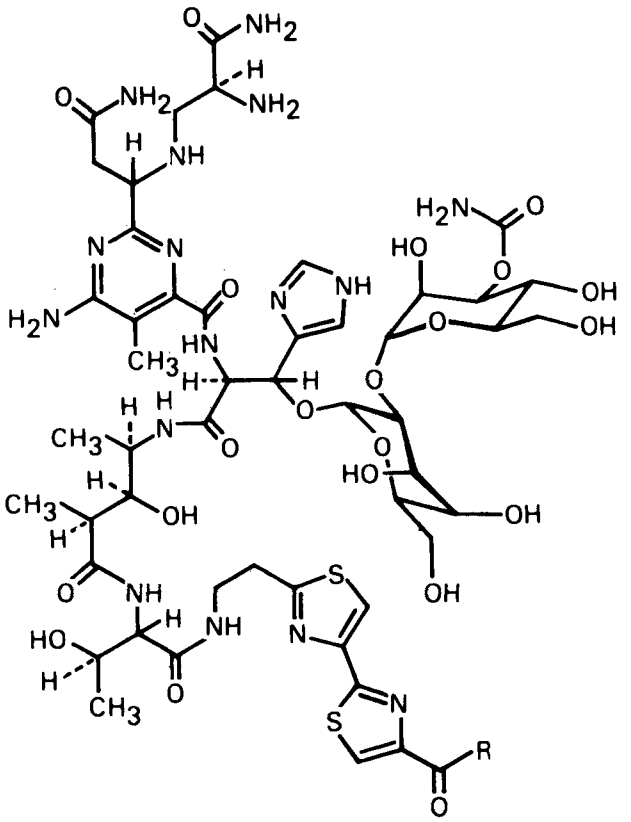

| bleomycin | R |
|---|---|
| demethyl-$A_2$ | NH—$CH_2$—$CH_2$—$CH_2$—S—$CH_3$ |
| $A_2$ | NH—$CH_2$—$CH_2$—$CH_2$—S=$(CH_3)_2$ |
| acid | OH |
| $B_2$ | NH—$(CH_2)_4$—NH—C(=NH)—$NH_2$ |
| $B_4$ | NH—$(CH_2)_4$—NH—C(=NH)—NH—$(CH_2)_4$—NH—C(=NH)—$NH_2$ |
| $A_5$ | NH—$(CH_2)_3$—NH—$(CH_2)_4$—$NH_2$ |



0022-3549/81/0800-0878$01.00/0
© 1981, American Pharmaceutical Association

(1977).
(6) D. Papahadjopoulos, G. Poste, W. J. Vail, and J. Biedler, *Cancer Res.*, **36**, 2988 (1976).
(7) C.-H. Huang, *Biochemistry*, **1**, 344 (1969).
(8) C.-Y. Chen and S. Schullery, *J. Biochem. Biophys. Methods*, **1**, 189 (1979).
(9) G. Gregoriadis, in "Methods in Enzymology," vol. 44, K. Mosbach, Ed., Academic, New York, N.Y., 1976, pp. 218, 227.
(10) T. C. Laurent and J. Killander, *J. Chromatogr.*, **14**, 317 (1964).
(11) G. Gregoriadis, *Nature*, **283**, 814 (1980).

**ACKNOWLEDGMENTS**

The authors thank Ms. E. Jacobsson for skillful assistance and Dr. J. Brewer, Dr. K. Granath, and Dr. L. Hagel for valuable comments and advice.

# High-Performance Liquid Chromatographic Determination of Components of Bleomycin Preparations

**A. ASZALOS ˣ, J. CRAWFORD, P. VOLLMER, N. KANTOR, and T. ALEXANDER**

Received September 8, 1980, from the *National Center for Antibiotics Analysis, Food and Drug Administration, Washington, DC 20204.* Accepted for publication January 6, 1981.

**Abstract** □ A fast and sensitive method was developed for the quantitative determination of at least 10 components of pharmaceutical bleomycin sulfate preparations. The method is based on the reversed-phase high-performance liquid chromatographic (HPLC) separation of the components on a μBondapak $C_{18}$ column with a mobile phase having a linear gradient of 10–40% methanol in aqueous 0.005 *M* 1-pentanesulfonic acid at pH 4.3. With this assay, the average standard deviations for components $A_2$ and $B_2$ are 0.92 and 0.87, respectively, for a 7.5–22.5 × $10^{-3}$-mg sample. Regulatory agencies presently use the official Code of Federal Regulations (CFR) method, which is based on CM-Sephadex column chromatography. It was demonstrated that this CFR method does not separate the bleomycin $A_2$ component from some other minor bleomycin components. After elution from the CM-Sephadex column, the "$A_2$ component" was separated into five components by the HPLC method. Bleomycin $A_2$ is stable under these HPLC conditions.

**Keyphrases** □ High-performance liquid chromatography—reversed phase, bleomycin assay, separation of bleomycin components □ Bleomycin—high-performance liquid chromatographic determination, separation of components □ Antineoplastics—bleomycin, high-performance liquid chromatographic analysis

Bleomycins (I) are a family of glycopeptide antibiotics obtained from the fermentation broth of *Streptomyces verticillus* (1). Bleomycins are effective against various human neoplasms, particularly against squamous cell carcinoma, sarcoma, and malignant lymphoma (2–4). Preparations used in the treatment of these neoplasms contain several bleomycins. The main components are bleomycins $A_2$ and $B_2$. Some minor components such as bleomycin acid, demethylbleomycin-$A_2$, and bleomycin $B_4$ also are present. Among these minor components, bleomycin $B_4$ is the most toxic (5).

The Code of Federal Regulations (CFR) (6) requires that bleomycin preparations for therapeutic use meet the following composition specifications: bleomycin $A_2$, not less than 60% and not more than 70%; bleomycin $B_2$, not less than 25% and not more than 32%; bleomycin $B_4$, not more than 1%; and bleomycins $A_2$ and $B_2$ combined, not less than 90% of the total bleomycins. The present established method is based on a lengthy CM-Sephadex column chromatographic procedure, essentially that described by Fujii *et al.* (7).

Reported high-performance liquid chromatographic (HPLC) methods were unsuitable for routine quantitative analysis. With one method (8), baseline resolution was incomplete; another method (9) was not designed for quantitative purposes; and a third method (10), which could be used to determine bleomycins $A_2$ and $B_2$, did not

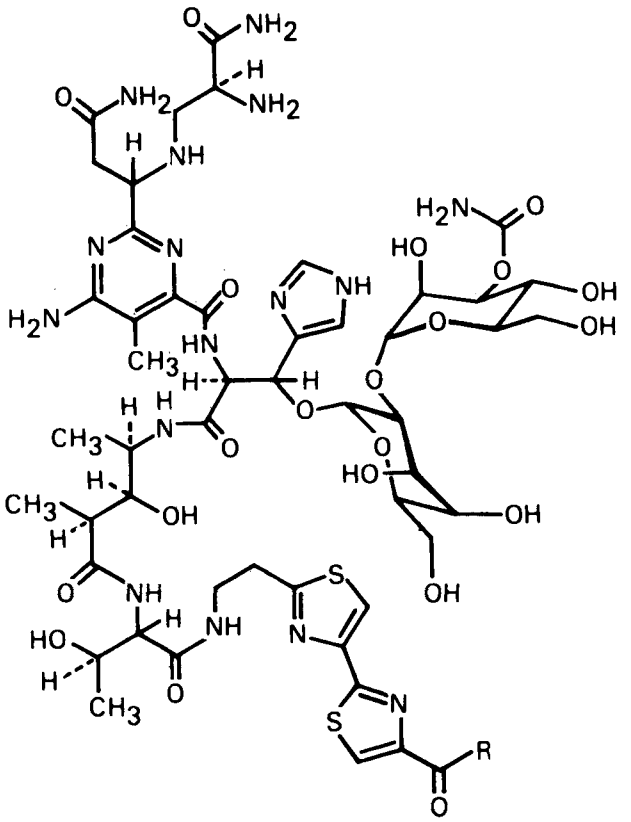

| bleomycin | R |
|---|---|
| demethyl-$A_2$ | NH—$CH_2$—$CH_2$—$CH_2$—S—$CH_3$ |
| $A_2$ | NH—$CH_2$—$CH_2$—$CH_2$—S=$(CH_3)_2$ |
| acid | OH |
| $B_2$ | NH—$(CH_2)_4$—NH—C(=NH)—$NH_2$ |
| $B_4$ | NH—$(CH_2)_4$—NH—C(=NH)—NH—$(CH_2)_4$—NH—C(=NH)—$NH_2$ |
| $A_5$ | NH—$(CH_2)_3$—NH—$(CH_2)_4$—$NH_2$ |



0022-3549/81/0800-0878$01.00/0
© 1981, American Pharmaceutical Association

detect the minor components. The developed HPLC assay is suitable for the fast, quantitative determination of at least 10 components found in commercial bleomycin preparations.

## EXPERIMENTAL

**Materials**—Spectrograde methanol was used throughout the experiments. Acetic acid[1], concentrated ammonium hydroxide[2], and 1-pentanesulfonic acid[3] were used without further purification. Solvents were deaerated under vacuum with stirring for 1 hr before use. Sterile bleomycin sulfate preparations[4] in vials containing 15 units of bleomycin activity were dissolved in 3 ml of deaerated water and stored at 5°.

**Apparatus**—A modular high-pressure liquid chromatograph was equipped with a constant-flow pump[5], a valve-type injector[5], and a fixed-wavelength (254-nm) UV detector[6]. A stainless-steel column (4.6 × 250 mm) was packed with fully porous 10-$\mu$m silica particles to which a monomolecular layer of octadecylsilane was chemically bonded. In this work, generically identical column packing materials from two different suppliers were used (referred to as Columns 1[7] and 2[8]). Columns were washed with methanol–water (1:1) after use each day and with methanol before each weekend. Calculations for the percentage of total UV absorbance at 254 nm were performed for each component by a microprocessor[9] with the peak area calculation program (Figs. 1 and 2). The microprocessor was set as follows: sensitivity, 10%; attenuator, 16; and initial peak width, 0.5.

**Analytical Procedure**—The sample size for injection was 3-9 $\mu$l of bleomycin solution. The solvent system consisted of 0.005 *M* 1-pentanesulfonic acid in 0.5% acetic acid deaerated aqueous solution, adjusted to pH 4.3 (concentrated ammonium hydroxide), and methanol with a linear gradient of 10–40% methanol. Gradient mixing time was 60 min, but chromatography was continued with the final gradient mixture (40% methanol) up to 75 min to allow for the appearance of demethylbleomycin-$A_2$, the last peak. The column pressure at a flow rate of 1.2–1.8 ml/min, depending on column conditions, was equivalent to the initial column pressure of 1600 psi.

The relative percent of each bleomycin component was calculated on the basis of the area under the peak by the microprocessor with the given parameters.

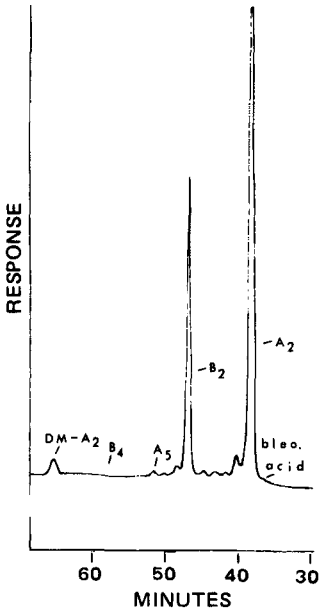


**Figure 1**—*HPLC separation profile of a bleomycin sulfate preparation obtained with Column 1 (6 $\mu$l of bleomycin solution injected). Key: bleo. acid, bleomycin acid; $A_2$, bleomycin $A_2$; $B_2$, bleomycin $B_2$; $A_5$, bleomycin $A_5$; $B_4$, bleomycin $B_4$; and DM-$A_2$, demethylbleomycin-$A_2$. Microprocessor quantitation indicates 58.29, 28.18, and 4.32 "relative %" composition for $A_2$, $B_2$, and demethyl-$A_2$, respectively.*

[1] Mallinckrodt Chemical Co., St. Louis, Mo.
[2] J. T. Baker Chemical Co., Phillipsburg, N.J.
[3] Eastman Organic Chemicals, Rochester, N.Y.
[4] Nippon-Kayaku Co. Ltd., Chugai Boyeki (America) Corp. Importers and Exporters, New York, N.Y.
[5] Model 6000 solvent delivery system and model 660 solvent programmer, Waters Associates, Milford, Mass.
[6] Model 440, Waters Associates, Milford, Mass.
[7] $\mu$Bondapak $C_{18}$, Waters Associates, Milford, Mass.
[8] Chromegabond MC-18, ES Industries, Marlton, N.J.
[9] Columbia Instrument Supergrator I.

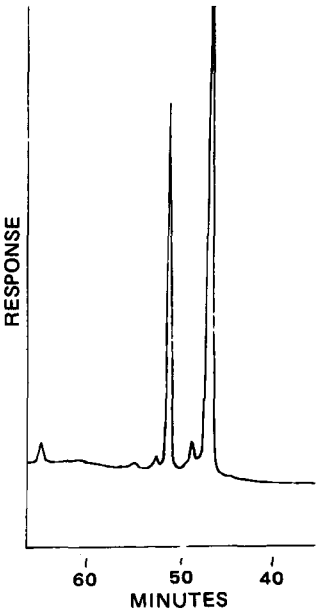


**Figure 2**—*HPLC separation profile of a bleomycin sulfate preparation obtained with Column 2 (6 $\mu$l of bleomycin solution injected). Relative peaks for separated components are the same as in Fig. 1. Microprocessor quantitation indicates 59.14, 29.62, and 4.09 "relative %" composition for $A_2$, $B_2$, and demethyl-$A_2$, respectively.*

## RESULTS AND DISCUSSION

In developing this HPLC method, different parameters such as solvent, column, pH, operating time, gradient composition, and flow rate were investigated for optimum separation. Mobile phases of acetonitrile, acetone, or methanol with aqueous solutions of perchloric acid or 1-pentanesulfonic acid in dilute acetic acid were studied. With aqueous 0.005 *M* 1-pentanesulfonic acid solution, adjusted to pH 4.3, and mixed with 10–40% methanol in a linear gradient, 10 or more components were

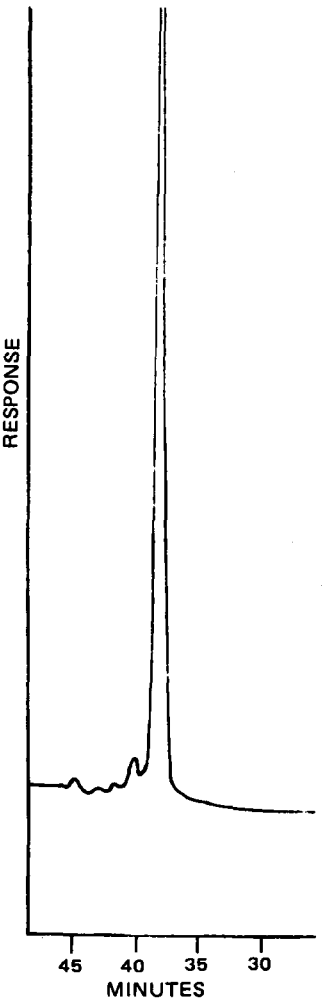


**Figure 3**—*HPLC separation profile obtained with Column 1 of the bleomycin "$A_2$ fraction" after elution from the CM-Sephadex column.*

**Table I—Comparison of the CFR and HPLC Methods for the Determination of Bleomycins $A_2$ and $B_2$ in Bleomycin Sulfate Preparations**

| Sample | Bleomycin A, % | | | Bleomycin B, % | | |
|---|---|---|---|---|---|---|
| | CFR Method | HPLC Method | *SD* | CFR Method | HPLC Method | *SD* |
| 1 | 68.43 (64.15)[a] | 62.30[b] | 0.46 | 28.33 | 28.10[b] | 0.80 |
| 2 | 67.60 (63.82)[a] | 63.16[c] | 1.12 | 28.54 | 29.49[c] | 1.25 |
| 3 | 66.52 | 59.50[d] | 1.26 | 30.85 | 28.48[d] | 0.77 |
| 4 | 65.78 | 60.33[b] | 0.85 | 31.39 | 29.89[b] | 0.66 |
| 5 | 69.27 | 65.12[e] | — | 26.63 | 29.30[e] | — |
| Average | | | 0.92 | | | 0.87 |

[a] Calculation after HPLC separation. [b] Average of 10 determinations. [c] Average of nine determinations. [d] Average of eight determinations. [e] Single determination.

detected. The last peak was observed at ~70 min, with a gradient mixing time of 60 min. Other gradient compositions and contours did not give satisfactory chromatograms. The same resolution of the 10 components was obtained between pH 4.0 and 6.0.

Another system that showed considerable promise was water, adjusted to pH 2.0 with perchloric acid, and mixed with 10–40% acetonitrile in a linear gradient. A separation profile like that in Fig. 2 was obtained, but the low pH of this solvent system made it impractical for routine use.

An initial column pressure of 1600 psi must be applied to obtain a flat baseline, suitable for area calculations with the microprocessor. Lower pressures result in baseline drift and poor area calculations. Typical separation profiles, obtained with Columns 1 and 2, are shown in Figs. 1 and 2, respectively. As used in this laboratory, Column 1 gave a better separation of the components. Specifically, the components between bleomycins $A_2$ and $B_2$ appeared as one peak with Column 2 but four peaks with Column 1. The quantitative results were comparable, however, for the bleomycin $A_2$, $B_2$, and demethyl-$A_2$ fractions from both columns; quantitative information for the $A_2$, $B_2$, and demethyl-$A_2$ fractions from the same sample is given for Columns 1 and 2 in the legends of Figs. 1 and 2, respectively.

The presumed identities of some individual peaks confirmed by coinjection of reference materials are shown in Fig. 1. No reference materials were available for the unidentified separated components.

Four bleomycin preparations were analyzed eight to 10 times each with Column 1 under the described HPLC conditions. These results (Table I), expressed as average percentages of the $A_2$ and $B_2$ components in bleomycin samples, were compared with those obtained by the official CFR method (6). The respective $A_2$ percentages obtained from the HPLC analyses were lower than those found by the CFR method. To explain this discrepancy, $A_2$ components isolated by the CFR method were collected from several column separations and combined, lyophilized, redissolved, and injected into the chromatograph. As shown in Fig. 3, the HPLC method separated this fraction into five components, with the major component having the retention time of bleomycin $A_2$. The amount of $A_2$ in this fraction was ~92% of the total bleomycin content of the fraction. After the $A_2$ percentages found by the CFR method were recalculated on the basis of the HPLC fraction separation, the official CFR column and HPLC results were in close agreement (Table I). This confirmation is significant since the accurate quantitation of bleomycins $A_2$ and $B_2$ in clinically used preparations is essential.

Bleomycin $A_2$ material collected from HPLC separations showed a single peak when rechromatographed by HPLC. This finding is evidence of the stability of bleomycin $A_2$ (and probably the other components) under these HPLC conditions.

Separate standard deviations for bleomycin $A_2$ and $B_2$ were calculated from multiple determinations of each component in four bleomycin samples (Table I). Calculations with these values give average standard deviations for components $A_2$ and $B_2$ of 0.92 and 0.87, respectively, and demonstrate good reproducibility for the HPLC assay.

## REFERENCES


(1) H. Umezawa, K. Maeda, T. Takeuchi, and Y. Okami, *J. Antibiot., Ser. A*, **19**, 200 (1966).

(2) T. Ichikawa, I. Nakano, and I. Hirokawa, *J. Urol.*, **102**, 699 (1969).

(3) I. Kimura, T. Onishi, I. Kunimasa, and J. Takano, *Cancer (Brussels)*, **29**, 59 (1972).

(4) C. D. Haas, C. A. Coltman, Jr., J. A. Gottlieb, A. Haut, J. K. Luce, R. W. Talley, B. Small, H. E. Wilson, and B. Hoogstraten, *ibid.*, **38**, 8 (1976).

(5) H. Umezawa, M. Ishizuka, K. Kimura, J. Iwanaga, and T. Takeuchi, *J. Antibiot.*, **21**, 592 (1968).

(6) "Code of Federal Regulations," Food and Drugs, Title 21, part 450.10a, U.S. Government Printing Office, Washington, D.C., 1980.

(7) A. Fujii, T. Takita, K. Maeda, and H. Umezawa, *J. Antibiot.*, **26**, 396 (1973).

(8) W. J. Rzeszotarski, W. C. Eckelman, and R. C. Reba, *J. Chromatogr.*, **124**, 88 (1976).

(9) C. R. Williams, *Proc. Anal. Div. Chem. Soc.*, **1977**, 242.

(10) T. T. Sakai, *J. Chromatogr.*, **161**, 389 (1978).

# Amino Acid Esters of Phenols as Prodrugs: Synthesis and Stability of Glycine, β-Aspartic Acid, and α-Aspartic Acid Esters of p-Acetamidophenol

**ILDIKO M. KOVACH *, IAN H. PITMAN ‡×, and TAKERU HIGUCHI**

Received August 22, 1980, from the *Department of Pharmaceutical Chemistry, University of Kansas, Lawrence, KS 66045.* Accepted for publication January 7, 1981. *Present address: Department of Chemistry, University of Kansas, Lawrence, KS 66045. ‡Present address: School of Pharmaceutics, Victorian College of Pharmacy, Parkville, Victoria, Australia, 3052.

**Abstract** □ pH–rate profiles were calculated for the hydrolysis of the glycine (II), β-aspartic acid (III), and α-aspartic acid (IV) esters of p-acetamidophenol (I) at 25° and $\mu$ = 1.0 *M*. The hydrolysis of esters II and III occurred predominantly *via* intermolecular reactions involving water, hydroxide ion, and the various ionic forms of the substrates. The hydrolysis of ester IV occurred predominantly *via* intramolecular reactions. The catalytic effects of formate, acetate, and phosphate ions as well as of tromethamine on the degradation on ester II were similar to their effects on the hydrolysis of ethyl dichloroacetate. The efficient catalysis of the hydrolysis of ester II in bicarbonate buffers was consistent with a mechanism that involved carbon dioxide and the formation and decomposition of a carbamate intermediate.

**Keyphrases** □ Prodrugs—of p-acetamidophenol, amino acid esters □ p-Acetamidophenol—amino acid esters as prodrugs, synthesis and analysis □ Phenols—amino acid esters as prodrugs, synthesis and analysis □ Amino acid esters—as prodrugs of p-acetamidophenol, synthesis and analysis

Amino acid esters of p-acetamidophenol (I) were proposed (1) as potentially useful prodrugs. Appropriate selection of the amino acid can yield derivatives having greater or less water solubility than p-acetamidophenol and a range of chemical stabilities with respect to transformation to the parent drug. When the amino acid is a normal dietary constituent, the transformation of the prodrug to I within the body will not yield a toxic byproduct.

Similar arguments can be used to support the investigation of amino acid esters of other phenolic drugs as prodrugs. This paper describes the synthesis and stability against degradation of the glycine (II), β-aspartic (III), and α-aspartic acid (IV) esters of I.

## RESULTS

**Characterization of Reactants**—The elemental analysis and NMR spectrum of the glycine (II) derivative of p-acetamidophenol (I) were completely consistent with the conclusion that it was the hydrobromide salt of II. The I esters of L-aspartic acid had elemental analyses and NMR spectra consistent with the conclusion that they were the hydrochloride salts of the isomers III and IV. Only one isomer could be obtained pure. This isomer was concluded to be ester III rather than ester IV because its pKa value (2.04) was closer to that of β-ethyl aspartate (2.00) (2) than it was to that of α-ethyl aspartate (3.04) (2). Its pKa value also was very close to the first pKa values of aspartic acid (1.88) (3) and histidine (1.78) (3), two molecules in which the carboxyl group adjacent to an ammonium group is the first to ionize. The greater reactivity of IV made it difficult to isolate and characterize.

**Decomposition of Esters II and III**—Esters II and III decomposed by hydrolysis in formate, acetate, and phosphate buffers. Plots of the observed first-order rate constants at each pH value, $k_{obs}$ values, *versus* the total concentration of buffer species, $[buffer]_T$, were linear over at least four buffer concentrations. Values of a buffer-independent first-order rate constant, $k_{hyd}$ values, were calculated from the *y* intercepts, when $[buffer]_T = 0$, of these plots. Values of $k_{hyd}$ are plotted *versus* pH in Fig. 1. Values of catalytic rate constants, $k_{cat}$, for the total buffer species were calculated in the case of hydrolysis of ester II from the slopes of the linear plots of $k_{obs}$ *versus* $[buffer]_T$.

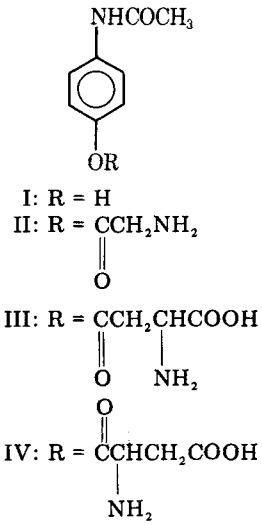


The relationship among $k_{obs}$, $k_{hyd}$, and $k_{cat}$ values is given by:

$$k_{obs} = k_{hyd} + k_{cat}[buffer]_T \quad \text{(Eq. 1)}$$

Values of $k_{cat}$ for decomposition of ester II are listed in Table I.

For phosphate catalysis, a plot of $k_{cat}/f_{EH^+}$ *versus* $f_b$ [where $f_{EH^+}$ and $f_b$ are the fraction of II that exists as its conjugate acid and the fraction of the buffer acid ($H_2PO_4^-$) that exists as its conjugate base ($HPO_4^{2-}$), respectively, for data at the various pH values] was essentially linear with a zero intercept when $f_b = 0$. Hence, the major reactions involved $HPO_4^{2-}$ ions and the conjugate acid of II. On the assumption that the other re-

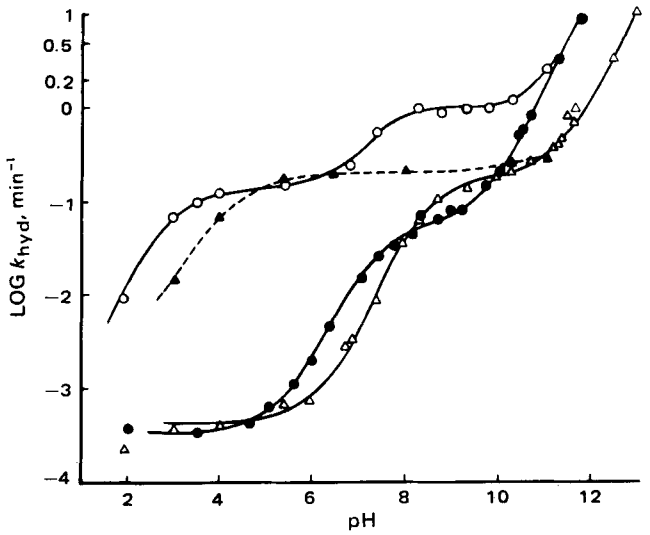


**Figure 1**—*Plots against pH of the logarithms of the buffer-independent pseudo-first-order rate constants,* $k_{hyd}$, *for the hydrolysis of esters II (●), III (△), and IV (○) and for the acid succinate of I (▲) in water at 25°,* $\mu$ *= 1.0 M. The lines were calculated as described in the text. The data for hydrolysis of the acid succinate of I were taken from Ref. 8.*

0022-3549/81/0800-0881$01.00/0
© 1981, American Pharmaceutical Association

**Table I—Catalytic Rate Constants, $k_{cat}$ (pH Dependent) and $k_b$ (pH Independent), for Oxyanion- and Tromethamine-Catalyzed Hydrolysis of *p*-Acetamidophenyl Glycinate at 25°, $\mu$ = 1.0 *M***

| Oxyanion | pH | $f_b$[a] | $f_{EH^+}$[b] | $10^3\,k_{cat}$, $M^{-1}$ min$^{-1}$ | $10^3\,k_b$, $M^{-1}$ min$^{-1}$ |
|---|---|---|---|---|---|
| Formate | 3.53 | 0.50 | 1.000 | 1.02 | 2.04 |
| Acetate | 5.08 | 0.80 | 1.000 | 4.14 | 5.18 |
| Phosphate | 5.60 | 0.15 | 1.000 | 19.50 | — |
| Phosphate | 6.00 | 0.30 | 1.000 | 38.00 | — |
| Phosphate | 6.38 | 0.50 | 0.927 | 49.60 | — |
| Phosphate | 7.08 | 0.83 | 0.710 | 85.20 | 120.00 |
| Tromethamine | 7.44 | 0.16 | 0.52 | 333.6 | — |
| Tromethamine | 8.18 | 0.50 | 0.16 | 354.0 | 4102 |

[a] Fraction of the buffer that exists as $HCO_3^-$, $CH_3COO^-$, $HPO_4^{2-}$, or tromethamine. The pKa values used in the calculations were the pH values of half-neutralized solutions of the acids or conjugate acids and were: $pKa^{HCO_2H}$, 3.53; $pKa^{CH_3COOH}$, 4.68; $pKa^{H_2PO_4^-}$, 6.38; and $pKa^{tromethamine}$, 8.18. [b] Fraction of ester II that exists as the conjugate acid (pKa = 7.44).

actions were similar, values of a pH-independent base catalysis constant, $k_b$ (which is equal to the value of the slope in the described type of plot), were calculated by dividing $k_{cat}$ values by the term $f_{EH^+}f_b$ (Table I).

The decomposition of ester II in tromethamine and carbonate buffers also was studied. In tromethamine buffers (pH 7.44 and 8.18), plots of $k_{obs}$ *versus* $[buffer]_T$ were linear, and $k_{cat}$ values were calculated in the manner described for oxyanion catalysis. At pH 9.22, a plot of $k_{obs}$ *versus* $[buffer]_T$ was paraboloid. This finding suggests that a reaction that was second order in tromethamine concentrations became important at higher pH. The reactions at higher pH were not studied further because they are unlikely to be important in biological systems.

The pH dependence of $k_{cat}$ values also was such that a plot of $k_{cat}/f_{EH^+}$ *versus* $f_b$ was linear with a zero intercept when $f_b = 0$. The value of the pH-independent rate constant, $k_b$, calculated from the slope of this line is given in Table I. This value is only approximate since $k_{cat}$ values were measured at two pH values only.

The hydrolysis of ester II in pH 6.00–8.85 buffers that contained various amounts of sodium bicarbonate was first order in sodium bicarbonate concentration. Phosphate buffers were used between pH 6 and 7, and tromethamine buffers were used at higher pH values. Plots of $k_{obs}$ for these reactions *versus* sodium bicarbonate concentration (up to $10^{-2}$ *M*) were linear, and the $k_{cat}$ values calculated from them are shown in Table II. At pH 6.0, this type of plot was linear up to $4 \times 10^{-3}$ *M* $NaHCO_3$. At higher concentrations, $k_{obs}$ values were independent of the sodium bicarbonate concentration. This behavior probably was caused by the fact that solutions at the higher concentrations were saturated with carbon dioxide.

**Decomposition of Ester IV**—The hydrolysis rate of ester IV was independent of the nature or composition of the buffer in all of the experiments. Hence, $k_{obs}$ values were concluded to be $k_{hyd}$ values (Fig. 1).

## DISCUSSION

The results of this study provide information on the stability *versus* degradation of three potentially useful prodrugs of *p*-acetamidophenol (I). However, analysis of the results also provides information about the effect of substituents in the acyl portion of phenolic esters on their hydrolysis rates. Such information can be used to design esters of other phenolic drugs as prodrugs.

**Mechanism of Water- and Hydroxide-Ion-Catalyzed Hydrolysis of Esters II–IV**—The line for ester II in Fig. 1 was calculated on the basis that the major reactions involved in its hydrolysis at pH 2–13 are:

$$EH^+ + H_2O \xrightarrow{k_A^{II}}$$
$$EH^+ + OH^- \xrightarrow{k_B^{II}}$$
$$E + OH^- \xrightarrow{k_C^{II}}$$

where E represents the ester neutral molecule and $EH^+$ is its conjugate acid in which the amino group is protonated. The rate law for these reactions is:

$$\frac{-d[E]_T}{dt} = k_{hyd}[E]_T = k_A^{II}[EH^+][H_2O] + k_B^{II}[EH^+][OH^-] + k_C^{II}[E][OH^-] \quad \text{(Eq. 2)}$$

where $[E]_T$ is the total concentration of ester at time *t*. The acid dissociation constant of the conjugate acid of ester II was determined to be $3.63 \times 10^{-8}$ at 25° and $\mu$ = 1.0 *M*. The values of $k_A^{II}$ (the water concentration was assumed to be 55.5 *M* in the computation of this second-order rate constant), $k_B^{II}$, and $k_C^{II}$ used to generate the line in Fig. 1 are included in Table III.

**Table II—Effect of pH on the Carbon Dioxide-Facilitated Decomposition of Ester II, $\mu$ = 1.0 *M*, 25°**

| pH | $k_{cat}$, $M^{-1}$ min$^{-1}$ | $f_E$[a] | $f_{CO_2}$[b] | $k_{cat}/f_E f_{CO_2}$, $M^{-1}$ min$^{-1}$ |
|---|---|---|---|---|
| 8.85 | 10.20 | 0.960 | 0.003 | 2951 |
| 8.60 | 9.60 | 0.940 | 0.006 | 1421 |
| 7.44 | 23.07 | 0.570 | 0.084 | 549.3 |
| 7.00 | 20.07 | 0.270 | 0.200 | 371.7 |
| 6.75 | 9.58 | 0.170 | 0.310 | 189.8 |
| 6.00 | 0.96 | 0.035 | 0.715 | 38.4 |

[a] Fraction of II that exists as a neutral molecule; pKa = 7.44. [b] Fraction of added sodium bicarbonate that exists as carbon dioxide or carbonic acid = 6.4.

The reaction pathway for the hydrolysis of II that is depicted as $EH^+ + OH^-$ is believed to predominate over the isokinetic pathway $E + H_2O$. This conclusion is based on the previously reported observation (4) that the second-order rate constant for the reaction between hydroxide ion and the methylbetaine methyl ester is virtually identical to that calculated for the reaction between $OH^-$ and the protonated glycine methyl ester. Only the latter compound could alternatively or concurrently be hydrolyzing by the isokinetic reaction; water catalyzed reaction of the neutral molecule. The similarity in the values of the second-order rate constants for the hydroxide-ion reaction strongly suggests that both compounds hydrolyze by the same mechanism.

Further support for this conclusion comes from the fact that the value of the ratio for ester II, $k_B^{II}/k_A^{II}$ ($3 \times 10^{10}$) is of the same order of magnitude as the ratio of the rate constants (5) for the specific base- and water-catalyzed hydrolysis of phenyl acetate ($10^{10}$). The leaving group tendencies of phenol (pKa 9.86) and I (pKa 9.49) are expected to be similar; therefore, the hydrolytic behavior of phenyl acetate appears to be a good model for the hydrolyses studied here. Since the ratio of $k_B^{II}/k_A^{II}$ for ester II is three times larger than the equivalent ratio for phenyl acetate, the presence of the positive charge in the cation of II probably favors hydroxide-ion attack more than it does water attack when these reactions are compared to the same reactions involving neutral phenyl acetate. Previous investigators (6, 7) observed a similar deviation when comparing the ratio of hydroxide-ion- and water-catalyzed hydrolysis rate constants for a series of $\alpha$-substituted *o*-nitrophenyl esters. They concluded that the enhancement for a reaction between hydroxide ion and a cationic ester could be accounted for better by postulating favorable electrostatic interactions in the transition state rather than by invoking electrostatic effects on collision frequency.

Comparison of the rate constants for the reaction between the neutral molecule of II and hydroxide ion ($k_C^{II}$) and between hydroxide ion and the acetate of I (8) indicates that the introduction of an amino group into the acetate (*i.e.*, an $\alpha$-amino group in the acyl moiety) increased the rate of this reaction 4.6 times. This figure is close to the fivefold increase in rate that follows the introduction of an amino group in the $\alpha$-position of ethyl acetate (4). Protonation of the amino group in ester II produced a further 100-fold increase in rate. Hence, the introduction of the $^+NH_3$ group into the acyl moiety of the acetate of I produced a 500-fold increase in the magnitude of the hydroxide-ion catalysis constant. This figure is considerably larger than that (150) found (9) for the introduction of $^+NH_3$ into the acyl portion of ethyl acetate. The difference in magnitude of these two figures is consistent with the generally accepted postulate that the rate of formation of a tetrahedral intermediate is the rate-determining step in the hydroxide-ion-catalyzed hydrolysis of phenolic esters (10), whereas the rate of breakdown of a tetrahedral intermediate also is in-

**Table III—Values of Microscopic Rate Constants [a] for Hydrolysis of Esters II and III in Aqueous Solutions at 25°, $\mu$ = 1.0 *M***

| Compound | $10^6\,k_A$[b], $M^{-1}$ min$^{-1}$ | $10^{-4}\,k_B$[c], $M^{-1}$ min$^{-1}$ | $10^{-2}\,k_C$[d], $M^{-1}$ min$^{-1}$ |
|---|---|---|---|
| II | 6.10 (±0.52) | 18.70 (±1.10) | 14.40 (±0.50) |
| III | 7.75 (±0.65) | 3.97 (±0.33) | 1.00 (±0.08) |

[a] Calculated by a curve-fitting technique from the data in Fig. 1. [b] For the reactions $EH^+ + H_2O \rightarrow$ in the case of ester II and $EH^\pm + H_2O \rightarrow$ in the case of ester III. [c] For the reactions $EH^+ + OH^- \rightarrow$ in the case of ester II and $EH^\pm + OH^- \rightarrow$ in the case of ester III. [d] For the reactions $E + OH^- \rightarrow$ in the case of ester II and $E^- + OH^- \rightarrow$ in the case of ester III.

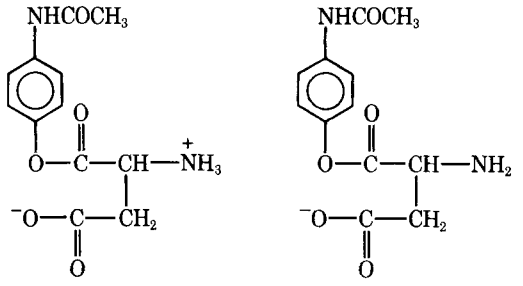

IV*a* IV*b*

volved in determining the hydrolysis rate of esters of more basic alcohols (11). Hence, a substituent such as $^+NH_3$, which acts primarily by stabilizing the transition state for tetrahedral intermediate formation (6, 7), should have a greater effect on the hydrolysis rate of phenolic esters than on esters of aliphatic alcohols.

The line for ester IV in Fig. 1 was calculated on the basis that the major reactions of the α-aspartic acid ester (IV) between pH 1.5 and 11.0 were:

$$EH^{\pm} \xrightarrow{k_A^{IV}} \text{products}$$
$$E^- \xrightarrow{k_B^{IV}} \text{products}$$

where $E^-$ and $EH^{\pm}$ are the zwitterion and anion of the ester, respectively. The rate law for these reactions is:

$$\frac{-d[E]_T}{dt} = k_{hyd}[E]_T = k_A^{IV}[EH^{\pm}] + k_B^{IV}[E^-] \qquad \text{(Eq. 3)}$$

The acid dissociation constants of ester IV could not be measured because of its extreme instability in water. However, it was expected that the values would be close to those of α-ethyl aspartic acid (2), *i.e.*, $9.12 \times 10^{-4}$ (for the cation ionizing to yield $EH^{\pm}$) and $3.16 \times 10^{-8}$ (for $EH^{\pm} \rightleftharpoons E^- + H^+$). The values of $k_A^{IV}$ and $k_B^{IV}$ that were used to calculate the curve in Fig. 1 are listed in Table IV.

The pH–rate profile for the hydrolysis of ester IV is markedly different from that of the esters II and III. At pH values slightly above the pKa of the carboxyl group of IV (~3.0), the decomposition rate of IV surpassed that of its isomer, III, almost 900 times. Also, the decomposition rate of IV was not catalyzed by any buffer species used in this study, and it was pH independent when the concentration of the zwitterion or the anion of IV was essentially constant. These phenomena can be accounted for best by postulating that the predominant reactions were intramolecular carboxylate-ion-catalyzed reactions involving the zwitterion IV*a* between pH 2 and 6 and the anion IV*b* between pH 6 and 11. The first-order rate constants for the first two reactions, $k_A^{IV}$ and $k_B^{IV}$, are given in Table IV.

Similar mechanisms previously were proposed (8, 12) to account for the hydrolysis of the acid succinate ester of phenols including *p*-acetamidophenol. The pH–rate profile for the latter reaction (9) is shown as the dashed line in Fig. 1.

The hydrolysis of ester IV is subject to intramolecular nucleophilic catalysis, and its hydrolysis rate is much faster than that of the ester II between pH 2 and 10. It was shown previously (13) that both α- and β-aspartic acid esters of ethanol hydrolyze more slowly than the glycinate ester and that the pH–rate profiles for all three compounds have similar shapes. These results suggest that the predominant hydrolysis reactions of the aliphatic alcohol esters are intermolecular reactions and that intramolecular nucleophilic catalysis is not significant in aspartic acid esters with such strongly basic leaving groups at $C_2H_5O^-$.

The line for ester III in Fig. 1 was calculated on the basis that the major reactions that occurred during its hydrolysis were:

$$EH^{\pm} + H_2O \xrightarrow{k_A^{III}} \text{products}$$
$$EH^{\pm} + OH^- \xrightarrow{k_B^{III}} \text{products}$$
$$E^- + OH^- \xrightarrow{k_C^{III}} \text{products}$$

where $E^-$ represents the anion of III and $E^{\pm}$ is its zwitterionic form. The acid dissociation constant of III was calculated to be $5.01 \times 10^{-9}$ at 25° and $\mu = 1.0\ M$. Values of the microscopic rate constants were calculated in the same way as the corresponding values for ester II (Table III).

The pH–rate profile for the hydrolysis of ester III is similar in shape to that for ester II and differs significantly from that for ester IV. Hence, it can be concluded that the predominant hydrolysis reactions of ester III involve inter- rather than intramolecular reactions. Apparently, the $^+NH_3$ or $NH_2$ substituent adjacent to the carboxylate group in the zwitterion or anion of III makes cyclization so unfavorable relative to the

**Table IV—Values of Microscopic Rate Constants [a] for Hydrolysis of Ester IV in Aqueous Solution at 25°, $\mu = 1.0\ M$**

| Reaction | Rate Constant | Value, $min^{-1}$ |
|---|---|---|
| $EH^{\pm} \rightarrow$ products | $k_A^{IV}$ | 0.135 |
| $E^- \rightarrow$ products | $k_B^{IV}$ | 1.06 |

[a] Calculated by a curve-fitting technique from the data in Fig. 1.

succinate or α-aspartic acid esters that the intramolecular catalyzed reaction is unfavorable relative to the intermolecular reactions. The $k_C^{III}$ and $k_B^{III}$ values are smaller than the $k_C^{II}$ and $k_B^{II}$ values to the extent that could be expected (14, 15) to result from moving the $NH_2$ or $^+NH_3$ group one carbon atom farther away from the ester carbonyl group.

**Buffer Catalysis of Ester II Hydrolysis**—The catalytic effects of oxy anions (and water) on the hydrolysis of II were similar to what was found previously (16) for the same species on the hydrolysis of esters activated in the acyl portion such as ethyl dichloroacetate. This result is demonstrated by the linearity of the plot (Fig. 2) of log $k_b$ values for the reactions of II *versus* the log $k_b$ values for the reactions of ethyl dichloroacetate (log $k_0$). Although the leaving group in the hydrolysis of II is a phenolate ion (*i.e.*, a relatively weak base), it is expected (10) that the rate of breakdown of a tetrahedral intermediate rather than the formation rate would be the rate determining step for nucleophilic catalysis in the reactions of II and ethyl dichloroacetate that are catalyzed by water and the oxy anions except hydroxide ion. Furthermore, on the basis of previous arguments (10, 16), water and formate ion probably are acting as general base catalysts, acetate ion probably is acting as both general base and nucleophilic catalysts, and phosphate ion and hydroxide ion probably are nucleophilic catalysts.

The second-order rate constant for aminolysis of the II cation by a molecule of neutral tromethamine fell close to the line in Fig. 2. Thus, the characteristics of this aminolysis reaction apparently are also similar to those (16) of the aminolysis of other aromatic esters or of aliphatic esters activated in the acyl portion.

The catalysis of the hydrolysis of II in sodium bicarbonate solutions can be accounted for on the basis of the sequence of reactions (Scheme I) proposed by Hay and Main (17) to account for the carbon dioxide-catalyzed hydrolysis of *p*-nitrophenyl esters of glycine and other α-amino acids. Hay and Main observed that values of $k_{cat}/f_E f_{CO_2}$ for reactions of *p*-nitrophenyl esters of α-amino acids were pH independent, and they concluded that a rate-determining reaction between the α-amino acid ester and carbon dioxide was followed by the rapid formation of a Leuchs anhydride and *p*-nitrophenol.

In contrast to this situation, values of $k_{cat}/f_E f_{CO_2}$ for reactions of ester II (Table II) in the presence of sodium bicarbonate were pH dependent throughout the 6.0–8.85 range. A plot of $f_E f_{CO_2}/k_{cat}$ *versus* the activity of hydrogen ion was linear ($r^2 = 0.999$) with an intercept of $5.43 \times 10^{-4}$ and a slope of $2.55 \times 10^4$ when $a_{H^+} = 0$.

This behavior can be accounted for by assuming that, under the experimental conditions, the concentration of carbamate remained essentially constant. This assumption leads to:

$$\frac{f_E f_{CO_2}}{k_{cat}} = \frac{k_3(k_{-1} + k_2) + k_{-1}k_{-2}a_{H^+}}{k_1 k_2 k_3} \qquad \text{(Eq. 4)}$$

where $f_{CO_2}$ is the fraction of bicarbonate buffer that exists as carbon dioxide and $f_E$ is the fraction of ester that exists as a neutral molecule.

This assumption requires that the decomposition rate of carbamate to yield the Leuchs anhydride and phenol is not much greater than the carbamate decomposition rate to yield reactants. Conversely, the conclusion that the formation rate of the carbamate from reactants is rate determining in the reactions of *p*-nitrophenyl esters infers that the decomposition of the carbamates to Leuchs anhydride and *p*-nitrophenol

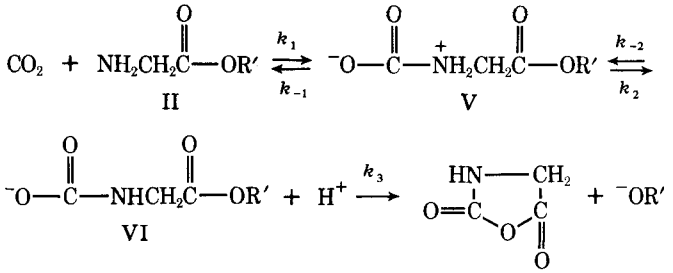

Leuchs anhydride

*Scheme I*

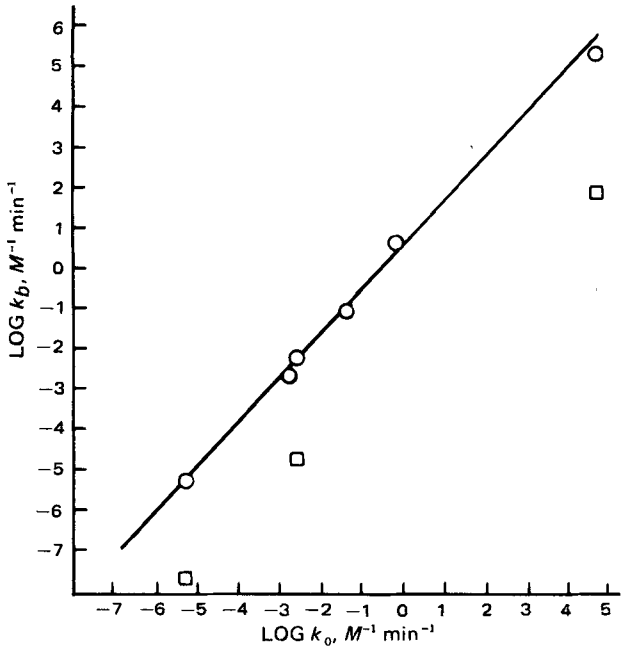


**Figure 2**—*Comparison of the second-order rate constants for the reactions of some general bases and nucleophiles with ester II* ($k_b$) (○) *to those for the reactions of the same reagents with ethyl dichloroacetate* ($k_0$). *The corresponding rate constants for the reactions of water, acetate ion, and hydroxide ion with phenyl acetate also are shown* (□).

in these reactions is substantially faster than its decomposition to yield reactants.

These conclusions are consistent with the expectation that *p*-nitrophenol is a better leaving group than *p*-acetamidophenol.

This efficient type of catalysis of amino acid ester hydrolysis by carbon dioxide is particularly interesting when considering the *in vivo* hydrolysis of amino acid esters of drugs since most biological fluids contain ~$3 \times 10^{-3}$ *M* $CO_2$.

## EXPERIMENTAL

**Materials**—All chemicals were reagent grade unless otherwise specified. Morpholine was dried over anhydrous calcium sulfate and distilled. Freshly boiled double-distilled water was used in all kinetic experiments.

***p*-Acetamidophenyl-*N*-carbobenzoxyglycinate (VII)**—A suspension of *N,N'*-dicyclohexylcarbodiimide (0.26 *M*) in dry methylene chloride was added to an equal volume in dry tetrahydrofuran of a solution of *p*-acetamidophenol (I), and the mixture was stirred at 0 ± 2° for 40 hr. Then *N,N'*-dicyclohexylurea, mp 22–29° [lit. (18) mp 29–30°], was filtered off (70% yield). Gradual reduction in volume of the filtrate under reduced pressure initially resulted in precipitation of I, which was filtered off, and then resulted in an ~1:1 mixture of *p*-acetamidophenol and VII. The filtrate finally yielded a syrup, which, after treatment with acetic acid to decompose excess *N,N'*-dicyclohexylcarbodiimide, filtration, and cooling, yielded more product. The crude ester, together with some I, was recrystallized from acetone, mp 140–142°.

**Hydrobromide of II**—A solution of hydrobromic acid (2–3 *M*) in acetic acid was prepared by bubbling the gas through the acid. The ester VII was dissolved in this solution (10 g/100 ml) and then stirred for 2 hr. Precipitation of the product was completed by the addition of ether–acetic anhydride (9:1). The crude product was washed with warm ether and acetone and recrystallized from methanol–acetone. The resulting product (80% yield) had a melting point of 228–230°; NMR ($D_2O$): δ 1.95 (s, 3H, $CH_3$), 4.05 (d, 2H, $CH_2$), 7.00 (d, 2H, aromatic H *ortho* to oxygen), and 7.24 (d, 2H, aromatic H *ortho* to amide).

*Anal.*—Calc. for $C_{10}H_{13}BrN_2O_3$: C, 41.5; H, 4.5; N, 9.7. Found: C, 41.3; H, 4.6; N, 9.5.

***N*-Carbobenzoxy-L-aspartic Acid Anhydride (VIII)**—One part of *N*-carbobenzoxy-L-aspartic acid, which had been dried and powdered, was mixed with three parts of acetic anhydride. The mixture was agitated for 1 hr and then allowed to react at room temperature for 15 hr. The product that precipitated when the solution was poured over ice was washed with cold water and ether. The waxy platelets had a melting point of 108–109°.

**α- and β-*p*-Acetamidophenyl-*N*-carbobenzoxy-L-aspartates (IX*a* and IX*b*)**—A solution of I in aqueous sodium hydroxide (equimolar) was cooled to 1°. A suspension of VIII in methylene chloride (1 mole of VIII to 2 moles of I) gradually was added to the cooled solution of *p*-acetamidophenoxide with constant stirring. The final ratios of water and methylene chloride in the mixture were 1:2. The mixture was stirred at 1° for 50 min, after which time the layers were separated. The aqueous layer was acidified with sufficient 5 *N* HCl to cause the separation of an oily layer and then was refrigerated. A pasty product, obtained following decantation of the supernatant liquid, was dried over phosphorus pentoxide *in vacuo*.

TLC of the product [on plates[1] impregnated with a 0.4 *M* formate buffer at pH 4; developed with ethyl acetate–butanol (4:1)] indicated that it contained I and two other compounds, which were subsequently identified as IX*a* and IX*b*. A 2% solution of the crude product in ethyl acetate was extracted in succession with pH 5, 0.4 *M* acetate–pH 6.3, 0.2 *M* sodium phosphate (5:1). TLC indicated that the more acidic buffer contained an almost pure sample of one of the isomeric esters. It was expected, and later confirmed, that this ester was the isomer with a pKa of 2.04 at 25°, and it was concluded to be IX*b*. Acidification of this solution yielded a white solid, mp 154–157°.

*Anal.*—Calc. for $C_{20}H_{20}N_2O_7$: C, 59.6; H, 5.0; N, 7.0. Found: C, 58.2; H, 4.9; N, 7.5.

The other buffer, upon acidification, yielded solids with lower melting points than IX*b*. TLC suggested that these solids were mixtures of IX*a* and IX*b*, but no successful method of separating them was found.

**Hydrochloride of III**—A catalyst consisting of 10% palladium-on-charcoal (18) was added to a 10% solution of IX*b* in dry methanol. Hydrogen was washed in dioxane and passed *via* a calcium chloride tube through the solution under moderate pressure for 5 hr. Precipitation of the product was completed by the addition of dry ether. The precipitated product was freed from the catalyst by elution with methanolic hydrochloric acid. Addition of ether to the eluent resulted in the precipitation of the hydrochloride of III which, after recrystallization from methanolic hydrochloride, had the following characteristics: mp 189–190°; NMR ($D_2O$): δ 1.95 (s, 3H, $CH_3$), 3.10 (d, 1H, $CH_2$), 3.25 (s, 1H, $CH_2$), 4.35 (q, 1H, CH), 7.00 (d, 2H, aromatic H *ortho* to oxygen), and 7.24 (d, 2H, aromatic H *ortho* to amide); pKa, 2.04 ± 0.06; $pKa_2$, 8.22 ± 0.06.

*Anal.*—Calc. for $C_{12}H_{15}ClN_2O_5$: C, 47.6; H, 5.0; N, 9.3. Found: C, 47.4; H, 5.0; N, 9.3.

**Mixture (50:50) of Hydrochlorides of III and IV**—When a mixture of the esters IX*a* and IX*b* was treated with hydrogen and catalyst in the manner previously described and the reaction mixture was filtered to remove excess catalyst and then reduced in volume, an ~50:50 mixture of the hydrochlorides of III and IV was recovered. This mixture had the same elemental analysis as the hydrochloride of III, but its NMR spectrum also contained peaks at δ 3.05 (d, 1H, $CH_2$), 3.19 (s, 1H, $CH_2$), and 4.67 (q, 1H, CH). The conclusion that the mixture was 50:50 was based on comparisons of the areas under the proton peaks.

**Acid Dissociation Constants**—Dissociation constants were measured at 25.0 ± 0.1° by using the potentiometric methods described previously (19).

**Rate Constants**—Rate constants were calculated from changes in UV absorbance at 282 or 242 nm that followed the mixing of solutions of the esters (usually 1–3 μl of aqueous solutions of II or III or a methanolic solution of III and IV) with aqueous buffers (2.5 or 5.0 ml). Reactions that had a half-life of <20 sec were followed on a stopped-flow spectrophotometer after equal volumes of aqueous solutions were mixed. The ionic strength of all reaction solutions was 1.0 *M* (adjusted with potassium chloride), and the temperature was maintained at 25.0 ± 0.1°. The buffers and pH ranges used were: formate, 1.9–4.1; acetate, 4.7–5.1; phosphate, 5.4–7.1; glycine, 9.8–10.5; tromethamine, 7.4–9.2; pyrophosphate, 7.7–9.0; morpholine, 8.3–9.3; carbonate, 9.85–10.7; and sodium hydroxide, >11.5. The initial substrate concentration was always $<10^{-3}$ *M*.

Pseudo-first-order rate constants for the hydrolyses of II and III were calculated from linear plots of log ($A - A_\infty$) *versus* time ($A$ and $A_\infty$ being the absorbance at a particular time and infinite time, respectively). Plots of log ($A - A_\infty$) *versus* time were biexponential for the hydrolysis of the mixtures of III and IV. Values of the rate constants for hydrolysis of III were calculated from the terminal slopes of such plots, and they agreed well with values that were determined using pure III. Values of the rate constants for hydrolysis of IV were calculated from the initial portions of the curves by using a feathering technique (20).

Rate constants were reproducible in at least three runs to within ±5%.

[1] Polygram Sil N-HR.

## REFERENCES

(1) I. M. Kovach, I. H. Pitman, and T. Higuchi, *J. Pharm. Sci.*, **64**, 1070 (1975).
(2) A. Pilbrant, *Acta Pharm. Suec.*, **6**, 37 (1969).
(3) "The Merck Index," 9th ed., Merck & Co., Rahway, N.J., 1976.
(4) M. R. Wright, *J. Chem. Soc. B*, **1968**, 548. *Ibid.*, **1969**, 707.
(5) T. C. Bruice and M. F. Mayahi, *J. Am. Chem. Soc.*, **82**, 3067 (1960).
(6) B. Holmquist and T. C. Bruice, *ibid.*, **94**, 2982 (1969).
(7) *Ibid.*, **91**, 2985 (1969).
(8) E. S. Rattie, E. G. Shami, L. W. Dittert, and J. V. Swintosky, *J. Pharm. Sci.*, **59**, 1738 (1970).
(9) R. P. Bell and F. J. Lindars, *J. Chem. Soc.*, **1954**, 4601.
(10) W. P. Jencks and N. Gilchrist, *J. Am. Chem. Soc.*, **90**, 2622 (1968).
(11) M. H. Bender, *ibid.*, **73**, 1626 (1951).
(12) E. Gaetjens and H. Morawetz, *ibid.*, **82**, 5328 (1960).
(13) A. Pilbrant, *Acta Pharm. Suec.*, **6**, 469 (1969).
(14) R. W. Hay and L. J. Porter, *Aust. J. Chem.*, **19**, 1197 (1966).
(15) R. W. Hay and L. J. Porter, *J. Chem. Soc. B*, **1967**, 1261.
(16) W. P. Jencks and J. Carriuolo, *J. Am. Chem. Soc.*, **83**, 1743 (1961).
(17) R. W. Hay and L. Main, *Aust. J. Chem.*, **21**, 155 (1968).
(18) E. J. Zahn and F. Diehl, *Z. Naturforsch.*, **12B**, 85 (1957).
(19) A. Albert and E. P. Serjeant, "Ionization Constants of Organic Acids and Bases," Methuen, London, England, 1962.
(20) A. A. Frost and R. G. Pearson, "Kinetics and Mechanism," Wiley, New York, N.Y., 1961.



## ACKNOWLEDGMENTS

Supported in part by grants from Warner-Lambert Research Institute and INTER$_x$ Research Corp.

I. H. Pitman was holder of National Institutes of Health Career Development Award KO4GH70100.


# Absorption and Bioavailability of Captopril in Mice and Rats after Administration by Gavage and in the Diet


**S. M. SINGHVI ˣ, K. J. KRIPALANI, A. V. DEAN, G. R. KEIM, J. S. KULESZA, F. S. MEEKER, Jr., J. J. ROSS, Jr., J. M. SHAW, and B. H. MIGDALOF**



Received June 27, 1980, from the *Departments of Drug Metabolism and Toxicology, Squibb Institute for Medical Research, New Brunswick, NJ 08903.* Accepted for publication January 6, 1981.



**Abstract** □ The absorption of captopril (I), a new antihypertensive agent, was studied in mice and rats at doses (50 and 1350 mg/kg) administered in the diet in chronic toxicological studies. $^{3}H$- or $^{35}S$-Labeled I was administered by gavage and in the diet to male and female animals in a two-way crossover study. Animals received daily doses of nonradiolabeled I in the diet for 25 days, except on Days 15 and 22 when radiolabeled I was administered either by gavage or in the diet. Absorption of the total radioactivity in 2-month-old mice averaged 49 and 48%, respectively, of the 50- and 1350-mg/kg doses given in the diet and 57 and 65%, respectively, of the doses given by gavage. The bioavailability of I in 2-month-old mice averaged 48 and 39% (diet) and 44 and 59% (gavage) of the 50- and 1350-mg/kg doses, respectively. In 2-month-old rats, absorption of the total radioactivity averaged 41% of the 50-mg/kg dose given in the diet. In 2- and 15-month-old rats, minimum absorption of the 1350-mg/kg dose averaged 36 and 45% (diet) and 51 and 71% (gavage), respectively; the minimum bioavailability averaged 29 and 29% (diet) and 39 and 44% (gavage), respectively. These studies demonstrate adequate absorption and bioavailability of I over a wide range of doses from the drug–diet mixtures and by young and old animals and also illustrate a useful experimental design for the estimation of relative oral absorption of a drug administered continuously in the diet over several days.



**Keyphrases** □ Captopril—absorption and bioavailability, gavage and dietary administration, mice and rats □ *Metabolism*—absorption and bioavailability of captopril, gavage and dietary administration, mice and rats □ Antihypertensives—absorption and bioavailability of captopril, gavage and dietary administration, mice and rats


Captopril (I), 1-[(2*S*)-3-mercapto-2-methyl-1-oxopropyl]-L-proline, is a potent and specific inhibitor of the enzyme that catalyzes the conversion of angiotensin I to angiotensin II (1) and was an orally effective antihypertensive agent in extensive clinical trials (2–4). The disposition of I in normal subjects was reported recently (5). Specific assays for determination of I as its *N*-ethylmaleimide derivative (II) also were reported (6, 7).

In oral toxicological and pathological studies over a 2-year period, I was administered daily in the diet to mice and rats at 50, 150, and 1350 mg/kg. The present study evaluated the effects of food and of repeated daily administration of 50- and 1350-mg/kg doses of I on its absorption and bioavailability in 2-month-old mice and rats and 15-month-old rats.

Investigations in animals and *in vitro* indicate that I is chemically unstable in biological fluids and undergoes rapid autoxidation to form III, the disulfide dimer of I, and other products. To prevent or minimize such processes, a procedure for immediate conversion of I to II in biological samples was established (5–7) (Scheme I). This procedure was utilized in the determination of nonlabeled I using GLC–mass spectrometry (7) and of radiolabeled I using thin-layer radiochromatography (6). Since radiolabeled I was necessary to determine absorption in the present study, thin-layer radiochromatography was used.

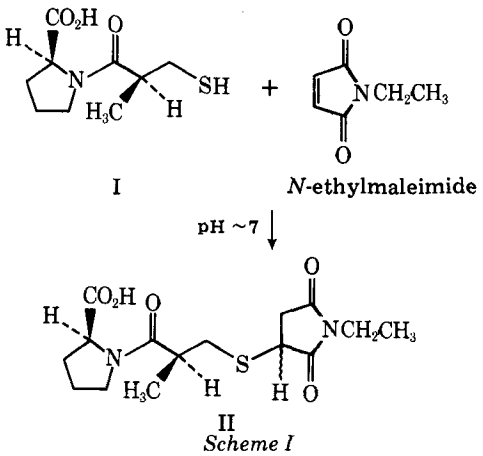


*Scheme I*



*© 1981, American Pharmaceutical Association*

## REFERENCES

(1) I. M. Kovach, I. H. Pitman, and T. Higuchi, *J. Pharm. Sci.*, **64**, 1070 (1975).
(2) A. Pilbrant, *Acta Pharm. Suec.*, **6**, 37 (1969).
(3) "The Merck Index," 9th ed., Merck & Co., Rahway, N.J., 1976.
(4) M. R. Wright, *J. Chem. Soc. B*, **1968**, 548. *Ibid.*, **1969**, 707.
(5) T. C. Bruice and M. F. Mayahi, *J. Am. Chem. Soc.*, **82**, 3067 (1960).
(6) B. Holmquist and T. C. Bruice, *ibid.*, **94**, 2982 (1969).
(7) *Ibid.*, **91**, 2985 (1969).
(8) E. S. Rattie, E. G. Shami, L. W. Dittert, and J. V. Swintosky, *J. Pharm. Sci.*, **59**, 1738 (1970).
(9) R. P. Bell and F. J. Lindars, *J. Chem. Soc.*, **1954**, 4601.
(10) W. P. Jencks and N. Gilchrist, *J. Am. Chem. Soc.*, **90**, 2622 (1968).
(11) M. H. Bender, *ibid.*, **73**, 1626 (1951).
(12) E. Gaetjens and H. Morawetz, *ibid.*, **82**, 5328 (1960).
(13) A. Pilbrant, *Acta Pharm. Suec.*, **6**, 469 (1969).
(14) R. W. Hay and L. J. Porter, *Aust. J. Chem.*, **19**, 1197 (1966).
(15) R. W. Hay and L. J. Porter, *J. Chem. Soc. B*, **1967**, 1261.
(16) W. P. Jencks and J. Carriuolo, *J. Am. Chem. Soc.*, **83**, 1743 (1961).
(17) R. W. Hay and L. Main, *Aust. J. Chem.*, **21**, 155 (1968).
(18) E. J. Zahn and F. Diehl, *Z. Naturforsch.*, **12B**, 85 (1957).
(19) A. Albert and E. P. Serjeant, "Ionization Constants of Organic Acids and Bases," Methuen, London, England, 1962.
(20) A. A. Frost and R. G. Pearson, "Kinetics and Mechanism," Wiley, New York, N.Y., 1961.



## ACKNOWLEDGMENTS

Supported in part by grants from Warner-Lambert Research Institute and INTER$_x$ Research Corp.

I. H. Pitman was holder of National Institutes of Health Career Development Award KO4GH70100.


# Absorption and Bioavailability of Captopril in Mice and Rats after Administration by Gavage and in the Diet


**S. M. SINGHVI ˣ, K. J. KRIPALANI, A. V. DEAN, G. R. KEIM, J. S. KULESZA, F. S. MEEKER, Jr., J. J. ROSS, Jr., J. M. SHAW, and B. H. MIGDALOF**



Received June 27, 1980, from the *Departments of Drug Metabolism and Toxicology, Squibb Institute for Medical Research, New Brunswick, NJ 08903.* Accepted for publication January 6, 1981.



**Abstract** □ The absorption of captopril (I), a new antihypertensive agent, was studied in mice and rats at doses (50 and 1350 mg/kg) administered in the diet in chronic toxicological studies. $^{3}H$- or $^{35}S$-Labeled I was administered by gavage and in the diet to male and female animals in a two-way crossover study. Animals received daily doses of nonradiolabeled I in the diet for 25 days, except on Days 15 and 22 when radiolabeled I was administered either by gavage or in the diet. Absorption of the total radioactivity in 2-month-old mice averaged 49 and 48%, respectively, of the 50- and 1350-mg/kg doses given in the diet and 57 and 65%, respectively, of the doses given by gavage. The bioavailability of I in 2-month-old mice averaged 48 and 39% (diet) and 44 and 59% (gavage) of the 50- and 1350-mg/kg doses, respectively. In 2-month-old rats, absorption of the total radioactivity averaged 41% of the 50-mg/kg dose given in the diet. In 2- and 15-month-old rats, minimum absorption of the 1350-mg/kg dose averaged 36 and 45% (diet) and 51 and 71% (gavage), respectively; the minimum bioavailability averaged 29 and 29% (diet) and 39 and 44% (gavage), respectively. These studies demonstrate adequate absorption and bioavailability of I over a wide range of doses from the drug–diet mixtures and by young and old animals and also illustrate a useful experimental design for the estimation of relative oral absorption of a drug administered continuously in the diet over several days.



**Keyphrases** □ Captopril—absorption and bioavailability, gavage and dietary administration, mice and rats □ *Metabolism*—absorption and bioavailability of captopril, gavage and dietary administration, mice and rats □ Antihypertensives—absorption and bioavailability of captopril, gavage and dietary administration, mice and rats


Captopril (I), 1-[(2*S*)-3-mercapto-2-methyl-1-oxopropyl]-L-proline, is a potent and specific inhibitor of the enzyme that catalyzes the conversion of angiotensin I to angiotensin II (1) and was an orally effective antihypertensive agent in extensive clinical trials (2–4). The disposition of I in normal subjects was reported recently (5). Specific assays for determination of I as its *N*-ethylmaleimide derivative (II) also were reported (6, 7).

In oral toxicological and pathological studies over a 2-year period, I was administered daily in the diet to mice and rats at 50, 150, and 1350 mg/kg. The present study evaluated the effects of food and of repeated daily administration of 50- and 1350-mg/kg doses of I on its absorption and bioavailability in 2-month-old mice and rats and 15-month-old rats.

Investigations in animals and *in vitro* indicate that I is chemically unstable in biological fluids and undergoes rapid autoxidation to form III, the disulfide dimer of I, and other products. To prevent or minimize such processes, a procedure for immediate conversion of I to II in biological samples was established (5–7) (Scheme I). This procedure was utilized in the determination of nonlabeled I using GLC–mass spectrometry (7) and of radiolabeled I using thin-layer radiochromatography (6). Since radiolabeled I was necessary to determine absorption in the present study, thin-layer radiochromatography was used.

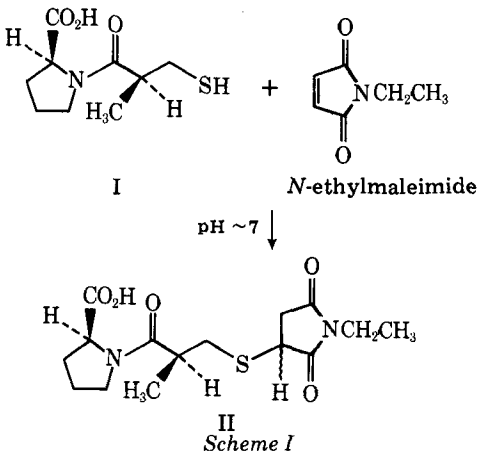


*Scheme I*



*© 1981, American Pharmaceutical Association*

## EXPERIMENTAL

**Materials**—$^{3}$H-Labeled I (uniformly labeled in the proline moiety) and $^{35}$S-labeled I had radiochemical and chemical purities of at least 95%, with a maximum of 5% of III present as an impurity. No other impurities were detected. To administer sufficient radioactivity for good quantitation, each dose contained a minimum of 5 μCi (range of 5–40 μCi). Since the doses ranged from 50 to 1350 mg/kg and since there was an approximate 10-fold difference between the average weights of mice and rats, the specific activities of radiolabeled I also varied greatly, from 0.06 to 1.0 μCi/mg for $^{3}$H-labeled I and from 2.7 to 8.9 μCi/mg for $^{35}$S-labeled I.

**Animals**—Male and female CD-1 outbred albino mice and CD outbred albino rats[1] were used. All mice were ~2 months old at the start of the study and weighed ~35 (males) and 27 (females) g. Two-month-old rats weighed ~260 (males) and 170 (females) g, and 15-month-old rats weighed 550 (males) and 330 (females) g. All animals had access to food and water *ad libitum* and were housed individually in metabolic cages throughout the study.

**Experimental Design**—For each dose level and age group, 16 animals (eight males and eight females) initially were given 14 consecutive daily doses of either 50 or 1350 mg of I/kg (nonradioactive) admixed with the diet. On Day 15, half of the animals (four males and four females) received radiolabeled drug (tritium or sulfur 35) in the diet; the other half received radiolabeled drug in aqueous solution by gavage. Administration of the nonradioactive drug–diet preparation was resumed on Day 16. On Day 22 (crossover), the animals that had received the radioactive drug in the diet on Day 15 were given the radioactive drug in aqueous solution by gavage; those that had received the drug in aqueous solution by gavage on Day 15 were given the radioactive drug in the diet. Administration of the nonradioactive drug–diet preparation was resumed for 3 days. The animals were given a drug-free diet on the days they received the radioactive drug by gavage.

Urine and feces were collected every 24 hr for 4 days after each radioactive dose. To minimize I oxidation, urine samples for the first 2 days after drug administration were collected in vessels containing 2 ml of a 2.5% aqueous solution of *N*-ethylmaleimide (5).

In an early study using 2-month-old rats, single 50-mg/kg doses of radiolabeled I were administered in the diet to six (three males and three females) animals and by intravenous route to four (two males and two females) animals. Thus, in that study, repeated administration of nonradiolabeled drug was not employed, and the animals did not receive radiolabeled I by gavage. Additionally, in separate studies in 2-month-old mice, single 50-mg/kg doses of radiolabeled I were given intravenously to eight (four males and four females) animals, and single 650-mg/kg doses of radiolabeled I were given intravenously to four males. In these studies, urine and feces also were collected for 4 days.

In experiments where 16 animals were used initially, a few animals that received the drug by gavage died of trauma due to misdosing during the first or the second phase of the study. Data were obtained for less than 16 animals.

**Preparation, Administration, and Assay of Dose**—*Nonradioactive I*—The drug–diet preparation was prepared fresh each week. Compound I was mixed with an appropriate amount of ground diet[2] in a mixer[3] to give a drug concentration that provided an estimated daily dose of 50 or 1350 mg/kg. Homogeneity and stability of the drug–diet mixture prepared by this procedure were satisfactory. The animals were offered this drug–diet preparation each day, except when receiving radioactive drug. Food consumption and body weights were determined daily.

*Radioactive I*—Animals were weighed just prior to dosing, and doses were administered based on those weights. For each animal, an accurately weighed amount of radiolabeled I, corresponding to 50 or 1350 mg of drug/kg, initially was combined with an appropriate amount of feed. The feed and drug were mixed thoroughly on glassine paper with a spatula. To facilitate essentially complete consumption of the drug–diet preparation, the total weight of the feed mixed with the radiolabeled drug was ~0.5 g less than the average daily consumption of feed during the 3 days prior to dosing with radiolabeled drug.

The drug–diet preparation was transferred to individual feeding cups and offered to the animal. The material adhering to the glassine paper and spatula and that remaining in the feeding cup after 24 hr were transferred with methanol to a volumetric flask and assayed in duplicate for total radioactivity. The amount of radiolabeled drug consumed with the feed by each animal was determined by subtracting the total amount of radioactivity found in the combined washings from the total radioactivity added initially to the feed. For dosing by gavage, a solution was prepared fresh by dissolving radiolabeled I in distilled water.

**Liquid Scintillation Counting**—The scintillation cocktail of Anderson and McClure (8) was used to count all samples, except feces, in studies using [$^{3}$H]captopril. This cocktail contained 0.2 g of 1,4-bis[2-(5-phenyloxazolyl)]benzene, 3 g of 2,5-diphenyloxazole, and 250 ml of a nonionic surfactant[4], which were brought to volume (1 liter) with xylene. A saturated solution of sodium pyruvate in methanol, acetic acid, and methanol in a ratio of 4:3:1 (by volume) was used to neutralize the contents of the vials before counting. Individual samples were prepared as will be described.

Urine (0.1 ml) was mixed with 0.5 ml of a tissue solubilizer[5], 15 ml of scintillation cocktail, and 0.1 ml of the neutralizing solution. In studies using [$^{35}$S]captopril, fecal samples were shaken with ~2–3 volumes of water for 16 hr. A portion of the suspension (0.2 g) was digested by shaking for 16 hr with 1.0 ml of the solubilizer. The digested sample was bleached with 1.0 ml of 20% benzoyl peroxide and mixed with 0.1 ml of the neutralizing solution and 15 ml of the scintillation cocktail.

Silica gel scrapings from TLC plates were mixed with 1.0 ml of water and counted in 15 ml of the scintillation cocktail.

Fecal homogenates of animals dosed with [$^{3}$H]captopril were combusted in a sample oxidizer[6]. The resulting tritiated water was trapped in 20 ml of scintillation cocktail[7].

All samples were counted in liquid scintillation spectrometers[8]. Counting efficiencies were determined with automatic external standardization and the use of previously prepared quench curves. To correct for the decay of sulfur 35 radioactivity (half-life of 87 days), suitably diluted aliquots of the dosing solutions were counted with each set of biological samples.

**Thin-Layer Radiochromatography**—A thin-layer radiochromatographic assay of I was described previously (5, 6). In the present study, aliquots (20–100 μl) of urine were chromatographed on 0.25-mm silica gel GF plates[9] in chloroform–ethyl acetate–acetic acid (4:5:3). Compounds I, II, and III were used as reference standards and were visualized by exposure to iodine vapor; their $R_f$ values were 0.55, 0.42, and 0.34, respectively. Each TLC plate was divided into three zones based on the location of the reference standards. The zone in the 0.4–0.6 $R_f$ range, which included I and II, was used to determine unchanged I in the sample.

**Data Analysis**—Estimates of absolute absorption of total radioactivity and absolute bioavailability of I were obtained using urinary excretion data; the percentages of the dose excreted in urine as total radioactivity and as unchanged I after oral administration of I were divided by similar data obtained following administration of a single comparable intravenous dose of radiolabeled I.

Statistical analyses were performed using the Student *t* test and analysis of variance. Where necessary, the overall means were adjusted for the unequal number of animals in the different groups.

## RESULTS

For rats and mice at 50- and 1350-mg/kg doses in the diet and by gavage, there were no statistically significant differences in amounts of radioactivity recovered in urine and feces between the sexes or between the two phases of the crossover. Therefore, the data for all animals (males and females) and for both phases of the crossover were combined for each mode of administration, and the overall mean excretion values were determined for mice (Table I) and rats (Table II). For both modes of administration and in both species, most excretion in urine and feces occurred during the first 48 hr after dosing. Between 48 and 96 hr, <3% of the administered radioactivity was excreted in the urine and feces of mice and <8% was excreted in the urine and feces of rats.

**Absorption and Bioavailability in Mice**—For the 50-mg/kg oral dose, mean recoveries of radioactivity in urine were 37.2% (diet) and 43.8% (gavage) of the dose (Table I). Following a single intravenous dose (50 mg/kg), excretion of radioactivity in the 0–96-hr urine was 76.3% of the dose. Thus, the absolute absorption values for the oral radioactive doses

[1] Charles River Breeding Laboratories, Wilmington, Mass.
[2] Purina Laboratory Chow, Ralston-Purina Co., St. Louis, Mo.
[3] Hobart Manufacturing Co., Troy, Ohio.

[4] Triton X-114, Ruger Chemical Co., Irvington, N.J.
[5] Soluene-350, Packard Instrument Co., Downers Grove, Ill.
[6] Packard model 306 automatic Tri-Carb oxidizer, Packard Instrument Co., Downers Grove, Ill.
[7] Monophase-40, Packard Instrument Co., Downers Grove, Ill.
[8] Packard Tri-Carb model 2425 or 3380, Packard Instrument Co., Downers Grove, Ill.
[9] Analtech Inc., Newark, Del.

**Table I—Absorption and Excretion of Total Radioactivity after Administration of Radiolabeled Captopril to Mice**

| Dose, mg/kg | Number of Mice | Route/Mode of Administration | Percent of Dose Excreted in 0–96 hr[a] | | | Absorption of Radioactivity, % |
|---|---|---|---|---|---|---|
| | | | Urine | Feces | Total | |
| 50 | 8 (4 M, 4 F) | Intravenous | 76.3 ± 2.29 | 13.8 ± 1.97 | 90.1 ± 1.56 | — |
| | 12 (7 M, 5 F) | *per os* (in diet) | 37.2 ± 5.16 | 48.0 ± 1.46 | 85.2 ± 5.71 | 48.8 ± 6.92 |
| | 12 (7 M, 5 F) | *per os* (by gavage) | 43.8 ± 3.68 | 47.3 ± 3.30 | 91.1 ± 1.43 | 57.4 ± 5.12 |
| 1350 | 4 M | Intravenous (650 mg/kg) | 89.8 ± 1.19 | 8.84 ± 0.72 | 98.7 ± 0.95 | — |
| | 16 (8 M, 8 F) | *per os* (in diet) | 42.8 ± 1.18 | 47.6 ± 1.61 | 90.4 ± 1.13 | 47.6 ± 1.46[b] |
| | 16 (8 M, 8 F) | *per os* (by gavage) | 58.7 ± 1.43 | 34.8 ± 2.22 | 93.5 ± 1.22 | 65.4 ± 1.81 |

[a] All values are the mean ± *SEM*. [b] Significantly less than the mean for the gavage dose ($p < 0.05$).

**Table II—Excretion of Total Radioactivity after Administration of Radiolabeled Captopril to Rats**

| Age, months | Dose, mg/kg | Number of Rats | Route/Mode of Administration | Percent of Dose Excreted in 0–96 hr[a] | | |
|---|---|---|---|---|---|---|
| | | | | Urine[b] | Feces | Total |
| 2 | 50 | 4 (2 M, 2 F) | Intravenous | 93.0 ± 1.34 | 9.0 ± 1.15 | 102.0 ± 0.23 |
| | | 6 (3 M, 3 F) | *per os* (in diet) | 37.7 ± 1.30 | 58.9 ± 2.55 | 96.5 ± 1.93 |
| | 1350 | 16 (8 M, 8 F) | *per os* (in diet) | 35.5[c] ± 1.19 | 61.5 ± 2.68 | 97.0 ± 1.96 |
| | | 13 (7 M, 6 F) | *per os* (by gavage) | 51.2 ± 1.80 | 41.4 ± 1.45 | 92.6 ± 1.02 |
| 15 | 1350 | 13 (7 M, 6 F) | *per os* (in diet) | 45.1[c] ± 1.66 | 50.8 ± 2.71 | 95.9 ± 2.64 |
| | | 12 (6 M, 6 F) | *per os* (by gavage) | 71.2 ± 2.98 | 24.5 ± 3.21 | 95.7 ± 2.23 |

[a] All values are the mean ± *SEM*. [b] These values represent minimum absorption of the orally administered dose. [c] Significantly less than the mean for the gavage dose ($p < 0.05$).

were 48.8% (diet) and 57.4% (gavage). These values were not statistically significantly different ($p > 0.05$). Unchanged I excreted in the 0–24-hr urine accounted for 19.4% (diet) and 18.0% (gavage) (Table III). After intravenous administration of a comparable dose, unchanged I in the urine accounted for 40.5% of the dose. Therefore, the absolute bioavailability values for I after oral administration of 50 mg/kg were 47.9% (diet) and 44.4% (gavage). These values were not significantly different ($p > 0.05$).

Based on relative urinary excretion (as a percentage of the radioactive dose) after oral (1350 mg/kg) and intravenous (650 mg/kg) administration, absorption of the oral radioactive 1350-mg/kg dose was 47.6% (diet) and 65.4% (gavage) (Table I)[10]. Thus, absorption of the 1350-mg/kg dose given in the diet was ~73% of that given by gavage. Based on the excretion of unchanged I in urine (0–48 hr) after oral and intravenous administration, the absolute bioavailability of I from the 1350-mg/kg oral dose was 39.2% (diet) and 58.6% (gavage) (Table III). The differences in the absorption and bioavailability values for the two modes of administration were statistically significant ($p < 0.05$).

**Absorption and Bioavailability in Rats**—The absolute absorption of the oral radioactive dose (50 mg/kg) in 2-month-old rats was 40.5% based on recoveries of radioactivity in 0–96-hr urine of 37.7% (diet) and 93.0% (intravenous) of the administered dose (Table II). At the time this study was done, an assay for I was not available and bioavailability estimates could not be obtained.

Excretion in the 0–96-hr urine (representing minimum absorption) after administration of 1350 mg/kg in 2-month-old rats accounted for 35.5% (diet) and 51.2% (gavage) of the dose (Table II). Unchanged I excreted in the 0–48-hr urine (representing minimum bioavailability) accounted for 28.9% (diet) and 39.4% (gavage) of the dose (Table IV).

In 15-month-old rats (1350-mg/kg dose), excretion in the 0–96-hr urine (representing minimum absorption) accounted for 45.1% (diet) and 71.2% (gavage) of the dose (Table II). Unchanged I excreted in the 0–48-hr urine accounted for 29.2% (diet) and 44.0% (gavage) of the dose (Table IV). The differences in minimum absorption values for the two modes of administration were statistically significant in both age groups ($p < 0.05$). The differences in minimum bioavailability values for the two modes of administration were statistically significant for the 2-month-old rats ($p < 0.05$) but not for the 15-month-old rats ($p > 0.05$).

Since urinary excretion of total radioactivity and unchanged I after parenteral administration of 1350 mg of the drug/kg was not determined in rats, the values reported for absorption and bioavailability of I represent minimum estimates.

## DISCUSSION

During chronic oral toxicological studies, test substances are administered to rodents either by gavage or by incorporation in the diet. Boyd (9) reported that administration of the entire daily dose to animals by gavage reveals the maximum toxic potential of chronic human dosing better than administration of a compound in the diet. However, in a more recent pharmacokinetic study in rats, continuous dietary administration of an orally absorbed cephalosporin, cefatrizine, produced higher peak plasma concentrations, longer exposure, and greater drug bioavailability than administration of the same daily dose given once a day orally by gavage (10). Furthermore, in many cases, the convenience of administering a drug in the diet and the elimination of trauma and dangers of pulmonary complications caused by intubation make dietary drug administration the preferred mode during long-term toxicological studies. Moreover, for a drug that is given more than once a day for therapeutic efficacy, dietary administration in toxicological studies mimics more closely the therapeutic dosage regimen and, thus, has a better chance of showing potential accumulation than single daily doses administered by gavage. On the other hand, administration by gavage provides maximum control over quantitation and the dosing time and might be more suitable for drugs with long half-lives and whose absorption is severely impaired by the presence of food.

The present studies demonstrate that the absorption and bioavailability of I in mice and rats were satisfactory at doses of 50 and 1350 mg/kg given in the diet during repeated daily administration. There were no apparent differences in the absorption and bioavailability of I between males and females of either species. The data suggest that the absorption

[10] The comparison between 1350-mg/kg po and 650-mg/kg iv doses was considered to be valid since (in separate studies) absorption of I in the dose range of 50–650 mg/kg was found to be dose independent. The maximum nontoxic intravenous dose in mice was 650 mg/kg.

**Table III—Bioavailability of Captopril after Administration of Radiolabeled Captopril to Mice**

| Dose, mg/kg | Number of Mice | Route/Mode of Administration | Percent of Dose Excreted in Urine: Total Radioactivity | Percent of Dose Excreted in Urine: Unchanged Captopril | Bioavailability, % |
|---|---|---|---|---|---|
| 50[a] | 8 (4 M, 4 F) | Intravenous | 74.0 ± 2.75 | 40.5 ± 4.26 | — |
| | 12 (7 M, 5 F) | *per os* (in diet) | 33.0 ± 5.10 | 19.4 ± 3.11 | 47.9 ± 9.18 |
| | 12 (7 M, 5 F) | *per os* (by gavage) | 41.0 ± 3.13 | 18.0 ± 1.98 | 44.4 ± 6.76 |
| 1350[b] | 4 M | Intravenous (650 mg/kg) | 89.4 ± 1.28 | 73.4 | — |
| | 16 (8 M, 8 F) | *per os* (in diet) | 41.6 ± 1.15 | 28.8 ± 1.77 | 39.2 ± 2.43[c] |
| | 16 (8 M, 8 F) | *per os* (by gavage) | 57.6 ± 1.35 | 43.1 ± 0.52 | 58.6 ± 0.73 |

[a] All values are the mean ± *SEM* for individual animals and represent the 0–24-hr urine. [b] The 0–48-hr urine was pooled for males and females separately. [c] Significantly less than the mean for the gavage dose ($p < 0.05$).

**Table IV—Urinary Excretion of Unchanged Captopril after Oral Administration of Radiolabeled Captopril (1350 mg/kg) to Rats**

| Age, months | Number of Rats | Route/Mode of Administration | Percent of Dose Excreted in 0–48-hr Urine[a]: Total Radioactivity | Percent of Dose Excreted in 0–48-hr Urine[a]: Unchanged Captopril[b] |
|---|---|---|---|---|
| 2 | 16 (8 M, 8 F) | *per os* (in diet) | 34.3 ± 0.98 | 28.9 ± 2.08[c] |
| | 13 (7 M, 6 F) | *per os* (by gavage) | 50.2 ± 1.78 | 39.4 ± 1.79 |
| 15 | 13 (7 M, 6 F) | *per os* (in diet) | 44.4 ± 1.62 | 29.2 ± 4.04 |
| | 12 (6 M, 6 F) | *per os* (by gavage) | 67.5 ± 2.50 | 44.0 ± 3.75 |

[a] All values are the mean ± *SEM;* the 0–48-hr urine was pooled for males and females separately in each group for thin-layer radiochromatography. [b] These values represent minimum bioavailability of the administered dose. [c] Significantly less than the mean for the gavage dose ($p < 0.05$).

and bioavailability of I were actually higher in 15-month-old rats than in 2-month-old rats. This observation indicates that animals were exposed to substantial amounts of I throughout the 2-year toxicological and pathological studies. In general, the absorption and bioavailability of I were greater after gavage doses than after the same doses given in the diet.

Although <19% (mice) and <39% (rats) of the administered dose were excreted as unchanged I in urine after oral administration, there was no evidence for any first-pass biotransformation or biliary excretion (and recycling) of I. In fact, the data in Table III indicate that the ratios of unchanged I to total radioactivity excreted in urine were comparable after oral and intravenous administration. In addition, fecal excretion after intravenous administration of I in rats (~9% of the dose) and in mice (~14% of the dose), in conjunction with biliary excretion of radioactivity determined in bile-cannulated rats (~10% of the dose) after oral administration of radiolabeled $I^{11}$, indicated little biliary excretion of I and its metabolites. Therefore, the lesser amount of unchanged I excreted in urine after oral administration as compared to intravenous administration appeared to be due to incomplete I absorption rather than first-pass biotransformation.

Repeated I administration did not significantly affect the extent of absorption or bioavailability of I in mice, based on a comparison of results obtained in the present studies with results obtained in previous studies in which single oral doses of I were given to fasted mice. The two-way crossover studies also illustrate a useful experimental design for the estimation of relative absorption of a drug administered continuously in the diet over several days. The effect of repeated administration on the absorption rate of I was not determined. However, all absorption and excretion measurements were carried out in animals that had received the drug for a minimum of 2 weeks.

[11] K. J. Kripalani and A. V. Dean, Squibb Institute, New Brunswick, NJ 08903, unpublished data.

## REFERENCES


(1) R. K. Ferguson, H. R. Brunner, G. A. Turini, H. Gavras, and D. N. McKinstry, *Lancet*, **1**, 775 (1977).

(2) D. B. Case, S. A. Atlas, J. H. Laragh, J. E. Sealey, P. A. Sullivan, and D. N. McKinstry, *Cardiovasc. Dis.*, **21**, 195 (1978).

(3) H. Gavras, H. R. Brunner, G. A. Turini, G. R. Kershaw, C. P. Tifft, S. Guttelod, I. Gavras, R. A. Vukovich, and D. N. McKinstry, *N. Engl. J. Med.*, **298**, 991 (1978).

(4) H. R. Brunner, H. Gavras, B. Waeber, G. R. Kershaw, G. A. Turini, R. A. Vukovich, and D. N. McKinstry, *Ann. Intern. Med.*, **90**, 19 (1979).

(5) K. J. Kripalani, D. N. McKinstry, S. M. Singhvi, D. A. Willard, R. A. Vukovich, and B. H. Migdalof, *Clin. Pharmacol. Ther.*, **27**, 636 (1980).

(6) B. H. Migdalof, S. M. Singhvi, and K. J. Kripalani, *J. Liq. Chromatogr.*, **3**, 857 (1980).

(7) P. T. Funke, E. Ivashkiv, M. F. Malley, and A. I. Cohen, *Anal. Chem.*, **52**, 1086 (1980).

(8) L. E. Anderson and W. O. McClure, *Anal. Biochem.*, **51**, 173 (1973).

(9) E. M. Boyd, *Can. Med. Assoc. J.*, **98**, 278 (1968).

(10) D. R. Van Harken and G. H. Hottendorf, *Toxicol. Appl. Pharmacol.*, **43**, 407 (1978).


## ACKNOWLEDGMENTS


Presented in part at the Basic Pharmaceutics Section, APhA Academy of Pharmaceutical Sciences, Anaheim meeting, April 1979.

The authors gratefully acknowledge Mr. J. Horvath, Mrs. A. Kowzun, Mrs. D. Miller, Mr. C. Mondi, Mr. D. Rothermal, and Ms. D. Tremblay for technical assistance, Mr. P. Egli for the synthesis of radiolabeled captopril, and Ms. R. Fand for statistical analysis of the data.

# High-Performance Liquid Chromatographic Analysis of Iodochlorhydroxyquin in Plasma

**F. W. EZZEDEEN *, A. N. MASOUD ‡, S. J. STOHS *x, and S. J. LERMAN §**

Received September 25, 1980, from the **Department of Biomedicinal Chemistry, the* ‡*Department of Anesthesiology, and the* §*Department of Pediatrics, University of Nebraska Medical Center, Omaha, NE 68105.* Accepted for publication January 7, 1981.

**Abstract** □ A simple isocratic high-performance liquid chromatographic procedure for the analysis of iodochlorhydroxyquin in human plasma is described. Protein was precipitated using perchloric acid, and the supernatant and precipitated protein fractions were extracted with ether. The ether phases were evaporated to dryness, reconstituted in mobile phase, and chromatographed. A reversed-phase microparticulate $C_{18}$ column, a precolumn, and a UV detector at 256 nm were used. A mobile phase containing 80% methanol and 20% 0.05 *M* phosphoric acid was employed at a flow rate of 1 ml/min. Quantitation of iodochlorhydroxyquin in the 1–15-μg/ml range in human plasma was demonstrated with a coefficient of variance of 0.1–0.06. Hydrocortisone, which is used in combination with iodochlorhydroxyquin in ointments and creams, does not interfere in the assay.

**Keyphrases** □ Iodochlorhydroxyquin—high-performance liquid chromatographic analysis, plasma □ Anti-infectives—iodochlorhydroxyquin, high-performance liquid chromatographic analysis, plasma □ High-performance liquid chromatography—analysis, iodochlorhydroxyquin, plasma

Iodochlorhydroxyquin[1] (I) has been widely used as an antidiarrheal, antimycotic, and antibacterial agent in many countries.

Tamura *et al.* studied patients with subacute myelo-opticoneuropathy and found I chelated with iron as a green pigment in the urine and feces and also free I crystals in the urine (1). Subacute myelo-opticoneuropathy was subsequently shown to be caused by the long-term oral treatment and high dosage use of I (1–3).

## BACKGROUND

Because of the toxicity associated with the oral usage of I, various analytical procedures have been developed for its determination in biological fluids. Electron-capture GLC, which requires expensive instrumentation and tedious and time-consuming derivatization, has been used (1, 4–8). Tsuji *et al.* (9) reported a method whereby I was chelated with aluminum and measured fluorometrically. A spectrophotometric method also was reported for the determination of I and its conjugates in the urine (10, 11). The spectrophotometric procedure is not sufficiently sensitive for the determination of the drug in plasma or serum. A complicated and time-consuming TLC procedure also was reported (12).

High-performance liquid chromatography (HPLC) has become an increasingly popular analytical technique in clinical and forensic laboratories. A procedure dealing with the separation and analysis of glucuronide and sulfate conjugates of I in urine using HPLC was reported previously (13) but was incapable of assaying for unconjugated I, even when present in high concentrations in the urine (13). The drug occurs predominantly in the unconjugated form in plasma (3).

A single oral dose of I of ~8 mg/kg in humans produces maximum serum levels of 3–6 μg/ml (8). Little research has been conducted on the percutaneous absorption of I. Fischer and Hartvig (14) treated four patients with widespread dermatitis of an unstated type with an ointment containing 3% I, and serum I levels were estimated by electron-capture GLC to be 0.8–1.2 μg/ml.

This report describes the analysis of therapeutic I concentrations in plasma using HPLC. The procedure combines sensitivity, specificity, and simplicity not attainable by previously described methods.

[1] 5-Chloro-7-iodo-8-quinolinol; Vioform, Ciba Pharmaceutical.

## EXPERIMENTAL

**Apparatus**—An isocratic HPLC system assembled in this laboratory consisted of a reciprocating minipump[2]; a stainless steel tube, 6.35 mm (0.25 in.) o.d. and 4.76 mm ($^3/_{16}$ in.) i.d. × 1 m, as a pulsation damper; a 34.5-MPa (5000 psi) pressure gauge[3]; a fixed-volume sample injector[4] with a 20-μl loop; and a variable-wavelength UV detector[5]. A multivoltage 25.40-cm strip-chart recorder[6] was connected to the UV detector.

A microparticulate reversed-phase chromatographic column, 250 × 2.6 mm, packed with ODS-HC-SIL-X-I[7], and a 5 × 40-mm guard column, RP-18-MPLC[8], were connected to the HPLC system. The following reagents were used: iodochlorhydroxyquin[1]; ether anhydrous analytical reagent[9]; methanol distilled in glass, residue free[10]; concentrated perchloric acid; anhydrous sodium sulfate; and water, which was deionized, demineralized, and glass distilled in this laboratory. Iodochlorhydroxyquin (mol. wt. 305.52) decomposed at ~170°, and no impurities were detected by HPLC.

**Standards**—Stock solutions of I were prepared in methanol and contained 1 mg/ml and 100 μg/ml. These solutions could be maintained in the refrigerator for at least 2 weeks without deterioration. Working solutions were prepared fresh daily. Dilutions were made using 80% methanol and 20% 0.05 *M* phosphoric acid to prepare the working standards, which were used to spike plasma samples and to calculate recovery from plasma samples after extraction.

**Extraction**—Aliquots of 1.0-ml plasma samples were transferred to 15-ml screw-capped and polytef-lined centrifuge tubes. Human blood bank plasma was used for all studies. Aliquots of I working standard were used to spike the plasma samples. After the tubes were shaken by hand for 1 min, 100 μl of concentrated perchloric acid was added to each tube; then the tubes were vortexed for another 30 sec and centrifuged[11] at 5000 rpm for 10 min at 15°. Approximately 0.5 ml of the supernatant fractions were extracted twice with 5 ml of ether in 15-ml glass culture tubes with polytef-lined screw caps by vortexing for 10 sec, and the phases were separated by centrifuging for 10 min at 15°.

The protein precipitates were extracted once with 10 ml of ethyl ether by vortexing for 1 min and centrifuged as already described. The ether extracts were dried over anhydrous sodium sulfate[9] and evaporated to dryness at 38° under a nitrogen stream[12]. The residue from each fraction was redissolved in 500 μl of the mobile phase, and 20 μl of each was injected onto the column.

**Chromatography**—The parameters used throughout this investigation included a reversed-phase column and precolumn as previously described, a 20-μl injector loop, and the recorder chart speed set at 0.254 mm (0.1 in.)/min. A mobile phase containing 80% methanol and 20% 0.05 *M* phosphoric acid was used at a flow rate of 1 ml/min. The mobile phase was filtered using a 0.2-μm filter[13], degassed under vacuum, and maintained at 40° during chromatography. The UV detector was set at 256 nm. The column was flushed at the end of each day with 100% methanol. Not more than 30 min was required for column equilibration prior to use each day.

[2] Milton Roy model 396-31.
[3] Laboratory Data Control, Riviera Beach, FL 33404.
[4] Rheodyne Inc., Berkeley, CA 94710.
[5] Spectro-Monitor III, Laboratory Data Control, Riviera Beach, FL 33404.
[6] Beckman Instruments, Palo Alto, CA 94304.
[7] Serial No. 1303, Perkin-Elmer, Norwalk, CT 06858.
[8] Manufactured by Brownlee Laboratories and obtained from Rheodyne Inc., Berkeley, CA 94710.
[9] Mallinckrodt, St. Louis, MO 63147.
[10] Burdick & Jackson Laboratories, Muskegon, MI 49442.
[11] Sorvall RC2-B refrigerated centrifuge, DuPont Co., Newton, CT 06470.
[12] SC/27R sample concentrator, Brinkmann Instruments, Westbury, NY 11590.
[13] Catalog No. EGWP-04700, Millipore Corp., Bedford, Mass.

0022-3549/81/0800-0889$01.00/0
© 1981, American Pharmaceutical Association

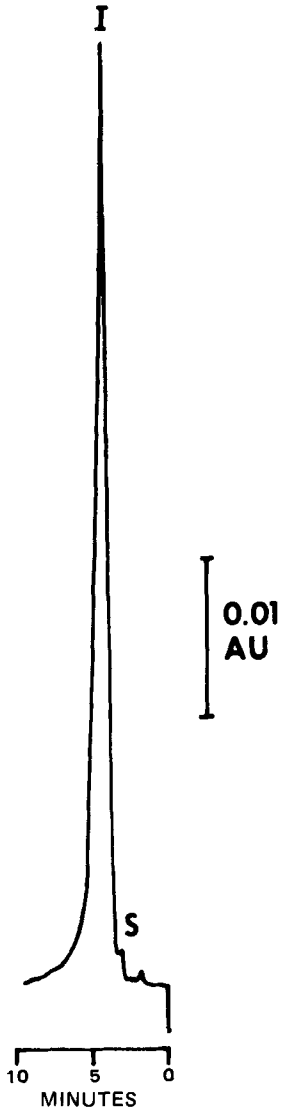


**Figure 1**—*Standard iodochlorhydroxyquin solution (2 μg/ml) dissolved in the mobile phase. The detector was set at 256 nm and 0.01 aufs. Other chromatographic conditions are described under* Experimental.

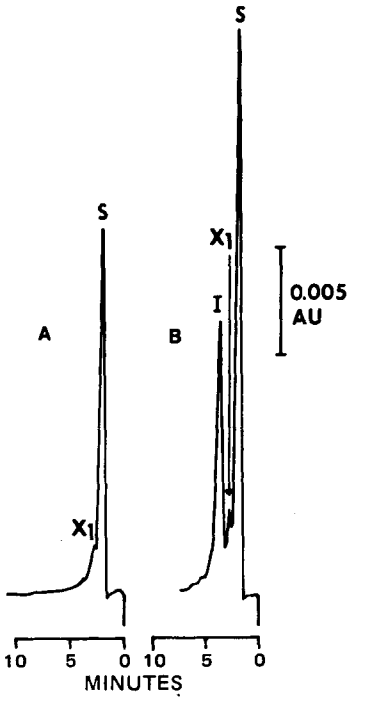


**Figure 2**—*The supernatant extraction from a plasma blank (A) and from plasma containing 5 μg/ml (B). The detector was set at 0.05 aufs, and other chromatographic conditions are as described in Fig. 1.*

## RESULTS AND DISCUSSION

Suitable retention of I was obtained when a mobile phase containing 80% methanol and 20% 0.05 *M* phosphoric acid was used with the described reversed-phase column. A typical chromatogram of standard I in the mobile phase is presented in Fig. 1. The capacity factor ($k'$) for I was 1.14, calculated according to the following:

$$k' = \frac{Rt_1 - Rt_0}{Rt_0} \qquad \text{(Eq. 1)}$$

where the retention time for I ($Rt_1$) was 3.75 min and the elution time of unretained compounds or the solvent front determined by injecting methanol onto the column ($Rt_0$) was 1.75 min.

Figure 2A is a chromatogram of an extracted plasma supernatant fraction without I addition. Figure 2B is a chromatogram of I extracted from a spiked plasma sample following protein precipitation using perchloric acid. Direct extraction of plasma by ether without protein precipitation resulted in the presence of unknown compounds that interfered with I upon chromatography. Preliminary studies revealed that large amounts of I were precipitated with the proteins. Therefore, both the acidified supernatant and precipitated protein fractions were extracted with ether. Extractions of I at pH values from 1 to 8 with ether, methylene dichloride, and carbon tetrachloride also were conducted. In addition, the use of ammonium sulfate as the protein precipitating agent was attempted, but the extraction efficiency of I was very poor. Ether extraction of both the supernatant and precipitated protein fractions following perchloric acid addition was most efficient and reproducible.

The representative chromatograms presented in Figs. 3A and 3B were obtained from ether-extracted protein precipitate fractions of human plasma (blank) and a plasma sample to which 5 μg of I/ml had been added, respectively. Two interfering substances were present in ether extractions of the precipitated protein fractions. The first of these compounds ($X_1$), which has a retention time close to I, was present in much larger concentrations in the extracts from the precipitated protein fraction (Fig. 3) as compared to the ether extracts of the supernatant fractions (Fig. 2). The second substance ($X_2$) was extracted from the precipitated protein fractions (Fig. 3) but not from the supernatant fractions (Fig. 2) and had a retention time of ~16 min.

Table I shows the percent recovery of I following extraction of the supernatant and precipitated protein fractions, as well as total recovery following the addition of 1–15 μg of I/ml to plasma. Each value represents the mean of three determinations with the standard deviation. The

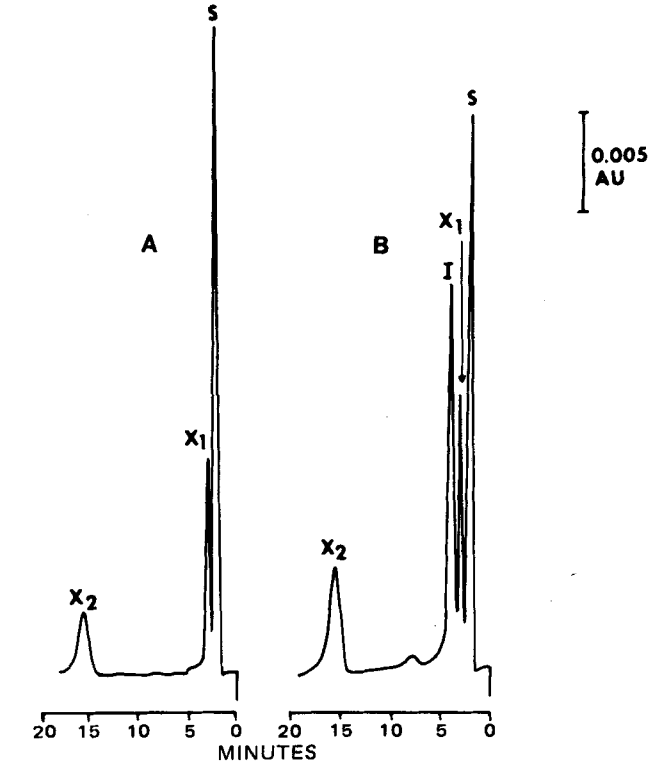


**Figure 3**—*Extraction of protein precipitate of a plasma blank (A) and of plasma containing 5 μg/ml (B). The detector was set at 0.05 aufs, and other chromatographic conditions are as described in Fig. 1.*

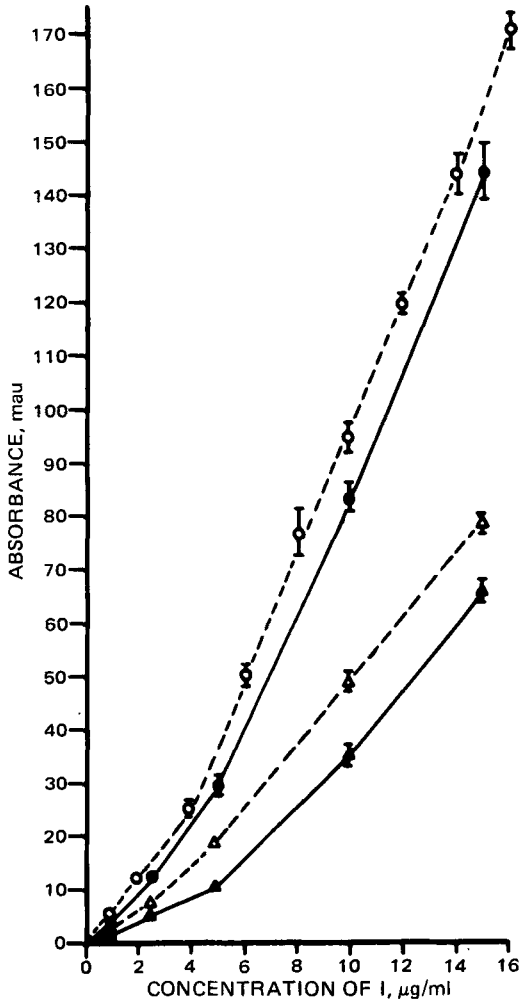


**Figure 4**—*Standard curve of iodochlorhydroxyquin. Key:* ▲—▲, *extracted supernatant fraction reconstituted in 500 μl of mobile phase;* △ - - △, *extracted precipitate fraction reconstituted in 500 μl of mobile phase;* ●—●, *mathematical summation of two aforementioned values; and* O - - O, *standard solutions diluted in the mobile phase. The peak height values were converted to reflect concentration in 500 μl to conform with values of extracted samples.*

coefficient of variance for each sample also is presented. From 28 to 41% of the total I added to plasma was recovered from the supernatant fraction, while 46–54% of I was recovered from the protein fraction. Total recovery of I was 77–91%.

The UV absorbance spectrum of I in the mobile phase exhibited two maxima at 256 ($\alpha = 0.15$) and 204 ($\alpha = 0.11$) nm. For optimum sensitivity, the detector was set at 256 nm. Standard solutions of I in the mobile phase were prepared at 1, 2, 4, 6, 8, 10, 12, 14, and 16 μg/ml, and 20-μl aliquots of each were injected. The standard curve for I is presented in Fig. 4. Each point on the graph represents the mean, and the bars represent the standard deviation of the mean for three injections. Some bars were omitted because the very small standard deviations of the mean could not be graphically represented.

The amounts of I extracted from the supernatant and precipitated protein fractions of plasma samples spiked with 1.0, 2.5, 5.0, 10.0, and 15.0 μg/ml of I are presented in Fig. 4. Concentrations of I higher than 15 μg/ml of plasma resulted in peak splitting for I upon HPLC. The reason for this effect is not known. The total I recovered at each concentration also is given in Fig. 4. Each point represents the mean, and the bars represent the standard deviation of the mean for three extractions. The correlation coefficients ($R$) for the standard curve for I, the extracted supernatant fraction, the extracted precipitated protein fraction, and the total extracted I were 0.995, 0.978, 0.995, and 0.992, respectively, where:

**Table I—Percent Recovery of Iodochlorhydroxyquin from Extracted Plasma** [a]

| Plasma Concentration, μg/ml | From Supernatant Fraction | From Precipitated Protein Fraction | Total |
|---|---|---|---|
| 1 | 30.0 ± 3.0 (0.17) | 54.0 ± 3.1 (0.09) | 84.0 ± 6.1 (0.12) |
| 2.5 | 30.8 ± 2.2 (0.11) | 45.9 ± 2.1 (0.07) | 76.7 ± 4.0 (0.08) |
| 5 | 28.0 ± 1.5 (0.09) | 48.9 ± 2.2 (0.07) | 76.9 ± 2.6 (0.06) |
| 10 | 35.8 ± 3.2 (0.17) | 50.4 ± 2.0 (0.07) | 86.2 ± 3.4 (0.07) |
| 15 | 41.3 ± 2.3 (0.08) | 49.5 ± 1.3 (0.04) | 90.8 ± 3.0 (0.06) |

[a] Each value is the mean with the standard deviation for three determinations. The values in parentheses are the coefficients of variance.

$$R = \frac{m\sigma_x}{\sigma_y} \qquad \text{(Eq. 2)}$$

The slope is:

$$m = \frac{\sum xy - \frac{\sum x \sum y}{N}}{\sum x^2 - \frac{(\sum x)^2}{N}} \qquad \text{(Eq. 3)}$$

where $\sigma$ is the standard deviation, $x$ is the concentration of I, $y$ is the peak height, and $N$ is the number of samples. The $y$ intercept is:

$$b = \frac{(\sum y - m)\sum x}{N} \qquad \text{(Eq. 4)}$$

The primary current application of I is as a topical antibacterial agent, and hydrocortisone is the drug most commonly found in creams and ointments in conjunction with I. Under the experimental conditions described, hydrocortisone elutes with the solvent front and is therefore easily resolved from I. The primary urinary metabolites of I are the glucuronide and sulfate conjugates; with the analytical system employed, these two compounds do not chromatograph.

The HPLC procedure described here provides a rapid and reproducible method for determining plasma I concentrations. Previously described methods are insufficiently sensitive to detect I in small plasma samples (10–12). Chromatography of I by direct ether extract was not possible due to interfering compounds. The most accurate and rapid assay for I was achieved by extracting the plasma supernatant fraction following protein precipitation with perchloric acid. Only a small amount of an unknown compound was extracted as compared to the extraction of two unknown compounds from the precipitated protein fraction.

## REFERENCES

(1) Z. Tamura, M. Yoshioka, T. Imarari, J. Fukaya, J. Kusaka, and K. Samejima, *Clin. Chim. Acta*, **47**, 13 (1973).

(2) Y. Toyokura and T. Takasu, *Jpn. J. Med. Sci. Biol.*, **28**, 87 (1975).

(3) Z. Tamura, *ibid.*, **28**, 69 (1975).

(4) D. B. Jack and W. Riess, *J. Pharm. Sci.*, **62**, 1929 (1973).

(5) P. H. Degen, W. Schneider, P. Vuillard, U. P. Geiger, and W. Riess, *J. Chromatogr.*, **117**, 407 (1976).

(6) P. Hartvig and C. Fagerlund, *ibid.*, **140**, 170 (1977).

(7) C. T. Chen, H. Kodama, Y. Egashora, K. Samejima, T. I. Manari, and Z. Tamura, *Chem. Pharm. Bull.*, **24**, 2007 (1976).

(8) C. T. Chen, K. Samejima, and Z. Tamura, *ibid.*, **24**, 97 (1976).

(9) A. Tsuji, T. Kinoshita, and F. Inuma, *ibid.*, **19**, 2209 (1971).

(10) L. Bergren and O. Hansson, *Clin. Pharmacol. Ther.*, **9**, 67 (1968).

(11) W. T. Haskins and G. W. Luttermoser, *J. Pharmacol. Exp. Ther.*, **109**, 201 (1953).

(12) P. D. Soldato, *J. Pharm. Sci.*, **66**, 1334 (1977).

(13) C. T. Chen, K. Hayukawa, T. Imanori, and Z. Tamura, *Chem. Pharm. Bull.*, **23**, 2173 (1975).

(14) T. Fischer and P. Hartvig, *Lancet*, **1**, 603 (1977).

# Influence of Serum Albumins on Decomposition Rates of *para*-Substituted 1-Phenyl-3-methyltriazenes and 5-(3-Methyl-1-triazeno)imidazole-4-carboxamide in Near Physiological Conditions

**FRANCO DELBEN *x, SERGIO PAOLETTI *, GIORGIO MANZINI *, and CARLO NISI ‡**

Received July 10, 1979, from the **Istituto di Chimica and the* ‡*Istituto di Chimica Farmaceutica, Università di Trieste, Trieste, Italy.*
Accepted for publication January 7, 1981.

**Abstract** □ The influence of human serum albumin on the decomposition rates of some arylmonomethyltriazenes in buffered aqueous solution was investigated. From the experimental data, a model for the triazene–albumin interaction was derived, and the thermodynamic parameters were systematically calculated by two independent methods. The results show marked dependence of the energetics of binding on the substituent in the triazene aromatic ring. For most of the triazenes studied, the binding with albumin was mainly enthalpy driven. Measurements also were performed using bovine and murine serum albumins.

**Keyphrases** □ Arylmonomethyltriazenes—decomposition rates, effect of human serum albumin □ Serum albumin, human—effect on decomposition rates of arylmonomethyltriazenes □ Binding kinetics—triazene–albumin interaction, decomposition rates □ Antitumor agents—arylmonomethyltriazenes, effect of human serum albumin on decomposition rates

Aryldimethyltriazenes are a class of compounds possessing antitumor (1–4), carcinogenic (5–7), and mutagenic (8–10) activities. Evidence exists that metabolites of these triazenes are responsible for their *in vivo* effects. Monomethyltriazenes, produced by oxidative *N*-demethylation of the parent dimethyl compounds, are considered as possible metabolic species active at a systemic level (2, 11, 12) since they can alkylate cellular components by hydrolysis (13). Arylmonomethyltriazenes decompose in aqueous solution buffered at near neutral pH values to the corresponding anilines, nitrogen, and carbon cation derivatives with pseudo-first-order kinetics (14).

Since the possibility of interaction between these drugs and serum components exists, the influence of serum albumins on the decomposition rates of some *para*-substituted 1-phenyl-3-methyltriazenes, 1-(2,4,6-trichloro)-phenyl-3-methyltriazene, and 5-(3-methyl-1-triazeno)-imidazole-4-carboxamide was studied. The last compound is possibly a metabolite of 5-(3,3-dimethyl-1-triazeno)-imidazole-4-carboxamide (NSC 45388), used in the treatment of malignant melanoma. Decomposition kinetic studies of these triazenes also were performed in the absence of serum albumins, because the reported data show a marked dependence of the decomposition rates of arylmonomethyltriazenes on the medium (15) and because accurate data in near physiological conditions are lacking.

Human serum albumin was systematically employed. Bovine and mouse serum albumins also were used for comparison and, in the latter case, to allow correlations between the present results and possible *in vivo* experiments.

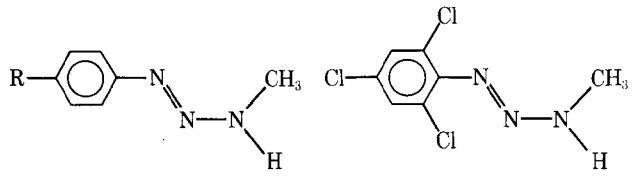

I–X



XI

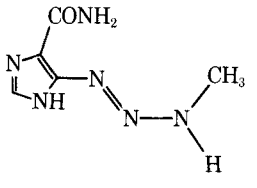

XII

## EXPERIMENTAL

**Chemistry**—The monomethyltriazenes (Table I) were synthesized by standard methods, *i.e.*, by coupling aryldiazonium chloride to two equivalents of methylamine in the presence of excess base, usually sodium carbonate. The coupling reactions, with the exceptions of VII and XI, were performed in the presence of large volumes of ether to extract the reaction products. To obtain very pure samples of I–VI and VIII, careful sublimation of small amounts of the raw materials, below their melting points, at ~0.2 torr was necessary. A chilling bath of dry ice–acetone was used to recover the recrystallized products; VII was purified by extracting the dried raw material with boiling ethyl acetate.

Purity of the monomethyltriazenes and the aromatic amines used as reference compounds was checked by NMR spectroscopy, elemental analysis, and TLC. Aluminum oxide and methanol–ethyl acetate–ligroin (3:2:1) or ethyl acetate–hexane (1:1) were used for TLC of monomethyltriazenes. The melting points were determined in open glass capillaries in a Büchi apparatus and were in accordance with the literature values. The references for the melting points are listed in Table I.

The solvents used for crystallizations were petroleum ether (bp 30–50°) for I, *n*-hexane for II–VI, ethyl acetate for VII, methanol for VIII, and benzene for IX.

**Materials**—The solvents used for TLC and crystallizations, as well as potassium dihydrogen *o*-phosphate and potassium hydroxide used in the preparation of buffer solutions, were reagent grade.

Serum albumins were crystallized and lyophilized human albumin, crystallized and lyophilized bovine serum albumin, mouse serum albumin fraction V powder, and crystallized and lyophilized egg albumin.

All serum albumins were used without further purification. Human and bovine serum albumin concentrations were determined spectrophotometrically using $E^{1\%}_{279} = 5.3$ and 6.6, respectively (22). Murine serum and egg albumin concentrations were determined by accurately weighing dried samples. Freshly prepared albumin, triazene, and buffer solutions were used.

**Methods**—All kinetic measurements were performed in 0.065 *M* phosphate buffer prepared using fresh, double-distilled water, specific conductivity $1.0 \times 10^{-6}\ \Omega^{-1}$/cm, adjusted to pH 7.40 at 25° by the addition of potassium hydroxide. The temperature dependence of pH of phosphate buffer solutions between 20 and 45° resulted in $2 \times 10^{-3}$ pH unit per degree. This temperature dependence was taken into account; *i.e.*, all results of the kinetic measurements performed at different tem-



*0022-3549/81/0800-0892$01.00/0*
*© 1981, American Pharmaceutical Association*

**Table I—Kinetic Data of the Pseudo-First-Order Decomposition of Monomethyltriazenes in Buffered Aqueous Solution [a]**

| Compound | R | Melting-Point Reference | $T$, °K | pH | $k \times 10^3$, $sec^{-1}$ |
|---|---|---|---|---|---|
| I | H | 17 | 294.9 | 7.405 | 4.78 |
| | | | 301.2 | 7.391 | 6.80 |
| | | | 310.8 | 7.371 | 11.3 |
| | | | 318.6 | 7.354 | 16.6 |
| II | $CH_3$ | 18 | 293.5 | 7.408 | 7.76 |
| | | | 303.0 | 7.388 | 13.1 |
| | | | 310.2 | 6.965 | 49.8 |
| | | | 310.2 | 7.179 | 32.5 |
| | | | 310.2 | 7.372 | 18.0 |
| | | | 310.2 | 7.711 | 9.50 |
| | | | 310.2 | 7.984 | 4.92 |
| | | | 310.7 | 7.371 | 20.2 |
| | | | 318.7 | 7.354 | 28.6 |
| III | F | 16 | 296.2 | 7.402 | 3.33 |
| | | | 299.7 | 7.395 | 4.03 |
| | | | 304.2 | 7.385 | 5.47 |
| | | | 310.0 | 7.372 | 7.61 |
| | | | 311.1 | 7.370 | 8.68 |
| | | | 314.8 | 7.362 | 11.05 |
| IV | Cl | 19 | 295.2 | 7.405 | 1.71 |
| | | | 303.2 | 7.387 | 2.79 |
| | | | 310.2 | 7.372 | 4.27 |
| | | | 318.3 | 7.354 | 6.62 |
| V | Br | 16 | 296.7 | 7.401 | 1.55 |
| | | | 303.2 | 7.387 | 2.39 |
| | | | 310.2 | 6.965 | 9.67 |
| | | | 310.2 | 7.192 | 6.00 |
| | | | 310.2 | 7.372 | 3.63 |
| | | | 310.2 | 7.711 | 1.80 |
| | | | 310.2 | 7.984 | 0.878 |
| | | | 316.2 | 7.359 | 5.36 |
| VI | I | 19 | 296.1 | 7.403 | 1.57 |
| | | | 302.3 | 7.389 | 2.32 |
| | | | 308.8 | 7.375 | 3.32 |
| | | | 313.7 | 7.364 | 4.41 |
| | | | 314.5 | 7.363 | 4.64 |
| VII | $CONH_2$ | 20 | 294.2 | 7.407 | 0.496 |
| | | | 303.2 | 7.387 | 0.965 |
| | | | 310.0 | 7.372 | 1.53 |
| | | | 317.9 | 7.355 | 2.48 |
| VIII | $COOCH_3$ | 19 | 294.2 | 7.407 | 0.383 |
| | | | 296.9 | 7.401 | 0.439 |
| | | | 302.2 | 7.389 | 0.692 |
| | | | 304.2 | 7.385 | 0.742 |
| | | | 310.2 | 7.372 | 1.11 |
| | | | 311.1 | 7.370 | 1.23 |
| | | | 315.4 | 7.361 | 1.65 |
| | | | 318.2 | 7.355 | 1.70 |
| IX | $SO_2CH_3$ | 2 | 302.9 | 7.388 | 0.318 |
| | | | 310.2 | 6.965 | 1.18 |
| | | | 310.2 | 7.192 | 0.824 |
| | | | 310.2 | 7.372 | 0.601 |
| | | | 310.2 | 7.711 | 0.351 |
| | | | 318.2 | 7.355 | 1.26 |
| X | $NO_2$ | 20 | 294.2 | 7.407 | 0.272 |
| | | | 295.3 | 7.007 | 0.468 |
| | | | 295.3 | 7.369 | 0.319 |
| | | | 295.3 | 7.917 | 0.241 |
| | | | 302.2 | 7.389 | 0.666 |
| | | | 303.9 | 6.986 | 1.18 |
| | | | 303.9 | 7.160 | 1.07 |
| | | | 303.9 | 7.348 | 0.879 |
| | | | 303.9 | 7.692 | 0.711 |
| | | | 303.9 | 7.896 | 0.715 |
| | | | 310.2 | 6.965 | 2.42 |
| | | | 310.2 | 7.192 | 1.98 |
| | | | 310.2 | 7.372 | 1.73 |
| | | | 310.2 | 7.711 | 1.69 |
| | | | 310.2 | 7.984 | 1.38 |
| | | | 318.2 | 7.355 | 3.50 |
| XI [b] | | | 296.7 | 7.401 | 11.7 |
| | | | 298.2 | 7.398 | 13.6 |
| | | | 302.7 | 7.388 | 23.4 |
| | | | 307.4 | 7.378 | 36.8 |
| | | | 312.4 | 7.367 | 55.0 |
| | | | 314.3 | 7.363 | 74.5 |
| XII | | 21 | 293.7 | 7.408 | 0.775 |
| | | | 302.2 | 7.389 | 2.31 |
| | | | 310.2 | 6.965 | 6.11 |
| | | | 310.2 | 7.192 | 5.89 |
| | | | 310.2 | 7.377 | 5.59 |
| | | | 310.2 | 7.984 | 5.36 |
| | | | 318.2 | 7.355 | 14.2 |

[a] Phosphate buffer, 0.065 $M$; ionic strength, 0.15 $M$. [b] This compound was a gift of Dr. G. F. Kolar, Institute for Toxicology and Chemotherapy, German Cancer Research Center, Heidelberg, West Germany.

peratures and pH values were interpolated at the common value of pH 7.40, using kinetic data determined as a function of pH between 7 and 8 for each triazene.

The decomposition reactions were followed spectrophotometrically at a fixed wavelength in the 310–350-nm range chosen to permit maximum variation of absorbance and minimum interference with the spectrum of the decomposition products. In each case, the spectrum at the end of the reaction was coincident with that of the corresponding aniline.

A freshly prepared solution ($\sim 4 \times 10^{-3}$ $M$) of monomethyltriazene in absolute ethanol was added to a known volume of aqueous phosphate buffer, in a quartz cell thermostated at ±0.05°, so that the ethanol–buffer volume ratio was 1:100 in all cases. The solution was stirred rapidly, and the absorbance was recorded as a function of time. The logarithm of the difference between the absorbance at time $t$ and at the final time was plotted *versus* $t$; from the straight line so obtained, the pseudo-first-order kinetic constant was calculated using the least-squares method.

At the wavelength used, serum albumins gave rise to very low scattering, which was constant with time and did not invalidate the measurements.

The treatment of experimental data was the same both in the absence and presence of albumin, even if the values of the molar absorptivities of free and bound triazene species ($\epsilon_F$ and $\epsilon_B$, respectively) might be different. This event does not invalidate the assumption of proportionality between the normalized optical density and the total triazene concentration during the kinetic measurements. An excess of $C_P$ (protein concentration) with respect to $C_B$ (bound triazene concentration) ensures near proportionality between $C_B$ and $C_F$ (free triazene concentration) and, therefore, between the optical density and $C_T$ (total triazene concentration):

$$\text{optical density} = \epsilon_B C_B + \epsilon_F C_F \qquad \text{(Eq. 1)}$$

and by use of Eqs. 5 and 6, it follows that:

$$\text{optical density} \propto (K_B C_P \epsilon_B + \epsilon_F) C_T = \text{constant } C_T \qquad \text{(Eq. 2)}$$

The possibility that the aniline produced by the decomposition reaction interferes with the triazene binding sites (*e.g.*, by competition) was tested. Some sequential kinetic measurements, performed in the same protein solution that allowed the aniline concentration to rise, gave constant half-lives, indicating that the effect of the aniline in this respect is negligible.

Linearization of data, when necessary, was performed by a computerized least-squares procedure.

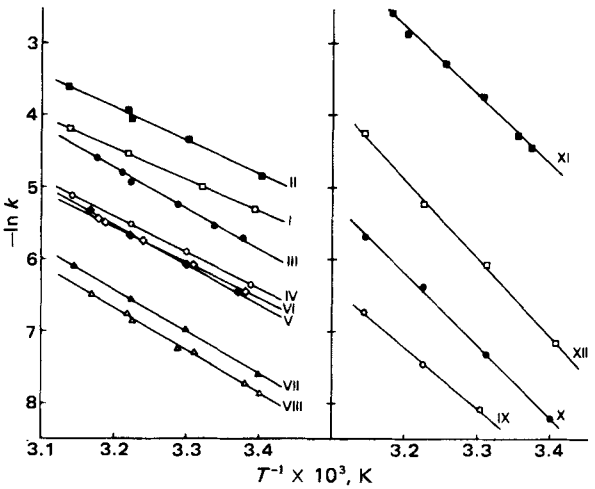


**Figure 1**—*Arrhenius plots for the monomethyltriazenes studied.*

**Table II—Kinetic Data of the Pseudo-First-Order Decomposition of Monomethyltriazenes [a]**

| Compound | $k \times 10^3$, $sec^{-1}$ | $t_{1/2}$, sec | ln $A$ [b] | $E$, kJ × $mole^{-1}$ [b] | $C_P \times 10^4$, $M$ | $k' \times 10^3$, $sec^{-1}$ | $t'_{1/2}$, sec | ln $A'$ [b] | $E'$, kJ × $mole^{-1}$ [b] |
|---|---|---|---|---|---|---|---|---|---|
| I | 10.2 | 68 | 9.8 ± 0.1 | 37.0 ± 0.1 | 1.05 | 8.6 | 81 | 12.2 ± 0.4 | 43.8 ± 1.1 |
| II | 17.7 | 39 | 10.0 ± 0.4 | 36.2 ± 1.1 | 1.20 | 11.5 | 60 | 13.1 ± 0.6 | 45.4 ± 1.6 |
| III | 7.56 | 92 | 12.9 ± 0.4 | 45.9 ± 1.1 | 0.98 | 6.36 | 109 | 13.2 ± 0.8 | 47.2 ± 2.1 |
| IV | 3.96 | 175 | 10.7 ± 0.1 | 41.9 ± 0.3 | 1.03 | 1.88 | 368 | 14.0 ± 0.3 | 52.4 ± 0.9 |
| V | 3.46 | 200 | 11.9 ± 0.2 | 45.3 ± 0.5 | 1.15 | 1.33 | 520 | 16.1 ± 1.8 | 58.9 ± 4.6 |
| VI | 3.40 | 204 | 10.3 ± 0.1 | 41.3 ± 0.4 | 1.00 | 0.99 | 698 | 19.1 ± 1.0 | 67.5 ± 2.5 |
| VII | 1.43 | 485 | 12.3 ± 0.2 | 48.7 ± 0.5 | 0.89 | 1.38 | 503 | 13.1 ± 0.1 | 50.6 ± 0.1 |
| VIII | 1.09 | 636 | 12.5 ± 0.4 | 49.8 ± 0.8 | 1.05 | 0.81 | 853 | 17.8 ± 0.2 | 64.1 ± 0.5 |
| IX | 0.589 | 1177 | 19.4 ± 0.6 | 69.3 ± 2.2 | — | — | — | — | — |
| X | 1.58 | 439 | 25.6 ± 0.7 | 82.7 ± 1.8 | 0.97 | 0.72 | 967 | 30.1 ± 2.0 | 96.6 ± 5.0 |
| XI | 47.6 | 15 | 27.6 ± 0.7 | 79.0 ± 1.7 | 1.00 | 11.6 | 60 | 17.7 ± 0.9 | 56.6 ± 2.3 |
| XII | 5.67 | 122 | 30.0 ± 0.6 | 90.8 ± 1.5 | 1.00 | 5.29 | 131 | — | — |

[a] The values of $k$, $t_{1/2}$, $k'$, and $t'_{1/2}$ refer to 37° and pH 7.40. The prime denotes the presence of human serum albumin; $C_P$ is the molar concentration of the protein. [b] Average ± *SD*.

## RESULTS AND DISCUSSION

The kinetic law of decomposition of the monomethyltriazenes studied, carried out at various temperatures in pH 7.4 phosphate buffer (ionic strength 0.15 *M*), proved to be pseudo-first order with respect to the triazene concentration in all cases (Table I). Corrections for the slight temperature effect on pH and, therefore, on $k$ were performed (see *Experimental*).

The Arrhenius plots of the kinetic data interpolated at pH 7.40 for all of the triazenes studied were fairly linear in the temperature range investigated (Fig. 1). By application of the empirical Arrhenius equation, $k = A \exp(-E/RT)$, to these kinetic measurements, the activation energies and the natural logarithm of the preexponential terms for the various triazenes were obtained (Table II).

The plot of log $k_{(R)}$ − log $k_{(H)}$ as a function of the Hammett constant $\sigma$ (23, 24) for the different *para*-R-substituted aryl derivatives gives a satisfactory straight line, except for X and, to a lesser extent, for IX (Fig. 2). The slope of such a straight line is negative, in agreement with the expected electrophilic character of the decomposition reaction, with $\rho = -2$ approximately.

The triazenes that follow the Hammett plot are characterized by relatively low and approximately similar activation energies and preexponential terms (36–50 kJ $mole^{-1}$ and 10–13, respectively), whereas higher $E$ and ln $A$ values have been found for XI and XII and for the two triazenes (IX and X) that do not follow this plot (69–91 kJ $mole^{-1}$ and 19–30, respectively). The peculiar behavior of IX and X is likely to be attributed to the different extent of protonation of these triazenes at pH 7.4 as compared to the other compounds. This protonation would affect their behavior with respect to acid catalysis.

The results of the kinetic measurements show that the presence of human serum albumin in solution causes a more or less marked lessening in the decomposition rates of the triazenes considered, without affecting the order of the reaction (Fig. 3 and Table III). Therefore, the reaction rate can be written as:

$$v = -\frac{dC_T}{dt} = k'C_T \qquad \text{(Eq. 3)}$$

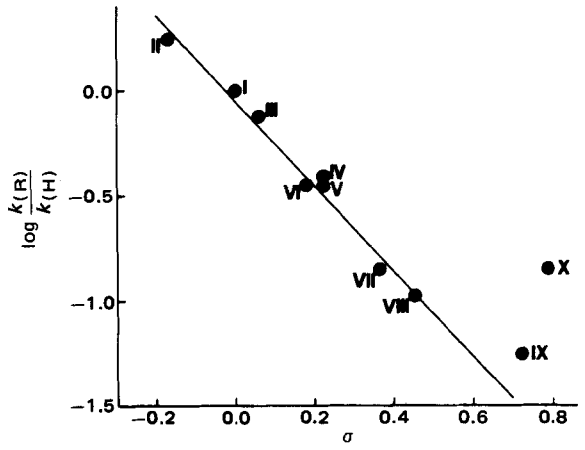


**Figure 2**—*Plot of* log $k_{(R)}$ −log $k_{(H)}$ versus *the Hammett constant,* $\sigma$, *for the various triazenes studied* ($\rho = -2$ *approximately).*

where $k'$ is the apparent kinetic constant in the presence of albumin ($k' < k$).

The observed lessening in the decomposition rates caused by serum albumin may be interpreted by assuming that: (*a*) the triazenes interact rapidly and reversibly with a binding site onto the protein, (*b*) it cannot decompose when bound to this site, and (*c*) the fraction of unbound triazene decomposes in the bulk of the solution with kinetic constant $k$.

On the basis of the first assumption, the stoichiometric constant of association between the triazene and the protein, $K_B$, may be defined as:

$$K_B = C_B/C_F(C_P - C_B) \qquad \text{(Eq. 4)}$$

Since in the present case $C_P$ is always greater than $C_T$ and $C_B$ generally is sufficiently smaller than $C_T$, $C_B$ can be neglected with respect to $C_P$, and it is possible to approximate:

$$\frac{C_B}{C_F} = K_B C_P \qquad \text{(Eq. 5)}$$

and, therefore:

$$C_F = C_T/(1 + K_B C_P) \qquad \text{(Eq. 6)}$$

This approximation induces a slight underestimation of the $K_B$ values, which is more relevant for the highest ones. This underestimation does

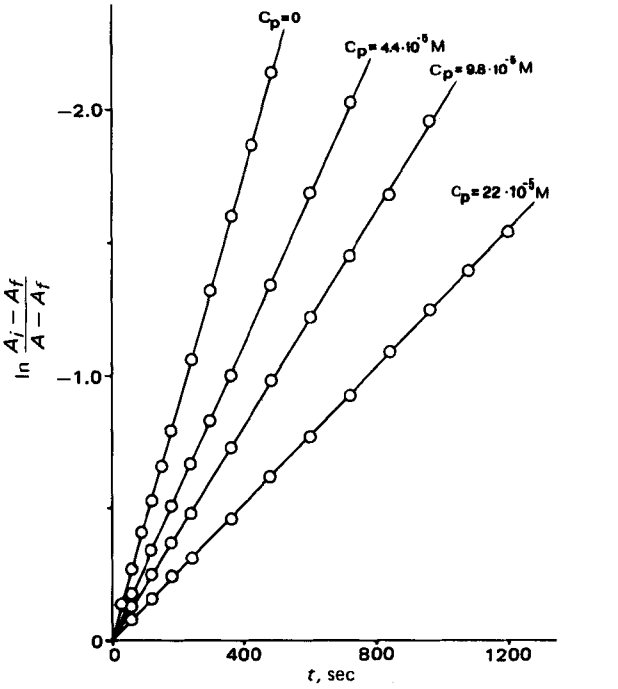


**Figure 3**—*Pseudo-first-order decomposition kinetics for 1-(*p*-chloro)-phenyl-3-methyltriazene at various human serum albumin concentrations at 37° and pH 7.40 (0.065 M potassium phosphate buffer);* $A_i$, $A_f$, *and* A *are the initial, final, and actual optical densities, respectively.*

**Table III—Kinetic Data of the Pseudo-First-Order Decomposition of Monomethyltriazenes in Buffered Aqueous Solution [a] in the Presence of Human Serum Albumin**

| Compound | $T$, °K | $C_P \times 10^4$, $M$ | pH | $k \times 10^3$, $sec^{-1}$ |
|---|---|---|---|---|
| I | 296.8 | 1.05 | 7.401 | 3.80 |
| | 302.9 | 1.05 | 7.388 | 5.73 |
| | 310.9 | 1.05 | 7.370 | 9.61 |
| | 317.7 | 1.05 | 7.356 | 13.4 |
| | 310.9 | 0.79 | 7.370 | 9.14 |
| | 310.9 | 1.59 | 7.370 | 8.29 |
| | 310.9 | 2.67 | 7.370 | 7.76 |
| II | 293.5 | 1.20 | 7.408 | 4.08 |
| | 302.7 | 1.20 | 7.388 | 7.20 |
| | 310.7 | 1.20 | 7.371 | 12.5 |
| | 310.2 | 0.70 | 7.372 | 13.3 |
| | 310.7 | 1.40 | 7.371 | 11.5 |
| | 311.2 | 2.80 | 7.370 | 8.47 |
| III | 299.7 | 0.98 | 7.395 | 3.14 |
| | 301.0 | 0.99 | 7.392 | 3.40 |
| | 305.6 | 0.98 | 7.382 | 5.01 |
| | 307.5 | 0.99 | 7.378 | 5.80 |
| | 311.1 | 0.98 | 7.370 | 6.83 |
| | 315.2 | 0.98 | 7.361 | 8.44 |
| | 310.3 | 0.49 | 7.372 | 7.26 |
| | 310.3 | 1.03 | 7.372 | 6.98 |
| | 310.3 | 2.05 | 7.372 | 5.50 |
| IV | 294.0 | 1.03 | 7.407 | 0.593 |
| | 303.0 | 1.03 | 7.387 | 1.20 |
| | 310.0 | 1.03 | 7.372 | 1.89 |
| | 318.0 | 1.03 | 7.355 | 3.43 |
| | 310.0 | 0.44 | 7.372 | 2.82 |
| | 310.0 | 0.98 | 7.372 | 2.03 |
| | 310.0 | 2.20 | 7.372 | 1.29 |
| V | 299.5 | 0.96 | 7.395 | 0.527 |
| | 303.4 | 1.15 | 7.387 | 0.854 |
| | 306.9 | 0.96 | 7.379 | 0.955 |
| | 310.2 | 1.10 | 7.372 | 1.47 |
| | 314.7 | 1.15 | 7.362 | 1.79 |
| | 310.2 | 0.55 | 7.372 | 1.90 |
| | 310.1 | 1.92 | 7.372 | 0.952 |
| | 310.2 | 2.20 | 7.372 | 0.982 |
| VI | 296.7 | 1.00 | 7.401 | 0.261 |
| | 302.7 | 1.00 | 7.388 | 0.424 |
| | 309.2 | 1.00 | 7.374 | 0.865 |
| | 313.9 | 1.00 | 7.364 | 1.22 |
| | 310.3 | 0.54 | 7.372 | 1.68 |
| | 310.3 | 1.08 | 7.372 | 0.960 |
| | 310.1 | 2.16 | 7.372 | 0.613 |
| VII | 294.0 | 0.89 | 7.407 | 0.468 |
| | 303.0 | 0.89 | 7.387 | 0.910 |
| | 318.0 | 0.89 | 7.355 | 2.52 |
| | 310.0 | 0.41 | 7.372 | 1.48 |
| | 310.0 | 1.50 | 7.372 | 1.41 |
| | 310.0 | 2.90 | 7.372 | 1.41 |
| VIII | 395.9 | 1.05 | 7.403 | 0.255 |
| | 303.7 | 1.05 | 7.386 | 0.532 |
| | 309.4 | 1.05 | 7.374 | 0.850 |
| | 316.0 | 1.05 | 7.359 | 1.49 |
| | 302.0 | 1.20 | 7.390 | 0.421 |
| | 318.0 | 1.20 | 7.355 | 1.21 |
| | 310.0 | 0.51 | 7.372 | 0.975 |
| | 310.0 | 1.20 | 7.372 | 0.844 |
| | 310.0 | 2.20 | 7.372 | 0.675 |
| | 310.0 | 4.00 | 7.372 | 0.505 |
| X | 294.0 | 0.97 | 7.407 | 0.091 |
| | 302.0 | 0.97 | 7.390 | 0.211 |
| | 318.0 | 0.97 | 7.355 | 1.77 |
| | 310.0 | 0.38 | 7.372 | 1.03 |
| | 310.0 | 0.86 | 7.372 | 0.831 |
| | 310.0 | 1.30 | 7.372 | 0.558 |
| | 310.0 | 2.40 | 7.372 | 0.425 |
| XI | 296.7 | 0.99 | 7.401 | 5.95 |
| | 297.9 | 1.00 | 7.399 | 5.42 |
| | 302.7 | 0.99 | 7.388 | 8.91 |
| | 307.4 | 1.00 | 7.378 | 11.5 |
| | 311.1 | 1.00 | 7.370 | 16.4 |
| | 316.8 | 1.00 | 7.358 | 23.4 |
| | 307.4 | 0.50 | 7.378 | 18.3 |
| XII | 310.0 | 1.20 | 7.372 | 5.32 |
| | 310.0 | 2.50 | 7.372 | 4.72 |

[a] Phosphate buffer, 0.065 $M$; ionic strength, 0.15 $M$.

not exceed 10% even in the less favorable case of the highest $K_B$ values ($\sim 2.10^4\ M^{-1}$), being slightly greater than the standard deviation due to random errors. This evaluation was done by choosing the values of $C_P$ and $C_T$ in the middle of their concentration range ($\sim 1.5 \times 10^{-4}$ and $2 \times 10^{-5}$ $M$, respectively).

A more rigorous treatment that avoids the approximation leading to Eq. 5 is given in the *Appendix*.

Following the previous assumptions, it is possible to state that:

$$v = -\frac{dC_T}{dt} = kC_F = kC_T/(1 + K_BC_P) \qquad \text{(Eq. 7)}$$

where $v$ is the decomposition rate. Therefore:

$$k' = k/(1 + K_BC_P) \qquad \text{(Eq. 8)}$$

and:

$$t'_{1/2} = t_{1/2}(1 + K_BC_P) \qquad \text{(Eq. 9)}$$

where $t'_{1/2}$ and $t_{1/2}$ are half-life times of the triazenes in the presence and absence of protein, respectively. Equations 8 and 9 are justified in the assumption that $C_P > C_T$.

For the triazenes considered, a plot of $t'_{1/2}/t_{1/2}$ *versus* $C_P$ gives a straight line with slope $K_B$ (Fig. 4). These $K_B$ values are reported in Table IV.

Another possible model, *i.e.*, a tight binding of the triazene onto the protein and the subsequent decomposition *in situ*, is ruled out since, in such a case, $k'$ would be independent of $C_P$ since $C_P$ is always greater than $C_T$ in the experiments.

The proposed theoretical scheme and the $K_B$ values deduced were confirmed by a series of independent kinetic measurements carried out for each triazene at constant $C_P$ and various temperatures between 20 and 45°.

Within the experimental accuracy (±3% approximately), the data also follow the Arrhenius equation in the presence of serum albumin, *i.e.*:

$$\ln k' = \ln A' - E'/RT \qquad \text{(Eq. 10)}$$

where the prime denotes the presence of albumin.

The activation parameters for all monomethyltriazenes studied are reported in Table II.

The introduction of the Arrhenius equation in Eq. 8 gives:

$$K_B = \frac{\frac{A}{A'}\exp\left(-\frac{E-E'}{RT}\right) - 1}{C_P} \qquad \text{(Eq. 11)}$$

Thus, Eq. 11 provides an independent way of obtaining $K_B$; the values so obtained are reported in Table IV. They are in agreement with those values determined from the measurements made as a function of $C_P$.

Moreover, from the temperature dependence of $K_B$, the binding enthalpies of the various triazene molecules onto the protein, $\Delta H_B$, can be estimated using the derivation of Eq. 11:

$$\Delta H_B = -\frac{\partial R \ln K_B}{\partial\left(\frac{1}{T}\right)} = \frac{(E-E')\frac{A}{A'}\exp\left(-\frac{E-E'}{RT}\right)}{\frac{A}{A'}\exp\left(-\frac{E-E'}{RT}\right) - 1}$$

$$= (E-E')\left(1 + \frac{1}{K_BC_P}\right) \qquad \text{(Eq. 12)}$$

Thus, by using $K_B$, the free energy of binding, $\Delta G_B$($\Delta G_B = -RT \ln K_B$), and $\Delta H_B$ values, the variation of binding entropy for the various triazenes can be obtained. Thermodynamic data are reported in Table IV. By inspection of these data, it can be seen that most of the triazenes considered interact with human serum albumin, mainly by an enthalpy-driven process, the entropic contribution to the $\Delta G_B$ values generally being quite low. This effect is more pronounced in VII and VIII, for which a larger enthalpy loss is paralleled by a strikingly larger entropy loss. Different behavior characterizes the trichloro-substituted compound, which completely reverses the signs of $\Delta H_B$ and $\Delta S_B$ and reveals a mainly entropy-driven binding to albumin, possibly related to a large desolvation of the triazene molecule in this process.

The smallest $K_B$ values are shown by triazenes VII and XII, the only compounds characterized by the presence of an amido group. Within the corresponding series of dimethyltriazenes, those carrying the carboxamide function are among the most active against experimental rodent tumors (4).

Kinetic measurements also were performed at constant temperature and in the presence of bovine and murine serum albumins. Although for the latter the quality of the measurements was limited by the low degree of purity of the available sample, in both cases the kinetics of reaction

**Table IV—Thermodynamic Data of Binding of Monomethyltriazenes by Human Serum Albumin at 37° in Phosphate Buffer (pH 7.40, Ionic Strength 0.15 $M$) [a]**

| Compound | $K_B \times 10^{-3}$, $M^{-1}$ | | $-\Delta G_B$, kJ × mole$^{-1}$ | | $-\Delta H_B$, kJ × mole$^{-1}$ | $\Delta S_B$, J × mole$^{-1}$ × °K$^{-1}$ |
|---|---|---|---|---|---|---|
| | Measurement 1[b] | Measurement 2[c] | Measurement 1[b] | Measurement 2[c] | | |
| I | 1.86 ± 0.13 | 2.2 ± 0.3 | 19.4 ± 0.2 | 19.9 ± 0.4 | 42 ± 7 | −70 ± 20 |
| II | 5.07 ± 0.06 | 4.9 ± 0.3 | 22.0 ± 0.1 | 21.9 ± 0.2 | 24 ± 5 | −10 ± 20 |
| III | 1.94 ± 0.18 | 2.6 ± 0.3 | 19.5 ± 0.2 | 20.3 ± 0.3 | 8 ± 15 | 40 ± 50 |
| IV | 10.8 ± 0.2 | 11.1 ± 0.2 | 24.0 ± 0.1 | 24.0 ± 0.1 | 20 ± 2 | 10 ± 10 |
| V | 13.3 ± 0.5 | 15.4 ± 0.5 | 24.5 ± 0.1 | 24.9 ± 0.1 | 22 ± 8 | 10 ± 20 |
| VI | 22.4 ± 0.9 | 30.7 ± 1.1 | 25.8 ± 0.1 | 26.6 ± 0.1 | 38 ± 4 | −40 ± 10 |
| VII | 0.34 ± 0.05 | 0.3 ± 0.1 | 15.0 ± 0.4 | 14.7 ± 0.9 | 65 ± 20 | −160 ± 60 |
| VIII | 2.84 ± 0.05 | 2.6 ± 0.2 | 20.5 ± 0.1 | 20.3 ± 0.2 | 62 ± 4 | −130 ± 10 |
| X | 13.4 ± 0.5 | 14.4 ± 1.1 | 24.5 ± 0.1 | 24.7 ± 0.2 | 25 ± 9 | 0 ± 30 |
| XI | 21.7 ± 0.4 | 22.1 ± 0.5 | 25.8 ± 0.1 | 25.8 ± 0.1 | −34 ± 4 | 190 ± 10 |
| XII | 0.70 ± 0.07 | — | 16.9 ± 0.3 | — | — | — |

[a] Average ± $SD$. [b] From kinetic measurements at 310 °K and various albumin concentration values. [c] From kinetic measurements at constant albumin concentration and various temperatures.

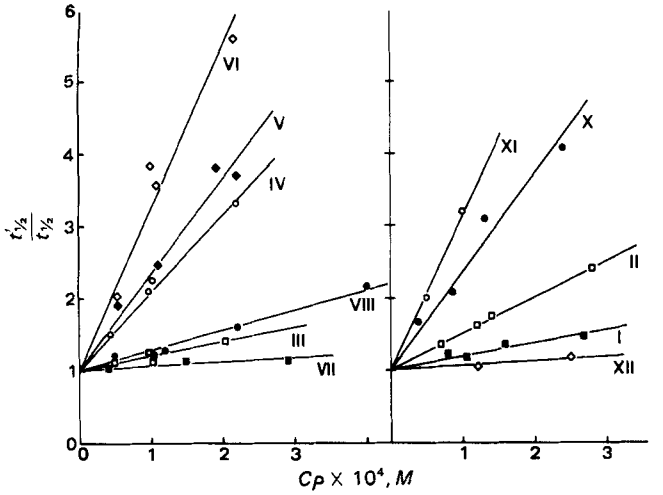


**Figure 4**—*Half-life times ratios, $t'_{1/2}/t_{1/2}$ (where the prime denotes the presence of human serum albumin) as a function of the protein concentration for the triazenes studied. The values refer to 37° and pH 7.40 (0.065 M potassium phosphate buffer).*

clearly remained pseudo-first order and the magnitude of the $K_B$ values was markedly similar to that obtained with human serum albumin. The kinetic and binding parameters are reported in Table V.

However, some kinetic experiments carried out in the presence of egg albumin showed no appreciable effect of this protein on the decomposition rates of the triazenes. This result, obtained in the presence of a protein similar to the serum albumins in some physicochemical properties and in amino acid composition but different in its biological role, confirms that the effect of the serum albumins on the decomposition rates of the triazenes is due to their specific binding abilities.

This protein binding can greatly influence the triazene half-life times in comparison with the values obtained in protein-free solutions. This interaction has to be taken into account in the attempt to correlate kinetic data *in vitro* with biological activities *in vivo*, although the extent of this interaction cannot be predicted easily on the basis of structural or physicochemical parameters.

A preliminary attempt to check, at least qualitatively, the influence of other serum components on the decomposition reactions and binding was performed using whole horse serum. The serum was diluted with phosphate buffer to reach a serum albumin concentration comparable with concentrations used in the previous experiments. The reaction still was pseudo-first order, and the half-lives were definitely close to those obtained in the presence of pure serum albumin (Table V). This result seems to indicate that the major part of the observed effect of the serum components on the triazene decomposition rates is to be attributed to the albumin fraction.

## APPENDIX

Exact solution of Eq. 4 for $C_F$, avoiding the simplifying condition $C_B \ll C_P$, leads to:

$$C_F = \tfrac{1}{2}\left[C_T - C_P - \frac{1}{K_B} + \sqrt{\left(C_P - C_T + \frac{1}{K_B}\right)^2 + \frac{4C_T}{K_B}}\right] \quad \text{(Eq. A1)}$$

The kinetic equation:

$$\frac{dC_T}{C_F} = \frac{dC_T}{\tfrac{1}{2}\left[C_T - C_P - \frac{1}{K_B} + \sqrt{\left(C_P - C_T + \frac{1}{K_B}\right)^2 + \frac{4C_T}{K_B}}\right]} = -k\,dt \quad \text{(Eq. A2)}$$

has to be integrated (from initial conditions: $C_T = C_{T,0}$ at $t = 0$).

This goal can be achieved considering that:

$$\frac{dC_T}{C_F} = \frac{dC_T}{dC_F}\frac{dC_F}{C_F} \quad \text{(Eq. A3)}$$

where:

$$\frac{dC_T}{dC_F} = \frac{C_F^2 + \frac{2C_F}{K_B} + \frac{1}{K_B}\left(C_P + \frac{1}{K_B}\right)}{\left(C_F + \frac{1}{K_B}\right)^2} \quad \text{(Eq. A4)}$$

so that:

$$\int_{C_{T,0}}^{C_T}\frac{dC_T}{C_F} = \int_{C_{F,0}}^{C_F}\left[\frac{C_F + \frac{2}{K_B} + \frac{1}{K_B C_F}\left(C_P + \frac{1}{K_B}\right)}{\left(C_F + \frac{1}{K_B}\right)^2}\right]dC_F = -k\int_0^t dt \quad \text{(Eq. A5)}$$

**Table V—Kinetic and Thermodynamic Data of the Decomposition of Monomethyltriazenes in Buffered Aqueous Solution in the Presence of Different Serum Albumins (0.065 $M$ Potassium Phosphate Buffer, pH 7.40, and 37°)**

| Compound | Protein-Free Solution, $t_{1/2}$, sec | Human Serum Albumin | | Bovine Serum Albumin | | Murine Serum Albumin | | Horse Serum, $t_{1/2}$, sec[c] |
|---|---|---|---|---|---|---|---|---|
| | | $t_{1/2}$, sec[a] | $K_B \times 10^{-3}$, $M^{-1}$ | $t_{1/2}$, sec[a] | $K_B \times 10^{-3}$, $M^{-1}$ | $t_{1/2}$, sec[b] | $K_B \times 10^{-3}$, $M^{-1}$ | |
| II | 39 | 70 | 5 | 85 | 8 | 85 | 8 | 100 |
| IV | 175 | 460 | 11 | 540 | 14 | 520 | 13 | 700 |
| VII | 485 | 510 | 0.3 | 500 | 0.2 | 490 | 0.1 | 700 |
| X | 439 | 1320 | 13 | 850 | 6 | 1050 | 10 | 1000 |
| XII | 122 | 135 | 0.7 | 145 | 1 | 120 | 0 | 130 |

[a] Values linearly interpolated at albumin concentration $1.5 \times 10^{-4}$ $M$. [b] Experimental values at protein concentration $1.5 \times 10^{-4}$ $M$. [c] Experimental values in whole horse serum diluted 1:4 with phosphate buffer.

Finally, the integrated function $F(C_F)$ results:

$$F(C_F) \equiv K_B C_P \left[\frac{1}{1 + K_B C_F} - \ln\left(C_F + \frac{1}{K_B}\right)\right] + (1 + K_B C_P) \ln C_F = F(C_{F,0}) - kt \quad \text{(Eq. A6)}$$

being obviously $C_F$ expressed as a function of $C_P$ by Eq. A1.

This formal treatment may easily be extended to the case of $n$ identical and independent binding sites present on the protein, simply by substituting $C_P$ by $nC_P$ in these expressions.

The mathematical treatment would be more complicated if nonidentical and possibly cooperative sites were present. Owing to the good agreement between experimental data and the described model, this last case was not considered.

In principle, Eq. A6 implies that the kinetic law for the decomposition of triazenes in the presence of albumin is not first order with respect to triazene concentration. It is easy to realize, by numerical substitution, that the deviation from first-order kinetics is almost negligible in the present case.

For several triazenes, it has been possible to plot the experimental data obtained for each triazene at constant temperature and various $C_P$ values in the form of the general function $F(C_F)$ *versus* $t$ (Eq. A6). All slopes at various $C_P$ values were matched successfully with the value for the kinetic constant, $k$, in the absence of protein by choosing the same $K_B$ value for each triazene. The same data, plotted according to the simplified form of Eq. 9, provided $K_B$ values in good agreement with those obtained by the more rigorous treatment.

## REFERENCES


(1) R. C. S. Audette, T. A. Connors, H. G. Mandel, K. Merai, and W. C. J. Ross, *Biochem. Pharmacol.*, **22,** 1855 (1973).

(2) T. A. Connors, P. M. Goddard, K. Merai, W. C. J. Ross, and D. E. V. Wilman, *ibid.*, **25,** 241 (1976).

(3) S. K. Carter, *Cancer Treat. Rep.*, **60,** 123 (1976).

(4) T. Giraldi, C. Nisi, T. A. Connors, and P. M. Goddard, *J. Med. Chem.*, **20,** 850 (1977).

(5) H. Druckrey, *Xenobiotica*, **3,** 271 (1973).

(6) R. Preussmann, S. Ivankovic, C. Landschütz, J. Gimmy, E. Flohr, and U. Griesbach, *Z. Krebsforsch.*, **81,** 285 (1974).

(7) S. Ivankovic, R. Port, and R. Preussmann, *ibid.*, **86,** 307 (1976).

(8) G. F. Kolar, R. Fahrig, and E. Vogel, *Chem.-Biol. Interact.*, **9,** 365 (1974).

(9) C. Malaveille, G. F. Kolar, and H. Bartsch, *Mutat. Res.*, **36,** 1 (1976).

(10) B. H. Venger, C. Hansch, G. J. Hatheway, and Y. U. Amrein, *J. Med. Chem.*, **22,** 473 (1979).

(11) D. L. Hill, *Cancer Res.*, **35,** 3106 (1975).

(12) P. Kleihaus, G. F. Kolar, and G. P. Margison, *ibid.*, **36,** 2189 (1976).

(13) K. Vaughan and M. F. G. Stevens, *Q. Rev.*, **7,** 377 (1978).

(14) V. Zvěřina, M. Remeš, J. Diviš, J. Marhold, and M. Matrka, *Collect. Czech. Chem. Commun.*, **38,** 251 (1973).

(15) N. S. Isaacs and E. Rannala, *J. Chem. Soc. Perkin II*, **1974,** 902.

(16) *Ibid.*, **1974,** 899.

(17) C. Süling, "Methoden der Organischen Chemie," vol. 10/3, G. Thieme, Stuttgart, West Germany, 1965, pp. 700, 701.

(18) E. H. White, A. A. Baum, and D. E. Eitel, "Organic Syntheses," coll. vol. 5, Wiley, New York, N.Y., 1973, pp. 797–800.

(19) M. Remeš, J. Diviš, V. Zvěřina, J. Marhold, and M. Matrka, *Cesk. Farm.*, **21,** 442 (1972).

(20) T. P. Ahern and K. Vaughan, *J. Chem. Soc., Chem. Commun.*, **1973,** 701.

(21) Y. F. Shealy and C. A. Krauth, *J. Med. Chem.*, **9,** 34 (1966).

(22) C. F. Chignell, *Mol. Pharmacol.*, **6,** 1 (1970).

(23) C. Hansch, A. Leo, S. H. Unger, K. H. Kim, D. Nikaitani, and E. J. Lien, *J. Med. Chem.*, **16,** 1207 (1973).

(24) C. D. Ritchie and W. F. Sager, *Progr. Phys. Org. Chem.*, **2,** 323 (1964).


## ACKNOWLEDGMENTS


Supported by the Consiglio Nazionale delle Ricerche, Rome, Italy.

The authors thank Dr. T. Giraldi for advice and suggestions and Mrs. G. Fabris for editorial assistance.


# Extreme Vertexes Design in Formulation Development: Solubility of Butoconazole Nitrate in a Multicomponent System


**SHABBIR T. ANIK ˣ and LAKSHMI SUKUMAR**



Received August 22, 1980, from the *Institute of Pharmaceutical Sciences, Syntex Research, Palo Alto, CA 94304.* Accepted for publication January 7, 1981.



**Abstract** □ The extreme vertexes design was shown to be an efficient method for the study of mixture problems, for generating points in the factor space that define a region for response surface analysis. By using this method, the solubility of butoconazole nitrate, an imidazole antifungal agent, was studied as a function of four components, polyethylene glycol 400, glycerin, polysorbate 60, and water, whose levels were subject to given constraints. A fifth component, poloxamer 407, was held constant. The design was used to generate 14 points in the region defined by the constraints. The $G$ efficiency of the design, with the assumption of a quadratic model for the response surface, was 79%. By using the solubilities determined at the 14 points and regression analysis, an equation was generated to characterize the response surface. Contour plots of the response surface illustrate the relationship of the solubility as a function of the components, and solubilities calculated at other points (in the region) agree well with the observed data.



**Keyphrases** □ Extreme vertexes design—formulation development, butoconazole nitrate solubility in a multicomponent system □ Formulation development—extreme vertexes design, butoconazole nitrate solubility in a multicomponent system □ Butoconazole nitrate—solubility, extreme vertexes design in formulation development □ Multicomponent systems—extreme vertexes design in formulation development, butoconazole nitrate solubility


A pharmaceutical formulation generally consists of a mixture of several components, whose levels may often be constrained by factors other than those directly determining its physical properties, such as irritation and cost. In developing this formulation, the component levels must be varied within these constraints to arrive at an optimum formulation with respect to several responses such as solubility, stability, and bioavailability. The conventional



© 1981, American Pharmaceutical Association

Finally, the integrated function $F(C_F)$ results:

$$F(C_F) \equiv K_B C_P \left[\frac{1}{1 + K_B C_F} - \ln\left(C_F + \frac{1}{K_B}\right)\right] + (1 + K_B C_P) \ln C_F = F(C_{F,0}) - kt \quad \text{(Eq. A6)}$$

being obviously $C_F$ expressed as a function of $C_P$ by Eq. A1.

This formal treatment may easily be extended to the case of $n$ identical and independent binding sites present on the protein, simply by substituting $C_P$ by $nC_P$ in these expressions.

The mathematical treatment would be more complicated if nonidentical and possibly cooperative sites were present. Owing to the good agreement between experimental data and the described model, this last case was not considered.

In principle, Eq. A6 implies that the kinetic law for the decomposition of triazenes in the presence of albumin is not first order with respect to triazene concentration. It is easy to realize, by numerical substitution, that the deviation from first-order kinetics is almost negligible in the present case.

For several triazenes, it has been possible to plot the experimental data obtained for each triazene at constant temperature and various $C_P$ values in the form of the general function $F(C_F)$ *versus* $t$ (Eq. A6). All slopes at various $C_P$ values were matched successfully with the value for the kinetic constant, $k$, in the absence of protein by choosing the same $K_B$ value for each triazene. The same data, plotted according to the simplified form of Eq. 9, provided $K_B$ values in good agreement with those obtained by the more rigorous treatment.

## REFERENCES


(1) R. C. S. Audette, T. A. Connors, H. G. Mandel, K. Merai, and W. C. J. Ross, *Biochem. Pharmacol.*, **22,** 1855 (1973).

(2) T. A. Connors, P. M. Goddard, K. Merai, W. C. J. Ross, and D. E. V. Wilman, *ibid.*, **25,** 241 (1976).

(3) S. K. Carter, *Cancer Treat. Rep.*, **60,** 123 (1976).

(4) T. Giraldi, C. Nisi, T. A. Connors, and P. M. Goddard, *J. Med. Chem.*, **20,** 850 (1977).

(5) H. Druckrey, *Xenobiotica*, **3,** 271 (1973).

(6) R. Preussmann, S. Ivankovic, C. Landschütz, J. Gimmy, E. Flohr, and U. Griesbach, *Z. Krebsforsch.*, **81,** 285 (1974).

(7) S. Ivankovic, R. Port, and R. Preussmann, *ibid.*, **86,** 307 (1976).

(8) G. F. Kolar, R. Fahrig, and E. Vogel, *Chem.-Biol. Interact.*, **9,** 365 (1974).

(9) C. Malaveille, G. F. Kolar, and H. Bartsch, *Mutat. Res.*, **36,** 1 (1976).

(10) B. H. Venger, C. Hansch, G. J. Hatheway, and Y. U. Amrein, *J. Med. Chem.*, **22,** 473 (1979).

(11) D. L. Hill, *Cancer Res.*, **35,** 3106 (1975).

(12) P. Kleihaus, G. F. Kolar, and G. P. Margison, *ibid.*, **36,** 2189 (1976).

(13) K. Vaughan and M. F. G. Stevens, *Q. Rev.*, **7,** 377 (1978).

(14) V. Zvěřina, M. Remeš, J. Diviš, J. Marhold, and M. Matrka, *Collect. Czech. Chem. Commun.*, **38,** 251 (1973).

(15) N. S. Isaacs and E. Rannala, *J. Chem. Soc. Perkin II*, **1974,** 902.

(16) *Ibid.*, **1974,** 899.

(17) C. Süling, "Methoden der Organischen Chemie," vol. 10/3, G. Thieme, Stuttgart, West Germany, 1965, pp. 700, 701.

(18) E. H. White, A. A. Baum, and D. E. Eitel, "Organic Syntheses," coll. vol. 5, Wiley, New York, N.Y., 1973, pp. 797–800.

(19) M. Remeš, J. Diviš, V. Zvěřina, J. Marhold, and M. Matrka, *Cesk. Farm.*, **21,** 442 (1972).

(20) T. P. Ahern and K. Vaughan, *J. Chem. Soc., Chem. Commun.*, **1973,** 701.

(21) Y. F. Shealy and C. A. Krauth, *J. Med. Chem.*, **9,** 34 (1966).

(22) C. F. Chignell, *Mol. Pharmacol.*, **6,** 1 (1970).

(23) C. Hansch, A. Leo, S. H. Unger, K. H. Kim, D. Nikaitani, and E. J. Lien, *J. Med. Chem.*, **16,** 1207 (1973).

(24) C. D. Ritchie and W. F. Sager, *Progr. Phys. Org. Chem.*, **2,** 323 (1964).


## ACKNOWLEDGMENTS


Supported by the Consiglio Nazionale delle Ricerche, Rome, Italy.

The authors thank Dr. T. Giraldi for advice and suggestions and Mrs. G. Fabris for editorial assistance.


# Extreme Vertexes Design in Formulation Development: Solubility of Butoconazole Nitrate in a Multicomponent System


**SHABBIR T. ANIK ˣ and LAKSHMI SUKUMAR**



Received August 22, 1980, from the *Institute of Pharmaceutical Sciences, Syntex Research, Palo Alto, CA 94304.* Accepted for publication January 7, 1981.



**Abstract** □ The extreme vertexes design was shown to be an efficient method for the study of mixture problems, for generating points in the factor space that define a region for response surface analysis. By using this method, the solubility of butoconazole nitrate, an imidazole antifungal agent, was studied as a function of four components, polyethylene glycol 400, glycerin, polysorbate 60, and water, whose levels were subject to given constraints. A fifth component, poloxamer 407, was held constant. The design was used to generate 14 points in the region defined by the constraints. The $G$ efficiency of the design, with the assumption of a quadratic model for the response surface, was 79%. By using the solubilities determined at the 14 points and regression analysis, an equation was generated to characterize the response surface. Contour plots of the response surface illustrate the relationship of the solubility as a function of the components, and solubilities calculated at other points (in the region) agree well with the observed data.



**Keyphrases** □ Extreme vertexes design—formulation development, butoconazole nitrate solubility in a multicomponent system □ Formulation development—extreme vertexes design, butoconazole nitrate solubility in a multicomponent system □ Butoconazole nitrate—solubility, extreme vertexes design in formulation development □ Multicomponent systems—extreme vertexes design in formulation development, butoconazole nitrate solubility


A pharmaceutical formulation generally consists of a mixture of several components, whose levels may often be constrained by factors other than those directly determining its physical properties, such as irritation and cost. In developing this formulation, the component levels must be varied within these constraints to arrive at an optimum formulation with respect to several responses such as solubility, stability, and bioavailability. The conventional



© 1981, American Pharmaceutical Association

approach is to vary one variable at a time until a satisfactory formulation is developed, which may or may not be the optimum. This process could conceivably involve numerous experiments. Therefore, methods are needed for choosing and determining the adequacy of various groups of possible experimental points.

In this regard, the use of factorial designs has been well established (1). However, classical factorial designs are not suitable for problems involving mixtures because of the constraint $\Sigma X_i = 1$, where $X_i$ is the level of the $i$th component; *i.e.*, the level of one component is fixed by the levels of the others. Furthermore, the classical factorial approach can result in large numbers of experimental points necessary to complete the design. To overcome these problems, McLean and Anderson (2) proposed the extreme vertexes design for mixture problems with upper and lower bounds. The advantages and disadvantages of this method were discussed and compared with other methods of experimental design (3–6).

The objective of this study was to demonstrate the utility of this design in pharmaceutical formulation development. The method is illustrated here by a solubility study of butoconazole nitrate, an antifungal agent, in a multicomponent system.

## THEORETICAL

The general procedure involves constructing, in $n$-dimensional component space, the hyperpolyhedron that defines the region of all possible formulations. This construction and the shape of the region are based on the constraints put on the various formulation components. The extreme vertexes are then just the collection of the vertexes of this hyperpolyhedron. To them are added the face centroids, the overall centroid, and, if necessary, the edge centroids (midpoints of the edges, generally included only for the longer edges).

When developing an experimental design, one generally has a particular model, such as linear, quadratic, or cubic, to be used for the response surface. Given a particular model, a reasonable subset of the derived set of possible formulations must be selected on which to do experimental work. If the full set is small enough, all points can be taken; but when the number of initial points is large, a method is necessary for the rational selection of an experimentally manageable subset of points. Several methods and parameters have been proposed to evaluate the quality and size of the design for a given model. Details of hyperpolyhedron generation, subset selection, and subset evaluation were reported previously (2, 4). The procedure used in this study to determine the design points is as follows.

Table I lists the components, their ranges, and all possible vertexes generated using the method in Ref. 2. Although there are five components, one component, poloxamer 407, was fixed at 0.1 (10%). Therefore, the problem is one of four variables whose sum equals 0.9. From the 32 vertexes generated, there are 10 allowable vertexes where the levels of the components fall within the specified ranges. Normalized distances (2) were calculated between adjacent vertexes of the hyperpolyhedron defined by these 10 allowable vertexes using Eq. 1 (Table II). The normalized distance between the $i$th and $j$th points, $d_{ij}$, is given by:

$$d_{ij} = \sum_{m=1}^{q} [(x_{im} - x_{jm})^2/(b_m - a_m)^2]^{1/2} \qquad \text{(Eq. 1)}$$

where $\mathbf{x}_i$ and $\mathbf{x}_j$ are the $q$-dimensional vectors defining the two points, $b_m$ and $a_m$ are the upper and lower bounds of the $m$th component, and $q$ is the number of variables (in this case four). Since points 3 and 29, 4 and 31, 5 and 13, and 6 and 15 are close to each other relative to the other points, they were replaced by their averages to give six extreme vertexes, which define the region in space shown in Fig. 1. This six-point design was then augmented by addition of centroids, using the method for

**Table I—All Possible Vertexes for the Given Four-Variable System [a]**

| Vertex | Component and Range: Polyethylene Glycol 400 (0.1–0.4) | Glycerin (0.1–0.4) | Polysorbate 60 (0–0.08) | Water (0.3–0.7) |
|---|---|---|---|---|
| 1[b] | 0.1 | 0.1 | 0 | 0.7 |
| 2[b] | 0.1 | 0.1 | 0.08 | 0.62 |
| 3[b] | 0.1 | 0.4 | 0 | 0.4 |
| 4[b] | 0.1 | 0.4 | 0.08 | 0.32 |
| 5[b] | 0.4 | 0.1 | 0 | 0.4 |
| 6[b] | 0.4 | 0.1 | 0.08 | 0.32 |
| 7 | 0.4 | 0.4 | 0 | 0.1 |
| 8 | 0.4 | 0.4 | 0.8 | 0.02 |
| 9 | 0.1 | 0.5 | 0 | 0.3 |
| 10[c] | 0.1 | 0.1 | 0 | 0.7 |
| 11 | 0.1 | 0.42 | 0.08 | 0.3 |
| 12 | 0.1 | 0.02 | 0.08 | 0.7 |
| 13[b] | 0.4 | 0.2 | 0 | 0.3 |
| 14 | 0.4 | — [d] | 0 | 0.7 |
| 15[b] | 0.4 | 0.12 | 0.08 | 0.3 |
| 16 | 0.4 | — [d] | 0.08 | 0.7 |
| 17 | 0.1 | 0.1 | 0.4 | 0.3 |
| 18[c] | 0.1 | 0.1 | 0 | 0.7 |
| 19 | 0.1 | 0.4 | 0.1 | 0.3 |
| 20 | 0.1 | 0.4 | — [d] | 0.7 |
| 21 | 0.4 | 0.1 | 0.1 | 0.3 |
| 22 | 0.4 | 0.1 | — [d] | 0.7 |
| 23 | 0.4 | 0.4 | — [d] | 0.3 |
| 24 | 0.4 | 0.4 | — [d] | 0.7 |
| 25 | 0.5 | 0.1 | 0 | 0.3 |
| 26[c] | 0.1 | 0.1 | 0 | 0.7 |
| 27 | 0.42 | 0.1 | 0.08 | 0.3 |
| 28 | 0.02 | 0.1 | 0.08 | 0.7 |
| 29[b] | 0.2 | 0.4 | 0 | 0.3 |
| 30 | — [d] | 0.4 | 0 | 0.7 |
| 31[b] | 0.12 | 0.4 | 0.08 | 0.3 |
| 32 | — [d] | 0.4 | 0.08 | 0.7 |

[a] All values are fractions of the mixture. Poloxamer 407 was fixed at 0.1. [b] Allowable vertexes. [c] Repeat points. [d] Values could not be calculated as sum of other components >1.

**Table II—Normalized Distances between Adjacent Extreme Vertexes**

| Vertex Pair[a] | Distance |
|---|---|
| 1, 2 | 1.02 |
| 1, 3 | 1.25 |
| 1, 5 | 1.25 |
| 2, 4 | 1.25 |
| 2, 6 | 1.25 |
| 3, 4 | 1.02 |
| 3, 29 | 0.42 |
| 4, 31 | 0.08 |
| 5, 6 | 1.02 |
| 5, 13 | 0.42 |
| 6, 15 | 0.08 |
| 13, 15 | 1.03 |
| 13, 29 | 0.94 |
| 15, 31 | 1.32 |
| 29, 31 | 1.03 |

[a] Numbers correspond to points in Table I.

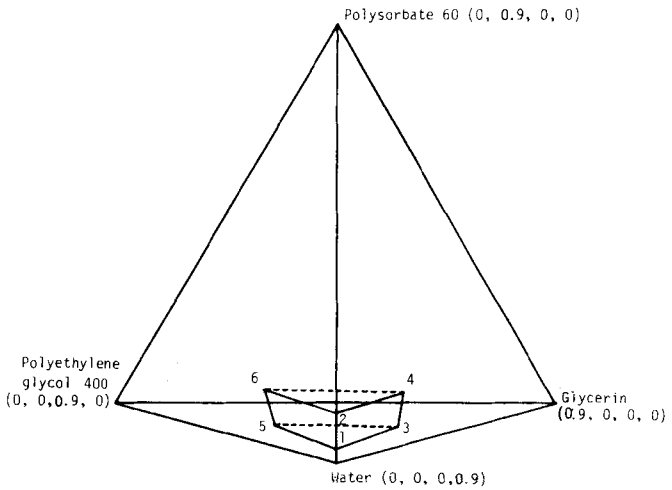


**Figure 1**—*Region defined by the extreme vertexes.*

**Table III—Final Design Used for Solubility Determinations and Their Respective Solubilities [a]**

| Number | Polyethylene Glycol 400 | Glycerin | Polysorbate 60 | Water | Solubility, mg/ml |
|---|---|---|---|---|---|
| Vertexes | | | | | |
| 1 | 0.1 | 0.1 | 0 | 0.7 | 3.0 |
| 2 | 0.1 | 0.1 | 0.08 | 0.62 | 7.3 |
| 3 | 0.15 | 0.4 | 0 | 0.35 | 4.9 |
| 4 | 0.11 | 0.4 | 0.08 | 0.31 | 8.4 |
| 5 | 0.4 | 0.15 | 0 | 0.35 | 8.6 |
| 6 | 0.4 | 0.11 | 0.08 | 0.31 | 12.7 |
| Centroids | | | | | |
| 7 | 0.1 | 0.1 | 0.04 | 0.66 | 5.1 |
| 8 | 0.4 | 0.13 | 0.04 | 0.33 | 10.8 |
| 9 | 0.13 | 0.4 | 0.04 | 0.33 | 6.6 |
| 10 | 0.216 | 0.216 | 0 | 0.468 | 4.4 |
| 11 | 0.203 | 0.203 | 0.08 | 0.414 | 7.9 |
| 12 | 0.255 | 0.255 | 0.08 | 0.31 | 9.4 |
| 13 | 0.275 | 0.275 | 0 | 0.35 | 5.8 |
| Overall centroid | | | | | |
| 14 | 0.21 | 0.21 | 0.04 | 0.44 | 6.3 |

[a] All values for the components are in fractions. Poloxamer 407 was fixed at 0.1.

centroids as in Ref. 2. Two face centroids, five edge centroids, and the overall centroid were calculated and added to the vertexes obtained above to result in the 14-point design shown in Table III.

For mixture experiments, the quadratic model (Eq. 2) is the most adequate for modeling the response surface (3). The response $Y$, in this case the solubility, is given by:

$$Y = \beta_0 + \sum_i \beta_i X_i + \sum_{1 \le i < j} \beta_{ij} X_i X_j \qquad \text{(Eq. 2)}$$

where $\beta$ is the fitted coefficient for each term and the $X$'s are the formulation component variables. (The quadratic model for mixture does not contain any squared terms due to the constraint $\Sigma X_i = 1$. In this case, a constant term is included since one component, poloxamer 407, is held constant.)

For a given model for characterizing the response surface, one can determine the quality or efficiency of the experimental design. One such criterion is the $G$ or global efficiency (4), which is defined by:

$$\%G = \frac{100p}{nv} \qquad \text{(Eq. 3)}$$

where $p$ is the number of parameters in the model, $n$ is the number of points in the design, and $v$ is $\max[\mathbf{x}(\mathbf{X}'\mathbf{X})^{-1}\mathbf{x}']$. The $\mathbf{x}$ is the $p$-dimensional vector of the model $\mathbf{Y} = \beta\mathbf{x}$ (*e.g.*, for the quadratic model discussed, $\mathbf{x}$ has the elements 1, $X_i$, $X_iX_j$); $\mathbf{X}$ is the $nxp$ matrix of the $\mathbf{x}$'s. For the quadratic model ($p = 11$ here since one component is constant), the values of $v$ and the $G$ efficiency of the 14-point design described are 0.989 and 79%, respectively. High efficiencies are generally not practical, and an efficiency of 50% or greater is ordinarily acceptable (4). Therefore, this design was used to generate the solubility data and response surface.

## EXPERIMENTAL

**Materials**—Polyethylene glycol 400[1] (I), glycerin[2] (II), polysorbate 60[2] (III), and poloxamer 407[3] (IV) were used as received.

**Solubility Determinations**—The drug was equilibrated in the respective solution for up to 7 days. At least two time points were taken for the solubility determinations. The solutions were filtered or centrifuged, and an aliquot of the filtrate or supernate was suitably diluted with methanol and assayed spectrophotometrically.

## RESULTS AND DISCUSSION

The results of the solubility measurements for the different solutions are given in Table III. The solubilities varied from 3 to 12.7 mg/ml and formed an acceptable range for response surface analysis. By using regression analysis[4], the data were fitted to the quadratic model defined by Eq. 2; Table IV gives the equation and regression parameters for the solubility equation:

**Table IV—Regression Parameters for the Solubility Equation [a]**

| Variable | Regression Coefficient | Standard Error | Probability >F |
|---|---|---|---|
| Intercept | 7.66 | | |
| I | 41.1 | 2.3 | 0.0001 |
| III | 30.6 | 6.1 | 0.0015 |
| Water | −4.2 | 1.2 | 0.0088 |
| (I) (II) | −59.9 | 4.8 | 0.0001 |
| (I) (III) | −39.3 | 11.7 | 0.0121 |
| (I) (water) | −74.2 | 6.5 | 0.0001 |
| (III) (water) | 23.3 | 9.4 | 0.0427 |

[a] I is polyethylene glycol 400, II is glycerin, and III is polysorbate 60 ($r^2 = 0.998$, $SE = 0.12$, $n = 14$).

$$\text{solubility} = 7.66 + 41.1\,(\text{I}) + 30.6\,(\text{III}) - 4.2\,(\text{water}) - 59.9\,(\text{I})(\text{II}) - 39.3\,(\text{I})(\text{III}) - 74.2\,(\text{I})(\text{water}) + 23.3\,(\text{III})(\text{water}) \qquad \text{(Eq. 4)}$$

This eight-parameter model gives the best fit to the data with all coefficients significant at the 95% confidence level. As might be expected, both polyethylene glycol 400 and polysorbate 60 have strong linear effects, which also were observed in solubility measurements with independent components. Several two-factor nonlinear terms show synergistic or antagonistic relationships between the different components and the solubility; however, a mechanistic interpretation of these terms must be done with caution since some coefficients are cross-correlated with the linear terms.

The equation, however, can be used for two purposes: (*a*) to calculate solubilities for any combination of components within the defined region, and (*b*) to generate contour plots of the response surface for delineating the behavior of the system within the region. Figure 2 shows a plot of calculated *versus* observed solubilities for some points within the region. The agreement is excellent over the entire solubility range; therefore, the equation may be used for calculating solubilities in any formulation of interest, which is of considerable value in development work.

Contour plots are useful for observing trends within the system, and they also provide a choice of alternative formulations for a given value of the response. Since this is a four-variable system, the effect of all four variables cannot be simultaneously represented. Hence, contour plots were made at the point of maximum solubility within the region, holding one component constant. The maximum solubility of 12.8 mg/ml is at polyethylene glycol 400 = 0.4, glycerin = 0.12, polysorbate 60 = 0.08, and water = 0.3, which is one vertex of the region. Figure 3 shows one such contour plot holding polysorbate 60 at 0.08. The equation below the figure describes the contours and is generated from the original equation by substituting polysorbate 60 = 0.08. The triangle in the center is the region of interest.

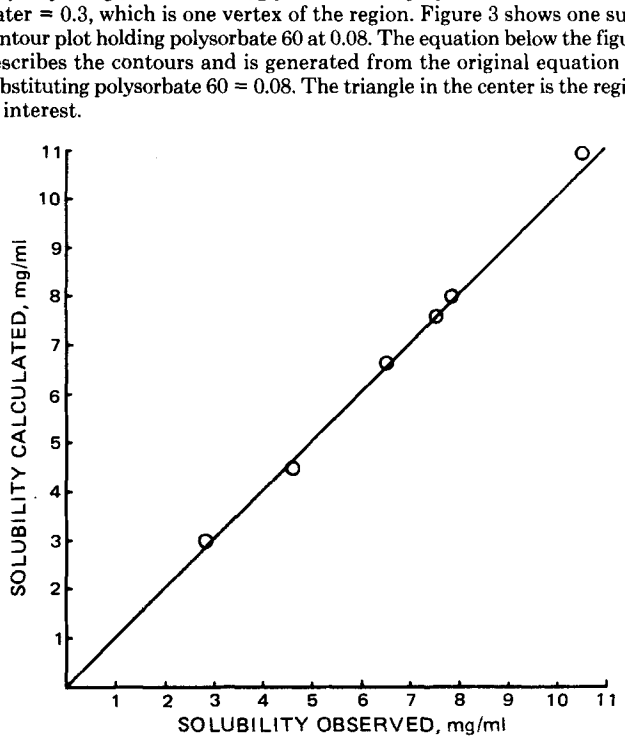


**Figure 2**—*Observed* versus *calculated solubilities (using the regression equation in Table IV).*

[1] Union Carbide Corp.
[2] Emery Industries.
[3] Pluronic F127, BASF Wyandotte Corp.
[4] Maximum $R^2$ improvement method, SAS Institute Program.

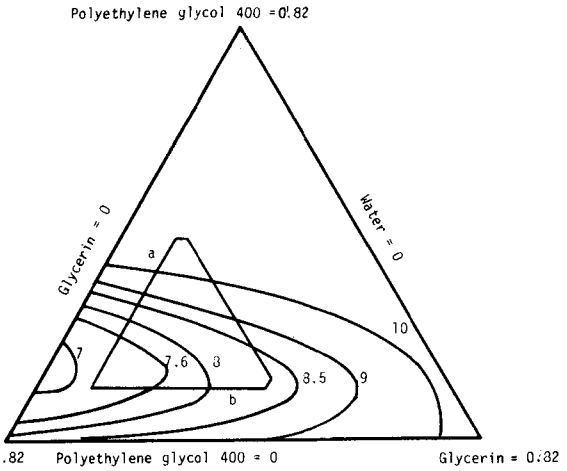


**Figure 3**—*Contour plot at polysorbate 60 = 0.08. Solubility = 10.1 + 38.0 (I) − 2.3 (water) − 59.9 (I)(II) − 74.2 (I)(water).*

The contour plot allows the formulator to choose any desirable solubility value and to determine the corresponding mixture. More importantly, it gives an overall picture of the response surface and the variation of the solubility as a function of the components. This, in turn, can be used to design a more robust formulation, that is, a region where the solubility does not vary greatly with small variations in component concentrations. Minor variations in production, therefore, would not result in drastic effects on the product. In addition, the following observations may be made from Fig. 3:

1. If one moves along the line glycerin = 0.1 (line a in Fig. 3) toward increasing polyethylene glycol 400, the solubility increases more slowly at lower polyethylene glycol 400 concentrations but increases more rapidly at higher levels.

2. If one moves along the line polyethylene glycol 400 = 0.1 (line b in Fig. 3) and replaces glycerin by water, the solubility changes only marginally. Hence, in changing the mixture from 40% glycerin to 10% glycerin by replacing with water, there is a change in solubility of only ~1 mg/ml. This information could be very useful if one were also concerned, for example, with the viscosity of the solution. The viscosity could be decreased considerably without compromising the solubility significantly.

Similar contour plots can be drawn holding different variables constant. These plots are not included here, but the interpretations are analogous to those made earlier.

From this analysis, it is evident that the extreme vertexes method in formulation development is a powerful approach to characterizing a formulation with a minimum number of experiments. (Factorial designs can be used for mixture problems only if one neglects the $n$th component, generally the least responsive, in generating the design. However, this approach may not give an optimum design.) This approach assumes even greater significance when more than one response must be studied since it allows optimization of the formulation with respect to the several responses simultaneously. This is easily done by overlapping contour plots of the different responses and choosing the region that satisfies all response criteria. An additional feature of the method is that one could first perform experiments only at the vertexes; if these experiments gave acceptable values for for the response, the design could be completed. Otherwise, the experimental region could be shifted to another area where the response might be more favorable, and the process could be repeated.

## REFERENCES

(1) G. E. P. Box, W. G. Hunter, and J. S. Hunter, "Statistics for Experimenters," Wiley, New York, N.Y., 1978.

(2) R. A. McLean and V. L. Anderson, *Technometrics*, **8**, 447 (1966).

(3) R. D. Snee, *J. Qual. Technol.*, **3**, 159 (1971).

(4) R. D. Snee, *Technometrics*, **17**, 149 (1975).

(5) R. D. Snee and D. W. Marquardt, *ibid.*, **18**, 19 (1976).

(6) R. D. Snee, *Chemtech*, **9**, 701 (1979).

## ACKNOWLEDGMENTS

Presented at the APhA Academy of Pharmaceutical Sciences, Washington, D.C., meeting, April 1980.

The authors thank Dr. Richard E. Jones for suggesting this method and for valuable discussions in the preparation of this manuscript and Dr. John Allen and Dr. Stefan Unger for some statistical computations.

# Radioimmunoassay of Flunisolide in Human Plasma

**C. NERENBERG and S. B. MATIN** ˣ

Received March 4, 1980, from the *Department of Analytical and Metabolic Chemistry, Syntex Research, Palo Alto, CA 94304.* Accepted for publication January 15, 1981.

**Abstract** □ A simple radioimmunoassay was developed for the measurement of flunisolide in human plasma or serum. Plasma extraction was not required. Antiserums were produced in rabbits by immunization against the flunisolide 21-hemisuccinate–bovine serum albumin conjugate. Cross-reactivities were determined for cortisol and a major metabolite of flunisolide and were 0.02 and 0.06%, respectively. Assay sensitivity is in the 100–200-pg/ml range. Accuracy studies gave regression lines of $y = 1.06x$, $r = 1.00$, for a 0.1-ml plasma aliquot and $y = 0.99x$, $r = 0.99$, for a 0.2-ml plasma aliquot. The accuracy of the method was estimated to be at least ±15%. The method was used to determine plasma concentration–time profiles in human subjects after the administration of a 1.0-mg iv dose.

**Keyphrases** □ Flunisolide—radioimmunoassay, human plasma or serum, plasma concentration–time profiles □ Corticoids—flunisolide, radioimmunoassay, human plasma or serum, plasma concentration–time profiles □ Radioimmunoassay—flunisolide, human plasma or serum

Flunisolide (6α-fluoro-11β,16α,17,21-tetrahydroxypregna-1,4-diene-3,20-dione cyclic 16,17-acetal with acetone, I) is a fast acting corticoid designed for use in the treatment of allergic rhinitis, asthma, and other respiratory disorders in humans (1–4).

Since the intended use of this drug was for the treatment of respiratory and upper respiratory disorders, its administration in an inhalation dosage form was a requirement. Since the amount of drug delivered by inhalation is generally small, the plasma levels achieved can be expected to be low.

This paper describes a selective and sensitive radioimmunoassay for the measurement of flunisolide in plasma or serum. This method was developed to provide data for the determination of certain pharmacokinetic parameters in humans, *e.g.*, plasma clearance, elimination half-life, and



*0022-3549/81/0800-0900$01.00/0*
*© 1981, American Pharmaceutical Association*

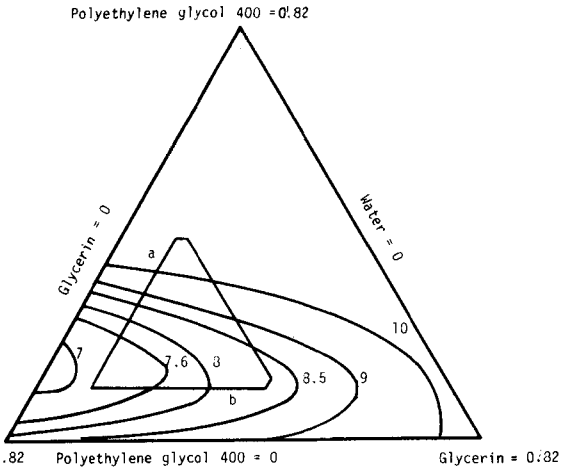


**Figure 3**—*Contour plot at polysorbate 60 = 0.08. Solubility = 10.1 + 38.0 (I) − 2.3 (water) − 59.9 (I)(II) − 74.2 (I)(water).*

The contour plot allows the formulator to choose any desirable solubility value and to determine the corresponding mixture. More importantly, it gives an overall picture of the response surface and the variation of the solubility as a function of the components. This, in turn, can be used to design a more robust formulation, that is, a region where the solubility does not vary greatly with small variations in component concentrations. Minor variations in production, therefore, would not result in drastic effects on the product. In addition, the following observations may be made from Fig. 3:

1. If one moves along the line glycerin = 0.1 (line a in Fig. 3) toward increasing polyethylene glycol 400, the solubility increases more slowly at lower polyethylene glycol 400 concentrations but increases more rapidly at higher levels.

2. If one moves along the line polyethylene glycol 400 = 0.1 (line b in Fig. 3) and replaces glycerin by water, the solubility changes only marginally. Hence, in changing the mixture from 40% glycerin to 10% glycerin by replacing with water, there is a change in solubility of only ~1 mg/ml. This information could be very useful if one were also concerned, for example, with the viscosity of the solution. The viscosity could be decreased considerably without compromising the solubility significantly.

Similar contour plots can be drawn holding different variables constant. These plots are not included here, but the interpretations are analogous to those made earlier.

From this analysis, it is evident that the extreme vertexes method in formulation development is a powerful approach to characterizing a formulation with a minimum number of experiments. (Factorial designs can be used for mixture problems only if one neglects the $n$th component, generally the least responsive, in generating the design. However, this approach may not give an optimum design.) This approach assumes even greater significance when more than one response must be studied since it allows optimization of the formulation with respect to the several responses simultaneously. This is easily done by overlapping contour plots of the different responses and choosing the region that satisfies all response criteria. An additional feature of the method is that one could first perform experiments only at the vertexes; if these experiments gave acceptable values for for the response, the design could be completed. Otherwise, the experimental region could be shifted to another area where the response might be more favorable, and the process could be repeated.

## REFERENCES

(1) G. E. P. Box, W. G. Hunter, and J. S. Hunter, "Statistics for Experimenters," Wiley, New York, N.Y., 1978.

(2) R. A. McLean and V. L. Anderson, *Technometrics*, **8**, 447 (1966).

(3) R. D. Snee, *J. Qual. Technol.*, **3**, 159 (1971).

(4) R. D. Snee, *Technometrics*, **17**, 149 (1975).

(5) R. D. Snee and D. W. Marquardt, *ibid.*, **18**, 19 (1976).

(6) R. D. Snee, *Chemtech*, **9**, 701 (1979).

## ACKNOWLEDGMENTS

Presented at the APhA Academy of Pharmaceutical Sciences, Washington, D.C., meeting, April 1980.

The authors thank Dr. Richard E. Jones for suggesting this method and for valuable discussions in the preparation of this manuscript and Dr. John Allen and Dr. Stefan Unger for some statistical computations.

# Radioimmunoassay of Flunisolide in Human Plasma

**C. NERENBERG and S. B. MATIN** ˣ

Received March 4, 1980, from the *Department of Analytical and Metabolic Chemistry, Syntex Research, Palo Alto, CA 94304.* Accepted for publication January 15, 1981.

**Abstract** □ A simple radioimmunoassay was developed for the measurement of flunisolide in human plasma or serum. Plasma extraction was not required. Antiserums were produced in rabbits by immunization against the flunisolide 21-hemisuccinate–bovine serum albumin conjugate. Cross-reactivities were determined for cortisol and a major metabolite of flunisolide and were 0.02 and 0.06%, respectively. Assay sensitivity is in the 100–200-pg/ml range. Accuracy studies gave regression lines of $y = 1.06x$, $r = 1.00$, for a 0.1-ml plasma aliquot and $y = 0.99x$, $r = 0.99$, for a 0.2-ml plasma aliquot. The accuracy of the method was estimated to be at least ±15%. The method was used to determine plasma concentration–time profiles in human subjects after the administration of a 1.0-mg iv dose.

**Keyphrases** □ Flunisolide—radioimmunoassay, human plasma or serum, plasma concentration–time profiles □ Corticoids—flunisolide, radioimmunoassay, human plasma or serum, plasma concentration–time profiles □ Radioimmunoassay—flunisolide, human plasma or serum

Flunisolide (6α-fluoro-11β,16α,17,21-tetrahydroxypregna-1,4-diene-3,20-dione cyclic 16,17-acetal with acetone, I) is a fast acting corticoid designed for use in the treatment of allergic rhinitis, asthma, and other respiratory disorders in humans (1–4).

Since the intended use of this drug was for the treatment of respiratory and upper respiratory disorders, its administration in an inhalation dosage form was a requirement. Since the amount of drug delivered by inhalation is generally small, the plasma levels achieved can be expected to be low.

This paper describes a selective and sensitive radioimmunoassay for the measurement of flunisolide in plasma or serum. This method was developed to provide data for the determination of certain pharmacokinetic parameters in humans, *e.g.*, plasma clearance, elimination half-life, and



*0022-3549/81/0800-0900$01.00/0*
*© 1981, American Pharmaceutical Association*

**Table I—Radioimmunoassay Protocol**

| Tube Number | Tube Description | Number of Replicates | Buffer, ml | Labeled Flunisolide, ml | Cold Flunisolide, ml | Plasma Unknowns, ml | Antiserums, ml | Total Volume, ml |
|---|---|---|---|---|---|---|---|---|
| 0 | Zero std. | 6 | 0.3 | 0.1 | — | 0.1[a] | 0.1 | 0.6 |
| 1 | 10 pg std. | 3 | 0.2 | 0.1 | 0.1 | 0.1 | 0.1 | 0.6 |
| 2 | 20 pg std. | 3 | 0.2 | 0.1 | 0.1 | 0.1 | 0.1 | 0.6 |
| 3 | 50 pg std. | 3 | 0.2 | 0.1 | 0.1 | 0.1 | 0.1 | 0.6 |
| 4 | 100 pg std. | 3 | 0.2 | 0.1 | 0.1 | 0.1 | 0.1 | 0.6 |
| 5 | 200 pg std. | 3 | 0.2 | 0.1 | 0.1 | 0.1 | 0.1 | 0.6 |
| 6 | 300 pg std. | 3 | 0.2 | 0.1 | 0.1 | 0.1 | 0.1 | 0.6 |
| 7 | 500 pg std. | 3 | 0.2 | 0.1 | 0.1 | 0.1 | 0.1 | 0.6 |
| 8 | 600 pg std. | 3 | 0.2 | 0.1 | 0.1 | 0.1 | 0.1 | 0.6 |
| N1, N2, *etc.* | Plasma–nonspecific traps | 3 | 0.4 | 0.1 | — | 0.1 | — | 0.6 |
| NB | Buffer–nonspecific trap | 3 | 0.5 | 0.1 | — | — | — | 0.6 |
| TC | Total counts | 3 | 0.5 | 0.1 | — | — | — | 0.6 |
| U1, U2, *etc.* | Unknowns | 3 or 6 | 0.3 | 0.1 | — | 0.1 | 0.1 | 0.6 |

[a] Standards and nonspecific traps received an aliquot of control plasma.

extent and rate of absorption. Other analytical methods such as GLC or GLC–mass spectrometry cannot be used for plasma level determinations because flunisolide is a thermally unstable compound.

## EXPERIMENTAL

**Materials**—Freund's complete and incomplete adjuvants were purchased in sealed glass ampuls[1]. Activated powdered charcoal[2] was used. The buffer was tris(hydroxymethyl)aminomethane–hydrochloric acid, 0.05 *M*, pH 7.2–7.4, with or without 0.1% gelatin. Flunisolide tritiated at the 1,2-positions with a specific activity of 39.9 Ci/mmole, the 21-hemisuccinate of flunisolide (II), and the flunisolide–bovine serum albumin conjugate were all synthesized in-house[3]. The 6$\beta$-hydroxy metabolite of flunisolide (6$\beta$,11$\beta$,16$\alpha$,17$\alpha$,21-pentahydroxypregna-1,4-diene-3,20-dione-16,17-acetonide) (III) used in the cross-reactivity experiment also was synthesized in-house[3].

**Antiserum Production**—The flunisolide–bovine serum albumin conjugate used for immunization was prepared by coupling II to bovine serum albumin with a water-soluble carbodiimide coupling reagent (5). The reaction mixture was dialyzed exhaustively against normal saline. The extent of conjugation was determined by measuring the protein concentration by the method of Lowry *et al.* (6), and the flunisolide residues were determined by UV absorption. The molar ratio was 57 moles of flunisolide/mole of bovine serum albumin.

An emulsion of the conjugate in saline was prepared by mixing with an equal volume of Freund's complete adjuvant. The bovine serum albumin concentration was 100 $\mu$g/ml, and 0.25 ml was injected subcutaneously into four sites in New Zealand White rabbits. Six weeks after the initial injection, all animals were placed on a regimen of weekly booster shots; the conjugate was prepared in incomplete Freund's adjuvant. After 6–8 months, antiserum dilutions of 1:10,000 to 1:30,000 yielded 50% binding or more. At this stage, assay development was begun.

**Radioimmunoassay**—Flunisolide standards for the standard curve were obtained by dilution of a stock solution of 10.0 mg of flunisolide in 10.0 ml of ethanol. A series of standard solutions, 20, 50, 100, 200, 300, 500, and 600 pg/0.1 ml, was prepared in tris(hydroxymethyl)aminomethane–hydrochloric acid buffer, pH 7.2, 0.05 *M*, without gelatin in 10.0-ml volumes and stored in the refrigerator. Gelatin was withheld from the buffer in the standards to give them a longer shelflife.

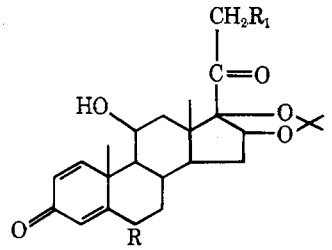


I: R = F, $R_1$ = OH
II: R = F, $R_1$ = $CO_2(CH_2)_2COOH$
III: R = OH, $R_1$ = OH

An ethanolic solution of the tritiated flunisolide was diluted with tris(hydroxymethyl)aminomethane–hydrochloric acid buffer, pH 7.2, 0.05 *M*, with 0.1% gelatin such that a 0.1-ml aliquot contained 8000–10,000 cpm. The solution was prepared in a volume sufficient for one assay and then was discarded. Radioisotope purity checks were carried out periodically on silica gel TLC plates[4] with chloroform–methanol–water (40:9:1) as the solvent system. To identify the radioactive band, cold reference standards were cospotted and identified under UV light. The $R_f$ values were ~0.4–0.5.

The antiserums were diluted in tris(hydroxymethyl)aminomethane–hydrochloric acid buffer, pH 7.2, 0.05 *M*, with 0.1% gelatin to yield a total binding of between 35 and 60%. Depending on the quality of the antiserum, this binding was achieved by diluting 1:10,000, 1:20,000, or 1:30,000; a 0.1-ml aliquot was added to each tube.

The charcoal stock suspension (1% in water) was diluted as required with tris(hydroxymethyl)aminomethane–hydrochloric acid, pH 7.2, 0.05 *M*, with 0.1% gelatin immediately before use. A 0.2-ml aliquot of the diluted charcoal suspension (0.4%) was added to blocks of 30–36 tubes at a time. The tubes were vortexed, and the 30-min time cycle was started. Midway through this cycle, charcoal was added to a second block of tubes and they were started on their 30-min cycle. This staggered array procedure was repeated until all tubes were processed. At the end of the 30-min cycle, each block of tubes was centrifuged immediately and sampled for counting.

The centrifuge used was refrigerated with a swingout head[5]. Liquid scintillation counting was done in a scintillation spectrometer[6], using commercially available scintillation fluid[7].

A typical radioimmunoassay protocol is given in Table I, and a stepwise procedure for setting up the assay is as follows. Buffer, tritiated flunisolide, standards, unknowns, antiserums, *etc.*, were added to the appropriate tubes (12 × 75-mm disposable culture tubes). After all additions had been made, the sides of the tubes were washed down by briefly vortexing (1–3 sec). The tubes were covered with sheets of waxed film[8] cut to fit the test tube racks and were incubated overnight at room temperature.

After overnight incubation, the tubes were placed in an ice bath for 2–3 hr. Then 0.2 ml of the charcoal suspension was added to blocks of 30–36 tubes. The tubes were vortexed for 6 sec, and the 30-min time cycle was started. After 30 min, the tubes were centrifuged at 2500 rpm for 4 min and immediately 0.5 ml of the supernate was transferred into scintillation vials. Then 10.0 ml of scintillation fluid was added, and the solutions were counted for 10 min.

**Data Processing**—Data processing was done with the aid of the Rodbard and LeWald Model I computer program (7), a logit–log trans-

[1] Difco Laboratories, Detroit, Mich.
[2] Norit A, Matheson, Coleman and Bell, Norwood, Ohio.
[3] Syntex Research, Palo Alto, Calif.
[4] Silica gel 60 F-254 plates, EM Laboratories, Elmsford, NY 10523.
[5] IEC model DPR-6000.
[6] Packard Tri-Carb model 3330.
[7] Aquasol or Oxifluor-$H_2O$, New England Nuclear.
[8] Parafilm.

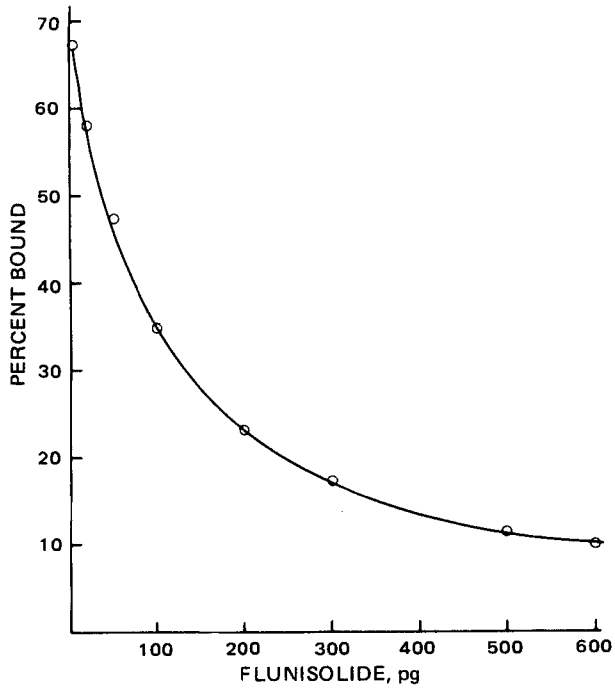


**Figure 1**—*Plot of a typical displacement curve (or standard curve). The antiserum dilution was 1:20,000. The binding–displacement reaction was carried out overnight at room temperature.*

formation that linearizes the sigmoid curve normally obtained in a displacement curve. However, the percent bound *versus* the flunisolide concentration can be plotted manually and the unknowns can be determined by interpolation. One advantage of this computer system is that it eliminates operator variation in plotting the standard curve and estimating the unknowns. It also increases the speed with which the computations can be made, especially if a teletype punched-tape system is coupled to the program.

**Accuracy and Precision**—Known amounts of flunisolide were added to plasma and serum, and then these samples were analyzed in triplicate.

## RESULTS AND DISCUSSION

The described method can be used to analyze flunisolide from human plasma directly without prior extraction or purification. This approach was possible because an aliquot of control plasma was added to all points in the standard curve, thereby making it chemically equivalent to that of the unknown samples. A typical standard curve is shown in Fig. 1. Since the control plasma was obtained from each subject prior to flunisolide dosing, it did not contain any endogenous flunisolide.

Pooled plasma from different subjects could be used, but the lower level of sensitivity was not achieved. This observed difference could be due to differences in plasma lipid content or other endogenous components. The exact nature of the component effecting this difference is not known. The effect of this difference is that the lower limit of sensitivity may have to be changed from 20 to 50 or 100 pg. If 50 pg becomes the lowest point on the standard curve that can be measured reliably, then for a 0.2-ml plasma aliquot the lower limit of sensitivity would change from 100 to 250 pg/ml; for a 0.1-ml plasma aliquot, it would change from 200 to 500 pg/ml.

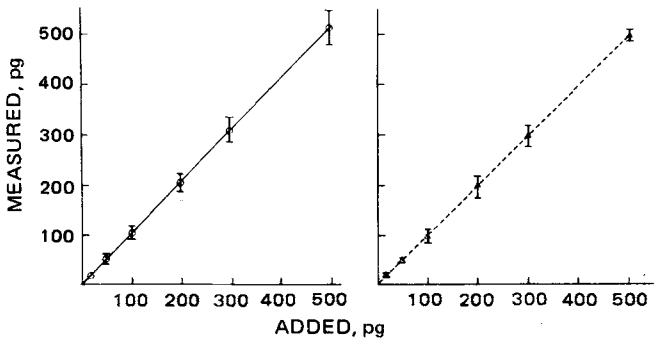


**Figure 2**—*Plots of accuracy measurements using 0.1- (left) and 0.2- (right) ml plasma aliquots. The regression line for the 0.1-ml curve was* y = *1.06*x, r = *1.00; for the 0.2-ml curve, it was* y = *0.99*x, r = *0.99.*

To obtain maximal sensitivity in a radioimmunoassay, certain assay conditions must be optimized. The first parameter to be optimized was the amount of charcoal required to effect the optimum separation of bound from free. This value was established by adding fixed amounts of tritiated flunisolide to a series of tubes containing buffer only and to another series of tubes containing buffer and 0.1 ml of plasma. Graded amounts of charcoal then were added in a constant-volume aliquot (0.2 ml) until the amount of free radioactivity remaining behind, *i.e.*, the nonspecific bound, was 2–4% for tubes containing buffer only and 4–8% for tubes containing an aliquot of plasma. In this laboratory, these conditions were met by using a 0.4% charcoal suspension.

Method sensitivity depends on the size of the aliquot subjected to analysis. If a 0.1-ml aliquot was used, then the lower limit of sensitivity corresponded to 200 pg/ml; for a 0.2-ml aliquot, it was 100 pg/ml. These limits were determined by the lowest concentration on the standard curve that could be reliably measured. With the present method, the lowest concentration that can be reliably measured is 20 pg/0.1-ml aliquot.

Method accuracy was determined by adding known amounts of flunisolide to blank plasma and then assaying these samples using 0.1- and 0.2-ml plasma aliquots. Accuracy measurements were carried out at six different concentrations and covered the entire range of the standard curve. The results were then averaged for each concentration and plotted as measured amounts *versus* added amounts (Fig. 2). The linearity of the plots and the fact that the slopes are essentially equal to unity with no intercept indicate that the measurements can be made accurately over

**Table II—Accuracy Experiments Carried Out in 0.1- and 0.2-ml Plasma Aliquots Showing the Ratios of Measured to Added Flunisolide**

| Flunisolide Added, pg/plasma aliquot (ml) | Flunisolide Measured[a], pg/plasma aliquot (ml) | Ratio $\frac{\text{Measured}}{\text{Added}}$ | Group *CV*, % |
|---|---|---|---|
| 20/0.1 | 22.7/0.1 | 1.14 | 4.0 |
| 20/0.1 | 20.7/0.1 | 1.04 | |
| 20/0.1 | 21.6/0.1 | 1.08 | |
| 20/0.1 | 21.2/0.1 | 1.06 | |
| 100/0.1 | 95.7/0.1 | 0.96 | 4.1 |
| 100/0.1 | 100.2/0.1 | 1.00 | |
| 100/0.1 | 91.4/0.1 | 0.91 | |
| 100/0.1 | 97.5/0.1 | 0.98 | |
| 300/0.1 | 289.2/0.1 | 0.96 | 6.7 |
| 300/0.1 | 330.4/0.1 | 1.10 | |
| 300/0.1 | 292.0/0.1 | 0.97 | |
| 300/0.1 | 290.7/0.1 | 0.97 | |
| 600/0.1 | 626.1/0.1 | 1.04 | 5.5 |
| 600/0.1 | 646.7/0.1 | 1.08 | |
| 600/0.1 | 690.4/0.1 | 1.15 | |
| 600/0.1 | 605.2/0.1 | 1.01 | |
| 20/0.2 | 15.9/0.2 | 0.84 | 15.5 |
| 20/0.2 | 19.3/0.2 | 0.97 | |
| 20/0.2 | 20.2/0.2 | 1.00 | |
| 20/0.2 | 24.4/0.2 | 1.22 | |
| 50/0.2 | 54.0/0.2 | 1.08 | 10.1 |
| 50/0.2 | 42.0/0.2 | 0.84 | |
| 50/0.2 | 49.0/0.2 | 0.98 | |
| 50/0.2 | 49.9/0.2 | 1.00 | |
| 100/0.2 | 92.3/0.2 | 0.92 | 3.7 |
| 100/0.2 | 90.4/0.2 | 0.90 | |
| 100/0.2 | 94.4/0.2 | 0.94 | |
| 100/0.2 | 86.0/0.2 | 0.86 | |
| 300/0.2 | 294.2/0.2 | 0.98 | 2.2 |
| 300/0.2 | 279.4/0.2 | 0.93 | |
| 300/0.2 | 285.2/0.2 | 0.95 | |
| 300/0.2 | 284.0/0.2 | 0.95 | |
| 500/0.2 | 498.8/0.2 | 1.00 | 3.5 |
| 500/0.2 | 499.0/0.2 | 1.00 | |
| 500/0.2 | 508.0/0.2 | 1.02 | |
| 500/0.2 | 470.9/0.2 | 0.94 | |

[a] Mean of triplicate determinations.

**Table III—Quality Control Experiments Carried Out with Each Experiment over 3 Months of Analysis**

| Sample | Plasma Aliquot, ml | Flunisolide Added: 100 pg/Plasma Aliquot, Picograms Measured ± *SD* | 100 pg/Plasma Aliquot, Ratio Measured / Added | 300 pg/Plasma Aliquot, Picograms Measured ± *SD* | 300 pg/Plasma Aliquot, Ratio Measured / Added |
|---|---|---|---|---|---|
| 1 | 0.20 | 92.4 ± 4.95 | 0.92 | 281.9 ± 3.04 | 0.94 |
| 2 | 0.20 | 98.2 ± 2.33 | 0.98 | 297.8 ± 12.66 | 0.99 |
| 3 | 0.20 | 95.8 ± 4.10 | 0.96 | 293.0 ± 12.94 | 0.98 |
| 4 | 0.10 | 113.5 ± 3.47 | 1.13 | 329.3 ± 11.29 | 1.10 |
| 5 | 0.10 | 94.0 ± 4.78 | 0.94 | 292.1 ± 10.75 | 0.97 |
| 6 | 0.10 | 93.0 ± 7.78 | 0.93 | 271.7 ± 6.43 | 0.91 |
| 7 | 0.10 | 102.4 ± 0.99 | 1.02 | 323.0 ± 8.06 | 1.08 |
| 8 | 0.10 | 103.1 ± 7.40 | 1.03 | 294.3 ± 11.10 | 0.98 |
| 9 | 0.10 | 91.4 ± 1.41 | 0.91 | 298.7 ± 17.68 | 1.00 |
| 10 | 0.10 | 104.9 ± 0.64 | 1.05 | 316.8 ± 16.60 | 1.06 |
| 11 | 0.10 | 93.5 ± 3.04 | 0.93 | 310.2 ± 7.99 | 1.03 |
| 12 | 0.10 | 97.3 ± 6.15 | 0.97 | 305.6 ± 2.40 | 1.02 |
| 13 | 0.10 | 94.2 ± 2.76 | 0.94 | 285.3 ± 10.04 | 0.95 |
| 14 | 0.10 | 102.2 ± 4.03 | 1.02 | 276.0 ± 9.69 | 0.92 |
| 15 | 0.20 | 92.7 ± 0.42 | 0.93 | 300.6 ± 2.33 | 1.00 |
| 16 | 0.20 | 92.6 ± 1.63 | 0.93 | 282.1 ± 1.63 | 0.94 |
| 17 | 0.20 | 84.2 ± 4.67 | 0.84 | 277.4 ± 11.24 | 0.92 |
| 18 | 0.20 | 95.5 ± 6.08 | 0.95 | 281.5 ± 11.17 | 0.94 |
| 19 | 0.20 | 91.2 ± 1.56 | 0.91 | 286.1 ± 9.26 | 0.95 |
| 20 | 0.20 | 84.9 ± 4.10 | 0.85 | 286.2 ± 14.50 | 0.95 |
| 21 | 0.20 | 90.3 ± 5.52 | 0.90 | 287.4 ± 3.25 | 0.96 |

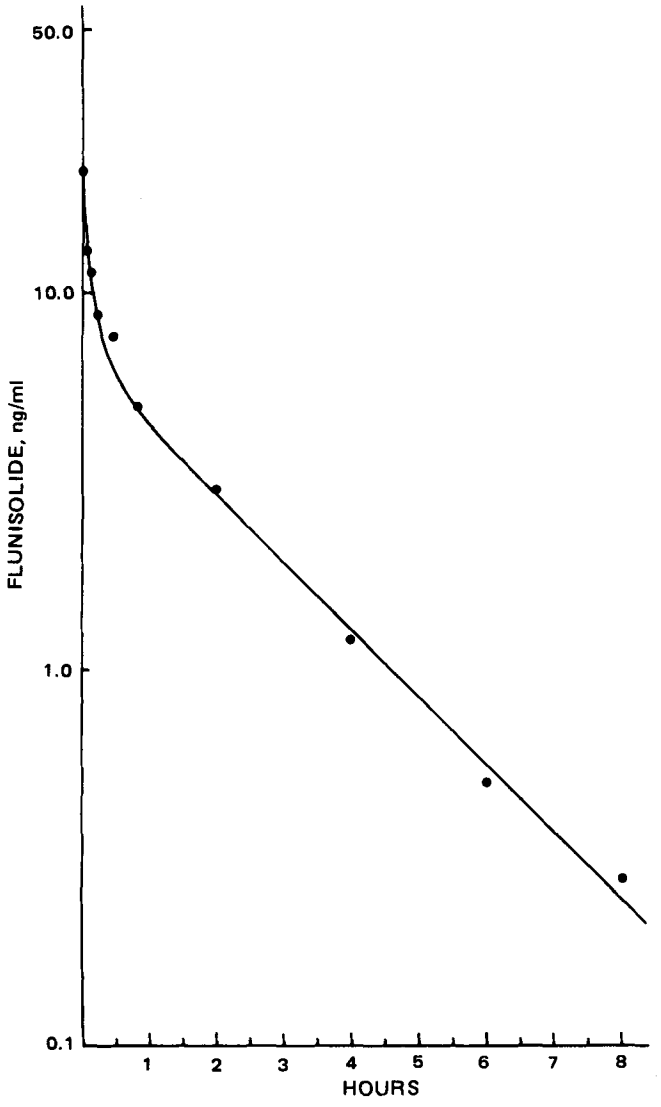


**Figure 3**—*Plasma concentration–time profile in human subjects after administration of a single 1.0-mg iv dose. Data are the average of 12 male volunteers.*

the concentration range tested. The results listed in Table II indicate that the method is capable of measuring within ±15%. The results of quality control experiments carried out during 3 months of routine analyses are given in Table III. The ratios of measured to added flunisolide show that an accuracy of ±15% is possible and can be maintained over time.

Assay validity also was tested by comparing plasma flunisolide levels determined by this method to the levels found by a carbon 14 radiochemical assay (8). A human male volunteer was given a 2.0-mg iv dose of flunisolide containing ~70 $\mu$Ci of $^{14}$C-labeled flunisolide. Blood samples were drawn at 0.5, 1.0, 3.0, 4.0, and 6.0 hr. The plasma was extracted with ethyl acetate, the extracts were evaporated to dryness, and the residue was subjected to TLC. The TLC plates were divided into 1-cm segments, and each segment was assayed for radioactivity. This procedure separated flunisolide from its metabolites. The plasma levels measured at each respective time point were 8.15, 6.07, 1.99, 1.27, and 0.47 ng/ml by radioimmunoassay and 8.26, 5.42, 2.02, 1.19, and 0.55 ng/ml by the radiochemical assay. The inherent variability of the radioimmunoassay is ±15%, and that of the radiochemical method combined with TLC can be as high as ±20%. Therefore, an absolute correlation by the two methods is not possible.

As in any radioimmunoassay, structurally related compounds can interfere. Cortisol is present endogenously at relatively high levels and is structurally related; the 6$\beta$-hydroxy compound is structurally related and is also the major metabolite of flunisolide. These compounds were chosen for cross-reactivity measurements. Cross-reactivities were determined from displacement curves generated for cortisol and the 6$\beta$-hydroxy metabolite of flunisolide, and these curves were compared to the flunisolide displacement curve. The concentration of each compound that corresponded to the 50% inhibition point on the flunisolide curve was then used to calculate the percent cross-reactivity. Cortisol and the 6$\beta$-hydroxy metabolite of flunisolide showed cross-reactivities of 0.02 and 0.06%, respectively.

The developed method was utilized to establish plasma concentration–time profiles in human subjects after the administration of a single 1.0-mg iv dose (8). Twelve male volunteers were used. Blood samples were taken at 2, 5, 10, and 30 min and at 1, 2, 4, 6, 8, and 24 hr and were analyzed in duplicate. The means, determined at each time point, were averaged for all subjects and plotted as concentration *versus* time (Fig. 3). The profile indicated that the method has sufficient sensitivity to be useful in various dosage form experiments.

## REFERENCES

(1) P. C. Turkeltaub, P. S. Norman, and S. Crepea, *J. Allergy Clin. Immunol.*, **55**, 120 (1975).

(2) D. Rajtora, J. K. Kammermeyer, J. Anuras, and H. B. Richerson, *ibid.*, **55**, 121 (1975).

(3) F. L. Bloom, R. H. Cohan, K. N. Leifer, D. L. Spangler, R. B. Rhoades, and H. J. Wittig, *Ann. Allergy*, **38**, 408 (1977).

(4) F. C. Lowell, J. L. Ohman, and M. Williams, *J. Allergy Clin. Immunol.*, **57**, 257 (1976).
(5) J. C. Sheehan and J. J. Hlarka, *J. Org. Chem.*, **21**, 439 (1956).
(6) O. H. Lowry, N. J. Rosebrough, A. L. Farr, and R. Randall, *J. Biol. Chem.*, **193**, 265 (1951).
(7) D. Rodbard and J. E. Lewald, *Acta Endocrinol. (Copenhagen), Suppl.*, **147**, 79 (1970).
(8) M. D. Chaplin, W. Rooks, II, E. W. Swenson, W. C. Cooper, C. Nerenberg, and N. I. Chu, *Clin. Pharmacol. Ther.*, **27**, 402 (1980).

**ACKNOWLEDGMENTS**

The authors acknowledge Dr. Howard Parnes for synthesis of the tritiated flunisolide and Dr. Pamela Burton for synthesis of the flunisolide hemisuccinate derivative and the flunisolide–bovine serum albumin conjugate. Acknowledgment is also made to Dr. Chaplin for the carbon 14 assay data, to Mr. William Leitch for production of the antiserum, and to Mr. W. Ho for assistance in the application of the method to studies in human subjects. The authors also thank Leigh Ann Wolfe for her assistance in the preparation of this manuscript.

# Fluoride Remineralization of Demineralized Bovine Tooth Enamel and Hydroxyapatite Pellets

**MASAKATSU YONESE *, JEFFREY L. FOX *, NAOKI NAMBU *, JOHN J. HEFFERREN ‡, and WILLIAM I. HIGUCHI *x**

Received June 30, 1980, from the **College of Pharmacy, University of Michigan, Ann Arbor, MI 48109*, and the ‡*American Dental Association, Chicago, IL 60611.* Accepted for publication January 26, 1981.

**Abstract** □ Both bovine enamel and hydroxyapatite pellets were remineralized in a fluoride-containing remineralization solution after prior demineralization for various lengths of time. In both the enamel and pellet systems, the degree of remineralization attainable was directly related to the extent of prior demineralization, although the demineralized material was never 100% recovered in remineralization. In some cases, fluoride levels up to several thousand parts per million were found at depths as great as 50 μm from the surface. The stoichiometry of the remineralized material and electron microprobe examination were consistent with the formation of fluoridated hydroxyapatite rather than calcium fluoride.

**Keyphrases** □ Fluoride—remineralization of demineralized bovine tooth enamel and hydroxyapatite pellets □ Remineralization—of demineralized bovine tooth enamel and hydroxyapatite pellets □ Hydroxyapatite pellets—remineralization along with demineralized bovine tooth enamel □ Teeth, bovine—remineralization of demineralized tooth enamel and hydroxyapatite pellets

Previous studies performed in these laboratories (1, 2) led to the development of a model for hydroxyapatite dissolution involving two distinct crystalline dissolution sites (3). This model is consistent with dissolution kinetic data and explains the observed morphology of hydroxyapatite dissolution at both the single-crystal level (4) and at the level of a compressed hydroxyapatite pellet or a block of tooth enamel (3).

In studying demineralization of remineralized enamel, it was noted (5, 6) that when enamel was demineralized under conditions where the medium was partially saturated with respect to hydroxyapatite, subsequent remineralization was successful; but when prior demineralization was carried out under more severe conditions, remineralization attempts gave poor results.

Since successful remineralization occurred under conditions where dissolution *via* only Site 1 would be expected, the hypothesis follows that this site might be the principal one for successful remineralization. This remineralization might consist chiefly of the filling of *c*-axis holes.

The present experiments were designed to test for the existence of a relationship between the amount of demineralization *via* Site 1 and the subsequent degree of remineralization attainable.

## EXPERIMENTAL

**Materials**—*Bovine Teeth*—Bovine incisors were used. Labial surfaces were ground with fine sandpaper to remove the pellicle.

*Hydroxyapatite Pellets*—Synthetic hydroxyapatite crystals, prepared using the procedure developed by Moreno *et al.* (7), were used in the preparation of pellets. About 50 mg of hydroxyapatite, preequilibrated in a humidity chamber containing saturated potassium nitrate aqueous solution to maintain the humidity at ~67%, was compressed in a die (0.62-cm diameter) under a force of 10,000 lb using a laboratory press.

**Buffer Solutions**—A solution 16% saturated (on a molar basis) with respect to the thermodynamic solubility of hydroxyapatite was used for demineralization. The solution was a 0.1 *M* acetate buffer containing 3.5 m*M* each of total calcium and total phosphate. The pH was adjusted to 4.5 with sodium hydroxide, and the ionic strength was adjusted to 0.5 with sodium chloride. For remineralization, a 0.1 *M* acetate buffer (pH 4.5) containing 12 m*M* of total calcium (including calcium 45 activity of 0.2 mCi/liter of solution), 12 m*M* total phosphate, 10 ppm of fluoride, and sodium chloride to adjust the ionic strength to 0.5 was used.

The ionic activity of hydroxyapatite, $K_{HAP}$ ($\equiv a_{Ca}^{10} a_{PO_4}^{6} a_{OH}^{2}$), of this buffer was $10^{-120}$. Although not saturated with respect to hydroxyapatite, this solution has a high enough degree of partial saturation so that hydroxyapatite dissolution would be expected to proceed slowly, if at all, based on previous work with solutions approaching this level of calcium and phosphate concentrations (3, 8).

**Demineralization**—A bovine tooth was covered with inlay wax except for 0.25 $cm^2$ of the labial surface. In the pellet experiments, a hydroxyapatite pellet with a surface area of 0.58 $cm^2$ was fixed on a small glass plate by the wax. Either the tooth or pellet then was demineralized in the 16% partially saturated buffer solution for 0.5–6 hr. The solution was shaken gently with a wrist-action shaker[1] and kept at 30°. The volume of the buffer solution was 10 ml/0.25 $cm^2$ of the sample surface.

**Remineralization**—The demineralized tooth or pellet then was given a remineralization treatment for 24–72 hr in 50 ml of the remineralization buffer solution. The solution was shaken gently and kept at 30° as remineralization proceeded.

**Etching and Scraping**—The remineralized sample then was etched in 1 ml of 0.5 *M* $HClO_4$ for successive periods of 15, 15, 30, 60, 120, 200, and 200 sec; the surface was washed with 1 ml of water after each etching step. The depths of the etched layers were estimated from the amounts of phosphate etched. Some hydroxyapatite pellets were scraped evenly

[1] Burrell Co.



*0022-3549/81/0800-0904$01.00/0*
*© 1981, American Pharmaceutical Association*

(4) F. C. Lowell, J. L. Ohman, and M. Williams, *J. Allergy Clin. Immunol.*, **57**, 257 (1976).
(5) J. C. Sheehan and J. J. Hlarka, *J. Org. Chem.*, **21**, 439 (1956).
(6) O. H. Lowry, N. J. Rosebrough, A. L. Farr, and R. Randall, *J. Biol. Chem.*, **193**, 265 (1951).
(7) D. Rodbard and J. E. Lewald, *Acta Endocrinol. (Copenhagen), Suppl.*, **147**, 79 (1970).
(8) M. D. Chaplin, W. Rooks, II, E. W. Swenson, W. C. Cooper, C. Nerenberg, and N. I. Chu, *Clin. Pharmacol. Ther.*, **27**, 402 (1980).

**ACKNOWLEDGMENTS**

The authors acknowledge Dr. Howard Parnes for synthesis of the tritiated flunisolide and Dr. Pamela Burton for synthesis of the flunisolide hemisuccinate derivative and the flunisolide–bovine serum albumin conjugate. Acknowledgment is also made to Dr. Chaplin for the carbon 14 assay data, to Mr. William Leitch for production of the antiserum, and to Mr. W. Ho for assistance in the application of the method to studies in human subjects. The authors also thank Leigh Ann Wolfe for her assistance in the preparation of this manuscript.

# Fluoride Remineralization of Demineralized Bovine Tooth Enamel and Hydroxyapatite Pellets

**MASAKATSU YONESE *, JEFFREY L. FOX *, NAOKI NAMBU *, JOHN J. HEFFERREN ‡, and WILLIAM I. HIGUCHI *x**

Received June 30, 1980, from the **College of Pharmacy, University of Michigan, Ann Arbor, MI 48109*, and the ‡*American Dental Association, Chicago, IL 60611.* Accepted for publication January 26, 1981.

**Abstract** □ Both bovine enamel and hydroxyapatite pellets were remineralized in a fluoride-containing remineralization solution after prior demineralization for various lengths of time. In both the enamel and pellet systems, the degree of remineralization attainable was directly related to the extent of prior demineralization, although the demineralized material was never 100% recovered in remineralization. In some cases, fluoride levels up to several thousand parts per million were found at depths as great as 50 μm from the surface. The stoichiometry of the remineralized material and electron microprobe examination were consistent with the formation of fluoridated hydroxyapatite rather than calcium fluoride.

**Keyphrases** □ Fluoride—remineralization of demineralized bovine tooth enamel and hydroxyapatite pellets □ Remineralization—of demineralized bovine tooth enamel and hydroxyapatite pellets □ Hydroxyapatite pellets—remineralization along with demineralized bovine tooth enamel □ Teeth, bovine—remineralization of demineralized tooth enamel and hydroxyapatite pellets

Previous studies performed in these laboratories (1, 2) led to the development of a model for hydroxyapatite dissolution involving two distinct crystalline dissolution sites (3). This model is consistent with dissolution kinetic data and explains the observed morphology of hydroxyapatite dissolution at both the single-crystal level (4) and at the level of a compressed hydroxyapatite pellet or a block of tooth enamel (3).

In studying demineralization of remineralized enamel, it was noted (5, 6) that when enamel was demineralized under conditions where the medium was partially saturated with respect to hydroxyapatite, subsequent remineralization was successful; but when prior demineralization was carried out under more severe conditions, remineralization attempts gave poor results.

Since successful remineralization occurred under conditions where dissolution *via* only Site 1 would be expected, the hypothesis follows that this site might be the principal one for successful remineralization. This remineralization might consist chiefly of the filling of *c*-axis holes.

The present experiments were designed to test for the existence of a relationship between the amount of demineralization *via* Site 1 and the subsequent degree of remineralization attainable.

## EXPERIMENTAL

**Materials**—*Bovine Teeth*—Bovine incisors were used. Labial surfaces were ground with fine sandpaper to remove the pellicle.

*Hydroxyapatite Pellets*—Synthetic hydroxyapatite crystals, prepared using the procedure developed by Moreno *et al.* (7), were used in the preparation of pellets. About 50 mg of hydroxyapatite, preequilibrated in a humidity chamber containing saturated potassium nitrate aqueous solution to maintain the humidity at ~67%, was compressed in a die (0.62-cm diameter) under a force of 10,000 lb using a laboratory press.

**Buffer Solutions**—A solution 16% saturated (on a molar basis) with respect to the thermodynamic solubility of hydroxyapatite was used for demineralization. The solution was a 0.1 *M* acetate buffer containing 3.5 m*M* each of total calcium and total phosphate. The pH was adjusted to 4.5 with sodium hydroxide, and the ionic strength was adjusted to 0.5 with sodium chloride. For remineralization, a 0.1 *M* acetate buffer (pH 4.5) containing 12 m*M* of total calcium (including calcium 45 activity of 0.2 mCi/liter of solution), 12 m*M* total phosphate, 10 ppm of fluoride, and sodium chloride to adjust the ionic strength to 0.5 was used.

The ionic activity of hydroxyapatite, $K_{HAP}$ ($\equiv a_{Ca}^{10} a_{PO_4}^{6} a_{OH}^{2}$), of this buffer was $10^{-120}$. Although not saturated with respect to hydroxyapatite, this solution has a high enough degree of partial saturation so that hydroxyapatite dissolution would be expected to proceed slowly, if at all, based on previous work with solutions approaching this level of calcium and phosphate concentrations (3, 8).

**Demineralization**—A bovine tooth was covered with inlay wax except for 0.25 $cm^2$ of the labial surface. In the pellet experiments, a hydroxyapatite pellet with a surface area of 0.58 $cm^2$ was fixed on a small glass plate by the wax. Either the tooth or pellet then was demineralized in the 16% partially saturated buffer solution for 0.5–6 hr. The solution was shaken gently with a wrist-action shaker[1] and kept at 30°. The volume of the buffer solution was 10 ml/0.25 $cm^2$ of the sample surface.

**Remineralization**—The demineralized tooth or pellet then was given a remineralization treatment for 24–72 hr in 50 ml of the remineralization buffer solution. The solution was shaken gently and kept at 30° as remineralization proceeded.

**Etching and Scraping**—The remineralized sample then was etched in 1 ml of 0.5 *M* $HClO_4$ for successive periods of 15, 15, 30, 60, 120, 200, and 200 sec; the surface was washed with 1 ml of water after each etching step. The depths of the etched layers were estimated from the amounts of phosphate etched. Some hydroxyapatite pellets were scraped evenly

[1] Burrell Co.



*0022-3549/81/0800-0904$01.00/0*
*© 1981, American Pharmaceutical Association*

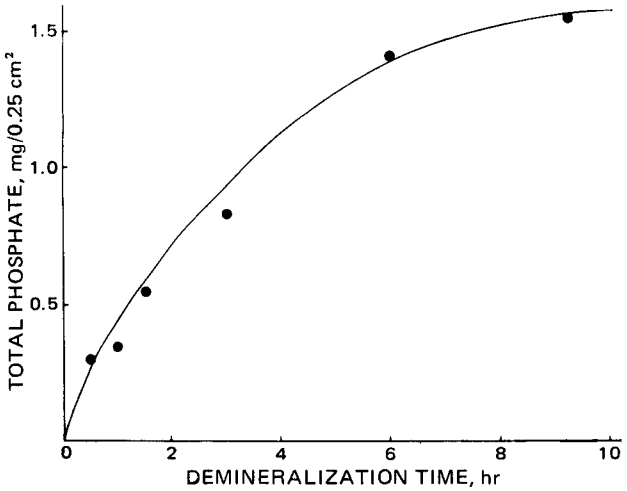


**Figure 1**—*Total phosphate dissolved from bovine tooth as a function of demineralization time.*

by a sharp razor in lieu of etching. The depths of the scraped layers were estimated from the weights of the powdered scrapings. This powder then was dissolved in perchloric acid and assayed to determine fluoride and calcium 45 concentrations.

**Analytical Techniques for Phosphate, Fluoride, Calcium, and Calcium 45**—Phosphate concentrations were determined by the method of Gee *et al.* (9), in which the phosphoammonium–molybdate complex formed is reduced by stannous chloride. The absorbance of the resulting blue color is determined after 15 min at 720 nm[2]. Fluoride concentrations were determined by a fluoride electrode[3] using a low level total ionic strength-adjusting buffer. Concentrations of calcium 45 were determined by a scintillation counter[4].

**Depth of Etchings**—The depths of the etched layers of the teeth and hydroxyapatite pellets were calculated from the amounts of phosphate removed in the etchings, assuming the density of the samples to be 2.95 g/ml. This information then was used to calculate the fluoride and calcium 45 content of the mineral per unit volume.

**Recovery of Demineralized Mineral by Remineralization**—The extent of remineralization is defined by the molar ratio of the total amount of fluoridated hydroxyapatite formed during remineralization to the amount of hydroxyapatite dissolved during demineralization. In this study, the molar ratio was defined as the cumulative calcium 45 taken up during remineralization to the calcium dissolved during demineralization.

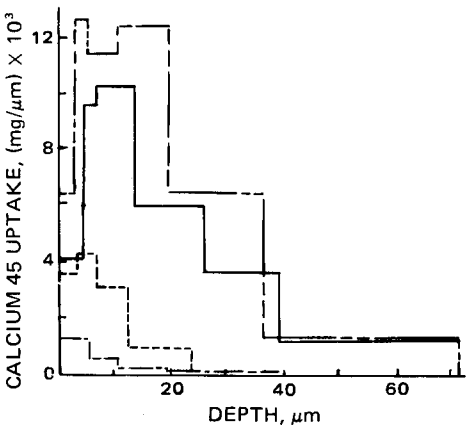


**Figure 2**—*Influence of demineralization time on 24-hr calcium 45 uptake profiles in bovine teeth. The D and R represent demineralization and remineralization, respectively. The lower subscripts represent the time in hours. Key: ——·——, $D_6$–$R_{24}$; —, $D_3$–$R_{24}$; ---, $D_1$–$R_{24}$; and —·—, $D_0$–$R_{24}$.*

[2] Hitachi 690 spectrophotometer.
[3] Model 94-09, Orion Co.
[4] Liquid scintillation system, Beckman Instruments.

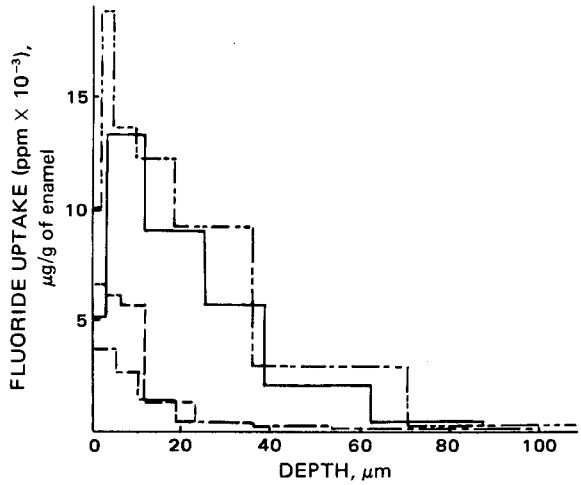


**Figure 3**—*Influence of demineralization time on 24-hr fluoride uptake profiles in bovine teeth. Key: ——·——, $D_6$–$R_{24}$; — , $D_3$–$R_{24}$; ---, $D_1$–$R_{24}$; and —·—, $D_0$–$R_{24}$.*

## RESULTS

**Effect of Demineralization on Remineralization**—Bovine teeth were demineralized in 10 ml of the 16% saturated buffer solution for 0–6 hr. Figure 1 shows the total phosphate (milligrams) dissolved per 0.25 cm² of surface. These results show that the buffer solution was not yet saturated with respect to hydroxyapatite after 6 hr of demineralization. That is, dissolution was still occurring.

To investigate the effects of demineralization on subsequent remineralization, the bovine teeth demineralized for 0–6 hr were remineralized for 24 hr. Figure 2 shows calcium 45 concentration profiles for these teeth. The calcium 45 concentration increases with increasing demineralization times, and the enamel not subjected to prior demineralization ($D_0$) was remineralized to a negligible extent. Figure 3 shows the fluoride concentration profiles of the same samples. Fluoride concentrations also increased with increasing demineralization times. However, the fluoride uptake of nondemineralized enamel was not negligible as was the calcium 45 uptake, probably as a result of a higher tendency for superficial ion exchange.

The fluoride concentration gradient of the teeth demineralized less than 1 hr decreased rapidly from the high levels at the surface to <500 ppm at a depth of only 20 μm, but the teeth demineralized more than 1.5 hr had much higher fluoride gradients, decreasing gradually to ~1000–2000 ppm of fluoride at depths of ~50–60 μm. These results are consistent with results in which teeth demineralized under mild conditions are rehardened or remineralized much easier than sound teeth (10, 11).

The effect of remineralization time on the calcium 45 and fluoride uptake was examined by remineralizing the teeth for 24 and 72 hr following 6 hr of demineralization. Figure 4 shows the resulting calcium 45 concentration profiles. They were nearly the same with remineralization being essentially complete at 24 hr.

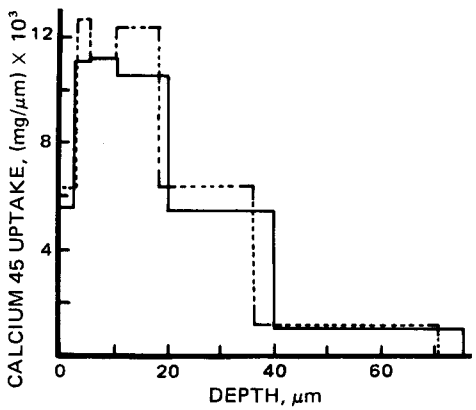


**Figure 4**—*Influence of remineralization time of calcium 45 uptake profiles in bovine teeth, showing that remineralization is essentially complete in 24 hr. Key: ---, $D_6$–$R_{24}$; and —, $D_6$–$R_{72}$.*

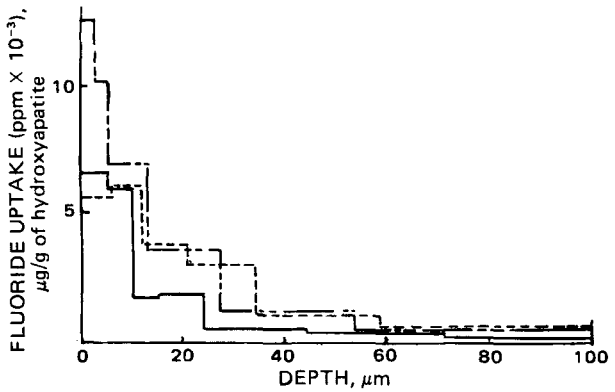


**Figure 5**—*Influence of demineralization time on 24-hr fluoride uptake profiles in hydroxyapatite pellets as measured by the perchloric acid etch technique. Key: —·—, $D_{3.0}$–$R_{24}$; ---, $D_{1.5}$–$R_{24}$; and —, $D_{0.0}$–$R_{24}$.*

To confirm that the demineralization/remineralization dependence seen in bovine teeth was indeed a result of hydroxyapatite behavior as expected from the model and not caused primarily by the enamel matrix, the remineralization of hydroxyapatite pellets was examined by the same method as used for the bovine teeth. Hydroxyapatite pellets were demineralized for 0, 1.5, or 3 hr. Figure 5 shows the fluoride concentration profiles obtained after remineralizing these pellets for 24 hr. The concentrations increased with increasing demineralization time in accord with the results obtained with bovine teeth. Although the calcium 45 uptake data are now shown, they were also coincident with the enamel data. However, fluoride and calcium 45 concentrations in the nondemineralized pellet were noticeably higher than those observed in enamel.

**Mineral Recovery by Remineralization**—The extent of mineral recovery was calculated in several experiments with bovine enamel and hydroxyapatite pellets (Fig. 6). In no case was the demineralized mineral completely replaced during remineralization.

**Form of Incorporated Fluoride**—If fluoridated hydroxyapatite was formed from the ions supplied by the remineralization solution, the molar ratio of calcium 45 to fluoride uptake should be 5.0; a ratio of 0.5 would be expected for the formation of calcium fluoride (I). Figure 7 shows the molar ratio of calcium 45 to fluoride uptake after 24 hr of remineralization for both bovine teeth and hydroxyapatite pellets as a function of demineralization time. The ratios were ~5.0, corresponding to the formation of fluoridated hydroxyapatite. However, for demineralization of <1.5 hr, the ratios were <5 but much higher than the 0.5 ratio expected from the formation of I. This discrepancy from 5.0 might be due to the formation of I to a small extent or to the ion exchanges of calcium and hydroxide ions of hydroxyapatite for calcium 45 and fluoride in the buffer solution.

In a remineralization study with hydroxyapatite powder using a remineralizing solution identical to that described earlier, it was shown by extraction with potassium hydroxide that the fluoride in the remineralized material is not in the form of I and is most likely apatitic (12).

As an independent check of the results obtained by the etching method,

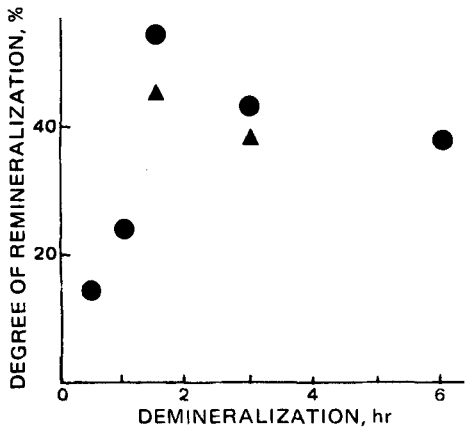


**Figure 6**—*Influence of demineralization time on the degree of subsequent remineralization. Key: ●, bovine tooth; and ▲, hydroxyapatite pellet.*

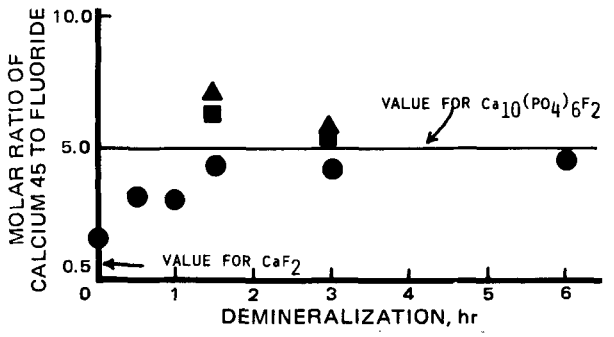


**Figure 7**—*Influence of demineralization time on the calcium 45 to fluoride molar ratio of the subsequently remineralized phase. Key: ●, bovine tooth (etching method); ■, hydroxyapatite pellet (etching method); and ▲, hydroxyapatite pellet (scraping method).*

the remineralization of hydroxyapatite pellets was investigated by the scraping method. Pellets remineralized for 24 hr following 1.5 or 3.0 hr of demineralization were scraped to a depth of ~60 μm, and the scrapings were analyzed for fluoride and calcium 45. The uptakes of fluoride and calcium 45 measured in this way were almost identical to those obtained by the etching method. The molar ratios of calcium 45 to fluoride uptake obtained from the etching and scraping techniques are shown in Fig. 7. The coincidence of the results of the two methods confirms the results obtained from the etching method. As a further check, electron microprobe determinations (calcium, phosphate, and fluoride) as a function of depth were carried out on sectioned, remineralized bovine teeth. The results were in good agreement with the perchloric acid method.

All experiments were carried out in duplicate, with the variation between the two trials typically on the order of 10–15%.

## DISCUSSION

In both bovine enamel and compressed hydroxyapatite pellets, there was a direct relationship between the amount of mineral lost during demineralization and the amount regained during remineralization for the time periods studied. In all cases, there was greater uptake of calcium 45 and fluoride in the pellet than in the bovine enamel. This difference is likely due to the higher porosity of the pellet. These results are consistent with the idea that when there is no prior demineralization, remineralization is restricted to available void spaces in the pellet or enamel. During demineralization, however, additional spaces are created (including *c*-axis holes in the crystals) in which remineralization can occur. It appears that remineralization is occurring both in the initial voids and in the voids created by demineralization.

The extent of remineralization after a 24-hr remineralization treatment was considerably less than 100% both for bovine teeth and hydroxyapatite pellets. However, in the real *in vivo* situation where teeth are continuously undergoing demineralization/remineralization cycles, the extent of remineralization must, on the average, be 100% unless there is an ongoing net growth of lesions.

It was expected that for longer demineralization times, the recovery during remineralization might be <100% because many more crystals would have time to dissolve completely, leaving no templates for subsequent remineralization. Work currently in progress in these laboratories, using microradiography as a tool for measuring mineral density profiles (13), has shown that this is the case. The described demineralization conditions result in a recession of the surface due to complete removal of ~40 μm of enamel, below which there is a lesion ~40 μm deep that is completely filled during the subsequent remineralization treatment.

This mechanism implies that for short demineralization times, nearly 100% recovery might be expected. In actuality, for the shortest demineralization times (<1.5 hr), the extent of remineralization was less than for some longer demineralization times. One possible explanation is that the starting enamel or pellet was not uniform and that the very first material removed in the demineralization was some more soluble phase that did not dissolve *via* the hole-forming mechanism presumably followed by hydroxyapatite under these conditions and, hence, did not leave any such templates for remineralization.

## CONCLUSIONS

Both bovine enamel and hydroxyapatite pellets were remineralized in a fluoride-containing remineralization solution after prior demineral-

alization for various lengths of time. In both the enamel and pellet systems, the degree of remineralization attainable was directly related to the extent of prior demineralization, although in no instance was the demineralized material 100% recovered in remineralization. Fluoride levels up to several thousand parts per million were found at depths as great as 50 μm from the surface in some cases. The stoichiometry of the remineralized material and electron microprobe examination were consistent with the formation of fluoridated hydroxyapatite rather than I. The detailed characterization of the behavior of the remineralized material is now being addressed in studies in these laboratories.

## REFERENCES


(1) M. S. Wu, W. I. Higuchi, J. L. Fox, and M. Friedman, *J. Dent. Res.*, **55**, 496 (1976).

(2) M. B. Fawzi, J. L. Fox, M. G. Dedhiya, W. I. Higuchi, and J. J. Hefferren, *J. Colloid Interface Sci.*, **67**, 304 (1978).

(3) J. L. Fox, W. I. Higuchi, M. B. Fawzi, and M. S. Wu, *ibid.*, **67**, 312 (1978).

(4) E. Griffith, A. Katdare, J. L. Fox, and W. I. Higuchi, *ibid.*, **67**, 331 (1978).

(5) T. Koulourides, P. Phantumvanite, E. C. Munksgaard, and T. Housch, *J. Oral Pathol.*, **3**, 185 (1974).

(6) M. F. Little and L. T. Steadman, *Arch. Oral Biol.*, **11**, 273 (1966).

(7) E. C. Moreno, T. M. Gregory, and W. E. Brown, *J. Res. Natl. Bur. Std.*, **72A**, 773 (1968).

(8) M. B. Fawzi, W. I. Higuchi, and J. J. Hefferren, *J. Dent. Res.*, **56**, 518 (1977).

(9) A. Gee, L. Domingues, and V. Deitz, *Anal. Chem.*, **26**, 1487 (1954).

(10) T. Koulourides and W. Pigman, *J. Dent. Res.*, **39**, 198 (1960).

(11) T. Koulourides, H. Cueto, and W. Pigman, *Nature*, **139**, 226 (1961).

(12) A. V. Katdare, J. L. Fox, D. J. Crommelin, and W. I. Higuchi, *J. Dent. Res., Spec. Issue A*, **59**, 501 (1980).

(13) D. Bergstrom, B. V. Iyer, J. L. Fox, and W. I. Higuchi, *ibid.*, **59**, 366 (1980).


## ACKNOWLEDGMENTS


Supported by National Institute of Dental Research Grants DE04600 and DE01830.

The authors thank Mr. John Lenke of the American Dental Association Laboratories, Chicago, Ill., for conducting electron microprobe determinations on remineralized enamel.


# Novel Topical Fluoride Delivery System I: Remineralization of Ground Bovine Teeth


**MASAKATSU YONESE *, BALA V. IYER *, JEFFREY L. FOX *, JOHN J. HEFFERREN ‡, and WILLIAM I. HIGUCHI *x**



Received June 30, 1980, from the **College of Pharmacy, University of Michigan, Ann Arbor, MI 48109*, and the ‡*American Dental Association, Chicago, IL 60611.* Accepted for publication January 26, 1981.



**Abstract** □ Laboratory studies were carried out on a newly conceived fluoride-containing remineralizing system with bovine teeth. The prototype fluoride delivery device involved micronized calcium fluoride maintained at the tooth surface with a cellulose film. Together with salivary calcium and phosphate (or simulated saliva), this system was able to generate and maintain the appropriate thermodynamic activity driving force for significant fluorapatite deposition in a reasonably short time (~48 hr).



**Keyphrases** □ Delivery devices—fluoride, remineralization of bovine teeth, effect of film thickness and particle size □ Fluoride—delivery devices for remineralization of bovine teeth, effect of film thickness and particle size on remineralization □ Remineralization—bovine teeth, fluoride delivery devices, effect of film thickness and particle size on remineralization □ Teeth, bovine—remineralization using fluoride delivery devices, effect of film thickness and particle size on remineralization


Recent *in vitro* studies in these laboratories (1) showed that the amount of fluoride incorporated in a remineralization treatment can be increased substantially if the tooth is demineralized carefully prior to the remineralization. This finding suggests that successful remineralization might be attained *in vivo* if the teeth could be demineralized to the same extent as in the *in vitro* experiments. This paper describes the initial studies in the development of a fluoride topical delivery system designed to achieve *in vivo* results similar to the results obtained *in vitro*.

*In vitro* remineralization can be very successful when the ionic activity product, $K_{FAP}$ ($a^{10}_{Ca^{2+}} a^{6}_{PO_4^{3-}} a^{2}_{F^-}$), is $\sim 10^{-108}$ (1). Less concentrated solutions provide less driving force for remineralization; more concentrated solutions may result in the rapid precipitation of calcium fluoride (I) or dicalcium phosphate dihydrate (II) in the prepared solutions themselves or in enamel pores, thereby blocking or retarding remineralization. It was decided to control the solution conditions at the enamel surface by supplying fluoride in the form of I suspended in a film adhering to the enamel surface.

Calculations have shown that mixtures of I and II or I alone in the film should result in solution compositions appropriate for remineralization at the enamel surface. Furthermore, the relatively low solubility of I limits the rate at which the suspended particles dissolve, so that fluoride applied in this way is inherently long acting, even with no moderation from the film. This fact makes the film design problem much simpler than when a more soluble fluoride source such as sodium fluoride is used and the film must then control the release rate. Therefore, the problem of film design is not to find a film with a narrowly prescribed set of properties but rather to find a film that can hold the particles of I in place while being porous to saliva and interfering minimally with particle dissolution.

## EXPERIMENTAL

**Materials and Methods**—Bovine teeth from 8-week-old, crate-fed, strictly kosher calves were obtained from packing houses in the Chicago area. These animals were chosen because each is subjected to rigidly controlled and uniform environmental conditions (including diet) and



*© 1981, American Pharmaceutical Association*

alization for various lengths of time. In both the enamel and pellet systems, the degree of remineralization attainable was directly related to the extent of prior demineralization, although in no instance was the demineralized material 100% recovered in remineralization. Fluoride levels up to several thousand parts per million were found at depths as great as 50 μm from the surface in some cases. The stoichiometry of the remineralized material and electron microprobe examination were consistent with the formation of fluoridated hydroxyapatite rather than I. The detailed characterization of the behavior of the remineralized material is now being addressed in studies in these laboratories.

## REFERENCES


(1) M. S. Wu, W. I. Higuchi, J. L. Fox, and M. Friedman, *J. Dent. Res.*, **55**, 496 (1976).

(2) M. B. Fawzi, J. L. Fox, M. G. Dedhiya, W. I. Higuchi, and J. J. Hefferren, *J. Colloid Interface Sci.*, **67**, 304 (1978).

(3) J. L. Fox, W. I. Higuchi, M. B. Fawzi, and M. S. Wu, *ibid.*, **67**, 312 (1978).

(4) E. Griffith, A. Katdare, J. L. Fox, and W. I. Higuchi, *ibid.*, **67**, 331 (1978).

(5) T. Koulourides, P. Phantumvanite, E. C. Munksgaard, and T. Housch, *J. Oral Pathol.*, **3**, 185 (1974).

(6) M. F. Little and L. T. Steadman, *Arch. Oral Biol.*, **11**, 273 (1966).

(7) E. C. Moreno, T. M. Gregory, and W. E. Brown, *J. Res. Natl. Bur. Std.*, **72A**, 773 (1968).

(8) M. B. Fawzi, W. I. Higuchi, and J. J. Hefferren, *J. Dent. Res.*, **56**, 518 (1977).

(9) A. Gee, L. Domingues, and V. Deitz, *Anal. Chem.*, **26**, 1487 (1954).

(10) T. Koulourides and W. Pigman, *J. Dent. Res.*, **39**, 198 (1960).

(11) T. Koulourides, H. Cueto, and W. Pigman, *Nature*, **139**, 226 (1961).

(12) A. V. Katdare, J. L. Fox, D. J. Crommelin, and W. I. Higuchi, *J. Dent. Res., Spec. Issue A*, **59**, 501 (1980).

(13) D. Bergstrom, B. V. Iyer, J. L. Fox, and W. I. Higuchi, *ibid.*, **59**, 366 (1980).


## ACKNOWLEDGMENTS


Supported by National Institute of Dental Research Grants DE04600 and DE01830.

The authors thank Mr. John Lenke of the American Dental Association Laboratories, Chicago, Ill., for conducting electron microprobe determinations on remineralized enamel.


# Novel Topical Fluoride Delivery System I: Remineralization of Ground Bovine Teeth


**MASAKATSU YONESE *, BALA V. IYER *, JEFFREY L. FOX *, JOHN J. HEFFERREN ‡, and WILLIAM I. HIGUCHI *x**



Received June 30, 1980, from the **College of Pharmacy, University of Michigan, Ann Arbor, MI 48109*, and the ‡*American Dental Association, Chicago, IL 60611.* Accepted for publication January 26, 1981.



**Abstract** □ Laboratory studies were carried out on a newly conceived fluoride-containing remineralizing system with bovine teeth. The prototype fluoride delivery device involved micronized calcium fluoride maintained at the tooth surface with a cellulose film. Together with salivary calcium and phosphate (or simulated saliva), this system was able to generate and maintain the appropriate thermodynamic activity driving force for significant fluorapatite deposition in a reasonably short time (~48 hr).



**Keyphrases** □ Delivery devices—fluoride, remineralization of bovine teeth, effect of film thickness and particle size □ Fluoride—delivery devices for remineralization of bovine teeth, effect of film thickness and particle size on remineralization □ Remineralization—bovine teeth, fluoride delivery devices, effect of film thickness and particle size on remineralization □ Teeth, bovine—remineralization using fluoride delivery devices, effect of film thickness and particle size on remineralization


Recent *in vitro* studies in these laboratories (1) showed that the amount of fluoride incorporated in a remineralization treatment can be increased substantially if the tooth is demineralized carefully prior to the remineralization. This finding suggests that successful remineralization might be attained *in vivo* if the teeth could be demineralized to the same extent as in the *in vitro* experiments. This paper describes the initial studies in the development of a fluoride topical delivery system designed to achieve *in vivo* results similar to the results obtained *in vitro*.

*In vitro* remineralization can be very successful when the ionic activity product, $K_{FAP}$ ($a^{10}_{Ca^{2+}} a^{6}_{PO_4^{3-}} a^{2}_{F^-}$), is $\sim 10^{-108}$ (1). Less concentrated solutions provide less driving force for remineralization; more concentrated solutions may result in the rapid precipitation of calcium fluoride (I) or dicalcium phosphate dihydrate (II) in the prepared solutions themselves or in enamel pores, thereby blocking or retarding remineralization. It was decided to control the solution conditions at the enamel surface by supplying fluoride in the form of I suspended in a film adhering to the enamel surface.

Calculations have shown that mixtures of I and II or I alone in the film should result in solution compositions appropriate for remineralization at the enamel surface. Furthermore, the relatively low solubility of I limits the rate at which the suspended particles dissolve, so that fluoride applied in this way is inherently long acting, even with no moderation from the film. This fact makes the film design problem much simpler than when a more soluble fluoride source such as sodium fluoride is used and the film must then control the release rate. Therefore, the problem of film design is not to find a film with a narrowly prescribed set of properties but rather to find a film that can hold the particles of I in place while being porous to saliva and interfering minimally with particle dissolution.

## EXPERIMENTAL

**Materials and Methods**—Bovine teeth from 8-week-old, crate-fed, strictly kosher calves were obtained from packing houses in the Chicago area. These animals were chosen because each is subjected to rigidly controlled and uniform environmental conditions (including diet) and



*© 1981, American Pharmaceutical Association*

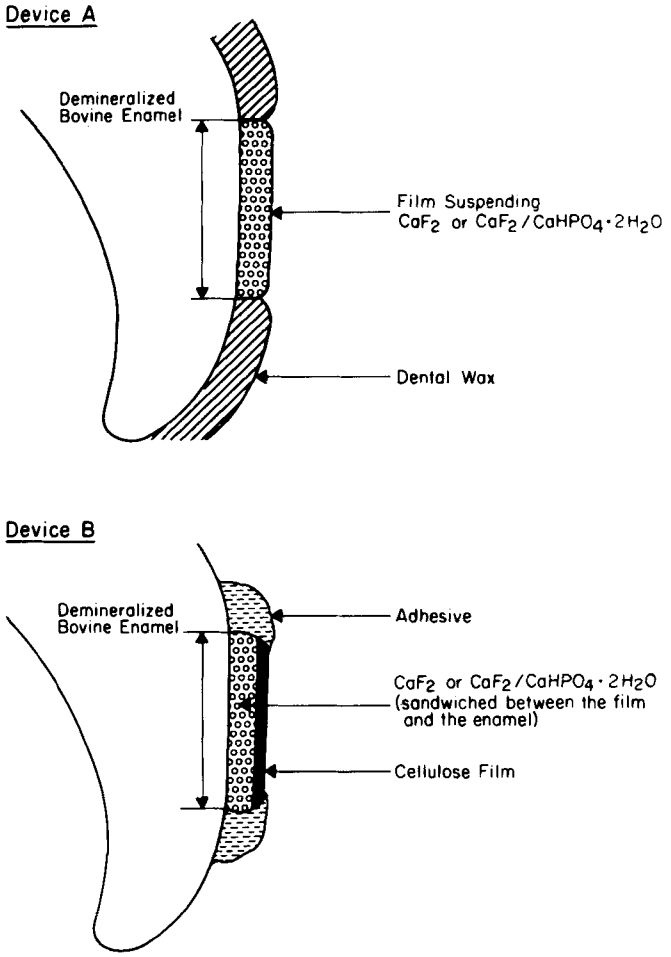


**Figure 1**—*Fluoride delivery devices.*

each is slaughtered at precisely the same age. Thus, each tooth has very nearly the same past history so there is little experimental variation from one tooth to another. In addition, these teeth provide large flat surfaces for kinetic studies and have no detectable fluoride (≪1 ppm in the enamel). All bovine teeth were ground with a rotating sandpaper (No. 600) to remove any pellicle and further reduce any sample to sample variation.

**Chemicals**—Ethylcellulose[1] and povidone[2] (average mol. wt. 10,000) were used as supplied from the manufacturer. The cellulose film was cut from dialysis tubing[3]. All other chemicals were analytical grade, and all water was distilled twice.

**Demineralization Experiments**—In the demineralization experiments, a tooth was covered by inlay wax except for ~0.25 $cm^2$ of the labial surface. The tooth then was demineralized in 10 ml of a 16% saturated buffer solution (0.1 *M* acetate buffer at pH 4.5, containing 3.5 m*M* total phosphate and total calcium, with the ionic strength adjusted to 0.5 by the addition of sodium chloride) with gentle shaking for 1–48 hr. The extent of demineralization was assessed by measuring the amount of phosphate dissolved. The solution was always kept at 30 ± 0.1°.

The attachment of fluoride delivery devices followed demineralization. Two kinds of devices were used (Fig. 1).

**Mixed Polymer Film with Suspended I or I–II (Fluoride Delivery Device A)**—Powders of I or II passed through either a 100-mesh sieve (150-μm openings) or a 270-mesh sieve (52-μm openings) were suspended in a 5% (w/v) ethanolic solution of the selected polymer mixture. The tooth was dipped for various times in the polymer solution. Before each dipping, the polymer solution on the tooth surface was dried so as not to drop off. Therefore, the film thickness could be controlled by the dipping times and was varied from 10 to 60 μm. After 2 min of drying, the tooth with the film was immersed in water for 30 min to permit ethanol to leach from the film.

[1] Ethocel, Dow Chemical Co.
[2] Matheson, Coleman and Bell.
[3] Spectrum Medical Industries.

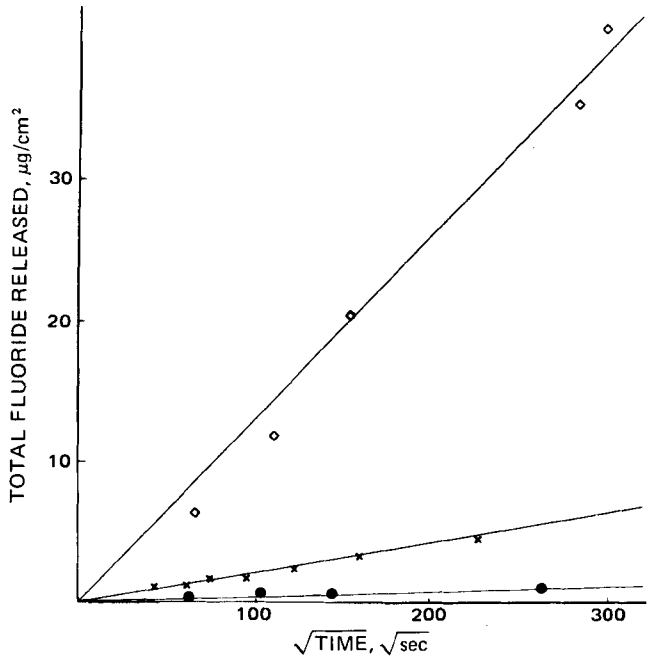


**Figure 2**—*Plots of Q* versus *the square root of time for determining the diffusivity of calcium fluoride in the polymeric films. Key:* ◇, *calcium fluoride–ethylcellulose–povidone (1:4:1);* ×, *calcium fluoride–ethylcellulose (1:5); and* ●, *calcium fluoride–ethylcellulose–glycerin (1:5:0.22).*

**Cellulose Film Containing Micronized I or I–II (Fluoride Delivery Device B)**—Powders of I and II passed through a 270-mesh sieve (52-μm openings) were mixed in various ratios. The mixture was scattered evenly on the surface (0.2 $cm^2$) and was covered by a cellulose film with its periphery fixed by adhesive[4]. The quantities used were 0.5 mg of I or 2 mg of a 1:6 mixture of I and II/0.2 $cm^2$.

**Remineralization Experiments**—In the remineralization experiments, the tooth with the attached fluoride delivery device was remineralized for 24–72 hr in buffer for remineralization (0.1 *M* acetate buffer at pH 4.5 containing 12 m*M* of total calcium and total phosphate with its ionic strength adjusted to 0.5 by the addition of sodium chloride). The buffer solution was shaken gently and kept at 30 ± 0.1° as in demineralization. A buffer solution volume of 100 ml was used so that the buffer composition during remineralization would not change significantly.

The remineralization in saliva was done in a test tube with enough saliva for dipping the tooth. The tooth was fixed at the tip of a small glass rod ~1–2 cm shorter in length than the test tube. The test tube was fixed on a rotating wheel (2 rpm) in an electric oven kept at 37°. This was accomplished in such a way that the tooth was prevented by the glass rod from moving down with the saliva as the tube rotated end-over-end and instead was immersed intermittently in the saliva. All remineralization experiments were done in duplicate.

The fluoride delivery system was removed after remineralization. For Device A, the film was dissolved by ethanol, which was renewed at least five times and shaken vigorously. For Device B, the film was peeled off carefully so as not to damage the tooth surface, and the tooth was washed with water to remove any I or II particles adhering to the surface. Then the surface was rewaxed, except for the remineralized area, and etched in 1 ml of 0.5 *M* $HClO_4$ for successive intervals of 30, 60, 120, 200, and 200 sec. The etched surface was washed with 1 ml of water after each etching step.

**Assay of Phosphate, Fluoride, and Calcium 45**—Phosphate, fluoride, and calcium 45 concentrations in each etching solution were analyzed when the tooth was remineralized in the buffer containing calcium 45. Phosphate and fluoride were analyzed when the tooth with the fluoride delivery device was remineralized in saliva.

Phosphate concentrations were determined by the method of Gee *et al.* (2) in which the phosphoammonium–molybdate complex formed was reduced by stannous chloride. The absorbance of the resulting blue color was determined after 15 min at 720 nm[5].

[4] Endur M, Ormco Co.
[5] Hitachi 690 spectrophotometer.

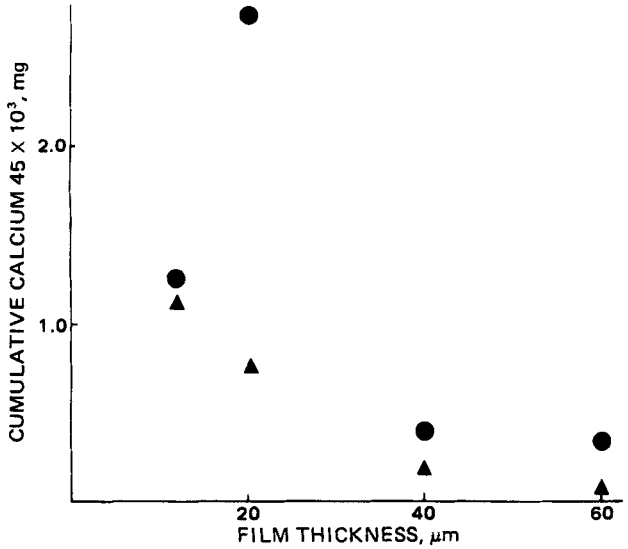


**Figure 3**—*Effect of film thickness and particle size on the cumulative uptake of calcium 45 with Device A. Teeth were demineralized for 6 hr and remineralized for 24 hr. Calcium fluoride particles passed through a 270- (●) or a 100- (▲) mesh sieve.*

Fluoride concentrations were determined by a combination fluoride electrode[6] using a low-level total ionic strength-adjusting buffer.

Calcium 45 was determined by a scintillation counter[7]. Nonradioactive calcium was measured by atomic absorption[8]. Because of possible phosphate interference, strontium chloride was added to each sample in the latter procedure.

**Apparent Diffusivity of I through Ethylcellulose, Ethylcellulose–Glycerin, and Ethylcellulose–Povidone Films**—When a solute is suspended in a film, its diffusivity, $D_e$, through the film can be obtained by measuring the amount of solute released from the film as a function of time according to (3):

$$Q = (2D_e t A C_s)^{1/2} \qquad \text{(Eq. 1)}$$

where $Q$ is the amount of solute released per unit area after time $t$, $A$ is the total amount of solute in the film per unit volume, and $C_s$ is the solubility of the solute in the film.

The diffusivities of I through ethylcellulose, ethylcellulose–glycerin, and ethylcellulose–povidone films were measured as follows. Calcium fluoride (I) was suspended in 0.3 ml of an ethanolic solution of the polymer or polymer mixture. The suspension was poured into a shallow (1-mm depth) cylindrical depression (0.88-cm radius) on a polytef disk and dried for 13 min in an electric oven at 50°. The film on the disk was then immersed into water that was stirred constantly and kept at 30°. The fluoride released from the film was determined at several sampling times with a fluoride electrode.

## RESULTS

**Fluoride Delivery Device A**—*Diffusivity of I in Polymer Films*—The plots for amounts of I released *versus* the square root of time for the three films are shown in Fig. 2. Effective diffusivities of I then were calculated from the slopes using Eq. 1. The values of $D_e$ for I in ethylcellulose, ethylcellulose–glycerin, and ethylcellulose–povidone films were $1.44 \pm 0.18 \times 10^{-10}$, $3.20 \pm 0.58 \times 10^{-12}$, and $2.20 \pm 0.25 \times 10^{-8}$ cm²/sec, respectively. Since the last film had a higher effective diffusivity and adhered to the tooth better, it was selected for Device A.

*Effects of Film Thickness and Particle Size of Suspended I on Remineralization*—The teeth demineralized for 6 hr ($D_6$) were covered by varying thicknesses (10–60 μm) of an ethylcellulose–povidone film containing I, which was sieved by a 100- or 270-mesh sieve (150- or 52-μm openings, respectively). Then these teeth were remineralized for 24 hr in buffer ($R_{24}$). Figure 3 shows the cumulative uptake of calcium 45 at depths up to 80 μm as a function of the film thickness. Fluoride uptake decreased with increasing film thickness for both particle sizes of I studied and were very small, with levels of only ~1/50 or less of those attained previously in solution remineralization experiments (1). Even in the system with smaller particles, appreciable uptake was not found. These results indicate that the diffusion of ions out of or through the film is the rate-limiting step for remineralization in this system and that the ionic activity product, $K_{FAP}$, simply does not reach a high enough value ($>10^{-108}$) in the tooth.

[6] Model 96-09, Orion Co.
[7] Liquid scintillation system, Beckman Instruments.
[8] Perkin-Elmer atomic absorption model 303.

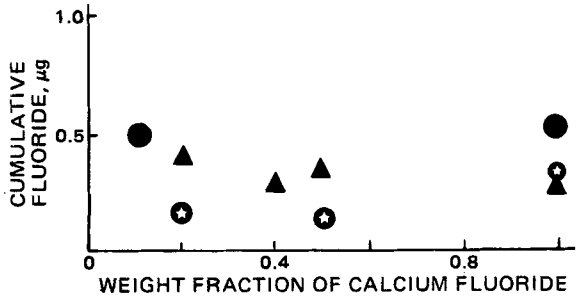


**Figure 4**—*Effect of ratio of calcium fluoride ($CaF_2$) to calcium phosphate dihydrate ($CaHPO_4 \cdot 2H_2O$) on cumulative fluoride uptake with Device A. Key: ●, $D_6$–$R_{24}$, 40-μm film thickness; ◘, $D_6$–$R_{72}$, 40-μm film thickness; and ▲, $D_{24}$–$R_{72}$, 40-μm film thickness.*

*Effects of Longer Remineralization Times and All Three Ion Sources*—Assuming that the solubility of I in the aqueous pores of the film phase is equal to its aqueous solubility implies that the fluoride concentration in the pores of the film is ~7 ppm. This concentration is high enough for the formation of fluoridated hydroxyapatite in the remineralization step, suggesting that higher permeabilities of the film to ions and longer remineralization times could increase the degree of remineralization. Furthermore, higher calcium and phosphate concentrations in the film might improve remineralization even if the permeability remains low. Therefore, the following experimental systems were examined.

Teeth demineralized for 6 or 24 hr were covered by a 40-μm film (ethylcellulose–povidone) containing mixtures of I and II and remineralized for 24 or 72 hr. Although a thinner film would present less of a barrier for ions to diffuse in from the external solution, the 40-μm film was selected to accommodate the particles that ranged in size up to ~50 μm. Figure 4 shows the cumulative fluoride uptake (in micrograms) to a depth of 89–90 μm as a function of the weight fraction of I in the I–II mixture. These results ranged from 0.2 to 0.5 μg and did not depend significantly on either the weight fraction of I or the demineralization and remineralization times. Fluoride concentrations in these teeth were much less than expected, a few hundred parts per million at a depth of ~40 μm.

**Fluoride Delivery Device B**—Calcium fluoride or a I–II mixture was dispersed on the surface of a demineralized tooth and covered by a cellulose film in which the ions were estimated to have an effective diffusivity of $\sim 10^{-6}$ cm²/sec. The tooth was remineralized for 24 hr in the reminer-

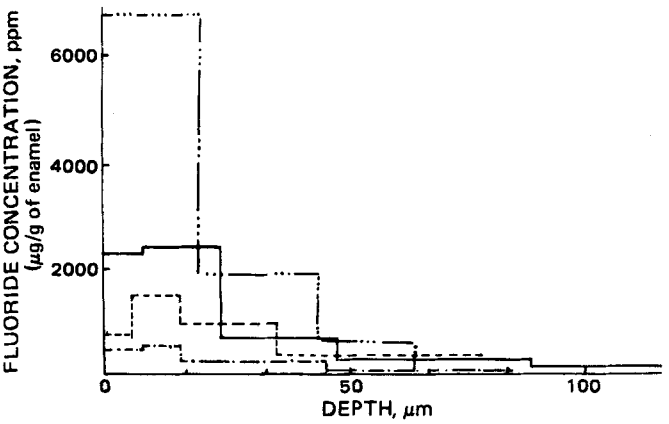


**Figure 5**—*Remineralization of ground bovine tooth using Device B in saliva and in remineralizing solution. Key: -···-, calcium fluoride with remineralization in saliva; —, calcium fluoride with remineralization in buffer solution; - - -, calcium fluoride and calcium phosphate dihydrate (1:6) with remineralization in saliva; and -·-, calcium fluoride and calcium phosphate dihydrate (1:6) with remineralization in buffer solution.*

alizing buffer solution. During remineralization, water, calcium, and phosphate diffuse through the cellulose film and through a region immediately adjacent to the tooth surface, which contains the micronized powders. Therefore, calcium and phosphate ions were supplied from both the buffer and the dissolution of these powders, while fluoride was supplied directly from the dissolution of I. The higher diffusivity of ions through the cellulose film and the lack of a polymer network on the tooth surface would be expected to lead to much more remineralization by Device B than was accomplished using Device A. Figure 5 shows the fluoride concentration profiles measured in the teeth remineralized with Device B. The results were considerably higher (1000–2000 ppm at depths as great as 40–50 μm) than the results obtained with Device A (<300 ppm). Furthermore, Device B containing only I was more effective in remineralizing the teeth than was Device B containing the I–II mixture, implying that calcium and phosphate readily diffused through the film from the solution.

The fluoride concentration profile of teeth remineralized in saliva instead of the buffer solution are shown in Fig. 5. The results were almost the same as those obtained from remineralization in the remineralizing buffer solution. As was the case when remineralizing with buffer solutions, the system containing I was much better than the I–II mixture. Even in saliva, an appreciable fluoride concentration was achieved using Device B.

## DISCUSSION

The results obtained with Device B show that satisfactory remineralization occurred when I was held in proximity to the tooth surface for 24 hr. These initial experiments with Device A, a prototype of a practical means for holding I near the tooth surface, show that the main problem to overcome is to find a polymer film that adheres to the tooth and from which I is released rapidly.

Since these studies showed that remineralization can be achieved in the model systems using bovine teeth, it then was verified that human teeth respond in similar manner (4, 5). These studies provide justification for proceeding in the development of the appropriate polymer system for use with Device A.

## SUMMARY

Delivery Device A, a possible prototype of a clinically feasible remineralization system, was not successful with the polymer systems studied. In each case, the film permeability was not high enough for ions to penetrate at a sufficient rate.

Delivery Device B, while not practical for clinical use, had a much higher permeability to ions than did Device A and was used to simulate behavior that might be expected from Device A if a more permeable film could be developed. Device B was quite effective in remineralizing teeth, yielding fluoride levels of ~1000 ppm at depths up to 50 μm, *even in saliva*. Calcium fluoride alone gave better results than the I–II mixtures studied.

These results imply that a practical clinical remineralization procedure based on Device A is feasible, with the primary problem being development of a suitable polymer film.

## REFERENCES

(1) M. Yonese, J. L. Fox, and W. I. Higuchi, AADR Abstract No. 50 (1978).

(2) A. Gee, L. Domingues, and V. Deitz, *Anal. Chem.*, **26**, 1487 (1954).

(3) T. Higuchi, *J. Pharm. Sci.*, **52**, 1145 (1963).

(4) M. Yonese, L. J. Abrahams, J. L. Fox, W. I. Higuchi, and G. Charbeneau, AADR Abstract No. 1114 (1979).

(5) L. J. Abrahams, M. Yonese, W. I. Higuchi, J. L. Fox, and G. T. Charbeneau, *J. Dent. Res.*, **59**, 583 (1980).

## ACKNOWLEDGMENTS

Supported by National Institute of Dental Research Grants DE04600 and DE02731.

# Novel Topical Fluoride Delivery System II: Remineralization of Human Teeth

**JEFFREY L. FOX, MASAKATSU YONESE, BALA V. IYER, LEWIS J. ABRAHAMS, and WILLIAM I. HIGUCHI** ˣ

Received June 30, 1980, from the *College of Pharmacy, University of Michigan, Ann Arbor, MI 48109.* Accepted for publication January 26, 1981.

**Abstract** □ A recently conceived calcium fluoride-containing remineralization system was tested using human teeth *in vitro*. The influence of several variables (surface pretreatment, demineralization time, and remineralization time) was studied. Appreciable levels of fluoride taken up by pumiced human teeth were found at depths up to 50 μm when remineralization was carried out in either the remineralizing solution or saliva. The successful performance of the delivery device in these laboratory studies is encouraging and indicates that the logical evolution of the crude devices studied thus far could lead to clinically practical fluoride delivery devices.

**Keyphrases** □ Delivery devices—fluoride, remineralization of human teeth *in vitro*, effect of surface treatment on remineralization □ Fluoride—delivery devices for remineralization of human teeth *in vitro*, effect of surface treatment on remineralization □ Remineralization—human teeth *in vitro*, fluoride delivery devices, effect of surface treatment on remineralization □ Teeth, human—remineralization *in vitro* using fluoride delivery devices, effect of surface treatment on remineralization

As a result of *in vitro* studies demonstrating the effectiveness of a controlled demineralization pretreatment in enhancing subsequent fluoride remineralization (1), investigations recently were initiated to develop techniques for a practical clinical remineralization procedure. In the previous study, Yonese *et al.* (2) worked with a delivery device that was capable of physically holding particles of calcium fluoride (I) adjacent to the tooth surface while remaining permeable to calcium, phosphate, and fluoride ions as well as water. This device was capable of depositing high levels of fluoride (1000–2000 ppm) at depths of up to 50 μm, using bovine enamel as a test substrate.

This paper demonstrates the effectiveness of demineralization–remineralization for human teeth and examines additional variables that are clinically relevant but that were not studied with the bovine teeth.

## EXPERIMENTAL

Human teeth removed for orthodontic reasons were obtained from dentists in the Chicago area.

The buffer solutions used for demineralization and remineralization were prepared as described previously (2). The demineralizing solution



0022-3549/81/0800-0910$01.00/0
© 1981, American Pharmaceutical Association

alizing buffer solution. During remineralization, water, calcium, and phosphate diffuse through the cellulose film and through a region immediately adjacent to the tooth surface, which contains the micronized powders. Therefore, calcium and phosphate ions were supplied from both the buffer and the dissolution of these powders, while fluoride was supplied directly from the dissolution of I. The higher diffusivity of ions through the cellulose film and the lack of a polymer network on the tooth surface would be expected to lead to much more remineralization by Device B than was accomplished using Device A. Figure 5 shows the fluoride concentration profiles measured in the teeth remineralized with Device B. The results were considerably higher (1000–2000 ppm at depths as great as 40–50 μm) than the results obtained with Device A (<300 ppm). Furthermore, Device B containing only I was more effective in remineralizing the teeth than was Device B containing the I–II mixture, implying that calcium and phosphate readily diffused through the film from the solution.

The fluoride concentration profile of teeth remineralized in saliva instead of the buffer solution are shown in Fig. 5. The results were almost the same as those obtained from remineralization in the remineralizing buffer solution. As was the case when remineralizing with buffer solutions, the system containing I was much better than the I–II mixture. Even in saliva, an appreciable fluoride concentration was achieved using Device B.

## DISCUSSION

The results obtained with Device B show that satisfactory remineralization occurred when I was held in proximity to the tooth surface for 24 hr. These initial experiments with Device A, a prototype of a practical means for holding I near the tooth surface, show that the main problem to overcome is to find a polymer film that adheres to the tooth and from which I is released rapidly.

Since these studies showed that remineralization can be achieved in the model systems using bovine teeth, it then was verified that human teeth respond in similar manner (4, 5). These studies provide justification for proceeding in the development of the appropriate polymer system for use with Device A.

## SUMMARY

Delivery Device A, a possible prototype of a clinically feasible remineralization system, was not successful with the polymer systems studied. In each case, the film permeability was not high enough for ions to penetrate at a sufficient rate.

Delivery Device B, while not practical for clinical use, had a much higher permeability to ions than did Device A and was used to simulate behavior that might be expected from Device A if a more permeable film could be developed. Device B was quite effective in remineralizing teeth, yielding fluoride levels of ~1000 ppm at depths up to 50 μm, *even in saliva*. Calcium fluoride alone gave better results than the I–II mixtures studied.

These results imply that a practical clinical remineralization procedure based on Device A is feasible, with the primary problem being development of a suitable polymer film.

## REFERENCES

(1) M. Yonese, J. L. Fox, and W. I. Higuchi, AADR Abstract No. 50 (1978).

(2) A. Gee, L. Domingues, and V. Deitz, *Anal. Chem.*, **26**, 1487 (1954).

(3) T. Higuchi, *J. Pharm. Sci.*, **52**, 1145 (1963).

(4) M. Yonese, L. J. Abrahams, J. L. Fox, W. I. Higuchi, and G. Charbeneau, AADR Abstract No. 1114 (1979).

(5) L. J. Abrahams, M. Yonese, W. I. Higuchi, J. L. Fox, and G. T. Charbeneau, *J. Dent. Res.*, **59**, 583 (1980).

## ACKNOWLEDGMENTS

Supported by National Institute of Dental Research Grants DE04600 and DE02731.

# Novel Topical Fluoride Delivery System II: Remineralization of Human Teeth

**JEFFREY L. FOX, MASAKATSU YONESE, BALA V. IYER, LEWIS J. ABRAHAMS, and WILLIAM I. HIGUCHI** ˣ

Received June 30, 1980, from the *College of Pharmacy, University of Michigan, Ann Arbor, MI 48109.* Accepted for publication January 26, 1981.

**Abstract** □ A recently conceived calcium fluoride-containing remineralization system was tested using human teeth *in vitro*. The influence of several variables (surface pretreatment, demineralization time, and remineralization time) was studied. Appreciable levels of fluoride taken up by pumiced human teeth were found at depths up to 50 μm when remineralization was carried out in either the remineralizing solution or saliva. The successful performance of the delivery device in these laboratory studies is encouraging and indicates that the logical evolution of the crude devices studied thus far could lead to clinically practical fluoride delivery devices.

**Keyphrases** □ Delivery devices—fluoride, remineralization of human teeth *in vitro*, effect of surface treatment on remineralization □ Fluoride—delivery devices for remineralization of human teeth *in vitro*, effect of surface treatment on remineralization □ Remineralization—human teeth *in vitro*, fluoride delivery devices, effect of surface treatment on remineralization □ Teeth, human—remineralization *in vitro* using fluoride delivery devices, effect of surface treatment on remineralization

As a result of *in vitro* studies demonstrating the effectiveness of a controlled demineralization pretreatment in enhancing subsequent fluoride remineralization (1), investigations recently were initiated to develop techniques for a practical clinical remineralization procedure. In the previous study, Yonese *et al.* (2) worked with a delivery device that was capable of physically holding particles of calcium fluoride (I) adjacent to the tooth surface while remaining permeable to calcium, phosphate, and fluoride ions as well as water. This device was capable of depositing high levels of fluoride (1000–2000 ppm) at depths of up to 50 μm, using bovine enamel as a test substrate.

This paper demonstrates the effectiveness of demineralization–remineralization for human teeth and examines additional variables that are clinically relevant but that were not studied with the bovine teeth.

## EXPERIMENTAL

Human teeth removed for orthodontic reasons were obtained from dentists in the Chicago area.

The buffer solutions used for demineralization and remineralization were prepared as described previously (2). The demineralizing solution



0022-3549/81/0800-0910$01.00/0
© 1981, American Pharmaceutical Association

consisted of an acetate buffer solution 16% saturated with respect to the thermodynamic solubility of hydroxyapatite (0.1 *M* acetate buffer containing 3.5 m*M* calcium and phosphate, adjusted to pH 4.5 by the addition of sodium hydroxide and to an ionic strength of 0.5 by the addition of sodium chloride). The remineralizing solution also was 0.1 *M* acetate buffer adjusted to pH 4.5 with an ionic strength of 0.5 *M*, but it contained 12 m*M* calcium and phosphate and 10 ppm of fluoride. All chemicals used in the buffers were reagent grade, and all water was distilled twice.

Dialysis bags[1] were used for the cellulose film in fabricating the fluoride delivery device.

The experimental procedures were similar to those reported previously (2). In these experiments, the fluoride delivery device was a cellulose film that physically held calcium fluoride (I) or a mixture of I and dicalcium phosphate dihydrate (II) against the tooth surface (Device B).

Teeth surfaces were conditioned in one of two ways. They were ground with rotating sandpaper (No. 400 first, followed by No. 600) to remove pellicle, or they were pumiced with a non-fluoride-containing pumice.

Prior to remineralization, the tooth received the following pretreatment. The tooth surface was covered by a dental inlay wax[2] except for a 0.25-$cm^2$ area on the front surface. Then the tooth was demineralized in 10 ml of the 16% partially saturated buffer solution for 0–48 hr while being shaken gently with a wrist-action shaker. The solution was kept at 30 ± 0.1°. The extent of demineralization was assessed by measurement of the amount of phosphate dissolved.

The fluoride delivery device was attached to the tooth surface prior to remineralization as follows. Calcium fluoride, sieved by a 270-mesh sieve (52-μm openings), was spread evenly on the tooth surface and covered by a cellulose film (0.2 $cm^2$ in area), the periphery of which was fixed in place by adhesive[3]. The teeth with the device attached were remineralized for 24–72 hr in the remineralizing buffer or in saliva. Details of the remineralization procedure were elaborated in the previous paper (2).

All experiments were done in duplicate except where noted, and the two trials generally were within 10–15% of each other. Results of one of the two are presented for clarity in the figures.

The fluoride delivery device was peeled off carefully from the adhesive to avoid damaging the tooth surface. Then the tooth surface was washed with water to remove the particles of I. The teeth were etched in 1 ml of 0.5 *M* $HClO_4$ in a small glass tube without stirring for successive intervals of 30, 60, 120, 200, and 200 sec. The etched surface was washed with 1 ml of water after each etching step. Concentrations of phosphate, fluoride, and calcium 45 in the etching solution were analyzed in the same manner as reported previously (2).

## RESULTS

**Effect of Pellicle on Remineralization**—In the previous experiments, bovine teeth were ground by rotating a fine sandpaper so as to remove the pellicle completely. However, during *in vivo* application of a clinically practical anticaries treatment, the pellicle might not be as readily removable. Therefore, the effects of the pellicle on demineralization and remineralization were investigated.

To test for a possible pellicle effect, one of three types of surface conditioning (grinding, pumicing, or simply washing) was done prior to demineralization. The conditioned tooth was demineralized in 16% partially saturated acetate buffer solution for 0–24 hr and then remineralized in the remineralizing solution. The fluoride delivery device was not used in this experiment.

Figure 1 shows the fluoride concentration profiles obtained for both ground and pumiced teeth. After grinding, the tooth demineralized for 2 hr had a high fluoride uptake while that of the nondemineralized tooth was much lower. The results were similar to those obtained previously with ground bovine teeth. The molar ratio of calcium 45 to fluoride uptake was near the value of 5.0 expected for completely fluoridated hydroxyapatite. For the pumiced teeth, however, the fluoride concentration profiles attained after demineralization–remineralization were lower and at about the same level as for the nondemineralized ground tooth. Thus, the type of surface conditioning greatly affected the degree of remineralization.

Figure 2 shows the cumulative fluoride uptake from the surface to a depth of ~80 μm as a function of the duration of demineralization. The fluoride uptake of both ground and pumiced teeth increased with the duration of demineralization, and the levels attained in the ground teeth were much greater than in the pumiced teeth.

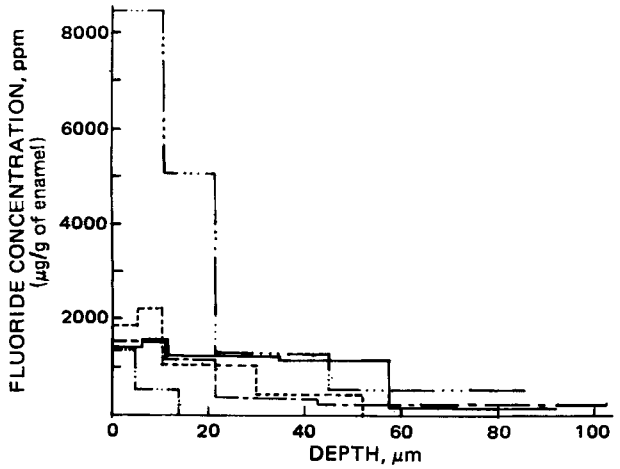


**Figure 1**—*Fluoride concentration profiles of ground and pumiced human teeth remineralized in buffer solution. Key:* - · · · -, $D_2$–$R_{24}$, *ground teeth;* — — —, $D_0$–$R_{24}$, *ground teeth;* - - -, $D_{24}$–$R_{24}$, *pumiced teeth;* —, $D_{16.5}$–$R_{24}$, *pumiced teeth; and* - · - · ·, $D_0$–$R_{24}$, *pumiced teeth. D and R represent demineralization and remineralization, respectively, and the lower subscripts represent the time in hours.*

**Remineralization with Device B in Buffer Solution**—Extrapolation of the data for the pumiced teeth in Fig. 2 suggests that prior demineralization for ~48 hr might be necessary to attain fluoride levels in pumiced teeth comparable to the levels attained in ground teeth demineralized for only 2 hr prior to remineralization. Therefore, all pumiced human teeth in these experiments were demineralized for 48 hr to achieve appreciable fluoride uptake. Figure 3 shows the fluoride concentration profiles of these pumiced human teeth after application of Device B containing only I. These teeth were remineralized for 24–72 hr in the acetate buffer. The fluoride concentrations in these teeth were 1000–2000 ppm at depths as great as 40 μm.

Figure 4 shows the cumulative fluoride uptake from the surface to about an 80-μm depth as a function of the remineralization time after application of Device B containing I or I and II (1:6). The device containing I alone appeared to be marginally more effective than the device containing I–II. Furthermore, fluoride uptake was almost independent of the duration of remineralization; a plateau was achieved after ~24 hr of remineralization, as in the previous study using bovine teeth (2).

As the next step in the approach to the *in vivo* situation, remineralization was carried out in saliva. The fluoride uptake concentration profiles of teeth remineralized in saliva are shown in Fig. 5. The fluoride uptake by the tooth remineralized for only 4 hr was very low, as expected. However, the teeth remineralized for 48 hr had fairly high fluoride levels up to a depth of ~50 μm.

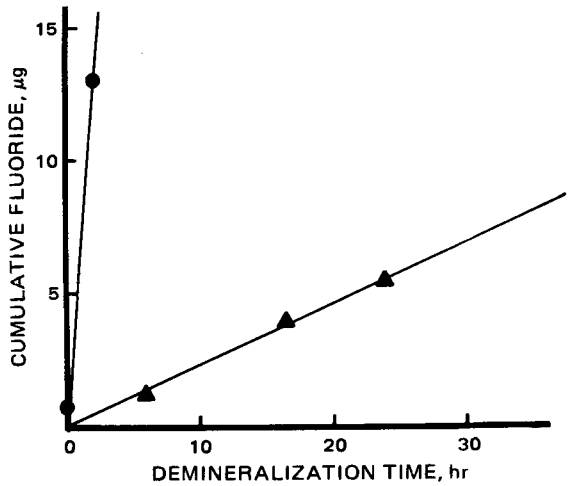


**Figure 2**—*Influence of surface treatment on cumulative fluoride uptake of human teeth demineralized for different time intervals. Key:* ●, *ground; and* ▲, *pumiced.*

[1] Spectrum Medical Industries, Los Angeles, Calif.
[2] Ivory inlay casting wax, Kerr Sybron Co.
[3] Endur M, Ormco Co.

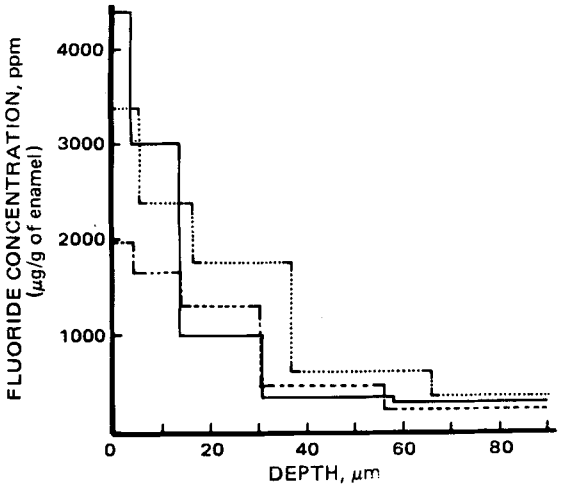


**Figure 3**—*Fluoride concentration profiles of pumiced human teeth treated with Device B containing calcium fluoride. Key: —, $D_{48}$–$R_{72}$; - · · · -, $D_{48}$–$R_{48}$; and - - - -, $D_{48}$–$R_{24}$.*

To determine whether loosely bound material at the tooth surface affects the interpretation of results, a tooth was brushed with a soft toothbrush[4] after remineralization (Fig. 5). The concentration peak seen at a depth of 5–20 μm in nonbrushed teeth was not present after brushing, implying that some relatively loose material may have been included in previous measurements of fluoride levels near the nonbrushed tooth surface. However, even in the brushed teeth, ~1000 ppm of fluoride was found at a depth of ~50 μm.

## DISCUSSION

Teeth used in this study were ground or pumiced prior to demineralization. A few trials also were conducted using teeth with no surface treatment and, therefore, with an intact pellicle. These teeth generally had poor fluoride uptake and considerably larger sample-to-sample variation and, therefore, were not studied further. Although ground teeth had much better fluoride uptake than pumiced teeth, the impracticality of grinding in a clinical setting also limited the number of experiments done with ground teeth. Furthermore, the length of prior demineralization of ground teeth was limited to only 2 hr because of the excessive loss of mineral occurring with longer demineralization times.

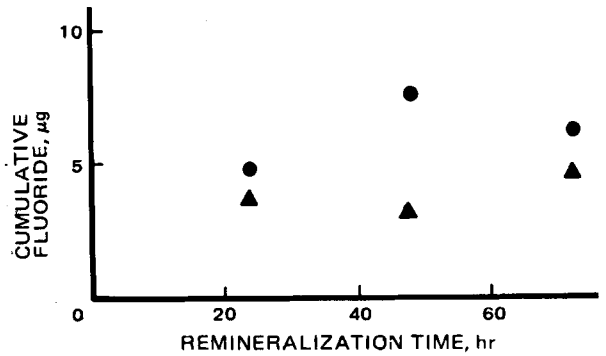


**Figure 4**—*Cumulative fluoride uptake of pumiced human teeth remineralized for different time intervals with Device B. Each point represents a single experiment. Key: ●, $D_{48}$–$R_T$, I alone; and ▲, $D_{48}$–$R_T$, I–II.*

[4] Colgate.

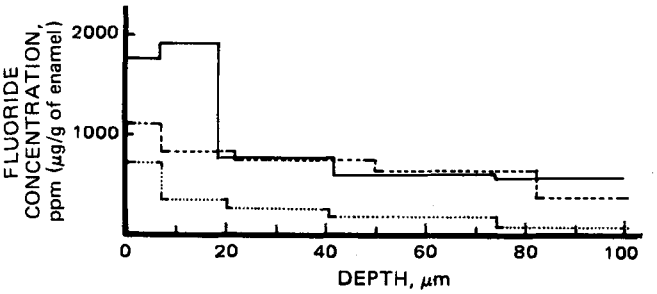


**Figure 5**—*Effect of brushing after remineralization on fluoride uptake of pumiced human teeth with Device B in saliva. Key: —, $D_{48}$–$R_{48}$, nonbrushed; - - -, $D_{48}$–$R_{48}$, brushed; and - · · · -, $D_{48}$–$R_4$, nonbrushed.*

The studies conducted with Device B show that the remineralization approach used has promise. In particular, the results show that remineralization is essentially complete after 24 hr of treatment and that appreciable fluoride levels are achieved at depths up to ~50 μm. Furthermore, the results are not greatly dependent on whether I alone or I–II is used. This finding may mean that there is considerable room to manipulate the formulation so that maximum efficiency of fluoride delivery is achieved. Although the mixture appeared to be slightly less effective in delivering fluoride than I alone, the efficiency was quite good (~3–5% of the total fluoride applied was deposited in the tooth).

The experiments conducted with saliva were encouraging, showing that saliva can be exploited as a source of calcium and phosphate even though a physical barrier exists between saliva and the tooth surface. Furthermore, this barrier prevents salivary proteins and other macromolecules from contacting the surface directly and possibly interfering with remineralization.

## SUMMARY

Although the surface conditioning of a tooth affects both remineralization and demineralization, human and bovine teeth have the same demineralization–remineralization behavior when the pellicle is removed by grinding. The degree of remineralization attainable increases in proportion to the amount of mineral removed during demineralization.

Appreciable fluoride levels by pumiced human teeth with Device B attached were found at depths of up to 50 μm when remineralization was carried out in either the remineralizing buffer solution or saliva.

The salient features of the fluoride delivery system used in this study were the use of a relatively insoluble fluoride salt (I), which is inherently long acting and also provides a source for calcium as well as fluoride, and the provision for a relatively long contact time (24–48 hr) so that the low fluoride levels provided by I could be sustained.

The successive performance of the delivery device in these laboratory studies is encouraging and indicates that the logical evolution of the crude devices studied thus far could likely lead to clinically practical fluoride delivery devices. Pilot *in vivo* studies (3) with Device B have already yielded results comparable to those obtained in these *in vitro* experiments.

## REFERENCES

(1) M. Yonese, J. L. Fox, and W. I. Higuchi, *J. Dent. Res., Spec. Issue A*, **57**, 87 (1978).

(2) M. Yonese, B. V. Iyer, J. L. Fox, J. J. Hefferren, and W. I. Higuchi, *ibid.*, **58**, 370 (1979).

(3) L. J. Abrahams, M. Yonese, W. I. Higuchi, J. L. Fox, and G. T. Charbeneau, *J. Dent. Res.*, **59**, 583 (1980).

## ACKNOWLEDGMENTS

Supported by National Institute of Dental Research Grants DE04600 and DE02731.

# Preparation of Spherical Matrixes of Prolonged-Release Drugs from Liquid Suspension

**Y. KAWASHIMA ˣ, H. OHNO, and H. TAKENAKA**

Received September 30, 1980, from the *Gifu College of Pharmacy, Mitahora, Gifu 502, Japan.* Accepted for publication January 28, 1981.

**Abstract** □ A simple and less expensive method for the preparation of spherical matrixes of prolonged-release drugs was developed from liquid suspension. The drugs dispersed in distilled water were agglomerated with a small amount of organic solution or melt of matrix material. The process, called a "solution" or "melting" method, depended on the state of matrix material. In the present study, sulfamethoxazole and sulfanilamide were agglomerated with white beeswax and ethylcellulose. Furthermore, the parameters affecting the average size and release behavior of the resultant matrixes were investigated. Increasing the amount of matrix material used yielded large matrixes and prolonged-release action. The drugs rendered hydrophobic by surface treatment produced larger matrixes that released drug more slowly than untreated drugs. The sizes of the matrixes decreased and became uniform with increasing agitation speed. The sulfamethoxazole matrixes with wax proved to be enteric coated since the release rate was fast in the alkaline test solution (pH 7.5) but slow in the acidic one (pH 1.2).

**Keyphrases** □ Spherical agglomeration—preparation of spherical matrixes of prolonged-release drugs from liquid suspension, sulfamethoxazole and sulfanilamide □ Prolonged-release drugs—preparation of spherical matrixes from liquid suspension, sulfamethoxazole and sulfanilamide □ Sulfamethoxazole—drug release behavior, preparation of spherical matrixes from liquid suspension □ Sulfanilamide—drug release behavior, preparation of spherical matrixes from liquid suspension

Previous investigators (1) found that the dispersed particles in liquid suspension were spherically agglomerated with a small amount of second immiscible liquid, which preferentially wetted the particles. By developing this research further, other investigators (2–4) established the "spherical agglomeration" technique as a favorable method for agglomeration of fine particles in liquid.

By using a modified spherical agglomeration technique, a simple and less expensive process was developed in the present study to prepare spherical matrixes of prolonged-release drugs as an alternative to spray-congealing methods (5–7). An organic solution (*e.g.*, benzene) or a melt of matrix material such as a wax-like material or ethylcellulose was used as a second immiscible liquid, *i.e.*, a collecting liquid. The parameters affecting micromeritic properties and drug release behavior of the resultant matrixes also were studied.

## EXPERIMENTAL

**Materials**—Sulfamethoxaxole[1], having geometric mean diameters of 6 and 380 μm and geometric standard deviations of 1.4 and 1.2 μm, respectively, was used. Fine sulfamethoxazole particles were supplied by pulverizing the coarse particles. Sulfanilamide[2] particles of a 297-μm geometric mean diameter with a geometric standard deviation of 1.1 μm also were used for agglomeration. White beeswax[3] and ethylcellulose[4] were used as matrix materials.

Surface-treated drugs were rendered strongly hydrophobic to increase their affinity with matrix material to attain a well-coated matrix. Surface treatment was done by allowing adsorption of palmitic acid[4] onto the drug surface. Adsorption was achieved by dispersing 10 g of particles in 200 ml of 3% palmitic acid–alcohol solutions and leaving the system for 2 days. The drugs adsorbed with palmitic acid were filtered and dried at 40° for 1 day. No significant changes in particle size after the treatment were observed.

**Preparation of Matrixes**—*Melting Method*—Sulfamethoxazole particles (10 g) were dispersed in 300 ml of distilled water contained in an 8 × 18.5-cm glass cylindrical vessel. The system was agitated at 241, 382, 620, and 1100 rpm by a turbine-type agitator with four blades, 4 cm in diameter, to examine the effect of agitation speed on product size. The agitator was set 1 cm from the bottom of the vessel.

The system was heated gradually to 90° by a mantel heater. When the system reached 90°, powdered white beeswax, weighing 1.25 or 1.5 g, was added to change the coating thickness of resultant matrixes. Then the system was agitated for 10 min at 90°. The molten white beeswax collected the dispersed drug and yielded spherical agglomerates. By removing the mantel heater, the system was cooled gradually to room temperature while stirring to harden the agglomerates. The resultant agglomerates were filtered and dried for 24 hr at 40°. The average diameter of the dried agglomerates was determined by a sieving method using standard sieves specified in the JP, the opening of which was nearly the same as that of the Tyler sieve. The size range varied from 16 to 84%.

*Solution Method*—A small amount of benzene solution of white beeswax or ethylcellulose was used instead of a white beeswax melt. Sulfamethoxazole particles (5 g) were agglomerated with 0.5, 1.3, or 3.0 ml of a 7% benzene solution of ethylcellulose. Then the system was agitated continuously at 620 rpm for 2 hr to evaporate the benzene and to harden the agglomerates. Sulfanilamide particles (10 g) were agglomerated with 4 or 8 ml of a 9.3% benzene solution of white beeswax. The resultant agglomerates were filtered and dried as described for the melting method.

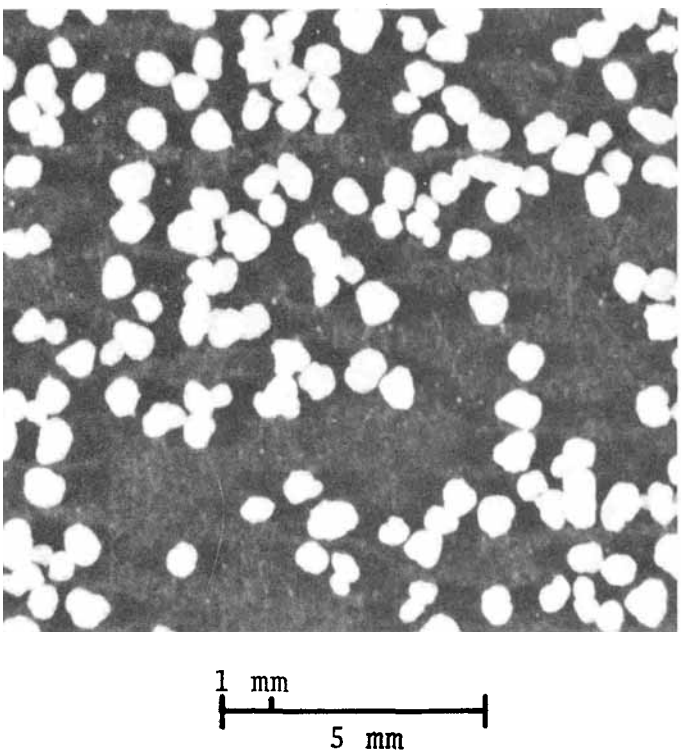


**Figure 1**—*Photomicrograph of sulfamethoxazole matrixes with white beeswax used for the release test.*

[1] Shionogi Pharmaceutical Co., Osaka, Japan.
[2] Nakarai Chemical Co., Tokyo, Japan.
[3] Miki Chemical Co., Tokyo, Japan.
[4] Kishida Chemical Co., Tokyo, Japan.

0022-3549/81/0800-0913$01.00/0
© 1981, American Pharmaceutical Association

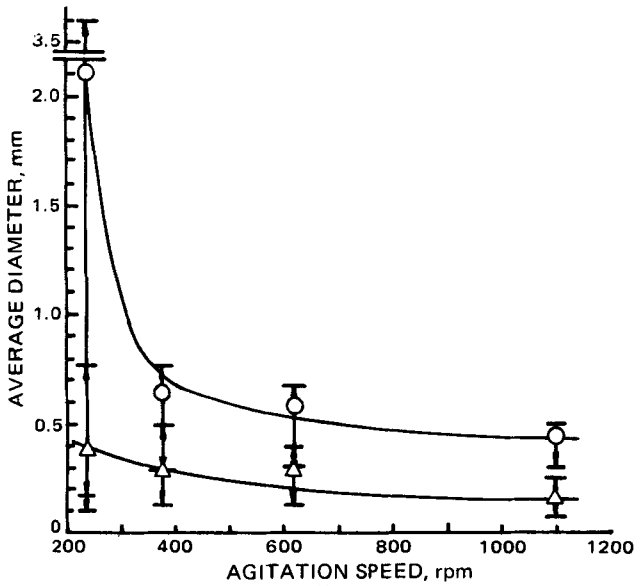


**Figure 2**—*Effect of agitation speed on the average diameter of matrixes. The material was pulverized sulfamethoxazole, and the collecting liquid was 1.5 g of a white beeswax melt. Key: ○, with surface treatment; and △, without surface treatment.*

**Drug Release Test of Agglomerates**—The dissolution tests were conducted by a beaker method. A USP rotating basket was modified by attaching a propeller to the top, which was used as an agitator. Thus, the adsorption of air bubbles to the basket was prevented and agitation was promoted. The agglomerates, fractionated to 500–1000 μm, were used to cancel the surface area effect on the dissolution rate.

The 90-mg test samples were added to 900 ml of distilled water or acidic (pH 1.2) or alkaline (pH 7.5) disintegration test solutions specified in the JP. Adhesion of agglomerates to the basket was slight. The system was controlled thermally at 37° and agitated at 150 rpm. At various adequate intervals, 2-ml aliquots were withdrawn from the system and filtered through a 0.2-μm filter[5]. The dissolved amounts of drug were determined spectrophotometrically at the UV wavelengths of 250 and 257 nm using a double-beam spectrophotometer[6].

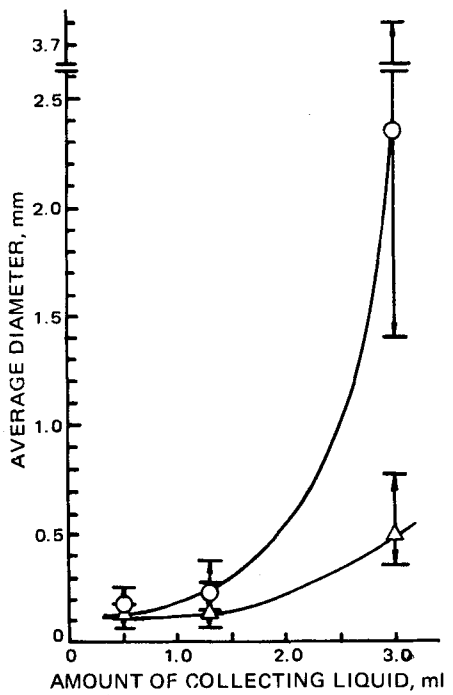


**Figure 3**—*Effect of collecting liquid on the average diameter of matrixes. The material was pulverized sulfamethoxazole, the collecting liquid was ethylcellulose solution, and the agitation speed was 1100 rpm. Key: ○, with surface treatment; and △, without surface treatment.*

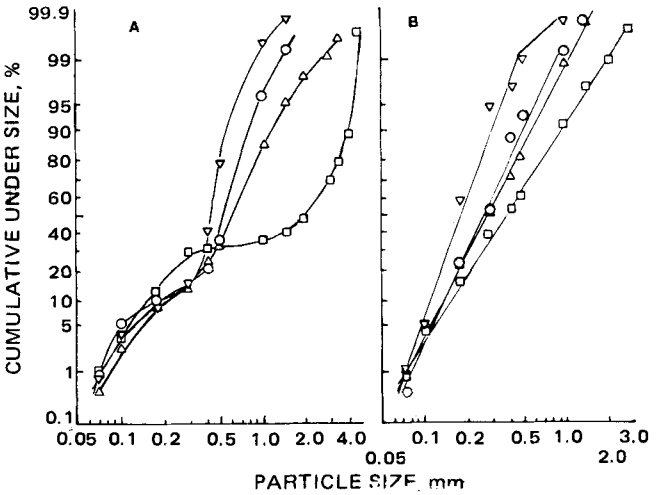


**Figure 4**—*Effect of surface treatment (A, with; and B, without) of raw materials and agitation speed on the size distribution of matrixes. The material was pulverized sulfamethoxazole, and the collecting liquid was 1.5 g of a white beeswax melt. Key: ▽, 1100 rpm; ○, 620 rpm; △, 382 rpm; and □, 241 rpm.*

## RESULTS AND DISCUSSION

**Parameters Affecting Agglomerate Particle Size**—The products prepared by this technique were fairly rounded spheres, varying from 50 μm to 4 mm in size. Products prepared by the melting method appeared to be coated with white beeswax (Fig. 1).

The effects of the agitation speed of the system on agglomerate size are shown in Fig. 2. The median diameters of the products of the fine sulfamethoxazole particles prepared by the melting method were plotted against the agitation speeds. With increasing agitation speed, the average size of the particle agglomerates without surface treatment decreased gradually from 380 to 150 μm. The surface-treated particles yielded larger agglomerates than particles without surface treatment. The surface-treated particles could be wetted easily by molten wax due to their strong hydrophobic properties, resulting in large agglomerates.

Agitation speed strongly affected the product size of the surface-treated particles. The average particle size decreased sharply from 2.1 to 0.62 mm when the agitation speed was increased from 241 to 382 rpm (Fig. 2). With the coarse sulfamethoxazole particle, the agitation speed similarly affected agglomerate size. However, there was little difference in product size between the particles with and without surface treatment. This result indicates that it is difficult to make the coarse particles hydrophobic by surface treatment because of their poor adsorption of palmitic acid.

The effects of the amount of collecting liquid on agglomerate size are seen in Fig. 3. The median diameter of the products of the fine sulfamethoxazole particles prepared by the solution method increased with the increasing amounts of benzene solutions of white beeswax used. This trend was evident for products of the surface-treated particles and may have been due to increased affinity with the collecting liquid caused by the hydrophobic nature of the particles. The increase in the agglomerate size caused by surface treatment was also confirmed with the sulfanilamide products.

The effects of surface treatment on the size distribution of the agglomerates of the fine sulfamethoxazole particles are seen in Fig. 4. The size distribution of the products without surface treatment was described by a log-normal form (Fig. 4B). The slope of the line, representing a geometric standard deviation, decreased with increasing agitation speed. This result suggests that the agglomerates of a fairly uniform size can be produced by increasing the agitation speed. The size distributions of the products of the surface-treated particles were not represented by a log-normal form (Fig. 4A), because they were heterogeneous mixtures containing some extraordinarily large particles, which increased in number at the lower agitation speed. At the lower stirring speed, the collecting liquid was not dispersed uniformly, resulting in a heterogeneous mixture. Furthermore, the adhesive force between the surface-treated particles

[5] Millipore.

[6] Hitachi model 556.

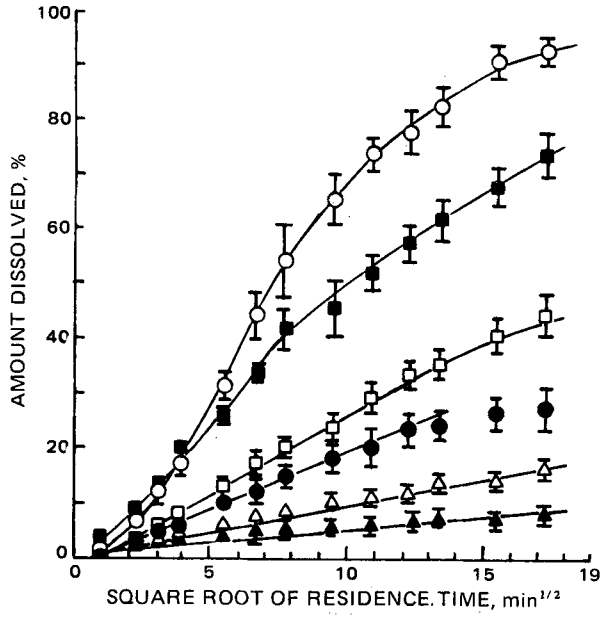


**Figure 5**—*Drug release patterns of sulfamethoxazole matrixes in distilled water. Key: ●, fine particle size, without surface treatment, 1.5 g of wax; △, coarse particle size, without surface treatment, 1.25 g of wax; ▲, coarse particle size, with surface treatment, 1.25 g of wax; □, fine particle size, with surface treatment, 1.3 ml of ethylcellulose solution; ■, fine particle size, without surface treatment, 1.3 ml of ethylcellulose solution; and ○, original sulfamethoxazole. Standard deviation bars for only representative batches are exhibited to avoid superimposing.*

might be stronger than the destructive force brought about by agitation. Therefore, once a large agglomerate was produced, it was rarely destroyed. Similar phenomena were observed for other products of sulfanilamide and sulfamethoxazole.

**Drug Release Behavior from Agglomerates**—Dissolution tests were undertaken to examine the prolonged-release behavior of the products. Dissolution behavior was represented by plotting the percentage of the drug released from the agglomerates on a semi-square root graph. The

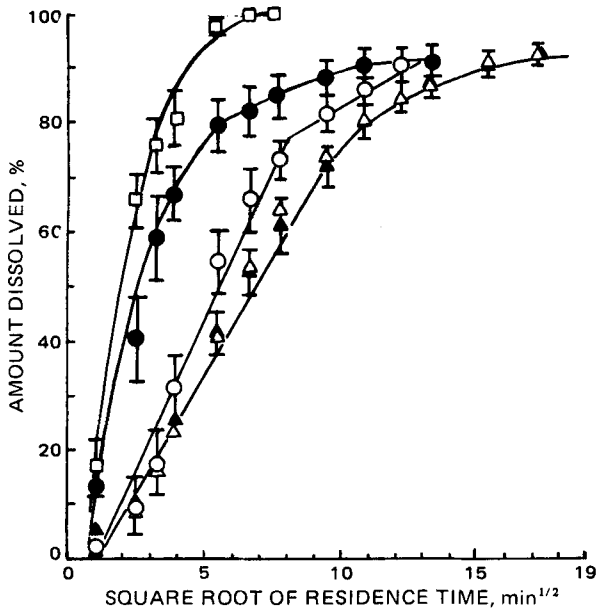


**Figure 6**—*Drug release patterns of sulfanilamide matrixes in distilled water. Key: ○, with surface treatment, 4 ml of collecting liquid; ●, without surface treatment, 4 ml of collecting liquid; △, with surface treatment, 8 ml of collecting liquid; ▲, without surface treatment, 8 ml of collecting liquid; and □, original sulfanilamide. Standard deviation bars for only representative batches are exhibited to avoid superimposing.*

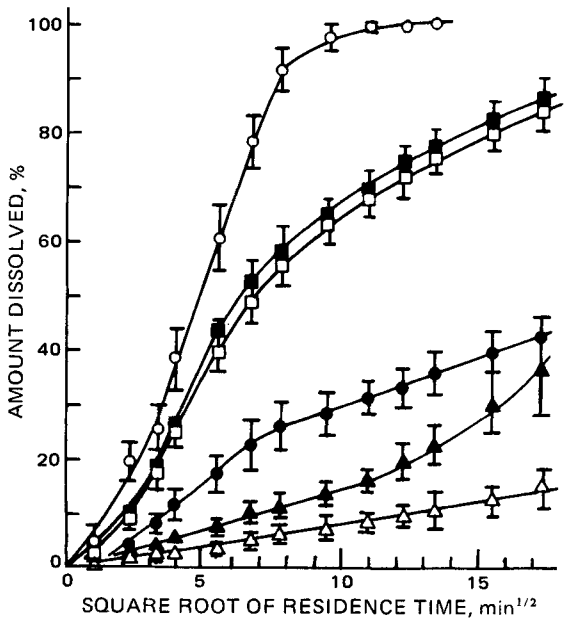


**Figure 7**—*Drug release patterns of sulfamethoxazole matrixes in acidic solution. Key: ●, fine particle size, without surface treatment, 1.5 g of wax; ▲, coarse particle size, without surface treatment, 1.25 g of wax; △, coarse particle size, with surface treatment, 1.25 g of wax; □, fine particle size, with surface treatment, 1.3 ml of ethylcellulose solution; ■, fine particle size, without surface treatment, 1.3 ml of ethylcellulose solution; and ○, original sulfamethoxazole. Standard deviation bars for only representative batches are exhibited to avoid superimposing.*

release behavior of the sulfamethoxazole and sulfanilamide products in distilled water is seen in Figs. 5 and 6, respectively. Compared with the original particles, all sulfamethoxazole products prepared by both the melting and solution methods released the drug slowly, although the release rates varied extensively, depending on the preparation condition (Fig. 5). The release patterns of the agglomerates with wax became fairly straight lines. This finding indicates that the release process obeys the

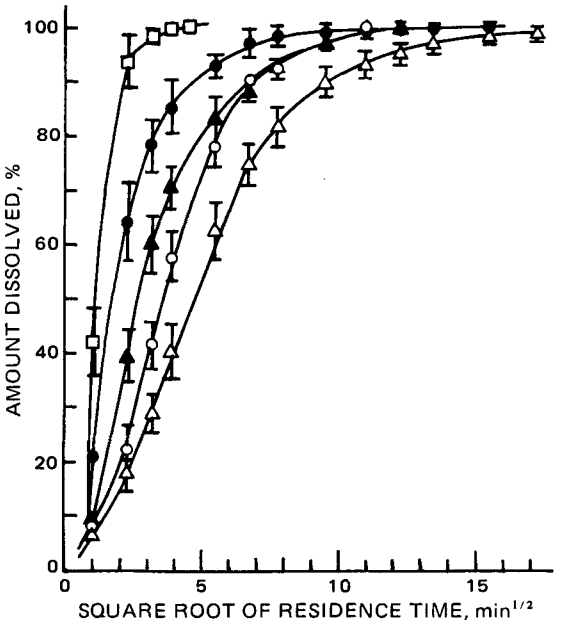


**Figure 8**—*Drug release patterns of sulfanilamide matrixes in acidic solution. Key: ○, with surface treatment, 4 ml of collecting liquid; ●, without surface treatment, 4 ml of collecting liquid; △, with surface treatment, 8 ml of collecting liquid; ▲, without surface treatment, 8 ml of collecting liquid; and □, original sulfanilamide. Standard deviation bars for only representative batches are exhibited to avoid superimposing.*

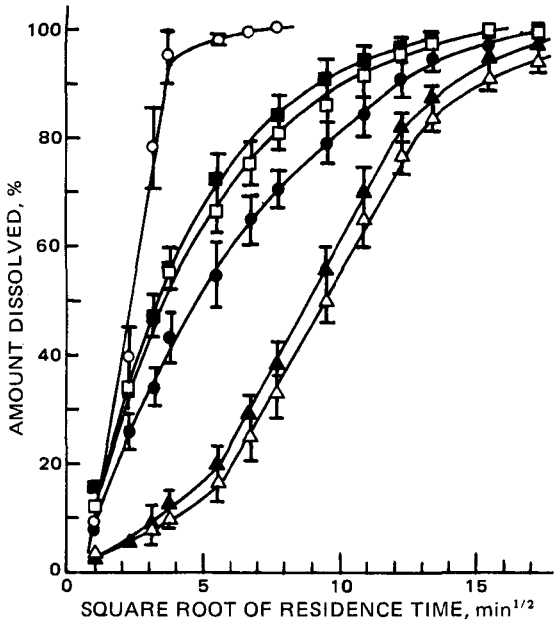


**Figure 9**—*Drug release patterns of sulfamethoxazole matrixes in alkaline solution. Key: ●, fine particle size, without surface treatment, 1.5 g of wax; ▲, coarse particle size, without surface treatment, 1.25 g of wax; △, coarse particle size, with surface treatment, 1.25 g of wax; □, fine particle size, with surface treatment, 1.3 ml of ethylcellulose solution; ■, fine particle size, without surface treatment, 1.3 ml of ethylcellulose solution; and ○, original sulfamethoxazole. Standard deviation bars for only representative batches are exhibited to avoid superimposing.*

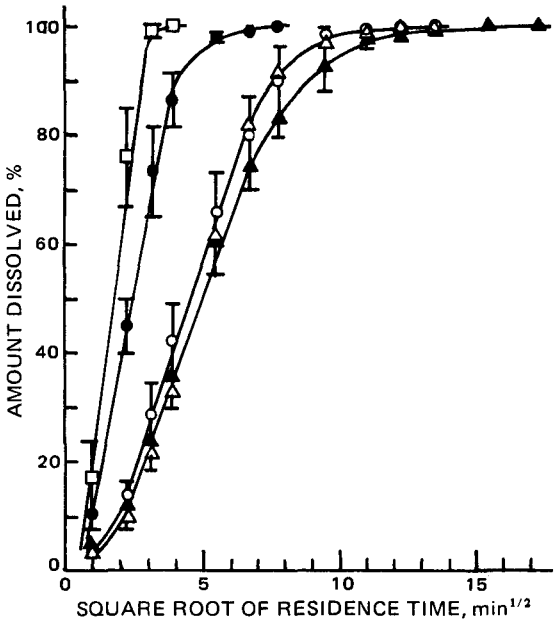


**Figure 10**—*Drug release patterns of sulfanilamide matrixes in alkaline solution. Key: ○, with surface treatment, 4 ml of collecting liquid; ●, without surface treatment, 4 ml of collecting liquid; △, with surface treatment, 8 ml of collecting liquid; ▲, without surface treatment, 8 ml of collecting liquid; and □, original sulfanilamide. Standard deviation bars for only representative batches are exhibited to avoid superimposing.*

Higuchi model (8), which explains the drug release process from a matrix as:

$$Q = [D(2A - C_s)C_s t]^{1/2} \quad \text{(Eq. 1)}$$

where $Q$ is the amount dissolved per unit area of exposure at time $t$, $A$ is the total volume of drug present in the matrix per unit volume, $C_s$ is the solubility of the drug in the external phase of the matrix, and $D$ is the diffusion constant. When $C_s \ll A$, Eq. 1 can be transformed to a more convenient form to exhibit the release patterns described in Figs. 5–10 (9):

$$C_r = 100[S_v(2DC_s t/A)^{1/2}] \quad \text{(Eq. 2)}$$

where $C_r$ is the percentage of the drug dissolved and $S_v$ is the specific surface area.

The surface treatment significantly delayed the drug release rate from the products. The product with surface treatment still retained 90% of the drug after a 5-hr exposure to the solvent. The size reduction of the raw materials adversely affected the prolonged-release action of the products (Fig. 5). This result may have been due to the fact that the fine particles can improve diffusivity in a matrix by their increased dissolution rate. The drug release rate of the agglomerate with ethylcellulose was faster than that of the agglomerates with wax, suggesting that the coating action of the ethylcellulose solution was weak compared with molten wax. The release pattern of the ethylcellulose product without surface treatment coincided with that of original sulfamethoxazole at the initial stage, although it deviated later. Figure 5 indicates that some uncoated drug on the product surface dissolved immediately on contact with the solvent, and the imbedded particles dissolved slowly at the later stage.

The release rates of the sulfanilamide products were faster than those of sulfamethoxazole (Fig. 6). The literature value of sulfanilamide solubility (10) is 7.5 g/liter (25°), whereas sulfamethoxazole is characterized as insoluble in the JP. The higher solubility of sulfanilamide, leading to the higher intrinsic dissolution rate, might be responsible for the increased release rate of sulfanilamide products. However, when a large amount of collecting liquid was used, the release pattern became a straight line with a decreased slope (Fig. 6). The surface treatment also delayed the release rate. Thus, it was confirmed that surface treatment of the raw materials and the amount of collecting liquid played an important role in controlling product release behavior.

The release patterns of the agglomerates in the acidic solution are displayed in Figs. 7 and 8. The release rates of the original and the agglomerates of sulfamethoxazole with ethylcellulose became faster than in distilled water (Fig. 7). While the release rates of the agglomerates with wax were almost the same as in distilled water, the release rates of both original sulfanilamide and its products (Fig. 8) were faster than in distilled water. The effects of the size and surface treatment of the raw materials on the release pattern of the products in Figs. 7 and 8 were similar to those in distilled water.

In the alkaline solution, the product release rates of both sulfamethoxazole and sulfanilamide were faster than in the other two media (Figs. 9 and 10). Enhancement of the release rate of sulfamethoxazole agglomerates with wax was particularly distinguished compared to the other products. The enteric-like action of the agglomerates with wax was proved by this finding. The fatty acid contained in the wax might be more soluble in the alkaline medium than in the acidic medium. In addition, the ester involved in the wax might be hydrolyzed more readily in the alkaline medium. These factors may promote the disintegration of the matrix and increase the release rate in the alkaline medium.

## REFERENCES

(1) H. M. Smith and I. E. Puddington, *Can. J. Chem.*, **38**, 1911 (1960).

(2) A. F. Sirianni, C. E. Capes, and I. E. Puddington, *Can. J. Chem. Eng.*, **47**, 166 (1969).

(3) C. E. Capes and J. P. Sutherland, *Ind. Eng. Chem. Process Des. Dev.*, **6**, 146 (1967).

(4) Y. Kawashima and C. E. Capes, *Powder Technol.*, **13**, 279 (1976).

(5) I. C. Robinson and C. H. Becker, *J. Pharm. Sci.*, **57**, 49 (1968).

(6) A. G. Cusimano and C. H. Becker, *ibid.*, **57**, 1104 (1968).

(7) I. S. Hamid and C. H. Becker, *ibid.*, **59**, 511 (1970).

(8) T. Higuchi, *ibid.*, **52**, 1145 (1963).

(9) H. Takenaka, Y. Kawashima, and S. Y. Lin, *Chem. Pharm. Bull.*, **27**, 3054 (1979).

(10) "The Merck Index," 9th ed., M. Windholz, Ed., Merck & Co., Rahway, N.J., 1976, p. 1155.

# GLC Analysis of Hydrocortisone, Triamcinolone Acetonide, and Desonide in Culture Media of Mouse and Human Dermal Fibroblasts Using Flame-Ionization Detection

**D. S-L. AU *, J. O. RUNIKIS ˣ, F. S. ABBOTT, and R. W. BURTON**

Received September 2, 1980, from the *Faculty of Pharmaceutical Sciences, University of British Columbia, Vancouver, British Columbia V6T 1W5, Canada.* Accepted for publication February 3, 1981. *Present address: College of Pharmacy, University of Houston, Houston, TX 77030.

**Abstract** □ A quantitative GLC assay with flame-ionization detection capable of detecting nanogram quantities of hydrocortisone, triamcinolone acetonide, and desonide in biological fluids was developed. This assay consisted of two extractions of the glucocorticoids from 1 *N* sodium chloride-treated cell culture media into ethyl acetate and subsequent double derivatization with methoxyamine and *N*-trimethylsilylimidazole. The chemical structures of methoxime–trimethylsilyl derivatives were confirmed by GLC–mass spectrometry. The methoxime–trimethylsilyl derivatives were stable for 24 hr. The applicability of this assay was demonstrated by studies of the glucocorticoid levels in L-929 and human dermal fibroblasts cell culture media over prolonged incubation (0–96 hr).

**Keyphrases** □ Glucocorticoids—GLC–mass spectrometric analysis of hydrocortisone, triamcinolone acetonide, and desonide in cell culture media □ GLC–mass spectrometry—analysis of hydrocortisone, triamcinolone acetonide, and desonide in cell culture media □ Hydrocortisone—GLC–mass spectrometric analysis, cell culture media □ Triamcinolone acetonide—GLC–mass spectrometric analysis, cell culture media □ Desonide—GLC–mass spectrometric analysis, cell culture media

Synthetic glucocorticoids vary in their clinical potencies as well as in their potential for causing dermal atrophy, a major adverse effect of long-term topical glucocorticoid therapy (1). Studies of the pathogenesis of this adverse effect have involved investigations of glucocorticoid effects on cell proliferation, protein synthesis, collagen synthesis, secretion of acid mucopolysaccharides, and other pleiotypic responses such as polyribosome formation and DNA synthesis (2, 3).

## BACKGROUND

Cultured dermal cells have been used previously as models, and the incubation of glucocorticoids with cultured cells lasted from hours to days. However, no reports of assays of glucocorticoids in cell culture media appear to have been published. It was assumed that the amounts of glucocorticoids dissolved represented their biologically active concentrations and that the metabolism of glucocorticoids during incubation was negligible. Therefore, development of a GLC assay should help to clarify the validity of such assumptions. Furthermore, with a quantitative GLC analysis of glucocorticoids in cultured cell systems, the relevant biochemical data of glucocorticoid effects can be more precisely interpreted, especially in terms of dose dependence.

The requirements for the estimation of glucocorticoids in biological systems are that sensitivity should be in the low nanogram range and that the technique should identify possible metabolites or decomposition products. Due to ready instrument availability, GLC using flame-ionization detection was selected for the determination of glucocorticoids in cell culture systems.

Few quantitative high-performance liquid chromatography (HPLC) (4–9) and GLC (10–12) assays have been reported for the analysis of synthetic glucocorticoids in biological fluids. One HPLC assay (4) achieved sensitivity as low as 0.05 ng of budesonide/ml of plasma in dogs with the aid of radioactive detection. Amounts as low as 2–4 ng of triamcinolone acetonide, triamcinolone, and prednisolone were detected in rat muscle by GLC using electron-capture detection and trimethylsilyl derivatization (12).

Martin and Amos (10) reported a GLC–mass spectrometric assay enabling the measurement of plasma concentrations of prednisone and prednisolone as methoxime–trimethylsilyl derivatives to nanogram per milliliter plasma levels. So far, methoxime–trimethylsilyl derivatization has not been applied to the assay of synthetic glucocorticoids except for prednisone and prednisolone (10), although it was used successfully for the assays of naturally occurring glucocorticoids (13). No specific assay techniques have been reported for desonide.

A GLC assay with flame-ionization detection was developed to quantitate hydrocortisone and synthetic glucocorticoids in cell culture media, using methoxime–trimethylsilyl derivatization.

## EXPERIMENTAL

**Materials**—Hydrocortisone[1] (I), triamcinolone[2] (II), triamcinolone acetonide[2] (III), and desonide[3] (IV) were obtained commercially. Progesterone[4] (V) was used as the internal standard. Methanol[5] and ethyl acetate[5] were distilled in glass, and pyridine[6] was silylating grade.

*Purity Confirmation of I–V*—All steroids were dried at 40° for 1 hr and at ambient temperature overnight in a vacuum oven before use. The weight lost due to the drying was <1% in all cases.

The melting points of these compounds were determined by both capillary melting-point determination[7] and differential scanning calorimetry[8]. The purities of I, IV, and V were satisfactory as received.

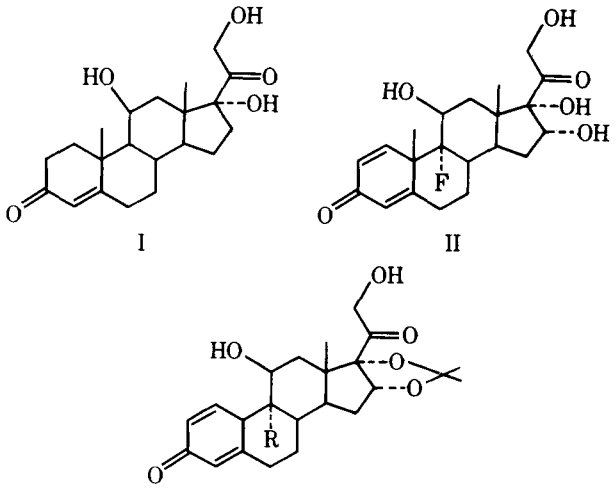


[1] Lot 402-9511, Pfizer Co., Montreal, Canada.
[2] Compound II was USP, code 2014, batch Z5040, and III was USP, code 45645, batch 431, Cyanamid of Canada Ltd., Montreal, Canada.
[3] Lot CS-1-37, Dome Laboratories, Division of Miles Laboratories, West Haven, Conn.
[4] Lot 113C-0190, Sigma Chemical Co., St. Louis, Mo.
[5] Caledon, Georgetown, Ontario, Canada.
[6] Pierce Chemical Co., Rockford, Ill.
[7] Thomas-Hoover apparatus, Arthur H. Thomas Co., Philadelphia, Pa.
[8] Model 1B, Perkin-Elmer, Norwalk, Conn.

0022-3549/81/0800-0917$01.00/0
© 1981, American Pharmaceutical Association

**Table I—Retention Time of Parent and Derivatized Glucocorticoids**

| Glucocorticoid | Retention Time[a], min: Underivatized Compound[b], 3% OV-17 | Methoxime–Trimethylsilyl Derivative, 3% OV-17 | Methoxime–Trimethylsilyl Derivative, 3% OV-7 |
|---|---|---|---|
| Progesterone | 1.31 | 1.38 | 2.57 |
| Prednisolone | — | 2.20 | — |
| Hydrocortisone | 4.09 | 2.10 | 4.50 |
| Triamcinolone | 5.04 | 3.53 | — |
| Desonide | 7.25 | 3.69 | 6.36 |
| Triamcinolone acetonide | 8.59 | 4.38 | 7.37 |

[a] Three or more values were averaged. [b] All compounds except progesterone gave more than one peak due to thermal decomposition. The value given is that of the major peak of each sample.

Samples II and III had to be recrystallized by dissolving the compound in methanol with the aid of steam and allowing the filtered resulting solution to stand in a hood for 3 days before collecting the crystals by filtration. The purities of all compounds were confirmed by HPLC.

*Methoxyamine Hydrochloride*[9]—This compound was dissolved in pyridine (100 mg/ml) (14) and stored in a conical reaction vial fitted with a polytef-lined valve[10] at 5° in a desiccator.

N-*Trimethylsilylimidazole*[11]—This compound was transferred to a conical reaction vial fitted with a polytef-lined valve immediately after each ampul was opened, and the vial was kept at 5° in a desiccator.

**Preparation of Derivatives**—*Methoxime–Trimethylsilyl Derivatives*—The procedure of Pfaffenberger and Horning (14) was adapted as follows. The test glucocorticoid (not more than 800 μg) was placed in a 1-ml conical reaction vial fitted with a polytef-lined screw cap[10]. Then 100 μl of methoxyamine hydrochloride–pyridine stock solution was added to dissolve the compound, and the resulting solution was incubated at 70° for 15 min. Then 100 μl of *N*-trimethylsilylimidazole was added, and silylation was conducted at 100° for 10–30 min, depending on the compound tested. An aliquot (1–2 μl) of the final reaction mixture (volume of 200 μl) was injected directly into the gas–liquid chromatograph or GLC–mass spectrometer.

tert-*Butyldimethylsilyl Derivatives*—The procedure was a modified version of previously reported methods (15–18). The test glucocorticoid (not more than 800 μg) was placed in a 1-ml conical reaction vial fitted with a polytef-lined screw cap. Then 100 μl of *tert*-butyldimethylsilyl chloride mixture[12] (1.0 mmole of *tert*-butyldimethylsilyl chloride and 2.5 mmoles of imidazole/ml of anhydrous *N,N*-dimethylformamide) was added to dissolve the compound, and the resulting solution was incubated at 100° for 1 hr. After the reaction, 100 μl of distilled water was added, and the derivatives were extracted into chloroform prior to GLC or GLC–mass spectrometric analysis.

**Differential Scanning Calorimetry**—A differential scanning calorimeter[8] was employed. All samples were crimped. The rate of temperature increase was 10°/min for each run.

**GLC**—The recording gas–liquid chromatograph[13] was equipped with a terminal[14] and a flame-ionization detector. The coiled glass column, 1.8 m × 2 mm i.d., contained 3% OV-7 coated onto 80–100-mesh Chromosorb W(HP).

All columns were conditioned at 100° for 15 hr, and then the oven temperature was programmed to increase by 0.1°/min up to 285°. The oven temperature was allowed to remain at 285° for ~15 hr to complete the conditioning process. The flow rate of carrier gas during conditioning was 10 ml/min.

The operating temperatures for routine analysis were: injection port, 265°; column, 285°; and detector, 300°. The gas flow rates were: carrier gas (helium), 60 ml/min; hydrogen, 40 ml/min; and air, 300 ml/min.

**GLC–Mass Spectrometry**—A computerized gas chromatograph–electron-impact mass spectrometer[15] was used to study the fragmentation pattern of the methoxime–trimethylsilyl derivatives for confirming their chemical structures. The following conditions were used for GLC: injection port temperature, 230°; column temperature, programmed from 200 to 260° at a rate of 10°/min; and carrier gas (helium) flow rate, 20 ml/min. The 2-m × 2-mm i.d. glass column was packed with 3% OV-17 coated onto 80–100-mesh Chromosorb W(HP). For the mass spectra, the ionization beam energy was 80 ev, the source analyzer temperature was 250°, and the separator was at 280°.

The modes of detection included total ion current and selected ion monitoring.

**Extraction**—The glucocorticoids were double extracted from the cell culture medium[16] containing 10% fetal calf serum as follows. Solid sodium chloride was added to decanted 5–10-ml aliquots of the medium to make it 1 *N*. The aqueous phase was extracted twice with an equal volume of glass-distilled ethyl acetate. After centrifugation to separate the layers, the organic extracts were combined and evaporated to dryness under a gentle nitrogen stream at ambient temperature. The residue was transferred to a 1-ml conical reaction vial containing 100 μl of internal standard (0.50 μg/ml in methanol) by rinsing three times with 0.2 ml of fresh ethyl acetate. The resulting mixture was evaporated to dryness and subjected to derivatization.

A white interface of precipitate occurred in the extraction of glucocorticoids from serum-containing media. The addition of sodium chloride to make a 1 *N* solution avoided this difficulty.

Ethyl acetate, ether, chloroform, and methylene chloride were evaluated for their extraction efficiency of glucocorticoids from serum-free and serum-containing media. Ethyl acetate was chosen because it had a high extraction efficiency and permitted easy withdrawal of the extracts.

Since the presence of serum in the medium decreased the extractability of glucocorticoids by single extraction, double extraction was used.

**Recovery Studies**—A series of known amounts of the test glucocorticoid solution in methanol (I, III, or IV) was added to individual centrifuge tubes and evaporated to dryness under a nitrogen stream. Five milliliters of 10% serum-containing medium, freshly prepared or decanted from control cells, was added to each glucocorticoid residue. The spiked samples were extracted as already described. Percentage recoveries were calculated from the standard curve of the glucocorticoid that was derivatized without extraction.

**Assays on Biological Samples**—*Human Dermal Fibroblasts*—Diploid dermal fibroblasts, isolated from explants of biopsies from 25–35-year-old males and stored at −193° in liquid nitrogen, were grown between the fourth and eighth subcultures in monolayer cultures to confluence in plastic culture plates.

*Mouse L-929 Dermal Fibroblasts*—Aneuploid mouse L-929 fibroblasts[17], originated from a chemically transformed clone in 1943 (19), were used. Both cultured cell lines were maintained in cell culture medium[16] (pH 6.8) supplemented with 10% fetal calf serum, 5 m*M* L-glutamine, 3.7 g of sodium bicarbonate/liter, 100 units of penicillin/ml, 100 μg of streptomycin/ml, and 0.25 μg of amphotericin B[18]/ml. The cells were incubated at 37° in carbon dioxide–air (5:95 v/v). The medium was changed twice weekly. Cellular morphology was examined regularly. Any plate with signs of infection, cellular degeneration, or poor growth was discarded.

**Treatment with Glucocorticoids**—Stock solutions of the test glucocorticoids ($10^3$ μg/ml in a propylene glycol vehicle) were prepared by mixing two volumes of propylene glycol (50% in methanol) and one volume of glucocorticoid solution in methanol ($10^3$ μg/ml) and then removing the methanol under vacuum. A control solution of the propylene glycol vehicle was prepared in a similar fashion.

Desired concentrations of 1 or 10 μg of glucocorticoid/ml of cell culture medium were prepared by adding 1 or 10 μl of the stock solutions/ml to the cell culture medium. The propylene glycol content of these glucocorticoid-treated media did not interfere with cell growth.

The stock solutions as well as the glucocorticoid-containing media were assayed before addition to the cells to ascertain the calculated and actual glucocorticoid concentrations. Some deviations of >15% of expected values were observed because of dilution errors. Only experimentally determined concentrations are reported here.

The glucocorticoid-treated medium was incubated for up to 96 hr with cells that had reached confluence in duplicate culture plates. The decanted media from the two plates containing 6–8 × $10^6$ cells were pooled and stored at −4° until analysis. The cells were harvested simultaneously for biochemical studies of glucocorticoid effects on cellular DNA (not reported here).

[9] Lot 04239.19, Pierce Chemical Co., Rockford, Ill.
[10] Reacti-vial with Teflon-lined Mininert valve, Pierce Chemical Co., Rockford, Ill.
[11] Lot 0211774, 10 × 1-g ampuls, Pierce Chemical Co., Rockford, Ill.
[12] Lot 18028, Applied Science Laboratories, State College, Pa.
[13] Model 5880A, Hewlett-Packard, Avondale, Pa.
[14] Model 18850A, Hewlett-Packard, Avondale, Pa.
[15] Varian MAT-111, Varian Associates, Palo Alto, Calif.
[16] Dulbecco Modified Eagle Medium.
[17] Passages 578 and 584, Flow Laboratories, McLean, Va.
[18] Fungizone.

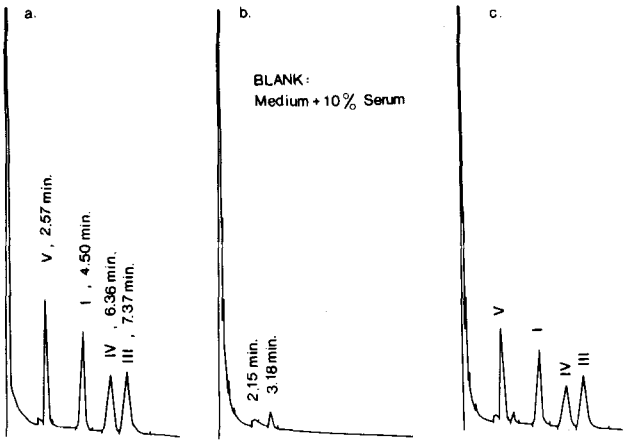


**Figure 1**—*Typical chromatograms of glucocorticoids and extracts. Key:* a, *extraction from methanol solutions;* b, *extraction from blank medium with 10% serum; and* c, *extraction from serum-containing medium.*

## RESULTS AND DISCUSSION

**Selection of Derivatizing Agents**—For initial experiments, *tert*-butyldimethylsilyl chloride was selected as a potential derivatizing reagent based on the advantages described in the literature (15–18). These advantages are: (*a*) high selectivity of the reaction, by which silylation occurs only at the unhindered C-21 hydroxyl group of the glucocorticoid; (*b*) increased stability of *tert*-butyldimethylsilyl ethers toward hydrolysis, which is $10^4$ times higher than that of trimethylsilyl ethers; and (*c*) the simplicity of the mass spectra of *tert*-butyldimethylsilyl ethers because these compounds give intense $(M - 57)^+$ ions. By monitoring this characteristic ion, mass spectrometry has the potential of being a sensitive and selective technique for quantitative analysis of glucocorticoids. The results obtained with this derivative, however, were generally disappointing, and further use of *tert*-butyldimethylsilyl chloride was discontinued. The *tert*-butyldimethylsilyl derivatives had unsatisfactory GLC properties, such as long retention times (longer than those of their parent compounds) and adsorption onto the column due to the remaining free functional groups.

The methoxime–trimethylsilyl derivatives of the test glucocorticoids proved to be superior to their corresponding *tert*-butyldimethylsilyl derivatives based on their satisfactory GLC properties, namely, short retention times and sharp symmetrical peaks with higher responses than their parent compounds.

**Column Selection**—Columns packed with 3% OV-7, OV-17, and OV-25 were examined for their suitability to resolve peaks of the internal standard, glucocorticoids, and any endogenous component in serum. The OV-7 and OV-17 columns gave superior elution profiles to the OV-25 column. However, with OV-17, the serum-associated endogenous peaks prevented satisfactory resolution of the peak of the internal standard, progesterone, a difficulty not present with the OV-7 column (Figs. 1*b* and 1*c*). Therefore, the OV-7 packing was selected, even though longer retention times were observed (Table I).

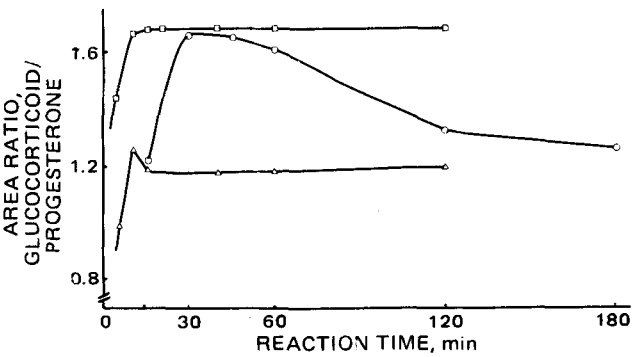


**Figure 2**—*Reaction kinetics of I–III at 100°. Plot of area ratio of derivatives formed to derivatized internal standard as a function of time. (The concentrations of I–III and their concentration ratios to the internal standard did not have to be the same.) Key:* △, *I;* □, *II; and* ○, *III.*

**Optimum Reaction Time for Silylation and Stability of Derivatives**—The optimum derivatization time of silylation was evaluated by reacting samples containing equivalent amounts of I–III for various times at 100°. Known amounts of separately derivatized methoxime internal standards then were added. The yield of the derivative, as observed by its area ratio to that of the internal standard, was monitored. The optimum yield was obtained when reaction times were 10, 15, and 30 min for I, II, and III, respectively (Fig. 2).

The methoxime–trimethylsilyl derivatives were stable in excess of 24 hr at 4° when stored in tightly capped reaction vials.

**Confirmation of Derivative Formation Using GLC–Mass Spectrometry**—The fragmentation patterns of derivatized I–IV when analyzed by electron-impact GLC–mass spectrometry confirmed the formation of methoxime–trimethylsilyl derivatives and V as the methoxime derivative (Figs. 3*a*–3*e*). Little information is available on fragmentation of the methoxime–trimethylsilyl derivatives of the synthetic glucocorticoids. Those of steroids present in rat adrenal gland extracts, primarily corticosterone derivatives, were reported by Prost and Maume (13). Their scheme of characteristic cleavages forms the basis for interpretation of the observed spectra (Figs. 3*a*–3*e*). The well-known losses of *O*-methoxy from *O*-methoxime groups and of silanol from trimethylsilyl groups (13, 20) were observed.

*Fragmentation Pattern of Hydrocortisone Derivative, Di(methoxime)-Tri(trimethylsilyl)-I*—The peak at *m/z* 636 (1.8%) corresponds to the molecular ion peak; other characteristic peaks were observed at *m/z* 605 (10.5%) $[(M - OCH_3)^+]$, 361 (3.5), 246 (6.1), 147 (7.0) $[(CH_3)_2Si = O^+ - Si(CH_3)_3]$ (21), 103 (11.4) $[CH_2 = O^+ - Si(CH_3)_3]$, 89 (12.3) $[O^+ - Si(CH_3)_3]$, and 73 (100) $[Si^+(CH_3)_3]$.

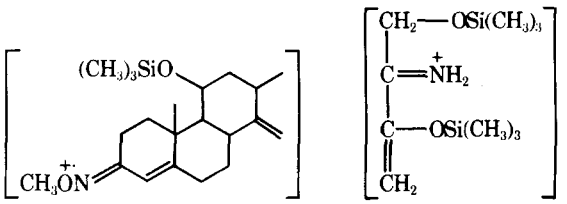


*m/z* 361 *m/z* 246

*Fragmentation Pattern of Triamcinolone Derivative, Di(methoxime)-Tetra(trimethylsilyl)-II*—The peak at *m/z* 739 (0.7%) corresponds to one less than the molecular ion $[(M - 1)^+]$. The characteristic peaks were 709 (3.0%) $[(M - OCH_3)^+]$, 689 (1.4) $[(M - OCH_3 - HF)^+]$, 618 (2.6) $[M - F - (CH_2{-}OSi(CH_3)_3)^+]$, 147 (8.8), 103 (12.3), and 73 (100).

*Fragmentation Pattern of Triamcinolone Acetonide Derivative, Mono(methoxime)-Di(trimethylsilyl)-III*—The peak at *m/z* 607 (0.4%) corresponds to the molecular ion. The characteristic peaks were 587 (1.1%) $[(M - HF)^+]$, 576 (1.6) $[(M - OCH_3)^+]$, 556 (10.7) $[(M - OCH_3 - HF)^+]$, 121 (9.0), 103 (18.1), and 73 (100).

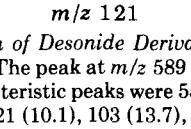


*m/z* 121

*Fragmentation Pattern of Desonide Derivative, Mono(methoxime)-Di(trimethylsilyl)-IV*—The peak at *m/z* 589 (0.8%) corresponds to the molecular ion. The characteristic peaks were 558 (4.9%) $[(M - OCH_3)^+]$, 468 (6.8) $[(M - 121)^+]$, 121 (10.1), 103 (13.7), and 73 (100).

*Fragmentation Pattern of Progesterone Derivative, Di(methoxime)-V*—The peak at *m/z* 372 (100%) corresponds to the molecular ion. The characteristic peaks were 341 (72.8%) $[(M - OCH_3)^+]$, 286 (29.5), 273 (46.2), 220 (11.5), 153 (57.4), 137 (40.2), 125 (65.6), 100 (75.5), and 87 (39.1).

**Resolution of Methoxime–Trimethylsilyl Derivatives on OV-7 and OV-17 Columns**—The GLC chromatograms of all four glucocorticoid derivatives appeared as single peaks when eluted from OV-7 columns (Figs. 1*a* and 1*c*). Compounds III and IV, however, resolved into two peaks, a minor peak A with a shorter retention time and occupying <10% of the peak area and a major peak B, when OV-17 packings were used due to the higher degree of resolution obtainable.

A GLC–mass spectrometric examination showed that the chemical structure of the derivative eluting as the minor peak A corresponded to mono(methoxime)–tri(trimethylsilyl)-IV, *m/z* 660, $[(M - 1)^+]$, whereas that of the major peak B corresponded to mono(methoxime)–di(trimethylsilyl)-IV, *m/z* 589 ($M^+$), as illustrated in Figs. 4*a* and 3*d*, respectively.

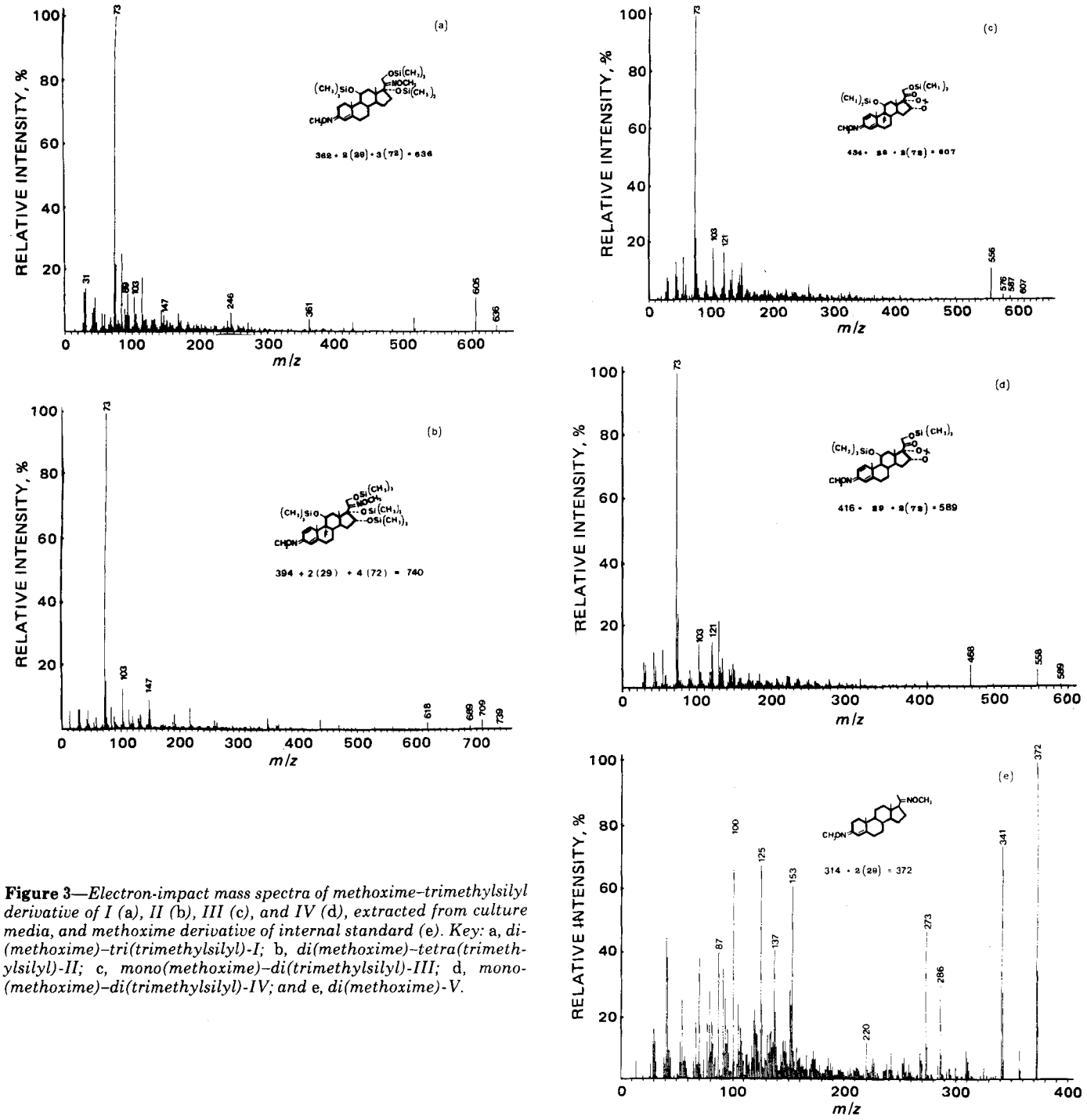


**Figure 3**—*Electron-impact mass spectra of methoxime–trimethylsilyl derivative of I* (a), *II* (b), *III* (c), *and IV* (d), *extracted from culture media, and methoxime derivative of internal standard* (e). *Key:* a, *di(methoxime)–tri(trimethylsilyl)-I;* b, *di(methoxime)–tetra(trimethylsilyl)-II;* c, *mono(methoxime)–di(trimethylsilyl)-III;* d, *mono(methoxime)–di(trimethylsilyl)-IV; and* e, *di(methoxime)-V.*

Formation of peak A is ascribed as being due to partial enolization of the keto group at C-20. The keto group at C-20 in IV as well as in III, in contrast to I and II, is hindered by the C-16,C-17 acetonide group and remains largely resistant to formation of the methoxime derivative. Under favorable conditions, such as exposure of the reaction mixtures to sunlight radiation and excess silylating reagent, some enolization can occur, which then would lead to the formation of the minor tri(trimethylsilyl) derivative observed.

Indirect evidence for the existence of the enolization reaction was obtained on exposure of the reaction mixture to sunlight. Sunlight is a catalyst for the enolization of various ketones (22). Exposure to sunlight increased the relative magnitude of peak A to peak B, as expected of a sunlight-catalyzed reaction. Removal of the reaction mixture from sunlight reversed the magnitude of peak A to its original levels, indicating the reversibility of sunlight-induced enolization. Prolonging the derivatization time led to an increase in peak A at the expense of the magnitude of peak B, suggesting the formation of A from B.

The fact that the chromatographic peaks from OV-7 columns represent two derivatization products of III and IV, however, did not interfere with the assay because the contributions by the tri(trimethylsilyl) derivatives were <10% of the area of the peaks and were in nearly constant ratio to those of the major di(trimethylsilyl) derivatives. The derivatization time should be kept at 30 min, and light should be excluded.

Compound III shared all of the previously mentioned characteristics of derivatization and gave mono(methoxime)–di(trimethylsilyl)-III, *m/z* 607 ($M^+$), as the major product and mono(methoxime)–tri(trimethylsilyl)-III, *m/z* 679 ($M^+$), as the minor product (Figs. 3*c* and 4*b*).

The presence of antibiotics in the medium showed no interference on the chromatograms.

**Calibration Curves**—Calibration curves were constructed for I, III, and IV extracted from medium containing 10% serum. The curves were linear within the ranges studied, namely, 40–1600 ng/μl of derivatized solution for I (equivalent to 1.6–65.8 μg/ml of medium), 60–1600 ng/μl of derivatized solution for III (equivalent to 2.4–63.7 μg/ml of medium),

**Table II—Estimation of I after Extraction from Spiked Medium Samples ($n$ = 3)**

| Amount Added to 5 ml of Serum-Containing Medium, μg | Weight Ratio[a] | Mean Peak Area Ratio[b] ± SD | Amount Recovered[c], μg | Mean Recovery ± SD, % |
|---|---|---|---|---|
| Mar. 1978 | | | | |
| 16.45 | 0.1347 | 0.1046 ± 0.0095 | 13.95 | 84.82 ± 6.86 |
| 24.67 | 0.2025 | 0.1444 ± 0.0021 | 18.69 | 75.75 ± 1.00 |
| 41.42 | 0.3372 | 0.2804 ± 0.0202 | 34.86 | 84.77 ± 5.84 |
| 61.68 | 0.5058 | 0.4393 ± 0.0281 | 53.75 | 87.15 ± 5.36 |
| 164.48 | 1.3480 | 1.1930 ± 0.0518 | 143.38 | 87.17 ± 3.71 |
| Aug. 1978 | | | | |
| 8.22 | 0.0667 | 0.0569 ± 0.0010 | 7.92 | 97.51 ± 5.52 |
| 16.45 | 0.1335 | 0.1406 ± 0.0076 | 18.39 | 111.82 ± 5.54 |
| 24.67 | 0.2003 | 0.1804 ± 0.0013 | 21.65 | 90.16 ± 4.39 |
| 41.12 | 0.3338 | 0.3550 ± 0.0222 | 44.11 | 107.28 ± 6.48 |
| 61.68 | 0.5006 | 0.4920 ± 0 0238 | 60.55 | 98.17 ± 4.63 |
| 82.24 | 0.6676 | 0.6486 ± 0.0211 | 79.34 | 96.47 ± 3.08 |
| 164.48 | 1.3351 | 1.3121 ± 0.0195 | 158.93 | 96.63 ± 1.42 |
| 328.96 | 2.6701 | 2.5330 ± 0.0465 | 305.40 | 92.84 ± 1.69 |

[a] Weight ratio of I/V (internal standard). [b] Peak area ratio of derivatized I/derivatized V. Mean values of triplicate samples, each determined by three measurements. [c] Calculated from the standard curve of I without extraction, $y = mx + c$, where $m = 1.026$ and $c = -0.009$ ($r^2 = 0.999$), and $y = mx + c$, where $m = 0.947$ and $c = -0.005$ ($r^2 = 0.998$) for extracted samples, as plotted for the mean area ratio *versus* weight ratio. The average mean recovery was 93.12 ± 9.74%.

and 20–300 ng/μl of derivatized solution for IV (equivalent to 0.80–12.0 μg/ml of medium) (Tables II–IV).

Two calibration curves of I were determined with a time lapse of 6 months between them. The relative standard deviation in slope values was 3.1%. The combined data gave a straight line of $y = 0.947x - 0.005$ with $r^2 = 0.998$, indicating satisfactory assay reproducibility.

Three calibration curves of III were determined within 1 year. The relative standard deviation of slope values was 7.6%. The combined data gave a straight line of $y = 0.553x + 0.012$ with $r^2 = 0.996$. The satisfactory reproducibility of the assay confirmed the validity of using the sum of double-peak areas, mono(methoxime)–di(trimethylsilyl)-III and mono(methoxime)–tri(trimethylsilyl)-III, based on the assumption that the yield ratio of these two peaks was a constant.

The recoveries of three glucocorticoids added in various amounts also were tabulated (Tables II–IV). The average mean recoveries were 93.12 ± 9.74, 85.64 ± 7.19, and 97.73 ± 4.72% for I, III, and IV, respectively.

Glucocorticoids generally are used in cell cultures at concentrations smaller than those used for preparing the calibration curves. However, these lower concentrations can be compensated readily by extracting >5 ml of the medium employed in the preparation of the calibration curves. On the other hand, the amounts used are realistic for assays of stock solution concentrates and similar solutions of pharmaceutical interest.

**Biological Data**—The applicability of the assay was demonstrated by determining the I, III, and IV levels in serum-containing cell culture medium after various incubation times with cultured human or mouse dermal fibroblasts (Tables V–VII).

The time profile of III indicated that its prolonged incubation of up

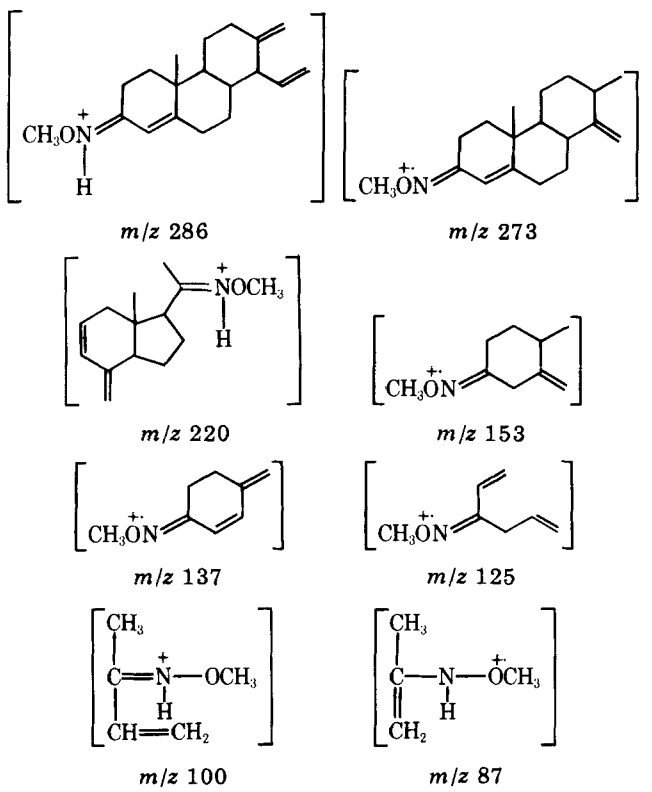


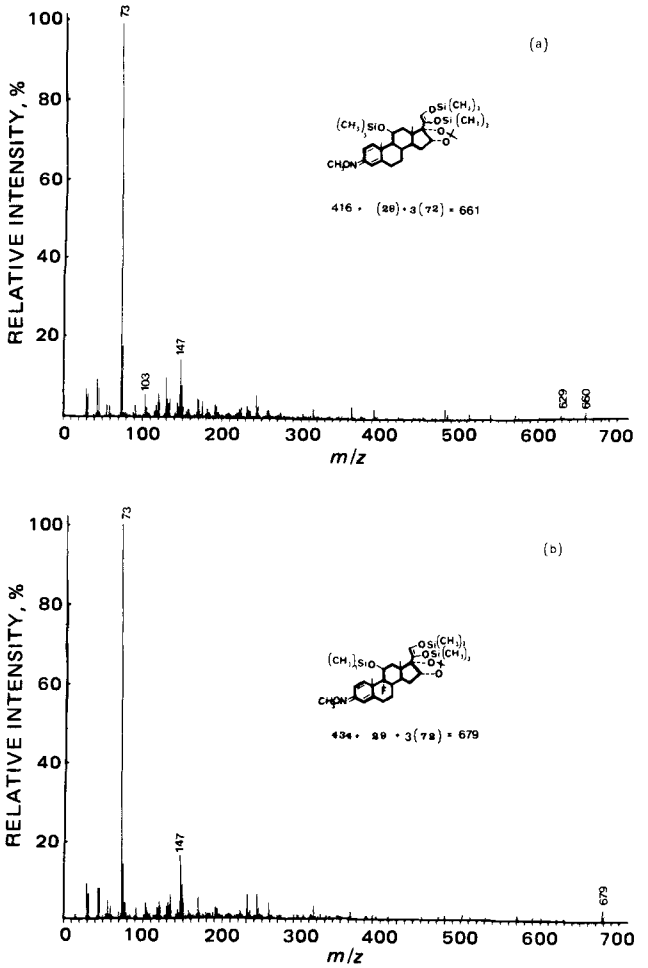


**Figure 4**—*Electron-impact mass spectra of mono(methoxime)–tri(trimethylsilyl)-IV* (a) *and mono(methoxime)–tri(trimethylsilyl)-III* (b).

**Table III—Estimation of III after Extraction from Spiked Medium Samples ($n$ = 3)**

| Amount Added to 5 ml of Serum-Containing Medium, μg | Weight Ratio[a] | Mean Peak Area Ratio[b] ± $SD$ | Amount Recovered[c], μg | Mean Recovery ± $SD$, % |
|---|---|---|---|---|
| Apr. 1978 | | | | |
| 25.92 | 0.1420 | 0.0725 ± 0.0125 | 22.75 | 87.75 ± 11.09 |
| 39.00 | 0.2137 | 0.1228 ± 0.0220 | 34.95 | 89.62 ± 12.36 |
| 64.80 | 0.3541 | 0.2142 ± 0.0089 | 57.13 | 88.17 ± 3.33 |
| 86.40 | 0.5314 | 0.2919 ± 0.0219 | 75.99 | 87.96 ± 6.15 |
| 129.13 | 0.7081 | 0.4082 ± 0.0311 | 104.23 | 80.65 ± 4.37 |
| 257.70 | 1.4120 | 0.8049 ± 0.0354 | 200.53 | 77.82 ± 2.49 |
| Oct. 1978 | | | | |
| 11.94 | 0.0969 | 0.0508 ± 0.0031 | 11.79 | 98.76 ± 4.25 |
| 15.92 | 0.1293 | 0.0694 ± 0.0012 | 14.84 | 93.21 ± 1.24 |
| 23.88 | 0.1938 | 0.1030 ± 0.0114 | 20.35 | 85.20 ± 7.82 |
| 39.80 | 0.3231 | 0.1778 ± 0.0001 | 32.60 | 81.92 ± 0.20 |
| 59.70 | 0.4846 | 0.2777 ± 0.0076 | 48.98 | 82.04 ± 2.08 |
| 79.60 | 0.6462 | 0.3628 ± 0.0053 | 62.92 | 79.05 ± 1.09 |
| 159.20 | 1.2922 | 0.7495 ± 0.0282 | 126.29 | 79.33 ± 2.90 |
| 318.4 | 2.5840 | 1.5506 ± 0.0356 | 257.58 | 80.90 ± 1.83 |
| Feb. 1979 | | | | |
| 11.94 | 0.1189 | 0.0659 ± 0.0040 | 11.63 | 97.37 ± 4.90 |
| 15.92 | 0.1586 | 0.0932 ± 0.0059 | 15.27 | 95.93 ± 4.95 |
| 23.88 | 0.2378 | 0.1435 ± 0.0111 | 21.99 | 92.08 ± 6.21 |
| 39.80 | 0.3964 | 0.2330 ± 0.0027 | 33.94 | 85.28 ± 0.91 |
| 59.70 | 0.5946 | 0.3556 ± 0.0253 | 50.32 | 84.28 ± 5.66 |
| 79.60 | 0.7928 | 0.5082 ± 0.0349 | 70.69 | 88.81 ± 5.86 |
| 159.2 | 1.5860 | 0.9127 ± 0.0962 | 124.72 | 78.34 ± 8.07 |
| 318.4 | 3.1710 | 1.6403 ± 0.0042 | 221.88 | 69.69 ± 0.17 |

[a] Weight ratio of III/V (internal standard). [b] Peak area ratio of derivatized III/derivatized V. Mean values of triplicate samples, each determined by three measurements. [c] Calculated from the standard curve of III without extraction, $y = mx + c$, where $m = 0.750$ and $c = -0.021$ ($r^2 = 0.990$), and $y = mx + c$, where $m = 0.553$ and $c = 0.012$ ($r^2 = 0.996$) for extracted samples, as plotted for the mean area ratio *versus* weight ratio. The average mean recovery was 85.64 ± 7.19%.

**Table IV—Estimation of IV after Extraction from Spiked Medium Samples ($n$ = 3)**

| Amount Added to 5 ml of Serum-Containing Medium, μg | Weight Ratio[a] | Mean Peak Area Ratio[b] ± $SD$ | Amount Recovered[c], μg | Mean Recovery ± $SD$, % |
|---|---|---|---|---|
| 4.0 | 0.0787 | 0.0395 ± 0.0030 | 3.95 | 98.77 ± 4.72 |
| 8.0 | 0.1625 | 0.1063 ± 0.0060 | 8.15 | 101.97 ± 4.70 |
| 12.0 | 0.2415 | 0.1693 ± 0.0057 | 12.12 | 101.03 ± 3.01 |
| 16.0 | 0.3252 | 0.2360 ± 0.0046 | 16.32 | 102.03 ± 1.81 |
| 24.0 | 0.4681 | 0.3500 ± 0.0078 | 23.49 | 97.91 ± 2.05 |
| 40.0 | 0.7254 | 0.5551 ± 0.0256 | 36.42 | 91.04 ± 4.03 |
| 60.0 | 1.0919 | 0.8473 ± 0.0907 | 54.81 | 91.36 ± 9.53 |

[a] Weight ratio of IV/V (internal standard). [b] Peak area ratio of derivatized IV/derivatized V. Mean values of triplicate samples, each determined by three measurements. [c] Calculated from the standard curve of IV without extraction, $y = mx + c$, where $m = 0.790$ and $c = -0.023$ ($r^2 = 0.999$), and $y = mx + c$, where $m = 0.713$ and $c = -0.0038$ ($r^2 = 0.999$) for extracted samples, as plotted for the mean area ratio *versus* weight ratio. The average mean recovery was 97.73 ± 4.72%.

**Table V—Levels of I in Media as a Function of Time after Incubation with Cultured Human Dermal Fibroblasts**

| Incubation Time, hr | $n$ | Concentration Assayed, μg/ml of medium | |
|---|---|---|---|
| | | A-2[a] (Percent Remaining Intact) | A-4[b] |
| 0 | 2 | 0.7307 ± 0.1338 (100.00 ± 18.31)[c] | — |
| 0.25 | 1 | — | 0.4621 |
| 2 | 2 | — | 0.3921 ± 0.0045 |
| 4 | 2 | 0.3892 ± 0.0345 (53.26 ± 4.72) | 0.5194 ± 0.0091 |
| 6 | 2 | — | 0.4737 ± 0.0091 |
| 8 | 2 | — | 0.4336 ± 0.0156 |
| 12 | 2 | — | 0.4364 ± 0.0130 |
| 24 | 2 | 0.3864 ± 0.0441 (52.88 ± 6.04) | 0.3464 ($n$ = 1) |
| 48 | 2 | — | 0.4545 ± 0.0497 |

[a] Human dermal fibroblasts, F.H. passage 6. [b] Human dermal fibroblasts, W.P. passage 4. [c] The concentration of I recovered from medium containing no cells was defined as 100% of intact drug.

to 83.5 hr with cultured mouse L-929 dermal fibroblasts did not decrease intact III in media. About 20% of III was removed from the culture medium by absorption and/or adsorption by cells 2 hr after administration of III. The levels of III at various incubation periods between 2 and 83.5 hr did not vary appreciably. A significant decrease of III after 94 hr was observed but unexplained.

To eliminate the possibility of decomposition, the stability of III in the medium upon incubation was studied at 37° in the absence of cells for 72 and 96 hr. There was no appreciable decomposition due to the incubation at 37°.

The levels of IV after 4 and 24 hr of incubation with mouse L-929 fibroblasts indicated ~20% loss of IV from the medium.

Therefore, for any biological effect of synthetic glucocorticoids observed at the dose level of 1 μg/ml of medium, the true bioavailable dose was probably not more than 0.2 μg/ml of medium.

The levels of I as a function of time were measured twice at various incubation intervals. The loss of I from the media due to cells was larger than that of the synthetic glucocorticoids. Compound I had rather constant levels when incubated between 0.25 and 48 hr.

**Metabolites**—No extra peaks were observed in samples incubated

**Table VI—Levels of III in Media as a Function of Time after Incubation with Cultured Mouse L-929 Dermal Fibroblasts**

| Incubation Time, hr | $n$ | Concentration Assayed, μg/ml of medium | Intact III Remaining in Media, % |
|---|---|---|---|
| 0 | 5 | 1.265 ● 0.0820 | 100.00 ± 6.48[a] |
| 2 | 2 | 1.032 ± 0.0029 | 81.58 ± 0.23 |
| 4 | 2 | 1.025 ± 0.0007 | 81.01 ± 0.06 |
| 8 | 2 | 1.030 ± 0.0101 | 81.45 ± 0.80 |
| 11 | 2 | 1.011 ± 0.0045 | 79.94 ± 0.36 |
| 24 | 2 | 1.060 ± 0.0050 | 83.77 ± 0.40 |
| 48 | 1 | 1.011 | 79.94 |
| 72 | 2 | 1.028 ± 0.0018 | 81.25 ± 0.14 |
| 83.5 | 2 | 1.079 ± 0.0300 | 85.29 ± 2.37 |
| 94 | 2 | 0.919 ± 0.022 | 72.67 ± 1.74 |

[a] The concentration of III recovered from medium containing no cells was defined as 100% of intact drug.

with cells for 0–108 hr, and there was no appreciable change in the magnitudes of endogenous peaks in the mixture due to the medium and 10% serum. It was proposed that no metabolite was apparently present unless its methoxime–trimethylsilyl derivative had the same retention time as the derivatized parent compound or that the amounts of metabolites were too small to be detected.

**Applicability of Methoxime–Trimethylsilyl Reaction to Other Glucocorticoids**—Another glucocorticoid, diflorasone diacetate, was derivatized under the same conditions. However, the reaction product gave four peaks in the gas–liquid chromatogram, indicating multiple derivatizing products, presumably due to the hydrolysis of acetates by hydrochloride generated in the reaction with methoxyamine hydrochloride and subsequent silylations at the C-17 and/or C-21 free hydroxyl groups. Therefore, diflorasone diacetate and probably other ester-containing glucocorticoids are not amenable to GLC analysis using the subsequent derivatization with methoxyamine hydrochloride and *N*-trimethylsilylimidazole.

Prednisolone could be derivatized to yield the di(methoxime)–tri(trimethylsilyl)prednisolone derivative with the same reaction procedure.

**Table VII—Levels of IV in Media as a Function of Time after Incubation with Cultured Mouse L-929 Dermal Fibroblasts**

| Incubation Time, hr | $n$ | Concentration Assayed, μg/ml of medium | Intact IV Remaining in Media, % |
|---|---|---|---|
| 0 | 4 | 0.6073 ± 0.0120 | 100.00 ± 1.98[a] |
| 4 | 2 | 0.5136 ± 0.1006 | 84.58 ± 11.70 |
| 24 | 2 | 0.4964 ± 0.0326 | 81.74 ± 5.37 |

[a] The concentration of IV recovered from medium containing no cells was defined as 100% of intact drug.

## REFERENCES


(1) W. D. Stewart, J. L. Danto, and S. Maddin, "Dermatology," 4th ed., Mosby, St. Louis, Mo., 1978, pp. 204–211.

(2) G. C. Priestley, *Br. J. Dermatol.*, **99,** 253 (1978).

(3) G. M. Tomkins, "Harvey Lectures 1972–1973, Series 68," Academic, New York, N.Y., pp. 37–65.

(4) A. Ryrfeldt, M. Tonnesson, L. Nilsson, and A. Wikby, *J. Steroid Biochem.*, **10,** 317 (1979).

(5) J. C. K. Loo, A. G. Butterfield, J. Moffat, and N. Jordan, *J. Chromatogr.*, **143,** 275 (1977).

(6) J. C. K. Loo and N. Jordan, *ibid.*, **143,** 314 (1977).

(7) A. M. DePaolis, G. Schnabel, S. E. Katz, and J. Rosen, *J. Assoc. Off. Anal. Chem.*, **60,** 210 (1977).

(8) W. Wortmann, C. Schnabel, and J. C. Touchstone, *J. Chromatogr.*, **84,** 396 (1973).

(9) G. Roth, A. Wikby, L. Nilsson, and A. Thalen, *J. Pharm. Sci.*, **69,** 766 (1980).

(10) S. B. Martin and B. Amos, *ibid.*, **67,** 923 (1978).

(11) P. A. Mason and R. Fraser, *J. Endocrinol.*, **64,** 277 (1975).

(12) P. M. Simpson, *J. Chromatogr.*, **77,** 161 (1973).

(13) M. Prost and B. F. Maume, in "Mass Spectrometry in Biochemistry and Medicine," A. Frigerio and N. Castagnoli, Eds., Raven, New York, N.Y., 1974, pp. 142, 143.

(14) C. D. Pfaffenberger and E. C. Horning, *J. Chromatogr.*, **112,** 581 (1975).

(15) *Gas Chromatogr. Newsl.*, **17,** 1 (1976).

(16) S. J. Gaskell and C. J. W. Brooks, *Biochem. Soc. Trans.*, **4,** 111 (1976).

(17) R. W. Kelly and P. L. Taylor, *Anal. Chem.*, **48,** 465 (1976).

(18) G. Phillipou, D. A. Bigham, and R. F. Seamark, *Steroids*, **26,** 516 (1975).

(19) "Control of Proliferation of Animal Cells," B. Clarkson and R. Baserga, Eds., Cold Spring Harbor Symposia, vol. 1, 1974, pp. 105–113.

(20) D. J. Harvey and P. Vouros, *Biomed. Mass Spectrom.*, **6,** 135 (1979).

(21) L. L. Engel and J. C. Orr, in "Biochemical Applications of Mass Spectrometry," G. R. Waller, Ed., Wiley–Interscience, New York, N.Y., 1972, p. 551.

(22) H. Hart, *Chem. Rev.*, **79,** 519 (1979).


## ACKNOWLEDGMENTS


Supported in part by Medical Research Council of Canada Grant 68-5295.

The authors are grateful to Dr. J. E. Axelson who generously allowed the use of the gas chromatograph.

# Micellar Solubilization of Cetaben Sodium in Surfactant and Lipid Solutions

**SAN-LAUNG CHOW** [x] **and BERNARD E. SIMS**

Received July 2, 1980, from the *Pharmaceutical/Mechanical R&D Section, Medical Research Division/Lederle Laboratories, American Cyanamid Company, Pearl River, NY 10965.* Accepted for publication January 27, 1981.

**Abstract** □ Cetaben sodium solubilities were evaluated by micellar solubilization in various surfactants and lipid solvents. At pH 8, the relationship between cetaben sodium solubility and surfactant concentration delineated apparent saturable kinetics; at pH 4.9, the relationship between the two parameters was linear. In the presence of 0.5% sodium taurocholate and polysorbate 80, cetaben sodium solubility increased as the medium pH was increased; however, in the presence of 0.5% poloxamer 188, cetaben sodium solubility revealed a hyperbola when the pH was changed from 4.9 to 8.0. Cetaben sodium solubility was enhanced greatly by mixed physiological surfactants, full-strength caprylic–capric monodiglycerides or monodiglycerides, when compared to a single surfactant system. Cetaben sodium solubility is influenced by pH, surfactant type, surfactant concentration, lipid solvent type, and the simultaneous presence of surfactants or phospholipids.

**Keyphrases** □ Cetaben sodium—micellar solubilization in surfactant and lipid solutions □ Solubility—micellization of cetaben sodium in surfactant and lipid solutions □ Surfactants—micellar solubilization of cetaben sodium □ Micellization—cetaben sodium solubilization in surfactant and lipid solutions □ Antiatherosclerotic agents—micellar solubilization of cetaben sodium in surfactant and lipid solutions

Cetaben sodium, sodium 4-(hexadecylamino)benzoate, is a new synthetic drug (1) highly effective in preventing and ameliorating the condition of atherosclerosis (2, 3). Cetaben sodium is an odorless, tasteless, white, soapy-textured powder; it is chemically stable under normal conditions and is not expected to present compatibility problems with the usual formulation excipients. However, cetaben sodium is practically insoluble in water at all pH values. As a consequence, analysis, bioavailability, and formulation problems have been encountered.

This paper reports findings that characterize some solubilities for cetaben sodium and describes the solubilization mechanism using surfactants and lipid solvents.

## EXPERIMENTAL

**Materials**—Cetaben sodium, >99% pure, was used as obtained[1]. Purified grade sodium taurocholate[2] was found to have <1% impurities by TLC (4). In some experiments, polysorbate 80[3] and poloxamer 188[4] were used as obtained as nonionic surfactants for solubilizing cetaben sodium. L-$\alpha$-Lecithin[5] (99% pure) and monoolein[6] and oleic acid[6] (>99% pure) were obtained commercially.

Caprylic–capric monodiglycerides[7], monodiglycerides[8], polyoxypropylene 15 stearyl ether[9], caprylic–capric triglycerides[10], triacetin[11], ethyl citrate[12], and medium-chain triglycerides oil[13] were used as lipid solvents as obtained. Analytical reagent grade monobasic and dibasic sodium phosphates[14] were used as buffer components. The total concentration of buffer solution was 65 m*M*. Micellar solutions of the surfactants in phosphate buffer were prepared by ultrasound irradiation for 5 min with a sonifier[15].

**Solubility Determinations**—An excess of cetaben sodium was added to 20 ml of micellar solutions contained in 50-ml amber screw-capped bottles. The bottles were shaken with a wrist-action shaker[16] for 48 hr in a shaker bath[17] (24 ± 0.1°). The time required for equilibration was established by a repetitive sampling technique. After equilibration, samples were filtered through 0.45-$\mu$m filters[18] held in adapters[19] and diluted appropriately if required. The samples were assayed for cetaben content by high-performance liquid chromatography (HPLC).

**Analysis**—Analytical determinations were carried out on an HPLC system consisting of a solvent-delivery unit[20], an injector[21], a 3.9-mm × 30-cm reversed-phase analytical column with 10-$\mu$m particles[22], a variable-wavelength UV detector[23], and a strip-chart recorder[24]. The mobile phase contained 90% methanol[25] in 2.5 m*M* ammonium acetate[25]. The system was operated at 280 nm and ambient temperature, and the mobile phase flow rate was 3 ml/min. Cetaben content was quantitated by comparing peak heights obtained from the chromatograms of experimental samples with those of chromatographed standards. Standard calibration plots of peak height *versus* concentration were linear in the concentration ranges studied.

## RESULTS AND DISCUSSION

**Influence of Surfactants on Cetaben Sodium Solubility**—Surfactants are one of the most important groups of formulation excipients used for pharmaceutical preparations. Their unique physicochemical properties have prompted considerable interest in their possible effects on drug absorption. However, these effects seem to be specific and not unique (5). Since dissolution usually is the rate-determining step for hydrophobic drug absorption, the influence of surfactants on cetaben solubility was investigated.

The solubilities of cetaben sodium in 0.5% sodium taurocholate, polysorbate 80, and poloxamer 188 at pH 4.9 were 0.028, 0.021, and 0.016 mg/ml, respectively; at pH 8, the solubilities were 0.468, 0.129, and 0.004 mg/ml, respectively. With the same surfactant concentration, cetaben sodium was solubilized in the following order: sodium taurocholate > polysorbate 80 > poloxamer 188. This cetaben solubilization is ascribed to the micellization of the drug by the surfactant systems. In such aqueous systems, micellization is due primarily to hydrophobic interactions between lipophilic moieties of the amphiphilic molecules (6).

A striking difference in solubility with respect to pH change also can be noted from these results, as will be discussed.

**Influence of pH on Cetaben Sodium Solubility**—The intralumenal intestinal pH varies under normal absorptive conditions and depends on the proximity of the absorbing segment to the pylorus. Therefore, the influence of pH on cetaben sodium solubility was evaluated. The pH of the aqueous media was varied from 4.9 to 8 by changing the relative amounts of the monobasic and dibasic salts of phosphate in the media.

With sodium taurocholate and polysorbate 80, a significant increase in the cetaben sodium solubility was observed as the medium pH was

[1] Metabolic Disease Research Section, Medical Research Division, American Cyanamid Co.
[2] Calbiochem Co., San Diego, Calif.
[3] Tween 80, Fisher Scientific Co., Fair Lawn, N.J.
[4] Pluronic F68, BASF Wyandotte Corp., Wyandotte, Mich.
[5] Type III-D from egg yolk, Sigma Chemical Co., St. Louis, Mo.
[6] Sigma Chemical Co., St. Louis, Mo.
[7] Capmul 8210, Capital City Products, Cleveland, Ohio.
[8] Arlacel 186, ICI, Wilmington, Del.
[9] Arlamol E, ICI, Wilmington, Del.
[10] Neobee M5, PVO, Boonton, N.J.
[11] Triacetin, Union Carbide, New York, N.Y.
[12] Pfizer Laboratories, New York, N.Y.
[13] MCT, Mead Johnson Laboratories, Evansville, Ind.
[14] J. T. Baker Chemical Co., Phillipsburg, N.J.
[15] Branson Ultrasonic Corp., Stamford, Conn.
[16] Model 75, Burrell Corp., Pittsburgh, Pa.
[17] Eberbach Corp., Ann Arbor, Mich.
[18] Millipore Corp., Bedford, Mass.
[19] Swinnex-25, Millipore Corp., Bedford, Mass.
[20] Model M6000A pump, Waters Associates, Milford, Mass.
[21] Model U6K, Waters Associates, Milford, Mass.
[22] $\mu$Bondapak $C_{18}$, Waters Associates, Milford, Mass.
[23] Model 450, Waters Associates, Milford, Mass.
[24] Omniscribe B-5000, Houston Instrument Division, Austin, Tex.
[25] Fisher Scientific Co., Fair Lawn, N.J.



*0022-3549/81/0800-0924$01.00/0*
*© 1981, American Pharmaceutical Association*

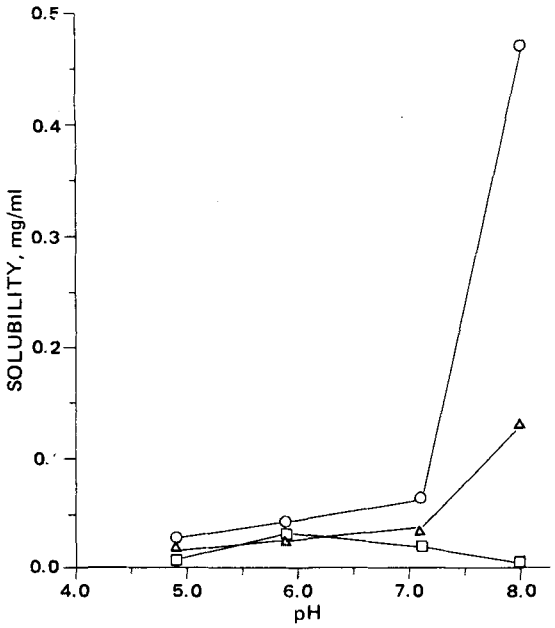


**Figure 1**—*Cetaben sodium solubilities in the presence of 0.5% (w/v) sodium taurocholate (○), polysorbate 80 (△), and poloxamer 188 (□) at pH 4.9, 5.9, 7.1, and 8.0.*

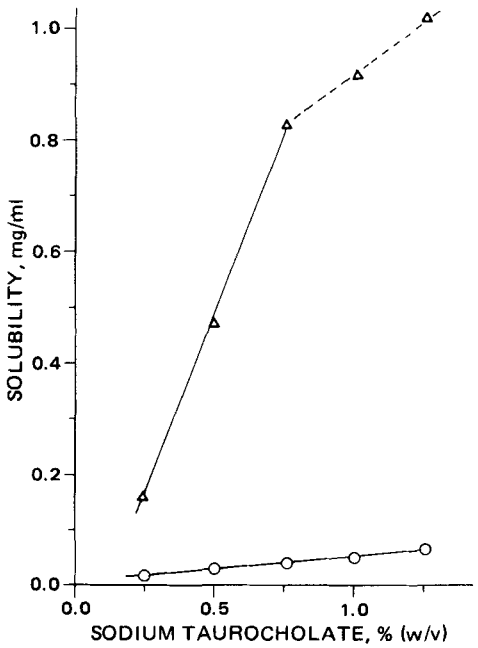


**Figure 2**—*Cetaben sodium solubilities in the presence of various strengths of sodium taurocholate at pH 4.9 (○) and 8.0 (△).*

increased (Fig. 1). Two separate mechanisms may account for this observation. The first mechanism is related to the ionization of cetaben itself. The apparent basic $pKa_1$ and acidic $pKa_2$ of cetaben were 2.6 and 5.3, respectively, in acetic acid when titrated with standardized perchloric acid that also was in acetic acid (7). Therefore, within pH 4.9–7.3, the proportion of cetaben in its anionic form increases as the hydrogen-ion concentration decreases, resulting in an increase in the aqueous solubility of cetaben as the pH is increased. The free acid form of cetaben had a much lower solubility than its sodium salt, indicating a consistency with the pH-partition hypothesis.

Changes in the critical micelle concentration (CMC) and micellar structure may offer another explanation for the changes in cetaben solubility under different pH conditions. Structurally, cetaben itself appears to have micellar properties. The alkaline pH conditions may enhance the mixed micellar formation, which results in a greater increase in cetaben solubility beyond pH 7.1–8. Bloor *et al.* (8) showed that the CMC for polysorbate 40 decreased with the pH increase as a result of the higher entropy change, which, in turn, was due to the greater degree of water structure at higher pH.

No evidence has proved or disproved the general applicability of these findings for surfactants other than polysorbate 40. Nevertheless, these postulations provide a possible explanation for the present experimental observations. It is likely that cetaben would partition more into the micellar phase resulting from a lower CMC at higher pH as compared to the lower pH conditions. The overall magnitude of the changes in cetaben solubility would depend entirely on the relative contribution of each mechanism. At pH values greater than 7.1, cetaben exists >98% as the anionic species. The sharp increase in cetaben solubility from pH 7.1 to 8 (Fig. 1) then is most likely due to changes in the CMC and micellar structure that are predominant under alkaline pH conditions.

In contrast to the sodium taurocholate and polysorbate 80 systems, the pH–solubility profile for poloxamer 188 delineated a hyperbola (Fig. 1). The described mechanisms still are applicable, except to the lowering of cetaben solubilities under alkaline pH values. This exception indicated that poloxamer 188 was not stable at alkaline conditions as compared to acidic conditions, a rationalization that was justified by a control experiment under the same experimental conditions using a UV spectral shift technique. As the medium pH becomes more alkaline, poloxamer 188 may degrade extensively, lose its surfactant properties, and, thus, cause the gradual dropping in cetaben solubility.

The complexity of the mixed micellar system makes analysis of the mechanisms contributing to the observed pH–solubility profiles difficult. The proposed mechanisms should be viewed as reasonable hypotheses explaining the present experimental observations. Further investigation should clarify the actual contribution of each mechanism to the overall pH–solubility profiles.

**Influence of Surfactant Concentration on Cetaben Sodium Solubility**—The low cetaben solubility requires surfactants for solubilization in an aqueous phase. To examine the effect of surfactant concentration on cetaben solubility, the surfactant concentration was increased in a stepwise fashion.

In the first series of experiments, the sodium taurocholate concentration was varied from 0.25 to 1.25% (w/v) at a constant pH of 4.9. The relationship between cetaben sodium solubility and sodium taurocholate concentration was linear (Fig. 2). This linearity suggests a typical solubilization plot for a micellar system where the solubility increases linearly with surfactant concentration beyond the CMC (9). As the surfactant concentration is increased, more drug is dissolved into the micellar phase (10). As a result, at higher sodium taurocholate concentrations, the amount of cetaben in the micellar phase would increase. Similar findings also were observed for nonionic surfactants, polysorbate 80, and poloxamer 188 (Figs. 3 and 4).

In the second series of experiments, all experimental conditions were kept the same but the medium pH was 8. The solubility–concentration profile delineated apparent saturable kinetics, revealing two linear segments with different slopes (Figs. 2–4). This change into two linear segments was statistically significant for sodium taurocholate and polysorbate 80 but not for poloxamer 188. The sudden change in slope could be due to size or shape changes in the micellar structure (11, 12). At

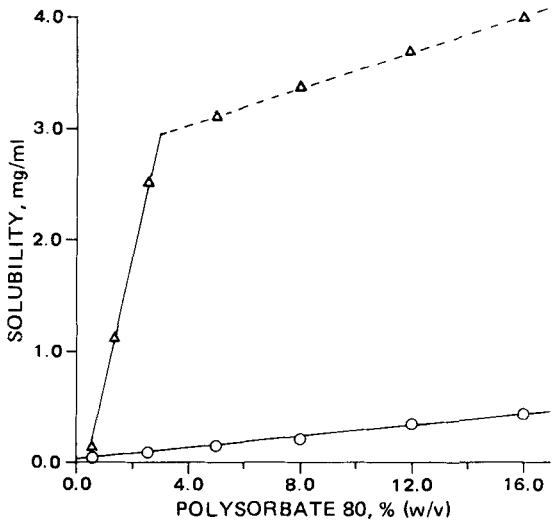


**Figure 3**—*Cetaben sodium solubilities in the presence of various strengths of polysorbate 80 at pH 4.9 (○) and 8.0 (△).*

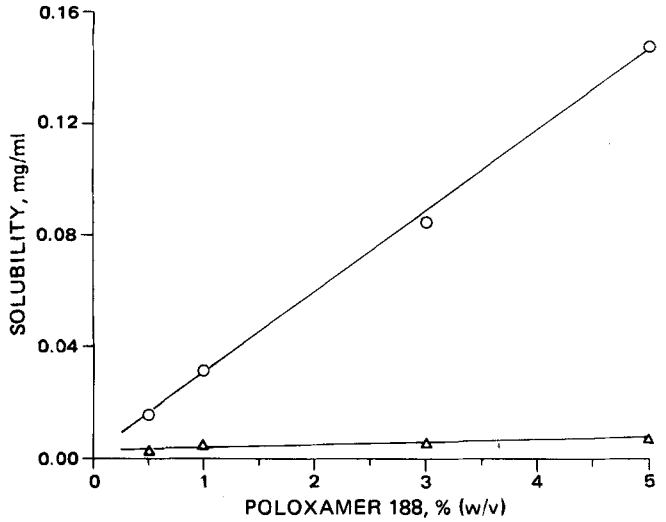


**Figure 4**—*Cetaben sodium solubilities in the presence of various strengths of poloxamer 188 at pH 4.9 (○) and 8.0 (△).*

concentrations higher than the CMC, micelles tend to coalesce into long rod-shaped micelles and cylindrical aggregates; finally, at very high concentrations, a phase transformation into lamellar structures takes place. Each transformation point varies and depends on the type of surfactant, the nature of surfactant, and the medium conditions.

**Influence of Mixed Physiological Surfactants on Cetaben Solubility**—Bile salts and phospholipids have been recognized as physiological surfactants important to lipid absorption (13, 14). The present study examined the effect of some physiological surfactants and mixed surfactant systems on cetaben sodium solubility.

Sodium taurocholate, lecithin, oleic acid, and monoolein were prepared in different proportions (Table I). Cetaben solubility was increased ninefold by taurocholate–monoolein, 23-fold by taurocholate–lecithin, 368-fold by taurocholate–oleic acid, 376-fold by taurocholate–oleic acid–lecithin, and 631-fold by taurocholate–oleic acid–monoolein when compared to taurocholate alone. Solubility enhancement can be attributed to an increased effective surface area when mixed disk micelles are formed (15). It also is possible that the inclusion of a second solubilizate may cause rearrangement of the mixed micelle structure, thereby altering the distribution coefficient favorable to solubilization (16).

**Influence of Lipid Solvents on Cetaben Solubility**—Lipid solvents

**Table I—Cetaben Sodium Solubilities in Solutions Containing Physiological Surfactants Prepared in Different Proportions**

| Surfactant | Molar Ratio[a], m*M* | Solubility, mg/ml | Solubility Ratio[b] |
|---|---|---|---|
| Taurocholate | 10 | 0.029 | 1 |
| Taurocholate–monoolein | 10:5 | 0.243 | 9 |
| Taurocholate–lecithin | 10:5 | 0.647 | 23 |
| Taurocholate–oleic acid | 62.5:3540 | 10.313 | 368 |
| Taurocholate–oleic acid–lecithin | 62.5:3540:0.78 | 10.547 | 376 |
| Taurocholate–oleic acid–monoolein | 62.5:3540:1.75 | 17.658 | 631 |

[a] The 10 m*M* was chosen because of its similarity to physiological concentrations of bile salts and its frequent use in previous studies. The ratios were chosen for convenience in preparation. [b] Solubility ratio = solubility in mixed surfactants/solubility in sodium taurocholate.

greatly enhance the bioavailability of hydrophobic compounds (10). Therefore, the effect of lipid solvents on cetaben solubility was studied to provide additional formulation information.

The selected lipid solvents were used at 100% strength. The solubilization capacity of lipid solvents for cetaben was in the following order: caprylic–capric monodiglycerides (23.191 mg/ml) > monodiglycerides (22.821 mg/ml) > triethyl citrate (0.61 mg/ml) > polyoxypropylene 15 stearyl ether (0.305 mg/ml) > medium-chain triglycerides (0.224 mg/ml) > caprylic–capric triglycerides (0.108 mg/ml) > triacetin (0.043 mg/ml).

Unlike solutions in aqueous media, micelles are formed by a stepwise aggregation rather than by a simple monomer–micelle equilibrium characteristic of aqueous systems (6, 17). The driving force behind aggregation and micellization in these nonaqueous media likely is due to dipole–dipole interactions between polar heads of the amphiphilic molecules (6).

Cetaben sodium is a promising antiatherosclerotic agent. Knowledge regarding the mechanism of its solubilization by surfactants and lipid solvents, as well as factors modifying its solubility, is essential for development of optimal formulation conditions.

## REFERENCES

(1) J. D. Albright, S. A. Schaffer, and R. G. Shepherd, *J. Pharm. Sci.*, **68**, 936(1979).

(2) W. Hollander, S. Prusty, S. Nagraj, B. Kirkpatrick, J. Paddock, and M. Colombo, *Atherosclerosis*, **31**, 307 (1978).

(3) A. S. Katocs, Jr., and S. A. Schaffer, *Fed. Proc. Fed. Am. Soc. Exp. Biol.*, **36**, 1160 (1977).

(4) J. J. Gregg, *J. Lipid. Res.*, **7**, 579 (1966).

(5) M. Gibaldi and S. Feldman, *J. Pharm. Sci.*, **59**, 579 (1970).

(6) A. S. Kertes, in "Micellization, Solubilization, and Microemulsions," K. L. Mittal, Ed., Plenum, New York, N.Y., 1977, p. 445.

(7) A. Albert and E. P. Serjeant, "The Determination of Ionization Constants," Chapman and Hall, London, England, 1971, p. 39.

(8) J. R. Bloor, J. C. Morrison, and C. T. Rhodes, *J. Pharm. Sci.*, **59**, 387 (1970).

(9) J. T. Carstensen, "Theory of Pharmaceutical Systems," vol. I, Academic, New York, N.Y., 1972, p. 41.

(10) W. J. Simmonds, in "Gastrointestinal Physiology," Physiology Series One, vol. 4, E. D. Jacobson and L. L. Shanbour, Eds., University Park Press, Baltimore, Md., 1974, p. 343.

(11) F. Wesoluch, A. T. Florence, F. Puisieux, and J. T. Carstensen, *Int. J. Pharm.*, **2**, 343 (1979).

(12) A. F. Hofmann and D. M. Small, *Annu. Rev. Med.*, **18**, 333 (1967).

(13) J. M. Dietschy and H. Westergaard, *J. Clin. Invest.*, **59**, 97 (1976).

(14) K. J. Isselbacher and R. K. Ockner, *Rev. Physiol. Biochem. Pharmacol.*, **71**, 107 (1974).

(15) R. O. Zimmerer, Jr., and S. Linderbaum, *J. Pharm. Sci.*, **68**, 581 (1979).

(16). F. Alhaique, D. Giacchetti, M. Marchetti, and F. M. Riccieri, *J. Pharm. Pharmacol.*, **29**, 401 (1977).

(17) P. L. Dubin, in "Abstracts of Papers of the American Chemical Society," vol. 174, American Chemical Society, Washington, D.C., 1977, topic 109.

## ACKNOWLEDGMENTS

Presented in part at the Basic Pharmaceutics Section, APhA Academy of Pharmaceutical Sciences, Washington, D.C., meeting, April 1980.

The authors thank Dr. Peter Bernardo and Dr. George Allen for support and encouragement.

# Powder Flow Studies III: Tensile Strength, Consolidation Ratio, Flow Rate, and Capsule-Filling-Weight Variation Relationships

**Z. T. CHOWHAN** ˣ **and I-CHANG YANG**

Received August 18, 1980, from *Syntex Research, Palo Alto, CA 94304.* Accepted for publication January 30, 1981.

**Abstract** □ The tensile strength of consolidated powder beds was studied by applying a series of loads to the surface of the powder beds in a tensile tester. The results were plotted as tensile strength *versus* consolidation pressure. The linearity of these plots suggests a direct relationship between tensile strength and consolidation pressure. The following plots gave linear relationships: (*a*) tensile strength *versus* consolidation ratio, (*b*) tensile strength *versus* coefficient of variation of the filled weight of the capsules, and (*c*) logarithm of the tensile strength *versus* logarithm of the flow rate. These results suggest a direct relationship between tensile strength and consolidation ratio and their usefulness in studying powder flow. The physical significance of the empirical equation used in consolidation studies was explored. A comparison of the empirical equation with a theoretically derived equation, under certain assumptions, suggests that the consolidation ratio is a function of the ratio of the initial volume to the net volume and a function of the coefficient of Rankine. The coefficient of Rankine is a function of the angle of internal friction in the static powder bed.

**Keyphrases** □ Tensile strength—powder flow behavior, relationship to consolidation ratio □ Powder flow—tensile strength, consolidation ratio relationships □ Consolidation ratio—powder flow behavior, relationship to tensile strength

The knowledge of powder behavior is important in understanding the powder properties during storage, transportation, mixing, granulating, capsule filling, and tableting. Tensile strength, defined as the force per unit area of a broken face required to split a powder compact, provides useful information on powder behavior. The effects of powder density, particle-size distribution, and interparticle forces were considered in developing a theory of the tensile strength of powders (1).

Theoretical developments in studying powder flow must make far-reaching simplifying assumptions because of the numerous parameters involved, such as size, shape, and surface texture. These developments, although interesting, are of limited practical utility.

## BACKGROUND

Recent studies (2, 3) reported the consolidation of loosely packed powders and powder mixtures in cylindrical containers by applying a series of loads. The results of simple measurements in which the decrease of powder volume was measured as a function of the compressive load were plotted as the logarithm of the change in volume *versus* the logarithm of the applied pressure. The slopes of these plots were similar, and the intercept (consolidation ratio) gave a linear relationship with the logarithm of the flow rate and the coefficient of variation of the filled weight of capsules produced on an automatic capsule-filling machine.

Simple consolidation measurements and the use of an empirical equation suggested a good relationship to flow properties of the powders and powder mixtures. A literature survey indicated a paucity of any relationship between powder flow behavior and tensile strength.

This paper reports linear relationships between (*a*) tensile strength and consolidation ratio, (*b*) tensile strength and coefficient of variation of the filled weight of capsules, and (*c*) logarithm of the tensile strength and logarithm of the flow rate. These results suggest a direct relationship between tensile strength and consolidation ratio and their usefulness in studying powder flow. A comparison of the empirical equation with a theoretically derived equation, under certain assumptions, suggests that the consolidation ratio is a function of the ratio of the initial volume to the net volume and a function of the coefficient of Rankine. The coefficient of Rankine is a function of the angle of internal friction in the static powder bed.

## EXPERIMENTAL

**Materials**—The drug[1], tromethamine salt of (±)-2-benzoyl-1-azabicyclo[3.3.0]octa-2,4-diene-6-carboxylic acid, was at least 99% pure. The excipients were spray-dried lactose USP[2], starch USP[3], and magnesium stearate USP[4].

**Mixing**—The powders of each formulation were mixed by the geometric dilution method on a piece of glassine paper. The powder mixture was screened through a 40-mesh screen to ensure proper mixing and to avoid powder agglomeration due to compaction. Three types of formulations were used. Drug and spray-dried lactose were mixed in the indicated proportions in the first formulation. The second formulation contained 0.5% magnesium stearate in addition to the drug and spray-dried lactose. The final formulation contained 10% starch, 0.5% magnesium stearate, spray-dried lactose, and drug in the indicated proportions. Powder mixing and all tensile strength measurements were carried out at 24 ± 1° and 40 ± 5% relative humidity.

**Tensile Strength**—The tensile strength of powder mixtures was determined by conducting a tensile test with an instrument[5] consisting of a main unit, an operational amplifier, and an $x$–$y$ recorder. The main unit included four major components: (*a*) a constant-speed motor for exerting a pulling force through a steel string to break the powder bed, (*b*) a cylindrical powder cell with one half fixed to the main unit and the other half movable by suspension onto a metal frame, (*c*) a strain gauge of 200-g force for the quantitative measurement of tensile stress required to break the powder bed, and (*d*) a linear, variable differential transformer for the measurement of powder bed displacement.

The operational amplifier contained a strain amplifier, a displacement meter, and an operational unit. The latter was designed to indicate only the actual load by subtracting the necessary blank load that varied with displacement.

Blank tests were run to ensure that there was no extra load between the two half-cells before the powder was loaded. An accurately weighed amount of the powder was charged evenly through the cell extension tube, and the compaction weight was inserted gently into this tube. After 20 sec, additional weights, from 100 g to 2 kg, were loaded, with 20 sec between each loading. The weights and the cell extension tube were unloaded after 5 min. A steady-state condition in the powder bed thus was reached. The pulling string connecting the powder cell through a strain gauge was tightened under suitable tension before the clamp of the two half-cells was released. Then the constant-speed motor switch was turned on to pull the movable half-cell.

During the breaking process, the $x$–$y$ recorder automatically recorded the tensile force profile over the total displacement of the two half powder beds. The peak value on the vertical axis of the tensile force–displacement curve gave the maximum tensile force of the powder. The area of breakage was normally 5 cm$^2$, provided the compaction weight descended to the proper position. Otherwise, the area was corrected for the powder bed thickness difference. The tensile strength of the powder bed was obtained by dividing the maximum tensile force with the area of powder bed breakage. Three determinations were made, and the mean and the standard deviation were calculated. Only results obtained from the tensile

[1] Institute of Organic Chemistry, Syntex Research, Palo Alto, Calif.
[2] Foremost Co., San Francisco, Calif.
[3] Staley Manufacturing Co., Decatur, Ill.
[4] Mallinckrodt Chemical Works, St. Louis, Mo.
[5] Cohetester, Hosokawa Micromeritics Laboratory, Osaka, Japan.

0022-3549/81/0800-0927$01.00/0
© 1981, American Pharmaceutical Association

**Table I—Tensile Strength of Powder Mixtures Containing Drug and Excipients at Various Consolidation Pressures**

| Percent Drug | Pressure, g/cm² | Tensile Strength, g/cm² | Slope | Intercept | Correlation Coefficient, r |
|---|---|---|---|---|---|
| 89.5 | 20.99 | 1.95 ± 0.026 | 0.03078 | 1.507 | 0.9897 |
| | 41.36 | 2.92 ± 0.11 | | | |
| | 66.84 | 3.74 ± 0.07 | | | |
| | 117.78 | 5.02 ± 0.32 | | | |
| 40 | 20.99 | 1.14 ± 0.098 | 0.0167 | 0.9686 | 0.9752 |
| | 41.36 | 1.81 ± 0.17 | | | |
| | 66.84 | 2.20 ± 0.08 | | | |
| | 117.78 | 2.85 ± 0.06 | | | |
| 20 | 20.99 | 0.58 ± 0.01 | 0.006122 | 0.4020 | 0.9776 |
| | 41.36 | 0.64 ± 0.06 | | | |
| | 66.84 | 0.74 ± 0.06 | | | |
| | 117.78 | 1.16 ± 0.07 | | | |
| 10 | 20.99 | 0.15 ± 0.04 | 0.00443 | 0.1039 | 0.9609 |
| | 41.36 | 0.30 ± 0.08 | | | |
| | 66.84 | 0.47 ± 0.05 | | | |
| | 117.78 | 0.59 ± 0.08 | | | |

fracture where the powder bed broke into two halves along the joint of the two half-cells were recorded.

## RESULTS AND DISCUSSION

The tensile strength results of powder mixtures containing 10, 20, 40, and 89.5% drug at various consolidation pressures are given in Table I and Fig. 1. The excipients in these powder mixtures were 10% starch, 0.5% magnesium stearate, and spray-dried lactose to make 100%. The results indicate that the tensile strength is related linearly to the consolidation pressure in the pressure range studied. The dimensionless slope of these lines may be regarded as material constant, which is a measure of the increase in cohesive forces between adjacent particles due to consolidation. The intercept indicates the cohesive forces in an unconsolidated powder bulk. For free-flowing powders, the intercept is zero.

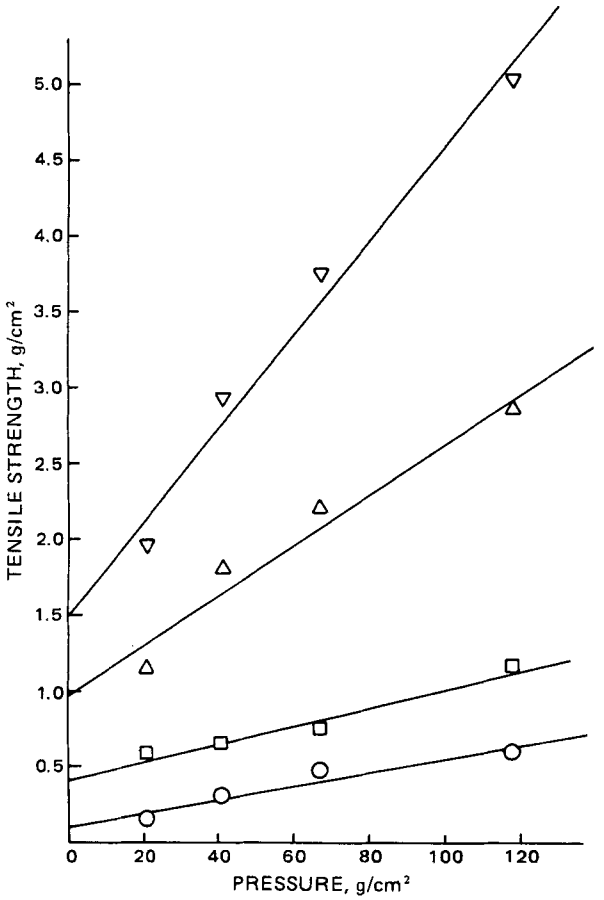


**Figure 1**—*Tensile strength of powder mixtures* versus *consolidation pressure plots showing linear relationships. Key:* ○, *10% drug;* □, *20% drug;* △, *40% drug; and* ▽, *89.5% drug.*

The profiles of the tensile strength *versus* percent drug at a constant consolidation pressure (66.84 g/cm²) are given in Fig. 2. The tensile strength of the mixtures containing 10 and 20% drug, lactose, and magnesium stearate was lower than that of mixtures containing drug, lactose, starch, and magnesium stearate and of mixtures containing drug and lactose. At higher drug concentrations, the tensile strength of the mixtures containing starch and magnesium stearate was higher than that of the mixtures containing only drug and lactose.

The consolidation ratio and the coefficient of variation of the filled weight of capsules reported previously (2) were plotted *versus* tensile strength (Fig. 3). The results indicate linear relationships between tensile strength and consolidation ratio and between tensile strength and coefficient of variation of the filled weight of the capsules. The logarithm of the flow rate reported earlier (3) and the logarithm of the tensile strength are plotted in Fig. 4. These results suggest that the tensile strength and consolidation ratio provide useful information of powder flow behavior.

The powder consolidation ratio was obtained (2) from the intercepts of the relative volume *versus* consolidation pressure plots according to:

$$\ln \frac{V_0 - V}{V} = m \ln \frac{P}{P_0} + I \qquad \text{(Eq. 1)}$$

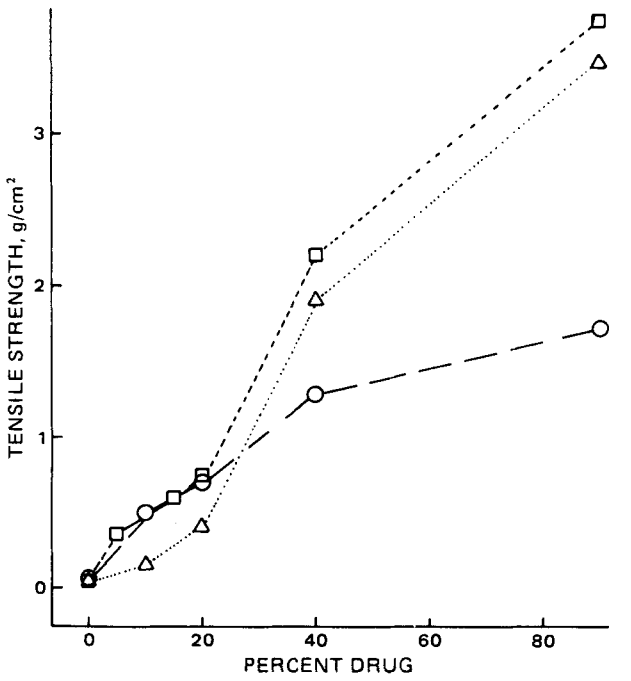


**Figure 2**—*Profiles of the tensile strength as a function of the formulation composition. Key:* ○, *drug and lactose mixture;* △, *drug, lactose, and 0.5% magnesium stearate mixture; and* □, *drug, lactose, 10% starch, and 0.5% magnesium stearate mixture.*

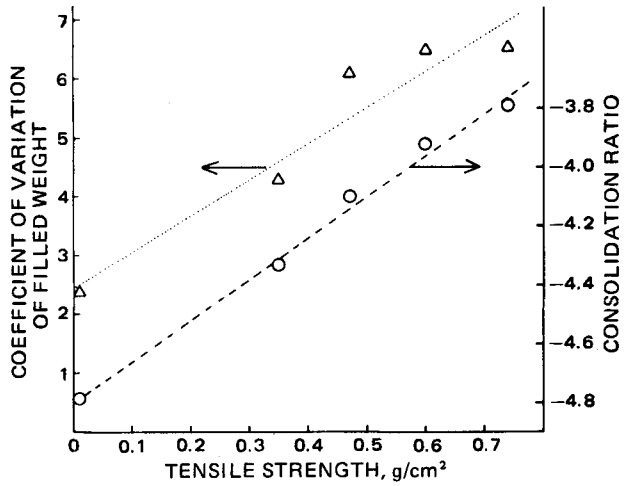


**Figure 3**—*Plots of the tensile strength* versus *consolidation ratio and coefficient of variation of the filled weight of the capsules. Key:* ○, r = *0.9964; and* △, r = *0.9583.*

where $V_0$ is the initial powder volume; $V$ is the powder volume at a given surface pressure, $P$; $P_0$ is the surface pressure $P$ (1 atmospheric pressure approximately equals 1 kg/cm$^2$); and $m$ and $I$ are constants.

By assuming $I = \ln C$, dividing both sides by $V_0$, and rearranging, Eq. 1 can be written as:

$$\frac{1}{V} - \frac{1}{V_0} = \frac{C}{V_0}\left(\frac{P}{P_0}\right)^m \qquad \text{(Eq. 2)}$$

Multiplying both sides by $V_\infty$, adding 1 to both sides, and rearranging give:

$$\frac{V - V_\infty}{V} = \frac{V_0 - V_\infty}{V_0} - \frac{CV_\infty}{V_0}\left(\frac{P}{P_0}\right)^m \qquad \text{(Eq. 3)}$$

where $V_\infty$ is the net volume of the powder.

Since porosity $n$ equals $(V - V_\infty)/V$ and the powder bed is assumed to be homogeneous, Eq. 3 can be written:

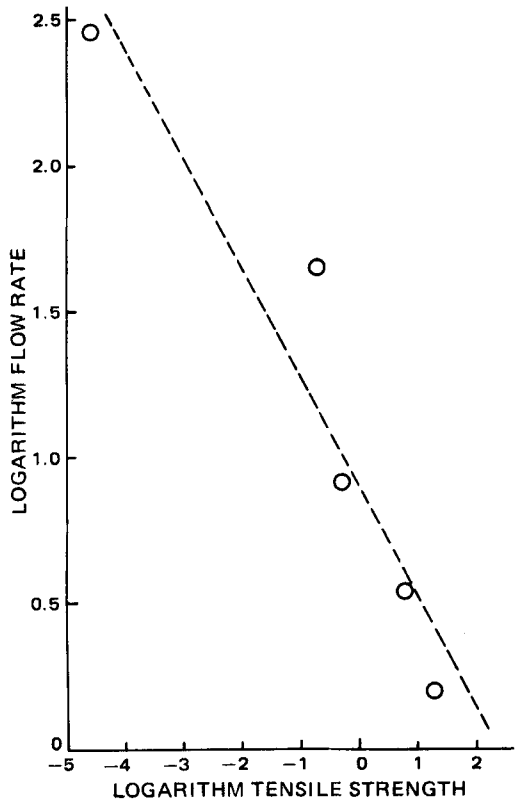


**Figure 4**—*Logarithm tensile strength* versus *logarithm flow rate showing a linear relationship* (r = *0.9523*).

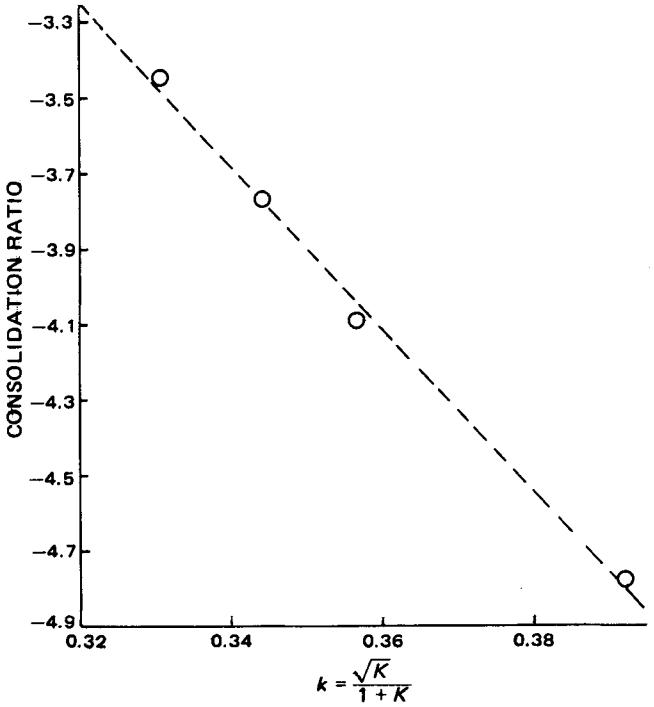


**Figure 5**—*Plots of consolidation on ratio* versus k *showing a linear relationship* (r = *−0.9980*).

$$n - n_0 = -\frac{CV_\infty}{V_0}\left(\frac{P}{P_0}\right)^m \qquad \text{(Eq. 4)}$$

Theories dealing with the pressure and volume change relationship have been reported in the field of powder technology. Kawakita and Ludde (4) obtained a theoretical compression equation using Mohr's circle of stress:

$$\Delta\phi = \frac{\sqrt{K}}{1 + K}\frac{d\sigma_1}{\sigma_1} \qquad \text{(Eq. 5)}$$

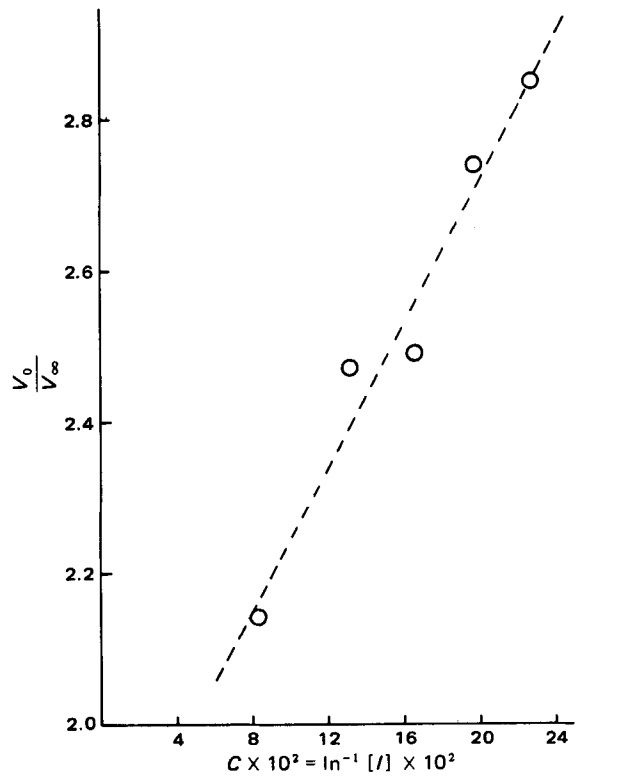


**Figure 6**—*Plots of* $V_0/V_\infty$ versus C *showing a linear relationship* (r = *0.9764*).

**Table II—Values of $\phi$, $K$, $k$, and $I$**

| Drug in Mixture, % | $\phi$ | $K$ | $k$ | $I$ |
|---|---|---|---|---|
| 40 | 48.6 | 0.1428 | 0.3307 | −3.45 |
| 20 | 46.5 | 0.1592 | 0.3442 | −3.77 |
| 10 | 44.5 | 0.1758 | 0.3566 | −4.09 |
| 0 | 38.4 | 0.2337 | 0.3918 | −4.78 |

where $\sigma_1$ is the maximum principal stress, $\phi$ is the angle of internal friction, and $K$ is the coefficient of Rankine (5) as given by:

$$K = \frac{1 - \sin \phi}{1 + \sin \phi} \quad \text{(Eq. 6)}$$

Thus, $\Delta\phi$ represents the probability of a packing change of the particles and is considered to be proportional to some quantities related to the state of packing in one of the several described manners. It was shown that various compression equations could be derived by making different assumptions about the properties that determine $\Delta\phi$.

If $\Delta\phi$ is proportional to the decrease in porosity and inversely proportional to the $m$th power of consolidation pressure, $-dn/P^m$, then:

$$-\frac{dn}{P^m} = k\frac{dP}{P} \quad \text{(Eq. 7)}$$

where $P$ is the consolidation pressure, $m$ is a constant, and $k$ is a function of the coefficient of Rankine.

Equation 7, on rearrangement, gives:

$$-dn = kP^{m-1}\,dP \quad \text{(Eq. 8)}$$

Integration of Eq. 8 from initial porosity $n_0$ to porosity $n$, corresponding to the zero initial consolidation pressure to the consolidation pressure $P$, gives:

$$n - n_0 = -\frac{k}{m}P^m \quad \text{(Eq. 9)}$$

Equation 9 is similar to Eq. 4, which is the modified form of Eq. 1. Equations 4 and 9 suggest that $C$ is a function of $(V/V_\infty)(k/m)$.

A previous study (2) showed that, for different powder mixtures of the same drug, $m$ was a constant. The value $k$ is a function of the coefficient of Rankine $K$ given by Eq. 6, and $\phi$ may be approximated from the angle of repose.

For the powder mixtures containing drug, spray-dried lactose, starch, and magnesium stearate, the values of $\phi$, $K$, $k$, and ln $C$ are given in Table II. A plot of $C$ *versus* $k$ gave a linear relationship with $r = -0.9666$. Figure 5 gives a plot of ln $C$ *versus* $k$. The excellent correlation ($r = -0.998$) indicates that ln $C$ is inversely proportional to $k$.

Figure 6 gives a plot of $V_0/V_\infty$ *versus* $C$ for the same powder mixture. A linear relationship ($r = 0.9809$) between $V_0/V_\infty$ *versus* $C$ suggests that these parameters are directly related.

The results of this study suggest that the consolidation ratio is a function of tensile strength and that both parameters are useful in studying flow behavior of powders and powder mixtures. The physical significance of the consolidation ratio was explored. The consolidation ratio is a function of the ratio of the initial volume to the net volume of the powder and of the coefficient of Rankine, which, in turn, is a function of the angle of internal friction in the static powder bed.

## REFERENCES


(1) D. C. Cheng, *Chem. Eng. Sci.*, **23**, 1405 (1968).

(2) Z. T. Chowhan and Y. P. Chow, *Int. J. Pharm.*, **4**, 317 (1980).

(3) Z. T. Chowhan and Y. P. Chow, *Drug Dev. Ind. Pharm.*, **6**, 1 (1980).

(4) K. Kawakita and K. Ludde, *Powder Technol.*, **4**, 61 (1970/71).

(5) W. J. Rankine, *Phil. Trans. R. Soc. London*, **146**, 9 (1856).


# Quantitation of Solvent Polarity Based on Molecular Structure


**LEMONT B. KIER**



Received October 27, 1980, from the *Department of Pharmaceutical Chemistry, Medical College of Virginia, Virginia Commonwealth University, Richmond, VA 23298.* Accepted for publication February 2, 1981.



**Abstract** □ A numerical index is proposed that ranks solvents according to their polarity. It is based entirely on structure, encoding the relative content of exterjacent electrons in the molecule. The index is the first-order valence molecular connectivity index, $^1\chi^v$. The index is modified for the number of isolated functional groups in the molecule. A comparison with solvent polarity indexes based on several experimental methods reveals a good relationship. The polarity index proposed can be quickly calculated, it does not depend on the availability of the actual molecule, and it permits prediction of solvent polarity or the polarity of mixtures.



**Keyphrases** □ Solvent polarity—quantitative method based on molecular structure ■ Polarity index—solvents, quantitative method based on molecular structure ■ Molecular structure—quantitative method for ranking solvent polarity


The term "solvent polarity" is widely used by chemists to characterize the observed manifestations of intermolecular interactions in a solution process. The processes may be chromatography, dissolution, or chemical reactions. The manifestations of the interactions are recorded as the separation or retention on stationary phases, the solubility, and the partitioning or reaction course and rate. Solvent polarity is a comparative term which the chemist uses intuitively to rank commonly employed compounds. This intuition, based on experience, permits the generalization that hydrocarbons are less polar than esters while alcohols are more polar than esters of the same molecular weight.

## BACKGROUND

The quantitation of solvent polarity is difficult in practice due to the variety of intermolecular forces that may operate between molecules in a given system. Much has been written about solution theory, but the forces influencing solvent–solute interactions can be summarized as those due to dispersion and dipolar and electron donor–acceptor properties (1).

Dispersion forces account for virtually all of the attractive energy between nonbonded atoms among hydrocarbons. These compounds are regarded as nonpolar when their solvent properties are characterized. Dipolar and electron donor–acceptor interactions influence the attractive energy among molecules possessing unsaturation or atoms other than carbon or hydrogen. Solvents possessing structures capable of these interactions are characterized as being polar. Thus, molecular structure governs solvent polarity, but this relationship has yet to be quantified in any simple way.




*0022-3549/81/0800-0930$01.00/0*



*© 1981, American Pharmaceutical Association*

**Table II—Values of $\phi$, $K$, $k$, and $I$**

| Drug in Mixture, % | $\phi$ | $K$ | $k$ | $I$ |
|---|---|---|---|---|
| 40 | 48.6 | 0.1428 | 0.3307 | −3.45 |
| 20 | 46.5 | 0.1592 | 0.3442 | −3.77 |
| 10 | 44.5 | 0.1758 | 0.3566 | −4.09 |
| 0 | 38.4 | 0.2337 | 0.3918 | −4.78 |

where $\sigma_1$ is the maximum principal stress, $\phi$ is the angle of internal friction, and $K$ is the coefficient of Rankine (5) as given by:

$$K = \frac{1 - \sin \phi}{1 + \sin \phi} \quad \text{(Eq. 6)}$$

Thus, $\Delta\phi$ represents the probability of a packing change of the particles and is considered to be proportional to some quantities related to the state of packing in one of the several described manners. It was shown that various compression equations could be derived by making different assumptions about the properties that determine $\Delta\phi$.

If $\Delta\phi$ is proportional to the decrease in porosity and inversely proportional to the $m$th power of consolidation pressure, $-dn/P^m$, then:

$$-\frac{dn}{P^m} = k\frac{dP}{P} \quad \text{(Eq. 7)}$$

where $P$ is the consolidation pressure, $m$ is a constant, and $k$ is a function of the coefficient of Rankine.

Equation 7, on rearrangement, gives:

$$-dn = kP^{m-1}\,dP \quad \text{(Eq. 8)}$$

Integration of Eq. 8 from initial porosity $n_0$ to porosity $n$, corresponding to the zero initial consolidation pressure to the consolidation pressure $P$, gives:

$$n - n_0 = -\frac{k}{m}P^m \quad \text{(Eq. 9)}$$

Equation 9 is similar to Eq. 4, which is the modified form of Eq. 1. Equations 4 and 9 suggest that $C$ is a function of $(V/V_\infty)(k/m)$.

A previous study (2) showed that, for different powder mixtures of the same drug, $m$ was a constant. The value $k$ is a function of the coefficient of Rankine $K$ given by Eq. 6, and $\phi$ may be approximated from the angle of repose.

For the powder mixtures containing drug, spray-dried lactose, starch, and magnesium stearate, the values of $\phi$, $K$, $k$, and ln $C$ are given in Table II. A plot of $C$ *versus* $k$ gave a linear relationship with $r = -0.9666$. Figure 5 gives a plot of ln $C$ *versus* $k$. The excellent correlation ($r = -0.998$) indicates that ln $C$ is inversely proportional to $k$.

Figure 6 gives a plot of $V_0/V_\infty$ *versus* $C$ for the same powder mixture. A linear relationship ($r = 0.9809$) between $V_0/V_\infty$ *versus* $C$ suggests that these parameters are directly related.

The results of this study suggest that the consolidation ratio is a function of tensile strength and that both parameters are useful in studying flow behavior of powders and powder mixtures. The physical significance of the consolidation ratio was explored. The consolidation ratio is a function of the ratio of the initial volume to the net volume of the powder and of the coefficient of Rankine, which, in turn, is a function of the angle of internal friction in the static powder bed.

## REFERENCES


(1) D. C. Cheng, *Chem. Eng. Sci.*, **23**, 1405 (1968).

(2) Z. T. Chowhan and Y. P. Chow, *Int. J. Pharm.*, **4**, 317 (1980).

(3) Z. T. Chowhan and Y. P. Chow, *Drug Dev. Ind. Pharm.*, **6**, 1 (1980).

(4) K. Kawakita and K. Ludde, *Powder Technol.*, **4**, 61 (1970/71).

(5) W. J. Rankine, *Phil. Trans. R. Soc. London*, **146**, 9 (1856).


# Quantitation of Solvent Polarity Based on Molecular Structure


**LEMONT B. KIER**



Received October 27, 1980, from the *Department of Pharmaceutical Chemistry, Medical College of Virginia, Virginia Commonwealth University, Richmond, VA 23298.* Accepted for publication February 2, 1981.



**Abstract** □ A numerical index is proposed that ranks solvents according to their polarity. It is based entirely on structure, encoding the relative content of exterjacent electrons in the molecule. The index is the first-order valence molecular connectivity index, $^1\chi^v$. The index is modified for the number of isolated functional groups in the molecule. A comparison with solvent polarity indexes based on several experimental methods reveals a good relationship. The polarity index proposed can be quickly calculated, it does not depend on the availability of the actual molecule, and it permits prediction of solvent polarity or the polarity of mixtures.



**Keyphrases** □ Solvent polarity—quantitative method based on molecular structure ■ Polarity index—solvents, quantitative method based on molecular structure ■ Molecular structure—quantitative method for ranking solvent polarity


The term "solvent polarity" is widely used by chemists to characterize the observed manifestations of intermolecular interactions in a solution process. The processes may be chromatography, dissolution, or chemical reactions. The manifestations of the interactions are recorded as the separation or retention on stationary phases, the solubility, and the partitioning or reaction course and rate. Solvent polarity is a comparative term which the chemist uses intuitively to rank commonly employed compounds. This intuition, based on experience, permits the generalization that hydrocarbons are less polar than esters while alcohols are more polar than esters of the same molecular weight.

## BACKGROUND

The quantitation of solvent polarity is difficult in practice due to the variety of intermolecular forces that may operate between molecules in a given system. Much has been written about solution theory, but the forces influencing solvent–solute interactions can be summarized as those due to dispersion and dipolar and electron donor–acceptor properties (1).

Dispersion forces account for virtually all of the attractive energy between nonbonded atoms among hydrocarbons. These compounds are regarded as nonpolar when their solvent properties are characterized. Dipolar and electron donor–acceptor interactions influence the attractive energy among molecules possessing unsaturation or atoms other than carbon or hydrogen. Solvents possessing structures capable of these interactions are characterized as being polar. Thus, molecular structure governs solvent polarity, but this relationship has yet to be quantified in any simple way.




*0022-3549/81/0800-0930$01.00/0*



*© 1981, American Pharmaceutical Association*

In contrast, several experimental observations have been used to construct a numerical ranking of solvent polarity. Hildebrand and Scott (2) reasoned that the molar heat of vaporization for the molar volume relates to the intermolecular interaction strength to give a value for a solubility parameter, $\delta$. Since the derivation of this polarity parameter is based on the assumption of the dominance of dispersion forces, it is less accurate for more specific dipolar forces.

Snyder (3) used the eluting power of solvents on stationary phases to arrive at an eluent strength parameter, $\epsilon^0$. The stationary phase is usually alumina, but other materials can be used with appropriate correction. Since the values for more polar solvents are quite close, the parameter is more discriminating for nonpolar solvents.

Rohrschneider (4) introduced a scale in which the solvent polarity, $P'$, is measured for GLC retention of butane and butadiene. The quality of the parameter increases with more polar solutes.

A polarity index, $Y$, measuring the ionizing power of a solvent from the solvolysis rates of several compounds, was devised (5). The charge transfer band of 1-alkylpyridinium iodide complexes was used (6) as a measure of the solvent polarity, $Z$. Finally, the dielectric constant has been associated with molecular polarity.

Each of these proposals is based on different sets of conditions and molecular behavior, although each is ultimately a function of molecular structure. This fact was recognized by Martin (7) who attempted the prediction of the chromatographic phase distribution of a molecule from structure fragment values. The method is limited to carefully defined functional groups.

The value of a polarity index lies in its ability to predict the relative polarity of a solvent for which experimental data are not available. A second potential value lies in the ability of an index to predict the polarity of a mixture of solvents from their individual values. Thus, a wide range of solvent polarity could be achieved from various proportions of two solvents with desirable physical, chemical, and toxicological properties.

## DERIVATION OF POLARITY INDEX FROM MOLECULAR STRUCTURE

**Structural Influences**—The structure of a molecule governs all physical and chemical phenomena. The solvent characteristics of a molecule depend on intermolecular interactions which, in turn, are dependent on structure. The generalization can be made that molecules classified as nonpolar according to any of the stated methods are molecules that possess few, if any, polar groups or bonds. Nonpolar molecules are distinguished by the absence of unsaturation or lone-pair electrons. Thus, pentane is universally regarded as nonpolar. It has only C–H and C–C bonds, which are devoid of electrons not axially directed between nuclei. In contrast, ether, with virtually the same molecular weight, is more polar. Ether has two lone pairs of electrons on the oxygen atom.

Similar comparisons between hexane and pentanol, cyclohexane and benzene, and methyl ethyl ketone and methyl acetate present the case that molecules, of about the same molecular weight, with $\pi$ and lone-pair electrons are more polar than those without them. This observation is not surprising since lone-pair electrons create significant dipoles capable of intermolecular interactions associated with polar solvents. The task then is to encode this structural information into a molecular index that will quantify solvent polarity from a purely structural basis.

**Calculation of Polarity Index**—The presence of $\pi$ and lone-pair electrons on an atom in its valence state was shown (8) to be encoded into the connectivity delta values, $\delta$ and $\delta^v$. These connectivity deltas are not to be confused with the Hildebrand–Scott polarity index (2). The valence delta, $\delta^v$, is assigned to an atom in its valence state according to the relationship $\delta^v = Z^v - h$, where $Z^v$ is the count of valence electrons and $h$ is the count of bonded hydrogen atoms. For atoms beyond the second quantum level, the expression $\delta^v = (Z^v - h)/(Z - Z^v)$, where $Z$ is the atomic number, is used (9). The simple delta value, $\delta$, is a count of all bonded atoms except hydrogen. It can be expressed as $\delta = \sigma - h$, where $\sigma$ is a count of all $\sigma$ electrons on the atom.

Since:

$$\delta^v = Z^v - h \qquad \text{(Eq. 1}a\text{)}$$

then:

$$\delta^v = \sigma + p + n - h \qquad \text{(Eq. 1}b\text{)}$$

where $p$ is a count of $\pi$ electrons and $n$ is a count of lone-pair electrons.

**Table I—Exterjacent Electrons *versus* ($^1\chi - {}^1\chi^v$)**

| Molecule | $^1\chi$ | $^1\chi^v$ | $\Delta^1\chi$ | Exterjacent Electrons |
|---|---|---|---|---|
| $CH_3CH_2CH_2CH_2CH_3$ | 2.414 | 2.414 | 0.0 | 0 |
| $CH_3CH_2CH_2CH_2NH_2$ | 2.414 | 2.115 | 0.299 | 2 |
| $CH_3CH_2CH_2CH_2OH$ | 2.414 | 2.023 | 0.391 | 4 |
| $CH_3CH_2OCH_2CH_3$ | 2.414 | 1.992 | 0.422 | 4 |
| $CH_3CH_2CH_2CH{=}O$ | 2.414 | 1.851 | 0.563 | 6 |
| $HOCH_2CH_2CH_2NH_2$ | 2.414 | 1.724 | 0.690 | 6 |
| $HOCH_2CH_2CH_2OH$ | 2.414 | 1.632 | 0.782 | 8 |
| $HOCH_2CH_2CH{=}O$ | 2.414 | 1.460 | 0.954 | 10 |
| $O{=}CHCH_2CH{=}O$ | 2.414 | 1.288 | 1.126 | 12 |

It follows that:

$$\delta^v - \delta = \sigma + p + n - h - \sigma + h \qquad \text{(Eq. 2}a\text{)}$$

$$\delta^v - \delta = p + n \qquad \text{(Eq. 2}b\text{)}$$

The count of $\pi$ and lone-pair electrons, called exterjacent electrons (8), is encoded in $\delta^v - \delta$.

By using these delta values assigned to each atom in a molecule, two molecular connectivity indexes are calculated by:

$$^1\chi = \Sigma(\delta_i\delta_j)^{-1/2} \qquad \text{(Eq. 3}a\text{)}$$

$$^1\chi^v = \Sigma(\delta_i^v\delta_j^v)^{-1/2} \qquad \text{(Eq. 3}b\text{)}$$

where $i$ and $j$ are each pair of bonded atoms and the summation is over the entire molecule.

The exterjacency on an atom, enumerated by $\delta^v - \delta$, can be encoded for the molecule by $^1\chi - {}^1\chi^v$. The subtraction of $\chi$ indexes is inverted since the reciprocal of the delta values is used in computing the molecular connectivity indexes. Kier and Hall (8) showed a derivation of the indexes from physical principles.

The effect on the calculated value of $^1\chi - {}^1\chi^v$ due to an increase of exterjacent electrons in a molecule is illustrated in Table I. With increasing numbers of exterjacent electrons in molecules in this series, the value of $^1\chi^v$ for the molecule decreases. For this series with a constant $^1\chi$ value, $^1\chi - {}^1\chi^v$ increases down the list.

In this series with a constant $^1\chi$ value, the $^1\chi - {}^1\chi^v$ value increases as the molecules increase in polarity. For molecules in an homologous series, for example the *n*-alkanols, the solvent polarity decreases with increasing size; however, the value of $^1\chi - {}^1\chi^v$ for such a series remains constant. To account for this effect, the use of $^1\chi - {}^1\chi^v$ to reflect solvent polarity must be modified by a term describing increasing molecular weight. This can be accomplished by diminishing the value of $^1\chi - {}^1\chi^v$ by $^1\chi$, which increases with size in an homologous series.

The index reflecting polarity thus may be described as:

$$\text{polarity} = {}^1\chi - {}^1\chi^v - {}^1\chi = -{}^1\chi^v \qquad \text{(Eq. 4)}$$

To restate this relationship, it is proposed that solvent polarity is inversely related to $^1\chi^v$. Table II shows the calculated values of $^1\chi^v$ for common solvents. Also included are other polarity indexes, $\epsilon^0(Al_2O_3)$, $\delta$, and $P'$, as well as the octanol–water partition coefficient, dielectric constant, and water solubility.

**Functional Group Number Weighting**—A number of molecules in Table II, such as ethylene glycol and dioxane, possess two isolated functional groups. These solvents are more polar than their monofunctional counterparts of about equal molecular weight, propanol and pyran. The two functional groups may be regarded as having twice the opportunity or probability of engaging in dipolar or electron donor–acceptor interactions with a solute.

For purposes of defining this solvent polarity index, a functional group is defined as an ensemble of atoms with exterjacent electrons that engage, as a unit, in essentially a single type of intermolecular interaction. Thus, the two oxygens and the carbon atom of an ester group constitute a functional group in this definition. Similarly, the three atoms of a nitro group represent one functional group in nitrobenzene. The six carbon $\pi$ electrons of the benzene ring also constitute a discrete functional group that acts in concert with the nitro group. Thus, nitrobenzene has two functional groups.

A nitrogen atom in pyridine participates in the $\pi$-electron annulus and contributes to van der Waals interaction. The nitrogen also may participate in hydrogen bonding through the lone-pair electrons. Thus, pyridine has two functional groups by this definition. To account for this, it is proposed that the calculated $^1\chi^v$ value be divided by a factor, $f$, describing the number of discrete, isolated functional groups. This method was

**Table II—Ranking of Solvent Polarity Using $^1\chi^v/f$ Index**

| Molecule | $^1\chi^v/f$ | $P'$[a] | Hildebrand–Scott $\delta$[b] | $\epsilon^0(Al_2O_3)$[c] | Octanol–Water log $P$[d] | Dielectric Constant[e] | Water Solubility[f], g/100 g |
|---|---|---|---|---|---|---|---|
| Cyclohexane | 3.000 | 0.0 | 8.2 | 0.04 | 3.44 | 2.0 | 0.01 |
| Hexane | 2.914 | 0.0 | 7.3 | 0.01 | — | 1.9 | Insoluble |
| Isopropyl ether | 2.781 | 2.2 | 7.0 | 0.28 | — | 3.9 | — |
| Chlorobenzene | 2.508 | 2.7 | 9.6 | 0.30 | 2.46 | 5.6 | 0.05 |
| Toluene | 2.411 | 2.3 | 8.9 | 0.29 | 2.80 | 2.4 | 0.05 |
| Carbon tetrachloride | 2.390 | 1.7 | 8.6 | 0.18 | 2.72 | 2.2 | 0.08 |
| Ethylene dichloride | 2.190 | 3.7 | 9.7 | 0.49 | 1.48 | 10.4 | — |
| Tetrahydrofuran | 2.077 | 4.2 | 9.1 | 0.45 | 0.73 | 7.6 | ∞ |
| Chloroform | 2.070 | 4.4 | 9.1 | 0.40 | 1.97 | 4.8 | 0.82 |
| Butanol | 2.023 | 3.9 | 11.3 | — | 0.88 | 12.5 | 7.45 |
| Benzene | 2.000 | 3.0 | 9.2 | 0.32 | 2.13 | 2.3 | 0.18 |
| Ether | 1.992 | 2.9 | 7.6 | 0.38 | 0.80 | 4.3 | 6 |
| Ethyl acetate | 1.904 | 4.3 | 8.6 | 0.58 | 0.70 | 6.0 | 8.1 |
| Methyl ethyl ketone | 1.765 | 4.5 | 9.3 | 0.51 | 0.27 | 18.5 | 24 |
| Methylene chloride | 1.690 | 3.4 | 9.6 | 0.42 | 1.25 | 8.9 | 1.3 |
| Propanol | 1.523 | 3.9 | 10.2 | 0.82 | 0.30 | 20.3 | ∞ |
| Carbon disulfide | 1.414 | 1.0 | 10.0 | 0.15 | — | 2.6 | 0.29 |
| Isopropanol | 1.413 | 4.2 | 10.2 | 0.82 | 0.05 | 19.9 | ∞ |
| Dimethylformamide | 1.388 | — | 11.5 | — | −1.01 | 36.7 | ∞ |
| Methyl acetate | 1.316 | — | 9.2 | 0.60 | 0.30 | 6.7 | — |
| Nitrobenzene | 1.250 | 4.5 | 11.1 | — | 1.85 | 34.8 | 0.19 |
| Acetone | 1.204 | 5.4 | 9.4 | 0.56 | −0.24 | 20.7 | ∞ |
| Benzonitrile | 1.192 | 4.6 | 10.7 | — | 1.56 | — | — |
| $\alpha$-Picoline | 1.135 | 4.8 | — | — | — | — | ∞ |
| Dioxane | 1.073 | 4.8 | 9.8 | 0.56 | −0.35 | 2.2 | ∞ |
| Ethanol | 1.023 | 5.2 | 11.2 | 0.88 | −0.30 | 24.6 | ∞ |
| Acetic acid | 0.928 | 6.2 | 12.4 | 1.00 | −0.25 | 6.2 | ∞ |
| Pyridine | 0.925 | 5.3 | 10.4 | 0.71 | 0.65 | 12.4 | ∞ |
| Nitromethane | 0.812 | 6.8 | 11.0 | 0.64 | −0.34 | 35.9 | 11.1 |
| Methoxyethanol | 0.757 | 5.7 | — | — | −0.77 | 16.9 | ∞ |
| Acetonitrile | 0.724 | 6.2 | 11.8 | 0.65 | −0.34 | 37.5 | ∞ |
| Ethanolamine | 0.678 | — | 13.5 | — | −1.31 | — | ∞ |
| Formamide | 0.569 | 7.3 | 17.9 | — | — | 109 | ∞ |
| Ethylene glycol | 0.566 | 5.4 | 13.5 | 1.11 | −1.93 | 37.7 | ∞ |
| Methanol | 0.447 | 6.6 | 12.9 | 0.95 | −0.65 | 32.7 | ∞ |
| Water | 0.0 | 9.0 | 21 | — | −1.38 | 80.2 | ∞ |

[a] Reference 4. [b] Reference 2. [c] Reference 3. [d] C. Hansch and A. Leo, "Substituent Constants for Correlation Analysis in Chemistry and Biology," Wiley, New York, N.Y., 1979. [e] "CRC Handbook of Chemistry and Physics," R. C. Weast and M. J. Astle, Eds., CRC Press, Boca Raton, Fla., 1979, E-56. [f] "Vogels' Textbook of Practical Organic Chemistry," 4th ed., B. S. Furniss, A. J. Hannaford, V. Rogers, P. Smith, and A. R. Tatchell, Eds., Longman Press, London, England, 1978, p. 1302.

applied to nitrobenzene, benzonitrile, $\alpha$-picoline, dioxane, pyridine, methoxyethanol, ethanolamine, and ethylene glycol (Table II).

The exception to this rule is the case where one or more halogen atoms is present on different carbon atoms, *i.e.*, ethylene dichloride. Chlorine does not make a significant contribution to a molecule in terms of enhancing its solvent polarity. Aryl and alkyl halides are classified among the more nonpolar solvents, *i.e.*, carbon tetrachloride, chlorobenzene, *etc.* Thus, the value of $^1\chi^v$ computed for a halogen-containing molecule would be used unmodified.

Table II lists 36 of the more common solvents, ranked according to increasing solvent polarity computed as a diminishing value of $^1\chi^v/f$. This polarity index, based solely on molecular structure, can be compared with the experimental polarity indexes derived by several methods. In addition, the table lists physical properties associated with solution phenomena. Several observations emerge from comparisons of these indexes.

## DISCUSSION

The diminishing value of $^1\chi^v/f$, associated with increasing solvent polarity, parallels the increase in the values of $P'$, $\delta$, and $\epsilon^0(Al_2O_3)$, with the $P'$ values having perhaps the best correlation. Each of these experimentally derived polarity indexes is based on different experimental methods; thus, a close correlation is not expected among them or with $^1\chi^v/f$. Nevertheless, for a broad definition of solvent polarity, $^1\chi^v/f$ performs quite well in comparison. The distinct advantage of using $^1\chi^v/f$ as a solvent polarity index is the fact that it is based exclusively on structure, so it is nonempirical. It can be computed quickly and simply for any molecule, including those that may not be available.

The physical properties in Table II correlate fairly well with $^1\chi^v/f$. The aqueous solubility is minimal for molecules with $^1\chi^v/f$ values above 2.0, intermediate for $^1\chi^v/f$ values of 1.5–2.0, and miscible for practically all molecules with $^1\chi^v/f$ values of $<\sim 1.5$.

There are exceptions to these observations, but generally the calculated $^1\chi^v/f$ index ranks the molecules according to solvent polarity as well as any of the experimental indexes, the advantage clearly being in the purely structural basis for the calculation.

An additional application of the $^1\chi^v/f$ solvent polarity index is obvious when binary solvent mixtures are considered. If it is assumed that when two nonreacting solvents are mixed the solvent polarity is an average of their polarities, weighted by their mole fractions, then it should be possible to calculate the solvent polarity of any mixture or, conversely, to design a solvent mixture with a specific solvent polarity. This latter course often is desirable when one solvent may possess unfavorable physical, chemical, or toxicological properties.

As an example, ether may have optimum solvent polarity for a particular application; however, its volatility and flammability preclude its use from safety considerations. It is desirable to reproduce approximately the $^1\chi^v/f = 1.992$ ether polarity with a mixture of two solvents. Calculations show that a 1:1 mixture of toluene and propanol has a $^1\chi^v/f$ value of 1.967, while a 2:1 mixture of methyl ethyl ketone and chlorobenzene has a $^1\chi^v/f$ value of 1.973.

Other applications of the index include the basis of selection of a relatively nonpolar solvent that is heavier or lighter than water or miscible, all with about the same polarity. Chloroform, butanol, and tetrahydrofuran, respectively, meet these specific criteria.

Finally, the index will prove useful in estimating the polarity of a molecule not commonly considered as a solvent or perhaps a polymeric structure such as the polyethers. Thus, the $^1\chi^v/f$ values lead to polarity rankings for some additional liquids: methylformamide, 1.024; diethylene glycol, 0.737; dimethoxy polyethylene glycol, $^1\chi^v/f$ approaches a limit of 1.10 with increasing size; morpholine, 1.142; various fluorinated ethanols, 0.0–0.5; glycerol, 0.569; and aniline, 1.100.

## REFERENCES

(1) B. L. Karger, L. R. Snyder, and C. Horvath, "An Introduction to Separation Science," Wiley, New York, N.Y., 1973.

(2) J. H. Hildebrand and R. L. Scott, "The Solubility of Nonelectrolytes," 3rd ed., Dover, New York, N.Y., 1964.

(3) L. R. Snyder, "Principles of Adsorption Chromatography," Dekker, New York, N.Y., 1968.

(4) L. Rohrschneider, "Advances in Chromatography," vol. IV, Dekker, New York, N.Y., 1968.
(5) E. Grunwald and S. Winstein, *J. Am. Chem. Soc.*, **70**, 846 (1948).
(6) E. Kosower, *ibid.*, **80**, 3253 (1958).
(7) A. J. P. Martin, *Biochem. Soc. Symp.*, **3**, 4 (1949).
(8) L. B. Kier and L. H. Hall, *J. Pharm. Sci.*, **70**, 583 (1981).
(9) L. B. Kier and L. H. Hall, *Eur. J. Med. Chem.*, **12**, 307 (1977).

# Structure–Activity Studies on Sulfamate Sweeteners II: Semiquantitative Structure–Taste Relationship for Sulfamate ($RNHSO_3^-$) Sweeteners—The Role of R

**WILLIAM J. SPILLANE ˣ and GRAINNE McGLINCHEY**

Received October 1, 1980, from the *Department of Chemistry, University College, Galway, Ireland.* Accepted for publication February 4, 1981.

**Abstract** □ With the use of Corey–Pauling–Koltun space-filling models, measurements of defined parameters ($x$, $y$, and $z$) were made of the R groups in a large number of carbosulfamates, $RNHSO_3^-$. The correlation between sweet and nonsweet sulfamates and the defined parameters for R is good. As a test, 12 new carbosulfamates were synthesized and tasted. The predictions of their sweetness or nonsweetness based on the correlation were >90% correct. To elicit a sweet taste, the R group of the sulfamate should have $x \geq 5.2$ Å and $\leq 7.2$ Å and $V$ (*i.e.*, $xyz$) $\leq 250$ Å$^3$ and probably $\geq 90$ Å$^3$. The receptor site is seen (as for aspartame) as a rather narrow cleft into which R has to fit "properly" or be "locked" so that the AH,B mechanism for initiating the sweet stimulae can operate. Possible applications of this approach are indicated.

**Keyphrases** □ Sweeteners—structure–activity analysis of sulfamates, the role of R side chains □ Sulfamates—sweeteners, structure–activity analysis, the role of R side chains □ Structure–activity relationships—the role of R side chain on sulfamate sweeteners

Synthetic studies of alternative sweeteners have been given impetus since the ban on cyclamates in 1970 and the apparently unresolved question of the toxicity of saccharin, the only synthetic sweetener presently used worldwide. These studies, aimed at the design of new synthetic sweeteners and a fuller understanding of sweetness, have led to the establishment of structure–taste relationships for some classes of alternative sweeteners (1–3).

Most workers have concentrated on the development of intraclass structure–taste relationships since there is good evidence that different classes of sweeteners act by binding at different receptor sites in the taste buds of the tongue (4). Thus, structure–taste information from one class is not transferable to another class.

## BACKGROUND

The structure–activity relationships of sulfamate sweeteners were reviewed in Part I of this study (5). Other investigators (6, 7), using Corey–Pauling–Koltun (CPK) space-filling atomic models, showed that the best $NHSO_3^-$ group conformation for sweet taste stimulation involved an angle ($\theta$) of 60° between the N–H and S–O bonds. The necessity of maintaining this optimal 60° torsional angle for sweetness explains why substitution of an $\alpha$-hydrogen by an alkyl group at C-1 of an alicyclic ring or aliphatic chain destroys sweetness. Similarly, the lack of sweetness of phenylsulfamate is ascribed to steric hindrance due to an *ortho*-hydrogen of the phenyl ring forcing the aminosulfonate group to adopt a conformation with $\theta \approx 0°$.

Pautet and Nofre (6) measured the lengths of various R groups in $RNHSO_3^-$ and found that for sweetness, R should lie between 5 and 7 Å. In their second paper (7), they suggested, on the basis of a few measurements, that R should have a "half-width" of <4 Å. While this approach is satisfactory for simpler aliphatic and alicyclic systems, it appeared to us to be inadequate for various substituted systems for several reasons:

1. Taste response is a function of the size, shape, and functionality of a molecule, *i.e.*, taste response = $f$(size, shape, functionality), and any assessment of size and shape should take into account the three-dimensional structure and conformation of the molecule.
2. Several molecules whose R groups have dimensions falling within the limits given by Pautet and Nofre (6, 7) were prepared (and tasted for sweetness), and it was found that they are not sweet (Table I, Compounds 15, 18, 47, and 49).

In the present work, 12 new sulfamates were synthesized. With the use of CPK space-filling models, measurements were taken on these and other sulfamates reported (and tasted) previously. A good correlation existed between sweet/nonsweet sulfamates and the defined parameters for R, so it is possible to predict whether unknown sulfamates will be sweet. Predictions based on the correlation were >90% correct for the 12 sulfamates synthesized.

## RESULTS AND DISCUSSION

Measurements were carried out on all known carbosulfamates for which taste data were available. Only those sulfamates whose lack of sweetness could be ascribed to a distortion of the angle $\theta$ from 60°, *e.g.*, those substituted at C-1 of a chain or a bridgehead (6, 7), were excluded.

Parameters $x$, $y$, and $z$ were defined and measured for each R group; from these values, a measure of the size or three-dimensional structure ($V$) of R is obtained from the product $xyz$ (see *Experimental*).

Table I lists the sulfamates on which measurements were made. The $x$, $y$, $z$, and $V$ parameters are given together with the literature references. The compounds are listed (Table I) in certain convenient groupings, *e.g.*, straight chain, branched, and increasing ring size.

In Fig. 1, a plot of $x$ (the "length" of R) against $V$ was made using the data for the previously reported sulfamates in Table I. The sulfamates synthesized in the present work (Compounds 15, 18, 20, 21, 35, 41, 43, and 45–49) and those about which predictions were made (Compounds 26–28) were excluded. Figure 1 reveals that nearly all of the sweet sulfamates fall into a rectangle (Fig. 1A) whose boundaries are reasonably well defined on three sides, being ~5.2 and ~7.2 Å on the $x$ axis and ~250 Å$^3$ on the $V$ axis. The fourth boundary appears to be $\leq 90$ Å$^3$ on the $V$ axis. Almost all of the sulfamates lying outside A are not sweet. Some bitter or faintly sweet sulfamates lie at or near one of the three defined boundaries.

Of the 12 sulfamates synthesized, it could be predicted on the basis of Table I and Fig. 1 that 10 of them would not be sweet and two of them would be sweet (*i.e.*, Compounds 46 and 48). Tasting indicated that these predictions were correct in 11 cases. The one exception was the apocamphane compound (Compound 48), which was bitter. All 12 compounds are shown in Fig. 2. Compound 48 might have been excluded since it is an example of a C-1 substituted sulfamate and, therefore, would not be expected to be sweet due to distortion of the angle $\theta$ from 60°. However, it is included because it is bitter and it does lie on a boundary.

0022-3549/81/0800-0933$01.00/0
© 1981, American Pharmaceutical Association

(4) L. Rohrschneider, "Advances in Chromatography," vol. IV, Dekker, New York, N.Y., 1968.
(5) E. Grunwald and S. Winstein, *J. Am. Chem. Soc.*, **70**, 846 (1948).
(6) E. Kosower, *ibid.*, **80**, 3253 (1958).
(7) A. J. P. Martin, *Biochem. Soc. Symp.*, **3**, 4 (1949).
(8) L. B. Kier and L. H. Hall, *J. Pharm. Sci.*, **70**, 583 (1981).
(9) L. B. Kier and L. H. Hall, *Eur. J. Med. Chem.*, **12**, 307 (1977).

# Structure–Activity Studies on Sulfamate Sweeteners II: Semiquantitative Structure–Taste Relationship for Sulfamate ($RNHSO_3^-$) Sweeteners—The Role of R

**WILLIAM J. SPILLANE ˣ and GRAINNE McGLINCHEY**

Received October 1, 1980, from the *Department of Chemistry, University College, Galway, Ireland.* Accepted for publication February 4, 1981.

**Abstract** □ With the use of Corey–Pauling–Koltun space-filling models, measurements of defined parameters ($x$, $y$, and $z$) were made of the R groups in a large number of carbosulfamates, $RNHSO_3^-$. The correlation between sweet and nonsweet sulfamates and the defined parameters for R is good. As a test, 12 new carbosulfamates were synthesized and tasted. The predictions of their sweetness or nonsweetness based on the correlation were >90% correct. To elicit a sweet taste, the R group of the sulfamate should have $x \geq 5.2$ Å and $\leq 7.2$ Å and $V$ (*i.e.*, $xyz$) $\leq 250$ Å$^3$ and probably $\geq 90$ Å$^3$. The receptor site is seen (as for aspartame) as a rather narrow cleft into which R has to fit "properly" or be "locked" so that the AH,B mechanism for initiating the sweet stimulae can operate. Possible applications of this approach are indicated.

**Keyphrases** □ Sweeteners—structure–activity analysis of sulfamates, the role of R side chains □ Sulfamates—sweeteners, structure–activity analysis, the role of R side chains □ Structure–activity relationships—the role of R side chain on sulfamate sweeteners

Synthetic studies of alternative sweeteners have been given impetus since the ban on cyclamates in 1970 and the apparently unresolved question of the toxicity of saccharin, the only synthetic sweetener presently used worldwide. These studies, aimed at the design of new synthetic sweeteners and a fuller understanding of sweetness, have led to the establishment of structure–taste relationships for some classes of alternative sweeteners (1–3).

Most workers have concentrated on the development of intraclass structure–taste relationships since there is good evidence that different classes of sweeteners act by binding at different receptor sites in the taste buds of the tongue (4). Thus, structure–taste information from one class is not transferable to another class.

## BACKGROUND

The structure–activity relationships of sulfamate sweeteners were reviewed in Part I of this study (5). Other investigators (6, 7), using Corey–Pauling–Koltun (CPK) space-filling atomic models, showed that the best $NHSO_3^-$ group conformation for sweet taste stimulation involved an angle ($\theta$) of 60° between the N–H and S–O bonds. The necessity of maintaining this optimal 60° torsional angle for sweetness explains why substitution of an $\alpha$-hydrogen by an alkyl group at C-1 of an alicyclic ring or aliphatic chain destroys sweetness. Similarly, the lack of sweetness of phenylsulfamate is ascribed to steric hindrance due to an *ortho*-hydrogen of the phenyl ring forcing the aminosulfonate group to adopt a conformation with $\theta \approx 0°$.

Pautet and Nofre (6) measured the lengths of various R groups in $RNHSO_3^-$ and found that for sweetness, R should lie between 5 and 7 Å. In their second paper (7), they suggested, on the basis of a few measurements, that R should have a "half-width" of <4 Å. While this approach is satisfactory for simpler aliphatic and alicyclic systems, it appeared to us to be inadequate for various substituted systems for several reasons:

1. Taste response is a function of the size, shape, and functionality of a molecule, *i.e.*, taste response = $f$(size, shape, functionality), and any assessment of size and shape should take into account the three-dimensional structure and conformation of the molecule.
2. Several molecules whose R groups have dimensions falling within the limits given by Pautet and Nofre (6, 7) were prepared (and tasted for sweetness), and it was found that they are not sweet (Table I, Compounds 15, 18, 47, and 49).

In the present work, 12 new sulfamates were synthesized. With the use of CPK space-filling models, measurements were taken on these and other sulfamates reported (and tasted) previously. A good correlation existed between sweet/nonsweet sulfamates and the defined parameters for R, so it is possible to predict whether unknown sulfamates will be sweet. Predictions based on the correlation were >90% correct for the 12 sulfamates synthesized.

## RESULTS AND DISCUSSION

Measurements were carried out on all known carbosulfamates for which taste data were available. Only those sulfamates whose lack of sweetness could be ascribed to a distortion of the angle $\theta$ from 60°, *e.g.*, those substituted at C-1 of a chain or a bridgehead (6, 7), were excluded.

Parameters $x$, $y$, and $z$ were defined and measured for each R group; from these values, a measure of the size or three-dimensional structure ($V$) of R is obtained from the product $xyz$ (see *Experimental*).

Table I lists the sulfamates on which measurements were made. The $x$, $y$, $z$, and $V$ parameters are given together with the literature references. The compounds are listed (Table I) in certain convenient groupings, *e.g.*, straight chain, branched, and increasing ring size.

In Fig. 1, a plot of $x$ (the "length" of R) against $V$ was made using the data for the previously reported sulfamates in Table I. The sulfamates synthesized in the present work (Compounds 15, 18, 20, 21, 35, 41, 43, and 45–49) and those about which predictions were made (Compounds 26–28) were excluded. Figure 1 reveals that nearly all of the sweet sulfamates fall into a rectangle (Fig. 1A) whose boundaries are reasonably well defined on three sides, being ~5.2 and ~7.2 Å on the $x$ axis and ~250 Å$^3$ on the $V$ axis. The fourth boundary appears to be $\leq 90$ Å$^3$ on the $V$ axis. Almost all of the sulfamates lying outside A are not sweet. Some bitter or faintly sweet sulfamates lie at or near one of the three defined boundaries.

Of the 12 sulfamates synthesized, it could be predicted on the basis of Table I and Fig. 1 that 10 of them would not be sweet and two of them would be sweet (*i.e.*, Compounds 46 and 48). Tasting indicated that these predictions were correct in 11 cases. The one exception was the apocamphane compound (Compound 48), which was bitter. All 12 compounds are shown in Fig. 2. Compound 48 might have been excluded since it is an example of a C-1 substituted sulfamate and, therefore, would not be expected to be sweet due to distortion of the angle $\theta$ from 60°. However, it is included because it is bitter and it does lie on a boundary.

0022-3549/81/0800-0933$01.00/0
© 1981, American Pharmaceutical Association

**Table I—Space Parameters for R Groups of Carbosulfamates**

| Compound | R | x, Å | y, Å | z, Å | V, Å³ | Reference |
|---|---|---|---|---|---|---|
| 1 | Ethyl | 4.36 | 3.71 | 4.06 | 66.0 | 16–18 |
| 2 | *n*-Propyl | 5.68 | 4.19 | 3.77 | 89.7 | 5, 16, 17 |
| 3 | *n*-Butyl | 6.88 | 4.38 | 3.77 | 113.0 | 16–19 |
| 4 | *n*-Pentyl | 8.12 | 4.62 | 3.77 | 142.0 | 16, 17 |
| 5 | 2-Methylbutyl | 6.68 | 5.54 | 5.28 | 195.0 | 20 |
| 6 | 3-Methylbuytl | 8.00 | 4.96 | 5.44 | 216.0 | 16 |
| 7 | Isobutyl | 5.40 | 4.80 | 6.08 | 158.0 | 5, 16, 19, 20 |
| 8 | Isopentyl | 5.64 | 5.12 | 6.24 | 180.0 | 20 |
| 9 | Isohexyl | 7.40 | 5.20 | 6.24 | 240.0 | 6 |
| 10 | Neopentyl | 5.40 | 5.68 | 6.08 | 186.0 | 16 |
| 11 | Cyclohexyl | 5.72 | 5.03 | 6.28 | 181.0 | 11 |
| 12 | 2-Methylcyclohexyl | 6.72 | 4.96 | 7.52 | 250.0 | 11 |
| 13 | 3-Methylcyclohexyl | 5.72 | 5.03 | 7.56 | 218.0 | 20 |
| 14 | 4-Methylcyclohexyl | 6.40 | 4.98 | 6.25 | 199.0 | 21 |
| 15 | 2,3-Dimethylcyclohexyl | 6.92 | 5.07 | 7.64 | 268.0 | —[a] |
| 16 | 2,6-Dimethylcyclohexyl | 7.04 | 5.00 | 8.64 | 304.0 | 21 |
| 17 | 2,5-Dimethylcyclohexyl | 6.96 | 5.07 | 8.64 | 305.0 | 20 |
| 18 | 3,3,5-Trimethylcyclohexyl | 5.32 | 6.64 | 7.76 | 274.0 | —[a] |
| 19 | 2-Ethylcyclohexyl | 7.08 | 5.00 | 8.80 | 314.0 | 21 |
| 20 | 4-*tert*-Butylcyclohexyl | 7.68 | 6.25 | 6.56 | 315.0 | —[a] |
| 21 | 4-*tert*-Pentylcyclohexyl | 8.16 | 6.69 | 6.32 | 345.0 | —[a] |
| 22 | Cyclopentyl | 5.32 | 4.88 | 5.96 | 155.0 | 21 |
| 23 | 2-Methylcyclopentyl | 5.32 | 4.88 | 6.72 | 174.0 | 20 |
| 24 | 3-Methylcyclopentyl | 6.40 | 5.24 | 6.28 | 211.0 | 19, 22 |
| 25 | Cyclobutyl | 5.04 | 4.48 | 5.44 | 123.0 | 5, 17 |
| 26 | 3-Methylcyclobutyl | 5.68 | 5.20 | 5.36 | 158.0 | —[b] |
| 27 | 2-Methylcyclobutyl | 5.40 | 5.20 | 6.00 | 168.0 | —[b] |
| 28 | Cyclobutylmethyl | 5.88 | 4.96 | 5.36 | 156.0 | —[b] |
| 29 | Cycloheptyl | 6.00 | 5.04 | 6.88 | 208.0 | 5, 21, 23 |
| 30 | Cyclooctyl | 6.64 | 5.04 | 7.36 | 246.0 | 21, 23 |
| 31 | Cycloonyl | 7.04 | 5.04 | 7.68 | 244.0 | 20 |
| 32 | Cyclododecyl | 7.64 | 5.20 | 8.80 | 350.0 | 5 |
| 33 | Cyclopentylmethyl | 6.96 | 4.90 | 6.00 | 205.0 | 24 |
| 34 | Cyclohexylmethyl | 7.80 | 5.04 | 6.36 | 250.0 | 20 |
| 35 | Cyclooctylmethyl | 8.24 | 5.12 | 7.76 | 327.0 | —[a] |
| 36 | 1-Cyclopentenyl | 5.16 | 4.08 | 7.36 | 155.0 | 25 |
| 37 | 2-Cyclohexenyl | 5.48 | 5.01 | 6.02 | 165.0 | 25 |
| 38 | 3-Cyclohexenyl | 5.48 | 5.30 | 6.27 | 182.0 | 25 |
| 39 | 2-Cycloheptenyl | 6.00 | 5.17 | 6.40 | 198.0 | 25 |
| 40 | 2-Cyclooctenyl | 6.88 | 5.25 | 6.92 | 250.0 | 25 |
| 41 | 4-Ethenylcyclohexyl | 7.88 | 5.11 | 6.36 | 256.0 | —[a] |
| 42 | Benzyl | 7.56 | 3.68 | 6.32 | 176.0 | 18, 19 |
| 43 | ac-Tetrahydro-1-naphthyl | 6.60 | 5.12 | 8.76 | 296.0 | —[a] |
| 44 | ac-Tetrahydro-2-naphthyl | 7.95 | 5.04 | 7.36 | 295.0 | 11 |
| 45 | 1-Indane | 6.40 | 5.04 | 8.72 | 281.0 | —[a] |
| 46 | 1-Norbornyl | 5.92 | 5.92 | 5.92 | 207.0 | —[a] |
| 47 | *cis*-Myrantyl | 6.80 | 7.68 | 6.28 | 328.0 | —[a] |
| 48 | 1-Apocamphane | 5.32 | 7.28 | 6.40 | 248.0 | —[a] |
| 49 | 2-Adamantyl | 6.76 | 6.53 | 6.96 | 307.0 | —[a] |
| 50 | 1-Adamantyl | 5.48 | 6.53 | 6.96 | 249.0 | 5 |

[a] Synthesized in the present work. [b] Not synthesized.

In Fig. 3, the 12 compounds are shown with those in Fig. 1 and three unknown compounds. On examination of Fig. 3, a quantitative assessment of the quality and predictive value of the correlation can be made. Of the 47 compounds synthesized and tasted (Compounds 26–28 can be excluded), there is only one nonsweet compound within area A and one sweet compound outside A if those actually on a boundary are ignored. Thus, the taste, *i.e.*, sweet/nonsweet, of 45 of the 47 compounds can be predicted correctly. This finding indicates that Fig. 3 has a 96% chance of correctly predicting the taste of unsynthesized sulfamates.

The correlation between sweet/nonsweet and the defined parameters for R is good and suggests that Fig. 3 can be used to predict whether certain unknown sulfamates will be sweet. Thus, its usefulness in the design of new sweet sulfamates is clear. For example, although Compound 25 is not sweet, it can be predicted that Compounds 26–28 will be sweet.

Plots of either *y* or *z versus V* did not give such a high correlation between sweet/nonsweet molecules and the magnitudes of *y*/*z* and *V*. A few known carbosulfamates were exluded in addition to the group specifically

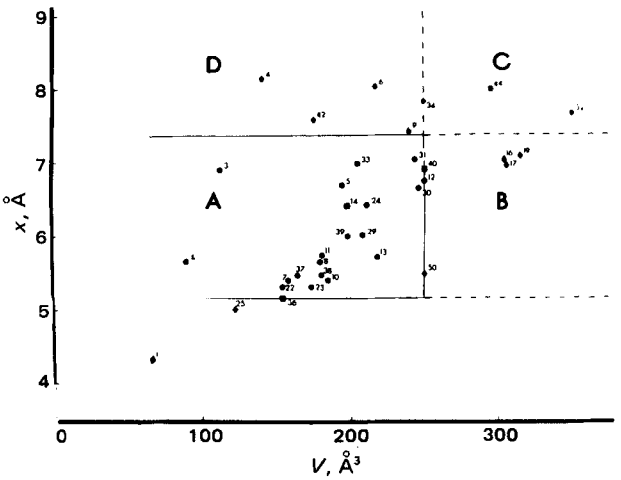


**Figure 1**—*Plot of the lengths of R (x)* versus V *for reported sulfamates. See Table I for key to compounds. Key:* ●, *sweet;* ♦, *nonsweet; and* ■, *bitter.*

mentioned at the beginning of this section. Thus, for example, *n*-hexylsulfamate and higher homologs were not considered since their *x* parameters ($x = 9.26$ Å for *n*-hexylsulfamate) would place them at the outer limits of the figures and, being nonsweet, they add nothing to the correlation. Some sulfamates that were not tasted were excluded.

The space-filling properties of R (as measured by *V* and *x*) are all important in determining whether or not a molecule is sweet; *V* is not a measure of the molecular volume of R, although the actual volumes of dipeptide ester sweeteners have been measured by immersion in 40% methanol using CPK models (8). The present authors found that the solvent penetrates into the hollows in the models; therefore, it was doubtful if this method could give an accurate assessment of volume (unless the models were hermetically sealed first). Recently, relative sweetness data for 33 dipeptide esters were correlated in a multiparameter equation involving parachor, hydrophobic, and STERIMOL parameters (9).

The *V* parameter can be regarded as the volume generated when *x*, *y*, and *z* are multiplied, *i.e.*, *V* gives the dimensions of the space or receptor site into which R will fit. Thus, although *V* is in part a function of *x*, both parameters are highly meaningful and allow one to explain why some sulfamates are sweet and others are not.

The absence of sweetness of some sulfamates (Fig. 3) can be explained if, as in the case of aspartame (10), the receptor site is seen as a rather narrow cleft (10 Å for aspartame) into which R has to be fitted. Thus, those molecules whose R groups have $5.2 \geq x \leq 7.2$ Å but $V > 250$ Å³ (Fig. 3B) are unable to fit into the receptor site and, therefore, cannot be "locked," and the AH,B mechanism for initiating the sweet stimulus cannot operate. Molecules with $x > 7.2$ Å are too long to fit into the receptor site (Fig. 3D), and molecules with $x > 7.2$ Å and $V > 250$ Å³ (Fig.

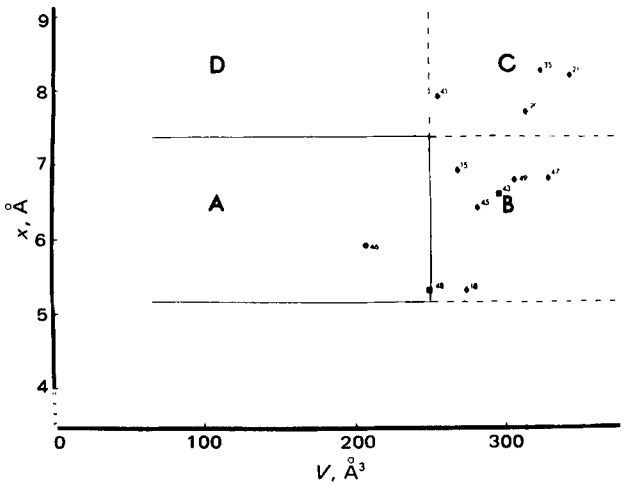


**Figure 2**—*Plot of lengths R (x)* versus V *for the 12 new sulfamates. See Table I for key to compounds. Key:* ●, *sweet;* ♦, *nonsweet; and* ■, *bitter.*

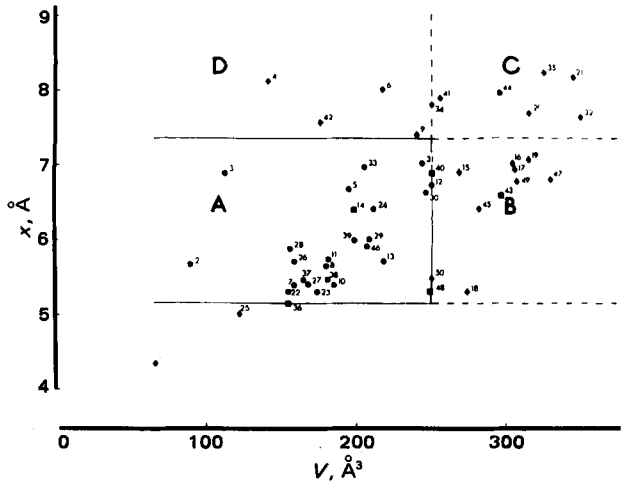


**Figure 3**—*Plot of the lengths of R (x) versus V for reported, newly synthesized, and some unknown (Compounds 26–28) sulfamates. See Table I for key to compounds. Key: ●, sweet; ♦, nonsweet; and ■, bitter.*

3C) are both too long and too large to be accommodated by the restricted three-dimensional geometry of the binding site. Finally, the few sulfamates with $x < 5.2$ Å and $V < 250$ Å$^3$ should give a poor fit at the binding site and might not be expected to be sweet.

The approach to structure–taste relationships developed here may be useful in developing such relationships for other types of sweeteners. An attempt is being made to extend it (both by syntheses and measurements on models) to include the large group of sulfamates whose R groups contain one or more heteroatoms. An advantage of the present method is that relative sweetness data are not required. If such data were available, additional patterns or trends might be discernible in Fig. 3. Seen on a broader canvas, the present approach might find application in the wider area of structure–activity relationship studies in chemoreception.

## EXPERIMENTAL

**Syntheses**—All of the sulfamates were synthesized either by reaction of the appropriate amines by the method of Audrieth and Sveda (11) or by the method of Boyland *et al.* (12). Many of the amines were prepared from the corresponding ketones by conversion to their oximes and subsequent sodium–ethanol reduction. All compounds were isolated as their sodium salts, except Compounds 43 and 48, which were purified as their ammonium salts. Compound 48 was prepared from camphor *via* camphorsulfonic acid, camphorsulfochloride, ketopinic acid (13), apocamphane-1-carboxylic acid (14), and 1-aminocamphane (15).

**Taste Analysis**—All of the sulfamates were tasted by four tasters who were asked to decide whether a solution was sweet or nonsweet, *i.e.*, tasteless or bitter. Prior to commencing, each taster took a concentrated solution of sodium *n*-propylsulfamate, which is very slightly sweet (5, 16). The methodology of the tasting process involved the following: (*a*) rinsing out the mouth with distilled water, (*b*) tasting a concentrated solution of the test sulfamate, (*c*) rinsing out the mouth with distilled water, and (*d*) tasting a concentrated solution of sodium *n*-propylsulfamate. (For many of the compounds taken from the literature and shown in Figs. 1–3, the taste data reported only indicated sweet or nonsweet results.)

**Measurements with Models**—The atoms making up each side-chain R were arranged in the most stretched conformation. For example, in Compound 12, the methyl group was put into an equatorial position; in Compound 15, the two methyl groups were put *trans* to one another. The side-chain R was positioned on a calibrated straight line (in the plane of the paper) so that the apex carbon (C-1) was superimposed on the zero mark and the remainder of the group was positioned on the line. The group R was clamped in this position, and the measurements ($x, y, z$) were made in this fixed position.

The length of R ($x$) could be read off the calibrated line or determined with a vernier. The width of R ($z$) was obtained by locating the widest points of the chain at right angles to the calibrated line in the $x, z$ plane and dropping perpendiculars from the $z$ axis to these points. The sum of the lengths of the two perpendiculars gave $z$. The height of R ($y$) was obtained by locating in the $x,y$ plane (at right angles to the plane of the paper) the highest point of R. Value $V$, in Å$^3$, is the volume generated by multiplication of $x$, $y$, and $z$. Where comparison was possible, measurements were usually within 10% of those previously reported (6, 7).

## REFERENCES

(1) G. A. Crosby, G. E. DuBois, and R. E. Wingard, Jr., in "Drug Design," vol. 8, Academic, New York, N.Y., 1979, chap. 5.

(2) B. Crammer and R. Ikan, *Chem. Soc. Rev.*, **6**, 431 (1977).

(3) "Sweetness and Sweeteners," G. G. Birch, L. F. Green, and C. B. Coulson, Eds., Applied Science, London, England, 1971.

(4) G. A. Crosby, G. E. DuBois, and R. E. Wingard, Jr., in "Drug Design," vol. 8, Academic, New York, N.Y., 1979, p. 231.

(5) G. A. Benson and W. J. Spillane, *J. Med. Chem.*, **19**, 869 (1976).

(6) F. Pautet and C. Nofre, *Z. Lebensm. Unters.-Forsch.*, **166**, 167 (1978).

(7) F. Pautet and C. Nofre, *Pharm. Acta Helv.*, **53**, 231 (1978).

(8) L. B. P. Brussel, H. G. Peer, and A. van der Heijden, *Z. Lebensm. Unters.-Forsch.*, **159**, 337 (1975).

(9) A. van der Heijden, L. B. P. Brussel, and H. G. Peer, *Chem. Senses Flavour*, **4**, 141 (1979).

(10) F. Lelj, T. Tancredi, P. A. Temussi, and C. Toniolo, *J. Am. Chem. Soc.*, **98**, 6669 (1976).

(11) L. F. Audrieth and M. Sveda, *J. Org. Chem.*, **9**, 89 (1944).

(12) E. Boyland, D. Manson, and S. F. D. Orr, *Biochem. J.*, **65**, 417 (1957).

(13) "Organic Synthesis," coll. vol. 5, H. E. Baumgarten, Ed., Wiley, New York, N.Y., 1973, pp. 194, 196, 689.

(14) E. J. Martin, *J. Am. Chem. Soc.*, **58**, 1438 (1936).

(15) "Organic Synthesis," coll. vol. 5, H. E. Baumgarten, Ed., Wiley, New York, N.Y., 1973, p. 273.

(16) C. Nofre and F. Pautet, *Bull. Soc. Chim. Fr.*, **1975**, 686.

(17) G. Hamprecht, D. Mangold, and K. H. Konig, German pat. 2,164,197 (1973).

(18) W. W. Thompson, U.S. pat. 2,805,124 (1957).

(19) H. Yamaguchi, Japanese pat. 13,056 (1963).

(20) B. Unterhalt and L. Böschemeyer, *Z. Lebensm. Unters.-Forsch.*, **149**, 227 (1972).

(21) *Ibid.*, **145**, 93 (1971).

(22) K. M. Beck and A. W. Weston, U.S. pat. 2,785,195 (1957).

(23) F. F. Blicke, H. E. Millson, Jr., and N. J. Doorenbos, *J. Am. Chem. Soc.*, **76**, 2498 (1954).

(24) C. Nofre and F. Pautet, French pat. 7,345,385 (1975).

(25) M. Avramoff and W. Taub, *Eur. J. Med. Chem.*, **13**, 81 (1978).

## ACKNOWLEDGMENTS

The authors thank the Department of Education (Ireland) for a grant to G. McGlinchey. This work was facilitated by gifts of sulfamate precursors from SSF (Dottikon, Switzerland) and Heico, Whittaker Corp.

# Investigation of Gel Structure of Aluminum Hydroxycarbonate Gel Using a Tension Cell

**EDWARD A. LIPKA *, JOSEPH R. FELDKAMP ‡, JOE L. WHITE ‡, and STANLEY L. HEM *x**

Received April 21, 1980, from the **Department of Industrial and Physical Pharmacy and the* ‡*Department of Agronomy, Purdue University, West Lafayette, IN 47907.* Accepted for publication February 6, 1981.

**Abstract** □ A tension cell was designed to measure the gel structure of aluminum hydroxycarbonate gel. Equilibrium measurements of the total water outflow *versus* applied tension give insight into the rigidity of the gel structure. Dynamic measurements of the rate of outflow of water at various applied tensions yield the capillary conductivity of the gel, which is related to the apparent surface area, particle size, and porosity. An aluminum hydroxycarbonate gel with a high apparent viscosity exhibited an increase in viscosity upon aging at 25°, which was accompanied by an increase in the equilibrium tension of the water phase, an increase in $\Delta\overline{G}_{H_2O}$, and a decrease in capillary conductivity. In contrast, the apparent viscosity of a low viscosity aluminum hydroxycarbonate gel, which was precipitated from the same reagents but with different precipitation temperature, pH, and stirring speed, exhibited a decrease in equilibrium water tension, a decrease in $\Delta\overline{G}_{H_2O}$, and an increase in capillary conductivity during aging at 25°.

**Keyphrases** □ Aluminum hydroxycarbonate gel—gel structure measurement using a tension cell □ Gels—aluminum hydroxycarbonate, gel structure measurement using a tension cell □ Tension cell—gel structure measurement of aluminum hydroxycarbonate gel

Many physical properties associated with aluminum hydroxycarbonate gel are simply a reflection of the particular structural arrangement of particles within the gel[1]. The specific structural arrangement is, in turn, a delicate function of various parameters such as particle size, shape, solids concentration, the nature and amount of any solutes present, and the various forces involved, *i.e.*, coulombic and van der Waals forces.

Viscosity is one of the most important physical properties of aluminum hydroxycarbonate gel. However, the viscosity of aluminum hydroxycarbonate gel varies widely, as evidenced by the availability of commercial aluminum hydroxycarbonate gels that are semisolids at 9% equivalent aluminum oxide content or that are pourable liquids at 9% equivalent aluminum oxide. The differences in apparent viscosity as well as the high water content of these systems suggest that considerable variation exists in the gel structure. For this reason, a series of experiments was performed utilizing a specially designed tension cell to obtain greater insight into the gel structure of aluminum hydroxycarbonate gel. The technique developed for this study was based on studies of clay systems (1) and offers the advantage of very little gel disruption during the experiment. The data obtained from the tension cell were compared to the results of more conventional measurements such as viscosity and rate of acid neutralization.

## EXPERIMENTAL

Conditions for the precipitation of aluminum hydroxycarbonate gel by the reaction of aluminum chloride, sodium carbonate, and sodium bicarbonate were varied (Table I) to produce two aluminum hydroxycarbonate gels of significantly different apparent viscosity. The aluminum hydroxycarbonate gel prepared using the conditions described by Kerkhof *et al.* (2) will be termed the high viscosity aluminum hydroxycarbonate gel, and the aluminum hydroxycarbonate gel prepared by Beekman's method (3) will be referred to as the low viscosity aluminum hydroxycarbonate gel.

X-ray[2] (4) and IR[3] (4) analysis confirmed that both the high and low viscosity aluminum hydroxycarbonate gels studied were amorphous aluminum hydroxycarbonate (5).

The rate of acid neutralization was determined by pH-stat titration[4] at pH 3.0 and 25° (6).

Rheograms were obtained using a rotational viscometer[5]. After being stirred to ensure homogeneity, the sample was extruded through a 15-gauge needle into a 600-ml beaker and allowed to stand for 1 hr with the spindle in place prior to the viscosity determination.

The tension cell was a modification of pressure cells used in soil sciences to study the interaction of water with solids (7–9). Preliminary experiments with a pressure cell indicated that pressures of 0.5 atm (68 cm of water) or greater, which are used to characterize water–soil interactions, are too large for studying aluminum hydroxycarbonate gel. To obtain accurately the small driving force needed, a cell capable of applying a small negative pressure or tension to the aluminum hydroxycarbonate gel was developed.

Figure 1 shows the construction of the tension cell. A glass cover fit loosely over the sample chamber to protect the sample and to minimize evaporation. The sample chamber was a plexiglass tube 6.35 cm i.d. × 6.985 cm o.d. × 17.145 cm in length. A 0.9525-cm notch was machined into the outside wall of the sample chamber so that the top base piece could be securely attached. A rubber O-ring and a 0.45-$\mu$m membrane filter were sandwiched between the sample chamber and the bottom base piece. An extracoarse sintered-glass disk, 6.19 × 0.476 cm, fit into the base and served as a filter support. The bottom base piece was machined so a trough system would aid the flow of water to the two outlet ports[6].

Figure 2 is a diagram of the complete tension cell apparatus. The tension cell was fastened to a movable plate[7], which could be accurately positioned by means of a screw gear and vernier system. Water from the samples was collected into a buret that was closed with a stopper containing a capillary which maintained atmospheric pressure in the buret. A three-way stopcock was incorporated in the outlet tubing.

It is essential that the volume comprising the membrane filter's pore volume, the sintered-glass disk's pore volume, and the outlet tubing be completely filled with water before the aluminum hydroxycarbonate gel sample is introduced into the sample chamber. The following procedure was followed in conducting the tension cell experiments:

1. The tension cell was filled from the bottom by adding water through the three-way stopcock. Water was allowed to fill the sample chamber to a height of ~8 cm.

2. The sample chamber cover was replaced with a large one-hole rubber stopper. With the three-way stopcock adjusted to connect the cell to the buret, pressure was applied through the hole in the rubber stopper to remove any air bubbles in the system. The rubber stopper was replaced with the glass cover, and the position of the outlet port was adjusted using the screw assembly so that the outlet port was level with the membrane filter. At this position, the water in the outlet port had a flat surface; *i.e.*, neither a meniscus or a drop was present. The system was allowed to equilibrate for 4–5 hr.

[1] A gel will be viewed as a continuous network of particles extending throughout the entire volume of the system which is, therefore, homogeneous in appearance.

[2] Kristalloflex 4 generator, type F diffractometer, Siemens AG, Karlsruhe, West Germany.

[3] Model 180, Perkin-Elmer Corp., Norwalk, Conn.

[4] PHM 26, TTT II, ABU 12 (2.5 ml), TTA 3, and SBR 2, Radiometer, Copenhagen, Denmark.

[5] Model RVT, Brookfield Engineering Laboratories, Stoughton, Mass.

[6] Swagelok 55-2-TA-OR-ST, Crawford Fitting Co., Solon, Ohio.

[7] Model B2504B-B2530B, Velmen, Bloomfield, N.Y.



*0022-3549/81/0800-0936$01.00/0*
*© 1981, American Pharmaceutical Association*

**Table I—Precipitation Parameters** [a]

| Type | Temperature | End-Point pH | Stirring Speed, rpm | Moles of Aluminum Chloride per Liter of Washed Gel | Moles of Sodium Carbonate per Liter of Washed Gel | Moles of Sodium Bicarbonate per Liter of Washed Gel |
|---|---|---|---|---|---|---|
| High viscosity | 25° | 6.5 | 500 | 0.75 | 0.315 | 0.805 |
| Low viscosity | 4° | 5.8 | 15 | 0.80 | 0.315 | 0.805 |

[a] The $AlCl_3$-$6H_2O$ (0.47 *M*) was added to a solution of 0.53 *M* $NaHCO_3$ and 0.23 *M* $Na_2CO_3$.

3. The stopcock was closed to prevent any water flow, and an accurately weighed sample was added to the chamber by extrusion through a 15-gauge needle.

4. The outlet port was raised so it was level with the top surface of the sample. A final adjustment was made in the position of the outlet port by opening the stopcock and adjusting the position of the outlet port to achieve a flat water surface at the outlet port. This was the zero-tension position. The sample was allowed to equilibrate for 30 min.

5. The tension cell was raised 2 cm, and the cumulative volume of water in the collection buret was recorded with time. To maintain a constant tension of 2 cm, the tension cell was raised 0.05 cm for every 1.5 ml of outflow. This manner of correction is permissible since it was observed in separate measurements that the volume change of the column of aluminum hydroxycarbonate gel is identical to the volume of water that has flowed from the aluminum hydroxycarbonate gel.

6. After the outflow from the sample was zero for 2 hr, the tension cell was raised by a predetermined increment (2-cm increments were used), and this step was repeated.

7. After the final tension increment, the sample remaining in the sample chamber was collected and accurately weighed. The sample was dried to constant weight at 110°. Loss during transfer never exceeded 0.05%.

## RESULTS AND DISCUSSION

Both equilibrium and dynamic measurements are possible through the use of the tension cell. Each contributes unique information concerning gel structure so that structural differences are readily ascertained.

In the case of the simple and more easily treated equilibrium data, where total water outflow is examined as a function of applied tension, the particular gel characteristic examined is structural rigidity. Since the volume of water outflow is equal to the volume change of the aluminum hydroxycarbonate gel during the experiment, the ability of a gel to resist collapse of its structural framework may be directly observed by measuring the amount of water released as a consequence of an applied tension. The experiment may be analyzed either in terms of simply plotting the equilibrium water content of the aluminum hydroxycarbonate gel as a function of applied tension or in terms of the following thermodynamic quantity (10–15):

$$\Delta\bar{G}_{H_2O} = -\bar{v}\rho g\tau \qquad \text{(Eq. 1)}$$

where $\bar{v}$ is the molar volume of water, $\rho$ is the density of water, $g$ is the gravitational constant, and $\tau$ is the tension increment. Thus, $\Delta\bar{G}_{H_2O}$ represents the work required per mole of water to remove water from the system with the accompanying compression of the particles into a smaller volume. If $\Delta\bar{G}_{H_2O}$ is large, the particles are pushed closer together only with difficulty due either to large cohesive forces between particles that prevent distortion of the gel structure or to repulsive forces (primarily coulombic repulsion) that prevent particle surfaces from approaching more closely. The latter force becomes much more pronounced only at higher solids concentrations.

Figure 3 shows the equilibrium water content of the high and low viscosity gels. As water was removed from either aluminum hydroxycarbonate gel, the further removal of water became increasingly more difficult. A greater rigidity of gel structure was indicated when the tension *versus* equilibrium water content curve rose more abruptly at low tension

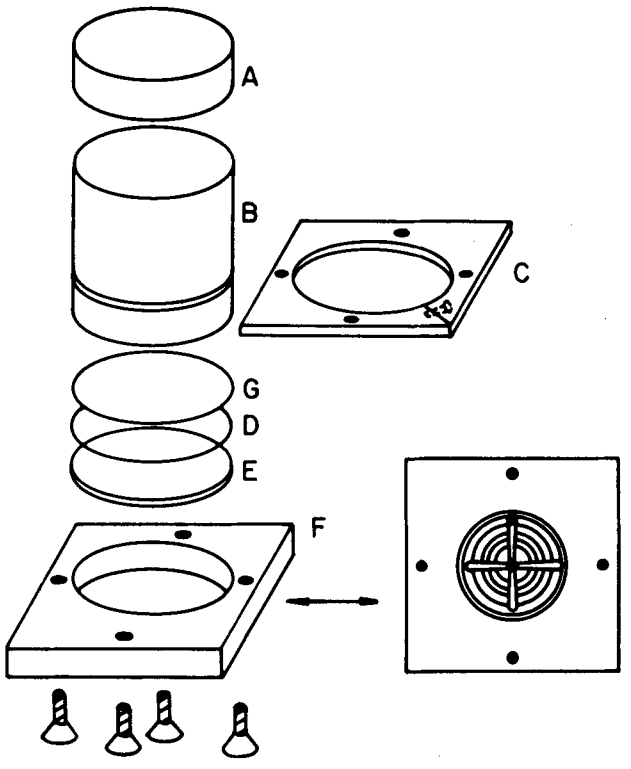


**Figure 1**—*Components of tension cell. Key: A, cover; B, sample chamber; C, top base; D, O-ring; E, sintered-glass disk; F, bottom base; and G, membrane filter.*

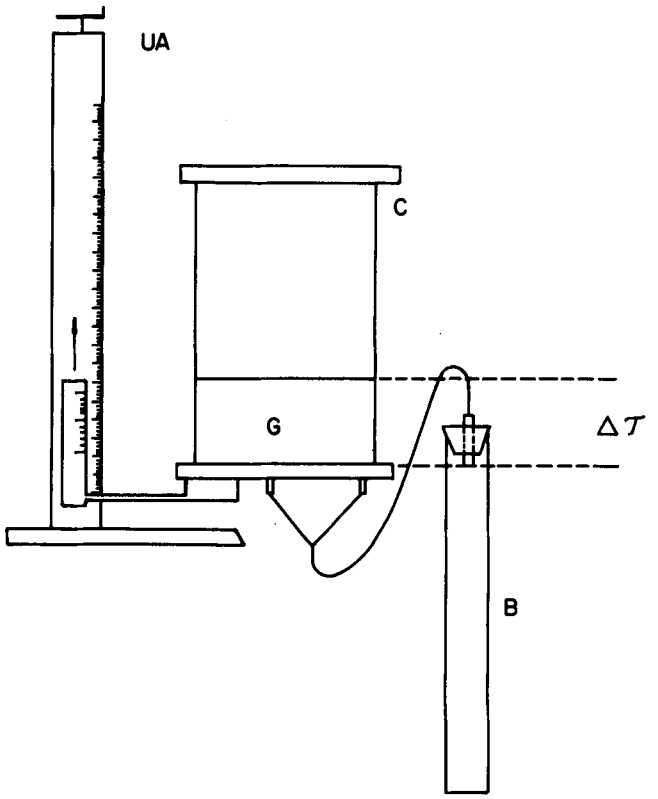


**Figure 2**—*Schematic of tension cell apparatus. Key: C, tension cell; UA, moveable plate assembly; B, collection buret; and G, sample gel.*

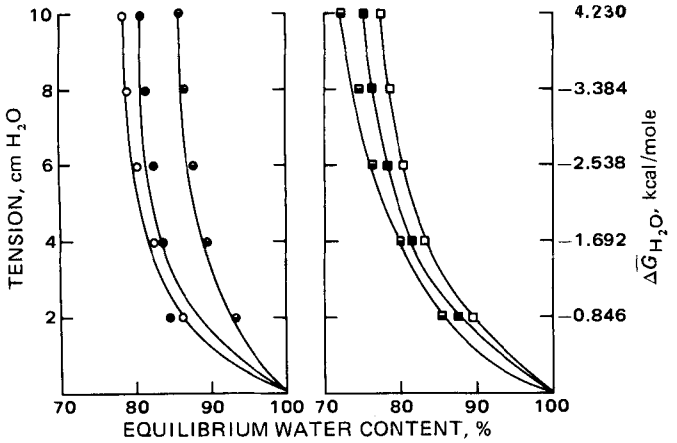


**Figure 3**—*Effect of equilibrium water content on the water tension and change in partial molar Gibbs free energy, $\Delta\bar{G}_{H_2O}$. The high viscosity gel was aged 2 (○), 6 (●), and 14 (◒) weeks at 25°. The low viscosity gel was aged 2 (□), 10 (■), and 14 (◨) weeks at 25°.*

values. The rigidity of the gel structure changed with age (Fig. 3). The high viscosity gel became considerably more rigid as it aged, whereas the low viscosity gel became less rigid with aging. These opposing trends demonstrate that different procedures of aluminum hydroxycarbonate gel preparation can lead to substantially different physical behavior both immediately after precipitation and during aging.

Dynamic measurements also are readily made with the tension cell. Darcy's law (1), which was developed to describe flow through porous media, provides the basis for analyzing the rate of water outflow at various applied tensions:

$$q = \frac{KA\tau}{L} \qquad \text{(Eq. 2)}$$

where $q$ is the rate of flow through the solid phase (cubic centimeters per minute); $K$ is the capillary conductivity (centimeters per minute); $A$ is the cross-sectional area of the solid phase (centimeters squared); $\tau$ is the driving potential, *i.e.*, tension head of water (centimeters); and $L$ is the length of the gel slab (centimeters).

The apparent surface area of the gel, particle size, and porosity all are interrelated. A qualitative measure of these parameters is provided by examining the relative ease with which water may flow through the system. This examination involves time-dependent measurements, whereas only equilibrium measurements were involved in evaluating structural rigidity of the gel structure. The rate of water outflow is measured so that an estimate of capillary conductivity, $K$, may be obtained (8, 9, 16). This quantity reflects the resistance to water flow offered by the gel particles. A large $K$ value implies a low resistance to water flow, which, in turn, indicates lower apparent surface area, larger particles, and higher porosity.

Figure 4 illustrates the capillary conductivity data obtained for the two aluminum hydroxycarbonate gels. With both gels, resistance to the flow of water through the system increased as the water content decreased. Opposite trends were again observed during aging. The high viscosity gel became more resistant to water flow as it aged, whereas the low viscosity gel allowed water to flow more rapidly through its interparticle space upon aging. Both the equilibrium and dynamic measurements indicate that as the gels age, their behavior with respect to water removal changes, which is an important property to consider in the use of aluminum hydroxycarbonate gel dosage forms. The different gel structures exhibited by the two aluminum hydroxycarbonates also will influence manufacturing processes in which the solids concentration is changed, such as in concentrating or washing.

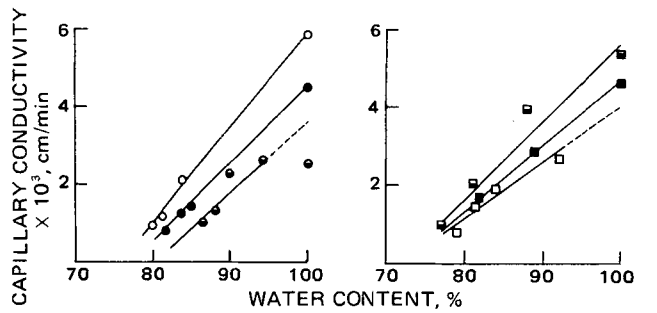


**Figure 4**—*Effect of water content on capillary conductivity. For clarity, the data points are represented by straight lines to emphasize the trends. The $R^2$ values for the straight lines range from 0.64 to 0.99. The high viscosity gel was aged 2 (○), 6 (●), and 14 (◒) weeks at 25°. The low viscosity gel was aged 2 (□), 10 (■), and 14 (◨) weeks at 25°.*

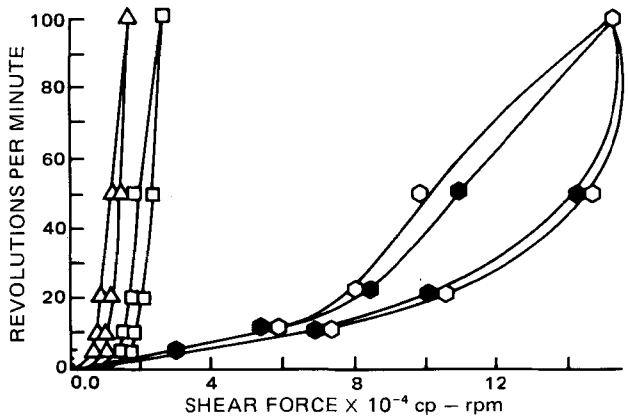


**Figure 5**—*Rheograms of the high viscosity gel during aging at 25°. Key: △, 1 day; □, 4 weeks; ●, 8 weeks; and ○, 12 weeks.*

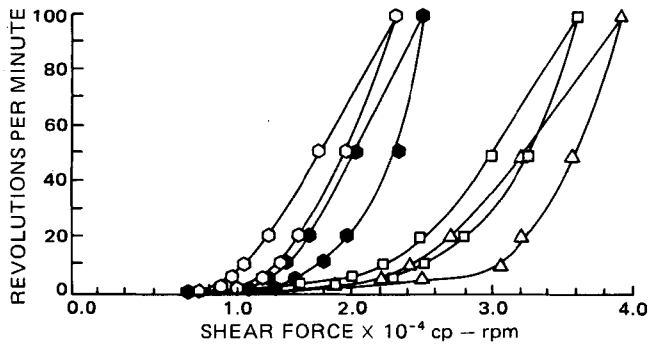


**Figure 6**—*Rheograms of the low viscosity gel during aging at 25°. Key: △, 1 day; □, 4 weeks; ●, 8 weeks; and ○, 12 weeks.*

The rheograms for both the high and low viscosity aluminum hydroxycarbonate gels (Figs. 5 and 6, respectively) indicate thixotropic, shear-thinning systems. The apparent viscosity of the high viscosity gel and the degree of hysteresis increased during aging. In contrast, the low viscosity gel exhibited a decrease in viscosity with aging but no change

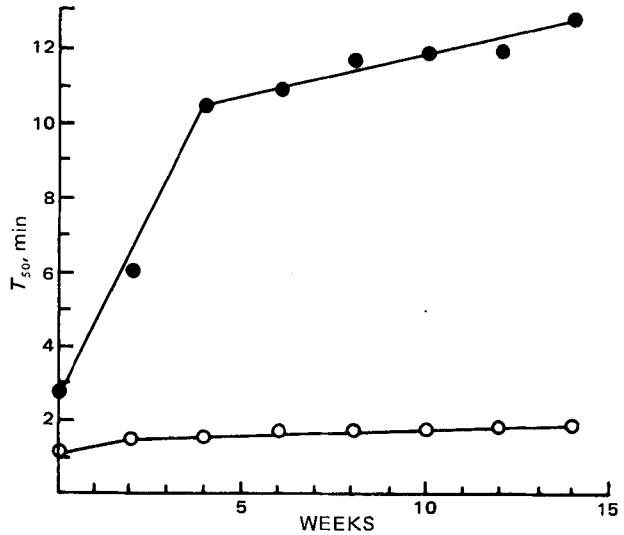


**Figure 7**—*Effect of aging at 25° on the rate of acid neutralization of the high viscosity gel (○) and the low viscosity gel (●).*

in the degree of hysteresis. These facts suggest a substantial increase in the cohesive forces operating between particles of the high viscosity gel and a decrease in the level of cohesion for the low viscosity gel.

Alteration of the degree of particle–particle cohesion due to changes in the level of particle charge was established previously (17). It was shown that additional charge provides sufficient coulombic repulsion to overcome the van der Waals attraction forces so that the apparent viscosity decreases. Examination of the rates of acid neutralization by the two aluminum hydroxycarbonate gels (Fig. 7) indicates a significant decrease in the rate of acid neutralization of the low viscosity gel but no appreciable change for the high viscosity gel. This behavior indicates that crystallinity develops in the low viscosity gel, eventually leading to the formation of a crystalline form of aluminum hydroxide such as gibbsite, which is free of carbonate (5, 18). The transformation to a carbonate-free aluminum hydroxide results in an increased zero point of charge (17) and, therefore, a buildup of charge on the low-viscosity gel. Thus, the apparent viscosity, gel structure rigidity, and resistance to water flow would be expected to decrease as was observed. With the high viscosity gel, the relatively stable rate of acid neutralization during the time period studied indicates that no buildup of charge occurs so that the natural tendency of a gel to form the most stable arrangement of particles with the maximum degree of particle–particle linking is observed. Thus, an increased apparent viscosity, an enhanced gel structure rigidity, and a decreased capillary conductivity are consistent with the proposed mechanism.

## CONCLUSIONS

The tension cell is useful for examining the physical state of a gel, especially when compared to other methods such as viscosity measurement where large inputs of mechanical energy in the form of shear stress may disrupt the gel structure. The tension cell is capable of providing meaningful data with a firm basis provided by thermodynamic and kinetic theory. The data reported here were obtained with considerable difficulty because of the necessity for position readjustment of the tension cell to maintain a constant tension, the long duration of the experiments, and the frequent tabulations of data required for the dynamic measurements. Early experiments, in which adjustments to maintain a constant tension during water outflow were not performed, did not produce satisfactory data. The manual adjustment of cell position to maintain a constant tension was essential in obtaining meaningful results. However, some of the scatter observed in Figs. 3 and 4 may have been due to unavoidable mechanical disturbances of the gel structure through the manual repositioning of the tension cell. Consequently, various methods for automating the tension cell are being tested so that acquiring the necessary data will be more convenient and more precise data may be obtained.

Future experiments are planned with the tension cell to give insight into various roles played by particle charge, size, and shape. The effects of surface charge and particle size on the compressibility of aluminum hydroxycarbonate gel are examined specifically in a subsequent report.

## REFERENCES


(1) D. Swartzendruber, in "The Flow of Water in Unsaturated Solids," R. J. M. De Weist, Ed., Academic, New York, N.Y., 1969, chap. 6.

(2) N. J. Kerkhof, J. L. White, and S. L. Hem, *J. Pharm. Sci.*, **66,** 1533 (1977).

(3) S. M. Beekman, U.S. pat. 3,773,917, (Nov. 20, 1973).

(4) S. L. Nail, J. L. White, and S. L. Hem, *J. Pharm. Sci.*, **64,** 1166 (1975).

(5) C. J. Serna, J. L. White, and S. L. Hem, *ibid.*, **67,** 1144 (1978).

(6) N. J. Kerkhof, R. K. Vanderlaan, J. L. White, and S. L. Hem, *ibid.*, **66,** 1528 (1977).

(7) L. A. Richards, *Soil Sci.*, **68,** 95 (1949).

(8) C. B. Tanner and D. E. Elrick, *Soil Sci. Soc. Am. Proc.*, **22,** 575 (1958).

(9) R. J. Reginato and C. H. M. van Bavel, *ibid.*, **26,** 1 (1962).

(10) D. M. Anderson and P. F. Low, *ibid.*, **22,** 99 (1958).

(11) P. F. Low, *Adv. Agron.*, **13,** 269 (1961).

(12) P. F. Low, *Soil Sci.*, **93,** 6 (1962).

(13) J. D. Oster and P. F. Low, *Soil Sci. Soc. Am. Proc.*, **28,** 605 (1964).

(14) I. Ravina and P. F. Low, *Clays Clay Miner.*, **20,** 109 (1972).

(15) H. A. Ruiz and P. F. Low, in "Proceedings of the 50th International Conference on Colloid Interface Science," M. Kerker, Ed., Academic, New York, N.Y., 1976, pp. 503–515.

(16) R. J. Kunze and D. Kirkham, *Soil Sci. Soc. Am. Proc.*, **26,** 421 (1962).

(17) J. R. Feldkamp, D. N. Shah, S. L. Meyer, J. L. White, and S. L. Hem, *J. Pharm. Sci.*, **70,** 638 (1981).

(18) S. L. Nail, J. L. White, and S. L. Hem, *ibid.*, **65,** 231 (1976).


## ACKNOWLEDGMENTS


Supported in part by a David Ross Fellowship to E. A. Lipka.

This report is Journal Paper 8071, Purdue University Agricultural Experiment Station, West Lafayette, IN 47907.

The authors thank Professor D. Swartzendruber for stimulating this research.


# Effect of Complex Formation between 4-Hexylresorcinol and Ethyl Myristate on Release Rate of 4-Hexylresorcinol from Petrolatum Base


**KATSUMI IGA, ANWAR HUSSAIN ˣ, and TOSHIO KASHIHARA**



Received April 7, 1980, from the *College of Pharmacy, University of Kentucky, Lexington, KY 40506.* Accepted for publication February 5, 1981.



**Abstract** □ The effect of ethyl myristate on the release rate of 4-hexylresorcinol from petrolatum base was studied at pH 7.4 and 37°. 4-Hexylresorcinol was analyzed spectrophotometrically at 278 nm. The release rate of hexylresorcinol from the ointments was directly proportional to the square root of time and depended on the percentage of ethyl myristate in the ointment base. For 0, 0.5, 1, 3, and 5% of ethyl myristate, the release rates were 29.6, 35.4, 38.3, 55.7, and 70.0 $\mu g/hr^{1/2}/cm^2$, respectively. The solubility of hexylresorcinol in the petrolatum base was determined as a function of ethyl myristate using partitioning techniques. The enhancement in hexylresorcinol solubility was rationalized on the basis of 1:1 and 1:2 complexes between hexylresorcinol and ethyl myristate. The complexation constants of these complexes were estimated to be 10 $M^{-1}$ and 206.1 $M^{-2}$, respectively. The diffusion coefficient of hexylresorcinol in the petrolatum base was estimated to be $1.31 \times 10^{-8}$ $cm^2/sec$.



**Keyphrases** □ Release rate—effect of ethyl myristate on release of 4-hexylresorcinol from petrolatum, quantitative analysis □ Ethyl myristate—effect on release rate of 4-hexylresorcinol from petrolatum, quantitative analysis □ 4-Hexylresorcinol—effect of ethyl myristate on release rate from petrolatum, quantitative analysis


Percutaneous absorption depends on both drug release from the vehicle and drug permeability through the skin. Drug release depends on physicochemical factors, such as the drug's solubility and diffusion coefficient in the vehicle.


*0022-3549/81/0800-0939$01.00/0*


*© 1981, American Pharmaceutical Association*

in the degree of hysteresis. These facts suggest a substantial increase in the cohesive forces operating between particles of the high viscosity gel and a decrease in the level of cohesion for the low viscosity gel.

Alteration of the degree of particle–particle cohesion due to changes in the level of particle charge was established previously (17). It was shown that additional charge provides sufficient coulombic repulsion to overcome the van der Waals attraction forces so that the apparent viscosity decreases. Examination of the rates of acid neutralization by the two aluminum hydroxycarbonate gels (Fig. 7) indicates a significant decrease in the rate of acid neutralization of the low viscosity gel but no appreciable change for the high viscosity gel. This behavior indicates that crystallinity develops in the low viscosity gel, eventually leading to the formation of a crystalline form of aluminum hydroxide such as gibbsite, which is free of carbonate (5, 18). The transformation to a carbonate-free aluminum hydroxide results in an increased zero point of charge (17) and, therefore, a buildup of charge on the low-viscosity gel. Thus, the apparent viscosity, gel structure rigidity, and resistance to water flow would be expected to decrease as was observed. With the high viscosity gel, the relatively stable rate of acid neutralization during the time period studied indicates that no buildup of charge occurs so that the natural tendency of a gel to form the most stable arrangement of particles with the maximum degree of particle–particle linking is observed. Thus, an increased apparent viscosity, an enhanced gel structure rigidity, and a decreased capillary conductivity are consistent with the proposed mechanism.

## CONCLUSIONS

The tension cell is useful for examining the physical state of a gel, especially when compared to other methods such as viscosity measurement where large inputs of mechanical energy in the form of shear stress may disrupt the gel structure. The tension cell is capable of providing meaningful data with a firm basis provided by thermodynamic and kinetic theory. The data reported here were obtained with considerable difficulty because of the necessity for position readjustment of the tension cell to maintain a constant tension, the long duration of the experiments, and the frequent tabulations of data required for the dynamic measurements. Early experiments, in which adjustments to maintain a constant tension during water outflow were not performed, did not produce satisfactory data. The manual adjustment of cell position to maintain a constant tension was essential in obtaining meaningful results. However, some of the scatter observed in Figs. 3 and 4 may have been due to unavoidable mechanical disturbances of the gel structure through the manual repositioning of the tension cell. Consequently, various methods for automating the tension cell are being tested so that acquiring the necessary data will be more convenient and more precise data may be obtained.

Future experiments are planned with the tension cell to give insight into various roles played by particle charge, size, and shape. The effects of surface charge and particle size on the compressibility of aluminum hydroxycarbonate gel are examined specifically in a subsequent report.

## REFERENCES


(1) D. Swartzendruber, in "The Flow of Water in Unsaturated Solids," R. J. M. De Weist, Ed., Academic, New York, N.Y., 1969, chap. 6.

(2) N. J. Kerkhof, J. L. White, and S. L. Hem, *J. Pharm. Sci.*, **66,** 1533 (1977).

(3) S. M. Beekman, U.S. pat. 3,773,917, (Nov. 20, 1973).

(4) S. L. Nail, J. L. White, and S. L. Hem, *J. Pharm. Sci.*, **64,** 1166 (1975).

(5) C. J. Serna, J. L. White, and S. L. Hem, *ibid.*, **67,** 1144 (1978).

(6) N. J. Kerkhof, R. K. Vanderlaan, J. L. White, and S. L. Hem, *ibid.*, **66,** 1528 (1977).

(7) L. A. Richards, *Soil Sci.*, **68,** 95 (1949).

(8) C. B. Tanner and D. E. Elrick, *Soil Sci. Soc. Am. Proc.*, **22,** 575 (1958).

(9) R. J. Reginato and C. H. M. van Bavel, *ibid.*, **26,** 1 (1962).

(10) D. M. Anderson and P. F. Low, *ibid.*, **22,** 99 (1958).

(11) P. F. Low, *Adv. Agron.*, **13,** 269 (1961).

(12) P. F. Low, *Soil Sci.*, **93,** 6 (1962).

(13) J. D. Oster and P. F. Low, *Soil Sci. Soc. Am. Proc.*, **28,** 605 (1964).

(14) I. Ravina and P. F. Low, *Clays Clay Miner.*, **20,** 109 (1972).

(15) H. A. Ruiz and P. F. Low, in "Proceedings of the 50th International Conference on Colloid Interface Science," M. Kerker, Ed., Academic, New York, N.Y., 1976, pp. 503–515.

(16) R. J. Kunze and D. Kirkham, *Soil Sci. Soc. Am. Proc.*, **26,** 421 (1962).

(17) J. R. Feldkamp, D. N. Shah, S. L. Meyer, J. L. White, and S. L. Hem, *J. Pharm. Sci.*, **70,** 638 (1981).

(18) S. L. Nail, J. L. White, and S. L. Hem, *ibid.*, **65,** 231 (1976).


## ACKNOWLEDGMENTS


Supported in part by a David Ross Fellowship to E. A. Lipka.

This report is Journal Paper 8071, Purdue University Agricultural Experiment Station, West Lafayette, IN 47907.

The authors thank Professor D. Swartzendruber for stimulating this research.


# Effect of Complex Formation between 4-Hexylresorcinol and Ethyl Myristate on Release Rate of 4-Hexylresorcinol from Petrolatum Base


**KATSUMI IGA, ANWAR HUSSAIN ˣ, and TOSHIO KASHIHARA**



Received April 7, 1980, from the *College of Pharmacy, University of Kentucky, Lexington, KY 40506.* Accepted for publication February 5, 1981.



**Abstract** □ The effect of ethyl myristate on the release rate of 4-hexylresorcinol from petrolatum base was studied at pH 7.4 and 37°. 4-Hexylresorcinol was analyzed spectrophotometrically at 278 nm. The release rate of hexylresorcinol from the ointments was directly proportional to the square root of time and depended on the percentage of ethyl myristate in the ointment base. For 0, 0.5, 1, 3, and 5% of ethyl myristate, the release rates were 29.6, 35.4, 38.3, 55.7, and 70.0 $\mu g/hr^{1/2}/cm^2$, respectively. The solubility of hexylresorcinol in the petrolatum base was determined as a function of ethyl myristate using partitioning techniques. The enhancement in hexylresorcinol solubility was rationalized on the basis of 1:1 and 1:2 complexes between hexylresorcinol and ethyl myristate. The complexation constants of these complexes were estimated to be 10 $M^{-1}$ and 206.1 $M^{-2}$, respectively. The diffusion coefficient of hexylresorcinol in the petrolatum base was estimated to be $1.31 \times 10^{-8}$ $cm^2/sec$.



**Keyphrases** □ Release rate—effect of ethyl myristate on release of 4-hexylresorcinol from petrolatum, quantitative analysis □ Ethyl myristate—effect on release rate of 4-hexylresorcinol from petrolatum, quantitative analysis □ 4-Hexylresorcinol—effect of ethyl myristate on release rate from petrolatum, quantitative analysis


Percutaneous absorption depends on both drug release from the vehicle and drug permeability through the skin. Drug release depends on physicochemical factors, such as the drug's solubility and diffusion coefficient in the vehicle.


*0022-3549/81/0800-0939$01.00/0*


*© 1981, American Pharmaceutical Association*

**Table I—Composition of the Ointments Used in the Release Rate Study**

| Ingredient | Percent of Ethyl Myristate | | | | |
|---|---|---|---|---|---|
| | 0.0 | 0.5 | 1.0 | 3.0 | 5.0 |
| White petrolatum, g | 10 | 10 | 10 | 10 | 10 |
| Hexylresorcinol, mg | 200 | 200 | 200 | 200 | 200 |
| Ethyl myristate, mg | — | 50 | 100 | 300 | 500 |

Simplified equations describing drug release from suspension (1) and solution (2) vehicles have been reported, and numerous studies (3–10) attempted to relate vehicle composition to the *in vitro* release rate. There is, however, relatively little quantitative information correlating the release rate with variations in physicochemical parameters produced by a compositional change in the vehicles. This investigation quantitatively and mechanistically examined the effect of ethyl myristate on the release rate of 4-hexylresorcinol from petrolatum.

## EXPERIMENTAL

**Ointment Preparation**—Table I shows the amounts of hexylresorcinol[1], ethyl myristate[2], and white petrolatum[3] used in ointment preparation. The ointments were prepared by warming hexylresorcinol and ethyl myristate at 40° in a 20-ml beaker. White petrolatum then was added, and the mixture was kept at 40° for 5 min until a homogeneous fluid mixture was obtained. A 5-ml sample of the liquid mixture was poured into a 20-ml polyethylene syringe from which the upper portion had been removed by cutting around the barrel at the 15-ml mark. The ointments were left in the syringe overnight at room temperature.

**Release Rate Measurements**—The half-syringe containing the ointment was attached to the USP dissolution apparatus and was immersed in a 60-ml glass tube containing 40 ml of 0.1 *M* phosphate buffer, pH 7.4, as shown in Fig. 1. The release rate of hexylresorcinol from the ointments was studied at 37° at a rotation speed of 50 rpm. At each sampling interval, the entire 40 ml of the dissolution medium was taken and replaced with 40 ml of fresh buffer. The hexylresorcinol concentration was determined spectrophotometrically[4] at 278 nm using a 10-cm cell.

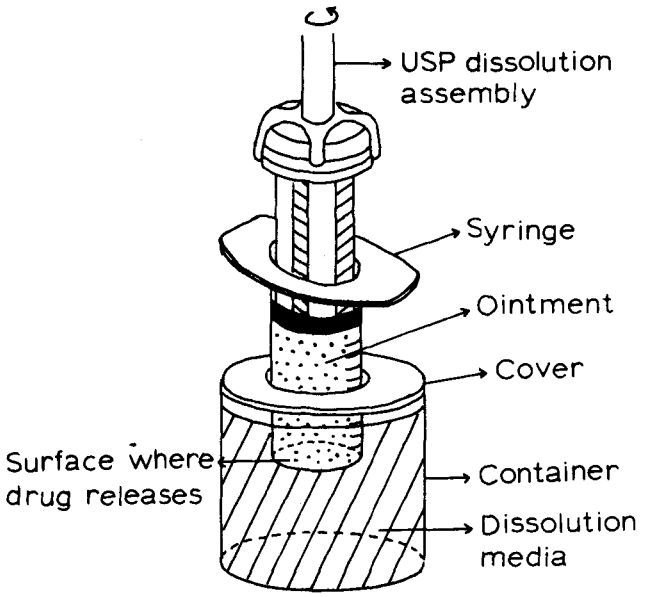


**Figure 1**—*Apparatus used for the determination of release rate of hexylresorcinol from ointment.*

[1] Curtin-Matheson, Cincinnati, Ohio.
[2] Sigma Chemical Co.
[3] Plough Inc.

**Table II—Composition and Ratio of the Aqueous and Ointment Layers Employed in the Partition Coefficient Determination**

| Aqueous Solution of Hexylresorcinol, ml | White Petrolatum, g | Ethyl Myristate Added to White Petrolatum, mg | Percent of Ethyl Myristate |
|---|---|---|---|
| 20 | 12 | — | 0 |
| 30 | 12 | 60 | 0.5 |
| 40 | 12 | 120 | 1 |
| 30 | 6 | 120 | 2 |
| 40 | 6 | 180 | 3 |
| 60 | 6 | 300 | 5 |

**Partition Coefficient of Hexylresorcinol in pH 7.4 Buffer and in White Petrolatum Containing Different Amounts of Ethyl Myristate**—Ethyl myristate and white petrolatum in the ratios shown in Table II were melted in a 200-ml beaker at 40° and were mixed thoroughly. An aqueous buffer solution containing 200 mg of hexylresorcinol in 500 ml of 0.1 *M* phosphate buffer, pH 7.4, also was prepared. Appropriate volumes of the hexylresorcinol solution (Table II) were added to the petrolatum–ethyl myristate mixtures, which were sonicated for 10 min in 200-ml beakers. The beaker then was shaken at 37° for 7 days, and the aqueous solution was filtered through a 0.45-μm filter[5]. Five milliliters of each filtrate was diluted to 50 ml with pH 7.4 phosphate buffer. The hexylresorcinol concentration was determined spectrophotometrically at 278 nm using a 10-cm cell.

The partition coefficient was calculated as follows:

$$\text{partition coefficient} = \frac{(\text{volume of aqueous layer})\,(\text{absorbance change, } A_0 - A, \text{ in aqueous layer})}{(\text{volume of ointment})\,(\text{absorbance in aqueous layer, } A)} \quad \text{(Eq. 1)}$$

where $A_0$ and $A$ are the initial and final absorbances of the solution, respectively. The volume of the ointment was calculated from the density and weight of the ointment.

## RESULTS AND DISCUSSION

The release profile of hexylresorcinol from the ointments is shown in Fig. 2 as a function of the ethyl myristate concentration. The release of hexylresorcinol from these ointments was proportional to the square root of time.

Higuchi (1) found that the release of drugs suspended in ointment bases obeys the following relationship:

$$Q = \sqrt{Dt(2A - C_s)C_s} \quad \text{(Eq. 2)}$$

where $Q$ is the amount released at time $t$ per unit area of exposure, $A$ is the drug concentration expressed in units per cubic centimeter, $C_s$ is the solubility of the drug in units per cubic centimeter in the external phase of the ointment, and $D$ is the diffusion constant of the drug molecule in the external phase.

Singh *et al.* (11) found that the square root of time dependency also was observed for the release of two interacting drugs incorporated in an inert matrix. These authors found that the release of the individual compounds in benzocaine–caffeine systems, as well as the sum of the two compounds, followed a linear relationship with the square root of time.

It can be shown that the release of hexylresorcinol from ointment bases containing different amounts of ethyl myristate also follows a square root of time dependency (see Eq. A8 under *Appendix*).

The exposed surface area for the release of hexylresorcinol was calculated from the diameter of the syringe (2.0 cm) to be 3.14 $cm^2$. The release rate of hexylresorcinol per unit area from the different ointment bases can be calculated by dividing the slopes of the lines in Fig. 2 by 3.14 $cm^2$. These values are listed in Table III as a function of ethyl myristate. The data indicate that the release rate of hexylresorcinol increased as the percent of ethyl myristate in the ointment increased. Thus, it is apparent that the enhancement in the hexylresorcinol release rate was due to the increase in hexylresorcinol solubility.

To obtain insight into the effect of ethyl myristate on hexylresorcinol solubility in petrolatum and on the nature of the interaction between the two agents, the total solubility of hexylresorcinol was determined in

[4] Varian model 118.
[5] Millipore Corp., Bedford, Mass.

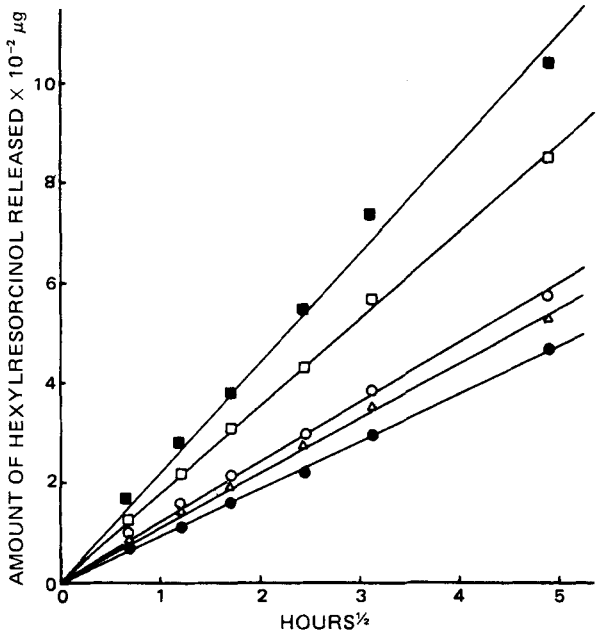


**Figure 2**—*Amount of hexylresorcinol released from ointment as a function of time*$^{1/2}$. *The amounts of ethyl myristate in the ointment were 0 (●), 0.5 (△), 1 (○), 3 (□), and 5 (■) %.*

petrolatum in the presence of ethyl myristate using partitioning. The partition coefficients of hexylresorcinol between the ointment bases and pH 7.4 buffer were calculated using Eq. 1 (Table IV and Fig. 3).

It is apparent from Fig. 3 that the partition coefficient of hexylresorcinol varied in a nonlinear fashion as a function of the ethyl myristate concentration. Previously, it was shown that the partition coefficient of hexylresorcinol between hexane containing various amounts of esters and pH 7.4 buffer also varied in a nonlinear fashion (12). Such behavior was rationalized on the basis of formation of 1:1 and 1:2 complexes between hexylresorcinol and the esters in hexane.

If a similar mechanism is operative in petrolatum, then the following relationships are valid:

$$HR_B \rightleftarrows HR$$

*Scheme I*

$$HR + EM \rightleftarrows HR\cdot EM$$

*Scheme II*

$$HR + 2EM \rightleftarrows HR\cdot EM_2$$

*Scheme III*

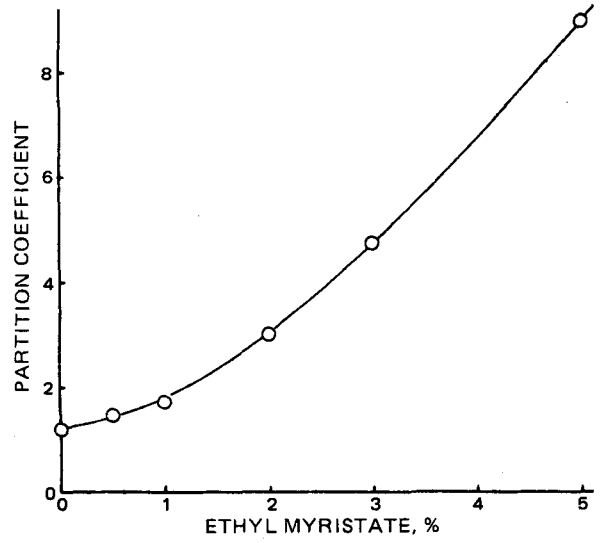


**Figure 3**—*Partition coefficient of hexylresorcinol between pH 7.4 buffer solution and ointment as a function of added ethyl myristate.*

**Table III—Dependency of the Release Rate of Hexylresorcinol on the Percentage of Ethyl Myristate Concentration in Petrolatum**

| Ethyl Myristate, % | Release Rate, $\mu g/hr^{1/2}/cm^2$ |
|---|---|
| 0.0 | 29.6 |
| 0.5 | 35.4 |
| 1.0 | 38.3 |
| 3.0 | 55.7 |
| 5.0 | 70.0 |

**Table IV—Dependency of the Partition Coefficient of Hexylresorcinol between pH 7.4 Buffer and Petrolatum on the Percentage of Added Ethyl Myristate**

| Ethyl Myristate, % | Partition Coefficient |
|---|---|
| 0 | 1.23 |
| 0.5 | 1.47 |
| 1 | 1.73 |
| 2 | 3.06 |
| 3 | 4.72 |
| 5 | 8.97 |

$$P_0 = \frac{(HR)}{(HR)_B} \quad \text{(Eq. 3)}$$

$$P = \frac{(HR)_T}{(HR)_B} \quad \text{(Eq. 4)}$$

$$K_{1:1} = \frac{(HR\cdot EM)}{(HR)(EM)} \quad \text{(Eq. 5)}$$

$$K_{1:2} = \frac{(HR\cdot EM_2)}{(HR)(EM)^2} \quad \text{(Eq. 6)}$$

$$(HR)_T = (HR) + (HR\cdot EM) + (HR\cdot EM_2) \quad \text{(Eq. 7)}$$

where $P_0$ and $P$ are the partition coefficients of hexylresorcinol between the buffer solution and the ointments without ethyl myristate and with ethyl myristate, respectively; $K_{1:1}$ and $K_{1:2}$ are the complexation constants of 1:1 and 1:2 complexes, respectively; and (HR), $(HR)_B$, $(HR)_T$, (HR·EM), ($HR\cdot EM_2$), and (EM) are the concentrations of free hexylresorcinol in the ointments, free hexylresorcinol in the buffer solution, total hexylresorcinol in the ointments, 1:1 complex of hexylresorcinol in the ointments, 1:2 complex of hexylresorcinol in the ointments, and free ethyl myristate in the ointments, respectively. The combination of Eqs. 3–7 results in:

$$\frac{P - P_0}{P_0} = K_{1:1}(EM) + K_{1:2}(EM)^2 \quad \text{(Eq. 8)}$$

Since a very dilute aqueous solution of hexylresorcinol was employed in the partitioning study, the concentration of the complexes can be considered to be small in comparison with the concentration of free ethyl myristate. It follows that (EM) = $(EM)_T$. Rearranging Eq. 8 results in:

$$\frac{P - P_0}{P_0(EM)_T} = K_{1:1} + K_{1:2}(EM)_T \quad \text{(Eq. 9)}$$

Table V shows the values of the left side of Eq. 9 as a function of $(EM)_T$. A plot of $(P - P_0)/P_0(EM)_T$ *versus* $(EM)_T$ should result in a straight line with the intercept of $K_{1:1}$ and the slope of $K_{1:2}$ as shown in Fig. 4. The values of $K_{1:1}$ and $K_{1:2}$ were 10 $M^{-1}$ and 206.1 $M^{-2}$, respectively. The apparent solubility of hexylresorcinol in the ointment bases can be estimated on the basis of the 1:1 and 1:2 complex formation from the values of the complexation constants ($K_{1:1}$, $K_{1:2}$) as follows.

**Table V—Relationship between Total Ethyl Myristate, $(EM)_T$, and $(P - P_0)/P_0(EM)_T$**

| $(EM)_T$, $M$ | $(P - P_0)/P_0(EM)_T$, $M^{-1}$ |
|---|---|
| $0.0 \times 10^{-2}$ | — |
| $1.53 \times 10^{-2}$ | 12.88 |
| $3.07 \times 10^{-2}$ | 13.29 |
| $6.14 \times 10^{-2}$ | 24.32 |
| $9.21 \times 10^{-2}$ | 30.89 |
| $15.31 \times 10^{-2}$ | 41.29 |

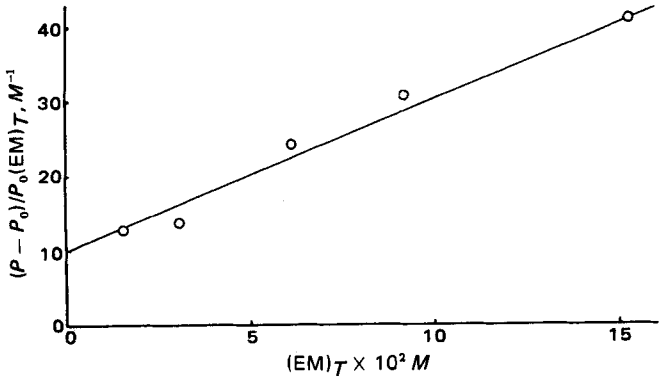


**Figure 4**—*Plot of* $(P - P_0)/P_0(EM)_T$ versus $(EM)_T$.

In the solubility system, $(HR)_T$ and (HR) can be written as:

$$(HR)_T = S_T \quad \text{(Eq. 10)}$$

$$(HR) = S_0 \quad \text{(Eq. 11)}$$

where $S_T$ and $S_0$ are the apparent and the original solubility of hexylresorcinol, respectively. Therefore, the total concentration of ethyl myristate and $S_T$ can be written as:

$$(EM)_T = (EM) + K_{1:1}(EM)S_0 + 2K_{1:2}(EM)^2S_0 \quad \text{(Eq. 12)}$$

$$S_T = S_0 + K_{1:1}(EM)S_0 + K_{1:2}(EM)^2S_0 \quad \text{(Eq. 13)}$$

Elimination of the $(EM)^2$ form gives an equation for the concentration of free ethyl myristate:

$$(EM) = \frac{1}{1 - K_{1:1}S_0}[(EM)_T - 2(S_T - S_0)] \quad \text{(Eq. 14)}$$

The combination of Eqs. 13 and 14 gives:

$$S_T = S_0 + \frac{K_{1:1}S_0}{1 - K_{1:1}S_0}[(EM)_T - 2(S_T - S_0)] + \frac{K_{1:2}S_0}{(1 - K_{1:1}S_0)^2}[(EM)_T - 2(S_T - S_0)]^2 \quad \text{(Eq. 15)}$$

The apparent solubility of hexylresorcinol in the ointment base can be estimated by using the determined values of $K_{1:1}$ and $K_{1:2}$ and $S_0$, which can be estimated as:

$$S_0 = P_0 \times S_B \quad \text{(Eq. 16)}$$

where $S_B$ is the solubility of hexylresorcinol in the buffer solution. The results shown in Table VI strongly suggest that the apparent solubility of hexylresorcinol in the ointment base increases in the presence of ethyl myristate and is due to the complex formation between hexylresorcinol and ethyl myristate.

**Table VI—Apparent Solubility of Hexylresorcinol in the Ointment Bases as a Function of Ethyl Myristate**

| Ethyl Myristate, % | Solubility of Hexylresorcinol in Ointments, $\mu g/cm^3$ |
|---|---|
| 0.0 | $0.680 \times 10^3$ |
| 0.5 | $0.801 \times 10^3$ |
| 1.0 | $0.987 \times 10^3$ |
| 2.0 | $1.479 \times 10^3$ |
| 3.0 | $2.121 \times 10^3$ |
| 5.0 | $3.753 \times 10^3$ |

**Table VII—Relationship between Added Ethyl Myristate and $\sqrt{C_s(2A - C_s)}$**

| Ethyl Myristate, % | $\sqrt{C_s(2A - C_s)}$, $\mu g/cm^3$ |
|---|---|
| 0.0 | $4.578 \times 10^3$ |
| 0.5 | $4.976 \times 10^3$ |
| 1.0 | $5.488 \times 10^3$ |
| 3.0 | $7.894 \times 10^3$ |
| 5.0 | $10.203 \times 10^3$ |

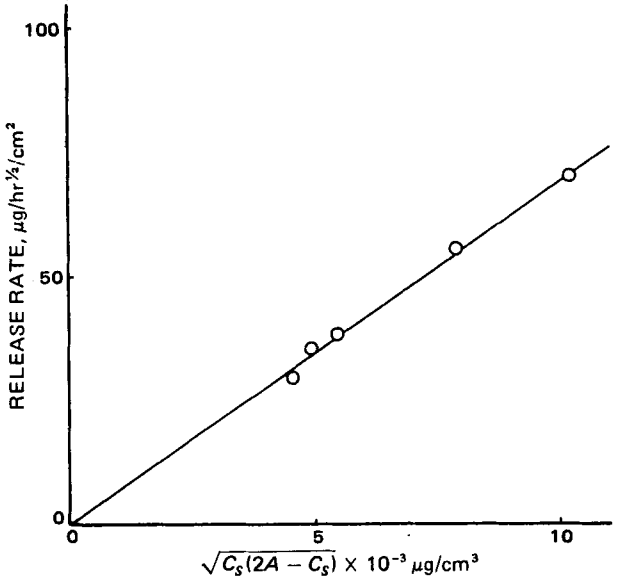


**Figure 5**—*Plot of release rate of hexylresorcinol from ointment* versus $\sqrt{C_s(2A - C_s)}$.

In Eq. 2, if the effective diffusion coefficient of hexylresorcinol in the ointments is the same, then the release rate depends only on the amount of hexylresorcinol and its apparent solubility in the ointments:

$$\text{release rate} = K\sqrt{C_s(2A - C_s)} \quad \text{(Eq. 17)}$$

where $K$ is a constant expressed as $\sqrt{D}$ and $A$ is 15.748 mg/cm³ on the basis of proper dimension. The calculated values of $\sqrt{C_s(2A - C_s)}$ are shown in Table VII.

Plots of the release rate *versus* $\sqrt{C_s(2A - C_s)}$ according to Eq. 17 should result in a straight line with a zero intercept as shown in Fig. 5. It is apparent from Fig. 5 that the enhancement in the release rate of hexylresorcinol is due only to the increase in hexylresorcinol solubility in the presence of ethyl myristate.

The calculated value of the effective diffusion coefficient, $D$, of hexylresorcinol in the ointment base was estimated from the slope of the line in Fig. 5 to be $1.31 \times 10^{-8}$ cm²/sec. By using the values of $D$ and $C_s$, the release rates of hexylresorcinol as a function of ethyl myristate were calculated using Eq. 2. These data (Fig. 6) show that good agreement was obtained between the calculated and experimental values.

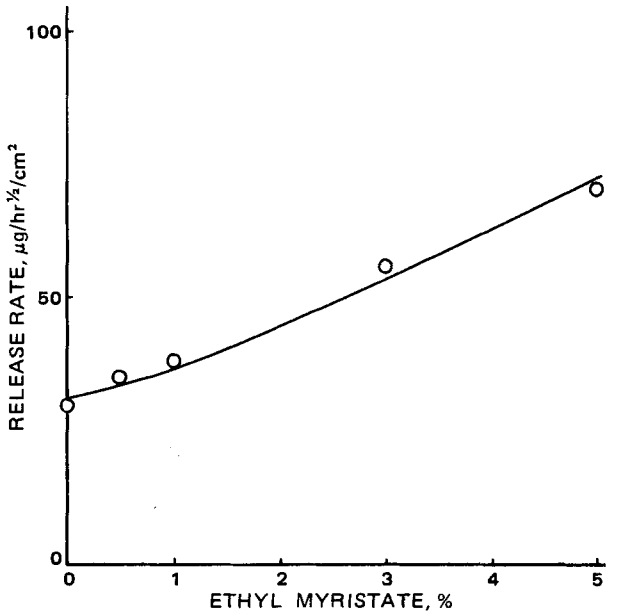


**Figure 6**—*Release rate of hexylresorcinol from ointment as a function of added ethyl myristate. Key:* ○, *experimental values; and* —, *calculated values.*

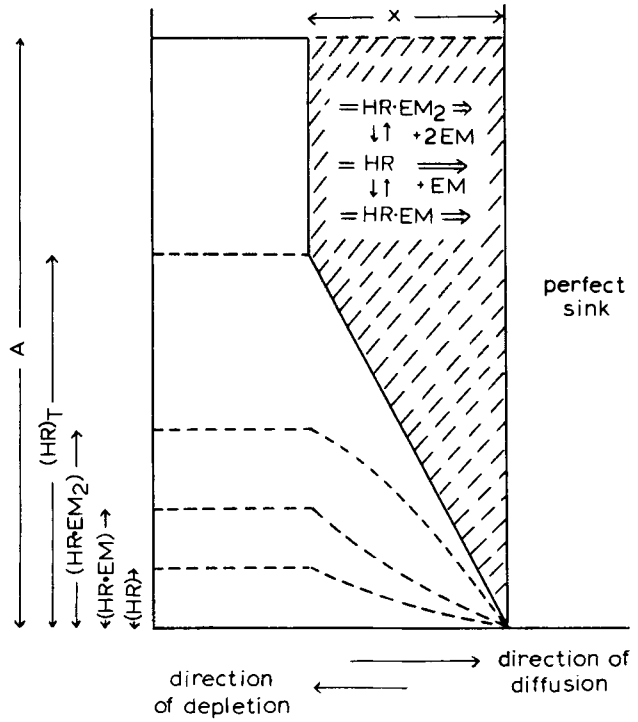


**Figure A1**—*Theoretical model describing the simultaneous release under sink conditions of HR, HR·EM, HR·EM$_2$, and (HR)$_T$ from petrolatum.*

## APPENDIX

In the diffusion layer, the following relationships are valid:

$$HR + EM \underset{k_{-1}}{\overset{k_1}{\rightleftharpoons}} HR{\cdot}EM$$

*Scheme AI*

$$HR + EM_2 \underset{k_{-2}}{\overset{k_2}{\rightleftharpoons}} HR{\cdot}EM_2$$

*Scheme AII*

where $k_1$, $k_{-1}$, $k_2$, and $k_{-2}$ are the rate constants for complexation. The combination of Fick's second law and reversible kinetic equations results in:

$$\frac{d(HR)}{dt} = D_1\frac{\partial^2(HR)}{\partial\chi^2} + k_{-1}(HR{\cdot}EM) + k_{-2}(HR{\cdot}EM_2) - k_1(HR)(EM) - k_2(HR)(EM)^2 \quad \text{(Eq. A1)}$$

$$\frac{d(HR{\cdot}EM)}{dt} = D_2\frac{\partial^2(HR{\cdot}EM)}{\partial\chi^2} + k_1(HR)(EM) - k_{-1}(HR{\cdot}EM) \quad \text{(Eq. A2)}$$

$$\frac{d(HR{\cdot}EM_2)}{dt} = D_3\frac{\partial^2(HR{\cdot}EM_2)}{\partial\chi^2} + k_2(HR)(EM)^2 - k_{-2}(HR{\cdot}EM_2) \quad \text{(Eq. A3)}$$

where $D_1$, $D_2$, and $D_3$ are the diffusion coefficients of HR, HR·EM, and HR·EM$_2$, respectively.

The mass balance equation for hexylresorcinol becomes:

$$(HR)_T = (HR) + (HR{\cdot}EM) + (HR{\cdot}EM_2) \quad \text{(Eq. A4)}$$

Differentiating with respect to time of Eq. A4 results in:

$$\frac{d(HR)_T}{dt} = \frac{d(HR)}{dt} + \frac{d(HR{\cdot}EM)}{dt} + \frac{d(HR{\cdot}EM_2)}{dt} \quad \text{(Eq. A5)}$$

The combination of Eqs. A1–A3 and A5 results in:

$$\frac{d(HR)_T}{dt} = D_1\frac{\partial^2(HR)}{\partial\chi^2} + D_2\frac{\partial^2(HR{\cdot}EM)}{\partial\chi^2} + D_3\frac{\partial^2(HR{\cdot}EM_2)}{\partial\chi^2} \quad \text{(Eq. A6)}$$

The diffusion coefficient of compounds is very insensitive to their molecular weights and only varies with $\sqrt[3]{1/\text{mol. wt.}}$. The molecular weights of hexylresorcinol, the 1:1 complex, and the 1:2 complex are 194, 440, and 716, respectively, and $\sqrt[3]{1/\text{mol. wt.}}$ values for the three compounds are 0.173, 0.131, and 0.112, respectively. Then $D_1 = D_2 = D_3 = D$, and Eq. A6 can be rewritten as:

$$\frac{d(HR)_T}{dt} = \frac{\partial^2(HR)_T}{\partial\chi^2} \quad \text{(Eq. A7)}$$

For such a system, the concentration profiles that may exist after the lapse of finite time can be drawn (Fig. A1).

As seen from Eqs. A1–A3 and A7 and Fig. A1, the concentration gradients of (HR), (HR·EM), and (HR·EM$_2$) do not give a straight line, but the concentration gradient of (HR)$_T$ gives a straight line and Eq. A8 can be used to calculate the release rate of hexylresorcinol in this system (1):

$$\text{release rate} = \sqrt{DC_s(2A - C_s)} \quad \text{(Eq. A8)}$$

## REFERENCES


(1) T. Higuchi, *J. Pharm. Sci.*, **50**, 874 (1961).

(2) W. I. Higuchi, *ibid.*, **51**, 802 (1962).

(3) J. Surowiecki, *Diss. Pharm. Pharmacol.*, XXIV, **4**, 407 (1972).

(4) J. Ostrenga, J. Haleblian, B. Poulsen, B. Ferrell, N. Mueller, and S. Shastri, *J. Invest. Dermatol.*, **56**, 392 (1971).

(5) C. W. Whitworth, *J. Pharm. Sci.*, **57**, 1540 (1968).

(6) C. W. Whitworth and R. E. Stephenson, *ibid.*, **60**, 48 (1971).

(7) M. Nakano and N. K. Patel, *ibid.*, **59**, 985 (1970).

(8) C. W. Whitworth and C. H. Becker, *ibid.*, **54**, 569 (1965).

(9) B. J. Poulsen, E. Young, V. Coquilla, and M. Katz, *ibid.*, **56**, 928 (1967).

(10) Z. T. Chowhan and R. Pritchard, *ibid.*, **64**, 754 (1975).

(11) P. Singh, S. J. Desai, A. P. Simonelli, and W. I. Higuchi, *ibid.*, **56**, 1548 (1967).

(12) E. Akaho, Ph.D. thesis, University of Kentucky, Lexington, Ky, 1979.

# High-Pressure Liquid Chromatographic Determination of Ibuprofen in Plasma

**ANWER ALI, SYED KAZMI, and FOTIOS M. PLAKOGIANNIS** ˣ

Received April 17, 1980, from the *Division of Pharmaceutics and Industrial Sciences, Arnold & Marie Schwartz College of Pharmacy and Health Sciences, Long Island University, Brooklyn, NY 11201.* Accepted for publication October 1, 1980.

**Abstract** □ A sensitive, simple, and rapid method for the quantitation of ibuprofen in plasma, using 1-(*p*-fluorobenzoyl)-5-methoxy-2-methylindole acetic acid as the internal standard, was developed. The method is based on reversed-phase high-pressure liquid chromatography with a mobile phase containing acetonitrile–0.1 *M* acetic acid (55:45 v/v). The chromatographic elution time was 8.5 min, and ibuprofen quantities as low as 0.1 μg/ml can be assayed. The suitability of the method is demonstrated.

**Keyphrases** □ Ibuprofen—analysis, high-pressure liquid chromatography, plasma □ Anti-inflammatory agents—ibuprofen, high-pressure liquid chromatographic analysis, plasma □ High-pressure liquid chromatography—analysis, ibuprofen in plasma

Ibuprofen is a nonsteroidal anti-inflammatory, antipyretic, and analgesic drug (1, 2) indicated for the relief of signs and symptoms of rheumatoid arthritis, osteoarthritis, and mild to moderate pain.

Relatively few methods are available for the measurement of blood ibuprofen levels. A paper chromatographic method involving separation and subsequent reaction with bromcresol purple was reported (3) but requires ~48 hr for completion. GLC methods, requiring extraction of the drug from plasma and tedious and time-consuming derivatization steps, were also reported (4, 5).

Recently, the use of paired-ion, reversed-phase, high-pressure liquid chromatography (HPLC) for quantitative drug analysis was demonstrated (6, 7). This paper reports a simple, rapid, and highly sensitive HPLC method for ibuprofen determination in plasma.

## EXPERIMENTAL

**Chemicals and Reagents**—Ibuprofen[1] and 1-(*p*-fluorobenzoyl)-5-methoxy-2-methylindole acetic acid[2] were the reference and internal standards, respectively. Chromatographic grade acetonitrile[3] and acetic acid[4] were used for the mobile phase preparation. All other reagents were analytical grade or better and were used as received.

**Animals**—Adult, male New Zealand rabbits, 2–3 kg, were studied.

**Mobile Phase**—Acetonitrile–0.1 *M* acetic acid (55:45 v/v) was used.

**Internal Standard Solution**—Ten milligrams of the internal standard, accurately weighed, was dissolved in a 10-ml volumetric flask and diluted to volume with methanol; this solution (1 ml) was diluted to 20 ml with methanol and used as the internal standard.

**Standard Solution**—Accurately weighed ibuprofen (100 mg) was dissolved in, and diluted to volume with, methanol in a 100-ml volumetric flask.

**Plasma Level Study**—To demonstrate the applicability of the procedure to the determination of plasma ibuprofen levels from a bioavailability study, suppositories containing 150 mg of ibuprofen were administered rectally to three rabbits. Blood samples (~3 ml) were removed by cardiac puncture at 0, 0.25, 0.5, 0.75, 1, 1.5, 2, 3, 4, 5, and 24 hr. The samples were placed into microcentrifuge tubes and centrifuged to obtain the plasma fraction. Plasma aliquots (0.5 ml) were processed along with spiked plasma standards.

For standard curves, blood samples were removed from the heart of nonmedicated rabbits, placed in centrifuge tubes, and centrifuged to obtain the plasma fraction. Plasma aliquots (0.5 ml) were pipetted into microtest tubes and spiked with ibuprofen to yield a final drug concentration of 0.1–50 μg/ml of plasma. To each microtest tube was added 0.1 ml of the internal standard. The mixture was mixed, diluted to 2.0 ml with methanol, and filtered through an organic filter[5].

**HPLC**—Samples were chromatographed on a high-pressure liquid chromatograph[6] equipped with a universal liquid chromatographic in-

**Table I—Recovery of Ibuprofen from Spiked Plasma** [a]

| Amount Added, μg/ml | Ibuprofen Found, % | *SD*, % |
|---|---|---|
| 50 | 100.4 | 0.21 |
| 25 | 99.2 | 0.38 |
| 10 | 98 | 0.98 |
| 5 | 96 | 1.98 |
| 2 | 105 | 2.50 |
| 1 | 104 | 0.80 |
| 0.9 | 95.5 | 0.90 |
| 0.5 | 96 | 0.80 |
| 0.2 | 110 | 0.80 |

[a] Each value is the average of five determinations.

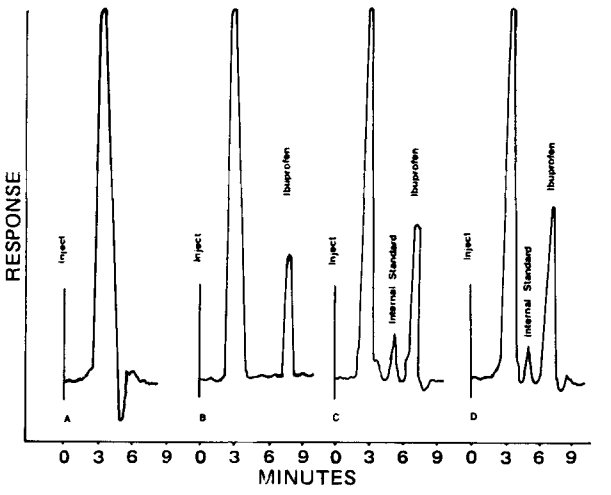


**Figure 1**—*High-pressure liquid chromatograms of blank plasma (A), blank plasma spiked with ibuprofen (B), blank plasma spiked with ibuprofen and the internal standard (C), and plasma obtained 60 min after ibuprofen administration and spiked with the internal standard (D).*

[1] The Upjohn Co, Kalamazoo, Mich.
[2] Merck Sharp & Dohme, West Point, Pa.
[3] Waters Associates, Milford, Mass.
[4] J. T. Baker Chemical Co., West Rochester, N.Y.
[5] Waters Associates, Milford, Mass.
[6] Model 440, Waters Associates, Milford, Mass.



*0022-3549/81/0800-0944$01.00/0*
*© 1981, American Pharmaceutical Association*

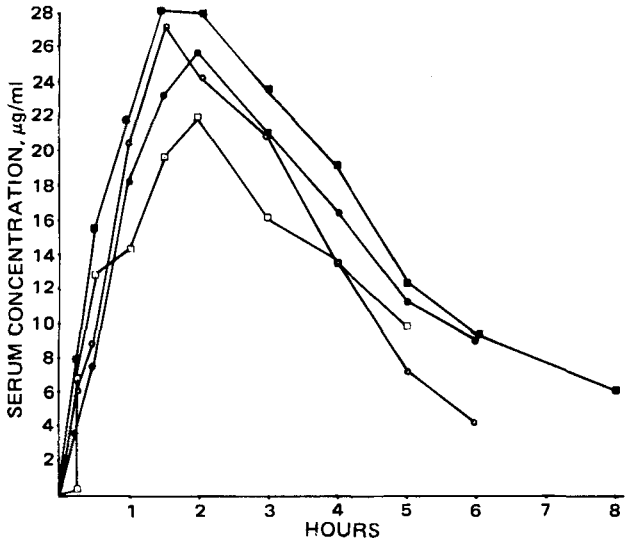


**Figure 2**—*Serum ibuprofen levels after administration of a 150-mg dose of a suppository of three different bases and one oral preparation. Key:* □, *theobroma oil;* ○, *polyethylene glycol 1540;* ●, *fatty acids; and* ■, *suspension.*

jector[5], a UV (254 nm) absorbance detector, and a strip-chart recorder. The deproteinated plasma samples were chromatographed at room temperature on a microparticulate ($\mu$Bondapak $C_{18}$) reversed-phase HPLC column (4 mm × 30 cm) with an eluting mobile phase of acetonitrile—0.1 *M* acetic acid (55:45 v/v). The flow rate was adjusted to 1 ml/min with an inlet pressure of ~1500 psi. The chart speed was 0.2 cm/min. The ratio of the peak height of ibuprofen to that of the internal standard was used to calculate the ibuprofen concentration, based on a calibration curve prepared from spiked plasma samples.

**Calculations**—Peak height ratios were obtained by dividing the peak height of ibuprofen by the peak height of the internal standard. Calibration curves from known ibuprofen concentrations in plasma were prepared by plotting the peak height ratios *versus* the ibuprofen concentration, expressed as micrograms per milliliter of plasma. Values of unknown concentrations of ibuprofen in plasma samples were read directly from the graph.

## RESULTS AND DISCUSSION

Typical chromatograms of blank rabbit plasma (A), blank rabbit plasma spiked with ibuprofen (B), blank rabbit plasma spiked with ibuprofen and internal standard (C), and plasma collected 60 min after administration of 150 mg of ibuprofen in a suppository or oral preparation and spiked with the internal standard (D) are shown in Fig. 1. Ibuprofen and the internal standard were well resolved and eluted with retention times of 8.5 and 5.5 min, respectively. No interference from metabolites was detected under these experimental conditions.

Table I illustrates recoveries of ibuprofen from plasma spiked with 0.1–50 $\mu$g/ml. The standard curve is the average of five determinations; the regression line slope was calculated to be 0.128 with a standard correlation matrix of 0.999, indicating excellent linearity.

The plasma ibuprofen time courses for four rabbits in a bioavailability study are shown in Fig. 2. The *AUC* values for the four formulations were 89.77, 74.38, 96.5, and 128.94 $\mu$g/ml/hr for 150 mg of ibuprofen in polyethylene glycol 1540, theobroma oil, esterified fatty acids ($C_{10}$–$C_{18}$)[7], and an oral suspension, respectively.

## REFERENCES

(1) S. S. Adams, E. E. Cliffe, B. Lessel, and J. S. Nicholson, *J. Pharm. Sci.*, **56**, 1686 (1967).

(2) S. S. Adams, K. F. McCullough, and J. S. Nicholson, *Arch. Int. Pharmacodyn. Ther.*, **178**, 115 (1969).

(3) S. S. Adams and E. E. Cliffe, *J. Pharm. Pharmacol.*, **17**, 173 (1965).

(4) G. Kaiser and J. Vaniessen, *J. Pharm. Sci.*, **63**, 219 (1974).

(5) R. F. N. Mills, S. S. Adams, E. E. Cliffe, W. Dickenson, and J. S. Nicholson, *Xenobiotica*, **3**, 589 (1973).

(6) "Paired Ion Chromatography," Bull. D61, Waters Associates, Milford, Mass., Dec. 1975.

(7) J. L. Day, L. Tterlikkis, R. Niemann, A. Mobley, and C. Spikes, *J. Pharm. Sci.*, **67**, 1027 (1978).

[7] Witepsol H-15, Kay-Fries Chemicals, Montvale, NJ 07645.

# Binding of Prostaglandins $E_1$ (Alprostadil), $E_2$ (Dinoprostone), $F_{1\alpha}$, and $F_{2\alpha}$ (Dinoprost) to Human Serum Proteins

**JOSEPH JUDIS**

Received October 20, 1978, from the *College of Pharmacy, University of Toledo, Toledo, OH 43606.* Accepted for publication January 13, 1981.

**Abstract** □ Prostaglandins $E_1$ (alprostadil), $E_2$ (dinoprostone), $F_{1\alpha}$, and $F_{2\alpha}$ (dinoprost) were characterized in terms of binding to human serum, albumin, γ-globulin II, β-globulin III, α-globulin IV-1, and α-globulin IV-4. By using equilibrium dialysis and tritium-labeled ligands, the percent binding for all four ligands was found to decrease in the following order: human serum, albumin, and α-globulin IV-4. For the other three proteins, the order was not consistent with the four ligands, and <10% binding was observed. In general, prostaglandins $E_1$ and $E_2$ showed a higher percent binding for all fractions than prostaglandins $F_{1\alpha}$ and $F_{2\alpha}$. All four ligands can be characterized as showing significant binding to human serum, albumin, and α-globulin IV-4.

**Keyphrases** □ Prostaglandins—binding to human serum proteins, equilibrium dialysis of radiolabeled prostaglandins □ Protein binding—prostaglandins $E_1$ (alprostadil), $E_2$ (dinoprostone), $F_{1\alpha}$, and $F_{2\alpha}$ (dinoprost) to human serum proteins, equilibrium dialysis of radiolabeled prostaglandins □ Binding, protein—binding of prostaglandins $E_1$ (alprostadil), $E_2$ (dinoprostone), $F_{1\alpha}$, and $F_{2\alpha}$ (dinoprost) to human serum proteins, equilibrium dialysis of radiolabeled prostaglandins □ Equilibrium dialysis—of radiolabeled prostaglandins $E_1$ (alprostadil), $E_2$ (dinoprostone), $F_{1\alpha}$, and $F_{2\alpha}$ (dinoprost) bound to human serum proteins

Since the discovery and description of the prostaglandins, a vast literature has evolved concerning their physiological and pharmacological actions (1). As circulating hormones, these compounds have different rates of disappearance from the circulation after injection. Presumably, the differences reflect differences in metabolic degradation rates (2, 3). The availability of a compound for metabolic degradation could be related to whether or not

0022-3549/81/0800-0945$01.00/0
© 1981, American Pharmaceutical Association

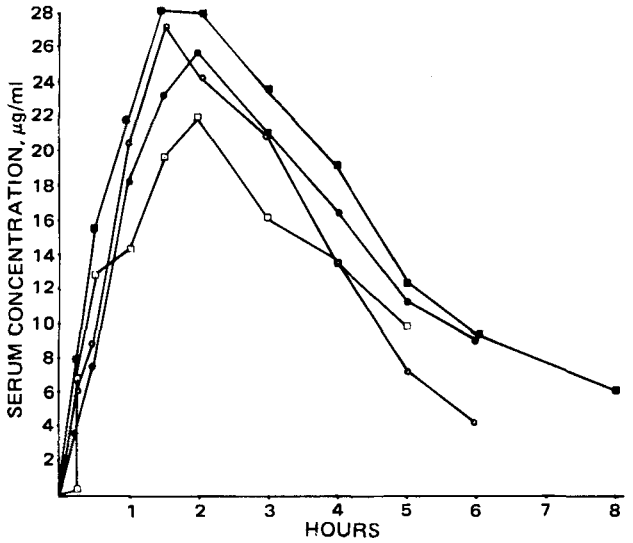


**Figure 2**—*Serum ibuprofen levels after administration of a 150-mg dose of a suppository of three different bases and one oral preparation. Key:* □, *theobroma oil;* ○, *polyethylene glycol 1540;* ●, *fatty acids; and* ■, *suspension.*

jector[5], a UV (254 nm) absorbance detector, and a strip-chart recorder. The deproteinated plasma samples were chromatographed at room temperature on a microparticulate ($\mu$Bondapak $C_{18}$) reversed-phase HPLC column (4 mm × 30 cm) with an eluting mobile phase of acetonitrile—0.1 *M* acetic acid (55:45 v/v). The flow rate was adjusted to 1 ml/min with an inlet pressure of ~1500 psi. The chart speed was 0.2 cm/min. The ratio of the peak height of ibuprofen to that of the internal standard was used to calculate the ibuprofen concentration, based on a calibration curve prepared from spiked plasma samples.

**Calculations**—Peak height ratios were obtained by dividing the peak height of ibuprofen by the peak height of the internal standard. Calibration curves from known ibuprofen concentrations in plasma were prepared by plotting the peak height ratios *versus* the ibuprofen concentration, expressed as micrograms per milliliter of plasma. Values of unknown concentrations of ibuprofen in plasma samples were read directly from the graph.

## RESULTS AND DISCUSSION

Typical chromatograms of blank rabbit plasma (A), blank rabbit plasma spiked with ibuprofen (B), blank rabbit plasma spiked with ibuprofen and internal standard (C), and plasma collected 60 min after administration of 150 mg of ibuprofen in a suppository or oral preparation and spiked with the internal standard (D) are shown in Fig. 1. Ibuprofen and the internal standard were well resolved and eluted with retention times of 8.5 and 5.5 min, respectively. No interference from metabolites was detected under these experimental conditions.

Table I illustrates recoveries of ibuprofen from plasma spiked with 0.1–50 $\mu$g/ml. The standard curve is the average of five determinations; the regression line slope was calculated to be 0.128 with a standard correlation matrix of 0.999, indicating excellent linearity.

The plasma ibuprofen time courses for four rabbits in a bioavailability study are shown in Fig. 2. The *AUC* values for the four formulations were 89.77, 74.38, 96.5, and 128.94 $\mu$g/ml/hr for 150 mg of ibuprofen in polyethylene glycol 1540, theobroma oil, esterified fatty acids ($C_{10}$–$C_{18}$)[7], and an oral suspension, respectively.

## REFERENCES

(1) S. S. Adams, E. E. Cliffe, B. Lessel, and J. S. Nicholson, *J. Pharm. Sci.*, **56**, 1686 (1967).

(2) S. S. Adams, K. F. McCullough, and J. S. Nicholson, *Arch. Int. Pharmacodyn. Ther.*, **178**, 115 (1969).

(3) S. S. Adams and E. E. Cliffe, *J. Pharm. Pharmacol.*, **17**, 173 (1965).

(4) G. Kaiser and J. Vaniessen, *J. Pharm. Sci.*, **63**, 219 (1974).

(5) R. F. N. Mills, S. S. Adams, E. E. Cliffe, W. Dickenson, and J. S. Nicholson, *Xenobiotica*, **3**, 589 (1973).

(6) "Paired Ion Chromatography," Bull. D61, Waters Associates, Milford, Mass., Dec. 1975.

(7) J. L. Day, L. Tterlikkis, R. Niemann, A. Mobley, and C. Spikes, *J. Pharm. Sci.*, **67**, 1027 (1978).

[7] Witepsol H-15, Kay-Fries Chemicals, Montvale, NJ 07645.

# Binding of Prostaglandins $E_1$ (Alprostadil), $E_2$ (Dinoprostone), $F_{1\alpha}$, and $F_{2\alpha}$ (Dinoprost) to Human Serum Proteins

**JOSEPH JUDIS**

Received October 20, 1978, from the *College of Pharmacy, University of Toledo, Toledo, OH 43606.* Accepted for publication January 13, 1981.

**Abstract** □ Prostaglandins $E_1$ (alprostadil), $E_2$ (dinoprostone), $F_{1\alpha}$, and $F_{2\alpha}$ (dinoprost) were characterized in terms of binding to human serum, albumin, γ-globulin II, β-globulin III, α-globulin IV-1, and α-globulin IV-4. By using equilibrium dialysis and tritium-labeled ligands, the percent binding for all four ligands was found to decrease in the following order: human serum, albumin, and α-globulin IV-4. For the other three proteins, the order was not consistent with the four ligands, and <10% binding was observed. In general, prostaglandins $E_1$ and $E_2$ showed a higher percent binding for all fractions than prostaglandins $F_{1\alpha}$ and $F_{2\alpha}$. All four ligands can be characterized as showing significant binding to human serum, albumin, and α-globulin IV-4.

**Keyphrases** □ Prostaglandins—binding to human serum proteins, equilibrium dialysis of radiolabeled prostaglandins □ Protein binding—prostaglandins $E_1$ (alprostadil), $E_2$ (dinoprostone), $F_{1\alpha}$, and $F_{2\alpha}$ (dinoprost) to human serum proteins, equilibrium dialysis of radiolabeled prostaglandins □ Binding, protein—binding of prostaglandins $E_1$ (alprostadil), $E_2$ (dinoprostone), $F_{1\alpha}$, and $F_{2\alpha}$ (dinoprost) to human serum proteins, equilibrium dialysis of radiolabeled prostaglandins □ Equilibrium dialysis—of radiolabeled prostaglandins $E_1$ (alprostadil), $E_2$ (dinoprostone), $F_{1\alpha}$, and $F_{2\alpha}$ (dinoprost) bound to human serum proteins

Since the discovery and description of the prostaglandins, a vast literature has evolved concerning their physiological and pharmacological actions (1). As circulating hormones, these compounds have different rates of disappearance from the circulation after injection. Presumably, the differences reflect differences in metabolic degradation rates (2, 3). The availability of a compound for metabolic degradation could be related to whether or not

0022-3549/81/0800-0945$01.00/0
© 1981, American Pharmaceutical Association

Table I—Binding of [$^3$H]Prostaglandins $E_1$, $E_2$, $F_{1\alpha}$, and $F_{2\alpha}$ to Human Serum Proteins [a]

| Serum Protein | | Percent of Prostaglandin Bound [b] | | | |
|---|---|---|---|---|---|
| Fraction | Concentration, mg/ml | $E_1$ | $E_2$ | $F_{1\alpha}$ | $F_{2\alpha}$ |
| Albumin | 40.0 | 81.40 (0.39) | 71.00 (2.57) | 63.3 (1.48) | 42.4 (0.92) |
| $\alpha$-Globulin IV-1 | 1.0 | 12.5 (0.46) | 8.96 (0.92) | 6.86 (0.29) | 5.13 (0.52) |
| $\alpha$-Globulin IV-4 | 5.0 | 55.00 (0.59) | 26.90 (0.58) | 31.0 (0.52) | 24.10 (2.12) |
| $\beta$-Globulin III | 7.0 | 5.04 (0.21) | 9.13 (0.64) | 3.17 (0.32) | 2.92 (0.15) |
| $\gamma$-Globulin II | 11.0 | 6.17 (0.43) | 7.12 (0.38) | 1.67 (0.12) | 0 |
| Human serum | — | 92.60 (0.09) | 80.10 (0.47) | 76.4 (2.56) | 70.9 (1.29) |

[a] Each system contained a total, in moles, of the following: prostaglandin $E_1$, $2.823 \times 10^{-8}$; prostaglandin $E_2$, $2.84 \times 10^{-8}$; prostaglandin $F_{1\alpha}$, $2.82 \times 10^{-8}$; and prostaglandin $F_{2\alpha}$, $2.83 \times 10^{-8}$. [b] Values in parentheses are standard deviations. Data were obtained using equilibrium dialysis method.

the compound is bound to a serum protein and the tightness of the binding (4). Prostaglandins bind to human plasma proteins, and some bind specifically to human serum albumin (2, 5–8).

Interest in serum protein binding capabilities of prostaglandins has centered on the quantitative analytical techniques in which prostaglandin must be quantitatively extractable from serum (8) and on factors involved in their physicochemical state as circulating hormones (2); knowledge of the latter is basic to the investigation of the pharmacological and pharmacokinetic properties of prostaglandins. Therefore, the percent binding of prostaglandins $E_1$ (alprostadil), $E_2$ (dinoprostone), $F_{1\alpha}$, and $F_{2\alpha}$ (dinoprost) to human serum proteins was examined.

## EXPERIMENTAL

**Methods**—Protein binding was measured using a previously described technique (9). Equilibrium dialysis was used to determine whether binding occurred between a ligand and a specific protein and the percent of ligand bound to the protein. Values reported are the averages of at least three replicates. This concentration range was selected to approximate the range of higher concentrations of prostaglandin $E_1$ used by Unger (8) in albumin binding studies. Radioactivity was determined in a liquid scintillation system[1].

**Materials**—[5,6-$^3$H(N)]Prostaglandin $E_1$[2], [5,6,8,11,12,14,15-$^3$H(N)]prostaglandin $E_2$[2], [5,6-$^3$H(N)]prostaglandin $F_{1\alpha}$[3], and [9-$^3$H]-prostaglandin $F_{2\alpha}$[3] had specific activities of 89.5, 117, 40, and 15 Ci/mmole, respectively. Crystalline human serum albumin and other human serum proteins were used as received[4]. A xylene-based phosphor solution[5] was used in all radioactivity determinations, and all other chemicals were reagent grade. Radiopurity was rechecked prior to use utilizing the methods indicated by the suppliers. A radiopurity of 99% was the minimum acceptable.

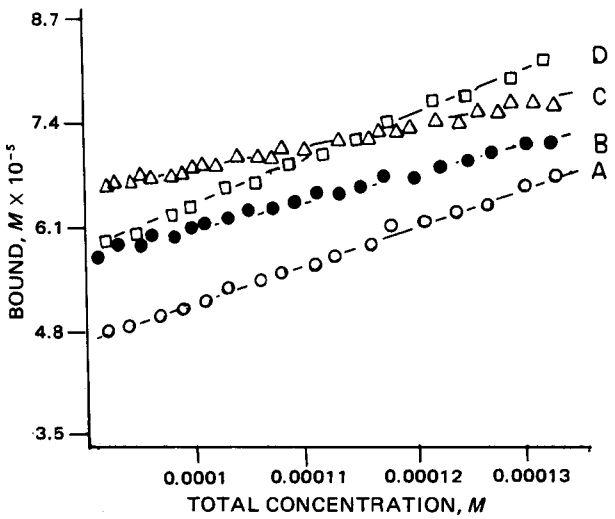


**Figure 1**—*Total concentration of ligand in the system* versus *bound concentration. Albumin concentration was 5.797 × $10^{-4}$ mole (40 mg/ml). Key: A, prostaglandin $F_{2\alpha}$; B, prostaglandin $F_{1\alpha}$; C, prostaglandin $E_1$; and D, prostaglandin $E_2$.*

## RESULTS AND DISCUSSION

The extent to which each prostaglandin was bound to whole human serum and several human serum proteins or fractions is tabulated in Table I. All four prostaglandins were bound to a significant extent (>70% binding) to whole human serum, and prostaglandins $E_1$ and $E_2$ were bound to a higher percentage than prostaglandins $F_{1\alpha}$ and $F_{2\alpha}$. This finding is in agreement with previous studies (5, 6) in which the affinity of prostaglandins for serum proteins decreased with an increase in the number of polar groups in the prostaglandin molecule.

The serum protein to which binding was greatest for all four compounds was albumin. All prostaglandins showed the next highest affinity for $\alpha$-globulin IV-4 and a relatively low affinity for the other serum protein fractions. $\alpha$-Globulin IV-4 contains corticosteroid binding globulin (10); although the latter protein cannot necessarily be implicated in the binding of prostaglandins to $\alpha$-globulin IV-4, the nonpolar nature of corticosteroids and prostaglandins suggests its possible involvement. Evidence for a prostaglandin $A_1$ binding protein in human plasma other than albumin has been presented (11).

There was a significant difference in the affinity of the E prostaglandins for human serum albumin compared to the F prostaglandins. With all four prostaglandins, the concentration of bound ligand increased in relation to the total ligand concentration in the system (Fig. 1).

Under the study conditions, prostaglandin instability was not a factor as demonstrated by Karim *et al.* (12). Membrane binding was determined in all experiments and was uniformly <5%. At least 95% of the counts per minute added could always be accounted for in the sum of the counts per minute in both sides of an equilibrium cell, indicating no significant binding to the plexiglass.

## REFERENCES

(1) "Prostaglandins: Physiological, Pharmacological and Pathological Aspects," S. Karim, Ed., University Park Press, Baltimore, Md., 1976.

(2) A. Raz, *Biochim. Biophys. Acta*, **280**, 602 (1972).

(3) H. Polet and L. Levine, *J. Biol. Chem.*, **250**, 351 (1975).

(4) M. Duchesne, A. Attallah, and J. B. Lee, *Biochem. Biophys. Res. Commun.*, **64**, 196 (1975).

(5) A. Atallah and G. C. Schussler, *Prostaglandins*, **4**, 479 (1973).

(6) A. Raz, *Biochem. J.*, **130**, 631 (1972).

(7) J. Gueriguian, *J. Pharmacol. Exp. Ther.*, **197**, 391 (1976).

(8) W. Unger, *J. Pharm. Pharmacol.*, **24**, 470 (1972).

(9) J. Judis, *J. Pharm. Sci.*, **66**, 802 (1977).

(10) U. Westphal, "Steroid–Protein Interactions," Springer–Verlag, New York, N.Y., 1971, p. 97.

(11) J. Gueriguian, *Fed. Proc. Fed. Am. Soc. Exp. Biol.*, **34**, 790 (1975).

(12) S. Karim, J. Devlin, and E. Hillier, *Eur. J. Pharmacol.*, **4**, 416 (1968).

## ACKNOWLEDGMENTS

The technical assistance of Mrs. Virginia Matusek is gratefully acknowledged.

[1] Beckman model LS-133.
[2] New England Nuclear Corp.
[3] Amersham Corp.
[4] ICN Life Sciences Group.
[5] PCS, Amersham Corp.

# Hepatic First-Pass Effect of Thiazinamium Methylsulfate (*N*-Methylpromethazine Methylsulfate) in Dogs

**JAN H. G. JONKMAN** *‡x, **HERMAN G. M. WESTENBERG** *§, and **EPPO VAN DER KLEYN** ¶

Received July 16, 1980, from the *Department of Pharmaceutical and Analytical Chemistry, State University of Groningen, Antonius Deusinglaan 2, 9713 AW Groningen, The Netherlands, the ‡Laboratory for Drug Analysis, Assen, The Netherlands, the §Department of Psychiatry, Academic Hospital, Utrecht, The Netherlands, and the ¶Department of Clinical Pharmacy, St. Radboud Hospital, University of Nijmegen, Nijmegen, The Netherlands. Accepted for publication January 26, 1981.

**Abstract** □ Plasma concentration–time curves are described for the intravenous infusion and portal vein infusion of the quaternary ammonium compound thiazinamium methylsulfate to dogs. Comparison of areas under the curve indicate that hepatic first-pass elimination occurred on the order of 25–50%.

**Keyphrases** □ Thiazinamium methylsulfate—hepatic first-pass effect in dogs, plasma concentration–time curves □ *N*-Methylpromethazine methylsulfate—hepatic first-pass effect in dogs, plasma concentration–time curves □ First-pass effect—thiazinamium methylsulfate, dogs, plasma concentration–time curves

Numerous drugs representing several therapeutic groups and chemical classes have been reported to be subject to either intestinal first-pass effect or hepatic first-pass effect (1–4). However, no evidence could be obtained from the literature concerning this phenomenon for quaternary ammonium compounds.

Recently, clinical pharmacokinetic studies on thiazinamium methylsulfate (*N*-methylpromethazine methylsulfate, I), a phenothiazine derivative containing a quaternary ammonium group, were reported (5–7). The drug has anticholinergic and antihistaminic properties and is used as a bronchodilator in patients suffering from generalized chronic obstructive lung diseases.

Absorption of the drug after oral administration was low (~10% of the dose), and considerable inter- and intrasubject variations in bioavailability were found. Such variations are often explained by the hepatic first-pass effect (8). The extent of a hepatic first-pass effect is often related to hepatic clearance (9). Since I is cleared largely by the liver (10), it was decided to investigate whether the hepatic first-pass effect also contributes to its incomplete bioavailability in the dog.

## EXPERIMENTAL

Dogs (Table I) were anesthetized by intravenous injection of pentobarbital sodium (30 mg/kg). Anesthesia was maintained by inhalation of oxygen, nitrous oxide, and halothane[1]. Each dog was used in two experiments with an interval of ~2 weeks.

In the first experiment, a slow continuous infusion of thiazinamium methylsulfate[2] (I) in sterile physiological salt solution was given in the vena cephalica antebrachii sinister for 100 min by pump (20 ml/hr). The dose rate was 1 mg/kg/hr. During and after the infusion, blood samples (~6 ml) were taken from the vena saphena parva dexter by a permanent cannula[3] at the time intervals indicated in Fig. 1.

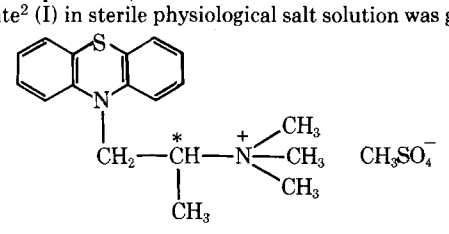

I

In the second experiment, the same procedure was repeated but the infusion was given in the vena porta (portal vein). The abdomen was opened, and a cannula was inserted *via* a side branch.

Plasma concentrations were determined by ion-pair extraction, followed by GLC separation and alkali flame-ionization detection (11).

The area under the plasma concentration–time curve (*AUC*) was measured by cutting and weighing a standard high-quality paper. The absolute bioavailability was calculated by dividing the *AUC* after portal vein infusion by the *AUC* after the intravenous infusion and was expressed as a percentage.

The pharmacokinetic parameters were calculated using the NONLIN program (12). A three-compartment body model was used, with zero-order input in the central compartment and final elimination from this compartment. The initial estimates of the parameters were determined graphically. Examination of the plot of the weighted residuals against time indicated that a weighting factor of $W = 1/\sqrt{y_i}$ resulted in the best fit.

**Table I—Data for the Four Dogs Used in the Experiment with Linear Infusion of I in the Portal Vein**

| Parameter | Dog 268 | Dog 343 | Dog 367 | Dog 515 |
|---|---|---|---|---|
| Breed | Labrador | Dalmatian | Labrador | Labrador |
| Sex | Female | Male | Female | Male |
| Weight, kg | 22 | 26 | 19 | 24 |
| Dose, mg/kg/hr | 1 | 1 | 1 | 1 |
| $F_{abs}$[a], % | 72.0 | 78.0 | 51.0 | 51.7 |

[a] Absolute bioavailability is expressed as a percentage of the dose.

## RESULTS AND DISCUSSION

The hepatic elimination of thiazinamium methylsulfate (I) during the first passage through the liver was investigated by determining the absolute bioavailability obtained after infusion of a drug-containing solution in the portal vein. In this way, the intestinal first-pass effect and the observed irregular and incomplete absorption were avoided. After intravenous infusion, plasma concentrations of ~600 ng/ml were obtained. After the infusion was stopped, plasma concentrations fell steeply (Fig. 1). The $(t_{1/2})_\alpha$ was estimated to be ~1 min, and the $(t_{1/2})_\beta$ was ~5–10 min; $(t_{1/2})_\gamma$, the elimination half-life, was ~6–7 hr. These figures should be considered as estimations because of the very steep decrease in plasma concentrations immediately after the infusion was stopped and the very low concentrations during the final elimination phase.

Studies in rats (10) indicated that the extremely rapid disappearance of the drug from the plasma was mainly due to both fast biliary elimination of the unchanged drug (3.8% of the dose) and rapid biotransformation to thiazinamium sulfoxide, which also can be excreted rapidly in the bile (16.1% of the dose). Two other metabolites also were excreted in bile (13.1 and 2.7% of the dose).

A substantial part of the dose in humans also was excreted in the bile [16.6% unchanged and 6.9% as the sulfoxide (13)].

After infusion in the portal vein, the plasma concentration–time curve rose somewhat slower than in the intravenous infusion. In Dogs 343 and 367, the plasma concentration–time curves reached a plateau level of

[1] Fluothane.
[2] Specia, Rhône Poulenc, Paris.
[3] Braunule, B. Braun, Melsungen, West Germany.

0022-3549/81/0800-0947$01.00/0
© 1981, American Pharmaceutical Association

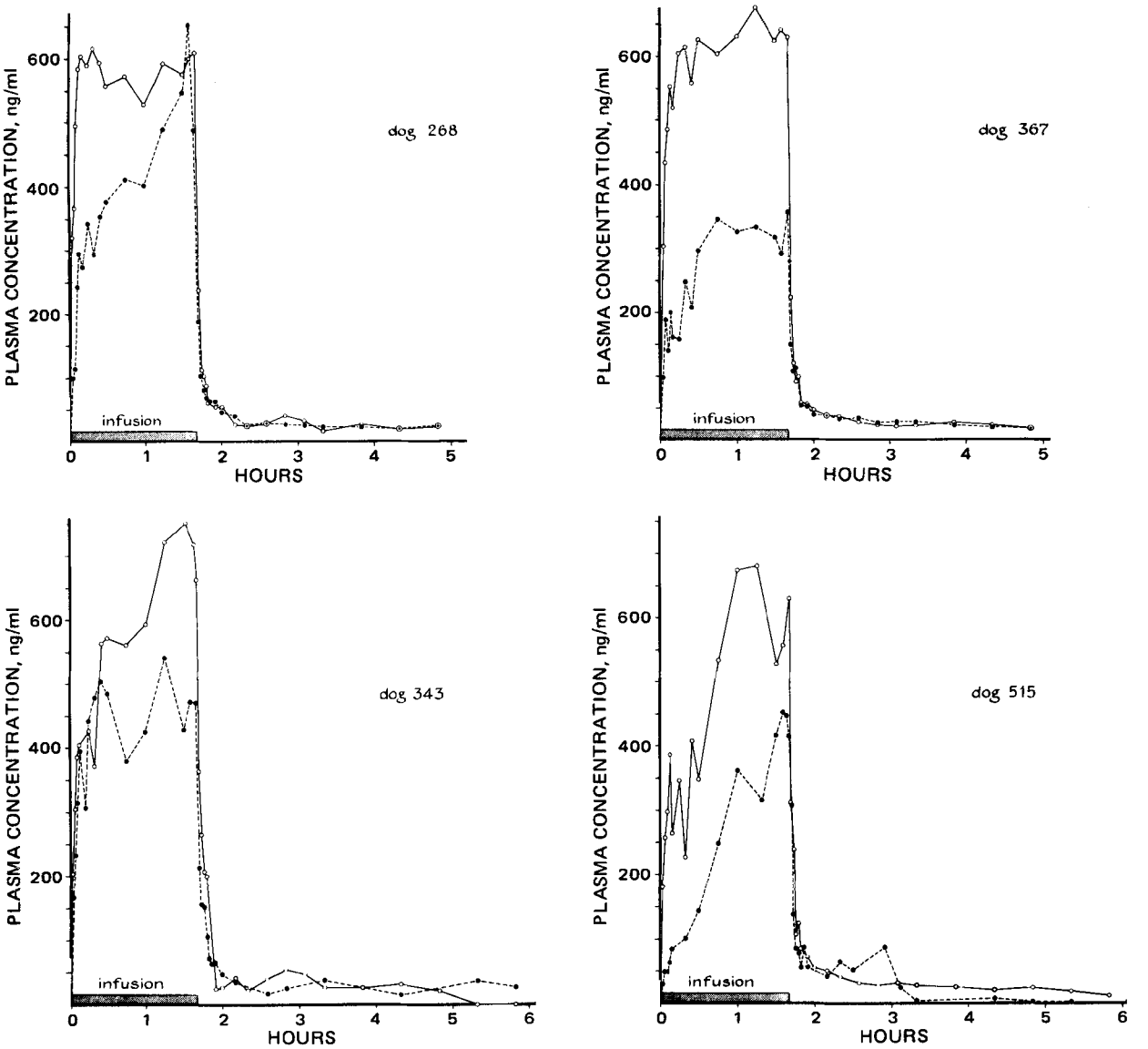


**Figure 1**—*Plasma concentrations in dogs during and after the infusion (1 mg/kg/hr) of I. Key: o—, intravenous infusion; and ●– –, infusion in portal vein.*

~300–400 ng/ml. The phenomenon can be explained by assuming that a substantial part of the drug offered to the liver by portal blood flow is extracted by this organ before the drug can enter the general circulation.

For Dogs 268 and 515, the curve was still going up at the end of the infusion time, suggesting that the biotransformation and/or elimination processes in the liver became saturated and were no longer able to remove the drug from the portal vein to the same extent as before.

The calculated absolute bioavailability ($F_{abs}$) after infusion in the portal vein varied from 51.0 to 78.0% (mean 63.2 ± 13.9 *SD*%), indicating a hepatic first-pass effect that removed 22.0–49.0% (mean 37.8 ± 14.9 *SD*%) of the dose before entering the general circulation.

Oguma *et al.* (14) found that, when valethamate bromide or scopolamine-*N*-butyl bromide (both quaternary ammonium compounds) was infused in the portal vein in the rat, biliary excretion was more pronounced than when infusion was given in a femoral vein. This result is an indirect indication of a hepatic first-pass effect. Gibaldi *et al.* (15) studied the metabolism of *N*,*N*-bis(phenylcarbamoylmethyl)dimethylammonium chloride, a quaternized lidocaine derivative, after intravenous and intraperitoneal administration and found that, during passage of drug through the liver after intraperitoneal administration, a fraction of the dose was irreversibly lost by metabolic conversion and subsequent biliary excretion (hepatic first-pass effect).

The results of this study on I are comparable with the observations of Taylor *et al.* (16) on the tertiary analog promethazine in rabbits. They reported a systemic availability of 59 ± 19% after promethazine injection into the portal vein. Although a different species is involved, the indication is that both the tertiary and the quaternary compound can be subjected extensively to a hepatic first-pass effect.

The results of the present study indicate that the low and variable bioavailability of an oral dose of I can be explained in part by an extensive hepatic first-pass effect.

## REFERENCES

(1) C. Jacquot, J. Cariou, J. R. Rapin, and Y. Cohen, in "Formulations and Preparations of Dosage Forms," J. Polderman, Ed., Elsevier, Amsterdam, The Netherlands, 1977, pp. 153–169.

(2) J. Caldwell and R. L. Smith, in *ibid.*, pp. 169–181.

(3) A. Bieder and J. Gaillot, in *ibid.*, pp. 181–195.

(4) M. Mayersohn, in "Principles and Perspectives in Drug Bioavailability," J. Blanchard, R. J. Sawchuk, and B. B. Brodie, Eds., S. Karger, Basel, Switzerland, 1979, pp. 248–255.

(5) J. H. G. Jonkman, L. E. van Bork, J. Wijsbeek, R. A. de Zeeuw, and N. G. M. Orie, *Clin. Pharmacol. Ther.*, **21**, 457 (1977).

(6) J. H. G. Jonkman, L. E. van Bork, J. Wijsbeek, A. S. Bolhuis-de Vries, R. A. de Zeeuw, N. G. M. Orie, and H. L. M. Cox, *J. Pharm. Sci.*, **68**, 69 (1979).

(7) J. H. G. Jonkman, L. E. van Bork, J. Wijsbeek, A. S. Bolhuis-de Vries, R. A. de Zeeuw, N. G. M. Orie, and H. L. M. Cox, *Int. J. Pharm.*, **3**, 55 (1979).

(8) J. T. Wilson, G. T. Atwood, and D. G. Shand, *Clin. Pharmacol.*

*Ther.*, **19**, 264 (1976).
(9) M. Rowland, *J. Pharm. Sci.*, **61**, 70 (1972).
(10) K. Neef, J. H. G. Jonkman, and D. K. F. Meyer, *ibid.*, **67**, 1147 (1978).
(11) J. H. G. Jonkman, J. Wijsbeek, S. Hollenbeek Brouwer-de Boer, R. A. de Zeeuw, L. E. van Bork, and N. G. M. Orie, *J. Pharm. Pharmacol.*, **27**, 849 (1975).
(12) C. M. Metzler, G. L. Elfring, and A. J. McEwen in "A Users Manual for NONLIN and Associated Programs," Upjohn Co., Kalamazoo, Mich., 1974.
(13) J. H. G. Jonkman, Ph.D. thesis, State University of Groningen, Groningen, The Netherlands, 1977.
(14) T. Oguma, T. Muramatsu, T. Iga, T. Fuwa, S. Awazu, and M. Hanano, *Chem. Pharm. Bull.*, **21**, 1554 (1973).
(15) M. Gibaldi, J. E. Axelson, and W. D. Conway, *J. Pharm. Sci.*, **64**, 359 (1975).
(16) G. Taylor and J. B. Houston, *J. Pharm. Pharmacol., Suppl.*, **31**, 40P (1979).

### ACKNOWLEDGMENTS

The authors are indebted to T. H. M. Arts, A. J. Peters, and P. G. H. Philips (Central Animal Laboratory, St. Radboud Hospital, University of Nijmegen) for technical assistance, and they gratefully acknowledge J. Konings (University of Nijmegen) for preparation of the illustrations.

# High-Performance Liquid Chromatographic Analysis of Triamterene and *p*-Hydroxytriamterene in Plasma

**GERALD J. YAKATAN *x and JOSEF E. CRUZ**

Received September 24, 1980, from the *Drug Dynamics Institute, College of Pharmacy, University of Texas at Austin, Austin, TX 78712.* Accepted for publication January 23, 1981. *Present address: Pharmaceutical Research Division, Warner-Lambert Company, Ann Arbor, MI 48105.

**Abstract** □ A rapid and sensitive high-performance liquid chromatographic assay was developed for triamterene and 6-*p*-hydroxytriamterene in plasma. Plasma (0.5 ml), after addition of the internal standard, was extracted with 10 ml of ether–isopropanol (95:5). After thorough mixing and separation of phases, the organic layer was evaporated to dryness under nitrogen. The residue was reconstituted with 500 μl of mobile phase [acetonitrile–water–acetic acid (60:39.5:0.5)], and 100 μl was injected into the chromatograph. Chromatographic separation was carried out on a $C_{18}$ μBondapak column at a flow rate of 1 ml/min. Detection of compounds in the column eluent was by UV absorption at 365 nm. The retention times for 6-*p*-hydroxytriamterene, triamterene, and the internal standard were 7.5, 9.0, and 12.0 min, respectively. The lower limit of detection for each compound was 20 ng/ml. Recoveries of triamterene and 6-*p*-hydroxytriamterene were 91–99 and 82–95%, respectively, over a 40–240-ng/ml range.

**Keyphrases** □ Triamterene—high-performance liquid chromatographic analysis, plasma □ *p*-Hydroxytriamterene—high-performance liquid chromatographic analysis, plasma □ Diuretics—high-performance liquid chromatographic analysis of triamterene and *p*-hydroxytriamterene, plasma □ High-performance liquid chromatographic analysis—triamterene and *p*-hydroxytriamterene, plasma

Triamterene, 2,4,7-triamino-6-phenylpteridine (I), is a natriuretic and a potassium-sparing diuretic. It is used mainly in combination with hydrochlorothiazide in the treatment of edema associated with congestive heart failure, cirrhosis of the liver, and the nephrotic syndrome.

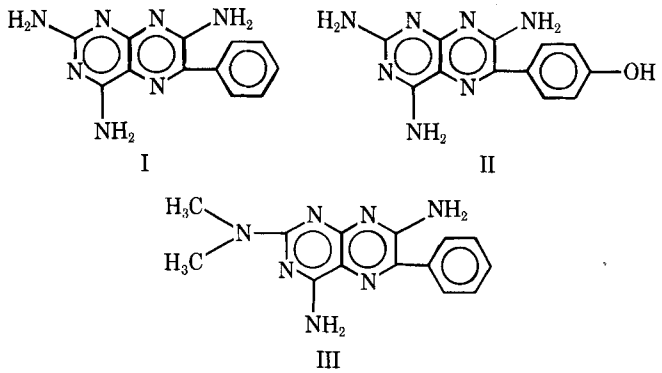

I



II



III

## BACKGROUND

Studies of plasma and urine concentrations of triamterene and its major metabolite, 2,4,7-triamino-6-*p*-hydroxyphenylpteridine (II), in humans and animals have been performed either with nonspecific fluorescence methods or more specific methods that require time-consuming and involved separation procedures (1–5). The separation techniques utilized have included paper chromatography (4), TLC (5), and liquid–liquid extraction (2, 6). One method (5) detected nanogram levels of the compounds, but the other methods lacked the sensitivity to measure nanogram concentrations of triamterene in plasma. A sensitive and specific assay is particularly desirable for study of triamterene pharmacokinetics since concentrations of the metabolite may be 10-fold those of the parent compound 30 min following oral administration (2).

Recently, two high-performance liquid chromatographic (HPLC) assays for triamterene in plasma were reported. One method (7) involved extraction of triamterene as its perchlorate ion-pair and subsequent normal-phase HPLC utilizing a fluorescence detector. Triamterene concentrations as low as 2 ng/ml could be detected, although the investigators did not employ an internal standard. The other method (8) involved extraction with ethyl acetate and subsequent reversed-phase HPLC with fluorescence detection; it had a sensitivity to 1 ng/ml. Neither research group attempted to quantitate metabolites.

This article describes a rapid, sensitive, and selective assay for triamterene and its major metabolite in plasma. The method involves a simple extraction of plasma with organic solvent and reversed-phase HPLC of the extract using UV detection.

## EXPERIMENTAL

**Reagents**—Acetonitrile[1] and methanol[1] were chromatography grade. Anhydrous ether[2], acetic acid[2], and isopropanol[2] were spectranalytical grade.

**Equipment**—A high-performance liquid chromatograph[3] with a syringe-loading sample injector[4], a recorder[5], and a variable-wavelength

[1] MCB Manufacturing Chemists Inc., Cincinnati, Ohio.
[2] Fisher Scientific Co., Fair Lawn, N.J.
[3] Tracor 950 chromatographic pump, Tracor Instruments, Austin, Tex.
[4] Model 7120, Rheodyne, Berkeley, Calif.
[5] OmniScribe, Houston Instruments, Austin, Tex.

0022-3549/81/0800-0949$01.00/0
© 1981, American Pharmaceutical Association

*Ther.*, **19**, 264 (1976).
(9) M. Rowland, *J. Pharm. Sci.*, **61**, 70 (1972).
(10) K. Neef, J. H. G. Jonkman, and D. K. F. Meyer, *ibid.*, **67**, 1147 (1978).
(11) J. H. G. Jonkman, J. Wijsbeek, S. Hollenbeek Brouwer-de Boer, R. A. de Zeeuw, L. E. van Bork, and N. G. M. Orie, *J. Pharm. Pharmacol.*, **27**, 849 (1975).
(12) C. M. Metzler, G. L. Elfring, and A. J. McEwen in "A Users Manual for NONLIN and Associated Programs," Upjohn Co., Kalamazoo, Mich., 1974.
(13) J. H. G. Jonkman, Ph.D. thesis, State University of Groningen, Groningen, The Netherlands, 1977.
(14) T. Oguma, T. Muramatsu, T. Iga, T. Fuwa, S. Awazu, and M. Hanano, *Chem. Pharm. Bull.*, **21**, 1554 (1973).
(15) M. Gibaldi, J. E. Axelson, and W. D. Conway, *J. Pharm. Sci.*, **64**, 359 (1975).
(16) G. Taylor and J. B. Houston, *J. Pharm. Pharmacol., Suppl.*, **31**, 40P (1979).

### ACKNOWLEDGMENTS

The authors are indebted to T. H. M. Arts, A. J. Peters, and P. G. H. Philips (Central Animal Laboratory, St. Radboud Hospital, University of Nijmegen) for technical assistance, and they gratefully acknowledge J. Konings (University of Nijmegen) for preparation of the illustrations.

# High-Performance Liquid Chromatographic Analysis of Triamterene and *p*-Hydroxytriamterene in Plasma

**GERALD J. YAKATAN *x and JOSEF E. CRUZ**

Received September 24, 1980, from the *Drug Dynamics Institute, College of Pharmacy, University of Texas at Austin, Austin, TX 78712.* Accepted for publication January 23, 1981. *Present address: Pharmaceutical Research Division, Warner-Lambert Company, Ann Arbor, MI 48105.

**Abstract** □ A rapid and sensitive high-performance liquid chromatographic assay was developed for triamterene and 6-*p*-hydroxytriamterene in plasma. Plasma (0.5 ml), after addition of the internal standard, was extracted with 10 ml of ether–isopropanol (95:5). After thorough mixing and separation of phases, the organic layer was evaporated to dryness under nitrogen. The residue was reconstituted with 500 μl of mobile phase [acetonitrile–water–acetic acid (60:39.5:0.5)], and 100 μl was injected into the chromatograph. Chromatographic separation was carried out on a $C_{18}$ μBondapak column at a flow rate of 1 ml/min. Detection of compounds in the column eluent was by UV absorption at 365 nm. The retention times for 6-*p*-hydroxytriamterene, triamterene, and the internal standard were 7.5, 9.0, and 12.0 min, respectively. The lower limit of detection for each compound was 20 ng/ml. Recoveries of triamterene and 6-*p*-hydroxytriamterene were 91–99 and 82–95%, respectively, over a 40–240-ng/ml range.

**Keyphrases** □ Triamterene—high-performance liquid chromatographic analysis, plasma □ *p*-Hydroxytriamterene—high-performance liquid chromatographic analysis, plasma □ Diuretics—high-performance liquid chromatographic analysis of triamterene and *p*-hydroxytriamterene, plasma □ High-performance liquid chromatographic analysis—triamterene and *p*-hydroxytriamterene, plasma

Triamterene, 2,4,7-triamino-6-phenylpteridine (I), is a natriuretic and a potassium-sparing diuretic. It is used mainly in combination with hydrochlorothiazide in the treatment of edema associated with congestive heart failure, cirrhosis of the liver, and the nephrotic syndrome.

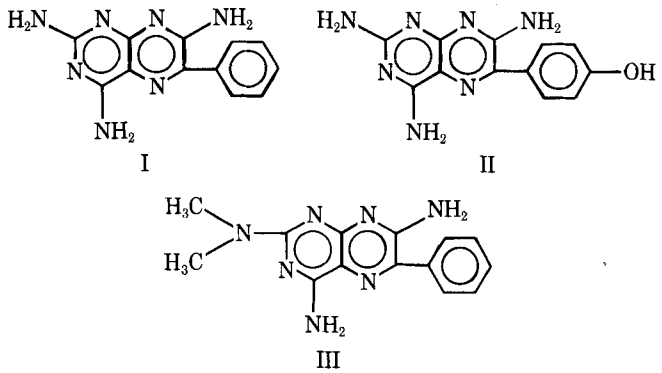

I



II



III

## BACKGROUND

Studies of plasma and urine concentrations of triamterene and its major metabolite, 2,4,7-triamino-6-*p*-hydroxyphenylpteridine (II), in humans and animals have been performed either with nonspecific fluorescence methods or more specific methods that require time-consuming and involved separation procedures (1–5). The separation techniques utilized have included paper chromatography (4), TLC (5), and liquid–liquid extraction (2, 6). One method (5) detected nanogram levels of the compounds, but the other methods lacked the sensitivity to measure nanogram concentrations of triamterene in plasma. A sensitive and specific assay is particularly desirable for study of triamterene pharmacokinetics since concentrations of the metabolite may be 10-fold those of the parent compound 30 min following oral administration (2).

Recently, two high-performance liquid chromatographic (HPLC) assays for triamterene in plasma were reported. One method (7) involved extraction of triamterene as its perchlorate ion-pair and subsequent normal-phase HPLC utilizing a fluorescence detector. Triamterene concentrations as low as 2 ng/ml could be detected, although the investigators did not employ an internal standard. The other method (8) involved extraction with ethyl acetate and subsequent reversed-phase HPLC with fluorescence detection; it had a sensitivity to 1 ng/ml. Neither research group attempted to quantitate metabolites.

This article describes a rapid, sensitive, and selective assay for triamterene and its major metabolite in plasma. The method involves a simple extraction of plasma with organic solvent and reversed-phase HPLC of the extract using UV detection.

## EXPERIMENTAL

**Reagents**—Acetonitrile[1] and methanol[1] were chromatography grade. Anhydrous ether[2], acetic acid[2], and isopropanol[2] were spectranalytical grade.

**Equipment**—A high-performance liquid chromatograph[3] with a syringe-loading sample injector[4], a recorder[5], and a variable-wavelength

[1] MCB Manufacturing Chemists Inc., Cincinnati, Ohio.
[2] Fisher Scientific Co., Fair Lawn, N.J.
[3] Tracor 950 chromatographic pump, Tracor Instruments, Austin, Tex.
[4] Model 7120, Rheodyne, Berkeley, Calif.
[5] OmniScribe, Houston Instruments, Austin, Tex.

0022-3549/81/0800-0949$01.00/0
© 1981, American Pharmaceutical Association

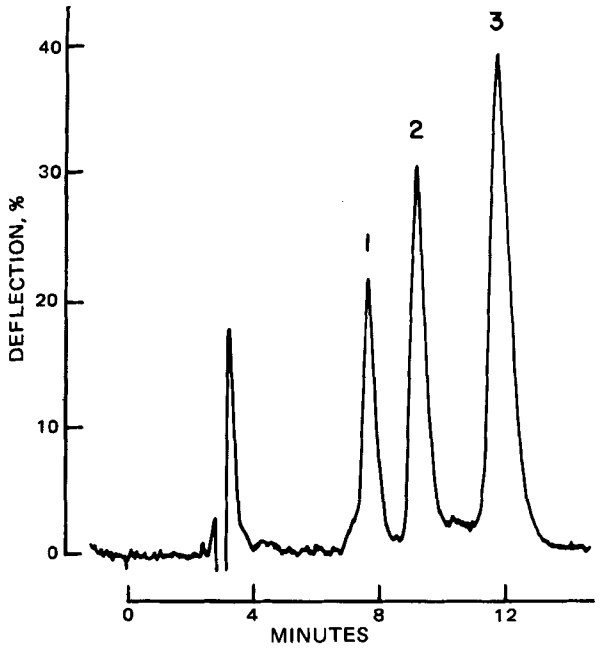


**Figure 1**—*Chromatogram of the extract of 0.5 ml of plasma containing 100 ng/ml each of 6-p-hydroxytriamterene (1) and triamterene (2) and 200 ng/ml of the internal standard (3). The extract was reconstituted with 500 μl of mobile phase, and 100 μl was injected.*

UV detector[6] were used. Chromatography was done on a μBondapak $C_{18}$ column[7].

**Assay Standards**—Stock methanol solutions of triamterene[8] (1 mg/100 ml), 6-*p*-hydroxytriamterene[9] (1 mg/100 ml), and the internal standard[8], 4,7-diamino-2-dimethylamino-6-phenylpteridine (1 mg/100 ml), were prepared and stored in light-resistant flasks to prevent photodecomposition. Plasma standards were prepared by adding appropriate amounts of methanol stock solutions to drug-free plasma to give final concentrations of 40–240 ng/ml of triamterene and 6-*p*-hydroxytriamterene and 200 ng/ml of the internal standard.

**Extraction**—To 0.5 ml of plasma in a silylated tube, 10 ml of anhydrous ether–isopropanol (95:5) was added. The tube contents were mixed with gentle agitation in an aliquot mixer[10] for 10 min and then centrifuged[11] for 20 min at 1300×*g* to separate the phases. The ether–isopropanol layer (top layer) was transferred to a sample concentrator[12] with a disposable Pasteur pipet and evaporated to dryness under nitrogen at ambient temperature. The dried extract was reconstituted with 500 μl of mobile phase, and 100 μl was injected into the chromatograph.

**Chromatography**—All chromatography was done at ambient temperature. The mobile phase was acetonitrile–distilled water–acetic acid (60:39.5:0.5). Prior to use, the mobile phase was filtered through a 10-μm polypropylene filter[13]. The flow rate was set at 1 ml/min, and the UV detector was set at 365 nm. The $\lambda_{max}$ values for triamterene, 6-*p*-hydroxytriamterene, and 4,7-diamino-2-dimethylamino-6-phenylpteridine were 365, 368, and 380 nm, respectively. The recorder was run at a chart speed of 0.635 cm/min.

**Quantitation**—Peak height ratios of triamterene or 6-*p*-hydroxytriamterene to the internal standard were obtained from the chromatograms and plotted against concentration or amount of drug to obtain calibration curves for each compound.

## RESULTS AND DISCUSSION

6-*p*-Hydroxytriamterene, triamterene, and the internal standard were separated and eluted in ~12 min; the retention times were 7.5, 9.0, and 12.0 min, respectively (Fig. 1). Extracts from blank plasma gave no interference from endogenous plasma components.

[6] Tracor 970, Tracor Instruments, Austin, Tex.
[7] Waters Associates, Milford, Mass.
[8] Smith Kline and French Laboratories, Philadelphia, Pa.
[9] Rohm & Haas, GmblH., Darmstadt, West Germany.
[10] Model 4651, Ames, Division of Miles Laboratories, Elkhart, Ind.
[11] Model TJ-6 centrifuge, Beckman Instruments, Palo Alto, Calif.
[12] Model SC/27R, Brinkmann Instruments, Westbury, N.Y.
[13] Gelman Filtration Products, Ann Arbor, Mich.

**Table I—Reproducibility of HPLC Assay of Triamterene and *p*-Hydroxytriamterene in Plasma**

| Concentration, ng/ml | Mean Peak Height Ratio | Mean Peak Height Ratio / Concentration | *RSD*, % |
|---|---|---|---|
| | Triamterene ($n$ = 5) | | |
| 40 | 0.1413 | 0.0035 | 6.44 |
| 80 | 0.2914 | 0.0036 | 8.44 |
| 120 | 0.4071 | 0.0034 | 7.30 |
| 200 | 0.6175 | 0.0031 | 7.37 |
| 240 | 0.8044 | 0.0034 | 2.86 |
| | 6-*p*-Hydroxytriamterene ($n$ = 4) | | |
| 40 | 0.0972 | 0.0024 | 18.88 |
| 80 | 0.2124 | 0.0026 | 5.84 |
| 120 | 0.2902 | 0.0024 | 4.56 |
| 200 | 0.4539 | 0.0023 | 7.45 |
| 240 | 0.5895 | 0.0025 | 5.45 |

Standard curves for both triamterene and 6-*p*-hydroxytriamterene were linear over the 40–240-ng/ml range. At least 20 ng/ml of each component could be detected when the dried plasma extract was reconstituted with 100 μl of mobile phase and most of the extract was injected into the chromatograph. The least-squares linear regression curves did not go through the origin, but the mean $y$ intercepts were not significantly different from zero (0.0099 for 6-*p*-hydroxytriamterene and 0.0235 for triamterene). Table I shows standard curve reproducibility for both triamterene and 6-*p*-hydroxytriamterene from analyses of plasma standards done on different days. By using the equations obtained from linear regression analyses of the data, triamterene and 6-*p*-hydroxytriamterene concentrations were calculated for each observed peak height ratio. The relative standard deviations were between 2 and 9% for both compounds with the exception of the metabolite at the 40-ng/ml level.

Recoveries of triamterene and 6-*p*-hydroxytriamterene from plasma extractions were assessed by comparing the peak height ratios of spiked plasma extracts with those of standard methanol solutions. The recoveries ranged from 82 to 95% for the metabolite and from 91 to 99% for triamterene over the concentration range studied.

4,7-Diamino-2-dimethylamino-6-phenylpteridine was chosen as the internal standard because it exhibited similar chromatographic behavior to triamterene. It eluted near the triamterene peak but was completely separated from triamterene and 6-*p*-hydroxytriamterene. Its retention time did not add significantly to the total analysis time, and its recovery from plasma by extraction was quantitative. This internal standard probably would not be present in the plasma of patients treated with triamterene and will not alter assay specificity.

The described HPLC procedure was developed to study triamterene and 6-*p*-hydroxytriamterene pharmacokinetics in dogs and humans. Unlike recently published procedures (7, 8), this assay quantitates both triamterene and the metabolite after direct extraction of plasma samples with organic solvent. Its simplicity and the short assay time are advantageous in the analyses of the large number of samples often encountered in pharmacokinetic and bioavailability studies. The small plasma volume needed for analysis is also an important consideration in such studies. These factors, coupled with the sensitivity and selectivity of the procedure, should provide an excellent technique for the study of the pharmacokinetics of triamterene and 6-*p*-hydroxytriamterene.

The assay described is not as sensitive as the recently published procedures (7, 8) since the UV absorption of the compounds is determined. An increase in sensitivity is expected by using fluorescence determination, and preliminary data suggest that the detection limit can be lowered to 1 ng/ml for each compound should such sensitivity be required.

Triamterene is often administered in combination with hydrochlorothiazide and other antihypertensives. The potential interference of these drugs was not evaluated since the procedure was developed to study the pharmacokinetics of triamterene and 6-*p*-hydroxytriamterene in dogs and humans not on antihypertensive therapy. However, the monitored UV wavelength is in a region that precludes interferences from the thiazides and many other compounds in the unlikely event that compounds of such widely differing structures are not adequately separated in the system described.

## REFERENCES

(1) A. W. Pruitt, J. L. McNay, and P. G. Dayton, *Drug Metab. Dispos.*, **3**, 30 (1975).

(2) A. W. Pruitt, J. S. Winkel, and P. G. Dayton, *Clin. Pharmacol. Ther.*, **21**, 610 (1977).
(3) W. I. Baba, G. R. Tudhope, and G. M. Wilson, *Br. Med. J.*, **2**, 756 (1962).
(4) S. T. Kau, B. V. Rama Sastry, J. D. Alvin, and M. T. Bush, *Drug Metab. Dispos.*, **3**, 345 (1975).
(5) B. Grebian, H. E. Geissler, and E. Mutschler, *Arzneim.-Forsch.*, **26**, 2125 (1976).
(6) P. G. Dayton, A. W. Pruitt, J. L. McNay, and J. Steinhorst, *Neuropharmacology*, **11**, 435 (1972).
(7) S. Sved, J. A. A. Sertie, and I. J. McGilveray, *J. Chromatogr.*, **162**, 474 (1979).
(8) R. R. Brodie, L. F. Chasseaud, T. Taylor, and L. M. Walmsley, *ibid.*, **164**, 527 (1979).

**ACKNOWLEDGMENTS**

Presented in part at the APhA Academy of Pharmaceutical Sciences, Washington, D.C., meeting, April 1980.

Supported in part by a grant-in-aid from the American Heart Association and by funds contributed in part by the Texas Affiliate.

The authors express their gratitude to Smith Kline and French Laboratories and to Rohm & Haas for authentic samples of triamterene and 6-*p*-hydroxytriamterene.

# Antimicrobial Activity of Phenolic Constituents of *Magnolia grandiflora* L.

**ALICE M. CLARK ˣ, FAROUK S. EL-FERALY, and WEN-SHYONG LI ***

Received December 8, 1980, from the *Department of Pharmacognosy, School of Pharmacy, University of Mississippi, University, MS 38677.* Accepted for publication January 14, 1981. *Present address: Taiwan Provincial Pingtung Institute of Agriculture, Pingtung, Taiwan, Republic of China.

**Abstract** □ Three phenolic constituents of *Magnolia grandiflora* L. were shown to possess significant antimicrobial activity using an agar well diffusion assay. Magnolol, honokiol, and 3,5′-diallyl-2′-hydroxy-4-methoxybiphenyl exhibited significant activity against Gram-positive and acid-fast bacteria and fungi. The minimum inhibitory concentrations were determined for each compound using a twofold serial dilution assay.

**Keyphrases** □ *Magnolia grandiflora* L.—antimicrobial activity of phenolic constituents, agar well diffusion assay □ Magnolol—phenolic constituent of *Magnolia grandiflora* L., antimicrobial activity □ Honokiol—phenolic constituent of *Magnolia grandiflora* L., antimicrobial activity □ 3,5′-Diallyl-2′-hydroxy-4-methoxybiphenyl—phenolic constituent of *Magnolia grandiflora* L., antimicrobial activity □ Antimicrobial activity—phenolic constituents of *Magnolia grandiflora* L., agar well diffusion assay

The search for new antibiotics is no longer restricted primarily to microbial products. Recently, constituents of higher plants have exhibited significant antimicrobial activity (1–4). The isolation and identification of magnolol (I), honokiol (II), and 3,5′-diallyl-2′-hydroxy-4-methoxybiphenyl (III) as phenolic constituents of the seeds of *Magnolia grandiflora* L. were reported (5). All three compounds have significant antifungal and antibacterial activity, and the details of this antimicrobial activity are described here.

## RESULTS AND DISCUSSION

Magnolol (I), honokiol (II), and 3,5′-diallyl-2′-hydroxy-4-methoxybiphenyl (III), phenolic constituents of *M. grandiflora* L. (5), showed significant antimicrobial activity against Gram-positive bacteria, an acid-fast bacterium, and yeast-like and filamentous fungi. All three compounds were tested qualitatively for activity using an agar well diffusion assay (Table I). The corresponding dimethyl ethers, IV and V, showed no significant activity.

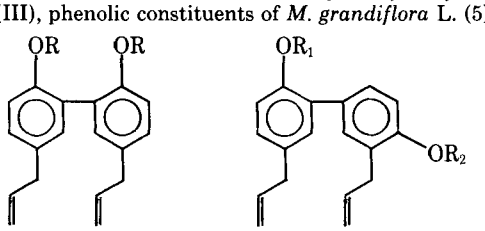


I: R = H
IV: R = $CH_3$

II: $R_1 = R_2 = H$
III: $R_1 = H$, $R_2 = CH_3$
V: $R_1 = R_2 = CH_3$

Streptomycin sulfate and amphotericin B also were tested to serve as standards for comparison. All three compounds (I–III) had activity comparable to the standards under the same test conditions.

The minimum inhibitory concentration (MIC) of each active compound was determined using a twofold serial dilution assay (Table II). All three compounds apparently were considerably more active than amphotericin B against *Trichophyton mentagrophytes* but not as active against *Candida albicans* and *Saccharomyces cerevisiae*. Methylation of one phenolic group of II to give III resulted in the loss of activity against *Aspergillus niger* and *C. albicans* but not against other fungi or bacteria. In fact, III was somewhat more active against *Staphylococcus aureus*, *Bacillus subtilis*, and *Mycobacterium smegmatis* than the dihydroxy compounds I and II. All three compounds possessed activity comparable to, or better than, streptomycin sulfate against *B. subtilis*, *S. aureus*, and *M. smegmatis*. Compounds I–III were also tested for activity against Gram-negative bacteria (*Escherichia coli* and *Pseudomonas aeruginosa*), but none showed any activity.

## EXPERIMENTAL

**Qualitative Antimicrobial Screening**—All compounds were tested for activity against the following microorganisms: *Bacillus subtilis* (ATCC 6633), *Staphylococcus aureus* (ATCC 6538), *Escherichia coli* (ATCC 10536), *Pseudomonas aeruginosa* (ATCC 15442), *Mycobacterium smegmatis* (ATCC 607), *Candida albicans* (ATCC 10231), *Saccharomyces cerevisiae* (ATCC 9763), *Aspergillus niger* (ATCC 16888), and *Trichophyton mentagrophytes* (ATCC 9972). Routine qualitative screening of compounds for antimicrobial activity was accomplished as previously described (1) except for the following modifications: plates for the assay were prepared by dispensing 25 ml of sterile agar medium into 100 × 15-mm sterile petri dishes; and using the quadrant streak method, the sterile agar plates were streaked with a dilution of the test organism (1 ml of broth culture in 9 ml of sterile water).

Antimicrobial activity was recorded as the width (in millimeters) of the inhibition zone measured from the edge of the agar well to the edge of the inhibition zone.

**Quantitative Antimicrobial Assay**—For compounds that showed significant activity in the qualitative screen, the MIC values were determined using the twofold serial dilution technique previously described (1). All compounds were initially tested using a concentration of 100 μg/ml in the first tube. After preliminary evaluation to determine the range of the MIC value, the concentrations in the first tube were de-

0022-3549/81/0800-0951$01.00/0
© 1981, American Pharmaceutical Association

(2) A. W. Pruitt, J. S. Winkel, and P. G. Dayton, *Clin. Pharmacol. Ther.*, **21**, 610 (1977).
(3) W. I. Baba, G. R. Tudhope, and G. M. Wilson, *Br. Med. J.*, **2**, 756 (1962).
(4) S. T. Kau, B. V. Rama Sastry, J. D. Alvin, and M. T. Bush, *Drug Metab. Dispos.*, **3**, 345 (1975).
(5) B. Grebian, H. E. Geissler, and E. Mutschler, *Arzneim.-Forsch.*, **26**, 2125 (1976).
(6) P. G. Dayton, A. W. Pruitt, J. L. McNay, and J. Steinhorst, *Neuropharmacology*, **11**, 435 (1972).
(7) S. Sved, J. A. A. Sertie, and I. J. McGilveray, *J. Chromatogr.*, **162**, 474 (1979).
(8) R. R. Brodie, L. F. Chasseaud, T. Taylor, and L. M. Walmsley, *ibid.*, **164**, 527 (1979).

**ACKNOWLEDGMENTS**

Presented in part at the APhA Academy of Pharmaceutical Sciences, Washington, D.C., meeting, April 1980.

Supported in part by a grant-in-aid from the American Heart Association and by funds contributed in part by the Texas Affiliate.

The authors express their gratitude to Smith Kline and French Laboratories and to Rohm & Haas for authentic samples of triamterene and 6-*p*-hydroxytriamterene.

# Antimicrobial Activity of Phenolic Constituents of *Magnolia grandiflora* L.

**ALICE M. CLARK ˣ, FAROUK S. EL-FERALY, and WEN-SHYONG LI ***

Received December 8, 1980, from the *Department of Pharmacognosy, School of Pharmacy, University of Mississippi, University, MS 38677.* Accepted for publication January 14, 1981. *Present address: Taiwan Provincial Pingtung Institute of Agriculture, Pingtung, Taiwan, Republic of China.

**Abstract** □ Three phenolic constituents of *Magnolia grandiflora* L. were shown to possess significant antimicrobial activity using an agar well diffusion assay. Magnolol, honokiol, and 3,5′-diallyl-2′-hydroxy-4-methoxybiphenyl exhibited significant activity against Gram-positive and acid-fast bacteria and fungi. The minimum inhibitory concentrations were determined for each compound using a twofold serial dilution assay.

**Keyphrases** □ *Magnolia grandiflora* L.—antimicrobial activity of phenolic constituents, agar well diffusion assay □ Magnolol—phenolic constituent of *Magnolia grandiflora* L., antimicrobial activity □ Honokiol—phenolic constituent of *Magnolia grandiflora* L., antimicrobial activity □ 3,5′-Diallyl-2′-hydroxy-4-methoxybiphenyl—phenolic constituent of *Magnolia grandiflora* L., antimicrobial activity □ Antimicrobial activity—phenolic constituents of *Magnolia grandiflora* L., agar well diffusion assay

The search for new antibiotics is no longer restricted primarily to microbial products. Recently, constituents of higher plants have exhibited significant antimicrobial activity (1–4). The isolation and identification of magnolol (I), honokiol (II), and 3,5′-diallyl-2′-hydroxy-4-methoxybiphenyl (III) as phenolic constituents of the seeds of *Magnolia grandiflora* L. were reported (5). All three compounds have significant antifungal and antibacterial activity, and the details of this antimicrobial activity are described here.

## RESULTS AND DISCUSSION

Magnolol (I), honokiol (II), and 3,5′-diallyl-2′-hydroxy-4-methoxybiphenyl (III), phenolic constituents of *M. grandiflora* L. (5), showed significant antimicrobial activity against Gram-positive bacteria, an acid-fast bacterium, and yeast-like and filamentous fungi. All three compounds were tested qualitatively for activity using an agar well diffusion assay (Table I). The corresponding dimethyl ethers, IV and V, showed no significant activity.

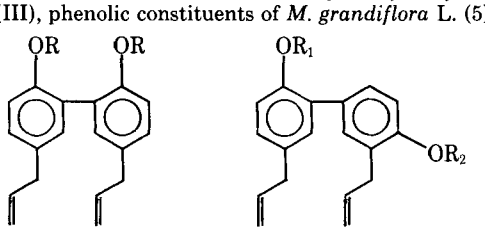


I: R = H
IV: R = $CH_3$

II: $R_1 = R_2 = H$
III: $R_1 = H$, $R_2 = CH_3$
V: $R_1 = R_2 = CH_3$

Streptomycin sulfate and amphotericin B also were tested to serve as standards for comparison. All three compounds (I–III) had activity comparable to the standards under the same test conditions.

The minimum inhibitory concentration (MIC) of each active compound was determined using a twofold serial dilution assay (Table II). All three compounds apparently were considerably more active than amphotericin B against *Trichophyton mentagrophytes* but not as active against *Candida albicans* and *Saccharomyces cerevisiae*. Methylation of one phenolic group of II to give III resulted in the loss of activity against *Aspergillus niger* and *C. albicans* but not against other fungi or bacteria. In fact, III was somewhat more active against *Staphylococcus aureus*, *Bacillus subtilis*, and *Mycobacterium smegmatis* than the dihydroxy compounds I and II. All three compounds possessed activity comparable to, or better than, streptomycin sulfate against *B. subtilis*, *S. aureus*, and *M. smegmatis*. Compounds I–III were also tested for activity against Gram-negative bacteria (*Escherichia coli* and *Pseudomonas aeruginosa*), but none showed any activity.

## EXPERIMENTAL

**Qualitative Antimicrobial Screening**—All compounds were tested for activity against the following microorganisms: *Bacillus subtilis* (ATCC 6633), *Staphylococcus aureus* (ATCC 6538), *Escherichia coli* (ATCC 10536), *Pseudomonas aeruginosa* (ATCC 15442), *Mycobacterium smegmatis* (ATCC 607), *Candida albicans* (ATCC 10231), *Saccharomyces cerevisiae* (ATCC 9763), *Aspergillus niger* (ATCC 16888), and *Trichophyton mentagrophytes* (ATCC 9972). Routine qualitative screening of compounds for antimicrobial activity was accomplished as previously described (1) except for the following modifications: plates for the assay were prepared by dispensing 25 ml of sterile agar medium into 100 × 15-mm sterile petri dishes; and using the quadrant streak method, the sterile agar plates were streaked with a dilution of the test organism (1 ml of broth culture in 9 ml of sterile water).

Antimicrobial activity was recorded as the width (in millimeters) of the inhibition zone measured from the edge of the agar well to the edge of the inhibition zone.

**Quantitative Antimicrobial Assay**—For compounds that showed significant activity in the qualitative screen, the MIC values were determined using the twofold serial dilution technique previously described (1). All compounds were initially tested using a concentration of 100 μg/ml in the first tube. After preliminary evaluation to determine the range of the MIC value, the concentrations in the first tube were de-

0022-3549/81/0800-0951$01.00/0
© 1981, American Pharmaceutical Association

**Table I—Antimicrobial Activity of Phenolic Constituents of *M. grandiflora* L.**

| Compound | Zone Diameter, mm | | | | | | |
|---|---|---|---|---|---|---|---|
| | *B. subtilis* | *S. aureus* | *M. smegmatis* | *C. albicans* | *S. cerevisiae* | *A. niger* | *T. mentagrophytes* |
| I | 8 | 7 | 15 | 6 | 12 | 6 | 17 |
| II | 9 | 10 | 12 | 6 | 12 | 8 | 20 |
| III | 7 | 6 | 13 | 2 | 15 | 1 | 15 |
| IV | 1 | 2 | — | — | 4 | — | 4 |
| V | — | — | — | — | 3 | — | 3 |
| Streptomycin sulfate | 10 | 7 | 17 | NT[a] | NT | NT | NT |
| Amphotericin B | NT | NT | NT | 4 | 5 | 3 | 4 |

[a] Not tested.

**Table II—Minimum Inhibitory Concentrations (Micrograms per Milliliter) of Phenolic Constituents of *M. grandiflora* L.[a]**

| Compound | *B. subtilis* | *S. aureus* | *M. smegmatis* | *C. albicans* | *S. cerevisiae* | *A. niger* | *T. mentagrophytes* |
|---|---|---|---|---|---|---|---|
| I | 5 (5) | 5 (5) | 5 (5) | 30 (30) | 10 (10) | 30 (30) | 2.5 (2.5) |
| II | 5 (5) | 10 (10) | 7.5 (7.5) | 30 (30) | 10 (10) | 30 (30) | 2.5 (2.5) |
| III | 2.5 (2.5) | 2.5 (2.5) | 2.5 (2.5) | NT[b] | 10 (10) | NT | 1.25 (1.25) |
| Streptomycin sulfate | 10 (10) | 10 (10) | 2.5 (1.25) | NT | NT | NT | NT |
| Amphotericin B | NT | NT | NT | 5 (5) | 2.5 (2.5) | 30 (30) | 15 (15) |

[a] Numbers in parentheses refer to values obtained on duplicate testing. [b] Not tested.

creased to either 30 or 60 μg/ml.

The MIC was taken as the lowest concentration that inhibited growth after 24 or 48 hr of incubation. Tubes inoculated with *B. subtilis* and *S. aureus* were incubated at 37° for 24 hr, while tubes inoculated with *M. smegmatis* were incubated at 37° for 48 hr. Tubes inoculated with fungi and yeasts were incubated at 30° for 48 hr. Streptomycin sulfate[1] and amphotericin B[2] were used as standard antibiotics for comparison with the phenolic compounds.

## REFERENCES


(1) C. D. Hufford, M. J. Funderburk, J. M. Morgan, and L. W. Robertson, *J. Pharm. Sci.*, **64**, 789 (1975).

(2) C. D. Hufford and W. L. Laswell, Jr., *Lloydia*, **41**, 156 (1978).

(3) L. A. Mitscher and A. Al-Shamma, *Annu. Rep. Med. Chem.*, **15**, 255 (1980).

(4) L. A. Mitscher, Y. H. Park, and D. Clark, *J. Natl. Prod.*, **43**, 259 (1980).

(5) F. S. El-Feraly and W.-S. Li, *Lloydia*, **41**, 442 (1978).


[1] Chas. Pfizer & Co., Groton, Conn.
[2] Calbiochem, San Diego, Calif.

## ACKNOWLEDGMENTS


Supported in part by the Research Institute of Pharmaceutical Sciences, School of Pharmacy, University of Mississippi.

The authors are grateful to Ms. Sue Johnson for technical assistance with the antimicrobial assay.


# Preparation and Antidiabetic Activity of Cyclic Sulfonylthiourea Derivatives


**RAAFAT SOLIMAN *x, HASSAN M. FEID-ALLAH §, and HOSNY F. MOHAMED ‡**



Received September 29, 1980, from the **Department of Pharmaceutical Chemistry and the* ‡*Department of Pharmacology, Faculty of Pharmacy, and the* §*Department of Chemistry, Faculty of Science, University of Alexandria, Alexandria, Egypt.* Accepted for publication January 21, 1981.



**Abstract** □ 3-Substituted 5-methyl-1-{*p*-[(3,5-dimethyl)pyrazol-1-yl]-, 5-methyl-1-{*p*-[(5-methyl-3-carboxy)pyrazol-1-yl]-, 1-{*p*-[(3-methyl-5-phenyl)pyrazol-1-yl]-, and 1-{*p*-[(3-methyl-4-bromo-5-phenyl)pyrazol-1-yl]benzenesulfonyl}-2-thiohydantoin and their 5-methyl-2-thiohydantoin and 5,6-dihydro-4(3*H*)-oxo-2(1*H*)-pyrimidinethione derivatives were prepared for evaluation as hypoglycemic agents. Biological testing showed that some of these compounds possessed antidiabetic activity.



**Keyphrases** □ Cyclic sulfonylthiourea derivatives—preparation and evaluation for antidiabetic activity, IR and PMR spectroscopy □ IR spectroscopy—identification of cyclic sulfonylthiourea derivatives, antidiabetic activity in mice □ Antidiabetic activity—synthesis and evaluation of cyclic sulfonylthiourea derivatives, identification by IR spectroscopy


In spite of the low hypoglycemic effect of substituted pyrazolesulfonylthiourea derivatives (1–3), their cyclic thio analogs showed potent antidiabetic activity (1). This finding initiated the synthesis of new cyclic pyrazolesulfonylthio analogs[1] for the evaluation of their antidiabetic effect.

## EXPERIMENTAL[2]

Substituted *p*-[(3,5-dimethyl)pyrazol-1-yl]-, *p*-[(5-methyl-3-carboxy)pyrazol-1-yl]-, *p*-[(3-methyl-5-phenyl)pyrazol-1-yl]-, and *p*-[(3-methyl-4-bromo-5-phenyl)pyrazol-1-yl]benzenesulfonylthiourea derivatives were prepared by the treatment of their corresponding *p*-sulfamylphenylpyrazole derivatives with the appropriate isothiocyanates.

[1] Application for a patent was made for compounds described in this report.
[2] Melting points were determined on a Kofler block and are uncorrected. IR spectra were determined as Nujol mulls with a Beckman IR-4210 spectrometer. PMR spectra was recorded on a Varian A-60 A spectrometer. Microanalyses were performed by the Microanalytical Unit, Faculty of Science, University of Cairo, Cairo, Egypt.




*0022-3549/81/0800-0952$01.00/0*


*© 1981, American Pharmaceutical Association*

**Table I—Antimicrobial Activity of Phenolic Constituents of *M. grandiflora* L.**

| Compound | Zone Diameter, mm | | | | | | |
|---|---|---|---|---|---|---|---|
| | *B. subtilis* | *S. aureus* | *M. smegmatis* | *C. albicans* | *S. cerevisiae* | *A. niger* | *T. mentagrophytes* |
| I | 8 | 7 | 15 | 6 | 12 | 6 | 17 |
| II | 9 | 10 | 12 | 6 | 12 | 8 | 20 |
| III | 7 | 6 | 13 | 2 | 15 | 1 | 15 |
| IV | 1 | 2 | — | — | 4 | — | 4 |
| V | — | — | — | — | 3 | — | 3 |
| Streptomycin sulfate | 10 | 7 | 17 | NT[a] | NT | NT | NT |
| Amphotericin B | NT | NT | NT | 4 | 5 | 3 | 4 |

[a] Not tested.

**Table II—Minimum Inhibitory Concentrations (Micrograms per Milliliter) of Phenolic Constituents of *M. grandiflora* L.[a]**

| Compound | *B. subtilis* | *S. aureus* | *M. smegmatis* | *C. albicans* | *S. cerevisiae* | *A. niger* | *T. mentagrophytes* |
|---|---|---|---|---|---|---|---|
| I | 5 (5) | 5 (5) | 5 (5) | 30 (30) | 10 (10) | 30 (30) | 2.5 (2.5) |
| II | 5 (5) | 10 (10) | 7.5 (7.5) | 30 (30) | 10 (10) | 30 (30) | 2.5 (2.5) |
| III | 2.5 (2.5) | 2.5 (2.5) | 2.5 (2.5) | NT[b] | 10 (10) | NT | 1.25 (1.25) |
| Streptomycin sulfate | 10 (10) | 10 (10) | 2.5 (1.25) | NT | NT | NT | NT |
| Amphotericin B | NT | NT | NT | 5 (5) | 2.5 (2.5) | 30 (30) | 15 (15) |

[a] Numbers in parentheses refer to values obtained on duplicate testing. [b] Not tested.

creased to either 30 or 60 μg/ml.

The MIC was taken as the lowest concentration that inhibited growth after 24 or 48 hr of incubation. Tubes inoculated with *B. subtilis* and *S. aureus* were incubated at 37° for 24 hr, while tubes inoculated with *M. smegmatis* were incubated at 37° for 48 hr. Tubes inoculated with fungi and yeasts were incubated at 30° for 48 hr. Streptomycin sulfate[1] and amphotericin B[2] were used as standard antibiotics for comparison with the phenolic compounds.

## REFERENCES


(1) C. D. Hufford, M. J. Funderburk, J. M. Morgan, and L. W. Robertson, *J. Pharm. Sci.*, **64**, 789 (1975).

(2) C. D. Hufford and W. L. Laswell, Jr., *Lloydia*, **41**, 156 (1978).

(3) L. A. Mitscher and A. Al-Shamma, *Annu. Rep. Med. Chem.*, **15**, 255 (1980).

(4) L. A. Mitscher, Y. H. Park, and D. Clark, *J. Natl. Prod.*, **43**, 259 (1980).

(5) F. S. El-Feraly and W.-S. Li, *Lloydia*, **41**, 442 (1978).


[1] Chas. Pfizer & Co., Groton, Conn.
[2] Calbiochem, San Diego, Calif.

## ACKNOWLEDGMENTS


Supported in part by the Research Institute of Pharmaceutical Sciences, School of Pharmacy, University of Mississippi.

The authors are grateful to Ms. Sue Johnson for technical assistance with the antimicrobial assay.


# Preparation and Antidiabetic Activity of Cyclic Sulfonylthiourea Derivatives


**RAAFAT SOLIMAN *x, HASSAN M. FEID-ALLAH §, and HOSNY F. MOHAMED ‡**



Received September 29, 1980, from the **Department of Pharmaceutical Chemistry and the* ‡*Department of Pharmacology, Faculty of Pharmacy, and the* §*Department of Chemistry, Faculty of Science, University of Alexandria, Alexandria, Egypt.* Accepted for publication January 21, 1981.



**Abstract** □ 3-Substituted 5-methyl-1-{*p*-[(3,5-dimethyl)pyrazol-1-yl]-, 5-methyl-1-{*p*-[(5-methyl-3-carboxy)pyrazol-1-yl]-, 1-{*p*-[(3-methyl-5-phenyl)pyrazol-1-yl]-, and 1-{*p*-[(3-methyl-4-bromo-5-phenyl)pyrazol-1-yl]benzenesulfonyl}-2-thiohydantoin and their 5-methyl-2-thiohydantoin and 5,6-dihydro-4(3*H*)-oxo-2(1*H*)-pyrimidinethione derivatives were prepared for evaluation as hypoglycemic agents. Biological testing showed that some of these compounds possessed antidiabetic activity.



**Keyphrases** □ Cyclic sulfonylthiourea derivatives—preparation and evaluation for antidiabetic activity, IR and PMR spectroscopy □ IR spectroscopy—identification of cyclic sulfonylthiourea derivatives, antidiabetic activity in mice □ Antidiabetic activity—synthesis and evaluation of cyclic sulfonylthiourea derivatives, identification by IR spectroscopy


In spite of the low hypoglycemic effect of substituted pyrazolesulfonylthiourea derivatives (1–3), their cyclic thio analogs showed potent antidiabetic activity (1). This finding initiated the synthesis of new cyclic pyrazolesulfonylthio analogs[1] for the evaluation of their antidiabetic effect.

## EXPERIMENTAL[2]

Substituted *p*-[(3,5-dimethyl)pyrazol-1-yl]-, *p*-[(5-methyl-3-carboxy)pyrazol-1-yl]-, *p*-[(3-methyl-5-phenyl)pyrazol-1-yl]-, and *p*-[(3-methyl-4-bromo-5-phenyl)pyrazol-1-yl]benzenesulfonylthiourea derivatives were prepared by the treatment of their corresponding *p*-sulfamylphenylpyrazole derivatives with the appropriate isothiocyanates.

[1] Application for a patent was made for compounds described in this report.
[2] Melting points were determined on a Kofler block and are uncorrected. IR spectra were determined as Nujol mulls with a Beckman IR-4210 spectrometer. PMR spectra was recorded on a Varian A-60 A spectrometer. Microanalyses were performed by the Microanalytical Unit, Faculty of Science, University of Cairo, Cairo, Egypt.




*0022-3549/81/0800-0952$01.00/0*


*© 1981, American Pharmaceutical Association*

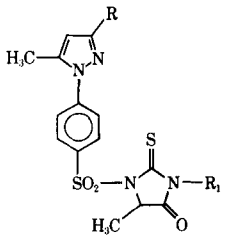

**Table I—3-Substituted 5-Methyl-1-{*p*-[(3,5-dimethyl)pyrazol-1-yl]- and [(5-Methyl-3-carboxy)pyrazol-1-yl]benzenesulfonyl}-2-thiohydantoins**

| Compound | R | $R_1$ | Yield, % | Melting Point | Formula | Analysis, % Calc. | Found |
|---|---|---|---|---|---|---|---|
| IIa | $CH_3$ | $CH_2$=$CHCH_2$ | 70 | 165° | $C_{18}H_{20}N_4O_3S_2$ | C 53.5 | 53.5 |
| | | | | | | H 5.0 | 5.3 |
| | | | | | | N 13.9 | 14.0 |
| | | | | | | S 15.8 | 15.6 |
| IIb | $CH_3$ | $CH_3(CH_2)_2$ | 65 | 216° | $C_{18}H_{22}N_4O_3S_2$ | C 53.2 | 53.4 |
| | | | | | | H 5.4 | 5.2 |
| | | | | | | N 13.8 | 13.7 |
| | | | | | | S 15.8 | 16.0 |
| IIc | $CH_3$ | $C_6H_{11}$ | 75 | 175° | $C_{21}H_{26}N_4O_3S_2$ | C 56.5 | 56.8 |
| | | | | | | H 5.8 | 6.0 |
| | | | | | | N 12.6 | 12.6 |
| | | | | | | S 14.3 | 14.0 |
| IId | $CH_3$ | $p$-$CH_3C_6H_4$ | 65 | 230° | $C_{22}H_{22}N_4O_3S_2$ | C 58.1 | 58.0 |
| | | | | | | H 4.8 | 5.0 |
| | | | | | | N 12.3 | 12.3 |
| | | | | | | S 14.1 | 14.1 |
| IIe | $CH_3$ | $C_6H_5CH_2$ | 70 | 140° | $C_{22}H_{22}N_4O_3S_2$ | C 58.1 | 57.9 |
| | | | | | | H 4.8 | 4.9 |
| | | | | | | N 12.3 | 12.5 |
| | | | | | | S 14.1 | 14.1 |
| IIIa | COOH | $CH_3(CH_2)_2$ | 65 | 210° | $C_{18}H_{20}N_4O_5S_2$ | C 49.5 | 49.7 |
| | | | | | | H 4.6 | 4.6 |
| | | | | | | N 12.8 | 13.0 |
| | | | | | | S 14.7 | 14.7 |
| IIIb | COOH | $CH_3(CH_2)_3$ | 70 | 144° | $C_{19}H_{22}N_4O_5S_2$ | C 50.7 | 51.0 |
| | | | | | | H 4.9 | 4.8 |
| | | | | | | N 12.4 | 12.5 |
| | | | | | | S 14.2 | 14.0 |
| IIIc | COOH | $C_6H_{11}$ | 65 | 171° | $C_{21}H_{24}N_4O_5S_2$ | C 52.9 | 53.1 |
| | | | | | | H 5.0 | 5.2 |
| | | | | | | N 11.8 | 12.0 |
| | | | | | | S 13.4 | 13.1 |

3-Substituted 5-methyl-1-{*p*-[(3,5-dimethyl)pyrazol-1-yl]- and 5-methyl-1-{*p*-[(5-methyl-3-carboxy)pyrazol-1-yl]benzenesulfonyl}-2-thiohydantoins (II and III, Scheme I) were prepared by refluxing an alcoholic solution of the appropriate thiourea derivative with ethyl $\alpha$-bromopropionate. The intermediate pseudothio derivatives underwent rapid rearrangement with the formation of 2-thiones. Their IR spectra showed a characteristic absorption band at 1120–1140 $cm^{-1}$, indicative of C=S, and at 1300 $cm^{-1}$, indicative of C–N (amide III band).

3-Substituted 1-{*p*-[(3-methyl-5-phenyl)pyrazol-1-yl]- and 1-{*p*-[(3-methyl-4-bromo-5-phenyl)pyrazol-1-yl]benzenesulfonyl}-2-thiohydantoin (VI and VII, Scheme II) and their 5-methyl-2-thiohydantoin (VIII and IX, Scheme II) and 5,6-dihydro-4(3*H*)-oxo-2(1*H*)-pyrimidinethione (X and XI, Scheme II) derivatives were prepared by refluxing an alcoholic solution of the appropriate thiourea derivative with ethyl bromoacetate, ethyl $\alpha$-bromopropionate, and ethyl $\beta$-bromopropionate, respectively. The intermediate pseudothio derivatives underwent rapid rearrangement with the formation of the 2-thiones.

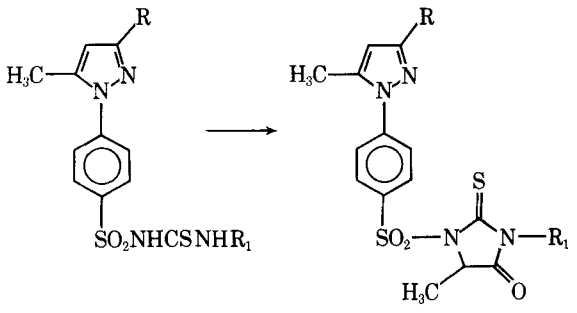

I

II: R = $CH_3$
III: R = COOH

*Scheme I*

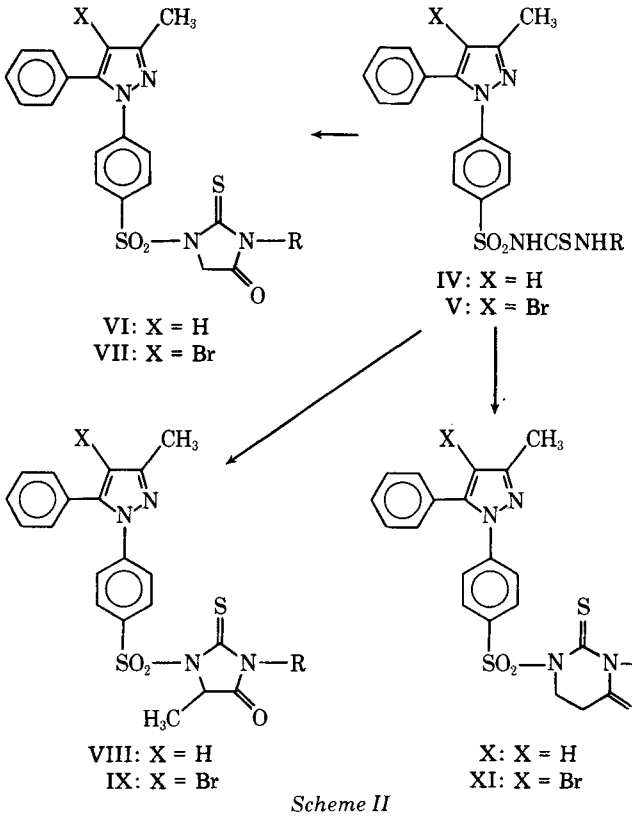

VI: X = H
VII: X = Br

IV: X = H
V: X = Br

VIII: X = H
IX: X = Br

X: X = H
XI: X = Br

*Scheme II*

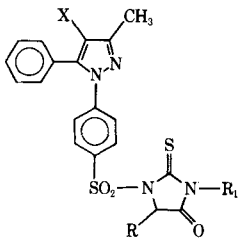

**Table II—3-Substituted 1-{*p*-[(3-Methyl-5-phenyl)pyrazol-1-yl] and [(3-Methyl-4-bromo-5-phenyl)pyrazol-1-yl]benzenesulfonyl}-2-thiohydantoins**

| Compound | R | $R_1$ | X | Yield, % | Melting Point | Formula | Analysis, % | Calc. | Found |
|---|---|---|---|---|---|---|---|---|---|
| VI*a* | H | $C_2H_5$ | H | 70 | 167° | $C_{21}H_{20}N_4O_3S_2$ | C | 57.3 | 57.4 |
| | | | | | | | H | 4.5 | 4.3 |
| | | | | | | | N | 12.7 | 12.6 |
| | | | | | | | S | 14.5 | 14.6 |
| VI*b* | H | $CH_2$=$CHCH_2$ | H | 50 | 175° | $C_{22}H_{20}N_4O_3S_2$ | C | 58.4 | 58.2 |
| | | | | | | | H | 4.4 | 4.4 |
| | | | | | | | N | 12.4 | 12.5 |
| | | | | | | | S | 14.2 | 14.0 |
| VI*c* | H | $CH_3(CH_2)_3$ | H | 60 | 115° | $C_{23}H_{24}N_4O_3S_2$ | C | 59.0 | 59.1 |
| | | | | | | | H | 5.1 | 5.2 |
| | | | | | | | N | 12.0 | 12.2 |
| | | | | | | | S | 13.7 | 13.4 |
| VI*d* | H | $C_6H_{11}$ | H | 70 | 215° | $C_{25}H_{26}N_4O_3S_2$ | C | 60.7 | 60.8 |
| | | | | | | | H | 5.3 | 5.1 |
| | | | | | | | N | 11.3 | 11.4 |
| | | | | | | | S | 13.0 | 13.2 |
| VI*e* | H | *p*-$CH_3C_6H_4$ | H | 65 | 168° | $C_{26}H_{22}N_4O_3S_2$ | C | 62.2 | 62.3 |
| | | | | | | | H | 4.4 | 4.5 |
| | | | | | | | N | 11.2 | 11.2 |
| | | | | | | | S | 12.7 | 12.8 |
| VI*f* | H | $C_6H_5CH_2$ | H | 55 | 222° | $C_{26}H_{22}N_4O_3S_2$ | C | 62.2 | 62.4 |
| | | | | | | | H | 4.4 | 4.2 |
| | | | | | | | N | 11.2 | 11.2 |
| | | | | | | | S | 12.7 | 12.9 |
| VII*a* | H | $C_2H_5$ | Br | 65 | 175° | $C_{21}H_{19}BrN_4O_3S_2$ | C | 48.6 | 48.7 |
| | | | | | | | H | 3.7 | 3.5 |
| | | | | | | | Br | 15.4 | 15.2 |
| | | | | | | | N | 10.8 | 11.0 |
| | | | | | | | S | 12.3 | 12.5 |
| VII*b* | H | $CH_3(CH_2)_3$ | Br | 60 | 162° | $C_{23}H_{23}BrN_4O_3S_2$ | C | 50.5 | 50.5 |
| | | | | | | | H | 4.2 | 4.1 |
| | | | | | | | Br | 14.6 | 14.2 |
| | | | | | | | N | 10.2 | 10.4 |
| | | | | | | | S | 11.7 | 11.8 |
| VII*c* | H | $C_6H_{11}$ | Br | 70 | 208° | $C_{25}H_{25}BrN_4O_3S_2$ | C | 52.4 | 52.5 |
| | | | | | | | H | 4.4 | 4.2 |
| | | | | | | | Br | 14.0 | 14.1 |
| | | | | | | | N | 9.8 | 9.6 |
| | | | | | | | S | 11.2 | 11.3 |
| VII*d* | H | *p*-$CH_3C_6H_4$ | Br | 70 | 240° | $C_{26}H_{21}BrN_4O_3S_2$ | C | 53.7 | 53.6 |
| | | | | | | | H | 3.6 | 3.4 |
| | | | | | | | Br | 13.8 | 13.7 |
| | | | | | | | N | 9.6 | 10.0 |
| | | | | | | | S | 11.0 | 11.2 |
| VII*e* | H | $C_6H_5CH_2$ | Br | 60 | 168° | $C_{26}H_{21}BrN_4O_3S_2$ | C | 53.7 | 53.6 |
| | | | | | | | H | 3.6 | 4.0 |
| | | | | | | | Br | 13.8 | 14.0 |
| | | | | | | | N | 9.6 | 9.5 |
| | | | | | | | S | 11.0 | 11.3 |
| VIII*a* | $CH_3$ | $C_2H_5$ | H | 60 | 194° | $C_{22}H_{22}N_4O_3S_2$ | C | 58.1 | 58.2 |
| | | | | | | | H | 4.8 | 4.7 |
| | | | | | | | N | 12.3 | 12.1 |
| | | | | | | | S | 14.1 | 14.2 |
| VIII*b* | $CH_3$ | $CH_3(CH_2)_3$ | H | 55 | 178° | $C_{24}H_{26}N_4O_3S_2$ | C | 59.8 | 60.0 |
| | | | | | | | H | 5.4 | 5.2 |
| | | | | | | | N | 11.6 | 11.4 |
| | | | | | | | S | 13.3 | 13.1 |
| VIII*c* | $CH_3$ | $C_6H_{11}$ | H | 65 | 198° | $C_{26}H_{28}N_4O_3S_2$ | C | 61.4 | 61.3 |
| | | | | | | | H | 5.5 | 5.6 |
| | | | | | | | N | 11.0 | 11.2 |
| | | | | | | | S | 12.6 | 12.5 |
| VIII*d* | $CH_3$ | *p*-$CH_3C_6H_4$ | H | 65 | 218° | $C_{27}H_{24}N_4O_3S_2$ | C | 62.8 | 62.4 |
| | | | | | | | H | 4.7 | 4.5 |
| | | | | | | | N | 10.9 | 11.0 |
| | | | | | | | S | 12.4 | 12.2 |
| IX*a* | $CH_3$ | $C_2H_5$ | Br | 65 | 215° | $C_{22}H_{21}BrN_4O_3S_2$ | C | 49.5 | 49.4 |
| | | | | | | | H | 3.9 | 4.1 |
| | | | | | | | Br | 15.0 | 15.1 |
| | | | | | | | N | 10.5 | 10.3 |
| | | | | | | | S | 12.0 | 12.3 |

**Table II—*Continued***

| Compound | R | $R_1$ | X | Yield, % | Melting Point | Formula | Analysis, % Calc. | Found |
|---|---|---|---|---|---|---|---|---|
| IX*b* | $CH_3$ | $CH_3(CH_2)_3$ | Br | 55 | 135° | $C_{24}H_{25}BrN_4O_3S_2$ | C 51.3 | 51.4 |
| | | | | | | | H 4.5 | 4.3 |
| | | | | | | | Br 14.3 | 14.2 |
| | | | | | | | N 10.0 | 10.2 |
| | | | | | | | S 11.4 | 11.1 |
| IX*c* | $CH_3$ | $C_6H_{11}$ | Br | 65 | 225° | $C_{26}H_{27}BrN_4O_3S_2$ | C 53.2 | 53.4 |
| | | | | | | | H 4.6 | 4.4 |
| | | | | | | | Br 13.6 | 13.7 |
| | | | | | | | N 9.5 | 9.3 |
| | | | | | | | S 10.9 | 11.2 |
| IX*d* | $CH_3$ | *p*-$CH_3C_6H_4$ | Br | 70 | 245° | $C_{27}H_{23}BrN_4O_3S_2$ | C 54.5 | 54.3 |
| | | | | | | | H 3.9 | 3.7 |
| | | | | | | | Br 13.4 | 13.1 |
| | | | | | | | N 9.4 | 9.7 |
| | | | | | | | S 10.8 | 11.0 |

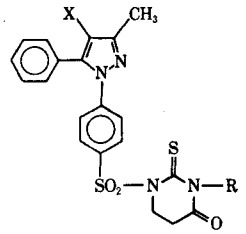


**Table III—3-Substituted 1-{*p*-[(3-Methyl-5-phenyl)pyrazol-1-yl] and 3-Methyl-4-bromo-5-phenyl)pyrazol-1-yl]benzenesulfonyl}-5,6-dihydro-4(3*H*)-oxo-2(1*H*)-pyrimidinethiones**

| Compound | R | X | Yield, % | Melting Point | Formula | Analysis, % Calc. | Found |
|---|---|---|---|---|---|---|---|
| X*a* | $CH_3(CH_2)_3$ | H | 60 | 165° | $C_{24}H_{26}N_4O_3S_2$ | C 59.8 | 59.8 |
| | | | | | | H 5.4 | 5.4 |
| | | | | | | N 11.6 | 11.2 |
| | | | | | | S 13.3 | 13.3 |
| X*b* | $C_6H_{11}$ | H | 70 | 228° | $C_{26}H_{28}N_4O_3S_2$ | C 61.4 | 61.4 |
| | | | | | | H 5.5 | 5.3 |
| | | | | | | N 11.0 | 11.2 |
| | | | | | | S 12.6 | 12.2 |
| X*c* | *p*-$CH_3C_6H_4$ | H | 65 | 255° | $C_{27}H_{24}N_4O_3S_2$ | C 62.8 | 62.6 |
| | | | | | | H 4.7 | 4.7 |
| | | | | | | N 10.9 | 10.7 |
| | | | | | | S 12.4 | 12.3 |
| X*d* | $C_6H_5CH_2$ | H | 65 | 220° | $C_{27}H_{24}N_4O_3S_2$ | C 62.8 | 62.5 |
| | | | | | | H 4.7 | 4.4 |
| | | | | | | N 10.9 | 11.1 |
| | | | | | | S 12.4 | 12.6 |
| XI*a* | $C_2H_5$ | Br | 70 | 222° | $C_{22}H_{21}BrN_4O_3S_2$ | C 49.5 | 49.4 |
| | | | | | | H 3.9 | 4.1 |
| | | | | | | Br 15.0 | 15.1 |
| | | | | | | N 10.5 | 10.4 |
| | | | | | | S 12.0 | 12.3 |
| XI*b* | $C_6H_{11}$ | Br | 65 | 230° | $C_{26}H_{27}BrN_4O_3S_2$ | C 53.2 | 53.3 |
| | | | | | | H 4.6 | 4.5 |
| | | | | | | Br 13.6 | 13.4 |
| | | | | | | N 9.5 | 9.6 |
| | | | | | | S 10.9 | 11.2 |
| XI*c* | *p*-$CH_3C_6H_4$ | Br | 70 | 198° | $C_{27}H_{23}BrN_4O_3S_2$ | C 54.5 | 54.2 |
| | | | | | | H 3.9 | 3.7 |
| | | | | | | Br 13.4 | 13.2 |
| | | | | | | N 9.4 | 9.3 |
| | | | | | | S 10.8 | 10.5 |
| XI*d* | $C_6H_5CH_2$ | Br | 65 | 225° | $C_{27}H_{23}BrN_4O_3S_2$ | C 54.5 | 54.3 |
| | | | | | | H 3.9 | 3.6 |
| | | | | | | Br 13.4 | 13.7 |
| | | | | | | N 9.4 | 9.2 |
| | | | | | | S 10.8 | 10.7 |

In addition to the two bands of the $-SO_2N<$ group at 1330–1355 and 1155–1180 $cm^{-1}$, the IR spectra of VI and VII revealed a secondary carbonyl amide absorption at 1740–1755 $cm^{-1}$ and a C=S band at 1100–1120 $cm^{-1}$.

The IR spectra of VIII and IX revealed, in addition to the two bands of the $-SO_2N<$ group at 1330–1350 and 1160–1190 $cm^{-1}$, a secondary carbonyl amide absorption at 1740–1752 $cm^{-1}$ and a C=S band at 1090–1110 $cm^{-1}$.

The IR spectra of X and XI revealed a secondary carbonyl amide absorption at 1640–1665 $cm^{-1}$ and a C=S band at 1080–1100 $cm^{-1}$ in addition to the two bands of the $-SO_2N<$ group at 1330–1350 and 1160–1180 $cm^{-1}$.

**Synthesis of II and III**—A mixture of *p*-[(3,5-dimethyl)- or *p*-[(5-methyl-3-carboxy)pyrazol-1-yl]benzenesulfonylthiourea (I, 0.01 mole) and ethyl α-bromopropionate (0.011 mole) in absolute ethanol (50 ml) was refluxed with stirring for 4–6 hr, concentrated, and allowed to crystallize. The products obtained were recrystallized from ethanol (Table I).

**Synthesis of VI and VII**—A mixture of *p*-[(3-methyl-5-phenyl)- or *p*-[(3-methyl-4-bromo-5-phenyl)pyrazol -1- yl]benzenesulfonylthiourea

**Table IV—Antidiabetic Activity of Substituted Cyclic Sulfonylthiourea Derivatives**

| Compound | Reduction in Plasma Glucose Level Compared with Control, % | Statistical Significance Value of $p$ |
|---|---|---|
| Phenformin | 10 | <0.01[a] |
| IIc | 1.5 | 0.05 |
| IIIc | 4.5 | <0.05[a] |
| VI*d* | 3.0 | <0.01[a] |
| VII*c* | 2.0 | 0.05 |
| VIII*c* | 8.0 | <0.01[a] |
| IX*c* | 4.0 | <0.01[a] |
| X*b* | 2.0 | 0.05 |
| XI*a* | 4.0 | <0.01[a] |

[a] Statistically significant.

(IV or V, 0.01 mole) and ethyl bromoacetate (0.011 mole) in absolute ethanol (50 ml) was refluxed with stirring for 4–6 hr, concentrated, and allowed to crystallize. The products obtained were recrystallized from ethanol (Table II).

**Synthesis of VIII and IX**—A mixture of IV or V (0.01 mole) and ethyl $\alpha$-bromopropionate (0.011 mole) in absolute ethanol (50 ml) was refluxed with stirring for 6–8 hr, concentrated, and allowed to crystallize. The products obtained were recrystallized from ethanol as colorless needles (Table II).

**Synthesis of X and XI**—A mixture of IV or V (0.01 mole) and ethyl $\beta$-bromopropionate (0.011 mole) in absolute ethanol (50 ml) was refluxed with stirring for 6–8 hr, concentrated, and allowed to crystallize. The products were recrystallized from 95% ethanol as colorless needles (Table III).

In addition to the aromatic protons at $\delta$ 7.0–8.1, the PMR spectra of VIc showed a multiplet at $\delta$ 0.8–1.7 for the $(CH_2)_3$ protons of the butyl group together with the methylene group of the cyclic ring, a singlet at $\delta$ 2.4 characteristic of the methyl group at C-3 of the pyrazole ring, a singlet at $\delta$ 1.3 for the $CH_3$ of the butyl group, and a singlet at $\delta$ 6.4 for the proton at C-4 of the pyrazole ring.

In addition to the aromatic protons at $\delta$ 6.8–7.9, the PMR spectra of XIc showed a singlet at $\delta$ 2.3 for the two methyl groups together with the two methylene groups of the cyclic ring.

## DISCUSSION

**Biological Testing**—Compounds IIc, IIIc, VI*d*, VIIc, VIII*c*, IX*c*, X*b*, and XI*a* were tested for hypoglycemic activity using alloxanized female albino mice weighing 20–25 g. Alloxan, 100 mg/kg of body weight, was injected into the tail vein in saline solution (10 mg/ml). Three days later, the mice were given the test compounds orally in suspension in 1% carboxymethylcellulose sodium at the rate of 0.2 mmole/kg of body weight.

Each day, four mice were used as a control group and one group of four mice was given the standard drug phenformin in a dose of 100 mg (0.4 mmole)/kg of body weight. Up to six groups of four mice received test compounds. Blood samples were taken at 0, 1, and 3 hr.

Blood was collected into 0.04% NaF solution. Glucose was determined by the microcolorimetric copper reduction technique of Haslewood and Strookman (4). Results are expressed as a percentage reduction of plasma glucose level compared to the control value.

**Statistical Significance**—Statistical significance was assessed using the Student $t$ test. Statistical significance was accepted where the calculated $t$ value exceeded the tabulated $t$ value at the 0.05 level.

From the data presented in Table IV, it is obvious that VIII possesses marked hypoglycemic activity. While IIIc, IX*c*, and XI*a* possess only moderate hypoglycemic activity, the potency of these compounds is more than their corresponding thiourea analogs.

## REFERENCES


(1) R. Soliman, *J. Med. Chem.*, **22**, 321 (1979).

(2) R. Soliman and H. M. Feid-Allah, *J. Pharm. Sci.*, **70**, 602 (1981).

(3) R. Soliman, H. M. Feid-Allah, S. K. El Sadany, and H. F. Mohamed, *ibid.*, **70**, 606 (1981).

(4) G. A. D. Haslewood and T. A. Strookman, *Biochem. J.*, **33**, 920 (1939).


# Synthesis of New Polyamine Derivatives for Cancer Chemotherapeutic Studies


**LOUIS T. WEINSTOCK *, WILLIAM J. ROST ‡x, and C. C. CHENG §**



Received July 28, 1980, from the **Midwest Research Institute, Kansas City, MO 64110*, the ‡*University of Missouri–Kansas City, Kansas City, MO 64110*, and the §*Mid-America Cancer Center, University of Kansas Medical Center, Kansas City, KS 66103.* Accepted for publication January 15, 1981.



**Abstract** □ Selected homologs, analogs, and acylated derivatives of spermine and spermidine, together with several heterocyclic and aromatic compounds containing a novoldiamine side chain, were prepared and evaluated biologically. Several compounds possessed activity against B-16 melanoma and human epidermoid carcinoma of the nasopharynx.



**Keyphrases** □ Polyamines—synthesis of derivatives, cancer chemotherapy □ Chemotherapy—synthesis of polyamine derivatives for cancer chemotherapy □ Derivatives—polyamines, synthesis, cancer chemotherapy


The importance of many naturally occurring polyamines, such as putrescine, spermidine, and spermine, to the growth of living cells is well established (1–4). It was reported recently that increased amounts of certain polyamines were found in rapidly proliferating biological systems (*e.g.*, chick embryo cells, rat regenerating liver cells, and wound-healing tissues) (5–10), as well as in neoplastic cells of animals and humans (11–16). The higher polyamine levels are believed to be contributed by ornithine decarboxylase activity in these tissues (17). Elevated polyamine levels also were detected in the urine of cancer patients (18–20). The high excretion level of polyamines declined when the patients were in remission, and chemotherapy treatment with methotrexate, cytosine arabinoside, 5-azacitidine, or fluorouracil resulted in polyamine depletion in tumor cells (21–23).

Since cellular protein synthesis is affected by polyamines at the transcription and translation level (24) and at least one role of polyamines is to organize the structure and activity of tRNA (25), it was postulated that properly designed analogs of polyamines could be useful in oncology studies. This concept was substantiated by previous reports (26–29) that some spermine and spermidine analogs of both synthetic and plant origin demonstrated inter-




*0022-3549/81/0800-0956$01.00/0*



© *1981, American Pharmaceutical Association*

**Table IV—Antidiabetic Activity of Substituted Cyclic Sulfonylthiourea Derivatives**

| Compound | Reduction in Plasma Glucose Level Compared with Control, % | Statistical Significance Value of $p$ |
|---|---|---|
| Phenformin | 10 | <0.01[a] |
| IIc | 1.5 | 0.05 |
| IIIc | 4.5 | <0.05[a] |
| VI*d* | 3.0 | <0.01[a] |
| VII*c* | 2.0 | 0.05 |
| VIII*c* | 8.0 | <0.01[a] |
| IX*c* | 4.0 | <0.01[a] |
| X*b* | 2.0 | 0.05 |
| XI*a* | 4.0 | <0.01[a] |

[a] Statistically significant.

(IV or V, 0.01 mole) and ethyl bromoacetate (0.011 mole) in absolute ethanol (50 ml) was refluxed with stirring for 4–6 hr, concentrated, and allowed to crystallize. The products obtained were recrystallized from ethanol (Table II).

**Synthesis of VIII and IX**—A mixture of IV or V (0.01 mole) and ethyl $\alpha$-bromopropionate (0.011 mole) in absolute ethanol (50 ml) was refluxed with stirring for 6–8 hr, concentrated, and allowed to crystallize. The products obtained were recrystallized from ethanol as colorless needles (Table II).

**Synthesis of X and XI**—A mixture of IV or V (0.01 mole) and ethyl $\beta$-bromopropionate (0.011 mole) in absolute ethanol (50 ml) was refluxed with stirring for 6–8 hr, concentrated, and allowed to crystallize. The products were recrystallized from 95% ethanol as colorless needles (Table III).

In addition to the aromatic protons at $\delta$ 7.0–8.1, the PMR spectra of VIc showed a multiplet at $\delta$ 0.8–1.7 for the $(CH_2)_3$ protons of the butyl group together with the methylene group of the cyclic ring, a singlet at $\delta$ 2.4 characteristic of the methyl group at C-3 of the pyrazole ring, a singlet at $\delta$ 1.3 for the $CH_3$ of the butyl group, and a singlet at $\delta$ 6.4 for the proton at C-4 of the pyrazole ring.

In addition to the aromatic protons at $\delta$ 6.8–7.9, the PMR spectra of XIc showed a singlet at $\delta$ 2.3 for the two methyl groups together with the two methylene groups of the cyclic ring.

## DISCUSSION

**Biological Testing**—Compounds IIc, IIIc, VI*d*, VIIc, VIII*c*, IX*c*, X*b*, and XI*a* were tested for hypoglycemic activity using alloxanized female albino mice weighing 20–25 g. Alloxan, 100 mg/kg of body weight, was injected into the tail vein in saline solution (10 mg/ml). Three days later, the mice were given the test compounds orally in suspension in 1% carboxymethylcellulose sodium at the rate of 0.2 mmole/kg of body weight.

Each day, four mice were used as a control group and one group of four mice was given the standard drug phenformin in a dose of 100 mg (0.4 mmole)/kg of body weight. Up to six groups of four mice received test compounds. Blood samples were taken at 0, 1, and 3 hr.

Blood was collected into 0.04% NaF solution. Glucose was determined by the microcolorimetric copper reduction technique of Haslewood and Strookman (4). Results are expressed as a percentage reduction of plasma glucose level compared to the control value.

**Statistical Significance**—Statistical significance was assessed using the Student $t$ test. Statistical significance was accepted where the calculated $t$ value exceeded the tabulated $t$ value at the 0.05 level.

From the data presented in Table IV, it is obvious that VIII possesses marked hypoglycemic activity. While IIIc, IX*c*, and XI*a* possess only moderate hypoglycemic activity, the potency of these compounds is more than their corresponding thiourea analogs.

## REFERENCES


(1) R. Soliman, *J. Med. Chem.*, **22**, 321 (1979).

(2) R. Soliman and H. M. Feid-Allah, *J. Pharm. Sci.*, **70**, 602 (1981).

(3) R. Soliman, H. M. Feid-Allah, S. K. El Sadany, and H. F. Mohamed, *ibid.*, **70**, 606 (1981).

(4) G. A. D. Haslewood and T. A. Strookman, *Biochem. J.*, **33**, 920 (1939).


# Synthesis of New Polyamine Derivatives for Cancer Chemotherapeutic Studies


**LOUIS T. WEINSTOCK *, WILLIAM J. ROST ‡x, and C. C. CHENG §**



Received July 28, 1980, from the **Midwest Research Institute, Kansas City, MO 64110*, the ‡*University of Missouri–Kansas City, Kansas City, MO 64110*, and the §*Mid-America Cancer Center, University of Kansas Medical Center, Kansas City, KS 66103.* Accepted for publication January 15, 1981.



**Abstract** □ Selected homologs, analogs, and acylated derivatives of spermine and spermidine, together with several heterocyclic and aromatic compounds containing a novoldiamine side chain, were prepared and evaluated biologically. Several compounds possessed activity against B-16 melanoma and human epidermoid carcinoma of the nasopharynx.



**Keyphrases** □ Polyamines—synthesis of derivatives, cancer chemotherapy □ Chemotherapy—synthesis of polyamine derivatives for cancer chemotherapy □ Derivatives—polyamines, synthesis, cancer chemotherapy


The importance of many naturally occurring polyamines, such as putrescine, spermidine, and spermine, to the growth of living cells is well established (1–4). It was reported recently that increased amounts of certain polyamines were found in rapidly proliferating biological systems (*e.g.*, chick embryo cells, rat regenerating liver cells, and wound-healing tissues) (5–10), as well as in neoplastic cells of animals and humans (11–16). The higher polyamine levels are believed to be contributed by ornithine decarboxylase activity in these tissues (17). Elevated polyamine levels also were detected in the urine of cancer patients (18–20). The high excretion level of polyamines declined when the patients were in remission, and chemotherapy treatment with methotrexate, cytosine arabinoside, 5-azacitidine, or fluorouracil resulted in polyamine depletion in tumor cells (21–23).

Since cellular protein synthesis is affected by polyamines at the transcription and translation level (24) and at least one role of polyamines is to organize the structure and activity of tRNA (25), it was postulated that properly designed analogs of polyamines could be useful in oncology studies. This concept was substantiated by previous reports (26–29) that some spermine and spermidine analogs of both synthetic and plant origin demonstrated inter-




*0022-3549/81/0800-0956$01.00/0*



© *1981, American Pharmaceutical Association*

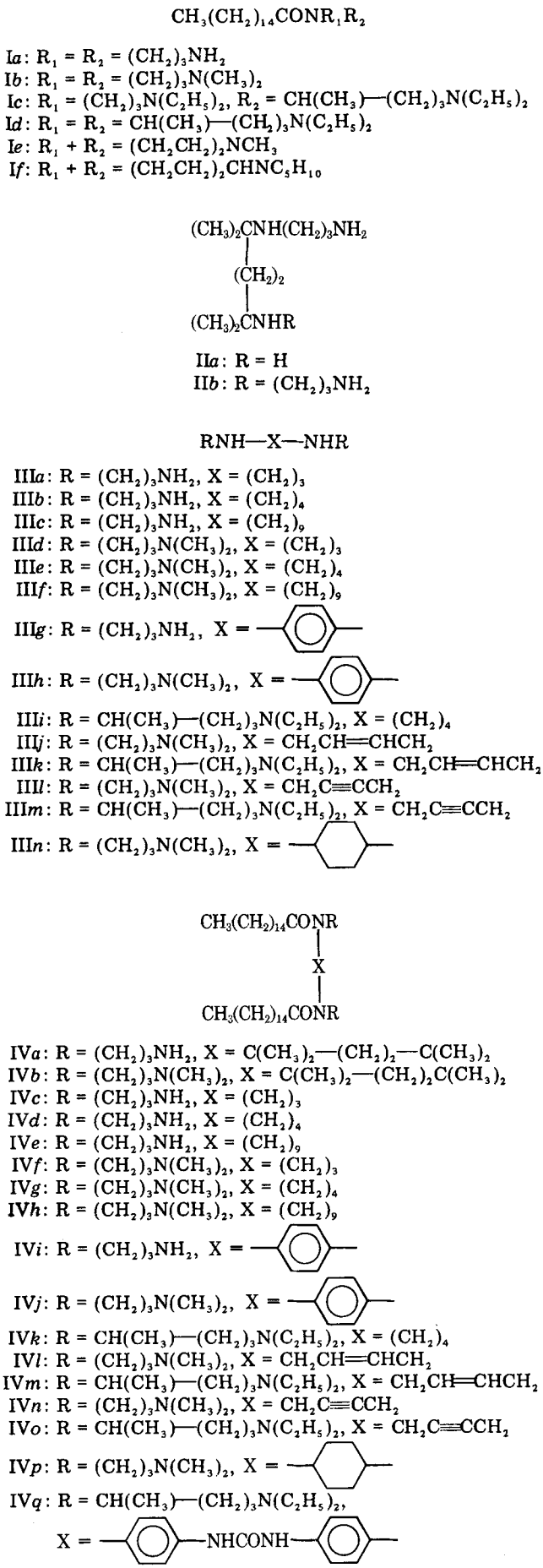


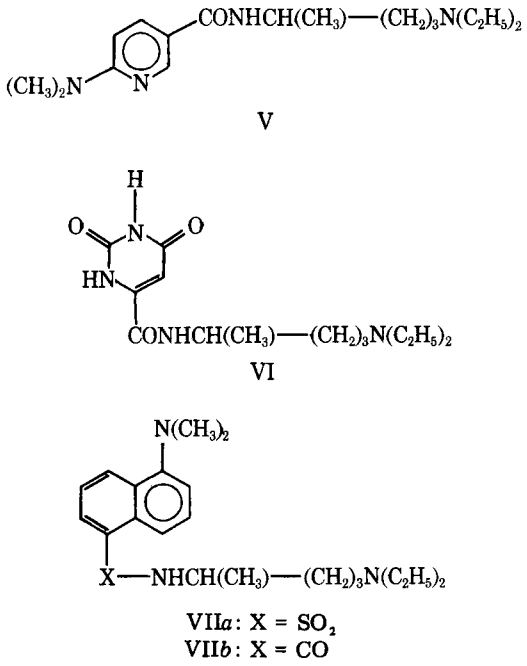


esting *in vitro* and *in vivo* antineoplastic activity. Based on the structure–activity relationship information provided by these investigators and the general biochemical and biological aspects of polyamines, selective analogs, homologs, and acylated derivatives of spermine and spermidine (I–IV), as well as several heterocyclic and aromatic compounds containing a novoldiamine side chain (V–VIII), were prepared and their biological activity was evaluated at the National Cancer Institute.

## EXPERIMENTAL

**Chemistry**—*N*,*N*-Bis(2-cyanoethyl)amine (VIII*a*), prepared by cyanoethylation of ammonia with acrylonitrile (30), was treated with palmitoyl chloride to yield the hexadecaneamide, VIII*b*. Catalytic reduction of VIII*b* with Raney nickel in ethanolic ammonia (31) gave I*a*, isolated as a dihydrochloride salt, mp 240–243° dec. The corresponding dimethyl homolog I*b* was obtained from I*a* and a mixture of formic acid and formamide, according to the method of Clarke *et al.* (32). Compounds Ic and I*d* were prepared by reductive alkylation of 5-diethylamino-2-pentanone (IX) with 3-diethylaminopropylamine (X*a*) and novoldiamine (XI), respectively, followed by acylation. Treatment of 1-methylpiperazine (XII) and 1,4′-bipiperidine (XIII) with palmitoyl chloride in tetrahydrofuran in the presence of triethylamine gave I*e* (isolated as a monohydrochloride salt, mp 150–152°) and I*f* (isolated as a free base, mp 68–69°), respectively.

The tetramethyl homologs of spermidine and spermine, II*a* (isolated as a diphosphate salt, mp 269–271°) and II*b* (disphosphate, mp 239–241°), were prepared by mono- and dicyanoethylation of 2,5-diamino-

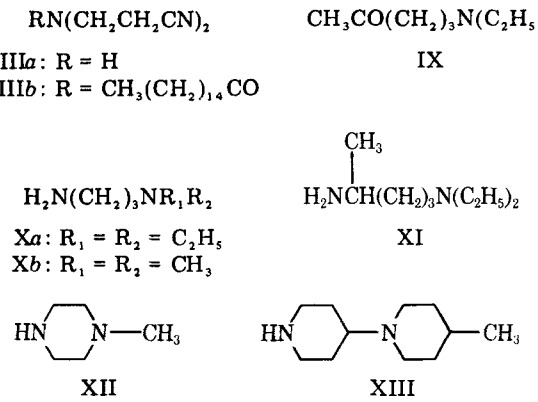

**Table I—Antineoplastic Activity Screening Results of Acylated and Some Unacylated Polyamines**

| Compound | P-388 Leukemia Dose, mg/kg | P-388 Leukemia T/C | B-16 Melanoma Dose, mg/kg | B-16 Melanoma T/C | KB Cell Culture $ED_{50}$, μg/ml |
|---|---|---|---|---|---|
| I*a* | 12.5 | 109 | — | — | 0.96 |
| I*b* | 6.25 | 101 | — | — | 0.024 |
| I*c* | 1.5 | 98 | 3.13 | 104 | 0.29 |
| I*d* | 6.25 | 99 | 3.13 | 91 | 0.026 |
| I*e* | 25.0 | 115 | — | — | 1.7 |
| I*f* | 300.0 | 100 | — | — | 100.0 |
| II*a* | 200.0 | 106 | — | — | — |
| II*b* | 3.13 | 115 | — | — | — |
| III*e* | 100.0 | 110 | — | — | 29.0 |
| III*i* | 25.0 | 92 | 50.0 | Toxic | 100.0 |
| | | | 25.0 | 224 | |
| | | | 12.5 | 125 | |
| | | | 6.5 | 133 | |
| | | | 3.13 | 125 | |
| III*k* | 3.13 | 100 | 6.25 | 105 | 100.0 |
| III*l* | 100.0 | 105 | — | — | 100.0 |
| III*m* | 3.13 | 108 | 1.56 | 105 | 2.2 |
| IV*a* | 6.25 | 114 | 12.5 | 111 | 16.0 |
| IV*b* | 25.0 | 98 | — | — | 2.3 |
| IV*c* | 25.0 | 109 | — | — | 2.0 |
| IV*d* | 400.0 | 111 | — | — | — |
| IV*e* | 50.0 | 97 | — | — | 100.0 |
| IV*f* | 1.56 | 106 | 1.56 | 106 | 2.6 |
| IV*g* | 12.5 | 90 | — | — | 2.3 |
| IV*h* | 3.13 | 108 | 6.25 | 118 | 12.0 |
| VI*i* | 100.0 | 98 | — | — | — |
| IV*j* | 3.0 | 101 | — | — | 8.9 |
| IV*k* | 25.0 | 93 | 3.13 | 104 | 26.0 |
| IV*l* | 6.25 | 113 | 50.0 | 155 | 2.2 |
| | | | 25.0 | 163 | |
| | | | 12.5 | 177 | |
| IV*m* | 12.5 | 102 | 3.13 | 98 | 2.4 |
| IV*n* | 25.0 | 95 | — | — | 2.5 |
| IV*o* | 50.0 | 101 | 12.5 | 106 | 0.63 |
| IV*p* | 3.13 | 90 | — | — | 18.0 |
| IV*q* | 100.0 | 93 | — | — | — |
| V | 25.0 | 123 | — | — | — |
| VI | 50.0 | 106 | — | — | — |
| VII*a* | 6.25 | 96 | 6.25 | 104 | — |
| XIV*b* | 100.0 | 128 | — | — | — |
| XVIII*a* | 12.5 | 117 | — | — | — |
| XVIII*b* | 25.0 | 98 | — | — | — |

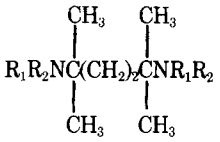

XIV*a*: $R_1 = R_2 = H$
XIV*b*: $R_1 = H$, $R_2 = (CH_2)_2CN$
XIV*c*: $R_1 = CH_3(CH_2)_{14}CO$, $R_2 = (CH_2)CN$

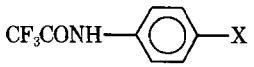

XV*a*: X = $NO_2$
XV*b*: X = $NH_2$
XV*c*: X = $NHCH(CH_3)—(CH_2)_3N(C_2H_5)_2$

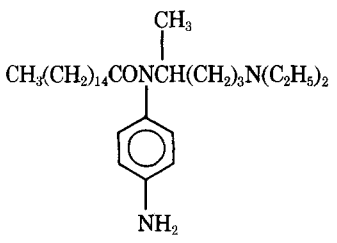

XVI

2,5-dimethylhexane (XIV*a*) with acrylonitrile, followed by catalytic hydrogenation. Acylation of the intermediate dinitrile XIV*b* with palmitoyl chloride and subsequent reduction yielded IV*a*, mp 70–73°. Reductive methylation (32) of IV*a* afforded IV*b*. Compounds IV*c* and IV*d* were prepared by similar sequential steps through intermediates III*a*–III*i* from the appropriate α,ω-diamines.

The unsaturated spermine analogs were prepared according to a reported method (33). Treatment of *trans*-1,4-dichloro-2-butene with 3-dimethylaminopropylamine (X*b*), followed by acylation of the intermediate diamine III*j*, yielded IV*l*, mp 58–60°. The novoldiamine analog IV*m* was prepared from III*k* in an analogous manner. Similarly, the corresponding butyne derivatives IV*n* (mp 40–41°) and IV*o* were prepared from 1,4-dichloro-2-butyne through the intermediates III*l* and III*m*, respectively. For the preparation of the cyclohexyl derivative IV*p*, the intermediate tetramine III*n* was obtained by reductive alkylation

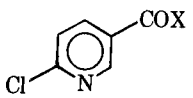

XVII*a*: X = OH
XVII*b*: X = $NHCH(CH_3)—(CH_2)_3N(C_2H_5)_2$

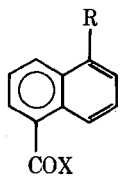

XVIII*a*: R = H, X = OH
XVIII*b*: R = $NO_2$, X = OH
XVIII*c*: R = $NO_2$, X = $NHCH(CH_3)—(CH_2)_3N(C_2H_5)_2$
XVIII*d*: R = $NH_2$, X = $NHCH(CH_3)—(CH_2)_3N(C_2H_5)_2$

of 1,4-cyclohexanedione and X*b*. Acylation of III*n* readily yielded IV*p*, mp 110–115°.

The urea derivative IV*q* was prepared as follows. *p*-Nitrotrifluoroacetanilide (XV*a*), prepared from *p*-nitroaniline and trifluoroacetic anhydride, was reduced to the corresponding amino derivative XV*b*. This reaction was followed by reductive alkylation with IX to give XV*c*. Acylation of XV*c* with palmitoyl chloride and subsequent hydrolysis with potassium carbonate gave the *p*-phenylenediamine derivative XVI. Treatment of XVI with diethylcarbamoyl chloride in pyridine, according to a reported method (34), yielded IV*q*, mp 313–315°.

Condensation of 6-chloronicotinic acid (XVII*a*) with novoldiamine in the presence of dicyclohexylcarbodiimide yielded the chloronicotinamide XVII*b*. Amination of XVII with aqueous dimethylamine gave V (monophosphate, mp 105–107° dec.). The orotamide derivative VI (mp 196–198°) was obtained by refluxing a mixture of novoldiamine and the methyl ester of orotic acid (35) in 2-methoxyethanol[1]. The naphthalenesulfonamide VII*a* (dihydrochloride, mp 77–80°) was prepared by treatment of dansyl chloride with novoldiamine. For the preparation of the naphthalenecarboxamide VII*b* (monophosphate, mp 211–214° dec.), the starting material 1-naphthoic acid (XVIII*a*) was nitrated according to previously reported methods (36, 37). Condensation of the resulting nitroacid XVIII*b* and XI, followed by hydrogenation and reductive alkylation, yielded VII*b*.

**Biological Activity**—Test results (Table I) were obtained from the National Cancer Institute. Biological screening was conducted in mice with leukemia P-388 and B-16 melanoma and an *in vitro* system with human epidermoid carcinoma of the nasopharynx (KB cell culture). (For the general procedure and data interpretation, see Refs. 38 and 39.)

None of the polyamines showed good activity against leukemia P-388. On the other hand, *N*,*N*′-bis(3-dimethylaminopropyl)-*N*,*N*′-bis(palmitoyl)-*trans*-1,4-diamino-2-butene (IV*l*) and *N*,*N*′-bis(5-diethylamino-2-pentyl)-1,4-butanediamine (III*i*) exhibited inhibitory activity against B-16 melanoma. Compound IV*l* gave test/control (T/C) values of 155, 163, and 177 at doses of 50, 25, and 12.5 mg/kg, respectively. Compound III*i* had a T/C value of 224 at 25 mg/kg but was toxic at 50 mg/kg.

For the KB cell culture, inhibitory activity was demonstrated when the $ED_{50}$ value was <6 μg/ml. Based on this criterion, several acylated and unacylated polyamines (I*a*–I*e*, III*m*, IV*b*, IV*c*, IV*f*, IV*g*, and IV*l*–IV*o*) demonstrated inhibitory activity. Three of the most active compounds (I*b*–I*d*) are all monoacylated polyamines that showed $ED_{50}$ values at concentrations of 0.024, 0.29, and 0.026 μg/ml, respectively.

## REFERENCES


(1) S. S. Cohen, "Introduction to the Polyamines", Prentice-Hall, Englewood Cliffs, N.J., 1971.

(2) H. Tabor and C. W. Tabor, in "Advances of Enzymology and Related Areas of Molecular Biology," vol. 36, A. Meister, Ed., Interscience, New York, N.Y., 1972, p. 203.

(3) U. Bachrach, "Function of Naturally Occurring Polyamines," Academic, New York, N.Y., 1973.

(4) J. Jänne, H. Pösö, and A. Raina, *Biochim. Biophys. Acta*, **473,** 241 (1978).

(5) C. M. Caldarera, B. Barbiroli, and G. Moruzzi, *Biochem. J.*, **97,** 84 (1965).

(6) W. G. Dykstra and E. J. Herbst, *Science*, **149,** 428 (1965).

(7) A. Raina, J. Janne, and M. Siimes, *Biochim. Biophys. Acta*, **123,** 197 (1966).

(8) A. Raina and T. Telaranta, *ibid.*, **138,** 200 (1967).

(9) D. H. Russell, *Fed. Proc. Fed. Am. Soc. Exp. Biol.*, **29,** 669 (1970).

(10) A. Mizutani, H. Inoue, and Y. Takeda, *Biochim. Biophys. Acta*, **338,** 183 (1974).

(11) D. H. Russell and C. C. Levy, *Cancer Res.*, **31,** 248 (1971).

(12) G. Anderson and O. Heby, *J. Natl. Cancer Inst.*, **48,** 165 (1972).

(13) U. Bachrach, S. Don, and H. Wiener, *Biochem. Biophys. Res. Commun.*, **55,** 1035 (1973).

(14) O. Heby, G. P. Sarna, L. J. Marton, M. Omine, S. Perry, and D. H. Russell, *Cancer Res.*, **33,** 2959 (1973).

(15) L. J. Morton, O. Heby, and C. B. Wilson, *Cancer*, **14,** 731 (1974).

(16) S. Don, H. Wiener, and U. Bachrach, *Cancer Res*, **35,** 194 (1975).

(17) D. V. Maudsley, *Biochem. Pharmacol.*, **28,** 153 (1979).

(18) D. H. Russell, C. C. Levy, S. C. Schimpff, and I. A. Hawk, *Cancer Res.*, **31,** 1555 (1971).

(19) A. Lipton, L. Sheehan, and H. A. Harvey, *Cancer*, **36,** 2351 (1975).

(20) T. P. Waalkers, C. W. Gehrke, D. C. Tormey, R. W. Zumwalt, J. N. Hueser, K. C. Juo, D. B. Lakings, D. L. Ahmann, and C. G. Moertel, *Cancer Chemother. Rep.*, **59,** 1103 (1975).

(21) D. H. Russell, *Cancer Res.*, **32,** 2459 (1972).

(22) O. Heby and D. H. Russell, *ibid.*, **33,** 159 (1973).

(23) D. H. Russell, W. B. Looney, C. J. Kovacs, H. A. Hopkins, L. J. Morton, S. M. LeGendre, and H. P. Morris, *ibid.*, **34,** 2382 (1974).

(24) I. D. Algranati and S. H. Goldenberg, *Trends Biochem. Sci.*, **2,** 272 (1977).

(25) S. S. Cohen, *Nature*, **274,** 209 (1978).

(26) M. Israel, J. S. Rosenfield, and E. J. Modest, *J. Med. Chem.*, **7,** 710 (1964).

(27) M. Israel, E. C. Zoll, N. Muhammad, and E. J. Modest, *ibid.*, **16,** 1 (1973).

(28) S. M. Kupchan, A. P. Davies, S. J. Bardoutis, H. K. Schnoes, and A. L. Burlingame, *J. Am. Chem. Soc.*, **89,** 5718 (1967); *J. Org. Chem.*, **34,** 3888 (1969).

(29) S. M. Kupchan, G. Bondesson, and A. P. Davies, *J. Med. Chem.*, **15,** 65 (1972).

(30) A. P. Terentyev, K. I. Chursina, and A. Kost, *J. Gen. Chem., USSR*, **21,** 115 (1951).

(31) R. L. Augustine, "Catalytic Hydrogenations," Dekker, New York, N.Y., 1965, p. 97.

(32) H. T. Clarke, H. B. Gillespie, and S. Z. Weisshaus, *J. Am. Chem. Soc.*, **55,** 4571 (1933).

(33) E. D. Parker, Ph.D. thesis, University of Texas, Austin, Tex., 1962; through *Diss. Abstr.*, **24,** 3959 (1964).

(34) L. M. Werbel, J. Battaglia, E. F. Elslager, and C. Younstrom, *J. Med. Chem.*, **13,** 592 (1970).

(35) G. D. Daves, Jr., F. Baiocchi, R. K. Robins, and C. C. Cheng, *J. Org. Chem.*, **26,** 2755 (1961).

(36) J. Ekstrand, *J. Prakt. Chem.*, **38,** 156 (1888).

(37) W. H. D. Morgan, *J. Chem. Soc.*, **1954,** 1716.

(38) R. I. Geren, N. H. Greenberg, M. M. MacDonald, A. M. Schumacker, and B. J. Abbott, *Cancer Chemother. Rep., Part 3*, **3,** 1 (1972).

(39) "Screening Data Summary Interpretation and Outline of Current Screen," Drug Evaluation Branch Instruction Booklet 14, Division of Cancer Treatment, National Cancer Institute, Bethesda, Md., 1978.


## ACKNOWLEDGMENTS


Supported in part by Contract N01-CM-33743 from the Division of Cancer Treatment, National Cancer Institute, National Institutes of Health.


[1] Methyl Cellosolve.

# Temperature-Dependent Effect of Edetate Disodium on Neomycin Stability

**N. A. HODGES** [x] **and PETA G. WALTON**

Received November 28, 1980, from the *Department of Pharmacy, Brighton Polytechnic, Sussex BN2 4GJ, England.* Accepted for publication January 26, 1981.

**Abstract** □ When heated at temperatures in excess of 100°, the stability of neomycin in aqueous ophthalmic formulations was improved by the addition of edetate disodium (0.01%). As the exposure temperature was reduced, the degree of stability enhancement diminished until the effect was reversed, and addition of edetate disodium was detrimental to neomycin stability in solutions stored at 30°.

**Keyphrases** □ Neomycin—stability in ophthalmic solutions containing edetate disodium □ Edetate disodium—temperature-dependent effect on neomycin stability □ Stability—neomycin in solutions containing edetate disodium

Edetate disodium (I) has been used to restrict metal-catalyzed oxidation of various drugs including several antibiotics (1–3). Neomycin (II), in common with other aminoglycoside antibiotics, is susceptible to atmospheric oxidation (4), and I has been recommended for inclusion in various neomycin preparations described in national formularies (5, 6). The factual basis for this recommendation is obscure, because few reports directly described the effects of I on the stability of II, although I has been included in formulations of fradiomycin (7), the principal components of which are neomycins B and C (8). The foregoing, together with observations during work on neomycin stability (9) that suggested I was of doubtful value in stabilizing neomycin at room temperatures, prompted the present study.

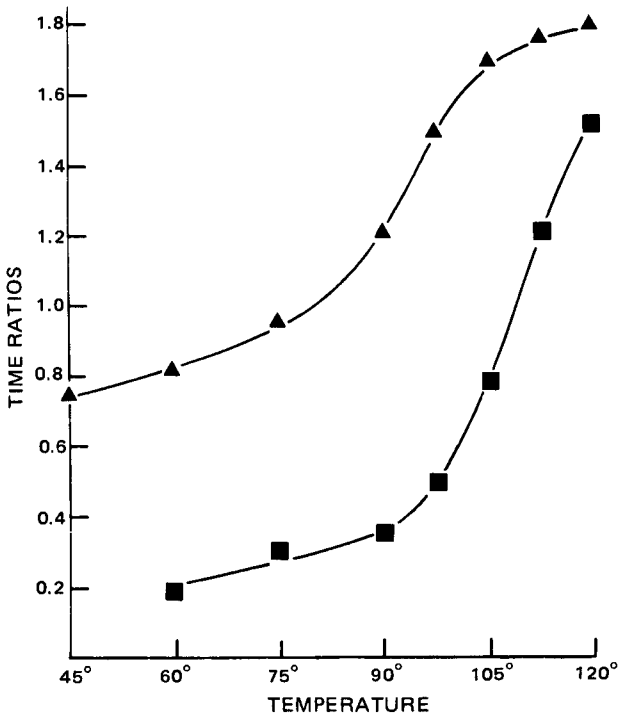


**Figure 1**—*Effect of heating temperature on the ratio of times required to achieve 15% (▲) or 50% (■) neomycin degradation in the presence and absence of edetate disodium.*

## EXPERIMENTAL

All reagents, apparatus, and procedures were described previously (9). The prepared 0.2 and 0.5% neomycin sulfate ophthalmic solutions contained 0.7% $Na_2HPO_4 \cdot 12H_2O$, 0.7% $NaH_2PO_4 \cdot 2H_2O$, and 0.002% phenylmercuric nitrate; 0.01% edetate disodium was included as required.

Initially, 3.5 ml of 0.2% neomycin solutions with and without I were sealed in neutral glass ampuls of nominal 5-ml capacity, leaving ~2 ml of airspace. The ampuls were heated by immersion in an oil bath at 120°, removed at suitable intervals, and rapidly cooled, and the contents were assayed. Plots of log percentage residual neomycin against time were constructed for solutions with and without I. Loss of neomycin did not consistently follow either zero- or first-order kinetics, and it was not possible to represent decomposition by a rate constant. For this reason, the effect of I inclusion was recorded as the ratio of times required to achieve either 15 or 50% neomycin loss in the presence and absence of I. This procedure was adopted also for 0.2% neomycin solutions heated between 45 and 112°.

The 0.5% neomycin solutions with and without edetate disodium were prepared to investigate the effect of changing the ratio of I to II and also to examine the stability of II at 100°, the temperature recommended for the BP process of heating with a bactericide (10). The solutions also were stored at 30°, and the stability of II was monitored.

Discoloration of solutions was recorded as absorbance at 450 nm.

## RESULTS AND DISCUSSION

The relationship between heating temperatures and the benefit resulting from inclusion of edetate disodium in the formulation is shown in Fig. 1. The beneficial effect, in terms of the time required for 50% neomycin loss, declined as the exposure temperature was reduced from 120 to 110°. Thereafter, the benefit was eliminated, and lowering the temperature further resulted in a progressively severe detrimental effect. A similar relationship was observed when a 15% fall in neomycin concentration was considered, but the advantage of edetate disodium inclusion was retained down to 80°. Thus, at temperatures between 80 and 110°, I afforded protection to II during the initial heating, but the reverse situation arose on prolonged exposure. In the 0.2% neomycin solutions, insufficient degradation occurred for values to be plotted at temperatures lower than 45 and 60° for 15 and 50% loss, respectively.

In the 0.5% neomycin solutions heated at 100°, the degradation rates down to ~70% of the initial concentration were almost identical in the

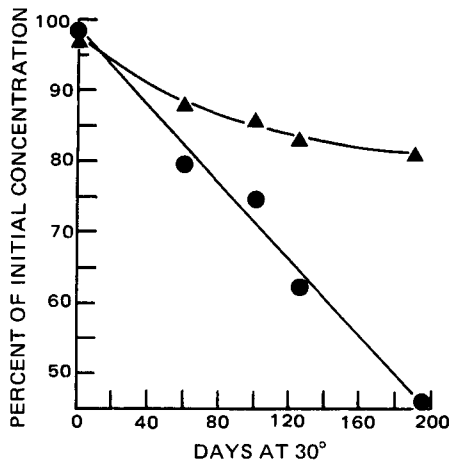


**Figure 2**—*Stability of 0.5% neomycin solutions with (●) and without (▲) edetate disodium during storage at 30°.*



*0022-3549/81/0800-0960$01.00/0*
*© 1981, American Pharmaceutical Association*

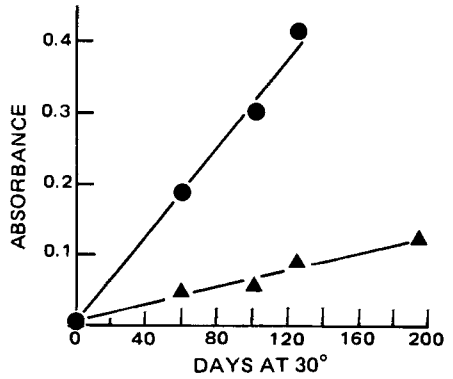


**Figure 3**—*Discoloration of 0.5% neomycin solutions with (●) and without (▲) edetate disodium during storage at 30°.*

solutions with and without I. Thereafter, the rate was slightly greater in the solution containing I (data not shown).

The fall in neomycin concentration and the associated discoloration of the solutions during storage at 30° are shown in Figs. 2 and 3. The data illustrated are for 10 ml of solution in amber ophthalmic dropper bottles. Solutions stored in ampuls at 30° gave qualitatively similar results, but the extent of degradation was somewhat less, due possibly to the smaller proportion of air to liquid in the ampuls. During prolonged storage, II was more stable in the absence rather than the presence of I. This pattern was reflected in the discoloration of the solutions.

Ethylenediaminetetraacetic acid or its disodium salt were observed previously to increase the degradation rate of epinephrine (11), physostigmine (12), and isoproterenol (13), which, like neomycin, all possess basic nitrogen groups in the molecule. With epinephrine (11) and isoproterenol (13), the diminished stability occurred at 37 and 60°, respectively, when ethylenediaminetetraacetic acid was present together with ferric ions at neutral pH values, although the mechanisms responsible for this effect have not been explained adequately. In the experimental system used in the present study, iron was not present other than as a contaminant of other chemicals or if it leached from glass. Furthermore, the same qualitative effects of edetate disodium inclusion were observed regardless of the neomycin batch, buffer concentration, color of the glass container, and presence or absence of phenylmercuric nitrate as a preservative.

The reported results show that inclusion of edetate disodium in neomycin ophthalmic formulations is likely to reduce the stability of the antibiotic during long-term storage at room temperatures. This effect is particularly important if the antibiotic solution is sterilized by filtration because the data indicate that the destabilization is operative even during the early storage period and that the initial protective effect observed at high temperatures is eliminated.

## REFERENCES

(1) Y. Kitano, N. Saegusa, S. Namikawa, E. Yoshikawa, and H. Kono, Japanese pat. 77, 31820 (Mar. 10, 1977).

(2) E. H. Girgis and A. A. Kassem, *J. Drug. Res.*, **5**, 189 (1973).

(3) M. C. Scrutton, *FEBS Lett.*, **78** (2), 216 (1977).

(4) R. M. Simone and R. P. Popino, *J. Am. Pharm. Assoc., Sci. Ed.*, **44**, 275 (1955).

(5) "British Pharmaceutical Codex," Pharmaceutical Press, London, England, 1973.

(6) "Australian Pharmaceutical Formulary and Handbook," Australasian Pharmaceutical Publishing Co., Melbourne, Australia, 1974.

(7) S. Makino, E. Hayashi, and K. Okamura, Japanese pat. 6247 ('60) (June 1, 1960).

(8) Y. Okami, in "Handbook on Microbiology Vol. III," A. I. Laskin and H. A. Lechevalier, Eds., C.R.C. Press, Cleveland, Ohio, 1973, p. 758.

(9) N. A. Hodges and J. Singh, *J. Pharm. Pharmacol.*, **30**, 737 (1978).

(10) "British Pharmacopoeia 1973," Her Majesty's Stationery Office, London, England, 1973, p. 241.

(11) S. Green, A. Mazur, and E. Shorr, *J. Biol. Chem.*, **220**, 237 (1956).

(12) J. Mørch, "Proceedings of the 17th Congress on Pharmaceutical Sciences," Leiden, The Netherlands, 1957; through T. D. Whittet, *Pharm. Acta Helv.*, **34**, 489 (1959).

(13) J. A. Clements, K. Hasson, and G. Smith, *J. Pharm. Pharmacol.*, **32**, 50P (1980).

# Physicochemical Properties of Magnesium Salicylate

**A. S. ALAM *x and D. GREGORIADES**

Received July 17, 1980, from the *Department of Preclinical Research, Rohm and Haas Company, Spring House, PA 19477.* Accepted for publication January 28, 1981. *Present address: American Critical Care, McGaw Park, IL 60085.

**Abstract** □ Magnesium salicylate tetrahydrate is a nonhygroscopic, crystalline powder, whereas anhydrous magnesium salicylate is amorphous and very hygroscopic. Magnesium salicylate tetrahydrate tablets formulated with gelatin as a binder showed a dissolution half-life ($t_{1/2}$) of 12 min, whereas a formulation using pregelatinized starch as a binder showed a $t_{1/2}$ of 33 min. The optimum level of calcium stearate in the formulation was determined by the oscilloscope tracings of compressional and ejectional forces from an instrumented rotary tableting machine. Increasing the level of calcium stearate from 1 to 1.5 and 2% resulted in dissolution $t_{1/2}$ values of 12, 18, and 21 min, respectively, and a higher incidence of softer tablets and capping.

**Keyphrases** □ Magnesium salicylate—physicochemical properties, tableted tetrahydrate and anhydrous forms, effect of calcium stearate on dissolution rate □ Calcium stearate—effect on dissolution rate of tableted magnesium salicylate □ Dissolution—effect of calcium stearate on magnesium salicylate tablets □ Analgesics—magnesium salicylate tablets, effect of calcium stearate on dissolution

Magnesium salicylate is a white powder with analgesic, antipyretic, and anti-inflammatory properties similar to those of aspirin (1). Although magnesium salicylate or combinations of magnesium salicylate with other analgesics have been widely used in various diseases, the physicochemical properties of magnesium salicylate are not well characterized. This study characterized the physicochemical properties of magnesium salicylate and determined the effect of several excipients on the dissolution rate from tablet formulations.

## EXPERIMENTAL

**Materials**—Magnesium salicylate tetrahydrate, anhydrous magnesium salicylate, lactose monohydrate, gelatin, pregelatinized starch, FD&C Red No. 3 aluminum lake, and calcium stearate were used for tablet preparations.

**Thermogravimetric Analysis**—Profiles of the tetrahydrate and anhydrous forms were obtained under nitrogen with a heating rate of 20°/min.

**X-Ray Diffraction**—Profiles of the tetrahydrate and anhydrous forms were determined using nickel-filtered radiation with a copper target, a range of 500, and time constant 5.

**Equilibrium Moisture Content**—Sulfuric acid–distilled water admixtures were prepared for the relative humidity chambers; 20, 40, 60,

0022-3549/81/0800-0961$01.00/0
© 1981, American Pharmaceutical Association

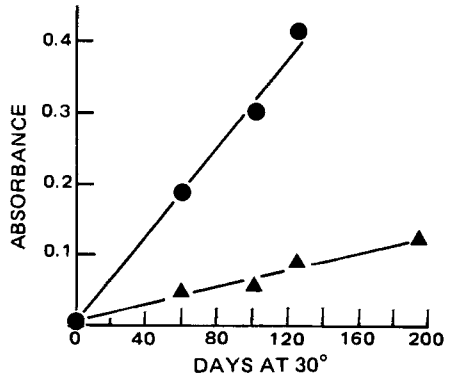


**Figure 3**—*Discoloration of 0.5% neomycin solutions with (●) and without (▲) edetate disodium during storage at 30°.*

solutions with and without I. Thereafter, the rate was slightly greater in the solution containing I (data not shown).

The fall in neomycin concentration and the associated discoloration of the solutions during storage at 30° are shown in Figs. 2 and 3. The data illustrated are for 10 ml of solution in amber ophthalmic dropper bottles. Solutions stored in ampuls at 30° gave qualitatively similar results, but the extent of degradation was somewhat less, due possibly to the smaller proportion of air to liquid in the ampuls. During prolonged storage, II was more stable in the absence rather than the presence of I. This pattern was reflected in the discoloration of the solutions.

Ethylenediaminetetraacetic acid or its disodium salt were observed previously to increase the degradation rate of epinephrine (11), physostigmine (12), and isoproterenol (13), which, like neomycin, all possess basic nitrogen groups in the molecule. With epinephrine (11) and isoproterenol (13), the diminished stability occurred at 37 and 60°, respectively, when ethylenediaminetetraacetic acid was present together with ferric ions at neutral pH values, although the mechanisms responsible for this effect have not been explained adequately. In the experimental system used in the present study, iron was not present other than as a contaminant of other chemicals or if it leached from glass. Furthermore, the same qualitative effects of edetate disodium inclusion were observed regardless of the neomycin batch, buffer concentration, color of the glass container, and presence or absence of phenylmercuric nitrate as a preservative.

The reported results show that inclusion of edetate disodium in neomycin ophthalmic formulations is likely to reduce the stability of the antibiotic during long-term storage at room temperatures. This effect is particularly important if the antibiotic solution is sterilized by filtration because the data indicate that the destabilization is operative even during the early storage period and that the initial protective effect observed at high temperatures is eliminated.

## REFERENCES

(1) Y. Kitano, N. Saegusa, S. Namikawa, E. Yoshikawa, and H. Kono, Japanese pat. 77, 31820 (Mar. 10, 1977).

(2) E. H. Girgis and A. A. Kassem, *J. Drug. Res.*, **5**, 189 (1973).

(3) M. C. Scrutton, *FEBS Lett.*, **78** (2), 216 (1977).

(4) R. M. Simone and R. P. Popino, *J. Am. Pharm. Assoc., Sci. Ed.*, **44**, 275 (1955).

(5) "British Pharmaceutical Codex," Pharmaceutical Press, London, England, 1973.

(6) "Australian Pharmaceutical Formulary and Handbook," Australasian Pharmaceutical Publishing Co., Melbourne, Australia, 1974.

(7) S. Makino, E. Hayashi, and K. Okamura, Japanese pat. 6247 ('60) (June 1, 1960).

(8) Y. Okami, in "Handbook on Microbiology Vol. III," A. I. Laskin and H. A. Lechevalier, Eds., C.R.C. Press, Cleveland, Ohio, 1973, p. 758.

(9) N. A. Hodges and J. Singh, *J. Pharm. Pharmacol.*, **30**, 737 (1978).

(10) "British Pharmacopoeia 1973," Her Majesty's Stationery Office, London, England, 1973, p. 241.

(11) S. Green, A. Mazur, and E. Shorr, *J. Biol. Chem.*, **220**, 237 (1956).

(12) J. Mørch, "Proceedings of the 17th Congress on Pharmaceutical Sciences," Leiden, The Netherlands, 1957; through T. D. Whittet, *Pharm. Acta Helv.*, **34**, 489 (1959).

(13) J. A. Clements, K. Hasson, and G. Smith, *J. Pharm. Pharmacol.*, **32**, 50P (1980).

# Physicochemical Properties of Magnesium Salicylate

**A. S. ALAM *x and D. GREGORIADES**

Received July 17, 1980, from the *Department of Preclinical Research, Rohm and Haas Company, Spring House, PA 19477.* Accepted for publication January 28, 1981. *Present address: American Critical Care, McGaw Park, IL 60085.

**Abstract** □ Magnesium salicylate tetrahydrate is a nonhygroscopic, crystalline powder, whereas anhydrous magnesium salicylate is amorphous and very hygroscopic. Magnesium salicylate tetrahydrate tablets formulated with gelatin as a binder showed a dissolution half-life ($t_{1/2}$) of 12 min, whereas a formulation using pregelatinized starch as a binder showed a $t_{1/2}$ of 33 min. The optimum level of calcium stearate in the formulation was determined by the oscilloscope tracings of compressional and ejectional forces from an instrumented rotary tableting machine. Increasing the level of calcium stearate from 1 to 1.5 and 2% resulted in dissolution $t_{1/2}$ values of 12, 18, and 21 min, respectively, and a higher incidence of softer tablets and capping.

**Keyphrases** □ Magnesium salicylate—physicochemical properties, tableted tetrahydrate and anhydrous forms, effect of calcium stearate on dissolution rate □ Calcium stearate—effect on dissolution rate of tableted magnesium salicylate □ Dissolution—effect of calcium stearate on magnesium salicylate tablets □ Analgesics—magnesium salicylate tablets, effect of calcium stearate on dissolution

Magnesium salicylate is a white powder with analgesic, antipyretic, and anti-inflammatory properties similar to those of aspirin (1). Although magnesium salicylate or combinations of magnesium salicylate with other analgesics have been widely used in various diseases, the physicochemical properties of magnesium salicylate are not well characterized. This study characterized the physicochemical properties of magnesium salicylate and determined the effect of several excipients on the dissolution rate from tablet formulations.

## EXPERIMENTAL

**Materials**—Magnesium salicylate tetrahydrate, anhydrous magnesium salicylate, lactose monohydrate, gelatin, pregelatinized starch, FD&C Red No. 3 aluminum lake, and calcium stearate were used for tablet preparations.

**Thermogravimetric Analysis**—Profiles of the tetrahydrate and anhydrous forms were obtained under nitrogen with a heating rate of 20°/min.

**X-Ray Diffraction**—Profiles of the tetrahydrate and anhydrous forms were determined using nickel-filtered radiation with a copper target, a range of 500, and time constant 5.

**Equilibrium Moisture Content**—Sulfuric acid–distilled water admixtures were prepared for the relative humidity chambers; 20, 40, 60,

0022-3549/81/0800-0961$01.00/0
© 1981, American Pharmaceutical Association

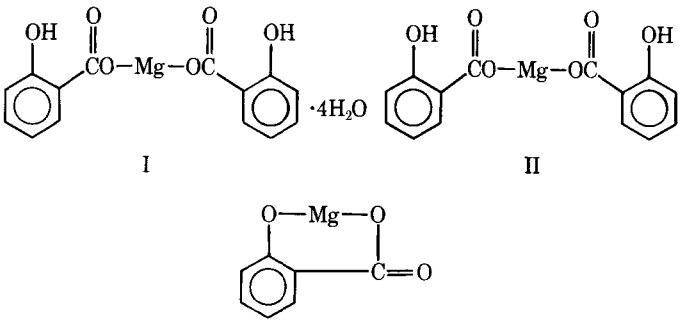

I II



III

and 80% relative humidities (RH) were obtained (2). The tetrahydrate and anhydrous forms were dried at 105°/4 hr/76 cm vac-vented, weighed into aluminum dishes, and placed in the humidity chambers at ambient room temperature. The dishes were weighed after 1, 2, and 3 weeks.

**Tablet Preparation**—Formulation A was prepared by granulating magnesium salicylate tetrahydrate, lactose, and colorant with 41% aqueous gelatin solution. Formulation B was prepared by adding water to the powder mix of magnesium salicylate tetrahydrate, lactose, pregelatinized starch, and colorant. The granulations were dried, sized in a hammermill, lubricated with calcium stearate, and compressed to a 1.83 × 0.74-cm capsule-shaped tablet on an instrumented rotary machine.

**Dissolution**—Tablet dissolution was determined by placing one tablet in the rotating-basket apparatus immersed in 900 ml of distilled water (3). The basket was rotated at 100 rpm. At 10, 20, 30, 60, and 120 min, a 1-ml sample was withdrawn, filtered through a 0.45-$\mu$m membrane filter, and diluted to 10 ml with distilled water; an aliquot was taken for UV absorbance at 296 nm. The amount dissolved was determined, and the cummulative percentage dissolved was calculated based on assayed values. Six individual tablets were run for each product. A NONLIN program (4) was used to calculate the apparent dissolution rate ($k_d$). The dissolution half-life ($t_{1/2}$) was determined by:

$$t_{1/2} = \frac{0.693}{k_d} \qquad \text{(Eq. 1)}$$

## RESULTS AND DISCUSSION

Magnesium salicylate tetrahydrate did not gain any moisture as reflected by the weights after 1, 2, and 3 weeks of storage of samples at 20, 40, 60, and 80% RH. Although the moisture gain for the 40% RH sample was higher, it was not significant. Anhydrous magnesium salicylate gained 1.7, 5.1, 12.2, and 21.5% of its weight, respectively, in these humidity chambers (Table I). Moisture equilibration was reached within 1 week of exposure in each chamber.

**Table I—Moisture Uptake (Percent) by Magnesium Salicylate Tetrahydrate and Anhydrous Magnesium Salicylate at Various Relative Humidity Storage**

| Product | Weeks | Relative Humidity 20% | 40% | 60% | 80% |
|---|---|---|---|---|---|
| Magnesium salicylate tetrahydrate | 1 | 0.05 | 0.03 | 0.08 | 0.06 |
| | 2 | 0.07 | 0.40 | 0.05 | 0.03 |
| | 3 | 0.06 | 0.90 | 0.60 | 0.04 |
| Anhydrous magnesium salicylate | 1 | 1.70 | 4.70 | 11.50 | 21.50 |
| | 2 | 1.70 | 4.80 | 11.90 | 21.80 |
| | 3 | 1.70 | 5.10 | 12.20 | 21.50 |

**Table II—Dissolution Profile[a] of Magnesium Salicylate Tetrahydrate Tablets**

| Formulation | $k_d \pm SD$, min$^{-1}$ | $t_{1/2} \pm SD$, min |
|---|---|---|
| A, 1% calcium stearate | 0.057 ± 0.012 | 12 ± 2.4 |
| A, 1.5% calcium stearate | 0.038 ± 0.007 | 18 ± 3.2 |
| A, 2% calcium stearate | 0.033 ± 0.007 | 21 ± 3.7 |
| B, 1% calcium stearate | 0.021 ± 0.003 | 33 ± 8.8 |

[a] USP apparatus, 100 rpm in distilled water, mean ± $SD$ of six tablets.

The thermogravimetric profile of magnesium salicylate tetrahydrate (I) showed a 20% weight loss between 75 and 200° (II) and a 35% weight loss between 200 and 350° (III), followed by a plateau region between 350 and 475°. Based on molecular weights and weight losses, the postulated products are as shown in Structures I–III.

X-ray diffraction results showed magnesium salicylate tetrahydrate to be crystalline, whereas anhydrous magnesium salicylate was amorphous. Based on these results, magnesium salicylate tetrahydrate was selected for tablet formulation.

Tablet dissolution data are shown in Table II. Although Formulations A and B were compressed to the same size, weight, thickness, and hardness, with equivalent compressional forces, the dissolution rates were different by as much as threefold. The $t_{1/2}$ values for Formulations A and B were 12 and 33 min, respectively. In both cases, the tablets did not disintegrate, and magnesium salicylate dissolved directly from the tablet matrix. It is postulated that the gelling properties of starch decreased the dissolution rate, whereas gelatin made the drug particles more hydrophilic; thus, the dissolution rate was increased (5).

The optimum calcium stearate level for Formulation A was determined by monitoring the oscilloscope tracings of compressional and ejectional forces during tableting (6). At 1% calcium stearate, tableting proceeded smoothly at the rate of 1500–1700 tablets/min, which was the maximum speed for the tablet machine. However, as the concentration of calcium stearate was increased to 1.5 and 2%, the resulting tablets became softer and showed a higher incidence of capping. Since calcium stearate is a hydrophobic lubricant, the $t_{1/2}$ value was affected adversely with the higher concentrations of lubricant. The dissolution $t_{1/2}$ values from Formulation A tablets containing 1, 1.5, and 2% calcium stearate were 12, 18, and 21 min, respectively.

## REFERENCES


(1) A. E. Swinyard, in "Remington's Pharmaceutical Sciences," 15th ed., Mack Publishing Co., Easton, Pa., 1975, p. 1050.

(2) A. S. Alam and E. L. Parrott, *J. Pharm. Sci.*, **61**, 265 (1972).

(3) "The United States Pharmacopeia," 19th rev., Mack Publishing Co., Easton, Pa., 1975, p. 651.

(4) W. J. Dixon, "Biomedical Computer Programs," University of California Press, Berkeley, Calif., 1975.

(5) S. Solvang and P. Finholt, *J. Pharm. Sci.*, **59**, 49 (1970).

(6) E. L. Knoechel, C. C. Sperry, and C. J. Lintner, *ibid.*, **56**, 116 (1967).


## ACKNOWLEDGMENTS


The authors thank Mr. H. Lindemeyer and Mr. J. Graham for analytical services, Mr. J. Ritts for computer analysis, and Dr. T. G. Brown, Jr., and Dr. W. E. Goode for interest and support.

# Succinimides with Oxyacetate Side Chain as Potential Anticonvulsant Agents

**J. A. OWOYALE ˣ, G. D. LAHAN, G. OSUIDE, and I. O. EDAFIOGHO**

Received September 8, 1980, from the *Department of Pharmacology and Pharmaceutical Chemistry, Ahmadu Bello University, Zaria-Nigeria.* Accepted for publication January 29, 1981.

**Abstract** □ Two new compounds, ethyl *N*-succinimidoxyacetate and methyl *N*-succinimidoxyacetate, were prepared by reacting a solution of freshly recrystallized *N*-hydroxysuccinimide in tetrahydrofuran with a mixture of the corresponding halogenated ester and triethylamine. The compounds possessed some anticonvulsant properties.

**Keyphrases** □ Succinimides—derivatives, anticonvulsant effects, synthesis and analysis □ Anticonvulsants—succinimide derivatives, synthesis and analysis □ Derivatives—of succinimides, synthesis and analysis

Aminooxyacetic acid is a potent anticonvulsant agent, but it causes convulsions at high doses. This convulsive tendency has been attributed to the unsubstituted amino group of this compound, which is very reactive with other groups, such as the aldehyde of pyridoxal phosphate (1). Two analogs of aminooxyacetic acid obtained by derivatizing its amino and carboxylic acid ends, ethyl *N*-phthalimidoxyacetate and methyl *N*-phthalimidoxyacetate, protected chicks against experimentally induced seizures (2, 3). In addition, ethyl *N*-phthalimidoxyacetate lacks the convulsant property of aminooxyacetic acid but is a less potent anticonvulsant (2).

With the aim of producing a very potent anticonvulsant, other cyclic imides were prepared, particularly hybrid compounds based on aminooxyacetic acid and such moieties that are normally associated with anticonvulsant properties. Accordingly, ethyl *N*-succinimidoxyacetate (I) and methyl *N*-succinimidoxyacetate (II) were synthesized, and their anticonvulsant activities were studied in the chick.

## RESULTS AND DISCUSSION

The synthesis of I and II was achieved in a one-step, self-indicating reaction. A light-blue color developed initially and disappeared at the end of the reaction. The major advantage of this reaction is that it proceeds at room temperature, especially since the starting material, *N*-hydroxysuccinimide, is usually hygroscopic and decomposes in warm water (4).

Results from preliminary pharmacological screening indicated that I and II possessed some anticonvulsant properties. Compounds I and II protected young chicks against electrically and chemically induced seizures. The details of the pharmacological screening will be reported elsewhere.

## EXPERIMENTAL

Melting points of the two compounds were determined by an electrothermal melting-point apparatus[1] and are uncorrected.

**Ethyl *N*-Succinimidoxyacetate (I)**—A solution of freshly recrystallized *N*-hydroxysuccinimide (1.15 g, 0.01 mole) in tetrahydrofuran (12 ml, 0.15 mole) was added to a mixture of ethyl bromoacetate (1.4 ml, 0.0125 mole) and triethylamine (2.1 ml, 0.015 mole). The reaction was allowed to proceed at room temperature for 12 hr, during which time the light-blue mixture became colorless. The reaction mixture was filtered, and the precipitate was washed with ether (5 × 20 ml).

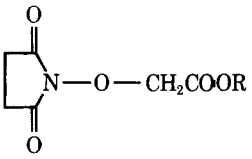

I: R = $C_2H_5$
II: R = $CH_3$

The combined filtrates were concentrated and the product was crystallized from ethanol to obtain 1.71 g of white fluffy flakes in an 85% yield, mp 80–81°; IR[2] (mineral oil): 1778, 1712 (C=O for succinimide), 1748 (C=O for ester), 1208, 1098 (C–O–C asymmetric and symmetric stretching for ester, respectively), ~2950, 2880 (C–H stretching), 1436, and 1372 (C–H asymmetric and symmetric deformation for $CH_2CH_3$, respectively) $cm^{-1}$; NMR[3] ($CDCl_3$): δ 2.70 (s, 4H, cyclic H), 4.60 (s, 2H, $-CH_2$), 4.17 (q, 2H, $J$ = 6 Hz, $CH_2$ ethyl), and 1.27 (t, 3H, $J$ = 6 Hz, $CH_3$ ethyl); TLC[4]: h$R_f$ 56.8.

*Anal.*[5]—Calc. for $C_8H_{11}NO_5$: C, 47.76; H, 5.51; N, 6.96. Found: C, 47.82; H, 5.50; N, 7.01.

**Methyl *N*-Succinimidoxyacetate (II)**—A solution of freshly recrystallized *N*-hydroxysuccinimide (1.15 g, 0.01 mole) in tetrahydrofuran (12 ml, 0.15 mole) was added to a mixture of methyl bromoacetate (1.1 ml, 0.0125 mole) and triethylamine (2.1 ml, 0.015 mole). The reaction was allowed to proceed at room temperature for 8 hr, during which time the light-blue mixture became colorless. The reaction mixture was filtered, and the white precipitate, heavily contaminated with triethylamine hydrobromide, was crystallized from ethanol to obtain 1.31 g of white crystals in a 70% yield.

A second crop of 0.13 g was obtained by concentrating the filtrate, and the total yield was 1.44 g (77%), mp 128–130°; IR (mineral oil): 1772, 1706 (C=O for succinimide), 1750 (C=O for ester), 1200, 1086 (C–O–C asymmetric and symmetric stretching for ester, respectively), ~2950, 2880 (C–H stretching), 1440, and 1370 (C–H asymmetric and symmetric deformation for $CH_3$, respectively) $cm^{-1}$; NMR ($CDCl_3$): δ 2.63 (s, 4H, cyclic H), 4.60 (s, 2H, $-CH_2$), and 3.63 (s, 3H, $CH_3$); TLC: h$R_f$ 53.7.

*Anal.*—Calc. for $C_7H_9NO_5$: C, 44.92; H, 4.85; N, 7.48. Found: C, 45.03; H, 4.88; N, 7.47.

**Screening**—Compounds I and II were screened for anticonvulsant properties by subjecting pretreated young chicks to electrically and chemically induced seizures. Maximal electroshock was delivered using electroshock equipment[6]; chemical seizures were achieved using aminooxyacetic acid, bicuculline, pentylenetetrazol, picrotoxin, and strychnine.

## REFERENCES

(1) G. Osuide, *Br. J. Pharmacol.*, **44**, 31 (1972).
(2) G. D. Lahan, G. Osuide, and F. Stansfield, *ibid.*, **67**, 441 (1979).
(3) G. Osuide, G. D. Lahan, J. A. Owoyale, and I. O. Edafiogho, *Nig. J. Pharm.*, **10**, 256 (1979).
(4) D. E. Ames and T. F. Grey, *J. Chem. Soc.*, **1**, 631 (1955).

[1] Model MF-370, A. Gallenkamp & Co. Ltd., London, England.

[2] Model SP700, Perkin-Elmer Corp., Norwalk, Conn.
[3] Varian A-60A, Varian Instruments, Palo Alto, Calif.
[4] TLC was run on Polygram SIL G/$UG_{254}$ using 10% methanol in chloroform.
[5] Elemental analyses were performed by Scandinavian MicroLaboratories, Herlev, Denmark.
[6] Model 7800, Ugo Basile ECT unit, Milan, Italy.

0022-3549/81/0800-0963$01.00/0
© 1981, American Pharmaceutical Association

# Antimicrobial Activity of Chlorhexidine Gluconate against Natural and Artificial Contamination during Simulation of In-Use Conditions

RAZA ALY

Received October 17, 1980, from the *Department of Dermatology, University of California, San Francisco, San Francisco, CA 94143.* Accepted for publication January 30, 1981.

**Abstract** □ Commercial bottles containing chlorhexidine gluconate (antimicrobial skin cleanser), whether exposed to room atmosphere or experimentally inoculated with *Staphylococcus aureus*, *Pseudomonas aeruginosa*, *Pseudomonas cepacia*, and *Proteus mirabilis*, did not exhibit microbial growth.

**Keyphrases** □ Chlorhexidine gluconate—antimicrobial activity, simulation of natural and artificial contamination □ Antimicrobial agents—chlorhexidine gluconate, simulation of contamination □ Skin cleanser—chlorhexidine gluconate, antimicrobial activity, simulation of contamination

Chlorhexidine gluconate has broad-spectrum antimicrobial activity against bacteria and several fungi (1–3). Although the antimicrobial activity of chlorhexidine when used on human skin is well documented, knowledge about bacterial contamination of commercial preparations during in-use conditions is lacking (4–6).

The present study was designed to determine the potential for bacterial contamination of a commercial chlorhexidine gluconate[1] skin cleanser by repeated exposure of opened bottles to room atmosphere over a prolonged period and to determine the potential for survival or growth of bacteria after repeated bacterial challenges with *Staphylococcus aureus*, *Pseudomonas aeruginosa*, *Pseudomonas cepacia*, and *Proteus mirabilis*. The test organisms were identified by cultural and biochemical reactions (7). Bottle-to-bottle transfers of the preparation were made to reflect certain in-use situations where residual product left in a used bottle is mixed with fresh product.

## EXPERIMENTAL

**Environmental Contamination**—Standard commercial bottles containing ~946 ml of the antimicrobial skin cleanser, tested and found free of contamination, were exposed to room atmosphere for 6 months by removing the tops daily and shaking for 5 min. Samples were taken weekly for the first 2 months and then at monthly intervals.

Two methods were utilized for determining bacterial contamination:

1. A 1-ml sample from each bottle was removed, diluted in trypticase soy broth containing 10% polysorbate 80[2] and 3% soy phosphatides[3] (neutralizer), and cultured on tryptic soy agar (containing 1% neutralizer). Culture plates were incubated at 37° for 48 hr.

2. A 20-ml aliquot was mixed with 250 ml of trypticase soy broth containing 0.3% neutralizer and then passed through a 0.45-μm filter disk. One-half of the filter was transferred to trypticase soy broth and the other half to thioglycollate broth. After 24 hr of incubation at 37°, 1 ml of each broth was cultured on tryptic soy agar.

**Experimental Contamination with *S. aureus*, *P. mirabilis*, *Ps. aeruginosa*, and *Ps. cepacia***—For a given test organism, the experimental contamination procedure comprised seven bacterial challenges and three bottle-to-bottle transfers over 25 weeks. A commercial bottle (Bottle 1) of the chlorhexidine gluconate preparation, previously tested and found to be free of bacteria, was challenged (C-1). The bottle contents were mixed, and the aliquots were tested at 10 min and after 1 week (just before C-2) for bacterial growth. Aliquots (25 ml) were removed *via* the delivery spout of the bottle, employing a hand pump to simulate in-use conditions, and were cultured for environmental contamination. The bottle then was challenged as before (C-2, 1 week). The aliquots were tested at 10 min and after 1 week (just before C-3) for bacterial growth. This contamination and testing for bacterial growth were repeated at 2 (C-3) and 3 (C-4) weeks. Challenge 5 (4 weeks) was performed as described, and the aliquot was tested for bacterial growth at 10 min only.

At this point, periodic bottle-to-bottle transfers of the preparations were begun to mimic certain in-use conditions, where fresh product was poured into a previously used bottle containing residual product with 1 ml containing $10^6$ viable bacteria (for a final concentration of $10^3$ bacteria/ml in the commercial bottle).

**First Transfer (4 Weeks)**—Forty milliliters from Bottle 1 was transferred aseptically into a new bottle (Bottle 2), previously tested and found free of bacteria. The aliquot was tested after 1 week (just before C-6) for bacterial growth. Bottle 2 was challenged (C-6, 5 weeks). The aliquot was tested at 10 min and also after 4 weeks (just before the second bottle-to-bottle transfer) for bacterial growth.

**Second Transfer (9 Weeks)**—Forty milliliters from Bottle 2 was transferred aseptically to a new bottle (Bottle 3). The aliquot was tested after 4 weeks (just before C-7) for bacterial growth. Bottle 3 was challenged (C-7, 13 weeks). The aliquot was tested at 10 min and also after 4 weeks (just before the third bottle-to-bottle transfer) for bacterial growth.

**Third Transfer (17 Weeks)**—Forty milliliters from Bottle 3 was transferred to a new bottle (Bottle 4). The aliquot was tested for bacterial growth after 8 weeks, concluding a total period of 25 weeks from the initial challenge.

## RESULTS AND DISCUSSION

No contamination was noted at the start of the study or after 5-min daily exposures and shaking of the product at room atmosphere for the 6-month duration of the environmental contamination. Delivery spouts of the bottles were cultured with a swab and were free of bacterial contamination.

Bottles of the products contaminated experimentally with *S. aureus*, *P. mirabilis*, *Ps. aeruginosa*, or *Ps. cepacia* were examined for 6 months for bacterial growth and were not contaminated. Delivery spouts also were free of bacterial contamination.

Chlorhexidine has excellent antimicrobial activity against Gram-positive and Gram-negative bacteria (1–6). Due to its broad-spectrum antimicrobial activities, chlorhexidine preparations have become widely used for disinfection.

## REFERENCES

(1) H. Beeuwkes, *J. Microbiol. Serol.*, **24**, 49 (1958).

(2) G. E. Davies, J. Francis, A. R. Martin, F. L. Rose, and G. Swain, *Br. J. Pharmacol.*, **9**, 192 (1954).

(3) C. A. Lawrence, *J. Am. Pharm. Assoc., Sci. Ed.*, **49**, 731 (1960).

(4) E. J. Lowbury, *Br. Med. J.*, **1**, 510 (1973).

(5) R. Aly and H. I. Maibach, *Appl. Environ. Microbiol.*, **37**, 610 (1979).

(6) R. Aly and H. I. Maibach, *Clin. Exp. Dermatol.*, **5**, 197 (1980).

(7) "Berge's Manual of Determinative Bacteriology," 8th ed., R. E. Buchanan and N. E. Gibbons, Eds., Williams & Wilkins, Baltimore, Md., 1974, pp. 221, 229, 328, 484.

[1] Hibiclins, ICI America.
[2] Tween 80, Sigma Chemical Co.
[3] Asolectin, Woodside, N.Y.



*0022-3549/81/0800-0964$01.00/0*
*© 1981, American Pharmaceutical Association*

# Analysis of Methoxsalen in Plasma by Reversed-Phase High-Performance Liquid Chromatography

**J. G. MONBALIU ˣ, M. T. ROSSEEL, and M. G. BOGAERT**

Received September 29, 1980, from the *Heymans Institute of Pharmacology, University of Ghent Medical School, De Pintelaan 135, B-9000 Ghent, Belgium.* Accepted for publication February 2, 1981.

**Abstract** □ A high-performance liquid chromatographic method for the determination of methoxsalen in plasma was developed. The method includes extraction from plasma of the drug and the internal standard (5-methoxypsoralen) into methylene chloride. Chromatography was performed on a reversed-phase $C_8$ column connected with a UV detector set at 254 nm. The mobile phase was methanol–acetonitrile–water (2:30:68). For a plasma sample of 0.25 ml, the maximal sensitivity was ~10 ng/ml. Accuracy was within 7.5% for therapeutic plasma levels, and the coefficient of variation varied between 4.3 and 0.9% for 28 and 300 ng/ml of plasma, respectively.

**Keyphrases** □ Methoxsalen—high-performance liquid chromatographic analysis, human plasma □ High-performance liquid chromatography—methoxsalen, human plasma □ Photosensitizer—methoxsalen, high-performance liquid chromatographic analysis, human plasma

Methoxsalen (8-methoxypsoralen), a furocoumarinic derivative, is used in conjunction with phototherapy in the treatment of psoriasis (1). Different methods of analysis of methoxsalen in plasma have been published. Fluorodensitometric methods (2, 3) are time consuming, and flame-ionization GLC (4) is not sensitive enough for measuring therapeutic plasma levels. Electron-capture GLC (5–7) and GLC–mass spectrometry (8) also have been described.

Since methoxsalen has a very high UV absorbance, a high-performance liquid chromatographic (HPLC) method with UV detection was developed. HPLC using a silica column also has been used (9, 10). HPLC on a reversed-phase column[1] was proposed (11), with the internal standard griseofulvin being added after the extraction. Reversed-phase HPLC on a $C_{18}$ column with trimethylpsoralen as the internal standard also was investigated (8, 12).

This report describes an HPLC method with a simple and rapid extraction procedure using a $C_8$ column and 5-methoxypsoralen as the internal standard.

## EXPERIMENTAL

**Reagents and Solvents**—Methoxsalen[2] (8-methoxypsoralen) and 5-methoxypsoralen[3] were used as received. Methylene chloride[4], methanol[5], and acetonitrile[5] were also used.

**Equipment**—A microprocessor-controlled high-performance liquid chromatograph[6] with a fixed-wavelength UV detector[7] (254 nm), an automatic injector, and a 10-μl sample loop were used.

Separations were performed on a reversed-phase column[8] (250 × 4.6 mm i.d.). The column was operated at 40°. Chromatograms were traced on a printer/plotter[6] at a chart speed of 0.5 cm/min.

**Chromatographic Conditions**—The mobile phase, methanol–acetonitrile–water (2:30:68), was pumped through the column at a flow rate of 1.5 ml/min at 500–1000 psi.

**Procedure**—To 250 μl of plasma in a 5-ml glass conical tube was added 200 ng of the internal standard, 5-methoxypsoralen (20 μl of a 0.001% methanol solution). The sample was extracted with 700 μl of methylene chloride for 30 sec on a mixer[9]. After centrifugation at 5000 rpm at 4° for 10 min, the organic phase was transferred to another 5-ml glass conical tube and evaporated to dryness at room temperature under nitrogen. The residue was stored at −20° until analysis. The extract was reconstituted in 20 μl of methanol just prior to chromatography, and 10 μl was injected.

**Absolute Recovery**—Absolute recovery of methoxsalen from plasma was determined by adding the internal standard after extraction and comparing peak height ratios with peak height ratios of a calibration curve. This calibration curve was obtained by injecting methanol solutions of methoxsalen at concentrations of 7.0, 36.0, and 50.0 ng/ml of plasma. Five replicates were analyzed at each concentration. The results are shown in Table I.

**Table I—Absolute Recovery of Methoxsalen from Plasma [a]**

| Quantity Added to 250 μl of Plasma, ng | Mean, % | Coefficient of Variation, % |
|---|---|---|
| 7.0 | 92.8 | 6.6 |
| 36.0 | 87.2 | 8.8 |
| 50.0 | 87.4 | 5.6 |

[a] $n = 5$.

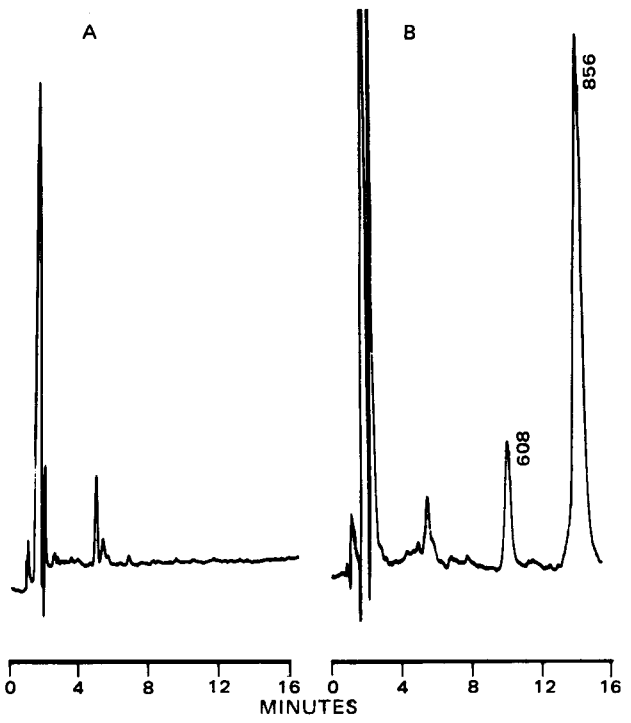


**Figure 1**—*Chromatogram of a 250-μl extract of human blank plasma (A) and of a 250-μl extract of human blank plasma spiked with 25 ng of methoxsalen* ($R_t$ *608 sec) and 200 ng of the internal standard* ($R_t$ *856 sec) (B).*

[1] μBondapak CN.
[2] Covor, Brussels, Belgium.
[3] Promedica, Paris, France.
[4] Pro analysis grade, Merck, Darmstadt, West Germany.
[5] Lichrosolv grade, Merck, Darmstadt, West Germany.
[6] Spectra Physics SP-8000, Eindhoven, The Netherlands.
[7] Spectra Physics SP-8200, Eindhoven, The Netherlands.
[8] Lichrosorb 10 RP 8, Chrompack, Merksem, Belgium.
[9] Vortex, Cenco Instruments Mij N. V., Breda, The Netherlands.

0022-3549/81/0800-0965$01.00/0
© 1981, American Pharmaceutical Association

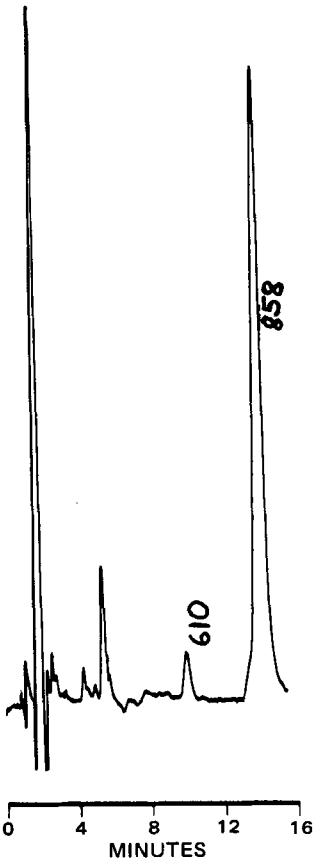


**Figure 2**—*Chromatogram of a 250-μl extract of plasma of a patient after oral intake of 30 mg of methoxsalen ($R_t$ 610 sec); the sample was spiked with 200 ng of the internal standard ($R_t$ 858 sec).*

tions containing 10–80 ng of methoxsalen and 100 ng of the internal standard.

## RESULTS AND DISCUSSION

The extraction gave good recoveries (87–93%) of methoxsalen from plasma (Table I).

Plasma standard curves were linear for concentrations ranging from 12 to 1000 ng/ml. The average slope for 16 standard curves, assayed over 5 months, was 0.008436 ± 0.000422 (mean ± *SD*), with an average correlation coefficient of 0.9980 ± 0.0023 (mean ± *SD*). For a plasma sample of 0.25 ml, the maximum sensitivity was ~10 ng/ml.

Within-run accuracy and precision were acceptable (Table II). For testing of the between-run reproducibility and accuracy, aliquots were taken 16 times over a 5-month period from a pool containing 100.0 ng of methoxsalen/ml of plasma; the average result was 102.4 ± 5.2 ng/ml (mean ± *SD*) ($n$ = 16).

**Table II—Within-Run Precision and Accuracy of Methoxsalen Assay**

| Quantity Added to 250 μl of Plasma, ng | Relative Error, % | Coefficient of Variation, % |
|---|---|---|
| 7 ($n$ = 4) | +7.5 | 4.3 |
| 36 ($n$ = 5) | +2.7 | 5.0 |
| 50 ($n$ = 5) | −2.9 | 2.6 |
| 75 ($n$ = 5) | −3.2 | 0.9 |

Figure 1A shows a representative chromatogram of an extract of human blank plasma. Figure 1B shows a chromatogram of human blank plasma spiked with methoxsalen and the internal standard. Both products were well resolved. Figure 2 shows a chromatogram of a plasma extract of a patient 130 min after the intake of 30 mg of methoxsalen, spiked with the internal standard.

The proposed method is suitable for plasma sample analysis for pharmacokinetic studies of methoxsalen in animals and humans. The extraction is simple and rapid, and only 700 μl of the extraction solvent is needed. This procedure is an improvement in comparison to other methods (8–12). The small volume of plasma used (250 μl) enables repeated sampling.

## REFERENCES

(1) L. Hodge and J. S. Comaish, *Drugs*, **13**, 288 (1977).

(2) M. J. Herfst, E. A. M. Koot-Gronsveld, and F. A. de Wolff, *Arch. Dermatol. Res.*, **262**, 1 (1978).

(3) S. G. Chakrabarti, D. A. Gooray, and J. A. Kenney Jr., *Clin. Chem.*, **24**, 1155 (1978).

(4) J. Gazith and H. Schaefer, *Biochem. Med.*, **18**, 102 (1977).

(5) J. Gazith, W. Schalla, and H. Schaefer, *Arch. Dermatol. Res.*, **263**, 215 (1978).

(6) J. Schmid and F. W. Koss, *J. Chromatogr.*, **146**, 498 (1978).

(7) H. Ehrsson, S. Eksborg, I. Wallin, N. Källberg, and G. Swanbeck, *ibid.*, **140**, 157 (1977).

(8) C. N. Hensby, *Clin. Exp. Dermatol.*, **3**, 355 (1978).

(9) C. V. Puglisi, J. A. F. de Silva, and J. C. Meyer, *Anal. Lett.*, **10**, 39 (1977).

(10) B. Ljunggren, D. M. Carter, J. Albert, and T. Reid, *J. Invest. Dermatol.*, **74**, 59 (1980).

(11) J. Kreuter and T. Higuchi, *J. Pharm. Sci.*, **68**, 451 (1979).

(12) L. M. L. Stolk, *Pharm. Weekbl. Sci. Ed.*, **2**, 29 (1980).

## ACKNOWLEDGMENTS

Supported by Grant 3.0007.80 from the Fund for Medical Scientific Research, Belgium.

# Simplified Physiologically Based Method to Estimate Steady-State Volume of Distribution

**Keyphrases** □ Pharmacokinetics—simplified physiologically based method to estimate steady-state volume of distribution □ Volume of distribution—estimation, simplified physiologically based method

*To the Editor:*

Until recently (1–4), few investigators studied the potential effect of arterial–venous plasma concentration differences on the determination of the apparent steady-state volume of distribution ($V_{ss}$) of drugs. When standard methods in linear pharmacokinetics were used, the calculated $V_{ss}$ values based on venous plasma data were invariably greater than those based on arterial data from the same animals (2–4). Differences as much as 2.4-fold were found.

From a physiological point of view, the driving force for elimination and distribution of a drug in the body should generally be its concentration in arterial plasma (especially for elimination by renal filtration) and not in peripheral venous plasma (commonly sampled for assay). Therefore, it seems appropriate to use the arterial data (if possible) for $V_{ss}$ calculations (1–3). A new arterial plasma area method for $V_{ss}$ determinations was proposed earlier (4).

In view of the difficulty and risk involved in arterial blood sampling, two physiologically based venous and excretion rate methods were derived (4).

Method I, the intravenous bolus injection method, is described by:

$$V_{ss} = \frac{\int_0^\infty (D - Ae_t/fe)\,dt}{AUC^V} \qquad \text{(Eq. 1)}$$

where $D$ is the bolus dose, $Ae_t$ is the cumulative urinary excretion of unchanged drug from time zero to $t$, $fe$ is the fraction of the dose excreted unchanged up to time infinity, and $AUC^V$ is the total area under the venous plasma drug concentration–time curve between time zero and time infinity. This method was verified experimentally[1].

Method II, the short-term intravenous infusion method, is described by:

$$V_{ss} = \frac{\int_0^\infty (D_t - Ae_t/fe)\,dt}{AUC^V} \qquad \text{(Eq. 2)}$$

where $D_t$ is the cumulative amount of drug infused up to time $t$.

Both Methods I and II require frequent and accurate urine collection and extensive blood sampling to estimate the $AUC^V$. This report describes a simpler physiologically based method, called the steady-state plasma–urinary method, for calculating $V_{ss}$.

By definition, $V_{ss}$ can be defined as (4 and references cited therein):

$$V_{ss} = \frac{A_{ss}}{C_{ss}} \qquad \text{(Eq. 3)}$$

where $A_{ss}$ is the amount of drug in the body at steady state following a constant-rate infusion and $C_{ss}$ is the steady-state plasma drug concentration. Therefore, $V_{ss}$ can be estimated after the attainment of steady state by:

$$V_{ss} = \frac{D_{ss} - (\text{total amount eliminated up to } t_{ss})}{C_{ss}} \qquad \text{(Eq. 4)}$$

$$V_{ss} = \frac{D_{ss} - Ae_{ss}Cl/Cl_R}{C_{ss}} \qquad \text{(Eq. 5)}$$

where $D_{ss}$ is the total amount of drug infused up to the steady state at time $t_{ss}$, $Ae_{ss}$ is the total cumulative amount of drug excreted unchanged up to time $t_{ss}$, $Cl$ is the total plasma drug clearance (*i.e.*, infusion rate/$C_{ss}$), and $Cl_R$ is the renal drug clearance. The value of $Cl_R$ can be determined by the conventional method, *i.e.*, urinary excretion rate at steady state divided by the $C_{ss}$. The times to reach various fractions of the steady-state plasma level during intravenous infusion initially can be estimated by a noncompartmental plasma area method described previously (5).

Equation 5 has several advantages over Eqs. 1 and 2. First, Eq. 5 requires only one or two venous blood samples at steady state. Second, all urinary samples can be pooled together (both convenient and economical in drug assay), except for the last one or two that are used for renal clearance measurement. Third, a loading bolus and/or loading infusion dose can be given to achieve the steady state rapidly with the final maintenance infusion; with Eq. 1 or 2, the study may have to be carried out for several half-lives. Fourth, the mathematical operation is much easier with Eq. 5. And fifth, it often may be more accurate to assay steady-state specimens due to higher concentrations. Furthermore, the described method is independent of the source of plasma sample since both arterial and venous (usually from a noneliminating leg or arm vein) plasma drug concentrations should be theoretically identical at steady state (4, 6, 7).

The limitation of the proposed method is that it can only be used for drugs excreted to some extent in the urine. Fluctuations in urine pH and flow rate should be minimized during the entire study period if either or both of them have been shown to significantly affect the renal clearance of drug. Several commonly used method to calculate $V_{ss}$ were recently reviewed (4, 8, 9). The use of the steady-state infusion method employing the measurement of plasma concentrations for calculating $V_{ss}$ were described previously (10–12). The recommended symbols in pharmacokinetics (12) are adopted in this communication.

(1) W. L. Chiou, in "Abstracts," APhA Academy of Pharmeceutical Sciences, Washington, D.C., meeting, Apr. 1978 (No. 15 in Basic Pharmaceutics Section).

(2) G. Lam and W. L. Chiou, in "Abstracts" APhA Academy of Pharmaceutical Sciences, San Antonio meeting, Nov. 1980 (No. 46 in Basic Pharmaceutics Section).

(3) G. Lam, M. L. Chen, M. G. Lee, and W. L. Chiou, presented at the APhA Academy of Pharmaceutical Sciences, St. Louis meeting, Mar. 1981.

(4) W. L. Chiou, *Int. J. Clin. Pharmacol. Ther. Toxicol.*, in press.

(5) W. L. Chiou, *J. Pharmacokinet. Biopharm.*, 8, 311 (1980).

[1] Unpublished data.

0022-3549/81/0800-0967$01.00/0
© 1981, American Pharmaceutical Association

(6) W. L. Chiou and G. Lam, *Int. J. Clin. Pharmacol. Ther. Toxicol.*, in press.
(7) W. L. Chiou, G. Lam, M. L. Chen, and M. G. Lee, *Res. Commun. Chem. Pathol. Pharmacol.*, **32**, 27 (1981).
(8) L. Z. Benet and R. L. Galeazzi, *J. Pharm. Sci.*, **68**, 1071 (1979).
(9) C. R. Kowarski and A. A. Kowarski, *ibid.*, **69**, 1222 (1980).
(10) M. Gibaldi, *ibid.*, **58**, 327 (1969).
(11) U. Klotz, *Clin. Pharmacokinet.*, **1**, 204 (1976).
(12) M. Rowland and G. Tucker, *J. Pharmacokinet. Biopharm.*, **8**, 497 (1980).

*Win L. Chiou* ˣ
*Gilbert Lam*
Department of Pharmacy
College of Pharmacy
University of Illinois Medical Center
Chicago, IL 60612

Received March 20, 1981.
Accepted for publication June 15, 1981.

## Modified USP Assay of Calcium Gluceptate

**Keyphrases** □ Calcium gluceptate—modified USP assay □ USP assay—modification for calcium gluceptate

*To the Editor:*

The USP assay procedure for calcium gluceptate consists of the complexometric estimation of calcium with ethylenediaminetetraacetic acid (1). To an accurately weighed amount of calcium gluceptate (~800 mg), 150 ml of water containing 2 ml of 3 *N* HCl is added. While stirring, ~25 ml of 0.05 *M* ethylenediaminetetraacetate disodium is added from a buret. Then 15 ml of 1 *N* NaOH and 300 mg of hydroxy naphthol blue indicator are added, and the titration is continued to a blue end-point.

A similar procedure is described for the assay of precipitated calcium carbonate, calcium chloride, calcium gluconate, calcium hydroxide, calcium lactate, and calcium levulinate and for the calcium content analysis of calcium pantothenate and racemic calcium pantothenate. Although each assay calls for the addition of hydrochloric acid, this step is only necessary where the calcium salt has a limited aqueous solubility (2, 3). Since calcium gluceptate is freely soluble in water (4), we suggest that the addition of hydrochloric acid should be omitted. Table I shows that assay results are not affected by the presence or absence of hydrochloric acid.

**Table I—Assay of Calcium Gluceptate in the Presence and Absence of Hydrochloric Acid**

| Calcium Gluceptate | Assay Value, %[a] | |
|---|---|---|
| | USP Method | Modified USP Method |
| Source A[b] | 96.80 ± 0.42 (96.55–97.43) | 96.82 ± 0.32 (96.54–97.10) |
| Source B[c] | 97.02 ± 0.39 (96.51–97.42) | 97.16 ± 0.21 (96.97–97.41) |
| Source C[d] | 101.15 ± 0.08 (101.04–101.24) | 100.86 ± 0.49 (100.14–101.17) |

[a] Mean ± *SD*, $n = 4$; range is given in parentheses. [b] Pfanstiehl. [c] Givaudan. [d] Italsintex.

The sodium hydroxide solution and the hydroxy naphthol blue indicator can be added to the calcium gluceptate solution at the beginning of the assay; thus, it is unnecessary to interrupt titration to make these additions. The estimation of calcium with ethylenediaminetetraacetic acid using hydroxy naphthol blue as the indicator is carried out at pH 12–13 (5). The addition of 15 ml of 1 *N* NaOH solution in the official assay brings the pH to this range. In the absence of hydrochloric acid, ~10 ml of 1 *N* NaOH solution would be sufficient to bring the pH to the required range. Thus, omitting the hydrochloric acid both simplifies the procedure and enables the amount of sodium hydroxide to be reduced.

We suggest that hydrochloric acid might be omitted in the assay of other freely soluble calcium salts.

(1) "The United States Pharmacopeia," 20th rev., United States Pharmacopeial Convention, Rockville, Md., 1980, p. 107.
(2) A. Q. Butler, F. A. Maurina, and F. A. Morecombe, *J. Pharm. Sci.*, **54**, 134 (1965).
(3) R. W. Goettsch, *ibid.*, **54**, 317 (1965).
(4) "The United States Pharmacopeia," 20th rev., United States Pharmacopeial Convention, Rockville, Md., 1980, p. 1125.
(5) A. Itoh and K. Ueno, *Analyst*, **95**, 583 (1970).

*R. Suryanarayanan*
*A. G. Mitchell* ˣ
Faculty of Pharmaceutical Sciences
University of British Columbia
2146 East Mall
Vancouver, B.C. V6T 1W5
Canada

Received February 9, 1981.
Accepted for publication April 27, 1981.
The authors thank Stanley Drug Products Ltd. for supplies of calcium gluceptate, and R. Suryanarayanan thanks the Science Council of British Columbia for a graduate research, engineering and technology award.

## Observed Artifacts due to Pellet Preparation in IR Spectrometry

**Keyphrases** □ IR spectrometry—observed artifacts due to pellet preparation □ Pellets—observed artifacts due to preparation, IR spectrometry

*To the Editor:*

IR spectrometry is required for identifying organic substances by most pharmacopeia and official compendia such as the USP XIX and the NF XIV (1, 2). The USP recommends: "Chemically identical substances of differing polymorphic forms often exhibit different infrared spectra when examined in the solid state. If a difference appears in the spectra, dissolve portions of both the sample and the reference standard in a suitable solvent, evaporate the solution to dryness, and repeat the test on the residues" (1). Differences resulting from polymorphism are considered to be the major reason for errors.

Certain secondary and tertiary amine derivatives such as bupivacaine, cinnarizine, and many butyrophenones have the same spectrum, in part or in whole, for their hydrochloride, hydrobromide, and free base forms when they are dissolved in methanol, ethanol, or isopropanol and if grinding with potassium bromide is prolonged.



*0022-3549/81/0800-0968$01.00/0*
*© 1981, American Pharmaceutical Association*

(6) W. L. Chiou and G. Lam, *Int. J. Clin. Pharmacol. Ther. Toxicol.*, in press.
(7) W. L. Chiou, G. Lam, M. L. Chen, and M. G. Lee, *Res. Commun. Chem. Pathol. Pharmacol.*, **32**, 27 (1981).
(8) L. Z. Benet and R. L. Galeazzi, *J. Pharm. Sci.*, **68**, 1071 (1979).
(9) C. R. Kowarski and A. A. Kowarski, *ibid.*, **69**, 1222 (1980).
(10) M. Gibaldi, *ibid.*, **58**, 327 (1969).
(11) U. Klotz, *Clin. Pharmacokinet.*, **1**, 204 (1976).
(12) M. Rowland and G. Tucker, *J. Pharmacokinet. Biopharm.*, **8**, 497 (1980).

*Win L. Chiou* ˣ
*Gilbert Lam*
Department of Pharmacy
College of Pharmacy
University of Illinois Medical Center
Chicago, IL 60612

Received March 20, 1981.
Accepted for publication June 15, 1981.

## Modified USP Assay of Calcium Gluceptate

**Keyphrases** □ Calcium gluceptate—modified USP assay □ USP assay—modification for calcium gluceptate

*To the Editor:*

The USP assay procedure for calcium gluceptate consists of the complexometric estimation of calcium with ethylenediaminetetraacetic acid (1). To an accurately weighed amount of calcium gluceptate (~800 mg), 150 ml of water containing 2 ml of 3 *N* HCl is added. While stirring, ~25 ml of 0.05 *M* ethylenediaminetetraacetate disodium is added from a buret. Then 15 ml of 1 *N* NaOH and 300 mg of hydroxy naphthol blue indicator are added, and the titration is continued to a blue end-point.

A similar procedure is described for the assay of precipitated calcium carbonate, calcium chloride, calcium gluconate, calcium hydroxide, calcium lactate, and calcium levulinate and for the calcium content analysis of calcium pantothenate and racemic calcium pantothenate. Although each assay calls for the addition of hydrochloric acid, this step is only necessary where the calcium salt has a limited aqueous solubility (2, 3). Since calcium gluceptate is freely soluble in water (4), we suggest that the addition of hydrochloric acid should be omitted. Table I shows that assay results are not affected by the presence or absence of hydrochloric acid.

**Table I—Assay of Calcium Gluceptate in the Presence and Absence of Hydrochloric Acid**

| Calcium Gluceptate | Assay Value, %[a] | |
|---|---|---|
| | USP Method | Modified USP Method |
| Source A[b] | 96.80 ± 0.42 (96.55–97.43) | 96.82 ± 0.32 (96.54–97.10) |
| Source B[c] | 97.02 ± 0.39 (96.51–97.42) | 97.16 ± 0.21 (96.97–97.41) |
| Source C[d] | 101.15 ± 0.08 (101.04–101.24) | 100.86 ± 0.49 (100.14–101.17) |

[a] Mean ± *SD*, $n = 4$; range is given in parentheses. [b] Pfanstiehl. [c] Givaudan. [d] Italsintex.

The sodium hydroxide solution and the hydroxy naphthol blue indicator can be added to the calcium gluceptate solution at the beginning of the assay; thus, it is unnecessary to interrupt titration to make these additions. The estimation of calcium with ethylenediaminetetraacetic acid using hydroxy naphthol blue as the indicator is carried out at pH 12–13 (5). The addition of 15 ml of 1 *N* NaOH solution in the official assay brings the pH to this range. In the absence of hydrochloric acid, ~10 ml of 1 *N* NaOH solution would be sufficient to bring the pH to the required range. Thus, omitting the hydrochloric acid both simplifies the procedure and enables the amount of sodium hydroxide to be reduced.

We suggest that hydrochloric acid might be omitted in the assay of other freely soluble calcium salts.

(1) "The United States Pharmacopeia," 20th rev., United States Pharmacopeial Convention, Rockville, Md., 1980, p. 107.
(2) A. Q. Butler, F. A. Maurina, and F. A. Morecombe, *J. Pharm. Sci.*, **54**, 134 (1965).
(3) R. W. Goettsch, *ibid.*, **54**, 317 (1965).
(4) "The United States Pharmacopeia," 20th rev., United States Pharmacopeial Convention, Rockville, Md., 1980, p. 1125.
(5) A. Itoh and K. Ueno, *Analyst*, **95**, 583 (1970).

*R. Suryanarayanan*
*A. G. Mitchell* ˣ
Faculty of Pharmaceutical Sciences
University of British Columbia
2146 East Mall
Vancouver, B.C. V6T 1W5
Canada

Received February 9, 1981.
Accepted for publication April 27, 1981.
The authors thank Stanley Drug Products Ltd. for supplies of calcium gluceptate, and R. Suryanarayanan thanks the Science Council of British Columbia for a graduate research, engineering and technology award.

## Observed Artifacts due to Pellet Preparation in IR Spectrometry

**Keyphrases** □ IR spectrometry—observed artifacts due to pellet preparation □ Pellets—observed artifacts due to preparation, IR spectrometry

*To the Editor:*

IR spectrometry is required for identifying organic substances by most pharmacopeia and official compendia such as the USP XIX and the NF XIV (1, 2). The USP recommends: "Chemically identical substances of differing polymorphic forms often exhibit different infrared spectra when examined in the solid state. If a difference appears in the spectra, dissolve portions of both the sample and the reference standard in a suitable solvent, evaporate the solution to dryness, and repeat the test on the residues" (1). Differences resulting from polymorphism are considered to be the major reason for errors.

Certain secondary and tertiary amine derivatives such as bupivacaine, cinnarizine, and many butyrophenones have the same spectrum, in part or in whole, for their hydrochloride, hydrobromide, and free base forms when they are dissolved in methanol, ethanol, or isopropanol and if grinding with potassium bromide is prolonged.



*0022-3549/81/0800-0968$01.00/0*
*© 1981, American Pharmaceutical Association*

(6) W. L. Chiou and G. Lam, *Int. J. Clin. Pharmacol. Ther. Toxicol.*, in press.
(7) W. L. Chiou, G. Lam, M. L. Chen, and M. G. Lee, *Res. Commun. Chem. Pathol. Pharmacol.*, **32**, 27 (1981).
(8) L. Z. Benet and R. L. Galeazzi, *J. Pharm. Sci.*, **68**, 1071 (1979).
(9) C. R. Kowarski and A. A. Kowarski, *ibid.*, **69**, 1222 (1980).
(10) M. Gibaldi, *ibid.*, **58**, 327 (1969).
(11) U. Klotz, *Clin. Pharmacokinet.*, **1**, 204 (1976).
(12) M. Rowland and G. Tucker, *J. Pharmacokinet. Biopharm.*, **8**, 497 (1980).

*Win L. Chiou* ˣ
*Gilbert Lam*
Department of Pharmacy
College of Pharmacy
University of Illinois Medical Center
Chicago, IL 60612

Received March 20, 1981.
Accepted for publication June 15, 1981.

## Modified USP Assay of Calcium Gluceptate

**Keyphrases** □ Calcium gluceptate—modified USP assay □ USP assay—modification for calcium gluceptate

*To the Editor:*

The USP assay procedure for calcium gluceptate consists of the complexometric estimation of calcium with ethylenediaminetetraacetic acid (1). To an accurately weighed amount of calcium gluceptate (~800 mg), 150 ml of water containing 2 ml of 3 *N* HCl is added. While stirring, ~25 ml of 0.05 *M* ethylenediaminetetraacetate disodium is added from a buret. Then 15 ml of 1 *N* NaOH and 300 mg of hydroxy naphthol blue indicator are added, and the titration is continued to a blue end-point.

A similar procedure is described for the assay of precipitated calcium carbonate, calcium chloride, calcium gluconate, calcium hydroxide, calcium lactate, and calcium levulinate and for the calcium content analysis of calcium pantothenate and racemic calcium pantothenate. Although each assay calls for the addition of hydrochloric acid, this step is only necessary where the calcium salt has a limited aqueous solubility (2, 3). Since calcium gluceptate is freely soluble in water (4), we suggest that the addition of hydrochloric acid should be omitted. Table I shows that assay results are not affected by the presence or absence of hydrochloric acid.

**Table I—Assay of Calcium Gluceptate in the Presence and Absence of Hydrochloric Acid**

| Calcium Gluceptate | Assay Value, %[a] | |
|---|---|---|
| | USP Method | Modified USP Method |
| Source A[b] | 96.80 ± 0.42 (96.55–97.43) | 96.82 ± 0.32 (96.54–97.10) |
| Source B[c] | 97.02 ± 0.39 (96.51–97.42) | 97.16 ± 0.21 (96.97–97.41) |
| Source C[d] | 101.15 ± 0.08 (101.04–101.24) | 100.86 ± 0.49 (100.14–101.17) |

[a] Mean ± *SD*, $n = 4$; range is given in parentheses. [b] Pfanstiehl. [c] Givaudan. [d] Italsintex.

The sodium hydroxide solution and the hydroxy naphthol blue indicator can be added to the calcium gluceptate solution at the beginning of the assay; thus, it is unnecessary to interrupt titration to make these additions. The estimation of calcium with ethylenediaminetetraacetic acid using hydroxy naphthol blue as the indicator is carried out at pH 12–13 (5). The addition of 15 ml of 1 *N* NaOH solution in the official assay brings the pH to this range. In the absence of hydrochloric acid, ~10 ml of 1 *N* NaOH solution would be sufficient to bring the pH to the required range. Thus, omitting the hydrochloric acid both simplifies the procedure and enables the amount of sodium hydroxide to be reduced.

We suggest that hydrochloric acid might be omitted in the assay of other freely soluble calcium salts.

(1) "The United States Pharmacopeia," 20th rev., United States Pharmacopeial Convention, Rockville, Md., 1980, p. 107.
(2) A. Q. Butler, F. A. Maurina, and F. A. Morecombe, *J. Pharm. Sci.*, **54**, 134 (1965).
(3) R. W. Goettsch, *ibid.*, **54**, 317 (1965).
(4) "The United States Pharmacopeia," 20th rev., United States Pharmacopeial Convention, Rockville, Md., 1980, p. 1125.
(5) A. Itoh and K. Ueno, *Analyst*, **95**, 583 (1970).

*R. Suryanarayanan*
*A. G. Mitchell* ˣ
Faculty of Pharmaceutical Sciences
University of British Columbia
2146 East Mall
Vancouver, B.C. V6T 1W5
Canada

Received February 9, 1981.
Accepted for publication April 27, 1981.
The authors thank Stanley Drug Products Ltd. for supplies of calcium gluceptate, and R. Suryanarayanan thanks the Science Council of British Columbia for a graduate research, engineering and technology award.

## Observed Artifacts due to Pellet Preparation in IR Spectrometry

**Keyphrases** □ IR spectrometry—observed artifacts due to pellet preparation □ Pellets—observed artifacts due to preparation, IR spectrometry

*To the Editor:*

IR spectrometry is required for identifying organic substances by most pharmacopeia and official compendia such as the USP XIX and the NF XIV (1, 2). The USP recommends: "Chemically identical substances of differing polymorphic forms often exhibit different infrared spectra when examined in the solid state. If a difference appears in the spectra, dissolve portions of both the sample and the reference standard in a suitable solvent, evaporate the solution to dryness, and repeat the test on the residues" (1). Differences resulting from polymorphism are considered to be the major reason for errors.

Certain secondary and tertiary amine derivatives such as bupivacaine, cinnarizine, and many butyrophenones have the same spectrum, in part or in whole, for their hydrochloride, hydrobromide, and free base forms when they are dissolved in methanol, ethanol, or isopropanol and if grinding with potassium bromide is prolonged.



*0022-3549/81/0800-0968$01.00/0*
*© 1981, American Pharmaceutical Association*

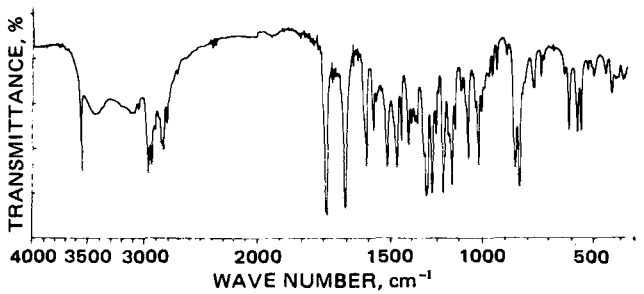


**Figure 1**—*Spectrum of moperone base; grinding with potassium bromide without any solvent.*

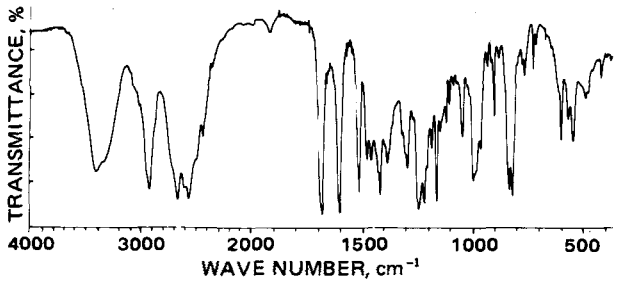


**Figure 2**—*Spectrum of moperone hydrochloride; grinding with potassium bromide without any solvent.*

In the case of amine hydrochloride, the exchange of chlorine ions with bromine ions was reported (3, 4). However, this explanation is unsatisfactory for the free base form. The presence of very intense absorption bands between 2650 and 2500 $cm^{-1}$, indicating nitrogen protonation, was confirmed (Figs. 1–3). In the case of moperone, the hydrobromide reextracted from the potassium bromide pellet by a minimum volume of methanol shows a final melting temperature of 184°, determined by thermomicroscopy, even though melting temperatures of the hydrobromide, hydrochloride, and free base forms are 186, 222, and 123°, respectively. It was reported (5) that amine salts having a protonated nitrogen atom of the $NH_3^+$, $NH_2^+$, or $NH^+$ type possess characteristic frequencies of 4000–2000 $cm^{-1}$.

The hydrobromide form of moperone (reextracted from potassium bromide pellets) was confirmed using X-ray diffraction. The spectra present the characteristic moperone hydrobromide pattern, including intense bands corresponding to *d* values of 0.64, 5.29, 5.16, 4.89, 4.78, 4.25, 3.68, and 3.61 Å. Identical results were obtained with pharmaceutical organic raw materials such as bupivacaine, cinnarizine, diethylpropion, diisopromine, fenfluramine, fluanisone, haloperidol, homatropine, and moperone.

The hydrobromide formation may be attributed to atmospheric carbon dioxide combined with the entropy of the system since the potassium bromide effect persists when sodium redistilled methanol or pyridine and potassium bromide solutions (pH 10) are used. Thus, it is important not to attribute the spectral consequences of this potassium bromide effect to the existence of a new polymorphic form.

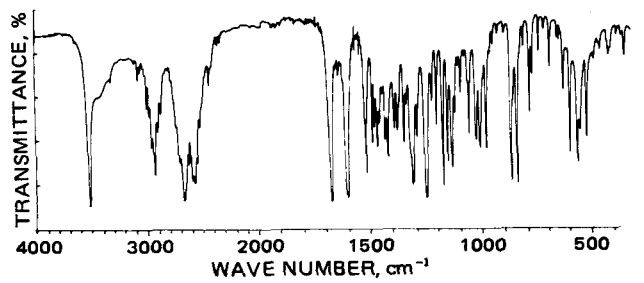


**Figure 3**—*Spectrum of moperone base or hydrochloride; grinding with potassium bromide and solvent.*

(1) The United States Pharmacopeia, 19th rev., Mack Publishing Co., Easton, Pa., 1975, p. 664.

(2) "The National Formulary," 14th ed., Mack Publishing Co., Easton, Pa., 1975, p. 1969.

(3) J. Carol, *J. Pharm. Sci.*, **50,** 451 (1961).

(4) S. C. Mutha and W. B. Ludeman, *ibid.*, **65,** 1400 (1976).

(5) W. E. Thompson, R. J. Warren, I. B. Eisdorfer, and J. E. Zarembo, *ibid.*, **54,** 1819 (1965).

*R. P. Bouche* ˣ
*M. Azibi*
*M. G. Draguet-Brughmans*
Faculté de Médecine–Ecole de Pharmacie
Laboratoire d'Analyse des Médicaments
Université Catholique de Louvain
73, avenue E. Mounier-BP. 7340
1200 Bruxelles, Belgium

Received December 1, 1980.
Accepted for publication May 21, 1981.

# First-Pass Clearance of Lidocaine in Healthy Volunteers and Epileptic Patients: Influence of Effective Liver Volume

**Keyphrases** □ Lidocaine—first-pass clearance in healthy volunteers and epileptic patients compared □ Bioavailability—lidocaine, compared in healthy volunteers and epileptic patients, influence of effective liver volume □ Hepatic retention—effect on first-pass clearance of lidocaine, healthy volunteers and epileptic patients compared

*To the Editor:*

Recent reports (1, 2) compared the absolute oral bioavailability of lidocaine in epileptic patients receiving chronic anticonvulsant drug therapy to that in normal healthy volunteers not receiving enzyme-inducing drugs. The authors of these reports concluded that the greater than twofold reduction in absolute availability observed in the epileptic patients was the result of increased hepatic first-pass metabolism caused by the chronic administration of anticonvulsant drugs.

The present study considers the possible impact of increased hepatic retention, rather than increased metabolic activity, on reduced bioavailability using the first-pass perfusion model presented in Scheme I. The model was used to simulate the effect of increased hepatoportal retention of lidocaine that could result from the induction of nonenzyme-related protein synthesis in the eliminating organ. The product of the liver volume ($V_H$) and liver retention ($R_H$) is the effective liver volume (3). Therefore, by definition, an increase in liver mass or hepatic tissue binding is reflected as an increase in hepatic organ clear-

0022-3549/81/0800-0969$01.00/0
© 1981, American Pharmaceutical Association

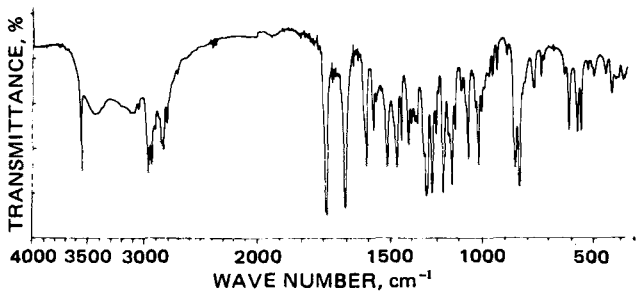


**Figure 1**—*Spectrum of moperone base; grinding with potassium bromide without any solvent.*

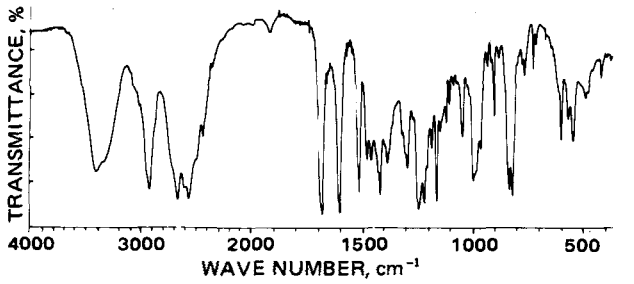


**Figure 2**—*Spectrum of moperone hydrochloride; grinding with potassium bromide without any solvent.*

In the case of amine hydrochloride, the exchange of chlorine ions with bromine ions was reported (3, 4). However, this explanation is unsatisfactory for the free base form. The presence of very intense absorption bands between 2650 and 2500 $cm^{-1}$, indicating nitrogen protonation, was confirmed (Figs. 1–3). In the case of moperone, the hydrobromide reextracted from the potassium bromide pellet by a minimum volume of methanol shows a final melting temperature of 184°, determined by thermomicroscopy, even though melting temperatures of the hydrobromide, hydrochloride, and free base forms are 186, 222, and 123°, respectively. It was reported (5) that amine salts having a protonated nitrogen atom of the $NH_3^+$, $NH_2^+$, or $NH^+$ type possess characteristic frequencies of 4000–2000 $cm^{-1}$.

The hydrobromide form of moperone (reextracted from potassium bromide pellets) was confirmed using X-ray diffraction. The spectra present the characteristic moperone hydrobromide pattern, including intense bands corresponding to *d* values of 0.64, 5.29, 5.16, 4.89, 4.78, 4.25, 3.68, and 3.61 Å. Identical results were obtained with pharmaceutical organic raw materials such as bupivacaine, cinnarizine, diethylpropion, diisopromine, fenfluramine, fluanisone, haloperidol, homatropine, and moperone.

The hydrobromide formation may be attributed to atmospheric carbon dioxide combined with the entropy of the system since the potassium bromide effect persists when sodium redistilled methanol or pyridine and potassium bromide solutions (pH 10) are used. Thus, it is important not to attribute the spectral consequences of this potassium bromide effect to the existence of a new polymorphic form.

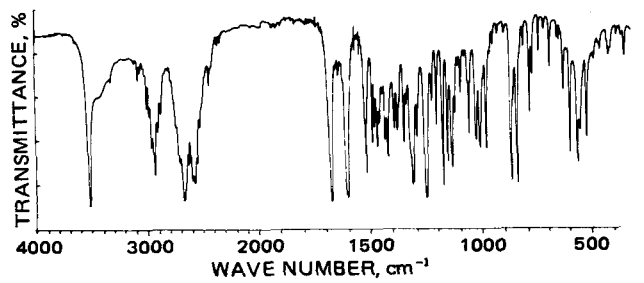


**Figure 3**—*Spectrum of moperone base or hydrochloride; grinding with potassium bromide and solvent.*

(1) The United States Pharmacopeia, 19th rev., Mack Publishing Co., Easton, Pa., 1975, p. 664.

(2) "The National Formulary," 14th ed., Mack Publishing Co., Easton, Pa., 1975, p. 1969.

(3) J. Carol, *J. Pharm. Sci.*, **50,** 451 (1961).

(4) S. C. Mutha and W. B. Ludeman, *ibid.*, **65,** 1400 (1976).

(5) W. E. Thompson, R. J. Warren, I. B. Eisdorfer, and J. E. Zarembo, *ibid.*, **54,** 1819 (1965).

*R. P. Bouche* ˣ
*M. Azibi*
*M. G. Draguet-Brughmans*
Faculté de Médecine–Ecole de Pharmacie
Laboratoire d'Analyse des Médicaments
Université Catholique de Louvain
73, avenue E. Mounier-BP. 7340
1200 Bruxelles, Belgium

Received December 1, 1980.
Accepted for publication May 21, 1981.

# First-Pass Clearance of Lidocaine in Healthy Volunteers and Epileptic Patients: Influence of Effective Liver Volume

**Keyphrases** □ Lidocaine—first-pass clearance in healthy volunteers and epileptic patients compared □ Bioavailability—lidocaine, compared in healthy volunteers and epileptic patients, influence of effective liver volume □ Hepatic retention—effect on first-pass clearance of lidocaine, healthy volunteers and epileptic patients compared

*To the Editor:*

Recent reports (1, 2) compared the absolute oral bioavailability of lidocaine in epileptic patients receiving chronic anticonvulsant drug therapy to that in normal healthy volunteers not receiving enzyme-inducing drugs. The authors of these reports concluded that the greater than twofold reduction in absolute availability observed in the epileptic patients was the result of increased hepatic first-pass metabolism caused by the chronic administration of anticonvulsant drugs.

The present study considers the possible impact of increased hepatic retention, rather than increased metabolic activity, on reduced bioavailability using the first-pass perfusion model presented in Scheme I. The model was used to simulate the effect of increased hepatoportal retention of lidocaine that could result from the induction of nonenzyme-related protein synthesis in the eliminating organ. The product of the liver volume ($V_H$) and liver retention ($R_H$) is the effective liver volume (3). Therefore, by definition, an increase in liver mass or hepatic tissue binding is reflected as an increase in hepatic organ clear-

0022-3549/81/0800-0969$01.00/0
© 1981, American Pharmaceutical Association

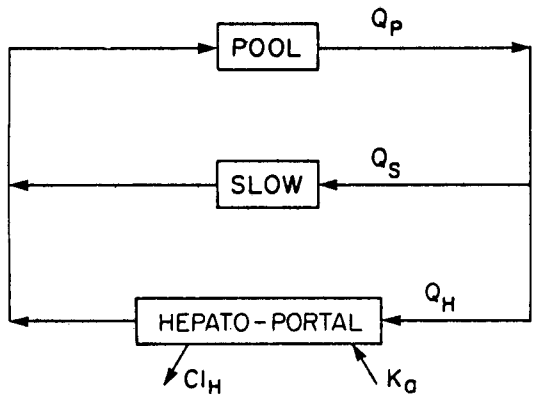


*Scheme I—First-pass perfusion model. The perfusion model contains three compartments: 1, the pool, which includes the serum and highly perfused noneliminating tissues where $V_P$ is the pool volume; 2, more slowly perfused noneliminating tissues where $V_SR_S$ is the effective volume of this more slowly equilibrating pool; and 3, the hepatoportal system, which is responsible for drug elimination and where $V_HR_H$ is the effective liver volume. Blood flow to the more slowly perfused organs and the hepatoportal system are described as $Q_S$ and $Q_H$, respectively, whereas the hepatic clearance is described as $Cl_H$.*

ance ($Cl_H$) as a result of an increase in the effective liver volume. Classic clearance concepts (4) dictate that changes in hepatic organ clearance ($Cl_H$) and hepatic blood flow ($Q_H$) result in changes in the first-pass extraction ($E$) and total body clearances ($Cl_B$) according to:

$$E = \frac{Cl_H}{Q_H + Cl_H} \quad \text{(Eq. 1)}$$

$$Cl_B = \frac{Q_H Cl_H}{Q_H + Cl_H} \quad \text{(Eq. 2)}$$

Hepatic organ clearance is generally assumed to mean metabolic clearance, although, in reality, it includes both metabolic activity and tissue retention in the liver due to tissue binding (3).

The experimental data was obtained from a previous report (1) in which six epileptic patients receiving chronic anticonvulsant therapy with known enzyme-inducing agents (*i.e.*, phenobarbital, primidone, carbamazepine, and phenytoin) and six healthy volunteers were studied. Each person was administered 86 mg of lidocaine base equivalents intravenously as the hydrochloride salt and ingested 608 mg of lidocaine base equivalents orally as the monohydrate salt on two separate occasions. Blood samples were withdrawn over 240 min to assess the pharmacokinetics of lidocaine in serum. Serum concentrations were determined by enzyme immunoassay (1).

The following differential equations describe the model presented in Scheme I and were used to simulate serum concentration–time data for oral and intravenous doses simultaneously using the nonlinear least-squares regression program NONLIN (5):

$$\frac{dC_P}{dt} = [(Q_S C_S/R_S) + (Q_H C_H/R_H) - Q_P C_P]/V_P \quad \text{(Eq. 3)}$$

$$\frac{dC_S}{dt} = [Q_S C_P - (Q_S C_S/R_S)]/V_S \quad \text{(Eq. 4)}$$

For the intravenous dose:

$$\frac{dC_H}{dt} = [Q_H C_P - (Q_H C_H/R_H) - (Cl_H C_H/R_H)]/V_H \quad \text{(Eq. 5)}$$

For the oral dose:

$$\frac{dC_H}{dt} = [k_a D e^{-kat} + Q_H C_P - (Q_H C_H/R_H) - (Cl_H C_H/R_H)]/V_H \quad \text{(Eq. 6)}$$

where $C_P$, $C_S$, and $C_H$ are the concentrations of lidocaine in the sampled compartment that contains the serum and the highly perfused tissues, more slowly perfused tissues, and hepatoportal system, respectively; $V_P$, $V_S$, and $V_H$ are the physiological volumes of these compartments; $Q_P$, $Q_S$, and $Q_H$ are the serum flow rate for these compartments; $R_S$ and $R_H$ are the retention factors for drug in the more slowly perfused tissues and the hepatoportal tissues, respectively; $Cl_H$ is the hepatic clearance rate; $k_a$ is the apparent absorption rate constant; and $D$ is the oral dose.

The parameters used in the simulations are presented in Table I. Both oral and intravenous data were simulated to determine the impact of increased effective linear volume on the pharmacokinetics of both administration routes.

The results of the simultations, together with the experimental data for the normal subjects and epileptic patients, are presented in Fig. 1. The differences between normal subjects and patients receiving enzyme-inducing agents can be adequately described by a perfusion model that allows only for a change in the effective liver volume rather than for changes in the enzyme activity *per se*.

Perucca and coworkers (1, 2) attributed reduced oral bioavailability of lidocaine in epileptic patients ingesting

**Table I—Pharmacokinetic Parameters Used in the Simulation of Lidocaine Serum Concentration–Time Data for Normal Healthy Volunteers and Epileptic Patients**

| Parameter | Normal Healthy Controls | Epileptic Patients |
|---|---|---|
| $k_a$, $min^{-1}$ | 0.145 | 0.145 |
| $V_P$, liters | 35 | 35 |
| $V_SR_S$, liters | 40 | 40 |
| $V_HR_H$, liters | 50 | 150 |
| $Q_S$, liters/min | 2.4 | 2.4 |
| $Q_H$, liters/min | 1.3 | 1.3 |
| $Cl_H$, liters/min | 2.3 | 6.2 |
| $Cl_B$, liters/min | 0.83 | 1.07 |
| $E$ | 0.64 | 0.83 |

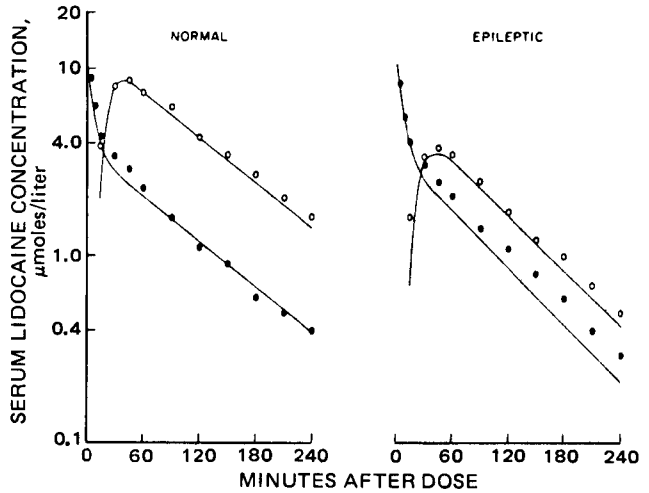


**Figure 1**—*Simulated and observed serum concentrations of lidocaine following intravenous (●) and oral (○) doses to epileptic patients receiving chronic anticonvulsant therapy and normal, healthy volunteers. The solid lines were simulated according to the model in Scheme I, assuming that the effective liver volume $V_HR_H$ was the only difference between the two study groups. (See Table I for parameters used in the simulation.)*

enzyme-inducing agents to a simple increase in hepatic first-pass metabolism. Although the existence of increased first-pass clearance was supported by the present analysis, the data suggest that an alternative mechanism, increased effective linear volume, may be responsible. Due to the increased retention of lidocaine in the liver as a result of increased effective liver volume, the first-pass clearance of lidocaine was much more extensive in epileptic patients than in normal volunteers.

Although the possibility exists for a reduction in the extent of lidocaine absorption in the epileptic patient, no evidence for a similar interaction could be found in the literature. In addition, it is highly unlikely that all of the anticonvulsant drugs used in this study should have the same effect on absorption. However, there is evidence (7–9) for the increase in effective liver volume observed in the present study. An increase in liver mass during anticonvulsant therapy, as well as an increase in binding affinity by the newly synthesized protein, has been postulated as possible mechanisms.

In conclusion, changes in the pharmacokinetics of drugs due to the chronic administration of enzyme-inducing agents has been attributed solely to increases in the intrinsic metabolic activity (6–9). Concomitant changes in blood flow are sometimes postulated as complementary mechanisms for increased clearance (9–11). However, one mechanism that has generally been overlooked is the effect of enzyme-inducing agents on the effective volume of the eliminating organ, *e.g.*, the liver and/or intestinal mucosa, by increasing tissue mass or tissue binding (10–12).

The results of the present analysis indicate that first-pass clearance may be a complex interaction of several pharmacokinetic parameters including blood flow, metabolic activity, and effective tissue volume. The complexity of this interaction may help to explain the apparent discrepancies between enzyme induction observed *in vitro* and *in vivo*.

(1) E. Perucca and A. Richens, *Br. J. Clin. Pharmacol.*, **8**, 21 (1979).

(2) E. Perucca, A. Hedges, K. A. Makki, and A. Richens, *ibid.*, **10**, 491 (1980).

(3) M. Rowland, L. Z. Benet, and G. G. Graham, *J. Pharmacokinet. Biopharm.*, **1**, 123 (1973).

(4) A. S. Nies, D. G. Shand, and G. R. Wilkinson, *Clin. Pharmacokinet.*, **1**, 135 (1976).

(5) C. M. Metzler, G. L. Elfring, and A. J. Mc Ewen, *Biometrics*, **30**, 512 (1974).

(6) G. Alvan, K. Piafsky, M. Lind, and C. von Bahr, *Clin. Pharmacol. Ther.*, **22**, 316 (1977).

(7) C. A. Difazio and R. E. Brown, *Anesthesiology*, **36**, 238 (1972).

(8) A. A. Lai and R. H. Levy, *J. Pharm. Sci.*, **68**, 416 (1979).

(9) M. S. Yates, C. R. Hiley, and D. J. Back, *Life Sci.*, **24**, 535 (1979).

(10) E. E. Ohnhaus, S. S. Thorgeirsson, D. S. Davies, and A. Breckenridge, *Biochem. Pharmacol.*, **20**, 2561 (1971).

(11) D. G. McDevitt, A. S. Nies, and G. R. Wilkinson, *ibid.*, **26**, 1247 (1979).

(12) R. Stegmann and M. H. Bickel, *Xenobiotica*, **12**, 737 (1977).

*Wayne A. Colburn*
Department of Pharmacokinetics and Biopharmaceutics
Hoffmann–La Roche Inc.
Nutley, NJ 07110

Received February 4, 1980.
Accepted for publication May 13, 1981.
The author thanks Mrs. W. Morley for preparation of the manuscript.

## Solubility and Partitioning V: Dependence of Solubility on Melting Point

**Keyphrases** □ Solubility—dependence on melting point, crystalline compounds □ Crystalline compounds—polycyclic aromatic hydrocarbons, dependence of solubility on melting point

*To the Editor:*

It is well known that the solubility (in any solvent) of a crystalline solute is at least partially dependent on certain properties of the crystal. The reduction in solubility that is attributable to solute crystallinity is given by:

$$\log \frac{X^C}{X^{SCL}} = \frac{-\Delta S_f(T_m - T)}{2.303RT} + \frac{\Delta C_p(T_m - T)}{2.303RT} - \frac{\Delta C_p}{2.303R} \ln\left(\frac{T_m}{T}\right) \quad \text{(Eq. 1)}$$

where $X^C$ and $X^{SCL}$ are the mole fractional solubilities of the crystalline solute and of the supercooled liquid, respectively; $T_m$ and $T$ are the melting point and temperature of interest, respectively (both in °K); $\Delta S_f$ is the entropy of fusion of the crystal; and $\Delta C_p$ is the difference in heat capacity between the crystal and the supercooled liquid.

The supercooled liquid, SCL, is the result of melting the crystal at the temperature of interest, which is assumed to be below the melting point. It is the equivalent to the "oil" form of the substance. In most cases, it is not possible to produce the oil or molten form below the melting point. For these cases, the supercooled liquid represents a hypothetical state.

To estimate the solubility of crystalline compounds, it is necessary to estimate the crystal–liquid solubility ratio, $X^C/X^{SCL}$. This estimation is normally facilitated by simplifying Eq. 1 to remove the $\Delta C_p$ terms. Two alternative approximations for $\Delta C_p$ are commonly used: $\Delta C_p = 0$ and $\Delta C_p = \Delta S_f$. These approximations lead to the following simplifications.

If $\Delta C_p = 0$:

$$\log \frac{X^C}{X^{SCL}} = -\frac{\Delta S_f(T_m - T)}{2.303RT} \quad \text{(Eq. 2)}$$

If $\Delta C_p = \Delta S_f$:

$$\log \frac{X^C}{X^{SCL}} = -\frac{\Delta S_f}{2.303R} \ln\left(\frac{T_m}{T}\right) \quad \text{(Eq. 3)}$$

Equation 2 was used by Yalkowsky and coworkers (1–4), whereas Eq. 3 was used by Martin *et al.* (5) and was recommended by Hildebrand *et al.* (6).

To verify one or the other of these approximations, it is necessary to find a set of crystalline solutes and a solvent for which $X^{SCL}$ is known. The crystalline polycyclic aromatic hydrocarbons (pah) in benzene are such a system. Since the solutes and solvent have no permanent dipoles, the major cohesive interactions will be the result of London dispersion forces. Dispersion forces are primarily dependent on polarizability, which is proportional to volume for hydrocarbons. Thus, the cohesive energy density of the solutes and the solvent is very similar, and the solutions are very nearly ideal. Because the components of an ideal solution are completely miscible (if they are liquids), it can be assumed that $X^{SCL} = 1.0$ for the polycyclic aromatic hydrocarbons in benzene.

It has been shown that the entropy of fusion of confor-

0022-3549/81/0800-0971$01.00/0
© 1981, American Pharmaceutical Association

enzyme-inducing agents to a simple increase in hepatic first-pass metabolism. Although the existence of increased first-pass clearance was supported by the present analysis, the data suggest that an alternative mechanism, increased effective linear volume, may be responsible. Due to the increased retention of lidocaine in the liver as a result of increased effective liver volume, the first-pass clearance of lidocaine was much more extensive in epileptic patients than in normal volunteers.

Although the possibility exists for a reduction in the extent of lidocaine absorption in the epileptic patient, no evidence for a similar interaction could be found in the literature. In addition, it is highly unlikely that all of the anticonvulsant drugs used in this study should have the same effect on absorption. However, there is evidence (7–9) for the increase in effective liver volume observed in the present study. An increase in liver mass during anticonvulsant therapy, as well as an increase in binding affinity by the newly synthesized protein, has been postulated as possible mechanisms.

In conclusion, changes in the pharmacokinetics of drugs due to the chronic administration of enzyme-inducing agents has been attributed solely to increases in the intrinsic metabolic activity (6–9). Concomitant changes in blood flow are sometimes postulated as complementary mechanisms for increased clearance (9–11). However, one mechanism that has generally been overlooked is the effect of enzyme-inducing agents on the effective volume of the eliminating organ, *e.g.*, the liver and/or intestinal mucosa, by increasing tissue mass or tissue binding (10–12).

The results of the present analysis indicate that first-pass clearance may be a complex interaction of several pharmacokinetic parameters including blood flow, metabolic activity, and effective tissue volume. The complexity of this interaction may help to explain the apparent discrepancies between enzyme induction observed *in vitro* and *in vivo*.

(1) E. Perucca and A. Richens, *Br. J. Clin. Pharmacol.*, **8**, 21 (1979).

(2) E. Perucca, A. Hedges, K. A. Makki, and A. Richens, *ibid.*, **10**, 491 (1980).

(3) M. Rowland, L. Z. Benet, and G. G. Graham, *J. Pharmacokinet. Biopharm.*, **1**, 123 (1973).

(4) A. S. Nies, D. G. Shand, and G. R. Wilkinson, *Clin. Pharmacokinet.*, **1**, 135 (1976).

(5) C. M. Metzler, G. L. Elfring, and A. J. Mc Ewen, *Biometrics*, **30**, 512 (1974).

(6) G. Alvan, K. Piafsky, M. Lind, and C. von Bahr, *Clin. Pharmacol. Ther.*, **22**, 316 (1977).

(7) C. A. Difazio and R. E. Brown, *Anesthesiology*, **36**, 238 (1972).

(8) A. A. Lai and R. H. Levy, *J. Pharm. Sci.*, **68**, 416 (1979).

(9) M. S. Yates, C. R. Hiley, and D. J. Back, *Life Sci.*, **24**, 535 (1979).

(10) E. E. Ohnhaus, S. S. Thorgeirsson, D. S. Davies, and A. Breckenridge, *Biochem. Pharmacol.*, **20**, 2561 (1971).

(11) D. G. McDevitt, A. S. Nies, and G. R. Wilkinson, *ibid.*, **26**, 1247 (1979).

(12) R. Stegmann and M. H. Bickel, *Xenobiotica*, **12**, 737 (1977).

*Wayne A. Colburn*
Department of Pharmacokinetics and Biopharmaceutics
Hoffmann–La Roche Inc.
Nutley, NJ 07110

Received February 4, 1980.
Accepted for publication May 13, 1981.
The author thanks Mrs. W. Morley for preparation of the manuscript.

## Solubility and Partitioning V: Dependence of Solubility on Melting Point

**Keyphrases** □ Solubility—dependence on melting point, crystalline compounds □ Crystalline compounds—polycyclic aromatic hydrocarbons, dependence of solubility on melting point

*To the Editor:*

It is well known that the solubility (in any solvent) of a crystalline solute is at least partially dependent on certain properties of the crystal. The reduction in solubility that is attributable to solute crystallinity is given by:

$$\log \frac{X^C}{X^{SCL}} = \frac{-\Delta S_f(T_m - T)}{2.303RT} + \frac{\Delta C_p(T_m - T)}{2.303RT} - \frac{\Delta C_p}{2.303R} \ln\left(\frac{T_m}{T}\right) \quad \text{(Eq. 1)}$$

where $X^C$ and $X^{SCL}$ are the mole fractional solubilities of the crystalline solute and of the supercooled liquid, respectively; $T_m$ and $T$ are the melting point and temperature of interest, respectively (both in °K); $\Delta S_f$ is the entropy of fusion of the crystal; and $\Delta C_p$ is the difference in heat capacity between the crystal and the supercooled liquid.

The supercooled liquid, SCL, is the result of melting the crystal at the temperature of interest, which is assumed to be below the melting point. It is the equivalent to the "oil" form of the substance. In most cases, it is not possible to produce the oil or molten form below the melting point. For these cases, the supercooled liquid represents a hypothetical state.

To estimate the solubility of crystalline compounds, it is necessary to estimate the crystal–liquid solubility ratio, $X^C/X^{SCL}$. This estimation is normally facilitated by simplifying Eq. 1 to remove the $\Delta C_p$ terms. Two alternative approximations for $\Delta C_p$ are commonly used: $\Delta C_p = 0$ and $\Delta C_p = \Delta S_f$. These approximations lead to the following simplifications.

If $\Delta C_p = 0$:

$$\log \frac{X^C}{X^{SCL}} = -\frac{\Delta S_f(T_m - T)}{2.303RT} \quad \text{(Eq. 2)}$$

If $\Delta C_p = \Delta S_f$:

$$\log \frac{X^C}{X^{SCL}} = -\frac{\Delta S_f}{2.303R} \ln\left(\frac{T_m}{T}\right) \quad \text{(Eq. 3)}$$

Equation 2 was used by Yalkowsky and coworkers (1–4), whereas Eq. 3 was used by Martin *et al.* (5) and was recommended by Hildebrand *et al.* (6).

To verify one or the other of these approximations, it is necessary to find a set of crystalline solutes and a solvent for which $X^{SCL}$ is known. The crystalline polycyclic aromatic hydrocarbons (pah) in benzene are such a system. Since the solutes and solvent have no permanent dipoles, the major cohesive interactions will be the result of London dispersion forces. Dispersion forces are primarily dependent on polarizability, which is proportional to volume for hydrocarbons. Thus, the cohesive energy density of the solutes and the solvent is very similar, and the solutions are very nearly ideal. Because the components of an ideal solution are completely miscible (if they are liquids), it can be assumed that $X^{SCL} = 1.0$ for the polycyclic aromatic hydrocarbons in benzene.

It has been shown that the entropy of fusion of confor-

0022-3549/81/0800-0971$01.00/0
© 1981, American Pharmaceutical Association

**Table I—Entropies of Fusion of Some Polycyclic Aromatic Hydrocarbons**

| | Reference 8 | Reference 9 | Reference 10 |
|---|---|---|---|
| Diphenyl | — | 13.2 | 13.0 |
| Naphthalene | 13.0 | 24.7 | 13.1 |
| Anthracene | 14.0 | 14.1 | 14.1 |
| Phenanthrene | 10.8 | 10.5 | 12.1 |
| Pyrene | 9.6 | 8.6 | — |
| Triphenylene | 12.7 | — | — |
| Chrysene | 11.8 | — | 14.9 |
| Fluorene | 11.6 | 12.1 | — |
| Acenaphthene | 14.3 | 14.4 | 13.6 |
| Fluoranthrene | 11.8 | — | — |

mationally rigid molecules is reasonably constant. Most large aromatic molecules have $\Delta S_f \simeq 13.5$ cal/°K/mole. The values of the entropy of fusion of some polycyclic aromatic hydrocarbons are shown in Table I.

Equations 2 and 3 can be tested by regression analysis of $X^{pah}_{benzene}$ as a function of $(T_m - T)/2.303RT$ and $\ln(T_m/T)/2.303R$, respectively, and comparison of the slopes with the expected value of 13.5 cal/°K/mole.

The values of $(T_m - T)/2.303RT$ and $\ln(T_m/T)/2.303R$ do not differ greatly for low melting solutes studied at room temperature. However, they can significantly deviate from one another at higher temperatures. The values of the two terms as a function of melting point at $T = 300$ and 400 °K are shown in Table II.

The solubilities of 14 polycyclic aromatic hydrocarbons in benzene as determined previously (7) at several temperatures are given in Table III. These data provide an excellent opportunity to test and compare the described equations. Table IV provides a summary of the least-squares regression analysis of the data in Table III against Eqs. 2 and 3. Both curves were forced through the origin.

It is apparent that both equations give excellent correlations with the data. The statistical parameters show better fit with Eq. 2, although the difference is not significant. The major difference between the two equations lies in the value of the slope. If the entropy of fusion of the polycyclic aromatic hydrocarbons is constant, as appears to be the case, the slope is equal to that value. The entropy of fusion calculated from Eq. 2 (16.19 cal/°K/mole) is much closer to the expected value of 13.5 cal/°K/mole than the slope of Eq. 3 (19.58 cal/°K/mole).

The slight difference between the slope obtained with Eq. 2 and 13.5 cal/°K/mole is probably due to a systematic change in cohesive energy density with increasing molecular size and, thus, with increasing melting point. This change would cause the larger and higher melting hydrocarbons to have $X^{SCL}$ progressively less than the ideal value of unity. It would also cause $X^C/X^{SCL}$ to appear to be artifactually high and thus increase the slope over the

**Table II—Dependence of $(T_m - T)/2.303RT$ and $\ln(T_m/T)/2.303R$ on $T_m$ and $T$**

| | $T$ = 300 °K | | $T$ = 400 °K | |
|---|---|---|---|---|
| $T_m$ | $\frac{(T_m - T)}{2.303RT}$ | $\frac{\ln(T_m/T)}{2.303RT}$ | $\frac{(T_m - T)}{2.303RT}$ | $\frac{\ln(T_m/T)}{2.303RT}$ |
| 300 | 0 | 0 | — | — |
| 400 | 0.07 | 0.06 | 0 | 0 |
| 500 | 0.15 | 0.11 | 0.05 | 0.05 |
| 600 | 0.22 | 0.15 | 0.11 | 0.09 |
| 700 | 0.29 | 0.19 | 0.16 | 0.12 |

**Table III—Solubility of Polycyclic Aromatic Hydrocarbons in Benzene**

| Solute | Melting Point ($T_m$), °K | Temperature ($T$), °K | Mole Fraction Solubility ($X$) |
|---|---|---|---|
| Diphenyl | 69 | 37.0 | 0.5118 |
| | 69 | 47.6 | 0.6478 |
| | 69 | 59.2 | 0.8195 |
| | 69 | 63.2 | 0.8916 |
| *o*-Terphenyl | 56 | 28.0 | 0.5852 |
| | 56 | 32.4 | 0.6442 |
| | 56 | 44.8 | 0.8012 |
| | 56 | 50.4 | 0.9013 |
| *m*-Terphenyl | 87 | 36.8 | 0.2827 |
| | 87 | 47.0 | 0.3338 |
| | 87 | 60.8 | 0.5466 |
| | 87 | 67.4 | 0.6407 |
| | 87 | 74.2 | 0.7571 |
| | 87 | 77.6 | 0.8344 |
| *p*-Terphenyl | 213 | 38.0 | 0.0071 |
| | 213 | 60.2 | 0.0156 |
| | 213 | 64.2 | 0.0178 |
| | 213 | 68.0 | 0.0204 |
| | 213 | 77.6 | 0.0279 |
| 1,3,5-Triphenylbenzene | 175 | 25.2 | 0.0299 |
| | 175 | 28.6 | 0.0351 |
| | 175 | 40.4 | 0.0483 |
| | 175 | 46.2 | 0.0562 |
| | 175 | 59.4 | 0.0795 |
| | 175 | 66.6 | 0.0960 |
| Naphthalene | 80 | 35.0 | 0.3766 |
| | 80 | 45.0 | 0.4806 |
| | 80 | 47.4 | 0.5094 |
| | 80 | 63.2 | 0.7119 |
| | 80 | 75.8 | 0.9180 |
| Anthracene | 218 | 35.8 | 0.0103 |
| | 218 | 42.4 | 0.0130 |
| | 218 | 50.6 | 0.0173 |
| | 218 | 59.6 | 0.0225 |
| | 218 | 70.2 | 0.0315 |
| Phenanthrene | 98 | 32.0 | 0.2239 |
| | 98 | 40.2 | 0.2836 |
| | 98 | 41.8 | 0.2990 |
| | 98 | 50.2 | 0.3750 |
| | 98 | 58.0 | 0.4572 |
| Pyrene | 150 | 32.4 | 0.0734 |
| | 150 | 58.6 | 0.1506 |
| | 150 | 66.8 | 0.1896 |
| | 150 | 76.2 | 0.2441 |
| | 150 | 84.6 | 0.3014 |
| Triphenylene | 198 | 39.4 | 0.0140 |
| | 198 | 47.6 | 0.0181 |
| | 198 | 63.8 | 0.0289 |
| | 198 | 69.4 | 0.0341 |
| | 198 | 82.8 | 0.0497 |
| Chrysene | 254 | 35.6 | 0.0021 |
| | 254 | 45.8 | 0.0032 |
| | 254 | 60.6 | 0.0052 |
| | 254 | 72.2 | 0.0079 |
| Fluorene | 113 | 33.6 | 0.1604 |
| | 113 | 54.4 | 0.2778 |
| | 113 | 58.4 | 0.3095 |
| | 113 | 69.4 | 0.4059 |
| | 113 | 72.8 | 0.4405 |
| Acenaphthene | 94 | 30.6 | 0.1815 |
| | 94 | 41.4 | 0.2540 |
| | 94 | 63.2 | 0.4731 |
| | 94 | 69.4 | 0.5552 |
| Fluoranthene | 110 | 44.8 | 0.2174 |
| | 110 | 56.0 | 0.3011 |
| | 110 | 64.4 | 0.3826 |
| | 110 | 77.2 | 0.5331 |

**Table IV—Summary of Regression Analyses**

| | Equation 2 | Equation 3 |
|---|---|---|
| Slope = $\Delta S_f$ | 16.19 | 19.58 |
| Correlation coefficient | 0.9945 | 0.9903 |
| Coefficient of variation | 13.49 | 17.91 |
| Standard deviation | 0.120 | 0.159 |
| Number of data points | 67 | 67 |

expected value. (If the analysis is restricted to hydrocarbons that melt at or below 150, the observed slopes are 13.96 for Eq. 2 and 15.40 for Eq. 3.)

Thus, it appears that Eq. 2 is more meaningful than Eq. 3 for quantitating the effects of solute crystallinity on solubility. This finding implies that the value of $\Delta C_p$ for the polycyclic aromatic hydrocarbons is closer to zero than it is to $\Delta S_f$. These results are in agreement with the results obtained for the aqueous solubility of a large number of organic nonelectrolytes of widely varying structure (1).

(1) S. H. Yalkowsky and S. C. Valvani, *J. Pharm. Sci.*, **69,** 912 (1980).

(2) S. H. Yalkowsky, G. L. Flynn, and T. G. Slunick, *ibid.*, **61,** 852 (1972).

(3) S. H. Yalkowsky and S. C. Valvani, *J. Chem. Eng. Data*, **24,** 127 (1979).

(4) S. H. Yalkowsky, R. J. Orr, and S. C. Valvani, *IEC Fundam.*, **18,** 351 (1979).

(5) A. Martin, J. Newberger, and A. Adjei, *J. Pharm. Sci.*, **69,** 487 (1980).

(6) J. H. Hildebrand, J. M. Prausnitz, and R. L. Scott, "Regular and Related Solutions," Van Nostrand Reinhold, New York, N.Y., 1970, p. 22.

(7) E. McLaughlin and H. A. Zainal, *J. Chem. Soc.*, **1959,** 863.

(8) F. Casellato, C. Vecchi, A. Grielli, and B. Casu, *Thermochim. Acta*, **6,** 361 (1973).

(9) R. D. Wauchope and F. W. Getzen, *J. Chem. Eng. Data*, **17,** 38 (1972).

(10) A. R. Ubbelohde, "The Molten State of Matter," Wiley, New York, N.Y., 1978, p. 148.

*Samuel H. Yalkowsky*
Pharmacy Research
The Upjohn Company
Kalamazoo, MI 49001

Received May 15, 1981.
Accepted for publication June 15, 1981.

# BOOKS

## REVIEWS

**Analytical Profiles of Drug Substances, Vol. 9.** Edited by KLAUS FLOREY. Academic, 111 Fifth Ave., New York, NY 10003. 1980. 618 pp. 15 × 23 cm.

This book is the ninth in a continuing series that covers the analytical aspects of specific drug entities. It was compiled under the auspices of the Pharmaceutical Analysis and Control Section of the Academy of Pharmaceutical Sciences. The individual profiles or monographs are much more complete than those found in the compendia. The information in the *Analytical Profiles* series not only includes compendial tests but also important supplemental information including synthesis, additional physical properties, data on stability, absorption, metabolism, and excretion, and various analytical methods. In general, each profile is a literature review, but IR, mass spectrometric, UV, and NMR spectra are reproduced along with appropriate crystallographic data. The coverage of the quantitative analytical procedures is usually very complete and includes dosage forms, biological fluids, foodstuffs where appropriate, and related information.

Volume 9 includes 19 new monographs: bacitracin, bretylium tosylate, carbamazepine, cefaclor, cefamandole nafate, cyproheptadine, dibenzepine hydrochloride, digoxin, doxorubicin, fluphenazine decanoate, gentamicin sulfate, haloperidol, khellin, lorazepam, methoxsalen, nadolol, nitrazepam, nitroglycerin, and trifluoperazine hydrochloride. In addition, the *Addendum* contains monographs for griseofulvin and methadone hydrochloride.

While praising *Analytical Profiles* in general, and Volume 9 in particular, this reviewer believes it is time for the editorial board to define more carefully what they want *Analytical Profiles* to become. Some of the drugs covered in Volume 9 are relatively new entities. Others, such as bacitracin, digoxin, haloperidol, khellin, and nitroglycerin, could be called classics. One would have thought that these drugs would have been covered years ago. It is not clear from reading the two monographs on griseofulvin and methadone hydrochloride in the *Addendum* what has been added. Furthermore, a review of the bibliography for griseofulvin shows 18 of 29 references published prior to 1969, six prior to 1974, four prior to 1979, and one unpublished paper authored by the individuals who wrote the monograph. Griseofulvin also appeared in Volume 8 of *Analytical Profiles*. What new information appears that was not published a year ago? This question is not answered. The other drug published in the *Addendum*, methadone hydrochloride, first appeared in Volumes 3 and 4 and probably is in need of updating. But, again, the updated information is not specified. Indeed, this monograph does not even reference the previous material found in Volumes 3 and 4.

The two drugs covered in the *Addendum* brings up another point. There does not seem to be a systematic plan to update the older monographs. With the rapid changes occurring in analytical methodology and instrumentation, such a plan seems to be imperative.

Nevertheless, this series meets a real need by bringing together a concise literature review of the analytical description of important drug entities. Volume 9 is no exception. Its purchase is recommended highly for appropriate libraries, workers in pharmaceutical analysis, and teachers of pharmaceutical chemistry who want to maintain excellent personal libraries.

*Reviewed by* John H. Block
*School of Pharmacy*
*Oregon State University*
*Corvallis, OR 97331*

---

**Clinical Pharmacokinetics: Concepts and Applications.** By MALCOLM ROWLAND and THOMAS N. TOZER. Lea & Febiger, 600 Washington Square, Philadelphia, PA 19106. 1980. 331 pp. 17 × 25 cm. Price U.S. $29.50 (Canada $35.50).

This book is an important contribution that will facilitate teaching a clinically relevant introductory course in pharmacokinetics. The goal of the authors was to fill a void which, in their own words, "has been the lack of a book that teaches the application of pharmacokinetics in drug therapy" to students, practitioners, and researchers. They are to be congratulated for achieving their goal.

The book is divided into four sections: Concepts, Disposition and Absorption Kinetics, Therapeutic Regimens, and Individualization. Each section is well supported with literature data and computer simulations. Chapters 5, 6, and 11 present a detailed, yet readable, description of clearance concepts (*i.e.*, the factors that determine steady-state plasma concentration). In contrast to most books written in the area of pharmacokinetics, college calculus is not needed to appreciate the textual material. Indeed, the authors remove much of the "mathematical fog" that has shrouded pharmacokinetics.

Several minor limitations to the text should be listed. Nonlinear kinetics is discussed quite briefly; *i.e.*, after reading the text, it is likely that

expected value. (If the analysis is restricted to hydrocarbons that melt at or below 150, the observed slopes are 13.96 for Eq. 2 and 15.40 for Eq. 3.)

Thus, it appears that Eq. 2 is more meaningful than Eq. 3 for quantitating the effects of solute crystallinity on solubility. This finding implies that the value of $\Delta C_p$ for the polycyclic aromatic hydrocarbons is closer to zero than it is to $\Delta S_f$. These results are in agreement with the results obtained for the aqueous solubility of a large number of organic nonelectrolytes of widely varying structure (1).

(1) S. H. Yalkowsky and S. C. Valvani, *J. Pharm. Sci.*, **69,** 912 (1980).

(2) S. H. Yalkowsky, G. L. Flynn, and T. G. Slunick, *ibid.*, **61,** 852 (1972).

(3) S. H. Yalkowsky and S. C. Valvani, *J. Chem. Eng. Data*, **24,** 127 (1979).

(4) S. H. Yalkowsky, R. J. Orr, and S. C. Valvani, *IEC Fundam.*, **18,** 351 (1979).

(5) A. Martin, J. Newberger, and A. Adjei, *J. Pharm. Sci.*, **69,** 487 (1980).

(6) J. H. Hildebrand, J. M. Prausnitz, and R. L. Scott, "Regular and Related Solutions," Van Nostrand Reinhold, New York, N.Y., 1970, p. 22.

(7) E. McLaughlin and H. A. Zainal, *J. Chem. Soc.*, **1959,** 863.

(8) F. Casellato, C. Vecchi, A. Grielli, and B. Casu, *Thermochim. Acta*, **6,** 361 (1973).

(9) R. D. Wauchope and F. W. Getzen, *J. Chem. Eng. Data*, **17,** 38 (1972).

(10) A. R. Ubbelohde, "The Molten State of Matter," Wiley, New York, N.Y., 1978, p. 148.

*Samuel H. Yalkowsky*
Pharmacy Research
The Upjohn Company
Kalamazoo, MI 49001

Received May 15, 1981.
Accepted for publication June 15, 1981.

# BOOKS

## REVIEWS

**Analytical Profiles of Drug Substances, Vol. 9.** Edited by KLAUS FLOREY. Academic, 111 Fifth Ave., New York, NY 10003. 1980. 618 pp. 15 × 23 cm.

This book is the ninth in a continuing series that covers the analytical aspects of specific drug entities. It was compiled under the auspices of the Pharmaceutical Analysis and Control Section of the Academy of Pharmaceutical Sciences. The individual profiles or monographs are much more complete than those found in the compendia. The information in the *Analytical Profiles* series not only includes compendial tests but also important supplemental information including synthesis, additional physical properties, data on stability, absorption, metabolism, and excretion, and various analytical methods. In general, each profile is a literature review, but IR, mass spectrometric, UV, and NMR spectra are reproduced along with appropriate crystallographic data. The coverage of the quantitative analytical procedures is usually very complete and includes dosage forms, biological fluids, foodstuffs where appropriate, and related information.

Volume 9 includes 19 new monographs: bacitracin, bretylium tosylate, carbamazepine, cefaclor, cefamandole nafate, cyproheptadine, dibenzepine hydrochloride, digoxin, doxorubicin, fluphenazine decanoate, gentamicin sulfate, haloperidol, khellin, lorazepam, methoxsalen, nadolol, nitrazepam, nitroglycerin, and trifluoperazine hydrochloride. In addition, the *Addendum* contains monographs for griseofulvin and methadone hydrochloride.

While praising *Analytical Profiles* in general, and Volume 9 in particular, this reviewer believes it is time for the editorial board to define more carefully what they want *Analytical Profiles* to become. Some of the drugs covered in Volume 9 are relatively new entities. Others, such as bacitracin, digoxin, haloperidol, khellin, and nitroglycerin, could be called classics. One would have thought that these drugs would have been covered years ago. It is not clear from reading the two monographs on griseofulvin and methadone hydrochloride in the *Addendum* what has been added. Furthermore, a review of the bibliography for griseofulvin shows 18 of 29 references published prior to 1969, six prior to 1974, four prior to 1979, and one unpublished paper authored by the individuals who wrote the monograph. Griseofulvin also appeared in Volume 8 of *Analytical Profiles*. What new information appears that was not published a year ago? This question is not answered. The other drug published in the *Addendum*, methadone hydrochloride, first appeared in Volumes 3 and 4 and probably is in need of updating. But, again, the updated information is not specified. Indeed, this monograph does not even reference the previous material found in Volumes 3 and 4.

The two drugs covered in the *Addendum* brings up another point. There does not seem to be a systematic plan to update the older monographs. With the rapid changes occurring in analytical methodology and instrumentation, such a plan seems to be imperative.

Nevertheless, this series meets a real need by bringing together a concise literature review of the analytical description of important drug entities. Volume 9 is no exception. Its purchase is recommended highly for appropriate libraries, workers in pharmaceutical analysis, and teachers of pharmaceutical chemistry who want to maintain excellent personal libraries.

*Reviewed by* John H. Block
*School of Pharmacy*
*Oregon State University*
*Corvallis, OR 97331*

---

**Clinical Pharmacokinetics: Concepts and Applications.** By MALCOLM ROWLAND and THOMAS N. TOZER. Lea & Febiger, 600 Washington Square, Philadelphia, PA 19106. 1980. 331 pp. 17 × 25 cm. Price U.S. $29.50 (Canada $35.50).

This book is an important contribution that will facilitate teaching a clinically relevant introductory course in pharmacokinetics. The goal of the authors was to fill a void which, in their own words, "has been the lack of a book that teaches the application of pharmacokinetics in drug therapy" to students, practitioners, and researchers. They are to be congratulated for achieving their goal.

The book is divided into four sections: Concepts, Disposition and Absorption Kinetics, Therapeutic Regimens, and Individualization. Each section is well supported with literature data and computer simulations. Chapters 5, 6, and 11 present a detailed, yet readable, description of clearance concepts (*i.e.*, the factors that determine steady-state plasma concentration). In contrast to most books written in the area of pharmacokinetics, college calculus is not needed to appreciate the textual material. Indeed, the authors remove much of the "mathematical fog" that has shrouded pharmacokinetics.

Several minor limitations to the text should be listed. Nonlinear kinetics is discussed quite briefly; *i.e.*, after reading the text, it is likely that

expected value. (If the analysis is restricted to hydrocarbons that melt at or below 150, the observed slopes are 13.96 for Eq. 2 and 15.40 for Eq. 3.)

Thus, it appears that Eq. 2 is more meaningful than Eq. 3 for quantitating the effects of solute crystallinity on solubility. This finding implies that the value of $\Delta C_p$ for the polycyclic aromatic hydrocarbons is closer to zero than it is to $\Delta S_f$. These results are in agreement with the results obtained for the aqueous solubility of a large number of organic nonelectrolytes of widely varying structure (1).

(1) S. H. Yalkowsky and S. C. Valvani, *J. Pharm. Sci.*, **69,** 912 (1980).

(2) S. H. Yalkowsky, G. L. Flynn, and T. G. Slunick, *ibid.*, **61,** 852 (1972).

(3) S. H. Yalkowsky and S. C. Valvani, *J. Chem. Eng. Data*, **24,** 127 (1979).

(4) S. H. Yalkowsky, R. J. Orr, and S. C. Valvani, *IEC Fundam.*, **18,** 351 (1979).

(5) A. Martin, J. Newberger, and A. Adjei, *J. Pharm. Sci.*, **69,** 487 (1980).

(6) J. H. Hildebrand, J. M. Prausnitz, and R. L. Scott, "Regular and Related Solutions," Van Nostrand Reinhold, New York, N.Y., 1970, p. 22.

(7) E. McLaughlin and H. A. Zainal, *J. Chem. Soc.*, **1959,** 863.

(8) F. Casellato, C. Vecchi, A. Grielli, and B. Casu, *Thermochim. Acta*, **6,** 361 (1973).

(9) R. D. Wauchope and F. W. Getzen, *J. Chem. Eng. Data*, **17,** 38 (1972).

(10) A. R. Ubbelohde, "The Molten State of Matter," Wiley, New York, N.Y., 1978, p. 148.

*Samuel H. Yalkowsky*
Pharmacy Research
The Upjohn Company
Kalamazoo, MI 49001

Received May 15, 1981.
Accepted for publication June 15, 1981.

# BOOKS

## REVIEWS

**Analytical Profiles of Drug Substances, Vol. 9.** Edited by KLAUS FLOREY. Academic, 111 Fifth Ave., New York, NY 10003. 1980. 618 pp. 15 × 23 cm.

This book is the ninth in a continuing series that covers the analytical aspects of specific drug entities. It was compiled under the auspices of the Pharmaceutical Analysis and Control Section of the Academy of Pharmaceutical Sciences. The individual profiles or monographs are much more complete than those found in the compendia. The information in the *Analytical Profiles* series not only includes compendial tests but also important supplemental information including synthesis, additional physical properties, data on stability, absorption, metabolism, and excretion, and various analytical methods. In general, each profile is a literature review, but IR, mass spectrometric, UV, and NMR spectra are reproduced along with appropriate crystallographic data. The coverage of the quantitative analytical procedures is usually very complete and includes dosage forms, biological fluids, foodstuffs where appropriate, and related information.

Volume 9 includes 19 new monographs: bacitracin, bretylium tosylate, carbamazepine, cefaclor, cefamandole nafate, cyproheptadine, dibenzepine hydrochloride, digoxin, doxorubicin, fluphenazine decanoate, gentamicin sulfate, haloperidol, khellin, lorazepam, methoxsalen, nadolol, nitrazepam, nitroglycerin, and trifluoperazine hydrochloride. In addition, the *Addendum* contains monographs for griseofulvin and methadone hydrochloride.

While praising *Analytical Profiles* in general, and Volume 9 in particular, this reviewer believes it is time for the editorial board to define more carefully what they want *Analytical Profiles* to become. Some of the drugs covered in Volume 9 are relatively new entities. Others, such as bacitracin, digoxin, haloperidol, khellin, and nitroglycerin, could be called classics. One would have thought that these drugs would have been covered years ago. It is not clear from reading the two monographs on griseofulvin and methadone hydrochloride in the *Addendum* what has been added. Furthermore, a review of the bibliography for griseofulvin shows 18 of 29 references published prior to 1969, six prior to 1974, four prior to 1979, and one unpublished paper authored by the individuals who wrote the monograph. Griseofulvin also appeared in Volume 8 of *Analytical Profiles*. What new information appears that was not published a year ago? This question is not answered. The other drug published in the *Addendum*, methadone hydrochloride, first appeared in Volumes 3 and 4 and probably is in need of updating. But, again, the updated information is not specified. Indeed, this monograph does not even reference the previous material found in Volumes 3 and 4.

The two drugs covered in the *Addendum* brings up another point. There does not seem to be a systematic plan to update the older monographs. With the rapid changes occurring in analytical methodology and instrumentation, such a plan seems to be imperative.

Nevertheless, this series meets a real need by bringing together a concise literature review of the analytical description of important drug entities. Volume 9 is no exception. Its purchase is recommended highly for appropriate libraries, workers in pharmaceutical analysis, and teachers of pharmaceutical chemistry who want to maintain excellent personal libraries.

*Reviewed by* John H. Block
*School of Pharmacy*
*Oregon State University*
*Corvallis, OR 97331*

---

**Clinical Pharmacokinetics: Concepts and Applications.** By MALCOLM ROWLAND and THOMAS N. TOZER. Lea & Febiger, 600 Washington Square, Philadelphia, PA 19106. 1980. 331 pp. 17 × 25 cm. Price U.S. $29.50 (Canada $35.50).

This book is an important contribution that will facilitate teaching a clinically relevant introductory course in pharmacokinetics. The goal of the authors was to fill a void which, in their own words, "has been the lack of a book that teaches the application of pharmacokinetics in drug therapy" to students, practitioners, and researchers. They are to be congratulated for achieving their goal.

The book is divided into four sections: Concepts, Disposition and Absorption Kinetics, Therapeutic Regimens, and Individualization. Each section is well supported with literature data and computer simulations. Chapters 5, 6, and 11 present a detailed, yet readable, description of clearance concepts (*i.e.*, the factors that determine steady-state plasma concentration). In contrast to most books written in the area of pharmacokinetics, college calculus is not needed to appreciate the textual material. Indeed, the authors remove much of the "mathematical fog" that has shrouded pharmacokinetics.

Several minor limitations to the text should be listed. Nonlinear kinetics is discussed quite briefly; *i.e.*, after reading the text, it is likely that

a student could not adequately adjust a patient's phenytoin dose. Since the authors have been involved in pioneering work in this field, it may be that such material will be included in an upcoming text to which they allude. However, in this reviewer's opinion, a more detailed treatment of nonlinear kinetics would have been useful.

Another significant defect of this text is that it is difficult to identify the primary source for some textual material. The source of the data contained in the tables and figures is identified. However, it is generally not possible to identify the source of information within the body of the text.

This book is well written and should be considered as a standard text for introductory courses in Pharmacy Baccalaureate and Doctor of Pharmacy programs and for freshman graduate courses in pharmaceutics and pharmacology.

*Reviewed by* David Lalka
*Department of Pharmaceutics*
*School of Pharmacy*
*State University of New York at Buffalo Amherst, NY 14260*

---

**Second Supplement to USP XX and NF XV.** Drug Standards Division, United States Pharmacopeial Convention, 12601 Twinbrook Parkway, Rockville, MD 20852. 245 pp. 20 × 29 cm. Price $8.00.

The *Second Supplement* is cumulative with the first one and contains changes that constitute revisions in the USP XX and NF XV effective May 1, 1981. Additions and deletions in the USP XX official monographs comprise the largest section, totaling 133 pages, whereas those in the General Requirements for Tests and Assays section are contained in 12 pages. Under General Information are selected portions of the regulations promulgated under the Controlled Substances Act and portions of the Poison Packaging Act and Regulations, of interest to students and practitioners in pharmacy and medicine. Changes in the official NF XV monographs comprise almost 20 pages and are followed by an appendix containing excerpts from federal regulations on antibiotics and an index to this supplement.

*Staff Review*

---

**Solid Pharmaceutics: Mechanical Properties and Rate Phenomena.** By JENS THURØ CARSTENSEN. Academic, 111 Fifth Ave., New York, NY 10003. 1980. 259 pp. 15 × 23 cm. Price $35.00.

This brief book, written in terse mathematical style, is an ambitious attempt to consolidate the more important research in the field of solid pharmaceutics. The first chapter contains an introduction to the characteristics of single-component systems, with emphasis on the properties of crystals. Chapter 2 deals with particulate solids and their dimensions and properties. Chapter 3 extends this treatment to two-component systems and includes such topics as blending and the effect of moisture on solids. The next two chapters are devoted to successive stages in the manufacture of tablets: precompression operations, including wet granulation, dry milling, tablet formulation, and lubrication, followed by compression and hardness testing. The book concludes with a section on the physical properties of solid dosage forms, particularly the dissolution of tablets and capsules and their chemical stability.

Solid pharmaceutics is perhaps the area in which the catholicity of the pharmaceutical sciences is most in evidence. In his scholarly treatment of the subject, Carstensen draws heavily on the literature of powder technology, crystallography, chemical engineering, polymer science, and metallurgy. Yet he does not hesitate to offer his own views on controversial subjects. In discussing the upward curvature observed in Hixson–Crowell plots of the cube root of mass *versus* time, he suggests that deviations from straight-line behavior can be attributed to the lack of isometry of most real particles. He then proceeds to show how one can introduce a shape factor to correct for this deviation. In discussing angle of repose, he points out that the equations usually employed predict that as the particle diameter becomes smaller, the angle of repose approaches an infinite value rather than the value most consistent with the physical model, 90°. To remedy this, the cohesional and frictional coefficients are expressed in terms of trial functions with proper boundary conditions and an equation is obtained based on the force diagram for a powder heap.

Particularly lucid is his treatment of Prout–Tompkins kinetics of solid-state decomposition. Carstensen also shows how the boundary conditions of the Prout–Tompkins model can be modified to treat data that follow first-order kinetics.

Where appropriate, the text is augmented with solved quantitative examples, copious tables of empirical data, and more than 100 beautifully drawn, uncluttered, line figures. Those familiar with Carstensen's earlier treatments of this subject, "Pharmaceutics of Solids and Solid Dosage Forms" and "Theory of Pharmaceutical Systems," will see some of the same figures and numerical examples in the present volume, but repetition has been kept to a minimum. The problems are relatively easy and are mainly computational exercises.

One may make some minor criticisms of the book, especially with regard to topics such as lyophilization and spray drying, which are given short shrift. Symbols often are introduced without definition, and unconventional symbols are substituted unnecessarily for more familiar ones. For example, in the Bragg equation, $R_0$ rather than $d$ is used for interplanar spacing. The Greek letter $\theta$ is used for time. More confusing, $F$ is used for the Helmholtz energy rather than $A$. Formerly, of course, $F$ was used in textbooks for the Gibbs free energy. There are a few errors. An exponent has been omitted in the Shotten–Hersey equation (V-3-24a). In the plot of water vapor pressure *versus* moles of water, one plateau for sodium phosphate is mislabeled (Fig. III-15). But these are minor points and in no way detract from my opinion that the author has treated a comprehensive set of difficult problems with excellent conceptual organization and clarity.

Pharmaceutical development scientists and graduate students who require a quantitative understanding of the operations related to the manufacture of solid dosage forms will find this slender volume very useful. It is not for casual reading, and the nonspecialist who wants a broad overview of the field will have to find it elsewhere.

*Reviewed by* J. Keith Guillory
*College of Pharmacy*
*University of Iowa*
*Iowa City, IA 52242*

a student could not adequately adjust a patient's phenytoin dose. Since the authors have been involved in pioneering work in this field, it may be that such material will be included in an upcoming text to which they allude. However, in this reviewer's opinion, a more detailed treatment of nonlinear kinetics would have been useful.

Another significant defect of this text is that it is difficult to identify the primary source for some textual material. The source of the data contained in the tables and figures is identified. However, it is generally not possible to identify the source of information within the body of the text.

This book is well written and should be considered as a standard text for introductory courses in Pharmacy Baccalaureate and Doctor of Pharmacy programs and for freshman graduate courses in pharmaceutics and pharmacology.

*Reviewed by* David Lalka
*Department of Pharmaceutics*
*School of Pharmacy*
*State University of New York at Buffalo Amherst, NY 14260*

---

**Second Supplement to USP XX and NF XV.** Drug Standards Division, United States Pharmacopeial Convention, 12601 Twinbrook Parkway, Rockville, MD 20852. 245 pp. 20 × 29 cm. Price $8.00.

The *Second Supplement* is cumulative with the first one and contains changes that constitute revisions in the USP XX and NF XV effective May 1, 1981. Additions and deletions in the USP XX official monographs comprise the largest section, totaling 133 pages, whereas those in the General Requirements for Tests and Assays section are contained in 12 pages. Under General Information are selected portions of the regulations promulgated under the Controlled Substances Act and portions of the Poison Packaging Act and Regulations, of interest to students and practitioners in pharmacy and medicine. Changes in the official NF XV monographs comprise almost 20 pages and are followed by an appendix containing excerpts from federal regulations on antibiotics and an index to this supplement.

*Staff Review*

---

**Solid Pharmaceutics: Mechanical Properties and Rate Phenomena.** By JENS THURØ CARSTENSEN. Academic, 111 Fifth Ave., New York, NY 10003. 1980. 259 pp. 15 × 23 cm. Price $35.00.

This brief book, written in terse mathematical style, is an ambitious attempt to consolidate the more important research in the field of solid pharmaceutics. The first chapter contains an introduction to the characteristics of single-component systems, with emphasis on the properties of crystals. Chapter 2 deals with particulate solids and their dimensions and properties. Chapter 3 extends this treatment to two-component systems and includes such topics as blending and the effect of moisture on solids. The next two chapters are devoted to successive stages in the manufacture of tablets: precompression operations, including wet granulation, dry milling, tablet formulation, and lubrication, followed by compression and hardness testing. The book concludes with a section on the physical properties of solid dosage forms, particularly the dissolution of tablets and capsules and their chemical stability.

Solid pharmaceutics is perhaps the area in which the catholicity of the pharmaceutical sciences is most in evidence. In his scholarly treatment of the subject, Carstensen draws heavily on the literature of powder technology, crystallography, chemical engineering, polymer science, and metallurgy. Yet he does not hesitate to offer his own views on controversial subjects. In discussing the upward curvature observed in Hixson–Crowell plots of the cube root of mass *versus* time, he suggests that deviations from straight-line behavior can be attributed to the lack of isometry of most real particles. He then proceeds to show how one can introduce a shape factor to correct for this deviation. In discussing angle of repose, he points out that the equations usually employed predict that as the particle diameter becomes smaller, the angle of repose approaches an infinite value rather than the value most consistent with the physical model, 90°. To remedy this, the cohesional and frictional coefficients are expressed in terms of trial functions with proper boundary conditions and an equation is obtained based on the force diagram for a powder heap.

Particularly lucid is his treatment of Prout–Tompkins kinetics of solid-state decomposition. Carstensen also shows how the boundary conditions of the Prout–Tompkins model can be modified to treat data that follow first-order kinetics.

Where appropriate, the text is augmented with solved quantitative examples, copious tables of empirical data, and more than 100 beautifully drawn, uncluttered, line figures. Those familiar with Carstensen's earlier treatments of this subject, "Pharmaceutics of Solids and Solid Dosage Forms" and "Theory of Pharmaceutical Systems," will see some of the same figures and numerical examples in the present volume, but repetition has been kept to a minimum. The problems are relatively easy and are mainly computational exercises.

One may make some minor criticisms of the book, especially with regard to topics such as lyophilization and spray drying, which are given short shrift. Symbols often are introduced without definition, and unconventional symbols are substituted unnecessarily for more familiar ones. For example, in the Bragg equation, $R_0$ rather than $d$ is used for interplanar spacing. The Greek letter $\theta$ is used for time. More confusing, $F$ is used for the Helmholtz energy rather than $A$. Formerly, of course, $F$ was used in textbooks for the Gibbs free energy. There are a few errors. An exponent has been omitted in the Shotten–Hersey equation (V-3-24a). In the plot of water vapor pressure *versus* moles of water, one plateau for sodium phosphate is mislabeled (Fig. III-15). But these are minor points and in no way detract from my opinion that the author has treated a comprehensive set of difficult problems with excellent conceptual organization and clarity.

Pharmaceutical development scientists and graduate students who require a quantitative understanding of the operations related to the manufacture of solid dosage forms will find this slender volume very useful. It is not for casual reading, and the nonspecialist who wants a broad overview of the field will have to find it elsewhere.

*Reviewed by* J. Keith Guillory
*College of Pharmacy*
*University of Iowa*
*Iowa City, IA 52242*

a student could not adequately adjust a patient's phenytoin dose. Since the authors have been involved in pioneering work in this field, it may be that such material will be included in an upcoming text to which they allude. However, in this reviewer's opinion, a more detailed treatment of nonlinear kinetics would have been useful.

Another significant defect of this text is that it is difficult to identify the primary source for some textual material. The source of the data contained in the tables and figures is identified. However, it is generally not possible to identify the source of information within the body of the text.

This book is well written and should be considered as a standard text for introductory courses in Pharmacy Baccalaureate and Doctor of Pharmacy programs and for freshman graduate courses in pharmaceutics and pharmacology.

*Reviewed by* David Lalka
*Department of Pharmaceutics*
*School of Pharmacy*
*State University of New York at Buffalo Amherst, NY 14260*

---

**Second Supplement to USP XX and NF XV.** Drug Standards Division, United States Pharmacopeial Convention, 12601 Twinbrook Parkway, Rockville, MD 20852. 245 pp. 20 × 29 cm. Price $8.00.

The *Second Supplement* is cumulative with the first one and contains changes that constitute revisions in the USP XX and NF XV effective May 1, 1981. Additions and deletions in the USP XX official monographs comprise the largest section, totaling 133 pages, whereas those in the General Requirements for Tests and Assays section are contained in 12 pages. Under General Information are selected portions of the regulations promulgated under the Controlled Substances Act and portions of the Poison Packaging Act and Regulations, of interest to students and practitioners in pharmacy and medicine. Changes in the official NF XV monographs comprise almost 20 pages and are followed by an appendix containing excerpts from federal regulations on antibiotics and an index to this supplement.

*Staff Review*

---

**Solid Pharmaceutics: Mechanical Properties and Rate Phenomena.** By JENS THURØ CARSTENSEN. Academic, 111 Fifth Ave., New York, NY 10003. 1980. 259 pp. 15 × 23 cm. Price $35.00.

This brief book, written in terse mathematical style, is an ambitious attempt to consolidate the more important research in the field of solid pharmaceutics. The first chapter contains an introduction to the characteristics of single-component systems, with emphasis on the properties of crystals. Chapter 2 deals with particulate solids and their dimensions and properties. Chapter 3 extends this treatment to two-component systems and includes such topics as blending and the effect of moisture on solids. The next two chapters are devoted to successive stages in the manufacture of tablets: precompression operations, including wet granulation, dry milling, tablet formulation, and lubrication, followed by compression and hardness testing. The book concludes with a section on the physical properties of solid dosage forms, particularly the dissolution of tablets and capsules and their chemical stability.

Solid pharmaceutics is perhaps the area in which the catholicity of the pharmaceutical sciences is most in evidence. In his scholarly treatment of the subject, Carstensen draws heavily on the literature of powder technology, crystallography, chemical engineering, polymer science, and metallurgy. Yet he does not hesitate to offer his own views on controversial subjects. In discussing the upward curvature observed in Hixson–Crowell plots of the cube root of mass *versus* time, he suggests that deviations from straight-line behavior can be attributed to the lack of isometry of most real particles. He then proceeds to show how one can introduce a shape factor to correct for this deviation. In discussing angle of repose, he points out that the equations usually employed predict that as the particle diameter becomes smaller, the angle of repose approaches an infinite value rather than the value most consistent with the physical model, 90°. To remedy this, the cohesional and frictional coefficients are expressed in terms of trial functions with proper boundary conditions and an equation is obtained based on the force diagram for a powder heap.

Particularly lucid is his treatment of Prout–Tompkins kinetics of solid-state decomposition. Carstensen also shows how the boundary conditions of the Prout–Tompkins model can be modified to treat data that follow first-order kinetics.

Where appropriate, the text is augmented with solved quantitative examples, copious tables of empirical data, and more than 100 beautifully drawn, uncluttered, line figures. Those familiar with Carstensen's earlier treatments of this subject, "Pharmaceutics of Solids and Solid Dosage Forms" and "Theory of Pharmaceutical Systems," will see some of the same figures and numerical examples in the present volume, but repetition has been kept to a minimum. The problems are relatively easy and are mainly computational exercises.

One may make some minor criticisms of the book, especially with regard to topics such as lyophilization and spray drying, which are given short shrift. Symbols often are introduced without definition, and unconventional symbols are substituted unnecessarily for more familiar ones. For example, in the Bragg equation, $R_0$ rather than $d$ is used for interplanar spacing. The Greek letter $\theta$ is used for time. More confusing, $F$ is used for the Helmholtz energy rather than $A$. Formerly, of course, $F$ was used in textbooks for the Gibbs free energy. There are a few errors. An exponent has been omitted in the Shotten–Hersey equation (V-3-24a). In the plot of water vapor pressure *versus* moles of water, one plateau for sodium phosphate is mislabeled (Fig. III-15). But these are minor points and in no way detract from my opinion that the author has treated a comprehensive set of difficult problems with excellent conceptual organization and clarity.

Pharmaceutical development scientists and graduate students who require a quantitative understanding of the operations related to the manufacture of solid dosage forms will find this slender volume very useful. It is not for casual reading, and the nonspecialist who wants a broad overview of the field will have to find it elsewhere.

*Reviewed by* J. Keith Guillory
*College of Pharmacy*
*University of Iowa*
*Iowa City, IA 52242*

A publication of the
American Pharmaceutical Association—
the National Professional Society
of Pharmacists

# JOURNAL OF PHARMACEUTICAL SCIENCES

## INDEX TO AUTHORS
## INDEX TO SUBJECTS

VOLUME 70
JANUARY TO DECEMBER, 1981

*Published monthly under the supervision of the Board of Trustees*

MARY H. FERGUSON
*Editor*

NANCY E. BROWN
*Production Editor*

JOHN PATRICK EVANS
*Copy Editor*

MICHAEL K. HAYES
*Copy Editor*

EDWARD G. FELDMANN
*Contributing Editor*

SAMUEL W. GOLDSTEIN
*Contributing Editor*

BELLE R. BECK
*Editorial Secretary*

EDWARD G. FELDMANN
*Acting Director of Publications*

EDITORIAL ADVISORY BOARD

John Autian
Norman R. Farnsworth
William J. Jusko
Herbert A. Lieberman
David E. Mann, Jr.
Ian W. Mathison
Gerald J. Papariello
Edward G. Rippie

JOURNAL OF PHARMACEUTICAL SCIENCES

SEPTEMBER 1981
VOLUME 70 NUMBER 9

RESEARCH ARTICLES

# Free Fatty Acid-Induced Platelet Aggregation: Studies with Solubilized and Nonsolubilized Fatty Acids

G. M. ZENTNER *, J. R. CARDINAL ‡, and S. W. KIM ‡x

Received September 15, 1980, from the *School of Pharmacy, University of Connecticut, Storrs, CT 06268, and the ‡College of Pharmacy, Department of Pharmaceutics, University of Utah, Salt Lake City, UT 84112. Accepted for publication February 13, 1981.

**Abstract** □ The aggregation response of washed porcine platelets to the sodium salts of stearic, oleic, palmitic, and myristic acids was analyzed turbidometrically. The fatty acids were prepared as aqueous suspensions and as taurocholate- or albumin-solubilized systems. The final concentration of fatty acid in the platelet preparation varied between 70 and 600 $\mu M$. This range was within or below the normal physiological limits of 300–1200 $\mu M$. Platelet aggregation was observed with both the suspended and taurocholate-solubilized fatty acids. The extent of platelet aggregate formation increased with the fatty acid concentration and chain length. With the exception of stearate, the taurocholate-solubilized fatty acids were more active than the suspensions. Albumin-solubilized fatty acids were devoid of platelet aggregating activity. Particle-size analysis of the solubilized fatty acids indicated that fatty acid precipitation had occurred subsequent to the addition of taurocholate-solubilized fatty acids to the platelets. This precipitation did not occur with the albumin-solubilized systems, suggesting that the fatty acids must assume a particulate physical state to induce aggregation. Platelet aggregation induced by fatty acids was not inhibited by 80 n$M$ epoprostenol, 75 $\mu M$ alprostadil, or 150 $\mu M$ indomethacin. This finding indicated that the fatty acid-induced platelet aggregation was independent of cyclic AMP-related calcium shift, cyclooxygenase–arachidonate, or granular nucleotide release mechanisms.

**Keyphrases** □ Fatty acids—induced platelet aggregation, solubilized and nonsolubilized fatty acids □ Platelets—free fatty acid-induced aggregation, solubilized and nonsolubilized fatty acids □ Coagulation—free fatty acid-induced platelet aggregation, solubilized and nonsolubilized fatty acids

Platelets are capable of several reactions necessary for participation in the hemostatic response. They "stick" to exposed subendothelial components and artificial surfaces (adhesion), as well as to one another (aggregation), in response to seemingly diverse stimuli. In addition, platelets release endogenous, pharmacologically active substances that accentuate adhesion, aggregation, and coagulation reactions. This reaction is referred to as platelet release. Thus, platelets can initiate and stimulate several phases of the overall coagulation process, although the aggregation reaction alone results in effective hemostatic blockage in small blood vessels and capillaries (1).

## BACKGROUND

Thrombin, collagen, adenosine diphosphate (ADP), epinephrine, and long chain ($>C_{14}$) unesterified fatty acids are compounds encountered *in vivo* that have been shown to initiate platelet aggregation (1–10). Platelets normally remain unaggregated in most disease-free individuals. That they aggregate in response to various threats to hemostasis suggests a delicate balance between circulating platelets and the aggregation-initiating substance(s). Disruption of this balance may result in either control or exacerbation of disease. For example, the normal response to vascular injury involves the production of thrombin and subsequent formation of a fibrin network (11). In this case, platelet aggregation induced by thrombin would be a disease controlling reaction through augmentation of thrombus formation to control bleeding. In contrast, disease states that result in elevated blood fatty acid levels are accompanied by an increased incidence of thromboembolism and platelet hyperaggregability in the absence of vascular injury (12–17). Here the platelet aggregation response exacerbates the disease condition.

The delicate balance between platelet aggregation or nonaggregation in response to a stimulus is exemplified by the platelet–fatty acid interaction. Numerous studies (6–10) have demonstrated hypercoagulability and platelet aggregation both *in vivo* and *in vitro* in response to administered fatty acid concentrations within the normal physiological range of 300–1200 $\mu M$. The fact that most individuals are free from platelet aggregation abnormalities when *in situ* fatty acid levels range from 300 to 1200 $\mu M$ suggests that the physical state of the administered free fatty acids is a critical determinant of aggregating activity.

It has been argued that the platelet aggregating activity of free fatty acids is related to micellar aggregates formed in aqueous solution (8–10, 18). Since the critical micellar temperature is >37° for most poorly soluble long chain fatty acids (19), a suspension state, rather than a micellar state, is anticipated. Inspection of data (7, 8, 10, 18) correlating platelet aggregating activity with free fatty acid chain length leads to the generalization that aggregating activity is negligible below $C_{14}$, with activity increasing markedly with chain lengths up to $C_{20}$; *i.e.*, the fatty acids least likely to form micelles exhibit the greatest platelet aggregating activity. This trend holds for both saturated and unsaturated fatty acids when the aggregation of washed platelet preparations *in vitro* is examined (9, 10, 20).

In the present study, the aggregation of washed porcine platelets was investigated as a function of the physical state of various fatty acid preparations. Final washed platelet fatty acid concentrations (70–600 $\mu M$) within normal physiological limits were examined (21, 22). The sodium salts of stearic, palmitic, myristic, and oleic acids were prepared

0022-3549/81/0900-0975$01.00/0
© 1981, American Pharmaceutical Association

as suspensions in buffered isotonic saline or as solubilized aqueous systems with either sodium taurocholate or albumin as the solubilizing agent. The effects of the nonspecific platelet aggregation inhibitors alprostadil, epoprostenol, and indomethacin (23) serve as a basis for mechanistic interpretations of the fatty acid-induced platelet aggregation reaction.

## EXPERIMENTAL

Slaughterhouse porcine blood was collected into polyethylene vessels containing 7.5 ml of 0.077 *M* edetate disodium[1] and 0.71 *M* anhydrous α-D-glucose[1]/92.5 ml of whole blood as an anticoagulant. The pH of the anticoagulant solution was adjusted to 7.4 with sodium hydroxide. Collected blood was placed into an ice bath until processed further.

Aqueous suspensions of oleic[1], palmitic[1], or myristic[1] acid were gently heated with a slight molar excess of aqueous sodium hydroxide to form the respective sodium salts. The pH values of these solutions were >10.0 after complete dissolution of the fatty acid. The solutions were cooled to room temperature; the insoluble fatty acid salt was collected and washed repeatedly with deionized water to remove excess sodium hydroxide. This product was vacuum dried at 30° for 24 hr. Sodium stearate[1] was used as received. All fatty acids were >99% pure as listed by the supplier.

Cholic acid[1] was recrystallized repeatedly from 95% ethanol. Purity was checked with UV spectroscopy and TLC, using isoamyl acetate[2]–propionic acid[2]–*n*-propanol[2]–water (40:30:20:10) as the developer. Taurine[1] was used as received. Sodium taurocholate was synthesized according to Lack *et al.* (24). The synthesized sodium taurocholate was found to be pure by TLC.

Epoprostenol[3] ($PGI_2$), alprostadil[3] ($PGE_1$), indomethacin[1], disodium adenosine diphosphate[1], fibrinogen[4] (porcine, fraction I), and albumin[1] (porcine, fraction V) were used as received. Reagents[1,2] in the phosphate, tromethamine, Tyrodes, and imidazole buffers were reagent grade and used as received.

Washed porcine platelets were prepared by Haslam's method (25) at 5°. Polycarbonate centrifuge tubes were used for all separations. Final suspension of platelets was in a 9:1 solution of 0.15 *M* NaCl and 0.15 *M* tromethamine buffer, pH 7.4. Platelets that did not resuspend immediately with gentle agitation were discarded. Platelets were counted and examined under phase contrast light microscopy[5] at 600× in a hemocytometer. The platelets were seen as individual entities without pseudopod formation, an observation that was confirmed by scanning electron microscopy[6] at 2K magnification. On this basis, the platelets were judged to be of normal morphology and in the unaggregated state. Platelet counts were adjusted to ~700,000/mm$^3$ for all aggregation experiments. Platelets prepared in this manner, and subsequently stored in an ice bath, remained viable for >6 hr without spontaneous aggregation.

The platelet aggregation reaction was followed turbidimetrically (26) with a commercially available aggregometer[7]. Aggregation was recorded as an increase in the monochromatic (600 nm) light transmittance of a washed platelet suspension with time. Results were relative to blanks containing all reagents except platelets. The 100% transmittance baseline was set with the blanks. Thus, the magnitude of the light transmittance was directly proportional to the extent of platelet aggregation.

For the aggregation experiments, 500 μl of washed porcine platelet suspension was added to a siliconized aggregation cell. Then 20 μl of 0.34 m*M* $CaCl_2$ and 40 μl of 0.11 mg of fibrinogen/ml were added. The system was equilibrated to 37° (~3 min) before proceeding. Under these conditions, the platelets did not aggregate spontaneously during 15 min of observation.

Aggregation was induced with either disodium adenosine diphosphate or fatty acid. Disodium adenosine diphosphate was prepared at a concentration of 2.4 m*M* in an isotonic imidazole–hydrochloric acid buffer, pH 6.8. The fatty acids were prepared at a concentration of 4 m*M* in isotonic phosphate buffer, pH 7.4, with and without 47 m*M* sodium taurocholate or 26 g % albumin as a solubilizing agent. Addition of 80 μl of the disodium adenosine diphosphate solution or 10–100 μl of the various fatty acid preparations to the calcium and fibrinogen equilibrated platelets marked the starting point of the aggregation reaction. Final reagent concentrations were 1.03 m*M* $Ca^{2+}$, 16 μg of fibrinogen/ml, 0.29 m*M* disodium adenosine diphosphate, 70–600 μ*M* fatty acid, 0.83–7.12 m*M* sodium taurocholate, and 4.0 g % albumin.

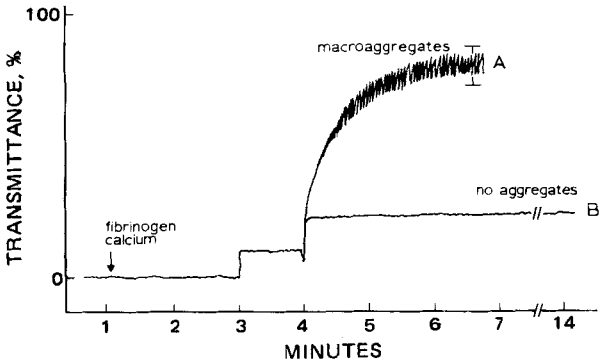


**Figure 1**—*ADP-induced platelet aggregation. Reagent concentrations were: A, 0.29 m*M *ADP; and B, 0.29 m*M *ADP with 75 μ*M *alprostadil or 80 n*M *epoprostenol. Each reagent was administered at 3 min.*

The effects of epoprostenol, alprostadil, and indomethacin on fatty acid-induced platelet aggregation were investigated. The prostaglandins were prepared in buffered solution at the respective pH values of maximum stability[3] immediately prior to addition to the platelets to minimize aqueous degradative effects. Indomethacin was freshly prepared each day. Epoprostenol was prepared at a concentration of 57.0 μ*M* in isotonic tromethamine buffer, pH 8.7. Alprostadil was prepared at a concentration of 0.5 m*M* in isotonic phosphate buffer, pH 7.4. Indomethacin was prepared at a concentration of 1.0 m*M* in Tyrodes' buffer, pH 7.4. The final concentrations in the platelet media were 80 n*M* epoprostenol, 75 μ*M* alprostadil, and 150 μ*M* indomethacin. Additions of these inhibitors to the platelets were made ~1 min prior to the fatty acid or disodium adenosine diphosphate additions.

Behavior of the solubilized fatty acid preparations in the aggregation cell was investigated under simulated conditions. The sodium taurocholate or albumin-solubilized fatty acid preparations were diluted to the same extent as in the aggregation cell. Isotonic phosphate buffer, pH 7.4, filtered three times through 0.22-μm microporous filters[8] was used as the diluent for all procedures. These samples were analyzed as a function of time and particle size with an electronic particle analysis instrument[9] equipped with a 30-μm aperture tube and a 100-μl manometer. The instrument was calibrated with 2.2-μm latex beads. The minimum detection limit was ~0.45 μm (diameter) under these conditions. Analysis of particle size with suspended fatty acid (nonsolubilized) preparation could not be completed due to the blockage of both the 30- and 100-μm aperture tubes. This finding indicated the presence of at least a small percentage of very large particles in these suspensions.

## RESULTS

The aggregation response to 0.29 m*M* ADP was followed turbidimetrically as shown in curve A of Fig. 1. This tracing was the average platelet aggregation response of five animals. The aggregation was immediate and monophasic, leading to macroscopic aggregates (macroaggregates) visible to the unaided eye. Higher concentrations of ADP did not result in further increases in light transmittance. Curve B shows that the addition of either 75 μ*M* alprostadil or 80 n*M* epoprostenol completely inhibited ADP-induced platelet aggregation. The stepwise increases in light transmittance at 3 and 4 min reflected the dilution of the washed platelet preparations by the reagent additions and did not represent aggregation. The imidazole–hydrochloric acid buffer system showed no intrinsic platelet aggregating activity.

The relative platelet aggregating activities of various fatty acid suspensions are compared in Fig. 2. There were no distinguishable differences in the average aggregation patterns elicited by the saturated (stearate) or monounsaturated (oleate) $C_{18}$ fatty acids at a final concentration of 600 μ*M*. Aggregation proceeded rapidly with production of large macroaggregates in a clear medium. The response to 600 μ*M* palmitate ($C_{16}$) differed from the $C_{18}$ fatty acids in the time course to macroaggregate formation. Though immediate in onset, the palmitate-induced aggregation proceeded somewhat slower than the stearate or

[1] Sigma Chemical Co., St. Louis, MO 63178.
[2] J. T. Baker Chemical Co., Phillipsburg, NJ 08865.
[3] Courtesy of The Upjohn Co., Kalamazoo, MI 49001.
[4] Nutritional Biochemicals Corp., Cleveland, OH 44128.
[5] Nikon Biophot, Nippon Kogaku Inc., Garden City, NY 11530.
[6] Cambridge Mark II A SEM, Cambridge, England.
[7] Model 335, Chronolog Corp., Havertown, PA 19083.
[8] Millipore Corp., Bedford, MA 01730.
[9] Coulter Counter model ZBI, Coulter Electronics, Hialeah, Fla.

**Table I—Final Sodium Taurocholate Concentrations in Relation to Solubilized Fatty Acid Concentrations**

| Final Solubilized Fatty Acid Concentrations, $\mu M$ | Final Sodium Taurocholate Concentrations, m$M$ |
|---|---|
| 600 | 7.12 |
| 320 | 3.85 |
| 170 | 2.01 |
| 70 | 0.83 |

oleate reactions. Myristate ($C_{14}$) was significantly less active than either the $C_{16}$ or $C_{18}$ fatty acid suspension. The aggregation response to myristate was minimal and did not result in visible aggregate formation. Thus, a general trend of aggregating activity increasing with chain length was observed when fatty acid suspensions were added to washed porcine platelets.

The data presented in Fig. 3 show the general relationship between fatty acid concentration and platelet aggregation. The speed and extent of palmitate-induced aggregation increased with fatty acid concentration. The 320 and 600 $\mu M$ additions resulted in macroaggregate formation. Generally, this trend was also followed by oleate and stearate. However, as anticipated from Fig. 2, the $C_{18}$ fatty acids were more active than equivalent amounts of palmitate, with macroaggregates formed at all concentrations examined (70–600 $\mu M$).

The platelet aggregating activities of equal concentrations of fatty acids in suspended and solubilized physical states were compared (Fig. 4). Sodium taurocholate was the solubilizing agent. The final taurocholate concentrations were related to the final fatty acid concentrations (Table I). Figure 4*a* shows that platelet macroaggregates formed more rapidly with taurocholate-solubilized 70 $\mu M$ oleate than with suspended 70 $\mu M$ oleate. Taurocholate-solubilized palmitate and myristate systems also were more active than the suspended counterparts at equivalent fatty acid concentrations (Figs. 4*b* and 4*c*). The 170 $\mu M$ palmitate and 600 $\mu M$ myristate suspensions elicited a weak platelet aggregation reaction. However, taurocholate-solubilized 170 $\mu M$ palmitate and 600 $\mu M$ myristate elicited platelet aggregation responses that led to macroaggregate formation. Comparisons between solubilized and suspended oleate, palmitate, and myristate at concentrations not shown in Fig. 4 followed this same trend; taurocholate-solubilized fatty acids were more active inducers of aggregation than the respective suspension counterparts. Sodium taurocholate alone was devoid of activity at all concentrations examined (Table I).

The suspended 70 $\mu M$ stearate system was more active than the taurocholate-solubilized 70 $\mu M$ stearate (Fig. 4*d*). At higher stearate concentrations, this same pattern was noted; however, macroaggregates were produced with both the taurocholate-solubilized and suspended forms. Thus, a reversal in the trend observed with the other fatty acids was noted with stearate.

The aggregating activities of taurocholate-solubilized oleate, stearate, palmitate, and myristate are compared in Fig. 5. Oleate (70 $\mu M$) elicited a rapid platelet aggregation response with macroaggregate production. Stearate, palmitate, and myristate were completely devoid of aggregating activity at this concentration.

The aggregation response to albumin-solubilized fatty acids is shown in Fig. 6. Turbidimetric tracings and light microscopy both indicated that platelet aggregation had not occurred in response to either albumin-solubilized 600 $\mu M$ oleate or palmitate. In the suspended state, these

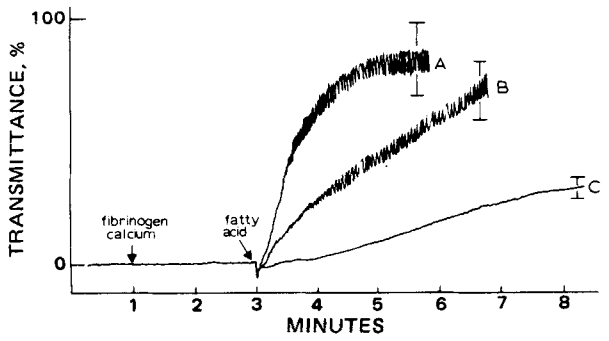


**Figure 2**—*Platelet aggregation response to 600 $\mu$M fatty acid suspensions as a function of chain length. Key: curve A, oleate or stearate ($C_{18}$); curve B, palmitate ($C_{16}$); and curve C, myristate ($C_{14}$).*

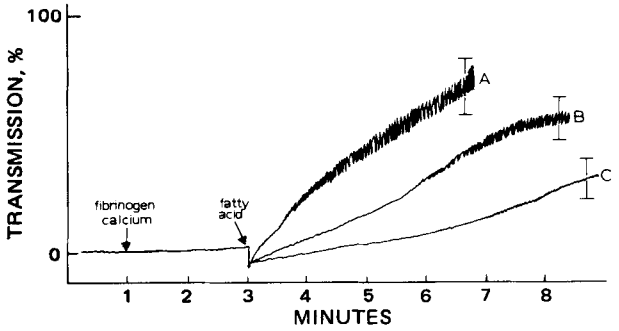


**Figure 3**—*Platelet aggregation as a function of the final suspended fatty acid concentration. Key: curve A, 600 $\mu$M palmitate; curve B, 320 $\mu$M palmitate; and curve C, 170 $\mu$M palmitate.*

concentrations of oleate and palmitate both elicited an immediate platelet aggregation response leading to macroaggregate formation (Fig. 2).

With macroaggregate production, the formation of a fibrous mucoid network subsequent to aggregate appearance was noted and was postulated to be fibrin. In platelet-free blanks, this network did not form. To

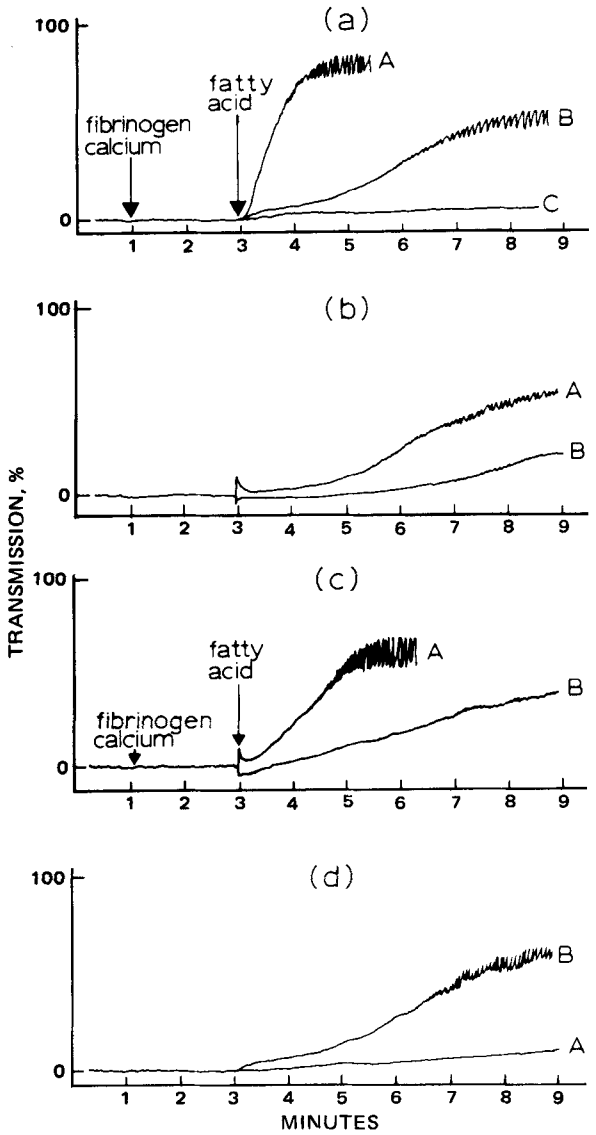


**Figure 4**—*Platelet aggregation as a function of the physical state of 70 $\mu$M oleate (a), 170 $\mu$M palmitate (b), 600 $\mu$M myristate (c), and 70 $\mu$M stearate (d). Key: curves A, sodium taurocholate-solubilized fatty acids; curves B, suspended fatty acids; and curve C, sodium taurocholate without fatty acid.*

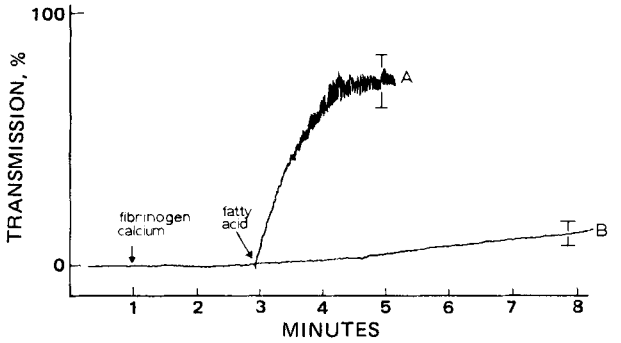


**Figure 5**—*Platelet aggregating activities of taurocholate-solubilized 70 μM fatty acids. Key: curve A, oleate; and curve B, stearate, palmitate, or myristate.*

determine its significance in relation to platelet aggregation, the calcium and fibrinogen requirements of washed porcine platelet aggregation were studied. Aggregation was induced with taurocholate-solubilized 170 *μM* oleate. Curve A in Fig. 7 shows that macroaggregate formation did not depend on fibrinogen. Without fibrinogen, the aggregation pattern was essentially identical to that with fibrinogen, although the fibrous mucoid network did not form in the absence of fibrinogen. Curve B of Fig. 7 reveals that calcium was required for aggregation. Without calcium, neither platelet aggregates nor the fibrous mucoid network formed. Although fibrinogen was not a requirement for aggregation, both fibrinogen and calcium were included in all trials to facilitate comparison with the predominant methodology in the literature.

The effects of alprostadil, epoprostenol, and indomethacin on platelet aggregation induced by suspended fatty acids are given in Fig. 8. A monophasic aggregation pattern leading to macroaggregate formation proceeded with or without the inhibitors. The time courses and extents of aggregation were not altered or inhibited by these agents.

The observed platelet aggregation patterns elicited by suspended or taurocholate-solubilized stearate are given in Fig. 9. Inhibitors were present as indicated. Aggregation activity increased with the taurocholate-solubilized stearate concentration up to 320 *μM*. The solubilized 600 *μM* system was somewhat less active than the solubilized 170 and 320 *μM* systems. However, macroaggregates formed with all but the taurocholate-solubilized 70 *μM* stearate system within the 10-min observation period. The platelet aggregation response to the taurocholate-solubilized stearate systems was unaltered by the inhibitors. The activity of the suspended stearate systems increased with concentration. Platelet aggregation induced by suspended stearate was more rapid than with taurocholate-solubilized stearate at all concentrations. The platelet response to suspended stearate was unaltered by the inhibitors; the possible exception was the aggregation induced by suspended 70 *μM* stearate. In this case, a decreased aggregation response was observed with both alprostadil and indomethacin. However, aggregate formation still was extensive.

Platelet aggregation patterns observed subsequent to additions of taurocholate-solubilized oleate are given in Fig. 10. Inhibitors were present as indicated. The 70 and 170 *μM* solubilized systems (Fig. 10*a*) induced a monophasic macroaggregate reaction. The response to the 320 and 600 *μM* solubilized oleate was anomalous. The 320 *μM* addition (Fig. 10*b*, curve A) elicited a biphasic response. Small aggregates appeared

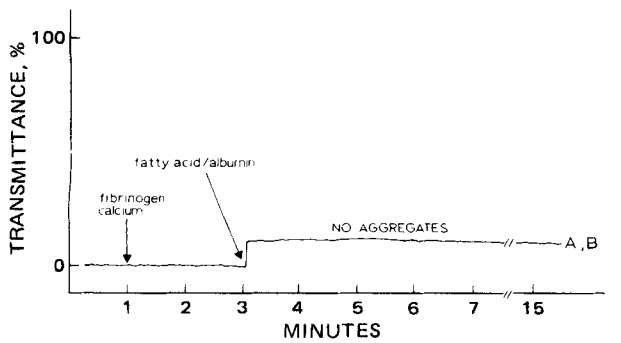


**Figure 6**—*Platelet aggregation response to albumin-solubilized fatty acids. Final fatty acid concentrations were: A, 600 μM oleate; and B, 600 μM palmitate. The final albumin concentration was 4 g %.*

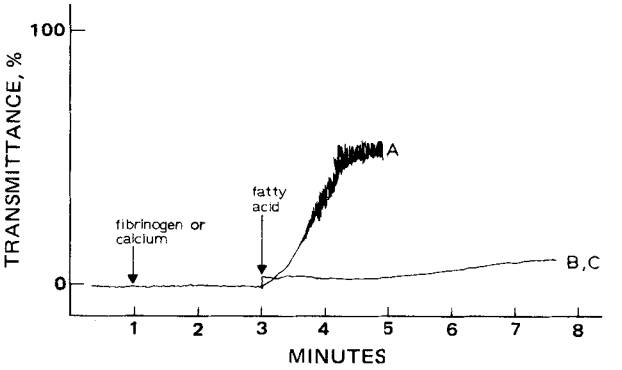


**Figure 7**—*Calcium and fibrinogen requirements of washed porcine platelet aggregation. Aggregation was induced with taurocholate-solubilized 170 μM oleate under the following conditions: curve A, 1 mM calcium without fibrinogen; curve B, 16 μg of fibrinogen/ml without calcium; and curve C, no calcium or fibrinogen.*

during the first phase and then disappeared during the second phase, leaving a clear solution devoid of visible aggregates. The 600 *μM* system elicited a monophasic response that also resulted in a clear, aggregate-free, solution.

Platelets were not visible in either of these clear solutions under 600× phase contrast light microscopy. Scanning electron micrographs at 2200× revealed unidentifiable debris. This finding was viewed as evidence for platelet lysis in response to the taurocholate-solubilized 320 and 600 *μM* oleate systems. This behavior was not observed with taurocholate alone or with any other taurocholate-solubilized fatty acid system examined. The aggregation inhibitors did not alter the observed responses to taurocholate-solubilized oleate except at the 320 *μM* concentration. Curve B of Fig. 10*b* reveals that epoprostenol actually enhanced the aggregate production. In the presence of epoprostenol, a monophasic response resulting in stable macroaggregate formation was observed.

The behavior of the taurocholate-solubilized oleate and stearate solutions was studied. Samples were diluted to the same concentrations used in the aggregation experiments and were examined with an electronic particle-size analyzer (Figs. 11 and 12). In all cases, the number of particles above 0.72 μm was negligible over the 10-min observation period. No particles were detected in the 4 m*M* fatty acid–47 m*M* sodium taurocholate stock solutions prior to dilution.

Dilution of a taurocholate-solubilized stock solution of oleate to 70 and 170 *μM* oleate resulted in rapid particle formation in the 0.45–0.72-μm diameter range. The taurocholate-solubilized 320 and 600 *μM* oleate systems precipitated much less. Particles were not detected in a 7.12 m*M* taurocholate system containing no fatty acid.

The behavior of taurocholate-solubilized stearate contrasted with oleate in that precipitation increased as the stearate concentration increased. However, in all cases, the extent of the stearate precipitation was less than with the taurocholate-solubilized 70 and 170 *μM* oleate systems.

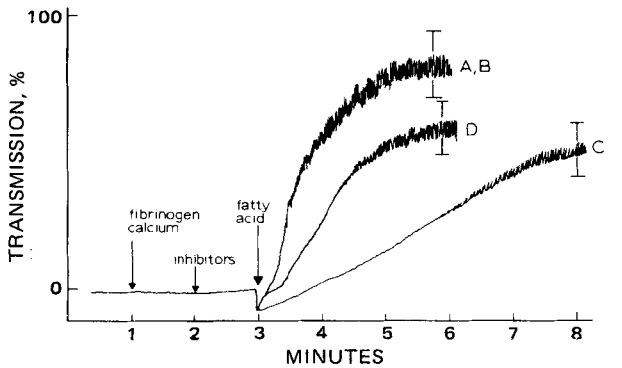


**Figure 8**—*Effects of alprostadil, epoprostenol, and indomethacin on platelet aggregation induced by suspended fatty acids. Key: curve A, 600 μM stearate with and without 75 μM alprostadil, 80 nM epoprostenol, or 150 μM indomethacin; curve B, 600 μM oleate with and without 150 μM indomethacin; curve C, 320 μM palmitate with and without 80 nM epoprostenol; and curve D, 170 μM oleate with and without 80 nM epoprostenol, 75 μM alprostadil, or 150 μM indomethacin.*

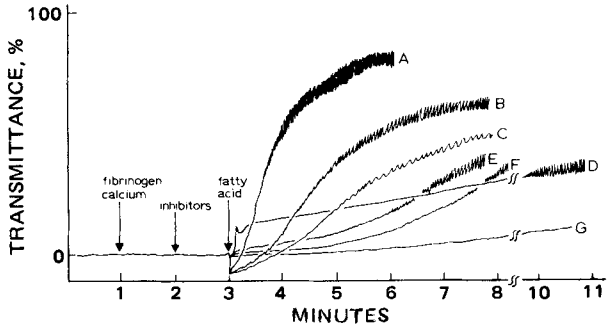


**Figure 9**—*Platelet aggregation as induced by taurocholate-solubilized and suspended stearate. Key (suspended stearate): curve A, 600 μM stearate with and without 75 μM alprostadil, 80 nM epoprostenol, or 150 μM indomethacin; curve B, 70 μM stearate; and curve C, 70 μM stearate with 75 μM alprostadil or 150 μM indomethacin. Key (taurocholate-solubilized stearate): curve D, 600 μM stearate with and without 80 nM epoprostenol; curve E, 320 μM stearate with and without 75 μM alprostadil, 80 nM epoprostenol, or 150 μM indomethacin; curve F, 170 μM stearate with and without 80 nM epoprostenol; and curve G, 70 μM stearate.*

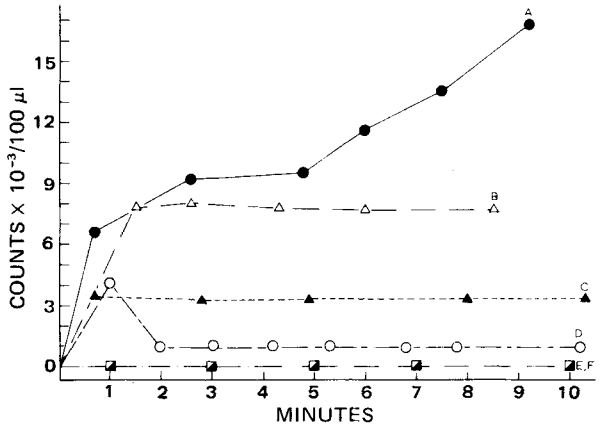


**Figure 11**—*Particle-size analysis of 4 mM oleate solubilized with either 47 mM sodium taurocholate or 26 g % albumin subsequent to dilution to 70 μM oleate/0.83 mM taurocholate (curve A), 170 μM oleate/2.01 mM taurocholate (curve B), 320 μM oleate/3.85 mM taurocholate (curve C), 600 μM oleate/7.12 mM taurocholate (curve D), 7.12 mM taurocholate (curve E), and 600 μM oleate/4 g % albumin (curve F). Size range was 0.45–0.72 μm in diameter.*

Prevention of fatty acid precipitation from the solubilized systems was possible if the final sodium taurocholate concentration was 47 m*M*. However, this concentration resulted in immediate and complete lysis of platelets. To alleviate this problem, it was necessary to replace taurocholate with another solubilizing agent, albumin, that would solubilize the fatty acids without lysing platelets. Particle-size analysis of albumin-solubilized oleate and palmitate (Figs. 11 and 12) indicated that no particle formation occurred above the 0.42-μm limit of detection. Light microscopy confirmed that the platelets were not lysed or visibly damaged by the albumin concentration employed.

## DISCUSSION

Porcine platelets resemble human platelets in several key areas (27): (*a*) membrane proteins; (*b*) monophasic aggregation induced by high concentrations of ADP; (*c*) potent inhibition of ADP, thrombin, and collagen-induced aggregation by alprostadil and inhibition of ADP by AMP; and (*d*) similar nucleotide content in the platelet storage granules. The present report indicates that the washed porcine platelet system can be used to distinguish the platelet aggregating activities of ADP and various fatty acids in suspended or solubilized physical states. Therefore, the porcine platelets were believed to be a reasonable *in vitro* model for the simulated study of human platelet behavior.

The platelet aggregation reaction is complex. To correlate the platelet responses to the many and varied aggregation inducing and inhibiting agents, a basic platelet reaction hypothesis has been proposed (23). Under this system, induction of platelet aggregation occurs with the interaction of inducing agents with receptor sites located on the platelet surface; changes thus induced lead to liberation of a transmitter substance [believed to be calcium ions (23, 28–30)] into the cytosol. The transmitter stimulates ATP-dependent contractile processes leading to aggregation.

Alprostadil and epoprostenol stimulate adenylate cyclase (1, 3, 31–33), which leads to increased production of cyclic adenosine monophosphate (AMP) in platelets. Elevated cyclic AMP results in platelet vesicular uptake of calcium ions from the cytosol (28, 30), which is accompanied by a reduction in platelet aggregation. Other work has shown that alprostadil can effectively inhibit platelet aggregation independent of cyclic AMP (34). The inhibitory effects of prostaglandins on platelet aggregation are thought to occur at the intermediate transmission step in the basic platelet reaction hypothesis and are, therefore, believed to be independent of the type of inducer (23). Literature data support this belief (1, 23, 29–31, 33) and suggest that epoprostenol is 30–40 times more potent than alprostadil (31).

Included in the basic platelet reaction hypothesis is the release of arachidonic acid from platelet membrane phospholipids through the action of phospholipase $A_2$ (31). The arachidonic acid then is converted into the cyclic endoperoxide prostaglandins $G_2$ and $H_2$ by cyclooxygenase. The endoperoxides react by alternate pathways to form thromboxane $A_2$ and epoprostenol. The endoperoxides and thromboxane $A_2$ are potent inducers of platelet aggregation while epoprostenol is a potent inhibitor (31, 35). It has been proposed that the balance among these compounds of common origin determines whether aggregation occurs *in vivo* (31). Indomethacin inhibits cyclooxygenase (36–38), thus preventing platelet aggregation associated with endoperoxide formation.

The aggregation response of the washed porcine platelets to 0.29 m*M* ADP was classically monophasic (Fig. 1), proceeding rapidly to macroaggregate production. The complete inhibition of this reaction by 75 μ*M* alprostadil or 80 n*M* epoprostenol agreed qualitatively with the literature (27, 39). However, on a quantitative basis, the ADP concentration was 10–20 times higher than normally used in *in vitro* aggregation studies (1, 3, 23, 29, 31, 34). This finding suggests that ADP-related aggregation was effectively eliminated by the prostaglandins.

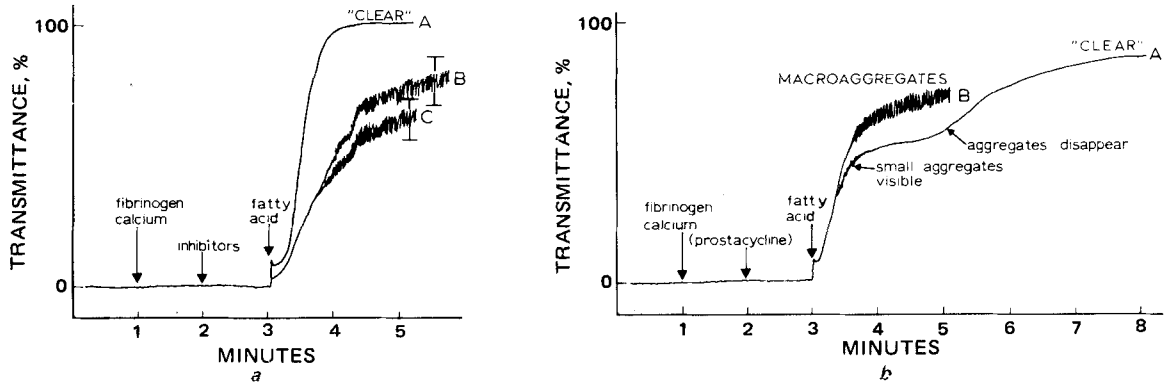


**Figure 10**—*Platelet aggregation as induced by taurocholate-solubilized oleate. Key for* a: *curve A, 600 μM oleate with and without 75 μM alprostadil; curve B, 170 μM oleate with and without 750 μM alprostadil, 80 nM epoprostenol, or 150 μM indomethacin; and curve C, 70 μM oleate with and without 75 μM alprostadil or 150 μM indomethacin. Key for* b: *curve A, 320 μM oleate; and curve B, 320 μM oleate with 80 nM epoprostenol.*

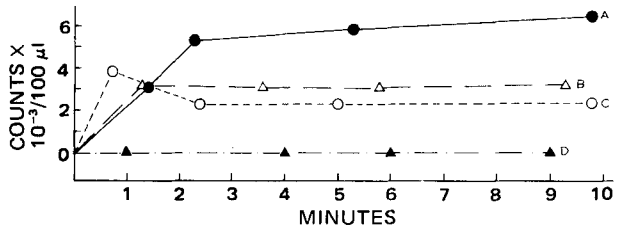


**Figure 12**—*Particle-size analysis of 4 mM stearate solubilized with 47 mM sodium taurocholate and 4 mM palmitate solubilized with 26 g % albumin subsequent to dilution to 600 µM stearate/7.12 mM taurocholate (curve A), 320 µM stearate/3.85 mM taurocholate (curve B), 70 µM stearate/0.83 mM taurocholate (curve C), and 600 µM palmitate/4 g % albumin (curve D). Size range was 0.45–0.72 µm in diameter.*

The platelet aggregating activity of the suspended fatty acid systems increased with both the fatty acid chain length and concentration (Figs. 2 and 3), in agreement with previous work (7, 8, 10, 18). Unsaturation of the hydrocarbon portion of the fatty acid molecule appeared to have no discernible effect on the platelet aggregation activity. This observation was in general agreement with other work where washed platelet aggregation was induced by fatty acids in suspension (9, 10, 20).

The effects of alprostadil, epoprostenol, and indomethacin on suspended fatty acid-induced platelet aggregation were examined (Figs. 8 and 9). With the possible exception of 70 *µM* stearate, these agents did not appear to alter the fatty acid-induced aggregation reaction, although they have been reported to inhibit collagen, thrombin, serotonin, epinephrine, vasopressin, ADP, and divalent cation ionophore-induced platelet aggregation (1, 23, 29–31, 34, 40, 41).

Simple correlation of platelet aggregating activity with the fatty acid chain length and concentration was not possible with the taurocholate-solubilized systems. Complex behavior was noted (Figs. 9 and 10), which differed markedly for the oleate as compared to the stearate systems.

A correlation of taurocholate-solubilized oleate-induced platelet aggregation with precipitate formation was found. The taurocholate-solubilized 70 and 170 *µM* oleate systems elicited immediate platelet aggregation reactions leading to platelet macroaggregates (Fig. 10). Immediate, extensive precipitate formation also was observed with these preparations (Fig. 11). The anomalous platelet response to taurocholate-solubilized 320 and 600 *µM* oleate was accompanied by a marked reduction in precipitate formation. Apparently, these latter systems remained solubilized to a greater extent, which may be attributed to the higher associated concentrations of taurocholate (Table I).

However, the platelet response to these preparations did not correlate strictly with taurocholate concentration. Taurocholate-solubilized 600 *µM* stearate (Fig. 9), myristate (Fig. 4), or palmitate or 7.12 m*M* taurocholate alone did not lyse platelets, although the final taurocholate concentration was equivalent to the solubilized oleate systems that lysed platelets. Thus, the platelet aggregating activity of the taurocholate-solubilized oleate systems appeared to depend on the formation of large numbers of particles subsequent to the addition to the washed platelet preparations. The biphasic response of the platelets to taurocholate-solubilized 320 *µM* oleate appeared to begin with platelet aggregation, ultimately ending in lysis (Fig. 10). This biphasic transition from the monophasic platelet aggregation response, elicited by the lower oleate concentrations, to the monophasic lysis of platelets by the higher oleate concentrations was a property unique to the taurocholate-solubilized oleate systems and corresponded directly with the extent of precipitation (Fig. 11).

All concentrations of taurocholate-solubilized stearate were less active than taurocholate-solubilized 70 and 170 *µM* oleate in the induction of platelet aggregation (Fig. 9). Precipitation from the stearate systems (Fig. 12) also was less extensive than from the oleate systems. Thus, although the taurocholate-solubilized oleate and stearate systems had differences in precipitation patterns and platelet aggregating activity, the development of a particulate physical state subsequent to taurocholate–fatty acid additions to washed platelets appeared to be important.

To investigate the dependence of fatty acid-induced platelet aggregation on a particulate physical state, oleate and palmitate were solubilized with albumin. The final albumin concentration subsequent to the addition to the washed platelets was 4 g %, which was sufficient to prevent precipitation of both 600 *µM* oleate and palmitate (Figs. 11 and 12). Under these conditions, the fatty acids were devoid of aggregating activity (Fig. 6) and did not lyse platelets, suggesting a particulate form of the free fatty acid was necessary to elicit the aggregation response.

The effects of alprostadil, epoprostenol, and indomethacin on the platelet response to taurocholate-solubilized oleate and stearate were examined (Figs. 9 and 10). These agents had no discernible effect on the platelet aggregation reaction except where induced by taurocholate-solubilized 320 *µM* oleate. In this case, epoprostenol appeared to enhance aggregation by preventing the second phase lysis (Fig. 10*b*). This increased resistance to cell damage associated with prostaglandin exposure was previously noted with red blood cells and gastric mucosal cells (42–45).

The ineffectiveness of alprostadil, epoprostenol, and indomethacin at inhibition of solubilized or suspended fatty acid-induced platelet aggregation suggested that the aggregation was independent of nucleotide release from endogenous storage granules within the platelets, cyclic AMP-related cytosol calcium shifts, and endoperoxide–thromboxane $A_2$ mechanisms. A particulate physical state for the fatty acids appeared to be prerequisite for platelet aggregating activity. The greater platelet aggregating activity, in general, of the taurocholate-solubilized systems (Fig. 4) suggests that specific particle-size and number requirements exist for optimal interaction, which are best achieved as the fatty acids precipitate out of the solubilized state. Based on normal particle growth kinetics, it is expected that the average particle size of these precipitates present during the aggregation process would be considerably smaller than the average particle size of the nonsolubilized suspensions.

Thus, fatty acid-induced platelet aggregation did not fit the scheme developed in the basic platelet reaction hypothesis (23). Rather, a direct physical interaction of fatty acid particles with platelets, leading to aggregation, appeared to be consistent with the observations. Although the precise role of calcium in these reactions remains unknown, the formation of calcium bridges between negatively charged fatty acid particles and negatively charged platelets (46) would account for both the particulate fatty acid physical state requirements and the ineffectiveness of the aggregation inhibiting agents.

## REFERENCES

(1) J. B. Smith and D. E. Macfarlane, in "The Prostaglandins," vol. 2, P. W. Ramwell, Ed., Plenum, New York, N.Y., 1974, p. 293.

(2) G. V. R. Born, *Ann. N.Y. Acad. Sci.*, **201**, 4 (1972).

(3) A. J. Barber, *Biochim. Biophys. Acta*, **444**, 579 (1976).

(4) C. B. Harbury, J. E. Hershgold, and S. L. Shrier, *Thromb. Diath. Haemorrh.*, **28**, 2 (1972).

(5) P. Didisheim and R. S. Mibashan, *ibid.*, **9**, 346 (1963).

(6) J. F. Mustard and M. A. Packham, *Pharmacol. Rev.*, **22**, 97 (1970).

(7) W. E. Connor, J. C. Hoak, and E. D. Warner, *J. Clin. Invest.*, **42**, 860 (1963).

(8) W. E. Connor, *ibid.*, **41**, 1199 (1962).

(9) V. Mahadevan, H. Singh, and W. O. Lundberg, *Proc. Soc. Exp. Biol. Med.*, **121**, 82 (1966).

(10) R. J. Prost-Dvojakovic and M. Samama, *Haemostasis*, **2**, 73 (1973).

(11) H. L. Nossel, in "Harrison's Principles of Internal Medicine," 9th ed., K. J. Isselbacher, R. D. Adams, E. Braunwald, R. G. Petersdorf, and J. D. Wilson, Eds., McGraw-Hill, New York, N.Y., 1980, p. 272.

(12) Y. Burstein, L. Berns, D. Heldenberg, Y. Kahn, B. Z. Werbin, and I. Tamir, *Am. J. Hematol.*, **4**, 17 (1978).

(13) E. L. Bierman, V. P. Dole, and T. N. Roberts, *Diabetes*, **6**, 475 (1957).

(14) A. G. Beckett and J. G. Lewis, *Lancet*, **2**, 14 (1960).

(15) P. S. Mueller and D. M. Watkin, *J. Lab. Clin. Med.*, **57**, 95 (1961).

(16) B. M. Rifkin, *J. Atheroscler. Res.*, **6**, 26 (1966).

(17) R. L. Burt, *Obstet. Gynecol.*, **15**, 460 (1960).

(18) W. E. Connor and J. C. F. Poole, *Q. J. Exp. Physiol.*, **46**, 1 (1961).

(19) P. Mukerjee and K. J. Mysels, "Critical Micelle Concentrations of Aqueous Surfactant Systems," National Standard Reference Data Series, National Bureau of Standards, Washington, D.C.

(20) J. C. Hoak, E. D. Warner, and W. E. Connor, *Circ. Res.*, **20**, 11 (1967).

(21) J. C. Hoak, W. E. Connor, and E. D. Warner, *Arch. Pathol.*, **81**, 136 (1966).

(22) "Documenta Geigy Scientific Tables," K. Diem and C. Lentner, Eds., Ciba-Geigy Corp., New York, N.Y., 1970, p. 600.

(23) H. Holmsen, *Ser. Haematol.*, **8**, 3 (1976).

(24) L. Lack, F. O. Dorrity, Jr., T. Walker, and G. D. Singletary, *J. Lipid Res.*, **14**, 367 (1973).
(25) R. J. Haslam, *Nature (London)*, **202**, 765 (1964).
(26) G. V. R. Born and M. J. Cross, *J. Physiol. (London)*, **168**, 178 (1963).
(27) W. J. Dodds, in "Platelets: A Multidisciplinary Approach," G. DeGaetano and S. Garattini, Eds., Raven, New York, N.Y., 1978.
(28) P. Massini, R. Kaser-Glanzmann, and E. F. Luscher, *Thromb. Haemostasis*, **40**, 212 (1978).
(29) R. L. Kinlough-Rathbone, M. A. Packham, H. J. Reimers, J. P. Cazenave, and J. F. Mustard, *J. Lab. Clin. Med.*, **90**, 707 (1977).
(30) R. J. Haslam, M. M. L. Davidson, J. E. B. Fox, and J. A. Lynham, *Thromb. Haemostasis*, **40**, 232 (1978).
(31) S. Moncada and J. R. Vane, in "Chemistry, Biochemistry and Pharmacological Activity of Prostanoids," S. M. Roberts and F. Scheinmann, Eds., Pergamon, New York, N.Y., 1979.
(32) E. W. Salzmann and H. Weisenberger, *Adv. Cyclic Nucleotide Res.*, **1**, 231 (1972).
(33) R. J. Haslam, *Ser. Haematol.*, **3**, 333 (1973).
(34) A. K. Sinha and R. W. Colman, *Science*, **200**, 202 (1978).
(35) J. Svensson, M. Hamberg, and B. Samuelsson, *Acta Physiol. Scand.*, **98**, 285 (1976).
(36) T. K. Bills, J. B. Smith, and M. J. Silver, *Biochim. Biophys. Acta*, **424**, 303 (1976).
(37) E. G. Lapetina, K. A. Chandrabose, and P. Cuatrecasas, *Proc. Natl. Acad. Sci. USA*, **75**, 818 (1978).
(38) M. Hamburg, J. Svensson, T. Wakabayashi, and B. Samuelsson, *ibid.*, **71**, 345 (1974).
(39) H. J. Berman, O. Tangen, D. Ausprunk, and H. Collins, *Bibl. Anat.*, **10**, 507 (1969).
(40) R. L. Kinlough-Rathbone, H. J. Reimers, and J. F. Mustard, *Science*, **192**, 1011 (1976).
(41) R. L. Kinlough-Rathbone, M. A. Packham, and J. F. Mustard, *Thromb. Res.*, **11**, 567 (1977).
(42) J. E. Allen and H. Rasmussen, *Science*, **174**, 512 (1971).
(43) H. Rasmussen and W. Lake, in "Prostaglandins in Hematology," M. J. Silver, J. B. Smith, and J. J. Kocsis, Eds., Spectrum, New York, N.Y., p. 187.
(44) J. E. Allen and H. Rasmussen, in "Prostaglandins in Cellular Biology," P. W. Ramwell and B. B. Pharriss, Eds., Plenum, New York, N.Y., 1972, p. 27.
(45) A. Robert, in "Practical Applications of Prostaglandins," S. M. M. Karim, Ed., University Park Press, Baltimore, Md., p. 95.
(46) G. V. F. Seaman, *Thromb. Diath. Haemorrh. (Suppl.)*, **26**, 53 (1967).

### ACKNOWLEDGMENTS

Presented in part at the APhA Academy of Pharmaceutical Sciences, Kansas City, Mo., meeting, November 1979.

Supported by National Institutes of Health Grant HL-17623.

S. W. Kim is a National Institutes of Health Research Career Development Awardee (HL-00272).

The authors thank Mr. J. C. McRea for assisting in the preparation of the prostaglandin solutions and Dr. D. Coleman for assisting in the scanning electron microscope observations.

# Pharmacokinetics of Sulfisoxazole Compared in Humans and Two Monogastric Animal Species

**ROBERT L. SUBER *§x, CHARLES LEE ‡, GEORGE TOROSIAN ‡, and GEORGE T. EDDS ***

Received September 24, 1980, from the **Department of Preventative Medicine and Toxicology and the* ‡*Department of Pharmaceutics, College of Pharmacy, University of Florida, Gainesville, FL 32610.* Accepted for publication February 6, 1981. §Present address: Pathology Services Project, National Center for Toxicological Research, Jefferson, AR 72079.

**Abstract** □ The pharmacokinetic profile of sulfisoxazole was studied and compared in dogs, swine, and humans. The trial was conducted over a 72-hr period after intravenous administration and a 96-hr period after oral administration in dogs and swine. In humans, the trial was conducted over an 8-hr period after oral administration. A two-compartment model system was used to define the pharmacokinetic profile. The mean half-lives for the distribution phase were 4.08, 1.30, and 0.56 hr in dogs, swine, and humans, respectively. For the elimination phase, the mean half-lives were 33.74, 46.39, and 7.40 hr in dogs, swine, and humans, respectively. The mean volume of the central compartment was approximately the same in dogs and swine, 10.6 and 10.5 liters, respectively. Humans had a smaller volume of distribution, 7.7 liters. The steady-state volumes of distribution were 17.2, 30.3, and 16.2 liters in dogs, swine, and humans, respectively. Dogs and swine excreted 42.2 and 30.7%, respectively, of the intravenous dose and 29.4 and 18.3%, respectively, of the oral dose. The bioavailability was 69.8% in dogs and 100.0% in swine. The fraction of drug bound ranged from 30 to 50% in dogs, 40 to 60% in swine, and 25 to 40% in humans.

**Keyphrases** □ Sulfisoxazole—pharmacokinetics in humans, dogs, and swine □ Pharmacokinetics—sulfisoxazole, comparison in humans, dogs, and swine □ Antibacterials—sulfisoxazole, pharmacokinetics in humans, dogs, and swine

Sulfisoxazole is an effective antibacterial agent often used in the treatment of urinary tract infections. Previous studies in dogs, swine, and cattle only measured blood levels of sulfisoxazole and sulfisoxazole acetyl following intravenous (1), subcutaneous (1), oral (2), and peritoneal (1) administrations. No detailed pharmacokinetic analyses were undertaken to characterize the absorption, distribution, metabolism, and excretion of sulfisoxazole in these animals. Likewise, human studies (3–5) of sulfisoxazole after single oral ingestion were limited to the measurement of blood concentrations of the parent drug and the acetyl metabolite. In one study (2), the steady-state blood level was measured following multiple-dose administration.

The first complete pharmacokinetic study in humans was conducted by Kaplan *et al.* (6) in which sulfisoxazole was administered intravenously, intramuscularly, and orally. Pharmacokinetic parameters were determined and availability was assessed. The present study compared sulfisozaxole pharmacokinetics in dogs, swine, and humans.

## EXPERIMENTAL

**Materials**—A 12.5% sulfisoxazole[1] solution was prepared with lithium hydroxide. The solution was filtered and placed in sterile 50-ml ampuls before use. Sulfisoxazole acetyl[2] was used as a reference standard for serum and urinary metabolite assay. All chemicals and solvents used in the high-performance liquid chromatographic (HPLC) assay were high purity solvents[3] and were filtered before use.

**Experimental Model**—The trial consisted of three female dogs (~2

[1] Hoffmann–La Roche, Nutley, N.J.
[2] Acetyl-$N^4$-sulfisoxazole, Hoffmann–La Roche, Nutley, N.J.
[3] Burdick & Jackson solvents, Bodman Chemical Co., Doraville, Ga.

0022-3549/81/0900-0981$01.00/0
© 1981, American Pharmaceutical Association

(24) L. Lack, F. O. Dorrity, Jr., T. Walker, and G. D. Singletary, *J. Lipid Res.*, **14**, 367 (1973).
(25) R. J. Haslam, *Nature (London)*, **202**, 765 (1964).
(26) G. V. R. Born and M. J. Cross, *J. Physiol. (London)*, **168**, 178 (1963).
(27) W. J. Dodds, in "Platelets: A Multidisciplinary Approach," G. DeGaetano and S. Garattini, Eds., Raven, New York, N.Y., 1978.
(28) P. Massini, R. Kaser-Glanzmann, and E. F. Luscher, *Thromb. Haemostasis*, **40**, 212 (1978).
(29) R. L. Kinlough-Rathbone, M. A. Packham, H. J. Reimers, J. P. Cazenave, and J. F. Mustard, *J. Lab. Clin. Med.*, **90**, 707 (1977).
(30) R. J. Haslam, M. M. L. Davidson, J. E. B. Fox, and J. A. Lynham, *Thromb. Haemostasis*, **40**, 232 (1978).
(31) S. Moncada and J. R. Vane, in "Chemistry, Biochemistry and Pharmacological Activity of Prostanoids," S. M. Roberts and F. Scheinmann, Eds., Pergamon, New York, N.Y., 1979.
(32) E. W. Salzmann and H. Weisenberger, *Adv. Cyclic Nucleotide Res.*, **1**, 231 (1972).
(33) R. J. Haslam, *Ser. Haematol.*, **3**, 333 (1973).
(34) A. K. Sinha and R. W. Colman, *Science*, **200**, 202 (1978).
(35) J. Svensson, M. Hamberg, and B. Samuelsson, *Acta Physiol. Scand.*, **98**, 285 (1976).
(36) T. K. Bills, J. B. Smith, and M. J. Silver, *Biochim. Biophys. Acta*, **424**, 303 (1976).
(37) E. G. Lapetina, K. A. Chandrabose, and P. Cuatrecasas, *Proc. Natl. Acad. Sci. USA*, **75**, 818 (1978).
(38) M. Hamburg, J. Svensson, T. Wakabayashi, and B. Samuelsson, *ibid.*, **71**, 345 (1974).
(39) H. J. Berman, O. Tangen, D. Ausprunk, and H. Collins, *Bibl. Anat.*, **10**, 507 (1969).
(40) R. L. Kinlough-Rathbone, H. J. Reimers, and J. F. Mustard, *Science*, **192**, 1011 (1976).
(41) R. L. Kinlough-Rathbone, M. A. Packham, and J. F. Mustard, *Thromb. Res.*, **11**, 567 (1977).
(42) J. E. Allen and H. Rasmussen, *Science*, **174**, 512 (1971).
(43) H. Rasmussen and W. Lake, in "Prostaglandins in Hematology," M. J. Silver, J. B. Smith, and J. J. Kocsis, Eds., Spectrum, New York, N.Y., p. 187.
(44) J. E. Allen and H. Rasmussen, in "Prostaglandins in Cellular Biology," P. W. Ramwell and B. B. Pharriss, Eds., Plenum, New York, N.Y., 1972, p. 27.
(45) A. Robert, in "Practical Applications of Prostaglandins," S. M. M. Karim, Ed., University Park Press, Baltimore, Md., p. 95.
(46) G. V. F. Seaman, *Thromb. Diath. Haemorrh. (Suppl.)*, **26**, 53 (1967).

### ACKNOWLEDGMENTS

Presented in part at the APhA Academy of Pharmaceutical Sciences, Kansas City, Mo., meeting, November 1979.

Supported by National Institutes of Health Grant HL-17623.

S. W. Kim is a National Institutes of Health Research Career Development Awardee (HL-00272).

The authors thank Mr. J. C. McRea for assisting in the preparation of the prostaglandin solutions and Dr. D. Coleman for assisting in the scanning electron microscope observations.

# Pharmacokinetics of Sulfisoxazole Compared in Humans and Two Monogastric Animal Species

**ROBERT L. SUBER *§x, CHARLES LEE ‡, GEORGE TOROSIAN ‡, and GEORGE T. EDDS ***

Received September 24, 1980, from the **Department of Preventative Medicine and Toxicology and the* ‡*Department of Pharmaceutics, College of Pharmacy, University of Florida, Gainesville, FL 32610.* Accepted for publication February 6, 1981. §Present address: Pathology Services Project, National Center for Toxicological Research, Jefferson, AR 72079.

**Abstract** □ The pharmacokinetic profile of sulfisoxazole was studied and compared in dogs, swine, and humans. The trial was conducted over a 72-hr period after intravenous administration and a 96-hr period after oral administration in dogs and swine. In humans, the trial was conducted over an 8-hr period after oral administration. A two-compartment model system was used to define the pharmacokinetic profile. The mean half-lives for the distribution phase were 4.08, 1.30, and 0.56 hr in dogs, swine, and humans, respectively. For the elimination phase, the mean half-lives were 33.74, 46.39, and 7.40 hr in dogs, swine, and humans, respectively. The mean volume of the central compartment was approximately the same in dogs and swine, 10.6 and 10.5 liters, respectively. Humans had a smaller volume of distribution, 7.7 liters. The steady-state volumes of distribution were 17.2, 30.3, and 16.2 liters in dogs, swine, and humans, respectively. Dogs and swine excreted 42.2 and 30.7%, respectively, of the intravenous dose and 29.4 and 18.3%, respectively, of the oral dose. The bioavailability was 69.8% in dogs and 100.0% in swine. The fraction of drug bound ranged from 30 to 50% in dogs, 40 to 60% in swine, and 25 to 40% in humans.

**Keyphrases** □ Sulfisoxazole—pharmacokinetics in humans, dogs, and swine □ Pharmacokinetics—sulfisoxazole, comparison in humans, dogs, and swine □ Antibacterials—sulfisoxazole, pharmacokinetics in humans, dogs, and swine

Sulfisoxazole is an effective antibacterial agent often used in the treatment of urinary tract infections. Previous studies in dogs, swine, and cattle only measured blood levels of sulfisoxazole and sulfisoxazole acetyl following intravenous (1), subcutaneous (1), oral (2), and peritoneal (1) administrations. No detailed pharmacokinetic analyses were undertaken to characterize the absorption, distribution, metabolism, and excretion of sulfisoxazole in these animals. Likewise, human studies (3–5) of sulfisoxazole after single oral ingestion were limited to the measurement of blood concentrations of the parent drug and the acetyl metabolite. In one study (2), the steady-state blood level was measured following multiple-dose administration.

The first complete pharmacokinetic study in humans was conducted by Kaplan *et al.* (6) in which sulfisoxazole was administered intravenously, intramuscularly, and orally. Pharmacokinetic parameters were determined and availability was assessed. The present study compared sulfisozaxole pharmacokinetics in dogs, swine, and humans.

## EXPERIMENTAL

**Materials**—A 12.5% sulfisoxazole[1] solution was prepared with lithium hydroxide. The solution was filtered and placed in sterile 50-ml ampuls before use. Sulfisoxazole acetyl[2] was used as a reference standard for serum and urinary metabolite assay. All chemicals and solvents used in the high-performance liquid chromatographic (HPLC) assay were high purity solvents[3] and were filtered before use.

**Experimental Model**—The trial consisted of three female dogs (~2

[1] Hoffmann–La Roche, Nutley, N.J.
[2] Acetyl-$N^4$-sulfisoxazole, Hoffmann–La Roche, Nutley, N.J.
[3] Burdick & Jackson solvents, Bodman Chemical Co., Doraville, Ga.

0022-3549/81/0900-0981$01.00/0
© 1981, American Pharmaceutical Association

Table I—Two-Compartment Pharmacokinetic Parameters in Dogs Administered Sulfisoxazole as a Single Intravenous Dose

| Subject | $t_{1/2,\alpha}$, hr | $t_{1/2,\beta}$, hr | $V_1$, liters | $V_2$, liters | $k_{12}$, $hr^{-1}$ | $k_{21}$, $hr^{-1}$ | $k_{10}$, $hr^{-1}$ | $Cl_T$, liters/hr |
|---|---|---|---|---|---|---|---|---|
| 1 | 4.61 | 35.18 | 9.03 | 2.95 | 0.0068 | 0.0208 | 0.1424 | 1.29 |
| 2 | 5.02 | 33.97 | 11.04 | 5.07 | 0.0103 | 0.0224 | 0.1258 | 1.39 |
| 3 | 3.70 | 36.28 | 9.55 | 6.87 | 0.0151 | 0.0210 | 0.1701 | 1.62 |
| 4 | 3.74 | 33.48 | 10.07 | 6.34 | 0.0143 | 0.0227 | 0.1689 | 1.70 |
| 5 | 3.92 | 29.87 | 14.07 | 10.77 | 0.0206 | 0.0269 | 0.1525 | 2.15 |
| 6 | 3.50 | 33.64 | 9.84 | 7.29 | 0.0169 | 0.0228 | 0.1791 | 1.76 |
| Mean | 4.08 | 33.74 | 10.60 | 6.55 | 0.0140 | 0.0228 | 0.1565 | 1.65 |
| *SD* | 0.60 | 2.17 | 1.83 | 2.59 | 0.0049 | 0.0022 | 0.0200 | 0.30 |

years old, 20.0 ± 1.0 kg), six female pigs (~3 months old, 20.0 ± 1.0 kg), and six male human volunteers (25–30 years old, 70–80 kg). The dogs were administered 100 mg of sulfisoxazole/kg by intravenous and oral routes in two replicates for each route with a 30-day rest period between administrations. The pigs also were administered 100 mg of sulfisoxazole/kg by intravenous and oral routes with a 21-day washout period. All animals were housed in metabolism cages and were maintained on a commercial diet[4] with *ad libitum* access to water.

Sulfisoxazole was administered both orally and intravenously as a 12.5% solution to dogs and swine. The human volunteers received 2.0 g of sulfisoxazole in a single oral dose. Due to the potential toxicity of intravenous administration of sulfisoxazole and its removal from the drug market, the Human Research Committee of the University of Florida would not allow intravenous administration to humans.

**Sampling Schemes**—For dogs and swine, blood samples were taken at 0.5, 1, 2, 3, 4.5, 6, 9, 12, 22, 32, 44, 56, and 72 hr after intravenous administration and at 0, 1, 2, 4, 6, 8, 10, 12, 14, 23, 32, 44, 56, 76, and 96 hr after oral administration. Total urine was collected daily by natural voiding for up to 4 days. Human blood samples were collected at 0, 1, 2, 4, 6, and 8 hr after oral administration. Urine was not collected in the human trial. Blood samples were taken from the cephalic vein in dogs and humans and *via* the anterior vena cava in swine. Serum and urine samples were frozen at −4° for up to 14 days before analysis.

**Assay for Sulfisoxazole and Sulfisoxazole Acetyl**—Sulfisoxazole and sulfisoxazole acetyl in plasma and urine were analyzed by a reversed-phase HPLC technique developed in these laboratories (7), using a 60% distilled water–40% methanol liquid phase with acetate buffer added to reduce the pH to 4.00. The detection limit for this assay was 10 ng/ml for both sulfisoxazole and the acetyl metabolite at 254 nm[5].

Serum samples were injected directly into the HPLC system, which was fitted with an in-line precolumn[6]. Unbound, unmetabolized sulfisoxazole and sulfisoxazole acetyl were extracted by cooling 25.0 ml of urine to 4° in an ice bath; sufficient 6 *M* HCl was added to reduce the pH to 3.0. After 5 min, 15.0 ml of chloroform[3] was added, the solution was removed from the ice bath, and extraction was completed in 5 min by swirling the solution once per minute. The chloroform was removed and evaporated under nitrogen, and the residue was reconstituted with methanol[3]. The peak height ratio was used to calculate the concentration of unbound, unmetabolized sulfisoxazole and sulfisoxazole acetyl with sulfathiazole as the internal standard.

Both serum and urine samples were spotted on TLC plates (8) to determine if other metabolites were present. All spots were accounted for without the elution of other metabolites.

**Plasma Protein Binding**—Human plasma samples, prepared at concentrations of 25, 50, 100, 200, 300, 400, and 500 μg of sulfisoxazole/ml, were dialyzed against 2.0 ml of pH 7.4 phosphate buffer. The dialysate was collected and analyzed for sulfisoxazole content. Protein binding of plasma samples collected from dogs, swine, and humans at various time intervals also was determined by equilibrium dialysis. The fraction of the drug bound was defined as $C_f/C_t$, where $C_f$ is the drug concentration in the dialysate and $C_t$ is the drug concentration in the plasma at the completion of equilibrium dialysis.

**Data Analysis**—A two-compartment open body model was applied to the analysis of plasma sulfisoxazole data after intravenous administration using a NONLIN program (9). Pharmacokinetic parameters, including $\alpha$, $\beta$, $k_{12}$, $k_{21}$, $k_{10}$, $V_1$, and $V_2$, were defined from the curve fitting. Plasma clearance was defined from the model as $k_{10}V_1$, where $V_1$ is the distribution volume of the central compartment. Renal clearance was defined as $f_e Cl_t$, where $f_e$ is the fraction of sulfisoxazole excreted unchanged in the urine. The volume of the peripheral compartment ($V_2$) was defined from the model $k_{12}V_1 = k_{21}V_2$.

Bioavailability of sulfisoxazole following solution administration to dogs and swine was determined by the urinary excretion method. The unchanged sulfisoxazole excreted in the urine in 72 hr was compared for oral and intravenous administration. The *AUC* (area under the plasma concentration–time curve) method was not applied to the determination of bioavailability in this investigation due to the discrepancies in terminal half-lives observed following intravenous and oral administration. This discrepancy could be due to the erratic absorption of the oral dose. The half-life of sulfisoxazole following oral administration to humans was determined from the log-linear slope of the plasma concentration–time curve. No attempt was made to assess the oral bioavailability in humans.

## RESULTS

In the 72-hr period following intravenous administration in the dog, sulfisoxazole levels showed biexponential decay (Fig. 1). The $\beta$-phase half-life in these animals had a mean of 33.74 hr, while the $\alpha$-phase half-life ranged from 3.5 to 5.0 hr (mean 4.08). Mean values for the volume of the central pool and the steady-state volume of distribution were 10.60 and 17.15 liters, respectively. Serum sulfisoxazole clearance ranged from 1.39 to 2.15 liters/hr (mean 1.65). The fraction of the dose eliminated unchanged was 42.2%. Renal clearance averaged 0.7 liter/hr. Pharmacokinetic parameters of the two-compartment model in dogs following intravenous sulfisoxazole administration are summarized in Table I.

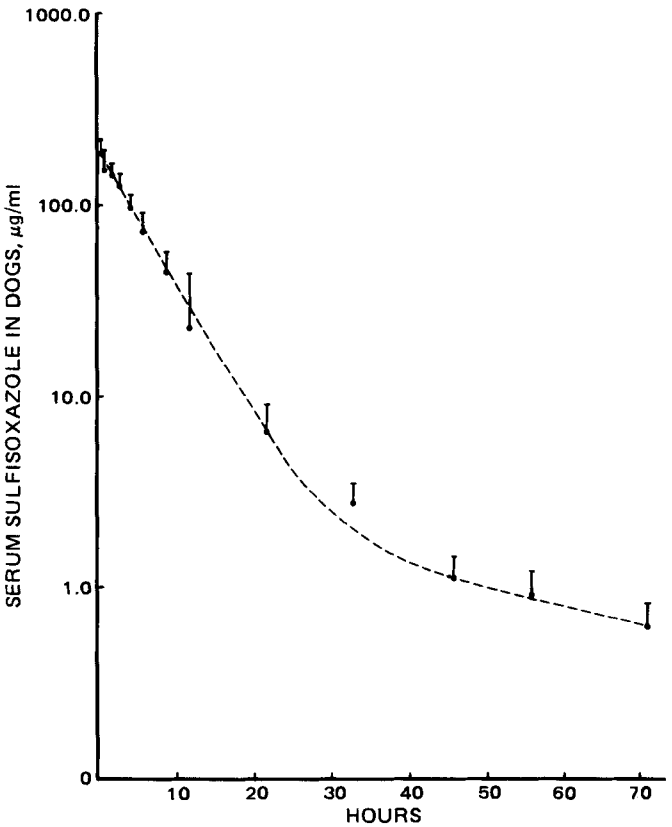


**Figure 1**—*Serum concentrations of unbound, unmetabolized sulfisoxazole in dogs.*

[4] Purina Dog Chow, Ralston-Purina Co., St. Louis, Mo., and 18% protein swine feed, University of Florida Swine Unit, Gainesville, Fla.

[5] Model 440 absorbance detector, Waters Associates, Milford, Mass.

[6] Corasil, Waters Associates, Milford, Mass.

Table II—Two-Compartment Pharmacokinetic Parameters in Swine Administered Sulfisoxazole as a Single Intravenous Dose

| Subject | $t_{1/2,\alpha}$, hr | $t_{1/2,\beta}$, hr | $V_1$, liters | $V_2$, liters | $k_{12}$, $hr^{-1}$ | $k_{21}$, $hr^{-1}$ | $k_{10}$, $hr^{-1}$ | $Cl_T$, liters/hr |
|---|---|---|---|---|---|---|---|---|
| 1 | 1.21 | 31.64 | 12.76 | 11.98 | 0.0214 | 0.0228 | 0.5509 | 7.03 |
| 2 | 1.36 | 36.67 | 15.65 | 24.65 | 0.0317 | 0.0202 | 0.4782 | 7.48 |
| 3 | 1.18 | 56.34 | 8.20 | 15.70 | 0.0247 | 0.0129 | 0.5631 | 4.62 |
| 4 | 1.31 | 64.77 | 9.58 | 33.12 | 0.0401 | 0.0116 | 0.4876 | 4.67 |
| 5 | 1.32 | 42.11 | 7.57 | 15.73 | 0.0293 | 0.0141 | 0.4931 | 3.73 |
| 6 | 1.40 | 46.82 | 9.09 | 17.49 | 0.0304 | 0.0158 | 0.4647 | 4.22 |
| Mean | 1.30 | 46.39 | 10.48 | 19.76 | 0.0296 | 0.0162 | 0.5063 | 5.29 |
| *SD* | 0.09 | 12.39 | 3.11 | 7.75 | 0.0064 | 0.0044 | 0.0406 | 1.56 |

The plasma levels in swine following intravenous administration also were biexponential (Fig. 2) and were analyzed by a two-compartment model. The $\alpha$- and $\beta$-phase half-lives in swine had means of 1.30 (range 1.18–1.40) and 53.33 (range 31.64–64.77) hr, respectively. The mean volumes were 10.48 and 30.24 liters for the central and steady-state pools, respectively. Plasma clearance ranged from 3.73 to 7.48 liters/hr (mean 5.29). Based on the percent of dose excreted unchanged (18.2%), the average renal clearance was 0.96 liter/hr. Pharmacokinetic constants of the two-compartment model in six swine following intravenous sulfisoxazole administration are recorded in Table II.

Following oral administration of sulfisoxazole to dogs, the peak plasma concentrations, ranging from 122.3 to 165.0 μg/ml, occurred at 1 hr. The peak time for swine occurred at 1 hr with much lower peak concentrations of 32.8–100.6 μg/ml. Sulfisoxazole acetyl reached a maximum of 12.1–20.0 μg/ml in 2–4 hr in all six pigs. The $\beta$-phase half-life of the acetyl metabolite was estimated to range from 23.2 to 37.9 hr with a mean of 31.0 ± 5.3 hr in pigs. Dogs either do not metabolize many aromatic amine compounds through acetylation or else possess a deacetylase that precludes analysis of the acetyl derivative (10). Sulfisoxazole acetyl was not observed in the urine or serum of dogs administered sulfisoxazole.

Following oral sulfisoxazole administration to humans, the plasma data were analyzed by a one-compartment model. Two-compartment analysis was not possible due to the lack of sampling in the 1st hr. The peak concentration of the unmetabolized sulfisoxazole occurred in <1 hr following oral administration, although the exact time was not known (Fig. 3). The rapid absorption of sulfisoxazole following oral administration was due to the drug being given as a solution. The $\beta$-phase half-life of sulfisoxazole ranged from 6.0 to 8.8 hr with a mean of 7.41 ± 0.59 hr. The half-life of sulfisoxazole in humans was not comparable to either the $\alpha$-phase or the $\beta$-phase half-life in dogs and swine; however, it was consistent with the $\beta$-phase half-life reported in a previous intravenous study in humans (6). The acetyl metabolite peaked at 4 hr and exhibited a longer $\beta$-phase half-life than the parent compound (Fig. 3). The mean biological half-life of sulfisoxazole acetyl was 14.1 ± 2.2 hr.

Table III records the percent of dose excreted as unchanged sulfisoxazole in the urine for the 96-hr period. Dogs and swine excreted 42.2 and 18.2% of the intravenous dose, respectively, during the trial period. In the oral trial, dogs excreted 29.4% of the dose compared to 18.3% excreted in swine.

Sulfisoxazole bioavailability (Table IV), 69.8 and 100% in dogs and swine, respectively, was determined from the unchanged drug excreted in the urine in 72 hr. Bioavailability of the drug in humans, although not available from this study due to a lack of corresponding intravenous data, was demonstrated to be complete (6).

In dogs, the fraction of the drug bound to plasma protein ranged from 30 to 50% in the sulfisoxazole concentration of 0–240 μg/ml (Table IV). In the same concentration range, sulfisoxazole was found to bind swine plasma protein from 40 to 60%. In humans, the bound fraction ranged from 25 to 40% in the concentration range of 80–200 μg/ml during the 8 hr following oral sulfisoxazole dosing. The *in vitro* binding of sulfisoxazole to blank human plasma in the range of 25–500 μg/ml was higher (38.9–63.0%) than *in vivo* binding and showed a concentration dependency. These *in vivo* plasma protein binding data were quite different from the

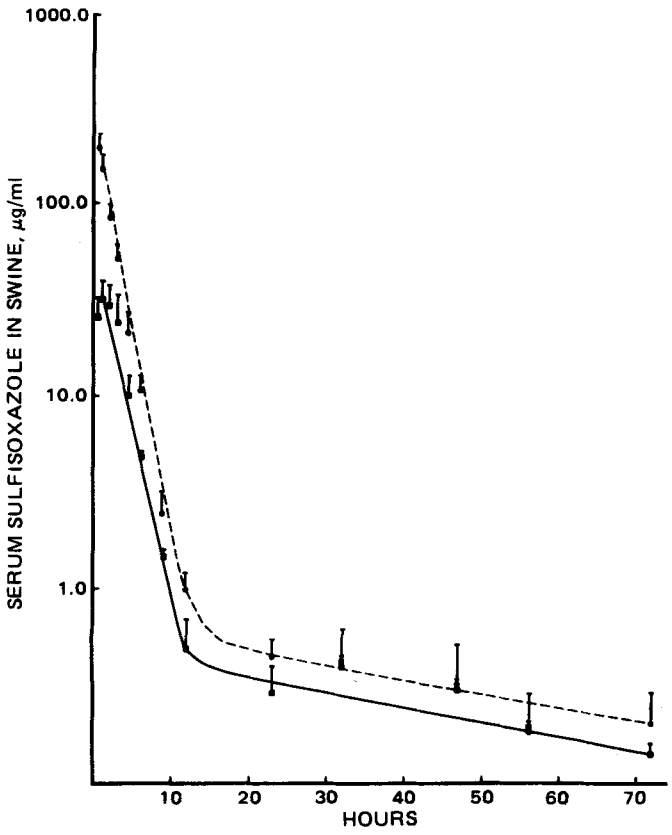


**Figure 2**—*Serum concentrations of unbound, unmetabolized sulfisoxazole (- - -) and sulfisoxazole acetyl (—) in swine.*

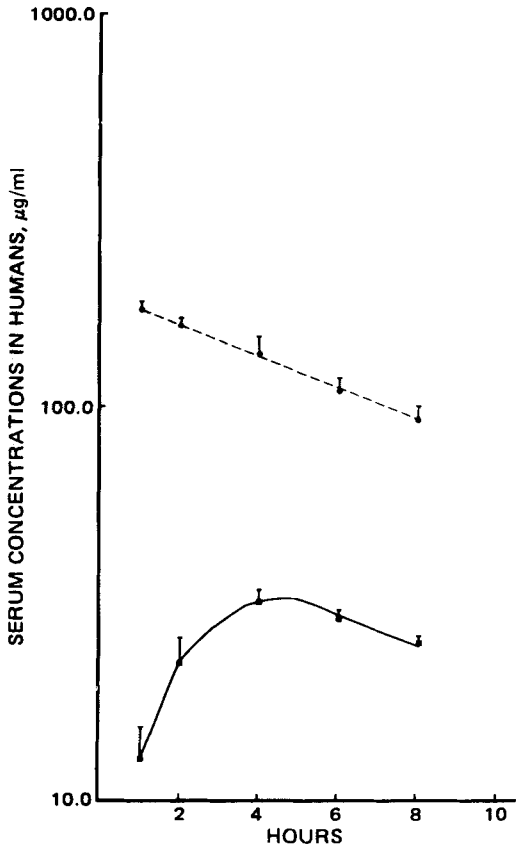


**Figure 3**—*Serum concentrations of unbound, unmetabolized sulfisoxazole (- - -) and sulfisoxazole acetyl (—) in humans.*

Table III—Comparison of the Percentage of Sulfisoxazole Dose Excreted Unchanged in the Urine in Dogs and Pigs in a 4-Day Period

| Hours | Dogs | | Pigs | |
|---|---|---|---|---|
| | Intravenous | Oral | Intravenous | Oral |
| 24 | 39.6 | 26.2 | 16.1 | 15.2 |
| 48 | 41.8 | 29.1 | 18.1 | 17.7 |
| 72 | 42.2 | — | 18.2 | — |
| 96 | — | 29.4 | — | 18.3 |

85% previously reported by Struller (11) but were consistent with the Randall *et al.* (2) report of 25%.

Table IV lists some mean pharmacokinetic parameters of sulfisoxazole in dogs, swine, and humans. Most of these parameters are significantly different from one another among species and can be used to evaluate the pharmacokinetic closeness of one species to another.

## DISCUSSION

The mean volume of the central compartment ($V_1$) was approximately the same in dogs (10.6 liters) and swine (10.5 liters). However, this value may become quite different when expressed in terms of lean body weight because of the much greater fat content in swine. This condition may explain the difference in the extrapolated initial concentration ($C_0$) of 192.0 μg/ml in dogs and 245.5 μg/ml in swine, although both species were given the same total dose. The $V_1$ value in humans was not available from this study; however, it could be derived from the Kaplan *et al.* (6) data as 7.7 liters, ~30% smaller than that of dogs. The $C_0$ was reported as 259.0 μg/ml in humans, a value 30% greater than that of dogs. The discrepancies in $V_1$ and $C_0$ are surprisingly consistent and compensated for each other in dogs and humans. This observation is in agreement with the dog being closer to humans with regard to fat content.

The difference in $C_0$ also can be explained in part by the peripheral volume ($V_2$) of 6.6 and 19.8 liters in dogs and swine, respectively. Humans had a $V_2$ value (8.5 liters) closer to that of dogs. The larger $V_2$ in swine could be due to the greater volume of total body water in young animals (12). Three-month-old swine were used in this experiment to eliminate the large volume of body fat found in adult animals.

The distribution ratio defined as $k_{21}/k_{12}$ was greatest in humans (2.3), followed by dogs (1.6) and swine (0.55), indicating that the drug returned from the peripheral compartment to the central compartment at a faster rate in humans than in swine (Table IV). This result was logically tied to the β-phase half-life of 7.4, 33.7, and 46.4 hr in humans, dogs, and swine, respectively, being in the reverse order to the $k_{21}/k_{12}$ ratio previously discussed. The ratio of $\beta/k_{10}$ (Table IV) was 0.03 in swine and 0.13 in dogs, and it was reported to be 0.66 in humans (6). This is in the same order as $k_{21}/k_{12}$, suggesting that more sulfisoxazole is available for elimination from the postdistributive phase in humans than in dogs and swine. This pattern also correlated reasonably with the β-phase half-life of the drug in these species.

By the end of the 72-hr intravenous trial in dogs, 42.2% of the dose was excreted in the urine as unchanged drug. At the end of 48 and 96 hr after oral administration, 29.1 and 29.4% of the dose were excreted, respectively, indicating that urinary excretion of the drug was complete at 72 hr. Therefore, oral sulfisoxazole bioavailability was determined by comparing the urinary excretion of the drug following these administration routes. Almost 70% of the dose was available to the general circulation after oral administration of the drug as a solution to dogs. The drug bioavailability in swine was determined in the same manner, and a value of almost 100% was obtained (Table IV). Dogs excreted 29.4% of the oral dose compared to 18.3% in swine, yet dogs actually exhibited less

Table IV—Comparison of Mean Pharmacokinetic Constants in Dogs, Swine, and Humans

| Constant[a] | Dogs | Swine | Humans |
|---|---|---|---|
| $k_{21}/k_{12}$ | 1.63 | 0.55 | 2.30[b] |
| $\beta/k$ | 0.13 | 0.03 | 0.66[b] |
| $F$, % | 69.8 | 100.0 | 97.5[b] |
| $r_p$, % | 30–50 | 40–60 | 25–40 |

[a] $F$ = bioavailability; $r_p$ = percent bound. [b] Reference 6.

oral drug absorption. Since both dogs and swine excreted only up to 42.2 and 18.2% of the intravenous dose, respectively, during the trial period, other metabolites probably are present but are not detected by the assay method used. Kaplan *et al.* (6) reported that 52.9% of the dose was excreted as unchanged sulfisoxazole in humans. No urinary data from the present study were available for comparison since the intravenous study was not conducted.

Following oral sulfisoxazole administration to swine and dogs, terminal half-lives deviated significantly from those following intravenous administration in each crossover study, particularly in dogs. This finding may indicate erratic drug absorption in both species, especially in dogs. This erratic absorption may contribute to the incomplete drug absorption in dogs. Different physiology of the GI system also may contribute to the different extent of drug absorption in dogs and swine.

Differences did exist for both α- and β-phase biological half-lives, bioavailability, plasma protein binding, and urinary excretion among all three species. No conclusion can be drawn as to which animal model is pharmacokinetically closer to humans. However, dogs appeared to be a better model than swine for studying the bilirubin toxicity induced by sulfisoxazole administration. The oral dose was responsible for increasing the free, unbound bilirubin in dogs without an increase in total bilirubin. This result did not occur in humans and swine. This topic will be the subject of a separate report.

## REFERENCES


(1) H. J. Florestano, M. E. Bahler, H. R. Blair, and G. R. Burch, *N. Am. Vet.*, **34**, 17 (1953).

(2) L. O. Randall, R. Engelberg, V. Ilieve, M. Row, H. Hoar, and T. H. McGavack, *Antibiot. Chemother.*, **6**, 877 (1954).

(3) P. C. Price and A. E. Hansen, *Tex. Rep. Biol. Med.*, **9**, 764 (1951).

(4) F. A. Svec, P. S. Rhoads, and J. H. Rohr, *Arch. Intern. Med.*, **85**, 83 (1950).

(5) E. H. Louglin and W. G. Mullin, *Antibiot. Chemother.*, **5**, 609 (1955).

(6) S. A. Kaplan, R. E. Weinfield, C. W. Abruzzo, and M. Lewis, *J. Pharm. Sci.*, **61**, 773 (1972).

(7) R. L. Suber and G. T. Edds, *J. Liq. Chromatogr.*, **3**, 257 (1980).

(8) E. G. C. Clarke, "Isolation and Identification of Drugs," Pharmaceutical Press, London, England, 1969, p. 549.

(9) C. M. Metzler, G. L. Elfring, and A. J. McGwen, *Biometrics*, **30**, 562 (Sept. 1974).

(10) B. Testa and P. Jenner, "Drug Metabolism: Chemical and Biochemical Aspects," Dekker, New York, N.Y., 1976, p. 317.

(11) T. H. Struller, *Antibiot. Chemother.*, **14**, 179 (1968).

(12) G. Zbiden, *Adv. Chem. Ser.*, **45**, 25 (1964).


## ACKNOWLEDGMENTS


Supported by Environmental Protection Agency Grant R 804570010.

# Tissue Distribution Studies of [$^{18}$F]Haloperidol, [$^{18}$F]-$\beta$-(4-Fluorobenzoyl)propionic Acid, and [$^{82}$Br]Bromperidol by External Scintigraphy

**G. A. DIGENIS *x, S. H. VINCENT *, C. S. KOOK *, R. E. REIMAN ‡, G. A. RUSS ‡, and R. S. TILBURY ‡**

Received October 1, 1980, from the **Divisions of Medicinal Chemistry and Nuclear Medicine, Colleges of Pharmacy and Medicine, University of Kentucky, Lexington, KY 40506*, and the ‡*Sloan-Kettering Institute for Cancer Research, New York, NY 10021.* Accepted for publication February 12, 1981.

**Abstract** □ Tissue distribution studies of [$^{18}$F]haloperidol and [$^{82}$Br]-bromperidol, two potent neuroleptic drugs, were performed in rats by serial sacrifice. The usefulness of external scintigraphy in obtaining tissue distribution data in large animals is demonstrated by the tissue distribution of [$^{18}$F]haloperidol in rhesus monkeys. Both serial sacrifice and external scintigraphic studies demonstrated that uptake of the two drugs after intravenous administration into their target organ, the brain, was very fast and that the ratio of brain to blood levels was high throughout the 2-hr observation. Bromperidol appeared to reach peak brain levels faster than its chloro analog, haloperidol. Both bromperidol and haloperidol concentrated overwhelmingly in the rat lung. Haloperidol also showed a high affinity for the monkey lung. The disposition pattern in rats of [$^{18}$F]-$\beta$-(4-fluorobenzoyl)propionic acid, an apparent intermediate in butyrophenone metabolism, was entirely different from that of the parent drugs. This metabolite did not concentrate in the rat brain.

**Keyphrases** □ Haloperidol, radiolabeled—tissue distribution studied in rats and rhesus monkeys using external scintigraphy and serial sacrifice □ Bromperidol, radiolabeled—tissue distribution studied in rats and rhesus monkeys using external scintigraphy and serial sacrifice □ Radionuclides—radiolabeled bromperidol and haloperidol, tissue distribution studied in rats and rhesus monkeys using external scintigraphy and serial sacrifice □ Neuroleptic agents—haloperidol and bromperidol, tissue distribution studied in rats and rhesus monkeys using external scintigraphy and serial sacrifice

The increased availability of short-lived radionuclides and radiopharmaceuticals and the growing accessibility of $\gamma$-counting facilities have made external scintigraphy a valuable analytical and diagnostic tool in radiopharmacy and nuclear medicine. Being noninvasive, external scintigraphy is particularly useful for providing information on the disposition of drugs in humans as well as in large mammals where large colonies of isogenic subjects are unavailable. Conventionally, such information is obtained by extrapolation from experimental animal data and measurements of blood and urine levels in humans. Such an approach neglects any inter- or intraspecies difference and assumes that drug levels in the target organ is proportional to blood levels. Unfortunately, this assumption may not be correct with certain neuroleptics of pharmacological interest. Such a discrepancy requires careful consideration, particularly when the dose regimen of a drug has to be adjusted on an individual basis.

External scintigraphic studies using compounds labeled with short-lived radionuclides provide at least a partial answer to this problem since such studies can provide information about tissue levels in humans. Additionally, repeated studies can be done using the same subjects, thus eliminating individual differences. *In vivo* distribution studies with compounds labeled with long-lived radioisotopes such as tritium and carbon 14 suffer from many disadvantages, the main one being that they are often inapplicable to humans.

External scintigraphy is particularly useful for short-term distribution and kinetic studies with compounds that are not metabolized extensively. This is particularly important since one main drawback of external scintigraphy is that it measures total radioactivity levels.

The present study attempted to demonstrate the usefulness of external scintigraphy and short-lived radionuclides as analytical tools in short-term tissue distribution studies of pharmaceutical drugs. Three butyrophenone compounds were chosen: haloperidol (II), $\beta$-(4-fluorobenzoyl)propionic acid (V), and bromperidol (VII).

## BACKGROUND

Butyrophenone neuroleptics are a class of compounds whose blood levels do not necessarily reflect levels in the target organ or therapeutic response. Janssen and Allewijn (1) reported that the neuroleptic activity of haloperidol and several other butyrophenones correlated well with the drug concentrations in the brain but suggested that blood levels need not be related to parameters of interest. Large individual differences also seem to exist in the serum levels attained after butyrophenone administration. Forsman and Ohman (2) examined the steady-state concentration of haloperidol in serum in relation to the daily dose and found up to 10-fold differences between individuals. Zingales (3) reported, in a study of 14 patients, that a patient who gave a poor response to haloperidol therapy always had the highest plasma levels. These and other findings suggest that a simple correlation might not exist between butyrophenone plasma and behavioral changes. Thus, tissue distribution studies should be conducted directly in humans to obtain a correlation between blood levels, brain levels, and central nervous system (CNS) activity.

Haloperidol (II) is the prototype of the butyrophenone neuroleptics and is widely used in the treatment of hypomania, mania, and acute and chronic schizophrenia (4). Bromperidol (VII) is the bromo analog of haloperidol and currently is used in clinical trials. Preliminary reports on its pharmacology indicated that VII may have a faster onset and a longer duration of action (5, 6). Therefore, it seemed of interest to study the tissue distribution patterns of II and VII and to compare the times taken to reach peak levels in the brain, the target organ. The tissue distribution of V, one of their pharmacologically inactive metabolites (7), also was studied and compared to that of II and VII.

Metabolism studies (1) with tritiated butyrophenone neuroleptics have shown that 2 hr after subcutaneous administration, 80% of the radioactivity in the brain of rats is due to intact drug. Hence, during short-term studies, it is expected that metabolites do not contribute significantly to radioactivity levels in the various tissues, particularly the brain.

Neuroleptics II and V were labeled with fluorine 18, whereas VII was labeled with bromine 82.

Fluorine 18 is a pure positron emitter (0.635 Mev, $\beta^+$) with a physical half-life of 110 min. The resulting 511 kev annihilation radiation is detected easily by conventional nuclear medicine instrumentation such as external scintigraphy. Bromine 82 has a longer half-life (35.4 hr), and it decays with the emission of a $\beta$-particle (444 kev maximum energy) followed by several $\gamma$-rays. The principal photon is centered around 777 kev. These high-energy $\gamma$-emissions cause a "shine through" effect that results in distorted scintiphotographs when bromine 82 is used for external scintigraphic studies (8). This problem can be avoided by using bromine 77. Bromine 82 was used for these experiments because it is commercially

0022-3549/81/0900-0985$01.00/0
© 1981, American Pharmaceutical Association

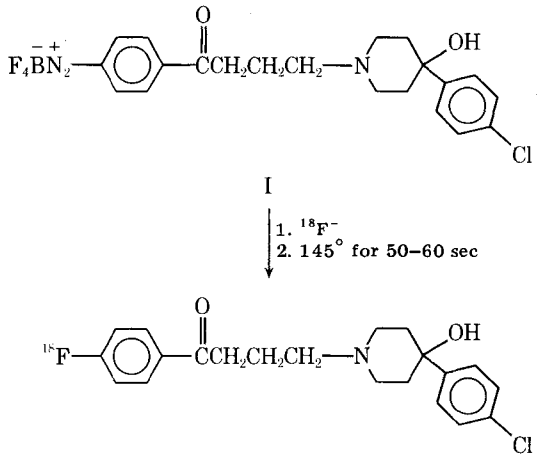


*Scheme I—Principal reaction in the preparation of [$^{18}$F]haloperidol ($^{18}$F-II).*

available. [$^{77}$Br]Bromperidol can be synthesized in the same manner as [$^{82}$Br]bromperidol.

The synthesis of [$^{18}$F]haloperidol and [$^{82}$Br]bromperidol was reported elsewhere (9, 10). The synthesis of $^{18}$F-labeled metabolite V and tissue distribution data of all three compounds in the rat and of [$^{18}$F]haloperidol in the rhesus monkey are reported here.

## EXPERIMENTAL

**Preparation of [$^{18}$F]Haloperidol ($^{18}$F-II)**—Production of the radionuclide fluorine 18, used for the synthesis of $^{18}$F-II, was accomplished by the irradiation of water with 22 Mev helium 3 particles produced by a cyclotron[1].

[$^{18}$F]Haloperidol was prepared from the diazonium tetrafluoroborate salt (I) (Scheme I) according to the previously published procedure (9). The specific activity of the purified product (column chromatography on neutral alumina) was 105 μCi/mg.

**Synthesis of β-(4-Fluorobenzoyl)propionic Acid (V)**—To 1.0 g (5.17 mmoles) of β-(4-aminobenzoyl)propionic acid (III) (11, 12) was added 9.0 ml of 18% HCl (Scheme II). The mixture was stirred vigorously and cooled to 5° in an ice bath. Then lithium tetrafluoroborate (1.59 g) in 3 ml of distilled water was added dropwise, followed by 3.0 ml of 10% $NaNO_2$. The solution was stirred vigorously for 15 min, and no precipitation was formed. The clear solution mixture was frozen in a dry ice–acetone bath and freeze dried for ~2 hr until most of the water was removed. The slurry was filtered through a sintered-glass funnel, cooled in dry ice, and washed with cold water. The brown solid (IV) was freeze dried again *in vacuo*.

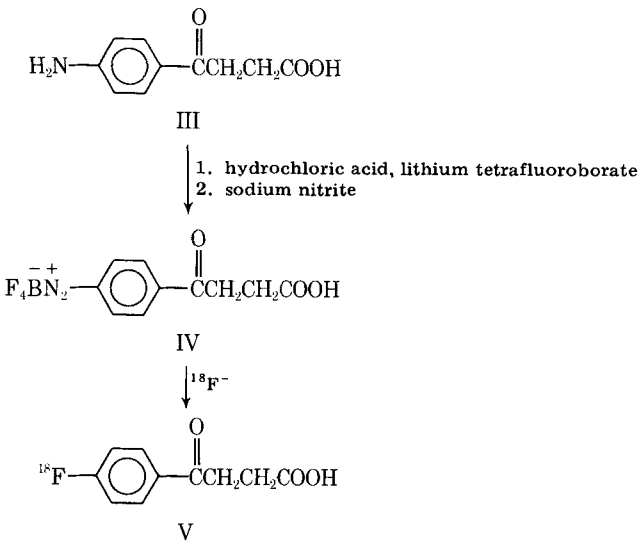


*Scheme II—Synthetic route for the preparation of [$^{18}$F]-β-(4-fluorobenzoyl)propionic acid ($^{18}$F-V).*

[1] Model CS-15, Sloan-Kettering Institute, New York, N.Y.

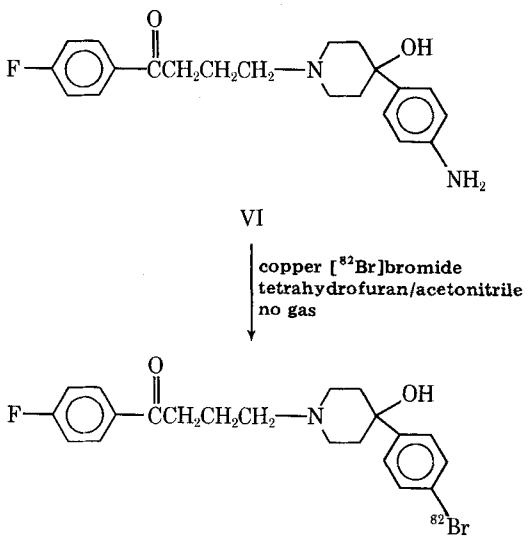


*Scheme III—Principal reaction in the preparation of [$^{82}$Br]bromperidol ($^{82}$Br-VII).*

The dry tetrafluoroborate salt (IV) subsequently was pyrolyzed in xylene–dioxane (3:1) at 145° for 15 min, and the solvent mixture was evaporated on a rotary evaporator to dryness. The dark-brown pyrolysate was then dissolved in 5% aqueous sodium hydroxide. The solution was filtered through a sintered-glass funnel, and the filtrate was acidified with 5% HCl until it was acidic to litmus paper. The acidic solution was then extracted with three 15-ml portions of chloroform. The extracts were combined, dried with sodium sulfate, and evaporated to dryness on the rotary evaporator to yield 0.48 g (47.3% yield) of V, mp 100–105° [lit. (13) mp 102–103°]. The identity of V was proven unequivocally by mixed melting point (100–105°) and comparative spectroscopic determinations (IR and NMR) with authentic V[2].

**Synthesis of [$^{18}$F]-β-(4-Fluorobenzoyl)propionic Acid ($^{18}$F-V)**—Fluorine 18 was produced by the Van de Graaff generator through the $^{20}Ne(d,\alpha) \rightarrow {}^{18}F$ nuclear reaction, at the end of which the glass target insert was washed with 7.5 ml of distilled water. The volume of the water was reduced to ~1 ml by heating at 110° and by blowing nitrogen gas into the solution. To the aqueous solution containing 17.2 mCi of fluorine 18 were added 50 mg of the diazonium salt (IV) and 2.0 ml of acetone. After standing for 5 min, the solvents were removed on the rotary evaporator at 50°. The residue was dried further in the freeze drier for 30 min, and the dried salt subsequently was pyrolyzed in xylene–dioxane (3:1) as already described.

The dark pyrolysate was dissolved in 5% NaOH, the solution was filtered, and the filtrate was acidified with 5% HCl. The acidic solution then was extracted with three 5-ml portions of chloroform. The extracts were combined, dried with sodium sulfate, and evaporated to dryness. The residue was washed with ether to yield 24.5 mg (123.2 μCi) of $^{18}$F-V. A radioscan of the thin-layer chromatogram of the product, developed in chloroform–cyclohexane–acetic acid (20:80:10) using a silica gel plate, showed that all activity was coincident with the spot of known V. The incorporation of fluorine 18 into the final product (V) was calculated to be 2.95%. The specific activity was 5.03 μCi/mg.

**Preparation of [$^{82}$Br]Bromperidol ($^{82}$Br-VII)**—[$^{82}$Br]Bromperidol was prepared from the aminoperidol VI according to the previously published procedure (10) (Scheme III). Copper(II) [$^{82}$Br]bromide was prepared *in situ* from potassium [$^{82}$Br]bromide obtained commercially[3]. The specific activity of the purified product (column chromatography on neutral alumina) was 440 μCi/mg.

***In Vivo* Distribution Studies**—*Animals*—Two mature healthy male rhesus monkeys and several male Sprague–Dawley rats, 300–500 g, were used. Monkeys A and B weighed 8.6 and 6.4 kg, respectively. The animals were allowed free access to food and water until the time of the experi-

[2] Aldrich Chemical Co., Milwaukee, Wis.
[3] New England Nuclear, Boston, Mass.

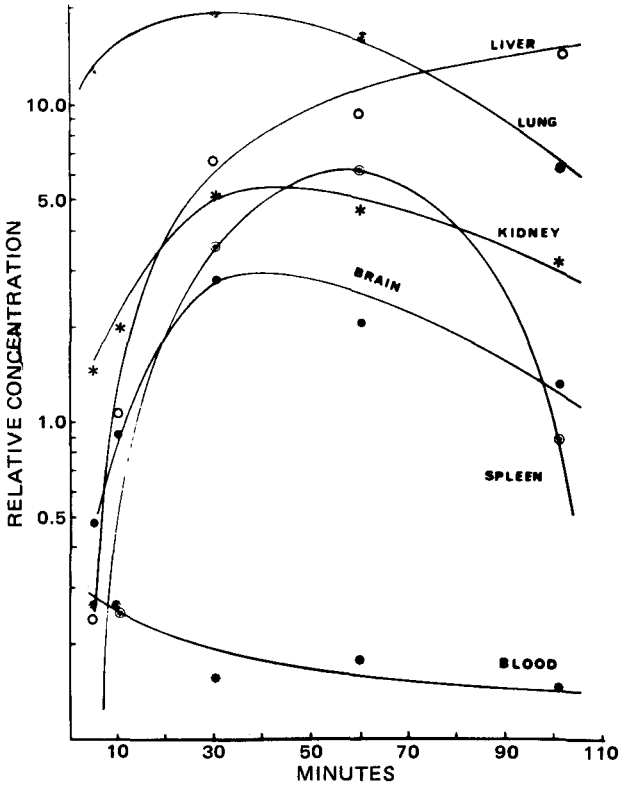


**Figure 1**—*Distribution of radioactivity following intravenous injection of [$^{18}$F]haloperidol (0.01 mg/kg, 0.8–0.9 μCi) in vital organs of the rat as a function of time. Each point represents average values from two rats. Relative concentration as defined by Woodard* et al. *(14) is: (counts of radioactivity in an organ/total radioactivity dose) × (weight of animal/weight of organ).*

ment. The monkeys were anesthetized with phencyclidine, and the rats were anesthetized with pentobarbital sodium solution.

*Dose and Route of Administration*—Solutions of [$^{18}$F]haloperidol ($^{18}$F-II), $^{18}$F-V and [$^{82}$Br]bromperidol ($^{82}$Br-VII) were prepared immediately after their synthesis. Both $^{18}$F-II and $^{82}$Br-VII were dissolved in an appropriate volume of solvent mixture containing propylene glycol, ethanol, and water at pH 4, and $^{18}$F-V was dissolved in the same solvent mixture at neutral pH. An aliquot of each solution was counted to determine the exact dose of radioactivity administered to the animals.

Monkey A was used for three rectilinear scans and received 0.52 mg of $^{18}$F-II/kg (300 μCi) in the left femoral vein. Monkey B was used for

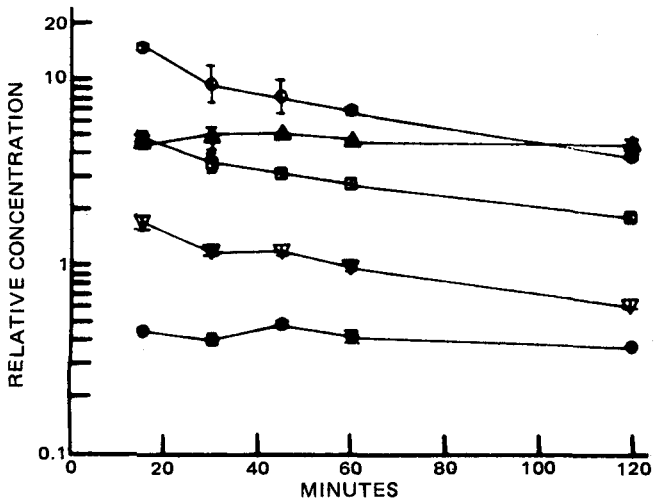


**Figure 2**—*Distribution of radioactivity following intravenous injection of [$^{82}$Br]bromperidol (0.2 mg/kg, 19–22 μCi) in various organs of the rat as a function of time. Each point represents average values in lungs (○), liver (▲), kidneys (□), brain (▽), and blood (●) from five rats.*

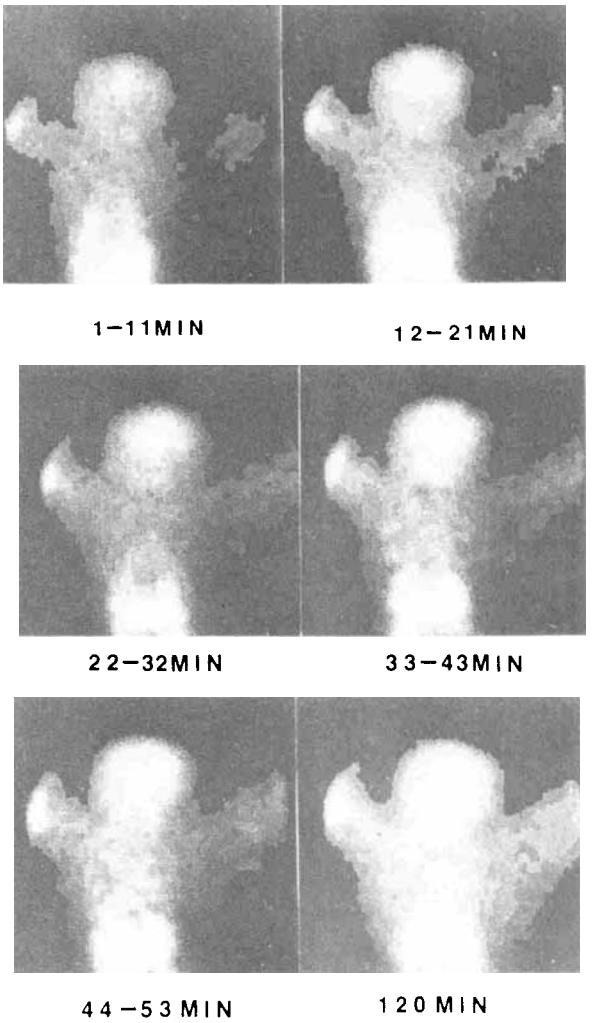


**Figure 3**—*Sequential computer-analyzed displays following intravenous injection of [$^{18}$F]haloperidol to a monkey, illustrating activity concentration in the brain and lung as a function of time.*

γ-camera scannings and received 1.05 mg of $^{18}$F-II/kg (200 μCi). The rats received 0.01 mg of $^{18}$F-II/kg (0.8–0.9 μCi), 0.01 mg of $^{18}$F-V/kg (0.02–0.04 μCi), or 0.2 mg of $^{82}$Br-VII/kg (19–22 μCi).

**Tissue Distribution Studies**—Following drug administration, the rats were sacrificed at various time intervals; a blood sample was withdrawn, followed by removal of the various organs. The samples were counted in a scintillation well-counter and corrected for decay. Radionuclide concentrations in the various organs were expressed by the relative retention method of Woodard *et al.* (14). Relative retention is defined as: (counts of radioactivity in an organ/total radioactivity dose) × (weight of animal/weight of organ). A high-energy γ-scanner was used for the rectilinear scans of Monkey A. The scans were performed 22, 82, and 142 min postinjection. Monkey B was used for the kinetic isotope distribution study with a γ-camera[4] (15).

## RESULTS

The distribution of $^{18}$F-II, $^{18}$F-V, and $^{82}$Br-VII in the vital organs of the rat as a function of time was determined by serial sacrifice of the animals. Figure 1 shows concentrations of fluorine 18 radioactivity (expressed as relative concentration) in various rat organs as a function of time after intravenous administration of $^{18}$F-II. A similar plot for the bromine 82 concentrations obtained after intravenous administration of $^{82}$Br-VII is shown in Fig. 2. The uptake of both II and VII into the target organ (brain) was very rapid. The bromine 82 concentration in the brain was already declining 15 min after administration, whereas the fluorine 18 concentration reached maximum levels 30 min after administration. Both II and VII were found to concentrate overwhelmingly in

[4] Total organ kinetic imaging monitor, TOKIM.

**Table I—Tissue Distribution of [$^{18}$F]Haloperidol ($^{18}$F-II) at Various Time Intervals in Monkey A [a]**

| Organ | Percent Activity | | |
|---|---|---|---|
| | 22 min | 82 min | 142 min |
| Brain | 2.3 | 2.7 | 2.2 |
| Lungs | 5.2 | 5.2 | 3.2 |
| Liver | 12.4 | 9.9 | 7.3 |
| Kidneys | 8.0 | 5.9 | 6.6 |

[a] Values represent percent activity in different areas (rectilinear scanning) over Monkey A. Loading dose was 0.52 mg/kg iv (300 μCi).

the lungs (Figs. 1 and 2, respectively), possibly due to their high lipophilicity. Their uptake by the liver also was very fast and continued throughout the observation period. Their blood levels, however, were relatively constant and much lower than the levels in the other organs. These data are in excellent agreement with those of Lewi *et al.* (16) who did experiments in rats with [$^{3}$H]haloperidol.

External imaging for the distribution of $^{18}$F-II in the monkey was accomplished using the γ-camera (15). Figure 3 shows sequential computer-analyzed displays obtained after intravenous administration of $^{18}$F-II. The results of the dynamic study are presented in Fig. 4. The uptake of II in the monkey lung was extremely rapid and reached a maximum level in the first 13 min. The initial uptake rate in the brain during this period also was fast. Between 10 and 20 min postinjection, the activity in the lungs did not change appreciably while that in the brain increased. After 20 min, the activity in the lung appeared to decrease (Fig. 4); a sharp decrease of activity was noted between 30 and 60 min. In contrast, however, the activity in the brain of the monkey did not change significantly over the same time interval. After 2 hr, the concentration of the drug and its metabolites was considerably decreased in the monkey lungs but remained at high levels in the brain (Fig. 3). In this connection, Janssen and Allewijn (1) showed that ~80% of the intact drug and 20% of its metabolites could be detected in the brain of the rat 2 hr after subcutaneous injection.

To obtain more information on the distribution of $^{18}$F-II, three rectilinear scans were performed on Monkey A at 22, 82, and 142 min postinjection with the high-energy γ-scanner. Areas on the scan images corresponding to brain, lungs, liver, and kidneys were analyzed for activity

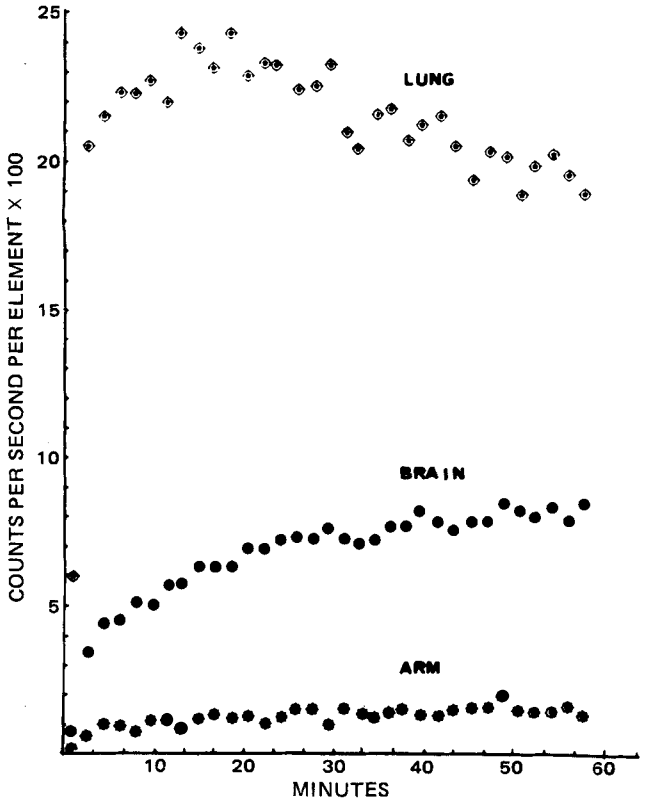


**Figure 4**—*Relative counts per second of [$^{18}$F]haloperidol (31.3 μCi/kg) in observed fields (head, lung, and arm) on Monkey B, obtained with the total organ kinetic imaging monitor technique (15).*

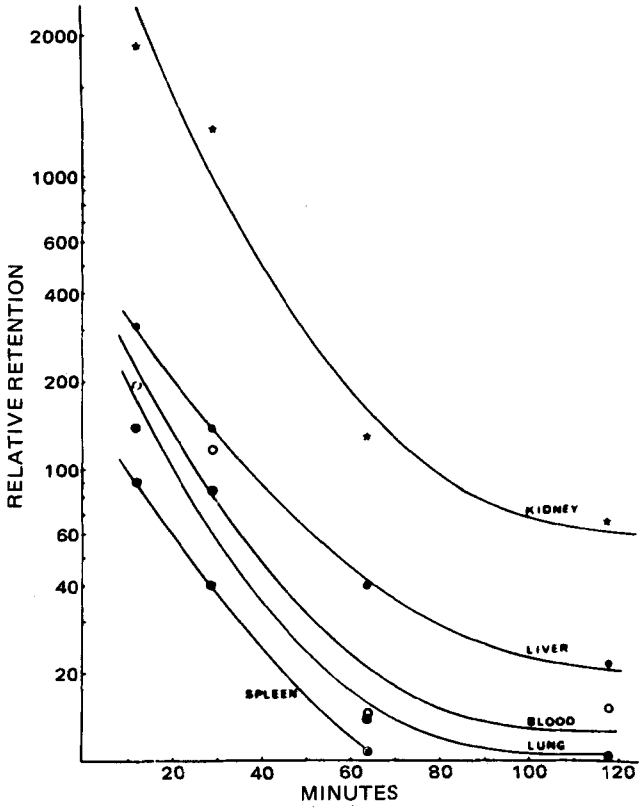


**Figure 5**—*Distribution of $^{18}$F-V (0.01 mg/kg, total radioactivity dose 2–4 × $10^{-2}$ μCi) in vital organs of the rat as a function of time. Each point represents average values from two rats.*

content by computer techniques. The percentage of the injected dose in each area was obtained by dividing the total counts in the selected areas by the counts from the whole body of the monkey. From Table I, it can be seen that the brain uptake of II in Monkey A approached near maximum level in 22 min and remained fairly constant with time. These results are consistent with those obtained with Monkey B utilizing kinetic imaging (Fig. 4). The activity in the lungs and liver reached a maximum within 22 min. After 82 min, the activity in these sites started to decrease. Here again, the results obtained with the scanner on Monkey A paralleled those obtained by imaging on Monkey B. From the computer printouts, it was estimated that ~34.6% of the total radioactive dose could be detected in the bladder of Monkey A 82 min after injection; 44.6% was found after 142 min.

The metabolite of II (V), which was synthesized utilizing a Schiemann-type reaction (Scheme II), was injected into rats. The rats were sacrificed at different times as in the distribution study of II. Each organ was assayed in the scintillation well-counter, and the counts were corrected for decay. The relative concentration of radioactivity in vital organs was calculated according to the method of Woodard *et al.* (14). From Fig. 5, it can be seen that a sharp drop in plasma levels was observed over a 1-hr period following intravenous injection of $^{18}$F-V, indicating a very fast distribution phase. The brain uptake was negligible, and the excretion rate from the kidney was very rapid. Elimination of V from the liver also was rapid.

## DISCUSSION

An attempt was made to demonstrate the usefulness of short-lived radioisotopes coupled with serial sacrifice and/or external scintigraphy in obtaining short-term distribution pharmacokinetic data. The tissue distribution of two butyrophenone neuroleptics and one of their metabolites in rats and monkeys was compared. The main emphasis was on the levels of these compounds in the target organ, the brain. As already discussed, brain levels are the apparent parameter of interest in butyrophenone therapy; in humans, these levels can only be measured using external scintigraphy.

The uptake of haloperidol (II) and bromperidol (VII) by rat brain was faster than the uptake of II by monkey brain. However, the uptake was relatively fast in both animals, with the monkey brain showing an ap-

parent slow but continuous accumulation of fluorine 18 radioactivity. The pattern observed in the monkey was quite similar to that reported for barbiturates and antipyrine (17). Unlike these compounds, however, II and VII exhibited very high brain to blood levels. These results seem to correlate well with the fast onset and prolonged duration of neuroleptic effects of II and VII. It is assumed that during the initial portion of the observation period, radioactivity levels reflect concentrations of intact drug. Literature data (1) indicate that this assumption is valid.

Data obtained in the rat seem to indicate that VII may enter the brain at a faster rate than II. This finding apparently is in agreement with the pharmacological observation that VII has a faster onset of action than II (5, 6). However, the dose of $^{82}$Br-VII administered to rats was much larger than that of $^{18}$F-II. Hence, the observed difference in the profiles of the brain levels of the two drugs also could be attributed to dose-dependent kinetics. Lewi *et al.* (16) obtained data that indicate that early uptake of II into the brain may be proportional to the administered dose. Studies involving brain uptake and dose-dependent kinetics of $^{18}$F-II and $^{82}$Br-VII utilizing external scintigraphy are in progress.

Compound V is an important intermediate in the metabolism of butyrophenone neuroleptics (7). It is believed to be the first metabolite formed during the oxidative *N*-dealkylation of these compounds. Compound V had negligible brain uptake and was eliminated rapidly from the liver and kidney after intravenous administration to rats (Fig. 5). However, this and subsequent metabolites accounted for ~20% of the radioactivity found in the brain of rats 2 hr after subcutaneous administration of $^{3}$H-II (1). Since V apparently is not partitioned into the brain, one may conclude from these findings that the metabolism of II and other butyrophenones may occur within the brain. If only the disappearance of radioactivity from the blood was followed, the relatively fast redistribution of V among the various tissues would be missed. External scintigraphy is a much more effective technique for following the tissue distribution of V since it allows continuous accumulation of data from the beginning of an experiment.

It is known that fluoride ions can replace the hydroxyl groups in hydroxyapatite crystals. Since the resulting fluoroapatite is more stable than hydroxyapatite, most fluoride ions administered to an animal concentrate in its skeleton. The present external scintigraphic studies with the monkey showed no accumulation of radioactivity in the area of the pelvis and knees. These anatomical areas were found to be regions of high free fluoride concentrations in rabbits (18). These data indicated that no $^{18}$F-labeled free fluoride was produced *in vivo* as a result of $^{18}$F-II administration. This finding strongly suggests that the carbon–fluorine 18 bond of the drug was not affected by its metabolism, a fact that is conversant with its high bond strength. Although the carbon–bromine bond is weaker than the carbon–fluorine bond, it is also believed that, during these experiments, there was no loss of bromine 82 from the aromatic ring of $^{82}$Br-VII as the bromide ion. This assumption was substantiated by Sargent *et al.* (8) who found that only 5% of the radioactivity excreted in the urine over 24 hr was due to inorganic bromide following the administration of [4-$^{82}$Br]bromodimethylphenylisopropylamine to human subjects.

## REFERENCES


(1) P. A. J. Janssen and F. T. Allewijn, *Arzneim.-Forsch.*, **19,** 199 (1969).

(2) A. Forsman and R. Ohman, *Nord. Psykiatr. Tidsskr.*, **28,** 441 (1974).

(3) I. A. Zingales, *J. Chromatogr.*, **54,** 15 (1971).

(4) C. J. E. Niemegeers and P. M. Laduron, *Proc. R. Soc. Med.*, **69,** Suppl. 1 (1976).

(5) C. J. E. Niemegeers and P. A. J. Janssen, *Arzneim.-Forsch.*, **24,** 45 (1974).

(6) W. Poldinger, E. Bures, and H. Haage, *Int. Pharmacopsychiatry*, **12,** 184 (1977).

(7) W. Soudijn, I. Van Wijngaarden, and F. Allewijn, *Eur. J. Pharmacol.*, **1,** 47 (1967).

(8) T. Sargent, D. A. Kalbhen, A. T. Shulgin, G. Braun, H. Stauffer, and N. Kusubov, *Neuropharmacology*, **14,** 165 (1975).

(9) C. S. Kook, M. F. Freed, and G. A. Digenis, *J. Med. Chem.*, **18,** 533 (1975).

(10) S. H. Vincent, M. B. Shambhu, and G. A. Digenis, *ibid.*, **23,** 75 (1980).

(11) J. P. Englis, R. C. Clapp, Q. P. Cole, and J. Krapcho, *J. Am. Chem. Soc.*, **67,** 2263 (1945).

(12) C. K. Chuang and Y. T. Huang, *Chem. Ber.*, **69B,** 1505 (1936).

(13) L. F. Fieser, E. Berliner, F. J. Bondhus, F. C. Chang, W. G. Dauben, M. G. Ettlinger, G. Fawaz, M. Fields, C. Heidelberger, H. Heymann, W. R. Vaughan, A. G. Wilson, E. Wilson, M. Wu, M. T. Leffler, K. E. Hamlin, E. J. Matson, E. E. Moore, M. B. Moore, and H. E. Zaugg, *J. Am. Chem. Soc.*, **70,** 3197 (1948).

(14) H. Q. Woodard, R. E. Bigler, and B. Freed, *J. Nucl. Med.*, **16,** 958 (1975).

(15) G. W. Monahan, W. J. Beattie, and J. S. Laughlin, *Phys. Med. Biol.*, **17,** 503 (1972).

(16) P. J. Lewi, J. J. P. Heykants, F. T. N. Allewijn, J. G. H. Dony, and P. A. J. Janssen, *Arzneim.-Forsch.*, **20,** 943 (1970).

(17) B. N. Ladu, H. G. Mandel, and E. L. Way, "Fundamentals of Drug Metabolism and Drug Disposition," Williams & Wilkins, Baltimore, Md., 1971, p. 83.

(18) A. Costeas, H. Q. Woodard, and J. S. Laughlin, *J. Nucl. Med.*, **11,** 43 (1970).


## ACKNOWLEDGMENTS


Supported in part by National Institute of Mental Health Grant 5RO1 MH31577-02.

The encouragement of Dr. John S. Laughlin of the Biophysics Laboratory, Sloan-Kettering Cancer Institute, is gratefully acknowledged.

# Radioimmunoassay of Carteolol in Human Plasma

**SOU-YIE CHU *x, SERGIO M. VEGA *, AKHTAR ALI ‡, and LAWRENCE T. SENNELLO ***

Received July 7, 1980, from the **Drug Metabolism Department and the* ‡*Radio-Labeling Service Department, Abbott Laboratories, North Chicago, IL 60064.* Accepted for publication February 12, 1981.

**Abstract** □ A radioimmunoassay for the direct measurement of carteolol, a new β-adrenoreceptor blocker, in human plasma was developed. Carteolol was acylated to form *O*-glutarylcarteolol, which was conjugated to bovine serum albumin to provide the immunogen. Antibody to carteolol was raised in New Zealand albino rabbits. The tracer was the radioiodinated derivative of *O*-glutarylcarteolol–tyrosine methyl ester conjugate. The method is highly sensitive, with a lower quantifiable concentration of ~0.4 ng of carteolol/ml using 0.1 ml of plasma, and has good specificity, with the major metabolite (8-hydroxycarteolol) showing only 0.2% cross-reactivity. It is reproducible, with relative standard deviations from triplicate standard curves being mostly within ±8%. The method is currently being used to monitor carteolol levels in clinical samples.

**Keyphrases** □ Radioimmunoassay—determination of carteolol in human plasma □ Carteolol—determination by radioimmunoassay, human plasma □ Antiadrenergics—carteolol, determination by radioimmunoassay, human plasma

Carteolol hydrochloride[1], 5-[3-(*tert*-butylamino)-2-hydroxypropoxy]-3,4-dihydrocarbostyril monohydrochloride, is a β-adrenoreceptor blocker currently under development as a candidate drug. A simple and sensitive fluorometric method was reported (1, 2) for the determination of its concentration in biological fluids. The lower quantifiable concentration was ~20 ng of carteolol (free base)/ml using 2 ml of plasma. This sensitivity is inadequate, especially for pharmacokinetic studies at anticipated therapeutic doses (*e.g.*, <20 mg qid). To provide the needed sensitivity, development of a radioimmunoassay for carteolol was undertaken. Antibody to carteolol was raised in rabbits by immunizing the animals with an immunogen prepared by covalently incorporating carteolol into bovine serum albumin. Radioimmunoassay using this antibody offered great sensitivity and specificity for the measurement of carteolol in plasma.

## EXPERIMENTAL

**Chemicals and Materials**—Commercial reagent grade solvents and chemicals were used. Chloramine-T solution (2.5 mg/ml) was prepared in 0.05 *M* phosphate buffer (pH 7.5). A 3.5-mg/ml solution of sodium metabisulfite also was prepared in the same buffer. The phosphate-buffered saline (saline buffer) was composed of 0.15 *M* NaCl and 0.01 *M* $NaH_2PO_4$–$K_2HPO_4$, pH 7.4.

**Chromatographic Analysis**—TLC was conducted using analytical (250 μm thick) and preparative (1000 μm) silica gel plates. The solvent system was usually ethyl acetate or chloroform–ethanol (2:1 v/v).

High-pressure liquid chromatographic (HPLC) separations were carried out using ion-pair or soap chromatography on reversed-phase columns[2]. The eluent for soap chromatography (soap eluent) was composed of 45% (v/v) acetonitrile, 0.02 *M* phosphoric acid, 0.02 *M* monobasic ammonium phosphate, and 0.15% (w/v) sodium lauryl sulfate. The typical ion-pair eluent was composed of 20% (v/v) acetonitrile, 10% tetrahydrofuran, 10% methanol, and 0.005 *M* *d*-camphorsulfonic acid. Preparative HPLC was conducted using a μBondapak $C_{18}$ column[3] (7.8 mm i.d.)

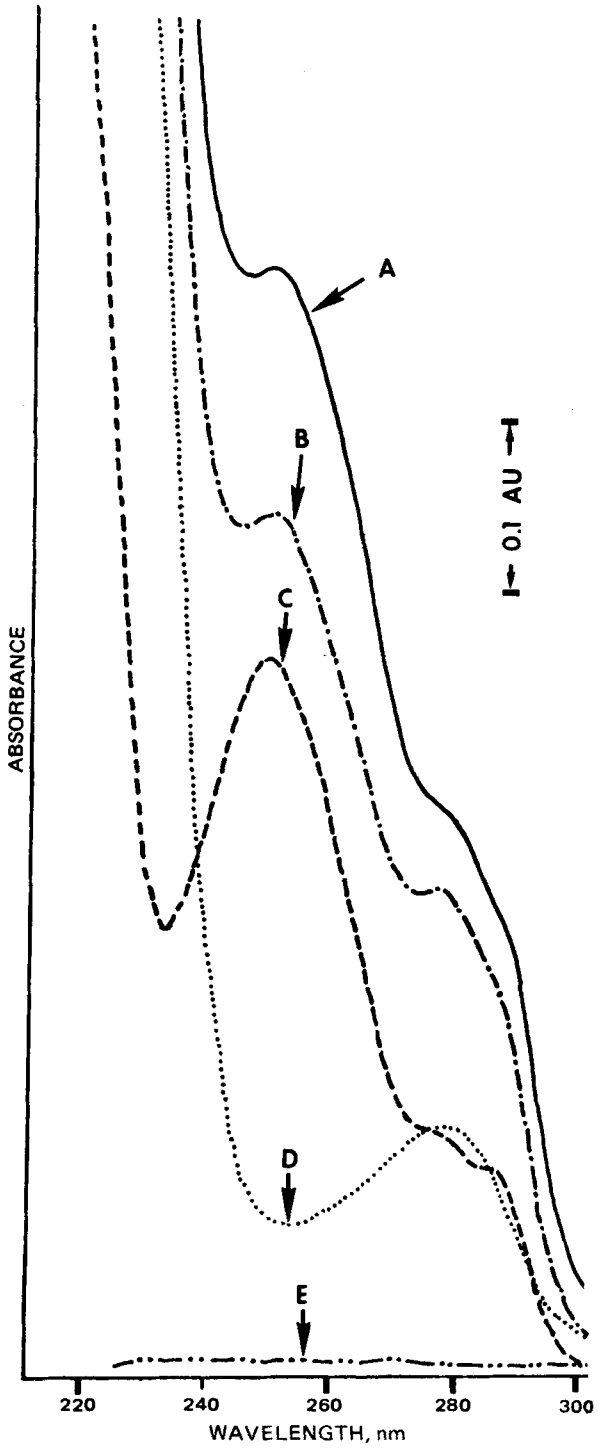


**Figure 1**—*UV absorption spectra of carteolol immunogen (A), mixture of I (20.6 μg/ml) and bovine serum albumin (242 μg/ml) (B), I (20.6 μg/ml) (C), bovine serum albumin (242 μg/ml) (D), and 0.05* M *tromethamine (pH 8.5) as background (E).*

[1] Abbott Laboratories, North Chicago, Ill.

[2] Zorbax C-8 (DuPont, Wilmington, Del.) or Spherisorb 5-μm ODS (Spectra-Physics, Santa Clara, Calif.).

[3] Waters Associates, Milford, Mass.



*0022-3549/81/0900-0990$01.00/0*
*© 1981, American Pharmaceutical Association*

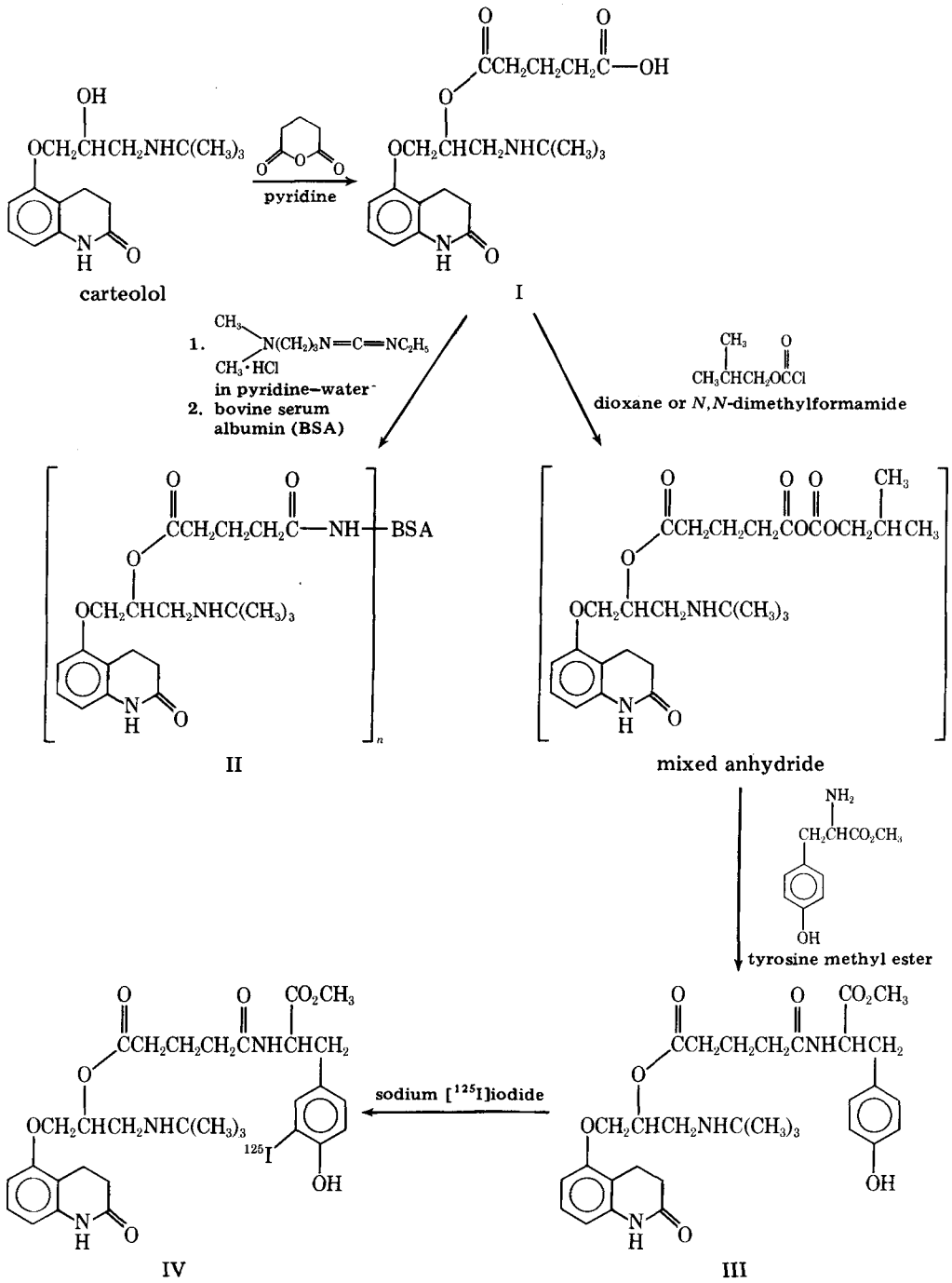


*Scheme I—Procedure for the preparation of carteolol immunogen and radioactive tracer.*

with an eluent of 18% (v/v) acetonitrile, 8% (v/v) tetrahydrofuran, and 0.005 *M* *d*-camphorsulfonic acid. Detection was accomplished by monitoring absorption at 254 nm.

**Preparation of Immunogen**—Scheme I shows the procedure for preparation of the immunogen and the radioactive tracer.

*Synthesis of* O-*Glutarylcarteolol (I)*—Carteolol (450 mg) and 210 mg of glutaric anhydride were dissolved in 7 ml of pyridine. The solution was allowed to stand overnight at room temperature and then was heated at 60° for 3 hr. The solvent was removed under reduced pressure on a rotary evaporator, and the residue was recrystallized from a mixture of ethanol and ethyl acetate. The product, after being air dried, was a colorless solid, mp 184–186°. The yield was 414 mg (66% of theory). The IR spectrum (potassium bromide pellet) showed a strong absorption band at 1740 $cm^{-1}$ (carbonyl absorption for carboxylic acid ester), indicating ester formation. The mass spectral data obtained using a direct-insert probe and electron-bombardment ionization gave the following major ions: *m/z* (ion, % relative abundance), 406.1 ($M^+$, 7.5), 391.0 (M − $CH_3$, 25.6), and 86.1 [$CH_2NHC(CH_3)_3$, 100]. PMR spectral data also were consistent with the proposed structure.

*Anal.*—Calc. for $C_{21}H_{30}N_2O_6$: C, 62.05; H, 7.44; N, 6.89. Found: C, 61.67; H, 7.68; N, 6.69.

*Preparation of Carteolol–Bovine Serum Albumin Conjugate (II)*—*O*-Glutarylcarteolol (200 mg) was dissolved in 4.0 ml of pyridine–water (1:1 v/v) with stirring. To the solution was added 240 mg of 1-ethyl-3-(3-dimethylaminopropyl)carbodiimide hydrochloride, and the mixture was stirred at room temperature for 30 min. A solution of 140 mg of bovine serum albumin in 5 ml of water then was added, and the mixture was stirred overnight.

The product was dialyzed in a cold room (~4°) against 2000 ml of saline buffer containing 5% (v/v) of dioxane and then twice against 2000 ml of water. A 0.50-ml aliquot of the dialyzed solution (~37 ml) was mixed with 1.5 ml of acetonitrile and subjected to HPLC analysis using the described soap eluent. The results showed no free I (< ~0.4 μg/ml) in the dialyzed solution. Another 0.5-ml aliquot was diluted 1:10 with 0.05 *M* trometh-

**Table I—Competition with Radioiodinated Carteolol Antigen for Antibody Binding Sites**

| Compound | Estimated $ID_{50}$, pg |
|---|---|
| Carteolol | 370 |
| Dehydrocarteolol | $25 \times 10^3$ |
| 8-Hydroxycarteolol | $230 \times 10^3$ |
| Isoproterenol | $>500 \times 10^3$ |
| 5-Hydroxy-3,4-dihydrocarbostyril | $>500 \times 10^3$ |
| Propranolol | No inhibition at $1 \times 10^6$ |

amine[4] and analyzed by UV spectrophotometry. The conjugated product had a UV spectrum (Fig. 1) nearly identical to that of a mixture of bovine serum albumin and I, showing an absorption maximum at 252 nm (similar to the carteolol derivative) and a shoulder at 278 nm (the absorption maximum for bovine serum albumin). It was estimated to contain an average of ~19 carteolol residues/bovine serum albumin molecule based on UV absorption data.

The remaining product solution was lyophilized to give 152.5 mg of white fluffy product, which was used for the immunization of rabbits.

**Preparation of $^{125}$I-Labeled Antigen**—*Preparation of O-Glutarylcarteolol-Tyrosine Methyl Ester Conjugate (III)*—*O*-Glutarylcarteolol (163 mg) was dissolved in 6 ml of hot *N,N*-dimethylformamide, and the solution was cooled in an ice water bath. To the chilled solution were added 100 μl of triethylamine and 80 μl of isobutyl chlorocarbonate. The mixture was stirred briefly on a vortex mixer and then allowed to stand in an ice water bath for 30 min with occasional stirring. To the reaction mixture was added a solution of 160 mg of tyrosine methyl ester in 4 ml of *N,N*-dimethylformamide, and the mixture was stirred briefly and allowed to stand at room temperature for ~2 hr. The solution then was evaporated to dryness, and the residue was dissolved in 2 ml of the described preparative HPLC eluent. Aliquots (~200 μl each) were chromatographed on a μBondapak $C_{18}$ column, and the fractions corresponding to the major UV-absorbing component were collected and used directly for subsequent radioiodination. The concentration of the product was estimated by comparison of its UV absorption at 252 nm to that of standard carteolol solutions (assuming approximately equal molar absorptivities for both compounds).

*Preparation of [$^{125}$I]-O-Glutarylcarteolol-Tyrosine Methyl Ester (IV)*—The procedure was similar to that described previously (3). In a disposable test tube were placed 10 μl of the III solution (~7.1 μg), 25 μl of 0.5 *M* phosphate buffer (pH 7.5), and 17 μl of sodium [$^{125}$I]iodide solution (4.0 mCi). To the solution was added 20 μl of chloramine-T solution, and the mixture was stirred for 60 sec. The reaction was terminated by the addition of 20 μl of sodium metabisulfite, and the solution was extracted with ethyl acetate (2 × 1.0 ml). The ethyl acetate solution (~95% total radioactivity) then was fractionated[5] with an eluent of 0.1% (v/v) acetic acid in ethanol. The effluent was collected in 1-ml fractions (Fig. 2). The peak fractions of the major radioactive component were pooled (1–2 mCi) and used in the radioimmunoassay. The radiochemical purity of this material was ~87% based on TLC and HPLC analyses. The compound was ~100% bound by the carteolol antiserum at a 1:200 dilution.

**Immunization**—New Zealand albino rabbits were used. A solution of II was prepared fresh in physiological saline at a concentration of 1 mg/ml and mixed thoroughly with an equal volume of Freund's complete adjuvant. One milliliter of the emulsion containing 0.5 mg of immunogen was injected into four footpads and two thighs of each rabbit. Each rabbit was immunized once a week for 4 weeks and then once every 2–6 weeks. Blood was obtained by cardiac puncture 6–14 days after the booster injections, allowed to clot overnight at 4°, and centrifuged at 2000 rpm for 20 min to yield the antiserum.

**Immunoassay Procedures**—*Preparation of Reagents*—The gelatin buffer used was saline buffer containing 0.1 mg of thimerosal/ml and 0.1% (w/v) pigskin gelatin. The radioactive tracer (usually with total radioactivity of ~1.5 mCi) was diluted to 100 ml with 0.002 *M* $H_3PO_4$ to form a stock solution, and the solution was refrigerated until used. A working solution of the tracer was prepared weekly by proper dilution (usually 1:100) of the stock solution with 0.002 *M* $H_3PO_4$.

A stock solution of carteolol standard was prepared at 1.0 mg/ml in distilled water, which was diluted 1:100 with gelatin buffer to form a working standard at 10 μg/ml. This latter solution was used to spike blank plasma. Typically, the working standard of carteolol was diluted 1:100 with blank plasma to give a plasma standard at 100 ng/ml, and this plasma sample then was diluted serially 1:2 with blank plasma to provide a set of plasma standards.

[4] J. T. Baker Chemical Co., Phillipsburg, N.J.

[5] A 1 × 17-cm Sephadex LH-20 column.

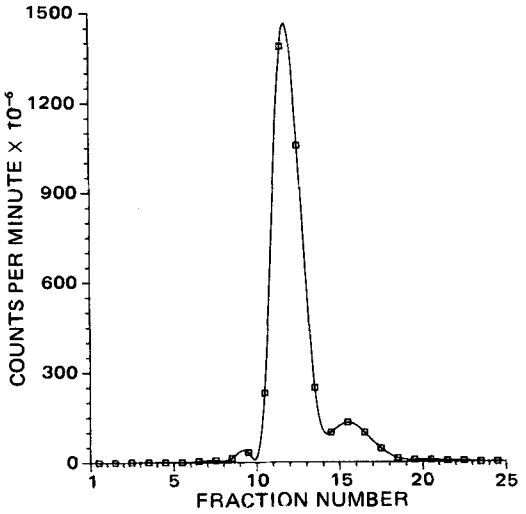


**Figure 2**—*Elution pattern of the radioiodination products on Sephadex LH-20 column. Fractions 12 and 13 were pooled and used as tracer in the radioimmunoassay.*

The antiserum from rabbits was diluted 1:4000 with gelatin buffer. An 18% (w/v) solution of polyethylene glycol 6000 in saline buffer was used to precipitate antibody-bound radioactivity.

*Assay*—A 100-μl aliquot of the diluted antiserum solution was added to 100 μl of plasma and 200 μl of gelatin buffer, followed by the addition of 100 μl of the tracer solution. The mixture was allowed to stand at ~4° overnight. To each sample was added 1.5 ml of polyethylene glycol 6000 solution, and the mixture was stirred briefly. The samples were centrifuged at 2500×*g* for 30 min at ~5°, and the supernate was decanted. The precipitate was mixed again with 1.5 ml of polyethylene glycol 6000 solution and centrifuged. After the supernate was decanted, the remainder was counted in a γ-counter.

A set of standard plasma samples was prepared in the concentration range to suit the intended analysis. A typical set included standards at 0, 0.17, 0.35, 0.69, 1.39, 2.77, 5.56, 11.11, 22.23, 44.46, and 88.91 ng/ml. These standards were carried through the radioimmunoassay in triplicate. The observed radioactivity counts (*B*) were divided by the counts from control plasma ($B_0$). A calibration curve was constructed using the mean ratios of $B/B_0$ *versus* the logarithms of plasma carteolol concentrations.

## RESULTS AND DISCUSSION

**Preparation of Immunogen**—To prepare the immunogen, carteolol hemiglutarate (I) was conjugated to bovine serum albumin. The hemisuccinate also was examined because hemisuccinate derivatives have been the most commonly used intermediates for the incorporation of haptens to carrier proteins (3–6). The *O*-succinylcarteolol showed only limited solubility in the common solvents such as water, methanol, eth-

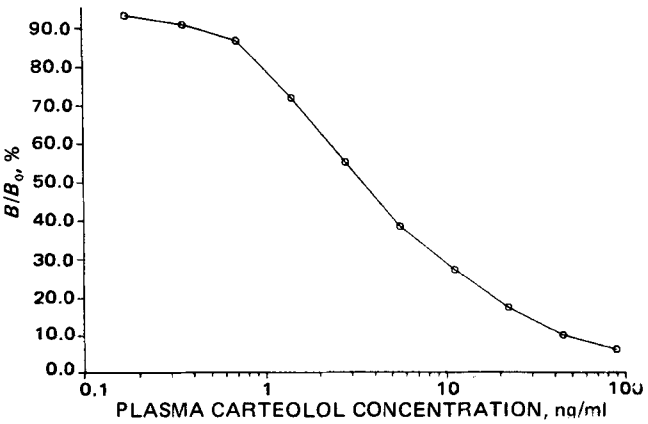


**Figure 3**—*Typical calibration curve for the radioimmunoassay.*

Table II—Within-Day and Day-to-Day Reproducibilities Using Mean Calculated Carteolol Levels (Nanograms per Milliliter) from the Radioimmunoassay

| Item | Theoretical Drug Concentration in Plasma, ng/ml | | | | | | | |
|---|---|---|---|---|---|---|---|---|
| | 0.35 | 0.69 | 1.39 | 2.77 | 5.56 | 11.11 | 22.23 | 44.46 |
| | | | | Day 1 | | | | |
| Mean ($n$ = 3) | 0.31 | 0.58 | 1.44 | 3.20 | 6.03 | 10.9 | 19.2 | 41.4 |
| *SD* | 0.02 | 0.04 | 0.06 | 0.12 | 0.21 | 0.34 | 0.24 | 1.44 |
| *RSD*, % | 6.5 | 6.1 | 4.1 | 3.9 | 3.6 | 3.1 | 1.2 | 3.5 |
| | | | | Day 2 | | | | |
| Mean ($n$ = 3) | 0.38 | 0.56 | 1.40 | 3.17 | 5.91 | 10.6 | 20.8 | 42.5 |
| *SD* | 0.02 | 0.05 | 0.02 | 0.17 | 0.22 | 0.12 | 0.72 | 2.03 |
| *RSD*, % | 6.1 | 8.4 | 1.4 | 5.4 | 3.7 | 1.1 | 3.5 | 4.8 |
| | | | | Day 3 | | | | |
| Mean ($n$ = 3) | 0.35 | 0.72 | 1.34 | 2.99 | 5.48 | 12.2 | 20.8 | 45.6 |
| *SD* | 0.01 | 0.06 | 0.11 | 0.23 | 0.54 | 1.43 | 1.13 | 0.97 |
| *RSD*, % | 3.2 | 8.5 | 8.2 | 7.8 | 9.8 | 11.7 | 5.4 | 2.1 |
| | | | | Average of the Nine Standard Curves | | | | |
| Mean ($n$ = 9) | 0.35 | 0.62 | 1.39 | 3.12 | 5.81 | 11.2 | 20.3 | 43.2 |
| *SD* | 0.03 | 0.09 | 0.08 | 0.19 | 0.40 | 1.04 | 1.06 | 2.30 |
| *RSD*, % | 9.6 | 13.8 | 5.4 | 5.9 | 6.9 | 9.2 | 5.2 | 5.3 |
| Percent theory | 99 | 90 | 100 | 113 | 105 | 101 | 91 | 97 |

anol, dioxane, *N*,*N*-dimethylformamide, tetrahydrofuran, and acetone. Several attempts to incorporate it to bovine serum albumin using the mixed anhydride method (3, 7), the carbodiimide procedure (8, 9), and the active ester method (*N*-hydroxysuccinimide) (10) were all unsuccessful. In contrast, the *O*-glutaryl derivative was quite soluble in these solvents and could be incorporated readily to bovine serum albumin.

**Immunization**—The production of carteolol antibody in rabbits was monitored periodically by checking the animal's serum for binding to the radioactive antigen. Antibody to carteolol could be found in the rabbit serum after six injections of the immunogen over 10 weeks. After the rabbits received eight or nine injections over 26–27 weeks, serums of very good antibody titers were obtained.

**Assay Procedures**—To obtain radioiodinated tracer, tyrosine methyl ester was conjugated to carteolol through the glutaryl group, using the mixed anhydride method. The reaction was complete after ~2 hr, based on HPLC analysis. Several attempts to obtain a solid product by solvent evaporation and crystallization all were unsuccessful. Preparative TLC also was unsuitable for purification of the product, because the isolated products following these treatments were always contaminated with carteolol. Thus, preparative HPLC was used to isolate the product. The fractionated product exhibited one absorption maximum at 252 nm and a shoulder at 278 nm, being consistent with the proposed structure. The product was hydrolyzed quite readily in neutral or alkaline media to give carteolol, providing additional support to the proposed structure.

One important step in radioimmunoassay is the separation of the antibody-bound and the free fractions of the radioactive antigen. Initially, a saturated ammonium sulfate solution was examined for this purpose according to the published radioimmunoassay procedure for propranolol (6). The nonspecific binding was unacceptably high. A 0.25% (w/v) suspension of activated charcoal in gelatin buffer also was unsatisfactory. Polyethylene glycol 6000 in saline buffer was subsequently tested and showed minimum nonspecific binding while providing good precipitation of the antibody–substrate complex. Thus, 1.5 ml of the polyethylene glycol reagent was adequate for 0.5 ml of the incubation mixture.

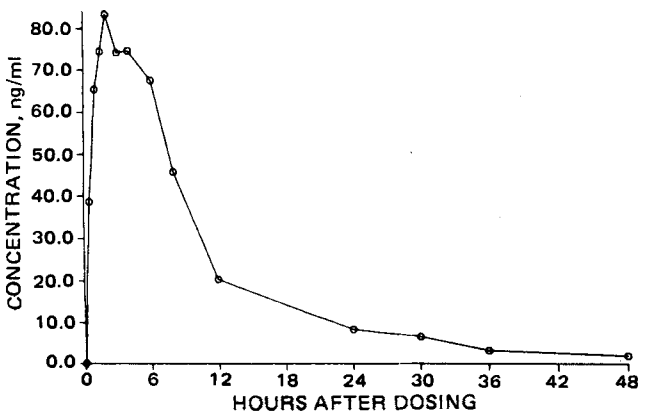


**Figure 4**—*Human plasma carteolol level–time profile determined by radioimmunoassay.*

Antibody specificity was tested against structurally related compounds by allowing each compound being used as a substitute for carteolol to compete with $^{125}$I-labeled antigen for antibody binding sites under the described radioimmunoassay conditions. The amount required to elicit 50% inhibition of initial binding ($ID_{50}$) was estimated by interpolation of the standard curve at $B/B_0$ of 50%. The results are summarized in Table I. The cross-reactivity was expressed as the ratio (percent) of the $ID_{50}$ for carteolol to that for the test compound. The only compound that showed significant cross-reactivity was dehydrocarteolol, being ~1.5%. This compound, however, is not a metabolite of carteolol. 8-Hydroxycarteolol, the major human metabolite, exhibited only very low cross-reactivity, <0.2%. Based on the available data, plasma 8-hydroxycarteolol levels within 12 hr after oral dosing are expected to be quite low compared to the corresponding parent drug levels. Thus, this metabolite should not interfere significantly in the radioimmunoassay of clinical samples.

Figure 3 shows a typical calibration curve generated according to the proposed radioimmunoassay procedure. Polypropylene and glass tubes were equally suitable for the assay. To assess day-to-day and within-day reproducibilities, standard plasma samples were prepared and carried through the radioimmunoassay procedure on 3 different days. On each day, three standard curves were prepared; each standard curve was derived from assays of triplicate samples. These $B/B_0$ ratios *versus* logarithms of concentrations were subjected to a least-squares best fit to a cubic equation using a computer program[1]. The $B/B_0$ ratios then were reinserted into the equation to calculate plasma concentration (Table II).

The radioimmunoassay procedure appears to be most suitable for the determination of plasma carteolol levels in the range of ~0.35–44.5 ng/ml. The daily replicate curves were quite reproducible, with the relative standard deviations ($n$ = 3) mostly within ±8%. The averages of the assayed carteolol levels from the nine standard curves were in good agreement with the theoretical concentrations, all being within 90–113% of theory. The relative standard deviations for these means were between ±5.2 and 13.8%, showing good day-to-day reproducibilities.

Figure 4 shows a plasma concentration–time curve obtained from the analysis of actual clinical samples from a male subject after receiving a 30-mg oral dose of carteolol hydrochloride. In summary, the proposed radioimmunoassay procedure is quite specific and has good within-day and day-to-day reproducibilities. The workup procedure is simple because it does not require solvent extraction or concentration steps. Most importantly, the method offers sensitivity that is far superior to previously reported methods. The lower quantifiable limit of this procedure is ~0.4 ng of carteolol/ml using 0.1 ml of plasma.

## REFERENCES

(1) S. Morita, Y. Irie, S. Sakuragi, H. Kohri, and H. Nishino, *Pharmacometrics*, **11**, 827 (1976).

(2) M. Kido, H. Mori, S. Masuda, H. Kohri, and K. Nakagawa, *Yakugaku Zasshi*, **97**, 1 (1977).

(3) G. C. Oliver, Jr., B. M. Parker, D. L. Brasfield, and C. W. Parker, *J. Clin. Invest.*, **47**, 1035 (1968).
(4) J. Landon and A. C. Moffat, *Analyst*, **101**, 225 (1976).
(5) A. L. Steiner, D. M. Kipnis, R. Utiger, and C. Parker, *Biochemistry*, **64**, 367 (1969).
(6) K. Kawashima, A. Levy, and S. Spector, *J. Pharmacol. Exp. Ther.*, **196**, 517 (1976).
(7) B. F. Erlanger, F. Borek, S. M. Beiser, and S. Lieberman, *J. Biol. Chem.*, **234**, 1090 (1959).
(8) J. C. Sheehan, J. Preston, and P. A. Cruickshank, *J. Am. Chem. Soc.*, **87**, 2492 (1965).
(9) G. E. Abraham and P. K. Grover, in "Principles of Competitive Protein-Binding Assays," W. D. Odell and W. H. Daughaday, Eds., Lippincott, Philadelphia, Pa., 1971, pp. 140–152.
(10) G. W. Anderson, J. E. Zimmerman, and F. M. Callahan, *J. Am. Chem. Soc.*, **85**, 3039 (1963).

**ACKNOWLEDGMENTS**

The authors thank Mrs. Susan Magic and Dr. Paulus Tsui for helpful discussions.

# Interactions of Cephalosporins and Penicillins with Nonpolar Macroporous Styrenedivinylbenzene Copolymers

**FRANCISCO SALTO ˣ and JULIO G. PRIETO**

Received December 1, 1980, from the *Departamento de Química, Facultad de Veterinaria, Universidad de León, León, Spain.* Accepted for publication February 11, 1981.

**Abstract** □ The conditions of sorption of penicillins and cephalosporins on nonionic macroporous copolymers of styrenedivinylbenzene were evaluated. By increasing the methanol concentration in the eluent, the sorption decreased. Salts exerted little influence on sorption. However, pH exerted a remarkable effect on sorption, and the capacity factor variations according to the pH are quantitatively described. Some typical separations are shown.

**Keyphrases** □ Cephalosporins—interactions with a nonpolar, macroporous styrenedivinylbenzene copolymer stationary phase □ Penicillins—interactions with a nonpolar, macroporous styrenedivinylbenzene copolymer stationary phase □ Capacity factors—cephalosporins and penicillins, interactions with a nonpolar, macroporous styrenedivinylbenzene copolymer stationary phase □ Antibiotics—cephalosporins and penicillins, interactions with a nonpolar, macroporous copolymer stationary phase

Nonionic polymers have come into use recently as nonpolar stationary phases in high-pressure liquid chromatography (HPLC), primarily because of the work of Pietrzyk and coworkers (1–5). The main advantages of these kinds of packing are their low cost, ability to function at any level, compatibility with most solvents, and high adsorbency properties.

Penicillins and cephalosporins are β-lactam antibiotics produced by acylation with different radicals of the amino groups of 7-aminocephalosporanic, 7-aminodeacetoxycephalosporanic, or 6-aminopenicillanic acids, which give cephalosporins, deacetoxycephalosporins, or penicillins, respectively. They are particularly suitable as models to study the effect of protonic equilibria on retention by nonpolar macroporous copolymers because of their structural similarities and, depending on the medium pH, they can be found in undissociated, anionic, cationic, or zwitterionic form.

In this study, a macroporous styrenedivinylbenzene copolymer[1] adsorbent with an average surface area of 780 $m^2/g$ and an average pore diameter of 50 Å (3) was used. The purposes of this work were to study the variables affecting the retention of penicillins and cephalosporins on resin copolymers and to demonstrate that the equations describing the retention of ionic solutes by the nonpolar stationary phases are applicable to the interactions of penicillins and cephalosporins with the copolymer. The results may assist in the development of new analytical methods and may improve β-lactam antibiotic extraction and purification methods; the optimum conditions of adsorption and elution may then be predicted.

## EXPERIMENTAL

7-Aminodeacetoxycephalosporanic acid (I), 7-phenylacetamidodeacetoxycephalosporin (II), cephalexin (III), cephradine (IV), 7-aminocephalosporanic acid (V), cephalosporin C (VI), cephalothin (VII), cephaloridine (VIII), cefazolin (IX), 6-aminopenicillanic acid (X), ampicillin (XI), penicillin G (XII), penicillin V (XIII), phenoxyethylpenicillin (XIV), 7-aminodeacetylcephalosporanic acid (XV), and deacetylcephalothin (XVI) were used as supplied[2].

The macroporous styrenedivinylbenzene copolymer[1] was supplied as spheres with an average size of ~500 μm. The resin particles were washed by extraction (soxhlet) with methanol and allowed to dry; they then were ground and sieved, with the 40–70-μm particles being selected (1). The size distribution of these particles was analyzed[3].

The chemicals were the highest commercial grade available and were used without any further purification. The buffer solutions were 0.05 *M* phosphate, and sodium sulfate was used to obtain the desired ionic strength. The mixtures of methanol–buffer solution were expressed in volume percent.

**Chromatographic Conditions**—A 2.5 × 600-mm steel column, equipped with suitable fittings and a 10-μm filter, was dry packed with the copolymer between 40 and 70 μm.

The liquid chromatograph was fitted with a pump[4], a 20-μl sample valve injector[5], a 250-nm UV detector[6], and a strip-chart recorder[7].

The chromatographed substances were prepared in the mobile phase at a concentration of 0.5 mg/ml, except for the penicillins, which were dissolved at a concentration of 3 mg/ml. In each case, a 20-μl aliquot was injected. The flow was maintained at 0.5 ml/min, and the sensitivity of the UV detector was set between 0.004 and 0.128 aufs, according to the absorptivity of the analyzed product.

The capacity factors ($k'$) were calculated in accordance with:

$$k' = \frac{V_R - V_0}{V_0} \qquad \text{(Eq. 1)}$$

[1] Amberlite XAD-4, Rohm & Haas Chemical Co.

[2] Courtesy of Antibióticos, S.A., Madrid, Spain.
[3] Sharples Micromerograph, Franklin Electronics, Bridgeport, Pa.
[4] Constametrik 00, Laboratory Data Control.
[5] Model 7120, Rheodyne.
[6] UV III monitor, Laboratory Data Control.
[7] Model XER, Sargent-Welch Scientific Co., Skokie, Ill.



*0022-3549/81/0900-0994$01.00/0*
*© 1981, American Pharmaceutical Association*

(3) G. C. Oliver, Jr., B. M. Parker, D. L. Brasfield, and C. W. Parker, *J. Clin. Invest.*, **47**, 1035 (1968).
(4) J. Landon and A. C. Moffat, *Analyst*, **101**, 225 (1976).
(5) A. L. Steiner, D. M. Kipnis, R. Utiger, and C. Parker, *Biochemistry*, **64**, 367 (1969).
(6) K. Kawashima, A. Levy, and S. Spector, *J. Pharmacol. Exp. Ther.*, **196**, 517 (1976).
(7) B. F. Erlanger, F. Borek, S. M. Beiser, and S. Lieberman, *J. Biol. Chem.*, **234**, 1090 (1959).
(8) J. C. Sheehan, J. Preston, and P. A. Cruickshank, *J. Am. Chem. Soc.*, **87**, 2492 (1965).
(9) G. E. Abraham and P. K. Grover, in "Principles of Competitive Protein-Binding Assays," W. D. Odell and W. H. Daughaday, Eds., Lippincott, Philadelphia, Pa., 1971, pp. 140–152.
(10) G. W. Anderson, J. E. Zimmerman, and F. M. Callahan, *J. Am. Chem. Soc.*, **85**, 3039 (1963).

**ACKNOWLEDGMENTS**

The authors thank Mrs. Susan Magic and Dr. Paulus Tsui for helpful discussions.

# Interactions of Cephalosporins and Penicillins with Nonpolar Macroporous Styrenedivinylbenzene Copolymers

**FRANCISCO SALTO ˣ and JULIO G. PRIETO**

Received December 1, 1980, from the *Departamento de Química, Facultad de Veterinaria, Universidad de León, León, Spain.* Accepted for publication February 11, 1981.

**Abstract** □ The conditions of sorption of penicillins and cephalosporins on nonionic macroporous copolymers of styrenedivinylbenzene were evaluated. By increasing the methanol concentration in the eluent, the sorption decreased. Salts exerted little influence on sorption. However, pH exerted a remarkable effect on sorption, and the capacity factor variations according to the pH are quantitatively described. Some typical separations are shown.

**Keyphrases** □ Cephalosporins—interactions with a nonpolar, macroporous styrenedivinylbenzene copolymer stationary phase □ Penicillins—interactions with a nonpolar, macroporous styrenedivinylbenzene copolymer stationary phase □ Capacity factors—cephalosporins and penicillins, interactions with a nonpolar, macroporous styrenedivinylbenzene copolymer stationary phase □ Antibiotics—cephalosporins and penicillins, interactions with a nonpolar, macroporous copolymer stationary phase

Nonionic polymers have come into use recently as nonpolar stationary phases in high-pressure liquid chromatography (HPLC), primarily because of the work of Pietrzyk and coworkers (1–5). The main advantages of these kinds of packing are their low cost, ability to function at any level, compatibility with most solvents, and high adsorbency properties.

Penicillins and cephalosporins are β-lactam antibiotics produced by acylation with different radicals of the amino groups of 7-aminocephalosporanic, 7-aminodeacetoxycephalosporanic, or 6-aminopenicillanic acids, which give cephalosporins, deacetoxycephalosporins, or penicillins, respectively. They are particularly suitable as models to study the effect of protonic equilibria on retention by nonpolar macroporous copolymers because of their structural similarities and, depending on the medium pH, they can be found in undissociated, anionic, cationic, or zwitterionic form.

In this study, a macroporous styrenedivinylbenzene copolymer[1] adsorbent with an average surface area of 780 $m^2/g$ and an average pore diameter of 50 Å (3) was used. The purposes of this work were to study the variables affecting the retention of penicillins and cephalosporins on resin copolymers and to demonstrate that the equations describing the retention of ionic solutes by the nonpolar stationary phases are applicable to the interactions of penicillins and cephalosporins with the copolymer. The results may assist in the development of new analytical methods and may improve β-lactam antibiotic extraction and purification methods; the optimum conditions of adsorption and elution may then be predicted.

## EXPERIMENTAL

7-Aminodeacetoxycephalosporanic acid (I), 7-phenylacetamidodeacetoxycephalosporin (II), cephalexin (III), cephradine (IV), 7-aminocephalosporanic acid (V), cephalosporin C (VI), cephalothin (VII), cephaloridine (VIII), cefazolin (IX), 6-aminopenicillanic acid (X), ampicillin (XI), penicillin G (XII), penicillin V (XIII), phenoxyethylpenicillin (XIV), 7-aminodeacetylcephalosporanic acid (XV), and deacetylcephalothin (XVI) were used as supplied[2].

The macroporous styrenedivinylbenzene copolymer[1] was supplied as spheres with an average size of ~500 μm. The resin particles were washed by extraction (soxhlet) with methanol and allowed to dry; they then were ground and sieved, with the 40–70-μm particles being selected (1). The size distribution of these particles was analyzed[3].

The chemicals were the highest commercial grade available and were used without any further purification. The buffer solutions were 0.05 *M* phosphate, and sodium sulfate was used to obtain the desired ionic strength. The mixtures of methanol–buffer solution were expressed in volume percent.

**Chromatographic Conditions**—A 2.5 × 600-mm steel column, equipped with suitable fittings and a 10-μm filter, was dry packed with the copolymer between 40 and 70 μm.

The liquid chromatograph was fitted with a pump[4], a 20-μl sample valve injector[5], a 250-nm UV detector[6], and a strip-chart recorder[7].

The chromatographed substances were prepared in the mobile phase at a concentration of 0.5 mg/ml, except for the penicillins, which were dissolved at a concentration of 3 mg/ml. In each case, a 20-μl aliquot was injected. The flow was maintained at 0.5 ml/min, and the sensitivity of the UV detector was set between 0.004 and 0.128 aufs, according to the absorptivity of the analyzed product.

The capacity factors ($k'$) were calculated in accordance with:

$$k' = \frac{V_R - V_0}{V_0} \qquad \text{(Eq. 1)}$$

[1] Amberlite XAD-4, Rohm & Haas Chemical Co.

[2] Courtesy of Antibióticos, S.A., Madrid, Spain.
[3] Sharples Micromerograph, Franklin Electronics, Bridgeport, Pa.
[4] Constametrik 00, Laboratory Data Control.
[5] Model 7120, Rheodyne.
[6] UV III monitor, Laboratory Data Control.
[7] Model XER, Sargent-Welch Scientific Co., Skokie, Ill.



*0022-3549/81/0900-0994$01.00/0*
*© 1981, American Pharmaceutical Association*

**Table I—Apparent pK'a Values of Investigated Substances Determined Potentiometrically at 20°, an Ionic Strength of 0.15, and 50% (v/v) Methanol**

| Compound | $pK'a_1$ | $pK'a_2$ |
|---|---|---|
| I | 3.63[a] | 5.16[a] |
| II | 4.41 | — |
| III | 4.51 | 6.97 |
| IV | 4.63 | 7.19 |
| V | 3.49[a] | 4.71[a] |
| VII | 4.32 | — |
| IX | 3.85 | — |
| X | 3.04[a] | 4.90[a] |
| XI | 4.11 | 6.84 |
| XII | 4.36 | — |
| XIII | 4.40 | — |
| XIV | 4.49 | — |

[a] Zero percent methanol (Ref. 6).

where $V_R$ is the elution volume of the chromatographic peak and $V_0$ is the column void volume, determined as the elution volume of a nonretained peak.

**Analysis of Experimental Data**—The numerical analysis of experimental data was carried out on a calculator[8] programmed for a nonlinear least-squares fit.

**Determination of pKa**—The apparent pKa values were potentiometrically determined previously (6) under the conditions of the mobile phases used, except for an ionic strength of 0.15, 50% water–methanol, and room temperature, which were determined in the present study.

## RESULTS AND DISCUSSION

The structures of the β-lactam substances studied were indicated previously (6).

The apparent pKa values for the penicillins and cephalosporins were studied in a 50% (v/v) methanol solution at an ionic strength of 0.15 and at room temperature (Table I).

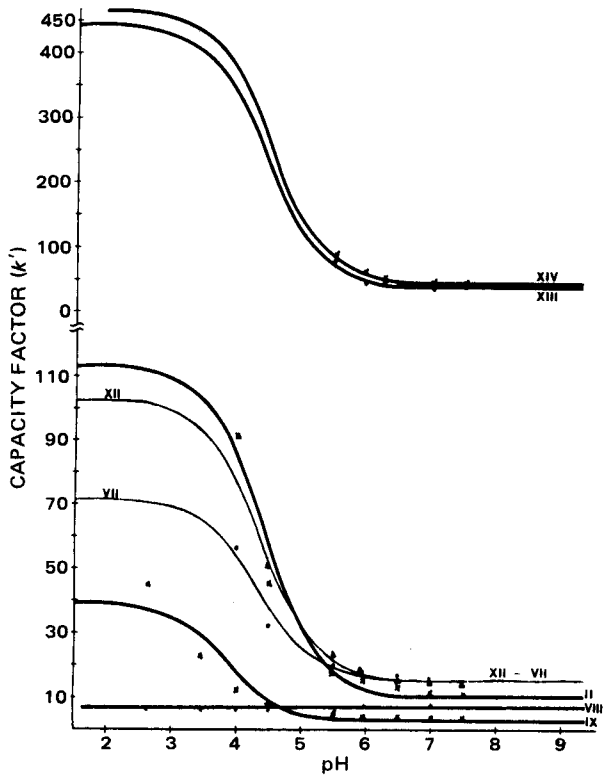


**Figure 1**—*Capacity factors, k', of acidic penicillins and cephalosporins on resin columns as a function of pH using mobile phases of 50% (v/v) methanol–0.05 M phosphate buffer at an ionic strength of 0.15. The continuous lines are the result of the nonlinear least-squares fit of the pairs of experimental k'/pH values to Eq. 2.*

[8] Texas Instruments TI-59.

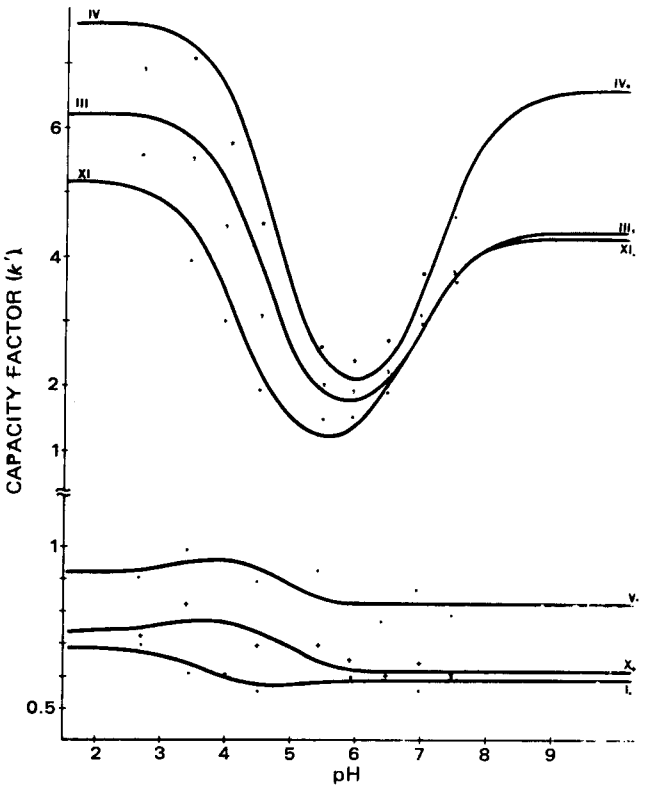


**Figure 2**—*Capacity factors, k', of amphoteric pencillins and cephalosporins on resin columns as a function of pH using mobile phases of 50% (v/v) methanol–0.05 M phosphate buffer at an ionic strength of 0.15. The continuous lines are the result of the nonlinear least-squares fit of the pairs of experimental k'/pH values to Eq. 3.*

Under the microscope, the resin particles were irregular in shape, with no dimension predominating over any other. The average size was ~55 μm. The size distribution analysis showed the particles to be 20–70 μm, with 50% (w/w) being <45 μm. The dry-packed column of resin showed an efficiency in which the height values of the theoretical plate were ~0.06 cm.

The peak tailings shown with the asymmetry factor calculated as 10% of the height of the peaks (7) were similar to those obtained with 30–70-μm octadecylsilica columns. Column permeability was relatively low. The values found for the permeability coefficient (8) were $\sim 4 \times 10^{-10}$ cm$^2$, considerably lower than those estimated by the Kozenzy–Carmen expression (8). This result is probably due to the unevenness of the resin particles since the smallest particles occupy the voids of the largest ones, thus giving a tighter packing than exists when all particles are of equal size.

**Effect of pH**—Although macroporous styrenedivinylbenzene copolymer permits the use of mobile phases at any pH, the instability of penicillins and cephalosporins in highly acidic or alkaline media limited this study to pH levels of 2.7–7.5.

The capacity factors of the penicillins and cephalosporins were studied on the resin column using 0.05 *M* phosphate buffer–methanol 50% (v/v) at different pH as the mobile phase (Figs. 1 and 2).

For nonpolar stationary phases, general equations have linked (6, 9) the variations of capacity factors of each solute ionic form. These general equations, worked out for nonpolar stationary phases and based on hydrophobic interactions, also are valid for describing variations in the capacity factors of penicillins and cephalosporins on macroporous styrenedivinylbenzene resins as a function of the mobile phase pH, as will be shown.

**Acidic Penicillins and Cephalosporins**—Cephalosporins and penicillins, inasmuch as they are weak acids, may be found in neutral, undissociated, or anionic form depending on the medium pH. The hydrophobic interactions of undissociated cephalosporins and penicillins with the nonpolar resin phase will be greater than for the corresponding ionic forms.

At high pH, distant from pKa, capacity factors are small and constant.

**Table II—Capacity Factors of Anionic ($k'_{-1}$) and Undissociated ($k'_0$) Forms of Penicillins and Cephalosporins in 50% (v/v) Methanol**

| | Compound | | | | | |
|---|---|---|---|---|---|---|
| | II | VII | IX | XII | XIII | XIV |
| $k'_0$ | 113 | 71.5 | 39.7 | 103 | 444 | 467 |
| $k'_{-1}$ | 10.0 | 15.6 | 2.66 | 15.2 | 39.5 | 43.3 |

**Table III—Capacity Factors of Anionic ($k'_{-1}$), Zwitterionic ($k'_0$), and Cationic ($k'_{+1}$) Forms of Amphoteric Penicillins and Cephalosporins in 50% (v/v) Methanol**

| | Compound | | |
|---|---|---|---|
| | III | IV | XI |
| $k'_0$ | 0.93 | 1.58 | 0.92 |
| $k'_{-1}$ | 4.69 | 6.59 | 4.32 |
| $k'_{+1}$ | 6.29 | 7.63 | 5.17 |

As the pH is lowered and approaches the pKa values, the anionic and the undissociated forms begin to coexist and the capacity factors increase. At acidic pH, where only the undissociated form may be found, the capacity factors are again constant and higher than those for high pH levels.

The quantitative description of the variations in the capacity factors with the concentration of hydronium ions may be expressed by (6, 9):

$$k' = \frac{k_0 + \frac{K_a}{[H^+]} k_{-1}}{1 + \frac{K_a}{[H^+]}} \qquad \text{(Eq. 2)}$$

where $k_0$ and $k_{-1}$ are the capacity factors of the dissociated and anionic forms, respectively; $K_a$ is the dissociation constant of penicillins or cephalosporins at 50% (v/v) methanol at an ionic strength of 0.05; and $[H^+]$ is the concentration of hydronium ions in the mobile phase.

In Fig. 1, the continuous line is the result of the nonlinear least-squares fit of experimental values of $k'$/pH to Eq. 2. An acceptable agreement exists between the theoretical provisions of Eq. 2 and the experimental values. All of the curves obtained have the same shape. The pH value at the inflection point is that of the pKa, and the pKa values found potentiometrically coincide favorably with those obtained from the curves in Fig. 1.

By applying the experimental data ($k'$/pH) to Eq. 2 using nonlinear least-squares fit, the capacity factors for the undissociated and anionic forms of each penicillin and cephalosporin studied were calculated (Table II).

**Amphoteric Penicillins and Cephalosporins**—The variations in the capacity factors of amphoteric cephalosporins and penicillins on stationary phases of nonpolar resins can be described by (6, 9):

$$k' = \frac{k_0 + k_{-1}\frac{K_{a_2}}{[H^+]} + k_{+1}\frac{[H^+]}{K_{a_1}}}{1 + \frac{K_{a_2}}{[H^+]} + \frac{[H^+]}{K_{a_1}}} \qquad \text{(Eq. 3)}$$

where $k_0$, $k_{-1}$, and $k_{+1}$ represent the capacity factors of zwitterionic, anionic, and cationic forms, respectively; and $K_{a_1}$ and $K_{a_2}$ represent the first and the second dissociation constants of penicillins or cephalosporins at 50% (v/v) methanol at an ionic strength of 0.05, respectively.

In Fig. 2, the continuous lines are obtained from the nonlinear least-squares fit of the experimental $k'$/pH values to Eq. 3. All of the curves obtained have the same shape, with the minimums coinciding with the pH value at the isoelectric point. The minimum of retention is due to the fact that the zwitterion form has a double charge (positive and negative), so the hydrophobic interactions with the resin are less than those of the anionic and cationic forms.

By applying the experimental $k'$/pH values to Eq. 3 by nonlinear least-squares fit, the capacity factors of the anionic, cationic, and zwitterionic forms of the cephalosporins and penicillins were calculated (Table III).

As expected, the capacity factors for the zwitterionic form are considerably smaller than those of the other molecular forms. The capacity factors of cationic forms are somewhat greater than those of anionic ones, which could imply that the undissociated carboxylic acid group contributes to adsorption more than does the uncharged amine group.

Being more polar then penicillins and cephalosporins, I, V, and X are less retained by the nonpolar column. The differences observed in the capacity factors with pH are small so the relative errors are large, which

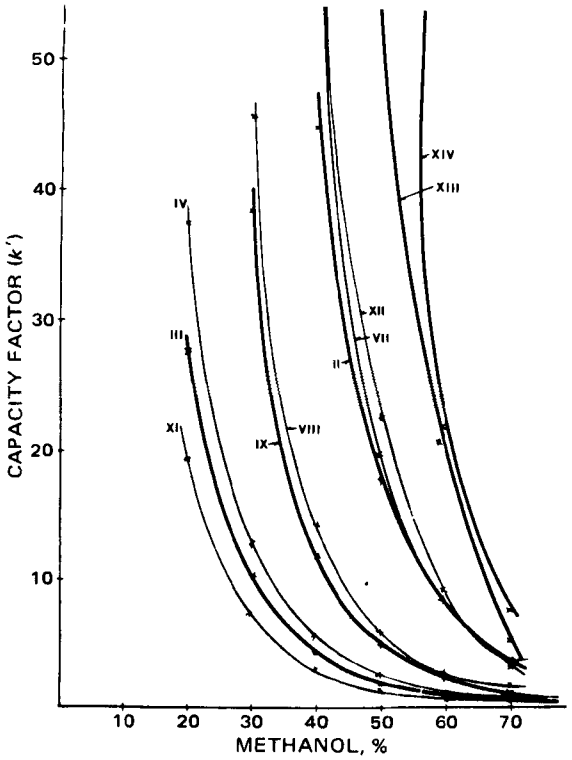


**Figure 3**—*Capacity factors, k', of penicillins and cephalosporins on resin columns using mobile phases of 0.05 M phosphate buffer at pH 5.5 and various methanol concentrations.*

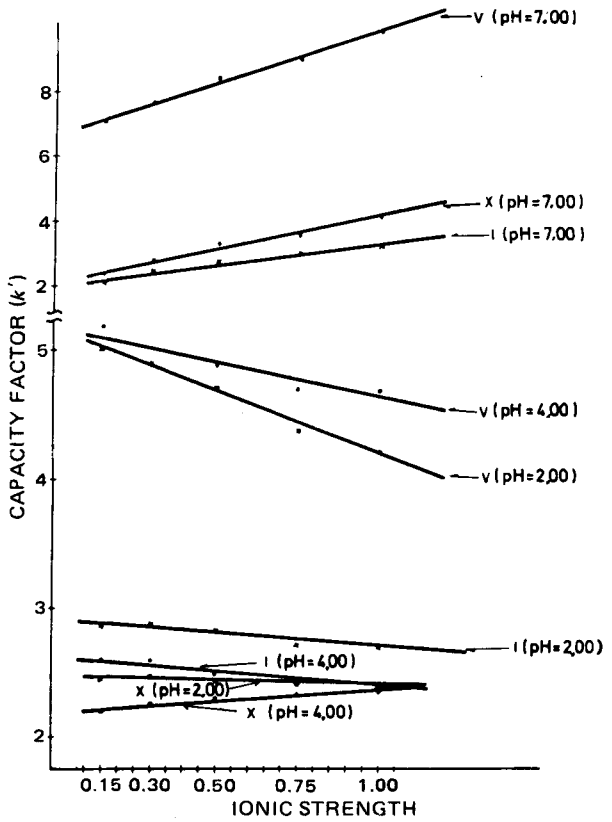


**Figure 4**—*Capacity factors, k', of I, V, and X on resin columns using mixtures of 0.05 M phosphate buffer at the pH indicated with 20% (v/v) methanol and variable ionic strengths as the mobile phases.*

Table IV—Capacity Factors of Anionic ($k'_{-1}$), Zwitterionic ($k'_0$), and Cationic ($k'_{+1}$) Forms of 7-Aminocephalosporanic (V), 6-Aminopenicillanic (X), and 7-Aminodeacetoxycephalosporanic (I) Acids in 50% (v/v) Methanol

| | Compound | | |
|---|---|---|---|
| | V | X | I |
| $k'_0$ | 1.0 | 0.78 | 0.56 |
| $k'_{-1}$ | 0.82 | 0.61 | 0.59 |
| $k'_{+1}$ | 0.92 | 0.73 | 0.69 |

implies that the application of Eq. 3 may be doubtful (Fig. 2). The results obtained for the capacity factors of the various forms are given in Table IV.

**Influence of Penicillin and Cephalosporin Structure on Capacity Factors**—Penicillin and cephalosporin nuclei are retained little by the nonpolar stationary phase of the resin. 7-Aminocephalosporanic acid (V), which has an acetoxy group in position 3 of the thiazine ring, is somewhat more retained than I and X. Acids I and X have very similar retention times, with that of the latter being somewhat greater.

Amphoteric α-aminophenylacetamide penicillins and cephalosporins have substantially higher capacity factors than their respective nuclei. Nevertheless, these factors are remarkably lower than those found for the acidic penicillins and cephalosporins. Within the group of amphoteric penicillins and cephalosporins, the least retained is ampicillin.

Within the deacetoxycephalosporins, cephradine is more retained than cephalexin, probaly due to the fact that the aromatic ring of cephalexin contributes to adsorption less than does the 2,4-cyclodihexene ring of cephradine.

Of the penicillins and cephalosporins studied that possess only one carboxylic group, the least retained is cephaloridine. In position 3 of the cephaloridine thiazine ring, the substitution of the pyridinic cation by the acetoxy group produces cephalothin, which, being much less polar, is retained considerably longer than cephaloridine. Cefazolin has intermediate capacity factors.

7-Aminocephalosporanic acid (V) and 6-aminopenicillanic acid (X), which have the same lateral chain and differ only as regards the nucleus, have very similar capacity factors. However, both V and X possess higher capacity factors than their respective nonacylated nuclei.

The introduction of phenoxy groups in the lateral chain of penicillins produces much higher capacity factors. Phenoxymethylpenicillin and phenoxyethylpenicillin are the most retained of those studied, the latter being somewhat retained owing to its slightly lesser polarity (Fig. 1).

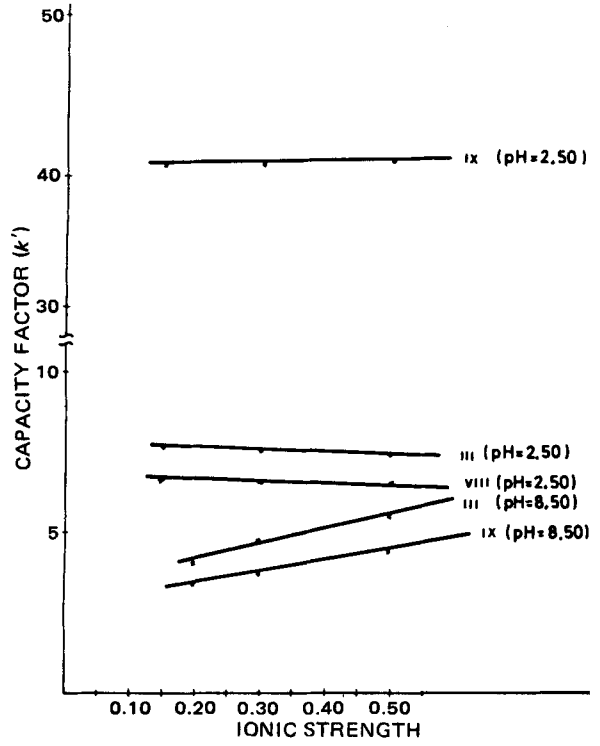


**Figure 5**—*Capacity factors, k', of some penicillins and cephalosporins on resin columns using mixtures of 0.05 M phosphate buffer at the pH indicated with 20% (v/v) methanol and variable ionic strengths as the mobile phases.*

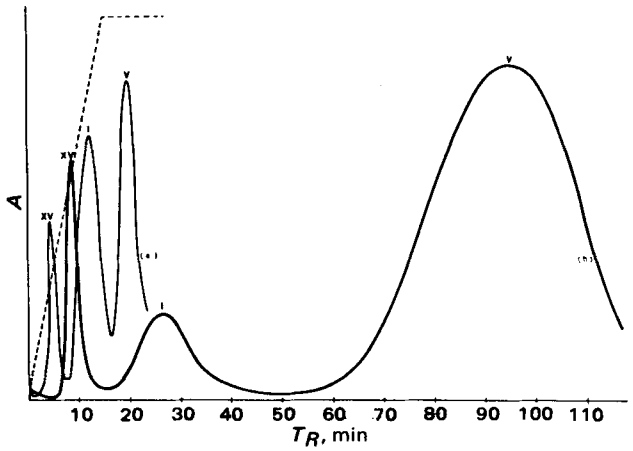


**Figure 6**—*Separation of 7-aminodeacetylcephalosporanic acid (XV), 7-aminocephalosporanic acid (V), and 7-aminodeacetoxycephalosporanic acid (I) on 2.5 × 600-mm resin columns. Key: a, 0.05 M phosphate buffer (pH 4.5) with 5% (v/v) methanol; and b, linear gradient elution (- - -) with 0.05 M phosphate buffer (pH 4.5) with from 5 to 30% (v/v) methanol.*

**Effect of Mobile Phase Methanol Content**—The retention of β-lactam substances by nonpolar macroporous styrenedivinylbenzene copolymers was studied using a mobile phase of 0.05 *M* phosphate buffer (pH 5.5), an ionic strength of 0.15, and different methanol contents.

As the methanol content of the mobile phase rose, the capacity factors decreased (Fig. 3). For the amphoteric substances I, III–V, X, and XI, the effect of the methanol content of the mobile phase on retention was not great, especially when compared with that of methanol on the retention of penicillins and cephalosporins having a single carboxyl group.

At pH 5.5, at which this study was conducted, amphoteric penicillins and cephalosporins are mainly in zwitterionic form whereas acidic penicillins and cephalosporins are principally anionic, so the polarity effect of the mobile phase is much greater on the latter than on the former.

In any event, III, IV, and XI had higher polarities than II and VII. Thus, it seems natural that mobile phase polarity should have a greater effect on the retention of less polar penicillins and cephalosporins.

**Effect of Mobile Phase Ionic Strength**—The effect of the ionic strength on the capacity factors of I, V, and X on resin was studied using mobile phases of 0.05 *M* phosphate buffer at pH 2.0, 4.0, and 7.0 with 20% (v/v) methanol. These pH levels were chosen to study the influence of the ionic strength on each ionic form (anionic at pH 7.0, zwitterionic at pH 4.0, and cationic at pH 2.0).

As shown in Fig. 4, the ionic strength had little influence on the capacity factors of I and X. A slight increase was observed in the retention of these acids as the ionic strength increased at alkaline pH, where both acids are anionic. For V, at pH 2.0 and 4.0, where it exists in cationic or zwitterionic form, respectively, the capacity factors were practically constant, with only a slight decrease as the ionic strength increased. At pH 7.0, the retention increased as the saline concentration increased. This phenomenon may be explained by the formation of ionic pairs between the carboxylate anion and the positive ions of the medium, which could alter their polar nature and/or the orientation of the molecules on the adsorbent surface.

The effect of the ionic strength on the retention of certain cephalosporins on nonpolar copolymers also was studied using mobile phases of 0.05 *M* phosphate buffer at pH 2.5 and 8.5 and a methanol content of 50% (v/v). The capacity factors of the cephalosporins studied varied little with the ionic strength of the mobile phase (Fig. 5). At pH 2.5, where the cefazolin is undissociated and cephalexin and cephaloridine are cationic, the capacity factors did not vary with increasing ionic strengh. At pH 8.5, where the cephalosporins are anionic, the representation $k'/\mu$ gives straight lines with a slightly positive slope. As in the previous case, a possible explanation could be the formation of ion-pairs as the ionic strength is increased, which could entail a rise in the contribution of the carboxylate anion on retention.

**Applications**—The results previously obtained were used to select the conditions for penicillin and cephalosporin separations.

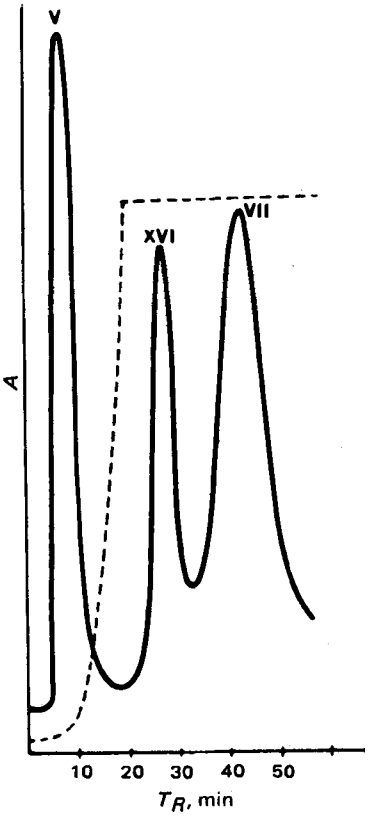


**Figure 7**—*Separation of 7-aminocephalosporanic acid (V), deacetylcephalothin (XVI), and cephalothin (VII) on resin columns; linear gradient elution (- - -) with 0.05 M phosphate buffer (pH 4.5) with from 35 to 60% (v/v) methanol.*

Figure 6 shows the separation from 7-aminocephalosporanic acid of two of its most frequent impurities, 7-aminodeacetoxycephalosporanic acid and deacetyl-7-aminocephalosporanic acid. The results obtained in an isocractic system and with gradient elution are shown in Figs. 6*a* and 6*b*, respectively.

Other examples of separation are shown in Figs. 7 and 8. In the former, cephalothin is separated from some of its possible impurities, 7-aminocephalosporanic acid and deacetylcephalothin. In the latter, cephalexin is separated from 7-aminodeacetoxycephalosporanic acid.

**Comparison of Stationary Phases of Nonionic Styrenedivinylbenzene Copolymers with Octadecylsilica**—The chromatographic interactions of penicillins and cephalosporins with the stationary phase of octadecylsilica were studied previously (6). From comparison of these results with those in the present work using polystyrenedivinylbenzene resins, the following conclusions can be drawn:

1. Polystyrenedivinylbenzene behaves as a reversed phase in a similar manner as the stationary phase of octadecylsilica. The same equations describe the capacity factor variations with pH for each stationary phase.

2. Even if the particle size for each column is similar, that of octadecylsilica has a theoretical plate height of about three times less than resin columns under the same conditions.

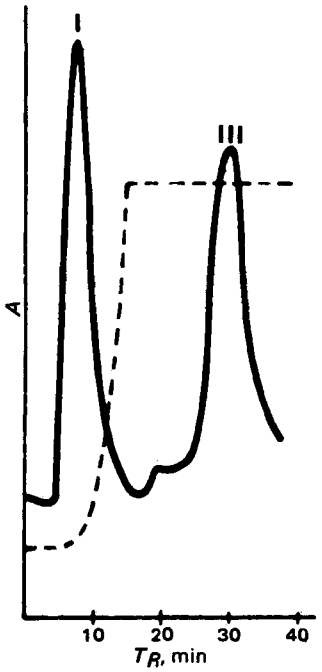


**Figure 8**—*Separation of 7-aminodeacetoxycephalosporanic acid (I) and cephalexin (III) on resin columns; linear gradient elution (- - -) with 0.05 M phosphate buffer (pH 4.5) with from 20 to 45% (v/v) methanol.*

3. The interactions among β-lactam antibiotics are more intense with resins than with octadecylsilica. Therefore, when using the resin column, a greater methanol content in the mobile phase is required than when the octadecylsilica column is used.

The octadecylsilica column is more appropriate for chromatographic separations of penicillins and cephalosporins than are columns of styrenedivinylbenzene copolymer. However, given the low cost of nonionic resins, adsorption–elution conditions may have many applications in extraction and purification processes of penicillins and cephalosporins.

## REFERENCES

(1) M. D. Grieser and D. J. Pietrzyk, *Anal. Chem.*, **45**, 1348 (1973).

(2) C. H. Chu and D. J. Pietrzyk, *ibid.*, **36**, 330 (1974).

(3) D. J. Pietrzyk and C. H. Chu, *ibid.*, **49**, 757 (1977).

(4) E. P. Kroeff and D. J. Pietrzyk, *ibid.*, **50**, 502 (1978).

(5) T. D. Rotsch, R. J. Sydor, and D. J. Pietrzyk, *J. Chromatogr. Sci.*, **17**, 339 (1979).

(6) F. Salto, J. G. Prieto, and T. Alemany, *J. Pharm. Sci.*, **69**, 501 (1980).

(7) J. J. Kirkland, H. J. Stoklosa, and J. C. H. Dilks, *J. Chromatogr. Sci.*, **15**, 303 (1977).

(8) L. R. Snyder and J. J. Kirkland, "Introduction to Modern Liquid Chromatography," Wiley, New York, N.Y., 1974, Appendixes I and II.

(9) D. J. Pietrzyk, E. P. Kroeff, and T. D. Rotsch, *Anal. Chem.*, **50**, 497 (1978).

# *In Vitro* Interaction of Quinidine with Kaolin and Pectin

**ARTHUR J. BUCCI *, STEVEN A. MYRE, HENRY S. I. TAN, and LATIF S. SHENOUDA ˣ**

Received October 20, 1980, from the *College of Pharmacy, University of Cincinnati Medical Center, Cincinnati, OH 45267.* Accepted for publication February 17, 1981. *Present address: College of Pharmacy, University of Rhode Island, Kingston, RI 02881.

**Abstract** □ The adsorption of quinidine onto kaolin was studied as a function of pH in aqueous solutions in which the ionic strength was adjusted to 0.1. The interaction of quinidine with pectin also was investigated in water and in phosphate buffer; the buffer pH and ionic strength were adjusted to 6.5 and 0.1, respectively. The *in vitro* results indicated that quinidine was adsorbed onto kaolin. At the highest concentration studied, the extent of adsorption increased from 3.64 mg of quinidine adsorbed/g of adsorbent at pH 2.4 to an average of 5.81 mg/g in the pH 5.5–7.5 range. In the presence of electrolytes, the interaction of quinidine with pectin was relatively small (3–13% bound) as compared to studies performed in water (66–90% bound). The data indicate that some quinidine may be adsorbed when this drug is administered concurrently with kaolin–pectin preparations.

**Keyphrases** □ Quinidine—interactions with kaolin and pectin, *in vitro* □ Kaolin—interactions with quinidine, *in vitro* □ Pectin—interactions with quinidine, *in vitro* □ Antiarrhythmic agents—quinidine, interactions with kaolin and pectin, *in vitro*

Quinidine is used in the treatment of cardiac arrhythmias, and its therapeutic effect is associated with maintaining serum levels of 2.0–6.0 μg/ml (1, 2). Side effects frequently encountered with these therapeutic levels include GI disturbances such as diarrhea (2–4). Pharmaceutical preparations containing both kaolin and pectin are available without prescription and frequently are used to treat diarrhea. Previous *in vitro* studies demonstrated that kaolin adsorbs various alkaloids (5), phenothiazines (6, 7), and cimetidine (8). *In vivo* studies showed that kaolin–pectin preparations concomitantly administered with lincomycin (9) or digoxin (10, 11) decreased the rate and the extent of absorption of these drugs.

Since kaolin adsorbs quinine *in vitro* (5), the cinchona alkaloid quinidine may be adsorbed by kaolin in the kaolin–pectin antidiarrheal preparations. Quinidine was reacted with polygalacturonic acid to form quinidine polygalacturonate (12). Since polygalacturonic acid is derived from pectin, complexation of quinidine with pectin also may occur, thus affecting the amount of quinidine available for absorption in the GI tract.

The purpose of this study was to determine the extent of quinidine adsorption onto kaolin as a function of physiological pH as well as the degree of quinidine–pectin interaction.

## EXPERIMENTAL

**Reagents**—Quinidine sulfate[1], 37% hydrochloric acid[2], monobasic sodium phosphate[3], dibasic sodium phosphate[3], anhydrous sodium sulfate[4], kaolin NF[4], and pectin[1] were used as received. The cellulose membrane tubing[5] employed had a molecular weight cutoff of 12,000–14,000.

**Analytical Method**—Quinidine sulfate concentrations in test solutions were determined using a fluorescence spectrophotometer[6] with a xenon power supply[7] and a recorder[8]. An excitation wavelength of 350 nm and an emission wavelength of 443 nm were used. By using a sensitivity setting of 4 and a concentration range of 0.2–1.0 μg/ml, a standard curve ($r$ = 0.999) was obtained as expressed by:

$$\%F = 100.0C + 0.175 \qquad \text{(Eq. 1)}$$

where $\%F$ is the emission intensity in percent and $C$ is the quinidine sulfate concentration in micrograms per milliliter. To minimize daily variation, a standard curve was obtained on a regular basis using controls subjected to the same conditions as the experimental samples.

**Determination of Equilibrium Time for Quinidine Adsorption onto Kaolin**—One-gram quantities of kaolin were weighed accurately into clean, dry, amber-glass bottles. Then 40.0 ml of quinidine sulfate solution was added. The quinidine concentrations in the time study were 5.0 and 40.0 mg/100 ml, representing the lowest and highest concentrations utilized. The bottles were capped tightly, placed in a thermostatically controlled water bath, and agitated at 37.0 ± 0.5°.

Samples were withdrawn at 6.0, 12.0, and 24.0 hr and were filtered immediately through a 0.22-μm membrane disposable filter[9]. The filtered solution was diluted and analyzed for the remaining quinidine sulfate content. Controls, containing identical concentrations of quinidine sulfate without kaolin, were treated in the same manner to check for any loss of quinidine due to degradation or adsorption onto the glassware and filter. A blank solution that contained kaolin without quinidine sulfate was prepared similarly.

**Kaolin Adsorption Studies**—The adsorption of quinidine onto kaolin was studied as a function of pH. Solution I consisted of 0.01 *M* HCl with a final pH of 2.4. Solutions II, III, and IV were phosphate buffers with final pH values of 5.5, 6.5, and 7.5, respectively. All solutions were adjusted to a final ionic strength of 0.10 by the addition of anhydrous sodium sulfate.

In all solutions studied, 40.0 ml of quinidine sulfate solution of 5.0, 10.0, 15.0, 20.0, 30.0, and 40 mg/100 ml was added to 1.0 g of kaolin in dry, amber-colored bottles. All samples were subjected to the same conditions and treated like those in the time study. All samples were left to equilibrate for 24.0 hr.

**Pectin Studies**—The interaction of quinidine with pectin was studied in water and in Solution III using membrane dialysis techniques similar to those reported previously (13, 14). Membrane bags were prepared from

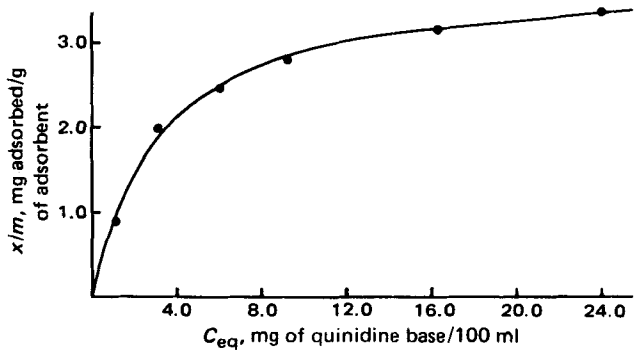


**Figure 1**—*Typical isotherm for the adsorption of quinidine onto kaolin in Solution I (pH 2.4) at 37°.*

[1] Sigma Laboratories, St. Louis, Mo.
[2] Mallinckrodt, St. Louis, Mo.
[3] Fisher Scientific Co., Fair Lawn, N.J.
[4] Matheson, Coleman and Bell, Norwood, Ohio.
[5] Spectropore-2, Spectrum Medical Laboratories, Los Angeles, Calif.
[6] Perkin-Elmer model 204.
[7] Perkin-Elmer model 150.
[8] Perkin-Elmer model 165.
[9] Millex, Millipore Corp., Bedford, Mass.

0022-3549/81/0900-0999$01.00/0
© 1981, American Pharmaceutical Association

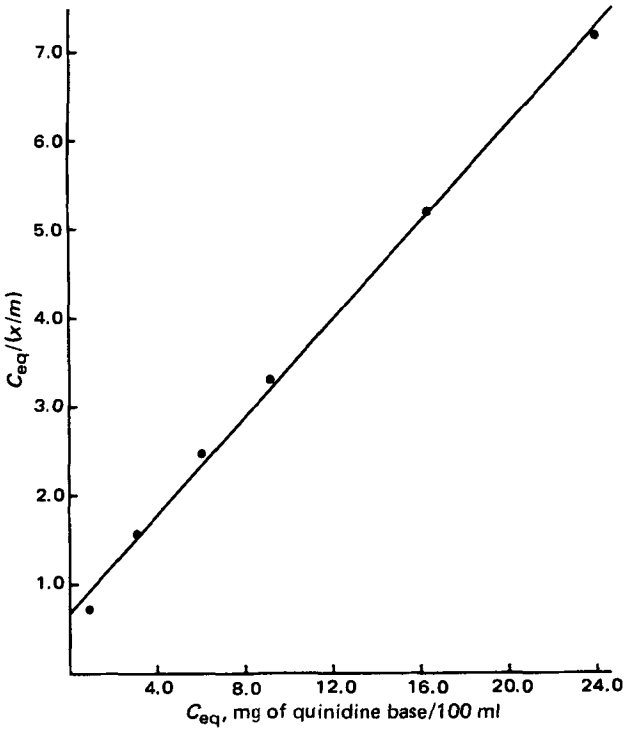


**Figure 2**—*Linear Langmuir plot for the adsorption of quinidine onto kaolin in Solution I (pH 2.4) at 37°, r = 0.999.*

cellulose tubing and were filled with 40.0 ml of pectin solution. Concentrations of 0.2, 0.4, 0.6, 0.8, and 1.0% pectin solution in water or in Solution III were used. The bags were clamped securely at the bottom and tied twice at the top to prevent leakage.

After inspection for leakage, the bags were immersed in a jar containing 60 ml of a 40.0-mg/100 ml quinidine sulfate solution either in water or in a buffered Solution III. The jars were capped tightly and placed in a shaking water bath thermostatically controlled to 37.0 ± 0.5°. The jars were allowed to agitate for 6.0 hr, a time previously determined as sufficient for achieving equilibrium. Additional membrane bags containing the appropriate solution were included in each study to check any loss of quinidine due to binding to the membrane and clamp.

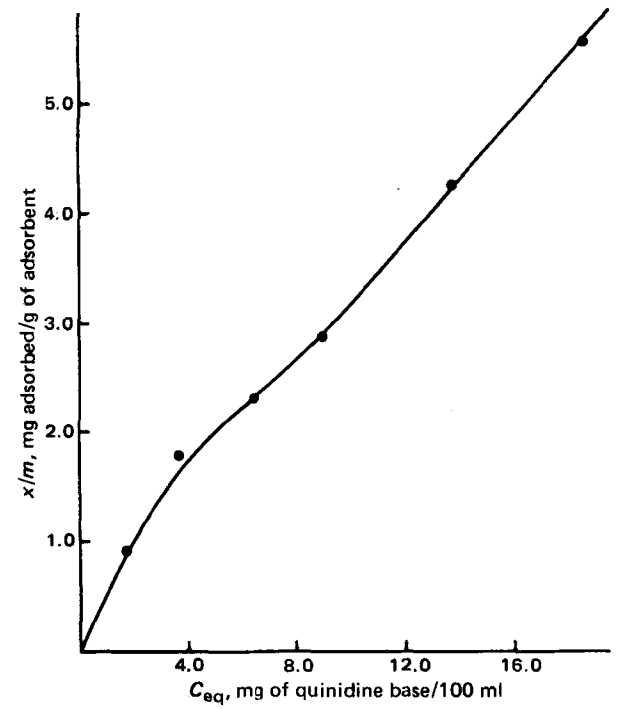


**Figure 3**—*Isotherm illustrating the adsorption of quinidine onto kaolin in Solution II (pH 5.5) at 37°.*

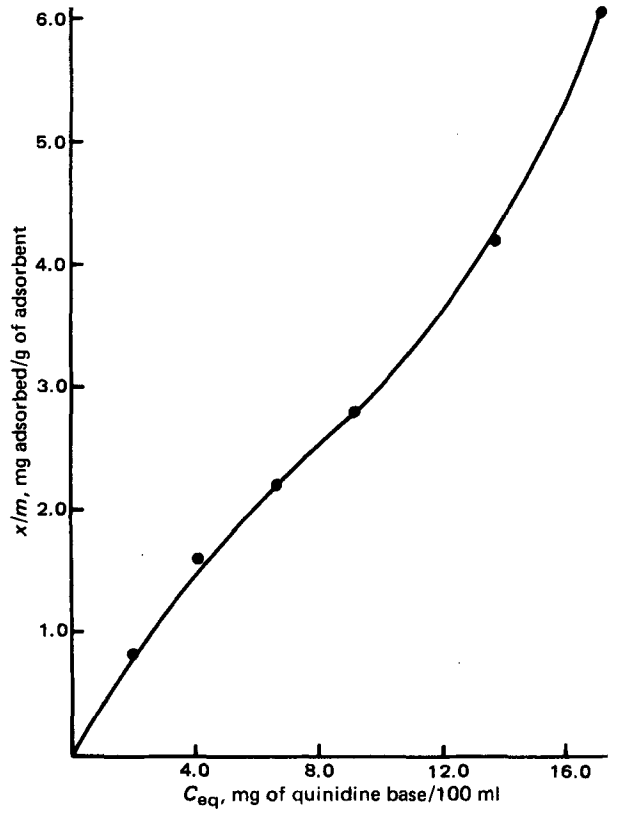


**Figure 4**—*Isotherm illustrating the adsorption of quinidine onto kaolin in Solution III (pH 6.5) at 37°.*

Four runs were performed for each pectin concentration. After achieving equilibrium and appropriate dilution, the quinidine sulfate contents both inside and outside the bag were determined spectrofluorometrically.

## RESULTS AND DISCUSSION

The kaolin time study indicated that equilibrium was achieved between 6.0 and 12.0 hr. To ensure equilibrium, all samples were allowed to agitate in the water bath for 24.0 hr. The membrane filter had no effect on the quinidine sulfate concentration based on assays performed prior to and after filtration. Furthermore, the lack of any significant decrease in the quinidine sulfate concentration in the controls indicated the apparent absence of adsorption of the drug onto the glassware and degradation during equilibration.

The results of the kaolin adsorption studies in Solution I were evaluated according to the Langmuir equation (Eq. 2):

$$\frac{x}{m} = \frac{k_1 k_2 C_{eq}}{1 + k_1 C_{eq}} \qquad \text{(Eq. 2)}$$

where $x/m$ is the weight, in milligrams, of quinidine base adsorbed per gram of kaolin; $C_{eq}$ is the concentration of quinidine base, in milligram percent, remaining in solution at equilibrium; $k_1$ is the adsorption coefficient; and $k_2$ is the maximum amount of drug adsorbed to form a monolayer under the experimental conditions. Figure 1 is a typical Langmuir isotherm obtained by plotting $x/m$ *versus* $C_{eq}$ and illustrates the formation of a quinidine monolayer on kaolin. Figure 2 is the fitted plot according to the following linear form of Langmuir:

$$C_{eq}/(x/m) = C_{eq}/k_2 + 1/k_1 k_2 \qquad \text{(Eq. 3)}$$

The maximum adsorptive capacity calculated from the slope of the line is 3.64 mg/g.

Ionic strength was adjusted with anhydrous sodium sulfate since preliminary studies showed that a high concentration of chloride ions, either in the form of hydrochloric acid (0.1 *M*) or sodium chloride for adjusting the ionic strenth to 0.1, caused quenching and interfered with the assay. The low concentration of hydrochloric acid (0.01 *M*) did not present any analytical problem. With quinidine sulfate concentrations up to 40.0 mg/100 ml, the results of adsorption studies in Solution II indicate that adsorption is not limited to the formation of a monolayer as

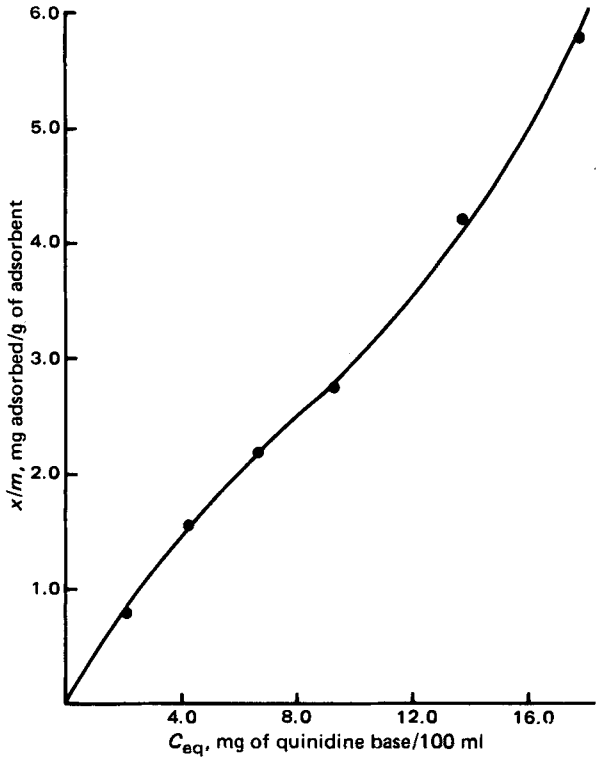


**Figure 5**—*Isotherm illustrating the adsorption of quinidine onto kaolin in Solution IV (pH 7.5) at 37°.*

observed in Solution I. This result is shown in Fig. 3, which indicates that multilayered adsorption occurred. Similar results were obtained from studies in Solutions III and IV (Figs. 4 and 5, respectively). Langmuir linearity was established for Solution II in quinidine sulfate concentrations between 1.0 and 3.0 mg/100 ml (Fig. 6). In this same low concentration range, linearity was not observed for Solutions III and IV.

These results indicate that adsorption of quinidine onto kaolin varies with pH. The apparent multilayered process that occurred in Solutions II–IV indicates that drug adsorption continues at higher pH values. Further experimentation is underway to explain this behavior.

Since increasing electrolyte concentrations may increase the adsorptive capacity of kaolin (7), it is not surprising that there are no apparent differences in the isotherms (Figs. 3–5) since the ionic strength was kept constant in all solutions. For example, at an initial concentration of 32.4 mg of quinidine base/100 ml (equivalent to 40 mg of quinidine sulfate/100 ml in solution) the calculated $x/m$ values are 5.57, 6.07, and 5.79 mg/g for Solutions II, III, and IV, respectively. Therefore, at quinidine sulfate concentrations up to 40.0 mg/100 ml, the amount of drug adsorbed per

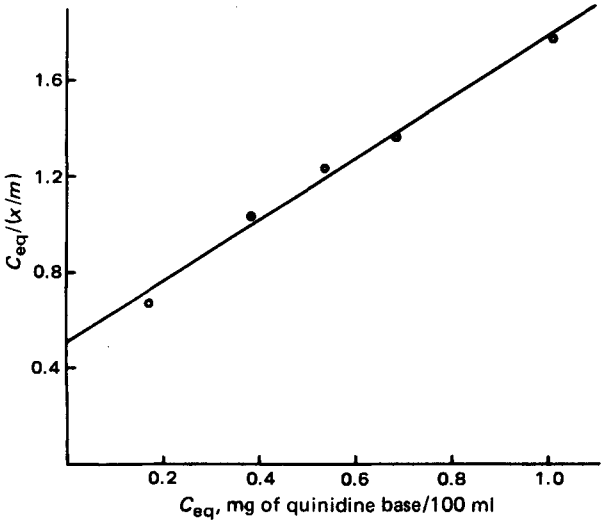


**Figure 6**—*Linear Langmuir plot for the adsorption of quinidine onto kaolin at low concentrations in Solution II (pH 5.5) at 37°, r = 0.994.*

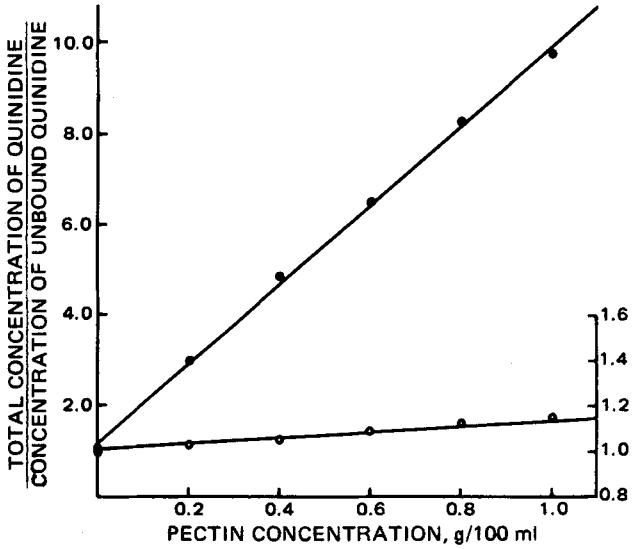


**Figure 7**—*Interaction between quinidine and pectin at 37°. Key: ●, water (r = 0.999); and ○, pH 6.4 buffer at an ionic strength of 0.1 (r = 0.998).*

gram of adsorbent increases as the pH is raised from acidic pH, simulating the stomach environment, to pH 5.5–7.5, which simulates the intestinal environment. The results of the present study parallel the findings of Remon *et al.* (15) who reported that the adsorption of quinidine onto kaolin increases with pH. Their results were obtained under different *in vitro* conditions with much higher quinidine sulfate concentrations. Thus, any firm comparisons between the two studies are difficult.

The data of the pectin study were analyzed by previously reported methods (14). The calculated coefficient of variation for identical runs was 1–4%. Figure 7 shows marked complexation between quinidine and pectin in unbuffered aqueous medium. The extent of binding of quinidine ranged between 66 and 90% at a pectin concentration between 0.2 and 1%. Binding was reduced markedly when the study was repeated in Solution III. The extent of binding ranged between 3 and 13% in the same pectin concentration range (Fig. 7). According to these data, complexation studies performed in water without electrolytes could be misleading. Studies utilizing electrolyte solutions, such as Solution III, may be more representative of an *in vivo* situation. The same pattern of interaction was observed by Remon *et al.* (15) who studied quinidine sulfate complexation with 1% pectin in water and in 0.01 *M* HCl. They reported that quinidine sulfate was 40% bound to pectin in water and was 5% bound in acidic solution. In the current study, ~90% of quinidine was bound by 1% pectin in water. This difference may be accounted for by the higher quinidine concentrations (500 mg/100 ml) used previously (15).

The results of this *in vitro* study indicate that kaolin is capable of adsorbing quinidine and that adsorption increases with pH. Pectin forms a complex with quinidine; however, the effect is less pronounced in Solution III than in water. Although complexation with pectin may afford a controlled and more uniform absorption of quinidine as shown for quinidine polygalacturonate (12), the data suggest that this effect may be minimal. Kaolin and pectin contained in antidiarrheal preparations may alter absorption of the drug from the GI tract. Relative bioavailability studies should be carried out to determine the significance of this interaction.

## REFERENCES

(1) R. H. Heissenbuttel and J. T. Bigger, *Am. Heart J.*, **80**, 453 (1970).

(2) B. F. Hoffman, M. R. Rosen, and A. L. Wit, *ibid.*, **89**, 804 (1975).

(3) D. M. Aviado and H. Salem, *J. Clin. Pharmacol.*, **15**, 477 (1975).

(4) I. S. Cohen, H. Jick, and S. I. Cohen, *Prog. Cardiovasc. Dis.*, **20**, 151 (1977).

(5) N. Evcim and M. Barr, *J. Am. Pharm. Assoc., Sci. Ed.*, **44**, 570 (1955).

(6) D. L. Sorby and E. M. Plein, *J. Pharm. Sci.*, **50**, 355 (1961).

(7) D. L. Sorby, E. M. Plein, and J. D. Benmaman, *ibid.*, **55**, 785 (1966).

(8) F. Ganjian, A. J. Cutie, and T. Jochsberger, *ibid.*, **69**, 352 (1980).
(9) J. G. Wagner, *Can. J. Pharm. Sci.*, **1**, 55 (1966).
(10) D. D. Brown and R. P. Juhl, *N. Engl. J. Med.*, **295**, 1034 (1976).
(11) K. S. Albert, J. W. Ayres, A. R. DiSanto, D. J. Weidler, E. Sakmar, M. R. Hallmark, R. G. Stoll, K. A. DeSante, and J. G. Wagner, *J. Pharm. Sci.*, **67**, 1582 (1978).
(12) A. Halpern, N. Shaftel, and A. J. Monte Bovi, *Am. J. Pharm.*, **130**, 190 (1958).
(13) I. M. Klotz, F. M. Walker, and R. B. Pivan, *J. Am. Chem. Soc.*, **68**, 1486 (1946).
(14) T. Higuchi and R. Kuramoto, *J. Am. Pharm. Assoc., Sci. Ed.*, **43**, 393 (1954).
(15) J. P. Remon, R. Van Severen, and P. Braeckman, *Pharm. Weekbl.*, **113**, 525 (1978).

# Quantification of Phencyclidine in Mainstream Smoke and Identification of Phenylcyclohex-1-ene as Pyrolysis Product

**A. S. FREEMAN and B. R. MARTIN** ˣ

Received September 2, 1980, from the *Department of Pharmacology, Virginia Commonwealth University, Medical College of Virginia, Richmond, VA 23298.* Accepted for publication February 12, 1981.

**Abstract** □ Parsley cigarettes containing [$^3$H]phencyclidine were machine smoked, and the mainstream smoke was trapped in glass wool filters. Radioactivity was extracted from these filters with chloroform. The average recoveries of radioactivity were 76, 85, 70, and 69% for cigarettes containing 3, 10, 30, and 50 mg of [$^3$H]phencyclidine hydrochloride, respectively. TLC and GLC–mass spectrometry were employed to identify and quantify compounds in the filter extracts. Approximately one-half of the recovered radioactivity represented a pyrolysis product, phenylcyclohex-1-ene. Formation of this product involved loss of piperidine from phencyclidine. Piperidine, which was not radiolabeled, also may appear in smoke intact. The remainder of the radiolabeled material represented unchanged phencyclidine. Therefore, the percentage of [$^3$H]phencyclidine delivered was ~40% of the amount smoked. This result was independent of puff frequency and quantity of phencyclidine hydrochloride smoked over the range tested. The [$^3$H]phencyclidine delivery was compared to the quantities of [$^3$H]-$\Delta^9$-tetrahydrocannabinol and [$^3$H]nicotine delivered in mainstream smoke. The recovery of unchanged [$^3$H]-$\Delta^9$-tetrahydrocannabinol from placebo marijuana cigarettes injected with a solution containing 3 mg of $\Delta^9$-tetrahydrocannabinol was 60%. Tobacco cigarettes injected with [$^3$H]nicotine yielded 70% unchanged nicotine in mainstream smoke.

**Keyphrases** □ Pyrolysis—formation of phenylcyclohex-1-ene from phencyclidine in smoke □ Phencyclidine—identification of pyrolysis product phenylcyclohex-1-ene in smoke □ Phenylcyclohex-1-ene—pyrolysis product of phencyclidine identified in smoke □ Smoke—identification of phenylcyclohex-1-ene, a pyrolysis product of phencyclidine

Phencyclidine [1-(1-phenylcyclohexyl)piperidine] has gained popularity as a drug of abuse, probably because it produces euphoria, dissociation, and hallucinations (1). Smoking phencyclidine-impregnated spices is currently a major method of abuse. The high temperature attained in a burning cigarette raises the possibility that phencyclidine may evolve pyrolysis products when smoked. Phencyclidine is converted to phenylcyclohex-1-ene in the gas chromatograph at low temperatures (2) (Scheme I), which may have led to the conclusion that phenylcyclohexene is a metabolite of phencyclidine (3). Preliminary results indicate that phenylcyclohexene also is formed during smoking (4). In this study, the amount of phencyclidine delivered in mainstream smoke was determined and the pyrolysis products were identified and quantified.

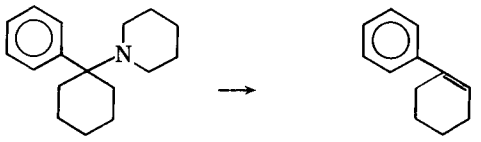


phencyclidine → phenylcyclohex-1-ene

*Scheme I*

## EXPERIMENTAL

**Drugs**—Phencyclidine hydrochloride[1], piperidinocyclohexane carbonitrile[1], [*phenyl*-1-$^3$H(*n*)]phencyclidine[1] (17 Ci/mmole), $\Delta^9$-tetrahydrocannabinol[1], and [1′,2′-$^3$H]-$\Delta^9$-tetrahydrocannabinol[1] (43 mCi/mmole) were used. [*pyrrolidinyl*-4′,4-$^3$H]Nicotine (4.7 Ci/mmole) was synthesized according to the procedure of Vincek *et al.* (5).

**Preparation of Cigarettes**—Cigarettes containing phencyclidine were prepared using commercially available parsley flakes[2], 55-mm cigarette tubes[3], and a cigarette machine[4]. Each cigarette (550–600 mg) was prepared immediately prior to its use by injection with 0.5 μCi of [$^3$H]-phencyclidine and 3, 10, 30, or 50 mg of phencyclidine hydrochloride in volumes of 50, 50, 150, or 200 μl of ethanol, respectively. Filterless cigarettes[5] (84 mm) were injected with 0.5 μCi of [$^3$H]nicotine in 50 μl of ethanol, and placebo marijuana cigarettes[1] were injected with 0.5 μCi of [$^3$H]-$\Delta^9$-tetrahydrocannabinol and 3 mg of $\Delta^9$-tetrahydrocannabinol in 50 μl of ethanol. All drug solutions were injected axially and evenly throughout the middle 35 mm of the cigarettes and allowed to dry before smoking.

**Procedure**—Cigarettes were inserted in a holder and attached to the smoking apparatus (Fig. 1). Smoking was effected by negative pressure provided by water aspiration, and smoke was collected on two contiguous filters (each consisting of 1–1.25 g of glass wool stuffed in 16 cm of 0.635-cm i.d. tubing[6]). Interfaced between the filters and vacuum source were an empty trap (for back-siphoning) and a trap containing 10 ml of chloroform.

Puffing was accomplished with an electric switching valve[7] that opened and closed the system to the vacuum every 5.8 sec. Puff frequency was altered by replacement of a capacitor in the circuit board controlling the valve. A vacuum regulator[8] was set to permit delivery of 45 ml of smoke/5.8-sec puff duration. After an entire cigarette was smoked, each

[1] National Institute on Drug Abuse.
[2] McCormick and Co., Baltimore, Md.
[3] Dominion Cigarette Tube Co., Montreal, Canada.
[4] Premier Supermatic, Central Tobacco Manufacturing Co. Ltd., Montreal, Canada.
[5] Pall Mall, American Tobacco Co., Richmond, Va.
[6] Tygon Tubing and Molded Products, Akron, Ohio.
[7] Skinner, New Britain, Conn.
[8] Fairchild, Winston-Salem, N.C.



*0022-3549/81/0900-1002$01.00/0*
© *1981, American Pharmaceutical Association*

(8) F. Ganjian, A. J. Cutie, and T. Jochsberger, *ibid.*, **69**, 352 (1980).
(9) J. G. Wagner, *Can. J. Pharm. Sci.*, **1**, 55 (1966).
(10) D. D. Brown and R. P. Juhl, *N. Engl. J. Med.*, **295**, 1034 (1976).
(11) K. S. Albert, J. W. Ayres, A. R. DiSanto, D. J. Weidler, E. Sakmar, M. R. Hallmark, R. G. Stoll, K. A. DeSante, and J. G. Wagner, *J. Pharm. Sci.*, **67**, 1582 (1978).
(12) A. Halpern, N. Shaftel, and A. J. Monte Bovi, *Am. J. Pharm.*, **130**, 190 (1958).
(13) I. M. Klotz, F. M. Walker, and R. B. Pivan, *J. Am. Chem. Soc.*, **68**, 1486 (1946).
(14) T. Higuchi and R. Kuramoto, *J. Am. Pharm. Assoc., Sci. Ed.*, **43**, 393 (1954).
(15) J. P. Remon, R. Van Severen, and P. Braeckman, *Pharm. Weekbl.*, **113**, 525 (1978).

# Quantification of Phencyclidine in Mainstream Smoke and Identification of Phenylcyclohex-1-ene as Pyrolysis Product

**A. S. FREEMAN and B. R. MARTIN** ˣ

Received September 2, 1980, from the *Department of Pharmacology, Virginia Commonwealth University, Medical College of Virginia, Richmond, VA 23298.* Accepted for publication February 12, 1981.

**Abstract** □ Parsley cigarettes containing [$^3$H]phencyclidine were machine smoked, and the mainstream smoke was trapped in glass wool filters. Radioactivity was extracted from these filters with chloroform. The average recoveries of radioactivity were 76, 85, 70, and 69% for cigarettes containing 3, 10, 30, and 50 mg of [$^3$H]phencyclidine hydrochloride, respectively. TLC and GLC–mass spectrometry were employed to identify and quantify compounds in the filter extracts. Approximately one-half of the recovered radioactivity represented a pyrolysis product, phenylcyclohex-1-ene. Formation of this product involved loss of piperidine from phencyclidine. Piperidine, which was not radiolabeled, also may appear in smoke intact. The remainder of the radiolabeled material represented unchanged phencyclidine. Therefore, the percentage of [$^3$H]phencyclidine delivered was ~40% of the amount smoked. This result was independent of puff frequency and quantity of phencyclidine hydrochloride smoked over the range tested. The [$^3$H]phencyclidine delivery was compared to the quantities of [$^3$H]-$\Delta^9$-tetrahydrocannabinol and [$^3$H]nicotine delivered in mainstream smoke. The recovery of unchanged [$^3$H]-$\Delta^9$-tetrahydrocannabinol from placebo marijuana cigarettes injected with a solution containing 3 mg of $\Delta^9$-tetrahydrocannabinol was 60%. Tobacco cigarettes injected with [$^3$H]nicotine yielded 70% unchanged nicotine in mainstream smoke.

**Keyphrases** □ Pyrolysis—formation of phenylcyclohex-1-ene from phencyclidine in smoke □ Phencyclidine—identification of pyrolysis product phenylcyclohex-1-ene in smoke □ Phenylcyclohex-1-ene—pyrolysis product of phencyclidine identified in smoke □ Smoke—identification of phenylcyclohex-1-ene, a pyrolysis product of phencyclidine

Phencyclidine [1-(1-phenylcyclohexyl)piperidine] has gained popularity as a drug of abuse, probably because it produces euphoria, dissociation, and hallucinations (1). Smoking phencyclidine-impregnated spices is currently a major method of abuse. The high temperature attained in a burning cigarette raises the possibility that phencyclidine may evolve pyrolysis products when smoked. Phencyclidine is converted to phenylcyclohex-1-ene in the gas chromatograph at low temperatures (2) (Scheme I), which may have led to the conclusion that phenylcyclohexene is a metabolite of phencyclidine (3). Preliminary results indicate that phenylcyclohexene also is formed during smoking (4). In this study, the amount of phencyclidine delivered in mainstream smoke was determined and the pyrolysis products were identified and quantified.

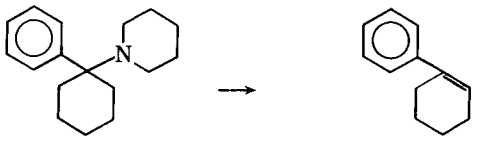


phencyclidine → phenylcyclohex-1-ene

*Scheme I*

## EXPERIMENTAL

**Drugs**—Phencyclidine hydrochloride[1], piperidinocyclohexane carbonitrile[1], [*phenyl*-1-$^3$H(*n*)]phencyclidine[1] (17 Ci/mmole), $\Delta^9$-tetrahydrocannabinol[1], and [1′,2′-$^3$H]-$\Delta^9$-tetrahydrocannabinol[1] (43 mCi/mmole) were used. [*pyrrolidinyl*-4′,4-$^3$H]Nicotine (4.7 Ci/mmole) was synthesized according to the procedure of Vincek *et al.* (5).

**Preparation of Cigarettes**—Cigarettes containing phencyclidine were prepared using commercially available parsley flakes[2], 55-mm cigarette tubes[3], and a cigarette machine[4]. Each cigarette (550–600 mg) was prepared immediately prior to its use by injection with 0.5 μCi of [$^3$H]-phencyclidine and 3, 10, 30, or 50 mg of phencyclidine hydrochloride in volumes of 50, 50, 150, or 200 μl of ethanol, respectively. Filterless cigarettes[5] (84 mm) were injected with 0.5 μCi of [$^3$H]nicotine in 50 μl of ethanol, and placebo marijuana cigarettes[1] were injected with 0.5 μCi of [$^3$H]-$\Delta^9$-tetrahydrocannabinol and 3 mg of $\Delta^9$-tetrahydrocannabinol in 50 μl of ethanol. All drug solutions were injected axially and evenly throughout the middle 35 mm of the cigarettes and allowed to dry before smoking.

**Procedure**—Cigarettes were inserted in a holder and attached to the smoking apparatus (Fig. 1). Smoking was effected by negative pressure provided by water aspiration, and smoke was collected on two contiguous filters (each consisting of 1–1.25 g of glass wool stuffed in 16 cm of 0.635-cm i.d. tubing[6]). Interfaced between the filters and vacuum source were an empty trap (for back-siphoning) and a trap containing 10 ml of chloroform.

Puffing was accomplished with an electric switching valve[7] that opened and closed the system to the vacuum every 5.8 sec. Puff frequency was altered by replacement of a capacitor in the circuit board controlling the valve. A vacuum regulator[8] was set to permit delivery of 45 ml of smoke/5.8-sec puff duration. After an entire cigarette was smoked, each

[1] National Institute on Drug Abuse.
[2] McCormick and Co., Baltimore, Md.
[3] Dominion Cigarette Tube Co., Montreal, Canada.
[4] Premier Supermatic, Central Tobacco Manufacturing Co. Ltd., Montreal, Canada.
[5] Pall Mall, American Tobacco Co., Richmond, Va.
[6] Tygon Tubing and Molded Products, Akron, Ohio.
[7] Skinner, New Britain, Conn.
[8] Fairchild, Winston-Salem, N.C.



*0022-3549/81/0900-1002$01.00/0*
© *1981, American Pharmaceutical Association*

Table I—Recovery of [$^3$H]Phencyclidine from Mainstream Smoke

| [$^3$H]Phencyclidine[a], mg | Radioactivity Recovered[b], % | Quantity Recovered[c], mg (micromoles) | |
|---|---|---|---|
| | | Phencyclidine | Phenylcyclohexene |
| 2.62 | 76 ± 4 | 1.43 (5.88) | 0.56 (3.54) |
| 8.73 | 84 ± 4 | 4.62 (19.01) | 2.71 (17.15) |
| 26.20 | 70 ± 4 | 11.19 (48.01) | 7.15 (45.20) |
| 43.63 | 69 ± 5 | 16.26 (66.92) | 13.84 (87.57) |

[a] Quantity of [$^3$H]phencyclidine injected into cigarettes that corresponds to 3, 10, 30, or 50 mg of the hydrochloride salt. [b] Means ± *SE* of $n = 3$. [c] Determined by TLC analysis.

filter tubing unit was washed with chloroform (40 ml), and 50-μl aliquots were placed in scintillation vials with 10 ml of aqueous counting scintillant[9]. A rinse of the cigarette holder was included in the wash of the first filter. Each sample was assayed for radioactivity in a scintillation counter[10]. Quench was corrected by external standardization.

**Temperature of Burning Cigarette**—A thermocouple[11] measured the temperature within a burning parsley cigarette. The temperature-sensitive electrode was inserted perpendicular to the long axis of the cigarette at its midpoint, and the temperature was recorded every 5 sec.

**TLC**—To quantify [$^3$H]phencyclidine and identify pyrolytic products, 150 μl of each chloroform wash of the glass wool was applied as a band to each of two 5 × 10-cm silica gel TLC plates[12] along with 5 μg of phencyclidine and phenylcyclohexene. One plate was developed in chloroform–methanol–concentrated ammonia (90:10:0.15), in which phencyclidine had an $R_f$ value of 0.42 and phenylcyclohexene moved with the solvent front. The other plate was developed in hexane–concentrated ammonia (5:0.04), in which phencyclidine remained at the origin and phenylcyclohexene had an $R_f$ value of 0.42. The bands were visualized by exposure to iodine vapor, and the plates then were divided into bands and scraped into scintillation vials containing 0.5 ml of methanol and 0.5 ml of water. The samples were sonicated for 30 min, and radioactivity was counted in 10 ml of counting fluid[13]. Counting efficiency was corrected by internal standardization using [$^3$H]toluene[14].

The [$^3$H]nicotine and [$^3$H]-$\Delta^9$-tetrahydrocannabinol smoke condensates were analyzed by TLC as already described. The solvent system for [$^3$H]nicotine was ether–acetone–concentrated ammonium hydroxide (4:1:0.15). The samples were cochromatographed with 3 μg of nicotine ($R_f$ 0.67), and the standard was visualized by spraying with Dragendorff solution. The [$^3$H]-$\Delta^9$-tetrahydrocannabinol samples were cospotted with 3 μg of $\Delta^9$-tetrahydrocannabinol. After development in 40–60% petroleum ether–ether (4:1), $\Delta^9$-tetrahydrocannabinol ($R_f$ 0.56) was visualized by spraying with 0.1% Fast Blue B in 1 *N* NaOH.

**GLC–Mass Spectrometry**—The instrument[15] was operated at an accelerating voltage of 1.55 kv, an electron energy of 70 ev, a separator temperature of 250°, an ion source temperature of 250°, and an injector temperature of 200°. The glass column (1 m × 2 mm) was packed with 3% (w/w) SP-2250 on 80–100-mesh Gas Chrom Q[16], and the carrier gas (helium) flow rate was 30 ml/min. The initial column temperature of 160° was increased to 180° immediately after phenylcyclohexene was eluted (0.95 min).

## RESULTS

The smoking interval for the average cigarette (smoked in its entirety) was ~6 min when a puff interval of 5.8 sec was used. The temperature at the midpoint of the parsley cigarettes ($n = 8$) reached a maximum of 671 ± 13°. The midpoint temperature was >400° for ~0.5 min (5 mm of cigarette burned), indicating that the cigarette components were subjected to high temperatures for a considerable time.

**Recovery of Radioactivity from Cigarettes**—After the smoking of a cigarette containing 3 mg of [$^3$H]phencyclidine hydrochloride, 76% of the radioactivity was found in the first filter and none was found in the second (Table I). Increasing the quantity of [$^3$H]phencyclidine hydrochloride in the cigarettes did not affect recovery. The possible effect of puff frequency on recovery also was investigated by increasing the interpuff interval from 5.8 to 30 sec. At the lower puff frequency, 67 ± 6% ($n = 3$) of the radioactivity in a cigarette containing 10 mg of [$^3$H]phencyclidine hydrochloride was recovered, which was slightly less than that recovered with the 5.8-sec interpuff interval.

**TLC Analysis**—In the solvent systems used, either phenylcyclohexene ran with the solvent front or phencyclidine remained at the origin. To ensure complete separation, the samples were chromatographed using two systems. The percentages of recovered radioactivity corresponding to phencyclidine and phenylcyclohexene were the same regardless of the TLC system employed.

All of the condensates contained appreciable quantities of phenylcyclohexene, which ranged from 37 to 54% of the recovered material (Table I). The percentage of phencyclidine converted to phenylcyclohexene increased somewhat as the quantity of phencyclidine was increased. Alteration of puff frequency produced no change in the relative amounts of phencyclidine and phenycyclohexene recovered. Experiments also were carried out to determine whether there was a constant delivery of radioactivity throughout the smoking process. Collection of smoke from the burning of the first third of the cigarette resulted in 16.3 ± 1% of the total recovered radioactivity; the second third accounted for 31 ± 5.6%, and the last third was 52.3 ± 7.0% of the total recovered ($n = 3$/group). The total recovery of the added [$^3$H]phencyclidine was 68 ± 5%.

**Identification and Quantification by GLC–Mass Spectrometry**—To identify phencyclidine and its pyrolytic products, mass spectra of standard compounds were recorded. Piperidinocyclohexane carbonitrile was injected into the GLC–mass spectrometer where it was readily converted to piperidinocyclohex-1-ene (6), which had a retention time of 0.8 min. Piperidinocyclohex-1-ene had a base peak at $m/z$ 164 and abundant ions at $m/z$ 150 (80% relative intensity), 136 (65%), and 122 (39%). Phenylcyclohexene (retention time 0.9 min) had a molecular ion at $m/z$ 158 (75%) and a base peak at $m/z$ 129. The mass spectrum of phencyclidine (retention time 3.7 min) was similar to that reported previously (2) in that $m/z$ 200 was the base peak and abundant ions were at $m/z$ 158 (57%), 129 (54%), and 91 (93%).

Three smoke condensates were selected randomly for continuous GLC–mass spectrometric scanning. Phencyclidine and phenylcyclohexene were present in all three samples, and no other pyrolysis products were identified. These same three samples also were analyzed by single-ion monitoring. Ions $m/z$ 129 and 200 were detected at the appropriate retention times for phenylcyclohexene and phencyclidine (Fig. 2), but there was no detectable $m/z$ 164 for piperidinocyclohex-1-ene. For quantitative purposes, separate calibration curves were constructed for phencyclidine and phenylcyclohexene in the 50–500-ng/μl concentration range by monitoring ions 200 and 129. The average ratio of phencyclidine to phenylclohexene in the three samples was 1.04 ± 0.02 on a molecular basis, which was in good agreement with the TLC analysis. Since phencyclidine is labile in the gas chromatograph (2), phencyclidine standards were analyzed for degradation products. Less than 0.5% of the phencyclidine was converted to phenylcyclohexene under the GLC–mass spectrometric conditions employed (Fig. 2).

**Recovery of Other Drugs of Abuse in Smoke**—Placebo marijuana cigarettes ($n = 3$) spiked with [$^3$H]-$\Delta^9$-tetrahydrocannabinol were smoked, and 94 ± 3% of the radioactivity was recovered in the first filter. Likewise, 73 ± 1% ($n = 3$) of the radioactivity in tobacco cigarettes in-

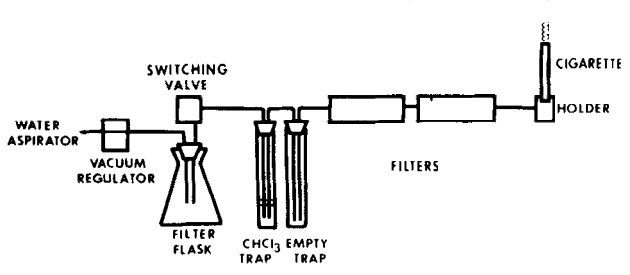


**Figure 1**—*Smoking apparatus.*

[9] ACS, Amersham Corp., Arlington Heights, Ill.
[10] Beckman Instruments, Palo Alto, Calif.
[11] Wahl Instruments, Culver City, Calif.
[12] Analtech, Newark, Del.
[13] Spectrafluor, Amersham Corp., Arlington Heights, Ill.
[14] New England Nuclear, Boston, Mass.
[15] Finnigan 4000 GLC–mass spectrometer, Finnigan, Sunnyvale, Calif.
[16] Applied Science Laboratories, State College, Pa.

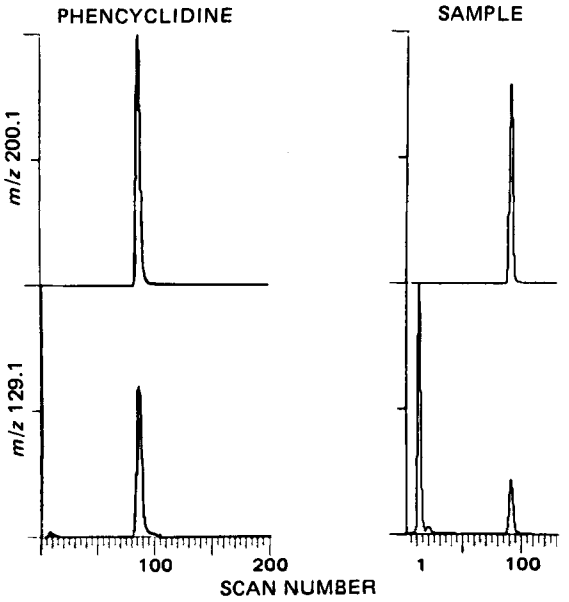


**Figure 2**—*Single-ion monitoring of phencyclidine and a sample.*

jected with [$^3$H]nicotine was recovered in the first filter. TLC analysis of the [$^3$H]-$\Delta^9$-tetrahydrocannabinol smoke condensate showed that 63% of the radioactivity was due to unchanged material so that 60% of the starting material was delivered in mainstream smoke. Ninety-five percent of the radioactivity recovered from the [$^3$H]nicotine cigarettes remained unchanged. Therefore, 70% of the original [$^3$H]nicotine was recovered from mainstream smoke.

## DISCUSSION

In cigarettes containing 3–50 mg of phencyclidine hydrochloride, an amount equivalent to that found in some street samples (7), ~40% of the starting material was recovered from mainstream smoke. The pyrolysis product, phenylcyclohexene, was present in concentrations comparable to those of phencyclidine. Therefore, the percentage of both compounds delivered in mainstream smoke was independent of the quantity of phencyclidine present. Since formation of phenylcyclohexene involves loss of the piperidine moiety from phencyclidine, it would be reasonable to assume that equimolar concentrations of piperidine also are delivered in smoke. Alteration of the puff frequency had little effect on the quantities of phencyclidine and phenylcyclohexene evolved, indicating minor importance of this variable on smoke composition.

This independence of smoke composition from the amount of drug and frequency of puffing suggests that illicit use of phencyclidine-containing cigarettes can be expected to yield amounts of phencyclidine and its pyrolysis product, phenylcyclohexene, similar to those found in this study. Also, the concentration of phencyclidine in mainstream smoke increased as the smoking period progressed, indicating that the drug condensed in the butt as smoking proceeded. This observation suggests that smokers are subjected to varying phencyclidine concentrations during the exposure period.

The recovery of phencyclidine in mainstream smoke was somewhat lower than that found for two other drugs of abuse. However, the recoveries of tetrahydrocannabinol and nicotine were higher than previously found (8, 9). The higher recoveries reported may be due, at least in part, to the high capacity of the glass wool filter to trap smoke components. The short cigarette–filter trap distance used, which approximated the actual smoking situation, minimized drug adsorption on the smoking apparatus. Moreover, cigarettes were burned in their entirety since no data are available concerning butt size of phencyclidine cigarettes. Undoubtedly, the length of cigarette that remains unsmoked varies considerably. The delivery of phencyclidine in smoke as reported in this study would be somewhat higher than the exposure to a smoker.

The relevance of phenylcyclohexene and piperidine intoxication and toxicity due to phencyclidine smoking has yet to be determined. Little is known of the pharmacological effects or toxicity of these products to which phencyclidine abusers are exposed. Preliminary results show the acute lethality of phenylcyclohexene to be an order of magnitude less than that of phencyclidine in rats and mice (4). Likewise, the acute toxicity of piperidine in rats appears to be 10-fold less than that of phencyclidine (10). The pyrolysis and delivery in smoke will be important considerations for experimentation involving inhalation of phencyclidine by smoking.

## REFERENCES

(1) E. D. Luby, B. D. Cohen, G. Rosenbaum, J. S. Gottlieb, and R. Kelley, *Arch. Neurol. Psychiatry*, **81**, 363 (1959).

(2) D. C. K. Lin, A. F. Fentiman, Jr., R. L. Foltz, R. D. Forney, Jr., and I. Sunshine, *Biomed. Mass Spectrom.*, **2**, 206 (1975).

(3) R. E. Ober, G. W. Gwynn, T. Chang, D. A. McCarthy, and A. J. Glazko, *Fed. Proc. Fed. Am. Soc. Exp. Biol.*, **22**, 539 (1963).

(4) B. R. Martin, A. S. Freeman, K. L. Kelly, V. M. Clayton, W. C. Vincek, and L. S. Harris, *ibid.*, **39**, 302 (1980).

(5) W. C. Vincek, B. R. Martin, M. D. Aceto, and E. R. Bowman, *J. Med. Chem.*, **23**, 960 (1980).

(6) C. Helisten and A. T. Shulgin, *J. Chromatogr.*, **117**, 232 (1976).

(7) G. D. Lundberg, R. C. Gupta, and S. H. Montgomery, *Clin. Toxicol.*, **9**, 503 (1976).

(8) J. E. Manno, G. F. Kiplinger, S. E. Haine, I. F. Bennett, and R. B. Forney, *Clin. Pharmacol. Ther.*, **11**, 808 (1970).

(9) I. Schmeltz, A. Wenger, D. Hoffmann, and T. C. Tso, *J. Agric. Food Chem.*, **27**, 602 (1979).

(10) H. F. Smyth, Jr., C. P. Carpenter, C. S. Weil, V. C. Pozzani, and J. A. Striegel, *Am. Ind. Hyg. Assoc. J.*, **23**, 95 (1962).

## ACKNOWLEDGMENTS

Supported by U.S. Public Health Service Grants DA-02396, DA-00490, and DA-07027.

The authors thank Dr. W. C. Vincek for helpful suggestions and Mr. Edward M. Dimen for technical assistance.

# Energy Relations in Compression of Polymeric Materials and Granulations

**HATEM FESSI *, JEAN-PAUL MARTY *, F. PUISIEUX *, and J. T. CARSTENSEN ‡x**

Received February 25, 1980, from the **Faculte de Pharmacie, Universite de Paris-Sud, 92290 Chatenay-Malabry, France*, and the ‡*School of Pharmacy, University of Wisconsin, Madison, WI 53706.* Accepted for publication February 12, 1981.

**Abstract** □ In tablet compression, a force, $F$, is exerted on a punch penetrating into a tablet die. For a stationary bottom punch, the force on the upper punch is a function, $F = f(x)$, of penetration and this value was previously determined empirically. Since differential energy is force, $f(x)$, multiplied by distance, $dx$, the integral $\int f(x)dx$ between limits should give the energy input into the tablet. The integral yields an expression where energy input is a linear function of the logarithm of the maximally applied pressure, $F^*$, a fact substantiated by the data presented.

**Keyphrases** □ Tablet compression—energy relations, polymeric materials and granulations □ Energy relationships—tablet compression, polymeric materials and granulations □ Parmentier–Führer equation—energy relations in tablet compression, polymeric materials and granulations

Many tablet properties (hardness, disintegration, dissolution, and thickness) are a function of the pressure at which the tablets are made, which essentially is the maximum pressure in the compression cycle. The energy input into the tablet is a more logical parameter for correlation with tablet properties but is less easily derived. The intent of this study was to obtain the pertinent correlations between the maximally applied pressure during the compression cycle and the energy imparted to the tablet in the compression step.

## EXPERIMENTAL

The tablet compositions listed in Table I were used. The polymers were polyvinyl alcohol[1], polyvinyl chloride[2], and a copolymer[3] of the two. Their respective particle sizes were 250–400 μm, <5 μm, and 80–125 μm. The three polymers were compressed first without additives and then as a granulation with the following composition: 20% diphenhydramine hydrochloride, 50% polymer, 1.5% povidone, and a quantity of tribasic calcium phosphate, *qs*. In the last three formulas listed, the polymer quantity was varied (to 60 and 70%) and the amount of tribasic calcium phosphate was reduced.

The granulations were made by mixing the tribasic calcium phosphate and the polymer and granulating with a 3.75% solution of povidone in isopropanol, except in one case where methylene chloride was used. The alcohol-wet granulations were dried in a small fluid bed drier[4] for 20 min at 60° and then were passed through an oscillating granulator through a 1-mm opening. The mesh fraction between 200 and 800 μm was obtained by sieving and was used for compression. Compression was carried out on a single-punch tablet machine[5] equipped with strain gauges for measuring upper and lower punch pressures and punch displacement. Compressions then were effected at a speed corresponding to one-sixtieth of a second per cycle, with upper punch pressures, $P$, of approximately 2, 3, 4, 5, and 6 tons, accurately monitored; 12-mm flat-faced punches were used.

## RESULTS AND DISCUSSION

In a tablet operation, powder first is introduced into the tablet die in loose packing (Fig. 1*a*) since it flows into the die and simply attains its cascaded density. Ideally, the penetration, $x$, of the upper punch starts at this point, denoted $x = -a$ (Fig. 2). The particles then rearrange to their closest packing (Fig. 1*b*), after which they are deformed elastically by further penetration of the upper punch. At a particular point ($x = 0$ in Fig. 2), the limit of elasticity is reached. From $x = -a$ to $x = 0$, the force, $F$, exerted by the upper punch is assumed here to be proportional to $x$ (although this assumption is not crucial).

At $x = 0$, the force has achieved a value of $F_0$; *i.e.*, up to the elastic limit, one may write:

$$F = F_0(x + a)/a \qquad -a \leqq x \leqq 0 \qquad \text{(Eq. 1)}$$

Beyond the elastic limit (1–10), substantial amounts of work, $A$, are required for further penetration of the upper punch, and particle fracture and/or plastic deformation take place (Fig. 1*c*). The deepest penetration is denoted $x = q$ (Fig. 2).

Parmentier (1) and Führer (2) suggested a force–displacement relationship that is hyperbolic; if it is confined to the $x \geqq 0$ region, it may be expressed as follows:

$$F = F'/(b - x) \qquad 0 \leqq x < b \qquad \text{(Eq. 2)}$$

where $F'$ is a constant and $b$ is an upper limit for $x$. It then follows

**Table I—Compounds Used and Least-Squares Fit Parameters from Fitting Areas of Energy Loop to Eq. 8**

| Formula | Correlation Coefficient | Slope, $F_0b$ | Intercept, $-F_0b \ln F_0$ | $F_0 \times 10^{-3}$, N |
|---|---|---|---|---|
| Polyvinyl chloride | 0.995 | 14.6 | −126 | 5.35 |
| Polyvinyl chloride + excipients[a] | 0.991 | 20.2 | −182 | 8.21 |
| Polyvinyl alcohol | 0.99 | 25.0 | −226 | 8.63 |
| Polyvinyl alcohol + excipients | 0.98 | 15.9 | −141 | 7.02 |
| Polyvinyl alcohol–polyvinyl chloride copolymer | 0.97 | 21.3 | −196 | 10.1 |
| Copolymer (50%) + excipients | 0.99 | 18.8 | −168 | 7.61 |
| Copolymer (60%) + excipients | 0.98 | 16.5 | −144 | 6.21 |
| Copolymer (70%) + excipients | 0.96 | 25.5 | −234 | 9.58 |
| Copolymer (50%) + excipients + methylene chloride | 0.96 | 19.1 | −170 | 7.68 |

[a] Excipients denote presence of diphenhydramine, povidone, and tribasic calcium phosphate; granulated with isopropanol unless otherwise stated.

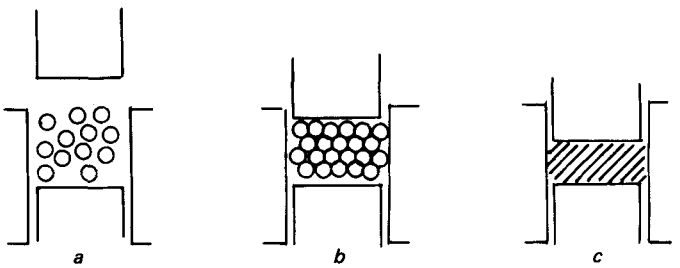


**Figure 1**—*The three basic steps in the tableting process: filling of die at cascaded density (a), rearrangement (b), and situation after plastic deformation and/or brittle fracture (c).*

[1] Rhodopas H, Rhone-Poulenc, France.
[2] Pevikon, 637P, Seppic, Paris, France.
[3] 15PVA/85PVC, Solvic, Solvay, France.
[4] Glatt, Basel, Switzerland.
[5] Frogerais type AO, Societe Edmond Frogerais, Vitry-sur-Seine, France.

0022-3549/81/0900-1005$01.00/0
© 1981, American Pharmaceutical Association

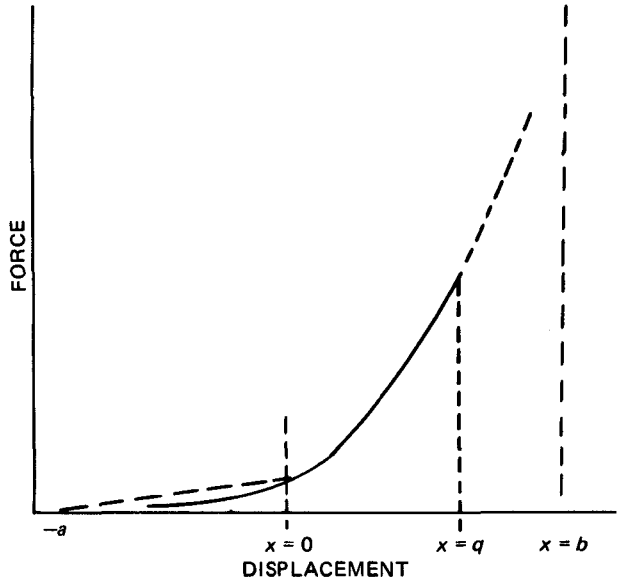


**Figure 2**—*Schematic of force–displacement cycle,* F = f(x).

that:

$$F' = F_0 b \qquad \text{(Eq. 3a)}$$

$$F = F_0 b/(b - x) \qquad \text{(Eq. 3b)}$$

The largest applied force, $F^*$ (corresponding to $x = q$), is given by:

$$F^* = F_0 b/(b - q) \qquad \text{(Eq. 4)}$$

The ideal graph then is as shown in Fig. 2. A typical experimental *F versus* $x$ plot is shown in Fig. 3.

In relating such data to the Parmentier–Führer equation (Eq. 2), it is noted that the value of $b$ is not known and the data in Fig. 3*b* are in the form:

$$\ln F = -Q \ln (b - x) + P \qquad \text{(Eq. 5)}$$

where $Q$ and $P$ are constants. If Eq. 2 holds, then $Q$ should equal −1. A best value of $b$ can be found by iteration as the value giving the least sum

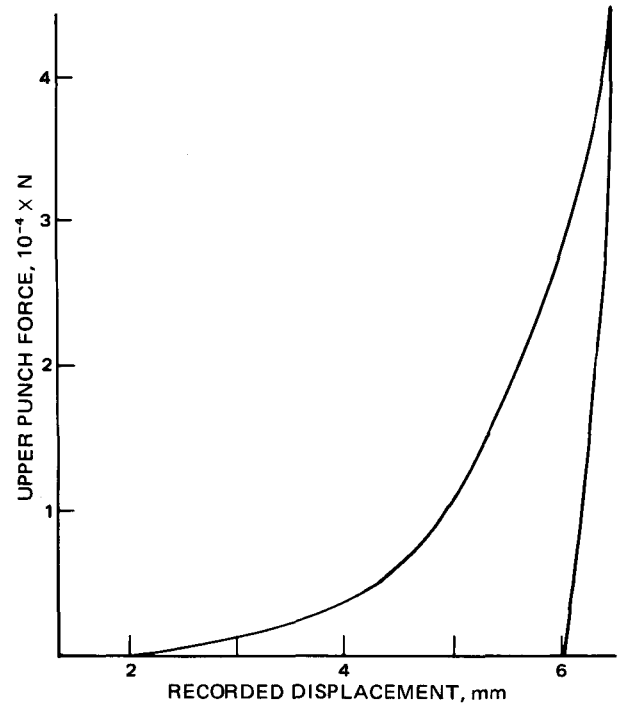


**Figure 3**—*Force–displacement cycle of granulation of polyvinyl acetate–polyvinyl chloride copolymer (50%) plus excipients. Compression maximum is 5 tons.*

**Table II—Data in Fig. 3 Treated According to Eq. 5**

| $x$, mm | $F$, $10^{-4}$ N | $\ln F \times 10^{-4}$, $y$ | $\ln (b - x)$ $b$ = 6.7 | $b$ = 6.5 | $b$ = 6.45 | $b$ = 6.55 | $b$ = 6.6 | $b$ = 6.9 |
|---|---|---|---|---|---|---|---|---|
| 3.65 | 0.28 | −1.27 | 1.05 | 0.98 | 0.96 | 0.99 | 1.01 | 1.12 |
| 5.50 | 1.4 | 0.34 | 0.18 | 0 | −0.05 | 0.05 | 0.095 | 0.34 |
| 5.95 | 2.28 | 0.82 | −0.29 | 0.60 | −0.69 | −0.51 | −0.43 | −0.05 |
| 6.3 | 3.44 | 1.24 | −0.92 | −1.61 | −1.90 | −1.39 | −1.20 | −0.51 |
| 6.35 | 4.48 | 1.50 | −1.05 | −1.90 | −2.30 | −1.61 | −1.39 | −0.60 |
| $(n-2)s^2_{yx}$ [a] | | | 0.21 | 0.42 | 0.54 | 0.26 | 0.29 | 0.68 |
| Slope $\alpha$ | | | −1.25 | −0.89 | −0.77 | −0.99 | −1.08 | −1.08 |
| Intercept | | | 0.27 | −0.03 | −0.09 | 0.04 | 1.11 | 0.42 |
| Correlation coefficient | | | −0.98 | −0.95 | −0.94 | −0.96 | −0.97 | −0.93 |

[a] Sum of deviations squared, *i.e.*, $(n-2)s^2_{yx} = \Sigma(y - \bar{y})^2 - \alpha^2(\Sigma\{x - \bar{x}\}^2)$.

of squares of ln $F$ regressed on ln $(b - x)$. This procedure is shown in Table II for the data of the type shown in Fig. 3. It is noted from Table II that the sum of squares is not exceedingly sensitive to the chosen value of $b$; *i.e.*, there is a broad minimum in the value of the sum of squares for $b$ values ranging from 6.45 to 6.7. The data treated according to Eq. 5 are shown graphically in Fig. 4. Based on the best-fit criteria, it would be somewhat difficult to choose one $b$ value over another in this range; what is important is that the range entails the slope $Q = -1$, which is the one dictated by Eq. 2.

The experimental zero point for $x$ is chosen judiciously but nevertheless arbitrarily. However, since the value of $b$ is obtained by iteration, this fact does not matter. If $x' = 0$ is chosen where $x$ is actually 2, then $b$ by iteration also would increase by a value of 2, and $(b - x)$ would have the same value as if $x$ had been accurately chosen.

The value of $b$ is related to (but not identical to) the true density, $\rho$, of the nonporous solid composition. True correspondence would exist if $\rho$ were pressure independent; however, $\rho$ is a function of $F$.

In compression (Figs. 1*b* and 1*c*), the work, $A$, done by the upper punch as it moves an infinitesimal distance, $dx$, against the powder mass is given by:

$$dA = F\,dx \qquad \text{(Eq. 6)}$$

The total work (energy imparted to the tablet during the compression step but excluding the decompression step) then is obtained by integration from zero to $x = q$, *i.e.*:

$$A = \int_0^q F_0 b/(b - x)dx = F_0 b[\ln b/(b - q)] \qquad \text{(Eq. 7)}$$

Introducing Eqs. 3*b* and 4 gives:

$$A = F_0 b \ln F^* - F_0 b \ln F_0 \qquad \text{(Eq. 8)}$$

As mentioned earlier, due to the floating nature of $b$, Eqs. 7 and 8 are independent of the experimental choice of $x = 0$.

Equation 8 predicts that a plot of the energy, $A$, as a function of ln $F$ should be linear and that the ratio of the slope to the intercept should be $-\ln F_0$. These energies were obtained as the areas under the curves of the type shown in Fig. 3. The data are indeed linear, as shown in Fig. 5, and the least-squares fit values of all formulas tested are shown in Table

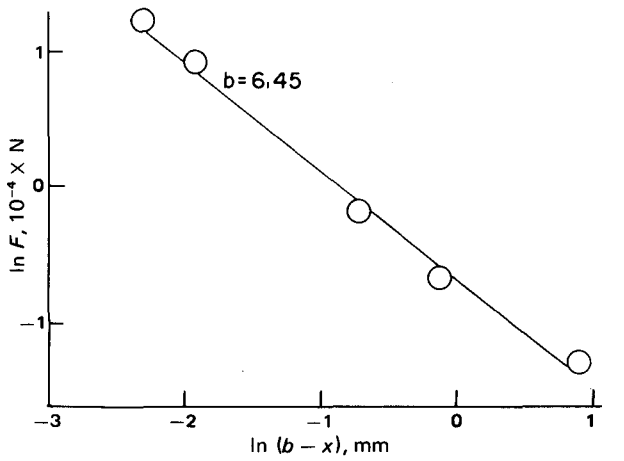


**Figure 4**—*Data in Fig. 3 (upper curve) treated according to Eq. 5.*

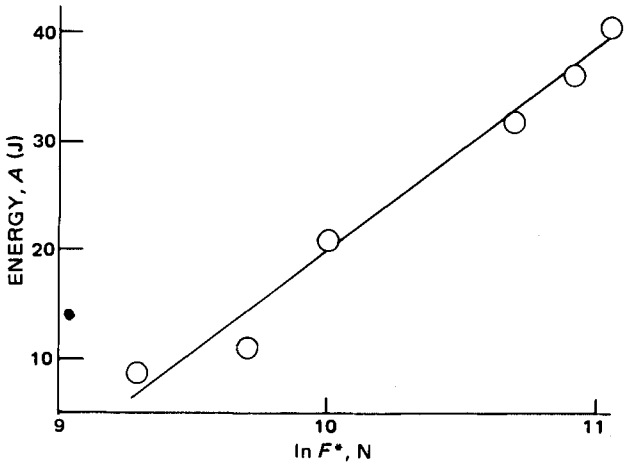


**Figure 5**—*Areas from plots of the type in Fig. 3 at six different pressures, plotted as a function of maximal pressure according to Eq. 6.*

I. The last column gives the $F_0$ value that is the smallest force necessary for actual displacement beyond the rearrangement step. It is seen from Table I that, for example, for "excipient + copolymer (50%)" (the case shown in Fig. 3), $F_0b$ ln $F_0$ = 168 J and $F_0b$ = 18.8 J. In other words, ln $F_0$ = 168/18.8 = 8.94, or $F_0$ = 6610 N. This value corresponds to an ordinate of 0.66 in Fig. 3, which corresponds to a "recorded" abscissa value (with arbitrary zero) of 4.5 mm.

Since $F_0b$ = 18.8, it follows that $b$ = 18.8/$F_0$ = 0.0028 m = 2.8 mm. Hence, in Fig. 3, the final asymptote would be at a recorded abscissa value of 4.5 + 2.8 = 7.3 mm (again recalling that the zero is somewhat arbitrary). At this point, the distance between the upper and lower punch would be 2.4 mm[6]. If the solid achieves its true density at $b$, then the true density can be deduced. The die has a diameter of 12 mm; *i.e.*, the volume between the upper and lower punch is equal to [$\pi$ (1.2$^2$/4) 0.24] = 0.27 cm$^3$.

[6] This value is obtained from knowledge of the lower punch position in relation to the arbitrary zero and does not account for possible compression of the presumably static lower punch.

The weight of the solids is 500 mg, so the true density would have a value of 0.5/0.27 = 1.84 g/cm$^3$, which is reasonable. Since compression can possibly (and presumably does) produce densities that are higher than the true densities at atmospheric pressure, the calculated figure only has interest in that it is of a reasonable magnitude. Furthermore, Eq. 8 deals with the energy input and assumes that the relaxation trace in Fig. 3 (the recovery) is vertical. This approximation becomes poorer the more pronounced the recovery after upper punch release.

## SUMMARY

The present study shows that the Parmentier–Führer equation for the value of the upper punch force as a function of displacement is useful and can be used to deduce mathematically energy *versus* maximum force relationships for energy input. These relationships were validated experimentally. The plots provide an estimate of the point in the displacement of the upper punch where the powder or granulation was rearranged to its closest packing.

## REFERENCES

(1) W. Parmentier, Ph.D. thesis, Technical University Carolo-Wilhemina zu Braunschweig, Braunschweig, West Germany, 1974, pp. 1–90.

(2) C. Führer, *Dtsch. Apoth.-Ztg.*, **105**, 1150 (1965).

(3) P. Toure, Ph.D. thesis, University of Paris-Sud, Chatenay-Malabry, France, 1979, p. 102.

(4) P. Toure, D. Duchene, F. Puisieux, and J. T. Carstensen, *Powder Technol.*, **26**, 213 (1980).

(5) J. T. Carstensen: "Rate Processes and Mechanical Properties in Solid Pharmaceutics," Academic, New York, N.Y., 1980, pp. 187–214.

(6) W. M. Long, *Powder Metall.*, **6**, 73 (1960).

(7) S. Leigh, J. E. Carless, and B. W. Burt, *J. Pharm. Sci.*, **56**, 888 (1967).

(8) J. J. Windheuser, J. Misra, S. P. Eriksen, and T. Higuchi, *ibid.*, **52**, 767 (1963).

(9) A. Obiorah, *Int. J. Pharm.*, **1**, 249 (1978).

(10) K. Marshall, "The Physics of Tablet Compression, 12th Arden House Conference, Feb. 2, 1977, Conference Notes," Colorcon, West Point, Pa., pp. 15, 16.

# Mevalonic Acid Analogs as Inhibitors of Cholesterol Biosynthesis

**C. ROWAN DeBOLD * and J. C. ELWOOD ˣ**

Received September 26,1980, from the *Department of Biochemistry, State University of New York, Upstate Medical Center, Syracuse, NY 13210.* Accepted for publication February 20, 1981. *Present address: Department of Medicine, Division of Endocrinology, Vanderbilt University School of Medicine, Nashville, TN 37232.

**Abstract** □ A series of 20 mevalonic acid analogs was synthesized and tested for their ability to inhibit cholesterol biosynthesis from [2-$^{14}$C]-mevalonate in rat liver homogenates. Removal of the 5-hydroxyl group from mevalonic acid produced an active inhibitor, 3-hydroxy-3-methylpentanoic acid. Removal of the 3-hydroxyl group, addition of an aromatic group in the 3-position, or insertion of a double bond reduced inhibitory activity. Compounds with an aromatic group or halide on the 5-position were active inhibitors. The most active inhibitor was 5-phenylpentanoic acid, with 50% inhibition at 0.064 m*M*.

**Keyphrases** □ Mevalonic acid—analogs synthesized as potential cholesterol biosynthesis inhibitors □ Cholesterol—inhibitors, synthesis and testing of mevalonic acid analogs □ Structure–activity relationships—mevalonic acid analogs as inhibitors of cholesterol biosynthesis

Considerable progress has been made in understanding the biosynthesis of cholesterol (1, 2). Mevalonic acid, the product of the major rate-limiting reaction of cholesterol biosynthesis, is converted to isopentenyl pyrophosphate by three enzymes, each requiring $Mg^{2+}$ and ATP. The first step is phosphorylation at position 5 by mevalonate kinase (EC 2.7.1.36). Next, 5-pyrophosphomevalonate is formed by phosphomevalonate kinase (EC 2.7.4.2). This product is decarboxylated and dehydrated by pyrophosphomevalonate decarboxylase (EC 4.1.1.33), possibly involving 3-phospho-5-pyrophosphomevalonate as an intermediate.

Interest has focused on these reactions for various reasons. For example, the role of cholesterol in atherosclerosis prompted a search for inhibitors of these reactions with the prospect of decreasing cholesterol synthesis (3–7). It also has been suggested that the decreased brain cholesterol levels seen in phenylketonuria may be due to inhibition of these steps by elevated levels of phenylalanine

0022-3549/81/0900-1007$01.00/0
© 1981, American Pharmaceutical Association

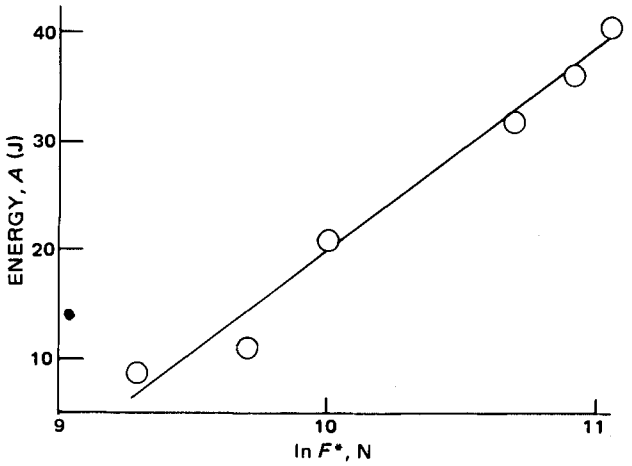


**Figure 5**—*Areas from plots of the type in Fig. 3 at six different pressures, plotted as a function of maximal pressure according to Eq. 6.*

I. The last column gives the $F_0$ value that is the smallest force necessary for actual displacement beyond the rearrangement step. It is seen from Table I that, for example, for "excipient + copolymer (50%)" (the case shown in Fig. 3), $F_0b$ ln $F_0$ = 168 J and $F_0b$ = 18.8 J. In other words, ln $F_0$ = 168/18.8 = 8.94, or $F_0$ = 6610 N. This value corresponds to an ordinate of 0.66 in Fig. 3, which corresponds to a "recorded" abscissa value (with arbitrary zero) of 4.5 mm.

Since $F_0b$ = 18.8, it follows that $b$ = 18.8/$F_0$ = 0.0028 m = 2.8 mm. Hence, in Fig. 3, the final asymptote would be at a recorded abscissa value of 4.5 + 2.8 = 7.3 mm (again recalling that the zero is somewhat arbitrary). At this point, the distance between the upper and lower punch would be 2.4 mm[6]. If the solid achieves its true density at $b$, then the true density can be deduced. The die has a diameter of 12 mm; *i.e.*, the volume between the upper and lower punch is equal to [$\pi$ (1.2$^2$/4) 0.24] = 0.27 cm$^3$.

[6] This value is obtained from knowledge of the lower punch position in relation to the arbitrary zero and does not account for possible compression of the presumably static lower punch.

The weight of the solids is 500 mg, so the true density would have a value of 0.5/0.27 = 1.84 g/cm$^3$, which is reasonable. Since compression can possibly (and presumably does) produce densities that are higher than the true densities at atmospheric pressure, the calculated figure only has interest in that it is of a reasonable magnitude. Furthermore, Eq. 8 deals with the energy input and assumes that the relaxation trace in Fig. 3 (the recovery) is vertical. This approximation becomes poorer the more pronounced the recovery after upper punch release.

## SUMMARY

The present study shows that the Parmentier–Führer equation for the value of the upper punch force as a function of displacement is useful and can be used to deduce mathematically energy *versus* maximum force relationships for energy input. These relationships were validated experimentally. The plots provide an estimate of the point in the displacement of the upper punch where the powder or granulation was rearranged to its closest packing.

## REFERENCES

(1) W. Parmentier, Ph.D. thesis, Technical University Carolo-Wilhemina zu Braunschweig, Braunschweig, West Germany, 1974, pp. 1–90.

(2) C. Führer, *Dtsch. Apoth.-Ztg.*, **105**, 1150 (1965).

(3) P. Toure, Ph.D. thesis, University of Paris-Sud, Chatenay-Malabry, France, 1979, p. 102.

(4) P. Toure, D. Duchene, F. Puisieux, and J. T. Carstensen, *Powder Technol.*, **26**, 213 (1980).

(5) J. T. Carstensen: "Rate Processes and Mechanical Properties in Solid Pharmaceutics," Academic, New York, N.Y., 1980, pp. 187–214.

(6) W. M. Long, *Powder Metall.*, **6**, 73 (1960).

(7) S. Leigh, J. E. Carless, and B. W. Burt, *J. Pharm. Sci.*, **56**, 888 (1967).

(8) J. J. Windheuser, J. Misra, S. P. Eriksen, and T. Higuchi, *ibid.*, **52**, 767 (1963).

(9) A. Obiorah, *Int. J. Pharm.*, **1**, 249 (1978).

(10) K. Marshall, "The Physics of Tablet Compression, 12th Arden House Conference, Feb. 2, 1977, Conference Notes," Colorcon, West Point, Pa., pp. 15, 16.

# Mevalonic Acid Analogs as Inhibitors of Cholesterol Biosynthesis

**C. ROWAN DeBOLD * and J. C. ELWOOD ˣ**

Received September 26,1980, from the *Department of Biochemistry, State University of New York, Upstate Medical Center, Syracuse, NY 13210.* Accepted for publication February 20, 1981. *Present address: Department of Medicine, Division of Endocrinology, Vanderbilt University School of Medicine, Nashville, TN 37232.

**Abstract** □ A series of 20 mevalonic acid analogs was synthesized and tested for their ability to inhibit cholesterol biosynthesis from [2-$^{14}$C]-mevalonate in rat liver homogenates. Removal of the 5-hydroxyl group from mevalonic acid produced an active inhibitor, 3-hydroxy-3-methylpentanoic acid. Removal of the 3-hydroxyl group, addition of an aromatic group in the 3-position, or insertion of a double bond reduced inhibitory activity. Compounds with an aromatic group or halide on the 5-position were active inhibitors. The most active inhibitor was 5-phenylpentanoic acid, with 50% inhibition at 0.064 m*M*.

**Keyphrases** □ Mevalonic acid—analogs synthesized as potential cholesterol biosynthesis inhibitors □ Cholesterol—inhibitors, synthesis and testing of mevalonic acid analogs □ Structure–activity relationships—mevalonic acid analogs as inhibitors of cholesterol biosynthesis

Considerable progress has been made in understanding the biosynthesis of cholesterol (1, 2). Mevalonic acid, the product of the major rate-limiting reaction of cholesterol biosynthesis, is converted to isopentenyl pyrophosphate by three enzymes, each requiring $Mg^{2+}$ and ATP. The first step is phosphorylation at position 5 by mevalonate kinase (EC 2.7.1.36). Next, 5-pyrophosphomevalonate is formed by phosphomevalonate kinase (EC 2.7.4.2). This product is decarboxylated and dehydrated by pyrophosphomevalonate decarboxylase (EC 4.1.1.33), possibly involving 3-phospho-5-pyrophosphomevalonate as an intermediate.

Interest has focused on these reactions for various reasons. For example, the role of cholesterol in atherosclerosis prompted a search for inhibitors of these reactions with the prospect of decreasing cholesterol synthesis (3–7). It also has been suggested that the decreased brain cholesterol levels seen in phenylketonuria may be due to inhibition of these steps by elevated levels of phenylalanine

0022-3549/81/0900-1007$01.00/0
© 1981, American Pharmaceutical Association

and its deaminated metabolites (8, 9). Furthermore, the development of specific inhibitors could be used to study the mechanism of these reactions and their importance as a secondary regulatory site of cholesterol synthesis. In addition, such inhibitors could help elucidate the mechanism and control of the recently observed nonsterol metabolic pathway of mevalonic acid (10, 11).

This paper describes the synthesis and testing of mevalonic acid analogs for their ability to inhibit the incorporation of [2-$^{14}$C]mevalonate into cholesterol by rat liver homogenates.

## EXPERIMENTAL[1]

All mevalonic acid analogs were either prepared in this laboratory or obtained commercially[2]. The 3-hydroxy esters were prepared by the Reformastki reaction (12). The products were purified by fractional vacuum distillation through a Vigreux column. The structures were verified by NMR spectroscopy. Elemental analyses were performed on those compounds for which there were no analytical data in the literature for comparison.

**Ethyl 3-(4-Chlorophenyl)-3-hydroxypentanoate (E-8)**—Compound E-8 was prepared by the careful dropwise addition of *p*-chloropropiophenone (15 g, 89 mmoles) and ethyl bromoacetate (15.5 g, 93 mmoles) in ether (20 ml) and benzene (20 ml) to granular zinc (11 g, 168 mmoles) while stirring mechanically. After the exothermic reaction subsided, the mixture was stirred and refluxed for 3 hr, cooled, acidified to pH 3 with 10% HCl, and extracted twice with chloroform.

The organic portions were combined, washed with 5% $NaHCO_3$, and dried over anhydrous magnesium sulfate, and the solvents were removed under reduced pressure. The residue was distilled, yielding 20 g (88%) of a colorless liquid, bp 111–112.5°/0.15 mm Hg; NMR ($CDCl_3$): $\delta$ 0.74 (t, 3H, $CH_3$), 1.09 (t, 3H, $CH_3$-ester), 1.78 (q, 2H, $CH_2$), 2.85 (s, 2H, $CH_2$=O), 4.08 (q, 2H, $COOCH_2$), 4.37 (s, 1H, OH), and 7.42 (s, 4H, aromatic) ppm.

*Anal.*—Calc. for $C_{13}H_{17}ClO_3$: C, 60.82; H, 6.67; Cl, 13.81. Found: C, 60.69; H, 6.74; Cl, 13.69.

**Ethyl 5-Chloro-3-hydroxy-3-phenylpentanoate (E-9)**—Compound E-9 was prepared by the slow addition of $\beta$-chloropropiophenone (5 g, 30 mmoles) and ethyl bromoacetate (4.95 g, 30 mmoles) in ether (13 ml) and benzene (13 ml) to zinc dust (1.9 g, 60 mmoles) while stirring mechanically. After the exothermic reaction subsided, the mixture was refluxed overnight and worked up as already described. Vacuum distillation yielded 4.0 g (52%) of a faint-yellow liquid (E-9), bp 120–122°/0.3 mm Hg; NMR ($CDCl_3$): $\delta$ 1.03 (t, 3H, $CH_3$), 2.27 (t, 2H, $CH_2$), 2.88 (s, 2H, $CH_2C$=O), 3.34 (m, 2H, $CH_2Cl$), 4.00 (q, 2H, $COOCH_2$), 4.54 (s, 1H, OH), and 7.33 (s, 5H, aromatic) ppm.

*Anal.*—Calc. for $C_{13}H_{17}ClO_3$: C, 60.82; H, 6.67; Cl, 13.81. Found: C, 60.51; H, 6.75; Cl, 13.88.

**Ethyl 3-Hydroxy-3-methylpentanoate (E-1)**—Methyl ethyl ketone (69 g, 0.96 mole) and ethyl bromoacetate (167 g, 1.0 mole) in ether (450 ml) were added to zinc dust (120 g, 1.84 moles) with mechanical stirring. The mixture was refluxed overnight and worked up as already described. Vacuum distillation yielded 108 g (70%) of a colorless liquid (E-1), bp 38–39°/0.015 mm Hg [lit. (13) bp 83–88°/13 mm].

**Ethyl 3-Hydroxy-3-phenylpentanoate (E-7)**—Propiophenone (33.5 g, 0.25 mole) and ethyl bromoacetate (42 g, 0.25 mole) in ether (50 ml) and benzene (50 ml) were added to zinc dust (33 g, 0.51 mole) with mechanical stirring. The mixture was refluxed overnight and worked up as already described. Distillation resulted in 35 g (63%) of a faint-pink liquid (E-7), bp 86.5–88°/0.15 mm Hg [lit. (14) bp 104°/0.5 mm].

**Ethyl $\Delta^2$-3-Methylpentenoate (E-2)**—The Emmons modification (15) of the Wittig reaction was used to prepare E-2. Ethyl bromoacetate (83.5 g, 0.5 mole) was added dropwise to a stirred solution of triethyl phosphite (83.1 g, 0.5 mole). After complete addition, the temperature was increased, and ethyl bromide began to distill off. As the liberation of ethyl bromide decreased, the temperature was increased slowly, finally remaining at 170–175° for 1 hr. The cooled solution was added dropwise to sodium ethoxide formed from the addition of absolute ethanol (23 g, 0.5 mole) to sodium ribbon (11.5 g, 0.5 mole) in tetrahydrofuran (300 ml) under nitrogen. Then, methyl ethyl ketone (36 g, 0.5 mole) was added slowly at a rate to keep the temperature below 35°.

After addition of the ketone, the mixture was stirred and refluxed overnight, cooled, and filtered. The precipitate was washed with ether, ethanol, and finally water. The aqueous phase was washed twice with ether. The combined organic phases were dried over anhydrous magnesium sulfate, and the solvents were removed under reduced pressure. Distillation yielded 48 g (68%) of a colorless liquid (E-2), bp 72–74°/23 mm Hg [lit. (16) bp 68°/14 mm]; NMR ($CDCl_3$): $\delta$ 1.06 (t, 3H, $CH_3$), 1.25 (t, 3H, $CH_3$-ester), 2.10 (m, 2H, $CH_2C$=), 2.16 (s, 3H, $CH_3C$=), 4.14 (q, 2H, $COOCH_2$), and 5.65 (s, 1H, HC=C) ppm.

**Methyl $\Delta^3$-3-Methylpentenoate (E-3)**—Kon and Linstead (17) claimed that ethyl $\Delta^3$-3-methylpentenoate could be selectively prepared by the dehydration of E-1 by heating in the presence of potassium hydrogen sulfate. However, this procedure resulted in a mixture of the $\Delta^2$- and $\Delta^3$-esters, as confirmed by NMR. Thus, the more complex procedure of Wagner (13) had to be utilized, which would specifically locate the double bond in the $\Delta^3$-position and result in the *trans*-isomer. Briefly, the procedure involved four steps: (*a*) aldol condensation of acetaldehyde and methyl ethyl ketone in the presence of base to yield 4-hydroxy-3-methylpentanone, (*b*) dehydration of the $\beta$-hydroxyketone to 3-methyl-3-penten-2-one, (*c*) formation of 3,4-dibromo-3-methyl-2-pentanone by the addition of bromine to the unsaturated ketone, and (*d*) Favorskii rearrangement of the $\alpha,\beta$-dibromoketone in the presence of sodium methoxide to form methyl $\Delta^3$-3-methylpentenoate (E-3) (25% yield), bp 47–50°/11 mm Hg [lit. (13) bp 74°/50 mm]; NMR ($CDCl_3$): $\delta$ 1.5 [m, 6H, ($CH_2C$=)$_2$], 3.0 (d, 2H, $CH_2$), 3.65 (s, 3H, $OCH_3$), and 5.42 (m, 1H, CH=C) ppm.

**Saponification of Esters**—Two general procedures similar to those of Stewart and Woolley (4) were used.

*Procedure 1*—To a stirred solution containing an ester (40 mmoles) in 80% ethanol (30 ml) at 60°, 40 ml of sodium hydroxide (1 *N*, 40 mmoles) was added dropwise over 90 min. After the mixture was stirred at 60° for 18 hr, the solvent was removed under reduced pressure. The remaining solution was extracted twice with ether, and the combined ether extractions were backwashed once with 5% $NaHCO_3$. The combined aqueous portion was acidified to pH 3 with 1 *N* HCl.

If the acid was a solid at room temperature, it precipitated out of the acidic solution and was collected by filtration and purified by recrystallization. If no precipitate formed, the aqueous solution was extracted twice with ether and twice with ethyl acetate. The combined organic extracts were washed with water until neutral, dried over anhydrous magnesium sulfate, and concentrated under reduced pressure. The residue was vacuum distilled.

*Procedure 2*—Because dehydration or isomerization was a problem during the saponification of E-1, E-2, E-3, a gentler procedure was used. The ester (40 mmoles) in 80% ethanol (60 ml) was cooled in an ice bath while 40 ml of sodium hydroxide (1 *N*, 40 mmoles) was added over 24 hr. The solution was stirred at room temperature for 1–2 days and the product was worked up as already described.

**3-(4-Chlorophenyl)-3-hydroxypentanoic Acid (A-8)**—Compound E-8 was hydrolyzed according to Procedure 1 producing A-8 (93%), which was recrystallized from benzene–hexane (1:1), mp 97–98°; NMR ($CDCl_3$): $\delta$ 0.71 (t, 3H, $CH_3$), 1.78 (q, 2H, $CH_2$), 2.91 (s, 2H, $CH_2C$=O), and 7.40 (s, 6H, aromatic, OH, COOH) ppm.

*Anal.*—Calc. for $C_{11}H_{13}ClO_3$: C, 57.79; H, 5.73; Cl, 15.50. Found: C, 57.67; H, 5.71; Cl, 14.88.

**3-Hydroxy-3-phenylpentano-5-lactone (E-10)**—Hydrolysis of E-9 by Procedure 1 unexpectedly resulted in a lactone, E-10. Recrystallization in ethyl acetate gave white crystals (56%), mp 133–135°; NMR ($CDCl_3$): $\delta$ 2.16 (broad, 2H, $CH_2$), 2.84 (s, 2H, $COCH_2$), 3.08 (s, 1H, OH, not present with $D_2O$), 4.44 (m, 2H, $OCH_2$), and 7.34 (s, 5H, aromatic) ppm.

*Anal.*—Calc. for $C_{11}H_{12}O_3$: C, 68.74; H, 6.29. Found: C, 68.48; H, 6.40; Cl, none.

**3-Hydroxy-3-phenylpentanoic Acid (A-7)**—Hydrolysis of E-7 by Procedure 1 resulted in A-7. Recrystallization from benzene gave white crystals (71%), mp 122–123° [lit. (14) mp 120–121°].

**$\Delta^2$-3-Ethoxybutenoic Acid (A-4)**—Hydrolysis of E-4 by Procedure 1 resulted in A-4. Recrystallization from absolute ethanol gave white crystals (31%), which decomposed on melting at 139–141° [lit. (18) mp 140°].

**3-Hydroxy-3-methylpentanoic Acid (A-1)**—Hydrolysis of E-1 by Procedure 2 resulted in A-1 (52%), bp 78–81°/0.02 mm Hg [lit. (3) bp 93–95°/0.03 mm].

**$\Delta^2$-3-Methylpentenoic Acid (A-2)**—Hydrolysis of E-2 by Procedure

[1] Melting points were determined on a Fisher-Johns apparatus and are uncorrected. NMR spectra were determined using a Varian A-60A spectrometer with tetramethylsilane as an internal standard. Elemental analyses were performed by Bristol Laboratories, Syracuse, N.Y.

[2] Compounds E-5, A-11, A-12, A-13, and A-14 were from Aldrich Chemical Co., and E-4 and A-6 were from Frinton Laboratory.

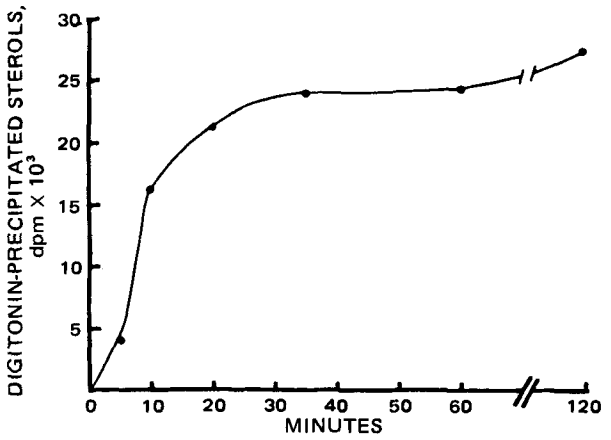


**Figure 1**—*Incorporation rate of [2-$^{14}$C]mevalonate into digitonin-precipitated sterols in rat liver homogenate. Each point represents the average of two determinations.*

2 resulted in A-2 (51%), which separated on standing into the *trans*-isomer (23%), mp 43–45° [lit. (19) mp 46–47°], and the *cis*-isomer (77%), bp 61°/0.55 mm Hg [lit. (20) bp 96°/5 mm]. Since complete separation could not be effected, a mixture of roughly equal parts of the isomers was used for testing in the homogenate system.

***trans*-$\Delta^3$-3-Methylpentenoic Acid (A-3)**—Hydrolysis of E-3 by Procedure 2 resulted in A-3 (97%), bp 51–53°/0.015 mm Hg [lit. (13) mp 35°]; NMR: $\delta$ 1.70 [m, 6H, $(CH_3C{=})_2$], 3.06 (d, 2H, $CH_2$), 5.45 (m, 1H, CH=C), and 11.56 (s, 1H, COOH) ppm.

***In Vitro* Assay of Cholesterol Biosynthesis**—The rat liver homogenates from mature male Wistar rats were prepared following the general procedures described previously (21). The homogenization medium consisted of 100 m*M* potassium phosphate, 30 m*M* nicotinamide, 4 m*M* magnesium chloride, 5 m*M* glutathione, and 1 m*M* ethylenediaminetetraacetic acid at pH 7.4. The final cofactor concentration[3] in each incubation flask was 2 m*M* ATP, 1 m*M* NAD, 1 m*M* NADP, 8 m*M* glucose-6-phosphate, and 2 units of glucose-6-phosphate dehydrogenase (baker's yeast, type XV).

To each 25-ml incubation flask were added 2 ml of homogenate, 0.1 ml of cofactor solution, and 0.1 ml of solution containing the compound to be tested. The acids were added as the potassium salt in water at pH 7.4, while the esters were added in 50% ethanol. Every compound was tested in duplicate. The appropriate controls, either water or 50% ethanol, also were run in duplicate in every assay. The assay was started by the addition of 0.1 ml of water containing the potassium salt of [2-$^{14}$C]mevalonate (0.1 $\mu$Ci, 0.0124 $\mu$mole) prepared from the dibenzylethylene ammonium salt[4]. Incubation continued for 20 min at 37° in a Dubnoff shaker at 100 oscillations/min. The incubation was terminated by the addition of 2 ml of 11% KOH (w/v) in ethanol.

The contents of each incubation flask were poured into 16 × 150-mm screw-capped tubes. Each flask was washed twice with 2-ml portions of 11% KOH (w/v) in ethanol, and the washings were added to the appropriate tube. Each sample was capped and saponified in a boiling water bath for 30 min. When the sample was cool, 7.5 ml of water and 2 ml of ethanol were added. The nonsaponifiable fraction containing the cholesterol was removed by three extractions with 9-ml portions of petroleum ether. This extraction procedure removed >99% of the cholesterol.

The procedure for the precipitation of cholesterol by digitonin was based on the method of Zak *et al.* (22). The digitonin precipitates were dissolved by warming in 2.0 ml of absolute methanol. A 1-ml aliquot was added to a toluene-based scintillation cocktail containing 2,5-diphenyloxazole (3.92 g/liter) and *p*-bis(*o*-methylstyryl)benzene (0.08 g/liter)[5].

## RESULTS AND DISCUSSION

The incorporation rate of [2-$^{14}$C]mevalonate into the digitonin-precipitated sterols by rat liver homogenates is shown in Fig. 1. Although digitonin precipitates all 3-$\beta$-hydroxysterols, this is almost entirely cholesterol in the liver. The incorporation rate was rapid for the first 20 min of incubation and leveled off by 30 min. By 120 min, ~25% of the biologically available optical isomer of mevalonic acid was incorporated into cholesterol. A 20-min incubation period was chosen for testing the inhibitory compounds because this point was at the end of the period of maximal sterol synthesis.

The effects of 20 mevalonic acid analogs on cholesterol biosynthesis from [2-$^{14}$C]mevalonate in rat liver homogenates were studied. All

**Table I—Effect of Aliphatic Mevalonic Acid Analogs on the Incorporation of [2-$^{14}$C]Mevalonate into Cholesterol by Rat Liver Homogenates**

| Compound[a] | Structure | Inhibition at 1 m*M*, % Ester[b] | Acid[c] |
|---|---|---|---|
| 1 | 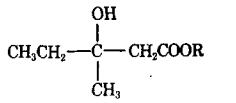 | 9.6[d] | 29.3 |
| 2 | 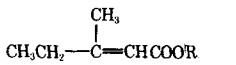 | 21.0 | 15.0 |
| 3 | 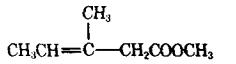 | 0 | 0 |
| 4 | 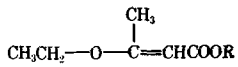 | 41.1 | 9.5 |
| 5 | 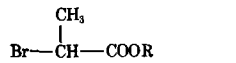 | 12.0 | — |
| 6 | 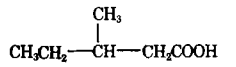 | — | 20.8 |

[a] In the text, compounds are identified with a number preceded by an E for an ester or an A for an acid. [b] R = $-CH_2CH_3$. [c] R = H. [d] Each number represents the average of at least two determinations.

**Table II—Effect of Aromatic Mevalonic Acid Analogs on the Incorporation of [2-$^{14}$C]Mevalonate into Cholesterol by Rat Liver Homogenates**

| Compound[a] | Structure | Inhibition at 1 m*M*, % Ester[b] | Acid[c] |
|---|---|---|---|
| 7 | 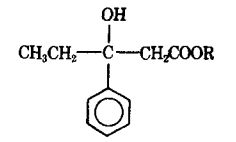 | 7.9[d] | 29.5[e] |
| 8 | 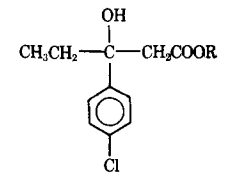 | 44.0 | 11.0 |
| 9 | 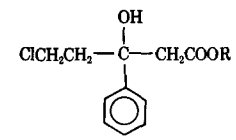 | 28.2 | — |
| 10 | 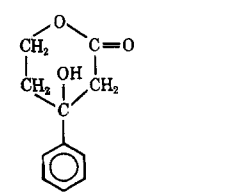 | 0[f] | — |

[a] In the text, compounds are identified with a number preceded by E for an ester or an A for an acid. [b] R = $-CH_2CH_3$. [c] R = H. [d] Each number represents the average of at least two determinations. [e] Percent stimulation. [f] Lactone.

[3] All cofactors were obtained from Sigma Chemical Co.
[4] New England Nuclear Corp.
[5] Radioactive samples were counted on a Packard Tri-Carb liquid scintillation spectrometer, model 2425.

**Table III—Effect of 5-Substituted Mevalonic Acid Analogs on the Incorporation of [2-$^{14}$C]Mevalonate into Cholesterol by Rat Liver Homogenates**

| Compound[a] | Structure | Inhibition of Acid at 1 m*M*, % |
|---|---|---|
| 11 | 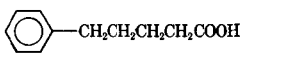 | 92.4[b] |
| 12 | 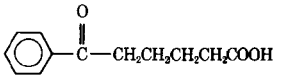 | 42.8 |
| 13 | $ClCH_2CH_2CH_2CH_2COOH$ | 15.2 |
| 14 | $BrCH_2CH_2CH_2CH_2COOH$ | 21.0 |

[a] In the text, compounds are identified with a number preceded by an A for acid. [b] Each number represents the average of at least two determinations.

compounds were initially tested at a concentration of 1 m*M*. Table I shows the series of analogs with a methyl group at position 3. Removal of the 5-hydroxyl group resulted in an effective inhibitor, 3-hydroxy-3-methylpentanoic acid (A-1). These data agree, in part, with those of Klimov *et al.* (23, 24), which showed that, in a series of mevalonic acid analogs with aromatic groups in position 2 or 3, the absence of a hydroxyl group in the 5-position increased the ability of the compound to inhibit cholesterol biosynthesis from [$^{14}$C]mevalonate in rat liver homogenates.

For bacterial and yeast assay systems, Stewart and Woolley (4, 5) concluded that the hydroxyl group at position 3 was necessary for highest antimevalonic activity. Table I shows that this conclusion also applies to the rat liver homogenate since several compounds (A-2, A-3, and A-6) that have similar structures to the active 3-hydroxyl inhibitor (A-1), but lack the 3-hydroxyl group, all showed lower activity.

Table I also shows that alterations of the backbone structure by introduction of a double bond at position 2 or 3 (A-2 or A-3) reduced inhibitory activity. These results confirm earlier work (3) that was questionable because the synthetic procedures used would not necessarily lead to the pure isomers and the structures were not proven adequately. On the other hand, Klimov *et al.* (23) found that a double bond at position 2 increased the activity compared to a saturated 3-hydroxyl analog. However, these data are not directly comparable since all compounds also contained an aromatic group at position 2 or 3.

The substitution of an aromatic group for the 3-methyl group produced inactive acids (A-7 and A-8) (Table II). In contrast, Klimov *et al.* (23) found increased activity of 3-hydroxyl compounds by adding a phenyl group to position 2 and/or a tolyl group to position 3. However, these data are not directly comparable since different aromatic groups were used.

In contrast to the acids, the ethyl esters of these 3-hydroxy-3-aromatic compounds showed considerable inhibitory activity. In general, there was little relationship between the activity of a compound as an ester and its activity as an acid. Compound E-10, resembling mevalonolactone with a phenyl ring replacing the 3-methyl group, was inactive.

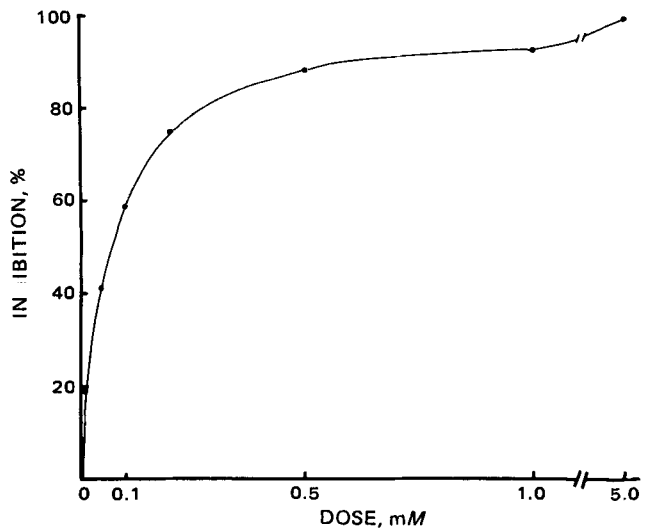


**Figure 2**—*Inhibition by 5-phenylpentanoic acid (A-11) of incorporation of [2-$^{14}$C]mevalonate into cholesterol by rat liver homogenates.*

Table III shows several compounds with an aromatic group or halide on the 5-carbon, all of which caused inhibition. The most active inhibitor was 5-phenylpentanoic acid (A-11), with 92.4% inhibition of cholesterol biosynthesis. Of the two 5-halogenated pentanoic acids, the bromo derivative was more inhibitory. Not all modifications of the 5-position yield inhibitors. Humber *et al.* (25) replaced the 5-hydroxyl group of mevalonic acid with a methoxy, ethoxy, or dimethylamino group and found that none of the compounds inhibited cholesterol biosynthesis in rat liver homogenates at concentrations of 1 m*M*.

The relationship between the dose and the effect of the most active compound, A-11, is shown in Fig. 2. There was 50% inhibition of cholesterol biosynthesis from labeled mevalonate in rat liver homogenates at a 0.064 m*M* concentration.

The results of this study show that A-11 is a very potent inhibitor of cholesterol biosynthesis from mevalonate in rat liver homogenates. Other investigators (3–6, 23, 24) tested mevalonic acid analogs that were effective inhibitors at concentrations of ≥1 m*M*. Compound A-11 showed significant inhibition of 20% at 0.01 m*M*, a 100-fold difference. The only compounds that rival its activity are 3,5-dihydroxy-3-fluoromethylpentanoic acid (26) and 3-hydroxy-3-methyl-6-phosphonohexanoic acid (7), which caused 50% inhibition of mevalonic acid metabolism at 0.07 and 0.145 m*M*, respectively.

## REFERENCES


(1) E. D. Beytía and J. W. Porter, *Ann. Rev. Biochem.*, **45,** 113 (1976).

(2) J. R. Sabine, "Cholesterol," Dekker, New York, N.Y., 1977, pp. 79–104.

(3) H. Weiss, E. Schiffman, and E. Titus, *J. Lipid Res.*, **2,** 258 (1961).

(4) J. M. Stewart and D. W. Woolley, *J. Am. Chem. Soc.*, **81,** 4951 (1959).

(5) J. M. Stewart and D. W. Woolley, *Biochemistry*, **3,** 1998 (1964).

(6) F. H. Hulcher, *Arch. Biochem. Biophys.*, **146,** 422 (1971).

(7) G. Popjak, T. S. Parker, V. Sarin, B. E. Tropp, and R. Engel, *J. Am. Chem. Soc.*, **100,** 8014 (1978).

(8) S. N. Shah, N. A. Peterson, and C. M. McKean, *Biochim. Biophys. Acta*, **187,** 236 (1969).

(9) S. Ranganathan and T. Ramasarma, *J. Neurochem.*, **22,** 987 (1974).

(10) J. Edmond and G. Popjak, *J. Biol. Chem.*, **249,** 66 (1974).

(11) A. M. Fogelman, J. Edmond, and G. Popjak, *ibid.*, **250,** 1771 (1975).

(12) M. W. Rathke, *Org. React.*, **22,** 423 (1975).

(13) R. B. Wagner, *J. Am. Chem. Soc.*, **71,** 3214 (1949).

(14) J. A. Barltroop, R. M. Acheson, P. G. Philpott, K. E. McPhee, and J. S. Hunt, *J. Chem. Soc.*, **1956,** 2928.

(15) W. S. Wadsworth and W. D. Emmons, *J. Am. Chem. Soc.*, **83,** 1733 (1961).

(16) G. A. R. Kon and K. S. Nargund, *J. Chem. Soc.*, **1932,** 2461.

(17) G. A. R. Kon and R. P. Linstead, *ibid.*, **1925,** 616.

(18) M. V. S. Sultanbawa and P. Veerevagu, *ibid.*, **1958,** 4113.

(19) R. B. Wagner and J. A. Moore, *J. Am. Chem. Soc.*, **72,** 974 (1950).

(20) G. A. R. Kon, R. P. Linstead, and J. M. Wright, *J. Chem. Soc.*, **1934,** 599.

(21) N. L. R. Bucher and K. McGarnahan, *J. Biol. Chem.*, **222,** 1 (1956).

(22) B. Zak, R. C. Dickerman, E. G. White, H. Burnett, and P. J. Cherney, *Am. J. Clin. Pathol.*, **24,** 1307 (1954).

(23) A. N. Klimov, E. D. Polyakova, A. L. Remizov, and L. A. Petrova, *Biokhimiya*, **32,** 88 (1967).

(24) A. N. Klimov, T. A. Klimova, L. A. Petrova, and E. D. Polyakova, *ibid.*, **36,** 851 (1971).

(25) L. G. Humber, M. Kraml, J. Dubuc, and R. Gaudry, *J. Med. Chem.*, **6,** 210 (1963).

(26) F. M. Singer, J. P. Januszka, and A. Borman, *Proc. Soc. Exp. Biol. Med.* **102,** 370 (1959).


## ACKNOWLEDGMENTS


Supported in part by the State University of New York Research Foundation (Biomedical Research Support Grant 211-E013-E).

A preliminary report of this work was presented at the 23rd annual meeting of the Australian Biochemical Society, an abstract of which has been published, *Proc. Aust. Biochem. Soc.*, **12,** 39 (1979).

# Antiproliferative Activity of Doxorubicin and Aminoanthraquinone Derivatives on Chinese Hamster Ovary Cells

**EDWIN M. UYEKI *, AKIRA NISHIO *, PHILIP J. WITTEK ‡, and C. C. CHENG *‡x**

Received October 14, 1980, from the **Department of Pharmacology and the* [1]*Mid-America Cancer Center, University of Kansas Medical Center, Kansas City, KS 66103.* Accepted for publication February 13, 1981.

**Abstract** □ A study of the antiproliferative activity of doxorubicin and several substituted aminoanthraquinone derivatives on Chinese hamster ovary cells was conducted. Doxorubicin and a derivative each inhibited cell proliferation at low concentrations, the latter being more potent than doxorubicin. A structure–activity relationship of these compounds is discussed in connection with an earlier postulated N–O–O triangulation hypothesis.

**Keyphrases** □ Aminoanthraquinone derivatives—synthesis and evaluation for antiproliferative activity, Chinese hamster ovary cells □ Doxorubicin—substituted aminoanthraquinone derivatives synthesized and evaluated for antiproliferative activity, Chinese hamster ovary cells □ Antiproliferative activity—aminoanthraquinone derivatives synthesized and evaluated for activity in Chinese hamster ovary cells □ Structure–activity relationships—substituted aminoanthraquinone derivatives synthesized and evaluated for antiproliferative activity

Based on a working hypothesis involving the recognition of a common N–O–O triangular pharmacophore among several antineoplastic agents (1, 2), 1,4-dihydroxy-5,8-bis{[2-(2-hydroxyethyl)amino]ethyl}amino-9,10-anthracenedione (I) was synthesized and found to possess outstanding antineoplastic activity in several experimental tumor systems (3, 4). Recently, a number of structural modification (5, 6), structure–activity (5, 7), pharmacological (7, 8), mechanistic (9, 10), and clinical trial (11) experiments were conducted. Since several analogs of I exhibited antineoplastic activity *in vivo* but do not contain the entire N–O–O triangular pattern, an *in vitro* study of their antiproliferative activity on Chinese hamster ovary cells was undertaken to obtain additional structure–activity relationship information.

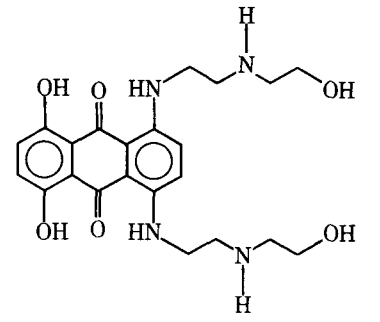

I

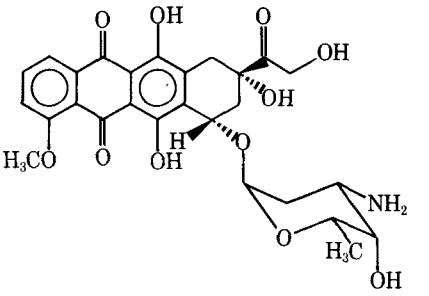

II

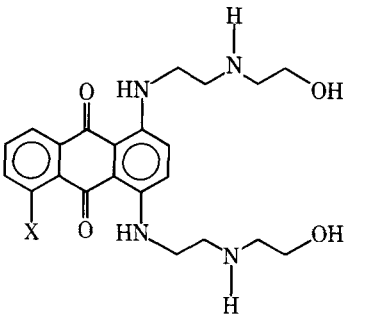

IIIa: X = H
IIIb: X = $NH_2$
IIIc: X = OH

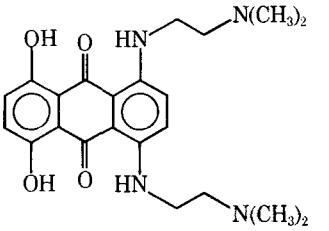

IV

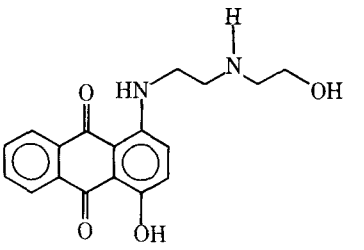

V

## EXPERIMENTAL

**Chemical Agents**—Seven compounds, including the antibiotic doxorubicin[1] (II), were evaluated. Preparation of I, IIIa, IV, and V was reported previously (3, 5).

*Preparation of 1-Amino-5,8-bis{[2-(2-hydroxyethyl)amino]ethyl}-amino-9,10-anthracenedione (IIIb)*—To a mixture of 8 g (0.031 mole) of 5-amino-2,3-dihydro-1,4-dihydroxy-9,10-anthracenedione (prepared by the reduction of 5-nitro-1,4-dihydroxy-9,10-anthracenedione in zinc and acetic acid) in 55 ml of 2-propanol at 50° was added 30 g (0.29 mole) of 2-[(2-aminoethyl)amino]ethanol with mechanical stirring under nitrogen. The resulting reaction mixture was stirred at 50° for 4.5 hr, during which time a precipitate formed. The mixture was cooled to room temperature and filtered.

The solid was washed with 2-propanol and ether and dried to give 8.3 g (60% yield) of the dihydro analog of the target compound, 1-amino-5,8-bis{[2-(2-hydroxyethyl)amino]ethyl}amino-9,10-dihydroxyanthracene, as gold-colored plates. Recrystallization from 2-propanol yielded an analytical sample, mp 135–145° dec.; UV: $\lambda_{max}$ (0.1 *N* HCl) 488 ($\epsilon$ 9800), 460 (15,300), 435 (11,700), and 252 (25,200) nm; $\lambda_{sh}$ (0.1 *N* HCl) 280 ($\epsilon$ 17,000) nm.

*Anal.*—Calc. for $C_{22}H_{31}N_5O_4$: C, 61.52; H, 7.28; N, 16.31. Found: C, 61.35; H, 7.11; N, 16.12.

The mother liquor from the initial filtration was allowed to stir uncovered for 10 days at room temperature. The solution gradually turned dark blue and deposited a blue gummy solid. Filtration of this material

[1] Supplied by Dr. Harry B. Wood, Jr., National Cancer Institute.

0022-3549/81/0900-1011$01.00/0
© 1981, American Pharmaceutical Association

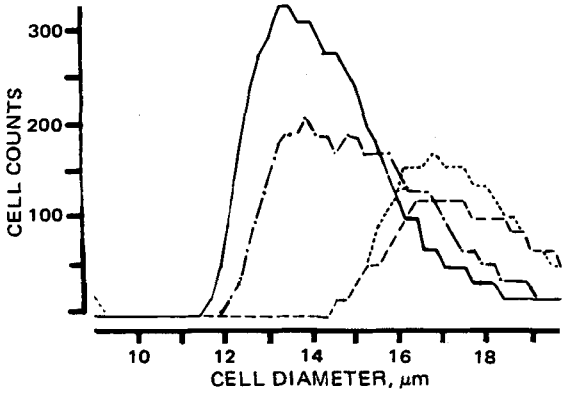


**Figure 1**—*Cell counts and cell-sizing data for I. The data were stored and processed in a microprocessor. Every point of each line represents the average value of I on triplicate cultures. Key: —, control; – –, 1000 nM; ·····, 200 nM; and -·-, 10 nM.*

and recrystallization from a mixture of methanol and 2-propanol gave 0.5 g (4% yield) of III*b* as a dark blue-black amorphous powder, mp 131–141° (dampening at 110°); UV: $\lambda_{max}$ (0.1 *N* HCl) 634 ($\epsilon$ 14,400), 590 (13,500), and 252 (27,500) nm; $\lambda_{sh}$ (0.1 *N* HCl) 550 ($\epsilon$ 7500) and 272 (14,500) nm.

*Anal.*—Calc. for $C_{22}H_{29}N_5O_4$: C, 61.81; H, 6.84; N, 16.38. Found: C, 61.53; H, 6.81; N, 16.04.

Compound III*b* could be obtained also from the dihydroanthraquinone product as follows. To 100 ml of refluxing nitrobenzene with magnetic stirring was added 5.0 g of the dihydroanthraquinone. After 20 min, the reaction mixture was allowed to cool, and 200 ml of ether was added. Filtration and drying of the solid product gave 3.4 g of III*b*.

*Preparation of 1-Hydroxy-5,8-bis{[2-(2-hydroxyethyl) amino]ethyl}amino-9,10-anthracenedione (IIIc)*—To 30 g (0.29 mole) of 2-[(2-aminoethyl)amino]ethanol at room temperature under nitrogen was added 8.5 g (0.033 mole) of 1,4,5-trihydroxy-2,3-dihydroanthraquinone in one portion with stirring. A slight exothermic reaction developed. The reaction mixture was stirred at room temperature for 3 hr and then was warmed at 50° for 1 hr. To this mixture was added 250 ml of 2-propanol, and the dark solution again was warmed to 50°. Air was bubbled into the reaction mixture for 4 hr at that temperature, and then it was cooled to 30° and filtered.

The solid was washed with 2-propanol followed by ether to give 4.0 g (28% yield) of III*c*, mp 118–122°. A second crop of 3.7 g (26% yield) was collected by addition of 400 ml of ether to the mother liquor. Recrystallization from propanol–ether gave an analytical sample of III*c* as a dark-blue amorphous powder, mp 120–125°; UV: $\lambda_{max}$ (0.1 *N* HCl) 636 ($\epsilon$ 9500), 593 (10,300), and 240 (23,800) nm; $\lambda_{sh}$ (0.1 *N* HCl) 550 ($\epsilon$ 6200) and 270 (11,900) nm.

*Anal.*—Calc. for $C_{22}H_{28}N_4O_5$: C, 61.67; H, 6.59; N, 13.08. Found: C, 61.65; H, 6.69; N, 13.09.

**Biological Methods**—Chinese hamster ovary cells[2] were grown in a

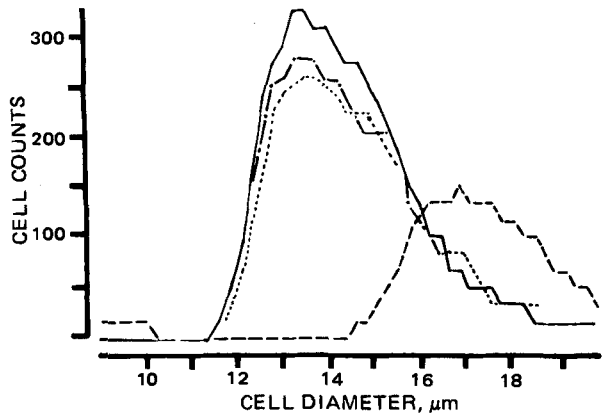


**Figure 2**—*Cell counts and cell-sizing data for II. Every point of each line represents the average value of II on triplicate cultures. Key: —, control; – –, 1000 nM; ·····, 200 nM; and -·-, 10 nM.*

[2] Supplied by Dr. Don Roufa, Kansas State University, Manhattan, Kans.

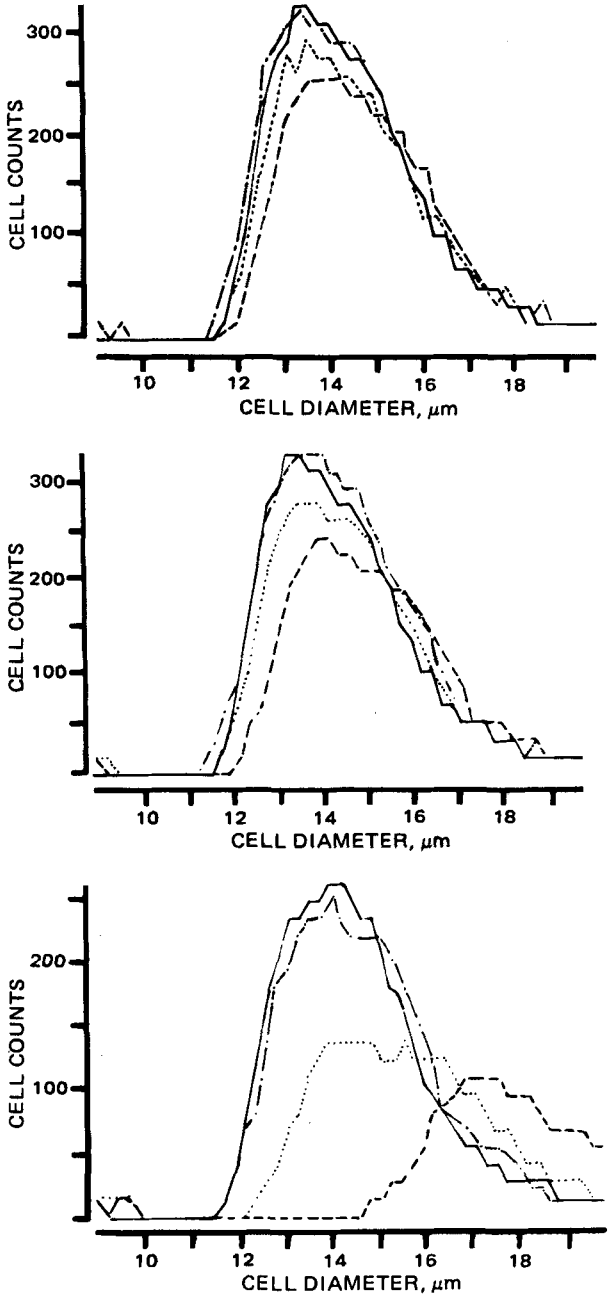


**Figure 3**—*Cell counts and cell-sizing data for III*a *(top), III*b *(middle), and III*c *(bottom). Every point of each line represents the average value of triplicate cultures. Key: —, control; – –, 1000 nM; ·····, 200 nM; and -·-, 10 nM.*

medium[3] supplemented with 10% newborn calf serum[4], selenium (30 n*M*), and insulin (10 ng/ml) and contained twice the glucose concentration (4 g/liter).

Cells were cultured at a concentration of 1–2 × $10^5$ cells/dish in 1 ml. All drug concentrations were in triplicate cultures. After overnight incubation, drugs were added and cultured for an additional 24 hr. Cells were trypsinized, diluted with the counting fluid, and analyzed with electronic cell-counting and cell-sizing equipment[5].

Data from 100 channels were stored on microprocessor disks and analyzed. Each line of the graphs (Figs. 1–5) represents the average of values obtained from triplicate cultures. The ordinate is expressed as the number of cell counts. The data from the cell-sizing equipment were calculated so that the abscissa represents cell diameter in micrometers. Hence, the

[3] Roswell Park Memorial Institute 1640; obtained from KC Biological, Lenexa, Kans.

[4] KC Biological, Lenexa, Kans.

[5] Isoton solution, a ZBI cell counter, and a 100-channel Channelyzer were obtained from Coulter Electronics, Hialeah, Fla.

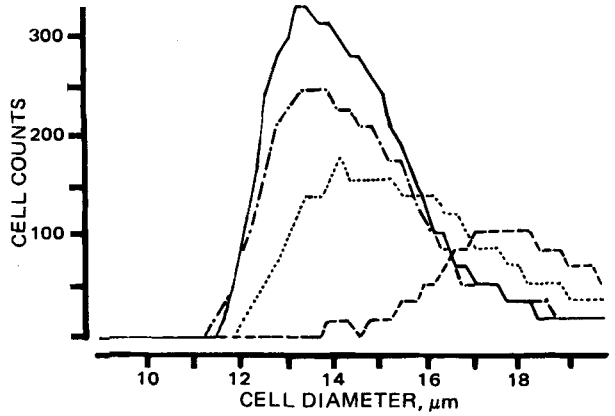


**Figure 4**—*Cell counts and cell-sizing data for IV. Every point of each line represents the average value of IV on triplicate cultures. Key: —, control; – –, 1000 nM; ·····, 200 nM; and –·–, 10 nM.*

data for each graph are given in terms of the number of cells for a given cell diameter.

## RESULTS

Cell counts and cell-sizing data for I and doxorubicin (II) are shown in Figs. 1 and 2, respectively. At 1000 n*M* ($1 \times 10^{-6}$ *M*), both I and II inhibited cell proliferation and shifted the population toward larger cells. In addition, I inhibited cell replication in concentrations as low as 10 n*M*, whereas II did not. However, at 10 n*M* I, the size distribution indicated a return to cells of a smaller diameter. Moreover, 10 n*M* I (72% of controls) was significantly lower than 200, 50, and 10 n*M* II, using Duncan's new multiple-range test at the 0.01 level of significance.

Compounds IIIc (Fig. 3) and IV (Fig. 4) showed activity comparable to II; *i.e.*, they were inhibitory at concentrations of 50 and 200 n*M* but not at 10 n*M*. At 200 and 1000 n*M*, IIIc and IV demonstrated that cell-size distributions shifted to a larger diameter.

Under similar culture conditions, V (Fig. 5), III*a*, and III*b* were much less effective, showing no statistically significant inhibition of cell proliferation compared with controls (Table I).

## DISCUSSION

Although both I and III*a* were reported to possess an inhibitory effect on cell survival and cell cycle progression in cultured mammalian cells (12–14), I appeared to be 200 times more potent than III*a* *in vitro* (12). Consequently, I and related aminoanthraquinones, as well as doxorubicin (II), were studied at concentrations between 1000 and 10 n*M* and the following results were obtained:

1. Compound I was significantly inhibitory to Chinese hamster ovary cell proliferation at concentrations as low as 10 n*M* I (Fig. 1).
2. Doxorubicin exhibited inhibitory activity as low as 50 n*M* (Fig. 2).
3. The other ring-dihydroxylated bis(aminoalkylamino)-substituted anthraquinone (IV) also was active at that concentration, but the magnitude of inhibition was not like that of I (Fig. 4).
4. The ring-monohydroxylated bis(aminoalkylamino)-substituted anthraquinone (III*c*) was active at 200 n*M* (Fig. 3).
5. Compound III*b* showed borderline activity at 1000 n*M* (Fig. 5).
6. Compounds III*a* and V (Fig. 5) were ineffective at the highest concentration (1000 n*M*) tested.

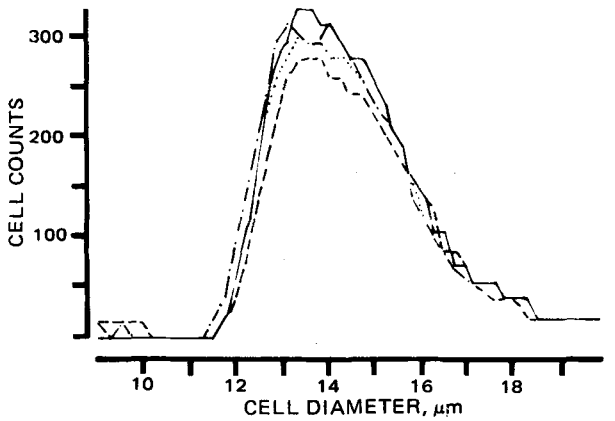


**Figure 5**—*Cell counts and cell-sizing data for V. Every point of each line represents the average value of V on triplicate cultures. Key: —, control; – –, 1000 nM; ·····, 200 nM; and –·–, 10 nM.*

**Table I—Antiproliferative Activity of Doxorubicin (II) and Analogs against Chinese Hamster Ovary Cells**

| Compound | Concentration, n*M* | Total Volume[a] × $10^6$ $\mu m^3$ | Percent of Controls[b] |
|---|---|---|---|
| Control | | 10.60 ± 0.36 (3) | |
| I | 1000 | 2.02 ± 0.74 (3) | 19* |
| | 200 | 2.55 ± 0.14 (3) | 24* |
| | 50 | 2.55 ± 0.11 (3) | 24* |
| | 10 | 7.67 ± 0.29 (3) | 72* |
| II | 1000 | 2.61 ± 0.11 (3) | 24* |
| | 200 | 9.13 ± 0.11 (3) | 86* |
| | 50 | 9.01 ± 0.21 (3) | 85* |
| | 10 | 9.48 ± 0.38 (3) | 89 |
| III*a* | 1000 | 9.40 ± 0.34 (3) | 88 |
| | 200 | 9.79 ± 0.90 (3) | 92 |
| | 50 | 9.95 ± 0.22 (3) | 93 |
| | 10 | 10.78 ± 0.17 (3) | 101 |
| III*b* | 1000 | 8.52 ± 0.77 (3) | 80 |
| | 200 | 9.82 ± 0.50 (3) | 92 |
| | 50 | 11.25 ± 0.52 (3) | 106 |
| | 10 | 11.24 ± 0.24 (3) | 106 |
| IV | 1000 | 1.46 ± 0.12 (3) | 13* |
| | 200 | 6.22 ± 0.61 (3) | 58* |
| | 50 | 9.27 ± 0.67 (3) | 87 |
| | 10 | 8.50 ± 0.15 (3) | 80 |
| V | 1000 | 9.53 ± 0.52 (3) | 89 |
| | 200 | 10.12 ± 0.32 (3) | 95 |
| | 50 | 10.63 ± 0.22 (3) | 100 |
| | 10 | 10.52 ± 0.24 (3) | 100 |
| Control | | 8.46 ± 0.26 (3) | |
| III*c* | 1000 | 1.35 ± 0.15 (3) | 15* |
| | 200 | 5.11 ± 0.10 (3) | 60* |
| | 50 | 7.17 ± 0.33 (3) | 84* |
| | 10 | 8.25 ± 0.19 (2) | 97 |

[a] Represents the area under the curve between 11.5 and 17.0 $\mu m$ in cell diameter; >95% of the cells from control cultures are included within these boundaries. Values are expressed as mean ±*SE* (number of determinations). [b] Values were analyzed, using analysis of variance and Duncan's new multiple-range test for significance. Asterisk represents differences between drug treated and controls at the 0.01 level of significance.

The importance of the N–O–O triangular pharmacophore to the antiproliferative activity of compounds of this type on Chinese hamster ovary cells was revealed since, theoretically, both I and IV possess two N–O–O sets, doxorubicin and IIIc possess one N–O–O set, and none of the other compounds contains this triangulation. The fact that III*b* showed borderline activity could be interpreted as due either to the presence of another electronegative element at the strategic position or to a gradual and incomplete replacement of the amino by a hydroxyl function under experimental conditions.

Most of the compounds studied showed good antineoplastic activity *in vivo*. Judging from the reports (3, 4, 7) that the dosage required for the unhydroxylated anthraquinones, such as III*a*, is at least 10 times higher than that required for the corresponding dihydroxyl analog, such as I, the possibility of *in vivo* hydroxylation to "complete" the N–O–O triangulation cannot be disregarded. In fact, chemical hydroxylation of 1,4-diamino-9,10-anthracenedione diboroacetate with an oxidizing agent such as sodium persulfate yielded the corresponding 5,8-dihydroxyl derivative (15), which further indicated that positions 5 and 8 are electronically preferred for hydroxylation.

## REFERENCES

(1) K. Y. Zee-Cheng and C. C. Cheng, *J. Pharm. Sci.*, **59**, 1630 (1970).

(2) R. H. Adamson, *Cancer Chemother. Rep. Part I*, **58**, 293 (1974).

(3) R. K. Y. Zee-Cheng and C. C. Cheng, *J. Med. Chem.*, **21**, 291 (1978).

(4) C. C. Cheng, G. Zbinden, and R. K. Y. Zee-Cheng, *J. Pharm. Sci.*, **68**, 393 (1979).

(5) R. K. Y. Zee-Cheng, E. G. Podrebarac, C. S. Menon, and C. C. Cheng, *J. Med. Chem.*, **22**, 501 (1979).
(6) K. C. Murdock, R. G. Child, P. F. Fabio, R. B. Angier, R. E. Wallace, F. E. Durr, and R. V. Citarella, *ibid.*, **22**, 1024 (1979).
(7) R. K. Johnson, R. K. Y. Zee-Cheng, W. W. Lee, E. M. Acton, D. W. Henry, and C. C. Cheng, *Cancer Treat. Rep.*, **63**, 425 (1979).
(8) R. E. Wallace, K. C. Murdock, R. B. Angier, and F. E. Durr, *Cancer Res.*, **39**, 1570 (1979).
(9) B. F. Kimler, *ibid.*, **40**, 42 (1980).
(10) T. W. Plumbridge, V. Knight, K. L. Patel, and J. R. Brown, *J. Pharm. Pharmacol.*, **32**, 78 (1980).
(11) D. D. Von Hoff, E. Pollard, J. Kuhn, E. Murray, and C. A. Coltman, Jr., *Cancer Res.*, **40**, 1516 (1980).
(12) F. Traganos, D. P. Evenson, L. Staiano-Coico, Z. Darzynkiewicz, and M. R. Melamed, *ibid.*, **40**, 671 (1980).
(13) D. P. Evenson, Z. Darzynkiewicz, L. Staiano-Coico, F. Traganos, and M. R. Melamed, *ibid.*, **39**, 2574 (1979).
(14) D. P. Evenson, F. Traganos, Z. Darzynkiewicz, L. Staiano-Coico, and M. R. Melamed, *J. Natl. Cancer Inst.*, **64**, 857 (1980).
(15) C. W. Greenhalgh, *Endeavour*, **35**, 134 (1976).

**ACKNOWLEDGMENTS**

Supported by Public Health Service Grant ES-02046 and a grant from the University of Kansas Endowment Association.

# Simultaneous Determination of Vitamins $B_1$, $B_2$, $B_6$, and Niacinamide in Multivitamin Pharmaceutical Preparations by Paired-Ion Reversed-Phase High-Pressure Liquid Chromatography

**RODERIC P. KWOK *x, W. P. ROSE *, RICK TABOR ‡, and THOMAS S. PATTISON ‡**

Received March 3, 1980, from the **Foremost-McKesson Research and Development Center, Dublin, CA 94566*, and the ‡*Forrest C. Shaklee Research Laboratories, Hayward, CA 94545.* Accepted for publication February 20, 1981.

**Abstract** □ A high-pressure liquid chromatographic procedure for the simultaneous determination of vitamins $B_1$, $B_2$, $B_6$, and niacinamide in multivitamin pharmaceutical preparations was developed and evaluated. The method uses paired-ion reversed-phase partition chromatography for baseline separation of the four water-soluble vitamins. This method was applied to the analysis of a multivitamin and multivitamin–multimineral tablets, and a technique was developed to reduce vitamin adsorption by the minerals. The results obtained by this method were compared with those obtained by the official methods. It was concluded that this method is fast, accurate, specific, and suitable for routine quality control use.

**Keyphrases** □ Vitamins, water soluble—simultaneous high-pressure liquid chromatographic analyses in multivitamin preparations □ High-pressure liquid chromatography—simultaneous analyses of various water-soluble vitamins in multivitamin preparations □ Multivitamin preparations—simultaneous high-pressure liquid chromatographic assay of various water-soluble vitamins

Progress in vitamin preparations is being impeded by methodological problems. Current official methods (1, 2) for the assay of water-soluble vitamins involve a complicated sample workup, tend to reproduce poorly because of the instability and pH sensitivity of the color development, and require that each vitamin be analyzed individually. These methods also are subject to interferences from various sources when analyzing samples with complex matrixes (3, 4).

High-pressure liquid chromatographic (HPLC) procedures for the simultaneous determination of water-soluble vitamins in pharmaceutical preparations have been described (5–7), but no mechanism has been developed to control vitamin adsorption by the minerals in multivitamin–multimineral tablets. This paper describes an HPLC procedure for the simultaneous determination of vitamins $B_1$, $B_2$, $B_6$, and niacinamide in multivitamin and multivitamin–multimineral tablets by paired-ion reversed-phase HPLC.

## EXPERIMENTAL

**Apparatus**—The HPLC system included two solvent pumps[1], a solvent programmer[2], a UV absorbance detector[3] at 280 nm, and an autoinjector[4]. A μBondapak phenyl (10 μm) 30-cm × 3.9-mm i.d. column and a 10-mv full-scale recorder[5] were used. Peak areas were determined using a laboratory data system[6]. The column temperature was regulated at 30° by a constant temperature bath[7]. A high-speed centrifuge was used[8], and the samples were disintegrated in a shaker bath[9] set at 60°.

**Materials and Reagents**—Thiamine hydrochloride, riboflavin, pyridoxine hydrochloride, and niacinamide were obtained as USP reference standards. 1-Hexanesulfonic acid was used as received[10]. Anhydrous citric acid[11] was obtained commercially and used without further purification. Solvents, all distilled-in-glass[12] grade, were obtained commercially. Commercial multivitamin preparations were obtained from local pharmacies.

**Preparation of Mobile Phases**—The two pumps used 0.0025 *M* 1-hexanesulfonic acid in water and in methanol, respectively. Prior to use, the mobile phases were degassed by vacuum filtration through a 0.5-μm pore, 47-mm diameter filter[13]. With a linear solvent program[14], a gradient was run at a constant flow rate of 2.0 ml/min for 18 min. Solvent conditions varied from 0 to 80% methanol in water. Five minutes was allowed between sample injections.

[1] Model 6000A, Waters Associates, Milford Mass.
[2] Model 660, Waters Associates, Milford, Mass.
[3] Model 440, Waters Associates, Milford Mass.
[4] WISP model 710A, Waters Associates, Milford Mass.
[5] Omniscribe, Houston Instrument, Houston, Tex.
[6] Model 3353, Hewlett-Packard, Palo Alto, Calif.
[7] FK2, Haak Inc., Saddle Brook, N.J.
[8] Sorvall RC-5B centrifuge fitted with SS-34 motor, DuPont Instruments, Wilmington, Del.
[9] Magni-Whirl water bath 15-453-400, Fisher Scientific Co., San Francisco, Calif.
[10] B-6 PIC reagent, Waters Associates, Milford Mass.
[11] Matheson, Coleman and Bell, Norwood, Ohio.
[12] Burdick & Jackson, Muskegon, Mich.
[13] Type LS, 47 mm, Millipore Corp. Bedford, Mass.
[14] Curve 6 on model 660 solvent programmer.



*0022-3549/81/0900-1014$01.00/0*
*© 1981, American Pharmaceutical Association*

(5) R. K. Y. Zee-Cheng, E. G. Podrebarac, C. S. Menon, and C. C. Cheng, *J. Med. Chem.*, **22**, 501 (1979).
(6) K. C. Murdock, R. G. Child, P. F. Fabio, R. B. Angier, R. E. Wallace, F. E. Durr, and R. V. Citarella, *ibid.*, **22**, 1024 (1979).
(7) R. K. Johnson, R. K. Y. Zee-Cheng, W. W. Lee, E. M. Acton, D. W. Henry, and C. C. Cheng, *Cancer Treat. Rep.*, **63**, 425 (1979).
(8) R. E. Wallace, K. C. Murdock, R. B. Angier, and F. E. Durr, *Cancer Res.*, **39**, 1570 (1979).
(9) B. F. Kimler, *ibid.*, **40**, 42 (1980).
(10) T. W. Plumbridge, V. Knight, K. L. Patel, and J. R. Brown, *J. Pharm. Pharmacol.*, **32**, 78 (1980).
(11) D. D. Von Hoff, E. Pollard, J. Kuhn, E. Murray, and C. A. Coltman, Jr., *Cancer Res.*, **40**, 1516 (1980).
(12) F. Traganos, D. P. Evenson, L. Staiano-Coico, Z. Darzynkiewicz, and M. R. Melamed, *ibid.*, **40**, 671 (1980).
(13) D. P. Evenson, Z. Darzynkiewicz, L. Staiano-Coico, F. Traganos, and M. R. Melamed, *ibid.*, **39**, 2574 (1979).
(14) D. P. Evenson, F. Traganos, Z. Darzynkiewicz, L. Staiano-Coico, and M. R. Melamed, *J. Natl. Cancer Inst.*, **64**, 857 (1980).
(15) C. W. Greenhalgh, *Endeavour*, **35**, 134 (1976).

**ACKNOWLEDGMENTS**

Supported by Public Health Service Grant ES-02046 and a grant from the University of Kansas Endowment Association.

# Simultaneous Determination of Vitamins $B_1$, $B_2$, $B_6$, and Niacinamide in Multivitamin Pharmaceutical Preparations by Paired-Ion Reversed-Phase High-Pressure Liquid Chromatography

**RODERIC P. KWOK *x, W. P. ROSE *, RICK TABOR ‡, and THOMAS S. PATTISON ‡**

Received March 3, 1980, from the **Foremost-McKesson Research and Development Center, Dublin, CA 94566*, and the ‡*Forrest C. Shaklee Research Laboratories, Hayward, CA 94545.* Accepted for publication February 20, 1981.

**Abstract** □ A high-pressure liquid chromatographic procedure for the simultaneous determination of vitamins $B_1$, $B_2$, $B_6$, and niacinamide in multivitamin pharmaceutical preparations was developed and evaluated. The method uses paired-ion reversed-phase partition chromatography for baseline separation of the four water-soluble vitamins. This method was applied to the analysis of a multivitamin and multivitamin–multimineral tablets, and a technique was developed to reduce vitamin adsorption by the minerals. The results obtained by this method were compared with those obtained by the official methods. It was concluded that this method is fast, accurate, specific, and suitable for routine quality control use.

**Keyphrases** □ Vitamins, water soluble—simultaneous high-pressure liquid chromatographic analyses in multivitamin preparations □ High-pressure liquid chromatography—simultaneous analyses of various water-soluble vitamins in multivitamin preparations □ Multivitamin preparations—simultaneous high-pressure liquid chromatographic assay of various water-soluble vitamins

Progress in vitamin preparations is being impeded by methodological problems. Current official methods (1, 2) for the assay of water-soluble vitamins involve a complicated sample workup, tend to reproduce poorly because of the instability and pH sensitivity of the color development, and require that each vitamin be analyzed individually. These methods also are subject to interferences from various sources when analyzing samples with complex matrixes (3, 4).

High-pressure liquid chromatographic (HPLC) procedures for the simultaneous determination of water-soluble vitamins in pharmaceutical preparations have been described (5–7), but no mechanism has been developed to control vitamin adsorption by the minerals in multivitamin–multimineral tablets. This paper describes an HPLC procedure for the simultaneous determination of vitamins $B_1$, $B_2$, $B_6$, and niacinamide in multivitamin and multivitamin–multimineral tablets by paired-ion reversed-phase HPLC.

## EXPERIMENTAL

**Apparatus**—The HPLC system included two solvent pumps[1], a solvent programmer[2], a UV absorbance detector[3] at 280 nm, and an autoinjector[4]. A μBondapak phenyl (10 μm) 30-cm × 3.9-mm i.d. column and a 10-mv full-scale recorder[5] were used. Peak areas were determined using a laboratory data system[6]. The column temperature was regulated at 30° by a constant temperature bath[7]. A high-speed centrifuge was used[8], and the samples were disintegrated in a shaker bath[9] set at 60°.

**Materials and Reagents**—Thiamine hydrochloride, riboflavin, pyridoxine hydrochloride, and niacinamide were obtained as USP reference standards. 1-Hexanesulfonic acid was used as received[10]. Anhydrous citric acid[11] was obtained commercially and used without further purification. Solvents, all distilled-in-glass[12] grade, were obtained commercially. Commercial multivitamin preparations were obtained from local pharmacies.

**Preparation of Mobile Phases**—The two pumps used 0.0025 *M* 1-hexanesulfonic acid in water and in methanol, respectively. Prior to use, the mobile phases were degassed by vacuum filtration through a 0.5-μm pore, 47-mm diameter filter[13]. With a linear solvent program[14], a gradient was run at a constant flow rate of 2.0 ml/min for 18 min. Solvent conditions varied from 0 to 80% methanol in water. Five minutes was allowed between sample injections.

[1] Model 6000A, Waters Associates, Milford Mass.
[2] Model 660, Waters Associates, Milford, Mass.
[3] Model 440, Waters Associates, Milford Mass.
[4] WISP model 710A, Waters Associates, Milford Mass.
[5] Omniscribe, Houston Instrument, Houston, Tex.
[6] Model 3353, Hewlett-Packard, Palo Alto, Calif.
[7] FK2, Haak Inc., Saddle Brook, N.J.
[8] Sorvall RC-5B centrifuge fitted with SS-34 motor, DuPont Instruments, Wilmington, Del.
[9] Magni-Whirl water bath 15-453-400, Fisher Scientific Co., San Francisco, Calif.
[10] B-6 PIC reagent, Waters Associates, Milford Mass.
[11] Matheson, Coleman and Bell, Norwood, Ohio.
[12] Burdick & Jackson, Muskegon, Mich.
[13] Type LS, 47 mm, Millipore Corp. Bedford, Mass.
[14] Curve 6 on model 660 solvent programmer.



*0022-3549/81/0900-1014$01.00/0*
*© 1981, American Pharmaceutical Association*

**Table I—Effect of Ferrous Gluconate and Magnesium Oxide on the Recovery of Pyridoxine Hydrochloride in 100 ml of 0.1 *N* HCl Solutions**

| Sample | Solution Composition: Amount of $B_6$, mg | Ferrous Gluconate, mg | Magnesium Oxide, mg | $B_6$, % recovery[a] | *SD* | *RSD*, % |
|---|---|---|---|---|---|---|
| Pyridoxine | 0.5 | — | — | 101 | 1.02 | 1.01 |
| Ferrous gluconate + magnesium oxide | — | 40 | 90 | None | — | — |
| Pyridoxine hydrochloride + ferrous gluconate | 0.5 | 40 | — | 80.43 | 1.01 | 1.26 |
| Pyridoxine hydrochloride + magnesium oxide | 0.5 | — | 90 | 59.00 | 5.31 | 9.00 |
| Pyridoxine hydrochloride + ferrous gluconate and magnesium oxide | 0.5 | 40 | 90 | 91.67 | 1.03 | 1.12 |

[a] $n = 5$.

**Table II—Water-Soluble Vitamins Found in Multivitamin–Multimineral Tablets[a] by Various Modes of Extraction**

| Vitamin, Label Claim | Percent of Label Claim: 0.1 *N* HCl | Dimethyl Sulfoxide | 1% Citric Acid in Dimethyl Sulfoxide |
|---|---|---|---|
| Thiamine hydrochloride, 2.1 mg/tablet | 96.6 ± 1.94 | 108.5 ± 7.54 | 100 ± 1.25 |
| Riboflavin, 2.4 mg/tablet | 81.2 ± 0.90 | 104.2 ± 1.80 | 100 ± 1.75 |
| Pyridoxine hydrochloride, 2.0 mg/tablet | 88.3 ± 1.70 | 84.2 ± 0.78 | 100 ± 1.58 |
| Niacinamide, 2.0 mg/tablet | 101.9 ± 3.26 | 100.6 ± 0.85 | 100 ± 3.11 |

[a] Vita Lea, Shaklee Corp.; each value is the mean ± *SD* of five determinations.

**Preparation of Standard Solutions**—Stock standard solutions of thiamine hydrochloride, pyridoxine hydrochloride, and niacinamide (0.5 mg/ml each) were prepared separately by dissolving accurately weighed USP reference standards in 0.1 *N* HCl. Due to poor solubility, only the riboflavin working standard solution was prepared in a more diluted form; <0.1 g accurately weighed USP reference standard was dissolved in 1000 ml of 0.1 *N* HCl, heated, and constantly stirred in a low actinic volumetric flask.

Different aliquots from each stock standard vitamin solution were combined and diluted with the riboflavin working standard solution. This procedure resulted in a working standard solution containing all four water-soluble vitamins at the desired concentration.

**Preparation of Sample Solutions**—*Multivitamin Tablets*—A suitable number of tablets containing no more than 10 mg of riboflavin were placed in a low actinic glass-stoppered erlenmeyer flask. Exactly 100 ml of 0.1 *N* HCl was pipetted into the flask, and the flask was stoppered and shaken for 45 min in a constant-temperature bath at 60°. The sample was allowed to cool to room temperature and then was centrifuged at 44,000×*g* for 18 min. Then 10 μl of the clear supernate was injected into the liquid chromatograph.

*Multivitamin–Multimineral Tablets*—A suitable number of tablets containing no more than 10 mg of riboflavin were placed in a low actinic glass-stoppered erlenmeyer flask. Exactly 100 ml of dimethyl sulfoxide containing 1% citric acid (anhydrous) was delivered into the flask. The solution then was shaken for 45 min in a constant-temperature bath at 60°. It was allowed to cool to room temperature and then was centrifuged at 44,000×*g* for 18 min. Then 10 μl of the clear supernate was injected into the liquid chromatograph.

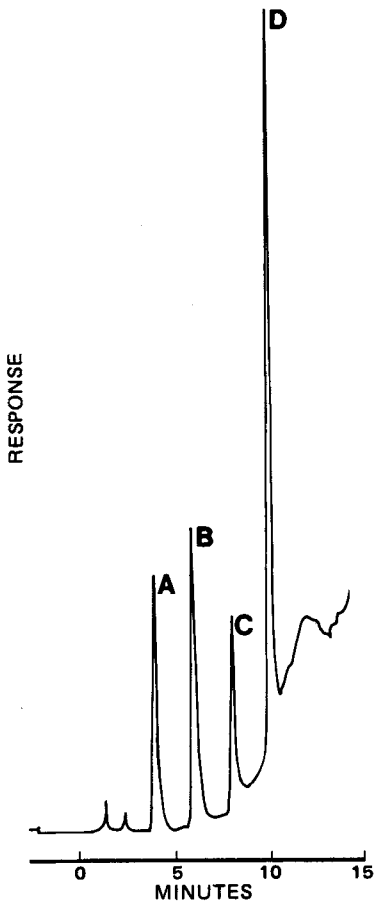


**Figure 1**—*Liquid chromatographic trace of a standard mixture of niacinamide (A), pyridoxine (B), thiamine (C), and riboflavin (D).*

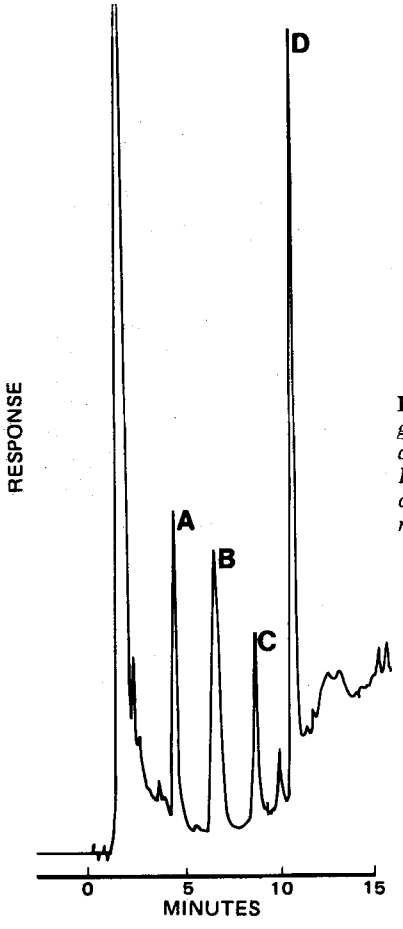


**Figure 2**—*Liquid chromatographic trace of the extract of a vitamin B complex tablet. Key: A, niacinamide; B, pyridoxine; C, thiamine; and D, riboflavin.*

**Table III—Recovery Results on Vitamins $B_1$, $B_2$, $B_6$, and Niacinamide**

| Sample | Percent Recovery[a], mean ± *SD* (% *RSD*) | | | |
|---|---|---|---|---|
| | $B_1$ | $B_2$ | $B_6$ | Niacinamide |
| Control multivitamin tablets[b] | None | None | None | None |
| Multivitamin tablets + added vitamins[c] | 100.8 ± 2.23 (2.21) | 102.1 ± 2.48 (2.43) | 104.3 ± 6.7 (6.43) | 102.1 ± 2.78 (2.72) |
| Control multivitamin–multimineral tablets[b] | None | None | None | None |
| Multivitamin–multimineral tablets + added vitamins[c] | 101.6 ± 2.21 (2.18) | 99.60 ± 2.01 (2.02) | 99.62 ± 2.92 (2.93) | 99.97 ± 1.45 (1.45) |

[a] Each value is the mean ± *SD* (% *RSD*) of six determinations. [b] Control tablets contain the complete formulation of B-Complex (multivitamin tablets) and Vita Lea (multivitamin–multimineral tablets) without vitamins $B_1$, $B_2$, $B_6$, and niacinamide. [c] Same as control tablets but with vitamins $B_1$, $B_2$, $B_6$, and niacinamide added directly to the flask.

**Table IV—Comparison of USP Method *versus* HPLC Method for the Analysis of Vitamins $B_1$ and $B_2$ in Multivitamin Products**

| Product[a] | Vitamin $B_1$ | | | | | Vitamin $B_2$ | | | | |
|---|---|---|---|---|---|---|---|---|---|---|
| | Formulation Amount | Found[b] | | | | Formulation Amount | Found | | | |
| | | HPLC | *SD* | USP | *SD* | | HPLC | *SD* | USP | *SD* |
| A | 66.42 mg/g | 65.91 | 0.56 | 66.5 | 1.83 | 70.72 mg/g | 70.66 | 0.27 | 72.9 | 1.36 |
| B | 1.178 mg/tablet | 1.151 | 0.02 | 1.248 | 0.04 | 1.143 mg/tablet | 1.172 | 0.018 | 1.245 | 0.026 |
| C | 9.45 mg/tablet | 9.63 | 0.35 | 8.73 | 0.90 | 8.415 mg/tablet | 8.597 | 0.110 | 7.910 | 0.129 |
| D | 0.678 mg/tablet | 0.687 | 0.003 | 0.695 | 0.009 | 0.718 mg/tablet | 0.716 | 0.002 | 0.674 | 0.010 |
| E | 10 mg/tablet | 10.5[c] | —[d] | —[d] | —[d] | 10 mg/tablet | 18.0[c] | —[d] | —[d] | —[d] |
| F | 11.6 mg/tablet | 11.9[c] | —[d] | —[d] | —[d] | 15 mg/tablet | 14.6[c] | —[d] | —[d] | —[d] |
| G | 3 mg/capsule | 3.1[c] | —[d] | —[d] | —[d] | 3 mg/capsule | 3.4[c] | —[d] | —[d] | —[d] |

[a] Key: A, Vita Lea Premixes (Shaklee); B, Vita Cal (Shaklee); C, B-Complex (Shaklee); D, Vita Lea (Shaklee); E, Super Thera-Vite M (Nature's Blend); F, Stress Formula (Value Rite); and G, B-Complex Capsules (Nature's Blend). [b] Each value is a mean ± *SD* of five determinations. [c] Single determination. [d] Not determined.

## RESULTS AND DISCUSSION

HPLC can provide a quick and accurate evaluation of multivitamin and multivitamin–multimineral tablets, and paired-ion reversed-phase HPLC is particularly attractive for determining water-soluble vitamins because polar constituents that dissolve in the aqueous mobile phase elute at or near the solvent front. Lipophilic constituents with very limited solubility in the aqueous mobile phase partition with the stationary phase, thereby eluting much later. Under these conditions, separation can be achieved. Thus, sample preparation time is greatly reduced and the accuracy of the method also is enhanced.

In the present study, 0.1 *N* HCl was used to extract the water-soluble vitamins from the multivitamin preparations. Dimethyl sulfoxide containing anhydrous citric acid was used to disperse the multivitamin–multimineral preparations since neither 0.1 *N* HCl nor dimethyl sulfoxide alone extracts pyridoxine completely. This may be due to adsorption of the vitamin by one or more of the minerals. Kwok *et al.* (8) established that vitamin A acetate adsorbs to ferrous gluconate and that a complexing agent can minimize this effect.

With a similar approach, it was demonstrated in these laboratories that, in 0.1 *N* HCl solution, pyridoxine hydrochloride adsorbs strongly to ferrous gluconate and magnesium oxide (Table I) and that a complexing agent like citric acid in dimethyl sulfoxide can minimize this effect (Table II). Thus, anhydrous citric acid was dissolved first in dimethyl sulfoxide to allow for the exposure to the minerals as soon as possible. Table I shows the effect of ferrous gluconate and magnesium oxide on pyridoxine hydrochloride in 0.1 *N* HCl solution. Table II demonstrates the percentage of recovery of all four water-soluble vitamins in multivitamin–multimineral tablets by different modes of extraction. It is obvious from Table II that 1% citric acid in dimethyl sulfoxide reduced the effect of ferrous gluconate and magnesium oxide to an insignificant level. The extraction of the other vitamins (thiamine, riboflavin, and niacinamide) was not impaired by the addition of the anhydrous citric acid in dimethyl sulfoxide.

Linearity of response over the range studied can be achieved using standard solutions. In these laboratories, the ratios of the concentration of the standard solution (expressed in nanograms per 10 microliters) to the area under the peak were consistent for all four water-soluble vitamins studied. These ratios were determined over 6 days, and their relative standard deviations were <1%. This finding indicates that the procedure can be used as a single-point standard for each vitamin.

Chromatographic traces of vitamin B standards, vitamin B complex, and the multivitamin–multimineral tablet extracts are presented in Figs. 1, 2, and 3, respectively. Using paired-ion reversed-phase HPLC, baseline

**Table V—Comparison of USP Method *versus* HPLC Method for Analysis of Vitamin $B_6$ and Niacinamide in Multivitamin Products**

| Product[a] | Vitamin $B_6$ | | | | | Niacinamide | | | | |
|---|---|---|---|---|---|---|---|---|---|---|
| | Formulation Amount | Found[b] | | | | Formulation Amount | Found | | | |
| | | HPLC | *SD* | USP | *SD* | | HPLC | *SD* | USP | *SD* |
| A | 54.21 mg/g | 54.33 | 1.40 | 54.9 | 1.24 | None | None | | None | |
| B | None | None | | None | | None | None | | None | |
| C | 11.97 mg/tablet | 11.37 | 0.15 | 9.27 | 0.23 | 99.00 mg/tablet | 98.60 | 3.31 | 97.20 | 4.40 |
| D | 0.670 mg/tablet | 0.668 | 0.013 | 0.680 | 0.019 | 5.49 mg/tablet | 5.54 | 0.06 | 5.18 | 0.30 |
| E | 5 mg/tablet | 4.7[c] | —[d] | —[d] | —[d] | 100 mg/tablet | 101.5[c] | —[d] | —[d] | —[d] |
| F | 5 mg/tablet | 5.1[c] | —[d] | —[d] | —[d] | 100 mg/tablet | 90.8[c] | —[d] | —[d] | —[d] |
| G | 0.5 mg/capsule | 0.9[c] | —[d] | —[d] | —[d] | 20 mg/capsule | 26.0[c] | —[d] | —[d] | —[d] |

[a] Key: A, Vita Lea Premixes (Shaklee); B, Vita Cal (Shaklee); C, B-Complex (Shaklee); D, Vita Lea (Shaklee); E, Super Thera-Vite M (Nature's Blend); F, Stress Formula (Value Rite); and G, B-Complex Capsules (Nature's Blend). [b] Each value is a mean ±*SD* of five determinations. [c] Single determination. [d] Not determined.

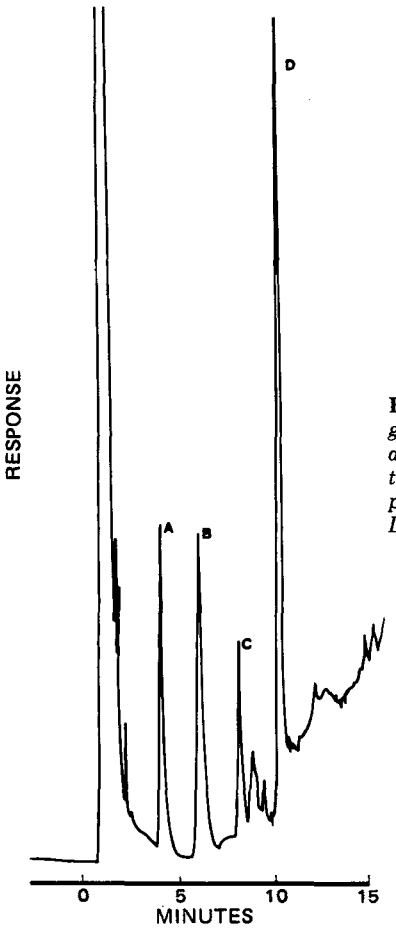


**Figure 3**—*Liquid chromatographic trace of the extract of a multivitamin–multimineral tablet. Key: A, niacinamide; B, pyridoxine; C, thiamine; and D, riboflavin.*

separation of all four water-soluble vitamins is possible (Figs. 1 and 2). There also is a baseline separation of the vitamins in the dimethyl sulfoxide extract (Fig. 3).

To validate the selectivity of the procedure, placebo formulations spiked with known amount of the vitamins were employed. The results are tabulated in Table III. All four vitamins were quantitatively recovered in both multivitamin and multivitamin–multimineral tablets.

To verify the applicability of this procedure further, various commercial multivitamin and multivitamin–multimineral tablets were assayed simultaneously by the HPLC and the USP methods (Tables IV and V). In each case, the precision of the HPLC procedure was greater than that of the current official procedure. This result may be attributed to the less complicated sample workup required by the former procedure. However, the results of the two methods compared favorably in terms of accuracy.

The described HPLC method appears to be attractive in terms of analysis time and should be adapted to various commercial products. The column lifetimes under these conditions of minimum sample preparation initially was a subject of concern. However, over 500 preparations were processed without change in the chromatographic characteristics of the system. This stability may be due in part to the small quantities of sample injected and in part to the proper care as recommended by the column supplier. The methodology for the HPLC determination of other vitamins is currently under investigation and will be published later.

## REFERENCES

(1) "The United States Pharmacopeia," 19th rev., Mack Publishing Co., Easton, Pa., 1975, pp. 341, 429, 442, 502.

(2) "The National Formulary," 14th ed., Mack Publishing Co., Easton, Pa., 1975, pp. 486, 984.

(3) V. D. Gupta and D. E. Cadwallader, *J. Pharm. Sci.*, **57**, 112 (1968).

(4) S. A. Ismaiel and D. A. Yassa, *Analyst*, **98**, 816 (1973).

(5) D. P. Wittmer and W. G. Haney, Jr., *J. Pharm. Sci.*, **63**, 588 (1974).

(6) S. P. Sood, D. P. Wittmer, S. A. Ismaiel, and W. G. Haney, *ibid*, **66**, 40 (1977).

(7) R. L. Kirchmeier and R. P. Upton, *ibid*, **67**, 1444 (1978).

(8) R. P. Kwok, T. Hudson, and S. Subramanian, in "Application of High Pressure Liquid Chromatographic Methods for Determination of Fat-Soluble Vitamins, A, D, E, and K in Foods & Pharmaceuticals," Association of Vitamin Chemists, Chicago, Ill., 1978.

# *In Vivo–In Vitro* Correlations with a Commercial Dissolution Simulator I: Methenamine, Nitrofurantoin, and Chlorothiazide

**MARTIN K. T. YAU and MARVIN C. MEYER** ˣ

Received October 20, 1980, from the *Division of Biopharmaceutics and Pharmacokinetics, Department of Pharmaceutics, College of Pharmacy, University of Tennessee Center for the Health Sciences, Memphis, TN 38163.* Accepted for publication February 20, 1981.

**Abstract** □ Dissolution profiles were determined for nine methenamine, 14 nitrofurantoin, and six chlorothiazide dosage forms using a dissolution simulator. Various *in vivo–in vitro* correlations were examined. The best correlation for methenamine was between the maximum urinary excretion rate and the time for 15% dissolution. A good correlation for the 50-mg nitrofurantoin tablets was also found between cumulative percent of drug excreted in 12 hr and the percent dissolved in 1 hr. There were no significant correlations for the 100-mg nitrofurantoin dosage forms. Good correlations were also observed for the 250- and 500-mg chlorothiazide tablets between the percent of drug dissolved in 1 min or the time for 15% dissolution and the maximum excretion rate.

**Keyphrases** □ Dissolution—profiles for methenamine, nitrofurantoin, and chlorothiazide, dissolution simulator □ Dissolution simulator—profiles for methenamine, nitrofurantoin, and chlorothiazide □ Methenamine—dissolution profile using dissolution simulator □ Nitrofurantoin—dissolution profile using dissolution simulator □ Chlorothiazide—dissolution profile using dissolution simulator

Many methods developed to study the *in vitro* dissolution properties of dosage forms have been reviewed previously (1). The primary objective of most efforts to develop *in vitro* dissolution procedures is to provide data that can be related to the performance of oral dosage forms when administered to human subjects. One sophisticated

0022-3549/81/0900-1017$01.00/0
© 1981, American Pharmaceutical Association

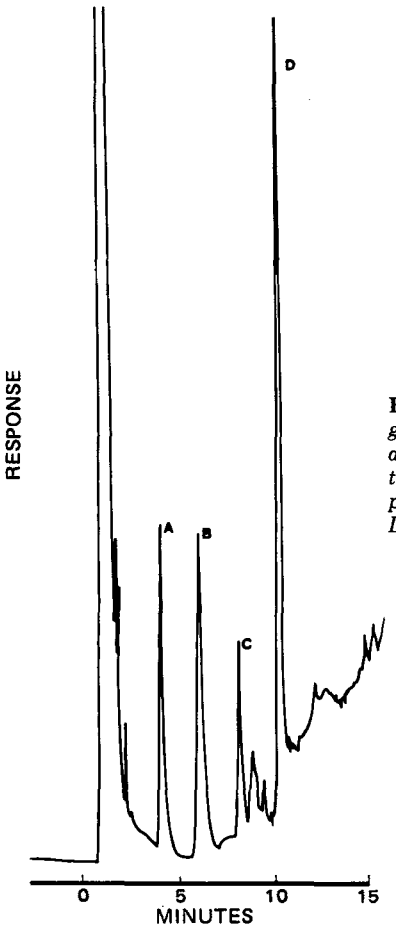


**Figure 3**—*Liquid chromatographic trace of the extract of a multivitamin–multimineral tablet. Key: A, niacinamide; B, pyridoxine; C, thiamine; and D, riboflavin.*

separation of all four water-soluble vitamins is possible (Figs. 1 and 2). There also is a baseline separation of the vitamins in the dimethyl sulfoxide extract (Fig. 3).

To validate the selectivity of the procedure, placebo formulations spiked with known amount of the vitamins were employed. The results are tabulated in Table III. All four vitamins were quantitatively recovered in both multivitamin and multivitamin–multimineral tablets.

To verify the applicability of this procedure further, various commercial multivitamin and multivitamin–multimineral tablets were assayed simultaneously by the HPLC and the USP methods (Tables IV and V). In each case, the precision of the HPLC procedure was greater than that of the current official procedure. This result may be attributed to the less complicated sample workup required by the former procedure. However, the results of the two methods compared favorably in terms of accuracy.

The described HPLC method appears to be attractive in terms of analysis time and should be adapted to various commercial products. The column lifetimes under these conditions of minimum sample preparation initially was a subject of concern. However, over 500 preparations were processed without change in the chromatographic characteristics of the system. This stability may be due in part to the small quantities of sample injected and in part to the proper care as recommended by the column supplier. The methodology for the HPLC determination of other vitamins is currently under investigation and will be published later.

## REFERENCES

(1) "The United States Pharmacopeia," 19th rev., Mack Publishing Co., Easton, Pa., 1975, pp. 341, 429, 442, 502.

(2) "The National Formulary," 14th ed., Mack Publishing Co., Easton, Pa., 1975, pp. 486, 984.

(3) V. D. Gupta and D. E. Cadwallader, *J. Pharm. Sci.*, **57**, 112 (1968).

(4) S. A. Ismaiel and D. A. Yassa, *Analyst*, **98**, 816 (1973).

(5) D. P. Wittmer and W. G. Haney, Jr., *J. Pharm. Sci.*, **63**, 588 (1974).

(6) S. P. Sood, D. P. Wittmer, S. A. Ismaiel, and W. G. Haney, *ibid*, **66**, 40 (1977).

(7) R. L. Kirchmeier and R. P. Upton, *ibid*, **67**, 1444 (1978).

(8) R. P. Kwok, T. Hudson, and S. Subramanian, in "Application of High Pressure Liquid Chromatographic Methods for Determination of Fat-Soluble Vitamins, A, D, E, and K in Foods & Pharmaceuticals," Association of Vitamin Chemists, Chicago, Ill., 1978.

# *In Vivo–In Vitro* Correlations with a Commercial Dissolution Simulator I: Methenamine, Nitrofurantoin, and Chlorothiazide

**MARTIN K. T. YAU and MARVIN C. MEYER** ˣ

Received October 20, 1980, from the *Division of Biopharmaceutics and Pharmacokinetics, Department of Pharmaceutics, College of Pharmacy, University of Tennessee Center for the Health Sciences, Memphis, TN 38163.* Accepted for publication February 20, 1981.

**Abstract** □ Dissolution profiles were determined for nine methenamine, 14 nitrofurantoin, and six chlorothiazide dosage forms using a dissolution simulator. Various *in vivo–in vitro* correlations were examined. The best correlation for methenamine was between the maximum urinary excretion rate and the time for 15% dissolution. A good correlation for the 50-mg nitrofurantoin tablets was also found between cumulative percent of drug excreted in 12 hr and the percent dissolved in 1 hr. There were no significant correlations for the 100-mg nitrofurantoin dosage forms. Good correlations were also observed for the 250- and 500-mg chlorothiazide tablets between the percent of drug dissolved in 1 min or the time for 15% dissolution and the maximum excretion rate.

**Keyphrases** □ Dissolution—profiles for methenamine, nitrofurantoin, and chlorothiazide, dissolution simulator □ Dissolution simulator—profiles for methenamine, nitrofurantoin, and chlorothiazide □ Methenamine—dissolution profile using dissolution simulator □ Nitrofurantoin—dissolution profile using dissolution simulator □ Chlorothiazide—dissolution profile using dissolution simulator

Many methods developed to study the *in vitro* dissolution properties of dosage forms have been reviewed previously (1). The primary objective of most efforts to develop *in vitro* dissolution procedures is to provide data that can be related to the performance of oral dosage forms when administered to human subjects. One sophisticated

0022-3549/81/0900-1017$01.00/0
© 1981, American Pharmaceutical Association

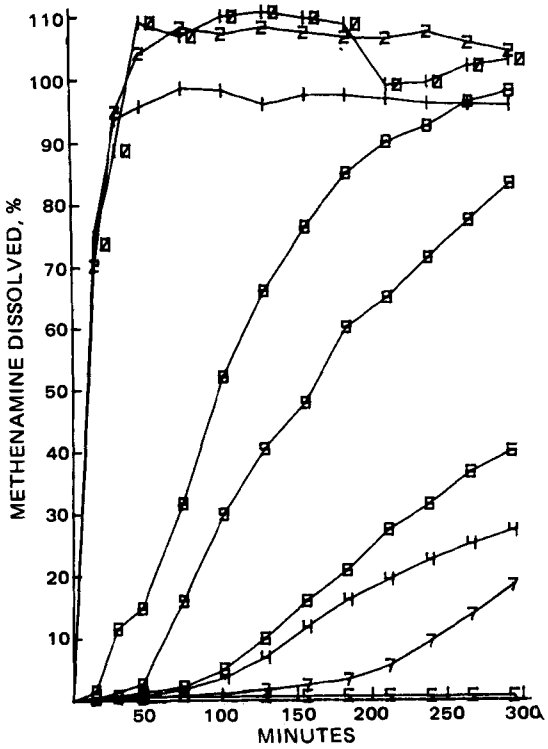


**Figure 1**—*Dissolution profiles for nine methenamine formulations. Each data point is the mean of two determinations. The simulated intestinal phase began after 32 min.*

instrument developed recently is a dissolution simulator[1], which is designed to be utilized in conjunction with an absorption simulator[2]. It is claimed (2) that these devices provide *in vitro* data that correlate well with *in vivo* bioavailability data. However, relatively little data demonstrating the applicability of these devices (3–5) have been published.

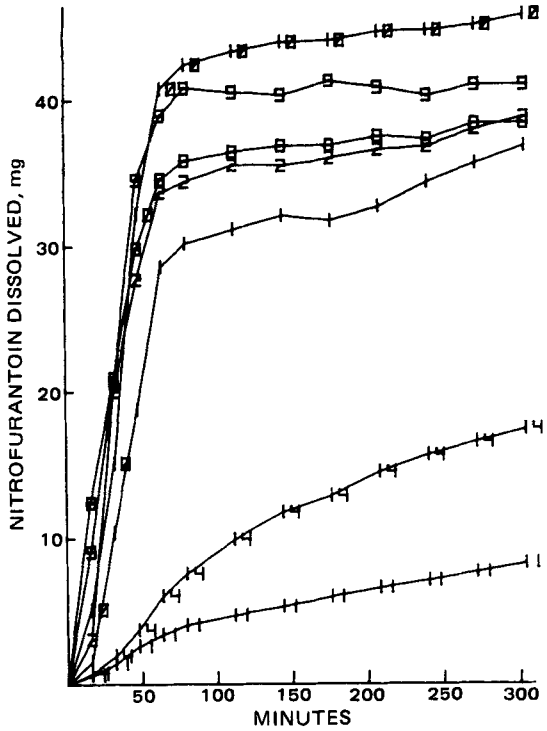


**Figure 2**—*Dissolution profiles for seven 50-mg nitrofurantoin formulations. Each data point represents the mean of two determinations. The intestinal phase began after 32 min.*

[1] SM 16752, Sartorius Filters, San Francisco, Calif.
[2] SM 16753, Sartorius Filters, San Francisco, Calif.

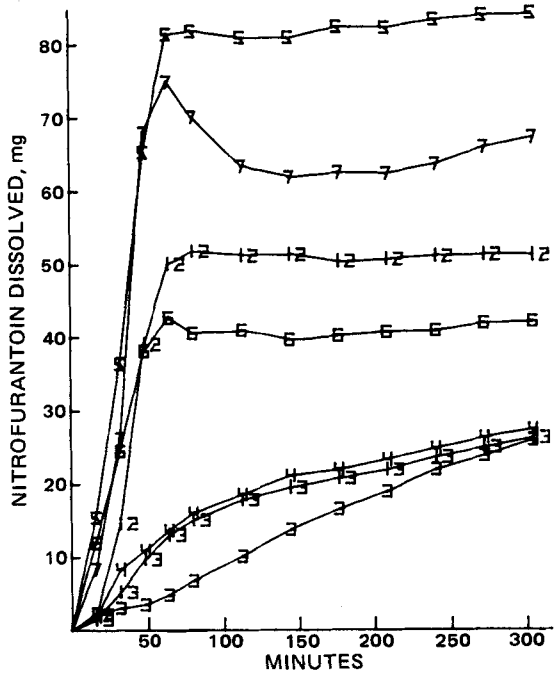


**Figure 3**—*Dissolution profiles for seven 100-mg nitrofurantoin formulations. Each data point represents the mean of two determinations. The intestinal phase began after 32 min.*

## BACKGROUND

The dissolution simulator is composed of two identical dissolution systems that permit the simultaneous evaluation of two dosage forms.

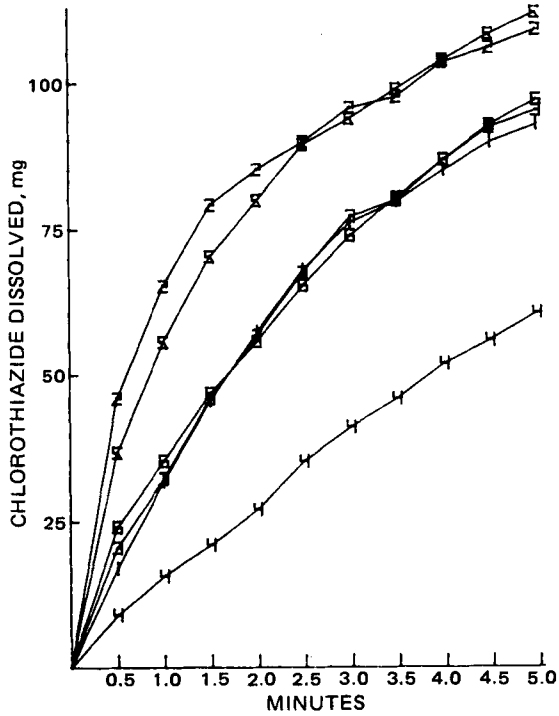


**Figure 4**—*Dissolution profiles for three 250-mg chlorothiazide tablet formulations (Products 1, 3, and 4) and three 500-mg chlorothiazide tablet formulations (Products 2, 5, and 6) in simulated gastric fluid. Each data point represents the mean of two determinations.*

The dissolution process takes place in two plastic cylinders. Dissolution fluid (100 ml) is placed in each cylinder, along with the dosage form and 70 g of glass beads. The cylinders rotate around a horizontal axis at 1.2 cpm to provide gentle agitation. The cylinder contents are maintained at 37°, and the pH of the dissolution fluid may be changed during the dissolution process by the addition of buffer salts. Samples ranging from 2.5 to 7.5 ml are automatically withdrawn and collected for analysis at sampling intervals of 0.5–60 min. The volume of dissolution fluid removed by sampling is replaced by fresh solution contained in a reservoir. The manufacturer recommends that the rate of sample withdrawal should be determined from data obtained in preliminary studies with the absorption simulator. The sampling rate for the dissolution simulator is directly related to the rate of drug diffusion in the absorption simulator.

The absorption simulator is essentially a dialysis cell designed to determine the diffusion rate of a drug, dissolved in either simulated gastric or intestinal fluid, across a membrane coated with a lipid substance into a pH 7.5 buffer. The diffusion rate is reported to be related to the rate of drug diffusion across the membranes of the GI tract.

Since little data were available to permit an evaluation of the correlation between *in vitro* dissolution data obtained with the dissolution simulator and the bioavailability of oral dosage forms in humans, a series of studies was initiated. The present study reports dissolution data for nine methenamine, 14 nitrofurantoin, and six chlorothiazide dosage forms. Each formulation was the subject of previous *in vivo* urinary excretion studies with healthy human subjects (6–8).

## EXPERIMENTAL

**Absorption Simulator Studies**—Each drug was dissolved in 100 ml of simulated gastric fluid (pH 1.1) containing hydrochloric acid, sodium chloride, and aminoacetic acid or in simulated intestinal fluid (pH 6.5) containing phosphate buffer. The initial drug concentrations were 200 μg/ml for the methenamine and chlorothiazide solutions and 100 μg/ml for the nitrofurantoin. A membrane with an effective surface area of 80 $cm^2$ was used for both the simulated gastric and intestinal phase diffusion studies. The composition of the lipid coating of the membrane was different for the two studies, but the nature of the coating was not available from the supplier.

The gastric and intestinal phase studies used artificial gastric and intestinal membranes[3]. The drug diffused from the gastric or intestinal phase, across the membrane, into the simulated plasma phase, which was a pH 7.5 phosphate buffer. At least three samples were collected from each phase at equal time intervals, and each study was done in duplicate. The resulting data were employed to calculate a diffusion rate constant, which was subsequently used to estimate an appropriate sampling rate for the dissolution simulator, according to a previous method (9).

**Dissolution Simulator Studies**—Each dosage form of the three drugs was initially placed into the simulated gastric fluid. The sampling rates for each drug were as follows: methenamine, 2.5 ml every 15 min for 30 min; nitrofurantoin, 2.5 ml every 16 min for 32 min; and chlorothiazide, 7.5 ml every 0.5 min for 5 min. At the end of the gastric phase, phosphate buffer was added to the dissolution fluid to increase the pH to 6.5 for methenamine and nitrofurantoin. Dissolution studies of the chlorothiazide formulations were only studied using the gastric phase. The sampling rates during this intestinal phase were as follows: methenamine, 2.5 ml every 5.5 min for 278 min; and nitrofurantoin, 2.5 ml every 16 min for 240 min. Two units of each drug formulation were studied. In addition, six tablets of one lot of nitrofurantoin were used to measure the reproducibility of the dissolution process.

The methenamine dosage forms, identified previously in a 10-subject study (6), consisted of a compressed tablet with 500 mg of methenamine base (Product 1), a suspension containing 50 mg of methenamine mandelate/ml (Product 2), a 500-mg methenamine hippurate tablet (Product 10), and six formulations of enteric-coated methenamine mandelate (Products 4–9). A 10th dosage form (Product 3), given as a solution in a previous study (6), was not included.

The nitrofurantoin dosage forms, included in earlier *in vivo* studies using 14 subjects (7), were six 50-mg tablets of microcrystalline drug (Products 1, 2, 8, 9, 11, and 14) and six 100-mg tablets of microcrystalline drug (Products 3–6, 12, and 13). A 50-mg macrocrystalline capsule (Product 10) and a 100-mg macrocrystalline capsule (Product 7) also were studied.

The chlorothiazide tablets contained either 250 (Products 1, 3, and 4) or 500 (Products 2, 5, and 6) mg of chlorothiazide and also were identified in an earlier study in which each dosage form was administered to a group of 12 subjects (8).

[3] Artificial gastric lipid barrier, SM 15701, and artificial intestinal lipid barrier, SM 15702, Sartorius Filters, San Francisco, Calif.

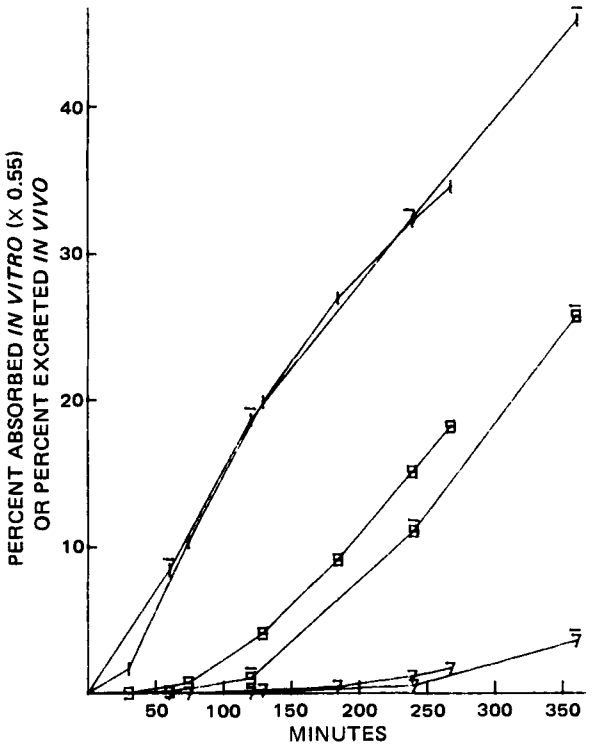


**Figure 5**—*Comparison of the total amount of methenamine withdrawn from the* in vitro *dissolution system (× 0.55) (Products 1, 7, and 9) and the cumulative amount of methenamine excreted in the* in vivo *studies (Products 1, 7, and 9) for three methenamine formulations. Each* in vitro *data point is the mean of two determinations. Each* in vivo *data point is the mean of 10 subjects.*

**USP Dissolution Tests**—Dissolution testing, using the USP rotating basket, was described previously for *in vivo* studies of the nitrofurantoin (7) and chlorothiazide (8) dosage forms. Studies using this dissolution apparatus were not conducted for the methenamine tablets.

**Analytical Methods**—Samples of methenamine solutions obtained with both the dissolution and absorption simulators were assayed by a colorimetric procedure based on a method developed to determine urine concentrations (10). Samples were diluted, and 0.5-ml aliquots were acidified with 0.5 ml of 6 *N* HCl and heated in a 70° water bath in a closed tube for 2 hr to hydrolyze the methenamine to formaldehyde. The solution was then cooled to 5°, and 1 ml of 0.1% tryptophan in 50% ethanol, 0.2 ml of 1% ferric chloride, and 1 ml of 90% sulfuric acid were added. The solution was heated for an additional 70 min at 70°.

After cooling to room temperature, the absorbance was determined at 575 nm and the methenamine concentration was calculated from a standard curve obtained by carrying aqueous solutions of known methenamine composition through the assay procedure. Preliminary studies indicated that the materials contained in the enteric coating of some of the products did not interfere in the assay at the dilution levels employed for the *in vitro* samples.

Nitrofurantoin samples obtained with either the absorption or dissolution simulator were diluted as necessary with pH 6.5 or 7.5 phosphate buffer, and the absorbance was determined at 278 nm. Standard curves also were prepared with nitrofurantoin solutions of known composition at pH 6.5 and 7.5.

Chlorothiazide samples were assayed at 278 nm after dilution with pH 6.5 or 7.5 phosphate buffer. Solutions of known chlorothiazide concentration also were assayed.

**Treatment of Dissolution Data**—Three types of data treatment were employed to evaluate the relationship between *in vitro* dissolution and *in vivo* urinary excretion data.

*Simulated Absorption Data*—The cumulative amount of drug excreted in the urine and the cumulative amount of dissolved drug withdrawn from the dissolution chamber were plotted *versus* time and were compared visually.

*General Correlations*—*In vivo* measurements, such as the cumulative

**Table I—Diffusion Characteristics and Sampling Rates Determined with the Absorption Simulator**

| Drug | $K_d \times 10^3$ cm/min$^{-1}$ (±SD) | | Calculated Time, between Samples, min[b] | | Actual Time between Samples, min | |
|---|---|---|---|---|---|---|
| | Gastric Phase[a] | Intestinal Phase[a] | Gastric Phase | Intestinal Phase | Gastric Phase | Intestinal Phase |
| Methenamine | 0.28 (0.12) | 0.64 (0.13) | 29.5 | 5.5 | 15.0 | 5.5 |
| Nitrofurantoin | 0.16 (0.01) | 0.34 (0.00) | 67.9 | 16.0 | 16.0 | 16.0 |
| Chlorothiazide | 0.12 (0.00) | 0.44 (0.04) | 110.0 | 9.8 | 0.5 | — |

[a] Diffusion rate constant, calculated according to Stricker (9). [b] Theoretical sampling rates for the dissolution simulator, calculated from the absorption simulator diffusion rate according to Stricker (9).

percent of drug excreted at specific times and maximum urinary excretion rates, were correlated with *in vitro* data such as the cumulative percent of drug dissolved and the time for a specific percent of drug to dissolve *in vitro*. The latter values for $T_{15\%}$, $T_{50\%}$, and $T_{70\%}$ were determined using the logarithmic-probability method of Sullivan *et al.* (11).

*Quadrant Analysis*—This relatively new approach (12, 13) utilizes *in vivo* data from individual subjects rather than just mean data from a group of subjects. The performance of each dosage form in each subject is evaluated relative to a reference dosage form. An arbitrary guideline, *e.g.*, 75%, is selected, and the percent of subjects exhibiting a relative bioavailability of at least 75% is determined and plotted *versus* the *in vitro* dissolution measurement of interest for each test dosage form. For example, if five out of 10 subjects exhibit a maximum urinary excretion rate for a test product that is at least 75% that of a reference product, 50% would be used for correlation with the *in vitro* measurement for that specific dosage form. The other formulations included in the *in vivo* and *in vitro* evaluations would be treated similarly to develop a possible correlation.

## RESULTS AND DISCUSSION

**Absorption Simulator**—The apparent first-order diffusion rate constants determined in simulated gastric and intestinal fluids using the absorption simulator are given in Table I. A direct comparison of the diffusion rates for a given drug in both gastric and intestinal fluid is not possible because the composition of the membranes was different for the two fluids.

The diffusion rate constants, which according to Stricker (9) are related to the *in vivo* drug absorption rate, were used to compute the optimum sampling intervals for the *in vitro* dissolution studies. The resulting sampling times are given in Table I. Since the dissolution simulator is supposed to involve dissolution studies using gastric fluid for 30 min to simulate gastric residence time, the calculated sampling intervals for methenamine, nitrofurantoin, and chlorothiazide were not appropriate. Thus, arbitrary sampling times were chosen for the gastric fluid dissolution studies of these drugs. In particular, the 0.5-min time used for chlorothiazide was based on a preliminary study that indicated that the gastric dissolution fluid was rapidly saturated with this drug within 5 min. Furthermore, because of the limited solubility of chlorothiazide, the dissolution study was terminated after 5 min.

The results obtained with the absorption simulator indicated that it was of little value for these three drugs in the determination of appropriate sampling intervals for the dissolution studies. While the absorption simulator may be useful in the study of diffusion characteristics of drugs through lipid membranes, such studies were beyond the scope of the present investigation.

**Dissolution Profiles**—Figures 1–4 illustrate the dissolution rate profiles for the various drug products as determined in the dissolution simulator. The enteric-coated methenamine formulations (Products 4–9) shown in Fig. 1 exhibited a delay in the onset of dissolution until the dissolution fluid pH was increased from 1.1 to 6.5. These dissolution profiles were utilized to develop the correlations described later with the previously determined *in vivo* data.

While the dissolution of only two units of each formulation was routinely studied for each drug, six tablets of one 50-mg nitrofurantoin product were used in one instance to evaluate the reproducibility of the dissolution process. The mean amount of nitrofurantoin dissolved after 16 min was 9.2 mg (range 8–11 mg); after 32 min, the mean was 21.3 mg (range 20–22 mg); and after 48 min, the mean was 34.7 mg (range 34–36 mg). Generally, this good agreement among the six replicates also was seen between the duplicate determinations for each formulation of the three drugs.

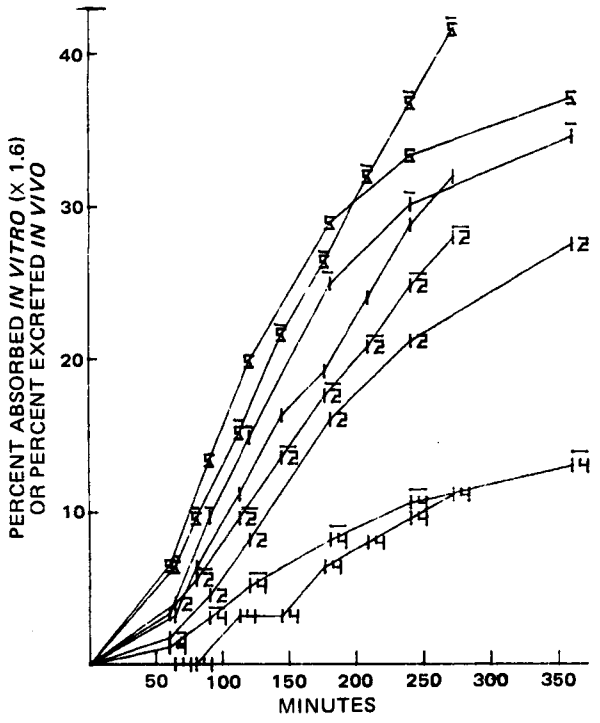


**Figure 6**—*Comparison of the total amount of nitrofurantoin withdrawn from the* in vitro *dissolution system (× 1.6) and the cumulative amount of nitrofurantoin excreted in the* in vivo *studies for four nitrofurantoin tablet formulations. Each* in vitro *data point (Products 1, 5, 12, and 14) is the mean of two determinations. Each* in vivo *data point (Products 1, 5, 12, and 14) is the mean of 14 subjects.*

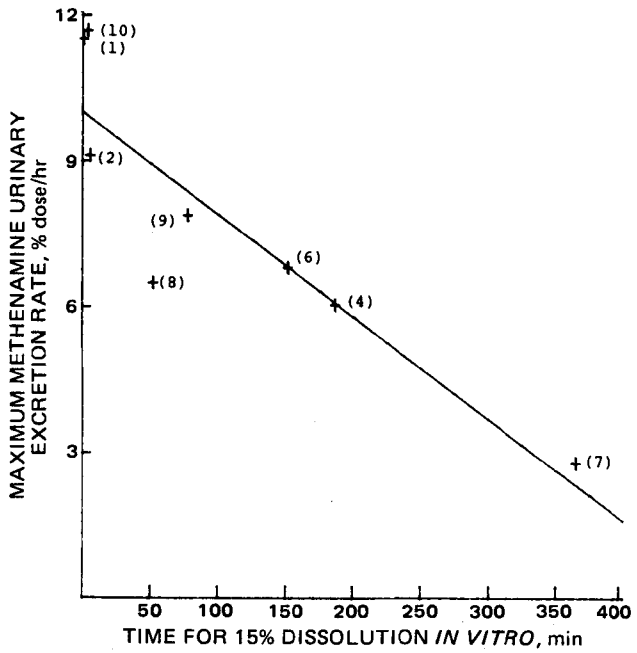


**Figure 7**—In vitro–in vivo *correlation for eight methenamine formulations,* $r = -0.894$ ($p < 0.01$). *Each data point represents the mean of two* in vitro *and 10* in vivo *values.*

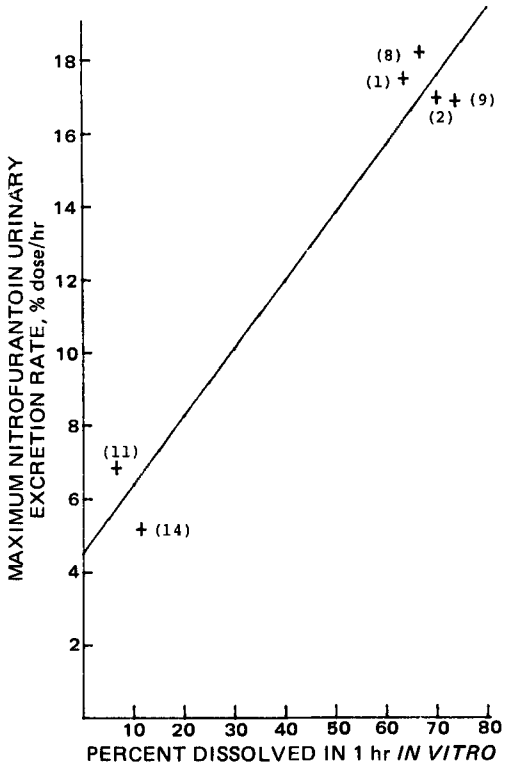


**Figure 8**—In vitro–in vivo *correlation for five 50-mg nitrofurantoin tablet formulations,* r = *0.976* (p < *0.01*). *Each data point represents the mean of two* in vitro *and 14* in vivo *values.*

**Simulated Absorption Profiles**—The dissolution simulator is reported by the manufacturer to be capable of providing data that can simulate *in vivo* absorption profiles (2). To evaluate this claim, plots were constructed of cumulative urinary excretion of each drug and the cumulative amount of dissolved drug withdrawn from the dissolution chamber at the corresponding times. Since the dissolution studies for the chlorothiazide tablets were carried out only for 5 min, simulation of *in vivo* data was not possible for these dosage forms.

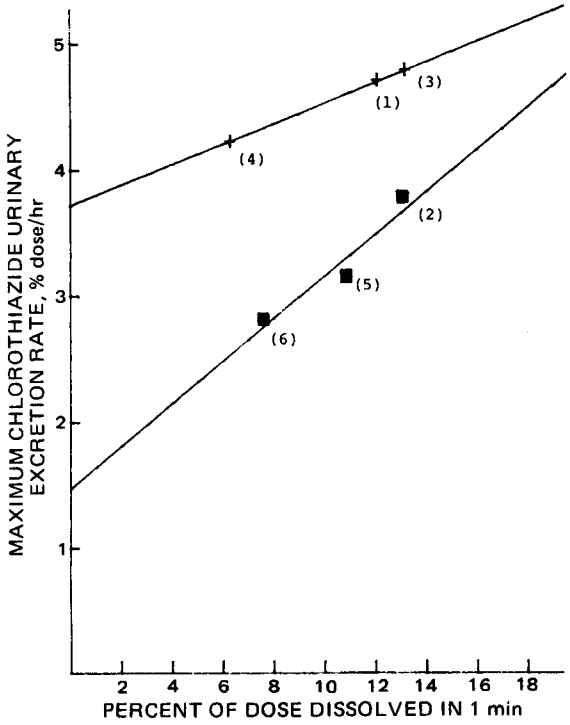


**Figure 9**—In vitro–in vivo *correlations for three 250- (+) and three 500- (■) mg chlorothiazide tablet formulations,* r = *0.999* (p < *0.05*) *and* r = *0.962* (p > *0.10*), *respectively. Each data point represents the mean of two* in vitro *and 12* in vivo *values.*

*Methenamine Tablets*—All data were expressed as the percent of dose to normalize for differences in methenamine content among products. Product 1, a compressed tablet of methenamine, was selected as a reference, and plots were made of the cumulative percent of dissolved drug withdrawn from the dissolution chamber and the mean cumulative percent of drug excreted in the urine of the 10 subjects receiving the drug in an earlier study (6). The *in vitro* curves paralleled the *in vivo* data but were somewhat higher. An empirical correction factor of 0.55, applied to the *in vitro* data, resulted in good correspondence between the two data sets.

The data shown in Fig. 5 illustrate the comparison between the *in vitro* data, corrected by a factor of 0.55, and the corresponding *in vivo* urinary excretion data for Product 9, with an intermediate dissolution rate, and Product 7, with a relatively slow dissolution rate. A similar good correspondence also was obtained for Products 4–6 and 10. The relationship between *in vitro* and *in vivo* data was not nearly as good for Products 2 and 8, with the *in vitro* data predicting greater urinary excretion than was actually seen.

*Nitrofurantoin Dosage Forms*—Figure 6 illustrates good correspondence between the *in vivo* and *in vitro* data for Products 1, 5, 12, and 14. Each *in vitro* data point was adjusted by a factor of 1.6, based on the observed parallelism for the *in vivo* and *in vitro* data for Product 9, which was taken as the reference product. Similar good correspondence was observed for Products 2 and 8, but there was a significant difference between the *in vivo* and *in vitro* data sets for Products 3, 4, 6, 11, and 13. As will be discussed, Products 7 and 10, the macrocrystalline capsules, exhibited dissolution characteristics that were quite different from the microcrystalline tablets. Therefore, these two dosage forms were not included with the microcrystalline formulations in this data treatment.

**General Correlations**—These correlations attempted to relate various *in vitro* and *in vivo* measurements. Only the best correlations will be discussed, although other correlations were examined.

*Methenamine Tablets*—The best correlation, $r = 0.928$ ($p < 0.01$), was seen between the area under the dissolution–time curve at 4.5 hr *versus* the cumulative percent excreted at 6 hr. When using $T_{15\%}$ as the *in vitro* measurement, good correlations were observed with the cumulative

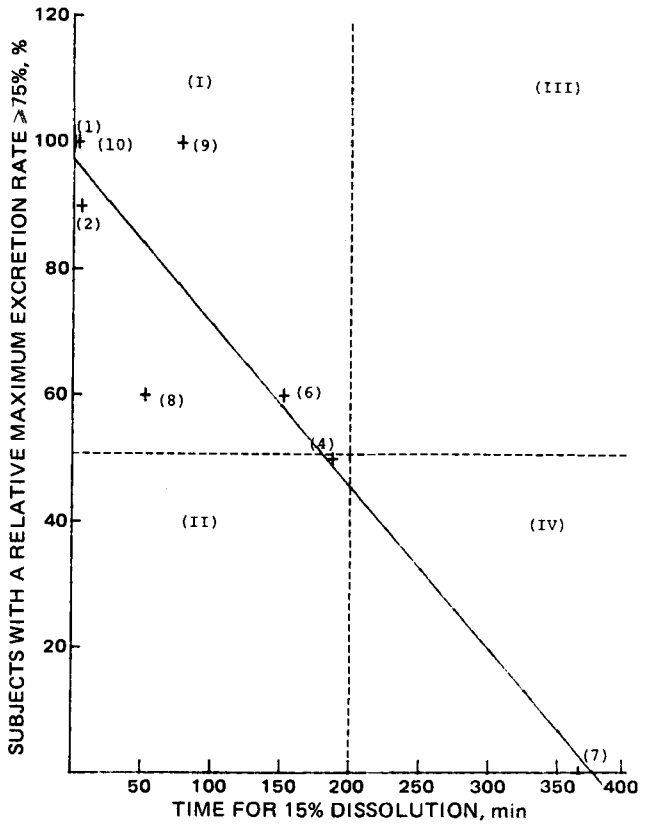


**Figure 10**—*Quadrant analysis for eight methenamine formulations,* r = *−0.93* (p < *0.01*). *Each data point represents the mean of two* in vitro *and 10* in vivo *values. Product 9 was the reference product.*

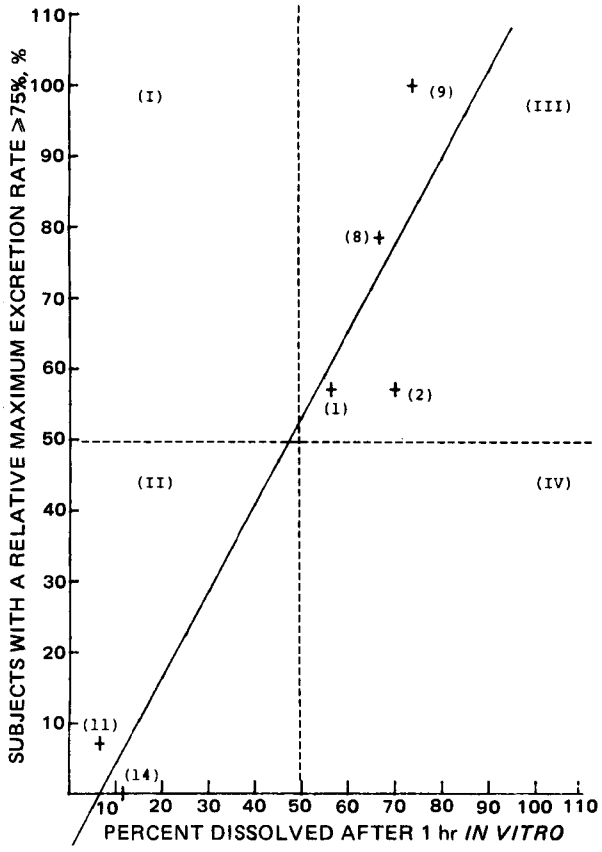


**Figure 11**—*Quadrant analysis for six 50-mg nitrofurantoin tablet formulations,* r = *0.943 (*p < *0.01). Each data point represents the mean of two* in vitro *and 14* in vivo *values. Product 9 was the reference product.*

percent excreted at 48 hr, $r = -0.875$ ($p < 0.01$), and the maximum excretion rate, $r = -0.894$ ($p < 0.01$) (Fig. 7). Since Products 4, 5, and 7 were <30% dissolved after 5 hr, correlations with $T_{\%}$ values beyond 15% could not be used. Product 5 is not illustrated because <1% of the drug had dissolved after 5 hr, and the tablet retained its original shape during the dissolution period.

*Nitrofurantoin*—Attempts to obtain *in vivo–in vitro* correlations that included Products 7 and 10 were not successful. Both dosage forms exhibited relatively good dissolution properties (Figs. 3 and 4). However, these two products ranked below eight of the other products in earlier bioavailability studies involving determination of cumulative urinary excretion. Thus, these two products, which represented capsule formulations of the macrocrystalline drug, were omitted from the correlations.

The percent of drug excreted in 12 hr and the maximum urinary excretion rate were correlated with the percent of drug dissolved at various times. Generally, the correlations with the 100-mg tablets were less satisfactory than with the 50-mg tablets. The correlation coefficient for the 100-mg tablets, using a variety of measurements, was <0.8 ($p < 0.10$), while correlation coefficients exceeded 0.93 ($p < 0.01$) for the 50-mg tablets. The best correlation for the 50-mg tablets is shown in Fig. 8, $r = 0.976$ ($p < 0.01$), using the maximum excretion rate and the percent of drug dissolved in 1 hr. Cumulative percent excreted in 12 hr also correlated well with the 1-hr dissolution value, $r = 0.960$ ($p < 0.01$). The poorer correlation with the 100-mg tablets may be due to the fact that the maximum excretion rates for the six tablets were much closer than for the 50-mg tablets. Previous investigators (14) noted a similar poorer correlation for 100-mg nitrofurantoin tablets, using the same lots as employed in the present study, but obtained *in vitro* data with a dissolution–dialysis system.

As part of the earlier *in vivo* studies (7), the individual tablets also were subjected to dissolution testing as described in USP XVIII. The present dissolution simulator data correlated much better than the earlier USP data for the 50-mg tablets, $r = 0.673$ ($p > 0.10$), although the degree of correlation was approximately the same for the 100-mg tablets using either the dissolution simulator, $r = 0.704$ ($p < 0.10$) or the USP rotating basket, $r = 0.793$ ($p < 0.10$).

*Chlorothiazide Tablets*—The data obtained for these dosage forms demonstrated one major limitation in the design of the dissolution simulator, namely that the total volume of dissolution fluid was limited to 100 ml. As shown in Fig. 4, this fluid was rapidly saturated with dissolving drug; as a result, dissolution was not continued beyond 5 min. The best correlations for both the 250- and 500-mg tablets were seen between the cumulative percent of drug dissolved in 1 min and the maximum excretion rate (Fig. 9). The data for the 250- and 500-mg tablets were not combined into a single correlation because the *in vivo* data did not exhibit a dose proportionality in urinary excretion, with a lower percent recovery for the 500-mg tablets (8).

The correlation was significant for the 250-mg tablets, $r = 0.999$ ($p < 0.05$), but not for the 500-mg tablets, $r = 0.962$ ($p < 0.10$). Good correlations, $r > 0.9$, existed between the maximum excretion rate or the cumulative percent excreted at 24 hr and $T_{15\%}$ or the percent dissolved at 2.5 min for the 250-mg tablets. However, these correlations were based on only three data points; the general applicability of the relationships need to be established for a larger group of dosage forms.

A good correlation, $r = 0.999$ ($p < 0.05$), also was obtained for the 250-mg tablets between the maximum excretion rate and the time for 30% dissolution using the USP rotating basket. However, for the 500-mg tablets, the correlation was much poorer for these same parameters, $r = 0.773$ ($p > 0.10$). Thus, on the basis of cost and convenience, the USP method is preferred over the dissolution simulator for the 250-mg tablets since both procedures result in comparable *in vitro–in vivo* correlations. However, the correlations for the 500-mg tablets were somewhat better for the dissolution simulator compared to the USP method.

**Quadrant Analysis**—This approach evaluates *in vivo* data using each subject as his or her own control, relating the bioavailability of a dosage form in a given subject to the performance of a reference dosage form in the same subject. For illustration, an arbitrary specification was selected such that 50% of the subjects participating in an *in vivo* study should exhibit a relative bioavailability of at least 75% for a test dosage form to be considered acceptable. The *in vivo* data were plotted *versus* an *in vitro* measurement for the individual dosage forms, and an *in vitro* dissolution specification was selected. While the *in vitro* specifications described for the three drugs under consideration are admittedly somewhat arbitrary,

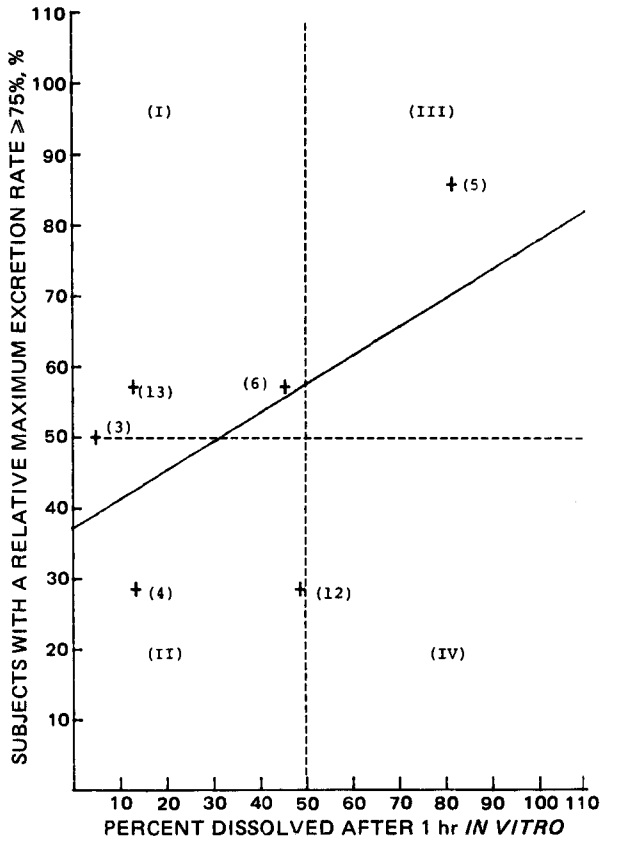


**Figure 12**—*Quadrant analysis for six 100-mg nitrofurantoin tablet formulations,* r = *0.557 (*p > *0.1). Each data point represents the mean of two* in vitro *and 14* in vivo *values. Product 9 was the reference product.*

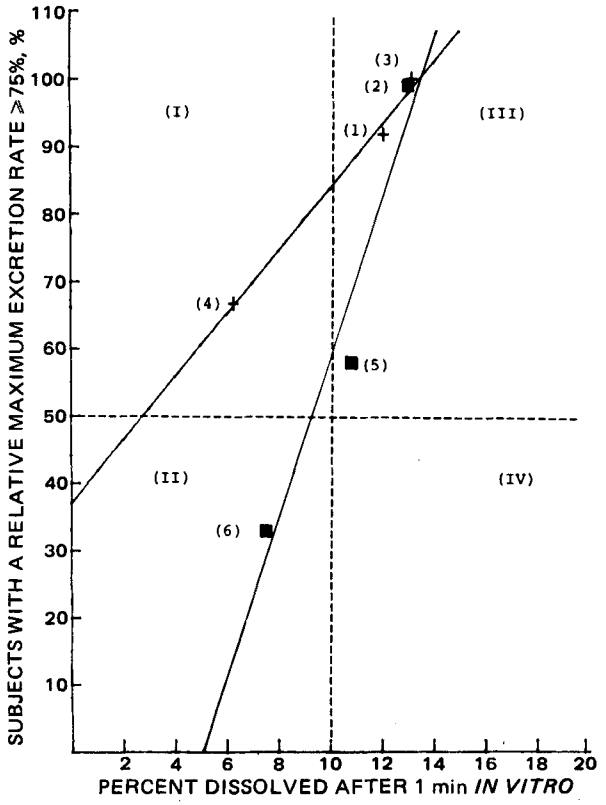


**Figure 13**—*Quadrant analysis for three 250- (+) and three 500- (■) mg chlorothiazide tablet formulations, r = 0.995 (p < 0.1) and r = 0.967 (p > 0.1), respectively. Each data point represents the mean of two* in vitro *and 12* in vivo *values.*

they serve to illustrate an alternative approach to setting such specifications.

*Methenamine*—Figure 10 illustrates the results of the quadrant analysis approach for methenamine. The selection of 200 min as the maximum permissible time to achieve 15% dissolution was based on the *in vivo* data, which indicated that Products 5 and 7 were unacceptable. Note that Product 5 does not appear in this figure since it did not achieve 15% dissolution within 6 hr. With the exception of Products 5 and 7, all other dosage forms were confined to Quadrant I and thus exhibited acceptable bioavailability and dissolution properties.

*Nitrofurantoin*—Figures 11 and 12 show the quadrant analysis for the 50- and 100-mg dosage forms, respectively. With the exception of Products 11 and 14, all other dosage forms represented in Fig. 11 were in Quadrant III and thus met both the *in vivo* and *in vitro* specifications. Using the same specifications for the 100-mg tablets illustrated in Fig. 12 did not yield a satisfactory result. Only Product 5 was in Quadrant III; Products 3, 6, and 13 failed the *in vitro* specification, although each exhibited adequate bioavailability. Furthermore, Product 12 nearly passed the dissolution requirement, although only 30% of the subjects exhibited a maximum urinary excretion rate that was at least 75% that of the reference product.

*Chlorothiazide*—A dissolution specification of 10% dissolution within 1 min was selected for the 250- and 500-mg tablets shown in Fig. 13. With this criterion, Product 4 exhibited an adequate excretion rate for the 250-mg tablets but failed the dissolution specification. For the 500-mg tablets, Product 6 failed both the *in vitro* and *in vivo* specifications. Because of the small number of dosage forms and the brief duration of the dissolution test, these data may be of limited value in establishing the utility of this approach as a predictor of the bioavailability of chlorothiazide dosage forms.

**Study Limitations**—All dissolution studies were carried out on production lots used in previous *in vivo* bioavailability studies. Thus, some formulations had been stored at room temperature for up to 4 years, and in some instances the expiration date indicated on the package had been exceeded. Furthermore, only a few tablets or capsules remained for many of the products, and it was not possible to reassay them for content and content uniformity. As a result, drug content and/or dissolution characteristics of these dosage forms may have changed since the earlier studies.

Evidence suggesting that significant changes in the characteristics of the dosage forms had not occurred may be obtained by comparing the extent of dissolution observed in the present studies with that obtained previously. The maximum amount of methenamine recovered during the dissolution studies with the dissolution simulator corresponded with the labeled quantity of drug in the product for those dosage forms that totally dissolved. With nitrofurantoin, a range of 7–80% of the labeled amount of drug was dissolved after 80 min in the dissolution simulator. In the earlier study (7), between 10 and 70% of the drug was dissolved after 90 min using the USP procedure. Furthermore, the two products with the slowest dissolution rate in the dissolution simulator were the same two products that dissolved the slowest in the previous study (7). Similarly, the extent of dissolution of the chlorothiazide tablets in the dissolution simulator was quite similar to the results obtained earlier (8) using the USP apparatus.

## CONCLUSIONS

The absorption simulator was evaluated as a tool to determine optimum sampling times for dissolution studies using the dissolution simulator. It was determined that the sampling times computed from the absorption simulator were not essential for the subsequent dissolution studies.

Reasonably good correlations generally were observed between the *in vitro* data obtained with the dissolution simulator and the *in vivo* data obtained in earlier human studies. However, the general applicability of the device to a wide variety of drugs is limited because only two dosage units can be tested simultaneously. Moreover, the 100-ml capacity of the dissolution system is insufficient for drugs with very low water solubility. The dissolution properties of the methenamine, chlorothiazide, and 50-mg nitrofurantoin tablets could all be satisfactorily correlated with one or more *in vivo* parameters. The correlations for the 100-mg nitrofurantoin tablets and the macrocrystalline nitrofurantoin capsule dosage forms were less satisfactory.

Attempts also were made to predict urinary excretion profiles using the *in vitro* data. After application of an adjustment factor, good predictions were seen for the majority of the methenamine dosage forms and seven of the 14 nitrofurantoin formulations. The method was not applicable for the chlorothiazide tablets.

Finally, *in vivo–in vitro* correlations were examined using a quadrant analysis approach. The method was shown to be of value in setting *in vitro* specifications that have at least some relevance to the *in vivo* performance of the dosage form.

## REFERENCES

(1) M. Pernarowski, in "Dissolution Technology," L. J. Leeson and J. T. Carstensen, Eds., Academy of Pharmaceutical Sciences, Washington, D.C., 1974, pp. 58–105.

(2) H. Stricker, "On the Relationship between Drug Absorption and Dissolution in the Gastro-Intestinal Tract (I)", Galenical Section of the Pharmaceutical Production Department of C. H. Boehringer Sohn. Ingelheim, distributed by Beckman Instruments, Anaheim, Calif.

(3) M. L. Huang and S. Huang, *J. Pharm. Sci.*, **66,** 608 (1977).

(4) V. F. Smolen, L. Ball, and M. Scheffler, *Pharm. Tech.*, 89 (June 1979).

(5) H. Johansen, "FIP 77 Abstracts," 37th International Congress of Pharmaceutical Sciences, The Hague, The Netherlands, Sept. 1977, p. 56.

(6) R. Gollamudi, A. B. Straughn, and M. C. Meyer, *J. Pharm. Sci.*, **70,** 596 (1981).

(7) M. C. Meyer, G. W. A. Slywka, R. E. Dann, and P. L. Whyatt, *ibid.*, **63,** 1693 (1974).

(8) A. B. Straughn, A. P. Melikian, and M. C. Meyer, *ibid.*, **68,** 1099 (1979).

(9) H. Stricker, *Drugs Made Ger.*, **16,** 80 (1973).

(10) R. Gollamudi, M. C. Meyer, and A. B. Straughn, *Biopharm. Drug Disposit.*, **1,** 27 (1979).

(11) T. J. Sullivan, E. Sakmar, and J. G. Wagner, *J. Pharmacokinet. Biopharm.*, **4,** 173 (1976).

(12) W. R. Fairweather, *ibid.*, **5,** 405 (1977).

(13) V. P. Shah, J. Hunt, V. K. Prasad, and B. E. Cabana, *Abstr. Acad. Pharm. Sci.*, **7,** 206 (1977).

(14) D. C. Papadimitriou and B. B. Sheth, *Drug Dev. Ind. Pharm.*, **4,** 373 (1978).

## ACKNOWLEDGMENTS

Adapted in part from a thesis submitted by M. K. T. Yau to the University of Tennessee Center for the Health Sciences in partial fulfillment of the Master of Science degree requirements.

Supported in part by U.S. Food and Drug Administration Contracts FDA 223-74-3097 and 223-77-3011 and the Tennessee Department of Public Health.

The use of the Sartorius absorption and dissolution simulators, provided by Sartorius Filters, is gratefully acknowledged.


# High-Performance Liquid Chromatographic Determination of Free Myxin and Its Reduction Product as Impurities in Cuprimyxin-Containing Creams


**G. MANIUS ˣ, R. TSCHERNE, R. VENTEICHER, and A. SECKER**



Received November 28, 1980, from the *Quality Control Department, Hoffmann–La Roche Inc., Nutley, NJ 07110.* Accepted for publication February 20, 1981.



**Abstract** □ A stability-indicating high-performance liquid chromatographic method was developed that can detect and quantitate low levels of the two most likely breakdown products of cuprimyxin. These degradation compounds, free myxin and its reduction product, can be determined in topical cream preparations in which cuprimyxin is formulated at the 0.5% (w/w) level. The method requires a simple two-step extraction, the addition of an internal standard, and chromatography on an amine-bonded column.



**Keyphrases** □ Myxin—high-performance liquid chromatographic assay in cuprimyxin-containing creams □ Cuprimyxin—high-performance liquid chromatographic determination of free myxin and its reduction product □ High-performance liquid chromatography—determination of free myxin and its reduction product in cuprimyxin-containing creams □ Antibacterial agents—high-performance liquid chromatographic determination of myxin and its reduction product in cuprimyxin-containing creams


Myxin (6-methoxy-1-phenazinol 5,10-dioxide) (I) was first isolated from the soil (1) and identified as a phenazine-type product from the broth of a myxobacter (2). Its correct structure was established by Weigele and Leimgruber (3), and it was realized in its most effective antimicrobial form as the cupric complex (II) (4, 5). When applied topically, II was found to have considerable antibacterial, antiyeast, and antifungal activity in veterinary applications without the irritation side effects experienced with I (6). It was formulated in a cream and tested *in vitro* against Gram-positive and Gram-negative bacterial and fungal pathogens (7) and yeast infections (8), *in vivo* as a cream for otic and ophthalmic infections (9), and as a suspension with hydrocortisone acetate for the treatment of otitis (10). The apparent biological mechanism of action involves alteration of the invading bacterial DNA template (11).

## BACKGROUND

A polarographic investigation found the electrochemical behavior of I to be a function of pH, reducing to 6-methoxy-1-phenazinol at pH < 3, to the anionic species 6-methoxyphenazinol at pH > 9, and to the intermediate 6-methoxy-1-phenazinol 10-oxide (III) at pH 3–9 (12). Compound III can be further reduced by intramolecular hydrogen bonding to 6-methoxy-1-phenazinol. The major degradation product of I in acid media and in pH 3–9 buffer solutions was found to be III[1]. Although the copper complex of II is readily dissociated in acid media to form I (Scheme I), pharmaceutical creams containing excess copper ions minimize dissociation when formulated at pH 5.7–6.2 (13).

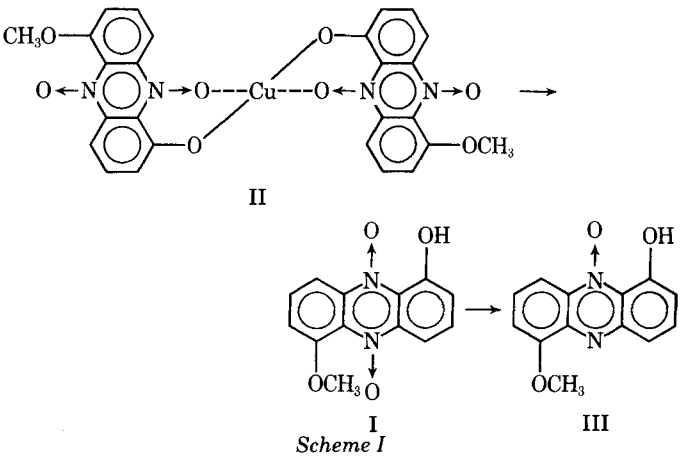


*Scheme I*

The rapid conversion of II to I was used to assay for II by measurement of the amount of I found spectrophotometrically[2] and by TLC (14). Microbiological assay methods for determining II directly from seeded agar plates also were reported[3].

The determination of I and III as probable impurities in formulations involving II is difficult for two reasons: (*a*) the relative ease of conversion of II to its free form (I), and (*b*) the inability to differentiate I and III spectrophotometrically. A separation technique that minimizes dissociation of the copper complex is essential. This paper describes the development of a high-performance liquid chromatographic (HPLC) method that meets these requirements.

## EXPERIMENTAL

**Apparatus**—A constant-flow solvent delivery system[4] was connected to a loop injector[5]. An amine-bonded silica column[6] was coupled to a spectrophotometric detector[7] set at 280 nm. A 10-mv recorder[8] was set at a chart speed of 50 cm/hr.

**Reagents and Chemicals**—Distilled-in-glass grade ethyl acetate[9] and heptane[9] and reagent grade acetic acid[10] were used. Samples and

[1] B. Z. Senkowski and J. E. Heveran, Hoffmann–La Roche Inc., Nutley, NJ 07110, 1971, unpublished data.

[2] M. Araujo, W. J. Mergens, and M. Osadca, Hoffmann–La Roche Inc., Nutley, NJ 07110, 1972, unpublished data.

[3] J. A. Bontempo and J. Unowsky, Hoffmann–La Roche Inc., Nutley, NJ 07110, 1969, unpublished data.

[4] Model 6000A, Waters Associates, Milford, Mass.

[5] Model U6K, Waters Associates, Milford, Mass.

[6] Chromegabond $NH_2$ (10 μm), 30 cm × 4.6 mm i.d., ES Industries, Marlton, N.J.

[7] Spectro Monitor II, LDC, Riviera Beach, Fla.

[8] Model 20, Varian Aerograph, Palo Alto, Calif.

[9] Burdick & Jackson Laboratories, Muskegon, Mich.

[10] J. T. Baker Chemical Co., Phillipsburg, N.J.




*0022-3549/81/0900-1024$01.00/0*



© *1981, American Pharmaceutical Association*

## ACKNOWLEDGMENTS

Adapted in part from a thesis submitted by M. K. T. Yau to the University of Tennessee Center for the Health Sciences in partial fulfillment of the Master of Science degree requirements.

Supported in part by U.S. Food and Drug Administration Contracts FDA 223-74-3097 and 223-77-3011 and the Tennessee Department of Public Health.

The use of the Sartorius absorption and dissolution simulators, provided by Sartorius Filters, is gratefully acknowledged.


# High-Performance Liquid Chromatographic Determination of Free Myxin and Its Reduction Product as Impurities in Cuprimyxin-Containing Creams


**G. MANIUS ˣ, R. TSCHERNE, R. VENTEICHER, and A. SECKER**



Received November 28, 1980, from the *Quality Control Department, Hoffmann–La Roche Inc., Nutley, NJ 07110.* Accepted for publication February 20, 1981.



**Abstract** □ A stability-indicating high-performance liquid chromatographic method was developed that can detect and quantitate low levels of the two most likely breakdown products of cuprimyxin. These degradation compounds, free myxin and its reduction product, can be determined in topical cream preparations in which cuprimyxin is formulated at the 0.5% (w/w) level. The method requires a simple two-step extraction, the addition of an internal standard, and chromatography on an amine-bonded column.



**Keyphrases** □ Myxin—high-performance liquid chromatographic assay in cuprimyxin-containing creams □ Cuprimyxin—high-performance liquid chromatographic determination of free myxin and its reduction product □ High-performance liquid chromatography—determination of free myxin and its reduction product in cuprimyxin-containing creams □ Antibacterial agents—high-performance liquid chromatographic determination of myxin and its reduction product in cuprimyxin-containing creams


Myxin (6-methoxy-1-phenazinol 5,10-dioxide) (I) was first isolated from the soil (1) and identified as a phenazine-type product from the broth of a myxobacter (2). Its correct structure was established by Weigele and Leimgruber (3), and it was realized in its most effective antimicrobial form as the cupric complex (II) (4, 5). When applied topically, II was found to have considerable antibacterial, antiyeast, and antifungal activity in veterinary applications without the irritation side effects experienced with I (6). It was formulated in a cream and tested *in vitro* against Gram-positive and Gram-negative bacterial and fungal pathogens (7) and yeast infections (8), *in vivo* as a cream for otic and ophthalmic infections (9), and as a suspension with hydrocortisone acetate for the treatment of otitis (10). The apparent biological mechanism of action involves alteration of the invading bacterial DNA template (11).

## BACKGROUND

A polarographic investigation found the electrochemical behavior of I to be a function of pH, reducing to 6-methoxy-1-phenazinol at pH < 3, to the anionic species 6-methoxyphenazinol at pH > 9, and to the intermediate 6-methoxy-1-phenazinol 10-oxide (III) at pH 3–9 (12). Compound III can be further reduced by intramolecular hydrogen bonding to 6-methoxy-1-phenazinol. The major degradation product of I in acid media and in pH 3–9 buffer solutions was found to be III[1]. Although the copper complex of II is readily dissociated in acid media to form I (Scheme I), pharmaceutical creams containing excess copper ions minimize dissociation when formulated at pH 5.7–6.2 (13).

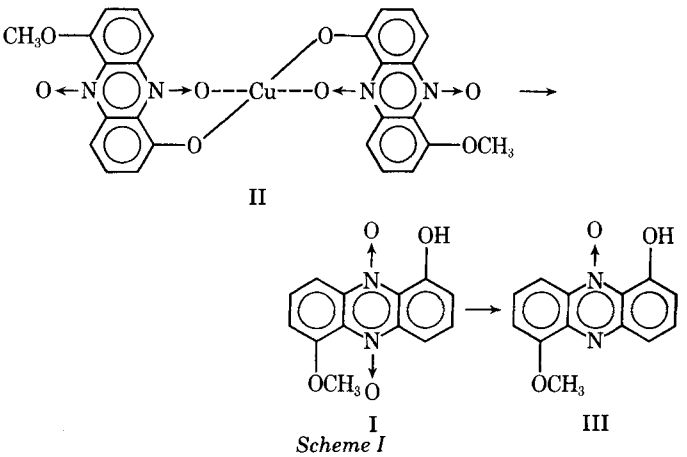


*Scheme I*

The rapid conversion of II to I was used to assay for II by measurement of the amount of I found spectrophotometrically[2] and by TLC (14). Microbiological assay methods for determining II directly from seeded agar plates also were reported[3].

The determination of I and III as probable impurities in formulations involving II is difficult for two reasons: (*a*) the relative ease of conversion of II to its free form (I), and (*b*) the inability to differentiate I and III spectrophotometrically. A separation technique that minimizes dissociation of the copper complex is essential. This paper describes the development of a high-performance liquid chromatographic (HPLC) method that meets these requirements.

## EXPERIMENTAL

**Apparatus**—A constant-flow solvent delivery system[4] was connected to a loop injector[5]. An amine-bonded silica column[6] was coupled to a spectrophotometric detector[7] set at 280 nm. A 10-mv recorder[8] was set at a chart speed of 50 cm/hr.

**Reagents and Chemicals**—Distilled-in-glass grade ethyl acetate[9] and heptane[9] and reagent grade acetic acid[10] were used. Samples and

[1] B. Z. Senkowski and J. E. Heveran, Hoffmann–La Roche Inc., Nutley, NJ 07110, 1971, unpublished data.

[2] M. Araujo, W. J. Mergens, and M. Osadca, Hoffmann–La Roche Inc., Nutley, NJ 07110, 1972, unpublished data.

[3] J. A. Bontempo and J. Unowsky, Hoffmann–La Roche Inc., Nutley, NJ 07110, 1969, unpublished data.

[4] Model 6000A, Waters Associates, Milford, Mass.

[5] Model U6K, Waters Associates, Milford, Mass.

[6] Chromegabond $NH_2$ (10 μm), 30 cm × 4.6 mm i.d., ES Industries, Marlton, N.J.

[7] Spectro Monitor II, LDC, Riviera Beach, Fla.

[8] Model 20, Varian Aerograph, Palo Alto, Calif.

[9] Burdick & Jackson Laboratories, Muskegon, Mich.

[10] J. T. Baker Chemical Co., Phillipsburg, N.J.




*0022-3549/81/0900-1024$01.00/0*



© *1981, American Pharmaceutical Association*

reference materials were obtained from the same source[11], except for the internal standard, 3-acetylindole[12].

**Mobile Phase**—A mixture of ethyl acetate–heptane–acetic acid (30:69.5:0.5) was prepared and run at a flow rate of 3.0 ml/min.

**Reference Standard Stock Solution**—Approximately 18 mg of I reference standard and 10 mg of III reference standard were weighed into a 500-ml volumetric flask and then dissolved and diluted to volume with ethyl acetate. A 10-ml aliquot was transferred into a 25-ml volumetric flask, which then was diluted to volume with heptane.

**Internal Standard Stock Solution I**—Approximately 80 mg of 3-acetylindole was weighed into a 500-ml volumetric flask and then dissolved and diluted to volume with ethyl acetate.

**Internal Standard Stock Solution II**—A 10-ml aliquot of internal standard stock solution I was transferred into a 25-ml volumetric flask, which then was diluted to volume with heptane.

**Working Reference Standard Solution**—Equal volumes of the reference standard stock solution and the internal standard stock solution II were pipetted.

**Extraction Solution**—The internal standard stock solution I (250 ml) was transferred into a 500-ml volumetric flask and diluted to volume with ethyl acetate.

**Sample Preparation**—Approximately 1.0 g of sample was weighed into a 50-ml centrifuge tube. Then 10 ml of the extraction solution was pipetted into the centrifuge tube, which was stoppered and shaken vigorously by hand until the sample was dispersed in the extracting solvent (~1 min). The tube then was centrifuged, and the liquid was decanted into a 25-ml volumetric flask. The extraction was repeated with 15 ml of a 2:3 ethyl acetate–heptane mixture, and the tube again was centrifuged. The liquid was decanted and combined with the first extraction, and the final volume was adjusted to 25 ml with heptane.

**Procedure**—The working reference standard solution (50 μl) was injected to determine retention times and relative response ratios. This injection was followed by 50-μl injections of the sample solutions. Peaks were quantitated by measurement of their heights in millimeters.

**Calculations**—The level of I in the sample was determined by the following:

$$\% \text{ (w/w) I in sample} = \frac{(H_I)(C_A)(25)(100)}{(H_A)(W)(RR)} \qquad \text{(Eq. 1)}$$

where $H_I$ and $H_A$ are the respective peak heights of I and 3-acetylindole in the sample solution, $C_A$ is the 3-acetylindole concentration in the sample solution, $W$ is the sample weight (milligrams), $RR$ is the relative response ratio, 25 is the dilution factor, and 100 is the conversion to percent.

The level of I as II was determined by:

$$\% \text{ (w/w) I as II} = \frac{(\% \text{ I in sample})(1.12)(100)}{(0.5)} \qquad \text{(Eq. 2)}$$

where 1.12 is the factor to convert I to II, 0.5 is the percent of II in the sample, and 100 is the conversion to percent.

The level of III was calculated in the same manner as I except that the 1.12 factor was omitted.

## RESULTS AND DISCUSSION

A representative chromatogram showing the elution of III, I, and the internal standard (IV) at 4, 7, and 10.5 min, respectively, is presented in Fig. 1. Table I lists data obtained on several lots of cream containing 0.5% II by weight. The data reflect double extractions of several samples encompassing a wide range of storage time.

Ethyl acetate was selected as the extracting solvent because of the high solubility of I and III and the very low solubility of II in it. In addition, ethyl acetate contributed only slightly to the dissociation of the copper complex. Conversely, solvents such as hexane and heptane incompletely dissolved I at the level required for preparation of the reference standard. Solvents such as methylene chloride, chloroform, and water produced dissociation of the complex, resulting in substantial amounts of I being formed for each extraction. Furthermore, ethyl acetate was complementary to heptane as a mobile phase in that it helped achieve reasonable retention times on the HPLC column.

Dissociation of the copper complex, facilitated by the nature of the cream, was singularly the most difficult aspect in developing the analytical method. For example, II was maintained as a 50% aqueous paste since it is subject to violent decomposition in the dry state (15). Investigations showed that extracts of the paste, even after several days of standing in contact with the paste, resulted in little I formation. Yet creams to which water was added as an extraction aid produced extensive amounts of I when extracted. It is believed that water in the presence of another ingredient in the cream, perhaps acid, causes this degradation.

**Table I—Levels of I and III in Creams Containing 0.5% II**

| Sample Lot | Age of Sample, months | I as Percentage of Cream | I as Percentage of II | III as Percentage of Cream | III as Percentage of II |
|---|---|---|---|---|---|
| A | 60 | 0.0055 | 1.2 | 0.015 | 3.0 |
| B | 52 | 0.0025 | 0.5 | 0.005 | 1.0 |
| C | 52 | 0.0072 | 1.6 | 0.038 | 7.5 |
| D | 47 | 0.0058 | 1.3 | 0.03 | 6.0 |
| E | 45 | 0.0055 | 1.2 | 0.036 | 7.1 |
| F | 25 | 0.0017 | 0.4 | 0.004 | 0.7 |
| G | 23 | 0.0045 | 1.0 | 0.002 | 0.4 |
| H | 16 | 0.0018 | 0.4 | 0.002 | 0.4 |
| I | 4 | 0.0025 | 0.5 | 0.007 | 1.4 |
| J | 3 | 0.0023 | 0.5 | 0.002 | 0.3 |
| K | 2 | 0.0038 | 0.9 | 0.001 | 0.2 |

Some dissociation of the complex was observed regardless of the solvent chosen to extract the cream. The extent was about the same for hexane as for ethyl acetate. A study[2] that included hexane, methanol, and ether found the stability of II in hexane to be the greatest. Of interest is the apparent equilibrium established so that a finite and consistent amount of I is always formed with each additional extraction. The level of I generated thus can be related to the extent of dissociation.

The destruction of the complex, at least within the framework of the cream matrix, is both time and heat dependent and, to a certain degree, water dependent. Therefore, it is necessary to proceed swiftly during and after extractions.

Allowing the extract to contact the paste for any length of time increases the likelihood of dissociation. Furthermore, conversion of I to III accelerates in solution. Similarly, the introduction of heat during the extraction, even from mechanical shaking or ultrasonication, resulted in an increased formation of I. Although the effect of water has already been cited, no difference was obtained for extractions that incorporated sodium sulfate. Therefore, its use is not obligatory. Extraction data are shown in Table II.

It was demonstrated[13] that II is more stable than I, except under acidic conditions whereupon the complex is irreversibly dissociated. The instability of I was observed in the reference solution, both visually, as a color change, and chromatographically, as a gradual diminishing of peak size over 1 day. If necessary, it may be better to prepare a new standard

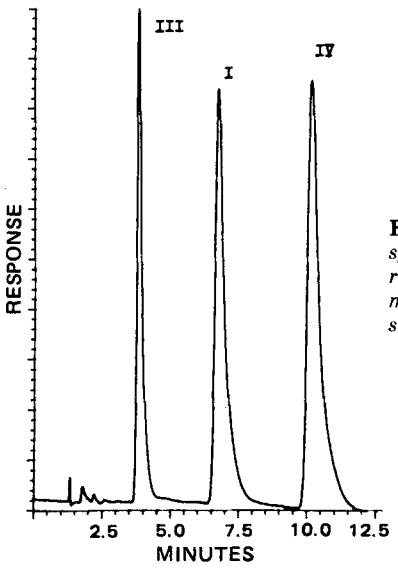


**Figure 1**—*Chromatogram of a synthetic mixture of the myxin reduction product (III), free myxin (I), and the internal standard (IV).*

[11] Hoffmann–La Roche Inc., Nutley, N.J.
[12] Aldrich Chemical Co., Milwaukee, Wis.

[13] C. Burke and J. E. Heveran, Hoffmann–La Roche Inc., Nutley, NJ 07110, 1971, unpublished data.

**Table II—Extraction Results of I as Percentage of II**

| Extract | Percentage I |
|---|---|
| Cream Extracts, Ultrasonication and Mechanical Shaking | |
| 1 | 0.9 |
| 2 | 0.5 |
| 3 | 0.5 |
| 4 | 0.5 |
| 5[a] | 1.2 |
| Cream Extracts, Manual Shaking | |
| 1 | 1.0 |
| 2 | 0.2 |
| 3 | 0.4 |
| 4 | 0.1 |
| 5 | 0.1 |
| 6 | 0.1 |
| 7 | 0.1 |
| 8[b] | 1.2 |
| Cream Extracts, Sodium Sulfate | |
| 1 | 1.0 |
| 2 | 0.3 |
| 3 | 0.2 |
| Cream Extracts, Water Dispersed | |
| 1 | 4.1 |
| 2 | 4.8 |
| 3 | 6.4 |
| 4 | 6.2 |
| II Paste | |
| 1 | 0.2 |
| 2 | <0.1 |
| 3 | <0.1 |
| 4 | <0.1 |
| 5[c] | 0.2 |

[a] Overnight standing of extract in contact with cream. [b] Overweekend standing of extract in contact with cream. [c] Overweekend standing of extract in contact with paste.

than to rely on a reduced value for reference response. The small amount (0.5%) of acetic acid added to the mobile phase to suppress solute ionization was not a factor and did not appear to convert any extracted II significantly.

Linearity studies performed on both I and III showed each to be completely linear within the concentration range selected, 0.0008–0.008 and 0.008–0.03 mg/ml, respectively. For I, the $y$ intercept was −0.07, the slope was 0.996, and the correlation coefficient was 1.000. For III, these values were 1.89, 1.49, and 0.999, respectively. An amount of I equivalent to 1.5% of II was added to 1 g of sample, which then was extracted. The recovery was 97.6%.

## REFERENCES


(1) E. A. Peterson, D. C. Gillespie, and F. D. Cook, *Can. J. Microbiol.*, **12,** 221 (1966).

(2) O. E. Edwards and D. C. Gillespie, *Tetrahedron Lett.*, **40,** 4867 (1966).

(3) M. Weigele and W. Leimgruber, *ibid.*, **8,** 715 (1967).

(4) W. Leimgruber, G. P. Maestrone, M. Mitrovic, and M. Weigele (to Hoffmann–La Roche Inc.), U.S. pat. 3,586,674 (June 22, 1971).

(5) W. Leimgruber, G. P. Maestrone, M. Mitrovic, and M. Weigele (to Hoffmann–La Roche Inc.), U.S. pat. 3,852,442 (Dec. 3, 1974).

(6) G. Maestrone, R. Darker, F. Hemrick, and M. Mitrovic, *Am. J. Vet. Res.*, **33,** 185 (1972).

(7) W. E. Snyder and G. Maestrone, *Vet. Med. Small Anim. Clin.*, **May 1976,** 585.

(8) G. Maestrone, E. Thompson, H. Yeisley, and M. Mitrovic, *ibid.*, **Dec. 1976,** 1681.

(9) G. Maestrone and M. Mitrovic, *Am. J. Vet. Res.*, **35,** 281 (1974).

(10) G. Maestrone and W. Brandt, *ibid.*, **40,** 285 (1979).

(11) S. M. Lesley and R. M. Behki, *Can. J. Microbiol.*, **17,** 1327 (1971).

(12) J. J. Donahue and S. Oliveri-Vigh, *Anal. Chim. Acta*, **63,** 415 (1973).

(13) M. H. Infeld and H. L. Newmark (to Hoffmann–La Roche Inc.), U.S. pat. 3,989,830 (Nov. 2, 1976).

(14) P. Haefelfinger and K. Häfelfinger, *Fresenius Z. Anal. Chem.*, **302,** 121 (1980).

(15) J. Berger, in "Kirk–Othmer Encyclopedia of Chemical Technology," vol. 3, 3rd ed., M. Grayson, Ed., Wiley, New York, N.Y., 1978, pp. 1–21.


# Mechanistic Studies on Transcorneal Permeation of Fluorometholone


**JAMES W. SIEG * and JOSEPH R. ROBINSON ˣ**



Received December 1, 1980, from the *School of Pharmacy, University of Wisconsin, Madison, WI 53706.* Accepted for publication February 19, 1981. *Present address: College of Pharmacy, University of Kentucky, Lexington, KY 40506.



**Abstract** □ The mechanism of corneal fluorometholone penetration was studied using albino rabbits, and the apparent rate and extent of steroid accumulation in the various cell layers of the cornea and aqueous humor were determined for normal and abraded eyes. The results are compared and contrasted to the mechanism previously reported for pilocarpine. Fluorometholone readily penetrates the intact corneal epithelium and accumulates in the hydrophilic stromal layers of the cornea. The kinetic profile is similar to that of pilocarpine and is largely a result of the precorneal dynamic processes. Pharmacokinetic parameters for each tissue were determined to establish an overall mechanism for corneal permeation of the steroid.



**Keyphrases** □ Fluorometholone—mechanistic studies on transcorneal permeation, compared with pilocarpine, rabbits □ Corneal permeation—transport mechanism, fluorometholone, compared with pilocarpine, rabbits □ Pharmacokinetics—fluorometholone compared with pilocarpine, mechanistic studies on transcorneal permeation, rabbits


The ocular penetration of steroids has been widely studied (1–8), but with emphasis primarily on quantitating specific tissue levels of drug rather than on establishing the mechanism for drug movement through the cornea. Previous work with pilocarpine defined the role of various corneal tissue layers in the permeation of a drug with both water and oil solubility (9), and the techniques can be used to study a representative steroid with low water solubility




*0022-3549/81/0900-1026$01.00/0*


*© 1981, American Pharmaceutical Association*

**Table II—Extraction Results of I as Percentage of II**

| Extract | Percentage I |
|---|---|
| Cream Extracts, Ultrasonication and Mechanical Shaking | |
| 1 | 0.9 |
| 2 | 0.5 |
| 3 | 0.5 |
| 4 | 0.5 |
| 5[a] | 1.2 |
| Cream Extracts, Manual Shaking | |
| 1 | 1.0 |
| 2 | 0.2 |
| 3 | 0.4 |
| 4 | 0.1 |
| 5 | 0.1 |
| 6 | 0.1 |
| 7 | 0.1 |
| 8[b] | 1.2 |
| Cream Extracts, Sodium Sulfate | |
| 1 | 1.0 |
| 2 | 0.3 |
| 3 | 0.2 |
| Cream Extracts, Water Dispersed | |
| 1 | 4.1 |
| 2 | 4.8 |
| 3 | 6.4 |
| 4 | 6.2 |
| II Paste | |
| 1 | 0.2 |
| 2 | <0.1 |
| 3 | <0.1 |
| 4 | <0.1 |
| 5[c] | 0.2 |

[a] Overnight standing of extract in contact with cream. [b] Overweekend standing of extract in contact with cream. [c] Overweekend standing of extract in contact with paste.

than to rely on a reduced value for reference response. The small amount (0.5%) of acetic acid added to the mobile phase to suppress solute ionization was not a factor and did not appear to convert any extracted II significantly.

Linearity studies performed on both I and III showed each to be completely linear within the concentration range selected, 0.0008–0.008 and 0.008–0.03 mg/ml, respectively. For I, the $y$ intercept was −0.07, the slope was 0.996, and the correlation coefficient was 1.000. For III, these values were 1.89, 1.49, and 0.999, respectively. An amount of I equivalent to 1.5% of II was added to 1 g of sample, which then was extracted. The recovery was 97.6%.

## REFERENCES


(1) E. A. Peterson, D. C. Gillespie, and F. D. Cook, *Can. J. Microbiol.*, **12,** 221 (1966).

(2) O. E. Edwards and D. C. Gillespie, *Tetrahedron Lett.*, **40,** 4867 (1966).

(3) M. Weigele and W. Leimgruber, *ibid.*, **8,** 715 (1967).

(4) W. Leimgruber, G. P. Maestrone, M. Mitrovic, and M. Weigele (to Hoffmann–La Roche Inc.), U.S. pat. 3,586,674 (June 22, 1971).

(5) W. Leimgruber, G. P. Maestrone, M. Mitrovic, and M. Weigele (to Hoffmann–La Roche Inc.), U.S. pat. 3,852,442 (Dec. 3, 1974).

(6) G. Maestrone, R. Darker, F. Hemrick, and M. Mitrovic, *Am. J. Vet. Res.*, **33,** 185 (1972).

(7) W. E. Snyder and G. Maestrone, *Vet. Med. Small Anim. Clin.*, **May 1976,** 585.

(8) G. Maestrone, E. Thompson, H. Yeisley, and M. Mitrovic, *ibid.*, **Dec. 1976,** 1681.

(9) G. Maestrone and M. Mitrovic, *Am. J. Vet. Res.*, **35,** 281 (1974).

(10) G. Maestrone and W. Brandt, *ibid.*, **40,** 285 (1979).

(11) S. M. Lesley and R. M. Behki, *Can. J. Microbiol.*, **17,** 1327 (1971).

(12) J. J. Donahue and S. Oliveri-Vigh, *Anal. Chim. Acta*, **63,** 415 (1973).

(13) M. H. Infeld and H. L. Newmark (to Hoffmann–La Roche Inc.), U.S. pat. 3,989,830 (Nov. 2, 1976).

(14) P. Haefelfinger and K. Häfelfinger, *Fresenius Z. Anal. Chem.*, **302,** 121 (1980).

(15) J. Berger, in "Kirk–Othmer Encyclopedia of Chemical Technology," vol. 3, 3rd ed., M. Grayson, Ed., Wiley, New York, N.Y., 1978, pp. 1–21.


# Mechanistic Studies on Transcorneal Permeation of Fluorometholone


**JAMES W. SIEG * and JOSEPH R. ROBINSON ˣ**



Received December 1, 1980, from the *School of Pharmacy, University of Wisconsin, Madison, WI 53706.* Accepted for publication February 19, 1981. *Present address: College of Pharmacy, University of Kentucky, Lexington, KY 40506.



**Abstract** □ The mechanism of corneal fluorometholone penetration was studied using albino rabbits, and the apparent rate and extent of steroid accumulation in the various cell layers of the cornea and aqueous humor were determined for normal and abraded eyes. The results are compared and contrasted to the mechanism previously reported for pilocarpine. Fluorometholone readily penetrates the intact corneal epithelium and accumulates in the hydrophilic stromal layers of the cornea. The kinetic profile is similar to that of pilocarpine and is largely a result of the precorneal dynamic processes. Pharmacokinetic parameters for each tissue were determined to establish an overall mechanism for corneal permeation of the steroid.



**Keyphrases** □ Fluorometholone—mechanistic studies on transcorneal permeation, compared with pilocarpine, rabbits □ Corneal permeation—transport mechanism, fluorometholone, compared with pilocarpine, rabbits □ Pharmacokinetics—fluorometholone compared with pilocarpine, mechanistic studies on transcorneal permeation, rabbits


The ocular penetration of steroids has been widely studied (1–8), but with emphasis primarily on quantitating specific tissue levels of drug rather than on establishing the mechanism for drug movement through the cornea. Previous work with pilocarpine defined the role of various corneal tissue layers in the permeation of a drug with both water and oil solubility (9), and the techniques can be used to study a representative steroid with low water solubility




*0022-3549/81/0900-1026$01.00/0*


*© 1981, American Pharmaceutical Association*

such as fluorometholone. This report compares and contrasts the corneal transport mechanism of fluorometholone to that established for pilocarpine.

## EXPERIMENTAL

**Materials**—Tritiated fluorometholone[1] was prepared using catalytic exchange. The specific activity of the steroid was 1.2 Ci/mmole, and the product was purified by vacuum distillation immediately prior to use.

Male albino rabbits, 2.0–2.5 kg, were fed a regular diet with unrestricted food and water.

**Preparation of Fluorometholone Solution**—A sufficient quantity of the tritiated steroid was added to sterile normal saline to make a $4 \times 10^{-5}$ *M* solution. The saline containing the steroid was equilibrated on a shaker bath at room temperature for 24 hr to ensure complete solution. The small amount of added tritiated steroid did not significantly alter the osmolarity of the saline solution.

**Removal of Corneal Epithelium**—The epithelial layer of the cornea was removed under local anesthesia to simulate an abraded eye or was harvested following death of the animals. In the first case, 2 drops of 0.5% tetracaine hydrochloride was used as a topical anesthetic prior to epithelium removal.

**Aqueous Humor Drug Concentration *versus* Time Profiles**—The techniques used were presented previously (1, 9). Unanesthetized animals were used, and a standard 50-$\mu$l dose was instilled with a microliter syringe. The dose was placed carefully onto the upper margin of the corneal surface and allowed to collect in the lower cul-de-sac.

At specified times following dosing, animals were sacrificed using an overdose of pentobarbital sodium. Eyes were rinsed with saline, and aqueous humor was aspirated from the anterior chamber. Aqueous humor samples (100 $\mu$l) were delivered into plastic liquid scintillation vials[2] containing refrigerated liquid scintillation counting solution[3]. The samples were counted using a scintillation spectrometer[4], and the data were converted to micrograms of steroid per milliliter of aqueous humor.

**Corneal Drug Concentration *versus* Time Profiles**—Cornea samples were taken immediately after aqueous humor was aspirated from the anterior chamber. Each cornea sample was rinsed with saline and blotted on tissue to remove excess water. The corneas were placed into tared combustion cones[5], and the wet weight was determined using an analytical balance. The cornea-containing combustion cone then was placed in a plastic vial[6] containing scintillation solution[7]. A tissue oxidizer[8] was used to burn each cornea, and samples were analyzed for steroid content. The final count for each sample was converted to micrograms of steroid per gram of cornea.

The only modification to this basic procedure occurred when only specific tissue layers of the cornea were monitored for steroid content; the described techniques were used.

## RESULTS

**Aqueous Humor Steroid Levels after Dosing with Fluorometholone Solution**—Aqueous humor steroid levels were monitored for 2 hr after topical instillation of fluorometholone solution into intact eyes (Fig. 1). A peak level was attained within 30 min. A semilog plot of the data gave a log-linear decline of concentration immediately following this peak, with an associated rate constant of 0.013 $min^{-1}$. Further pharmacokinetic analysis yielded an apparent absorption rate constant of 0.07 $min^{-1}$. In addition, estimates of the area under the curve for up to 2 hr postinstillation indicated that at least 20–30% of the instilled dose ultimately reached the aqueous humor.

**Corneal Steroid Concentration following Dosing with Fluorometholone Solution**—The corneal fluorometholone levels for the various tissue layers of intact eyes are presented in Figs. 1 and 2. The steroid reached a peak concentration in the whole intact cornea (Fig. 1) within 5 min; this result also was reflected by the data for the corneal epithelium (Fig. 2). A semilog plot of the data for the epithelium showed that drug concentration in this tissue was biphasic with two linear elim-

[1] New England Nuclear Corp., Boston, MA 02118.
[2] Mini-Vial, Research Products International Corp.
[3] Aquasol, New England Nuclear, Boston, MA 02118.
[4] Model 2002, Packard Instrument Co.
[5] Combusto-cone, Packard Instrument Co.
[6] The Vial, Research Products International Corp.
[7] Monophase-40, Packard Instrument Co.
[8] Model 306, Packard Instrument Co.

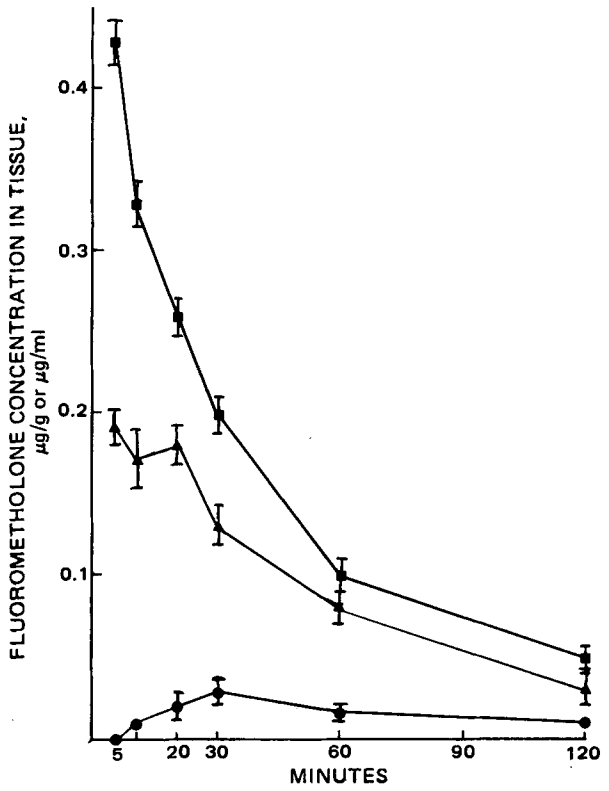


**Figure 1**—*Concentration of steroid in ocular tissues after dosing intact eyes with $4 \times 10^{-5}$ M fluorometholone solution. Key: ●, aqueous humor; ■, intact cornea; and ▲, stroma–endothelium.*

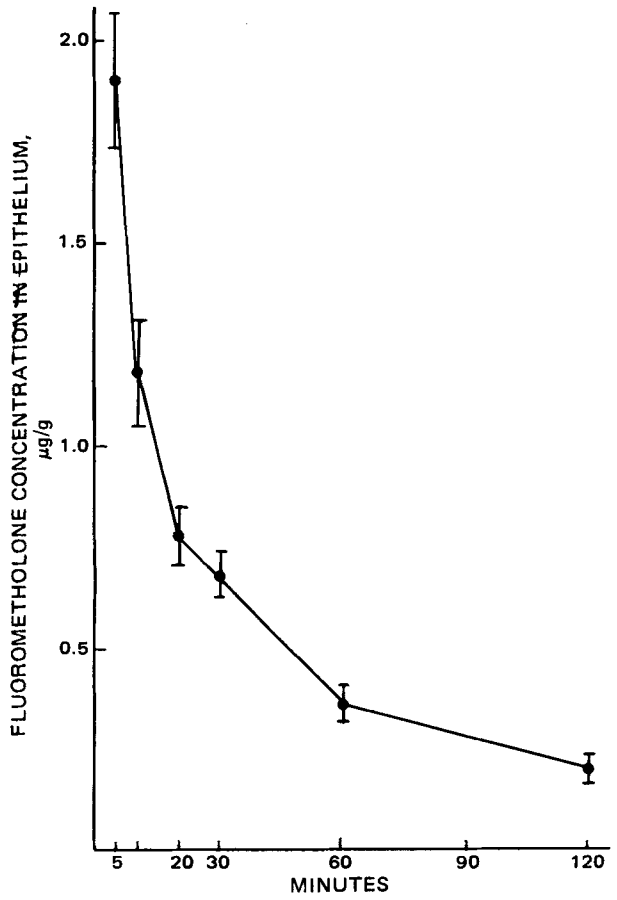


**Figure 2**—*Concentration of steroid in the epithelium after dosing intact eyes with $4 \times 10^{-5}$ M fluorometholone solution.*

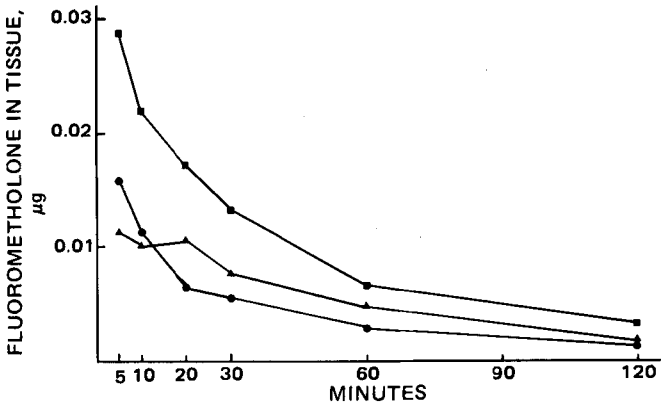


**Figure 3**—*Amount of steroid in ocular tissues after dosing intact eyes with 4 × $10^{-5}$ M fluorometholone solution. Key: ●, epithelium; ■, intact cornea; and ▲, stroma–endothelium.*

ination segments. This finding is almost identical to that previously seen with pilocarpine (9). The first-phase elimination rate constant was 0.06 $min^{-1}$, and the terminal phase rate constant was 0.014 $min^{-1}$.

The steroid also quickly reached the stroma–endothelium of the intact eye and built up to a relatively high concentration when compared with the aqueous humor levels. These levels decreased with an associated rate constant of 0.16 $min^{-1}$ and remained higher than the respective aqueous humor concentrations at all times up to 2 hr after dosing.

The amount of steroid in each tissue was also calculated using the experimentally determined tissue weights. Data of this type often can provide a clearer understanding of drug movement through the various ocular tissues. Although drug concentration is the driving force for drug permeation through these tissues, the large differences in tissue weights and distribution volumes sometimes give a misleading representation of the actual amount of drug involved. A comparison of the various amount *versus* time profiles can be made by referring to Fig. 3. The amount of fluorometholone in the epithelium fell below that in the stroma–endothelium rather quickly, even though the epithelial concentration remained higher at all times up to 2 hr. These differences are due to the almost 10-fold difference in weights between these two tissue layers.

**Ocular Penetration of Fluorometholone in Abraded Eyes**—The concentration of fluorometholone in aqueous humor and the cornea following topical instillation of a 4 × $10^{-5}$ *M* solution into intact and abraded eyes is presented in Figs. 4 and 5. Removal of the epithelium increased the aqueous humor levels of fluorometholone by ~60%, even though the peak was shifted from 30 min in intact eyes to ~10 min in abraded eyes. In addition, the elimination rate from the aqueous humor was about twice that obtained for intact eyes, being ~0.027 $min^{-1}$. The net result of these effects was that the areas under the curve for intact and abraded eyes were nearly identical.

## DISCUSSION

A true solution of the drug was selected as the dosing system to avoid slow absorption of undissolved drug in a suspension. Thus, the $t_{1/2}$ of fluorometholone in aqueous humor was ~54 min for intact eyes. This amount corresponds well with the turnover rate of aqueous humor, and

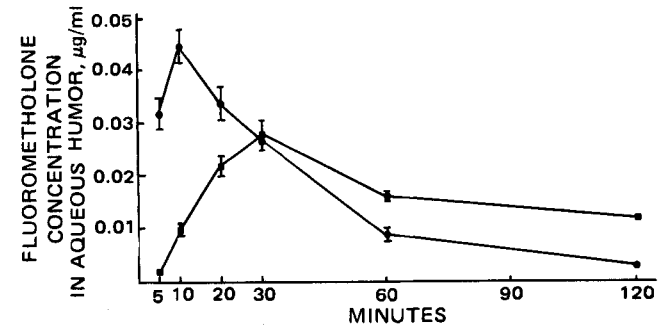


**Figure 4**—*Aqueous humor steroid concentration in intact (●) and abraded (○) eyes after dosing with 4 × $10^{-5}$ M fluorometholone solution.*

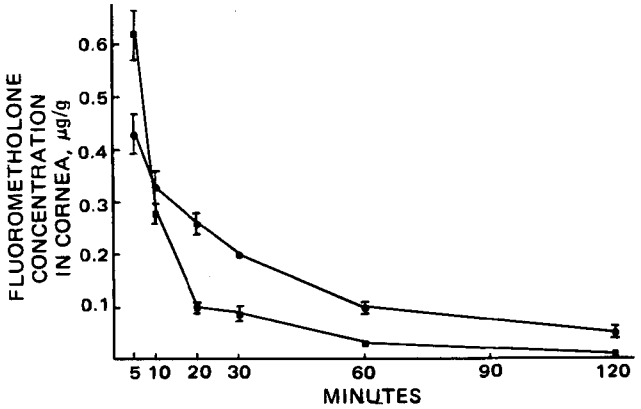


**Figure 5**—*Corneal steroid concentration in intact (●) and abraded (○) eyes after dosing with 4 × $10^{-5}$ M fluorometholone solution.*

presumably removal of fluorometholone from the anterior chamber is governed by this mechanism. However, previous corneal transport studies with fluorometholone suspensions reported a $t_{1/2}$ of ~100 min (10) because they did not extend beyond absorption of the suspension to obtain the true elimination rate constant.

The peak times for fluorometholone in the ocular tissues were similar to those previously obtained for pilocarpine (9). This observation would be somewhat puzzling when the vastly different water solubilities of these two drugs are considered. However, the effect of the parallel elimination process in the precorneal area on the observed apparent kinetic constants for ocular drug permeation already has been extensively discussed (9, 11). This parallel loss process is responsible for the apparent peak times and is essentially the same for both fluorometholone and pilocarpine.

The kinetic constants obtained for the various tissues are consistent with a mechanism consisting of a series of first-order absorption and elimination steps occurring in a succession of compartments with little or no lateral drug diffusion. The first-phase absorption rate constant calculated from the epithelium data was ~0.5 $min^{-1}$ for fluorometholone. This value again coincides well with the apparent absorption rate constant derived from previous rinsing studies and further reinforces the premise that this apparent kinetic constant is a direct reflection of the precorneal drainage process ($k_d$ = 0.545 $min^{-1}$). The first-phase corneal

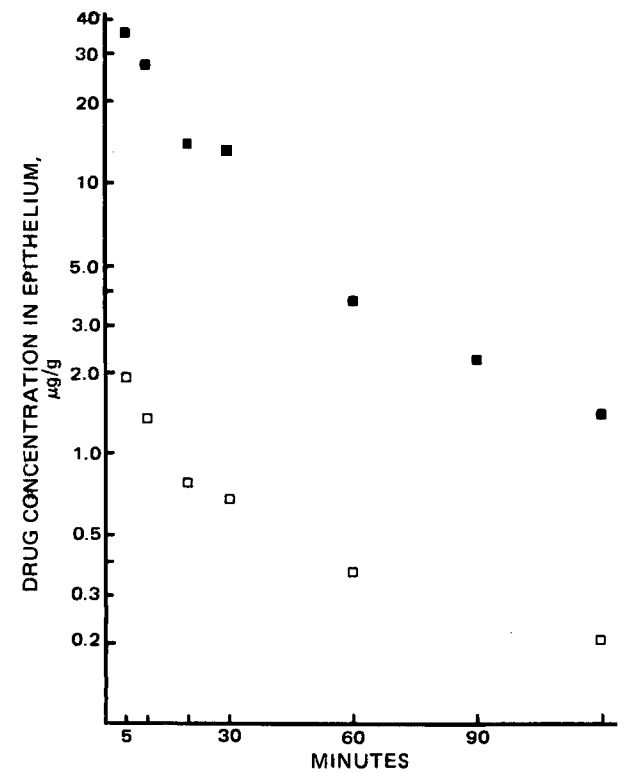


**Figure 6**—*Epithelial concentration* versus *time profiles for pilocarpine (▲) and fluorometholone (△).*

**Table I—Percent of Total Corneal Drug Content Present in Epithelium at Various Times after Dosing with Pilocarpine and Fluorometholone Solutions**

| Minutes | Percent in Epithelium | |
|---|---|---|
| | Pilocarpine | Fluorometholone |
| 5 | 92 | 56 |
| 10 | 85 | 52 |
| 20 | 68 | 40 |
| 30 | 72 | 42 |
| 60 | 67 | 45 |
| 120 | 73 | 44 |

elimination rate constant (0.06 $min^{-1}$) corresponds well with the apparent absorption rate constant into the aqueous humor (0.07 $min^{-1}$). In addition, the terminal phase elimination rate constant (0.014 $min^{-1}$) is almost equal to the measured aqueous humor elimination rate constant (0.013 $min^{-1}$).

The stroma–endothelium acts as a separate, distinct compartment from the aqueous chamber in the case of fluorometholone, unlike the situation for pilocarpine where free diffusion of drug between the aqueous humor and the stroma–endothelium occurred (9). The differences may be ascribed to possible binding of the steroid to some substance in the stroma (*e.g.*, collagen) or to an involvement of the endothelium. Owing to the oil solubility of fluorometholone, it is not unlikely that the drug may directly enter the cell membranes of the endothelium and pass *via* a transcellular route. On the other hand, being relatively fat insoluble, pilocarpine may pass directly into the anterior chamber *via* the intercellular spaces or pores. The difference in the elimination rate constants is particularly significant for the aqueous humor and cornea when comparing intact and abraded eyes. The increased elimination rate for abraded eyes suggests that the steroid leaves these tissues largely by back-diffusion into the tear film when the epithelium is not present. This effect was not apparent in the previous studies with pilocarpine. The extent of back-diffusion might argue against a protein binding mechanism for fluorometholone in the stroma in favor of a role for the endothelium.

The true absorption rate constant for pilocarpine is small, ~0.002 $min^{-1}$ (9). The data for fluorometholone indicate a much larger true rate constant for the steroid. The initial precorneal conditions were similar for both drugs, yet the total bioavailability of fluorometholone from solution was much greater. Nearly 30% of the instilled fluorometholone dose appeared to penetrate the cornea as opposed to only ~3% of pilocarpine. This finding suggests that the true rate constant for absorption into the epithelium is about 10 times higher than that of pilocarpine, or on the order of 0.02 $min^{-1}$. However, this still would not change the observed apparent absorption rate constant (0.5 $min^{-1}$) since the overriding influence is the rate constant for drainage. Thus, even though the apparent rate constant is the sum of all rate constants in the precorneal area, the increased magnitude of $k_{true}$ for fluorometholone is not sufficient to show up in the experimental measurement of $k_{apparent}$.

The results of the abraded eye studies (Fig. 4) show that the epithelium is not as great a barrier for fluorometholone as for pilocarpine. Thus, removal of the epithelium only increased the peak aqueous humor concentration by ~60%, whereas the observed increase with pilocarpine was a factor of 7 (9). This observation was noted previously (5) in an *in vitro* perfusion study where a three- to fourfold increase in corneal permeability was noted for water-soluble steroids and little or no increase was observed for lipid-soluble corticosteroids such as fluorometholone. This effect is also apparent when the percent of total corneal drug content present in the epithelium is calculated and compared for both drugs (Table I). Drug disposition in the cornea clearly favors the epithelium for pilocarpine, whereas fluorometholone distributes somewhat equally between the epithelium and stroma–endothelium. Previous work with pilocarpine showed the epithelium acting as both a barrier and a reservoir for pilocarpine, but this effect is less prominent with fluorometholone.

The epithelial drug concentration–time profile for fluorometholone is biphasic when plotted semilogarithmically. Similar circumstances exist for pilocarpine; in fact, the two drugs have remarkably similar profiles for this tissue (Fig. 6). Except for the absolute magnitude of the tissue concentrations, the shapes of the profiles are virtually identical. When the vastly different physical properties of fluorometholone and pilocarpine are considered, it seems likely that the explanation for this similarity is linked to some process involving the ocular tissues rather than to some specific property of both drugs.

## REFERENCES


(1) J. W. Sieg and J. R. Robinson, *J. Pharm. Sci.*, **64**, 931 (1975).

(2) C. Short, R. H. Keates, E. F. Donovan, M. Wyman, and W. Murdick, *Arch. Ophthalmol.*, **75**, 689 (1966).

(3) W. V. Cox, A. Kupferman, and H. M. Leibowitz, *ibid.*, **88**, 308 (1972).

(4) A. Kupferman, M. V. Pratt, K. Suckewer, and H. M. Leibowitz, *ibid.*, **91**, 373 (1974).

(5) D. S. Hull, J. E. Hine, H. F. Edelhauser, and R. A. Hyndiuk, *Invest. Ophthalmol.*, **13**, 457 (1974).

(6) I. H. Leopold, J. L. Sawyer, and H. Green, *Arch. Ophthalmol.*, **54**, 916 (1955).

(7) K. Green and S. J. Downs, *Invest. Ophthalmol.*, **13**, 316 (1974).

(8) C. Rosenblum, R. E. Dengler, Jr., and R. F. Geoffroy, *Arch. Ophthalmol.*, **77**, 234 (1967).

(9) J. W. Sieg and J. R. Robinson, *J. Pharm. Sci.*, **65**, 1816 (1976).

(10) A. Kupferman and H. M. Leibowitz, *Arch. Ophthalmol.*, **93**, 425 (1975).

(11) J. W. Sieg, M. C. Makoid, and J. R. Robinson, *J. Pharm. Sci.*, **65**, 150 (1976).


## ACKNOWLEDGMENTS


Supported in part by a grant from Allergan Pharmaceuticals, Irvine, Calif.

# Combined High-Performance Liquid Chromatographic Procedure for Measuring 4-Hydroxypropranolol and Propranolol in Plasma: Pharmacokinetic Measurements following Conventional and Slow-Release Propranolol Administration

**O. H. DRUMMER ˣ, J. McNEIL, E. PRITCHARD, and W. J. LOUIS**

Received November 3, 1980, from the *Clinical Pharmacology & Therapeutics Unit, Austin Hospital, University of Melbourne, Heidelberg, 3084, Victoria, Australia.* Accepted for publication February 17, 1981.

**Abstract** □ An assay is described for the simultaneous determination of propranolol and its active metabolite, 4-hydroxypropranolol, in human plasma. Both compounds were separated from an ethereal extract by high-performance liquid chromatography employing a $C_{18}$ bonded-phase column. Detection of the effluent was by fluorescence. Suitable fluorescent spectrometers and wavelength settings that allow optimum detection of both compounds have been described. The limit of sensitivity was 2 ng/ml for both propranolol and 4-hydroxypropranolol. Mean peak plasma levels of propranolol and 4-hydroxypropranolol in six patients receiving a single dose of a slow-release 160-mg formulation of propranolol were 28 and 6 ng/ml, respectively. These levels were about one-tenth the level obtained following a single conventionally prepared dose of propranolol (160 mg). Peak levels were delayed and plasma levels of propranolol persisted for a longer period with the slow-release formulation. Area under the curve estimates suggested that the bioavailability of the slow-release formulation following single-dose administration was about one-third that of the conventional preparation.

**Keyphrases** □ High-performance liquid chromatography—simultaneous assay of propranolol and 4-hydroxypropranolol, conventional and slow-release formulations compared □ Propranolol—high-performance liquid chromatographic assay with 4-hydroxypropranolol, conventional and slow-release formulations compared □ Pharmacokinetics—propranolol, conventional and slow-release formulations compared □ Bioavailability—propranolol, conventional and slow-release formulations compared

4-Hydroxypropranolol is formed by hepatic microsomal enzymes (1) following oral administration of propranolol (2). This active metabolite possesses β-adrenoceptor blocking activity (2–4). To date, GLC and high-performance liquid chromatographic (HPLC) methods involving the simultaneous detection of both 4-hydroxypropranolol and propranolol (5–12) have not been satisfactory. Sample preparation has not been uniform, and the selection of suitable fluorometric detection systems and the conditions for chromatography have varied considerably.

The present method provides a sensitive HPLC assay for the simultaneous measurement of propranolol and its active metabolite. Preliminary pharmacokinetic studies on the administration of conventional and slow-release oral propranolol formulations were conducted.

## EXPERIMENTAL

**Materials**—4-Hydroxypropranolol[1], propranolol hydrochloride[2], labetalol hydrochloride[3], ether[4], sodium metabisulfite[5], sodium carbonate[5], and monobasic potassium phosphate[6] were used.

**Apparatus**—A constant-flow high-performance liquid chromatograph[7] was equipped with a universal injector[8], a fluorometer[9], and a spectrofluorometer[10]. The stainless steel 30-cm long × 3.9-mm i.d. column was obtained prepacked[11].

**Chromatography**—The mobile phase consisted of 50% methanol[12] in 10 m*M* monobasic potassium phosphate buffer adjusted to pH 3.4 with 5 *M* HCl. It was pumped at a flow rate of 1.5 ml/min (1500 psi).

The retention volumes for 4-hydroxypropranolol, labetalol, and propranolol were 6.0, 7.2, and 9.0 ml, respectively.

The column eluate was monitored on a fluorometer set at excitation[13] and emission[14] wavelengths of 310 and 380 nm, respectively, which were optimal for 4-hydroxypropranolol fluorescence. When a spectrofluorometer was used, the wavelengths were set to be optimal for propranolol, at 295 and 360 nm, respectively. The bandpass was 20 nm. When propranolol levels were >10 ng/ml, a second fluorometer using excitation and emission wavelengths of 310[13] and 334[15] nm, respectively, occasionally was substituted for the spectrofluorometer.

Sensitivity settings on the fluorometer usually were maintained on high gain and lamp power settings; attenuations varied from ×2 to ×5 while the spectrofluorometer sensitivity range (0.3–1.0 μ*A*) gave a full-scale deflection.

**Standards**—Fresh solutions of propranolol and the internal standard, labetalol, were prepared weekly as aqueous solutions at concentrations of 1 and 4 μg/ml, respectively. Solutions of 4-hydroxypropranolol were prepared daily in water containing 1 m*M* HCl and 2% (w/v) sodium metabisulfite. For preparation of plasma standards, drug-free plasma was spiked with known amounts of aqueous stock solutions of both 4-hydroxypropranolol and propranolol in the 0–2000-ng/ml of plasma concentration range.

**Controls**—Control heparinized plasma containing 60 ng of 4-hydroxypropranolol/ml and 100 ng of propranolol/ml was prepared and stored until use in 1-ml aliquots at −20°.

**Procedure**—Labetalol (400 ng, 100 μl) was added to chromium trioxide-washed glass tubes containing 1 ml of unknown plasma, plasma standards, or control plasma. To each tube, 100 μl of freshly prepared sodium metabisulfite (20% w/v), 1 ml of sodium carbonate (1 *M*, pH 10.2), and 8 ml of ether then were added in turn. The tubes were stoppered, gently shaken for 10 min on a reciprocating automatic shaker[16], and centrifuged at 2000 rpm for 10 min. The ether phase was transferred to a fresh tube and evaporated to dryness under a gentle nitrogen stream in a water bath kept at ambient temperature. The residue was reconstituted with 100 μl of chromatography mobile phase, transferred to a microfuge tube[17], and centrifuged[18] for 4 min. An aliquot of the supernate (50 μl) then was injected into the liquid chromatograph.

**Quantitation**—Calibration curves were constructed for both 4-hydroxypropranolol and propranolol by calculating the peak height ratios of both components to the peak height of labetalol and plotting these ratios against the amount of standard added to each tube. For routine

[1] Courtesy of Dr. C. Proctor, ICI Pty. Ltd.
[2] Sigma Chemical Co., St. Louis, MO.
[3] Gift from Glaxo Australia Pty. Ltd.
[4] May & Baker, Dagenham, England.
[5] Merck, Darnstadt, West Germany.
[6] Ajax Chemicals, Sydney, Australia.
[7] M6000A, Waters Associates, Sydney, Australia.
[8] U6K, Waters Associates.
[9] Fluorichrom, Varian Pty. Ltd.
[10] Farrand Optical Co., Valhalla, N.Y.
[11] μBondapak $C_{18}$, Waters Associates.
[12] Liquid chromatography grade, Waters Associates.
[13] Filter 310 I, Varian Pty. Ltd.
[14] Filters 3.75 and 4.76, Varian Pty. Ltd.
[15] Filter 334 I, Varian Pty. Ltd.
[16] Paton Industries, South Australia, Australia.
[17] Eppendorf, Hamburg, West Germany.
[18] Mettich, Tuttlingen, West Germany.



*0022-3549/81/0900-1030$01.00/0*
*© 1981, American Pharmaceutical Association*

**Table I—Assay Parameters for Measurement of 4-Hydroxypropranolol and Propranolol from Plasma**

| Parameter | 4-Hydroxy-propranolol | Propranolol |
|---|---|---|
| Detection limit, ng | 2 | 2 |
| Recovery, % | 75 ± 4 ($n$ = 20) | 68 ± 3 ($n$ = 23) |
| Reproducibility within-day, % | 6 ($n$ = 5) | 7 ($n$ = 5) |
| Reproducibility day-to-day, % | 21 ($n$ = 27) | 12 ($n$ = 19) |

assays, the peak height ratios of drug to the internal standard obtained from a plasma standard containing 50 ng of 4-hydroxypropranolol/ml, 100 ng of propranolol/ml, and 400 ng of labetalol/ml were used to calculate the concentrations of propranolol and 4-hydroxypropranolol in unknown plasma. An aliquot of control plasma was included in each batch to ensure day-to-day reproducibility.

**Clinical Study**—Six healthy volunteers, mean age of 21.8 ± 0.2 years and weight of 62 ± 4 kg, participated in the double-blind crossover study. After an overnight fast, each subject was given a single oral dose of propranolol. Three subjects were given a conventional 160-mg formulation, and the other three were given a slow-release 160-mg formulation. Venous blood samples (10 ml) were taken prior to drug administration and then at 0.33, 0.66, 1.0, 1.5, 2.0, 2.5, 3.0, 4.0, 5.0, 6.0, 8.0, 12, and 24 hr. One week later, the same volunteers were given the other formulation of propranolol (160 mg of conventional or slow-release formulation) and a similar set of blood samples were taken.

**Pharmacokinetic Analysis**—Area under the concentration–time curves were calculated by the trapezoidal method and extrapolated to infinity by dividing the final concentration point (24 hr) by the slope of the terminal phase.

## RESULTS AND DISCUSSION

Both propranolol and 4-hydroxypropranolol exhibit natural fluorescence, allowing their separation by liquid chromatography and detection with a fluorescence detector. The excitation wavelengths (205 or 295 nm) are the same for both compounds, but the fluorescence emission spectra of propranolol and 4-hydroxypropranolol differ in that the wavelength maximum for emission in aqueous solution are 360 and 435 nm, respectively. Thus, there is a need for compromise in setting the wavelength of the detector to balance the loss of sensitivity for propranolol when the wavelength chosen is maximal for its metabolite.

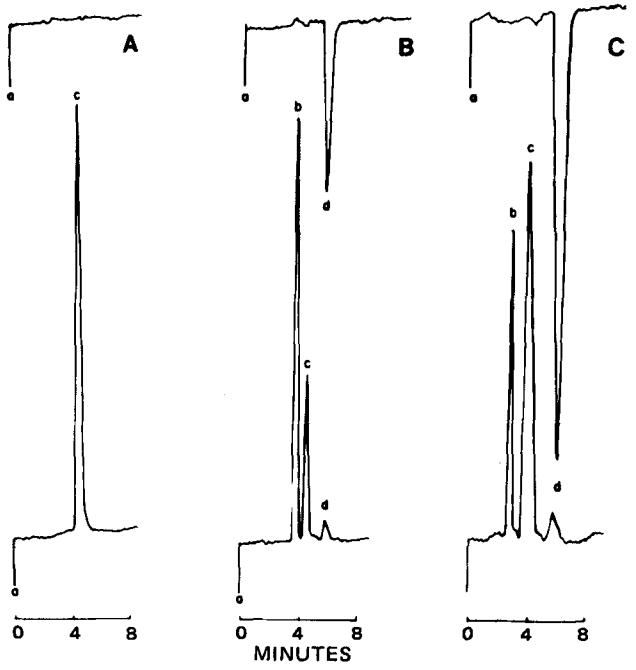


**Figure 1**—*High performance liquid chromatographs for: (A) a blank plasma extract, (B) an aqueous injection of 50-ng amounts of 4-hydroxypropranolol, propranolol, and (C) an extract of a patient plasma sample after receiving a single oral dose of conventional propranolol (propranolol level = 229 ng/ml; 4-hydroxypropranolol level = 47 ng/ml). Key: a, injection site; b, 4-hydroxypropranolol; c, labetalol; and d, propranolol.*

**Table II—Stability of 4-Hydroxypropranolol and Propranolol in Serum when Stored Frozen at −20°**

| Weeks of Storage | 4-Hydroxypropranolol, ng/ml | Propranolol, ng/ml |
|---|---|---|
| 1 | 66 | 88 |
| 2 | 59 | 79 |
| 3 | 61 | 94 |
| 4 | 60 | 91 |
| 5 | 64 | 90 |
| 9 | 62 | 90 |
| Mean ($SD$) | 62 ± 3 ($n$ = 21) | 90 ± 3 ($n$ = 19) |

Previous assay methods partially overcame this problem by using deuterium light sources, setting the excitation wavelength at 205 nm (5), and introducing a 340-nm cutoff filter for emission. Other assays (7, 9) using inefficient fluorometers suffered from inadequate sensitivity. Some investigators (8, 11) overcame the sensitivity problem by measuring each compound separately. This time-consuming process required injecting each extract twice, once at the chosen wavelengths for 4-hydroxypropranolol and then with the detector set at wavelengths optimal for propranolol. A recent study (12) avoided multiple injections; but to detect the 4-hydroxypropranolol and propranolol peaks, it was necessary to change the emission wavelength manually during each chromatographic run. This procedure is not suited for processing more than a few samples and does not lend itself to automatic injection techniques.

The present assay allows simultaneous detection of both compounds using an inexpensive tungsten light source. A filter fluorometer with an interference filter for the excitation light (310 nm) was used in conjunction with a combination of cutoff filters for emission, thus allowing light with a wavelength of >380 nm to be transmitted. This filter combination was optimal for 4-hydroxypropranolol fluorescence but still allowed satisfactory measurement of propranolol. The detection limit for 4-hydroxypropranolol was 2 ng/ml of plasma; for propranolol, it was 20 ng/ml (Table I). At these concentrations, peaks three times the baseline noise were obtained.

When more sensitive conditions were required for propranolol, a spectrofluorometer was connected in series with the fluorometer and set at wavelengths optimal for propranolol (295 nm/360 nm). Under these

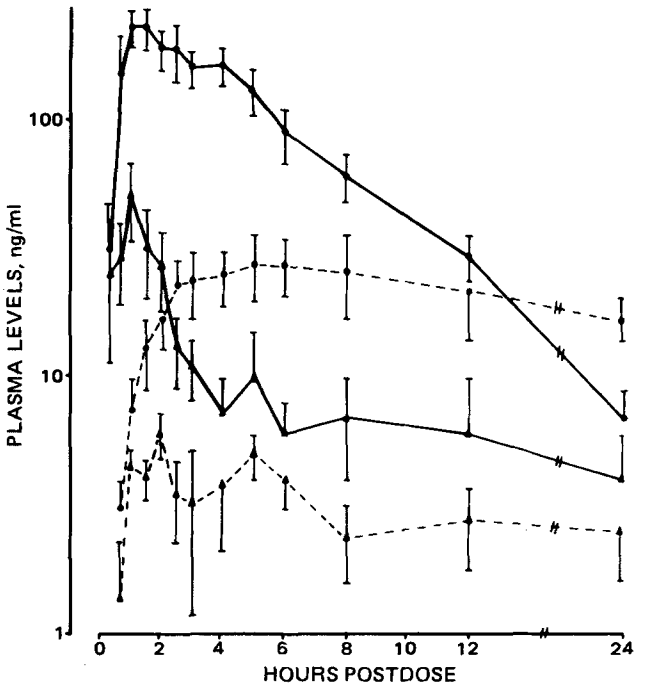


**Figure 2**—*Semilogarithmic plot of the mean plasma 4-hydroxypropranolol and propranolol levels* versus *time following single oral doses of a conventional propranolol formulation (160 mg) and a slow-release preparation (160 mg). Key: ●—●, propranolol (conventional); ●---●, propranolol (slow release); ▲—▲, 4-hydroxypropranolol (conventional); and ▲---▲, 4-hydroxypropranolol (slow release).*

conditions, the detection limit for propranolol was 2 ng/ml of plasma. 4-Hydroxypropranolol was not detected in the latter system due to the relatively narrow bandpass (20 nm) on the spectrofluorometer and the higher emission wavelengths for this compound.

If a spectrofluorometer is not available, a second fluorometer can be set at 310 nm/334 nm with interference filters; a sensitivity of 10 ng/ml for propranolol is obtained.

Methanol–10 m*M* phosphate buffer, pH 3.4 (50:50), was used as the mobile phase for reversed-phase chromatography on this bonded column and gave excellent resolution between 4-hydroxypropranolol, labetalol, and propranolol with retention volumes of 6.0, 7.2, and 9.0 ml, respectively. This separation was more reproducible than that reported with other published mobile phases, *e.g.*, acetic acid (7–10, 13) or phosphoric acid (6, 12, 14), and less harmful to the column than heptane–sulfonic acid (8).

Conjugation as the glucuronidate or sulfate is a major route of elimination of both propranolol and 4-hydroxypropranolol (15). Although the present assay method was designed primarily to measure the biologically active unconjugated drug, modification of the procedure utilizing an enzyme-catalyzed hydrolysis step prior to extraction with ether allows measurement of total propranolol and 4-hydroxypropranolol. This procedure has been well characterized (9, 12).

Figures 1A and 1B show liquid chromatograms for a blank plasma extract and an aqueous injection of 50-ng amounts of each compound. Figure 1C represents a patient plasma extract with 4-hydroxypropranolol and propranolol levels of 47 and 229 ng/ml, respectively. The upper tracing in each case represents the tracing for propranolol obtained on the spectrofluorometer. No other peaks interfered with the peaks for propranolol and 4-hydroxypropranolol. However, prazosin and quinidine interfered with the peaks for the internal standard. In the presence of either drug, 4-methylpropranolol is a suitable alternative internal standard (6).

Calibration curves were constructed by spiking drug-free plasma with aqueous solutions in the concentration range of 0–100 ng/ml for 4-hydroxypropranolol and of 0–2000 ng/ml for propranolol. The peak heights of both drugs were divided by the peak height for labetalol (internal standard) and plotted against concentration. Both drugs exhibited linear calibration curves with intercepts through the origin.

Reproducibility for both drugs was evaluated by performing replicate assays of the control plasma containing both drugs. Within-day variability was 6 and 7% for 4-hydroxypropranolol and propranolol, respectively. When the same control plasma was assayed over 5 weeks, values of 21 and 12% were obtained (Table I). The stability of 4-hydroxypropranolol was cited as a major problem (5, 8), so although sodium metabisulfite was added as a stabilizer to the plasma prior to extracting, it was feared that the plasma stored frozen without stabilizer might deteriorate with time. When control plasma was assayed at weekly intervals over 9 weeks, no deterioration was evident (Table II). This result was confirmed by Taburet *et al.* (8), who found that the metabolite was stable for at least 4 weeks at −20°.

No data have been published on plasma level profiles of both unconjugated propranolol and 4-hydroxypropranolol following oral administration of a slow-release propranolol formulation. The mean (±*SEM*) plasma concentrations of these two compounds were compared in six volunteers receiving, on separate occasions 1 week apart, a single oral 160-mg dose of propranolol in a conventional formulation and a 160-mg slow-release preparation (Fig. 2). Peak levels of propranolol after the conventional formulation were 236 ± 38 ng/ml at 60 min, consistent with previous reports (7, 16). Peak levels for the slow-release preparations were considerably lower and delayed (28 ± 8 ng/ml, obtained 5 hr postdose).

The slow-release formulation was not associated with an increased rate of formation of the active metabolite 4-hydroxypropranolol. In fact, in all patients, peak levels (conventional, 51 ± 17 ng/ml; slow release, 6 ± 1 ng/ml) and area under the curve values (*AUC*) (conventional, 218 ± 17 ng hr/ml; slow release, 141 ± 32 ng hr/ml) for the 4-hydroxy metabolite were considerably less following single doses of the slow-release formulation. The persistence of propranolol in plasma for >24 hr with the slow-release formulation suggests that drug accumulation may occur with chronic daily therapy and that attainment of steady state may require several days of treatment. Calculation of the bioavailability for the slow-release preparation by extrapolation of the 24-hr data is likely to overestimate the *AUC*. Nevertheless, bioavailability of the slow-release preparation was poor; corresponding propranolol *AUC* estimations suggest that the bioavailability of single doses of the slow-release formulation was at least 2.9 times lower than that of the conventional preparation. The association of low propranolol levels and low levels of the 4-hydroxy metabolites is consistent with the suggestion that high 4-hydroxypropranolol levels are formed only in the presence of high concentrations of the parent drug in the liver (17).

## REFERENCES


(1) J. D. Fitzgerald and S. R. O'Donnell, *Br. J. Pharmacol.*, **43,** 222 (1971).

(2) C. R. Cleaveland and D. G. Shand, *Clin. Pharmacol. Ther.*, **13,** 181 (1971).

(3) J. W. Paterson, M. E. Conolly, C. T. Dollery, A. Hayes, and R. G. Cooper, *Pharmacol. Clin.*, **2,** 127 (1970).

(4) G. L. Tindell, T. Walle, and T. E. Gaffney, *Life Sci.*, **11,** 1029 (1972).

(5) T. Walle, J. Morrison, K. Walle, and E. Conradi, *J. Chromatogr.*, **114,** 351 (1975).

(6) R. L. Nation, G. W. Peng, and W. L. Chiou, *ibid.*, **145,** 429 (1978).

(7) D. W. Schneck, J. F. Pritchard, and A. H. Hayes, Jr., *Res. Commun. Chem. Pathol. Pharmacol.*, **24,** 3 (1979).

(8) A. M. Taburet, A. A. Taylor, J. R. Mitchell, D. E. Rollins, and J. L. Pool, *Life Sci.*, **24,** 209 (1979).

(9) J. F. Pritchard, D. W. Schneck, and A. H. Hayes, Jr., *J. Chromatogr.*, **162,** 47 (1979).

(10) G. Nygard, W. H. Shelver, and S. K. W. Khalil, *J. Pharm. Sci.*, **68,** 379 (1979).

(11) W. D. Mason, E. N. Amick, and O. H. Weddle, *Anal. Lett.*, **10,** 515 (1977).

(12) M. Loo and S. Riegelman, *J. Chromatogr.*, **183,** 213 (1980).

(13) A. J. J. Wood, K. Carr, E. E. Vestal, S. Balcher, G. R. Wilkinson, and D. G. Shand, *Br. J. Clin. Pharmacol.*, **6,** 345 (1978).

(14) G. J. Schmidt and F. L. Vandemark, *Chromatogr. Newsl.*, **5,** 42 (1977).

(15) T. Walle, E. C. Conradi, U. K. Walle, T. C. Fagan, and T. E. Gaffney, *Clin. Pharmacol. Ther.*, **27,** 22 (1980).

(16) D. A. Routledge and D. G. Shand, *Clin. Pharmacokinet.*, **4,** 73 (1979).

(17) D. W. Schneck, J. F. Pritchard, T. P. Gibson, J. E. Vary, and A. H. Hayes, Jr., *Clin. Pharmacol. Ther.*, **27,** 744 (1980).


## ACKNOWLEDGMENTS


The authors thank the Life Assurance Medical Research Foundation and Imperial Chemical Industries for their support for these studies.

# Thermochemical Investigations of Nearly Ideal Binary Solvents VII: Monomer and Dimer Models for Solubility of Benzoic Acid in Simple Binary and Ternary Solvents

**WILLIAM E. ACREE, Jr., and GARY L. BERTRAND** ˣ

Received November 10, 1980, from the *Department of Chemistry, University of Missouri-Rolla, Rolla, MO 65401.* Accepted for publication March 2, 1981.

**Abstract** □ Solubilities are reported for benzoic acid at 25.0° in binary mixtures of carbon tetrachloride with cyclohexane, *n*-hexane, or *n*-heptane and of cyclohexane with *n*-hexane or *n*-heptane and in ternary mixtures of carbon tetrachloride–cyclohexane–*n*-hexane and carbon tetrachloride–cyclohexane–*n*-heptane. Solubilities also are reported for benzoic acid in some binary solvents at 30.0° and for *m*-toluic acid in binary mixtures of cyclohexane and *n*-hexane at 25.0°. The results are compared to the predictions of equations developed previously for solubility in systems of purely nonspecific interactions, with the benzoic acids considered as either monomeric or dimeric molecules in solution. The dimer model gave more accurate predictions, with a maximum deviation of 4.4% between observed and predicted solubilities in all systems studied. Solubility maxima were predicted and observed for benzoic and *m*-toluic acids in cyclohexane–*n*-hexane and for benzoic acid in cyclohexane–*n*-heptane. The application of these solubility relationships to liquid–liquid partition coefficients is discussed.

**Keyphrases** □ Binary solvents—thermochemical study of monomer and dimer models for benzoic acid solubility □ Benzoic acid—thermochemical study, monomer and dimer models for solubility in simple binary and ternary solvents □ Solubility—benzoic acid in simple binary and ternary solvents, monomer and dimer models □ Thermochemistry—monomer and dimer models for solubility of benzoic acid in simple binary and ternary solvents

The use of mixed solvents for influencing solubility and multiphase partitioning has great potential application in pharmaceutical research. Maximum realization of this potential depends on the development of equations that predict solubilities or partition coefficients in mixed solvents from the properties of the individual components. This study continued the testing (1–4) of applications and limitations of the nearly ideal binary solvent (NIBS) model for predicting solution enthalpies (1, 2), solubilities (3), and gas–liquid partition coefficients (4) of solutes in binary solvent mixtures relative to their properties in pure solvents.

## BACKGROUND

The NIBS model predicts that any partial molar thermodynamic excess property of a solute at infinite dilution in a binary solvent is a volume fraction average (a weighted mole fraction average gives somewhat better predictions for solution enthalpies) of its properties at infinite dilution in a pure solvent, with a correction for solvent "unmixing" by the presence of the solute. This model gives good predictions for solute properties in systems of nonspecific interactions, but it fails for systems with specific solvent–solvent or solvent–solute interactions. The solubility equations have been successfully applied to solubilities as high as 0.3 mole fraction (3) for solutes that do not self-associate or form solvent–solute complexes.

Benzoic acid presents an interesting test for these equations because of its very strong self-association in "inert" solvents, even at high dilution. Calculations with reported dimerization constants in cyclohexane (5), carbon tetrachloride (5, 6), and benzene (5, 7, 8) indicate that <4% of the benzoic acid molecules are monomers at saturation at 25°. Thus, this approach should give relatively poor predictions of the solubility of benzoic acid in terms of a monomer model, but it has a reasonable chance of success if a dimer model is used.

The dimer model may be an oversimplification, however, since Krishnan *et al.* (8) presented evidence for trimers of benzoic acid in benzene. The reported equilibrium constants for benzoic acid at saturation in benzene at 25° led to estimates that 2.5% of the benzoic acid molecules are monomers, 66% are dimers, and the remainder are trimers. To avoid the complications of trimeric forms, the present study was confined to solvents in which benzoic acid is considerably less soluble than in benzene.

During this work, the nearly ideal binary solvent model was found to predict maxima for benzoic acid solubility in mixtures of cyclohexane with *n*-hexane or *n*-heptane. Such maxima are usually explained with solubility parameter theory (9) in terms of the solubility parameter of the solute lying between the solubility parameters of the solvents. However, all estimates of the solubility parameters of benzoic acid monomers or dimers give values greater than any of the solvents studied, so these measurements provide a test of the more general applicability of the present approach. Similar predictions for maximum solubility of *m*-toluic acid also were tested.

The equations for solubility in binary solvents were expanded to include ternary solvents. Since these equations require excess free energy data (data that are often not available), an approximation was developed from the original nearly ideal binary solvent model for estimating the excess properties of a multicomponent system from the properties of the contributing binary systems. The resultant equations give good predictions for the solubility of benzoic acid in two simple ternary solvents.

## EXPERIMENTAL

Benzoic acid (99%) was dried at 60° for several hours, mp 122.5 ± 0.5° [lit. (10) mp 122.4°]. *m*-Toluic acid (99%) was recrystallized twice from aqueous ethanol and dried at 80°, mp 109.5 ± 0.5° [lit. (10) mp 111–113°]. The recrystallized acid was titrated to a thymol blue end-point with freshly standardized sodium methoxide solution by the method of Fritz and Lisicki (11), except toluene was substituted for benzene. The purity of the *m*-toluic acid was calculated to be 100.1 ± 0.5%. Cyclohexane (99+%), *n*-heptane (99+%), and *n*-hexane (99%) were stored over molecular sieves (Type 4A) and distilled shortly before use. Carbon tetrachloride (99+%) was purified by the method of Scatchard *et al.* (12), stored in contact with mercury under an argon atmosphere, and distilled shortly before use.

Solvent mixtures were prepared by weight with sufficient accuracy to allow calculation of compositions to 0.0001 mole fraction. Solvents and excess carboxylic acid were placed in brown glass containers and allowed to equilibrate in a constant-temperature bath at 25.00 ± 0.01 or 30.00 ± 0.01°, maintained constant to ±0.002°, for several days. The attainment of equilibrium was verified by repetitive measurements after several

**Table I—Solubilities of Benzoic Acid and *m*-Toluic Acid in Pure Solvents**

| Solute(s) | Solvent | Temperature | $10^2 X_s^{sat}$ |
|---|---|---|---|
| Benzoic acid | *c*-$C_6H_{12}$ | 25.0° | 1.15 |
| | *c*-$C_6H_{12}$ | 30.0° | 1.46 (1.43[a]) |
| Benzoic acid | *n*-$C_6H_{14}$ | 25.0° | 1.00 |
| | *n*-$C_6H_{14}$ | 30.0° | 1.26 |
| Benzoic acid | *n*-$C_7H_{16}$ | 25.0° | 1.14 |
| | *n*-$C_7H_{16}$ | 30.0° | 1.47 |
| Benzoic acid | $CCl_4$ | 25.0° | 4.92 (4.99[b]) |
| | $CCl_4$ | 30.0° | 5.98 |
| *m*-Toluic acid | *c*-$C_6H_{12}$ | 25.0° | 1.27 |
| | *n*-$C_6H_{14}$ | 25.0° | 1.17 |

[a] Reference 15. [b] Reference 16.

0022-3549/81/0900-1033$01.00/0
© 1981, American Pharmaceutical Association

**Table II—Solubility of Benzoic Acid in Binary Solvents at 25.0 and 30.0°: Comparison of the Predictions of Monomer and Dimer Models in Eqs. 1 and 2**

| Temperature | Solvent 1 | Solvent 2 | $X_1^0$ | $10^2\,X_s^{sat\,a}$ | Percent Deviation (Monomer Model)[b], Eq. 1 or 2 | Percent Deviation (Dimer Model)[b] Eq. 1 | Eq. 2 |
|---|---|---|---|---|---|---|---|
| 25.0° | $c$-$C_6H_{12}$ | $CCl_4$ | 0.1847 | 3.89 | −4.3 | −0.9 | −0.9 |
| | | | 0.3681 | 3.07 | −8.1 | −3.5 | −3.5 |
| | | | 0.5207 | 2.46 | −8.2 | −3.3 | −3.3 |
| | | | 0.6226 | 2.12 | −8.0 | −4.0 | −4.0 |
| | | | 0.8084 | 1.56 | −4.2 | −1.6 | −1.6 |
| 25.0° | $n$-$C_7H_{16}$ | $CCl_4$ | 0.1784 | 3.75 | −6.5 | −1.6 | −1.2 |
| | | | 0.2303 | 3.47 | −7.9 | −2.1 | −1.0 |
| | | | 0.3348 | 2.95 | −8.9 | −2.5 | −0.5 |
| | | | 0.3930 | 2.70 | −9.2 | −2.7 | −1.4 |
| | | | 0.3932 | 2.69 | −9.0 | −2.5 | −1.2 |
| | | | 0.4708 | 2.40 | −9.0 | −2.8 | −1.4 |
| | | | 0.5433 | 2.14 | −7.8 | −2.0 | −0.6 |
| | | | 0.7013 | 1.70 | −5.8 | −1.4 | −0.4 |
| 30.0° | $n$-$C_7H_{16}$ | $CCl_4$ | 0.2421 | 4.23 | −8.4 | −2.5 | −1.4 |
| | | | 0.4269 | 3.22 | −9.6 | −3.2 | −1.8 |
| | | | 0.6237 | 2.41 | −7.6 | −2.6 | −1.4 |
| | | | 0.7346 | 2.06 | −5.3 | −1.5 | −0.8 |
| 25.0° | $n$-$C_6H_{14}$ | $CCl_4$ | 0.1550 | 3.95 | −6.4 | −1.5 | −1.1 |
| | | | 0.3419 | 2.97 | −10.4 | −3.1 | −2.3 |
| | | | 0.4408 | 2.51 | −10.4 | −2.7 | −1.9 |
| | | | 0.5951 | 1.95 | −9.4 | −2.7 | −2.0 |
| | | | 0.8028 | 1.37 | −4.9 | −1.1 | −0.7 |
| 30.0° | $n$-$C_6H_{17}$ | $CCl_4$ | 0.2255 | 4.83 | −9.6 | −2.9 | −2.4 |
| | | | 0.3078 | 3.91 | −10.8 | −3.5 | −2.9 |
| | | | 0.4556 | 3.04 | −11.0 | −3.4 | −2.7 |
| | | | 0.6438 | 2.26 | −9.1 | −2.2 | −1.5 |
| | | | 0.7564 | 1.85 | −6.5 | −2.0 | −1.5 |
| 25.0° | $c$-$C_6H_{12}$ | $n$-$C_6H_{14}$ | 0.2573 | 1.08 | −1.8 | 0.0 | +0.3 |
| | | | 0.4699 | 1.13 | −3.0 | 0.0 | +0.5 |
| | | | 0.5342 | 1.15 | −4.1 | −0.9 | −0.5 |
| | | | 0.6566 | 1.18 | −4.9 | −1.6 | −1.3 |
| | | | 0.8044 | 1.17 | −2.6 | 0.0 | +0.2 |
| 30.0° | $c$-$C_6H_{12}$ | $n$-$C_6H_{14}$ | 0.2341 | 1.36 | −2.8 | −0.9 | −0.7 |
| | | | 0.2845 | 1.38 | −3.2 | −1.1 | −0.9 |
| | | | 0.5059 | 1.46 | −4.8 | −1.8 | −1.4 |
| | | | 0.6670 | 1.50 | −5.1 | −2.0 | −1.7 |
| | | | 0.7821 | 1.51 | −4.4 | −1.8 | −1.5 |
| 25.0° | $c$-$C_6H_{12}$ | $n$-$C_7H_{16}$ | 0.2781 | 1.19 | −2.1 | −0.3 | +0.2 |
| | | | 0.4602 | 1.21 | −3.0 | −0.6 | +0.1 |
| | | | 0.5713 | 1.21 | −3.2 | −1.0 | 0.0 |
| | | | 0.6825 | 1.22 | −4.0 | −1.7 | −1.0 |
| | | | 0.8142 | 1.19 | −2.2 | −0.6 | −0.1 |

[a] $X_s^{sat}$ is calculated as if the solute is monomeric. [b] Percent deviation = $100 \ln (X_s^{sat})_{calc}/(X_s^{sat})_{obs}$.

additional days. Acid solubility was determined by transferring a weight aliquot through a coarse filter into a flask containing blank nonaqueous titration solvent. The solutions were titrated with freshly standardized sodium methoxide solution to the thymol blue end-point, giving solubilities reproducible to within 1%.

Solubilities in pure solvents (Table I), in binary solvents (Tables II and III), and in ternary solvents (Table IV) are reported as formal mole fractions, calculated as though the solute were monomeric, and solvent compositions ($X_i^0$) are calculated as if the solute were not present. Table I results are in good agreement with previously reported values.

## DISCUSSION

**Monomer and Dimer Models for Solubility in Binary Solvents**—The following two equations for solubility in systems of nonspecific interactions were developed from the general equation (3), depending on whether a regular solution model (Eq. 1) or Flory–Huggins model (Eq. 2) is used:

$$RT \ln(a_s^{solid}/X_s^{sat}) = (1 - \Phi_s^{sat})^2[\Phi_1^0(\Delta\overline{G}_s^e{}^*_{X_1^0=1} + \Phi_2^0(\Delta\overline{G}_s^e)^*_{X_2^0=1} - \overline{V}_s(X_1^0\overline{V}_1 + X_2^0\overline{V}_2)^{-1}(\Delta\overline{G}_{12}^e)] \quad \text{(Eq. 1)}$$

$$RT\left[\ln(a_s^{solid}/\Phi_s^{sat}) - (1 - \Phi_s^{sat})\left(1 - \frac{\overline{V}_s}{(X_1^0\overline{V}_1 + X_2^0\overline{V}_2)}\right)\right] = (1 - \Phi_s^{sat})^2[\Phi_1^0(\Delta\overline{G}_s^{fh})^*_{X_1^0=1} + \Phi_2^0(\Delta\overline{G}_s^{fh})^*_{X_2^0=1} - \overline{V}_s(X_1^0\overline{V}_1 + X_2^0\overline{V}_2)^{-1}(\Delta\overline{G}_{12}^{fh})] \quad \text{(Eq. 2)}$$

in which $\overline{V}_i$ is the molar volume of a pure liquid, $X_i$ is the mole fraction, $\Phi_i$ is the volume fraction, $\Delta\overline{G}_{12}^e$ is the molar excess Gibbs free energy of the mixed solvent, and:

$$\Delta\overline{G}_{12}^{fh} = \Delta\overline{G}_{12}^e + RT[\ln(X_1^0\overline{V}_1 + X_2^0V_2) - X_1^0\ln(\overline{V}_1) - X_2^0\ln(\overline{V}_2)] \quad \text{(Eq. 3)}$$

The superscript (0) indicates that the solvent mole fraction or volume fraction is calculated as if the solute were not present. The activity of the solid solute ($a_s^{solid}$), relative to the supercooled liquid (also equal to the mole fraction solubility in an ideal solution), can be calculated from the melting point ($T_m$) and the molar enthalpy of fusion ($\Delta H_s^{fus}$):

$$\ln(a_s^{solid}) = \int_{T_m}^{T} (\Delta H_s^{fus}/RT^2)\,dT \quad \text{(Eq. 4)}$$

The use of these equations for solubility predictions in mixed solvents is as follows. The quantities $(\Delta\overline{G}_s^e)^*_{X_1^0=1}$ or $(\Delta\overline{G}_s^{fh})^*_{X_1^0=1}$ are calculated from the mole fraction or volume fraction solubility of the solute in the pure solvents (the asterisk indicates that these are approximations of infinite dilution properties). Then these properties are used in the appropriate equation to calculate the solubility as $X_s^{sat}$ or $\Phi_s^{sat}$ in a solvent mixture, using a reiterative process. The quantity $(1 - \Phi_s^{sat})$ is taken as unity in

**Table III—Solubility of *m*-Toluic Acid in Cyclohexane (1) + *n*-Hexane at 25°**

| $X_1^0$ | $10^2\,X_s^{sat}$ | Percent Deviation (Monomer Model), Eq. 1 or 2 | Percent Deviation (Dimer Model) Eq. 1 | Eq. 2 |
|---|---|---|---|---|
| 0.2380 | 1.27 | −4.3 | −2.0 | −1.7 |
| 0.4028 | 1.33 | −6.4 | −3.0 | −2.6 |
| 0.6121 | 1.37 | −7.2 | −3.3 | −2.8 |
| 0.8239 | 1.36 | −5.6 | −2.8 | −2.5 |

Table IV—Solubility of Benzoic Acid in Ternary Solvents at 25.0°: Comparison of Predictions of the Dimer Model in Eqs. 13 and 14

| Solvent 1 | Solvent 2 | Solvent 3 | $X_1^0$ | $X_2^0$ | $10^2 X_s^{sat}$ | Percent Deviation (Dimer Model) Eq. 13 | Eq. 14 |
|---|---|---|---|---|---|---|---|
| $CCl_4$ | $c$-$C_6H_{12}$ | $n$-$C_6H_{14}$ | 0.1109 | 0.4951 | 1.37 | −1.5 | −1.2 |
| | | | 0.2099 | 0.1836 | 1.50 | −2.5 | −2.0 |
| | | | 0.1903 | 0.6665 | 1.58 | −2.2 | −1.9 |
| | | | 0.3084 | 0.3713 | 1.86 | −1.2 | −3.3 |
| | | | 0.4225 | 0.4807 | 2.27 | −4.4 | −4.3 |
| | | | 0.5273 | 0.1011 | 2.49 | −4.0 | −3.2 |
| | | | 0.6766 | 0.1774 | 3.20 | −2.9 | −1.6 |
| $CCl_4$ | $c$-$C_6H_{12}$ | $n$-$C_7H_{16}$ | 0.1144 | 0.5450 | 1.41 | −1.3 | +0.8 |
| | | | 0.1891 | 0.2337 | 1.54 | −2.1 | −1.1 |
| | | | 0.1795 | 0.6927 | 1.56 | −2.6 | −2.1 |
| | | | 0.2216 | 0.1952 | 1.60 | −1.8 | −0.8 |
| | | | 0.3205 | 0.3927 | 1.90 | −2.8 | −1.8 |
| | | | 0.4754 | 0.4457 | 2.43 | −3.6 | −3.2 |
| | | | 0.5426 | 0.0991 | 2.55 | −4.1 | −2.8 |
| | | | 0.6973 | 0.1740 | 3.26 | −2.6 | −1.9 |

the first approximation, and convergence is rapid unless the solubility is quite large.

Applications of the monomer and dimer models to these equations are straightforward, taking the molecular weight, molar volume, and molar enthalpy of fusion of the dimer to be exactly twice the values for the monomer[1], and lead to the relationships:

$$(a_{ss}^{solid}) = (a_s^{solid})^2, ss = \text{dimer} \quad \text{(Eq. 5)}$$

$$X_{ss}^{sat} = X_s^{sat}/(2 - X_s^{sat}) \quad \text{(Eq. 6)}$$

$$\overline{V}_{ss} = 2\overline{V}_s \quad \text{(Eq. 7)}$$

$$\Phi_{ss}^{sat} = \Phi_s^{sat} \quad \text{(Eq. 8)}$$

Activities and molar volumes used in these calculations are given in Table V. The same molar volumes are used for calculations at 25 and 30° since, in the original equations, molar volumes are used as approximations of temperature-independent parameters. The major difference between the monomer and dimer models appears to be due to the different values calculated for the activity of the solid; while important for absolute predictions of solubilities, this effect is relatively unimportant for predictions of solubility in mixed solvents from values in pure solvents. For example, the predictions of Eqs. 1 and 2 are completely independent of the value assigned to the activity of the solid for solutes of very low solubility. The important difference between these models is in the ratio of the molar volume of the solute to that of the solvent, operating on the excess free energy of solvent mixing.

The results of calculations with monomer and dimer models in Eqs. 1 and 2 are given in Tables II and III as percentage deviations between calculated and observed values. The dimer model is definitely superior to the monomer model, and Eq. 2 is slightly more accurate than Eq. 1 for benzoic acid and $m$-toluic acid in these systems. While none of these models gives predictions within experimental uncertainty for these solutes, the accuracy of the dimer model is comparable to that of the monomer model for solutes such as iodine, naphthalene, and benzil, which are not considered to be capable of self-association. The limitation here appears to be due to the very simple solution model on which the equations are based rather than on the exact description of the chemical species in solution. The monomer model, however, is such a poor description of the real condition of carboxylic acid solutions that predictions are limited by the accuracy of the description.

**Solubility in Multicomponent Solvents**—Rigorous development of the multicomponent forms of Eqs. 1 and 2 from the original model (3) leads to equations containing the excess free energy $(\Delta\overline{G}_1^e \ldots N)$ of the multicomponent system. Since data of this type are available for very few ternary systems and fewer systems of higher order, an approximation is necessary. The following equations, based on the original model, give very good predictions for simple multicomponent systems (13):

$$(\Delta\overline{G}_1^e \ldots N) = \sum_{i=1}^{N-1} \sum_{j>i}^{N} (X_1^0 + X_j^0)(\Phi_i^0 + \Phi_j^0)(\Delta\overline{G}_{ij}^e)^* \quad \text{(Eq. 9)}$$

$$(\Delta\overline{G}_1^{fh} \ldots N) = \sum_{i=1}^{N-1} \sum_{ji}^{N} (X_i^0 + X_j^0)(\Phi_i^0 + \Phi_j^0)(\Delta\overline{G}_{ij}^{fh})^* \quad \text{(Eq. 10)}$$

with:

$$X_i^* = X_i^0/(X_i^0 + X_j^0) \quad \text{(Eq. 11)}$$

$$(\Delta\overline{G}_{ij}^{fh})^* = (\Delta\overline{G}_{ij}^e)^* + RT[\ln(X_i^*\overline{V}_i + X_j^*\overline{V}_j) - X_i^*\ln(\overline{V}_i) - X_j^*\ln(\overline{V}_j)] \quad \text{(Eq. 12)}$$

and $(\Delta\overline{G}_{ij}^e)^*$ is the excess Gibbs free energy of the binary solvent mixture at composition $X_i^*$. The solubility equations for a solid solute then become:

$$RT\ln(a_s^{solid}/X_s^{sat}) = (1 - \Phi_s^{sat})^2 \left[\sum_{i=1}^{N} \Phi_i^0(\Delta\overline{G}_s^e)_{X_i^0=1}^* - (\overline{V}_s/\overline{V}_m)(\Delta\overline{G}_1^e \ldots N)\right] \quad \text{(Eq. 13)}$$

and:

$$RT\left[\ln(a_s^{solid}/\Phi_s^{sat}) - (1 - \Phi_s^{sat})\left(1 - \frac{V_s}{\overline{V}_m}\right)\right] = (1 - \Phi_s^{sat})^2 \times \left[\sum_{i=1}^{N} \Phi_i^0(\Delta\overline{G}_s^{fh})_{X_i^0=1} - (\overline{V}_s/\overline{V}_m)(\Delta\overline{G}_1^{fh} \ldots N)\right] \quad \text{(Eq. 14)}$$

with:

$$\overline{V}_m = \sum_{i=1}^{N} X_i^0\overline{V}_i \quad \text{(Eq. 15)}$$

These equations, while unfortunately rather complex, are rigorous within the model and are easily adaptable to computerized calculations. An important feature of Eqs. 9 and 10 is the ability to use binary data in any form, independent of the form of the equation by which the binary data may be represented. As previously noted (4), the contribution of the binary or multicomponent mixing term may be negligible if the system is nearly ideal and the molar volume of the solute is small in comparison

Table V—Solvent and Solute Properties Used in Calculations

| | Temperature | $a_i^{solid}$ | $\overline{V}_i$, cm³/mole |
|---|---|---|---|
| Solute | | | |
| Benzoic acid (monomer) | 25° | 0.2275[a] | 104.38[a] |
| | 30° | 0.2468[a] | 104.38 |
| Benzoic acid (dimer) | 25° | 0.0518 | 208.76 |
| | 30° | 0.0609 | 208.76 |
| $m$-Toluic acid (monomer) | 25° | 0.2489[b] | 121.8[c] |
| $m$-Toluic acid (dimer) | 25° | 0.0620 | 243.6 |
| Solvent | | | |
| Carbon tetrachloride | — | — | 97.08 |
| Cyclohexane | — | — | 108.76 |
| $n$-Hexane | — | — | 131.57 |
| $n$-Heptane | — | — | 147.48 |
| Solvent Mixture | | | $(\Delta\overline{G}_{12}^e)^d$ |
| $c$-$C_6H_{12}$ + $CCl_4$ | | | Ref. 17 |
| $n$-$C_6H_{14}$ + $CCl_4$ | | | Ref. 18 |
| $n$-$C_7H_{16}$ + $CCl_4$ | | | Ref. 19 |
| $c$-$C_6H_{12}$ + $n$-$C_6H_{14}$ | | | Ref. 20 |
| $c$-$C_6H_{12}$ + $n$-$C_7H_{16}$ | | | Ref. 21 |

[1] The enthalpy of fusion is actually for the transition of the solid to a mixture of monomers and dimers; but for consistency in these calculations, the melt is considered to be completely monomeric for the monomer model and completely dimeric for the dimer model.

[a] Reference 22. [b] Estimated from data in Ref. 10. [c] Estimated by approximating the difference between the molar volumes of $m$-toluic acid and benzoic acid as the difference between toluene and benzene. [d] The excess Gibbs free energy was assumed to be the same at 25 and 30°.

to the solvents. Large solute molecules magnify the contribution of the unmixing term and, in the application to multicomponent solvents, also magnify the errors in the approximations of Eqs. 9 and 10. Thus, Eqs. 13 and 14 can be expected to become increasingly less accurate with increasing complexity of the solvent mixture. For the simple ternary solvents studied, the dimer model predicts solubilities of benzoic acid as accurately as in binary solvents. The results of calculations with the monomer model are not shown since they were very similar to results for binary systems and considerably less accurate than those of the dimer model.

The authors have serious doubts about the applicability of these equations to the solubility of benzoic acids in mixtures of aromatic and aliphatic solvents, partly because of the possible existence of trimers in aromatic solvents. Of more concern, however, is the possibility of specific $\pi$–$\pi$ interactions between the solvent and solute, which would violate the basic assumptions of the NIBS model.

## CONCLUSIONS

The dimer model of the nearly ideal binary solvent equation gives very good predictions for the solubility of benzoic and *m*-toluic acids in these simple solvent mixtures and should be equally applicable to solubilities of most monofunctional carboxylic acids in multicomponent systems of nonspecific solvent–solvent and solvent–solute interactions. The solubility of solid phenol in systems of this type is expected to obey similar equations based on a trimer model (14), but the solubility of gaseous phenol at high dilution (or the Henry's law constant) should be best described by a monomer model. Extraction equilibria present an interesting case in that the appropriate model may depend on the concentration range studied.

The nearly ideal binary solvent equations cannot be rigorously developed for liquid–liquid extraction in systems of practical importance because of the thermodynamic complexity of these systems, but equations developed for idealized systems may have some practical applicability. The simplest system of this type involves the distribution of a solute between two completely immiscible liquid phases, one phase consisting of a mixture of solvents and a reference phase in which the activity coefficient of the solute may be expected to remain fairly constant over the concentration range studied. For solutions sufficiently dilute to allow approximation of $(1 - \Phi_s)$ as unity, Eq. 2 becomes:

$$\ln(K_s)_m \approx \sum_{i=1}^{N} \Phi_i^0 \ln(K_s)_{X_i^0=1} + (\overline{V}_s/\overline{V}_m)(RT)^{-1}(\Delta\overline{G}_1^{fh} \ldots N) \qquad \text{(Eq. 16)}$$

with the distribution coefficient ($K_s$) based on molar (moles per liter) concentrations ($C_s$):

$$(K_s)_m = (C_s)_m/(C_s)_{\text{reference}} \qquad \text{(Eq. 17)}$$

The distribution of benzoic acid between water (reference) and mixtures of inert solvents should be best described by a dimer model ($\overline{V}$ = 209 cm$^3$/mole) at high concentrations and by a monomer model ($\overline{V}_s$ = 104 cm$^3$/mole) in very dilute solutions. Experiments are being conducted to determine whether the presence of water in the organic phase interferes with these predictions.

## REFERENCES


(1) E. L. Taylor and G. L. Bertrand, *J. Solution Chem.*, **3,** 479 (1974).

(2) T. E. Burchfield and G. L. Bertrand, *ibid.*, **4,** 205 (1975).

(3) W. E. Acree, Jr., and G. L. Bertrand, *J. Phys. Chem.*, **81,** 1170 (1977).

(4) *Ibid.*, **83,** 2385 (1979).

(5) G. Allen, J. G. Watkinson, and K. H. Webb, *Spectrochim. Acta*, **22,** 807 (1966).

(6) P. K. Glasoe, S. Hallock, M. Hove, and J. M. Duke, *ibid.*, **27A,** 2309 (1971).

(7) E. M. Woolley and N. S. Zaugg, *Anal. Calorim.*, **3,** 479 (1974).

(8) T. Krishnan, W. C. Duer, S. Goldman, and J.-L. Fortier, *Can. J. Chem.*, **57,** 530 (1979).

(9) J. H. Hildebrand, J. H. Prausnitz, and R. L. Scott, "Regular and Related Solutions," Van Nostrand Reinhold, New York, N.Y., 1970.

(10) R. C. Weast, "Handbook of Chemistry and Physics," 52nd ed., Chemical Rubber Co., Cleveland, Ohio, 1971.

(11) J. S. Fritz and N. M. Lisicki, *Anal. Chem.*, **23,** 589 (1951).

(12) G. Scatchard, S. E. Wood, and J. M. Mochel, *J. Am. Chem. Soc.*, **61,** 3206 (1936).

(13) W. E. Acree, Jr., Ph.D. dissertation, University of Missouri–Rolla, Rolla, Mo., 1981.

(14) E. M. Woolley, J. G. Travers, B. P. Erno, and L. G. Hepler, *J. Phys. Chem.*, **75,** 3591 (1971).

(15) C. K. Hancock, J. N. Pawloski, and J. P. Idoux, *J. Org. Chem.*, **31,** 3801 (1966).

(16) A. Seidell, "Solubility of Inorganic, Metalorganic, and Organic Compounds," 3rd ed., Van Nostrand, New York, N.Y., 1940.

(17) J. R. Goates, R. J. Sullivan, and J. B. Ott, *J. Phys. Chem.*, **63,** 589 (1959).

(18) D. V. S. Jain, V. K. Gupta, and B. S. Lark, *Indian J. Chem.*, **8,** 815 (1970).

(19) T. G. Bissell and A. G. Williamson, *J. Chem. Thermodyn.*, **7,** 131 (1975).

(20) I. P.-C. Li, B. C.-Y. Lu, and E. C. Chen, *J. Chem. Eng. Data*, **18,** 305 (1973).

(21) K. L. Young, R. A. Mentzer, R. A. Greenkorn, and K. C. Chao, *J. Chem. Thermodyn.*, **9,** 979 (1977).

(22) M. J. Chertoff and A. N. Martin, *J. Am. Pharm. Assoc., Sci. Ed.*, **49,** 444 (1960).


## ACKNOWLEDGMENTS


Supported by National Science Foundation Grant CHE 79-21534.

# Instantaneous Input Hypothesis in Pharmacokinetic Studies

**WIN L. CHIOU ˣ, GILBERT LAM, MEI-LING CHEN, and MYUNG G. LEE**

Received December 1, 1980, from the *Department of Pharmacy, College of Pharmacy, University of Illinois at the Medical Center, Chicago, IL 60612.* Accepted for publication February 20, 1981.

**Abstract** □ Observed venous plasma concentrations of furosemide, propranolol, griseofulvin, and theophylline at 0.33 and 0.66 min after intravenous bolus injections to unanesthetized dogs were compared with those extrapolated using the instantaneous input hypothesis. At 0.33 min, extrapolated/observed plasma level ratios as high as 20.5, 65.5, 226, and 1.17 were found for these four drugs, respectively. Venous plasma levels peaked at 1 min postinjection in all studies. Total plasma areas ($AUC_{0\to\infty}$) estimated using the instantaneous input principle were higher by as much as 6.0, 6.8, and 19.6% for propranolol, griseofulvin, and furosemide, respectively, when compared with experimental data. The effect on theophylline was negligible. These results suggest the need for cautious interpretation of some venous pharmacokinetic data. More studies in animals and humans are required to assess the magnitude of deviation from the instantaneous input hypothesis for drugs in general.

**Keyphrases** □ Pharmacokinetics—instantaneous input hypothesis, comparison with conventional extrapolation method, dogs □ Instantaneous input hypothesis—comparison with conventional extrapolation method, dogs □ Venous pharmacokinetics—instantaneous input hypothesis and conventional extrapolation method compared, dogs

In pharmacokinetic studies, venous plasma (blood or serum) level data, usually obtained 1–30 min (1–3) after a rapid intravenous bolus injection, often are employed to fit a polyexponential equation, $\sum_{i=1}^{n} A_i e^{-\lambda_i t}$. The obtained equation, also called the disposition function, then is used for pharmacokinetic analysis (1–10). This method assumes that, after injection, the drug is instantaneously distributed into an initial apparent volume of distribution or the volume of the central compartment as defined in the multicompartmental mammillary modeling analysis. The initial volume of distribution or the volume of the central compartment is calculated by dividing the dose by the extrapolated plasma concentration at time zero, $C_p^0$, which, in turn, is calculated by the summation of the polyexponential coefficients, $\sum_{i=1}^{n} A_i$. The total area under the plasma concentration–time curve from zero to infinite time, $AUC_{0\to\infty}^{ext}$, usually is obtained by:

$$AUC_{0\to\infty}^{ext} = \sum_{i=1}^{n} \frac{A_i}{\lambda_i} \qquad \text{(Eq. 1)}$$

In Eq. 1, the plasma area from time zero to the first plasma concentration point is, in essence, estimated by the extrapolation based on experimental data obtained later.

The present report compares experimentally obtained plasma concentrations and plasma areas between time zero and 1 min with those estimated by the conventional extrapolation method.

## EXPERIMENTAL

**Intravenous Bolus Studies**—Propranolol[1], furosemide[2], theophylline[3], and griseofulvin[4] were studied in mongrel male conditioned dogs, 18.7–23.7 kg. The drug in solution was injected through an indwelling catheter placed in the cephalic vein. Blood samples were withdrawn from a permanent cannula placed in the femoral vein *via* the saphenous vein. Bolus injection was completed in 10 sec for propranolol and furosemide and in 20 sec for theophylline and griseofulvin. Normal saline, 3–5 ml, was used immediately to flush the catheter to ensure complete drug delivery.

Blood samples were collected before injection and at 0.33, 0.66, 1, 2, 3, 6, 9, 15, 30, 45, 90, 120, 150, 180, 210, 240, 300, and 360 min postinjection. They were centrifuged immediately and stored frozen prior to analysis. The midpoint of injection was set as time zero. Concentrations of drugs in plasma were quantitated by the specific and sensitive high-performance liquid chromotagraphic methods developed previously in this laboratory (11–14).

Two dogs were studied for each drug; five dogs were used in the entire study. At least 3–5 days elapsed between studies for each dog. The doses and body weights of the dogs are summarized in Table I.

**Data Analysis**—Plasma data from 1 min were fitted to either a two- or three-exponential equation by using a nonlinear least-squares regression program, NONLIN (15), on a digital computer. Plasma data were weighted by the reciprocal concentration squared.

## RESULTS AND DISCUSSION

The coefficients and exponents of the polyexponential disposition function based on the NONLIN computer analysis are summarized in Table I. Goodness of fit is supported by the $r^2$ values, which were all very close to 1.000 (Table I). There is good agreement between the experimental data and the computer-generated curves (Figs. 1–4). However, the plasma concentrations found at 0.33 and 0.66 min were lower than those estimated by the extrapolation method from the polyexponential decay equations in all studies. The differences between the observed and extrapolated levels at 0.33 min are summarized in Table II. Ratios of the extrapolated to observed concentrations up to 20.5, 65.5, and 226 were found for furosemide, propranolol, and griseofulvin, respectively (Table

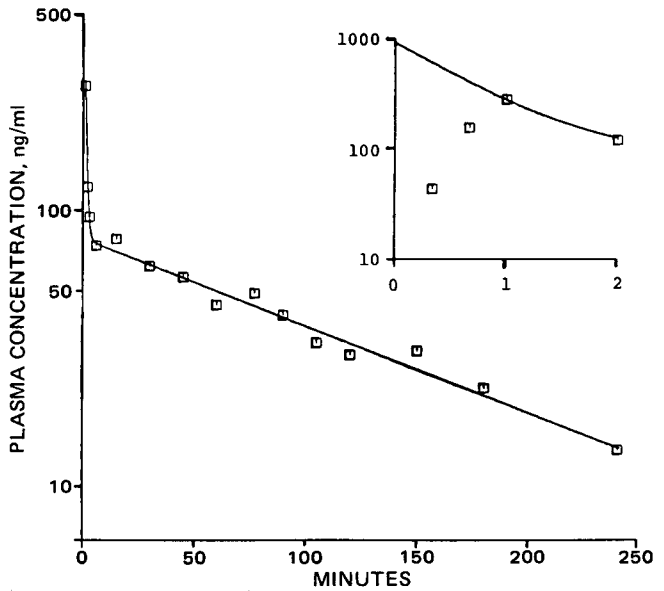


**Figure 1**—*Venous plasma concentration profile of propranolol following an intravenous bolus injection of 10 mg of propranolol hydrochloride to Dog 2. The solid line was generated by the NONLIN computer program. The insert shows the profile in the first 2 min.*

[1] Propranolol hydrochloride (10 mg/ml), Ayerst Laboratories, New York, N.Y.
[2] Lasix injection (10 mg/ml), Hoechst-Roussel Co., Somerville, N.J.
[3] Aminophylline injection (500 mg/5 ml), Elkins Sinn Co., Cherry Hill, N.J.
[4] Powder (Ayerst Laboratories, New York, N.Y.) dissolved in polyethylene glycol 400 (60 mg/1.5 ml).

0022-3549/81/0900-1037$01.00/0
© 1981, American Pharmaceutical Association

**Table I—Polyexponential Disposition Function Using Nonlinear Least-Squares Regression Analysis of Plasma Concentration Data from 1 Min**

| Drug | Dose, mg | Dog[a] | $A_1$, μg/ml | $A_2$, μg/ml | $A_3$, μg/ml | $\lambda_1$, $min^{-1}$ | $\lambda_2$, $min^{-1}$ | $\lambda_3$, $min^{-1}$ | $r^2$ |
|---|---|---|---|---|---|---|---|---|---|
| Propranolol | 8.8 | 1 | 0.842 | 0.0785 | — | 1.43 | 0.00726 | — | 0.998 |
| | 8.8 | 2 | 0.887 | 0.0922 | 0.0571 | 0.737 | 0.0321 | 0.0103 | 1.000 |
| Furosemide | 40 | 2 | 28.5 | 9.04 | 1.12 | 0.955 | 0.153 | 0.0261 | 1.000 |
| | 40 | 3 | 28.4 | 5.49 | 0.764 | 1.12 | 0.125 | 0.0230 | 1.000 |
| Theophylline | 400 | 3 | 95.6 | 21.8 | — | 0.613 | 0.0028 | — | 0.996 |
| | 400 | 4 | 7.37 | 20.3 | — | 0.319 | 0.0026 | — | 0.998 |
| Griseofulvin | 60 | 3 | 9.71 | 3.35 | 1.47 | 1.79 | 0.187 | 0.0188 | 1.000 |
| | 60 | 5 | 5.92 | 1.31 | 0.691 | 0.515 | 0.0357 | 0.0091 | 1.000 |

[a] Body weights for Dogs 1–5 were 18.7, 20.3, 19.2, 23.7, and 21.3 kg, respectively.

**Table II—Comparisons of Observed and Extrapolated Plasma Concentrations at 0.33 min and Actual and Extrapolated Total Plasma Areas after Intravenous Bolus Injection to Dogs**

| Drug | Dog | Observed Plasma Level at 0.33 min, μg/ml | Extrapolated Plasma Level at 0.33 min, μg/ml | Extrapolated/ Observed Plasma Level Ratio at 0.33 min | $AUC^{ext}_{0\to\infty}$, min μg/ml | $AUC^{act}_{0\to\infty}$, min μg/ml | Percent Overestimation in Plasma Area |
|---|---|---|---|---|---|---|---|
| Propranolol | 1 | 0.0430 | 0.600 | 14.0 | 11.41 | 11.00 | 3.75 (4.86)[a] |
| | 2 | 0.0129 | 0.842 | 65.5 | 9.62 | 9.08 | 5.97 |
| Furosemide | 2 | 3.22 | 30.5 | 9.48 | 131.9 | 113.5 | 16.2 (17.9)[a] |
| | 3 | 1.25 | 25.6 | 20.5 | 102.5 | 85.7 | 19.6 |
| Theophylline | 3 | 88.0 | 99.7 | 1.13 | 7933 | 7920 | 0.17 (0.13)[a] |
| | 4 | 22.9 | 26.9 | 1.17 | 7835 | 7829 | 0.08 |
| Griseofulvin | 3 | 0.989 | 9.96 | 10.1 | 101.5 | 95.0 | 6.81 (5.38)[a] |
| | 5 | 0.0308 | 6.97 | 226 | 124.2 | 119.4 | 4.72 |

[a] Mean of the two dog studies.

II). For theophylline, the difference at 0.33 min was relatively much smaller (13 and 17%). The inserts in Figs. 1–4 show the experimental and extrapolated plasma level profiles of the individual dog study for the first 2 min postdosing.

In dogs, the peak plasma levels occurred at 1 min after intravenous injection; but in preliminary studies using anesthetized rabbits, peak plasma (from femoral vein) levels for procainamide (16) and griseofulvin occurred at 2 min after a rapid intravenous bolus injection.

The overestimations of the initial plasma concentrations from the extrapolation of the polyexponential equation probably could be attributed to several factors, such as the lag time due to drug transport from the injection site to the sampling site (17), mixing of the drug in the blood circulation, and drug extraction by the sampling tissue through diffusion across capillary walls. The last factor was supported by the fact that drug concentrations in plasma of blood collected simultaneously from the femoral artery of the same leg were higher than those in venous plasma (16). It has been stated (17) that the zero-time plasma concentration at the normal sampling site immediately after intravenous injection theoretically should be zero. The present data (Figs. 1–4) appear to support this statement.

The areas under the plasma curve between time zero and 1 min after injection were calculated by the "extrapolated" integration method (Eq. 2) and also by the linear trapezoidal rule method using experimentally observed plasma concentrations and assuming zero drug concentration at time zero:

$$AUC^{ext}_{0\text{–}1\ min} = \sum_{i=1}^{n} \frac{A_i}{\lambda_i}(1 - e^{-\lambda_i t}) \qquad \text{(Eq. 2)}$$

where $t$ was set to be 1 min. The overestimation of the plasma area in the first 1 min ($\Delta AUC$) by the extrapolation method is assumed to be equal

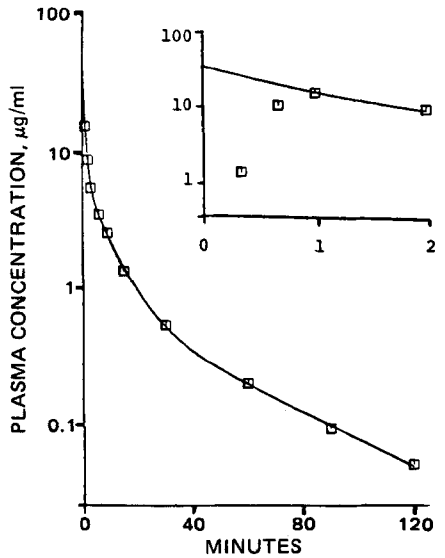


**Figure 2**—*Venous plasma concentration profile of furosemide following an intravenous bolus injection of 40 mg to Dog 3.*

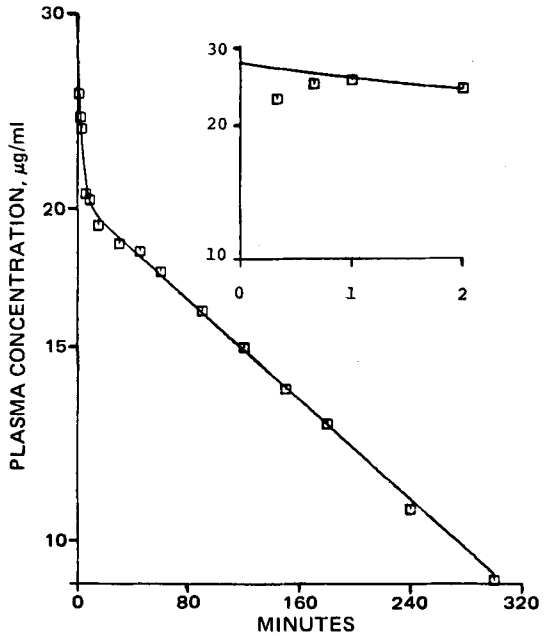


**Figure 3**—*Venous plasma concentration profile of theophylline following an intravenous bolus injection of 400 mg to Dog 4.*

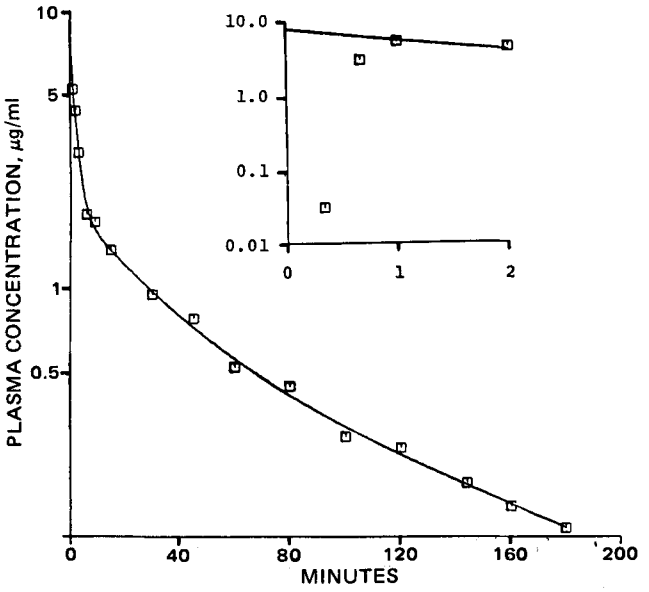


**Figure 4**—*Venous plasma concentration profile of griseofulvin following an intravenous bolus injection of 60 mg to Dog 5.*

to the difference between the areas estimated by the described two methods. The "correct" (actual) total plasma area, $AUC^{act}_{0\to\infty}$, may be calculated by:

$$AUC^{act}_{0\to\infty} = AUC^{ext}_{0\to\infty} - \Delta AUC \qquad \text{(Eq. 3)}$$

Therefore, the percentage of overestimation in plasma area for the first 1 min by the extrapolation method as compared with the actual total plasma area can be calculated by:

$$\%\ \text{overestimation} = \frac{\Delta AUC}{AUC^{act}_{0\to\infty}} \times 100 \qquad \text{(Eq. 4)}$$

The results of the analyses for the four drugs are summarized in Table II. The mean overestimations for theophylline, propranolol, griseofulvin, and furosemide were 0.13, 4.86, 5.38, and 17.9%, respectively.

The plasma concentration and area data within the 1st min after intravenous injection are different from the prediction using the conventional polyexponential disposition function or multicompartmental mammillary modeling analysis. These results appear to indicate that a very intensive early blood sampling schedule may be required to characterize accurately the plasma level profile during the early period. Although the four drugs studied have markedly different physicochemical properties (two weak acids, one weak base, and one neutral compound), more studies in animals and humans are needed to assess the general magnitude of deviation from the instantaneous input hypothesis.

These findings may have some significant implications in pharmacokinetic studies. For example, the difference between the actual and the extrapolated total plasma area for furosemide in Dog 3 was 19.6% (Table II). This value would result in a difference of 19.7% in the calculated total body clearance (467 *versus* 390 ml/min based on dose/$AUC_{0\to\infty}$). By using the extrapolated total plasma area as a reference, the absolute bioavailability from a completely bioavailable dosage form (assuming correct plasma area measurement) in this dog can be calculated as only ~80%. Furosemide in solution or tablet was reported to be incompletely absorbed (usually <73%) in humans (18–22), although the total diuretic response (relationship with plasma level or dose appears to be complicated, Ref. 22) was often the same following oral or intravenous administration of the same dose (18, 19, 21). If the phenomenon observed in the two dogs in the present study happened similarly in humans, then the absolute bioavailability of furosemide might be greater than reported. Further studies are required to prove this hypothesis.

The results of the present study support the contention (23, 24) that the constant blood withdrawal method may be useful to determine accurately the $AUC_{0\to\infty}$ after an intravenous bolus injection, especially in humans. Furthermore, the extensive blood sampling procedure can be avoided (23–25).

## REFERENCES

(1) W. L. Chiou and S. Riegelman, *J. Pharm. Sci.*, **58,** 1500 (1969).
(2) *Ibid.*, **60,** 1376 (1971).
(3) W. L. Chiou, *ibid.*, **69,** 867 (1980).
(4) L. Z. Benet, *ibid.*, **61,** 536 (1972).
(5) M. Gibaldi and D. Perrier, in "Pharmacokinetics," Dekker, New York, N.Y., 1975.
(6) J. G. Wagner, in "Fundamentals of Clinical Pharmacokinetics," Drug Intelligence Publications, Hamilton Press, Hamilton, Ill., 1976.
(7) J. G. Wagner, *J. Pharmacokinet. Biopharm.*, **4,** 443 (1976).
(8) L. Z. Benet and R. L. Galeazzi, *J. Pharm. Sci.*, **68,** 1071 (1979).
(9) W. L. Chiou, *ibid.*, **69,** 57 (1980).
(10) W. L. Chiou, *J. Pharmacokinet. Biopharm.*, **8,** 311 (1980).
(11) R. L. Nation, G. W. Peng, and W. L. Chiou, *J. Chromatogr.*, **145,** 429 (1978).
(12) *Ibid.*, **162,** 88 (1979).
(13) G. W. Peng, M. A. F. Gadalla, and W. L. Chiou, *Clin. Chem.*, **24,** 357 (1978).
(14) R. L. Nation, G. W. Peng, V. Smith, and W. L. Chiou, *J. Pharm. Sci.*, **67,** 805 (1978).
(15) C. M. Metzler, G. L. Elfring, and A. J. McEwen, in "A User's Manual for Nonlin and Associated Program," Upjohn Co., Kalamazoo, Mich., 1976.
(16) G. Lam and W. L. Chiou, in "Abstracts for Papers Presented at the APhA Academy of Pharmaceutical Sciences," San Antonio meeting, Nov. 9–13, 1980.
(17) W. L. Chiou, *J. Pharmacokinet. Biopharm.*, **7,** 527 (1979).
(18) M. R. Kelly, R. E. Cutler, A. W. Forrey, and B. M. Kimpel, *Clin. Pharmacol. Ther.*, **15,** 178 (1974).
(19) R. A. Branch, C. J. C. Roberts, M. Homeida, and D. Levine, *Br. J. Clin. Pharmacol.*, **4,** 121 (1977).
(20) W. J. Tilstone and A. Fine, *Clin. Pharmacol. Ther.*, **23,** 644 (1978).
(21) L. Z. Benet, *J. Pharmacokinet. Biopharm.*, **7,** 1 (1979).
(22) R. E. Cutler and A. D. Blair, *Clin. Pharmacokinet.*, **4,** 279 (1979).
(23) B. Vogelstein, A. A. Kowarski, and P. S. Lietman, *Clin. Pharmacol. Ther.*, **22,** 131 (1977).
(24) C. R. Kowarski and A. A. Kowarski, *J. Pharm. Sci.*, **67,** 875 (1978).
(25) *Ibid.*, **69,** 1222 (1980).

# Aminoglutethimide Bioavailability, Pharmacokinetics, and Binding to Blood Constituents

THOMAS A. THOMPSON ˣ, JEANNETTE D. VERMEULEN, WILLIAM E. WAGNER, Jr., and ANNE R. LE SHER

Received December 1, 1980, from the *Research Department, Pharmaceuticals Division, Ciba-Geigy Corporation, Ardsley, NY 10502.* Accepted for publication March 2, 1981.

**Abstract** □ The bioavailability of aminoglutethimide tablets was examined using a spectrophotometric assay. For six subjects receiving 500 mg of aminoglutethimide as an oral solution, the average peak concentration was 6.2 μg/ml with a median time of 0.8 hr. The corresponding average peak concentration for tablet administration was 5.9 μg/ml with a median time of 1.5 hr. Average values for the area under the curve (*AUC*) extrapolated to infinity were 89.0 and 96.8 μg hr/ml for the solution and tablets, respectively. The tablets had a 9% larger mean for the *AUC* than the solution and a 5% lower value for the mean maximum concentration. The bioavailability of the tablets is considered equal to that of oral solution. Data for individual concentration *versus* time curves were treated by nonlinear least-squares curve fitting. A two-compartment model with first-order absorption gave an acceptable fit for most data sets, but the individual absorption rate coefficients were not reliably determined. Values were estimated for plasma clearance, renal clearance, and volume of distribution. The distribution of aminoglutethimide between plasma and cells of human blood was examined *in vitro*; the drug concentration in cells was 1.4–1.7 times the concentration in plasma. The binding of aminoglutethimide to plasma proteins of human blood was measured by equilibrium dialysis at starting concentrations of 5 and 10 μg/ml. The binding ranged from 21.3 to 25.0% without concentration dependence.

**Keyphrases** □ Aminoglutethimide—bioavailability, pharmacokinetics, binding to blood constituents □ Bioavailability—aminoglutethimide, pharmacokinetics, binding to blood constituents □ Pharmacokinetics—aminoglutethimide, bioavailability, binding to blood constituents

Aminoglutethimide, α-(*p*-aminophenyl)-α-ethylglutarimide, is an inhibitor of adrenal corticosteroid biogenesis (1) used for the treatment of Cushing's syndrome (2). The urinary excretion of aminoglutethimide in humans was measured and accounted for 39 and 54% of 250- and 500-mg oral doses, respectively (3). Acetamidoglutethimide was reported as a metabolite in human urine (4). An assay procedure for aminoglutethimide in plasma and information about its half-life, clearance, and compliance in patients were reported previously (5). The purposes of the present study were to evaluate the bioavailability of a commercial dosage form[1], to explore the pharmacokinetics, and to measure the binding of aminoglutethimide to blood constituents.

## EXPERIMENTAL

**Clinical Study Protocols**—Eight healthy adult male volunteers, 25–54 years of age, were given a copy of the appropriate protocol and full information about the drug; they signed statements of informed consent. Each subject was screened regarding general health and history of drug hypersensitivity and underwent a physical examination, urine analysis, and a hematologic and blood chemistry analysis. The subjects ranged in height from 173 to 188 cm and in weight from 64 to 91 kg. Each subject was instructed to avoid any medication during the study and during the preceding week. The consumption of alcoholic beverages was prohibited during and for 3 days preceding the study.

Two subjects participated in a pilot study, and six others participated in a random crossover bioavailability study with a washout period of 14 days.

[1] Cytadren, 250-mg tablets, E-10447, Ciba-Geigy Corp.

Aminoglutethimide (500 mg) was administered in the morning after an overnight fast. No food or liquid other than water was permitted until 2 hr after drug administration, when a simple standard breakfast was allowed. Samples (10 ml) of venous blood were collected[2] at 0, 0.25, 0.50, 0.75, 1, 2, 3, 4, 5, 6, 12, 24, and 48 hr in the pilot study and at 0, 0.33, 0.66, 1, 1.5, 2, 2.5, 3, 6, 9, 12, 15, and 24 hr in the bioavailability study. The heparinized blood samples were centrifuged, and the plasmas were separated. Saliva production was stimulated during the bioavailability study by having the subjects chew a small piece of paraffin[3], and 2-ml saliva samples were obtained at the same time that the 0-, 1-, 2-, 3-, 6-, 9-, and 12-hr blood samples were drawn. Total urines were collected during the pilot study at intervals ending at 2, 4, 6, 12, 24, and 48 hr. Samples were frozen until analysis.

**Assay Methodology**—Plasma, urine, and saliva samples were analyzed for aminoglutethimide by the quantitative spectrophotometric method described previously, which involves extraction with chloroform and reaction with diazotized *p*-dimethylaminobenzaldehyde (5). The method was tested before use by analysis of control samples to which aminoglutethimide had been added. Frozen samples of human control plasma were thawed, pooled, and centrifuged to remove solids. Syringes[4] were used to add 0, 23, 30, 52, 57, 80, and 160 μl of a 1-μg/μl solution of aminoglutethimide in ethanol to seven 40-ml centrifuge tubes. The alcohol was evaporated, and 10.0 ml of plasma was added to each tube. Polytef-lined screw-capped tubes were rotated for 15 min. Approximately 2.5 ml of each concentration of aminoglutethimide in plasma was placed in triplicate into vials. Two blanks were added, and the vials then were number coded in random sequence. All samples were frozen as soon as prepared and stored at −10° pending analysis.

The specificity of the method was examined with respect to the metabolite acetamidoglutethimide and three other metabolites isolated from rat urine[5]. Aliquots (8, 25, and 40 μl) of a 1-μg/μl solution of each metabolite were placed in duplicate into test tubes, evaporated, redissolved in ethanol, and analyzed without extraction.

The stability of aminoglutethimide in plasma during frozen storage at −10° was examined. Aminoglutethimide was added to plasma from control volunteers to provide concentrations of 5, 10, and 15 μg/ml. Replicate aliquots of each concentration and blank were placed into separate vials. One set was analyzed immediately; the other sets were stored in a freezer pending analysis after 1, 5, 15, and 30 days.

**Binding Methodology**—For the whole blood distribution experiments, a 2.0-mg/ml stock solution of aminoglutethimide in ethanol was diluted 10-fold with 0.9% saline. The resulting 0.2-mg/ml solution was added to heparinized whole blood obtained within 2 hr from three healthy human volunteers. Concentrations of 0, 5, and 10 μg/ml were prepared and equilibrated in a shaking water bath for 30 min at 37°. Plasma was prepared by centrifugation and stored overnight in a freezer pending analysis. The concentration of drug in cells was calculated as follows:

$$\mu g/ml \text{ in cells} = \frac{\mu g/ml \text{ in blood} - \mu g/ml \text{ in plasma}}{\text{hematocrit}} + \mu g/ml \text{ in plasma} \quad \text{(Eq. 1)}$$

Binding of aminoglutethimide by plasma proteins was measured by equilibrium dialysis against pH 7.4 isotonic buffer. Aminoglutethimide in ethanol (1.0 mg/ml) was added to heparinized plasma from different individuals to produce 5- and 10-μg/ml concentrations. The dialysis buffer was prepared by mixing 8.7 ml of 5.4 g/liter $KH_2PO_4$ with 30.4 ml of 10.7 g/liter $Na_2HPO_4 \cdot 7H_2O$, adding 4.5 g of NaCl, and diluting to 500 ml. The pH was adjusted to 7.4. Dialysis membranes were prepared for

[2] Becton-Dickinson green-topped Vacutainers were used.
[3] Parafilm M, American Can Co., Greenwich, CT 06830.
[4] Hamilton.
[5] Metabolites of aminoglutethimide were obtained from Mr. Hp. Egger, Ciba-Geigy Corp., Ardsley, NY 10502.



0022-3549/81/0900-1040$01.00/0
© 1981, American Pharmaceutical Association

**Table I—Number of Subjects Having Treatment Emergent Signs and Symptoms during Aminoglutethimide Administration**

| Sign or Symptom | Ethanolic Solution | | | Tablets | | |
|---|---|---|---|---|---|---|
| | Mild | Moderate | Severe | Mild | Moderate | Severe |
| Dizziness | 1 | 4 | — | 1 | — | — |
| Light headedness | — | — | — | 2 | — | — |
| Sedation | 1 | — | — | 2 | 1 | — |
| Headache | 1 | — | — | — | — | — |

use by boiling in distilled water for 5 min and rinsing thoroughly. The membranes were stored under water in a refrigerator. Dialysis was carried out for 18 hr using 5-ml cells in a shaking water bath at 37°. Aliquots (2.0 ml) of both the dialyzed plasma and buffer were analyzed for aminoglutethimide.

**Data Evaluation**—The bioavailability of the aminoglutethimide tablets was evaluated by comparison of the area under the curve ($AUC$) extrapolated to infinity for plasma concentration curves resulting from two 250-mg tablets and from 500 mg of aminoglutethimide dissolved in a special vehicle containing 10% ethanol, 30% propylene glycol, and 10% glycerin. The $AUC$ values were obtained by application of the trapezoidal rule. Peak plasma concentrations ($C_{max}$), times of peak concentration ($T_{max}$), and half-lives ($T_{1/2}$) also were examined.

**Pharmacokinetic Analysis**—Nonlinear least-squares curve fitting was carried out using AUTOAN and NONLIN computer programs. Values for clearance and the volume of distribution were calculated as follows, where $t_1 - t_2$ is elapsed time:

$$\text{renal clearance} = \frac{\text{amount excreted } t_1 - t_2}{AUC\ t_1 - t_2} \quad \text{(Eq. 2)}$$

$$\text{plasma clearance} = \text{dose}/AUC \quad \text{(Eq. 3)}$$

$$V_c = \frac{\text{dose}}{(AUC)\,(K_{el})} \quad \text{(Eq. 4)}$$

$$V_\beta = 1.44 V_c K_{el} T_{1/2\beta} \quad \text{(Eq. 5)}$$

$$V_{ss} = V_c \frac{K_{21} + K_{12}}{K_{21}} \quad \text{(Eq. 6)}$$

## RESULTS AND DISCUSSION

**Assay Validation**—The assay procedure was tested by blind analysis of a group of 20 samples of human plasma to which known amounts of aminoglutethimide from 2.3 to 16 μg/ml had been added. Replicates and blank samples were included. The samples were analyzed in random sequence, and the concentrations were unknown to the analyst until later. The mean and standard deviation for the percent recovery in the blind validation experiment were 97.4 ± 3.8, demonstrating good accuracy and precision. Plasma calibration standards of three different concentrations were freshly prepared and analyzed on 14 occasions during several months. The mean of slopes for the standard curves and also the mean analytical response for each drug level had relative deviations of 2%, showing excellent agreement.

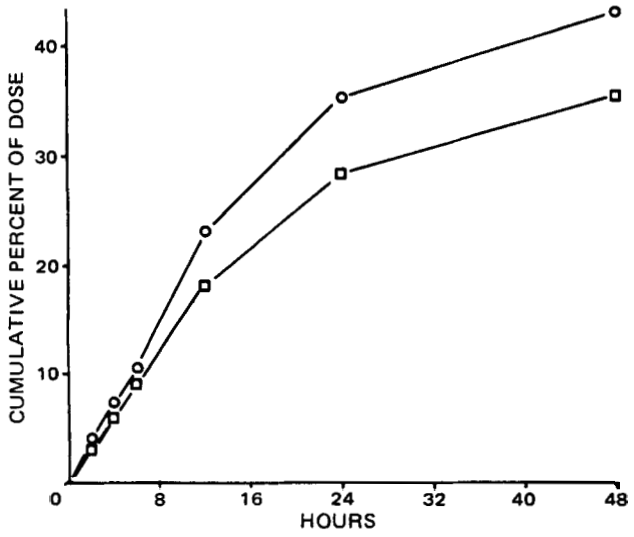


**Figure 1**—*Urinary excretion of aminoglutethimide by two subjects after two 250-mg tablets.*

**Table II—Renal Clearance of Aminoglutethimide**

| Subject | Interval, hr | $R_c$, ml/min | Mean ± $SD$ |
|---|---|---|---|
| 1 | 0–2 | 24 | 30.4 ± 5.9 |
| | 2–4 | 25 | |
| | 4–6 | 31 | |
| | 6–12 | 38 | |
| | 12–24 | 34 | |
| 2 | 0–2 | 33 | 37.6 ± 8.4 |
| | 2–4 | 28 | |
| | 4–6 | 36 | |
| | 6–12 | 50 | |
| | 12–24 | 41 | |

The stability of aminoglutethimide in plasma during frozen storage was examined. Aminoglutethimide was added to human control plasma to obtain concentrations of 5.0, 10.0, and 15.0 μg/ml. Aliquots were analyzed after 0, 1, 5, 15, and 30 days of frozen storage, and the percent recoveries ranged from 96 to 103% with no apparent trend. All samples in the bioavailability study were analyzed before 30 days of storage had elapsed.

The assay is applicable to urine and saliva as well as to plasma. Five 2.0-ml aliquots of human urine to which 2.5–15.0 μg/ml of aminoglutethimide had been added were analyzed to test the procedure. The average recovery and standard deviation were 91.4 ± 3.2%. A similar recovery experiment with saliva gave 99.4 ± 1.1%.

Acetamidoglutethimide and three metabolites of unknown structure from rat urine did not cause any response in the assay.

**Clinical Observations**—Each subject completed the study as planned. Table I shows that no severe signs or symptoms appeared, although four subjects complained of moderate dizziness after receiving aminoglutethimide in ethanolic solution. This effect probably resulted from ingestion of ethanol while fasting. In no case did the symptoms prevent the subjects from performing their usual activities.

**Cumulative Percent of Dose Excreted**—The cumulative percent of aminoglutethimide excreted unchanged in urine was measured for the two subjects who ingested two 250-mg tablets in the pilot experiment (Fig. 1). Renal excretion of unchanged drug proceeded slowly and accounted for 35.0–42.6% of the dose during 48 hr. These values are in accord with those reported previously (3). Urine was not obtained in the six-subject bioavailability experiment.

**Renal Clearance**—Renal clearance was calculated for the two subjects for whom both urine and plasma samples were obtained (Table II). The values suggest that aminoglutethimide may be processed renally by glomerular filtration with passive tubular reabsorption of some filtered drug.

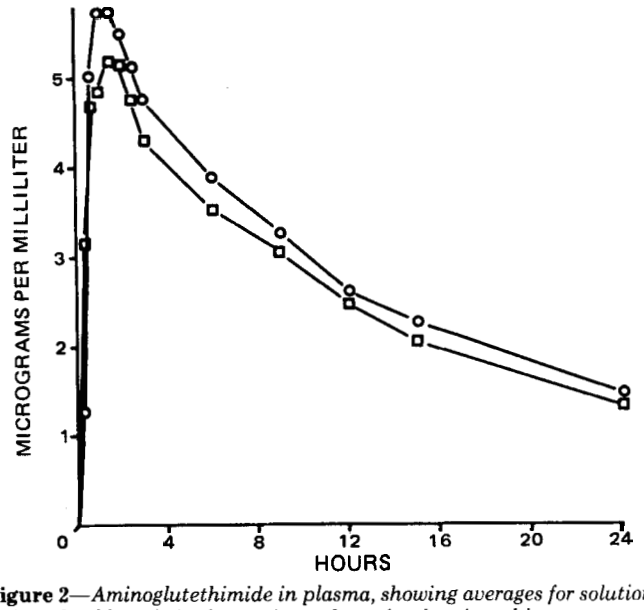


**Figure 2**—*Aminoglutethimide in plasma, showing averages for solution (□) and tablets (○) after 500-mg doses in the six-subject crossover study.*

**Table III—Concentration Maximum, Half-Life, and Area under the Curve for Aminoglutethimide in Plasma**

| Subject | 500 mg in Solution | | | | Two 250-mg Tablets | | | |
|---|---|---|---|---|---|---|---|---|
| | $C_{max}$, μg/ml | $T_{max}$, hr | $T_{1/2\beta}$, hr | $AUC_{0-\infty}$, μg hr/ml | $C_{max}$, μg/ml | $T_{max}$, hr | $T_{1/2}$, hr | $AUC_{0-\infty}$, μg hr/ml |
| 3 | 5.3 | 2.0 | 9 | 70 | 5.9 | 1.5 | 10 | 88 |
| 4 | 5.0 | 2.0 | 12 | 88 | 5.8 | 1.5 | 12 | 93 |
| 5 | 7.4 | 0.7 | 14 | 101 | 5.8 | 0.7 | 13 | 97 |
| 6 | 7.2 | 0.3 | 16 | 96 | 5.6 | 1.5 | 15 | 101 |
| 7 | 4.9 | 1.0 | 12 | 74 | 6.1 | 1.0 | 13 | 95 |
| 8 | 7.1 | 0.7 | 12 | 105 | 6.3 | 1.5 | 12 | 107 |
| Mean | 6.2 | 1.1 | 12.5 | 89 | 5.9 | 1.3 | 12.5 | 97 |
| *SD* | 1.2 | 0.7 | 2.3 | 14 | 0.2 | 0.3 | 1.6 | 7 |
| Median | — | 0.8 | — | — | — | 1.5 | — | — |

**Table IV—Pharmacokinetic Parameters from Computer Modeling of Aminoglutethimide Plasma Data**

| Dosage Form | Subject | $r^2$ | $K_A$ | $K_{21}$ | $K_{el}$ | $K_{12}$ | $C_0$ | Lag Time |
|---|---|---|---|---|---|---|---|---|
| Tablet | 3 | 1.000 | 2.800 | 1.917 | 0.1097 | 1.053 | 9.6 | 0.3 |
| | 4 | 1.000 | 2.212 | 0.334 | 0.0719 | 0.085 | 6.8 | 0.1 |
| | 5 | 0.999 | 10.750 | 1.284 | 0.0676 | 0.284 | 6.4 | 0.3 |
| | 6 | 0.999 | 2.718 | 0.477 | 0.0747 | 0.297 | 7.6 | 0.2 |
| | 7 | 0.999 | 2.841 | 0.494 | 0.0839 | 0.298 | 8.1 | 0.3 |
| | 8 | 0.999 | 4.341 | 0.097 | 0.0590 | 0.026 | 6.9 | 0.3 |
| Solution | 3 | 0.835 | 0.395 | 0.115 | 0.2496 | 0.266 | 22.6 | 0.8 |
| | 4 | 0.998 | 2.632 | 0.283 | 0.0609 | 0.009 | 5.4 | 0.2 |
| | 5 | 0.999 | 9.659 | 0.359 | 0.0797 | 0.249 | 8.3 | 0.3 |
| | 6 | 0.991 | 8.590 | 0.336 | 0.0810 | 0.173 | 6.8 | None |
| | 7 | 0.999 | 3.440 | 0.678 | 0.0816 | 0.291 | 6.2 | 0.1 |
| | 8 | 0.998 | 3.906 | 0.210 | 0.0690 | 0.064 | 7.6 | None |

**Plasma Concentration–Time Curves**—The concentration–time curves were similar for all subjects. Maximum concentrations of 4.9–7.4 μg/ml were found 0.3–2.0 hr after ingestion of 500 mg of aminoglutethimide in solution, and two 250-mg tablets resulted in peak concentrations of 5.6–6.3 μg/ml occurring 0.7–1.5 hr after ingestion (Table III). An initially rapid decline was followed by a slower decline having a half-life of 9–16 hr for the solution and 10–15 hr for the tablets.

A graph of the average plasma concentrations (Fig. 2) shows similar, but not superimposable curves. The tablets had a 9% larger average for the *AUC* than the solution (Table III). A difference in *AUC* of this magnitude has little practical significance, and the tablet formulation may be considered bioequivalent to the solution. It is common practice to assess the absorption efficiency of tablets relative to an oral solution by calculating a ratio of average *AUC* values. According to pharmacokinetic theory, the ratio of areas equals a ratio of the fraction of each dose absorbed if the plasma clearance ($C_p$) is the same (6). The tablets and solution had average $C_p$ values of 86.2 and 95.7 ml/min, respectively. Since the tablets and solution were administered at the same dose level in a random crossover pattern, the apparent differences in $C_p$ and *AUC* values probably are artifacts of the data. The $C_{max}$ value for the solution was 5% larger than for the tablets, and the average terminal half-life value was 12.5 hr for both the tablets and solution. This value for aminoglutethimide half-life agrees well with the average 13.3 hr reported for an initial dosage of six patients (6). The time of peak concentration was slightly earlier for solution, 0.8 hr *versus* 1.5 hr for tablets.

**Table V—Plasma Clearance and Volumes of Distribution for Aminoglutethimide**

| Dosage Form | Subject | $C_p$, ml/min | $V_c$, liters | $V_\beta$, liters | $V_{ss}$, liters |
|---|---|---|---|---|---|
| Tablet | 3 | 94 | 51.8 | 82.4 | 80.2 |
| | 4 | 89 | 74.8 | 92.7 | 93.8 |
| | 5 | 86 | 76.2 | 97.2 | 93.2 |
| | 6 | 82 | 66.3 | 107.7 | 107.6 |
| | 7 | 88 | 62.7 | 99.2 | 100.5 |
| | 8 | 78 | 79.2 | 80.6 | 100.6 |
| | Mean | 86.2 | 68.50 | 93.30 | 95.98 |
| | *SD* | 5.6 | 10.30 | 10.37 | 9.36 |
| Solution | 3 | 119 | 28.6 | 92.7 | 94.8 |
| | 4 | 94 | 93.3 | 98.0 | 96.3 |
| | 5 | 82 | 62.1 | 99.0 | 105.2 |
| | 6 | 86 | 64.3 | 121.1 | 97.4 |
| | 7 | 114 | 82.8 | 116.5 | 118.3 |
| | 8 | 79 | 69.0 | 82.1 | 90.0 |
| | Mean | 95.7 | 66.68 | 101.57 | 100.33 |
| | *SD* | 17.0 | 22.14 | 14.71 | 10.09 |

Nonlinear least-squares curve fitting of plasma data using AUTOAN and NONLIN computer programs with equal weighting of data gave equations of acceptable fit using a two-compartment model with first-order absorption. Values for the squared correlation coefficient were >0.99 in all but one instance (Table IV). However, the standard deviations for the individual absorption rate constants were too great for meaningful evaluation of this parameter.

Values for $C_p$ are shown in Table V. The observed average $C_p$ values of 86.2 and 95.7 ml/min indicate a moderate clearance rate. Table V also shows values for principal volume of distribution parameters. In the absence of intravenous data, the dose was assumed to be completely absorbed. The values for clearance and volumes of distribution are overestimated if this assumption is incorrect.

**Binding to Blood Cells and Plasma Proteins**—The distribution of aminoglutethimide between plasma and cells of human blood was calculated after *in vitro* equilibration of drug with heparinized blood and analysis of the drug in plasma. The concentration of aminoglutethimide in cells was 1.4–1.7 times the concentration in plasma. The binding of aminoglutethimide *in vitro* to plasma proteins of three subjects was measured by equilibrium dialysis at 37°. Initial drug concentrations of 5 and 10 μg/ml showed binding of 21.3–25.0%. No concentration-dependent trend was apparent.

**Saliva Concentrations**—Saliva samples were obtained to determine whether saliva assay is an acceptable alternative to plasma assay. Saliva production was stimulated by chewing a small piece of paraffin. Paraffin was reported to absorb significant amounts of propranolol and indomethacin (7), and a preliminary test for glutethimide absorption was carried out as described previously (7). Little or no absorption was found. However, the concentrations of aminoglutethimide found in saliva of the bioavailability subjects were too low for the analytical method. Measurable concentrations were found in only a few samples, and no correlation with plasma concentrations was apparent.

## REFERENCES


(1) R. N. Dexter, L. M. Fishman, R. L. Ney, and G. W. Liddle, *J. Clin. Endocrinol. Metab.*, **27**, 473 (1967).

(2) R. I. Misbin, J. Canary, and D. Willard, *J. Clin. Pharmacol.*, **16**, 645 (1976).

(3) J. S. Douglas and P. J. Nicholls. *J. Pharm. Pharmacol., Suppl.*,

115S, 17, (1965).
(4) J. S. Douglas and P. J. Nicholls, *ibid.*, *Suppl.*, 150P, **24**, (1972).
(5) F. T. Murray, S. Santner, E. Samojlik, and R. J. Santen, *J. Clin. Pharmacol.*, **19**, 704 (1979).
(6) J. G. Wagner, in "Fundamentals of Clinical Pharmacokinetics," Drug Intelligence Publications, Hamilton, Ill., 1975, p. 347.
(7) E. A. Taylor, T. L. Kaspi, and P. Turner, *J. Pharm. Pharmacol.*, **30**, 813 (1978).

# High-Performance Liquid Chromatographic Assay for Nanogram Determination of Chlorpromazine and Its Comparison with a Radioimmunoassay

**K. K. MIDHA *x, J. K. COOPER *, I. J. McGILVERAY ‡, A. G. BUTTERFIELD ‡, and J. W. HUBBARD §**

Received June 6, 1980, from the **College of Pharmacy, University of Saskatchewan, Saskatoon, Saskatchewan S7N 0W0, Canada*, the *‡Drug Research Laboratories, Health Protection Branch, Health and Welfare Canada, Ottawa, Ontario K1A 0L2, Canada*, and the *§Faculty of Pharmacy, University of Manitoba, Winnipeg, Manitoba R3T 2N2, Canada.* Accepted for publication February 17, 1981.

**Abstract** □ A specific and sensitive high-performance liquid chromatographic (HPLC) method for the quantitative determination of plasma chlorpromazine concentrations is described. The procedure is capable of determining 1 ng of chlorpromazine/ml and is adequate for following plasma concentration–time profiles after 7-mg single intravenous doses. After a simple organic extraction of the drug and an internal standard (mesoridazine) from plasma, the organic layer was transferred to a vial and evaporated to dryness at 55° under nitrogen. The residue was dissolved in 200 μl of HPLC grade acetonitrile. Aliquots (70–100 μl) were chromatographed, and the drug was quantitated in the range of 1–15 ng/ml of plasma using a fixed-wavelength UV detector. Plasma concentrations determined by the method were compared with those obtained by a previously reported radioimmunoassay specific for chlorpromazine and *N*-desmethylchlorpromazine. The two methods agreed favorably with a correlation coefficient of 0.993 and a slope of 0.994.

**Keyphrases** □ Chlorpromazine—high-performance liquid chromatographic analysis in plasma and comparison with a radioimmunoassay □ Psychotropic agents—chlorpromazine, high-performance liquid chromatographic analysis □ Antipsychotic phenothiazines—chlorpromazine, high-performance liquid chromatographic analysis and radioimmunoassay comparison

Chlorpromazine is widely used in the treatment of certain psychiatric disorders (1). It undergoes extensive metabolism, and several of its metabolites (2) are considered to be psychoactive. Some of the metabolites can be quantitated in plasma; in some studies, the ratio of plasma concentrations of active to inactive metabolites was correlated with clinical improvement in schizophrenic patients (3–5).

The various chemical methods of quantitation that have been used include GLC with electron-capture detection (6), GLC with mass spectrometric detection (7, 8), fluorescent labeling with dansyl chloride (9), labeled derivative formation (10), and TLC of a quaternary ammonium derivative formed by reaction with 9-bromomethylacridine, followed by UV photolysis and spectrofluorometric determination (11). These methods may have adequate sensitivity to determine plasma concentrations following therapeutic dosage regimens, but they are generally cumbersome and not easily amenable to routine clinical monitoring.

The radioimmunoassay procedures are generally simple, sensitive, and readily applicable to routine analysis. Although sensitive, radioimmunoassays generally are suspect from the aspect of specificity. In the case of chlorpromazine radioimmunoassay (12–14), this specificity concern is augmented by the extremely large number of identified metabolites. To verify the specificity of the radioimmunoassay procedure reported previously (14), which was based on proper designing of the antibody (15), high-performance liquid chromatographic (HPLC) assay, specific and sensitive to 1 ng/ml of plasma, was developed. This HPLC assay is described and compared with the radioimmunoassay reported earlier (14).

## EXPERIMENTAL

**Materials**—Chlorpromazine hydrochloride[1], prochlorperazine[1], mesoridazine besylate[2], 2-chlorophenothiazine[3], chlorpromazine sulfoxide[4], 7-hydroxychlorpromazine sulfoxide[4], *N*-monodesmethylchlorpromazine[4], *N*-monodesmethylchlorpromazine sulfoxide[4], *N*-didesmethylchlorpromazine[4], *N*-didesmethylchlorpromazine sulfoxide[4], and chlorpromazine *N*-oxide[4] were used. All solvents were HPLC grade[5], and all other chemicals were commercial analytical reagent grade.

**Apparatus**—A liquid chromatographic pump[6] and a valve-loop injector[7] fitted with a 1000-μl loop were connected to a fixed-wavelength detector[8] operated at 254 nm. The detector was attenuated to 0.005 aufs for chlorpromazine and to 0.5 aufs for the internal standard.

**Column**—A 250 × 3.2-mm i.d. column, packed with 5-μm cyano-bonded column packing[9], was used at ambient temperature with a mobile phase flow rate of 1.6 ml/min.

**Mobile Phase**—The mobile phase consisted of 10% aqueous 0.015 *M* sodium acetate–acetic acid buffer (pH 6.5) and 90% acetonitrile. It was degassed by refluxing for 5 min and transferred to the solvent reservoir.

**Internal Standard**—A stock solution of mesoridazine besylate (1000 μg/ml, calculated as free base) was prepared in double-distilled water, stored in the absence of UV light at 4°, and used throughout the experiments. Dilutions of 50 μg/ml were prepared weekly and used for analysis.

**Preparation of Standard Curves**—An aqueous solution of chlorpromazine hydrochloride (100 μg/ml, calculated as free base) was prepared weekly in double-distilled deionized water and stored in the ab-

[1] Poulenc Ltd., Montreal, Quebec, Canada.
[2] Sandoz Pharmaceuticals, Dorval, Quebec, Canada.
[3] Aldrich Chemical Co., Montreal, Quebec, Canada.
[4] Donated by Dr. A. A. Manian, National Institute of Mental Health, Rockville, Md.
[5] Fisher Scientific Co., Montreal, Quebec, Canada.
[6] Model 110A, Altex, Beckman Instruments, Toronto, Ontario, Canada.
[7] Model 7120, Rheodyne, Technical Marketing Associates, Ottawa, Ontario, Canada.
[8] Model 440, Waters Associates, Mississauga, Ontario, Canada.
[9] Spherisorb CN, Altex, Beckman Instruments, Toronto, Ontario, Canada.

0022-3549/81/0900-1043$01.00/0
© 1981, American Pharmaceutical Association

115S, 17, (1965).
(4) J. S. Douglas and P. J. Nicholls, *ibid.*, *Suppl.*, 150P, **24**, (1972).
(5) F. T. Murray, S. Santner, E. Samojlik, and R. J. Santen, *J. Clin. Pharmacol.*, **19**, 704 (1979).
(6) J. G. Wagner, in "Fundamentals of Clinical Pharmacokinetics," Drug Intelligence Publications, Hamilton, Ill., 1975, p. 347.
(7) E. A. Taylor, T. L. Kaspi, and P. Turner, *J. Pharm. Pharmacol.*, **30**, 813 (1978).

# High-Performance Liquid Chromatographic Assay for Nanogram Determination of Chlorpromazine and Its Comparison with a Radioimmunoassay

**K. K. MIDHA *x, J. K. COOPER *, I. J. McGILVERAY ‡, A. G. BUTTERFIELD ‡, and J. W. HUBBARD §**

Received June 6, 1980, from the **College of Pharmacy, University of Saskatchewan, Saskatoon, Saskatchewan S7N 0W0, Canada*, the *‡Drug Research Laboratories, Health Protection Branch, Health and Welfare Canada, Ottawa, Ontario K1A 0L2, Canada*, and the *§Faculty of Pharmacy, University of Manitoba, Winnipeg, Manitoba R3T 2N2, Canada.* Accepted for publication February 17, 1981.

**Abstract** □ A specific and sensitive high-performance liquid chromatographic (HPLC) method for the quantitative determination of plasma chlorpromazine concentrations is described. The procedure is capable of determining 1 ng of chlorpromazine/ml and is adequate for following plasma concentration–time profiles after 7-mg single intravenous doses. After a simple organic extraction of the drug and an internal standard (mesoridazine) from plasma, the organic layer was transferred to a vial and evaporated to dryness at 55° under nitrogen. The residue was dissolved in 200 μl of HPLC grade acetonitrile. Aliquots (70–100 μl) were chromatographed, and the drug was quantitated in the range of 1–15 ng/ml of plasma using a fixed-wavelength UV detector. Plasma concentrations determined by the method were compared with those obtained by a previously reported radioimmunoassay specific for chlorpromazine and *N*-desmethylchlorpromazine. The two methods agreed favorably with a correlation coefficient of 0.993 and a slope of 0.994.

**Keyphrases** □ Chlorpromazine—high-performance liquid chromatographic analysis in plasma and comparison with a radioimmunoassay □ Psychotropic agents—chlorpromazine, high-performance liquid chromatographic analysis □ Antipsychotic phenothiazines—chlorpromazine, high-performance liquid chromatographic analysis and radioimmunoassay comparison

Chlorpromazine is widely used in the treatment of certain psychiatric disorders (1). It undergoes extensive metabolism, and several of its metabolites (2) are considered to be psychoactive. Some of the metabolites can be quantitated in plasma; in some studies, the ratio of plasma concentrations of active to inactive metabolites was correlated with clinical improvement in schizophrenic patients (3–5).

The various chemical methods of quantitation that have been used include GLC with electron-capture detection (6), GLC with mass spectrometric detection (7, 8), fluorescent labeling with dansyl chloride (9), labeled derivative formation (10), and TLC of a quaternary ammonium derivative formed by reaction with 9-bromomethylacridine, followed by UV photolysis and spectrofluorometric determination (11). These methods may have adequate sensitivity to determine plasma concentrations following therapeutic dosage regimens, but they are generally cumbersome and not easily amenable to routine clinical monitoring.

The radioimmunoassay procedures are generally simple, sensitive, and readily applicable to routine analysis. Although sensitive, radioimmunoassays generally are suspect from the aspect of specificity. In the case of chlorpromazine radioimmunoassay (12–14), this specificity concern is augmented by the extremely large number of identified metabolites. To verify the specificity of the radioimmunoassay procedure reported previously (14), which was based on proper designing of the antibody (15), high-performance liquid chromatographic (HPLC) assay, specific and sensitive to 1 ng/ml of plasma, was developed. This HPLC assay is described and compared with the radioimmunoassay reported earlier (14).

## EXPERIMENTAL

**Materials**—Chlorpromazine hydrochloride[1], prochlorperazine[1], mesoridazine besylate[2], 2-chlorophenothiazine[3], chlorpromazine sulfoxide[4], 7-hydroxychlorpromazine sulfoxide[4], *N*-monodesmethylchlorpromazine[4], *N*-monodesmethylchlorpromazine sulfoxide[4], *N*-didesmethylchlorpromazine[4], *N*-didesmethylchlorpromazine sulfoxide[4], and chlorpromazine *N*-oxide[4] were used. All solvents were HPLC grade[5], and all other chemicals were commercial analytical reagent grade.

**Apparatus**—A liquid chromatographic pump[6] and a valve-loop injector[7] fitted with a 1000-μl loop were connected to a fixed-wavelength detector[8] operated at 254 nm. The detector was attenuated to 0.005 aufs for chlorpromazine and to 0.5 aufs for the internal standard.

**Column**—A 250 × 3.2-mm i.d. column, packed with 5-μm cyano-bonded column packing[9], was used at ambient temperature with a mobile phase flow rate of 1.6 ml/min.

**Mobile Phase**—The mobile phase consisted of 10% aqueous 0.015 *M* sodium acetate–acetic acid buffer (pH 6.5) and 90% acetonitrile. It was degassed by refluxing for 5 min and transferred to the solvent reservoir.

**Internal Standard**—A stock solution of mesoridazine besylate (1000 μg/ml, calculated as free base) was prepared in double-distilled water, stored in the absence of UV light at 4°, and used throughout the experiments. Dilutions of 50 μg/ml were prepared weekly and used for analysis.

**Preparation of Standard Curves**—An aqueous solution of chlorpromazine hydrochloride (100 μg/ml, calculated as free base) was prepared weekly in double-distilled deionized water and stored in the ab-

[1] Poulenc Ltd., Montreal, Quebec, Canada.
[2] Sandoz Pharmaceuticals, Dorval, Quebec, Canada.
[3] Aldrich Chemical Co., Montreal, Quebec, Canada.
[4] Donated by Dr. A. A. Manian, National Institute of Mental Health, Rockville, Md.
[5] Fisher Scientific Co., Montreal, Quebec, Canada.
[6] Model 110A, Altex, Beckman Instruments, Toronto, Ontario, Canada.
[7] Model 7120, Rheodyne, Technical Marketing Associates, Ottawa, Ontario, Canada.
[8] Model 440, Waters Associates, Mississauga, Ontario, Canada.
[9] Spherisorb CN, Altex, Beckman Instruments, Toronto, Ontario, Canada.

0022-3549/81/0900-1043$01.00/0
© 1981, American Pharmaceutical Association

**Table I—HPLC Retention Times of Chlorpromazine and Its Metabolites**

| Compound | Retention Time, min |
|---|---|
| Chlorpromazine | 1.90 |
| Chlorpromazine sulfoxide | 6.50 |
| 7-Hydroxychlorpromazine | 2.70 |
| 7-Hydroxychlorpromazine sulfoxide | 9.14 |
| *N*-Monodesmethylchlorpromazine | 5.86 |
| *N*-Monodesmethylchlorpromazine sulfoxide | 19.16 |
| *N*-Didesmethylchlorpromazine | 3.48 |
| *N*-Didesmethylchlorpromazine sulfoxide | 9.64 |
| Chlorpromazine *N*-oxide | 6.10 |

**Table II—HPLC Estimation of Chlorpromazine Added to Plasma [a]**

| Added, ng | *n* | Mean Peak Height Ratio × $10^2$ | *SD* | *RSD* [b] |
|---|---|---|---|---|
| 1.0 | 10 | 0.101 | 0.004 | 3.96 |
| 2.5 | 5 | 0.250 | 0.009 | 3.60 |
| 5.0 | 5 | 0.498 | 0.021 | 4.21 |
| 7.5 | 5 | 0.758 | 0.012 | 1.58 |
| 10.0 | 10 | 0.995 | 0.028 | 2.81 |
| 15.0 | 5 | 1.418 | 0.026 | 1.84 |

[a] $y = mx$, where $m = 0.0975 \pm 0.0011$; $r^2 = 0.999$. [b] Mean = 3.00.

sence of UV light at 4°. Appropriate final dilutions of 1.0, 2.5, 5.0, 7.5, 10.0, and 15.0 ng/ml were made directly in plasma just prior to analysis.

**Extraction of Samples**—Plasma samples were extracted using a modification of a method previously used for GLC–mass spectrometric analysis (8).

To a 15-ml centrifuge tube[10] were added 2 ml of plasma, 1 ml of aqueous internal standard (50 μg of mesoridazine), and 0.1 ml of 1 *N* HCl. The sample was mixed[11] for 30 sec, and 4 ml of HPLC grade isopropanol then was added. The sample was mixed[12] for an additional 5 min and then centrifuged[13] at 5000 rpm for 20 min at 0°. The supernate was poured into another tube[10], and the pH was adjusted to 12.5 with 200 μl of 5 *N* NaOH. After mixing[12] for 10 sec, 4 ml of HPLC grade *n*-heptane was added. The sample was mixed[12] for an additional 10 min and centrifuged[14] at 2500 rpm at room temperature.

The upper organic layer then was transferred by pasteur pipet to a 5-ml conical vial[15]. The sample was evaporated[16] to dryness under nitrogen and then cooled to room temperature. Then 200 μl of acetonitrile was added, and the sample was mixed[12] for 2 min. The clear yellow solution was transferred by pasteur pipet to a 1-ml screw-capped disposable vial. For analysis, 75–100 μl was injected into the chromatograph.

**Plasma Level Study**—Two normal healthy volunteers, 64 and 87 kg, participated in a clinically supervised study. The antecubital veins on both arms of each subject were catheterized by means of infusion sets[17]. The intravenous solutions were prepared by diluting a commercial injectable preparation[18] with 50 ml of normal saline solution. The solutions were infused over a 2-min period *via* the left catheter. The 64-kg subject received 10 mg, and the other subject received 7 mg of chlorpromazine as the hydrochloride. Blood samples were collected in heparinized tubes[19] without touching the rubber stoppers. After centrifugation, the plasma was removed and stored at 4° until just prior to analysis.

**Recovery Study**—For the determination of chlorpromazine recovery, blank plasma was spiked with 2.5 and 5.0 ng of chlorpromazine/ml as the hydrochloride salt and the samples were analyzed as already described.

The absolute peak heights obtained from the standards were compared with those of fresh standards of chlorpromazine free base in acetonitrile.

**Quantitation**—Spiked plasma extracts were chromatographed, and standard curves were constructed by plotting the ratios of chlorpromazine to internal standard peak heights *versus* the concentration of the drug (nanograms per milliliter of plasma). Calibration standards were chromatographed each day when the unknown samples were analyzed. The concentrations of the unknown samples were determined by comparison of the peak height ratios to the standard curve obtained that day.

## RESULTS AND DISCUSSION

Under the described conditions, chlorpromazine and the internal standard (mesoridazine) gave sharp and symmetrical peaks that eluted in 8 min (Fig. 1B). No interference from endogenous plasma constituents was observed, as can be seen from the chromatogram obtained when the method was applied to blank plasma (Fig. 1A). Figure 1B shows a chromatogram of a spiked plasma sample containing 2.5 ng of chlorpromazine/ml and 50 μg of mesoridazine. Figure 1C shows a chromatogram of a 5-hr postdose plasma sample (2 ml) from the volunteer who received 7 mg of chlorpromazine intravenously, the chlorpromazine concentration being estimated as 6.5 ng/ml. The specificity of the method was established further by chromatographing all available metabolites under the assay conditions. Several of these metabolites are considered to be major metabolic components in humans. All of the metabolites tested eluted at retention times different from those of chlorpromazine and mesoridazine (Table I).

Mass spectral analyses of collected peaks from chromatographed plasma extracts of bulk plasma samples from dosed volunteers and spiked blank plasma were identical, suggesting that there was no interference from chlorpromazine metabolites that were not tested.

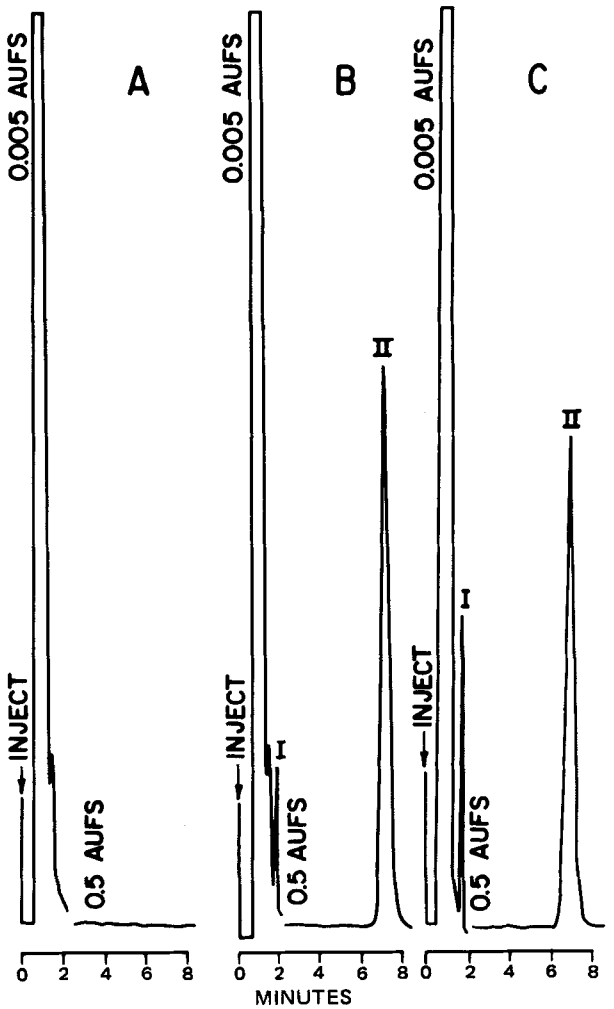


**Figure 1**—*Chromatograms of an extract of 2 ml of plasma. Key: A, blank; B, spiked with chlorpromazine (2.5 ng/ml) and the internal standard mesoridazine (25 μg/ml); and C, sample from a volunteer 5 hr postdose (7 mg iv) estimated to contain 6.5 ng of chlorpromazine/ml. Peak I is chlorpromazine, and peak II is mesoridazine.*

[10] Corex, Fisher Scientific Co., Montreal, Quebec, Canada.
[11] Vortex Genie, Fisher Scientific Co., Montreal, Quebec, Canada.
[12] Evapomix, Fisher Scientific Co., Montreal, Quebec, Canada.
[13] Sorval RC2-B refrigerated centrifuge, Ivan Sorvall Inc., Newton, CT 06470.
[14] IEC model HNS, Fisher Scientific Co., Montreal, Quebec, Canada.
[15] Reacti-vial, Chromatographic Specialties, Brockville, Ontario, Canada.
[16] Thermolyne Dri-Bath, Fisher Scientific Co., Montreal, Quebec, Canada.
[17] Butterfly, Abbott Laboratories Ltd., Montreal, Quebec, Canada.
[18] Largactil, Poulenc Ltd., Montreal, Quebec, Canada.
[19] Vacutainers, Becton Dickinson and Co., Mississauga, Ontario, Canada.

**Table III—Recovery of Chlorpromazine from Plasma**

| Nanograms Added to 1 ml of Plasma | $n$ | Mean Nanograms Recovered | Percent Recovery, mean ± $SD$ |
|---|---|---|---|
| 5.00 | 8 | 1.73 | 34.59 ± 0.57 |
| 2.5 | 6 | 0.86 | 34.31 ± 0.76 |

During the development of this assay, one major problem was the loss of chlorpromazine during plasma precipitation, drug extraction, or solvent evaporation. This problem was reported previously (16–18), and a simple method requiring minimum sample manipulation was sought to overcome it. Precipitation of plasma proteins was the process chosen because it would improve recovery of chlorpromazine by facilitating its release from high affinity bound plasma protein sites (19). Of the various reagents tried for plasma protein precipitation, trichloroacetic acid and acetonitrile resulted in complete occlusion of chlorpromazine. Precipitation with methanol was abandoned since evaporation was required before chlorpromazine could be extracted into nonpolar organic solvents. The use of isopropanol not only precipitated plasma proteins without occlusion of the drug but also reduced its loss due to adsorption and/or absorption onto the surfaces of the glass tubes used. Furthermore, the miscibility of isopropanol with a nonpolar solvent like heptane avoided the evaporation step completely. Mixtures of isopropanol and heptane were successfully used for extracting chlorpromazine and its metabolites from plasma (8).

The problem of the loss of chlorpromazine at the lower nanogram levels (≤10 ng) still existed and was visibly evident from the negative intercepts of the standard curves compiled using 50 ng of prochlorperazine/ml as the internal standard. To avoid the loss of chlorpromazine due to adsorption and/or absorption onto glass surfaces, the concentration of the internal standard was raised to 600 ng/ml in the hope that it would saturate the adsorption and/or absorption sites. This amount did not rectify the problem completely since the standard curves still showed some negative intercepts. A further increase in the prochlorperazine concentration resulted in a peak that interfered with that of chlorpromazine. This peak was thought to be due to a small impurity present in the prochlorperazine used.

A solution of 10 μg of 2-chlorophenothiazine used as an antioxidant (11) along with 50 ng of prochlorperazine was tried to solve the described problem. However, on chromatographic analysis, the peak due to 2-chlorophenothiazine tailed into that of chlorpromazine. Ultimately, the use of mesoridazine as an internal standard at a concentration of 50 μg appeared to prevent adsorption and/or absorption as indicated by the lack of negative intercept observed with other internal standards tried. It also provided an acceptable retention time with no interference from plasma constitutents.

Table II shows a composite standard curve for the quantitation of chlorpromazine from plasma. The curve is linear with a negligible intercept over the concentration range of 1–15 ng/ml. The ratio of chlorpromazine to mesoridazine plotted against chlorpromazine concentration gave a straight line passing through the origin ($r^2$ = 0.999). A mean slope

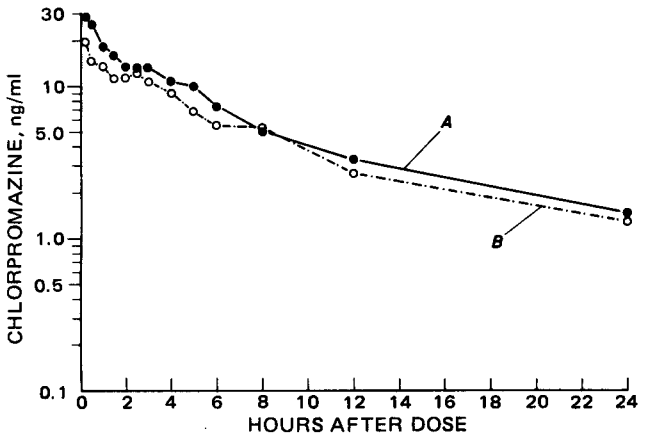


**Figure 2**—*Chlorpromazine concentrations in the plasma of two normal healthy volunteers. Key: A, volunteer (64 kg) who received 10 mg of an injectable chlorpromazine; and B, volunteer (87 kg) who received 7 mg of the same preparation.*

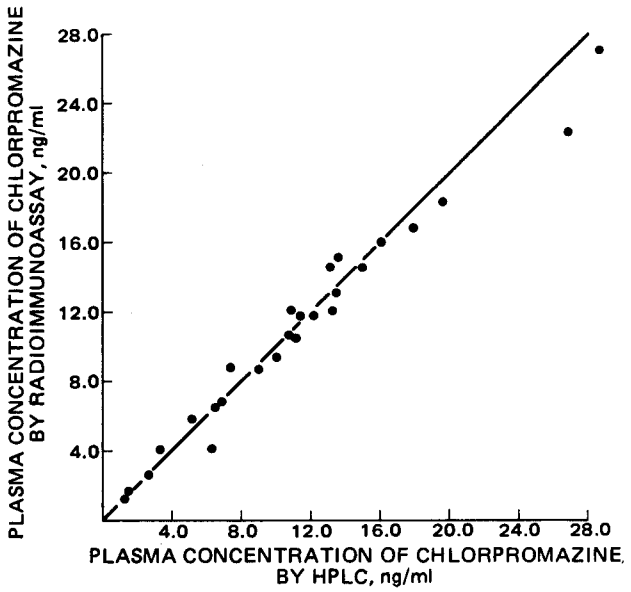


**Figure 3**—*Plot of plasma chlorpromazine concentration in humans by radioimmunoassay (14)* versus *plasma concentration of chlorpromazine measured by the described HPLC method;* n = *26,* $r^2$ = *0.993, and slope = 0.994.*

value of 0.0975 ± 0.0011 was obtained. This linearity of the curve was observed to 30 ng/ml, the highest concentration tested. For plasma samples containing concentrations of >30 ng/ml, aliquots smaller than 2 ml should be extracted.

The sensitivity of the described assay 1 ng/ml of plasma was adequate for following plasma concentration–time profiles of subjects receiving low single intravenous doses of the drug (7–10 mg). However, it was not adequate for following plasma profiles in volunteers who were orally administered single low doses (up to 25 mg) of the drug.

The overall recovery of chlorpromazine is given in Table III. Results were from at least six determinations at the 2.5- and 5.0-ng/ml plasma levels. A mean percent recovery of 34.45 ± 0.67 was obtained. Although the recoveries of chlorpromazine in the present assay are low, they are reproducible. Attempts to improve the recovery of the drug led to either added complexities or irreproducibility.

Application of the described HPLC procedure to plasma concentration determinations in subjects who received single intravenous doses of chlorpromazine[17] (7 or 10 mg) is shown in Fig. 2. As can be seen, the method is of sufficient sensitivity to analyze specimens obtained as late as 24 hr after this low single intravenous dose.

The described HPLC procedure was compared to the earlier radioimmunoassay procedure in which the antibody used cross-reacted only with chlorpromazine and *N*-desmethylchlorpromazine (14). There was excellent agreement between the values obtained by the two methods (Fig. 3). The correlation coefficient ($r^2$) of 0.993 and the slope value of 0.994 were obtained for 26 samples from the two volunteers, analyzed by the two methods. This excellent correlation suggests that *N*-desmethylchlorpromazine is not a major metabolite following single low intravenous doses.

The described HPLC procedure is precise, accurate, and specific for the drug. Furthermore, it is of sufficient sensitivity to determine plasma levels following single intravenous doses (7 or 10 mg) of the drug and should be suitable for single- or multiple-dose pharmacokinetic or bioavailability studies. It compared favorably with a correlation coefficient of 0.99 with the radioimmunoassay procedure reported earlier, thereby suggesting that both procedures are suitable for therapeutic monitoring of patients undergoing treatment with chlorpromazine. However, it may not have the sensitivity for following plasma profiles in volunteers who are orally administered single doses of up to 25 mg of the drug.

## REFERENCES

(1) C. Swett, *J. Clin. Psychiatry*, **40,** 464 (1979).

(2) I. S. Forrest, D. E. Green, M. T. Serra, F. C. Chao, and K. O. Loeffler, *Commun. Psychopharmacol.*, **2,** 131 (1978).

(3) G. Sakalis, T. L. Chan, G. Sathananthan, N. Schooler, S. Goldberg, and S. Gershon, *ibid.*, **1,** 156 (1977).

(4) O. T. Phillipson, J. M. McKeown, J. Baker, and A. F. Healey, *Br. J. Psychiatry*, **131**, 172 (1977).
(5) A. V. P. Mackay, A. F. Healey, and J. Baker, *Br. J. Clin. Pharmacol.*, **1**, 425 (1974).
(6) S. H. Curry, *Psychopharmacol. Commun.*, **2**, 1 (1976).
(7) C. G. Hammar, B. Holmstedt, and R. Ryhage, *Anal. Biochem.*, **25**, 532 (1968).
(8) G. Alfredsson, B. Wode-Helgodt, and G. Sedvall, *Psychopharmacology*, **48**, 123 (1976).
(9) I. S. Forrest, S. D. Rose, L. G. Brookes, B. Halpern, V. A. Bacon, and L. A. Silberg, *Aggressologie*, **12**, 127 (1970).
(10) D. H. Efron, S. R. Harris, A. A. Manian, and L. E. Gaudette, *Psychopharmacologia*, **19**, 207 (1971).
(11) P. N. Kaul, L. R. Whitfield, and M. L. Clark, *J. Pharm. Sci.*, **65**, 689 (1976).
(12) M. Shostak, in "The Phenothiazines and Structurally Related Drugs," I. S. Forrest, C. J. Carr, and E. Usdin, Eds., Raven, New York, N.Y., 1974.
(13) K. Kawashima, R. Dixon, and S. Spector, *Eur. J. Pharmacol.*, **32**, 195 (1975).
(14) K. K. Midha, J. C. K. Loo, J. W. Hubbard, M. L. Rowe, and I. J. McGilveray, *Clin. Chem.*, **25**, 166 (1979).
(15) J. W. Hubbard, K. K. Midha, I. J. McGilveray, and J. K. Cooper, *J. Pharm. Sci.*, **67**, 1563 (1978).
(16) I. S. Forrest, P. E. Green, M. J. Serra, and K. O. Loeffler, *Proc. West. Pharmacol. Soc.*, **19**, 125 (1976).
(17) P. N. Kaul, M. W. Conway, and M. L. Clark, in "The Phenothiazines and Structurally Related Drugs," I. S. Forrest, C. J. Carr, and E. Usdin, Eds., Raven, New York, N.Y., 1974, p. 391.
(18) P. Turano, W. J. Turner, and D. Donato, in *ibid.*, Raven, New York, N.Y., 1974, p. 315.
(19) P. R. A. May and T. Van Putten, *Arch. Gen. Psychiatry*, **35**, 1081 (1978).

### ACKNOWLEDGMENTS

Presented in part at the American Society of Pharmacology and Experimental Therapeutics meeting, Portland, Oreg., August 1979.

# Analysis of Pilocarpine and Isopilocarpine in Ophthalmic Solutions by UV Spectrophotometry–Polarimetry

**BRITT S. SCOTT ˣ, DANNY L. DUNN, and EDWIN D. DORSEY**

Received September 12, 1980, from *New Product Research/Analytical Chemistry, Alcon Laboratories, Inc., Fort Worth, TX 76101.* Accepted for publication March 4, 1981.

**Abstract** □ An improved analytical method was developed that simultaneously quantitates pilocarpine and isopilocarpine in the presence of each other and pilocarpic acid. Pilocarpine and isopilocarpine are first separated from any pilocarpic acid present in the sample by eluting with water-washed chloroform through a column packed with acid-washed diatomaceous earth. The concentrations of pilocarpine and isopilocarpine then are determined by a combination of UV spectrophotometric and polarimetric measurements. UV absorbance is measured at the absorption maximum (215 nm), and optical rotation is measured at the 254-nm line of mercury. Standard curve and standard recovery data are presented. The method is applicable to several commercially available ophathalmic solutions of pilocarpine and is compared to both the USP colorimetric method and a high-performance liquid chromatographic method.

**Keyphrases** □ Pilocarpine—analysis in the presence of isopilocarpine and pilocarpic acid, ophthalmic solutions □ Isopilocarpine—analysis in the presence of pilocarpine and pilocarpic acid, ophthalmic solutions □ UV spectrophotometry—analysis of pilocarpine and isopilocarpine, ophthalmic solutions □ Polarimetry—analysis of pilocarpine and isopilocarpine, ophthalmic solutions

Pilocarpine is an alkaloid used in the treatment of glaucoma to lower intraocular pressure. It has been reported to isomerize into isopilocarpine or to form pilocarpic acid reversibly in basic solution (1, 2). Both processes result in a loss of pharmacological activity (3, 4).

## BACKGROUND

Several satisfactory nonspecific methods have been developed for the analysis of pilocarpine (5–11), but only recently have numerous specific analytical methods been reported (1, 2, 12–17). Two procedures combine colorimetry and polarimetry (1, 12); the first measures a chromium complex of pilocarpine (5), and the second measures an iron complex of the hydroxamic acid of pilocarpine (8). While both methods are theoretically sound in that the colorimetric methods should quantitate total pilocarpine and isopilocarpine and the polarimetric measurements should determine the amount of pilocarpine, these methods are not widely used for routine analysis.

One specific NMR spectrometry method, requiring a 100-MHz instrument, distinguishes between pilocarpine, isopilocarpine, pilocarpic acid, isopilocarpic acid, and pilocarpate and isopilocarpate ions (2). However, this procedure is not designed for multiple analyses and requires expensive instrumentation and reagents. A GLC method that separates pilocarpine and isopilocarpine was also described, but it involves a tedious derivatization of pilocarpine prior to analysis (13). Several specific high-performance liquid chromatographic (HPLC) methods for the quantitation of pilocarpine and isopilocarpine were reported (14–17) and were discussed previously (18).

The present report describes a specific procedure involving a combination of column chromatography, UV spectrophotometry, and polarimetry to analyze for pilocarpine and isopilocarpine in the presence of each other and pilocarpic acid. Validation data for the procedure and data resulting from the analysis of commercially available ophthalmic solutions by this and two other analytical methods are presented.

## EXPERIMENTAL

**Reagents**—USP reference standard pilocarpine nitrate, USP grade pilocarpine hydrochloride[1], and ACS reagent grade isopilocarpine nitrate[2], hydrochloric acid, dibasic potassium phosphate, monobasic potassium phosphate, water-washed chloroform, and acid-washed diatomaceous earth[3] were used.

**Solutions**—The following were used: 0.1 *M* HCl and pH 5.8 potassium phosphate buffer (prepared by mixing one volume of 1 *M* dibasic potassium phosphate with nine volumes of 1 *M* monobasic potassium phosphate and adjusting to pH 5.8 with the appropriate potassium phosphate solution).

**Equipment**—A UV spectrophotometer[4], polarimeter[5], and 60-MHz NMR instrument[6] were used.

**Optical Rotation Measurements**—Stock solutions of pilocarpine hydrochloride and isopilocarpine nitrate were prepared in 0.1 *M* HCl. From these stock solutions, a series of solutions was prepared in concentrations ranging from 0.17 to 1.70 mg/ml of pilocarpine or isopilo-

[1] Quimitra S. A., Merck.
[2] Aldrich Chemical Co.
[3] Celite 545, Johns-Manville Product Corp.
[4] Beckman model ACTA CV with matched 1-cm quartz cells.
[5] Perkin-Elmer model 241 MC with a 100 × 4-mm i.d. cell.
[6] Varian model EM360A.



*0022-3549/81/0900-1046$01.00/0*
© *1981, American Pharmaceutical Association*

(4) O. T. Phillipson, J. M. McKeown, J. Baker, and A. F. Healey, *Br. J. Psychiatry*, **131**, 172 (1977).
(5) A. V. P. Mackay, A. F. Healey, and J. Baker, *Br. J. Clin. Pharmacol.*, **1**, 425 (1974).
(6) S. H. Curry, *Psychopharmacol. Commun.*, **2**, 1 (1976).
(7) C. G. Hammar, B. Holmstedt, and R. Ryhage, *Anal. Biochem.*, **25**, 532 (1968).
(8) G. Alfredsson, B. Wode-Helgodt, and G. Sedvall, *Psychopharmacology*, **48**, 123 (1976).
(9) I. S. Forrest, S. D. Rose, L. G. Brookes, B. Halpern, V. A. Bacon, and L. A. Silberg, *Aggressologie*, **12**, 127 (1970).
(10) D. H. Efron, S. R. Harris, A. A. Manian, and L. E. Gaudette, *Psychopharmacologia*, **19**, 207 (1971).
(11) P. N. Kaul, L. R. Whitfield, and M. L. Clark, *J. Pharm. Sci.*, **65**, 689 (1976).
(12) M. Shostak, in "The Phenothiazines and Structurally Related Drugs," I. S. Forrest, C. J. Carr, and E. Usdin, Eds., Raven, New York, N.Y., 1974.
(13) K. Kawashima, R. Dixon, and S. Spector, *Eur. J. Pharmacol.*, **32**, 195 (1975).
(14) K. K. Midha, J. C. K. Loo, J. W. Hubbard, M. L. Rowe, and I. J. McGilveray, *Clin. Chem.*, **25**, 166 (1979).
(15) J. W. Hubbard, K. K. Midha, I. J. McGilveray, and J. K. Cooper, *J. Pharm. Sci.*, **67**, 1563 (1978).
(16) I. S. Forrest, P. E. Green, M. J. Serra, and K. O. Loeffler, *Proc. West. Pharmacol. Soc.*, **19**, 125 (1976).
(17) P. N. Kaul, M. W. Conway, and M. L. Clark, in "The Phenothiazines and Structurally Related Drugs," I. S. Forrest, C. J. Carr, and E. Usdin, Eds., Raven, New York, N.Y., 1974, p. 391.
(18) P. Turano, W. J. Turner, and D. Donato, in *ibid.*, Raven, New York, N.Y., 1974, p. 315.
(19) P. R. A. May and T. Van Putten, *Arch. Gen. Psychiatry*, **35**, 1081 (1978).

### ACKNOWLEDGMENTS

Presented in part at the American Society of Pharmacology and Experimental Therapeutics meeting, Portland, Oreg., August 1979.

# Analysis of Pilocarpine and Isopilocarpine in Ophthalmic Solutions by UV Spectrophotometry–Polarimetry

**BRITT S. SCOTT ˣ, DANNY L. DUNN, and EDWIN D. DORSEY**

Received September 12, 1980, from *New Product Research/Analytical Chemistry, Alcon Laboratories, Inc., Fort Worth, TX 76101.* Accepted for publication March 4, 1981.

**Abstract** □ An improved analytical method was developed that simultaneously quantitates pilocarpine and isopilocarpine in the presence of each other and pilocarpic acid. Pilocarpine and isopilocarpine are first separated from any pilocarpic acid present in the sample by eluting with water-washed chloroform through a column packed with acid-washed diatomaceous earth. The concentrations of pilocarpine and isopilocarpine then are determined by a combination of UV spectrophotometric and polarimetric measurements. UV absorbance is measured at the absorption maximum (215 nm), and optical rotation is measured at the 254-nm line of mercury. Standard curve and standard recovery data are presented. The method is applicable to several commercially available ophathalmic solutions of pilocarpine and is compared to both the USP colorimetric method and a high-performance liquid chromatographic method.

**Keyphrases** □ Pilocarpine—analysis in the presence of isopilocarpine and pilocarpic acid, ophthalmic solutions □ Isopilocarpine—analysis in the presence of pilocarpine and pilocarpic acid, ophthalmic solutions □ UV spectrophotometry—analysis of pilocarpine and isopilocarpine, ophthalmic solutions □ Polarimetry—analysis of pilocarpine and isopilocarpine, ophthalmic solutions

Pilocarpine is an alkaloid used in the treatment of glaucoma to lower intraocular pressure. It has been reported to isomerize into isopilocarpine or to form pilocarpic acid reversibly in basic solution (1, 2). Both processes result in a loss of pharmacological activity (3, 4).

## BACKGROUND

Several satisfactory nonspecific methods have been developed for the analysis of pilocarpine (5–11), but only recently have numerous specific analytical methods been reported (1, 2, 12–17). Two procedures combine colorimetry and polarimetry (1, 12); the first measures a chromium complex of pilocarpine (5), and the second measures an iron complex of the hydroxamic acid of pilocarpine (8). While both methods are theoretically sound in that the colorimetric methods should quantitate total pilocarpine and isopilocarpine and the polarimetric measurements should determine the amount of pilocarpine, these methods are not widely used for routine analysis.

One specific NMR spectrometry method, requiring a 100-MHz instrument, distinguishes between pilocarpine, isopilocarpine, pilocarpic acid, isopilocarpic acid, and pilocarpate and isopilocarpate ions (2). However, this procedure is not designed for multiple analyses and requires expensive instrumentation and reagents. A GLC method that separates pilocarpine and isopilocarpine was also described, but it involves a tedious derivatization of pilocarpine prior to analysis (13). Several specific high-performance liquid chromatographic (HPLC) methods for the quantitation of pilocarpine and isopilocarpine were reported (14–17) and were discussed previously (18).

The present report describes a specific procedure involving a combination of column chromatography, UV spectrophotometry, and polarimetry to analyze for pilocarpine and isopilocarpine in the presence of each other and pilocarpic acid. Validation data for the procedure and data resulting from the analysis of commercially available ophthalmic solutions by this and two other analytical methods are presented.

## EXPERIMENTAL

**Reagents**—USP reference standard pilocarpine nitrate, USP grade pilocarpine hydrochloride[1], and ACS reagent grade isopilocarpine nitrate[2], hydrochloric acid, dibasic potassium phosphate, monobasic potassium phosphate, water-washed chloroform, and acid-washed diatomaceous earth[3] were used.

**Solutions**—The following were used: 0.1 *M* HCl and pH 5.8 potassium phosphate buffer (prepared by mixing one volume of 1 *M* dibasic potassium phosphate with nine volumes of 1 *M* monobasic potassium phosphate and adjusting to pH 5.8 with the appropriate potassium phosphate solution).

**Equipment**—A UV spectrophotometer[4], polarimeter[5], and 60-MHz NMR instrument[6] were used.

**Optical Rotation Measurements**—Stock solutions of pilocarpine hydrochloride and isopilocarpine nitrate were prepared in 0.1 *M* HCl. From these stock solutions, a series of solutions was prepared in concentrations ranging from 0.17 to 1.70 mg/ml of pilocarpine or isopilo-

[1] Quimitra S. A., Merck.
[2] Aldrich Chemical Co.
[3] Celite 545, Johns-Manville Product Corp.
[4] Beckman model ACTA CV with matched 1-cm quartz cells.
[5] Perkin-Elmer model 241 MC with a 100 × 4-mm i.d. cell.
[6] Varian model EM360A.



*0022-3549/81/0900-1046$01.00/0*
© *1981, American Pharmaceutical Association*

carpine. Several solutions containing both pilocarpine and isopilocarpine were also prepared. The pilocarpine and isopilocarpine concentrations of these solutions varied inversely at intervals of 20% and ranged from 0.00 to 1.70 mg/ml. The total concentration was kept at a constant 1.70 mg/ml.

The optical rotation of each solution was measured as will be described under *Procedure*.

**Standard Preparation**—Approximately 100 mg of pilocarpine hydrochloride or the pilocarpine nitrate equivalent was accurately weighed into a 10.0-ml volumetric flask. The standard was dissolved and diluted to volume with purified water. After mixing, a 2.0-ml aliquot was pipetted into a 250-ml beaker.

**Commercial Product Preparation**—Sufficient sample to contain the equivalent of 20 mg of pilocarpine hydrochloride was pipetted into a 250-ml beaker.

**Standard Curve Preparation**—Aqueous stock solutions of pilocarpine and isopilocarpine were prepared similarly to those already described, and appropriate volumes were pipetted into 250-ml beakers. The resulting concentrations of the optical rotation solutions ranged from 0.35 to 1.04 mg/ml for the pilocarpine standard curve.

The total pilocarpine–isopilocarpine concentration of the combined solutions was 0.68 mg/ml. Again, the pilocarpine and isopilocarpine concentrations varied inversely (at intervals of 25%).

**Standard Addition Sample Preparation**—A series of pilocarpine nitrate samples containing ~17 mg as pilocarpine free base was prepared. Isopilocarpine nitrate was added to the pilocarpine solutions in intervals of 2%. The amount of isopilocarpine in the standard addition samples ranged from 2 to 10%.

**Procedure**—Six milliliters of pH 5.8 buffer was added to each standard and sample in the 250-ml beakers and thoroughly mixed. Approximately 12 g of acid-washed diatomaceous earth was added to each beaker and mixed well by stirring with a spatula. The contents of each beaker were transferred into separate glass chromatographic columns containing a pledget of glass wool at the bottom. Each beaker was then dry washed with ~3 g of acid-washed diatomaceous earth, which was also transferred to the columns. Another pledget of glass wool was placed at the top of each column. The contents of the columns were packed by gentle tapping, and the carpines were eluted with 200 ml of water-washed chloroform into separate 250-ml separators containing 25.0 ml of 0.1 *M* HCl. The separators were then vigorously shaken for 1 min.

The optical rotations of the acid layers and a 0.1 *M* HCl blank were measured at 254 nm, using a mercury vapor lamp. The optical rotation of the blank was subtracted from all other optical rotation measurements. Two milliliters of each optical rotation solution was then accurately diluted to 100.0 ml with 0.1 *M* HCl. The UV absorbance of these solutions was measured at the peak maximum (215 nm) by scanning from 245 to 205 nm after the spectrophotometer was zeroed at 215 nm with a 0.1 *M* HCl blank. Pilocarpine and isopilocarpine concentrations, as percent label pilocarpine, were calculated using the following:

$$C_p = (R/a_p - 0.165A/e_p)/0.835 \quad \text{(Eq. 1a)}$$

$$\%\ \text{label pilocarpoine} = 100\ C_p/C_t \quad \text{(Eq. 1b)}$$

$$\text{isopilocarpine (expressed as \% label pilocarpine)} = 100\ (AC_{std}/A_{std}C_t) - \%\ \text{label pilocarpine} \quad \text{(Eq. 1c)}$$

where all concentrations are those of the optical rotation solutions, in milligrams per milliliter, and:

$C_p$ = calculated pilocarpine concentration in sample
$R$ = degrees of optical rotation of sample
$a_p = R_{std}/C_{std}$
$R_{std}$ = degrees of optical rotation of standard
$C_{std}$ = pilocarpine concentration in standard
$A$ = absorbance of sample
$e_p = A_{std}/C_{std}$
$A_{std}$ = absorbance of standard
$C_t$ = theoretical pilocarpine concentration in sample

## RESULTS AND DISCUSSION

**Optical Rotation**—Pilocarpine and isopilocarpine both have the same molar absorptivity at their absorbance maximum of 215 nm, *i.e.*, $\log \epsilon = 3.77$ (19). Although both compounds rotate light in a positive manner in aqueous solution at 254 nm, pilocarpine exhibits a larger optical rotation than isopilcarpine. These two physical characteristics form the basis for the present analytical method.

**Table I—Analysis of Isopilocarpine at Levels Commonly Found in Pilocarpine Ophthalmic Solutions**

| Theoretical Pilocarpine, % | Experimental Pilocarpine, % | Theoretical Isopilocarpine, % | Experimental Isopilocarpine, % |
|---|---|---|---|
| 98.0 | 97.9, 98.0 | 2.0 | 2.2, 3.1 |
| 96.0 | 95.7, 95.3 | 4.0 | 4.0, 4.5 |
| 94.4 | 94.1, 93.9 | 5.6 | 6.2, 6.6 |
| 92.3 | 92.3, 90.9 | 7.7 | 7.9, 8.1 |
| 90.5 | 90.6, 90.6 | 9.5 | 9.6, 8.6 |

Three sets of aqueous standards, containing either pilocarpine, isopilocarpine, or a mixture of both, were prepared, and the optical rotations were measured. A least-squares analysis of the optical rotation *versus* concentration gave a correlation coefficient for pilocarpine of 1.0000 and a $y$ intercept of −0.0018°. The relative standard deviation was 1.01%, and the slope was 1.330°/mg/ml. The correlation coefficient for the isopilocarpine data was 0.9993, and the $y$ intercept was 0.0012°. The relative standard deviation was 2.07%, and the slope was 0.219°/mg/ml. The optical rotations of the pilocarpine and isopilocarpine solutions were additive, and the observed optical rotations of the pilocarpine–isopilocarpine mixtures agreed well with predicted values (99.2 ± 0.9%)[7].

**Calculations**—Equations for determining the pilocarpine and isopilocarpine content of the solutions were derived based on the UV and optical rotation measurements of pilocarpine and isopilocarpine standards. The derivations are as follows:

$$R = R_p + R_i \quad \text{(Eq. 2a)}$$

$$R = a_pC_p + a_iC_i \quad \text{(Eq. 2b)}$$

At a constant temperature and wavelength:

$$ya_p = a_i \quad \text{(Eq. 3)}$$

From the slopes of the pilocarpine and isopilocarpine optical rotation curves:

$$a_p = 1.330°/\text{mg/ml} \quad \text{(Eq. 4a)}$$

$$a_i = 0.219°/\text{mg/ml} \quad \text{(Eq. 4b)}$$

So:

$$y = a_i/a_p = 0.219/1.330 = 0.165 \quad \text{(Eq. 5)}$$

Thus:

$$R = a_p(C_p + 0.165C_i) \quad \text{(Eq. 6)}$$

Since:

$$A = A_p + A_i \quad \text{(Eq. 7)}$$

And then:

$$A = e_pC_p + e_iC_i \quad \text{(Eq. 8)}$$

Since:

$$e_p = e_i \quad \text{(Eq. 9)}$$

$$A = e_p(C_p + C_i) \quad \text{(Eq. 10)}$$

$$C_i = (A/e_p) - C_p \quad \text{(Eq. 11)}$$

So:

$$R = a_p[C_p + 0.165(A/e_p - C_p)] \quad \text{(Eq. 12a)}$$

$$R = a_p(C_p + 0.165A/e_p - 0.165C_p) \quad \text{(Eq. 12b)}$$

$$R = a_p[C_p(1 - 0.165) + 0.165A/e_p] \quad \text{(Eq. 12c)}$$

Therefore:

$$C_p = (R/a_p - 0.165A/e_p)/0.835 \quad \text{(Eq. 13)}$$

and:

$$\%\ \text{label pilocarpine} = 100\ C_p/C_t \quad \text{(Eq. 14)}$$

Isopilocarpine, expressed as percent label pilocarpine, equals the concentration of total carpine as determined by UV analysis after elution

[7] Mean ± *SD*.

Table II—Determination of Pilocarpine and Isopilocarpine in Commercially Available Pilocarpine Ophthalmic Solutions

| Sample Concentration as Hydrochloride, % | Pilocarpine Analysis[a], % | | | Isopilocarpine Analysis[a], % | |
|---|---|---|---|---|---|
| | UV–Polarimetry | HPLC[b] | USP[c] | UV–Polarimetry | HPLC[c] |
| 2 | 97, 99 | 98, 99 | 99, 99 | 0.0, 1.0 | 0.9, 1.0 |
| 1 | 96, 95 | 94, 96 | 95, 96 | 2.7, 4.4 | 1.4, 1.4 |
| 2 | 99, 100 | 102, 101 | 103, 104 | 3.7, 3.9 | 3.7, 3.6 |
| 2 | 99, 98 | 101, 100 | 100, 98 | 0.0, 0.8 | 0.7, 0.8 |

[a] Percent label as pilocarpine salt. [b] Reference 18. [c] The USP procedure is the colorimetric method described in Ref. 8.

from the column, minus the pilocarpine concentration as already determined:

isopilocarpine, as % label pilocarpine

$$= 100\,(AC_{std}/A_{std}C_t) - \%\text{ label pilocarpine} \quad \text{(Eq. 15)}$$

where all concentrations are those of the optical rotation solutions, in milligrams per milliliter, subscripts $p$ refer to pilocarpine, subscripts $i$ refer to isopilocarpine, and:

$R$ = degrees of optical rotation
$a = R/C$
$C$ = sample concentration
$e = A/C$
$A$ = absorbance
$C_{std}$ = pilocarpine concentration in standard
$A_{std}$ = absorbance of standard
$C_t$ = theoretical pilocarpine concentration in sample.

The pilocarpic acid concentration can then be calculated by subtracting the total carpine concentration from the total imidazole concentration, which can be obtained without chromatographic separation from the direct UV comparison of sample and standard dilutions. All concentrations in this calculation are expressed as percent label pilocarpine.

**Analysis of Pilocarpine and Isopilocarpine**—Pilocarpine standard solutions with concentrations of 0.007–0.021 mg/ml (0.34–1.04 mg/ml for the optical rotation concentrations) were analyzed by this procedure. A least-squares analysis of the absorbance plotted *versus* the concentration gave a correlation coefficient of 0.9996 and a $y$ intercept of 0.014 absorbance unit. The relative standard deviation was 2.16%. The average log $\epsilon$ was 3.77, which agreed well with the published value (19). The correlation coefficient for the optical rotation plotted *versus* concentration was 0.9999 with a $y$ intercept of −0.0071°, and the relative standard deviation was 0.48%. Complete elution of pilocarpine from the column was indicated by the good agreement of the observed optical rotation values with the predicted optical rotation values (102.0 ± 0.5%)[7].

A standard curve containing known mixtures of pilocarpine and isopilocarpine was evaluated using USP reference standard pilocarpine nitrate as the standard. The concentration of pilocarpine and isopilocarpine ranged inversely from 0 to 100% at intervals of 25%. The results showed that the method was specific for pilocarpine and isopilocarpine in the presence of each other; the experimental values agreed within 3% of the theoretical percent label.

A series of pilocarpine samples was analyzed after making standard additions of isopilocarpine ranging in concentration from 2 to 10% of the amount of pilocarpine present. The results showed that isopilocarpine can be analyzed accurately at levels commonly found in pilocarpine ophthalmic solutions. The results for pilocarpine and isopilocarpine were within 1% of the theoretical amount present (Table I).

Eluting the pilocarpine solutions through an acid-washed diatomaceous earth column with chloroform leaves methylcellulose (7) and most other interfering excipients of commercially available ophthalmic solutions, as well as pilocarpic and isopilocarpic acids (carpic acids) and pilocarpate and isopilocarpate ions (carpate ions), on the column. The pH 5.8 phosphate buffer prevents pilocarpine protonation, which, in turn, ensures that it will not be retained by the column. The retention of carpic acids and carpate ions by the column was confirmed by analyzing a sodium hydroxide-hydrolyzed solution of pilocarpine hydrochloride by NMR spectrometry (2) and the described UV–optical rotation method. This method detected 13% pilocarpine and 49% isopilocarpine, equal to 62% total carpines. NMR analysis detected 60% total carpines (pilocarpine plus isopilocarpine) and 40% total carpate ions. The results from these two methods were consistent and confirmed that carpic acids and carpate ions are not eluted from the column.

**Analysis of Commercially Available Pilocarpine Solutions**—Commercially available pilocarpine ophthalmic solutions were analyzed by the described method, a normal-phase HPLC method (18), and the USP colorimetric method (9). These solutions contained excipients commonly found in ophthalmic formulations such as benzalkonium chloride, chlorobutanol, disodium edetate, sodium acetate, citric acid, boric acid, menthol, camphor, and hydroxypropyl methylcellulose. Overall, the results of the UV–polarimetric method were in good agreement with the results from the HPLC and USP colorimetric methods. With the described procedure, the total pilocarpine and isopilocarpine content of the formulations approximately equaled the value obtained by the nonspecific USP colorimetric method, as expected (Table II). Thus, this method exhibits specificity and appears to be an improved analytical procedure for pilocarpine in ophthalmic solutions.

The only inconsistent results among the three methods were obtained on a 2% pilocarpine nitrate formulation containing polyvinyl alcohol and chlorobutanol. Average pilocarpine percent label values of 106, 94, and 127% were obtained for the UV–polarimetry, HPLC, and USP methods, respectively. The UV–polarimetry and HPLC methods produced average results for isopilocarpine of 2.0 and 1.2% label, respectively.

## REFERENCES


(1) R. A. Anderson and S. D. FitzGerald, *Australas. J. Pharm.*, **48**, S108 (1967).

(2) M. A. Nunes and E. Brochmann-Hanssen, *J. Pharm. Sci.*, **63**, 716 (1974).

(3) R. K. Hill and S. Barcza, *Tetrahedron*, **22**, 2889 (1966).

(4) R. A. Anderson and J. B. Cowle, *Br. J. Ophthalmol.*, **52**, 607 (1968).

(5) I. S. Shupe, *J. Assoc. Off. Agr. Chem.*, **24**, 757 (1941).

(6) J. W. Webb, R. S. Kelley, and A. J. McBay, *J. Am. Pharm. Assoc., Sci. Ed.*, **41**, 278 (1952).

(7) J. Levine and E. Horrocks, *J. Assoc. Off. Agr. Chem.*, **43**, 233 (1960).

(8) E. Brochmann-Hanssen, P. Schmid, and J. D. Benmaman, *J. Pharm. Sci.*, **54**, 783 (1965).

(9) "The United States Pharmacopeia," 19th rev., Mack Publishing Co., Easton, Pa., 1975, pp. 385, 386.

(10) I. S. Gibbs and M. M. Tuckerman, *J. Pharm. Sci.*, **59**, 395 (1970).

(11) S. W. Dziedzic, S. E. Gitlow, and D. L. Krohn, *ibid.*, **65**, 1262 (1976).

(12) J. B. Murray, *Proc. Soc. Anal. Chem.*, **7**, 107 (1970).

(13) W. F. Bayne, L.-C. Chu, and F. T. Tao, *J. Pharm. Sci.*, **65**, 1724 (1976).

(14) T. Urbanyi, A. Piedmont, E. Willis, and G. Manning, *ibid.*, **65**, 257 (1976).

(15) J. D. Weber, *J. Assoc. Off. Anal. Chem.*, **59**, 1409 (1976).

(16) A. Noordam, K. Waliszewski, C. Olieman, L. Maat, and H. C. Beyerman, *J. Chromatogr.*, **153**, 271 (1978).

(17) J. J. O'Donnell, R. Sandman, and M. V. Drake, *J. Pharm. Sci.*, **69**, 1096 (1980).

(18) D. L. Dunn, B. S. Scott, and E. D. Dorsey, *ibid.*, **70**, 446 (1981).

(19) "Handbook of Chemistry and Physics," 57th ed., R. C. Weast, Ed., CRC Press, Cleveland, Ohio, 1976, p. C-439.


## ACKNOWLEDGMENTS


The authors greatly appreciate the assistance of Satoru Numajiri, Alcon Medicinal Chemistry, in the preparation of the hydrolyzed pilocarpine solution, Karen Haggard, New Product Research/Analytical Chemistry, for technical assistance in analyzing samples, and Linda Brammer and William Jones, New Product Research/Analytical Chemistry, for assistance and advice.

# Interspecies Difference in Drug Protein Binding–Temperature and Protein Concentration Dependency: Effect on Calculation of Effective Protein Fraction

YASUTAKA IGARI *x, YUICHI SUGIYAMA *, SHOJI AWAZU ‡, and MANABU HANANO *

Received November 13, 1979, from the *Faculty of Pharmaceutical Sciences, University of Tokyo, Bunkyo-ku, Tokyo, Japan, and the ‡Division of Biopharmacy, Tokyo College of Pharmacy, Horinouchi, Hachioji-shi, Tokyo, Japan. Accepted for publication March 2, 1981.

**Abstract** □ The effects of temperature and protein concentration on the binding of thiopental to bovine and rat serum albumin and to rat plasma were examined using flow and equilibrium dialysis techniques. The effects of temperature and protein concentration were peculiar to each species. The binding of thiopental to rat serum albumin or rat plasma was sensitive to temperatures between 4 and 37°, whereas the binding to bovine serum albumin was sensitive to a protein concentration difference of 0.1–4.44%. Therefore, the effective protein fraction is affected by various sets of binding parameters of albumins determined under various temperatures and protein concentrations. Thus, a semipredictive method for plasma or tissue binding may be unsuccessful unless proper binding parameters are used.

**Keyphrases** □ Thiopental—effects of temperature and protein concentration on plasma and tissue binding, interspecies differences □ Effective protein fraction—effects of temperature and protein concentration, interspecies differences □ Drug protein binding—effects of temperature and protein concentration, interspecies differences □ Dialysis—equilibrium and flow techniques, effects of temperature and protein concentration on plasma and tissue binding, interspecies differences

Drug protein binding has an important role in drug distribution, disposition, and excretion. Numerous reports have dealt with drug protein binding under various conditions of drug level, protein concentration, and temperature. Some authors (1–3) adopted experimental conditions different from physiological ones, such as a lower temperature or lower plasma protein concentration. In addition, they discussed *in vivo* situations based on the inadequate experimental data obtained in this way.

## BACKGROUND

Recently, important critical information on these points was reported (4–6). Shen and Gibaldi (6) provided significant criticism on a previous report (7) that dealt with the application of *in vitro* drug protein binding data to the prediction of an *in vivo* situation utilizing a physiologically based pharmacokinetic model. To construct a physiologically based pharmacokinetic model, both tissue and plasma protein binding are important. However, tissue and organs are not as accessible as plasma for the determination of drug protein binding.

Dedrick and Bischoff (7) proposed the concept of the effective protein fraction to depict tissue binding, taking into consideration that little information was available on the binding of barbiturates to tissues. They calculated effective protein fractions based on the binding data of various rabbit organ homogenates at an initial drug concentration of 0.5 m*M* using the binding parameters (8) of 1% bovine serum albumin for barbiturates. However, Shen and Gibaldi (6) concluded that the use of the effective protein fraction in developing pharmacokinetic models for drug distribution might not be feasible for the following reasons:

1. Binding parameters were assumed to be constant over the concentration range of both bovine serum albumin and rabbit organ homogenate.
2. Interspecies differences were not considered.

Nevertheless, since the concept of the effective protein fraction is useful for the prediction of drug distribution in tissues where there is a shortage of information on tissue binding, the effects of protein concentration and temperature on drug protein binding were studied here using bovine and rat serum albumin and rat plasma. By considering these effects and interspecies differences, a semipredictive method for plasma protein or tissue binding was tested by measuring binding levels in plasma or a homogenized tissue sample.

Thiopental, which was studied previously (6, 7), was chosen as the model drug for the present study. Flow dialysis was used to assess protein binding of thiopental to bovine and rat serum albumin and rat plasma, while equilibrium dialysis was used for the rat plasma and homogenized rat tissue samples.

## EXPERIMENTAL

**Chemicals**—Rat serum albumin[1] and bovine serum albumin[2] were Fraction V powder. Stock albumin solutions were prepared by dissolving serum albumin powder in 0.05 *M* tromethamine buffer (I) adjusted to pH 7.4 with hydrochloric acid. Thiopental sodium[3] was prepared fresh daily.

**Quantitation of Thiopental**—Standards were carried through the entire procedure. A previous method (9) was used with slight modification (*i.e.*, dual-wavelength measurement[4] and *n*-heptane were employed). The recoveries from extraction were >90% and linear within the concentration range used.

**Rat Plasma and Tissue Sample**—Plasma was obtained by centrifuging, 30 min after intravenous injection of heparin, the fresh blood of a male Wistar rat (250–300 g) fed a normal laboratory diet. After the body was perfused with cold saline, the muscle was excised, rinsed in ice-cold saline, blotted, weighed, cut into small pieces, and homogenized by a motor-driven polytef glass homogenizer in 0.05 *M* I to yield 25% (w/v) homogenate. Rat plasma and homogenized muscle sample were predialyzed through cellulose dialysis tubing against 100 volumes of I at pH 7.4 for 18–24 hr at 4° with stirring. Little volume change was found during predialysis.

**Dialysis**—Flow dialysis of serum albumin solutions and rat plasma were carried out according to a reported method (10) using I at pH 7.4. Flow rates of I were 25 ml/hr at 37° and 12 ml/hr at 4°, respectively. Thiopental permeability through cellulose dialysis membrane remained almost constant before and after each experiment, which was checked by carrying out dialysis using I at pH 7.4 instead of protein solution.

Equilibrium dialyses of rat plasma and homogenized rat tissue samples were carried out according to the method of Sugiyama *et al.* (11) using I at pH 7.4. Equilibrium was established by 12 hr of dialysis at 37° and by 24 hr of dialysis at 4°, respectively. Equilibrium dialyses of homogenized tissue were carried out only at 4°.

**Data Analysis**—Results from binding experiments presented in Figs. 1–4 were subjected to curve fitting to Eq. 1 by a digital computer program (12):

$$r = \frac{n_1 k_1 C_f}{1 + k_1 C_f} + \frac{n_2 k_2 C_f}{1 + k_2 C_f} \qquad \text{(Eq. 1)}$$

where $k_1$ and $k_2$ are the association constants corresponding to $n_1$ and $n_2$, the number of primary and secondary binding sites; $C_f$ is the free drug concentration, and $r$ is the molar ratio of the bound drug to the binding protein assuming a molecular weight of 69,000. Results from binding experiments presented in Figs. 5 and 6 were subjected to curve fitting to Eq. 2 by means of a digital computer program (12). Data were weighted with the reciprocals of their variance:

[1] Pentex.
[2] Armour Pharmaceutical Co., Phoenix, Az.
[3] Tanabe, Tokyo, Japan.
[4] Hitachi 356 UV spectrometer.

0022-3549/81/0900-1049$01.00/0
© 1981, American Pharmaceutical Association

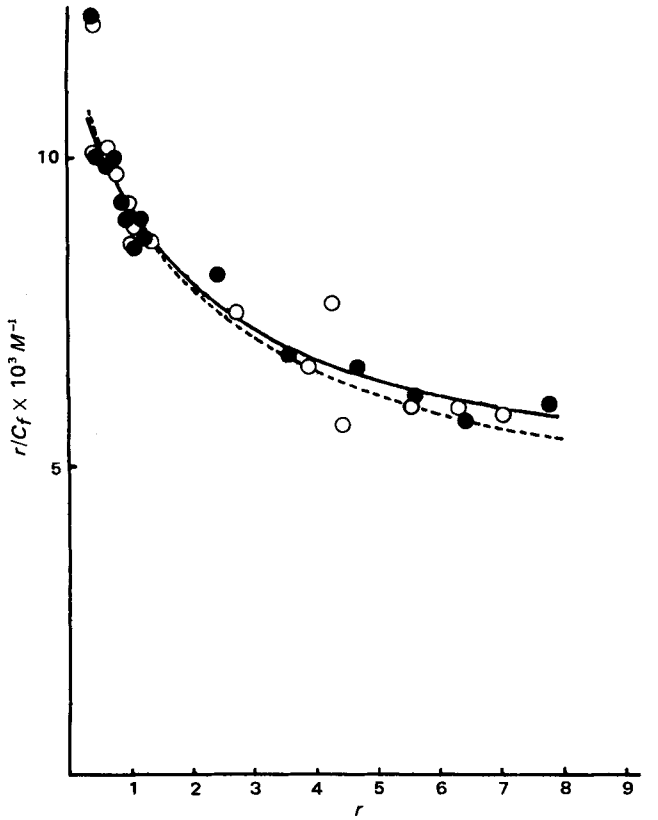


**Figure 1**—*Effect of temperature on thiopental binding to 1% (w/v) bovine serum albumin in 0.05* M *tromethamine buffer at pH 7.4 by flow dialysis [4° (●) and 37° (○)]. Each point represents the mean of three experiments. The smooth curves at 37° (- - -) and 4° (—) are the best fit to these data using the predetermined values for the number of sites* $n_1 = 1.0$ *and* $n_2 = 83.4$.

$$C_b = \frac{n_1(P)k_1C_f}{1 + k_1C_f} + \frac{n_2(P)k_2C_f}{1 + k_2C_f} \qquad \text{(Eq. 2)}$$

where $(P)$ is the protein concentration and $C_b$ is the bound drug concentration in plasma or tissue homogenates. Value $n_1(P)$ or $n_2(P)$ is presumed to be the composite parameter.

The $n_1$ and $n_2$ values obtained from experiments using each protein source at various protein concentrations and temperatures were averaged and constrained, and revised sets of $k_1$ and $k_2$ values were derived corresponding to the constrained average $\bar{n}_1$ and $\bar{n}_2$ values according to a previous report (5).

## RESULTS

**Comparison of Two Dialysis Methods**—Figure 5 displays, in the form of a Scatchard plot, the binding of thiopental to rat plasma at 4° assessed by flow and equilibrium dialyses. At low thiopental concentrations, there was a slight difference in binding, probably due to the sensitivity limit of the analytical technique, especially in the flow dialysis experiment. (Flow dialysis was employed mainly for the advantages of reduced incubation time and smaller volume of protein sample compared to equilibrium dialysis.)

**Thiopental Binding to Bovine Serum Albumin**—The effects of temperature and protein concentration on thiopental binding to bovine serum albumin were examined. As shown in Fig. 1, there was little, if any, temperature dependency of thiopental binding to 1% (w/v) bovine serum albumin between 4 and 37°, especially at low thiopental concentrations. Thiopental binding to 1 and 4% (w/v) bovine serum albumin at 37° is shown in Fig. 2. At low thiopental concentrations, there was a protein concentration dependency of thiopental binding to bovine serum albumin. In addition, thiopental binding to a range of bovine serum albumin at an initial thiopental concentration of 1 m$M$ was examined (Fig. 2, inset). This relationship resembles that presented previously (6). Thus, it seems that bovine serum albumin is sensitive to albumin concentration and practically insensitive to temperatures between 4 and 37°.

**Thiopental Binding to Rat Plasma**—Figure 6 presents the data on thiopental binding to undiluted rat plasma at 4 and 37°. Figure 7 represents thiopental binding to undiluted rat plasma and 50 and 25% (v/v) diluted rat plasma at 37°. These data imply that the characteristics of thiopental binding to rat plasma are contrary to those of bovine serum albumin, *i.e.*, very sensitive to temperatures between 4 and 37° and practically insensitive to protein concentration within at least a fourfold dilution of rat plasma.

**Table I—Thiopental Binding to Rat Serum Albumin and Bovine Serum Albumin**

| Serum Albumin Concentration | Temperature | $k_1$[a] | $k_2$[a] | $n_1$[b] | $n_2$[b] |
|---|---|---|---|---|---|
| Rat | | | | | |
| 1% (w/v) | 4° | 40.9 | 1.31 | 1.0[c] | 8.0[c] |
| 1% (w/v) | 37° | 19.4 | 0.806 | 1.0[c] | 8.0[c] |
| 4% (w/v) | 37° | 20.1 | 0.990 | 1.0[c] | 8.0[c] |
| Bovine | | | | | |
| 1% (w/v) | 4° | 5.84 | 0.068 | 1.0[c] | 83.4[d] |
| 1% (w/v) | 37° | 6.31 | 0.0654 | 1.0[c] | 83.4[d] |
| 4% (w/v) | 37° | 1.62 | 0.636 | 1.0 | 11.6 |

[a] Association constant ($\times 10^3\ M^{-1}$). [b] The number of binding sites. [c] Predetermined and constrained (see text).

**Thiopental Binding to Rat Serum Albumin**—Thiopental binding to 1 and 4% (w/v) rat serum albumin and to 1% (w/v) rat serum albumin at 4 and 37° is shown in Figs. 3 and 4, respectively. These data suggest similar binding characteristics of rat serum albumin to those of rat plasma, *i.e.*, sensitive to temperatures between 4 and 37° and practically insensitive to protein concentrations between 1 and 4% (w/v).

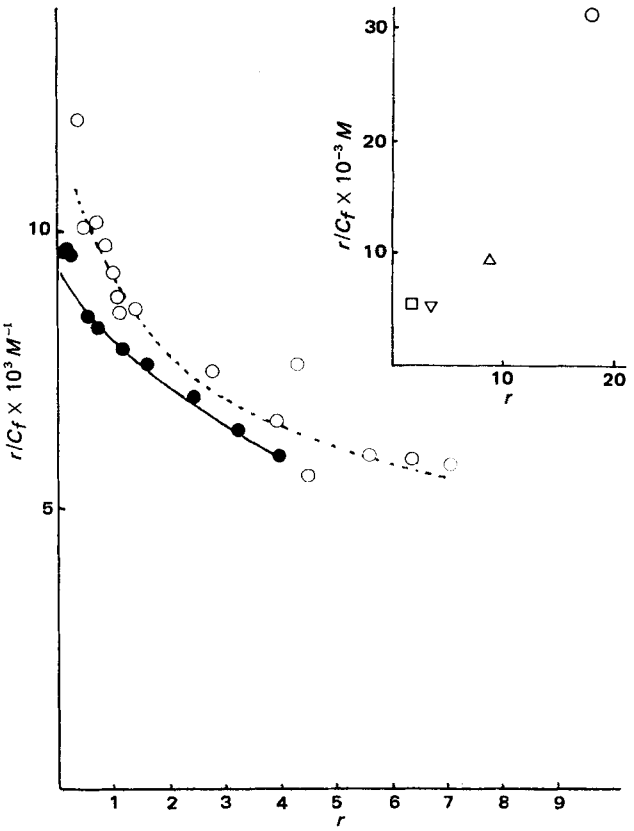


**Figure 2**—*Effect of protein concentration on thiopental binding to bovine serum albumin in 0.05* M *tromethamine buffer at pH 7.4 and 37° by flow dialysis [1% w/v (○) and 4% w/v (●)]. Each point represents the mean of three experiments. The data points and the smooth curve for 1% (w/v) bovine serum albumin are the same as those in Fig. 1. The smooth curve for 4% (w/v) bovine serum albumin (—) is the best fit to these data. [Inset: Scatchard plot for the binding of a single thiopental concentration (1 m*M*) to a bovine serum albumin concentration range in 0.05* M *tromethamine buffer at pH 7.4 and 37° by flow dialysis. Each data point represents the mean of two experiments. Key: ○, 0.1% (w/v); △, 0.5% (w/v); ▽, 1.74% (w/v); and □, 4.44% (w/v)].*

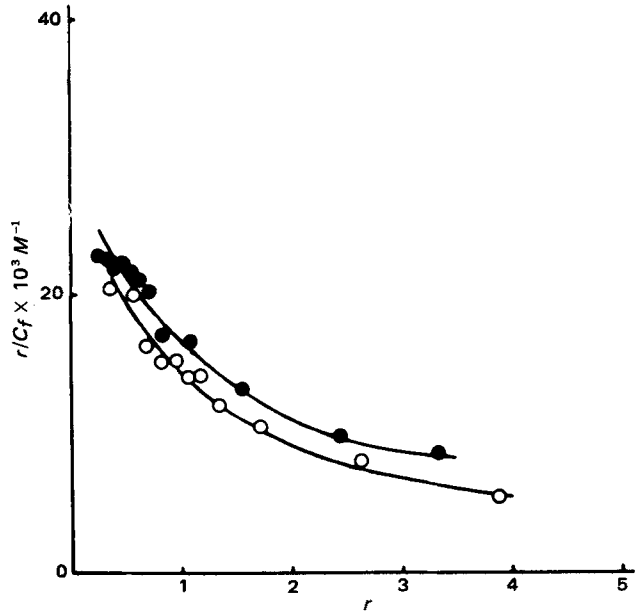


**Figure 3**—*Effect of protein concentration on thiopental binding to rat serum albumin at 37° in 0.05* M *tromethamine buffer at pH 7.4 [1% w/v (○) and 4% w/v (●)]. Each point represents the mean of three experiments. The smooth curves are the best fit to these data using the predetermined values for the number of sites* $n_1 = 1.0$ *and* $n_2 = 8.0$. *Flow dialysis was used.*

**Binding Parameters**—For the binding parameters of thiopental binding to rat serum albumin of 1% (w/v) at 4 and 37° and of 4% (w/v) at 37°, $n_1$ and $n_2$ values first were calculated without constraint and then averaged ($\bar{n}_1 = 1.0 \pm 0.221$ and $\bar{n}_2 = 8.0 \pm 3.52$). Then a revised set of $k_1$ and $k_2$ values was derived for each experiment corresponding to the constrained $\bar{n}_1$ and $\bar{n}_2$ values. In this way, the values for the number of binding sites were predetermined and constrained. The binding data for thiopental to rat plasma were analyzed in the same manner as for rat serum albumin [$\bar{n}_1(P) = 0.136 \pm 0.0251$ and $\bar{n}_2(P) = 2.42 \pm 1.12$ (m$M$)]. However, for bovine serum albumin, because of protein concentration-dependent binding, the constrained average $\bar{n}_1$ and $\bar{n}_2$ values were not proper for deriving revised sets of $k_1$ and $k_2$ values since the residual sum of squares became significantly larger than that derived without constraint. Therefore, the binding data of thiopental to 1% (w/v) bovine serum albumin at 4 and 37° were analyzed in the same manner as for rat serum albumin [$\bar{n}_1$ = 1.0(1.57 and 0.431) and $\bar{n}_2$ = 83.4(101.0 and 65.8)]

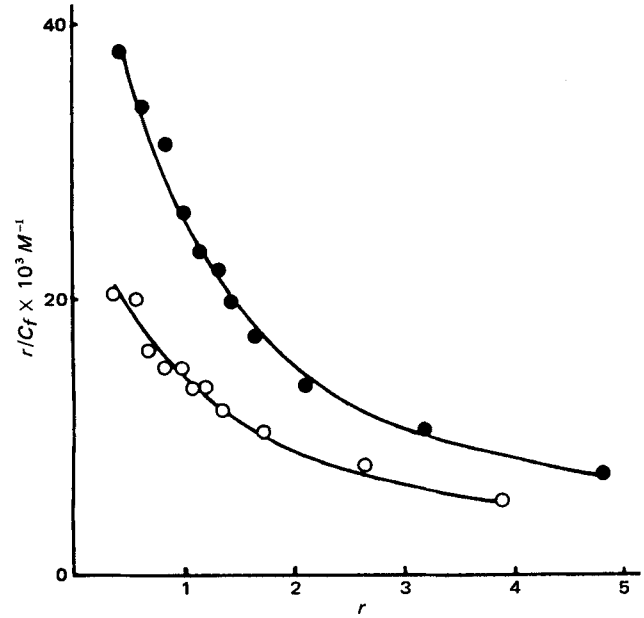


**Figure 4**—*Effect of temperature on thiopental binding to 1% (w/v) rat serum albumin in 0.05* M *tromethamine buffer at pH 7.4 by flow dialysis [4° (●) and 37° (○)]. Each point represents the mean of three experiments. The smooth curves are the best fit using the predetermined values for the number of sites* $n_1 = 1.0$ *and* $n_2 = 8.0$. *Flow dialysis was used.*

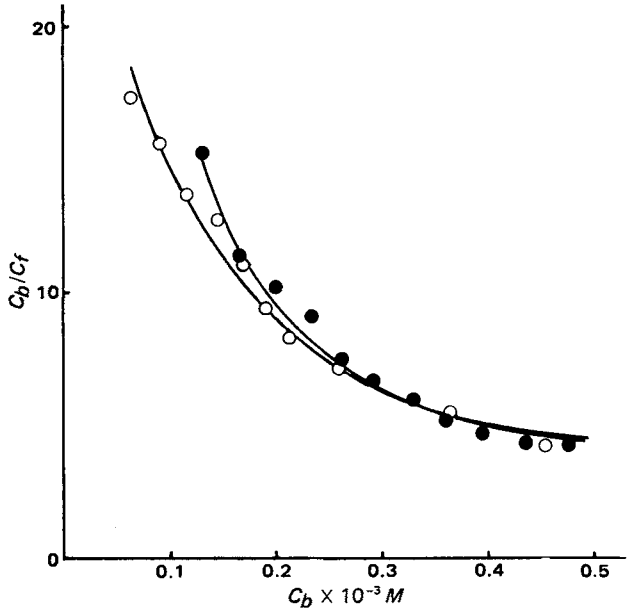


**Figure 5**—*Scatchard plots for the binding of thiopental to rat plasma at 4° by flow dialysis (●) and equilibrium dialysis (○). Each point represents the mean of three experiments. The smooth curves are the best fit to these data using the predetermined values for the binding capacities [*$n_1(P) = 0.136$ *and* $n_2(P) = 2.42$ *(m*M*)].*

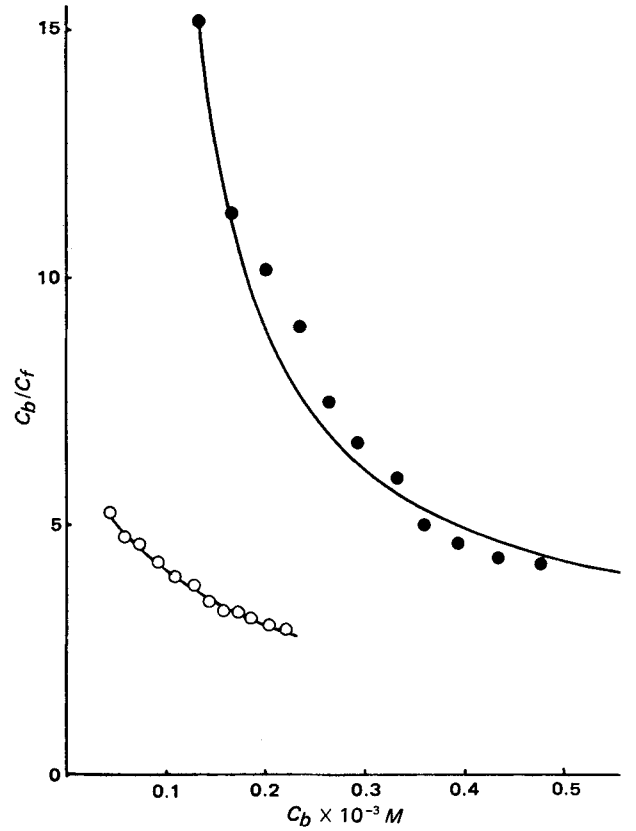


**Figure 6**—*Effect of temperature on thiopental binding to rat plasma by flow dialysis [4° (●) and 37° (○)]. Each point represents the mean of three experiments. The smooth curves are the best fit to these data using the predetermined values for the number of sites [*$n_1(P) = 0.136$ *and* $n_2(P) = 2.42$ *(m*M*)]. The smooth curve and the data points for rat plasma at 4° are the same as those in Fig. 5.*

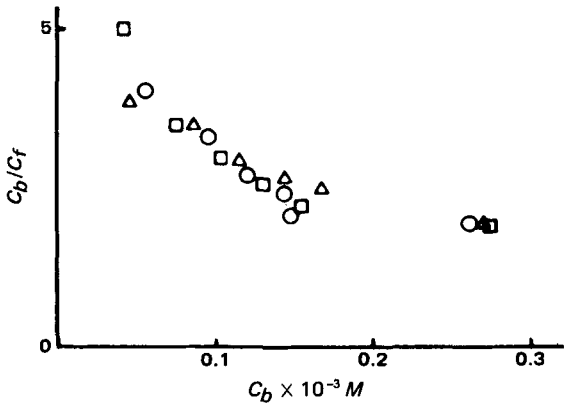


**Figure 7**—*Scatchard plots for the binding of thiopental to rat plasma at 37° by flow dialysis. Key: ○, 25% (v/v); △, 50% (v/v); and □, undiluted. Diluted rat plasma was prepared by adding 0.05 M tromethamine buffer at pH 7.4. Dilution factors of 2 for 50% (v/v) and 4 for 25% (v/v) rat plasma were corrected respectively. Each point represents the mean of three experiments.*

and then revised sets of $k_1$ and $k_2$ values were derived corresponding to the constrained average $\bar{n}_1$ and $\bar{n}_2$ values.

For the binding data for thiopental to bovine serum albumin of 4% (w/v) at 37°, $n_1$ was assigned a value of 1.0, obtained from the data analysis of the other two experimental results of bovine serum albumin. Then a revised set of $n_2$, $k_1$, and $k_2$ values was derived corresponding to the constrained $n_1$ value since $n_1$ became negative without constraining. The residual sum of squares was not significantly larger than the residual sum of squares in the other cases. The results are summarized in Tables I and II.

**Prediction of Tissue Binding Utilizing Binding Parameters of Serum Albumin**—Dedrick and Bischoff (7) proposed the concept of effective protein fraction using the binding parameters of 1% bovine serum albumin and the bound fraction of rabbit organ homogenates at an initial drug concentration of 0.5 m$M$ previously reported (8). In the absence of additional information, Dedrick and Bischoff (7) combined these data to express thiopental content in various tissues as:

$$C_t = (1 - f_p)C_f + f_p X \qquad \text{(Eq. 3)}$$

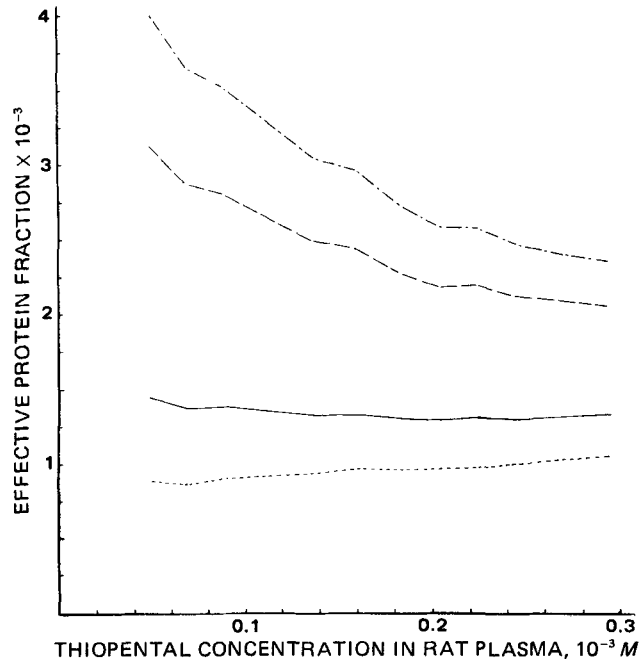


**Figure 8**—*Total thiopental concentration in rat plasma* versus *effective protein fractions* ($f_p$) *calculated according to Eq. 3 using the binding parameters of 4% (w/v) rat serum albumin at 37° (—), 1% (w/v) rat serum albumin at 4° (- - -), 4% (w/v) bovine serum albumin at 37° (- - -), and 1% (w/v) bovine serum albumin at 37° (– –).*

**Table II—Thiopental Binding to Rat Plasma** [a]

| Temperature | Dialysis | $k_1$ [b] | $k_2$ [b] |
|---|---|---|---|
| 37° | Flow | 32.8 | 0.686 |
| 4° | Flow | 320.6 | 1.57 |
| 4° | Equilibrium | 173.3 | 1.65 |

[a] The binding capacity, predetermined and constrained (see text), was $n_1(P)$ = 0.136 and $n_2(P)$ = 2.42 (m$M$) in all cases. [b] Association constant ($\times 10^3\ M^{-1}$).

where $C_t$ is the total drug concentration [assumed to be present initially in rabbit organ homogenate, *i.e.*, 0.5 m$M$ (7)], $C_f$ is the free drug concentration, $X$ is the bound drug concentration described using the binding parameters of 1% bovine serum albumin in the form of Eq. 1, and $f_p$ is a dimensionless parameter of the effective protein fraction.

Thus, the values of the effective protein fraction for tissues were calculated at an initial drug concentration of 0.5 m$M$, but the assumption (7) that the values of the effective protein fraction were constant at all drug concentrations has not been proved. In the present study, comparable precise information on plasma and tissue binding were available, so the relationship between the effective protein fraction and the drug concentration was investigated. Figure 8 displays the $f_p$ values calculated according to Eq. 3 at various thiopental concentrations in rat plasma. The $f_p$ values based on the binding parameters of other than 4% (w/v) rat serum albumin at 37° proved to be dependent on thiopental concentrations in rat plasma. In particular, the binding parameters of bovine serum albumin gave decreasing $f_p$ values with increasing thiopental concentrations in rat plasma. Hence, a $f_p$ value calculated at one thiopental concentration in rat plasma could not readily be extrapolated to another. However, since the concept of the effective protein fraction is useful only when little information is available, the predicted thiopental binding to rat plasma or tissue homogenate based on a single $f_p$ value and on the binding parameters of serum albumin was compared with the observed data.

Figure 9 shows the simulation curves calculated according to Eq. 3 using the $f_p$ values at thiopental concentrations of 0.160 m$M$ in rat plasma (A) and 0.391 m$M$ in muscle homogenate (B). As can be expected from the results shown in Fig. 8, the simulated curves based on the binding parameters other than 4% rat serum albumin at 37° diverted slightly from the observed data (Fig. 9A). In Fig. 9B, the simulated curves based on the binding parameters of bovine serum albumin rather than of rat serum albumin seem to give better prediction for rat muscle homogenate thiopental binding. However, at low thiopental concentrations (those of pharmacological interest), a single $f_p$ value can give good prediction with both serum albumins. Therefore, the effective protein fraction should be calculated from the bound fraction of plasma or tissue homogenate samples measured within a drug concentration range (especially free drug concentration) of pharmacological interest. The $f_p$ value calculated at a pharmacologically meaningless drug concentration will give a wrong prediction when compared to the observed data for meaningful concentrations (Fig. 9B inset) and may lead to failure in construction of physiologically based pharmacokinetic models.

## DISCUSSION

As already pointed out (6), extrapolation of thiopental binding data for one concentration of bovine serum albumin to another will produce errors because of protein concentration-dependent binding. Thus, in the present study, the values of effective protein fractions (Fig. 8) decreased 42% for 4% bovine serum albumin and 35% for 1% bovine serum albumin with increasing thiopental concentrations in rat plasma. Similar results were obtained by calculating the values of effective protein fractions from the binding data of salicylate to human plasma (13) as well as the binding parameters of salicylate to human serum albumin (14). The calculated values of effective protein fractions of 1% human serum albumin at salicylate concentrations of 100 and 300 μg/ml were nearly equal, but the effective protein fractions of 0.1% human serum albumin changed twofold. If it is assumed that the association constants of 0.1% human serum albumin are equal to those of 1% human serum albumin, the effective protein fractions of 0.1% human serum albumin become nearly equal at 100 and 300 μg/ml of salicylate. Thus, the effects of protein concentration-dependent drug protein binding on the calculation of effective protein fraction will be ascribed to the change of association constants and/or the number of binding sites. Therefore, protein concentration-dependent drug protein binding greatly affects the effective protein fraction.

The present study shows that there was little, if any, temperature effect

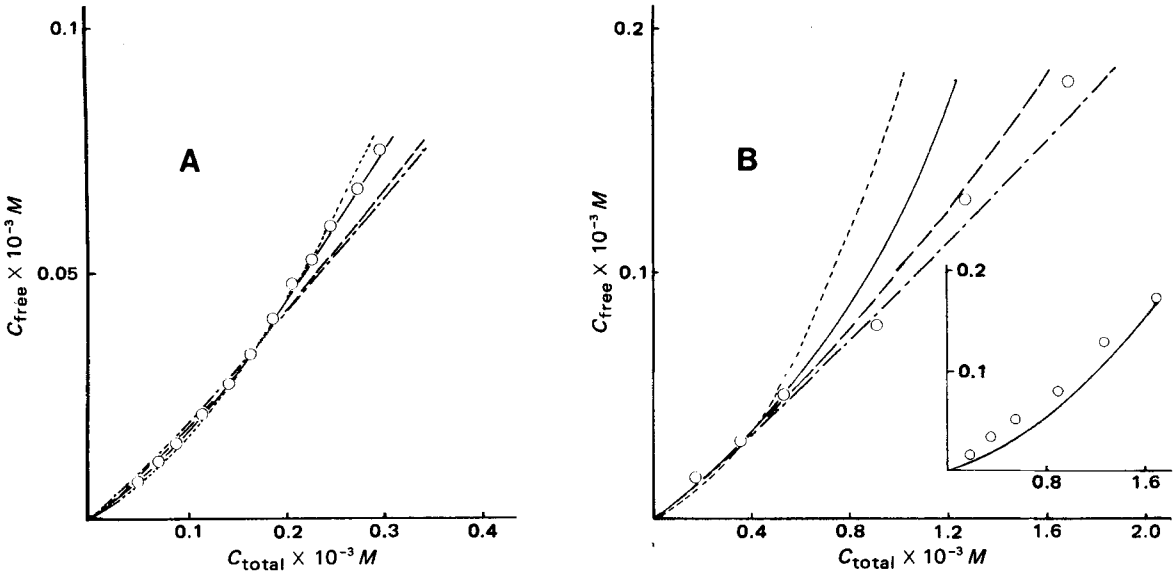


**Figure 9**—*Simulation curves calculated according to Eq. 3 using the $f_p$ values for thiopental concentration of 0.160 mM in rat plasma (A) and of 0.391 mM in muscle homogenate (B) and the binding parameters of 4% rat serum albumin at 37° (—), 1% rat serum albumin at 4° (- - -), 4% bovine serum albumin at 37° (- - - -), and 1% bovine serum albumin at 37° (– –). Each point (○) represents the mean of three experiments. [B, inset: simulation curves calculated according to Eq. 3 using the binding parameters of 4% rat serum albumin and the $f_p$ values for thiopental concentrations of 0.391 mM ($f_p$ = 0.00357) and 1.86 mM ($f_p$ = 0.00534).]*

on thiopental binding to bovine serum albumin but that temperature greatly affected thiopental binding to rat serum albumin and rat plasma. As shown in Fig. 8, because of the temperature effect on thiopental binding to rat serum albumin, the binding parameters obtained at 4° different from body temperature gave concentration-dependent effective protein fractions. Similar results are expected for the binding of salicylate to human serum albumin (5) whose association constants are highly dependent on temperature.

The binding parameters of rat serum albumin gave a better fit to the observed rat plasma binding data than those of bovine serum albumin (Figs. 8 and 9A). The binding parameters of bovine serum albumin gave a better fit to the observed muscle homogenate binding data than those of rat serum albumin (Fig. 9B). Thus, interspecies and tissue differences in drug protein binding (other than temperature and protein concentration effects) should be considered.

The concept of the effective protein fraction is not applicable to the *in vivo* situation when there is a significant protein concentration effect on drug tissue homogenate binding or when the binding profile of the tissue homogenate differs greatly from that of serum albumin. Furthermore, the homogenated tissue sample does not always reflect the *in vivo* situation. The concept of the effective protein fraction is not a perfect method for predicting tissue binding. However, since it is difficult to measure tissue binding in a direct and perfect manner at present, appropriate use of the effective protein fraction will facilitate the development of useful physiologically based pharmacokinetic models.

Consequently, *in vitro* binding experiments for predicting *in vivo* situations would be best performed at approximate body temperature, using physiological protein levels, and at free drug concentrations in the pharmacologically useful range. In addition, interspecies differences in drug protein binding should be considered.

## REFERENCES

(1) C. F. Chignell and D. K. Starkweather, *Pharmacology*, **5**, 235 (1971).

(2) D. T. Witiak and M. W. Whitehouse, *Biochem. Pharmacol.*, **18**, 971 (1969).

(3) J. N. McArthur, P. D. Dawkins, and M. J. H. Smith, *J. Pharm. Pharmacol.*, **23**, 32 (1971).

(4) C. J. Bowmer and W. E. Lindup, *Biochem. Pharmacol.*, **27**, 937 (1978).

(5) J. F. Zarolinski, S. Keresztes-Nagy, R. L. Mais, and Y. T. Oester, *ibid.*, **23**, 1767 (1974).

(6) D. Shen and M. Gibaldi, *J. Pharm. Sci.*, **63**, 1698 (1974).

(7) R. L. Dedrick and K. B. Bischoff, *Chem. Eng. Prog. Symp. Ser.*, **64**, 32 (1968).

(8) L. R. Goldbaum and P. K. Smith, *J. Pharmacol. Exp. Ther.*, **111**, 197 (1954).

(9) B. B. Brodie, L. C. Mark, E. M. Papper, P. A. Lief, E. Bernstein, and E. A. Rovenstein, *ibid.*, **98**, 85 (1950).

(10) S. P. Colowick and F. C. Womack, *J. Biol. Chem.*, **244**, 774 (1969).

(11) Y. Sugiyama, T. Iga, S. Awazu, and M. Hanano, *J. Pharmacobiol. Dyn.*, **2**, 193 (1979).

(12) T. Nakagawa and Y. Koyanagi, "SALS, a computer program for statistical analysis with least squares fitting," Library Program of the University of Tokyo Computer Center, Tokyo, Japan, 1978.

(13) A. H. Anton and W. T. Corey, *Acta Pharmacol. Toxicol., Suppl. 3*, **29**, 134 (1971).

(14) S. W. Boobis and C. F. Chignell, *Biochem. Pharmacol.*, **28**, 751 (1979).

# Nitroglycerin Pharmacokinetics after Intravenous Infusion in Normal Subjects

E. F. McNIFF *, A. YACOBI ‡, F. M. YOUNG-CHANG §, L. H. GOLDEN §, A. GOLDFARB §, and HO-LEUNG FUNG *x

Received December 8, 1980, from the *Department of Pharmaceutics, State University of New York at Buffalo, Amherst, NY 14260, the ‡American Critical Care, McGaw Park, IL 60085, and the §Millard Fillmore Hospital, Gates Circle, Buffalo, NY 14209. Accepted for publication March 2, 1981.

**Abstract** □ The purpose of this investigation was to examine the pharmacokinetics of nitroglycerin in normal volunteers after intravenous drug administration. Eight subjects (including one subject on two occasions) received a dose of ~0.6 mg iv of nitroglycerin at a rate of 18 μg/min. Plasma concentrations of intact drug during and after the infusion were determined using a GLC method. Intra- and intersubject variability in nitroglycerin plasma kinetics was substantial. Generally, however, plasma nitroglycerin disposition was characterized by: (*a*) a large apparent plasma clearance (0.3–1 liter/min/kg), (*b*) a large volume of distribution (~3 liters/kg), and (*c*) a rapid plasma half-life (~3 min). From the apparent volume of distribution obtained, plasma drug can be estimated to account for only ~1.3% of total drug in the body. Minor fluctuations in tissue distribution, which can be produced by a myriad of external and internal stimuli, could cause dramatic fluctuation in plasma nitroglycerin concentrations and, hence, in the calculated pharmacokinetic parameters. For example, in two subjects studied, plasma nitroglycerin concentrations oscillated to such an extent that pharmacokinetic analysis could not be performed. In some subjects, steady-state concentrations were not observed in spite of the apparent short plasma half-life, and rebound in plasma concentrations during the postinfusion phase were evident. These phenomena were also observed in other kinetic studies involving organic nitrates.

**Keyphrases** □ Nitroglycerin—pharmacokinetics, intravenous infusion in normal subjects □ Pharmacokinetics—nitroglycerin, intravenous infusion in normal subjects □ Vasodilators—nitroglycerin, pharmacokinetics, intravenous infusion in normal subjects

Sublingual nitroglycerin has been used extensively for the relief of acute attacks of angina pectoris. Recently, intravenous nitroglycerin was shown to be effective in patients with congestive heart failure following myocardial infarction, for the treatment of coronary artery spasm in patients with variant forms of angina, for the reduction of arterial hypertension during coronary artery bypass, and for the induction of controlled hypotension during surgery.

## BACKGROUND

Although the hemodynamic response to nitroglycerin infusion has been studied extensively, little is known about nitroglycerin pharmacokinetics. Wei and Reid (1) reported plasma nitroglycerin concentrations in patients receiving intravenous infusions, but their data were limited to measurements of single plasma concentrations obtained after a 1-hr infusion. Recently, Armstrong *et al.* (2) studied nitroglycerin pharmacokinetics from arterial blood samples in patients with congestive cardiac failure. Their pharmacokinetic calculations of clearance and the volume of distribution also were based on one steady-state nitroglycerin concentration obtained at the time of the maximum infusion rate. Data was not presented to confirm that steady state was indeed achieved.

Nitroglycerin is known to have a high affinity for plastic materials used in intravenous infusion bags and administration sets (3–5). A significant fraction of the dose can be lost to the delivery system during intravenous nitroglycerin infusion, thus leading to significant errors in the estimation of pharmacokinetic parameters. Since the available literature on nitroglycerin kinetics (1, 2) does not make explicit reference to this factor, pharmacokinetic parameters generated from these reports may be subject to additional degrees of uncertainty.

The present investigation examined the pharmacokinetics of intravenously administered nitroglycerin in normal subjects. Methodological problems were avoided by preequilibrating the infusion administration sets with nitroglycerin solution and determining the actual dose infused into each subject directly from the nitroglycerin concentration in the infusion solution immediately before and after drug administration. Plasma nitroglycerin concentrations were determined during and after infusion. Additionally, noninvasive hemodynamic parameters were monitored during the study.

## EXPERIMENTAL

Eight healthy, nonsmoking, male adult volunteers underwent normal screening for vital signs, ECG, and laboratory parameters. Exclusion criteria included: (*a*) history of abnormalities of the cardiovascular, renal, or hepatic systems, blood, GI tract, or endocrine organs or any other significant disease state; (*b*) drug addiction including chronic marijuana use or alcoholism; and (*c*) chronic use of any medication.

**Screening for Nitroglycerin Hypersensitivity**—Prior to the study and at least 1 week before receiving the nitroglycerin infusion, each subject was prescreened for nitroglycerin hypersensitivity. This screening was done by sublingual administration of 0.15-mg doses of nitroglycerin[1] at 0, 7.5, 15.0, and 22.5 min for a total dose of 0.6 mg. Subjects who did not show any adverse reactions or nitrate hypersensitivity were included.

**Preparation of Infusion Solutions**—Nitroglycerin[2] was supplied in 10-ml ampuls containing 5 mg of nitroglycerin in a buffered solution of 10% ethanol. Five milliliters of this solution was added to 100 ml of normal saline (0.9%) in a glass intravenous container just prior to use.

**Saturation of Infusion Tubing**—Nitroglycerin adsorption to the infusion tubing was minimized by using a short length of tubing and preinfusion to saturate adsorption sites. The infusion solution was drawn first into a 50-ml glass syringe, which then was connected with the infusion tubing[3]. With an infusion pump[4], 10 ml was infused through the tubing at a rate of 0.382 ml/min, which then was increased to 0.764 ml/min until an additional 4 ml flowed through the tubing. The final 2 ml from this preinfusion procedure was collected for drug content assay (preinfusion sample). Following completion of the infusion into the subject, another 2-ml sample of the infusion solution was collected (postinfusion sample). The concentration of nitroglycerin in these two samples was compared with a sample taken directly from the glass intravenous bottle.

**Drug Administration**—Nitroglycerin solution was infused into a peripheral forearm vein through a polytef catheter[5] at a flow rate of 0.764 ml/min for 32 min. The nitroglycerin concentration in the infusion solutions was ~22 μg/ml, and the infusion rate was ~18 μg/min. The actual rate and the total amount of nitroglycerin administered to each subject were calculated from the assayed concentration of the infusion solutions.

**Blood Samples**—Disposable plastic syringes, previously determined not to cause drug loss (5), were used to draw blood samples through a peripheral vein cannula[5] in the arm not used for infusion. Following blood withdrawal, the cannula was flushed with heparin (100 U/ml) in 0.9% sodium chloride. Samples (5 ml) were drawn at 0 (just prior to infusion), 10, 20, 32, 34, 36, 38, 42, 47, 52, 62, and 77 min. Following transfer to silanized glass culture tubes and immediate centrifugation, the plasma was

[1] USP tablets, 0.15 mg (1/400 gr), lot 2GL77A Eli Lilly & Co., Indianapolis, Ind.
[2] Nitroglycerin solution, lot no. 19743 clinical trial material, American Critical Care, McGaw Park, Ill.
[3] K50 extension tubing, 50.8 cm, Pharmaseal, Toa Alta, Puerto Rico.
[4] Model 940, Harvard Apparatus, Millis, Mass.
[5] Angiocath, 20 ga × 1¼ in., The Deseret Co., Sandy, Utah.



0022-3549/81/0900-1054$01.00/0
© 1981, American Pharmaceutical Association

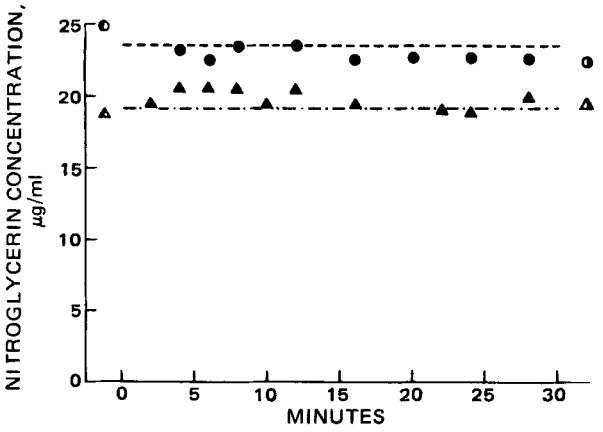


**Figure 1**—*Nitroglycerin concentration in infusion solutions during two simulated runs. Key to Run 1 samples: ◐, preinfusion; ●, during infusion; ◑, postinfusion; and ---, calculated infusion concentration. Key to Run 2 samples: ▲, preinfusion; ▲, during infusion; ▲, postinfusion; and –.–., calculated infusion concentration.*

separated and placed on ice until transported to the assay laboratory for storage at −20°. Sample analysis was performed as soon as possible and generally no later than 1 month after collection. These collection and storage conditions previously were shown to preserve nitroglycerin adequately (6).

**Hemodynamic Monitoring**—To ensure subject safety, hemodynamic status was determined periodically throughout the study. Blood pressure was determined by sphygmomanometry, and heart rate was measured manually or by an ECG monitoring device.

**Assay**—Plasma samples were assayed in duplicate according to a previously reported (7) GLC procedure. To increase sensitivity, the volumes of the plasma sample and the extraction solvent were increased to 0.5 ml. Caprylene was the internal standard. Recovery of nitroglycerin (~90%) was not affected by this modification.

A kinetic assay procedure (8, 9) was used to measure the nitroglycerin concentration of the infusion solutions.

**Calculations**—The actual infusion rate ($k_0$) for each subject was obtained by multiplication of the flow rate (0.764 ml/min) by the average of the nitroglycerin concentration in the preinfusion and postinfusion samples. In instances where no postinfusion sample was taken, the preinfusion concentration was used. The product of $k_0$ and the infusion time (32 min) yielded the total dose of nitroglycerin administered to each subject. Rebound in nitroglycerin plasma concentration occurred in several subjects, usually 10–20 min after infusion was terminated.

Estimates of pharmacokinetic parameters were obtained by using only those postinfusion data points that decreased in concentration chronologically. The elimination rate constant ($K$) was estimated by linear regression of the postinfusion log nitroglycerin plasma concentration *versus* time plot under such conditions. The area under the plasma nitroglycerin concentration *versus* time curve during the infusion period ($AUC_{0-32}$) was obtained using the spline method on a desk-top computer[6]. The postinfusion area ($AUC_{32-\infty}$) was computed by dividing the plasma nitroglycerin concentration at 32 min ($C_{32}$) by the estimated elimination rate constant. The total area then was obtained from the sum:

$$AUC_{0-\infty} = AUC_{0-32} + AUC_{32-\infty} \quad \text{(Eq. 1)}$$

The apparent systemic clearance ($Cl_s$) was calculated from:

$$Cl_s = \frac{\text{dose}}{AUC_{0-\infty}} \quad \text{(Eq. 2)}$$

and the apparent volume of distribution ($V_d$) was computed as:

$$V_d = \frac{Cl_s}{K} \quad \text{(Eq. 3)}$$

An additional estimate of the systemic clearance of nitroglycerin was obtained from:

$$Cl_s^* = \frac{k_0}{C_{32}} \quad \text{(Eq. 4)}$$

[6] Model 9825A, Hewlett-Packard, Fort Collins, Colo.

**Table I—Nitroglycerin Concentration (Micrograms per Milliliter) in Infusion Solutions**

| Subject[a] | Bottle Concentration | Preinfusion Sample | Postinfusion Sample | Calculated Infusion Concentration |
|---|---|---|---|---|
| 3 | 22.2 | 21.3 | 27.4 | 24.4 |
| 4 | 24.7 | 20.4 | 20.3 | 20.4 |
| 5A | 24.5 | 21.0 | 22.5 | 21.8 |
| 5B | 23.5 | 24.8 | —[b] | 24.8[c] |
| 6 | 25.6 | 22.2 | 36.1 | 29.2 |
| 7 | 22.3 | 19.7 | 23.2 | 21.4 |
| 8 | 22.5 | 21.5 | 21.6 | 21.5 |
| 9 | 23.4 | 24.4 | —[b] | 24.4[c] |
| 10 | 22.0 | 18.1 | —[b] | 18.1[c] |
| Mean | 23.4 | 22.6 | 25.2 | 22.8 |
| ±*SD* | 1.3 | 2.7 | 5.9 | 3.2 |

[a] Numbers arranged in chronological order of study. [b] Not determined; see text for explanation. [c] Concentration in preinfusion sample used.

## RESULTS

An *in vitro* experiment was conducted to determine whether the adopted regimen for the saturation of the infusion tubing was adequate in delivering a constant nitroglycerin concentration during dosing. Figure 1 shows the results of two separate runs in which the infusion systems were presaturated as described and the concentration of nitroglycerin emerging from the infusion system during a simulated infusion was determined as a function of time. It is apparent that the procedure produced a relatively stable effluent nitroglycerin concentration during the 32 min of infusion. The infusion concentration calculated from the mean of the preinfusion and postinfusion samples appeared to represent the actual infusion concentration adequately. The mean of the absolute difference

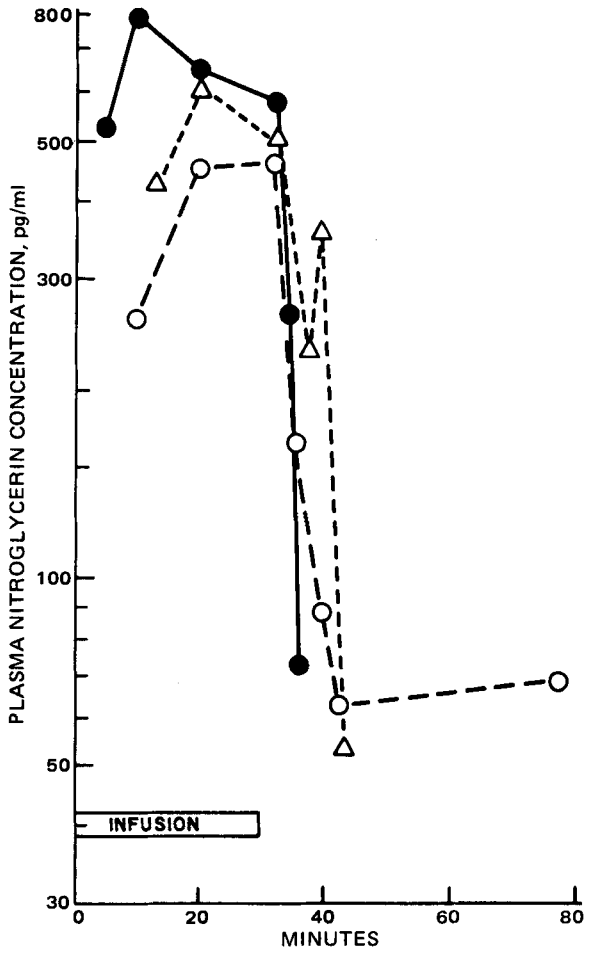


**Figure 2**—*Plasma nitroglycerin concentrations after intravenous administration to Subjects 5B (●), 7 (○), and 8 (△).*

**Table II—Pharmacokinetic Data Obtained after Intravenous Nitroglycerin Infusion in Normal Subjects**

| Subject | Infusion Rate, μg/min | Dose, μg | $K$, $min^{-1}$ | $t_{1/2}$, min | $V_d$, liters/kg | $Cl_s = \frac{D}{AUC}$, liters/min/kg | $Cl^* = \frac{k_0}{C_{32}}$, liter/min/kg | Apparent Steady State Achieved |
|---|---|---|---|---|---|---|---|---|
| 5B | 18.9 | 605 | 0.52 | 1.3 | 1.7 | 0.31 (29.8)[a] | 0.33 | Yes |
| 7 | 16.4 | 524 | 0.21 | 3.3 | 2.4 | 0.49 (37.7) | 0.43 | Yes |
| 8 | 16.5 | 527 | 0.19 | 3.7 | 2.9 | 0.54 (31.3) | 0.57 | Yes |
| 3 | 18.6 | 596 | 0.25 | 2.8 | 4.1 | 1.02 (73.4) | 0.67 | No |
| 4 | 15.5 | 496 | 0.18 | 3.8 | 5.2 | 0.94 (60.2) | 0.66 | No |
| 5A | 16.6 | 531 | 0.31 | 2.2 | 2.4 | 0.74 (71.0) | 0.47 | No |
| 9 | 18.6 | 598 | 0.31 | 2.2 | 4.1 | 1.03 (78.3) | 0.90 | No |
| 6 | 18.2 | 584 | — | — | — | — | — | -- |
| 10 | 21.5 | 688 | — | — | — | — | — | -- |
| Mean | 17.9 | 573 | 0.28 | 2.8 | 3.3 | 0.72 (54.5) | 0.58 | |
| ±*SD* | 1.8 | 59 | 0.12 | 0.9 | 1.2 | 0.28 (21.1) | 0.19 | |

[a] Number in parentheses represents total body clearance ($Cl_s$ × body weight), liters per minute.

of each sample concentration from the calculated infusion concentration was 2.8 and 4.1% for Runs 1 and 2, respectively.

Nitroglycerin concentrations in the infusion bottle, preinfusion, and postinfusion samples are shown in Table I. Analysis of variance (one way) showed that there was no statistical difference ($p > 0.35$) between these concentrations. Thus, the infusion system was apparently saturated with respect to adsorption, and the administered dose can be estimated from the infusion concentrations as described.

Subject 1 experienced nausea and fainting after the test sublingual doses were administered and was excused from the intravenous study. Subject 2 was not affected by the sublingual doses but was so nervous during the intravenous study that blood samples could not be easily withdrawn. No pharmacokinetic data were obtained from this subject.

Subjects 3–10 completed the study without any undesirable effects. Subject 5 was studied twice, separated by a period of 4 months. Intersubject variability in plasma nitroglycerin concentrations was quite large. Based on the shape of the plasma nitroglycerin concentration *versus* time profile, the data can be conveniently divided into three groups. Group A included three profiles (Fig. 2) in which steady-state nitroglycerin concentration was apparently achieved. Group B consisted of four profiles (Fig. 3) in which no steady state was apparent. Group C included two profiles (Fig. 4) in which plasma nitroglycerin concentrations were fluctuating erratically such that pharmacokinetic analysis was impossible.

Table II summarizes the individual data and the estimated pharmacokinetic parameters. The systemic clearance values were calculated according to both Eqs. 2 and 4. When an apparent steady state in plasma concentration was achieved during the infusion period, the two methods yielded essentially identical values. When an apparent steady state was not achieved, the value calculated by dose/$AUC$ was always larger than that obtained by $k_0/C_{32}$. Irrespective of the calculation method, the systemic nitroglycerin clearance was extremely rapid (~0.3–1 liter/min/kg). The apparent volume of distribution at 3.3 liters/kg also was high. Since plasma volume is ~42 ml/kg (10), the apparent volume of distribution for nitroglycerin was ~80 times the plasma volume.

Except in Subjects 6 and 10, nitroglycerin elimination was rapid; an average half-life of ~3 min was observed. In several subjects, an apparent rebound in plasma nitroglycerin concentration occurred at ~15 min after the infusion was stopped (Figs. 2–4). Fortunately, this phenomenon occurred generally after the washout elimination phase had gone through two or three apparent half-lives. Thus, pharmacokinetic analysis of the remaining infusion data could be performed without these later time points.

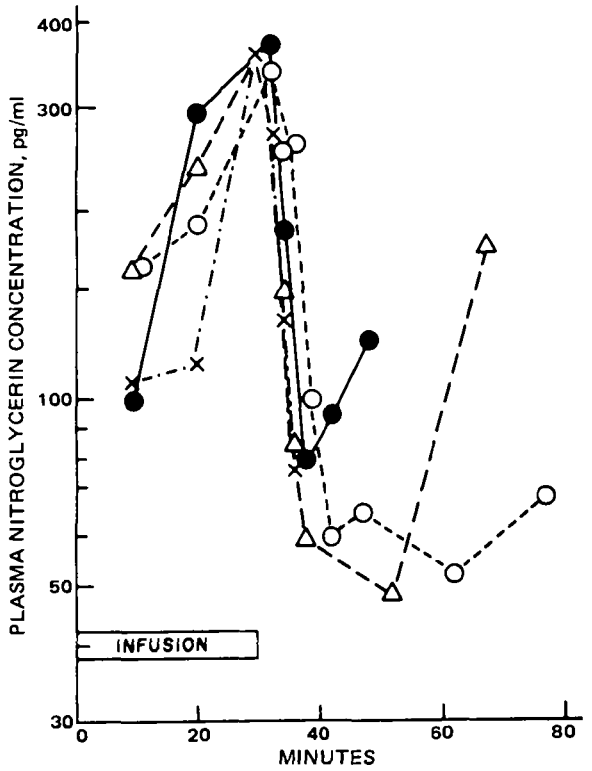


**Figure 3**—*Plasma nitroglycerin concentrations after intravenous administration to Subjects 3 (●), 4 (○), 5A (△), and 9 (×).*

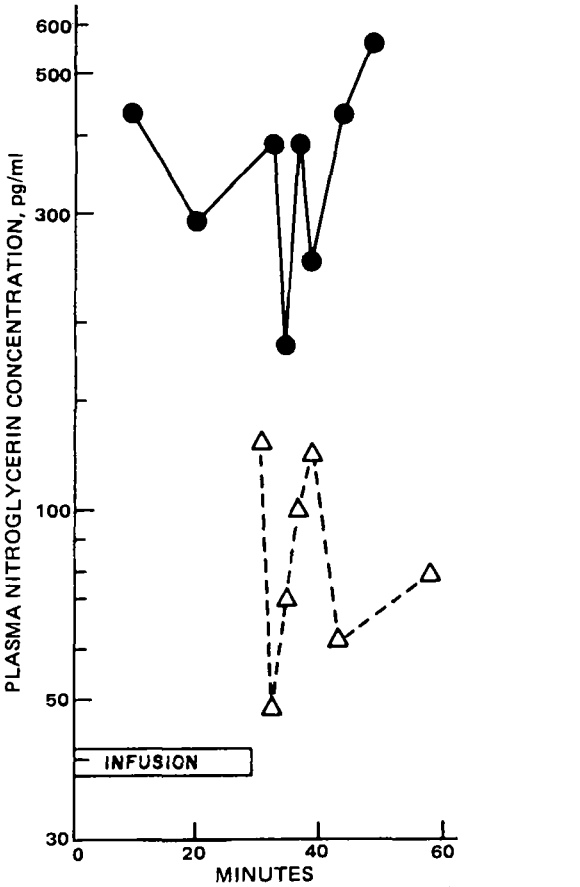


**Figure 4**—*Plasma nitroglycerin concentrations after intravenous administration to Subjects 6 (●) and 10 (△).*

**Table III—Mean Heart Rate and Systolic and Diastolic Blood Pressure in Seven Normal Subjects [a] following Intravenous Infusion of 0.6 mg of Nitroglycerin during 30 min**

| Parameter | Mean | *SD* |
|---|---|---|
| Heart rate per minute | | |
| Preinfusion, control | 67.7 | 14.0 |
| Postinfusion, maximum | 75.4 | 14.9 |
| Postinfusion, minimum | 61.4 | 11.1 |
| Systolic blood pressure, mm/Hg | | |
| Preinfusion, control | 117.1 | 20.6 |
| Postinfusion, maximum | 118.7 | 16.8 |
| Postinfusion, minimum | 106.0 | 15.3 |
| Diastolic blood pressure, mm/Hg | | |
| Preinfusion, control | 76.6 | 10.4 |
| Postinfusion, maximum | 80.3 | 8.8 |
| Postinfusion, minimum | 72.6 | 9.3 |

[a] In two subjects, these parameters were monitored but not reported.

In the early part of this study, the cannula used for infusion was removed from the subjects as soon as possible. This step was taken ~15 min after cessation of the infusion. Initial data analysis suggested that removal of the cannula might be coincidental with the rebound in plasma drug concentrations. It was reasoned that manipulation of the cannula during removal might cause disturbance and release of tissue bound drug near the infusion site or of a small volume of infusion solution from the cannula into plasma, resulting in transient increases in plasma nitroglycerin concentrations. To test this hypothesis, Subject 5 was used again and Subjects 9 and 10 were studied without disturbing the infusion cannula during the entire postinfusion sampling period. Inspection of the respective plasma concentration profiles indicates that this procedure had no apparent effect. In fact, Subject 10 was one of the two subjects whose plasma kinetics showed the most fluctuation. In cases where the infusion cannula remained in place during the postinfusion sampling period, no postinfusion sample of the dosing solution was collected.

The dose infused (0.6 mg over 0.5 hr) did not produce any significant changes in heart rate or systolic and diastolic blood pressures in the subjects (Table III).

## DISCUSSION

Plasma nitroglycerin kinetics are characterized by rapid disappearance and an apparently large plasma clearance. The plasma half-life of nitroglycerin determined from this study (2.8 ± 0.9 min, mean ± *SD*) is in good agreement with values reported by Armstrong *et al.* (2, 11) for arterial samples after intravenous administration (1.9 min) and after sublingual nitroglycerin dosing (4.4 min). Recently, these authors also reported (12) a half-life of *in vitro* nitroglycerin degradation in human blood of ~6 min at 37°. Therefore, *in vivo* blood (plasma) elimination of nitroglycerin is at least a result of both blood degradation and organ metabolism, the latter most probably by the liver (13).

The apparent plasma clearance determined in this study ranged from 0.31 to 1.03 liters/min/kg, corresponding to values of total body clearance of 29.8–78.3 liters/min. Although there are some methodological differences among this study and previous ones (1, 2), the apparent systemic clearance values determined from each of the three studies were all quite high (Table IV).

The data of Armstrong *et al.* (2) require some additional comments. These authors utilized arterial samples, and preliminary reports (14, 15) suggested that arterial nitroglycerin concentrations might be substantially higher than those found in peripheral veins. The somewhat lower systemic clearance values obtained by these authors are consistent with this suggestion. In addition, their patients were classified into two groups. Patients in Group 1 were generally responsive to hemodynamic management with nitroglycerin infusion, while those in Group 2 seemed to be refractory to nitroglycerin treatment. Group 1 patients received a lower infusion rate than patients in Group 2 (15–94 *versus* 59–440 μg/min, respectively) and showed higher ($p < 0.005$) systemic clearances (13.8 *versus* 3.6 liters/min, respectively). Based on the infusion rate, it is perhaps more appropriate to compare results from the normal subjects in the present study with those of Group 1 patients from the previous study.

Substantial intersubject variability in nitroglycerin kinetics was observed in the present study. The plasma nitroglycerin concentrations of Subjects 5B (second trial), 7, and 8 seemed to reach apparent steady state during the 32-min infusion. The good agreement obtained between $Cl_s$ values calculated from Eqs. 2 and 4 confirmed that steady state was achieved. The average clearance from these three subjects was 0.45 liter/min/kg, which agreed well with a value of 28 liters/min (0.4 liter/min/kg assuming an average body weight of 70 kg) reported previously (11) following sublingual nitroglycerin administration.

In contrast, the plasma nitroglycerin concentrations of Subjects 3, 4, 5A (first trial), and 9 did not approach apparent steady-state values. In these cases, the clearance value estimated with the *AUC* was much larger than that calculated using $k_0/C_{32}$ and also larger than that found with the first group. This result suggests that a significant portion of the area may be unaccounted for in these subjects. The estimated plasma half-lives in these subjects, however, were not dissimilar from those found with the first group, nor were they substantially different from values of 4.4 min reported after sublingual nitroglycerin (11) and of 1.9 min in arterial samples (2) after intravenous infusion. Nevertheless, a terminal disposition phase that is below the present limits of detection possibly may exist. The presence of a prolonged $\beta$-phase is consistent with the lack of attainment of steady-state plasma concentrations in these subjects. However, Subject 5 behaved differently in two separate trials: in the first trial (5A), steady state was achieved while in the second trial (5B), it was not. This information suggests that plasma nitroglycerin kinetics could vary substantially.

By using the apparent clearance values obtained, an apparent volume of distribution of 3.3 ± 1.2 liters/kg (mean ± *SD*) can be estimated. By using a plasma volume of 42 ml/kg (10), the amount of nitroglycerin residing in the plasma compartment can account for 1.3% of the total body load. Minor fluctuations in nitroglycerin content in the nonplasma (tissue) compartment, which may result from a host of internal and external stimuli, could cause dramatic fluctuations in plasma nitroglycerin concentrations. In Subjects 6 and 10, such wide fluctuations in plasma nitroglycerin concentrations occurred that no pharmacokinetic analysis was possible. Coincidentally, there was difficulty in placing the intravenous catheter in these two subjects. It is interesting to speculate that the release of endogenous substances after minor tissue damage may have some effect on the tissue distribution of nitroglycerin.

Although this study was not designed to examine the hemodynamic response to nitroglycerin infusion in detail, no significant change was observed in the monitored parameters. This finding is not surprising in view of the small doses and low infusion rates employed. In fact, nitroglycrin has been infused in normal subjects at rates as high as 200 μg/min with no significant adverse hemodynamic effect (16).

The observation of apparent rebound and oscillations in plasma nitrate concentrations in some subjects is not unique to this study. A similar phenomenon (17) was recently reported following intravenous infusion of isosorbide dinitrate. Because of its extensive tissue distribution, rapid plasma clearance of nitroglycerin during the postinfusion period may lead to a nonequilibrium redistribution of tissue drug back to the plasma compartment. The situation may be analogous to that observed for serum procainamide concentrations in patients immediately after hemodialysis (18). In that case, rebound and oscillations of procainamide concentra-

**Table IV—Comparison of Study Methods and Pharmacokinetic Parameters Obtained among Three Investigations**

| | Wei and Reid (1) | Armstrong *et al.* (2) | Present |
|---|---|---|---|
| Subjects | Patients with acute myocardial infarction | Patients with congestive heart failure | Normal volunteers |
| *n* | 5 | 16 | 8 |
| Apparent infusion rate, μg/min | 37.5–175 | 15–440 | 15–22 |
| Blood sampling site | Vein (unspecified) | Radial artery | Antecubital vein |
| Calculated systemic clearance, liters/min | 14–146 | 7.0–24.7[a]<br>0.9–6.4[b] | 29.8–78.3 |
| Mean elimination half-life, min | — | 1.9 | 2.8 |

[a] Responsive group as defined in Ref. 2. [b] Nonresponsive group as defined in Ref. 2.

tions were attributed to shifts of drug into and out of various body compartments following drug clearance by hemodialysis (18).

Finally, the very large apparent plasma nitroglycerin clearance observed in this and other studies (1, 2) after intravenous administration warrants some comments. The apparent plasma clearance is not only greater than liver plasma flow but it also exceeds cardiac output. Physiologically, it is difficult to conceive how any drug can be cleared, in reality, faster than cardiac output. However, several possibilities might have led to the present experimental observation.

First, the dose actually infused into each subject was substantially less than that used in the pharmacokinetic calculation. For the apparent plasma nitroglycerin clearance to equal cardiac output [~7 liters/min for a 70-kg man at rest (19)], the dose infused would have to be ~10–25% of the dose used in calculation. This wide divergence in dose is considered unlikely because of the great care taken in the present study to minimize and account for drug adsorption in the infusion sets and because nitroglycerin concentrations emerging at the end of the infusion line were actually determined before and after infusion.

Second, there is substantial nitroglycerin degradation in the blood itself due to spontaneous hydrolysis or enzymatic breakdown. Armstrong *et al.* (12) gave a $t_{1/2}$ of 6 min for *in vitro* nitroglycerin degradation in human blood at 37°. If it can be assumed that this half-life reflects *in vivo* spontaneous blood degradation, the contribution of this process to the total apparent clearance will be $0.693/6 \times 69 \simeq 8.0$ ml/min/kg [using a blood volume of 69 ml/kg of body weight (10)], which is ~1% of the total apparent clearance (Table II). Even if the half-life of *in vivo* blood degradation is assumed to be equal to the systemic *in vivo* plasma half-life ($t_{1/2}$ = 3 min, Table II), the maximum contribution of spontaneous blood degradation to the apparent clearance will still be only ~2%.

Third, the *AUC* used in the calculation of clearance does not represent the total *AUC; i.e.*, a much longer secondary or tertiary plasma half-life exists but cannot be experimentally determined because of assay limitations. However, in the present study the plasma nitroglycerin concentrations in three subjects appeared to have reached steady state within the short infusion period of 15 min. In these subjects, a hidden and prolonged half-life probably does not exist.

Fourth, when the drug is infused into the systemic circulation, a first-pass removal process possibly may be present in the vascular bed so that the infused dose is not totally available to the systemic circulation. In other words, the vascular bed functions as a first-pass extraction tissue towards an intravenous dose of nitroglycerin in much the same way that the liver serves as a first-pass extraction organ for an oral dose. If this assumption is correct, then the apparent clearance values obtained will have to be corrected by an apparent bioavailability factor, which is less than unity. The demonstration of substantial differences in arterial *versus* venous nitroglycerin concentrations (14, 15) is not inconsistent with the hypothesis that blood vessels can clear nitroglycerin. Experiments conducted in rats (20) suggested that first-pass vessel uptake of nitroglycerin does occur. The apparent bioavailability factor, however, was not quantitated. The extent of the contribution of this phenomenon to the observed clearance value in humans also is unknown at present.

In conclusion, nitroglycerin kinetics in humans are characterized by apparent extensive tissue distribution and rapid plasma clearance. Because of these factors, plasma nitroglycerin concentrations may be subjected to high intra- and intersubject variabilities. This does not necessarily mean, however, that the effects produced by intravenous nitroglycerin also may be highly variable. Indeed, data from this laboratory (20) suggested that the presumed target tissue of nitroglycerin, the blood vessels, has a much higher concentration of drug compared to plasma. The systemic pharmacological effects of nitroglycerin may be better related to drug concentrations in the blood vessels than to those in plasma. Studies are in progress to characterize the pharmacokinetics of nitroglycerin in these presumed target tissues.

## REFERENCES


(1) J. T. Wei and P. R. Reid, *Circulation*, **59**, 588 (1979).

(2) P. W. Armstrong, J. A. Armstrong, and G. S. Marks, *ibid.*, **62**, 160 (1980).

(3) P. A. Cossum, M. S. Roberts, A. J. Galbraith, and G. W. Boyd, *Lancet*, **2**, 349 (1978).

(4) D. M. Baaske, A. H. Amann, D. M. Wagenknecht, M. Mooers, J. E. Carter, H. J. Hoyt, and R. G. Stoll, *Am. J. Hosp. Pharm.*, **37**, 201 (1980).

(5) B. L. McNiff, E. F. McNiff, and H.-L. Fung, *ibid.*, **36**, 173 (1979).

(6) G. A. Maier, A. Poliszczuk, and H.-L. Fung, *Int. J. Pharm.*, **4**, 75 (1979).

(7) S. K. Yap, E. F. McNiff, and H.-L. Fung, *J. Pharm. Sci.*, **67**, 682 (1978).

(8) H.-L. Fung, P. Dalecki, E. Tse, and C. T. Rhodes, *ibid.*, **62**, 696 (1973).

(9) S. K. Yap, C. T. Rhodes, and H.-L. Fung, *Am. J. Hosp. Pharm.*, **32**, 1039 (1975).

(10) "Scientific Tables, Documenta Geigy," 7th ed., J. R. Geigy, S. A., Basel, Switzerland, 1970.

(11) P. W. Armstrong, J. A. Armstrong, and G. S. Marks, *Circulation*, **59**, 585 (1979).

(12) J. A. Armstrong, S. E. Slaughter, G. S. Marks, and P. W. Armstrong, *Can. J. Physiol. Pharmacol.*, **58**, 459 (1980).

(13) G. A. Maier, C. Arena, and H.-L. Fung, *Biochem. Pharmacol.*, **29**, 646 (1980).

(14) J. F. Brymer, P. L. Stetson, J. A. Walton, Jr., B. Lucchesi, and B. Pitt, *Clin. Res.*, **27**, 229A (1979).

(15) P. W. Armstrong, J. A. Armstrong, and G. S. Marks, *Circulation*, **62**(III), 326 (1980).

(16) B. Christenson, I. Nordenfelt, H. Westling, and T. White, *Scand. J. Clin. Lab. Invest.*, **23**, 49 (1969).

(17) T. Taylor, L. F. Chasseaud, E. Doyle, A. Darragh, D. A. O'Kelly, and D. Fitzgerald, *Biopharm. Drug Dispos.*, **1**, 149 (1980).

(18) T. P. Gibson, E. J. Matusik, and W. A. Briggs, *Clin. Pharmacol. Ther.*, **19**, 206 (1976).

(19) J. T. Shepard and P. M. Vanhoutte, in "The Human Cardiovascular System, Facts and Concepts," Raven, New York, N.Y., 1979.

(20) A. Kamiya and H.-L. Fung, in "Abstracts of Papers presented before the APhA Academy of Pharmaceutical Sciences," 11(No. 1), 78 (1981).


## ACKNOWLEDGMENTS


Supported in part by National Institutes of Health Grants GM 20852 and 5T32 GM 07145 (E. F. McNiff). Support by American Critical Care is gratefully acknowledged.

# Synthesis of *N*-Glycosylthioureas, *N*-Glycosylrhodanines, and *N*-Glycosyl-2-aminothiazoles and Their Antimicrobial Activity

**WILLIAM O. FOYE** ˣ **and SEUNG HO AN**

Received December 5, 1980, from the *Samuel M. Best Research Laboratory, Massachusetts College of Pharmacy and Allied Health Sciences, Boston, MA 02115.* Accepted for publication March 4, 1981.

**Abstract** □ A method for obtaining *N*-β-D-glucopyranosylthioureas was found in the aminolysis of *N*-(2,3,4,6-tetra-*O*-acetyl-β-D-glucopyranosyl)-5-aralkylidenerhodanines. Aminolysis of the triacetylated or tribenzoylated ribosylrhodanines generally did not give ribosylthioureas but resulted in glycosidic cleavage, although *N*-(2,3,5-tri-*O*-benzoyl-β-D-ribofuranosyl)thioureas were obtained using morpholine and hydroxylamine. Ring closure of *N*-β-D-glucopyranosylthiourea with ethyl bromopyruvate gave ethyl 2-(*N*-β-D-glucopyranosyl)aminothiazole-4-carboxylate, and ammonolysis led to the corresponding 4-carboxamide. Antimicrobial screening against five microorganisms showed that *N*-(2,3,5-tri-*O*-acetyl-β-D-ribofuranosyl)rhodanine and the glucosylaminothiazole-4-carboxylate had the broadest spectrum of inhibitory activity, although the thioureas usually showed inhibition of some organisms.

**Keyphrases** □ *N*-Glycosylthioureas, rhodanines, and 2-aminothiazoles—synthesis, screened for antimicrobial activity □ Glucopyranosylthioureas—synthesis, screened for antimicrobial activity □ Antimicrobial activity—*N*-glycosylthioureas, *N*-glycosylrhodanines, and *N*-glycosyl-2-aminothiazoles

A method for obtaining *N*-β-D-glucopyranosylthiourea in good yield was previously reported (1). It involved the ammonolysis in methanol of *N*-(2,3,4,6-tetra-*O*-acetyl-β-D-glucopyranosyl)-5-aralkylidenerhodanines (I), resulting in deacetylation, ring cleavage, and formation of the thiourea (II). Fischer (2) synthesized tetra-*O*-acetyl-

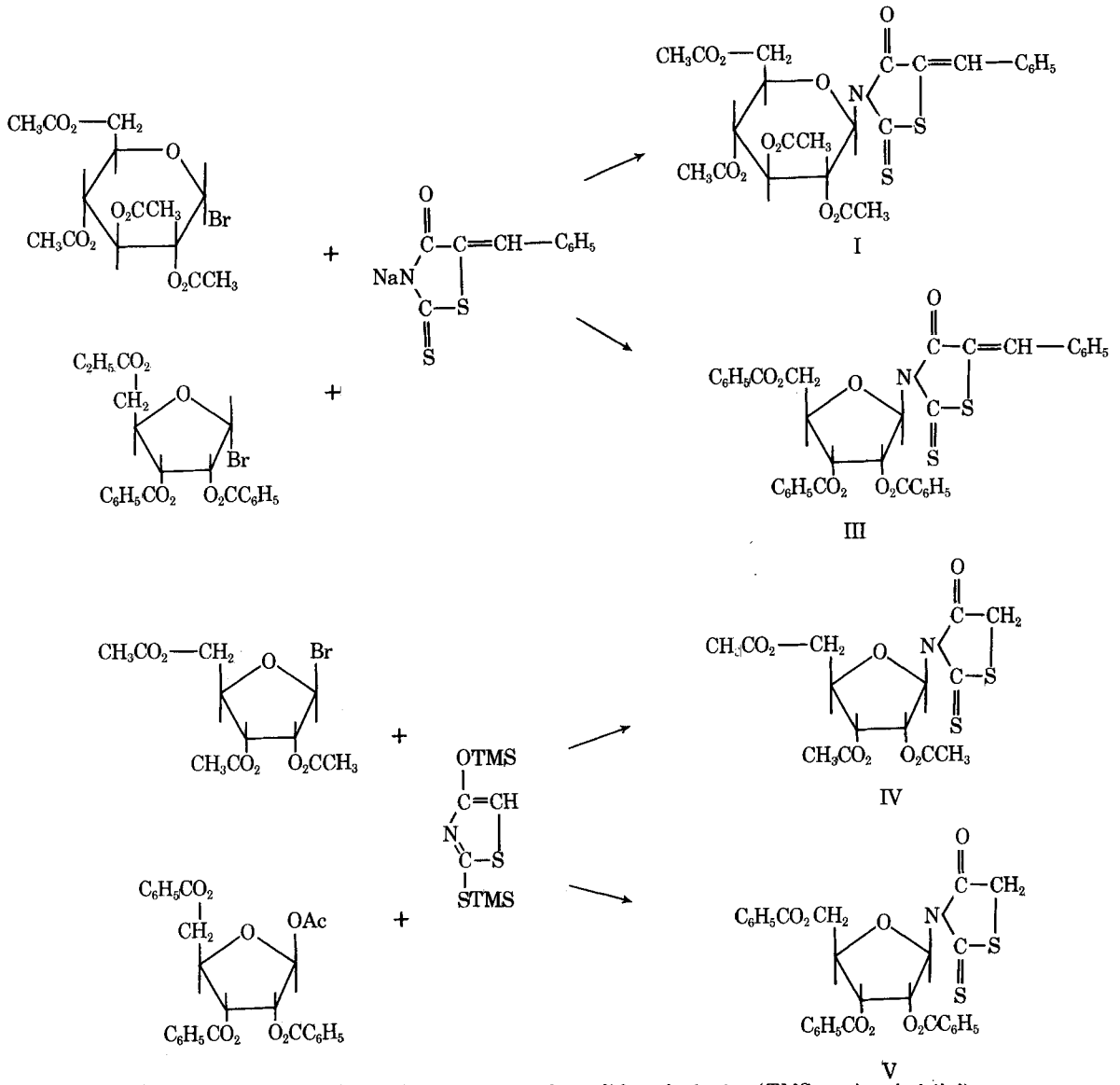

*Scheme I—Glycosylation of rhodanine and 5-benzylidenerhodanine (TMS = trimethylsilyl).*

0022-3549/81/0900-1059$01.00/0
© 1981, American Pharmaceutical Association

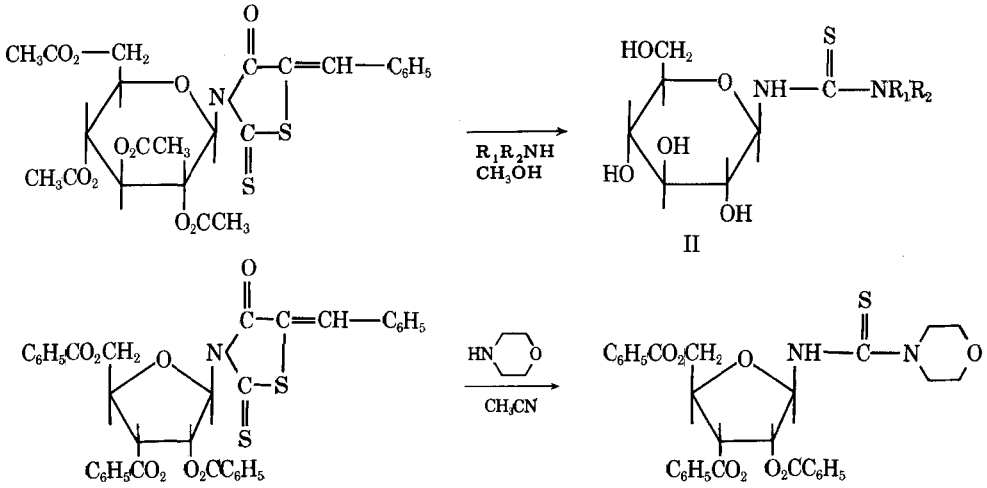

*Scheme II—Aminolysis of glycosyl-5-benzylidenerhodanines.*

glucopyranosylthiourea from tetra-*O*-acetylglucopyranosylisothiocyanate and ammonia and obtained the deacetylated product in good yield. Other investigators utilized the Fischer procedure to obtain deacetylated glucopyranosylthioureas but got only poor yield (3) or none at all (4). Fusion of glucose and thiourea resulted in a very low yield of glucopyranosylthiourea (5).

A logical extension of this reaction is the use of amines, in place of ammonia, to obtain *N*-substituted glucopyranosylthioureas. Such compounds have potential as antibacterial, antiviral, and anticancer agents. A number of thioureas have demonstrated activity as antiviral (6, 7) and as antibacterial–antifungal (8, 9) agents. Rhodanine and its derivatives have shown antibacterial (10) and antifungal (11) activities, as well as antiviral activity against Echovirus 12 (12) and activity as inhibitors of neuraminidases (13). To provide compounds with anticancer potential, attempts were made to prepare ribosyl derivatives of both rhodanine and the thioureas; ring closure of the glucosylthiourea to glucosylthiazoles also was performed.

## DISCUSSION

**Chemistry**—The glycosylrhodanines (I and III) were synthesized by glycosidation of 5-benzylidenerhodanine sodium salt with either 2,3,4,6-tetra-*O*-acetyl-α-D-glucopyranosyl bromide or 2,3,5-tri-*O*-benzoyl-D-ribofuranosyl bromide in acetone or acetonitrile. Yields of 65–82% were obtained. Another procedure, particularly useful for obtaining ribosylrhodanines, involved reaction of a silylated rhodanine with either 2,3,5-tri-*O*-acetyl-β-D-ribofuranosyl bromide or 1-*O*-acetyl-2,3,5-tri-*O*-benzoyl-β-D-ribofuranose in the presence of stannic chloride. With unsubstituted rhodanine, 92 and 93% yields of the triacetyl (IV) and tribenzoyl (V) derivatives were realized, respectively; with the 5-benzylidene derivatives, 57 and 65% yields were obtained, respectively. Silylation was carried out using hexamethyldisilazane, chlorotrimethylsilane, and toluene. The glycosylation reactions are shown in Scheme I.

Aminolysis of *N*-(2,3,4,6-tetra-*O*-acetyl-β-D-glucopyranosyl)-5-benzylidenerhodanine was carried out using an excess of various amines in methanol in a pressure bottle at room temperature for 1–4 days. Yields of 41–92% of the glucosylthioureas were obtained (Table I). The by-products, α-mercaptocinnamyl amides (13) and acetamides, were separated by column chromatography where fractional recrystallization was unsuccessful. The $R_f$ values for the thioureas and the by-products are listed in Table II. Aminolysis of *N*-(2,3,5-tri-*O*-benzoyl-β-D-ribofuranosyl)-5-benzylidenerhodanine was attempted with several amines, using the same procedure. Ribosylthioureas were not obtained, apparently because of the instability of the glycosidic linkage. In the case of morpholine, however, *N*-(2,3,5-tri-*O*-benzoyl-β-D-ribofuranosyl)morpholine-4-thiocarboxamide (VI) was isolated. When this compound was treated with methanolic ammonia, cleavage of the glycosidic linkage was again observed, and morpholine-4-thiocarboxamide was isolated. An *N*-(2,3,5-tri-*O*-benzoyl-β-D-ribofuranosyl)thiourea was also isolated on reaction with hydroxylamine and triethylamine, but the ethoxythiourea was the product. Aminolysis of *N*-(2,3,5-tri-*O*-acetyl-β-D-ribofuranosyl)-5-benzylidenerhodanine and *N*-(2,3,5-tri-*O*-acetyl-β-D-ribofuranosyl)rhodanine using several amines again resulted in glycosidic cleavage. Aminolyses are shown in Scheme II.

The *N*-β-D-glucopyranosylthiourea prepared from I (R = benzylidene) and methanolic ammonia was treated with ethyl bromopyruvate to give ethyl 2-(*N*-β-D-glucopyranosyl)aminothiazole-4-carboxylate (VII) in a 92% yield (Scheme III). Ammonolysis of this compound in methanol gave the corresponding 4-carboxamide (VIII).

IR spectra of the glucosylthioureas revealed broad, hydrogen-bonded hydroxyl groups at 3300–3500 $cm^{-1}$ and the appearance of NH at 1520–1570, C=S at 1060–1080, and a β-glycosidic linkage at 890–920 $cm^{-1}$. The characteristic acetylglucopyranosylrhodanine peaks at 1750 (acetyl C=O), 1675–1700 (rhodanine C=O), and 1240 (C=S) $cm^{-1}$ were absent. The PMR spectra showed an absence of acetyl hydrogens in the 1.9–2.1-ppm region. A peak for the anomeric proton appeared at 5.07–5.40 ppm ($J$ = 8–9 Hz), which also indicated a β-configuration (14). The NH

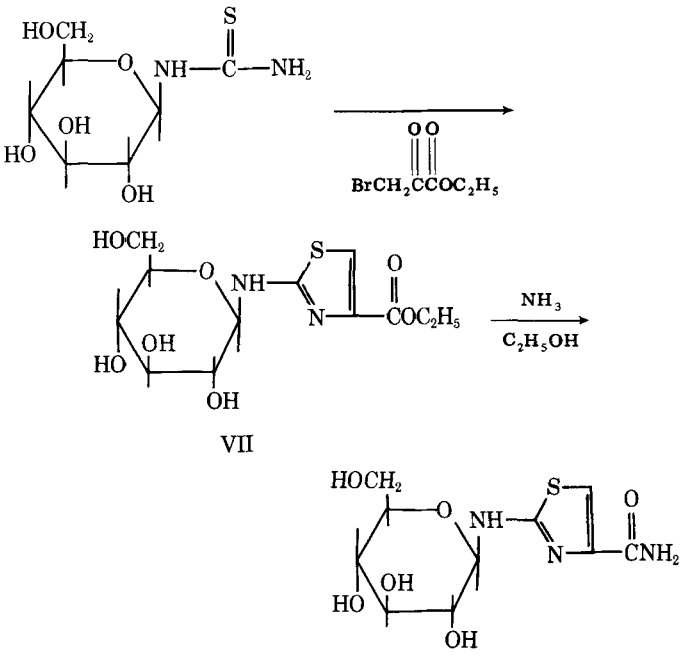

*Scheme III—Synthesis of 2-(glucosyl)aminothiazoles.*

**Table I—Physical Properties of *N*-β-D-Glucopyranosylthioureas**

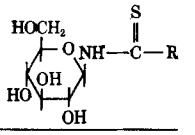

| R | Formula | Melting Point | Yield, % | $[\alpha]_D^{25}$ (Solvent) | Analysis, % | Calc. | Found |
|---|---|---|---|---|---|---|---|
| $NH_2$ | $C_7H_{14}N_2O_5S$ | 207–209° dec. | 87 | −34.85° (water) | C | 35.29 | 34.92 |
| | | | | | H | 5.92 | 6.20 |
| | | | | | N | 11.76 | 11.54 |
| | | | | | S | 13.46 | 13.38 |
| $N(CH_3)_2$ | $C_9H_{18}N_2O_5S \cdot \frac{1}{6} H_2O$ | 183–184° dec. | 70 | −4.40° (dimethylformamide) | C | 40.14 | 40.34 |
| | | | | | H | 6.86 | 6.76 |
| | | | | | N | 10.40 | 9.94 |
| | | | | | S | 11.90 | 11.75 |
| $N(C_2H_5)_2$ | $C_{11}H_{22}N_2O_5S \cdot H_2O$ | 106–109° dec. | 81 | −11.0° (water) | C | 42.29 | 42.57 |
| | | | | | H | 7.74 | 7.66 |
| | | | | | N | 8.96 | 8.87 |
| | | | | | S | 10.26 | 10.34 |
| $NH(CH_2)_3CH_3$ | $C_{11}H_{22}N_2O_5S \cdot \frac{2}{3} (CH_3)_2CO$ | 94–96° dec. | 80 | −15.4° (water) | C | 46.87 | 46.40 |
| | | | | | H | 7.83 | 7.68 |
| | | | | | N | 8.41 | 8.42 |
| | | | | | S | 9.63 | 9.60 |
| $NHCH_2CH{=}CH_2$ | $C_{10}H_{18}N_2O_5S \cdot (CH_3)_2CO$ | 95–97° dec. | 44 | −25.8° (water) | C | 46.41 | 45.95 |
| | | | | | H | 7.19 | 7.09 |
| | | | | | N | 8.33 | 8.18 |
| | | | | | S | 9.53 | 9.36 |
| $NHCH_2C_6H_5$ | $C_{14}H_{20}N_2O_5S \cdot (CH_3)_2CO$ | 97–100° dec. | 64 | −19.1° (water) | C | 52.83 | 52.69 |
| | | | | | H | 6.78 | 6.56 |
| | | | | | N | 7.28 | 7.21 |
| | | | | | S | 8.30 | 8.10 |
| $NHCH_2CH_2C_6H_5$ | $C_{15}H_{22}N_2O_5S$ | 87–89° dec. | 78 | −19.0° (water) | C | 52.62 | 52.35 |
| | | | | | H | 6.48 | 6.42 |
| | | | | | N | 8.18 | 7.90 |
| | | | | | S | 9.36 | 9.61 |
| 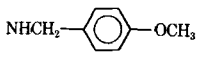 | $C_{15}H_{22}N_2O_6S$ | 82–85° dec. | 73 | −20.3° (water) | C | 50.27 | 50.35 |
| | | | | | H | 6.19 | 6.14 |
| | | | | | N | 7.82 | 7.69 |
| | | | | | S | 8.96 | 9.13 |
| 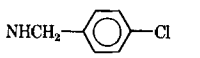 | $C_{14}H_{19}ClN_2O_5S$ | 83–84° dec. | 62 | +6.2° (dimethylformamide) | C | 46.35 | 46.31 |
| | | | | | H | 5.28 | 5.40 |
| | | | | | Cl | 9.77 | 9.63 |
| | | | | | N | 7.72 | 7.77 |
| | | | | | S | 8.84 | 8.88 |
| 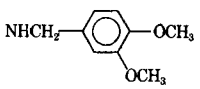 | $C_{16}H_{24}N_2O_7S$ | 105° dec. | 92 | −1.3° (methanol) | C | 49.47 | 50.00 |
| | | | | | H | 6.23 | 5.92 |
| | | | | | N | 7.21 | 7.06 |
| | | | | | S | 8.25 | 8.35 |
| | $C_{10}H_{18}N_2O_5S \cdot (CH_3)_2CO$ | 95–97° dec. | 44 | −25.8° (water) | C | 46.41 | 45.95 |
| | | | | | H | 7.19 | 7.09 |
| | | | | | N | 8.33 | 8.18 |
| | | | | | S | 9.53 | 9.36 |
| 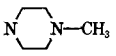 | $C_{12}H_{23}N_3O_5S$ | 175–177° dec. | 50 | −12.2° (water) | C | 44.84 | 44.94 |
| | | | | | H | 7.21 | 7.20 |
| | | | | | N | 13.07 | 12.97 |
| | | | | | S | 9.98 | 10.13 |
| | $C_{11}H_{20}N_2O_6S \cdot H_2O$ | 179–181° | 79 | −8.2° (dimethylformamide) | C | 40.48 | 40.54 |
| | | | | | H | 6.80 | 6.69 |
| | | | | | N | 8.56 | 8.58 |
| | | | | | S | 9.82 | 9.65 |
| | $C_{11}H_{20}N_2O_5S_2$ | 148–151° dec. | 40 | +3.05° (dimethylformamide) | C | 40.72 | 40.54 |
| | | | | | H | 6.21 | 6.38 |
| | | | | | N | 8.63 | 8.31 |
| | | | | | S | 19.77 | 19.44 |

glycoside peak appeared at 7.25–8.40 ppm ($J$ = 8 Hz) and was replaceable with deuterium oxide.

The ribosylrhodanines and ribosylthioureas gave the expected IR absorptions, with benzoyl C=O stretching frequencies appearing at 1725–1730 $cm^{-1}$ for the benzoylribose compounds and acetyl C=O stretching appearing at 1750 $cm^{-1}$ for the acetyl derivatives. The C=S stretching vibration appeared at 1230–1270 $cm^{-1}$ in the rhodanine ring and at 1110–1115 $cm^{-1}$ in the thioureas. The C=O stretching vibration in the ribosylrhodanines was at 1720–1740 $cm^{-1}$, a higher frequency than that for the C=O of the 5-substituted rhodanines (1675–1700 $cm^{-1}$).

The most characteristic PMR peaks of the ribosylrhodanines were of the benzylidene CH or 5-$CH_2$ of the rhodanine ring, appearing as singlets at 7.67–7.78 or 3.90–4.19 ppm, respectively. The anomeric proton was seen as a doublet ($J$ = 2–4 Hz) at 6.15–6.77 ppm. The anomeric proton of the ribosylthioureas was found as a broad singlet at 5.80–5.86 ppm, and the NH glycosidic proton appeared at 8.40–9.10 ppm. In general, the β-glycosidic linkages of heterocyclic ribosides have been observed (15) rather than the α-forms. The three protons on C-4 and C-5 of the ribose ring overlapped as a multiplet at 3.57–4.70 ppm.

The anomeric proton of the glucosylaminothiazoles was unclear in the PMR spectrum. The NH proton appeared at 8.20 ppm ($J$ = 8 Hz), and the C-5 proton of the thiazole ring was seen as a singlet at 7.30–7.62 ppm. The methylene protons of the glucosyl moiety appeared as a multiplet at 3.50 ppm.

**Antimicrobial Activity**—Antimicrobial activities were observed by the agar plate screening method using *Staphylococcus aureus*, *Escherichia coli*, *Pseudomonas aeruginosa*, *Candida albicans*, and *Aspergillus niger*. These organisms represent a Gram-positive and two Gram-negative bacteria, a yeast, and a mold, respectively. Compounds showing some inhibitory activity were then measured by the serial tube dilution method previously described (1) to obtain minimal inhibitory concentrations (Table III).

Most prepared compounds showed inhibitory activity against *S. aureus*. All glucosylthioureas showing inhibitory activity were derived from primary amines, except those prepared from piperidine and dimethylamine, indicating that antimicrobial activity tends to decrease as the degree of substitution on the thiourea nitrogen increases.

A good percentage of the compounds were inhibitory to *C. albicans* and *A. niger*, *N*-β-D-glucopyranosyl-*N'*-butylthiourea being the most active against these organisms. Ethyl 2-(*N*-β-D-glucopyranosyl)aminothiazole-4-carboxylate showed inhibitory activity against four organisms, comparable to that from rhodanine, but not against *A. niger*. The glucosylthioureas derived from diethylamine, *N*-methylpiperazine, morpholine, and thiomorpholine did not show any antimicrobial activity. This result could be due to poor solubility, except in the case of diethylamine.

Among the ribosylrhodanines and ribosylthioureas, none of the benzoyl-protected compounds revealed any activity. *N*-(2,3,5-Tri-*O*-acetyl-β-D-ribofuranosyl)rhodanine was active against all five organisms, however, possibly because of *in vivo* hydrolysis of the acetyl groups. The corresponding 5-benzylidene derivative was active against only *S. aureus* and *C. albicans*.

The best activity of the compounds reported here was shown by *N*-(2,3,5-tri-*O*-acetyl-β-D-ribofuranosyl)rhodanine, which had comparable activity to that of rhodanine itself. Nearly as broad antimicrobial activity was found with ethyl 2-(*N*-β-D-glucopyranosyl)aminothiazole-4-carboxylate, which showed comparable activity against four organisms and slightly better activity against *S. aureus* than rhodanine itself. The thioureas generally were inhibitory against two or three of the five organisms observed.

## EXPERIMENTAL[1]

**Glucopyranosylthioureas: *N*-β-D-Glucopyranosyl-*N'*-butylthiourea** — *N*-(2,3,4,6-Tetra-*O*-acetyl-β-D-glucopyranosyl)-5-(3,4-dimethoxybenzylidene)rhodanine (1) (1 g, 0.0016 mole) was added to a solution of *n*-butylamine (1.08 g, 0.016 mole) in 50 ml of methanol in a pressure bottle. The reaction mixture was stirred at room temperature for 20 hr with the pressure bottle well closed. The mixture was filtered, and the filtrate was evaporated to dryness *in vacuo* below 30°.

The residue was dissolved in the minimum amount of acetone and stored at 5° for 18 hr. The white precipitate was filtered, washed with acetone, and dried *in vacuo* at room temperature, yielding 0.426 g (80%), mp 94–96° dec.; $[\alpha]_D^{25}$ −15.4° (*c*, 0.54); IR (KBr): 3500–3300 (OH, NH), 3100 (NH), 1550 (NH), 1080 (C=S), and 900 (β-form) $cm^{-1}$; NMR (dimethyl sulfoxide-$d_6$ + $D_2O$): δ 5.07 (d, H1, *J* = 8 Hz), 3.52 (m, 2H6), 3.17 (m, $NCH_2$), 1.40 (m, 4H, $CH_2CH_2$), and 0.96 (m, 3H, $CH_3$) ppm.

*Anal.*—Calc. for $C_{11}H_{22}N_2O_5S \cdot \frac{2}{3}(CH_3)_2CO$: C, 46.87; H, 7.83; N, 8.41; S, 9.63. Found: C, 46.40; H, 7.68; N, 8.42; S, 9.60.

**Ethyl 2-(*N*-β-D-Glucopyranosyl)aminothiazole-4-carboxylate Hydrobromide**—Ethyl bromopyruvate (8.99 g, 0.047 mole) was added to a suspension of *N*-β-D-glucopyranosylthiourea (10 g, 0.042 mole) in 120 ml of hot ethanol, and the mixture was heated for 30 min. The resulting solution was evaporated to dryness *in vacuo*, and the residue was crystallized from ethanol–acetone, filtered, and dried *in vacuo* at room temperature, yielding 16.03 g (91.9%) of white powder, mp 162–163° dec.; $[\alpha]_D^{25}$ −48.4° (*c*, 1.1); IR (KBr): 3500–3300 (OH, NH), 3160 (NH), 1725 (C=O), 1090 (β-ring), and 895 (β-form) $cm^{-1}$; NMR (dimethyl sulfoxide-$d_6$): δ 7.62 (s, H5), 6.09 (bs, OH, NH), 4.24 (q, $CH_2$), 3.51 (m, 2H6′), and 1.30 (t, $CH_3$) ppm.

*Anal.*—Calc. for $C_{12}H_{18}N_2O_7S \cdot HBr$: C, 34.71; H, 4.61; N, 6.75; S, 7.72. Found: C, 34.88; H, 4.71; N, 6.72; S, 7.92.

**2- (*N*-β-D-Glucopyranosyl)aminothiazole-4-carboxamide**—Ethyl 2-(*N*-β-D-glucopyranosyl)aminothiazole-4-carboxylate hydrobromide (4.15 g, 0.01 mole) was added to a solution of methanol (50 ml) saturated with ammonia at 0° in a pressure bottle. The mixture was stirred at room temperature for 48 hr in the stoppered bottle and then evaporated to dryness *in vacuo*. The residue was mixed with a small amount of ethyl acetate and chromatographed on a silica gel column (2.54 × 20 cm) using acetone as the first solvent (300 ml) and methanol as the second (300 ml).

The methanol effluent was concentrated to 75 ml, and ethyl acetate (500 ml) was added. The creamy-yellow precipitate was filtered and dried *in vacuo* at room temperature, yielding 2.77 g (76%), mp 96° dec.; $[\alpha]_D^{25}$ −22.2° (*c*, 1.4); IR (KBr): 3500–3300 (OH, NH), 1660 (NH), 1080 (β-ring), and 895 (β-form) $cm^{-1}$; NMR (dimethyl sulfoxide-$d_6$): δ 8.20 (d, NH, *J* = 8 Hz), 7.30 (s, H5), and 3.50 (m, 2H6′) ppm.

*Anal.*—Calc. for $C_{10}H_{15}N_3O_6S \cdot 2H_2O \cdot \frac{1}{2}C_2H_5OH$: C, 36.26; H, 6.09; N, 11.53; S, 8.80. Found: C, 36.41; H, 5.72; N, 11.92; S, 8.84.

***N*-(2,3,5-Tri-*O*-acetyl-β-D-ribofuranosyl)rhodanine**—To a suspension of rhodanine (1.34 g, 0.01 mole) in toluene (25 ml), hexamethyldisilazane (4 ml, 0.02 mole) and chlorotrimethylsilane (10 ml, 0.08 mole) were added. The mixture was refluxed 2 hr with exclusion of moisture. It was filtered, and the filtrate was evaporated to a syrup *in vacuo*. A solution of 2,3,5-tri-*O*-acetyl-D-ribofuranosyl bromide (16) (3.2 g, 0.01 mole) in acetonitrile was added at 0°, along with molecular sieves (8–12 mesh, 1 g) and stannic chloride (0.29 ml, 0.0025 mole) in acetonitrile (10 ml). The mixture was stirred at 0° for 3 hr and filtered, and the filtrate was evaporated to a syrup.

This syrup was dissolved in chloroform (50 ml) and filtered. The chloroform solution was washed with 10% potassium iodide solution (50 ml) and water (50 ml). The resulting solution was dried (sodium sulfate), evaporated to a thin syrup, and dried below 25° *in vacuo*, yielding 3.61 g (92%) of amorphous material; $[\alpha]_D^{25}$ +34.9° (*c*, 1.86, chloroform); IR (KBr): 1750 (C=O), 1380 (ring $CH_2$), 1240–1220 (C=S), and 890 (β-form) $cm^{-1}$; NMR (chloroform-$d_1$): δ 6.37 (d, H1′, *J* = 3.5 Hz), 5.80 (m, H2′), 5.45 (m, H3′), 4.30 (m, 3H4′,5′), 3.95 (s, 2H5), and 2.15 (9H, s, $3CH_3$) ppm.

*Anal.*—Calc. for $C_{14}H_{17}NO_8S_2$: C, 42.96; H, 4.38; N, 3.58; S, 16.38. Found: C, 42.76; H, 4.43; N, 3.71; S, 16.08.

***N*-(2,3,5-Tri-*O*-acetyl-β-D-ribofuranosyl)-5-benzylidenerhodanine**—A solution of 1,2,3,5-tetra-*O*-acetyl-β-D-ribofuranose (3.18 g, 0.01 mole) in dry methylene chloride (20 ml) was added at −60° to dry methylene chloride (40 ml) saturated with dry hydrogen bromide. The mixture was protected from moisture and allowed to warm to room temperature. The solvent was removed *in vacuo* below 30°, and the residue was evaporated with dry toluene (20 ml).

**Table II—$R_f$ Values for Reactants and Products in the Synthesis of Glucosylthioureas[a]**

| Amine | $R_f$ Values: Rhodanine Derivative[b] | Thiourea Derivative | Cinnamamide | Acetamide |
|---|---|---|---|---|
| $NH_3$ | 0.72 | 0.41 | 0.67 | 0.56 |
| | 0.94[c] | 0.10[c] | 0.27[c] | 0.83[c] |
| $NH(CH_3)_2$ | 0.91 | 0.50 | 0.71 | — |
| $NH(C_2H_5)_2$ | 0.86 | 0.65 | | |
| $NH_2(CH_2)_3CH_3$ | 0.87 | 0.72 | 0.62 | |
| $NH_2CH_2CH{=}CH_2$ | 0.88 | 0.71 | 0.56 | |
| $NH_2CH_2C_6H_5$ | 0.87 | 0.76 | 0.53 | 0.33 |
| $NH_2CH_2CH_2C_6H_5$ | 0.90 | 0.75 | 0.56 | 0.27 |
| 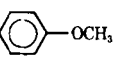 | 0.81 | 0.65 | 0.49 | 0.31[d] |
| 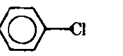 | 0.91 | 0.67 | 0.83 | |
| 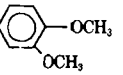 | 0.82 | 0.54 | 0.74 | |
|  | 0.85 | 0.66 | | |
| 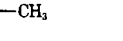 | 0.84 | 0.15 | 0.41 | 0.31 |
|  | 0.89 | 0.57 | | |
|  | 0.87 | 0.72 | 0.69 | 0.18[d] |

[a] Solvent system: acetone–butanol–water (5:4:1); silica gel plate. [b] *N*-(2,3,4,6-Tetra-*O*-acetyl-β-D-glucopyranosyl)-5-benzylidenerhodanine. [c] Aluminum oxide plate. [d] $R_f$ value of amine.

[1] Melting points were determined in capillaries with a Mel-Temp block and are uncorrected. IR absorption spectra were recorded with a Perkin-Elmer 457A grating spectrophotometer. NMR spectra were determined with a Varian T60 spectrometer with tetramethylsilane as the internal standard. Optical rotations were measured with a Perkin-Elmer 241MC polarimeter and a Carl Zeiss polarimeter. Elemental analyses were performed by Dr. F. B. Strauss, Oxford, England. TLC was carried out on Eastman silica gel plates with fluorescent indicator or alumina plates. For the glycosides, an efficient solvent system was *n*-butanol–acetone–water (4:5:1).

Rhodanine, the amines, 1,2,3,5-tetra-O-acetyl-β-D-ribofuranose, 1-*O*-acetyl-2,3,5-tri-*O*-benzoyl-β-D-ribofuranose, 1,1,1,3,3,3-hexamethyldisilazane, chlorotrimethylsilane, and stannic chloride were supplied by Aldrich Chemical Co. Silica gel and alumina for column chromatography were supplied by Fisher Scientific Co. Anhydrous ammonia, hydrogen bromide, and dimethylamine were obtained from Matheson Gas Products. The amines were purified by distilling with zinc powder prior to use. Solvents were dried with 3- or 4-Å molecular sieves.

**Table III—Antimicrobial Activities**

| R | Minimum Inhibitory Concentration, *M* | | | | |
|---|---|---|---|---|---|
| | *S. aureus* | *E. coli* | *P. aeruginosa* | *C. albicans* | *A. niger* |
| 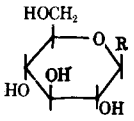 | | | | | |
| | $10^{-4}$ | — | — | $10^{-3}$ | $10^{-2}$ |
| | $10^{-2}$ | — | — | — | — |
| | $10^{-3}$ | — | — | $10^{-4}$ | $10^{-3}$ |
| | $10^{-4}$ | — | — | — | — |
| | — | $10^{-2}$ | $10^{-2}$ | — | — |
| | $10^{-3}$ | — | — | — | — |
| 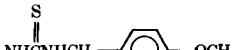 | $10^{-2}$ | — | — | $10^{-3}$ | $10^{-2}$ |
| 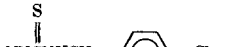 | $10^{-3}$ | $10^{-2}$ | — | $10^{-2}$ | — |
| 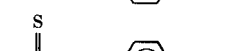 | $10^{-2}$ | — | — | $10^{-2}$ | — |
| | $10^{-2}$ | — | $10^{-3}$ | — | — |
| | $10^{-4}$ | $10^{-3}$ | $10^{-3}$ | $10^{-3}$ | — |
| 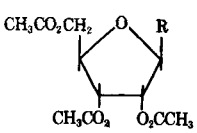 | | | | | |
| 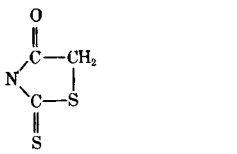 | $10^{-3}$ | $10^{-3}$ | $10^{-2}$ | $10^{-3}$ | $10^{-3}$ |
| 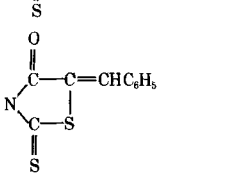 | $10^{-3}$ | — | — | $10^{-2}$ | — |
| Rhodanine | $10^{-3}$ | $10^{-3}$ | $10^{-3}$ | $10^{-3}$ | $10^{-2}$ |

The sodium salt of 5-benzylidenerhodanine was prepared by adding 5-benzylidenerhodanine (2.21 g, 0.01 mole) to a suspension of sodium hydride (0.24 g, 0.01 mole) in anhydrous ether (40 ml) (prepared from 57% sodium hydride oil suspension by removing mineral oil with hexane under nitrogen). The mixture was stirred at room temperature until no hydrogen was evolved. The solvent was removed by evaporation, and the residue was dried *in vacuo*.

To a suspension of the sodium salt of 5-benzylidenerhodanine (2.43 g, 0.01 mole) in acetonitrile (70 ml) was added a solution of 2,3,5-tri-*O*-acetyl-D-ribofuranosyl bromide (16) (3.39 g, 0.01 mole) in acetonitrile (30 ml), followed by 7 g of molecular sieves (8–12 mesh). The mixture was stirred at room temperature for 4 days. The insoluble material was filtered and washed with acetonitrile, and the combined filtrates were evaporated *in vacuo* below 30°. The residue was dissolved in chloroform (50 ml), and the solution was washed with 10% potassium iodide solution (20 ml) and water (40 ml), dried (sodium sulfate), and evaporated to a thin syrup.

The residue was dissolved in the minimum amount of methanol and chromatographed on an alumina column (neutral, 2.54 × 20 cm) with methanol as the eluant. The fast moving component was collected (150 ml) and evaporated to dryness. The residue was dissolved in the minimum amount of 95% ethyl alcohol and stored at −20°, and the crystals were collected and dried *in vacuo* at room temperature, yielding 2.76 g (57%),

mp 89–92°; $[\alpha]_D^{25}$ −78.5° (*c*, 2.42, chloroform); IR (KBr): 1750 (C=O), 1250–1220 (C=S), 900 (β-form), and 780 (=CH) $cm^{-1}$; NMR (chloroform-$d_1$): δ 7.67 (s, =CH), 7.45 (s, 5H, aromatic), 6.52 (d, H1′, $J$ = 3 Hz), 5.95 (m, H2′), 5.65 (m, H3′), 4.35 (m, 3H4′,5′), and 2.15 (9H, s, $3CH_3$) ppm.

*Anal.*—Calc. for $C_{21}H_{21}NO_8S_2$: C, 52.60; H, 4.41; N, 2.92; S, 13.37. Found: C, 52.41; H, 4.63; N, 2.83; S, 13.23.

***N*-(2,3,5-Tri-*O*-benzoyl-β-D-ribofuranosyl)rhodanine**—To a suspension of rhodanine (0.64 g, 0.005 mole) in toluene (20 ml), hexamethyldisilazane (2 ml, 0.01 mole) and chlorotrimethylsilane (5 ml, 0.04 mole) were added. The mixture was stirred at 65° for 2 hr with exclusion of moisture. It was then filtered and evaporated to a thin syrup. A solution of 1-*O*-acetyl-2,3,4-tri-*O*-benzoyl-β-D-ribofuranose (2.52 g, 0.005 mole) in ethylene dichloride (10 ml) was added, and stannic chloride (0.44 ml, 0.0037 mole) in ethylene dichloride (10 ml) was added dropwise with stirring at 0°. The mixture was diluted with 15 ml of ethylene dichloride, and the resulting mixture was neutralized with saturated sodium bicarbonate solution (70 ml).

The emulsion was filtered over a layer of sand–diatomaceous earth, and the organic phase was separated, extracted with 10% potassium iodide solution (60 ml), washed with water (60 ml), and dried (sodium sulfate). The separated organic layer was evaporated to a semisolid below 30° and dried *in vacuo* at room temperature, yielding 2.69 g (93%); $[\alpha]_D^{25}$ −17.5° (*c*, 0.86, chloroform); IR (KBr): 1750–1720 (C=O), 1450 (ring $CH_2$), 1280–1240 (C=S), and 890 (β-form) $cm^{-1}$; NMR (chloroform-$d_1$): δ 8.00–7.10 (m, 15H, aromatic), 6.65 (d, H1′, $J$ = 3 Hz), 6.28 (m, H2′), 6.00 (m, H3′), 4.68 (m, 3H4′,5′), and 3.90 (s, 2H5) ppm.

*Anal.*—Calc. for $C_{29}H_{23}N_2O_8S$: C, 60.32; H, 4.01; N, 2.42; S, 11.10. Found: C, 60.12; H, 4.24; N, 2.26; S, 10.89.

***N*-(2,3,5-Tri-*O*-benzoyl -β- D-ribofuranosyl)-5-benzylidenerhodanine**—To a solution of 5-benzylidenerhodanine (1.77 g, 0.08 mole) in acetonitrile (50 ml) was added 2,3,5-tri-*O*-benzoyl-D-ribofuranosyl bromide (17) (4.1 g, 0.008 mole), followed by 3.2 ml of 10% NaOH. The mixture was stirred at room temperature for 6 days and then was filtered and evaporated to a semisolid *in vacuo* below 30°. The residue was triturated with methanol (15 ml) to give a yellow precipitate, which was filtered and chromatographed on alumina (neutral) with methanol as the eluant. The first effluent (100 ml) was collected and evaporated. The resulting precipitate was filtered and dried *in vacuo* at room temperature, yielding 3.46 g (65%), mp 146–148°; $[\alpha]_D^{25}$ −128.6° (*c*, 1.0, tetrahydrofuran); IR (KBr): 1730 (C=O), 1270–1250 (C=S), and 770 (=CH) $cm^{-1}$; NMR (dimethyl sulfoxide-$d_6$): δ 8.10–7.50 (m, 20H, aromatic), 7.78 (s, =CH), 6.77 (d, H1′, $J$ = 2 Hz), 6.28 (m, 2H2′,3′), and 4.70 (m, 3H4′,5′) ppm.

*Anal.*—Calc. for $C_{36}H_{27}NO_8S_2$: C, 64.95; H, 4.09; N, 2.10; S, 9.63. Found: C, 65.20; H, 4.48; N, 1.83; S, 9.82.

***N*-(2,3,5-Tri-*O*-benzoyl -β- D-ribofuranosyl)morpholine-4-thiocarboxamide**—To a suspension of *N*-(2,3,5-tri-*O*-benzoyl-β-D-ribofuranosyl)-5-benzylidenerhodanine (3.32 g, 0.005 mole) in acetonitrile (40 ml) were added 0.5 ml of water and then morpholine (4.38 g, 0.05 mole) in small portions with stirring over 10 min. The solution was stirred at room temperature for 2 days, and a small amount of precipitate was filtered. The filtrate was evaporated to a syrup and dried *in vacuo*. The residue was dissolved in the minimum amount of acetone and chromatographed on silica gel with acetone as the eluant. The fast moving band was collected (50 ml) and evaporated to dryness *in vacuo* at room temperature, yielding 2.86 g (96%), mp 75–77°; $[\alpha]_D^{25}$ −19.5° (*c*, 2.3, chloroform); IR (KBr): 1725 (C=O), 1115 (C=S), and 880 (β-form) $cm^{-1}$; NMR (dimethyl sulfoxide-$d_6$): δ 9.10 (bs, NH), 7.70 (m, 15H, aromatic), 5.86 (bs, H1′), 3.80 (m, 2H5′), 3.68 (m, 4H, $CH_2OCH_2$), and 3.54 (m, 4H, $CH_2NCH_2$) ppm.

*Anal.*—Calc. for $C_{31}H_{30}N_2O_8S$: C, 63.04; H, 5.12; N, 4.74; S, 5.43. Found: C, 63.12; H, 5.67; N, 4.89; S, 5.64.

***N*-(2,3,5-Tri-*O*-benzoyl -β- D-ribofuranosyl)-*N*′-ethoxythiourea**—A solution of *N*-(2,3,5-tri-*O*-benzoyl-β-D-ribofuranosyl)-5-benzylidenerhodanine (1.66 g, 0.0025 mole) in acetonitrile (40 ml) was treated with pulverized hydroxylamine hydrochloride (0.7 g, 0.01 mole), and triethylamine (1.4 ml, 0.01 mole) was added dropwise with stirring over 5 min. The mixture was stirred for 1 hr, the precipitate was filtered, and the filtrate was treated with ethyl acetate (100 ml) to give a precipitate. This precipitate was filtered, and the filtrate was extracted with 0.1 *N* HCl (40 ml), water (100 ml), and saturated sodium chloride solution (50 ml). It was dried (sodium sulfate) and evaporated, and the residue was chromatographed on alumina (neutral), using 2-propanol as the first solvent (200 ml) and methanol as the second (200 ml).

The methanol effluent was evaporated to 40 ml to give a yellow precipitate, which was filtered and dried at room temperature *in vacuo*, yielding 1.32 g (93%), mp 106° dec.; $[\alpha]_D^{25}$ −13.2° (*c*, 1.1, chloroform); IR (KBr): 1725 (C=O), 1270 (C—O), and 1120 (C=S) $cm^{-1}$; NMR (chloroform-$d_1$): δ 8.40 (bs, NH), 7.88–7.30 (m, 15H, aromatic), 5.80 (bs, H1′), 4.05 (q, $CH_2$), 3.95 (m, 2H5′), and 1.14 (t, $CH_3$) ppm.

*Anal.*—Calc. for $C_{29}H_{28}N_2O_8S$: C, 61.69; H, 5.00; N, 4.96; S, 5.68. Found: C, 61.88; H, 4.76; N, 4.88; S, 5.62.

**Antimicrobial Activity**—Tests were first carried out by the agar plate method, using 20–30 mg of each compound and measuring the zones of inhibition. The organisms used were *S. aureus* (ATCC 6538), *E. coli* (ATCC 11229), *P. aeruginosa* (ATCC 15442), *C. albicans* (ATCC 10259), and *A. niger* (ATCC 1015). Portions of four or five discrete colonies of the organisms were inoculated into 10.0 ml of a suitable broth medium and streaked on agar plates. Trypticase soy agar (BBL) was used for bacteria, and Sabouraud maltose agar (BBL) was used for the yeast and mold. Incubations were at 37° for 24–48 hr for the bacteria and at 25° for 48–72 hr for the yeast and mold.

Minimum inhibitory concentrations by the serial tube dilution procedure were carried out for the compounds found active by the agar plate procedure as previously described (1). Inhibitory concentrations were expressed in moles.

## REFERENCES


(1) W. O. Foye and P. Tovivich, *J. Pharm. Sci.*, **66**, 1607 (1977).

(2) E. Fischer, *Chem. Ber.*, **47**, 1377 (1914).

(3) F. Micheel and W. Brunkhorst, *ibid.*, **88**, 481 (1955).

(4) H. Takahashi, N. Nimura, and H. Ogura, *Chem. Pharm. Bull.*, **27**, 1130 (1979).

(5) S. B. Helferich and W. Kosche, *Chem. Ber.*, **59B**, 69 (1926).

(6) A. S. Galabov, E. H. Velichkova, and G. N. Vassilev, *Chemotherapy*, **23**, 81 (1977).

(7) A. Kreutzberger and H. H. Schroeders, *Arch. Pharm.*, **309**, 25 (1976).

(8) E. G. Delegan, I. V. Smolanka, V. S. Petrus, and V. N. Plakhotnyvk, *Fiziol. Akt. Veshchestva*, **8**, 70 (1976).

(9) T. Noguchi, K. Kohmoto, and K. Kato, U.S. pat. 4,020,095 (1976).

(10) T. Zsolnai, *Arzneim.-Forsch.*, **19**, 558 (1969).

(11) G. Matolcsy, B. Bordas, and M. Hamran, *Acta Phytopathol.*, **4**, 345 (1969).

(12) H. J. Eggers, M. A. Koch, A. Furst, G. D. Daves, Jr., J. J. Wilczynski, and K. Folkers, *Science*, **167**, 294 (1970).

(13) T. H. Haskell, F. E. Peterson, D. Watson, N. R. Plessas, and T. Culbertson, *J. Med. Chem.*, **13**, 697 (1970).

(14) R. W. Lenz and J. P. Heeschen, *J. Polym. Sci.*, **51**, 247 (1961).

(15) J. A. Montgomery and H. J. Thomas, *J. Org. Chem.*, **36**, 1962 (1971).

(16) R. A. Earl and L. R. Townsend, *J. Carbohyd. Nucleosides Nucleotides*, **1**, 77 (1974).

(17) J. D. Stevens, R. K. Ness, and H. G. Fletcher, Jr., *J. Org. Chem.*, **33**, 1806 (1968).


## ACKNOWLEDGMENTS


Abstracted from a thesis submitted by S. H. An to the Massachusetts College of Pharmacy and Allied Health Sciences in partial fulfillment of Doctor of Philosophy degree requirements.

Supported by funds from the John R. and Marie K. Sawyer Memorial Fund, Massachusetts College of Pharmacy and Allied Health Sciences, and the Society of Cosmetic Chemists.

# Effective Therapy of Enteric Hyperoxaluria: *In Vitro* Binding of Oxalate by Anion-Exchange Resins and Aluminum Hydroxide

**M. F. LAKER** * **and A. F. HOFMANN** ˣ

Received August 11, 1980, from the *Division of Gastroenterology, Department of Medicine, University of California at San Diego Medical Center, San Diego, CA 92103.* Accepted for publication March 2, 1981. *Present address: Department of Clinical Biochemistry, Royal Victoria Infirmary, Newcastle-upon-Tyne NE1 4LP, England.

**Abstract** □ Hyperabsorption of dietary oxalate is a major factor in the pathogenesis of enteric hyperoxaluria and a frequent complication of inflammatory bowel disease and ileojejunal bypass surgery. Successful treatment requires reduction in oxalate intake or inhibition of absorption of dietary oxalate by oral ingestion of oxalate binding agents. To identify such agents, oxalate binding by anion-exchange resins, gums, and aluminum hydroxide was measured under conditions that simulated those present in the intestinal lumen. Of the agents tested, those that bound oxalate best were colestipol and aluminum hydroxide. Strongly basic anion-exchange resins readily bound oxalate only in the absence of chloride. These results suggest that colestipol and aluminum hydroxide administration might reduce dietary oxalate absorption in patients with enteric hyperoxaluria.

**Keyphrases** □ Oxalate—*in vitro* binding by various anion-exchange resins and aluminum hydroxide □ Binding agents—*in vitro* binding of oxalate by anion-exchange resins and aluminum hydroxide □ Enteric hyperoxaluria—dietary oxalate, *in vitro* binding by anion-exchange resins and aluminum hydroxide

Nephrolithiasis is a frequent complication of inflammatory bowel disease (1, 2), ileal resection (3–5), and ileojejunal bypass (6, 7). The stones are usually composed of calcium oxalate; hyperoxaluria, which often occurs in patients with ileal dysfunction, is a major predisposing factor.

Enteric hyperoxaluria is due, at least in part, to enhanced absorption of dietary oxalate (8, 9). The pathogenesis of this condition is complex and probably involves alterations in the physical state of dietary oxalate in the intestinal lumen as well as an increase in colonic permeability to the oxalate anion. In hyperoxaluric patients, malabsorbed fatty acids are thought to prevent normal precipitation of oxalate in the gut by preferentially binding intraluminal calcium to form insoluble calcium soaps (10, 11). Free oxalate then is absorbed in increased amounts, in part because the permeability of the colon to the oxalate anion is increased by abnormally elevated intraluminal concentrations of bile acids and fatty acids (12–14).

This explanation suggests that enteric hyperoxaluria can be treated successfully by decreasing dietary oxalate, the free oxalate concentration in the intestinal lumen, or the colonic permeability. To decrease intraluminal oxalate, agents capable of binding or precipitating oxalate could be administered. To decrease the concentration of fatty acids or bile acids in the colonic lumen, fat intake could be reduced or bile acid or fatty acid binding resins could be administered.

## BACKGROUND

In this study the *in vitro* binding of oxalate by a number of nonabsorbable substances was examined. Cholestyramine, a nonabsorbable ion-exchange resin already reported to bind oxalate *in vitro* (9, 15), was used successfully by some investigators (3, 9), but not others (7, 16), to reduce oxalate excretion in patients with enteric hyperoxaluria. Aluminum antacids are essentially nonabsorbable and also were reported to decrease oxalate excretion in patients with enteric hyperoxaluria (11). However, since both cholestyramine and aluminum hydroxide are potent binders of bile acids (17–20) and fatty acids (21) *in vitro*, their ability to diminish urinary oxalate excretion in patients with enteric hyperoxaluria might result from bile acid or fatty acid binding in the colon, which would diminish the enhanced mucosal permeability, thus reducing the increased oxalate absorption. This effect on mucosal permeability might contribute more to diminishing oxalate absorption than that attributable to intraluminal oxalate binding. Thus, an unequivocal interpretation of clinical investigations of agents capable of binding not only oxalate but also bile acids and fatty acids is impossible.

Information is needed on the relative affinity *in vitro* of these binding agents for oxalate. Binding studies with these and several other potential therapeutic agents for oxalate are reported here. Binding of oxalate by calcium was not studied since the solubility product of calcium oxalate is well known and since calcium administration to patients with enteric hyperoxaluria has been reported to increase urinary calcium excretion, which may be undesirable in patients at risk for nephrolithiasis (22, 23).

## EXPERIMENTAL

**Adsorbents**—The adsorbents investigated were ion-exchange resins, an uncharged hydrophobic resin, guar gum, and various types of aluminum hydroxide.

Three types of strongly basic anion-exchange resins were used. The first ($SB_r$) is a widely used bead resin with quaternary ammonium groups attached to a styrene–divinyl benzene copolymer lattice[1]. The second, cholestyramine[2], is chemically identifical to $SB_r$ but was milled to reduce its particle size; it is marketed as a hypocholesterolemic agent. The third ($SB_d$) is a resin used for ion-exchange gel permeation chromatography; it consists of dextran beads containing quaternary ammonium groups[3].

Three weakly basic anion-exchange resins also were used. The first, colestipol[4], is a synthetic ion-exchange resin prepared by cross-linking tetraethylenepentamine with epichlorohydrin; the polymer, which has primary and secondary amine groups, is marketed as a hypocholesterolemic agent. The second ($WB_r$), a widely used bead resin, contains mostly tertiary amine groups on an epoxy lattice[5]. The third ($WB_c$), diethylaminoethylcellulose containing diethylamine groups on a cellulose lattice, is used for ion-exchange chromatography of proteins[6].

The uncharged hydrophobic resin ($UH_r$) consisted of beads of divinyl–benzene styrene copolymer with a macroreticular surface[7]. Guar gum[8] is a natural gum containing primary and secondary amino groups.

Aluminum hydroxide was used both in the form of proprietary antacid preparations ($AHPF_1$[9] and $AHPF_2$[10]) and as dried powder[11]. Three types

[1] Dowex-1, Dow Chemical Co. (sold as AG1-X4 by Bio-Rad Laboratories, Richmond, Calif.).
[2] Provided by Mead Johnson Co., Evansville, Ind.
[3] QAE-Sephadex, Pharmacia, Inc., Piscataway, N.J.
[4] Provided by The Upjohn Co., Kalamazoo, Mich.
[5] Dowex-3, Dow Chemical Co. (sold as AG3-X4A by Bio-Rad Laboratories, Richmond, Calif.).
[6] DEAE Cellulose, Schleicher and Schuell, Keene, N.H.
[7] XAD-2, Rohm & Haas, Philadelphia, Pa. (purchased from Mallinckrodt, St. Louis, Mo.).
[8] Bradford Co., Los Angeles, Calif.
[9] Amphogel (AHCFI), Wyeth Laboratories.
[10] Alternagel (AHCFII), Stuart Pharmaceuticals.
[11] Three aluminum hydroxide preparations (Reheis, Barcroft, and Chattem) were generously supplied by the Rorer Group through the courtesy of John Eckman.

0022-3549/81/0900-1065$01.00/0
© 1981, American Pharmaceutical Association

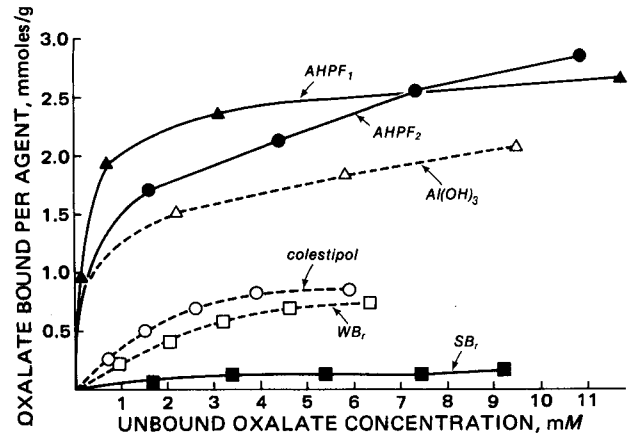


**Figure 1**—*Equilibrium isotherms for oxalate binding to anion-exchange resins and aluminum hydroxide in histidine buffer (pH 6.5, 37°; 0.15 M chloride ion).*

of aluminum hydroxide powder were studied.

Ion-exchange resins were conditioned before use by stirring with two volumes of 1 *N* NaOH, decanting the supernate, and washing the resin with distilled water. The resin was converted to the chloride form by stirring with two volumes of 1 *N* HCl. After repeated washings with glass-distilled water until the supernate was no longer acidic (pH > 6), resins were dried at room temperature.

Next, $UH_r$ was conditioned by washing with methanol followed by distilled water and then was stored in water. The dextran- and cellulose-based ion exchangers, as well as the guar gum, were preswollen in buffered saline solution (150 m*M* NaCl, 20 m*M* L-histidine, pH 6.5).

Aluminum hydroxide preparations were used without initial conditioning.

**Adsorption Studies**—Oxalate binding was studied by incubating 50 mg of adsorbent (wet weight for $UH_r$, volume containing 50 mg of aluminum hydroxide for $AHPF_1$ and $AHPF_2$, and dry weight for the other adsorbents) with 10 ml of oxalate-containing solution. The solutions contained varying amounts of unlabeled oxalic acid (2–25 m*M*), a constant amount of [$^{14}$C]oxalic acid[12] (20 μCi/liter), sodium chloride (150 m*M*), and L-histidine (20 m*M*). The pH was adjusted to 6.5 with hydrochloric acid.

Premixed solutions and adsorbents were added to 20 ml-glass serum storage vials, which were sealed with butyl rubber septa and crimped aluminum closures. The sealed bottles were kept in a 37° oven and continuously rotated. Samples were centrifuged, and the supernate was aspirated; its radioactivity was determined by liquid scintillation counting (0.2 ml was mixed with 10 ml of scintillant[13]). Each study was performed in duplicate.

The binding affinity of each adsorbent for oxalate was characterized by using adsorption isotherms to summarize the data (24). The amount of oxalate bound at equilibrium was determined for several starting

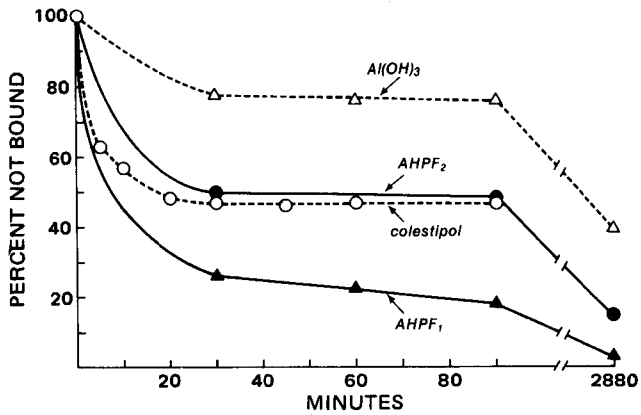


**Figure 2**—*Kinetics of oxalate binding to aluminum hydroxide or colestipol (pH 6.5, 37°; 0.15 M chloride ion).*

[12] New England Nuclear, Boston, Mass.
[13] Ready-Solv HP, Beckman Instruments, Fullerton, Calif.

**Table I—Oxalate Binding at Equilibrium by Selected Adsorbents in the Presence of Isotonic Saline or Simulated Intestinal Content (Containing Fatty Acid and Bile Acid Anions)**

| Adsorbent | Incubation Solution Oxalate Concentration, m*M* | Oxalate Bound, mmoles/g of adsorbent: With 0.15 *M* Saline | With Simulated Intestinal Content | Reduction in Binding, % |
|---|---|---|---|---|
| $SB_r$ | 10 | 0.16 | 0.10 | 37 |
| $WB_r$ | 10 | 0.74 | 0.52 | 30 |
| Colestipol | 10 | 0.85 | 0.44 | 48 |
| $AHPF_1$ | 25 | 2.38 | 0.74 | 69 |
| Aluminum hydroxide powder | 25 | 1.84 | 0.10 | 94 |

concentrations (2–10 m*M* for resins and 5–25 m*M* for aluminum hydroxide preparations). Specimens in which adsorbent and isotope were omitted were included as controls. The kinetics of oxalate binding were studied by repeated sampling of containers with a single oxalate concentration (7.5 m*M*).

To test whether oxalate binding to $SB_r$ was influenced by the presence of chloride ion in the incubation medium, oxalate binding to $SB_r$ was defined in the absence of chloride ion. Thus, $SB_r$ was incubated with 10 ml of a solution containing 7.5 m*M* oxalic acid, [$^{14}$C]oxalic acid (20 μCi/liter), and 20 m*M* L-histidine, and the pH was adjusted to 6.5. Oxalate binding at equilibrium was determined as already described.

To determine whether bile acid or fatty acid anions that are present in intestinal content in humans might competitively inhibit oxalate binding, oxalate binding was measured in simulated intestinal content (25). The incubation solution contained 130 m*M* sodium chloride, 20 m*M* L-histidine, 7.5 m*M* glycocholic acid, 7.5 m*M* chenylglycine, 2.5 m*M* taurocholic acid, 2.5 m*M* chenyltaurine, 6.7 m*M* monoolein, and 13.3 m*M* oleic acid; the pH of the solution was adjusted to 6.5 (19). Unlabeled oxalate (10 m*M* for resins and 25 m*M* for aluminum hydroxide preparations) and [$^{14}$C]oxalic acid (20 μCi/liter) were included. Vials were sampled until equilibrium of binding was achieved.

Experiments also were carried out to determine whether substances present in the liquid component of one of the two proprietary formulations of aluminum hydroxide ($AHPF_1$) influenced oxalate binding. An aliquot was centrifuged, and the supernatant fraction was removed. The aluminum hydroxide was resuspended in water and recentrifuged, with the supernate being discarded, and this procedure was repeated three times. The initial supernate was then mixed with aluminum hydroxide powder. The equilibrium binding was studied with the dried $AHPF_1$ residue as well as the suspension of aluminum hydroxide powder, the oxalate concentration in the incubation mixture being 15 mmoles/liter.

## RESULTS

**Equilibrium Isotherms**—Colestipol and $WB_r$ had a greater affinity for oxalate than $SB_r$ (Fig. 1). Binding to $SB_d$ or $WB_c$ (not shown) was considerably less than that to $SB_r$. The weak binding of oxalate to $SB_r$ was due to the chloride ion in the medium; when chloride ion was omitted, binding increased threefold.

In addition, aluminum hydroxide, either as a proprietary antacid formulation or as a dried powder, readily bound oxalate. Binding of oxalate to $AHPF_1$ was identical whether the suspension or the washed solid phase obtained by centrifugation was used. Thus, all binding was attributable to particulate aluminum hydroxide. The binding isotherms for all aluminum hydroxide powders were similar, so only data for one of them are shown. No binding by guar gum or $UH_r$ was detected, and $WB_c$ only bound oxalate weakly (7%).

In Table I, oxalate binding by selected adsorbents in the presence or absence of simulated intestinal content is compared. Less oxalate was bound by all the adsorbents tested when constituents of intestinal content, *i.e.*, bile acid and fatty acid anions, were included. The decrease was most marked for aluminum hydroxide preparations, with $AHPF_1$ binding only 31% and aluminum powder binding only 5% of the amount of oxalate adsorbed in the absence of intestinal content. Oxalate binding to colestipol and $WB_r$ was also less in simulated intestinal content, being 52 and 70%, respectively, of that observed when chloride was the only anion present.

**Binding Kinetics**—Oxalate was adsorbed more rapidly by colestipol

and $WB_r$ (not shown) than by aluminum hydroxide (Fig. 2). The binding to aluminum hydroxide had two rates. Initially, there was rapid uptake, binding being more rapid for proprietary antacid formulations of aluminum hydroxide than for the powders. For both adsorbents, several days were required for equilibrium to be obtained.

## DISCUSSION

These results indicate that oxalate, in the presence of simulated intestinal content, binds better to aluminum hydroxide and weak anion-exchange resins (colestipol and $WB_r$) than to a strongly basic ion-exchange resin. They also show that the binding is rapid to ion-exchange resins but consists of a slow and fast component for aluminum hydroxide.

Although cholestyramine has been reported to be an effective oxalate adsorbent *in vitro* (11, 16), the data suggest that effective binding occurs only if chloride is omitted from the incubation. This could explain the findings of Caspary *et al.* (16) who demonstrated that cholestyramine did not bind oxalate *in vivo*. The data suggest that the reported efficacy of this resin in the treatment of enteric hyperoxaluria (3, 9) is due more to its binding of bile acid and fatty acids than to its binding of oxalate. Such binding should diminish colonic permeability to oxalate, which would be interpreted as reducing its absorption.

Colestipol and $WB_r$ bound less oxalate when bile acids and fatty acids were present in the incubation mixture; however, both resins were effective binding agents under experimental conditions simulating those present in the small intestinal lumen.

Aluminum hydroxide preparations had a greater capacity than colestipol or $WB_r$ for oxalate binding but required much longer for equilibrium to be reached, a factor that could diminish clinical efficacy. Although the commercial antacid preparations bound oxalate more rapidly than the dry powder preparations, similar amounts were bound by the two forms of oxalate within 30 min. Whether these differing rates of binding *in vitro* have clinical significance is unknown.

These *in vitro* binding data indicate that both aluminum antacids and weakly basic anion exchange resins might prove effective in adsorbing oxalate within the intestinal lumen and thus act to diminish the hyperoxaluria occurring in patients with intestinal disease. Preliminary clinical studies support these *in vitro* binding studies (26). Nonetheless, several recent reports (27, 28) claimed that oral calcium reduces oxalate absorption and that urinary calcium levels do not show a reciprocal increase.

Although hyperoxaluria contributes to nephrolithiasis in such patients, other factors, such as diminished urinary volume (29) and hypocitraturia (30, 31), are involved. Thus, reduction in oxalate excretion is only one of several alternative approaches for reducing the lithogenicity of urine.

## REFERENCES


(1) J. J. Deren, J. G. Porush, M. F. Levitt, and M. J. Khilnani, *Ann. Intern. Med.*, **56,** 843 (1962).

(2) E. A. Gelzayd, R. I. Breuer, and J. B. Kirsner, *Am. J. Dig. Dis.*, **13,** 1027 (1968).

(3) L. H. Smith, H. Fromm, and A. F. Hofmann, *N. Engl. J. Med.*, **286,** 1371 (1972).

(4) W. H. Admirand, D. L. Earnest, and H. E. Williams, *Trans. Assoc. Am. Physicians*, **84,** 307 (1971).

(5) R. H. Dowling, G. A. Rose, and D. J. Sutor, *Lancet*, **1,** 1103 (1971).

(6) S. S. Dickstein and B. Frame, *Surg. Gynecol. Obstet.*, **136,** 257 (1973).

(7) J. P. O'Leary, W. C. Thomas, and E. R. Woodward, *Am. J. Surg.*, **127,** 142 (1974).

(8) V. S. Chadwick, K. Modha, and R. H. Dowling, *N. Engl. J. Med.*, **289,** 172 (1973).

(9) J. Q. Stauffer, M. H. Humphreys, and G. J. Weir, *Ann. Intern. Med.*, **79,** 383 (1973).

(10) D. L. Earnest, G. Johnson, H. E. Williams, and W. H. Admirand, *Gastroenterology*, **66,** 1114 (1974).

(11) D. L. Earnest, *Am. J. Clin. Nutr.*, **30,** 72 (1977).

(12) J. W. Dobbins and H. J. Binder, *Gastroenterology*, **70,** 1096 (1976).

(13) J. W. Dobbins and H. J. Binder, *N. Engl. J. Med.*, **296,** 298 (1977).

(14) M. Hatch, R. W. Freel, A. M. Goldner, and D. L. Earnest, *Gastroenterology*, **78,** 1180 (1980).

(15) H. J. Binder, *ibid.*, **67,** 441 (1974).

(16) W. F. Caspary, J. Tonissen, and P. G. Lankisch, *Acta Hepato-Gastroenterol.*, **24,** 193 (1977).

(17) R. A. Willson, A. F. Hofmann, and G. G. R. Kuster, *Gastroenterology*, **66,** 95 (1974).

(18) W. H. Johns and T. R. Bates, *J. Pharm. Sci.*, **58,** 179 (1969).

(19) J. Clain, J.-R. Malagelada, V. Chadwick, and A. F. Hofmann, *Gastroenterology*, **73,** 556 (1977).

(20) A. F. Llewellyn, G. H. Tomkin, and G. M. Murphy, *Pharm. Acta Helv.*, **52,** 1 (1977).

(21) W. H. Johns and T. R. Bates, *J. Pharm. Sci.*, **59,** 329 (1970).

(22) D. L. Earnest, H. E. Williams, and W. H. Admirand, "Transactions of the Association of American Physicians," vol. 88, William J. Dornan, Collingdale, Pa., 1975, pp. 224, 234.

(23) E. Barilla, C. Notz, D. Kennedy, and C. Y. C. Pak, *Am. J. Med.*, **64,** 579 (1978).

(24) J. J. Kipling, "Adsorption from Solutions of Non-Electrolytes," Academic, New York, N.Y., 1965, chap. 7.

(25) G. P. van Berge Henegouwen and A. F. Hofmann, *Gastroenterology*, **73,** 300 (1977).

(26) M. F. Laker and A. F. Hofmann, *ibid.*, **78,** 1202 (1980) (abstract).

(27) J. Holst Pedersen and J. Steen, *Scand. J. Gastroenterol.*, **14,** 97 (1979).

(28) E. Hylander, S. Jarnum, and K. Nielsen, *ibid.*, **15,** 349 (1980).

(29) L. H. Smith, P. G. Werness, D. M. Wilson, and S. F. Phillips, *Clin. Res.*, **28,** 486A (1980) (abstract).

(30) J. P. O'Leary, W. C. Thomas, Jr., and E. R. Woodward, *Am. J. Surg.*, **127,** 142 (1974).

(31) D. Rudman, J. L. Dedonis, M. T. Fountain, J. B. Chandler, G. G. Gerron, G. A. Fleming, and M. H. Kutner, *N. Engl. J. Med.*, **303,** 657 (1980).


## ACKNOWLEDGMENTS


Supported by a grant-in-aid from the National Foundation for Ileitis and Colitis, by National Institutes of Health Grant AM 21506, and by grants-in-aid from the Rorer Group, Eli Lilly & Co., Herbert Falk GmbH, and Canada Packers, Ltd. Additional support was received from the Research (Endowments) Committee of St. Thomas's Hospital, London, England.

# Disposition of Sulfadimethoxine in Cattle: Inclusion of Protein Binding Factors in a Pharmacokinetic Model

**D. W. A. BOURNE *§, M. BIALER *¶, L. W. DITTERT *‖, M. HAYASHI **, G. RUDAWSKY ‡, G. D. KORITZ ‡, and R. F. BEVILL ‡x**

Received June 11, 1979, from the **College of Pharmacy, University of Kentucky, Lexington, KY 40506*, and the ‡*College of Veterinary Medicine, University of Illinois, Champaign–Urbana, IL 61801.* Accepted for publication March 5, 1981. §Present address: Department of Pharmacy, University of Queensland, St. Lucia, 4067, Queensland, Australia. ¶Present address: School of Pharmacy, Hebrew University, Jerusalem, Israel. ‖Present address: School of Pharmacy, University of Pittsburgh, Pittsburgh, PA 15261. **Present address: Tokyo College of Pharmacy, Tokyo, Japan.

**Abstract** □ Sulfadimethoxine was administered intravenously and orally to four cattle, and plasma and urine samples were collected at various times postdose. Modeling these data with a linear pharmacokinetic model gave unsatisfactory fits, and the data were subsequently fitted to a one-compartment model with saturable protein binding. The saturable protein binding model included the usual linear excretion and elimination processes as well as protein binding parameters. The values obtained *in vivo* for the binding constant, $5.01 \times 10^4\ M^{-1}$, and the total protein concentration, $7.89 \times 10^{-4}\ M$, compared favorably with previously reported *in vitro* values. These results indicate that protein binding can be successfully included in a pharmacokinetic model.

**Keyphrases** □ Sulfadimethoxine—protein binding, pharmacokinetics, cattle □ Protein binding—sulfadimethoxine, pharmacokinetics, cattle □ Pharmacokinetics—sulfadimethoxine, protein binding, cattle

Sulfadimethoxine is a long-acting sulfonamide with bacteriostatic activity against a variety of organisms, and commercial preparations are available for use in chickens, turkeys, dogs, cats, horses, cattle, and humans. Because of the widespread use of sulfonamides, a problem of drug residues in edible food tissues has developed.

To understand the kinetics of sulfonamides in food-producing animals, the disposition of various sulfonamides was investigated in a number of species (1–4). The present study involves the disposition of sulfadimethoxine in cattle after intravenous and oral administration. Previous studies (5–7) investigated sulfadimethoxine kinetics in cattle; however, none of these reports included excretion of metabolites into urine or the extensive binding of sulfadimethoxine to plasma proteins.

## EXPERIMENTAL

**Animals**—Four crossbred heifers[1], 10–12 months old and 161–202 kg, were used. The four animals were weighed and placed in slot-floored metabolism units 3 days prior to drug administration. They received a grain–concentrate mixture in limited amounts and grass, hay, and water *ad libitum* during the acclimatization and experimental periods; however, feed was withheld 24 hr prior to oral dosing. To facilitate urine collection, Foley retention catheters[2] were placed in the urinary bladder of each animal 24 hr prior to drug administration.

**Drugs**—Sulfadimethoxine[3] was prepared as a 12.5% solution in sterile distilled water. Complete solution of sulfadimethoxine was aided with a sufficient quantity of sodium hydroxide.

**Dosing Procedure**—Sulfadimethoxine (107 mg/kg of body weight) was administered by rapid intravenous drip into the left jugular vein of each animal. After a washout period of ~3 months, sulfadimethoxine (107 mg/kg of body weight) was administered to each animal *via* stomach tube.

**Sample Collection**—Blood and urine samples were collected at 0, 0.5, 1, 2, 3, 4, 6, 8, 10, 12, 16, 24, 36, 48, 60, 72, 84, 96, 108, and 120 hr following drug administration. Blood samples were taken from the right jugular vein in heparinized syringes and centrifuged at 3000 rpm for 7 min. The plasma was collected and stored at 4° until assay; all plasma samples were assayed within 1 week. The total volume of urine excreted during each sampling period was recorded before aliquots were taken. Urine samples were stored at −20° until assay.

**Assay Methods**—The plasma sulfadimethoxine concentration was determined spectrophotometrically following color formation with Bratton–Marshall reagents (2, 8). The concentrations of sulfadimethoxine and metabolites in urine were determined spectrophotometrically following separation by TLC and color formation, as previously described (2).

## RESULTS AND DISCUSSION

**Analytical Data following Intravenous Administration**—The average plasma concentration *versus* time data obtained following intravenous sulfadimethoxine administration to cattle (Table I and Fig. 1) appeared to fall biexponentially with a terminal rate constant of ~0.065 $hr^{-1}$ (biological half-life of 10.7 hr). The area under the average plasma concentration *versus* time curve from 0 to 120 hr was 3030 mg hr/liter.

The average excretion rate of unchanged sulfadimethoxine into urine *versus* time data (Fig. 1) also appeared to fall biexponentially but with

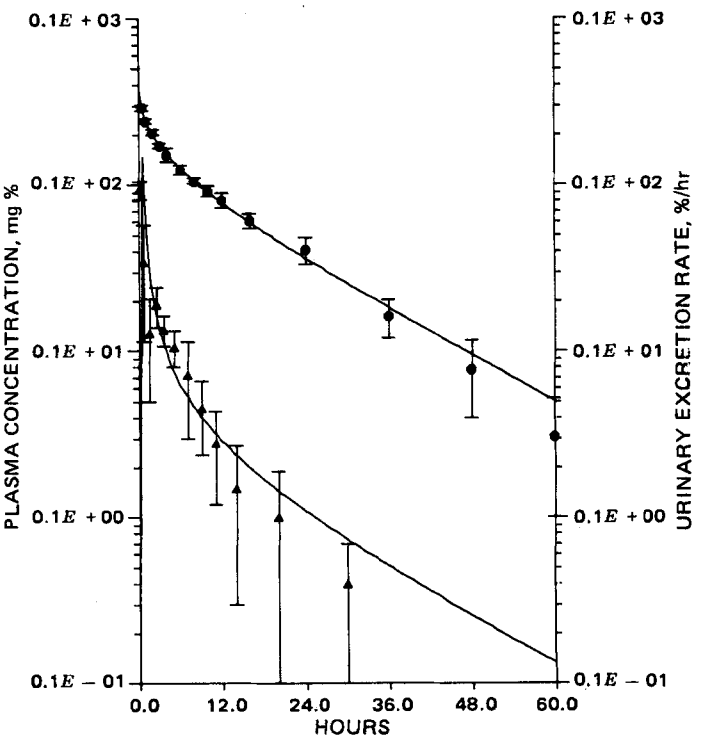


**Figure 1**—*Semilog plot of plasma concentration (●) versus time and rate of excretion of unchanged sulfadimethoxine in urine (▲) versus time following intravenous sulfadimethoxine administration. Points are the experimentally observed averages (SD as error bars) for four cattle, and lines were calculated.*

[1] Randomly selected from a group of heifers obtained from producers in the vicinity of Urbana, Ill.
[2] Bardex, 24 Fr, C. R. Bard Inc., Murray Hill, N.J.
[3] Lot 117102, Hoffmann-La Roche, Nutley, N.J.



*0022-3549/81/0900-1068$01.00/0*
*© 1981, American Pharmaceutical Association*

**Table I—Average Plasma Concentration of Sulfadimethoxine and Cumulative Amount of Sulfadimethoxine, Acetylsulfadimethoxine, and Polar Metabolite Excreted in Urine following Intravenous Sulfadimethoxine Administration**

| Hours | Plasma Concentration, mg/100 ml | Cumulative Amount Excreted in Urine, % of dose | | |
|---|---|---|---|---|
| | | Sulfadimethoxine | Acetylsulfadimethoxine | Polar Metabolite |
| 0.5 | 29.3 ± 1.2[a] | 4.7 ± 0.6 | 1.8 ± 0.4 | 0.2 ± 0.1 |
| 1.0 | 24.3 ± 0.9 | 6.4 ± 1.6 | 4.5 ± 0.5 | 0.3 ± 0.1 |
| 2.0 | 20.8 ± 0.8 | 7.7 ± 2.3 | 10.4 ± 1.3 | 0.6 ± 0.3 |
| 3.0 | 17.3 ± 0.6 | 9.6 ± 2.6 | 16.9 ± 1.6 | 0.9 ± 0.4 |
| 4.0 | 15.3 ± 1.4 | 11.0 ± 2.5 | 22.2 ± 2.1 | 1.2 ± 0.5 |
| 6.0 | 12.4 ± 0.8 | 13.1 ± 2.5 | 30.2 ± 1.7 | 1.9 ± 0.6 |
| 8.0 | 10.6 ± 0.4 | 14.5 ± 3.1 | 34.8 ± 2.8 | 2.3 ± 0.6 |
| 10.0 | 9.2 ± 0.6 | 15.4 ± 3.3 | 38.7 ± 3.4 | 2.4 ± 0.6 |
| 12.0 | 8.2 ± 0.8 | 16.0 ± 3.6 | 41.6 ± 3.4 | 2.6 ± 0.7 |
| 16.0 | 6.1 ± 0.7 | 16.6 ± 3.9 | 45.3 ± 4.5 | 2.8 ± 0.8 |
| 24.0 | 4.1 ± 0.7 | 17.4 ± 4.1 | 49.8 ± 5.3 | 3.0 ± 1.0 |
| 36.0 | 1.6 ± 0.4 | 17.9 ± 4.4 | 52.8 ± 6.3 | 3.4 ± 1.4 |
| 48.0 | 0.8 ± 0.4 | 17.9 ± 4.4 | 53.8 ± 7.0 | 3.5 ± 1.7 |
| 60.0 | 0.3 ± 0.2 | —[b] | 54.4 ± 7.4 | 3.7 ± 2.0 |
| 72.0 | —[c] | —[b] | —[d] | 3.8 ± 2.2 |
| 84.0 | —[c] | —[b] | —[d] | 4.0 ± 2.4 |
| 96.0 | —[c] | —[b] | —[d] | —[e] |
| 108.0 | —[c] | —[b] | —[d] | —[e] |
| 120.0 | —[c] | —[b] | —[d] | —[e] |

[a] One standard deviation ($n = 4$). [b] No further sulfadimethoxine was detected in urine after 48 hr. [c] Less than 0.1 mg/100 ml. [d] No further acetylsulfadimethoxine was detected in urine after 60 hr. [e] No further polar metabolite was detected in urine after 84 hr.

a slope quite different from that of the plasma data, especially at early time points. The total cumulative amounts of unchanged sulfadimethoxine, acetylsulfadimethoxine, and a polar metabolite excreted into urine were 17.9, 54.4, and 4.0% of the administered dose, respectively (Table I and Fig. 2).

Similar results were obtained for all four individual animals. Results for one animal are shown in Fig. 3.

**Analytical Data following Oral Administration**—The average plasma concentration *versus* time data obtained following oral sulfadimethoxine administration to cattle are shown in Table II and Fig. 4. The peak plasma concentration was 114 mg/liter at 10 hr, and the area under the plasma concentration–time curve from 0 to 120 hr was 4458 mg hr/liter. The total cumulative amounts of unchanged sulfadimethoxine, acetylsulfadimethoxine, and a polar metabolite excreted into urine were 6.3, 35.6, and 2.1% of the administered dose, respectively (Table II).

**Selection of Pharmacokinetic Model**—On the basis of plasma concentration data alone, a three-compartment linear model was used

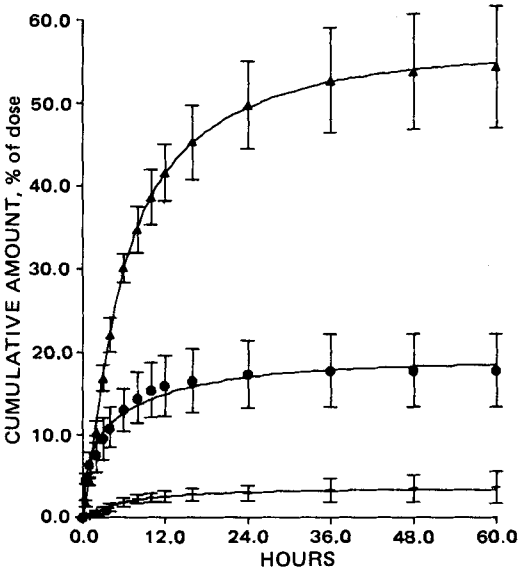


**Figure 2**—*Plot of cumulative amounts of sulfadimethoxine (●), acetylsulfadimethoxine (▲), and polar metabolite (+) excreted into urine* versus *time. Points are the experimentally observed averages for four cattle, and lines were calculated.*

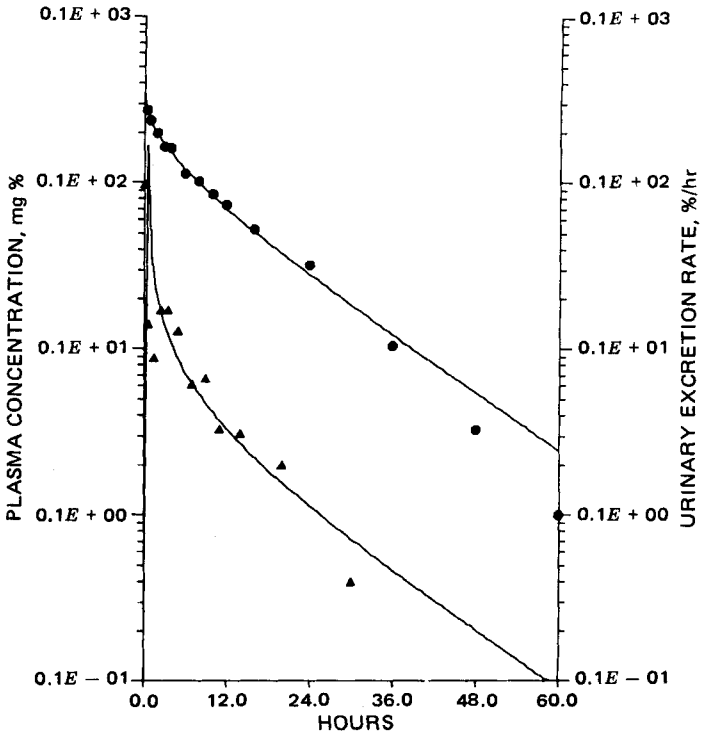


**Figure 3**—*Semilog plot of plasma concentration (●)* versus *time and rate of excretion of unchanged sulfadimethoxine in urine (▲)* versus *time following intravenous administration to one animal. Points were experimentally observed, and lines were calculated.*

to describe the elimination kinetics of sulfadimethoxine in cattle (7). However, a linear model, including the three-compartment model described previously, would predict that the plasma data and the urinary rate of excretion data would appear parallel when plotted semilogarithmically. If linear first-order kinetics apply, the rate of excretion at any time is directly proportional to the plasma concentration. The results obtained (Fig. 1) suggest that there is no constant proportionality between plasma concentration and the rate of excretion data at each time point measured so a simple linear model may not be sufficient to explain the data.

**Table II—Average Plasma Concentration of Sulfadimethoxine and Cumulative Amount of Sulfadimethoxine, Acetylsulfadimethoxine, and Polar Metabolite Excreted in Urine following Oral Sulfadimethoxine Administration**

| Hours | Plasma Concentration, mg/100 ml | Cumulative Amount Excreted in Urine, % of dose | | |
|---|---|---|---|---|
| | | Sulfadimethoxine | Acetylsulfadimethoxine | Polar Metabolite |
| 0.5 | 1.8 ± 1.4[a] | 0.0 | 0.0 | 0.0 |
| 1.0 | 4.0 ± 2.0 | 0.1 ± 0.1 | 0.1 ± 0.1 | 0.0 |
| 2.0 | 7.6 ± 2.0 | 0.1 ± 0.2 | 0.5 ± 0.4 | 0.1 ± 0.0 |
| 3.0 | 9.3 ± 1.7 | 0.2 ± 0.2 | 1.1 ± 0.6 | 0.1 ± 0.0 |
| 4.0 | 10.5 ± 1.5 | 0.3 ± 0.3 | 2.1 ± 0.9 | 0.2 ± 0.1 |
| 6.0 | 11.1 ± 1.0 | 0.5 ± 0.4 | 3.9 ± 2.4 | 0.4 ± 0.2 |
| 8.0 | 11.1 ± 0.7 | 0.8 ± 0.8 | 5.6 ± 4.6 | 0.6 ± 0.1 |
| 10.0 | 11.4 ± 1.0 | 0.9 ± 0.9 | 7.2 ± 4.6 | 0.8 ± 0.1 |
| 12.0 | 10.5 ± 0.9 | 0.9 ± 0.9 | 8.2 ± 4.5 | 0.9 ± 0.2 |
| 16.0 | 9.1 ± 1.1 | 1.1 ± 1.0 | 9.8 ± 5.3 | 0.9 ± 0.2 |
| 24.0 | 8.6 ± 1.0 | 2.0 ± 1.5 | 18.2 ± 7.3 | 0.9 ± 0.2 |
| 36.0 | 6.3 ± 1.4 | 4.6 ± 1.2 | 27.7 ± 5.1 | 1.0 ± 0.5 |
| 48.0 | 4.0 ± 0.9 | 5.9 ± 1.3 | 32.7 ± 3.8 | 1.2 ± 0.7 |
| 60.0 | 2.1 ± 0.6 | 6.1 ± 1.2 | 34.5 ± 3.6 | 1.3 ± 1.0 |
| 72.0 | 1.1 ± 0.5 | 6.2 ± 1.3 | 35.1 ± 3.8 | 1.5 ± 1.3 |
| 84.0 | 0.6 ± 0.6 | 6.3 ± 1.3 | 35.4 ± 4.1 | 1.6 ± 1.6 |
| 96.0 | 0.2 ± 0.1 | —[b] | 35.6 ± 4.4 | 1.7 ± 1.8 |
| 108.0 | —[c] | —[b] | —[d] | 1.8 ± 1.9 |
| 120.0 | —[c] | —[b] | —[d] | 1.9 ± 2.1 |
| 132.0 | —[c] | —[b] | —[d] | 2.1 ± 2.6 |
| 144.0 | —[c] | —[b] | —[d] | 2.1 ± 2.6 |

[a] One standard deviation ($n = 4$). [b] No further sulfadimethoxine was detected in urine after 84 hr. [c] Less than 0.1 mg/100 ml. [d] No further acetylsulfadimethoxine was detected in urine after 96 hr.

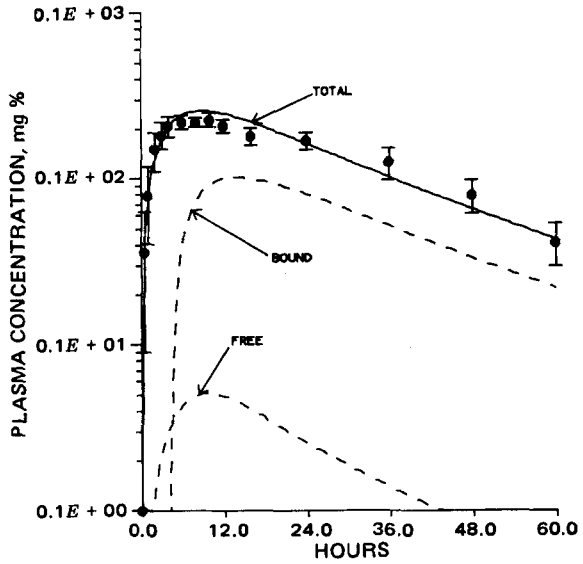


**Figure 4**—*Semilog plot of plasma concentration (●) versus time following oral sulfadimethoxine administration. Points are the experimentally observed averages for four cattle, and lines were calculated. The points and the solid line were multiplied by 2 to separate these values from the dashed lines representing free and bound drug concentrations.*

Sulfadimethoxine is extensively bound to bovine serum albumin, and the percentage of drug bound to protein decreases as the total concentration of drug in plasma increases (6). Since only free drug can be removed by the kidney or metabolized, protein binding of sulfadimethoxine should extensively affect sulfadimethoxine disposition. Kruger-Thiemer *et al.* (9) proposed a number of pharmacokinetic models involving protein binding of sulfonamides in humans. By means of computer simulations, these authors fit the plasma concentration *versus* time data to a pharmacokinetic model involving protein binding.

In view of the extensive protein binding of sulfadimethoxine in bovine plasma, it was decided that a model involving protein binding could be used to fit the data. A one-compartment model (Scheme I) was selected as the simplest model involving reversible protein binding.

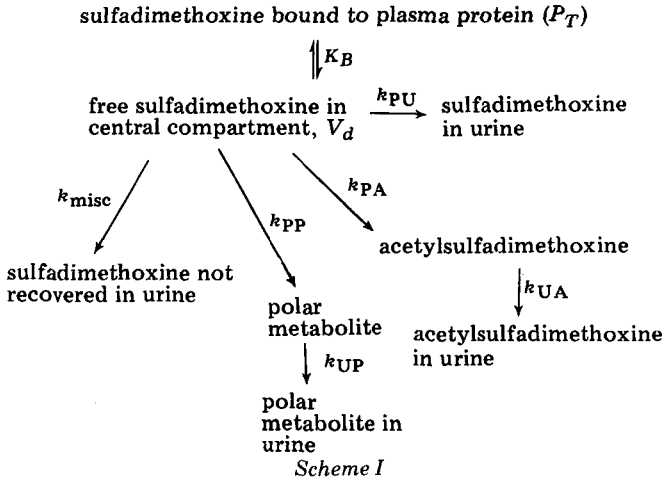


*Scheme I*

Value $K_B$ is the protein binding constant, $P_T$ is the total concentration of protein binding sites, and $V_d$ is the apparent volume of distribution.

Because drug and metabolite concentrations in urine were measured, this model includes metabolism of sulfadimethoxine and excretion of the two metabolites. All transfer processes in this model are linear, obeying first-order kinetics, with protein binding described by:

$$K_B = \text{[drug bound to protein]/[free drug][free protein binding sites]} \quad \text{(Eq. 1)}$$

The data were also fitted to linear two- and three-compartment models (Schemes II and III, respectively) so that a statistical evaluation of the model shown in Scheme I could be made.

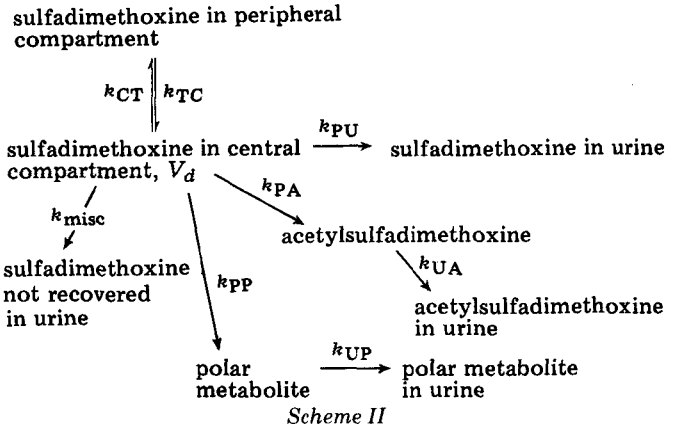


*Scheme II*

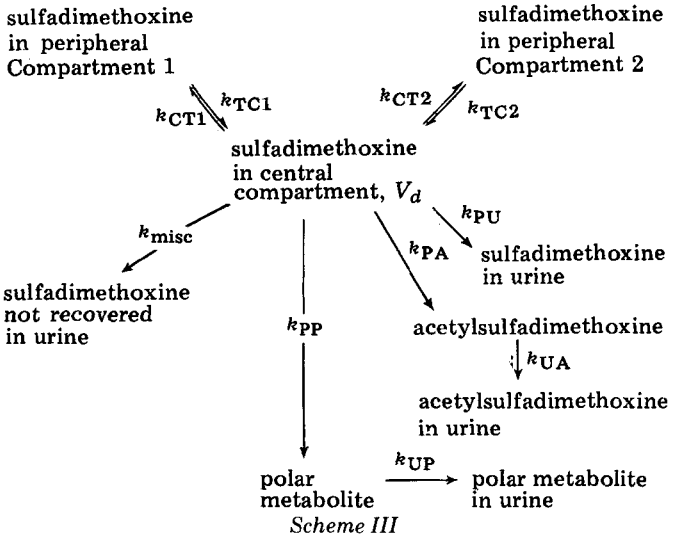


*Scheme III*

**Fitting Data to Pharmacokinetic Model**—*Intravenous Study*—The plasma and urine data obtained following intravenous administration of sulfadimethoxine were fitted simultaneously to the model shown in Scheme I and to the linear models shown in Schemes II and III using the digital computer program NONLIN.

An initial estimate of the overall elimination rate constant, $k_{el}$ ($= k_{PU} + k_{PA} + k_{PP} + k_{misc}$) (Scheme I), was obtained from the slope of the early rate of urinary excretion of unchanged sulfadimethoxine *versus* time data and the estimated concentration of free sulfadimethoxine present at zero time. This value for $k_{el}$ was separated into values for the individual rate constants ($k_{PU}$, $k_{PA}$, $k_{PP}$, and $k_{misc}$) by means of the total cumulative amounts of sulfadimethoxine excreted as unchanged drug, acetyl metabolite, or polar metabolite into urine data (1).

The free sulfadimethoxine concentration in plasma at different total concentrations was calculated from the data of Silvestri *et al.* (6) and was used to obtain initial estimates of the binding equilibrium constant, $K_B$, and the total concentration of protein binding sites, $P_T$. The initial fitting of the data was carried out with all of the parameters, except $k_{UA}$ and $k_{UP}$, held fixed at the initial estimate values. Once best fit values of $k_{UA}$ and $k_{UP}$ were obtained, the fitting was continued with progressively more of the parameters allowed to vary, *i.e.*, $k_{PU}$, $k_{PA}$, $k_{PP}$, $k_{misc}$, $K_B$, and then $P_T$. The final best fit values for all parameters of the model in Scheme I are presented in Table III. The close agreement between the model and the experimental data is shown in Figs. 1–3, 5, and 6. The lines were generated using the model shown in Scheme I with the best fit parameter values of Table III.

Initial estimates for $k_{el}$, $k_{CT}$, and $k_{TC}$ (Scheme II) and $k_{el}$, $k_{CT1}$, $k_{TC1}$, $k_{CT2}$, and $k_{TC2}$ (Scheme III) were obtained by "feathering" the plasma concentration–time data. Initial estimates for the other parameters of the linear models were obtained as already described. The fitting process was completed for each model using the average and individual animal data.

The Akaike criterion (11) was used to compare the proposed model,

**Table III—Values of Pharmacokinetic Parameters Obtained Using Scheme I following Intravenous Sulfadimethoxine Administration**

| Parameter | Animal 1 | 2 | 3 | 4 | Average | Mean ± *SD* |
|---|---|---|---|---|---|---|
| $k_{PU}$, $hr^{-1}$ | 1.399 | 0.382 | 0.104 | 0.173 | 0.443 | 0.515 ± 0.601 |
| $k_{PA}$, $hr^{-1}$ | 4.300 | 1.061 | 0.448 | 0.322 | 1.311 | 1.533 ± 1.873 |
| $k_{PP}$, $hr^{-1}$ | 0.276 | 0.0452 | 0.0191 | 0.0374 | 0.0824 | 0.0944 ± 0.122 |
| $k_{misc}$, $hr^{-1}$ | 1.448 | 0.333 | 0.152 | 0.157 | 0.518 | 0.523 ± 0.623 |
| $k_{el}$, $hr^{-1}$ | 7.423 | 1.821 | 0.723 | 0.689 | 2.354 | 2.664 ± 3.216 |
| $K_B$, $M^{-1}$ | $10.53 \times 10^4$ | $4.66 \times 10^4$ | $2.88 \times 10^4$ | $1.96 \times 10^4$ | $5.12 \times 10^4$ | $5.01 \times 10^4 \pm 3.85 \times 10^4$ |
| $P_T$, $M$ | $10.65 \times 10^{-4}$ | $8.48 \times 10^{-4}$ | $6.04 \times 10^{-4}$ | $6.40 \times 10^{-4}$ | $8.69 \times 10^{-4}$ | $7.89 \times 10^{-4} \pm 2.13 \times 10^{-4}$ |
| $k_{UA}$, $hr^{-1}$ | 0.552 | 0.433 | 0.516 | 0.940 | 0.412 | 0.610 ± 0.225 |
| $k_{UP}$, $hr^{-1}$ | 1.023 | 0.399 | 1.128 | 0.232 | 0.396 | 0.696 ± 0.446 |
| $V_d$, liters | 49.2 | 63.8 | 47.6 | 53.6 | 47.4 | 53.6 ± 7.3 |
| $V_d$, liter/kg | 0.306 | 0.316 | 0.317 | 0.321 | 0.279 | 0.315 ± 0.006 |
| AIC[a] $P_T$ | 141 | 110 | 182 | 76 | 56 | — |
| AIC 2C | 223 | 198 | 247 | 200 | 219 | — |
| AIC 3C | 227 | 202 | 252 | 205 | 206 | — |

[a] Akaike Information Criteria.

**Table IV—Values of Pharmacokinetic Parameters Obtained Using Scheme I following Oral Sulfadimethoxine Administration**

| Parameter | Animal 1 | 2 | 3 | 4 | Average | Mean ± *SD* |
|---|---|---|---|---|---|---|
| $k_{PU}$, $hr^{-1}$ | 0.490 | 0.129 | 0.0500 | 0.0276 | 0.129 | 0.17 ± 0.22 |
| $k_{PA}$, $hr^{-1}$ | 2.847 | 0.993 | 0.262 | 0.273 | 0.970 | 1.1 ± 1.2 |
| $k_{PP}$, $hr^{-1}$ | 0.0695 | 0.0648 | 0.0106 | 0.0089 | 0.0409 | 0.039 ± 0.033 |
| $k_{misc}$, $hr^{-1}$ | 0.825 | 0.266 | 0.860 | 0.0912 | 0.322 | 0.32 ± 0.35 |
| $k_{el}$, $hr^{-1}$ | 4.232 | 1.452 | 0.409 | 0.400 | 1.462 | 1.62 ± 1.81 |
| $k_{UA}$, $hr^{-1}$ | 6.76 | 0.251 | 2.47 | 0.0944 | 0.376 | 2.4 ± 3.1 |
| $k_{UP}$, $hr^{-1}$ | 50.0 | 50.0 | 43.7 | 48.7 | 40.1 | 48.1 ± 3.0 |
| Bioavailability | 0.553 | 0.632 | 0.530 | 0.650 | 0.550 | 0.591 ± 0.059 |
| $k_a$, $hr^{-1}$ | 0.413 | 0.113 | 0.155 | 0.154 | 0.187 | 0.209 ± 0.138 |

incorporating protein binding parameters (Scheme I) with the linear models (Schemes II and III). In each case, the one-compartment saturable protein binding model gave a better fit than either of the two linear models (Table III). The appropriateness of the chosen model is further supported by the reasonable values obtained for $K_B$ and $P_T$. The average value of $K_B$ obtained in the present study, $5.01 \times 10^4\ M^{-1}$, compares favorably with values reported by other workers using bovine serum albumin *in vitro*, $1.5\text{–}25 \times 10^4\ M^{-1}$ (12–14). In addition, the average value of $P_T$, $7.89 \times 10^{-4}\ M$, compares well with the plasma albumin concentrations previously reported, $4.5\text{–}4.7 \times 10^{-4}\ M$ (15, 16).

*Oral Study*—The plasma and urine data obtained following oral administration of sulfadimethoxine were fitted to the model shown in Scheme I, with an added first-order absorption step. The initial estimate of the absorption rate constant, $k_a$, was determined by the method of residuals. The bioavailability was calculated as 0.59. When calculated by comparison of the total amount of drug recovered in urine following intravenous and oral administration, ~47% of the dose was absorbed. The ratio of the area under the plasma concentration–time curve could not be used in this study as a measure of bioavailability since the model was nonlinear. The model is consistent with the observed higher area under the curve following the oral dose compared with the intravenous dose. The values of the parameters of Scheme I obtained from the intravenous study were used as initial estimates in fitting the oral study data with the NONLIN computer program. The final best fit values obtained are

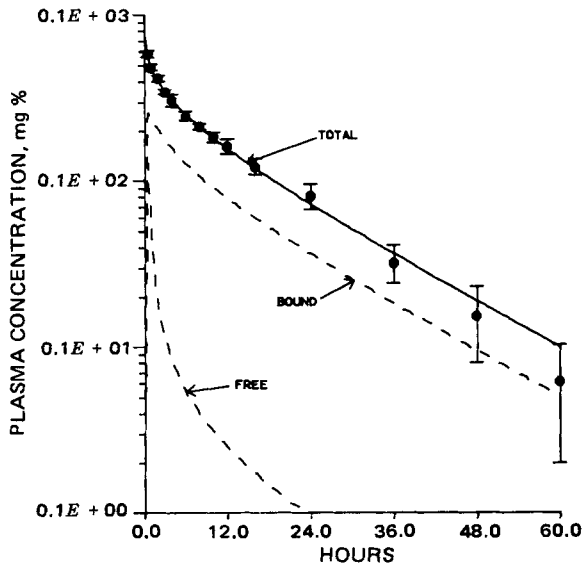


**Figure 5**—*Semilog plot of plasma concentration (●) versus time following intravenous sulfadimethoxine administration. Points are the experimentally observed averages for four cattle, and lines were calculated. The points and the solid line were multiplied by 2 to separate these values from the dashed lines representing free and bound drug concentrations.*

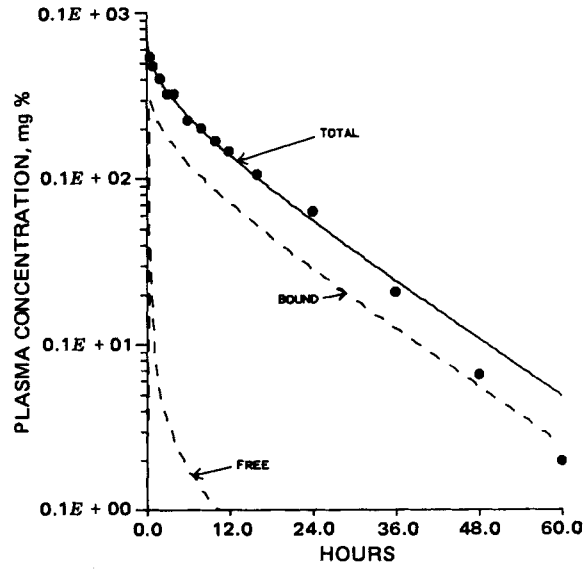


**Figure 6**—*Semilog plot of plasma concentration (●) versus time following intravenous sulfadimethoxine administration to one animal. Points were experimentally observed, and lines were calculated. The points and the solid line were multiplied by 2 to separate these values from the dashed lines representing free and bound drug concentrations.*

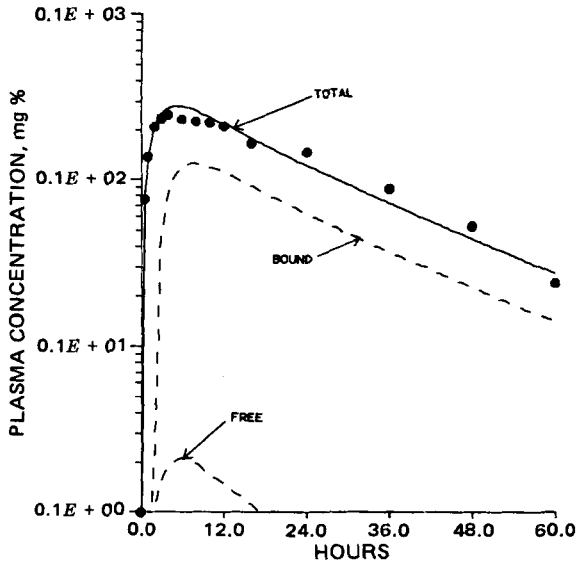


**Figure 7**—*Semilog plot of plasma concentration (●) versus time following oral sulfadimethoxine administration to one animal. Points were experimentally observed, and lines were calculated. The points and the solid line were multiplied by 2 to separate these values from the dashed lines representing free and bound drug concentrations.*

presented in Table IV. The lines in Figs. 4 and 7 were calculated using the best fit values of the parameters.

## REFERENCES

(1) D. W. A. Bourne, R. F. Bevill, R. M. Sharma, R. P. Gural, and L. W. Dittert, *Am. J. Vet. Res.*, **38**, 967 (1977).

(2) R. F. Bevill, R. M. Sharma, S. H. Meachum, S. C. Wozniak, D. W. A. Bourne, and L. W. Dittert, *ibid.*, **38**, 973 (1977).

(3) G. D. Koritz, R. F. Bevill, D. W. A. Bourne, and L. W. Dittert, *ibid.*, **39**, 481 (1978).

(4) D. W. A. Bourne, L. W. Dittert, G. D. Koritz, and R. F. Bevill, *J. Pharmacokinet. Biopharm.*, **6**, 123 (1978).

(5) C. M. Stowe and C. S. Sisodia, *Am. J. Vet. Res.*, **24**, 525 (1963).

(6) R. Silvestri, P. Magnifico, and S. Glatstein, *ibid.*, **28**, 1783 (1967).

(7) H. G. Boxenbaum and S. A. Kaplan, *J. Pharmacokinet. Biopharm.*, **3**, 257 (1975).

(8) J. S. Annino, in "Standard Methods of Clinical Chemistry," vol. 3, Academic, New York, N.Y., 1961, pp. 200–206.

(9) E. Kruger-Thiemer, W. Diller, and P. Bunger, *Antimicrob. Agents Chemother.*, **5**, 183 (1965).

(10) C. M. Metzler, G. L. Elfind, and A. J. McEwen, "A User's Manual for NONLIN and Associated Programs, Research Biostatistics," Upjohn Co., Kalamazoo, Mich., 1974.

(11) K. Yamaki, T. Nakagawa, and T. Uno, *J. Pharmacokinet. Biopharm.*, **6**, 165 (1978).

(12) P.-L. Hsu, J. K. H. Ma, H. W. Jun, and L. A. Luzzi, *J. Pharm. Sci.*, **63**, 27 (1974).

(13) M. Nakagaki, N. Koga, and H. Terada, *Yakugaku Zasshi*, **84**, 516 (1964).

(14) I. Moriguchi, S. Wada, and J. Nishizawa, *Chem. Pharm. Bull.*, **16**, 601 (1968).

(15) M. S. Spector, "Handbook of Biological Data," Saunders, Philadelphia, Pa., 1956.

(16) E. Genazzani and G. Pagnini, *Am. J. Vet. Res.*, **24**, 1212 (1963).

## ACKNOWLEDGMENTS

Supported by Food and Drug Administration Grant 223-74-178.

# Quantitative Determination of Conjugated Estrogens in Formulations by Capillary GLC

**G. K. PILLAI and K. M. McERLANE ˣ**

Received December 15, 1980, from the *Faculty of Pharmaceutical Sciences, University of British Columbia, Vancouver, British Columbia, V6T 1W5 Canada.* Accepted for publication March 4, 1981.

**Abstract** □ A rapid capillary GLC method for the analysis of conjugated estrogen tablets and injectable formulations is described. The method involves the hydrolytic cleavage of the sodium sulfate ester conjugates by sulfatase enzyme. The free phenolic steroids are reacted sequentially with hydroxylamine hydrochloride and *N,O*-bis(trimethylsilyl)trifluoroacetamide. The resulting dual derivatives are analyzed on a 15-m glass capillary column wall coated with a cyanopropylmethyl silicone phase.

**Keyphrases** □ Estrogens, conjugated—quantitative determinations by capillary GLC □ GLC, capillary—quantitative determination of conjugated estrogens □ Steroids—conjugated estrogens, quantitative determination by capillary GLC

Conjugated estrogens is the official name (1) given to a group of closely related steroids derived from the urine of pregnant mares. These naturally occurring, water-soluble salts have been used since 1942 for the treatment of estrogen deficiency symptoms associated with menopause. Only recently, however, have the structures of these steroids been collectively reported (2) and quantitative methods developed (3, 4). For many years, the accepted method of analysis was that contained in USP XVIII (5), which specified colorimetric methods and limits for the major steroids, estrone and equilin, as well as for total estrogen content. An absorbancy ratio requirement was included in the identification tests for an unspecified steroid.

Recent revisions of the USP/NF (1) included a GLC identification test based on a published method (3) but retained the iron–kober chromogenic reagent for the assay of estrone, equilin, and total estrogen content. The identification test requires a prominent peak for one steroid, 17α-dihydroequilin, and this substance probably is the steroid monitored by the previous USP (5) identification test.

## BACKGROUND

A consequence of the broad and nonquantitative specifications for the major and minor steroids is that compendial standards may not ensure pharmaceutical equivalence. More rigorous specifications for the indi-



*0022-3549/81/0900-1072$01.00/0*
*© 1981, American Pharmaceutical Association*

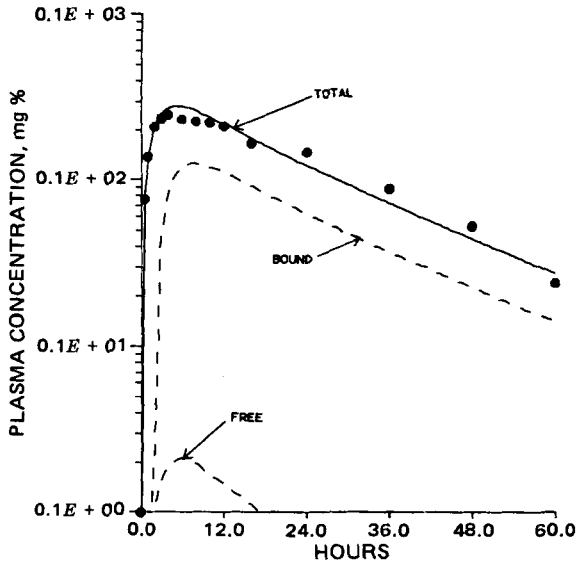


**Figure 7**—*Semilog plot of plasma concentration (●) versus time following oral sulfadimethoxine administration to one animal. Points were experimentally observed, and lines were calculated. The points and the solid line were multiplied by 2 to separate these values from the dashed lines representing free and bound drug concentrations.*

presented in Table IV. The lines in Figs. 4 and 7 were calculated using the best fit values of the parameters.

## REFERENCES

(1) D. W. A. Bourne, R. F. Bevill, R. M. Sharma, R. P. Gural, and L. W. Dittert, *Am. J. Vet. Res.*, **38**, 967 (1977).

(2) R. F. Bevill, R. M. Sharma, S. H. Meachum, S. C. Wozniak, D. W. A. Bourne, and L. W. Dittert, *ibid.*, **38**, 973 (1977).

(3) G. D. Koritz, R. F. Bevill, D. W. A. Bourne, and L. W. Dittert, *ibid.*, **39**, 481 (1978).

(4) D. W. A. Bourne, L. W. Dittert, G. D. Koritz, and R. F. Bevill, *J. Pharmacokinet. Biopharm.*, **6**, 123 (1978).

(5) C. M. Stowe and C. S. Sisodia, *Am. J. Vet. Res.*, **24**, 525 (1963).

(6) R. Silvestri, P. Magnifico, and S. Glatstein, *ibid.*, **28**, 1783 (1967).

(7) H. G. Boxenbaum and S. A. Kaplan, *J. Pharmacokinet. Biopharm.*, **3**, 257 (1975).

(8) J. S. Annino, in "Standard Methods of Clinical Chemistry," vol. 3, Academic, New York, N.Y., 1961, pp. 200–206.

(9) E. Kruger-Thiemer, W. Diller, and P. Bunger, *Antimicrob. Agents Chemother.*, **5**, 183 (1965).

(10) C. M. Metzler, G. L. Elfind, and A. J. McEwen, "A User's Manual for NONLIN and Associated Programs, Research Biostatistics," Upjohn Co., Kalamazoo, Mich., 1974.

(11) K. Yamaki, T. Nakagawa, and T. Uno, *J. Pharmacokinet. Biopharm.*, **6**, 165 (1978).

(12) P.-L. Hsu, J. K. H. Ma, H. W. Jun, and L. A. Luzzi, *J. Pharm. Sci.*, **63**, 27 (1974).

(13) M. Nakagaki, N. Koga, and H. Terada, *Yakugaku Zasshi*, **84**, 516 (1964).

(14) I. Moriguchi, S. Wada, and J. Nishizawa, *Chem. Pharm. Bull.*, **16**, 601 (1968).

(15) M. S. Spector, "Handbook of Biological Data," Saunders, Philadelphia, Pa., 1956.

(16) E. Genazzani and G. Pagnini, *Am. J. Vet. Res.*, **24**, 1212 (1963).

## ACKNOWLEDGMENTS

Supported by Food and Drug Administration Grant 223-74-178.

# Quantitative Determination of Conjugated Estrogens in Formulations by Capillary GLC

**G. K. PILLAI and K. M. McERLANE ˣ**

Received December 15, 1980, from the *Faculty of Pharmaceutical Sciences, University of British Columbia, Vancouver, British Columbia, V6T 1W5 Canada.* Accepted for publication March 4, 1981.

**Abstract** □ A rapid capillary GLC method for the analysis of conjugated estrogen tablets and injectable formulations is described. The method involves the hydrolytic cleavage of the sodium sulfate ester conjugates by sulfatase enzyme. The free phenolic steroids are reacted sequentially with hydroxylamine hydrochloride and *N,O*-bis(trimethylsilyl)trifluoroacetamide. The resulting dual derivatives are analyzed on a 15-m glass capillary column wall coated with a cyanopropylmethyl silicone phase.

**Keyphrases** □ Estrogens, conjugated—quantitative determinations by capillary GLC □ GLC, capillary—quantitative determination of conjugated estrogens □ Steroids—conjugated estrogens, quantitative determination by capillary GLC

Conjugated estrogens is the official name (1) given to a group of closely related steroids derived from the urine of pregnant mares. These naturally occurring, water-soluble salts have been used since 1942 for the treatment of estrogen deficiency symptoms associated with menopause. Only recently, however, have the structures of these steroids been collectively reported (2) and quantitative methods developed (3, 4). For many years, the accepted method of analysis was that contained in USP XVIII (5), which specified colorimetric methods and limits for the major steroids, estrone and equilin, as well as for total estrogen content. An absorbancy ratio requirement was included in the identification tests for an unspecified steroid.

Recent revisions of the USP/NF (1) included a GLC identification test based on a published method (3) but retained the iron–kober chromogenic reagent for the assay of estrone, equilin, and total estrogen content. The identification test requires a prominent peak for one steroid, 17α-dihydroequilin, and this substance probably is the steroid monitored by the previous USP (5) identification test.

## BACKGROUND

A consequence of the broad and nonquantitative specifications for the major and minor steroids is that compendial standards may not ensure pharmaceutical equivalence. More rigorous specifications for the indi-



*0022-3549/81/0900-1072$01.00/0*
*© 1981, American Pharmaceutical Association*

**Table I—Assay [a] of a Multiple-Injection Vial**

| Component | 1 | 2 | 3 | 4 | Mean ± *SD* | Percentage |
|---|---|---|---|---|---|---|
| 17α-Estradiol | 0.0210 | 0.0204 | 0.0209 | 0.0206 | 0.0207 ± 0.0002 | 2.82 |
| 17β-Estradiol | 0.0072 | 0.0085 | 0.0143 | 0.0144 | 0.0111 ± 0.0037 | 1.51 |
| 17α-Dihydroequilin | 0.1177 | 0.1209 | 0.1157 | 0.1244 | 0.1196 ± 0.0038 | 16.29 |
| 17β-Dihydroequilin | 0.0076 | 0.0084 | 0.0084 | 0.0083 | 0.0081 ± 0.0003 | 1.10 |
| Estrone | 0.3472 | 0.3593 | 0.3519 | 0.3478 | 0.3515 ± 0.0055 | 47.87 |
| Equilin | 0.1626 | 0.1674 | 0.1675 | 0.1673 | 0.1662 ± 0.0024 | 22.64 |
| 17α-Dihydroequilenin | 0.0130 | 0.0113 | 0.0098 | 0.0083 | 0.0106 ± 0.0020 | 1.44 |
| 17β-Dihydroequilenin | 0.0014 | 0.0011 | 0.0005 | 0.0003 | 0.0008 ± 0.0005 | 0.11 |
| Equilenin | 0.0491 | 0.0463 | 0.0433 | 0.0431 | 0.0454 ± 0.0028 | 6.18 |
| Total, mg | 0.7268 | 0.7431 | 0.7323 | 0.7345 | 0.7342 | |
| Total × 1.38, mg | 1.0029 | 1.0254 | 1.0105 | 1.0136 | 1.0131 | |

[a] Amount is expressed as milligrams of each steroid in a 1.0-mg aliquot. Amount of conjugated estrogens found = 1.0131 ± 0.0093 mg.

vidual steroids are needed, especially in view of the widely varying potencies of each steroid in the mixture. For example, 17β-estradiol, although a minor component, exhibits 12 times the potency of the major steroid, estrone (6). Many methods have attempted to resolve all of the components of this relatively complex mixture, including paper chromatography (7–9), TLC (10–14), high-performance liquid chromatography (15–18), and GLC (2–4, 19–23). Of these, two GLC methods were capable of resolving most of the components and were applied toward quantitation of the pharmaceutical product (3, 4). However, both methods suffer from either long chromatographic times and poor column stability (3) or the need for dual injections and lack of resolution of 17β-estradiol from 17α-dihydroequilin (4). In addition, the quantitation of the estrogens was further hindered by the presence of an impurity subsequently identified as equol (21). This impurity, if not removed prior to analysis, would interfere with both GLC methods (3, 4). This interference has necessitated the removal of this impurity by a lengthy extraction step (4).

As an alternative to packed column chromatographic analysis of the equine estrogens, capillary columns were recently used (24). However, the method did not significantly improve the resolution of estrone and equilin and did not address the problem of resolution of 17β-estradiol from 17α-dihydroequilin. Similar efforts in this laboratory resulted in the complete resolution of all known equine estrogens present in conjugated estrogens using a highly polar capillary column (25). The present study was based on the capillary column separation reported earlier (25) but included a quantitative determination of all known estrogens as well as a reported impurity, equol, in tablet and injectable formulations.

## EXPERIMENTAL

A gas chromatograph[1] equipped with a capillary inlet system, a flame-ionization detector, and a data terminal[2] was used for all measurements.

A commercial 15-m × 0.25-mm borosilicate column[3] wall coated with cyanopropylmethyl silicone liquid phase (Silar 10C) was used with a helium carrier gas flow of 0.8 ml/min through the column and a split vent flow of 40 ml/min. The column inlet pressure was 10 psi. The injector and detector temperatures were both 250°; the oven temperature was programmed from 170° for 7 min, heated at 2.3°/min to 220°, and maintained at this temperature for 5 min.

GLC–mass spectral data[4] were obtained with electron-impact ionization at 70 ev.

**Materials**—Reagent grade chloroform, acetic acid, sodium acetate, and anhydrous sodium sulfate were used. *N,O*-Bis(trimethylsilyl)trifluoroacetamide[5] and pyridine[5] were silylation grade. Sulfatase enzyme[6], ethinyl estradiol[7], hydroxylamine hydrochloride[8], and equine estrogens[9] were used as received.

**Sample Extraction and Preparation**—*Tablets*—Twenty tablets were weighed and powdered, and an amount equivalent to 1 mg of conjugated estrogens was weighed into a 50-ml, polytef-lined, screw-capped culture tube. To this tube was added 15 ml of an acetate buffer (0.02 *M*, pH 5.2), and the tube was shaken mechanically for 20 min. An amount equivalent to 2000 units of sulfatase enzyme was added, and the contents were incubated in a water bath at 45° for 30 min with occasional shaking. Then 0.2 ml of the internal standard, ethinyl estradiol, was added in 10 ml of chloroform, and the tube was shaken mechanically for an additional 30 min.

After centrifugation at 2000 rpm for 15 min, the chloroform layer was separated as completely as possible and filtered through a bed of anhydrous sodium sulfate. The filtrate, 3 ml at a time, was evaporated to dryness under a clean nitrogen stream in a 5-ml conical vial[10]. To the residue was added 200 μl of a 2% solution of hydroxylamine hydrochloride in dry pyridine. The polytef-lined screw-capped vial was heated in an aluminum block[11] at 70° for 30 min. The excess pyridine in the vial was evaporated under a gentle stream of clean, dry nitrogen, 150 μl of *N,O*-bis(trimethylsilyl)trifluoroacetamide and 50 μl of dry pyridine were added, and the vial was heated at 70° for an additional 10 min. Then 2 μl of the resulting solution was injected directly into the gas chromatograph. Peak identification was confirmed by comparison of retention times with those of pure standards.

*Injectable Formulation*—The contents of a 25-mg multiple injection vial were dissolved in an acetate buffer and brought to volume in a 50-ml volumetric flask with acetate buffer. An aliquot equivalent to 1 mg of conjugated estrogens was processed as described.

## RESULTS AND DISCUSSION

Conjugated estrogens exist in the pharmaceutical product as the sodium salts of the sulfate esters. For GLC analysis, it was necessary to hydrolyze these esters to their free phenolic forms. Two hydrolysis methods were used previously. The first method (2) involved the use of hydrochloric acid at elevated temperature, and the second consisted of

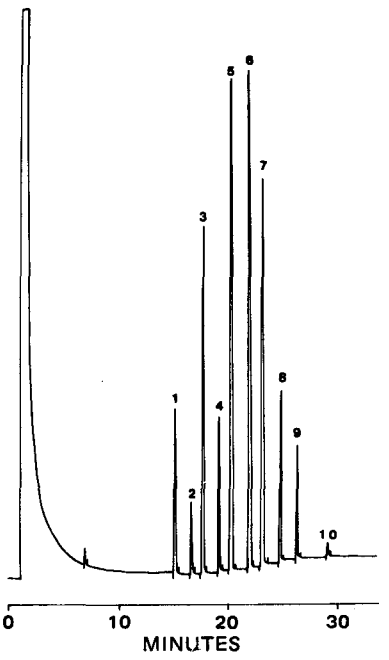


**Figure 1**—*Chromatogram of a standard mixture of equine estrogens as their oxime–trimethylsilyl derivatives. Key: 1, 17α-estradiol; 2, 17β-estradiol; 3, 17α-dihydroequilin; 4, 17β-dihydroequilin; 5, ethinyl estradiol (internal standard); 6, estrone; 7, equilin; 8, 17α-dihydroequilenin; 9, 17β-dihydroequilenin; and 10, equilenin.*

[1] Model 5830 A, Hewlett-Packard, Avondale, Pa.
[2] Model 18850A, Hewlett-Packard, Avondale, Pa.
[3] Alltech Associates, Rockford, Ill.
[4] Varian Mat 111 mass spectrometer, Hewlett-Packard 5700A gas chromatograph, and Varian 621/L computer.
[5] Pierce Chemical Co., Rockford, Ill.
[6] Type H-2, Sigma Chemical Co., St. Louis, Mo.
[7] Sigma Chemical Co., St. Louis, Mo.
[8] British Drug Houses, London, England.
[9] Ayerst Pharmaceuticals, Montreal, Canada.
[10] Reacti-Vial, Pierce Chemical Co., Rockford, Ill.
[11] Reacti-Therm heating module, Pierce Chemical Co., Rockford, Ill.

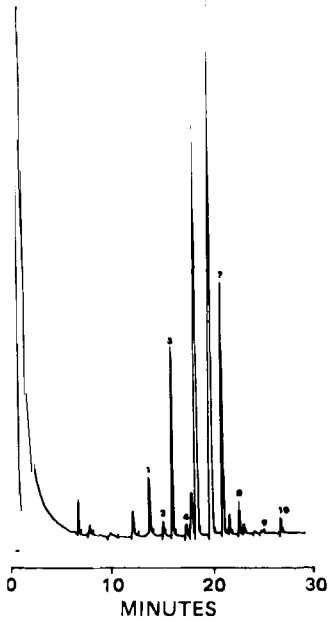


**Figure 2**—*Chromatogram of equine estrogens as their oxime–trimethylsilyl derivatives derived from a multiple-injection vial. Key: 1, 17α-estradiol; 2, 17β-estradiol; 3, 17α-dihydroequilin; 4, 17β-dihydroequilin; 5, ethinyl estradiol (internal standard); 6, estrone; 7, equilin; 8, 17α-dihydroequilenin; 9, 17β-dihydroequilenin; and 10, equilenin.*

incubation with sulfatase enzyme (3). The use of hydrochloric acid to hydrolyze steroid sulfates is known to cause steroid transformations (26, 27); and since it was considered essential to measure the original components of the mixture without creating artifacts during workup, acid hydrolysis could not be used. Although optimum conditions for the use of the sulfatase enzyme were established previously (4), it was considered necessary to ascertain that phosphates, suspected to be present in one formulation, did not inactivate the enzyme. Accordingly, a series of enzyme concentrations was incubated with identical aliquots of this tablet formulation, and an optimum enzyme quantity of 2000 units was found to yield maximum estrogen quantities. Above this value, no increase in estrogen levels was noted.

A prior examination of derivative combinations and capillary column phases led to the development of an excellent separation of all known equine estrogens as a dual derivative (25). Among the derivatives evaluated, an oxime–trimethylsilyl combination was most suitable.

As shown in Fig. 1, the chromatogram obtained for the oxime–trimethylsilyl derivatives exhibited excellent resolution of the equine estrogens. The potent steroid, 17β-estradiol, was well resolved from 17α-dihydroequilin, as was estrone from equilin. These two steroid pairs presented the greatest problems in previous chromatographic methods. In addition, the total chromatographic time was shortened as compared to the values, 55 (4) and 70 (3) min, reported earlier.

The chromatographic properties of samples obtained from hydrolysis of commercial formulations of conjugated estrogens are shown in Figs.

**Figure 3**—*Chromatogram of equine estrogens as their oxime–trimethylsilyl derivatives derived from a 2.5-mg tablet. Key: 1, 17α-estradiol; 2, 17β-estradiol; 3, 17α-dihydroequilin; 4, 17β-dihydroequilin; 5, ethinyl estradiol (internal standard); 6, estrone; 7, equilin; 8, 17α-dihydroequilenin; 9, 17β-dihydroequilenin; 10, equilenin; 11, equol; and 12, ethyl phthalate.*

**Table II—Composition of Commercial Formulations Containing Conjugated Estrogens** [a]

| Component | Sample: 25-mg Multiple-Injection Vial | Sample: 2.5-mg Tablet |
|---|---|---|
| 17α-Estradiol | 2.82 | 0.66 |
| 17β-Estradiol | 1.06 | 0.12 |
| 17α-Dihydroequilin | 16.23 | 2.87 |
| 17β-Dihydroequilin | 1.11 | 0.23 |
| Estrone | 48.07 | 62.01 |
| Equilin | 22.45 | 26.95 |
| 17α-Dihydroequilenin | 1.65 | 1.12 |
| 17β-Dihydroequilenin | 0.11 | 0.12 |
| Equilenin | 6.49 | 6.51 |
| Equol | — | 3.85 |

[a] These results represent the percentage of each conjugated estrogen; each value is the average of two assays. The formulations are from two different manufacturers.

2 and 3. Unlike the chromatogram shown in Fig. 1 and those reported for the commercial products using conventional packed columns, these chromatograms exhibit evidence of several additional minor components. One may be 9-dehydroestrone; however, a reference standard for this material was not available for comparison. The two commercial formulations display significant qualitative and quantitative differences. The formulation shown in Fig. 3 contained ethyl phthalate (retention time, 7.32 min) and equol (retention time, 22.07 min). The identities of these two extraneous substances were confirmed by comparison of their GLC and mass spectral characteristics. Ethyl phthalate is a probable residue from the tablet film-coating process, while equol was previously reported (21) as a contaminant of equine estrogens in some formulations. Since the present method can resolve equol from the equine steroids, prewash of the unhydrolyzed sample with benzene (4) is unnecessary since equol will not interfere with quantitation. Elimination of this purification step further reduces the total analysis time.

The subsequent quantitation of the separated equine estrogens was accomplished by determining the relative response ratios of samples of each individual equine estrogen as compared to the internal standard, ethinyl estradiol. At least six aliquots of each steroid, at levels bracketing the anticipated quantity in the mixture, were analyzed with a constant amount of internal standard. For all determinations, the correlation between the peak area ratios and concentrations was ≥0.998. The precision of the assay was checked by duplicate injections of four aliquots taken from a single 50-ml solution prepared from a multiple-injection vial. Each of the four aliquots was separately hydrolyzed, extracted, derivatized, and assayed. The mean and standard deviation of each steroid and the total are given in Table I.

Quantitation of conjugated estrogens in some available formulations provided the data shown in Table II; unlike with previous methods (3, 4), the quantity of 17β-estradiol now can be determined with certainty. In addition, it was found that the quantity of equilenin was double the amounts reported earlier, perhaps because of the increase in sensitivity due to the shorter retention time in the present chromatographic assay.

## REFERENCES

(1) "The United States Pharmacopeia," 20th rev., United States Pharmacopeial Convention, Rockville, Md., 1980, p. 298.

(2) R. Roman, C. A. Yates, J. F. Miller, and W. J. A. VandenHeuvel, *Can. J. Pharm. Sci.*, **10**, 8 (1974).

(3) R. Johnson, R. Masserano, R. Haring, B. Kho, and G. Schilling, *J. Pharm. Sci.*, **64**, 1007 (1975).

(4) K. M. McErlane and N. M. Curran, *ibid.*, **66**, 523 (1977).

(5) "The United States Pharmacopeia," 18th rev., Mack Publishing Co., Easton, Pa., 1970.

(6) O. Gisvold, in "Textbook of Organic Medicinal and Pharmaceutical Chemistry," 3rd ed., C. O. Wilson and O. Gisvold, Eds., Lippincott, Philadelphia, Pa., 1956, p. 578.

(7) E. Heftmann, *Science*, 111, 571 (1950).

(8) J. E. Cox, *J. Chromatogr.*, **61**, 193 (1971).

(9) E. Heftmann, *J. Am. Chem. Soc.*, **73**, 851 (1951).

(10) G. J. Kroll, G. R. Boyden, R. H. Moody, J. C. Comeau, and B. T. Kho, *J. Chromatogr.*, **61**, 187 (1971).

(11) K. M. Rajkowski and G. D. Broadhead, *ibid.*, **89**, 374 (1974).

(12) L. E. Crocker and B. A. Lodge, *ibid.*, **62**, 158 (1971).

(13) *Ibid.*, **69**, 419 (1978).

(14) I. Schroeder, G. Lopez-Sanchez, J. C. Medina-Acevedo, and M. del Carmen Espinosa, *J. Chromatogr. Sci.*, **13**, 37 (1975).
(15) A. G. Butterfield, B. A. Lodge, and N. J. Pound, *ibid.*, **11**, 401 (1973).
(16) R. W. Roos, *ibid.*, **14**, 505 (1976).
(17) G. Capitano and R. Tscherne, *J. Pharm. Sci.*, **68**, 311 (1979).
(18) P. I. Mussey, D. C. Collins, and J. R. K. Prudy, *Steroids*, **31**, 583 (1978).
(19) I. Schroeder, J. C. Medina-Acevedo, and G. Lopez-Sanchez, *J. Chromatogr. Sci.*, **10**, 183 (1972).
(20) K. M. McErlane, *ibid.*, **12**, 97 (1974).
(21) G. Carrignan, N. M. Curran, B. A. Lodge, and K. M. McErlane, *Can. J. Pharm. Sci.*, **13**, 73 (1978).
(22) R. N. Johnson, R. P. Masserano, B. T. Kho, and W. P. Adams, *J. Pharm. Sci.*, **67**, 1218 (1978).
(23) W. P. Adams, J. Hasegawa, R. N. Johnson, and R. C. Haring, *ibid.*, **68**, 986 (1979).
(24) J. S. Zweig, R. Roman, W. B. Hagerman, and W. J. A. VandenHeuvel, *HRC CC, J. High Resolut. Chromatogr. Chromatogr. Commun.*, **3**, 169 (1980).
(25) G. K. Pillai and K. M. McErlane, *ibid.*, **4**, 70 (1981).
(26) C. A. Muehlbaecher and E. K. Smith, *Clin. Chem.*, **16**, 158 (1970).
(27) L. P. Cawley, B. O. Musser, W. Faucette, S. Beckloff, and H. Learned, *ibid.*, **11**, 1009 (1965).

## ACKNOWLEDGMENTS

Supported by a grant from the Natural, Applied and Health Sciences, University of British Columbia.

The authors thank Ayerst Pharmaceuticals, Montreal, Canada, for their gift of equine estrogens, and Dr. B. Lodge, Health Protection Branch, Ottawa, Canada, for a reference sample of equol. The authors are grateful to Mr. R. Burton for the mass spectral analysis.

# Thiourea and Thiosemicarbazide Derivatives Structurally Related to Hexestrol: Synthesis and Anticancer and Other Pharmacological Properties

**A.-MOHSEN M. E. OMAR ‡x, A. M. FARGHALY *, A. A. B. HAZZAI *, N. H. ESHBA *, F. M. SHARABI ‡, and T. T. DAABEES ‡**

Received May 16, 1980, from the **Department of Pharmaceutical Chemistry and the* ‡*Department of Pharmacology, Faculty of Pharmacy, University of Alexandria, Alexandria, Egypt.* Accepted for publication November 24, 1980.

**Abstract** □ Two novel series of thio compounds bearing internal structural modifications of hexestrol were synthesized as potential anticancer agents. The first contains several *N*-substituted thiourea functions, and the second contains various $N^4$-substituted-3-thiosemicarbazide moieties in place of one α-ethyl group of hexestrol dimethyl ether. The products showed no antileukemic activity in the P-388 lymphocytic leukemia system and did not exhibit any anticonvulsant or estrogenic properties.

**Keyphrases** □ Hexestrol—structurally related thiourea and thiosemicarbazide derivatives as anticancer agents □ Anticancer drugs, potential—compounds related to hexestrol, screened against P-388 lymphocytic leukemia □ Thioureas—synthesis, hexestrol derivatives, evaluation of anticonvulsant and anticancer activities □ Thiosemicarbazide—synthesis of hexestrol derivatives, evaluation of anticonvulsant and anticancer activities

Concurrent with ongoing studies of the cyclodesulfurization of thio compounds into various heterocyclic derivatives (1), related studies have been concerned with the synthesis of thio compounds derived from menadione (2), phthiocol (2), steroids (3), diethylstilbestrol (4), and theophylline (5), the biologically active nuclei, for various pharmacological purposes. Extending these studies to compounds containing thio functions as internal modifications of hexestrol, the thio derivatives IV–XI and XIV–XVIII (Scheme I) were prepared and tested for anticancer, estrogenic, and anticonvulsant activities.

## RESULTS AND DISCUSSION

**Chemistry**—1,2-Bis(*p*-methoxyphenyl)butylamine (II), required as the starting material, was prepared through conversion of α-ethyldesoxyanision (I) into the corresponding oxime (6), using hydroxylamine hydrochloride and potassium acetate in ethanol, followed by reduction of the product with aluminum amalgam in aqueous ethanol (7). The amine (II) was reacted with the equivalent amount of alkyl-, aryl-, or aralkylisothiocyanates (III) in refluxing ethanol to give *N*-[1,2-bis(*p*-methoxyphenyl)butyl]-*N'*-substituted thioureas (IV–XI) in high yields (Table I).

The treatment of the amine (II) with ethyl bromoacetate and sodium carbonate in anhydrous acetone gave the glycinate ester (XII), which was heated with excess hydrazine hydrate to yield the $N^{\alpha}$-[1,2-bis(*p*-methoxyphenyl)butyl]-α-aminoacetohydrazide (XIII). Heating equimolar amounts of this acid hydrazide and the selected isothiocyanate derivatives (III) in refluxing ethanol gave the required 4-substituted-1-{$N^{\alpha}$-[1,2-bis(*p*-methoxyphenyl)butyl]-α-aminoacetyl}-3-thiosemicarbazides (XIV–XVIII) (Scheme I and Table I). The products were identified by the appearance of four bands at 1550–1525, 1345, 1320–1305, and 945–910 $cm^{-1}$, characteristic for the –N–C=S amides of I, II, III, and IV, respectively, in the IR spectra (5, 8).

The PMR spectra of representative examples of the thiourea derivatives IV, VIII, and IX and the thiosemicarbazides XIV, XV, and XVII showed the common protons resonating at various shifts (Table II). In addition to these signals, the other NH proton of the thiourea part was identified at various shifts depending on the substituent present. It appeared as a triplet at δ 5.90 ppm for the allyl derivative (IV), as a singlet at δ 8.11 ppm for the *m*-tolyl derivative (VIII), and as a multiplet at δ 6.11 ppm for the benzyl thiourea (XI). Likewise, the $N^4$-H proton of the thiosemicarbazides appeared as a broad multiplet at δ 6.59 and 6.54 ppm for XIV and XV, respectively, and as a singlet at δ 8.57 ppm for XVII.

The mass spectrum of *N*-[1,2-bis(*p*-methoxyphenyl)butyl]-*N'*-benzylthiourea (XI) did not show the molecular ion peak at *m/z* 434. However, it indicated that the compound had undergone fragmentation through two pathways (Scheme II). The first pathway produced ions A and B at *m/z* 284 and 150, while the second pathway gave ions C and D at *m/z* 269 and 165, respectively. These four ions, on further fragmentation, produced various daughter ions (Scheme II), of which the tropylium ion at *m/z* 91 was almost as intense as the base peak at *m/z* 78. The mass spectrum of the thiosemicarbazide (XVII) did not show the molecular ion peak at *m/z* 506, but it showed the base peak at *m/z* 208 (see *Experimental*).

0022-3549/81/0900-1075$01.00/0
© 1981, American Pharmaceutical Association

(14) I. Schroeder, G. Lopez-Sanchez, J. C. Medina-Acevedo, and M. del Carmen Espinosa, *J. Chromatogr. Sci.*, **13**, 37 (1975).
(15) A. G. Butterfield, B. A. Lodge, and N. J. Pound, *ibid.*, **11**, 401 (1973).
(16) R. W. Roos, *ibid.*, **14**, 505 (1976).
(17) G. Capitano and R. Tscherne, *J. Pharm. Sci.*, **68**, 311 (1979).
(18) P. I. Mussey, D. C. Collins, and J. R. K. Prudy, *Steroids*, **31**, 583 (1978).
(19) I. Schroeder, J. C. Medina-Acevedo, and G. Lopez-Sanchez, *J. Chromatogr. Sci.*, **10**, 183 (1972).
(20) K. M. McErlane, *ibid.*, **12**, 97 (1974).
(21) G. Carrignan, N. M. Curran, B. A. Lodge, and K. M. McErlane, *Can. J. Pharm. Sci.*, **13**, 73 (1978).
(22) R. N. Johnson, R. P. Masserano, B. T. Kho, and W. P. Adams, *J. Pharm. Sci.*, **67**, 1218 (1978).
(23) W. P. Adams, J. Hasegawa, R. N. Johnson, and R. C. Haring, *ibid.*, **68**, 986 (1979).
(24) J. S. Zweig, R. Roman, W. B. Hagerman, and W. J. A. VandenHeuvel, *HRC CC, J. High Resolut. Chromatogr. Chromatogr. Commun.*, **3**, 169 (1980).
(25) G. K. Pillai and K. M. McErlane, *ibid.*, **4**, 70 (1981).
(26) C. A. Muehlbaecher and E. K. Smith, *Clin. Chem.*, **16**, 158 (1970).
(27) L. P. Cawley, B. O. Musser, W. Faucette, S. Beckloff, and H. Learned, *ibid.*, **11**, 1009 (1965).

## ACKNOWLEDGMENTS

Supported by a grant from the Natural, Applied and Health Sciences, University of British Columbia.

The authors thank Ayerst Pharmaceuticals, Montreal, Canada, for their gift of equine estrogens, and Dr. B. Lodge, Health Protection Branch, Ottawa, Canada, for a reference sample of equol. The authors are grateful to Mr. R. Burton for the mass spectral analysis.

# Thiourea and Thiosemicarbazide Derivatives Structurally Related to Hexestrol: Synthesis and Anticancer and Other Pharmacological Properties

**A.-MOHSEN M. E. OMAR ‡x, A. M. FARGHALY *, A. A. B. HAZZAI *, N. H. ESHBA *, F. M. SHARABI ‡, and T. T. DAABEES ‡**

Received May 16, 1980, from the **Department of Pharmaceutical Chemistry and the* ‡*Department of Pharmacology, Faculty of Pharmacy, University of Alexandria, Alexandria, Egypt.* Accepted for publication November 24, 1980.

**Abstract** □ Two novel series of thio compounds bearing internal structural modifications of hexestrol were synthesized as potential anticancer agents. The first contains several *N*-substituted thiourea functions, and the second contains various $N^4$-substituted-3-thiosemicarbazide moieties in place of one α-ethyl group of hexestrol dimethyl ether. The products showed no antileukemic activity in the P-388 lymphocytic leukemia system and did not exhibit any anticonvulsant or estrogenic properties.

**Keyphrases** □ Hexestrol—structurally related thiourea and thiosemicarbazide derivatives as anticancer agents □ Anticancer drugs, potential—compounds related to hexestrol, screened against P-388 lymphocytic leukemia □ Thioureas—synthesis, hexestrol derivatives, evaluation of anticonvulsant and anticancer activities □ Thiosemicarbazide—synthesis of hexestrol derivatives, evaluation of anticonvulsant and anticancer activities

Concurrent with ongoing studies of the cyclodesulfurization of thio compounds into various heterocyclic derivatives (1), related studies have been concerned with the synthesis of thio compounds derived from menadione (2), phthiocol (2), steroids (3), diethylstilbestrol (4), and theophylline (5), the biologically active nuclei, for various pharmacological purposes. Extending these studies to compounds containing thio functions as internal modifications of hexestrol, the thio derivatives IV–XI and XIV–XVIII (Scheme I) were prepared and tested for anticancer, estrogenic, and anticonvulsant activities.

## RESULTS AND DISCUSSION

**Chemistry**—1,2-Bis(*p*-methoxyphenyl)butylamine (II), required as the starting material, was prepared through conversion of α-ethyldesoxyanision (I) into the corresponding oxime (6), using hydroxylamine hydrochloride and potassium acetate in ethanol, followed by reduction of the product with aluminum amalgam in aqueous ethanol (7). The amine (II) was reacted with the equivalent amount of alkyl-, aryl-, or aralkylisothiocyanates (III) in refluxing ethanol to give *N*-[1,2-bis(*p*-methoxyphenyl)butyl]-*N'*-substituted thioureas (IV–XI) in high yields (Table I).

The treatment of the amine (II) with ethyl bromoacetate and sodium carbonate in anhydrous acetone gave the glycinate ester (XII), which was heated with excess hydrazine hydrate to yield the $N^{\alpha}$-[1,2-bis(*p*-methoxyphenyl)butyl]-α-aminoacetohydrazide (XIII). Heating equimolar amounts of this acid hydrazide and the selected isothiocyanate derivatives (III) in refluxing ethanol gave the required 4-substituted-1-{$N^{\alpha}$-[1,2-bis(*p*-methoxyphenyl)butyl]-α-aminoacetyl}-3-thiosemicarbazides (XIV–XVIII) (Scheme I and Table I). The products were identified by the appearance of four bands at 1550–1525, 1345, 1320–1305, and 945–910 $cm^{-1}$, characteristic for the –N–C=S amides of I, II, III, and IV, respectively, in the IR spectra (5, 8).

The PMR spectra of representative examples of the thiourea derivatives IV, VIII, and IX and the thiosemicarbazides XIV, XV, and XVII showed the common protons resonating at various shifts (Table II). In addition to these signals, the other NH proton of the thiourea part was identified at various shifts depending on the substituent present. It appeared as a triplet at δ 5.90 ppm for the allyl derivative (IV), as a singlet at δ 8.11 ppm for the *m*-tolyl derivative (VIII), and as a multiplet at δ 6.11 ppm for the benzyl thiourea (XI). Likewise, the $N^4$-H proton of the thiosemicarbazides appeared as a broad multiplet at δ 6.59 and 6.54 ppm for XIV and XV, respectively, and as a singlet at δ 8.57 ppm for XVII.

The mass spectrum of *N*-[1,2-bis(*p*-methoxyphenyl)butyl]-*N'*-benzylthiourea (XI) did not show the molecular ion peak at *m/z* 434. However, it indicated that the compound had undergone fragmentation through two pathways (Scheme II). The first pathway produced ions A and B at *m/z* 284 and 150, while the second pathway gave ions C and D at *m/z* 269 and 165, respectively. These four ions, on further fragmentation, produced various daughter ions (Scheme II), of which the tropylium ion at *m/z* 91 was almost as intense as the base peak at *m/z* 78. The mass spectrum of the thiosemicarbazide (XVII) did not show the molecular ion peak at *m/z* 506, but it showed the base peak at *m/z* 208 (see *Experimental*).

0022-3549/81/0900-1075$01.00/0
© 1981, American Pharmaceutical Association

Table I—*N*-1,2-Bis(*p*-methoxyphenyl)butyl-*N'*-substituted Thioureas (IV–XI), Thiosemicarbazide Derivatives (XIV–XVII), and Results of Their Screening for Anticonvulsant Activity

| Compound | Yield, % | Melting Point | Molecular Formula | Analysis, % | Calc. | Found | Anticonvulsant[a] Protection, % | Anticonvulsant[a] Mortality, % |
|---|---|---|---|---|---|---|---|---|
| IV | 85 | 151–152° | $C_{22}H_{28}N_2O_2S$ | C | 68.71 | 68.50 | 10 | 60 |
| | | | | H | 7.34 | 7.20 | | |
| | | | | N | 7.29 | 7.30 | | |
| | | | | S | 8.34 | 8.60 | | |
| V | 82 | 114–116° | $C_{23}H_{32}N_2O_2S$ | C | 68.96 | 68.70 | —[b] | —[b] |
| | | | | H | 8.05 | 7.80 | | |
| | | | | N | 7.00 | 7.00 | | |
| | | | | S | 8.00 | 7.90 | | |
| VI | 70 | 122–123° | $C_{25}H_{28}N_2O_2S$ | C | 71.39 | 71.30 | —[b] | —[b] |
| | | | | H | 6.71 | 6.80 | | |
| | | | | N | 6.66 | 6.20 | | |
| | | | | S | 7.62 | 7.80 | | |
| VII | 84 | 142–144° | $C_{26}H_{30}N_2O_2S$ | C | 71.85 | 71.85 | 20 | 50 |
| | | | | H | 6.96 | 6.80 | | |
| | | | | N | 6.45 | 6.80 | | |
| | | | | S | 7.38 | 7.30 | | |
| VIII | 81 | 127–128° | $C_{26}H_{30}N_2O_2S$ | C | 71.85 | 71.90 | 0 | 80 |
| | | | | H | 6.96 | 7.00 | | |
| | | | | N | 6.45 | 6.10 | | |
| | | | | S | 7.38 | 7.50 | | |
| IX | 76 | 147–149° | $C_{25}H_{27}ClN_2O_2S$ | C | 65.99 | 65.70 | 40 | 50 |
| | | | | H | 5.98 | 5.80 | | |
| | | | | Cl | 7.79 | 7.70 | | |
| | | | | N | 6.16 | 5.70 | | |
| | | | | S | 7.05 | 7.20 | | |
| X | 68 | 175–176° | $C_{25}H_{27}BrN_2O_2S$ | C | 60.12 | 60.10 | 20 | 70 |
| | | | | H | 5.45 | 5.80 | | |
| | | | | Br | 16.00 | 16.00 | | |
| | | | | N | 5.61 | 5.30 | | |
| | | | | S | 6.42 | 6.50 | | |
| XI | 90 | 119–120° | $C_{26}H_{30}N_2O_2S$ | C | 71.85 | 71.60 | 0 | 90 |
| | | | | H | 6.96 | 6.80 | | |
| | | | | N | 6.45 | 6.10 | | |
| | | | | S | 7.38 | 7.10 | | |
| XIV | 90 | 110–111° | $C_{24}H_{32}N_4O_3S$ | C | 63.13 | 62.80 | 0 | 90 |
| | | | | H | 7.06 | 6.60 | | |
| | | | | N | 12.27 | 11.80 | | |
| | | | | S | 7.02 | 7.50 | | |
| XV | 76 | 134–135° | $C_{25}H_{36}N_4O_3S$ | C | 63.53 | 63.60 | 10 | 30 |
| | | | | H | 7.68 | 7.50 | | |
| | | | | N | 11.86 | 12.00 | | |
| | | | | S | 6.76 | 6.60 | | |
| XVI | 87 | 148–150° | $C_{27}H_{32}N_4O_3S$ | C | 65.82 | 65.80 | —[b] | —[b] |
| | | | | H | 6.55 | 6.60 | | |
| | | | | N | 11.38 | 11.40 | | |
| | | | | S | 6.57 | 7.10 | | |
| XVII | 85 | 139–141° | $C_{28}H_{34}N_4O_3S$ | C | 66.37 | 66.10 | 50 | 40 |
| | | | | H | 6.76 | 6.10 | | |
| | | | | N | 11.06 | 11.30 | | |
| | | | | S | 6.33 | 6.00 | | |
| XVIII | 70 | 151–152° | $C_{28}H_{34}N_4O_3S$ | C | 66.37 | 65.95 | 10 | 60 |
| | | | | H | 6.76 | 6.60 | | |
| | | | | N | 11.06 | 10.90 | | |
| | | | | S | 6.33 | 7.00 | | |

[a] The compounds, in doses equivalent to 100 mg of meprobamate/kg, were suspended in gum acacia and orally given to albino mice (seven to 11 mice for each compound). The percent protection and percent mortality were determined as previously reported (5). [b] Not tested.

**Biological**—Compounds IV, V, VII, IX–XI, and XIV–XVIII did not exhibit any anticancer activity when tested in the P-388 lymphocytic leukemia system (9). In addition, the testing of representative examples of the products for other pharmacological properties revealed that they lacked estrogenic (Table III) and anticonvulsant (Table I) activities.

As revealed in the literature, various compounds possessing anticancer (10) and other pharmacological properties can be produced through chemical modifications involving the replacement of the one or two $\alpha$-ethyl groups of hexestrol by ethylidenyl (10–12), cyclopropyl (13), aryl (14, 15), or substituted amide (16, 17) moieties. As a supplementary modification of hexestrol, the designed compounds contained the thiourea and the thiosemicarbazide functions. The thiosemicarbazide compounds are known to produce anticancer activity when attached to certain heterocyclic compounds (18–21).

The inactivity of the products in the P-388 lymphocytic leukemia system has provided another example (9) of the inability of these thio functions, due to the variation of structures, to form the tridentate ligands (22) necessary for blocking DNA synthesis in tumor cells. The thio groups were too bulky relative to the $\alpha$-ethyl groups in hexestrol to allow IV and XIV to bind to the receptors; hence, they did not exhibit estrogenic activity (3). The results of anticonvulsant screening for XVII (5), which indicated 50% protection, confirmed the failure of related types of these compounds to fulfill the structural requirement for a proper anticonvulsant agent.

## EXPERIMENTAL[1]

**1,2-Bis(*p*-methoxyphenyl)butylamine (II)**—Aluminum amalgam, prepared from aluminum (22 g) and mercuric chloride (17.5 g) as reported (7), was treated with the solution of the oxime (12 g, 0.04 mole) in ethanol (220 ml) and distilled water (220 ml). The reaction mixture was stirred for 48 hr and filtered, and the residue was washed with ethanol (2 × 200 ml). Ethanol was distilled off from the combined filtrate and washings, and the residue was extracted with ether (4 × 100 ml). The ether extracts

[1] All melting points are uncorrected. IR spectra were measured as Nujol mulls on a Beckman 4210 IR spectrophotometer. NMR and mass spectra were measured on a Perkin-Elmer R 32 and a AEI-MS-50, respectively.

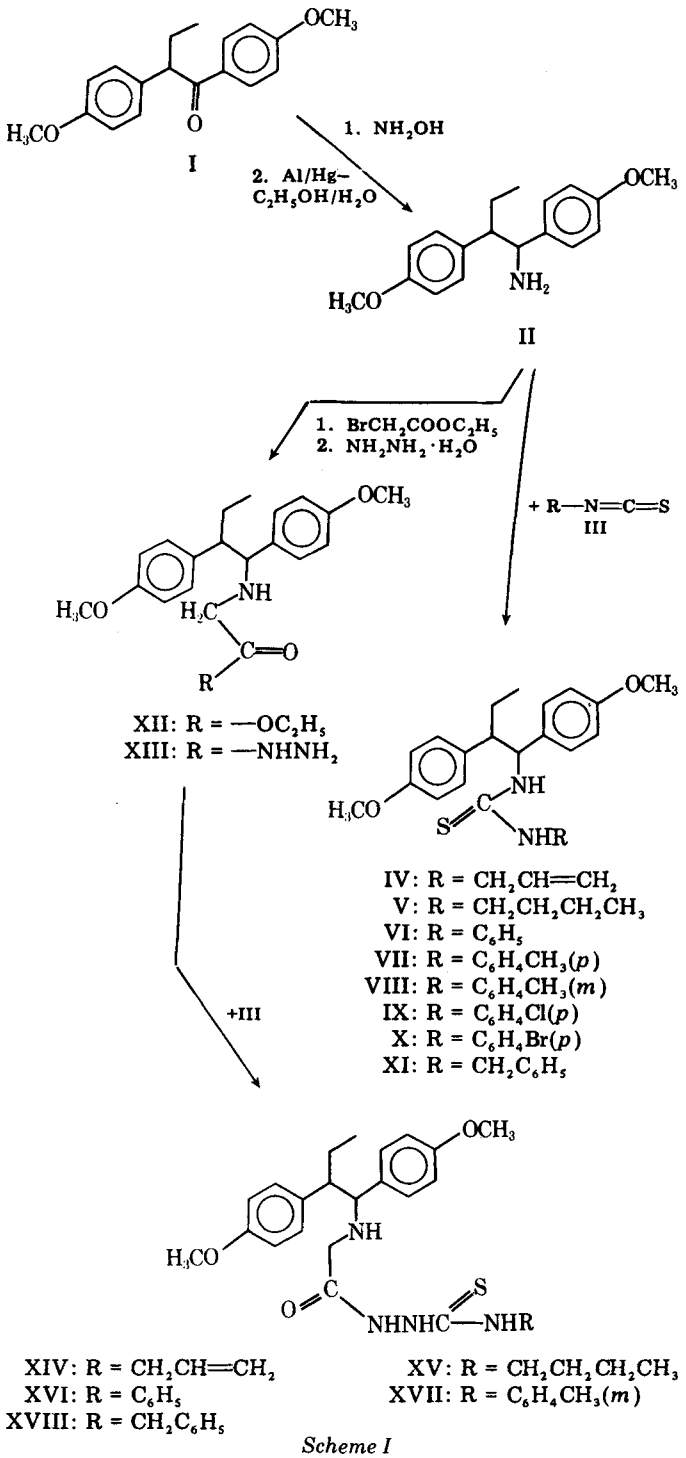


*Scheme I*

were dried (anhydrous sodium sulfate) and evaporated to leave an oil, which soon solidified. Crystallization from light petroleum (bp 60–80°) gave 8.6 g (75% yield) of white needles, mp 94–95° [lit. (23) mp 94–95.5°].

***N*-[1,2-Bis(*p*-methoxyphenyl)butyl]-*N'*-substituted Thioureas (IV–XI)**—A solution of II and the equivalent amount of the appropriate alkyl-, aryl-, or aralkylisothiocyanate (III) in ethanol was heated under reflux for 30 min. The solvent was evaporated, and the residue was scratched with drops of light petroleum (bp 40–60°) or an ether–light petroleum mixture to deposit into a solid. The products were crystallized from a benzene–light petroleum mixture and identified by elemental analysis, IR, PMR (Table II), and mass spectra; IR (mineral oil): 3400–3330 and 3310–3220 (NH), 1610, 1585, and 1510 (C=C aromatic), and 1550–1525, 1345, 1320–1305, and 945–910 $cm^{-1}$ (–N–C=S, amide I, II, III, and IV bands, respectively). Yields and physical constants of the products are recorded in Table I. The mass spectrum of XI showed

**Table II—Signals of the Common Protons in the PMR Spectra of the Thioureas IV, VIII, and XI and the Thiosemicarbazide Derivatives XIV, XV, and XVII**

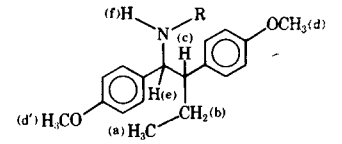


| Compound | Chemical Shift[a], δ ppm ($CDCl_3$) | | | | | | |
|---|---|---|---|---|---|---|---|
| | H(a) | H(b) | H(c) | H(d) | H(d') | H(e) | H(f) |
| IV | 0.70 t | 1.54 q | 2.77 q | 3.80 s | 3.80 s | 5.00 m | 6.34 d |
| VIII | 0.70 t | 1.56 m | 2.76 m | 3.75 s[b] | 3.78 s | 5.69 t | 6.30 d |
| XI | 0.75 t | 1.55 m | 2.77 m | 3.75 s[b] | 3.87 s | 5.00 m | 6.70 m |
| XIV | 0.60 t | 1.36 m | 2.72 m | 3.88 s | 3.88 s | 3.58 m | —[c] |
| XV | 0.60 t | — | 2.74 m | 3.84 s | 3.84 s | 3.53 m | —[c] |
| XVII | 0.58 t | 1.33 m | 2.70 m | 3.72 s[b] | 3.75 s | 3.54 m | —[c] |

[a] s = singlet, d = doublet, t = triplet, q = quartet, and m = multiplet. [b] The difference in the chemical shift between the (d) and (d') group protons is due to the presence of the protons of the methoxyl group (d) in the positive shielding area caused by the anisotropic effect of the aryl substituents in the thio chains of these compounds. [c] H(f) in the thiosemicarbazides appeared between 0.90 and 1.82 ppm mixed with the methylenic protons.

*m/z* (relative abundance %) $M^{\cdot}$ at 434 absent, 284 (2), 269 (46), 240 (6), 165 (6), 150 (8), 149 (42), 136 (42), 135 (9), 134 (9), 133 (5), 121 (31), 107 (9), 106 (16), 91 (99), and 78 (100).

***N*$^{\alpha}$-[1,2-Bis(*p*-methoxyphenyl)butyl] -α- aminoacetohydrazide (XIII)**—A solution of ethyl bromoacetate (2.24 g, 0.0134 mole) in dry acetone (10 ml) was added dropwise (during 30 min) onto a well-stirred mixture of II (3.45 g, 0.012 mole) and anhydrous sodium carbonate in dry acetone (40 ml). The mixture was heated under reflux while stirring for 8 hr, allowed to cool, and then filtered. The filtrate was evaporated to leave an oily residue, which was dissolved in benzene (50 ml). The benzene solution was washed successively with 10% aqueous HCl (2 × 25 ml), sodium carbonate solution, and water. Benzene was evaporated to leave 3.78 g (84%) of a viscous oil, which was homogeneous on TLC and used directly in the subsequent experiments: IR (mineral oil): 3340 (NH), 1740 (C=O), 1610, 1585, and 1510 (C=C, aromatic), 1300 (δ NH), and 1250, 1175, and 1040 (C–O–C) $cm^{-1}$.

The mixture of ester XII (3 g, 0.0081 mole) and hydrazine hydrate (15 ml) was heated for 3 hr at 90–110° (external temperature). The mixture was poured onto excess water to separate the oil, which was extracted with benzene (2 × 50 ml). The benzene extract was washed with water, dried (anhydrous sodium sulfate), and evaporated. The oil left (2.57 g, 89%) was homogeneous on TLC and used directly for preparation of the thiosemicarbazides; IR (liquid film): 3350 (NH), 1670 (C=O), 1615, 1585, and 1510 (C=C aromatic), 1305 (δ NH), and 1250, 1180, and 1040 (C–O–C) $cm^{-1}$.

**4-Substituted -1- {*N*$^{\alpha}$-[1,2-bis(*p*-methoxy)butyl] -α- aminoacetyl}-3-thiosemicarbazides (XIV–XVIII)**—The mixture of the acid hydrazide XIII (0.71 g, 0.002 mole) and an equimolar amount of the appropriate alkyl-, aryl-, or aralkylisothiocyanate (III) in dry benzene (20 ml) was heated under reflux for 2.5 hr. The solvent was removed, and the residue was boiled in light petroleum while being scratched to deposit into solid. Crystallization from benzene–light petroleum gave the required thiosemicarbazides (XIV–XVIII) (Table I). The products were identified by microanalysis and IR, PMR (Table II), and mass spectra. The mass spectrum for the *m*-tolylthiosemicarbazide (XVII) showed *m/z* (relative abundance %) $M^{\cdot}$ at 506 absent, 325 (3), 296 (2), 269 (12), 268 (6), 208

**Table III—Results of Estrogenic Activities**

| Compound | Doses, μmoles/kg | Number of Animals | Uterine Weight, mg/100 g of body weight ± *SE* | *p* Value[a] |
|---|---|---|---|---|
| Ovariectomized control | 0 | 5 | 56.4 ± 6.1 | — |
| Hexestrol | 2 | 4 | 123.5 ± 9.5 | <0.001 |
| | 8 | 4 | 155.0 ± 19.4 | <0.01 |
| IV | 2 | 4 | 46.1 ± 7.5 | NS |
| | 8 | 4 | 45.8 ± 2.9 | NS |
| | 32 | 4 | 48.6 ± 3.4 | NS |
| XIV | 2 | 4 | 49.9 ± 7.2 | NS |
| | 8 | 4 | 53.8 ± 3.2 | NS |
| | 32 | 4 | 98.6 ± 15.5 | <0.02 |

[a] NS = not significant.

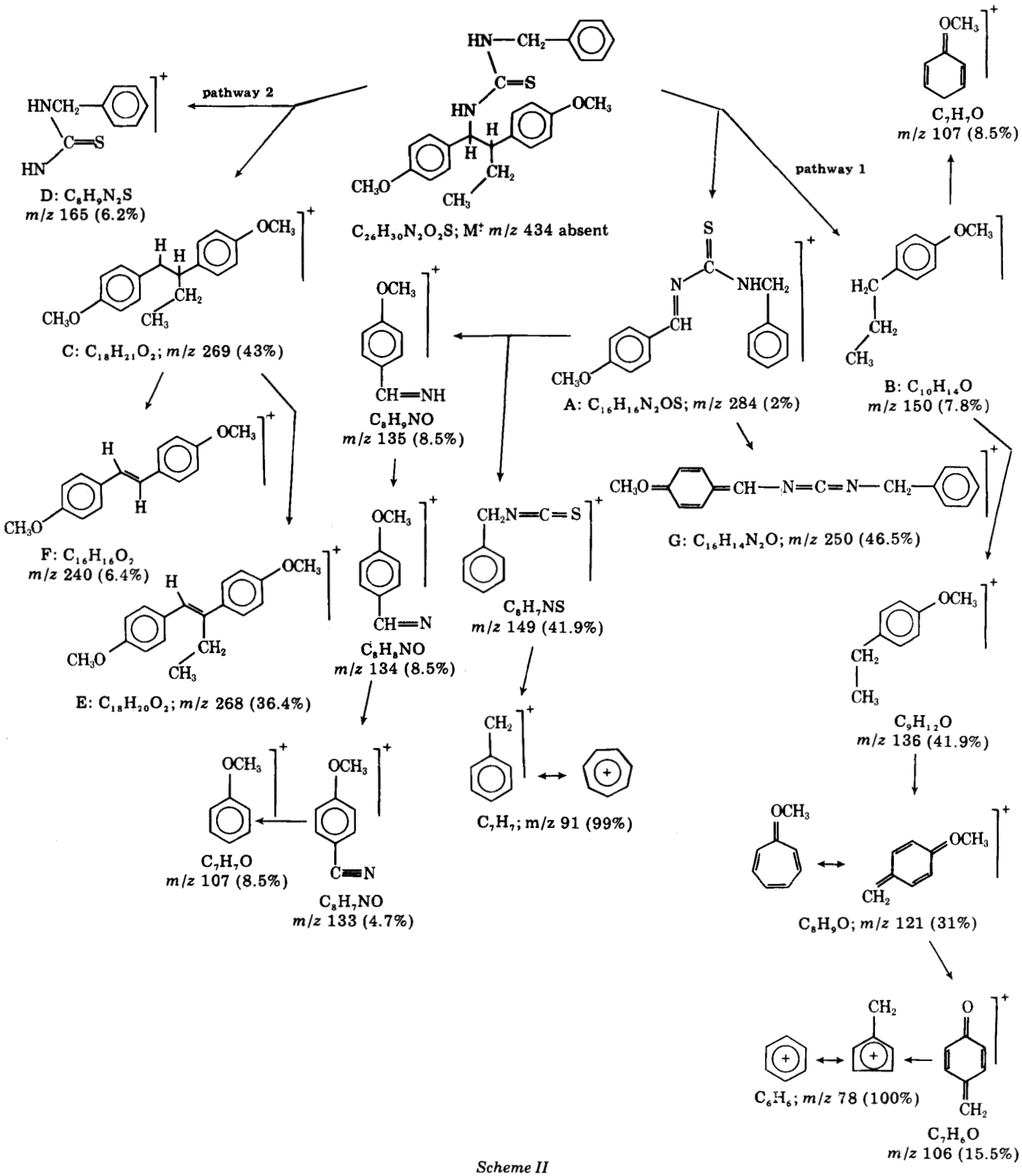


*Scheme II*

(100), 193 (20), 150 (35), 149 (99), 148 (64), 136 (46), 135 (9), 134 (8), 133 (4), 121 (61), 117 (22), 116 (16), 107 (36), 106 (34), 91 (99), 85 (28), 83 (44), and 78 (12).

## REFERENCES


(1) A.-M. M. E. Omar, F. A. Ashour, and J. Bourdais, *J. Heterocyl. Chem.*, **16**, 1435 (1979).

(2) A.-M. M. E. Omar and N. S. Habib, *Pharmazie*, **33**, 81 (1978).

(3) A.-M. M. E. Omar, S. M. El-Khawass, A. B. Makar, N. M. Bakry, and T. T. Daabees, *ibid.*, **33**, 577 (1978).

(4) E. I. Ibrahim, A.-M. M. E. Omar, M. A. Khalil, M. A. Makar, M. R. I. Soliman, and T. T. Daabees, *ibid.*, **35**, 82 (1980).

(5) A.-M. M. E. Omar, F. A. Ashour, A. B. Makar, and M. R. I. Soliman, *ibid.*, **34**, 110 (1979).

(6) P. P. T. Sah, *J. Chin. Chem. Soc.* (*Taipei*), **13**, 111 (1946); through

*Chem. Abstr. Jpn.*, **41**, 5870a (1947).
(7) R. M. Shafik, R. Soliman, and A. M. Hassan, *J. Pharm. Sci.*, **67**, 991 (1978).
(8) A.-M. M. E. Omar and S. A. Osman, *Pharmazie*, **28**, 30 (1973).
(9) E. A. Ibrahim, A.-M. M. E. Omar, and M. A. Khalil, *J. Pharm. Sci.*, **69**, 1348 (1980).
(10) M. A. Kornitsckii and L. A. Cherkasskii, *Vopr. Onkol.*, **16**, 84 (1970); through *Chem. Abstr. Jpn.*, **73**, 710p (1970).
(11) E. R. Clark and S. R. O'Donnell, *J. Chem. Soc.*, **1965**, 6509.
(12) D. J. Collins and J. J. Hobbs, *Aust. J. Chem.*, **23**, 119 (1970).
(13) J. G. Bennett, Jr., and S. C. Bunce, *J. Org. Chem.*, **25**, 73 (1960).
(14) Wm. S. Merrell Co., British pat. 822,954 (1959); through *Chem. Abstr. Jpn.*, **54**, 8740c (1960).
(15) T. Giannina, M. Butler, F. Popick, and B. Steinetz, *Contraception*, **3**, 347 (1971); through *Chem. Abstr. Jpn.*, **75**, 45219t (1971).
(16) S. H. Zaheer, P. B. Sattur, and P. P. Rao, *Ann. Chem.*, **691**, 55 (1966).
(17) N. K. Kochetkov and N. V. Dudykina, *Zh. Obshch. Khim.*, **29**, 4078 (1959); through *Chem. Abstr. Jpn.*, **54**, 20982h (1960).
(18) K. C. Agrawal, S. Clayman, and A. C. Sartorelli, *J. Pharm. Sci.*, **65**, 297 (1976).
(19) W. E. Antholine, J. N. Knight, and D. H. Petering, *J. Med. Chem.*, **19**, 339 (1976).
(20) J. A. Crim and G. Petering, *Cancer Res.*, **27**, 1268 (1967).
(21) I. Anthonini, F. Claudi, F. Franchetti, M. Grifantini, and S. Martelli, *J. Med. Chem.*, **20**, 447 (1977).
(22) F. A. Frensh and E. J. Blaur, *Cancer Res.*, **25**, 1454 (1965).

**ACKNOWLEDGMENTS**

Supported in part by Pharco Pharmaceuticals, Cairo, Egypt.

The authors thank the members of the Drug Research and Development Division of Cancer Research, National Cancer Institute, for screening the compounds and the members of the Microanalytical Unit, Faculty of Science, University of Cairo, for microanalytical data.

## NOTES

# Pharmacokinetic Linearity of Desipramine Hydrochloride

**D. WEINER ˣ, D. GARTEIZ, M. CAWEIN, T. DUSEBOUT, G. WRIGHT *, and R. OKERHOLM**

Received July 10, 1980, from the *Merrell Dow Pharmaceuticals Inc., Subsidiary of the Dow Chemical Company, Cincinnati, OH 45215.* Accepted for publication February 2, 1981. *Present address: A. H. Robins Co., Richmond, VA 23220.

**Abstract** □ The pharmacokinetic linearity of two single oral doses of desipramine hydrochloride was examined in a parallel study involving 30 subjects. Fourteen subjects received 75 mg (3 × 25 mg) of desipramine hydrochloride, and 16 subjects received 150 mg (1 × 150 mg). An open one-compartment model with a lag time to the start of absorption was used to examine the pharmacokinetic linearity. The results of the study suggest that the kinetics are linear in the dose range studied.

**Keyphrases** □ Desipramine hydrochloride—pharmacokinetic linearity, bioavailability, comparison of two tablet dose levels, humans □ Pharmacokinetic linearity—desipramine hydrochloride, humans □ Tricyclic antidepressants—desipramine hydrochloride, pharmacokinetic linearity, bioavailability, comparison of two tablet dose levels, humans

Tricyclic antidepressants are widely used in the treatment of depression. Recent studies (1–9) showed a relationship between steady-state plasma tricyclic levels and therapeutic response. Several investigations (10–14) were undertaken to find a means of predicting steady-state plasma tricyclic antidepressant concentrations based on plasma levels obtained after a single dose, thus avoiding time-consuming dosage titration to therapeutic plasma levels. These studies indicated that steady-state plasma levels can be predicted accurately by the area under the plasma concentration curve (*AUC*) following a single dose or by a single plasma level obtained 24, 48, or 72 hr after dosing.

This study determined the pharmacokinetic linearity of two single doses of desipramine hydrochloride[1], providing additional evidence that the steady-state predictions are reasonable.

## EXPERIMENTAL

**Subjects**—Thirty healthy male volunteers were randomized into two parallel treatment groups; 14 received 75 mg (three 25-mg tablets) of desipramine hydrochloride and 16 received one 150-mg tablet. The subjects were 19–40 years of age and 47–78 kg. All subjects were within 10% of their ideal weight.

**Protocol**—Each subject received the prescribed dose at 8:00 am. A 15-ml blood sample (vacuum blood-drawing tubes[2] containing lithium heparin as anticoagulant) was drawn just prior to dosing (time zero) and at 0.5, 1, 2, 3, 4, 6, 8, 10, 12, 14, 24, 36, 48, and 72 hr postdosing. No solid food was permitted from 8:00 pm of the preceding day until 12:00 noon of the dose day, at which time a standard lunch was served. A low-fat dinner was served at 6:00 pm; after collection of the 24-hr sample, the subject resumed eating *ad libitum*. A parallel design was employed instead of a crossover design since the elimination half-life for desipramine can be long and variable (15).

**Analytical Method**—The separated plasma was kept frozen until it was assayed. Desipramine was measured using a GLC–mass spectrometric technique adapted from Pantarotto *et al.* (16). The method involved the addition of the internal standard (nortriptyline) and extraction of the alkalinized plasma with *n*-hexane. The extract was reacted with acetic anhydride and pyridine without prior evaporation. The acetylated extract then was evaporated to dryness, and the residue was dissolved in ethanol. An aliquot was injected into the apparatus with selected-ion monitoring at *m/z* 305 and 308.

**Calculations**—Pharmacokinetic parameters were computed for each dosage level corresponding to an open one-compartment model with a lag time (17) using:

$$C(t) = \frac{FD}{V}\frac{K_a}{(K_a - K_e)}\left[e^{-K_e(t-L)} - e^{-K_a(t-L)}\right] \qquad \text{(Eq. 1)}$$

where $D$ is the administered oral dose, $F$ is the fraction of the dose absorbed, $V$ is the apparent volume of distribution, $K_a$ is the apparent first-order absorption rate constant, $K_e$ is the first-order elimination rate constant, $L$ is the lag time to the start of absorption, and $t$ is the time

[1] Norpramin, Merrell Dow Pharmaceuticals.

[2] Kimble-Terumo Venoject tubes.

0022-3549/81/0900-1079$01.00/0
© 1981, American Pharmaceutical Association

*Chem. Abstr. Jpn.*, **41**, 5870a (1947).
(7) R. M. Shafik, R. Soliman, and A. M. Hassan, *J. Pharm. Sci.*, **67**, 991 (1978).
(8) A.-M. M. E. Omar and S. A. Osman, *Pharmazie*, **28**, 30 (1973).
(9) E. A. Ibrahim, A.-M. M. E. Omar, and M. A. Khalil, *J. Pharm. Sci.*, **69**, 1348 (1980).
(10) M. A. Kornitsckii and L. A. Cherkasskii, *Vopr. Onkol.*, **16**, 84 (1970); through *Chem. Abstr. Jpn.*, **73**, 710p (1970).
(11) E. R. Clark and S. R. O'Donnell, *J. Chem. Soc.*, **1965**, 6509.
(12) D. J. Collins and J. J. Hobbs, *Aust. J. Chem.*, **23**, 119 (1970).
(13) J. G. Bennett, Jr., and S. C. Bunce, *J. Org. Chem.*, **25**, 73 (1960).
(14) Wm. S. Merrell Co., British pat. 822,954 (1959); through *Chem. Abstr. Jpn.*, **54**, 8740c (1960).
(15) T. Giannina, M. Butler, F. Popick, and B. Steinetz, *Contraception*, **3**, 347 (1971); through *Chem. Abstr. Jpn.*, **75**, 45219t (1971).
(16) S. H. Zaheer, P. B. Sattur, and P. P. Rao, *Ann. Chem.*, **691**, 55 (1966).
(17) N. K. Kochetkov and N. V. Dudykina, *Zh. Obshch. Khim.*, **29**, 4078 (1959); through *Chem. Abstr. Jpn.*, **54**, 20982h (1960).
(18) K. C. Agrawal, S. Clayman, and A. C. Sartorelli, *J. Pharm. Sci.*, **65**, 297 (1976).
(19) W. E. Antholine, J. N. Knight, and D. H. Petering, *J. Med. Chem.*, **19**, 339 (1976).
(20) J. A. Crim and G. Petering, *Cancer Res.*, **27**, 1268 (1967).
(21) I. Anthonini, F. Claudi, F. Franchetti, M. Grifantini, and S. Martelli, *J. Med. Chem.*, **20**, 447 (1977).
(22) F. A. Frensh and E. J. Blaur, *Cancer Res.*, **25**, 1454 (1965).

**ACKNOWLEDGMENTS**

Supported in part by Pharco Pharmaceuticals, Cairo, Egypt.

The authors thank the members of the Drug Research and Development Division of Cancer Research, National Cancer Institute, for screening the compounds and the members of the Microanalytical Unit, Faculty of Science, University of Cairo, for microanalytical data.

## NOTES

# Pharmacokinetic Linearity of Desipramine Hydrochloride

**D. WEINER ˣ, D. GARTEIZ, M. CAWEIN, T. DUSEBOUT, G. WRIGHT *, and R. OKERHOLM**

Received July 10, 1980, from the *Merrell Dow Pharmaceuticals Inc., Subsidiary of the Dow Chemical Company, Cincinnati, OH 45215.* Accepted for publication February 2, 1981. *Present address: A. H. Robins Co., Richmond, VA 23220.

**Abstract** □ The pharmacokinetic linearity of two single oral doses of desipramine hydrochloride was examined in a parallel study involving 30 subjects. Fourteen subjects received 75 mg (3 × 25 mg) of desipramine hydrochloride, and 16 subjects received 150 mg (1 × 150 mg). An open one-compartment model with a lag time to the start of absorption was used to examine the pharmacokinetic linearity. The results of the study suggest that the kinetics are linear in the dose range studied.

**Keyphrases** □ Desipramine hydrochloride—pharmacokinetic linearity, bioavailability, comparison of two tablet dose levels, humans □ Pharmacokinetic linearity—desipramine hydrochloride, humans □ Tricyclic antidepressants—desipramine hydrochloride, pharmacokinetic linearity, bioavailability, comparison of two tablet dose levels, humans

Tricyclic antidepressants are widely used in the treatment of depression. Recent studies (1–9) showed a relationship between steady-state plasma tricyclic levels and therapeutic response. Several investigations (10–14) were undertaken to find a means of predicting steady-state plasma tricyclic antidepressant concentrations based on plasma levels obtained after a single dose, thus avoiding time-consuming dosage titration to therapeutic plasma levels. These studies indicated that steady-state plasma levels can be predicted accurately by the area under the plasma concentration curve (*AUC*) following a single dose or by a single plasma level obtained 24, 48, or 72 hr after dosing.

This study determined the pharmacokinetic linearity of two single doses of desipramine hydrochloride[1], providing additional evidence that the steady-state predictions are reasonable.

## EXPERIMENTAL

**Subjects**—Thirty healthy male volunteers were randomized into two parallel treatment groups; 14 received 75 mg (three 25-mg tablets) of desipramine hydrochloride and 16 received one 150-mg tablet. The subjects were 19–40 years of age and 47–78 kg. All subjects were within 10% of their ideal weight.

**Protocol**—Each subject received the prescribed dose at 8:00 am. A 15-ml blood sample (vacuum blood-drawing tubes[2] containing lithium heparin as anticoagulant) was drawn just prior to dosing (time zero) and at 0.5, 1, 2, 3, 4, 6, 8, 10, 12, 14, 24, 36, 48, and 72 hr postdosing. No solid food was permitted from 8:00 pm of the preceding day until 12:00 noon of the dose day, at which time a standard lunch was served. A low-fat dinner was served at 6:00 pm; after collection of the 24-hr sample, the subject resumed eating *ad libitum*. A parallel design was employed instead of a crossover design since the elimination half-life for desipramine can be long and variable (15).

**Analytical Method**—The separated plasma was kept frozen until it was assayed. Desipramine was measured using a GLC–mass spectrometric technique adapted from Pantarotto *et al.* (16). The method involved the addition of the internal standard (nortriptyline) and extraction of the alkalinized plasma with *n*-hexane. The extract was reacted with acetic anhydride and pyridine without prior evaporation. The acetylated extract then was evaporated to dryness, and the residue was dissolved in ethanol. An aliquot was injected into the apparatus with selected-ion monitoring at *m/z* 305 and 308.

**Calculations**—Pharmacokinetic parameters were computed for each dosage level corresponding to an open one-compartment model with a lag time (17) using:

$$C(t) = \frac{FD}{V}\frac{K_a}{(K_a - K_e)}\left[e^{-K_e(t-L)} - e^{-K_a(t-L)}\right] \qquad \text{(Eq. 1)}$$

where $D$ is the administered oral dose, $F$ is the fraction of the dose absorbed, $V$ is the apparent volume of distribution, $K_a$ is the apparent first-order absorption rate constant, $K_e$ is the first-order elimination rate constant, $L$ is the lag time to the start of absorption, and $t$ is the time

[1] Norpramin, Merrell Dow Pharmaceuticals.

[2] Kimble-Terumo Venoject tubes.

0022-3549/81/0900-1079$01.00/0
© 1981, American Pharmaceutical Association

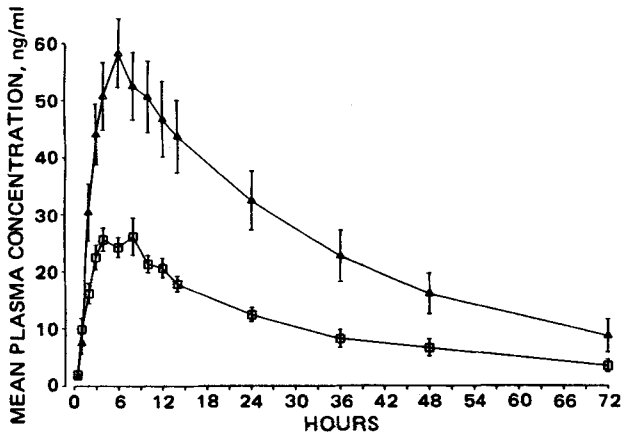


**Figure 1**—*Concentration of desipramine in plasma (mean ± SE). Key: □, desipramine hydrochloride, 3 × 25 mg; and △, desipramine hydrochloride, 150 mg.*

postdosing. These calculations were performed using the computer program NONLIN (18).

The distributions of $F/V$, $K_a$, $K_e$, and $L$ for the two dose groups were compared statistically by the Mann–Whitney U test (19). The elimination half-life, $t_{1/2}$, was calculated as $0.693/K_e$. No analysis was performed on $t_{1/2}$ since the results would be identical to those reported on $K_e$ using this statistical method. If the kinetics of the compound are linear in the dose range studied, the distributions of $F/V$, $K_a$, $K_e$, and $L$ are expected to be the same for both dose groups.

The $AUC$ (nanogram hours per milliliter) was calculated using the trapezoidal rule. Statistical analysis of the $AUC$, $C_{max}$ (nanograms per milliliter), and $t_{max}$ (hours) data was performed on the logarithms of the values using a two-sample $t$-test. Homogeneity of variance was verified by Cochran's test (20). The mean $AUC$ and $C_{max}$ values for the 150-mg group were expressed as a percentage of the 75-mg group mean by taking the antilog of the difference in log means. If the kinetics are linear in the dose range studied, the expected 150-mg mean would be ~200% of the 75-mg mean for $AUC$ and $C_{max}$ but equal to the 75-mg mean for $t_{max}$.

## RESULTS

The mean plasma concentrations are displayed for the two dose groups in Fig. 1, and the relevant pharmacokinetic data are listed in Table I.

The lag time estimated for the 75-mg dose ranged from 0 to 0.78 hr, while that for the 150-mg dose ranged from 0.39 to 0.77 hr. A statistically significant longer lag time for the 150-mg group resulted. However, this result probably has no clinical significance since maintenance therapy is required with tricyclic antidepressants.

The apparent $K_a$ calculated from this data ranged from 0.210 to 1.733 hr for 29 of the 30 subjects; the other subject had an estimated apparent $K_a$ of 13.548. There was no statistically significant difference in the apparent $K_a$ values for the two groups, but the value from the one individual resulted in a relatively high mean and standard error for the apparent $K_a$ of the 75-mg dose. If the value for this subject is deleted, the corresponding values are 0.69 ± 0.13 (mean ± $SE$).

The half-lives estimated for 28 of the 30 subjects ranged from 9.76 to 34.65 hr; the other two half-lives were 4.85 and 69.30 hr. There was no statistically significant difference in the half-lives between the two groups. These half-lives agreed quite well with the previously reported half-lives of 17.1 ± 5.3 hr (mean ± $SD$, range 12.5–24.7 hr) following a 1-mg/kg dose of desipramine (29.75 ± 4.89 mg, mean ± $SD$) (11) and of 20.0 ± 1.5 hr (mean ± $SD$, range 12–30) following a 100-mg dose of desipramine (21).

There were no statistically significant differences among $F/V$, $K$, or $t_{max}$ for the two dose groups.

The 150-mg dose produced significantly higher mean $AUC$ and $C_{max}$ values than did the 75-mg dose. The mean $AUC$ for the 150-mg group, when expressed as a percentage of the 75-mg mean, was 219% with 95% confidence limits of 151–318%. The corresponding mean ratio for $C_{max}$ was 199% with 95% confidence limits of 150–263%.

These results indicate that the kinetics of desipramine hydrochloride are linear in the 75–150-mg range and provide additional evidence that the earlier steady-state predictions based on levels after a single dose are meaningful.

**Table I—Pharmacokinetic Parameters (Mean ± *SE*)**

| Parameter | 75 mg ($n$ = 14) | 150 mg ($n$ = 16) |
|---|---|---|
| $F/V$, $ml^{-1} \times 10^3$ | 0.45 ± 0.05 | 0.47 ± 0.04 |
| $K_a$, $hr^{-1}$ | 1.61 ± 0.93[a] | 0.50 ± 0.06 |
| $K_e$, $hr^{-1}$ | 0.048 ± 0.008 | 0.040 ± 0.004 |
| $t_{1/2}$, hr | 19.7 ± 4.0 | 18.4 ± 1.8 |
| $L$[b], hr | 0.46 ± 0.05 | 0.62 ± 0.03 |
| $AUC$[c], ng hr/ml | 771.7 ± 87.3 | 1854.0 ± 307.0 |
| $C_{max}$[c], ng/hr | 30.7 ± 3.2 | 60.9 ± 5.9 |
| $t_{max}$, hr | 6.1 ± 0.7 | 5.9 ± 0.5 |

[a] Values are 0.69 ± 0.13 when one subject is deleted. [b] $p < 0.02$. [c] $p < 0.001$.

## REFERENCES

(1) A. H. Glassman and J. M. Perel, *Arch. Gen. Psychiatry*, **28**, 649 (1973).

(2) D. Luchins and J. Anath, *J. Nerv. Ment Dis.*, **162**, 430 (1976).

(3) R. A. Braithwaite, R. Goulding, G. Theano, J. Bailey, and A. Coppen, *Lancet*, **1**, 1297 (1972).

(4) M. Asberg, B. Cronholm, F. Sjoqvist, and D. Tuck, *Br. Med. J.*, **3**, 331 (1971).

(5) P. Kragh-Sorensen, M. Asberg, and C. Eggert-Hansen, *Lancet*, **1**, 113 (1973).

(6) V. E. Ziegler, P. J. Clayton, J. R. Taylor, B. T. Co, and J. T. Biggs, *Clin. Pharmacol. Ther.*, **20**, 458 (1976).

(7) A. H. Glassman, J. M. Perel, M. Shostak, S. J. Kantor, and J. L. Fleiss, *Arch. Gen. Psychiatry*, **34**, 197 (1977).

(8) V. E. Ziegler, B. T. Co, J. R. Taylor, P. J. Clayton, and J. T. Biggs, *Clin. Pharmacol. Ther.*, **19**, 795 (1976).

(9) L. F. Gram, N. Reisby, I. Ibsen, A. Nagy, S. Dencker, P. Bech, G. O. Petersen, and J. Christiansen, *Clin. Pharmacol. Ther.*, **19**, 318 (1976).

(10) B. Alexanderson, *Eur. J. Clin. Pharmacol.*, **5**, 44 (1972).

(11) *Ibid.*, **5**, 1 (1972).

(12) T. B. Cooper and G. M. Simpson, *Am. J. Psychiatry*, **135**, 333 (1978).

(13) S. A. Montgomery, R. McAuley, D. B. Montgomery, R. A. Braithwaite, and S. Dawling, *Clin. Pharmacokinet.*, **4**, 129 (1979).

(14) D. Brunswick, J. Amsterdam, J. Mendels, and S. Stern, *Clin. Pharmacol. Ther., Part One*, **25**, 605 (1979).

(15) D. Alexanderson and F. Sjoqvist, in "Pharmacology and the Future of Man Proceedings," 5th International Congress Pharmacology, San Francisco, Calif., 1972, 3, pp. 150–162.

(16) C. Pantarotto, G. Belvedere, L. Burti, and A. Frigerio, "Advances in Mass Spectrometry in Biochemistry and Medicine," vol. 1, Spectrum, New York, N.Y., 1976.

(17) M. Gibaldi and D. Perrier, "Pharmacokinetics," Dekker, New York, N.Y., 1975, p. 36.

(18) C. M. Metzler, G. L. Elfring, and A. J. McEwen, *Biometrics*, **1974** 562.

(19) S. Siegel, "Nonparametric Statistics for the Behavioral Sciences," McGraw-Hill, New York, N.Y., 1956, pp. 116–127.

(20) B. J. Winer, "Statistical Principles in Experimental Design," McGraw-Hill, New York, N.Y., 1971, pp. 208, 209.

(21) W. Z. Potter, A. P. Zavadil, III, I. J. Kopin, and F. K. Goodwin, *Arch. Gen. Psychiatry*, **37**, 314 (1980).

## ACKNOWLEDGMENTS

The authors gratefully acknowledge the technical assistance of G. O. Breault, J. F. Tessier, W. Krueger, and L. Adams, Analytical Development Corp., in the plasma desipramine determinations and Dr. Ronald Schoenwald for useful comments.

# Transport in Quantitative Structure–Activity Relationships VI: Relationship between Transport Rate Constants and Partition Coefficients

**HAN van de WATERBEEMD ˣ, PAUL van BAKEL, and ADRI JANSEN**

Received October 20, 1980, from the *Department of Pharmacochemistry, Subfaculty of Pharmacy, University of Leyden, 2300 RA Leyden, The Netherlands.* Accepted for publication February 2, 1981.

**Abstract** □ The transport rate constant of a drug partitioned in a two-phase system from an aqueous to an organic phase ($k_1^{obs}$) and vice versa ($k_2^{obs}$) is a function of the partition coefficient $P$ and of a solvent system-dependent parameter $\beta$. Drug transport is shown to be independent of molecular structure for a number of arbitrary compounds.

**Keyphrases** □ Drug transport—relationship between drug transport rate constants and partition coefficients □ Partition coefficients—relationship between drug transport rate constants and partition coefficients □ Structure–activity relationships—relationship between drug transport rate constants and partition coefficients

Partition coefficients ($P$) often are used as parameters in quantitative structure–activity relationships. A quadratic log $P$ term also is necessary in many relationships to obtain good statistics. The appearance of quadratic terms has been attributed to the influence of drug transport from the site of application to the site of action (1). However, partition coefficients are equilibrium constants, and transport is kinetic in nature. Thus, the relationship between the kinetic and equilibrium parameters of partitioning is important.

## BACKGROUND

Recently, it was shown that relationships exist between transport rates and partition coefficients (2, 3). A new transport model was developed to explain these relationships (2, 3).

A kinetic approach of this interfacial drug transport model reveals the following bilinear relationships between transport rate constants ($k^{obs}$) and $P$:

$$\log k_1^{obs} = \log P - \log\left(\frac{k_{org}}{k_{aq}}P + 1\right) + \log k_{org} \qquad \text{(Eq. 1)}$$

$$\log k_2^{obs} = -\log\left(\frac{k_{org}}{k_{aq}}P + 1\right) + \log k_{org} \qquad \text{(Eq. 2)}$$

where $k_1^{obs}$ is the observed rate constant for the drug transport from water to an organic solvent, $k_2^{obs}$ is the observed rate constant for the reverse process, and $k_{org}$ and $k_{aq}$ are the diffusion rate constants of the drug through the two adjacent stagnant layers, which are assumed to be at an interface. The $\beta$ value, known from Kubinyi's bilinear model (4, 5), appears to be identical to the quotient of $k_{org}$ and $k_{aq}$ (2, 3).

Moreover, it can be understood from this theory how drug transport in a biological system can be described with partition coefficients and why bilinear and parabolic relationships are found experimentally (6). This new interfacial drug transfer model is related closely to other literature models (6).

The theoretical equations were tested with a series of 30 sulfonamide derivatives, and it was demonstrated that $\beta$ under fixed conditions is a constant for a certain two-phase solvent system (3). In the $n$-octanol–water system, and in the chosen vessel and at a certain fixed temperature and stirring rate, the experimental regression equations are:

$$\log k_1^{obs} = \log P - \log(0.412P + 1) - 3.985$$
$$n = 30 \quad r = 0.990 \quad F = 1397 \quad s = 0.045 \qquad \text{(Eq. 3)}$$

$$\log k_2^{obs} = -\log(0.411P + 1) - 3.985$$
$$n = 30 \quad r = 0.998 \quad F = 6218 \quad s = 0.046 \qquad \text{(Eq. 4)}$$

From these experimental equations, it is concluded that the transport model and the theoretically found relationships between transport rate constants and $P$ have a physicochemical reality at least for a series of congeneric compounds. It was concluded previously that the effective volumes of the compounds of this sulfonamide series are all very similar. Differences in intrinsic molecular volume and polarity of the compounds are obviously compensated by a change in solvent association of the solute (3). It is tempting to assume that a compensation mechanism of intrinsic radius, polarity, and charge distribution holds for other compounds with variations even in the molecular skeleton. The present paper describes the results of transport rate measurements of compounds with variations in structure, size, and lipophilicity, including ion-pairs and partly ionized compounds.

## EXPERIMENTAL

Transport rate constants were determined with the apparatus and method previously described (7).

Partition coefficients were taken from the literature (8) or were determined by UV detection[1] after shaking appropriate amounts of mutually saturated solvents and allowing overnight separation.

All chemicals were available commercially and were analytical grade.

## RESULTS AND DISCUSSION

The observed ($k^{obs}$) and calculated ($k^{cal}$) transport data are given in Table I. Apparent partition coefficients ($P_{app}$) were used to calculate the rate constants with Eqs. 3 and 4. The observed rate constants and apparent partition coefficients of ion-pairs and ionic compounds are dependent on the initial concentration (9). The data are plotted in Fig. 1. All points are situated very near to the curves calculated for the sulfon-

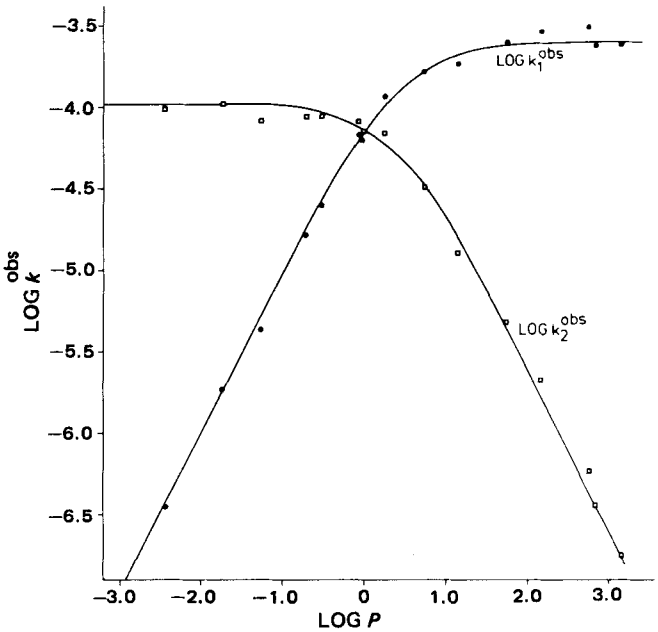


**Figure 1**—*Log* $k^{obs}$ *versus log P curves for the compounds of Table I. The plotted data are the log* $k^{obs}$ *values, and the drawn curves were calculated with Eqs. 3 and 4.*

[1] Gilford spectrophotometer 250.

0022-3549/81/0900-1081$01.00/0
© 1981, American Pharmaceutical Association

**Table I—Transport Data of Various Compounds in *n*-Octanol–Water [a,b]**

| Compound | Molecular Weight | log $P_{oct}^{app}$ | log $k_1^{obs}$ | log $k_1^{calc}$ | $\Delta_1^{obs-calc}$ | log $k_2^{obs}$ | log $k_2^{calc}$ | $\Delta_2^{obs-calc}$ | $C_0$[c], moles per liter |
|---|---|---|---|---|---|---|---|---|---|
| Ephedrine hydrochloride | 202 | −2.45 | −6.444 | −6.436 | −0.008 | −4.020 | −3.986 | −0.034 | $5.0 \times 10^{-5}$ |
| Adrenaline bitartrate | 333 | −1.75 | −5.725 | −5.738 | 0.013 | −3.978 | −3.988 | 0.010 | $3.0 \times 10^{-5}$ |
| Berberine chloride | 372 | −1.28 | −5.369 | −5.274 | −0.095 | −4.089 | −3.994 | −0.095 | $6.2 \times 10^{-2}$ |
| Sulfanilamide | 172 | −0.72[d] | −4.781 | −4.738 | −0.043 | −4.061 | −4.018 | −0.043 | $1.1 \times 10^{-4}$ |
| Benzilonium *n*-hexanesulfonate | 518 | −0.55 | −4.593 | −4.578 | −0.015 | −4.048 | −4.033 | −0.015 | $2.5 \times 10^{-3}$ |
| Benzilonium *n*-heptanesulfonate | 532 | −0.03 | −4.199 | −4.156 | −0.043 | −4.170 | −4.126 | −0.044 | $2.5 \times 10^{-3}$ |
| Caffeine | 194 | −0.07[d] | −4.156 | −4.186 | 0.030 | −4.086 | −4.115 | 0.029 | $2.0 \times 10^{-4}$ |
| Antipyrine | 188 | 0.23[d] | −3.925 | −3.985 | 0.060 | −4.155 | −4.215 | 0.060 | $5.8 \times 10^{-5}$ |
| Aminopyrine | 231 | 0.71 | −3.783 | −3.768 | −0.015 | −4.495 | −4.479 | −0.016 | $1.4 \times 10^{-4}$ |
| Triamcinolone | 394 | 1.16[d] | −3.732 | −3.667 | −0.065 | −4.892 | −4.826 | −0.066 | $6.7 \times 10^{-5}$ |
| Benzocaine | 165 | 1.73 | −3.590 | −3.619 | 0.029 | −5.320 | −5.348 | 0.028 | $9.0 \times 10^{-5}$ |
| Benzene | 78 | 2.15[d] | −3.518 | −3.607 | 0.089 | −5.668 | −5.756 | 0.088 | $9.4 \times 10^{-3}$ |
| Toluene | 92 | 2.73[d] | −3.499 | −3.602 | 0.103 | −6.229 | −6.331 | 0.102 | $3.0 \times 10^{-3}$ |
| Diazepam | 285 | 2.82[d] | −3.613 | −3.601 | −0.012 | −6.432 | −6.420 | −0.012 | $2.3 \times 10^{-5}$ |
| *p*-Xylene | 106 | 3.15[d] | −3.605 | −3.601 | −0.004 | −6.755 | −6.750 | −0.005 | $1.7 \times 10^{-3}$ |

[a] The log $k^{calc}$ calculated from Eqs. 3 and 4. [b] Stirring rate was 0.667 $sec^{-1}$, and temperature was 20 ± 0.1° (7). [c] Initial concentration in aqueous or organic phase (7). [d] Taken from Ref. 8.

amide derivatives (3) (Eqs. 3 and 4). The regression equations for the compounds of Table I are:

$$\log k_1^{obs} = \log P - \log (0.364P + 1) - 4.010 \quad \text{(Eq. 5)}$$
$$n = 15 \quad r = 0.999 \quad F = 4401 \quad s = 0.051$$

$$\log k_2^{obs} = -\log (0.358P + 1) - 4.016 \quad \text{(Eq. 6)}$$
$$n = 15 \quad r = 0.999 \quad F = 5375 \quad s = 0.051$$

When the data of the compounds of Table I are combined with the data of the sulfonamide derivatives, the regression equations are:

$$\log k_1^{obs} = \log P - \log (0.386P + 1) - 3.999 \quad \text{(Eq. 7)}$$
$$n = 45 \quad r = 0.997 \quad F = 7332 \quad s = 0.047$$

$$\log k_2^{obs} = -\log (0.385P + 1) - 4.002 \quad \text{(Eq. 8)}$$
$$n = 45 \quad r = 0.998 \quad F = 12{,}055 \quad s = 0.047$$

Because $\beta$ can only be determined with a relative standard deviation of ~10% (3, 10), it can be concluded that Eqs. 5–8 do not differ significantly and that all compounds behave as belonging to one series with regard to partitioning.

Since diffusion rate constants through the stagnant layers largely determine the overall transport rates, dependency on the radius of the molecules is expected (Stokes–Einstein relation). However, because this effect was not observed, it was concluded that the effective molecular radii of the sulfonamide derivatives all are very similar (3). This fact also holds for other compounds. These observations show that the absolute magnitude of transport rate constants in a two-phase system is not dependent on the intrinsic molecular size of a compound.

In conclusion, transport rate constants of drug partitioning in a chosen two-phase system are determined by the partition coefficient ($P$) and the solvent system parameter ($\beta$). This $\beta$ value, which equals $k_{org}/k_{aq}$, is a new parameter that can be calculated from the plateau values of a log $k^{obs}$/log $P$ curve (3).

Drug transport in biological systems includes a series of interphase aqueous environment to membrane transfers and vice versa. For each transfer process, a certain $\beta$ value can be defined; thus, it is interesting to know the factors that determine this parameter. It is assumed that the stagnant layers at an interface are more or less structured (3) and that this structuring originates from a mutual influencing of the two adjacent phases (water–organic solvent or water–membrane). Polarity and polarizability of the solvents seem to be important properties. Investigations on this subject are in progress. Studies on the partitioning kinetics of drugs will produce more knowledge of the transport properties of drugs, which then can result in improved pharmacokinetic parameters of drugs (11, 12) and the successful application of quantitative structure–activity relationships.

## REFERENCES


(1) R. F. Rekker, "The Hydrophobic Fragmental Constant," Elsevier, Amsterdam, The Netherlands, 1977, p. 4.

(2) J. T. M. van de Waterbeemd, C. A. A. van Boeckel, A. C. A. Jansen, and K. W. Gerritsma, *Eur. J. Med. Chem.*, **15**, 279 (1980).

(3) J. T. M. van de Waterbeemd, C. A. A. van Boeckel, R. L. F. M. de Seraux, A. C. A. Jansen, and K. W. Gerritsma, *Pharm. Weekbl. Sci. Ed.*, in press.

(4) H. Kubinyi, *Arzneim.-Forsch.*, **26**, 1991 (1976).

(5) H. Kubinyi, *J. Pharm. Sci.*, **67**, 262 (1978).

(6) J. T. M. van de Waterbeemd and A. C. A. Jansen, *Pharm. Weekbl. Sci. Ed.*, in press.

(7) J. T. M. van de Waterbeemd, A. C. A. Jansen, and K. W. Gerritsma, *ibid.*, **2**, 73 (1980).

(8) C. Hansch and A. Leo, "Substituent Constants for Correlation Analysis in Chemistry and Biology," Wiley–Interscience, New York, N.Y., 1979.

(9) B. C. Lippold and G. F. Schneider, *Arzneim.-Forsch.*, **25**, 843 (1975).

(10) H. Kubinyi and O.-H. Kehrhahn, *ibid.*, **28**, 598 (1978).

(11) J. K. Seydel, D. Trettin, H. P. Cordes, O. Wassermann, and M. Malyusz, *J. Med. Chem.*, **23**, 607 (1980).

(12) B. Testa and B. Salvesen, *J. Pharm. Sci.*, **69**, 497 (1980).

# Simultaneous Determination of Hydrochlorothiazide and Triamterene in Capsule Formulations by High-Performance Liquid Chromatography

G. N. MENON ˣ and L. B. WHITE

Received December 8, 1980, from the *Department of Analytical Research, Abbott Laboratories, North Chicago, IL 60064.* Accepted for publication February 20, 1981.

**Abstract** □ A stability-indicating, high-performance liquid chromatographic method is presented for the simultaneous determination of hydrochlorothiazide and triamterene in two-component capsule formulations. An aliquot of the sample is dissolved in a mixture of acetonitrile and aqueous acetic acid, mixed with *m*-hydroxyacetophenone as an internal standard, and chromatographed on octadecylsilane bonded to microparticulate silica using 80% acetate buffer (pH 5.0, 0.004 *M*)–15% acetonitrile–5% methanol as the mobile phase. The relative standard deviations are ±1.1–1.6% for hydrochlorothiazide and ±1.7–2.2% for triamterene for two formulations. Recoveries of the two drugs added to placebos ranged from 98.4 to 101.7%.

**Keyphrases** □ Hydrochlorothiazide—simultaneous determination by high-performance liquid chromatography with triamterene, capsule formulations □ Triamterene—simultaneous determination by high-performance liquid chromatography with hydrochlorothiazide, capsule formulations □ High-performance liquid chromatography—simultaneous determination of hydrochlorothiazide and triamterene, capsule formulations

A combination dosage form of triamterene and hydrochlorothiazide is indicated in the treatment and management of edema and hypertension. Several methods are available for the assay of hydrochlorothiazide, alone (1–3) or in combination with other drugs such as methyldopa (4), hydralazine (5), reserpine (5, 6), and furosemide (7), and other diuretic–antihypertensive drugs of the thiazide family (8). These methods range from nonspecific approaches such as titrimetry, spectrophotometry, and polarography to specific determinations by high-performance liquid chromatography (HPLC). Triamterene has been assayed by absorption spectroscopy, fluorescence, and TLC fluorometry (9–11).

While separation of triamterene and hydrochlorothiazide from other diuretic–antihypertensive drugs by HPLC was reported (12, 13), no details are available for the specific assay of the two drugs in a dosage form. Furthermore, there are no indications in the literature whether the HPLC separations obtained are specific for the intact drug substances only. A direct method for the simultaneous determination of triamterene and hydrochlorothiazide, used to study the dissolution rate of a tablet dosage form (14), also does not differentiate between the drugs and their respective degradation products.

This paper reports a simple, rapid, and precise stability-indicating assay for triamterene and hydrochlorothiazide in capsule formulation by HPLC.

## EXPERIMENTAL

**Instrumentation**—The chromatographic system was equipped with a dual-piston reciprocating pump[1], a universal injector[2], and a variable-wavelength detector[3]. The separation was performed on a 30-cm × 4-mm i.d. column containing microparticulate-bonded (10-μm) octadecylsilane material[4]. The chromatographic peaks were electronically integrated and recorded[5].

**Mobile Phase**—A solution of 20 ml of 0.2 *M* sodium acetate[6] adjusted to pH 5.0 with acetic acid was mixed with 780 ml of water, 150 ml of acetonitrile[7], and 50 ml of methanol[7]. The solution was filtered, degassed under vacuum, and used as the mobile phase.

**Internal Standard Solution**—A solution of *m*-hydroxyacetophenone[8] (3 mg/ml) in acetronitrile–water (1:1) was used as the internal standard.

**Standard Preparation**—A stock solution of hydrochlorothiazide was prepared using 100 mg of USP reference standard dissolved in 200 ml of acetonitrile. Stock triamterene solution was prepared by adding 25 ml of acetonitrile, followed by 4 ml of acetic acid, to 100 mg of USP reference standard, slurrying well, dissolving, and diluting to 100 ml with water.

A working standard solution was prepared by mixing 5 ml of each stock solution with 10 ml of the internal standard solution and diluting to 100 ml with water.

**Sample Preparation**—An aliquot of a powder blend from 10 capsules of a commercial formulation[9], equivalent to 50 mg of hydrochlorothiazide and 100 mg of triamterene, was slurried with 25 ml of acetonitrile followed by 4 ml of acetic acid. The mixture was shaken well for 5 min, mixed with 10 ml of internal standard solution, dissolved, and diluted to 100 ml with water. A portion of the solution was filtered through a polycarbonate membrane[10] using a filter assembly[11] and was analyzed.

**Analysis**—The chromatographic conditions used for the analysis were; flow rate, 2 ml/min; detector, 273 nm, 0.1 aufs; injection volume, 40 μl; and temperature, ambient.

Quantitative determinations were made by comparison of the peak area ratios of hydrochlorothiazide and triamterene to the *m*-hydroxyacetophenone from a sample injection to the corresponding area ratios from a standard injection.

## RESULTS AND DISCUSSION

The HPLC system described by Honigberg *et al.* (13) provided excellent separation of hydrochlorothiazide and triamterene in a commercial formulation[9]. However, when formulations degraded by acid and alkali reflux were examined, a degradation product of triamterene eluted on the shoulder of the hydrochlorothiazide peak. Therefore, the mobile phase was modified to provide for adequate resolution of the various components of degraded formulations.

Figure 1 shows a typical chromatogram from the analysis of a formulation. The detection wavelength of 273 nm was chosen so that the peak area ratios of both drugs to the internal standard were close to unity.

Triamterene is only slightly soluble in water and forms insoluble complex salts with mineral acids (15). The complexes formed with acetic acid are reportedly (15) more soluble than the inorganic acid complexes. The use of acetic acid and the order of addition of the solvents are critical in the rapid dissolution of the formulation.

Hydrochlorothiazide is susceptible to both acid and alkaline hydrolysis and yields formaldehyde and 4-amino-6-chloro-*m*-benzenedisulfonamide

[1] Model 6000A, Waters Associates, Milford, Mass.
[2] Model U6K, Waters Associates, Milford, Mass.
[3] Model SF 770 Spectroflow monitor, Schoeffel, Westwood, N.J.
[4] μBondapak $C_{18}$, Waters Associates, Milford, Mass.
[5] Model 3385A automation system, Hewlett-Packard, Avondale, Pa.
[6] Analytical reagent, Mallinckrodt, St. Louis, Mo.
[7] Distilled in glass, Burdick & Jackson, Muskegon, Mich.
[8] Aldrich Chemical Co., Milwaukee, Wis.
[9] Dyazide®, Smith Kline and French Laboratories, Philadelphia, Pa.
[10] Nuclepore Corp., Pleasanton, Calif.
[11] Swinnex, Millipore Corp., Bedford, Mass.

0022-3549/81/0900-1083$01.00/0
© 1981, American Pharmaceutical Association

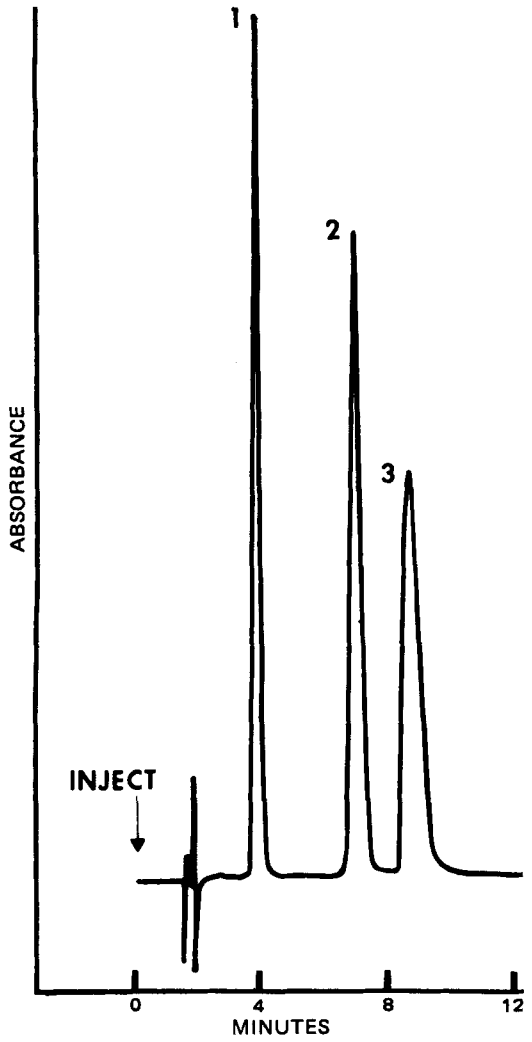


**Figure 1**—*Chromatogram of typical commercial capsule formulation. Key: 1, hydrochlorothiazide; 2, m-hydroxyacetophenone; and 3, triamterene.*

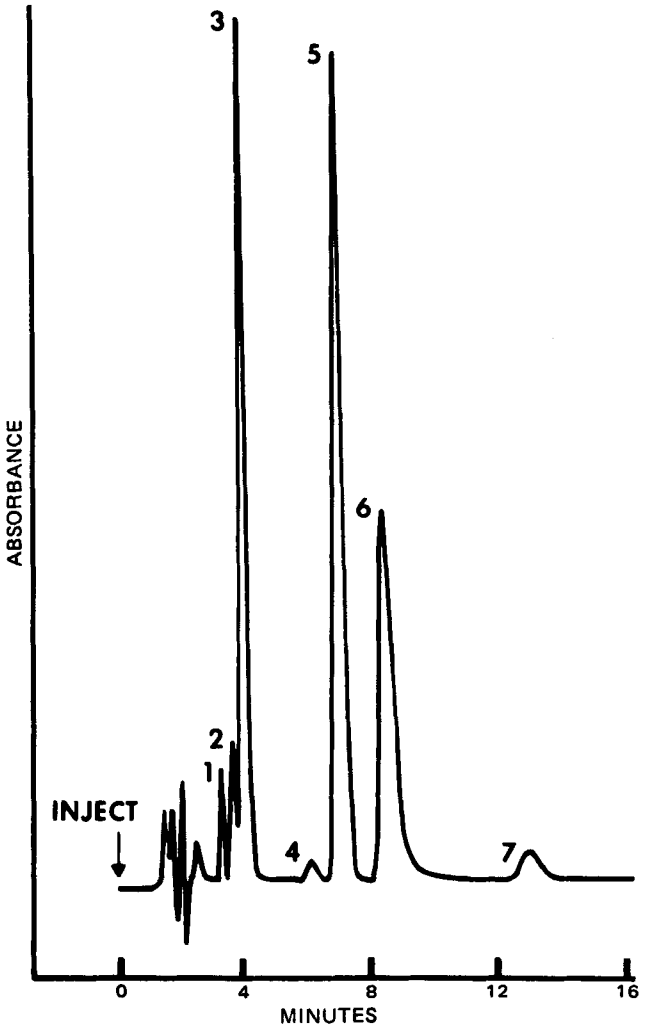


**Figure 2**—*Chromatogram of acid- and alkali-degraded commercial formulation. Key: 1, 4-amino-6-chloro-m-benzenedisulfonamide; 2, 4, and 7, degradation products of triamterene; 3, hydrochlorothiazide; 5, m-hydroxyacetophenone; and 6, triamterene.*

on degradation (16, 17). Although the degradation products of triamterene are not described in the literature, hydrolysis with 5 *N* HCl reportedly produced the 4-hydroxy and 7-hydroxy analogs of triamterene (18). Samples of the formulation were refluxed in 1 *N* HCl, 1 *N* NaOH, and water to observe the hydrolytic effects and resultant changes in the chromatogram. In a separate experiment, triamterene alone was subjected to similar hydrolytic stress for 3 hr. No degradation of triamterene was observed on water reflux, although total degradation resulted on base reflux and ~50% degradation occurred under acid reflux.

Figure 2 shows a chromatogram obtained from the injection of a mixture of acid- and alkali-degraded formulation. Alkali reflux of triamterene produced predominantly peak 7 with minor amounts of peak 2. Acid reflux resulted in larger amounts of peaks 2 and 4 with a trace of peak 7. The refluxed solutions were filtered and neutralized. Upon neutralization, precipitates formed in both the acid and base hydrolyzates. These precipitates were analyzed by HPLC, mass spectrometry, and spectrophotometry. By mass spectrometry, both precipitates showed *m/z* 254 but with different fragmentation patterns, suggesting that they were positional isomers of the hydroxy analogs of triamterene (Scheme I).

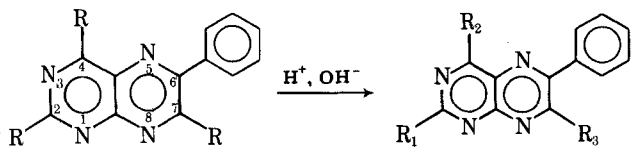


triamterene: R = $NH_2$
peak 7 analog: $R_1$ = OH, $R_2$ = $R_3$ = $NH_2$ in alkali
peak 4 analog: $R_2$ = OH, $R_1$ = $R_3$ = $NH_2$ in acid
peak 2 analog: $R_3$ = OH, $R_1$ = $R_2$ = $NH_2$ in acid

*Scheme I*

Based on the spectral properties in acidic and basic media and comparison to the synthetic hydroxypteridines prepared by Spickett and Timmis (18), peak 7 (the major alkaline degradation product) was identified as 4,7-diamino-2-hydroxy-6-phenylpteridine and peak 4 was identified as 2,7-diamino-4-hydroxy-6-phenylpteridine. Peak 2 probably is the 7-hydroxy analog isolated (18) upon acid hydrolysis of 2,4,7-triamino-6-phenylpteridine. Since peak 2 elutes earlier, the compound may have higher solubility than the 4- and 2-hydroxy compounds and is not precipitated on neutralization of the hydrolyzates. The major degradation pathways are represented in Scheme I.

The mass spectra of the identified compounds are in agreement with the proposed assignments. Since all components are adequately resolved from each other and the internal standard, the method indicates the

**Table I—HPLC Analysis of Hydrochlorothiazide–Triamterene Capsule Formulations**

| Parameter | Hydrochlorothiazide | | Triamterene | |
|---|---|---|---|---|
| | Product I[a] | Product II[b] | Product I[a] | Product II[b] |
| Number of analyses | 9 | 9 | 9 | 9 |
| Milligrams per capsule (mean) | 25.8 | 25.5 | 51.0 | 51.3 |
| RSD, % | ±1.6 | ±1.1 | ±2.2 | ±1.7 |

[a] Dyazide®, Smith Kline and French Laboratories, Philadelphia, Pa. [b] Abbott Laboratories, North Chicago, Ill.

stability of the drugs in the formulation. None of these degradation products was detected in a formulation subjected to high-temperature stability testing.

The linearity of the detector response was established for hydrochlorothiazide in the range of 15–30 mg/capsule ($r$ = 1.000, $y$-intercept = 0.002) and for triamterene in the range of 30–70 mg/capsule ($r$ = 1.000, $y$-intercept = 0.04). Standard addition–recovery experiments performed in two different placebos at various drug levels showed recoveries of 98.4–101.7% for hydrochlorothiazide ($n$ = 12, $CV$ = ±1.2%) and 99.5–102.0% for triamterene ($n$ = 12, $CV$ = ±0.9%).

The reproducibility of the method was demonstrated by performing replicate analyses on a commercial formulation[9] and another experimental formulation with different excipients. The statistical data generated from these analyses are presented in Table I.

In conclusion, HPLC provides a rapid and precise method for the quantitative determination of hydrochlorothiazide and triamterene in a combination oral dosage form. The method is sensitive to the degradation products of these drugs and is free from interference due to excipients in the products examined.

## REFERENCES


(1) A. I. Cohen, B. T. Keeler, N. H. Coy, and H. L. Yale, *Anal. Chem.*, **34**, 216 (1962).

(2) A. B. DeLeo and M. J. Stern, *J. Pharm. Sci.*, **55**, 173 (1966).

(3) F. R. Fazzari, *J. Assoc. Off. Anal. Chem.*, **53**, 582 (1970).

(4) R. Chu, *ibid.*, **54**, 603 (1971).

(5) T. Urbanyi and A. O'Connell, *Anal. Chem.*, **44**, 565 (1972).

(6) A. G. Butterfield, E. G. Lovering, and R. W. Sears, *J. Pharm. Sci.*, **67**, 650 (1978).

(7) H. Abdine, M. A. H. El Sayed, and Y. M. El Sayed, *J. Assoc. Off. Anal. Chem.*, **61**, 6975 (1978).

(8) E. Kkolos and J. Walker, *Anal. Chim. Acta*, **80**, 117 (1975).

(9) L. Guetrello and J. Dobrecky, *Rev. Farm.*, **111**, 13 (1969); through *Chem. Abstr.*, **71**, 64116 (1969).

(10) E. Densivil and J. Vismans, *Pharm. Weekbl.*, **105**, 1441 (1970).

(11) W. Bruehl and E. Schmid, *Arzneim-Forsch.*, **20**, 485 (1970).

(12) R. E. Moskalyk, R. A. Locock, L. G. Chatten, A. M. Veltman, and M. F. Bielech, *J. Pharm. Sci.*, **64**, 1406 (1975).

(13) I. L. Honigberg, J. T. Stewart, A. P. Smith, and D. W. Hester, *ibid.*, **64**, 1201 (1975).

(14) J. K. C. Yen, *Can. J. Pharm. Sci.*, **5**, 112 (1970).

(15) L. W. Dittert, T. Higuchi, and D. R. Reese, *J. Pharm. Sci.*, **53**, 1325 (1964).

(16) T. Yamana and Y. Mizukami, *Yakugaku Zasshi*, **85**, 1057 (1965).

(17) J. A. Mollica, C. R. Rehm, and J. B. Smith, *J. Pharm. Sci.*, **58**, 635 (1969).

(18) R. G. W. Spickett and G. M. Timmis, *J. Chem. Soc.*, **1954**, 2887.


## ACKNOWLEDGMENTS


The authors acknowledge the assistance of Mr. R. D. Cox, Mr. J. Webster, Mr. R. J. Mauritz, and Ms. S. L. Mueller in obtaining validation and structural data.


# Test for Reproducibility of Metered-Dose Aerosol Valves for Pharmaceutical Solutions


**A. CUTIE [§x], J. BURGER [*], C. CLAWANS [‡], D. DOLINSKY [§], W. FEINSTEIN [*], B. GUPTA [‡], A. GRUENEBERG [¶], and J. SCIARRA [§]**



Received September 8, 1980, from [§]*Arnold & Marie Schwartz College of Pharmacy and Health Sciences, Brooklyn, NY 11201*, the [*]*Whitehall International, Division of American Home Products Corporation, New York, NY 10017*, the [‡]*Schering Corporation, Bloomfield, NJ 07003*, and the [¶]*USV Laboratories Division, Tuckahoe, NY 10707.* Accepted for publication February 9, 1981.



**Abstract** □ Seven independent testing sites received metered-dose aerosols containing a standard test solution to assess a newly designed protocol for studying the reproducibility of metered-dose aerosol valves. In accordance with the rather small sampling protocol design, the amount of product dispensed per actuation was measured over the life of the aerosol at designated regions of actuation. A statistical analysis of the data collected at each testing site clearly indicated that the testing protocol is sufficiently reliable and workable for assessing the reproducibility of valve delivery for a given lot of metered-dose valves.



**Keyphrases** □ Aerosols—testing procedure for establishing the reproducibility of metered-dose valves □ Inhalation products—testing procedure for establishing the reproducibility of metered-dose aerosol valves □ Valve delivery—metered-dose aerosols, testing procedure for establishing reproducibility


Test methods, including specific gravity, net contents, vapor pressure, moisture content, spray patterns, and particulate-size determinations, have been established for determining the acceptance of metered-dose aerosol valves for pharmaceutical use (1–4). Reproducibility of the dosage delivered may be determined by assay techniques which establish the amount of active (5). Although USP XX (6) includes metered-dose inhalation products in the monographs and establishes some standards with which these metered-dose products must comply, little has been done in establishing a uniform test procedure for all metered-dose products.

The Aerosol Specification Committee[1] elected to establish a simple and uniform test method for metered-dose aerosol valves by examining the uniformity of valve delivery (amount of solution delivered by the valve) within a valve and between individual valves in any given lot. The procedure outlined in this study provides a means for manufacturers to assess the reproducibility of valve delivery for a given lot of metered-dose valves throughout the life of the product.

## EXPERIMENTAL

**Aerosol Test Solutions**—Pharmaceutical test solutions were prepared by taking 0.10% by weight of isopropyl myristate[2] and adding it to a mixture of 24.90% by weight of trichloromonofluoromethane (Propellant

[1] Of the Industrial Pharmacy Technology Section, Academy of Pharmaceutical Sciences, American Pharmaceutical Association.

[2] Givaudan Corp., Clifton, N.J.


*0022-3549/81/0900-1085$01.00/0*


*© 1981, American Pharmaceutical Association*

stability of the drugs in the formulation. None of these degradation products was detected in a formulation subjected to high-temperature stability testing.

The linearity of the detector response was established for hydrochlorothiazide in the range of 15–30 mg/capsule ($r$ = 1.000, $y$-intercept = 0.002) and for triamterene in the range of 30–70 mg/capsule ($r$ = 1.000, $y$-intercept = 0.04). Standard addition–recovery experiments performed in two different placebos at various drug levels showed recoveries of 98.4–101.7% for hydrochlorothiazide ($n$ = 12, $CV$ = ±1.2%) and 99.5–102.0% for triamterene ($n$ = 12, $CV$ = ±0.9%).

The reproducibility of the method was demonstrated by performing replicate analyses on a commercial formulation[9] and another experimental formulation with different excipients. The statistical data generated from these analyses are presented in Table I.

In conclusion, HPLC provides a rapid and precise method for the quantitative determination of hydrochlorothiazide and triamterene in a combination oral dosage form. The method is sensitive to the degradation products of these drugs and is free from interference due to excipients in the products examined.

## REFERENCES


(1) A. I. Cohen, B. T. Keeler, N. H. Coy, and H. L. Yale, *Anal. Chem.*, **34**, 216 (1962).

(2) A. B. DeLeo and M. J. Stern, *J. Pharm. Sci.*, **55**, 173 (1966).

(3) F. R. Fazzari, *J. Assoc. Off. Anal. Chem.*, **53**, 582 (1970).

(4) R. Chu, *ibid.*, **54**, 603 (1971).

(5) T. Urbanyi and A. O'Connell, *Anal. Chem.*, **44**, 565 (1972).

(6) A. G. Butterfield, E. G. Lovering, and R. W. Sears, *J. Pharm. Sci.*, **67**, 650 (1978).

(7) H. Abdine, M. A. H. El Sayed, and Y. M. El Sayed, *J. Assoc. Off. Anal. Chem.*, **61**, 6975 (1978).

(8) E. Kkolos and J. Walker, *Anal. Chim. Acta*, **80**, 117 (1975).

(9) L. Guetrello and J. Dobrecky, *Rev. Farm.*, **111**, 13 (1969); through *Chem. Abstr.*, **71**, 64116 (1969).

(10) E. Densivil and J. Vismans, *Pharm. Weekbl.*, **105**, 1441 (1970).

(11) W. Bruehl and E. Schmid, *Arzneim-Forsch.*, **20**, 485 (1970).

(12) R. E. Moskalyk, R. A. Locock, L. G. Chatten, A. M. Veltman, and M. F. Bielech, *J. Pharm. Sci.*, **64**, 1406 (1975).

(13) I. L. Honigberg, J. T. Stewart, A. P. Smith, and D. W. Hester, *ibid.*, **64**, 1201 (1975).

(14) J. K. C. Yen, *Can. J. Pharm. Sci.*, **5**, 112 (1970).

(15) L. W. Dittert, T. Higuchi, and D. R. Reese, *J. Pharm. Sci.*, **53**, 1325 (1964).

(16) T. Yamana and Y. Mizukami, *Yakugaku Zasshi*, **85**, 1057 (1965).

(17) J. A. Mollica, C. R. Rehm, and J. B. Smith, *J. Pharm. Sci.*, **58**, 635 (1969).

(18) R. G. W. Spickett and G. M. Timmis, *J. Chem. Soc.*, **1954**, 2887.


## ACKNOWLEDGMENTS


The authors acknowledge the assistance of Mr. R. D. Cox, Mr. J. Webster, Mr. R. J. Mauritz, and Ms. S. L. Mueller in obtaining validation and structural data.


# Test for Reproducibility of Metered-Dose Aerosol Valves for Pharmaceutical Solutions


**A. CUTIE [§x], J. BURGER [*], C. CLAWANS [‡], D. DOLINSKY [§], W. FEINSTEIN [*], B. GUPTA [‡], A. GRUENEBERG [¶], and J. SCIARRA [§]**



Received September 8, 1980, from [§]*Arnold & Marie Schwartz College of Pharmacy and Health Sciences, Brooklyn, NY 11201*, the [*]*Whitehall International, Division of American Home Products Corporation, New York, NY 10017*, the [‡]*Schering Corporation, Bloomfield, NJ 07003*, and the [¶]*USV Laboratories Division, Tuckahoe, NY 10707.* Accepted for publication February 9, 1981.



**Abstract** □ Seven independent testing sites received metered-dose aerosols containing a standard test solution to assess a newly designed protocol for studying the reproducibility of metered-dose aerosol valves. In accordance with the rather small sampling protocol design, the amount of product dispensed per actuation was measured over the life of the aerosol at designated regions of actuation. A statistical analysis of the data collected at each testing site clearly indicated that the testing protocol is sufficiently reliable and workable for assessing the reproducibility of valve delivery for a given lot of metered-dose valves.



**Keyphrases** □ Aerosols—testing procedure for establishing the reproducibility of metered-dose valves □ Inhalation products—testing procedure for establishing the reproducibility of metered-dose aerosol valves □ Valve delivery—metered-dose aerosols, testing procedure for establishing reproducibility


Test methods, including specific gravity, net contents, vapor pressure, moisture content, spray patterns, and particulate-size determinations, have been established for determining the acceptance of metered-dose aerosol valves for pharmaceutical use (1–4). Reproducibility of the dosage delivered may be determined by assay techniques which establish the amount of active (5). Although USP XX (6) includes metered-dose inhalation products in the monographs and establishes some standards with which these metered-dose products must comply, little has been done in establishing a uniform test procedure for all metered-dose products.

The Aerosol Specification Committee[1] elected to establish a simple and uniform test method for metered-dose aerosol valves by examining the uniformity of valve delivery (amount of solution delivered by the valve) within a valve and between individual valves in any given lot. The procedure outlined in this study provides a means for manufacturers to assess the reproducibility of valve delivery for a given lot of metered-dose valves throughout the life of the product.

## EXPERIMENTAL

**Aerosol Test Solutions**—Pharmaceutical test solutions were prepared by taking 0.10% by weight of isopropyl myristate[2] and adding it to a mixture of 24.90% by weight of trichloromonofluoromethane (Propellant

[1] Of the Industrial Pharmacy Technology Section, Academy of Pharmaceutical Sciences, American Pharmaceutical Association.

[2] Givaudan Corp., Clifton, N.J.


*0022-3549/81/0900-1085$01.00/0*


*© 1981, American Pharmaceutical Association*

**Table I—Means and Ranges of the Amount of Material Delivered per Actuation for Each Site (21- and 22-Actuation Study)**

| Actuations | Site I | | Site II | | Site III | | Site IV | |
|---|---|---|---|---|---|---|---|---|
| | $\bar{X}$ | Range | $\bar{X}$ | Range | $\bar{X}$ | Range | $\bar{X}$ | Range |
| 1 | 71.5 | 60.7–84.8 | 26.8 | 9.1–77.9 | 23.6 | 14.9–30.5 | 28.6 | 13.0–64.0 |
| 2 | 73.2 | 57.3–99.9 | 74.9 | 70.3–84.7 | 74.3 | 70.2–77.1 | 74.1 | 68.5–78.6 |
| 3 | 74.8 | 61.9–87.0 | 76.1 | 72.3–77.6 | 74.2 | 71.8–76.5 | 74.0 | 65.5–78.2 |
| 4 | 71.0 | 60.6–76.9 | 76.4 | 75.1–77.5 | 75.5 | 72.1–77.7 | 80.0 | 74.5–77.3 |
| 5 | 76.0 | 75.5–77.3 | 76.5 | 74.9–78.0 | 75.0 | 73.2–75.8 | 72.2 | 56.8–77.3 |
| 6 | 75.4 | 72.5–78.0 | 77.2 | 75.3–80.0 | 74.4 | 72.7–75.6 | 76.3 | 74.5–77.7 |
| 7 | 77.1 | 72.0–86.7 | 76.8 | 75.6–77.7 | 75.6 | 74.1–77.1 | 77.6 | 74.8–77.3 |
| 8 | 73.7 | 67.5–76.1 | 76.7 | 75.4–77.6 | 75.1 | 72.4–77.5 | 75.7 | 72.2–78.9 |
| 9 | 74.8 | 72.2–76.7 | 76.6 | 75.3–76.8 | 74.6 | 73.1–76.8 | 74.6 | 74.2–75.9 |
| 10 | 76.6 | 71.6–87.2 | 76.7 | 75.6–77.2 | 74.5 | 71.4–77.1 | 75.1 | 73.0–76.8 |
| 26 | 74.1 | 72.2–76.5 | 75.5 | 74.5–76.3 | 70.5 | 63.8–75.1 | 72.5 | 64.0–76.5 |
| 27 | 77.4 | 72.7–86.0 | 76.5 | 74.9–79.2 | 73.1 | 71.5–74.0 | 74.7 | 73.5–75.7 |
| 28 | 69.9 | 62.4–75.3 | 75.2 | 74.1–75.9 | 73.9 | 72.2–75.4 | 74.1 | 72.9–75.4 |
| 29 | 73.6 | 71.5–76.5 | 75.1 | 73.4–77.1 | 73.2 | 71.7–74.6 | 47.7 | 72.8–76.1 |
| 76 | 74.5 | 73.2–74.8 | 72.5 | 74.1–75.7 | 72.5 | 71.2–75.3 | 73.3 | 71.8–75.2 |
| 77 | 74.3 | 72.7–76.1 | 73.6 | 74.7–75.1 | 73.6 | 72.0–75.5 | 73.9 | 73.3–75.1 |
| 78 | 74.4 | 73.0–75.7 | 73.7 | 73.2–75.4 | 73.7 | 73.1–76.3 | 73.9 | 71.7–76.5 |
| 79 | 74.0 | 73.0–74.7 | 73.7 | 74.4–76.2 | 73.7 | 72.8–75.6 | 73.8 | 73.0–75.0 |
| 117 | 72.8 | 71.7–75.3 | 73.8 | 66.6–82.1 | 73.8 | 72.8–75.1 | 72.4 | 68.6–73.7 |
| 178 | 74.1 | 74.0–75.9 | 74.1 | 60.7–76.0 | 74.1 | 72.9–75.8 | 71.2 | 62.4–73.6 |
| 179 | 72.4 | 70.0–75.5 | 72.8 | 67.8–75.5 | 72.8 | 70.7–75.7 | 69.3 | 56.0–74.5 |
| 180 | 68.4 | 63.2–76.5 | 70.3 | 63.7–80.0 | 70.3 | 58.1–75.4 | 65.1 | 33.6–73.7 |
| Mean | 73.1 | | 72.8 | | 71.4 | | 71.6 | |

**Table II—Means and Ranges of the Amount of Material Delivered per Actuation for Each Site (14-Actuation Study)**

| Actuations | Site I | | Site II | | Site III | | Site IV | | Site V | |
|---|---|---|---|---|---|---|---|---|---|---|
| | $\bar{X}$ | Range | $\bar{X}$ | Range | $\bar{X}$ | Range | $\bar{X}$ | Range | $\bar{X}$ | Range |
| 7 | 74.2 | 73.6–77.6 | 75.6 | 75.2–76.2 | 75.2 | 74.1–76.6 | 76.0 | 73.1–77.3 | 75.4 | 73.1–78.6 |
| 8 | 75.8 | 72.3–77.9 | 75.4 | 74.6–75.9 | 76.2 | 75.0–77.9 | 76.0 | 74.6–76.9 | 76.6 | 75.3–80.2 |
| 9 | 75.5 | 74.5–76.9 | 75.5 | 74.8–76.3 | 75.2 | 74.6–76.3 | 76.6 | 75.6–77.8 | 77.2 | 76.2–80.1 |
| 10 | 75.3 | 73.9–77.3 | 74.8 | 74.0–75.7 | 75.8 | 74.0–76.5 | 75.9 | 74.9–77.0 | 76.0 | 75.4–77.4 |
| 81 | 76.6 | 73.7–79.3 | 75.0 | 74.2–76.7 | 75.8 | 74.1–77.2 | 75.8 | 75.0–76.9 | 75.4 | 73.3–79.1 |
| 82 | 78.1 | 73.6–90.0 | 75.3 | 74.5–76.3 | 75.1 | 75.1–76.4 | 74.5 | 73.7–75.1 | 75.5 | 74.7–79.2 |
| 83 | 75.4 | 74.1–78.0 | 75.0 | 73.8–75.8 | 76.0 | 74.6–78.8 | 75.0 | 74.4–75.8 | 86.4 | 74.6–129.1 |
| 84 | 75.7 | 74.2–78.5 | 74.0 | 72.2–75.3 | 75.7 | 74.1–78.4 | 75.3 | 75.0–75.8 | 75.2 | 71.7–80.1 |
| 85 | 75.4 | 73.9–77.7 | 75.1 | 74.4–75.6 | 76.1 | 74.2–77.9 | 75.1 | 74.9–76.2 | 74.8 | 74.9–78.1 |
| 166 | 76.8 | 74.8–78.4 | 74.8 | 74.1–75.5 | 74.8 | 74.2–75.5 | 74.0 | 70.5–75.9 | 75.0 | 74.1–77.1 |
| 167 | 75.1 | 73.8–76.7 | 74.6 | 73.1–76.1 | 74.6 | 73.4–75.2 | 74.5 | 72.5–75.0 | 75.2 | 74.2–78.2 |
| 168 | 75.0 | 72.2–76.4 | 75.3 | 74.6–75.9 | 74.9 | 74.2–76.2 | 74.9 | 74.3–76.0 | 75.2 | 73.3–78.4 |
| 169 | 75.6 | 74.2–76.5 | 75.1 | 73.8–76.6 | 75.1 | 73.9–76.5 | 74.9 | 74.0–75.8 | 75.6 | 73.4–78.3 |
| 170 | 75.9 | 74.6–78.3 | 75.9 | 73.6–76.6 | 75.3 | 74.4–75.8 | 75.1 | 74.0–76.0 | 75.4 | 73.1–78.5 |
| Mean | 75.7 | | 75.1 | | 75.4 | | 75.2 | | 76.4 | |

11[3]), 50.00% by weight of dichlorodifluoromethane (Propellant 12[4]), and 25% by weight of dichlorotetrafluoroethane (Propellant 114[5]). This solution was prepared by the cold fill process, and a suitable metered container was used.

**Aerosol Components**—In the initial study (Protocol I), an experimental 63-μl aerosol valve[6] was used. In each subsequent study (Protocol II), a valve with a 50-μl metering chamber[6] and stainless steel stem was used. Fifteen-milliliter aluminum aerosol containers[6] and standard button actuators[6] were employed in all studies.

**Preparation of Samples**[7]—In a thermostatically controlled chill tank maintained at −32°, isopropyl myristate was mixed with trichloromonofluoromethane. By using gravity-fed metering equipment with an electrically controlled solenoid shutoff, this solution was filled by volume and time into the aluminum container. The filling machine reservoir was maintained at a constant volume and temperature, thus allowing for precise volume fills in the container *via* a predetermined timed opening of the filler tube. At a second similar filling station, at 2:1 blend of Propellants 12 and 114, maintained at −37°, was metered into the aluminum container to the appropriate volume. Aerosol valves (without diptubes) were placed on the aluminum cans and crimped. The completed cans then were tested for leaks by immersing each for 3–5 min in a water bath maintained at 55°. Cans showing evidence of leaks (production of gas bubbles) were removed and discarded.

**Sampling Procedure**—After filling, leak testing, and spray testing, the containers were packed in the inverted position (valve down) into nested cardboard shippers. In a random manner, one shipper (containing 100 cans) was sent by parcel post to each testing site[8] where the cartons were stored at ambient conditions with the cans inverted (valve down).

**Testing Procedure**—To minimize possible variation due to the multicentric nature of the studies, the following protocols were utilized at each site.

*Protocol I*—Five cans were selected from the 100 cans supplied. With the actuator kept in place, the container was weighed accurately to ±0.1 mg. The valve was actuated once, and then the container was reweighed and the weight loss was recorded. Single actuations were repeated, and the weight loss was recorded for each individual actuation up to and including 10 actuations. The time interval was recorded between each actuation. The valve was actuated again for Actuations 11–25, with 3 sec between each actuation. The container was weighed, and single actuations were repeated. The weight loss of each individual actuation was recorded up to and including Actuation 29. The valve was actuated again for Actuations 30–75, with 3 sec between each actuation. The container was weighed, and single actuations were repeated. The weight loss was recorded for each individual actuation up to and including Actuation 79. The valve was actuated again for Actuations 80–176, with 3 sec between each actuation and 1 min before dispensation of Actuations 80, 91, 101, and 111. The container was weighed, and single actuations were repeated. The weight loss of each individual actuation up to and including Actuation 180 was recorded.

*Protocol II*—Five cans were selected from the 100 cans supplied. With

[3] Freon 11, E. I. du Pont de Nemours & Co., Wilmington, Del.
[4] Freon 12, E. I. du Pont de Nemours & Co., Wilmington, Del.
[5] Freon 114, E. I. du Pont de Nemours & Co., Wilmington, Del.
[6] Riker Laboratories, Northridge, Calif.
[7] Prepared by Armstrong Laboratories, Division of ATI, West Roxbury, Mass.
[8] Designated by the Aerosol Specification Committee.

**Table III—Analysis of Variance for 22-Actuation Study**

| Source of Variance | Sum of Squares | Degrees of Freedom | Mean Square | $F$ | Probability |
|---|---|---|---|---|---|
| Between cans | | | | | |
| Sites | 190.20 | 3 | 63.40 | <1.00 | NS[a] |
| Cans within sites | 1745.76 | 16 | 109.11 | | |
| Within cans | | | | | |
| Actuation | 1303.17 | 1 | 1303.17 | 17.59 | $p < 0.01$ |
| Actuations × sites | 456.42 | 3 | 152.14 | 2.05 | NS[a] |
| Actuation × cans within sites | 1185.60 | 16 | 74.10 | | |

[a] Not significant.

**Table IV—Analysis of Variance for 21-Actuation Study**

| Source of Variance | Sum of Squares | Degrees of Freedom | Mean Square | $F$ | Probability |
|---|---|---|---|---|---|
| Between cans | | | | | |
| Sites | 28.56 | 3 | 9.52 | <1.00 | NS[a] |
| Cans within sites | 2420.16 | 16 | 151.26 | | |
| Within cans | | | | | |
| Actuations | 135.26 | 1 | 135.26 | 2.51 | NS[a] |
| Actuations × sites | 101.16 | 3 | 33.72 | <1.00 | NS[a] |
| Actuations × cans within sites | 860.96 | 16 | 53.81 | | |

[a] Not significant.

the actuator kept in place, the container was weighed accurately to ±0.1 mg. The valve was actuated six times. After 30 sec, the weight of the container was recorded. Single actuations were repeated, and the weight loss was recorded for each individual actuation up to and including Actuation 10. The time interval between each actuation was recorded. The valve was actuated again at a rate of one actuation every 2 sec until one-half of the total labeled actuations minus five. (In this study, Actuation 80 was one-half of the total actuations minus five.) After 5–7 min (to allow temperature equilibrium), single actuations were repeated, and the weight loss was recorded for each individual actuation up to and including Actuation 85. The valve again was actuated at a rate of one actuation every 2 sec until five less than the total labeled actuations. (In this study, Actuation 165 was five less than the total actuations.) The wait of 5–7 min and single actuations were repeated, and the weight loss was recorded for each individual actuation up to and including Actuation 170.

In both protocols, relative humidity, temperature, condensation on can (if any), misdirected sprays, and amount accumulated on actuator (by weighing the actuator before and after rinsing with plenty of water) were reported. All actuations were performed with the cans inverted.

## RESULTS AND DISCUSSION

The means and ranges of the amount of material delivered through the metered-dose valve utilizing Protocols I and II are given in Tables I and II, respectively. Both protocols were designed to assess the amount of material actuated by a metered valve under testing during each region of product use. The regions specifically evaluated were the initial doses actuated and actuations when the aerosol container was approximately 10, 30, 50, 70, and 95% empty. No attempt was made to access the valve's performance just prior to container emptying (tail off) since it varied considerably, depending on the contents remaining in the container and the experimenter's technique (container agitation, angle of container, *etc.*).

Two separate analyses of variance were performed on the data presented in Table I to determine the influence of testing sites (laboratory conditions and technician performance) and actuation number on the amount of material actuated. The analyses were performed using two-factor analysis of variance with repeated measures on one factor (7) and a computer program[9] for repeated-measured analysis of variance. Conservative degrees of freedom were utilized in the statistical analysis of the data because of the repeated, nonindependent nature of the actuations.

[9] Bio-Medical Computer Program-P Series, BMDP Computer Center, Pittsburgh, PA 15238.

**Table V—Analysis of Variance for 14-Actuation Study**

| Source of Variance | Sum of Squares | Degrees of Freedom | Mean Square | $F$ | Probability |
|---|---|---|---|---|---|
| Between cans | | | | | |
| Sites | 72.44 | 4 | 18.11 | 0.89 | NS[a] |
| Cans within sites | 408.00 | 20 | 20.40 | | |
| Within cans | | | | | |
| Actuations | 22.62 | 13 | 1.74 | 0.008 | NS[a] |
| Sites × actuations | 707.72 | 52 | 13.61 | 0.063 | NS[a] |
| Actuations × cans within sites | 56,409.60 | 260 | 216.96 | | |

[a] Not significant.

The first analysis was a four-site by 22-actuation design (Protocol I) with actuations as the repeated factor. The 22 actuations outlined in Protocol I consisted of measurements of Actuations 1–10, 26–29, 76–79, and 177–180. The results given in Table III clearly indicate no significant effect for the test sites, a significant effect for actuations, and no significant interaction between sites and actuations. Therefore, there were no differences between sites, but there were differences between successive actuations.

Since the significant effect for actuation was thought to be due to the unique effects of the first actuation (valve priming), a second analysis was performed. It was identical to the previous one, except that the data for the first actuation were omitted. This procedure resulted in a four-site by 21-actuation design. The results presented in Table IV clearly indicate no significant effects for sites or actuations and no significant interactions. Therefore, when the unique first actuation was omitted, there were no differences between sites and no differences between successive actuations.

One analysis of variance was performed on the data in Table II. The data collected utilizing Protocol II (14-actuation study) when analyzed statistically indicated no difference in the milligrams of solution actuated between sites, between actuations, or in the site by actuation interaction (Table V).

## CONCLUSIONS

The statistical analysis of data clearly indicated that the protocols described are not influenced by the experimenter or the test site at which the study was conducted. The abbreviated procedure involving only 14 actuation measurements outlined in Protocol II also yielded the same results as the 21-actuation study and is practical for assessing the reproducibility of valve delivery for a given lot of metered-dose valves.

## REFERENCES


(1) "Aerosol Guide," Chemical Specialties Manufacturers Association, Washington, D.C., 1971.

(2) B. Tollin, "The Determination of Particle Size of Aerosols, A Review," Selected Pharmaceutical Research References, vol. I, Smith Kline and French Laboratories, Philadelphia, Pa., 1960.

(3) J. Kanig and H. Mintzer, Aerosol Technicomment, vol. III, no. 2, Aerosol Techniques Inc., Milford, Conn., 1960.

(4) I. Porush, C. G. Thiel, and J. G. Young, *J. Am. Pharm. Assoc., Sci. Ed.*, **49**, 70 (1960).

(5) J. G. Young, I. Porush, C. G. Thiel, S. Cohen, and C. H. Stimmel, *ibid.*, **49**, 72 (1960).

(6) "The United States Pharmacopeia," 20 ed., United States Pharmacopeial Convention, Rockville, Md., 1980, p. 1024.

(7) B. J. Winer, "Statistical Principles in Experimental Design," McGraw-Hill, New York, N.Y., 1971, p. 518.


## ACKNOWLEDGMENTS


The authors thank Dr. Lewis P. Amsel, Dr. Irv Porush, Dr. William Gorman, Mr. Gary Hall, Mr. Harvey Mintzer, and Mr. Simon Welch for technical assistance and advice.

# Synthesis and Skeletal Muscle Relaxant Activity of 3-(Aminoacyl)-1-[[[5-(substituted phenyl)-2-furanyl]methylene]amino]-2,4-imidazolidinediones

**F. L. WESSELS** [x], **K. O. ELLIS, and R. L. WHITE, Jr.**

Received September 2, 1980, from the *Research & Development Department, Norwich-Eaton Pharmaceuticals, Division of Morton-Norwich Products, Inc., Norwich, NY 13815.* Accepted for publication February 17, 1981.

**Abstract** □ A series of 3-(aminoacyl)-1-[[[5-(substituted phenyl)-2-furanyl]methylene]amino]-2,4-imidazolidinediones was synthesized and evaluated for skeletal muscle relaxant activity. All compounds were active by the intravenous route, and nine of 11 were active orally. One compound was very active when evaluated by the mouse Straub tail and rotarod tests; its efficacy index ($ED_{50}$ rotarod/$ED_{50}$ Straub tail) was 2.0, while its therapeutic index ($LD_{50}/ED_{50}$ Straub tail) was >225.

**Keyphrases** □ 3-Aminoacyl-substituted 2,4-imidazolidinediones—synthesis and evaluation for skeletal muscle relaxant activity, mice □ Dantrolene sodium—related compounds synthesized and evaluated for skeletal muscle relaxant activity, mice □ Skeletal muscle relaxant activity—dantrolene sodium-related compounds synthesized and evaluated for activity, mice □ Muscle, skeletal—relaxant properties evaluated in dantrolene-related compounds, mice

Several 2,4-imidazolidinediones have skeletal muscle relaxant activity (1). One member of this series, dantrolene[1], caused skeletal muscle relaxation by a unique mechanism, acting directly on the skeletal muscle (2, 3). It has been hypothesized that dantrolene sodium induces muscle relaxation by inhibiting the release of $Ca^{2+}$ from the sarcoplasmic reticulum (4, 5).

This paper presents the syntheses (6) and skeletal muscle relaxant activity of a series of 3-aminoacyl compounds related to dantrolene.

## EXPERIMENTAL[2]

The imidazolidinediones selected as starting materials were prepared by a literature method (1). The title compounds (Table I) were prepared by the general procedure shown in Scheme I and as exemplified by the following typical reaction.

**3 -(3-Aminopropionyl)-1-[[[5-(4-nitrophenyl)-2-furanyl]methylene]amino]-2,4-imidazolidinedione Hydrochloride (IIIa)**—*N-tert*-Butoxycarbonyl-β-alanine (14 g, 0.075 mole) in dimethylformamide (350 ml) was cooled to 0°, and triethylamine (21 ml, 0.15 mole) was added rapidly. The solution was maintained at from −5 to −10° while isobutyl chlorocarbonate (10.5 ml, 0.075 mole) was added. The stirred solution was kept at −5° for 10 min, and then solid 1-[[[5-(4-nitrophenyl)-2-furanyl]methylene]amino]-2,4-imidazolidinedione (21 g, 0.068 mole) was added over 5 min. The temperature was maintained at from −5 to 0° for 30 min, and then the solution was stirred for 1 hr without cooling. The dimethylformamide solution was poured into a stirred solution of ice water (3.0 liters) containing concentrated hydrochloric acid (50 ml). The resulting yellow solid was collected and air dried. Recrystallization from acetonitrile (2.5 liters) yielded 17 g (51%) of intermediate product, mp 213–214°.

The 3-[3-(*N-tert*-butoxycarbonylamino)-1-oxopropyl-1-[[[5-(4-nitrophenyl)-2-furanyl]methylene]amino]-2,4-imidazolidinedione (17 g, 0.035 mole) was added to 3% hydrochloric acid–acetic acid (400 ml) at 15°, and the mixture was stirred for 5 hr. The mixture was filtered, and the collected solid was washed with nitromethane (200 ml) and ether (100 ml). The solid was dried in a 60° oven overnight, yielding 14 g of IIIa (94%, 48% overall), mp 211–212°; IR: 2.8–4.0 (broad N–H), 5.6, 5.7, 5.8, 6.25, 6.6, and 7.5 μ.

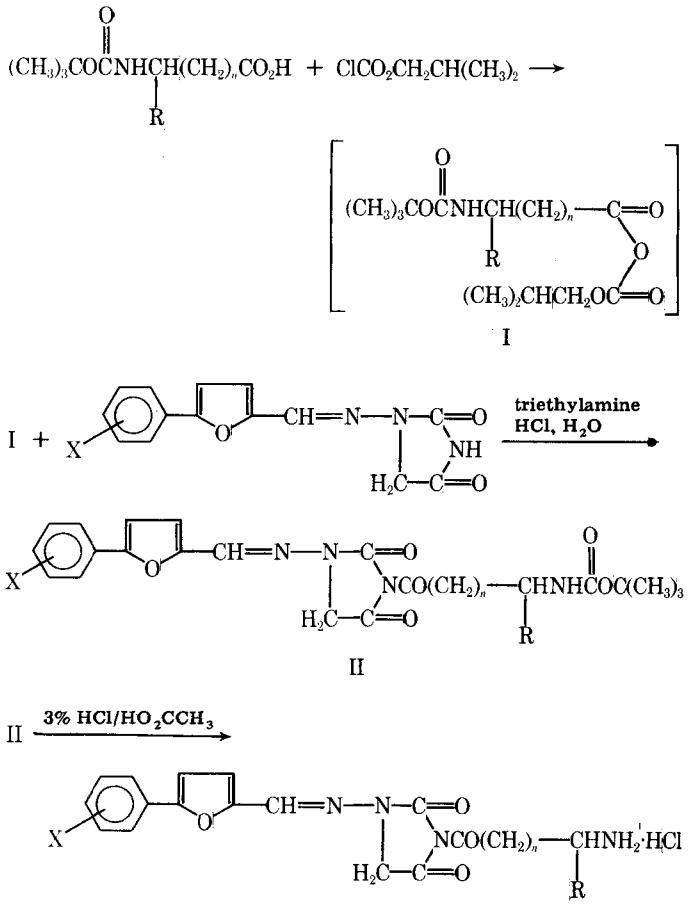


IIIa–IIIk

*Scheme I—See Table I for specific values for X, R, and n.*

**Pharmacology**—*Gross Observation*—Groups of three unfasted male mice[3], 20–27 g, were used. The drugs were administered perorally at doses of 50–800 mg/kg as a 2% concentration suspended in 0.5% methylcellulose 4000 cps[4]. Gross observation for pharmacological effects were made for 2 hr, utilizing a rating of drug effect signs similar to that described by Irwin (7). Muscle relaxation was rated on a scale from 0 to 4: 0, no effect; 1, slight; 2, moderate; 3, marked; and 4, extreme.

*Pithed Rat Gastrocnemius Muscle Preparation*—The method used for direct stimulation of the gastrocnemius muscle in rats[5] ($n$ = 4) was the same as that described previously (8). The test drugs were administered intravenously at logarithmically spaced doses in tetrahydrofurfuryl alcohol[6] or dimethyl sulfoxide[7]. Solvent effects accounted for a <20% decrease in the twitch response at the highest volume tested.

*Rotarod Testing in Mice*—A method similar to that described by

[1] Morton-Norwich Products.

[2] Melting points were taken in a Mel-Temp apparatus in open capillary tubes and are uncorrected. IR spectra were determined as Nujol mulls on a Perkin-Elmer 137B spectrophotometer.

[3] Taconic Farms, TAC:(SW)fBr.

[4] Methocel, Dow Chemical Co.

[5] Taconic Farms, TAC:SD/NfBr.

[6] Eastman Kodak Co.

[7] McKesson and Robbins.



*0022-3549/81/0900-1088$01.00/0*
*© 1981, American Pharmaceutical Association*

**Table I—Physical Properties of IIIa–IIIk**

| Compound | X | n | R | Yield, % | Melting Point | Formula | Analysis, % | Calc. | Found | IR of Carbonyls, μ |
|---|---|---|---|---|---|---|---|---|---|---|
| IIIa | 4-$NO_2$ | 1 | H | 48 | 211–212° | $C_{17}H_{15}N_5O_6$·HCl | C | 48.41 | 48.44 | 5.6, 5.7, 5.8 |
| | | | | | | | H | 3.82 | 3.95 | |
| | | | | | | | N | 16.61 | 16.92 | |
| IIIb | 3-Cl, 4-Cl | 1 | H | 45 | 199–202° | $C_{17}H_{14}Cl_2N_4O_4$·HCl | C | 45.81 | 45.81 | 5.55, 5.7, 5.8 |
| | | | | | | | H | 3.39 | 3.33 | |
| | | | | | | | N | 12.57 | 12.45 | |
| IIIc | 4-F | 1 | H | 28 | 195–197° | $C_{17}H_{14}FN_4O_4$·HCl | C | 51.72 | 51.96 | 5.6, 5.7, 5.8 |
| | | | | | | | H | 4.08 | 4.18 | |
| | | | | | | | N | 14.19 | 13.94 | |
| IIId | 4-Cl | 1 | H | 82 | 242–245° | $C_{17}H_{15}ClN_4O_4$·HCl | C | 49.77 | 49.90 | 5.55, 5.7, 5.8 |
| | | | | | | | H | 3.69 | 3.87 | |
| | | | | | | | N | 13.66 | 13.48 | |
| IIIe | 3-Cl, 4-Cl | 0 | $CH_3$ | 25 | 192–196° | $C_{17}H_{14}Cl_2N_4O_4$·HCl | C | 45.81 | 45.98 | 5.55, 5.7, 5.8 |
| | | | | | | | H | 3.39 | 3.41 | |
| | | | | | | | N | 12.57 | 12.65 | |
| IIIf | 4-CN | 1 | H | 62 | 193–194° | $C_{18}H_{15}N_5O_4$·HCl | C | 53.08 | 53.55 | 5.55, 5.65, 5.8 |
| | | | | | | | H | 4.01 | 4.05 | |
| | | | | | | | N | 17.43 | 17.30 | |
| IIIg | 3-Cl, 4-Cl | 4 | H | 28 | 205–207° | $C_{20}H_{20}Cl_2N_4O_4$·HCl | C | 49.24 | 49.24 | 5.5, 5.65, 5.8 |
| | | | | | | | H | 4.34 | 4.30 | |
| | | | | | | | N | 11.49 | 11.51 | |
| IIIh | 3-Cl, 4-Cl | 0 | $C_6H_5CH_2$ | 52 | 152–160° | $C_{23}H_{18}Cl_2N_4O_4$·HCl | C | 52.94 | 52.66 | 5.6, 5.7, 5.8 |
| | | | | | | | H | 3.67 | 3.85 | |
| | | | | | | | N | 10.74 | 10.67 | |
| IIIi | 4-$OCH_3$ | 1 | H | 40 | 190° dec. | $C_{18}H_{18}N_4O_5$·HCl | C | 53.14 | 53.41 | 5.6, 5.7, 5.85 |
| | | | | | | | H | 4.71 | 4.93 | |
| | | | | | | | N | 13.77 | 13.77 | |
| IIIj | 3-Cl, 4-F | 1 | H | 28 | 191–193° | $C_{17}H_{14}ClFN_4O_4$·HCl | C | 47.57 | 47.50 | 5.55, 5.7, 5.8 |
| | | | | | | | H | 3.52 | 3.88 | |
| | | | | | | | N | 13.05 | 13.00 | |
| IIIk | 3-$CF_3$, 4-Cl | 1 | H | 49 | 198–199° | $C_{18}H_{14}ClF_3N_4O_4$·HCl | C | 45.11 | 45.26 | 5.5, 5.7, 5.8 |
| | | | | | | | H | 3.15 | 3.43 | |
| | | | | | | | N | 11.69 | 11.45 | |

[a] Compounds IIIa–IIIk showed the higher energy absorptions of the ring C=O at 5.55–5.6 μ upon acylation and loss of tautomerism; in contrast, the starting material for IIIa, for example, exhibited C=O values at 5.68 and 5.85 μ(1).

**Table II—Skeletal Muscle Relaxant Activity of a Series of 3-(Aminoacyl)-1-[[[5-(substituted phenyl)-2-furanyl]methylene]amino]-2,4-imidazolidinediones**

| Compound | Gastrocnemius Twitch Tension, % inhibition[a] | Maximum Muscle Relaxation Score[b] (at mg/kg po) | Straub Tail $ED_{50}$[c,i] | Rotarod $ED_{50}$[d,i] | Muscle Relaxant Efficacy Index[e] | $LD_{50}$[f,i] | Therapeutic Index[g] |
|---|---|---|---|---|---|---|---|
| IIIa | −87 (1.5) | 4 (400) | 18 (33–37) | 33.6 (21–49) | 2.0 | >4000 | >225 |
| IIIb | −70 (4.5) | 3 (200) | 38 (22–64) | 19.7 (14–28) | 0.5 | 460 (449–471) | 11 |
| IIIc | −45 (1.7) | 2 (800) | 90 (58–138) | 18.3 (2–66) | 0.2 | 226 (221–244) | 3 |
| IIId | −81 (2.2) | 2 (800) | 201 (104–362) | 17.1 (12–24) | 0.1 | 646 (525–763) | 3 |
| IIIe | −69 (0.4) | 4 (400) | 70 (34–159) | 64.2 (34–99) | 0.9 | 1055 (785–1391) | 15 |
| IIIf | −86 (1.6) | 2 (800) | 367 (206–491) | 27.5 (18–42) | 0.4 | 155 (115–196) | 0.4 |
| IIIg | −74 (2.6) | 3 (400) | 48 (32–72) | <5.0 | <0.1 | — | — |
| IIIh | −65 (1.8) | 0 (200) | — | — | — | — | — |
| IIIi | −50 (3.3) | 0 (800) | — | — | — | — | — |
| IIIj | −74 (2.6) | 3 (800) | 291 (116–76972) | 33.0 (29–38) | 0.1 | 314 (290–329) | 1.1 |
| IIIk | −74 (1.3) | 3 (800) | 85 (55–128) | 19.0 (13–29) | 0.2 | 589 (<560–>682) (indeterminate) | 6.9 |
| Dantrolene sodium | −80 (1.0) | 4 (400) | 37 (20–66) | 62.0 (27–262) | 1.7 | 1370 (888–1853)[h] | 37 |
| Clodanolene sodium | −78 (3.7) | 4 (400) | 22 (7–60) | 22.0 (17–37) | 1.7 | 742 (299–1204)[h] | 38 |

[a] Percent inhibition of electrically induced contractions of the rat gastrocnemius muscle at a cumulative dose of 36.6 mg/kg iv. The figure in parentheses is the standard error of the mean. [b] Where 1 = slight, 2 = moderate, 3= marked, and 4= severe drug effect as measured by gross observation in mice and the dose (in parentheses) at which this occurred. [c] Intraperitoneal dose of drug causing inhibition of morphine-induced Straub tail in 50% of the mice. [d] Intraperitoneal dose of drug causing loss of motor coordination (rotarod) in 50% of the mice. [e] $ED_{50}$ rotarod/$ED_{50}$ Straub tail. [f] Intraperitoneal dose of drug causing death in 50% of the mice within 72 hr. [g] $LD_{50}/ED_{50}$ Straub tail. [h] See Ref. 8. [i] The figures in parentheses are the 95% confidence limits. Muscle relaxant testing was not completed on compounds which were not effective orally (IIIh, IIIi) or in which the Rotarod $ED_{50}$ was below the Straub Tail $ED_{50}$ (IIIg).

Dunham and Miya (9) was used to test the effect of drugs on motor coordination. Male mice[3] ($n$ = 10/group) were trained to walk the revolving rod (20 rpm) for over 1 min. The test drugs were administered intraperitoneally in 0.5% methylcellulose at logarithmically spaced doses to the previously trained mice, and performance trials were conducted 30 min following drug administration. The inability of an animal to stay on the rotarod for more than 30 sec was considered a positive drug effect. The $ED_{50}$ values (rotarod) (the drug dose that caused 50% of the animals to fall off the rotarod within 30 sec) were calculated using the method of Litchfield and Wilcoxon (10).

*Straub Tail in Mice*—The method used in these experiments was similar to that reported by Ellis and Carpenter (11). Male mice[3] ($n$ = 10/group) were used for Straub tail testing. The drugs were administered intraperitoneally in 0.5% methylcellulose 20 min after morphine[8] (15 mg/kg sc) injection. The drugs were judged effective if they caused the elevated Straub tail to lay flat on the table. The compounds were administered in logarithmically spaced doses, and $ED_{50}$ values (dose of the

[8] Mallinckrodt.

drug causing the elevated tail to lay flat in 50% of the animals) were obtained by the method of Litchfield and Wilcoxon (10).

*$LD_{50}$ in Mice*—The test compounds were administered perorally in 0.5% methylcellulose to groups of unfasted male mice[3] ($n$ = 10/group). The animals were held in cages for 72 hr, and the deaths were recorded. The $LD_{50}$ values (drug dose causing death in 50% of the animals) were calculated using the method of Litchfield and Wilcoxon (10).

## RESULTS AND DISCUSSION

The synthesized compounds (6) exhibited a better absorption and solubility profile than the parent compound, dantrolene. Eleven compounds were synthesized and evaluated for skeletal muscle relaxant activity (Table II). In the pithed rat gastrocnemius muscle preparation, all compounds were effective intravenous skeletal muscle relaxants (>50% inhibition of the electrically induced twitch contraction) (Table II).

Compounds III*a* and III*f* were also potent inhibitors of the gastrocnemius twitch tension. These compounds were the most effective in that the maximal inhibition of the twitch response was 86–87% whereas dantrolene sodium and clodanolene sodium only yielded a maximal inhibition of 80%.

Gross observation in mice identified nine of the 11 compounds as orally effective muscle relaxants. Among these nine (muscle relaxant score of >1 at doses up to 800 mg/kg), III*a* and III*e* were the most effective, producing muscle relaxant scores of 4. Compounds III*b*, III*g*, III*j*, and III*k* were slightly less effective, producing muscle relaxant scores of 3; III*b* produced a 3 level of muscle relaxation at 200 mg/kg.

Lowering of the Straub tail previously was shown (11) to result from relaxation of the sacrococcygeal muscles at the base of the tail. Several different drugs can produce this muscle relaxation (11). However, the muscle relaxant properties of a drug are useful only when they can be separated in a dose-dependent manner from its neurotoxic properties (motor incoordination). Motor incoordination is an unacceptable consequence of skeletal muscle relaxant therapy and, therefore, is a limiting factor in determining muscle relaxant efficacy. In the Straub tail model, the muscle relaxant dose is identified as St $ED_{50}$; the motor incoordination dose is identified with the rotarod test (Rr $ED_{50}$). Comparing these two doses as a ratio, $ED_{50}$ rotarod:$ED_{50}$ Straub tail, gives an indication of the separation between the two dose ranges (*i.e.*, the greater the ratio, the more separation between the two doses).

Compound III*a* yielded a muscle relaxant efficacy index of 2.0, and all other compounds produced muscle relaxant efficacy indexes of <1.0. Additionally, when III*a* was evaluated for acute toxicity, no deaths were seen up to 4000 mg/kg, and the resultant therapeutic index was >225.

The difference in muscle relaxant efficacy indexes between III*a* and other muscle relaxants of this type (dantrolene sodium and clodanolene sodium), including the compounds in Table II, is small but consistent. Compound III*a* is a potent, direct-acting skeletal muscle contraction antagonist (inhibition of the directly induced gastrocnemius twitch tension). The muscle relaxant efficacy index and acute therapeutic index values reflect a high degree of efficacy and safety.

## REFERNECES


(1) H. R. Snyder, Jr., C. S. Davis, R. K. Bickerton, and R. P. Halliday, *J. Med. Chem.*, **10**, 807 (1967).

(2) L. J. Honkomp, R. P. Halliday, and F. L. Wessels, *Pharmacologist*, **12**, 301 (1970).

(3) K. O. Ellis and J. F. Carpenter, *Fed. Proc. Fed. Am. Soc. Exp. Biol.*, **30**, 670 (1971).

(4) K. O. Ellis and J. F. Carpenter, *Naunyn-Schmiedebergs Arch. Pharmacol.*, **275**, 83 (1972).

(5) K. O. Ellis and S. H. Bryant, *ibid.*, **274**, 107 (1972).

(6) R. L. White, Jr., U.S. pat. 4,001,222 (Jan. 4, 1977).

(7) S. Irwin, *Pyschopharmacologia*, **13**, 222 (1968).

(8) K. O. Ellis and F. L. Wessels, *Arzneim.-Forsch.*, **28**, 1100 (1978).

(9) N. W. Dunham and T. S. Miya, *J. Am. Pharm. Assoc., Sci. Ed.*, **46**, 208 (1957).

(10) J. T. Litchfield, Jr., and F. Wilcoxon, *J. Pharmacol. Exp. Ther.*, **96**, 99 (1949).

(11) K. O. Ellis and J. F. Carpenter, *Neuropharmacology*, **13**, 211 (1974).


## ACKNOWLEDGMENTS


The authors are indebted to Ms. C. J. Weinheimer and Ms. L. Cooley for the synthesis of some of the compounds, to Ms. C. Jeffrey and Ms. D. George for the microanalyses, and to Mrs. Mildred Hazard for typing the manuscript. The technical assistance of Ms. R. Turrell in obtaining the pharmacological data is also greatly appreciated.


# Formation of Methyl Ester of Salicyluric Acid during Quantitation of Salicyluric Acid in Urine by High-Pressure Liquid Chromatography


**R. O. DAY *§, S. H. DROMGOOLE *x, D. E. FURST *, C. HIGNITE ‡, and H. E. PAULUS ***



Received July 31, 1980, from the **Department of Medicine, School of Medicine, University of California, Los Angeles, Los Angeles, CA 90024*, and the ‡*Department of Clinical Pharmacology, Veterans Administration Hospital, Kansas City, MO 66103.* Accepted for publication February 4, 1981.


§Present address: Department of Clinical Pharmacology, St. Vincent's Hospital, Darlinghurst, 20010, N.S.W., Australia.



**Abstract** □ The formation of the methyl ester of salicyluric acid was observed during the quantitation of salicyluric acid and other salicylate metabolites in urine by high-pressure liquid chromatography. This methyl ester formation caused artificially low values for salicyluric acid and high values for salicylic acid.



**Keyphrases** □ Salicyluric acid—methylation during high-pressure liquid chromatography □ Methylation—salicyluric acid in urine, high-pressure liquid chromatography □ High-pressure liquid chromatography—salicyluric acid in urine, methylation


Several high-pressure liquid chromatographic (HPLC) assays for salicylic acid and its metabolites, salicyluric acid and gentisic acid, in serum and urine were reported recently (1–8). Review of these methods indicates that certain precautions must be taken to prevent sublimation losses of salicylic acid during evaporation (6) and decom-




*0022-3549/81/0900-1090$01.00/0*


*© 1981, American Pharmaceutical Association*

drug causing the elevated tail to lay flat in 50% of the animals) were obtained by the method of Litchfield and Wilcoxon (10).

*$LD_{50}$ in Mice*—The test compounds were administered perorally in 0.5% methylcellulose to groups of unfasted male mice[3] ($n$ = 10/group). The animals were held in cages for 72 hr, and the deaths were recorded. The $LD_{50}$ values (drug dose causing death in 50% of the animals) were calculated using the method of Litchfield and Wilcoxon (10).

## RESULTS AND DISCUSSION

The synthesized compounds (6) exhibited a better absorption and solubility profile than the parent compound, dantrolene. Eleven compounds were synthesized and evaluated for skeletal muscle relaxant activity (Table II). In the pithed rat gastrocnemius muscle preparation, all compounds were effective intravenous skeletal muscle relaxants (>50% inhibition of the electrically induced twitch contraction) (Table II).

Compounds III*a* and III*f* were also potent inhibitors of the gastrocnemius twitch tension. These compounds were the most effective in that the maximal inhibition of the twitch response was 86–87% whereas dantrolene sodium and clodanolene sodium only yielded a maximal inhibition of 80%.

Gross observation in mice identified nine of the 11 compounds as orally effective muscle relaxants. Among these nine (muscle relaxant score of >1 at doses up to 800 mg/kg), III*a* and III*e* were the most effective, producing muscle relaxant scores of 4. Compounds III*b*, III*g*, III*j*, and III*k* were slightly less effective, producing muscle relaxant scores of 3; III*b* produced a 3 level of muscle relaxation at 200 mg/kg.

Lowering of the Straub tail previously was shown (11) to result from relaxation of the sacrococcygeal muscles at the base of the tail. Several different drugs can produce this muscle relaxation (11). However, the muscle relaxant properties of a drug are useful only when they can be separated in a dose-dependent manner from its neurotoxic properties (motor incoordination). Motor incoordination is an unacceptable consequence of skeletal muscle relaxant therapy and, therefore, is a limiting factor in determining muscle relaxant efficacy. In the Straub tail model, the muscle relaxant dose is identified as St $ED_{50}$; the motor incoordination dose is identified with the rotarod test (Rr $ED_{50}$). Comparing these two doses as a ratio, $ED_{50}$ rotarod:$ED_{50}$ Straub tail, gives an indication of the separation between the two dose ranges (*i.e.*, the greater the ratio, the more separation between the two doses).

Compound III*a* yielded a muscle relaxant efficacy index of 2.0, and all other compounds produced muscle relaxant efficacy indexes of <1.0. Additionally, when III*a* was evaluated for acute toxicity, no deaths were seen up to 4000 mg/kg, and the resultant therapeutic index was >225.

The difference in muscle relaxant efficacy indexes between III*a* and other muscle relaxants of this type (dantrolene sodium and clodanolene sodium), including the compounds in Table II, is small but consistent. Compound III*a* is a potent, direct-acting skeletal muscle contraction antagonist (inhibition of the directly induced gastrocnemius twitch tension). The muscle relaxant efficacy index and acute therapeutic index values reflect a high degree of efficacy and safety.

## REFERNECES


(1) H. R. Snyder, Jr., C. S. Davis, R. K. Bickerton, and R. P. Halliday, *J. Med. Chem.*, **10**, 807 (1967).

(2) L. J. Honkomp, R. P. Halliday, and F. L. Wessels, *Pharmacologist*, **12**, 301 (1970).

(3) K. O. Ellis and J. F. Carpenter, *Fed. Proc. Fed. Am. Soc. Exp. Biol.*, **30**, 670 (1971).

(4) K. O. Ellis and J. F. Carpenter, *Naunyn-Schmiedebergs Arch. Pharmacol.*, **275**, 83 (1972).

(5) K. O. Ellis and S. H. Bryant, *ibid.*, **274**, 107 (1972).

(6) R. L. White, Jr., U.S. pat. 4,001,222 (Jan. 4, 1977).

(7) S. Irwin, *Pyschopharmacologia*, **13**, 222 (1968).

(8) K. O. Ellis and F. L. Wessels, *Arzneim.-Forsch.*, **28**, 1100 (1978).

(9) N. W. Dunham and T. S. Miya, *J. Am. Pharm. Assoc., Sci. Ed.*, **46**, 208 (1957).

(10) J. T. Litchfield, Jr., and F. Wilcoxon, *J. Pharmacol. Exp. Ther.*, **96**, 99 (1949).

(11) K. O. Ellis and J. F. Carpenter, *Neuropharmacology*, **13**, 211 (1974).


## ACKNOWLEDGMENTS


The authors are indebted to Ms. C. J. Weinheimer and Ms. L. Cooley for the synthesis of some of the compounds, to Ms. C. Jeffrey and Ms. D. George for the microanalyses, and to Mrs. Mildred Hazard for typing the manuscript. The technical assistance of Ms. R. Turrell in obtaining the pharmacological data is also greatly appreciated.


# Formation of Methyl Ester of Salicyluric Acid during Quantitation of Salicyluric Acid in Urine by High-Pressure Liquid Chromatography


**R. O. DAY *§, S. H. DROMGOOLE *x, D. E. FURST *, C. HIGNITE ‡, and H. E. PAULUS ***



Received July 31, 1980, from the **Department of Medicine, School of Medicine, University of California, Los Angeles, Los Angeles, CA 90024*, and the ‡*Department of Clinical Pharmacology, Veterans Administration Hospital, Kansas City, MO 66103.* Accepted for publication February 4, 1981.


§Present address: Department of Clinical Pharmacology, St. Vincent's Hospital, Darlinghurst, 20010, N.S.W., Australia.



**Abstract** □ The formation of the methyl ester of salicyluric acid was observed during the quantitation of salicyluric acid and other salicylate metabolites in urine by high-pressure liquid chromatography. This methyl ester formation caused artificially low values for salicyluric acid and high values for salicylic acid.



**Keyphrases** □ Salicyluric acid—methylation during high-pressure liquid chromatography □ Methylation—salicyluric acid in urine, high-pressure liquid chromatography □ High-pressure liquid chromatography—salicyluric acid in urine, methylation


Several high-pressure liquid chromatographic (HPLC) assays for salicylic acid and its metabolites, salicyluric acid and gentisic acid, in serum and urine were reported recently (1–8). Review of these methods indicates that certain precautions must be taken to prevent sublimation losses of salicylic acid during evaporation (6) and decom-




*0022-3549/81/0900-1090$01.00/0*


*© 1981, American Pharmaceutical Association*

position of salicyluric acid to salicylic acid by microorganisms (3, 4). There are no reports of the methylation of salicyluric acid during its quantitation in biological fluids.

In measuring salicylic acid and its metabolites in urine by HPLC, it was observed that salicyluric acid was methylated as a consequence of sample preparation. Because similar alteration of the salicyluric acid may occur in other laboratories during quantitation, the methylated product was identified by GLC–mass spectrometry. The conditions under which this product is formed and methods to prevent its formation are described.

## EXPERIMENTAL

**Reagents**—Methanol[1], ether[2], *o*-methoxybenzoic acid[3] (*o*-anisic acid), sodium salicylate[3], salicyluric acid[3] (*o*-hydroxyhippuric acid), and gentisic acid[3] were used.

Stock standard solutions of sodium salicylate (5 mg/ml), salicyluric acid (10 mg/ml), and gentisic acid (2 mg/ml) were prepared by dissolving the compounds in small volumes of ethanol and bringing to volume with pH 7 phosphate buffer (0.1 *M*). The stock solutions were kept frozen at 0° until required. Working standards of sodium salicylate (500, 250, and 50 μg/ml), salicyluric acid (1000, 500, and 100 μg/ml), and gentisic acid (200, 100, and 20 μg/ml) were made in fresh, blank urine.

**Procedures**—Urine (1 ml), to which 1 ml of a standard solution of *o*-methoxybenzoic acid (100 μg/ml) in pH 7 phosphate buffer (0.1 *M*) had been added, was acidified with 0.6 *M* HCl (1 ml) and extracted into 5 ml of ether by shaking for 5 min. Following centrifugation, the aqueous layer was frozen in acetone–dry ice, and the ether layer was collected. The ether was evaporated to dryness at 10° with air or nitrogen. The residue was resuspended in 0.75 ml of anhydrous methanol or a mixture of 85% water containing 1.6% acetic acid and 15% methanol. Samples were placed in 1-ml capped vials[4] and injected into the HPLC system *via* an automatic sampler[5] fitted with a 20-μl injection loop. The flush time was 30 sec, and the run time was 20 min. A 15-cm × 4.6-mm i.d. reversed-phase column[6] and a 5-cm × 2.1-mm i.d. precolumn[7] were used to separate salicylic acid and its metabolites. The mobile phase of 85% water (containing 1.6% acetic acid) and 15% methanol was pumped[8] at 2.5 ml/min. Peaks were detected by a UV detector[9] (310 nm) coupled to a recorder[10] and peak integrator[11].

To determine the conditions under which salicyluric acid was altered, salicyluric acid dissolved in water was taken through the described sample preparation but with the following changes: (*a*) the evaporated ether extract was dissolved in methanol for up to 3 weeks before injection onto the column; (*b*) the ether extract was blown to dryness with air or nitrogen; and (*c*) the residue following ether evaporation was resuspended either in methanol or 85% water (containing 1.6% acetic acid) and 15% methanol.

Aliquots of water and urine samples were extracted with ether in the presence and absence of hydrochloric acid, and the ether extracts were added to test tubes containing salicyluric acid prior to drying with nitrogen or air. The resulting residues then were redissolved in methanol and allowed to stand for up to 2 weeks before analysis.

The structure of the altered salicyluric acid was identified by GLC and mass spectrometry following repeated collection and lyophilization of the unknown chromatographic peak. The trimethylsilyl derivative of this sample was prepared by dissolving the residue in an excess (0.5 ml) of pyridine–*N*,*O*-bis(trimethylsilyl)trifluoroacetamide–trimethylchlorosilane (10:10:1). The mixture then was warmed for 5 min at 90°. An aliquot of the trimethylsilyl derivative was injected onto a GLC column (2 m × 2 mm i.d.), packed with 4% OV-17 on Gas Chrom Q[12] (100–120 mesh), programmed from 80 to 300° at 10.0°/min. The altered product of salicyluric acid then was identified by mass spectrometry[13].

Preparation of the methyl esters of salicyluric acid, gentisic acid, *o*-methoxybenzoic acid, and salicylic acid was attempted by bubbling hydrogen chloride through methanolic solutions of these chemicals for 5 min. The acidified methanolic solutions then were taken to dryness, and the residues were redissolved in 1.0 ml of methanol and subjected to HPLC using the described conditions. The methyl ester of salicylic acid was not formed under these conditions; complete esterification of *o*-methoxybenzoic acid and salicyluric acid was achieved, but gentisic acid esterification was only partially complete.

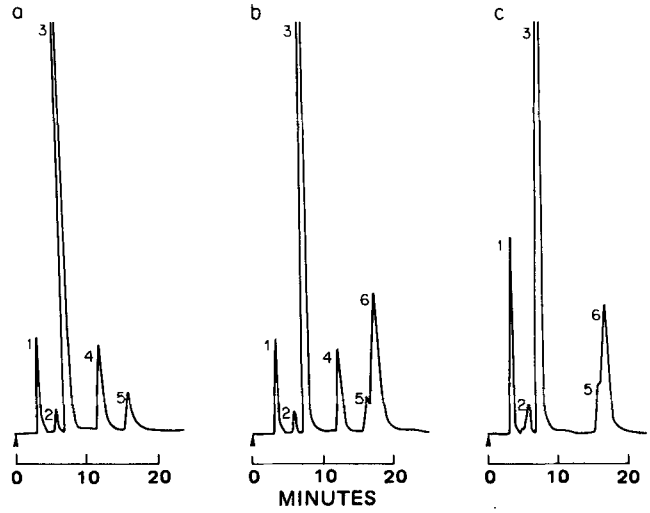


**Figure 1**—*Chromatograms of salicylic acid and its metabolites in urine under different experimental conditions: urine extract in methanol (a) immediately after the addition of methanol, (b) after allowing the methanolic extract to stand at room temperature for 8 hr, and (c) after the evaporation of ether with air. Key: 1, gentisic acid; 2, glucuronide of salicylic acid; 3, salicyluric acid; 4,o-methoxybenzoic acid; 5, salicylic acid; and 6, methyl salicylurate. The arrows indicate the points of injection.*

## RESULTS AND DISCUSSION

Quantitation of salicylic acid and its metabolites in urine gave accurate and reproducible results. Nitrogen was used to remove the ether at 10°, and the methanolic residue was immediately injected into the chromatograph. The sensitivity of the method was 5 μg/ml for salicylic acid, 5 μg/ml for salicyluric acid, and 2 μg/ml for gentisic acid. The coefficients of variation for repeated measurements of salicylic acid at 50 μg/ml, for salicyluric acid at 100 μg/ml, and for gentisic acid at 20 μg/ml were 2.6, 0.7, and 1.5%, respectively. These figures are similar to those previously reported (1, 4).

A typical HPLC tracing is shown in Fig. 1*a*. The retention times for gentisic acid, salicyluric acid, *o*-methoxybenzoic acid, and salicylic acid were 4, 8.4, 13, and 17.5 min, respectively.

The small peak that eluted between the gentisic acid and salicyluric acid peaks was probably one of the salicyl glucuronides since it disappeared following incubation of the urine with β-glucuronidase.

Occasionally, a peak that interfered with the salicylic acid peak was observed (Figs. 1*b* and 1*c*). This effect became apparent when extracted urine samples were prepared for HPLC (by the addition of methanol) well in advance of their actual injection onto the column *via* the automatic sample injector accessory. Interference also was observed if the ethereal extracts of urine were evaporated to dryness with air. The appearance and extent of this interference were variable. Sequential HPLC analysis of the salicylic acid, salicyluric acid, and gentisic acid standards in urine or water indicated that this peak was due to changes in the salicyluric acid standard.

When the salicyluric acid standard was extracted into ether from urine or water, interference occurred under the following experimental conditions: (*a*) if air or nitrogen was used to evaporate the ether; (*b*) if methanol was used to resuspend the residue from the ether evaporation; (*c*) if the residue from the ether evaporation stood in methanol for more

[1] Burdick & Jackson Laboratories, Muskegon, Mich.
[2] Nanograde, Mallinckrodt, St. Louis, Mo.
[3] Aldrich Chemical Co., Milwaukee, Wis.
[4] Wheaton Scientific, Millville, N.J.
[5] Model 500, Altex Scientific, Berkeley, Calif.
[6] Ultrasphere-ODS, Altex Scientific, Berkeley, Calif.
[7] Perisorb RP-18, 30–40 μm, Merck, Darmstadt, West Germany.
[8] Model 110A, Altex Scientific, Berkeley, Calif.
[9] Model 100-10 spectrophotometer, Hitachi Scientific Instruments, Mountain View, Calif.
[10] Model 250-2, two channel, Curken Scientific, Danbury, Conn.
[11] Model 485, Varian Instrument Division, Palo Alto, Calif.
[12] Supelco Inc., Bellefonte, Pa.
[13] Model 3300 with 6000 data system, Finnigan Corp., Sunnyvale, Calif.

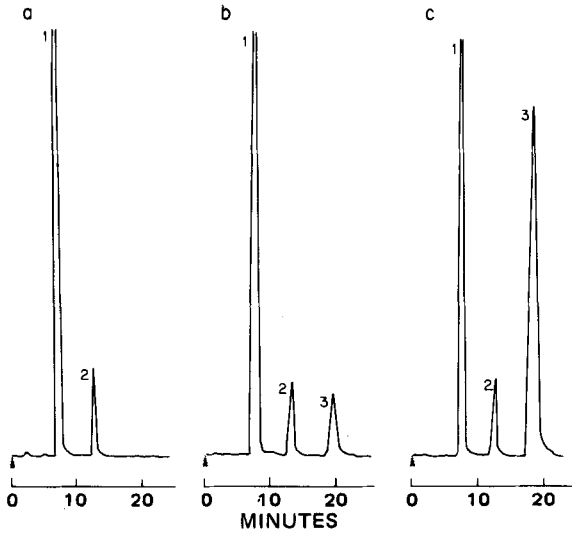


**Figure 2**—*Chromatograms of the salicyluric acid standard (1 mg/ml) under different experimental conditions: ether extract of salicyluric acid standard after standing in (a) 85% water containing 1.6% acetic acid–15% methanol for 10 days, (b) methanol for 6 hr, and (c) methanol for 21 days. The salicyluric acid concentration decreased 47%. Key: 1, salicyluric acid; 2, o-methoxybenzoic acid; and 3, methyl salicylurate. The arrows indicate the points of injection.*

than 2 hr; or (*d*) if hydrochloric acid was used to acidify the ester extract.

The time course and extent of changes in the standards were quite variable (Fig. 2*a*), but salicyluric acid levels decreased ~20% after the samples had stood in methanol for 6 hr (Fig. 2*b*). The maximum observed decrease in salicyluric acid levels was 47% after the salicyluric acid ether extract (1000 μg/ml) had stood in methanol for 21 days (Fig. 2*c*). However, there was no alteration of the salicyluric acid standard dissolved in methanol for up to 3 weeks.

The interfering peak was collected after repeated injection and subjected to GLC–mass spectrometry for identification. Examination of the electron-impact mass spectra revealed that this peak was the methyl ester of salicyluric acid.

Like many esterification reactions, the conversion of salicyluric acid to methyl salicylurate is catalyzed by small amounts of acid. In addition, dehydration of the residue upon ether evaporation also may promote the methyl salicylurate formation. Dehydration by ether secondary to the formation of an azeotrope with water is well known. These effects favor ester formation between the carboxyl group of glycine and methanol under anhydrous conditions (Scheme I). In the ether extract, methanol is in large excess and the equilibrium is driven to the right (*i.e.*, methyl salicylurate is formed).

The formation of the ester can be prevented by adding water (which shifts the equilibrium to the left) or by adding another carbonyl group (*e.g.*, acetic acid), which competes with salicyluric acid for ester formation. Use of nitrogen gas and a limited time of exposure of salicyluric acid to methanol also help to control the ester formation with salicyluric acid.

Alternatively, salicyluric acid esterification can be circumvented if diluted urine (after centrifugation and filtration) is injected directly onto the column. However, with the HPLC column and solvent system employed, resolution of the gentisic acid peak from other endogenous substances in urine was not satisfactory without extraction.

Although some previous reports discussed precautions to prevent sublimation losses of salicylic acid and decomposition of salicyluric acid to salicylic acid by microorganisms (3, 6), there are no reports on the formation of methyl ester of salicyluric acid.

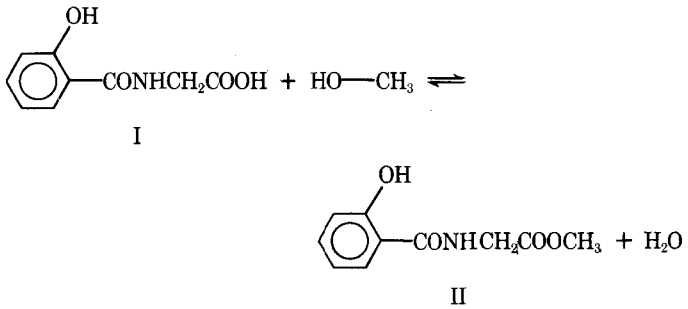


*Scheme I—Mechanism of the formation of methyl salicylurate (II) from salicyluric acid (I).*

One method (1) employed ether for urine extraction, but the ethereal residue was dissolved in methanol–water–acetic acid (50:60:1), which inhibits formation of methyl salicylurate.

Esterification of gentisic acid, salicyluric acid, and *o*-methoxybenzoic acid occurred when hydrogen chloride gas was bubbled through methanolic solutions of these compounds. The retention times of these esters were 17.3, 17.4, and 41.4 min, respectively. The methyl ester of salicylic acid was not formed under these conditions.

However, the absence of interference peaks other than the peak corresponding to methyl salicylurate and the lack of change of the gentisic acid and salicylic acid standards during the ethereal extraction of standards in urine or water indicate that esterification of gentisic acid and *o*-methoxybenzoic acid did not occur.

It is obvious from the chromatograms in which the formation of methyl salicylurate was not inhibited (Figs. 1*b* and 1*c*) that an underestimation of salicyluric acid and an overestimation of salicylic acid are possible since large amounts of methyl salicylurate can appear as a single peak of salicylic acid.

## REFERENCES

(1) I. Bekersky, H. G. Boxenbaum, M. H. Whitson, C. V. Puglisi, R. Pocelink, and S. A. Kaplan, *Anal. Lett.*, **10**, 539 (1977).

(2) D. Blair, B. H. Rumack, and R. G. Peterson, *Clin. Chem.*, **24**, 1543 (1978).

(3) B. E. Cham, D. Johns, F. Bochner, D. M. Imhoff, and M. Rowland, *ibid.*, **25**, 1420 (1979).

(4) B. E. Cham, F. Bochner, D. M. Imhoff, D. Johns, and M. Rowland, *ibid.*, **26**, 111 (1980).

(5) M. M. Lubran, S. N. Steen, and R. L. Smith, *Ann. Clin. Lab. Sci.*, **9**, 501 (1979).

(6) G. W. Peng, M. A. F. Gadalla, V. Smith, A. Peng, and W. L. Chiou, *J. Pharm. Sci.*, **67**, 710 (1978).

(7) C. P. Terweij-Groen, T. Vahlkamp, and J. D. Kraak, *J. Chromatogr.*, **145**, 115 (1978).

(8) J. N. Miceli, M. K. Aravind, S. N. Cohen, and A. K. Done, *Clin. Chem.*, **25**, 1002 (1979).

## ACKNOWLEDGMENTS

Supported by Grant from the U.S. Public Health Service (No. AM 26473), the Arthritis Foundation, the Southern California Chapter of the Arthritis Foundation, and the Dorothy and Thomas Leavy Trust Fund.

R. O. Day was supported by the National Health and Medical Research Council of Australia, and C. Hignite was supported by the Medical Service of the Veteran's Administration.

The authors are indebted to Dr. Gerhard Levy for his advice and assistance during the preparation of this manuscript.

# Direct Linear Plotting Method for Estimation of Pharmacokinetic Parameters

**Keyphrases** □ Pharmacokinetics—direct linear plotting method of parameter estimation □ Direct linear plotting method—estimation of pharmacokinetic parameters

*To the Editor:*

Recently, a method was described (1) for estimating the parameters of a single-compartment linear pharmacokinetic model following intravenous bolus dose administration. This method is based on the following relationship:

$$\ln C = \ln C_0 - Kt \qquad \text{(Eq. 1)}$$

where $C_t$ is the concentration at some time, $t$, after bolus administration of a drug that results in an initial concentration of $C_0$ and $K$ is the first-order elimination rate constant. This equation may be rearranged to yield:

$$\ln C_0 = \ln C + Kt \qquad \text{(Eq. 2)}$$

For each $C$, $t$ data point, a straight line could be generated. The equation is of the general form:

$$Y = b + XM \qquad \text{(Eq. 3)}$$

where $Y$ is $\ln C_0$, $b$ is $\ln C$, $X$ is $K$, and $M$ is $t$. By using a pair of data values ($C_1$, $t_1$ and $C_2$, $t_2$), two such lines can be generated. The $X$-axis coordinate of the point of intersection of these lines provides an estimate for the $K$ parameter ($K_i$), and the $Y$-axis coordinate of this point of intersection provides an estimate of $\ln C_0$ ($\ln C_{0i}$). Thus, $K_i$ can be calculated according to:

$$K_i = \frac{\ln C_2 - \ln C_1}{t_1 - t_2} \qquad \text{(Eq. 4)}$$

and $C_{0i}$ is calculated by substituting $K_i$ into Eq. 2 and using values for either data point ($C_1$, $t_1$ or $C_2$, $t_2$), *e.g.*:

$$\ln C_{0i} = t_1 K_i + \ln C_1 \qquad \text{(Eq. 5)}$$

When more than two sets of data are available, the $K_i$ and $\ln C_{0i}$ values must be calculated for all possible combinations of data pairs. The median of all calculated $K_i$ values provides the best estimate of $K$, and the median of all calculated $\ln C_{0i}$ values provides the best estimate of $\ln C_0$. The selection of median values minimizes the effect of outliers on the parameter estimate; *i.e.*, an estimate that differed greatly from the true parameter would markedly affect the mean of all estimates but would have no greater effect on the median than would an estimate that was only slightly different than the true parameter value. This series of calculations and comparisons is readily performed by the microcomputer.

It is not the purpose of this communication to justify the use of the direct linear plotting (DLP) method of parameter estimation. Previous findings (1) indicate that this method is superior to standard nonlinear regression (with and without weighting correction) when the assumption of equal variance for all experimental data points is violated; *i.e.*, when outliers are present. However, in the absence of outliers, simple unweighted nonlinear regression performs best. Non-normal distribution of error might be expected when analytical results are periodically affected by a large magnitude. For example, a micropipet that periodically dispenses only 30–50% of the labeled volume would result in a non-normal distribution of errors. In this situation, parameter estimation using the DLP method would be favored.

**Table I—Pharmacokinetic Parameter Estimates**

| Parameter | Actual Value | Regression Estimate | Regression Percent Error | DLP Estimate | DLP Percent Error |
|---|---|---|---|---|---|
| $A$ | 50 | 81.4 | 62.8 | 56.9 | 13.8 |
| $\alpha$ | 0.8 | 1.05 | 31.2 | 0.85 | 6.2 |
| $B$ | 10 | 10.12 | 1.2 | 8.9 | −11.0 |
| $\beta$ | 0.08 | 0.078 | −2.5 | 0.073 | −8.7 |

This communication describes a program written for the microcomputer[1], using BASIC language, which facilitates the application of the DLP method of parameter estimation. In addition, the program allows for sequential parameter estimates (stripping). This program allows extension of the DLP method to polyexponential equations. As output, the program provides standard exponential (unweighted) regression values for $C_0$ and the rate constant $K$, the correlation coefficient, and estimated values for all observed concentration data. The program then provides $K_i$ and $C_{0i}$ values for all intersections already described and provides the numbers of intersection values that are

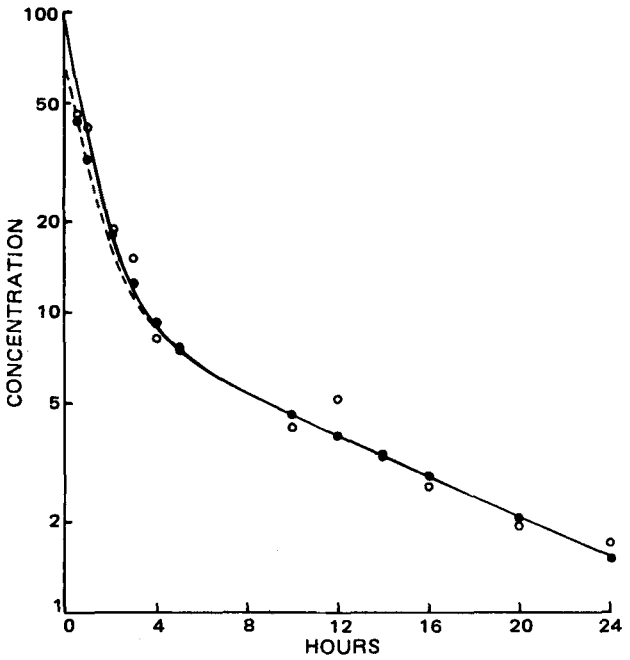


**Figure 1**—*Simulated concentration* versus *time data without error (●) and including error (○). The solid line is the best fit line obtained by stepwise unweighted nonlinear regression analysis. The broken line is the best fit line obtained by stepwise application of the DLP method.*

[1] APPLE II plus, DOS 3.2.1.

0022-3549/81/0900-1093$01.00/0
© 1981, American Pharmaceutical Association

less than and greater than the given value. Thus, the median parameters are selected by the user. Once selected, these intersection values are used to calculate predicted concentration values for each observed value.

The performance of the DLP program is shown in the following example. Concentrations expected at time 0.5, 1, 1.5, 2.0, 3, 4, 5, 10, 12, 14, 16, 20, and 24 hr were simulated for the biexponential equation:

$$C_t = 50e^{-0.8t} + 10e^{-0.08t} \quad \text{(Eq. 6)}$$

Error with a coefficient of variation of either 5 or 20% was randomly assigned to the simulated concentrations such that four of the 12 observations were affected by the larger error. The results are shown in Fig. 1. The program was used to strip the curve. Concentrations observed between 10 and 24 hr were used for the $\beta$-phase, and those between 0.5 and 5 hr were used for the $\alpha$-phase. The results of parameter estimation using sequential regression (stripping) and the DLP method are shown in Table I. In this example, DLP produced better estimates of $A$ and $\alpha$ (13.8 and 6.2% error) than did sequential regression analysis (62.8 and 31.2% error). Estimates of $B$ and $\beta$ were somewhat better using regression (1.2 and −2.5% error) than with the DLP method (13.8 and 6.2% error). The large errors made by regression analysis in estimating $A$ and $\alpha$ indicate that DLP estimates for the entire curve were superior.

The determination of the importance of the DLP method of parameter estimation in pharmacokinetics will require further experimentation. It is hoped that the described program will facilitate this process.

(1) L. Endrenyi and H.-Y. Tang, *Comp. Biomed. Res.*, **13**, 430 (1980).

*Jeffrey R. Koup*
Department of Pharmacy Practice
School of Pharmacy
University of Washington
Seattle, WA 98195

Received March 24, 1981.
Accepted for publication June 18, 1981.

# BOOKS

## REVIEWS

**Introduction to Pharmaceutical Dosage Forms.** By HOWARD C. ANSEL. Lea & Febiger, Washington Square, Philadelphia, PA 19106. 1981. 408 pp. 18.5 × 26 cm.

The format and presentation of this third edition are the same as in the previous one, but the material has been revised to the current official compendia. The book is intended "to introduce the beginning pharmacy students to medicinal and pharmaceutic substances, the methods of their incorporation into pharmaceutical dosage forms, and the utilization of these forms in patient care."

The discussions on heritage, terminology, code of ethics, regulations, and drug substances should satisfactorily orient beginning students in their first professional course in pharmacy. The appendix defines drug categories and discusses measurements, and tables of official preparations are given. Pharmaceutical products are logically treated from the viewpoint of administration route, and the classes of pharmaceutical preparations also are discussed. Numerous photographs illustrate equipment, processing, and packaging.

However, the presentation of dosage form design in terms of biopharmacy, formulation, and practice is inadequate. Whether the curriculum of a college is arranged to present a preparations–physical pharmacy sequence or a technology series of courses, the scope of this text restricts its use to an orientation course because of its superficial presentation of theory and pharmacy principles and limited discussion of techniques and manufacturing principles.

*Reviewed by* Eugene L. Parrott
*College of Pharmacy*
*University of Iowa*
*Iowa City, IA 52242*

---

**Pharmaceutical Calculations,** 2nd Ed. By JOEL L. ZATZ. John Wiley & Sons, 605 Third Ave., New York, NY 10016. 1981. 388 pp. 13.3 × 25 cm. Price $17.50.

Pharmaceutical calculations continues to be one of the most frustrating subjects to teach in any pharmacy curriculum. The complete accuracy required in answering many problems, the mixing of different metrology systems, the frequent use of conversions, and the simultaneous introduction of pharmaceutical terminology confound many students. This ongoing dilemma has resulted in pharmaceutical calculations being taught and evaluated in a variety of ways at different schools of pharmacy. No single textbook can solve the distress frequently associated with calculations, but Joel Zatz's second edition goes a long way to making it all more bearable.

The book is longer than the first edition by 77 pages because it now has an appendix containing instruction and problems on temperature conversion, alcohol proof strength, and sodium chloride equivalents in addition to the inclusion of alligation and a greatly expanded section on milliequivalents.

The cover of the book describes the structure of the text succinctly: "The progression of topics within each chapter and in the overall structure of the book constitutes a programmed format that permits self-paced learning and builds upon previously learned concepts to reinforce understanding. Students participate actively and are able to concentrate on calculations that are most difficult for them. Emphasis is on practical approaches to meeting accuracy requirements in filling prescriptions and manufacturing."

This book is designed to fit into the usual first general pharmacy course, to serve as a text in a calculations course or as a self-instruction text apart from the formal classroom, or to be an aid for review, and it does all of these well.

It is difficult to find much about the text to criticize. About all one can say is that it does not contain a section on commercial arithmetic which some instructors prefer to include in their course, and there are a few prescription problems for oral preparations containing amaranth (Red No. 2) which was banned in time to have been deleted from the new edition.

In conclusion, while working examples from the text, the reviewer finds it refreshing to solve for "j" (for Joel?) rather than to always hunt for the usual unknown "x."

*Reviewed* by E. Roy Hammarlund
*School of Pharmacy*
*Department of Pharmaceutics*
*University of Washington*
*Seattle, WA 98195*

less than and greater than the given value. Thus, the median parameters are selected by the user. Once selected, these intersection values are used to calculate predicted concentration values for each observed value.

The performance of the DLP program is shown in the following example. Concentrations expected at time 0.5, 1, 1.5, 2.0, 3, 4, 5, 10, 12, 14, 16, 20, and 24 hr were simulated for the biexponential equation:

$$C_t = 50e^{-0.8t} + 10e^{-0.08t} \quad \text{(Eq. 6)}$$

Error with a coefficient of variation of either 5 or 20% was randomly assigned to the simulated concentrations such that four of the 12 observations were affected by the larger error. The results are shown in Fig. 1. The program was used to strip the curve. Concentrations observed between 10 and 24 hr were used for the $\beta$-phase, and those between 0.5 and 5 hr were used for the $\alpha$-phase. The results of parameter estimation using sequential regression (stripping) and the DLP method are shown in Table I. In this example, DLP produced better estimates of $A$ and $\alpha$ (13.8 and 6.2% error) than did sequential regression analysis (62.8 and 31.2% error). Estimates of $B$ and $\beta$ were somewhat better using regression (1.2 and −2.5% error) than with the DLP method (13.8 and 6.2% error). The large errors made by regression analysis in estimating $A$ and $\alpha$ indicate that DLP estimates for the entire curve were superior.

The determination of the importance of the DLP method of parameter estimation in pharmacokinetics will require further experimentation. It is hoped that the described program will facilitate this process.

(1) L. Endrenyi and H.-Y. Tang, *Comp. Biomed. Res.*, **13**, 430 (1980).

*Jeffrey R. Koup*
Department of Pharmacy Practice
School of Pharmacy
University of Washington
Seattle, WA 98195

Received March 24, 1981.
Accepted for publication June 18, 1981.

# BOOKS

## REVIEWS

**Introduction to Pharmaceutical Dosage Forms.** By HOWARD C. ANSEL. Lea & Febiger, Washington Square, Philadelphia, PA 19106. 1981. 408 pp. 18.5 × 26 cm.

The format and presentation of this third edition are the same as in the previous one, but the material has been revised to the current official compendia. The book is intended "to introduce the beginning pharmacy students to medicinal and pharmaceutic substances, the methods of their incorporation into pharmaceutical dosage forms, and the utilization of these forms in patient care."

The discussions on heritage, terminology, code of ethics, regulations, and drug substances should satisfactorily orient beginning students in their first professional course in pharmacy. The appendix defines drug categories and discusses measurements, and tables of official preparations are given. Pharmaceutical products are logically treated from the viewpoint of administration route, and the classes of pharmaceutical preparations also are discussed. Numerous photographs illustrate equipment, processing, and packaging.

However, the presentation of dosage form design in terms of biopharmacy, formulation, and practice is inadequate. Whether the curriculum of a college is arranged to present a preparations–physical pharmacy sequence or a technology series of courses, the scope of this text restricts its use to an orientation course because of its superficial presentation of theory and pharmacy principles and limited discussion of techniques and manufacturing principles.

*Reviewed by* Eugene L. Parrott
*College of Pharmacy*
*University of Iowa*
*Iowa City, IA 52242*

---

**Pharmaceutical Calculations,** 2nd Ed. By JOEL L. ZATZ. John Wiley & Sons, 605 Third Ave., New York, NY 10016. 1981. 388 pp. 13.3 × 25 cm. Price $17.50.

Pharmaceutical calculations continues to be one of the most frustrating subjects to teach in any pharmacy curriculum. The complete accuracy required in answering many problems, the mixing of different metrology systems, the frequent use of conversions, and the simultaneous introduction of pharmaceutical terminology confound many students. This ongoing dilemma has resulted in pharmaceutical calculations being taught and evaluated in a variety of ways at different schools of pharmacy. No single textbook can solve the distress frequently associated with calculations, but Joel Zatz's second edition goes a long way to making it all more bearable.

The book is longer than the first edition by 77 pages because it now has an appendix containing instruction and problems on temperature conversion, alcohol proof strength, and sodium chloride equivalents in addition to the inclusion of alligation and a greatly expanded section on milliequivalents.

The cover of the book describes the structure of the text succinctly: "The progression of topics within each chapter and in the overall structure of the book constitutes a programmed format that permits self-paced learning and builds upon previously learned concepts to reinforce understanding. Students participate actively and are able to concentrate on calculations that are most difficult for them. Emphasis is on practical approaches to meeting accuracy requirements in filling prescriptions and manufacturing."

This book is designed to fit into the usual first general pharmacy course, to serve as a text in a calculations course or as a self-instruction text apart from the formal classroom, or to be an aid for review, and it does all of these well.

It is difficult to find much about the text to criticize. About all one can say is that it does not contain a section on commercial arithmetic which some instructors prefer to include in their course, and there are a few prescription problems for oral preparations containing amaranth (Red No. 2) which was banned in time to have been deleted from the new edition.

In conclusion, while working examples from the text, the reviewer finds it refreshing to solve for "j" (for Joel?) rather than to always hunt for the usual unknown "x."

*Reviewed* by E. Roy Hammarlund
*School of Pharmacy*
*Department of Pharmaceutics*
*University of Washington*
*Seattle, WA 98195*

less than and greater than the given value. Thus, the median parameters are selected by the user. Once selected, these intersection values are used to calculate predicted concentration values for each observed value.

The performance of the DLP program is shown in the following example. Concentrations expected at time 0.5, 1, 1.5, 2.0, 3, 4, 5, 10, 12, 14, 16, 20, and 24 hr were simulated for the biexponential equation:

$$C_t = 50e^{-0.8t} + 10e^{-0.08t} \quad \text{(Eq. 6)}$$

Error with a coefficient of variation of either 5 or 20% was randomly assigned to the simulated concentrations such that four of the 12 observations were affected by the larger error. The results are shown in Fig. 1. The program was used to strip the curve. Concentrations observed between 10 and 24 hr were used for the $\beta$-phase, and those between 0.5 and 5 hr were used for the $\alpha$-phase. The results of parameter estimation using sequential regression (stripping) and the DLP method are shown in Table I. In this example, DLP produced better estimates of $A$ and $\alpha$ (13.8 and 6.2% error) than did sequential regression analysis (62.8 and 31.2% error). Estimates of $B$ and $\beta$ were somewhat better using regression (1.2 and −2.5% error) than with the DLP method (13.8 and 6.2% error). The large errors made by regression analysis in estimating $A$ and $\alpha$ indicate that DLP estimates for the entire curve were superior.

The determination of the importance of the DLP method of parameter estimation in pharmacokinetics will require further experimentation. It is hoped that the described program will facilitate this process.

(1) L. Endrenyi and H.-Y. Tang, *Comp. Biomed. Res.*, **13**, 430 (1980).

*Jeffrey R. Koup*
Department of Pharmacy Practice
School of Pharmacy
University of Washington
Seattle, WA 98195

Received March 24, 1981.
Accepted for publication June 18, 1981.

# BOOKS

## REVIEWS

**Introduction to Pharmaceutical Dosage Forms.** By HOWARD C. ANSEL. Lea & Febiger, Washington Square, Philadelphia, PA 19106. 1981. 408 pp. 18.5 × 26 cm.

The format and presentation of this third edition are the same as in the previous one, but the material has been revised to the current official compendia. The book is intended "to introduce the beginning pharmacy students to medicinal and pharmaceutic substances, the methods of their incorporation into pharmaceutical dosage forms, and the utilization of these forms in patient care."

The discussions on heritage, terminology, code of ethics, regulations, and drug substances should satisfactorily orient beginning students in their first professional course in pharmacy. The appendix defines drug categories and discusses measurements, and tables of official preparations are given. Pharmaceutical products are logically treated from the viewpoint of administration route, and the classes of pharmaceutical preparations also are discussed. Numerous photographs illustrate equipment, processing, and packaging.

However, the presentation of dosage form design in terms of biopharmacy, formulation, and practice is inadequate. Whether the curriculum of a college is arranged to present a preparations–physical pharmacy sequence or a technology series of courses, the scope of this text restricts its use to an orientation course because of its superficial presentation of theory and pharmacy principles and limited discussion of techniques and manufacturing principles.

*Reviewed by* Eugene L. Parrott
*College of Pharmacy*
*University of Iowa*
*Iowa City, IA 52242*

---

**Pharmaceutical Calculations,** 2nd Ed. By JOEL L. ZATZ. John Wiley & Sons, 605 Third Ave., New York, NY 10016. 1981. 388 pp. 13.3 × 25 cm. Price $17.50.

Pharmaceutical calculations continues to be one of the most frustrating subjects to teach in any pharmacy curriculum. The complete accuracy required in answering many problems, the mixing of different metrology systems, the frequent use of conversions, and the simultaneous introduction of pharmaceutical terminology confound many students. This ongoing dilemma has resulted in pharmaceutical calculations being taught and evaluated in a variety of ways at different schools of pharmacy. No single textbook can solve the distress frequently associated with calculations, but Joel Zatz's second edition goes a long way to making it all more bearable.

The book is longer than the first edition by 77 pages because it now has an appendix containing instruction and problems on temperature conversion, alcohol proof strength, and sodium chloride equivalents in addition to the inclusion of alligation and a greatly expanded section on milliequivalents.

The cover of the book describes the structure of the text succinctly: "The progression of topics within each chapter and in the overall structure of the book constitutes a programmed format that permits self-paced learning and builds upon previously learned concepts to reinforce understanding. Students participate actively and are able to concentrate on calculations that are most difficult for them. Emphasis is on practical approaches to meeting accuracy requirements in filling prescriptions and manufacturing."

This book is designed to fit into the usual first general pharmacy course, to serve as a text in a calculations course or as a self-instruction text apart from the formal classroom, or to be an aid for review, and it does all of these well.

It is difficult to find much about the text to criticize. About all one can say is that it does not contain a section on commercial arithmetic which some instructors prefer to include in their course, and there are a few prescription problems for oral preparations containing amaranth (Red No. 2) which was banned in time to have been deleted from the new edition.

In conclusion, while working examples from the text, the reviewer finds it refreshing to solve for "j" (for Joel?) rather than to always hunt for the usual unknown "x."

*Reviewed* by E. Roy Hammarlund
*School of Pharmacy*
*Department of Pharmaceutics*
*University of Washington*
*Seattle, WA 98195*

A publication of the
American Pharmaceutical Association—
the National Professional Society
of Pharmacists

# JOURNAL OF PHARMACEUTICAL SCIENCES

## INDEX TO AUTHORS
## INDEX TO SUBJECTS

VOLUME 70
JANUARY TO DECEMBER, 1981

*Published monthly under the supervision of the Board of Trustees*

MARY H. FERGUSON
*Editor*

NANCY E. BROWN
*Production Editor*

JOHN PATRICK EVANS
*Copy Editor*

MICHAEL K. HAYES
*Copy Editor*

EDWARD G. FELDMANN
*Contributing Editor*

SAMUEL W. GOLDSTEIN
*Contributing Editor*

BELLE R. BECK
*Editorial Secretary*

EDWARD G. FELDMANN
*Acting Director of Publications*

EDITORIAL ADVISORY BOARD

John Autian
Norman R. Farnsworth
William J. Jusko
Herbert A. Lieberman
David E. Mann, Jr.
Ian W. Mathison
Gerald J. Papariello
Edward G. Rippie

JOURNAL OF PHARMACEUTICAL SCIENCES

OCTOBER 1981
VOLUME 70 NUMBER 10

RESEARCH ARTICLES

# Solid-State Decomposition of Alkoxyfuroic Acids

**J. T. CARSTENSEN *x and ROHIT KOTHARI ‡**

Received November 10, 1980, from the **School of Pharmacy, University of Wisconsin, Madison, WI 53706*, and ‡*Ryker Laboratories, St. Paul, MN 55100.* Accepted for publication March 6, 1981.

**Abstract** □ A series of alkoxyfuroic acids with alkyl lengths of $n$ = 8–18 was synthesized, and the solid-state decomposition was studied. Bawn kinetics were adhered to, and the solid and liquid decomposition rate constants were established; they followed an Arrhenius relationship well, with energy of activations and preexponential factors being a function of the chain length. There was a break in this correlation between $n$ = 14 and $n$ = 16. The liquefaction points were of the expected correlation with inverse temperature. The isokinetic temperature ($T_i$) fell fairly well on the line demonstrated for other compound series.

**Keyphrases** □ Solid-state decomposition—alkoxyfuroic acids with alkyl chain lengths of $n$ = 8–18 □ Alkoxyfuroic acids—Arrhenius relationship, energy of activation and preexponential factors as a function of chain length □ Bawn kinetics—solid and liquid decomposition rate constants of alkoxyfuroic acids

Chemical decomposition of pure solids has been discussed sporadically in the literature, the principal publications being those of Prout and Tompkins (1) and Bawn (2). The reactions are usually dictated to a great extent by physical (*e.g.*, active site propagation) rather than chemical steps, resulting in high activation energies (300–400 kJ) when the reaction is one where:

$$\text{solid} \rightarrow \text{solid} + \text{gas}$$

*Scheme I*

This reaction (Scheme I) was essentially covered by Prout and Tompkins, whereas the reaction (Scheme II) treated by Bawn is:

$$\text{solid} \rightarrow \text{liquid} + \text{gas}$$

*Scheme II*

Several reactions of this latter type were reported in the pharmaceutical literature (3–6). In these reactions (Scheme II), it was shown that the part occurring in the solid is not necessarily dictated by active site propagation and that chemical factors are much more prevalent (5) than when Scheme I applies. Chemical substituent effects have, for instance, been demonstrated (3–5).

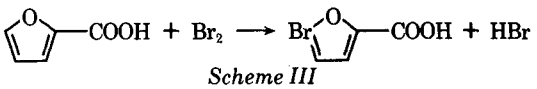

*Scheme III*

The work described in this report deals with chemical substituent (chain length) effects in a series of alkyloxyfuroic acids. One of these acids (7) was previously shown to be a hypolipidemic agent.

## EXPERIMENTAL

**Synthesis**—The compounds studied were 5-alkyloxy-2-furoic acids, *i.e.*, RCOOH, where R = $C_nH_{2n+1}$–O–($C_4H_2O$)– and where $n$ = 8, 10, 12, 14, 16, and 18. The syntheses were carried out by the method described by Parker *et al.* (7) with a few modifications. Furoic acid was first brominated to give 5-bromofuroic acid, using carbon tetrachloride as a solvent (Scheme III).

A 2-liter round-bottom flask, fitted with a reflux condenser, drying tube, and magnetic stirrer, was charged with 250 g of furoic acid and 1.2 liters of carbon tetrachloride. The mixture was stirred until all of the furoic acid was dissolved. The solution was heated to 40°, and then 500 g of bromine was added slowly through a funnel directly fitted to the flask. The reaction mixture was then refluxed on a water bath for 5 hr. At the end of the refluxing period, carbon tetrachloride was distilled off.

The product of the reaction was dissolved in boiling water and filtered hot. Upon cooling, the bromosubstituted acid precipitated. It was further purified by recrystallization from hot water. To eliminate any dibromofuroic acid that might have formed, the barium salt was prepared as follows. For each gram of the product, 25 cm$^3$ of water was added and made strongly alkaline with ammonium hydroxide; 1 g of barium chloride was added with some activated charcoal. After 15 min, the solution was filtered. The filtrate was acidified with hydrochloric acid; the 5-bromofuroic acid, which precipitated out, was recrystallized from hot water. The yield was 60%, mp 186°, in agreement with the melting point obtained by Whittaker (8).

The 5-alkyloxy-2-furoic acid was next synthesized from the bromofuroic acid in two stages as shown in Schemes IV and V.

A reaction flask was charged with 1 liter of toluene, and ~0.1 liter of the solvent was distilled off to dry. The toluene remaining was cooled to 40° under nitrogen, and 0.33 mole of $n$-alkanol and 0.45 mole of sodium hydride (as a 50% dispersion in oil) were added. The mixture was refluxed

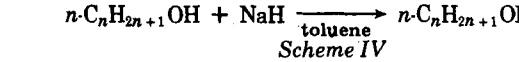

*Scheme IV*

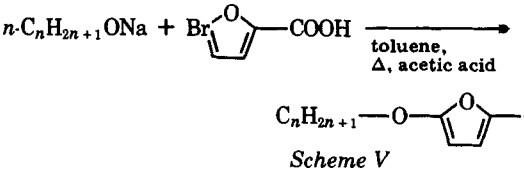

*Scheme V*

0022-3549/81/1000-1095$01.00/0
© 1981, American Pharmaceutical Association

**Table I—Properties of 5-Alkyloxy-2-furoic Acids**

| $n$[a] | Melting Point | Heat of Fusion, $\Delta H_f$, Obtained from Kinetic Data, kJ/mole | $\Delta H_{DTA}$ from Thermal Analysis, kJ/mole | $q = \Delta H_f - \Delta H_{DTA}$, kJ/mole | Density, g/cm$^3$ [b] | Crude Yield, % | Recrystallized Yield, % |
|---|---|---|---|---|---|---|---|
| 8 | 127° | 111 | 29 | 82 | 1.28 | 60 | 47 |
| 10 | 125° | 53 | —[c] | —[c] | 1.23 | 40 | 30 |
| 12 | 122° | 72 | 41.2 | 31 | 1.13 | 72 | 63 |
| 14 | 119° | 68 | 31.6 | 36 | 1.13 | 72 | 63 |
| 16 | 118° | 63 | —[c] | —[c] | 1.11 | 35 | 23 |
| 18 | 117° | 73 | 36 | 37 | — | 58 | 50 |
| 5-BFA[d] | 186° | | | | | 75 | 70 |

[a] $n$ = alkyl length. [b] Densities done by pycnometry. In the case of $n$ = 18, the material wets very poorly in solvents in which it is poorly soluble and density data are not available. [c] Decomposition pertubates thermogram too much in these cases to draw conclusions. [d] 5-Bromofuroic acid.

for 3 hr and then cooled under nitrogen to 40–45°. A suspension of 0.2 mole of 5-bromofuroic acid in 0.2 liter of dry toluene was added rapidly. The reaction mixture was held at 60° for ~1 hr to ensure that the balance of the sodium hydride had reacted to form the sodium salt of the acid. It was then heated at reflux temperature for 16 hr.

The mixture was cooled to 30°, and 1.2 liters of ether was added, followed by 0.3 liter of 15% acetic acid. Stirring was continued for ~30 min. The organic portion was separated with the help of a separator and then was washed three times with either distilled water or saturated sodium chloride solution. The solution was dried with calcium chloride, and then the drying agent was removed by vacuum filtration. Most of the ether was stripped off with the help of a flask-evaporator and a hot water bath held at 45°. The concentrated solution was chilled in a freezer for 12–15 hr.

The precipitated solid was filtered off and washed with cold toluene. The crude product was dissolved in hot 2-butanone or acetone, and then activated charcoal was added. The mixture was stirred for a few minutes and filtered while hot. This solution was cooled gradually to 5°, and the recrystallized product was filtered off after a few hours. Recrystallization was carried out at least three times to ensure purity. The compounds were identified with the help of NMR and mass spectra and, where possible, differential scanning calorimetry. Melting points were determined and are listed in Table I.

**Kinetic Studies**—Kinetic studies were carried out by preparing a sample *in vacuo* in a sample bulb with an attached mercury manometer such as was described previously (3, 6). The whole assembly was placed in a tall thermostatically controlled bath with either water or mineral oil as the medium; temperature control was ±0.2°. The amount of gas pressure at any time can be deduced from a knowledge of the volume, mercury height, and density of mercury at the temperature in question and can then be converted to number of moles of gas produced.

Condensation characteristics and mass spectra of the gas confirmed it to be carbon dioxide. Since, in the manner described, the decomposition takes place in a system that is evacuated but that contains mercury vapor in the headspace, several control studies were done in break-seal tubes (3) to ascertain that the mercury vapor did not affect reaction rates.

**Vapor Pressure Studies**—Since the possibility exists that the decomposition of a solid at constant volume occurs in the vapor phase, the vapor pressure of the various solids was determined. The Knudsen effusion method was used (9–12). In this method, the rate of vapor loss through a small orifice is measured gravimetrically under conditions of free molecular flow; the vapor pressure is calculated directly from the proportionality between the rate of mass loss and the vapor pressure.

The Knudsen cells used were aluminum crucibles with a lid placed on the top in conjunction with an "O" ring. A small orifice (0.5-mm diameter) was drilled in the lid. The mean value of the orifice diameter was determined microscopically. The fidelity of the method was checked by determining vapor pressures of a compound (benzoic acid) with well-established vapor pressure values (13). The cells were placed on the pan of an electrobalance in a vacuum chamber such as was described previously (14).

To determine the decomposition rate constant in the vapor phase, a 2-liter bulb was equipped with a break-seal tube. The amount of alkoxyfuroic acid necessary to (just) saturate the bulb at 95° was calculated from the vapor pressure *versus* temperature curve. This amount was then added to the bulb as a methanol solution. The solvent was then evaporated off (on the vacuum rack) at room temperature, and the nonbreak-seal end was fused off. The bulb was placed at 95°, and the amount of carbon dioxide evolved after 1 week was determined, in this case by means of a McLeod gauge with a 1:10,000 ratio of compression capacity.

## RESULTS AND DISCUSSION

The general pattern is that the solid decomposes by some means and that a liquid decomposition product is formed. There are three main feasible models that could account for this reaction.

In Model A, the solid (RCOOH) evaporates and decomposes in the vapor phase to RH and $CO_2$, and RH condenses. Decomposition in the solid state is negligible.

In Model B, the solid (RCOOH) decomposes in the solid state and, in addition to carbon dioxide, forms liquid RH in which RCOOH is insoluble. [Prout–Tompkins kinetics (1)].

In Model C, the solid (RCOOH) decomposes in the solid state and, in addition to carbon dioxide, forms liquid RH in which RCOOH is soluble [Bawn kinetics (2)].

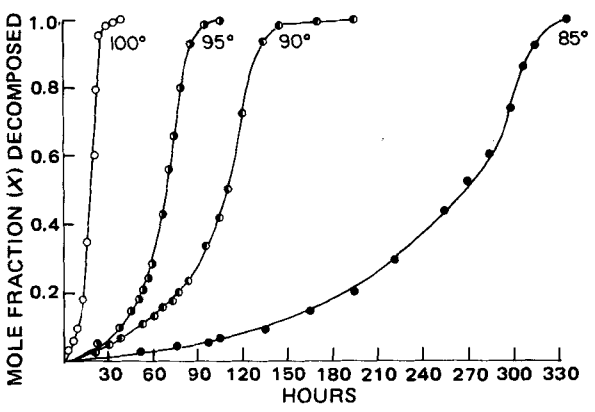


**Figure 1**—*Decomposition of octyloxy furanoic acid at various temperatures. Key:* ●, *85°;* ◐, *90°,* ◑, *95°; and* ○, *100°.*

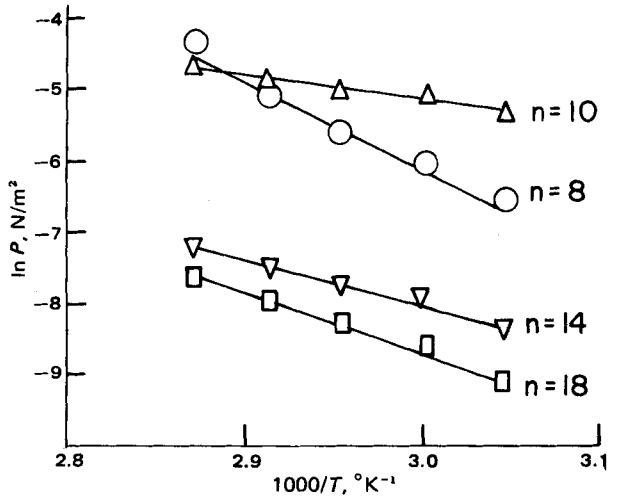


**Figure 2**—*Vapor pressures as a function of temperature. Only four of the alkoxyfuroic acids are plotted to avoid crowding. Key:* ○, n = *8;* △, n = *10;* ▽, n = *14; and* □, n = *18.*

**Table II—Mole Fraction ($X_s$) at Complete Liquefaction**

| Temperature ($T$) | $n$[a] | | | | | |
|---|---|---|---|---|---|---|
| | 8 | 10 | 12 | 14 | 16 | 18 |
| 127° | 0 | 0 | | | | |
| 125° | | | 0 | | | |
| 119° | | | | 0 | | |
| 118° | | | | | 0 | |
| 117° | | | | | | 0 |
| 100° | 0.60 | 0.59 | 0.56 | 0.48 | 0.65 | 0.70 |
| 95° | 0.73 | 0.68 | 0.65 | 0.62 | 0.72 | 0.74 |
| 90° | 0.84 | 0.75 | 0.76 | 0.76 | 0.80 | 0.80 |
| 85° | 0.91 | 0.80 | 0.83 | 0.78 | 0.90 | 0.89 |
| Eq. 8, $N$[b] | 4 | 4 | 4 | 4 | 3[b] | 4 |
| Correlation coefficient | −0.997 | −0.999 | −0.997 | −0.990 | −0.994 | −0.957 |
| Slope | −13,355 | −6360 | −8655 | −8117 | −7580 | −8824 |
| Intercept | 34.9 | 16.1 | 22.4 | 21.1 | 19.3 | 22.5 |
| $\Delta H_f$, kJ | 111 | 53 | 72 | 68 | 63 | 73 |
| $T_0$, °K | 383 | 394 | 386 | 385 | 393 | 391 |
| $T_0$, °C | 110 | 121 | 113 | 112 | 120 | 118 |

[a] $n$ = alkyl length. [b] Number of points used. In the case of $n$ = 16, only the first 3 points were used since the point at 85° appears to be a (slight) outlier.

There is also the possibility of Model B or C in combination with Model A.

For Model A, Scheme VI applies:

$$\text{RCOOH(solid)} \rightarrow \text{RCOOH(vapor)} \rightarrow \text{RH} + \text{CO}_2$$

*Scheme VI*

If $A$ denotes the amount of intact RCOOH, then by denoting its vapor pressure as $P$:

$$dA/dt = -k'P \qquad \text{(Eq. 1)}$$

Since $P$ is simply a function of temperature, the reaction, carried out isothermally, would be zero order, with a rate constant of:

$$k_0 = k'P \qquad \text{(Eq. 2}a\text{)}$$

A typical decomposition curve is shown in Fig. 1. It is obvious from visual inspection that the decomposition is not zero order. Furthermore, the decomposition rate constants in the gas phase were found in the worst case ($n$ = 8) to be of the order of $3 \times 10^{-3}$ hr$^{-1}$ at 95°. Vapor pressure curves are shown in Fig. 2. For $n$ = 8, the pressure at 95° was $89 \times 10^{-3}$ Pa ($\sim 9 \times 10^{-7}$ atm). The headspace ($V$) of the bulb/manometer was ~100 cm$^3$, so that ($N$ denoting moles):

$$dN/dt = (V/RT)\, dP/dt = (V/RT)k'P \qquad \text{(Eq. 2}b\text{)}$$

which, with the previous figures, amounts to $0.9 \times 10^{-11}$ mole/hr or (the molecular weight for $n$ = 8 being 228) $2 \times 10^{-6}$ mg/100 hr. Hence, Model A can be ruled out.

During the decomposition as time progresses, more and more liquid is present and less and less solid exists. At a particular point, no more solid is present and the entire sample is liquid. If Model B is correct, then this point should correspond to 100% decomposition. But this is not the case; this point occurs, on the average, at 75% decomposition. Hence, the parent compound (RCOOH) has a finite solubility, $S$ moles/mole RH, and Model C seems to be a more feasible model. The mathematical consequences of the model are as follows (6). If $X$ denotes mole fraction decomposed, if $k_s$ is the decomposition rate constant of RCOOH in the solid state, and if $k_l$ is the decomposition rate constant of RCOOH in solution in RH, then:

$$\ln(1 + AX) = \alpha t \qquad \text{(Eq. 3)}$$

where $A$ is an adjustable parameter and $t$ is time. The value of $A$ is given by:

$$A = \alpha/k_s \qquad \text{(Eq. 4)}$$

and:

$$\alpha = k_l S - k_s S - k_s \qquad \text{(Eq. 5)}$$

$S$ can be determined from the time, $t_s$, at which the system becomes completely liquid. If the amount decomposed at this point is $X_s$, then the amount not decomposed is $1 - X_s$ and, hence, the solubility is

$$S = (1 - X_s)/X_s \text{ moles/mole} \qquad \text{(Eq. 6)}$$

Beyond time $t_s$, the system is a solution and should adhere to first-order kinetics, *i.e.*:

$$\ln[(1 - X)/(1 - X_s)] = -k(t - t_s) \qquad \text{(Eq. 7)}$$

For Model C to apply, it is necessary that: (*a*) the data below time $t_s$ can be linearized *via* Eq. 3; (*b*) the data above time $t_s$ can be linearized by suitable liquid kinetic schemes; and (*c*) the value of $k_l$ found from this latter scheme when inserted in Eq. 5, together with the solubility $S = (1 - X_s)/X_s$ and $k_s$ from Eq. 4, gives a value of $\alpha$ in agreement with the value of $\alpha$ from Eq. 3. If the above statements hold, then a double check of the model is established for its correctness. Of course, a model is never

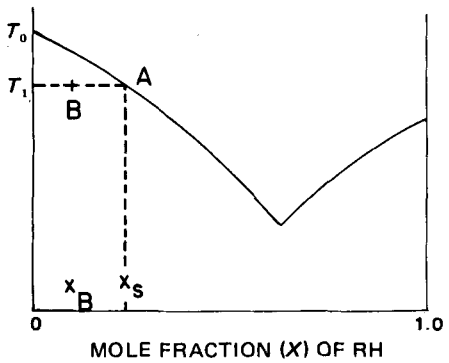


**Figure 3**—*Melting-point diagram of RCOOH and RH. If the decomposition is carried out at* $T_1$, *then at a certain time* ($t_B$) *a decomposition corresponding to* $X_B$ *will have occurred. The amounts of solid and liquid will be determined by the weight arm rule. At a particular point in time* ($t_s$), *the last solid will disappear. This point corresponds to point A* ($x_s$, $T_1$), *which is part of the melting-point curve.*

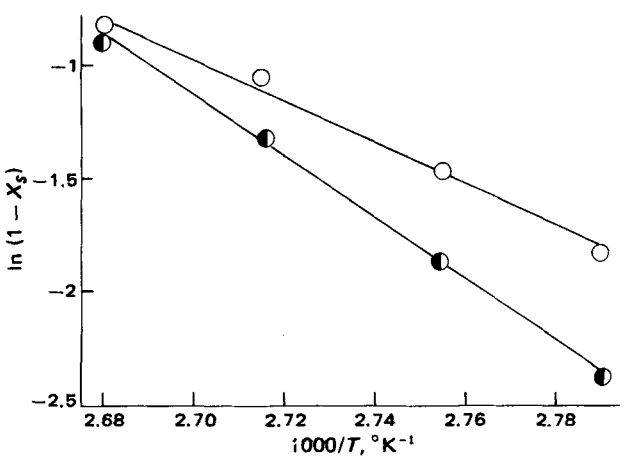


**Figure 4**—$X_s$ *plotted as a function of 1000/*T. *Key:* ○, n = *10; and* ◐, n = *8.*

**Table III—Least-Squares Fit Data According to Eq. 3.**

| $n$ | Temperature | $A$ | $C$ | $D$ | $k_s$, $10^4$ hr$^{-1}$ | $R$ |
|---|---|---|---|---|---|---|
| 8 | 85° | 18.904 | 0.00858 | 0.00009 | 4.5 | 0.994 |
| 8 | 90° | 10.973 | 0.0160 | 0.00008 | 14.6 | 0.992 |
| 8 | 95° | 14.021 | 0.0435 | 0.00009 | 31.0 | 0.991 |
| 8 | 100° | 12.579 | 0.106 | 0.00008 | 83.9 | 0.994 |
| 10 | 85° | 20.289 | 0.00758 | 0.00002 | 3.7 | 0.990 |
| 10 | 90° | 22.716 | 0.0283 | 0.00007 | 12.5 | 0.991 |
| 10 | 95° | 18.814 | 0.0438 | 0.00008 | 23.3 | 0.992 |
| 10 | 100° | 23.188 | 0.150 | 0.00008 | 64.5 | 0.994 |
| 12 | 85° | 62.094 | 0.00915 | 0.00005 | 3.5 | 0.990 |
| 12 | 90° | 39.795 | 0.0402 | 0.00007 | 10.1 | 0.992 |
| 12 | 95° | 41.035 | 0.07842 | 0.00009 | 19.1 | 0.993 |
| 12 | 100° | 47.860 | 0.245 | 0.00007 | 51.2 | 0.990 |
| 14 | 85° | 22.456 | 0.00679 | 0.00007 | 3.0 | 0.997 |
| 14 | 90° | 72.127 | 0.05965 | 0.00006 | 8.3 | 0.998 |
| 14 | 95° | 123.577 | 0.1661 | 0.00007 | 13.4 | 0.992 |
| 14 | 100° | 175.312 | 0.556 | −0.00010 | 31.7 | 0.990 |
| 16 | 85° | 30.196 | 0.00835 | 0.00004 | 2.8 | 0.990 |
| 16 | 90° | 48.866 | 0.0460 | 0.00009 | 9.4 | 0.993 |
| 16 | 95° | 42.389 | 0.0859 | −0.00004 | 20.3 | 0.992 |
| 16 | 100° | 54.795 | 0.358 | 0.0000 | 65.4 | 0.997 |
| 18 | 85° | 24.460 | 0.00859 | 0.00007 | 3.5 | 0.998 |
| 18 | 90° | 71.224 | 0.0453 | 0.00009 | 6.4 | 0.999 |
| 18 | 95° | 51.261 | 0.0726 | 0.00009 | 14.2 | 0.998 |
| 18 | 100° | 77.328 | 0.476 | −0.00008 | 61.6 | 0.997 |

[a] $n$ = alkyl lengths.

"proven"; it is simply established that the data generated do not conflict with it. Therefore, it is prudent to check the adherance in as many ways as possible to guarantee that the model is self-consistent.

It is obvious that the values of $t_s$ and $X_s$ are important, and some elaboration on this point will be made prior to testing the remaining points regarding Model C. If one considers a eutectic diagram (*e.g.*, Fig. 3), then it is obvious that at a given temperature, $T_1$, the point $(X_s, T_1)$ is part of the melting-point curve, provided the two compounds, RCOOH and RH, form a simple melting-point diagram to the left of the eutectic point without solid solution formation.

The left eutectic diagrams, constructed from $T$ *versus* $X_s$ data, are given in Table II. The heat of fusion of RCOOH should be obtainable from these curves since:

$$\ln(1 - X_s) = \frac{(-\Delta H_f)(T_0 - T_s)}{RT_0T_s}$$

$$= (-\Delta H_f/R)[(1/T_s) - (1/T_0)] \quad \text{(Eq. 8)}$$

where $T_0$ is the melting point of RCOOH and $T$ is the temperature corresponding to the particular $X_s$ in consideration; $R$ is the gas constant (8.3143 J mole$^{-1}$ degree$^{-1}$). Examples of data plotted according to Eq. 8 are shown in Fig. 4. Least-squares fit parameters are shown on the bottom of Table II. The $\Delta H_f$ value is obtained by multiplying the slope by −8.31, and $T_0$ is minus the slope divided by the intercept. It should correspond to the melting point and, except for $n$ = 8, this correlation is reasonably good.

The $\Delta H_f$ values obtained in this fashion are shown in Table I to enable comparison with data to be developed later. When differential thermal analysis (DTA) is applied, a $\Delta H$ value is obtained that is the heat of fusion for stable compounds. It is derived from the area under the endotherm. For compounds that decompose below their melting point, however, the $\Delta H$ value obtained from this area is the difference between the heat absorbed ($\Delta H_f$) due to melting and the heat evolved ($q$) due to the reaction, *i.e.*:

$$\Delta H_{DTA} = \Delta H_f - q \quad \text{(Eq. 9)}$$

Therefore, the enthalpy of reaction ($-q$) can be deduced, and values of $\Delta H_{DTA}$ and $q$ are listed in Table I. There were cases ($n$ = 10 and $n$ = 16) where the reaction taking place concurrent with or before melting made the thermograms so poorly reproducible that they are not reported here. The values for $q$ should be viewed in this light as well. For $n$ = 8, the melting point obtained from the kinetic data (Eq. 8) differs from that obtained by differential thermal analysis by several degrees. However, the latter is questionable rather than the former. The values of $\Delta H_f$ and $q$ are not germane to the further development; they are included here simply for completeness and to indicate that ancillary values obtained in the study did not conflict with the proposed model.

As an example of the fits obtained *via* Eq. 3, the data shown by direct plotting in Fig. 1 were transposed *via* Eq. 3 and are shown in Fig. 5. The fit is good. Least-squares fit parameters obtained by iteration of Model A for all of the data are shown in Table III in the form:

$$\ln(1 + Ax) = Ct + D \quad \text{(Eq. 10)}$$

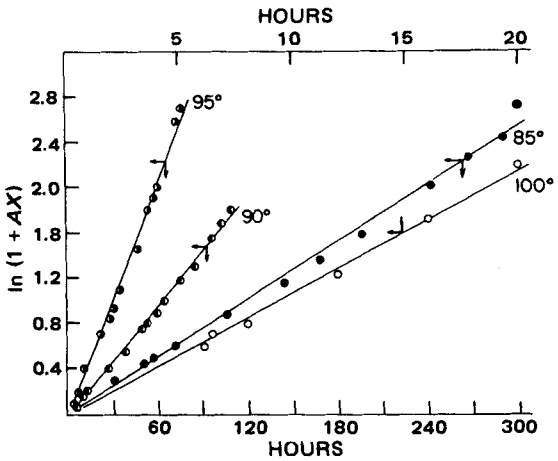


**Figure 5**—*Data from Fig. 1 plotted according to Eq. 3. Key:* ●, *85°;* ◐, *90°;* ◑, *95°; and* ○, *100°. Note dual scales.*

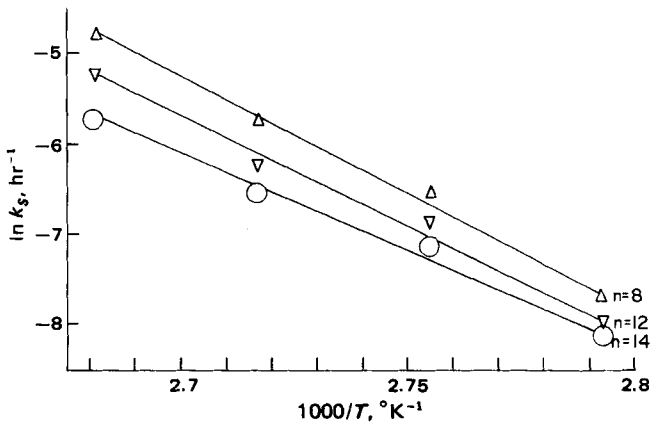


**Figure 6**—*Arrhenius plot of* $k_s$ *(hr*$^{-1}$*). For graphical clarity, only* n = *8 (*△*),* n = *12 (*▽*), and* n = *14 (*○*) are shown.*

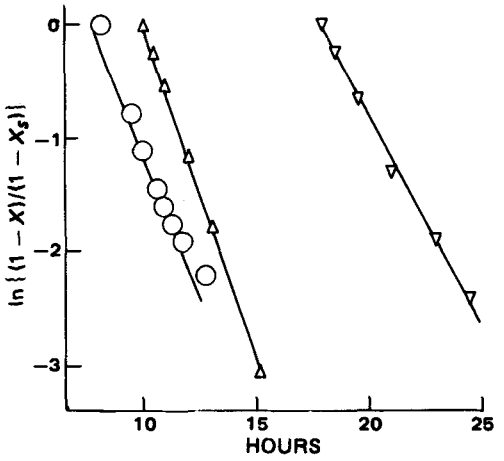


**Figure 7**—*First-order kinetics after the point where complete liquefaction has occurred. Key:* ▽, n = *10;* ○, n = *14; and* △, n = *16 (all at 100°).*

It is noted from the table that the $D$ values are small (<0.0001) at the same time as $R$, the correlation coefficient, is high (never <0.99). Hence, $C$ becomes synonymous with $\alpha$ in Eq. 3, allowing calculation of $k_s$ *via* Eq. 4. The values of $k_s$ obtained in this fashion are shown in Table III.

The temperature dependence of the $k_s$ values is, according to the Arrhenius equation:

$$\ln k_s = -(E_a/R)(1/T) + \ln Z \qquad \text{(Eq. 11)}$$

where $E_a$ is the activation energy and $Z$ is a preexponential factor. This is exemplified in Fig. 6 (linearity is obvious upon visual inspection). Least-squares fit parameters are shown in Table IV, and the high correlation coefficients are indicative of the good fits.

As mentioned, the data in Table III ($A = \alpha/k_s$ and $C = \alpha$) in conjunction with the values from Table II [$S = (1 - X_s)/X_s$] will allow calculation of the decomposition rate in solution, $k_l$ hr$^{-1}$. The parts of the curves beyond $t_s$ can be used directly to calculate the first-order decomposition rate of RCOOH in solution in RH. An example is shown in Fig. 7; the linearity is graphically obvious, supporting the assumption of first-order kinetics in solution, *i.e.*, confirming Eq. 7. The reproducibility is fair at best (±10% for the rate constants). The rate constants obtained in this fashion are denoted simply $k$ (Table V). The correlation coefficients confirm the visually observed linearity.

If the proposed model is correct, then $k$ and $k_l$ should be identical. They were plotted in linear fashion (Fig. 8); again, the linearity with a zero intercept is implied by:

$$k = A_1 k + B_1 \qquad \text{(Eq. 12)}$$

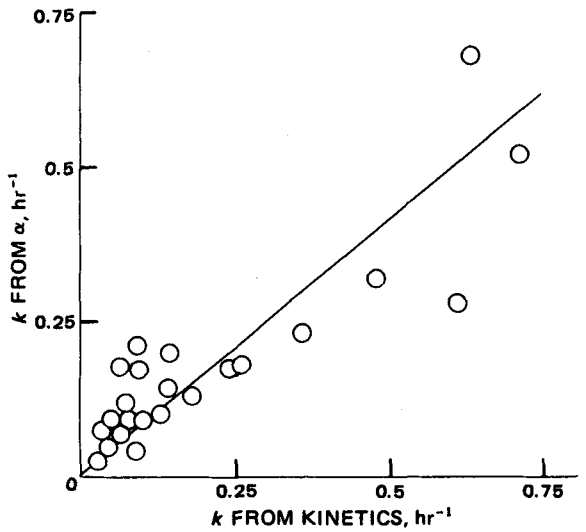


**Figure 8**—*Solution decomposition rate constants* ($k_l$) *derived from* $\alpha$ *as a function of solution decomposition rate constants* ($k$) *found experimentally.*

**Table IV—Arrhenius Parameters for the Alkoxyfuroic Acids.**

| $n^a$ | $10^{-5}\,E_a$, J/mole | $Z$ |
|---|---|---|
| 8 | 2.2 | $3.69\ 10^{27}$ |
| 10 | 2.0 | $2.62\ 10^{26}$ |
| 12 | 1.9 | $5.09\ 10^{24}$ |
| 14 | 1.7 | $9.9\ 10^{20}$ |
| 16 | 2.3 | $3.8\ 10^{29}$ |
| 18 | 2.1 | $6.78\ 10^{26}$ |

[a] $n$ = alkyl length.

**Table V—Solution Decomposition Rate Constants (Hour$^{-1}$) for the Alkoxyfuranoic Acids (RCOOH) in Solution in RH as a Function of Reciprocal Temperature Eq. 11**

| $n^a$ | Correlation Coefficient, $R^2$ | Intercept (ln $Z'$) | Slope ($-E_a/R$) | $E_a$, kJ/mole | $Z$ |
|---|---|---|---|---|---|
| 8 | 0.972 | 22.89 | −9,113 | 76 | $0.87 \times 10^{10}$ |
| 10 | 0.984 | 51.01 | −19,513 | 162 | $1.42 \times 10^{22}$ |
| 12 | 0.969 | 50.15 | −19,083 | 159 | $6.02 \times 10^{21}$ |
| 14 | 0.933 | 55.78 | −20,903 | 174 | $1.68 \times 10^{24}$ |
| 16 | 0.925 | 55.66 | −21,006 | 176 | $1.49 \times 10^{24}$ |
| 18 | 0.911 | 50.96 | −19,239 | 160 | $1.35 \times 10^{22}$ |

[a] $n$ = alkyl length.

where $A_1$ should be unity and $B_1$ should be zero. The least-squares fit values in Fig. 8 are $A_1 = 0.83 \pm 0.22$ and $B_1 = 0.17 \pm 0.25$, so the figure does not contradict the proposed model. The overall correlation coefficient is 0.975.

The $k_l$ or $k$ values should be treatable by the Arrhenius equation (Fig. 9). The least-squares fit parameters for these relations are shown in Table V.

Pothisiri and Carstensen (4) suggested that the temperature at which $k_l = k_s$ ($T_i$) is related to the melting point ($T_m$) in log–log fashion. Data from the present study are pooled with data from Ref. 4, in Fig. 10, and the correlation seems to hold with the alkoxyfuroic acids as well as previously reported compounds. Since the furoic acids have melting temperatures close to one another, they have been averaged, as has $T_i$ (Fig. 10). With the small number of compounds at present, this is, at best, a rank-order correlation.

An attempt was made to correlate the kinetic parameters with substituent properties (chain length) in Fig. 11. Both $E_a$ and $Z$ decreased

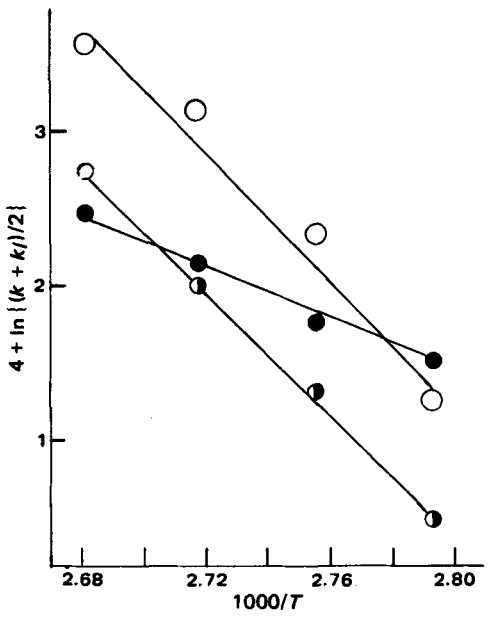


**Figure 9**—*Logarithm of the solution decomposition rate constants of RCOOH in solution in RH plotted as a function of 1000/T (°K$^{-1}$). Key:* ●, n = *8;* ◑, n = *10; and* ○, n = *14. The remainder are left out for graphical clarity.*

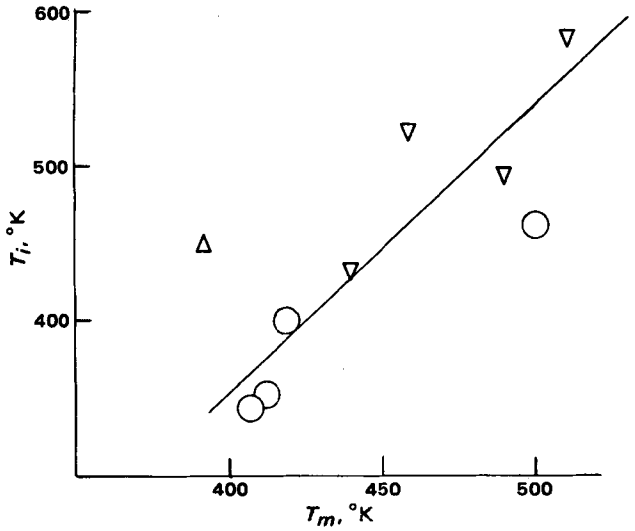


**Figure 10**—*Data from Refs. 3 (∇) and 4 (○) plotted together with the average* $T_m$ *and* $T_i$ *values (△) from this study. (Average* $T_m$ *= 394 ± 4 °K and, average* $T_i$ *= 450 ± 50 °K.)*

with increasing chain length up to $n$ = 14, after which there was an upward break in the curve. This discontinuity did not exist in other properties of the series (vapor pressures, densities, and enthalpies of fusion and reaction). No explanation is offered for this break at present.

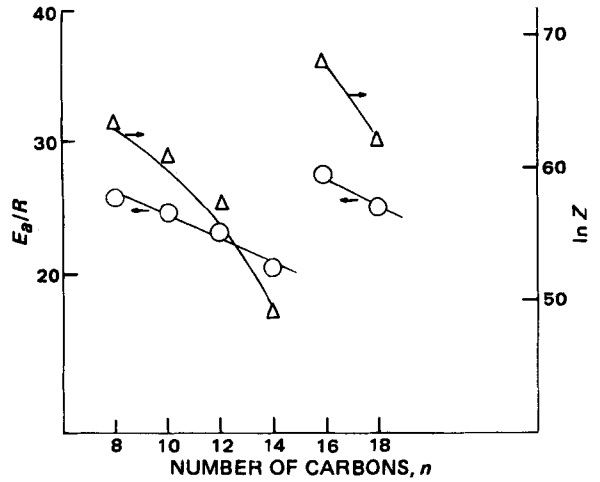


**Figure 11**—$E_a/R$ *and ln Z from Eq. 11 (Table IV) plotted* versus n. *The values for* n = *14 are slightly (4%) lower than previously reported (6) due to increased precision in this study (multiple runs).*

The effect of particle size was estimated by micronizing a sample ($n$ = 14). At 85°, this sample had a value of $k_s = 3.3 \times 10^{-4}$/hr as opposed to $3.3 \times 10^{-4}$/hr for a nonmicronized sample; therefore the effect of particle size was not pronounced. All samples tested were not milled, *i.e.*, were in the recrystallized state, and had surface areas, measured by nitrogen adsorption, of ~1 $m^2/g$.

A final note on reproducibility is in order. Data were duplicated with parameter values obtained from 10 sets that differed by no more than 5%. The effect of the use of a mercury manometer as contrasted to the use of break-seal tubes was also tested (in five cases) with duplication within the previously mentioned error.

Therefore, it is fairly conclusive that the alkoxyfuroic acids decompose as shown in Scheme II, and solid and liquid decomposition rate constants have been established. The liquefaction characteristics are in accordance with what would be expected from melting-point diagrams with a reasonable correlation. Energy of activation is a function of chain length, as is the preexponential factor. There is a break in this correlation curve at $n$ = 14/16. The isokinetic temperature ($T_i$) falls fairly well on the correlation line established for other compounds.

## REFERENCES

(1) E. G. Prout and F. C. Tompkins, *Trans. Faraday Soc.*, **40,** 488 (1944).

(2) C. E. H. Bawn, in "Chemistry of the Solid State," W. E. Garner, Ed., Butterworths, London, England, 1955, p. 254.

(3) J. T. Carstensen and M. N. Musa, *J. Pharm. Sci.*, **61,** 1112 (1972).

(4) P. Pothisiri and J. T. Carstensen, *ibid.*, **64,** 1931 (1975).

(5) J. T. Carstensen and P. Pothisiri, *ibid.*, **64,** 37 (1975).

(6) J. T. Carstensen and R. C. Kothari, *ibid.*, **69,** 123 (1980).

(7) R. A. Parker, T. Karyia, J. M. Grisar, and V. Petrow, *J. Med. Chem.*, **20,** 781 (1977).

(8) R. M. Whittaker, *Rec. Trav. Chim.*, **52,** 352 (1933).

(9) M. Knudsen, *Ann. Phys.*, **28,** 999 (1909).

(10) *Ibid.*, **29,** 179 (1909).

(11) M. J. Pikal and A. L. Lukes, *J. Pharm. Sci.*, **65,** 1269 (1976).

(12) *Ibid.*, **65,** 1278 (1976).

(13) M. Davies and B. Kybett, *Trans. Faraday Soc.*, **61,** 1608 (1963).

(14) L. VanCampen, G. Zografi, and J. T. Carstensen, *Int. J. Pharm.*, **5,** 1 (1980).

## ACKNOWLEDGMENTS

Presented in part at the APhA Academy of Pharmaceutical Sciences, San Antonio meeting, November 1980.

Abstracted in part from a thesis submitted by R. Kothari to the University of Wisconsin in partial fulfillment of the Doctor of Philosophy degree requirements.

Supported in part by a research grant from Hoffmann–La Roche, Nutley, NJ 07110.

The authors thank Dr. J. Sheridan, Hoffmann–La Roche, Nutley, N.J., and Dr. M. A. Zoglio and Dr. R. A. Parker, Merrell-National Laboratories, Cincinnati, Ohio, for technical assistance.

# Mechanism of Interaction between Polyols and Aluminum Hydroxide Gel

**DHIREN N. SHAH *, JOE L. WHITE ‡, and STANLEY L. HEM *x**

Received November 21, 1980, from the **Department of Industrial and Physical Pharmacy and the* ‡*Department of Agronomy, Purdue University, West Lafayette, IN 47907.* Accepted for publication March 6, 1981.

**Abstract** □ IR spectroscopy and changes in the rate of acid neutralization were used to study the interaction between various polyols and aluminum hydroxide. Hydrogen bonding is responsible for this interaction, although structural requirements limit the polyols that interact with aluminum hydroxide. Mannitol and sorbitol, both linear polyols, interacted with sulfate-containing aluminum hydroxide gel and aluminum hydroxycarbonate gel, while inositol, a cyclic polyol, did not interact. The adsorbed polyol has the favorable effect of inhibiting the polymerization reaction that occurs on aging and the negative effect of reducing the rate of acid neutralization. Thus, the specific polyol and concentration must be carefully selected to maximize the desired effect of stabilizing the gel structure. The presence of mannitol in the reaction medium during precipitation did not significantly enhance gel structure stability, probably because the mannitol was desorbed during the washing process as a consequence of the weak adsorption forces.

**Keyphrases** □ Aluminum hydroxide—mechanism of interaction with polyols □ Polyols—mechanism of interaction with aluminum hydroxide □ Spectroscopy, IR—mechanism of interaction between polyols and aluminum hydroxide gel □ Structure stability—mechanism of interaction between polyols and aluminum hydroxide gel

The use of a polyol such as sorbitol to improve the stability of aluminum hydroxide antacid formulations, a widely followed practice, has been the object of numerous studies and patents (1–8). Although these reports demonstrated the beneficial effects of polyols, the molecular basis of the interaction has not been described. This study examined the mechanism of interaction between polyols and aluminum hydroxide gel and the factors that affect the optimum use of polyols in antacid formulations.

## EXPERIMENTAL

Aluminum hydroxycarbonate gel was obtained commercially. A sulfate-containing aluminum hydroxide gel containing 3.4% equivalent aluminum oxide (0.33 *M*) was precipitated by the reaction of aluminum sulfate and strong ammonia solution NF (NF XV) (9). To determine the effect of the presence of mannitol at the time of precipitation, a series of precipitations of a sulfate-containing aluminum hydroxide gel containing 1.5% equivalent aluminum oxide (0.147 *M*) was carried out as described but with either 0.22 or 0.588 *M* mannitol dissolved in the aluminum sulfate solution prior to precipitation. The sulfate-containing aluminum hydroxide gel was divided into two portions. One portion was washed in the usual manner with three volumes of deionized water, and the second portion was not washed. The lower concentration of equivalent aluminum oxide was required due to the limited solubility of mannitol (0.99 *M* in water) (10).

The ease of mannitol desorption from the sulfate-containing aluminum hydroxide gel was determined by preparing a suspension containing 0.22 *M* mannitol and 0.147 *M* equivalent aluminum oxide. The mixture was centrifuged at 15,000 rpm (27,000×*g*) for 30 min. The clear supernate was decanted, weighed, and assayed for mannitol by a microcolorimetric method (11). The solid phase was resuspended in double-distilled water to the original volume, and the procedure was repeated five times.

Sorbitol, mannitol, and inositol were selected for the IR study because each is a six-carbon polyol containing one hydroxide per carbon. Sorbitol and mannitol are linear, while inositol is cyclic. The deuteration procedure of Hamill and Freudenberg (12) was adopted since the polyols are water soluble, nonvolatile, and stable in aqueous solution up to 100°. Deuterium oxide (30 g) was added to 5 g of polyol, and the solution was maintained at 70° for 72 hr followed by lyophilization[1]. The preparation of deuterated sorbitol was not successful since a glass was always obtained during lyophilization (13). The IR spectra of the deuterated mannitol and deuterated inositol were compared to those of mannitol and inositol. The OH:OD frequency ratio was 1.35 for each hydroxyl band, which confirmed that deuteration had occurred (14).

The interaction between the deuterated polyols and aluminum hydroxycarbonate gel or sulfate-containing aluminum hydroxide gel was studied by preparing a suspension containing 0.50 *M* deuterated polyol and 0.33 *M* equivalent aluminum oxide. The suspensions were allowed to mix for 1 hr, and a sample was air dried. IR spectra were recorded[2] using potassium bromide pellets (1 mg of sample/300 mg of potassium bromide). The positions of the hydroxy and deuteroxy stretching bands were determined using an abscissa expansion of 5× with a wave number marker at every 10 $cm^{-1}$ and an ordinate expansion of either 1× or 10×.

The rate of acid neutralization of suspensions containing 0.50 *M* polyol and 0.33 *M* equivalent aluminum oxide was determined by pH-stat titration[3] at pH 3.0 and 25° (15) during aging at 40°. The effect of polyol concentration on the rate of acid neutralization was studied by determining the pH-stat titrigrams of a series of suspensions containing 0.098 *M* equivalent aluminum oxide and varying molar ratios of polyol. The lower concentration of equivalent aluminum oxide was necessary due to the low solubility of inositol (0.78 *M*) (10).

The soluble aluminum content of aluminum hydroxycarbonate gels containing various amounts of mannitol was determined by centrifugation at 15,000 rpm (27,000×*g*) for 30 min and measurement of the aluminum content of the supernate by atomic absorption spectroscopy[4] (16).

## RESULTS AND DISCUSSION

Amphoteric compounds such as aluminum hydroxide usually exhibit hydroxyl stretching frequencies at 3660–2900 $cm^{-1}$ (17). The hydroxyl stretching frequencies of polyols occur at 3450–3200 $cm^{-1}$ (18). An interaction between aluminum hydroxide and a polyol that involves the hydroxyls of either the aluminum hydroxide or the polyol would be difficult to study by IR spectroscopy because the hydroxyl stretching frequencies overlap. This problem is aggravated by the occurrence of hydroxyl stretching vibrations of adsorbed water in the same region. However, the interaction between deuterated polyols and aluminum hydroxide can be directly studied by IR spectroscopy since deuteroxy stretching frequencies of deuterated polyols occur between 2550 and 2370 $cm^{-1}$. Aluminum hydroxide does not exhibit any IR absorption bands in the 2600–2400-$cm^{-1}$ region. There appears to be no hydrogen–deuterium exchange between the deuterated polyols and the aluminum hydroxycarbonate gel at these experimental temperatures. Since the preparation of the potassium bromide pellets required air drying the sample, there is the question of whether the dehydration process changes the apparent nature of the interaction. The fact that no shift was observed for the inositol–aluminum hydroxide systems suggests that the shifts observed for mannitol were not an artifact.

Figure 1 shows that both the frequency and relative intensity of the deuteroxy stretching bands of deuterated mannitol are significantly altered by the aluminum hydroxycarbonate gel. The free deuteroxyl band of deuterated mannitol occurred at the highest frequency, *i.e.*, 2525 $cm^{-1}$, and the intermolecularly bonded deuteroxyl peaks occurred at the lower frequencies, *i.e.*, 2495, 2448, and 2415 $cm^{-1}$ (19, 20). Adsorption of deu-

[1] Virtis Research Equipment, Gardiner, N.Y.
[2] Model 180, Perkin-Elmer Co., Norwalk, Conn.
[3] PHM 26, TTT 11, ABU 12 (2.5 ml), TTA 3, and SBR 2, Radiometer, Copenhagen, Denmark.
[4] Model 290B, Perkin-Elmer Co., Norwalk, Conn.

0022-3549/81/1000-1101$01.00/0
© 1981, American Pharmaceutical Association

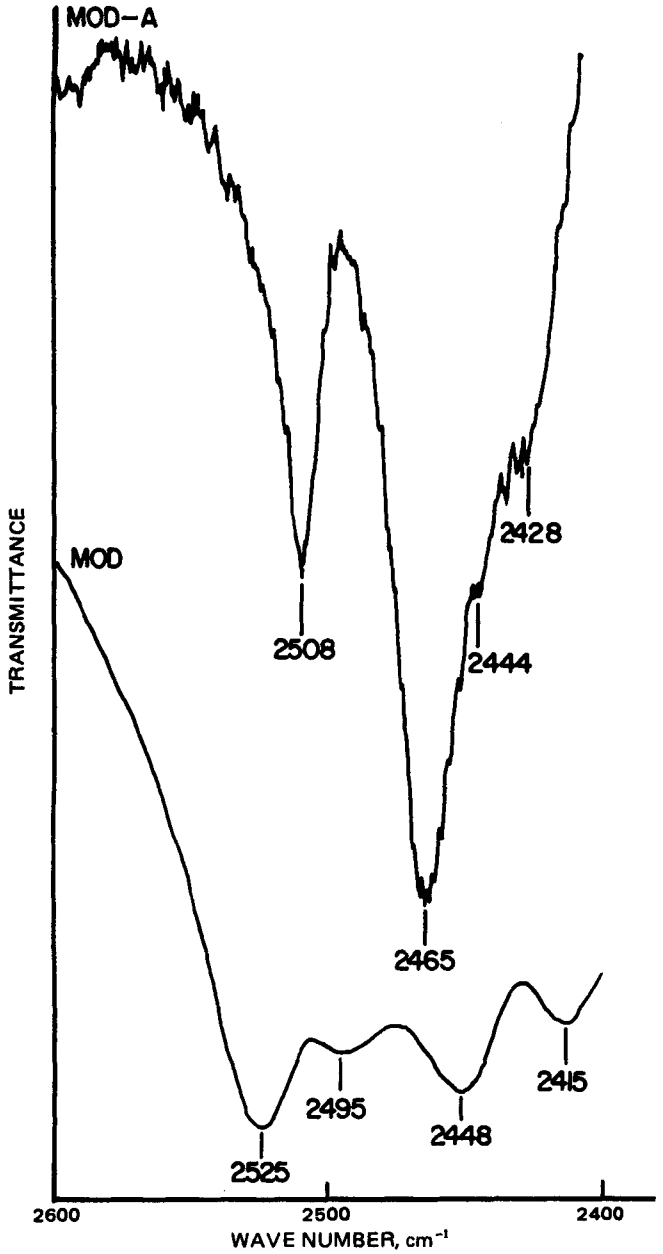


**Figure 1**—*Deuteroxy stretching bands of deuterated mannitol (MOD) and deuterated mannitol in the presence of aluminum hydroxycarbonate gel (MOD-A). Ordinate expansion is 1× for MOD and 10× for MOD-A.*

terated mannitol by aluminum hydroxycarbonate gel as a consequence of hydrogen bonding would be expected to cause the free deuteroxyl band to shift to a lower frequency, as observed in Fig. 1. The band at 2525 $cm^{-1}$ shifted to 2508 $cm^{-1}$, which suggests weak hydrogen bonding. However, the bands arising from intermolecular hydrogen bonds would be expected to shift to higher frequencies when monolayer adsorption occurs. From Fig. 1, it appears that the major intermolecular vibration at 2448 $cm^{-1}$ shifted upward to 2465 $cm^{-1}$ and that the 2415 band shifted to appear as a shoulder in the 2430-$cm^{-1}$ region of the deuterated mannitol–aluminum hydroxycarbonate gel system. Thus, the complex changes observed in the IR spectrum of deuterated mannitol in the presence of aluminum hydroxycarbonate gel reflect the adsorption of deuterated mannitol onto the aluminum hydroxycarbonate surface.

A similar change in the IR spectrum of deuterated mannitol occurred in the presence of sulfate-containing aluminum hydroxide gel with the deuteroxy stretching bands appearing at 2516, 2476, 2450, and 2414 $cm^{-1}$ as a consequence of adsorption.

The carbonate stretching bands of aluminum hydroxycarbonate at 1521 and 1467 $cm^{-1}$ were not affected by the presence of deuterated mannitol, suggesting that the coordinated carbonate is not involved in

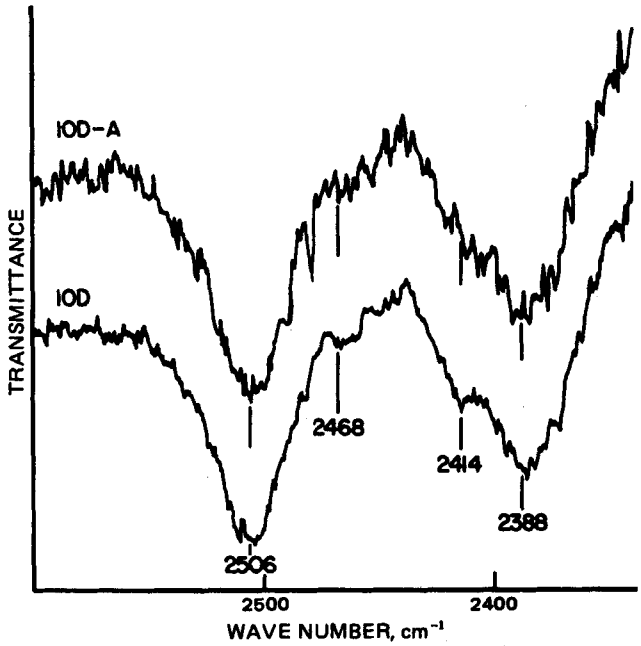


**Figure 2**—*Deuteroxy stretching bands of deuterated inositol (IOD) and deuterated inositol in the presence of aluminum hydroxycarbonate gel (IOD-A). Ordinate expansion is 10×.*

the interaction with mannitol. However, the sulfate stretching frequency of the sulfate-containing aluminum hydroxide gel shifted from 1130 to 1110 $cm^{-1}$ in the presence of deuterated mannitol. IR evidence indicates that carbonate is strongly coordinated to aluminum in aluminum hydroxycarbonate gel while sulfate is weakly coordinated to aluminum in sulfate-containing aluminum hydroxide gel (21). The apparent absence of interaction of deuterated mannitol with coordinated carbonate in aluminum hydroxycarbonate gel may be due to the strong coordination of carbonate to aluminum, which would not be substantially affected by hydrogen bonding with deuterated mannitol. The weaker sulfate–aluminum bond in sulfate-containing aluminum hydroxide gel is affected by hydrogen bonding with deuterated mannitol, and a 20 $cm^{-1}$-shift in the frequency of the sulfate bond was observed.

The hypothesis that the interaction between mannitol and aluminum hydroxide is due to hydrogen bonding is further supported by the observation that the soluble aluminum content of aluminum hydroxycarbonate gel was 0.3% and did not change when mannitol was added to the gel in a molar ratio of 0.5–4 *M* mannitol per equivalent aluminum oxide. Thus, the interaction between mannitol and aluminum hydroxycarbonate gel is not strong enough to solubilize aluminum.

The IR spectrum of deuterated inositol was not affected by the aluminum hydroxycarbonate gel (Fig. 2), thus indicating that no interaction occurs between inositol and aluminum hydroxide. However, the deuteroxy stretching frequencies of deuterated inositol (2506, 2468, 2414, and 2388 $cm^{-1}$) were all lower than those observed for deuterated mannitol (2525, 2495, 2448, and 2415 $cm^{-1}$). Thus, intermolecular association of inositol is expected to be greater than for mannitol.

IR evidence for the interaction of mannitol with aluminum hydroxide gel and the absence of an interaction with inositol is supported by the change in acid reactivity of mixtures of aluminum hydroxycarbonate gel and polyols during aging. The pH-stat titrigrams of the aluminum hydroxycarbonate gel (0.33 *M* equivalent aluminum oxide) and mixtures of the aluminum hydroxycarbonate gel containing 0.5 *M* mannitol, sorbitol, or inositol showed that all four samples reacted completely in ~60 min (Fig. 3), although the rate of acid neutralization was slightly slower in the mixtures containing sorbitol or mannitol. The pH-stat titrigrams of the aluminum hydroxycarbonate gel and the inositol-containing mixture were significantly affected by aging at 40° for 1 week. As seen in Fig. 3, ~20% of the aluminum hydroxycarbonate gel reacted very slowly at pH 3, suggesting that extensive polymerization of the aluminum hydroxy polymers had occurred (22). In contrast, the mixtures containing mannitol or sorbitol reacted completely after aging at 40° for 1 week, although the reaction rate decreased, requiring 90 min for complete neutralization. Thus, sorbitol and mannitol were effective in minimizing polymerization in aluminum hydroxycarbonate gel while inositol did not show any effect on the structural changes during aging.

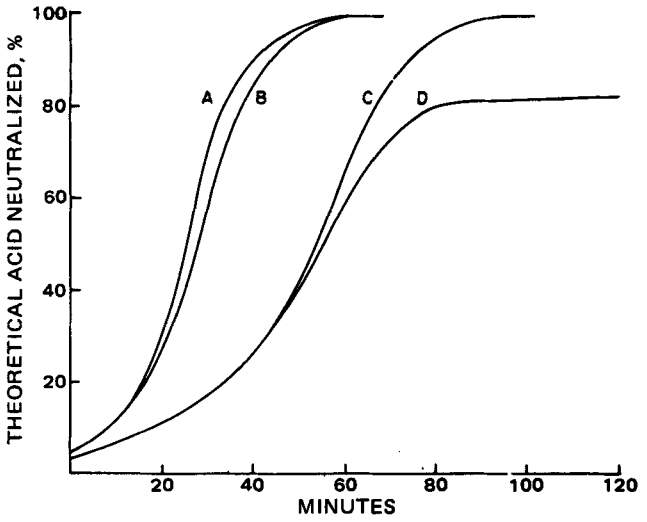


**Figure 3**—*Effect of polyols on the rate of acid neutralization of aluminum hydroxycarbonate gel (AHC). Key: A, initial pH-stat titrigram of AHC and inositol-containing AHC; B, initial pH-stat titrigram of sorbitol-containing AHC and mannitol-containing AHC; C, 1 week, 40° titrigram of sorbitol-containing AHC and mannitol-containing AHC; and D, 1 week, 40° titrigram of AHC and inositol-containing AHC.*

Therefore, the hydrogen bonding of polyols with aluminum hydroxide is an important reaction because the adsorbed polyol appears to interfere with the polymerization reaction and, consequently, the structural changes that ultimately lead to the inactive crystalline forms of aluminum hydroxide are minimized. However, the reaction between polyols and aluminum hydroxide gel is not universal. The difference in the effect of mannitol and sorbitol in comparison to inositol may be due to differences in the conformation of the polyol or in the strength of its intermolecular forces. Mannitol and sorbitol are both linear polyols, while inositol is related to cyclohexane. A linear conformation may permit more extensive hydrogen bonding to the aluminum hydroxide surface than is possible with cyclic polyols because of steric factors and the position of hydrogen

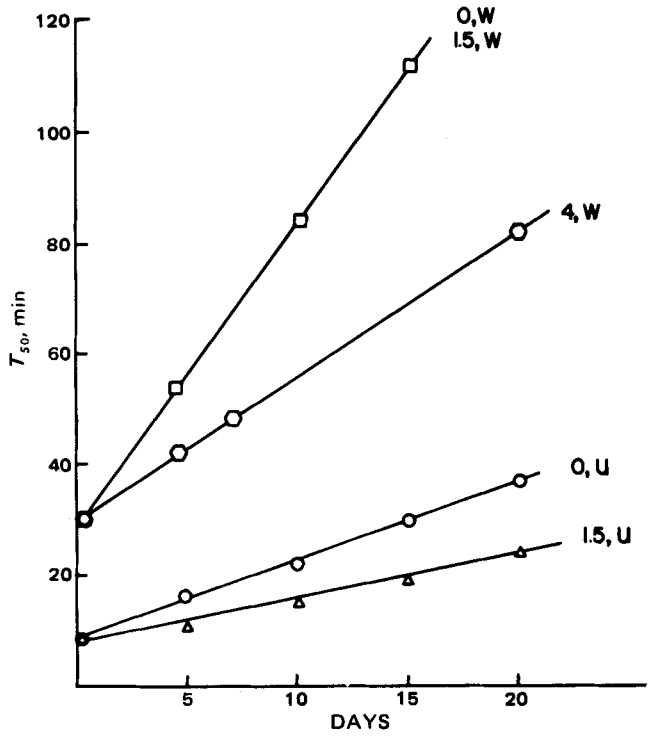


**Figure 4**—*Change in the rate of acid neutralization during aging at 25° of sulfate-containing aluminum hydroxide gels precipitated in the presence of 0, 1.5, and 4* M *mannitol per equivalent aluminum oxide. Key:* W, *washed; and* U, *unwashed.*

**Table I—Effect of Polyols on the Rate of Acid Neutralization of Aluminum Hydroxycarbonate Gel Containing 0.98 *M* Equivalent Aluminum Oxide**

| Polyol Added | $T_{50}$, min | | | |
|---|---|---|---|---|
| | 0.3 *M* polyol | 1.3 *M* polyol | 2.3 *M* polyol | 3.3 *M* polyol |
| Control[a] | 26 | 26 | 26 | 26 |
| Mannitol | 26 | 28 | 30 | 44 |
| Sorbitol | 26 | 28 | 30 | 44 |
| Inositol | 26 | 26 | 26 | 26 |

[a] Aluminum hydroxycarbonate gel.

bonding sites. The melting points of sorbitol, mannitol, and inositol are 110, 168, and 225°, respectively (10). The higher melting point and lower deuteroxy-stretching frequencies of inositol suggest the presence of strong intermolecular forces. Thus, the tendency of inositol toward self-association may be greater than the tendency toward adsorption by aluminum hydroxide.

The polyol concentration used to stabilize aluminum hydroxide must be carefully selected because the adsorbed polyol, in addition to interfering with polymerization, may also slow the rate of reaction with protons and thus reduce the rate of acid neutralization. Evidence of this effect was seen (Fig. 3) as a slight reduction in the rate of acid neutralization occurred when sorbitol or mannitol was added to the aluminum hydroxycarbonate gel. This effect is seen clearly in Table I where the rate of acid neutralization of aluminum hydroxycarbonate gel, as measured by the time required to neutralize 50% of the sample ($T_{50}$), increases in direct relationship to the concentration of mannitol or sorbitol. In the presence of high levels of mannitol or sorbitol, the $T_{50}$ increased from 26 to 44 min. In contrast, inositol did not affect the rate of acid neutralization.

Since changes in the aluminum hydroxide gel structure occur most rapidly immediately after precipitation (23), it may be advisable to incorporate a polyol in the reaction medium to achieve the maximum rate of acid neutralization. Thus, a sulfate-containing aluminum hydroxide gel was precipitated in the presence of varying amounts of mannitol. As seen in Fig. 4, the sulfate-containing aluminum hydroxide gel precipitated in the presence of a molar ratio of 1.5 *M* mannitol per equivalent aluminum oxide aged at the same rate as the control. However, the rate of loss of acid reactivity was substantially reduced when the sulfate-containing aluminum hydroxide gel was precipitated in the presence of a molar ratio of 4 *M* mannitol per equivalent aluminum oxide.

It was hypothesized, based on the hydrogen bonding mechanism indicated by the IR study, that the washing procedure removed most of the mannitol, and this hypothesis is supported by the desorption profile shown in Fig. 5. Most of the mannitol was removed by the first volume of wash water, and only ~30% of the added mannitol remained after the described washing procedure. The rate of acid neutralization of the unwashed sulfate-containing aluminum hydroxide gel was much greater

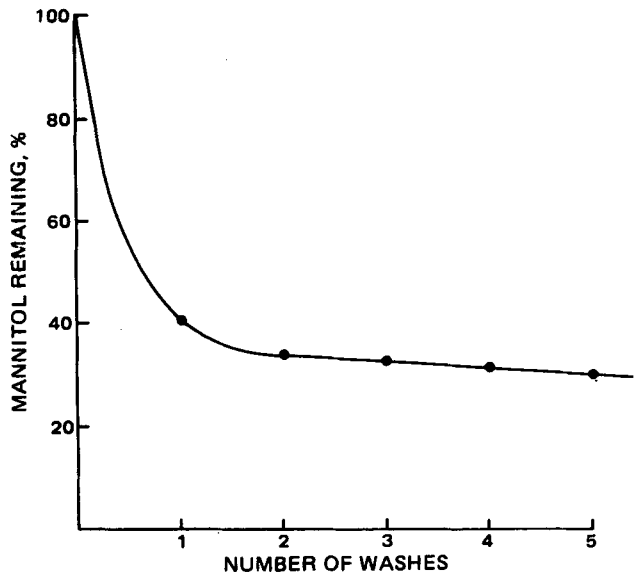


**Figure 5**—*Desorption of mannitol during washing with distilled water.*

than that of the washed portion, and the rate of loss of acid reactivity during aging was also reduced. This behavior confirms the strong stabilizing effect of anions (23). However, the unwashed portion that was precipitated in the presence of a molar ratio of 1.5 *M* mannitol per equivalent aluminum oxide showed the smallest decrease in the rate of acid neutralization during aging. The interaction between polyols and aluminum hydroxide gel apparently is too weak to recommend the incorporation of mannitol or sorbitol in the reaction medium. However, the results suggest the addition of mannitol or sorbitol immediately after washing.

## REFERENCES


(1) J. R. Gwilt, J. L. Livingstone, and A. Robertson, *J. Pharm. Pharmacol.*, **10**, 770 (1958).

(2) E. T. Hinkel, Jr., M. P. Fisher, and M. L. Tainter, *J. Am. Pharm. Assoc., Sci. Ed.*, **48**, 384 (1959).

(3) B. K. Davison and R. E. Schaffer, *J. Pharm. Pharmacol.*, **13**, 1195 (1976).

(4) S. L. Nail, J. L. White, and S. L. Hem, *J. Pharm. Sci.*, **65**, 1195 (1976).

(5) C. E. Alford, U.S. pat. 2,999,790 (1961).

(6) L. C. Greene, A. Misher, and W. E. Smith, U.S. pat. 3,591,680 (1971).

(7) R. Persson and J. Sjoergren, German pat. 1,467,767 (1968); through *Chem. Abstr.*, **73**, P38544a (1970).

(8) A. M. Rubino and J. J. Margress, U.S. pat. 4,112,072 (1978).

(9) S. L. Hem, E. J. Russo, S. M. Bahal, and R. S. Levi, *J. Pharm. Sci.*, **59**, 317 (1970).

(10) "The Merck Index," 9th ed., Merck & Co., Rahway, N.J., 1976.

(11) J. M. Bailey, *J. Lab. Clin. Med.*, **54**, 158 (1959).

(12) W. H. Hamill and W. Freudenberg, *J. Am. Chem. Soc.*, **57**, 1427 (1935).

(13) A. P. Mackenzie, *Bull. Parenter. Drug Assoc.*, **20**, 101 (1966).

(14) K. Nakanishi and P. H. Solomon, "Infrared Absorption Spectroscopy," 2nd ed., Holden-Day, San Francisco, Calif., 1977, p. 63.

(15) N. J. Kerkhof, R. K. Vanderlaan, J. L. White, and S. L. Hem, *J. Pharm. Sci.*, **66**, 1528 (1977).

(16) M. K. Wang, J. L. White, and S. L. Hem, *ibid.*, **69**, 668 (1980).

(17) Y. I. Ryskin, in "The Infrared Spectra of Minerals," V. C. Farmer, Ed., Mineralogical Society, London, England, 1974, p. 146.

(18) "Atlas of Spectral Data and Physical Constants for Organic Compounds," J. G. Grasselli, Ed., CRC Press, Cleveland, Ohio, 1973, p. B-644.

(19) K. Nakanishi and P. H. Solomon, "Infrared Absorption Spectroscopy," 2nd ed., Holden-Day, San Francisco, Calif., 1977, pp. 25–27.

(20) C. N. R. Rao, "Chemical Applications of Infrared Spectroscopy," Academic, New York, N.Y., 1963, pp. 175–180.

(21) C. J. Serna, J. L. White, and S. L. Hem, *Soil Sci. Soc. Am. Proc.*, **41**, 1009 (1977).

(22) S. L. Nail, J. L. White, and S. L. Hem, *J. Pharm. Sci.*, **65**, 1188 (1976).

(23) N. J. Kerkhof, J. L. White, and S. L. Hem, *ibid.*, **64**, 940 (1975).


## ACKNOWLEDGMENTS


This report is Journal Paper 8324, Purdue University Agricultural Experiment Station, West Lafayette, IN 47907.


# Effect of Age and Gender on Disposition of Temazepam


**MARCIA DIVOLL, DAVID J. GREENBLATT ˣ, JEROLD S. HARMATZ, and RICHARD I. SHADER**



Received December 12, 1980, from the *Division of Clinical Pharmacology, Departments of Psychiatry and Medicine, Tufts University School of Medicine and New England Medical Center Hospital, Boston, MA 02111.* Accepted for publication March 5, 1981.



**Abstract** □ Thirty-two male and female volunteers, 24–84 years of age, ingested single 30-mg doses of temazepam, a 3-hydroxy-1,4-benzodiazepine derivative used as a hypnotic agent. Kinetics of total and unbound temazepam were determined from multiple plasma temazepam concentrations measured during 48 hr after the dose. The temazepam elimination half-life ranged from 8 to 38 hr and was longer in women than in men (16.8 *versus* 12.3 hr, $p < 0.05$). Likewise, clearance of total temazepam (assuming complete absorption) was higher in men than in women (1.35 *versus* 1.02 ml/min/kg, $p < 0.025$). Neither half-life nor clearance was significantly related to age. The volume of distribution of total temazepam (mean 1.40 liters/kg) was unrelated to age or gender. Temazepam was extensively protein bound, with a mean free fraction of 2.6% (range 1.7–3.4%). The free fraction increased with age ($r = 0.45$, $p = 0.01$), partly due to the inverse relation of the free fraction to plasma albumin concentration ($r = -0.34$, $p = 0.06$) and the age-related decline in plasma albumin ($r = -0.49$, $p < 0.005$). After correction for individual differences in binding, clearance of unbound temazepam in men was higher than in women (50.5 *versus* 39.7 ml/min/kg, $0.05 < p < 0.1$), and it tended to decline with age in both sexes ($r = -0.44$ and $-0.43$, respectively, $p = 0.1$).



**Keyphrases** □ Temazepam—effect of age and gender on disposition and elimination □ Tranquilizers—temazepam, effect of age and gender on disposition and elimination □ Hypnotics—temazepam, effect of age and gender on disposition and elimination


Temazepam (I) is a 3-hydroxy-1,4-benzodiazepine derivative used as a hypnotic agent. The major metabolic pathway of temazepam in humans involves conjugation with glucuronic acid at position 3, yielding a water-soluble glucuronide metabolite that is excreted in the urine (1). Since the aging process may alter drug pharmacokinetics, this study was undertaken to assess the disposition and elimination of temazepam in young and elderly volunteers.

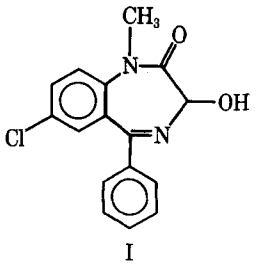


I

## EXPERIMENTAL

**Subjects**—Thirty-two healthy male and female volunteers, 24–84 years of age, participated after giving written informed consent. They were divided into four groups of young male, young female, elderly male, and elderly female subjects (Table I). All young subjects were free of any identifiable medical disease and were taking no medications. Elderly individuals were ambulatory, active, and in general good health. Five elderly subjects were taking medications for the treatment of cardiovascular disease that was clinically stable and compensated.




*0022-3549/81/1000-1104$01.00/0*


*© 1981, American Pharmaceutical Association*

than that of the washed portion, and the rate of loss of acid reactivity during aging was also reduced. This behavior confirms the strong stabilizing effect of anions (23). However, the unwashed portion that was precipitated in the presence of a molar ratio of 1.5 *M* mannitol per equivalent aluminum oxide showed the smallest decrease in the rate of acid neutralization during aging. The interaction between polyols and aluminum hydroxide gel apparently is too weak to recommend the incorporation of mannitol or sorbitol in the reaction medium. However, the results suggest the addition of mannitol or sorbitol immediately after washing.

## REFERENCES


(1) J. R. Gwilt, J. L. Livingstone, and A. Robertson, *J. Pharm. Pharmacol.*, **10**, 770 (1958).

(2) E. T. Hinkel, Jr., M. P. Fisher, and M. L. Tainter, *J. Am. Pharm. Assoc., Sci. Ed.*, **48**, 384 (1959).

(3) B. K. Davison and R. E. Schaffer, *J. Pharm. Pharmacol.*, **13**, 1195 (1976).

(4) S. L. Nail, J. L. White, and S. L. Hem, *J. Pharm. Sci.*, **65**, 1195 (1976).

(5) C. E. Alford, U.S. pat. 2,999,790 (1961).

(6) L. C. Greene, A. Misher, and W. E. Smith, U.S. pat. 3,591,680 (1971).

(7) R. Persson and J. Sjoergren, German pat. 1,467,767 (1968); through *Chem. Abstr.*, **73**, P38544a (1970).

(8) A. M. Rubino and J. J. Margress, U.S. pat. 4,112,072 (1978).

(9) S. L. Hem, E. J. Russo, S. M. Bahal, and R. S. Levi, *J. Pharm. Sci.*, **59**, 317 (1970).

(10) "The Merck Index," 9th ed., Merck & Co., Rahway, N.J., 1976.

(11) J. M. Bailey, *J. Lab. Clin. Med.*, **54**, 158 (1959).

(12) W. H. Hamill and W. Freudenberg, *J. Am. Chem. Soc.*, **57**, 1427 (1935).

(13) A. P. Mackenzie, *Bull. Parenter. Drug Assoc.*, **20**, 101 (1966).

(14) K. Nakanishi and P. H. Solomon, "Infrared Absorption Spectroscopy," 2nd ed., Holden-Day, San Francisco, Calif., 1977, p. 63.

(15) N. J. Kerkhof, R. K. Vanderlaan, J. L. White, and S. L. Hem, *J. Pharm. Sci.*, **66**, 1528 (1977).

(16) M. K. Wang, J. L. White, and S. L. Hem, *ibid.*, **69**, 668 (1980).

(17) Y. I. Ryskin, in "The Infrared Spectra of Minerals," V. C. Farmer, Ed., Mineralogical Society, London, England, 1974, p. 146.

(18) "Atlas of Spectral Data and Physical Constants for Organic Compounds," J. G. Grasselli, Ed., CRC Press, Cleveland, Ohio, 1973, p. B-644.

(19) K. Nakanishi and P. H. Solomon, "Infrared Absorption Spectroscopy," 2nd ed., Holden-Day, San Francisco, Calif., 1977, pp. 25–27.

(20) C. N. R. Rao, "Chemical Applications of Infrared Spectroscopy," Academic, New York, N.Y., 1963, pp. 175–180.

(21) C. J. Serna, J. L. White, and S. L. Hem, *Soil Sci. Soc. Am. Proc.*, **41**, 1009 (1977).

(22) S. L. Nail, J. L. White, and S. L. Hem, *J. Pharm. Sci.*, **65**, 1188 (1976).

(23) N. J. Kerkhof, J. L. White, and S. L. Hem, *ibid.*, **64**, 940 (1975).


## ACKNOWLEDGMENTS


This report is Journal Paper 8324, Purdue University Agricultural Experiment Station, West Lafayette, IN 47907.


# Effect of Age and Gender on Disposition of Temazepam


**MARCIA DIVOLL, DAVID J. GREENBLATT ˣ, JEROLD S. HARMATZ, and RICHARD I. SHADER**



Received December 12, 1980, from the *Division of Clinical Pharmacology, Departments of Psychiatry and Medicine, Tufts University School of Medicine and New England Medical Center Hospital, Boston, MA 02111.* Accepted for publication March 5, 1981.



**Abstract** □ Thirty-two male and female volunteers, 24–84 years of age, ingested single 30-mg doses of temazepam, a 3-hydroxy-1,4-benzodiazepine derivative used as a hypnotic agent. Kinetics of total and unbound temazepam were determined from multiple plasma temazepam concentrations measured during 48 hr after the dose. The temazepam elimination half-life ranged from 8 to 38 hr and was longer in women than in men (16.8 *versus* 12.3 hr, $p < 0.05$). Likewise, clearance of total temazepam (assuming complete absorption) was higher in men than in women (1.35 *versus* 1.02 ml/min/kg, $p < 0.025$). Neither half-life nor clearance was significantly related to age. The volume of distribution of total temazepam (mean 1.40 liters/kg) was unrelated to age or gender. Temazepam was extensively protein bound, with a mean free fraction of 2.6% (range 1.7–3.4%). The free fraction increased with age ($r = 0.45$, $p = 0.01$), partly due to the inverse relation of the free fraction to plasma albumin concentration ($r = -0.34$, $p = 0.06$) and the age-related decline in plasma albumin ($r = -0.49$, $p < 0.005$). After correction for individual differences in binding, clearance of unbound temazepam in men was higher than in women (50.5 *versus* 39.7 ml/min/kg, $0.05 < p < 0.1$), and it tended to decline with age in both sexes ($r = -0.44$ and $-0.43$, respectively, $p = 0.1$).



**Keyphrases** □ Temazepam—effect of age and gender on disposition and elimination □ Tranquilizers—temazepam, effect of age and gender on disposition and elimination □ Hypnotics—temazepam, effect of age and gender on disposition and elimination


Temazepam (I) is a 3-hydroxy-1,4-benzodiazepine derivative used as a hypnotic agent. The major metabolic pathway of temazepam in humans involves conjugation with glucuronic acid at position 3, yielding a water-soluble glucuronide metabolite that is excreted in the urine (1). Since the aging process may alter drug pharmacokinetics, this study was undertaken to assess the disposition and elimination of temazepam in young and elderly volunteers.

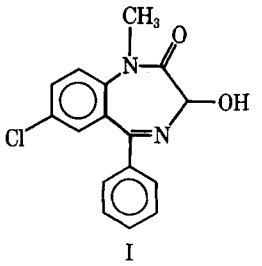


I

## EXPERIMENTAL

**Subjects**—Thirty-two healthy male and female volunteers, 24–84 years of age, participated after giving written informed consent. They were divided into four groups of young male, young female, elderly male, and elderly female subjects (Table I). All young subjects were free of any identifiable medical disease and were taking no medications. Elderly individuals were ambulatory, active, and in general good health. Five elderly subjects were taking medications for the treatment of cardiovascular disease that was clinically stable and compensated.




*0022-3549/81/1000-1104$01.00/0*


*© 1981, American Pharmaceutical Association*

**Table I—Subject Characteristics and Pharmacokinetics of Temazepam**

| Parameter | Mean Values (Range) Young Male ($n$ = 7) | Young Female ($n$ = 7) | Elderly Male ($n$ = 8) | Elderly Female ($n$ = 10) |
|---|---|---|---|---|
| Subject characteristics | | | | |
| Age, years | 29.0 (24–39) | 29.7 (28–33) | 69.1 (60.0–76.0) | 69.8 (62.0–84.0) |
| Weight, kg | 71.4 (63.6–79.5) | 61.4 (52.7–70.5) | 77.2 (64.5–90.9) | 61.8 (52.7–75.0) |
| Smoking, cigarettes/day | 8.2 (0–20) | 8.4 (0–28) | 0 | 5.0 (0–20) |
| Albumin, g/100 ml | 4.7[a] (4.5–4.9) | 4.5 (3.8–5.3) | 4.1[a] (3.6–4.7) | 4.3 (3.7–4.8) |
| Kinetics of total (free plus bound) temazepam | | | | |
| Peak plasma temazepam concentration, ng/ml | 430.0 (293–585) | 483.0 (359–754) | 371.0 (222–687) | 409.0 (251–610) |
| Weight-normalized peak concentration, $\mu g/ml \times kg$ | 30.3 (21.4–38.6) | 29.4 (22.8–45.3) | 28.5 (15.9–56.2) | 25.0 (13.2–32.5) |
| Time of peak concentration, hours after dose | 2.18 (0.75–4.0) | 2.75 (0.75–4.0) | 1.84 (0.75–4.0) | 4.65 (1.0–12.0) |
| Elimination half-life, hr | 12.8 (9.4–23.3) | 16.2 (10.1–25.3) | 11.9 (8.3–14.2) | 17.2 (8.9–37.9) |
| Volume of distribution, liters/kg | 1.53 (0.67–2.8) | 1.40 (1.20–1.76) | 1.32 (0.89–2.08) | 1.39 (0.68–2.30) |
| Clearance, ml/min/kg | 1.36 (0.82–1.72) | 1.10 (0.59–1.54) | 1.35 (0.73–2.45) | 0.97 (0.70–1.48) |
| Kinetics of unbound temazepam | | | | |
| Free fraction, % | 2.54 (1.66–4.18) | 2.30 (1.74–2.93) | 3.12 (2.25–3.89) | 2.75 (2.21–3.40) |
| Unbound $V_d$, liters/kg | 68.0 (32.2–168.7) | 61.5 (46.7–81.6) | 43.2 (23.7–65.4) | 50.8 (30.8–91.3) |
| Unbound clearance, ml/min/kg | 57.2 (37.2–83.7) | 46.8 (27.4–70.1) | 44.7 (19.8–81.7) | 35.4 (24.0–45.1) |

[a] $p < 0.005$ for young *versus* elderly of the same sex.

**Procedure**—After an overnight fast, subjects ingested a single 30-mg capsule of temazepam[1] with 100–200 ml of tap water. They remained fasting until 3 hr after drug ingestion. Venous blood samples were drawn into heparinized tubes from an indwelling butterfly cannula (kept patent by flushing with dilute heparin solution) or by venipuncture prior to the dose and at the following postdosage times: 0.25, 0.5, 0.75, 1.0, 1.5, 2, 2.5, 3, 4, 6, 8, 12, 24, 30, 36, and 48 hr. Plasma was separated and stored at −20° until the time of assay.

**Sample Analysis**—Temazepam concentrations in all plasma samples were determined by electron-capture GLC after addition of a benzodiazepine analog (3-hydroxyprazepam) as the internal standard (2).

The free fraction (percent unbound) was determined by equilibrium dialysis at 37° (3) of a single sample drawn in the nonfasting state. Since heparin may influence the free fraction of benzodiazepines, no subject received heparin systemically for at least 24 hr prior to sampling. Duplicate 2-ml plasma samples were spiked to contain 500 ng/ml of unlabeled temazepam and 20 nCi/ml of tritiated temazepam (62.5 μCi/mg). The radioactivity was determined in a liquid scintillation counter[2]. The mean coefficient of variation between duplicate samples was <6%. Binding was independent of the total plasma temazepam concentration over a range of 160–4160 ng/ml.

**Pharmacokinetic and Statistical Analysis**—Each set of data points was analyzed by iterative nonlinear least-squares regression techniques (4). Data points were fitted to the following two functions:

$$C = B(e^{-\beta t} - e^{-k_a t}) \quad \text{(Eq. 1)}$$

$$C = -(A + B)e^{-k_a t} + Ae^{-\alpha t} + Be^{-\beta t} \quad \text{(Eq. 2)}$$

where $C$ is the plasma temazepam concentration at time $t$ after dosage; $A$ and $B$ are hybrid intercept terms; and $k_a$, $\alpha$, and $\beta$ are hybrid exponents representing phases of drug absorption, distribution, and elimination, respectively. When necessary, both equations were modified by addition of a lag time prior to the start of first-order absorption. The choice between Eqs. 1 and 2 as functions of best fit was determined by scatter of actual data points about the fitted function and by comparison of weighted residual errors (5).

The hybrid exponent $\beta$ was used to calculate the apparent elimination half-life ($t_{1/2\beta}$). The area under the 48-hr plasma concentration curve was calculated using the trapezoidal rule; to this value was added the extrapolated residual area from the final concentration point to infinity, yielding the total area under the plasma concentration curve ($AUC$). The extrapolated area accounted for an average of 9.8% (range 2.6–36.8%) of the total $AUC$.

When neither Eq. 1 nor 2 provided an adequate fit of the data, $t_{1/2\beta}$ was calculated using the terminal log-linear portion of the plasma concentration curve. The total $AUC$ was calculated as described.

Although absolute bioavailability of temazepam is not known, previous studies of lorazepam, a structurally similar 3-hydroxy-1,4-benzodiazepine derivative, indicated that absolute systemic availability of orally administered drug is close to 100% (6, 7). Accordingly, it was assumed that the entire 30-mg temazepam dose reached the systemic circulation (100% bioavailability). Total clearance was calculated as the administered dose divided by the $AUC$, and the apparent volume of distribution ($V_d$) using the area method was calculated as total clearance divided by $\beta$. The volume of distribution and clearance of unbound temazepam were calculated as the quotient of total $V_d$ or clearance divided by the unbound fraction.

## RESULTS

Peak plasma temazepam concentrations ranged from 222 to 754 ng/ml. Peak concentrations were not significantly influenced by age, although they tended to be higher in women then in men and lower in elderly than in young of both sexes (Table I). After normalization for weight, peak plasma concentrations were similar among groups. Temazepam was slowly absorbed, with the time of peak concentrations ranging from 0.75 to 12.0 hr after dosage. The mean time of peak concentration among the four groups ranged from 1.8 to 4.7 hr after dosage and was not significantly influenced by age or gender. Iterative analysis provided satisfactory solutions in only 11 of the 32 subjects (Fig. 1).

The $V_d$ value for temazepam ranged from 0.7 to 2.3 liters/kg. Mean values for the four groups (1.32–1.53 liters/kg) were very close regardless of age or sex.

Within sexes, age was not significantly related to temazepam half-life or clearance (Figs. 2 and 3). However, $t_{1/2\beta}$ was significantly longer in women (mean 16.8 hr) than in men (12.3 hr) regardless of age ($p < 0.05$). Likewise, clearance of total temazepam was lower in women than in men regardless of age (1.02 *versus* 1.35 ml/min/kg, $p < 0.025$).

The free fraction of temazepam ranged from 1.67 to 4.18% and increased significantly with age ($r = 0.45$, $p < 0.02$) (Fig. 4). Elderly of both

[1] Restoril, Sandoz, East Hanover, N.J.
[2] Beckman Instruments.

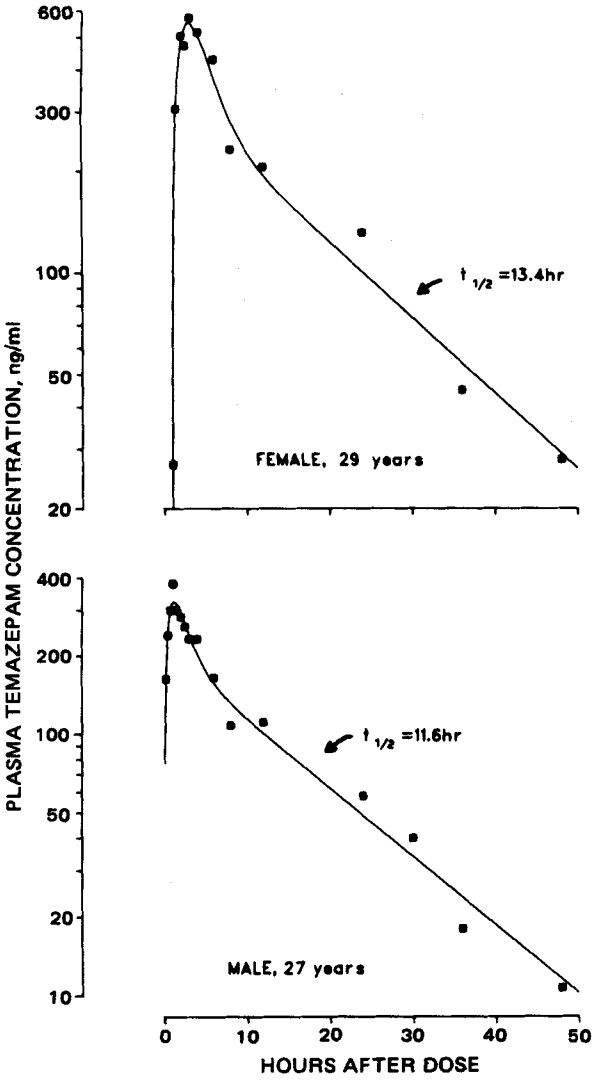


**Figure 1**—*Plasma temazepam concentrations in two representative subjects who displayed first-order absorption. Solid lines are pharmacokinetic functions determined by nonlinear least-squares regression analysis.*

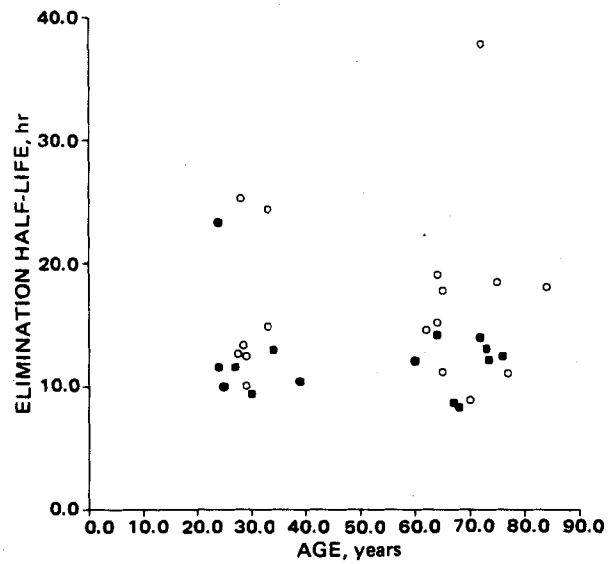


**Figure 2**—*Relation of age to temazepam elimination half-life in males and females. Key:* ■, *male* (r = −0.17); *and* O, *female* (r = 0.11).

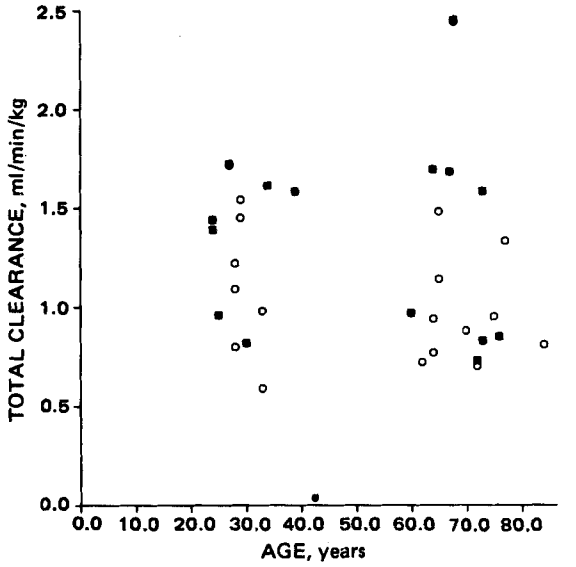


**Figure 3**—*Relation of age to clearance of total temazepam in males and females. Key:* ■, *male* (r = −0.04); *and* O, *female* (r = −0.23).

sexes had a higher free fraction than did the young subjects. The increased free fraction of temazepam in the elderly was partly explained by plasma albumin concentrations, which declined significantly with age ($r = -0.49$, $p < 0.01$).

Values of unbound $V_d$ were lower in the elderly than in the young subjects of both sexes, but the differences were not significant (Table I). Clearance of unbound temazepam declined with age in both sexes (Table I and Fig. 5), although differences did not reach statistical significance. As in the case of clearance of total temazepam, unbound clearance was higher in men than in women (50.5 *versus* 39.7 ml/min/kg, $0.05 < p < 0.1$).

## DISCUSSION

Previous studies with benzodiazepines that undergo oxidative biotransformation (such as chlordiazepoxide, diazepam, and desmethyldiazepam) suggest that metabolic clearance may be impaired among the elderly, particularly in elderly males (8–13). However, for benzodiazepines that undergo glucuronide conjugation (such as oxazepam and lorazepam), the aging process has minimal, if any, effect on metabolic disposition (6, 14–16).

In the present study, the absorption of temazepam from the GI tract was relatively slow. The time of peak concentration averaged 3 hr after dosage and was not significantly influenced by age or sex.

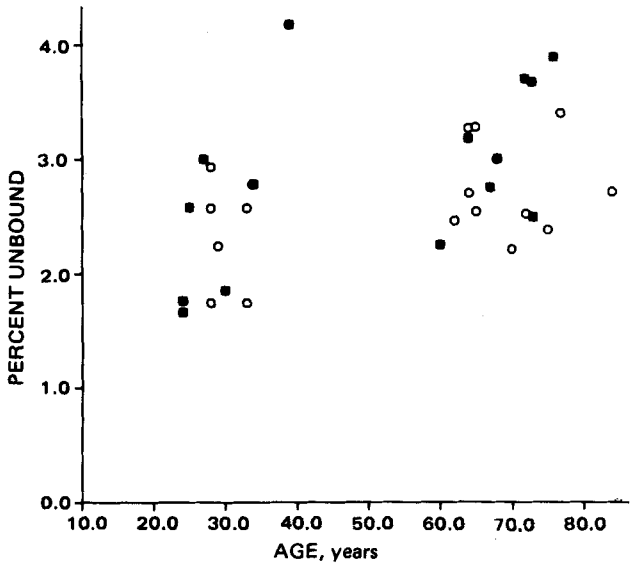


**Figure 4**—*Relation of age to temazepam protein binding in males and females. Key:* ■, *male* (r = 0.53); *and* O, *female* (r = 0.43).

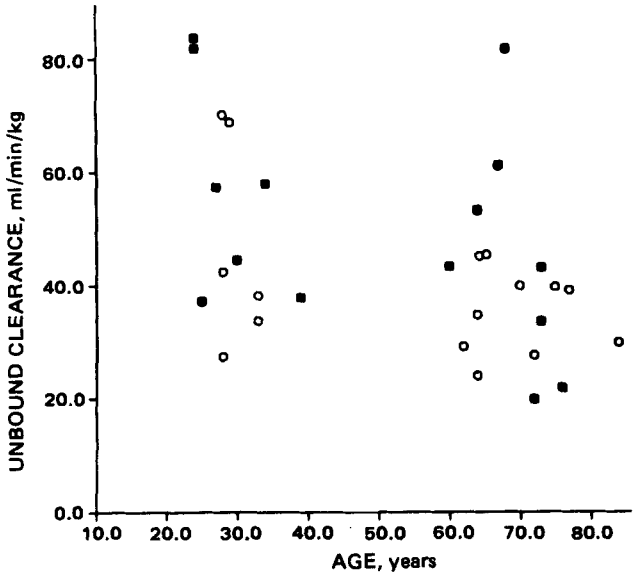


**Figure 5**—*Relation of age to clearance of unbound temazepam in males and females. Key: ■, male (r = −0.43); and ○, female (r = −0.44).*

The apparent elimination half-life of temazepam was somewhat longer than suggested by previous reports (17, 18). The mean value of $t_{1/2\beta}$ was 14.7 hr (range of 8–38 hr). Women had longer $t_{1/2\beta}$ times than men regardless of age. An essentially identical relation of gender to $t_{1/2\beta}$ was observed in a previous study of oxazepam (16).

The relation of clearance of total temazepam to age and sex also was very similar to that observed with oxazepam. Temazepam clearance was higher in men than in women and was essentially uninfluenced by age. However, the effect of age on clearance of unbound temazepam was partly obscured by an age-related increase in the free fraction. After correction for individual differences in temazepam protein binding, unbound clearance was reduced, but not significantly, in the elderly of both sexes, although it was still higher in men than in women of corresponding age. Neither age nor sex significantly influenced the volume of distribution of total or unbound temazepam, but unbound $V_d$ values tended to be smaller in the elderly than in the young of both sexes.

The effect of age and sex on temazepam distribution and clearance closely resembles the findings of previous studies of oxazepam and lorazepam, two other 3-hydroxy-1,4-benzodiazepines biotransformed by glucuronide conjugation (6, 16). The results contrast strikingly with studies of benzodiazepines transformed by oxidative pathways such as chlordiazepoxide, diazepam, and desmethyldiazepam. Clearance of these compounds declines with increasing age, and the extent of distribution increases with age. For diazepam and desmethyldiazepam, the age-related decline in clearance is more striking in men than in women (8, 13). Distribution of these two compounds is related to sex as well as age, with larger $V_d$ values associated both with increasing age and female sex.

Thus, the relation of age to benzodiazepine disposition is not easily generalized since it may be dependent on the metabolic pathway of the drug in question as well as the gender composition of the study population.

## REFERENCES

(1) H. J. Schwarz, *Br. J. Clin. Pharmacol.*, **8**, 23S (1979).

(2) M. Divoll and D. J. Greenblatt, *J. Chromatogr.*, **222**, 125 (1981).

(3) E. Woo and D. J. Greenblatt, *J. Pharm. Sci.*, **68**, 466 (1979).

(4) D. J. Greenblatt, M. D. Allen, D. S. MacLaughlin, D. H. Huffman, J. S. Harmatz, and R. I. Shader, *J. Pharmacokinet. Biopharm.*, **7**, 159 (1979).

(5) H. G. Boxenbaum, S. Riegelman, and R. M. Elashoff, *ibid.*, **2**, 123 (1974).

(6) D. J. Greenblatt, M. D. Allen, A. Locniskar, J. S. Harmatz, and R. I. Shader, *Clin. Pharmacol. Ther.*, **26**, 103 (1979).

(7) D. J. Greenblatt, R. I. Shader, K. Franke, D. S. MacLaughlin, J. S. Harmatz, M. Divoll, A. Werner, and E. Woo, *J. Pharm. Sci.*, **68**, 57 (1979).

(8) D. J. Greenblatt, M. D. Allen, J. S. Harmatz, and R. I. Shader, *Clin. Pharmacol. Ther.*, **27**, 301 (1980).

(9) J. Kanto, M. Maenpaa, R. Mantyla, R. Sellman, and E. Valovirta, *Anesthesiology*, **51**, 154 (1979).

(10) R. K. Roberts, G. R. Wilkinson, R. A. Branch, and S. Schenker, *Gastroenterology*, **75**, 479 (1978).

(11) R. I. Shader, D. J. Greenblatt, J. S. Harmatz, K. Franke, and J. Koch-Weser, *J. Clin. Pharmacol.*, **17**, 709 (1977).

(12) U. Klotz and P. Muller-Seydlitz, *Br. J. Clin. Pharmacol.*, **7**, 119 (1979).

(13) M. D. Allen, D. J. Greenblatt, J. S. Harmatz, and R. I. Shader, *Clin. Pharmacol. Ther.*, **28**, 196 (1980).

(14) H. J. Shull, G. R. Wilkinson, R. Johnson, and S. Schenker, *Ann. Intern. Med.*, **84**, 420 (1976).

(15) J. W. Kraus, P. V. Desmond, J. P. Marshall, R. F. Johnson, S. Schenker, and G. R. Wilkinson, *Clin. Pharmacol. Ther.*, **24**, 411 (1978).

(16) D. J. Greenblatt, M. Divoll, J. S. Harmatz, and R. I. Shader, *J. Pharmacol. Exp. Ther.*, **215**, 86 (1980).

(17) L. M. Fuccella, *Br. J. Clin. Pharmacol.*, **8**, 31S (1979).

(18) P. Bittencourt, A. Richens, P. A. Toseland, J. F. C. Wicks, and A. N. Latham, *ibid.*, **8**, 37S (1979).

## ACKNOWLEDGMENTS

Supported in part by Grant MH-34223 from the U.S. Public Health Service, by Grant 77-611 from the Foundations' Fund for Research in Psychiatry, and by a grant-in-aid from Sandoz, East Hanover, N.J.

The authors are grateful for the assistance of Lawrence J. Moschitto, Lornna L. Jason, and Dr. Dean S. MacLaughlin.

# Pharmacokinetics of Captopril in Dogs and Monkeys

**S. M. SINGHVI ˣ, A. E. PETERSON, J. J. ROSS, Jr., J. M. SHAW, G. R. KEIM, and B. H. MIGDALOF**

Received September 12, 1980, from the *Departments of Drug Metabolism and Toxicology, Squibb Institute for Medical Research, New Brunswick, NJ 08903.* Accepted for publication March 4, 1981.

**Abstract** □ [$^{14}$C]Captopril was given as a priming dose, followed by constant intravenous infusion for 4 or 6 hr, to three anesthetized dogs and three anesthetized monkeys. Blood, urine, and bile samples were collected during and after drug infusion. Pharmacokinetic evaluations were carried out exclusively on data obtained for unchanged captopril. The average total body clearance ($Cl_T$) and the renal clearance ($Cl_R$) of captopril, in milliliters per kilogram per hour, were 605 and 341 in the dog and 1135 and 944 in the monkey. The biliary clearance of captopril was negligible in both species. The greater difference between the $Cl_R$ and $Cl_T$ values in the dog compared to that in the monkey was the result of more extensive metabolism of captopril by the dog. Since almost all of the radioactive dose was recovered in urine in both species, captopril and its metabolites were almost exclusively eliminated by the kidneys. One primary reason that body and renal clearance values of captopril were much greater in the monkey than in the dog was that the net tubular secretion of captopril was about three times greater in the monkey (82%) than in the dog (28%). The volume of distribution of captopril was higher in the monkey (3.6 liters/kg) than in the dog (2.5 liters/kg); the volume of the central compartment was about the same (0.5 liter/kg) for both species. The terminal half-life value was slightly higher in the dog (2.8 hr) than in the monkey (2.2 hr).

**Keyphrases** □ Captopril—pharmacokinetics in dogs and monkeys using radiolabeled drug, continuous intravenous infusion □ Pharmacokinetics—captopril in dogs and monkeys, continuous intravenous infusion □ Antihypertensives—pharmacokinetics of captopril in dogs and monkeys, continuous intravenous infusion

Captopril, 1-[(2*S*)-3-mercapto-2-methyl-1-oxopropyl]-L-proline, is a potent, orally active, specific inhibitor of the enzyme that catalyzes the conversion of angiotensin I to angiotensin II (1). It also was shown clinically to be an effective antihypertensive agent (2–4). This study determined the pharmacokinetics of captopril in dogs and monkeys using [$^{14}$C]captopril.

## BACKGROUND

Captopril, a thiol compound, is chemically unstable in biological samples and undergoes rapid autoxidation to form the disulfide dimer of the parent compound and other unidentified products (5, 6). To prevent or minimize such processes, captopril was converted to its *N*-ethylmaleimide derivative in blood, urine, and bile during or immediately after sample collection (5, 6).

In previous blood level studies in animals and humans, captopril was administered orally, and difficulty was encountered in estimating its biological half-life and other pharmacokinetic parameters. This difficulty was partly because of the lack of a sensitive specific assay and partly because of an apparent nonlinearity in the terminal portions of semilogarithmic plots of blood levels *versus* time. It was anticipated that efforts to obtain pharmacokinetic parameters following a single intravenous bolus dose of captopril would have been hampered by the same problems. Consequently, to obtain better pharmacokinetic information, it was decided to study captopril pharmacokinetics in dogs and monkeys during steady-state conditions achieved by continuous intravenous infusion.

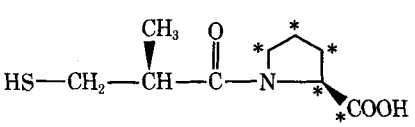

I(* = sites labeled with carbon 14)

## EXPERIMENTAL

**Materials**—[$^{14}$C]Captopril was universally labeled with carbon 14 in the proline moiety. Radiochemical and chemical purities were each ~98%; ~2% of [$^{14}$C]captopril disulfide was present as an impurity. A nonionic surfactant[1], a tissue solubilizer[2], and *N*-ethylmaleimide[3] were used. Other chemicals were reagent grade and were obtained commercially.

**Animals**—Three male adult purebred beagles (9–11 kg) and three male adult rhesus monkeys (6–8 kg) were used.

**Procedure**—The study design was identical for dogs and monkeys. Each animal was fasted overnight, hydrated orally with water (25 ml/kg for dogs; 15 ml/kg for monkeys), anesthetized with intravenous pentobarbital sodium (30 mg/kg), intubated with an endotracheal catheter, and maintained under anesthesia by constant intravenous infusion of pentobarbital sodium (2.7 mg/kg/hr).

For determination of creatinine clearance, a priming dose of 60 mg of creatinine/kg was injected intravenously followed by 18 mg/kg/hr in the infusate. The infusate also contained phosphate-buffered 5% mannitol (pH 7.4) to maintain adequate urine flow. After the start of the infusion, the animal was surgically prepared for the collection of bile and urine. The cystic duct was ligated, and the common bile duct was cannulated near its junction with the duodenum; then both ureters were cannulated for urine collection. Urine and bile were collected for consecutive 30-min periods, and a blood sample was withdrawn at the midpoint of each collection period. After two consecutive control periods, [$^{14}$C]captopril priming and constant infusion doses were started simultaneously.

For the first dog and monkey, the priming and infusion doses (Tables I and II) were selected using data obtained from preliminary studies; the infusions were continued for 4 hr. Subsequently, the doses were determined based on results from the first animal of each species such that the steady-state concentrations of unchanged captopril in the blood of the next two animals of each species were approximately the same as the first (0.2 μg/ml). The doses for the last two dogs and monkeys were as follows: a priming dose of 0.4 mg/kg (dog) and 1.0 mg/kg (monkey) over a 1-min period and constant infusion of 0.1 mg/kg/hr (dog) and 0.2 mg/kg/hr (monkey) for 6 hr. [$^{14}$C]Captopril was infused using a constant infusion pump[4]. After the end of the infusion of [$^{14}$C]captopril, the 5% mannitol infusion was continued, and the animal was kept under anesthesia for an additional 8 hr. The 5% mannitol infusate contained creatinine and pentobarbital sodium and was infused throughout the study using another constant infusion pump[4].

Urine and bile were collected every 30 min during [$^{14}$C]captopril infusion, for 3 hr after the end of infusion, and then every 1 hr for the next 5 hr. A blood sample was withdrawn at the midpoint of each collection. All samples were treated with *N*-ethylmaleimide and analyzed for total radioactivity and unchanged captopril.

**Analytical Methods**—A thin-layer radiochromatographic assay for captopril in blood and urine was described previously (5, 6). Bile and urine samples were analyzed in an identical manner. This method is quite specific for unchanged captopril and has a limit of detection of ~10 ng/ml. The scintillation cocktail of Anderson and McClure (7) was used to count blood and bile samples. The tissue solubilizer[2] was added to solubilize whole blood and bile samples. Urine samples were counted directly in Bray's liquid scintillation counting solution[5].

All samples were counted in liquid scintillation spectrometers[6]. These counters were regularly normalized for valid utilization of automatic external standardization ratios for determination of disintergrations per minute. Known standards were counted to verify the accuracy of the instruments. Counting efficiency was determined using automatic ex-

[1] Triton X-114, Ruger Chemical Co., Irvington, N.J.
[2] Soluene-350, Packard Instrument Co., Downers Grove, Ill.
[3] Eastman Kodak, Rochester, N.Y.
[4] Sigmamotor, Middleport, N.Y.
[5] National Diagnostics, Parsippany, N.J.
[6] Packard Tri-Carb liquid scintillation spectrometers, model 2425 or 3380, Packard Instrument Co.



*0022-3549/81/1000-1108$01.00/0*
*© 1981, American Pharmaceutical Association*

**Table I—Pharmacokinetic Parameters Obtained in Anesthetized Dogs during and after Infusion of [$^{14}$C]Captopril**

| Pharmacokinetic Parameter | Infusion Data[a] Animal H8-113 | H6-117 | H8-23 | Average | Postinfusion Data Animal H8-113 | H6-117 | H8-23 | Average | Overall Average, ±*SD* |
|---|---|---|---|---|---|---|---|---|---|
| Steady-state blood level, μg/ml | 0.20 | 0.17 | 0.21 | 0.19 | — | — | — | — | 0.19 ± 0.02 |
| Priming dose, mg/kg | 1.37 | 0.42 | 0.44 | — | — | — | — | — | — |
| Infusion dose, mg/kg/hr | 0.10 | 0.12 | 0.12 | — | — | — | — | — | — |
| Body clearance, ml/kg/hr | 516 | 718 | 545 | 593 | 560 | 754 | 540 | 618 | 605 ± 103 |
| Renal clearance, ml/kg/hr | 364 | 444 | 233 | 347 | 343[b] | 428[b] | 235[b] | 335 | 341 ± 91 |
| Biliary clearance, ml/kg/hr | 0.40 | 0.41 | 0.55 | 0.45 | — | — | — | — | 0.45 ± 0.08 |
| Creatinine clearance, ml/kg/hr | 282 | 328 | 148 | 253 | — | — | — | — | 253 ± 94 |
| Renal clearance/body clearance | 0.71 | 0.62 | 0.43 | 0.59 | 0.61 | 0.57 | 0.44 | 0.54 | 0.56 ± 0.11 |
| Renal clearance/creatinine clearance | 1.29 | 1.35 | 1.57 | 1.40 | — | — | — | — | 1.40 ± 0.15 |
| Net tubular secretion, %[c] | 22 | 26 | 36 | 28 | — | — | — | — | 28 ± 7 |
| Apparent volume of distribution, liters/kg | 4.06[d] | 2.41 | 2.86 | 2.63 | 2.18 | 2.59 | 2.22 | 2.33 | 2.45 ± 0.28 |
| Volume of central compartment, liters/kg | — | — | — | — | 0.63 | 0.43 | 0.40 | 0.49 | 0.49 ± 0.13 |
| Half-life ($t_{1/2}\beta$), hr | 5.44[d] | 2.33 | 3.61 | 2.97 | 2.71 | 2.38 | 2.84 | 2.64 | 2.77 ± 0.51 |
| $\alpha$, hr$^{-1}$ | — | — | — | — | 1.52 | 2.60 | 2.62 | 2.25 | 2.25 ± 0.63 |
| $\beta$, hr$^{-1}$ | — | — | — | — | 0.26 | 0.29 | 0.24 | 0.26 | 0.26 ± 0.03 |
| $k_{12}$, hr$^{-1}$ | — | — | — | — | 0.45 | 0.71 | 1.03 | 0.73 | 0.73 ± 0.29 |
| $k_{21}$, hr$^{-1}$ | — | — | — | — | 0.44 | 0.43 | 0.47 | 0.45 | 0.45 ± 0.02 |
| $k_{el}$, hr$^{-1}$ | — | — | — | — | 0.89 | 1.75 | 1.37 | 1.34 | 1.34 ± 0.43 |
| $k_e$, hr$^{-1}$ | — | — | — | — | 0.54 | 1.00 | 0.59 | 0.71 | 0.71 ± 0.25 |

[a] Mean of the last three (Dog H8-113) or eight (Dogs H6-117 and H8-23) consecutive 30-min infusion periods, considered to be at steady-state. [b] Calculated using all data obtained during and after the infusion of [$^{14}$C]captopril (see Fig. 2). [c] Represents minimum net tubular secretion since captopril protein binding was assumed to be zero (see text for details). [d] These values were considered to be unreliable because true steady-state was not achieved in this dog; not included in the average.

**Table II—Pharmacokinetic Parameters Obtained in Anesthetized Monkeys during and after Infusion of [$^{14}$C]Captopril**

| Pharmacokinetic Parameter | Infusion Data[a] Animal 5-31 | 8-7 | 8-1 | Average | Postinfusion Data Animal 5-31 | 8-7 | 8-1 | Average | Overall Average ±*SD* |
|---|---|---|---|---|---|---|---|---|---|
| Steady-state blood level, μg/ml | 0.22 | 0.16 | 0.27 | 0.22 | — | — | — | — | 0.22 ± 0.06 |
| Priming dose, mg/kg | 2.52 | 0.93 | 0.97 | — | — | — | — | — | — |
| Infusion dose, mg/kg/hr | 0.20 | 0.20 | 0.22 | — | — | — | — | — | — |
| Body clearance, ml/kg/hr | 915 | 1316 | 823 | 1018 | 1262 | 1551 | 941 | 1251 | 1135 ± 285 |
| Renal clearance, ml/kg/hr | 997 | 1174 | 672 | 948 | 1017[b] | 1150[b] | 653[b] | 940 | 944 ± 229 |
| Biliary clearance, ml/kg/hr | 0.20 | 0.16 | 0.18 | 0.18 | — | — | — | — | 0.18 ± 0.02 |
| Creatinine clearance, ml/kg/hr | 200 | 197 | 114 | 170 | — | — | — | — | 170 ± 49 |
| Renal clearance/body clearance | 1.09 | 0.89 | 0.82 | 0.93 | 0.81 | 0.74 | 0.69 | 0.75 | 0.83 ± 0.14 |
| Renal clearance/creatinine clearance | 4.98 | 5.84 | 6.04 | 5.56 | — | — | — | — | 5.56 ± 0.56 |
| Net tubular secretion, %[c] | 80 | 83 | 83 | 82 | — | — | — | — | 82 ± 1.7 |
| Apparent volume of distribution, liters/kg | 3.92 | 2.55 | 2.52 | 3.00 | 4.67 | 5.19 | 2.91 | 4.26 | 3.63 ± 1.14 |
| Volume of central compartment, liters/kg | — | — | — | — | 0.70 | 0.50 | 0.34 | 0.51 | 0.51 ± 0.18 |
| Half-life ($t_{1/2}\beta$), hr | 2.97 | 1.33 | 2.12 | 2.14 | 2.57 | 2.32 | 2.15 | 2.35 | 2.24. ± 0.55 |
| $\alpha$, hr$^{-1}$ | — | — | — | — | 2.66 | 3.64 | 3.91 | 3.40 | 3.40 ± 0.66 |
| $\beta$, hr$^{-1}$ | — | — | — | — | 0.27 | 0.30 | 0.32 | 0.30 | 0.30 ± 0.03 |
| $k_{12}$, hr$^{-1}$ | — | — | — | — | 0.73 | 0.49 | 1.03 | 0.75 | 0.75 ± 0.27 |
| $k_{21}$, hr$^{-1}$ | — | — | — | — | 0.40 | 0.35 | 0.46 | 0.40 | 0.40 ± 0.06 |
| $k_{el}$, hr$^{-1}$ | — | — | — | — | 1.80 | 3.10 | 2.74 | 2.55 | 2.55 ± 0.67 |
| $k_e$, hr$^{-1}$ | — | — | — | — | 1.45 | 2.30 | 1.92 | 1.89 | 1.89 ± 0.21 |

[a] Mean of the last four (Monkey 5-31) or six (Monkeys 8-7 and 8-1) consecutive 30-min infusion periods, considered to be at steady-state. [b] Calculated using all data obtained during and after the infusion of [$^{14}$C]Captopril (see Fig. 2). [c] Represents minimum net tubular secretion since captopril protein binding was assumed to be zero (see text for details).

ternal standardization. The color and chemical quenching of the samples were corrected by using appropriately prepared quench curves. All samples were prepared and analyzed in duplicate and were counted for a minimum of 3000 counts, which resulted in a counting error of <1.8%.

**Data Analysis**—Pharmacokinetic parameters for captopril were calculated from data obtained during the infusion and postinfusion phases of the study, using relationships given in the *Appendix*.

## RESULTS

In all animals, blood pressure, heart rate, and respiration rate were monitored; no major changes were observed in any of these parameters during the infusion of [$^{14}$C]captopril. The creatinine clearance, a measure of the glomerular filtration rate, also was found to be reasonably constant during the infusion period.

Pharmacokinetic evaluations were carried out exclusively on data obtained for unchanged captopril in blood, urine, and bile during the steady-state period and the postinfusion phase. A typical semilogarithmic plot of concentrations of unchanged captopril in blood *versus* time is shown in Fig. 1. In all animals, the blood levels followed a similar pattern as a function of time; the levels were initially high due to the priming dose, steady-state levels were reached toward the end of the infusion period, and the blood levels declined biexponentially during the postinfusion period. This biexponential decline of blood captopril concentrations indicates that the drug exhibits characteristics of a two-compartment open model, with elimination occurring from the central compartment.

The priming and infusion doses of [$^{14}$C]captopril given to the first dog (H8-113) and the first monkey (5-31) were selected using limited data available from previous blood level studies, which were not designed to estimate pharmacokinetic parameters. Because of the relatively short duration of infusion and deficiencies in the priming and infusion doses initially selected, true steady-state conditions were either just approached or attained for only a limited time in the first dog and first monkey. Based on the information derived from these two animals, the priming and infusion doses of [$^{14}$C]captopril were modified to attain rapid steady-state conditions in an additional two dogs (H6-117 and H8-23) and two monkeys (8-7 and 8-1).

For the latter animals, the infusion period for [$^{14}$C]captopril was extended from the 4 hr used in the earlier study to 6 hr to maintain steady-state conditions for a longer period. As a result, good steady-state conditions were attained for the last two dogs and two monkeys. Most results for these animals were comparable to those obtained for the first animal of each species. Therefore, with few exceptions, the results of the various pharmacokinetic parameters were averaged for all three animals

**Table III—Excretion of Total Radioactivity and Unchanged Captopril in the Urine and Bile of Anesthetized Dogs and Monkeys following Infusion of [$^{14}$C]Captopril**

| Excretion | Component | Percent of Dose Excreted[a] | | | | | | | |
|---|---|---|---|---|---|---|---|---|---|
| | | Dog | | | | Monkey | | | |
| | | H8-113 | H6-117 | H8-23 | Average ± *SD* | 5-31 | 8-7 | 8-1 | Average ± *SD* |
| Urine | Total radioactivity | 92.8 | 95.2 | 83.8 | 90.6 ± 6.0 | 91.7 | 99.9 | 90.6 | 94.1 ± 5.1 |
| | Captopril | 58.1 | 61.3 | 39.4 | 52.9 ± 11.8 | 80.6 | 86.7 | 75.8 | 81.0 ± 5.5 |
| Bile | Total radioactivity | 0.78 | 2.65 | 3.45 | 2.29 ± 1.37 | 0.31 | 0.49 | 0.47 | 0.42 ± 0.10 |
| | Captopril | 0.04 | 0.05 | 0.09 | 0.06 ± 0.03 | 0.01 | 0.02 | 0.02 | 0.017 ± 0.006 |
| Total (urine and bile) | Total radioactivity | 93.6 | 97.9 | 87.3 | 92.9 ± 5.3 | 92.0 | 100.4 | 91.1 | 94.5 ± 5.1 |
| | Captopril | 58.1 | 61.4 | 39.5 | 53.0 ± 11.8 | 80.6 | 86.7 | 75.8 | 81.0 ± 5.5 |

[a] Cumulative excretion for entire duration of the study (4- or 6-hr infusion period plus 8-hr postinfusion).

(Tables I and II). Since pharmacokinetic parameters calculated from both steady-state and postinfusion data were comparable for each animal, overall averages of all the parameters also were calculated.

Average clearance values (milliliters per kilogram per hour) obtained in the dog were 605 (body clearance, $Cl_T$), 341 (renal clearance, $Cl_R$), and 0.45 (biliary clearance, $Cl_B$) (Table I). Average creatinine clearance ($Cl_{Cr}$) was 253 ml/kg/hr. A comparison of the $Cl_R$ and $Cl_{Cr}$ values indicated an average minimum net tubular secretion of captopril of 28% in the dog. Net tubular secretion values were calculated by assuming no reversible (physicochemical) binding of captopril to plasma proteins and, therefore, represent minimum estimates. Since *N*-ethylmaleimide used for stabilizing captopril hemolyzes blood, plasma could not be obtained for determination of protein binding. However, *in vitro* studies done in this laboratory showed that, while captopril forms chemically reversible covalent bonds with plasma proteins, its physicochemical (noncovalent) binding to plasma proteins is negligible (8). The average volume of distribution ($V_d$) in the dog was 2.5 liters/kg, while the volume of the central compartment ($V_1$) averaged ~0.5 liter/kg. The average terminal half-life ($t_{1/2}\beta$) in blood in the dog was ~2.8 hr (Table I).

In the monkey, the average clearance values, in milliliters per kilogram per hour were 1135 ($Cl_T$), 944 ($Cl_R$), 0.2 ($Cl_B$), and 170 ($Cl_{Cr}$) (Table II). With the assumption of negligible physicochemical binding of captopril to plasma proteins, a comparison of $Cl_R$ and $Cl_{Cr}$ indicated an average minimum net tubular secretion of 82%. The average $V_d$ and $V_1$ values were 3.6 and 0.5 liters/kg, respectively. The average $t_{1/2}\beta$ value in the monkey was 2.2 hr (Table II).

Renal clearance ($Cl_R$) values for all animals also were calculated by using all data obtained and plotting the urinary excretion rate of unchanged captopril *versus* the blood concentration of captopril at the midpoint of urinary collection periods. A typical plot is shown in Fig. 2. These data provided excellent linearity, as indicated by correlation coefficient ($r^2$) values of >0.97 for all animals. The slopes of these lines represented the renal clearance values, and the intercept values were close to the expected value of zero. The values obtained for $Cl_R$ by this method were similar to those obtained using only the steady-state data (Tables I and II).

The excretion data (Table III) showed that averages of 91% (dog) and 94% (monkey) of the administered dose were recovered in urine, while biliary excretion accounted for only 2.3% (dog) and 0.4% (monkey) of the administered dose.

## DISCUSSION

The disposition of captopril in humans after oral administration of [$^{14}$C]captopril was reported recently (5); at the time the present study in animals was conducted, captopril pharmacokinetics in humans following intravenous administration of the drug had not been determined. Based on the disposition data obtained in humans after oral administration of [$^{14}$C]captopril, there was a lack of correlation between the pharmacokinetics and pharmacodynamics of the drug (5). Although unchanged captopril was not detected in the blood after 6 hr, other studies in hypertensive patients had demonstrated good control of blood pressure with a three-times-daily dosing regimen (5). Thus, this study in dogs and monkeys was initiated to gain a better understanding of captopril pharmacokinetics and to provide information for properly designing pharmacokinetic studies in humans.

Captopril appears to exhibit characteristics of a two-compartment open model in both the dog and monkey. In both species, the values for biliary clearance were negligible. Although the hepatic clearance of captopril could not be directly calculated, negligible biliary clearance of captopril indicated that the difference between the total body clearance and renal clearance of captopril in both species was primarily due to the metabolic

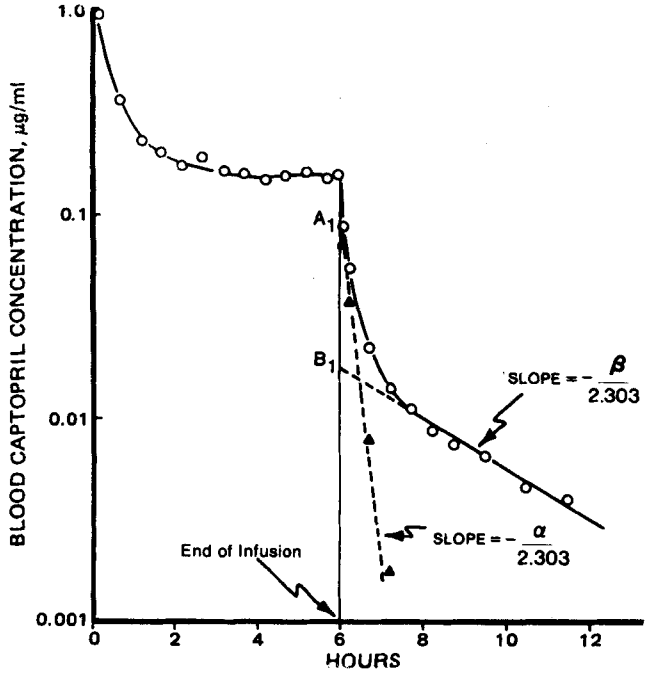


**Figure 1**—*Concentration of unchanged captopril in blood during and after infusion of [$^{14}$C]captopril into an anesthetized monkey (8-7).*

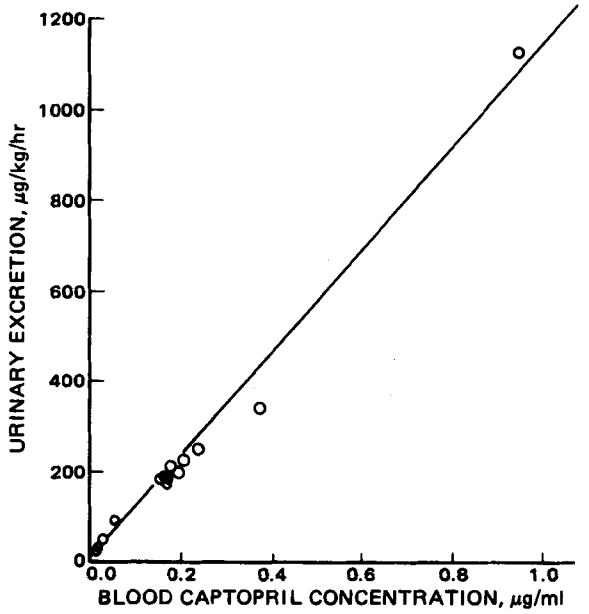


**Figure 2**—*Renal clearance of captopril in an anesthetized monkey (8-7) during and after infusion of [$^{14}$C]captopril. Slope ($Cl_R$) = 1150 ml/kg/hr, y-intercept = 1.8 μg/kg/hr, and correlation coefficient ($r^2$) = 0.990.*

clearance of captopril. Since almost all of the radioactive dose was recovered in urine in both species, captopril and its metabolites were almost exclusively eliminated by the kidneys.

A comparison of the disposition data in humans (5) and in dogs and monkeys (this study) indicated that the majority of the radioactivity excreted in urine in these species was unchanged captopril. In addition, the major elimination route of captopril in humans was *via* the kidneys. Based on a comparison of fecal excretion of radioactivity in normal subjects (5) and in patients with impaired renal function (9) after oral administration of [$^{14}$C]captopril, nonrenal elimination of captopril and its metabolites did not increase under conditions of reduced kidney function. Thus, to avoid any toxic side effects from accumulation of captopril or its metabolites, smaller doses or longer intervals between doses of captopril may be necessary in patients with renal impairment.

The volume of distribution of captopril was higher in the monkey (3.6 liters/kg) than in the dog (2.5 liters/kg); the volume of the central compartment ($V_1$) was about the same (0.5 liter/kg) for both species. The values for distribution rate constants ($k_{12}$ and $k_{21}$) were comparable for both species. However, the overall elimination rate constant ($k_{el}$) in the monkey (2.6 $hr^{-1}$) was about twice that found in the dog (1.3 $hr^{-1}$) due to the higher renal clearance in the monkey. The renal excretion rate constant ($k_e$) in the monkey (1.9 $hr^{-1}$) was also more than twice that found in the dog (0.7 $hr^{-1}$).

The body and renal clearance values of captopril in the monkey were much greater than the corresponding values for the dog, primarily because the net tubular secretion of captopril was three times higher in the monkey than in the dog. The volumes of distribution of captopril in the dog (2.5 liters/kg) and monkey (3.6 liters/kg) indicated extensive distribution of captopril throughout the body.

A comparison of the urinary excretion data between the dog and monkey (Table III) indicated that, while the average amount of total radioactivity excreted in urine during the entire experiment was approximately the same for both animals, the average amount of unchanged captopril excreted in urine was much higher in the monkey. In fact, the average ratios of $Cl_R$ and $Cl_T$ in the dog (0.56, Table I) and monkey (0.83, Table II) were in excellent agreement with the fractions of the administered dose excreted in urine as unchanged drug in these animals (0.53 and 0.81, respectively) (Table III). Thus, the greater difference between $Cl_R$ and $Cl_T$ values in the dog compared to that in the monkey can be explained by the fact that a relatively larger fraction of a given dose of captopril was eliminated by a nonrenal mechanism (metabolism) in the dog than in the monkey. Biliary excretion accounted for only 2.3% (dog) and 0.4% (monkey) of the dose (Table III). Average fecal excretion of radioactivity in unanesthetized dogs and monkeys after single intravenous doses of [$^{14}$C]captopril (2.5 mg/kg) was also <2%[7]. These data indicate that the low biliary excretion observed in anesthetized animals was not due to the administration of a general anesthetic. Thus, in both species, the major route for elimination from the body was *via* the kidneys.

The terminal half-life value was slightly higher in the dog than in the monkey. Problems in estimating the captopril half-life were encountered in previous studies in which apparent curvilinearity of semilogarithmic plots of blood concentrations *versus* time had been observed after oral administration of captopril in humans and animals (5, 10). This curvilinearity was tentatively attributed to formation of reversible disulfide bonds of captopril with proteins. By using a steady-state design for the present study, meaningful estimates of the half-life and other pharmacokinetic parameters were obtained, and the problems of curvilinearity in the semilogarithmic plots of blood concentrations *versus* time encountered after administration of single captopril doses were avoided.

## APPENDIX

**Total body clearance ($Cl_T$)** is the volume of blood cleared of drug per unit time, which is a measure of the rate at which infused compound is cleared or removed from the blood by all mechanisms:

$$Cl_T = \frac{\text{infusion rate}}{\text{blood concentration}} \qquad \text{(Eq. A1)}$$

**Renal clearance ($Cl_R$)** is the volume of blood cleared of drug by the kidney and excreted in the urine per unit time:

$$Cl_R = \frac{\text{renal excretion rate of compound}}{\text{blood concentration}} \qquad \text{(Eq. A2)}$$

Equation A2 is also used to calculate the creatinine clearance (a measure of glomerular filtration rate) when creatinine is infused along with the drug.

**Biliary clearance ($Cl_B$)** is the volume of blood cleared of drug by the bile per unit time:

$$Cl_B = \frac{\text{biliary excretion rate}}{\text{blood concentration}} \qquad \text{(Eq. A3)}$$

**Renal clearance/body clearance** reflects the contribution of renal excretion to the body clearance of drug. The deviation from 1.0 reflects the contribution of nonrenal mechanisms to the body clearance of the compound.

**Renal clearance ($Cl_R$)/creatinine clearance ($Cl_{Cr}$)** reflects the mode of drug excretion by the kidney. A ratio of <1.0 suggests glomerular filtration and net tubular reabsorption. A ratio of >1.0 suggests glomerular filtration and net tubular secretion.

**Apparent volume of distribution ($V_d$)** is the theoretical volume of water occupied by drug in the body, assuming uniform distribution and a concentration equal to that found in the blood:

$$V_d = \frac{\text{total compound in body}}{\text{blood concentration}} \qquad \text{(Eq. A4)}$$

**Terminal half-life ($t_{1/2}\beta$)** is an estimate of the time required by all mechanisms to clear half of the drug from the body:

$$t_{1/2}\beta = \frac{\text{volume of distribution}}{\text{body clearance}} \times 0.693 \qquad \text{(Eq. A5)}$$

Postinfusion blood concentration data can also be used to calculate some parameters calculated by using steady-state data as well as some parameters that cannot be calculated by using data obtained during the infusion period. The following relationships were used to calculate various pharmacokinetic parameters (with the assumption that the compound shows characteristics of a two-compartment open model):

$$C = A \exp(-\alpha t') + B \exp(-\beta t') \qquad \text{(Eq. A6)}$$

$$A = \frac{A_1 \alpha T}{1 - \exp(-\alpha T)} \qquad \text{(Eq. A7)}$$

$$B = \frac{B_1 \beta T}{1 - \exp(-\beta T)} \qquad \text{(Eq. A8)}$$

$$k_{21} = \frac{A\beta + B\alpha}{A + B} \qquad \text{(Eq. A9)}$$

$$k_{el} = \frac{\alpha\beta}{k_{21}} \qquad \text{(Eq. A10)}$$

$$k_{12} = \alpha + \beta - k_{21} - k_{el} \qquad \text{(Eq. A11)}$$

$$V_1 = \frac{\text{total dose infused}}{A + B} \qquad \text{(Eq. A12)}$$

$$V_d = \frac{\text{total dose infused}}{AUC \times \beta} \qquad \text{(Eq. A13)}$$

$$Cl_T = V_1 \times k_{el} = V_d\beta \qquad \text{(Eq. A14)}$$

$$k_e = \frac{Cl_R}{V_1} \qquad \text{(Eq. A15)}$$

$$Cl_T = Cl_R + Cl_H + Cl_0 \qquad \text{(Eq. A16)}$$

$$Cl_H = Cl_B + Cl_M \qquad \text{(Eq. A17)}$$

$$t' = t - T \qquad \text{(Eq. A18)}$$

where $A_1$ and $B_1$ are intercepts on the concentration axis at the point when the infusion is stopped (Fig. 1) and:

$C$ = concentration of drug at any time during the postinfusion period
$T$ = time of infusion
$t$ = time since the start of the infusion
$V_1$ = volume of the central compartment
$V_d$ = apparent volume of distribution
$Cl_H$ = hepatic clearance
$Cl_M$ = metabolic clearance
$Cl_0$ = clearance by other unknown routes
$AUC$ = area under the blood concentration *versus* time curve
$k_{12}$ and $k_{21}$ = distribution rate constants
$k_{el}$ = overall elimination rate constant
$k_e$ = renal excretion rate constant

[7] S. M. Singhvi and K. J. Kripalani, unpublished data.

Renal or biliary clearance can be calculated by plotting the rate of urinary excretion or biliary excretion against the blood concentration at the midpoint of each urinary or biliary collection, respectively. The resulting slopes represent each corresponding clearance value (Fig. 2 illustrates the calculation of renal clearance). However, $Cl_H$, $Cl_M$, and $Cl_0$ cannot be calculated by conventional methods.

Percent net tubular secretion can be calculated using the following relationship:

$$\text{percent net tubular secretion} = \frac{Cl_R - Cl_{cr} \times \text{fraction of unbound compound}}{Cl_R} \times 100 \qquad \text{(Eq. A19)}$$

## REFERENCES


(1) R. K. Ferguson, H. R. Brunner, G. A. Turini, H. Gavras, and D. N. McKinstry, *Lancet*, **1**, 775 (1977).

(2) D. B. Case, S. A. Atlas, J. H. Laragh, J. E. Sealey, P. A. Sullivan, and D. N. McKinstry, *Progr. Cardiovasc. Dis.*, **21**, 195 (1978).

(3) H. Gavras, H. R. Brunner, G. A. Turini, G. R. Kershaw, C. P. Tifft, S. Cuttelod, I. Gavras, R. A. Vukovich, and D. N. McKinstry, *N. Engl. J. Med.*, **298**, 991 (1978).

(4) H. R. Brunner, H. Gavras, B. Waeber, G. R. Kershaw, G. A. Turini, R. A. Vukovich, and D. N. McKinstry, *Ann. Intern. Med.*, **90**, 19 (1979).

(5) K. J. Kripalani, D. N. McKinstry, S. M. Singhvi, D. A. Willard, R. A. Vukovich, and B. H. Migdalof, *Clin. Pharmacol. Ther.*, **27**, 636 (1980).

(6) B. H. Migdalof, S. M. Singhvi, and K. J. Kripalani, *J. Liq. Chromatogr.*, **3**, 857 (1980).

(7) L. E. Anderson and W. A. McClure, *Anal. Biochem.*, **51**, 173 (1973).

(8) K. Wong, S. J. Lan, and B. H. Migdalof, *Pharmacologist*, **21**, 173 (1979).

(9) A. J. Rommel, A. M. Pierides, and A. F. Heald, *Clin. Pharmacol. Ther.*, **27**, 282 (1980).

(10) S. M. Singhvi, A. E. Peterson, J. M. Shaw, and B. H. Migdalof, *Fed. Proc. Fed. Am. Soc. Exp. Biol.*, **39**, 538 (1980).


## ACKNOWLEDGMENTS


The authors gratefully acknowledge the technical assistance of Mr. C. J. Mondi and Mr. R. J. Ratoff and the editorial assistance of Dr. J. Dreyfuss and Dr. P. L. Sibley. The synthesis of radiolabeled captopril was carried out by Mr. P. Egli.


# Quantitation of Daunorubicin, Doxorubicin, and Their Aglycones by Ion-Pair Reversed-Phase Chromatography


**A. CAROL HANEKE ˣ, J. CRAWFORD, and A. ASZALOS**



Received January 23, 1981, from the *Food and Drug Administration, National Center for Antibiotics Analysis, Washington, DC 20204.* Accepted for publication March 9, 1981.



**Abstract** □ A fast and sensitive high-pressure liquid chromatographic method was developed for the quantitation of doxorubicin, daunorubicin, and their aglycones in pharmaceutical preparations. Because its higher pH extends column life while permitting determination of impurities, this system represents an improvement over previously published methods. It utilizes a $C_{18}$ bonded silica gel column and a solvent system consisting of methanol–0.01 *M* monobasic ammonium phosphate aqueous solution (65:35) at pH 4.0 and 1600 psi of pressure. The accuracy of the doxorubicin and daunorubicin determinations, expressed as the coefficient of variation, is 1.65 and 1.27%, respectively. The aglycones can be determined with a precision of <1.3%.



**Keyphrases** □ Doxorubicin—high-pressure liquid chromatographic assay, quantitation of impurities □ Daunorubicin—high-pressure liquid chromatographic assay, quantitation of impurities □ High-pressure liquid chromatography—quantitation of doxorubicin, daunorubicin, and their aglycones □ Antibiotics—quantitation of doxorubicin, daunorubicin, and their aglycones by high-pressure liquid chromatography


Doxorubicin (adriamycin) is an anthracycline antibiotic (I) consisting of the tetracyclic quinoid aglycone doxorubicinone (adriamycinone) in a glycosidic linkage to the amino sugar daunosamine (1, 2). Doxorubicin has been shown to be effective against various human neoplasms (3, 4). Pharmaceutical preparations of doxorubicin contain several impurities such as daunorubicin, daunorubicinone, and doxorubicinone, as well as other minor contaminants. Some of these impurities, particularly daunorubicin and daunorubicinone, are present because doxorubicin is prepared from daunorubicin by chemical synthesis (5), and the parent compound and its impurities are carried through to the product during the manufacturing process.

Daunorubicin (II) is a recently approved drug used in the treatment of acute leukemia and certain solid tumors in humans (6, 7). Daunorubicin preparations contain impurities such as daunorubicinone, which may be carried through the isolation process of the drug from the fermentation broth (8). It is important that the potency of both doxorubicin and daunorubicin be determined because clinical treatment relies on an accurate dosage schedule (9). It is equally important to determine the impurities in these pharmaceutical preparations, particularly the aglycone content, because these impurities are mutagenic and have no antitumor activity (10).

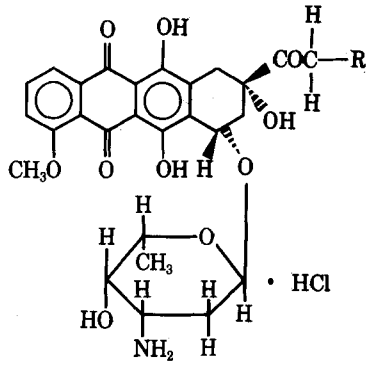

I: R = OH
II: R = H




*0022-3549/81/1000-1112$01.00/0*



*© 1981, American Pharmaceutical Association*

Renal or biliary clearance can be calculated by plotting the rate of urinary excretion or biliary excretion against the blood concentration at the midpoint of each urinary or biliary collection, respectively. The resulting slopes represent each corresponding clearance value (Fig. 2 illustrates the calculation of renal clearance). However, $Cl_H$, $Cl_M$, and $Cl_0$ cannot be calculated by conventional methods.

Percent net tubular secretion can be calculated using the following relationship:

$$\text{percent net tubular secretion} = \frac{Cl_R - Cl_{cr} \times \text{fraction of unbound compound}}{Cl_R} \times 100 \qquad \text{(Eq. A19)}$$

## REFERENCES


(1) R. K. Ferguson, H. R. Brunner, G. A. Turini, H. Gavras, and D. N. McKinstry, *Lancet*, **1**, 775 (1977).

(2) D. B. Case, S. A. Atlas, J. H. Laragh, J. E. Sealey, P. A. Sullivan, and D. N. McKinstry, *Progr. Cardiovasc. Dis.*, **21**, 195 (1978).

(3) H. Gavras, H. R. Brunner, G. A. Turini, G. R. Kershaw, C. P. Tifft, S. Cuttelod, I. Gavras, R. A. Vukovich, and D. N. McKinstry, *N. Engl. J. Med.*, **298**, 991 (1978).

(4) H. R. Brunner, H. Gavras, B. Waeber, G. R. Kershaw, G. A. Turini, R. A. Vukovich, and D. N. McKinstry, *Ann. Intern. Med.*, **90**, 19 (1979).

(5) K. J. Kripalani, D. N. McKinstry, S. M. Singhvi, D. A. Willard, R. A. Vukovich, and B. H. Migdalof, *Clin. Pharmacol. Ther.*, **27**, 636 (1980).

(6) B. H. Migdalof, S. M. Singhvi, and K. J. Kripalani, *J. Liq. Chromatogr.*, **3**, 857 (1980).

(7) L. E. Anderson and W. A. McClure, *Anal. Biochem.*, **51**, 173 (1973).

(8) K. Wong, S. J. Lan, and B. H. Migdalof, *Pharmacologist*, **21**, 173 (1979).

(9) A. J. Rommel, A. M. Pierides, and A. F. Heald, *Clin. Pharmacol. Ther.*, **27**, 282 (1980).

(10) S. M. Singhvi, A. E. Peterson, J. M. Shaw, and B. H. Migdalof, *Fed. Proc. Fed. Am. Soc. Exp. Biol.*, **39**, 538 (1980).


## ACKNOWLEDGMENTS


The authors gratefully acknowledge the technical assistance of Mr. C. J. Mondi and Mr. R. J. Ratoff and the editorial assistance of Dr. J. Dreyfuss and Dr. P. L. Sibley. The synthesis of radiolabeled captopril was carried out by Mr. P. Egli.


# Quantitation of Daunorubicin, Doxorubicin, and Their Aglycones by Ion-Pair Reversed-Phase Chromatography


**A. CAROL HANEKE ˣ, J. CRAWFORD, and A. ASZALOS**



Received January 23, 1981, from the *Food and Drug Administration, National Center for Antibiotics Analysis, Washington, DC 20204.* Accepted for publication March 9, 1981.



**Abstract** □ A fast and sensitive high-pressure liquid chromatographic method was developed for the quantitation of doxorubicin, daunorubicin, and their aglycones in pharmaceutical preparations. Because its higher pH extends column life while permitting determination of impurities, this system represents an improvement over previously published methods. It utilizes a $C_{18}$ bonded silica gel column and a solvent system consisting of methanol–0.01 *M* monobasic ammonium phosphate aqueous solution (65:35) at pH 4.0 and 1600 psi of pressure. The accuracy of the doxorubicin and daunorubicin determinations, expressed as the coefficient of variation, is 1.65 and 1.27%, respectively. The aglycones can be determined with a precision of <1.3%.



**Keyphrases** □ Doxorubicin—high-pressure liquid chromatographic assay, quantitation of impurities □ Daunorubicin—high-pressure liquid chromatographic assay, quantitation of impurities □ High-pressure liquid chromatography—quantitation of doxorubicin, daunorubicin, and their aglycones □ Antibiotics—quantitation of doxorubicin, daunorubicin, and their aglycones by high-pressure liquid chromatography


Doxorubicin (adriamycin) is an anthracycline antibiotic (I) consisting of the tetracyclic quinoid aglycone doxorubicinone (adriamycinone) in a glycosidic linkage to the amino sugar daunosamine (1, 2). Doxorubicin has been shown to be effective against various human neoplasms (3, 4). Pharmaceutical preparations of doxorubicin contain several impurities such as daunorubicin, daunorubicinone, and doxorubicinone, as well as other minor contaminants. Some of these impurities, particularly daunorubicin and daunorubicinone, are present because doxorubicin is prepared from daunorubicin by chemical synthesis (5), and the parent compound and its impurities are carried through to the product during the manufacturing process.

Daunorubicin (II) is a recently approved drug used in the treatment of acute leukemia and certain solid tumors in humans (6, 7). Daunorubicin preparations contain impurities such as daunorubicinone, which may be carried through the isolation process of the drug from the fermentation broth (8). It is important that the potency of both doxorubicin and daunorubicin be determined because clinical treatment relies on an accurate dosage schedule (9). It is equally important to determine the impurities in these pharmaceutical preparations, particularly the aglycone content, because these impurities are mutagenic and have no antitumor activity (10).

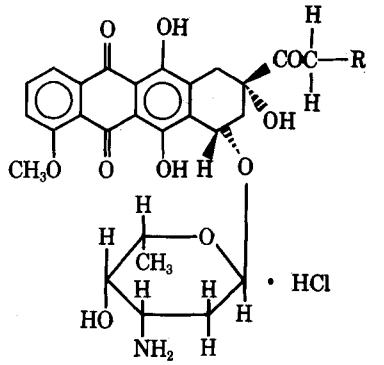

I: R = OH
II: R = H




*0022-3549/81/1000-1112$01.00/0*



*© 1981, American Pharmaceutical Association*

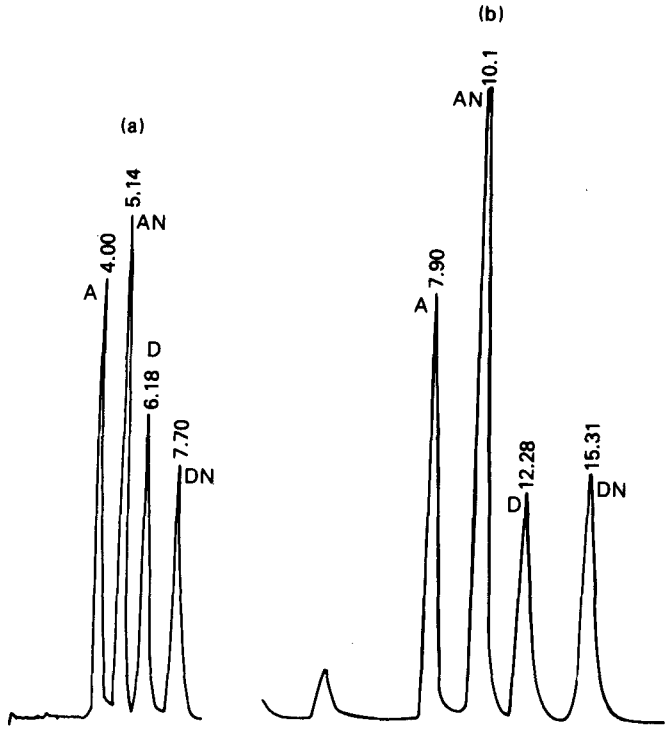


**Figure 1**—*HPLC separation profile of daunorubicin (D), doxorubicin (A), daunorubicinone (DN), and doxorubicinone (AN) with $C_{18}$ bonded silica gel, methanol–0.01 M monobasic ammonium phosphate aqueous solution (65:35), pH 4.0, and flow rate of 2 ml/min (a) and 1 ml/min (b). Numbers given are retention times in minutes.*

## BACKGROUND

The *Code of Federal Regulations* (CFR) (11) specifies that high-pressure liquid chromatography (HPLC) be used to establish the composition of doxorubicin and daunorubicin preparations but does not require determination of the aglycones. The official method utilizes a pH 2.0 mobile phase, which can adversely affect the useful life of the chromatographic column and may also hydrolyze daunorubicin to its aglycone and daunosamine during the long analytical process.

Most previously published HPLC procedures for the analyses of these drugs are suitable only for the estimation of doxorubicin and its metabolites in plasma (12–15). Some also use a detrimental pH 2 mobile phase (12, 13). Others use a quaternary (14) or a gradient (15) solvent system and do not provide rapid quantitation of pharmaceutical preparations of doxorubicin or daunorubicin. A low pH system was used by Eksborg (16), who achieved good separations of daunorubicin, doxorubicin, and their C-13 hydroxylated metabolites by HPLC (16). Other methods were developed to determine daunorubicin and its C-13 hydroxylated metabolite in plasma (17, 18). However, none of these published methods was designed to quantitate doxorubicinone and daunorubicinone.

This report describes a new HPLC method for the quantitative determination of daunorubicin, doxorubicin, and their aglycones in pharmaceutical preparations.

## EXPERIMENTAL

**Reagents**—Spectrograde methanol and deionized water were used throughout the experiments. Monobasic ammonium phosphate[1], acetic acid[2], and heptanesulfonic acid[3] were used without further purification. Daunorubicin[4] and doxorubicin[5] were obtained commercially. Daunorubicinone and doxorubicinone were prepared as described previously (19 and 2, respectively) and checked for purity by melting-point, IR, and TLC [single spot at $R_f$ 0.92 and 0.78, respectively; methanol–chloroform–formic acid (15:85:2); silica gel] analyses.

[1] Fisher Scientific Co., Pittsburgh, Pa.
[2] Mallinckrodt Chemical Co., St. Louis, Mo.
[3] Eastman Chemicals, Rochester, N.Y.
[4] Rhodia Inc., New York, N.Y.
[5] Farmitalia, Milan, Italy.

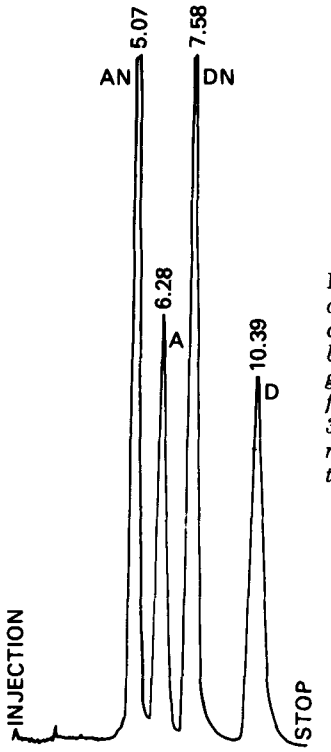


**Figure 2**—*HPLC separation profile of daunorubicin (D), doxorubicin (A), daunorubicinone (DN), and doxorubicinone (AN) with $C_{18}$ bonded silica gel, methanol–0.005 M heptanesulfonic acid aqueous solution (62.5:37.5), pH 3.5, and flow rate of 2 ml/min. Numbers indicate retention times in minutes.*

**Apparatus**—A modular high-pressure liquid chromatograph[6] was equipped with a constant-flow pump, a valve-type injector[7], and a 254-nm fixed-wavelength detector[8]. Data were recorded and reduced by a microprocessor[9] set for peak area calculations at a chart speed of 0.5 cm/min and attenuation of 128.

**Chromatographic Conditions**—A 25-cm × 4.6-mm i.d. stainless steel column, packed with 10-μm particle-size $C_{18}$ reversed-phase packing material[10], was used for all assays. The isocratic mobile phase consisted of 650 ml of methanol and 350 ml of water to which was added 1.15 g of monobasic ammonium phosphate dissolved in 5 ml of acetic acid (final pH 4.0). The mobile phase was filtered through a 0.2-μm filter and degassed by vacuum for 20 min. The flow rate was 2 ml/min, which produced a pressure of ~1600 psi. All separations were performed at ambient temperature. A 5-μl sample was injected into the chromatograph.

Before the assay was begun, a resolution factor for the system was determined at ambient temperature with a flow rate of 1.0 ml/min. To facilitate measurements of peak width, the detector was set to give at least 50% response full scale and a chart speed of 2 cm/min. The column was purged with mobile phase until a steady baseline was established. Then 5 mg of doxorubicin and 5 mg of doxorubicinone were accurately weighed into a 10-ml volumetric flask and diluted to volume with methanol. Then 5 μl of this solution was injected into the chromatograph. The retention time for the doxorubicin and the doxorubicinone peaks should be ~470 and 600 sec, respectively.

The resolution factor ($R_s$) is calculated as follows:

$$R_s = 2(t_2 - t_1)/(W_1 + W_2) \qquad \text{(Eq. 1)}$$

where $(t_2 - t_1)$ is the difference in retention times measured in centimeters at peak maxima between the doxorubicin and the doxorubicinone peaks and $W_2$ and $W_1$ are the peak widths at the base of the peaks in centimeters.

A resolution factor of 2.2 is recommended. Experiments evaluated in statistical terms were performed eight to 10 times each.

**Sample Preparation**—*Vials*—To obtain a concentration of 0.5 mg/ml, the finished products were diluted as follows: 4, 8, or 10 ml of methanol was added to a 10-, 20-, or 50-mg vial, respectively. Then 2, 2, or 1 ml of the resulting solution was transferred to a 10-ml volumetric flask and diluted to volume with methanol. Dilution factors were 20, 40, or 100 ml, respectively. A 5-μl sample size was used. Peak areas of the

[6] Model 6001A, Waters Associates, Milford, Mass.
[7] Model U6K, Waters Associates, Milford, Mass.
[8] Model 240, Waters Associates, Milford, Mass.
[9] Integrator 3380A, Hewlett-Packard Co., Palo Alto, Calif.
[10] μBondapak, Waters Associates, Milford, Mass.

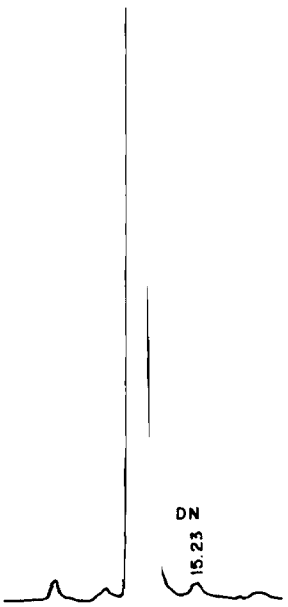


**Figure 3**—*Chromatogram of daunorubicinone estimated at 0.5% of the parent compound with the HPLC conditions given under* Experimental *for estimation of the aglycones. Numbers indicate retention times in minutes.*

samples were compared to those of the standard, and the concentrations were calculated as follows:

$$\text{mg/vial} = \frac{A_u \times W_s \times DF \times P}{A_s \times 1000\ \mu\text{g/mg}} \quad \text{(Eq. 2)}$$

where $A_u$ is area of the sample peak, $W_s$ is milligrams per milliliter of the standard, $DF$ is the dilution factor in milliliters, $P$ is purity of the standard in micrograms per milligram, and $A_s$ is area of the standard peak.

*Bulk Samples*—The standard and bulk samples were diluted with methanol to a concentration of 0.5 mg/ml, and a 5-$\mu$l sample size was used. Peak area data of the bulk samples were compared to those of the standard and calculated as follows:

$$\mu\text{g/mg} = \frac{A_u \times W_s \times P}{A_s \times W_u} \quad \text{(Eq. 3)}$$

where $W_u$ is milligrams per milliliter of the sample.

**Estimation of Aglycones**—The aglycone determination for each drug was developed for the range in which they usually occur in the preparations analyzed (0.5–3.0% of the parent compound). Because of the relatively low aglycone concentrations in the preparations and the limitations of the microprocessor in calculating relatively small areas, the attenuation was changed to 32 and the flow rate was changed to 1.0 ml/min to ensure good precision.

## RESULTS AND DISCUSSION

Optimal HPLC conditions established for this assay consisted of a mobile phase acidity of 3.5–7.0 to ensure a reasonably long column lifetime, a turnaround time of <15 min to enable high productivity, and a resolution factor of at least 2.0 for accurate quantitation.

Figure 1 shows the optimum HPLC profile achieved with the best ammonium sulfate solvent system. The pH was 4.0 and retention times for the last appearing peaks were 8 and 15 min at 2- and 1-ml/min flow rates, respectively. The resolutions for the first two peaks were 2.4 (Fig. 1*a*) and 2.7 (Fig. 1*b*) at 2- and 1-ml/min flow rates, respectively. Figure 2 shows the optimum HPLC profile achieved with the heptanesulfonic acid system. The separation time was slightly over 10 min, the pH was 3.5, and the resolution was 2.1 for the first two peaks with a 2-ml/min flow rate. No correlation between resolution and pH, flow rate (column pressure), or percent methanol could be found for either solvent system. However, the resolution was generally poorer at higher pH values.

Since the ammonium sulfate solvent system at pH 4.0 and 65% methanol gave slightly superior resolution and acidity than the heptanesulfonic acid solvent system, it was used for the rest of the study. This system was evaluated for quantitative estimation of doxorubicin, daunorubicin, and their aglycones. The aglycones were assayed at low levels relative to the parent compound since pharmaceutical preparations contain small amounts of these substances.

**Table I—Comparative Results by the Ammonium Sulfate and the CFR Methods**

| Sample | Ammonium Sulfate Method | | CFR Method | |
|---|---|---|---|---|
| | % | μg/mg | % | μg/mg |
| Standard | 100.0 | 912 | 100.0 | 912 |
| Sample A: 1 | 97.5 | 889 | 97.6 | 890 |
| 2 | 97.8 | 892 | 97.5 | 890 |
| 3 | 98.2 | 896 | 98.7 | 901 |
| Sample B: 1 | 98.7 | 900 | 98.0 | 894 |
| 2 | 97.9 | 893 | 97.7 | 891 |
| 3 | 98.1 | 896 | 99.2 | 904 |
| Sample C: 1 | 98.0 | 894 | 99.6 | 908 |
| 2 | 96.2 | 879 | 97.0 | 885 |
| 3 | 97.9 | 892 | 99.1 | 904 |

Doxorubicin was assayed in the 1–5-μg/injection range. There is a linear relation between the peak area and the quantity of doxorubicin injected within this range. A standard curve must be determined for every combination of parameters. The standard deviation of these results was 0.71%, and the coefficient of variation was 1.65%. Similar results, a standard deviation of 0.77% and a coefficient of variation of 1.27%, were obtained for daunorubicin.

Doxorubicin preparations are dispensed in 10- and 50-mg vials. Daunorubicin is obtained as a bulk preparation or in 20-mg vials. Both drugs are dissolved in methanol to obtain a 0.5-mg/ml solution, and a 5-μl sample is injected. The content of the vials can be calculated as shown in the *Experimental* section.

The precision for the estimation of doxorubicinone in the presence of a relatively large amount of doxorubicin and of daunorubicinone in the presence of a relatively large quantity of daunorubicin, expressed as standard deviation, is 1.27%. A linear relationship is shown between peak area data and the quantity of the algycones injected. Assay of these aglycones in either preparation is possible under these experimental conditions provided a standard curve is determined for each new combination of parameters. Figure 3 shows a chromatogram of the assay of daunorubicinone at 0.5% of the parent compound.

Several pharmaceutical preparations were assayed by the new ammonium sulfate method, and the results (Table I) were compared to those obtained by the CFR method, which uses an internal standard. Comparison of these data shows that results fall within a desirable range and that the proposed new method produces assay values comparable to those found by the official method. The average coefficient of variation is 0.70% for these measurements. The aglycone content was also determined for two bulk preparations used in this study; Samples A and B contained 0.34 and 0.49% daunorubicinone, respectively.

## REFERENCES

(1) F. Arcamone, A. DiMarco, and S. Penco, German offen. pat. 2,510,866 (1975).

(2) F. Arcamone, A. G. Franceschi, S. Penco, and A. Selva, *Tetrahedron Lett.*, **1969**, 1007.

(3) S. K. Carter, *J. Natl. Cancer Inst.*, **55**, 1265 (1975).

(4) "International Symposium on Adriamycin," S. K. Carter, A. DiMarco, M. Ghione, I. H. Krakoff, and G. Mathe, Eds., Springer Verlag, New York, N.Y., 1972.

(5) F. Arcamone, A. G. Franceschi, and S. Penco, U.S. pat. 3,803,124 (1974).

(6) C. Tan, H. Tasaka, K. Yu, M. L. Murphy, and D. A. Karnofsky, *Cancer*, **20**, 333 (1967).

(7) H. S. Schwartz and P. M. Kanter, *Cancer Chemother. Rep. Part 3*, **8**, 107 (1975).

(8) A. DiMarco, M. Gaetani, P. Orezze, B. M. Scarpinato, R. Silvestrini, M. Soldati, T. Dasdia, and L. Valentini, *Nature*, **201**, 706 (1964).

(9) R. A. Minow, R. S. Benjamin, E. T. Lee, and J. A. Gottlieb, *Cancer*, **39**, 1397 (1977).

(10) C. Cordaro, T. Cebula, and J. Ramsey, FDA/PRT Semiannual Report, AIC-R-29, Apr. 14, 1980.

(11) Code of Federal Regulations, 21 Food and Drug 436.322.

(12) R. N. Pierce and P. I. Jatlow, *J. Chromatogr.*, **164**, 471 (1979).

(13) S. Eksborg, H. Ehrssom, and I. Anderson, *ibid.*, **164**, 479 (1979).

(14) J. H. Peters and J. F. Murray, Jr., *J. Liq. Chromatogr.*, **2**, 45 (1979).

(15) M. Israel, W. J. Pegg, P. M. Wilkinson, and M. B. Garnick, *ibid.*, **1**, 795 (1978).
(16) S. Eksborg, *J. Chromatogr.*, **149**, 225 (1978).
(17) R. Hulhoven and J. P. Desager, *ibid.*, **125**, 369 (1976).
(18) R. Baurain, A. Zenebergh, and A. Troulet, *ibid.*, **157**, 331 (1978).
(19) F. Arcamone, G. Franceschi, P. Orezze, G. Cassinelli, W. Barkieri, and R. Mondelli, *J. Am. Chem. Soc.*, **86**, 5334 (1964).

# Extended Hildebrand Solubility Approach: Methylxanthines in Mixed Solvents

**A. MARTIN *x, A. N. PARUTA ‡, and A. ADJEI ***

Received July 24, 1980, from the **Drug Dynamics Institute, College of Pharmacy, University of Texas, Austin, TX 78712*, and the ‡*College of Pharmacy, University of Rhode Island, Kingston, RI 02881.* Accepted for publication March 16, 1981.

**Abstract** □ The solubility profiles of theobromine, theophylline, and caffeine at 25° were examined in binary solvent systems including dioxane–formamide, water–polyethylene glycol 400, and glycerin–propylene glycol. Theobromine solubility was studied in dioxane–water mixtures, a solvent system that was investigated earlier for the solubility of theophylline and caffeine. Solubilities were calculated in these polar systems by a regression method, based on an extension of the Hildebrand–Scatchard equation of regular solution theory. A linear relationship between the mixed solvent solubility parameter, $\delta_1$, and dielectric constant, $\epsilon$, was introduced earlier and was confirmed in the present study. In addition, it was observed that a regression of log(activity coefficient) on $\epsilon$ in a second or higher degree polynomial provides reasonable solubility values for the methylxanthines in mixed solvents. A direct regression of molal or mole fraction (but not molar) solubility against $\delta_1$, $\epsilon$, or against volume percent of one or the other solvent in a binary solvent mixture provided a suitable measure of solubility for these crystalline drugs in mixed polar solvents. The drug's solubility parameter as determined from peak solubility in mixed polar solvents varied somewhat, depending on the specific solvent system employed. It is suggested that a drug may exhibit one (or more) solubility parameters in nonpolar solutions and multiple solubility parameters in polar systems. The extended solubility approach serves for the back-calculation of solubilities in mixed solvent systems, even though the solubility parameter of the solute may vary from one solvent system to the next.

**Keyphrases** □ Methylxanthines—solubility profiles using extended Hildebrand–Scatchard equation □ Solubility—methylxanthines in mixed solvents, extended Hildebrand–Scatchard equation □ Hildebrand–Scatchard equation—modified, solubility profiles of methylxanthines in mixed solvents

Previous reports (1–3) introduced an approach to estimate the solubility of drugs in mixed and pure solvent systems. The method employs the equation:

$$-\log X_2 = \frac{\Delta S^f_m}{R}\log\frac{T_m}{T} + \frac{V_2\phi_1^2}{2.303RT}(\delta_1-\delta_2)^2 + \frac{V_2\phi_1^2}{2.303RT}2(\delta_1\delta_2 - W) \quad \text{(Eq. 1a)}$$

or:

$$-\log X_2 = \frac{\Delta S^f_m}{R}\log\frac{T_m}{T} + \frac{V_2\phi_1^2}{2.303RT}(\delta_1^2+\delta_2^2-2W) \quad \text{(Eq. 1b)}$$

where $X_2$ is the mole fraction solubility of the drug, $\Delta S^f_m$ is the entropy of fusion, $R$ is the molar gas constant, $T_m$ is the melting point of the compound in Kelvin degrees, $T$ is the absolute temperature at which the solubility is measured, $V_2$ is the molar volume of the drug as a hypothetical supercooled liquid solute at temperature $T$, $\phi_1$ is the volume fraction of the solvent, $\delta_1$ and $\delta_2$ are the solubility parameters of the solvent and solute, and $W$ is the solute–solvent interaction energy. Subscript 1 is used for solvent and subscript 2 for solute. The $W$ value is computed for the drug in each solvent mixture, using Eq. 1*b*. It may, in turn, be back-calculated employing a power series regression in $\delta_1$ to estimate mole fraction or molal solubilities. By knowing the density of the solution at a particular temperature, it is also possible to convert these calculations to molar solubilities. The term $V_2\phi_1^2/2.303RT$ is designated in this study by the symbol $A$. The present work tests the extended Hildebrand solubility approach (as this method is called) with various binary solvent mixtures.

## EXPERIMENTAL

The sources and treatment of methylxanthines and some of the solvents used were given previously (2, 3)[1]. Additional solvents employed in the present study were propylene glycol[2], polyethylene glycol 400[2], and glycerin[2]. Pertinent physicochemical properties of the xanthine derivatives are recorded in Table I. The solubilities of the drugs were determined in a shaker bath employing 20-ml screw-capped vials containing an excess of the drug at 25 ± 0.2°. Equilibrium occurred well before 96 hr. Samples were withdrawn after 96 hr and filtered through a 0.22-$\mu$m filter, and aliquots were removed and diluted for spectrophotometric assay. Runs were carried out in quadruplicate, and the four results were averaged. Densities of the saturated solutions and of the solvent mixtures were determined in quadruplicate at 25 ± 0.2° in 10-ml pycnometers.

## RESULTS AND DISCUSSION

Theobromine was dissolved in mixtures of dioxane and water at 25°. The solubility profile is shown in Fig. 1. Table II contains the data used to plot the back-calculation line of Fig. 1, including $W_{calc}$ and $A$ values. Solution densities and dielectric constants are also recorded in Table II.

**Ideal Solubility in Relation to Maximum Solubility in Real Systems**—The ideal mole fraction solubility of theobromine at 25° is 0.0029, a value well below the ideal solubilities of theophylline (0.0190) and caffeine (0.0685) at 25° (Table I and Fig. 1) because of the greater $\Delta H^f_m$ value and high melting point (348°) of theobromine. The peak solubility of theobromine in the best dioxane–water mixture (~70% dioxane) is well below ideal solubility (Fig. 1), as observed previously for caffeine and theophylline. This phenomenon was noted by Gordon and Scott (4) and by others (5, 6). Scatchard *et al.* (7) observed that the value of $C_{12}$ (an-

[1] Reference 2 states that mean molar volumes of the binary solvent mixtures are calculated from Eq. 17, in which each molecular weight was multiplied by the mole fraction of that solvent in the mixture. This is an error; the quantity used in Refs. 2 and 3 and in the present study is volume fraction rather than mole fraction.
[2] Fisher Scientific.

0022-3549/81/1000-1115$01.00/0
© 1981, American Pharmaceutical Association

(15) M. Israel, W. J. Pegg, P. M. Wilkinson, and M. B. Garnick, *ibid.*, **1**, 795 (1978).
(16) S. Eksborg, *J. Chromatogr.*, **149**, 225 (1978).
(17) R. Hulhoven and J. P. Desager, *ibid.*, **125**, 369 (1976).
(18) R. Baurain, A. Zenebergh, and A. Troulet, *ibid.*, **157**, 331 (1978).
(19) F. Arcamone, G. Franceschi, P. Orezze, G. Cassinelli, W. Barkieri, and R. Mondelli, *J. Am. Chem. Soc.*, **86**, 5334 (1964).

# Extended Hildebrand Solubility Approach: Methylxanthines in Mixed Solvents

**A. MARTIN *x, A. N. PARUTA ‡, and A. ADJEI ***

Received July 24, 1980, from the **Drug Dynamics Institute, College of Pharmacy, University of Texas, Austin, TX 78712*, and the ‡*College of Pharmacy, University of Rhode Island, Kingston, RI 02881.* Accepted for publication March 16, 1981.

**Abstract** □ The solubility profiles of theobromine, theophylline, and caffeine at 25° were examined in binary solvent systems including dioxane–formamide, water–polyethylene glycol 400, and glycerin–propylene glycol. Theobromine solubility was studied in dioxane–water mixtures, a solvent system that was investigated earlier for the solubility of theophylline and caffeine. Solubilities were calculated in these polar systems by a regression method, based on an extension of the Hildebrand–Scatchard equation of regular solution theory. A linear relationship between the mixed solvent solubility parameter, $\delta_1$, and dielectric constant, $\epsilon$, was introduced earlier and was confirmed in the present study. In addition, it was observed that a regression of log(activity coefficient) on $\epsilon$ in a second or higher degree polynomial provides reasonable solubility values for the methylxanthines in mixed solvents. A direct regression of molal or mole fraction (but not molar) solubility against $\delta_1$, $\epsilon$, or against volume percent of one or the other solvent in a binary solvent mixture provided a suitable measure of solubility for these crystalline drugs in mixed polar solvents. The drug's solubility parameter as determined from peak solubility in mixed polar solvents varied somewhat, depending on the specific solvent system employed. It is suggested that a drug may exhibit one (or more) solubility parameters in nonpolar solutions and multiple solubility parameters in polar systems. The extended solubility approach serves for the back-calculation of solubilities in mixed solvent systems, even though the solubility parameter of the solute may vary from one solvent system to the next.

**Keyphrases** □ Methylxanthines—solubility profiles using extended Hildebrand–Scatchard equation □ Solubility—methylxanthines in mixed solvents, extended Hildebrand–Scatchard equation □ Hildebrand–Scatchard equation—modified, solubility profiles of methylxanthines in mixed solvents

Previous reports (1–3) introduced an approach to estimate the solubility of drugs in mixed and pure solvent systems. The method employs the equation:

$$-\log X_2 = \frac{\Delta S^f_m}{R}\log\frac{T_m}{T} + \frac{V_2\phi_1^2}{2.303RT}(\delta_1-\delta_2)^2 + \frac{V_2\phi_1^2}{2.303RT}2(\delta_1\delta_2 - W) \quad \text{(Eq. 1a)}$$

or:

$$-\log X_2 = \frac{\Delta S^f_m}{R}\log\frac{T_m}{T} + \frac{V_2\phi_1^2}{2.303RT}(\delta_1^2+\delta_2^2-2W) \quad \text{(Eq. 1b)}$$

where $X_2$ is the mole fraction solubility of the drug, $\Delta S^f_m$ is the entropy of fusion, $R$ is the molar gas constant, $T_m$ is the melting point of the compound in Kelvin degrees, $T$ is the absolute temperature at which the solubility is measured, $V_2$ is the molar volume of the drug as a hypothetical supercooled liquid solute at temperature $T$, $\phi_1$ is the volume fraction of the solvent, $\delta_1$ and $\delta_2$ are the solubility parameters of the solvent and solute, and $W$ is the solute–solvent interaction energy. Subscript 1 is used for solvent and subscript 2 for solute. The $W$ value is computed for the drug in each solvent mixture, using Eq. 1*b*. It may, in turn, be back-calculated employing a power series regression in $\delta_1$ to estimate mole fraction or molal solubilities. By knowing the density of the solution at a particular temperature, it is also possible to convert these calculations to molar solubilities. The term $V_2\phi_1^2/2.303RT$ is designated in this study by the symbol $A$. The present work tests the extended Hildebrand solubility approach (as this method is called) with various binary solvent mixtures.

## EXPERIMENTAL

The sources and treatment of methylxanthines and some of the solvents used were given previously (2, 3)[1]. Additional solvents employed in the present study were propylene glycol[2], polyethylene glycol 400[2], and glycerin[2]. Pertinent physicochemical properties of the xanthine derivatives are recorded in Table I. The solubilities of the drugs were determined in a shaker bath employing 20-ml screw-capped vials containing an excess of the drug at 25 ± 0.2°. Equilibrium occurred well before 96 hr. Samples were withdrawn after 96 hr and filtered through a 0.22-$\mu$m filter, and aliquots were removed and diluted for spectrophotometric assay. Runs were carried out in quadruplicate, and the four results were averaged. Densities of the saturated solutions and of the solvent mixtures were determined in quadruplicate at 25 ± 0.2° in 10-ml pycnometers.

## RESULTS AND DISCUSSION

Theobromine was dissolved in mixtures of dioxane and water at 25°. The solubility profile is shown in Fig. 1. Table II contains the data used to plot the back-calculation line of Fig. 1, including $W_{calc}$ and $A$ values. Solution densities and dielectric constants are also recorded in Table II.

**Ideal Solubility in Relation to Maximum Solubility in Real Systems**—The ideal mole fraction solubility of theobromine at 25° is 0.0029, a value well below the ideal solubilities of theophylline (0.0190) and caffeine (0.0685) at 25° (Table I and Fig. 1) because of the greater $\Delta H^f_m$ value and high melting point (348°) of theobromine. The peak solubility of theobromine in the best dioxane–water mixture (~70% dioxane) is well below ideal solubility (Fig. 1), as observed previously for caffeine and theophylline. This phenomenon was noted by Gordon and Scott (4) and by others (5, 6). Scatchard *et al.* (7) observed that the value of $C_{12}$ (an-

[1] Reference 2 states that mean molar volumes of the binary solvent mixtures are calculated from Eq. 17, in which each molecular weight was multiplied by the mole fraction of that solvent in the mixture. This is an error; the quantity used in Refs. 2 and 3 and in the present study is volume fraction rather than mole fraction.
[2] Fisher Scientific.

0022-3549/81/1000-1115$01.00/0
© 1981, American Pharmaceutical Association

**Table I—Properties of Theophylline, Caffeine, and Theobromine**

| Property | Theophylline | Caffeine | Theobromine |
|---|---|---|---|
| Heat of fusion[a] at melting point, cal/mole | 7097 | 5044 | 9819 |
| Melting point[b], °K | 547.65 | 512.15 | 621.15 |
| Molecular weight[c], g/mole | 180.18 | 194.19 | 180.18 |
| Molar volume[d] at 25°, ml/mole | 124.0 | 144.0 | 124.0 |
| Solubility parameter[e], $(cal/cm^3)^{1/2}$ | 14.0 | 13.8 | 14.0 |
| Ideal mole fraction solubility, $X_2^i$ at 25° [f] | 0.01896 | 0.06845 | 0.00291 |
| Solubility (mole/liter) in: | | | |
| Dioxane | 0.03032 | 0.09656 | 0.00518 |
| Water | 0.04083 | 0.12438 | 0.00183 |
| *N,N*-Dimethylformamide | 0.20173 | 0.16433 | 0.00854 |
| Hexane | 0.00083 | 0.00003 | 0.00015 |
| UV absorption spectra, $\lambda_{max}$[g] | 270 | 273 | 273 |
| Molar absorptivity[g], *E* 1%, 1 cm | 530 | 519 | 550 |

[a] Determined by differential scanning calorimetry using Perkin-Elmer DSC model 1B. [b] Melting temperatures of the xanthines determined using Perkin-Elmer DSC model 1B. [c] Molecular weights of the xanthines obtained from the manufacturer's specifications and correlated with results using mass spectrometry. [d] Molar volume of the xanthines (ml/mole) determined using an arithmetic mean of the apparent molar volume in dioxane–water mixtures, and solute molar volumes from group contribution methods (Ref. 18). [e] Solute solubility parameters, $(cal/cm^3)^{1/2}$ calculated using a graphical solubility method (Ref. 22) and a group contribution method (Ref. 18). [f] $\log X_2^i = (\Delta S_m^f/R) \log (T/T_m)$. [g] Ref. 23.

other symbol used for $W$) was 5% greater than $\delta_1\delta_2$ for benzene in methanol at 0.5 mole fraction and 8% greater than $\delta_1\delta_2$ for carbon tetrachloride in methanol, signifying strong solute–solvent interaction in these mixtures. The mole fraction solubility of theobromine in the optimum water–dioxane mixture is 0.00075 or 74% below ideal (Fig. 1) suggesting self-association of solvent, solute, or both.

The differences, Δ, between ideal and actual interaction energies of the three methylxanthines in these optimum mixtures are given in Table III. The solute–solvent interaction energy, $W$, is included together with

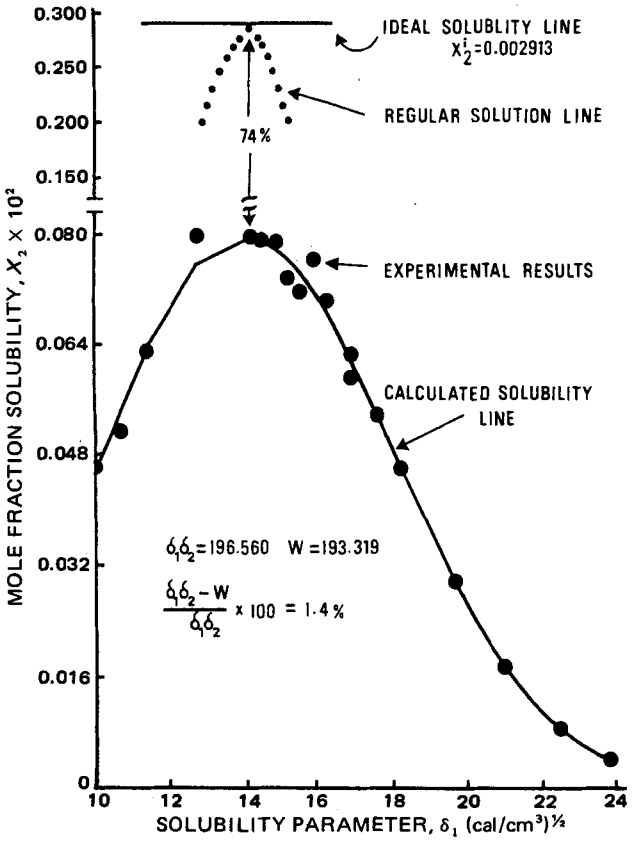


**Figure 1**—*Mole fraction solubility of theobromine in dioxane–water mixtures at 25°. Key: • • •, peak region of the regular solution curve; ●, observed solubilities; and —, back-calculated solubility using Eq. 2a of Table IV.*

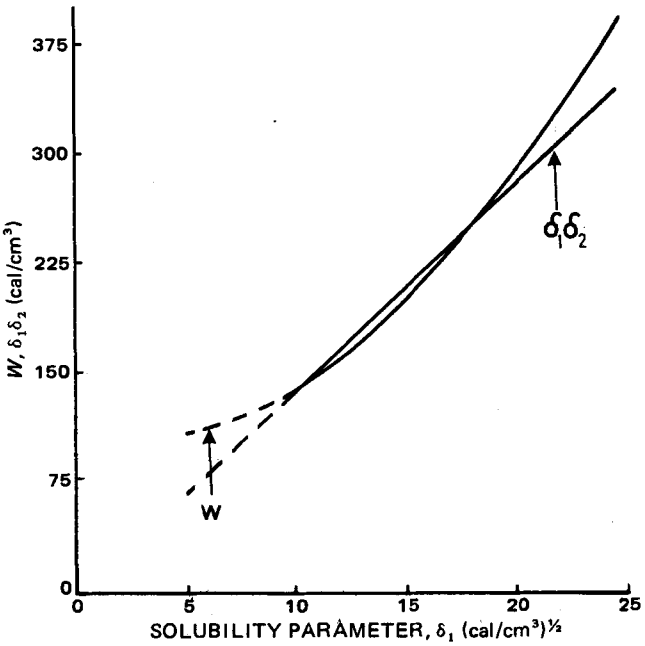


**Figure 2**—*Relationship of* W *and* $\delta_1\delta_2$, *for theophylline in dioxane* ($\delta_1$ = *10.0) and water* ($\delta_2$ = *23.5) mixture at 25°.*

$\delta_1\delta_2$, the interaction term that would be applicable if the systems behaved as regular solutions. The ratio, $K$, of $W$ to $\delta_1\delta_2$ at peak solubility is found in the last column of Table III. These data indicate that a difference of 1.4% between the geometric mean $\delta_1\delta_2$ and $W$ results in a 74% decrease in expected solubility for theobromine in dioxane–water.

Figure 2 shows the slightly curved line obtained when $W$ is plotted against $\delta_1$. The geometric mean, $\delta_1\delta_2$, is plotted on the same graph against $\delta_1$ to depict graphically the relationship of $W$ to $\delta_1\delta_2$ for theophylline across the mixtures of dioxane ($\delta_1$ = 10.0) to water ($\delta_1$ = 23.5). This small difference in interaction energy, ($\Delta = \delta_1\delta_2 - W$) of Eq. 1*a*, in xanthine–dioxane–water systems accounts for the fact that maximum solubility of the real system does not reach $X_2^i$, the ideal value of peak solubility.

The extended Hildebrand equation differs from the Hildebrand equation in the use of $W$ to replace $\delta_1\delta_2$, and Fig. 2 provides a graphical demonstration of why the original Hildebrand approach cannot be used to estimate solubilities of drugs in polar solvent mixtures. In Fig. 2, $\delta_1\delta_2$

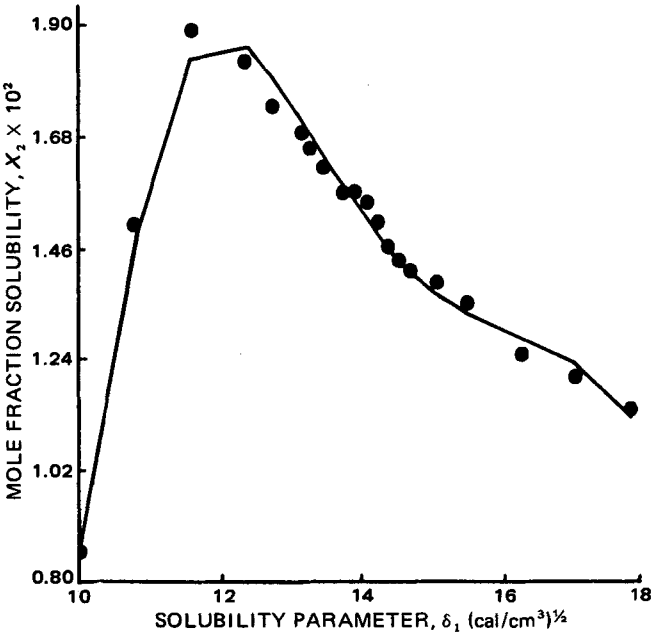


**Figure 3**—*Mole fraction solubility of caffeine in dioxane–formamide mixtures at 25°. Key: ●, observed solubilities; and —, back-calculated solubility based on Eqs. 5a and 5b of Table V.*

**Table II—Observed [a] and Calculated [b] Solubilities of Theobromine [c] in Dioxane–Water Mixtures at 25°.**

| Volume Percent Water, $100\phi_w$ | Solution Density | $A$ [e] | $\delta_1$ [f] | $\epsilon_1$ [g] | $W_{calc}$ | log $\alpha_2/A$ | $X_{2_{obs}} \times 10^6$ [a] | $X_{2_{calc}} \times 10^6$ [b] | Percent Difference |
|---|---|---|---|---|---|---|---|---|---|
| 100 | 0.9976 | 0.09084 | 23.45 | 78.54 | 362.316 | 21.42037 | 33 | 33 | −1.0 |
| 90 | 1.0808 | 0.09082 | 22.11 | 69.28 | 333.734 | 17.43588 | 76 | 77 | −1.5 |
| 80 | 1.0148 | 0.09077 | 20.76 | 62.63 | 306.457 | 13.76552 | 164 | 157 | 4.6 |
| 70 | 1.0230 | 0.09072 | 19.42 | 52.02 | 280.888 | 11.21233 | 280 | 276 | 1.5 |
| 60 | 1.0293 | 0.09067 | 18.07 | 43.13 | 256.645 | 9.21972 | 425 | 428 | −0.7 |
| 50 | 1.0350 | 0.09064 | 16.73 | 37.09 | 234.088 | 7.90106 | 560 | 582 | −3.9 |
| 40 | 1.0388 | 0.09062 | 15.39 | 27.46 | 213.031 | 7.01479 | 674 | 699 | −3.8 |
| 30 | 1.0381 | 0.09062 | 14.04 | 20.54 | 193.334 | 6.48362 | 753 | 746 | 1.0 |
| 20 | 1.0370 | 0.09065 | 12.70 | 12.52 | 175.289 | 6.51980 | 747 | 707 | 5.4 |
| 10 | 1.0336 | 0.09071 | 11.33 | 5.72 | 158.391 | 7.61277 | 594 | 595 | −0.1 |
| 0 | 1.0290 | 0.09077 | 10.01 | 2.13 | 143.594 | 9.00030 | 444 | 452 | −1.9 |

[a] Data selected from solubilities determined at 25° using 18 solvent mixtures. [b] Calculated solubilities obtained by regressing $W$ *versus* $\delta_1$ in a third-degree power series (cubic). The cubic equation is Eq. 3*a* of Table IV. Essentially the same $X_{2_{calc}}$ values are obtained by regressing $W$ or log $\alpha_2/A$ on $\phi_w$ using Eq. 8*a* or 8*b* or by regressing $W$ or log $\alpha_2/A$ on $\epsilon_1$ (equations not shown). [c] $\delta_2 = 14.0$ (cal/cm$^3$)$^{1/2}$. [d] $X_2^i = 0.002913$, $-\log X_2^i = 2.5357$, $\Delta H_m^f = 9819$ cal/mole, $\Delta S_m^f = 15.81$ eu, and $V = 124$ ml/mole. [e] $V_2\phi_1^2/2.303RT$. [f] Solubility parameter obtained from Ref. 24 and by use of Eq. 14 of Ref. 2. [g] Experimentally determined dielectric constants of solvent mixtures at 25°.

is linear across the range of $\delta_1$ values while the correct value, $W$, produces a curve that passes through the $\delta_1\delta_2$ line. Only at two points where the straight line intersects the curve may the Hildebrand $\delta_1\delta_2$ values be used satisfactorily to predict the drug solubility.

**Predicting Solubility Using Regression Analysis**—As with theophylline and caffeine, theobromine solubility may be depicted using the extended solubility approach, *i.e.*, the regression of $W$ or log $\alpha_2/A$ on $\delta_1$ in a power series as reported earlier (1–3). The appropriate second degree (quadratic), third degree (cubic), and fourth degree (quartic) equations for theobromine in dioxane–water at 25° are given in Table IV. The solid line in Fig. 1, representing back-calculated solubilities of theobromine in dioxane–water mixtures, was obtained with Eq. 2*a* and demonstrates a good fit to experimental data. As observed in Eqs. 2*a*, 3*a*, and 4*a* of Table IV, when regressing $W$ *versus* $\delta_1$, five or six places should be retained after the decimal point for satisfactory results. In the log $\alpha_2/A$ *versus* $\delta_1$ equations (Eqs. 2*b*, 3*b*, and 4*b*), five or six places after the decimal points are also needed. The same remarks apply to Eqs. 5 and 6 of Table V. In Eqs. 8*a* and 8*b*, three places after the decimal point are adequate.

The question of when it is appropriate to use a quadratic *versus* a cubic or quartic equation is not easily answered without an analysis of variance. Statistical analysis of the solubility data will be presented in a separate report. Use of the extended solubility approach has shown that the data of some solubility studies (*e.g.*, theobromine in dioxane–water, Table II and Fig. 1) are satisfactorily reproduced with a quadratic equation. The solubility of caffeine in dioxane–water was better reproduced using a cubic equation and, for added refinement, a quartic equation (3). A fifth-degree equation was not necessary in any case studied thus far.

**Methylxanthines in Other Solvent Systems**—To examine the extended solubility approach in mixed solvents other than dioxane–water, solubilities of the three methylxanthines were measured at 25° in dioxane–formamide (Fig. 3), glycerin–propylene glycol (Fig. 4), and polyethylene glycol 400–water mixtures (Fig. 5). The quadratic regression equations of $W$ *versus* $\delta_1$ and log $\alpha_2/A$ *versus* $\delta_1$ used to obtain the back-calculated curves of Figs. 3 and 4 are found in Table V (Eqs. 5 and 6).

The original Hildebrand equation (4, 8) predicts that the solubility of a compound, the solubility parameter of which lies between the $\delta$ values of the two solvents of a binary mixture, will exhibit a peak where the solubility parameter of the mixed solvent, $\delta_1$, equals that of the solute, $\delta_2$. When $\delta_2$ of the solute is found on one side or the other of the solubility parameters of pure liquids that are combined to form the solvents, no peak is expected. For example, maximum solubility of theophylline is not found in the mixture of propylene glycol ($\delta_1 = 15.0$) and glycerin ($\delta_1 = 17.7$) since the solubility parameter of theophylline ($\delta_2 = 14.0$) does not fall between the $\delta$ values of these two solvents. However, this fact does not prevent the use of the extended Hildebrand solubility approach to calculate solubilities in solvent combinations such as glycerin and propylene glycol (Fig. 4).

**Solvation**—The solubilities of the three xanthines reach maxima below the ideal solubilities in dioxane–water mixtures. This failure to attain ideal solubility was attributed to solvent clustering (4), but a satisfactory explanation on a molecular basis has not been provided.

Solubility in excess of the ideal value is generally accepted as a manifestation of complexation between the solute and solvent and is commonly called solvation. Theophylline in the binary solvent of polyethylene glycol 400–water provides an example of solvation. Here the solubility rises to a maximum value of $X_2 = 0.0309$ (Fig. 5). In contrast to $W$ values for the xanthines in dioxane–water mixtures (Table III), $W$ for theophylline in polyethylene glycol 400–water is greater than $\delta_1\delta_2$ at maximum solubility. The $K$ value, which is equal to $W/\delta_1\delta_2$, is 1.0074 in this case.

The percent difference between maximum actual and ideal mole fraction solubility for theophylline in polyethylene glycol 400–water is 63%, whereas the difference, $\Delta = \delta_1\delta_2 - W$, is only 0.7%. Comparison of these results with the values in Table III again demonstrates that a very small difference between $\delta_1\delta_2$ and $W$ may result in a large difference between ideal and actual solubilities.

Thus, for real systems, drug solubility maxima in mixed solvents may be greater than, equal to, or less than ideal solubility, and $K = W/\delta_1\delta_2$ may have values greater than, equal to, or less than unity. When $K = 1.0$, a solution cannot necessarily be referred to as regular. In polar systems, the condition $W = \delta_1\delta_2$ may arise more or less by chance as observed in Fig. 2, where the $\delta_1\delta_2$ lines crosses $W$ at two points owing, perhaps, to a balancing of opposing intermolecular forces; thus, the conditions set forth by Hildebrand (8) for a regular solution would not obtain.

For solubilities greater than ideal, the sign of the logarithmic activity coefficients becomes negative ($\alpha_2 < 1$), and the computer program used to obtain $W_{calc}$ must take this fact into account. The $W$ calculated by regression always yields a positive log $\alpha_2$, and the computer is pro-

**Table III—Comparison of Observed Peak and Ideal Solubility Values of Caffeine, Theophylline, and Theobromine in Dioxane–Water Mixtures at 25°**

| Compound | $\delta_2$, (cal/cm$^3$)$^{1/2}$ | Ideal Solubility $X_2^i$ | Observed Peak Solubility $X_2$ | $\frac{X_2^i - X_2}{X_2^i} \times 100\%$ | $\delta_1\delta_2$ (cal/cm$^3$) | W, (cal/cm$^3$) | $\Delta$ [a] $= \delta_1\delta_2 - W$ (Percent Difference) | $K$ [a] $= W/\delta_1\delta_2$ |
|---|---|---|---|---|---|---|---|---|
| Caffeine | 13.8 | 0.0685 | 0.0282 | 59% | 193.200 | 191.715 | 1.485 (0.8%) | 0.9923 |
| Theophylline | 14.0 | 0.0190 | 0.0144 | 24% | 204.400 | 203.590 | 0.810 (0.4%) | 0.9960 |
| Theobromine | 14.0 | 0.0029 | 0.00075 | 74% | 196.000 | 193.319 | 2.681 (1.4%) | 0.9863 |

[a] The quantity $K$ was first suggested by E. Walker, J. Appl. Chem., 2, 470 (1952). The large differences between $X_2$ and $X_2^i$ resulting from very small differences $\Delta$ between $W$ and $\delta_1\delta_2$ were pointed out by Walker for polymer solutions.

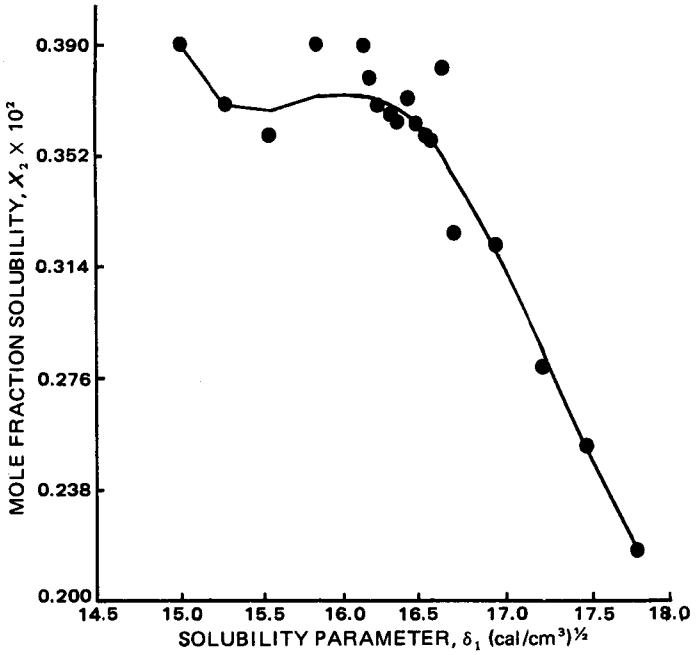


**Figure 4**—*Mole fraction solubility of theophylline in glycerin–propylene glycol mixtures at 25°. Key: ●, observed solubilities; and —, back-calculated solubility based on Eqs. 6a and 6b of Table V.*

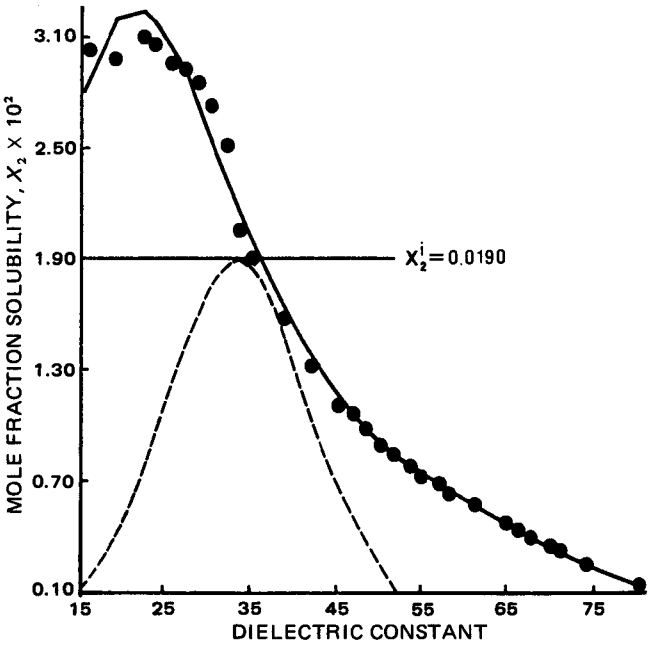


**Figure 5**—*Mole fraction solubility of theophylline in polyethylene glycol 400–water mixtures at 25°. Key: ●, observed solubilities; —, back-calculated solubility obtained by regressing W against solvent dielectric constant values based on Eqs. 7a and 7b of Table V; and ---, Hildebrand regular solution curve, which reaches a peak at $X_2^i$ at a solubility parameter of 14.*

grammed to reverse this sign when the calculated solubility $X_2$ is greater than $X_2^i$.

**Solubility Parameters and Dielectric Constant**—Other investigators (9–12) studied the solubility of methylxanthines and other classes of drugs as a function of the dielectric constants, $\epsilon_1$, of pure and mixed solvents. Employing 25 solvents of known $\delta_1$ and $\epsilon_1$ values, Paruta *et al.* (13) obtained:

$$\delta_1 = 7.5 + 0.22\epsilon_1 \qquad \text{(Eq. 9)}$$

to relate solvent solubility parameters to the solvent dielectric constant. The work leading to Eq. 9 (13) was repeated in the present study, regressing $\delta_1$ values of 35 liquids from various classes against dielectric constants obtained from a standard reference source (14), and the following was obtained:

$$\delta_1 = 8.3 + 0.19\epsilon_1 \qquad \text{(Eq. 10)}$$

In the particular series used in the current solubility analysis, $\delta_1$ values were regressed for each class of solvent against $\epsilon_1$ values. The resulting expression, Eqs. 11–13, with appropriate coefficients are found in Table VI. These linear expressions allow the conversion from $\delta_1$ to $\epsilon_1$ and vice versa in mixed solvent systems when studying solubility profiles expressed in terms of either solubility parameters or dielectric constants. While Eqs. 9 and 10 do not provide exact correspondence between $\delta_1$ and $\epsilon_1$ in specific solvent systems as do Eqs. 11–13, they do afford simple relationships for quick conversion between $\delta_1$ and $\epsilon_1$.

Since $\delta_1$ and $\epsilon_1$ are linearly related, it should be possible to regress log $\alpha_2/A$ or $W$ in a power series against $\epsilon_1$; $W$ and log $\alpha_2/A$ are regressed *versus* $\epsilon_1$ for theophylline in polyethylene glycol 400–water mixtures (Eqs. 7, Table V). The back-calculated solubility curve, Eq. 7b, for theophylline in this mixed solvent system is shown in Fig. 5. Figure 5 demonstrates that results showing mole fraction or molal solubility plotted against dielectric constant may be calculated using the extended solubility approach. Eq. 7b gives better results than Eq. 7a.

**Volume Fraction and Molar Volume**—However, neither $\delta_1$ nor $\epsilon_1$ are necessary to predict solubility. An earlier report (3) demonstrated that $W$, $\delta_1$, and $\delta_2$ may be by-passed and that a drug's solubility in a binary solvent may be back-calculated at a particular temperature based only on the volume fraction or percent of one solvent in another. (Molar

**Table IV—Equations Obtained from Regression of $W$ and Log $\alpha_2/A$ in Second-(Quadratic), Third-(Cubic), and Fourth-Degree (Quartic) Power Series on $\delta_1$ for Theobromine in Dioxane–Water Mixtures at 25°**

| | $W$ *versus* $\delta_1$ | Equation | Log $\alpha_2/A$ *versus* $\delta_1$ | Equation |
|---|---|---|---|---|
| Quadratic | $78.761046 + 2.294693\delta_1 + 0.417790\delta_1^2$ | 2*a* | $38.477909 - 4.589386\delta_1 + 0.164419\delta_1^2$ | 2*b* |
| Cubic | $81.160844 + 1.827037\delta_1 + 0.446860\delta_1^2 - 0.000579\delta_1^3$ | 3*a* | $33.678312 - 3.654074\delta_1 + 0.106281\delta_1^2 + 0.001158\delta_1^3$ | 3*b* |
| Quartic | $65.378019 + 5.948237\delta_1 + 0.055798\delta_1^2 + 0.015432\delta_1^3 - 0.000239\delta_1^4$ | 4*a* | $65.243960 - 11.896473\delta_1 + 0.888405\delta_1^2 - 0.030865\delta_1^3 + 0.000478\delta_1^4$ | 4*b* |

**Table V—Caffeine, Theophylline, and Theobromine in Solvent Mixtures at 25°: Quadratic Equations Obtained from Regression of $W$ and Log $\alpha_2/A$ *versus* $\delta$, $\epsilon_1$, and $\phi_w$**

| Mixture | $W$ *versus* $\delta_1$ | Equation | Log $\alpha_2/A$ *versus* $\delta_1$ | Equation |
|---|---|---|---|---|
| Caffeine in dioxane–formamide | $82.90558 + 1.36517\delta_1 + 0.44882\delta_1^2$ | 5*a* | $24.62885 - 2.73034\delta_1 + 0.10236\delta_1^2$ | 5*b* |
| Theophylline in glycerin–propylene glycol | $16.539654 + 9.924499\delta_1 + 0.182719\delta_1^2$ | 6*a* | $162.920693 - 19.848998\delta_1 + 0.634562\delta_1^2$ | 6*b* |
| **Mixture** | $W$ *versus* $\epsilon_1$ | **Equation** | Log $\alpha_2/A$ *versus* $\epsilon_1$ | **Equation** |
| Theophylline in polyethylene glycol 400–water | $129.56925 + 1.29791\epsilon_1 + 0.02046\epsilon_1^2$ | 7*a* | $6.781325 - 0.347859\epsilon_1 + 0.005543\epsilon_1^2$ | 7*b* |
| **Mixture** | $W$ *versus* $\phi_w$ (Volume Fraction of Water in Mixed Solvent) | **Equation** | Log $\alpha_2/A$ *versus* $\phi_w$ (Volume Fraction in Mixed Solvent) | **Equation** |
| Theobromine in Dioxane–Water | $143.453 + 143.768\phi_w + 75.088\phi_w^2$ | 8*a* | $9.164 - 18.042\phi_w + 30.184\phi_w^2$ | 8*b* |

**Table VI—Regression of $\delta_1$ *versus* $\epsilon_1$ for Solvent Mixtures at 25°**

| Mixed Solvent System | Regression Equation of $\delta_1$ *versus* $\epsilon_{25°}$ for Mixed Solvents[a] | Equation | $n$ | $r^2$ |
|---|---|---|---|---|
| Dioxane–water | $\delta_1 = 10.332\ (\pm 0.182) + 0.171\ (\pm 0.016)\epsilon_1$ | 11 | 18 | 0.995 |
| Glycerin–propylene glycol | $\delta_1 = 9.615\ (\pm 0.544) + 0.185\ (\pm 0.014)\epsilon_1$ | 12 | 11 | 0.986 |
| Polyethylene glycol 400–water | $\delta_1 = 7.541\ (\pm 0.156) + 0.196\ (\pm 0.004)\epsilon_1$ | 13 | 20 | 0.999 |

[a] Values in parentheses are ±1 *SE*.

volume of the solvent mixture may also be regressed against log $\alpha_2/A$ to reproduce experimental solubilities.) For theobromine in pure dioxane, pure water, and mixtures of this solvent pair, an equation relating log $\alpha_2/A$ and $\phi_w$, the volume fraction of water, is given as Eq. 8*b* in Table V. The log $\alpha_2/A$ and volume percent of water required for this calculation are found in Table II. With the value of $A$ (Table II) at a solvent volume fraction, *e.g.*, 0.40 or 40% water, log $\alpha_{2_{calc}} = 0.61427$ is obtained. This term, together with $-\log X_2^i = 2.5357$, yields $-\log X_2$. Changing the sign and taking the antilog provide the predicted solubility, $X_2 = 7.08 \times 10^{-4}$ at 25° for theobromine in water–dioxane mixtures having a $\delta_1$ value fo 15.39 and a dielectric constant of 27.46 (40% water–60% dioxane); $X_{2_{obs}}$ is equal to $6.74 \times 10^{-4}$. If one wishes to obtain the drug's solubility at another temperature, both $-\log X_2^i$ and $A$ will have new values. Densities of the solutions will also change with temperature.

If only molal or weight percent solubility data are accessible, together with volume percent of the liquids in a binary solvent, ideal solubility and $A$ values being lacking, quadratic equations can be obtained by regressing concentrations *versus* $\delta_1$, $\epsilon_1$, or $\phi_w$ to give fairly accurate back-calculations of solubility across the entire range of the solvent mixture. If the solubility is expressed in molarity, however, the method cannot be used directly. Instead, densities must be used to convert molarity to molality or mole fraction before regression *versus* $\delta_1$, $\epsilon_1$, or the solvent volume fraction can be conducted.

**Multiple Solubility Parameters of a Solute**—The peak solubility of caffeine in dioxane–formamide (Fig. 3) is found at a solvent $\delta_1$ value of 12, rather than the value of 13.8 observed for caffeine in dioxane–water systems. If the point of maximum solubility, where $\delta_1 \cong \delta_2$, is taken as a definition of $\delta_2$ for the drug molecule, then two $\delta$ values (12.0 and 13.8) must be accepted for caffeine. Other workers observed more than one solubility parameter for a solute. Hildebrand and Scott (15) found it necessary to adjust the $\delta_2$ value of iodine from 13.1 to 14.9 to account for variations in solute characteristics in some nonpolar and polar solvents; the solubility parameter ordinarily reported for iodine is 14.1. On investigating the solubility of sulfur in various solvents, Hildebrand and Scott (16) reported $\delta_2$ values for sulfur from ~11.5 to 14.5, although most of the values were in the 12–13 range.

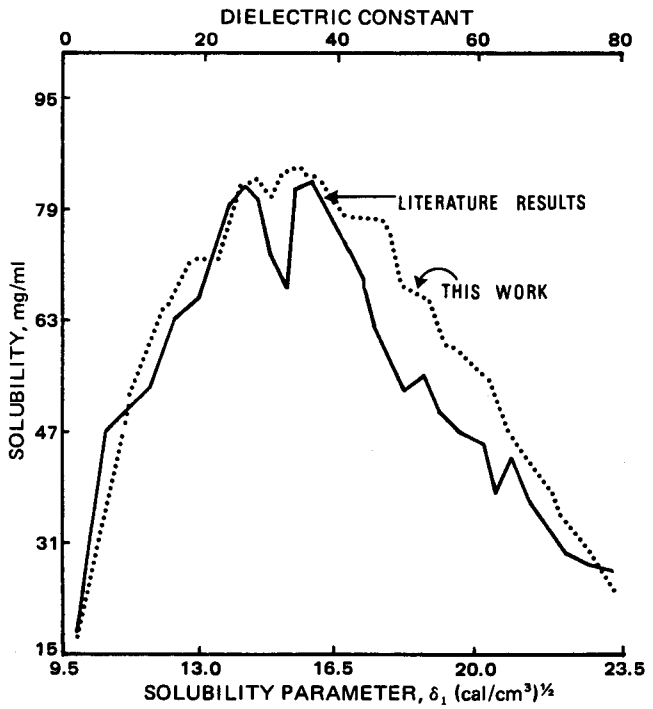


**Figure 6**—*Caffeine in dioxane–water mixtures at 25°. Solubility profiles were obtained from two studies (Ref. 2 is this work and Ref. 11 is literature results). The $\delta_2$ value at peak solubility occurs at ~$\delta_1$ = 15.*

Baker (17) found that solvents partitioned between amorphous and crystalline regions of semicrystalline polymers in solution. Based on solubility and swelling studies, he distinguished three distinct solubility parameters for a polymer. For example, the solubility parameters for butyl rubber at 25° were 7.15, 8.46, and 9.51. For atactic polypropylene at 40°, the $\delta_2$ values were 7.01, 8.07, and 9.38. Other reports (11, 12) showed that methylxanthines in various binary solvent systems exhibited peak solubilities at different solvent dielectric constants. Therefore, it is not surprising that the $\delta_2$ of caffeine obtained from peak solubilities in binary solvents varies according to the solvent mixture employed.

Although the studies reported here are preliminary, it appears from current work that drugs exhibit multiple solubility parameters (one or several for the solute in nonpolar and moderately polar solvents and multiple values in highly solvating and complexing solvents). Fortunately, multiple $\delta_2$ values for a drug do not adversely affect the extended solubility approach. The appropriate $\delta_2$ value is obtained from the method of Fedors (18), the maximum in the solubility profile for a dioxane–water system, or a regression method reported elsewhere (19, 20). The solute solubility parameter, $\delta_2$, so determined is then used with $W$ and $\delta_1$ of the solvent mixture to back-calculate solubilities.

The physicochemical phenomenon on which multiple solute values are based is difficult to explain. Hoy (21) suggested that solutes may behave in a "chameleon-like" manner, adapting to the solvent environment in which they are found. For example, carboxylic acids interact through hydrogen bonds with alcohols and water in these highly polar solvents, whereas such acids self-associate in nonpolar solvents. Therefore, the solubility parameters of these solutes would be expected to have different values in various pure and mixed solvents.

The shape and position of the peak in a solubility profile are altered when solubility is plotted as molarity or milligrams per milliliter instead of mole fraction. The solubility profile for caffeine in dioxane–water mixtures, obtained in this work and from the literature (11), is plotted against $\delta_1$ and $\epsilon_1$ in Fig. 6. The solubility values from the two studies vary somewhat but produce essentially the same profiles. The $\delta_2$ value from the peak solubility of a milligrams per milliliter *versus* $\delta_1$ plot, as seen here, would be ~15, as contrasted to a value of 13.8 obtained from a plot of mole fraction solubility of caffeine in dioxane–water mixtures.

## CONCLUSIONS

The extended solubility approach was shown to apply to three methylxanthines, theophylline, caffeine, and theobromine, in a number of binary solvent systems. It was suggested (1–3) that $W$, the solute–solvent interaction energy, may be regressed in a second, third, or fourth degree power series in terms of the pure or mixed solvent solubility parameter, $\delta_1$, to reproduce the experimental solubility curve. Direct regression of log $\alpha_2/A$ on $\delta_1$, together with a knowledge of $A$ and the drug's ideal solubility at the temperature of the experiment, provides a method for accurately reproducing solubilities of drugs in binary solvent mixtures. In an earlier study (3), it was possible to regress log $\alpha_2/A$ on $\phi_i$, where $\phi_i$ is the volume fraction of one of the two solvents in a binary solvent mixture. In the present report, the linear relationship between $\delta_1$ and $\epsilon_1$, first reported by Paruta *et al.* (13), was confirmed for various solvent systems. For the purpose of predicting solubility, it is possible to regress log $\alpha_2/A$ or $W$ directly *versus* $\epsilon_1$ in a quadratic or higher power series, as shown here. These various approaches yield back-calculated mole fraction solubility within experimental error.

The apparent success of the extended Hildebrand solubility approach to date suggests that Eq. 1, an extension of the Hildebrand equation without the restriction of the geometric mean, provides a satisfactory empirical representation for the solubility of drugs in polar binary solvent systems. In this method, $W$ is obtained from solubility data and then back-calculated by regressing $W$ against $\delta_1$, $\phi_i$, or $\epsilon_1$. This technique may not appear to be fruitful in affording *ab initio* predictions of solubilities or providing fundamental information about solvent–solute interaction since solubility data are required for the method. However, the form of the empirical equation appears to be correct for handling relatively polar

as well as nonpolar systems. An effort is being made to obtain $W$ without solubility data, with the possibility of finding a physicochemical basis for $W$ and/or a group contribution method for estimating this solvent–solute interaction term.

It is interesting to observe in Table III and in Figs. 1 and 5 that small (fractional to 1 or 2%) differences between $\delta_1\delta_2$, the geometric mean, and $W$, the correct adhesive energy density, may cause large differences (25–75%) between ideal and real solubilities. It will challenge the investigator to measure and calculate energies within 5–50 cal/mole required for an independent measure of $W$ for accurate estimation of solubilities. The prediction of solubility using $W$ from group contributions would represent a step toward a better understanding of the behavior of drug molecules in polar and nonpolar solvent systems.

## REFERENCES


(1) A. Martin, J. Newburger, and A. Adjei, *J. Pharm. Sci.*, 68(10), IV (1979).

(2) *Ibid.*, **69**, 487 (1980).

(3) A. Adjei, J. Newburger, and A. Martin, *J. Pharm. Sci.*, **69**, 659 (1980).

(4) L. J. Gordon and R. L. Scott, *J. Am. Chem. Soc.*, **74**, 4138 (1952).

(5) M. J. Chertkoff and A. Martin, *J. Am. Pharm. Assoc., Sci. Ed.*, **49**, 444 (1960).

(6) F. A. Restaino and A. Martin, *J. Pharm. Sci.*, **53**, 636 (1964).

(7) G. Scatchard, S. E. Wood, and J. M. Mochel, *J. Am. Chem. Soc.*, **68**, 1959 (1946).

(8) J. H. Hildebrand and R. L. Scott, "The Solubility of Nonelectrolytes," 3rd ed., Dover, New York, N.Y., 1964.

(9) A. N. Paruta, B. J. Sciarrone, and N. G. Lordi, *J. Pharm. Sci.*, **54**, 838 (1965).

(10) A. N. Paruta and B. B. Sheth, *ibid.*, **55**, 896 (1966).

(11) A. N. Paruta and S. A. Irani, *ibid.*, **55**, 1055 (1966).

(12) *Ibid.*, **55**, 1060 (1966).

(13) A. N. Paruta, B. J. Sciarrone, and N. G. Lordi, *J. Pharm. Sci.*, **51**, 704 (1962).

(14) R. C. Weast, "Handbook of Chemistry and Physics," CRC Press, Cleveland, Ohio, 1978.

(15) J. H. Hildebrand and R. L. Scott, "The Solubility of Nonelectrolytes," 3rd ed., Dover, New York, N.Y., 1964, p. 274.

(16) *Ibid.*, p. 280.

(17) E. G. Baker, presented at the International Symposium on Macromolecular Chemistry, International Union of Pure and Applied Chemistry, Toronto, Canada, 1968.

(18) R. F. Fedors, *Polym. Eng. Sci.*, **14**, 147 (1974).

(19) G. Cavé, R. Kothari, F. Puisieux, A. Martin, and J. T. Carstensen, *Int. J. Pharm.*, **5**, 267 (1980).

(20) A. Martin and J. Carstensen, *J. Pharm. Sci.*, **70**, 170 (1981).

(21) K. Hoy, *J. Paint Technol.*, **42**, 76 (1970).

(22) K. C. James, C. T. Ng, and P. R. Noyce, *J. Pharm. Sci.*, **65**, 656 (1976).

(23) "Isolation and Identification of Drugs," E. G. C. Clark, Ed., Pharmaceutical Press, London, England, 1974, pp. 234, 567, 568.

(24) K. Hoy, B. A. Price, and R. A. Martin, "Tables of Solubility Parameters," Union Carbide, Tarrytown, N.Y., 1975.


## ACKNOWLEDGMENTS


Supported in part by an endowed professorship to A. Martin by Mr. Coulter Sublett.

The authors acknowledge the assistance of P. L. Wu, who obtained the regression equation of $\delta_1$ *versus* dielectric constant and T. Velasquez for solubility determinations of theophylline in mixtures of polyethylene glycol and water. They also thank Terri Shrode and Nancy Irvin for secretarial assistance.


# Degradation Kinetics and Mechanism of Aminocephalosporins in Aqueous Solution: Cefadroxil


**AKIRA TSUJI *x, EMI NAKASHIMA *, YOSHIHARU DEGUCHI *, KAZUNORI NISHIDE *, TAKAYOSHI SHIMIZU §, SUMIO HORIUCHI §, KIYOYASU ISHIKAWA §, and TSUKINAKA YAMANA ‡**



Received December 12, 1980, from the **Faculty of Pharmaceutical Sciences and the* ‡*Hospital Pharmacy, Kanazawa University, Takaramachi, Kanazawa 920, Japan,* and the §*Nonclinical Research Laboratories, Bristol Banyu Manufacturing Co., Ltd., Kota-cho, Nukata-Gun, Aichi 444-01, Japan.* Accepted for publication March 3, 1981.



**Abstract** □ The degradation kinetics and mechanism of a new, orally effective cephalosporin derivative, cefadroxil, in aqueous solution were investigated at pH 2.51–11.5 at 35° and ionic strength 0.5. The degradation rates were determined by high-pressure liquid chromatography. At constant pH and temperature, the degradation followed first-order kinetics and a log $k$–pH profile was presented. The shape of the rate–pH profile resembled that for cephalexin or cephradine under the same conditions. Citrate and phosphate buffers enhanced general acid and base catalysis of the degradation. In aqueous solution, cefadroxil was shown to degrade by three parallel reactions: (*a*) intramolecular aminolysis by the C-7 side-chain amino group on the $\beta$-lactam moiety, (*b*) water-catalyzed or spontaneous hydrolysis, and (*c*) $\beta$-lactam cleavage by the nucleophilic attack of hydroxide ion. In neutral and weak alkaline solutions, the main degradation products were two piperazine-2,5-diones and 3-hydroxy-4-methyl-2(5*H*)-thiophenone, the former being formed from Reaction *a*, while the latter arose *via* the degradation pathways of Reactions *b* and/or *c*.



**Keyphrases** □ Cefadroxil—degradation kinetics and mechanism, high-pressure liquid chromatography, pH–rate profile, intramolecular aminolysis to produce piperazinediones, buffer and temperature effects □ Degradation kinetics—cefadroxil, high-pressure liquid chromatography assay, pH–rate profile, intramolecular aminolysis to produce piperazinediones, buffer and temperature effects □ pH–rate profile—cefadroxil, degradation kinetics and mechanism, intramolecular aminolysis to produce piperazinediones, buffer and temperature effects □ Piperazinediones—cefadroxil degradation kinetics and mechanism, intramolecular aminolysis


A previous study (1) determined the degradation kinetics of a series of cephalosporins in aqueous solution at 35° and ionic strength 0.5. The degradation of cephalosporins possessing an $\alpha$-amino group in their C-7 side chain, such as cephalexin, cephradine, and cephaloglycin, was facilitated by the intramolecular attack of the amino group to the reactive $\beta$-lactam moiety at neutral pH (1–4). The relative instability of cephaloglycin under physio-




*0022-3549/81/1000-1120$01.00/0*


*© 1981, American Pharmaceutical Association*

as well as nonpolar systems. An effort is being made to obtain $W$ without solubility data, with the possibility of finding a physicochemical basis for $W$ and/or a group contribution method for estimating this solvent–solute interaction term.

It is interesting to observe in Table III and in Figs. 1 and 5 that small (fractional to 1 or 2%) differences between $\delta_1\delta_2$, the geometric mean, and $W$, the correct adhesive energy density, may cause large differences (25–75%) between ideal and real solubilities. It will challenge the investigator to measure and calculate energies within 5–50 cal/mole required for an independent measure of $W$ for accurate estimation of solubilities. The prediction of solubility using $W$ from group contributions would represent a step toward a better understanding of the behavior of drug molecules in polar and nonpolar solvent systems.

## REFERENCES


(1) A. Martin, J. Newburger, and A. Adjei, *J. Pharm. Sci.*, 68(10), IV (1979).

(2) *Ibid.*, **69**, 487 (1980).

(3) A. Adjei, J. Newburger, and A. Martin, *J. Pharm. Sci.*, **69**, 659 (1980).

(4) L. J. Gordon and R. L. Scott, *J. Am. Chem. Soc.*, **74**, 4138 (1952).

(5) M. J. Chertkoff and A. Martin, *J. Am. Pharm. Assoc., Sci. Ed.*, **49**, 444 (1960).

(6) F. A. Restaino and A. Martin, *J. Pharm. Sci.*, **53**, 636 (1964).

(7) G. Scatchard, S. E. Wood, and J. M. Mochel, *J. Am. Chem. Soc.*, **68**, 1959 (1946).

(8) J. H. Hildebrand and R. L. Scott, "The Solubility of Nonelectrolytes," 3rd ed., Dover, New York, N.Y., 1964.

(9) A. N. Paruta, B. J. Sciarrone, and N. G. Lordi, *J. Pharm. Sci.*, **54**, 838 (1965).

(10) A. N. Paruta and B. B. Sheth, *ibid.*, **55**, 896 (1966).

(11) A. N. Paruta and S. A. Irani, *ibid.*, **55**, 1055 (1966).

(12) *Ibid.*, **55**, 1060 (1966).

(13) A. N. Paruta, B. J. Sciarrone, and N. G. Lordi, *J. Pharm. Sci.*, **51**, 704 (1962).

(14) R. C. Weast, "Handbook of Chemistry and Physics," CRC Press, Cleveland, Ohio, 1978.

(15) J. H. Hildebrand and R. L. Scott, "The Solubility of Nonelectrolytes," 3rd ed., Dover, New York, N.Y., 1964, p. 274.

(16) *Ibid.*, p. 280.

(17) E. G. Baker, presented at the International Symposium on Macromolecular Chemistry, International Union of Pure and Applied Chemistry, Toronto, Canada, 1968.

(18) R. F. Fedors, *Polym. Eng. Sci.*, **14**, 147 (1974).

(19) G. Cavé, R. Kothari, F. Puisieux, A. Martin, and J. T. Carstensen, *Int. J. Pharm.*, **5**, 267 (1980).

(20) A. Martin and J. Carstensen, *J. Pharm. Sci.*, **70**, 170 (1981).

(21) K. Hoy, *J. Paint Technol.*, **42**, 76 (1970).

(22) K. C. James, C. T. Ng, and P. R. Noyce, *J. Pharm. Sci.*, **65**, 656 (1976).

(23) "Isolation and Identification of Drugs," E. G. C. Clark, Ed., Pharmaceutical Press, London, England, 1974, pp. 234, 567, 568.

(24) K. Hoy, B. A. Price, and R. A. Martin, "Tables of Solubility Parameters," Union Carbide, Tarrytown, N.Y., 1975.


## ACKNOWLEDGMENTS


Supported in part by an endowed professorship to A. Martin by Mr. Coulter Sublett.

The authors acknowledge the assistance of P. L. Wu, who obtained the regression equation of $\delta_1$ *versus* dielectric constant and T. Velasquez for solubility determinations of theophylline in mixtures of polyethylene glycol and water. They also thank Terri Shrode and Nancy Irvin for secretarial assistance.


# Degradation Kinetics and Mechanism of Aminocephalosporins in Aqueous Solution: Cefadroxil


**AKIRA TSUJI *x, EMI NAKASHIMA *, YOSHIHARU DEGUCHI *, KAZUNORI NISHIDE *, TAKAYOSHI SHIMIZU §, SUMIO HORIUCHI §, KIYOYASU ISHIKAWA §, and TSUKINAKA YAMANA ‡**



Received December 12, 1980, from the **Faculty of Pharmaceutical Sciences and the* ‡*Hospital Pharmacy, Kanazawa University, Takaramachi, Kanazawa 920, Japan,* and the §*Nonclinical Research Laboratories, Bristol Banyu Manufacturing Co., Ltd., Kota-cho, Nukata-Gun, Aichi 444-01, Japan.* Accepted for publication March 3, 1981.



**Abstract** □ The degradation kinetics and mechanism of a new, orally effective cephalosporin derivative, cefadroxil, in aqueous solution were investigated at pH 2.51–11.5 at 35° and ionic strength 0.5. The degradation rates were determined by high-pressure liquid chromatography. At constant pH and temperature, the degradation followed first-order kinetics and a log $k$–pH profile was presented. The shape of the rate–pH profile resembled that for cephalexin or cephradine under the same conditions. Citrate and phosphate buffers enhanced general acid and base catalysis of the degradation. In aqueous solution, cefadroxil was shown to degrade by three parallel reactions: (*a*) intramolecular aminolysis by the C-7 side-chain amino group on the $\beta$-lactam moiety, (*b*) water-catalyzed or spontaneous hydrolysis, and (*c*) $\beta$-lactam cleavage by the nucleophilic attack of hydroxide ion. In neutral and weak alkaline solutions, the main degradation products were two piperazine-2,5-diones and 3-hydroxy-4-methyl-2(5*H*)-thiophenone, the former being formed from Reaction *a*, while the latter arose *via* the degradation pathways of Reactions *b* and/or *c*.



**Keyphrases** □ Cefadroxil—degradation kinetics and mechanism, high-pressure liquid chromatography, pH–rate profile, intramolecular aminolysis to produce piperazinediones, buffer and temperature effects □ Degradation kinetics—cefadroxil, high-pressure liquid chromatography assay, pH–rate profile, intramolecular aminolysis to produce piperazinediones, buffer and temperature effects □ pH–rate profile—cefadroxil, degradation kinetics and mechanism, intramolecular aminolysis to produce piperazinediones, buffer and temperature effects □ Piperazinediones—cefadroxil degradation kinetics and mechanism, intramolecular aminolysis


A previous study (1) determined the degradation kinetics of a series of cephalosporins in aqueous solution at 35° and ionic strength 0.5. The degradation of cephalosporins possessing an $\alpha$-amino group in their C-7 side chain, such as cephalexin, cephradine, and cephaloglycin, was facilitated by the intramolecular attack of the amino group to the reactive $\beta$-lactam moiety at neutral pH (1–4). The relative instability of cephaloglycin under physio-




*0022-3549/81/1000-1120$01.00/0*


*© 1981, American Pharmaceutical Association*

logical conditions was attributed to this phenomenon, its half-life being only ~5 hr. Although cephalexin and cephradine react similarly, they were much more stable than cephaloglycin under the same conditions. Because of the intramolecular aminolysis of these aminocephalosporins in aqueous solution, stable piperazinediones were formed (1–3, 5–7).

This paper describes the degradation kinetics and mechanisms of a new, orally effective cephalosporin antibiotic, cefadroxil (I), which shows essentially the same antibacterial spectrum as cephalexin (8). It is structurally similar to cephalexin, differing only in the hydroxylation of the phenyl side chain.

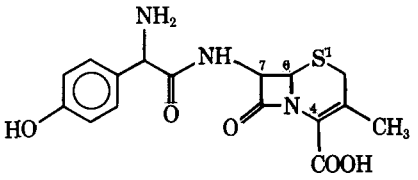

I

## EXPERIMENTAL[1]

**Materials**—Cefadroxil monohydrate (947 μg/mg) was used without further purification. Buffers and all other chemicals were reagent grade.

**Buffers**—Citrate and phosphate buffers (pH 2.51–5.82 and 6.00–7.20, respectively) were used for the kinetic study. At pH > 7.20, a pH-stat[2] was used to maintain a constant pH. All buffers of the kinetic solutions were adjusted with potassium chloride to an ionic strength of 0.5. The pH was measured[2] at the temperature of the kinetic study.

**Kinetic Procedures**—All kinetic experiments were carried out at 35 ± 0.1° and ionic strength 0.5 unless otherwise stated. Accurately weighed cefadroxil was dissolved in an appropriate buffer or 0.5 *M* potassium chloride solution preheated to the desired temperature to give an initial concentration of $5 \times 10^{-3}$ *M*. The fast reaction was performed in a glass-stoppered 100-ml volumetric flask. Where the half-life was >1 day, the degradation buffer solution was sealed in 5-ml ampuls. Samples were withdrawn at suitable intervals, cooled in an ice bath, diluted with distilled water if necessary, and analyzed.

The degradation rate of cefadroxil was followed by measuring the remaining drug concentration by a reversed-phase high-pressure liquid chromatographic (HPLC) method. In addition to the HPLC determination of the overall degradation rate of cefadroxil, the decrease in the concentration of the primary amino group in cefadroxil during the degradation was followed by a colorimetric assay.

**Analytical Procedures**—*HPLC*—The liquid chromatograph[3] was equipped with a UV detector[4] set at 254 nm and a 4.0 × 300-mm stainless steel column prepacked with octadecylsilane chemically bonded on totally porous silica gel[5]. The mobile phase was 2% (or 3%) acetonitrile–98% (or 97%) 0.01 *M* ammonium acetate aqueous solution. Chromatography was performed at ambient temperatures, and samples were eluted at a flow rate of 2 ml/min. Peak heights were measured, and the concentrations were calculated from the calibration curves obtained daily.

*Colorimetric Assay*—The primary amino group was quantitated by using the trinitrobenzenesulfonic acid assay of Satake *et al.* (9) in a modified form used previously (3) for cephalexin degradation.

A 500-μl aliquot of the degradation solution containing cefadroxil was added to 2 ml of a 0.2 *M* phosphate buffer at pH 7.6. Thereafter, 2 ml of a 0.2% (w/v) aqueous solution of 2,4,6-trinitrobenezenesulfonic acid was added; after standing for 30 min in darkness at room temperature, the absorbance of the resulting orange solution was measured[6] at 420 nm against a blank consisting of 500 μl of reaction solution without cefadroxil, 2 ml of phosphate buffer, and 2 ml of trinitrobenzenesulfonic acid solution treated similarly.

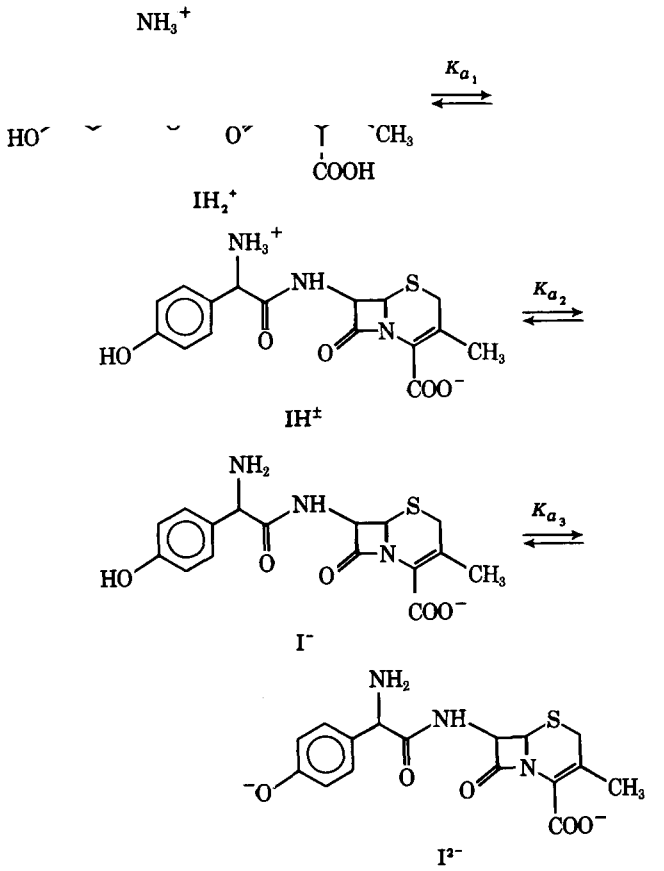

*Scheme I*

*Determination of Ionization Constants*—The apparent ionization constants, $pK_{a_1}$ and $pK_{a_2}$, for the dissociation of carboxylic acid and the α-ammonium group of cefadroxil (Scheme I) were determined to be 2.64 ± 0.03 and 7.30 ± 0.03, respectively, by the potentiometric titration of 0.01 *M* antibiotic aqueous solution at an ionic strength of 0.5 and 35°. The $pK_{a_3}$ value for the phenolic group of cefadroxil was determined spectrophotometrically (10). The calculation was made from the change in absorbance[6] at 250 nm for $5 \times 10^{-5}$ *M* cefadroxil solution adjusted to ionic strength 0.5 with potassium chloride at various pH values and 35° to give $pK_{a_3} = 9.69 \pm 0.06$.

**TLC**—TLC was conducted on precoated silica gel plates 0.25-mm thick. Developing solvents were: Solvent A, chloroform–ethyl acetate–acetic acid–water (4:4:4:1); Solvent B, methyl isobutyl ketone–acetic acid–water (7:2:1); Solvent C, toluene–butanol–acetic acid–water (4:4:3:1); and Solvent D, ethyl acetate–isopropanol–water (10:7:5). The chromatograms were visualized by exposing the plates to iodine vapor.

**Isolation and Identification of Degradation Products in Basic Aqueous Solution**—Cefadroxil (2.5 g) in 0.1 *M* disodium phosphate solution (50 ml) was kept at 60° for 1 hr at pH 9.1. The reaction mixture gave four spots on TLC. Acidification with dilute hydrochloric acid and subsequent fractionation as shown in Scheme II gave the product II (25 mg) and a mixture of IV and V slightly contaminated with III (370 mg).

*Product II*—Recrystallization from chloroform–hexane yielded the pure compound, mp 118–119.5°; IR: 3370 (OH), 1690 (thiolactone), and 1630 (olefin) $cm^{-1}$; PMR (deuterochloroform): δ 2.09 (s, 3H, $CH_3$), 3.74 (s, 2H, $CH_2$), and 6.10 (s, 1H, OH) ppm; UV (water-methanol, 9:1): $\lambda_{max}$ 246, 255 (shoulder), 246, and 304 nm (0.1 *N* NaOH added).

*Anal.*—Calc. for $C_5H_6O_2S$: C, 46.14; H, 4.65. Found: C, 45.83; H, 4.61.

[1] IR spectra were run in potassium bromide using a Hitachi 215 spectrophotometer. UV spectra were recorded with a Shimadzu UV-300 spectrophotometer. PMR spectra were obtained, unless otherwise stated, in deuterated dimethyl sulfoxide on a Hitachi R-24B (60 MHz) spectrometer with chemical shifts measured relative to tetramethylsilane. Elemental analyses were carried out at the Central Analysis Center, Nagoya City University, Japan. Preparative TLC was conducted on Merck precoated TLC plates (silica gel 60 F254, 0.5- or 2 mm thick). Visualization was done with iodine vapor. Melting points were determined on a heat block melting-point apparatus and are uncorrected.

[2] pH-Stat titrator assembly consisting of TTT2 titrator and ABU12b autoburet, Radiometer, Copenhagen, Denmark, and PHM26 pH meter, Radiometer, Copenhagen, Denmark.

[3] Model FLC-A700, Japan Spectroscopic Co., Tokyo, Japan.

[4] Model UVIDEC-100, Japan Spectroscopic Co., Tokyo, Japan.

[5] μBondapak $C_{18}$, Waters Associates, Milford, Mass.

[6] Double-beam spectrophotometer, UV-200, Shimadzu, Kyoto, Japan.

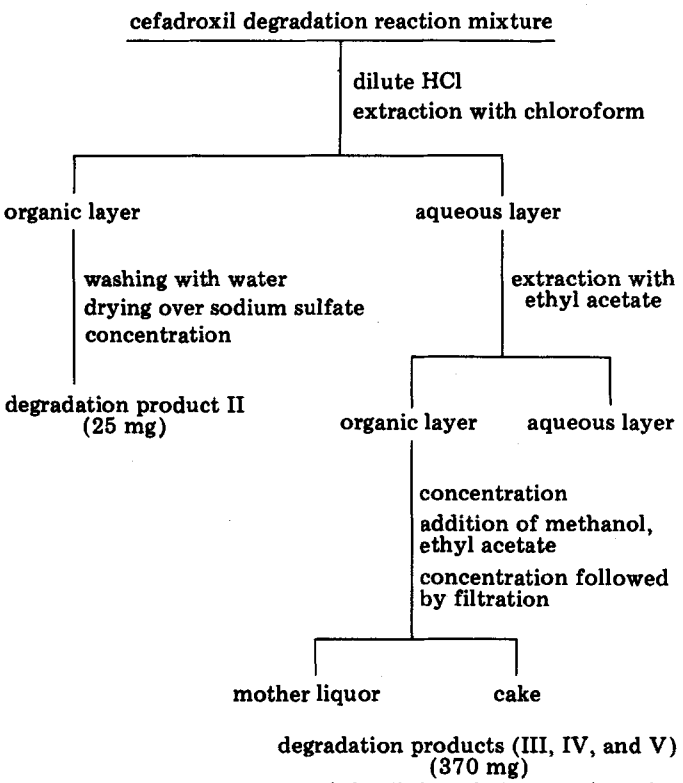


*Scheme II—Fractionation of cefadroxil degradation reaction mixture.*

*Mixture of Products of IV and V*—IR: 3500–3000 (OH, NH), 1710 (shoulder, carboxyl), and 1660 (amide) $cm^{-1}$; PMR ($d_5$-pyridine): δ 1.43 (d, 8 Hz) and 2.41 (s) ppm (~2:1); PMR ($d_5$-pyridine–deuterium oxide): δ 1.44 (s) and 2.45 (s) ppm; PMR (deuterium oxide–potassium carbonate): δ 1.21 (s) ppm; UV (methanol): $\lambda_{max}$ 225 and 273 nm; TLC: $R_f$ (Solvent D) 0.62 (III, trace), 0.55 (IV), and 0.45 (V).

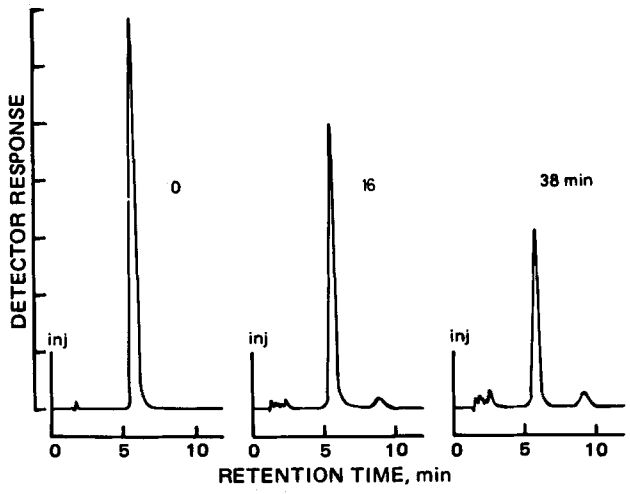


**Figure 1**—*Changes in the high-pressure liquid chromatogram during cefadroxil degradation at pH 11.50, 35°, and ionic strength 0.5 with time. The mobile phase was 2% acetonitrile–98% 0.01 M ammonium acetate, and samples were eluted at a flow rate of 2 ml/min.*

**Degradation Products in Organic Solvent System**—A suspension of cefadroxil (10 g) in methanol (250 ml) was refluxed for 3 hr while acetonitrile (100 ml) was added dropwise. Evaporation of the solvent *in vacuo* followed by the addition of chloroform (400 ml) to the residue yielded a precipitate (7.6 g), which was identified by IR and TLC as the mixture of IV and V slightly contaminated with III.

**Methyl Esters of Products IV and V**—The mixture of IV and V (7.5 g) was dissolved in warm methanol. After cooling, an ethereal solution (150 ml) of diazomethane, generated from *N*-methyl-*N*-nitroso-*p*-tolu-

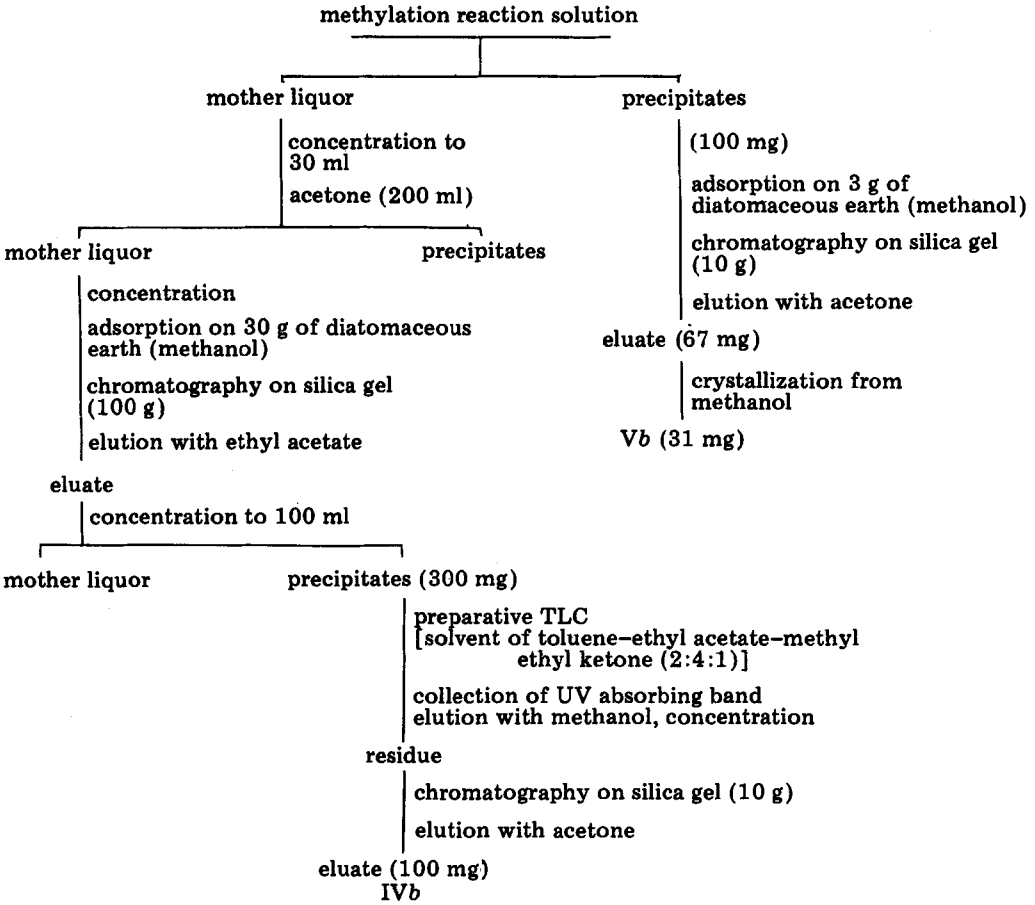


*Scheme III—Fractionation of the methylation reaction solution of cefadroxil degradation products.*

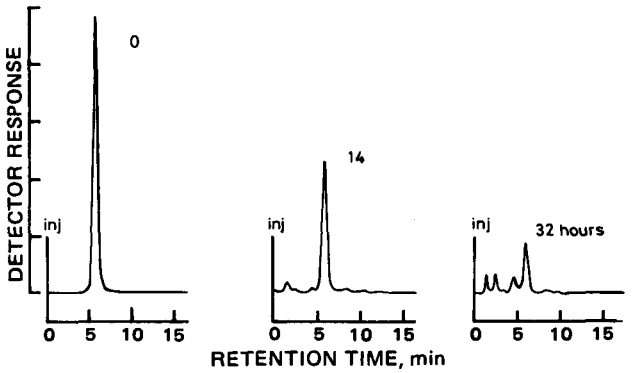


**Figure 2**—*Changes in the high-pressure liquid chromatogram during cefadroxil degradation at pH 7.20 (0.15 M phosphate), 35°, and ionic strength 0.5 with time. The mobile phase was 2% acetonitrile–98% 0.01 M ammonium acetate, and samples were eluted at a flow rate of 2 ml/min.*

enesulfonamide (30 g), was added dropwise over 1 hr. The precipitate (2.2 g) was filtered, and a part (100 mg) was chromatographed on silica gel (10 g) with acetone as the eluent to give pure ester V*b* (67 mg), mp 212–213°; IR: 3500–3000 (OH, NH), 1730 (ester), and 1680 (amide) $cm^{-1}$; PMR: δ 1.20 (d, $J$ = 7 Hz, 3H), ~3 (m, 3H), 3.80 (s, 3H), 4.05 (m, 1H), 5.03 (s, 1H), 5.41 (m, 1H), 6.78 (d, $J$ = 9 Hz, 4H), 7.85 (d, 1H, exchangeable), 8.38 (s, 1H, exchangeable), and 9.31 (b, 1H, exchangeable) ppm; UV: $\lambda_{max}$ 226 and 276 nm.

*Anal.*—Calc. for $C_{17}H_{19}N_3O_5S$: C, 54.10; H, 5.07; N, 11.13. Found: C, 53.98; H, 5.00; N, 10.68.

The filtrate was separated as shown in Scheme III to give a small amount of ester IV*b*. Recrystallization from methanol yielded 100 mg of the pure ester, mp 214–215°; IR: 3500–3000 (OH, NH), 1720 (ester), and 1660 (amide) $cm^{-1}$; PMR: δ 2.04 (s, 3H), 3.05–3.5 (m, 2H), 4.25–4.6 (m, 2H), 4.85 (s, 1H), 6.55–7.3 (d, J = 9 Hz, 4H), 8.21 (s, 1H, exchangeable), 8.71 (s, 1H, exchangeable), and 9.37 (b, 1H, exchangeable) ppm; UV (methanol): $\lambda_{max}$ 230 and 277 nm.

*Anal.*—Calc. for $C_{17}H_{19}N_3O_5S$: C, 54.10; H, 5.07; N, 11.13. Found: C, 53.53; H, 5.05; N, 10.93.

***N*-Acetylcefadroxil (VI)**—A suspension of cefadroxil (3 g) in acetic anhydride (200 ml) was stirred at ambient temperature for 15 hr. The precipitate was filtered and washed with water to yield pure VI (1.7 g, 53.3%) after recrystallization from methanol, mp 217–220° (dec.); IR: 3500–3000 (OH, NH), 1765 (β-lactam), 1735 (shoulder, carboxyl), and 1655 (amide) $cm^{-1}$; PMR: δ 1.88 (s, 3H, acetyl), 1.98 (s, 3H, 3-methyl), 3.0–3.7 (dd, $J$ = 18 Hz, 2H, 2-$CH_2$), 4.93 (d, $J$ = 5 Hz, 1H, 6-CH), 5.4–5.7 (broad, 3H, benzylic and 7-CH), 6.5–7.4 (dd, $J$ = 8 Hz, 4H, aromatic), 8.35 (d, $J$ = 9 Hz, 1H, 7-NH), 9.07 (d, $J$ = 9 Hz, 1H, NH of acetamide), and 9.3 (broad, 1H, phenolic) ppm; UV (water): $\lambda_{max}$ 228 and 263 nm.

*Anal.*—Calc. for $C_{18}H_{19}N_3O_6S$: C, 53.33; H, 4.72; N, 10.36. Found: C, 52.84; H, 4.33; N, 9.94.

## RESULTS AND DISCUSSION

**Order of Degradation and Observed Rate Constants**—The kinetics of cefadroxil degradation was followed by the HPLC method using an appropriate buffer system or a pH-stat to maintain a constant pH. Typical chromatograms of basic (pH 11.50, pH-stat) and neutral (pH 7.20, 0.15 *M* phosphate buffer) reaction mixtures, sampled at suitable time intervals, are shown in Figs. 1 and 2, indicating that the degradation products can be separated from the parent compound. Figure 3 shows the logarithmic plots of the residual cefadroxil concentration *versus* time at pH 11.50 for three different initial concentrations of 1, 5, and $10 \times 10^{-3}$ *M*. The observed pseudo-first-order rate constants were almost identical to the overall degradation of cefadroxil calculated from the slopes and were independent of initial drug concentration.

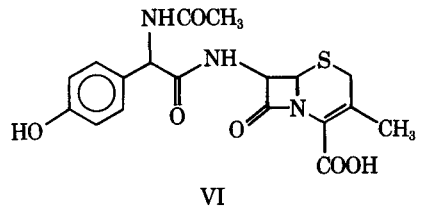


VI

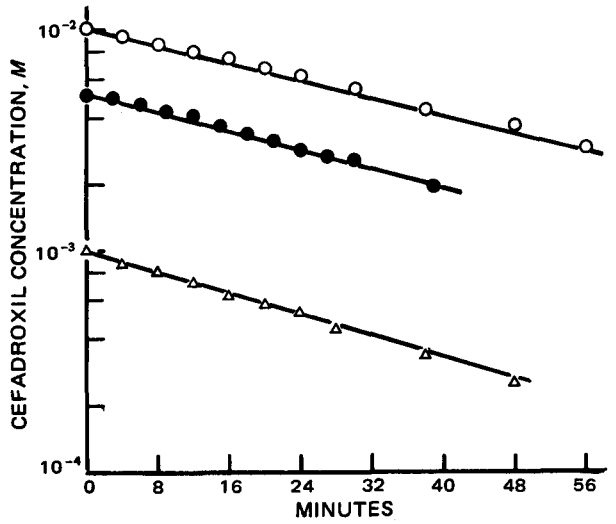


**Figure 3**—*Apparent first-order plots for cefadroxil degradation at three different concentrations (○, 1 × $10^{-2}$ M; ●, 5 × $10^{-3}$ M; and △, 1 × $10^{-3}$ M) at pH 11.50, 35°, and ionic strength 0.5, determined by HPLC assay.*

Similar semilogarithmic plots of the percent residual cefadroxil *versus* time were reasonably linear under various pH conditions (Fig. 4). These results indicate that the degradation of cefadroxil at constant pH, temperature, and ionic strength follows simple first-order kinetics with respect to cefadroxil. The observed rate constants and the buffer systems are listed in Table I.

**Catalytic Effect of Buffer Systems**—The catalytic effect of the two buffer systems used in the kinetic studies was determined at constant pH, temperature (35°), ionic strength ($\mu$ = 0.5), and drug concentration ($5 \times 10^{-3}$ *M*); only the buffer concentration was varied. This experiment was done at several pH values within the effective range for each buffer employed. The results (Figs. 5 and 6) show that the observed first-order rate constants increased linearly with an increase in the buffer concentrations at a constant pH in all cases.

Figure 5 shows the catalytic effect of citrate buffers between pH 2.51 and 5.82. The observed rate constant in the citrate buffer was actually a summation of several catalytic rate constants catalyzed by the buffer species plus the rate constant at zero buffer concentration. Accordingly, the observed rate constants, $k_{obs}$, may be expressed by:

$$k_{obs} = k_{pH} + k_{H_3A}[H_3A] + k_{H_2A^-}[H_2A^-] + k_{HA^{2-}}[HA^{2-}] + k_{A^{3-}}[A^{3-}] \quad \text{(Eq. 1)}$$

where $k_{pH}$ represents the rate constant at zero buffer concentration; other $k$ values are the second-order rate constants imposed by citrate buffer; $[H_3A]$, $[H_2A^-]$, $[HA^{2-}]$, and $[A^{3-}]$ are the concentrations of undissociated citric acid, dihydrogen citrate ion, monohydrogen citrate ion, and citrate ion, respectively.

The total citrate concentration, $[Cit]_T$, is shown as:

$$[Cit]_T = [H_3A] + [H_2A^-] + [HA^{2-}] + [A^{3-}] \quad \text{(Eq. 2)}$$

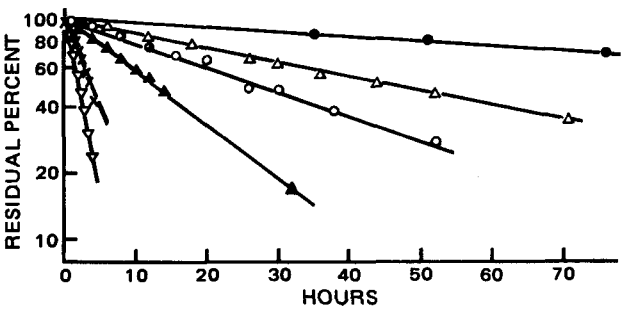


**Figure 4**—*Apparent first-order plots for the degradation of 5 × $10^{-3}$ M cefadroxil at various pH values, 35°, and ionic strength 0.5, determined by HPLC assay. Key: ●, pH 5.82 (0.11 M citrate buffer); △, pH 6.00 (0.10 M phosphate buffer); ○, pH 6.00 (0.2 M phosphate buffer); ▲, pH 7.20 (0.15 M phosphate buffer); ×, pH 10.50 (pH-stat); and ▽, pH 10.75 (pH-stat).*

**Table I—Effects of Buffer Concentration and pH on the Pseudo-First-Order Rate Constants for Cefadroxil Degradation at 35° and Ionic Strength 0.5**

| pH (Buffer) | $10^3 k_{obs}$, $hr^{-1}$ | | | | $10^3 k_{pH}$, $hr^{-1}$ |
|---|---|---|---|---|---|
| | 0.05 *M* | 0.10 *M* | 0.15 *M* | 0.20 *M* | |
| 2.51 (Citrate) | 0.937 | 0.987 | 1.03 | 0.979 | 0.950 |
| 3.11 (Citrate) | 1.06 | 1.03 | 1.13 | 1.18 | 0.950 |
| 3.71 (Citrate) | 1.10 | 1.25 | 1.34 | 1.48 | 0.950 |
| 4.31 (Citrate) | 1.28 | 1.58 | 1.92 | 2.17 | 0.970 |
| 4.91 (Citrate) | 1.69 | 2.33 | 2.99 | 3.58 | 1.02 |
| 5.82 (Citrate) | 2.64 (0.037 *M*) | 3.81 (0.073 *M*) | 4.98 (0.110 *M*) | 6.09 (0.146 *M*) | 1.47 |
| 6.00 (Phosphate) | 8.27 | 14.3 | 21.8 | 25.5 | 1.50 |
| 6.58 (Phosphate) | 16.6 | 26.8 | 37.8 | 48.7 | 4.50 |
| 7.00 (pH-stat) | — | — | — | — | 6.52 |
| 7.00 (pH-stat) | — | — | — | — | 37.1 (50°) |
| 7.00 (pH-stat) | — | — | — | — | 92.6 (60°) |
| 7.20 (Phosphate) | 15.5 (0.03 *M*) | 25.7 (0.06 *M*) | 40.3 (0.10 *M*) | 55.7 (0.15 *M*) | 7.50 |
| 8.46 (pH-stat) | — | — | — | — | 16.0 |
| 9.00 (pH-stat) | — | — | — | — | 22.0 |
| 9.70 (pH-stat) | — | — | — | — | 60.1 |
| 10.50 (pH-stat) | — | — | — | — | 177 |
| 10.75 (pH-stat) | — | — | — | — | 361 |
| 11.50 (pH-stat) | — | — | — | — | 590 (30°) |
| 11.50 (pH-stat) | — | — | — | — | 1470 |
| 11.50 (pH-stat) | — | — | — | — | 2180 (40°) |
| 11.50 (pH-stat) | — | — | — | — | 7560 (50°) |

The dissociation constants of citric acid can be written as:

$$K_1^{cit} = \frac{[H_2A^-]a_{H^+}}{[H_3A]} \quad \text{(Eq. 3)}$$

$$K_2^{cit} = \frac{[HA^{2-}]a_{H^+}}{[H_2A^-]} \quad \text{(Eq. 4)}$$

$$K_3^{cit} = \frac{[A^{3-}]a_{H^+}}{[HA^{2-}]} \quad \text{(Eq. 5)}$$

From Eqs. 1–5, the following overall rate expression, $k_{obs}$, was obtained:

$$k_{obs} = k_{pH} + [Cit]_T \frac{k_{H_3A}(a_{H^+})^3 + k_{H_2A^-}K_1^{cit}(a_{H^+})^2 + k_{HA^{2-}}K_1^{cit}K_2^{cit}a_{H^+} + k_{A^{3-}}K_1^{cit}K_2^{cit}K_3^{cit}}{(a_{H^+})^3 + K_1^{cit}(a_{H^+})^2 + K_1^{cit}K_2^{cit}a_{H^+} + K_1^{cit}K_2^{cit}K_3^{cit}} \quad \text{(Eq. 6)}$$

In this case, no attempt was made to elucidate the catalytic constants with respect to the protonated and zwitterionic species of cefadroxil. By using the dissociation constants of citric acid, $pK_1^{cit} = 3.08$, $pK_2^{cit} = 4.75$, and $pK_3^{cit} = 5.40$ (11), the citrate catalytic constants at 35° were found from Eq. 6 and the slopes in Fig. 5 to be $k_{H_3A} = 9.70 \times 10^{-5}\ M^{-1}\ hr^{-1}$, $k_{H_2A^-} = 1.85 \times 10^{-3}\ M^{-1}\ hr^{-1}$, $k_{HA^{2-}} = 1.86 \times 10^{-2}\ M^{-1}\ hr^{-1}$, and $k_{A^{3-}} = 9.47 \times 10^{-2}\ M^{-1}\ hr^{-1}$.

Figure 6 shows the phosphate buffer effect between pH 6.00 and 7.20. Within this pH range, only the mono- and dihydrogen phosphate ions are significant. The overall rate expression can be given for the phosphate buffer effect as:

$$k_{obs} = k_{pH} + [Ph]_T \frac{k_{H_2PO_4^-}a_{H^+} + k_{HPO_4^{2-}}K_2^{Ph}}{a_{H^+} + K_2^{Ph}} \quad \text{(Eq. 7)}$$

where $k_{HPO_4^{2-}}$ and $k_{H_2PO_4^-}$ are the catalytic rate constants by mono- and dihydrogen ion species of phosphate and $[Ph]_T$ is the total phosphate concentration. By using the dissociation constant of the dihydrogen phosphate ion, $pK_2^{Ph} = 6.59$ at 35°, $\mu = 0.5$ (12), the catalytic rate constants on the degradation of cefadroxil were obtained from Eq. 7 and the slopes in Fig. 6 to be $k_{H_2PO_4^-} = 6.80 \times 10^{-2}\ M^{-1}\ hr^{-1}$ and $k_{HPO_4^{2-}} = 0.378\ M^{-1}\ hr^{-1}$.

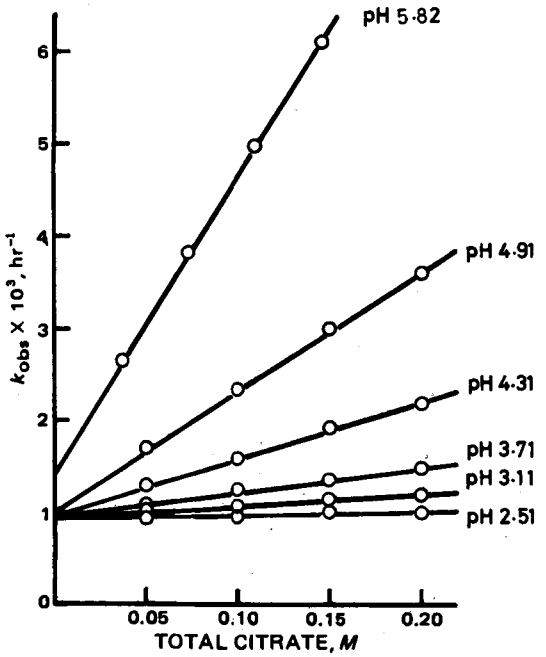


**Figure 5**—*Plots of pseudo-first-order rate constant* versus *total citrate buffer concentration for cefadroxil degradation at various pH values, 35°, and ionic strength 0.5.*

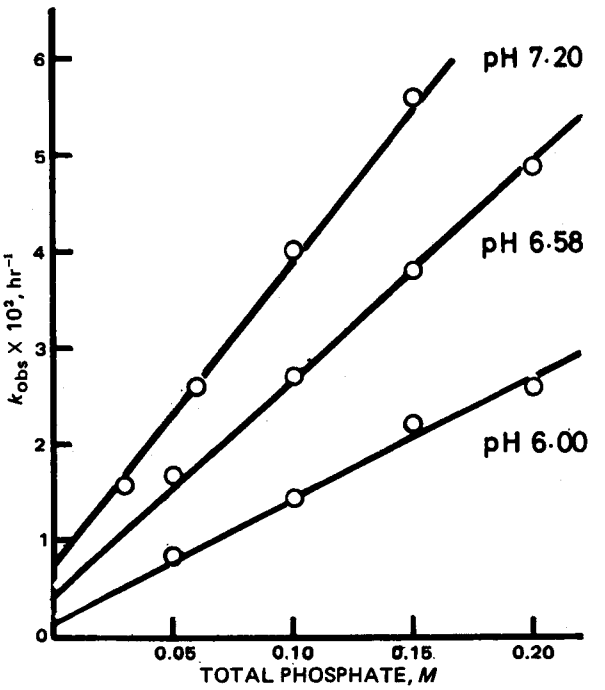


**Figure 6**—*Plots of pseudo-first-order rate constant* versus *total phosphate buffer concentration for cefadroxil degradation at various pH values, 35°, and ionic strength 0.5.*

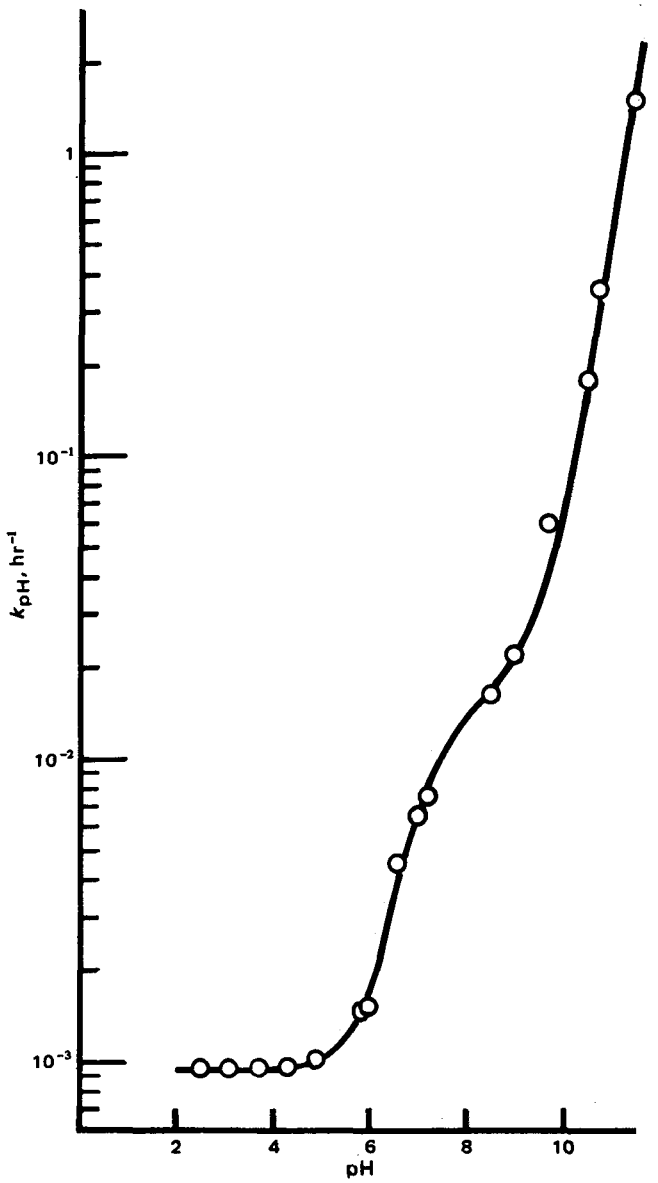


**Figure 7**—*Log $k_{pH}$–pH profile for cefadroxil degradation in aqueous solution at 35° and ionic strength 0.5, where $k_{pH}$ is the apparent first-order rate constant for the degradation in buffer-free solutions or in buffers showing no effect on the degradation rate. The line represents the curve calculated from Eq. 10 and the constants in Table II; the points are experimental values.*

**pH–Rate Profile**—The pH dependence of the overall first-order rate constant, $k_{pH}$, of cefadroxil degradation at 35° and ionic strength 0.5 is shown in Fig. 7. The rate constants used in construction of the graph were obtained from the intercepts of the graphs of $k_{obs}$ *versus* total buffer concentrations at various pH values (Figs. 5 and 6). The results from runs performed with a pH-stat were incorporated (Table I).

In the pH range studied, the amphoteric antibiotic cefadroxil exists in four different ionic forms: as a cation ($IH_2^+$), a zwitterion ($IH^\pm$), an anion ($I^-$), and a dianion ($I^{2-}$), the apparent pKa values of $IH_2^+$, $IH^\pm$, and $I^-$ being 2.64, 7.30, and 9.69, respectively (35°, $\mu$ = 0.5) (Scheme I).

Figure 7 shows that at pH > 10, the observed rate of the degradation increased rapidly and uniformly with increasing pH. Since the slope of this straight-line portion of the log $k_{pH}$ *versus* pH profile is unity, the dissociation of the phenolic moiety apparently has no effect on the $\beta$-lactam cleavage, and the specific hydroxide-ion-catalyzed reactions of anionic and dianionic cefadroxil take place at the same rate in this pH region and account exclusively for the total cefadroxil degradation.

At pH values near $pKa_2$, there was an ascending sigmoid dependence of $k_{pH}$ on pH, followed by a rapid rate decrease as the pH decreased. This inflection indicates that the dissociation equilibria of the side-chain amino group influenced the degradation rate. Below pH 5, the degradation rate of cefadroxil was pH independent and not influenced by the dissociation of the 4-carboxylic acid group ($pKa_1$ = 2.64). This observation implies that the overall degradation consists chiefly of the water-catalyzed reactions of both cationic and zwitterionic cefadroxil. The hydrogen-ion-catalyzed cefadroxil degradation was negligible compared to the water-catalyzed reaction above pH 2.5.

The total shape of the log $k_{pH}$–pH profile of cefadroxil is very similar to that for cephalexin or cephradine (1) and suggests that the rate expression given in Eq. 8 also holds true for the overall degradation of cefadroxil:

$$\frac{d[I]_T}{dt} = -[k_0(f_{IH_2^+} + f_{IH^\pm}) + (k_b + k_{OH}K_w/a_{H^+})(f_{I^-} + f_{I^{2-}})][I]_T \quad \text{(Eq. 8)}$$

where $k_0$ represents the first-order rate constant for water-catalyzed degradation of both cationic and zwitterionic cefadroxil; $k_b$ represents the first-order rate constant for the spontaneous (or water-catalyzed) degradation of the ionic and dianionic species of cefadroxil; $k_{OH}$ represents the second-order rate constant for specific hydroxide-ion-catalyzed degradation of all anionic species; $K_w$ is the autoprotolytic constant; $f_{IH_2^+}$, $f_{IH^\pm}$, $f_{I^-}$, and $f_{I^{2-}}$ represent the mole fractions of the cationic, zwitterionic, anionic, and dianionic species of amphoteric cefadroxil, respectively; and $[I]_T$ is the total cefadroxil concentration.

By introducing the first-order expression:

$$-\frac{d[I]_T}{dt} = k_{pH}[I]_T \quad \text{(Eq. 9)}$$

the following pseudo-first-order rate expression is derived since only the dissociation of the 7-side chain amino group could influence the degradation rate:

$$k_{pH} = k_0\frac{a_{H^+}}{a_{H^+} + K_{a_2}} + (k_b + k_{OH}K_w/a_{H^+})\frac{K_{a_2}}{a_{H^+} + K_{a_2}} \quad \text{(Eq. 10)}$$

The theoretical degradation rate constant of cefadroxil was calculated for the pH of 2.5–11.5 range. By employing $K_w = 2.09 \times 10^{-14}$ at 35° (13), the various rate constants listed in Table II were best satisfied. In Fig. 7, the line represents the theoretical curve calculated by substituting these $k$ values into Eq. 10 while the points show the experimental results. The good agreement indicates that this equation adequately describes the kinetics of total cefadroxil degradation.

**Degradation Products in Neutral and Alkaline Solutions**—The thin-layer chromatogram of the degradation reaction solution of cefadroxil, conducted in a basic phosphate buffer at pH 9.1 at 60° for 1 hr, revealed four spots other than cefadroxil. These spots were tentatively named products II, III, IV, and V according to their $R_f$ values on TLC. Closer inspection of the chromatogram showed the major products to be IV and V.

Products III, IV, and V also were detected in the degradation carried out in methanol–acetonitrile, which suggests that the main degradation process is almost identical in the two solutions, but no trace of II was observed.

Attempts to isolate and characterize the reaction mixture met with difficulties and proved only partially successful. Treatment of the mixture as shown in Scheme II yielded II and a mixture of IV and V slightly contaminated with III. Further separation of the latter mixture under repetitive chromatography was successful.

The structural elucidation of II was achieved based on spectral data. The PMR spectrum revealed simple patterns composed of three singlet signals at $\delta$ 2.09, 3.74, and 6.10 ppm, with signal areas in the ratio of 3:2:1, respectively. Furthermore, the IR spectrum exhibited three characteristic absorptions at 3370, 1690, and 1630 cm$^{-1}$, which suggests the presence of an enol lactone. The UV spectrum showed absorbances at 246 and 255 nm, the latter showing a typical bathochromic shift to 304 nm on the addition of a base. This finding led to the determination of II as the thiol lactone, 3-hydroxyl-4-methyl-2-(5*H*)-thiophenone. Elemental analysis data supported the structure.

Compound II is reported in the literature as the degradation product of cephalexin in experiments conducted at pH 7.4 (6) and 3.3 (7).

The mixture of IV and V, the major products, displayed no peaks corresponding to a $\beta$-lactam in its IR spectrum, strongly indicating that the $\beta$-lactam was cleaved. The PMR spectrum in $d_5$-pyridine revealed,

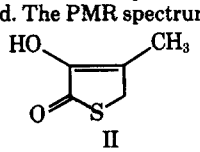


II

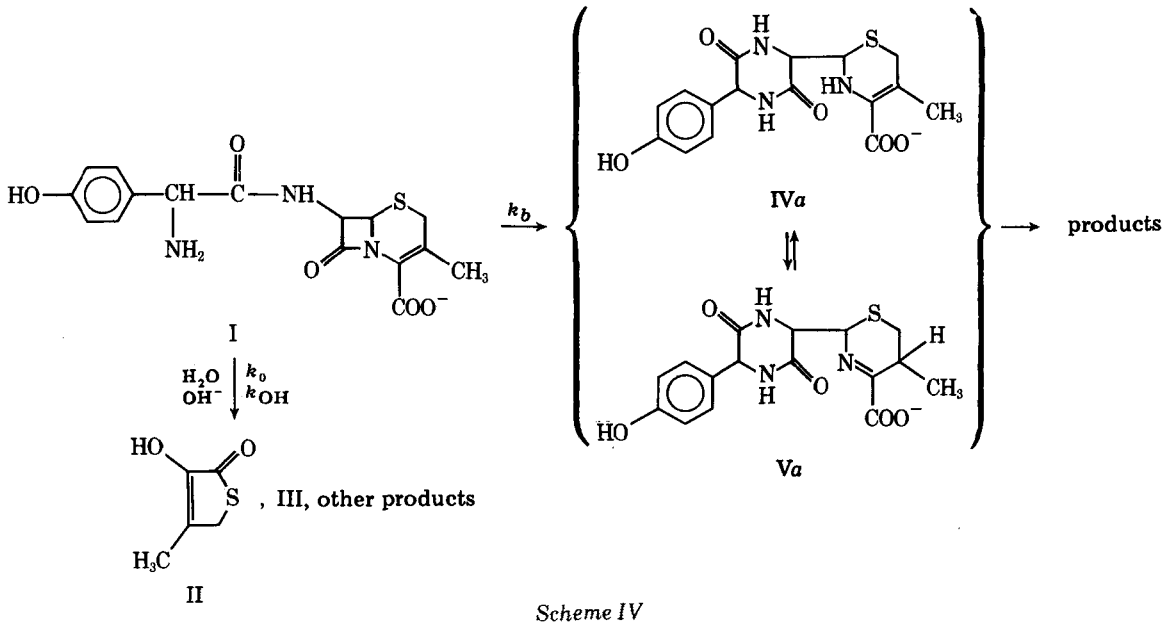


*Scheme IV*

among others, two signals ascribable to methyl groups at δ 1.58 (doublet) and 2.23 (singlet) ppm, the approximate ratio of the integrated signal areas being 2:1. This finding suggests the existence of two different methyl groups in the mixture, most likely one attached to a secondary carbon atom and the other attached to a double bond. Moreover, since the mixture showed no reaction with dinitrobenzenesulfonic acid, the lack of free amino groups is evident. From these results, it was speculated that the mixture is composed of the piperazinedione derivatives, IV*a* and V*a*.

Further information on the structure of the components was gained by derivatizing the mixture to the respective methyl esters with diazomethane in methanol. Chromatographic separations as shown in Scheme III proved successful in isolating each derivative.

The PMR spectrum of the major product, V*b*, showed a doublet signal at δ 1.20 ppm ascribable to a methyl group on a secondary carbon atom coupling with a vicinal proton. On addition of deuterium oxide, the signals centered at δ 4.05 and 5.41 ppm showing complex coupling patterns simplify, making it reasonable to assign the former to the proton on C-7 and the latter to the proton on C-6 showing longrange coupling with protons on C-2 and/or C-3. The IR spectrum revealed peaks for ester carbonyl (1730 $cm^{-1}$) and superimposed amide carbonyls (1680 $cm^{-1}$), while the UV spectrum showed absorbances at 226 and 276 nm, assigned to the phenol group. All data proved to be consistent with the proposed structure, a piperazinedione derivative with the double bond at the C-4, C-5-position.

The minor product, IV*b*, exhibited IR and UV spectra closely resembling those of V*b*. The PMR spectrum revealed a singlet at δ 2.04 ppm, which was the decisive factor in determining its structure as the piperazinedione derivative with the double bond at the C-3, C-4-position.

Elemental analyses for the two esters supported the illustrated structures. The characterization of the methyl derivatives led to the conclusion that the major degradation products of cefadroxil in basic aqueous solution have structures IV*a* and V*a*, as illustrated in Scheme IV.

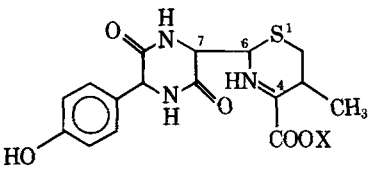

V*a*: X = H
V*b*: X = $CH_3$

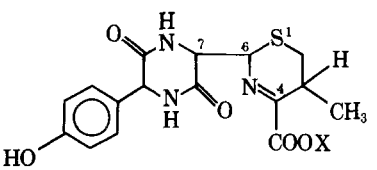

IV*a*: X = H
IV*b*: X = $CH_3$

**Mechanism of Reaction Involving Side-Chain α-Amino Group**—The shape of the pH–rate profile of cefadroxil in the neutral pH region may be accounted for by the following three mechanisms (Scheme V): (*a*) intramolecular nucleophilic attack of unprotonated side-chain amino groups on the β-lactam carbonyl moiety, (*b*) intramolecular general base catalysis by the amino group inducing the attack of a water molecule on the β-lactam moiety, and (*c*) intramolecular general acid catalysis by the protonated amino group inducing the attack of hydroxide ion on the β-lactam moiety. These mechanisms are kinetically indistinguishable.

Mechanism *a* is markedly different from the other two in the formation of piperazine-2,5-dione products, whose structures are shown here as IV*a* or V*a*. Cohen *et al.* (5) reported the isolation of a piperazinedione product similar to V*a* from an aqueous sodium carbonate solution of cephradine. Recently, the piperazinedione was isolated from an aqueous phosphate solution of cephalexin kept at 35° and pH 7.6 for 24 hr (6). In this study, the structural speculation of the mixture of IV*a* and V*a* for the precipitated products from the basic solution of cefadroxil and the successful

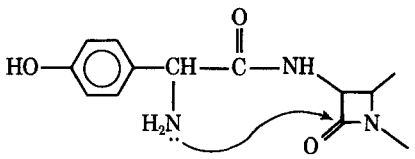

Mechanism a

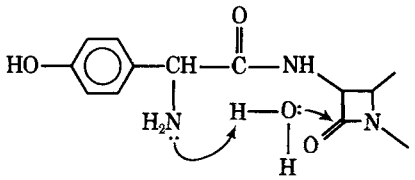

Mechanism b

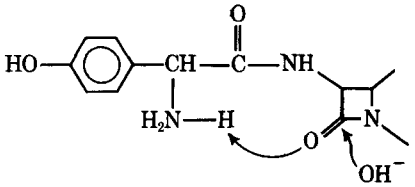

Mechanism c

*Scheme V*

Table II—Dissociation Constants and Rate Constants [a] for the Degradation of Aminocephalosporins at 35° and Ionic Strength 0.5

| Antibiotic | $pKa_1$ | $pKa_2$ | $10^3 k_0$, $hr^{-1}$ | $10^2 k_b$, $hr^{-1}$ | $10^{-2} k_{OH}$, $M^{-1} hr^{-1}$ |
|---|---|---|---|---|---|
| Cefadroxil | 2.64 | 7.30 | 0.941 | 1.61 | 2.54 |
| Cephalexin[b] | 2.56 | 6.88 | 1.15 | 1.01 | 2.64 |
| Cephradine[b] | 2.53 | 7.30 | 1.10 | 0.740 | 3.98 |
| Cephaloglycin[b] | 1.91 | 6.90 | 5.00 | 13.5 | 13.1 |

[a] Rate constants are defined in Eq. 10. [b] Reference 1.

isolation and identification of their methyl esters (IV*b* and V*b*) supported the occurrence of Mechanism *a*.

Additional evidences for the intramolecular aminolysis reaction (Mechanism *a*) were obtained. Figure 8 shows the first-order plots of the disappearance of amino groups by following the decrease in the concentration of primary amino groups in cefadroxil solution during its degradation in 0.15 *M* phosphate buffer at pH 7.20, 35°, and $\mu = 0.5$, the plots being obtained by the Guggenheim method (14). Total disappearance followed by the HPLC method for the same samples is also shown in Fig. 8. The apparent first-order rate constants obtained from the two methods are in reasonable agreement, suggesting that the loss of cefadroxil is accompanied by a parallel loss of its amino group. Furthermore, when *N*-acetylcefadroxil (VI) was heated in a neutral phosphate buffer, no reaction was observed on TLC, indicating that the degradation required a free amino group attacking the β-lactam moiety.

These results lead to the conclusion that the degradation of cefadroxil proceeding at neutral and basic pH was dominated by a spontaneous aminolysis (Mechanism *a*) rather than water-catalyzed aminolysis to produce the piperazinediones IV*a* and V*a*.

**Equilibrium between Degradation Products**—PMR spectral studies of the mixture of IV*a* and V*a* suggested the existence of an equilibrium between them. PMR spectra in $d_5$-pyridine showed a doublet at δ 1.21 ppm which, on addition of deuterium oxide, changed to a broad singlet; no change was observed with the singlet at δ 2.01 ppm, clearly indicating the presence of an equilibrium shown in Scheme IV where the C-3 proton was easily exchanged by deuterium oxide through the migration of the double bond. Further evidence for the equilibrium was obtained when the degradation of cefadroxil in potassium carbonate–deuterium oxide solution was monitored by PMR. The spectrum showed the singlet at δ 2.01 ppm, assigned to the methyl group of cefadroxil, gradually disappearing with time while a new singlet assignable to a secondary methyl group appeared. This change indicates the double bond migration, probably to the 4,5-position, to predominantly yield V*a* and exhibits the same behavior found for cephradine (5) and cephalexin (1).

Similar migration of the double bond was also observed between the methyl esters, IV*b* and V*b*. In the PMR spectra of IV*b* in $d_6$-dimethyl sulfoxide, the addition of deuterium oxide and trifluoroacetic acid to the sample resulted in the appearance of new signal peaks, corresponding to the spectrum of V*b*, which increased in area until an apparent equilibrium was reached. Integration of peak areas showed that the equilibrium was attained at a ratio of 3:1 with IV*b* predominating.

This result was confirmed by conducting the same experiment, this time starting with V*b*, which showed the appearance and increase of small peaks corresponding to IV*b* until a similar equilibrium was reached in favor of IV*b*. Furthermore, data obtained from TLC of the esters in acidic conditions also supported the existence of an equilibrium.

**Available Evidence for Formation of II and a Possible Degradation Pathway in Aqueous Solution**—The degradation product II was isolated or confirmed from the cefadroxil degradation solutions in water and in 0.1 *M* dibasic sodium phosphate solution at pH 9.1. However, when cefadroxil was degraded in neutral organic solvents, no formation of II was observed on TLC. Bundgaard (6) reported the isolation of 3-hydroxy-4-methyl-2(5*H*)-thiophenone (II) from the degradation solution of cephalexin in 0.5 *M* phosphate buffer at pH 7.5 and proposed

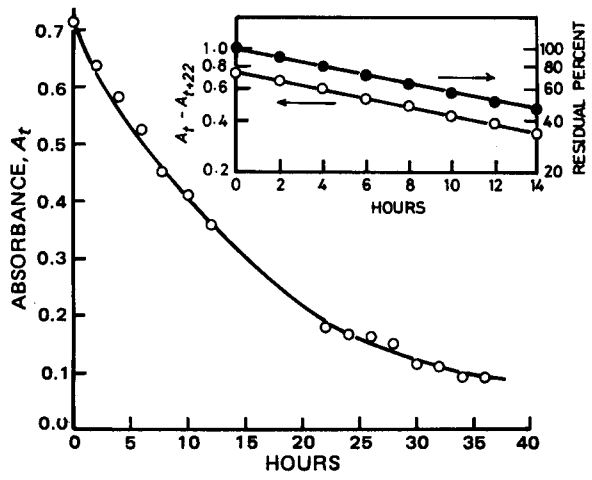


**Figure 8**—*Time courses for primary amino group disappearance during cefadroxil ($5 \times 10^{-3}$ M) degradation in 0.15 M phosphate buffer (pH 7.20) at 35° and ionic strength 0.5. Absorbance refers to the absorbances produced by subjecting equal aliquots of the reaction solution to the trinitrobenzenesulfonic acid assay. The inset shows the first-order plots of the data (○) obtained by Guggenheim treatment (22-hr intervals) in comparison with the HPLC assay (●) of the same samples.*

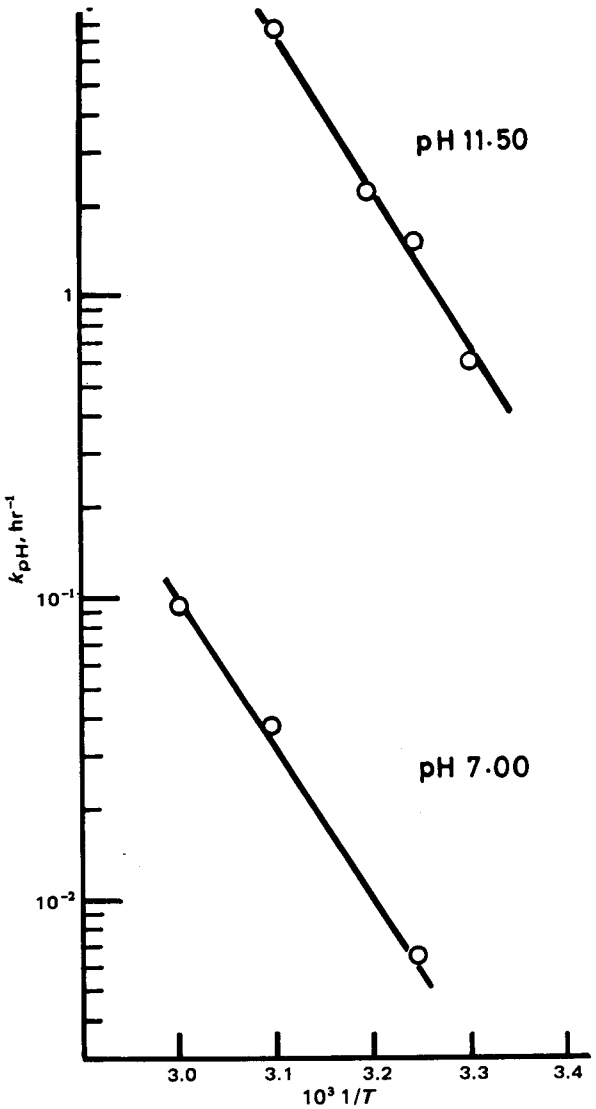


**Figure 9**—*Arrhenius plots for the apparent first-order rate constants, $k_{pH}$, for cefadroxil degradation at pH 7.00 and 11.50 and ionic strength 0.5. The pH values were maintained by a pH-stat.*

that this thiophene derivative might be transformed from the piperazinedione product.

To clarify the possible formation of II from IV*a* or V*a*, the product mixture IV*a* and V*a* was heated in an alkaline phosphate solution. Several secondary degradation products were detectable on TLC, but none had the same $R_f$ value as II. The results suggest that product II does not form *via* IV*a* and V*a* but is directly formed from cefadroxil *via* a different pathway.

Product III was difficult to isolate in amounts sufficient to characterize it; its formation was confirmed in neutral and basic degradation solutions of cefadroxil.

A possible route to account for the observed formation of II, III, IV*a*, and V*a* is shown in Scheme IV.

**Temperature Dependency**—Rate constants for the overall disappearance of cefadroxil were obtained from 35 to 60° at pH 7.00 and 11.50. The pH of the reaction solution was maintained constant by the use of a pH-stat. The Arrhenius plots are shown in Fig. 9. From these data, the apparent activation energies at pH 7.00 and 11.50 was determined to be 21.4 and 23.8 kcal/mole, respectively.

In aqueous solution at pH 7.00 and 35°, cefadroxil degraded *via* intramolecularly catalyzed reaction ($k_b$ reaction) to an extent of 83% and *via* a water-catalyzed $\beta$-lactam opening ($k_0$ reaction) to an extent of 17%.

At pH 11.50, the hydroxide-ion catalyzed degradation proceeded exclusively, the contribution of the $k_b$ reaction being only 0.1%. The apparent activation energy of 23.8 kcal/mole at this alkaline pH may include the heat of ionization of water, 13.1 kcal/mole (13). The net activation enthalpy, $\Delta H^{\neq}$, of hydroxide-ion-catalyzed degradation of cefadroxil was calculated to be 10.5 kcal/mole at 35°.

**Comparative Stability Among Aminocephalosporins**—Table II lists various rate constants defined by Eq. 10 for the degradation of cephaloglycin, cephalexin, and cephradine determined previously under the same kinetic conditions. It is apparent that the stability pattern of cefadroxil resembles that of cephalexin and cephradine over all pH regions.

A comparison of the specific rate constants of $k_0$, $k_b$, and $k_{OH}$ for the four aminocephalosporins shows that the $\beta$-lactam moiety of cephaloglycin, which has an acetoxymethyl group in the C-3 position, is about four to five times more susceptible to attack of both water and hydroxide ion and eight to 18 times more reactive to intramolecular attack by the C-7 side-chain amino group than that of cephalosporins possessing a methyl group at the C-3 position, *i.e.*, cefadroxil, cephalexin, and cephradine. The difference in reactivity between cephaloglycin and the other three antibiotics may be ascribed to the difference in the inductive ability of their C-3 substituents and/or leavability of the C-3 moiety, as suggested previously for cephalosporin degradations (1, 3, 15–18).

## REFERENCES


(1) T. Yamana and A. Tsuji, *J. Pharm. Sci.*, **65**, 1563 (1976).

(2) T. Yamana, A. Tsuji, K. Kanayama, and O. Nakano, *J. Antibiot.*, **27**, 1000 (1974).

(3) H. Bundgaard, *Arch. Pharm. Chemi. Sci. Ed.*, **4**, 25 (1976).

(4) E. S. Rattie, D. E. Guttman, and L. J. Ravin, *Arzneim.-Forsch.*, **28**, 944 (1978).

(5) A. I. Cohen, P. T. Funke, and M. S. Puar, *J. Pharm. Sci.*, **62**, 1559 (1973).

(6) H. Bundgaard, *Arch. Pharm. Chemi Sci. Ed.*, **5**, 149 (1977).

(7) A. Dinner, *J. Med. Chem.*, **20**, 963 (1977).

(8) R. E. Buck and K. E. Price, *Antimicrob. Agents Chemother.*, **11**, 324 (1977).

(9) K. Satake, T. Okuyama, M. Ohashi, and T. Shinoda, *J. Biochem. (Tokyo)*, **47**, 654 (1960).

(10) A. Albert and E. P. Serjeant, "The Determination of Ionization Constants," Chapman and Hall, London, England, 1971.

(11) M. A. Schwartz, A. P. Granatek, and F. H. Buckwalter, *J. Pharm. Sci.*, **51**, 523 (1962).

(12) T. Yamana, A. Tsuji, E. Kiya, and E. Miyamoto, *ibid.*, **66**, 861 (1977).

(13) H. S. Harned and W. J. Hamer, *J. Am. Chem. Soc.*, **55**, 2194 (1933).

(14) E. A. Guggenheim, *Phil. Mag.*, **2**, 538 (1926).

(15) R. B. Hermann, *J. Antibiot.*, **26**, 223 (1973).

(16) J. M. Indelicato, T. T. Norvilas, R. R. Pfeiffer, W. J. Wheeler, and W. L. Wilham, *J. Med. Chem.*, **17**, 523 (1974).

(17) D. B. Boyd, R. B. Hermann, D. E. Presti, and M. M. Marsh, *ibid.*, **18**, 408 (1975).

(18) H. Bundgaard, *Arch. Pharm. Chemi. Sci. Ed.*, **3**, 94 (1975).


# Alterations in Integrity of Goldfish Membrane Induced by Edetate Disodium


**P. J. CASCELLA ˣ, E. G. HUPPLER, II, and J. D. JOHNSON**



Received October 20, 1980, from the *College of Pharmacy, South Dakota State University, Brookings, SD 57007.* Accepted for publication March 5, 1981.



**Abstract** □ The effect of the chelating agent edetate disodium on the integrity of the goldfish membrane was examined. The time to produce death in goldfish exposed to secobarbital sodium was used as a reflection of membrane integrity. Although a minimum edetate disodium concentration was necessary to induce alterations in integrity, no direct relationship between the effect and concentration of the chelating agent was evident. The chelating agent's effect appeared to be an enhancement of the transport of the ionized drug form. The change in membrane integrity existed at least 24 hr after theoretical exposure to edetate disodium, but cyclic alterations in integrity could not be ruled out. The effect on integrity was also demonstrated to be nonpermanent, and the apparent loss in integrity was partially restored by calcium but not by magnesium.



**Keyphrases** □ Permeability—effect of edetate disodium on goldfish membrane □ Edetate disodium—effect on membrane permeability, goldfish □ Chelating agents—edetate disodium, effect on membrane permeability, goldfish


Edetic acid is a chelating agent capable of changing transfer rates of certain substances across membrane barriers (1–4). It was reported (1) that the sodium salt of edetic acid was capable of enhancing the absorption of heparin and synthetic heparinoids from the GI tract of rats and dogs and that these results were consistent with another investigation (2) in the monkey, dog, cat, rabbit, and human. Feldman and Gibaldi (3) demonstrated that edetic acid was capable of affecting the transfer rate of salicylate, but not salicylamide, across the everted rat intestine. They concluded that edetic acid was capable of altering the barrier for water-soluble, but not lipid-soluble, compounds. It was also demonstrated (4) that the sodium salt of edetic acid was capable of increasing phenolsulfonphthalein absorption in rats.

Although edetic acid is capable of changing the permeability of membranes to various compounds, the exact nature of the mechanism involved is unknown. Regardless of the mechanism, numerous studies have been performed to see if the effects of the chelating agent can be reversed. Windsor and Cronheim (1) found that the magnesium and




*0022-3549/81/1000-1128$01.00/0*


*© 1981, American Pharmaceutical Association*

that this thiophene derivative might be transformed from the piperazinedione product.

To clarify the possible formation of II from IV*a* or V*a*, the product mixture IV*a* and V*a* was heated in an alkaline phosphate solution. Several secondary degradation products were detectable on TLC, but none had the same $R_f$ value as II. The results suggest that product II does not form *via* IV*a* and V*a* but is directly formed from cefadroxil *via* a different pathway.

Product III was difficult to isolate in amounts sufficient to characterize it; its formation was confirmed in neutral and basic degradation solutions of cefadroxil.

A possible route to account for the observed formation of II, III, IV*a*, and V*a* is shown in Scheme IV.

**Temperature Dependency**—Rate constants for the overall disappearance of cefadroxil were obtained from 35 to 60° at pH 7.00 and 11.50. The pH of the reaction solution was maintained constant by the use of a pH-stat. The Arrhenius plots are shown in Fig. 9. From these data, the apparent activation energies at pH 7.00 and 11.50 was determined to be 21.4 and 23.8 kcal/mole, respectively.

In aqueous solution at pH 7.00 and 35°, cefadroxil degraded *via* intramolecularly catalyzed reaction ($k_b$ reaction) to an extent of 83% and *via* a water-catalyzed $\beta$-lactam opening ($k_0$ reaction) to an extent of 17%.

At pH 11.50, the hydroxide-ion catalyzed degradation proceeded exclusively, the contribution of the $k_b$ reaction being only 0.1%. The apparent activation energy of 23.8 kcal/mole at this alkaline pH may include the heat of ionization of water, 13.1 kcal/mole (13). The net activation enthalpy, $\Delta H^{\neq}$, of hydroxide-ion-catalyzed degradation of cefadroxil was calculated to be 10.5 kcal/mole at 35°.

**Comparative Stability Among Aminocephalosporins**—Table II lists various rate constants defined by Eq. 10 for the degradation of cephaloglycin, cephalexin, and cephradine determined previously under the same kinetic conditions. It is apparent that the stability pattern of cefadroxil resembles that of cephalexin and cephradine over all pH regions.

A comparison of the specific rate constants of $k_0$, $k_b$, and $k_{OH}$ for the four aminocephalosporins shows that the $\beta$-lactam moiety of cephaloglycin, which has an acetoxymethyl group in the C-3 position, is about four to five times more susceptible to attack of both water and hydroxide ion and eight to 18 times more reactive to intramolecular attack by the C-7 side-chain amino group than that of cephalosporins possessing a methyl group at the C-3 position, *i.e.*, cefadroxil, cephalexin, and cephradine. The difference in reactivity between cephaloglycin and the other three antibiotics may be ascribed to the difference in the inductive ability of their C-3 substituents and/or leavability of the C-3 moiety, as suggested previously for cephalosporin degradations (1, 3, 15–18).

## REFERENCES


(1) T. Yamana and A. Tsuji, *J. Pharm. Sci.*, **65**, 1563 (1976).

(2) T. Yamana, A. Tsuji, K. Kanayama, and O. Nakano, *J. Antibiot.*, **27**, 1000 (1974).

(3) H. Bundgaard, *Arch. Pharm. Chemi. Sci. Ed.*, **4**, 25 (1976).

(4) E. S. Rattie, D. E. Guttman, and L. J. Ravin, *Arzneim.-Forsch.*, **28**, 944 (1978).

(5) A. I. Cohen, P. T. Funke, and M. S. Puar, *J. Pharm. Sci.*, **62**, 1559 (1973).

(6) H. Bundgaard, *Arch. Pharm. Chemi Sci. Ed.*, **5**, 149 (1977).

(7) A. Dinner, *J. Med. Chem.*, **20**, 963 (1977).

(8) R. E. Buck and K. E. Price, *Antimicrob. Agents Chemother.*, **11**, 324 (1977).

(9) K. Satake, T. Okuyama, M. Ohashi, and T. Shinoda, *J. Biochem. (Tokyo)*, **47**, 654 (1960).

(10) A. Albert and E. P. Serjeant, "The Determination of Ionization Constants," Chapman and Hall, London, England, 1971.

(11) M. A. Schwartz, A. P. Granatek, and F. H. Buckwalter, *J. Pharm. Sci.*, **51**, 523 (1962).

(12) T. Yamana, A. Tsuji, E. Kiya, and E. Miyamoto, *ibid.*, **66**, 861 (1977).

(13) H. S. Harned and W. J. Hamer, *J. Am. Chem. Soc.*, **55**, 2194 (1933).

(14) E. A. Guggenheim, *Phil. Mag.*, **2**, 538 (1926).

(15) R. B. Hermann, *J. Antibiot.*, **26**, 223 (1973).

(16) J. M. Indelicato, T. T. Norvilas, R. R. Pfeiffer, W. J. Wheeler, and W. L. Wilham, *J. Med. Chem.*, **17**, 523 (1974).

(17) D. B. Boyd, R. B. Hermann, D. E. Presti, and M. M. Marsh, *ibid.*, **18**, 408 (1975).

(18) H. Bundgaard, *Arch. Pharm. Chemi. Sci. Ed.*, **3**, 94 (1975).


# Alterations in Integrity of Goldfish Membrane Induced by Edetate Disodium


**P. J. CASCELLA ˣ, E. G. HUPPLER, II, and J. D. JOHNSON**



Received October 20, 1980, from the *College of Pharmacy, South Dakota State University, Brookings, SD 57007.* Accepted for publication March 5, 1981.



**Abstract** □ The effect of the chelating agent edetate disodium on the integrity of the goldfish membrane was examined. The time to produce death in goldfish exposed to secobarbital sodium was used as a reflection of membrane integrity. Although a minimum edetate disodium concentration was necessary to induce alterations in integrity, no direct relationship between the effect and concentration of the chelating agent was evident. The chelating agent's effect appeared to be an enhancement of the transport of the ionized drug form. The change in membrane integrity existed at least 24 hr after theoretical exposure to edetate disodium, but cyclic alterations in integrity could not be ruled out. The effect on integrity was also demonstrated to be nonpermanent, and the apparent loss in integrity was partially restored by calcium but not by magnesium.



**Keyphrases** □ Permeability—effect of edetate disodium on goldfish membrane □ Edetate disodium—effect on membrane permeability, goldfish □ Chelating agents—edetate disodium, effect on membrane permeability, goldfish


Edetic acid is a chelating agent capable of changing transfer rates of certain substances across membrane barriers (1–4). It was reported (1) that the sodium salt of edetic acid was capable of enhancing the absorption of heparin and synthetic heparinoids from the GI tract of rats and dogs and that these results were consistent with another investigation (2) in the monkey, dog, cat, rabbit, and human. Feldman and Gibaldi (3) demonstrated that edetic acid was capable of affecting the transfer rate of salicylate, but not salicylamide, across the everted rat intestine. They concluded that edetic acid was capable of altering the barrier for water-soluble, but not lipid-soluble, compounds. It was also demonstrated (4) that the sodium salt of edetic acid was capable of increasing phenolsulfonphthalein absorption in rats.

Although edetic acid is capable of changing the permeability of membranes to various compounds, the exact nature of the mechanism involved is unknown. Regardless of the mechanism, numerous studies have been performed to see if the effects of the chelating agent can be reversed. Windsor and Cronheim (1) found that the magnesium and




*0022-3549/81/1000-1128$01.00/0*


*© 1981, American Pharmaceutical Association*

**Table I—Effect of Recovery Time on Time of Death of Goldfish Exposed to Edetate Disodium and 0.1 m*M* Secobarbital Sodium Solution**

| Recovery | Treatment | | | Control | | | Significance |
|---|---|---|---|---|---|---|---|
| | Mean Time | *SD* | *n*[a] | Mean Time | *SD* | *n* | |
| Zero | 14.86 | 4.26 | 10 | 26.93 | 5.20 | 8 | $p < 0.05$ |
| 30 min | 15.19 | 2.78 | 9 | 18.96 | 4.60 | 9 | NS[b] |
| 24 hr | 19.17 | 2.32 | 8 | 24.63 | 4.09 | 8 | $p < 0.05$ |
| 48 hr | 21.80 | 6.19 | 10 | 22.07 | 4.73 | 8 | NS |
| 72 hr | 37.60 | 4.83 | 9 | 40.23 | 5.55 | 9 | NS |

[a] *n* = number of fish. [b] Not significant ($p > 0.05$).

**Table II—Effect of Concentration of Edetate Disodium on Time of Death of Goldfish in 0.1 m*M* Secobarbital Sodium Solution**

| Concentration of Edetate Disodium, mg/ml | Treatment | | | Control | | | Significance |
|---|---|---|---|---|---|---|---|
| | Mean Time of Death, min | *SD* | *n*[a] | Mean Time of Death min | *SD* | *n* | |
| 0.05 | 26.29 | 4.36 | 10 | 25.72 | 4.10 | 9 | NS[b] |
| 0.10 | 26.29 | 3.97 | 10 | 32.73 | 7.49 | 10 | $p < 0.05$ |
| 0.15 | 19.51 | 2.84 | 10 | 26.32 | 2.62 | 10 | $p < 0.05$ |
| 0.20 | 23.03 | 1.79 | 10 | 32.27 | 8.07 | 10 | $p < 0.05$ |
| 0.25 | 15.19 | 1.10 | 7 | 19.80 | 4.76 | 8 | $p < 0.05$ |
| 0.30 | 17.29 | 2.11 | 7 | 20.15 | 2.49 | 7 | $p < 0.05$ |
| 0.40 | 18.25 | 4.61 | 10 | 22.62 | 4.61 | 10 | $p < 0.05$ |

[a] *n* = number of fish. [b] Not significant ($p > 0.05$).

calcium salts of edetic acid were incapable of increasing absorption, and Tidball (4) reported that rinsing with magnesium salts fully restored normal permeability. It was also reported (3) that neither calcium nor magnesium was capable of restoring normal permeability of the rat intestinal membrane.

A previous report (5) presented preliminary findings of the effect of edetate disodium on the goldfish membrane. It was considered of interest to examine the effects of edetic acid on the goldfish since they have been used in a number of studies (6–9) for the assessment of absorption and toxicity of numerous compounds. Goldfish offer an advantage over other experimental animals in that they can be exposed to chelating agents for relatively long periods of time. It also is reasonably easy to assess the effects on the membrane at different times after exposure. This report is a followup of our preliminary findings.

## EXPERIMENTAL

**Recovery Time Studies**—Goldfish (*Carassius auratus*), 1–3 g, were placed in groups of five in tanks containing 2 liters of edetate disodium[1] (0.2 mg/ml). The solutions were made with glass-distilled[2] water and were adjusted[3] to pH 7.4 using 0.1 *N* NaOH or HCl. The fish were left in the solutions for 24 hr and then were placed for varying periods in recovery tanks containing 2 liters of glass-distilled water adjusted to pH 7.4. Individual fish were then placed into beakers containing 200 ml of 0.1 m*M* secobarbital sodium[4] in a 0.05 *M* phosphate buffer, pH 7.4. Cessation of gill and mouth movements was noted, and the time to death was computed.

Controls were run for each group following the procedure for the edetate disodium-treated fish, except that the chelating agent was omitted from the treatment tank.

All investigations were performed at (20 ± 2°).

**Concentration Studies**—Five fish (1–3 g) were placed in tanks containing 2 liters of edetate disodium (varying concentrations) in glass-distilled water adjusted to pH 7.4 using 0.1 *N* NaOH or HCl. The fish were left in the tanks for 24 hr and then placed for 24 hr in a recovery tank containing 2 liters of glass-distilled water adjusted to pH 7.4. Individual fish were then placed in beakers containing 200 ml of 0.1 m*M* secobarbital sodium in 0.05 *M* phosphate buffer, pH 7.4. Cessation of gill and mouth movements was noted, and the time to death was computed.

Controls were run in the same manner as described previously. All experiments were performed at 20 ± 2°.

**pH Study**—Five fish (1–3 g) were placed in tanks containing 2 liters of 0.2 mg of edetate disodium/ml (adjusted to pH 7.4) in glass-distilled water for 24 hr. Individual fish were then immediately placed (zero recovery) in beakers containing 200 ml of 0.1 m*M* secobarbital sodium solution buffered to pH 6.4, 7.4, or 8.4 with 0.05 *M* phosphate buffer. Again, time to death was calculated.

Controls were run in the same manner as already described and all experiments were performed at 20 ± 2°.

**Calcium and Magnesium Study**—Five fish (1–3 g) were placed in tanks containing 2 liters of 0.2 mg of edetate disodium/ml (adjusted to pH 7.4) in glass-distilled water for 24 hr. Fish were then placed in recovery tanks for 24 hr. The recovery tanks contained either 2 liters of glass-distilled water or 2 liters of a 1 m*M* solution of calcium chloride or magnesium chloride. All tanks were adjusted to pH 7.4. After 24 hr, individual fish were placed in beakers containing 200 ml of a 0.1 m*M* secobarbital sodium solution buffered to pH 7.4 with 0.05 *M* phosphate buffer. Time to death was computed.

Controls were run by placing fish in glass-distilled water for 48 hr (water was changed at the end of 24 hr) and then placing individual fish in secobarbital solution as described.

All experiments were performed at 20 ± 2°.

## RESULTS AND DISCUSSION

The results of the recovery time study are summarized in Table I. As is evident from the control data, there appears to be a large amount of day-to-day variation in response. This is evident from the control segment of the table, since the controls are essentially the same procedure, one should expect similar results. However, the mean time of deaths, ranged from 18.96 to 40.23 min.

Comparisons between the treated and control fish (which were performed at the same time) were made within each block of the table using a Student *t* test. A significant difference ($p < 0.05$) existed between the treated and control fish for the 0- and 24-hr recovery studies. There was no significant difference for the 30-min and 48- and 72-hr recovery studies. Although the reason for the lack of a significant difference at the 30-min recovery study is unknown, it is consistent with previous results (5). If it is assumed that the amount of secobarbital necessary to produce death is the same between treated and control fish, then the significant difference for the 24-hr recovery study implies that alterations in membrane permeability induced by edetate disodium may exist for a substantial time after theoretical exposure of the membrane to the chelating agent, at least in the described system. The effect of the chelating agent on membrane permeability is not permanent, however, as evident from the 48- and 72-hr recovery treatments.

[1] Fisher Scientific Co., Fair Lawn, N.J.
[2] Corning Model AG-1B.
[3] Heath Model EU-302A.
[4] Robinson Laboratory, San Francisco, Calif.

**Table III—Difference between the Mean of Each Control and Individual Observations of Each Treatment**

| Observation | Edetate Disodium Concentration, mg/ml | | | | | |
|---|---|---|---|---|---|---|
| | 0.10 | 0.15 | 0.20 | 0.25 | 0.30 | 0.40 |
| 1 | 6.44 | 10.49 | 7.69 | 5.49 | 4.85 | 6.44 |
| 2 | −0.29 | 9.75 | 9.55 | 3.35 | 0.40 | −3.18 |
| 3 | 10.38 | 9.57 | 10.35 | 4.02 | 6.27 | 4.82 |
| 4 | 9.51 | 7.47 | 11.10 | 3.85 | 1.59 | 6.14 |
| 5 | 11.00 | 7.04 | 7.32 | 4.48 | 1.97 | 5.00 |
| 6 | 3.68 | 5.22 | 11.97 | 6.62 | 3.57 | 5.42 |
| 7 | 1.88 | 1.67 | 8.47 | 4.43 | 1.34 | 5.42 |
| 8 | 4.85 | 3.10 | 6.70 | — | — | 4.09 |
| 9 | 10.58 | 6.80 | 8.34 | — | — | 3.49 |
| 10 | 5.11 | 6.97 | 10.87 | — | — | 6.10 |
| Mean | 6.31 | 6.81 | 9.24 | 4.61 | 2.86 | 4.27 |
| *SD* | 3.95 | 2.85 | 1.79 | 1.11 | 2.12 | 2.81 |

**Table IV—Effect of Calcium and Magnesium on Enhanced Permability Induced by Edetate Disodium**

| Group | Treatment[a] A | | | Treatment[b] B | | |
|---|---|---|---|---|---|---|
| | Mean Time of Death | *n*[c] | *SD* | Mean Time of Death | *n* | *SD* |
| I | 29.23 | 10 | 4.43 | 29.95 | 10 | 5.87 |
| II | 19.70 | 9 | 4.63 | 19.15 | 10 | 1.45 |
| III | 19.63 | 10 | 3.76 | 23.24 | 10 | 4.06 |

[a] Group III contained a 1 m*M* magnesium chloride solution. [b] Group III contained a 1 m*M* calcium chloride solution. [c] *n* = number of fish.

The results of the concentration of edetate disodium on time of death study are listed in Table II. A significant difference ($p < 0.05$) existed between each treatment and control, except for the lowest concentration of the chelating agent. To determine the effect of chelating agent concentration on time of death, the effect of day-to-day variation should be eliminated since the studies were performed on different days. This correction was made for the data in which the treatments were significantly different from the controls, *i.e.*, all but the lowest concentration of edetate disodium, by subtracting each individual observation of the treatments from the mean of each control performed at the same time as the treatment (Table III).

An analysis of variance for unequal data sets was performed on the differences for each concentration, and the result indicated a significant difference ($p < 0.05$) between the means. The means were analyzed using the Newman–Keuls method with a harmonic mean of the sample size to compensate for unequal data sets. These results indicated a difference between the treatment concentrations of 0.10, 0.15, and 0.20 mg/ml with the 0.30-mg/ml treatment. There was also a difference between the 0.2-mg/ml concentration and the 0.25- and 0.40-mg/ml treatments. A plot of the mean differences *versus* concentration of treatment (Fig. 1) shows that despite significant differences between the treatments, no direct relationship between concentration of edetate disodium and effect was apparent.

Experiments were also performed to determine if the effect of edetate disodium on membrane permeability could be reversed by exposing the fish to calcium or magnesium chloride solutions. In each experiment, the times of death of three groups of fish in secobarbital sodium were determined. The first group was the control, the second group was treated with edetate disodium and placed in a recovery tank for 24 hr, and the third group was exposed to the chelating agent and then placed in a recovery tank containing calcium or magnesium chloride for 24 hr before being placed in the secobarbital sodium solution. All groups were studied at the same time, and the results are summarized in Table IV.

An analysis of variance was performed, and the results indicated a significant difference between the means for both studies. Analysis of the means using the Newman–Keuls method indicated that, in the magnesium chloride study, the control was significantly different from the edetate disodium group and the edetate disodium/magnesium chloride group. No difference existed between the edetate disodium and the edetate disodium/magnesium chloride group. Thus, it appears that magnesium is incapable of restoring membrane integrity under these experimental conditions. In the calcium chloride study, a significant difference ($p < 0.05$) existed between all three treatments. Thus, it appears that calcium is able to restore, at least partially, the apparent loss of membrane integrity induced by edetate disodium.

In previous experiments (5) fish also were treated with edetate disodium and then exposed to secobarbital sodium buffered to varying pH values. While the treated fish seemed to fit the model proposed by Levy and Gucinski (10) for the absorption of secobarbital sodium, the controls did not. It was decided to repeat the pH study using a 24-hr treatment, zero recovery. The results of both studies are listed in Table V. Comparisons were made within each block using a Student *t* test, and there was no significant difference between treatments and control at pH 6.4 regardless of the treatment. In the 24-hr treatment, 30-min recovery, there was no significant difference at any pH. In the 24-hr treatment, zero recovery and the 24-hr treatment, 24-hr recovery, there were significant differences at pH 7.4 and 8.4.

Since secobarbital is a weak acid with a pKa of 7.9, it appears that the chelating agent changes membrane permeability to the ionized drug form since there was a significant difference between treated and control animals only at pH values (7.4 and 8.4) where the drug appreciably existed as the ionized form. The apparent increase in membrane permeability to the ionized drug form is not enough to compensate for the reduction in the absorption of the unionized form since the times to produce death increased with increasing buffer pH. Linear regression was performed on the reciprocal of the mean time of death *versus* the fraction of drug unionized for the 24-hr treatment zero recovery study and its controls.

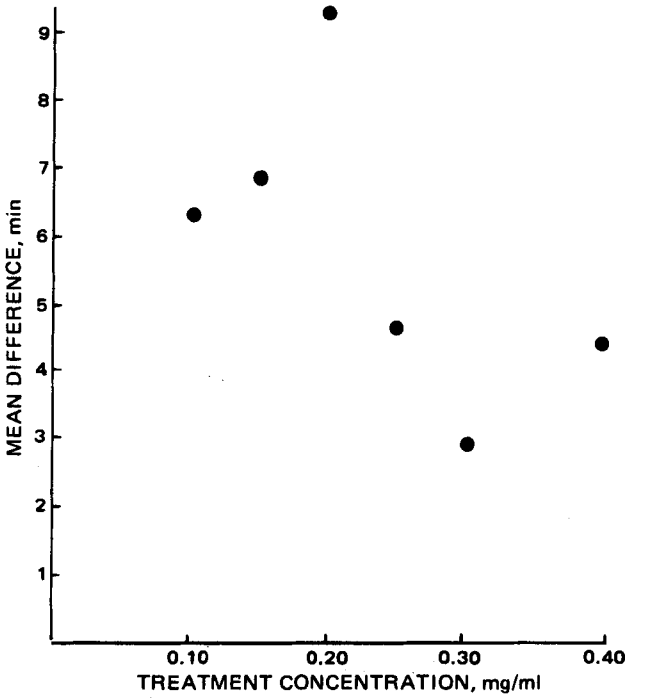


**Figure 1**—*Plot of the mean differences* versus *concentration of the chelating agent treatments.*

Table V—Effect of pH and Recovery Time on Time of Death of Goldfish Treated with Edetate Disodium and Exposed to 0.1 m*M* Secobarbital Sodium

| | pH 6.4 | | | pH 7.4 | | | pH 8.4 | | |
|---|---|---|---|---|---|---|---|---|---|
| | Mean Time ± *SD*, min | *n*[a] | Significance | Mean Time ± *SD*, min | *n* | Significance | Mean Time ± *SD*, min | *n* | Significance |
| Treatment[b] | 18.58 ± 3.54 | 5 | NS[c] | 18.74 ± 0.98 | 7 | $p < 0.05$ | 39.11 ± 5.93 | 3 | $p < 0.05$ |
| Control[d] | 19.76 ± 1.95 | 5 | | 21.88 ± 2.87 | 10 | | 51.77 ± 5.05 | 4 | |
| Treatment[e] | 14.88 ± 0.99 | 10 | NS | 20.21 ± 3.74 | 10 | NS | 52.29 ± 9.70 | 10 | NS |
| Control[f] | 13.49 ± 2.51 | 10 | | 23.89 ± 5.80 | 10 | | 62.30 ± 16.93 | 10 | |
| Treatment[g] | 18.73 ± 5.92 | 10 | NS | 23.03 ± 1.79 | 10 | $p < 0.05$ | 58.83 ± 17.31 | 10 | $p < 0.05$ |
| Control[h] | 15.80 ± 3.51 | 5 | | 32.27 ± 8.07 | 10 | | 97.84 ± 22.19 | 10 | |

[a] *n* = number of fish. [b] 24-hr treatment, zero recovery. [c] Not significant ($p > 0.05$). [d] 24-hr blank, zero recovery. [e] 24-hr treatment, 30-min recovery. [f] 24-hr blank, 30-min recovery. [g] 24-hr treatment, 24-hr recovery. [h] 24-hr blank, 24-hr recovery.

The predicted least-squares equations are, respectively:

$$1/t = 0.0413f_u + 0.0170 \quad (r = 0.9660) \quad \text{(Eq. 1}a\text{)}$$

and:

$$1/t = 0.0443f_u + 0.0093 \quad (r = 0.9906) \quad \text{(Eq. 1}b\text{)}$$

According to the Levy–Gucinski model (10) concerning the absorption of the ionized and unionized forms of drug in goldfish, a plot of reciprocal time of response ($1/t$) as a function of the fraction of drug unionized should be linear with a slope equal to $K_b(K_u - K_i)$ and an intercept equal to $K_bK_i$.

$$1/t = K_bK_i + K_b(K_u - K_i)f_u \quad \text{(Eq. 2)}$$

where $K_b$ is a constant equal to the quotient of the secobarbital concentration to which the fish were exposed divided by the amount of barbiturate in the fish at death; $K_i$ and $K_u$ are the first-order rate constants for the ionized and unionized drug forms, respectively. Upon inspection of the data, two discrepancies appear. The controls fit the model reasonably well while the treated animals do so to a lesser degree. In both cases, however, curvature of a form representing an inverted exponential cannot be ruled out. The intercepts of both plots are also not significantly different ($p > 0.05$) from zero. Whether these discrepancies represent a breakdown of the model or assumptions of the model as specified by Levy and Gucinski or simply a large amount of statistical variation cannot be discerned at this time. However, due to these discrepancies, the analysis as performed earlier (5), using the ratio of slope to intercept to evaluate the ratios of $K_u$:$K_i$ was not performed. Regardless of the model that characterizes the absorption of secobarbital sodium under these experimental conditions, it appears from Table V that edetate disodium changes membrane permeability to the ionized form of the drug and that the effect can be present 24 hr after theoretical exposure to the chelating agent.

## REFERENCES


(1) E. Windsor and G. E. Cronheim, *Nature*, **190**, 263 (1961).

(2) M. A. Seidell, E. Windsor, and A. Surtshin, *Clin. Res.*, **8**, 246 (1960).

(3) S. Feldman and M. Gibaldi, *J. Pharm. Sci.*, **58**, 967 (1969).

(4) C. S. Tidball, *Am. J. Physiol.*, **206**, 243 (1964).

(5) P. J. Cascella and P. D. Kindelspire, *J. Pharm. Sci.*, **69**, 972 (1980).

(6) G. Levy and J. A. Anello, *ibid.*, **57**, 101 (1968).

(7) G. Levy, K. E. Miller, and R. H. Reuning, *ibid.*, **55**, 394 (1966).

(8) C. H. Nightingale, M. Tse, and E. I. Stupak, *ibid.*, **61**, 1948 (1972).

(9) S. Feldman, M. DeFrancisco, and P. J. Cascella, *ibid.*, **64**, 1713 (1975).

(10) G. Levy and S. P. Gucinski, *J. Pharmacol. Exp. Ther.*, **146**, 80 (1964).


## ACKNOWLEDGMENTS


The authors thank Paul Kindelspire for laboratory assistance and Dr. Lee Tucker for suggestions concerning the statistical analysis.


# Effect of Various Vehicles and Vehicle Volumes on Oral Absorption of Triamterene in Rats


**THOMAS F. PATTON ˣ and PAMELA GILFORD**



Received October 6, 1980, from the *Department of Pharmaceutical Chemistry, University of Kansas, Lawrence, KS 66044.* Accepted for publication March 10, 1981.



**Abstract** □ The oral bioavailability of triamterene in rats was investigated after its administration as a suspension in lipid and aqueous vehicles in addition to a lactic acid solution. Triamterene is poorly soluble in both aqueous and lipid vehicles. A 1-ml oral dose volume showed that lipid vehicles may provide some enhancement of oral availability compared with aqueous suspensions. However, when the vehicle volume was reduced to a realistic dosage form volume for the rat, peanut oil and aqueous suspensions were indistinguishable from each other with respect to peak height, peak time, and overall bioavailability. For a given vehicle small vehicle volumes resulted in a better relative oral availability than did large vehicle volumes.



**Keyphrases** □ Triamterene—poor solubility in lipid and aqueous vehicles □ Vehicle volume—small *versus* large vehicle volumes in oral availability in rats □ Oral bioavailability—parameters of triamterene administered as suspensions in lipid and aqueous vehicles and lactic acid solution


The rate and extent of absorption of orally administered drugs are influenced by factors within the GI environment, such as the solubility and extent of drug ionization, gastric emptying, intestinal motility, and stimulation of bile flow. The relative contribution of each factor to oral availability is often difficult to distinguish. The vehicle into which a



© 1981, American Pharmaceutical Association

Table V—Effect of pH and Recovery Time on Time of Death of Goldfish Treated with Edetate Disodium and Exposed to 0.1 m*M* Secobarbital Sodium

| | pH 6.4 | | | pH 7.4 | | | pH 8.4 | | |
|---|---|---|---|---|---|---|---|---|---|
| | Mean Time ± *SD*, min | *n*[a] | Significance | Mean Time ± *SD*, min | *n* | Significance | Mean Time ± *SD*, min | *n* | Significance |
| Treatment[b] | 18.58 ± 3.54 | 5 | NS[c] | 18.74 ± 0.98 | 7 | $p < 0.05$ | 39.11 ± 5.93 | 3 | $p < 0.05$ |
| Control[d] | 19.76 ± 1.95 | 5 | | 21.88 ± 2.87 | 10 | | 51.77 ± 5.05 | 4 | |
| Treatment[e] | 14.88 ± 0.99 | 10 | NS | 20.21 ± 3.74 | 10 | NS | 52.29 ± 9.70 | 10 | NS |
| Control[f] | 13.49 ± 2.51 | 10 | | 23.89 ± 5.80 | 10 | | 62.30 ± 16.93 | 10 | |
| Treatment[g] | 18.73 ± 5.92 | 10 | NS | 23.03 ± 1.79 | 10 | $p < 0.05$ | 58.83 ± 17.31 | 10 | $p < 0.05$ |
| Control[h] | 15.80 ± 3.51 | 5 | | 32.27 ± 8.07 | 10 | | 97.84 ± 22.19 | 10 | |

[a] *n* = number of fish. [b] 24-hr treatment, zero recovery. [c] Not significant ($p > 0.05$). [d] 24-hr blank, zero recovery. [e] 24-hr treatment, 30-min recovery. [f] 24-hr blank, 30-min recovery. [g] 24-hr treatment, 24-hr recovery. [h] 24-hr blank, 24-hr recovery.

The predicted least-squares equations are, respectively:

$$1/t = 0.0413f_u + 0.0170 \quad (r = 0.9660) \quad \text{(Eq. 1}a\text{)}$$

and:

$$1/t = 0.0443f_u + 0.0093 \quad (r = 0.9906) \quad \text{(Eq. 1}b\text{)}$$

According to the Levy–Gucinski model (10) concerning the absorption of the ionized and unionized forms of drug in goldfish, a plot of reciprocal time of response ($1/t$) as a function of the fraction of drug unionized should be linear with a slope equal to $K_b(K_u - K_i)$ and an intercept equal to $K_bK_i$.

$$1/t = K_bK_i + K_b(K_u - K_i)f_u \quad \text{(Eq. 2)}$$

where $K_b$ is a constant equal to the quotient of the secobarbital concentration to which the fish were exposed divided by the amount of barbiturate in the fish at death; $K_i$ and $K_u$ are the first-order rate constants for the ionized and unionized drug forms, respectively. Upon inspection of the data, two discrepancies appear. The controls fit the model reasonably well while the treated animals do so to a lesser degree. In both cases, however, curvature of a form representing an inverted exponential cannot be ruled out. The intercepts of both plots are also not significantly different ($p > 0.05$) from zero. Whether these discrepancies represent a breakdown of the model or assumptions of the model as specified by Levy and Gucinski or simply a large amount of statistical variation cannot be discerned at this time. However, due to these discrepancies, the analysis as performed earlier (5), using the ratio of slope to intercept to evaluate the ratios of $K_u$:$K_i$ was not performed. Regardless of the model that characterizes the absorption of secobarbital sodium under these experimental conditions, it appears from Table V that edetate disodium changes membrane permeability to the ionized form of the drug and that the effect can be present 24 hr after theoretical exposure to the chelating agent.

## REFERENCES


(1) E. Windsor and G. E. Cronheim, *Nature*, **190**, 263 (1961).

(2) M. A. Seidell, E. Windsor, and A. Surtshin, *Clin. Res.*, **8**, 246 (1960).

(3) S. Feldman and M. Gibaldi, *J. Pharm. Sci.*, **58**, 967 (1969).

(4) C. S. Tidball, *Am. J. Physiol.*, **206**, 243 (1964).

(5) P. J. Cascella and P. D. Kindelspire, *J. Pharm. Sci.*, **69**, 972 (1980).

(6) G. Levy and J. A. Anello, *ibid.*, **57**, 101 (1968).

(7) G. Levy, K. E. Miller, and R. H. Reuning, *ibid.*, **55**, 394 (1966).

(8) C. H. Nightingale, M. Tse, and E. I. Stupak, *ibid.*, **61**, 1948 (1972).

(9) S. Feldman, M. DeFrancisco, and P. J. Cascella, *ibid.*, **64**, 1713 (1975).

(10) G. Levy and S. P. Gucinski, *J. Pharmacol. Exp. Ther.*, **146**, 80 (1964).


## ACKNOWLEDGMENTS


The authors thank Paul Kindelspire for laboratory assistance and Dr. Lee Tucker for suggestions concerning the statistical analysis.


# Effect of Various Vehicles and Vehicle Volumes on Oral Absorption of Triamterene in Rats


**THOMAS F. PATTON ˣ and PAMELA GILFORD**



Received October 6, 1980, from the *Department of Pharmaceutical Chemistry, University of Kansas, Lawrence, KS 66044.* Accepted for publication March 10, 1981.



**Abstract** □ The oral bioavailability of triamterene in rats was investigated after its administration as a suspension in lipid and aqueous vehicles in addition to a lactic acid solution. Triamterene is poorly soluble in both aqueous and lipid vehicles. A 1-ml oral dose volume showed that lipid vehicles may provide some enhancement of oral availability compared with aqueous suspensions. However, when the vehicle volume was reduced to a realistic dosage form volume for the rat, peanut oil and aqueous suspensions were indistinguishable from each other with respect to peak height, peak time, and overall bioavailability. For a given vehicle small vehicle volumes resulted in a better relative oral availability than did large vehicle volumes.



**Keyphrases** □ Triamterene—poor solubility in lipid and aqueous vehicles □ Vehicle volume—small *versus* large vehicle volumes in oral availability in rats □ Oral bioavailability—parameters of triamterene administered as suspensions in lipid and aqueous vehicles and lactic acid solution


The rate and extent of absorption of orally administered drugs are influenced by factors within the GI environment, such as the solubility and extent of drug ionization, gastric emptying, intestinal motility, and stimulation of bile flow. The relative contribution of each factor to oral availability is often difficult to distinguish. The vehicle into which a



© 1981, American Pharmaceutical Association

**Table I—Mean Plasma Concentration (Nanograms per Milliliter) of Triamterene in Rats [a] following an Oral Dose of 10 mg/kg in a 1-ml Vehicle Volume**

| Hours | Lactic Acid Solution | Aqueous Suspension | Peanut Oil Suspension | Oleic Acid Suspension | Triolein Suspension |
|---|---|---|---|---|---|
| 0.5 | 196 (28)[b] | 257 (82) | 178 (29) | 65 (8) | 141 (56) |
| 1.0 | 236 (29) | 267 (106) | 185 (11) | 166 (60) | 164 (53) |
| 1.5 | 350 (38) | 174 (49) | 338 (50) | 152 (23) | 220 (2) |
| 2.0 | 368 (52) | 179 (54) | 282 (52) | 224 (61) | 189 (50) |
| 2.5 | 371 (43) | 123 (27) | 294 (41) | 162 (36) | 130 (17) |
| 3.0 | 448 (50) | 114 (33) | 231 (52) | 144 (16) | 102 (11) |
| 4.0 | 404 (87) | 99 (28) | 206 (39) | 129 (13) | 132 (24) |
| 5.0 | 351 (107) | 61 (17) | 202 (31) | 138 (41) | 140 (33) |
| 6.0 | 168 (62) | 62 (14) | 194 (31) | 111 (24) | 116 (30) |
| 12.0 | 127 (43) | 51 (6) | 104 (24) | 202 (62) | 69 (13) |
| 24.0 | 40 (2) | 37 (15) | 40 (1) | 201 (50) | 59 (14) |

[a] Mean of four rats. [b] Numbers in parentheses are the standard errors of the means.

drug is incorporated and the vehicle volume administered may affect all of these factors in addition to any interactions the vehicle may have with the drug itself.

## BACKGROUND

A traditional problem in oral drug delivery has been the relatively low bioavailability exhibited by many poorly water-soluble drugs. Considerable research has centered on the possible enhancement of the oral bioavailability of such drugs by their incorporation into various lipid vehicles. It is unclear whether lipid vehicles may affect oral bioavailability through some biochemical and/or physiological effects, whether solubilization of the drug is the mechanism, or a combination of these factors is operative.

Crounse (1) demonstrated an increase in griseofulvin bioavailability when administered with a high fat diet to humans. Griseofulvin bioavailability in rats also was enhanced when administered in various corn oil vehicles (2, 3). Indoxole bioavailability was increased in both humans (4) and rats (5) when administered in lipid vehicles. Sulfisoxazole (6) and dicumarol (7) are other examples of drugs whose bioavailability is enhanced in lipid vehicles.

Grisafe and Hayton (8) concluded that triglycerides had the ability to enhance the oral absorption of griseofulvin due to the enhanced dissolution and not directly to the lipid-induced increases in absorption. Solubilization of poorly water-soluble drugs as a method of improving oral bioavailability was confirmed by other investigators (9–11).

Yamahira *et al.* (12–14) recently demonstrated that the volume of vehicle in which the drug is administered can influence the results obtained in oral bioavailability studies. It was concluded that many oral bioavailability studies, particularly those with rats, used unrealistically large vehicle volumes. Yamahira *et al.* (13) developed a reproducible method of administering very small vehicle volumes (2–20 μl) to rats to eliminate the physiological effects caused by large vehicle volumes.

In the present study, the effects of various vehicles and vehicle volumes were correlated to the oral absorption of the poorly soluble, potassium-sparing diuretic, triamterene, in rats.

## EXPERIMENTAL

**Materials**—Pure triamterene powder[1] was used to prepare all drug suspensions and solutions. Five drug vehicles were studied initially: water, peanut oil[2], triolein[3], lactic acid[4], and oleic acid[5]. All solvents for chromatography were high-performance liquid chromatographic (HPLC) grade[6], and other reagents were analytical grade[6].

The suspensions used initially were at concentrations of 4.0 mg/ml. Ten-milliliter aliquots were transferred to 15-ml screw-capped tubes and shaken for 30 min on a mixer[7] with a modified shaker head. Five drops of surfactant[8] were added to the aqueous suspensions. For the solution vehicle, triamterene was dissolved in an 8% lactic acid solution. In subsequent studies, peanut oil and aqueous suspensions were prepared as described at a concentration of 45 mg/ml. The range of solubilities of triamterene in all vehicles (other than the lactic acid solutions) was $10^{-4}$–$10^{-5}$ *M*.

**Table II—Mean Peak Plasma Concentration, Mean Time of Peak Concentration, and Mean *AUC* in Rats [a] following an Oral Dose of 10 mg/kg of Triamterene in a 1-ml Vehicle Volume**

| Vehicle | Mean Peak Plasma Concentration, ng/ml | Mean Time of Peak Concentration, hr | Mean *AUC*, 0–24 hr, ng hr/ml |
|---|---|---|---|
| Lactic acid solution | 510 (55) | 3.75 (0.48) | 4184 (915) |
| Aqueous suspension | 286 (104) | 0.62 (0.12) | 1647 (288) |
| Peanut oil suspension | 348 (44) | 2.50 (0.61) | 3219 (43) |
| Oleic acid suspension | 266 (86) | 2.50 (0.54) | 4744 (842) |
| Triolein suspension | 249 (42) | 2.62 (0.83) | 2214 (294) |

[a] Means calculated from four individual experiments in four different rats in a balanced incomplete block design.

**Animal Studies**—Initial studies evaluated five vehicles in a balanced incomplete block design. Ten rats were each randomly assigned to receive two of the formulations, and each formulation was tested in four rats. A 1-week washout period was allowed before a rat was used again.

Male rats[9], 250–300 g, were fasted for 12 hr prior to dosing with 10 mg of triamterene/kg, suspended or dissolved in the various vehicles. Immediately prior to dosing, suspensions were removed from the shaker and the appropriate dose was drawn into a tuberculin syringe[10]. The volume was adjusted to 1 ml with the requisite vehicle, and the syringe was shaken again.

Lightly ether-anesthetized animals were dosed with a 76-mm intubation needle[11] attached to the tuberculin syringe. Blood samples were taken by tail clipping while the animals were restrained in plexiglass cages[11]. Blood samples were obtained every 0.5 hr for 3 hr; then every hour until 6 hr, and then at 12 and 24 hr. In later studies, a 9-hr sample was added.

Whole blood (~350-μl samples) was collected in heparinized caraway capillary tubes[12], blown into 1.5-ml microcentrifuge tubes[13], and spun for 3 min[14]. Plasma aliquots (100 μl) were placed in 4-ml polypropylene tubes[15] with fitted caps. Plasma samples were frozen until analysis.

Later studies compared peanut oil and aqueous suspensions administered in a 20-μl volume in a complete crossover study in four rats. The washout period was 1 week. To administer the 20-μl volume, the procedure of Yamahira *et al.* (13) was adopted with some modifications. The suspensions were prepared at concentrations of 45 mg/ml so that each rat received 0.9 mg in the 20-μl volume. The dosing system consisted of 19-gauge flexible tubing with a luer-lock end[16] sleeved with polyethylene tubing for rigidity.

A 50-μl syringe[16] was used to draw the dose, and the tubing was calibrated to double check the volume. Each dose was followed by a small volume of air injected through the tubing to ensure that no material re-

[1] Smith Kline and French, Philadelphia, Pa.
[2] Planters, Standard Brands, New York, N.Y.
[3] Seventy-five percent practical grade, Sigma Chemicals, St. Louis, Mo.
[4] Eighty-five percent laboratory grade, Fisher Scientific Co., Fair Lawn, N.J.
[5] Purified, Fisher Scientific Co., Fair Lawn, N.J.
[6] Fisher Scientific Co., Fair Lawn, N.J.
[7] Vortex Genie, Scientific Industries, Bohemia, N.Y.
[8] Tween 85, ICI America, Wilmington, Del.
[9] Sprague-Dawley, Madison, Wis.
[10] Monoject, Sherwood Medical Industries, Deland, Fla.
[11] Perfektum, Popper and Sons, New Hyde Park, N.Y.
[12] Dade Division, American Hospital Supply, Miami, Fla.
[13] Centaur Sciences, Stamford, Conn.
[14] Eppendorf microcentrifuge, Brinkmann Instruments, Westbury, N.Y.
[15] Elkay Products, Shrewsbury, Mass.
[16] Hamilton Co., Reno, Nev.

Table III—Plasma Concentration of Triamterene following an Oral Dose of 0.9 mg to Rats in a 20-μl Vehicle Volume in a Complete Crossover Study

| Hours | Rat 1, ng/ml | Rat 2, ng/ml | Rat 3, ng/ml | Rat 4, ng/ml |
|---|---|---|---|---|
| | | Peanut Oil Suspension | | |
| 0.5 | 96 | 201 | 95 | 138 |
| 1.0 | 202 | 248 | 152 | 154 |
| 1.5 | 236 | 222 | 190 | 134 |
| 2.0 | 281 | 276 | 289 | 148 |
| 2.5 | 284 | 277 | 281 | 110 |
| 3.0 | 178 | 212 | 188 | 127 |
| 4.0 | 124 | 148 | 164 | 136 |
| 5.0 | 162 | 99 | 168 | 108 |
| 6.0 | 90 | 81 | 116 | 161 |
| 9.0 | 76 | 54 | 72 | 75 |
| 12.0 | 76 | 68 | 52 | 60 |
| 24.0 | 77 | 45 | 65 | 39 |
| | | Aqueous Suspension | | |
| 0.5 | 213 | 160 | 216 | 167 |
| 1.0 | 147 | 252 | 314 | 182 |
| 1.5 | 201 | 142 | 292 | 233 |
| 2.0 | 223 | 222 | 308 | 213 |
| 2.5 | 149 | 222 | 244 | 191 |
| 3.0 | 234 | 179 | 208 | 180 |
| 4.0 | 200 | 194 | 118 | 228 |
| 5.0 | 150 | 86 | 90 | 122 |
| 6.0 | 136 | 218 | 80 | 84 |
| 9.0 | 110 | 92 | 180 | 70 |
| 12.0 | 72 | 96 | 52 | 68 |
| 24.0 | 51 | 99 | 94 | 48 |

mained on the inside. This dosing system was checked with the actual suspensions used and was found to provide reproducible doses within ±10%.

**Analytical Procedure**—The analytical procedure was a modification of the method of Sved *et al.* (15). Plasma samples were thawed, 0.2 ml of perchloric acid was added, and the sample was mixed. Methylisobutylketone[17] (0.8-ml), which had been saturated with 1 *M* $HClO_4$, was then added, and the sample was mixed again. Sample tubes were then capped and shaken for 20 min, samples were centrifuged for 10 min, and the methylisobutylketone layer was removed and refrigerated in glass vials. Standards were prepared by adding appropriate concentrations of triamterene to 100 μl of blank plasma and extracted in the same manner. This extraction procedure provided ~90% recovery when compared to standards prepared directly in methylisobutylketone in a plasma concentration range of 10–850 ng/ml.

HPLC[18] was used to analyze the extracted plasma samples. Fifty-microliter injections were made onto the column[19], and the flow rate was 2 ml/min. No attempts were made to quantitate metabolites. The system operated at 1000 psi at a fluorometer setting of 335-nm excitation and 470-nm emission. The mobile phase consisted of methylene chloride–hexane–methanol–perchloric acid (55:35:10:0.1). Concentrations were quantitated by comparing peak height to the standards developed for each set of samples.

## RESULTS

In the first series of experiments, 10 mg of triamterene/kg was administered to rats in 1 ml of the following vehicles: solution in 8% lactic acid, aqueous suspension, oleic acid suspension, triolein suspension, and peanut oil suspension. Ten rats were randomly assigned to a balanced incomplete block design in which each rat received two formulations in trials separated by 1 week. Each formulation was administered four times to four different rats.

Table I shows the mean plasma concentrations with associated standard errors for each formulation in the four rats at each sampling time. Table II shows the mean peak concentration, mean time of peak concentration, and mean area under the plasma concentration–time curve (0–24 hr) computed by trapezoidal integration from the four individual experiments with each formulation[20].

[17] Mallinckrodt, Paris, Ky.

[18] The chromatographic system consisted of a 6000 A pump and U6K universal injector (Waters Associates, Milford, Mass.) coupled to an FS 970 fluorometer (Schoeffel Instrument Corp., Westwood, N.J.).

[19] Lichrosorb Si-60-7 (250 × 4.6 mm), Chrompak, Whittier, Calif.

[20] Although the oleic acid suspension resulted in the largest *AUC*, this result is biased by the 12- and 24-hr time points in which plasma concentrations began to increase again. This observation is currently not explained and is being reevaluated.

Table IV—Mean Peak Plasma Concentration, Mean Time of Peak Concentration, and Mean *AUC* in Rats[a] following an Oral Dose of 0.9 mg of Triamterene in a 20-μl Vehicle Volume

| Vehicle | Mean Peak Plasma Concentration, ng/ml | Mean Time of Peak Plasma Concentration, hr | Mean *AUC*, ng hr/ml |
|---|---|---|---|
| Aqueous suspension | 258 (19) | 1.62 (0.47) | 2560 (169) |
| Peanut oil suspension | 251 (32) | 2.00 (0.35) | 2162 (103) |

[a] Means calculated from four individual experiments in four different rats in a complete crossover study; none of the means in any column are significantly different ($\alpha = 0.05$)..

The data of Tables I and II show a trend with peanut oil suspensions toward higher plasma triamterene levels and an overall increase in the availability of triamterene when compared to the aqueous suspensions. These findings led to a further investigation of peanut oil as a potential vehicle for enhancing the oral availability of triamterene. A second series of experiments, in a complete crossover study, was conducted in which the peanut oil suspension was compared to aqueous suspensions in four rats, also at a dose of 10 mg/kg in a 1-ml volume. The specific results of this study are not shown here; however, it confirmed the potential of peanut oil as a vehicle to enhance the oral availability of triamterene.

The third series of experiments was conducted to evaluate the oral availability of triamterene using aqueous and peanut oil suspensions in a realistic dosage form vehicle volume. In this study, 20 μl of peanut oil or aqueous suspensions of triamterene containing 45 mg of drug/ml were administered to four rats in a complete crossover design. Each rat received 0.9 mg of triamterene in a 20-μl dose volume, which represents a realistic dosage form volume when scaled to the size of the rat (13). Table III shows the individual plasma triamterene levels measured in the four rats with both aqueous and peanut oil suspensions. Figure 1 shows a plot of the mean plasma level at each time point for both the aqueous and peanut oil suspensions, and Table IV shows the mean peak concentrations, time of peak concentration, and mean *AUC* (0–24 hr).

## DISCUSSION

In the initial study with the 1-ml vehicle volume, the three lipid vehicles exhibited a trend toward a later peak time and maintained higher plasma levels for a longer time when compared to aqueous suspensions. With all formulations tested, a rather large intersubject variability was noted. This finding was consistent with what other investigators observed following triamterene administration (16). Such variability coupled with the small number of trials (four) performed with each vehicle made it difficult to evaluate statistical differences among the vehicles even though the trends were clear. Additionally, any differences among the lipid vehicles with respect to triamterene availability cannot be explained on the basis of drug solubility in the vehicles. Even with oleic acid, which was the suspension vehicle in which triamterene was most soluble, <1% of the administered drug was in solution.

The lactic acid solution clearly provided the highest plasma triamterene levels of the vehicles evaluated with a 1-ml dosing volume. As previously noted, the oleic acid vehicle resulted in the largest *AUC*, al-

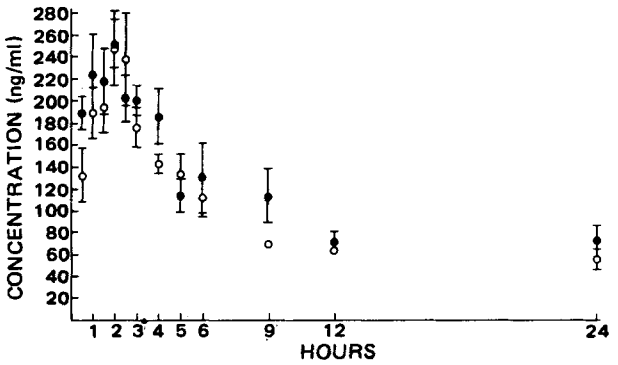


**Figure 1**—*Mean plasma levels of triamterene in rats following oral administration of 0.9 mg in a 20-μl vehicle volume in a complete crossover study. Key:* ○, *peanut oil suspension; and* ●, *aqueous suspension. Bars represent standard error of the mean.*

though this result was biased by the 12- and 24-hr time points. Oleic acid was not investigated further in this study, although Noguchi *et al.* (17) concluded that oleic acid may be a useful vehicle to sustain the release of poorly water-soluble drugs, thus, prolonging their effects.

In the last series of this study, the oral availability of triamterene was evaluated from peanut oil and aqueous suspensions in which the dosing volume was reduced to 20 $\mu$l. Peanut oil was selected for comparison with the aqueous vehicle based on results from the initial study. In that study, the peanut oil vehicle provided a similar peak plasma level as the aqueous suspension, although peak levels occurred somewhat later. The decline from peak levels was slower for peanut oil than for the aqueous suspension, resulting in a larger overall *AUC* for peanut oil suspensions. Finally, the intersubject variability in the initial study was smallest with the peanut oil suspensions. It was thus concluded that peanut oil might be a promising vehicle for formulating triamterene and improving its oral availability.

The results (Tables III and IV and Fig. 1) of the two-way crossover study, comparing peanut oil and aqueous suspensions of triamterene, did not confirm the initial optimism regarding peanut oil as a vehicle when administered in realistic dosage form vehicle volumes. A weighted unpaired $t$-test revealed no significant differences between the aqueous and peanut oil vehicles with respect to peak plasma concentration, peak time, or *AUC* ($\alpha = 0.05$). These results suggest that any enhanced availability in the peanut oil vehicle, which was suggested by the initial study, may have been due to physiological effects on the GI tract caused by the relatively large vehicle volume used. Such effects appeared to be eliminated when the dosage form vehicle volumes were used.

A further aspect of these studies is the comparison of the doses used in both the large and small volume experiments. In the 1-ml administered volume study, each rat received ~2.5 mg of triamterene; in the 20-$\mu$l volume study, the administered dose was ~0.9 mg. The $t$-test revealed that neither peak height nor peak time was significantly different between these two studies ($\alpha = 0.5$). However, with the aqueous suspension, the *AUC* for the 20-$\mu$l dose volumes was greater ($p < 0.05$) than with the 1-ml volume. With the peanut oil suspensions, the *AUC* for the 20-$\mu$l dose volume was significantly less than with the 1-ml volume ($p < 0.001$) but, in absolute terms, was reduced by one-third compared with the dosage reduction of a factor of ~3. Clearly, the larger dose volumes for both peanut oil and aqueous suspensions adversely affected the oral availability of triamterene. The precise mechanism of this effect is unexplained, although it is probably due to some alteration of physiological processes within the GI tract caused by the large vehicle volumes.

The results indicated that the methodology used to evaluate the effects of various vehicles on the GI absorption of drugs must be carefully considered. The results of *in situ* perfusion studies and those employing large vehicle volumes may not be directly applicable to an actual dosage form. With triamterene, a drug poorly soluble in both aqueous and lipid vehicles, a large volume of lipid vehicle may provide some enhancement of oral availability when compared to aqueous vehicles. At least with peanut oil, however, when the vehicle volume is reduced to a realistic dosage form volume, the potential advantage is lost. Furthermore, small vehicle volumes result in better relative oral availability for triamterene than do large vehicle volumes. Such a finding might be considered with regard to the administration of triamterene in conjunction with some foods.

## REFERENCES


(1) R. G. Crounse, *J. Invest. Dermatol.*, **37**, 529 (1961).

(2) M. Kraml, J. Dubue, and D. Beall, *Can. J. Biochem.*, **40**, 1449 (1962).

(3) P. J. Carrigan and T. R. Bates, *J. Pharm. Sci.*, **62**, 1476 (1973).

(4) J. G. Wagner, E. S. Gerard, and D. G. Kaiser, *Clin. Pharmacol. Ther.*, **7**, 610 (1966).

(5) D. G. Kaiser, E. M. Glenn, R. H. Johnson, and R. L. Johnson, *J. Pharmacol. Exp. Ther.*, **155**, 174 (1967).

(6) S. E. Swenson, W. L. DeLorenzo, R. Engelberg, M. Spooner, and L. O. Randell, *Antibiot. Med.*, **2**, 148 (1956).

(7) D. C. Bloedow and W. L. Hayton, *J. Pharm. Sci.*, **65**, 328 (1976).

(8) J. A. Grisafe and W. L. Hayton, *ibid.*, **67**, 895 (1978).

(9) V. Stella, J. Haslam, N. Yata, H. O'Kada, S. Lindenbaum, and T. Higuchi, *ibid.*, **67**, 1375 (1978).

(10) J. Kreuter and T. Higuchi, *ibid.*, **68**, 451 (1979).

(11) V. Alvisi, C. Longhini, B. Bagni, F. Portaluppi, M. Ruina, and C. Fersini, *Arzneim-Forsch.*, **29**, 1047 (1979).

(12) Y. Yamahira, T. Noguchi, H. Takenaka, and T. Maeda, *J. Pharmacokinet. Dyn.*, **1**, 160 (1978).

(13) Y. Yamahira, T. Noguchi, T. Noguchi, H. Takenaka, and T. Maeda, *ibid.*, **2**, 52 (1979).

(14) Y. Yamahira, T. Noguchi, H. Takenaka, and T. Maeda, *Int. J. Pharm.*, **3**, 23 (1979).

(15) S. Sved, J. A. A. Sertie, and I. J. McGilveray, *J. Chromatogr.*, **162**, 474 (1979).

(16) A. W. Pruitt, J. S. Winkel, and P. G. Dayton, *Clin. Pharmacol. Ther.*, **21**, 610 (1977).

(17) T. Noguchi, K. Taniguchi, S. Muranishi, and H. Sezaki, *Chem. Pharm. Bull.*, **25**, 434 (1977).


## ACKNOWLEDGMENTS


Supported by grants from R. P. Scherer Corp. and Inter$_x$ Research Corp.


# Compression Properties of Granulations Made with Binders Containing Different Moisture Contents


**Z. T. CHOWHAN** ˣ **and Y. P. CHOW**



Received June 27, 1980, from the *Institute of Pharmaceutical Sciences, Syntex Research, Palo Alto, CA 94304.* Accepted for publication March 5, 1981.



**Abstract** □ The role of the granulation moisture content on compression properties of granules made with selected binders was studied. The results suggested that, at lower pressures, higher moisture-containing granules were slightly more compressible than lower moisture-containing granules. However, at higher pressures, the reverse was true because of the water lubrication effect. At lower moisture levels, the crushing strength of the tablets was dependent on the binder; at higher moisture levels, binder differences became less significant.



**Keyphrases** □ Compression—effect of moisture content on granulations made with various binders □ Granulations—effect of moisture content on compression properties, various binders □ Binders—various, effect of moisture content on compression properties of granulations


The compression behavior of four pharmaceutical powders of widely different particle-size distribution and shape was reported previously (1). It was shown that the Heckel (2) and Cooper–Eaton (3) equations can be used




*0022-3549/81/1000-1134$01.00/0*


*© 1981, American Pharmaceutical Association*

though this result was biased by the 12- and 24-hr time points. Oleic acid was not investigated further in this study, although Noguchi *et al.* (17) concluded that oleic acid may be a useful vehicle to sustain the release of poorly water-soluble drugs, thus, prolonging their effects.

In the last series of this study, the oral availability of triamterene was evaluated from peanut oil and aqueous suspensions in which the dosing volume was reduced to 20 $\mu$l. Peanut oil was selected for comparison with the aqueous vehicle based on results from the initial study. In that study, the peanut oil vehicle provided a similar peak plasma level as the aqueous suspension, although peak levels occurred somewhat later. The decline from peak levels was slower for peanut oil than for the aqueous suspension, resulting in a larger overall *AUC* for peanut oil suspensions. Finally, the intersubject variability in the initial study was smallest with the peanut oil suspensions. It was thus concluded that peanut oil might be a promising vehicle for formulating triamterene and improving its oral availability.

The results (Tables III and IV and Fig. 1) of the two-way crossover study, comparing peanut oil and aqueous suspensions of triamterene, did not confirm the initial optimism regarding peanut oil as a vehicle when administered in realistic dosage form vehicle volumes. A weighted unpaired $t$-test revealed no significant differences between the aqueous and peanut oil vehicles with respect to peak plasma concentration, peak time, or *AUC* ($\alpha = 0.05$). These results suggest that any enhanced availability in the peanut oil vehicle, which was suggested by the initial study, may have been due to physiological effects on the GI tract caused by the relatively large vehicle volume used. Such effects appeared to be eliminated when the dosage form vehicle volumes were used.

A further aspect of these studies is the comparison of the doses used in both the large and small volume experiments. In the 1-ml administered volume study, each rat received ~2.5 mg of triamterene; in the 20-$\mu$l volume study, the administered dose was ~0.9 mg. The $t$-test revealed that neither peak height nor peak time was significantly different between these two studies ($\alpha = 0.5$). However, with the aqueous suspension, the *AUC* for the 20-$\mu$l dose volumes was greater ($p < 0.05$) than with the 1-ml volume. With the peanut oil suspensions, the *AUC* for the 20-$\mu$l dose volume was significantly less than with the 1-ml volume ($p < 0.001$) but, in absolute terms, was reduced by one-third compared with the dosage reduction of a factor of ~3. Clearly, the larger dose volumes for both peanut oil and aqueous suspensions adversely affected the oral availability of triamterene. The precise mechanism of this effect is unexplained, although it is probably due to some alteration of physiological processes within the GI tract caused by the large vehicle volumes.

The results indicated that the methodology used to evaluate the effects of various vehicles on the GI absorption of drugs must be carefully considered. The results of *in situ* perfusion studies and those employing large vehicle volumes may not be directly applicable to an actual dosage form. With triamterene, a drug poorly soluble in both aqueous and lipid vehicles, a large volume of lipid vehicle may provide some enhancement of oral availability when compared to aqueous vehicles. At least with peanut oil, however, when the vehicle volume is reduced to a realistic dosage form volume, the potential advantage is lost. Furthermore, small vehicle volumes result in better relative oral availability for triamterene than do large vehicle volumes. Such a finding might be considered with regard to the administration of triamterene in conjunction with some foods.

## REFERENCES


(1) R. G. Crounse, *J. Invest. Dermatol.*, **37**, 529 (1961).

(2) M. Kraml, J. Dubue, and D. Beall, *Can. J. Biochem.*, **40**, 1449 (1962).

(3) P. J. Carrigan and T. R. Bates, *J. Pharm. Sci.*, **62**, 1476 (1973).

(4) J. G. Wagner, E. S. Gerard, and D. G. Kaiser, *Clin. Pharmacol. Ther.*, **7**, 610 (1966).

(5) D. G. Kaiser, E. M. Glenn, R. H. Johnson, and R. L. Johnson, *J. Pharmacol. Exp. Ther.*, **155**, 174 (1967).

(6) S. E. Swenson, W. L. DeLorenzo, R. Engelberg, M. Spooner, and L. O. Randell, *Antibiot. Med.*, **2**, 148 (1956).

(7) D. C. Bloedow and W. L. Hayton, *J. Pharm. Sci.*, **65**, 328 (1976).

(8) J. A. Grisafe and W. L. Hayton, *ibid.*, **67**, 895 (1978).

(9) V. Stella, J. Haslam, N. Yata, H. O'Kada, S. Lindenbaum, and T. Higuchi, *ibid.*, **67**, 1375 (1978).

(10) J. Kreuter and T. Higuchi, *ibid.*, **68**, 451 (1979).

(11) V. Alvisi, C. Longhini, B. Bagni, F. Portaluppi, M. Ruina, and C. Fersini, *Arzneim-Forsch.*, **29**, 1047 (1979).

(12) Y. Yamahira, T. Noguchi, H. Takenaka, and T. Maeda, *J. Pharmacokinet. Dyn.*, **1**, 160 (1978).

(13) Y. Yamahira, T. Noguchi, T. Noguchi, H. Takenaka, and T. Maeda, *ibid.*, **2**, 52 (1979).

(14) Y. Yamahira, T. Noguchi, H. Takenaka, and T. Maeda, *Int. J. Pharm.*, **3**, 23 (1979).

(15) S. Sved, J. A. A. Sertie, and I. J. McGilveray, *J. Chromatogr.*, **162**, 474 (1979).

(16) A. W. Pruitt, J. S. Winkel, and P. G. Dayton, *Clin. Pharmacol. Ther.*, **21**, 610 (1977).

(17) T. Noguchi, K. Taniguchi, S. Muranishi, and H. Sezaki, *Chem. Pharm. Bull.*, **25**, 434 (1977).


## ACKNOWLEDGMENTS


Supported by grants from R. P. Scherer Corp. and Inter$_x$ Research Corp.


# Compression Properties of Granulations Made with Binders Containing Different Moisture Contents


**Z. T. CHOWHAN** ˣ **and Y. P. CHOW**



Received June 27, 1980, from the *Institute of Pharmaceutical Sciences, Syntex Research, Palo Alto, CA 94304.* Accepted for publication March 5, 1981.



**Abstract** □ The role of the granulation moisture content on compression properties of granules made with selected binders was studied. The results suggested that, at lower pressures, higher moisture-containing granules were slightly more compressible than lower moisture-containing granules. However, at higher pressures, the reverse was true because of the water lubrication effect. At lower moisture levels, the crushing strength of the tablets was dependent on the binder; at higher moisture levels, binder differences became less significant.



**Keyphrases** □ Compression—effect of moisture content on granulations made with various binders □ Granulations—effect of moisture content on compression properties, various binders □ Binders—various, effect of moisture content on compression properties of granulations


The compression behavior of four pharmaceutical powders of widely different particle-size distribution and shape was reported previously (1). It was shown that the Heckel (2) and Cooper–Eaton (3) equations can be used




*0022-3549/81/1000-1134$01.00/0*


*© 1981, American Pharmaceutical Association*

**Table I—Tablet Formulations [a]**

| Ingredient | Formulation A | B | C | D | E |
|---|---|---|---|---|---|
| Ticlopidine hydrochloride | 250 | 250 | 250 | 250 | 250 |
| Lactose | 91.25 | 91.25 | 91.25 | 91.25 | 99.05 |
| Starch | 39.00 | 39.00 | 39.00 | 39.00 | 39.00 |
| Magnesium stearate | 1.95 | 1.95 | 1.95 | 1.95 | 1.95 |
| Methylcellulose | 7.8 | — | — | — | — |
| Povidone | — | 7.8 | — | — | — |
| Pregelatinized starch | — | — | 7.8 | — | — |
| Hydroxypropyl methylcellulose | — | — | — | 7.8 | — |

[a] Milligrams of ingredient per tablet.

to quantify the compression parameters of powders, provided that various experimental conditions are considered.

The relative density *versus* pressure plots of the granulations made with powder mixtures by wet granulation did not give a typical relationship (4), as previously explained (2). A break in the linear portion of the Heckel plots at a pressure range of ~1200–1900 kg/cm$^2$ was explained largely on the basis of the water lubrication effect at higher pressures. At lower pressures, where the water lubrication effect did not occur, the relative density–pressure plots (2) and the Cooper–Eaton plots (3) were used to calculate the apparent material constants and the coefficients of the Cooper–Eaton equation. Excellent correlation between the apparent material constant ($C_1$) of the Heckel equation and the coefficient ($k_2$) of the Cooper–Eaton equation and the tablet crushing strength suggested the usefulness of these studies for proper binder selection when designing tablet formulations.

This paper reports the role of moisture content on compression properties of granulations made with selected binders.

## EXPERIMENTAL

**Materials**—Ticlopidine hydrochloride[1] (I) was at least 98% pure. The excipients, crystalline lactose[2], starch[3], magnesium stearate[4], povidone[5], methylcellulose[6], hydroxypropyl methylcellulose[7], and pregelatinized starch[3], were all USP grade.

**Granulation**—The formulations are listed in Table I. Compound I and lactose were mixed together in a small planetary mixer for 5 min. For Formulation C, pregelatinized starch was also mixed with I and lactose and granulated with purified water by mixing for 5 min. For Formulations A, B, and D, the binder was dispersed or dissolved in the same amount of water as was used in granulating Formulation C. The I–lactose mixture (39 g) was granulated with 15 ml of the granulating solution by mixing for 5 min.

For Formulation E, the I–lactose mixture was granulated with 15 ml of purified water. The wet granulation was passed through a 1.4-mm aperture and dried in a forced-air oven at 40° until the desired moisture levels were obtained. The dried granulation was screened through a 1.2-mm aperture. Starch and magnesium stearate then were blended with the granulation for 5 min.

**Compression**—For each compression, 390 mg of the granulation was used[8]. The die and punches were 10.32 mm in diameter, and the punches were flat-faced. The contact time of the upper punch with the granulation was less than 5 sec. Immediately after compression and ejection, the height of the compact was measured accurately and the volume and density of the compact were calculated. Three determinations were made for each data point. The mean volumes of compression, along with the standard deviations at given pressures for granulations made with the selected binders, are given in Table II.

**Tablet Crushing Strength**—The compact hardness was determined[9] immediately after compression. For each hardness determination, three compacts were tested and the mean was calculated.

**Moisture Determination**—An aluminum dish was dried in a forced-air oven at 60° for 30 min. The dish was then equilibrated to room temperature, and the sample was accurately weighed into the dish and

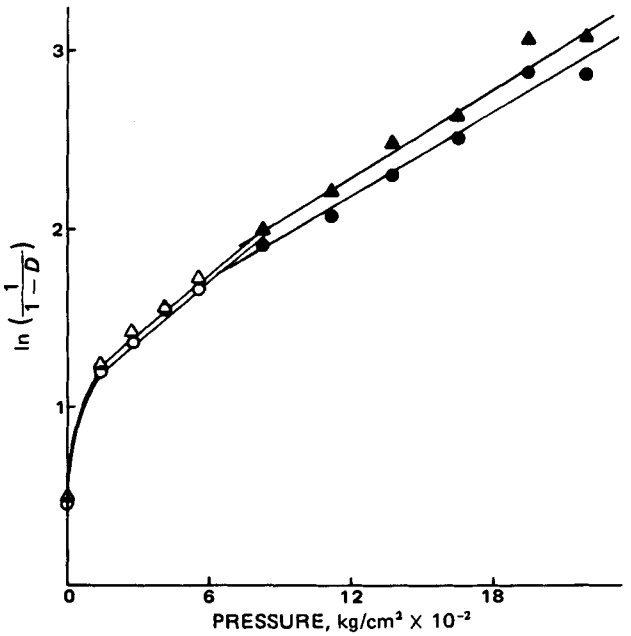


**Figure 1**—*Plots of ln[1/(1 − D)] versus pressure using granulations made with povidone (△,▲) and methylcellulose (○,●) as binders. The moisture contents at the time of compression were 1.12% for povidone granules and 0.89% for methylcellulose granules.*

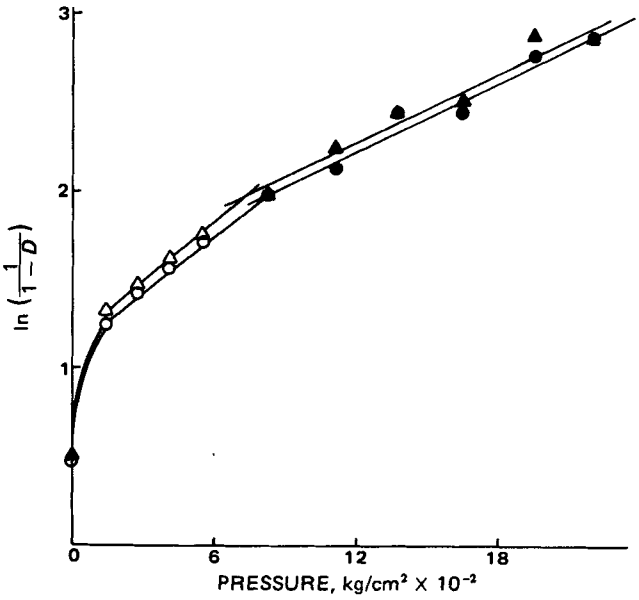


**Figure 2**—*Plots of ln[1/(1 − D)] versus pressure using granulations made with pregelatinized starch (○, ●) and without a binder (△,▲). The moisture contents at the time of compression were 0.79% for pregelatinized starch granules and 0.77% for granules made without a binder.*

[1] 5-(o-Chlorobenzyl)-4,5,6,7-tetrahydrothieno-[3,2-c]pyridine hydrochloride, Sanofi Research Co., New York, NY 10019.
[2] Regular grade, Foremost Co., San Francisco, CA 94104.
[3] Staley Manufacturing Co., Decatur, IL 62525.
[4] Mallinckrodt Chemical Co., St. Louis, MO 63134.
[5] GAF Corp., New York, NY 10020.
[6] Methocel A-15, Dow Chemical Co., Midland, MI 48640.
[7] Pharmacoat 606, Shinetsu Chemical Co., Tokyo, Japan.
[8] Model b Carver laboratory press, Fred S. Carver Inc., Summit, NJ 07901.
[9] Schleuniger-2E hardness tester, Vector Corp., Marion, IA 52302.

**Table II—Mean Volumes [a] of Compression for Granulations Made with Selected Binders Containing Different Moisture Contents**

| Pressure, kg/cm² | Methylcellulose | | Povidone | | Pregelatinized Starch | | Hydroxypropyl Methylcellulose | | | No Binder | |
|---|---|---|---|---|---|---|---|---|---|---|---|
| | 2.44% Moisture | 0.89% Moisture | 2.23% Moisture | 1.12% Moisture | 2.02% Moisture | 0.79% Moisture | 3.35% Moisture | 2.32% Moisture | 0.75% Moisture | 1.95% Moisture | 0.77% Moisture |
| 135.9 | 0.395 ± 0.004 | 0.414 ± 0.002 | 0.393 ± 0.000 | 0.405 ± 0.002 | 0.399 ± 0.004 | 0.401 ± 0.002 | 0.389 ± 0.002 | 0.401 ± 0.000 | 0.412 ± 0.002 | 0.389 ± 0.004 | 0.382 ± 0.002 |
| 271.9 | 0.369 ± 0.000 | 0.389 ± 0.002 | 0.365 ± 0.004 | 0.380 ± 0.004 | 0.369 ± 0.002 | 0.380 ± 0.002 | 0.367 ± 0.002 | 0.378 ± 0.006 | 0.384 ± 0.002 | 0.372 ± 0.002 | 0.361 ± 0.002 |
| 407.8 | 0.355 ± 0.002 | 0.367 ± 0.002 | 0.350 ± 0.002 | 0.365 ± 0.000 | 0.352 ± 0.000 | 0.363 ± 0.002 | 0.352 ± 0.002 | 0.357 ± 0.002 | 0.369 ± 0.002 | 0.357 ± 0.002 | 0.346 ± 0.002 |
| 543.7 | 0.346 ± 0.000 | 0.357 ± 0.002 | 0.340 ± 0.002 | 0.350 ± 0.000 | 0.342 ± 0.002 | 0.350 ± 0.002 | 0.340 ± 0.002 | 0.350 ± 0.002 | 0.361 ± 0.000 | 0.346 ± 0.002 | 0.338 ± 0.002 |
| 815.6 | 0.331 ± 0.002 | 0.340 ± 0.002 | 0.321 ± 0.002 | 0.333 ± 0.002 | 0.329 ± 0.002 | 0.333 ± 0.002 | 0.329 ± 0.004 | 0.333 ± 0.002 | 0.342 ± 0.000 | 0.331 ± 0.002 | 0.325 ± 0.002 |
| 1359.3 | 0.314 ± 0.002 | 0.321 ± 0.004 | 0.310 ± 0.004 | 0.314 ± 0.002 | 0.312 ± 0.000 | 0.314 ± 0.002 | 0.314 ± 0.002 | 0.316 ± 0.002 | 0.321 ± 0.002 | 0.314 ± 0.002 | 0.312 ± 0.000 |
| 1631.2 | 0.310 ± 0.002 | 0.314 ± 0.002 | 0.306 ± 0.002 | 0.310 ± 0.002 | 0.308 ± 0.002 | 0.314 ± 0.002 | — | 0.312 ± 0.002 | 0.312 ± 0.002 | 0.312 ± 0.000 | 0.306 ± 0.000 |
| 2174.9 | 0.304 ± 0.002 | 0.360 ± 0.000 | 0.299 ± 0.002 | 0.301 ± 0.000 | 0.306 ± 0.002 | 0.304 ± 0.000 | 0.360 ± 0.002 | 0.308 ± 0.002 | 0.308 ± 0.002 | 0.304 ± 0.002 | 0.304 ± 0.002 |

[a] In cubic centimeters (mean ± *SD*).

dried in the oven at 60° until it reached a constant weight. The moisture content was calculated from the sample weight before and after drying.

**Bulk Density**—The powder was slowly sifted into a 50-ml graduated cylinder through a plastic funnel. The powder weight ($W$) and volume ($V$) were recorded to calculate the bulk density ($\gamma_b = W/V$).

**True Density**—The true density of the granules was calculated from the true density of the individual components in the formulation. The method of density matching (5) was used to determine the true density of individual components. A few milligrams of the powder was added to the test tubes containing different combinations of carbon tetrachloride and hexane mixtures. The powder–solvent mixture was shaken on a vortex mixer, centrifuged, and allowed to stand for 30 min. The true density of the powder was the same as the density of the solvent mixture in which the powder remained suspended. The density of the solvent mixture was determined with a pycnometer at 23° using water to calibrate the volume.

## RESULTS AND DISCUSSION

The relative density *versus* pressure plots of the granulations made with selected binders at different moisture levels are given in Figs. 1 and 2 (moisture content, 0.77–1.12%) and 3 and 4 (moisture content, 1.95–2.44%). The relative density *versus* pressure plots of the granulations made with hydroxypropyl methylcellulose at different moisture levels are given in Fig. 5.

As reported previously (4), the relative density *versus* pressure plots of the granulations made with powder mixtures do not give a typical relationship, as explained by Heckel (2). According to the Heckel equation (Eq. 1), plots of $\ln [1/(1-D)]$ *versus* pressure ($P$) give, on extrapolation, the material constant ($C$), which is identified with the reciprocal yield pressure of the material, and the intercept ($I$), which is identified with the movement of particles during the initial stages of compaction:

$$\ln\left(\frac{1}{1-D}\right) = CP + I \qquad \text{(Eq. 1)}$$

where $D$ (relative density of the compact) is obtained by dividing the bulk density at a given pressure by the true density (calculated). However, bulk density was determined on granules before compression (no pressure).

The break in the relative density *versus* pressure plots (Figs. 1–5) could be attributed largely to the water lubrication effect. At higher pressures, the small amount of water in the granulation is squeezed out to the surface of the die wall and thus reduces the die wall friction. However, at lower pressures, the small amount of water in the granules remains in the

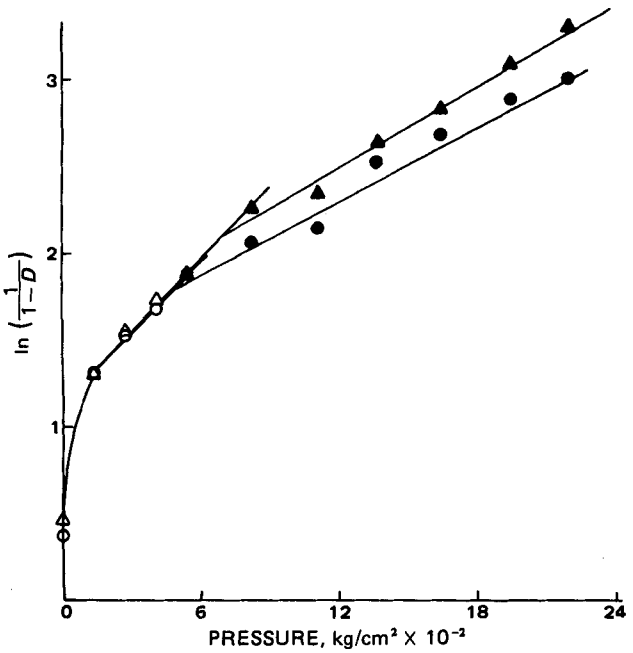


**Figure 3**—*Plots of ln[1/(1 − D)]* versus *pressure using granulations made with povidone (△,▲) and methylcellulose (○,●) as binders. The moisture contents at the time of compression were 2.23% for povidone granules and 2.44% for methylcellulose granules.*

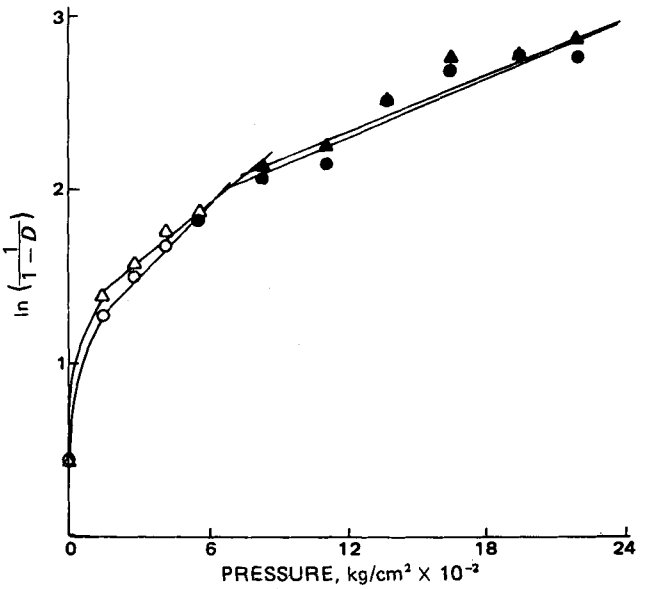


**Figure 4**—*Plots of ln[1/(1 − D)]* versus *pressure using granulations made with pregelatinized starch (○,●) and without a binder (△,▲). The moisture contents at the time of compression were 2.02% for pregelatinized starch granules and 1.95% for granules made without a binder.*

**Table III—Values of Bulk Density, Calculated True Density, and Densification of the Granules Made with Selected Binders Containing Different Moisture Contents**

| Binder | Moisture Content, % | Bulk Density, g/ml | Calculated True Density | $D_0$ | $D_a$ | $D_b$ |
|---|---|---|---|---|---|---|
| None | 0.77 | 0.538 | 1.357 | 0.396 | 0.702 | 0.306 |
| | 1.95 | 0.490 | 1.354 | 0.362 | 0.723 | 0.361 |
| Methyl- | 0.89 | 0.490 | 1.355 | 0.362 | 0.647 | 0.285 |
| cellulose | 2.44 | 0.420 | 1.348 | 0.312 | 0;692 | 0.380 |
| Povidone | 1.12 | 0.521 | 1.348 | 0.386 | 0.671 | 0.285 |
| | 2.23 | 0.512 | 1.345 | 0.381 | 0.690 | 0.309 |
| Pregelatinized | 0.79 | 0.516 | 1.357 | 0.380 | 0.669 | 0.289 |
| starch | 2.02 | 0.477 | 1.351 | 0.353 | 0.695 | 0.342 |
| Hydroxypropyl | 0.75 | 0.499 | 1.355 | 0.368 | 0.688 | 0.320 |
| methylcellulose | 2.32 | 0.457 | 1.348 | 0.339 | 0.677 | 0.338 |
| | 3.35 | 0.446 | 1.346 | 0.331 | 0.696 | 0.365 |

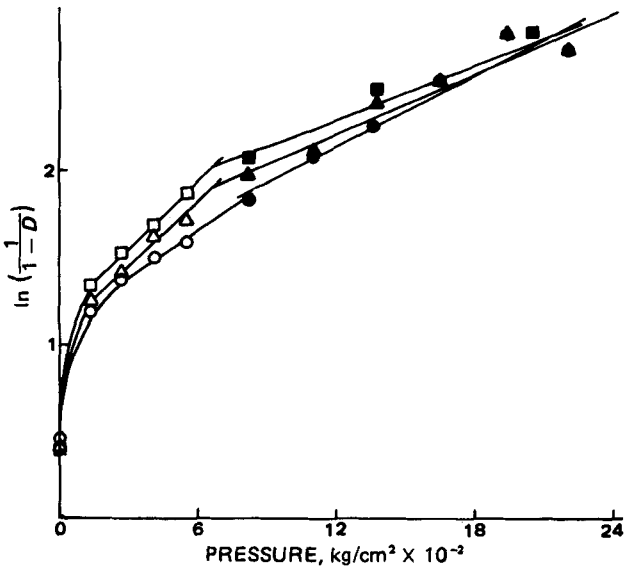


**Figure 5**—*Plots of ln[1/(1 − D)] versus pressure using granulations made with hydroxypropyl methylcellulose as a binder. The moisture contents at the time of compression were 3.35% (□,■), 2.32% (△,▲), and 0.75% (○,●).*

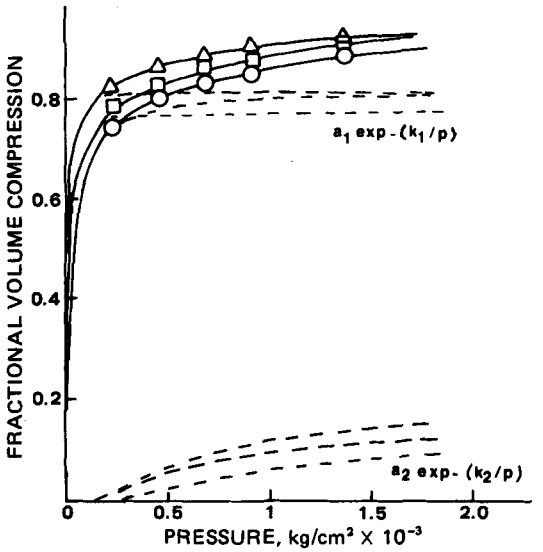


**Figure 6**—*Fractional volume compression versus pressure plots of the granulation made with hydroxypropyl methylcellulose dried to different moisture contents. Key: ○, 0.75% moisture; □, 2.32% moisture; and △, 3.35% moisture. Dotted lines indicate calculated results of Eq. 4.*

granulation and the powder mixtures behave as a single material. In view of the water lubrication effect, the first part of the relative density–pressure plots could be analyzed by the Heckel equation.

Table III gives the values of the bulk density and the calculated true density of the granules made with selected binders containing different moisture contents and the three-stage densification values, $D_0$, $D_a$, and $D_b$. These values represent the three-stage densification process that takes place: filling the die ($D_0$), individual particle movement and rearrangement ($D_b$), and particle deformation after interparticle bonding becomes appreciable ($D_a$).

The $D_a$ value was obtained from the measured intercept value, $I$ (Eq. 1), and the relationship:

$$D_a = 1 - e^{-I} \qquad \text{(Eq. 2)}$$

The $D_b$ value was obtained from the experimental bulk density, $D_0$:

$$D_b = D_a - D_0 \qquad \text{(Eq. 3)}$$

In agreement with previous results (1, 2, 4), $D_a$ values were higher than $D_b$ values, indicating that more densification occurred by granule deformation than by rearrangement and granule movement. However, these values did not show significant effect due to differences in the type of binder or the percent moisture content. The concentration of binders in these formulations was even lower than that used previously (4).

At lower moisture levels (0.75–1.12%), the values of the apparent material constant, $C_1$ (Table IV), suggest that granules made with methylcellulose, povidone, and pregelatinized starch are more compressible than granules made with hydroxypropyl methylcellulose and without a binder. However, at higher moisture levels (1.95–2.44%), the values of the ap-

**Table IV—Values of the Apparent Material Constants, $C_1$ and $C_2$, and Intercept $I$ of Compacts Made from Granules Containing Different Binders**

| Binder | Moisture Content, % | $C_1$, $(kg/cm^2)^{-1} \times 10^4$ | $I$ | Correlation Coefficient | $C_2$, $(kg/cm^2)^{-1} \times 10^4$ | Correlation Coefficient |
|---|---|---|---|---|---|---|
| None | 0.77 | 10.11 | 1.212 | 0.999 | 6.77 | 0.979 |
| | 1.95 | 11.07 | 1.282 | 0.994 | 5.99 | 0.968 |
| Methylcellulose | 0.89 | 11.33 | 1.042 | 0.994 | 7.68 | 0.984 |
| | 2.44 | 11.98 | 1.179 | 0.991 | 7.59 | 0.986 |
| Povidone | 1.12 | 11.41 | 1.111 | 0.999 | 8.98 | 0.983 |
| | 2.23 | 14.10 | 1.170 | 0.995 | 8.96 | 0.992 |
| Pregelatinized | 0.79 | 11.26 | 1.107 | 1.000 | 6.89 | 0.982 |
| starch | 2.02 | 11.73 | 1.186 | 0.987 | 6.83 | 0.969 |
| Hydroxypropyl | 0.75 | 8.24 | 1.164 | 0.998 | 7.31 | 0.963 |
| methylcellulose | 2.32 | 11.96 | 1.129 | 0.989 | 6.58 | 0.956 |
| | 3.35 | 13.31 | 1.190 | 1.000 | 5.92 | 0.988 |

**Table V—Values of $a_1$, $a_2$, $k_1$, and $k_2$ of the Compacts Made from Granulations Containing Different Binders**

| Binder | Moisture Content, % | $a_1$ | $a_2$ | $k_1$, kg/cm² | $k_2$, kg/cm² |
|---|---|---|---|---|---|
| None | 0.77 | 0.77 | 0.23 | 2.05 | 482.37 |
| | 1.95 | 0.82 | 0.17 | 3.03 | 355.76 |
| Methylcellulose | 0.89 | 0.76 | 0.24 | 4.25 | 386.61 |
| | 2.44 | 0.83 | 0.14 | 2.63 | 245.97 |
| Povidone | 1.12 | 0.74 | 0.27 | 1.00 | 393.22 |
| | 2.23 | 0.82 | 0.15 | 9.53 | 324.32 |
| Pregelatinized starch | 0.79 | 0.75 | 0.25 | 0.71 | 420.18 |
| | 2.02 | 0.82 | 0.16 | 7.53 | 315.87 |
| Hydroxypropyl methylcellulose | 0.75 | 0.80 | 0.17 | 10.10 | 469.58 |
| | 2.32 | 0.81 | 0.18 | 2.55 | 392.55 |
| | 3.35 | 0.82 | 0.19 | 0.07 | 368.38 |

**Table VI—Crushing Strength Change after Overnight Exposure to Ambient Room Conditions in Tablets Compressed at 815 kg/cm²**

| Binder | Moisture Content, % | Initial Crushing Strength, Strong–Cobb units | Crushing Strength after Overnight Exposure, Strong–Cobb units |
|---|---|---|---|
| Pregelatinized starch | 2.02 | 7.77 ± 0.55 | 7.73 ± 0.32 |
| Povidone | 2.23 | 7.6 ± 0.6 | 10.77 ± 0.38 |
| Methylcellulose | 2.44 | 7.77 ± 2.59 | 10.93 ± 0.42 |
| Hydroxypropyl methylcellulose | 2.32 | 7.80 ± 0.17 | 9.33 ± 0.68 |
| None | 1.95 | 5.27 ± 1.06 | 4.27 ± 0.86 |

parent material constant, $C_1$ (Table IV), suggest that granules made with povidone are more compressible than granules made with other binders.

The $C_2$ values, representing the slope of the second linear region (Table IV), were obtained under the assumption that the compact above a certain pressure ($P$) compresses under the water lubrication effect, thus giving a higher yield pressure. At lower moisture content, the $C_2$ values suggest that the granules made with methylcellulose and povidone are more compressible than granules made with other binders. At higher moisture contents, the $C_2$ values suggest that methylcellulose and povidone are also slightly more compressible than granules made with other binders.

In general, the $C_1$ values indicate that the granulations containing lower moisture levels are slightly less compressible than those containing higher moisture levels. However, the $C_2$ values suggest that the lower moisture-containing granules are slightly more compressible than the higher moisture-containing granules. At higher applied pressures, granules containing more moisture may exhibit a barrier to compression due to the water lubrication effect, thus making these granules more difficult to compress.

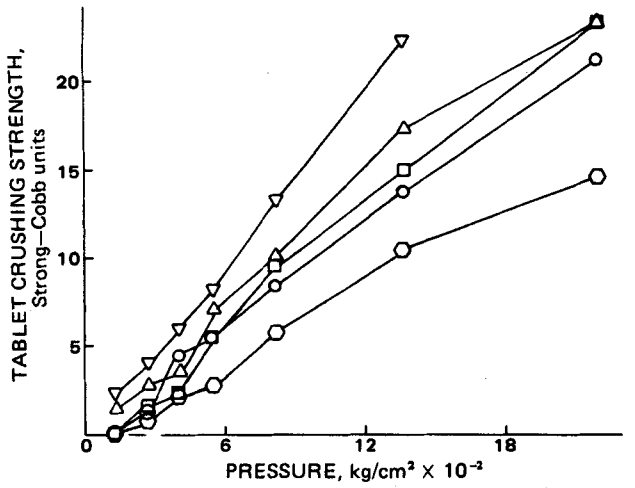


**Figure 7**—*Tablet crushing strength* versus *pressure profiles of tablets compressed from granulations made with different binders. The moisture contents of the granules at the time of compression were 0.89% (methylcellulose) (▽); 0.79% (pregelatinized starch) (△); 1.12% (povidone) (○); 0.75% (hydroxypropyl methylcellulose) (○); and 0.77% (no binder) (□).*

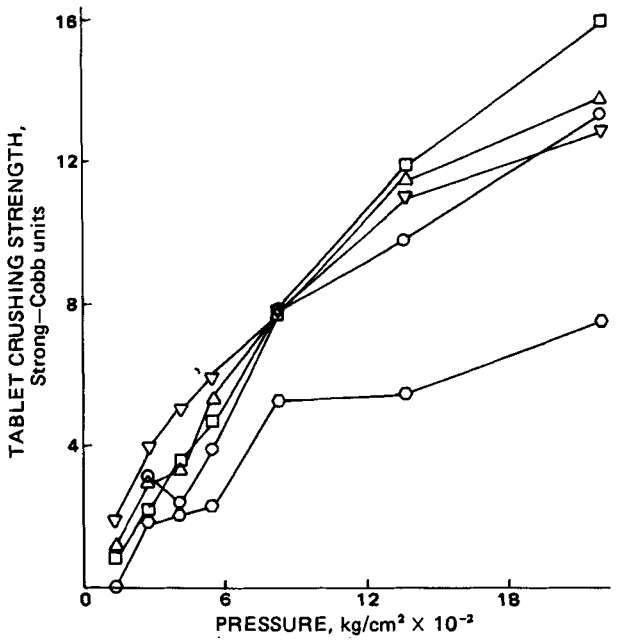


**Figure 8**—*Tablet crushing strength* versus *pressure profiles of tablets compressed from granulations made with different binders. The moisture contents of the granules at the time of compression were 2.23% (povidone) (□); 2.02% (pregelatinized starch) (△); 2.32% (hydroxypropyl methylcellulose) (○); 2.44% (methylcellulose) (▽); and 1.95% (no binder) (○).*

Cooper and Eaton (3) analyzed compression behavior of ceramic powders by assuming two largely independent probabilistic processes, the filling of large holes and the filling of small pores. The Cooper–Eaton equation (Eq. 4) relates the fractional value compression, $V^*$, to the applied pressure, $P$:

$$V^* = \frac{V_0 - V}{V_0 - V_\infty} = a_1 \exp - (k_1/P) + a_2 \exp - (k_2/P) \quad \text{(Eq. 4)}$$

where:

$V_0$ = initial total volume when no holes are filled
$V$ = compact volume
$V_\infty$ = compact volume when all holes of all types are filled
$a_1$ and $a_2$ = dimensionless coefficients indicating a fraction of the theoretical compression that would be achieved at infinite pressure by each particular process
$k_1$ and $k_2$ = coefficients with units of pressure where the particular process is most probable

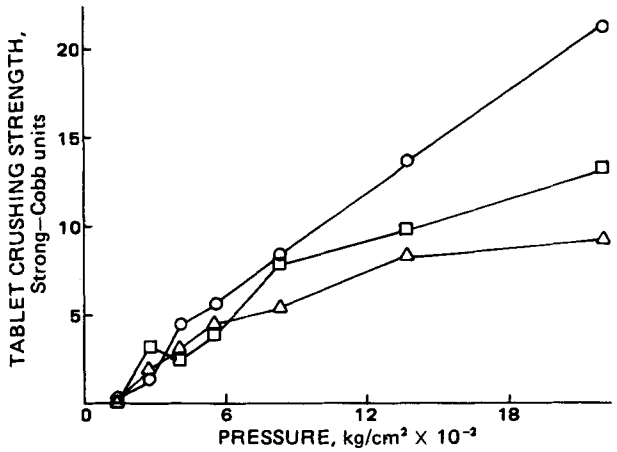


**Figure 9**—*Tablet crushing strength* versus *pressure profiles of tablets compressed from granulations made with hydroxypropyl methylcellulose. The moisture contents of the granules at the time of compression were 0.75% (○), 2.32% (□), and 3.55% (△).*

The fractional volume compression *versus* applied pressure plots up to the first linear region of the relative density *versus* pressure plots were used to calculate the coefficients of the Cooper–Eaton equation (Table V). Figure 6 gives the fractional volume compression *versus* pressure plots of the granulation made with hydroxypropyl methylcellulose and dried to different moisture contents. The experimental data were fitted to the results of the calculations using Eq. 4. The values of the coefficients were obtained from the best-fit curves.

The larger values of the dimensionless coefficient $a_1$ compared to $a_2$ (Table V) suggest that a large percentage of compression was achieved by filling large holes. The sum of coefficients $a_1$ and $a_2$ ranged from 0.97 to 1.01, indicating that compression is achieved by the two probabilistic processes of filling large and small holes by rearrangement, fragmentation, and plastic flow.

The coefficient $k_1$ gives the pressure needed to fill the large holes. This process occurs primarily by particles sliding past one another, which may require elastic deformation or even slight fracturing or plastic flow of particles. This process occurs at low pressures and is reflected in small $k_1$ values (Table V).

The coefficient $k_2$ indicates the pressure needed to fill small voids that are substantially smaller than the original particles. These voids can be filled by plastic flow or by fragmentation. This process requires high pressure, which is reflected in large $k_2$ values (Table V). Thus, $k_2$ provides more information about granulation compressibility since, during the rearrangement process, granules do not produce hard compacts. The $k_2$ values given in Table V indicate that, at lower moisture contents, methylcellulose- and povidone-containing granules are more compressible than granules made with the other binders. At higher moisture contents, methylcellulose-containing granules are more compressible than granules made with other binders. The $k_2$ values also suggest that the higher moisture-containing granules are more compressible than those of lower moisture content. This finding is in complete agreement with the $C_1$ values of the Heckel plots (Table IV), which suggest that the high moisture granules compress more easily than the low moisture ones.

The tablet crushing strength *versus* pressure profiles of granulations made with the selected binders containing different moisture contents are given in Figs. 7–9. At lower moisture contents (0.75–1.12%), methylcellulose-containing tablets gave higher crushing strengths than those made with granules containing other binders. The tablets made from granules without a binder were lower in crushing strength than the tablets made from granules containing binders.

At higher moisture levels (1.95–2.44%), differences in tablet crushing strength due to the binders were small (Fig. 8). Povidone-containing granules were better in crushing strength only at high pressure. Granules without a binder showed lower tablet crushing strengths compared to those with different binders.

Figure 9 compares the tablet crushing strength *versus* pressure profiles of the tablets compressed from granulations made with hydroxypropyl methylcellulose at different moisture levels. These results clearly show that the lower moisture-containing granules gave a higher crushing strength compared to the higher moisture-containing granules and that these differences became more pronounced as pressure was increased.

At higher moisture levels, it is important to consider the moisture-induced crushing strength increase phenomenon (6). Table VI gives the initial crushing strength and the crushing strength after a 24-hr exposure to ambient room conditions of tablets compressed at a given pressure. The crushing strength of tablets containing povidone, methylcellulose, and hydroxypropyl methylcellulose increased after overnight exposure to ambient room conditions. Pregelatinized starch-containing tablets did not show any change in crushing strength after overnight exposure to ambient room conditions. In the absence of a binder, the tablet crushing strength actually decreased after overnight exposure to ambient room conditions.

## REFERENCES


(1) Z. T. Chowhan and Y. P. Chow, *Int. J. Pharm.*, **5**, 139 (1980).

(2) R. W. Heckel, *Trans. Metall. Soc. AIME*, **221**, 671, 1001 (1961).

(3) A. R. Cooper and L. E. Eaton, *J. Am. Ceram. Soc.*, **45**, 97 (1962).

(4) Z. T. Chowhan and Y. P. Chow, *Int. J. Pharm. Technol. Prod. Manuf.*, **2**, 29 (1981).

(5) G. Oster and M. Yamamoto, *Chem. Rev.*, **63**, 257 (1963).

(6) Z. T. Chowhan and L. Palagyi, *J. Pharm. Sci.*, **67**, 1385 (1978).


# Leaching of 2-(2-Hydroxyethylmercapto)benzothiazole into Contents of Disposable Syringes


**MARISA C. PETERSEN *, JOHN VINE ‡, JOHN J. ASHLEY ‡, and ROGER L. NATION *x**



Received November 17, 1980, from the **Perinatal Pharmacology Laboratory, Foundation 41, The Women's Hospital, Crown Street, Surry Hills, 2010 Australia*, and the ‡*Department of Pharmacy, University of Sydney, Sydney, Australia.* Accepted for publication March 6, 1981.



**Abstract** □ A contaminant was found to leach into the contents of two brands of disposable syringes. It was identified as 2-(2-hydroxyethylmercapto)benzothiazole and is believed to be formed during manufacture of the syringes as a result of a reaction between 2-mercaptobenzothiazole, a rubber vulcanization accelerator, and ethylene oxide, used for sterilization. The contaminant was isolated from the rubber plunger-seal and identified using mass, NMR, and UV spectroscopic methods. The amount of contaminant appearing in the contents of syringes was measured; up to 140 μg was found under clinically relevant conditions. This finding has important implications with respect to the use of these syringes for drug administration and for the collection of blood for drug analyses.



**Keyphrases** □ 2-(2-Hydroxyethylmercapto)benzothiazole—leaching into contents of disposable syringes, isolation, identification, and quantitation □ Syringes, disposable—leaching of 2-(2-hydroxyethylmercapto)benzothiazole, isolation, identification, and quantitation □ Contaminants—2-(2-hydroxyethylmercapto)benzothiazole, leaching from disposable syringes


Several previous reports described the problems associated with the leaching of compounds from plastic infusion bags and giving sets and from blood collection tubes. The measurement of drug levels in blood and plasma samples for toxicological, therapeutic monitoring, or pharmacokinetic purposes may be hampered by such contaminants. In addition, the accumulation of plasticizers in patients' organs after transfusion of blood from plastic storage bags was reported (1).

Recently, contamination of blood collected in evacuated


*0022-3549/81/1000-1139$01.00/0*


*© 1981, American Pharmaceutical Association*

The fractional volume compression *versus* applied pressure plots up to the first linear region of the relative density *versus* pressure plots were used to calculate the coefficients of the Cooper–Eaton equation (Table V). Figure 6 gives the fractional volume compression *versus* pressure plots of the granulation made with hydroxypropyl methylcellulose and dried to different moisture contents. The experimental data were fitted to the results of the calculations using Eq. 4. The values of the coefficients were obtained from the best-fit curves.

The larger values of the dimensionless coefficient $a_1$ compared to $a_2$ (Table V) suggest that a large percentage of compression was achieved by filling large holes. The sum of coefficients $a_1$ and $a_2$ ranged from 0.97 to 1.01, indicating that compression is achieved by the two probabilistic processes of filling large and small holes by rearrangement, fragmentation, and plastic flow.

The coefficient $k_1$ gives the pressure needed to fill the large holes. This process occurs primarily by particles sliding past one another, which may require elastic deformation or even slight fracturing or plastic flow of particles. This process occurs at low pressures and is reflected in small $k_1$ values (Table V).

The coefficient $k_2$ indicates the pressure needed to fill small voids that are substantially smaller than the original particles. These voids can be filled by plastic flow or by fragmentation. This process requires high pressure, which is reflected in large $k_2$ values (Table V). Thus, $k_2$ provides more information about granulation compressibility since, during the rearrangement process, granules do not produce hard compacts. The $k_2$ values given in Table V indicate that, at lower moisture contents, methylcellulose- and povidone-containing granules are more compressible than granules made with the other binders. At higher moisture contents, methylcellulose-containing granules are more compressible than granules made with other binders. The $k_2$ values also suggest that the higher moisture-containing granules are more compressible than those of lower moisture content. This finding is in complete agreement with the $C_1$ values of the Heckel plots (Table IV), which suggest that the high moisture granules compress more easily than the low moisture ones.

The tablet crushing strength *versus* pressure profiles of granulations made with the selected binders containing different moisture contents are given in Figs. 7–9. At lower moisture contents (0.75–1.12%), methylcellulose-containing tablets gave higher crushing strengths than those made with granules containing other binders. The tablets made from granules without a binder were lower in crushing strength than the tablets made from granules containing binders.

At higher moisture levels (1.95–2.44%), differences in tablet crushing strength due to the binders were small (Fig. 8). Povidone-containing granules were better in crushing strength only at high pressure. Granules without a binder showed lower tablet crushing strengths compared to those with different binders.

Figure 9 compares the tablet crushing strength *versus* pressure profiles of the tablets compressed from granulations made with hydroxypropyl methylcellulose at different moisture levels. These results clearly show that the lower moisture-containing granules gave a higher crushing strength compared to the higher moisture-containing granules and that these differences became more pronounced as pressure was increased.

At higher moisture levels, it is important to consider the moisture-induced crushing strength increase phenomenon (6). Table VI gives the initial crushing strength and the crushing strength after a 24-hr exposure to ambient room conditions of tablets compressed at a given pressure. The crushing strength of tablets containing povidone, methylcellulose, and hydroxypropyl methylcellulose increased after overnight exposure to ambient room conditions. Pregelatinized starch-containing tablets did not show any change in crushing strength after overnight exposure to ambient room conditions. In the absence of a binder, the tablet crushing strength actually decreased after overnight exposure to ambient room conditions.

## REFERENCES


(1) Z. T. Chowhan and Y. P. Chow, *Int. J. Pharm.*, **5**, 139 (1980).

(2) R. W. Heckel, *Trans. Metall. Soc. AIME*, **221**, 671, 1001 (1961).

(3) A. R. Cooper and L. E. Eaton, *J. Am. Ceram. Soc.*, **45**, 97 (1962).

(4) Z. T. Chowhan and Y. P. Chow, *Int. J. Pharm. Technol. Prod. Manuf.*, **2**, 29 (1981).

(5) G. Oster and M. Yamamoto, *Chem. Rev.*, **63**, 257 (1963).

(6) Z. T. Chowhan and L. Palagyi, *J. Pharm. Sci.*, **67**, 1385 (1978).


# Leaching of 2-(2-Hydroxyethylmercapto)benzothiazole into Contents of Disposable Syringes


**MARISA C. PETERSEN *, JOHN VINE ‡, JOHN J. ASHLEY ‡, and ROGER L. NATION *x**



Received November 17, 1980, from the **Perinatal Pharmacology Laboratory, Foundation 41, The Women's Hospital, Crown Street, Surry Hills, 2010 Australia*, and the ‡*Department of Pharmacy, University of Sydney, Sydney, Australia.* Accepted for publication March 6, 1981.



**Abstract** □ A contaminant was found to leach into the contents of two brands of disposable syringes. It was identified as 2-(2-hydroxyethylmercapto)benzothiazole and is believed to be formed during manufacture of the syringes as a result of a reaction between 2-mercaptobenzothiazole, a rubber vulcanization accelerator, and ethylene oxide, used for sterilization. The contaminant was isolated from the rubber plunger-seal and identified using mass, NMR, and UV spectroscopic methods. The amount of contaminant appearing in the contents of syringes was measured; up to 140 μg was found under clinically relevant conditions. This finding has important implications with respect to the use of these syringes for drug administration and for the collection of blood for drug analyses.



**Keyphrases** □ 2-(2-Hydroxyethylmercapto)benzothiazole—leaching into contents of disposable syringes, isolation, identification, and quantitation □ Syringes, disposable—leaching of 2-(2-hydroxyethylmercapto)benzothiazole, isolation, identification, and quantitation □ Contaminants—2-(2-hydroxyethylmercapto)benzothiazole, leaching from disposable syringes


Several previous reports described the problems associated with the leaching of compounds from plastic infusion bags and giving sets and from blood collection tubes. The measurement of drug levels in blood and plasma samples for toxicological, therapeutic monitoring, or pharmacokinetic purposes may be hampered by such contaminants. In addition, the accumulation of plasticizers in patients' organs after transfusion of blood from plastic storage bags was reported (1).

Recently, contamination of blood collected in evacuated


*0022-3549/81/1000-1139$01.00/0*


*© 1981, American Pharmaceutical Association*

tubes[1] with a compound identified as tris(2-butoxyethyl)-phosphate was reported (2). Leaching of this compound into blood causes a decrease in plasma protein binding and redistribution to the red blood cells of several drugs including propranolol (3), imipramine (4), alprenolol (4), quinidine (5), and lidocaine (6). Consequently, the measured plasma concentrations of these drugs were spuriously low. Tris(2-butoxyethyl) phosphate, leached into blood samples from collection tubes, interfered directly with the analysis of postmortem specimens (2) and with GLC analysis of theophylline (7). Another plasticizer, di(2-ethylhexyl) phthalate, also was reported to interfere with a GLC assay for disopyramide (8).

During recent work involving the development of a high-performance liquid chromatographic (HPLC) assay for blood and plasma corticosteroids (9), a large chromatographic peak interfered with the assay. The absence of the interfering compound in samples collected directly into a glass container indicated that it originated in the collection system and was not due to endogenous material or contamination of the reagents used in extraction. The compound originated in the disposable syringes used for blood collection.

The identification of the source of the compound, its isolation, and the elucidation of its chemical structure are reported here.

## EXPERIMENTAL

**Identification of Contaminant Source**—Three brands of disposable plastic syringes (A[2], B[3], and C[4]) were used. Initially, one syringe of each brand (10–12-ml capacity) was filled through a 19-gauge needle[5] with freshly distilled water (10 ml) and allowed to stand for 2 min. Another sample of water (10 ml) was allowed to stand for 2 min in a blood storage tube containing ammonium heparin (100 U/10 ml) and separation granules[6]. From each of these sources 1 ml (10%) of the water was extracted with methylene chloride[7], which was then concentrated at 45° and chromatographed as described previously for plasma samples (9). The reversed-phase HPLC column[8], with a mobile phase of methanol–water (60:40) at a flow rate of 1.25 ml/min, was coupled to a UV detector set at 254 nm. An aliquot (1 ml) of distilled water, which had been measured directly into a glass extraction tube, was also analyzed as already described.

To pinpoint the source of contamination, this procedure was repeated with three Brand A syringes, three Brand C syringes, and three samples of water measured into glass extraction tubes. In addition, the barrels of three Brand A syringes with the plungers removed and needles crimped were each filled with 10 ml of distilled water, and three rubber plunger-seals from Brand A syringes were removed and immersed in beakers containing 10 ml of distilled water. The syringes and components were in contact with the water for 2 min, and 1 ml was assayed.

To establish that the contaminant was extracted from the syringes into blood as well as into water and to confirm that the chromatographic peak observed in plasma samples was not an endogenous compound, the following experiment was performed. Blood was drawn from a single subject through a cannula[9] and three-way tap[10] using the three brands of syringes in turn. The total blood volume (15 ml) was drawn within 3 min. The blood was transferred to three heparinized plastic tubes for centrifugation; in each case, 1 ml of the resulting plasma was assayed.

**Identification of Contaminant**—To facilitate identification of the compound of interest, several syringes of each brand were allowed to stand, containing water, for 10 min. The water was subsequently extracted, the concentrated extract was chromatographed, and the fraction of the HPLC eluate corresponding to the peak of interest was collected. The fractions from each brand of syringe were pooled separately and evaporated to dryness in a 45° water bath under a nitrogen stream. The residues were dissolved in 1 ml of distilled water and extracted with methylene chloride. The extracts then were concentrated. To provide sufficient sample for NMR studies, derivatization procedures, and UV spectroscopy, ~500 μg of the contaminant was collected by pooling the HPLC fractions from 20 Brand A syringes (35-ml capacity) as already described.

GLC–mass spectrometric analyses were carried out on a chemical-ionization mass spectrometer[11] interfaced to a gas chromatograph[12]. The glass GLC column (0.91 m × 2 mm i.d.) was packed with a phenyl methyl silicone phase[13] and was programmed from 150 to 200° at 10°/min. Injection port and interface temperatures were maintained at 260°. Methane chemical-ionization mass spectra were generated by using methane as both the GLC carrier and chemical-ionization reactant gas. A flow rate of 20 ml/min generated an ion source pressure of 130 Pa. Deuterium oxide chemical-ionization mass spectra were generated by introducing deuterium oxide into the methane plasma *via* a variable leak (10). Ammonia chemical-ionization mass spectra were obtained by using helium as the GLC carrier gas at a flow rate of 20 ml/min and adding ammonia through a makeup T piece at the end of the column. The ammonia flow rate was adjusted to give an ion source pressure of 130 Pa. The electron beam energy for chemical ionization was 110 ev, and the ion source and analyzer regions of the mass spectrometer were operated at 60–100°. An interactive data system[14] was used for data acquisition and processing.

High-resolution electron-impact mass spectra were obtained[15] using the direct insertion probe inlet and an electron beam energy of 70 ev.

Derivatization reactions were carried out by dividing a methylene chloride extract from Brand A syringes into two portions and evaporating each to dryness. One portion was treated with 10 μl of a silylation reagent[16] by heating at 50° for 1 hr. The other portion was treated with excess freshly distilled ethereal diazomethane for 15 min at room temperature and then evaporated to a volume of <50 μl in a water bath at 40°.

2-(2-Hydroxyethylmercapto)benzothiazole (II) was synthesized from 2-mercaptobenzothiazole (I) and 2-chloroethanol according to the method of Sexton (11). The product, recrystallized twice from benzene, had a melting point of 56–57° [lit. (11) 56–58°].

**Quantitation of Contaminant**—Once the compound leaching from the syringes had been identified and synthesized, the recrystallized product was used as a standard to measure how much contaminant was leached from syringes under several sets of conditions. Brand A syringes were used for all three parts of this experiment.

1. Several syringes (2 and 10 ml) were filled with various volumes of distilled water and allowed to stand for 5 min before an aliquot was injected directly onto the HPLC column.

2. Seven syringes (20 ml) were each filled with 10 ml of distilled water and allowed to stand for 4–300 min before an aliquot was injected onto the column.

3. The effect of two different vehicles that are used for parenteral dosage forms was examined. A pediatric formulation, which consisted of 25 μg of digoxin/ml of propylene glycol (40%)–alcohol (10.5%)–water[17], was studied because the contaminant displayed lipophilic tendencies in its solvent extraction and HPLC characteristics and, therefore, was expected to partition more favorably into a less polar solvent than water and because the presence of the contaminant may have one of its most serious implications in infant therapy. Water (1 ml) was drawn into each of three 2-ml syringes and allowed to stand for 2, 5, or 12.5 min, and the digoxin formulation (1 ml) was drawn into each of four 2-ml syringes and allowed to stand for 1, 2, 5, or 11 min. Aliquots were injected directly into the chromatograph, and an injection also was made of the digoxin dosage form, which had not been in contact with the plastic syringes.

## RESULTS

**Source of Contaminant**—The interfering peak observed when developing an HPLC assay for plasma samples had a retention time of 6.5

[1] Vacutainer, Becton-Dickinson, Rutherford, N.J.
[2] Monoject, Sherwood Medical Industries, Deland, Fla.,
[3] Terumo, Terumo Aust. Pty. Ltd., Melbourne, Australia.
[4] Pharma-Plast, A.H.S./Aust. Pty. Ltd., Balgowlah, Australia.
[5] Monoject brand.
[6] Disposable Products Pty. Ltd., Sydney, Australia.
[7] GR grade, Merck, Darmstadt, West Germany.
[8] RP-8, Brownlee, Santa Clara, Calif.
[9] Dwellcath, Tuta Laboratories, Sydney, Australia.
[10] Pharma-Plast brand.
[11] Model 3200, Finnigan Corp., Sunnyvale, Calif.
[12] Model 9500, Finnigan Corp., Sunnyvale, Calif.
[13] Three percent OV-17 on Chromosorb W AW DMCS, 120–140 mesh, Applied Science Laboratories, State College, Pa.
[14] Model 6110, Finnigan Corp., Sunnyvale, Calif.
[15] AEI MS-9 mass spectrometer, Kratos Ltd., Manchester, England.
[16] TRI-SIL, Pierce Chemical Co., Rockford, Ill.
[17] Lanoxin pediatric injection, Wellcome Australasia, Rosebery, Australia.

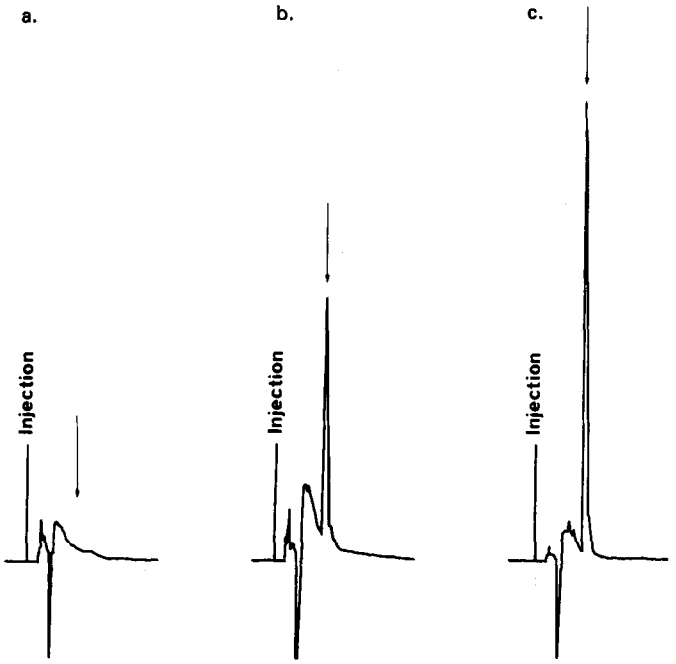


**Figure 1**—*HPLC traces of extracts of distilled water that had been standing in Brand C (sensitivity 0.05 aufs) (a), Brand B (0.02 aufs) (b), and Brand A (0.05 aufs) (c) syringes. The arrow marks retention time of 6.5 min.*

min under the chromatographic conditions described previously (9). When water was allowed to stand in the syringes and blood storage tubes for 2 min and aliquots were analyzed, a large chromatographic peak was again observed at 6.5 min in the extracts of the water from Brands A and B syringes. Extracts of the water from the blood storage tube and the Brand C syringe had chromatograms identical to that of the extract of the water that had been measured directly into the glass extraction tube.

Figure 1 illustrates the magnitude of the interfering peak observed when 10% of the water in the A–C syringes was extracted and chromatographed. Brand B syringes released less of the compound chromatographing at 6.5 min than did the A syringes. Later studies in which all of the water in the syringe was extracted showed that the A and B syringes also released into the water compounds that chromatographed with retention times of 3.8 and 4.7 min but with peak heights ~5% that of the peak at 6.5 min. These peaks were not seen in extracts of water from the C syringe.

In turn, plasma (1 ml) harvested from blood collected into the three brands of syringes was extracted and chromatographed. No peak was observed at 6.5 min when a C syringe had been used to collect the blood, but large peaks were seen in the extracts of plasma collected in A and B syringes.

The results of the experiment in which various parts of the Brand A syringe were allowed to contact the water are summarized in Table I. Although these results were semiquantitative, the severalfold differences in the heights of the peaks indicated that the contaminant was probably being leached from the rubber seal on the plunger. The average height of the peak resulting from only the syringe barrel contacting the water was <10% of the height of the peak resulting from the intact syringe being filled with water. In contrast, the peak resulting from extraction of water in which the plunger-seal had been immersed was three times greater than the peak from the intact syringe.

**Identification of Contaminant**—GLC–mass spectral analysis of the fraction collected from HPLC after extraction of the contents of Brand A syringes revealed a single GLC peak with a retention time of 2.2 min. The presence of a molecular ion at *m/z* 211 in the electron-impact mass spectrum of this GLC peak and a protonated molecular ion ($MH^+$) at *m/z* 212, together with methane adduct ions at *m/z* 240 ($M + C_2H_5^+$) and 252 ($M + C_3H_5^+$) in the methane chemical-ionization mass spectrum (Fig. 2), suggested a molecular weight of 211. Confirmation was obtained from the ammonia chemical ionization mass spectrum, which contained a single ion peak at *m/z* 212. The observation of a $MH^+$ ion in the ammonia spectrum indicated that the compound was a stronger gas phase base than ammonia (12).

The relative abundances of the isotopic ion peaks at *m/z* 212, 213, and

**Table I—Height [a] of the Contaminant Peak after 2 Min of Contact between Water and Brand A Syringe Components**

| | Intact Syringe | Barrel Only | Plunger-Seal |
|---|---|---|---|
| | 404 | 34 | 875 |
| | 384 | 37 | 1250 |
| | 416 | 28 | 1500 |
| Mean | 401 | 33 | 1208 |
| Relative percent | 100 | 8.2 | 301 |

[a] All peak heights measured in millimeters and normalized to 0.01 aufs.

214 in the ammonia chemical-ionization mass spectrum, measured accurately using the selected ion monitoring mode, were 100, 11.81, and 9.40 (average of five measurements), respectively, which indicated the empirical formula $C_9H_9NOS_2$ (calculated isotopic abundances: 100, 11.91, and 9.44, respectively). This result was confirmed by high-resolution electron-impact mass spectrometry (measured mass 211.0128, calculated for $C_9H_9NOS_2$ 211.0125). The deuterium oxide chemical-ionization mass spectrum contained a quasimolecular ion at *m/z* 214. However, ionization of the molecule by addition of a $D^+$ ion would be expected to give an ion at *m/z* 213. Therefore, the observation of *m/z* 214 in the spectrum showed that the molecule contains one exchangeable hydrogen atom (13). The appearance of an ion peak at *m/z* 194 in both the methane (Fig. 2*b*) and deuterium oxide chemical-ionization mass spectra ($MH^+ - H_2O$ and $MD^+ - D_2O$, respectively) indicated the presence of a hydroxyl group, which would account for the exchangeable hydrogen atom.

Treatment of the compound with the silylation reagent and analysis by GLC–mass spectrometry showed a single product with a molecular weight of 283, corresponding to a monotrimethylsilylated derivative. The compound, however, failed to react with diazomethane and, therefore, must be an aliphatic alcohol rather than a phenol or carboxylic acid.

The base peak in the electron impact mass spectrum (Fig. 2*a*) was at *m/z* 167, and the relative abundances of the isotope peaks at *m/z* 168 and 169 indicated that this ion still contained the two sulfur atoms. In many respects, the spectrum below *m/z* 170 resembled that of I. The relative abundances of the ions at *m/z* 166, 140, 123, 108, 91, 69, and 45 in the spectrum of the compound were quite similar to those reported for I (14).

On the basis of the mass spectral data, II was indicated. Although the major fragment ions in both the electron-impact and chemical-ionization mass spectra could be rationalized in terms of this structure (Schemes I and II), other isomers in which the side chain was attached to the phenyl ring could not be excluded. However, these isomers can be excluded on the basis of NMR spectroscopic data.

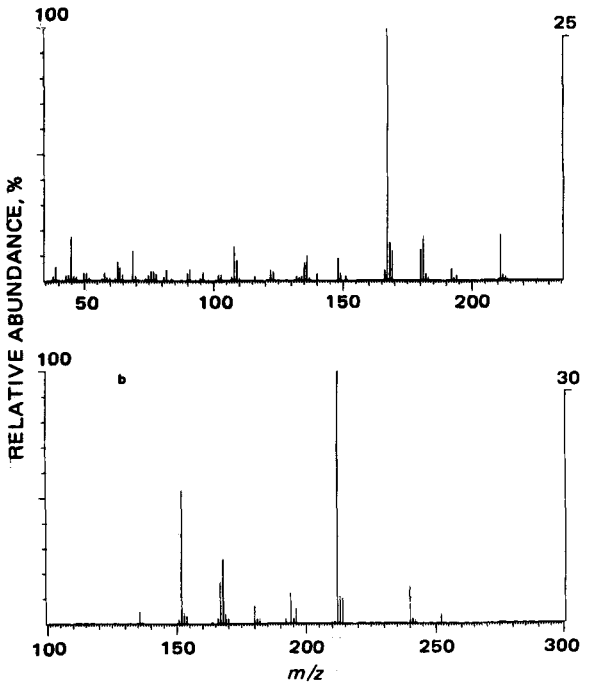


**Figure 2**—*Mass spectra of the contaminant identified as 2-(2-hydroxyethylmercapto)benzothiazole (II). Key: a, electron impact; and b, methane chemical ionization.*

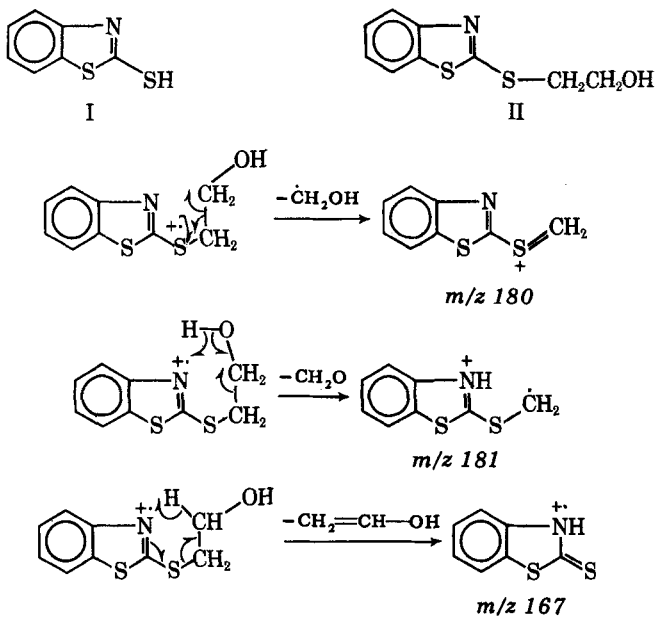


*Scheme I—Electron-impact-induced fragmentation of II.*

The NMR spectrum (recorded at 58°) contained signals at δ 7.15–7.85 (m, 4H, aromatic CH), 3.94 (m, 2H, $CH_2$–O–), 3.45 (t, 2H, $CH_2$–S–), and 3.03 (t, 1H, OH, removed by exchange in $D_2O$). Significantly, no signal could be attributed to a C-2 proton. In the NMR spectrum of benzothiazole, this signal occurred as a sharp singlet at δ 8.95. Moreover, the splitting pattern of the four aromatic protons in the spectrum of the compound extracted from syringes was very similar to that observed for the four protons on the phenyl ring of benzothiazole. Therefore, it was concluded that the side chain must be attached to C-2 of the benzothiazole ring as shown in II. In keeping with this structure, irradiation at δ 3.03 caused the signal at δ 3.94 to change to a triplet, and irradiation at δ 3.94 caused the signal at δ 3.45 to collapse to a singlet.

This structure was also supported by UV spectrophotometric data in that the observed absorption maxima ($\lambda_{max}$) at 224 and 279 nm were almost identical to the maxima reported for 2-(methylmercapto)benzothiazole ($\lambda_{max}$ 224 and 280 nm) (15).

As final proof, 2-(2-hydroxyethylmercapto)benzothiazole (II) was synthesized using the method of Sexton (11). The mass, NMR, UV, and IR spectra and chromatographic retention times (GLC and HPLC) of the authentic compound were identical to those of the compound extracted from the Brand A syringes. The mass spectra (electron-impact and chemical ionization) and GLC and HPLC retention times of the compound extracted from the A and B syringes were identical; therefore, it was concluded that both brands released II into their contents.

**Table II—Amount of 2-(2-Hydroxyethylmercapto)benzothiazole (II) in Various Volumes of Water Allowed to Stand in Brand A Syringes for 5 Min**

| 2-ml Syringe | | | 10-ml Syringe | | |
|---|---|---|---|---|---|
| Volume, ml | μg/ml | μg | Volume, ml | μg/ml | μg |
| 0.5 | 3.78 | 1.89 | 2.0 | 3.59 | 7.18 |
| 1.0 | 1.57 | 1.57 | 5.0 | 1.65 | 8.26 |
| 2.0 | 0.98 | 1.97 | 10.0 | 0.89 | 8.87 |

**Table III—Amount of 2-(2-Hydroxyethylmercapto)-benzothiazole (II) Leached with Time into Water (10 ml) from 20-ml Brand A Syringes [a]**

| Minute | II, μg |
|---|---|
| 4 | 13.8 |
| 9 | 16.1 |
| 30 | 34.0 |
| 60 | 53.2 |
| 150 | 93.0 |
| 240 | 108.7 |
| 300 | 139.5 |

[a] Each data point represents analysis of water from a different syringe.

**Quantitation of II**—The amount of II found in the contents of the syringe after 5 min was similar for a given syringe capacity regardless of the volume of water in the barrel (Table II). As may be expected, the 10-ml syringes, with a greater surface area of rubber exposed to the liquid, released more II (mean 8.1 μg) than the 2-ml syringes (mean 1.8 μg). In a 20-ml syringe, the amount of II in the water increased as the contact time between the rubber and water increased, even up to 5 hr when 140 μg was found (Table III). Compound II moved quickly into the water from the rubber, as was shown by the presence of several micrograms of II in the syringe contents after only 4–5 min (Tables II and III). Table IV shows the amounts of II that leached into 1 ml of water and 1 ml of the digoxin formulation after various times. The results were very similar for the two solvents and followed the trends established in the previous experiments.

These data (Tables III and IV) suggest that the appearance of II in the syringe contents is not limited by the extent of its solubility in the solvent, but it is more likely to be restricted by the rate at which it can move out of the rubber matrix.

## DISCUSSION

The early experiments, designed to identify the source of the contaminant, indicated that II was coming from the rubber seal on the plunger of Brands A and B syringes. This finding was consistent with their structure since both brands have soft rubber seals while Brand C does not. Compound II is not commonly used in rubber manufacture, but

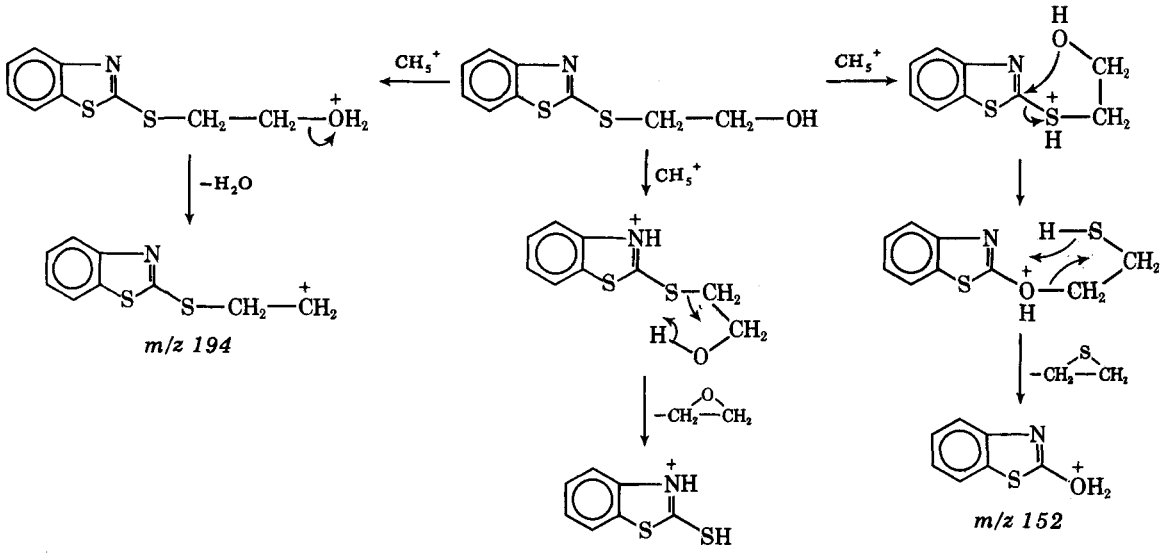


*Scheme II—Methane chemical-ionization-induced fragmentation of II.*

Table IV—Amount of 2-(2-Hydroxyethylmercapto)-benzothiazole (II) in the Contents of 2-ml Brand A Syringes Containing Different Solvents

| Distilled Water, 1 ml | | Digoxin Formulation, 1 ml | |
|---|---|---|---|
| Minute | II, μg | Minute | II, μg |
| 2 | 1.25 | 1 | 1.05 |
| 5 | 1.95 | 2 | 1.31 |
| 12.5 | 3.34 | 5 | 2.83 |
| | | 11 | 3.26 |

it has been reported to be a reaction product of I, a widely used vulcanization accelerator, and ethylene oxide (16), used in this case for sterilization of the syringes. A sample of I had the same HPLC retention time (4.7 min) as the later of the two smaller peaks found in the chromatograms of extracts from A and B syringes, supporting the view that II is formed from I.

Rubbers formulated with I were reported to present stability problems when subjected to γ-radiation (17), so syringes containing I in rubber components are likely to be sterilized with ethylene oxide. One brand of syringe that has a rubber plunger-seal and is sterilized by ethylene oxide[18] did not leach I and II into water. This brand has been reported as nontoxic to amniotic fluid cell cultures whereas other brands have been associated with cultures that fail to thrive (18, 19).

More information is available on the toxicity of I than on that of II. Compound I was identified as one of the allergens responsible for allergies to the rubber in clothing and shoes (20) and also was reported to be mutagenic in fruit flies (21) and embryotoxic in rats (22). The toxicity of I and II was studied in cell lines and in mice by Guess and O'Leary (16). Using a suggested standard of toxicity rating, they reported that both compounds would be rated as highly toxic in mice when given by the parenteral route and moderately toxic when ingested. They also suggested that care should be exercised if these compounds could gain access to the systemic circulation and reported that II was more toxic than I when administered parenterally or orally.

While II was first noticed because of its appearance in blood samples, its transfer from the rubber seal to solutions administered parenterally must be considered. Although no toxicity data are reported for II in humans, the introduction of microgram quantities of even a moderately toxic foreign compound into the body should be recognized and, if possible, avoided. The results indicate that the amount of II leaching into the syringe contents increases with the time of exposure to the rubber and with the capacity of the syringe, but it is essentially independent of the volume of liquid in the syringe. When 10 ml of water was allowed to remain in a 20-ml syringe for 5 hr, 140 μg of II was measured in the contents. This may be a cause for concern with obstetric and surgical patients undergoing epidural anesthesia since additional anesthetic solution is often left in a disposable syringe until further pain relief is required several hours later. When such relief is required, the solution containing accumulated II is injected into the epidural space, in close proximity to the cerebrospinal fluid. Compound II may also accumulate in patients who receive several injections while in the hospital or in patients who are on chronic parenteral medication, *e.g.*, diabetics.

The inadvertent administration of II may be of particular importance in hospitalized infants, especially premature infants, children, and patients with impaired elimination. Total parenteral nutrition for infants in some intensive care nurseries is administered from a disposable syringe (10 ml), which may have been filled several hours previously in the aseptic supply area. In this situation, relatively large amounts of II may be administered intravenously.

Brand A syringes were reported previously as the source of a contaminant that interfered in chromatographic assays for chlorpheniramine (23) and oxazepam (24). In this laboratory, II was first noticed as a large chromatographic peak that interfered with plasma steroid assays (9), making accurate measurement of plasma hydrocortisone and betamethasone levels impossible. Such interference results in a considerable waste of time and materials until the source of the contaminant is identified and a more suitable brand of syringe is used. Moreover, such interference may be present but not recognized if the contaminant cochromatographs with a drug, resulting in an overestimate of drug concentration (24). This situation clearly has the potential to compromise the conclusions drawn from pharmacokinetic and therapeutic monitoring data, with possible implications for clinical management. Alteration of plasma protein binding and distribution between blood components of some drugs has been caused by the contamination of blood samples (25). This more subtle effect has serious implications since it results in spuriously low plasma drug level measurements. The possibility that II could interfere in a similar way must also be considered when blood is collected in disposable syringes.

The presence of contaminants may be overlooked if the compounds do not possess characteristics that cause them to interfere with assays in general use. There may be several other compounds leaching out of syringes, closures, blood collection tubes, and other plastic and rubber apparatus which have not yet been recognized but may have similar implications toxicologically and analytically.

[18] Plastipak, Becton-Dickinson, Rutherford, N.J.

## REFERENCES


(1) R. J. Jaeger and R. J. Rubin, *N. Engl. J. Med.*, **287**, 1114 (1972).

(2) S. J. Dickson, A. W. Missen, and G. J. Down, *Forensic Sci.*, **4**, 155 (1974).

(3) R. H. Cotham and D. Shand, *Clin. Pharmacol. Ther.*, **18**, 535 (1975).

(4) O. Borga, K. M. Piafsky, and O. G. Nilsen, *Clin. Pharmacol. Ther.*, **22**, 539 (1977).

(5) D. Fremstad and K. Bergerud, *Acta Pharmacol. Toxicol.*, **39**, 570 (1976).

(6) W. W. Stargel, C. R. Roe, P. A. Routledge, and D. G. Shand, *Clin. Chem.*, **25**, 617 (1979).

(7) C. J. Least, G. F. Johnson, and H. M. Solomon, *Clin. Chem.*, **22**, 765 (1976).

(8) D. K. Dubetz, N. N. Brown, W. D. Hooper, M. J. Eadie, and J. H. Tyrer, *Br. J. Clin. Pharmacol.*, **6**, 279 (1978).

(9) M. C. Petersen, R. L. Nation, and J. J. Ashley, *J. Chromatogr.*, **183**, 131 (1980).

(10) D. J. Morgan, M. P. Smyth, J. Thomas, and J. H. Vine, *Xenobiotica*, **7**, 365 (1977).

(11) W. A. Sexton, *J. Chem. Soc.*, **1939**, 470.

(12) I. Dzidic and J. A. McCloskey, *Org. Mass Spectrom.*, **6**, 939 (1972).

(13) D. F. Hunt, G. N. McEwan, and R. A. Upham, *Anal. Chem.*, **44**, 1292 (1972).

(14) B. J. Millard and H. F. Temple, *Org. Mass Spectrom.*, **1**, 285 (1968).

(15) R. A. Morton and A. L. Stubbs, *J. Chem. Soc.*, **1939**, 1321.

(16) W. L. Guess and R. K. O'Leary, *Toxicol. Appl. Pharmacol.*, **14**, 221 (1969).

(17) M. A. Zakirova, A. S. Kuzminskii, and T. G. Degteva, *Kauch. Rezina*, **28**, 8 (1969); through *Chem. Abstr. Jpn.*, **72**, 67977d (1970).

(18) S. G. Purvis-Smith, M. A. Jones, and W. Wertelecki, *Lancet*, **I**, 993 (1978).

(19) K. L. Garver, S. L. Marchese, and E. G. Boas, *N. Engl. J. Med.*, **295**, 286 (1976).

(20) F. Saito and Y. Yamatuta, *Nippon Hifuka Gakkai Zasshi*, **82**, 763 (1972); through *Chem. Abstr. Jpn.*, **78**, 150970r (1973).

(21) Y. A. Revazova, *Toksikol. Nov. Khim. Veshchestv, Vnedryaemykh Rezin. Shinnuyu Prom*, Meditsina, Moscow, USSR., 1968, pp 196–203; through *Chem. Abstr. Jpn.*, **71**, 47071e (1969).

(22) S. E. Aleksandrov, *Tezisy Dokl. Nauchn. Sess. Khim. Tekhnol. Org. Soedin. Sery Sernistykh Neftei, 13th*, Zinatne, Riga, USSR., 1974, pp 98–9; through *Chem. Abstr. Jpn.*, **85**, 117605x (1976).

(23) N. K. Athanikar, G. W. Peng, R. L. Nation, S-M. Huang, and W. L. Chiou, *J. Chromatogr.*, **162**, 367 (1979).

(24) D. J. Greenblatt, J. S. Harmatz, and R. I. Shader, *Pharmacology*, **16**, 26 (1978).

(25) K. M. Piafsky, *Clin. Pharmacokinet.*, **5**, 246 (1980).


## ACKNOWLEDGMENTS


The authors thank Jacki Winyard for skilled technical assistance and Marion Pozniak and Yvonne Molloy for typing this manuscript.

# Apomorphine: Bioavailability and Effect on Stereotyped Cage Climbing in Mice

ROBERT V. SMITH *x, ALLEN E. KLEIN *,
RICHARD E. WILCOX ‡, and WILLIAM H. RIFFEE ‡

Received October 6, 1980, from the *Drug Dynamics Institute and the ‡Division of Pharmacology, College of Pharmacy, University of Texas at Austin, Austin, TX 78712. Accepted for publication March 20, 1981.

**Abstract** □ Plasma levels of apomorphine and its conjugates were studied following intravenous, intraperitoneal, and oral administrations to mice. Following hydrolysis, apomorphine and its conjugates were assayed by high-performance liquid chromatography. The absolute bioavailability of apomorphine was 4%. A significant first-pass effect due to extensive conjugation in the liver was postulated based on calculated bioavailabilities and comparison of plasma levels of apomorphine and its conjugates following oral, intraperitoneal, and intravenous administrations. Apomorphine-induced stereotypical cage climbing in mice was investigated following administration of apomorphine by the three routes. Analysis of time-course data obtained from the cage-climbing experiments indicated an absolute bioavailability of 16% for apomorphine.

**Keyphrases** □ Apomorphine—bioavailability, effect on stereotyped cage climbing, mice □ Bioavailability—apomorphine, intravenous, intraperitoneal, and oral administration □ Behavior—apomorphine-induced cage climbing in mice, intravenous, intraperitoneal, and oral administration □ Emetics—apomorphine, bioavailability, effect on stereotyped cage climbing in mice

Recently, there has been considerable interest in the pharmacology and clinical utility of apomorphine (I). Its ability as an antiparkinsonian (1, 2) was noted at least 15 years before the clinical adoption of levodopa (3). More recent studies confirmed the clinical efficacy of subcutaneously administered apomorphine in the treatment of parkinsonism (4). Activity is observed when I is given to humans orally (5); however, the necessary dosage differential between these two administration routes is reportedly greater than an order of magnitude (5).

In addition to its potential use as an antiparkinsonian, I has been implicated in the treatment of Huntington's chorea (6, 7), tardive dyskinesia (8, 9), spasmodic torticollis (9), Gilles de la Tourette's syndrome (10), schizophrenia (11–13), and thalamic pain (14). The clinical application of I, however, is confounded by its apparent poor, oral absorption (5), short duration of action (4, 5), and chemical instability (15).

## BACKGROUND

Prodrugs may provide a viable alternative to the use of apomorphine (I) *per se*. Its *O,O'*-diesters, II–VI, were previously prepared and tested in mice and rats (16–20). When injected intraperitoneally, these compounds showed prolonged pharmacological effects typical of I. Furthermore, the duration of I-like effects appear to follow rank-order rates of hydrolyses expected for II–VI. However, only indirect evidence has been provided to correlate the pharmacological activity of I prodrugs with circulating blood levels of I (18–20).

The disposition of I in mice following intravenous administration was also studied (21, 22). Similarly to humans, the results in mice indicate a relatively short half-life for I. Recent studies (23) confirmed these earlier data (21, 22). Significant first-pass effects were suggested from experiments with $^3$H-labeled I and measurements of total and ethyl acetate-extracted radioactivity in mouse plasma following intravenous, intraperitoneal, and oral administrations (23).

In the present experiments, plasma analyses of I and its conjugates by high-performance liquid chromatography (HPLC) were conducted to document more carefully the bioavailability of I in mice. In addition, comparisons were made between chromatographically measured I and murine stereotyped cage climbing (24–26). The latter pharmacological test is dopaminergic in nature (27) and is possibly an effective model for predicting the antiparkinsonian activity of drugs like I (26). It was hoped that possible blood level-pharmacological correlations might be useful in future evaluations of I prodrugs.

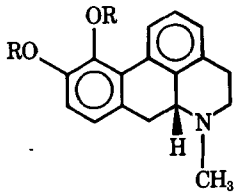


I: R = H
II: R = $CH_3CO$
III: R = $CH_3CH_2CO$
IV: R = $(CH_3)_2CHCO$
V: R = $(CH_3)_3CCO$
VI: R = $C_6H_5CO$

## EXPERIMENTAL

**Reagents**—All organic solvents used in the HPLC procedures were distilled-in-glass grade[1]. Water was deionized and double distilled from glass. *R*-(−)-Apomorphine hydrochloride hemihydrate[2] [98% pure as determined by UV spectrophotometry (28)], *N*-*n*-propylnorapomorphine[3], boldine[4], [$^3$H]apomorphine[5] (specific activity 31.3 Ci/mmole), and ascorbic acid[6] were used as obtained. β-Glucuronidase (bacterial type II; 51,300 modified Fishman units/g) was used as received[7], following activation by addition of ~0.05 ml of chloroform/ml of enzyme solution. All other solvents and reagents were analytical reagent grade.

**HPLC Analyses**—HPLC assays for apomorphine (I) in plasma were performed in duplicate as previously reported (29, 30) but with the following modifications: a 7-cm × 2.1-mm i.d. guard column[8] was installed before the analytical column, and the citrate–phosphate buffer (29, 30), was replaced by 0.05 *M* acetate buffer (pH 3.25) containing 0.001 *M* sodium lauryl sulfate. Analyses of I glucuronides were accomplished after enzymatic hydrolysis. In these instances, 200-μl plasma samples were mixed with 400 μl of a pH 6.8 buffer solution (0.07 *M* phosphate buffer with 8.7 m*M* ascorbic acid) and 50 μl of a β-glucuronidase solution, equivalent to 130 Fishman units.

The enzyme solution was incubated for 30 min at 37°, and the incubation conditions were chosen since a 15-min incubation time under nearly identical conditions was reported to be sufficient for the complete hydrolysis of *N*-*n*-propylnorapomorphine glucuronide at a concentration level of 45 μg/ml (31). Incubation was terminated by the addition of 1.5 ml of acetonitrile solution containing 2 μg of boldine/ml as an internal standard. This solution was vortexed for 5 sec and centrifuged for 10 min at 1230×*g*. An 800-μl portion of the supernate was then transferred to a 1-ml siliated vial[9], evaporated, and assayed according to an earlier method (29). The amount of conjugated I in a sample was determined as the difference between the assay for free I, and the total assay, which includes I glucuronides.

[1] Li Chrosolv, E. Merck, Darmstadt, West Germany, or Burdick & Jackson Laboratories, Muskegon, Mich.
[2] McFarland Smith, Edinburgh, Scotland.
[3] Sterling Winthrop Research Institute, Rensselaer, N.Y.
[4] ICN Pharmaceuticals, Cleveland, Ohio.
[5] New England Nuclear, Boston, Mass.
[6] Fisher Chemical Co., Pittsburgh, Pa.
[7] Sigma Chemical Co., St. Louis, Mo.
[8] Co-Pell ODS, Whatman, Clifton, N.J.
[9] Reactivial, Pierce Chemical Co., Rockford, Ill.



0022-3549/81/1000-1144$01.00/0
© 1981, American Pharmaceutical Association

**Table I—Plasma Levels of Apomorphine and Its Conjugates following Administration to Mice**

| | Plasma Concentration, μg/ml[a] | | | | | | | |
|---|---|---|---|---|---|---|---|---|
| | Intraveneous | | | | | | | |
| | 7.5 mg/kg | | 15 mg/kg | | Intraperitoneal, 50 mg/kg | | Oral, 50 mg/kg | |
| Minutes | Apomorphine | Conjugates | Apomorphine | Conjugates | Apomorphine | Conjugates | Apomorphine | Conjugates |
| 3 | 2.7 | 0.0 | 4.0 | 0.0 | 3.1 | 7.3 | 0.5 | 4.0 |
| 5 | 2.3 | 0.0 | 3.4 | 0.7 | 5.0 | 22.9 | 1.0 | 9.5 |
| 10 | 0.5 | 2.2 | 2.5 | 2.0 | 3.1 | 22.0 | 0.7 | 12.6 |
| 15 | 0.0 | 1.0 | 2.0 | 2.8 | 4.2 | 22.7 | 0.0 | 7.0 |
| 30 | 0.5 | 0.0 | 0.7 | 2.6 | 0.8 | 14.6 | 0.0 | 5.4 |
| 45 | 0.0 | 0.9 | 0.0 | 0.7 | 0.0 | 7.4 | 0.0 | 8.8 |
| 60 | 0.0 | 0.0 | 0.0 | 1.0 | 0.0 | 1.8 | 0.0 | 3.3 |
| 90 | 0.7 | 0.0 | 0.0 | 0.9 | 0.0 | 0.8 | 0.0 | 1.9 |
| 120 | 0.0 | 0.0 | 0.0 | 0.0 | 0.0 | 2.4 | 0.0 | 2.4 |

[a] As determined by HPLC; average of five or six animals per data point. Values of <0.4 μg/ml (limit of assay sensitivity) were determined as zero.

**Table II—Bioavailability Parameters for Apomorphine as Determined by HPLC**

| | Parent Drug[a] | | | Conjugates[a] | | |
|---|---|---|---|---|---|---|
| Route/Dose, mg/kg | $AUC_{0-90}$, μg min/ml | $C_{max}$, μg/ml | $t_{max}$, min | $AUC_{0-90}$, μg min/ml | $C_{max}$, μg/ml | $t_{max}$, min |
| iv/15[b] | 49 | 4.0 | 3 | 94 | 2.8 | 15 |
| iv/7.5[b] | 29 | 2.7 | 3 | 31 | 2.2 | 10 |
| po/50[c] | 7 | 1.0 | 5 | 369 | 12.6 | 10 |
| ip/50[d] | 70 | 5.0 | 5 | 610 | 22.9 | 12 |

[a] Obtained from HPLC analyses of pooled plasma of five or six mice at each study time (see *Experimental*). [b] Percent parent drug circulating ($AUC$ parent drug/$AUC$ parent drug + $AUC$ conjugates × 100) = 34%. (iv/15) and 48% (iv/7.5). [c] Percent parent drug circulating = 2%. [d] Percent parent drug circulating = 10%; calculated from results with [$^3$H]apomorphine (ip/50), 10% (ether extraction), and 16% (ethyl acetate extraction).

**Assay of [$^3$H]Apomorphine in Plasma**—Two 100-μl portions of a plasma sample were each mixed with 1 ml of 0.5 *M* phosphate buffer (pH 7.0) saturated with sodium chloride. The solutions were extracted with 4.0 ml of ether or ethyl acetate by vortexing for 5 min and then were centrifuged at 1230×*g* for 20 min. A 2.0-ml portion of each organic layer was mixed with 18.0 ml of scintillation cocktail[10], and 0.5 ml of each aqueous layer was mixed with 9.5 ml of the cocktail. The solutions were counted[11] at 40% efficiency.

**Bioavailability Studies**—All investigations were conducted with experimentally naive male CD-1 albino mice[12], 20–36 g. Throughout the studies, access to food and water was provided *ad libitum*. Animals were maintained on a 12-hr light–dark cycle (lights on at 6 am and off at 6 pm), and all testing was done between 9 am and 5 pm. Only one plasma sample or one videotaping of stereotypic cage climbing was evaluated from each mouse after dosing; however, each data point was obtained by averaging analyses of pooled plasma samples or stereotyped behavior of five or six animals.

Dose levels of 50 mg of I/kg were administered orally and intraperitoneally, and 15 and 7.5 mg/kg were given intravenously. For the radiochemical study, a 50-mg of I/kg ip dose was given equivalent to ~100 Ci/kg of [$^3$H]apomorphine. Apomorphine was administered orally as an aqueous solution by intubation into the stomach *via* a suitable needle attached to a syringe; intraperitoneal and intravenous doses were given by injection.

Blood samples (400 μl) were taken from the infraorbital sinus (32) into heparanized tubes at 0, 3, 5, 10, 15, 30, 45, 60, 90, and 120 min following I administration and were immediately centrifuged. For chromatographic assay samples, 40 μl of a 150 m*M* ascorbic acid solution was added as an antioxidant to every 1–1.5 ml of plasma pooled from five or six mice per time interval following administration. For selected time periods, up to three replicate samples were collected by the pooled plasma method to evaluate the reproducibility of results. The samples were stored at −15° until analyzed. This temperature and the use of ascorbic acid prevents significant decomposition of I for up to 10 weeks (33). All chromatographic assays were completed within 2 weeks of sampling. For the radioactive samples, 100-μl portions of plasma from each mouse were immediately extracted and/or counted directly within 48 hr. Five [$^3$H]-apomorphine samples were collected for each time period.

**Stereotyped Cage Climbing**—A modification of a previous procedure (24) was used. For a 1-hr habituation period, the mice were placed into cylindrical cages, 12 cm in diameter × 14 cm high, with walls of vertical bars, 2 mm in diameter and 1 cm apart, surmounted by fine wire mesh. Immediately prior to the administration of I (2.0 and 7.5 mg/kg iv, 2.0 and 4.0 mg/kg ip, or 50 mg/kg po) or isotonic saline (intraperitoneally), behavior was videotaped to establish a baseline of activity for each animal. Beginning 3 min after drug administration, the behavior of each animal was videotaped and later rated "blind" by methods previously described (26).

**Calculations**—Bioavailability of oral and intraperitoneal doses compared to the intravenous dose was calculated as the ratios of the corresponding areas under the experimental curves ($AUC$) obtained by cutting and weighing. Areas beyond the last sampling point were initially obtained by extrapolating the apparent concentration decay phase of the individual experimental plasma concentration *versus* time curves to infinite time (34). In the final analyses (Table II), $AUC$ values for the 0–90-min period were obtained because of negligible plasma levels of drug and conjugates for most routes at 120 min. Bioavailability was calculated by dividing $AUC_{po}$ by $AUC_{iv}$ after multiplication by the intravenous–oral

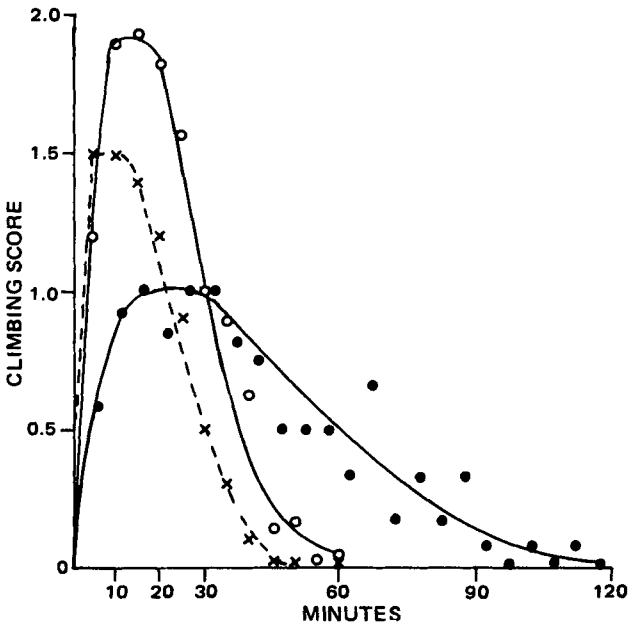


**Figure 1**—*Time course of murine cage climbing following administration of apomorphine. Key:* ○, *2.0 mg/kg iv;* ×, *4 mg/kg ip; and* ●, *50 mg/kg po.*

[10] Ready-Solo GP, Beckman Instruments, Fullerton, Calif.
[11] LS 8000 scintillation counter, Beckman Instruments, Fullerton, Calif.
[12] Charles River Laboratories, Wilmington, Mass.

dose ratio. Peak serum concentrations ($C_{max}$), maximum cage-climbing scores, and times of the peak concentration or score ($t_{max}$) were obtained from the individual plasma level or stereotypic behavior *versus* time curves.

## RESULTS AND DISCUSSION

Plasma samples obtained from mice dosed with apomorphine (I) by intravenous, intraperitoneal, and oral routes were analyzed by HPLC (29, 30). Only parent drug was detected in plasma ether extracts, confirming preliminary results obtained by TLC with [$^3$H]apomorphine (23). The major metabolite(s) behaved as an *O*-glucuronide(s) from analyses of plasma fractions treated with β-glucuronidase. The importance of *O*-glucuronidation in the metabolism of I in mice was reported previously (21, 35).

The data in Tables I and II reveal that I is largely present in plasma in its conjugate form, especially after intraperitoneal and oral administrations. Furthermore, experiments utilizing [$^3$H]apomorphine and both ether and ethyl acetate extractions provided measurements of I and its apparent conjugates (following intraperitoneal administration) that were consistent with those in the HPLC determinations. In no experiments were the mono-*O*-methyl ethers of I, apocodeine (VII), and isoapocodeine (VIII) detected as metabolites.

Compounds VII and VIII are readily determined by the HPLC system utilized (36) and are formed *in vitro* when I is incubated with rat liver catechol-*O*-methyltransferase preparations fortified with *S*-adenosylmethionine (37–39). Furthermore, *in vivo* experiments (stereotyped behavior) in rats with I and catechol-*O*-methyltransferase inhibitors seem to suggest a role for VII and/or VIII in the metabolism of I (39). Indeed, Symes *et al.* (40) found elevated brain levels of I in rats pretreated with pyrogallol and tropolone, both catechol-*O*-methyltransferase inhibitors. However, these authors acknowledged that pyrogallol and tropolone may serve as inhibitors of apomorphine *O*-glucuronidation. The mono-*O*-methylation of I is perhaps species specific or is of little apparent quantitative significance in the mouse.

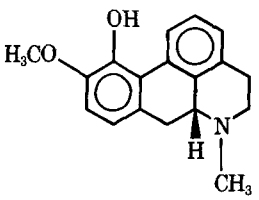


VII

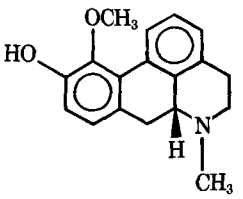


VIII

The absolute bioavailability of I following oral administration [(*AUC* parent drug po/dose po)/(*AUC* parent drug iv/dose iv) × 100] averaged 4%, which confirms similar results obtained using [$^3$H]apomorphine (23). Thus, there appears to be a significant first-pass effect when I is administered orally to mice. The relative amount of unconjugated I found in plasma after intraperitoneal administration was higher than that observed after oral administration but was relatively lower than the levels of parent drug found after intravenous dosing. The percent of circulating parent drug followed the order intravenous > intraperitoneal > oral, and the results with intraperitoneal dosing were confirmed by experiments with [$^3$H]apomorphine (Table II). This finding probably indicates considerable portal uptake after intraperitoneal administration as suggested previously (41).

Despite the apparent rapid and extensive conjugation of I in the mouse, its bioavailability as measured by the extent of absorption of drug plus conjugates [(*AUC* parent drug po + *AUC* conjugates po/dose)/[*AUC* parent drug iv + *AUC* conjugates iv/dose) × 100] averages nearly 90%. Thus, the poor pharmacological activity observed following oral administration of I to mice is likely related to the efficient conjugation to an apparently inactive (or poorly active) conjugate. Similar conjugations and analogous first-pass effects may be the cause of reportedly poor oral activity of I in rats (16) and humans (5).

**Stereotyped Cage Climbing**—Apomorphine-induced stereotypical cage climbing was studied after intravenous, oral, and intraperitoneal administrations. Cage climbing in mice is an unusual, but apparently specific, response to certain dopaminergic agents (25–27). Treated mice respond by "verticalization" in which two or four paws remain clutching to the vertical bars of specially designed cylindrical cages (24). The cage climbing response is accurately and reproducibly rated by the videotape methodology previously described (26).

**Table III—Time Course Measurements of Apomorphine-Induced Cage Climbing in Mice**

| Route/Dose, mg/kg | $t_{max}$ | *AUC*, units/min |
|---|---|---|
| iv/7.5 | 10 | 240 |
| iv/2.0 | 15 | 86 |
| po/50 | 15 | 286 |
| ip/4 | 10 | 32 |
| ip/2 | 10 | 16 |

The time courses of I-induced cage climbing for representative doses of I are depicted in Fig. 1. Responses occurred almost immediately following administration, while maximum ratings were observed (Table III) within a few minutes of the $t_{max}$ determined for I by HPLC. Thus, the behavioral response appears to mimic the time course–blood levels of I in mice (21–23). The potentiation of I-induced stereotypical behavior in rodents by compounds that can serve as inhibitors of *O*-glucuronidation or catechol-*O*-methyltransferase also supports this proposal[13] (39, 40).

The relative *AUC* values (Table III) observed for the time course of cage climbing after different administration routes nicely parallel the data determined radiochemically and by HPLC and also by previous radiochemical assays (23). An absolute bioavailability measurement for I can be calculated using the stereotyped cage climbing data in Table III [*i.e.*, (*AUC*-cage climb po/dose po)/(*AUC*-cage climb iv/dose iv) × 100]. When averaged over the available data, the absolute bioavailability of I was calculated as 16%, which is of a similar order of magnitude as the 4% found after HPLC analyses.

As an extension of the data presented, it appears that murine cage climbing may be useful in evaluating the *in vivo* release of I from its prodrugs. Before this evaluation, however, correlations should be sought between chemical analyses of I released *in vivo* and stereotyped cage climbing produced by prodrugs. Evaluations of this type are currently being investigated and will be the subject of a future report.

## REFERENCES

(1) R. S. Schwab, L. V. Amador, and J. Y. Lettvin, *Trans. Am. Neurol. Assoc.*, **76**, 231 (1951).

(2) V. G. Vernier and K. R. Unna, *J. Pharmacol. Exp. Ther.*, **103**, 365 (1951).

(3) G. C. Cotzias, M. H. Van Woert, and I. M. Schiffer, *N. Engl. J. Med.*, **276**, 374 (1967).

(4) G. C. Cotzias, P. S. Papavasiliou, C. Fehling, B. Kaufman, and I. Mena, *ibid.*, **282**, 31 (1970).

(5) G. C. Cotzias, P. S. Papavasiliou, E. S. Tolosa, J. S. Mendez, and M. Bell-Midura, *ibid.*, **294**, 567 (1976).

(6) I. Shoulson and T. N. Chase, *Annu. Rev. Med.*, **26**, 415 (1975).

(7) E. S. Tolosa and S. B. Sparber, *Life Sci.*, **15**, 1371 (1974).

(8) C. D. Marsden, D. Tarsy, and R. J. Baldessarini, in "Psychiatric Aspects of Neurologic Disease," D. F. Benson and D. Blumir, Eds., Grune and Stratton, New York, N.Y., 1975, pp. 219–265.

(9) E. S. Tolosa, *Arch. Neurol.*, **35**, 459 (1978).

(10) M. Feinberg and B. J. Carroll, *Arch. Gen. Psychiatry*, **36**, 979 (1979).

(11) C. A. Tamminga, M. H. Schaffer, R. C. Smith, and J. M. Davis, *Science*, **200**, 567 (1978).

(12) R. C. Smith, C. T. Tamminga, and J. M. Davis, *J. Neurol. Trans.*, **40**, 171(1977).

(13) F. Brambilla, S. Scarone, M. Ponzano, C. Maffei, P. Nobile, C. Rovere, and A. Guastalla, *Neuropsychobiology*, **5**, 185 (1979).

(14) D. P. Miley, A. A. Abrams, J. H. Atkinson, and D. S. Janowsky, *Am. J. Psychiatry*, **135**, 1230 (1978).

(15) R. E. Wilcox, D. W. Humphrey, W. H. Riffee, and R. V. Smith, *J. Pharm. Sci.*, **69**, 974 (1980).

(16) R. J. Baldessarini, K. G. Walton, and R. J. Borgman, *Neuropharmacology*, **14**, 725 (1975).

(17) R. J. Borgman, R. J. Baldessarini, and K. G. Walton, *J. Med. Chem.*, **19**, 717 (1976).

(18) R. J. Baldessarini, K. G. Walton, and R. J. Borgman, *Neuropharmacology*, **15**, 471 (1976).

(19) R. J. Baldessarini, N. S. Kula, K. G. Walton, and R. J. Borgman, *Psychopharmacology*, **53**, 45 (1977).

[13] Similar observations were made in the authors' laboratories for murine cage climbing; R. E. Wilcox, W. H. Riffee, and R. V. Smith, unpublished observations.

(20) R. J. Baldessarini, A. E. Boyd, III, N. S. Kula, and R. J. Borgman, *Psychoneuroendocrinology*, **4**, 173 (1979).
(21) P. N. Kaul, E. Brockmann-Hanssen, and E. L. Way, *J. Pharm. Sci.*, **50**, 248 (1961).
(22) A. M. Burkman, R. E. Notari, and W. K. Van Tyle, *J. Pharm. Pharmacol.*, **26**, 493 (1974).
(23) R. V. Smith, R. E. Wilcox, W. H. Soine, W. H. Riffee, R. J. Baldessarini, and N. S. Kula, *Res. Commun. Chem. Pathol. Pharmacol.*, **24**, 483 (1979).
(24) P. Protais, J. Costentin, and J. C. Schwartz, *Psychopharmacology*, **50**, 1 (1976).
(25) W. H. Riffee, R. E. Wilcox, and R. V. Smith, *Eur. J. Pharmacol.*, **54**, 723 (1979).
(26) R. E. Wilcox, W. H. Riffee, and R. V. Smith, *Pharmacol. Biochem. Behav.*, **10**, 161 (1979).
(27) R. E. Wilcox, W. H. Riffee, and R. V. Smith, *ibid.*, **11**, 653 (1979).
(28) W. H. Soine, P. Salgo, and R. V. Smith, *J. Labelled Compd. Radiopharm.*, **16**, 597 (1979).
(29) R. V. Smith, D. W. Humphrey, S. Szeinbach, and J. C. Glade, *Anal. Lett.*, **12**, 371 (1979).
(30) R. V. Smith, A. E. Klein, A. M. Clark, and D. W. Humphrey, *J. Chromatogr.*, **179**, 195 (1979).
(31) R. V. Smith, A. E. Klein, and D. O. Thompson, *Mikrochim. Acta*, 151 (1980) I.
(32) B. H. Migdalof, *Drug Metab. Rev.*, **5**, 295 (1976).
(33) R. V. Smith, D. W. Humphrey, and R. E. Wilcox, *Res. Commun. Chem. Pathol. Pharmacol.*, **27**, 183 (1980).
(34) J. W. Crow, M. Gibaldi, and G. Levy, *J. Pharm. Sci.*, **68**, 958 (1979).
(35) P. N. Kaul and M. W. Conway, *ibid.*, **60**, 93 (1971).
(36) R. V. Smith, J. C. Glade, and D. W. Humphrey, *J. Chromatogr.*, **172**, 520 (1979).
(37) J. G. Cannon, R. V. Smith, A. Modiri, S. P. Sood, R. J. Borgman, M. A. Aleem, and J. P. Long, *J. Med. Chem.*, **15**, 273 (1972).
(38) G. M. McKenzie and H. L. White, *Biochem. Pharmacol.*, **22**, 2329 (1973).
(39) K. Missala, S. Lal, and T. L. Sourkes, *Eur. J. Pharmacol.*, **22**, 54 (1973).
(40) A. L. Symes, S. Lal, and T. L. Sourkes, *J. Pharm. Pharmacol.*, **27**, 947 (1975).
(41) G. Levy and M. Gibaldi, in "Handbook of Experimental Pharmacology," Vol. XXVIII Part 3, J. R. Gillette and J. R. Mitchell, Eds., Springer-Verlag, New York, N.Y., 1974, pp. 1–34.

**ACKNOWLEDGMENTS**

Supported by Grants NS-12259 (R. V. Smith) and NS-06114 (R. E. Wilcox) from the National Institute for Neurological and Communicative Disorders and Stroke and Grant MH-33442 (W. H. Riffee and R. E. Wilcox) from the National Institute of Mental Health. Assistance was also obtained through a starter grant (R. E. Wilcox) from the University Research Institute (BRSG-Program).

The authors are grateful to Julie A. Anderson, Astreida Ducreux-P., and Dawn T. Sanchez-Barona for technical assistance and to the Sterling Winthrop Research Institute, Rensselaer, N.Y., for their generous gift of *N*-*n*-propylnorapomorphine.

# Antitumor Agents XLII: Comparison of Antileukemic Activity of Helenalin, Brusatol, and Bruceantin and Their Esters on Different Strains of P-388 Lymphocytic Leukemic Cells

**IRIS H. HALL ˣ, K. H. LEE, M. OKANO, D. SIMS, T. IBUKA, Y. F. LIOU, and Y. IMAKURA**

Received September 8, 1980, from the *Division of Medicinal Chemistry, School of Pharmacy, University of North Carolina, Chapel Hill, NC 27514.* Accepted for publication March 6, 1981.

**Abstract** □ Based on the fact that some known antineoplastic agents possess an ester moiety within their structure, the esters of helenalin, a sesquiterpene lactone, and of brusatol and bruceantin, quassinoids, were synthesized and tested for antileukemic activity in the P-388 screen. These agents gave different T/C % values dependent on the P-388 lymphocytic leukemia strain and the host strain of mice used. Later studies demonstrated that the agents caused different degrees of inhibition of nucleic acid and protein synthesis in the various P-388 strains. The higher the degree of inhibition of precursor incorporation into the nucleic acid or protein, the higher was the T/C % value obtained in a given P-388 strain. The study demonstrates the lack of consistency of P-388 lymphocytic leukemia cell lines used in various laboratories and indicates that the inbred strain of mice is a critical factor in the tolerance of drug toxicity and, thus, T/C % obtained.

**Keyphrases** □ P-388 lymphocytic leukemic cells—antileukemic activity of helenalin, brusatol, and bruceantin and their esters □ Antileukemic agents—comparison of helenalin, brusatol, and bruceantin and their esters □ Helenalin—comparison with brusatol, bruceantin, and their esters, antileukemic activity □ Brusatol—comparison with helenalin and bruceantin and their esters, antileukemic activity □ Bruceantin—comparison with helenalin and brusatol and their esters, antileukemic activity

The naturally occurring sesquiterpene lactones continue to provide numerous examples of structures exhibiting significant cytotoxic antitumor activity (1). In general, they have proven to be potent inhibitors of Walker 256 carcinosarcoma growth in rats and Ehrlich ascites carcinoma growth in mice and marginal inhibitors of P-388 lymphocytic leukemia in mice (2). For example, eupaformosanin (3), molephantinin (4), phantomolin (5), eupahyssopin (6), and helenalin (I) (7) all demonstrated highly significant inhibitory activity in the Walker 256 carcinosarcoma survival system with a T/C value of ≧300% at the low dose of 2.5 mg/kg (T/C >140% required for significant activity). However, in the P-388 murine lymphocytic leukemia screen, an *in vivo* test system currently used as a standard method by the National Cancer Institute (NCI) for evaluating compounds of natural origin, these compounds

0022-3549/81/1000-1147$01.00/0
© 1981, American Pharmaceutical Association

(20) R. J. Baldessarini, A. E. Boyd, III, N. S. Kula, and R. J. Borgman, *Psychoneuroendocrinology*, **4**, 173 (1979).
(21) P. N. Kaul, E. Brockmann-Hanssen, and E. L. Way, *J. Pharm. Sci.*, **50**, 248 (1961).
(22) A. M. Burkman, R. E. Notari, and W. K. Van Tyle, *J. Pharm. Pharmacol.*, **26**, 493 (1974).
(23) R. V. Smith, R. E. Wilcox, W. H. Soine, W. H. Riffee, R. J. Baldessarini, and N. S. Kula, *Res. Commun. Chem. Pathol. Pharmacol.*, **24**, 483 (1979).
(24) P. Protais, J. Costentin, and J. C. Schwartz, *Psychopharmacology*, **50**, 1 (1976).
(25) W. H. Riffee, R. E. Wilcox, and R. V. Smith, *Eur. J. Pharmacol.*, **54**, 723 (1979).
(26) R. E. Wilcox, W. H. Riffee, and R. V. Smith, *Pharmacol. Biochem. Behav.*, **10**, 161 (1979).
(27) R. E. Wilcox, W. H. Riffee, and R. V. Smith, *ibid.*, **11**, 653 (1979).
(28) W. H. Soine, P. Salgo, and R. V. Smith, *J. Labelled Compd. Radiopharm.*, **16**, 597 (1979).
(29) R. V. Smith, D. W. Humphrey, S. Szeinbach, and J. C. Glade, *Anal. Lett.*, **12**, 371 (1979).
(30) R. V. Smith, A. E. Klein, A. M. Clark, and D. W. Humphrey, *J. Chromatogr.*, **179**, 195 (1979).
(31) R. V. Smith, A. E. Klein, and D. O. Thompson, *Mikrochim. Acta*, 151 (1980) I.
(32) B. H. Migdalof, *Drug Metab. Rev.*, **5**, 295 (1976).
(33) R. V. Smith, D. W. Humphrey, and R. E. Wilcox, *Res. Commun. Chem. Pathol. Pharmacol.*, **27**, 183 (1980).
(34) J. W. Crow, M. Gibaldi, and G. Levy, *J. Pharm. Sci.*, **68**, 958 (1979).
(35) P. N. Kaul and M. W. Conway, *ibid.*, **60**, 93 (1971).
(36) R. V. Smith, J. C. Glade, and D. W. Humphrey, *J. Chromatogr.*, **172**, 520 (1979).
(37) J. G. Cannon, R. V. Smith, A. Modiri, S. P. Sood, R. J. Borgman, M. A. Aleem, and J. P. Long, *J. Med. Chem.*, **15**, 273 (1972).
(38) G. M. McKenzie and H. L. White, *Biochem. Pharmacol.*, **22**, 2329 (1973).
(39) K. Missala, S. Lal, and T. L. Sourkes, *Eur. J. Pharmacol.*, **22**, 54 (1973).
(40) A. L. Symes, S. Lal, and T. L. Sourkes, *J. Pharm. Pharmacol.*, **27**, 947 (1975).
(41) G. Levy and M. Gibaldi, in "Handbook of Experimental Pharmacology," Vol. XXVIII Part 3, J. R. Gillette and J. R. Mitchell, Eds., Springer-Verlag, New York, N.Y., 1974, pp. 1–34.

**ACKNOWLEDGMENTS**

Supported by Grants NS-12259 (R. V. Smith) and NS-06114 (R. E. Wilcox) from the National Institute for Neurological and Communicative Disorders and Stroke and Grant MH-33442 (W. H. Riffee and R. E. Wilcox) from the National Institute of Mental Health. Assistance was also obtained through a starter grant (R. E. Wilcox) from the University Research Institute (BRSG-Program).

The authors are grateful to Julie A. Anderson, Astreida Ducreux-P., and Dawn T. Sanchez-Barona for technical assistance and to the Sterling Winthrop Research Institute, Rensselaer, N.Y., for their generous gift of *N*-*n*-propylnorapomorphine.

# Antitumor Agents XLII: Comparison of Antileukemic Activity of Helenalin, Brusatol, and Bruceantin and Their Esters on Different Strains of P-388 Lymphocytic Leukemic Cells

**IRIS H. HALL ˣ, K. H. LEE, M. OKANO, D. SIMS, T. IBUKA, Y. F. LIOU, and Y. IMAKURA**

Received September 8, 1980, from the *Division of Medicinal Chemistry, School of Pharmacy, University of North Carolina, Chapel Hill, NC 27514.* Accepted for publication March 6, 1981.

**Abstract** □ Based on the fact that some known antineoplastic agents possess an ester moiety within their structure, the esters of helenalin, a sesquiterpene lactone, and of brusatol and bruceantin, quassinoids, were synthesized and tested for antileukemic activity in the P-388 screen. These agents gave different T/C % values dependent on the P-388 lymphocytic leukemia strain and the host strain of mice used. Later studies demonstrated that the agents caused different degrees of inhibition of nucleic acid and protein synthesis in the various P-388 strains. The higher the degree of inhibition of precursor incorporation into the nucleic acid or protein, the higher was the T/C % value obtained in a given P-388 strain. The study demonstrates the lack of consistency of P-388 lymphocytic leukemia cell lines used in various laboratories and indicates that the inbred strain of mice is a critical factor in the tolerance of drug toxicity and, thus, T/C % obtained.

**Keyphrases** □ P-388 lymphocytic leukemic cells—antileukemic activity of helenalin, brusatol, and bruceantin and their esters □ Antileukemic agents—comparison of helenalin, brusatol, and bruceantin and their esters □ Helenalin—comparison with brusatol, bruceantin, and their esters, antileukemic activity □ Brusatol—comparison with helenalin and bruceantin and their esters, antileukemic activity □ Bruceantin—comparison with helenalin and brusatol and their esters, antileukemic activity

The naturally occurring sesquiterpene lactones continue to provide numerous examples of structures exhibiting significant cytotoxic antitumor activity (1). In general, they have proven to be potent inhibitors of Walker 256 carcinosarcoma growth in rats and Ehrlich ascites carcinoma growth in mice and marginal inhibitors of P-388 lymphocytic leukemia in mice (2). For example, eupaformosanin (3), molephantinin (4), phantomolin (5), eupahyssopin (6), and helenalin (I) (7) all demonstrated highly significant inhibitory activity in the Walker 256 carcinosarcoma survival system with a T/C value of ≧300% at the low dose of 2.5 mg/kg (T/C >140% required for significant activity). However, in the P-388 murine lymphocytic leukemia screen, an *in vivo* test system currently used as a standard method by the National Cancer Institute (NCI) for evaluating compounds of natural origin, these compounds

0022-3549/81/1000-1147$01.00/0
© 1981, American Pharmaceutical Association

**Table I—Antineoplastic Activity of Sesquiterpene Lactones and Quassinoids against P-388-UNC Lymphocytic Leukemia Cell Growth in $BDF_1$ Mice**

| Compound | Dose, mg/kg/day ip | Average Days Survived of T/C | T/C % |
|---|---|---|---|
| I | 60[a] | 3.0/9.66 | 31 |
| | 15 | 11.9/9.66 | 123 |
| | 8 | 15.4/9.66 | 162 |
| | 3 | 12.9/9.66 | 134 |
| II | 60[a] | 5.8/9.66 | 60 |
| | 30 | 16.2/9.66 | 168 |
| | 15 | 25.2/9.66 | 261 |
| | 8 | 13.8/9.66 | 143 |
| | 3 | 13.8/9.66 | 143 |
| III | 0.6 | 14.2/9.5 | 149 |
| | 0.3 | 14.3/9.5 | 150 |
| | 0.25 | 14.5/9.5 | 153 |
| | 0.125 | 15.0/9.5 | 158 |
| | 0.100 | 12.8/9.5 | 134 |
| IV | 1.0 | 20.2/9.5 | 213 |
| | 0.6 | 25.8/9.5 | 272 (197) |
| | 0.3 | 20.4/9.5 | 215 |
| | 0.25 | 15.5/9.5 | 163 |
| | 0.125 | 11.0/9.5 | 116 |
| | 0.100 | 11.0/9.5 | 116 |
| V | 0.6 | 25.2 | 217 |

[a] Toxic at this dose.

failed to give T/C values higher than 147% at the maximum dose level of 25 mg/kg/day (1) (T/C >125% required for significant activity).

## BACKGROUND

In this laboratory, previous systematic investigation of the structure–activity relationships among the sesquiterpene lactones and related compounds indicated the importance of the bifunctional alkylating enone O=C—C=$CH_2$ system and the ester moiety for enhanced cytotoxic antitumor activity (1). For example, the bifunctional alkylating helenalin (I), which contains a $\beta$-unsubstituted cyclopentenone and an $\alpha$-methylene-$\gamma$-lactone, is more potent than the corresponding 2,3-dihydrohelanalin or 11,13-dihydrohelenalin (plenolin) in its *in vitro* cytotoxicity (8) and *in vivo* antitumor activity (2). Cytotoxicity is also enhanced by introduction of a lipophilic ester side chain to helenalin and related derivatives (9).

The importance of the ester group that contributes to the enhanced *in vivo* antitumor activity is also seen in many other naturally occurring antitumor agents including the germacranolides eupaformosanin, molephantinin, phantomolin, and eupahyssopin as well as the quassinoid bruceantin (10), the diterpene taxol (11), the alkaloids indicine *N*-oxide (12), homoharringtonine (13), vincristine (14), and vinblastine (14), the macrolide maytansine (15), and the fungal metabolites anguidin (16), actinomycin D (dactinomycin) (17), and mitomycin C (18). The latter compounds (19) possess high *in vivo* antileukemic activity against the P-388 lymphocytic leukemia growth.

This evidence, coupled with the fact that polyfunctionality is a common structural feature in many of the described antileukemic agents, led to the hypothesis that a polyfunctional alkylating-type compound originating from the combination of bifunctional or monofunctional alkylating active species *via* an ester linkage might be highly active as an antileukemic agent. Thus, esters of helenalin, brusatol, and bruceantin were synthesized and examined for their antileukemic activity against P-388 lymphocytic leukemia cell growth. Those results are now reported utilizing two different strains of P-388 lymphocytic leukemia cells along with the effects of these esters on key enzymes of nucleic acid and protein synthesis.

## EXPERIMENTAL

**Source of Compounds**—Helenalin (I) was isolated from *Balduina angustifolia* by the methods of Lee *et al.* (20). Treatment of I with malonyl dichloride in dry benzene by the general method gave rise to crystalline bis(helenalinyl)malonate[1] [II, $C_{33}H_{36}O_{10}$, mp 217–218°], resulting in a molecule with four alkylating centers. Brusatol (III) was obtained by treating bruceoside A, a quassinoid glycoside isolated from *Brucea javanica*, with 3 *N* $H_2SO_4$–methanol (1:1) to hydrolyze the glycosidic

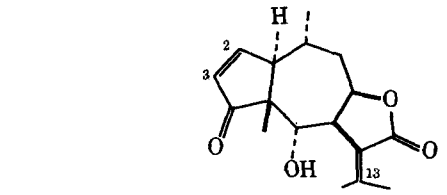

I

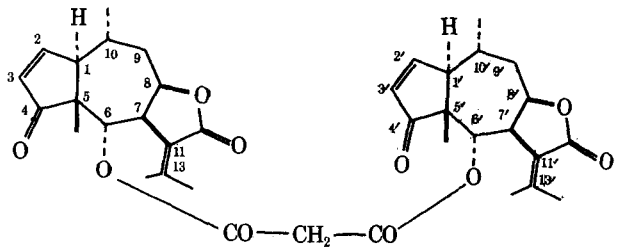

II

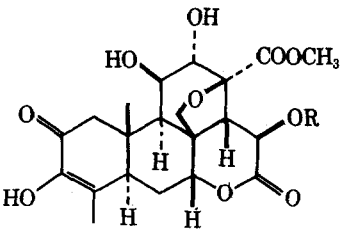

III: R = COCH = C(CH$_3$)(CH$_3$)

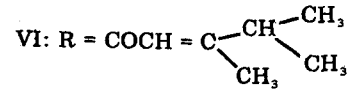

VI: R = COCH = C(CH$_2$CH$_3$)(CH$_3$)

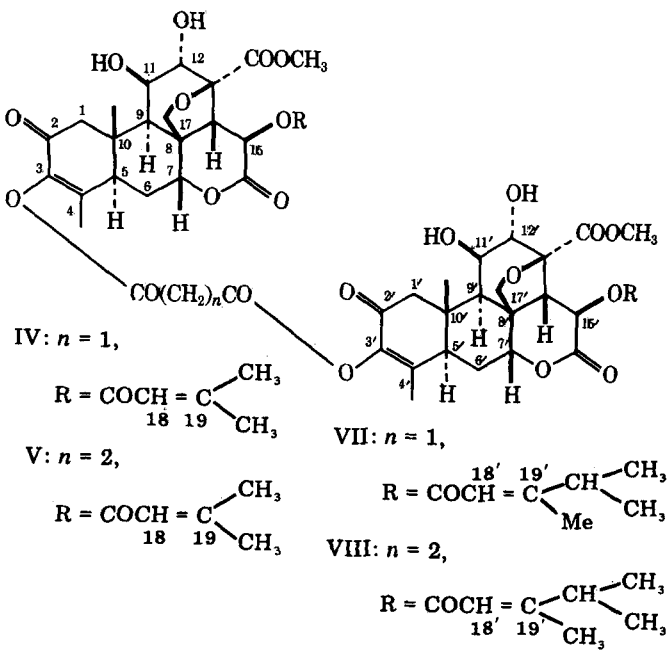

IV: $n$ = 1, R = COCH = C(CH$_3$)(CH$_3$) (18, 19)

V: $n$ = 2, R = COCH = C(CH$_3$)(CH$_3$) (18, 19)

VII: $n$ = 1, R = COCH = C(CH$_2$CH$_3$)(CH$_3$) (18′, 19′; Me)

VIII: $n$ = 2, R = COCH = C(CH$_2$CH$_3$)(CH$_3$) (18′, 19′)

[1] The UV, IR, and NMR spectra data of II, IV, V, VII, and VIII were in accord with assigned structure.

**Table II—Antineoplastic Activity of Sesquiterpene Lactones and Quassinoids against P-388-UNC and P-388-NIH Lymphocytic Leukemia Cell Growth**

| Compound | Dose, mg/kg/day ip | P-388-UNC, T/C % | | P-388-NIH, T/C % | |
|---|---|---|---|---|---|
| | | CDF | $BDF_1$ | CDF | $BDF_1$ |
| I | 15 | 123 | — | 134 | — |
| | 8 | 168 | — | 154 | 162 |
| | 3 | 134 | 158 | 138 | 152 |
| II | 15 | — | — | toxic | toxic |
| | 8 | 145 | 168 | 129 | 145 |
| | 3 | 143 | — | 138 | 130 |
| III | 1.0 | 152 (toxic) | 234 | 162 (toxic) | 176 |
| | 0.6 | 149 | 152 | 152 | 156 |
| IV | 0.6 | 188 | 197 | 125 | 135 |
| V | 0.6 | 168 | 207 | 133 | 161 |
| VI | 1.0 | 168 | 258 | 162 | 176 |
| | 0.6 | 146 | — | — | — |
| VII[a] | 1.2 | — | 111 | — | — |
| | 0.6 | 138 | 139 | 125 | 139 |
| | 0.3 | — | 109 | — | — |
| VIII | 1.2 | — | 164 | — | 168 |
| | 0.6 | 132 | 153 | 144 | 151 |
| | 0.3 | — | 150 | — | — |
| 5-Fluorouracil | 12.5 | 162 | 166 | 186 | 209 |

[a] P-388-NIH contractors: 163 (3.0), 165 (1.5), 146 (0.75), and 128 (0.38).

**Table III—*In Vitro* Effects (Percent of Control) of Sesquiterpene Lactones and Quassinoids on P-388-UNC and P-388-NIH Lymphocytic Leukemia Cell Metabolism**

| Compounds | P-388-UNC | | | P-388-NIH | | |
|---|---|---|---|---|---|---|
| | DNA | RNA | Protein | DNA | RNA | Protein |
| I, 20 μmoles | 15 ± 2[a] | 85 ± 3[a] | 68 ± 9[a] | 10 ± 5[a] | 84 ± 6[a] | 79 ± 3[a] |
| II, 20 μmoles | 38 ± 3[a] | 55 ± 4[a] | 50 ± 4[a] | 38 ± 4[a] | 52 ± 5[a] | 75 ± 10[b] |
| III, 10 μmoles | 48 ± 4[a] | 44 ± 2[a] | 45 ± 3[a] | 47 ± 4[a] | 71 ± 5[a] | 80 ± 6[b] |
| IV, 10 μmoles | 54 ± 7[a] | 52 ± 5[a] | 17 ± 13[a] | 46 ± 5[a] | 90 ± 7[a] | 65 ± 5[a] |
| V, 10 μmoles | 36 ± 4[a] | 41 ± 6[a] | 26 ± 4[a] | 41 ± 3[a] | 71 ± 5[a] | 75 ± 3[a] |
| VI, 10 μmoles | 38 ± 2[a] | 47 ± 6[a] | 58 ± 3[a] | 35 ± 3[a] | 71 ± 3[a] | 85 ± 2[b] |
| VII, 10 μmoles | 45 ± 8[a] | 66 ± 3[a] | 60 ± 3[a] | 43 ± 4[a] | 67 ± 4[a] | 75 ± 4[a] |
| VIII, 10 μmoles | 52 ± 4[a] | 78 ± 4[a] | 68 ± 3[a] | 52 ± 5[a] | 74 ± 6[a] | 77 ± 2[a] |
| 0.05% Polysorbate 80 (control) | 100 ± 6 | 100 ± 5 | 100 ± 4 | 100 ± 7 | 100 ± 5 | 100 ± 8 |
| Emetine, 50 μmoles | — | — | 60 ± 3[a] | — | — | 61 ± 4[a] |
| Pyrocatechol violet, 50 μmoles | — | — | 60 ± 5[a] | — | — | 62 ± 4[a] |
| Value dpm/$10^6$ cells ($n$ = 6) | 36,777 | 38,615 | 76,518 | 39,564 | 45,309 | 79,103 |

[a] $p \leq 0.001$. [b] $p \leq 0.005$.

linkage (21–23). Bruceantin (VI) was also synthesized from bruceoside A (24–25).

Brusatol (III) (22–24) and bruceantin (VI) were treated similarly with malonyl dichloride and succinyl chloride in dry pyridine to yield, after purification of the reaction products by preparative TLC, the corresponding bis(brusatolyl)malonate[1] [IV, $C_{55}H_{64}O_{24}\cdot H_2O$, mp 191–193°], bis(brusatolyl)succinate[1] [V, $C_{56}H_{66}O_{24}$, mp 248–250°], bis(bruceantinyl)malonate[1] [VII, $C_{59}H_{72}O_{24}$, mp 193–195°], and bis(bruceantinyl)-succinate[1] [VIII, $C_{60}H_{74}O_{24}$, mp 250° dec.][2].

**Biological**—*P-388 Lymphocytic Leukemia Antitumor Screen*—The P-388 lymphocytic leukemia-UNC tumor line was originally obtained from Mason Research Institute through NCI and has been maintained in this laboratory in DBA/2 male donor mice for ~2 years. The P-388 lymphocytic leukemia-NIH was obtained in April 1980 from the same source. The eight test compounds with the standard 5-fluorouracil were administered to both the P-388-UNC and P-388-NIH strains as follows. $BDF_1$ or CDF male mice (~20 g) were administered $10^6$ P-388 lymphocytic leukemia cells intraperitoneally on Day 0 (26). Test compounds were homogenized in 0.05% polysorbate 80–water and administered intraperitoneally daily.

*KB Tissue Cytotoxic Assay*—KB (human epidermoid carcinoma of the mouth) cells were maintained in minimum essential medium and 10% fetal calf serum containing the antibiotics penicillin and streptomycin (26). The method of Huang *et al.* (27) was utilized for the cytotoxic assay in microtest tissue culture plates.

*P-388 Lymphocytic Leukemia Cell Metabolism*—$BDF_1$ male mice (~22 g) were innoculated with $10^6$ P-388 tumor cells as previously described. On day 9, the cells were collected from the peritoneal cavity. *In vitro* incorporation studies were conducted using $10^6$ P-388-UNC or P-388-NIH cells, minimum essential medium, and 1 μCi of thymidine (6-$^3$H, 21.8 Ci/mmole), uridine (6-$^3$H, 22.4 Ci/mmole), or L-leucine [4,5-$^3$H(N) 56.5 Ci/mmole] in a total volume of 1 ml, which was incubated for 90 min at 37° (28). Compounds I and II were tested at a final concentration of 20 μmoles, and III–VIII were tested at a 10-μmole concentration.

The thymidine incorporation into DNA assays were terminated with 0.5 *N* perchloric acid containing 1% pyrophosphate. Radiolabeled DNA was collected on glass fiber paper (GF/F) by vacuum suction. RNA and protein incorporation studies were terminated with trichloroacetic acid, and the acid-insoluble macromolecule was collected on nitrocellulose membrane filters. The filter papers were placed in scintillation vials and counted in a toluene–octoxynol scintillation fluid (29).

## RESULTS AND DISCUSSION

Initially, the antileukemic activity was determined in the P-388-UNC lymphocytic leukemia screen. The T/C % value for II at 15 mg/kg/day was exceedingly high, *e.g.*, T/C % = 261 in $BDF_1$ male mice. The quassinoid esters of III were then examined and, as can be seen in Table I, IV at 0.6 mg/kg resulted in T/C % values of 272 and 197 and V resulted in a T/C % value of 217 in $BDF_1$ male mice.

Compounds I–V followed a dose–response curve against P-388-UNC lymphocytic leukemia growth in $BDF_1$ mice. The $ED_{50}$ for helenalin (I) in the KB cytotoxic assay was 0.188 compared to the literature value (28) of 0.19 μg/ml. Bis(helenalinyl)malonate (II) afforded an $ED_{50}$ of 0.08 μg/ml. The $ED_{50}$ values for the quassinoids were also impressive, with III, IV, VI, and VIII equal to 0.31, 0.025, 0.056, and 0.275 μg/ml, respectively.

In an attempt to confirm these unexpected high results, II, IV, and V were submitted to NCI for retesting and evaluation. The two contract screening agencies used by NCI were unable to obtain results >12 mg/kg in CDF mice for I and II; but at 3 and 0.39 mg/kg, T/C % values of 130[3] and 120[4], respectively, were obtained. Compound IV was also submitted to the same two contract screeners[3], whose studies resulted in T/C %

[2] Unpublished results.

[3] Southern Research.

values of 131, 135, and 131 at 3, 1.5, and 0.75 mg/kg, respectively. The second contract screener[4] found II, III, and IV totally inactive in their P-388 lymphocytic leukemia screen in CDF mice.

Since these results were somewhat baffling, a new sample of P-388 lymphocytic leukemia cells, noted as P-388-NIH, was obtained[5]. The compounds were retested against P-388-UNC and P-388-NIH leukemia growth in CDF and $BDF_1$ male mice with dosing from Days 1 to 9. These results are shown in Table II along with the data for two new compounds, *i.e.*, the malonate (VII) and succinate (VIII) ester of bruceantin. Bruceantin (VI) is a quassinoid in Phase II clinical trial. These data confirmed previous observation by this laboratory in $BDF_1$ male mice using the P-388-UNC strain, whereas data for P-388-NIH in CDF mice were comparable with the contractor's results. However, a difference could be observed between $BDF_1$ and CDF donor mice and the resulting T/C % values. Apparently, the $BDF_1$ male mice were able to tolerate the higher doses of I–III and VI, thus affording higher T/C % values than when administered to CDF mice. In fact, in a previous report (29) on DBA/2 male mice, testing above 0.5 mg/kg with III in the P-388 screen resulted in deaths. The inbred hybrid strain of mice may be a critical factor since mice used for the study in Table I were bred in this laboratory ($C_{57}B1/6$ female × DBA/2j male), whereas those used in Table II were obtained commercially[6]. When VII was tested[3] at 3, 1.5, 0.75, and 0.38 mg/kg, T/C % values of 163, 165, 146, and 128, respectively, were obtained, which were within the scope of data presented in Table II.

The two sets of conflicting data pose the question of whether P-388-UNC is a different strain of P-388 lymphocytic leukemia cells resulting from some alteration or mutation. Thus, since the sesquiterpene lactones and quassinoids were known to affect nucleic acid and protein synthesis in tumor cells, these parameters were examined in the P-388-UNC and P-388-NIH strains of cells from $BDF_1$ mice.

Table III indicates that *in vitro* DNA synthesis was affected approximately the same degree by I and II in the two strains of P-388 cells. RNA synthesis was inhibited by I and II equally in the P-388-UNC and P-388-NIH cells. Protein synthesis, however, was inhibited at a much higher rate in the P-388-UNC strain than the P-388-NIH strain (*e.g.*, compare II at 50 and 25% inhibition, respectively). Examination of II–VIII showed that the degree of inhibition of DNA synthesis was of the same magnitude in both strains of P-388 cells for a given compound. The RNA synthesis inhibition by III–VI was much higher in the P-388-UNC strain compared to the P-388-NIH strain, resulting in ~24–38% higher inhibition of RNA synthesis, with IV demonstrating the largest difference (*i.e.*, 48% in the P-388-UNC strain and 10% in the P-388-NIH strain).

Protein synthesis inhibition was also decidedly different between the two different strains for III–VI. Compound III afforded a 20% inhibition in the P-388-NIH and a 55% inhibition in the P-388-UNC strain. Compound IV demonstrated a difference of 35% compared to 83% inhibition, V showed a difference of 25% compared to 72%, and VI showed a difference of 15% compared to 42% in the respective strains. Compounds VI and VIII demonstrated approximately the same T/C % values in the two strains of P-388 cells, and the effects of the two compounds on RNA and protein synthesis was comparable in the two strains of cells. The standard emetine and pyrocatechol violet at 5 μmoles demonstrated the same degrees of protein inhibition in the two strains of P-388 cells.

These studies indicate that the P-388-UNC and P-388-NIH strains of P-388 lymphocytic leukemia cells are different in their metabolic response to certain chemical agents and the difference may be responsible for diverse values obtained in the antineoplastic screen. The P-388-UNC strain appears to be particularly sensitive to sesquiterpene lactone and quassinoid-type structure but less sensitive to 5-fluorouracil. Furthermore, the strain of mice used may be critical for the T/C % values obtained, depending on the tolerance of the mice to the particular toxic effects of the chemical agent.

[4] Battelle Memorial Institute.
[5] Mason Research Institute.
[6] Jackson Laboratories.

## REFERENCES


(1) K. H. Lee, "Program and Abstracts of the 16th National Medicinal Chemistry Symposium," American Chemical Society, Kalamazoo, Mich. 1978, pp. 44–58.

(2) I. H. Hall, K. H. Lee, C. O. Starnes, S. ElGebaly, T. Ibuka, Y. S. Wu, T. Kimura, and M. Haruna, *J. Pharm. Sci.*, **67**, 1235 (1978).

(3) K. H. Lee, T. Kimura, M. Haruna, A. T. McPhail, K. D. Onan, and H. C. Huang, *Phytochemistry*, **16**, 1068 (1977).

(4) K. H. Lee, T. Ibuka, H. C. Huang, and D. L. Harris, *J. Pharm. Sci.*, **64**, 1077 (1975).

(5) A. T. McPhail, K. D. Onan, K. H. Lee, T. Ibuka, M. Kozuka, T. Shingu, and H. C. Huang, *Tetrahedron Lett.*, **1974**, 2739.

(6) K. H. Lee, T. Kimura, M. Okamoto, C. M. Cowherd, A. T. McPhail, and K. D. Onan, *ibid.*, **1976**, 1051.

(7) K. H. Lee, M. Haruna, H. C. Huang, B. S. Wu, and I. H. Hall, *J. Pharm. Sci.*, **66**, 1194 (1977).

(8) K. H. Lee, H. Furukawa, and E. S. Huang, *J. Med. Chem.*, **15**, 609 (1972).

(9) K. H. Lee, R. Meck, C. Piantadosi, and E. S. Huang, *ibid.*, **16**, 299 (1973).

(10) S. M. Kupchan, R. W. Britton, J. A. Lacadie, M. F. Ziegler, and C. W. Sigel, *J. Org. Chem.*, **40**, 648 (1975).

(11) M. C. Wani, H. L. Taylor, M. E. Wall, P. Coggon, and A. T. McPhail, *J. Am. Chem. Soc.*, **93**, 2325 (1971).

(12) A. R. Mattocks, *J. Chem. Soc. (C)*, **1967**, 329.

(13) R. G. Powell, D. Weisleder, and C. R. Smith, Jr., *J. Pharm. Sci.*, **61**, 1227 (1972).

(14) I. S. Johnson, J. G. Armstrong, M. Gorman, and J. P. Burnett, *Cancer Res.*, **23**, 1390 (1963).

(15) S. M. Kupchan, Y. Komoda, W. A. Court, G. J. Thomas, R. M. Smith, A. Karim, C. J. Gilmore, R. C. Haltiwanger, and R. F. Bryan, *J. Am. Chem. Soc.*, **94**, 1354 (1972).

(16) W. Loeffler, R. Mauli, M. E. Ruesch, and H. Staehelin, *Chem. Abstr.*, **62**, 5856d (1965).

(17) A. Goldin and R. K. Johnson, *Cancer Chemother. Rep. Pt. 1*, **58**, 63 (1974).

(18) C. L. Stevens, K. G. Taylor, M. E. Munk, W. S. Marshall, K. Noll, G. D. Shah, L. G. Shah, and K. Uzu, *J. Med. Chem.*, **8**, 1 (1964).

(19) H. B. Wood, Jr., "Chemical Structures of Current Interest to the Division of Cancer Treatment—Drugs with Clinical Activity and Some Unique Compounds in Development," Drug Synthesis and Chemistry Branch, National Cancer Institute, Jan. 1977.

(20) K. H. Lee, D. C. Anuforo, E. S. Huang, and C. Piantadosi, *J. Pharm. Sci.*, **61**, 626 (1972).

(21) K. Y. Sim, J. J. Sims, and T. A. Geissman, *J. Org. Chem.*, **33**, 429 (1968).

(22) K. H. Lee, Y. Imakura, and H. C. Huang, *J. Chem. Soc., Chem. Commun.*, **1977**, 69.

(23) K. H. Lee, Y. Imakura, Y. Sumida, R. Y. Wu, I. H. Hall, and H. C. Huang, *J. Org. Chem.*, **44**, 2180 (1979).

(24) S. M. Kupchan, R. W. Britton, J. A. Lacadie, M. F. Ziegler, and C. W. Sigel, *ibid.*, **40**, 648 (1975).

(25) M. Okano and K. H. Lee, *J. Org. Chem.*, in press.

(26) R. I. Geran, N. H. Greenberg, M. M. MacDonald, A. M. Schumacher, and B. J. Abbott, *Cancer Chemother. Rep., Part 3*, **3**, 1 (1972).

(27) E. S. Huang, K. H. Lee, C. Piantadosi, T. A. Geissman, and J. S. Pagano, *J. Pharm. Sci.*, **61**, 1960 (1972).

(28) G. R. Pettit, J. C. Budzinski, G. M. Cragg, P. Brown, and L. D. Johnston, *J. Med. Chem.*, **17**, 1013 (1974).

(29) I. H. Hall, K. H. Lee, S. A. ElGebaly, Y. Imakura, Y. Sumida, and R. Y. Wu, *J. Pharm. Sci.*, **68**, 883 (1979).


## ACKNOWLEDGMENTS


Supported by American Cancer Society Grant CH-19 and National Institutes of Health Grants CA-17625 and CA-22929 awarded to K. H. Lee and I. H. Hall.

The authors thank Larry Carpenter and Jill Maness for technical assistance.

# GLC Analysis of Menthol, Phenol, Benzocaine, and Pyrilamine Maleate in Aerosol Spray Lotion

**FABRIZIO DE FABRIZIO**

Received November 12, 1980, from *Adcock Ingram Laboratories Limited, P.O. Box 2368, Johannesburg 2000, South Africa.* Accepted for publication February 12, 1981. * Present address Atomic Energy Board (Chemical Division), Private Bag X256, Pretoria 0001, South Africa.

**Abstract** □ A GLC method is presented for the quantitative determination of menthol, phenol, benzocaine, and pyrilamine maleate. The propellent was exhausted from a pressurized can, and an aliquot of the alcoholic base was weighed. After the addition of the internal standard diluted with chloroform, 1 μl of the mixture was injected in the chromatograph with a flame-ionization detector and a glass column packed with 2.5% OV-225. Average recoveries were 100.3 ± 1.4, 100.0 ± 1.4, 101.3 ± 1.5, and 101.5 ± 1.5% for menthol, phenol, benzocaine, and pyrilamine maleate, respectively.

**Keyphrases** □ Aerosols—GLC analysis of menthol, phenol, benzocaine, and pyrilamine maleate □ GLC—analysis of menthol, phenol, benzocaine, and pyrilamine maleate in aerosol form □ Sprays—GLC analysis of menthol, phenol, benzocaine, and pyrilamine maleate

Menthol (I), phenol (II), benzocaine (III), and pyrilamine maleate (IV) are found in various preparations, such as creams, lotions, and dusting powders, used for the treatment of allergic conditions and analgesic applications. While analyses have been reported for the quantitation of I–III singly and in combination with other drugs in topical products, no analytical procedure was found for IV in lotion or cream form.

Douglas (1) used GLC to determine I, II, and methyl salicylate in several commercial preparations. Quantitative determinations of III by colorimetric (2), high-performance liquid chromatographic (HPLC) (3), and GLC (4) methods also were reported. Ghanekar and Gupta (5) used HPLC to determine the maleates of IV, chlorpheniramine, brompheniramine, and pheniramine. The method presented here permits the simultaneous determination and identification of the components analyzed with a single injection.

## EXPERIMENTAL

**Materials**—A gas chromatograph[1] with a flame-ionization detector was fitted with a 1.8-m × 3-mm i.d. column packed with 2.5% OV-225 on Chromosorb W, 80–100 mesh. The reagents[2] chloroform, menthol, phenol, and dichloroxylenol[3] were used.

**Solution Preparation**—The stock standard solution was prepared by dissolving, per milliliter of chloroform, 7.9 mg of menthol, 7.9 mg of phenol, 7.8 mg of benzocaine[4], and 10.9 mg of pyrilamine maleate[4]. In 50 ml of chloroform was dissolved 1000 mg of dichloroxylenol, the internal standard solution.

**Standard Preparation**—Stock standard preparation (3 ml) was pipetted into a 50-ml volumetric flask, and 2 ml of the internal standard solution was added and diluted to the mark with chloroform. Then 1 μl was injected into the chromatograph.

**Table I—Standard Preparation**

| Trial | Recovery, % I | II | III | IV |
|---|---|---|---|---|
| 1 | 100.2 | 100.6 | 100.6 | 101.0 |
| 2 | 101.6 | 101.9 | 103.2 | 103.0 |
| 3 | 100.5 | 100.5 | 99.6 | 99.1 |
| 4 | 99.5 | 100.0 | 103.4 | 101.2 |
| 5 | 101.6 | 101.3 | 99.3 | 100.2 |
| 6 | 100.9 | 100.9 | 102.5 | 100.2 |
| 7 | 99.5 | 99.0 | 102.8 | 102.9 |
| 8 | 97.9 | 98.8 | 100.7 | 103.0 |
| 9 | 100.0 | 97.8 | 101.0 | 103.5 |
| 10 | 100.6 | 100.0 | 100.3 | 100.7 |
| Mean | 100.3 | 100.0 | 101.3 | 101.5 |
| *SD* | ±1.1 | ±1.4 | ±1.5 | ±1.5 |

**Sample Preparation**—A pressurized can was cooled in the freezer of an ordinary refrigerator for 1 hr. The can was removed and pierced in the shoulder plate (valve site). The propellent ejection was regulated by holding the piercing device into the perforated hole. When the propellent[5] pressure had ceased, the top of the can was cut, and the alcoholic base[6] was poured into a 250-ml conical flask. The flask was shaken mechanically for 20 min. All operations were carried out under a semiclosed hood. An aliquot of liquid (~2.5 ml) was weighed into a 50-ml volumetric flask, and 2 ml of the internal standard solution was added and diluted to volume with chloroform. Then 1 μl was injected into the chromatograph.

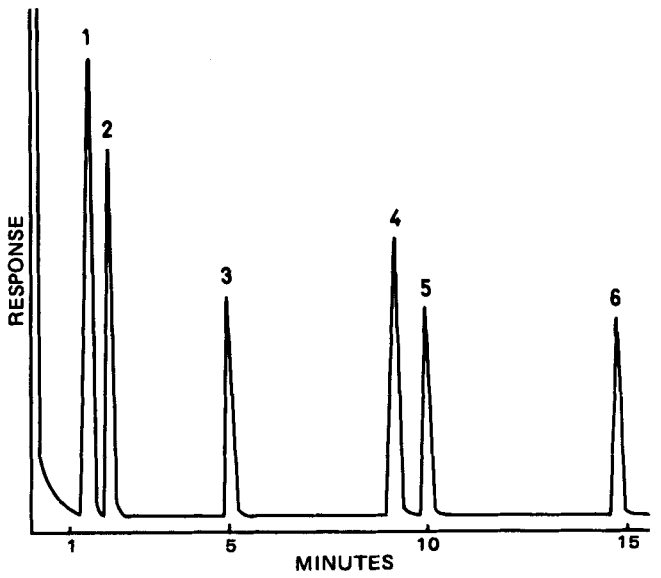


**Figure 1**—*Representative gas chromatogram, Key: 1, menthol; 2, phenol; 3, internal standard; 4, acetylated lanolin alcohol; 5, benzocaine; and 6, pyrilamine maleate.*

[1] Hewlett-Packard 5840-A.
[2] Unless otherwise specified, all reagents were from British Drug Houses.
[3] Pfaltz & Bauer.
[4] USP reference standard.
[5] Dichlorofluoromethane (Arcton 12), Imperial Chemical Industry Ltd.
[6] The preparation, excluding the propellent, contained, per gram, 13.3 mg of I, 13.3 mg of II, 12.5 mg of III, 18.3 mg of IV, ethanol, Myglyol, Crodolan LA, and Cetiol HE.

0022-3549/81/1000-1151$01.00/0
© 1981, American Pharmaceutical Association

**Table II—Response Factors of I–IV with Respect to the Internal Standard [a]**

| Solution, % | Component | Response Factor | *RSD*, % |
|---|---|---|---|
| 80 | I | 2.06 | 0.78 |
| | II | 1.79 | 0.71 |
| | III | 1.40 | 1.11 |
| | IV | 0.99 | 0.64 |
| 100 | I | 2.05 | 1.02 |
| | II | 1.81 | 0.82 |
| | III | 1.41 | 1.00 |
| | IV | 0.99 | 1.74 |
| 120 | I | 2.10 | 0.90 |
| | II | 1.84 | 1.14 |
| | III | 1.43 | 1.68 |
| | IV | 1.04 | 1.43 |

[a] Three solutions were prepared, and 18 measurements were made.

**Table III—Precision Study of a Commercial Preparation**

| Parameter | Compound I | II | III | IV |
|---|---|---|---|---|
| Theoretical content, mg/g | 13.3 | 13.3 | 12.5 | 18.3 |
| $\bar{X}$ ($n$ = 8) | 13.0 | 13.1 | 12.3 | 18.3 |
| *RSD*, % | 0.75 | 0.76 | 1.2 | 1.2 |

## RESULTS AND DISCUSSION

The recovery study was conducted by preparing a standard solution containing the internal standard and all of the ingredients in amounts as found in the commercial product. The solution was determined 10 times. The results (Table I) show that active ingredients can be separated (Fig. 1) and analyzed by direct injection into the chromatograph. Eventual interferences from other ingredients were investigated by preparing a solution that excluded the active components. The chromatogram of this solution showed a peak of one component[7] with a retention time at ~9.15 min, which did not interfere. Peaks of less volatile compounds[8] appeared between 25 and 28 min. Therefore, it was convenient to allow the instrument to run periodically for 30 min during the analysis.

The ratios of the area per weight of substance to the area per weight of internal standard were calculated for the active components over a range of 80–120% of the label claim. Results for three solutions (80, 100, and 120%) are reported in Table II. Several liquid phases were tried to accommodate compounds of different polarity in the same chromatogram. The response factors throughout the concentration range studied attest to the usefulness of OV-225 as the liquid phase.

Since the procedure was planned only to determine the active ingredients contained in the alcoholic base, it appeared preferable to remove first the propellent from the rest of the sample at a temperature (~0°) where the alcoholic vapor tension was considerably reduced. The residual propellent was eliminated by shaking the decanted sample for 20 min. Precision also was examined by analyzing a production lot commercial preparation. Results are reproduced in Table III.

The method presented is reasonably fast, and precision is consistent with accuracy.

## REFERENCES


(1) C. C. Douglas, *J. Assoc. Off. Anal. Chem.*, **55**, 610 (1972).

(2) S. Belal, M. A. El-Sayed, A. El-Nenaey, and S. A. Soliman, *Talanta*, **25**, 290 (1980).

(3) V. D. Gupta and S. Sachanandani, *J. Pharm. Sci.*, **66**, 897 (1977).

(4) F. L. Fricke, *J. Assoc. Off. Anal. Chem.*, **55**, 1162 (1972).

(5) A. G. Ghanekar and V. D. Gupta, *Am. J. Hosp. Pharm.*, **34**, 651 (1977).


[7] Acetylated lanolin alcohol (Crodalan).

[8] Polyol fatty acid esters (Cetiol HE) and triglyceride mixture of saturated fatty acids (Myglyol 812).

# Optical Characterization of a Low Solubility Organic Compound


**H. E. HUBER**



Received April 7, 1980, from *Merrell Research Center, Merrell-National Laboratories, Division of Richardson-Merrell Inc., Cincinnati, OH 45215.* Accepted for publication March 5, 1981.



**Abstract** □ The X, Y, and Z principal vibration directions along with the principal refractive indexes, optic angle, optical sign, birefringence, optical orientation, and crystal system for the low solubility compound 5-(tetradecyloxy)-2-furancarboxylic acid were determined with a polarizing microscope and spindle stage. The X and Z principal vibration directions are not coincident with the $a$ and $c$ crystallographic axes; however, the Y direction is considered to be coincident with the $b$ axis. Therefore, the crystal is assigned to the monoclinic crystal system. The bladed/lath-shaped crystals rest on one of the two large orthopinacoid (100) faces and present the microscopist with a single plane of optical symmetry. A $\beta$ refractive index of 1.555 is observed with the crystal axis of elongation parallel to the polarizer, and a $\gamma'$ of ~1.600–1.660 is observed in the contiguous extinction position. Determination of the optic angle, principal vibration directions, and principal refractive indexes was facilitated by mounting the crystals on a spindle stage for rotation about the $b$ crystallographic axis (optic normal).



**Keyphrases** □ 5-(Tetradecyloxy)-2-furancarboxylic acid—optical characterization using a polarizing microscope and spindle stage □ Optical characterization—low solubility compound, 5-(tetradecyloxy)-2-furancarboxylic acid □ Crystallography—optical characterization of a low solubility organic compound, 5-(tetradecyloxy)-2-furancarboxylic acid


Control of dosage formulation in the clinic by conventional aqueous dissolution methods was not possible with 5-(tetradecyloxy)-2-furancarboxylic acid[1] (I) because of its poor solubility in alcohol and/or water. A high concentration of surfactant and water was eventually utilized for the solvent, but other controls were necessary to ensure that changes in the crystalline structure between lots did not occur. Long-chain fatty acid compounds such as this one are well known for their polymorphic character (1).

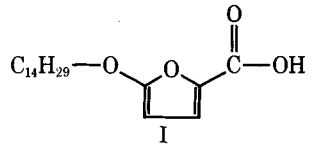


I

[1] RMI 14,514, Merrell Research Center.




*0022-3549/81/1000-1152$01.00/0*



© *1981, American Pharmaceutical Association*

**Table II—Response Factors of I–IV with Respect to the Internal Standard [a]**

| Solution, % | Component | Response Factor | *RSD*, % |
|---|---|---|---|
| 80 | I | 2.06 | 0.78 |
| | II | 1.79 | 0.71 |
| | III | 1.40 | 1.11 |
| | IV | 0.99 | 0.64 |
| 100 | I | 2.05 | 1.02 |
| | II | 1.81 | 0.82 |
| | III | 1.41 | 1.00 |
| | IV | 0.99 | 1.74 |
| 120 | I | 2.10 | 0.90 |
| | II | 1.84 | 1.14 |
| | III | 1.43 | 1.68 |
| | IV | 1.04 | 1.43 |

[a] Three solutions were prepared, and 18 measurements were made.

**Table III—Precision Study of a Commercial Preparation**

| Parameter | Compound I | II | III | IV |
|---|---|---|---|---|
| Theoretical content, mg/g | 13.3 | 13.3 | 12.5 | 18.3 |
| $\bar{X}$ ($n$ = 8) | 13.0 | 13.1 | 12.3 | 18.3 |
| *RSD*, % | 0.75 | 0.76 | 1.2 | 1.2 |

## RESULTS AND DISCUSSION

The recovery study was conducted by preparing a standard solution containing the internal standard and all of the ingredients in amounts as found in the commercial product. The solution was determined 10 times. The results (Table I) show that active ingredients can be separated (Fig. 1) and analyzed by direct injection into the chromatograph. Eventual interferences from other ingredients were investigated by preparing a solution that excluded the active components. The chromatogram of this solution showed a peak of one component[7] with a retention time at ~9.15 min, which did not interfere. Peaks of less volatile compounds[8] appeared between 25 and 28 min. Therefore, it was convenient to allow the instrument to run periodically for 30 min during the analysis.

The ratios of the area per weight of substance to the area per weight of internal standard were calculated for the active components over a range of 80–120% of the label claim. Results for three solutions (80, 100, and 120%) are reported in Table II. Several liquid phases were tried to accommodate compounds of different polarity in the same chromatogram. The response factors throughout the concentration range studied attest to the usefulness of OV-225 as the liquid phase.

Since the procedure was planned only to determine the active ingredients contained in the alcoholic base, it appeared preferable to remove first the propellent from the rest of the sample at a temperature (~0°) where the alcoholic vapor tension was considerably reduced. The residual propellent was eliminated by shaking the decanted sample for 20 min. Precision also was examined by analyzing a production lot commercial preparation. Results are reproduced in Table III.

The method presented is reasonably fast, and precision is consistent with accuracy.

## REFERENCES


(1) C. C. Douglas, *J. Assoc. Off. Anal. Chem.*, **55**, 610 (1972).

(2) S. Belal, M. A. El-Sayed, A. El-Nenaey, and S. A. Soliman, *Talanta*, **25**, 290 (1980).

(3) V. D. Gupta and S. Sachanandani, *J. Pharm. Sci.*, **66**, 897 (1977).

(4) F. L. Fricke, *J. Assoc. Off. Anal. Chem.*, **55**, 1162 (1972).

(5) A. G. Ghanekar and V. D. Gupta, *Am. J. Hosp. Pharm.*, **34**, 651 (1977).


[7] Acetylated lanolin alcohol (Crodalan).

[8] Polyol fatty acid esters (Cetiol HE) and triglyceride mixture of saturated fatty acids (Myglyol 812).

# Optical Characterization of a Low Solubility Organic Compound


**H. E. HUBER**



Received April 7, 1980, from *Merrell Research Center, Merrell-National Laboratories, Division of Richardson-Merrell Inc., Cincinnati, OH 45215.* Accepted for publication March 5, 1981.



**Abstract** □ The X, Y, and Z principal vibration directions along with the principal refractive indexes, optic angle, optical sign, birefringence, optical orientation, and crystal system for the low solubility compound 5-(tetradecyloxy)-2-furancarboxylic acid were determined with a polarizing microscope and spindle stage. The X and Z principal vibration directions are not coincident with the $a$ and $c$ crystallographic axes; however, the Y direction is considered to be coincident with the $b$ axis. Therefore, the crystal is assigned to the monoclinic crystal system. The bladed/lath-shaped crystals rest on one of the two large orthopinacoid (100) faces and present the microscopist with a single plane of optical symmetry. A $\beta$ refractive index of 1.555 is observed with the crystal axis of elongation parallel to the polarizer, and a $\gamma'$ of ~1.600–1.660 is observed in the contiguous extinction position. Determination of the optic angle, principal vibration directions, and principal refractive indexes was facilitated by mounting the crystals on a spindle stage for rotation about the $b$ crystallographic axis (optic normal).



**Keyphrases** □ 5-(Tetradecyloxy)-2-furancarboxylic acid—optical characterization using a polarizing microscope and spindle stage □ Optical characterization—low solubility compound, 5-(tetradecyloxy)-2-furancarboxylic acid □ Crystallography—optical characterization of a low solubility organic compound, 5-(tetradecyloxy)-2-furancarboxylic acid


Control of dosage formulation in the clinic by conventional aqueous dissolution methods was not possible with 5-(tetradecyloxy)-2-furancarboxylic acid[1] (I) because of its poor solubility in alcohol and/or water. A high concentration of surfactant and water was eventually utilized for the solvent, but other controls were necessary to ensure that changes in the crystalline structure between lots did not occur. Long-chain fatty acid compounds such as this one are well known for their polymorphic character (1).

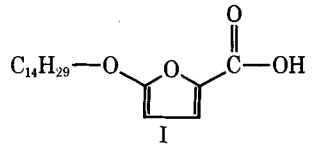


I

[1] RMI 14,514, Merrell Research Center.




*0022-3549/81/1000-1152$01.00/0*



© *1981, American Pharmaceutical Association*

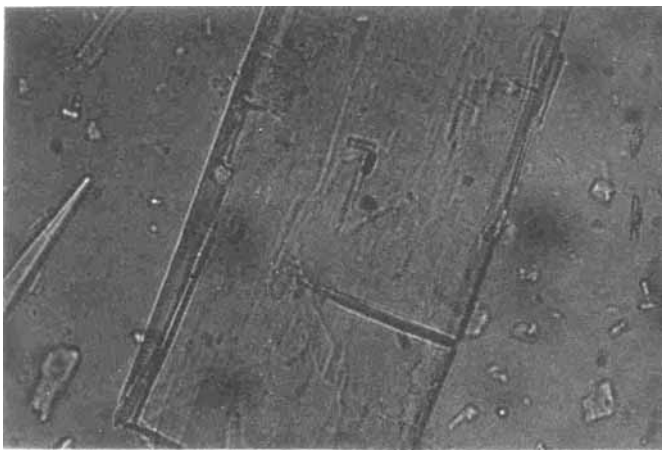


**Figure 1**—*Photomicrograph of I crystals obtained with the tungsten filament lamp at 4 amp and 0.25-sec exposure time. No filters were used. Crystals were mounted in 1.460 Cargille fluid, A 1/5 series.*

## BACKGROUND

Some investigators (2–4) attempted to control this variable with differential scanning calorimetry or related thermal methods, and others utilized X-ray diffraction. In a few isolated reports (5–7), a combination of these methods, along with optical crystallographic characterizations, was used.

Once the crystal is characterized, optical methods offer many advantages for routine identification of other lots. Optical values are quite specific for a substance, and most microscopic examinations can be performed with a minimum of time and effort. The number of discriminating optical parameters that can be used is usually numerous; consequently, one or more can be selected as conditions or limitations dictate.

An optical characterization of I is presented here and was utilized along with surface area measurements to control potential crystal changes. An X-ray diffraction profile was determined as part of the total crystal characterization; however, only optical methods are utilized for routine examination.

Geologists and chemists have long relied on optical methods for ready identification and, in some cases, composition determinations of unknown mineral or chemical samples. Each substance has a unique atomic arrangement and, therefore, unique optical properties. Optical determinative data for organic compounds are limited compared to those for inorganic materials; however, the data available indicate that the same specificity applies.

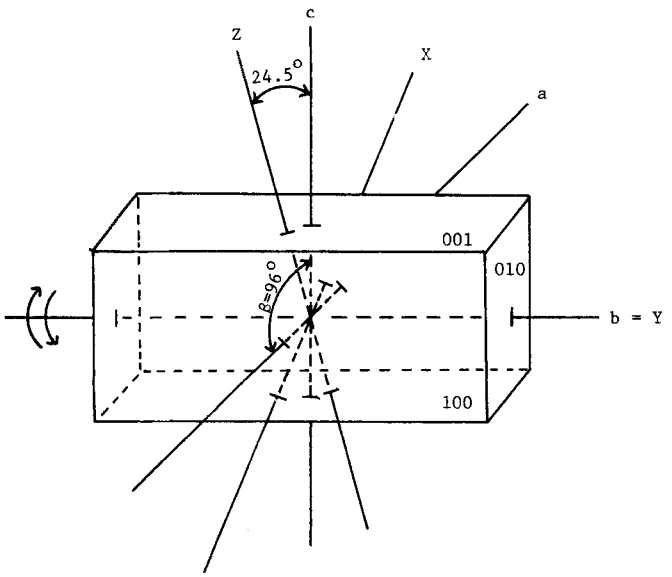


**Figure 2**—*Optical orientation of I in relation to its crystallographic axes.*

**Table I—Optical Properties Obtained for I**

| Parameter | Value |
|---|---|
| Refractive indexes (5893A – D line 25°) | |
| $\alpha$ | 1.470 ± 0.002 |
| $\beta$ | 1.555 ± 0.002 |
| $\gamma$ | 1.670 ± 0.002 |
| Birefringence | 0.200 |
| Optic axial angle (5893A – D line 25°) | $2V = 81° \pm 2.0$ |
| Optical axial plane | 010 |
| Sign of double refraction | Positive |
| Extinction | Parallel |
| Crystal system | Monoclinic |
| Elongation sign | ± |

Microscopic slide mounts of unmilled I exhibited 100–500-μm lath-shaped crystals (Fig. 1) that appeared suitable for the study. By utilizing polarizing microscopic procedures, optical crystallographic characterization of I was successfully performed.

## EXPERIMENTAL

Compound I was obtained by crystallization from methyl ethyl ketone. One lot of crystals was used for the crystal characterization study, and other lots were examined to verify that the optical data were consistent.

**Equipment**—A trinocular widefield microscope[2] was fitted with a polarizing substage condenser, an analyzer in the body tube, strain free 0.40 and 0.65 N.A. objectives, and a 12-v, 60-w tungsten filament lamp. A regulating transformer permitted the load to be varied up to a maximum of 6 amp. Photomicrographs were obtained with a 35-mm camera[2] mounted on the vertical ocular. Film[3] was 35-mm black and white with an ASA of 125. A second monocular, polarizing microscope[2] with an adjustable Bertrand lens and iris in the body tube, strain-free objectives up to 0.85 N.A., and a tungsten filament lamp with heat filters also was used.

The stage was a simple, inexpensive device described previously (8) in which a crystal is attached to a spindle and rotated about a single axis perpendicular to the microscope axis.

**Microscopic Examination**—An amount of powder adhering to the point of a dissecting needle was tapped onto the surface of a microscope slide, and the index of refraction fluid was applied with a glass applicator. The powder was mixed with fluid, and a cover slip was added. The slide was then examined with a polarized light microscope using orthoscopic and conoscopic optic conditions. (For an extensive and detailed description of microscopic procedures for optical crystallographic studies, see Refs. 9–11 or any of the numerous publications available on the

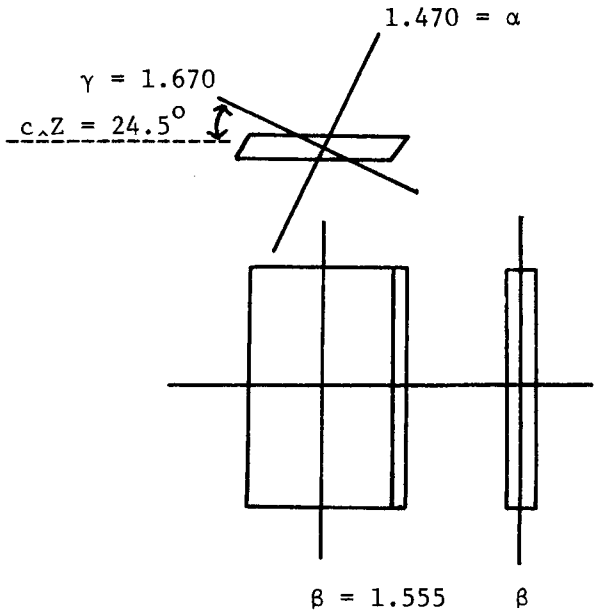


**Figure 3**—*Orthographic projection of typical crystal of I.*

[2] Leitz.
[3] Kodak PX135.

subject.) Spindle stage examination of crystals followed that described previously (8, 11).

## RESULTS AND DISCUSSION

Preliminary orthoscopic examination revealed that the lath-shaped crystals (Fig. 1) exhibited a single plane of optical symmetry from which a single $\beta$ refractive index value could be obtained. The crystals were quite thin, and most grains lay on the 100 orthopinacoid.

To obtain $\beta$ and $\gamma$ refractive index values, the crystals were mounted (Fig. 2) onto a spindle stage. The crystals were rotated on their $b$-axis to orientations that presented the principal vibration directions, and refractive index values were determined by immersion in various fluids.

Crystals could not be oriented to provide a 010 end view, and therefore, a $\beta$-angle could not be observed or measured microscopically. Subsequent data reported from X-ray diffraction methods gave a value of 96°. An orthographic projection of a typical crystal of I is shown in Fig. 3, and Table I presents the optical properties.

## REFERENCES


(1) A. N. Martin, "Physical Pharmacy," 2nd ed., Lea & Febiger, Philadelphia, Pa., 1973, p. 82.

(2) J. Haleblian and W. McCrone, *J. Pharm. Sci.*, **58**, 911 (1969).

(3) Y. Matsuda, S. Kawaguchi, H. Kobayashi, and J. Nishijo, *J. Pharm. Pharmacol.*, **32**, 579 (1980).

(4) E. Nuernberg and A. Werthmann, *Pharm. Ind.*, **40**, 1061 (1978).

(5) H. A. Rose, *Anal. Chem.*, **27**, 1841 (1955).

(6) W. C. McCrone, *ibid.*, 26, 1662 (1954).

(7) J. Donnay and H. Ondik, "Crystal Data Determinative Tables, Vols. I & III," 3rd ed., U.S. Department of Commerce, National Bureau of Standards and the Joint Committee on Powder Diffraction Standards, Washington, D.C., 1972 (vol. I), 1978 (vol. III).

(8) R. E. Wilcox, *Am. Mineral.*, **44**, 1272 (1959).

(9) F. D. Bloss, "An Introduction to the Methods of Optical Crystallography," Holt, Rinehart and Winston, New York, N.Y., 1961.

(10) T. R. P. Gibb, Jr., "Optical Methods of Chemical Analysis," 1st ed., McGraw-Hill, New York, N.Y., 1942.

(11) E. E. Wahlstrom, "Optical Crystallography," 5th ed., Wiley, New York, N.Y.


## ACKNOWLEDGMENTS


The author is grateful for the assistance and facilities provided by Dr. Harvey Sunderman, Department of Geology, University of Cincinnati, Cincinnati, Ohio, and for the X-ray diffraction data obtained by Dr. Ralph J. Hinch, Jr., Walter McCrone Associates, Chicago, Ill.


# Synthesis of Dehydroepiandrosterone Sulfatide and 16$\alpha$-Halogenated Steroids


**MAGID ABOU-GHARBIA, LAURA PASHKO, ARTHUR SCHWARTZ, and DANIEL SWERN** ˣ



Received December 8, 1980, from the *Fels Research Institute and Department of Chemistry, Temple University, Philadelphia, PA 19122.* Accepted for publication March 5, 1981.



**Abstract** □ Dehydroepiandrosterone sulfatide was prepared in a 68% yield by the reaction of 5-androstene-3$\beta$-ol-17-one 3-sulfate (silver salt) with dipalmitoyl $\alpha$-iodopropylene glycol. The sulfatide was found to be a more potent inhibitor of human glucose-6-phosphate dehydrogenase than dehydroepiandrosterone. 16$\alpha$-Halogenated steroids also were prepared by direct halogenation of the steroid or indirect halogenation of an appropriate steroidal intermediate. Among various halogenated steroids, 16$\alpha$-bromoepiandrosterone was ~50 times as potent as dehydroepiandrosterone as an inhibitor of glucose-6-phosphate dehydrogenase.



**Keyphrases** □ Dehydroepiandrosterone sulfatide—synthesis, tested as glucose-6-phosphate dehydrogenase inhibitor □ 16$\alpha$-Halogenated derivatives of epiandrosterone—synthesis, tested as glucose-6-phosphate dehydrogenase inhibitors □ Glucose-6-phosphate dehydrogenase—synthesis of dehydroepiandrosterone sulfatide and 16$\alpha$-halogenated steroids


Of the naturally occurring steroids that had been tested, dehydroepiandrosterone (I) proved to be an outstanding noncompetitive inhibitor of glucose-6-phosphate dehydrogenase (1, 2). The sulfated form of I (I$a$) is a major adrenal secretory product in humans. Approximately 99% of the plasma form of this steroid is sulfated, while the remainder is unconjugated steroid. The plasma concentration of the sulfated form of I exceeds that of any other steroidal hormone, yet its biological role is unknown. (Most investigators refer to the conjugated form as the sulfate.)

According to Oertel and coworkers (3, 4), the sulfated form of the hormone found in human plasma is I-sulfatide (II), the ester of sulfatidic acid, which must be isolated under extremely mild conditions because of its lability. In

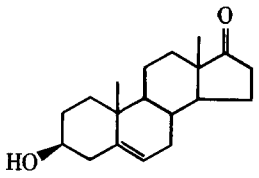


I

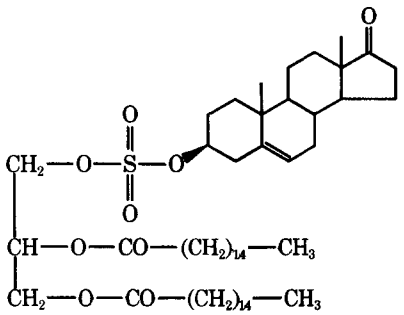


II

the search for analogs of considerably higher potency than I or II in inhibiting glucose-6-phosphate dehydrogenase to diminish or eliminate undesirable side effects of high dosage dehydroepiandrosterone therapy, the sulfatide (II) and 16$\alpha$-halogenated derivatives of epiandrosterone were synthesized.

## RESULTS AND DISCUSSION

Dipalmitoyl-L-$\alpha$-iodopropylene glycol (III) was prepared in an 80% yield by facile acylation of L-$\alpha$-iodopropylene glycol with two equivalents




*0022-3549/81/1000-1154$01.00/0*


*© 1981, American Pharmaceutical Association*

subject.) Spindle stage examination of crystals followed that described previously (8, 11).

## RESULTS AND DISCUSSION

Preliminary orthoscopic examination revealed that the lath-shaped crystals (Fig. 1) exhibited a single plane of optical symmetry from which a single $\beta$ refractive index value could be obtained. The crystals were quite thin, and most grains lay on the 100 orthopinacoid.

To obtain $\beta$ and $\gamma$ refractive index values, the crystals were mounted (Fig. 2) onto a spindle stage. The crystals were rotated on their $b$-axis to orientations that presented the principal vibration directions, and refractive index values were determined by immersion in various fluids.

Crystals could not be oriented to provide a 010 end view, and therefore, a $\beta$-angle could not be observed or measured microscopically. Subsequent data reported from X-ray diffraction methods gave a value of 96°. An orthographic projection of a typical crystal of I is shown in Fig. 3, and Table I presents the optical properties.

## REFERENCES


(1) A. N. Martin, "Physical Pharmacy," 2nd ed., Lea & Febiger, Philadelphia, Pa., 1973, p. 82.

(2) J. Haleblian and W. McCrone, *J. Pharm. Sci.*, **58**, 911 (1969).

(3) Y. Matsuda, S. Kawaguchi, H. Kobayashi, and J. Nishijo, *J. Pharm. Pharmacol.*, **32**, 579 (1980).

(4) E. Nuernberg and A. Werthmann, *Pharm. Ind.*, **40**, 1061 (1978).

(5) H. A. Rose, *Anal. Chem.*, **27**, 1841 (1955).

(6) W. C. McCrone, *ibid.*, 26, 1662 (1954).

(7) J. Donnay and H. Ondik, "Crystal Data Determinative Tables, Vols. I & III," 3rd ed., U.S. Department of Commerce, National Bureau of Standards and the Joint Committee on Powder Diffraction Standards, Washington, D.C., 1972 (vol. I), 1978 (vol. III).

(8) R. E. Wilcox, *Am. Mineral.*, **44**, 1272 (1959).

(9) F. D. Bloss, "An Introduction to the Methods of Optical Crystallography," Holt, Rinehart and Winston, New York, N.Y., 1961.

(10) T. R. P. Gibb, Jr., "Optical Methods of Chemical Analysis," 1st ed., McGraw-Hill, New York, N.Y., 1942.

(11) E. E. Wahlstrom, "Optical Crystallography," 5th ed., Wiley, New York, N.Y.


## ACKNOWLEDGMENTS


The author is grateful for the assistance and facilities provided by Dr. Harvey Sunderman, Department of Geology, University of Cincinnati, Cincinnati, Ohio, and for the X-ray diffraction data obtained by Dr. Ralph J. Hinch, Jr., Walter McCrone Associates, Chicago, Ill.


# Synthesis of Dehydroepiandrosterone Sulfatide and 16$\alpha$-Halogenated Steroids


**MAGID ABOU-GHARBIA, LAURA PASHKO, ARTHUR SCHWARTZ, and DANIEL SWERN** ˣ



Received December 8, 1980, from the *Fels Research Institute and Department of Chemistry, Temple University, Philadelphia, PA 19122.* Accepted for publication March 5, 1981.



**Abstract** □ Dehydroepiandrosterone sulfatide was prepared in a 68% yield by the reaction of 5-androstene-3$\beta$-ol-17-one 3-sulfate (silver salt) with dipalmitoyl $\alpha$-iodopropylene glycol. The sulfatide was found to be a more potent inhibitor of human glucose-6-phosphate dehydrogenase than dehydroepiandrosterone. 16$\alpha$-Halogenated steroids also were prepared by direct halogenation of the steroid or indirect halogenation of an appropriate steroidal intermediate. Among various halogenated steroids, 16$\alpha$-bromoepiandrosterone was ~50 times as potent as dehydroepiandrosterone as an inhibitor of glucose-6-phosphate dehydrogenase.



**Keyphrases** □ Dehydroepiandrosterone sulfatide—synthesis, tested as glucose-6-phosphate dehydrogenase inhibitor □ 16$\alpha$-Halogenated derivatives of epiandrosterone—synthesis, tested as glucose-6-phosphate dehydrogenase inhibitors □ Glucose-6-phosphate dehydrogenase—synthesis of dehydroepiandrosterone sulfatide and 16$\alpha$-halogenated steroids


Of the naturally occurring steroids that had been tested, dehydroepiandrosterone (I) proved to be an outstanding noncompetitive inhibitor of glucose-6-phosphate dehydrogenase (1, 2). The sulfated form of I (I$a$) is a major adrenal secretory product in humans. Approximately 99% of the plasma form of this steroid is sulfated, while the remainder is unconjugated steroid. The plasma concentration of the sulfated form of I exceeds that of any other steroidal hormone, yet its biological role is unknown. (Most investigators refer to the conjugated form as the sulfate.)

According to Oertel and coworkers (3, 4), the sulfated form of the hormone found in human plasma is I-sulfatide (II), the ester of sulfatidic acid, which must be isolated under extremely mild conditions because of its lability. In

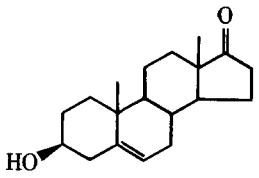


I

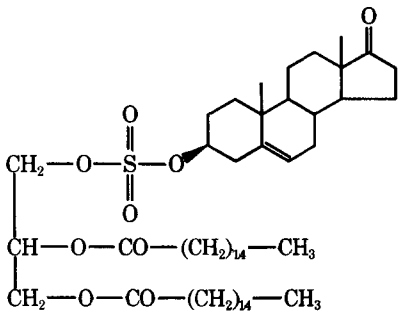


II

the search for analogs of considerably higher potency than I or II in inhibiting glucose-6-phosphate dehydrogenase to diminish or eliminate undesirable side effects of high dosage dehydroepiandrosterone therapy, the sulfatide (II) and 16$\alpha$-halogenated derivatives of epiandrosterone were synthesized.

## RESULTS AND DISCUSSION

Dipalmitoyl-L-$\alpha$-iodopropylene glycol (III) was prepared in an 80% yield by facile acylation of L-$\alpha$-iodopropylene glycol with two equivalents




*0022-3549/81/1000-1154$01.00/0*


*© 1981, American Pharmaceutical Association*

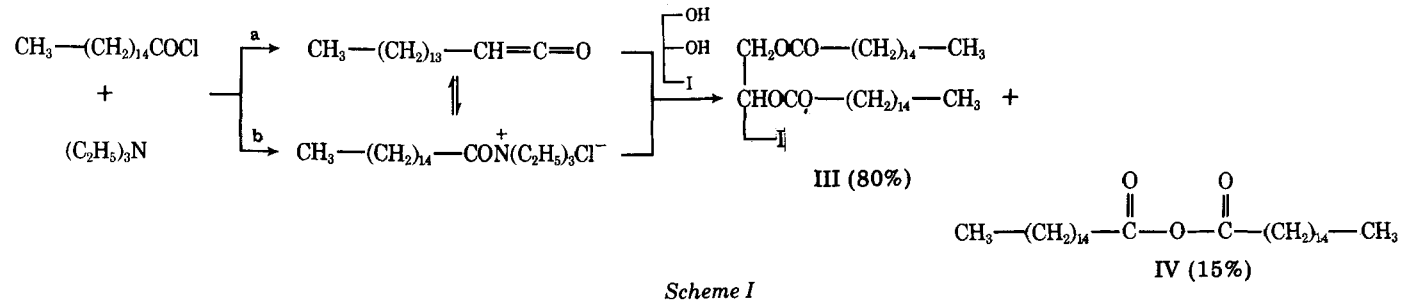


*Scheme I*

of palmitoyl chloride in the presence of triethylamine (Scheme I). Reaction of carboxylic acid halides in the presence of triethylamine has been found (5, 6) to involve two pathways, an elimination pathway (a) involving a ketene intermediate and a substitution route (b) involving an acyl ammonium salt intermediate. The product palmitic anhydride (IV) also was isolated in a 15% yield. When quinoline was used instead of triethylamine, as suggested in the literature (7), only 67% of the diglyceride, in addition to 25% of palmitic acid, was formed after a reaction time of 7 days.

Dehydroepiandrosterone sulfatide (II) was then prepared in a 68% yield by alkylation of the sulfate (silver salt) (I*b*) with the iododiglyceride (III) in dry benzene (Scheme II). The sulfatide (II) was found to be a more potent inhibitor of human glucose-6-phosphate dehydrogenase than I*a* itself. It is a labile material and decomposes readily within a few days, even at −5°, to the sulfate with loss of biological activity.

The fact that $\alpha$-substitution at the C-16-position enhances biological activity of certain steroids, coupled with the intention to find more potent and stable compounds, led to the preparation of 16$\alpha$-halo derivatives of epiandrosterone (8–10). 16$\alpha$-Chloro, bromo, and fluoro derivatives were prepared from epiandrosterone according to reaction sequence shown in Scheme III.

Treatment of epiandrosterone with isoamyl nitrite in basic medium afforded 16-oximino-17-ketone (V). The observed melting point, 218–219°, does not agree with the value of 245–247° reported by Mateos *et al.* (11) but is in agreement with that reported earlier by Huffman and Lott (12). IR spectra and elemental analyses of V were consistent with the structure shown.

Treatment of V with sodium hydroxide, ammonia, and sodium hypochlorite (11, 13–15) yielded the yellow 16-diazo compound (VI), which, upon treatment with the appropriate hydrogen halide (hydrochloric, hydrobromic, and hydrofluoric acids) afforded the corresponding colorless 16$\alpha$-halo derivative. Hydriodic acid, however, reduced the diazo compound to epiandrosterone. The 16$\alpha$-configuration was established by comparing the melting points of the products with those reported in the literature (16–20) and by independent synthesis.

The 16$\alpha$-fluoro derivative was also prepared (but in only a 28% yield) by a halogen-exchange technique by refluxing the corresponding bromo derivative (VII*a*) with five equivalents of anhydrous silver fluoride in toluene–isopropanol for 48 hr. The 16$\alpha$-bromo derivative (VII*a*) was independently prepared in a 60% yield by refluxing epiandrosterone with cupric bromide in methanol for 24 hr (17).

The 16$\alpha$-iodo derivative (VII*d*) was prepared by direct iodination of the enol diacetate (VIII) with iodine in the presence of mercuric acetate or with *N*-iodosuccinimide, followed by hydrolysis of the 3$\beta$-acetoxy derivative (IX) with concentrated hydrochloric acid (Scheme IV). Overall yields of VIII to VII*d* were 89%.

16$\alpha$-Iodo steroids were first synthesized in 1973 *via* the 17-bromo-16,17-epoxy derivative or by a halogen-exchange procedure (16). The current procedure is more convenient since the starting materials are commercially available and yields are higher.

Contrary to expectation, VII*a* was the most active halogenated derivative of the four; it is ~50 times as active as dehydroepiandrosterone in inhibiting glucose-6-phosphate dehydrogenase in mouse and human red blood cells. Compound VII*a* is also ~50 times as active in antagonizing the *O*-tetradecanoylphorbol acetate-induced stimulation in the rate of DNA synthesis in mouse skin. A dose of 0.4 mg/kg ip of VII*a* is about as active as 20 mg of dehydroepiandrosterone/kg.

Compounds VII*b* and VII*d* were less active than VII*a*; VII*c* was inactive.

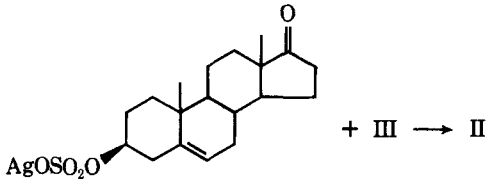


Ib

*Scheme II*

## EXPERIMENTAL[1]

**Dipalmitoyl-L-$\alpha$-iodopropylene Glycol (III)**—All apparatus was flame dried; strictly dry conditions were used throughout the study. To a stirred solution of dry, redistilled triethylamine (3.64 ml, 26 mmoles) and L-$\alpha$-iodopropylene glycol (2.7 g, 13.5 mmoles) in dry chloroform (15 ml) at 0°, a solution of palmitoyl chloride (7.42 g, 26 mmoles) in *n*-pentane (50 ml) was added dropwise. The reaction mixture was then stirred for 3 hr at 0°, and the precipitated triethylamine hydrochloride was removed by filtration. The solvent was evaporated from the filtrate under reduced pressure, and the residual solid was digested with hot absolute methanol. The insoluble material was filtered and recrystallized from acetone to afford 1.92 g (15% yield) of the by-product palmitic anhydride (IV), mp 61–63°; IR (KBr): $\nu_{max}$ 1745 and 1800 cm$^{-1}$ [–C(=O)–O–(C=O)–].

The hot methanol filtrate was cooled, and the solid that precipitated was separated by filtration and recrystallized from petroleum ether (bp 30–60°)–methanol (1:1) to afford 7.4 g (80% yield) of the diglyceride (III), mp 46–48°; IR (KBr): $\nu_{max}$ 1730 and 1745 cm$^{-1}$ [–O–C(=O)–]; $^1$H-NMR ($CDCl_3$): $\delta$ 0.65–1.10 (t, 6H), 1.1–2.00 (m, 52H), 2.20–2.45 (m, 4H), 3.30 (d, 2H), 4.2–4.35 (d, 2H), and 4.9–5.2 (q, 1H).

*Anal.*—Calc. for $C_{35}H_{67}IO_4$: C, 61.92; H, 9.94; I, 18.69. Found: C, 61.96; H, 10.04; I, 18.58.

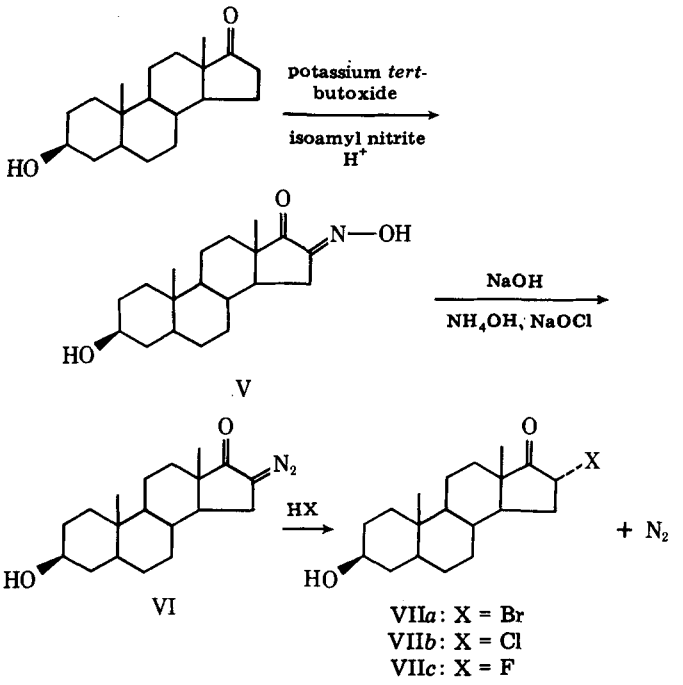


*Scheme III*

[1] Melting points were determined on a Thomas-Hoover Unimelt apparatus and are uncorrected. IR spectra were recorded on a Unicam SP-1000 spectrophotometer. The $^1$H-NMR spectra were determined using an XL-100 instrument and tetramethylsilane as the internal standard. Elemental analyses were performed by Galbraith Laboratories, Knoxville, Tenn.

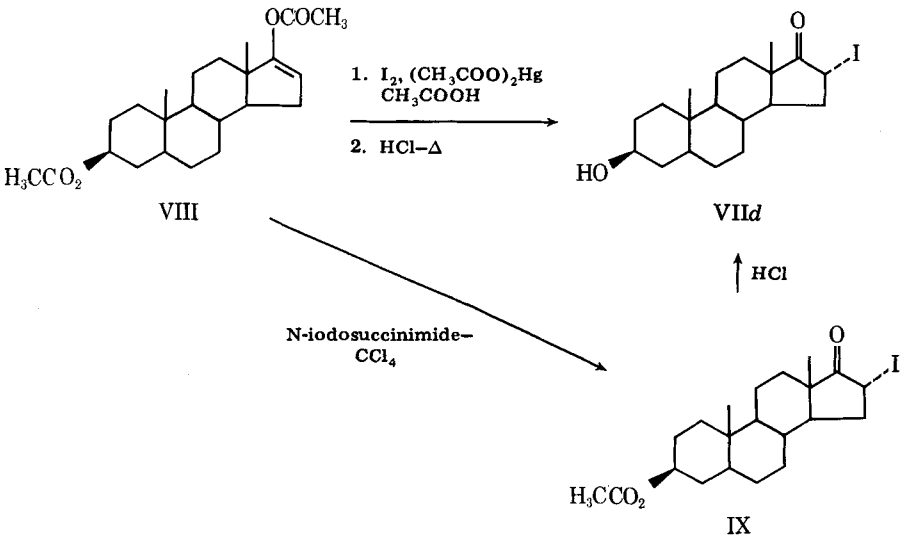


*Scheme IV*

Replacement of triethylamine by quinoline was unsatisfactory; the yield of III was only 67% after 7 days of reaction time. Palmitic acid was obtained in a 25% yield; it was separated as its sodium salt by neutralization with sodium carbonate solution. The acid was regenerated by acidification with 6 *N* HCl, mp 58–60°; IR (KBr): $\nu_{max}$ 1700 $cm^{-1}$ [–C(=O)–OH].

**Dehydroepiandrosterone Sulfatide (II)**—A mixture of the diglyceride III (0.37 g, 0.54 mole) and dehydroepiandrosterone sulfate silver salt (0.28 g, 0.860 mmole) (*Ib*) was refluxed in dry benzene (15 ml) for 2 hr. Silver iodide was separated by filtration while hot and washed with dry benzene (10 ml), and the combined benzene filtrates were evaporated to dryness under reduced pressure. The residual yellow solid was washed with cold petroleum ether and dried, mp 66–68°, yield 68%; IR (KBr): $\nu_{max}$ 1730 and 1745 $cm^{-1}$ {[–O–C(=O)–] and cyclic O=C–}; $^1$H-NMR ($CDCl_3$): absence of signal at $\delta$ 3.3 for III and appearance of signal at $\delta$ 4.45 (m, 1H, vinylic).

*Anal.*—Calc. for $C_{54}H_{90}O_9S$: C, 70.85; H, 9.90. Found: C, 70.81; H, 9.43.

**Androstan-3β-ol-16-oximino-17-one (V)**—To a fresh solution of potassium *tert*-butoxide, prepared from potassium (3.8 g, 100 mmoles) and anhydrous *tert*-butyl alcohol (120 ml), epiandrosterone (3.6 g, 12.4 mmoles) was added with vigorous stirring. The mixture was refluxed under nitrogen until a clear yellow solution was obtained and then cooled, and isoamyl nitrite (6.3 ml) was added over 2 hr. The reaction mixture was poured into water (1 liter), acidified with 6 *N* HCl, and then stored at 5° overnight. The separated crude ketooxime (V) was filtered, washed with water, and recrystallized from methanol to afford 3.0 g (68% yield) of V, mp 218–219° [lit. (11) mp 245–247° and (12) mp 218–219°]; IR (KBr): $\nu_{max}$ 1630 (C=N), 1740 (C=O), 3200 (N–OH), and 3400 (OH) $cm^{-1}$.

*Anal.*—Calc. for $C_{19}H_{29}NO_3$: C, 71.43; H, 9.15; N, 4.38. Found: C, 71.18; H, 9.32; N, 4.30.

**5α-Androstan-3β-hydroxy-16α-bromo-17-one (VII*a*)**—Compound VII*a* was prepared in a 60% yield by bromination of epiandrosterone with cupric bromide and in a 72% yield from the diazoketone (VII) following reported procedures (11), mp 158–160° [lit. (11) mp 164–165°]; IR (KBr): $\nu_{max}$ 1740 (C=O) and 3400 (OH) $cm^{-1}$.

*Anal.*—Calc. for $C_{19}H_{29}BrO_2$: C, 61.78; H, 7.79; Br, 21.69. Found: C, 61.60; H, 8.01; Br, 21.87.

**5α-Androstan-3β-hydroxy-16α-chloro-17-one (VII*b*)**—Compound VII*b* was prepared in a 70% yield from the diazoketone (VI) following a reported procedure, mp 178–180° [lit. (11) mp 170–171°]; IR (KBr): $\nu_{max}$ 1750 (C=O) and 3450 (OH) $cm^{-1}$.

**5α-Androstan-3β-hydroxy-16α-fluoro-17-one (VII*c*)**—Compound VII*c* was prepared in a 20% yield from the diazoketone (VI) and pyridine–hydrofluoric acid and in a 28% yield by refluxing VII*d* with five equivalents of anhydrous silver fluoride in toluene–isopropanol (3:1) for 48 hr, mp 177–179°; IR (KBr): $\nu_{max}$ 1760 (C=O) and 3400 (OH) $cm^{-1}$; mass spectra: *m/z* 308 ($M^+$, *m/z* calc. 308).

*Anal.*—Calc. for $C_{19}H_{29}FO_2$: F, 6.15. Found: F, 5.87.

**5α-Androstan-3β-hydroxy-16α-iodo-17-one (VII*d*)**—*Method A* (21)—To a stirred solution of the enol diacetate (VIII) (20) (496 mg, 1.3 mmoles) in acetic acid (18 ml) containing mercuric acetate (10 mg), iodine (580 mg) dissolved in acetic acid (20 ml) was added over 2 hr. Stirring was continued for an additional hour, and the mixture was then poured into cold water (50 ml) and extracted with chloroform. The extract was washed successively with aqueous potassium iodide, sodium bicarbonate, and water. Evaporation of the chloroform afforded 481 mg (89% yield) of VII*d*, mp 170–172° [lit. (16) mp 173–175°]; IR (KBr): $\nu_{max}$ 1730 (C=O) and 3450 (OH) $cm^{-1}$.

*Anal.*—Calc. for $C_{19}H_{29}IO_2$: C, 54.80; H, 7.02; I, 30.48. Found: C, 55.17; H, 7.00; I, 30.77.

*Method B*—*N*-Iodosuccinimide (0.2 g, 0.88 mmole) was added to a solution of the enol diacetate (VIII) (200 mg, 0.53 mmole) in dioxane (15 ml); after slight warming to ensure complete dissolution, the reaction mixture was left in the dark for 24 hr. Potassium iodide solution was added to the reaction mixture, followed by excess 10% aqueous sodium thiosulfate solution. The reaction mixture was extracted with chloroform, dried, and evaporated. The white solid residue was recrystallized from methanol–ether to afford 208 mg (86% yield) of the 3β-acetoxy-16α-iodo derivative (IX), mp 147–148° [lit. (16) mp 144–147°]; IR (KBr): $\nu_{max}$ 1735 [O–C(=O)–$CH_3$] and 1740 (C=O) $cm^{-1}$. To a solution of 250 mg of IX in methanol (10 ml) at room temperature, 37% HCl (1 ml) was added. After the mixture stood at room temperature overnight, VII*d* was separated by filtration, mp 170–172° (mixed melting point with sample prepared by Method A showed no depression).

## REFERENCES

(1) A. G. Schwartz, *Cancer Res.*, **39**, 1129 (1979).

(2) P. H. Marks and J. Banks, *Proc. Natl. Acad. Sci., USA*, **46**, 447 (1960).

(3) G. W. Oertel and P. Benes, *J. Steroid Biochem.*, **3**, 493 (1972).

(4) P. Benes, M. Schirazi, and G. W. Oertel, *Steroids Lipids Res.*, **4**, 285 (1973).

(5) W. E. Truce and P. S. Bailey, Jr., *J. Org. Chem.*, **34**, 1341 (1969).

(6) W. E. Truce, R. N. Bavry, and P. S. Bailey, Jr., *Tetrahedron Lett.*, **1968**, 5651.

(7) N. Z. Stanacev and M. Kates, *Can. J. Biochem. Phys.*, **38**, 297 (1960).

(8) G. P. Bueller, W. F. Johns, D. L. Cook, and R. A. Edgren, *J. Am. Chem. Soc.*, **80**, 1769 (1958).

(9) G. P. Mueller and W. F. Johns, *J. Org. Chem.*, **26**, 2403 (1961).

(10) R. Ranieri and H. R. Levy, *Biochemistry*, **9**, 2234 (1970).

(11) J. L. Mateos, O. Chao, and H. Flores, *Tetrahedron*, **19**, 1051 (1963).

(12) M. N. Huffman and M. H. Lott, *J. Biol. Chem.*, **207**, 431 (1954).

(13) M. O. Forster, *J. Chem. Soc.*, **107**, 260 (1915).

(14) M. P. Cava and E. Moroz, *J. Am. Chem. Soc.*, **84**, 115 (1962).

(15) J. Meinwald, G. G. Curtis, and P. G. Gassman, *ibid.*, **84**, 116 (1962).

(16) P. Catsoulacos and A. Hassner, *Bull. Soc. Chim.*, **2**, 717 (1973).
(17) E. R. Glazier, *J. Org. Chem.*, **27**, 2937 (1962).
(18) C. W. Shoppee, R. H. Jenkins, and G. H. R. Summer, *Collect. Czech. Chem. Commun.*, **23**, 3049 (1958).
(19) J. Fajkos and F. Sorm, *ibid.*, **24**, 766 (1959).
(20) E. R. Glazin, *J. Org. Chem.*, **27**, 4397 (1962).
(21) N. S. Leeds, D. K. Fukushima, and T. F. Gallagher, *J. Am. Chem. Soc.* **76**, 2943 (1954).

**ACKNOWLEDGMENTS**

Presented in part at the ISF-AOCS World Congress, New York, N.Y., April 1980.

Supported by National Institutes of Health Grants CA-14661 and AG-00368.

M. Abou-Gharbia was supported by Grant CA-09214 from the National Cancer Institute. Partial support was obtained from the Samuel S. Fels Fund, Fels Research Institute, and Temple University.

# Dosage Form Design for Improvement of Bioavailability of Levodopa V: Absorption and Metabolism of Levodopa in Intestinal Segments of Dogs

**KUNIHIRO SASAHARA ˣ, TAKASHI NITANAI, TAEKO HABARA, TADASHI MORIOKA, and EIICHI NAKAJIMA**

Received November 10, 1980, from the *Product Development Laboratories, Sankyo Company, Ltd., 1-2-58, Hiromachi, Shinagawa, Tokyo, Japan.* Accepted for publication March 10, 1981.

**Abstract** □ Plasma levels of levodopa, total dopamine, and residual amounts of levodopa and its metabolites at the administered site were analyzed following administration of single 100-mg doses of levodopa in solution into isolated segments of the duodenum, jejunum, and ileum of the dog. The largest area under the plasma concentration–time curve (*AUC*) of levodopa during the 1.0-hr study was obtained following administration in the duodenum, followed by the jejunum and ileum. In addition, the residual amounts of levodopa and its metabolites detected at the administration sites were: ileum, 23%; jejunum, 7%; and duodenum, <1%. The largest *AUC* of total dopamine was obtained following administration in the jejunum, followed by the ileum and duodenum. This order was consistent with the order of levodopa decarboxylase enzyme activity reported previously. Therefore, it can be concluded that the major absorption site of levodopa in the intestine resides in the upper small intestine. Levodopa in 10-, 50-, and 100-mg doses was administered into isolated duodenal segments. The *AUC* of levodopa increased nonlinearly with increasing dose. Negligible amounts of both levodopa and its metabolites were observed in the segment at 1.0 hr after administration, indicating that the duodenal absorption of levodopa was not saturable within the dose range tested.

**Keyphrases** □ Levodopa—absorption and metabolism, intestinal segments, dogs, bioavailability, dosage form design □ Dosage form design—bioavailability of levodopa, absorption and metabolism in dog intestinal segments □ Bioavailability—levodopa, dosage form design, absorption and metabolism in dog intestinal segments

It was previously reported (1) that the reduced bioavailability of levodopa following oral administration was primarily due to levodopa metabolism by levodopa decarboxylase in the intestinal tissue, with the most enzyme activity in the jejunum and the least in the duodenum. The present investigation attempted to validate these findings by a study of levodopa absorption from intestinal segments.

## EXPERIMENTAL

**Major Absorption Site of Levodopa in Intestine of Dogs**—Nine healthy male mongrel dogs, 11.1–13.9 kg, were fasted for ~16 hr and anesthetized with 25-mg/kg iv doses of pentobarbital sodium. They were divided into three equal groups according to the segment to be ligated. After the dog was fixed on its back, a laparotomy was performed on each dog, and a 20-cm segment of the duodenum, the jejunum, or the ileum was ligated. A single 100-mg dose of levodopa was injected as a 1% solution[1] into the ligated segment of each dog. Blood samples were withdrawn with a heparinized syringe from the brachial or femoral vein.

At 0, 2, 5, 15, 30, and 60 min after dosing, blood samples were withdrawn and processed as described previously (2). The animals were killed by exsanguination at 1 hr after levodopa administration, and the ligated loop was washed with saline and then three times with 0.04 *N* $HClO_4$ solution. The irrigating solution was assayed for residual amounts of levodopa and its metabolites.

**Influence of Levodopa Dose on Absorption and Metabolism of Levodopa in Duodenum of Dogs**—Nine healthy male mongrel dogs, 10.2–13.5 kg, were fasted for ~16 hr and anesthetized as described previously. After the dog was fixed on its back, a laparotomy was performed and a 20-cm segment of the duodenum was ligated. Ten-milligram doses of levodopa in a 0.2% solution[1] were injected into the duodenal loops of the first three dogs, 50-mg doses in a 0.5% solution[1] were injected into the duodenal loops of the second three dogs, and 100-mg doses in a 1.0% solution[1] were injected into the duodenal loops of the third group.

Blood samples were withdrawn with a heparinized syringe from the hepatoportal vein at 0, 2, 5, 15, 30, and 60 min after administration. Blood samples and the irrigating solution obtained from the final wash of the ligated loops were processed as already described.

**Assay of Levodopa and Its Metabolites in Plasma and in Administered Site**—Levodopa and its metabolite in plasma were determined according to a reported method (3). Residual amounts of levodopa and its metabolites in the dosing site of the intestine were determined according to the method reported previously (1).

## RESULTS

**Major Absorption Site of Intestine of Levodopa in Dogs**—The average plasma levels of levodopa and total dopamine[2] are shown in Fig. 1 following administration of single 100-mg doses of levodopa to the duodenum, jejunum, and ileum. The highest plasma levodopa levels were obtained after duodenal administration; peak concentrations of 9.5 ± 1.9 mg/liter were observed at 5 min. Plasma levodopa levels following administration to the jejunum reached the peak levels of 5.0 ± 0.8 mg/liter at 15 min. Plasma levodopa levels following administration to the ileum were not only lowest but also increased so slowly that they reached peak levels of only 3.2 ± 0.3 mg/liter at 30 min after administration.

The average *AUC* of levodopa up to 1.0 hr after administration is shown in Fig. 2. The *AUC* of levodopa after administration to the ileum was approximately one-half that observed after duodenal administration.

[1] The 0.2, 0.5, and 1% levodopa solutions were prepared by dissolving levodopa in the buffer solution containing 0.2% sodium bicarbonate and 0.5% polyvinyl acetate (~pH 8.0).

[2] Total dopamine = unconjugated dopamine + conjugated dopamine.

0022-3549/81/1000-1157$01.00/0
© 1981, American Pharmaceutical Association

(16) P. Catsoulacos and A. Hassner, *Bull. Soc. Chim.*, **2**, 717 (1973).
(17) E. R. Glazier, *J. Org. Chem.*, **27**, 2937 (1962).
(18) C. W. Shoppee, R. H. Jenkins, and G. H. R. Summer, *Collect. Czech. Chem. Commun.*, **23**, 3049 (1958).
(19) J. Fajkos and F. Sorm, *ibid.*, **24**, 766 (1959).
(20) E. R. Glazin, *J. Org. Chem.*, **27**, 4397 (1962).
(21) N. S. Leeds, D. K. Fukushima, and T. F. Gallagher, *J. Am. Chem. Soc.* **76**, 2943 (1954).

**ACKNOWLEDGMENTS**

Presented in part at the ISF-AOCS World Congress, New York, N.Y., April 1980.

Supported by National Institutes of Health Grants CA-14661 and AG-00368.

M. Abou-Gharbia was supported by Grant CA-09214 from the National Cancer Institute. Partial support was obtained from the Samuel S. Fels Fund, Fels Research Institute, and Temple University.

# Dosage Form Design for Improvement of Bioavailability of Levodopa V: Absorption and Metabolism of Levodopa in Intestinal Segments of Dogs

**KUNIHIRO SASAHARA ˣ, TAKASHI NITANAI, TAEKO HABARA, TADASHI MORIOKA, and EIICHI NAKAJIMA**

Received November 10, 1980, from the *Product Development Laboratories, Sankyo Company, Ltd., 1-2-58, Hiromachi, Shinagawa, Tokyo, Japan.* Accepted for publication March 10, 1981.

**Abstract** □ Plasma levels of levodopa, total dopamine, and residual amounts of levodopa and its metabolites at the administered site were analyzed following administration of single 100-mg doses of levodopa in solution into isolated segments of the duodenum, jejunum, and ileum of the dog. The largest area under the plasma concentration–time curve (*AUC*) of levodopa during the 1.0-hr study was obtained following administration in the duodenum, followed by the jejunum and ileum. In addition, the residual amounts of levodopa and its metabolites detected at the administration sites were: ileum, 23%; jejunum, 7%; and duodenum, <1%. The largest *AUC* of total dopamine was obtained following administration in the jejunum, followed by the ileum and duodenum. This order was consistent with the order of levodopa decarboxylase enzyme activity reported previously. Therefore, it can be concluded that the major absorption site of levodopa in the intestine resides in the upper small intestine. Levodopa in 10-, 50-, and 100-mg doses was administered into isolated duodenal segments. The *AUC* of levodopa increased nonlinearly with increasing dose. Negligible amounts of both levodopa and its metabolites were observed in the segment at 1.0 hr after administration, indicating that the duodenal absorption of levodopa was not saturable within the dose range tested.

**Keyphrases** □ Levodopa—absorption and metabolism, intestinal segments, dogs, bioavailability, dosage form design □ Dosage form design—bioavailability of levodopa, absorption and metabolism in dog intestinal segments □ Bioavailability—levodopa, dosage form design, absorption and metabolism in dog intestinal segments

It was previously reported (1) that the reduced bioavailability of levodopa following oral administration was primarily due to levodopa metabolism by levodopa decarboxylase in the intestinal tissue, with the most enzyme activity in the jejunum and the least in the duodenum. The present investigation attempted to validate these findings by a study of levodopa absorption from intestinal segments.

## EXPERIMENTAL

**Major Absorption Site of Levodopa in Intestine of Dogs**—Nine healthy male mongrel dogs, 11.1–13.9 kg, were fasted for ~16 hr and anesthetized with 25-mg/kg iv doses of pentobarbital sodium. They were divided into three equal groups according to the segment to be ligated. After the dog was fixed on its back, a laparotomy was performed on each dog, and a 20-cm segment of the duodenum, the jejunum, or the ileum was ligated. A single 100-mg dose of levodopa was injected as a 1% solution[1] into the ligated segment of each dog. Blood samples were withdrawn with a heparinized syringe from the brachial or femoral vein.

At 0, 2, 5, 15, 30, and 60 min after dosing, blood samples were withdrawn and processed as described previously (2). The animals were killed by exsanguination at 1 hr after levodopa administration, and the ligated loop was washed with saline and then three times with 0.04 *N* $HClO_4$ solution. The irrigating solution was assayed for residual amounts of levodopa and its metabolites.

**Influence of Levodopa Dose on Absorption and Metabolism of Levodopa in Duodenum of Dogs**—Nine healthy male mongrel dogs, 10.2–13.5 kg, were fasted for ~16 hr and anesthetized as described previously. After the dog was fixed on its back, a laparotomy was performed and a 20-cm segment of the duodenum was ligated. Ten-milligram doses of levodopa in a 0.2% solution[1] were injected into the duodenal loops of the first three dogs, 50-mg doses in a 0.5% solution[1] were injected into the duodenal loops of the second three dogs, and 100-mg doses in a 1.0% solution[1] were injected into the duodenal loops of the third group.

Blood samples were withdrawn with a heparinized syringe from the hepatoportal vein at 0, 2, 5, 15, 30, and 60 min after administration. Blood samples and the irrigating solution obtained from the final wash of the ligated loops were processed as already described.

**Assay of Levodopa and Its Metabolites in Plasma and in Administered Site**—Levodopa and its metabolite in plasma were determined according to a reported method (3). Residual amounts of levodopa and its metabolites in the dosing site of the intestine were determined according to the method reported previously (1).

## RESULTS

**Major Absorption Site of Intestine of Levodopa in Dogs**—The average plasma levels of levodopa and total dopamine[2] are shown in Fig. 1 following administration of single 100-mg doses of levodopa to the duodenum, jejunum, and ileum. The highest plasma levodopa levels were obtained after duodenal administration; peak concentrations of 9.5 ± 1.9 mg/liter were observed at 5 min. Plasma levodopa levels following administration to the jejunum reached the peak levels of 5.0 ± 0.8 mg/liter at 15 min. Plasma levodopa levels following administration to the ileum were not only lowest but also increased so slowly that they reached peak levels of only 3.2 ± 0.3 mg/liter at 30 min after administration.

The average *AUC* of levodopa up to 1.0 hr after administration is shown in Fig. 2. The *AUC* of levodopa after administration to the ileum was approximately one-half that observed after duodenal administration.

[1] The 0.2, 0.5, and 1% levodopa solutions were prepared by dissolving levodopa in the buffer solution containing 0.2% sodium bicarbonate and 0.5% polyvinyl acetate (~pH 8.0).

[2] Total dopamine = unconjugated dopamine + conjugated dopamine.

0022-3549/81/1000-1157$01.00/0
© 1981, American Pharmaceutical Association

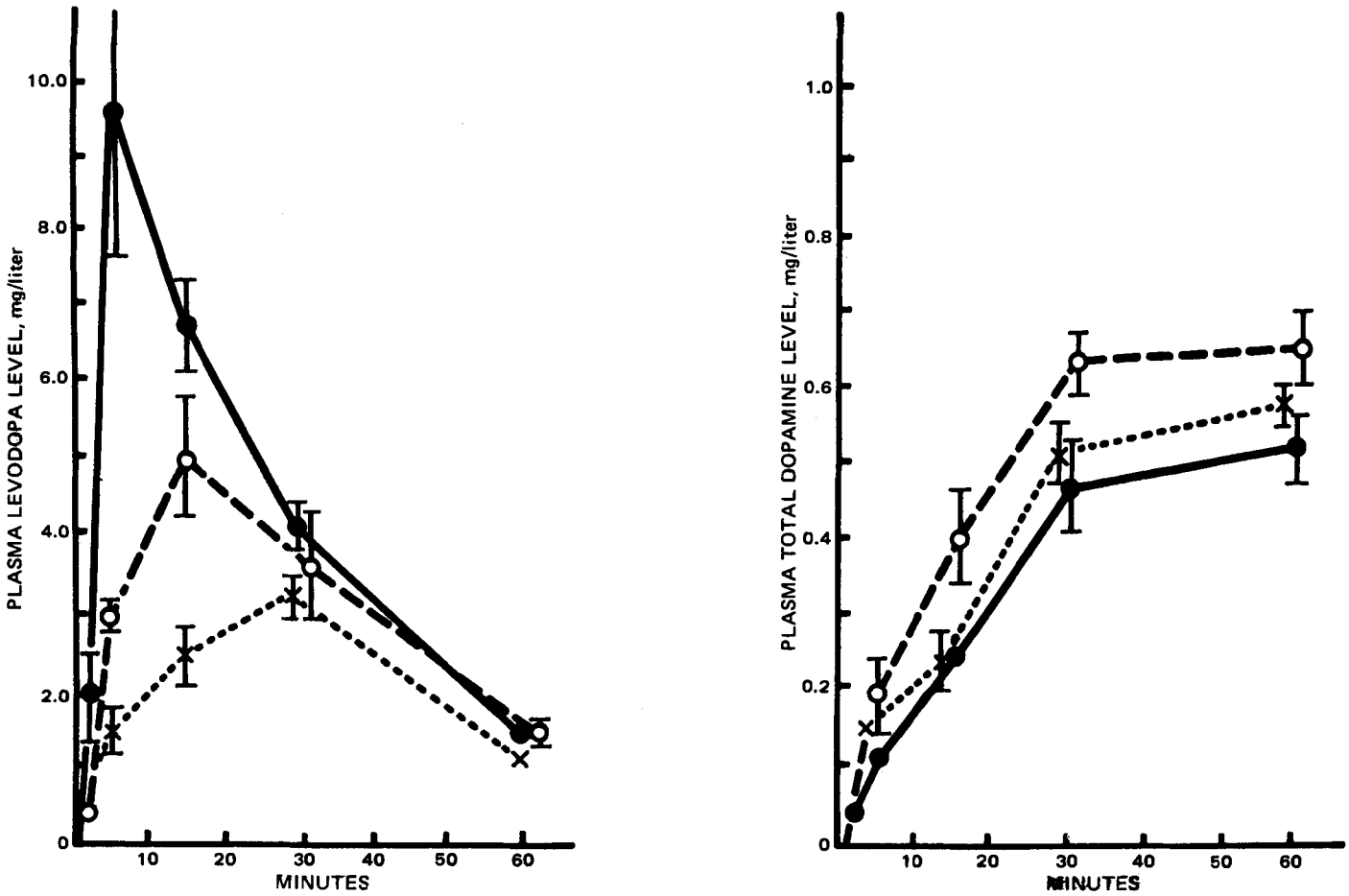


**Figure 1**—*Average plasma levels of levodopa (± SE) and total dopamine (± SE) following administration of single 100-mg dose of levodopa to dog duodenum (●), jejunum (○), and ileum (×).*

However, plasma levels of total dopamine increased slowly and reached the peak levels at 30–60 min after administration, irrespective of the administration site. The highest plasma levels of total dopamine were observed following administration to the jejunum, followed by the ileum and duodenum. This order did not correspond with the order of plasma levodopa levels.

The residual amounts of levodopa and its metabolites recovered from the segment are shown in Table I. These results showed that the residual amounts of levodopa and its metabolites were proportional to the order of plasma levodopa levels. Virtually all drug was absorbed from the duodenal segments, and negligible amounts of metabolites of levodopa were detected. Therefore, it was concluded that the major absorption site of levodopa is the duodenum.

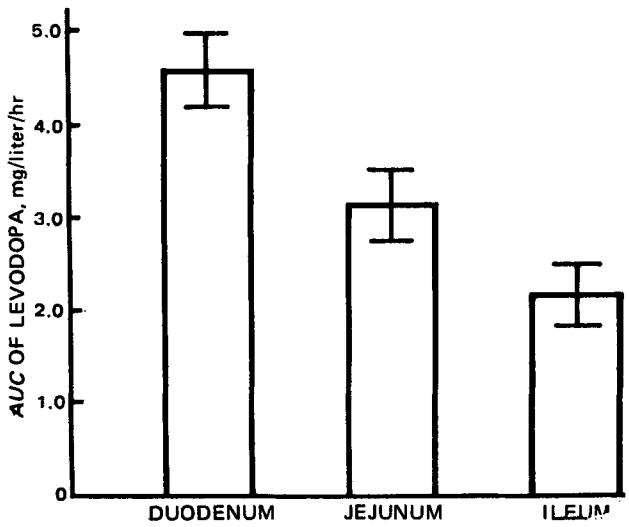


**Figure 2**—*Average* AUC *of levodopa (± SE) up to 1.0 hr after administration of single 100-mg doses of levodopa to dog duodenum, jejunum, and ileum.*

**Influence of Levodopa Dose on Absorption and Metabolism of Levodopa in Duodenum in Dogs**—The average plasma levels of levodopa and total dopamine following administration of single 10-, 50-, and 100-mg doses of levodopa to the duodenum of three dogs are shown in Fig. 3. As the administered dose increased, plasma levodopa levels in the hepatoportal vein appeared to be disproportionally high. In addition, the absorption rate from the duodenum was rapid since the peak time of plasma levodopa levels was observed at 2 min after dosing. However, total dopamine revealed an inverse situation; *i.e.*, as the dose increased, the relative plasma levels of total dopamine were progressively less. The relationship between the levodopa dose administered and the observed *AUC* of levodopa and the observed *AUC* of total dopamine up to 1.0 hr after dosing are shown in Fig. 4. These findings and the fact that levodopa obeys linear kinetics in the body after drug absorption (4) may indicate that metabolism of levodopa to dopamine by levodopa decarboxylase in the dog duodenum proceeds by a capacity-limited process.

The amounts of levodopa and its metabolites remaining at the ad-

**Table I—Percentage of Residual Amounts to the Administered Dose at the Administered Site at 1.0 hr after Administration of Single 100-mg Dose of Levodopa to Dog Duodenum, Jejunum, and Ileum** [a]

| Site | Levodopa | Total Dopamine | Total[b] |
|---|---|---|---|
| Duodenum | 0.8 ± 0.4[c] | 0.1 ± 0.03 | 0.9 ± 0.4 |
| Jejunum | 6.6 ± 0.4 | 0.7 ± 0.1 | 7.2 ± 0.4 |
| Ileum | 21.8 ± 1.8 | 1.0 ± 0.1 | 23.1 ± 1.7 |

[a] 3,4-Dihydroxyphenylacetic acid and homovanillic acid were not detected. [b] Sum of levodopa, total dopamine, 3,4-dihydroxyphenylacetic acid, and homovanillic acid. [c] Average ± *SE*, $n = 3$.

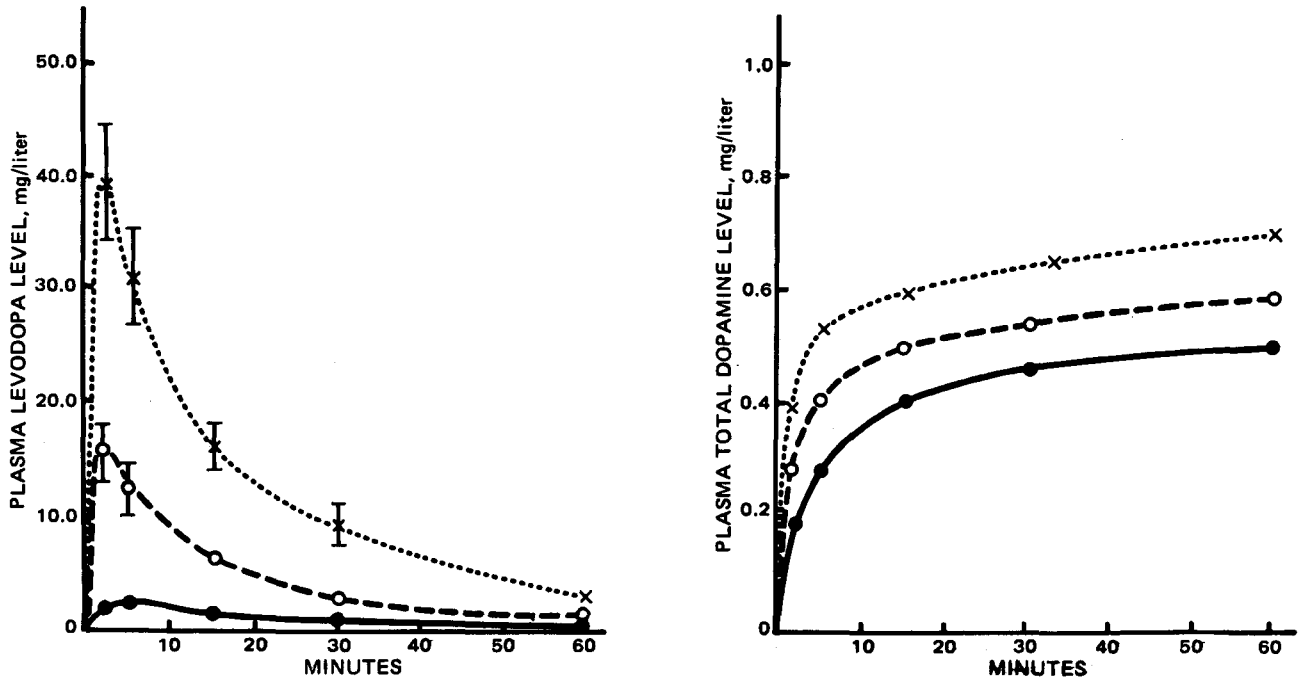


**Figure 3**—*Average plasma levels of levodopa (± SE) and total dopamine (± SE) following administration of single 10- (●), 50- (○), and 100-mg (×) doses of levodopa to dog duodenum.*

ministered site at 1.0 hr after administration were 1% of the administered dose, indicating that levodopa is completely absorbed within 1.0 hr after administration even at the largest dose studied.

## DISCUSSION

It was previously reported (5–7) that the shorter the transit time through the stomach, the higher the observed plasma levodopa levels. These reports suggested that the upper small intestine might play an important role in levodopa absorption *via* the oral route. Analogously, the major site of oral absorption of other amino acids has been shown to be the upper small intestine (8, 9). The isolated intestinal studies carried out in the present investigation showed that the major absorption site of levodopa was the duodenum and that complete absorption occurred in the dose range studied. The inverse relationship between the observed plasma levels of levodopa and total dopamine shown in Fig. 1 is consistent with the fact that activity of levodopa decarboxylase is the lowest in the duodenum and increases in the lower sections of the small intestine (1).

However, previous studies (4) reported that levodopa bioavailability

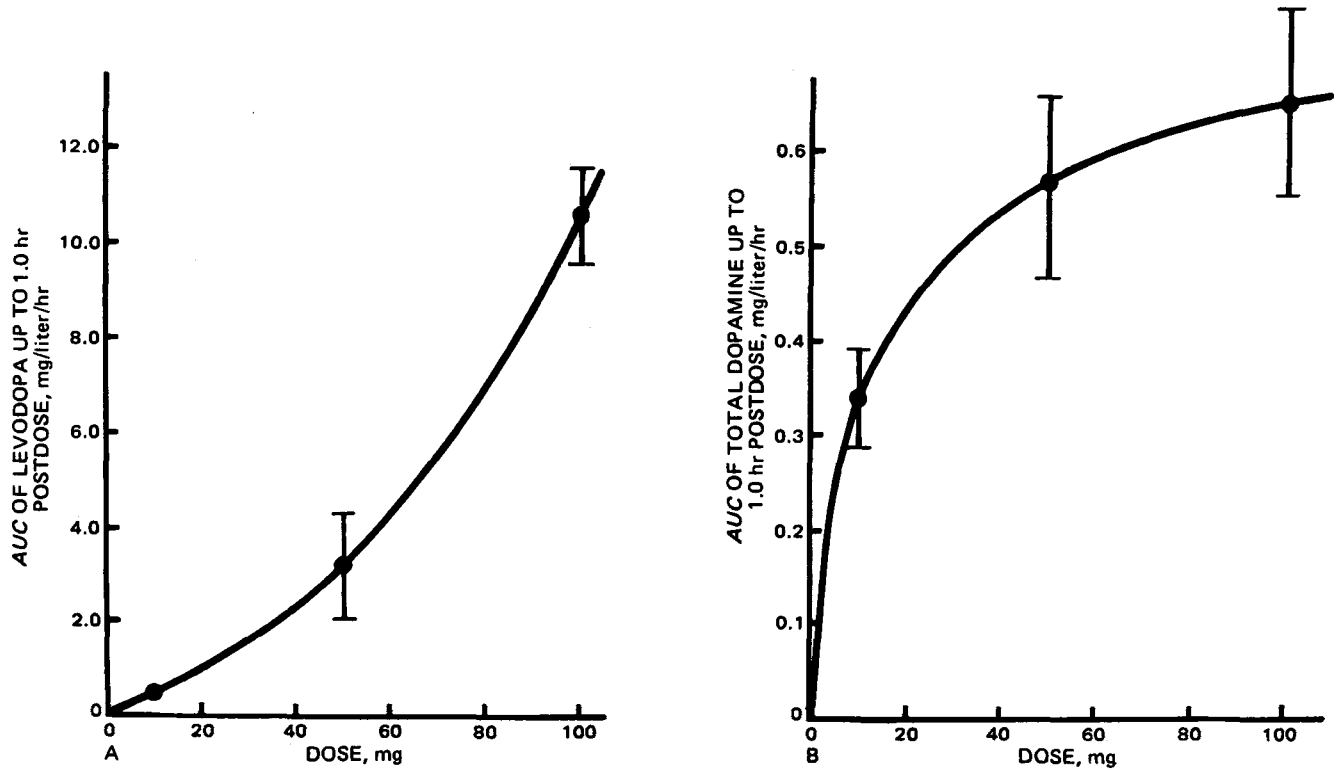


**Figure 4**—*Relationship between the levodopa dose administered and the observed* AUC *of levodopa (A) and the observed* AUC *of total dopamine (B) up to 1.0 hr after dosing.*

in the intact dog was dose dependent and that administration of 10-, 50-, and 100-mg doses of levodopa to the duodenum led to the same results shown in Fig. 3. Yet negligible amounts of levodopa remained in the duodenal segment, and plasma levodopa levels resulted from saturable metabolism of levodopa to dopamine by the levodopa decarboxylase enzyme system in the duodenal tissue. Calimlim *et al.* (10) noted that the levodopa metabolites produced in the stomach may be responsible for nausea and vomiting. Their study and the present results indicate that levodopa bioavailability might be improved with an enteric-coated preparation that releases levodopa in high concentration at the upper small intestine.

## REFERENCES


(1) K. Sasahara, T. Nitanai, T. Habara, T. Kojima, Y., Kawahara, T. Morioka, and E. Nakajima, *J. Pharm. Sci.*, **70**, 730 (1981).

(2) K. Sasahara, T. Nitanai, T. Morioka, and E. Nakajima, *ibid.*, **69**, 261 (1980).

(3) K. Sasahara, T. Nitanai, T. Habara, A. Ninomiya, T. Morioka, and E. Nakajima, *Ann. Rep. Sankyo Res. Lab.*, **30**, 65 (1978).

(4) K. Sasahara, T. Nitanai, T. Habara, T. Morioka, and E. Nakajima, *J. Pharm. Sci.*, **69**, 1374 (1980).

(5) A. Leon and H. Spiegel, *J. Clin. Pharmacol.*, **12**, 263 (1972).

(6) D. N. Wade, P. T. Mearrich, D. J. Birkett, and J. L. Morris, *Aust. N. Z. M. Med.*, **4**, 138 (1974).

(7) P. T. Mearrick, D. N. Wade, D. J. Birkett, and J. L. Morris, *ibid.*, **4**, 144 (1974).

(8) R. P. Spencer, *Am. J. Clin. Nutr.*, **22**, 292 (1969).

(9) D. M. Matheus and L. Laster, *Gut*, **6**, 411 (1965).

(10) L. R. Calimlim, C. A. Dujoune, J. P. Morgan, I. Lasagne, and J. R. Boamcjome, *Eur. J. Clin. Invest.*, **1**, 313 (1971).


## ACKNOWLEDGMENTS


Presented in part at the Pharmaceutics Section, 97th Meeting of the Pharmaceutical Society of Japan, Tokyo meeting, April 1977.

The authors thank Dr. T. Higuchi for valuable discussions, Dr. H. Negoro, Dr. S. Akagi, and Dr. T. Miki for promotion of the research project, Dr. S. Riegelman for constructive comments on the manuscript, and Mrs. S. Tsutsumi for typing the manuscript.


# Blood Collection Technique: No Effect on *In Vitro* Protein Binding of Prednisolone


**MARIO L. ROCCI, JR., and WILLIAM J. JUSKO** ˣ



Received November 28, 1980, from the *Clinical Pharmacokinetics Laboratory, Department of Pharmaceutics, School of Pharmacy, State University of New York at Buffalo*, and the *Millard Fillmore Hospital, Buffalo, NY 14209.* Accepted for publication March 25, 1981.



**Abstract** □ The effect of the blood collection vessel and systemic heparin administration on *in vitro* protein binding of prednisolone was examined in blood collected from human subjects. No differences in the fractional binding of prednisolone were found in plasma from plain glass culture tubes, heparinized culture tubes, and two types of red- and green-top commercial vacuum tubes. Thus, these blood collection techniques do not alter serum or plasma albumin and transcortin binding of prednisolone.



**Keyphrases** □ Binding—prednisolone, effect of blood collection techniques □ Tris(2-butoxyethyl)phosphate—leached substance altering protein binding of selected drugs □ Prednisolone—protein binding in blood collection techniques


Blood collection techniques can affect the binding of ligands to serum proteins (1–7). Heparin administration stimulates lipoprotein lipase release *in vivo* (8), and this enzyme can increase the serum concentrations of nonesterified fatty acids *in vivo* (8) and *in vitro* (9). These fatty acids displace drugs from their binding sites on albumin (10). Heparin also has been shown to alter the plasma protein binding of several drugs when used to prevent blood clotting *in vitro* (6). Tris(2-butoxyethyl)phosphate, a substance leached from some stoppers, also alters the protein binding of selected drugs (1–4). Weak bases that bind to $\alpha_1$-acid glycoprotein are principally affected (2).

This study examined the effect of blood collection on the protein binding of prednisolone. This synthetic glucocorticoid is bound in serum by three proteins: transcortin, albumin, and $\alpha_1$-acid glycoprotein, although the latter contributes minimally to the overall binding of this steroid *in vivo* (11). The limited capacity of transcortin for binding prednisolone results in a nonlinear relationship between prednisolone free fraction and serum concentration, with increases in the free fraction occurring at higher concentrations. This binding pattern contributes greatly to the nonlinear disposition of this compound in humans (12). In addition, the unbound drug appears to be the pharmacologically active moiety (11). Thus, accurate binding measurements are essential when examining prednisolone pharmacokinetics.

## EXPERIMENTAL

**Study Design**—Four healthy adult males (nonsmokers), ages 24–37 years, were studied. A "scalp vein" infusion set[1] was inserted into an arm vein, and an intravenous drip of normal saline was infused at a rate of 0.5 ml/min to maintain the collection line open for 2 hr. At the end of this period, 10 ml of blood was collected into each of five tubes: (*a*) a plain glass culture tube, (*b*) a red-top commercial tube[2], (*c*) a green-top commercial tube with heparin[2], (*d*) another red-top commercial tube[3], and (*e*) a culture tube containing 0.2 ml of 1000-units/ml heparin injection[4]. Contact between the blood samples and stoppers from the two types of commercial tubes was assured through inversion of these tubes.

After initial blood collection, a dilute heparin solution in normal saline (20 units/ml) was connected to the infusion set to prevent clotting of the collection line. At 2, 2.5, 3, 3.5, and 4 hr, 5 ml of the heparin solution was flushed through the line to simulate heparin administration during intermittent blood sample collection. At 4 hr, blood was collected in various tubes as described.

All samples were maintained at 25° for 1 hr and then centrifuged; the plasma (or serum) was harvested and frozen (−20°) prior to analysis.

**Analysis**—Prednisolone containing trace quantities of [$^3$H]prednisolone[5] (specific activity 53 mCi/mmole) was added to each sample to produce concentrations of 100 ng/ml. The protein binding of prednisolone was assessed using equilibrium dialysis for 16 hr at 37° and radioactivity analysis as previously described (13).

**Statistics**—A two-way analysis of variance was performed (14) to differentiate between the effect of systemic heparin administration and the effect of the collection container on prednisolone protein binding. An interaction term was included so that the combined effects of these factors could be assessed.

[1] Pharmaseal Laboratories, Glendale, Calif.
[2] Vacutainer, Becton-Dickinson, Rutherford, N.J.
[3] Venoject, Kimble-Terumo, Elkton, Md.
[4] Lipo-Hepin, Riker Laboratories, Northridge, Calif.
[5] New England Nuclear, Boston, Mass.




*0022-3549/81/1000-1160$01.00/0*


*© 1981, American Pharmaceutical Association*

in the intact dog was dose dependent and that administration of 10-, 50-, and 100-mg doses of levodopa to the duodenum led to the same results shown in Fig. 3. Yet negligible amounts of levodopa remained in the duodenal segment, and plasma levodopa levels resulted from saturable metabolism of levodopa to dopamine by the levodopa decarboxylase enzyme system in the duodenal tissue. Calimlim *et al.* (10) noted that the levodopa metabolites produced in the stomach may be responsible for nausea and vomiting. Their study and the present results indicate that levodopa bioavailability might be improved with an enteric-coated preparation that releases levodopa in high concentration at the upper small intestine.

## REFERENCES


(1) K. Sasahara, T. Nitanai, T. Habara, T. Kojima, Y., Kawahara, T. Morioka, and E. Nakajima, *J. Pharm. Sci.*, **70**, 730 (1981).

(2) K. Sasahara, T. Nitanai, T. Morioka, and E. Nakajima, *ibid.*, **69**, 261 (1980).

(3) K. Sasahara, T. Nitanai, T. Habara, A. Ninomiya, T. Morioka, and E. Nakajima, *Ann. Rep. Sankyo Res. Lab.*, **30**, 65 (1978).

(4) K. Sasahara, T. Nitanai, T. Habara, T. Morioka, and E. Nakajima, *J. Pharm. Sci.*, **69**, 1374 (1980).

(5) A. Leon and H. Spiegel, *J. Clin. Pharmacol.*, **12**, 263 (1972).

(6) D. N. Wade, P. T. Mearrich, D. J. Birkett, and J. L. Morris, *Aust. N. Z. M. Med.*, **4**, 138 (1974).

(7) P. T. Mearrick, D. N. Wade, D. J. Birkett, and J. L. Morris, *ibid.*, **4**, 144 (1974).

(8) R. P. Spencer, *Am. J. Clin. Nutr.*, **22**, 292 (1969).

(9) D. M. Matheus and L. Laster, *Gut*, **6**, 411 (1965).

(10) L. R. Calimlim, C. A. Dujoune, J. P. Morgan, I. Lasagne, and J. R. Boamcjome, *Eur. J. Clin. Invest.*, **1**, 313 (1971).


## ACKNOWLEDGMENTS


Presented in part at the Pharmaceutics Section, 97th Meeting of the Pharmaceutical Society of Japan, Tokyo meeting, April 1977.

The authors thank Dr. T. Higuchi for valuable discussions, Dr. H. Negoro, Dr. S. Akagi, and Dr. T. Miki for promotion of the research project, Dr. S. Riegelman for constructive comments on the manuscript, and Mrs. S. Tsutsumi for typing the manuscript.


# Blood Collection Technique: No Effect on *In Vitro* Protein Binding of Prednisolone


**MARIO L. ROCCI, JR., and WILLIAM J. JUSKO** ˣ



Received November 28, 1980, from the *Clinical Pharmacokinetics Laboratory, Department of Pharmaceutics, School of Pharmacy, State University of New York at Buffalo*, and the *Millard Fillmore Hospital, Buffalo, NY 14209.* Accepted for publication March 25, 1981.



**Abstract** □ The effect of the blood collection vessel and systemic heparin administration on *in vitro* protein binding of prednisolone was examined in blood collected from human subjects. No differences in the fractional binding of prednisolone were found in plasma from plain glass culture tubes, heparinized culture tubes, and two types of red- and green-top commercial vacuum tubes. Thus, these blood collection techniques do not alter serum or plasma albumin and transcortin binding of prednisolone.



**Keyphrases** □ Binding—prednisolone, effect of blood collection techniques □ Tris(2-butoxyethyl)phosphate—leached substance altering protein binding of selected drugs □ Prednisolone—protein binding in blood collection techniques


Blood collection techniques can affect the binding of ligands to serum proteins (1–7). Heparin administration stimulates lipoprotein lipase release *in vivo* (8), and this enzyme can increase the serum concentrations of nonesterified fatty acids *in vivo* (8) and *in vitro* (9). These fatty acids displace drugs from their binding sites on albumin (10). Heparin also has been shown to alter the plasma protein binding of several drugs when used to prevent blood clotting *in vitro* (6). Tris(2-butoxyethyl)phosphate, a substance leached from some stoppers, also alters the protein binding of selected drugs (1–4). Weak bases that bind to $\alpha_1$-acid glycoprotein are principally affected (2).

This study examined the effect of blood collection on the protein binding of prednisolone. This synthetic glucocorticoid is bound in serum by three proteins: transcortin, albumin, and $\alpha_1$-acid glycoprotein, although the latter contributes minimally to the overall binding of this steroid *in vivo* (11). The limited capacity of transcortin for binding prednisolone results in a nonlinear relationship between prednisolone free fraction and serum concentration, with increases in the free fraction occurring at higher concentrations. This binding pattern contributes greatly to the nonlinear disposition of this compound in humans (12). In addition, the unbound drug appears to be the pharmacologically active moiety (11). Thus, accurate binding measurements are essential when examining prednisolone pharmacokinetics.

## EXPERIMENTAL

**Study Design**—Four healthy adult males (nonsmokers), ages 24–37 years, were studied. A "scalp vein" infusion set[1] was inserted into an arm vein, and an intravenous drip of normal saline was infused at a rate of 0.5 ml/min to maintain the collection line open for 2 hr. At the end of this period, 10 ml of blood was collected into each of five tubes: (*a*) a plain glass culture tube, (*b*) a red-top commercial tube[2], (*c*) a green-top commercial tube with heparin[2], (*d*) another red-top commercial tube[3], and (*e*) a culture tube containing 0.2 ml of 1000-units/ml heparin injection[4]. Contact between the blood samples and stoppers from the two types of commercial tubes was assured through inversion of these tubes.

After initial blood collection, a dilute heparin solution in normal saline (20 units/ml) was connected to the infusion set to prevent clotting of the collection line. At 2, 2.5, 3, 3.5, and 4 hr, 5 ml of the heparin solution was flushed through the line to simulate heparin administration during intermittent blood sample collection. At 4 hr, blood was collected in various tubes as described.

All samples were maintained at 25° for 1 hr and then centrifuged; the plasma (or serum) was harvested and frozen (−20°) prior to analysis.

**Analysis**—Prednisolone containing trace quantities of [$^3$H]prednisolone[5] (specific activity 53 mCi/mmole) was added to each sample to produce concentrations of 100 ng/ml. The protein binding of prednisolone was assessed using equilibrium dialysis for 16 hr at 37° and radioactivity analysis as previously described (13).

**Statistics**—A two-way analysis of variance was performed (14) to differentiate between the effect of systemic heparin administration and the effect of the collection container on prednisolone protein binding. An interaction term was included so that the combined effects of these factors could be assessed.

[1] Pharmaseal Laboratories, Glendale, Calif.
[2] Vacutainer, Becton-Dickinson, Rutherford, N.J.
[3] Venoject, Kimble-Terumo, Elkton, Md.
[4] Lipo-Hepin, Riker Laboratories, Northridge, Calif.
[5] New England Nuclear, Boston, Mass.




*0022-3549/81/1000-1160$01.00/0*


*© 1981, American Pharmaceutical Association*

Table I—Mean (±*SD*) Percent *In Vitro* Binding of Prednisolone in Serum Samples Obtained in Various Collection Tubes before and after Systemic Heparin Administration

| Tube | Before Heparin | After Heparin |
|---|---|---|
| Glass culture | 84.6 (1.6) | 84.7 (5.0) |
| Commercial[a] (red top) | 83.3 (3.7) | 86.5 (4.4) |
| Heparinized commercial[a] (green top) | 83.6 (2.2) | 84.6 (4.8) |
| Commercial[b] (red top) | 79.9 (6.0) | 84.2 (7.0) |
| Glass culture with heparin (200 units/0.2 ml) | 86.6 (1.2) | 87.2 (2.7) |

[a] Vacutainer. [b] Venoject.

## RESULTS AND DISCUSSION

The extent of prednisolone binding *in vitro* in the serum (or plasma) samples from the various collection tubes before and after systemic heparin administration is presented in Table I. There were no significant differences in the fractional binding of prednisolone in samples obtained from the various collection tubes ($F = 1.12$). In addition, heparin infusion had no significant effect on the fractional binding of prednisolone ($F = 2.84$). No dual interactions occurred between the collection vessel and heparin administration ($F = 0.67$).

Therefore, heparin administration has no effect on the *in vitro* binding of prednisolone at low steroid concentrations. A low concentration of prednisolone was chosen for these studies to reflect binding to transcortin, a protein that has not been assessed in relation to such potential binding displacement. Changes in the binding at this concentration would result in the greatest relative increase in the free fraction when compared to higher steroid concentrations where ~50–60% of prednisolone is bound (15). Elevation of free fatty acid levels by heparin increases the free fraction of drugs such as phenytoin, warfarin (10), and quinidine (5). The lipase responsible for the release of these fatty acids is active *in vitro* and can introduce a further artifact in the binding measurements *via in vitro* release of these displacing agents (9).

Heparin affects the binding of warfarin, salicylic acid, and phenytoin when used as an anticoagulant *in vitro* (6). The lack of significant differences in prednisolone binding among heparinized and nonheparinized samples obtained prior to systemic heparin administration indicates that the *in vitro* presence of heparin is not of major concern when conducting prednisolone binding and disposition studies.

The leaching of tris(2-butoxyethyl)phosphate from the stoppers of one tube[2] increased the free fraction of basic drugs including propranolol (1), alprenolol (3), and quinidine (4). Prednisolone is a neutral molecule and thus is not affected by the presence of tris(2-butoxyethyl)phosphate. Therefore, the use of heparin and commercial tubes does not appear to pose a problem when examining the protein binding of prednisolone.

## REFERENCES


(1) R. H. Cotham and D. Shand, *Clin. Pharmacol. Ther.*, **18**, 535 (1975).

(2) O. Borgå, K. M. Piafsky, and O. G. Nilsen, *ibid.*, **21**, 539 (1977).

(3) K. M. Piafsky and O. Borgå, *Lancet*, **2**, 963 (1976).

(4) D. Fremstad and K. Bergerud, *Acta Pharmacol. Toxicol.*, **39**, 570 (1976).

(5) K. M. Kessler, R. C. Leech, and J. F. Spann, *Clin. Pharmacol. Ther.*, **25**, 204 (1979).

(6) V. W. Wiegand, J. T. Slattery, K. L. Hintze, and G. Levy, *Life Sci.*, **25**, 471 (1979).

(7) M. Wood, D. G. Shand, and A. J. J. Wood, *Clin. Pharmacol. Ther.*, **25**, 103 (1979).

(8) J. R. E. Fraser, R. R. H. Lovell, and P. J. Nestel, *Clin. Sci.*, **20**, 351 (1961).

(9) K. M. Giacomini, S. E. Swezey, J. C. Giacomini, and T. F. Blaschke, *Life Sci.*, **27**, 771 (1980).

(10) R. Gugler, D. W. Shoeman, and D. L. Azarnoff, *Pharmacology*, **12**, 160 (1974).

(11) P. O. Ballard, *Monogr. Endocrinol.*, **12**, 25 (1975).

(12) W. J. Jusko and J. Q. Rose, *Ther. Drug Monit.*, **2**, 169 (1980).

(13) M. L. Rocci, Jr., N. F. Johnson, and W. J. Jusko, *J. Pharm. Sci.*, **69**, 977 (1980).

(14) J. L. Bruning and B. L. Kintz, "Computational Handbook of Statistics," Scott, Foresman, Glenview, Ill., 1977, pp. 48–54.

(15) G. P. Lewis, W. J. Jusko, C. W. Burke, and L. Graves, *Lancet*, **2**, 778 (1971).


## ACKNOWLEDGMENTS


Supported in part by Grant 24211 from the National Institute of General Medical Sciences, National Institutes of Health.


# Sodium Chloride Equivalents, Cryoscopic Properties, and Hemolytic Effects of Certain Medicinals in Aqueous Solution IV: Supplemental Values


**E. ROY HAMMARLUND**



Received February 18, 1981, from the *Department of Pharmaceutics, School of Pharmacy, University of Washington, Seattle, WA 98195.* Accepted for publication March 23, 1981.



**Abstract** □ A supplemental table of sodium chloride equivalents and freezing-point depressions at various concentrations for 29 substances in aqueous solution is presented. Also listed is the isosmotic concentration of each material that can form such a solution. The degree of hemolysis of human erythrocytes was determined in 12 different isosmotic solutions, and the data are presented to supplement the previously published values. While four isosmotic solutions prevented hemolysis, eight others did not.



**Keyphrases** □ Sodium chloride equivalents—data for 29 drugs □ Cryoscopic properties—data for 29 drugs □ Hemolytic effects—data for 29 drugs □ Medicinals—sodium chloride equivalents, cryoscopic properties, and hemolytic effects determined for 29 drugs


The sodium chloride equivalents and freezing-point depressions for 499 substances in aqueous solution were determined experimentally and reported previously (1–5). Furthermore, the degree of hemolysis of fresh human erythrocytes in certain aqueous isosmotic solutions was studied using the hemolytic method (3–6).

The current investigation studied some additional available substances not included in earlier cryoscopic and


0022-3549/81/1000-1161$01.00/0


© 1981, American Pharmaceutical Association

Table I—Mean (±*SD*) Percent *In Vitro* Binding of Prednisolone in Serum Samples Obtained in Various Collection Tubes before and after Systemic Heparin Administration

| Tube | Before Heparin | After Heparin |
|---|---|---|
| Glass culture | 84.6 (1.6) | 84.7 (5.0) |
| Commercial[a] (red top) | 83.3 (3.7) | 86.5 (4.4) |
| Heparinized commercial[a] (green top) | 83.6 (2.2) | 84.6 (4.8) |
| Commercial[b] (red top) | 79.9 (6.0) | 84.2 (7.0) |
| Glass culture with heparin (200 units/0.2 ml) | 86.6 (1.2) | 87.2 (2.7) |

[a] Vacutainer. [b] Venoject.

## RESULTS AND DISCUSSION

The extent of prednisolone binding *in vitro* in the serum (or plasma) samples from the various collection tubes before and after systemic heparin administration is presented in Table I. There were no significant differences in the fractional binding of prednisolone in samples obtained from the various collection tubes ($F = 1.12$). In addition, heparin infusion had no significant effect on the fractional binding of prednisolone ($F = 2.84$). No dual interactions occurred between the collection vessel and heparin administration ($F = 0.67$).

Therefore, heparin administration has no effect on the *in vitro* binding of prednisolone at low steroid concentrations. A low concentration of prednisolone was chosen for these studies to reflect binding to transcortin, a protein that has not been assessed in relation to such potential binding displacement. Changes in the binding at this concentration would result in the greatest relative increase in the free fraction when compared to higher steroid concentrations where ~50–60% of prednisolone is bound (15). Elevation of free fatty acid levels by heparin increases the free fraction of drugs such as phenytoin, warfarin (10), and quinidine (5). The lipase responsible for the release of these fatty acids is active *in vitro* and can introduce a further artifact in the binding measurements *via in vitro* release of these displacing agents (9).

Heparin affects the binding of warfarin, salicylic acid, and phenytoin when used as an anticoagulant *in vitro* (6). The lack of significant differences in prednisolone binding among heparinized and nonheparinized samples obtained prior to systemic heparin administration indicates that the *in vitro* presence of heparin is not of major concern when conducting prednisolone binding and disposition studies.

The leaching of tris(2-butoxyethyl)phosphate from the stoppers of one tube[2] increased the free fraction of basic drugs including propranolol (1), alprenolol (3), and quinidine (4). Prednisolone is a neutral molecule and thus is not affected by the presence of tris(2-butoxyethyl)phosphate. Therefore, the use of heparin and commercial tubes does not appear to pose a problem when examining the protein binding of prednisolone.

## REFERENCES


(1) R. H. Cotham and D. Shand, *Clin. Pharmacol. Ther.*, **18**, 535 (1975).

(2) O. Borgå, K. M. Piafsky, and O. G. Nilsen, *ibid.*, **21**, 539 (1977).

(3) K. M. Piafsky and O. Borgå, *Lancet*, **2**, 963 (1976).

(4) D. Fremstad and K. Bergerud, *Acta Pharmacol. Toxicol.*, **39**, 570 (1976).

(5) K. M. Kessler, R. C. Leech, and J. F. Spann, *Clin. Pharmacol. Ther.*, **25**, 204 (1979).

(6) V. W. Wiegand, J. T. Slattery, K. L. Hintze, and G. Levy, *Life Sci.*, **25**, 471 (1979).

(7) M. Wood, D. G. Shand, and A. J. J. Wood, *Clin. Pharmacol. Ther.*, **25**, 103 (1979).

(8) J. R. E. Fraser, R. R. H. Lovell, and P. J. Nestel, *Clin. Sci.*, **20**, 351 (1961).

(9) K. M. Giacomini, S. E. Swezey, J. C. Giacomini, and T. F. Blaschke, *Life Sci.*, **27**, 771 (1980).

(10) R. Gugler, D. W. Shoeman, and D. L. Azarnoff, *Pharmacology*, **12**, 160 (1974).

(11) P. O. Ballard, *Monogr. Endocrinol.*, **12**, 25 (1975).

(12) W. J. Jusko and J. Q. Rose, *Ther. Drug Monit.*, **2**, 169 (1980).

(13) M. L. Rocci, Jr., N. F. Johnson, and W. J. Jusko, *J. Pharm. Sci.*, **69**, 977 (1980).

(14) J. L. Bruning and B. L. Kintz, "Computational Handbook of Statistics," Scott, Foresman, Glenview, Ill., 1977, pp. 48–54.

(15) G. P. Lewis, W. J. Jusko, C. W. Burke, and L. Graves, *Lancet*, **2**, 778 (1971).


## ACKNOWLEDGMENTS


Supported in part by Grant 24211 from the National Institute of General Medical Sciences, National Institutes of Health.


# Sodium Chloride Equivalents, Cryoscopic Properties, and Hemolytic Effects of Certain Medicinals in Aqueous Solution IV: Supplemental Values


**E. ROY HAMMARLUND**



Received February 18, 1981, from the *Department of Pharmaceutics, School of Pharmacy, University of Washington, Seattle, WA 98195.* Accepted for publication March 23, 1981.



**Abstract** □ A supplemental table of sodium chloride equivalents and freezing-point depressions at various concentrations for 29 substances in aqueous solution is presented. Also listed is the isosmotic concentration of each material that can form such a solution. The degree of hemolysis of human erythrocytes was determined in 12 different isosmotic solutions, and the data are presented to supplement the previously published values. While four isosmotic solutions prevented hemolysis, eight others did not.



**Keyphrases** □ Sodium chloride equivalents—data for 29 drugs □ Cryoscopic properties—data for 29 drugs □ Hemolytic effects—data for 29 drugs □ Medicinals—sodium chloride equivalents, cryoscopic properties, and hemolytic effects determined for 29 drugs


The sodium chloride equivalents and freezing-point depressions for 499 substances in aqueous solution were determined experimentally and reported previously (1–5). Furthermore, the degree of hemolysis of fresh human erythrocytes in certain aqueous isosmotic solutions was studied using the hemolytic method (3–6).

The current investigation studied some additional available substances not included in earlier cryoscopic and


0022-3549/81/1000-1161$01.00/0


© 1981, American Pharmaceutical Association

**Table I—Sodium Chloride Equivalents and Freezing-Point Depressions [a]**

| Chemical | Concentration of Solution, sodium chloride Equivalents | | | | | At Isosmotic Concentration | |
|---|---|---|---|---|---|---|---|
| | 0.5% | 1% | 2% | 3% | 5% | | |
| Amikacin base | 0.06 | 0.05 | 0.05 | 0.05 | 0.05 | — | — |
| | 0.016° | 0.031° | 0.062° | 0.091° | 0.153° | — | — |
| Benzquinamide hydrochloride | 0.14 | 0.14 | 0.13 | 0.12 | — | — | — |
| | 0.041° | 0.079° | 0.150° | 0.216° | — | — | — |
| Bretylium tosylate | 0.16 | 0.14 | 0.13 | 0.12 | 0.11 | — | — |
| | 0.043° | 0.081° | 0.148° | 0.208° | 0.327° | — | — |
| Calcium gluceptate | 0.12 | 0.12 | 0.11 | 0.10 | 0.10 | — | — |
| | 0.037° | 0.068° | 0.124° | 0.178° | 0.275° | — | — |
| Carbazochrome salicylate | 0.38 | 0.36 | 0.36 | — | — | 0.35 | 2.57%[b] |
| | 0.106° | 0.210° | 0.410° | — | — | 0.52° | 2.57% |
| Cefamandole nafate[c] | 0.16 | 0.14 | 0.12 | 0.11 | 0.10 | — | — |
| | 0.045° | 0.079° | 0.137° | 0.187° | 0.290° | — | — |
| Cefazolin sodium | 0.14 | 0.13 | 0.12 | 0.11 | 0.11 | — | — |
| | 0.042° | 0.074° | 0.132° | 0.190° | 0.303° | — | — |
| Cefoxitin sodium[c] | 0.18 | 0.16 | 0.15 | 0.14 | 0.13 | — | — |
| | 0.050° | 0.092° | 0.166° | 0.238° | 0.384° | — | — |
| Cephapirin sodium | 0.14 | 0.13 | 0.13 | 0.13 | 0.12 | 0.11 | 7.80% |
| | 0.038° | 0.075° | 0.149° | 0.222° | 0.361° | 0.52° | 7.80% |
| Dobutamine hydrochloride | 0.20 | 0.18 | 0.16 | — | — | — | — |
| | 0.053° | 0.101° | 0.188° | — | — | — | — |
| Dopamine hydrochloride | 0.30 | 0.30 | 0.29 | 0.29 | — | 0.29 | 3.11% |
| | 0.085° | 0.170° | 0.335° | 0.502° | — | 0.52° | 3.11% |
| Etidocaine hydrochloride | 0.18 | 0.18 | 0.18 | 0.18 | 0.18 | 0.18 | 5.08% |
| | 0.051° | 0.102° | 0.204° | 0.306° | 0.510° | 0.52° | 5.08% |
| Isoetharine hydrochloride | 0.24 | 0.23 | 0.22 | 0.21 | — | 0.21 | 4.27% |
| | 0.068° | 0.132° | 0.250° | 0.368° | — | 0.52° | 4.27% |
| Ketamine hydrochloride | 0.21 | 0.21 | 0.21 | 0.21 | — | 0.21 | 4.29% |
| | 0.061° | 0.122° | 0.244° | 0.366° | — | 0.52° | 4.29% |
| Leucovorin calcium | 0.06 | 0.05 | 0.05 | 0.04 | 0.04 | — | — |
| | 0.013° | 0.026° | 0.052° | 0.077° | 0.126° | — | — |
| Metoclopramide hydrochloride | 0.16 | 0.15 | 0.13 | 0.12 | 0.11 | — | — |
| | 0.045° | 0.084° | 0.155° | 0.216° | 0.315° | — | — |
| Metrizamide | 0.04 | 0.04 | 0.03 | 0.03 | — | — | — |
| | 0.010° | 0.020° | 0.040° | 0.060° | — | — | — |
| Nalbuphine hydrochloride | 0.16 | 0.15 | 0.14 | — | — | — | — |
| | 0.045° | 0.085° | 0.158° | — | — | — | — |
| Oxymorphone hydrochloride | 0.16 | 0.16 | 0.15 | 0.14 | 0.13 | — | — |
| | 0.044° | 0.088° | 0.168° | 0.244° | 0.382° | — | — |
| Piperacillin sodium[c] | 0.11 | 0.11 | 0.11 | 0.10 | — | — | — |
| | 0.032° | 0.063° | 0.123° | 0.175° | — | — | — |
| Potassium thiocyanate | 0.61 | 0.59 | — | — | — | 0.59 | 1.52% |
| | 0.180° | 0.341° | — | — | — | 0.52° | 1.52% |
| Propantheline bromide[c] | 0.11 | 0.11 | — | — | — | — | — |
| | 0.032° | 0.064° | — | — | — | — | — |
| Propranolol hydrochloride[c] | 0.20 | 0.20 | 0.20 | — | — | — | — |
| | 0.060° | 0.122° | 0.230° | — | — | — | — |
| Sodium nitroprusside | 0.30 | 0.29 | 0.28 | 0.28 | — | 0.27 | 3.30% |
| | 0.086° | 0.167° | 0.322° | 0.475° | — | 0.52° | 3.30% |
| Sodium thiocyanate | 0.71 | 0.71 | — | — | — | 0.71 | 1.27% |
| | 0.205° | 0.410° | — | — | — | 0.52° | 1.27% |
| Terbutaline sulfate | 0.14 | 0.14 | 0.14 | 0.14 | 0.13 | 0.13 | 6.75% |
| | 0.042° | 0.082° | 0.161° | 0.238° | 0.390° | 0.52° | 6.75% |
| Ticarcillin disodium | 0.20 | 0.20 | 0.20 | 0.19 | — | 0.19 | 4.62% |
| | 0.056° | 0.113° | 0.226° | 0.339° | — | 0.52° | 4.62% |
| Timolol maleate | 0.14 | 0.13 | 0.12 | — | — | — | — |
| | 0.038° | 0.077° | 0.146° | — | — | — | — |
| Tobramycin | 0.08 | 0.07 | 0.07 | 0.07 | 0.06 | — | — |
| | 0.019° | 0.038° | 0.075° | 0.112° | 0.187° | — | — |

[a] Top value is sodium chloride equivalent, and bottom value is freezing-point depression. [b] Isosmotic concentration, % w/v. [c] Solution foams readily.

hemolytic investigations. Results are presented in tables to supplement the previous data.

## EXPERIMENTAL

**Cryoscopic Measurements**—The method used to measure the freezing points of the solutions was the same as that already reported; all freezing-point data were obtained with a cryoscopic osmometer (4).

The freezing-point measurements were corrected for the amount of disengaged ice; −0.52° was used as the comparative freezing point for aqueous 0.9% reagent grade sodium chloride solution, which is isotonic and isosmotic with blood and tears. The materials studied were of the official grade of purity or better, and the grade of purity of the donated specialty preparations complied with the manufacturer's specifications.

**Hemolysis of Human Erythrocytes**—Colorimetric hemoglobin determinations were made to indicate the degree of hemolysis for solutions that could be made isosmotic. The method (3–6) utilized a 45-min incubation period of erythrocytes in the isosmotic solution, followed by centrifugation of the erythrocytes and ghosts and determination of absorbance *versus* a standard at 540 nm in a colorimeter.

## RESULTS AND DISCUSSION

Table I lists the sodium chloride equivalents and freezing-point depressions at various concentrations for the 29 substances investigated. To use these data, one should employ the sodium chloride equivalent that represents the concentration nearest to the desired final concentration of the medicinal substance used. Because of general interest in colligative properties of medicinal solutions, freezing-point depressions and sodium chloride equivalents are included for several substances that are not necessarily used as isotonic or isosmotic solutions. Sodium chloride equivalents and isosmotic concentrations are reported to the nearest 0.01.

Table II—Hemolysis of Erythrocytes in Isosmotic Solutions

| Substances | Isosmotic Concentration, % w/v | Hemolysis, % | Approximate pH |
|---|---|---|---|
| Carbazochrome salicylate | 2.57 | 82[a] | 9.4 |
| Cefazolin sodium | 8.77 | 0 | 4.6 |
| Cephapirin sodium | 7.80 | 3[b] | 6.7[c] |
| Dopamine hydrochloride | 3.11 | 6 | 4.6 |
| Etidocaine hydrochloride | 5.08 | 100 | 4.3 |
| Isoetharine hydrochloride | 4.27 | 8 | 4.1 |
| Ketamine hydrochloride | 4.29 | 41 | 3.3 |
| Potassium thiocyanate | 1.52 | 0 | 6.3 |
| Sodium nitroprusside | 3.30 | 50[d] | 9.1 |
| Sodium thiocyanate | 1.27 | Trace | 5.0 |
| Terbutaline sulfate | 6.75 | 11 | 4.1 |
| Ticarcillin disodium | 4.62 | Trace | 5.2 |

[a] Solution turned orange. [b] Solution turned yellow. [c] The pH was determined after addition of erythrocytes. [d] Solution turned red brown.

The percent of hemolysis found for the 12 isosmotic solutions studied, the isosmotic concentration used for each, and the solution's approximate pH before the addition of erythrocytes are listed in Table II. Any noticeable change in appearance of the erythrocytes or the solution was indicated. Of the 12 compounds studied, only four isosmotic solutions prevented hemolysis of human erythrocytes.

A compilation of the 305 substances whose isosmotic solutions were studied using the present hemolytic method shows that 144 failed to prevent hemolysis while 161 prevented hemolysis. Care must be taken not to equate isotonicity and isosmoticity without knowledge of the corresponding data whenever a biological membrane is utilized. This aspect was discussed previously (2, 4, 6–9).

Earlier studies (3–5) showed apparent aggregation of some substances in aqueous solution. In the present study, the cryoscopic graphs of cefamandole nafate and cefoxitin sodium (whose aqueous solutions foamed considerably) showed a slight discontinuity at 1%, suggesting that some aggregation may have taken place above that concentration; however, this phenomenon was not as distinct as with the previously reported drugs. Likewise, solutions of piperacillin sodium, propantheline bromide, and propranolol foamed considerably, suggesting that their surface tensions also were lowered; however, a plot of their cryoscopic graphs did not indicate aggregation. A sufficient number of compounds in the total study did tend to aggregate in solution, which suggests that this interfacial phenomenon may play a role in drug action by affecting biological activity. Associations taking place in the complex biological medium undoubtedly affect the thermodynamic activity of a given drug at the molecular level and, therefore, warrant increased study.

## REFERENCES


(1) E. R. Hammarlund and K. Pedersen-Bjergaard, *J. Am. Pharm. Assoc., Sci. Ed.*, **47**, 107 (1958).

(2) E. R. Hammarlund, J. F. Deming, and K. Pedersen-Bjergaard, *J. Pharm. Sci.*, **54**, 160 (1965).

(3) E. R. Hammarlund and G. L. Van Pevenage, *ibid.*, **55**, 1448 (1966).

(4) W. E. Fassett, T. S. Fuller, and E. R. Hammarlund, *ibid.*, **58**, 1540 (1969).

(5) C. Sapp, M. Lord, and E. R. Hammarlund, *ibid.*, **64**, 1884 (1975).

(6) E. R. Hammarlund and K. Pedersen-Bjergaard, *ibid.*, **50**, 24 (1961).

(7) J. Daussett and L. Contu, *Ann. Rev. Med.*, **18**, 55 (1967).

(8) A. R. Freeman and M. A. Spertes, *Biochem. Pharmacol.*, **11**, 161 (1962); **12**, 47 (1963); **12**, 1235 (1963).

(9) T. F. Williams, C. C. Fordham, III, W. Hollander, Jr., and L. G. West, *J. Clin. Invest.*, **38**, 1587 (1959).


## ACKNOWLEDGMENTS


The author is grateful to the manufacturers for supplying the trademarked substances used and to undergraduate pharmacy students Susan Denny, Sze Wah Lau, Alan Liu, and Carol Mandau for carrying out many of the determinations.


# Improved Liquid Chromatographic Assay for Serum Fluorouracil Concentrations in the Presence of Ftorafur


**C. L. HORNBECK *x, R. A. FLOYD ‡, J. C. GRIFFITHS *, and J. E. BYFIELD §**



Received January 5, 1981, from the * *Department of Laboratory Services and the* ‡ *Department of Pharmacy, Veterans Administration Medical Center, San Diego, CA 92161*, and the § *Division of Radiation Oncology, University of California Medical Center, San Diego, CA 92103.* Accepted for publication March 23, 1981.



**Abstract** □ An improved liquid chromatographic assay for serum ftorafur and fluorouracil is shown to be routine, sensitive, and reproducible using 200 μl of serum. Dilute ammonium acetate buffer at pH 10.2 is used for solubilization of the evaporated ethyl acetate extract for injection into the liquid chromatograph. A stability study indicated little or no *in vitro* formation of fluorouracil from ftorafur under the conditions described. Low serum fluorouracil levels were found after administration of therapeutic doses of ftorafur.



**Keyphrases** □ Liquid chromatographic assay—improved results for fluorouracil in presence of ftorafur □ Ftorafur—stability study, no *in vitro* formation of fluorouracil □ Anticancer agent—ftorafur potential for treatment of GI cancers


The recent development of an oral dosage form of the antineoplastic ftorafur [$R_1S$-*1*-(tetrahydro-2-furanyl)-5-fluorouracil] (I) has added new potential for the treatment of GI cancers on an outpatient basis. Ftorafur is generally considered to be a prodrug for fluorouracil (II), which, in turn, derives its cytotoxicity from its structural resemblance to uracil (IV). Inspection of the structure of I, II, and IV reveals the structural similarities between these molecules, and comparison of I and III indicates the unusual tetrahydrofuranyl ring of ftorafur.

## BACKGROUND

During initial human studies with bolus ftorafur, investigators reported circulating levels of fluorouracil greater than those found after continuous intravenous infusion of fluorouracil (1, 2). In addition, there is some clinical similarity between bolus ftorafur and infusional fluorouracil in terms of patient toxicity (3). These findings suggested that the cytotoxic mechanism of ftorafur was probably due to the slow release of fluorouracil into the systemic circulation.

However, in a more recent study with bolus ftorafur, very low circulating levels of fluorouracil were reported and fluorouracil was not detected in the serum 8 hr after ftorafur administration (4). This report suggested that the high fluorouracil levels reported previously were the result of *in vitro* breakdown of ftorafur or perhaps its more labile dehydro metabolite (5). This metabolite is thought to differ from ftorafur by only a double bond located in an undetermined position in the furanyl ring


*0022-3549/81/1000-1163$01.00/0*


*© 1981, American Pharmaceutical Association*

Table II—Hemolysis of Erythrocytes in Isosmotic Solutions

| Substances | Isosmotic Concentration, % w/v | Hemolysis, % | Approximate pH |
|---|---|---|---|
| Carbazochrome salicylate | 2.57 | 82[a] | 9.4 |
| Cefazolin sodium | 8.77 | 0 | 4.6 |
| Cephapirin sodium | 7.80 | 3[b] | 6.7[c] |
| Dopamine hydrochloride | 3.11 | 6 | 4.6 |
| Etidocaine hydrochloride | 5.08 | 100 | 4.3 |
| Isoetharine hydrochloride | 4.27 | 8 | 4.1 |
| Ketamine hydrochloride | 4.29 | 41 | 3.3 |
| Potassium thiocyanate | 1.52 | 0 | 6.3 |
| Sodium nitroprusside | 3.30 | 50[d] | 9.1 |
| Sodium thiocyanate | 1.27 | Trace | 5.0 |
| Terbutaline sulfate | 6.75 | 11 | 4.1 |
| Ticarcillin disodium | 4.62 | Trace | 5.2 |

[a] Solution turned orange. [b] Solution turned yellow. [c] The pH was determined after addition of erythrocytes. [d] Solution turned red brown.

The percent of hemolysis found for the 12 isosmotic solutions studied, the isosmotic concentration used for each, and the solution's approximate pH before the addition of erythrocytes are listed in Table II. Any noticeable change in appearance of the erythrocytes or the solution was indicated. Of the 12 compounds studied, only four isosmotic solutions prevented hemolysis of human erythrocytes.

A compilation of the 305 substances whose isosmotic solutions were studied using the present hemolytic method shows that 144 failed to prevent hemolysis while 161 prevented hemolysis. Care must be taken not to equate isotonicity and isosmoticity without knowledge of the corresponding data whenever a biological membrane is utilized. This aspect was discussed previously (2, 4, 6–9).

Earlier studies (3–5) showed apparent aggregation of some substances in aqueous solution. In the present study, the cryoscopic graphs of cefamandole nafate and cefoxitin sodium (whose aqueous solutions foamed considerably) showed a slight discontinuity at 1%, suggesting that some aggregation may have taken place above that concentration; however, this phenomenon was not as distinct as with the previously reported drugs. Likewise, solutions of piperacillin sodium, propantheline bromide, and propranolol foamed considerably, suggesting that their surface tensions also were lowered; however, a plot of their cryoscopic graphs did not indicate aggregation. A sufficient number of compounds in the total study did tend to aggregate in solution, which suggests that this interfacial phenomenon may play a role in drug action by affecting biological activity. Associations taking place in the complex biological medium undoubtedly affect the thermodynamic activity of a given drug at the molecular level and, therefore, warrant increased study.

## REFERENCES


(1) E. R. Hammarlund and K. Pedersen-Bjergaard, *J. Am. Pharm. Assoc., Sci. Ed.*, **47**, 107 (1958).

(2) E. R. Hammarlund, J. F. Deming, and K. Pedersen-Bjergaard, *J. Pharm. Sci.*, **54**, 160 (1965).

(3) E. R. Hammarlund and G. L. Van Pevenage, *ibid.*, **55**, 1448 (1966).

(4) W. E. Fassett, T. S. Fuller, and E. R. Hammarlund, *ibid.*, **58**, 1540 (1969).

(5) C. Sapp, M. Lord, and E. R. Hammarlund, *ibid.*, **64**, 1884 (1975).

(6) E. R. Hammarlund and K. Pedersen-Bjergaard, *ibid.*, **50**, 24 (1961).

(7) J. Daussett and L. Contu, *Ann. Rev. Med.*, **18**, 55 (1967).

(8) A. R. Freeman and M. A. Spertes, *Biochem. Pharmacol.*, **11**, 161 (1962); **12**, 47 (1963); **12**, 1235 (1963).

(9) T. F. Williams, C. C. Fordham, III, W. Hollander, Jr., and L. G. West, *J. Clin. Invest.*, **38**, 1587 (1959).


## ACKNOWLEDGMENTS


The author is grateful to the manufacturers for supplying the trademarked substances used and to undergraduate pharmacy students Susan Denny, Sze Wah Lau, Alan Liu, and Carol Mandau for carrying out many of the determinations.


# Improved Liquid Chromatographic Assay for Serum Fluorouracil Concentrations in the Presence of Ftorafur


**C. L. HORNBECK *x, R. A. FLOYD ‡, J. C. GRIFFITHS *, and J. E. BYFIELD §**



Received January 5, 1981, from the * *Department of Laboratory Services and the* ‡ *Department of Pharmacy, Veterans Administration Medical Center, San Diego, CA 92161*, and the § *Division of Radiation Oncology, University of California Medical Center, San Diego, CA 92103.* Accepted for publication March 23, 1981.



**Abstract** □ An improved liquid chromatographic assay for serum ftorafur and fluorouracil is shown to be routine, sensitive, and reproducible using 200 μl of serum. Dilute ammonium acetate buffer at pH 10.2 is used for solubilization of the evaporated ethyl acetate extract for injection into the liquid chromatograph. A stability study indicated little or no *in vitro* formation of fluorouracil from ftorafur under the conditions described. Low serum fluorouracil levels were found after administration of therapeutic doses of ftorafur.



**Keyphrases** □ Liquid chromatographic assay—improved results for fluorouracil in presence of ftorafur □ Ftorafur—stability study, no *in vitro* formation of fluorouracil □ Anticancer agent—ftorafur potential for treatment of GI cancers


The recent development of an oral dosage form of the antineoplastic ftorafur [$R_1S$-*1*-(tetrahydro-2-furanyl)-5-fluorouracil] (I) has added new potential for the treatment of GI cancers on an outpatient basis. Ftorafur is generally considered to be a prodrug for fluorouracil (II), which, in turn, derives its cytotoxicity from its structural resemblance to uracil (IV). Inspection of the structure of I, II, and IV reveals the structural similarities between these molecules, and comparison of I and III indicates the unusual tetrahydrofuranyl ring of ftorafur.

## BACKGROUND

During initial human studies with bolus ftorafur, investigators reported circulating levels of fluorouracil greater than those found after continuous intravenous infusion of fluorouracil (1, 2). In addition, there is some clinical similarity between bolus ftorafur and infusional fluorouracil in terms of patient toxicity (3). These findings suggested that the cytotoxic mechanism of ftorafur was probably due to the slow release of fluorouracil into the systemic circulation.

However, in a more recent study with bolus ftorafur, very low circulating levels of fluorouracil were reported and fluorouracil was not detected in the serum 8 hr after ftorafur administration (4). This report suggested that the high fluorouracil levels reported previously were the result of *in vitro* breakdown of ftorafur or perhaps its more labile dehydro metabolite (5). This metabolite is thought to differ from ftorafur by only a double bond located in an undetermined position in the furanyl ring


*0022-3549/81/1000-1163$01.00/0*


*© 1981, American Pharmaceutical Association*

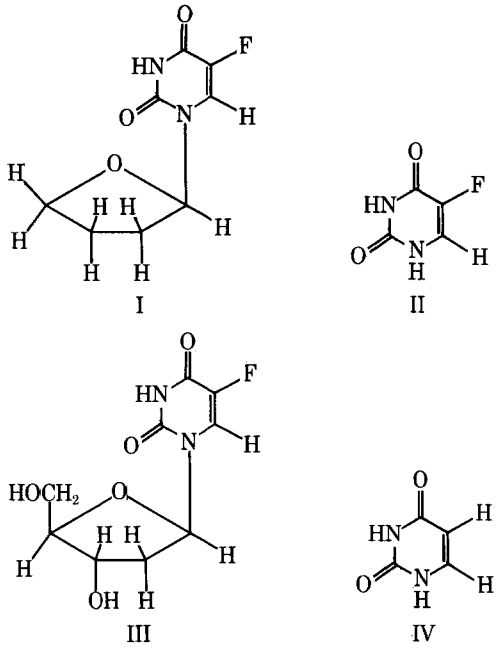


(5, 6). In view of these divergent results and the importance of determining whether serum fluorouracil levels resulting from ftorafur administration could be related to patient efficacy and toxicity as indicated with infusional fluorouracil (7), levels of circulating fluorouracil were determined in patients on bolus ftorafur protocols (6).

In initial attempts to adopt existing liquid chromatographic assays for ftorafur and fluorouracil in this laboratory, great difficulty was experienced in obtaining results either routinely or reproducibly for fluorouracil. These problems were caused mainly by interfering peaks of varying sizes from serum to serum and partly by peak broadening with the use of methanol as the injection solvent. To overcome these difficulties, an assay originally developed by other researchers (8) was modified. The modified assay is very sensitive and reproducible and is readily adaptable to routine therapeutic drug monitoring of fluorouracil in the presence of ftorafur and its labile metabolite, dehydroftorafur. A stability study revealed little or no formation of *in vitro* fluorouracil during assay or storage, and patient serum data confirm low levels of circulating fluorouracil with ftorafur doses as high as 5 g/m$^2$.

## EXPERIMENTAL

**Subjects and Clinical Protocols**—Blood samples were taken from five patients with various GI carcinomas during 15 treatment cycles of a Phase I clinical trial of combined ftorafur and radiation therapy. Each cycle consisted of total daily ftorafur doses of 1.5–2.0 g/m$^2$ for 5 days and concurrent daily radiation doses of 250 rads starting on the 2nd day for 4 days. Each cycle was followed by 9 days of rest before the next treatment cycle. Ftorafur was administered orally three times daily with meals, and the serum samples were drawn 1–4 hr after the midday dose. One patient was given a single intravenous 2-hr infusion of 5.0 g of ftorafur/m$^2$. Blood samples were taken periodically during and for up to 24 hr after the infusion. All serum samples were frozen at −20° until analysis.

**Reagents and Apparatus**—Analytical standards of ftorafur[1], fluorouracil[2], and thymidine[2] were used as supplied. All solvents were nanograde quality.

The analysis of serum fluorouracil, ftorafur, and dehydroftorafur was performed on a microprocessor-controlled high-performance liquid chromatograph[3] equipped with a variable-wavelength detector, automatic sampling system, and a 4-mm × 30-cm reversed-phase column[4]. The column was run at ambient temperatures at a flow rate of 2 ml/min. The elution solvent varied from 3 to 6% methanol in 0.01 *M* aqueous sodium acetate (pH 4.0), yielding retention times of 2.9, 23, and 27 min for fluorouracil, ftorafur, and dehydroftorafur, respectively. The variable UV

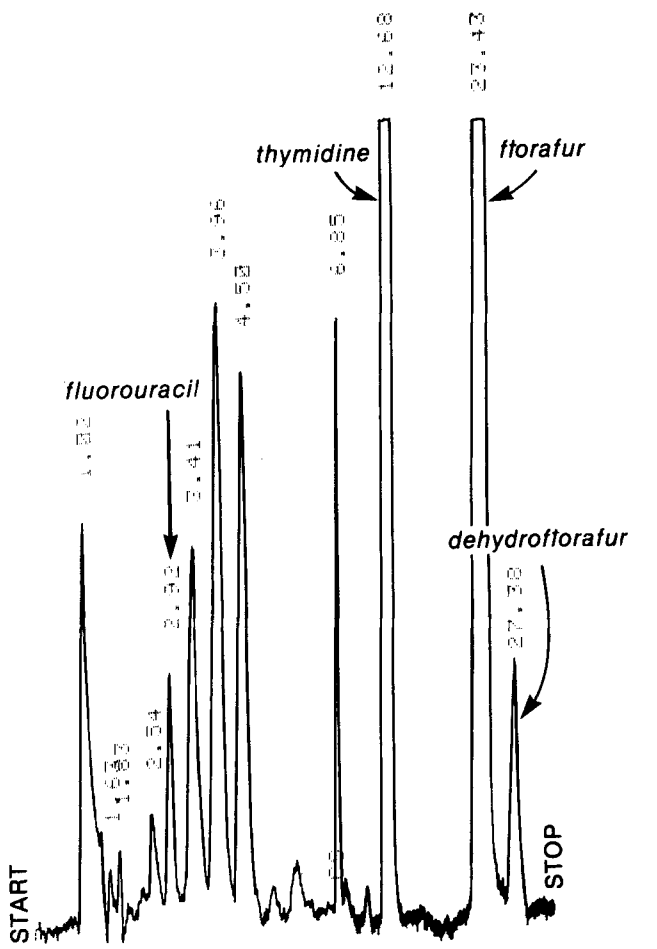


**Figure 1**—*Liquid chromatographic profile of a patient serum using 100 μl of 0.01* M *ammonium acetate (pH 10.2) as the injection solvent for the evaporated ethyl acetate extract of 200 μl of serum. Chart speed was changed from 0.8 to 0.15 cm/min at 6.5 min.*

detector was set at a sample wavelength of 270 nm and a reference wavelength of 330 nm with full-scale absorbance set at 0.003 unit.

**Extraction Procedure**—To a 10-ml screw-capped disposable glass tube were added 200 μl of serum; either 100 μl of water, fluorouracil, or ftorafur solution; 40 μl of thymidine internal standard (100 μg/ml serum); 40 μl of 0.5 *M* sodium phosphate buffer; and 6 ml of ethyl acetate. The tubes were shaken vigorously for 3 min and centrifuged at 2000 rpm for 15 min (1000×*g*). The organic phase was transferred to a second 10-ml tube and evaporated to dryness under nitrogen at 50°. Then 100 μl of 0.01 *M* ammonium acetate (pH 10.2) was added to the dried extract, and the tube was sonicated for 30 min. The extract was transferred to a microvial and capped, and 25 μl was injected into the liquid chromatograph.

Along with patient samples and the control, each assay included two duplicate reference standards for fluorouracil at concentrations of either 50 or 100 ng/ml and two ftorafur reference standards at concentrations of 50 and 100 μg/ml for quantitation of both ftorafur and dehydroftorafur. When filtration was used as a substitute for extraction and concentration, serum was passed through centriflow-membrane filters[5] before injection into the liquid chromatograph.

## RESULTS AND DISCUSSION

The most important modification to the original assay (8) is the use of 0.01 *M* ammonium acetate at pH 10.2 instead of methanol to take up the dried ethyl acetate extract. This approach leads to other modifications by taking advantage of the anionic form of the fluoropyrimidines occurring at alkaline pH. Many materials extracted by ethyl acetate are not soluble in the aqueous pH 10.2 solvent. With the modified procedure, the

[1] Division of Cancer Treatment, National Cancer Institute, National Institutes of Health, Bethesda, MD 20014.
[2] Sigma Chemical Co., St. Louis, MO 63178.
[3] Model 1084B, Hewlett-Packard, Avondale, PA 19311.
[4] μBondapak $C_{18}$, Waters Associates, Milford, MA 01757.
[5] Type CF50A, Amicon Corp., Lexington, MA 02173.

extraction ratio of ethyl acetate to serum can be increased from 8:1 to 16:1; this change increases the recovery of fluorouracil from ~50 to 70% and still eliminates interferences with the fluorouracil peak.

Figure 1 is a typical serum profile. When methanol is used as the injection solvent, mixing occurs more slowly, which effectively broadens peaks not well retained by the column. These faster eluting peaks are much sharper with the use of the aqueous solvent. This increased peak definition, combined with cleaner spectra and greater fluorouracil recovery, results in a lower and constant serum requirement of 200 μl from which concentrations as low as 10 ng/ml of fluorouracil can be reliably and routinely detected. Many blank serum samples as well as patient serum samples have been tested with this procedure, and none produced interfering peaks.

The procedure offers two other benefits that are not clearly demonstrated in Fig. 1. Thymidine in microgram amounts was proven to be a reliable internal standard for the fluoropyrimidines after numerous runs showed that very few peaks of any size other than ftorafur and dehydroftorafur eluted after ~7–8 min from injection. Naturally occurring thymidine appears in low nanogram amounts in serum and contributes <1% to the much higher amounts of thymidine spiked into serum. Another advantage is a decrease in solubilization of less polar and more strongly retained compounds extracted by ethyl acetate. These materials are soluble in methanol and often become interferences in subsequent injections into the liquid chromatograph. This decrease in slowly eluting peaks allows a far more reliable use of automated injection capabilities. Ten to 20 samples can be processed for injection in 2–3 hr, and the liquid chromatograph can be programmed to inject automatically day or night.

To determine truly representative systemic fluorouracil levels in the presence of ftorafur, it is important to demonstrate that the fluorouracil concentration measured is not a result of the breakdown of ftorafur or the more labile dehydroftorafur during storage or assay. Briefly, ftorafur and dehydroftorafur did not contribute *in vitro* to fluorouracil concentrations in serum when stored at −20° for up to 6 weeks or when stored for up to 10 hr in 0.01 *M* ammonium acetate (pH 10.2) at room temperature. No fluorouracil could be detected after extraction and chromatography of purified ftorafur spiked into blank serum. A negligible fluorouracil concentration was detected after extraction and chromatography of dehydroftorafur spiked into blank serum; however, the dehydroftorafur had been concentrated by lyophilization during which conversion of dehydroftorafur to fluorouracil previously was demonstrated.

Storage and reproducibility were conveniently checked by monitoring the control samples included in daily assays. These samples were from a ftorafur patient serum, which had been divided into 200-μl aliquots and frozen at −20° until assayed. Day-to-day variations in the fluorouracil levels of 10 of these aliquots were small and random, indicating that no measurable fluorouracil originated from ftorafur and dehydroftorafur for up to 6 weeks of storage at −20°. The coefficient of variation for the control samples was 4.8% for fluorouracil at a mean concentration of 44 ng/ml. The mean and coefficient of variation for ftorafur were 64 μg/ml and 5.8%, respectively, while the corresponding values for dehydroftorafur were 1.1 μg/ml and 9.4%.

The contribution to fluorouracil from ftorafur at a concentration of ~100 μg/ml was negligible during extraction and chromatography. This result was determined by injecting a very concentrated aqueous solution of ftorafur into the liquid chromatograph to separate it from any contaminating fluorouracil. The ftorafur peak was collected, and an aliquot of the unconcentrated and fluorouracil-free ftorafur solution was spiked into a blank serum to give a concentration of ~100 μg/ml. The spiked serum was extracted and chromatographed as usual; no measurable fluorouracil peak was found in the elution profile.

Since a purified and concentrated form of dehydroftorafur was not available, it was not possible to repeat an identical experiment with the metabolite. Therefore, dehydroftorafur had to be isolated from fluorouracil and ftorafur by liquid chromatography of patient serum. For isolation of dehydroftorafur, the column elution buffer was changed from sodium acetate to ammonium acetate; the collected dehydroftorafur fraction was immediately titrated to pH ~10 for concentration by lyophilization. The reconstituted dehydroftorafur was spiked into a blank serum to give an approximate concentration of 1 μg/ml. Extraction and chromatography of the spiked serum resulted in a small 5-fluorouracil concentration of 15 ng/ml. However, it previously had been shown that similar lyophilization of ftorafur resulted in measurable fluorouracil formation. Since dehydroftorafur is even more labile, this would indicate that the formation of fluorouracil was a result of the lyophilization step, which is not part of the routine assay. In addition, serum dehydroftorafur concentrations have been typically <5% of ftorafur serum concentrations.

**Table I—Mean and Standard Deviation of the Serum Concentrations for the Three Fluoropyrimidines Monitored in Five Patients on Oral Ftorafur Chemotherapy [a]**

| Patient | Total Daily Dose, g/m² | Ftorafur, μg/ml | Dehydroftorafur, μg/ml | Fluorouracil, ng/ml | n [b] |
|---|---|---|---|---|---|
| BH | 1.5 | 76 ± 14 | 0.87 ± 0.35 | 70 ± 15 | 6 |
| RJ | 1.5 | 50 ± 14 | 0.76 ± 0.31 | 63 ± 17 | 8 |
| RW | 1.5 | 96 ± 35 | — | 45 ± 36 | 9 |
| FT | 2.0 | 79 ± 15 | — | 64 ± 22 | 7 |
| NR | 2.0 | 73 ± 23 | 1.6 ± 0.45 | 76 ± 30 | 10 |

[a] Ftorafur range = 34–147 μg/ml. Fluorouracil range = 9–133 ng/ml. [b] Number of serum samples monitored.

If the instrument is used unattended in the automatic injection mode, the last sample to be injected will sit in the pH 10.2 solution for up to 10 hr more than the first sample injected. To test this situation, multiple extractions were performed on another patient serum having a ftorafur concentration of 124 μg/ml and a dehydroftorafur concentration of 1.5 μg/ml. The dried extracts were brought up in the pH 10.2 buffer, and the samples were injected so that 10 hr elapsed from the first to last injection. The initial concentration of fluorouracil measured in this sample was 53 ng/ml, and only small random changes (coefficient of variation of 4.3%) were seen over the 10-hr period in the three fluoropyrimidine concentrations. These results were routinely confirmed several times by placing the first sample injected behind the last sample for automatic reinjection.

Table I shows the average serum levels for five patients treated with several cycles of concurrent radiation and oral ftorafur chemotherapy. On a molar basis, the dosages are approximately equivalent to the 5-day dosage of fluorouracil given during direct intravenous infusion of 25 mg/kg/24 hr. This dosage of fluorouracil generates serum fluorouracil levels starting near 100 ng/ml to >500 ng/ml (9). The highest serum fluorouracil concentrations achieved in the ftorafur patients were comparatively low, and only three of the 40 values exceeded 100 ng/ml. In a different protocol, Patient BH was given a single intravenous bolus dose of 5.0 g/m² of ftorafur and serum levels of the three fluoropyrimidines were monitored for 24 hr after the dose. This dose was more than three times this patient's daily 1.5 g/m² of oral ftorafur given during the regular 5-day cycle. The ftorafur level at 2 hr was 250 μg/ml with a fluorouracil level of 150 ng/ml. At 24 hr, the ftorafur concentration had dropped to 90 μg/ml with a fluorouracil level of only 85 ng/ml.

Serum fluorouracil concentrations in the 1–2-μg/ml range were reported for up to 24 hr after a ftorafur intravenous bolus dose of 5 g/m² (2). However, the latter data were acquired using a somewhat different method. The serum had been filtered through a 50,000 molecular weight cutoff filter and injected directly into the liquid chromatograph with water as the column eluant. As a check on methodological differences, the 2- and 24-hr serum samples from Patient BH were repeated using the filtration method with 0.1 *M* sodium acetate, 5% methanol (pH 4.0), or water as the column eluant. Both 200- and 1000-ng/ml fluorouracil standards were run concurrently with these samples, which demonstrated fluorouracil peaks smaller than the 200-ng/ml standard with both column eluants.

The assay is sensitive and reproducible, and there appears to be little or no *in vitro* formation of fluorouracil during storage or assay under the conditions described. With just minor variations, the assay is now routinely used to monitor fluorouracil serum and cerebrospinal fluid concentrations in fluorouracil infusion patients instead of the more complex GLC–mass spectrometric assay used previously (7, 10). Ftorafur patient data indicate that ftorafur does not release fluorouracil into the serum in concentrations comparable to levels seen during fluorouracil infusion regimens. Furthermore, the data indicate that fluorouracil does not accumulate in the serum to infusional fluorouracil levels during repeated 5-day oral administration of therapeutic doses of ftorafur.

## REFERENCES

(1) E. B. Hills, V. C. Godefroi, I. A. O'Leary, M. Burke, D. Andrzejewski, W. Brukwinski, and J. P. Horwitz, *J. Pharm. Sci.*, **66**, 1497 (1977).

(2) J. A. Benvenuto, K. Lu, S. W. Hall, R. S. Benjamin, and T. L. Loo, *Cancer Res.*, **38**, 3867 (1978).

(3) M. Valdivieso, G. P. Bodey, J. A. Gottlieb, and E. J. Freireich, *ibid.*, **36**, 1821 (1976).
(4) J. L. Au, A. T. Wu, M. A. Friedman, and W. Sadee, *Cancer Treat. Rep.*, **63**, 343 (1979).
(5) J. L. Au and W. Sadee, *Cancer Res.*, **39**, 4289 (1979).
(6) C. L. Hornbeck, J. C. Griffiths, R. A. Floyd, N. C. Ginther, J. E. Byfield, and T. R. Sharp, *Cancer Treat. Rep.*, **65**, 69 (1981).
(7) R. A. Floyd, C. L. Hornbeck, J. E. Byfield, J. C. Griffiths, T. R. Sharp, and S. Frankel, *Cancer Chemother. Pharmacol.*, in press.
(8) A. T. Wu, J. L. Au, and W. Sadee, *Cancer Res.*, **38**, 210 (1978).
(9) R. A. Floyd, J. C. Griffiths, C. L. Hornbeck, S. Frankel, T. Sharp, and J. Byfield, *Am. Soc. Clin. Oncol. (Proc.)*, **21**, 395 (1980).
(10) T. Marunaka, Y. Umeno, K. Yoshida, M. Nagamachi, Y. Minami, and S. Fujii, *J. Pharm. Sci.*, **69**, 1296 (1980).

# High-Performance Liquid Chromatographic Assay of Tolbutamide and Carboxytolbutamide in Human Plasma

**GURSHARAN RAGHOW and MARVIN C. MEYER ˣ**

Received October, 10, 1980, from the *Division of Biopharmaceutics and Pharmacokinetics, Department of Pharmaceutics, College of Pharmacy, University of Tennessee Center for the Health Sciences, Memphis, TN 38163.* Accepted for publication March 4, 1981.

**Abstract** □ A high-performance liquid chromatographic method was developed for the simultaneous measurement of tolbutamide and its major metabolite, carboxytolbutamide, in plasma. The assay involves the ether extraction of 1 ml of plasma, using chlorpropamide as an internal standard. The extract is dried, the residue is taken up in acetonitrile, and 5 μl is injected into a reversed-phase column. The mobile phase consisted of 35% acetonitrile and 65% 0.05 *M* phosphoric acid buffer (pH 3.9). A fixed-wavelength detector was set at 254 nm. The sensitivity limits for the tolbutamide and carboxytolbutamide assay were 2 and 0.1 μg/ml, respectively. The ratio of carboxytolbutamide to tolbutamide in plasma obtained from a subject given a 500-mg tolbutamide tablet was ~1:20.

**Keyphrases** □ Tolbutamide—simultaneous high-performance liquid chromatographic assay with carboxytolbutamide, human plasma □ Carboxytolbutamide—simultaneous high-performance liquid chromatographic assay with tolbutamide, human plasma □ High-performance liquid chromatography—simultaneous assay of tolbutamide and carboxytolbutamide

Tolbutamide is an oral hypoglycemic agent used for the chronic treatment of diabetes mellitus of the maturity-onset type. After oral administration to humans, ~85% of the dose is excreted in the urine as the carboxy metabolite (1-butyl-3-*p*-carboxyphenylsulfonylurea) and the hydroxymethyl metabolite (1-butyl-3-*p*-hydroxymethylphenylsulfonylurea) (1), both inactive.

## BACKGROUND

The pharmacokinetics of tolbutamide in patients is highly variable, with apparent half-lives ranging from ~2 to 25 hr (2, 3). Because of this variability, it was suggested that plasma tolbutamide concentrations should be determined in patients receiving this drug (2, 4). The bioavailability of tolbutamide after oral administration was shown to be influenced by the salt form (5), the surface area (6), and the excipients present in the formulation (7). These observations are particularly significant since changes in the serum glucose concentrations show a good relationship to the time course of tolbutamide in plasma (5, 7). Therefore, an assay method for tolbutamide and its metabolites would be useful in pharmacogenetic studies, therapeutic drug monitoring, and bioavailability studies.

Colorimetric (8–12) and UV (13) methods lack sensitivity and specificity. Methods involving GLC (14–17) require derivatization of the drug. More recently, high-performance liquid chromatographic (HPLC) methods were developed (18, 19). One method (18) is suitable for the determination of tolbutamide and its major metabolite, carboxytolbutamide, but does not use an internal standard and is not sensitive enough to quantitate the low metabolite levels reported previously (20). Another method (19) uses chlorpropamide as an internal standard but does not measure carboxytolbutamide simultaneously.

## EXPERIMENTAL

**Reagents and Chemicals**—Tolbutamide[1], carboxytolbutamide[1], chlorpropamide[2], ether[3], acetonitrile[3], hydrochloric acid[4], and phosphoric acid[5] were used.

**HPLC**—Deionized water (1 ml) and 1 ml of chlorpropamide internal standard (30 μg/ml) were added to 1 ml of plasma in a 20-ml centrifuge tube with a polytef-lined screw cap. After mixing, 0.1 ml of 1.3 *N* HCl was added; the mixture was extracted with 10 ml of ether for 15 min by gentle shaking on a platform shaker. After centrifugation at −10° for 15 min at 3000 rpm, the ether layer was transferred to a 15-ml conical tube and evaporated under nitrogen at 40°. The residue was taken up in 100 μl of acetonitrile and vortexed for 30 sec, and 5 μl was injected into the HPLC system.

The HPLC system consisted of a sample injector[6], a mobile phase pump[7] operated at 2.5 ml/min (2000 psi), a reversed-phase column[8], a fixed-wavelength UV absorbance detector[9] at 254 nm (aufs 0.01), and a recorder[10] operated at 0.5 cm/min. The mobile phase consisted of 35% acetonitrile and 65% 0.05 *M* phosphoric acid buffer (pH 3.9). Column temperature was maintained at 28°. After each use, the column was washed with water followed by methanol to avoid damage by the buffer in the mobile phase.

**Preparation of Standard Curves**—A standard solution was prepared to contain 100 μg of tolbutamide/ml and 5 μg of carboxytolbutamide/ml in 0.1 *N* NaOH. Aliquots of this solution were diluted with deionized water to yield standards containing 2, 5, 10, 20, 40, 60, and 80 μg of tolbutamide/ml and 0.1, 0.25, 0.5, 1, 2, 3, and 4 μg of carboxytolbutamide/ml. The internal standard solution contained 30 μg of chlorpropamide/ml in 0.0005 *N* NaOH. One milliliter of the tolbutamide–carboxytolbutamide solution and 1 ml of the chlorpropamide solution were added to 1 ml of pooled human plasma, and the mixture was assayed. Standard curves were prepared using duplicate samples at each concentration by plotting peak height ratio (tolbutamide to internal standard or carboxytolbutamide to internal standard) *versus* drug or metabolite concentration.

**Stability Studies**—Three 20-ml samples of pooled plasma were spiked with 20 ml of water, 20 ml of an aqueous standard containing 10 μg of tolbutamide/ml and 0.5 μg of carboxytolbutamide/ml, or 20 ml of an aqueous standard containing 80 μg of tolbutamide/ml and 4 μg of carboxytolbutamide/ml. Each portion of spiked plasma was separated into individual 8-ml portions and stored frozen at −10° for subsequent assay after 1, 2, and 4 weeks. A sample of each also was assayed immediately after preparation.

[1] Provided by The Upjohn Co., Kalamazoo, Mich.
[2] Provided by Pfizer, Brooklyn, N.Y.
[3] Burdick & Jackson Laboratories, Muskegon, Mich.
[4] Fisher Scientific Co., Fair Lawn, N.J.
[5] Mallinckrodt, Paris, Ky.
[6] Model U6K, Waters Associates, Milford Mass.
[7] Model M6000, Waters Associates, Milford, Mass.
[8] μBondapak $C_{18}$, Waters Associates, Milford, Mass.
[9] Model 440, Waters Associates, Milford, Mass.
[10] Recordall Series 5000, Fisher Scientific Co., St. Louis, Mo.



*0022-3549/81/1000-1166$01.00/0*
*© 1981, American Pharmaceutical Association*

(3) M. Valdivieso, G. P. Bodey, J. A. Gottlieb, and E. J. Freireich, *ibid.*, **36**, 1821 (1976).
(4) J. L. Au, A. T. Wu, M. A. Friedman, and W. Sadee, *Cancer Treat. Rep.*, **63**, 343 (1979).
(5) J. L. Au and W. Sadee, *Cancer Res.*, **39**, 4289 (1979).
(6) C. L. Hornbeck, J. C. Griffiths, R. A. Floyd, N. C. Ginther, J. E. Byfield, and T. R. Sharp, *Cancer Treat. Rep.*, **65**, 69 (1981).
(7) R. A. Floyd, C. L. Hornbeck, J. E. Byfield, J. C. Griffiths, T. R. Sharp, and S. Frankel, *Cancer Chemother. Pharmacol.*, in press.
(8) A. T. Wu, J. L. Au, and W. Sadee, *Cancer Res.*, **38**, 210 (1978).
(9) R. A. Floyd, J. C. Griffiths, C. L. Hornbeck, S. Frankel, T. Sharp, and J. Byfield, *Am. Soc. Clin. Oncol. (Proc.)*, **21**, 395 (1980).
(10) T. Marunaka, Y. Umeno, K. Yoshida, M. Nagamachi, Y. Minami, and S. Fujii, *J. Pharm. Sci.*, **69**, 1296 (1980).

# High-Performance Liquid Chromatographic Assay of Tolbutamide and Carboxytolbutamide in Human Plasma

**GURSHARAN RAGHOW and MARVIN C. MEYER ˣ**

Received October, 10, 1980, from the *Division of Biopharmaceutics and Pharmacokinetics, Department of Pharmaceutics, College of Pharmacy, University of Tennessee Center for the Health Sciences, Memphis, TN 38163.* Accepted for publication March 4, 1981.

**Abstract** □ A high-performance liquid chromatographic method was developed for the simultaneous measurement of tolbutamide and its major metabolite, carboxytolbutamide, in plasma. The assay involves the ether extraction of 1 ml of plasma, using chlorpropamide as an internal standard. The extract is dried, the residue is taken up in acetonitrile, and 5 μl is injected into a reversed-phase column. The mobile phase consisted of 35% acetonitrile and 65% 0.05 *M* phosphoric acid buffer (pH 3.9). A fixed-wavelength detector was set at 254 nm. The sensitivity limits for the tolbutamide and carboxytolbutamide assay were 2 and 0.1 μg/ml, respectively. The ratio of carboxytolbutamide to tolbutamide in plasma obtained from a subject given a 500-mg tolbutamide tablet was ~1:20.

**Keyphrases** □ Tolbutamide—simultaneous high-performance liquid chromatographic assay with carboxytolbutamide, human plasma □ Carboxytolbutamide—simultaneous high-performance liquid chromatographic assay with tolbutamide, human plasma □ High-performance liquid chromatography—simultaneous assay of tolbutamide and carboxytolbutamide

Tolbutamide is an oral hypoglycemic agent used for the chronic treatment of diabetes mellitus of the maturity-onset type. After oral administration to humans, ~85% of the dose is excreted in the urine as the carboxy metabolite (1-butyl-3-*p*-carboxyphenylsulfonylurea) and the hydroxymethyl metabolite (1-butyl-3-*p*-hydroxymethylphenylsulfonylurea) (1), both inactive.

## BACKGROUND

The pharmacokinetics of tolbutamide in patients is highly variable, with apparent half-lives ranging from ~2 to 25 hr (2, 3). Because of this variability, it was suggested that plasma tolbutamide concentrations should be determined in patients receiving this drug (2, 4). The bioavailability of tolbutamide after oral administration was shown to be influenced by the salt form (5), the surface area (6), and the excipients present in the formulation (7). These observations are particularly significant since changes in the serum glucose concentrations show a good relationship to the time course of tolbutamide in plasma (5, 7). Therefore, an assay method for tolbutamide and its metabolites would be useful in pharmacogenetic studies, therapeutic drug monitoring, and bioavailability studies.

Colorimetric (8–12) and UV (13) methods lack sensitivity and specificity. Methods involving GLC (14–17) require derivatization of the drug. More recently, high-performance liquid chromatographic (HPLC) methods were developed (18, 19). One method (18) is suitable for the determination of tolbutamide and its major metabolite, carboxytolbutamide, but does not use an internal standard and is not sensitive enough to quantitate the low metabolite levels reported previously (20). Another method (19) uses chlorpropamide as an internal standard but does not measure carboxytolbutamide simultaneously.

## EXPERIMENTAL

**Reagents and Chemicals**—Tolbutamide[1], carboxytolbutamide[1], chlorpropamide[2], ether[3], acetonitrile[3], hydrochloric acid[4], and phosphoric acid[5] were used.

**HPLC**—Deionized water (1 ml) and 1 ml of chlorpropamide internal standard (30 μg/ml) were added to 1 ml of plasma in a 20-ml centrifuge tube with a polytef-lined screw cap. After mixing, 0.1 ml of 1.3 *N* HCl was added; the mixture was extracted with 10 ml of ether for 15 min by gentle shaking on a platform shaker. After centrifugation at −10° for 15 min at 3000 rpm, the ether layer was transferred to a 15-ml conical tube and evaporated under nitrogen at 40°. The residue was taken up in 100 μl of acetonitrile and vortexed for 30 sec, and 5 μl was injected into the HPLC system.

The HPLC system consisted of a sample injector[6], a mobile phase pump[7] operated at 2.5 ml/min (2000 psi), a reversed-phase column[8], a fixed-wavelength UV absorbance detector[9] at 254 nm (aufs 0.01), and a recorder[10] operated at 0.5 cm/min. The mobile phase consisted of 35% acetonitrile and 65% 0.05 *M* phosphoric acid buffer (pH 3.9). Column temperature was maintained at 28°. After each use, the column was washed with water followed by methanol to avoid damage by the buffer in the mobile phase.

**Preparation of Standard Curves**—A standard solution was prepared to contain 100 μg of tolbutamide/ml and 5 μg of carboxytolbutamide/ml in 0.1 *N* NaOH. Aliquots of this solution were diluted with deionized water to yield standards containing 2, 5, 10, 20, 40, 60, and 80 μg of tolbutamide/ml and 0.1, 0.25, 0.5, 1, 2, 3, and 4 μg of carboxytolbutamide/ml. The internal standard solution contained 30 μg of chlorpropamide/ml in 0.0005 *N* NaOH. One milliliter of the tolbutamide–carboxytolbutamide solution and 1 ml of the chlorpropamide solution were added to 1 ml of pooled human plasma, and the mixture was assayed. Standard curves were prepared using duplicate samples at each concentration by plotting peak height ratio (tolbutamide to internal standard or carboxytolbutamide to internal standard) *versus* drug or metabolite concentration.

**Stability Studies**—Three 20-ml samples of pooled plasma were spiked with 20 ml of water, 20 ml of an aqueous standard containing 10 μg of tolbutamide/ml and 0.5 μg of carboxytolbutamide/ml, or 20 ml of an aqueous standard containing 80 μg of tolbutamide/ml and 4 μg of carboxytolbutamide/ml. Each portion of spiked plasma was separated into individual 8-ml portions and stored frozen at −10° for subsequent assay after 1, 2, and 4 weeks. A sample of each also was assayed immediately after preparation.

[1] Provided by The Upjohn Co., Kalamazoo, Mich.
[2] Provided by Pfizer, Brooklyn, N.Y.
[3] Burdick & Jackson Laboratories, Muskegon, Mich.
[4] Fisher Scientific Co., Fair Lawn, N.J.
[5] Mallinckrodt, Paris, Ky.
[6] Model U6K, Waters Associates, Milford Mass.
[7] Model M6000, Waters Associates, Milford, Mass.
[8] μBondapak $C_{18}$, Waters Associates, Milford, Mass.
[9] Model 440, Waters Associates, Milford, Mass.
[10] Recordall Series 5000, Fisher Scientific Co., St. Louis, Mo.



*0022-3549/81/1000-1166$01.00/0*
*© 1981, American Pharmaceutical Association*

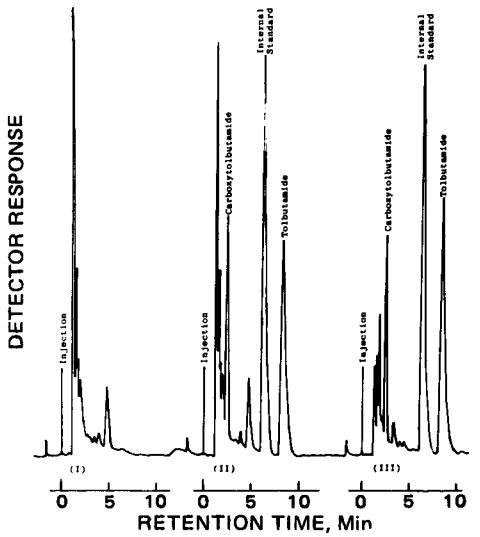


**Figure 1**—*Chromatograms for plasma extracts. Key: I, blank pooled plasma; II, pooled plasma spiked with 40 μg of tolbutamide/ml, 2 μg of carboxytolbutamide/ml, and 30 μg of chlorpropamide/ml as the internal standard; and III, plasma sample obtained from human subject 4 hr after a 500-mg oral dose of tolbutamide, with chlorpropamide added as internal standard.*

**Human Study**—A healthy male volunteer received a single commercially available 500-mg tolbutamide tablet. Blood samples (10 ml) were obtained just before and at 0.5, 1, 2, 3, 4, 6, and 24 hr after drug administration. These samples were assayed for tolbutamide and carboxytolbutamide levels using the described procedures.

## RESULTS AND DISCUSSION

Tolbutamide, carboxytolbutamide, and chlorpropamide each exhibited a 235-nm wavelength of maximum absorbance when present in the mobile phase. A wavelength of 254 nm was selected to permit utilization of a fixed-wavelength detector. The absorptivities of tolbutamide, carboxytolbutamide, and chlorpropamide in the mobile phase were 3.2, 27.9, and 9.3 liters/g cm, respectively, at 254 nm.

Typical chromatograms for extracted plasma are shown in Fig. 1 for a pooled plasma sample containing no drug, a pooled plasma sample containing 40 μg of tolbutamide/ml and 2 μg of carboxy metabolite/ml, and a plasma sample obtained from a subject 4 hr after a 500-mg oral dose of tolbutamide. Chlorpropamide (30 μg/ml) was added to the latter two samples. The metabolite, internal standard, and drug peaks were well resolved with retention times of 1.8, 5.6, and 7.8 min, respectively. A peak with a retention time of 4.0 min appeared in extracts of pooled plasma but did not interfere in the assay, provided the mobile phase was carefully maintained at pH 3.9. This peak did not appear in the plasma samples freshly obtained from a human subject. The recoveries of tolbutamide, the carboxy metabolite, and chlorpropamide were ~99, 80, and 60%, respectively, relative to a direct HPLC assay of aqueous standards. Thus, the greater sensitivity of the assay for carboxytolbutamide was due to absorptivity differences rather than extraction efficiency.

Standard curves prepared for both tolbutamide and the carboxy metabolite exhibited excellent linearity over the concentration ranges employed for each material. The least-squares slope, intercept, and correlation coefficient for the tolbutamide calibration curve were 0.0140, 0.0052, and 0.9999, respectively. The same values for the carboxy metabolite were 0.303, −0.013, and 0.9999, respectively. The precision of the assay for tolbutamide and carboxytolbutamide was determined by the analysis of six replicate samples at each of three concentrations. Plasma samples containing 10, 40, and 80 μg of tolbutamide/ml exhibited relative standard deviations of 1.8, 0.5, and 0.4%, respectively. Plasma samples containing 0.5, 2.0, and 4.0 μg of carboxytolbutamide/ml exhibited relative standard deviations of 7.9, 2.2, and 1.4%, respectively. The lower limits of sensitivity were 2 μg/ml for tolbutamide and 0.1 μg/ml for the carboxy metabolite. Analysis of the spiked pooled plasma samples that had been stored frozen for 1, 2, and 4 weeks indicated no significant loss of tolbutamide or the carboxy metabolite over that period.

Figure 2 summarizes the tolbutamide and carboxy metabolite concentrations determined in a subject who received a 500-mg of tolbutamide

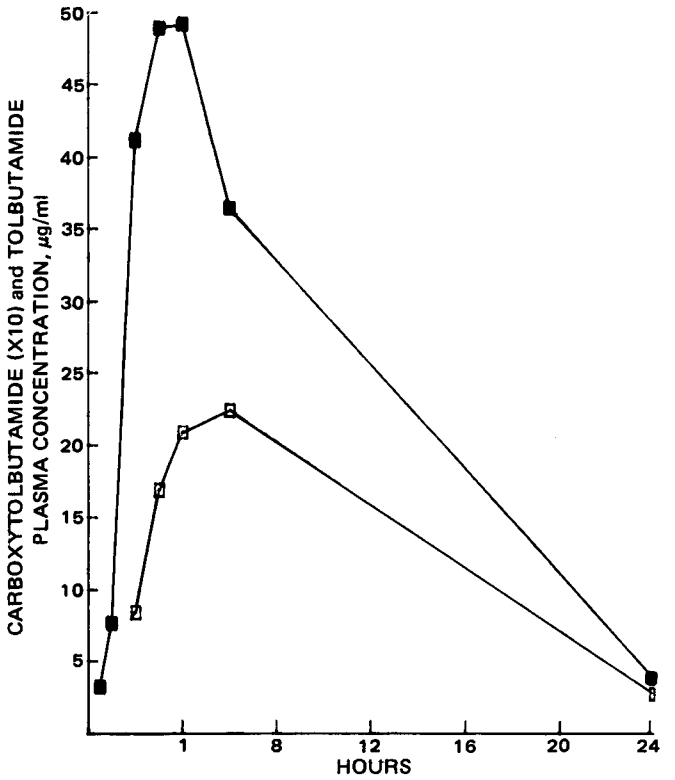


**Figure 2**—*Plasma concentrations of tolbutamide (■) and carboxytolbutamide (□) following administration of a 500-mg oral dose of tolbutamide to a human subject.*

tablet. The peak plasma tolbutamide concentration of 49 μg/ml was in the range of peak levels reported in other studies with human subjects who received 500-mg oral doses of the drug (17, 21). The peak plasma carboxy metabolite concentration was 2.2 μg/ml, which was ~1/20 the tolbutamide concentration. Matin and Knight (20) found a ratio of ~50:1 for tolbutamide to the carboxy metabolite after administration of a 1-g iv dose to a diabetic patient. They also reported the presence of a hydroxymethyl metabolite in this patient. The concentration of the metabolite paralleled that of the carboxy metabolite but was ~50% that of the major metabolite. Since an authentic sample of the hydroxymethyl metabolite was unavailable, it was not possible to determine the potential for this compound to interfere in the present assay or to be quantitated by the assay. However, chromatograms obtained with the assay did not reveal any evidence of an additional peak that could be attributed to this metabolite.

Based on these data, the reported method exhibits adequate sensitivity and specificity for single-dose bioavailability studies as well as for the monitoring of plasma tolbutamide concentrations in patients. In addition, the method is applicable to pharmacokinetic studies of the drug and its primary metabolite. It also should be applicable to the determination of plasma chlorpropamide concentrations with tolbutamide as the internal standard.

## REFERENCES

(1) R. C. Thomas and G. J. Ikeda, *J. Med. Chem.*, **9**, 507 (1966).
(2) J. Scott and P. L. Poffenbarger, *Diabetes*, **28**, 41 (1979).
(3) E. A. Sotaniemi and E. Huhti, *Am. Clin. Res.*, **6**, 146 (1974).
(4) A. Melander, G. Sartor, E. Wahlin, B. Schersten, and P. O. Bitzen, *Br. Med. J.*, **1**, 142 (1978).
(5) E. Nelson, E. L. Knoechel, W. E. Hamlin, and J. G. Wagner, *J. Pharm. Sci.*, **51**, 509 (1962).
(6) E. Nelson, S. Long, and J. G. Wagner, *J. Pharm. Sci.*, **53**, 1224 (1964).
(7) A. B. Varley, *J. Am. Med. Assoc.*, **206**, 1745 (1968).
(8) H. Spingler, *Klin. Wochenschr.*, **35**, 533 (1957).
(9) R. H. Carmichael, *Clin. Chem.*, **5**, 597 (1959).
(10) T. Chulski, *J. Lab. Clin. Med.*, **53**, 490 (1959).
(11) W. Kern, *Anal. Chem.*, **35**, 50 (1963).
(12) S. B. Matin and M. Rowland, *J. Pharm. Pharmacol.*, **25**, 186 (1973).

(13) J. Sibasaki, R. Konishi, T. Ueki, and T. Morishita, *Chem. Pharm. Bull.*, **21**, 1747 (1973).
(14) K. Sabih and K. Sabih, *J. Pharm. Sci.*, **59**, 782 (1970).
(15) J. A. Taylor, *Clin. Pharmacol. Ther.*, **13**, 710 (1972).
(16) T. J. Toolan and R. L. Wagner, Jr., *Ann. N.Y. Acad. Sci.*, **74**, 449 (1959).
(17) K. K. Midha, I. J. McGilveray, and C. Charette, *J. Pharm. Sci.*, **65**, 576 (1976).
(18) R. L. Nation, G. W. Peng, and W. L. Chiou, *J. Chromatogr.*, **146**, 121 (1978).
(19) S. Sved, I. J. McGilveray, and N. Beaudoin, *J. Pharm. Sci.*, **65**, 1356 (1976).
(20) S. B. Matin and J. B. Knight, *Biomed. Mass Spectrom.*, **1**, 323 (1974).
(21) K. A. DeSante, in "Tolbutamide Tablets USP Upjohn," Bioavailability Study BA 17–2, Upjohn Co., Kalamazoo, Mich., 1977.

**ACKNOWLEDGMENTS**

Supported in part by the Tennessee Department of Public Health and FDA Contract 223-77-3097.

# Human Blood Preservation: Effect on *In Vitro* Protein Binding

**ANDRÉ J. JACKSON ˣ, ANN K. MILLER, and PREM K. NARANG**

Received September 8, 1980, from the *Clinical Pharmacokinetics Laboratory, School of Pharmacy, University of Maryland, Baltimore, MD 21201.* Accepted for publication March 23, 1981.

**Abstract** □ *In vitro* plasma protein binding for phenytoin, meperidine, and bretylium tosylate was affected by the type of preserved human blood used for its estimation. Fresh heparinized plasma and serum gave equivalent fractions bound at the concentrations studied for all three drugs. However, the *in vitro* plasma binding of phenytoin and meperidine decreased ~9–50% when estimated in fresh citrated plasma or commercially available lyophylized human serum at the concentration levels investigated. The fraction of bretylium tosylate bound to plasma protein decreased ~30–40% when estimated in fresh citrated plasma but was unchanged when estimated in the lyophylized human serum.

**Keyphrases** □ Binding, plasma protein—effect of blood preservation, humans □ Blood—preservation, effect on *in vitro* plasma protein binding □ Pharmacokinetics—effect of human blood preservation on *in vitro* protein binding

The influence of plasma protein binding on the distribution and elimination of drugs was recently reviewed (1). Accurate evaluation of the fraction of drug bound is essential for a thorough understanding of a drug's pharmacokinetics. Plasma/serum protein binding is normally estimated using several *in vitro* techniques such as equilibrium dialysis, ultrafiltration, gel filtration, differential spectrophotometry, and electrophoresis (2). Several investigators determined plasma protein binding in fresh plasma from subjects participating in pharmacokinetic studies (3, 4), and other sources of blood were utilized in other studies. A frequently reported source is fresh blood bank plasma (5, 6). Blood bank plasma is normally preserved with a standard anticoagulant/preservative, citrate phosphate dextrose USP. However, the presence of preservative has been implicated in lowering the protein binding of quinidine (5). Therefore, it is important that the effect of blood constituents and preservatives be evaluated.

The purpose of this investigation was to determine if a standard anticoagulant/preservative would interfere with the binding of other drugs and the suitability of a commercially available lyophilized serum[1] as a substitute for blood bank plasma when large volumes of plasma/serum are required. The drugs studied, phenytoin, meperidine, and bretylium tosylate, are chemically different and have been reported[2] to exhibit a binding of 90, 60, and 10%[2], respectively (3, 7).

## EXPERIMENTAL

Blood was obtained from one healthy male volunteer, 27 years of age, who was not using any medication. Blood was collected in a clean glass flask containing either 400 IU of heparin/20 ml of blood or 63 ml of citrate phosphate dextrose/450 ml of blood. The blood to be used as serum was collected in clean glass test tubes and allowed to clot. Lyophilized serum[1], reconstituted according to the manufacturer's suggestion, was used as the commercial source of lyophilized human serum.

**Table I—Effect of Blood Preservation Procedure on Fraction of Drug Bound** [a]

| Drug | Concentration, μg/ml | Fresh Plasma Heparin | Fresh Plasma Citrate | Fresh Serum | Lyophilized Serum |
|---|---|---|---|---|---|
| Phenytoin | 15.0 | 0.89 (0.90, 0.88) | 0.80 (0.76, 0.84) | 0.89 (0.89, 0.89) | 0.80 (0.79, 0.81) |
| | 5.0 | 0.90 (0.89, 0.90) | 0.81 (0.79, 0.83) | 0.90 (0.91, 0.89) | 0.80 (0.80, 0.80) |
| Meperidine | 0.98 | 0.58 (0.56, 0.60) | 0.25 (0.23, 0.27) | 0.54 (0.52, 0.56) | 0.26 (0.22, 0.30) |
| | 0.12 | 0.60 (0.58, 0.62) | 0.27 (0.22, 0.28) | 0.58 (0.52, 0.62) | 0.23 (0.18, 0.28) |
| Bretylium | 1.2 | 0.13 (0.14, 0.12) | 0.04 (0.04, 0.04) | 0.10 (0.12, 0.09) | 0.12 (0.12, 0.12) |
| tosylate | 0.3 | 0.11 (0.12, 0.11) | 0.06 (0.06, 0.05) | 0.11 (0.10, 0.12) | 0.10 (0.08, 0.12) |

[a] Mean of two determinations; individual values are given in parentheses.

A standard solution of [$^{14}$C]meperidine, [$^{14}$C]bretylium tosylate, or [$^{14}$C]phenytoin was added to plasma at two concentrations within the respective therapeutic ranges. Protein binding was then determined by equilibrium dialysis. The samples were dialyzed across a cellophane membrane against phosphate buffer (0.067 *M*, pH 7.4) at 37° using a dialysis cell. Equilibrium was achieved for each drug by 24 hr. A control

[1] Sera Chem, Fisher Scientific, Orangeburg, NY 10962.
[2] A. Yacobi, personal communication, American Critical Care, McGaw Park, IL.



0022-3549/81/1000-1168$01.00/0
© 1981, American Pharmaceutical Association

(13) J. Sibasaki, R. Konishi, T. Ueki, and T. Morishita, *Chem. Pharm. Bull.*, **21**, 1747 (1973).
(14) K. Sabih and K. Sabih, *J. Pharm. Sci.*, **59**, 782 (1970).
(15) J. A. Taylor, *Clin. Pharmacol. Ther.*, **13**, 710 (1972).
(16) T. J. Toolan and R. L. Wagner, Jr., *Ann. N.Y. Acad. Sci.*, **74**, 449 (1959).
(17) K. K. Midha, I. J. McGilveray, and C. Charette, *J. Pharm. Sci.*, **65**, 576 (1976).
(18) R. L. Nation, G. W. Peng, and W. L. Chiou, *J. Chromatogr.*, **146**, 121 (1978).
(19) S. Sved, I. J. McGilveray, and N. Beaudoin, *J. Pharm. Sci.*, **65**, 1356 (1976).
(20) S. B. Matin and J. B. Knight, *Biomed. Mass Spectrom.*, **1**, 323 (1974).
(21) K. A. DeSante, in "Tolbutamide Tablets USP Upjohn," Bioavailability Study BA 17–2, Upjohn Co., Kalamazoo, Mich., 1977.

**ACKNOWLEDGMENTS**

Supported in part by the Tennessee Department of Public Health and FDA Contract 223-77-3097.

# Human Blood Preservation: Effect on *In Vitro* Protein Binding

**ANDRÉ J. JACKSON ˣ, ANN K. MILLER, and PREM K. NARANG**

Received September 8, 1980, from the *Clinical Pharmacokinetics Laboratory, School of Pharmacy, University of Maryland, Baltimore, MD 21201.* Accepted for publication March 23, 1981.

**Abstract** □ *In vitro* plasma protein binding for phenytoin, meperidine, and bretylium tosylate was affected by the type of preserved human blood used for its estimation. Fresh heparinized plasma and serum gave equivalent fractions bound at the concentrations studied for all three drugs. However, the *in vitro* plasma binding of phenytoin and meperidine decreased ~9–50% when estimated in fresh citrated plasma or commercially available lyophylized human serum at the concentration levels investigated. The fraction of bretylium tosylate bound to plasma protein decreased ~30–40% when estimated in fresh citrated plasma but was unchanged when estimated in the lyophylized human serum.

**Keyphrases** □ Binding, plasma protein—effect of blood preservation, humans □ Blood—preservation, effect on *in vitro* plasma protein binding □ Pharmacokinetics—effect of human blood preservation on *in vitro* protein binding

The influence of plasma protein binding on the distribution and elimination of drugs was recently reviewed (1). Accurate evaluation of the fraction of drug bound is essential for a thorough understanding of a drug's pharmacokinetics. Plasma/serum protein binding is normally estimated using several *in vitro* techniques such as equilibrium dialysis, ultrafiltration, gel filtration, differential spectrophotometry, and electrophoresis (2). Several investigators determined plasma protein binding in fresh plasma from subjects participating in pharmacokinetic studies (3, 4), and other sources of blood were utilized in other studies. A frequently reported source is fresh blood bank plasma (5, 6). Blood bank plasma is normally preserved with a standard anticoagulant/preservative, citrate phosphate dextrose USP. However, the presence of preservative has been implicated in lowering the protein binding of quinidine (5). Therefore, it is important that the effect of blood constituents and preservatives be evaluated.

The purpose of this investigation was to determine if a standard anticoagulant/preservative would interfere with the binding of other drugs and the suitability of a commercially available lyophilized serum[1] as a substitute for blood bank plasma when large volumes of plasma/serum are required. The drugs studied, phenytoin, meperidine, and bretylium tosylate, are chemically different and have been reported[2] to exhibit a binding of 90, 60, and 10%[2], respectively (3, 7).

## EXPERIMENTAL

Blood was obtained from one healthy male volunteer, 27 years of age, who was not using any medication. Blood was collected in a clean glass flask containing either 400 IU of heparin/20 ml of blood or 63 ml of citrate phosphate dextrose/450 ml of blood. The blood to be used as serum was collected in clean glass test tubes and allowed to clot. Lyophilized serum[1], reconstituted according to the manufacturer's suggestion, was used as the commercial source of lyophilized human serum.

**Table I—Effect of Blood Preservation Procedure on Fraction of Drug Bound** [a]

| Drug | Concentration, μg/ml | Fresh Plasma Heparin | Fresh Plasma Citrate | Fresh Serum | Lyophilized Serum |
|---|---|---|---|---|---|
| Phenytoin | 15.0 | 0.89 (0.90, 0.88) | 0.80 (0.76, 0.84) | 0.89 (0.89, 0.89) | 0.80 (0.79, 0.81) |
| | 5.0 | 0.90 (0.89, 0.90) | 0.81 (0.79, 0.83) | 0.90 (0.91, 0.89) | 0.80 (0.80, 0.80) |
| Meperidine | 0.98 | 0.58 (0.56, 0.60) | 0.25 (0.23, 0.27) | 0.54 (0.52, 0.56) | 0.26 (0.22, 0.30) |
| | 0.12 | 0.60 (0.58, 0.62) | 0.27 (0.22, 0.28) | 0.58 (0.52, 0.62) | 0.23 (0.18, 0.28) |
| Bretylium | 1.2 | 0.13 (0.14, 0.12) | 0.04 (0.04, 0.04) | 0.10 (0.12, 0.09) | 0.12 (0.12, 0.12) |
| tosylate | 0.3 | 0.11 (0.12, 0.11) | 0.06 (0.06, 0.05) | 0.11 (0.10, 0.12) | 0.10 (0.08, 0.12) |

[a] Mean of two determinations; individual values are given in parentheses.

A standard solution of [$^{14}$C]meperidine, [$^{14}$C]bretylium tosylate, or [$^{14}$C]phenytoin was added to plasma at two concentrations within the respective therapeutic ranges. Protein binding was then determined by equilibrium dialysis. The samples were dialyzed across a cellophane membrane against phosphate buffer (0.067 *M*, pH 7.4) at 37° using a dialysis cell. Equilibrium was achieved for each drug by 24 hr. A control

[1] Sera Chem, Fisher Scientific, Orangeburg, NY 10962.
[2] A. Yacobi, personal communication, American Critical Care, McGaw Park, IL.



0022-3549/81/1000-1168$01.00/0
© 1981, American Pharmaceutical Association

dialysis was run at each concentration. Following equilibration, aliquots of the buffer and plasma compartments were sampled and analyzed by liquid scintillation spectrometry. Sample efficiency was estimated by external standardization.

## RESULTS AND DISCUSSION

Data presented in Table I indicate agreement of the binding values in fresh serum and heparinized plasma with those reported earlier[2] (3, 7). However, the binding of all three drugs significantly decreased in the fresh blood bank plasma, thereby indicating drug displacement from binding sites by the citrate phosphate dextrose preservative. The decreased binding was not due to a change in pH since the pH was maintained at 7.4 after addition of the preservative. The binding of phenytoin and meperidine was also lowered in lyophilized serum while that of bretylium tosylate was not affected. The manufacturer reports that salicylates are added to lyophilized serum. Therefore, a possible explanation may be a change in protein conformation due to freezing and reconstitution, which would affect the more heavily bound drugs (phenytoin and meperidine) or competitive interaction with the salicylates. Bretylium tosylate would be least affected since it is only 10% bound.

Based on these results, studies done with commercial lyophilized serum should be verified by binding studies in fresh plasma/serum. Furthermore, when blood bank plasma is used for binding studies, the type of preservative used should be stated to allow rigorous evaluation of the pharmacokinetic parameters related to the free fraction and to facilitate duplication of protein binding studies.

## REFERENCES


(1) J. J. Vallner, *J. Pharm. Sci.*, **66**, 447 (1977).

(2) C. Davidson, in "Fundamentals of Drug Metabolism and Drug Disposition," B. LaDu, H. Mandel, and E. Way, Eds., Williams & Wilkins, Baltimore, Md., 1971, pp. 63–74.

(3) U. Klotz, T. S. McHorse, G. R. Wilkinson, and S. Schenker, *Clin. Pharmacol. Ther.*, **16**, 667 (1974).

(4) L. E. Mather, G. T. Tucker, A. E. Pflug, M. J. Lindop, and C. Wilkerson, *ibid.*, **17**, 21 (1975).

(5) E. Woo and D. J. Greenblatt, *J. Pharm. Sci.*, **68**, 466 (1979).

(6) P. H. Hinderling, J. Bres, and E. R. Garrett, *ibid.*, **63**, 1684 (1974).

(7) V. W. Weigan, K. L. Hintze, J. T. Slattery, and G. Levy, *Clin. Pharmacol. Ther.*, **27**, 297 (1980).


# Acyclic Puromycin Analogs: 9-[(2-Phenylalanylamidoethoxy)methyl]adenine and 9-(3-Phenylalanylamidopropyl)adenine


**JAMES L. KELLEY[x], CARL A. MILLER, and HOWARD J. SCHAEFFER**



Received January 29, 1981 from *Wellcome Research Laboratories, Research Triangle Park, NC 27709.*
Accepted for publication April 1, 1981.



**Abstract** □ Two acyclic puromycin analogs, in which the 2′- and 5′-hydroxymethyl groups or the 2′-hydroxyl and 5′-hydroxyethoxy portions of the cyclic carbohydrate ring were excised, were synthesized and evaluated for inhibition of an *in vitro* protein-synthesizing system and for antiviral and antibacterial activity. No puromycin-like activity was seen with these conformationally free compounds.



**Keyphrases** □ Puromycin—acyclic analogs, synthesis and analysis, evaluation for inhibition of protein synthesis and antiviral and antibacterial activity □ Analogs—of puromycin, acyclic, synthesis and analysis, evaluation for inhibition of protein synthesis and antiviral and antibacterial activity □ Antineoplastics—puromycin, synthesis and analysis of acyclic analogs, evaluation for inhibition of protein synthesis and antiviral and antibacterial activity


A program initiated to synthesize nucleoside analogs, in which the cyclic carbohydrate moiety is replaced by an acyclic side chain, led to the discovery of the potent antiherpetic drug acyclovir, 9-[(2-hydroxyethoxy)methyl]-guanine[1] (1). This approach to nucleoside modification has been extended to the synthesis of two acyclic analogs of the broad spectrum antibiotic puromycin (I). This nucleoside antibiotic, which is an inhibitor of protein biosynthesis, has not been useful in the treatment of human disease because of its nephrotoxicity (2). It was shown (3–5), however, that toxicity could be alleviated by removal of the 5′-hydroxy group.

This paper reports an approach to separation of toxicity from activity involving the synthesis of distinct fragments of puromycin in which parts of the cyclic carbohydrate moiety are excised. Elimination of the 2′- and 5′-hydroxymethyl groups (dotted lines in I) or the 2′-hydroxyl and 5′-hydroxyethoxy portions (broken lines) would leave side chains as in II*a* or II*b*, respectively[2]. Both II*a* and II*b* can assume a conformation that is superimposable on puromycin, but they lack the 5′-hydroxyl group implicated in puromycin toxicity (3, 6). Open chain analogs similar to

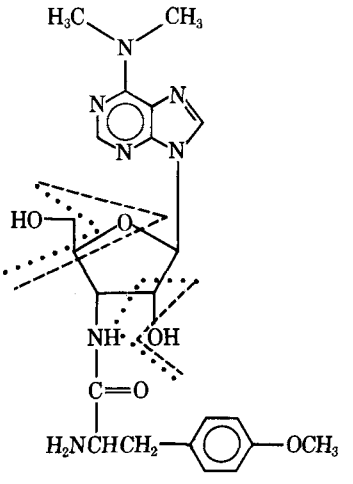

I

[1] Zovirax.

[2] In this work, the readily available DL-phenylalanine was used since the phenylalanyl analog of puromycin is nearly as active as puromycin (7, 8). In addition, the *N* 6-methyl groups of puromycin were shown to be unnecessary for puromycin-like activity (9).


0022-3549/81/1000-1169$01.00/0


© 1981, American Pharmaceutical Association

dialysis was run at each concentration. Following equilibration, aliquots of the buffer and plasma compartments were sampled and analyzed by liquid scintillation spectrometry. Sample efficiency was estimated by external standardization.

## RESULTS AND DISCUSSION

Data presented in Table I indicate agreement of the binding values in fresh serum and heparinized plasma with those reported earlier[2] (3, 7). However, the binding of all three drugs significantly decreased in the fresh blood bank plasma, thereby indicating drug displacement from binding sites by the citrate phosphate dextrose preservative. The decreased binding was not due to a change in pH since the pH was maintained at 7.4 after addition of the preservative. The binding of phenytoin and meperidine was also lowered in lyophilized serum while that of bretylium tosylate was not affected. The manufacturer reports that salicylates are added to lyophilized serum. Therefore, a possible explanation may be a change in protein conformation due to freezing and reconstitution, which would affect the more heavily bound drugs (phenytoin and meperidine) or competitive interaction with the salicylates. Bretylium tosylate would be least affected since it is only 10% bound.

Based on these results, studies done with commercial lyophilized serum should be verified by binding studies in fresh plasma/serum. Furthermore, when blood bank plasma is used for binding studies, the type of preservative used should be stated to allow rigorous evaluation of the pharmacokinetic parameters related to the free fraction and to facilitate duplication of protein binding studies.

## REFERENCES


(1) J. J. Vallner, *J. Pharm. Sci.*, **66**, 447 (1977).

(2) C. Davidson, in "Fundamentals of Drug Metabolism and Drug Disposition," B. LaDu, H. Mandel, and E. Way, Eds., Williams & Wilkins, Baltimore, Md., 1971, pp. 63–74.

(3) U. Klotz, T. S. McHorse, G. R. Wilkinson, and S. Schenker, *Clin. Pharmacol. Ther.*, **16**, 667 (1974).

(4) L. E. Mather, G. T. Tucker, A. E. Pflug, M. J. Lindop, and C. Wilkerson, *ibid.*, **17**, 21 (1975).

(5) E. Woo and D. J. Greenblatt, *J. Pharm. Sci.*, **68**, 466 (1979).

(6) P. H. Hinderling, J. Bres, and E. R. Garrett, *ibid.*, **63**, 1684 (1974).

(7) V. W. Weigan, K. L. Hintze, J. T. Slattery, and G. Levy, *Clin. Pharmacol. Ther.*, **27**, 297 (1980).


# Acyclic Puromycin Analogs: 9-[(2-Phenylalanylamidoethoxy)methyl]adenine and 9-(3-Phenylalanylamidopropyl)adenine


**JAMES L. KELLEY[x], CARL A. MILLER, and HOWARD J. SCHAEFFER**



Received January 29, 1981 from *Wellcome Research Laboratories, Research Triangle Park, NC 27709.*
Accepted for publication April 1, 1981.



**Abstract** □ Two acyclic puromycin analogs, in which the 2′- and 5′-hydroxymethyl groups or the 2′-hydroxyl and 5′-hydroxyethoxy portions of the cyclic carbohydrate ring were excised, were synthesized and evaluated for inhibition of an *in vitro* protein-synthesizing system and for antiviral and antibacterial activity. No puromycin-like activity was seen with these conformationally free compounds.



**Keyphrases** □ Puromycin—acyclic analogs, synthesis and analysis, evaluation for inhibition of protein synthesis and antiviral and antibacterial activity □ Analogs—of puromycin, acyclic, synthesis and analysis, evaluation for inhibition of protein synthesis and antiviral and antibacterial activity □ Antineoplastics—puromycin, synthesis and analysis of acyclic analogs, evaluation for inhibition of protein synthesis and antiviral and antibacterial activity


A program initiated to synthesize nucleoside analogs, in which the cyclic carbohydrate moiety is replaced by an acyclic side chain, led to the discovery of the potent antiherpetic drug acyclovir, 9-[(2-hydroxyethoxy)methyl]-guanine[1] (1). This approach to nucleoside modification has been extended to the synthesis of two acyclic analogs of the broad spectrum antibiotic puromycin (I). This nucleoside antibiotic, which is an inhibitor of protein biosynthesis, has not been useful in the treatment of human disease because of its nephrotoxicity (2). It was shown (3–5), however, that toxicity could be alleviated by removal of the 5′-hydroxy group.

This paper reports an approach to separation of toxicity from activity involving the synthesis of distinct fragments of puromycin in which parts of the cyclic carbohydrate moiety are excised. Elimination of the 2′- and 5′-hydroxymethyl groups (dotted lines in I) or the 2′-hydroxyl and 5′-hydroxyethoxy portions (broken lines) would leave side chains as in II*a* or II*b*, respectively[2]. Both II*a* and II*b* can assume a conformation that is superimposable on puromycin, but they lack the 5′-hydroxyl group implicated in puromycin toxicity (3, 6). Open chain analogs similar to

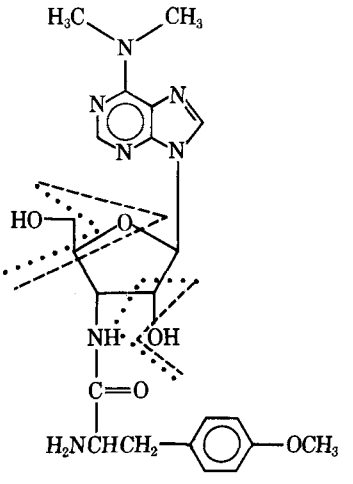

I

[1] Zovirax.

[2] In this work, the readily available DL-phenylalanine was used since the phenylalanyl analog of puromycin is nearly as active as puromycin (7, 8). In addition, the *N* 6-methyl groups of puromycin were shown to be unnecessary for puromycin-like activity (9).


0022-3549/81/1000-1169$01.00/0


© 1981, American Pharmaceutical Association

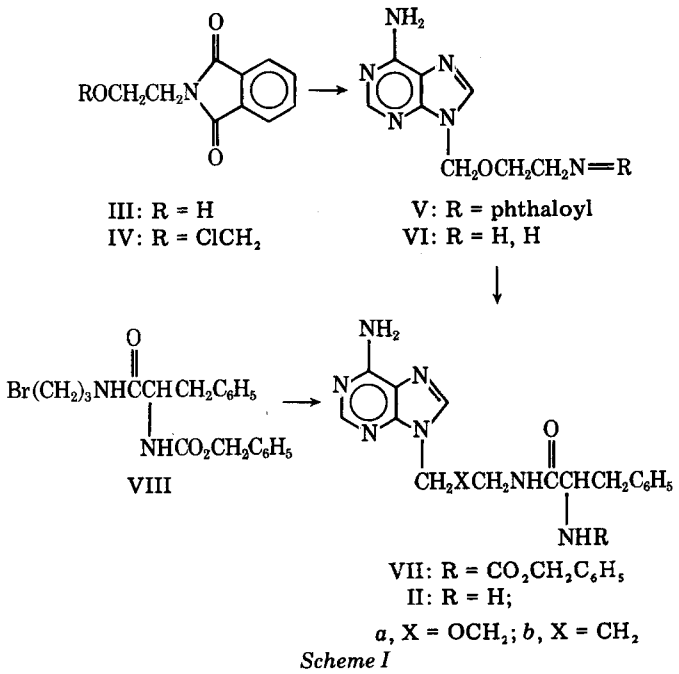


*Scheme I*

IIb but containing a 2′-hydroxyl group were reported to have powerful (10) or moderate (11, 12) puromycin-like activity. Evidence on the importance of a 2′-hydroxyl group for puromycin-like activity is conflicting (13–16).

The present paper reports the synthesis of two acyclic analogs of puromycin that lack the 5′- and 2′-hydroxyl groups. These compounds were tested for inhibition of an *in vitro* protein-synthesizing system and for antiviral and antibacterial activity.

## RESULTS AND DISCUSSION

The acyclic puromycin analogs IIa and IIb were synthesized as outlined in Scheme I. Chloromethylation (17) of III gave IV, which was reacted with adenine to give V. Identity of the product as a 9-substituted adenine was indicated from the UV spectrum (18). Cleavage of the phthaloyl group gave VI, which was coupled with DL-*N*-carbobenzoxyphenylalanine using the mixed anhydride method (19) to give VIIa. Hydrogenolysis of VIIa gave the acyclic puromycin analog IIa. For preparation of IIb, adenine was alkylated with VIII, followed by cleavage of the carbobenzoxy moiety with hydrogen bromide in acetic acid.

Both IIa and IIb were tested against an *Escherichia coli*-$f_2$-RNA protein-synthesizing system and were inactive at $10^{-4}$ *M*. Under the same conditions, puromycin showed 50% inhibition at $10^{-6}$ *M*. The lack of puromycin-like activity in IIa or IIb further substantiates the earlier conclusion that a conformationally rigid system, such as that provided by a cyclopentane ring, is necessary for puromycin-like activity (4, 11, 20).

All six of the 9-substituted adenines, V, VI, VIIa, VIIb, IIa, and IIb, were tested by means of plaque inhibition tests against three DNA viruses (vaccinia virus, adenovirus type 5, and herpes simplex virus type 1) and six RNA viruses (influenza NWS, measles, Bunyamwera, Semliki Forest, rhino 1B, and corona) (1, 21, 22). Compounds IIb, VIIa, and VIIb showed weak activity at 50 μg/disk against one DNA virus, herpes simplex type 1, although none were sufficiently active to warrant secondary testing. None of the compounds was active at 50 μg/disk against the RNA viruses.

The six adenines were also tested for *in vitro* antibacterial activity (23) against *Streptococcus pyrogenes* (CN10), *Streptococcus faecalis* (CN478), *Staphylococcus aureus* (CN491), *E. coli* (CN314), *Salmonella typhosa* (CN512), *Shigella dysenteriae* (CN1513), *Klebsiella pneumoniae* (CN3632), *Enterobacter aerogenes* (2200/86), *Enterobacter cloacae* (2200/87), *Citrobacter freundii* (2200/77), *Proteus vulgaris* (CN329), *Proteus mirabilis* (S2409), *Pseudomonas aeruginosa* (CN200), and *Candida albicans* (CN1863). None of the compounds was inhibitory at 100 μg/ml.

## EXPERIMENTAL

***N*-[(2-Chloromethoxy)ethyl]phthalimide (IV)**—A stirred dispersion of 19.12 g (0.10 mole) of III and 3.00 g (0.10 mole) of paraformaldehyde in 250 ml of ethylene dichloride was saturated with dry hydrogen chloride at −10°. After 4 hr, the solution was dried with calcium chloride, filtered, and spin-evaporated *in vacuo* to afford a white solid (21.94 g, 91%), mp 69–72°. Recrystallization from ether gave the analytical sample, mp 69–70°; NMR ($CDCl_3$): δ 7.80 (m, 4H, aromatic H), 5.45 (s, 2H, $ClCH_2O$), and 3.95 (s, 4H, $CH_2CH_2$).

*Anal.*—Calc. for $C_{11}H_{10}ClNO_3$: C, 55.1; H, 4.21; N, 5.85. Found: C, 55.9; H, 4.34; N, 5.84.

**9-[(2-Phthalimidoethoxy)methyl]adenine (V)**—This compound was prepared from adenine and IV as described for VIIb on a 100-mmole scale, except that the reaction solution was poured over 2 liters of ice water; the product was collected by filtration to yield 20.0 g (59%), mp 252–256°. A portion was recrystallized twice from 2-methoxyethanol and once from dimethylformamide to give the analytical sample, mp 256–258°; UV: $\lambda_{max}^{0.1\ N\ HCl}$ 258 nm (ε 10,800); UV: $\lambda_{max}^{0.1\ N\ NaOH}$ 259 nm (ε 15,000); NMR (trifluoroacetic acid): δ 9.20 (s, 1H, purine H), 8.70 (s, 1H, purine H), 7.98 (s, 4H, aromatic H), 6.03 (s, 2H, $NCH_2O$), and 4.17 (s, 4H, $CH_2CH_2$).

*Anal.*—Calc. for $C_{16}H_{14}N_6O_3$: C, 56.8; H, 4.17; N, 24.8. Found: C, 56.8; H, 4.28; N, 24.7.

**9-[(2-Aminoethoxy)methyl]adenine (VI)**—A mixture of 3.38 g (10 mmoles) of V, 1.0 ml (20 mmoles) of hydrazine hydrate, 250 ml of ethanol, and 75 ml of 2-methoxyethanol was refluxed with stirring for 4 hr. The cooled reaction mixture was spin-evaporated *in vacuo*. The residual solid was dispersed in 100 ml of 1 *N* HCl, stirred at ambient temperature for 0.5 hr, and then left overnight at 0°. The mixture was filtered and thoroughly washed with water. The combined filtrates were spin-evaporated *in vacuo* to give a residue, which was dissolved in 100 ml of water and stirred with ion-exchange resin[3] until a negative silver nitrate test was obtained. The mixture was filtered and spin-evaporated *in vacuo* to give a white powder (1.25g, 60%), mp 168–170°. Recrystallization from 2-propanol gave analytically pure material (0.80 g, 38%), mp 170–171°; UV: $\lambda_{max}^{0.1\ N\ HCl}$ 256 nm (ε 13,900); UV: $\lambda_{max}^{0.1\ N\ NaOH}$ 259 nm (ε 14,100); NMR (dimethyl sulfoxide-$d_6$): δ 8.31 (s, 1H, purine H), 8.22 (s, 1H, purine H), 7.34 (broad s, 2H, purine $NH_2$), 5.60 (s, 2H, $NCH_2O$), 3.48 (t, 2H, $OCH_2CH_2$), 2.64 (t, 2H, $CH_2CH_2N$), and 1.60 (broad s, 2H, aliphatic $NH_2$).

*Anal.*—Calc. for $C_8H_{12}N_6O$: C, 46.1; H, 5.81; N, 40.4. Found: C, 46.3; H, 5.86; N, 40.2.

**9 - [(2 - *N* - Carbobenzoxyphenylalanylamidoethoxy)methyl]-adenine (VIIa)**—To a stirred, ice bath cooled solution of 7.78 g (26.0 mmoles) of DL-*N*-carbobenzoxyphenylalanine and 2.62 g (26.0 mmoles) of triethylamine in 100 ml of tetrahydrofuran was added 2.70 g (25.0 mmoles) of ethyl chloroformate. A precipitate formed within a few minutes; after 1 hr, 2.70 g (13.0 mmoles) of VI was added. After 2 hr at ambient temperature, 20 ml of water was added and the reaction was spin-evaporated *in vacuo*. The residue was dissolved in 250 ml of chloroform and washed with four 50-ml portions of water, four 50-ml portions of 5% aqueous sodium bicarbonate, 50 ml of water, and 50 ml of brine. Then it was dried and spin-evaporated *in vacuo*.

The product was slurried in 2-propanol and collected (5.25 g, 82%), mp 207–208°. The analytical sample was recrystallized from 2-propanol, mp 208–210°; UV: $\lambda_{max}^{0.N\ HCl}$ 257 nm (ε 14,000); UV: $\lambda_{max}^{0.1\ N\ NaOH}$ 259 nm (ε 14,600); NMR (dimethyl sulfoxide-$d_6$): δ 8.26 (s, 1H, purine H), 8.17 (s, 1H, purine H), 8.10 (t, 1H, $CH_2NH$), 7.45 (d, 1H, CHNH), 7.28 and 7.23 (s, 12H, aromatic H, $NH_2$), 5.53 (s, 2H, $NCH_2O$), 4.93 (s, 2H, $OCH_2C_6H_5$), 4.19 (m, 1H, CH), 3.47 (m, 2H, $OCH_2CH_2$), 3.22 (m, 2H, $CH_2CH_2NH$), and 2.90 and 2.70 (m, 2H, $CHCH_2C_6H_5$).

*Anal.*—Calc. for $C_{25}H_{27}N_7O_4$: C, 61.3; H, 5.56; N, 20.0. Found: C, 61.5; H, 5.62; N, 20.0.

**9- [(2-Phenylalanylamidoethoxy)methyl]adenine Fumarate (IIa)**—A mixture of 0.98 g (2.0 mmoles) of VIIa dissolved in 50 ml of acetic acid and 0.30 g of 10% palladium-on-carbon was shaken in the presence of hydrogen at 2–3 atm for 3 hr. The mixture was filtered and spin-evaporated *in vacuo*. The residual oil was combined with 0.232 g (2.0 mmoles) of fumaric acid in 10 ml of ethanol, warmed to effect solution, and allowed to cool (0.660 g, 93%), mp 188–189° (effervescent). The analytical sample was recrystallized from ethanol, mp 190–191° (effer-

[3] Melting points were taken in capillary tubes on a Mel-Temp block and are uncorrected. NMR data were recorded on Varian XL-100-15-FT and T-60 spectrometers with tetramethylsilane as an internal standard. UV spectra were obtained on a Unicam SP 800 spectrophotometer. Each analytical sample had spectral data compatible with its assigned structure and moved as a single spot on TLC.

vescent); UV: $\lambda_{max}^{0.1N\ HCl}$ 257 nm ($\epsilon$ 12,000); UV: $\lambda_{max}^{0.1\ N\ NaOH}$ 259 nm ($\epsilon$ 12,200); NMR (dimethyl sulfoxide-$d_6$): $\delta$ 8.26 (s, 1H, purine H), 8.17 (s, 1H, purine H), 8.11 (t, 1H, $CH_2NH$), 7.29 (s, 2H, purine $NH_2$), 7.21 (s, 5H, aromatic H), 6.51 (s, 1H, fumarate CH), 5.52 (s, 2H, $NCH_2O$), ~5.5 (broad s, $CHNH_2$, fumarate OH), 3.54 (m, 1H, CH), 3.44 (m, 2H, $OCH_2CH_2$), 3.19 (m, 2H, $CH_2NH$), and 2.91 and 2.71 (m, 2H, $CH_2C_6H_5$).

*Anal.*—Calc. for $C_{17}H_{21}N_7O_2 \cdot 0.5\ C_4H_4O_4$: C, 55.2; H, 5.61; N, 23.7. Found: C, 54.9; H, 5.73; N, 23.5.

**3 - *N* - Carbobenzoxyphenylalanylamidopropyl Bromide (VIII)**—To a stirred, ice–salt bath cooled solution of 29.93 g (0.10 mol) of DL-*N*-carbobenzoxyphenylalanine and 10.12 g (0.10 mole) of triethylamine in 325 ml of chloroform was added 10.85 g (0.10 mole) of ethyl chloroformate in 20 ml of chloroform. After 0.25 hr, a solution of 21.89 g (0.10 mole) of 3-bromopropylamine hydrobromide in 70 ml of water was added, followed by 25 ml of 4 *N* NaOH with vigorous stirring. After 96 hr at ambient temperature, the two layers were separated. The chloroform layer was washed with two 50-ml portions of 0.1 *N* HCl, two 50-ml portions of water, and once with brine. It then was dried and spin-evaporated *in vacuo*. The residual solid was slurried with hexane and collected (22.25 g, 53%), mp 123–125°. A portion was recrystallized from ethyl acetate–hexane to give the analytical sample, mp 125–126° (resolidified and remelted 129–130°).

*Anal.*—Calc. for $C_{20}H_{23}BrN_2O_3$: C, 57.3; H, 5.53; N, 6.68. Found: C, 57.3; H, 5.46; N, 6.60.

**9-(3-*N*-Carbobenzoxyphenylalanylamidopropyl)adenine Hydrochloride (VII*b*)**—To a stirred, ice bath cooled dispersion of 1.81 g (45.2 mmoles) of sodium hydride (60.2% dispersion in mineral oil) in 70 ml of dimethylformamide was added 6.08 g (45.0 mmoles) of adenine. After 10 min, the cold bath was removed and the mixture was stirred at ambient temperature for 1 hr, when salt formation was complete. A solution of 19.08 g (45.5 mmoles) of VIII in 100 ml of dimethylformamide was added; after 42 hr at ambient temperature, the reaction was filtered and spin-evaporated *in vacuo*. The residue was partitioned between 600 ml of 5% methanol in chloroform and 50 ml of water, and the layers were separated.

The organic phase was washed with two 100-ml portions of water and once with brine. It then was dried and spin evaporated *in vacuo*. The residue was dissolved in ethanol and diluted with hydrogen chloride-saturated ethanol to give a crystalline product (14.20 g, 62%), mp 195–197°. The analytical sample was obtained from ethanol, mp 196–197°; UV $\lambda_{max}^{0.1\ N\ HCl}$ 262 nm ($\epsilon$ 12,200); UV: $\lambda_{max}^{0.1\ N\ NaOH}$ 262 nm ($\epsilon$ 12,200); NMR (dimethylsulfoxide-$d_6$): $\delta$ 8.45 (s, 2H, purine H), 8.20 (t, 1H, $CH_2NH$), 7.57 (d, 1H, $CHNH$), 7.26 (s, 10H, aromatic H), 4.95 (s, 2H, $OCH_2C_6H_5$), ~4.2 (m, 5H, $NH_2$, purine $CH_2$, CH), 3.0–2.8 (m, 4H, $CH_2NH$, $CHCH_2C_6H_5$), and 1.92 (m, 2H, $CH_2CH_2CH_2$).

*Anal.*—Calc. for $C_{25}H_{28}ClN_7O_3$: C, 58.8; H, 5.53; N, 19.2. Found: C, 59.2; H, 5.61; N, 19.1.

**9-(3-Phenylalanylamidopropyl)adenine (II*b*)**—To a stirred solution of 8.16 g (16.0 mmoles) of VII*b* in 100 ml of acetic acid was added 30 ml of 30–32% hydrogen bromide in acetic acid. After 18 hr, the reaction mixture was diluted with 500 ml of ether, the solvent was decanted, and the solids were washed with ether. The crude hydrobromide was dissolved in water and passed through a column containing an excess of ion-exchange resin[3]. The eluates were spin-evaporated *in vacuo* to give a syrup, which crystallized under ether and was recrystallized from 2-propanol (2.57 g, 47%), mp 143–145°. The analytical sample had a melting point of 145–146°; UV: $\lambda_{max}^{0.1\ N\ HCl\ +\ 10\%\ C_2H_5OH}$ 259 nm ($\epsilon$ 13,700); UV: $\lambda_{max}^{0.1\ N\ NaOH\ +\ 10\%\ C_2H_5OH}$ 261 nm ($\epsilon$ 13,700); NMR (dimethyl sulfoxide-$d_6$): $\delta$ 8.13 (s, 1H, purine H), 8.10 (s, 1H, purine H), 7.96 (t, 1H, $CH_2NH$), 7.22 (s, 7H, aromatic H and purine $NH_2$), 4.04 (t, 2H, purine $CH_2$), 3.39 (q, 1H, CH), 3.03 (q, 2H, $CH_2NH$), 2.92 and 2.65 (m, 2H, $CH_2C_6H_5$), 1.88 (m, 2H, $CH_2CH_2CH_2$), and 1.65 (s, 2H, $CHNH_2$).

*Anal.*—Calc. for $C_{17}H_{21}N_7O$: C, 60.2; H, 6.24; N, 28.9. Found: C, 60.0; H, 6.23; N, 28.8.

**Inhibition of Protein Synthesis Assay**—For measurement of protein synthesis, extracts were prepared from cells of *E. coli* D10 by the method of Nirenberg (24) as modified by Godson and Sinsheimer (25). RNA was prepared from bacteriophage-$f_2$ as described previously (26). Reaction mixtures (0.1 ml) were prepared as described (24) with [4,5-$^3$H]-L-leucine[4] as the radioactive amino acid. Compounds to be tested were added as neutral solutions. The reaction was started by addition of 10 $\mu$g of $f_2$-RNA. After incubation at 37° for 10 min, the reaction was stopped by the addition of sodium hydroxide to a final concentration of 0.1 *M*. After a further 15 min at 37°, 10 volumes of 10% trichloroacetic acid were added; then the mixture was heated at 85° for 20 min and cooled. The precipitates were collected on filters[5] and washed with 5% trichloroacetic acid, and the precipitated radioactivity was counted as described previously (27). In each trial, puromycin[6] was tested as a standard inhibitor and gave 50% inhibition at ~$10^{-6}$ *M*.

[3] Rexyn 201(OH).

[4] New England Nuclear.

[5] Millipore.

[6] Nutritional Biochemical Corp.

## REFERENCES


(1) H. J. Schaeffer, L. Beauchamp, P. de Miranda, G. B. Elion, D. J. Bauer, and P. Collins, *Nature*, **272**, 583 (1978).

(2) D. Nathans, in "Antibiotics," vol. I, D. Gottlieb and P. D. Shaw, Eds., Springer-Verlag, New York, N.Y., 1967, pp. 259–277.

(3) R. G. Almquist and R. Vince, *J. Med. Chem.*, **16**, 1396 (1973).

(4) S. Daluge and R. Vince, *ibid.*, **15**, 171 (1972).

(5) R. Vince, R. G. Almquist, C. L. Ritter, F. N. Shirota, and H. T. Nagasawa, *Life Sci.*, **18**, 345 (1976).

(6) E. Kmetec and A. Tirpack, *Biochem. Pharmacol.*, **19**, 1493 (1970).

(7) D. Nathans and A. Neidle, *Nature (London)*, **197**, 1076 (1963).

(8) B. L. Hutchings in "Chemistry and Biology of Purines," CIBA Foundation Symposium, G. E. W. Wolstenholme and C. M. O'Conner, Eds., Little, Brown, Boston, Mass. 1957, p. 177.

(9) F. W. Lichtenthaler, E. Cuny, T. Morina, and I. Rychlik, *Chem. Ber.*, **112**, 2588 (1979).

(10) B. P. Gottikh, A. A. Kraevskii, M. K. Kukhanova, A. A., Yatsyna, A. M. Kritsyn, and V. L. Florentiev, *Mol. Biol. Rep.*, **1**, 173 (1973).

(11) R. Vince and R. G. Isakson, *J. Med. Chem.*, **16**, 37 (1973).

(12) A. Holy, J. Cerna, and I. Rychlik, *Nucleic Acid Res.*, **1**, 1221 (1974).

(13) I. Rychlik, J. Cerna, S. Chladek, J. Zemlicka, and Z. Haladova, *J. Mol. Biol.*, **43**, 13 (1969).

(14) M. K. Kukhanova, V. A. Pozdnyakov, L. V. Nikolaeva, A. A. Kraevskii, Y. U. Mitin, and B. P. Gottikh, *Mol. Biol. (Moscow)*, **8**, 389 (1974); through *Chem. Abstr.*, **81**, 14700m (1974).

(15) J. Robins, R. A. Jones, and M. MacCross, *Biochemistry*, **13**, 553 (1974).

(16) M. Sprinzl and F. Cramer, *Proc. Natl. Acad. Sci. USA*, **72**, 3049 (1975).

(17) A. J. Hill and D. T. Keach, *J. Am. Chem. Soc.*, **48**, 257 (1926).

(18) N. J. Leonard and J. A. Deyrup, *ibid.*, **84**, 2148 (1962).

(19) G. W. Anderson, J. E. Zimmerman, and F. M. Callahan, *ibid.*, **89**, 5012 (1967).

(20) R. Vince and S. Daluge, *J. Med. Chem.*, **20**, 930 (1977).

(21) F. C. Herrmann, *Proc. Soc. Exp. Biol. Med.*, **107**, 142 (1961).

(22) B. Rada, D. Blašković, F. Sorm, and J. Skoda, *Experientia*, **16**, 487 (1960).

(23) S. R. M. Bushby and G. H. Hitchings, *Br. J. Pharmacol. Chemother.*, **33**, 72 (1968).

(24) M. W. Nirenberg, "Methods in Enzymology," vol. VI, Academic, New York, N.Y., 1963, p. 17.

(25) G. N. Godson and R. L. Sinsheimer, *Biochim. Biophys. Acta*, **149**, 476 (1967).

(26) R. F. Gesteland and H. Boedtker, *J. Mol. Biol.*, **8**, 496 (1964).

(27) R. J. Harvey, *J. Bacteriol.*, **101**, 574 (1970).


## ACKNOWLEDGMENTS


The authors are indebted to Dr. R. J. Harvey for the inhibition of protein synthesis test results, to Dr. D. J. Bauer and his group for the antiviral testing, to Dr. S. R. M. Bushby for the antibacterial screening. They also thank Dr. B. S. Hurlbert and his staff for the elemental analyses and 60-MHz NMR spectra, Mr. Aris Ragouzeous for assistance with the 100-MHz NMR analysis, and Mrs. A. Melton for excellent technical assistance. J. L. Kelley thanks Dr. B. Roth and Dr. S. Daluge for helpful discussions.

# Phenobarbital Solubility in Propylene Glycol–Glycerol–Water Systems

**MAMDOUH A. MOUSTAFA, ABDULLA M. MOLOKHIA ˣ, and M. WAFIK GOUDA**

Received January 5, 1981, from the *Department of Pharmaceutics, College of Pharmacy, University of Riyadh, Riyadh, Saudi Arabia.* Accepted for publication March 20, 1981.

**Abstract** □ Phenobarbital solubility in various binary and ternary propylene glycol–glycerol–water solvent systems was determined. Phenobarbital concentrations several times those of the ethanol-containing USP and BPC elixirs were obtained. From log solubility–solvent composition plots, a general equation was developed for phenobarbital solubility prediction in propylene glycol–water, glycerol–water, and propylene glycol–glycerol–water solvent systems. Solubility predictions using another equation, based on linear log solubility–dielectric constant relationships, were limited by the need to use different constants for different solvent blends. Heats of solution for phenobarbital determined in selected solvent blends as well as in USP and BPC elixirs varied within a very narrow range, suggesting similar solute–solvent interactions.

**Keyphases** □ Phenobarbital—solubility in various binary and ternary solvent systems □ Solubility—phenobarbital in binary and ternary solvent systems □ Solvent systems—various binary and ternary, phenobarbital solubility

Ethanol-free liquid preparations of phenobarbital and other drugs are needed for the treatment of alcoholic patients, children, the elderly, and peptic ulcer patients. Furthermore, ethanol is not a pharmacologically inert solvent, and its interactions with various drugs are well known (1). Ethanol is used in many prescription and nonprescription liquid preparations in proportions up to 90% (2, 3). It is used in drug products as a solvent, preservative, and stabilizer and for its pharmacological effects. Other compounds may be used in place of ethanol except when it is used as a solvent.

Various formulas were suggested as alternatives to official formulas for phenobarbital elixir (4–9). Most formulas, however, contained ethanol in proportions varying from 15 to 40%. Some solubilized systems of phenobarbital also were prepared and tested for stability and *in vitro* availability (10, 11). In the present study, phenobarbital solubility was determined in binary and ternary propylene glycol–glycerol–water systems, and solubility data were correlated to physicochemical properties of solvents and the solute. This study should provide a model for the development of ethanol-free pharmaceutical solutions of drugs that currently include ethanol in their formulations.

## EXPERIMENTAL

**Materials**—Phenobarbital[1], propylene glycol[2], and glycerin[2] were used as supplied.

**Solubility Studies**—Excess quantities of phenobarbital were placed in 50-ml glass-stoppered flasks with 30 ml of the solvent system. The flasks were shaken in a thermostatically controlled water bath[3] until saturation. Four different temperatures were used; the temperature control was better than ±0.2°. Samples of the saturated solutions were pipeted, filtered through a 0.8-μm membrane filter[4], suitably diluted with the same solvent, and assayed for phenobarbital. In all solvent systems, 0.01 *N* HCl was used instead of water to suppress phenobarbital ionization.

**Assay**—Phenobarbital was assayed spectrophotometrically[5] according to a previously described method (12). A calibration curve was established for phenobarbital in every solvent blend.

## RESULTS AND DISCUSSION

Equilibrium solubility data of phenobarbital in aqueous solvent blends containing different proportions of glycerol and/or propylene glycol are shown in Fig. 1. Phenobarbital concentrations up to 45 mg/ml (~10 times the concentration of USP or BPC elixirs) were obtained. The contribution of propylene glycol to the increase in phenobarbital solubility was greater than that of glycerol. Log solubility–solvent composition plots for both propylene glycol–water and glycerol–water systems (Fig. 2) were straight lines. Literature data (13) indicate that, in a propylene glycol–water system, the logarithm of the solubility of some drugs is linearly related to the fraction of propylene glycol present by:

$$\log S_t = \log S_0 + \alpha f \qquad \text{(Eq. 1)}$$

where $S_t$ is the drug solubility in the solvent mixture, $f$ is the volume fraction of propylene glycol, $S_0$ is the drug solubility in water, and $\alpha$ is a constant characteristic of the system under study.

Results in Fig. 2 show that Eq. 1 applies to the solubility of phenobarbital in glycerol–water and propylene glycol–water. Values for the constants ($\alpha$) for propylene glycol and glycerol as calculated from the

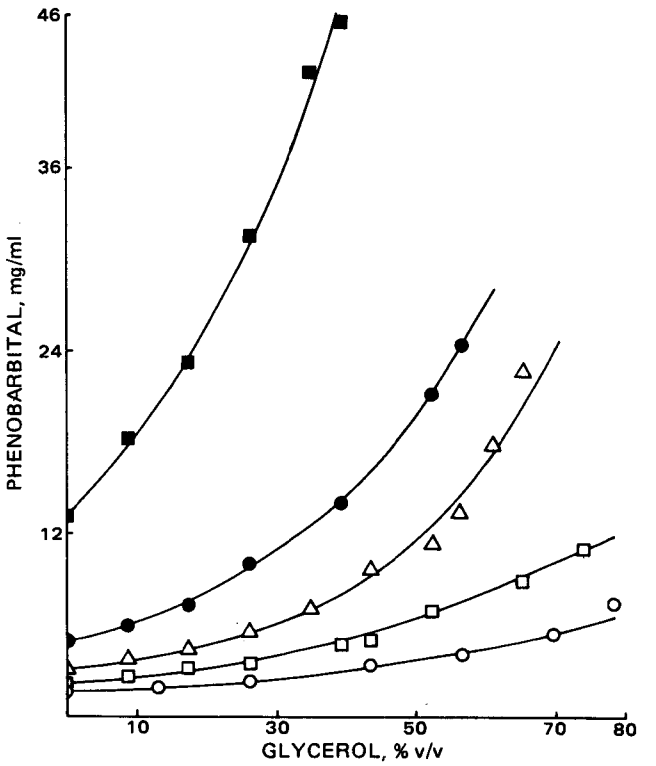


**Figure 1**—*Phenobarbital solubility in propylene glycol (PG)–glycerol–water systems at 32°. Key: ○, 0% PG; □, 10% PG; △, 20% PG; ●, 30% PG; and ■, 50% PG.*

[1] B.D.H. Chemicals Ltd., Poole, England.
[2] E. Merck, Darmstadt, West Germany.
[3] Kotterman, type 3407, Hanigsen, West Germany.
[4] Millipore Corp., Bedford, Mass.
[5] Pye-Unicam SP 600, Cambridge, England.



0022-3549/81/1000-1172$01.00/0
© 1981, American Pharmaceutical Association

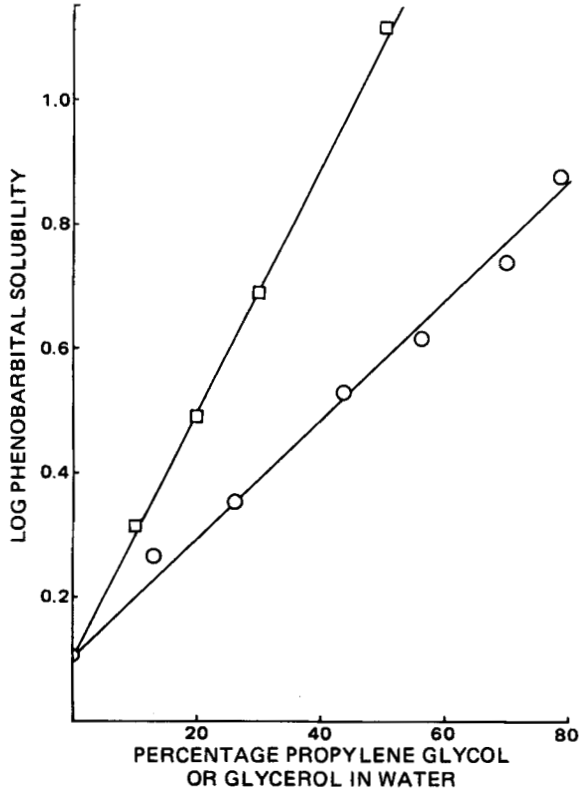


**Figure 2**—*Phenobarbital solubility in propylene glycol–water (PG–W) and glycerol–water (G–W) binary systems at 32°. Key: ○, G–W; and □, PG–W.*

slopes of the lines (Fig. 2) were 19.88 and $10.88 \times 10^{-3}$, respectively. In an attempt to extend the approach to the solubility of phenobarbital in propylene glycol–glycerol–water, the following equation was developed:

$$\log S_t = \log S_0 + \alpha_1 f_1 + \alpha_2 f_2 + \beta f_1^2 f_2 \qquad \text{(Eq. 2)}$$

where $\alpha_1$ and $\alpha_2$ are the constants for propylene glycol and glycerol, respectively, and $f_1$ and $f_2$ are the volume fractions of both solvents. The term $\beta f_1^2 f_2$ was determined from the fitting of some experimental solubility data to Eq. 2. It accounts for the increase in solubility due to solvent

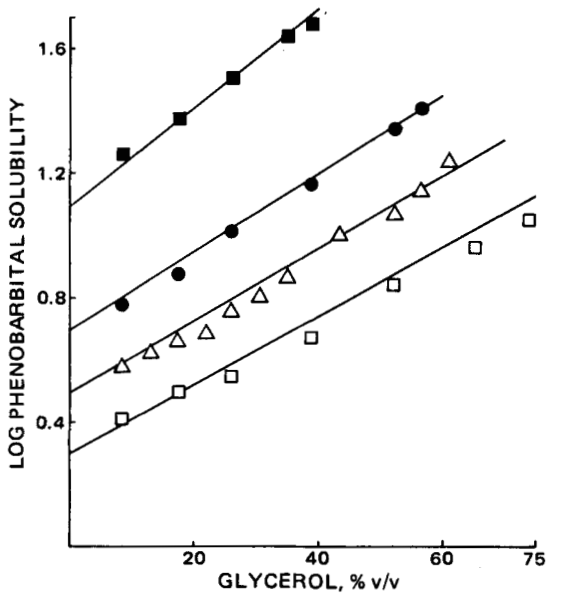


**Figure 3**—*Agreement of experimental solubility of phenobarbital in propylene glycol–glycerol–water (PG–G–W) ternary systems with values predicted from Eq. 2. Key: —, theoretical; □, 10% PG; △, 20% PG; ●, 30% PG; and ■, 50% PG.*

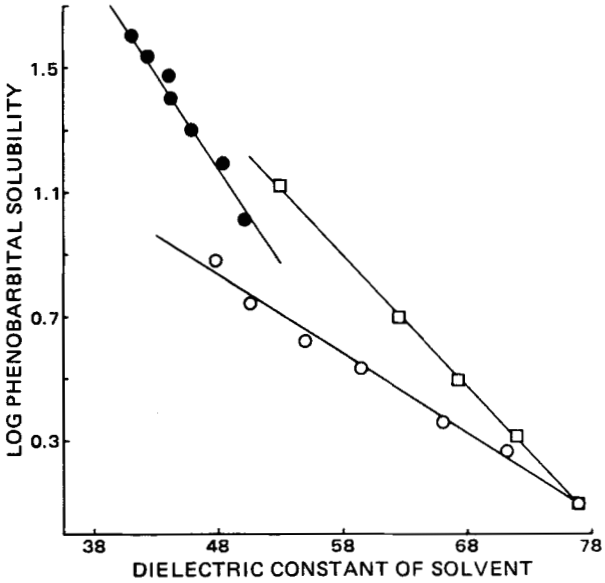


**Figure 4**—*Relationship of phenobarbital solubility to the dielectric constant of the solvent system. Key: ○, glycerol–water; □, propylene glycol–water; and ●, propylene glycol–glycerol–water.*

interactions. When $f_1$ and $f_2$ are equal to zero, Eq. 2 reduces to:

$$\log S_t = \log S_0 \qquad \text{(Eq. 3)}$$

which is the logarithm of phenobarbital solubility in 0.01 $N$ HCl.

When $f_1$ is variable and $f_2 = 0$, Eq. 2 is reduced to:

$$\log S_t = \log S_0 + \alpha_1 f_1 \qquad \text{(Eq. 4)}$$

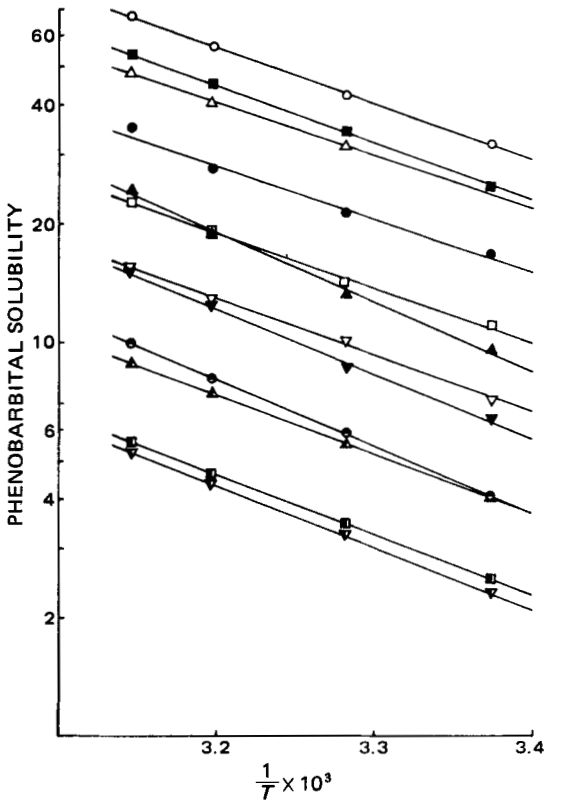


**Figure 5**—*Effect of temperature on phenobarbital solubility (propylene glycol, PG; glycerol, G; and water, W). Key: ○, BPC elixir; ■, 50% polyethylene glycol 400–50% W; △, 50% PG–26% G–24% W; ●, 30% PG–52% G–18% W; □, 30% PG–39% G–31% W; ▲, 50% PG–50% W; ▽, 30% PG–26% G–44% W; ▼, USP elixir; ◓, 30% PG–9% G–61% W; ◭, 20% PG–26% G–54% W; ◧, 10% PG–26% G–64% W; and ▼, 44% G–56% W.*

which describes the solubility of phenobarbital in propylene glycol–water.

When $f_1 = 0$ and $f_2$ is variable, Eq. 2 reduces to:

$$\log S_t = \log S_0 + \alpha_2 f_2 \qquad \text{(Eq. 5)}$$

which describes the solubility of phenobarbital in glycerol–water binary systems. Figure 3 shows the fitting of theoretical lines calculated on the basis of Eq. 2 to experimental points determined in the present study. The good fit suggests the possible use of such an equation for solubility predictions in ternary propylene glycol–glycerol–water systems.

Gorman and Hall (14) reported a linear relationship between the logarithm of secobarbital solubility and the dielectric constant of the binary solvent systems which have similar bonding characteristics: ethanol–water, glycerol–water, and propylene glycol–water. In the present investigation, the log solubility–dielectric constant (calculated) relationship for phenobarbital in propylene glycol–water and glycerol–water was also linear (Fig. 4). When this approach was extended to phenobarbital solubility in propylene glycol–glycerol–water, an essentially linear relationship was observed (Fig. 4). However, this linearity does not seem to extend to solvent systems containing high proportions of water since the line does not intersect with the other two lines at 100% water solvent composition. This result does not allow for solubility predictions over a wide range of solvent compositions as is possible when Eq. 2 is utilized.

The effect of temperature on phenobarbital solubility in 12 selected solvent systems was studied. Equilibrium solubilities were determined at 23, 32, 40, and 45 ± 0.2°, and the log solubility–$1/T$ relationships were plotted (Fig. 5). The heats of solution calculated from Fig. 5 varied in the relatively narrow range of 6–8 kcal/mole for the different solvent systems. The relatively nonpolar phenobarbital molecule is believed to dissolve in the relatively polar solvent blends through hydrogen bonding of the electronegative oxygen of the phenobarbital carbonyl groups to the hydrogen of hydroxyl groups in water, glycerol, or propylene glycol. The close values of heats of solution suggest similar types of solution mechanism and bonding.

Results of the present investigation showed that phenobarbital solubility can be effected through the use of mixed ethanol-free solvents to produce concentrations well above those required to formulate a phenobarbital elixir. The correlation of solubility data to specific solvent contributions enabled solubility predictions from a knowledge of solvent composition. Evaluation of the stability and bioavailability of phenobarbital in these solvent systems will be reported later.

## REFERENCES


(1) "Evaluations of Drug Interactions," 2nd ed., American Pharmaceutical Association, Washington, D.C., 1976.

(2) G. E. Dukes, J. G. Kuhn, and R. P. Evens, *Am. Fam. Physician*, **16**, 97 (1977).

(3) N. C. Petroni and A. A. Cardoni, *Drug Ther.*, **8**, 72 (1978).

(4) G. M. Krause and J. M. Cross, *J. Am. Pharm. Assoc., Sci. Ed.*, **40**, 137 (1951).

(5) R. A. Anderson, *Austr. J. Pharm.*, **30**, 96 (1949).

(6) A. Urdang and E. E. Leuallen, *J. Am. Pharm. Assoc., Sci. Ed.*, **45**, 425 (1956).

(7) C. F. Peterson and R. E. Hopponen, *ibid.*, **42**, 540 (1953).

(8) N. C. Zacharias, *Can. Pharm. J.*, **84**, 608 (1951).

(9) T. L. Breon and A. N. Paruta, *J. Pharm. Sci.*, **59**, 1306 (1970).

(10) V. F. Naggar, M. A. Moustafa, S. A. Khalil, and M. M. Motawi, *Can. J. Pharm. Sci.*, **7**, 112 (1972).

(11) S. A. Khalil, M. A. Moustafa, V. F. Naggar, and M. M. Motawi, *ibid.*, **7**, 109 (1972).

(12) T. Higuchi and E. Brochmann-Hanssen, "Pharmaceutical Analysis," Interscience, New York, N.Y., 1961, p. 231.

(13) S. Yalkowsky, G. L. Flynn, and G. L. Amidon, *J. Pharm. Sci.*, **61**, 983 (1972).

(14) W. G. Gorman and G. D. Hall, *ibid.*, **53**, 1017 (1964).


## ACKNOWLEDGMENTS


Presented at the APhA Academy of Pharmaceutical Sciences, San Antonio meeting, November 1980.

The authors thank Mr. I. D. Marlow for technical assistance.


# COMMUNICATIONS

## Single-Point Maintenance Dose Prediction: Role of Interindividual Differences in Clearance and Volume of Distribution in Choice of Sampling Time


**Keyphrases** ☐ Pharmacokinetics—single-point maintenance dose prediction, theoretical analysis ☐ Single-point maintenance dose prediction—pharmacokinetics, theoretical analysis


*To the Editor:*

Experimental observations of very strong correlations between a single determination of concentration after the first dose of a drug and the eventual steady-state concentration have been observed experimentally for lithium, nortriptyline, imipramine, and desipramine (1–5). Such a relationship also exists for drugs with short half-lives based on simulations and clinical studies of chloramphenicol and theophylline (6–8).

If a single determination of concentration after the first dose of drug correlates with the eventual steady-state concentration, then, over the linear range, this correlation provides the basis for the prediction of maintenance dose necessary to achieve a desired steady-state concentration. In an attempt to clarify this very powerful method of maintenance dose prediction, a theoretical analysis of the relationship was carried out to determine the: (*a*) source




*0022-3549/81/1000-1174$01.00/0*


*© 1981, American Pharmaceutical Association*

which describes the solubility of phenobarbital in propylene glycol–water.

When $f_1 = 0$ and $f_2$ is variable, Eq. 2 reduces to:

$$\log S_t = \log S_0 + \alpha_2 f_2 \qquad \text{(Eq. 5)}$$

which describes the solubility of phenobarbital in glycerol–water binary systems. Figure 3 shows the fitting of theoretical lines calculated on the basis of Eq. 2 to experimental points determined in the present study. The good fit suggests the possible use of such an equation for solubility predictions in ternary propylene glycol–glycerol–water systems.

Gorman and Hall (14) reported a linear relationship between the logarithm of secobarbital solubility and the dielectric constant of the binary solvent systems which have similar bonding characteristics: ethanol–water, glycerol–water, and propylene glycol–water. In the present investigation, the log solubility–dielectric constant (calculated) relationship for phenobarbital in propylene glycol–water and glycerol–water was also linear (Fig. 4). When this approach was extended to phenobarbital solubility in propylene glycol–glycerol–water, an essentially linear relationship was observed (Fig. 4). However, this linearity does not seem to extend to solvent systems containing high proportions of water since the line does not intersect with the other two lines at 100% water solvent composition. This result does not allow for solubility predictions over a wide range of solvent compositions as is possible when Eq. 2 is utilized.

The effect of temperature on phenobarbital solubility in 12 selected solvent systems was studied. Equilibrium solubilities were determined at 23, 32, 40, and 45 ± 0.2°, and the log solubility–$1/T$ relationships were plotted (Fig. 5). The heats of solution calculated from Fig. 5 varied in the relatively narrow range of 6–8 kcal/mole for the different solvent systems. The relatively nonpolar phenobarbital molecule is believed to dissolve in the relatively polar solvent blends through hydrogen bonding of the electronegative oxygen of the phenobarbital carbonyl groups to the hydrogen of hydroxyl groups in water, glycerol, or propylene glycol. The close values of heats of solution suggest similar types of solution mechanism and bonding.

Results of the present investigation showed that phenobarbital solubility can be effected through the use of mixed ethanol-free solvents to produce concentrations well above those required to formulate a phenobarbital elixir. The correlation of solubility data to specific solvent contributions enabled solubility predictions from a knowledge of solvent composition. Evaluation of the stability and bioavailability of phenobarbital in these solvent systems will be reported later.

## REFERENCES


(1) "Evaluations of Drug Interactions," 2nd ed., American Pharmaceutical Association, Washington, D.C., 1976.

(2) G. E. Dukes, J. G. Kuhn, and R. P. Evens, *Am. Fam. Physician*, **16**, 97 (1977).

(3) N. C. Petroni and A. A. Cardoni, *Drug Ther.*, **8**, 72 (1978).

(4) G. M. Krause and J. M. Cross, *J. Am. Pharm. Assoc., Sci. Ed.*, **40**, 137 (1951).

(5) R. A. Anderson, *Austr. J. Pharm.*, **30**, 96 (1949).

(6) A. Urdang and E. E. Leuallen, *J. Am. Pharm. Assoc., Sci. Ed.*, **45**, 425 (1956).

(7) C. F. Peterson and R. E. Hopponen, *ibid.*, **42**, 540 (1953).

(8) N. C. Zacharias, *Can. Pharm. J.*, **84**, 608 (1951).

(9) T. L. Breon and A. N. Paruta, *J. Pharm. Sci.*, **59**, 1306 (1970).

(10) V. F. Naggar, M. A. Moustafa, S. A. Khalil, and M. M. Motawi, *Can. J. Pharm. Sci.*, **7**, 112 (1972).

(11) S. A. Khalil, M. A. Moustafa, V. F. Naggar, and M. M. Motawi, *ibid.*, **7**, 109 (1972).

(12) T. Higuchi and E. Brochmann-Hanssen, "Pharmaceutical Analysis," Interscience, New York, N.Y., 1961, p. 231.

(13) S. Yalkowsky, G. L. Flynn, and G. L. Amidon, *J. Pharm. Sci.*, **61**, 983 (1972).

(14) W. G. Gorman and G. D. Hall, *ibid.*, **53**, 1017 (1964).


## ACKNOWLEDGMENTS


Presented at the APhA Academy of Pharmaceutical Sciences, San Antonio meeting, November 1980.

The authors thank Mr. I. D. Marlow for technical assistance.


# COMMUNICATIONS

## Single-Point Maintenance Dose Prediction: Role of Interindividual Differences in Clearance and Volume of Distribution in Choice of Sampling Time


**Keyphrases** ☐ Pharmacokinetics—single-point maintenance dose prediction, theoretical analysis ☐ Single-point maintenance dose prediction—pharmacokinetics, theoretical analysis


*To the Editor:*

Experimental observations of very strong correlations between a single determination of concentration after the first dose of a drug and the eventual steady-state concentration have been observed experimentally for lithium, nortriptyline, imipramine, and desipramine (1–5). Such a relationship also exists for drugs with short half-lives based on simulations and clinical studies of chloramphenicol and theophylline (6–8).

If a single determination of concentration after the first dose of drug correlates with the eventual steady-state concentration, then, over the linear range, this correlation provides the basis for the prediction of maintenance dose necessary to achieve a desired steady-state concentration. In an attempt to clarify this very powerful method of maintenance dose prediction, a theoretical analysis of the relationship was carried out to determine the: (*a*) source




*0022-3549/81/1000-1174$01.00/0*


*© 1981, American Pharmaceutical Association*

and magnitude of the error involved with the estimate, (*b*) general applicability of the method to other drugs, and (*c*) limits of the method's application (9). It was observed that the method yielded a good estimate of clearance in an individual which did not seem to be affected by interindividual variation in the volume of distribution (10).

The analysis described the inverse relationship between the concentration ($C^*$) observed at some time ($t^*$) after the first dose ($D^*$) and the maintenance dose ($D_m$) required to obtain a desired steady-state drug concentration ($\overline{C}_{ss}$):

$$1/D_m = \Psi C^* \qquad \text{(Eq. 1)}$$

where:

$$\Psi = \frac{e^{Kt^*}}{\overline{C}_{ss} K \tau D^*} \qquad \text{(Eq. 2)}$$

where $K$ is the elimination rate constant of the drug in an individual patient and $\tau$ is the dosing interval. It was previously noted (9) that $\Psi$ (the proportionality factor in Eq. 1 as defined by Eq. 2) would vary among individuals but in such a manner that, at a certain $t^*$, the variability would not allow estimates of $D_m$ that would yield $\overline{C}_{ss}$ values within 10–20% of the target value.

The purpose of this communication is to extend this analysis into areas not completely dealt with previously:

1. Since $K$ is a function of clearance ($Cl$) and volume of distribution ($V$), how does $\Psi$ vary as a function of interindividual variability in these independent parameters?
2. Why is $\Psi$ relatively constant throughout a population?
3. What factors determine the optimum value of $t^*$?

To answer these questions, it is first necessary to recast $\Psi$ as a function of clearance and volume of distribution through the relationship:

$$K = Cl/V \qquad \text{(Eq. 3)}$$

Therefore:

$$\Psi = \frac{V e^{(Cl/V)t^*}}{Cl \overline{C}_{ss} \tau D^*} \qquad \text{(Eq. 4)}$$

The portion of $\Psi$ that varies among the population is $(V/Cl)e^{(Cl/V)t^*}$. Ideally, $\Psi$ would not vary from one individual to another, but since $Cl$ and $V$ vary throughout the population, $\Psi$ will vary among individuals. However, $\Psi$ is minimally affected by interindividual differences in $Cl$ and $V$ when its partial first derivatives with respect to these independent variables are simultaneously close to zero. The partial first derivatives are equal to zero when:

$$(Cl/V)t^* = 1 \qquad \text{(Eq. 5)}$$

or:

$$t^* = V/Cl = 1/K \qquad \text{(Eq. 6)}$$

Thus, $\Psi$ is insensitive to interindividual differences in $Cl$ and $V$ when $(Cl/V)t^*$ is in the neighborhood of 1.

It is important to remember that $\Psi$ does not vary simply as a function of $Cl$ or $V$ among individuals but actually varies as a function of their ratio, $K$. Therefore, it is appropriate to consider the intersubject variability of $\Psi$ as a function of $K$ and to consider the influence of interindividual variability in $K$ on the value of $\Psi$ as defined by Eq. 2.

Since $K$ varies among individuals, the true value of $\Psi$ also varies throughout the popultion. However, under certain conditions, $\Psi$ varies much less than $K$. The variability in $K$ causes minimum fluctuations in $\Psi$ if $K$ and $e^{Kt^*}$ vary in proportion to one another (Eq. 2). When the exponent ($x$) of $e^x$ is in the neighborhood of 1, the value of $e^x$ varies in rough proportion to $x$. As seen in Table I, a fourfold variation in $x$ centered around 1 produces less than a 15% variation in the function $e^x/x$ about its mean value.

**Table I—Effect of Varying the Value of $x$ about 1 on the Value of the Function $e^x/x$**

| $x$ | $e^x$ | $e^x/x$ | Ratio[a] |
|---|---|---|---|
| 0.50 | 1.65 | 3.30 | 1.01 |
| 1.25 | 2.79 | 2.79 | 0.86 |
| 2.00 | 7.39 | 3.69 | 1.13 |
| Mean | | 3.26 | |

[a] Ratio of $e^x/x$ for each value of $x$ to the mean value.

Equation 2 is of the form $e^x/(x/t^*)$ where $x = (Cl/V)t^* = Kt^*$. When the value of $t^*$ in Eq. 6 is substituted into Eq. 2, the value of the exponent is 1. When $x$ increases, $e^x$ increases in rough proportion, and the value of the ratio in Eq. 2 does not change greatly. Therefore, $\Psi$ does not vary greatly with $K$ as long as $Kt^*$ remains in the neighborhood of 1.

In addition, from the steps leading to Eq. 6, it is seen that the value of $\Psi$ is insensitive to interindividual changes in $Cl$ and $V$ when $(Cl/V)t^*$ (*i.e.*, $Kt^*$) is in the neighborhood of 1. Since $t^*$ is chosen and fixed in the single-point method of maintenance dose prediction and since $K$ varies among individuals, changes in $Cl$ and $V$ increasingly affect $\Psi$ as $Kt^*$ moves away from 1. If the influence of interindividual differences in $Cl$ and $V$ are to be kept at a minimum for the majority of the population and if the mathematical properties of Eq. 2 are to be taken advantage of, $t^*$ should be chosen as the mean (or mode) value of $1/K$.

When $t^*$ is chosen in this manner, $\Psi$ varies minimally with changes in $K$ and the method gives estimates of maintenance doses based on a population average value of $\Psi$ that are minimally affected by interindividual variability in $Cl$ and $V$. These considerations can be extended to any one-compartment drug for which a clinically acceptable value of $t^*$ (perhaps not >24 hr) can be chosen such that $Kt^*$ can be kept in the neighborhood of 1 throughout the population. This approach is presently being extended to multicompartment drugs and the prediction of steady-state concentrations of metabolites of therapeutic interest.


(1) T. B. Cooper, P.-E. E. Bergner, and G. M. Simpson, *Am. J. Psychiatry*, **130**, 601, (1973).

(2) T. B. Cooper and G. M. Simpson, *ibid.*, **133**, 440 (1976).

(3) *Ibid.*, **135**, 333 (1978).

(4) R. Braithwaite, S. Montgomery, and S. Dawling, *Clin. Pharmacol. Ther.*, **23**, 303 (1978).

(5) D. J. Brunswick, J. D. Amsterdam, J. Mendels, and S. L. Stern, *ibid.*, **25**, 605 (1979).

(6) J. R. Koup, C. M. Sack, A. L. Smith, and M. Gibaldi, *Clin. Pharmacokinet.*, **5**, 460 (1980).

(7) J. R. Koup, C. M. Sack, A. L. Smith, W. M. Neely, and M. Gibaldi, *ibid.*, **6**, 83 (1981).

(8) G. G. Shapiro, J. R. Koup, C. T. Furukawa, W. E. Pierson, M. Gibaldi, D. Fuquay, and C. W. Bierman, *Pediatrics*, in press.

(9) J. T. Slattery, M. Gibaldi, and J. R. Koup, *Clin. Pharmacokinet.*, **5**, 377 (1980).

(10) J. R. Koup, J. T. Slattery, and M. Gibaldi, *Res. Commun. Chem. Pathol. Pharmacol.*, **25**, 559 (1979).

*John T. Slattery*
Department of Pharmaceutics
University of Washington
Seattle, WA 98105

Received February 18, 1981.
Accepted for publication June 10, 1981.
Discussions with Dr. René Levy and Dr. Milo Gibaldi are gratefully acknowledged.

# Correlation of Water Solubility with Octanol–Water Partition Coefficient

**Keyphrases** □ Solubility—water, correlation with octanol–water partition coefficient □ Partition coefficient—octanol–water, correlation with water solubility □ Melting-point effect—correlation between water solubility and octanol–water partition coefficient

*To the Editor:*

Yalkowsky and Valvani (1) made a valuable analysis of the melting-point effect on the solubility of solid compounds and discussed the correlation between water solubility ($S$) and the octanol–water partition coefficient ($P$). Regression equations between log $S$ and log $P$ were constructed using log $P$ values calculated primarily from molecular fragment constants developed by Nys and Rekker (2).

We have found several points relevant to the Yalkowsky–Valvani analysis (1). First, part of their conclusions for a particular class of compounds was based on a linear regression between the values of log $S_{obs}$ and log $P_{estim}$ obtained from the correlation equation for that class of compounds. Regression of this kind must, in principle, yield log $S_{obs}$ = 1.0 log $S_{estim}$ with an intercept equal to 0.0. The correlation coefficient will then be a measure of how well log $S_{obs}$ fits log $S_{estim}$. For reasons unspecified, this condition was not met in their Eqs. 32–36.

Second, the calculated values of log $P$ for some low solubility compounds are highly imprecise. For instance, the values of log $P$, 5.05, 5.79, and 6.53, estimated for 1,2,3,5-tetra-, penta-, and hexachlorobenzene, respectively, in their Table VI, are considerably greater than the corresponding experimental values of 4.46 (3), 4.94 (3), and 5.50 (4). It is surprising that the molar solubilities (log $S$) predicted from these calculated log $P$ values and the solute melting points ($MP$) fall into close agreement with the experimental log $S$. If experimental log $P$ values are entered into the correlation derived by Yalkowsky *et al.* (5) for the compounds in Table VI, *i.e.*, log $S = -0.9874 \log P - 0.0095(MP) + 0.7178$, the estimated $S$ values then deviate appreciably from the experimental data.

It is understood that log $P$ values calculated by various fragment approaches are only as accurate as the values used to define each fragment. At this time, the rules to calculate log $P$ values are empirically derived. This approach has led to numerous correction factors for such things as branching, flexibility, chain length, bond unsaturation, and substituent polarity. In general, the fragment approach works reasonably well for simple low molecular weight molecules. It tends to be less accurate for more complex molecules.

Third, Yalkowsky and Valvani assumed that the effect of octanol–water mutual saturation on the partition coefficient was small and thus ignored it in their treatment. Banerjee *et al.* (3) also reported no observable effect of octanol–water mutual saturation. Although this effect is expected to be small for compounds with relatively high solubilities in both octanol and water, it becomes significant for solutes with limited solubilities. Consequently, it would be a factor in the correlation of log $S$ *versus* log $P$ at the low $S$ (high $P$) region.

The significance of octanol–water mutual saturation may be evaluated by comparing experimental $P$ values with those calculated from solute solubilties in octanol and water for some high melting solid compounds. Because of the high melting-point effect, solids have limited solubilities in both solvents and their partition coefficients can be determined directly from the ratios of solute solubilties in the two solvents. Note that at low (mole fraction) concentrations, solute activity coefficients are essentially constant and the log $P$ of a solute would be practically constant at all concentrations.

We selected *p,p'*-dichlorodiphenyltrichloroethane (I)[1], hexachlorobenzene (II)[2], and anthracene (III) for illustration. The experimental and estimated octanol–water partition coefficients and the determined solubilities in water, octanol, and water-saturated octanol for these compounds are given in Table I. If it is assumed that mutual saturation has no effect on solute partitioning, the partition coefficients should be equal to the ratios of solute solubilties in pure octanol and water ($S_o/S_w$); *i.e.*, log $P$ = 6.88 for I, 5.85 for II, and 4.73 for III. These calculated $P$ values are larger than the experimental values by factors of 3.3, 2.2, and 1.9 for I, II, and III, respectively. The difference between experimental and calculated $P$ values results presumably from an alteration of the solute solubilities in the two solvents due to their mutual saturation.

**Table I—Solubilities and Octanol–Water Partition Coefficients of I, II, and III**

| Compound | Melting Point | $S_w$ (μg/liter)[a] | $S_o$ (g/liter) | $S_{o/w}$ (g/liter) | log $S_o/S_w$ | log $P_{exp}$ | log $P_{est}$[b] |
|---|---|---|---|---|---|---|---|
| I | 108.5° | 5.5 (25°)[c]<br>5.0 (20°) | 41.5 (24°) | 31.9 (24°) | 6.88 | 6.36 | — |
| II | 230° | 5.0 (25°)[c] | 3.53 (23°) | 2.65 (23°) | 5.85 | 5.50 | 6.53 |
| III | 216° | 45 (25°)[d] | 2.44 (23°) | 2.22 (23°) | 4.73 | 4.45[e] | 4.63 |

[a] Key: $S_w$, solubility in water; $S_o$, solubility in octanol; $S_{o/w}$, solubility in water-saturated octanol; and $P_{exp}$, experimental octanol–water partition coefficient. [b] Estimated values from fragment constants given in Ref. 1. [c] Reference 7. [d] Reference 8. [e] Reference 6.

[1] Commonly referred to as DDT.
[2] Commonly referred to as HCB.

(10) J. R. Koup, J. T. Slattery, and M. Gibaldi, *Res. Commun. Chem. Pathol. Pharmacol.*, **25**, 559 (1979).

*John T. Slattery*
Department of Pharmaceutics
University of Washington
Seattle, WA 98105

Received February 18, 1981.
Accepted for publication June 10, 1981.
Discussions with Dr. René Levy and Dr. Milo Gibaldi are gratefully acknowledged.

# Correlation of Water Solubility with Octanol–Water Partition Coefficient

**Keyphrases** □ Solubility—water, correlation with octanol–water partition coefficient □ Partition coefficient—octanol–water, correlation with water solubility □ Melting-point effect—correlation between water solubility and octanol–water partition coefficient

*To the Editor:*

Yalkowsky and Valvani (1) made a valuable analysis of the melting-point effect on the solubility of solid compounds and discussed the correlation between water solubility ($S$) and the octanol–water partition coefficient ($P$). Regression equations between log $S$ and log $P$ were constructed using log $P$ values calculated primarily from molecular fragment constants developed by Nys and Rekker (2).

We have found several points relevant to the Yalkowsky–Valvani analysis (1). First, part of their conclusions for a particular class of compounds was based on a linear regression between the values of log $S_{obs}$ and log $P_{estim}$ obtained from the correlation equation for that class of compounds. Regression of this kind must, in principle, yield log $S_{obs}$ = 1.0 log $S_{estim}$ with an intercept equal to 0.0. The correlation coefficient will then be a measure of how well log $S_{obs}$ fits log $S_{estim}$. For reasons unspecified, this condition was not met in their Eqs. 32–36.

Second, the calculated values of log $P$ for some low solubility compounds are highly imprecise. For instance, the values of log $P$, 5.05, 5.79, and 6.53, estimated for 1,2,3,5-tetra-, penta-, and hexachlorobenzene, respectively, in their Table VI, are considerably greater than the corresponding experimental values of 4.46 (3), 4.94 (3), and 5.50 (4). It is surprising that the molar solubilities (log $S$) predicted from these calculated log $P$ values and the solute melting points ($MP$) fall into close agreement with the experimental log $S$. If experimental log $P$ values are entered into the correlation derived by Yalkowsky *et al.* (5) for the compounds in Table VI, *i.e.*, log $S = -0.9874 \log P - 0.0095(MP) + 0.7178$, the estimated $S$ values then deviate appreciably from the experimental data.

It is understood that log $P$ values calculated by various fragment approaches are only as accurate as the values used to define each fragment. At this time, the rules to calculate log $P$ values are empirically derived. This approach has led to numerous correction factors for such things as branching, flexibility, chain length, bond unsaturation, and substituent polarity. In general, the fragment approach works reasonably well for simple low molecular weight molecules. It tends to be less accurate for more complex molecules.

Third, Yalkowsky and Valvani assumed that the effect of octanol–water mutual saturation on the partition coefficient was small and thus ignored it in their treatment. Banerjee *et al.* (3) also reported no observable effect of octanol–water mutual saturation. Although this effect is expected to be small for compounds with relatively high solubilities in both octanol and water, it becomes significant for solutes with limited solubilities. Consequently, it would be a factor in the correlation of log $S$ *versus* log $P$ at the low $S$ (high $P$) region.

The significance of octanol–water mutual saturation may be evaluated by comparing experimental $P$ values with those calculated from solute solubilties in octanol and water for some high melting solid compounds. Because of the high melting-point effect, solids have limited solubilities in both solvents and their partition coefficients can be determined directly from the ratios of solute solubilties in the two solvents. Note that at low (mole fraction) concentrations, solute activity coefficients are essentially constant and the log $P$ of a solute would be practically constant at all concentrations.

We selected *p,p'*-dichlorodiphenyltrichloroethane (I)[1], hexachlorobenzene (II)[2], and anthracene (III) for illustration. The experimental and estimated octanol–water partition coefficients and the determined solubilities in water, octanol, and water-saturated octanol for these compounds are given in Table I. If it is assumed that mutual saturation has no effect on solute partitioning, the partition coefficients should be equal to the ratios of solute solubilties in pure octanol and water ($S_o/S_w$); *i.e.*, log $P$ = 6.88 for I, 5.85 for II, and 4.73 for III. These calculated $P$ values are larger than the experimental values by factors of 3.3, 2.2, and 1.9 for I, II, and III, respectively. The difference between experimental and calculated $P$ values results presumably from an alteration of the solute solubilities in the two solvents due to their mutual saturation.

**Table I—Solubilities and Octanol–Water Partition Coefficients of I, II, and III**

| Compound | Melting Point | $S_w$ (μg/liter)[a] | $S_o$ (g/liter) | $S_{o/w}$ (g/liter) | log $S_o/S_w$ | log $P_{exp}$ | log $P_{est}$[b] |
|---|---|---|---|---|---|---|---|
| I | 108.5° | 5.5 (25°)[c]<br>5.0 (20°) | 41.5 (24°) | 31.9 (24°) | 6.88 | 6.36 | — |
| II | 230° | 5.0 (25°)[c] | 3.53 (23°) | 2.65 (23°) | 5.85 | 5.50 | 6.53 |
| III | 216° | 45 (25°)[d] | 2.44 (23°) | 2.22 (23°) | 4.73 | 4.45[e] | 4.63 |

[a] Key: $S_w$, solubility in water; $S_o$, solubility in octanol; $S_{o/w}$, solubility in water-saturated octanol; and $P_{exp}$, experimental octanol–water partition coefficient. [b] Estimated values from fragment constants given in Ref. 1. [c] Reference 7. [d] Reference 8. [e] Reference 6.

[1] Commonly referred to as DDT.
[2] Commonly referred to as HCB.

Water (2.3 $M$) dissolved in octanol (6) reduces solute solubility in octanol, while octanol ($4.5 \times 10^{-3}$ $M$) in water (9) enhances solute solubility in water. To support this point, the solubilities of these three compounds in water-saturated octanol are shown to be reduced by ~10–30% because of water saturation. These results suggest that octanol in water promotes water solubility by ~75% for III, 70% for II, and 150% for I.

Based on these findings, the use of experimental partition coefficients probably would improve the reliability of the log $S$–log $P$ correlation at the high $P$ region.


(1) S. H. Yalkowsky and S. C. Valvani, *J. Pharm. Sci.*, **69**, 912 (1980).

(2) G. G. Nys and R. F. Rekker, *Eur. J. Med. Chem.*, **9**, 361 (1974).

(3) S. Banerjee, S. H. Yalkowsky, and S. C. Valvani, *Environ. Sci. Technol.*, **14**, 1227 (1980).

(4) C. T. Chiou and D. W. Schmedding, in "Test Protocols for Environmental Fate and Movement of Toxicants," Association of Official Analytical Chemists, Arlington, Va., 1981, p. 28.

(5) S. H. Yalkowsky, R. J. Orr, and S. C. Valvani, *Ind. Eng. Chem. Fundam.*, **18**, 351 (1979).

(6) A. Leo, C. Hansch, and D. Elkins, *Chem. Rev.*, **71**, 525 (1971).

(7) L. Weil, G. Duré, and K. Quentin, *Z. Wasser-Abwasser Forsch.*, **7**, 169 (1974).

(8) W. E. May, in "Petroleum in the Marine Environment," L. Petrakis and F. T. Weiss, Eds., Advances in Chemistry Series, 185, 143 (1980).

(9) R. Collander, *Acta Chem. Scand.*, **5**, 774 (1951).



*Cary T. Chiou* [x]
*David W. Schmedding*
Environmental Health Sciences Center
Oregon State University
Corvallis, OR 97331

*John H. Block*
School of Pharmacy
Oregon State University
Corvallis, OR 97331



Received February 23, 1981.
Accepted for publication May 21, 1981.

Supported by U.S. Public Health Grants ES-00210 and ES-02400 and Environmental Protection Agency Grant CR-808046 from the EPA Environmental Research Laboratory, Corvallis, OR.


## Correlation of Water Solubility with Octanol–Water Partition Coefficient: A Response


**Keyphrases** □ Solubility—water, correlation with octanol–water partition coefficient, response □ Partition coefficient—octanol–water, correlation with water solubility, response □ Melting-point effect—correlation between water solubility and octanol–water partition coefficient, response


*To the Editor:*

The preceding paper (1) raised three concerns about our recent paper (2) which we shall now attempt to alleviate.

The first concern of Chiou *et al.* (1) is that Eqs. 32–36 of Ref. 2 do not have slopes of unity and intercepts of zero. The reason for this apparent discrepancy was mentioned briefly in the paragraph preceding Eq. 37 of Ref. 2 but will be discussed more completely here.

**Table I—Aqueous Molar Solubility ($S_w$) and Octanol–Water Partition Coefficients ($PC$) of Tetra-, Penta-, and Hexachlorobenzenes**

| Compound | Melting point | Experimental log $PC$ | log $S_w$ Observed[a] | log $S_w$ Predicted by Eq. 2 |
|---|---|---|---|---|
| 1,2,3,5-Tetrachlorobenzene | 54° | 4.46[b] | −4.79 | −4.46 |
| Pentachlorobenzene | 86° | 4.94[b] | −5.65 | −5.35 |
| Hexachlorobenzene | 230° | 5.50[c] | −7.76 | −7.67 |

[a] Reference 2. [b] Reference 3. [c] Reference 1.

Equation 30 of Ref. 2 was developed on the basis of the theoretical relationships between solubility, partition coefficient, melting point, and entropy of fusion. Solubility data for five classes of compounds were compared to the predictions based on:

$$\log S_w \cong -\log PC - 0.01MP + 1.05 \qquad \text{(Eq. 1)}$$

Only if this theoretical equation perfectly predicted all of the solubilities would the slope be unity and the intercept zero.

In most cases, the slopes were not significantly different from unity; however, the intercepts tended to be slightly negative rather than zero. This trend shows a systematic overestimation of solubility by a factor of ~3. This finding indicated that while the theoretical equation was not perfect, it did provide a basis for assessing the role of the partition coefficient and the melting point in controlling aqueous solubility.

Each of the five classes of compounds represents a fairly small data set (in most cases covering only a few orders of magnitude in solubility). The slopes and intercepts are thus more subject to errors in the log $S_w$ measurements and/or the log $PC$ estimation than is the whole data set, which covers almost nine orders of magnitude. The empirical equation for rigid molecules (Eq. 39 of Ref. 2) is:

$$\log S_w = -1.05 \log PC - 0.012MP + 0.87 \qquad \text{(Eq. 2)}$$

When Eq. 2 is used to estimate solubilities, it gives a slope and intercept of unity and zero, respectively. This final equation rather than the ones based on the smaller data sets should be used to estimate aqueous solubilities.

Second, Chiou *et al.* (1) point out that log $PC$ calculations tend to be imprecise for low solubility compounds and seem surprised that the calculated values work better for estimating aqueous solubility than their own experimentally determined values. The reason for this situation is again statistical. For the reasons already described, it is best to use Eq. 2 to estimate solubility. When this is done, the experimental log $PC$ values of Chiou *et al.* (1) will yield calculated solubilities that are in excellent agreement with the observed values as shown in Table I.

The regression equations were obtained by correlating aqueous solubility with melting points and calculated values of log $PC$. If experimental log $PC$ values were available, the regression coefficient of log $PC$ as well as the intercept probably would be somewhat altered. Thus, systematic errors in estimating log $PC$ are compensated for by the choice of the coefficient of log $PC$.

Water (2.3 $M$) dissolved in octanol (6) reduces solute solubility in octanol, while octanol ($4.5 \times 10^{-3}$ $M$) in water (9) enhances solute solubility in water. To support this point, the solubilities of these three compounds in water-saturated octanol are shown to be reduced by ~10–30% because of water saturation. These results suggest that octanol in water promotes water solubility by ~75% for III, 70% for II, and 150% for I.

Based on these findings, the use of experimental partition coefficients probably would improve the reliability of the log $S$–log $P$ correlation at the high $P$ region.


(1) S. H. Yalkowsky and S. C. Valvani, *J. Pharm. Sci.*, **69**, 912 (1980).

(2) G. G. Nys and R. F. Rekker, *Eur. J. Med. Chem.*, **9**, 361 (1974).

(3) S. Banerjee, S. H. Yalkowsky, and S. C. Valvani, *Environ. Sci. Technol.*, **14**, 1227 (1980).

(4) C. T. Chiou and D. W. Schmedding, in "Test Protocols for Environmental Fate and Movement of Toxicants," Association of Official Analytical Chemists, Arlington, Va., 1981, p. 28.

(5) S. H. Yalkowsky, R. J. Orr, and S. C. Valvani, *Ind. Eng. Chem. Fundam.*, **18**, 351 (1979).

(6) A. Leo, C. Hansch, and D. Elkins, *Chem. Rev.*, **71**, 525 (1971).

(7) L. Weil, G. Duré, and K. Quentin, *Z. Wasser-Abwasser Forsch.*, **7**, 169 (1974).

(8) W. E. May, in "Petroleum in the Marine Environment," L. Petrakis and F. T. Weiss, Eds., Advances in Chemistry Series, 185, 143 (1980).

(9) R. Collander, *Acta Chem. Scand.*, **5**, 774 (1951).



*Cary T. Chiou* [x]
*David W. Schmedding*
Environmental Health Sciences Center
Oregon State University
Corvallis, OR 97331

*John H. Block*
School of Pharmacy
Oregon State University
Corvallis, OR 97331



Received February 23, 1981.
Accepted for publication May 21, 1981.

Supported by U.S. Public Health Grants ES-00210 and ES-02400 and Environmental Protection Agency Grant CR-808046 from the EPA Environmental Research Laboratory, Corvallis, OR.


## Correlation of Water Solubility with Octanol–Water Partition Coefficient: A Response


**Keyphrases** □ Solubility—water, correlation with octanol–water partition coefficient, response □ Partition coefficient—octanol–water, correlation with water solubility, response □ Melting-point effect—correlation between water solubility and octanol–water partition coefficient, response


*To the Editor:*

The preceding paper (1) raised three concerns about our recent paper (2) which we shall now attempt to alleviate.

The first concern of Chiou *et al.* (1) is that Eqs. 32–36 of Ref. 2 do not have slopes of unity and intercepts of zero. The reason for this apparent discrepancy was mentioned briefly in the paragraph preceding Eq. 37 of Ref. 2 but will be discussed more completely here.

**Table I—Aqueous Molar Solubility ($S_w$) and Octanol–Water Partition Coefficients ($PC$) of Tetra-, Penta-, and Hexachlorobenzenes**

| Compound | Melting point | Experimental log $PC$ | log $S_w$ Observed[a] | log $S_w$ Predicted by Eq. 2 |
|---|---|---|---|---|
| 1,2,3,5-Tetrachlorobenzene | 54° | 4.46[b] | −4.79 | −4.46 |
| Pentachlorobenzene | 86° | 4.94[b] | −5.65 | −5.35 |
| Hexachlorobenzene | 230° | 5.50[c] | −7.76 | −7.67 |

[a] Reference 2. [b] Reference 3. [c] Reference 1.

Equation 30 of Ref. 2 was developed on the basis of the theoretical relationships between solubility, partition coefficient, melting point, and entropy of fusion. Solubility data for five classes of compounds were compared to the predictions based on:

$$\log S_w \cong -\log PC - 0.01MP + 1.05 \qquad \text{(Eq. 1)}$$

Only if this theoretical equation perfectly predicted all of the solubilities would the slope be unity and the intercept zero.

In most cases, the slopes were not significantly different from unity; however, the intercepts tended to be slightly negative rather than zero. This trend shows a systematic overestimation of solubility by a factor of ~3. This finding indicated that while the theoretical equation was not perfect, it did provide a basis for assessing the role of the partition coefficient and the melting point in controlling aqueous solubility.

Each of the five classes of compounds represents a fairly small data set (in most cases covering only a few orders of magnitude in solubility). The slopes and intercepts are thus more subject to errors in the log $S_w$ measurements and/or the log $PC$ estimation than is the whole data set, which covers almost nine orders of magnitude. The empirical equation for rigid molecules (Eq. 39 of Ref. 2) is:

$$\log S_w = -1.05 \log PC - 0.012MP + 0.87 \qquad \text{(Eq. 2)}$$

When Eq. 2 is used to estimate solubilities, it gives a slope and intercept of unity and zero, respectively. This final equation rather than the ones based on the smaller data sets should be used to estimate aqueous solubilities.

Second, Chiou *et al.* (1) point out that log $PC$ calculations tend to be imprecise for low solubility compounds and seem surprised that the calculated values work better for estimating aqueous solubility than their own experimentally determined values. The reason for this situation is again statistical. For the reasons already described, it is best to use Eq. 2 to estimate solubility. When this is done, the experimental log $PC$ values of Chiou *et al.* (1) will yield calculated solubilities that are in excellent agreement with the observed values as shown in Table I.

The regression equations were obtained by correlating aqueous solubility with melting points and calculated values of log $PC$. If experimental log $PC$ values were available, the regression coefficient of log $PC$ as well as the intercept probably would be somewhat altered. Thus, systematic errors in estimating log $PC$ are compensated for by the choice of the coefficient of log $PC$.

The third concern raised by Chiou *et al.* (1) is the lack of a correction for the mutual miscibility of water and octanol. They show three examples that indicate an error as high as 0.3–0.5 in log *PC* for very nonpolar solutes. This magnitude of error is not of particular concern. It is well within the error normally encountered in determining experimental values for both log $S_w$ and log *PC* for hydrophobic compounds and certainly within the limitations of Eq. 2.

The conclusion of Chiou *et al.* (1) is that experimental values for log *PC* should be used to improve the reliability of the log $S_w$ − log *PC* correlation in the high log *PC* region. While this may be true, it is somewhat impractical. The value of Eq. 2 is that it provides a simple means of estimating log $S_w$ from nothing more than a knowledge of the melting point of the solute and a group contribution estimate of its partition coefficient. The measurement of accurate partition coefficients greater than 10,000 (log *PC* > 4) is far more difficult and subject to error than the measurement of log $S_w$.

(1) C. T. Chiou, D. W. Schmedding, and J. H. Block, *J. Pharm. Sci.*, **70**, 1176 (1981).
(2) S. H. Yalkowsky and S. C. Valvani, *ibid.*, **69**, 912 (1980).
(3) S. Banerjee, S. H. Yalkowsky, and S. C. Valvani, *Environ. Sci. Technol.*, **14**, 1227 (1980).

*Samuel H. Yalkowsky* ˣ
*Shri C. Valvani*
Pharmacy Research
The Upjohn Company
Kalamazoo, MI 49001

Received May 26, 1981.
Accepted for publication July 2, 1981.

# BOOKS

## REVIEWS

**Controlled Release Technologies: Methods, Theory, and Applications.** Edited by AGIS F. KYDONIEUS. CRC Press, 2000 N.W. 24th St., Boca Raton, FL 33431. 1980. Vol. I, 261 pp., and Vol. II, 273 pp. 17 × 26 cm. Price U.S. $69.95 each (Foreign $79.95).

*Controlled Release Technologies* is contained in two volumes, with a contributors list that reads like a "who's who" in the field of controlled-release products. In the prefix, the editor indicates that "technologies described in these two volumes depend almost exclusively on the use of polymers and polymer technology" and that, although "applications, advantages and fundamental concepts of controlled release have been the subject of many symposia and several books dealing with formulations, all known delivery systems have not been assembled for consideration as they are in these volumes." The editor is entirely correct on this point.

Volume I contains six chapters dealing with fundamental concepts of controlled release, monolithic polymer devices, monolithic elastomeric material, membrane systems, multilayered laminated structures, and controlled release from ultramicroporous triacetate. Volume II contains 13 chapters including topics on erodible matrixes and biodegradative controlled release of pesticides from polymeric substances, polymers containing pendent pesticide substituents, microencapsulation using coacervation phase separation techniques with pharmaceutical and agricultural applications, the Wurster process, microencapsulation using physical methods, controlled-vapor release from hollow fibers, delivery of active agents by osmosis, starch and other polyols as encapsulating matrixes for pesticides, pine craft lignin as a pesticide delivery system, and other controlled-release technologies and applications.

Most chapters provide a brief description of the theory of preparing controlled-release devices but omit specific examples of formulations or preparation techniques which the "novice" could employ to make the products described. This may be because much of such information is proprietary, or it may be because the authors have assumed that the average reader will already have some knowledge in this area. Chapter 3 in Volume I is an exception in that many interesting product formulations have been presented. The volumes were published in 1980, and the editor's introductory comments were signed and dated 1978. Thus, most chapters do not contain references more recent than 1976, but the literature prior to this time is well covered and a large number of excellent references are provided with each chapter.

In addition, Chapter 13 of Volume II, which deals with "other controlled release technologies and applications," contains a series of tables listing U.S. patent numbers, companies holding the patents, titles of controlled-release systems, applications for the controlled-release systems, active agents involved, and the controlled-release method employed. These tables are quite informative.

The authors have done a good job of presenting polymeric controlled-release technology for drugs, insecticides, pesticides, herbicides, and antifouling formulations. Many chapters contain a brief mathematical description for active ingredient release theory followed by an

The third concern raised by Chiou *et al.* (1) is the lack of a correction for the mutual miscibility of water and octanol. They show three examples that indicate an error as high as 0.3–0.5 in log *PC* for very nonpolar solutes. This magnitude of error is not of particular concern. It is well within the error normally encountered in determining experimental values for both log $S_w$ and log *PC* for hydrophobic compounds and certainly within the limitations of Eq. 2.

The conclusion of Chiou *et al.* (1) is that experimental values for log *PC* should be used to improve the reliability of the log $S_w$ − log *PC* correlation in the high log *PC* region. While this may be true, it is somewhat impractical. The value of Eq. 2 is that it provides a simple means of estimating log $S_w$ from nothing more than a knowledge of the melting point of the solute and a group contribution estimate of its partition coefficient. The measurement of accurate partition coefficients greater than 10,000 (log *PC* > 4) is far more difficult and subject to error than the measurement of log $S_w$.

(1) C. T. Chiou, D. W. Schmedding, and J. H. Block, *J. Pharm. Sci.*, **70**, 1176 (1981).
(2) S. H. Yalkowsky and S. C. Valvani, *ibid.*, **69**, 912 (1980).
(3) S. Banerjee, S. H. Yalkowsky, and S. C. Valvani, *Environ. Sci. Technol.*, **14**, 1227 (1980).

*Samuel H. Yalkowsky* ˣ
*Shri C. Valvani*
Pharmacy Research
The Upjohn Company
Kalamazoo, MI 49001

Received May 26, 1981.
Accepted for publication July 2, 1981.

# BOOKS

## REVIEWS

**Controlled Release Technologies: Methods, Theory, and Applications.** Edited by AGIS F. KYDONIEUS. CRC Press, 2000 N.W. 24th St., Boca Raton, FL 33431. 1980. Vol. I, 261 pp., and Vol. II, 273 pp. 17 × 26 cm. Price U.S. $69.95 each (Foreign $79.95).

*Controlled Release Technologies* is contained in two volumes, with a contributors list that reads like a "who's who" in the field of controlled-release products. In the prefix, the editor indicates that "technologies described in these two volumes depend almost exclusively on the use of polymers and polymer technology" and that, although "applications, advantages and fundamental concepts of controlled release have been the subject of many symposia and several books dealing with formulations, all known delivery systems have not been assembled for consideration as they are in these volumes." The editor is entirely correct on this point.

Volume I contains six chapters dealing with fundamental concepts of controlled release, monolithic polymer devices, monolithic elastomeric material, membrane systems, multilayered laminated structures, and controlled release from ultramicroporous triacetate. Volume II contains 13 chapters including topics on erodible matrixes and biodegradative controlled release of pesticides from polymeric substances, polymers containing pendent pesticide substituents, microencapsulation using coacervation phase separation techniques with pharmaceutical and agricultural applications, the Wurster process, microencapsulation using physical methods, controlled-vapor release from hollow fibers, delivery of active agents by osmosis, starch and other polyols as encapsulating matrixes for pesticides, pine craft lignin as a pesticide delivery system, and other controlled-release technologies and applications.

Most chapters provide a brief description of the theory of preparing controlled-release devices but omit specific examples of formulations or preparation techniques which the "novice" could employ to make the products described. This may be because much of such information is proprietary, or it may be because the authors have assumed that the average reader will already have some knowledge in this area. Chapter 3 in Volume I is an exception in that many interesting product formulations have been presented. The volumes were published in 1980, and the editor's introductory comments were signed and dated 1978. Thus, most chapters do not contain references more recent than 1976, but the literature prior to this time is well covered and a large number of excellent references are provided with each chapter.

In addition, Chapter 13 of Volume II, which deals with "other controlled release technologies and applications," contains a series of tables listing U.S. patent numbers, companies holding the patents, titles of controlled-release systems, applications for the controlled-release systems, active agents involved, and the controlled-release method employed. These tables are quite informative.

The authors have done a good job of presenting polymeric controlled-release technology for drugs, insecticides, pesticides, herbicides, and antifouling formulations. Many chapters contain a brief mathematical description for active ingredient release theory followed by an

abundance of practical examples. There are many useful illustrations in graphical and tabular form as well as numerous high quality photographs. All art work is top quality. These volumes will be useful to scientists and students involved in controlled-release technologies.

*Reviewed by* James W. Ayres
*School of Pharmacy*
*Oregon State University*
*Corvallis, OR 97331*

---

**Recent Developments in Mass Spectrometry in Biochemistry and Medicine, 6.** Edited by ALBERTO FRIGERIO and MALCOLM McCAMISH. Elsevier, 52 Vanderbilt Ave., New York, NY 10017. 1980. 553 pp. 16 × 24 cm. Price $83.00.

This volume is a compilation of the papers from the *Proceedings of the 6th International Symposium on Mass Spectrometry in Biochemistry and Medicine*, Venice, June 1979. It contains 52 papers from a variety of mass spectrometric applications. Similar to the previous series, this volume attempts to bring together the latest information on the application of mass spectrometry and research development and methodology of mass spectrometry. This objective is met in the area of the latest applications in biochemistry and medicine.

This book discusses various applicational aspects from experts in the field and is quite up-to-date. Examples of its applications in lipids, prostaglandins, protein sequencing, biogenic amines, metabolite identification, pharmacokinetics, placental drug transfer, and physiological exchange of endogenous substances are of interest to readers at intermediate to advanced levels in mass spectrometry. It is particularly useful to less sophisticated readers who want to get a glimpse of the field without purchasing the previous volumes of the proceedings. Perhaps disappointing to some experienced researchers is the deficiency in certain aspects of applications such as the use of stable isotopes in pharmacology and pharmacokinetics. This may reflect a lack of participation of certain segment of the biomedical researchers in the symposium.

In the area of latest developments in instrumentation and methodology, it has somewhat short-changed the reader. Several areas such as mass spectrometry–mass spectrometry (multiple mass spectrometry), ion-cyclotron mass spectrometry, and high-pressure liquid chromatography–mass spectrometer interface are not covered. Nonetheless, several chapters in this area are quite valuable, *e.g.*, the description of the Kratos MS 80, the laser microprobe mass analyzer and its applications, low- and high-pressure negative chemical-ionization mass spectrometry, and the disposable surface probe.

This book is divided into six general classifications, including qualitative and quantitative studies of endogenous and exogenous compounds, instrumentation and methodology, and environmental studies. These classifications, although somewhat artificial, are quite helpful in locating quickly a particular area of interest. However, it is not understood why a paper that discusses the application of the electron-capture detector in liquid chromatography without any reference to mass spectrometry was included in this book (pp. 317–330).

This book contains an author index but not a subject index. The former does not serve much purpose because no affiliations of the authors are provided in this index and the name of the author can already be found in the table of contents. The latter, if available, is usually more useful in helping readers locate the subject of interest. However, this book is a reasonably up-to-date reference book on mass spectrometry.

*Reviewed by* Kenneth K. Chan
*School of Pharmacy*
*University of Southern California*
*Los Angeles, CA 90033*

**Applied Biopharmaceutics and Pharmacokinetics.** By LEON SHARGEL and ANDREW B. C. YU. Appleton-Century-Crofts, 292 Madison Ave., New York, NY 10017. 1980. 253 pp. 16 × 24 cm. Price $18.50.

This book, intended primarily for undergraduate students in pharmacy and allied health professions, emphasizes pharmacokinetic principles rather than biopharmaceutics. The first two chapters review elementary mathematics and kinetics, and the next three chapters introduce one-compartment and multicompartment pharmacokinetic models. Chapter 6 briefly discusses biopharmaceutics, including absorption mechanisms and dosage form dissolution. Chapters 7–11 deal with absorption kinetics, bioavailability, clearance, hepatic elimination, and protein binding. Chapters 12, 13, and 14 consider intravenous infusions, multiple-dose administration, and nonlinear pharmacokinetics, Chapters 15 and 16 discuss clinical pharmacokinetics, and Chapter 17 describes the kinetics of pharmacological effects.

The book is quite readable, with numerous illustrations. Most chapters contain practice problems, along with detailed solutions. In addition, questions are included at the end of each chapter, and answers are provided in the *Appendix*. One major attribute of the book is the step-by-step illustrations given for some of the more common pharmacokinetic manipulations (*e.g.*, method of residuals, Wagner–Nelson method, and Loo–Riegelman calculation). Only a limited number of references are provided, and they are generally in the form of a bibliography at the end of each chapter.

The text appears relatively free from errors, although several incorrect equations were found, and some generalizations were made that were not as widely applicable as the text seemed to imply. On the whole, the book provides a reasonable introduction to the material, although the somewhat superficial discussion of some topics could mislead someone utilizing the text without a thorough understanding of the limitation and pitfalls in the approaches. However, the book would be suitable as an introductory undergraduate text for a course taught by an instructor experienced in pharmacokinetics.

*Reviewed by Marvin C. Meyer*
*Department of Pharmaceutics*
*College of Pharmacy*
*University of Tennessee*
*Center for the Health Sciences*
*Memphis, TN 38163*

---

**Progress in Drug Metabolism, Vol. 5.** Edited by J. W. BRIDGES and L. F. CHASSEAUD. Wiley, 605 Third Ave., New York, NY 10016. 1980. 358 pp. 15 × 23 cm. Price $85.00.

This volume is the fifth in a series concerned with various aspects of drug metabolism. This volume is similar to the previous four volumes in that five to six major, current, and timely topics are reviewed. These topics are not necessarily directly related other than that they are concerned with the general topic of drug metabolism.

Chapter 1 deals with the distribution and role of cytochrome P-450 in extrahepatic organs and in prostaglandin metabolism. Steroidogenic organs also are extensively reviewed. The chapter does not include recent investigations involving cytochrome P-450 in the intestine and colon, and most references are pre-1978, although the volume was published in late 1980.

Chapter 2 addresses a topic on which relatively little information exists, namely species variations in xenobiotic metabolizing enzymes. The chapter is restricted to hepatic metabolism, primarily involving microsomal monoxygenases, epoxide hydratase, and glucuronyltransferase. No information is provided on interspecies variation within hepatic and extrahepatic tissues.

abundance of practical examples. There are many useful illustrations in graphical and tabular form as well as numerous high quality photographs. All art work is top quality. These volumes will be useful to scientists and students involved in controlled-release technologies.

*Reviewed by* James W. Ayres
*School of Pharmacy*
*Oregon State University*
*Corvallis, OR 97331*

---

**Recent Developments in Mass Spectrometry in Biochemistry and Medicine, 6.** Edited by ALBERTO FRIGERIO and MALCOLM McCAMISH. Elsevier, 52 Vanderbilt Ave., New York, NY 10017. 1980. 553 pp. 16 × 24 cm. Price $83.00.

This volume is a compilation of the papers from the *Proceedings of the 6th International Symposium on Mass Spectrometry in Biochemistry and Medicine*, Venice, June 1979. It contains 52 papers from a variety of mass spectrometric applications. Similar to the previous series, this volume attempts to bring together the latest information on the application of mass spectrometry and research development and methodology of mass spectrometry. This objective is met in the area of the latest applications in biochemistry and medicine.

This book discusses various applicational aspects from experts in the field and is quite up-to-date. Examples of its applications in lipids, prostaglandins, protein sequencing, biogenic amines, metabolite identification, pharmacokinetics, placental drug transfer, and physiological exchange of endogenous substances are of interest to readers at intermediate to advanced levels in mass spectrometry. It is particularly useful to less sophisticated readers who want to get a glimpse of the field without purchasing the previous volumes of the proceedings. Perhaps disappointing to some experienced researchers is the deficiency in certain aspects of applications such as the use of stable isotopes in pharmacology and pharmacokinetics. This may reflect a lack of participation of certain segment of the biomedical researchers in the symposium.

In the area of latest developments in instrumentation and methodology, it has somewhat short-changed the reader. Several areas such as mass spectrometry–mass spectrometry (multiple mass spectrometry), ion-cyclotron mass spectrometry, and high-pressure liquid chromatography–mass spectrometer interface are not covered. Nonetheless, several chapters in this area are quite valuable, *e.g.*, the description of the Kratos MS 80, the laser microprobe mass analyzer and its applications, low- and high-pressure negative chemical-ionization mass spectrometry, and the disposable surface probe.

This book is divided into six general classifications, including qualitative and quantitative studies of endogenous and exogenous compounds, instrumentation and methodology, and environmental studies. These classifications, although somewhat artificial, are quite helpful in locating quickly a particular area of interest. However, it is not understood why a paper that discusses the application of the electron-capture detector in liquid chromatography without any reference to mass spectrometry was included in this book (pp. 317–330).

This book contains an author index but not a subject index. The former does not serve much purpose because no affiliations of the authors are provided in this index and the name of the author can already be found in the table of contents. The latter, if available, is usually more useful in helping readers locate the subject of interest. However, this book is a reasonably up-to-date reference book on mass spectrometry.

*Reviewed by* Kenneth K. Chan
*School of Pharmacy*
*University of Southern California*
*Los Angeles, CA 90033*

**Applied Biopharmaceutics and Pharmacokinetics.** By LEON SHARGEL and ANDREW B. C. YU. Appleton-Century-Crofts, 292 Madison Ave., New York, NY 10017. 1980. 253 pp. 16 × 24 cm. Price $18.50.

This book, intended primarily for undergraduate students in pharmacy and allied health professions, emphasizes pharmacokinetic principles rather than biopharmaceutics. The first two chapters review elementary mathematics and kinetics, and the next three chapters introduce one-compartment and multicompartment pharmacokinetic models. Chapter 6 briefly discusses biopharmaceutics, including absorption mechanisms and dosage form dissolution. Chapters 7–11 deal with absorption kinetics, bioavailability, clearance, hepatic elimination, and protein binding. Chapters 12, 13, and 14 consider intravenous infusions, multiple-dose administration, and nonlinear pharmacokinetics, Chapters 15 and 16 discuss clinical pharmacokinetics, and Chapter 17 describes the kinetics of pharmacological effects.

The book is quite readable, with numerous illustrations. Most chapters contain practice problems, along with detailed solutions. In addition, questions are included at the end of each chapter, and answers are provided in the *Appendix*. One major attribute of the book is the step-by-step illustrations given for some of the more common pharmacokinetic manipulations (*e.g.*, method of residuals, Wagner–Nelson method, and Loo–Riegelman calculation). Only a limited number of references are provided, and they are generally in the form of a bibliography at the end of each chapter.

The text appears relatively free from errors, although several incorrect equations were found, and some generalizations were made that were not as widely applicable as the text seemed to imply. On the whole, the book provides a reasonable introduction to the material, although the somewhat superficial discussion of some topics could mislead someone utilizing the text without a thorough understanding of the limitation and pitfalls in the approaches. However, the book would be suitable as an introductory undergraduate text for a course taught by an instructor experienced in pharmacokinetics.

*Reviewed by Marvin C. Meyer*
*Department of Pharmaceutics*
*College of Pharmacy*
*University of Tennessee*
*Center for the Health Sciences*
*Memphis, TN 38163*

---

**Progress in Drug Metabolism, Vol. 5.** Edited by J. W. BRIDGES and L. F. CHASSEAUD. Wiley, 605 Third Ave., New York, NY 10016. 1980. 358 pp. 15 × 23 cm. Price $85.00.

This volume is the fifth in a series concerned with various aspects of drug metabolism. This volume is similar to the previous four volumes in that five to six major, current, and timely topics are reviewed. These topics are not necessarily directly related other than that they are concerned with the general topic of drug metabolism.

Chapter 1 deals with the distribution and role of cytochrome P-450 in extrahepatic organs and in prostaglandin metabolism. Steroidogenic organs also are extensively reviewed. The chapter does not include recent investigations involving cytochrome P-450 in the intestine and colon, and most references are pre-1978, although the volume was published in late 1980.

Chapter 2 addresses a topic on which relatively little information exists, namely species variations in xenobiotic metabolizing enzymes. The chapter is restricted to hepatic metabolism, primarily involving microsomal monoxygenases, epoxide hydratase, and glucuronyltransferase. No information is provided on interspecies variation within hepatic and extrahepatic tissues.

abundance of practical examples. There are many useful illustrations in graphical and tabular form as well as numerous high quality photographs. All art work is top quality. These volumes will be useful to scientists and students involved in controlled-release technologies.

*Reviewed by* James W. Ayres
*School of Pharmacy*
*Oregon State University*
*Corvallis, OR 97331*

---

**Recent Developments in Mass Spectrometry in Biochemistry and Medicine, 6.** Edited by ALBERTO FRIGERIO and MALCOLM McCAMISH. Elsevier, 52 Vanderbilt Ave., New York, NY 10017. 1980. 553 pp. 16 × 24 cm. Price $83.00.

This volume is a compilation of the papers from the *Proceedings of the 6th International Symposium on Mass Spectrometry in Biochemistry and Medicine*, Venice, June 1979. It contains 52 papers from a variety of mass spectrometric applications. Similar to the previous series, this volume attempts to bring together the latest information on the application of mass spectrometry and research development and methodology of mass spectrometry. This objective is met in the area of the latest applications in biochemistry and medicine.

This book discusses various applicational aspects from experts in the field and is quite up-to-date. Examples of its applications in lipids, prostaglandins, protein sequencing, biogenic amines, metabolite identification, pharmacokinetics, placental drug transfer, and physiological exchange of endogenous substances are of interest to readers at intermediate to advanced levels in mass spectrometry. It is particularly useful to less sophisticated readers who want to get a glimpse of the field without purchasing the previous volumes of the proceedings. Perhaps disappointing to some experienced researchers is the deficiency in certain aspects of applications such as the use of stable isotopes in pharmacology and pharmacokinetics. This may reflect a lack of participation of certain segment of the biomedical researchers in the symposium.

In the area of latest developments in instrumentation and methodology, it has somewhat short-changed the reader. Several areas such as mass spectrometry–mass spectrometry (multiple mass spectrometry), ion-cyclotron mass spectrometry, and high-pressure liquid chromatography–mass spectrometer interface are not covered. Nonetheless, several chapters in this area are quite valuable, *e.g.*, the description of the Kratos MS 80, the laser microprobe mass analyzer and its applications, low- and high-pressure negative chemical-ionization mass spectrometry, and the disposable surface probe.

This book is divided into six general classifications, including qualitative and quantitative studies of endogenous and exogenous compounds, instrumentation and methodology, and environmental studies. These classifications, although somewhat artificial, are quite helpful in locating quickly a particular area of interest. However, it is not understood why a paper that discusses the application of the electron-capture detector in liquid chromatography without any reference to mass spectrometry was included in this book (pp. 317–330).

This book contains an author index but not a subject index. The former does not serve much purpose because no affiliations of the authors are provided in this index and the name of the author can already be found in the table of contents. The latter, if available, is usually more useful in helping readers locate the subject of interest. However, this book is a reasonably up-to-date reference book on mass spectrometry.

*Reviewed by* Kenneth K. Chan
*School of Pharmacy*
*University of Southern California*
*Los Angeles, CA 90033*

**Applied Biopharmaceutics and Pharmacokinetics.** By LEON SHARGEL and ANDREW B. C. YU. Appleton-Century-Crofts, 292 Madison Ave., New York, NY 10017. 1980. 253 pp. 16 × 24 cm. Price $18.50.

This book, intended primarily for undergraduate students in pharmacy and allied health professions, emphasizes pharmacokinetic principles rather than biopharmaceutics. The first two chapters review elementary mathematics and kinetics, and the next three chapters introduce one-compartment and multicompartment pharmacokinetic models. Chapter 6 briefly discusses biopharmaceutics, including absorption mechanisms and dosage form dissolution. Chapters 7–11 deal with absorption kinetics, bioavailability, clearance, hepatic elimination, and protein binding. Chapters 12, 13, and 14 consider intravenous infusions, multiple-dose administration, and nonlinear pharmacokinetics, Chapters 15 and 16 discuss clinical pharmacokinetics, and Chapter 17 describes the kinetics of pharmacological effects.

The book is quite readable, with numerous illustrations. Most chapters contain practice problems, along with detailed solutions. In addition, questions are included at the end of each chapter, and answers are provided in the *Appendix*. One major attribute of the book is the step-by-step illustrations given for some of the more common pharmacokinetic manipulations (*e.g.*, method of residuals, Wagner–Nelson method, and Loo–Riegelman calculation). Only a limited number of references are provided, and they are generally in the form of a bibliography at the end of each chapter.

The text appears relatively free from errors, although several incorrect equations were found, and some generalizations were made that were not as widely applicable as the text seemed to imply. On the whole, the book provides a reasonable introduction to the material, although the somewhat superficial discussion of some topics could mislead someone utilizing the text without a thorough understanding of the limitation and pitfalls in the approaches. However, the book would be suitable as an introductory undergraduate text for a course taught by an instructor experienced in pharmacokinetics.

*Reviewed by Marvin C. Meyer*
*Department of Pharmaceutics*
*College of Pharmacy*
*University of Tennessee*
*Center for the Health Sciences*
*Memphis, TN 38163*

---

**Progress in Drug Metabolism, Vol. 5.** Edited by J. W. BRIDGES and L. F. CHASSEAUD. Wiley, 605 Third Ave., New York, NY 10016. 1980. 358 pp. 15 × 23 cm. Price $85.00.

This volume is the fifth in a series concerned with various aspects of drug metabolism. This volume is similar to the previous four volumes in that five to six major, current, and timely topics are reviewed. These topics are not necessarily directly related other than that they are concerned with the general topic of drug metabolism.

Chapter 1 deals with the distribution and role of cytochrome P-450 in extrahepatic organs and in prostaglandin metabolism. Steroidogenic organs also are extensively reviewed. The chapter does not include recent investigations involving cytochrome P-450 in the intestine and colon, and most references are pre-1978, although the volume was published in late 1980.

Chapter 2 addresses a topic on which relatively little information exists, namely species variations in xenobiotic metabolizing enzymes. The chapter is restricted to hepatic metabolism, primarily involving microsomal monoxygenases, epoxide hydratase, and glucuronyltransferase. No information is provided on interspecies variation within hepatic and extrahepatic tissues.

abundance of practical examples. There are many useful illustrations in graphical and tabular form as well as numerous high quality photographs. All art work is top quality. These volumes will be useful to scientists and students involved in controlled-release technologies.

*Reviewed by* James W. Ayres
*School of Pharmacy*
*Oregon State University*
*Corvallis, OR 97331*

---

**Recent Developments in Mass Spectrometry in Biochemistry and Medicine, 6.** Edited by ALBERTO FRIGERIO and MALCOLM McCAMISH. Elsevier, 52 Vanderbilt Ave., New York, NY 10017. 1980. 553 pp. 16 × 24 cm. Price $83.00.

This volume is a compilation of the papers from the *Proceedings of the 6th International Symposium on Mass Spectrometry in Biochemistry and Medicine*, Venice, June 1979. It contains 52 papers from a variety of mass spectrometric applications. Similar to the previous series, this volume attempts to bring together the latest information on the application of mass spectrometry and research development and methodology of mass spectrometry. This objective is met in the area of the latest applications in biochemistry and medicine.

This book discusses various applicational aspects from experts in the field and is quite up-to-date. Examples of its applications in lipids, prostaglandins, protein sequencing, biogenic amines, metabolite identification, pharmacokinetics, placental drug transfer, and physiological exchange of endogenous substances are of interest to readers at intermediate to advanced levels in mass spectrometry. It is particularly useful to less sophisticated readers who want to get a glimpse of the field without purchasing the previous volumes of the proceedings. Perhaps disappointing to some experienced researchers is the deficiency in certain aspects of applications such as the use of stable isotopes in pharmacology and pharmacokinetics. This may reflect a lack of participation of certain segment of the biomedical researchers in the symposium.

In the area of latest developments in instrumentation and methodology, it has somewhat short-changed the reader. Several areas such as mass spectrometry–mass spectrometry (multiple mass spectrometry), ion-cyclotron mass spectrometry, and high-pressure liquid chromatography–mass spectrometer interface are not covered. Nonetheless, several chapters in this area are quite valuable, *e.g.*, the description of the Kratos MS 80, the laser microprobe mass analyzer and its applications, low- and high-pressure negative chemical-ionization mass spectrometry, and the disposable surface probe.

This book is divided into six general classifications, including qualitative and quantitative studies of endogenous and exogenous compounds, instrumentation and methodology, and environmental studies. These classifications, although somewhat artificial, are quite helpful in locating quickly a particular area of interest. However, it is not understood why a paper that discusses the application of the electron-capture detector in liquid chromatography without any reference to mass spectrometry was included in this book (pp. 317–330).

This book contains an author index but not a subject index. The former does not serve much purpose because no affiliations of the authors are provided in this index and the name of the author can already be found in the table of contents. The latter, if available, is usually more useful in helping readers locate the subject of interest. However, this book is a reasonably up-to-date reference book on mass spectrometry.

*Reviewed by* Kenneth K. Chan
*School of Pharmacy*
*University of Southern California*
*Los Angeles, CA 90033*

**Applied Biopharmaceutics and Pharmacokinetics.** By LEON SHARGEL and ANDREW B. C. YU. Appleton-Century-Crofts, 292 Madison Ave., New York, NY 10017. 1980. 253 pp. 16 × 24 cm. Price $18.50.

This book, intended primarily for undergraduate students in pharmacy and allied health professions, emphasizes pharmacokinetic principles rather than biopharmaceutics. The first two chapters review elementary mathematics and kinetics, and the next three chapters introduce one-compartment and multicompartment pharmacokinetic models. Chapter 6 briefly discusses biopharmaceutics, including absorption mechanisms and dosage form dissolution. Chapters 7–11 deal with absorption kinetics, bioavailability, clearance, hepatic elimination, and protein binding. Chapters 12, 13, and 14 consider intravenous infusions, multiple-dose administration, and nonlinear pharmacokinetics, Chapters 15 and 16 discuss clinical pharmacokinetics, and Chapter 17 describes the kinetics of pharmacological effects.

The book is quite readable, with numerous illustrations. Most chapters contain practice problems, along with detailed solutions. In addition, questions are included at the end of each chapter, and answers are provided in the *Appendix*. One major attribute of the book is the step-by-step illustrations given for some of the more common pharmacokinetic manipulations (*e.g.*, method of residuals, Wagner–Nelson method, and Loo–Riegelman calculation). Only a limited number of references are provided, and they are generally in the form of a bibliography at the end of each chapter.

The text appears relatively free from errors, although several incorrect equations were found, and some generalizations were made that were not as widely applicable as the text seemed to imply. On the whole, the book provides a reasonable introduction to the material, although the somewhat superficial discussion of some topics could mislead someone utilizing the text without a thorough understanding of the limitation and pitfalls in the approaches. However, the book would be suitable as an introductory undergraduate text for a course taught by an instructor experienced in pharmacokinetics.

*Reviewed by Marvin C. Meyer*
*Department of Pharmaceutics*
*College of Pharmacy*
*University of Tennessee*
*Center for the Health Sciences*
*Memphis, TN 38163*

---

**Progress in Drug Metabolism, Vol. 5.** Edited by J. W. BRIDGES and L. F. CHASSEAUD. Wiley, 605 Third Ave., New York, NY 10016. 1980. 358 pp. 15 × 23 cm. Price $85.00.

This volume is the fifth in a series concerned with various aspects of drug metabolism. This volume is similar to the previous four volumes in that five to six major, current, and timely topics are reviewed. These topics are not necessarily directly related other than that they are concerned with the general topic of drug metabolism.

Chapter 1 deals with the distribution and role of cytochrome P-450 in extrahepatic organs and in prostaglandin metabolism. Steroidogenic organs also are extensively reviewed. The chapter does not include recent investigations involving cytochrome P-450 in the intestine and colon, and most references are pre-1978, although the volume was published in late 1980.

Chapter 2 addresses a topic on which relatively little information exists, namely species variations in xenobiotic metabolizing enzymes. The chapter is restricted to hepatic metabolism, primarily involving microsomal monoxygenases, epoxide hydratase, and glucuronyltransferase. No information is provided on interspecies variation within hepatic and extrahepatic tissues.

Chapter 3 deals with the pharmacokinetics and metabolism of an extensive array of nonsteroidal anti-inflammatory agents including salicylates, arylacetic acids, arylpropionic acids, and *N*-heterocycles. The importance of understanding the basic pharmacokinetic properties of these drugs is emphasized. Some evidence is presented that nonsteroidal anti-inflammatory agents concentrate in inflamed tissues, but the underlying mechanisms and implications are poorly understood. Most references involve work completed prior to 1978.

Chapter 4 is concerned with the monitoring of drug disposition by immunoassay, providing a basic introduction to radioimmunoassays. In addition, there is an extensive discussion on enzyme immunoassays and also luminescent (fluorescent) immunoassays. An enormous amount of literature is now available on the immunoassay of drugs. The authors have provided a distillation and update of information on the background of immunoassays, including theories and applications ranging from practical to research uses.

Chapter 5 deals with the pharmacokinetics and metabolism of industrial chemicals. Because of the large scope of this topic, the authors restricted their discussion to the use of pharmacokinetics involved in toxicological evaluation of styrene, 2,4,5-trichlorophenoxyacetic acid, and 1,4-dioxane. Also discussed is the use of pharmacokinetic concepts and risk assessment using vinylidene chloride and tetrachloroethylene as model compounds. The examples used stress the importance of integrating chronic toxicity bioassay results with the pharmacokinetics and resulting macromoleculecular events in assessing the risk of exposure to chemicals.

The nature of the topics covered in this volume is extremely broad, as has been the case with previous volumes. The volume provides a useful addition to the review and evaluation of the literature concerned with drug metabolism. A major drawback of the volume is its price. However, Volume 5 certainly is an important addition to the library of these involved in the field of drug metabolism.

*Reviewed by* Sidney J. Stohs
*College of Pharmacy*
*University of Nebraska Medical Center*
*Omaha, NE 68105*

A publication of the
American Pharmaceutical Association—
the National Professional Society
of Pharmacists

# JOURNAL OF PHARMACEUTICAL SCIENCES

## INDEX TO AUTHORS
## INDEX TO SUBJECTS

VOLUME 70
JANUARY TO DECEMBER, 1981

*Published monthly under the supervision of the Board of Trustees*

MARY H. FERGUSON
*Editor*

NANCY E. BROWN
*Production Editor*

JOHN PATRICK EVANS
*Copy Editor*

MICHAEL K. HAYES
*Copy Editor*

EDWARD G. FELDMANN
*Contributing Editor*

SAMUEL W. GOLDSTEIN
*Contributing Editor*

BELLE R. BECK
*Editorial Secretary*

EDWARD G. FELDMANN
*Acting Director of Publications*

EDITORIAL ADVISORY BOARD

John Autian
Norman R. Farnsworth
William J. Jusko
Herbert A. Lieberman
David E. Mann, Jr.
Ian W. Mathison
Gerald J. Papariello
Edward G. Rippie

JOURNAL OF PHARMACEUTICAL SCIENCES

NOVEMBER 1981
VOLUME 70 NUMBER 11

*LITERATURE SURVEY*

# Topical Drug Delivery to Cattle and Sheep

**IAN H. PITMAN[x] and SUSAN J. ROSTAS**

Received from the *School of Pharmaceutics, Victorian College of Pharmacy Ltd., Parkville, Victoria 3052 Australia.*

**Keyphrases** □ Topical drug delivery—to cattle and sheep, literature survey □ Cattle—topical drug delivery, literature survey □ Sheep—topical drug delivery, literature survey

CONTENTS

*The Barriers* ..... 1185
Hair and Wool ..... 1185
Skin Topography ..... 1185
Gross Structure of Sheep and Cattle Skins ..... 1185
Emulsion ..... 1186
*Barrier Variability* ..... 1186
Exposure to Solvents ..... 1186
Skin Temperature ..... 1186
Season ..... 1187
Breed ..... 1187
Body Region ..... 1187
Other Factors ..... 1187
*Absorption Mechanisms* ..... 1188
*Pour-On and Spot-On Formulations* ..... 1191
Retention of Drugs on Skin ..... 1192
Solvent Systems and Methods of Application ..... 1192
*Future Work* ..... 1192
*References* ..... 1192

Twenty-one years ago, Rogoff and Kohler (1) demonstrated that the application of 100 ml of a concentrated solution of the organophosphorus insecticide crufomate (I) (Table I) to a small area of a cow's skin could control cattle grubs. Compound I is a systemic insecticide (2), and its mode of action is believed to involve its absorption across the skin into the cow's systemic circulation and, hence, distribution throughout the body, thus interacting with cattle grubs as they migrate through the tissues. Confirmation of drug absorption came from the observation that a slight depression of erythrocyte cholinesterase activity followed drug administration (1). This type of dosage form is referred to as a "pour-on" or "spot-on". It is a liquid formulation (solution, emulsion, or suspension) intended to be applied to a small area of an animal's skin to promote drug absorption into the bloodstream. The concentration of drug in a spot-on is higher than that in a pour-on; consequently, a smaller dosage is used.

The realization that drugs can be introduced topically into the bloodstream has stimulated the search for topical drug delivery systems to control internal and external parasites and to deliver nutrients, metabolic regulators, and hormonal regulators.

Systemic insecticides can be used to control external parasites if the latter are bloodsuckers (*e.g.*, sucking louse *Linognathus vituli*) or if drug is secreted onto the skin *via* sweat or sebaceous glands.

Although the goal of delivering drugs to the systemic circulation *via* the topical route has only been actively researched during the past 21 years, the farm industry has many years of experience in the application of drugs to the hair, wool, and skin of domestic animals by way of dips, dusts, and sprays. However, these dosage forms usually contain a much smaller drug concentration than dosage forms such as pour-ons that are intended to promote systemic delivery. Consequently, because the driving force for Fickian diffusion across a membrane such as skin is the concentration gradient across the membrane, these dosage forms usually act by bringing the drug into contact with an external parasite rather than by promoting absorption.

For example, it is common practice to treat cattle grubs in beef cattle with a dip containing 0.25% I or a spray containing 0.375% I. The usual strengths of the pour-ons and spot-ons of I are 8 and 12%, respectively. Similarly, it is common practice to treat horn flies (*Haematobia irritans*) in beef cattle with back rubbers[1] (burlap soaked with a mixture of an insecticide in an oil such as diesel fuel wrapped around a wire or cable) containing 1% coumafos (II) (3), dust bags[1] (doubled burlap bags containing powdered drug) containing 1 or 5% II, sprays containing 0.06%

[1] They apply drug to the animal's coat when the animal rubs against them.

0022-3549/81/1100-1181$01.00/0
© 1981, American Pharmaceutical Association

**Table I—Some Veterinary Antiparasite Drugs [a]**

| Compound Number | Generic Name | Trade Names | Structure | Melting Point | Solubility: Water | Solubility: Organic Solvents |
|---|---|---|---|---|---|---|
| I | Crufomate | Dowco 132, Montrel, Ruelene | 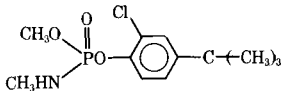 | 60–60.5° | pi[b] | S[c]: acetone, benzene, carbon tetrachloride; pi:light petroleum |
| II | Coumafos | Co-ral, *etc.* | 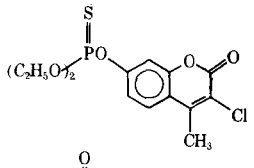 | 91° | pi | PS[d]: acetone, chloroform, corn oil |
| III | Dichlorvos | Atgard, *etc.* | 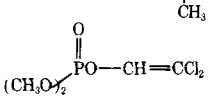 | Liquid | 1 g/100 ml | M[e]: alcohol, most nonpolar molecules |
| IV | Levamisole | Levasole, Nemicide, Citarin-L | 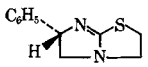 | 60–61.5° | — | — |
| V | Tetramisole hydrochloride | Citarin, Nilverm | ± isomer of IV 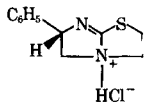 | 264–265° | 21 g/100 ml | S: methanol, propylene, glycol; SpS[f]: ethanol; SS[g]: chloroform, hexane, acetone |
| VI | Trichlorfon | Dylox | 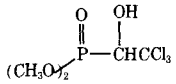 | 83–84° | 15.4 g/100 ml | Chloroform: 75 g/100 ml; ether: 17 g/100 ml; benzene: 15.2 g/100 ml; VSS[h]: pentane, hexane |
| VII | Ronnel | Viozene | 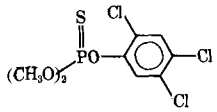 | 41° | 0.004 g/100 ml | FS[i]: acetone, carbon tetrachloride, ether, methylene chloride, kerosene |
| VIII | Phosmet | Imidan | 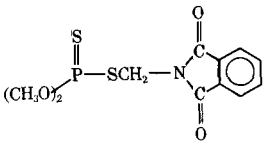 | 71.9° | 25 ppm | Organic solvents |
| IX | Chlorpyrifos | Dowco 179 | 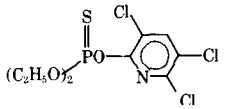 | 1–42° | 2 ppm | Isooctane: 79% W/W; methanol: 43% W/W; FS: other organics |
| X | Chlorfenvinphos | — | 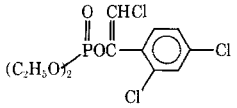 | Liquid | VSpS[j] (dec. at pH >7) | FS: organics |
| XI | Dioxation | Navadel | 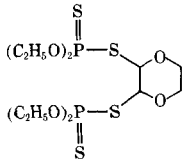 | Liquid | pi | PS: hexane |
| XII | Crotoxyfos | Ciodrin | 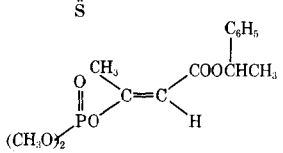 | Liquid | 0.1% | SS: kerosene, saturated hydrocarbons; S: acetone, chloroform, ethanol, highly chlorinated hydrocarbons |
| XIII | Famophos | Warbex | 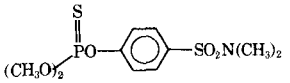 | 52.5–53.5° | — | — |
| XIV | Methidathion | Supracide | 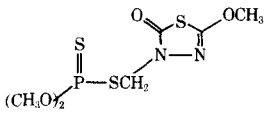 | 39–40° | <1% | S: most organics |
| XV | Temefos | Lapor | 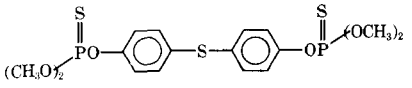 | | — | |

**Table I**—*Continued*

| Compound Number | Generic Name | Trade Names | Structure | Melting Point | Solubility | |
|---|---|---|---|---|---|---|
| | | | | | Water | Organic Solvents |
| XVI | Tetrachlorvinfos | Rabon | 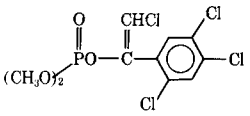 | 97–98° | 11 ppm | Xylene: <15%; chloroform: 40–50% |
| XVII | Malathion | Malamar 50, Prioderm | 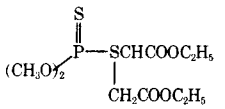 | 2.9° | 145 ppm (hydrolyzed pH >7 or <5) | Soluble in most organics |
| XVIII | Dichlofenthion | Nemacide, Bromex | 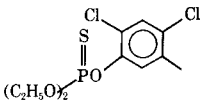 | Liquid | SS | M: most organics |
| XIX | Fenthion | Tiguvon | 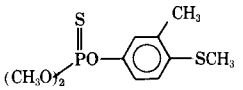 | Liquid | 55 mg/liter | M: most organics |
| XX | Difluron | — | 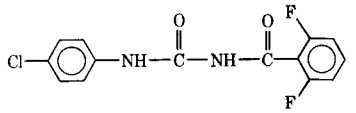 | — | — | — |
| XXI | Bromopfos | — | 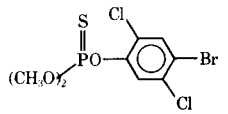 | — | — | — |
| XXII | Ethyl bromopfos | — | 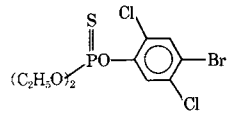 | — | — | — |
| XXIII | Chlormadinone | — | 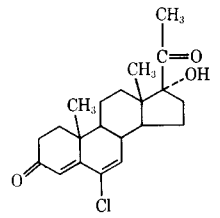 | — | — | — |
| XXIV | 4,5,6-Trichloro-7-(diethylsulfamoyl)-2-(trifluoromethyl) benzimidazole | — | 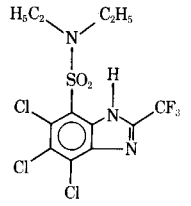 | — | — | — |

[a] From "The Merck Index" 9th ed., Merck & Co., Rahway, N.J., 1976. [b] pi = practically insoluble. [c] S = soluble. [d] PS = partially soluble. [e] M = miscible. [f] SpS = sparingly soluble. [g] SS = slightly soluble. [h] VSS = very slightly soluble. [i] FS = freely soluble. [j] VSpS = very sparingly soluble.

II (3), or dips containing 0.06% II. The usual strength for a pour-on of II is 4%.

Another example of a drug delivery system that acts primarily by bringing drug into contact with the pest rather than promoting absorption is polyvinyl chloride strips impregnated with dichlorvos (III) and attached to the legs of cattle to control cattle grub by killing ovipositing flies, eggs, or newly hatched larvae (4).

Although these dosage forms are not necessarily intended to promote systemic absorption, they may do so with harmful effects to the animals under abnormal conditions. For example, if sheep are driven too far or too fast or are confined to a woolshed to protect them from rain after dipping, overheating can occur, thereby increasing the skin temperature sufficiently to promote the absorption of the dip chemicals (5).

Most of this review will be concerned with topical delivery of drugs into the systemic circulation rather than with delivery onto the skin to promote local contact with ectoparasites. However, an understanding of the permeability of cattle and sheep skins to drugs will provide a basis for preventing drug absorption (thus reducing toxicity to the host animal), prolonging drug action, and promoting drug delivery.

The topical route of systemic delivery is attractive to the farming industry because:

1. It is less labor intensive to apply a drug to an animal's skin than to administer more conventional dosage forms such as drenches, injections, and inocculations.
2. The drug is introduced into the bloodstream without

having to traverse the GI tract where it can be extensively metabolized or bound to proteins and other GI tract contents or where its transit time is unpredictable.

3. The dose for each animal can be regulated much more closely than when drugs are added to feed or are presented as licks.

4. When properly formulated, these systems are likely to cause less trauma and tissue damage than injections or drenches and are less likely to interfere with nutritional status.

The pour-on or spot-on dosage form is particularly attractive since it can be applied rapidly and easily to an animal's skin and the cost of equipment is much less than that required for spraying or dipping. However, it has been argued that the pour-on technique can be more expensive than spraying when large numbers of cattle are to be treated, the application lacks the shampooing effect of a shower treatment, and the operator is exposed to the grave risk of absorbing toxic materials from handling concentrated drug products that have been specifically formulated to promote absorption (6). This latter point was recently investigated (7), with the conclusion that experienced veterinarians can use commercially available organophosphorus pour-ons without absorbing enough drug to depress blood cholinesterase activity. This safety aspect may not be so high with inexperienced operators.

It has long been recognized that topical drug administration to humans has many advantages. As the result of a workable understanding of the barrier properties and transport mechanisms of human skin and of the influence of the physicochemical properties of drugs, vehicles, and other formulation excipients on the absorption process, pharmaceutical scientists can now produce topical dosage forms for humans that demonstrate well-controlled drug delivery. Some excellent reviews were written on these subjects (8–12). The discovery that the cells of the human stratum corneum, the dead keratinized epithelium that comprises the outer 0.001 cm of the skin, are the rate-determining barrier to human skin absorption has led to the design and performance of numerous *in vitro* experiments using isolated skin.

At present, the barrier properties of sheep and cattle skins are not well understood. One report (13) suggested that drugs are much more likely to traverse sheep and cattle skins by way of skin appendages (*i.e.*, hair follicles, sweat and sebaceous glands, and ducts) rather than through the cells of the stratum corneum as in humans, in spite of the fact that both sheep (14) and cattle (15) skins have a substantial stratum corneum. However, more work is necessary to clarify this point.

The next section of this review describes the gross structure of cattle and sheep skins and the physicochemical properties that these barriers are likely to present to diffusing drug molecules. This section is followed by a discussion of the possible changes in the barrier properties of skin as the result of season, temperature, age, sex, humidity, *etc.* Another section is concerned with useful parameters for understanding the permeability character-

**Table II—Thickness of Cattle and Sheep Skins**

| Animal | Breed | Body Region (Season) | Thickness, mm | | | | | Reference |
|---|---|---|---|---|---|---|---|---|
| | | | Whole Skin | Stratum Corneum | Uncornified Epidermis | Papillary Layer of Dermis | Reticular Layer of Dermis | |
| Cattle | Ayrshire Bullock | D T-L[a] (winter) | — | $3.09 \times 10^{-2}$ | $3.11 \times 10^{-2}$ | — | — | 15 |
| | Devon | Midside (unknown) | 8.15 | — | — | — | — | 36 |
| | Hereford | Midside (unknown) | 6.77 | — | — | — | — | 36 |
| | Zebu Cross | Midside (unknown) | 6.43 | — | — | 1.40 | 4.56 | 36 |
| | Australian Illawarra Shorthorn | Midside (unknown) | 6.23 | — | — | — | — | 36 |
| | Friesian | Midside (unknown) | 6.08 | — | — | — | — | 36 |
| | Zebu | Midside (unknown) | 5.77 | — | — | 0.98 | 4.45 | 36 |
| | Aberdeen Angus | Midside (unknown) | 5.75 | — | — | — | — | 36 |
| | Shorthorn | Midside (unknown) | 5.69 | — | — | 1.70 | 4.08 | 36 |
| | Jersey | Midside (unknown) | 5.46 | — | — | — | — | 36 |
| | Jersey | Upper thorax (summer) | 3.5 | — | — | — | — | 37 |
| | Jersey | Upper thorax (spring) | 4.7 | — | — | — | — | 37 |
| | Sahiwals | Upper thorax (summer) | 4.7 | — | — | — | — | 37 |
| | Sahiwals | Upper thorax (spring) | 5.7 | — | — | — | — | 37 |
| Sheep | Finnish Landrace/Dorset Horn | D T-L (winter) | — | $3.14 \times 10^{-2}$ | $1.67 \times 10^{-2}$ | | | |
| | Southdown | Various (unknown) | 2.7 | — | — | — | — | 22 |
| | Shropshire | Various (unknown) | — | — | $2.7 \times 10^{-2}$[b] | — | — | 22 |
| | Merino | Various (unknown) | — | — | $4.2 \times 10^{-2}$[b] | — | — | 22 |

[a] Dorsal thoraco-lumbar. [b] Reported as average total epidermal thickness.

istics of membranes and the conclusions about cattle and sheep skin permeability that can be drawn from some *in vitro* studies. The review concludes with an examination of reports of field and laboratory experiences with veterinary topical drug delivery systems (primarily pour-ons and spot-ons) and suggestions for future work.

## THE BARRIERS

**Hair and Wool**—The first absorption barrier encountered by drug molecules following their application to the skins of cattle and sheep is the hair or wool coat. There are ~2000 hair fibers/cm$^2$ in cattle (16, 17), although this number is affected by the animal's breed, sex, weight, age, and body region. Each fiber grows out of hair follicles, which, in cattle, are randomly distributed over the animal's body. Each follicle has a sweat gland, a sebaceous gland, and an arrector pili muscle associated with it. The hairs of European cattle leave the skin at an average angle of 61–62° (18), whereas those of Asian and African cattle tend to leave at an average angle of slightly less than 60° (19).

The hair and wool follicles in sheep, and consequently the hair and wool fibers, are not randomly distributed over the body but are in definite groups containing one to five primary follicles (20), which have a sebaceous gland, a sweat gland, an arrector pili muscle, and a number of secondary follicles, which have only sebaceous glands. Merino sheep were reported to have 300–400 primary follicles/cm$^2$ and 6000–10,000 secondary follicles/cm$^2$ in wool-growing regions (*i.e.*, midside, midback, and flank) of the body (21). The average density of primary follicles does not change appreciably on the hair-growing regions, but the densities of secondary follicles are markedly reduced. Differences in follicle densities and in ratios of numbers of primary and secondary follicles with breed were discussed elsewhere (20, 21).

Because hair and wool fibers are composed of the modified protein keratin, they possess chemically reactive groups such as thiol, amino, and carboxyl groups and hydrophobic regions. Thus, they can react with and change (frequently reduce) the thermodynamic activity of drugs that they contact. Many chemicals bind strongly to wool (23–28), and a similar situation must be expected with cattle hair.

However, sheep wool and, to a lesser extent, cattle hair are coated with an emulsion of sweat and sebum that is formed in the follicle infundibula where the sweat and sebaceous glands empty their secretions. Wool fibers appear to have an almost continuous coat of this emulsion (29) [frequently referred to as the yolk (30)], while only the lower parts of cattle hairs are similarly coated (29). This emulsion rapidly dissolves many chemicals that are applied to the coat or skin of animals (31, 32), and diffusion within the emulsion, either up or down the fibers, always competes with diffusion of molecules through the skin (33, 34).

Consequently, an understanding of the nature of the emulsion and the manner in which it varies with breed, sex, climate, season, and nutritional state is fundamental to an understanding of topical drug delivery.

**Skin Topography**—Scanning electron micrographs of cattle and sheep skins reveal that the surfaces consist of roughly hexagonal squama punctuated by hair or wool fibers and their associated follicle pores (29). The pores are not open and clear but are protected by a conical mass, which appears to be composed of squama and a convex amorphous material. The latter is believed to be a partially dehydrated or modified form of the emulsion of sweat and sebum that is formed in the follicle infundibula. As mentioned previously, the convex amorphous material also coats most of the wool fibers and the lower parts of cattle hairs. Globules or strips of this material are also present at the junctions of the interfollicular squama in both cattle and sheep skin; in the latter, a significant amount is present on the squama surfaces.

**Gross Structure of Cattle and Sheep Skins**—Like other mammals, the skin of cattle (35) and sheep (20, 22) consists of a cornified stratum corneum, an uncornified "living" epidermis, and a dermis differentiated in the cow and, to a much smaller extent, sheep (20) into papillary and reticular layers. The relative thicknesses of the various skin layers in different animal breeds are given in Table II.

The most reliable studies of the structure of the stratum corneum have employed cryostat sections (14, 15). This technique causes much less damage to the stratum corneum than does a histological technique, which involves dehydration and embedding in paraffin.

The stratum corneum of cattle appears to consist primarily of vertical columns of cells (15). The outer two-thirds of the stratum corneum cells, but not the lower third, the uncornified epidermis, or the sweat glands, are permeated by an emulsion believed to be the emulsified sweat mentioned earlier. It is proposed that the emulsion is formed in the follicle infundibula and oozes to the surface through the outer layers of the stratum corneum and the follicle pore (15).

The entire stratum corneum of sheep is permeated by emulsion, and an intact film of emulsion ~$0.90 \times 10^{-2}$ mm thick covers its outer surface (14). The lower half of the stratum corneum ($1.6 \times 10^{-2}$ mm) consists of vertical columns of densely packed flattened cells, whereas the outer half consists of a loosely knit structure.

The papillary layer of the dermis has a depth of 1–2 mm in cattle (Table II) but is much thinner in sheep (20). It is composed of fine collagenous fibers interwoven with fine elastic and reticular fibers. The reticular layer is a broad zone of coarse collagenous fibers. Goldsberry and Colhoun (38) suggested that the transition zone between the papillary and reticular layers of dermis in cattle occurs around the hair follicle bulb, whereas Jenkinson (35) suggested that the two layers meet in the region of the sebaceous gland. In any case, in both sheep and cattle, the sebaceous gland is associated with the upper portions of the hair follicle and the sweat glands are below the follicle bulb (22, 35). In both species, the ducts of the sweat glands open into the infundibula of the hair follicles (primary follicles in sheep) slightly above the entry point of the sweat ducts (22, 35, 38).

The blood supply to the skin is particularly important to drug delivery because once the drug comes into contact with a capillary network, it has the opportunity of entering the blood and being carried away from the skin. Entry into the blood is likely to be rapid unless the drug molecule is very hydrophobic (39).

Blood supply to mammalian skin was reviewed previously (35). Briefly, the hair bulb, the sebaceous gland, the

sweat gland, and especially the hair follicles are richly supplied by blood in both cattle and sheep. These blood vessels also permeate the papillary layer of the dermis.

**Emulsion**—It was previously stated that the hair and wool fibers, the infundibula of the hair and wool follicles, the junctions of squama of the stratum corneum, and all (in the case of sheep) or part (cattle) of the stratum corneum are permeated by an emulsion which oozes up from the follicle infundibula. The chemical components of the emulsion vary from animal to animal and with such factors as the time of year and climate, but most lipids in the emulsion arise from the secretions of the sebaceous glands (14, 15, 40). Minor components are likely to arise from desquamating squama (*i.e.*, keratin), cell debris, bacterial excreta, and blood. The likely components of the emulsion are listed in Table III (41–43). Thus, the solvent properties of the emulsion and its ability to solubilize and modify the thermodynamic activity of topically applied drugs will be determined by the relative concentrations of the various constituents.

In addition, the viscosity of the emulsion and thus its ability to support molecular diffusion will vary with its water content. This latter parameter will be influenced by the activity of the sweat gland, but it also has been inferred (29) that the emulsion may lose water by evaporation as it permeates through the layers of the stratum corneum. Future physicochemical studies must elucidate the solubility characteristics of skin emulsions under conditions likely to be encountered by sheep and cattle.

## BARRIER VARIABILITY

**Exposure to Solvents**—Lloyd *et al.* (44) showed that cattle skin can be clipped coarsely or finely without removing more than four cell layers of the stratum corneum. However, washing the skin with ether removed all but three stratum corneum layers (44). This effect is almost certainly involved in the marked erythema that ether causes on bovine skin (45), and it predisposes the skin to infection by *Dermatophilus congolensis* (46). Methanol washing of cattle skin had a much smaller effect on stratum corneum thickness (44) and on the incidence of infection (46). The susceptibility of cattle skin to infection also was increased by washing with light petroleum (47) or following intense water spraying (48); in sheep skin, it was increased by heavy rain (49).

The development of erythema and susceptibility to infection probably are caused by removal of the outer squama of the stratum corneum and, in particular, removal of the emulsion from the skin surface, from the junctions of squama, and from hair pores. Consequently, treatment of skin with these solvents, as well as with detergents, is likely to affect its permeability, and the extent to which this occurs is worthy of investigation.

Lipid solvents and dimethyl sulfoxide treatment of cattle and sheep skin at 20° apparently stimulates the secretory cells of the sweat glands and promotes cutaneous water loss (50). Hence, as well as removing skin lipids, the application of organic solvents to the skin is likely to lead to increased hydration of the stratum corneum and changes in the composition and viscosity of any emulsion that remains associated with the skin.

The resistance of cattle skin to infection returned 24 hr after washing with ether (46), although only one lipid layer (*i.e.*, layer of stratum corneum cells) had been replaced in that time (44). It is thus likely that replacement of emulsion in the junctions between the squama is well underway by 24 hr (46).

**Table III—Major Constituents of Skin Emulsion**

| Source | Constituents |
|---|---|
| Sebaceous gland | Monoester waxes, diester waxes, squalene, cholesterol, cholesterol esters, phospholipids, triglyceride esters of fatty acids, free fatty acids, corticosteroids |
| Sweat gland | Water, sodium ions, potassium ions, calcium ions, magnesium ions, chloride ions, lactate ions, free amino acids, water-soluble proteins, epinephrine |
| Blood | Albumin, transferrin, immunoglobulins IgA, G, and M |

The precise effects of these changes cannot be predicted at this stage. They will depend on the mechanism by which drug molecules are absorbed and on the chemical properties of each drug.

**Skin Temperature**—Elevation of temperature increases the molecular diffusion rate by lowering its activation energy. However, temperature changes also influence skin permeability by changing the activity of sweat glands and the composition of their secretions. The results of these changes are expressed as changes in the composition and viscosity of the skin emulsion and in the degree of skin hydration.

The temperature of sheep and cattle skins is influenced by ambient temperature, radiation, convection, evaporation, shivering, and exercise (43). The skin surface temperature of cattle in the shade does not vary appreciably from one area of the body to another (43). However, the coat type and skin color are important when the animal is in sunlight. Thus, an 8° temperature difference has been reported between black-haired (heat-absorbing) and white-haired (heat-reflecting) regions (51).

The effect of ambient temperature on domestic animal skin permeability is likely to be more profound than it is on human skin. This difference arises partly because humans, especially those receiving dermal treatment, are unlikely to expose their skin to the wide range of temperatures (*e.g.*, 0–50°) that animal skins may be exposed to. In addition, animal skin temperatures tend to change much more dramatically with changing environment than do human skin temperatures. For example, the surface temperature of cattle was observed (52) to vary from 34.5 to 40° when ambient temperature was increased from 15 to 40°. The temperature of the skin of sheep varied from 31 to 38.5° when ambient temperature was varied from 20 to 40°. Rectal temperatures varied from 38.2 to 40.2° throughout the same range of ambient temperatures.

The greater efficiency of the human skin thermoregulatory process could arise because of the greater rate of human sweating (2000 $g^{-2}$/hr) as against sheep (32 $g^{-2}$/hr) or cattle (588 $g^{-2}$/hr) (53).

Increases in ambient temperature increase the rate and volume of secretion of sweat in cattle (54, 55) and in shorn (53, 56) and unshorn (56) sheep. This factor may profoundly affect the aqueous content and viscosity of the emulsion because heat has only a minor effect on the output or composition of sebum (57) unless it is prolonged for >3 days (57, 58).

In addition to the higher output of sebum when high

temperatures were maintained for long periods, the relative concentration of linoleic acid (and other free fatty acids) in the sebum increased (57, 58). The importance of this finding to dermal drug delivery results from the fact that linoleic acid reduced the increased water loss from the skin of rats that was induced by fatty acid deficiency (59, 60) and is thus likely to affect skin permeability to other compounds.

Low humidity at a constant temperature caused an increase in the concentrations of palmitic and myristic acids in sebum of cattle (57).

**Season**—Most changes observed in the structure and anatomy of animal skins as a result of seasonal changes follow a predictable pattern. Smith and Jenkinson (45) found that the sebum output by Ayrshire cattle in Ayre was slightly lower in winter than at other times of the year. However, the situation may be different in hot climates because it was reported (61) that sebum secretion in cattle (Shorthorns, Friesans, and Egyptian cattle) in Egypt was greater in winter than in summer. Similarly, Nay and Hayman (62) reported that the sweat gland volume, as well as the papillary layer and skin thickness of cattle, was greater in winter than in summer. The increased size of the sweat gland indicates that it is less active in winter than in the summer (63). Amakiri (64) reported that the thickness of the total skin, the stratum corneum, and the epidermis of cattle in Nigeria was slightly thicker during the rainy season than during the dry season. The direct relationship between sweat gland volume and papillary layer thickness observed for cattle appears to be quite general (62).

**Breed**—Table II reveals differences in both total skin thickness and thickness of various skin layers for cattle of different breeds.

Differences also occur in the density of hair follicles with different breeds of cattle and sheep. The hair follicle density of a large number of breeds of cattle with different body weight, age, sex, and growth rate follows the rule (65):

$$D = kW^{-0.67} \quad \text{(Eq. 1)}$$

where $D$ is the density of hair follicles and $W$ is the animal weight. The constant $k$ varies slightly with breed. It was observed that the density of hair follicles for Hereford and Shorthorn cattle was similar to those of Africander crossbreeds provided all the animals had similar weights (65). However, Brahman cattle had 20% more follicles per unit area than animals of the other breeds with similar weights.

The rule expressed in Eq. 1 accounts for the observations that cattle between 1 and 2 years of age had denser coats than older cattle of the same breed and that coats were densest in times of drought (*i.e.*, when the animals were lighter) (66).

Differences in follicle densities and in ratios of the number of primary to secondary follicles in different breeds of sheep have been studied (20, 21). Jenkinson and Nay (18, 19) found that the ratio of length ($L$) to diameter ($D$) of sweat glands ($L/D$) and the depths of the hair follicle ($FD$) varied in a regular manner between breeds of cattle. These authors characterized three skin types: Type 1, where $L/D < 8.0$ and $FD < 1.5$ mm (Jersey cattle and most Asian and African cattle); Type II, where $L/D > 12$ and $FD > 2$ mm (many Scottish highland breeds); and Type III, where $L/D > 12$ and $FD < 1.5$ mm (some South American breeds).

Tropical cattle (*e.g.*, Asian, African, and South American breeds) frequently have smaller sweat gland volumes than European breeds (19, 64), perhaps because the glands are more active. Values of various average parameters for cattle from different continents are given in Table IV.

The complexity of this topic is illustrated by the observation that Hereford × Shorthorn cattle sweated at a higher rate than Brahman × Shorthorns under mild conditions but at a lower rate when under stress (67).

**Body Region**—The hair and wool follicle densities and types of fibers in sheep and cattle vary significantly with the region of the body examined. The body of a sheep can generally be divided into wool-growing regions and hair-growing regions. The approximate location of these regions in numerous breeds is described in Table V (20). The epidermis of the skin is thinner on wool-growing areas (30 μm) than in hair-growing regions (500 μm) (20). Similarly, while there is an area of uniform skin thickness in the middle of a sheep's back on either side of and parallel to the vertebral column (22), there is also a steep dorsoventral gradient in skin thickness on either side of the medial dorsal line. The thicker skin is over the vertebral column, near the tail along the back of the sheep and towards the neck in older sheep.

As already mentioned, the wool follicles can be primary (with a sweat gland and a sebaceous gland) or secondary (with a sebaceous gland only). It was reported (20) that the sebaceous and sweat glands are larger in the hair- than in the wool-growing regions.

These observations suggest that whether drugs cross sheep skin *via* the cells of the epidermis or *via* the skin appendages, the permeability of the skin of wool-growing areas (thinner epidermis and more follicles) would be greater than that of haired skin. One factor that could reverse this expectation would be the greater potential of the dense wool coat, relative to the thinner hair coat, to react with applied drugs.

A study of the density of sweat glands and, thus, of hair follicles of Ayrshire cattle (16) indicated that the highest density (2500 $cm^{-2}$) was in skin of the axilla and neck and that the lowest was in the lower limbs (1000 $cm^{-2}$). Table VI describes the areas that had above or below average density of sweat glands and area of secretory surface per square centimeter of skin.

The thickest epidermis on Hereford and Aberdeen Angus cattle was found to be where the follicle density was lowest (*e.g.*, the epidermis of the muzzle was 150–200 cells thick (38). The thinnest epidermis in Herefords was located laterally on the thorax, neck gluteal region, and upper forelegs. In three of four Aberdeen Angus, the thinnest epidermis was on the dorsal part of the body. Such information is useful for predicting the best area of an animal's body for appropriate drug application.

**Other Factors**—Various additional factors are likely to influence skin permeability, and more factors probably will be revealed by carefully controlled studies of skin absorption.

The influence of sex has not been explored, although it was reported that sebum output was greater in castrated male Ayrshire calves than in females (45) and that male

**Table IV—Sweat Glands and Hair Follicles of Cattle [a]**

| Parameter | European | Asian | African | South American |
|---|---|---|---|---|
| Sweat gland length, μm | 928 ± 276 | 738 ± 87 | 695 ± 223 | 972 ± 394 |
| Sweat gland diameter, μm | 107 ± 21 | 87 ± 18 | 85 ± 18 | 90 ± 15 |
| L/D [b] | 8.8 ± 2.5 | 8.6 ± 3.1 | 8.4 ± 3.0 | 10.8 ± 3.9 |
| Sweat gland volume, $\mu m^3 \times 10^{-6}$ | 9.0 ± 5.2 | 4.9 ± 3.7 | 4.3 ± 2.5 | 6.7 ± 4.3 |
| Follicle length, mm | 2.0 ± 0.3 | 1.5 ± 0.3 | 1.6 ± 0.2 | 1.7 ± 0.2 |
| Follicle diameter, μm | 44.2 ± 8.1 | 47.3 ± 8.0 | 53.5 ± 7.3 | 54.2 ± 8.1 |
| Follicle depth, mm | 1.8 ± 0.3 | 1.3 ± 0.2 | 1.4 ± 0.2 | 1.5 ± 0.2 |
| FL/FDM [c] | 46.4 ± 9.7 | 32.4 ± 9.1 | 30.2 ± 6.6 | 32.5 ± 5.9 |

[a] Data from Refs. 18 and 19. [b] Sweat gland length/sweat gland diameter. [c] Follicle length/follicle diameter.

Aberdeen Angus cattle had thicker skins than females (38).

The nutritional status of the animal is also likely to be important. Thus, when wheat-fed sheep had their diet supplemented abomasally with methionine, there was a thickening of the epidermis, poor formation and improper keratinization of wool fibers, and, subsequently, a gross thickening of the outer root sheath (68). Similarly, it was reported (69) that vitamin A deficiency in cattle resulted in hyperkeratosis, leading to substantial skin thickening in the upper two-thirds of the animal's body. The vitamin A deficiency in this case was believed to be caused by ingestion of chlorinated naphthalenes, which were used as lubricants in animal food-processing equipment.

## ABSORPTION MECHANISMS

There is abundant evidence (Table VII) that many chemicals are transported across sheep and cattle skins in sufficient amounts and at sufficient rates to bring about expected pharmacological responses. However, none of the studies involving topical drug delivery to live animals provided solid evidence about absorption mechanisms. In addition, while some data are available on drug transport across excised sheep (70) and cattle (13, 71–74) skins in *in vitro* experiments, few reliable correlations were found between *in vitro* permeability parameters and *in vivo* behavior. Consequently, any speculations about absorption mechanisms at this time are highly tenuous. However, such speculations are useful in that they may create guidelines for the design and execution of needed investigations into this subject.

The speculations that follow are based mainly on knowledge of the mechanisms of drug transport across human skin (10–12, 76, 77), knowledge of the comparative anatomy and physiology of cattle and sheep skins, and conclusions drawn from a limited number of *in vitro* measurements of skin permeability (13, 70–74). The major speculations or hypotheses about cattle and sheep skin penetration are:

1. Bulk transport of neutral molecules with small to medium size molecular weights occurs largely *via* skin appendages (hair or wool follicles and associated ducts and glands) rather than the transcellular pathway which predominates in human skin penetration.

2. The rate and extent of drug absorption across the skin is significantly influenced by the composition and physical properties of the sebum–sweat emulsion associated with the skin.

**Table V—Wool- and Hair-Growing Regions in Sheep**

| Regions | Body Area |
|---|---|
| Wool growing | Midside, midflank, flank |
| Hair growing | Inguinal junction, inguen, axilla, scrotum, cheek, chin, dorsal nose, manus (proximal and distal), pes, pinna |

Most neutral molecules cross human skin by passive diffusion through cells of the interfollicular region rather than through the skin appendages (hair follicles and sweat ducts) (10, 12), even though neutral molecules with small to medium molecular weights have greater diffusivity in the appendages than in the stratum corneum. [The diffusion constants for water were reported to be $0.3–1.2 \times 10^{-5}$, $6–12 \times 10^{-5}$, and $2 \times 10^{-10}$ $cm^2$/min in human hair follicles, sweat ducts, and stratum corneum, respectively (10).] It is believed that bulk transport across human skin occurs *via* the skin cells rather than the appendages because the surface area occupied by the latter is only $10^{-3}$ of the surface area of the skin (12).

It seems reasonable that transappendagial transport would be more important in transport across cattle and sheep skins because they contain a higher density of appendages than human skin. While a square centimeter of human skin contains an average of 40–70 hair follicles and 200–250 sweat ducts, the same area of cattle skin contains ~2000 hair follicles (16, 17) with their associated sweat and sebaceous glands and ducts; sheep skins can contain up to 10,000 follicles with their associated ducts (20, 21).

The resistance to penetrating molecules, $R$, offered by multilayered human skin that consists of a stratum corneum (with resistance $R_S$), a viable epidermis (with resistance $R_E$), and a dermis (with resistance $R_D$) is given by (10):

$$R = R_S + R_E + R_D \qquad \text{(Eq. 2)}$$

Equation 2 can be restated as:

$$R = \frac{1}{k_p} = \frac{\delta S}{D_S K_S} + \frac{\delta E}{D_E K_E} + \frac{\delta D}{D_D K_D} \qquad \text{(Eq. 3)}$$

where:

$k_p$ = permeability constant of skin
$\delta_i$ = thickness of $i$th layer
$D_i$ = diffusion constant of penetrant in $i$th layer
$K_i$ = $i$th layer–vehicle partition coefficient of penetrant

Studies on the penetration of excised human skin by small to medium molecular weight molecules (10, 12) revealed that the first terms in Eqs. 2 and 3 describe the process. Thus, for a homologous series of straight-chain aliphatic alcohols with one to eight carbon atoms, the stratum corneum was the rate-determining barrier. Variations in the thickness or other properties of the viable epidermis or dermis had no effect on the rate of penetration. A similar situation applied to the penetration of levamisole (IV) through excised human skin specimens

**Table VI—Relative Density of Sweat Glands and Area of Secretory Surface per Square Centimeter of Skin for Ayrshire Cattle [a]**

| | Density of Sweat Glands, $cm^{-2}$ | Area of Secretory Surface per Square Centimeter of Skin, $cm^{-2}$ |
|---|---|---|
| Above average | Neck ventral, neck lateral, axilla | Neck ventral, axilla, upper hindleg |
| Below average | Back sacral, gluteus, lower hindleg | Forehead, back sacral, lower foreleg, gluteus, lower hindleg |

[a] From Ref. 16.

whose thicknesses varied from 1.3 to 0.8 mm (13). The average thickness of the human stratum corneum is 0.001 mm (11); therefore, all skin specimens in this experiment contained a uniform thickness of stratum corneum and varying thicknesses of viable epidermis and dermis.

However, the rate of penetration of IV through excised cattle (13) and sheep (71) skins with thicknesses that varied from 1.7 to 0.7 mm was dependent on the total skin thickness. The stratum corneum of cattle (15) and sheep (14) skin was reported to be 3.09 and $3.14 \times 10^{-2}$ mm, respectively, so all skin samples examined in these studies had their stratum corneums intact.

This evidence suggests that the rate-determining barrier to cattle and sheep skin penetration is not the stratum corneum but the whole skin. In the case of sheep skin penetration, it is known that the entire stratum corneum is penetrated by an emulsion of sebum and sweat (14). Hence, in this case, it may be argued that molecules indeed penetrate the stratum corneum *via* lipid regions in which they have similar diffusivity to that in the medium surrounding the cells in the epidermis and dermis. However, it was noted that the lower one-third of the stratum corneum of cattle skin (~0.01 mm) is not permeated by the emulsion (15), thus presenting a similar barrier to penetration as that of the human stratum corneum.

Another possible explanation is that levamisole passes rapidly through the stratum corneum and its rate of clearance into the lower skin layers is rate determining. Higuchi (77) estimated that very lipophilic molecules (*i.e.*, those with activity coefficients of $10^3$ or $10^5$) in infinitely dilute solutions in water would encounter rate-determining clearance from the stratum corneum into the more aqueous

**Table VII—Summary of Dermal Drug Delivery Studies**

| Study | Animal | Drugs | Purpose | Comments | Reference |
|---|---|---|---|---|---|
| 1 | Cattle | I, II, VIII, IX, X, XI, XII, XXI, XXII | Pour-on against southern cattle tick | VIII and IX superior | 78 |
| 2 | Cattle | VII | Bioavailability | | 79 |
| 3 | Cattle | I | Pour-on against GI parasites | Poor against abomasal parasites; erratic against intestinal parasites | 80 |
| 4 | Cattle | I | Pour-on versus spray, intramuscular and intraperitoneal injections against *Hypoderma* spp. | All dosage forms >93% effective | 84 |
| 5 | Cattle | XIX | Pour-on against cattle lice | 62.3–97.8% effective | 88 |
| 6 | Cattle | IX | Pour-on against cattle lice | Effective | 89 |
| 7 | Cattle | VIII, IX, XIV, XV | Pour-ons against long-nosed sucking lice | Most effective for a short term | 6 |
| 8 | Cattle | XIII | Pour-on versus intramuscular injection against cattle grub | Equivalent | 90 |
| 9 | Cattle | I | Pour-on against nematodes | Erratic results except against *H. placei* | 91 |
| 10 | Cattle | 44 compounds | Screen for systemic activity | Variable | 92 |
| 11 | Cattle | I | Spray *versus* pour-on against cattle grub | Pour-on superior | 1 |
| 12 | Cattle | XIII, XIV, XIX | Comparison of XIV with XIII and XIX against cattle lice | XIV at 4 mg/kg equivalent to XIII at 16.5 mg/kg, XIX at 4.5 mg/kg | 93 |
| 13 | Cattle | II | Comparison of pour-on and intramuscular injection *via* spray | Pour-on and intramuscular injection superior | 94 |
| 14 | Cattle | I | Pour-on anthelmintic | Effective against five nematodes, ineffective against four nematodes | 95 |
| 15 | Cattle | II | Bioavailability of spray | Little absorbed | 83 |
| 16 | Cattle, sheep | VII | Bioavailability | — | 96 |
| 17 | Cattle | I, II, VI, VII, VIII, XVIII, *etc.* | Comparison of pour-ons against cattle grub | Variable results | 97 |
| 18 | Cattle | I, VI, VIII | Spray and pour-on of VIII *versus* sprays of I and VI against cattle grub | All exceed $LD_{90}$ | 98 |
| 19 | Cattle | I, II, VI | Pour-ons *versus* dusts and sprays against horn flies | Dusts and pour-ons superior to sprays | 99 |
| 20 | Cattle, sheep | 10 compounds | Saturated sprays and pour-ons against cattle ticks | Maximum protection: sheep, 3 weeks, cattle, 1 day | 100 |
| 21 | Cattle | XX | Bioavailability from 1% suspension | No absorption | 101 |
| 22 | Cattle | XXIII | Pour-on for estrus synchronization | Equivalent to oral | 102 |
| 23 | Cattle | IV | Toxicity study | All complications corrected in 1–4 weeks | 103 |
| 24 | Cattle | IV | Anthelmintic trial of pour-on | Variable results but comparable to orthodox methods | 104 |
| 25 | Cattle | IV | Spot-on against round worms | Effective | 105 |
| 26 | Cattle | IV | Spot-on against lung and GI worms | Effective | 85 |
| 27 | Cattle | IV | Pour-on against nematodes | Equivalent to oral and subcutaneous dosage forms | 80 |
| 28 | Cattle, sheep | IV | Pour-on against nematodes | Effective | 86 |
| 29 | Sheep, goats | XIX | Pour-on against lice and keds | Effective against goats, hairy and wool/hair sheep; less effective against wool sheep | [a] |
| 30 | Sheep | XXIII | Pour-on against *Fasciola hepatica* | Worms in liver reduced 99–100% in 3 weeks | 87 |

[a] H. J. J. Terblanche, Bayer, South Africa (Pty.) Ltd. personal communication.

skin layers (*i.e.*, epidermis and dermis). This situation, which is essentially the same as one where the last two terms in Eqs. 2 and 3 predominate, was discussed by other investigators (10, 12, 39). However, it is unlikely that IV, which has a partition coefficient of only 5.2 between water and toluene (70), is sufficiently lipophilic to experience rate-determining clearance from the stratum corneum. The data on human skin penetration (13), where the stratum corneum was established to be the rate-determining barrier, also suggest that IV is not highly lipophilic. Thus, these *in vitro* results support the conclusion that IV penetrates cattle skin *via* skin appendages.

Further confirmation comes from the value calculated for the diffusion constants for IV in cattle skin ($2.1 \times 10^{-5}$ $cm^2$/min) (13) and sheep skin ($2.5 \times 10^{-5}$ $cm^2$/min) (71). These values are much closer to those reported for water diffusing through human hair follicles ($0.3–1.2 \times 10^{-5}$ $cm^2$/min) (10) or sweat ducts ($6.0–12.0 \times 10^{-5}$ $cm^2$/min) (10) than to the value calculated for water ($3–4 \times 10^{-8}$ $cm^2$/min) (10) or IV ($1.9 \times 10^{-9}$ $cm^2$/min) (13) penetrating through the stratum corneum.

Additional support comes from considering the effect that dimethyl sulfoxide has on penetration through cattle skin (71), sheep skin (70), and human skin (11). The dramatic accelerating effect that dimethyl sulfoxide has on the penetration of many molecules through human skin is in marked contrast to its effect on levamisole penetration through excised cattle and sheep skins where it slightly decreased penetration rates relative to those from aqueous solvents. Because this accelerating effect has been ascribed to dimethyl sulfoxide's ability to alter temporarily the structure of the stratum corneum, it can be concluded that drugs do not penetrate cattle and sheep skins by this route. The decrease in penetration rate through cattle and sheep skins caused by dimethyl sulfoxide is believed to result from its reduction of the thermodynamic activity of the drug in the applied formulation (70).

If the transappendagial route is the major means of bulk transport through cattle and sheep skins, it does not necessarily follow that the total skin thickness, depth of follicle, or length of sweat or sebaceous ducts would greatly influence penetration rates in live animals as they apparently do in excised skin. The hair follicles and ducts are richly supplied by blood, and drug molecules are likely to pass rapidly through the capillary walls and be carried away by the blood as they diffuse through the appendages.

If transappendagial penetration predominates in cattle and sheep skins and transcellular penetration predominates in human skin, some procedures that have been adopted to promote human skin penetration will not necessarily be effective in promoting cattle and sheep skin penetration. The procedures in question were well reviewed (10–12, 76), and they include hydration of the skin and the use of stratum corneum modifiers such as dimethyl sulfoxide or surfactants.

However, other procedures such as maximization of the concentration gradient or, more accurately, the thermodynamic activity gradient of a drug across the rate-determining barrier and of the rate-determining barrier–vehicle partition coefficient will be equally important in promoting cattle and sheep skin penetration as in promoting any Fickian diffusion process (77). Thus, if molecules diffuse through the skin appendages and these present a homogeneous barrier, the flux $J$ is given by:

$$J = \frac{D_A K_A}{\delta_A} \Delta C_S = k_{P,A} \Delta C_S \qquad \text{(Eq. 4)}$$

where:

$D_A$ = diffusion constant of penetrant molecules in appendages
$K_A$ = appendage–vehicle partition coefficient of penetrant
$\delta_A$ = thickness of appendages that must be traversed
$\Delta C_S$ = external concentration difference
$k_{P,A}$ = permeability constant of penetrant molecules in appendages

Poulsen (76) and others (10–12) discussed how an understanding of the density of the stratum corneum (because $D \propto 1/\text{viscosity}$) and its solvent and physicochemical properties have been utilized to control dermal delivery to humans. Similar approaches are necessary to promote dermal delivery to cattle and sheep but will necessitate an understanding of the viscosity and physicochemical properties of the appendagial pathways.

Anatomical and physiological studies of cattle and sheep skins, discussed earlier, indicate that the nature of the skin emulsion formed from sebum and sweat holds the clue to skin permeability. The emulsion forms in the infundibula of the follicles and, in oozing through follicle pores and through all (in sheep) or the upper layers (in cattle) of the stratum corneum, results in the deposition of emulsified sebum around the emerging fibers and, to a greater (in sheep) or lesser (in cattle) extent, on the wool and hair fibers. This emulsion probably is the medium through which molecules must pass to reach a point where they can diffuse through capillaries into the blood.

If this conclusion is correct, seasonal changes in the composition of the emulsion that result from previously discussed seasonal changes in sweat and sebum output are the reason why drugs appear to penetrate cattle skin faster in summer than in winter. *In vitro* studies on penetration of levamisole (IV) through excised cattle skin revealed that the drug penetrated 10 times faster through skin harvested in summer than through skin harvested in winter (71). A similar conclusion was drawn from measurements of blood levels of IV in cattle following application of trial pour-on formulations in summer and winter (71). Another possible example of reduced skin permeability in winter as compared to summer was the report (78) that a pour-on phosmet (VIII) at 40 mg/kg gave excellent control of Southern Cattle Tick when applied to cattle in Australia in March (early fall) or September or October (spring) but poor control in May (winter).

Preliminary results indicate that the penetration barrier (*i.e.*, in all probability, the emulsion) is a relatively polar solvent for penetrant molecules. Thus, studies of the penetration of IV through excised cattle skin (71) indicated that the partition coefficient of IV from aqueous solutions where it existed primarily as a neutral molecule was 0.84. The substitution of water by less polar solvents (*i.e.*, better solvents for IV) resulted in an apparent reduction in the skin–solvent partition coefficients. Dedek (72) concluded that polar organophosphorus compounds (*i.e.*, those with

relatively high water solubility) penetrate cattle skin most rapidly from solvents with low polarity, whereas nonpolar Compounds penetrate most rapidly from polar solvents.

Before a definitive correlation of these results with the solvent properties of the barrier can be made, it must be established (77) that diffusion in the barrier rather than clearance from it into an aqueous environment is rate determining for the organophosphorus compounds. Nevertheless, Dedek and coworkers (72–74) set out useful guidelines for formulation of topical drug delivery systems. The solubilities of some insecticides are given in Table I. Values of 738 compounds are in Ref. 75.

An additional problem arises if diffusion through the emulsion is the preferred pathway for drug absorption. Hence, if a dosage form is designed so that the drug has a favorable emulsion–vehicle partition coefficient, the drug will also have a strong tendency to diffuse up the emulsion coat on the hair and wool fibers in competition with its diffusion into the lower skin layers. This phenomenon could reduce the rate of skin penetration, but it could also lead to relatively sustained release of a drug over an extended period because the surface emulsion would act as a drug depot.

It must be reemphasized that the foregoing discussion is highly speculative and is included to stimulate experimental approaches towards elucidation of absorption mechanisms.

## POUR-ON AND SPOT-ON FORMULATIONS

Table VII lists some trials performed with pour-on or spot-on formulations on cattle and sheep. While there is a substantial body of evidence that topical drug delivery can be effective, the studies provided little information on the absorption mechanism and thus little information that could be used as a basis for designing future topical drug delivery systems. Some of the reasons for this sorry state of affairs are:

1. Failure to report the solvents used in trials. All but three of the reports tabulated in Table VII failed to mention the solvents used. Words such as "a suitable solvent," "a rapidly evaporating solvent," "a slowly evaporating solvent," or "an emulsifiable solvent" were used. Therefore, it is not possible to ascertain whether the failure of certain trials arose because the partition coefficient between the penetration barrier and the solvent or vehicle was so unfavorable that the rate and extent of absorption (*i.e.*, the bioavailability) were unacceptably low or because the drug was not active systemically. Furthermore, it is known that many organic solvents damage skin. This effect could increase drug bioavailability to a point where it gave an acceptable therapeutic response but produced unacceptable inflammation or lesions due to bacterial proliferation.

Without knowing the solvent used, it is also impossible to separate skin damage caused by residual drug from that possibly caused by the solvent. An example of the problems caused by failure to specify the solvents used in the formulations is provided by a report (78) of a comparison of nine pour-on formulations of organophosphorus insecticides against the Southern Cattle Tick in Australian Illawarra Shorthorns (Study 1 in Table VII). Because the solvents were not mentioned, it was impossible to evaluate why phosmet (VIII) at 40 mg/kg and chlorpyrifos (IX) at 60 mg/kg gave better tick control than the other seven products or why IX caused severe hair loss and skin burns while the VIII formulation did not.

2. Failure to restrain animals so that they cannot lick themselves or other animals. Drugs applied to the skin of animals can enter the systemic circulation by transdermal absorption or orally if the animals ingest the drug by licking. In many cases, drugs were applied to animals in such a way that they could not lick them off themselves (*e.g.*, drugs applied to cattle on the dorsal midline extending backward from the withers), but frequently no steps were taken to prevent the animals from licking drug from other animals.

The danger of this latter event leading to erroneous results is illustrated by a study (79) (Study 2 in Table VII) in which ronnel (VII) was applied on the dorsal midline of cattle from the hip forward and drug concentrations in the blood and other tissues were monitored as a function of time. The animals were yoked and their tails were tied for the first 10 days to prevent any oral ingestion; they were then allowed to run free. The blood levels of VII passed through a maximum after 36 hr and then fell away exponentially until about Day 11 when there was a dramatic increase in blood levels, eventually reaching a blood concentration that was 50% higher than the initial maximum. This phenomenon resulted from oral ingestion of drug after the animals were allowed to run free.

No difference in efficiency of a levamisole pour-on against nematodes in cattle was observed between restrained and free cattle (80). This result could arise because levamisole, as would be expected from the *in vitro* skin permeability studies (13), is very rapidly absorbed.

While it is appreciated that commercially useful pour-on formulations will be applied to free running animals, care must be exercised in judging the effectiveness of a formulation on the basis of trials where oral ingestion of topically applied drugs is possible.

3. The use of imprecise end-points to evaluate products. The ideal end-point for the evaluation of a drug delivery system is the therapeutic or pharmacological response that it is intended to elicit. However, as illustrated by Poole and Dooley (81) (Study 3 in Table VII), great care must be exercised in selecting the correct end-point. These authors discussed the effectiveness of a crufomate pour-on as an anthelmintic against GI parasites in cattle on the basis of both the egg count per gram of feces and the helminth counts at necropsy. The latter parameter indicated that the dosage form had no anthelmintic effect on abomasal helminths and had eratic efficacy on intestinal parasites. This finding was in contrast to an earlier report (82) that concluded, on the basis of egg counts per gram of feces only, that the treatment was effective against a variety of GI parasites in cattle. The authors (81) pointed out that ova in the feces indicated only the presence of an ovulating female helminth and should be used only as a diagnostic tool.

Because it is wasteful and often not possible to carry out necropsies to evaluate anthelmintic activities of pour-on formulations, it seems highly desirable to obtain blood level *versus* time profiles for drugs following dermal application and to use this information as a basis for developing new formulations.

These points illustrate the need to use caution in interpreting currently available reports on the effectiveness of pour-on formulations.

**Retention of Drugs on Skin**—Some reports indicated that a number of topically applied drugs persist on the skin or coat of animals for long periods and that only a fraction of the applied dose is absorbed (poor bioavailability). For example, the application of a 4% formulation of $^{32}P$-labeled VII in paraffin oil to cattle (Study 2 in Table VII) resulted in the appearance in the blood of an organosoluble fraction (undegraded drug and an oxygen analog) and water-soluble breakdown products (79). The maximum concentration of the organosoluble fraction was reached in 48 hr in restrained animals and had fallen to zero by Day 9. However, an appreciable amount of radioactivity was still present on the skin and hair after 10 weeks.

Although only very small amounts of $^{32}P$-labeled II were absorbed by cattle following the use of a dilute spray solution (in 20% xylene–octoxynol[2]), high levels of unchanged drug could still be detected on the skin after several weeks (83) (Study 4 in Table VII). Similarly, high levels of I were present on the skin of cattle 30 days after treatment with both a spray and pour-on made by diluting an emulsifiable concentrate of drug with water (84) (Study 5 in Table VII). These phenomena presumably result from chemical interactions of the drugs with the hair fibers or the skin proteins as discussed previously.

The ways in which these phenomena are likely to vary with the chemical properties of the drug are illustrated by reports that the bioavailability of IV from a pour-on (80) and spot-on (85) formulation was as good as or better than that from an oral formulation (Studies 6 and 7 in Table VII).

**Solvent Systems and Methods of Application**—Although many investigators have failed to report the exact solvent systems used in individual studies, there are frequent references to generic solvents. Pour-on formulations often consist of a suspension of a wettable powder in water or light mineral oils. Manufacturers do not usually reveal the formulation of the wettable powders, but they are generally composed of a wetting agent, a dispersing agent, and a clay or other inert carrier together with the drug. The wettable powder is employed to maximize the rate of dissolution of solid drug following its application to the skin.

Suspensions are also sometimes prepared in light liquid paraffin or other light mineral oils or oil-based water-immiscible drug solutions.

Light mineral oils are usually poor solvents for drugs, but they are often included in suspensions or solutions to hold the drug on the animal's skin. Some other solvent systems that have been described are 10% dimethyl sulfoxide-aromatic hydrocarbon (86), 10% cyclohexanol–aromatic hydrocarbon (86), dimethyl sulfoxide–amyl alcohol (1:4) (87), and various isopropanol-based solvents that contain light mineral oils, surfactants, or aromatic and nonaromatic solvents.

Water-insoluble compounds are often formulated as an emulsifiable concentrate. The emulsifiable concentrate contains one or more surfactant and produces an emulsion or micellar solution, with the water-insoluble drug in the nonaqueous phase, when mixed with water.

Various methods have been described for applying topical drug delivery systems. The simplest and most commonly used method is to pour the drug solution from a beaker or similar vessel onto the skin of the animal. Application of drugs to sheep skin has been achieved by parting the wool and dispensing the formulation from a needleless syringe (86).

One study (104) reported that the area of cattle skin to which IV had been applied was kept damp for several days. However, the effect of this procedure on penetration rates was not recorded.

One report (96) highlighted the fact that VII was absorbed more effectively from shorn than from unshorn areas of sheep skin.

## FUTURE WORK

There is an urgent need to establish firmly whether a relationship exists between the permeability of excised cattle and sheep skins to drug formulations in *in vitro* experiments and the permeability of the skins in live animals. Such relationships have been established (10, 12) for human skin penetration, and this fact has led to the production of a vast amount of quantitative information about the process.

If no direct relationship is found, it will suggest that such factors as the rate of production of sebum or sweat, the rate of blood flow, and even the rate at which keratinized epithelial cells are shed by the skin of live animals may be involved in the dermal drug delivery process. If this is the case, experiments must be carried out on live animals under various conditions to permit a rational approach to controlled dermal delivery. These experiments must be performed under conditions where applied drugs cannot be ingested and where their chance of being removed by rain or other environmental forces is minimized.

If the permeability of excised skin is directly related to *in vivo* behavior, the task of characterizing the absorption mechanism will be easier. The experimental methods already developed to study human skin penetration (13) can be applied to obtain quantitative information about the effects of breed, season, climate, age, nutritional status, and formulation on the transdermal delivery process.

## REFERENCES


(1) W. M. Rogoff and P. H. Kohler, *J. Econ. Entomol.*, **53**, 814 (1960).

(2) R. O. Drummond and O. H. Graham, *ibid.*, **59**, 723 (1966).

(3) H. G. Kinzer, *Vet. Med. Rev.*, **71**, 83 (1971).

(4) L. M. Hunt, M. L. Beadles, B. K. Shelley, B. N. Gilbert, and R. O. Drummond, *J. Econ. Entomol.*, **73**, 32 (1980).

(5). J. S. Healey, *The Agricultural Gazette of New South Wales*, Dec. 1970.

(6). P. R. Kettle and J. M. Lukies, *N. Z. Vet. J.*, **27**, 78 (1979).

(7) V. B. Beat and D. P. Morgan, *J. Am. Vet. Med. Assoc.*, **170**, 812 (1977).

(8) H. D. Calvery, J. H. Draize, and E. P. Lang, *Physiol. Rev.*, **26**, 510 (1946).

(9) S. Rothman, *J. Lab. Clin. Med.*, **28**, 1305 (1943).

(10) R. J. Scheuplein and I. H. Blank, *Physiol. Rev.*, **51**, 702 (1971).

(11) M. Katz and B. J. Poulsen, in "Handbook of Experimental Pharmacology," vol. 28, part 1, B. B. Brodie and J. Gillette, Eds.,


[2] Triton X-100.

Springer-Verlag, Berlin, Germany, 1971, pp. 103–174.
(12) R. J. Scheuplein, *J. Invest. Dermatol.*, **67,** 31 (1976).
(13) I. H. Pitman and S. J. Rostas, *J. Pharm. Sci.*, in press.
(14) D. H. Lloyd, S. F. Amakiri, and D. M. Jenkinson, *Res. Vet. Sci.*, **26,** 180 (1979).
(15) D. H. Lloyd, W. D. B. Dick, and D. M. Jenkinson, *ibid.*, **26,** 172 (1979).
(16) J. D. Findlay and S. H. Yang, *J. Agric. Soc.*, **40,** 126 (1950).
(17) S. F. Amakiri, *Anim. Prod.*, **18,** 285 (1974).
(18) D. M. Jenkinson and T. Nay, *Aust. J. Biol. Sci.*, **25,** 585 (1972).
(19) *Ibid.*, **26,** 259 (1973).
(20) A. G. Lyne and D. E. Hollis, *Aust. J. Biol. Sci.*, **21,** 499 (1968).
(21) M. L. Ryder, *J. Agric. Sci.*, **49,** 275 (1957).
(22) G. P. Kozlowski and M. L.Calhoun, *Am. J. Vet. Res.*, **30,** 1267 (1969).
(23) M. R. Freney, M. Lipson, and N. P. H. Graham, *Counc. Sci. Ind. Res. Aust. Bull.*, **108,** 27 (1941).
(24) J. Hambrack and S. Wilken-Jorden Onderstepoort, *J. Vet. Sci. Anim. Husb.*, **2,** 271 (1934).
(25) I. R. Harrison and C. A. Johnson, *Nature (London)*, **181,** 1267 (1958).
(26) I. R. Harrison and C. A. Johnson, *Ann. Appl. Biol.*, **49,** 588 (1961).
(27) I. Hoffman, R. B. Carson, and R. F. Morris, *Can. J. Anim. Sci.*, **43,** 303 (1963).
(28) M. Lipson and R. J. Hope, in "Proceedings of the International Wool Textile Research Conference," Australia, 1955, C.S.I.R.O., Melbourne, 1956, Vol. E, p. 523.
(29) D. M. Jenkinson and D. H. Lloyd, *Br. Vet. J.*, **135,** 376 (1979).
(30) A. N. Sinclair, *Vet. Rev.*, **24,** 95 (1977).
(31) A. F. Machin, *J. Sci. Food Agric.*, **5,** 330 (1956).
(32) A. F. Machin, *Soc. Chem. Ind. Monogr.*, **21,** 81 (1966).
(33) A. N. Sinclair, *Aust. Vet. J.*, **39,** 81 (1963).
(34) A. N. Sinclair, "University of Sydney Post Graduate Foundation in Veterinary Science Review No. 8," 1970.
(35) D. M. Jenkinson, in "Comparative Physiology and Pathology of the Skin," E. J. Rook and C. S. Walton, Eds., Blackwell, Oxford, England, 1965, pp. 591–608.
(36) D. F. Dowling, *Aust. J. Agric. Res.*, **6,** 776 (1955).
(37) R. H. Hayman, J. W. V. Beeston, T. E. Allen, and T. Nay, *J. Agric. Sci.*, **67,** 345 (1966).
(38) S. Goldsberry and M. L. Calhoun, *Am. J. Vet. Res.*, **20,** 61 (1959).
(39) G. L. Flynn and S. H. Yalkowsky, *J. Pharm. Sci.*, **61,** 838 (1972).
(40) M. E. Smith and S. U. Ahmed, *Res. Vet. Sci.*, **21,** 250 (1976).
(41) D. M. Jenkinson, D. H. Lloyd, and R. M. Mabon, *ibid.*, **21,** 124 (1976).
(42) D. M. Jenkinson, D. H. Lloyd, and R. M. Mabon, *J. Comp. Pathol. Ther.*, **89,** 43 (1979).
(43) D. M. Jenkinson, *Proc. R. Soc. Edinburgh*, **79B,** 3 (1980).
(44) D. H. Lloyd, W. D. B. Dick, and D. M. Jenkinson, *Res. Vet. Sci.*, **26,** 250 (1979).
(45) M. E. Smith and D. M. Jenkinson, *J. Agric. Sci.*, **84,** 57 (1975).
(46) D. H. Lloyd and D. M. Jenkinson, *Br. Vet. J.*, **136,** 122 (1980).
(47) D. S. Roberts, *Aust. J. Agric. Res.*, **14,** 492 (1963).
(48) T. A. Nobel, U. Kloffer, and F. Neumann, in "Dermatophilis Infection in Animals and Man," D. H. Lloyd and K. C. Sellers, Eds., Academic, London, England, 1976.
(49) P. K. C. Austwick, in *ibid.*
(50) P. G. Hiley, Y. S. Pan, D. Robertshaw, and J. E. Vercoe, *Aust. J. Biol. Sci.*, **30,** 197 (1977).
(51) J. A. Clark and K. Cena, *Dtsch. Tieraerztl. Wochenschr.*, **79,** 292 (1972).
(52) W. R. Beakley, and J. D. Findlay, *J. Agric. Sci.*, **45,** 353 (1955).
(53) A. H. Brook and B. F. Short, *Aust. J. Agric. Res.*, **11,** 577 (1960).
(54) K. A. Ferguson and D. F. Dowling, *Aust. J. Agric. Res.*, **6,** 640 (1955).
(55) D. M. Jenkinson, *Br. J. Dermatol.*, **88,** 397 (1973).
(56) K. G. Johnson, *J. Physiol.*, **235,** 523 (1973).
(57) M. E. Smith, R. C. Noble, and D. M. Jenkinson, *Res. Vet. Sci.*, **19,** 253 (1975).
(58) W. Y. Poon, D. M. Jenkinson, R. C. Noble, and J. H. Moore, *ibid.*, **25,** 234 (1978).
(59) P. J. Hartop and C. Prottey, *Br. J. Dermatol.*, **95,** 255 (1976).
(60) C. Prottey, P. J. Hartop, J. G. Black, and J. I. McCormack, *ibid.*, **94,** 13 (1976).
(61) M. M. Shapie and M. M. A. El Khair, *UAR J. Anim. Prod.*, **10,** 81 (1970).
(62) T. Nay and R. H. Hayman, *Aust. J. Agric. Res.*, **14,** 294 (1963).
(63) R. H. Hayman and T. Nay, *ibid.*, **9,** 385 (1958).
(64) S. F. Amakiri, *Res. Vet. Sci.*, **17,** 351 (1974).
(65) H. G. Turner, T. Nay, and G. T. French, *Aust. J. Agric. Res.*, **13,** 960 (1962).
(66) H. B. Carter and D. F. Dowling, *ibid.*, **5,** 745 (1954).
(67) A. V. Schleger and H. G. Turner, *ibid.*, **16,** 92 (1965).
(68) R. E. Chapman and P. R. Reis, *Aust. J. Biol. Sci.*, **31,** 161 (1978).
(69) A. N. Worden, in "Comparative Physiology and Pathology of the Skin," A. J. Rook and G. P. Walton, Eds., Blackwell, Oxford, England, 1965.
(70) L. M. Ponting and I. H. Pitman, *Aust. J. Pharm. Sci.*, 8 15 (1979).
(71) I. H. Pitman and S. J. Rostas, to be published.
(72) W. Dedek, *Stud. Environ. Sci.*, **7,** 47 (1980).
(73) W. Dedek and H. Schwarz, *S C I Monogr* **29,** 120 (1968).
(74) W. Dedek, K. Wenzel, and H. Schwarz, *Arch. Exp. Vet. Med.*, **29,** 857 (1975); K. Wenzel and W. Dedek, *Pharmazie*, **31,** 402 (1976).
(75) F. A. Gunter, W. E. Westlake, and P. S. Jaglan, *Res. Rev.*, **20,** 1 (1968).
(76) B. J. Poulsen, in "Drug Design," vol. IV, E. J. Ariens, Ed., Academic, New York, N.Y., 1973.
(77) T. Higuchi, in "Design of Biopharmaceutical Properties through Pro-drugs and Analogs," E. B. Roche, Ed., American Pharmaceutical Association, Washington, D.C., 1977.
(78) F. C. Loomis, A. Noorderilaven, and W. J. Roulston, *J. Econ. Entomol.*, **65,** 1638 (1972).
(79) M. Avrahami, M. H. Clear, and A. R. Ritchie, *N.Z. J. Exp. Agric.*, **2,** 115 (1974).
(80) C. Curr, *Aust. Vet. J.*, **53,** 425 (1977).
(81) J. B. Poole and K. L. Dooley, *Am. J. Vet. Res.*, **33,** 1063 (1972).
(82) ACD Information Bulletin No. 117, Dow Chemical Co., Midland, Mich., July 1960.
(83) J. N. Kaplanis, E. D. Hopkins, and G. H. Treiber, *J. Agric. Food Chem.*, **7,** 483 (1959).
(84) M. A. Khan, *Vet. Rec.*, **93,** 528 (1973).
(85) H. Dorn and M. Federmann, *Vet. Med. Rec.*, **1,** 5 (1976).
(86) P. J. Brooker and J. Goose, *Vet. Rec.*, **96,** 249 (1975).
(87) P. J. Brooker, J. Goose, and A. Percival, Ger. Offen. 2,408,736 (1974).
(88) H. Neuhauser, *Vet. Med. Rev.*, **4,** 348 (1974).
(89) K. D. McMartin, *Down Earth*, **33,** 18 (1977).
(90) E. C. Loomis and R. C. Schock, *J. Med. Entomol.*, **14,** 649 (1978).
(91) H. Herlich, D. A. Porter, and R. S. Isenstein, *Vet. Med.*, **56,** 219 (1961).
(92) R. O. Drummond and T. M. Whetstone, *J. Econ. Entomol.*, **67,** 237 (1974).
(93) R. J. Hart, W. A. Cavey, B. Moore, and M. B. Strong, *Austr. Vet. J.*, **55,** 575 (1979).
(94) R. O. Drummond and O. H. Graham, *J. Econ. Entomol.*, **55,** 255 (1962).
(95) C. J. Hatton, *Down Earth*, **33,** 10 (1977).
(96) V. Shanks, *N.Z. J. Exp. Agric.*, **3,** 37 (1975).
(97) R. O. Drummond and O. H. Graham, *J. Econ. Entomol.*, **59,** 723 (1966).
(98) R. O. Drummond, T. M. Whetstone, B. K. Skelley, and C. C. Barrett, *ibid.*, **70,** 176 (1977).
(99) C. K. Dorsey, J. O. Heishman, and C. H. Taylor, *ibid.*, **55,** 425 (1962).
(100) J. D. Tenquist, D. F. Wright, and H. P. Skyrme, *N.Z. J. Exp. Agric.*, **3,** 281 (1975).
(101) G. W. Ive, *J. Agric. Food Chem.*, **28,** 81 (1978).
(102) W. Busch, D. Flick, P. Heber, and H. Köhler, *Arch. Exp. Vet.*, **28,** 737 (1974).
(103) F. Inderbitzin and J. Eckert, *Prakt. Tieraerzl.*, **58,** 579 (1977); through *Vet. Bull.*, **48,** 230 (1978).
(104) D.ap T. Rowlands and J. Berger, *J.S. Afr. Vet. Assoc.*, **48,** 85 (1977).

(105) H. O. Gomez Castro and M. A. Gonzalez Gomez, *Vet. Med. Rev.*, 1, 87 (1977).

ACKNOWLEDGMENTS

Supported in part by a grant from the Wool Research Trust Fund–Australian Wool Corp.

The authors thank ICI Australia Ltd. and, in particular, Mrs. Helen Owens for assistance in conducting a computer search of the literature.

RESEARCH ARTICLES

# Pharmacokinetics of Sustained Serum Methotrexate Concentrations Secondary to Gastrointestinal Obstruction

**WILLIAM E. EVANS ˣ, ANASTASIOS TSIATIS, WILLIAM R. CROM, GARRETT M. BRODEUR, THOMAS C. COBURN, and CHARLES B. PRATT**

Received October 14, 1980, from the *Clinical Pharmacokinetics Laboratory, Biostatistics Section, Department of Diagnostic Imaging*, and the *Department of Hematology-Oncology, St. Jude Children's Research Hospital, Memphis, TN 38101.*
Accepted for publication March 30, 1981.

**Abstract** □ A physiological pharmacokinetic model for methotrexate was refined and used to simulate serum methotrexate concentrations after high dose (5000 mg/m$^2$) intravenous infusions with fixed normal values for all model parameters except the GI transit rate. There was good agreement between simulated and measured values when model simulations with the normal GI transit rate were compared to values measured following 109 doses administered to 27 patients with normal GI function. When model simulations were performed using GI transit rates representing 75, 50, and 10% of normal, there was a marked prolongation of the terminal serum methotrexate half-life, which was directly related to the reduction in the transit rate. When simulations were performed with GI transit reduced by 50%, the maximum amount of methotrexate in the GI lumen was 25% higher and occurred 4 hr later. Model simulations of serum methotrexate concentrations, using a GI transit rate reduced by 50%, were also in good agreement with serum concentrations measured in two patients with partial GI obstruction. These data establish a pharmacokinetic basis for previous clinical observations indicating sustained serum methotrexate concentrations in patients with GI obstructions and exemplify the utility of physiological pharmacokinetic models in assessing the potential effects of clinical variables on drug disposition.

**Keyphrases** □ Methotrexate—sustained serum concentrations in patients with GI obstruction, pharmacokinetics □ Pharmacokinetics—sustained serum methotrexate concentrations in patients with GI obstruction □ Model simulations—sustained serum methotrexate concentrations in patients with GI obstruction, pharmacokinetics

High dose methotrexate with leucovorin rescue is widely used as adjuvant therapy for osteosarcoma and in the treatment of acute leukemia, non-Hodgkin's lymphoma, head and neck carcinoma, and other solid tumors. However, the administration of high dose methotrexate leucovorin rescue carries with it the risk of severe toxicity, which may be fatal. A national survey (1) conducted prior to 1977 revealed a 6% incidence of mortality attributed to high dose methotrexate. For this reason, efforts have been made to identify factors that predispose to toxicity and to establish guidelines that reduce the risk of morbidity and mortality associated with high dose methotrexate therapy.

Previous studies indicated that certain clinical characteristics such as renal dysfunction, dehydration, pleural effusions, and ascites (2–7) are associated with a higher risk of toxicity following high dose methotrexate leucovorin rescue, presumably due to delayed methotrexate plasma clearance. One study (6) reported slower methotrexate elimination from plasma of two patients who had GI obstruction, in the absence of any previously described clinical features associated with delayed clearance. The present study was undertaken to establish the pharmacokinetic basis for sustained serum methotrexate concentrations in patients with GI obstruction.

## EXPERIMENTAL

**Pharmacokinetic Model**—The flow-limited physiological pharmacokinetic model of Bischoff *et al.* (8) (Scheme I) was used to simulate methotrexate concentrations in serum and tissues following high dose methotrexate intravenous infusions. Volume terms, flow rates, distribution ratios, rate constants, and transit times (*Appendix*) were those previously described by Bischoff *et al.* (8), unless otherwise stated. The volume terms and plasma flow rates were scaled to patient weight or body surface area by the equations shown in the *Appendix*, which were derived from previously published data (8, 9).

Previously published human studies (10–13) characterizing the renal clearance of methotrexate in patients with normal renal function established that the net renal clearance of methotrexate is serum concentration dependent. Glomerular filtration, tubular secretion, and tubular reabsorption are all components of methotrexate renal clearance (12), establishing the basis for saturable processes at high serum concentrations with the resulting lower net renal clearance. Therefore, net clearance probably is determined by both first-order (filtration) and saturable (secretion, reabsorption) processes. However, the rate constants ($V_{max}$ and $K_M$) for tubular secretion and reabsorption of methotrexate have not been established in humans. Therefore, net renal clearance of methotrexate was calculated from the least-squares linear regression of net renal clearance on log serum concentrations, using the published data summarized in Table I. The regression line was described by the equation $Cl_R$ (milliliters per minute per meter$^2$) = 92.0 − (13.8)(ln $C_p$), where $r^2$ = 0.81.

Secretion of methotrexate into bile from the liver was modified to represent a saturable process with $V_{max}$ = 1000 μg/min and $K_M$ = 5 μg/ml. Therefore, the ratio of $V_{max}$ to $K_M$ (200) was the same as that used by Bischoff *et al.* (8), but the differential equation permitted saturation of biliary secretion at high serum concentrations. As described in the original model-development work by Bischoff *et al.* (8), the biliary ex-



*0022-3549/81/1100-1194$01.00/0*
*© 1981, American Pharmaceutical Association*

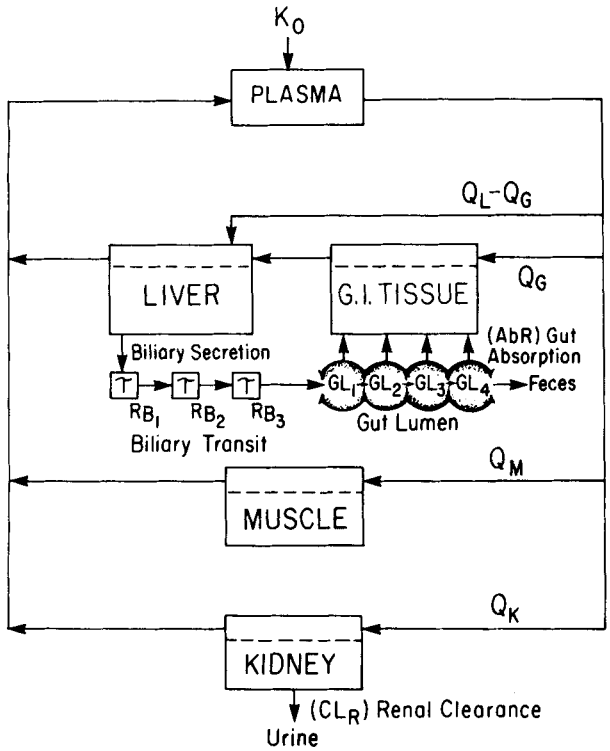


*Scheme I—Scheme of physiological pharmacokinetic model for methotrexate simulations (modified from Ref. 8).*

cretion parameter is a conjectural value to create the best fit to data from normal subjects. The assignment of $V_{max}$ and $K_M$ values in the present study represents a conservative approach by limiting the maximum velocity of drug entry into the GI compartment. GI blood flow ($Q_G$) was reduced from 82% of liver blood flow (as used by Bischoff) to 66% of liver blood flow. This value is more physiological since only ~80% of portal blood flow originates in the GI tract (14) and total portal blood flow is ~82% of hepatic blood flow (*i.e.*, 0.80 × 0.82 = 0.66). All other model parameters, including strong specific tissue binding constants, multicompartment models of biliary transit and gut lumen transit, and zero-order gut absorption, were the same as previously described (8).

A set of differential equations (*Appendix*) describing the mass balances of each model compartment was used to simulate the methotrexate concentration in each compartment as a function of time. These differential equations were simultaneously solved by a numerical method using the Runge–Kutta (15) algorithm.

Simulations of methotrexate serum and tissue concentrations were made using the previously described ("normal") values for all model parameters except GI transit time. To assess the influence of GI obstruction on serum disposition of methotrexate, model simulations were made using GI transit rates ($K_f$) of 0.001, 0.00075, 0.0005, and 0.0001 $min^{-1}$, representing 100, 75, 50, and 10% of the normal transit rate, respectively. All model simulations were for a 6-hr constant-rate intravenous infusion of 5000 mg of methotrexate/$m^2$.

For comparison, serum methotrexate concentrations measured following 109 infusions administered to 27 patients (6–30-hr concentrations) and 38 infusions administered to 21 of these patients (36–78-hr concentrations) are shown with model simulations. All of these patients had normal renal, hepatic, and GI function and had none of the previously described clinical features that predispose to toxicity. The clinical and laboratory evaluations of these patients were previously described in detail (6). Serum methotrexate concentrations measured in two patients with GI obstruction are also shown for comparison. The clinical and laboratory findings in these two patients were previously described (6). Both patients had partial small bowel obstructions secondary to tumor compression at the time of high dose methotrexate administration. Roentgenographic documentation of these GI obstructions is presented in Fig. 1.

Methotrexate serum concentrations for all of these patients were determined in duplicate by at least two methods: a radioenzymatic assay using dihydrofolate reductase (New England Enzyme) and an enzyme immunoassay (SYVA). These assays were shown to produce results comparable to a high-pressure liquid chromatographic assay and to cross-react <4% with the major methotrexate metabolite, 7-hydroxymethotrexate (16).

**Table I—Net Renal Clearance of Methotrexate**

| Net Renal Clearance, ml/min/$m^2$ | Mean Serum Concentration, $\mu M$ |
|---|---|
| 118 | 0.45[a] |
| 103 | ~0.2[b] |
| 78 | ~1.0[c] |
| 65 | 10.0[a] |
| 59 | ~10.0[d] |
| 20–50 | ~100.0[e] |

[a] Evans *et al.* (unpublished data). [b] Reference 12. [c] Reference 11. [d] Reference 13. [e] Reference 10.

## RESULTS

As shown in Fig. 2, there was good agreement between simulated and measured serum methotrexate concentrations in patients with normal renal, hepatic, and GI function, using normal model parameters. Figure 2 also shows simulations with GI transit rates reduced by 25, 50, and 90%. These model simulations demonstrate a marked decrease in the rate of decline in serum concentrations beginning ~24–30-hr postinfusion. The prolongation of methotrexate half-life during this time interval was directly related to the reduction in the GI transit rate (Table II). These simulations also demonstrate that the GI transit rate has little influence on serum methotrexate half-life during the first 24 hr postinfusion. This finding is not surprising since most methotrexate is eliminated *via* renal clearance during this time interval and the amount of methotrexate undergoing enterohepatic circulation is relatively small.

There was good agreement between serum methotrexate concentrations measured in the two patients with GI obstruction and model simulations with the GI transit rate reduced by 50% (Fig. 3).

The simulated amounts (milligrams) of methotrexate in the GI lumen at selected times postinfusion, calculated as:

$$A_{MTX_{GL}} = \frac{(C_{GL_1} + C_{GL_2} + C_{GL_3} + C_{GL_4})}{4} V_{GL} \qquad \text{(Eq. 1)}$$

are summarized in Table III for model simulations using the normal GI transit rate and a transit rate reduced by 50%. As shown, the maximum amount of methotrexate in the GI lumen was ~25% higher and occurred 4 hr later when the GI transit rate was reduced by 50%. More importantly, the amount of methotrexate in the GI lumen declined more slowly when GI transit was reduced. By 48 hr, the amount of methotrexate was approximately four times higher when the GI transit was reduced 50% and more than 10-fold higher by 96 hr. Moreover, the amount of methotrexate in the GI lumen at 72 hr (with reduced transit) was comparable to conventional (25 mg/$m^2$) oral doses of methotrexate, although it represents <1% of the administered dose.

## DISCUSSION

A previous study (6) suggested that GI obstruction could result in a prolonged serum methotrexate half-life following administration of high dose methotrexate. Since prolongation of methotrexate elimination places patients administered high dose methotrexate at increased risk for severe toxicity (6, 7, 17), it is important to establish the clinical variables that may alter methotrexate disposition. This has been done for clinical features such as renal dysfunction (11, 18), pleural effusion (2, 5), and ascites (5). Although an earlier report described (6) previous clinical observations of sustained serum methotrexate concentrations in patients with GI obstruction, the theoretical basis for these observations had not been established.

In the present study, a previously described physiological pharmacokinetic model (8) for methotrexate disposition was used to assess the effect of the GI transit rate on methotrexate disposition. The original model assumes that methotrexate is not metabolized. However, subsequent studies have established that methotrexate is metabolized to 7-hydroxymethotrexate and studies in this laboratory[1] indicate that nonrenal clearance of methotrexate in children is ~15 ml/min/$m^2$. Metabolic clearance was assumed to be negligible for the present study, and was the same for all model simulations (0 ml/min/$m^2$).

By using model parameters that were refined from the original model

[1] W. E. Evans *et al.*, unpublished data.

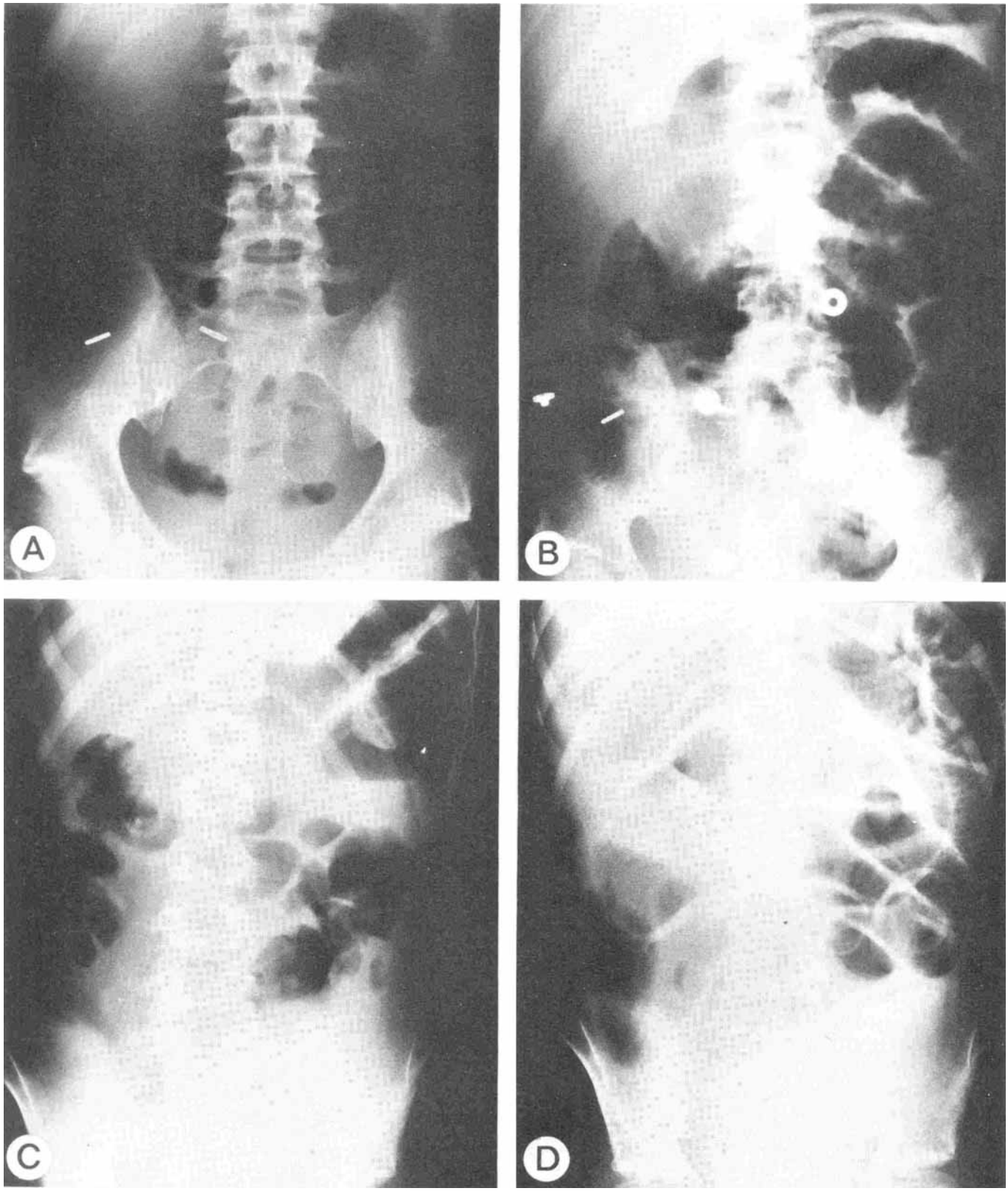


**Figure 1**—*Abdominal roentgenograms of the two patients with partial GI obstructions. Key: A, Patient 1, 9 days prior to high dose methotrexate; B, Patient 1, 6 days following methotrexate; C, Patient 2, 2 days prior to high dose methotrexate; and D, Patient 2, 19 days following methotrexate. Both sets of roentgenograms demonstrate partial GI obstruction during the evaluation period.*

(8), simulations were produced with all model parameters held constant except for the GI transit rate. These simulations demonstrated that greater amounts of methotrexate accumulate in the intestinal lumen when GI transit is reduced. The simulated amount of methotrexate in the GI lumen decreased more slowly when GI transit was reduced such that the amount in the lumen was more than 10-fold higher at 96 hr when transit was reduced by 50%. Moreover, the reduction of the GI transit rate and the resulting increased accumulation of methotrexate resulted in a prolongation of the terminal serum methotrexate half-life, which was directly related to the extent of reduction in GI transit. Model simulations

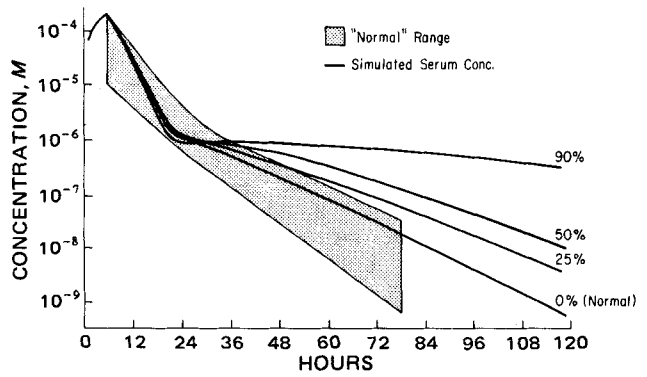


**Figure 2**—*Simulation of methotrexate serum concentrations* versus *time (solid line) by physiological pharmacokinetic model using normal GI transit rate and transit rate reduced by 25, 50, and 90% from normal. Shaded area represents range of serum concentrations measured following 109 doses administered to 27 patients (6–24-hr measurements) and 38 doses administered to 21 patients (25–78-hr measurements).*

with GI transit rate reduced by 50% were comparable to serum concentrations measured in two patients with partial GI obstructions.

These data indicate that the prolongation of serum methotrexate half-life produced by GI obstruction can result in serum methotrexate concentrations being sustained at cytotoxic levels beyond the period of conventional leucovorin rescue. These data also provide the theoretical basis for previously described (19) changes in methotrexate disposition in a patient with vincristine-induced ileus. The observed difference in simulated serum methotrexate concentrations when the GI transit rate was reduced 25% suggests that only a modest compromise in GI function could affect methotrexate disposition and provides a potential mechanism for other drug interactions.

The importance of altered GI function for a drug such as methotrexate, which is eliminated <5% in the feces, is related to the fact that the high dosage of methotrexate administered (*i.e.*, 5000 mg/m$^2$) produces serum concentrations (*i.e.*, $10^{-3}$ *M*) exceeding the minimum cytotoxic concentration (*i.e.*, $\sim 10^{-8}$ *M*) by ~100,000-fold. Thus, perturbation of an excretory pathway that eliminates only a small percentage of the administered dose becomes important. Moreover, reduction in GI transit would result in a more localized accumulation of methotrexate presented to the GI lumen, which produces more rapid saturation of the limited absorptive sites and thereby prolongs reabsorption. Thus, fecal elimination is retarded and reabsorption is delayed, resulting in sustained serum methotrexate concentrations.

The importance of the actual site of GI obstruction was not addressed in the present study, which assumed a consistent reduction in transit rate throughout the GI tract. It is conceivable that partial or complete obstruction in the upper portion of the small bowel might result in a greater localization of methotrexate (*versus* colonic obstruction), while complete obstruction at any site may lead to other clinical complications that could alter methotrexate disposition (*i.e.*, vomiting, malnutrition, *etc.*). These

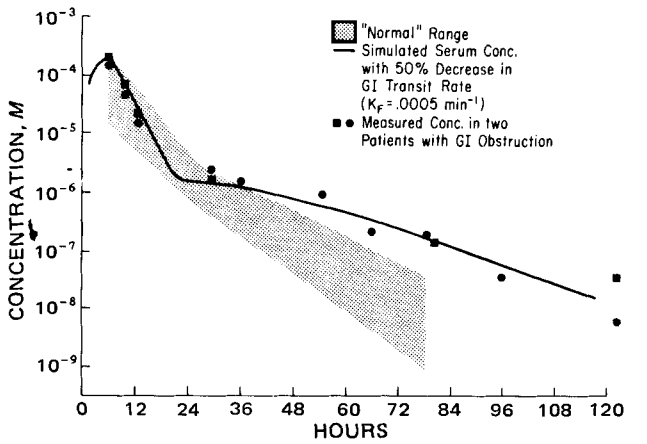


**Figure 3**—*Simulations of methotrexate serum concentrations* versus *time (solid line) by physiological pharmacokinetic model when GI transit rate is reduced by 50% from normal. Shaded area is as described in Fig. 2.*

**Table II—Terminal Serum Half-Life of Methotrexate from Simulated Data**

| GI Transit, min$^{-1}$ (Percent of Normal) | Half-Life, hr |
|---|---|
| 0.001 (100%) | 8.4 |
| 0.00075 (75%) | 9.8 |
| 0.0005 (50%) | 14.0 |
| 0.0001 (10%) | 39.0 |

questions await further study, as does the clinical significance of potential drug-induced alterations in GI motility.

## APPENDIX

The symbols used are:

$AbR$ = absorption rate, micrograms per minute
$aR$ = strong specific binding, micrograms per gram
$C$ = concentration, micrograms per milliliter or micrograms per gram
$Cl_R$ = renal clearance, milliliters per minute
$K_f$ = transit rate in gut lumen, minute$^{-1}$ (reciprocal of transit time)
$K_M$ = Michaelis–Menten constant, micrograms per milliliter
$K_{0(t)}$ = drug infusion rate, micrograms per minute
$Q$ = plasma flow rate, milliliters per minute
$R$ = tissue-to-plasma equilibrium distribution ratio for linear binding
$r$ = drug transport rate in bile, micrograms per minute
$t$ = time, minutes
$V$ = volume, milliliters
$V_{max}$ = maximum rate of saturable process, micrograms per minute
$Wt$ = body weight, kilograms
$\tau$ = nominal residence time in bile transit subcompartments, minutes

The subscripts used are:

$G$ = GI tissue
$GL$ = gut lumen
$K$ = kidney
$L$ = liver
$M$ = muscle
$P$ = plasma
1, 2, 3, 4 = gut lumen or bile subcompartments

The differential equations for the physiological model are as follows.

For plasma:

$$\frac{dC_P}{dt} = \frac{K_{0(t)} + Q_L\frac{C_L}{aR_L} + Q_K\frac{C_K}{aR_K} + Q_M\frac{C_M}{R_M} - (Q_L + Q_K + Q_M)C_P}{V_P} \quad \text{(Eq. A1)}$$

For kidneys:

$$\frac{dC_K}{dt} = \frac{Q_K\left(C_P - \frac{C_K}{aR_K}\right) - Cl_R\frac{C_K}{aR_K}}{V_K} \quad \text{(Eq. A2)}$$

For the liver:

$$\frac{dC_L}{dt} = \frac{(Q_L - Q_G)\left(C_P - \frac{C_L}{aR_L}\right) + Q_G\left(\frac{C_G}{aR_G} - \frac{C_L}{aR_L}\right) - \frac{V_{max_L}C_L/aR_L}{K_{M_L} + C_L/aR_L}}{V_L} \quad \text{(Eq. A3)}$$

For muscle:

$$\frac{dC_M}{dt} = \frac{Q_M\left(C_P - \frac{C_M}{R_M}\right)}{V_M} \quad \text{(Eq. A4)}$$

For GI tissue:

$$\frac{dC_G}{dt} = \frac{Q_G\left(C_P - \frac{C_G}{aR_G}\right) + AbR_{GL}}{V_G} \quad \text{(Eq. A5)}$$

**Table III—Amount of Methotrexate Accumulated in GI Lumen from Simulated Data for 1.0-m² Patient**

| Hours | GI Transit Rate, $min^{-1}$: 0.001 (Normal), mg | 0.0005 (50% Normal), mg |
|---|---|---|
| Peak[a] | 444 | 553 |
| 24 | 319 | 496 |
| 48 | 37 | 148 |
| 72 | 5 | 36 |
| 96 | 0.7 | 8 |

[a] Sixteen hours for normal GI transit and 20 hr for 50% reduced GI transit.

For the gut lumen:

$$\frac{dC_{GL_1}}{dt} = \frac{4r_{B_3} - (4\,K_f V_{GL} C_{GL_1}) - AbR_{GL_1}}{V_{GL}} \quad \text{(Eq. A6}a\text{)}$$

$$\frac{dC_{GL_2}}{dt} = \frac{4K_f V_{GL}(C_{GL_1} - C_{GL_2}) - AbR_{GL_2}}{V_{GL}} \quad \text{(Eq. A6}b\text{)}$$

$$\frac{dC_{GL_3}}{dt} = \frac{4K_f V_{GL}(C_{GL_2} - C_{GL_3}) - AbR_{GL_3}}{V_{GL}} \quad \text{(Eq. A6}c\text{)}$$

$$\frac{dC_{GL_4}}{dt} = \frac{4K_f V_{GL}(C_{GL_3} - C_{GL_4}) - AbR_{GL_4}}{V_{GL}} \quad \text{(Eq. A6}d\text{)}$$

The gut absorption rate is given by

$$AbR_{GL_i} = \frac{V_{\max_{GL}} C_{GL_i}}{K_{M_{GL}} + C_{GL_i}} \qquad i = 1, \ldots, 4 \quad \text{(Eq. A7}a\text{)}$$

$$AbR_{GL} = \frac{AbR_{GL_1} + AbR_{GL_2} + AbR_{GL_3} + AbR_{GL_4}}{4} \quad \text{(Eq. A7}b\text{)}$$

The biliary transit rate is given by:

$$\frac{dr_{B_3}}{dt} = \frac{r_{B_2} - r_{B_3}}{\tau} \quad \text{(Eq. A8}a\text{)}$$

$$\frac{dr_{B_2}}{dt} = \frac{r_{B_1} - r_{B_2}}{\tau} \quad \text{(Eq. A8}b\text{)}$$

$$\frac{dr_{B_1}}{dt} = \frac{\dfrac{V_{\max_L C_L/aRL}}{K_{M_L} + C_L/aR_L} - r_{B_1}}{\tau} \quad \text{(Eq. A8}c\text{)}$$

Renal clearance is given by:

$$Cl_R = BSA92.0 - (13.8)\,(\ln C_P) \quad \text{(Eq. A9)}$$

where:

$V_{\max_L} = 1000\ \mu g/min$
$K_{M_L} = 5\ \mu g/ml$
$V_{\max_{GL}} = 1900\ \mu g/min$
$K_{M_{GL}} = 200\ \mu g/ml$
$\tau = 10$
$R_K = 3.0$
$R_G = 1.0$
$R_L = 3.0$
$R_M = 0.15$

$$aR_K = R_K + \frac{0.3}{C_P}$$

$$aR_G = R_G + \frac{0.1}{C_P}$$

$$aR_L = R_L + \frac{0.4}{C_P}$$

$K_f = 0.001\ min^{-1}$ (normal value)

Volume equal:

$$V_P = 44 \cdot Wt^{0.99}\ \text{(plasma)} \quad \text{(Eq. A10}a\text{)}$$

$$V_K = 7.5 \cdot Wt^{0.85}\ \text{(kidneys)} \quad \text{(Eq. A10}b\text{)}$$

$$V_L = 34 \cdot Wt^{0.87}\ \text{(liver)} \quad \text{(Eq. A10}c\text{)}$$

$$V_G = 49 \cdot Wt^{0.94}\ \text{(GI)} \quad \text{(Eq. A10}d\text{)}$$

$$V_{GL} = 49 \cdot Wt^{0.94}\ \text{(GI lumen)} \quad \text{(Eq. A10}e\text{)}$$

$$V_M = 500 \cdot Wt\ \text{(muscle)} \quad \text{(Eq. A10}f\text{)}$$

where $V$ is in milliliters and $Wt$ is in kilograms.

Organ plasma flow equals:

$$Q_K = 24.5 \cdot Wt^{0.792}\ \text{(kidneys)} \quad \text{(Eq. A11}a\text{)}$$

$$Q_L = 29.96 \cdot Wt^{0.767}\ \text{(liver)} \quad \text{(Eq. A11}b\text{)}$$

$$Q_G = 0.66 \cdot Q_L\ \text{(GI)} \quad \text{(Eq. A11}c\text{)}$$

$$Q_M = 18.17 \cdot Wt^{0.738}\ \text{(muscle)} \quad \text{(Eq. A11}d\text{)}$$

where $Q$ is in milliliters/minutes and $Wt$ is in kilograms.

## REFERENCES


(1) D. D. Von Hoff, J. S. Penta, L. J. Helman, and M. Slavik, *Cancer Treat. Rep.*, **61**, 745 (1977).

(2) W. E. Evans and C. B. Pratt, *Clin. Pharmacol. Ther.*, **23**, 68 (1978).

(3) N. Jaffe and D. Traggis, *Cancer Chemother. Rep. Part 3*, **6**(1), 31 (1975).

(4) H. Chan, W. E. Evans, and C. B. Pratt, *Cancer Treat. Rep.*, **61**, 797 (1977).

(5) S. H. Wan, D. H. Huffman, and D. L. Azarnoff, *Cancer Res.*, **34**, 3487 (1974).

(6) W. E. Evans, C. B. Pratt, R. H. Taylor, L. F. Barker, and W. R. Crom, *Cancer Chemother. Pharmacol.*, **3**, 161 (1979).

(7) M. H. N. Tattersall, L. M. Parker, S. W. Pitman, and E. Frei, III, *Cancer Chemother. Rep. Part 3*, **6**, 25 (1975).

(8) K. B. Bischoff, R. L. Dedrick, D. S. Zaharko, and J. A. Longstreth, *J. Pharm. Sci.*, **60**, 1128 (1971).

(9) K. B. Bischoff, *Cancer Chemother. Rep. Part 1*, **59**, 777 (1975).

(10) D. D. Shen and D. L. Azarnoff, *Clin. Pharmacokinet.*, **3**, 1 (1978).

(11) D. H. Huffman, S. H. Wan, D. L. Azarnoff, D. L., and B. Hoogstraten, *Clin. Pharmacol. Ther.*, **14**, 572 (1973).

(12) D. G. Liegler, E. S. Henderson, M. A. Hahn, and V. T. Oliverio, *ibid.*, **10**, 849 (1969).

(13) W. H. Isacoff, P. F. Morrison, J. Arorsty, K. L. Willis, J. B. Block, and T. L. Lincoln, *Cancer Treat. Rep.*, **61**, 1665 (1977).

(14) A. C. Guyton, "Textbook of Medical Physiology," Saunders, Philadelphia, Pa., 1976.

(15) "Introductory Computer Methods and Numerical Analysis," R. H. Pennington, Ed., Macmillan, New York, N.Y., 1965.

(16) R. G. Buice, W. E. Evans, J. Karas, C. A. Nicholas, P. Sidhu, A. B. Straughn, M. C. Meyer, and W. R. Crom, *Clin. Chem.*, **26**, 1902 (1980).

(17) R. G. Stoller, K. R. Hande, S. A. Jacobs, S. A. Rosenberg, and B. A. Chabner, *N. Engl. J. Med.*, **297**, 630 (1977).

(18) M. V. Freeman, *J. Pharmacol. Exp. Ther.*, **122**, 154 (1958).

(19) D. Ridgway, D. C. Renholds, R. C. Neerhart, and L. J. Wolff, *Cancer*, **46**, 2571 (1980).


## ACKNOWLEDGMENTS


Presented in part at the Eighth Annual Meeting of the American College of Clinical Pharmacology, Washington, D.C., May 1980.

Supported in part by Cancer Center Support (CORE) Grant CA 21765, by Solid Tumor Program Project Grant CA 23099, and by ALSAC.

The authors acknowledge the assistance of Dr. Gary C. Yee, Dr. Joseph A. Sinkule, and Mr. Larry F. Barker in the conduct and analysis of this study and Ms. Linda Rawlinson and Ms. Fabrienne Holloway in preparing this manuscript.

# Concentration of Perfluorohexyl Bromide in Dog Plasma and Selected Tissues

**MAUREEN SCRIME and JEROME EDELSON** ˣ

Received February 19, 1981, from the *Department of Drug Metabolism and Disposition, Sterling-Winthrop Research Institute, Rensselaer, NY 12144.* Accepted for publication April 2, 1981.

**ABSTRACT** □ Beagle dogs received single perfluorohexyl bromide doses, either 30.2 g/kg po or 3.8 g/kg intratracheally. The apparent first-order plasma half-life during the terminal elimination phase was ~8 hr after oral treatment and >8 hr after intratracheal administration. Tissue analysis showed the highest mean concentration of the compound in abdominal fat 1 week after intratracheal administration. One dog had detectable levels in abdominal fat 4 weeks after treatment by either administration route.

**Keyphrases** □ Perfluorohexyl bromide—tissue and blood plasma levels in dogs after oral and intratracheal administration □ Fluorocarbons—perfluorohexyl bromide, tissue and blood plasma levels in dogs after oral and intratracheal administration □ Radiopaque contrast agents—perfluorocarbons, perfluorohexyl bromide, tissue and plasma levels in dogs after oral and intratracheal administration

Perfluorocarbon compounds were recently investigated for their potential use as radiopaque diagnostic agents. Perfluorooctyl bromide and perfluorohexyl bromide (I) are the least toxic of these compounds (1–11). Among the most frequently performed radiodiagnostic procedures with these two compounds are bronchography, alveolography (4, 5), and gastroenterography (4, 7).

## BACKGROUND

One desirable property in contrast agents used in bronchography and alveolography is rapid elimination from the lungs. Radiopaque agents currently available for bronchography and alveolography are retained in the lungs for long periods; thus, they may irritate pulmonary tissues and cause varying degrees of damage (5). Vaporization of the perfluorocarbons at body temperature (4), a property not characteristic of other radiopaque agents, predisposes them to efficient elimination from the lungs. Although mucocilliary clearance is involved in elimination of the "neat" perfluorocarbons, evaporation plays the major role in elimination from the lungs (4, 5). Radiographic measurements demonstrated the elimination time from the lungs to be 30–60 min for I, as compared to 3–6 hr for the octyl derivative (4).

Good quality radiogastroenterograms have been obtained with these compounds since low viscosity and low surface tension allow them to flow freely into tiny folds and orifices (4, 6, 7). Visualization and delineation were similar for the two compounds (4). However, by vaporizing in the bowel, I provided a unique gas-contrast resolution, which allowed exceptional mucosal definition (4, 7, 8).

Elimination of the octyl derivative after oral and intratracheal administration to beagle dogs was reported (11). High concentrations of this compound were found in abdominal fat 4 weeks after medication. The present study presents elimination characteristics of I in plasma and selected tissues after oral and intratracheal administration to beagle dogs.

## EXPERIMENTAL

**Animal Procedure**—Two groups of beagle dogs, six males and six females in each group, received either a 30.2-g/kg po dose or a 3.8-g/kg intratracheal dose of I[1]. A gastric tube was used for oral administration. The intratracheal dose was instilled under light thiopental[2] anesthesia (35 mg/kg iv); a gastric tube was inserted into the trachea until it reached a point several centimeters above the bifurcation of the right and left bronchi.

Blood samples were drawn at various intervals from the femoral vein. Potassium oxalate was used as the anticoagulant. The blood was promptly centrifuged at 2500 rpm for 10 min, and the plasma was separated and stored until analysis.

Two males and females from each group were anesthetized and killed by pentobarbital sodium[2] overdose (45 mg/kg iv) 7, 14, and 28 days after treatment. Samples of the abdominal fat, gonads, adrenals, mesenteric and thoracic lymph nodes, and lungs were stored in glass jars at −4° until assay. Previous studies showed that the highest levels of the octyl derivative were found in these tissues (5, 11). Bile samples were collected from the intratracheally tested group only.

**Extraction Procedure**—Plasma samples, 1 ml each, were extracted with 1 ml of isooctane containing 0.25 μg of tetrachlorodifluoroethane[3], the internal standard for the assay. The mixture was mechanically shaken for 10 min and centrifuged for 10 min at 2500 rpm. A sample of the organic phase, 2.5 μl, was analyzed by GC.

Tissue samples, up to 2 g of frozen tissue depending on the sample size, were minced with a scalpel and placed into a 5-ml polyethylene homogenization vessel[4]. A known volume of isooctane containing the internal standard, approximately two volumes per gram of tissue, was added, and the mixture was homogenized for 1 min. The homogenization vessel was submerged in an ice bath during homogenization. The homogenate was centrifuged at 2500 rpm for 10 min, and 2.5 μl of the organic phase was assayed.

Known amounts of I were added to samples of normal, control dog plasma and tissue; these samples were freshly prepared and used as standards. They were extracted and assayed as described.

**GC**—All samples were analyzed using a gas chromatograph equipped

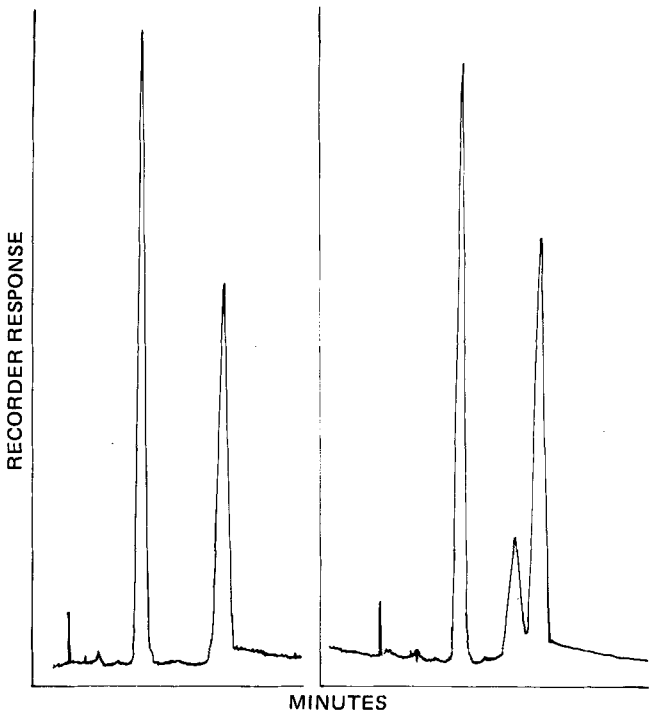


**Figure 1**—*Chromatogram of extracted dog plasma containing the internal standard (left) and the same sample containing 190 ng of I/ml (right).*

[1] E. I. du Pont de Nemours, Wilmington, Del.
[2] Abbott, North Chicago, Ill.
[3] Freon 112, E.I. du Pont de Nemours, Wilmington, Del.
[4] Sorvall, Norwalk, Conn.

0022-3549/81/1100-1199$01.00/0
© 1981, American Pharmaceutical Association

**Table I—Tissue I Concentrations (Micrograms per Gram) in Beagle Dogs that Received 30.2 g/kg po**

| Dog Number, Sex, and Weight (kg) | Lung | Fat | Thoracic Lymph | Mesenteric Lymph | Adrenals | Ovaries | Testes |
|---|---|---|---|---|---|---|---|
| | | | 1 Week | | | | |
| 1, M, 9.3 | 0.02 | 1.6 | 0.65 | 0.11 | 0.02 | — | <MQL[a] |
| 2, M, 10.1 | <MQL | 0.79 | 0.15 | <MQL | <MQL | — | <MQL |
| 3, F, 7.5 | <MQL | 0.08 | 0.03 | <MQL | 0.02 | <MQL | — |
| 4, F, 7.0 | <MQL | 1.8 | 0.28 | 0.06 | 0.04 | <MQL | — |
| | | | 2 Weeks | | | | |
| 5, M, 10.2 | <MQL | 0.07 | <MQL | <MQL | <MQL | — | <MQL |
| 6, M, 10.6 | <MQL | 0.06 | <MQL | <MQL | <MQL | — | <MQL |
| 7, F, 8.3 | <MQL | 0.08 | <MQL | <MQL | <MQL | <MQL | — |
| 8, F, 7.8 | <MQL | <MQL | <MQL | <MQL | <MQL | <MQL | — |
| | | | 4 Weeks | | | | |
| 9, M, 9.8 | <MQL | 0.09 | <MQL | <MQL | <MQL | — | <MQL |
| 10, M, 9.2 | <MQL | <MQL | <MQL | <MQL | <MQL | — | <MQL |
| 11, F, 7.3 | <MQL | <MQL | <MQL | <MQL | <MQL | <MQL | — |
| 12, F, 7.5 | <MQL | <MQL | <MQL | <MQL | <MQL | <MQL | — |

[a] Mean minimum quantifiable level (MQL) was 0.01 μg/g.

with a $^{63}$Ni-electron-capture detector[5], an automatic sampler, and an integrator. The silanized glass column, 1.8 m × 3 mm i.d., was packed with 80–100-mesh, porous polymer beads[6]. The oven was operated in the isocratic mode at 175°; both the injection port and detector temperatures were 250°. The flow rate of the carrier gas, a mixture of 7% methane in argon[7], was 40 ml/min. Under these conditions, the retention times of I and the internal standard were 6.5 and 7.8 min, respectively.

## RESULTS AND DISCUSSION

Figure 1 shows typical chromatograms of plasma extracted by the described procedure. The relationship between the relative peak area ratio and the concentration of I was linear up to 200 ng/ml; the computer estimated the standard line by a least-squares method. The concentration in the unknown sample was calculated from the equation for the extracted standards line. The minimum quantifiable level, defined as that value whose 80% confidence limit just encompassed zero, was 10 ng/ml or gram of tissue.

The mean plasma concentrations of I following oral and intratracheal administration are shown on Figs. 2 and 3, respectively. The apparent first-order terminal elimination half-life following oral administration of I was ~8 hr, as determined by linear regression on the logarithm of the plasma concentration and sample time data ($r$ = 0.993). By the intratracheal route, the decline in plasma I concentration did not appear to follow first-order kinetics (Fig. 3); plasma levels were higher than observed after oral treatment, indicating greater absorption by this administration route.

In the orally dosed group, the only tissue in which I was detected beyond the 1st week was abdominal fat (Table I). No detectable level of I was found in the gonads, and only one low level was found in a 1-week lung sample. The tissue values were highly variable. In the intratracheally dosed dogs, the highest levels of I were seen in the abdominal fat (Table II); I was not detected in bile or ovaries, and only one low level was found in the testes. After 1 week, detectable levels of I were found only in abdominal fat and lymph nodes. Only one dog still had low levels of I in abdominal fat, by either treatment route, 4 weeks after medication. The octyl derivative, which was administered at similar doses in the previous study (11), also was detected in abdominal fat 4 weeks after medication.

The level of I detected in the one beagle 4 weeks after oral medication was 2% of the mean level of the octyl derivative detected in the eight animals in the previous oral study. Similarly, the level of I detected in the one dog 4 weeks after intratracheal administration was 1% of the mean level of the octyl derivative detected in the four animals that were treated by intratracheal administration of the octyl derivative in the previous study. Levels of I in abdominal fat of the remaining dogs, 4 weeks after treatment, were below the minimum quantifiable level of the assay.

Thus, detectable levels of both the octyl- and hexylperfluorocarbon compounds were seen 4 weeks after oral and intratracheal administration to beagle dogs. Levels of I observed were 1–2% those of the octyl derivative, indicating that the higher vapor pressure of I facilitated elimination from the body.

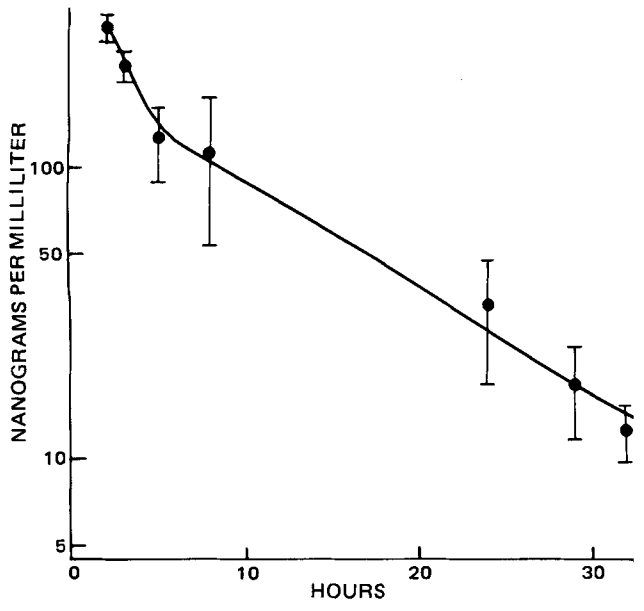


**Figure 2**—*Plasma concentrations in beagle dogs after oral administration of 30.2 g of I/kg;* n = *12. The vertical bar represents 2* SE.

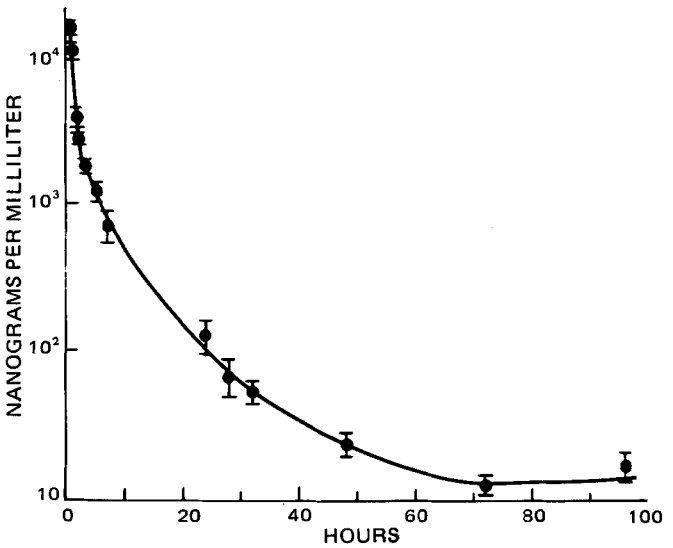


**Figure 3**—*Plasma concentrations in beagle hounds after intratracheal administration of 3.8 g of I/kg;* n = *12. The vertical bar represents 2* SE.

[5] Model 5710A, Hewlett-Packard, Avondale, Pa.
[6] Porapak QS, Waters Associates, Framingham, Mass.
[7] Linde, New York, N.Y.

Table II—Tissue I Concentrations (Micrograms per Gram) in Beagle Dogs that Received 3.8 g/kg intratracheally

| Dog Number, Sex, and Weight (kg) | Lung | Fat | Thoracic Lymph | Mesenteric Lymph | Bile | Adrenals | Ovaries | Testes |
|---|---|---|---|---|---|---|---|---|
| | | | | 1 Week | | | | |
| 1, M, 10.4 | 0.01 | 6.5 | 0.30 | 0.70 | <MQL[a] | 0.11 | — | <MQL |
| 2, M, 9.2 | 0.01 | 0.96 | 0.26 | 0.09 | <MQL | 0.12 | — | 0.01 |
| 3, F, 7.3 | 0.01 | 2.5 | 0.31 | 0.11 | <MQL | 0.07 | <MQL | — |
| 4, F, 8.6 | <MQL | 0.86 | <MQL | 0.14 | <MQL | 0.05 | <MQL | — |
| | | | | 2 Weeks | | | | |
| 5, M, 10.0 | <MQL | 0.67 | <MQL | 0.28 | <MQL | <MQL | — | <MQL |
| 6, M, 9.3 | <MQL | <MQL | <MQL | <MQL | <MQL | <MQL | — | <MQL |
| 7, F, 8.2 | <MQL | 0.16 | <MQL | 0.02 | <MQL | <MQL | —[b] | — |
| 8, F, 6.6 | <MQL | 0.67 | 0.03 | 0.05 | <MQL | <MQL | <MQL | — |
| | | | | 4 Weeks | | | | |
| 9, M, 10.7 | <MQL | <MQL | <MQL | <MQL | <MQL | <MQL | — | <MQL |
| 10, M, 9.9 | <MQL | <MQL | <MQL | <MQL | <MQL | <MQL | — | <MQL |
| 11, F, 8.2 | <MQL | <MQL | <MQL | <MQL | <MQL | <MQL | <MQL | — |
| 12, F, 6.9 | <MQL | 0.06 | <MQL | <MQL | <MQL | <MQL | <MQL | — |

[a] Mean minimum quantifiable level (MQL) was 0.01 μg/g. [b] No sample.


## REFERENCES

(1) D. M. Long, M. Liu, P. S. Szanto, and P. Alrenga, *Chest*, **61S**, 64 (1972).

(2) D. M. Long, M. Liu, P. S. Szanto, and P. Alrenga, *Rev. Surg.*, **29**, 71 (1972).

(3) A. S. Arambulo, M. Liu, A. L. Rosen, G. Dobben, and D. M. Long, *Drug Dev. Commun.*, **1**, 73 (1974).

(4) D. M. Long, M. Liu, P. S. Szanto, D. P. Alrenga, M. M. Patel, M. V. Rios, and L. M. Nyhus, *Radiology*, **105**, 323. (1972).

(5) M. S. Liu and D. M. Long, *Invest. Radiol.*, **11**, 479 (1976).

(6) M. S. Liu, G. D. Dobben, P. B. Szanto, D. P. Alrenga, U. Khin, A. S. Arambulo, and R. Forrest, *ibid.*, **11**, 319 (1976).

(7) M. S. Liu and D. M. Long, *Radiology*, **122**, 71 (1977).

(8) D. Enzmann and S. W. Young, *J. Comp. Assist. Tomogr.*, **3**, 622 (1979).

(9) M. Hussain, S. Niazi, A. Arambulo, and D. M. Long, *J. Pharm. Sci.*, **66**, 907 (1977).

(10) M. L. Miller, J. D. Stinnett, and L. C. Clark, Jr., *J. Reticuloendothel. Soc.*, **27**, 105 (1980).

(11) F. H. Lee, M. Scrime, and J. Edelson, *J. Pharm. Sci.*, **67**, 1038 (1978).



## ACKNOWLEDGMENTS

The authors thank M. P. Kullberg and the Department of Toxicology, Sterling-Winthrop Research Institute, for their assistance.


# Dose-Dependent Protein Binding and Disposition of Prednisolone in Rabbits


**MARIO L. ROCCI, Jr., and WILLIAM J. JUSKO** ˣ



Received November 28, 1980, from the *Department of Pharmaceutics, School of Pharmacy, State University of New York at Buffalo, Amherst, NY 14260.* Accepted for publication March 25, 1981.



**Abstract** □ An animal model was sought that would mimic humans with regard to the dose-dependent pharmacokinetics of prednisolone. Four rabbits were each given 0.5 and 10 mg iv of prednisolone, and timed blood samples were obtained. Plasma prednisolone and prednisone concentrations were assayed by high-performance liquid chromatography, and protein binding was assessed using equilibrium dialysis at 37°. Increases in the systemic clearance, volume of distribution at steady state, mean residence time (in three of four rabbits), and variance of residence time occurred as dose was increased. As in humans, prednisolone was partly converted to prednisone in the rabbit. Transcortin and albumin concentrations and their affinity constants for binding prednisolone were also similar to humans.



**Keyphrases** □ Prednisolone—dose-dependent protein binding and pharmacokinetics, rabbits □ Binding, protein—prednisolone, pharmacokinetics, rabbits □ Pharmacokinetics—prednisolone, protein binding, rabbits


Prednisolone and its pharmacologically inactive prodrug, prednisone, are synthetic glucocorticoids widely used in the treatment of various disease entities including asthma, shock, and nephrotic syndrome. Jusko and Rose (1) demonstrated nonlinear pharmacokinetics of these compounds in humans, characterized by increases in their total plasma clearance with increases in dose. Furthermore, the serum protein binding of prednisolone is nonlinear at therapeutic serum concentrations owing to the existence of two binding proteins (2). This binding appears to explain most, but not all, of the nonlinearity in prednisolone pharmacokinetics in humans (1).

To assess mechanisms contributing to this nonlinear disposition, an animal model is needed that mimics humans with regard to the serum protein binding and disposition of prednisolone. The serum protein binding of prednisolone was previously examined in rat, rabbit, canine, and human serum (3), with the rabbit being most like the human in type and degree of nonlinear binding. This study further evaluated the rabbit as an animal model for dose-dependent disposition of prednisolone.

## EXPERIMENTAL

**Methods**—Four New Zealand White rabbits, 3.0–3.9 kg, received 0.5- and 10-mg iv equivalent doses of prednisolone as the sodium succinate.


0022-3549/81/1100-1201$01.00/0


© 1981, American Pharmaceutical Association

Table II—Tissue I Concentrations (Micrograms per Gram) in Beagle Dogs that Received 3.8 g/kg intratracheally

| Dog Number, Sex, and Weight (kg) | Lung | Fat | Thoracic Lymph | Mesenteric Lymph | Bile | Adrenals | Ovaries | Testes |
|---|---|---|---|---|---|---|---|---|
| | | | | 1 Week | | | | |
| 1, M, 10.4 | 0.01 | 6.5 | 0.30 | 0.70 | <MQL[a] | 0.11 | — | <MQL |
| 2, M, 9.2 | 0.01 | 0.96 | 0.26 | 0.09 | <MQL | 0.12 | — | 0.01 |
| 3, F, 7.3 | 0.01 | 2.5 | 0.31 | 0.11 | <MQL | 0.07 | <MQL | — |
| 4, F, 8.6 | <MQL | 0.86 | <MQL | 0.14 | <MQL | 0.05 | <MQL | — |
| | | | | 2 Weeks | | | | |
| 5, M, 10.0 | <MQL | 0.67 | <MQL | 0.28 | <MQL | <MQL | — | <MQL |
| 6, M, 9.3 | <MQL | <MQL | <MQL | <MQL | <MQL | <MQL | — | <MQL |
| 7, F, 8.2 | <MQL | 0.16 | <MQL | 0.02 | <MQL | <MQL | —[b] | — |
| 8, F, 6.6 | <MQL | 0.67 | 0.03 | 0.05 | <MQL | <MQL | <MQL | — |
| | | | | 4 Weeks | | | | |
| 9, M, 10.7 | <MQL | <MQL | <MQL | <MQL | <MQL | <MQL | — | <MQL |
| 10, M, 9.9 | <MQL | <MQL | <MQL | <MQL | <MQL | <MQL | — | <MQL |
| 11, F, 8.2 | <MQL | <MQL | <MQL | <MQL | <MQL | <MQL | <MQL | — |
| 12, F, 6.9 | <MQL | 0.06 | <MQL | <MQL | <MQL | <MQL | <MQL | — |

[a] Mean minimum quantifiable level (MQL) was 0.01 μg/g. [b] No sample.


## REFERENCES

(1) D. M. Long, M. Liu, P. S. Szanto, and P. Alrenga, *Chest*, **61S**, 64 (1972).

(2) D. M. Long, M. Liu, P. S. Szanto, and P. Alrenga, *Rev. Surg.*, **29**, 71 (1972).

(3) A. S. Arambulo, M. Liu, A. L. Rosen, G. Dobben, and D. M. Long, *Drug Dev. Commun.*, **1**, 73 (1974).

(4) D. M. Long, M. Liu, P. S. Szanto, D. P. Alrenga, M. M. Patel, M. V. Rios, and L. M. Nyhus, *Radiology*, **105**, 323. (1972).

(5) M. S. Liu and D. M. Long, *Invest. Radiol.*, **11**, 479 (1976).

(6) M. S. Liu, G. D. Dobben, P. B. Szanto, D. P. Alrenga, U. Khin, A. S. Arambulo, and R. Forrest, *ibid.*, **11**, 319 (1976).

(7) M. S. Liu and D. M. Long, *Radiology*, **122**, 71 (1977).

(8) D. Enzmann and S. W. Young, *J. Comp. Assist. Tomogr.*, **3**, 622 (1979).

(9) M. Hussain, S. Niazi, A. Arambulo, and D. M. Long, *J. Pharm. Sci.*, **66**, 907 (1977).

(10) M. L. Miller, J. D. Stinnett, and L. C. Clark, Jr., *J. Reticuloendothel. Soc.*, **27**, 105 (1980).

(11) F. H. Lee, M. Scrime, and J. Edelson, *J. Pharm. Sci.*, **67**, 1038 (1978).



## ACKNOWLEDGMENTS

The authors thank M. P. Kullberg and the Department of Toxicology, Sterling-Winthrop Research Institute, for their assistance.


# Dose-Dependent Protein Binding and Disposition of Prednisolone in Rabbits


**MARIO L. ROCCI, Jr., and WILLIAM J. JUSKO** ˣ



Received November 28, 1980, from the *Department of Pharmaceutics, School of Pharmacy, State University of New York at Buffalo, Amherst, NY 14260.* Accepted for publication March 25, 1981.



**Abstract** □ An animal model was sought that would mimic humans with regard to the dose-dependent pharmacokinetics of prednisolone. Four rabbits were each given 0.5 and 10 mg iv of prednisolone, and timed blood samples were obtained. Plasma prednisolone and prednisone concentrations were assayed by high-performance liquid chromatography, and protein binding was assessed using equilibrium dialysis at 37°. Increases in the systemic clearance, volume of distribution at steady state, mean residence time (in three of four rabbits), and variance of residence time occurred as dose was increased. As in humans, prednisolone was partly converted to prednisone in the rabbit. Transcortin and albumin concentrations and their affinity constants for binding prednisolone were also similar to humans.



**Keyphrases** □ Prednisolone—dose-dependent protein binding and pharmacokinetics, rabbits □ Binding, protein—prednisolone, pharmacokinetics, rabbits □ Pharmacokinetics—prednisolone, protein binding, rabbits


Prednisolone and its pharmacologically inactive prodrug, prednisone, are synthetic glucocorticoids widely used in the treatment of various disease entities including asthma, shock, and nephrotic syndrome. Jusko and Rose (1) demonstrated nonlinear pharmacokinetics of these compounds in humans, characterized by increases in their total plasma clearance with increases in dose. Furthermore, the serum protein binding of prednisolone is nonlinear at therapeutic serum concentrations owing to the existence of two binding proteins (2). This binding appears to explain most, but not all, of the nonlinearity in prednisolone pharmacokinetics in humans (1).

To assess mechanisms contributing to this nonlinear disposition, an animal model is needed that mimics humans with regard to the serum protein binding and disposition of prednisolone. The serum protein binding of prednisolone was previously examined in rat, rabbit, canine, and human serum (3), with the rabbit being most like the human in type and degree of nonlinear binding. This study further evaluated the rabbit as an animal model for dose-dependent disposition of prednisolone.

## EXPERIMENTAL

**Methods**—Four New Zealand White rabbits, 3.0–3.9 kg, received 0.5- and 10-mg iv equivalent doses of prednisolone as the sodium succinate.


0022-3549/81/1100-1201$01.00/0


© 1981, American Pharmaceutical Association

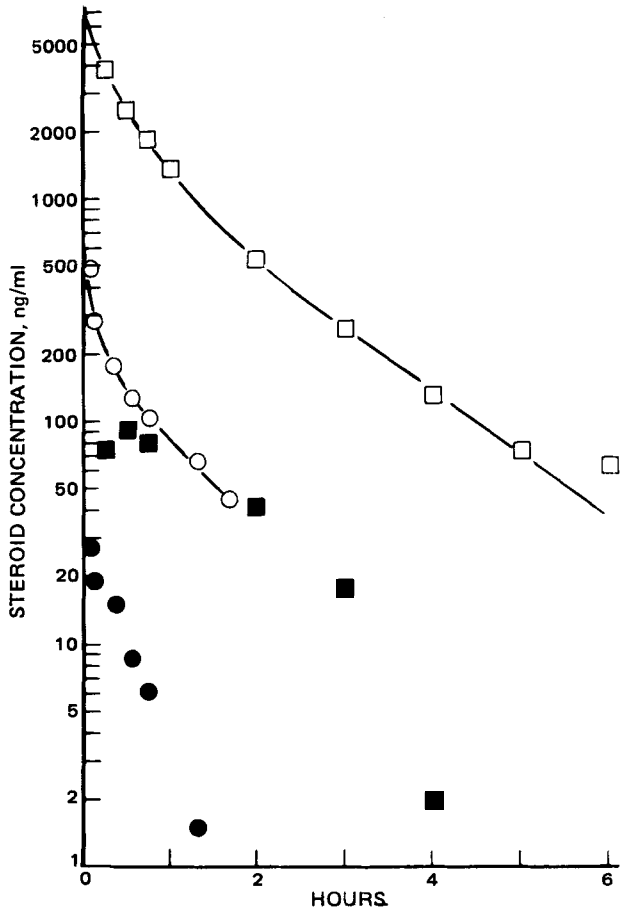


**Figure 1**—*Serum concentration* versus *time profiles of prednisolone (○,□) and prednisone (●,■) after 0.5 mg of prednisolone (○,●) and 10 mg of prednisolone (□,■) intravenously in Rabbit 2.*

A balanced crossover design was used, with 2 weeks between crossover. Rabbit body weight did not change appreciably over the experimental period. The drug was administered into the lower left marginal ear vein over 15 sec. Blood samples (~3 ml) were obtained from the right lower marginal ear vein just prior to dosing and at 0.08, 0.17, 0.25, 0.5, 0.75, 1, 2, 3, 4, 6, and 8 hr following drug administration.

**Sample Analysis**—Serum samples were analyzed for prednisolone and prednisone using the high-performance liquid chromatographic (HPLC) technique described earlier (4). Serum protein binding of prednisolone was evaluated at 37° by equilibrium dialysis with [$^3$H]-prednisolone. Details of the protein binding technique and data analysis were presented previously (3).

**Pharmacokinetics**—The area under the curve for prednisone ($AUC_P$) and prednisolone ($AUC_{Pn}$), the systemic clearance ($Cl_T$), mean residence time ($MRT$), variance of the residence time ($VRT$), and volume of distribution at steady state ($V_D^{ss}$) were obtained through use of the LAGRAN computer program, which provides model-independent estimates of these pharmacokinetic parameters based on area/moment analysis[1].

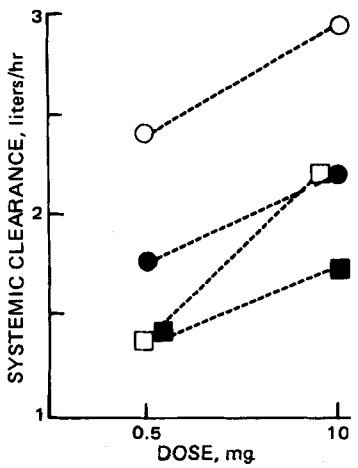


**Figure 2**—*Systemic clearance ($Cl_T$) of prednisolone as a function of dose. The stippled lines connect $Cl_T$ values from the same rabbit.*

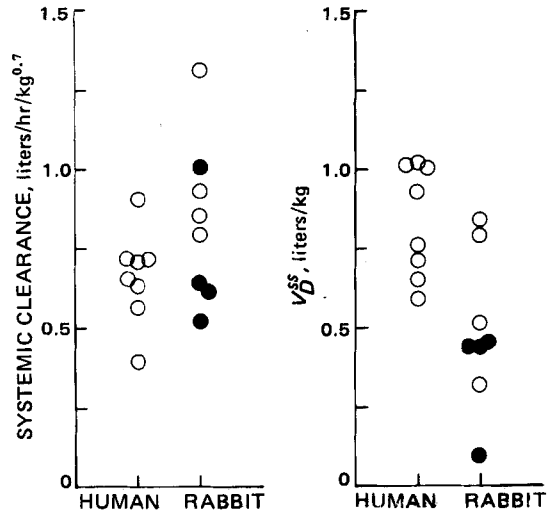


**Figure 3**—*Rabbit $Cl_T$ values (animal scale-up) and $V_D^{ss}$ values compared to those observed in humans. The solid and open symbols in the rabbit data represent values from the low and high dose studies. Human data are from Rose* et al. *(6).*

The free drug clearance ($Cl_{T,free}$) and the transcortin (CBG) free drug clearance ($Cl_{T,CBG\text{-}free}$) of prednisolone were computed using:

$$Cl_{T,free} = \text{dose}/AUC_{Pn,free} \quad \text{(Eq. 1)}$$

$$Cl_{T,CBG\text{-}free} = \text{dose}/AUC_{Pn,CBG\text{-}free} \quad \text{(Eq. 2)}$$

where $AUC_{Pn,free}$ and $AUC_{Pn,CBG\text{-}free}$ are the areas under the serum concentration *versus* time curves of free and CBG-free prednisolone.

Approximate extraction ratios of prednisolone by kidney ($E_K$) and liver ($E_L$) tissues were obtained as the ratio of $Cl_T$ to kidney plasma flow ($Q_K$) and liver plasma flow ($Q_L$). The values of $Q_K$ and $Q_L$ used in the computation were 55 and 70 ml/min (5).

## RESULTS

**Prednisolone Disposition**—Typical serum concentration–time profiles for prednisolone and prednisone after low and high doses of prednisolone are presented for Rabbit 2 in Fig. 1. Prednisolone disposition was biphasic in nature, with metabolism of prednisolone to prednisone occurring at each dose. The systemic clearance of prednisolone ($Cl_T$) at the two doses is shown in Fig. 2. A significant increase ($p < 0.02$) in $Cl_T$ occurred with the increase in dose. The mean ($\pm SD$) $Cl_T$ values after low and high intravenous doses were 1.72 (±0.48) and 2.25 (±0.52) ml/min, respectively. The approximate $E_K$ and $E_L$ values obtained using the mean $Cl_T$ values were 0.036 and 0.028, respectively. There was no dose dependence in prednisolone clearance when corrected for albumin and

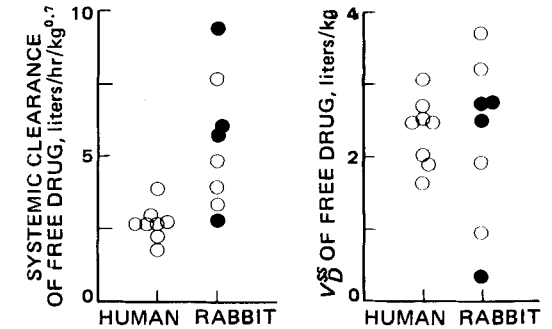


**Figure 4**—*Rabbit $Cl_T$ and $V_D^{ss}$ values for unbound prednisolone compared to human values (corrected for animal scale-up). The solid and open symbols in the rabbit data represent values from the low and high dose studies. Human data are from Rose* et al. *(6).*

[1] M. L. Rocci and W. J. Jusko, to be published.

**Table I—Essential Characteristics of Prednisolone Disposition**

| Rabbit | Body Weight, kg | Dose, mg | Total Plasma Clearance, $Cl_T$, liters/hr/kg | Free Drug Clearance, $Cl_{T,free}$, liters/hr/kg | CBG-Free Drug Clearance, $Cl_T$, $CBG_{free}$, liters/hr/kg | $AUC_P/AUC_{Pn}$ | Volume of Distribution at Steady State, $V_D^{ss}$, liters/kg | Mean Residence Time, $MRT$, hr | Variance of Residence Time, $VRT$, hr |
|---|---|---|---|---|---|---|---|---|---|
| 1 | 3.2 | 0.5 | 0.75 | 6.59 | 1.27 | 0.040 | 0.44 | 0.59 | 0.39 |
| | 3.2 | 10.0 | 0.92 | 5.31 | 1.03 | 0.028 | 0.84 | 0.92 | 1.38 |
| 2 | 3.4 | 0.5 | 0.51 | 3.94 | 0.87 | 0.060 | 0.46 | 0.89 | 1.16 |
| | 3.4 | 10.0 | 0.64 | 3.32 | 0.74 | 0.052 | 0.79 | 1.23 | 2.18 |
| 3 | 3.9 | 0.5 | 0.35 | 1.85 | 0.54 | — | 0.10 | 0.29 | 0.11 |
| | 3.9 | 10.0 | 0.56 | 2.20 | 0.65 | 0.044 | 0.32 | 0.57 | 0.68 |
| 4 | 3.0 | 0.5 | 0.46 | 4.3 | 0.95 | — | 0.44 | 0.95 | 1.14 |
| | 3.0 | 10.0 | 0.56 | 2.8 | 0.63 | 0.076 | 0.51 | 0.91 | 1.51 |
| Significance[a] (between doses) | | — | $p < 0.02$ | NS[a] | NS | — | $p < 0.05$ | NS | $p < 0.02$ |

[a] NS = not significant.

transcortin binding ($Cl_{T,free}$) nor in the clearance corrected for only transcortin binding ($Cl_{T,CBG\text{-}free}$) (Table I).

Significant increases in the volumes of distribution at steady state ($V_D^{ss}$) and the variance of residence time ($VRT$) were observed at the higher prednisolone dose. In contrast, the mean residence time ($MRT$) increased with dose in only three of four rabbits. This total change in $MRT$ was not statistically significant (Table I).

Figure 3 illustrates $V_D^{ss}$ and $Cl_T$ using animal scale-up corrections (5) for the rabbit compared to the human (6). There was no significant difference in the $Cl_T$ values between species. In contrast, $V_D^{ss}$ values were significantly higher in the human than in the rabbit ($p < 0.01$). Comparison of $Cl_T$ and $V_D^{ss}$ for unbound prednisolone between humans and rabbits using animal scale-up corrections demonstrated no significant species difference in $V_D^{ss}$, while the $Cl_T$ values for free prednisolone were significantly higher in the rabbit ($p < 0.05$) (Fig. 4).

**Protein Binding**—A plot of percent bound *versus* postequilibrium dialysis serum prednisolone concentrations for a rabbit is presented in Fig. 5. The mean (±$SD$) serum albumin concentration and the binding affinity constant obtained from computer fitting of the binding data (2) were 5.51 (±0.46) × $10^{-4}$ $M$ and 6.24 (±1.5) × $10^3$ $M^{-1}$, respectively. The mean (±$SD$) transcortin concentration and binding affinity constant, also obtained through computer fitting, were 4.70 (±2.4) × $10^{-7}$ $M$ and 2.84 (±2.16) × $10^7$ $M^{-1}$, respectively. The binding parameters obtained in each rabbit are compared in Figs. 6 and 7 with values obtained from a study (6) performed in normal healthy volunteers.

## DISCUSSION

The pharmacokinetic parameters derived from these disposition studies are dose and time average values since the disposition of prednisolone is nonlinear, as indicated by the increase in $Cl_T$, $V_D^{ss}$, $MRT$, and $VRT$ with dose. Interconversion between these corticosteroids occurs as well, providing an additional confounding influence on the pharmacokinetic parameters obtained in the present investigation. Such interconversion of prednisone and prednisolone was demonstrated in humans (1, 6) and in the isolated perfused rat kidney (7). The increases in $Cl_T$ and $V_D^{ss}$, as well as the formation of prednisone after intravenous doses of prednisolone, are all characteristic of the disposition of this steroid in humans (1). Corrections of $Cl_T$ for total protein binding and transcortin binding partially eliminates the differences in $Cl_T$ between low and high doses of prednisolone. This result also was observed in the human and suggests that nonlinear protein binding largely produces dose-dependent changes in $Cl_T$ (6).

The dose-dependent increase in $V_D^{ss}$ is consistent with the changes in protein binding that occur as a function of serum prednisolone concentration (Fig. 4). High prednisolone doses produce higher initial serum concentrations. The reduced binding of prednisolone at these high concentrations (Fig. 4) results in increased distribution of prednisolone to tissues, as reflected by an increase in $V_D^{ss}$.

Further support for the importance of protein binding in prednisolone disposition is provided by the low extraction ratios of prednisolone by the kidney and liver, suggesting that only drug not bound to serum proteins is available to these tissues (*i.e.*, restrictive clearance). The extraction ratios calculated in the present investigation are overestimates of the true extraction ratios since total and not individual organ clearances were used. The $E_K$ value, however, agrees very well with those (mean = 0.044) obtained during prednisolone perfusion in isolated rat kidneys (7).

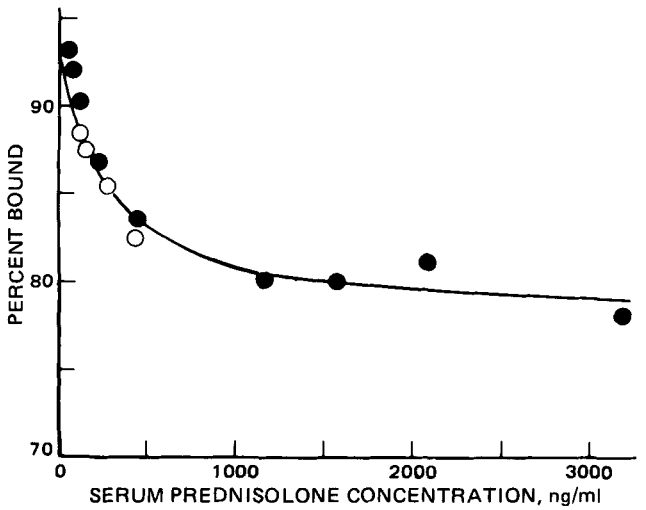


**Figure 5**—*Percent of prednisolone bound* versus *postdialysis serum prednisolone concentration after low (○) and high (●) intravenous prednisolone doses. The solid line represents the nonlinear least-squares regression line for the protein binding data using a modified Rosenthal relationship for two classes of binding sites (see Ref. 2).*

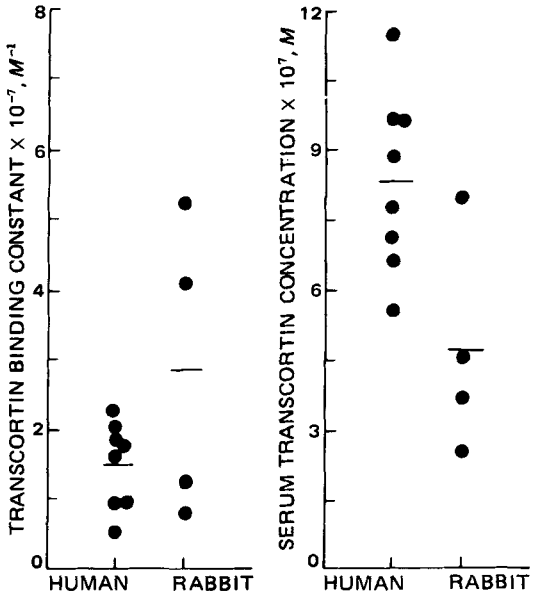


**Figure 6**—*Serum transcortin concentrations and binding affinity constants for prednisolone in the rabbit and in normal healthy human volunteers (from Ref. 6).*

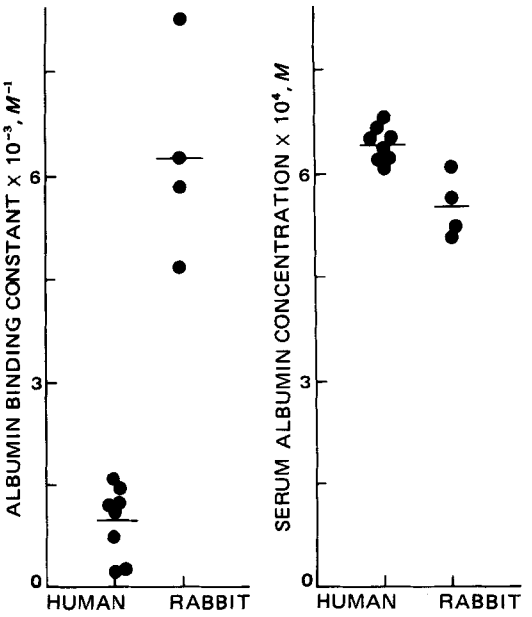


**Figure 7**—*Serum albumin concentrations and binding affinity constants for prednisolone in the rabbit and in normal healthy volunteers (from Ref. 6).*

Adolph (8) demonstrated that many metabolic and physiological properties among mammals are proportional to some exponential power of their body weight, and Dedrick (9) indicated that the exponent is usually in the 0.7–0.8 range. Excellent agreement between humans and rabbits was observed in the $Cl_T$ values normalized for weight raised to the 0.7 power (Fig. 3). In addition, $V_D^{ss}$ values, although significantly different between species, are in the same general range. The absence of significant interspecies differences in $V_D^{ss}$ for unbound prednisone (corrected for animal scale-up) (Fig. 4) suggests that differences in binding between species accounts for the differences in $V_D^{ss}$ observed for total drug. The significantly higher free $Cl_T$ in the rabbit (Fig. 4) should not be a major complication in its use as a model since the interspecies difference in this parameter is not large. While the doses used for these comparisons are not equivalent, the dose range examined in the rabbit (0.15–2.98 mg/kg) encompasses the dose (0.52 mg/kg) employed in the human studies (6). This comparison establishes that the normalized $Cl_T$ and $V_D^{ss}$ values in the rabbit are reasonably similar to those observed in humans and further demonstrates the applicability of the rabbit in mimicking prednisolone disposition in humans.

The relative changes in $Cl_T$ and $V_D^{ss}$ with prednisolone dose are greater in the human than in the rabbit. Rose *et al.* (6) observed that both $Cl_T$ and $V_D^{ss}$ approximately doubled over an eightfold dose range. The relative increases in $Cl_T$ and $V_D^{ss}$ with dose in the present study averaged 33 and 102%, respectively. These increases were observed over a 20-fold dose range. The lesser magnitude of the changes in $Cl_T$ and $V_D^{ss}$ in the rabbit may be due to less pronounced nonlinearity of prednisolone plasma binding (2).

The apparent increase in *MRT* (in three of the four rabbits studied) at the higher dose directly reflects an increase in the average persistence time of prednisolone in the body. The fractional increase in $V_D^{ss}$ at the higher dose exceeds the relative increase in $Cl_T$ that occurs as the dose is increased. Since $MRT = V_D^{ss}/Cl_T$, the net effect of these changes is an increase in *MRT*. The increase in *VRT* with dose indicates a wider spread of residence time of the mass of drug molecules at the higher dose. This finding appears to be congruous with the enhanced $Cl_T$ and the larger $V_D^{ss}$ that occur at the higher dose. Increases in $Cl_T$ serve to diminish the residence time of prednisolone, while more extensive tissue distribution of prednisolone prolongs the residence time. Concomitant increases in each of these processes would increase the variance (spread) of the residence times of the drug molecules.

The transcortin and albumin serum concentrations and affinity constants for prednisolone binding in rabbits are in the same general range as those determined in normal healthy volunteers after the 40-mg iv dose of prednisolone phosphate (Figs. 6 and 7). This finding confirms the similarity in prednisolone binding between human and rabbit reported previously (3). The apparent superposition of the binding data after low and high prednisolone doses suggests that prednisolone does not compete with prednisone or other metabolites for protein binding sites on transcortin and albumin. The concentrations of these potential displacers is higher after larger prednisolone doses. Competitive binding studies are required, however, to definitively ascertain whether such competition actually occurs.

In conclusion, the rabbit appears to be a suitable model for prednisolone disposition in humans. This species is also desirable from a technical standpoint in that blood samples are easily obtainable and may be taken in sufficient volume to permit examination of serum prednisolone protein binding in addition to HPLC assay for total serum prednisolone and prednisone concentrations.

## REFERENCES

(1) W. J. Jusko and J. Q. Rose, *Ther. Drug Monit.*, **2**, 169 (1980).

(2) A. A. Sandberg, W. R. Slaunwhite, Jr., and H. N. Antoniades, *Rec. Prog. Horm. Res.*, **13**, 209 (1957).

(3) M. L. Rocci, Jr., N. F. Johnson, and W. J. Jusko, *J. Pharm. Sci.*, **69**, 977 (1980).

(4) J. Q. Rose and W. J. Jusko, *J. Chromatogr.*, **162**, 273 (1979).

(5) K. B. Bischoff, R. L. Dedrick, D. S. Zaharko, and J. A. Longstreth, *J. Pharm. Sci.*, **60**, 1128 (1971).

(6) J. Q. Rose, A. M. Yurchak, and W. J. Jusko, *J. Pharmacokinet. Biopharm.*, **9**, 1 (1981).

(7) M. L. Rocci, Jr., S. J. Szefler, M. Acara, and W. J. Jusko, *Drug Metab. Disp.*, **9**, 177 (1981).

(8) E. F. Adolph, *Science*, **109**, 579 (1949).

(9) R. L. Dedrick, *J. Pharmacokinet. Biopharm.*, **1**, 435 (1973).

## ACKNOWLEDGMENTS

Supported in part by Grant 24211 from the National Institute of General Medical Sciences, National Institutes of Health.

# High-Pressure Liquid Chromatographic Determination of Anthralin in Ointments

**JEAN-CLAUDE CARON** ˣ **and BRAHAM SHROOT**

Received January 9, 1981, from the *Centre International de Recherches Dermatologiques, Sophia Antipolis, F-06565 Valbonne, France.* Accepted for publication March 23, 1981.

**Abstract** □ Anthralin concentration was determined in different ointments by high-pressure liquid chromatography, and results were compared with those of the USP assay technique. Significant differences existed between the claimed and the actual levels of anthralin in some preparations. Varying quantities of anthralin breakdown products were found, and their concentrations appear to be related to the nature of the formulation.

**Keyphrases** □ Anthralin—high-pressure liquid chromatographic determination in ointments □ High-pressure liquid chromatography—determination of anthralin in ointments □ Ointments—high-pressure liquid chromatographic determination of anthralin

Anthralin, applied percutaneously in various formulations, has been used in the treatment of psoriasis for over 100 years (1). This reactive chemical entity can undergo predictable chemical changes in the vehicle, depending on the presence of basic ingredients and/or oxygen. The end-products are claimed to be inactive in the chemotherapy of psoriasis (2). Ponec-Waelsch and Hulsebosch (3) postulated that anthralin and zinc hydroxide interact in zinc oxide pastes (Lassars' paste). These workers, however, used UV spectrophotometry for the assay and, as discussed recently (4), quantification of the breakdown products can only be estimated following prior separation of the compounds by TLC.

High-pressure liquid chromatography (HPLC), a selective, sensitive, reproducible, and rapid assay procedure, seemed a better choice for this assay and is compared in the present study to the standard USP method (5).

## EXPERIMENTAL

**Materials**—Acetic acid[1] was analytical reagent grade; isooctane, isopropyl ether, methanol, chloroform, and *n*-hexane were HPLC grade[2] and were used as received after filtration and degassing.

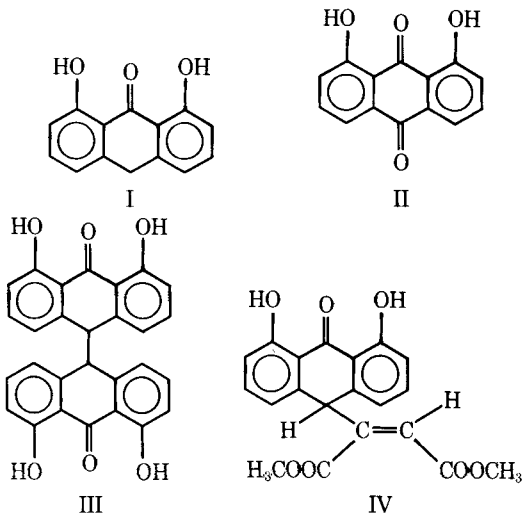


[1] Prolabo Normapur.
[2] Merck.

1,8-Dihydroxy-9-anthrone (anthralin, I) was purified by column chromatography. Its chemical derivatives, 1,8-dihydroxy-9,10-anthraquinone (quinone, II) and 1,8,1′,8′-tetrahydroxy-10,10′-dianthrone (dimer, III) (6), and the internal standard, 1,8-dihydroxy-9-anthron-10-yl maleic acid dimethyl ester (IV) (7), were synthesized[3] following published procedures.

**Instrumentation**—Two high-pressure liquid chromatographs were used. One was equipped with a septumless injector[4], a reciprocating pump[5], a normal-phase 25-cm column[6], a UV-visible detector[7] set at 254 nm, and a strip-chart recorder[8]. The other chromatograph[9] was equipped with a reversed-phase 25-cm column[10] also set at 254 nm (referenced at 500 nm). The mobile phases compositions and conditions used are listed in Table I. Under these conditions, the response of each compound was linear in the working range (1–50 μg/ml).

**Products Investigated**—Commercially available samples were used, except in one case where the formulation was obtained directly from the

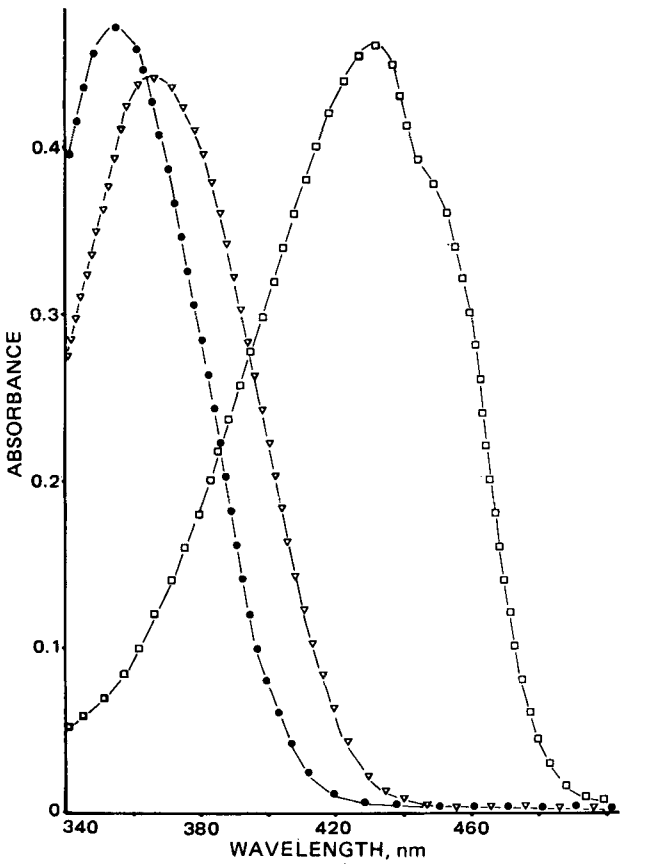


**Figure 1**—*Visible spectra at 10 μg/ml in chloroform of anthralin (●), the dimer (▽), and the quinone (□). Molar absorptivities (ε) at 345 and 432 nm are, respectively, 10,650 and 100 for anthralin, 16,970 and 220 for the dimer, and 1680 and 10,890 for the quinone.*

[3] Laboratoirès de Recherches Fondamentales, L'Oréal, Aulnay-sous-Bois, France.
[4] Waters Associates model U6K.
[5] Waters Associates model 6000A.
[6] Merck Lichrosorb RT 250-4-5 μm-Si60.
[7] Waters Associates model 440.
[8] Omniscribe.
[9] Hewlett-Packard model 1084 B.
[10] Merck Lichrosorb RT 250-4-5 μm-RP18.

0022-3549/81/1100-1205$01.00/0
© 1981, American Pharmaceutical Association

**Table I—Analytical Conditions and Chromatographic Properties Observed in HPLC Separation of Anthralin, the Quinone, and the Dimer**

| Packing | Analytical Conditions | Compound | Retention Time, min |
|---|---|---|---|
| Normal phase ($SiO_2$) | Mobile phase (percent volume); isooctane (44.5), isopropyl ether (49.9), methanol (5.4), acetic acid (0.2); flow: 1 ml/min; pressure: 81 bars; temperature: 30° | Anthralin | 3.70 |
| | | Quinone | 3.35 |
| | | Dimer | 4.52 |
| | | Internal standard | 5.25 |
| Reversed phase ($C_{18}$) | Mobile phase (percent volume): water (24.9), methanol (74.9), acetic acid (0.2); flow: 2 ml/min; pressure: 254 bars; temperature: 60° | Anthralin | 4.90 |
| | | Quinone | 4.52 |
| | | Dimer | 8.42 |
| | | Internal standard | 3.68 |

pharmacy of a local hospital. The ointment bases and theoretical concentrations of anthralin are given in Table II.

**Analytical Procedure**—Ointment theoretically corresponding to ~200 μg of anthralin was weighed and spiked with exactly 200 μg of internal standard in the appropriate solvent (chloroform or *n*-hexane) from a freshly prepared (1 mg/ml) stock solution.

The extraction was performed by shaking the mixture for 15 min on a vortex mixer in the presence of 5 ml of chloroform or *n*-hexane and filtering the resulting solution through a solvent-resistant filter[11]. An aliquot (1 ml) of this solution was then evaporated to dryness under nitrogen at room temperature, and the residue was redissolved in the same amount of the elution solvent and subjected to HPLC analysis.

## RESULTS AND DISCUSSION

The USP describes an assay procedure for the quantification of anthralin as the starting material for the preparation of ointments or in the ointment itself. This method is based on the absorbances at 354 and 432 nm but suffers from overlapping and interference between the absorption maxima of anthralin, dimer, and quinone (Fig. 1). In contrast, the described method allows the quantification of anthralin and its major oxidation products in the presence of each other (Fig. 2).

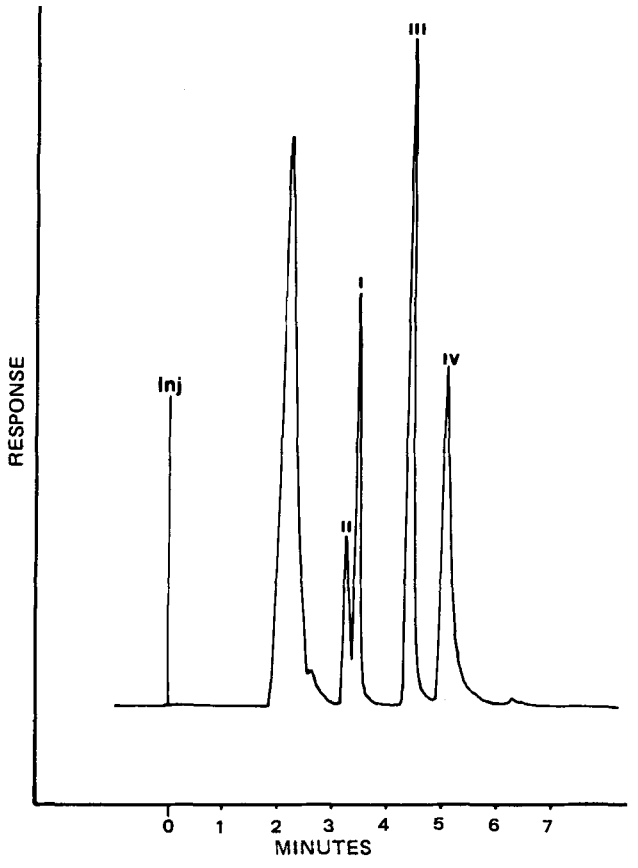


**Figure 2**—*Example of the chromatogram of a formulation extract (Sample 11) obtained on a silica gel phase.*

[11] Millipore FHLP 013, 0.5 μm.

Table III lists the results obtained by HPLC and USP techniques for the percentages of anthralin in the formulations studied.

Table IV lists the results obtained for anthralin, the quinone, and the dimer, with chloroform as the extraction solvent, on the two chromatographic systems; for solubility reasons, *n*-hexane is unsuitable as an extraction solvent for the dimer.

In nine out of the 12 formulations studied, 100 ± 5% of the material could be accounted for. Since the possible variation in the original anthralin used by the manufacturers could not be estimated, in cases where significantly less products was found, the extraction procedure was verified by adding increasing amounts of pure anthralin standard to the ointment before extraction.

The possibility of anthralin decomposition during extraction can be rejected since the standard deviation in the results obtained by the two extraction procedures was the same as the error in the analytical procedures itself. Decomposition during chromatography on either system can also be rejected since the normal and reversed-phase results are in good agreement.

Consequently, the difference between the theoretical and actual concentrations of anthralin in the ointment is related to the vehicle itself, in particular the zinc oxide pastes (Base D, Table III). Three out of the four such preparations (Samples 9, 11, and 12) contained <40% of the theoretical amount of anthralin; in two cases, a marked tendency towards the formation of the corresponding dimer (81 and 91%) was noted.

For Base C (Sample 10), low overall recovery was obtained with the highest amount of quinone. This low recovery can be explained by the

**Table II—Composition of Vehicles and Theoretical Anthralin Concentration of Ointments**

| Cream Base | Anthralin Concentration, % | Code |
|---|---|---|
| Powder-in-cream urea | 0.1 | A |
| Oil-in-water cream | 0.1 | B |
| Anhydrous water washable | 0.2 | C |
| Zinc oxide–petrolatum–salicylic acid–lanolin–starch | 0.2 | D |
| Zinc oxide–petrolatum–salicylic acid–starch | 0.22 | D |
| Oil-in-water cream | 0.25 | B |
| Zinc oxide–petrolatum–salicylic acid starch | 0.44 | D |
| Salicylic acid–cetyl alcohol–sodium lauryl sulfate–paraffin–petrolatum | 0.44 | E |
| Oil-in-water cream | 0.5 | B |

**Table III—Percentage of Anthralin [a] Related to the Theoretical Amount Compared to USP Assay Results**

| Sample | Base Code | Anthralin, % HPLC | Anthralin, % USP |
|---|---|---|---|
| 1 | A | 90.8 ± 2.5 | 113 |
| 2 | B | 90.1 ± 1.2 | 105 |
| 3 | B | 79.8 ± 2.5 | 94 |
| 4 | B | 71.5 ± 1.9 | 103 |
| 5 | D | 70.4 ± 2.4 | 85 |
| 6 | E | 70.2 ± 2.3 | 109 |
| 7 | E | 68.4 ± 1.8 | 112 |
| 8 | B | 66.0 ± 2.5 | 106 |
| 9 | D | 37.1 ± 2.1 | 53 |
| 10 | C | 26.9 ± 1.2 | 82 |
| 11 | D | 18.8 ± 1.3 | 79 |
| 12 | D | 3.3 ± 1.6 | 74 |

[a] Average of results obtained with chloroform and *n*-hexane extractions with the two chromatographic systems.

Table IV—Percentage of Recovery of Anthralin and Its Decomposition Products [a]

| Sample | Anthralin, % | Dimer, % | Quinone, % | Total Recovery, % |
|---|---|---|---|---|
| 1 | 88.5 | 7.2 | 1 | 96.7 |
| 2 | 92 | 9 | 2 | 103.0 |
| 3 | 80.9 | 15.5 | 2.2 | 98.6 |
| 4 | 72.6 | 25 | 1.3 | 98.9 |
| 5 | 71.2 | 4.7 | 1.1 | 77.0 |
| 6 | 70.5 | 25.1 | 1.8 | 97.4 |
| 7 | 69.0 | 22.4 | 1.7 | 93.1 |
| 8 | 67.4 | 29.5 | 1 | 97.9 |
| 9 | 39.0 | 10.4 | 1.2 | 50.6 |
| 10 | 29.8 | 2.5 | 12.9 | 45.2 |
| 11 | 17.3 | 81.1 | 5.9 | 104.3 |
| 12 | 4.4 | 90.9 | 5.1 | 100.4 |

[a] Chloroform extraction; average of data obtained using both chromatographic systems.

formation of high molecular weight materials, and an HPLC method is currently being developed for the analysis of these products.

The surprising disparity between the USP and HPLC assay results can be rationalized when the data in Table IV are considered. Although both methods rely on UV absorption, the USP technique cannot quantify the dimer and merely includes it with the anthralin level. However, a discrepancy between the results is still evident after correcting the USP data for the presence of dimer.

The majority of these ointments contained ~70% (range 44–92%) of the theoretical amount of anthralin, the remaining 30% being various quantities of the dimer, quinone, and, perhaps, high molecular weight materials.

The need to check anthralin and its preparations must be emphasized, and the danger of further decomposition of samples in use cannot be ignored.

## REFERENCES


(1) B. Squire, *Br. Med. J.*, **1**, 546 (1877). *Ibid.*, **1**, 199 (1877). B. Squire, *Arch. Dermatol. Synphilol.*, **10**, 332 (1877).

(2) A. Krebs and H. Schaltegger, *Hautarzt*, **20**, 204 (1969).

(3) M. Ponec-Waelsch and H. J. Hulsebosch, *Arch. Dermatol. Forsch.*, **249**, 141 (1974).

(4) H. M. Elsabbagh, C. W. Whitworth, and L. C. Schramm, *J. Pharm. Sci.*, **68**, 388 (1979).

(5) "The United States Pharmacopeia," 20th rev., United States Pharmacopeial Convention, Rockville, Md., 1980, p. 48.

(6) B. L. van Duuren, A. Segal, S.-S. Tseng, G. M. Rusch, G. Loewengart, U. Mate, D. Roth, A. Smith, S. Melchionne, and I. Seidman, *J. Med. Chem.*, **21**, 26 (1978).

(7) O. F. Schultz and G. Fry, *Arch. Pharm. (Weinheim)*, **310**, 776 (1977).


## ACKNOWLEDGMENTS


Presented in part at the Anthralin Symposium, Sophia Antipolis, France, October 1980.

The authors are indebted to Mr. J. Maignan for the preparation and purification of the anthralin derivatives. They also thank Professor H. Schaefer for advice and encouragement, and Dr. R. Baran, Hopital des Brousailles, Cannes, France, for supplying one formulation.


# High-Performance Liquid Chromatographic Determination of Stereoselective Disposition of Carprofen in Humans


**J. K. STOLTENBORG *, C. V. PUGLISI ‡, F. RUBIO *, and F. M. VANE *x**



Received January 26, 1981, from the **Department of Biochemistry and Drug Metabolism and the* ‡*Department of Pharmacokinetics and Biopharmaceutics, Hoffmann-La Roche Inc., Nutley, NJ 07110.* Accepted for publication March 25, 1981.



**Abstract** □ A high-performance liquid chromatographic (HPLC) assay was developed for the determination of the ratios of the (*S*)-(+) and (*R*)-(−) enantiomers of the anti-inflammatory drug carprofen in blood, urine, and feces. The procedure relies on: (*a*) extraction and purification of carprofen from biological fluids, (*b*) reaction of carprofen with (*S*)-(−)-α-methylbenzylamine to form the two diastereomeric (S)-(−)-α-methylbenzylamides *via* the 1,1′-carbonyldiimidazole intermediate, (*c*) purification of the reaction mixture by extraction of the diastereomeric derivatives into hexane at pH 11, and (*d*) analysis of the diastereomeric derivatives by HPLC with UV detection. The (*S*)-(+):(*R*)-(−) ratios in the blood of three subjects receiving single 100-mg oral doses of carprofen were greater than unity up to 16 hr after dosing. The mean ± *SD* of the ratios in the early blood samples (0.5, 1, and 2 hr) was 1.21 ± 0.09, while the mean of the ratios in the later blood samples (4, 6, 8, 12, and 16 hr) was slightly higher (1.48 ± 0.17). The blood level fall-off curves for the (*S*)-(+) and (*R*)-(−) enantiomers were similar in each of the three subjects for the 4–16-hr period. The carprofen enantiomers were excreted stereoselectively by humans. An excess of the (*S*)-(+) enantiomer relative to the (*R*)-(−) enantiomer was excreted in the urine as the ester glucuronide, while unchanged (*R*)-(−) enantiomer predominated in the feces. The total urinary plus fecal excretion of the enantiomers (0–96 hr) revealed only a slight excess of the (*S*)-(+) enantiomer over the (*R*)-(−) enantiomer, which amounted to 2.1–4.9% of the dose. Since the amount of carprofen (free and glucuronide) excreted in 96 hr by the three subjects only accounted for 62–72% of the dose, no definitive statement could be made relative to the possible inversion of the carprofen chiral center.



**Keyphrases** □ Carprofen—stereoselective disposition determination in humans using high-performance liquid chromatography □ Anti-inflammatory agents—carprofen, metabolism in humans, and rats, high-performance liquid chromatography □ High-performance liquid chromatography—determination of stereoselective disposition of carprofen in humans


Carprofen [(D,L)-6-chloro-α-methylcarbazole-2-acetic acid] is presently undergoing extensive clinical evaluation as a nonsteroidal anti-inflammatory agent. The possible stereoselective disposition of carprofen is of interest since it is a racemic compound with a chiral center at the α-carbon position. Other α-methylarylacetic acids have been shown to undergo stereoselective disposition and inversion at the α-carbon (1–5).

A TLC procedure was previously developed (6) for the quantitation of the enantiomers of [$^{14}$C]carprofen as their diastereomeric (*S*)-(−)-α-methylbenzylamides. This TLC procedure has been used to study stereoselective elimi-



© 1981, American Pharmaceutical Association

Table IV—Percentage of Recovery of Anthralin and Its Decomposition Products [a]

| Sample | Anthralin, % | Dimer, % | Quinone, % | Total Recovery, % |
|---|---|---|---|---|
| 1 | 88.5 | 7.2 | 1 | 96.7 |
| 2 | 92 | 9 | 2 | 103.0 |
| 3 | 80.9 | 15.5 | 2.2 | 98.6 |
| 4 | 72.6 | 25 | 1.3 | 98.9 |
| 5 | 71.2 | 4.7 | 1.1 | 77.0 |
| 6 | 70.5 | 25.1 | 1.8 | 97.4 |
| 7 | 69.0 | 22.4 | 1.7 | 93.1 |
| 8 | 67.4 | 29.5 | 1 | 97.9 |
| 9 | 39.0 | 10.4 | 1.2 | 50.6 |
| 10 | 29.8 | 2.5 | 12.9 | 45.2 |
| 11 | 17.3 | 81.1 | 5.9 | 104.3 |
| 12 | 4.4 | 90.9 | 5.1 | 100.4 |

[a] Chloroform extraction; average of data obtained using both chromatographic systems.

formation of high molecular weight materials, and an HPLC method is currently being developed for the analysis of these products.

The surprising disparity between the USP and HPLC assay results can be rationalized when the data in Table IV are considered. Although both methods rely on UV absorption, the USP technique cannot quantify the dimer and merely includes it with the anthralin level. However, a discrepancy between the results is still evident after correcting the USP data for the presence of dimer.

The majority of these ointments contained ~70% (range 44–92%) of the theoretical amount of anthralin, the remaining 30% being various quantities of the dimer, quinone, and, perhaps, high molecular weight materials.

The need to check anthralin and its preparations must be emphasized, and the danger of further decomposition of samples in use cannot be ignored.

## REFERENCES


(1) B. Squire, *Br. Med. J.*, **1**, 546 (1877). *Ibid.*, **1**, 199 (1877). B. Squire, *Arch. Dermatol. Synphilol.*, **10**, 332 (1877).

(2) A. Krebs and H. Schaltegger, *Hautarzt*, **20**, 204 (1969).

(3) M. Ponec-Waelsch and H. J. Hulsebosch, *Arch. Dermatol. Forsch.*, **249**, 141 (1974).

(4) H. M. Elsabbagh, C. W. Whitworth, and L. C. Schramm, *J. Pharm. Sci.*, **68**, 388 (1979).

(5) "The United States Pharmacopeia," 20th rev., United States Pharmacopeial Convention, Rockville, Md., 1980, p. 48.

(6) B. L. van Duuren, A. Segal, S.-S. Tseng, G. M. Rusch, G. Loewengart, U. Mate, D. Roth, A. Smith, S. Melchionne, and I. Seidman, *J. Med. Chem.*, **21**, 26 (1978).

(7) O. F. Schultz and G. Fry, *Arch. Pharm. (Weinheim)*, **310**, 776 (1977).


## ACKNOWLEDGMENTS


Presented in part at the Anthralin Symposium, Sophia Antipolis, France, October 1980.

The authors are indebted to Mr. J. Maignan for the preparation and purification of the anthralin derivatives. They also thank Professor H. Schaefer for advice and encouragement, and Dr. R. Baran, Hopital des Brousailles, Cannes, France, for supplying one formulation.


# High-Performance Liquid Chromatographic Determination of Stereoselective Disposition of Carprofen in Humans


**J. K. STOLTENBORG *, C. V. PUGLISI ‡, F. RUBIO *, and F. M. VANE *x**



Received January 26, 1981, from the **Department of Biochemistry and Drug Metabolism and the* ‡*Department of Pharmacokinetics and Biopharmaceutics, Hoffmann-La Roche Inc., Nutley, NJ 07110.* Accepted for publication March 25, 1981.



**Abstract** □ A high-performance liquid chromatographic (HPLC) assay was developed for the determination of the ratios of the (*S*)-(+) and (*R*)-(−) enantiomers of the anti-inflammatory drug carprofen in blood, urine, and feces. The procedure relies on: (*a*) extraction and purification of carprofen from biological fluids, (*b*) reaction of carprofen with (*S*)-(−)-α-methylbenzylamine to form the two diastereomeric (S)-(−)-α-methylbenzylamides *via* the 1,1′-carbonyldiimidazole intermediate, (*c*) purification of the reaction mixture by extraction of the diastereomeric derivatives into hexane at pH 11, and (*d*) analysis of the diastereomeric derivatives by HPLC with UV detection. The (*S*)-(+):(*R*)-(−) ratios in the blood of three subjects receiving single 100-mg oral doses of carprofen were greater than unity up to 16 hr after dosing. The mean ± *SD* of the ratios in the early blood samples (0.5, 1, and 2 hr) was 1.21 ± 0.09, while the mean of the ratios in the later blood samples (4, 6, 8, 12, and 16 hr) was slightly higher (1.48 ± 0.17). The blood level fall-off curves for the (*S*)-(+) and (*R*)-(−) enantiomers were similar in each of the three subjects for the 4–16-hr period. The carprofen enantiomers were excreted stereoselectively by humans. An excess of the (*S*)-(+) enantiomer relative to the (*R*)-(−) enantiomer was excreted in the urine as the ester glucuronide, while unchanged (*R*)-(−) enantiomer predominated in the feces. The total urinary plus fecal excretion of the enantiomers (0–96 hr) revealed only a slight excess of the (*S*)-(+) enantiomer over the (*R*)-(−) enantiomer, which amounted to 2.1–4.9% of the dose. Since the amount of carprofen (free and glucuronide) excreted in 96 hr by the three subjects only accounted for 62–72% of the dose, no definitive statement could be made relative to the possible inversion of the carprofen chiral center.



**Keyphrases** □ Carprofen—stereoselective disposition determination in humans using high-performance liquid chromatography □ Anti-inflammatory agents—carprofen, metabolism in humans, and rats, high-performance liquid chromatography □ High-performance liquid chromatography—determination of stereoselective disposition of carprofen in humans


Carprofen [(D,L)-6-chloro-α-methylcarbazole-2-acetic acid] is presently undergoing extensive clinical evaluation as a nonsteroidal anti-inflammatory agent. The possible stereoselective disposition of carprofen is of interest since it is a racemic compound with a chiral center at the α-carbon position. Other α-methylarylacetic acids have been shown to undergo stereoselective disposition and inversion at the α-carbon (1–5).

A TLC procedure was previously developed (6) for the quantitation of the enantiomers of [$^{14}$C]carprofen as their diastereomeric (*S*)-(−)-α-methylbenzylamides. This TLC procedure has been used to study stereoselective elimi-



© 1981, American Pharmaceutical Association

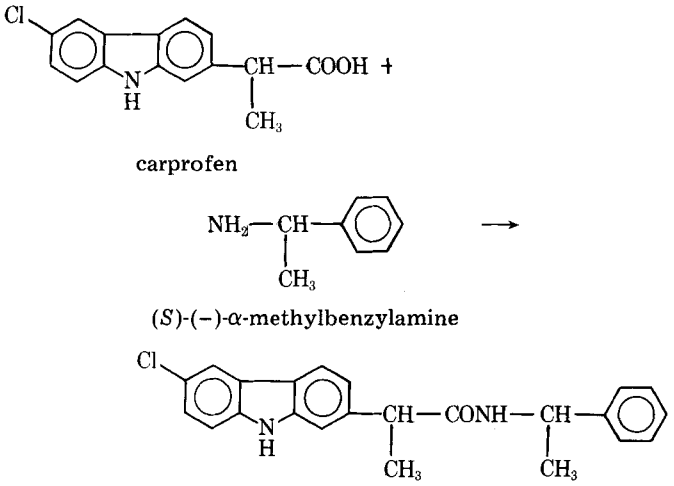

carprofen

(*S*)-(−)-α-methylbenzylamine

(*R,S*) and (*S,S*) diastereomeric amides of carprofen
*Scheme I*

nation of [$^{14}$C]carprofen in rats (6) and humans (7). In the rat, the (*R*)-(−) enantiomer is eliminated from the blood and secreted in the bile as the ester glucuronide at a rate approximately twice that of the (*S*)-(+) enantiomer. Concurrently, the (*S*)-(+) isomer, the pharmacologically more active enantiomer (8), persists longer in rat blood. Preliminary data suggested a preferred urinary elimination of the (*S*)-(+) enantiomer as the ester glucuronide and a preferred fecal elimination of the (*R*)-(−) enantiomer in humans (7).

This report describes a high-performance liquid chromatographic (HPLC) assay for the determination of the (*S*)-(+):(*R*)-(−) ratios of carprofen in biological fluids by measuring the diastereomeric (*S*)-(−)-α-methylbenzylamide derivatives of carprofen. Whereas the radio-TLC stereospecific assay depends on labeled carprofen for quantitation, the HPLC assay can be used to evaluate clinical specimens from studies using nonlabeled drugs. This stereospecific HPLC assay, in conjunction with other assays (9, 10) for total carprofen, was used to study the stereoselective disposition of carprofen in humans.

## EXPERIMENTAL

**Materials**—The procedure relies on the reaction of racemic carprofen with (*S*)-(−)-α-methylbenzylamine[1] to form the (*R,S*) and (*S,S*) diastereomers (Scheme I). However, the synthetic analytical standards, I and II, were prepared by reacting the carprofen enantiomers with (*R*)-(+)-α-methylbenzylamine. Therefore, standards I and II are the antipodes, respectively, of the (*R,S*) and (*S,S*) diastereomers formed in the carprofen reaction procedure. A solution of 32.5 mg of 1,1′-carbonyldiimidazole[1]/ml of chloroform was prepared daily.

*Carprofen*—Carprofen ($C_{15}H_{12}ClNO_2$) has a molecular weight of 273.72. A stock solution of 1 mg/ml in ethanol was prepared. Carprofen[2] labeled with carbon 14 in the α-position was used in certain experiments as indicated. The original specific activity of 9.91 μCi/mg was diluted in solution with appropriate amounts of unlabeled compound.

For the (*S*)-(+) enantiomer the specific rotation in methanol was $[\alpha]_D^{23}$ +53.7°; for the (R)-(−) enantiomer, the specific rotation in methanol was $[\alpha]_D^{23}$ −54.2°.

*Standard I*[3] [(S,R)-N-(*2-Phenethyl*)-α-*methyl*(*6-chloro-9H-carbazol-2-yl*)*acetamide*]—Standard I ($C_{23}H_{21}ClN_2O$) has a molecular weight of 376.88, mp 238–239°. It dissolved slowly in the HPLC solvent system (0.75% $CH_3OH$ in methylene chloride) at concentrations greater than 0.5 mg/ml.

*Standard II*[3] [(R,R)-N-(*2-Phenethyl*)-α-*methyl*(*6-chloro-9H-carbazol-2-yl*)*acetamide*]—Standard II ($C_{23}H_{21}ClN_2O$) has a molecular weight of 376.88, mp 191–193°. It was soluble in the HPLC solvent system at concentrations of 1.0 mg/ml.

*Reagents*—The following analytical reagent grade chemicals were used: 1 and 0.6 *N* NaOH, 0.1 and 6 *N* HCl, 1 and 0.2 *M* sodium acetate buffer (pH 5), 1 *M* potassium phosphate buffer (monobasic) (pH 7), 0.2 *N* $NH_4OH$ (pH 11), acetic acid, formic acid, methanol, ethanol (anhydrous), chloroform (stabilized with 0.75% ethanol), methylene chloride, UV quality hexane, and ether[4] (anhydrous).

*TLC*—TLC plates were precoated with silica gel 60F-254[5]. Filter paper[6] was used for lining the TLC tanks. A shortwave UV lamp was used for visualization of spots.

**Extraction and Purification of Carprofen from Biological Samples**—*Blood*—Five-milliliter aliquots of blood were adjusted to pH 5 with 2 ml of 1 *M* acetate buffer and extracted twice with 12 ml of ether. The blood–ether mixtures were shaken for 10 min in a reciprocating shaker[7] at 60–80 strokes/min and centrifuged[8] at 2400 rpm for 5 min at room temperature. The combined ether layers were evaporated to dryness with nitrogen in a 30–40° water bath[9]. The extract residues were dissolved

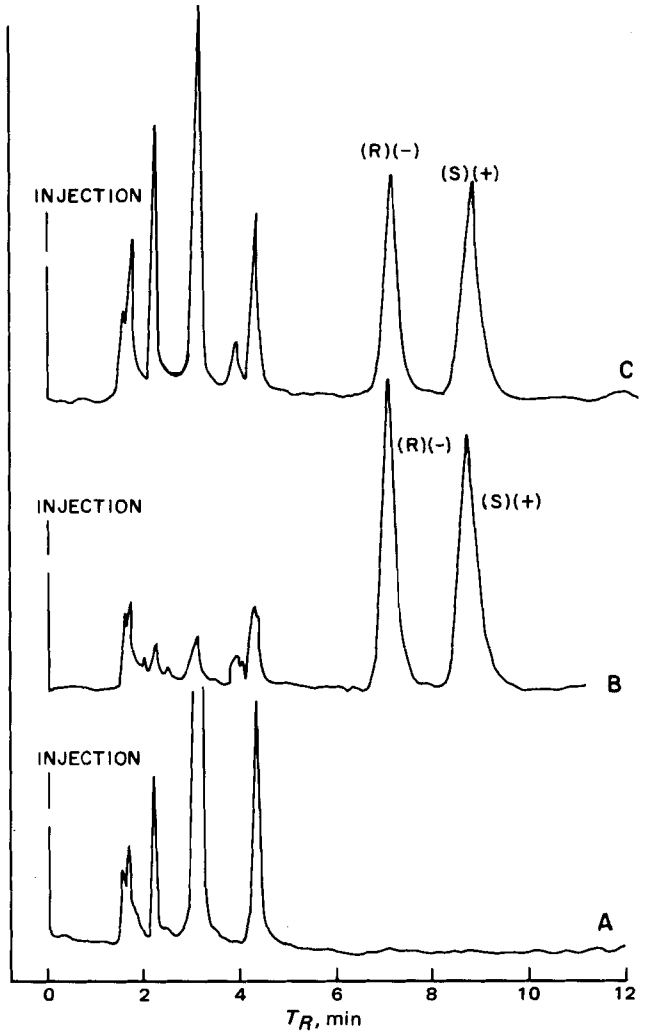


**Figure 1**—*HPLC (UV detection) of the products from the reaction with (S)(−)-α-methylbenzylamine. Key (A), reagent blank; B, standard carprofen; and C, control human urine spiked with carprofen. Peaks labeled (R)-(−) and (S)-(+) are the diastereomeric amides of the (R)-(−) and (S)-(+) enantiomers of carprofen, respectively.*

[1] Aldrich Chemical Co.
[2] $^{14}$C-Labeled carprofen was provided by Dr. A. Liebman and Dr. R. Muccino, Chemical Research Department, Hoffmann–LaRoche.
[3] Mr. L. Berger and Mr. A. Corraz, Chemical Research Department, Hoffmann–LaRoche, synthesized the analytical standards I and II.
[4] J. T. Baker Chemical Co.
[5] Brinkmann Instruments.
[6] Whatman No. 1.
[7] Eberbach.
[8] Model K, IEC Corp.
[9] Organomation Associates N-EVAP.

**Table I—HPLC ($N = 3$ [a]) Determination of the (*S*)-(+):(*R*)-(−) Values for Varying Amounts of Standard Carprofen**

| Amount of Carprofen Reacted, μg | (*S*)-(+):(*R*)-(−) Value Found | CV, % |
|---|---|---|
| 5 | 1.00 ± 0.03 | 3.0 |
| 10 | 1.01 ± 0.01 | 1.0 |
| 15 | 1.01 ± 0.01 | 1.0 |
| 20 | 1.01 ± 0.01 | 1.0 |
| Average | | 1.5% |

[a] Number of separate reactions on different days.

in 100 μl of ethanol and spotted on the TLC plate as 3-cm wide streaks.

The plate was developed with chloroform—acetic acid (90:10) until the solvent reached 14 cm from the origin. The UV-absorbing band corresponding to carprofen ($R_f$ 0.54) was well separated from biological impurities ($R_f$ 0.61). The silica gel containing carprofen was scraped off the plate and, after addition of 3 ml of 0.2 *M* acetate buffer (pH 5), was extracted twice with 5 ml of ether. The combined ether layers were evaporated to dryness.

*Urine*—Aliquots of 2–5 ml of urine were adjusted to pH 11 by the addition of 1 ml of 1 *N* NaOH. After standing 2 hr at room temperature to cleave the ester glucuronides, the solution was adjusted to pH 5 and the deconjugated carprofen was extracted twice with 10 ml of ether as already described. The ethanolic extract was spotted on a TLC plate, and the plate was developed using chloroform–ethanol–formic acid (90:10:5). Carprofen ($R_f$ 0.50) was extracted from the silica gel as previously described. When it was necessary to extract 10 ml of urine, two 5-ml aliquots were extracted in separate tubes and the extracts were combined before TLC analysis.

*Feces*—Feces were homogenized in ~10 volumes of ethanol–water (70:30), and a 10-ml aliquot of each homogenate was diluted with 5 ml of 1 *M* acetate buffer (pH 5). The resulting ethanolic suspension was extracted once with 20 ml of hexane–ether (3:2). The supernatant fraction was back-extracted with 5 ml of 0.6 *N* NaOH. After centrifugation, the hexane–ether phase was discarded. The alkaline layer was washed with 10 ml of ether and, after centrifugation, the ether was discarded. Then 0.5 ml of 6 *N* HCl and 2 ml of 1 *M* phosphate buffer (pH 7) were added to the alkaline extract. This solution was extracted twice with 10 ml of ether.

The residue of this ether extract was dissolved in 7.5 ml of ethanol–0.1 *N* HCl (4:1). This solution was washed twice with 10 ml of hexane, and the hexane was discarded after each washing. The ethanol–hydrochloric acid layer was diluted with 7.5 ml of water and extracted once with 15 ml of hexane–ether (3:2). The residue of the hexane–ether extract was dissolved in ethanol and spotted on a TLC plate. The plate was developed using chloroform–ethanol–acetic acid (90:10:1). Carprofen ($R_f$ 0.40) did not resolve from endogenous biological impurities in this system, necessitating redevelopment in another solvent system; chloroform–methanol–concentrated ammonium hydroxide (70:30:1) separated carprofen ($R_f$ 0.12) from the biological impurities. Carprofen was extracted from the silica gel as already described.

**Derivatization Procedure (Scheme I)**—The derivatization procedure is based on the method used by VanGiessen and Kaiser (11) for the GLC determination of the enantiomers of ibuprofen, an α-methylarylacetic acid. Carprofen standards were processed in duplicate with each series of unknowns in concentrations comparable to the expected carprofen concentrations in the unknowns (1.4–30 μg). The reaction was performed in 15-ml conical glass-stoppered centrifuge tubes. To the dried residues of the standards and the unknowns, 0.1 ml of the 1,1′-carbonyldiimidazole solution was added. Each tube was rotated to permit the reactant to contact the residue completely. The mixture was allowed to stand at room temperature for 5 min, then 10 μl of acetic acid and 25 μl of (*S*)-(−)-α-methylbenzylamine were added stepwise, and the solution was mixed well with a vibrating mixer. The solution was centrifuged briefly and then was allowed to react at room temperature for 20 min.

After completion of the reaction, 3 ml of 0.2 *N* $NH_4OH$ (pH 11) and 5 ml of hexane were added. The tubes were stoppered tightly, shaken for 10 min in a reciprocating shaker at 60–80 strokes/min, and centrifuged for 5 min. A 4.5-ml aliquot of the hexane extract was transferred to a 15-ml conical centrifuge tube and evaporated to dryness under nitrogen in a 30–40° water bath. After drying thoroughly for 5 min in a desiccator *in vacuo*, the residue was dissolved in 0.5– 2.0 ml of the HPLC mobile phase and a 10-μl aliquot was injected into the liquid chromatograph.

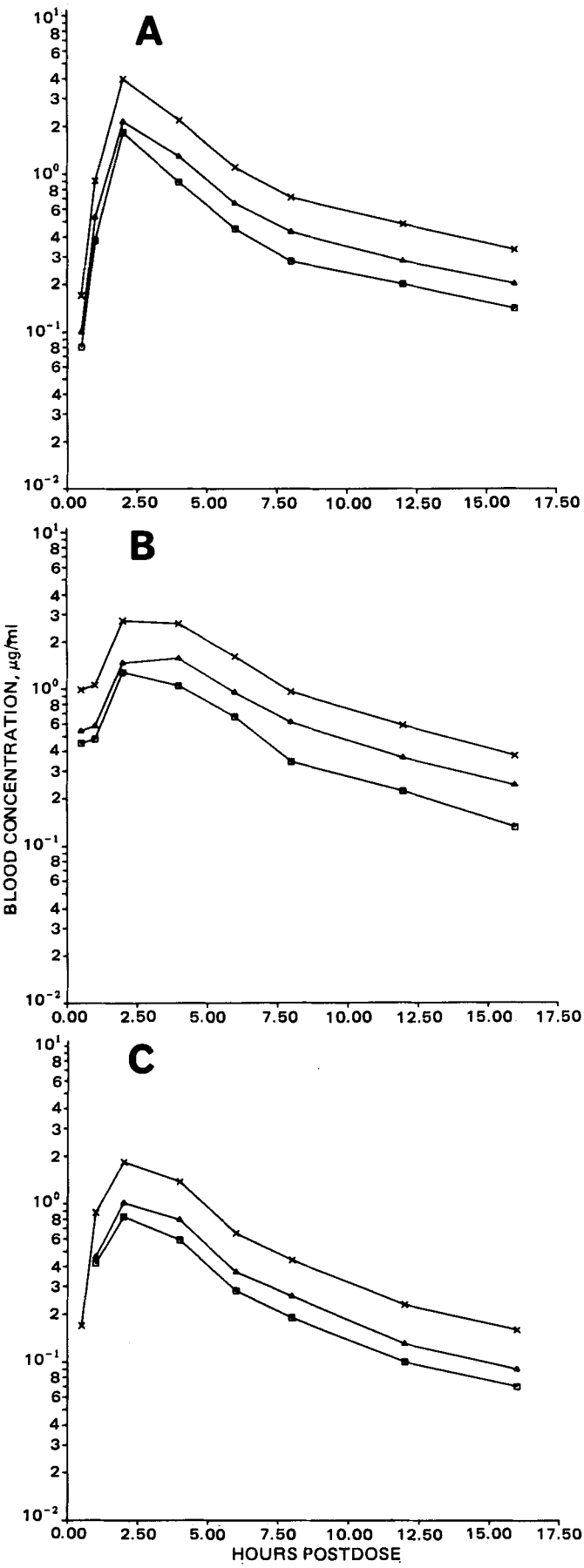


**Figure 2**—*Blood levels of carprofen (×) and of its (S)-(+) (△) and (R)-(−) (□) enantiomers in three subjects, each receiving 100 mg of carprofen. Key: A, Subject III/14; B, subject V/41; and C, subject V/42.*

**Table II—HPLC Determination of the (*S*)-(+):(*R*)-(−) Values of Synthetic Mixtures of (*S*)-(+) and (*R*)-(−) Carprofen Enantiomers in Human Blood and Urine**

| Sample | (*S*)-(+):(*R*)-(−) Value Added | Total Added, μg | Volume of Biological Sample, ml | (*S*)-(+):(*R*)-(−) Value Found ± *SD* | *n*[a] | *CV*, % |
|---|---|---|---|---|---|---|
| External standards | 0.34 | 17.5 | — | 0.33 ± 0.001 | 2 | 0.3 |
| | 1.07 | 19.4 | — | 1.11 ± 0.017 | 2 | 1.5 |
| | 1.99 | 29.8 | — | 2.00 ± 0.005 | 2 | 0.3 |
| Human blood | 1.07 | 10.1 | 5.0 | 1.11 ± 0.03 | 3 | 2.7 |
| | 1.50 | 10.5 | 5.0 | 1.5 ± 0.04 | 3 | 2.7 |
| | 1.99 | 10.8 | 5.0 | 2.02 ± 0.03 | 3 | 1.5 |
| Human urine | 0.49 | 21.6 | 1.0 | 0.48 ± 0.01 | 2 | 2.1 |
| | 1.07 | 23.3 | 1.0 | 1.08 ± 0.01 | 2 | 1.0 |
| | 1.50 | 24.2 | 1.0 | 1.39 ± 0.03 | 2 | 2.2 |

[a] *n* = number of replicate samples. Each reaction sample was analyzed twice by HPLC.

**Table III—Comparison of the HPLC Method with UV Detection and the Radio-TLC Method in Determining (*S*)-(+):(*R*)-(−) Values in Human Urine (Subject II) after a Single 50-mg Oral Dose of [$^{14}$C]Carprofen**

| Excretion period, hour | HPLC–UV | Radio-TLC |
|---|---|---|
| 0–2 | 1.25 | 1.30 |
| 2–4 | 1.26 | 1.34 |
| 4–6 | 1.27 | 1.27 |
| 6–9 | 1.16 | 1.16 |
| 9–12 | 1.19 | 1.20 |
| 12–24 | 1.27 | 1.24 |
| 24–48 | 1.01 | 0.986 |

[a] Average (*S*)-(+):(*R*)-(−) values are based on duplicate determinations of each specimen by each method.

**HPLC Analysis of Diastereomeric Derivatives of Carprofen**—*Column*—A 25-cm × 4.6-mm i.d. stainless steel column containing 10-μm silica gel[10] was used along with a guard column[11]. To maintain good performance, the column was sequentially washed (2.0 ml/min) with 200 ml of methanol, 200 ml of methylene chloride, 200 ml of *n*-heptane, and 60 ml of methylene chloride.

*Instrumental Parameters*—The liquid chromatograph[12] was equipped with a UV absorbance detector[13] operated at 254 nm and a solvent delivery system[14]. A fluorescence detector[15], operated at 240 nm for excitation and at wavelengths greater than 350 nm[16] for emission, was used for a limited number of HPLC analyses. The isocratic mobile phase was a mixture of 0.75% $CH_3OH$ in methylene chloride at a head pressure of 450 psi and at a constant flow rate of 2.0 ml/min. Solvents were routinely filtered and degassed[17] immediately before use.

The UV detector sensitivity was $1 \times 10^{-2}$ aufs, and the fluorescence detector sensitivity was 0.1 μA.F.s. The chart speed on the recorder[18] was 2.5 cm/min. A full-scale pen response was obtained with an injection of 75 ng of each diastereomer when operating in either detection mode. Under these conditions, the (*R*,*S*) diastereomer and standard I had the same retention time of 6.4 min with $k' = 5.1$. The (*S*,*S*) diastereomer and standard II had the same retention time of 7.6 min with $k' = 6.7$.

*Analytical Standards*—Separate stock solutions of standards I and II were prepared by dissolving 5.000 mg of the former and 5.041 mg of the latter in 500 ml of 0.75% $CH_3OH$ in methylene chloride. The stock solutions were diluted with this same solvent to prepare solutions of 5, 10, 25, 50, and 75 ng/10 μl. Ten-microliter aliquots of these solutions were injected as external standards for establishing the HPLC parameters. The computed UV peak areas, as well as peak heights, were plotted *versus* concentration, and the UV detector was shown to respond linearly and equivalently to both diastereomers.

*Quantitation and Calculations*—Free and total carprofen concentrations were determined in urine and feces of subjects given [$^{14}$C]carprofen by the radiometric method (6). Free carprofen in blood was quantitated by HPLC (9). UV detection and computer integration of the areas under the (*S*,*S*) and (*R*,*S*) diastereomer peaks were used to determine the (*S*)-(+):(*R*)-(−) ratios, which were applied to the carprofen concentrations to determine the concentrations of the individual carprofen enantiomers.

[10] Whatman Partisil 10 adsorbent.
[11] Whatman HC Pellosil packing (38 μm silica gel).
[12] Model ALC/GPC 204, Waters Associates.
[13] Model 440, Waters Associates.
[14] Model 6000A, Waters Associates.
[15] Schoeffel model FS-970.
[16] Corning No. 0-52 filter.
[17] All-glass filter apparatus, 47 mm, Millipore Corp.
[18] Hewlett-Packard model 7132A.

## RESULTS AND DISCUSSION

**Characteristics of Stereospecific Carprofen Assay**—Typical chromatograms for a reagent blank, standard carprofen, and spiked human urine are shown in Fig. 1. To minimize the presence of UV-absorbing impurities and to obtain adequate HPLC separation of the diastereomers, it was necessary to modify the procedures described in the original radio-TLC method (6). Extraction of the reaction product into hexane from an alkaline aqueous phase (instead of ether at pH 5) removed certain acidic and more polar by-products and provided a product sufficiently pure for direct HPLC analysis. The concentration of early eluting UV-absorbing impurities that interfered with the (*R*)-(−)-carprofen diastereomeric amide peak could be reduced satisfactorily by reacting carprofen with half the amount of each reagent used previously (6).

[$^{14}$C]Carprofen was used to determine the overall formation of the diastereomeric amides. The radioactivity determined in the reaction extract indicated that the reaction yield was 62.3 ± 2.9% (*SD*), equivalent to the yield found with the original procedure (6).

The overall percent recovery of carprofen from urine after extraction, preparative TLC, a second extraction, derivatization, and final extraction was 39.3 ± 2.3% (*SD*) with a detection limit of 0.6 μg/ml when 10 ml was extracted. The feces assay had a recovery of 29.2 ± 3.75% with a detection limit of 0.6 μg/ml of homogenate when a 10-ml aliquot of homogenate was extracted. The blood assay had a recovery of 41.5 ± 8.3% with a limit of detection of 0.27 μg/ml when a 5-ml aliquot was extracted.

Table I presents the statistical evaluation of the (*S*)-(+):(*R*)-(−) values found for carprofen reacted over a range of concentrations. The results show that the method is reproducible. Therefore, modification of the derivatization and extraction procedure did not affect overall yield and reproducibility.

To check the accuracy and precision of the method, biological samples spiked with carprofen were analyzed. The following mean (*S*)-(+):(*R*)-(−) ratios (±*SD*) were found at the indicated concentrations of carprofen: 0.27 μg/ml in blood, 1.03 ± 0.05 ($n = 4$); 0.83 μg/ml in blood, 0.98 ± 0.04 ($n = 9$); 1.0 μg/ml in urine, 0.99 ± 0.02 ($n = 7$); 2 μg/ml in urine, 0.99 ± 0.01 ($n = 3$); and 22 μg/ml of fecal homogenate, 1.02 ± 0.03 ($n = 3$). In addition, blood and urine were spiked with synthetic mixtures of carprofen enantiomers with varying (*S*)-(+):(*R*)-(−) ratios. The coefficients of variation of the ratios found were ≤2.7% (Table II). These results indicate that the method is accurate and precise.

Fluorescence detection was used for determining the (*S*)-(+):(*R*)-(−) values in a limited number of samples. Carprofen standards of 10 and 20 μg were reacted, and the diastereomers were quantitated by computer-integration of the peak areas or by measurement of peak heights. The (*S*)-(+):(*R*)-(−) values had a mean of 0.987 ± 0.012 (± *SD*) ($n = 22$). Fluorescence detection shows promise as an alternative detection mode, especially when UV contaminants are present.

**Application to Biological Specimens**—To compare the radio-TLC and HPLC methods, urine samples from a subject who had ingested 50 mg of [$^{14}$C]carprofen (0.5 μCi/mg) were analyzed by both methods. The (*S*)-(+):(*R*)-(−) ratios obtained by the two methods were nearly identical (Table III).

Blood specimens were obtained from three human subjects who were

**Table IV—Determination of (*S*)-(+):(*R*)-(−) Values in Human Blood following a Single 100-mg Oral Dose of Carprofen [a]**

| Subject | Hours after Administration | | | | | | | |
|---|---|---|---|---|---|---|---|---|
| | 0.5 | 1.0 | 2.0 | 4.0 | 6.0 | 8.0 | 12.0 | 16.0 |
| III/14 | 1.23 | 1.40 | 1.16 | 1.45 | 1.46 | 1.52 | 1.41 | 1.40 |
| V/41 | 1.19 | 1.22 | 1.15 | 1.51 | 1.35 | 1.77 | 1.65 | 1.92 |
| V/42 | NA[b] | 1.08 | 1.22 | 1.35 | 1.31 | 1.38 | 1.40 | 1.36 |

[a] Ratios for Subjects III/14 and V/41 were determined by the HPLC method, and the ratios for Subject V/42 were determined using a fluorometric TLC procedure. For the latter subject, carprofen was extracted by the standard procedure from 9–11 ml aliquots of blood containing 0.2–1.8 μg of carprofen. After cleanup of carprofen by extraction with sodium hydroxide and by TLC, the diastereomeric derivatives were formed, separated by TLC, and extracted from the silica gel bands with 2.5 ml of ethanol–1% acetic acid. Comparison of the fluorescence intensities measured at 370 nm (emitting wavelength) after activating at 295 nm resulted in the fluorescence (*S*)-(+):(*R*)-(−) ratios for racemic carprofen of 0.986 ± 0.002. [b] Not analyzed.

**Table V—Urinary and Fecal Excretion of Carprofen and Its Individual Enantiomers in Three Human Subjects Following Single 50-mg Doses of [$^{14}$C] Carprofen**

| Excreta | Excretion Period, hr | Carprofen and Enantiomer Excretion in Percent of Dose | | | | | | | | | | | | | | |
|---|---|---|---|---|---|---|---|---|---|---|---|---|---|---|---|---|
| | | Subject I | | | | | Subject II | | | | | Subject III | | | | |
| | | Total Carbon 14 | Total[a] (T) or Free (F) Carprofen | (*S*)-(+):(*R*)-(−) | (*S*)-(+) | (*R*)-(−) | Total Carbon 14 | Total[a] (T) or Free (F) Carprofen | (*S*)-(+):(*R*)-(−) | (*S*)-(+) | (*R*)-(−) | Total Carbon 14 | Total[a] (T) or Free (F) Carprofen | (*S*)-(+):(*R*)-(−) | (*S*)-(+) | (*R*)-(−) |
| Urine | 0–24 | 57.6 | 53.5 T | 1.2[b] | 29.2 | 24.3 | 62.4 | 53.4 T | 1.3[b] | 30.2 | 23.2 | 44.8 | 39.7 | 1.3[b] | 22.4 | 17.3 |
| | 24–48 | 9.6 | 8.3 T | 1.0 | 4.2 | 4.2 | 5.7 | 4.6 T | 1.0 | 2.3 | 2.3 | 7.7 | 6.3 | 1.1 | 3.3 | 3.0 |
| | 48–72 | 4.2 | 3.3 T | 0.7 | 1.4 | 1.9 | 2.4 | 2.0 T | NA[c] | NA | NA | 2.5 | 2.0 | 1.0 | 1.0 | 1.0 |
| | 0–72 | 71.4 | 65.1 T | | 34.8 | 30.4 | 70.5 | 60.0 T | | 32.5[d] | 25.5[d] | 55.0 | 48.0 | | 26.7 | 21.3 |
| Feces | 0–24 | ND[e] | ND | NA | NA | NA | 3.0 | 2.0 F | NA | NA | NA | 1.0 | NA | NA | NA | NA |
| | 24–48 | 3.6 | 2.0 F | 0.4 | 0.6 | 1.4 | 1.0 | 0.3 F | 0.3 | 0.1 | 0.2 | 19.6 | 10.0 | 0.4 | 1.2 | 2.9 |
| | 48–72 | 3.1 | 2.0 F | 0.4 | 0.6 | 1.4 | 4.4 | 2.0 F | 0.3 | 0.5 | 1.5 | 8.5 | 3.0 | 0.5 | 0.7 | 1.6 |
| | 72–96 | 5.1 | 3.0 F | NA | NA | NA | 4.3 | 2.0 F | 0.3 | 0.5 | 1.5 | 3.5 | 1.0 | 0.5 | 0.4 | 1.1 |
| | 0–96[d] | 11.8 | 7.0 F | | 1.2 | 2.8 | 12.7 | 6.3 F | | 1.1 | 3.2 | 32.6 | 14.0 | | 2.3 | 5.6 |
| Total (urine and Feces)[d] | | 83.2 | 72.1 F | | 36.0 | 33.2 | 83.2 | 66.3 F | | 33.6 | 28.7 | 87.6 | 62.0 | | 29.0 | 26.9 |

[a] Free carprofen plus ester glucuronide. [b] The (*S*)(+):(*R*)-(−) values were determined for the excretion periods 0–2, 2–4, 4–6, 6–9, 9–12, and 12–24. The mean (*S*-)(+):(*R*)-(−) values for 0–24 hr are presented. The standard deviation was ±0.1 in each case. [c] Not analyzed. [d] These sums for carprofen and its enantiomers are minimum values because not all samples over the time period were analyzed. However, the samples not analyzed contained little radioactivity so their absence should not significantly affect the total excretion values. [e] Not detected.

each administered a single oral dose of 100 mg of carprofen[19]. Intact carprofen had been shown by Rubio *et al.* (10) to be the predominant component in human plasma during the first 12 hr after single-dose administration. Data on the enantiomeric ratios in the blood are presented in Table IV. The (*S*)-(+) enantiomer exceeded the (*R*)-(−) enantiomer at all time points, which is consistent with previous results (7). In addition, there was a small increase in the (*S*)-(+):(*R*)-(−) ratios with respect to time. The mean (± *SD*) of the ratios in the 4–16-hr blood samples was 1.48± 0.17, which was significantly higher ($p < 0.001$, Student *t* test) than the mean (± *SD*) of 1.21 ± 0.09 found for the early blood samples (0.5–2 hr). The relatively constant (*S*)-(+):(*R*)-(−) ratios in the 4–16-hr blood samples from the three human subjects resulted in parallel fall-off curves for the two enantiomers (Fig. 2). This finding suggests that assays for total carprofen would reflect the concentration of the pharmacologically more active (*S*)-(+) enantiomer, at least during this time period.

Previously a larger increase in (*S*)-(+):(*R*)-(−) ratios was seen in the blood of two rats given carprofen intravenously (6). The 1-hr blood samples had ratios of 1.14 and 1.21, while the 6-hr blood samples had ratios of 2.09 and 2.39. In these rats, the (*R*)-(−) enantiomer was eliminated from the blood at a rate approximately twice that of the (*S*)-(+) isomer. Therefore, the stereoselective disposition of carprofen is more pronounced in rats than in humans.

Rubio *et al.* (10) reported that three human subjects administered single oral 50-mg doses of [$^{14}$C]carprofen excreted (0–120 hr) a mean (± *SD*) of 2.8 ± 0.5% of the dose in the urine as free carprofen and 63.1 ± 10.8% as carprofen ester glucuronide. In the feces, a mean of 7% of the dose was recovered as directly extractable intact carprofen. Similar results were obtained by Ray *et al.* (12) after administration of single 100-mg doses of [$^{14}$C]carprofen to three human subjects.

Urine and fecal samples from the Rubio *et al.* study (10) were analyzed by the stereospecific assay (Table V). In all urine samples collected between 0 and 24 hr, the (*S*)-(+) enantiomer exceeded the (*R*)-(−) enantiomer; after 24 hr, urinary (*S*)-(+):(*R*)-(−) values were close to unity with the exception of the 48–72-hr urine of Subject I where the ratio was 0.7. The (*R*)-(−) enantiomer of free carprofen predominated in all fecal samples between 24 and 96 hr. These data demonstrate the stereoselective excretion of carprofen by humans.

Other α-methylarylacetic acids that are structurally related to carprofen undergo stereoselective inversion. Cicloprofen undergoes (*R*)-(−) to (*S*)-(+) inversion in rats (2, 3), monkeys (2), and dogs (4), and both ibuprofen (1) and benoxaprofen (5) undergo (*R*)-(−) to (*S*)-(+) inversion in humans. In each case, inversion was unequivocally demonstrated by the administration of the (*R*)-(−) enantiomer. Only the racemic mixture of carprofen has been given to humans. The amount of the (*S*)-(+) enantiomer of carprofen in the total urinary and fecal excretion exceeded the amount of the (*R*)-(−) enantiomer by only 2.1–4.9% of the dose (Table V). The data did not show any significant amount of stereoselective inversion of carprofen. However, since excreted carprofen accounted for only 62–72% of the administered dose, stereoselective inversion cannot be excluded as a possibility.

[19] Three normal volunteers, each receiving a single 100-mg dose of carprofen, were part of a study conducted by Dr. James D. Moore, University of Montana Foundation, Deer Lodge, Mont.

## REFERENCES


(1) D. G. Kaiser, G. J. VanGiessen, R. J. Reischer, and W. J. Wechter, *J. Pharm. Sci.*, **65**, 269 (1976).

(2) S. J. Lan, K. J. Kripalani, A. V. Dean, P. Egli, L. T. DiFazio, and E. C. Schreiber, *Drug Metab. Dispos.*, **4**, 330 (1976).

(3) A. V. Dean, S. J. Lan, K. J. Kripalani, L. T. DiFazio, and E. C. Schreiber, *Xenobiotica*, **7**, 549 (1977).

(4) K. J. Kripalani, A. Z. El-Abdin, A. V. Dean, and E. C. Schreiber, *ibid.*, **6**, 159 (1976).

(5) R. J. Bopp, J. F. Nash, A. S. Ridolfo, and E. R. Shepard, *Drug Metab. Dispos.*, **7**, 356 (1979).

(6) J. M. Kemmerer, F. A. Rubio, R. M. McClain, and B. A. Koechlin, *J. Pharm. Sci.*, **68**, 1274 (1979).

(7) J. Kemmerer, B. A. Koechlin, and F. Rubio, *Fed. Proc. Fed. Am. Soc. Exp. Biol.*, **37**, Abstr. 2075, 605 (1978).

(8) Z. N. Gaut, H. Baruth, L. O. Randall, C. Ashley, and J. R. Paulsrud, *Prostaglandins*, **10**, 59 (1975).

(9) C. V. Puglisi, J. C. Meyer, and J. A. F. deSilva, *J. Chromatogr.*, **136**, 391 (1977).

(10) F. Rubio, S. Seawall, R. Pocelinko, B. DeBarbieri, W. Benz, L. Berger, L. Morgan, J. Pao, T. H. Williams, and B. Koechlin, *J. Pharm. Sci.*, **69**, 1245 (1980).
(11) G. J. VanGiessen and D. G. Kaiser, *ibid.*, **64**, 798 (1975).
(12) J. E. Ray, D. N. Wade, and G. G. Graham, *Clin. Exp. Pharmacol. Phys.*, **6**, 175 (1979).

**ACKNOWLEDGMENTS**

The authors thank Dr. Lester Weissman, Department of Clinical Pharmacology, and Dr. James D. Moore, University of Montana Foundation, for the blood samples. They also thank Dr. M. A. Schwartz for constructive suggestions and Mrs. Kathleen Heusser and Mrs. Carole Eggert for assistance in preparation of this manuscript.

# Hydration and Percutaneous Absorption II: Influence of Hydration on Water and Alkanol Permeation through Swiss Mouse Skin; Comparison with Hairless Mouse

**CHARANJIT R. BEHL *x and MICHAEL BARRETT**

Received January 5, 1981, from the *College of Pharmacy, University of Michigan, Ann Arbor, MI 48109.* Accepted for publication March 16, 1981. *Present address: Pharmaceutical Research, Roche Laboratories, Hoffmann–La Roche Inc., Nutley, NJ 07110.

**Abstract** □ *In vitro* permeation studies with biological membranes often involve long, aqueous maceration of the tissue. The present investigation examined the possible effects of hydration on barrier integrity of Swiss mouse skin, using water, methanol, ethanol, and butanol as permeants and a previously developed procedure involving multiple, sequential permeation runs on each piece of skin. The permeation rate of water increased almost linearly up to 30 hr of hydration and then tended to level off. Transport rates of methanol and ethanol increased asymptotically and then plateaued at ~15 hr. These results contrast with earlier findings on hairless mouse skin where the permeabilities of these three compounds were unaffected by aqueous immersion. The permeation rate of butanol also increased during the first 15 hr of hydration but gradually declined over the next 25 hr. This result again contrasts with the hairless mouse species in which butanol permeability doubled in 10 hr and then plateaued. The species differences in the hydration profiles appear related to the vastly dissimilar pellages and, in the Swiss mouse, may indicate greater involvement of the transfollicular pathway.

**Keyphrases** □ Hydration—effect on water and alkanol permeation through Swiss mouse skin, comparison with hairless mouse □ Absorption, percutaneous—effect of hydration on water and alkanol permeation through Swiss mouse skin, comparison with hairless mouse □ Permeability—effect of hydration on water and alkanol absorption through Swiss mouse skin, comparison with hairless mouse

A previous study (1) on the influence of long aqueous immersion (hydration) on the permeability properties of hairless mouse skin used a method involving sequenced, *in vitro* diffusional experiments on each skin membrane. Hydration-related alterations of the permeation behaviors of a series of compounds were systematically investigated, and the observed effects were related to the physicochemical properties of the permeants and mass transport mechanism. The permeabilities of water, methanol, and ethanol were not affected by immersion of the skin in normal saline. The permeabilities of butanol and hexanol doubled and reached asymptotes in 10 hr of hydration. The permeation rate of heptanol only increased by ~50%, while octanol showed an initial 50% increase followed by a 25% decline to assume an invariant rate with a net 25% hydration-induced alteration.

In view of the experimental and possible mechanistic significance of the hydration-induced permeability alterations, the present study compared the influence of hydration on the skin permeability of the Swiss mouse, to that of the hairless mouse. The results obtained proved the skins of the two species to be exceedingly different in their chemical barrier properties, both in terms of absolute rates of permeation of the low molecular weight alcohols and in their hydration sensitivities.

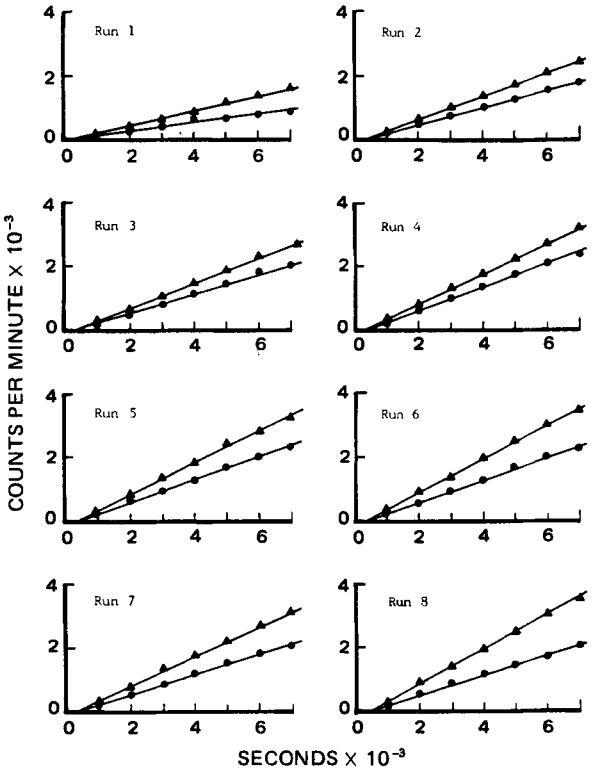


**Figure 1**—*Series of receiver concentration* versus *time profiles for eight sequential permeation runs on a single skin. This figure is one set of data from the methanol (▲)–butanol (●) series detailed in the text. Key: Run 1, $t_0$ = 0 hr; Run 2, $t_0$ = 5 hr; Run 3, $t_0$ = 10 hr; Run 4, $t_0$ = 15 hr; Run 5, $t_0$ = 20 hr; Run 6, $t_0$ = 25 hr; Run 7, $t_0$ = 30 hr; and Run 8, $t_0$ = 43 hr.*

## EXPERIMENTAL

**Chemicals**—[$^3$H]Water[1], [$^3$H]methanol[1], [$^{14}$C]ethanol[2], and [$^{14}$C]-butanol[2] were used as received. The radiochemicals were diluted into 0.9%

[1] New England Nuclear, Boston, MA 02218.
[2] International Chemical and Nuclear Corp., Irvine, CA 92715.



0022-3549/81/1100-1212$01.00/0
© 1981, American Pharmaceutical Association

(10) F. Rubio, S. Seawall, R. Pocelinko, B. DeBarbieri, W. Benz, L. Berger, L. Morgan, J. Pao, T. H. Williams, and B. Koechlin, *J. Pharm. Sci.*, **69**, 1245 (1980).
(11) G. J. VanGiessen and D. G. Kaiser, *ibid.*, **64**, 798 (1975).
(12) J. E. Ray, D. N. Wade, and G. G. Graham, *Clin. Exp. Pharmacol. Phys.*, **6**, 175 (1979).

**ACKNOWLEDGMENTS**

The authors thank Dr. Lester Weissman, Department of Clinical Pharmacology, and Dr. James D. Moore, University of Montana Foundation, for the blood samples. They also thank Dr. M. A. Schwartz for constructive suggestions and Mrs. Kathleen Heusser and Mrs. Carole Eggert for assistance in preparation of this manuscript.

# Hydration and Percutaneous Absorption II: Influence of Hydration on Water and Alkanol Permeation through Swiss Mouse Skin; Comparison with Hairless Mouse

**CHARANJIT R. BEHL *x and MICHAEL BARRETT**

Received January 5, 1981, from the *College of Pharmacy, University of Michigan, Ann Arbor, MI 48109.* Accepted for publication March 16, 1981. *Present address: Pharmaceutical Research, Roche Laboratories, Hoffmann–La Roche Inc., Nutley, NJ 07110.

**Abstract** □ *In vitro* permeation studies with biological membranes often involve long, aqueous maceration of the tissue. The present investigation examined the possible effects of hydration on barrier integrity of Swiss mouse skin, using water, methanol, ethanol, and butanol as permeants and a previously developed procedure involving multiple, sequential permeation runs on each piece of skin. The permeation rate of water increased almost linearly up to 30 hr of hydration and then tended to level off. Transport rates of methanol and ethanol increased asymptotically and then plateaued at ~15 hr. These results contrast with earlier findings on hairless mouse skin where the permeabilities of these three compounds were unaffected by aqueous immersion. The permeation rate of butanol also increased during the first 15 hr of hydration but gradually declined over the next 25 hr. This result again contrasts with the hairless mouse species in which butanol permeability doubled in 10 hr and then plateaued. The species differences in the hydration profiles appear related to the vastly dissimilar pellages and, in the Swiss mouse, may indicate greater involvement of the transfollicular pathway.

**Keyphrases** □ Hydration—effect on water and alkanol permeation through Swiss mouse skin, comparison with hairless mouse □ Absorption, percutaneous—effect of hydration on water and alkanol permeation through Swiss mouse skin, comparison with hairless mouse □ Permeability—effect of hydration on water and alkanol absorption through Swiss mouse skin, comparison with hairless mouse

A previous study (1) on the influence of long aqueous immersion (hydration) on the permeability properties of hairless mouse skin used a method involving sequenced, *in vitro* diffusional experiments on each skin membrane. Hydration-related alterations of the permeation behaviors of a series of compounds were systematically investigated, and the observed effects were related to the physicochemical properties of the permeants and mass transport mechanism. The permeabilities of water, methanol, and ethanol were not affected by immersion of the skin in normal saline. The permeabilities of butanol and hexanol doubled and reached asymptotes in 10 hr of hydration. The permeation rate of heptanol only increased by ~50%, while octanol showed an initial 50% increase followed by a 25% decline to assume an invariant rate with a net 25% hydration-induced alteration.

In view of the experimental and possible mechanistic significance of the hydration-induced permeability alterations, the present study compared the influence of hydration on the skin permeability of the Swiss mouse, to that of the hairless mouse. The results obtained proved the skins of the two species to be exceedingly different in their chemical barrier properties, both in terms of absolute rates of permeation of the low molecular weight alcohols and in their hydration sensitivities.

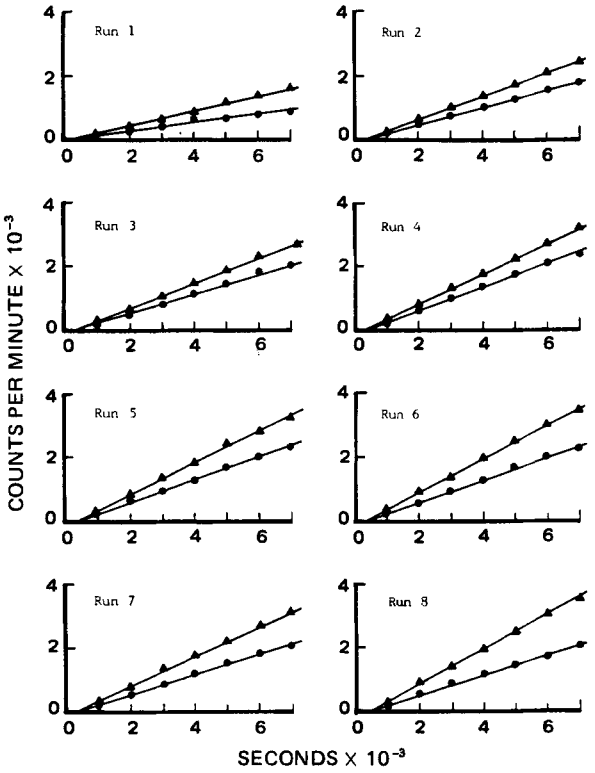


**Figure 1**—*Series of receiver concentration* versus *time profiles for eight sequential permeation runs on a single skin. This figure is one set of data from the methanol (▲)–butanol (●) series detailed in the text. Key: Run 1, $t_0$ = 0 hr; Run 2, $t_0$ = 5 hr; Run 3, $t_0$ = 10 hr; Run 4, $t_0$ = 15 hr; Run 5, $t_0$ = 20 hr; Run 6, $t_0$ = 25 hr; Run 7, $t_0$ = 30 hr; and Run 8, $t_0$ = 43 hr.*

## EXPERIMENTAL

**Chemicals**—[$^3$H]Water[1], [$^3$H]methanol[1], [$^{14}$C]ethanol[2], and [$^{14}$C]-butanol[2] were used as received. The radiochemicals were diluted into 0.9%

[1] New England Nuclear, Boston, MA 02218.
[2] International Chemical and Nuclear Corp., Irvine, CA 92715.



0022-3549/81/1100-1212$01.00/0
© 1981, American Pharmaceutical Association

**Table I—Summary of Hydration Effect Data for Water**

| Hours of Hydration | $P \times 10^3$, cm/hr Mouse 1 (33.0 g) | Mouse 2 (38.0 g) | Mouse 3 (33.0 g) | Mouse 4 (36.5 g) | Mouse 5 (35.5 g) | Average $P \times 10^3 \pm SD$, cm/hr |
|---|---|---|---|---|---|---|
| 0 | 5.1 | 2.2 | 5.6 | 1.9 | 5.3 | 4.0 ± 1.8 |
| 5 | 6.1 | 2.8 | 6.2 | 6.3 | 4.0 | 5.1 ± 1.6 |
| 10 | 6.3 | 3.6 | 6.6 | 7.4 | 5.9 | 6.0 ± 1.4 |
| 15 | 7.1 | 4.5 | 7.4 | 8.3 | 9.5 | 7.4 ± 1.9 |
| 20 | 8.1 | 5.1 | 8.9 | 10.6 | 11.9 | 8.9 ± 2.6 |
| 25 | 8.6 | 5.7 | 9.3 | 10.6 | 13.7 | 9.6 ± 2.9 |
| 30 | 8.9 | 8.6 | 10.5 | 11.7 | 14.9 | 10.9 ± 2.6 |
| 48 | 9.7 | 8.2 | 11.6 | 11.4 | 17.7 | 11.7 ± 3.6 |

**Table II—Summary of Hydration Effect Data for Methanol**

| Hours of Hydration | $P \times 10^3$, cm/hr Mouse 1 (34.5 g) | Mouse 2 (36.0 g) | Mouse 3 (38.0 g) | Mouse 4 (34.0 g) | Mouse 5 (33.0 g) | Average $P \times 10^3 \pm SD$, cm/hr |
|---|---|---|---|---|---|---|
| 0 | 2.6 | 5.7 | 9.8 | 6.3 | 2.7 | 5.4 ± 3.0 |
| 5 | 4.2 | 7.1 | 10.0 | 8.5 | 2.7 | 6.5 ± 3.0 |
| 10 | 5.6 | 7.7 | 10.8 | 9.8 | 3.2 | 7.4 ± 3.1 |
| 15 | 7.3 | 9.6 | 12.2 | 12.1 | 3.9 | 9.0 ± 3.5 |
| 20 | 7.9 | 9.8 | 12.4 | 12.7 | 4.1 | 9.4 ± 3.5 |
| 25 | 7.6 | 10.7 | 13.2 | 13.3 | 4.2 | 9.8 ± 3.9 |
| 30 | 7.6 | 11.0 | 11.9 | 12.9 | 4.1 | 9.5 ± 3.6 |
| 43 | 7.2 | 11.0 | 13.4 | 13.0 | 4.2 | 9.8 ± 4.0 |

sodium chloride irrigation solution[3] (saline) for permeation experiments. The final chemical concentration in the diffusional medium was $\leq 10^{-4}$ *M*.

**Animals**—Male Swiss mice[4], albino out bred of Skh:Icr strains, had free access to food and water, and bedding was changed at least once a week.

**Hair Removal**—All skins used in the diffusion experiments were denuded of hair. Usual depilation methods, *i.e.*, shaving and chemical depilation, were avoided because they might seriously alter the barrier properties (2, 3). Hair from the abdominal surface of the freshly sacrificed mouse was removed by the nondestructive and nonirritating procedure of close cropping with a pair of surgical scissors.

**Permeation Procedure**—Two-compartment glass diffusion cells (1) were employed to determine skin permeability. All membranes sandwiched between the half-cells were full-thickness skin sections excised from the abdominal surfaces of Swiss mice, freshly sacrificed by spinal cord dislocation. Mouse age was tightly confined (~180 days) to avoid age-related effects (4). The external medium of the diffusion cell was saline, and the half-cell contents were stirred at 150 rpm. All experiments were carried out at 37°. The concentration in the receiver chamber (dermis side) was monitored with time for ~2 hr.

Complete hydration profiles were obtained on each skin by carrying out eight sequential experiments, with rinsing between runs (1). The

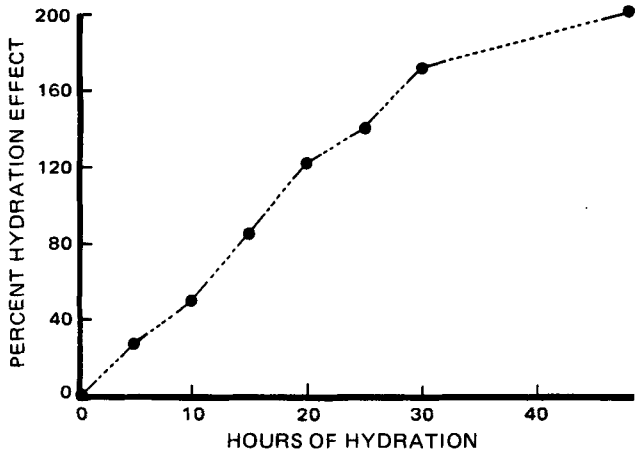


**Figure 2**—*Plot of hydration effects* versus *hydration time for water.*

[3] Abbott Laboratories, North Chicago, IL 60064.

[4] Skin Cancer Hospital, Temple University, Philadelphia, PA 19104.

**Table III—Summary of Hydration Effect Data for Ethanol**

| Hours of Hydration | $P \times 10^3$, cm/hr Mouse 1 (33.0 g) | Mouse 2 (38.0 g) | Mouse 3 (33.0 g) | Mouse 4 (36.5 g) | Mouse 5 (35.5 g) | Average $P \times 10^3 \pm SD$, cm/hr |
|---|---|---|---|---|---|---|
| 0 | 3.7 | 1.7 | 4.3 | 3.5 | 2.7 | 3.2 ± 1.0 |
| 5 | 4.4 | 2.7 | 4.7 | — | 4.8 | 4.2 ± 1.0 |
| 10 | 4.8 | 3.2 | 4.8 | 4.6 | 5.9 | 4.7 ± 1.0 |
| 15 | 5.2 | 3.3 | 5.3 | 5.4 | 8.1 | 5.5 ± 1.7 |
| 20 | 5.3 | 3.5 | 5.9 | 4.0 | 10.1 | 5.8 ± 2.6 |
| 25 | 5.0 | 4.3 | 5.2 | 4.3 | 11.0 | 6.0 ± 2.8 |
| 30 | 5.6 | 4.2 | 5.5 | 4.9 | 11.4 | 6.3 ± 2.9 |
| 48 | 4.7 | 3.6 | 5.7 | 4.8 | 10.9 | 5.9 ± 2.9 |

**Table IV—Summary of Hydration Effect Data for Butanol**

| Hours of Hydration | $P \times 10^3$, cm/hr Mouse 1 (33.0 g) | Mouse 2 (38.0 g) | Mouse 3 (33.0 g) | Mouse 4 (36.5 g) | Mouse 5 (35.5 g) | Average $P \times 10^3 \pm SD$, cm/hr |
|---|---|---|---|---|---|---|
| 0 | 8.3 | 6.1 | 8.7 | 9.0 | 5.7 | 7.6 ± 1.5 |
| 5 | 14.4 | 10.4 | 12.8 | 15.5 | 8.2 | 12.3 ± 3.0 |
| 10 | 15.7 | 11.6 | 14.6 | 16.8 | 8.7 | 13.5 ± 3.3 |
| 15 | 18.8 | 14.7 | 16.6 | 20.6 | 10.9 | 16.3 ± 3.8 |
| 20 | 20.3 | 13.5 | 14.8 | 19.7 | 9.7 | 15.6 ± 4.4 |
| 25 | 19.1 | 14.0 | 13.7 | 19.6 | 10.1 | 15.3 ± 4.0 |
| 30 | 18.6 | 14.6 | 11.8 | 19.5 | 9.5 | 14.8 ± 4.3 |
| 43 | 16.3 | 11.9 | 13.4 | 18.3 | 8.9 | 13.8 ± 3.7 |

permeant concentration was determined radioisotopically using a liquid scintillation counter[5] with Aquasol[1] as the cocktail. A technique of dual labels was employed to study the permeation of $^3$H- and $^{14}$C-labeled penetrants simultaneously (4).

**Data Analysis**—The data were plotted as the receiver compartment concentration as a function of time. Each permeability coefficient was calculated from (1):

$$P = \frac{V}{A}\frac{(dC/dt)}{\Delta C} \qquad \text{(Eq. 1)}$$

where

$P$ = permeability coefficient (centimeters per hour)
$A$ = diffusional area (~0.6 cm$^2$)
$\Delta C$ = concentration difference across the membrane, which was taken to be equal to the donor concentration (counts per minute per cm$^3$)
$V$ = receiver half-cell volume (1.4 ml)
$dC/dt$ = steady-state slope (counts per minute per cubic centimeter per hour)

## RESULTS AND DISCUSSION

Figure 1 contains eight subplots obtained in sequential permeation experiments carried out on one piece of skin over 43 hr with [$^3$H]methanol and [$^{14}$C]butanol as the dual permeants. Under the experimental conditions, the linear relationship between the receiver concentration and time (which develops in each run) is representative of a quasi steady-state

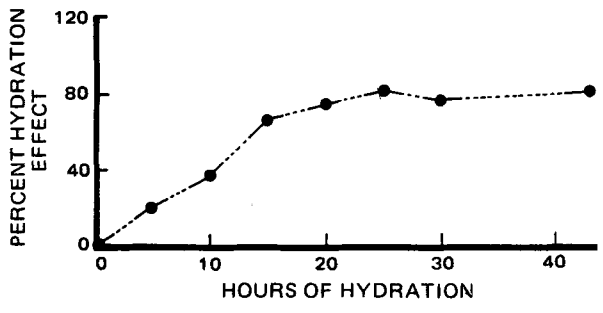


**Figure 3**—*Plot of hydration effects* versus *hydration time for methanol.*

[5] Model LS 9000, Beckman Instruments, Fullerton, Calif.

**Table V—Summary of Hydration Effects**

| Hours of Hydration | Percent Hydration Effect[a] | | | |
|---|---|---|---|---|
| | Water | Methanol | Ethanol | Butanol |
| 0 | 0.0 | 0.0 | 0.0 | 0.0 |
| 5 | 27.5 | 20.4 | 31.3 | 61.8 |
| 10 | 50.0 | 37.0 | 46.9 | 77.6 |
| 15 | 85.0 | 66.7 | 71.9 | 114.5 |
| 20 | 122.5 | 74.1 | 81.3 | 105.3 |
| 25 | 140.0 | 81.5 | 87.5 | 101.3 |
| 30 | 172.5 | 75.9 | 96.9 | 94.7 |
| 43[b] or 48[c] | 192.5 | 81.5 | 84.4 | 81.6 |

[a] Equation 2. [b] Methanol and butanol. [c] Water and ethanol.

transport process. Slopes of these linear segments were used to compute the permeability coefficients (Eq. 1).

Five mice were used for each of the four penetrants, and eight sequential experiments were run on each skin, yielding a total of 160 diffusion experiments. Permeability coefficients computed from 20 figures analogous to Fig. 1 are reported in Tables I–IV for water, methanol, ethanol, and butanol, respectively. Rather large animal-to-animal variations in the permeability coefficients were found for all four permeants. Similar variability was observed in earlier studies with the hairless mouse skin (1, 4). However, within a given piece of skin, permeabilities changed systematically and stereotypically for a given compound. The "percent hydration effect" was calculated from:

$$\text{percent hydration effect} = \frac{P\text{ (at a given hydration time)} - P\text{ (at zero hydration)}}{P\text{ (at zero hydration)}} \times 100 \quad \text{(Eq. 2)}$$

These derived numbers are given in Table V. To illustrate the hydration influences, the results (percentage changes) were plotted as a function of hydration time (Figs. 2–5).

Of all the permeants studied in the Swiss mouse skin, water experienced the largest increase in permeability during the aqueous immersion. Figure 2 shows that the percentage increase in permeability rose almost linearly up to 30 hr of immersion but then showed signs of leveling off. The hydration sensitivity for water was markedly different than that reported for the hairless species (1) where water penetration rates were not significantly altered by the soaking treatment. Methanol's permeability also increased with time of immersion but only up to ~20 hr. Beyond this point, the net hydration increase remained essentially invariant at 78.3 ± 3.8% (average of data at 20, 25, 30, and 48 hr of hydration). Ethanol exhibited similar behavior, with an asymptote value of 87.5 ± 6.7% (average of data at 20, 25, 30, and 48 hr of hydration). The close parallelism in the hydration profiles of methanol and ethanol may imply that both solutes penetrate the Swiss mouse skin *via* a common route. The results represent a great departure from hairless mouse data (1), which indicate no hydration-induced alterations for either methanol or ethanol.

Butanol's permeability through Swiss mouse skin also rose during the first 15 hr of aqueous immersion. Data gathered beyond this time are difficult to interpret since butanol's permeability appears to decline between 15 and 43 hr in an almost linear manner. The absolute permeability coefficients at 15 and 43 hr are not statistically separable. However, the lack of a statistically supported difference may be the result of interanimal variability since all five Swiss mouse skins showed an approximate 20% decline in butanol's permeability coefficient over 15–43 hr. Moreover, the butanol data were obtained using the dual-label procedure with methanol as the copermeant, and the permeability coefficient

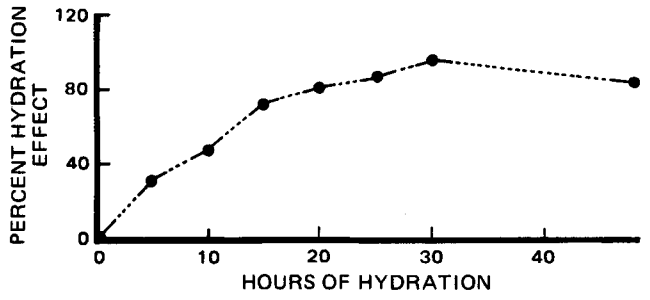


**Figure 4**—*Plot of hydration effects* versus *hydration time for ethanol.*

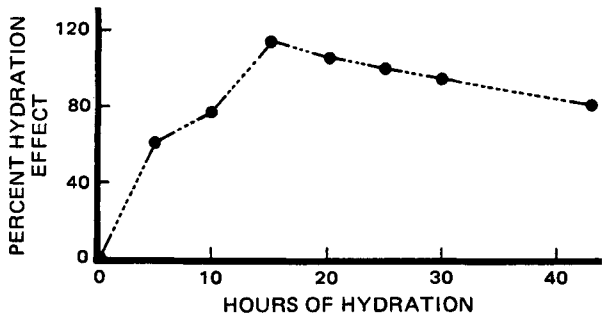


**Figure 5**—*Plot of hydration effects* versus *hydration time for butanol.*

for methanol was invariant past ~20 hr. It was tentatively concluded that when hydrating conditions are sustained past 15 hr, there is a small but real depreciation of the permeability coefficient of butanol. For hairless mouse skin, butanol's permeability coefficient doubled over the initial 10-hr immersion and then remained constant (1). Thus, with the lower alkanols and water, the skin of the Swiss species behaved qualitatively differently from that of hairless species.

**Possible Explanation of Observed Hydration Profiles**—*Water, Methanol, and Ethanol*—It was pointed out (4) that the polar solutes (water, methanol, and ethanol) do not appear to permeate the skin of the hairless mouse by the main lipoidal pathway, presumably located within the stratum corneum, but use an alternative parallel diffusional route of either transfollicular or transepidermal origin. In the mature hairless mouse, most follicles are cystic, the atrophied remains of an early coat of hair, and are not visually prominent. However, the Swiss mouse is abundantly covered with actively cycling hair follicles containing prominent hairs. Given this difference between the two species, it might be expected for a follicularly placed polar pathway that hydrophilic permeants would have greatly enhanced permeabilities through Swiss mouse skin. The permeability coefficients for water, methanol, and ethanol were indeed several times larger in the Swiss species than in the hairless species, particularly when compared in the fully hydrated states.

The qualitative differences in hydration sensitivities between the two types of mice are of even greater significance. Water gradually plasticized some critical phase of the Swiss mouse skin and opened it to more facile diffusion of the small polar solutes. In contrast, the permeabilities of water, methanol, and ethanol through hairless mouse skin were unaffected by long immersion. Quantitative considerations aside, there is obviously some fundamental difference in tissue structure and the barrier mechanism. These changes may be due to an enhanced follicular mechanism in the Swiss mouse. In this case, gradual hydration and softening of the sebaceous medium would explain the overall effects. However, the skin is integrated tissue and increased follicular density and hair prominency have been associated with a less well-formed horny layer. Thus, the critical changes possibly are associated with different degrees and qualities of cornification.

*Butanol*—Permeation of butanol was reported (1,4) to occur transepidermally by partitioning into the lipoid components of the stratum corneum of hairless mouse skin. This process is believed to occur in the Swiss species as well. Therefore, the hydration-related permeability changes in the Swiss species could be due to some modification of the lipoidal pathway in the stratum corneum. However, the exact mechanism for either species is unknown.

**Significance of Present Studies**—The influence of hydration needs to be considered in the design of skin permeation studies, and the exact state of hydration should be reported. This study suggests a possible means of factoring transepidermal and the transfollicular pathways. Given the possible association of the hair follicles and hydration-induced alterations in skin permeability, clinically different results of the occlusive dressing might be expected between hairy and nonhairy human surfaces.

## REFERENCES

(1) C. R. Behl, G. L. Flynn, T. Kurihara, N. Harper, W. Smith, W. I. Higuchi, N. F. H. Ho, and C. L. Pierson, *J. Invest. Dermatol.*, **75**, 346 (1980).

(2) L. Park, C. R. Behl, and G. L. Flynn, in "Abstracts," 128th Annual Meeting, American Pharmaceutical Association, St. Louis, Mo., Mar. 30, 1981 (Basic Pharmaceutics Abstract 23).

(3) P. Campbell, T. Watanabe, and S. K. Chanderasekaran, *Fed. Proc. Fed. Soc. Exp. Biol.*, **35**, 639 (1976).

(4) C. R. Behl, G. L. Flynn, T. Kurihara, W. M. Smith, N. Harper, O. G. Gatmaitan, C. L. Pierson, W. I. Higuchi, and N. F. H. Ho, in "Abstracts," 126th APS Annual Meeting, American Pharmaceutical Association, Anaheim, Calif., Apr. 21–26, 1979 (Basic Pharmaceutics Abstracts 82).

**ACKNOWLEDGMENTS**

Presented in part at the Basic Pharmaceutics Section, APhA Academy of Pharmaceutical Sciences, Washington, D.C. meeting, April 1980 (Abstract 35).

Supported in part by National Institutes of Health Grant GM 24611.

# Stability-Indicating High-Performance Liquid Chromatographic Analysis of Lidocaine Hydrochloride and Lidocaine Hydrochloride with Epinephrine Injectable Solutions

**SIGMUND M. WARASZKIEWICZ ˣ, E. A. MILANO, and R. DiRUBIO**

Received December 12, 1980, from *Astra Pharmaceutical Products, Inc., Worcester, MA 01606.* Accepted for publication March 24, 1981.

**Abstract** □ A reversed-phase, high-performance liquid chromatographic (HPLC) procedure, which is specific and quantitative for lidocaine hydrochloride, epinephrine, and methylparaben, was developed for the analysis of lidocaine hydrochloride and lidocaine hydrochloride with epinephrine solutions for injection. Epinephrine sulfonic acid and adrenochrome are separated in this system. Also separated are lidocaine and methylparaben and their respective degradation products, 2,6-xylidine and *p*-hydroxybenzoic acid. The analysis requires that three detectors (two UV and one electrochemical) be connected in series. By using this arrangement, lidocaine hydrochloride and methylparaben are quantitated by UV at 254 and 280 nm, respectively, while epinephrine is quantitated electrochemically. The method is simple, accurate, precise, and rapid. No sample preparation or internal standard is necessary, and only a 2-μl sample volume is required for analysis. Chromatographic conditions include a μBondapak CN column and a mobile phase of 0.01 *M* 1-octanesulfonic acid sodium salt, 0.1 m*M* edetate disodium, 2% acetic acid, 2% acetonitrile, and 1% methanol in water.

**Keyphrases** □ High-performance liquid chromatography—specific and quantitative stability-indicating procedure for lidocaine hydrochloride, epinephrine, and methylparaben □ Lidocaine hydrochloride—injectable solutions of epinephrine using stability-indicating high-performance liquid chromatography □ Epinephrine—high-performance liquid chromatographic procedure for assaying components of injectable solutions □ Methylparaben—high-performance liquid chromatography for assaying components of injectable solutions

A literature review indicated that the various colorimetric and fluorometric methods utilized for the analysis of epinephrine in local anesthetic solutions all have problems associated with them (1, 2). The colorimetric methods generally are not stability indicating. Epinephrine sulfonic acid and bisulfite interfere with the development of the color, resulting in a lack of specificity for intact epinephrine.

A fluorometric procedure, based on the trihydroxyindole reaction first observed by Loew (3) and later modified (4, 5), is specific for epinephrine but is subject to many variables such as time, temperature, pH, presence of bisulfite, and the composition of the final alkaline/ascorbate reagent. The current USP (6) method for assaying epinephrine in lidocaine hydrochloride injectable solutions is a fluorometric procedure; although the method is specific for epinephrine, its application requires a great deal of experience and technique. The fluorometric procedure for the analysis of epinephrine in lidocaine hydrochloride injectable solutions has been automated (7) but is subject to interferences.

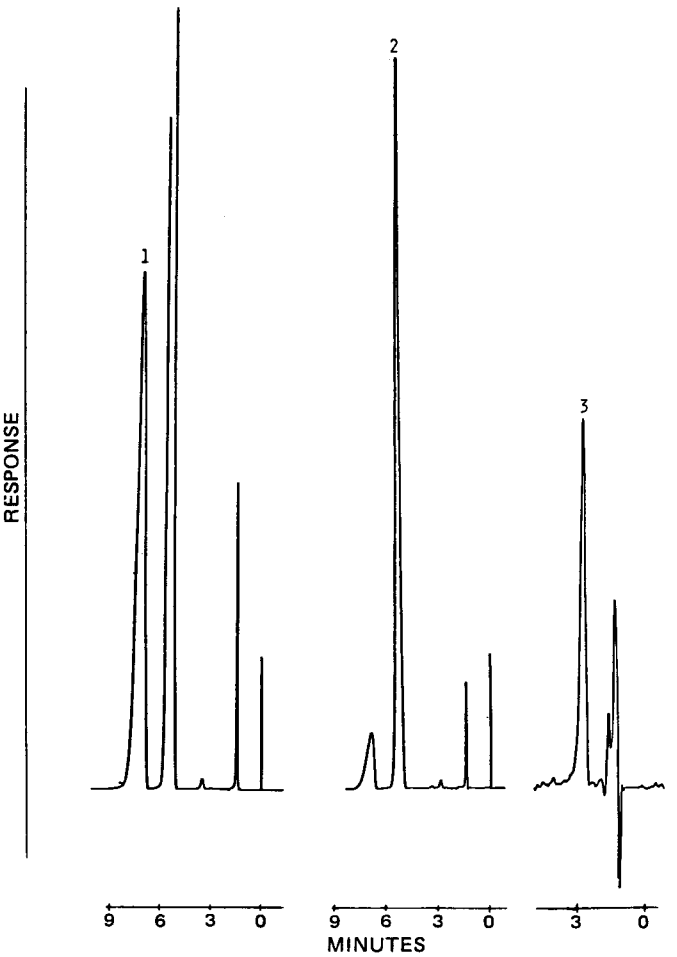


**Figure 1**—*Representative chromatograms of a 2-μl injection of a 2% lidocaine hydrochloride with 1:100,000 epinephrine solution, showing simultaneous detection of lidocaine (1) with UV detector at 254 nm, methylparaben (2) with UV detector at 280 nm, and epinephrine (3) with electrochemical detector at +0.90 v.*

0022-3549/81/1100-1215$01.00/0
© 1981, American Pharmaceutical Association

(3) P. Campbell, T. Watanabe, and S. K. Chanderasekaran, *Fed. Proc. Fed. Soc. Exp. Biol.*, **35**, 639 (1976).

(4) C. R. Behl, G. L. Flynn, T. Kurihara, W. M. Smith, N. Harper, O. G. Gatmaitan, C. L. Pierson, W. I. Higuchi, and N. F. H. Ho, in "Abstracts," 126th APS Annual Meeting, American Pharmaceutical Association, Anaheim, Calif., Apr. 21–26, 1979 (Basic Pharmaceutics Abstracts 82).

**ACKNOWLEDGMENTS**

Presented in part at the Basic Pharmaceutics Section, APhA Academy of Pharmaceutical Sciences, Washington, D.C. meeting, April 1980 (Abstract 35).

Supported in part by National Institutes of Health Grant GM 24611.

# Stability-Indicating High-Performance Liquid Chromatographic Analysis of Lidocaine Hydrochloride and Lidocaine Hydrochloride with Epinephrine Injectable Solutions

**SIGMUND M. WARASZKIEWICZ ˣ, E. A. MILANO, and R. DiRUBIO**

Received December 12, 1980, from *Astra Pharmaceutical Products, Inc., Worcester, MA 01606.* Accepted for publication March 24, 1981.

**Abstract** □ A reversed-phase, high-performance liquid chromatographic (HPLC) procedure, which is specific and quantitative for lidocaine hydrochloride, epinephrine, and methylparaben, was developed for the analysis of lidocaine hydrochloride and lidocaine hydrochloride with epinephrine solutions for injection. Epinephrine sulfonic acid and adrenochrome are separated in this system. Also separated are lidocaine and methylparaben and their respective degradation products, 2,6-xylidine and *p*-hydroxybenzoic acid. The analysis requires that three detectors (two UV and one electrochemical) be connected in series. By using this arrangement, lidocaine hydrochloride and methylparaben are quantitated by UV at 254 and 280 nm, respectively, while epinephrine is quantitated electrochemically. The method is simple, accurate, precise, and rapid. No sample preparation or internal standard is necessary, and only a 2-μl sample volume is required for analysis. Chromatographic conditions include a μBondapak CN column and a mobile phase of 0.01 *M* 1-octanesulfonic acid sodium salt, 0.1 m*M* edetate disodium, 2% acetic acid, 2% acetonitrile, and 1% methanol in water.

**Keyphrases** □ High-performance liquid chromatography—specific and quantitative stability-indicating procedure for lidocaine hydrochloride, epinephrine, and methylparaben □ Lidocaine hydrochloride—injectable solutions of epinephrine using stability-indicating high-performance liquid chromatography □ Epinephrine—high-performance liquid chromatographic procedure for assaying components of injectable solutions □ Methylparaben—high-performance liquid chromatography for assaying components of injectable solutions

A literature review indicated that the various colorimetric and fluorometric methods utilized for the analysis of epinephrine in local anesthetic solutions all have problems associated with them (1, 2). The colorimetric methods generally are not stability indicating. Epinephrine sulfonic acid and bisulfite interfere with the development of the color, resulting in a lack of specificity for intact epinephrine.

A fluorometric procedure, based on the trihydroxyindole reaction first observed by Loew (3) and later modified (4, 5), is specific for epinephrine but is subject to many variables such as time, temperature, pH, presence of bisulfite, and the composition of the final alkaline/ascorbate reagent. The current USP (6) method for assaying epinephrine in lidocaine hydrochloride injectable solutions is a fluorometric procedure; although the method is specific for epinephrine, its application requires a great deal of experience and technique. The fluorometric procedure for the analysis of epinephrine in lidocaine hydrochloride injectable solutions has been automated (7) but is subject to interferences.

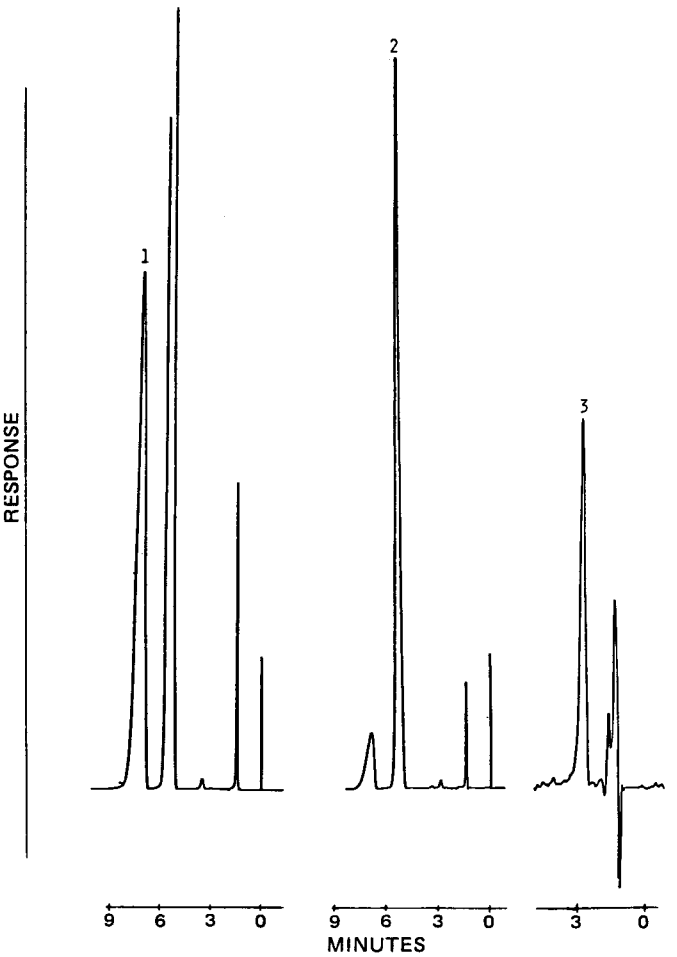


**Figure 1**—*Representative chromatograms of a 2-μl injection of a 2% lidocaine hydrochloride with 1:100,000 epinephrine solution, showing simultaneous detection of lidocaine (1) with UV detector at 254 nm, methylparaben (2) with UV detector at 280 nm, and epinephrine (3) with electrochemical detector at +0.90 v.*

0022-3549/81/1100-1215$01.00/0
© 1981, American Pharmaceutical Association

A high-performance liquid chromatographic (HPLC) method for epinephrine in local anesthetic solutions, which utilized a UV detector, was developed in this laboratory, but it lacked the specificity and sensitivity needed to be stability indicating. The development of electrochemical detectors for HPLC (8) and their subsequent application in the analysis of catecholamines in biological systems (9, 10) opened an entirely new possibility for the analysis of epinephrine in local anesthetic preparations. By coupling the electrochemical detector in series with a UV detector, it was possible to develop a specific, stability-indicating method that not only allowed for improved analysis of epinephrine but also permitted the simultaneous analysis of methylparaben and lidocaine hydrochloride (Fig. 1).

## EXPERIMENTAL

**Apparatus**—Analyses were performed on a liquid chromatograph[1] equipped with a 6000-psi solvent delivery system[2] and a septumless injector[3]. Detection of methylparaben and lidocaine was carried out with a dual-channel fixed-wavelength UV detector[4]. The methylparaben was quantitated at 280 nm, and the lidocaine hydrochloride was quantitated at 254 nm. Detection of epinephrine was carried out with a glassy carbon thin-layer detector cell[5] operated with an amperometric controller[6] at a potential of +0.90 v relative to a silver–silver chloride reference electrode[7]. The inlet of the electrochemical detector was connected to the outlet of the UV detector. The prepacked column[8] (30 cm × 4 mm i.d.) was operated at ambient temperature at a flow rate of 2.0 ml/min.

**Reagents**—1-Octanesulfonic acid sodium salt[9], edetate disodium[10], acetic acid[11], acetonitrile[12], methanol[13], methylparaben[14], and lidocaine hydrochloride monohydrate USP[15] were used as received. Epinephrine bitartrate USP reference standard[16] was dried in a vacuum desiccator over silica gel for at least 3 hr before use and subsequently stored in a desiccator over silica gel.

**Mobile Phase**—The mobile phase consisted of 0.01 *M* 1-octanesulfonic acid sodium salt, 0.1 m*M* edetate disodium, 2% (v/v) acetic acid, 2% (v/v) acetonitrile, and 1% (v/v) methanol in high quality distilled water. To minimize random electrical noise spikes from the electrochemical detector, the mobile phase should be degassed daily by filtering through a 0.45-μm filter[17] connected to an aspirator.

**Stock Solutions**—*Epinephrine*[18]—An appropriate quantity (Table I) of epinephrine bitartrate USP reference standard was weighed accurately into the appropriate size volumetric flask, 0.01 *N* HCl was added, and the solution was diluted to volume with 0.01 *N* HCl and mixed. The solution is stable for 1 week if refrigerated.

*Methylparaben*—In a 250-ml volumetric flask, 625 mg of methylparaben (accurately weighed) was added to 10 ml of acetonitrile and stirred until completely dissolved. The solution was diluted to volume with distilled water and mixed. Then the solution was cooled to room temperature and diluted to volume with distilled water. Occasionally, upon standing, some methylparaben crystallized out; it was redissolved by heating, but care was taken to recool to room temperature before pipetting for preparation of the standards.

*Lidocaine Hydrochloride*[18]—An appropriate quantity (Table I) of lidocaine hydrochloride monohydrate USP was weighed accurately into a 100-ml volumetric flask and distilled water was added; then the solution was diluted to volume with distilled water and mixed.

**Table I—Weight Guidelines for the Preparation of Stock Solutions and Standards for Various Lidocaine Hydrochloride–Epinephrine Products**

| Sample | Stock Solution | Recommended Dilution | Resulting Concentration |
|---|---|---|---|
| | Epinephrine[a] | | |
| 1:50,000 | ~18 mg/100 ml of 0.01 *N* HCl | 5:25 | ~20 μg/ml |
| 1:100,000 | ~23 mg/250 ml of 0.01 *N* HCl | 5:25 | ~10 μg/ml |
| 1:200,000 | ~23 mg/500 ml of 0.01 *N* HCl | 5:25 | ~5.0 μg/ml |
| | Methylparaben[b] | | |
| 1.00 mg/ml | ~625 mg/250 ml of distilled water | 10:25 | ~1.0 mg/ml |
| | Lidocaine Hydrochloride[c] | | |
| 0.5% | ~1.56 g/100 ml of distilled water | 9:25 (8:25) | ~5.3 (~4.7), mg/ml |
| 1.0% | ~3.11 g/100 ml of distilled water | 9:25 (8:25) | ~10.5 (~9.4), mg/ml |
| 1.5% | ~4.67 g/100 ml of distilled water | 9:25 (8:25) | ~15.8 (~14.1), mg/ml |
| 2.0% | ~6.22 g/100 ml of distilled water | 9:25 (8:25) | ~21.0 (~18.7), mg/ml |

[a] Epinephrine (μg/ml) = [epinephrine bitartrate (mg)/volume (ml)] × (183.21/333.30) × (5/25) × 1000. [b] Methylparaben (mg/ml) = [methylparaben (mg)/250] × (10/25). [c] Lidocaine hydrochloride (mg/ml) = [lidocaine HCl · $H_2O$ (g)/100] × (270.8/288.8) × [9(8)/25] × 1000.

**Standard Solutions**—Two standards (one at ~95% and one at ~105% of the expected lidocaine hydrochloride concentration) are required for the quantitation of the lidocaine hydrochloride if calculated utilizing peak heights. (Preliminary data indicated that only one standard is necessary if peak areas are utilized for the quantitation.)

*Standard I*—Five milliliters of the appropriate (Table I) epinephrine stock solution, 10 ml of methylparaben stock solution, and 9 ml of the appropriate (Table I) lidocaine hydrochloride stock solution were pipetted into a 25-ml volumetric flask, diluted to volume with distilled water, and mixed.

*Standard II*—Five milliliters of the epinephrine stock solution used for Standard I, 10 ml of methylparaben stock solution, and 8 ml of the lidocaine hydrochloride stock solution used for Standard I were pipetted into a 25-ml volumetric flask, diluted to volume with distilled water, and mixed.

The lidocaine hydrochloride monohydrate salt was used to prepare the stock solutions, but the final concentrations of the standards are reported as anhydrous lidocaine hydrochloride.

**Chromatography**—The column was conditioned with mobile phase for 0.5 hr at a flow rate of 2 ml/min before use. The electrochemical detector was turned on 0.5 hr before use. Standard I (2 μl) was injected repeatedly until the peak height response for all peaks of interest was reproducible to ±1–2%. The retention times of epinephrine, methylparaben, and lidocaine are ~3, ~5, and ~7 min, respectively. The flow rate was varied slightly to compensate for minor column-to-column differences. Two-microliter injections of the standards and samples were made, ensuring that each series of samples was bracketed by an injection of Standards I and II.

**Calculations**—The following calculations were used.

1. epinephrine (micrograms per milliliter) = (peak height of epinephrine in sample divided by average peak height of epinephrine in Standards I and II) × concentration of epinephrine in standards (micrograms per milliliter)

2. methylparaben (milligrams per milliliter) = (peak height of methylparaben in sample divided by average peak height of methylparaben in Standards I and II) × concentration of methylparaben in standards (milligrams per milliliter)

For lidocaine hydrochloride (milligrams per milliliter)[19], the equation of the line is determined where $Y_I$ and $Y_{II}$ are the peak heights for lidocaine hydrochloride in Standards I and II and $X_I$ and $X_{II}$ are the concentrations (milligrams per milliliter) of lidocaine hydrochloride in Standards I and II, respectively. The peak height ($Y_s$) for lidocaine hy-

[1] Model ALC/GPC 204, Waters Associates, Milford, MA 01757.
[2] Model 6000A, Waters Associates, Milford, MA 01757.
[3] Model U6K, Waters Associates, Milford, MA 01757.
[4] Model 440, Waters Associates, Milford, MA 01757.
[5] Model TL-5, Bioanalytical Systems, West Lafayette, IN 47906.
[6] Model LC-4, Bioanalytical Systems, West Lafayette, IN 47906.
[7] Model RC-2, Bioanalytical Systems, West Lafayette, IN 47906.
[8] μBondapak CN, 10 μm, Waters Associates, Milford, MA 01757.
[9] Eastman Kodak Co., Rochester, NY 14650.
[10] Analytical reagent grade, Mallinckrodt Chemical Works, St. Louis, MO 63134.
[11] Analytical reagent grade, J. T. Baker Chemical Co., Phillipsburg, NJ 08865.
[12] Low UV, distilled in glass, Burdick & Jackson Laboratories, Muskegon, MI 49442.
[13] Anhydrous, distilled in glass, Burdick & Jackson Laboratories, Muskegon, MI 49442.
[14] J. T. Baker Chemical Co., Phillipsburg, NJ 08865.
[15] Astra Pharmaceutical Products, Worcester, MA 01606.
[16] USP–NF Reference Standards, Rockville, MD 20852.
[17] Type HA, Millipore Corp., Bedford, MA 01730.
[18] Appropriate dilutions of the stock solutions may be made instead of separate stock solutions for each concentration.
[19] This entire calculation can be performed on any calculator capable of linear regression analysis.

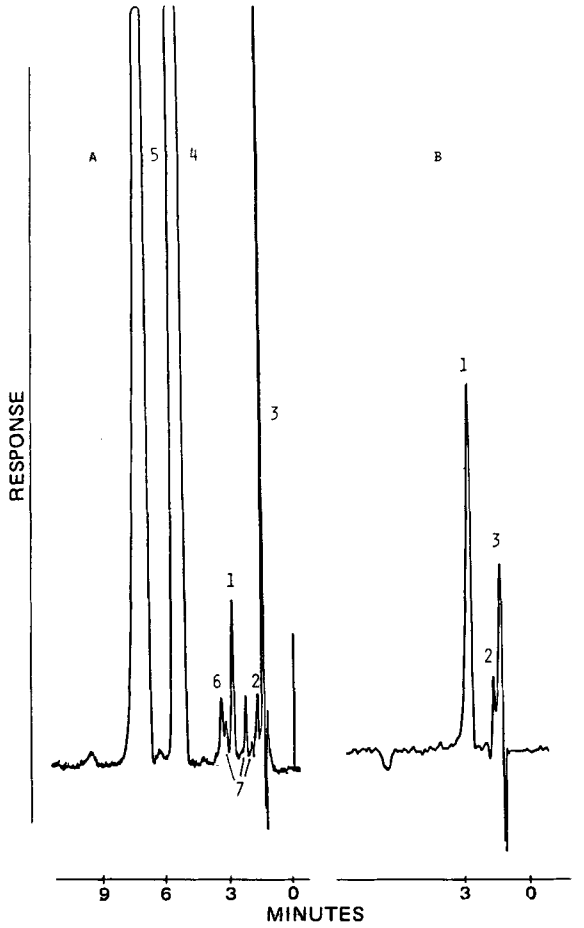


**Figure 2**—*(A) Representative chromatogram of a 2-μl injection of a 2% lidocaine hydrochloride with 1:100,000 epinephrine solution with UV detector at 280 nm and 0.005 aufs. Key: 1, epinephrine; 2, epinephrine sulfonic acid; 3, sodium metabisulfite; 4, methylparaben; 5, lidocaine hydrochloride; 6,* p*-hydroxybenzoic acid; and 7, package extractables and unknowns. (B) Representative chromatogram of a 2-μl injection of the same solution as in A with electrochemical detector at +0.90 v and 50 na/v. Key: 1, epinephrine; 2, epinephrine sulfonic acid; and 3, sodium metabisulfite.*

drochloride in the sample is substituted into the equation, which is solved for the concentration ($X_s$).

## RESULTS

**Precision**—The precision (reproducibility), reported as the relative standard deviation, was better than ±1% for epinephrine, methylparaben, and lidocaine hydrochloride as determined on 10 replicate injections.

**Linearity**—The linearity of response was determined by preparing samples containing known quantities of the components of interest in a range from ~80–120% of the theoretical labeled quantity at each concentration[20]. All calibration curves were linear, with correlations coefficient >0.99.

**Accuracy**—Accuracy was determined by preparing simulated samples containing known quantities of the components of interest along with all excipients. The percent recoveries were determined by four different operators on two liquid chromatographs over 1 week, indicating that a day-to-day accuracy of ±1% could be obtained routinely: epinephrine, 99.9 ± 0.6% (98.1–100.9%), $n$ = 34; methylparaben, 99.8 ± 0.5% (99.0–100.6%), $n$ = 8; and lidocaine hydrochloride, 100.2 ± 0.9% (98.4–101.8%), $n$ = 30.

**Specificity**—Simulated samples to which the potential degradation products had been added were injected, and the chromatograms were recorded. The potential degradation products were separated from the components of interest (Table II), indicating that the HPLC method is stability indicating.

**Table II—HPLC Retention Values for Epinephrine, Methylparaben, Lidocaine Hydrochloride, and Their Potential Degradation Products**

| Compound | Retention Time, min | $k'$ |
|---|---|---|
| Epinephrine sulfonic acid | 1.8 | 0.29 |
| Adrenochrome | 2.2 | 0.57 |
| Epinephrine | 3.0 | 1.14 |
| *p*-Hydroxybenzoic acid | 3.2 | 1.29 |
| Methylparaben | 5.0 | 2.57 |
| 2,6-Xylidine | 4.4 | 2.14 |
| Lidocaine hydrochloride | 6.8 | 3.86 |

Further proof of this stability-indicating capability was obtained by subjecting production batches[21] of lidocaine hydrochloride with epinephrine injection to various conditions of stress[22] and assaying for epinephrine, methylparaben, and lidocaine hydrochloride. The results indicated that the major degradation products were those that had been proposed (Table II) and also that any other unknown degradation products did not interfere with the assays.

A comparison of the chromatograms obtained from analysis of the same solution[23] with the UV and electrochemical detectors clearly showed the advantages gained in specificity and sensitivity from the electrochemical detectors. Not only the degradation products but also the package extractables interfered with the accurate quantitation of epinephrine with the UV detector (Fig. 2).

An electrochemically active peak was observed that eluted from the column immediately after epinephrine (Fig. 3). This peak was identified

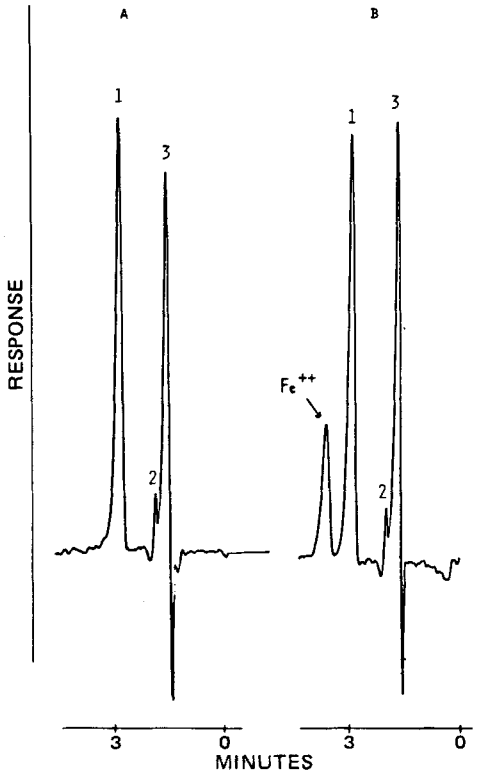


**Figure 3**—*Representative chromatograms of a 2-μl injection of a 2% lidocaine hydrochloride with 1:100,000 epinephrine solution. Key: A, with 0.1 m*M *disodium edetate in the mobile phase; B; without disodium edetate; 1, epinephrine; 2, epinephrine sulfonic acid; and 3, sodium metabisulfite.*

[20] Epinephrine concentrations were 1:50,000; 1:100,000; and 1:200,000. The methylparaben concentration was 1.00 mg/ml. The lidocaine hydrochloride concentrations were 0.5, 1.0, and 2.0%. The method was developed so that solutions containing 0.5–2.0% lidocaine hydrochloride could be assayed without any sample preparation. If the lidocaine hydrochloride concentration in a sample to be assayed is >2.0%, an appropriate dilution with distilled water should be made so that the lidocaine hydrochloride concentration is between 0.5 and >2.0%.

[21] Astra Pharmaceutical Products, Worcester, MA 01606.

[22] Autoclaving for 5, 10, and 20 cycles, storage for 1 month at 80 and 110°, exposure to atmospheric oxygen, addition of 12 ppm of aluminum, and an increase in the pH of the solution.

[23] Product at its expiration date.

**Table III—Comparison of the HPLC Method with the USP XX or Current Methodology**

| Assay | Number of Batches Assayed | Percent Difference[a] |
|---|---|---|
| Epinephrine | 115 | −0.3 (USP–HPLC) |
| Methylparaben | 87 | +2.5 (UV–HPLC) |
| Lidocaine hydrochloride | 87 | −2.3 (USP–HPLC) |

[a] Mean percent difference for batches assayed.

as $Fe^{2+}$ (11) and did not interfere with the assay. However, addition of 0.1 m*M* edetate disodium to the mobile phase resulted in complete elimination of the $Fe^{2+}$ peak with no other effect on the chromatogram.

**Comparison of HPLC Method with USP or Current Methodology**—Production samples[21] of lidocaine hydrochloride with epinephrine in injectable solutions, which included vials, ampuls, and dental cartridges from batches < 1 month old to batches at their expiration date, were assayed by HPLC, fluorometry (epinephrine), titrimetry (lidocaine hydrochloride), and spectrophotometry (methylparaben). All analyses were performed on individual dosage units (if enough solution was available) or on aliquots from a pool of several dosage units (if one unit was inadequate). The results (Table III) indicate good agreement between the methods.

## DISCUSSION

The HPLC procedure provides a significant advance over existing methodology for assaying components in epinephrine-containing local anesthetic injectable solutions. Three of the major components (epinephrine, lidocaine hydrochloride, and methylparaben) of these types of dosage forms may be assayed simultaneously in one injection. The current methodology requires separate analytical procedures for each component.

The small sample size (2 μl) allows replicate analysis of the three components from individual dosage units. The current methodology in some cases requires units to be pooled to obtain a sufficient sample for analysis.

No preparation of the sample is necessary. The dosage unit is opened, a 2-μl aliquot is removed with a 10-μl syringe, and the sample is injected into the chromatograph. The current methodology requires extensive sample preparation for each component.

The HPLC method is selective and specific for all three components and is stability indicating.

Although both the HPLC and current methodology may be automated, the HPLC method offers a distinct advantage since only one setup of automated equipment is needed. The current methodology requires three separate and different automated setups since the procedure for each component is different. The HPLC methodology can be used to assay other local anesthetic injectable solutions such as prilocaine hydrochloride, etidocaine hydrochloride, mepivacaine hydrochloride, and bupivacaine hydrochloride with little or no change in the mobile phase.

## REFERENCES


(1) "Analytical Profiles of Drug Substances," vol. 7, K. Florey, Ed., Academic, New York, N.Y., 1978, p. 193.

(2) J. R. Doty, *Anal. Chem.*, **20,** 1166 (1948).

(3) O. Loew, *Biochem. Z.*, **85,** 2955 (1918).

(4) H. Hellberg, *Sv. Farm. Tidskr.*, **64,** 493 (1960).

(5) V. K. Prasad, R. A. Ricci, B. C. Nunning, and A. P. Granatek, *J. Pharm. Sci.*, **62,** 1130 (1973).

(6) "The United States Pharmacopeia," 20th rev., United States Pharmacopeial Convention, Rockville, Md., 1979, p. 449.

(7) H. Tarlin, M. Hudson, and M. Sahn, *J. Pharm. Sci.*, **65,** 1463 (1976).

(8) W. R. Heineman and P. T. Kissinger, *Anal. Chem.*, **50,** 166R (1978).

(9) R. M. Riggin and P. T. Kissinger, *ibid.*, **49,** 2109 (1977).

(10) T. P. Moyer and N. Jiang, *J. Chromatogr.*, **153,** 365 (1978).

(11) H. Hashimoto and Y. Maruyama, *ibid.*, **152,** 387 (1978).


## ACKNOWLEDGMENTS


The authors thank Mr. Allard Edhorn, Dr. Peter Kissinger, and Dr. Ronald Shoup for valuable discussions on electrochemical detectors. They also thank Mr. Gerard Boyce and Mr. Bruce Manning for encouragement and Ms. Debbie Soloski and Ms. Patricia Murray for assistance in the comparison of the methods.


# GC and GC–Mass Spectrometric Determination of *p*-Hydroxyphenobarbital Extracted from Plasma, Urine, and Hepatic Microsomes


**I. M. KAPETANOVIĆ *x and H. J. KUPFERBERG**



Received September 10, 1980, from the *Epilepsy Branch, National Institute of Neurological and Communicative Disorders and Stroke, Bethesda, MD 20205.* Accepted for publication March 19, 1981.


*Present address: Laboratory of Neurosciences, Gerontology Research Center, National Institute on Aging, Baltimore City Hospital, Baltimore, MD 21224.



**Abstract** □ Analytical methodology was developed for the quantitation of *p*-hydroxyphenobarbital extracted from plasma, urine, and hepatic microsomes. *p*-Hydroxyphenobarbital was derivatized with an appropriate *n*-alkyl iodide in the presence of a methanolic base in aprotic solvent medium. The peralkylated derivatives were stable indefinitely and were quantitated by the sensitive and selective method of GC nitrogen-selective detection and/or selected ion monitoring. The accuracy, precision, and cross verification of all methods were good. The analysis was subsequently used to study the effects of other drugs on phenobarbital biodisposition.



**Keyphrases** □ *p*-Hydroxyphenobarbital—determination by GC and GC–mass spectrometry in urine, plasma, and hepatic microsomes □ Phenobarbital—quantitation of *p*-hydroxyphenobarbital by GC and GC–mass spectrometry in urine, plasma, and hepatic microsomes □ GC—nitrogen-selective detection of *p*-hydroxyphenobarbital in urine, plasma, and hepatic microsomes


Phenobarbital (I) is commonly used in the treatment of epilepsy, and *p*-hydroxyphenobarbital (II) is its major metabolite. Even though *p*-hydroxyphenobarbital is considered to be devoid of antiepileptic activity, its quantitation is important when studying phenobarbital biodisposition. During a study on the mechanisms of val-




*0022-3549/81/1100-1218$01.00/0*


*© 1981, American Pharmaceutical Association*

**Table III—Comparison of the HPLC Method with the USP XX or Current Methodology**

| Assay | Number of Batches Assayed | Percent Difference[a] |
|---|---|---|
| Epinephrine | 115 | −0.3 (USP–HPLC) |
| Methylparaben | 87 | +2.5 (UV–HPLC) |
| Lidocaine hydrochloride | 87 | −2.3 (USP–HPLC) |

[a] Mean percent difference for batches assayed.

as $Fe^{2+}$ (11) and did not interfere with the assay. However, addition of 0.1 m*M* edetate disodium to the mobile phase resulted in complete elimination of the $Fe^{2+}$ peak with no other effect on the chromatogram.

**Comparison of HPLC Method with USP or Current Methodology**—Production samples[21] of lidocaine hydrochloride with epinephrine in injectable solutions, which included vials, ampuls, and dental cartridges from batches < 1 month old to batches at their expiration date, were assayed by HPLC, fluorometry (epinephrine), titrimetry (lidocaine hydrochloride), and spectrophotometry (methylparaben). All analyses were performed on individual dosage units (if enough solution was available) or on aliquots from a pool of several dosage units (if one unit was inadequate). The results (Table III) indicate good agreement between the methods.

## DISCUSSION

The HPLC procedure provides a significant advance over existing methodology for assaying components in epinephrine-containing local anesthetic injectable solutions. Three of the major components (epinephrine, lidocaine hydrochloride, and methylparaben) of these types of dosage forms may be assayed simultaneously in one injection. The current methodology requires separate analytical procedures for each component.

The small sample size (2 μl) allows replicate analysis of the three components from individual dosage units. The current methodology in some cases requires units to be pooled to obtain a sufficient sample for analysis.

No preparation of the sample is necessary. The dosage unit is opened, a 2-μl aliquot is removed with a 10-μl syringe, and the sample is injected into the chromatograph. The current methodology requires extensive sample preparation for each component.

The HPLC method is selective and specific for all three components and is stability indicating.

Although both the HPLC and current methodology may be automated, the HPLC method offers a distinct advantage since only one setup of automated equipment is needed. The current methodology requires three separate and different automated setups since the procedure for each component is different. The HPLC methodology can be used to assay other local anesthetic injectable solutions such as prilocaine hydrochloride, etidocaine hydrochloride, mepivacaine hydrochloride, and bupivacaine hydrochloride with little or no change in the mobile phase.

## REFERENCES


(1) "Analytical Profiles of Drug Substances," vol. 7, K. Florey, Ed., Academic, New York, N.Y., 1978, p. 193.

(2) J. R. Doty, *Anal. Chem.*, **20,** 1166 (1948).

(3) O. Loew, *Biochem. Z.*, **85,** 2955 (1918).

(4) H. Hellberg, *Sv. Farm. Tidskr.*, **64,** 493 (1960).

(5) V. K. Prasad, R. A. Ricci, B. C. Nunning, and A. P. Granatek, *J. Pharm. Sci.*, **62,** 1130 (1973).

(6) "The United States Pharmacopeia," 20th rev., United States Pharmacopeial Convention, Rockville, Md., 1979, p. 449.

(7) H. Tarlin, M. Hudson, and M. Sahn, *J. Pharm. Sci.*, **65,** 1463 (1976).

(8) W. R. Heineman and P. T. Kissinger, *Anal. Chem.*, **50,** 166R (1978).

(9) R. M. Riggin and P. T. Kissinger, *ibid.*, **49,** 2109 (1977).

(10) T. P. Moyer and N. Jiang, *J. Chromatogr.*, **153,** 365 (1978).

(11) H. Hashimoto and Y. Maruyama, *ibid.*, **152,** 387 (1978).


## ACKNOWLEDGMENTS


The authors thank Mr. Allard Edhorn, Dr. Peter Kissinger, and Dr. Ronald Shoup for valuable discussions on electrochemical detectors. They also thank Mr. Gerard Boyce and Mr. Bruce Manning for encouragement and Ms. Debbie Soloski and Ms. Patricia Murray for assistance in the comparison of the methods.


# GC and GC–Mass Spectrometric Determination of *p*-Hydroxyphenobarbital Extracted from Plasma, Urine, and Hepatic Microsomes


**I. M. KAPETANOVIĆ *x and H. J. KUPFERBERG**



Received September 10, 1980, from the *Epilepsy Branch, National Institute of Neurological and Communicative Disorders and Stroke, Bethesda, MD 20205.* Accepted for publication March 19, 1981.


*Present address: Laboratory of Neurosciences, Gerontology Research Center, National Institute on Aging, Baltimore City Hospital, Baltimore, MD 21224.



**Abstract** □ Analytical methodology was developed for the quantitation of *p*-hydroxyphenobarbital extracted from plasma, urine, and hepatic microsomes. *p*-Hydroxyphenobarbital was derivatized with an appropriate *n*-alkyl iodide in the presence of a methanolic base in aprotic solvent medium. The peralkylated derivatives were stable indefinitely and were quantitated by the sensitive and selective method of GC nitrogen-selective detection and/or selected ion monitoring. The accuracy, precision, and cross verification of all methods were good. The analysis was subsequently used to study the effects of other drugs on phenobarbital biodisposition.



**Keyphrases** □ *p*-Hydroxyphenobarbital—determination by GC and GC–mass spectrometry in urine, plasma, and hepatic microsomes □ Phenobarbital—quantitation of *p*-hydroxyphenobarbital by GC and GC–mass spectrometry in urine, plasma, and hepatic microsomes □ GC—nitrogen-selective detection of *p*-hydroxyphenobarbital in urine, plasma, and hepatic microsomes


Phenobarbital (I) is commonly used in the treatment of epilepsy, and *p*-hydroxyphenobarbital (II) is its major metabolite. Even though *p*-hydroxyphenobarbital is considered to be devoid of antiepileptic activity, its quantitation is important when studying phenobarbital biodisposition. During a study on the mechanisms of val-




*0022-3549/81/1100-1218$01.00/0*


*© 1981, American Pharmaceutical Association*

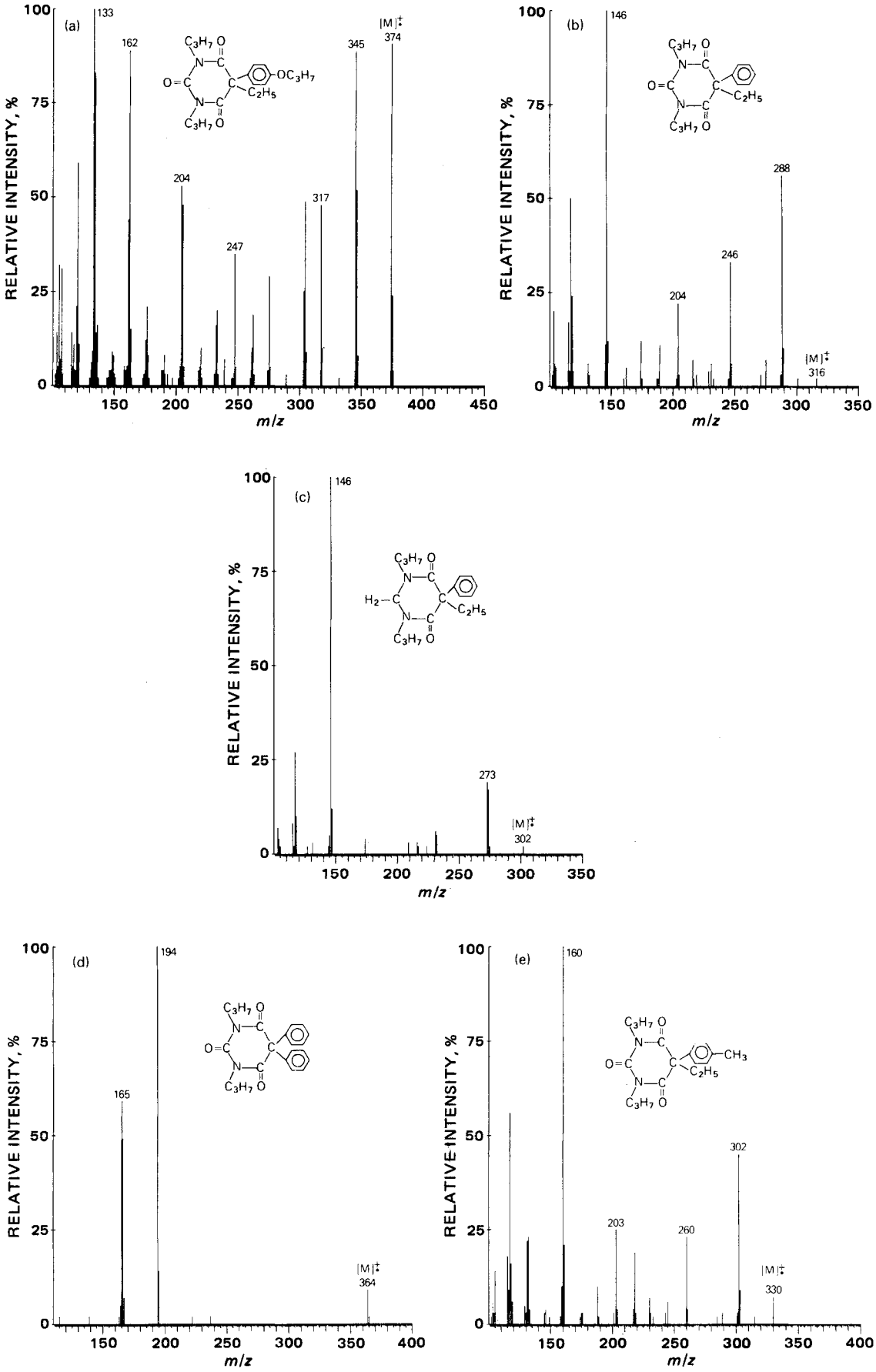


**Figure 1**—*Electron-impact mass spectra of propylated reference compounds and internal standards. Key:* a, p-*hydroxyphenobarbital;* b, *phenobarbital;* c, *primidone;* d, *diphenylbarbituric acid; and* e, p-*methylphenobarbital.*

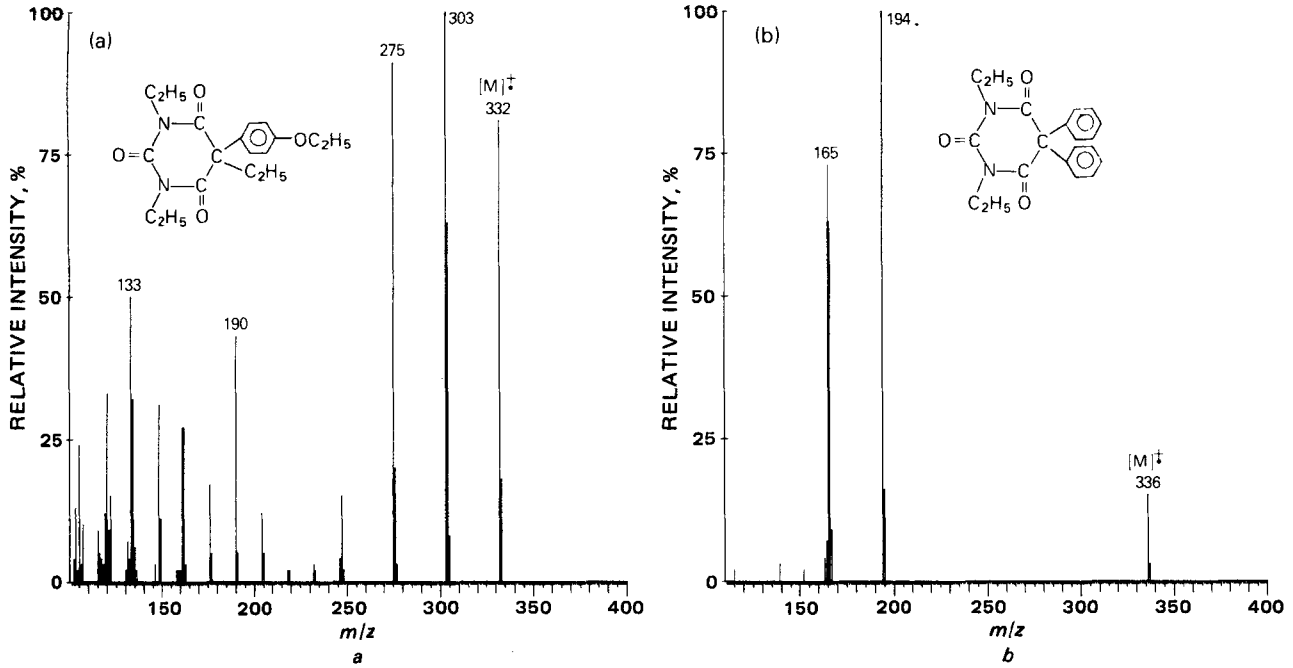


**Figure 2**—*Electron-impact spectra of ethylated* p-*hydroxyphenobarbital* (a) *and diphenylbarbituric acid* (b).

proate-caused elevation of plasma phenobarbital levels, it became necessary to quantitate *p*-hydroxyphenobarbital extracted from plasma, urine, and hepatic microsomes. The reported procedures for its quantitation lacked sensitivity or selectivity, and some methods had additional drawbacks. For example, countercurrent distribution and TLC in conjunction with liquid scintillation (1) are laborious and require the use of a radioactive tracer. TLC methods (2, 3) usually require a separate means of detection. GC methods using on-column methylation (4) can yield incomplete derivatization, and they also accelerate column degradation; furthermore, samples are not very stable once the alkylating base is added. The high-pressure liquid chromatographic method (5) has limited sensitivity due to a relatively poor extinction coefficient of unionized barbiturates.

Therefore, a GC nitrogen-selective detection method was developed for the determination of *p*-hydroxyphenobarbital. The nitrogen-selective detector is commercially available and is a reasonably priced accessory for the gas chromatograph. Its simplicity of operation is similar to that of the regular flame-ionization detector, but its sensitivity and selectivity are superior. The barbiturates were derivatized to optimize their chromatographic sep-

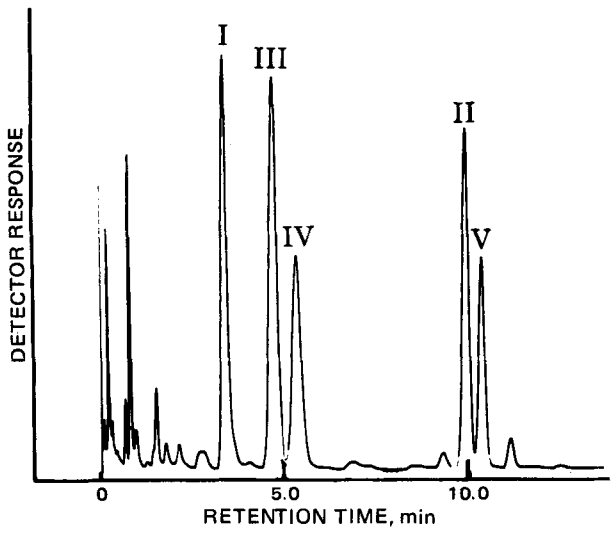


**Figure 3**—*Gas chromatogram of propylated human urine (hydrolyzed) extract using nitrogen–phosphorus flame-ionization detector. Levels of phenobarbital (I),* p-*hydroxyphenobarbital (II), and primidone (IV) were 34.6, 40.3, and 31.9 μg/ml, respectively. Diphenylbarbituric acid (V, 25 μg/ml) and* p-*methylphenobarbital (III, 50 μg/ml) were the internal standards.*

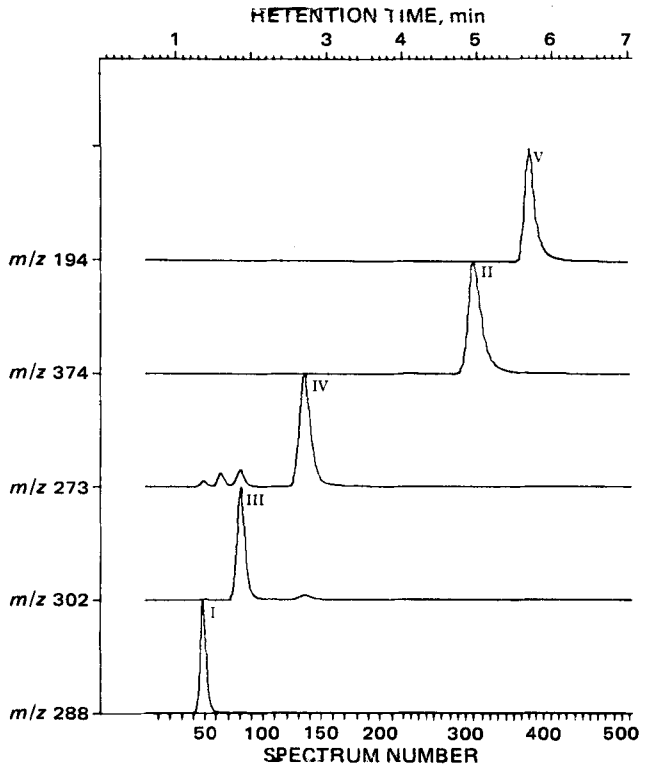


**Figure 4**—*Selected ion monitoring (electron-impact mode) tracing of propylated human urine (hydrolyzed) extract. For additional details, see Fig. 3.*

**Table I—Accuracy and Precision of Determination of Urinary *p*-Hydroxyphenobarbital (II), Phenobarbital (I), and Primidone (IV)**

| Actual II, I and IV, μg/ml | Experimental[a], μg/ml | | |
|---|---|---|---|
| | II | I | IV |
| 10.00 | 10.08 ± 0.27 | 9.12 ± 0.28 | 10.32 ± 0.24 |
| 100.00 | 100.40 ± 1.23 | 101.10 ± 1.54 | 97.60 ± 1.72 |

[a] Values expressed as mean ± *SD* of four determinations.

aration and to stabilize them. Derivatization was performed by modification of a reported alkylation procedure for barbiturates (6).

These analytical methods were satisfactorily employed for *in vitro* animal experiments and *in vivo* human studies dealing with valproate-phenobarbital interaction (7–9).

## EXPERIMENTAL

**Instrumentation**—The gas chromatograph[1] was equipped with a flame-ionization detector and a nitrogen–phosphorus flame-ionization detector. The injection port and detector temperatures were 260 and 300°, respectively. Helium was used as the carrier at a flow rate of 30 ml/min.

The dodecapole mass spectrometer[2] was equipped with electron-impact and chemical-ionization sources and was coupled to the gas chromatograph[3] by a glass-lined single-stage jet separator. Data acquisition and reduction were computer automated[4]. The temperatures of the injection port, transfer line, and ion source were 300, 300, and 180°, respectively. In the electron-impact mode, helium was used as the carrier at a flow rate of 25 ml/min; the operating pressure of the ion source was $3.7 \times 10^{-6}$ torr, and the mass spectrometer was operated with an electron energy of 70 ev. In the chemical-ionization mode, methane was used as the carrier at a flow rate of 15 ml/min and as a reagent gas. The operating pressure of the ion source was 0.4 torr, and an ionizing energy of 250 ev was used to produce the reactant ions.

**Materials**—All organic solvents[5] were used as obtained after their purity was checked. Reference compounds (phenobarbital[6], primidone[6], and *p*-hydroxyphenobarbital[7]) and internal standards (*p*-methylphenobarbital[7] and 5,5-diphenylbarbituric acid[8]) were also checked for purity before use. Methyl, ethyl, *n*-propyl, and *n*-butyl iodides[9] and tetraethylammonium hydroxide (25% methanolic solution[9]) were used as obtained.

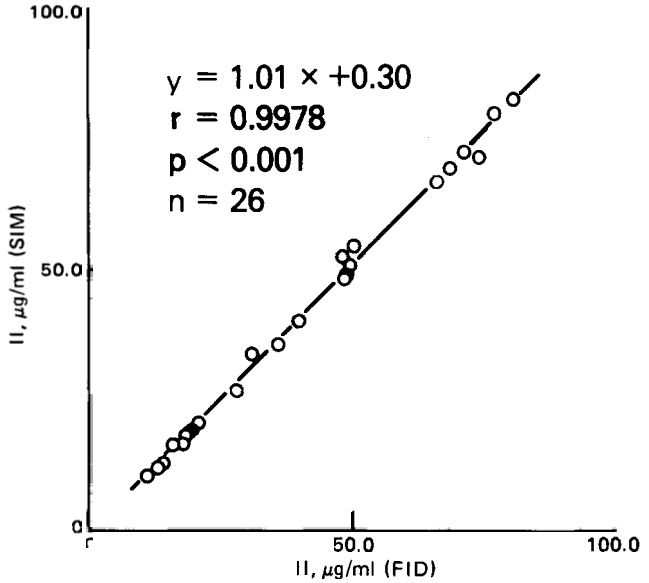


**Figure 5**—*Relationship between selected ion monitoring (SIM) at electron-impact mode and GC nitrogen–phosphorus flame-ionization detector (FID) methods for quantitation of urinary* p-*hydroxyphenobarbital (II).*

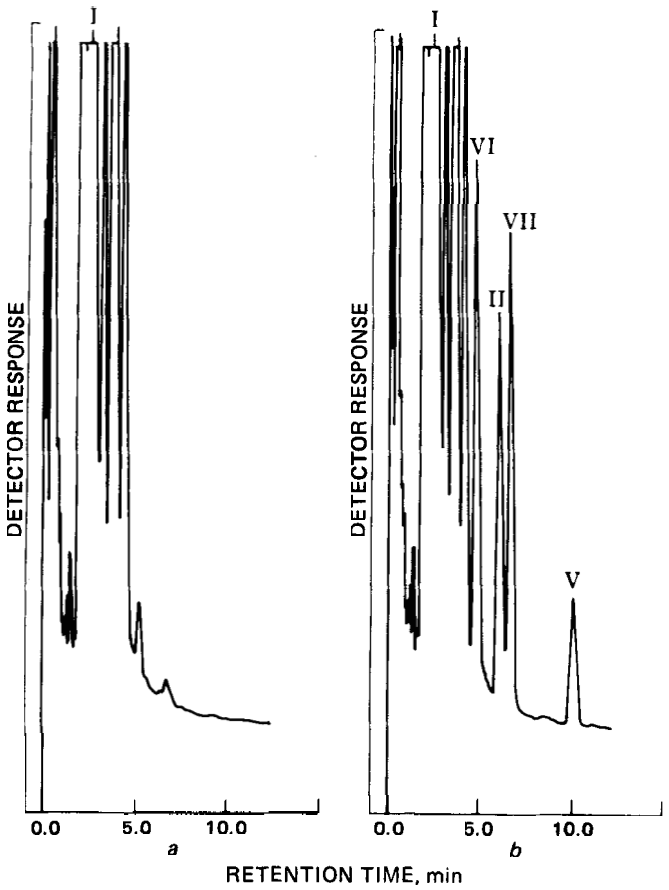


**Figure 6**—*Gas chromatogram of extract from microsomal blank (a) and microsomal phenobarbital reaction mixture containing phenobarbital (b) using nitrogen–phosphorus flame-ionization detector. The reaction occurred in the presence of 4 mM phenobarbital, and 0.875 μg of* p-*hydroxyphenobarbital was formed. Diphenylbarbituric acid (0.50 μg) was the internal standard. Peaks VI and VII represent other metabolites of phenobarbital. The microsomal blank was run parallel to the microsomal phenobarbital reaction, but NADPH was added after termination of the reaction and no internal standard was added. The chromatogram of the blank shows a lack of interferences for* p-*hydroxyphenobarbital and diphenylbarbituric acid.*

Silanized GC glass columns[10] for heated on-column injection were packed with commercially available packings[10].

Sodium salt of phenobarbital[11] was used for animal treatment.

A commercial source of β-glucuronidase–arylsulfatase and NADPH was used[12].

All other chemicals were reagent grade.

**Human Subjects**—The subjects were epileptic patients[13] who consented to participate in a clinical study of drug–drug interactions in antiepileptic therapy. Blood samples were obtained at 7 am, just prior to administration of the patients' morning medication (including phenobarbital and/or primidone); 24-hr urine samples were also collected. For the clinical study, blood and urine samples were obtained while the plasma barbiturate levels were at steady state.

**Animals**—Adult male Holtzman rats[14], ~200 g, were injected intra-

[1] Hewlett-Packard model 5840A.
[2] Hewlett-Packard model 5982A.
[3] Hewlett-Packard model 5700 series.
[4] Hewlett-Packard model 5934A data system.
[5] Burdick & Jackson Laboratories, Muskegon, Mich.
[6] USPC, Rockville, Md.
[7] Aldrich Chemical Co., Milwaukee, Wis.
[8] Generous gift from Dr. A. Raines, Department of Pharmacology, School of Medicine and Dentistry, Georgetown University, Washington, DC 20007.
[9] Eastman Chemical Co., Rochester, NY.
[10] Supelco, Bellefonte, Pa.
[11] Merck & Co., Rahway, N.J.
[12] Boehringer-Mannheim Biochemicals, Indianapolis, Ind.
[13] Admitted to the Clinical Center, National Institutes of Health.
[14] Charles River, Wilmington, Mass.

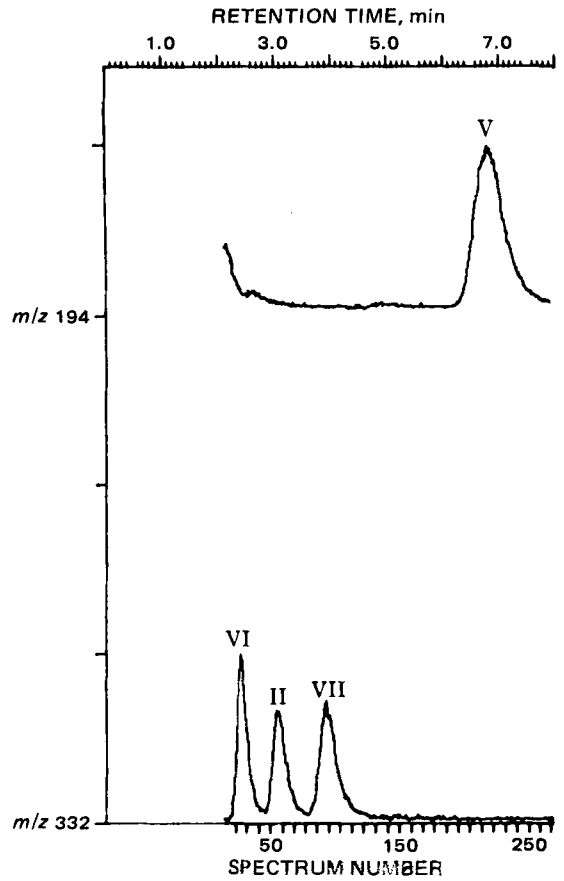


**Figure 7**—*Selected ion monitoring (electron-impact mode) tracing of ethylated extract from microsomal phenobarbital metabolic reaction. For additional details, see Fig. 6.*

peritoneally with aqueous phenobarbital sodium solution (75 mg/kg) on 3 consecutive days. The rats were then sacrificed, and hepatic microsomes were prepared as previously described (10).

**Microsomal Reactions**—Microsomal reactions were carried out in 0.1 *M* potassium phosphate buffer (pH 7.50) in the presence of 1.83 nmoles of microsomal cytochrome P-450 and various concentrations of the substrate, phenobarbital. Following preequilibration of the samples at 37° for 1 min, reaction was initiated with NADPH (final NADPH concentration in the reaction mixture was 0.25 m*M*). The samples were incubated at 37° for 8 min in 5 ml of reaction mixture.

**Plasma Extraction**—Stock methanolic solutions of reference compounds and internal standards were kept at 4° and were stable on storage. Methanolic solutions of reference compounds (10–200 μl) were added to the tubes to be used for standards, and methanolic solutions of internal standards were added to all of the tubes. Methanol was evaporated, using a rotary evaporator with aspirator vacuum[15]. Blank plasma or plasma from phenobarbital-treated subjects (1 ml) was added to the appropriate tubes. Spiked plasma standards were extracted along with the patients' samples.

For the determination of total (free plus conjugated) *p*-hydroxyphenobarbital, the samples were hydrolyzed. Free *p*-hydroxyphenobarbital was determined by omitting the hydrolysis. For determination of total *p*-hydroxyphenobarbital, 0.2 ml of 0.5 *M* sodium acetate buffer (pH 5.00) was added, followed by 50 μl of β-glucuronidase–arylsulfatase, and samples were incubated at 37° for 20–24 hr. To hydrolyzed and nonhydrolyzed samples, 1 ml of 1 *M* monobasic potassium phosphate was added; samples were then extracted with 7 ml of ethyl acetate, using a reciprocating shaker. Following centrifugation (~2000 rpm), the ethyl acetate phase was collected and washed with 2 ml of 0.1 *N* HCl and evaporated to dryness. Hexane was added to the residue, and the samples were extracted with 5 ml of acetonitrile. Hexane was used to remove endogenous lipoidal substances. The acetonitrile phase was collected and evaporated to dryness, and the residue was ready for derivatization.

**Urine Extraction**—The hydrolysis of urine samples was analogous to that of the plasma samples. Hydrolyzed and nonhydrolyzed urine samples were extracted in the same manner as the plasma samples.

[15] Buchler Instruments, Fort Lee, N.J.

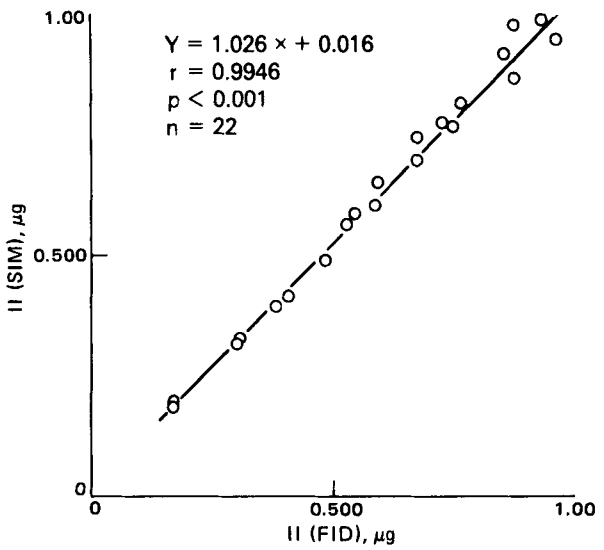


**Figure 8**—*Relationship between selected ion monitoring (SIM) (electron-impact mode) and GC nitrogen–phosphorus flame-ionization detector (FID) methods for quantitation of* p*-hydroxyphenobarbital (II) formed in microsomal reaction.*

**Microsome Extraction**—Microsomal reactions were terminated by the addition of 7 ml of cold benzene (or toluene). For consistency, phenobarbital was added such that its final concentration prior to the addition of benzene was always the same. Aqueous and organic phases were mixed by hand inversion, samples were centrifuged, and the benzene layer was discarded. The samples were then washed again with 7 ml of benzene. A double benzene wash was employed to eliminate some of the large excess of phenobarbital, which would otherwise swamp the peak corresponding to the relatively small amounts of generated *p*-hydroxyphenobarbital. *p*-Hydroxyphenobarbital was not extractable into benzene under these conditions. Following the benzene washes, diphenylbarbituric acid (the internal standard) was added, and the samples were extracted with 7 ml of ethyl acetate; the ethyl acetate phase was collected and evaporated to dryness.

**Derivatization Reactions**—The derivatization reaction was essentially the same for the extracts from plasma, urine, and microsomes. The main difference was in the choice of the *n*-alkyl iodide; the selection of alkyl iodide was made to optimize chromatographic separations. Ethyl iodide was selected for derivatization of plasma and microsomal extracts, whereas *n*-propyl iodide was used for urinary extracts. To the residue from the extract were added 200 μl of acetonitrile and 50 μl of methanolic (25%) tetraethylammonium hydroxide, and the sample was mixed well. The appropriate *n*-alkyl iodide (25 μl) was added, and the sample was mixed again and placed in a water bath at 60° for 60 min, the optimum conditions for all derivatizations.

At the end of this time, 7 ml of chloroform was added, and the sample was washed sequentially with 2 ml of 0.1 *N* HCl, 0.1 *N* NaOH, and deionized water. The washed chloroform phase was evaporated to dryness, and the residue was dissolved in methanol or isoamyl acetate for analysis. Derivatized samples were stable at 4° or at room temperature for at least 2 months.

The major modification of the reported derivatization procedure for barbiturates (6) was the use of a different aprotic solvent. Acetonitrile was selected instead of *N*,*N*-dimethylacetamide because the former is more easily removed by evaporation. It has also been shown (11) that acetone serves equally as well as *N*,*N*-dimethylacetamide in alkylation of the phenolic group; but because higher temperatures were required for propylation of *p*-hydroxyphenobarbital, the low boiling point of acetone precluded its use. It was confirmed that acetonitrile or 2-butanone serves equally as well as *N*,*N*-dimethylacetamide in the derivatization of *p*-hydroxyphenobarbital or other barbiturates, and all three were superior to a protic solvent such as methanol.

**Analysis**—The samples were analyzed on a gas chromatograph equipped with a nitrogen–phosphorus flame-ionization detector (urine and microsomes) or a gas chromatograph–mass spectrometer–computer system (plasma). Quantitation was done using peak heights (urine and microsomes) or selected ion monitoring using peak areas (plasma).

Cross-verification of the analytical methods was carried out on the gas

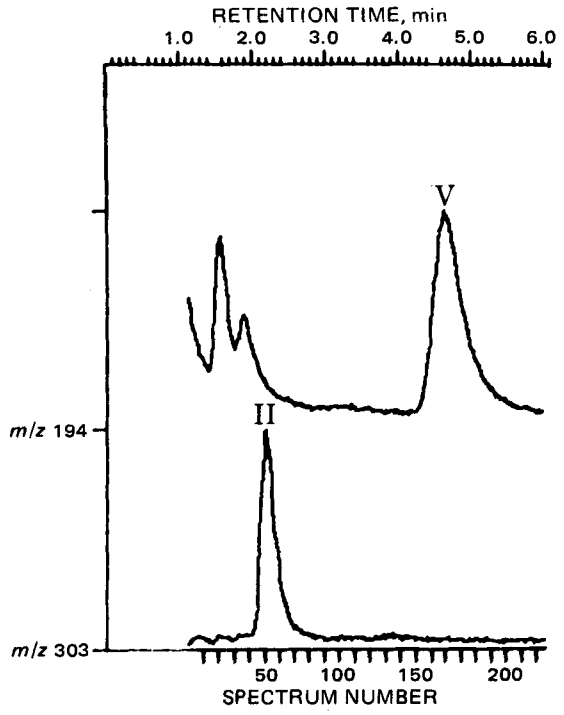


**Figure 9**—*Selected ion monitoring (electron-impact mode) tracing of ethylated human plasma (nonhydrolyzed) extract. The* p*-hydroxyphenobarbital level was 0.29 μg/ml. Diphenylbarbituric acid (0.50 μg/ml) was the internal standard.*

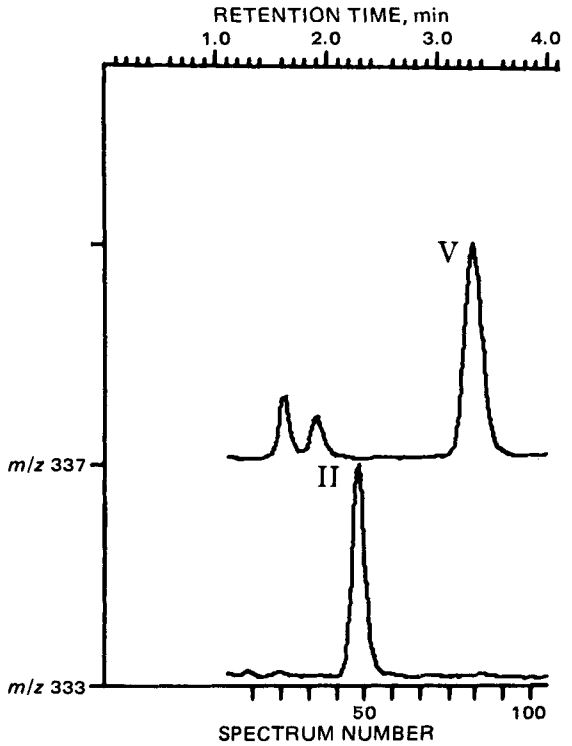


**Figure 10**—*Selected ion monitoring (chemical-ionization mode) tracing of ethylated human plasma (nonhydrolyzed) extract. For additional details, see Fig. 9.*

chromatograph–mass spectrometer–computer system. Quantitation was done by selected ion monitoring, using peak areas expressed as percent relative to internal standard. The selected ion monitoring technique was used to optimize sensitivity and specificity.

All samples, including the standards, were always injected in random order; some samples were injected in duplicate. Reproducibility between duplicate injections was always >95%. Random samples were analyzed in duplicate on the same day and on different days, and reproducibility was also >95%.

*Urine Analysis*—The gas chromatograph was equipped with a glass column (1.8 m × 2 mm i.d.) packed with 3% SE-30 on 100–120-mesh Gas Chrom Q. Oven temperature was maintained at 205° for 6 min, followed by temperature programming at 10°/min to 250°. Analysis of urinary *p*-hydroxyphenobarbital also allowed simultaneous quantitation of phenobarbital and primidone. *p*-Methylphenobarbital (III) was the internal standard for phenobarbital and primidone (IV); diphenylbarbituric acid (V) was the internal standard for *p*-hydroxyphenobarbital.

For verification of the analytical method, the gas chromatograph–mass spectrometer–computer system, operated in the electron-impact mode, was equipped with a glass column (0.9 m × 2 mm i.d.) packed with 3% SP 2250 DA on 100–120-mesh Supelcoport. Oven temperature was maintained at 200° for 4 min and then was programmed at 32°/min to 250°. The ions of *m/z* 374, 288, 273, 194, and 302 were monitored for propylated *p*-hydroxyphenobarbital (Fig. 1*a*), phenobarbital (Fig. 1*b*), primidone (Fig. 1*c*), diphenylbarbituric acid (Fig. 1*d*), and *p*-methylphenobarbital (Fig. 1*e*), respectively.

*Microsome Analysis*—The gas chromatograph was equipped with a glass column (1.8 m × 2 mm i.d.) packed with 2% OV3 on 100–120-mesh Supelcoport, and the analysis was done isothermally at 210°. Of the several packings tested, this one gave the most satisfying resolution for the peaks of interest. Diphenylbarbituric acid was the internal standard.

The gas chromatograph–mass spectrometer–computer system used for verification of the analytical method was operated in the electron-impact mode and was fitted with a glass column (0.9 m × 2 mm i.d.) packed with 3% SP 2250 DA on 100–120-mesh Supelcoport. The analysis was done isothermally at 190°. The ions of *m/z* 332 and 194 were monitored for *p*-hydroxyphenobarbital (Fig. 2*a*) and diphenylbarbituric acid (Fig. 2*b*), respectively.

*Plasma Analysis*—The gas chromatograph–mass spectrometer–computer system, operated in the electron-impact mode, was equipped with a glass column (0.9 m × 2 mm i.d.) packed with 3% SP 2250 DA on 100–120-mesh Supelcoport, and the analysis was done isothermally at 200°. Diphenylbarbituric acid was the internal standard. The ions of *m/z* 303 and 194 were monitored for *p*-hydroxyphenobarbital and diphenylbarbituric acid, respectively.

The analytical method was verified by a gas chromatograph–mass spectrometer–computer system operated in the chemical-ionization mode, using a glass column (1.2 m × 2 mm i.d.) packed with 3% OV-1 on Gas Chrom Q. The analysis was done isothermally at 220°. The ions of *m/z* 333 and 337 were monitored for *p*-hydroxyphenobarbital and diphenylbarbituric acid, respectively. The monitored ions corresponded to the quasimolecular ions for the two compounds, and they both were the base peak as well.

## RESULTS AND DISCUSSION

**Urine**—The capability of monitoring urinary phenobarbital and primidone along with *p*-hydroxyphenobarbital by this method is convenient because phenobarbital is a major metabolite of primidone, a closely related antiepileptic agent. Thus, if primidone is administered, its urinary output can be quantitated at the same time as its primary and secondary metabolites, phenobarbital and *p*-hydroxyphenobarbital, respectively. A gas chromatogram (Fig. 3) and selected ion monitoring tracing (Fig. 4) of urinary *p*-hydroxyphenobarbital, phenobarbital, and primidone are illustrated. Standard curves were set up for all three barbiturates, and the concentrations selected for all three ranged from 10 to 100 μg/ml. This range bracketed the range of experimental values for all three barbiturates.

Representative standard curves obtained from the GC nitrogen–phosphorus flame-ionization detector data exhibited the following linear least-squares regression equations and correlation coefficients ($r^2$): $y = 0.0204x + 0.006$ and $r^2 = 0.9996$ for *p*-hydroxyphenobarbital; $y = 0.0313x + 0.072$ and $r^2 = 0.9995$ for phenobarbital; and $y = 0.0167x + 0.004$ and $r^2 = 0.9965$ for primidone. Furthermore, the accuracy and precision of the method were evaluated by quadruplicate analyses of spiked samples; the results (Table I) demonstrated good accuracy and precision.

There was a good correlation between the GC nitrogen–phosphorus flame-ionization detector and selected ion monitoring methods for quantitation of urinary *p*-hydroxyphenobarbital (Fig. 5). A similar correlation was also obtained for the quantitation of phenobarbital and primidone in the urine. The 24-hr urinary output of phenobarbital, free *p*-hydroxyphenobarbital, and total (free plus conjugated) *p*-hydroxyphenobarbital from a patient on a therapeutic regimen of phenobarbital alone (180 mg/day) was 33.0 ± 4.9 μg/ml, 27.3 ± 2.7 mg, and 60.9 ± 4.1

mg, respectively (mean ± *SD* of five determinations). The urinary output of phenobarbital is reported in concentration units rather than in absolute amount of excreted phenobarbital because the amount of urinary phenobarbital is dependent on urinary volume, which is not the case for free or conjugated *p*-hydroxyphenobarbital.

**Microsomes**—A gas chromatogram (Fig. 6*b*) and selected ion monitoring tracing (Fig. 7) of *p*-hydroxyphenobarbital generated in the microsomal reaction are illustrated. A representative standard curve obtained from the GC nitrogen–phosphorus flame-ionization detector data was described by the linear least-squares regression equation as $y = 3.34x + 0.005$, $r^2 = 0.9993$. The standards ranged from 0.10 to 1.00 μg of *p*-hydroxyphenobarbital and bracketed the range of experimental values. The accuracy and precision of the method were measured by quadruplicate analyses of spiked samples. The results were 0.098 ± 0.001 and 1.04 ± 0.03 μg of *p*-hydroxyphenobarbital for samples spiked with 0.10 and 1.00 μg of *p*-hydroxyphenobarbital, respectively (mean ± *SD* of four determinations).

There was good correlation between the GC nitrogen–phosphorus flame-ionization detector and selected ion monitoring methods for quantitation of *p*-hydroxyphenobarbital in the microsomal phenobarbital metabolic reaction (Fig. 8). In the microsomal oxidative metabolism of phenobarbital, two metabolites in addition to *p*-hydroxyphenobarbital were detected (peaks VI and VII in Figs. 6*b* and 7). Compound VI was subsequently shown to correspond to *m*-hydroxyphenobarbital on the basis of the same retention times as those of the synthetic reference compound[16] in several chromatographic systems. Furthermore, ratios for the relative abundance of several ions for this metabolite were virtually identical to those of the reference compound, as determined by the gas chromatograph–mass spectrometer–computer system. Compound VII, however, could possibly be the *ortho* analog on the basis of some limited electron-impact mass spectrometric data. However, a complete mass spectrometric analysis was not performed, and the reference standard was not available. Thus, the identity of VII remains speculative. The values for $K_m$ and $V_{max}$, the kinetic parameters for *p*-hydroxylation of phenobarbital, were determined to be 1.16 m*M* and 0.325 nmole of *p*-hydroxyphenobarbital formed $min^{-1}$ $nmole^{-1}$ of P-450, respectively.

**Plasma**—Occasional interferences were encountered in the analysis of plasma *p*-hydroxyphenobarbital by the GC nitrogen–phosphorus flame-ionization detector method. Since it proved difficult to eliminate them satisfactorily with column packing phases of different polarities, a more specific selected ion monitoring method was developed. Selected ion monitoring tracings in the electron-impact mode (Fig. 9) and chemical ionization mode (Fig. 10) for the analysis of plasma *p*-hydroxyphenobarbital are illustrated. A representative standard curve obtained from the selected ion monitoring (electron-impact) data was described by the linear least-squares equation as $y = 49.68x + 0.017$, $r^2 = 0.9978$. The standards ranged from 0.25 to 1.50 μg/ml of *p*-hydroxyphenobarbital and bracketed the range of experimental values. The accuracy and precision of the method were evaluated by quadruplicate analyses of spiked samples. The results were 0.268 ± 0.014 and 1.05 ± 0.03 μg/ml of *p*-hydroxyphenobarbital for samples spiked with 0.250 and 1.00 μg/ml of *p*-hydroxyphenobarbital, respectively.

There was good correlation between the electron-impact and chemical-ionization modes of the selected ion monitoring method. For example, quadruplicate analyses of a plasma sample yielded mean (±*SD*) levels of 0.344 ± 0.008 and 0.338 ± 0.014 μg/ml of *p*-hydroxyphenobarbital in the electron-impact and chemical-ionization modes, respectively. Plasma levels of free *p*-hydroxyphenobarbital and total (free plus conjugated) *p*-hydroxyphenobarbital in a patient maintained on a therapeutic regimen of phenobarbital alone (180 mg/day) were 0.516 ± 0.022 and 0.763 ± 0.057 μg/ml, respectively (mean ± *SD* of four determinations).

[16] Generous gift from Dr. K. H. Dudley, Department of Pharmacology, School of Medicine, University of North Carolina, Chapel Hill, N.C.

## REFERENCES


(1) J. Alvin, T. McHorse, A. Hoyumpa, M. T. Bush, and S. Schenker, *J. Pharmacol. Exp. Ther.*, **192**, 224 (1975).

(2) S. S. Levin, M. F. Schwartz, D. Y. Cooper, and J. C. Touchstone, *J. Chromatogr.*, **154**, 349 (1978).

(3) R. Subramanian, S. Rajeswari, T. R. Chandrasekar, and V. N. Visvanatha Rao, *Curr. Sci.*, **48**, 399 (1979).

(4) N. Kållberg, S. Agurell, Ö. Ericsson, E. Bucht, B. Jalling, and L. O. Boréus, *J. Clin. Pharmacol.*, **9**, 161 (1975).

(5) R. W. Dykeman and D. J. Ecobichon, *J. Chromatogr.*, **162**, 104 (1979).

(6) R. H. Greeley, *Clin. Chem.*, **20**, 192 (1974).

(7) I. M. Kapetanović, H. J. Kupferberg, R. J. Porter, and J. K. Penry, *Pharmacologist*, **21**, 208 (1979).

(8) I. M. Kapetanović, H. J. Kupferberg, R. J. Porter, and J. K. Penry, in "Antiepileptic Therapy: Advances in Drug Monitoring," S. I. Johannessen, P. L. Morselli, C. E. Pippenger, A. Richens, D. Schmidt, and H. Meinardi, Eds., Raven, New York, N.Y., 1980, p. 373.

(9) I. M. Kapetanović and H. J. Kupferberg, *Fed. Proc. Fed. Am. Soc. Exp. Biol.*, **39**, 1099 (1980).

(10) J. L. Blumer and J. J. Mieyal, *J. Biol. Chem.*, **253**, 1159 (1978).

(11) I. M. Kapetanović, J. S. Dutcher, and J. M. Strong, *Anal. Chem.*, **49**, 1843 (1977).


## ACKNOWLEDGMENTS


The authors thank Dr. R. J. Porter, Dr. E. Schulman, Dr. W. Theodore, and Dr. J. K. Penry for selecting and clinically managing the patients from the Clinical Epilepsy Section, Experimental Therapeutics Branch, National Institute of Neurological and Communicative Disorders and Stroke, and Ms. B. J. Hessie for editorial assistance.

# Solubility Behavior of Phenolic Compounds in Hexane–Ethyl Acetate, Hexane–Ethyl Myristate, and Hexane–Ethyl Pivalate Cosolvent Systems

**EIICHI AKAHO *, KATSUMI IGA ‡, JAN KRAAL §, and ANWAR HUSSAIN ¶ x**

Received February 1, 1980, from the *School of Pharmacy, Kobe-Gakuin University, Tarumi-ku, Kobe, Japan,* ‡*Takeda Chemical Industries, Ltd., Tokyo, Japan,* and the §*College of Dentistry and the* ¶*College of Pharmacy, University of Kentucky, Lexington, KY 40506.* Accepted for publication March 19, 1981.

**Abstract** □ Interactions of phenolic compounds 4-hexylresorcinol and 3,4-dimethylphenol with esters were studied using hexane–ester cosolvent systems by both phase solubility and partitioning methods. The data obtained by the phase solubility method were variable and could not be analyzed by any mathematical model. The data obtained by the partitioning method, however, strongly suggest that 4-hexylresorcinol forms 1:1 and 1:2 complexes with the esters in hexane, while 3,4-dimethylphenol forms only 1:1 complexes with the same esters.

**Keyphrases** □ Phenolic compounds—interaction with esters using hexane–ester cosolvent systems, phase solubility and partitioning methods □ Phase solubility—interaction of phenolic compounds with esters □ 4-Hexylresorcinol—formation of 1:1 and 1:2 complexes with esters in hexane □ 3,4-Dimethylphenol—formation of 1:1 complexes with esters

In a previous investigation (1), the permeability coefficient of 4-hexylresorcinol through an ethylene–vinyl acetate copolymer membrane varied in a nonlinear fashion as a function of the vinyl acetate content of the copolymers. In the same study, the partition coefficient of the drug in the membrane varied nonlinearly as a function of the vinyl acetate content. The results were rationalized on the basis that the dihydroxy compound forms 1:1 and 1:2 complexes with the vinyl acetate portion of the copolymers.

A study was undertaken to determine the solubility behavior of 4-hexylresorcinol in hexane–ethyl acetate cosolvent systems; hexane and ethyl acetate represent the polyethylene and the vinyl acetate portions of the copolymer, respectively. Additional data in other cosolvent systems, hexane–ethyl myristate and hexane–ethyl pivalate, also were studied. To obtain further insight on the mechanism of interaction of 4-hexylresorcinol in the described cosolvent systems, the solubility of a monohydroxy compound, 3,4-dimethylphenol, also was studied.

## EXPERIMENTAL

**Materials**—4-Hexylresorcinol[1] and 3,4-dimethylphenol[2] were crystallized from hot benzene. Ethyl myristate, ethyl acetate, and ethyl pivalate, reagent grades, were purified by distillation.

**Phase Solubility Study**—To each 1.0 g of the phenols placed in respective 10-ml volumetric flasks, a 10-ml solution containing 1.5–30 × $10^{-2}$ *M* of the esters in hexane was added. The flasks were shaken for 48 hr in a water bath shaker at 25°. The solutions were centrifuged, exactly 1 ml of supernate was pipetted into a volumetric flask, and the volume was completed to the mark with hexane. Further dilutions were carried out when necessary to obtain an absorbance range within the Beer's law region. The absorbance of the solutions was determined spectrophotometrically[3] at 277.5 nm. The solubilities of the phenols were calculated using a standard curve constructed for them in hexane. This procedure was previously reported (2).

[1] Curtin-Matheson Scientific, Cincinnati, Ohio.
[2] Aldrich Chemical Co., Milwaukee, Wis.
[3] Cary 118, Varian Associates, Palo Alto, Calif.

**Partitioning Study**—Two hundred milligrams of the phenol was dissolved in 1 liter of phosphate buffer (0.1 *M*, pH 7.5), and exactly 5 ml of the aqueous solution was pipetted into a 15-ml test tube with a stopper. Exact volumes (between 2 and 5 ml) of the solutions containing 1.5–30 × $10^{-2}$ *M* of the esters in hexane were added to the test tubes, which then were shaken for 10 min. After the test tubes were centrifuged, the aqueous layer was taken and the absorbance of the solution was determined spectrophotometrically without dilution at 277.5 nm. The partition coefficients (*PC*) were calculated from the change in UV absorbance at 277.5 nm in the aqueous layer before and after the partition:

$$PC = \frac{(\text{volume of aqueous layer})(A_0 - A)}{(\text{volume of organic layer})(A)} \qquad \text{(Eq. 1)}$$

where $A_0 - A$ is the absorbance change in the aqueous layer and $A$ is the absorbance in the aqueous layer.

## RESULTS AND DISCUSSION

Tables I, II, and III show the total solubility of 4-hexylresorcinol as a function of the ethyl acetate, ethyl myristate, and ethyl pivalate concentrations in hexane, respectively. Figure 1 shows the solubility diagrams of the drug in the three cosolvent systems and demonstrates that the solubility increased in a nonlinear fashion as a function of the added esters and that the solubility behavior was different in the three cosolvent systems.

To characterize these systems mathematically, it was first assumed that 4-hexylresorcinol forms 1:1 and 1:2 complexes with esters according

**Table I—Solubility of 4-Hexylresorcinol in Ethyl Acetate–Hexane**

| Concentration of Total Ethyl Acetate in Hexane, × $10^2$ *M* | Total Solubility of 4-Hexylresorcinol, × $10^3$ *M* |
|---|---|
| 0 | 4.5 |
| 2.27 | 4.5 |
| 4.54 | — |
| 6.80 | 5.7 |
| 9.08 | 4.9 |
| 11.4 | 5.2 |
| 22.7 | 410 |
| 34.1 | 779 |
| 45.4 | 820 |

**Table II—Solubility of 4-Hexylresorcinol in Ethyl Myristate–Hexane**

| Concentration of Total Ethyl Acetate in Hexane, × $10^2$ *M* | Total Solubility of 4-Hexylresorcinol, × $10^3$ *M* |
|---|---|
| 0 | 4.5 |
| 0.61 | 5.7 |
| 1.22 | 6.5 |
| 1.84 | 7.7 |
| 2.45 | 6.9 |
| 3.01 | 12.3 |
| 6.14 | 40.2 |
| 9.21 | 48.7 |
| 12.28 | 82.8 |
| 30.7 | 362 |

0022-3549/81/1100-1225$01.00/0
© 1981, American Pharmaceutical Association

**Table III—Solubility of 4-Hexylresorcinol in Ethyl Pivalate–Hexane**

| Concentration of Total Ethyl Pivalate in Hexane, $\times 10^2$ *M* | Total Solubility of 4-Hexylresorcinol, $\times 10^3$ *M* |
|---|---|
| 1.53 | 4.7 |
| 3.06 | 4.7 |
| 4.59 | 5.2 |
| 6.12 | 5.2 |
| 7.7 | 6.3 |
| 15.3 | 153 |
| 23.0 | — |
| 30.6 | 291 |

to Eqs. 2 and 3 (3, 4):

$$HR_0 + E_0 = HR - E \quad \text{(Eq. 2)}$$

$$HR_0 + 2E_0 = HR - E_2 \quad \text{(Eq. 3)}$$

$$K_{1:1} = \frac{[HR - E]}{[HR_0][E_0]} \quad \text{(Eq. 4)}$$

$$K_{1:2} = \frac{[HR - E_2]}{[HR_0][E_0]^2} \quad \text{(Eq. 5)}$$

where $[HR_0]$, $[E_0]$, $[HR - E]$, and $[HR - E_2]$ represent the concentrations of free 4-hexylresorcinol, free ester, the 1:1 complex, and the 1:2 complex, respectively.

The total concentration of 4-hexylresorcinol, $[HR_T]$, and the total concentration of the ester, $[E_T]$, can be written according to:

$$[HR_T] = [HR_0](1 + K_{1:1}[E_0] + K_{1:2}[E_0]^2) \quad \text{(Eq. 6)}$$

$$[E_T] = [E_0] + K_{1:1}[E_0][HR_0] + 2K_{1:2}[E_0]^2[HR_0] \quad \text{(Eq. 7)}$$

Elimination of $[E_0]^2$ from Eq. 7 by using Eq. 6 gives:

$$[E_0] = \frac{1}{1 - K_{1:1}[HR_0]}\{[E_T] - 2([HR_T] - [HR_0])\} \quad \text{(Eq. 8)}$$

The combination of Eqs. 6 and 8 to eliminate $[E_0]$ gives:

$$[HR_T] = [HR_0] + \frac{K_{1:1}[HR_0]}{1 - K_{1:1}[HR_0]}\{[E_T] - 2([HR_T] - [HR_0])\} + \frac{K_{1:2}[HR_0]}{(1 - K_{1:1}[HR_0])^2}\{[E_T] - 2([HR_T] - [HR_0])\}^2 \quad \text{(Eq. 9)}$$

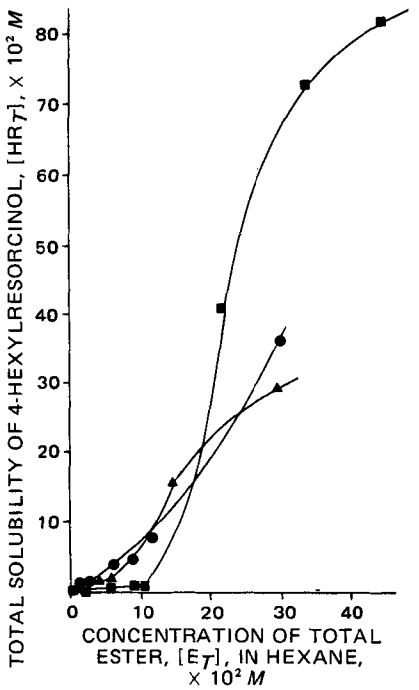


**Figure 1**—*Plot of the total solubility of 4-hexylresorinol, $[HR_T]$, as a function of the total ester concentration $[E_T]$, in hexane at 25°. Key: ■, ethyl acetate; ●, ethyl myristate; and ▲, ethyl pivalate.*

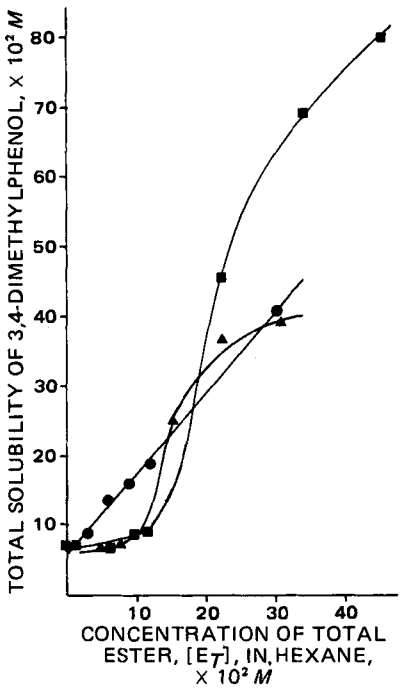


**Figure 2**—*Plot of the total solubility of 3,4-dimethylphenol as a function of the total ester concentration, $[E_T]$, in hexane at 25°. Key: ■, ethyl acetate; ●, ethyl myristate; and ▲, ethyl pivalate.*

Bringing $[HR_0]$ to the left side of Eq. 9 and dividing both sides of Eq. 9 by $[E_T] - 2([HR_T] - [HR_0])$ gives:

$$\frac{[HR_T] - [HR_0]}{[E_T] - 2([HR_T] - [HR_0])} = \frac{K_{1:1}[HR_0]}{1 - K_{1:1}[HR_0]} + \frac{K_{1:2}[HR_0]}{(1 - K_{1:1}[HR_0])^2}\{[E_T] - 2([HR_T] - [HR_0])\} \quad \text{(Eq. 10)}$$

A plot of the left-hand side of Eq. 10 *versus* $[E_T] - 2([HR_T] - [HR_0])$ should give a straight line with a positive intercept. However, the phase solubility data plotted according to Eq. 10 gave a negative intercept value, and the concentration of the free ester, $[E_0]$, calculated from Eq. 8 also gave a negative value. This result was evident from the data in Tables I–III where at $30 \times 10^{-2}$ *M* esters in hexane, the total solubility of 4-hexylresorcinol was equivalent or slightly greater than that of the ester added.

Other assumptions based on the formation of dimer or higher order complexes failed to explain the solubility behavior of 4-hexylresorcinol in these systems. Similarly, the phase solubility diagrams of 3,4-di-

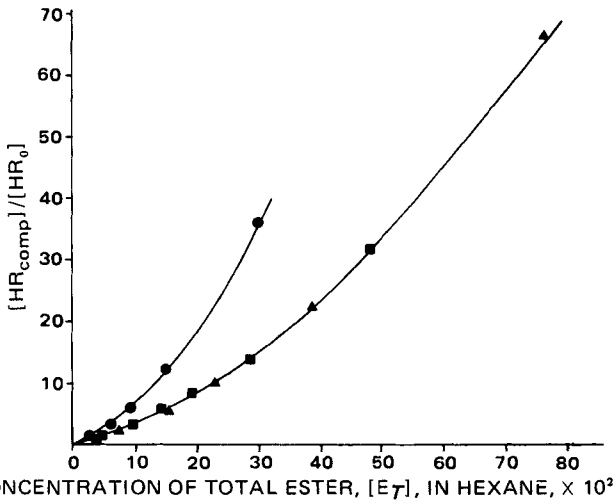


**Figure 3**—*Plot of $[HR_{comp}]/[HR_0]$ as a function of the total ester concentration, $[E_T]$, in hexane ($[HR_{comp}] = [HR_T] - [HR_0]$). Key: ■, ethyl acetate; ●, ethyl myristate; and ▲, ethyl pivalate.*

**Table IV—Extent of Complex Formation between 4-Hexylresorcinol and Ethyl Acetate in Hexane Determined by Partitioning Study**

| Concentration of Total Ethyl Acetate, $\times 10^2$ M | Partition Coefficient | $\frac{[HR_{comp}]}{[HR_0]}$ |
|---|---|---|
| 0 | 0.754 | 0 |
| 4.80 | 1.97 | 1.48 |
| 9.61 | 3.46 | 3.36 |
| 14.4 | 5.57 | 6.03 |
| 19.2 | 7.55 | 8.52 |
| 28.5 | 12.1 | 14.2 |
| 48.1 | 25.7 | 31.5 |

**Table V—Extent of Complex Formation between 4-Hexylresorcinol and Ethyl Myristate in Hexane Determined by Partitioning Study**

| Concentration of Total Ethyl Myristate, $\times 10^2$ M | Partition Coefficient | $\frac{[HR_{comp}]}{[HR_0]}$ |
|---|---|---|
| 0 | 0.754 | 0 |
| 1.53 | 1.33 | 0.674 |
| 3.07 | 1.90 | 1.40 |
| 6.14 | 3.45 | 3.35 |
| 9.21 | 5.48 | 5.91 |
| 15.0 | 10.7 | 12.4 |
| 30.1 | 29.5 | 36.2 |

**Table VI—Extent of Complex Formation between 4-Hexylresorcinol and Ethyl Pivalate in Hexane Determined by Partitioning Study**

| Concentration of Total Ethyl Pivalate, $\times 10^2$ M | Partition Coefficient | $\frac{[HR_{comp}]}{[HR_0]}$ |
|---|---|---|
| 0 | 0.754 | 0 |
| 3.84 | 1.56 | 0.962 |
| 7.68 | 2.66 | 2.361 |
| 15.4 | 5.26 | 5.63 |
| 23.0 | 9.23 | 10.6 |
| 38.4 | 18.6 | 22.5 |
| 76.4 | 54.3 | 66.6 |

methylphenol were different in the three cosolvent systems (Fig. 2). It is known that the monohydroxy compound forms a 1:1 complex with esters. If that is the case, then one should observe a linear increase in the total solubility of the phenol as a function of added esters in hexane. In Fig. 2, the increase in the solubility of 3,4-dimethylphenol as a function of added esters in hexane is nonlinear for ethyl pivalate and ethyl acetate and appears to be linear for ethyl myristate.

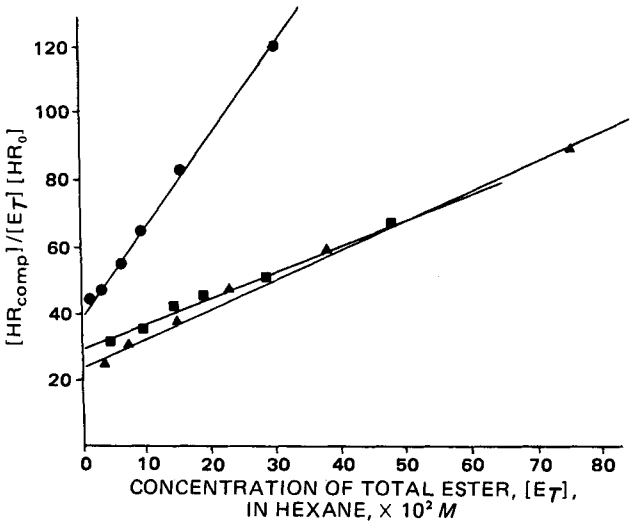


**Figure 4**—*Plot of $[HR_{comp}]/[HR_0][E_T]$ as a function of the total ester concentration, $[E_T]$, in hexane according to Eq. 16 ($[HR_{comp}] = [HR_T] - [HR_0]$). Key: ■, ethyl acetate; ●, ethyl myristate; and ▲, ethyl pivalate.*

Further examination of the equilibrated systems showed that, in addition to the supernatant and crystalline phases, an oily third phase existed. It was assumed that the abnormalities in the phase solubility diagrams of 4-hexylresorcinol and 3,4-dimethylphenol were due to the formation of a eutectic phase between the low-melting-point phenols and the esters. It is known that low-melting-point phenols form a eutectic mixture upon their interaction with a low-melting-point proton acceptor.

The irreproducibility of the phase solubility data of 4-hexylresorcinol led to a study to characterize the nature of the complexes formed using partitioning methods. The data obtained for 4-hexylresorcinol in the three cosolvent systems are shown in Tables IV–VI. The concentration of free 4-hexylresorcinol, $[HR_0]$, in hexane was obtained as follows:

$$[HR_0] = (PC \text{ at } 0\% \text{ ester})\,[HR_{H_2O}] \quad \text{(Eq. 11)}$$

where $PC$ at 0% ester is the partition coefficient of 4-hexylresorcinol at zero ester concentration, $[HR_{H_2O}]$ is the aqueous phase concentration, and the concentration of 4-hexylresorcinol in the complex is equal to $[HR_T] - [HR_0]$. A plot of $([HR_T] - [HR_0])/[HR_0]$ *versus* added ester is shown in Fig. 3 for ethyl acetate, ethyl myristate, and ethyl pivalate. As seen in Fig. 3, the increase in the total drug concentration as a function of added esters showed a positive curvature. The ratio of the free form, $[HR_0]$, and the complex form of 4-hexylresorcinol, $[HR_{comp}]$, in the organic layer is:

$$\frac{[HR_{comp}]}{[HR_0]} = \frac{[HR_T] - [HR_0]}{[HR_0]} \quad \text{(Eq. 12)}$$

$[HR_T] - [HR_0]$ is given from Eq. 6; *i.e.*,

$$[HR_T] - [HR_0] = K_{1:1}[E_0][HR_0] + K_{1:2}[HR_0][E_0]^2 \quad \text{(Eq. 13)}$$

Substituting the $[HR_T] - [HR_0]$ value from Eq. 12 in Eq. 13 gives:

$$\frac{[HR_{comp}]}{[HR_0]} = K_{1:1}[E_0] + K_{1:2}[E_0]^2 \quad \text{(Eq. 14)}$$

Dividing both sides of Eq. 14 by $[E_0]$ gives:

$$\frac{[HR_{comp}]}{[HR_0][E_0]} = K_{1:1} + K_{1:2}[E_0] \quad \text{(Eq. 15)}$$

Since the partitioning study used very dilute solutions of 4-hexylresorcinol, the concentrations of the complexes also are fairly small. Even if 100% of 4-hexylresorcinol complexes with esters, it is reasonable to replace the concentration of the free ester, $[E_0]$, by the concentration of the total ester concentration, $[E_T]$:

$$\frac{[HR_{comp}]}{[HR_0][E_T]} = K_{1:1} + K_{1:2}[E_T] \quad \text{(Eq. 16)}$$

A plot of $[HR_{comp}]/[HR_0][E_T]$ *versus* $[E_T]$ provides a straight line with a slope of $K_{1:2}$ and an intercept of $K_{1:1}$. The experiments were repeated

**Table VII—Stability Constants of 4-Hexylresorcinol and 3,4-Dimethylphenol in Hexane–Ester Systems**

| Ester | 4-Hexylresorcinol $K_{1:1}$[a], $M^{-1}$ | 4-Hexylresorcinol $K_{1:2}$[b], $M^{-2}$ | 3,4-Dimethylphenol, $K_{1:1}$, $M^{-1}$ |
|---|---|---|---|
| Ethyl acetate | 28 | 80 | 9.24 |
| Ethyl pivalate | 21 | 100 | 9.18 |
| Ethyl myristate | 40 | 266 | 15.5 |

[a] Stability constant of 1:1 complex. [b] Stability constant of 1:2 complex.

**Table VIII—Extent of Complex Formation between 3,4-Dimethylphenol and Ethyl Acetate Determined by Partitioning Study**

| Total Concentration of 3,4-Dimethylphenol, $\times 10^2$ M | Partition Coefficient | $\frac{[DMP_{comp}]}{[DMP_0]}$ |
|---|---|---|
| 0 | 1.37 | — |
| 4.80 | 1.96 | 0.44 |
| 9.16 | 2.53 | 0.85 |
| 19.23 | 3.86 | 1.83 |
| 28.48 | 5.00 | 2.67 |
| 48.07 | 7.60 | 4.57 |

**Table IX—Extent of Complex Formation between 3,4-Dimethylphenol and Ethyl Myristate Determined by Partitioning Study**

| Total Concentration of 3,4-Dimethylphenol, $\times 10^2 M$ | Partition Coefficient | $\frac{[DMP_{comp}]}{[DMP_0]}$ |
|---|---|---|
| 0 | 1.37 | — |
| 1.53 | 1.73 | 0.27 |
| 3.07 | 1.96 | 0.43 |
| 6.14 | 2.61 | 0.91 |
| 9.21 | 3.31 | 1.43 |
| 15.03 | 4.57 | 2.35 |
| 30.00 | 7.94 | 4.83 |

for various cosolvent systems, and each showed a straight-line relationship between the two parameters (Fig. 4). The stability constants, $K_{1:1}$ and $K_{1:2}$, for each ester were calculated from Fig. 4 and are shown in Table VII. It is evident from these results that 4-hexylresorcinol forms not only 1:1 but also 1:2 complexes with esters in hexane. The stability constant values obtained for ethyl myristate were somewhat higher than those for the other esters. This result is probably due to the fact that ethyl myristate has a larger hydrocarbon chain, which results in a better interaction with the hydrophobic portion of phenols.

To ascertain whether the formation of 1:2 complexes is due to the involvement of the two hydroxy groups of 4-hexylresorcinol, the partitioning study was repeated with 3,4-dimethylphenol. The data obtained from this study are shown in Tables VIII–X. A plot of $[DMP_{comp}]/[DMP_0][E_T]$ *versus* the total ester concentration is shown in Fig. 5; $[DMP_{comp}]$ is the concentration of 3,4-dimethylphenol in the complex form, and $[DMP_0]$ is the concentration of the free form.

**Table X—Extent of Complex Formation between 3,4-Dimethylphenol and Ethyl Pivalate Determined by Partitioning Study**

| Total Concentration of 3,4-Dimethylphenol, $\times 10^2 M$ | Partition Coefficient | $\frac{[DMP_{comp}]}{[DMP_0]}$ |
|---|---|---|
| 0 | 1.37 | — |
| 3.82 | 1.78 | 0.30 |
| 7.68 | 2.33 | 0.70 |
| 15.36 | 3.33 | 1.44 |
| 23.04 | 4.32 | 2.17 |
| 38.40 | 6.63 | 3.86 |

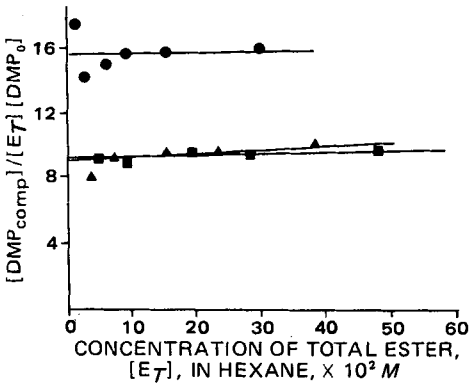


**Figure 5**—*Plot of $[DMP_{comp}]/[DMP_{free}][E_T]$ as a function of the total ester concentration, $[E_T]$, in hexane; $[DMP_{comp}]$ and $[DMP_{free}]$ represent the concentrations of complexed and free forms of 3,4-dimethylphenol, respectively. ($[DMP_{comp}] = [DMP_T] - [DMP_0]$). Key: ■, ethyl acetate; ●, ethyl myristate; and ▲, ethyl pivalate.*

As seen in Fig. 5, the monohydroxy compound forms only a 1:1 complex with the esters. The stability constants calculated from Fig. 5 are given in Table VII. The results of this study substantiate the conclusion that the diffusion of 4-hexylresorcinol through ethylene–vinyl acetate copolymers involved the formation of 1:1 and 1:2 complexes between the drug and the vinyl acetate portion of the copolymers.

## REFERENCES

(1) E. Akaho, Ph.D. dissertation, University of Kentucky, Lexington, Ky. 1979.

(2) H. B. Kostenbauder and T. Higuchi, *J. Am. Pharm. Assoc. Sci. Ed.*, **45**, 518 (1956).

(3) T. Higuchi, J. H. Richards, S. S. Dacis, A. Kamada, J. P. How, M. Nakano, N. I. Nakano, and I. H. Pitman, *J. Pharm. Sci.*, **58**, 661 (1969).

(4) H. Fung and T. Higuchi, *ibid.*, **60**, 1782 (1971).

# High-Performance Liquid Chromatographic Analysis of Chemical Stability of 5-Aza-2′-deoxycytidine

**KUN-TSAN LIN*x, RICHARD L. MOMPARLER*‡, and GEORGES E. RIVARD***

Received December 17, 1979, from the *Centre de Recherche Pédiatrique, Hôpital Sainte-Justine, and the ‡Département de Pharmacologie, Université de Montréal, Montréal, Québec, Canada H3T 1C5. Accepted for publication March 31, 1981.

**Abstract** □ The chemical stability of 5-aza-2′-deoxycytidine (I) in acidic, neutral, and alkaline solutions was analyzed by high-performance liquid chromatography. In alkaline solution, I underwent rapid reversible decomposition to *N*-(formylamidino)-*N*′-β-D-2-deoxyribofuranosylurea (II), which decomposed irreversibly to form 1-β-D-2′-deoxyribofuranosyl-3-guanylurea (III). The pseudo-first-order rate constants for this reaction were determined. The decomposition of I in alkaline solution was identical to that reported previously for the related analog, 5-azacytidine. However, in neutral solution (or water), there was a marked difference in the decomposition of I and 5-azacytidine. The same decomposition products were formed from 5-azacytidine in neutral solution as in alkaline solution. However, in neutral solution, I decomposed to II and three unknown compounds that were chromophoric at 254 nm. Compound I was most stable when stored in neutral solution at low temperature.

**Keyphrases** □ 5-Aza-2′-deoxycytidine—analysis of chemical stability using high-performance liquid chromatography □ Antileukemic agents—5-aza-2′-deoxycytidine, analysis of chemical stability using high-performance liquid chromatography □ High-performance liquid chromatography—analysis of chemical stability of 5-aza-2′-deoxycytidine

5-Aza-2′-deoxycytidine (I), a nucleoside antimetabolite, is a very active antileukemic agent in mice (1, 2) and a potent cytotoxic agent against neoplastic cells *in vitro* (2, 3). This antimetabolite is related to 5-azacytidine, an agent currently used in the clinical treatment of acute leukemia (4).



*0022-3549/81/1100-1228$01.00/0*
*© 1981, American Pharmaceutical Association*

**Table IX—Extent of Complex Formation between 3,4-Dimethylphenol and Ethyl Myristate Determined by Partitioning Study**

| Total Concentration of 3,4-Dimethylphenol, $\times 10^2 M$ | Partition Coefficient | $\frac{[DMP_{comp}]}{[DMP_0]}$ |
|---|---|---|
| 0 | 1.37 | — |
| 1.53 | 1.73 | 0.27 |
| 3.07 | 1.96 | 0.43 |
| 6.14 | 2.61 | 0.91 |
| 9.21 | 3.31 | 1.43 |
| 15.03 | 4.57 | 2.35 |
| 30.00 | 7.94 | 4.83 |

for various cosolvent systems, and each showed a straight-line relationship between the two parameters (Fig. 4). The stability constants, $K_{1:1}$ and $K_{1:2}$, for each ester were calculated from Fig. 4 and are shown in Table VII. It is evident from these results that 4-hexylresorcinol forms not only 1:1 but also 1:2 complexes with esters in hexane. The stability constant values obtained for ethyl myristate were somewhat higher than those for the other esters. This result is probably due to the fact that ethyl myristate has a larger hydrocarbon chain, which results in a better interaction with the hydrophobic portion of phenols.

To ascertain whether the formation of 1:2 complexes is due to the involvement of the two hydroxy groups of 4-hexylresorcinol, the partitioning study was repeated with 3,4-dimethylphenol. The data obtained from this study are shown in Tables VIII–X. A plot of $[DMP_{comp}]/[DMP_0][E_T]$ *versus* the total ester concentration is shown in Fig. 5; $[DMP_{comp}]$ is the concentration of 3,4-dimethylphenol in the complex form, and $[DMP_0]$ is the concentration of the free form.

**Table X—Extent of Complex Formation between 3,4-Dimethylphenol and Ethyl Pivalate Determined by Partitioning Study**

| Total Concentration of 3,4-Dimethylphenol, $\times 10^2 M$ | Partition Coefficient | $\frac{[DMP_{comp}]}{[DMP_0]}$ |
|---|---|---|
| 0 | 1.37 | — |
| 3.82 | 1.78 | 0.30 |
| 7.68 | 2.33 | 0.70 |
| 15.36 | 3.33 | 1.44 |
| 23.04 | 4.32 | 2.17 |
| 38.40 | 6.63 | 3.86 |

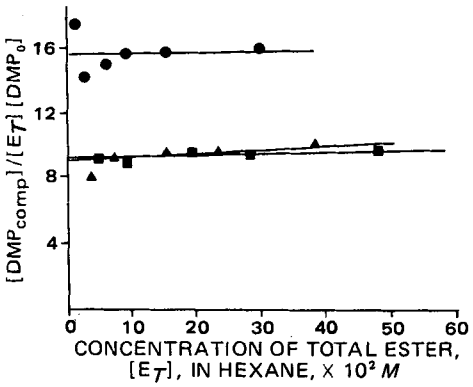


**Figure 5**—*Plot of $[DMP_{comp}]/[DMP_{free}][E_T]$ as a function of the total ester concentration, $[E_T]$, in hexane; $[DMP_{comp}]$ and $[DMP_{free}]$ represent the concentrations of complexed and free forms of 3,4-dimethylphenol, respectively. ($[DMP_{comp}] = [DMP_T] - [DMP_0]$). Key: ■, ethyl acetate; ●, ethyl myristate; and ▲, ethyl pivalate.*

As seen in Fig. 5, the monohydroxy compound forms only a 1:1 complex with the esters. The stability constants calculated from Fig. 5 are given in Table VII. The results of this study substantiate the conclusion that the diffusion of 4-hexylresorcinol through ethylene–vinyl acetate copolymers involved the formation of 1:1 and 1:2 complexes between the drug and the vinyl acetate portion of the copolymers.

## REFERENCES

(1) E. Akaho, Ph.D. dissertation, University of Kentucky, Lexington, Ky. 1979.

(2) H. B. Kostenbauder and T. Higuchi, *J. Am. Pharm. Assoc. Sci. Ed.*, **45**, 518 (1956).

(3) T. Higuchi, J. H. Richards, S. S. Dacis, A. Kamada, J. P. How, M. Nakano, N. I. Nakano, and I. H. Pitman, *J. Pharm. Sci.*, **58**, 661 (1969).

(4) H. Fung and T. Higuchi, *ibid.*, **60**, 1782 (1971).

# High-Performance Liquid Chromatographic Analysis of Chemical Stability of 5-Aza-2′-deoxycytidine

**KUN-TSAN LIN*x, RICHARD L. MOMPARLER*‡, and GEORGES E. RIVARD***

Received December 17, 1979, from the *Centre de Recherche Pédiatrique, Hôpital Sainte-Justine, and the ‡Département de Pharmacologie, Université de Montréal, Montréal, Québec, Canada H3T 1C5. Accepted for publication March 31, 1981.

**Abstract** □ The chemical stability of 5-aza-2′-deoxycytidine (I) in acidic, neutral, and alkaline solutions was analyzed by high-performance liquid chromatography. In alkaline solution, I underwent rapid reversible decomposition to *N*-(formylamidino)-*N*′-β-D-2-deoxyribofuranosylurea (II), which decomposed irreversibly to form 1-β-D-2′-deoxyribofuranosyl-3-guanylurea (III). The pseudo-first-order rate constants for this reaction were determined. The decomposition of I in alkaline solution was identical to that reported previously for the related analog, 5-azacytidine. However, in neutral solution (or water), there was a marked difference in the decomposition of I and 5-azacytidine. The same decomposition products were formed from 5-azacytidine in neutral solution as in alkaline solution. However, in neutral solution, I decomposed to II and three unknown compounds that were chromophoric at 254 nm. Compound I was most stable when stored in neutral solution at low temperature.

**Keyphrases** □ 5-Aza-2′-deoxycytidine—analysis of chemical stability using high-performance liquid chromatography □ Antileukemic agents—5-aza-2′-deoxycytidine, analysis of chemical stability using high-performance liquid chromatography □ High-performance liquid chromatography—analysis of chemical stability of 5-aza-2′-deoxycytidine

5-Aza-2′-deoxycytidine (I), a nucleoside antimetabolite, is a very active antileukemic agent in mice (1, 2) and a potent cytotoxic agent against neoplastic cells *in vitro* (2, 3). This antimetabolite is related to 5-azacytidine, an agent currently used in the clinical treatment of acute leukemia (4).



*0022-3549/81/1100-1228$01.00/0*
*© 1981, American Pharmaceutical Association*

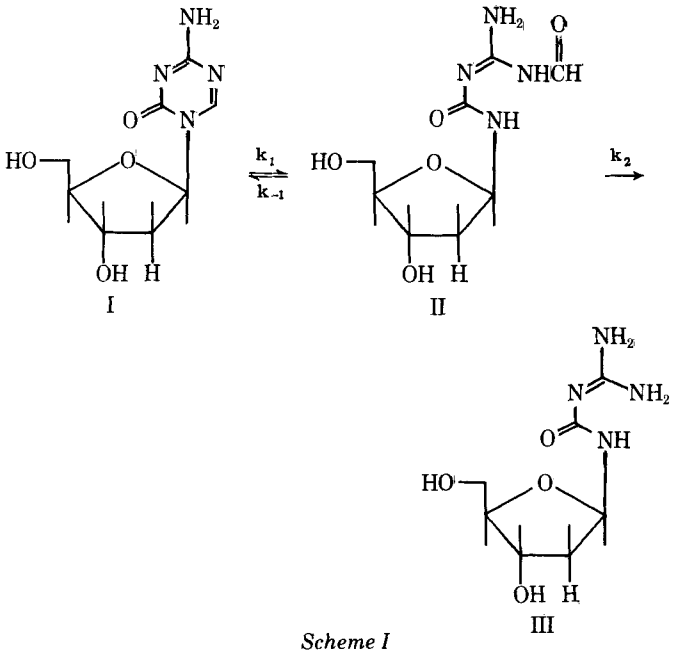

*Scheme I*

## BACKGROUND

One major problem encountered in the clinical formulation of 5-azacytidine is its chemical instability, leading to solutions of decreasing potency on storage. The chemical stability of 5-azacytidine was first studied by Píthová *et al.* (5), who demonstrated that in alkaline solution the triazine ring of 5-azacytidine opens and loses a formyl group to form 1-β-D-ribofuranosyl-3-guanylurea. These workers proposed that the intermediate compound in this reaction was *N*-(formylamidino)-*N'*-β-D-ribofuranosylurea, but they were unable to isolate it using paper chromatography because of its chemical instability. Beisler (6), using high-performance liquid chromatography (HPLC), isolated and identified this intermediate compound and showed that it could be partially converted back to 5-azacytidine.

The chemical decomposition of I at alkaline pH (Scheme I) presumably follows the same reaction steps as described previously for 5-azacytidine. In alkaline solutions, I undergoes a reversible hydrolytic reaction to form *N*-(formylamidino)-*N'*-β-D-2-deoxyribofuranosylurea (II), which, by the irreversible loss of the formyl group, forms 1-β-D-2'-deoxyribofuranosyl-3-guanylurea (III).

The present study investigated the decomposition of I in acidic, neutral, and alkaline solutions and at different temperatures to illustrate the chemical stability of this compound.

## EXPERIMENTAL

5-Aza-2'-deoxycytidine (I) was synthesized[1] by modification of an earlier method (7).

**Method of Analysis**—HPLC[2] was performed with a variable-wavelength detector by monitoring at 220 or 254 nm. Analytical and preparative work was accomplished with a 300 × 3.9-mm i.d. commercially packed octadecylsilane column[3], which was eluted at a flow rate of 2 ml/min with 10 m*M* potassium phosphate buffer (pH 6.8). For analytical and preparative work, 20- and 500-μl injector loops, respectively, were used.

Stock solutions of 10 m*M* I in water were stored at −70°. Aliquots of this solution were thawed quickly and stored at 1–2°. The following buffers were used for the pH stability studies: phosphoric acid, pH 2.2; phosphoric acid–potassium phosphate, pH 3.2; sodium acetate buffer, pH 4.5 and 5.7; potassium phosphate buffer, pH 6.4 and 7.0; and sodium borate, pH 8.5, 9.2, 9.8, and 10.4. Compound II was prepared by addition of 20 μl of 0.5 *M* sodium borate, pH 10.4, to a 1.0-ml solution of 10 m*M* I. The mixture was incubated for 2 min at 24° and then neutralized with 20 μl of 1.0 *M* $KH_2PO_4$, and a 500-μl sample was injected onto the column for isolation of II.

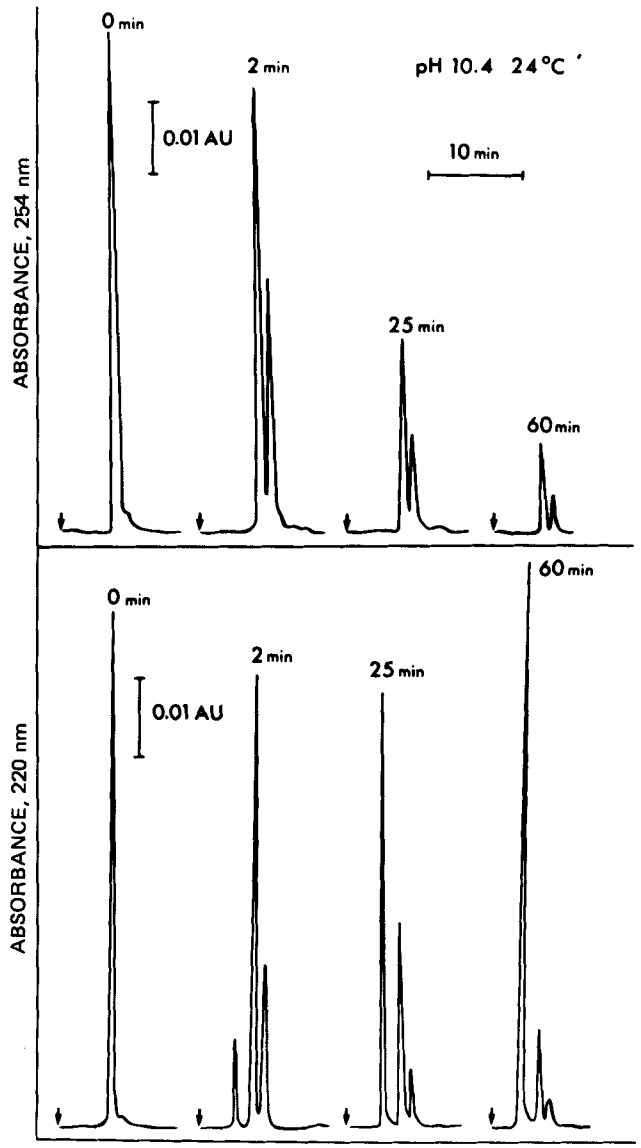


**Figure 1**—*Decomposition of I at pH 10.4 and 24°. Compound I (1.0 mM) was dissolved in 10 mM borate buffer (pH 10.4). At the indicated times, an aliquot of the solution was neutralized with phosphate buffer and analyzed by HPLC at 254 and 220 nm.*

**Kinetic Experiments**—A series of tubes containing 10 μl of 0.5 *M* stock sodium borate buffer were incubated at 37° for 10 min. Then 100 μl of isolated II (in 10 m*M* potassium phosphate, pH 6.8) was added to each tube to start the reaction. At timed intervals, an aliquot was withdrawn, and 20 μl was injected onto the column. The absorbance at 220 nm was recorded, and the relative concentration of the observed degradation products was characterized by peak heights. Similar experimental procedures were followed for the kinetic study on 5-azacytidine[4].

## RESULTS

The decomposition of I at pH 10.4 and 24° as determined by HPLC is shown in Fig. 1. Measurement of the absorbance of the column eluate at 254 nm initially showed a single major peak (I) with a $t_R$ value of 5.5 min. With time, a second peak (II) appeared with a $t_R$ value of 6.6 min. Both peaks showed a gradual decrease in peak size with time. At 220 nm, the column eluate initially showed a single major peak (I) with a $t_R$ = 5.5 min. With time, peak II ($t_R$ = 6.6 min) and peak III ($t_R$ = 3.5 min) became evident. At 60 min, most of I decomposed to peak III.

[1] By Dr. A. Piskala, Institute of Organic Chemistry and Biochemistry, Czechoslovak Academy of Science, 16610 Prague 6, Czechoslovakia.

[2] Model 110 pump and Hitachi variable-wavelength detector, Altex Scientific, Berkeley, Calif.

[3] μBondapak $C_{18}$, Waters Associates, Framingham, Mass.

[4] Drug Synthesis and Chemistry Branch, Division of Cancer Treatment, National Cancer Institute, Bethesda, Md.

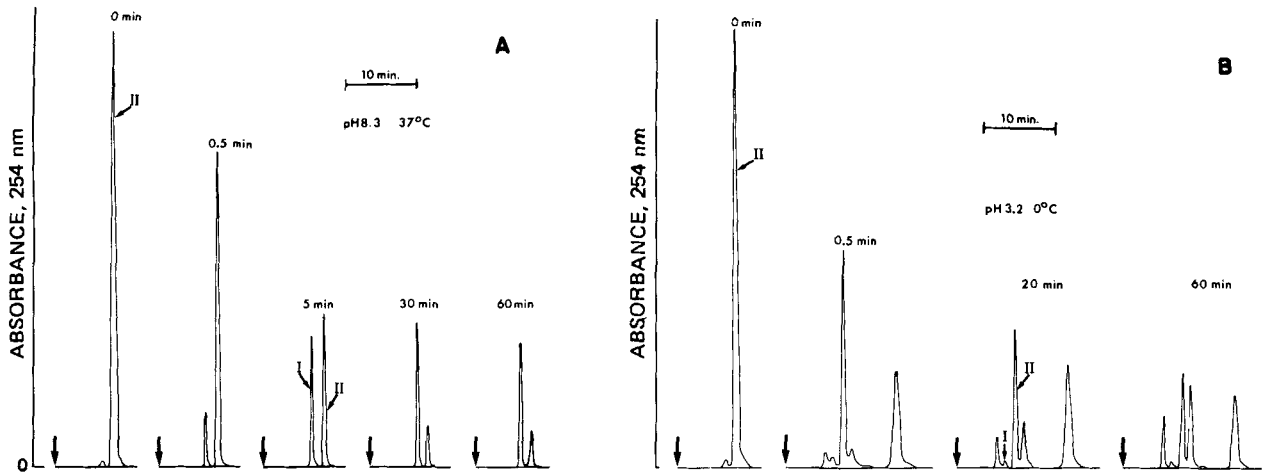


**Figure 2**—*Conversion of II to I at pH 8.3, 37° (A), and to unidentified compounds at pH 3.2, 0° (B). Peak II was isolated by HPLC and placed in 20 mM potassium phosphate buffer (at final pH 8.3 or 3.2). At the indicated times, aliquots of this solution were analyzed by HPLC.*

When II was isolated and placed at pH 8.3 and 37°, I appeared rapidly, indicating that II could be converted to I (Fig. 2A). However, when II was placed in an acidic solution (pH 3.2), it did not produce I; three unidentified peaks at 254 nm were observed. The latter reaction was very rapid, even at 0° (Fig. 2B).

The decomposition of I and 5-azacytidine when stored in water and in pH 7.4 phosphate buffer at 24° for 24 hr is compared in Fig. 3. Absorbance measurements at 254 nm of the column eluate showed five major peaks for I and two major peaks for 5-azacytidine. At 220 nm, the column eluate showed seven major peaks for I and three major peaks for 5-azacytidine.

The decomposition rates of I in acidic, neutral, and basic solutions at 24 and 37° are shown in Figs. 4A and 4B, respectively. Compound I decomposed more rapidly at pH 2.2, 8.5, and 9.2 than at pH 5.7, 6.4, and 7.0. The decomposition rate of I was the slowest at pH 7.0. At pH 2.2 a peak with the same $t_R$ value (2.3 min) as 5-azacytosine appeared on the chromatogram. The decomposition rate of I was very temperature dependent. For example, at pH 7.0, the decomposition rate was about sevenfold greater at 37 than at 24°.

A kinetic study at pH 8.1 and 9.5 was then carried out with II as the starting substance. According to Scheme I, the pseudo-first-order rate constants $k_1$, $k_{-1}$, and $k_2$ were determined using the following differential

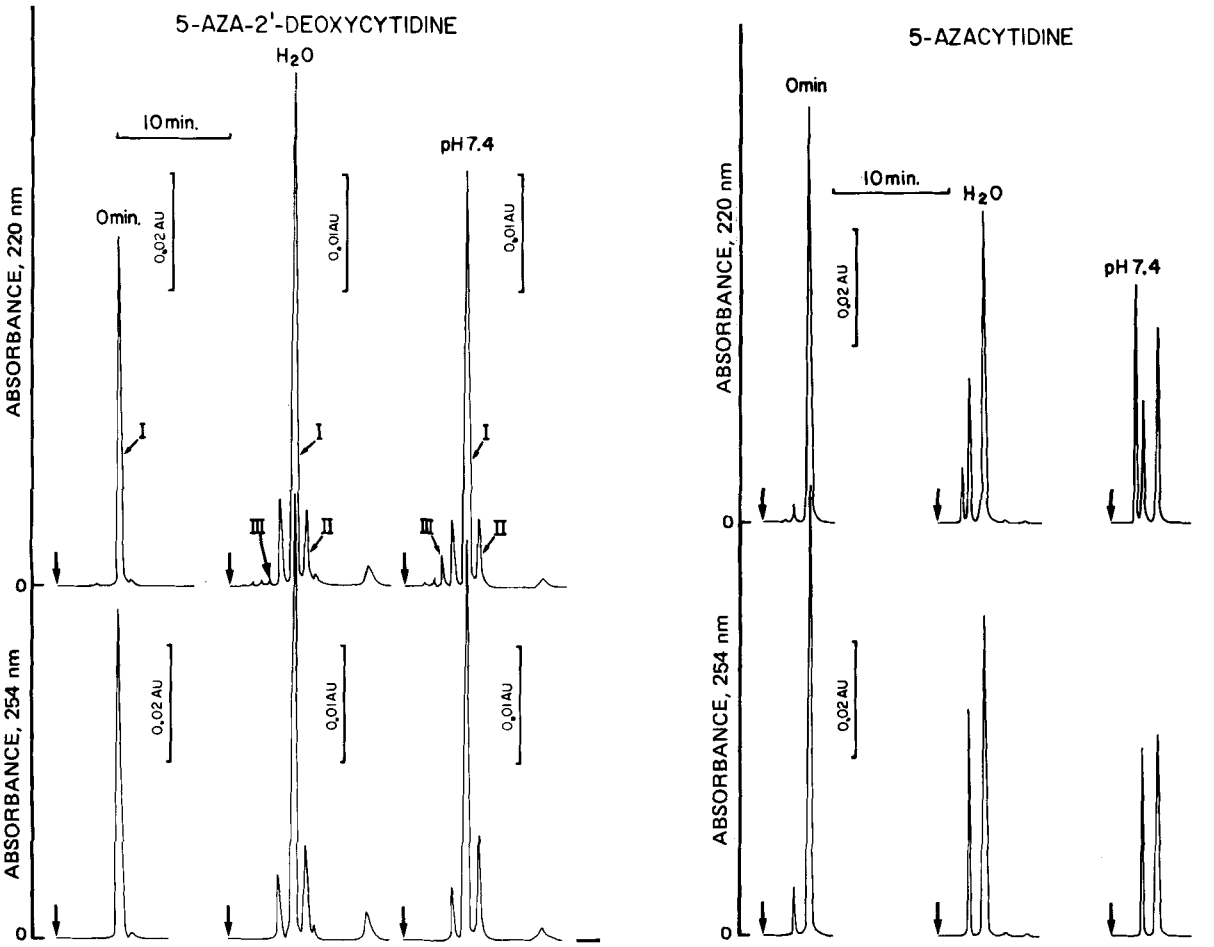


**Figure 3**—*Decomposition of I and 5-azacytidine in pH 7.4 phosphate buffer and water. 5-Azacytidine (0.5 mM) and I (0.5 mM) were dissolved in 10 mM potassium phosphate (pH 7.4) and water and incubated at 24°. At the indicated times, aliquots of these solutions were analyzed by HPLC at 254 and 220 nm.*

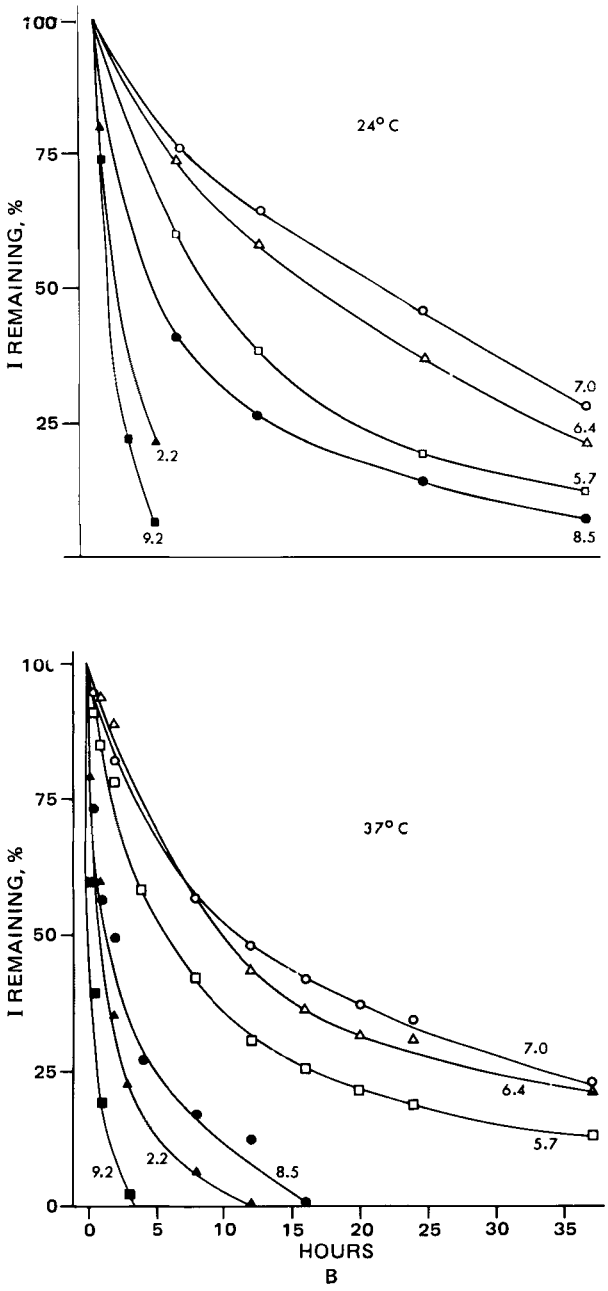


**Figure 4**—*Effect of pH and temperature on the stability of I. Compound I (1.0 mM) was dissolved in 10 mM of the appropriate buffer with the indicated pH and incubated at either 24° (top) or 37° (bottom). At the indicated times, an aliquot of the solution was neutralized with phosphate buffer and analyzed by HPLC.*

equations (8):

$$I_t = k_{-1} II_0 \left( \frac{1}{B-A} e^{-At} + \frac{1}{A-B} e^{-Bt} \right) \quad \text{(Eq. 1)}$$

$$II_t = II_0 \left( \frac{k_1 - A}{B-A} e^{-At} + \frac{k_1 - B}{A-B} e^{-Bt} \right) \quad \text{(Eq. 2)}$$

$$III_t = II_0 \left( 1 - \frac{k_2(k_1 - A)}{A(B-A)} e^{-At} - \frac{k_2(k_1 - B)}{B(A-B)} e^{-Bt} \right) \quad \text{(Eq. 3)}$$

Here $A$ and $B$ are roots of the following quadratic equation taken with the reverse signs:

$$X^2 + X(k_1 + k_2 + k_{-1}) + k_1 k_2 = 0 \quad \text{(Eq. 4)}$$

The rate constants thus obtained are presented in Table I and were used to generate time–concentration profiles for I–III. Normalized experimental data obtained by HPLC were superimposed on these generated time–concentration profiles (Fig. 5). Similar procedures were used for the kinetic study of 5-azacytidine, and the results are shown in Table I and Figs. 6 and 7.

**Table I—Rate Constants for the Alkaline Decomposition of I and 5-Azacytidine at 37°**

| Compound and pH[a] | Pseudo-First-Order Rate Constant, $min^{-1}$ | | |
|---|---|---|---|
| | $k_1$ | $k_2$ | $k_{-1}$ |
| 5-Azacytidine, 9.5 | $2.0 \times 10^{-1}$ | $2.2 \times 10^{-1}$ | $6.0 \times 10^{-1}$ |
| 5-Azacytidine, 8.1 | $1.7 \times 10^{-2}$ | $2.0 \times 10^{-2}$ | $5.6 \times 10^{-2}$ |
| I, 9.5 | $2.2 \times 10^{-1}$ | $2.8 \times 10^{-1}$ | $7.5 \times 10^{-1}$ |

[a] The pH value was determined at 37° in a separate tube by mixing one volume of 0.5 *M* stock sodium borate buffer with 10 volumes of 10 m*M* potassium phosphate (pH 6.8).

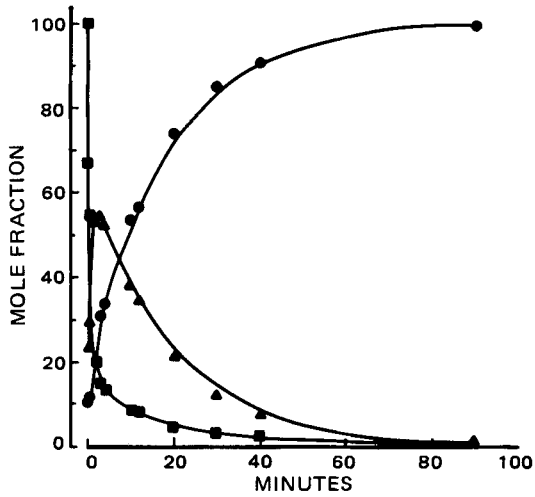


**Figure 5**—*Time–concentration profile of decomposition for I at pH 9.5 and 37°. Key: ▲, normalized data for I; ■, normalized data for II; and ●, normalized data for III. Solid lines were generated by computer for ▲, ■, and ● using rate constants determined independently.*

## DISCUSSION

The hydrolysis of 5-azacytidine in alkaline solution and water results in the opening of the triazine ring between C-6 and N-1 to form *N*-(formylamidino)-*N'*-β-D-ribofuranosylurea in a reversible reaction; when this latter compound loses the formyl group, it irreversibly forms 1-β-D-ribofuranosyl-3-guanylurea (5, 6). By using quantum chemical cal-

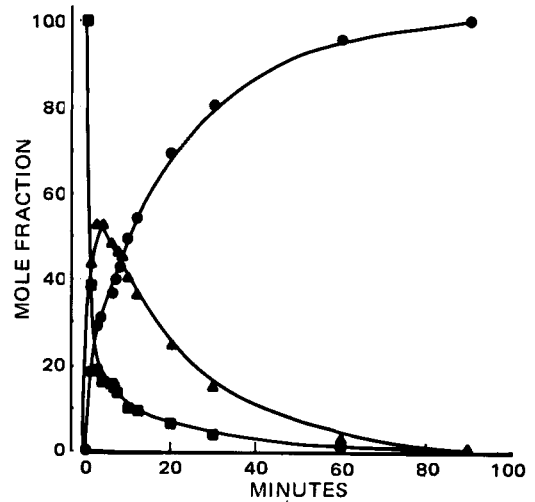


**Figure 6**—*Time–concentration profile of decomposition for 5-azacytidine at pH 9.5 and 37°. Key: ▲, normalized data for 5-azacytidine; ■, normalized data for N-(formylamidino)-N'-β-D-ribofuranosylurea; and ● normalized data for 1-β-D-ribofuranosyl-3-guanylurea. Solid lines were generated by computer for ▲, ■, and ● using rate constants determined independently.*

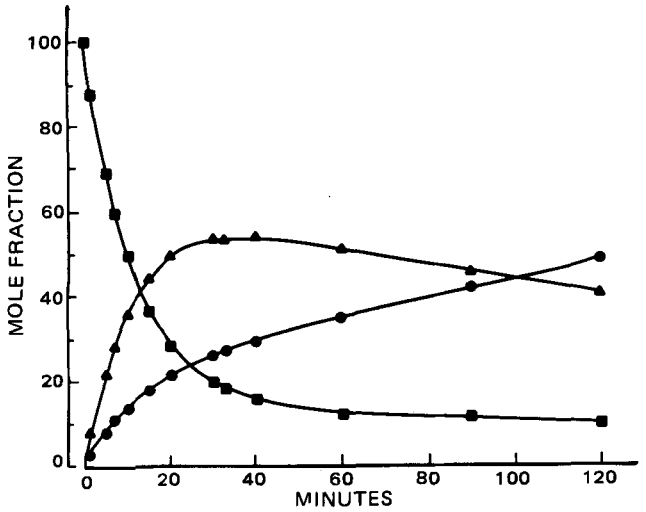


**Figure 7**—*Time–concentration profile of decomposition for 5-azacytidine at pH 8.1 and 37°. Key: ▲, normalized data for 5-azacytidine; ■, normalized data for* N-*(formylamidino)-*N′*-β-*D*-ribofuranosylurea; and ●, normalized data for 1-β-*D*-ribofuranosyl-3-guanylurea. Solid lines were generated by computer for ▲, ■, and ● using rate constants determined independently.*

culations, it was shown (5) that the electron density at C-6 of 5-azacytosine is much lower than cytosine, making this position more susceptible to nucleophilic attack by a hydroxyl ion.

From the structural similarity of 5-azacytidine and I, it would seem that I would decompose in alkaline solution according to Scheme I. This study supports this reaction scheme in alkaline solution. As shown in Fig. 1, the decomposition of peak I ($t_R$ = 5.5 min) at pH 10.4 produced peak II ($t_R$ = 6.6 min) when the column eluate was monitored at 254 nm. Peak III was not observed on this chromatogram because guanylurea derivatives are nonchromophoric at 254 nm (5, 6).

However, at 220 nm, peak III ($t_R$ = 3.5 min) became apparent following the decomposition of II to III. When peak II was isolated, it had the same $UV_{max}$ of 238 nm as reported previously (6) for *N*-(formylamidino)-*N*′-β-ribofuranosylurea. The hydrolysis of I in alkaline solution produced an initial increase in absorbance[5] at 238 nm, supporting the formation of II, since the formylguanylurea derivative has a much higher extinction coefficient than 5-azacytosine derivatives at this wavelength (6). The conversion of II to I (Fig. 2A) indicates that this reaction is reversible, which is in agreement with other observations (5, 6) for 5-azacytidine.

There were marked differences in the decomposition of I and 5-azacytidine in phosphate buffer (pH 7.4) and water (Fig. 3). In these solvents, 5-azacytidine decomposed to form formylguanylurea and guanylurea derivatives, as reported previously (6). However, the decomposition of I in phosphate buffer or water was very different from that of 5-azacytidine as shown by the presence of five (254 nm) and seven (220 nm) peaks on the chromatograms of I. Two of these peaks represent I and II, whereas the other peaks were not identified. These unidentified peaks could also be produced rapidly by placing II at pH 3.2 (Fig. 2B), even at 0°. These unidentified compounds were not the intermediates that eventually formed III, since they were not converted to III when placed in alkaline buffer, as would happen to I and II under the same conditions.

Determination of the pseudo-first-order rate constants for I and 5-azacytidine at pH 9.5 and 37° demonstrated that both compounds decomposed at comparable rates, although the formylguanylurea derivative for ribose appeared to be slightly more stable than that of deoxyribose (Table I). A 22-fold decrease in the hydroxyl-ion concentration (pH 9.5–8.1) reduced all three rate constants for 5-azacytidine equally by about 11-fold. Lowering the pH from 9.5 to 8.1 also greatly reduced the conversion rate of II to I and to III (Figs. 5 and 8). The kinetic data obtained for I at pH 8.1 did not quite fit in Eqs. 1–3 because apparently some of the decomposition did not follow Scheme I precisely due to the formation of minor unidentified peaks. Thus the rate constants were not determined. These unidentified peaks became increasingly prominent as the pH was lowered, and there was virtually no conversion of II to I at pH <4.6. (Fig. 2B).

[5] R. L. Momparler, unpublished data.

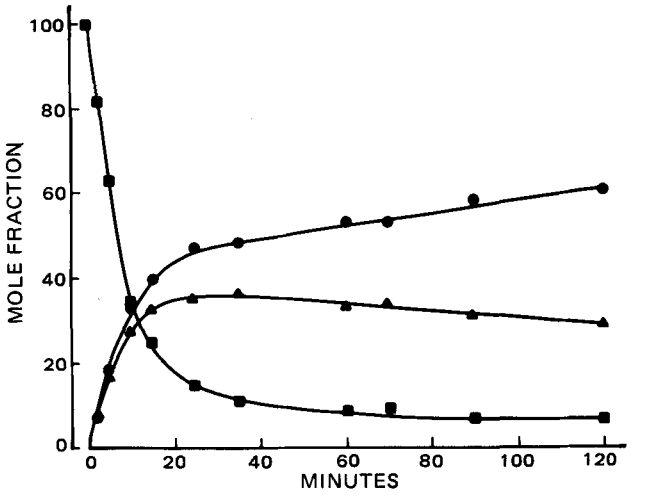


**Figure 8**—*Time–concentration profile of decomposition for I at pH 8.1 and 37°. Key: ▲, normalized data for I; ■, normalized data for II; and ●, normalized data for III.*

Comparison of the overall stability profile of I in aqueous buffer solution at various pH levels showed that I was most stable at neutral pH and at low temperature (Fig. 4). The instability of I at high pH could be explained on the basis that the opening of the triazine ring ($k_1$) and the breakage of an amide bond ($k_2$) is facilitated by a hydroxyl ion. Reduction in pH would slow down both these events and thus stabilize I. However, I became increasing unstable as the pH was gradually reduced below 7.0. This result might be due to the increase in the rate of ring opening as well as to the instability of II in acidic solutions; thus, once ring opening took place and produced II, the latter broke down to the unidentified peaks more rapidly and minimized the reversal back to I (Fig. 2B). In strong acidic solution (with pH <2.2), breakage of the glycolytic bond of I occurred, producing 5-azacytosine[6] as reported previously for I (9) and for 5-azacytidine (5, 10).

The effect of pH and temperature on the chemical stability of 5-azacytidine was studied by Chan *et al.* (11), who observed that this compound is most stable at pH 7.0 and that its rate of decomposition increases in solutions of high or low pH and with temperature.

## REFERENCES

(1) F. Šorm and J. Veselý, *Neoplasma*, **15,** 339 (1968).

(2) R. L. Momparler and F. A. Gonzales, *Cancer Res.*, **38,** 2673 (1978).

(3) R. L. Momparler and J. Goodman, *ibid.*, **37,** 1636 (1977).

(4) W. R. Volger, D. S. Miller, and J. W. Keller, *Blood*, **48,** 331 (1976).

(5) P. Píthová, A. Pískala, J. Pitha, and F. Šorm, *Collect. Czech. Chem. Commun.*, **30,** 2801 (1965).

(6) J. A. Beisler, *J. Med. Chem.*, **21,** 204 (1978).

(7) J. Pliml and F. Šorm, *Collect. Czech. Chem. Commun.*, **29,** 2576 (1964).

(8) N. M. Rodiguin and E. N. Rodiguina, "Consecutive Chemical Reactions," Van Nostrand, Princeton, N.J., 1979.

(9) A. Pískala, M. Synackova, H. Tomankova, P. Fiedler, and V. Zizkovsky, *Nucleic Acid Res.*, **4,** s109 (1978).

(10) R. E. Notari and J. L. DeYoung, *J. Pharm. Sci.*, **64,** 1148 (1975).

(11) K. K. Chan, D. D. Giannini, J. A. Staroscik, and W. Sadee, *ibid.*, **68,** 807 (1979).

## ACKNOWLEDGMENTS

Supported by U.S. Public Health Service Grant CA23340 from the National Cancer Institute.

The authors thank Suzanne Beaudet for assistance in preparation of this manuscript.

[6] Unpublished observations.

# Distribution, Metabolism, and Elimination of Phenobarbital in Rats: Physiologically Based Pharmacokinetic Model

**J. M. ENGASSER* ˣ, F. SARHAN ‡, C. FALCOZ *, M. MINIER *, P. LETOURNEUR *, and G. SIEST ‡**

Received February 15, 1980, from the **Laboratoire des Sciences du Génie Chimique, CNRS-ENSIC, 1, rue Grandville, 54042 Nancy Cedex, France*, and the ‡*Laboratoire de Biochimie Pharmacologique, Faculté de Pharmacie, 7, rue Albert Lebrun, 54001 Nancy, France.*
Accepted for publication March 26, 1981.

**Abstract** □ The distribution, metabolism, and elimination kinetics at two different doses of phenobarbital were examined in rats. After intravenous injection, phenobarbital distributed very rapidly to the liver and kidneys, less rapidly to the muscle and gut, and much more slowly to the brain. At the higher dose, a concentration rebound was observed 1 hr after injection. In addition, phenobarbital distributed unevenly in various organs as a result of a different extent of drug binding. A physiologically based model, including enterohepatic cycling and diffusion resistances between blood and tissue, is proposed for phenobarbital pharmacokinetics. It satisfactorily describes phenobarbital distribution in rats at the two doses and allows an evaluation of fundamental physicobiochemical parameters such as drug–tissue binding constants, blood–tissue transport coefficients, metabolism, and elimination rate constants.

**Keyphrases** □ Phenobarbital—physiologically based model for distribution, metabolism, and elimination kinetics in rats □ Models, pharmacokinetic—for phenobarbital distribution, metabolism, and elimination, rats □ Pharmacokinetics—model for phenobarbital distribution, metabolism, and elimination, rats

Physiologically based models are being used more frequently in pharmacokinetic studies (1, 2). Based on anatomical and physiological characteristics and on drug physicochemical parameters, these models greatly facilitate pharmacokinetic data interpretation and allow extrapolation outside the data range and to other species. Physiological models are of greatest interest for the determination of basic physicobiochemical parameters relating to drug disposition and action and for the rational design of drug posology. Their potential was recently illustrated for anticancer drugs (2) and for digoxin (3), thiopental (4, 5), and pesticides (6).

The present study, which examined the distribution, metabolism, and elimination of phenobarbital following intravenous injection in rats, proposes a physiologically based pharmacokinetic model for phenobarbital. The drug, known to have different pharmacological action (sedative, hypnotic, and antiepileptic) depending on its concentration level in the brain, is also a powerful inducer of hepatic metabolizing enzymes (7). A physiological model considering phenobarbital diffusion to the brain, metabolism in the liver, binding to proteins and tissues, renal elimination, and intestinal resorption following biliary excretion can satisfactorily describe phenobarbital distribution and fate in rats.

## EXPERIMENTAL

Male Sprague–Dawley rats[1], 200–240 g, were injected intravenously with an isotonic sodium chloride solution of phenobarbital sodium[2]. Two doses, 30 and 50 mg/kg, were used. At different times after injection in the tail vein, the rats were decapitated, and blood and tissues were collected. After blood centrifugation at 9000 rpm, plasma was separated. Tissues and plasma were then stored at −14° until analysis.

Phenobarbital was extracted from plasma, urine, and bile using a one-step extraction procedure with chloroform; drug extraction from tissues and feces was performed with a previously described, two-step procedure with chloroform (8). Phenobarbital was then assayed in a gas chromatograph equipped with a nitrogen selective detector (9) to improve assay specificity and sensitivity. Analysis sensitivity is <1 μg of phenobarbital/sample.

For the evaluation of urinary excretion, rats were placed in metabolic cages. Urine, free from fecal contamination, was collected at timed intervals and then assayed for phenobarbital. The biliary excretion of phenobarbital was determined on bile duct-cannulated rats previously anesthetized with ether.

Drug binding to plasma proteins was measured with an equilibrium dialysis system[3]. When using 1-ml polytef[4] dialysis cells with cellulose membranes[5], binding equilibrium can be rapidly achieved. Experiments were performed with undiluted plasma adjusted to pH 7.35 by carbogen (5% carbon dioxide, 95% oxygen) bubbled on one side of the membrane and an isotonic phosphate buffer (pH 7.35), initially spiked with phenobarbital, on the other side. Phenobarbital binding to the membrane was <5%. A total plasma concentration of 10–110 μg/ml was investigated.

## RESULTS

Figure 1 shows the measured distribution of phenobarbital in the blood, liver, brain, muscle, intestine, and kidneys at the two injected doses of 50 and 30 mg/kg. Each point represents the mean obtained for five rats, with a standard deviation between 15 and 20%. The following pharmacokinetic characteristics can be observed. First, while phenobarbital distributed very rapidly in the liver and kidneys, it entered more slowly in brain, muscle, and intestine, probably because of mass transport limitations. The slowness of drug diffusion was particularly pronounced in the brain where the maximum concentration was reached only after 1 hr at the two investigated doses.

Second, a concentration rebound was observed in blood and several organs, ~1 hr after drug injection, at least at the higher dose. This phenomenon may be the result of enterohepatic cycling[6]. A biliary excretion of unchanged phenobarbital (~110 μg in the 1st hr at the high dose) was indeed observed in bile duct-cannulated rats.

Third, during the elimination phase, the concentration remained at different levels in the various organs, with the liver presenting the highest phenobarbital affinity. This result suggests different binding extents by plasma proteins and tissues.

Further insight into the kinetics of the limiting processes is obtained by plotting the ratio of the drug concentration over the administered dose. As seen in Fig. 2 for the various tissues, the points corresponding to the two doses come close together, indicating that phenobarbital pharmacokinetics can be considered dose independent at the investigated concentrations. Consequently, in a first approximation, first-order transport, metabolism, and excretion processes, as well as linear phenobarbital binding to plasma proteins and tissues, may be assumed.

[1] Domaine des Oncins, Saint-Germain sur l'Arbresle, France.
[2] Merck.
[3] Dianorm apparatus, Diachema, Birmenstorf, Zurich, Switzerland.
[4] Teflon.
[5] Spectrapor 2, Spectrum Medical Industries, Los Angeles, Calif.
[6] J. Caldwell, J. E. Croft, and R. L. Smith, St. Mary's Hospital Medical School, London, England, to be published.

0022-3549/81/1100-1233$01.00/0
© 1981, American Pharmaceutical Association

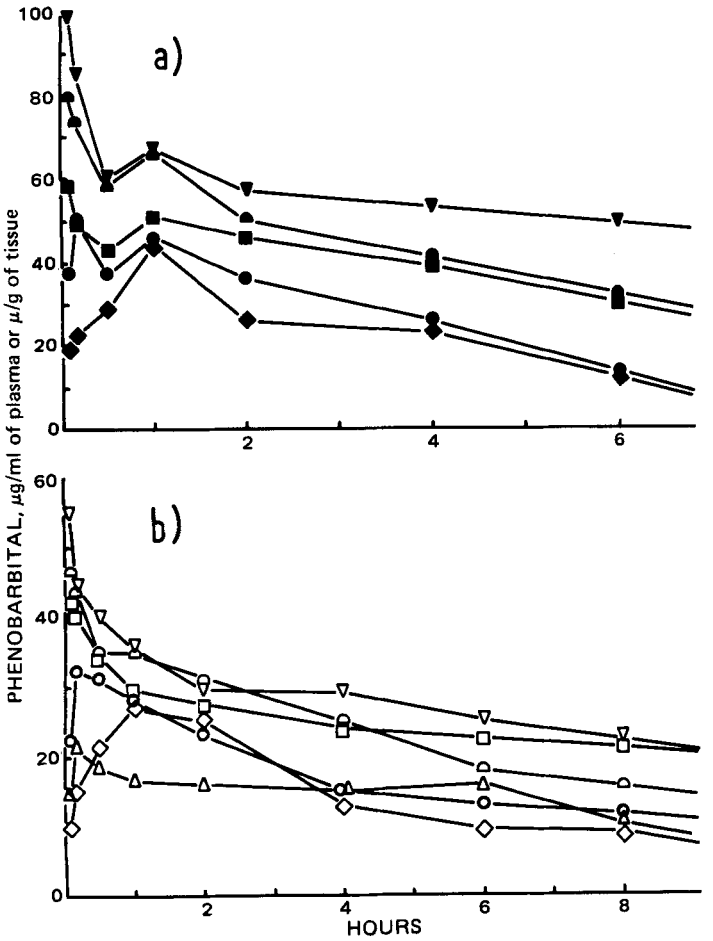


**Figure 1**—*Time evolution of phenobarbital distribution in rat tissues after intravenous injection of 50 (a) and 30 (b) mg/kg. Key (solid symbols for a and open symbols for b): ◓, ◔, plasma; ◆, ◇, brain; ▼, ▽, liver; ■, □, kidneys; and ●, ○, muscle; △, gut.*

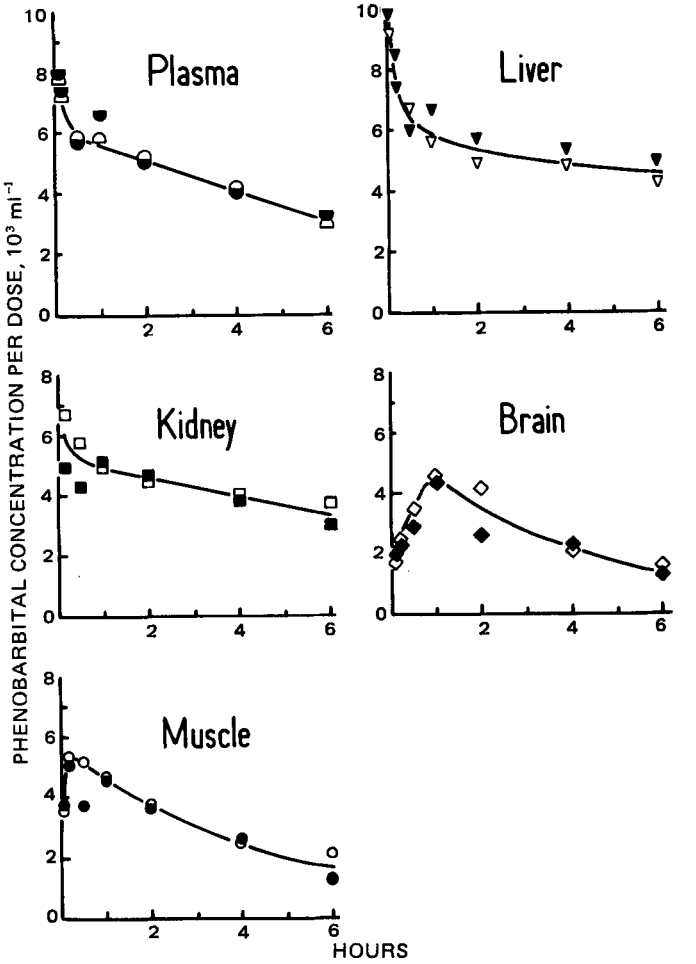


**Figure 2**—*Variation with time of the ratio of phenobarbital concentration over the administered dose in various rat tissues as calculated from Fig. 1 Key: solid symbols, 50 mg/kg; and open symbols, 30 mg/kg.*

The kinetics of urinary excretion were independently determined by simultaneously measuring the rate of urinary excretion and plotting the results as a function of drug plasma concentration. Figure 3 shows that the elimination rate was proportional to plasma concentration for concentrations of <30 μg/ml, with, however, the rate falling off at higher levels. During the first 24 hr, the total amount of excreted unchanged phenobarbital was ~10% of the administered dose.

## THEORY

**Flow-Sheet Diagram**—In its basic structure, the model in Scheme I is similar to models previously proposed for other drugs (4, 10). It depicts the main organs (brain, liver, gut, kidneys, and muscles) represented by a physiological compartment and connected by the blood network. Moreover, each organ and tissue is subdivided into the flowing blood and the tissue region. Tissues not experimentally considered are lumped into an additional compartment, called "remaining distribution volume," analogous to the distribution volume concept introduced in classical pharmacokinetics.

In view of the previous experimental results, the model also takes into account the enterohepatic cycle. The progress of the biliary-secreted drug towards the gut is handled by a plug flow compartment with a given residence time. Since the intestinal resorption of phenobarbital is relatively fast, the excreted drug is assumed to be directly transferred to the gut tissue.

In addition, this model includes some diffusional limitations between the perfusing blood and the brain, muscle, and intestinal tissues. In other organs, drug membrane transport is fast enough to assume equilibrium between blood and tissue.

To account for drug elimination, the model also considers drug metabolism in the liver tissue and urinary excretion in the kidney.

**Injection**—To represent intravenous administration of the drug, the injection function $Dg(t)$ proposed by Bischoff and Dedrick (4) was used such that:

$$g(t) = \frac{30}{\theta}\left(\frac{t}{\theta}\right)^2\left(1 - \frac{t}{\theta}\right)^2 \qquad \text{(Eq. 1)}$$

where $g(t)$ is a normalized impulse function (minutes$^{-1}$), $\theta$ is the injection duration (minutes), and $D$ is the total dose (micrograms).

**Drug Binding to Plasma Proteins**—The total blood concentration can be expressed as:

$$C^*_{Bl} = (1 - \text{HEM})\, C^*_P + \text{HEM}\, C^*_{BlC} \qquad \text{(Eq. 2)}$$

where:

$C^*_{Bl}$ = total blood concentration (micrograms per milliliter)
$C^*_P$ = total plasma concentration
$C^*_{BlC}$ = total blood cell concentration.
HEM = hematocrit (dimensionless)

It was observed experimentally that for phenobarbital the total blood concentration is equal to the total plasma concentration, *i.e.*:

$$C^*_{Bl} = C^*_P = C^*_{BlC} \qquad \text{(Eq. 3)}$$

Blood may thus be assimilated to plasma.

In the plasma, it is necessary to distinguish between the free and bound drug concentration:

$$C^*_P = C_P + C'_P \qquad \text{(Eq. 4)}$$

where $C_P$ is the free plasma concentration, and $C'_P$ is the bound plasma concentration.

According to drug binding experiments, there is a linear relationship between plasma bound and free phenobarbital concentrations, *i.e.*:

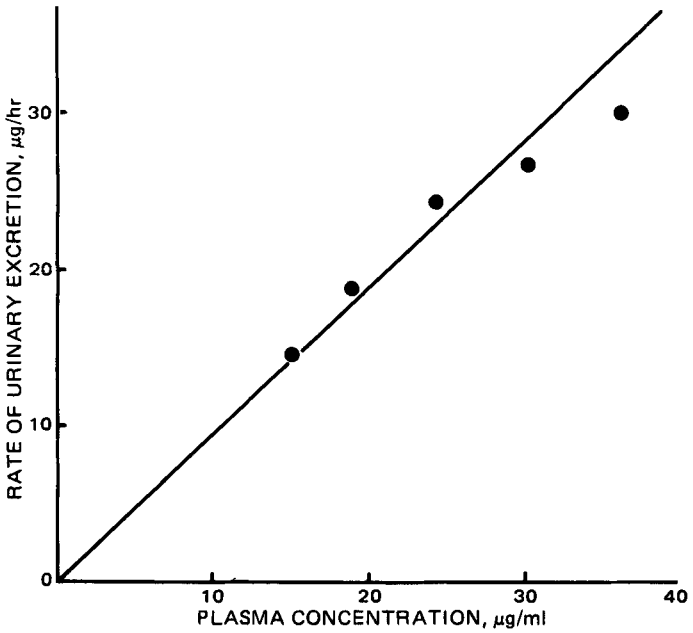


**Figure 3**—*Rate of urinary phenobarbital excretion as a function of plasma concentration after a 30-mg/kg iv dose. The rate was calculated from the quantity of phenobarbital excreted over 2 hr, and the corresponding plasma concentration is the one at the middle of the collection period. The urinary elimination rate constant was evaluated from the slope of the line drawn through the experimental points.*

$$C'_P = b_P C_P \qquad \text{(Eq. 5)}$$

where $b_P$ represents the plasma binding constant. Accordingly, the total plasma concentration is simply related to the free concentration by:

$$C^*_P = (1 + b_P)C_p \qquad \text{(Eq. 6)}$$

**Drug Binding to Tissues**—As previously proposed (4), the total tissue concentration is expressed as:

$$C^*_T = f_T C_T + (1 - f_T)C'_T \qquad \text{(Eq. 7)}$$

where:

$C^*_T$ = total tissue concentration
$C_T$ = free tissue concentration
$C'_T$ = bound tissue concentration
$f_T$ = water fraction of tissue (dimensionless)

Preliminary binding experiments with diluted muscles, as well as other results (11) with rat lung and liver slices, suggest a linear relationship for phenobarbital tissue binding, *i.e.*:

$$C'_T = b_T C_T \qquad \text{(Eq. 8)}$$

where $b_T$ is the binding constant of the tissue. Under these conditions:

$$C^*_T = [f_T + (1 - f_T)b_T]C_T \qquad \text{(Eq. 9)}$$

According to Eqs. 6 and 9, for blood and tissues the total concentration, $C^*$, is proportional to the free concentration, $C$:

$$C^* = \Phi C \qquad \text{(Eq. 10)}$$

where:

$$\Phi = f + (1 - f)b \qquad \text{(Eq. 11)}$$

The proportionality constant, $\Phi$, represents the binding ability of blood and tissues (12).

**Blood–Tissue Distribution**—In organs where the transport of drug between blood and tissue is very fast, equal free concentrations in plasma and tissue were assumed, *i.e.*:

$$C_T = C_P \qquad \text{(Eq. 12)}$$

However, in brain, muscle, and gut, drug transport between blood and tissue may represent a limiting process. Under these conditions the transport rate is expressed as:

$$r_t = H(C_P - C_T) \qquad \text{(Eq. 13)}$$

where $r_t$ is the drug transport rate from plasma to tissue (μg/min), and $H$ is the drug transport coefficient or tissue permeability (ml/min).

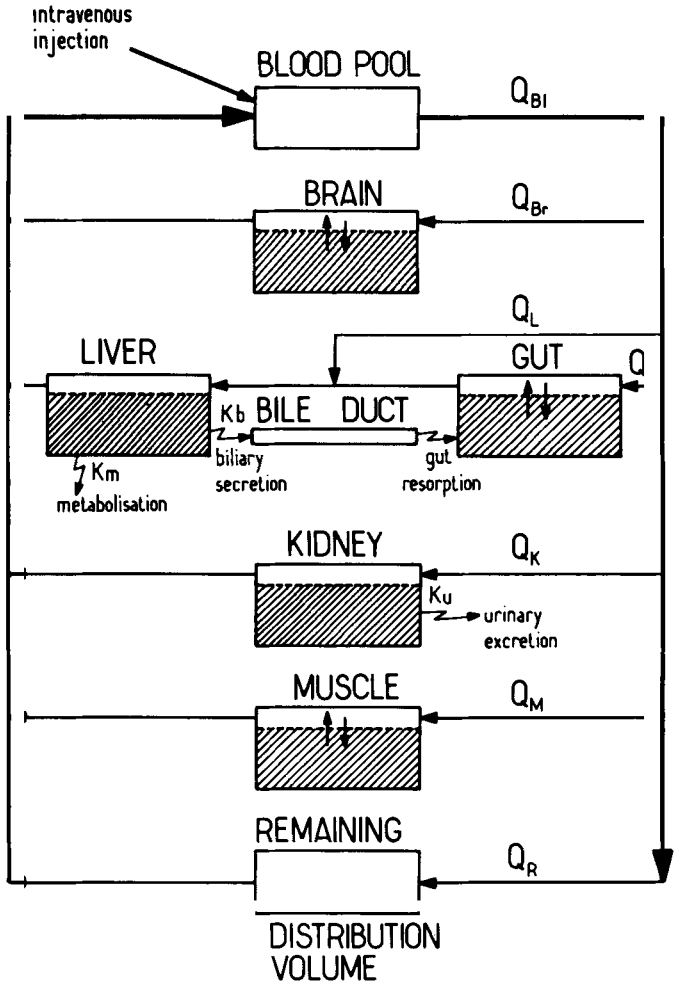


*Scheme I—Physiological pharmacokinetic model for phenobarbital.*

**Drug Elimination Processes**—Phenobarbital elimination by urinary excretion, hepatic metabolism, and biliary excretion is assumed to be a first-order process and thus is represented by:

$$r_e = KC_T \qquad \text{(Eq. 14)}$$

where:

$r_e$ = elimination rate (μg/min)
$K$ = elimination (excretion or metabolism) rate constant (ml/min)
$C_T$ = free concentration in elimination tissue (μg/ml)

The total amount of drug, $E$ (in micrograms), excreted in a given organ is equal to:

$$E = \int_0^t KC_T\,dt \qquad \text{(Eq. 15)}$$

where $t$ is time (minutes).

**Mass Balance Equations**—The resulting mass balance equations for the various compartments are as follows (notation is given in the *Appendix*).

For blood:

$$V_{Bl}\Phi_{Bl}\frac{dC_{Bl}}{dt} = Dg(t) + \Phi_{Bl}\,[Q_{Br}C_{Br,Bl} + (Q_L + Q_G)C_{L,Bl} + Q_K C_{K,Bl} + Q_M C_{M,Bl} + Q_R C_R - Q_{Bl}C_{Bl}] \qquad \text{(Eq. 16a)}$$

where:

$$Q_R = Q_{Bl} - Q_{Br} - Q_L - Q_G - Q_K - Q_M \qquad \text{(Eq. 16b)}$$

**Table I—Values of parameters for a Standard 200-g Male Rat [a]**

| Compartment | Physiological Parameters: Volume, ml: Tissue | Volume, ml: Blood [b] | Blood Flow, ml/min | Water Fraction [c] ($f$) | Pharmacokinetic Parameters: Binding: Constant ($b$) | Binding: Ability ($\Phi$) | Transfer Coefficient, ml/min | Elimination Constant, ml/min |
|---|---|---|---|---|---|---|---|---|
| Blood | | 13 | 58(*) | — | 1.1 | 2.1 | | |
| Brain | 2 | 0.022 | 2 | 0.80 | 1.1 | 1. | 0.15 | |
| Gut | 5.6 | 0.23 | 8.5 | 0.76 | 1.7 | 1.2 | 20 | $K_b = 1$ |
| Liver | 6.7 | 0.7 | 1 | 0.75 | 6.7 | 2.4 | | $K_m = 0.4$ |
| Kidneys | 2.3 | 0.21 | 8.5 | 0.80 | 6.1 | 2. | | $K_u = 0.04$ |
| Muscle | 93 | 0.4 | 10 | 0.78 | 3.6 | 1.6 | 50 | |
| Remaining distribution volume | | 55 | 28 [d] | | | | | |

[a] References 3, 5, and 13–23. [b] Blood permitted to ooze from tissue (13). [3] From dog values (5). [d] Calculated from difference between total cardiac output (*) and the sum of the tissue blood flows.

For brain blood:

$$V_{Br,Bl}\Phi_{Bl}\frac{dC_{Br,Bl}}{dt} = Q_{Br}\Phi_{Bl}(C_{Bl} - C_{Br,Bl}) + H_{Br}(C_{Br,T} - C_{Br,Bl}) \quad \text{(Eq. 17a)}$$

For brain tissue:

$$V_{Br,T}\Phi_{Br}\frac{dC_{Br,T}}{dt} = H_{Br}(C_{Br,Bl} - C_{Br,T}) \quad \text{(Eq. 17b)}$$

For gut blood:

$$V_{G,Bl}\Phi_{Bl}\frac{dC_{G,Bl}}{dt} = Q_G\Phi_{Bl}(C_{Bl} - C_{G,Bl}) + H_G(C_{G,T} - C_{G,Bl}) \quad \text{(Eq. 18a)}$$

For gut tissue:

$$V_{G,T}\Phi_G\frac{dC_{G,T}}{dt} = H_G(C_{G,Bl} - C_{G,T}) + K_bC_{L,T}^{(t-T_{del})} \quad \text{(Eq. 18b)}$$

where $C_{L,T}^{(t-T_{del})}$ is the free tissular liver concentration at time $(t - T_{del})$.

For liver:

$$C_{L,Bl} = C_{L,T} = C_L \quad \text{(Eq. 19a)}$$

$$(V_{L,Bl}\Phi_{Bl} + V_{L,T}\Phi_L)\frac{dC_L}{dt} = \Phi_{Bl}[Q_GC_{G,Bl} + Q_LC_{Bl} - (Q_G + Q_L)C_L] - (K_m + K_b)C_L \quad \text{(Eq. 19b)}$$

For kidney:

$$C_{K,Bl} = C_{K,T} = C_K \quad \text{(Eq. 20a)}$$

$$(V_{K,Bl}\Phi_{Bl} + V_{K,T}\Phi_K)\frac{dC_K}{dt} = Q_K\Phi_{Bl}(C_{Bl} - C_K) - K_uC_K \quad \text{(Eq. 20b)}$$

For muscle blood:

$$V_{M,Bl}\Phi_{Bl}\frac{dC_{M,Bl}}{dt} = Q_M\Phi_{Bl}(C_{Bl} - C_{M,Bl}) + H_M(C_{M,T} - C_{M,Bl}) \quad \text{(Eq. 21a)}$$

For muscle tissue:

$$V_{M,T}\Phi_M\frac{dC_{M,T}}{dt} = H_M(C_{M,Bl} - C_{M,T}) \quad \text{(Eq. 21b)}$$

For the remaining distribution volume:

$$V_R\frac{dC_R}{dt} = Q_R(C_{Bl} - C_R) \quad \text{(Eq. 22)}$$

The resulting set of nonlinear differential equations is solved simultaneously with a fourth-order Runge–Kutta method on a digital computer.

**Values of Parameters**—The various anatomic and physiological parameters, blood flow rates, tissue volumes, and water fractions for a 200-g male rat are summarized in Table I. The remaining distribution volume was determined by fitting the theoretical curves to the experimental results.

For the intravenous drug injection, a value of 0.25 min for $\theta$ is representative of the experimental conditions.

The plasma binding constant $b_P$ was experimentally determined as 1.1, which corresponds to a proportionality constant, $\Phi p$, of 2.1 between the total and free plasma concentration. The binding constants $b_T$ for the tissues as defined in Eq. 8 were obtained by curve fitting. They were most precisely determined from the different drug levels in the elimination phase, as experimentally observed in Fig. 1. The resulting values of $b_T$ and the tissue binding ability $\Phi_T$, *i.e.*, the proportionality constant between total and free concentration, are shown in Table I.

The urinary elimination constant, $K_u$, defined in Eq. 20*b* as the proportionality constant between the rate of urinary elimination and the free tissue, *i.e.*, free plasma, concentration in the kidney can be simply evaluated from the slope of the line obtained on Fig. 3 as 0.04 ml/min.

The metabolism rate constant $K_m$, which, according to Eq. 14, relates the rate of metabolism to the free liver tissue concentration, was estimated by dividing the amount of drug metabolized, ~80% of the dose, during the first 24 hr by the area under the free plasmatic concentration *versus* time curve (assuming equal free plasma and free liver tissue concentration):

$$K_m = (1 + b_P)\frac{\int_0^{24} K_mC_L\,dt}{\int_0^{24} C_P\,dt} \quad \text{(Eq. 23)}$$

This evaluation procedure yields a value of 0.4 ml/min for $K_m$.

As previously suggested (12), the passage of the drug through the enterohepatic cycle was approximated in Eq. 18*b* by a delay time, $T_{del}$, which approximates the drug travel through the bile and down the small intestine before absorption in the gut tissue. This residence time, $T_{del}$, through the enterohepatic cycle was adjusted to 55 min to obtain a concentration rebound ~1 hr after drug injection. The magnitude of the biliary excretion constant, $K_b$, which directly determines the height of the concentration rebound, was chosen as 1 ml/min.

Finally, blood–tissue transfer coefficients in brain, muscle, and gut were determined by fitting the theoretical curves to the experimentally observed tissue concentrations during the distribution phase. The corresponding values are given in Table I.

## DISCUSSION

The theoretical drug distribution curves in the various compartments obtained with the previously defined model are shown in Fig. 4. The two sets of curves corresponding to the two injected doses of 30 and 50 mg/kg were calculated with the same physiological and pharmacokinetic parameters (Table I).

Although in its present state the model does not perfectly describe the observed phenobarbital distribution, it appears satisfactory in many respects. It is the simplest possible model based on the animal anatomy and taking into account key physiological parameters such as protein and tissue binding, liver metabolism, renal excretion, bile excretion, intestinal reabsorption, and tissue diffusion. This model, which only entails simple first-order physical and chemical rate processes, can especially account for the slow drug penetration in the brain, for the concentration rebound 1 hr after injection, and for different tissue drug levels during the elimination phase. Moreover, for several tissues it adequately predicts drug levels at two different doses, at least at the lower dose.

The present model can be improved to get a close agreement with experimental observation. The model does not precisely describe, at the two doses, the relatively narrow peak or its exact height in the brain tissue. The introduction into the model of a simple reversible mass transfer process through the brain–blood barrier accounts for the relatively slow drug entry into the brain but also results in slow drug release during the elimination phase. The observed rapid phenobarbital concentration decrease in the brain may be explained and modeled by some more

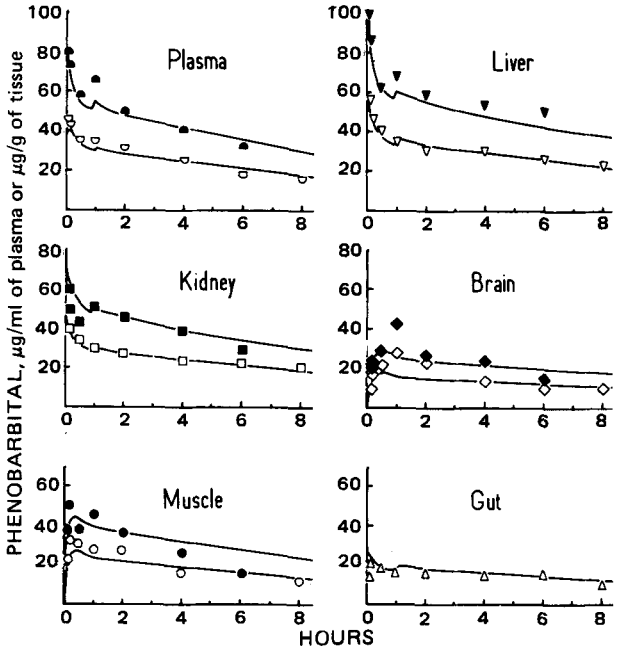


**Figure 4**—*Calculated time distribution of phenobarbital in various rat tissues, using the physiologically based pharmacokinetic model at 50 and 30 mg/kg. The corresponding experimental points are taken from Fig. 1. Key: solid symbols, 50 mg/kg; and open symbols, 30 mg/kg.*

complex asymmetric transport process, which greatly favors drug transport, at least during the elimination phase. Some active drug secretion from brain tissue to the peripheral blood was experimentally demonstrated for triamterene (24) and salicylic acid (25).

Another observation concerns the enterohepatic cycle, which was introduced in the model to explain the phenobarbital concentration rebound. Similar rebounds were observed in rats with morphine (27), phenolphthalein (28), and phenytoin metabolites (29). The lag time ranged from 4 to 6 hr, accounting, in addition to hepatic formation and biliary excretion, for the intestinal hydrolysis of the glucurono conjugate prior to reabsorption of the compound; this rebound did not occur with bile duct-cannulated rats (28, 29).

As demonstrated by the present model, despite continuous bile flow in the rat, phenobarbital biliary excretion followed by intestinal reabsorption can partly account for the concentration rebound observed at the higher dose ~1 hr after drug injection. This phenomenon can be theoretically obtained by considering a mean residence time of ~55 min of the drug through bile and intestine before reabsorption, provided the excreted drug concentration is sufficiently high. Autoradiographic studies with [$^{14}$C]phenobarbital[7] demonstrated an intensive enterohepatic recycling. On the other hand, Caldwell *et al.*[6] found that ~35% of an intraperitoneal [$^{14}$C]phenobarbital dose was excreted by the bile while only 1% was recovered in the feces during the first 24 hr. Moreover, unmetabolized phenobarbital seems to represent about one-third of the total gut content radioactivity. Personal experiments and other work (26) on bile duct-cannulated rats confirm the biliary excretion of unmodified phenobarbital.

However, according to this model based on a simple delay time through the enterohepatic cycle, an approximate 10-fold greater amount of phenobarbital than that experimentally observed has to be excreted in the bile to account for the observed peak height. Thus, further experiments are necessary to quantify the mechanism of biliary excretion. Moreover, if enterohepatic cycling is the actual phenomenon responsible for the concentration rebound, a more detailed representation of the cycle may be needed to improve model validity.

According to Fig. 4, phenobarbital elimination at the high dose is slightly faster than that predicted by simple first-order renal excretion and liver metabolism. A better quantitative understanding of the various elimination processes represents another prerequisite for better physiological modeling.

In the present model, a remaining distribution volume was introduced to represent all nonspecified organs and tissues. This distribution volume can account for the approximate 30% of the dose that distributes elsewhere than in blood, liver, brain, muscle, gut, and kidneys. According to autoradiographic results[7] for phenobarbital, the remaining distribution volume corresponds primarily to fat, lungs, and the heart, providing that in all tissues, except for the intestine and gut contents, there are no metabolites but only unchanged drug[6].

In conclusion, a relatively simple model based on the animal physiology and physicochemical drug parameters to a first approximation describes the main characteristics of phenobarbital pharmacokinetics. This model has many features similar to physiological models recently proposed for other compounds (3, 6, 10, 30).

[7] A. Rico, École Nationale Vétérinaire, Toulouse, France, unpublished data.

## APPENDIX

$b$ = linear binding constant (dimensionless)
$C$ = free drug concentration (micrograms per milliliter of water)
$C'$ = bound drug concentration (micrograms per gram of dry matter)
$C^*$ = total drug concentration (micrograms per milliliter of blood or micrograms per gram of tissue)
$D$ = dose (micrograms)
$E$ = total amount eliminated by one-way metabolism, bile, or urine during a period of time (micrograms)
$f$ = fraction of water (dimensionless)
$g(t)$ = normalized impulse injection function (minutes$^{-1}$)
$H$ = transport coefficient between blood and tissue (milliliters per minute)
HEM = hematocrit (dimensionless)
$K$ = elimination constant by metabolism ($K_m$), bile ($K_b$), or urine ($K_u$) (milliliters per minute)
$r_e$ = elimination rate (micrograms per minute)
$r_t$ = drug transport rate from plasma to tissue (micrograms per minute)
$t$ = time (minute)
$T_{del}$ = step-delay time accounting for the biliary excretion (minute)
$V$ = volume (milliliter)
$\Phi$ = global binding coefficient for blood or tissue (dimensionless)
$\theta$ = injection duration (minute)
$Bl$ = blood pool
$BlC$ = blood cells
$Br$ = brain
$G$ = gut
$K$ = kidneys
$L$ = liver
$M$ = muscle
$P$ = plasma
$R$ = remaining distribution volume
$T$ = tissue
$X,Bl$ = blood compartment of the considered organ or tissue $X$
$X,T$ = tissue compartment of the considered organ or tissue $X$

## REFERENCES

(1) K. J. Himmelstein and R. J. Lutz, *J. Pharmacokinet. Biopharm.*, **7**, 127 (1979).

(2) H.-S. G. Chen and J. F. Gross, *Cancer Chemother. Pharmacol.* **2**, 85, (1979).

(3) L. I. Harrison and M. Gibaldi, *J. Pharm. Sci.*, **66**, 1679 (1977).

(4) K. B. Bischoff and R. L. Dedrick, *ibid.*, **57**, 1346 (1968).

(5) C. N. Chen and J. D. Andrade, *ibid.*, **65**, 717 (1976).

(6) D. B. Tuey and H. B. Matthews, *Drug Metab. Dispos.*, **5**, 444 (1977).

(7) C. Ioannides and D. V. Parke, *J. Pharm. Pharmacol.*, **27**, 739 (1975).

(8) R. Khodjett, R. Khil, A.-M. Batt, G. Siest, C. Tridon, and M. Weber, *Pathol. Biol.*, **23**, 409 (1975).

(9) F. Sarhan, J. M. Ziegler, A. Nicolas, and G. Siest, *J. Chromatogr.*, **183**, 505 (1980).

(10) C. N. Chen, D. L. Coleman, J. D. Andrade, and A. R. Temple, *J. Pharm. Sci.*, **67**, 38 (1978).

(11) T. M. Ludden, L.S. Schanker, and R. C. Lanman, *Drug Metab. Dispos.*, **4**, 8 (1976).

(12) K. B. Bischoff, R. L. Dedrick, and D. S. Zaharko, *J. Pharm. Sci.*, **59**, 149 (1970).

(13) P. L. Altman and D. S. Dittmer, "Biological Handbooks, Respiration and Circulation," Federation of American Societies for Experimental Biology, Bethesda, Maryland, 1971.
(14) A. Bonaccorsi, E. Dejana, and A. Quintana, *J. Pharmacol. Methods*, **1**, 321 (1978).
(15) I. C. Caldwell, S. Mahmood, and M. Weatherall, *J. Pharmacokinet. Biopharm.*, **6**, 521 (1978).
(16) H. H. Donaldson, "The Rat: Data and Reference Tables," 2nd ed., Wistar Institute of Anatomy and Biology, Philadelphia, Pa., 1924.
(17) D. O. Foster and M. L. Frydman, *Can. J. Physiol. Pharmacol.*, **56**, 97 (1978).
(18) A. Gjedde, J. J. Caronna, B. Hindfelt, and F. Plum, *Am. J. Physiol.*, **229**, 113 (1975).
(19) E. E. Ohnhaus and J. T. Locher, *Eur. J. Pharmacol.*, **31**, 161 (1975).
(20) Y. Sasaki and H. N. Wagner, *J. Appl. Physiol.*, **30**, 879 (1971).
(21) W. S. Spector, "Handbook of Biological Data," Saunders, Philadelphia, Pa., 1956.
(22) L. Takács, L. A. Debreckzni, and C. Farsang, *J. Appl. Physiol.*, **38**, 696 (1975).
(23) F. Vetterlein, R. Halfter, and G. Schmidt, *Arzneim-Forsch*, **29**, 747 (1979).
(24) A. W. Pruitt, J. L. McNay, and P. G. Dayton, *Drug Metab. Dispos.*, **3**, 30 (1975).
(25) M. A. Gonzalez, T. N. Tozer, and D. T. T. Chang, *J. Pharm. Sci.*, **64**, 99 (1975)
(26) D. Y. Cooper, H. Schleyer, S. S. Levin, J. C. Touchstone, R. H. Eisenhardt, H. M. Vars, O. Rosenthal, H. Rastigar, and A. Harken, in "The Introduction of Drug Metabolism," R. W. Estabrook and E. Lindenlaub, Eds., Symposia Medica Hoechst, Verlag, Stuttgart, West Germany, 1979, pp. 253–256.
(27) B. E. Dahlström and L. K. Paalzow, *J. Pharmacokinet. Biopharm.*, **6**, 505 (1978).
(28) W. A. Colburn, P. C. Hirom, R. J. Parker, and P. Milburn, *Drug Metab. Dispos.*, **7**, 100 (1979).
(29) A. M. El-Hawari and G. L. Plaa, *ibid.*, **6**, 59 (1978).
(30) M. Mintun, K. J. Himmelstein, R. L. Schroder, M. Gibaldi, and D. D. Shen, *J. Pharmacokinet. Biopharm.*, **8**, 373 (1980).

# Solubility Behavior of Barbituric Acids in Aqueous Solution of Sodium Alkyl Sulfonate as a Function of Concentration and Temperature

**C. VAUTION *, C. TREINER ‡ ×, F. PUISIEUX *, and J. T. CARSTENSEN §**

Received January 5, 1981, from the *Laboratoire de Pharmacie Galénique, Faculté de Pharmacie, Rue Jean Baptiste Clément, 92290 Chatenay Malabry, France*, the ‡ *Laboratoire d'Electrochimie, Université Pierre et Marie Curie, 4 Place Jussieu, Bâtiment F, 75005, Paris, France*, and the § *School of Pharmacy, University of Wisconsin, Madison, WI 53706.* Accepted for publication March 25, 1981.

**Abstract** □ The solubility of 13 barbituric acids was determined in aqueous solutions of sodium alkyl sulfonate. The effects of concentration and temperature were investigated, and the thermodynamic functions of the solubilization process were calculated. An analysis of the location of a solubilized species within a micelle is suggested in terms of the sign and amplitude of the standard entropy of solubilization, which is strongly positive for micelle penetration and negative for adsorption. A solubilization mechanism through adsorption onto the micellar surface is suggested for most of the barbituric acids studied. The enthalpy/entropy compensation phenomenon was identical for barbituric acids in ionic and nonionic (polyoxyethylene lauryl ether) surfactant solutions with a compensation temperature of 270 °K, indicating common behavior of these compounds with respect to micellar solubilization. The concept of molecular surface area was used to correlate the free energy of solubilization of the solutes to their size and structure. A linear relationship was found with an excellent correlation factor for the alkane derivatives of the 5-ethyl-barbituric acids. The specific behavior of some of the barbituric acids investigated is discussed.

**Keyphrases** □ Solubility—barbituric acids in aqueous sodium alkyl sulfonate, thermodynamics □ Thermodynamics—solubility of barbituric acids in aqueous sodium alkyl sulfonate □ Barbituric acids—solubility in aqueous sodium alkyl sulfonate, thermodynamics

The increase in solubility of poorly soluble preservatives in water by the addition of surfactants has been the subject of a large number of studies (1, 2). This phenomenon is related to the formation of micelles in water, but the availability of the preservative as an active agent is highly dependent on the molecular attachment site, and this subject is still a controversial matter. Opposite views have been proposed for barbituric acids, such as adsorption at the micelle interface (3) or incorporation into the micelle hydrocarbon core (4). However, for simpler molecules like acetone or urea, which may be considered model compounds for barbituric acids, thermodynamic evidence shows that these molecules hardly penetrate the micelle interior, at least at the critical micelle concentration (CMC) and for ionic micelles (5, 6).

## BACKGROUND

Studies on the solubilization of barbituric acids have been mostly (7) restricted to the influence of nonionic surfactants (3, 4, 8–10). Few of these studies were concerned with the determination of thermodynamic functions such as free energy, enthalpy, and entropy (3). In fact, few papers have been published on this subject for compounds other than barbituric acids (3, 11, 12).

The present work investigated the solubilization properties of sodium alkyl sulfonate. Its biodegradability and nontoxic properties, even at high surfactant concentration, make it an interesting surfactant in formulation problems (13). The barbituric acids are useful compounds in this respect since the possibility of changing, almost at will, the radicals attached to the malonylurea ring permits the study of the influence of shape and structure on the solubilization process. Thus, previous studies (14) on the molecular surface area concept and the investigation of the effects of temperature on barbituric solutions have indicated the use of the entropy function to deduce the chemical environment of compounds solubilized by micelles.

## EXPERIMENTAL

**Materials**—Sodium alkyl sulfonate[1] was composed of 90.7% (by weight) monosulfonated detergent, 8.8% polysulfonated compound, and 0.5% unsulfonated product. The monosulfonated compound was a mixture of $C_{14}H_{29}SO_3Na$ and $C_{15}H_{31}SO_3Na$, so a molecular weight of 323 was adopted in the concentration calculations. The CMC of the detergent

[1] Produits chimiques de la Montagne Noire, 81100, Castres, France.



0022-3549/81/1100-1238$01.00/0
© 1981, American Pharmaceutical Association

(13) P. L. Altman and D. S. Dittmer, "Biological Handbooks, Respiration and Circulation," Federation of American Societies for Experimental Biology, Bethesda, Maryland, 1971.
(14) A. Bonaccorsi, E. Dejana, and A. Quintana, *J. Pharmacol. Methods*, **1**, 321 (1978).
(15) I. C. Caldwell, S. Mahmood, and M. Weatherall, *J. Pharmacokinet. Biopharm.*, **6**, 521 (1978).
(16) H. H. Donaldson, "The Rat: Data and Reference Tables," 2nd ed., Wistar Institute of Anatomy and Biology, Philadelphia, Pa., 1924.
(17) D. O. Foster and M. L. Frydman, *Can. J. Physiol. Pharmacol.*, **56**, 97 (1978).
(18) A. Gjedde, J. J. Caronna, B. Hindfelt, and F. Plum, *Am. J. Physiol.*, **229**, 113 (1975).
(19) E. E. Ohnhaus and J. T. Locher, *Eur. J. Pharmacol.*, **31**, 161 (1975).
(20) Y. Sasaki and H. N. Wagner, *J. Appl. Physiol.*, **30**, 879 (1971).
(21) W. S. Spector, "Handbook of Biological Data," Saunders, Philadelphia, Pa., 1956.
(22) L. Takács, L. A. Debreckzni, and C. Farsang, *J. Appl. Physiol.*, **38**, 696 (1975).
(23) F. Vetterlein, R. Halfter, and G. Schmidt, *Arzneim-Forsch*, **29**, 747 (1979).
(24) A. W. Pruitt, J. L. McNay, and P. G. Dayton, *Drug Metab. Dispos.*, **3**, 30 (1975).
(25) M. A. Gonzalez, T. N. Tozer, and D. T. T. Chang, *J. Pharm. Sci.*, **64**, 99 (1975)
(26) D. Y. Cooper, H. Schleyer, S. S. Levin, J. C. Touchstone, R. H. Eisenhardt, H. M. Vars, O. Rosenthal, H. Rastigar, and A. Harken, in "The Introduction of Drug Metabolism," R. W. Estabrook and E. Lindenlaub, Eds., Symposia Medica Hoechst, Verlag, Stuttgart, West Germany, 1979, pp. 253–256.
(27) B. E. Dahlström and L. K. Paalzow, *J. Pharmacokinet. Biopharm.*, **6**, 505 (1978).
(28) W. A. Colburn, P. C. Hirom, R. J. Parker, and P. Milburn, *Drug Metab. Dispos.*, **7**, 100 (1979).
(29) A. M. El-Hawari and G. L. Plaa, *ibid.*, **6**, 59 (1978).
(30) M. Mintun, K. J. Himmelstein, R. L. Schroder, M. Gibaldi, and D. D. Shen, *J. Pharmacokinet. Biopharm.*, **8**, 373 (1980).

# Solubility Behavior of Barbituric Acids in Aqueous Solution of Sodium Alkyl Sulfonate as a Function of Concentration and Temperature

**C. VAUTION *, C. TREINER ‡ ×, F. PUISIEUX *, and J. T. CARSTENSEN §**

Received January 5, 1981, from the *Laboratoire de Pharmacie Galénique, Faculté de Pharmacie, Rue Jean Baptiste Clément, 92290 Chatenay Malabry, France*, the ‡ *Laboratoire d'Electrochimie, Université Pierre et Marie Curie, 4 Place Jussieu, Bâtiment F, 75005, Paris, France*, and the § *School of Pharmacy, University of Wisconsin, Madison, WI 53706.* Accepted for publication March 25, 1981.

**Abstract** □ The solubility of 13 barbituric acids was determined in aqueous solutions of sodium alkyl sulfonate. The effects of concentration and temperature were investigated, and the thermodynamic functions of the solubilization process were calculated. An analysis of the location of a solubilized species within a micelle is suggested in terms of the sign and amplitude of the standard entropy of solubilization, which is strongly positive for micelle penetration and negative for adsorption. A solubilization mechanism through adsorption onto the micellar surface is suggested for most of the barbituric acids studied. The enthalpy/entropy compensation phenomenon was identical for barbituric acids in ionic and nonionic (polyoxyethylene lauryl ether) surfactant solutions with a compensation temperature of 270 °K, indicating common behavior of these compounds with respect to micellar solubilization. The concept of molecular surface area was used to correlate the free energy of solubilization of the solutes to their size and structure. A linear relationship was found with an excellent correlation factor for the alkane derivatives of the 5-ethyl-barbituric acids. The specific behavior of some of the barbituric acids investigated is discussed.

**Keyphrases** □ Solubility—barbituric acids in aqueous sodium alkyl sulfonate, thermodynamics □ Thermodynamics—solubility of barbituric acids in aqueous sodium alkyl sulfonate □ Barbituric acids—solubility in aqueous sodium alkyl sulfonate, thermodynamics

The increase in solubility of poorly soluble preservatives in water by the addition of surfactants has been the subject of a large number of studies (1, 2). This phenomenon is related to the formation of micelles in water, but the availability of the preservative as an active agent is highly dependent on the molecular attachment site, and this subject is still a controversial matter. Opposite views have been proposed for barbituric acids, such as adsorption at the micelle interface (3) or incorporation into the micelle hydrocarbon core (4). However, for simpler molecules like acetone or urea, which may be considered model compounds for barbituric acids, thermodynamic evidence shows that these molecules hardly penetrate the micelle interior, at least at the critical micelle concentration (CMC) and for ionic micelles (5, 6).

## BACKGROUND

Studies on the solubilization of barbituric acids have been mostly (7) restricted to the influence of nonionic surfactants (3, 4, 8–10). Few of these studies were concerned with the determination of thermodynamic functions such as free energy, enthalpy, and entropy (3). In fact, few papers have been published on this subject for compounds other than barbituric acids (3, 11, 12).

The present work investigated the solubilization properties of sodium alkyl sulfonate. Its biodegradability and nontoxic properties, even at high surfactant concentration, make it an interesting surfactant in formulation problems (13). The barbituric acids are useful compounds in this respect since the possibility of changing, almost at will, the radicals attached to the malonylurea ring permits the study of the influence of shape and structure on the solubilization process. Thus, previous studies (14) on the molecular surface area concept and the investigation of the effects of temperature on barbituric solutions have indicated the use of the entropy function to deduce the chemical environment of compounds solubilized by micelles.

## EXPERIMENTAL

**Materials**—Sodium alkyl sulfonate[1] was composed of 90.7% (by weight) monosulfonated detergent, 8.8% polysulfonated compound, and 0.5% unsulfonated product. The monosulfonated compound was a mixture of $C_{14}H_{29}SO_3Na$ and $C_{15}H_{31}SO_3Na$, so a molecular weight of 323 was adopted in the concentration calculations. The CMC of the detergent

[1] Produits chimiques de la Montagne Noire, 81100, Castres, France.



0022-3549/81/1100-1238$01.00/0
© 1981, American Pharmaceutical Association

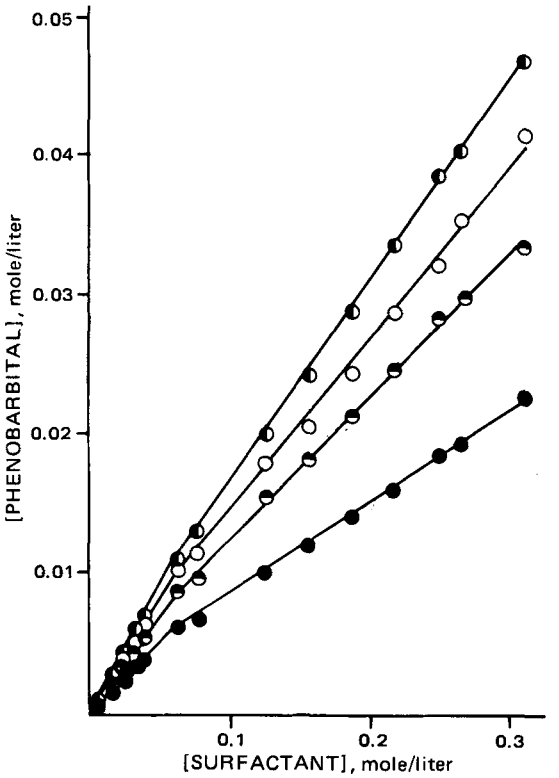


**Figure 1**—*Variation of the solubility of phenobarbital with sodium alkyl sulfonate concentration at various temperatures. Key:* ◐, *55°;* ○, *45°;* ◓, *35°; and* ●, *25°.*

used was 0.0039 mole/liter, as determined from conductivity measurements at 25°. Highly pure sodium dodecyl sulfate[2] was used without purification. Its CMC at 25° was 0.0081 mole/liter, in excellent agreement with literature values (15).

The barbituric acids were from different sources[3]. Their melting points and solubilities in water at 25° are presented in Table I, although some solubility values in water may be slightly in error due to impurities. However, since the major interest was in partition coefficients, *i.e.*, in ratio of concentrations with and without the added surfactant, the influence of the impurities on the partition coefficient values should be negligible.

**Solubility Measurements**—The barbiturate solution with the added surfactant was equilibrated for 240 hr (10 days) at a given temperature, and controlled to within ±0.1°. The suspension was filtered and diluted, and the concentration of solubilized solute was determined with a UV spectrophotometer[4].

**Solubility Calculations**—The pH of the solutions was determined and used with the pKa of each barbituric acid to correct for the variation of solubility due to the pH change of the solution, which occurs with the addition of alkyl sulfonate (16). The classic formula was used:

$$S = S_0 (1 + 10^{pH-pKa}) \qquad \text{(Eq. 1)}$$

where $S$ and $S_0$ are the total amount of barbituric acid and the intrinsic solubility of the undissociated acid, respectively.

## RESULTS AND DISCUSSION

An example of the variation of barbituric acid solubilization with the surfactant concentration is presented at several temperatures in Fig. 1. This behavior was typical of all barbituric acids studied with alkyl sulfonate but had not been observed with nonionic surfactants. It has been interpreted as the result of the presence of mixed micelles of monosulfonated and polysulfonated sodium alkyl sulfonate above the concentration $C_2$ (17). Below this value, the only micelles present are formed from monosulfonated molecules. The present report concerns only the first part of these curves, *i.e.*, the initial slope above the CMC. In Fig. 1, the maximum concentration of solubilized material is plotted for convenience as a function of the concentration of surfactant used minus the CMC.

In all cases, solubilization increased with increased surfactant concentration in water and with temperature. To quantify, the relative variation of the solubilized solute in water and in the micellar solutions, an apparent distribution coefficient such as:

$$K = \frac{S_m - S_w}{S_w C} \qquad \text{(Eq. 2)}$$

is defined where $S_m$ and $S_w$ are the saturation molarities of solubilized barbituric acid in the micellar solution and in water, respectively, and $C$ is the excess of surfactant above the CMC in moles per liter. The maximum surfactant concentration used in the determination of $K$ was ~0.04 mole/liter (1.3 g/100 ml of solution).

In each case, $K$ was calculated using at least eight experimental points with a least-squares method. As shown in Table II, $K$ decreased as temperature increased, which means that the increase in solubility was faster in water than in the micellar solution. This finding agrees with previous findings (3) for barbituric acids in nonionic polyoxyethylene lauryl ether aqueous solutions but contradicts the results of Ismail *et al.* (10) for the same solutes with the nonionic polyoxyethylene derivative surfactants used (monoalkyl ether, monostearate, and polysorbate).

**Thermodynamic Functions and Location of Solubilized Material in Micelles**—To discuss the thermodynamic properties of the solutions, the free energy of solubilization may be calculated as:

$$\Delta G_s^\circ = -RT \ln K \qquad \text{(Eq. 3)}$$

where $K$ is an apparent distribution coefficient, uncorrected for volume effects (5).

The standard enthalpy of solubilization is defined by:

$$\partial \frac{\ln K}{\partial T} = \frac{\Delta H_s^\circ}{RT^2} \qquad \text{(Eq. 4)}$$

and:

$$\Delta G_s^\circ = \Delta H_s^\circ - T\Delta S_s^\circ \qquad \text{(Eq. 5)}$$

where $\Delta S_s^\circ$ is the standard entropy of solubilization. The results of these calculations are given in Table II. The precision of $\Delta H_s^\circ$ is not very good when obtained from indirect determinations (4). Thus, $\Delta H_s^\circ$ values should be considered reliable within ±300 cal/mole, while $\Delta S_s^\circ$ values are accurate to ±1.0 entropy units.

The same thermodynamic functions are examined in more extreme cases in Table III, using the standard thermodynamic functions of hydrocarbon transfer (18) from water to an aqueous anionic surfactant solution (such as sodium lauryl sulfate of molarity $c$ = 0.06 mole/liter).

Thus:

$$\Delta G_t^\circ = -RT \frac{S}{S^\circ} \qquad \text{(Eq. 6)}$$

As expected, $\Delta G_t^\circ$ is more negative the larger the solute molecule since

**Table I—Some Physical Properties of Barbituric Acids**

| Acid | Melting Point | $S_w$, mole/liter | Molecular Surface Area[d], Å$^2$ |
|---|---|---|---|
| Barbital[b] | 186° | 0.00401 | 102.6 |
| Vinbarbital[b] | 165° | 0.00487 | 142.0 |
| Butabarbital[b] | 168° | 0.00407 | 140.3 |
| Butethal[b] | 125° | 0.0213 | 138.8 |
| Pentobarbital[b] | 125° | 0.00407 | 158.4 |
| Amobarbital[b] | 156–158° | 0.00217 | 160.1 |
| Allobarbital[c] | 175° | 0.00865 | 89.2 |
| Aprobarbital[d] | 145° | 0.0194 | 117.2 |
| Butalbital[d] | 140° | 0.00759 | 135.3 |
| Secobarbital[d] | 95° | 0.00441 | 151.7 |
| Phenobarbital[b] | 175° | 0.00517 | 152.4 |
| Heptabarbital[b] | 175° | 0.00100 | 156.7 |
| Reposal[b] | 213° | 0.00168 | 150.0 |

[a] Molecular surface areas of side chains on the malonylurea ring. [b] A 5-ethylbarbituric acid. [c] A 5-diallylbarbituric acid. [d] A 5-allylbarbituric acid.

[2] Merck "pro analysis."

[3] Barbital, Expandia, Paris; vinbarbital, Schmoller et Bompard, Grasse; butabarbital, Expandia; butobarbital, Rhone Poulenc Chimie, Courbevoie; pentobarbital, Expandia; amobarbital, Expandia; allobarbital, Soprotec, Paris; aprobarbital Expandia; itobarbital, Rhone Poulenc Chimie; secobarbital, Expandia; phenobarbital, Cooperation pharmaceutique française, Paris; heptabarbital, Laboratoire Geigy, Rueil-Malmaison; and reposal, Laboratoire Martinet, Vernouillet, Dreux.

[4] Beckman model 25.

**Table II—Partition Coefficients and Thermodynamic Parameters [a] for Barbituric Acids as a Function of Temperature (Molar Scale)**

| Acid | $t$ | $K$, moles$^{-1}$ | $\Delta G_s^\circ$, cal/mole | $\Delta H_s^\circ$, cal/mole | $\Delta S_s^\circ$, cal/mole/deg |
|---|---|---|---|---|---|
| Barbital | 25° | 3.8 | −790 | −2600 | −6.0 |
| | 35° | 3.5 | −770 | | −5.9 |
| | 45° | 3.2 | −720 | | −5.9 |
| | 55° | 2.5 | −600 | | −6.0 |
| Vinbarbital | 35° | 16.0 | −1700 | −700 | +3.2 |
| | 45° | 16.0 | −1750 | | +3.2 |
| | 55° | 14.8 | −1760 | | +3.1 |
| Butabarbital | 25° | 22.4 | −1840 | −3100 | −4.3 |
| | 35° | 17.8 | −1760 | | −4.4 |
| | 45° | 15.3 | −1720 | | −4.4 |
| | 55° | 13.8 | −1710 | | −4.3 |
| Butethal | 35° | 19.4 | −1820 | −2100 | −0.9 |
| | 45° | 17.5 | −1810 | | −0.8 |
| | 55° | 15.7 | −1790 | | −0.6 |
| Pentobarbital | 25° | 39.3 | −2170 | −1100 | +3.7 |
| | 35° | 39.4 | −2230 | | +3.5 |
| | 55° | 33.4 | −2290 | | +3.6 |
| Amobarbital | 25° | 51.6 | −2340 | −1700 | +2.1 |
| | 35° | 48.0 | −2370 | | +2.0 |
| | 45° | 43.0 | −2380 | | +2.0 |
| Allobarbital | 25° | 9.2 | −1310 | −2200 | −2.9 |
| | 35° | 8.5 | −1310 | | −2.8 |
| | 45° | 7.3 | −1250 | | −2.9 |
| | 55° | 5.9 | −1150 | | −3.1 |
| Aprobarbital | 25° | 14.4 | −1580 | −2700 | −3.6 |
| | 35° | 10.1 | −1420 | | −4.0 |
| | 45° | 9.8 | −1440 | | −3.8 |
| | 55° | 9.3 | −1450 | | −3.7 |
| Butalbital | 25° | 21.4 | −1810 | −2600 | −2.6 |
| | 35° | 19.4 | −1820 | | −2.5 |
| | 45° | 16.3 | −1760 | | −2.6 |
| | 55° | 14.6 | −1750 | | −2.5 |
| Secobarbital | 25° | 80.6 | −2600 | −4100 | −5.9 |
| | 35° | 60.7 | −2510 | | −6.0 |
| | 45° | 50.3 | −2480 | | −5.9 |
| | 55° | 40.6 | −2420 | | −5.9 |
| Phenobarbital | 25° | 22.7 | −1850 | −3800 | −6.5 |
| | 35° | 18.6 | −1790 | | −6.5 |
| | 45° | 12.7 | −1660 | | −6.6 |
| Heptabarbital | 25° | 33.5 | −2080 | −2000 | +0.3 |
| | 35° | 27.7 | −2030 | | +0.1 |
| | 45° | 26.5 | −2070 | | +0.2 |
| | 55° | 24.2 | −2060 | | +0.3 |
| Reposal | 25° | 117.6 | −2820 | −1600 | +4.2 |
| | 35° | 103.9 | −2840 | | +4.2 |
| | 45° | 97.2 | −2890 | | +4.2 |
| | 55° | 92.2 | −2950 | | +4.2 |

[a] Throughout this paper, 1 cal = 4.184 J.

dispersion forces and the hydrophobic effect both increase in magnitude when the surface of contact between the solute and the solvent molecules (here the micelles) increases.

The standard enthalpy of transfer, $\Delta H_t^\circ$, is close to zero and is also size dependent, but the entropy of transfer is strongly positive. Since hydrocarbons dissolve in the micelle interior, the positive entropy change upon solubilization seems a good thermodynamic characteristic of the penetration of a solute from an aqueous to a nonaqueous environment. The cases of ammonium chloride and hydrochloric acid were chosen to illustrate the behavior of a polar or an ionic hydrophilic solute (19). [Methane is presented to illustrate the thermodynamics of transfer of a hydrocarbon from water to an organic component (20). It shows that all thermodynamic functions are of the same order of magnitude whether the transfer is from water to a micellar phase or to an organic solvent in the case of penetration. The same reasoning may be applied to a polar solute.] Table III shows that, for a hydrophilic solute transferred from an aqueous to an organic environment, $\Delta G_t^\circ$ is positive and $\Delta S_t^\circ$ is negative. Since ammonium chloride or hydrochloric acid prefers water to the organic phase (19), a negative entropy change is associated with nonpenetration of the solute into the organic phase (which can be a micelle). Thus, $\Delta G_s^\circ < 0$ and $\Delta S_s^\circ > 0$ are associated with the penetration into a micelle interior, and $\Delta G_s^\circ > 0$ and $\Delta S_s^\circ < 0$ are associated with an interaction of the solute with the micelle without penetration, *i.e.*, through an adsorption phenomenon.

**Table III—Thermodynamic Standard Transfer Functions for Various Solutes from Water to Organic solvents at 25° (Mole Fraction Scale)**

| Solute | Organic Solvent | $\Delta G_t^\circ$, cal/mole | $\Delta H_t^\circ$, cal/mole | $\Delta S_t^\circ$, cal/mole/deg |
|---|---|---|---|---|
| Pentane[a] | Micellar solution[b] | −5720 | −1100 | +15.6 |
| Butane[a] | Micellar solution[b] | −5130 | 0 | +17.2 |
| Propane[a] | Micellar solution[b] | −4230 | +1000 | +17.5 |
| Ethane[a] | Micellar solution[b] | −3450 | +2000 | +18.3 |
| Methane[c] | Ethanol | −2650 | +1960 | +15.4 |
| Methane[c] | Cyclohexane | −2280 | +2380 | +15.6 |
| Ammonium chloride[d] | Ethanol | +5010 | −2830 | −26.3 |
| Hydrochloric acid | Ethanol | +4320 | −5400 | −32.6 |

[a] Reference 18. [b] Aqueous sodium lauryl sulfate solution; $c$ = 0.06 mole/liter. [c] Reference 20. [d] Reference 19.

**Table IV—Partition Coefficients and Thermodynamic Parameters for Butethal in Aqueous Sodium Lauryl Sulfate Solutions (Molar Scale)**

| $t$ | $K$, mole$^{-1}$ | $\Delta G_s^\circ$, cal/mole | $\Delta H_s^\circ$, cal/mole | $\Delta S_s^\circ$, cal/mole/deg |
|---|---|---|---|---|
| 25° | 29.0 | −1990 | −3040 | −3.5 |
| 35° | 24.0 | −1950 | | −3.5 |
| 45° | 21.0 | −1930 | | −3.5 |
| 55° | 18.0 | −1880 | | −3.5 |

Examination of the barbituric acids shows that $\Delta H_s^\circ$ is negative in all cases and $\Delta S_s^\circ$ is negative or zero for nine out of 13 barbiturates. Thus, it may be concluded that solubilization occurs in an environment of mixed water and nonpolar molecules, depending on the particular solute, but with a preference for a predominantly aqueous phase.

To compare solutes dissolved in sodium lauryl sulfate and alkyl sulfonate solutions, the solubilization of butethal was studied at four temperatures in very pure samples of sodium lauryl sulfate. The results were analyzed as for the alkyl sulfonate solutions (Table IV). They are similar in both surfactant solutions. The $\Delta G_s^\circ$ values are equal within experimental error, and only the dependence of $K$ with temperature is slightly different with alkyl sulfonate and sodium lauryl sulfate. The $\Delta H_s^\circ$ and $\Delta S_s^\circ$ values are both somewhat more negative in the alkyl sulfonate solutions, a good example of enthalpy/entropy compensation. In addition, the thermodynamic functions are very much the same in the nonionic polyoxyethylene lauryl ether solutions (deduced from dialysis measurements at several temperatures) and in the anionic alkyl sulfonate solutions. For example, $\Delta G_s^\circ$ is systematically more negative by only ~20% in the nonionic solution[5]. This finding should be the result of a number of compensation effects. If, as was previously suggested (3) for polyoxyethylene lauryl ether and as presently proposed for alkyl sulfonate, solubilization occurs through adsorption for barbituric acids in these surfactant solutions, the situations at each micelle surface must be quite different. In particular, the role of the adsorbed sodium counterions in the latter case should be clarified.

**Enthalpy/Entropy Compensation Phenomenon**—Ionic and nonionic surfactants as solubilizing agents also can be compared by considering the enthalpy/entropy compensation phenomenon. It occurs in most solutions but presents amazing regularities for aqueous solutions. Lumry and Rajendar (21) described the phenomenon by an equation of the type:

$$\Delta H_s^\circ = \alpha + T_c \Delta S_s^\circ \qquad \text{(Eq. 7)}$$

where $\alpha$ and $T_c$ are constants. This equation holds for a given solute in various media or for a series of different solutes in a given medium. The compensation temperature ($T_c$) is equal to an average value of 285 °K for most aqueous or predominantly aqueous systems, indicating a common mechanism in a given solution process when essentially water molecules are involved. [In organic solvents, Eq. 7 is known as the Barclay–Butler plot (22) with $T_c \approx 910$ °K.]

Figure 2 presents the correlation found for the barbituric acids used in this work and those of Ikeda *et al.* (3) with polyoxyethylene lauryl ether. If the results for barbital and reposal in the ionic solutions and for

[5] The same situation was described with phenobarbital in ionic and nonionic surfactant solutions (7). Unfortunately, the authors did not publish the actual data but only corresponding curves.

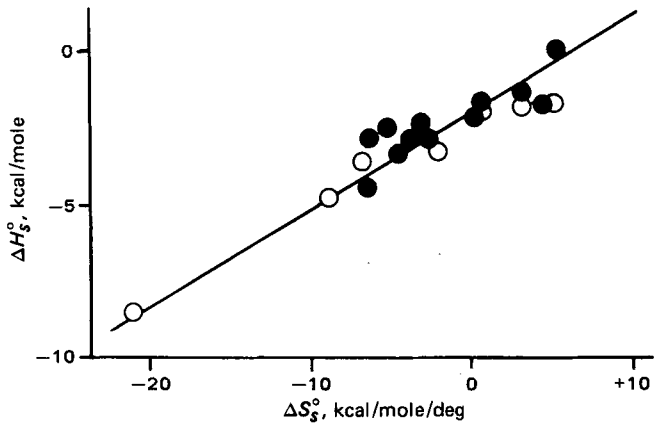


**Figure 2**—*Enthalpy/entropy compensation plot for barbituric acids in sodium alkyl sulfonate (●), ionic, and polyoxyethylene lauryl ether (○), nonionic, aqueous solutions at 25°.*

secobarbital in the nonionic solutions are discarded, a linear regression on the remaining 18 barbituric acid solutions may be represented at 25° by:

$$\Delta H_s^\circ = -2020 + 269\ \Delta S_s^\circ \qquad \text{(Eq. 8)}$$

with a correlation coefficient of $r^2 = 0.98$. The $T_c$ value of 269 °K is in agreement with the average 285 °K.

The Humphreys and Rhodes distribution coefficients at several temperatures were also analyzed for benzoic acid in aqueous solutions of *n*-alkylpolyoxyethylene surfactants. Benzoic acid is considered as being mostly adsorbed on the micelle surface (23). The derived thermodynamic functions are presented at 25° in Table V. The $\Delta H_s^\circ$ and $\Delta S_s^\circ$ values are situated on the same line as for the other systems in Fig. 3.

Although speculation on the meaning of the compensation temperature in terms of chemical compensation has been criticized (24), the fact that, for the same chemical process (*i.e.*, solubilization by adsorption onto micellar surfaces), a single line is obtained on a $\Delta H_s^\circ$ *versus* $\Delta S_s^\circ$ plot should be considered. In the case of benzoic acid, $\Delta S_s^\circ$ becomes less negative as the number of oxyethylene group increases, which may be interpreted as an increase in penetration of the benzoic molecule within the micelle mantle. However, $\Delta S_s^\circ$ remains negative for the four surfactants, indicating that adsorption still predominates for this system.

**Solubilization and Molecular Surface Area Concept**—Many approaches have been tested, from the crudest models that correlate distribution coefficients with the number of carbon atoms on the barbituric acid molecule [with corrections for the position of radicals and the malonylurea rings (25)], to the more general approach of Hansch and Anderson (26), who correlated drug activity with the distribution coefficient in octanol–water mixtures, to others who use the regular solution theory to find an index of drug activity (27). An attractive alternative to these approaches may be found in the concept of molecular surface area, as proposed by Herman (14) and extensively used in the case of slightly soluble series of organic compounds in water (28–30). It is based on the idea that, provided no specific interactions take place between solute and solvent molecules and the solute is sufficiently diluted so that solute–solute interactions are negligible, the molecular surface of contact between solute and solvent molecules is proportional to their free energy of interaction. Thus, the logarithm of solubility should be a linear function of the molecular surface area. Implicitly, it is assumed that the same correlation will not be found for any series of compounds. Thus, alkanes, alkynes, or aromatic derivatives may be found on different straight lines.

**Table V—Partition Coefficients and Thermodynamic Parameters for Benzoic Acid in Nonionic Surfactant Solutions at 25° (Molar Scale)**

| Surfactant[a] | *K*, mole | $\Delta G_s^\circ$, cal/mole | $\Delta H_s^\circ$, cal/mole | $\Delta S_s^\circ$, cal/mole/deg |
|---|---|---|---|---|
| $C_{16}E_{16}$ | 50.07 | −2320 | −3700 | −4.7 |
| $C_{16}E_{30}$ | 45.55 | −2260 | −3100 | −2.9 |
| $C_{16}E_{40}$ | 32.72 | −2070 | −3100 | −3.7 |
| $C_{16}E_{96}$ | 27.43 | −1960 | −2300 | −1.2 |

[a] *n*-Alkylpolyethylene $C_nE_m$, where $n$ = number of carbon atoms and $m$ = number of polyoxyethylene groups.

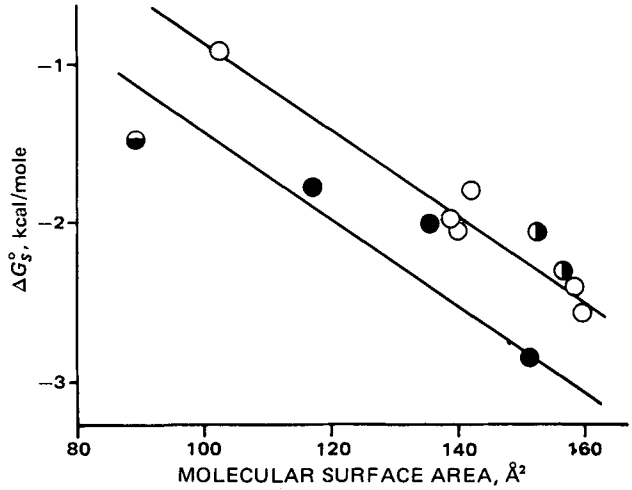


**Figure 3**—*Variation of the standard free energy of solubilization of barbituric acids with the molecular surface area of their substituted groups at 25°. Key: ○, 5-ethyl (linear); ◑, 5-ethyl (cyclic); ●, 5-allyl; and ◒, 5-diallyl.*

Valvani *et al.* (29) proposed a simplified version of the elaborate method of evaluation of molecular surface area by Herman (14), and the present study used their results whenever possible (28). The heptabarbital ring has been considered as being equivalent to that of cycloheptane (29) minus one methylene group (a quaternary carbon atom has no molecular surface area) and minus the difference between one methylene and one CH group. It was assumed that the molecular surface areas of phenobarbital and cyclobarbital were equivalent to that of a benzene ring minus one methylene group. The molecular surface area of malonylurea was not accounted for since it was assumed to play the same role for each barbituric acid. The results of these calculations are presented in Table I. (Reposal was not calculated because of too many geometrical unknowns. However, a value of ~150 Å² is plausible.)

Figures 3 and 4 correlate $\Delta G_s^\circ$ (which is proportional to the logarithm of a ratio of solubilities) and molecular surface area at 25 and 55°. For the eight 5-ethylbarbituric acids, a linear correlation is found at 25° with a standard deviation of $\sigma = 117$ and $r^2 = 0.980$. (If phenobarbital is ignored, $\sigma = 101$ and $r^2 = 0.990$.) At 55°, the correlation is even better if phenobarbital is ignored, with $\sigma = 70$ and $r^2 = 0.995$. This result is as good as the correlation found, for example, between the logarithm of the partition coefficients of alkylbenzenes in octanol–water mixtures and their molecular surface area (28). The standard deviation is of the order of magnitude of the experimental error or better. The three 5-monoallylbarbituric acids stand on a parallel to the preceding line, and the one 5-diallylbarbituric acid is at a still more negative $\Delta G_s^\circ$ value. This behavior was observed with other types of correlations, such as those involving the solubility and melting point of a given series of compounds (31).

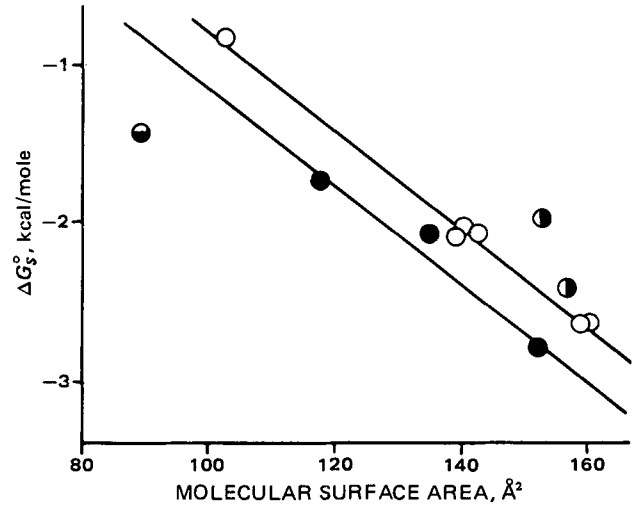


**Figure 4**—*Variation of the standard free energy of solubilization of barbituric acids with the molecular surface area of their substituted groups at 55°. See Fig. 3 for key.*

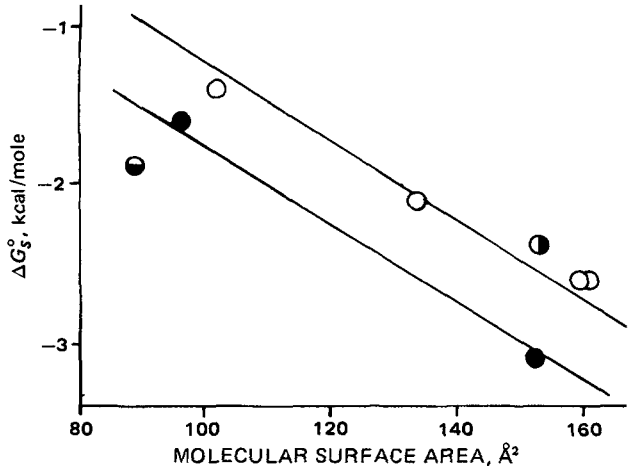


**Figure 5**—*Variation of the standard free energy of solubilization of barbituric acids with the molecular surface area of their substituted groups at 25°, polyoxyethylene lauryl ether solutions. See Fig. 3 for key.*

Comparison of these results with those of Ikeda *et al.* (3) in polyoxyethylene lauryl ether aqueous solutions (Fig. 5) shows the standard deviation of fit for the five 5-ethyl derivatives is $\sigma = 53$ with $r^2 = 0.996$. It also seems that the two monoallyl and the one diallyl derivatives are in the same position with respect to the 5-ethyl line in polyoxyethylene lauryl ether and alkyl sulfonate solutions.

Since the common behavior of these solutes in nonionic and ionic surfactant solutions has been stressed, some differences should now be pointed out. Some authors noted the specific interaction between phenobarbital and oxyethylene groups at high surfactant concentrations and low temperatures (3, 4), leading to precipitation of this barbituric acid. Such behavior is not found with alkyl sulfonate. However, some specificity is apparent with the observation that, for phenobarbital, $\Delta G_s^\circ$ moves off the line corresponding to the 5-ethyl derivatives as the temperature increases. This effect, which is small, is difficult to interpret since specific effects usually decrease as temperature increases. (The correlation between $\Delta G_s^\circ$ and molecular surface area is better at 55° than at 25° for the 5-ethylbarbituric acids.) Reposal is more soluble than one might expect from its molecular surface area, although it is the only compound for which precise molecular surface area evaluation could not be made. Finally, a rough correlation may be observed between $\Delta G_s^\circ$ and $\Delta S_s^\circ$ in a direction indicating that the micellar solubilization is favored by the penetration of the solubilized compounds in the micelle interior. Thus, barbital with the less negative $\Delta G_s^\circ$ value and reposal with the most negative $\Delta G_s^\circ$ value have the most negative and the most positive $\Delta S_s^\circ$ values, respectively. This observation again points out that micellar solubilization is essentially an entropy-related phenomenon.

In conclusion, although this study used an impure surfactant product, the self-consistency of the results, when compared with pure sodium lauryl sulfate solutions or with the nonionic solutions, and the correlations found with the molecular surface area approach justify the general conclusions proposed.

## REFERENCES

(1) J. W. McBain and E. Hutchinson, "Solubilization," Academic, New York, N.Y., 1955.

(2) P. H. Elworthy, A. T. Florence, and C. B. McFarlane, "Solubilization by Surface Active Agents," Chapman and Hall, London, England, 1968.

(3) K. Ikeda, K. Kato, and T. Kukamoto, *Chem. Pharm. Bull.*, **19**, 2510 (1971).

(4) M. W. Gouda, A. A. Ismail, and M. M. Motawi, *J. Pharm. Sci.*, **59**, 1402 (1970).

(5) M. F. Emerson and A. Holtzer, *J. Phys. Chem.*, **71**, 3320 (1967).

(6) C. Treiner, A. Le Besnerais, and C. Micheletti, "Thermodynamic Behaviour of Electrolytes in Mixed Solvents II," W. F. Furter, Ed., Advances in Chemistry Series, American Chemical Society, Washington, D.C., 1979, p. 177.

(7) V. F. Naggar, M. A. Moustapha, S. A. Khalil, and M. M. Motawi, *Can. J. Pharm. Sci.*, **7**, 112 (1972).

(8) A. A. Ismail, M. W. Gouda, and M. M. Motawi, *J. Pharm. Sci.*, **59**, 220 (1970).

(9) N. N. Salib, A. A. Ismail, and A. S. Geneidi, *Pharm. Ind.*, **36**, 108 (1974).

(10) A. A. Ismail, M. W. Gouda, and M. M. Motawi, *ibid.*, **36**, 735 (1974).

(11) K. J. Humphreys and C. T. Rhodes, *J. Pharm. Sci.*, **57**, 79 (1968).

(12) B. W. Barry and D. I. D. El Eini, *J. Pharm. Pharmacol.*, **28**, 210 (1976).

(13) R. DeLourne and L. Marcou, *Labo. Pharma.*, **225**, 572 (1976).

(14) R. B. Herman, *J. Phys. Chem.*, **76**, 2574 (1972).

(15) P. Mukerjee and K. J. Mysels, "Critical Micelle Concentration of Aqueous Surfactant Systems," Systems NSRDS-NBS 36, U.S. Government Printing Office, Washington, D.C., 1971.

(16) R. H. Gumtow, *Am. J. Pharm. Ed.*, **31**, 515 (1967).

(17) C. Vaution, J. Paris, F. Puisieux, and J. T. Carstensen, *Int. J. Pharm.*, **1**, 349 (1978).

(18) A. Wishnia, *J. Phys. Chem.*, **67**, 2079 (1963).

(19) M. H. Abraham and A. F. D. De Namor, *J. Chem. Soc. Faraday Trans. I*, **74**, 2101 (1978).

(20) A. Ben-Naim and M. Yaacobi, *J. Phys. Chem.*, **78**, 170 (1974).

(21) R. Lumry and S. Rajendar, *Biopolymers*, **9**, 1125 (1970).

(22) Krishnan and H. L. Friedman, "Solute/Solvent Interactions," vol. II, J. F. Coetzee and C. D. Ritchie, Eds., Dekker, New York, N.Y., 1976.

(23) P. Mukerjee, J. R. Cardinal, and N. R. Descu, "Micellization, Solubilization and Microemulsions," K. L. Mittal, Ed., Plenum, New York, N.Y. 1977, vol. I.

(24) R. R. Krug, W. G. Hunter, and R. A. Grieger, *Nature*, **261**, 566 (1976).

(25) D. J. Lamb and J. Harris, *J. Am. Pharm. Assoc., Sci. Ed.*, **49**, 583 (1960).

(26) C. Hansch and S. M. Anderson, *J. Med. Chem.*, **10**, 745 (1967).

(27) S. A. Khalil, M. A. Moustapha, and O. Y. Abdallah, *Can. J. Pharm. Sci.*, **11**, 121 (1976).

(28) S. H. Yalkowsky and S. C. Valvani, *J. Med. Chem.*, **19**, 727 (1976).

(29) S. C. Valvani, S. H. Yalkowsky, and G. L. Amidon, *J. Phys. Chem.*, **80**, 829 (1976).

(30) S. H. Yalkowsky and S. C. Valvani, *J. Chem. Eng. Data*, **24**, 127 (1979).

(31) M. Almgren, F. Grieser, J. R. Powell, and J. K. Thomas, *ibid.*, **24**, 285 (1979).

# Theoretical Comparison of Release Rates of Drugs into Sink and Nonsink Conditions

**RICHARD H. GUY *x, and JONATHAN HADGRAFT ‡**

Received October 6, 1980, from the **School of Pharmacy, University of California, San Francisco, CA 94143*, and the ‡*Department of Pharmacy, University of Nottingham, University Park, Nottingham NG7 2RD, England.* Accepted for publication March 30, 1981.

**Abstract** □ Theoretical expressions were derived that show how drug release rates are modified by sink and nonsink conditions. The effect of basic physicochemical parameters and the relevance to *in vitro* testing are discussed.

**Keyphrases** □ Theoretical release profiles—drug release rates modified by sink and nonsink conditions □ Release rates—theoretical comparison of drug release into sink and nonsink conditions

The release characteristics of formulations are often determined in sink conditions, usually produced either with a continuous supply of fresh receptor solution or by devising an experiment where there is a large receptor volume compared to the donor phase. Mathematical equations were previously derived to describe drug release into sink conditions for certain physical situations (1–6), and experimental confirmation of the results was obtained (7–12). For some cases, the assumption that drug release takes place into sink conditions is an adequate representation of the *in vivo* situation, but nonsink conditions would be more appropriate under certain circumstances. Furthermore, experimental constraints may prevent the attainment of sink conditions *in vitro* and, consequently, a mathematical description of the nonsink situation is necessary.

In this paper, drug release into sink and nonsink conditions is theoretically compared and the manner in which the volume of the receptor phase affects the drug release rate is demonstrated. The relevant diffusion equations are solved for a nonspecific general situation using the method of Laplace transformation. The style of the mathematical approach parallels that of several recent reports (13–17).

## THEORETICAL

**The Model**—The formulation is assumed to release drug at a diffusion-controlled rate into a well-stirred receptor volume. The concentration profile of drug in the formulation and the receptor compartment then have the form shown in Fig. 1.

The cumulative amount of drug that penetrates into the receptor compartment at time $t$ is given by:

$$M_t = D_d A \int_0^t (dc_d/dx)_{x=0}\, dt \qquad \text{(Eq. 1)}$$

where $D_d$ is the diffusion coefficient of the drug in the formulation and $A$ is the surface area across which release takes place.

To simplify solution of the diffusion equations, three normalized variables are defined (18):

$$U = c/c_0 \qquad \text{(Eq. 2)}$$

$$X = x/l \qquad \text{(Eq. 3)}$$

$$T = D_d t/l^2 \qquad \text{(Eq. 4)}$$

where $c_0$ is the initial drug concentration in the donor phase and $l$ is the thickness of the donor phase. With these variables, it is possible to rewrite Eq. 1 to give:

$$M_t = Alc_0 \int_0^T (\partial U_d/\partial X)_0\, dT \qquad \text{(Eq. 5)}$$

To facilitate solution of the diffusion equations, it is also assumed that diffusion occurs in only one dimension and that the diffusion coefficient is concentration independent.

Diffusion in the donor phase is then described by Fick's second law of diffusion, which, in terms of the normalized variables, is expressed as:

$$\partial U_d/\partial T = \partial^2 U_d/\partial X^2 \qquad \text{(Eq. 6)}$$

This differential equation is solved by using Laplace transforms with boundary conditions appropriate to sink and nonsink conditions.

**Sink Conditions**—For sink conditions, drug is continuously removed from the surface of the formulation, producing the boundary conditions:

$$T \geq 0 \qquad U_{d,X=0} = 0 \qquad \text{(Eq. 7)}$$

$$T = 0 \qquad U_d = 1 \qquad \text{(Eq. 8)}$$

$$(\partial U_d/\partial X)_1 = 0 \qquad \text{(Eq. 9)}$$

The physical significance of Eqs. 7–9 may be explained as follows. Equation 7 describes the sink condition. For all values of $T$ (the normalized time variable), the concentration at the surface of the formulation ($X = 0, x = 0$) is zero. Equation 8 shows that there is initially a uniform drug concentration in the donor phase (*i.e.*, at $t = 0, c = c_0$ and $U_d = 1$). Finally, Eq. 9 indicates that there is only a finite quantity of drug in the donor phase; *i.e.*, it is not being replenished by any reservoir at $x = l (X = 1)$.

The Laplace transform of Eq. 6:

$$s\bar{U}_d - 1 = \partial^2 \bar{U}_d/\partial X^2 \qquad \text{(Eq. 10)}$$

has the general solution:

$$\bar{U}_d = A \cosh s^{1/2}X + B \sinh s^{1/2}X + s^{-1} \qquad \text{(Eq. 11)}$$

By using boundary conditions Eqs. 7 and 9, the coefficients $A$ and $B$ may be eliminated to give:

$$(\partial \bar{U}_d/\partial X)_0 = s^{-1/2} \tanh s^{1/2} \qquad \text{(Eq. 12)}$$

Thus:

$$M_t = Alc_0 \mathcal{L}^{-1} (s^{-3/2} \tanh s^{1/2}) \qquad \text{(Eq. 13)}$$

which is identical to a previous problem (Eq. 15 of Ref. 14) and which has

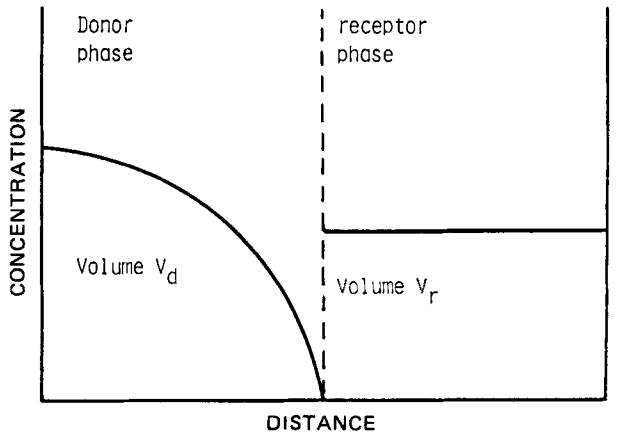


**Figure 1**—*Concentration profile of drug in the receptor and donor phases at some time t after the start of the experiment.*

0022-3549/81/1100-1243$01.00/0
© 1981, American Pharmaceutical Association

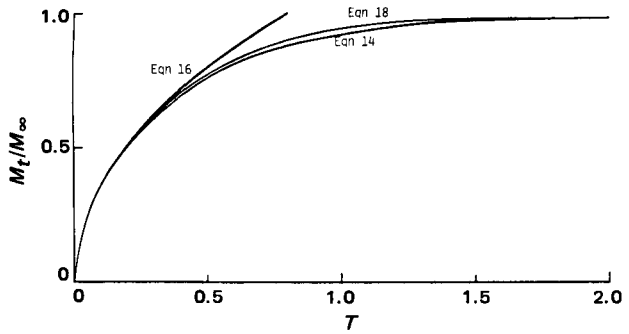


**Figure 2**—*Release profile generated from Eqs. 14, 16, and 18 for sink conditions.*

a solution:

$$M_t = M_\infty \left[1 - 8/\pi^2 \sum_{n=1}^{\infty} \{(2n-1)^{-2} \exp[-(2n-1)^2\pi^2 T/4]\}\right] \quad \text{(Eq. 14)}$$

where $M_\infty = AlC_0$ and is the initial total amount of drug.

It is also possible to derive simplified expressions by approximating the hyperbolic term in Eq. 13 and then taking the inverse transform.

For short times $T < 1$, $s > 1$, $\tanh s^{1/2} \simeq 1$ (19):

$$M_t \simeq M_\infty \mathcal{L}^{-1}(s^{-3/2}) \quad \text{(Eq. 15)}$$

$$M_t \simeq 2M_\infty T^{1/2}\pi^{-1/2} \quad \text{(Eq. 16)}$$

At long times $T > 1$, $s < 1$, $\coth s^{1/2} \simeq s^{-1/2} + s^{1/2}/3$ (19):

$$M_t \simeq 3M_\infty \mathcal{L}^{-1}[s^{-1}(s+3)^{-1}] \quad \text{(Eq. 17)}$$

$$M_t \simeq M_\infty[1 - \exp(-3T)] \quad \text{(Eq. 18)}$$

**Nonsink Conditions**—For these release characteristics, the drug concentration is allowed to build up in the receptor phase and the condition described by Eq. 7 is no longer valid. At the interface between the formulation and the receptor compartment, fast interfacial kinetics are assumed, which provide the new boundary condition:

$$K = U_{r,0}/U_{d,0} \quad \text{(Eq. 19)}$$

where $K$ is a partition coefficient.

Solution of the diffusion equation is identical to that previously described. A finite quantity of drug is still present, and the boundary condition Eq. 9 is still valid. The difference arises during the elimination of the coefficients $A$ and $B$ in the general solution, Eq. 11.

The coefficients are eliminated by considering the buildup of concentration in the receptor phase, which is related to the amount diffused at time $t$ by:

$$c_r = M_t/V_r \quad \text{(Eq. 20)}$$

Substitution of Eq. 5 gives:

$$c_r = AlC_0V_r^{-1}\mathcal{L}^{-1}[s^{-1}(\partial\overline{U}_d/\partial X)_0] \quad \text{(Eq. 21)}$$

Thus:

$$\overline{U}_{d,0} = Al(KV_r)^{-1}s^{-1}(\partial\overline{U}_d/\partial X)_0 \quad \text{(Eq. 22)}$$

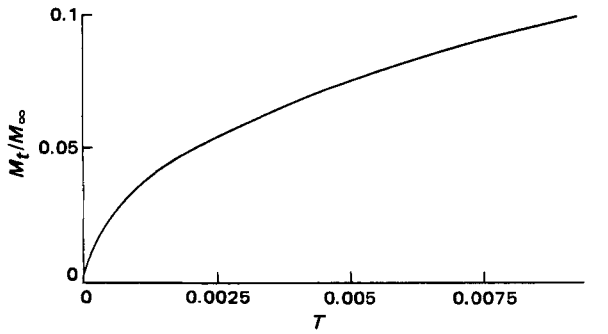


**Figure 3**—*Release profile given from Eq. 26 with* Q = *1, showing the short time pattern for nonsink conditions.*

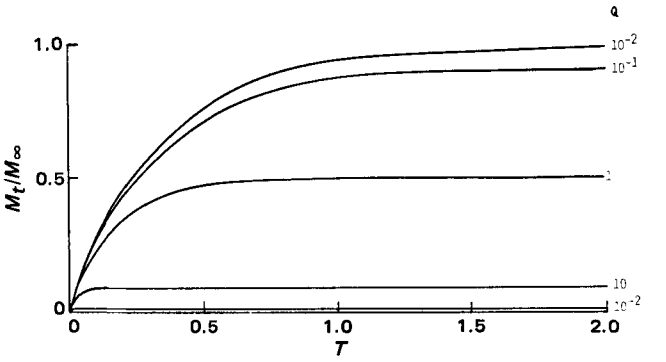


**Figure 4**—*Release profile from Eq. 28 with various values of* Q, *showing the long time pattern for nonsink conditions.*

Differentiation of Eq. 11 and use of the boundary condition Eq. 9 give:

$$(\partial\overline{U}_d/\partial X)_0 = (\overline{U}_{d,0} - s^{-1})s^{1/2}\tanh s^{1/2} \quad \text{(Eq. 23)}$$

and $(\partial\overline{U}_d/\partial X)_0$ may be eliminated by combination of Eqs. 22 and 23. Hence:

$$c_r = KAlc_0\mathcal{L}^{-1}[s^{-1}(s^{1/2}V_rK\coth s^{1/2} + Al)^{-1}] \quad \text{(Eq. 24)}$$

Simple inversion of this equation is not possible, and approximations are made for long and short time release profiles.

**Short Time Approximation**—At short times $T < 1$, $s > 1$, the coth function in Eq. 24 may be approximated (19):

$$c_r = Alc_0V_r^{-1}\mathcal{L}^{-1}[s^{-1}(s^{1/2} + Al/V_rK)^{-1}] \quad \text{(Eq. 25)}$$

This function may be most readily inverted by separation into partial fractions followed by inversion of the individual fractions (19):

$$M_t = M_\infty Q^{-1}[1 - \exp(Q^2T)\,\mathrm{erfc}\,(QT^{1/2})] \quad \text{(Eq. 26)}$$

where $Q = Al/V_rK$.

**Long Time Approximation**—For $T > 1$, $s < 1$, and $\coth s^{1/2} \simeq s^{-1/2} + s^{1/2}/3$, Eq. 24 becomes:

$$c_r = KAlc_0\mathcal{L}^{-1}\{s^{-3/2}[V_rK(s^{1/2} + s^{1/2}/3) + Als^{-1/2}]^{-1}\} \quad \text{(Eq. 27)}$$

which may be inverted:

$$M_t = M_\infty(1+Q)^{-1}\{1 - \exp[-3(1+Q)T]\} \quad \text{(Eq. 28)}$$

**Comparison of Sink *versus* Nonsink Conditions**—It is now possible to obtain a direct comparison of the two sets of conditions using the approximations at short and long times. At short times, Eqs. 26 and 16 produce:

$$\frac{M_{t,ns}}{M_{t,s}} = \frac{\pi^{1/2}[1 - \exp(Q^2T)\mathrm{erfc}(QT^{1/2})]}{2QT^{1/2}} \quad \text{(Eq. 29)}$$

and this complex expression describes the ratio of the amount released at time $t$ from nonsink compared to sink conditions.

The equivalent ratio for long times is given by combining Eqs. 28 and 18:

$$\frac{M_{t,ns}}{M_{t,s}} = \frac{1 - \exp[-3(1+Q)T]}{(1+Q)[1 - \exp(-3T)]} \quad \text{(Eq. 30)}$$

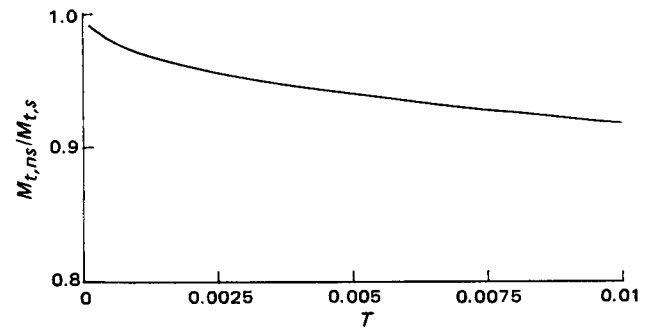


**Figure 5**—*Comparison of sink* versus *nonsink conditions at short times.*

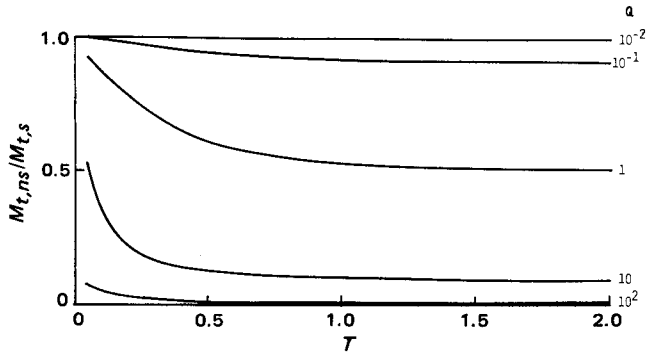


**Figure 6**—*Comparison of sink* versus *nonsink conditions at long times.*

## DISCUSSION

Figure 2 shows the release profile generated using the full solution given by Eq. 14. The figure also shows Eqs. 16 and 18, the two approximations. It is apparent that Eq. 16 is correct up to values of $T \sim 0.5$; from this time onwards, Eq. 18 is applicable.

No unique mathematical expression is obtainable to describe the nonsink conditions. Therefore, concentration is focused on long and short time approximations because it is not possible to predict accurately the release profile for $T$ values approximating to unity. Figure 3 shows the short time approximation given by Eq. 26 for $Q = 1$. The curve generated shows a smooth release pattern not unlike that given by the more simple $t^{1/2}$ approximation applicable to sink conditions. However, there are slight differences as $T$ increases, as shown in Fig. 3. This result would be expected at short periods of time since there is no appreciable concentration buildup in the receptor phase.

The long time approximation, given by Eq. 28, is plotted in Fig. 4. The variation with $Q$ is indicated, and a series of simple first-order curves is obtained. The curves approach the limit, as $T \rightarrow \infty$, of $(1 + Q)^{-1}$, as predicted by Eq. 28. When $Q < 1$, the nonsink limit approaches the long time limit for sink conditions, as expected. This situation corresponds to the experimental conditions of a large receptor volume or large partition coefficient.

Figure 5 compares sink and nonsink conditions at short times for $Q = 1$. At extremely short times, the ratio is unity, as expected. However, as $T$ increases, the deviation from unity becomes more marked and the effect of nonsink conditions becomes apparent. As expected, this general deviation is more pronounced at long times (Fig. 6) and is most noticeable for large values of $Q$ corresponding to small values of the volume of the receptor phase and low partition coefficient.

## REFERENCES


(1) T. Higuchi, *J. Pharm. Sci.*, **50,** 874 (1961).

(2) *Ibid.*, **52,** 1145 (1963).

(3) T. J. Roseman and W. I. Higuchi, *J. Pharm. Sci.*, **59,** 353 (1970).

(4) S. J. Desai, P. Singh, A. P. Simonelli, and W. I. Higuchi, *ibid.*, **55,** 1124 (1966).

(5) P. Singh, S. J. Desai, A. P. Simonelli, and W. I. Higuchi, *ibid.*, **56,** 1542 (1967).

(6) *Ibid.*, **56,** 1548 (1967).

(7) S. J. Desai, A. P. Simonelli, and W. I. Higuchi, *J. Pharm. Sci.*, **54,** 1459 (1965).

(8) J. B. Schwartz, A. P. Simonelli, and W. I. Higuchi, *ibid.*, **57,** 274 (1968).

(9) B. Farhadieh, S. Borodkin, and J. D. Buddenhagen, *ibid.*, **60,** 209 (1971).

(10) *Ibid.*, **60,** 212 (1971).

(11) H. Lapidus and N. G. Lordi, *J. Pharm. Sci.*, **55,** 840 (1966).

(12) *Ibid.*, **57,** 1292 (1968).

(13) W. J. Albery and J. Hadgraft, *J. Pharm. Pharmacol.*, **31,** 129 (1979).

(14) J. Hadgraft, *Int. J. Pharm.*, **2,** 177 (1979).

(15) *Ibid.*, **2,** 265 (1979).

(16) *Ibid.*, **4,** 229 (1980).

(17) R. H. Guy and J. Hadgraft, *Int. J. Pharm.*, **6,** 321 (1980).

(18) J. Crank, "The Mathematics of Diffusion," Oxford University Press, Oxford, England, 1975.

(19) M. Abramovitz and I. A. Stegun, "Handbook of Mathematical Functions," Dover Publications, New York, N.Y., 1980.


# Physicochemical and Analytical Characteristics of Itanoxone


**HENRI COUSSE ˣ, GILBERT MOUZIN, JEAN-PAUL RIBET, and JEAN-CLAUDE VEZIN**



Received March 5, 1980, from the *P. Fabre S.A. Research Center, 17 Avenue Jean Moulin, 81106 Castres, France.* Accepted for publication March 27, 1981.



**Abstract** □ The analytical and spectroscopic characteristics of itanoxone were determined. These data can be used to identify or assay this new drug.



**Keyphrases** □ Itanoxone—physicochemical and analytical characteristics of itanoxone □ Spectroscopy—itanoxone, physicochemical and analytical characteristics □ Hyperlipidemic agents—itanoxone, physicochemical and analytical characteristics □ Hyperuricemic agents—itanoxone, physicochemical and analytical characteristics


Itanoxone is the internationally designated name (1) for 4-[4′-(2-chlorophenyl)phenyl]-4-oxo-2-methylenebutanoic acid (I). This compound has pharmacological and clinical properties (2) suitable for the treatment of hyperlipidemia (3–5) and hyperuricemia (6). Theoretical impurities of I (7) and an industrial purification process (8) were studied previously. This paper considers some physical and physicochemical properties of I.

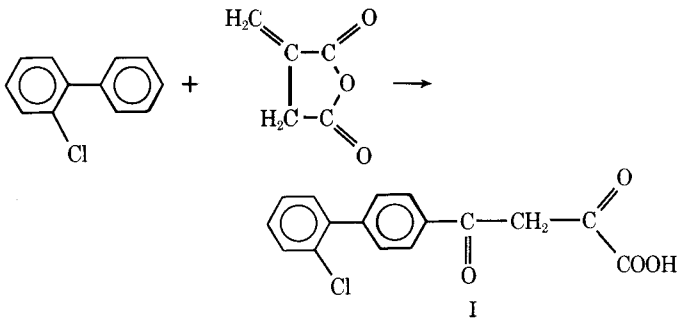


*Scheme I*

## EXPERIMENTAL

**Synthesis**—Itanoxone (I) was synthetized by the Friedel–Crafts reaction between itaconic anhydride and 2-chlorobiphenyl (9, 10) (Scheme I).


*0022-3549/81/1100-1245$01.00/0*


*© 1981, American Pharmaceutical Association*

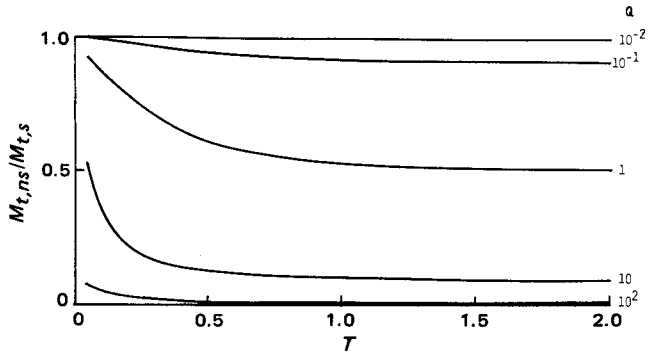


**Figure 6**—*Comparison of sink* versus *nonsink conditions at long times.*

## DISCUSSION

Figure 2 shows the release profile generated using the full solution given by Eq. 14. The figure also shows Eqs. 16 and 18, the two approximations. It is apparent that Eq. 16 is correct up to values of $T \sim 0.5$; from this time onwards, Eq. 18 is applicable.

No unique mathematical expression is obtainable to describe the nonsink conditions. Therefore, concentration is focused on long and short time approximations because it is not possible to predict accurately the release profile for $T$ values approximating to unity. Figure 3 shows the short time approximation given by Eq. 26 for $Q = 1$. The curve generated shows a smooth release pattern not unlike that given by the more simple $t^{1/2}$ approximation applicable to sink conditions. However, there are slight differences as $T$ increases, as shown in Fig. 3. This result would be expected at short periods of time since there is no appreciable concentration buildup in the receptor phase.

The long time approximation, given by Eq. 28, is plotted in Fig. 4. The variation with $Q$ is indicated, and a series of simple first-order curves is obtained. The curves approach the limit, as $T \rightarrow \infty$, of $(1 + Q)^{-1}$, as predicted by Eq. 28. When $Q < 1$, the nonsink limit approaches the long time limit for sink conditions, as expected. This situation corresponds to the experimental conditions of a large receptor volume or large partition coefficient.

Figure 5 compares sink and nonsink conditions at short times for $Q = 1$. At extremely short times, the ratio is unity, as expected. However, as $T$ increases, the deviation from unity becomes more marked and the effect of nonsink conditions becomes apparent. As expected, this general deviation is more pronounced at long times (Fig. 6) and is most noticeable for large values of $Q$ corresponding to small values of the volume of the receptor phase and low partition coefficient.

## REFERENCES


(1) T. Higuchi, *J. Pharm. Sci.*, **50,** 874 (1961).

(2) *Ibid.*, **52,** 1145 (1963).

(3) T. J. Roseman and W. I. Higuchi, *J. Pharm. Sci.*, **59,** 353 (1970).

(4) S. J. Desai, P. Singh, A. P. Simonelli, and W. I. Higuchi, *ibid.*, **55,** 1124 (1966).

(5) P. Singh, S. J. Desai, A. P. Simonelli, and W. I. Higuchi, *ibid.*, **56,** 1542 (1967).

(6) *Ibid.*, **56,** 1548 (1967).

(7) S. J. Desai, A. P. Simonelli, and W. I. Higuchi, *J. Pharm. Sci.*, **54,** 1459 (1965).

(8) J. B. Schwartz, A. P. Simonelli, and W. I. Higuchi, *ibid.*, **57,** 274 (1968).

(9) B. Farhadieh, S. Borodkin, and J. D. Buddenhagen, *ibid.*, **60,** 209 (1971).

(10) *Ibid.*, **60,** 212 (1971).

(11) H. Lapidus and N. G. Lordi, *J. Pharm. Sci.*, **55,** 840 (1966).

(12) *Ibid.*, **57,** 1292 (1968).

(13) W. J. Albery and J. Hadgraft, *J. Pharm. Pharmacol.*, **31,** 129 (1979).

(14) J. Hadgraft, *Int. J. Pharm.*, **2,** 177 (1979).

(15) *Ibid.*, **2,** 265 (1979).

(16) *Ibid.*, **4,** 229 (1980).

(17) R. H. Guy and J. Hadgraft, *Int. J. Pharm.*, **6,** 321 (1980).

(18) J. Crank, "The Mathematics of Diffusion," Oxford University Press, Oxford, England, 1975.

(19) M. Abramovitz and I. A. Stegun, "Handbook of Mathematical Functions," Dover Publications, New York, N.Y., 1980.


# Physicochemical and Analytical Characteristics of Itanoxone


**HENRI COUSSE ˣ, GILBERT MOUZIN, JEAN-PAUL RIBET, and JEAN-CLAUDE VEZIN**



Received March 5, 1980, from the *P. Fabre S.A. Research Center, 17 Avenue Jean Moulin, 81106 Castres, France.* Accepted for publication March 27, 1981.



**Abstract** □ The analytical and spectroscopic characteristics of itanoxone were determined. These data can be used to identify or assay this new drug.



**Keyphrases** □ Itanoxone—physicochemical and analytical characteristics of itanoxone □ Spectroscopy—itanoxone, physicochemical and analytical characteristics □ Hyperlipidemic agents—itanoxone, physicochemical and analytical characteristics □ Hyperuricemic agents—itanoxone, physicochemical and analytical characteristics


Itanoxone is the internationally designated name (1) for 4-[4′-(2-chlorophenyl)phenyl]-4-oxo-2-methylenebutanoic acid (I). This compound has pharmacological and clinical properties (2) suitable for the treatment of hyperlipidemia (3–5) and hyperuricemia (6). Theoretical impurities of I (7) and an industrial purification process (8) were studied previously. This paper considers some physical and physicochemical properties of I.

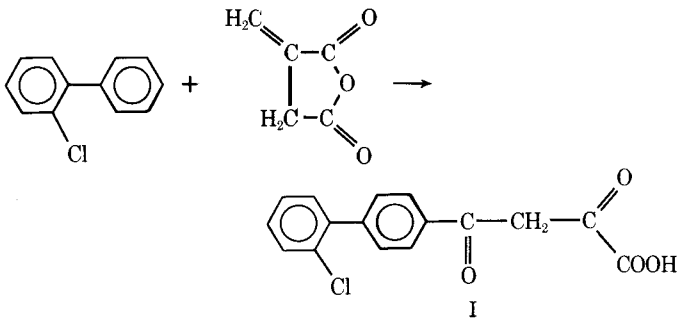


*Scheme I*

## EXPERIMENTAL

**Synthesis**—Itanoxone (I) was synthetized by the Friedel–Crafts reaction between itaconic anhydride and 2-chlorobiphenyl (9, 10) (Scheme I).


*0022-3549/81/1100-1245$01.00/0*


*© 1981, American Pharmaceutical Association*

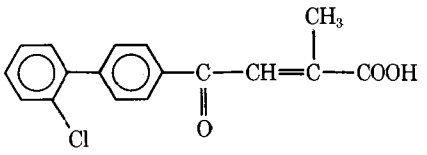

II

**Apparatus**—A GLC chromatograph[1] was equipped with a glass 3 m × 4-mm i.d. column, packed with 10% (w/w) Carbowax 20 *M* on Chromosorb W.A.W. (60–80 mesh). The carrier gas was nitrogen at 50 ml/min, the column temperature was 130°, and the injection detector temperature was 200°. Potentiometric measurements were made with a titration device[2] fitted with a combined electrode[3]. Melting points were determined on a hot stage[4] and were not corrected.

PMR spectra were recorded at 40° on a spectrometer[5] using solutions in dimethyl sulfoxide-$d_6$ containing tetramethylsilane as the internal standard. IR spectra were measured on a spectrophotometer[6] using potassium bromide pellets at ~1% (w/w) concentration. A mass spectrometer[7] with the probe at 160° and an ionizing voltage of 70 ev, was used.

**Identification and Assay of Impurities**—Secondary products of I were described previously (7), but that report did not include tests and detection limits for impurities. The solvents used in the reaction and during recrystallization were determined by GLC. Traces of aluminum from the aluminum chloride catalyst were identified by emission spectrography[8] (low voltage alternating arc, carbon electrodes) (11).

**Determination of pKa**—The pKa values were determined by potentiometric titration using a glass electrode. A water-jacketed beaker connected to a circulating water bath maintained the temperature of the titrating vessel at 25°. Stirring was accomplished by introducing a slow nitrogen stream under the surface of the solution to be titrated.

The titrant of carbonate-free potassium hydroxide (0.100 *N* KOH) was delivered from a micrometer syringe; for each addition of titrant, the pH was measured and the pKa was determined from the half-neutralization point.

**Solubility Conditions**—The solubilities, expressed in percentage (weight/volume), were determined as follows. The solvent and solute were placed in 50-ml test tubes with a suitable amount of undissolved I. The tubes were stoppered and shaken for 1 hr at 25 ± 1° to avoid isomerization of I into II (7). The tubes were then centrifugated, and the liquid was filtered through a sintered-glass funnel. The clear liquid was diluted and spectrophotometrically[9] assayed for I.

**Partition Coefficients**—Itanoxone was partitioned between buffer solutions saturated with organic solvents and organic solvent saturated with buffer solutions. Usually 50 ml of buffer solution containing a known amount of solute was shaken with an equal volume of organic solvent. The sample was maintained at 25 ± 1° and mechanically[10] shaken for 1.5 hr until equilibrium was obtained (12, 13). After stirring, the two phases were separated by centrifugation at 3000 rpm for 30 min. The amount of I in the water layer was determined spectrophotometrically.

## RESULTS AND DISCUSSION

**Assay of Impurities**—Methylene chloride reaction solvent and dimethylformamide recrystallization solvent had retention times of 1.5 and 3.5 min, respectively. Under these conditions, solvent amounts of <0.05% (w/w) were detected in itanoxone (I). The most sensitive rays characteristic of aluminum (11) were not observed in the spectrum of I. The lower limit of detection sensitivity of metal in I is 0.02 μg.

**Melting Points**—Itanoxone occurs as a white crystalline powder in the monoclinic system (14) with an instantaneous melting point of 212 ± 1°. It is overlapped by the standard melting points of saccharin and dicyanodiamide.

**Determination of pKa**—In view of the low solubility of I in water, the pKa value was determined at 25° by extrapolation from a series of dissociation constants in water–dioxane mixtures evaluated by potentiometry. The results are expressed by introducing an experimental parameter, $g(S)$, which is characteristic of each solvent (15). This quantity takes care of all types of solvent–solute interactions, such as hydrogen bonding and structural effects, and its measurement gives the magnitude of solvent effects on acid–base reactions. Measurement of the dissociation constant of itanoxone, ${}^{S}K_I$, and of salicylic acid, ${}^{S}K_{\text{ref}}$, used as the standard compound in each $S$ medium indicates that the difference between both pKa values is a linear function of $g(S)$ according to the formula:

$$\text{p}{}^{S}K_{a\text{I}} - \text{p}{}^{S}K_{a\text{ref}} = \alpha + \beta g(S) \qquad \text{(Eq. 1)}$$

in which $\alpha$ and $\beta$ are constants dependent only on I. Itanoxone transfer between water and dioxane may be expressed by:

$$\log {}^{\text{water}}T^{\text{dioxane}}(\text{I}) = \log C_{\text{sat}}^{\text{water}}(\text{I}) - \log C_{\text{sat}}^{\text{dioxane}}(\text{I}) \qquad \text{(Eq. 2)}$$

where $C_{\text{sat}}^{\text{water}}(\text{I})$ and $C_{\text{sat}}^{\text{dioxane}}(\text{I})$ are the solubilities (weight/volume) of I in water–dioxane. Thus, $\log {}^{\text{water}}T^{\text{dioxane}}$ (I) is proportional to the solvent variable $g(S)$:

$$\log {}^{\text{water}}T^{\text{dioxane}}(\text{I}) = f(\text{I}) \times g(S) \qquad \text{(Eq. 3)}$$

where $f(\text{I})$ is a constant characteristic of I. The measurement of solubility of I in water–dioxane enables the calculation of values proportional to the solvent variable $g(S)$. The agreed convention is then expressed as:

$$g(S) = -\log {}^{\text{water}}T^{\text{dioxane}}(\text{I}) \qquad \text{(Eq. 4)}$$

For each $g(S)$ calculation, the relative water and dioxane contents of the medium must be considered.

Extrapolation to pure water gives $g(S) = 0$. Any $g(S)$ is given by:

$$g(S) = -\log {}^{\text{water}}T^{\text{dioxane}}(\text{I}) = -\log a(0.019)/b(3.9) \qquad \text{(Eq. 5)}$$

where $a$ and $b$ represent the water and dioxane contents, respectively.

The values of $g(S)$ for different percentage volumes of dioxane and the pKa values of salicylic acid (the reference compound) are shown in Table

**Table I—Dissociation Constants in Water–Dioxane Mixtures**

| Dioxane, % (v/v) | $g(S)$ | $\text{pKa}_{\text{ref}}$[a] | $\text{pKa}_{\text{I}}$[b] | $\text{pKa}_{\text{I}} - \text{pKa}_{\text{ref}}$ |
|---|---|---|---|---|
| 0.6 | 2.49 | 4.60 | 6.68 | 2.08 |
| 0.8 | 2.92 | 5.50 | 7.55 | 2.05 |
| 0.9 | 3.26 | 6.40 | 8.38 | 1.98 |

[a] The pKa of salicylic acid. [b] The pKa of itanoxone.

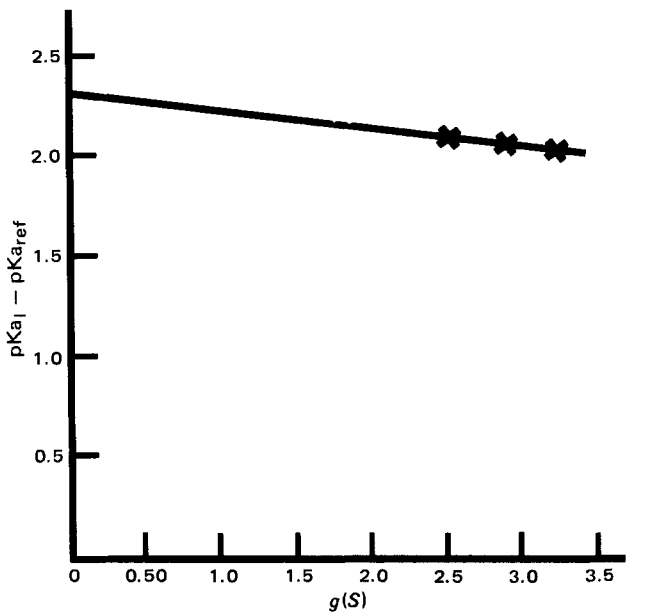


**Figure 1**—*Determination of pKa of itanoxone by extrapolation. The solid line gives the difference between $pKa_I$ and $pKa_{ref}$ determined on the same water–dioxane media* versus g(S) *($pKa_I = pKa_{ref} + 2.3 = 3.0 + 2.3 = 5.30$).*

[1] Girdel 3000, Giravions Dorand, Suresnes, France.
[2] Mettler Instruments, Greifensee, Zürich, Switzerland.
[3] Tacussel TCBG II/HS, Solea, Villeurbanne, France.
[4] Kofler, C. Reichert AG, Wein XVII, Austria.
[5] Model R-24B, Hitachi Perkin-Elmer, Hitachi Ltd., Tokyo, Japan.
[6] Model 177, Perkin-Elmer Ltd., Beaconsfield, Buckinghamshire, England.
[7] Ribermag R-10-10B, Nermag S. A., Rueil-Malmaison, France.
[8] Model E-478, Hilger spectrograph.
[9] Model DK-2A, Beckman Instruments, GMBH, München 45, West Germany.
[10] New Brunswick Scientific Co., Edison, N.J.

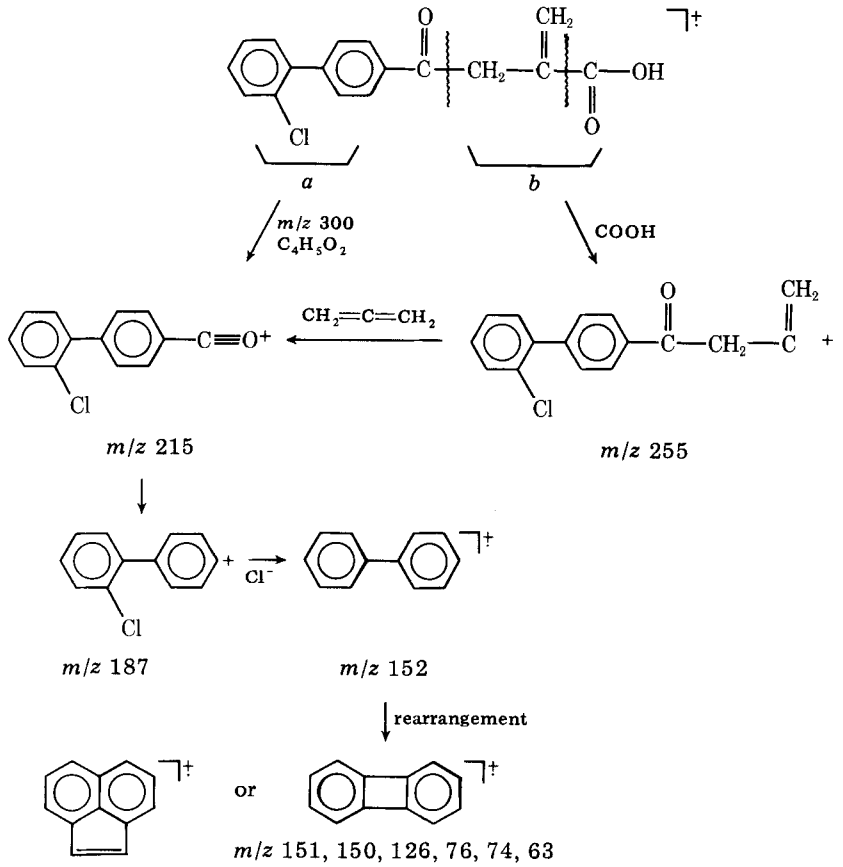


*Scheme II—Fragmentation mechanism.*

I. The difference between the two pKa values is a linear function of $g(S)$. The determination of the pKa of I in water by extrapolation of measurements made on water–dioxane mixtures is plotted *versus* $g(S)$ determined for each water–dioxane system (Fig. 1). The pKa of salicylic acid determined in water is 3.0. The pKa of I determined in water–dioxane with extrapolation of the results to zero dioxane concentration is 3.0 + 2.3 = 5.30.

**Solubility**—The maximum values are expressed in Table II as percentage (weight/volume). This technique cannot be used for ketonic solvents having absorptions in the same range.

**Partition Coefficients**—The I concentration was determined in the aqueous phase by UV spectroscopy at 265 nm. The apparent partition coefficient is calculated by the formula:

$$\text{Apparent partition coefficient} = \frac{C_{\text{octanol}}}{C_{\text{buffer}}} = \frac{(C_1 - C_2) \times a}{C_2 \times b} \quad \text{(Eq. 6)}$$

where $C_1$ and $C_2$ are the I concentrations (weight/volume) in the aqueous phase before and after equilibration, respectively, and $a$ and $b$ are the volumes of the aqueous and octanol phases, respectively. By working at a fixed pH and knowing the pKa for I, the partition coefficient can be determined using:

$$\text{Partition coefficient} = \frac{C_{\text{octanol}}}{C_{\text{buffer}}\,(1 - \alpha)} \quad \text{(Eq. 7)}$$

where $\alpha$ is the degree of ionization. Details are given in Table III.

For a good extraction yield of I from biological media such as blood and urine, it is imperative to use an acidic pH. Under these conditions, 98% of the drug is extracted from the aqueous phase during the first extraction. Ethyl acetate is recommended to reduce emulsion effects.

The TLC procedure reported previously (7) was used to demonstrate that I did not isomerize during the 1–1.5 hr needed to determine solubility or partition coefficients. In the media used to determine solubilities and partition coefficients, traces of II were detected after the 2nd hr of TLC. The amount of II ranged from 0.1 to 0.3%, depending on the solvent. Isomerization continued, but the lack of II in the first 2 hr confirmed the validity of solubility and partition data.

**IR Spectroscopy**—The IR spectrum revealed characteristic bands (16) that agreed with the suggested structure: 3000–3080 (aromatic and ethylenic CH), 2910 (aliphatic CH), 1690 (C=O acid), 1675 (C=O conjugated ketone), and 1630 (ethylenic C=C) $cm^{-1}$ (Fig. 2).

**UV Spectroscopy**—The spectrum was obtained in ethanolic solution using 1-cm quartz cells, $\lambda_{max}$ 265 ($\epsilon$ 18,350 ± 30) nm.

**PMR Spectroscopy**—Assignments (17) were: $\delta$ 4.1 (s, 2H, $COCH_2$), 5.75 (d, 1H, $J$ = 1.2 Hz, *trans*-*H*C=CCOOH), 6.3 (d, 1H, $J$ = 1.2 Hz, *cis*-*H*C=CCOOH), 7.3–7.7 (m, 6H, aromatic protons), 8.05 (d, 2H, $J$ = 8 Hz, aromatic protons *ortho* to C=O), and 11–13.5 (s, 1H, COOH) ppm.

**Table II—Solubilities at 20°, Percent (weight/volume)**

| Solvent | Solubility, g/100 ml |
|---|---|
| *n*-Hexane | 0.00025 |
| Water | 0.019 |
| Chloroform | 0.15 |
| Ether | 0.17 |
| Acetonitrile | 0.20 |
| Ethyl acetate | 0.24 |
| Methanol | 0.39 |
| Ethanol | 0.50 |
| *n*-Octanol | 0.75 |
| Dioxane | 3.9 |
| Tetrahydrofuran | 4.34 |
| Dimethylformamide | 28.5 |
| Dimethyl sulfoxide | 38.4 |

**Table III—Itanoxone Partition Coefficients between *n*-Octanol and Buffered Solutions**

| Buffer Solution | Apparent Partition Coefficient[a] | Partition Coefficient | Log $P$ |
|---|---|---|---|
| pH 10[b] | 2.12 | 2120 | 7.66 (0.021) |
| pH 7.4[c] | 16.6 | 2075 | 7.64 (0.020) |
| pH 2.2[d] | 2098 | 2100 | 7.65 (0.043) |

[a] All determinations were done in triplicate, and the average value for log $P$ was determined. Values in parentheses indicate standard deviations. [b] Ammonium chloride buffer (0.05 $M$). [c] Phosphate buffer (0.05 $M$). [d] Potassium chloride buffer (0.05$M$).

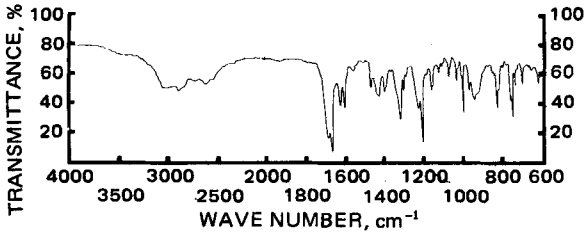


**Figure 2**—*IR spectrum of itanoxone*

The exchangeable acid proton appeared faintly in dimethyl sulfoxide-$d_6$, but a very marked singlet was obtained in pyridine-$d_5$ at 9.9 ppm.

**Mass Spectroscopy**—The molecular peak was observed at *m/z* 300, corresponding to the molecular mass of the product. The most characteristic fragments of I gave a series of peaks at *m/z* 302, 300, 277, 255, 217, 215, 152, and 76. The peak at *m/z* 302 corresponded to the chlorine 37 isotope. The isotopic peaks at p + 2 were also observed in the various fragments containing chlorine.

Fragmentation is shown in Scheme II. The $C_{12}H_8$ ion (*m/z* 152) (18, 19) was followed by the series of ions at *m/z* 151, 150, 126, 76, 75, 74, and 63. The relative intensities of these ions in the spectrum of I were very close to those in the Cornu–Massot catalog (20) for diphenylene and acenaphthene. This result indicates that the ion obtained after the removal of C=O and the chlorine atom rearranges to give a radical ion with a structure close to diphenylene or acenaphthene.

## REFERENCES

(1) "International General Designation," *Chron. Org. Mond. Santé*, **33** (3), list 41-8 (1975).

(2) H. Cousse, G. Mouzin, J. P. Rieu, and A. Delhon (to P. Fabre S. A.), French pat. 2,300,551 (1975).

(3) A. Bizzi, M. T. Tacconi, E. Veneroni, and M. Cini, "7th International Congress of Pharmacology," Paris, France, 1978.

(4) A. Delhon, J. P. Tarayre, H. Lauressergues, and S. Casadio, "International Conference on Atherosclerosis," Milan, Italy, Nov. 1975.

(5) J. Lubetzki and A. Mose, "International Conference on Atherosclerosis," Milan, Italy, Nov. 1975.

(6) F. Mazoyer (to P. Fabre S.A.), U.S. pat. 105,420 (1979).

(7) J. P. Rieu, G. Mouzin, H. Cousse, and A. Boucherle, *J. Pharm. Sci.*, **69**, 49 (1980).

(8) H. Cousse, P. Hascoet, G. Mouzin, and J. P. Rieu, French pat. 79.245.82 (1979).

(9) H. Cousse, G. Mouzin, and J. P. Rieu, (to P. Fabre S.A.), French pat. 2,265,409 (1974) and U.S. pat. 4,058,558 (1977).

(10) H. Cousse, G. Mouzin, and J. P. Rieu, Swiss pat. 595,322 (1975).

(11) P. Pascal, "Traité de Chimie Minérale, Masson et Cie," Paris, France, 1932.

(12) C. Hansch, R. M. Muir, T. Fujita, P. P. Maloney, F. Geiger, and M. Streich, *J. Am. Chem. Soc.*, **85**, 2817, (1963).

(13) T. Fujita, J. Iwasa, and C. Hansch, *ibid.*, **86**, 5175, (1964).

(14) R. Roques, H. Cousse, G. Mouzin, *Acta Crystallogr.*, in press.

(15) R. Gaboriaud, J. C. Halle, and P. Letellier, *Bull. Soc. Chim. Fr.*, **1976**, 1093.

(16) L. J. Bellamy, "The Infrared Spectra of Complex Molecules," 2nd ed., Methuen, London, England, 1966.

(17) M. L. Martin and G. L. Martin, "Manual of Nuclear Magnetic Resonance," Azoulay, Paris, France, 1971.

(18) F. W. McLafferty, "Interpretation of Mass Spectra," 2nd ed., Benjamin, Mass., 1973.

(19) S. Safe, *Org. Mass Spectrom.*, **5**, 1221 (1971).

(20) A. Cornu and R. Massot, "Compilation of Mass Spectral Data," Heyden and Son, 1966.

# Effect of Docusate Sodium on Drug Release from a Controlled-Release Dosage Form

**WALTER G. CHAMBLISS, ROBERT W. CLEARY, RICHARD FISCHER, ALAN B. JONES, PAUL SKIERKOWSKI, W. NICHOLES, and ARTHUR H. KIBBE** ˣ

Received December 22, 1980, from the *Department of Pharmaceutics, University of Mississippi, University, MS 38677.* Accepted for publication April 1, 1981.

**Abstract** □ This study was designed to determine the effect of a clinically used surfactant, docusate sodium, on the release of chlorpheniramine from a controlled-release dosage form (encapsulated coated pellets). *In vivo* treatments consisted of the controlled-release capsule alone or with 200 mg of docusate sodium. Plasma chlorpheniramine levels were determined, and the *AUC* was calculated. No significant difference in *AUC* values was observed between the two treatments. At a concentration below the CMC, docusate sodium enhanced the *in vitro* drug release rate. The surfactant exerted a greater effect on the release of the first one-third of the drug contained in nonwax-coated pellets. At the CMC, 0.02% (w/v), docusate sodium rapidly entrapped chlorpheniramine in micelles. The overall enhanced dissolution rate *in vivo* may have been offset by micellar drug entrapment.

**Keyphrases** □ Docusate sodium—effect on drug release from a controlled-release dosage form □ Controlled-release formulations—effect of docusate sodium on drug release □ Surfactants—effect on drug release of controlled-release dosage forms

Most long-acting oral dosage forms utilize a physical barrier to decrease the rate of drug release into the GI tract. The wax coating on the pellets of a controlled-release capsule serves as this barrier (1).

Disintegration of the wax coat is thought to be controlled by the penetration of moisture through pores (2). The pH of the medium reportedly does not affect disintegration (3) although surface tension is thought to be important. The surface tension of intestinal fluid is less than gastric fluid due to bile salts in the intestines. This lowered surface tension may lead to the release of more drug into the intestinal fluids (2). The effect of lowered surface tension in the GI tract on the release of drug from wax-coated pellets has not been reported.

## BACKGROUND

Numerous studies have been performed to determine the effect of surfactants on drug absorption, mainly with surfactants that promote oral absorption of a poorly absorbed drug. The exact mechanism by which docusate sodium and other surfactants enhance drug absorption is unknown. The most popular theory has been that surfactants directly alter membrane permeability of the GI tract (4–14). Although the mechanism of this "hyperabsorptive state" is unknown, most investigators believe that the surfactant disrupts the integrity of the epithelial membrane in a reversible fashion (4–11). The removal of proteins (12, 13) and phos-



*0022-3549/81/1100-1248$01.00/0*
*© 1981, American Pharmaceutical Association*

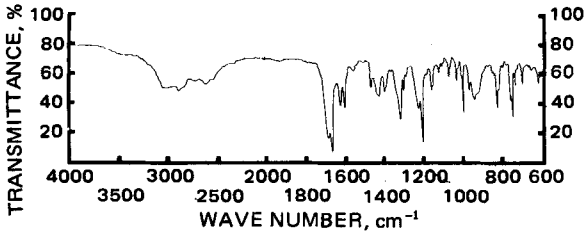


**Figure 2**—*IR spectrum of itanoxone*

The exchangeable acid proton appeared faintly in dimethyl sulfoxide-$d_6$, but a very marked singlet was obtained in pyridine-$d_5$ at 9.9 ppm.

**Mass Spectroscopy**—The molecular peak was observed at *m/z* 300, corresponding to the molecular mass of the product. The most characteristic fragments of I gave a series of peaks at *m/z* 302, 300, 277, 255, 217, 215, 152, and 76. The peak at *m/z* 302 corresponded to the chlorine 37 isotope. The isotopic peaks at p + 2 were also observed in the various fragments containing chlorine.

Fragmentation is shown in Scheme II. The $C_{12}H_8$ ion (*m/z* 152) (18, 19) was followed by the series of ions at *m/z* 151, 150, 126, 76, 75, 74, and 63. The relative intensities of these ions in the spectrum of I were very close to those in the Cornu–Massot catalog (20) for diphenylene and acenaphthene. This result indicates that the ion obtained after the removal of C=O and the chlorine atom rearranges to give a radical ion with a structure close to diphenylene or acenaphthene.

## REFERENCES

(1) "International General Designation," *Chron. Org. Mond. Santé*, **33** (3), list 41-8 (1975).

(2) H. Cousse, G. Mouzin, J. P. Rieu, and A. Delhon (to P. Fabre S. A.), French pat. 2,300,551 (1975).

(3) A. Bizzi, M. T. Tacconi, E. Veneroni, and M. Cini, "7th International Congress of Pharmacology," Paris, France, 1978.

(4) A. Delhon, J. P. Tarayre, H. Lauressergues, and S. Casadio, "International Conference on Atherosclerosis," Milan, Italy, Nov. 1975.

(5) J. Lubetzki and A. Mose, "International Conference on Atherosclerosis," Milan, Italy, Nov. 1975.

(6) F. Mazoyer (to P. Fabre S.A.), U.S. pat. 105,420 (1979).

(7) J. P. Rieu, G. Mouzin, H. Cousse, and A. Boucherle, *J. Pharm. Sci.*, **69**, 49 (1980).

(8) H. Cousse, P. Hascoet, G. Mouzin, and J. P. Rieu, French pat. 79.245.82 (1979).

(9) H. Cousse, G. Mouzin, and J. P. Rieu, (to P. Fabre S.A.), French pat. 2,265,409 (1974) and U.S. pat. 4,058,558 (1977).

(10) H. Cousse, G. Mouzin, and J. P. Rieu, Swiss pat. 595,322 (1975).

(11) P. Pascal, "Traité de Chimie Minérale, Masson et Cie," Paris, France, 1932.

(12) C. Hansch, R. M. Muir, T. Fujita, P. P. Maloney, F. Geiger, and M. Streich, *J. Am. Chem. Soc.*, **85**, 2817, (1963).

(13) T. Fujita, J. Iwasa, and C. Hansch, *ibid.*, **86**, 5175, (1964).

(14) R. Roques, H. Cousse, G. Mouzin, *Acta Crystallogr.*, in press.

(15) R. Gaboriaud, J. C. Halle, and P. Letellier, *Bull. Soc. Chim. Fr.*, **1976**, 1093.

(16) L. J. Bellamy, "The Infrared Spectra of Complex Molecules," 2nd ed., Methuen, London, England, 1966.

(17) M. L. Martin and G. L. Martin, "Manual of Nuclear Magnetic Resonance," Azoulay, Paris, France, 1971.

(18) F. W. McLafferty, "Interpretation of Mass Spectra," 2nd ed., Benjamin, Mass., 1973.

(19) S. Safe, *Org. Mass Spectrom.*, **5**, 1221 (1971).

(20) A. Cornu and R. Massot, "Compilation of Mass Spectral Data," Heyden and Son, 1966.

# Effect of Docusate Sodium on Drug Release from a Controlled-Release Dosage Form

**WALTER G. CHAMBLISS, ROBERT W. CLEARY, RICHARD FISCHER, ALAN B. JONES, PAUL SKIERKOWSKI, W. NICHOLES, and ARTHUR H. KIBBE** ˣ

Received December 22, 1980, from the *Department of Pharmaceutics, University of Mississippi, University, MS 38677.* Accepted for publication April 1, 1981.

**Abstract** □ This study was designed to determine the effect of a clinically used surfactant, docusate sodium, on the release of chlorpheniramine from a controlled-release dosage form (encapsulated coated pellets). *In vivo* treatments consisted of the controlled-release capsule alone or with 200 mg of docusate sodium. Plasma chlorpheniramine levels were determined, and the *AUC* was calculated. No significant difference in *AUC* values was observed between the two treatments. At a concentration below the CMC, docusate sodium enhanced the *in vitro* drug release rate. The surfactant exerted a greater effect on the release of the first one-third of the drug contained in nonwax-coated pellets. At the CMC, 0.02% (w/v), docusate sodium rapidly entrapped chlorpheniramine in micelles. The overall enhanced dissolution rate *in vivo* may have been offset by micellar drug entrapment.

**Keyphrases** □ Docusate sodium—effect on drug release from a controlled-release dosage form □ Controlled-release formulations—effect of docusate sodium on drug release □ Surfactants—effect on drug release of controlled-release dosage forms

Most long-acting oral dosage forms utilize a physical barrier to decrease the rate of drug release into the GI tract. The wax coating on the pellets of a controlled-release capsule serves as this barrier (1).

Disintegration of the wax coat is thought to be controlled by the penetration of moisture through pores (2). The pH of the medium reportedly does not affect disintegration (3) although surface tension is thought to be important. The surface tension of intestinal fluid is less than gastric fluid due to bile salts in the intestines. This lowered surface tension may lead to the release of more drug into the intestinal fluids (2). The effect of lowered surface tension in the GI tract on the release of drug from wax-coated pellets has not been reported.

## BACKGROUND

Numerous studies have been performed to determine the effect of surfactants on drug absorption, mainly with surfactants that promote oral absorption of a poorly absorbed drug. The exact mechanism by which docusate sodium and other surfactants enhance drug absorption is unknown. The most popular theory has been that surfactants directly alter membrane permeability of the GI tract (4–14). Although the mechanism of this "hyperabsorptive state" is unknown, most investigators believe that the surfactant disrupts the integrity of the epithelial membrane in a reversible fashion (4–11). The removal of proteins (12, 13) and phos-



*0022-3549/81/1100-1248$01.00/0*
*© 1981, American Pharmaceutical Association*

**Table I—Accumulative *AUC* (Micrograms Minutes per Milliliter) of Chlorpheniramine from Subjects Receiving 12 mg of Chlorpheniramine in a Controlled-Release Capsule with (Treatment B) or without (Treatment A) 200 mg of Docusate Sodium**

| | Subject 1 | | | Subject 2 | | |
|---|---|---|---|---|---|---|
| | Treatment | | Area | Treatment | | Area |
| Min | A | B | Change | A | B | Change |
| 40 | 8.79 | 5.79 | −3.90 | 5.23 | 5.48 | +0.25 |
| 80 | 18.10 | 13.13 | −4.97 | 12.30 | 12.28 | −0.02 |
| 160 | 37.10 | 26.60 | −10.50 | 24.24 | 25.02 | +0.78 |
| 240 | 54.79 | 40.59 | −14.20 | 41.63 | 37.26 | −4.37 |
| 480 | 107.48 | 88.24 | −19.24 | 107.68 | 71.90 | −35.78 |
| | Subject 3 | | | Subject 4 | | |
| | Treatment | | Area | Treatment | | Area |
| Min | A | B | Change | A | B | Change |
| 40 | 6.36 | 8.07 | +1.71 | 7.36 | 8.89 | +1.53 |
| 80 | 13.03 | 19.32 | +6.29 | 17.95 | 18.20 | +0.25 |
| 160 | 25.40 | 37.69 | +12.29 | 37.03 | 33.89 | −3.13 |
| 240 | 38.16 | 57.00 | +18.84 | 56.08 | 52.25 | −3.83 |
| 480 | 69.54 | 105.08 | +35.54 | 113.73 | 107.61 | −6.12 |
| | Subject 5 | | | Subject 6 | | |
| | Treatment | | Area | Treatment | | Area |
| Min | A | B | Change | A | B | Change |
| 40 | 9.27 | 7.14 | −2.13 | 10.49 | 7.18 | −3.31 |
| 80 | 19.28 | 19.22 | −0.06 | 20.91 | 18.63 | −2.28 |
| 160 | 42.24 | 41.76 | −0.48 | 40.51 | 48.93 | +8.42 |
| 240 | 64.28 | 63.05 | −1.23 | 57.38 | 76.46 | +19.08 |
| 480 | 118.70 | 131.47 | +12.77 | 99.03 | 156.60 | +57.57 |
| | Subject 7 | | | | | |
| | Treatment | | Area | | | |
| Min | A | B | Change | | | |
| 40 | 9.18 | 10.87 | +1.69 | | | |
| 80 | 19.41 | 21.32 | +1.91 | | | |
| 160 | 41.00 | 39.46 | −1.54 | | | |
| 240 | 62.11 | 69.09 | +6.98 | | | |
| 480 | 112.21 | 145.95 | +33.74 | | | |

pholipids (13, 14) from the membrane by surfactants may alter permeability. "Plasticization" of the membrane by the action of surfactant molecules in the lipoidal epithelium has also been suggested as a possible mechanism for altered permeability (7).

Gouda and colleagues (4–8) determined that the effect of docusate sodium on drug absorption was concentration related. The critical micelle concentration (CMC) was closely related to the critical concentration for the enhancement of drug absorption. The CMC for docusate sodium was reported to be 0.02–0.03% (w/v) (15). Surfactants can trap drug molecules in micelles that form in surfactant concentrations above the CMC. Since micelles are thought to be too large to diffuse across the mucosal membrane, drugs trapped by micelles are not available for absorption (16).

## EXPERIMENTAL

***In Vivo***—A 2 × 2 Latin square design was used to study the effect of coadministration of 200 mg of docusate sodium on the GI absorption of chlorpheniramine released from a controlled-release capsule[1]. Seven subjects were randomly assigned to two different groups. Study days were separated by 7 days to allow adequate drug clearance of the previous dose.

All subjects were adult males, 22–34 years of age, who were within 10% of their ideal body weight. Since the drugs were not administered on a milligram per killigram basis, only subjects weighing 72–80 kg were used. In addition, all subjects had prestudy test results within the normal laboratory limits.

Subjects fasted for 12 hr prior to drug administration and were allowed water *ad. libitum*. Blood samples were drawn through a 21-gauge heparin lock inserted into a vein on the dorsal side of the forearm. Treatment A consisted of 12 mg of chlorpheniramine in controlled-release capsule dosage form[1]. Treatment B consisted of the chlorpheniramine capsule and two 100-mg docusate sodium capsules[2]. Drugs were ingested with 240 ml of water. Blood samples (7.5 ml) were drawn at 0, 10, 20, 40, 80, 160, 240, 360, and 480 min. Plasma was immediately separated and kept frozen until assayed.

**Assay Procedure**—The procedure of Chiou *et al.* (17) was modified and used for the assay of chlorpheniramine in plasma. Samples were analyzed by a high-performance liquid chromatograph[3] equipped with a reversed-phase column[4] and a UV detector set at 264 nm[5]. The mobile phase consisted of 20% acetonitrile in phosphate buffer (0.075 *M* monobasic ammonium phosphate in 0.016 *M* phosphoric acid). Chlorpheniramine and the internal standard, brompheniramine, had average retention times of 9.64 and 12.75 min, respectively, at a flow rate of 1 ml/min.

Aliquots (200 μl) of the plasma samples were added to 5-ml centrifuge tubes containing 10 μl of brompheniramine solution (3.67 μg of brompheniramine free base/ml of 0.5% phosphoric acid). Then 200 μl of 60% methanol in 0.2 *M* sodium acetate buffer was added, followed by vortexing for 10 sec. The samples were centrifuged at 400×*g* for 10 min.

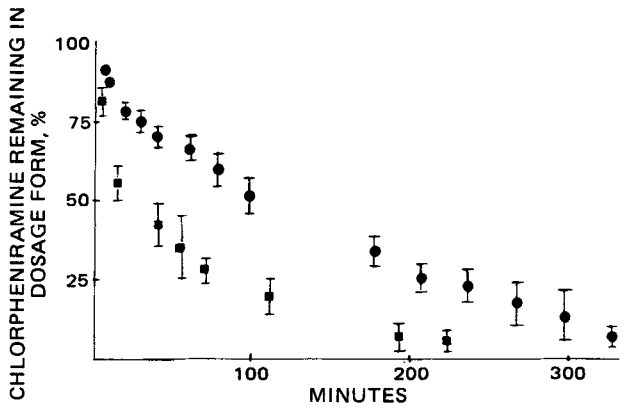


**Figure 1**—*Linear* in vitro *dissolution profile of 12 mg of chlorpheniramine released from the controlled-release dosage form into 0.1* N *HCl containing 0.01% (w/v) docusate sodium (Group II, ■) or no docusate sodium (Group I, ●).*

[1] Teldrin Spansule, 12 mg, Lot X566573, Smith Kline & French.
[2] Colace capsules, 100 mg, lot MJN73, Mead Johnson.
[3] Varian model 4200.
[4] μBondapak $C_{18}$, Waters Associates.
[5] Tracor model 970.

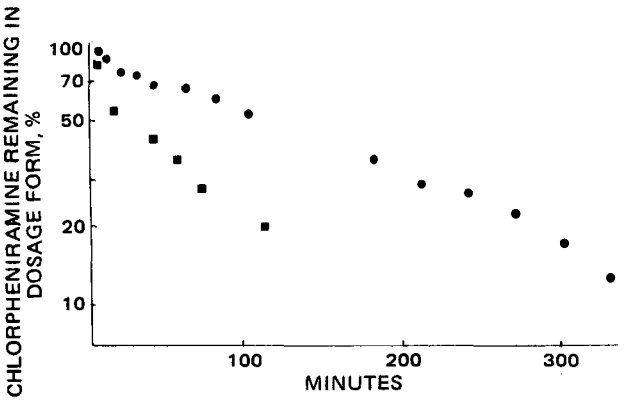


**Figure 2**—*Semilogarithmic* in vitro *dissolution profile of 12 mg of chlorpheniramine released from the controlled-release dosage form into 0.1* N *HCl containing 0.01% (w/v) docusate sodium (Group II, ■) or no docusate (Group I, ●).*

Duplicate 20-μl injections of the supernate were analyzed by high-performance liquid chromatography (HPLC).

The ratio of the area units of the chlorpheniramine peak to the area units of the brompheniramine peak was used to determine the plasma chlorpheniramine concentration from the standard curve. Linearity ($r$ = 0.992) on the standard curve was observed from 0.0088 mg to 0.352 mg/ml of pooled plasma.

***In Vitro***—A USP rotating-basket dissolution apparatus[6] was used for all dissolution studies. The controlled-release capsule was placed into the 40-mesh rotating basket and lowered into 500 ml of 0.1 *N* HCl (Group I, no docusate sodium; Group II, 0.01% (w/v) docusate sodium). The dissolution medium was maintained at 37 ± 0.2°. The basket was lowered to a position 2 cm from the bottom of the vessel and rotated at 100 rpm. Aliquots of 3.0 ml were removed from the point midway between the cylindrical edge of the basket and the wall of the vessel.

Samples from Group I were immediately transferred to a cell and analyzed for chlorpheniramine by UV spectroscopy[7] at 264 nm. Samples from Group I were drawn at 0, 5, 10, 20, 30, 40, 60, 80, 100, 180, 210, 240, 270, 300, 330, 360, 390, 420, 450, 540, and 720 min. Samples from Group II were transferred to a 5-ml centrifuge tube and centrifuged at 400×*g* for 10 min. Centrifugation was necessary because the surfactant solubilized the wax, resulting in an opaque suspension. The supernate was transferred to a cell and analyzed at 264 nm. Sampling times for Group II were 0, 5, 15, 40, 55, 70, 110, 190, 220, 250, 280, 355, 540, and 720 min. All samples were returned to the dissolution medium, but samples from Group II were first remixed with centrifuged material.

**Micellar Entrapment Study**—A single study was performed to determine the effect of surfactant concentration on chlorpheniramine availability. Chlorpheniramine powder USP (12 mg) was added to the dissolution vessel which contained 500 ml of 0.1 *N* HCl and either 0.01 or 0.02% (w/v) of docusate sodium. The solutions were agitated by the rotation of the dissolution basket at 100 rpm. Aliquots of 3.0 ml were removed at 0, 1, 3, 4, 6, 9, and 11 min. The samples were immediately transferred to a cell and the amount of free chlorpheniramine was determined by UV detection at 264 nm.

## RESULTS AND DISCUSSION

***In Vivo***—The plasma concentrations for each subject were plotted *versus* time, and the areas under the curves (*AUC*) were calculated by the trapezoidal rule. Table I shows the *AUC* for each subject at 40, 80, 160, 240, and 480 min. The mean *AUC* and the standard deviations are given in Table II. A $t$ test ($p$ = 0.1) revealed no significant difference between the mean *AUC* obtained after administration of Treatments A (no docusate sodium) or B (200 mg of docusate sodium) at each time period. A paired $t$ test was performed on the mean change in area from Treatment A to B for each time. No significant difference was observed at $p$ = 0.1.

***In Vitro* Dissolution**—Figures 1 and 2 contain graphs of the percent of total drug remaining in the dosage form *versus* time on linear and semilogarithmic graph paper, respectively. Each data point represents the average of four trials. As shown in Fig. 2, the drug was released in a first-order process in both groups. The data (percent remaining *versus* time) were analyzed by the NONLIN subroutine of the AUTOAN computer program (18) to determine if the dissolution profile was best described by a mono- or polyexponential equation. The data from both groups were best described by a biexponential equation.

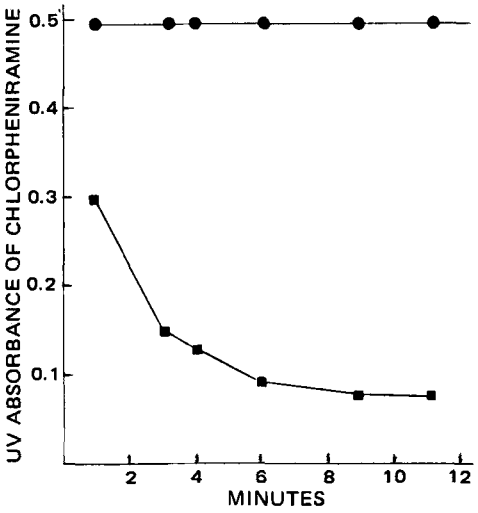


**Figure 3**—*Micellar entrapment of chlorpheniramine in 0.1* N *HCl containing 0.01% (●) or 0.02% (■) w/v of docusate sodium.*

The results of the analysis are shown in Table III. As expected, the initial dissolution rate constants, $k_1$, from both groups were greater than the corresponding terminal rate constants, $k_2$. The first phase of drug release provides the loading dose at a rapid rate. The second rate constant, $k_2$, is associated with the slower rate at which the maintenance dose is released.

The overall effect that docusate sodium had on drug release from the controlled-release capsule may be observed by comparing the dissolution rate constants calculated for each group. Both initial and terminal rates of drug release were increased by the surfactant. The initial rate constant, $k_1$, was tripled (from $1.25 \times 10^{-2}$ to $3.92 \times 10^{-2}$ $min^{-1}$) in the presence of the surfactant. The terminal rate constant, $k_2$, was doubled (from $5.85 \times 10^{-3}$ to $1.19 \times 10^{-2}$ $min^{-1}$) by the surfactant. The ratio of $k_1$ to $k_2$ was increased by the surfactant from a value of 2.14 to 3.29. This finding suggests that the surfactant exerted a greater effect on the initial drug release than on the release of the maintenance dose.

One-third of chlorpheniramine contained in the controlled-release capsule was in nonwax-coated pellets, with the remainder of the drug contained in pellets coated with varying thicknesses of wax. Table IV contains the dissolution data divided into two segments, which roughly correspond to the amounts of drug contained in these two types of pellets. The times given in Table IV were determined from regression analysis of the dissolution data using the biexponential equations described in Table III. A value of 95% released was chosen for the last group due to the difficulty of accurately determining the time at which 100% of the drug had been released from the dosage form.

The $\Delta T$ values in Table IV represent the time required for chlorpheniramine to be released from each pellet group. The $\Delta T$ value for the first one-third of the drug was simply the time required for 33.33% to be released from the dosage form. The $\Delta T$ value for the release of drug from wax-coated pellets (33.33–95%) was determined by subtracting $\Delta T$ for the first one-third from the total time required to release 95% of the drug. The surfactant decreased the required release time from both pellet groups. However, as shown by the ratio of $\Delta T$ from Group I to $\Delta T$ from Group II in Table IV, the surfactant had a greater effect on the amount

**Table II—Mean *AUC* (Micrograms Minutes per Milliliter) ± *SD* from Subjects Receiving 12 mg of Chlorpheniramine in a Controlled-Release Capsule with (Treatment B) or without (Treatment A) 200 mg of Docusate Sodium**

| Minutes | Treatment A | Treatment B | Mean Area Change |
|---|---|---|---|
| 40 | 8.10 ± 1.85 | 7.62 ± 1.87 | −0.48 ± 2.30 |
| 80 | 17.28 ± 3.31 | 17.44 ± 3.39 | +0.16 ± 3.49 |
| 160 | 35.36 ± 7.46 | 36.19 ± 8.45 | +0.83 ± 7.53 |
| 240 | 53.49 ± 9.92 | 56.53 ± 14.38 | +3.04 ± 12.52 |
| 480 | 104.05 ± 16.41 | 115.26 ± 30.78 | +11.21 ± 33.38 |

[6] Erweka type DT.
[7] Varian Techtron 635.

Table III—Results of Regression Analysis Used to Determine Lines of Best Fit from Dissolution Data

| Group[a] | Time Interval, min | $r$ | $y$-Intercept, % | $k_1$, $min^{-1}$ | $k_2$, $min^{-1}$ |
|---|---|---|---|---|---|
| I | 0–20 | 0.995 | 98.82 | $1.25 \times 10^{-2}$ | — |
| I | 30–390 | 0.995 | 95.67 | — | $5.85 \times 10^{-3}$ |
| II | 0–15 | 0.999 | 100.27 | $3.92 \times 10^{-2}$ | — |
| II | 15–190 | 0.995 | 67.35 | — | $1.19 \times 10^{-2}$ |

[a] Group I = 12 mg of chlorpheniramine released from a controlled-release capsule into 0.1 *N* HCl, and Group II = 12 mg of chlorpheniramine released from a controlled-release capsule into 0.1 *N* HCl containing 0.01% (w/v) docusate sodium.

Table IV—Time Required for a Fixed Amount of Chlorpheniramine to be Released from the Controlled-Release Capsule

| Percent Released | Group I[a] Time, min | Group I[a] $\Delta T$[c], min | Group II[b] Time, min | Group II[b] $\Delta T$, min | Ratio, $\Delta T_I/\Delta T_{II}$ |
|---|---|---|---|---|---|
| 33.33 | 64.22 | 64.22 | 10.62 | 10.62 | 6.05 |
| 95.00 | 502.10 | 437.88 | 218.07 | 207.47 | 2.11 |

[a] Dissolution of 12 mg of chlorpheniramine released from the controlled-release capsule into 0.1 *N* HCl. [b] Dissolution of 12 mg of chlorpheniramine released from the controlled-release capsule into 0.1 *N* HCl containing 0.01% (w/v) docusate sodium. [c] Amount of time required for chlorpheniramine to be released from each pellet group.

of time required for the first one-third of the drug to be released. This ratio decreased from 6.05 for the nonwax-coated pellet group to 2.11 for the wax-coated pellet group.

Figure 3 shows the results of the micellar entrapment study. Below the CMC, the amount of free chlorpheniramine in solution was not altered. However, in 0.1 *N* HCl containing 0.02% (w/v) docusate sodium, the amount of free chlorpheniramine decreased rapidly over a short time. This finding demonstrated that the micelles formed in the surfactant solution at the CMC apparently have a high affinity for the chlorpheniramine molecules. Drugs trapped in surfactant micelles must be released from the micelle before crossing the mucosal membrane. Therefore, micellar entrapment *in vivo* could delay or decrease drug absorption. The concentration of docusate sodium that was in contact with the controlled-release capsule in the *in vivo* study probably exceeded the CMC.

## CONCLUSIONS

The availability of chlorpheniramine maleate from a controlled-release capsule was not significantly altered *in vivo* by the coadministration of 200 mg of docusate sodium. No significant difference in the *AUC* at 40, 80, 160, 240, and 480 min was observed between the administration of the capsule alone or with docusate sodium.

Docusate sodium enhanced the *in vitro* rate of chlorpheniramine release from the dosage form. The initial drug release rate tripled and the release of the remainder of the drug doubled in the presence of the surfactant. Micelles formed in the dissolution medium at the CMC of docusate sodium were shown to bind rapidly to chlorpheniramine.

There are several possible explanations as to why the enhanced drug release rate was not observed *in vivo*. The surfactant concentration *in vivo* may have exceeded the CMC of docusate sodium. Although the drug release rate may have been enhanced, micellar entrapment of the drug molecules may have occurred. Drug molecules trapped by surfactant micelles are generally considered to be too large to be absorbed from the GI tract. The overall effect of the surfactant on drug release from the dosage form may have been negated by micellar entrapment. The surfactant also was observed to exert its major effect *in vitro* on the release of the loading dose. The nonwax-coated pellets in the controlled-release capsule are designed for the rapid release of the loading dose *in vivo*. Rapid therapeutic blood levels of chlorpheniramine were obtained in this study both in the presence and absence of the surfactant. Initial therapeutic levels of the drug were obtained so fast that any enhancement of initial drug release due to surfactant was not discernible.

The effect of docusate sodium on the absorption of a solution of chlorpheniramine maleate is not known. Investigation of this effect would show whether micellar entrapment of the drug by 200 mg of docusate sodium occurs *in vivo*. Additional insights into the *in vivo* effects of the surfactant on drug release from the dosage form would be gained by decreasing the amount of surfactant administered to the subjects. The effect of premicellar concentrations of the surfactant could be observed.

Although the *in vivo* study showed no significant difference in the *AUC* after administration of the controlled-release capsule alone or with the surfactant, generalizations should not be made. The effect of a surfactant on drug absorption is highly dependent on the drug being studied. Surfactants have been shown to increase, decrease, or have no effect on the absorption of a drug already released from the dosage form. Other drugs contained in similar long-acting oral dosage forms may show marked changes in drug absorption when exposed *in vivo* to a surfactant.

## REFERENCES


(1) J. Lazarus and J. Cooper, *J. Pharm. Sci.*, **50**, 722 (1961).

(2) M. Robinson, in "The Theory and Practice of Industrial Pharmacy," 2nd ed., L. Lachman, H. A. Lieberman, and J. L. Lieberman, Eds., Lea & Febiger, Philadelphia, Pa., 1976, p. 449.

(3) E. Parrot, in "Prescription Pharmacy," 2nd ed., J. Sprowls, Ed., Lippincott, Philadelphia, Pa., 1970, p. 153.

(4) M. W. Gouda, *Can J. Pharm. Sci.*, **9**, 37 (1974).

(5) M. W. Gouda, S. Malik, and D. Canaham, *J. Pharm. Sci.*, **64**, 987 (1975).

(6) M. W. Gouda, S. Malik, and S. Khalil, *Can. J. Pharm. Sci.*, **10**, 24 (1975).

(7) M. W. Gouda, N. Khalafallah, and S. Khalil, *J. Pharm. Sci.*, **64**, 991 (1975).

(8) M. W. Gouda, S. Gamal, A. Ebian, and S. Khalil, *Can. J. Pharm. Sci.*, **13**, 16 (1978).

(9) G. Levy and J. A. Anello, *J. Pharm. Sci.*, **57**, 101 (1968).

(10) W. Davis, R. Pfeiffer, and J. Quay, *ibid.*, **59**, 960 (1970).

(11) G. Levy, in "Prescription Pharmacy," J. Sprowls, Ed., Lippincott, Philadelphia, Pa., 1970, p. 73.

(12) S. Feldman and M. Reinhard, *J. Pharm. Sci.*, **65**, 1460 (1976).

(13) S. Feldman, M. Reinhard, and C. Wilson, *ibid.*, **62**, 1961 (1973).

(14) A. Mattocks and S. Penzotti, *ibid.*, **61**, 475 (1972).

(15) P. Mukerjee and K. Mysels, in "Critical Micelle Concentrations of Aqueous Surfactant Systems," U.S. Department of Commerce–National Bureau of Standards, Washington, D.C. 1971, p. 136.

(16) M. Gibaldi, in "The Theory and Practice of Industrial Pharmacy," 2nd ed., L. Lachman, H. A. Lieberman, and J. L. Kanig, Eds., Lea & Febiger, Philadelphia, Pa., 1976, p. 108.

(17) W. Chiou, N. Athanika, G. Peng, R. Nation, and S. Huang, *J. Chromatogr.*, **162**, 367 (1979).

(18) "Decision-Making Pharmacokinetic Computer Program," Publication Distribution Service, University of Michigan, Ann Arbor, Mich., 1974.


## ACKNOWLEDGMENTS


Supported by the Research Institute of Pharmaceutical Sciences.

# Interaction of Povidone with Aromatic Compounds II: Evaluation of Ionic Strength, Buffer Concentration, Temperature, and pH by Factorial Analysis

**J. A. PLAIZIER-VERCAMMEN** ˣ **and R. E. De NÈVE**

Received April 28, 1980, from the *Faculteit Geneeskunde en Farmacie, Vrije Universiteit Brussel, Laarbeeklaan, 103 B-1090 Brussels, Belgium.* Accepted for publication April 1, 1981.

**Abstract** □ The interaction of a series of ligand molecules, all consisting of substituted benzoic and nicotinic acid derivatives, and povidone was studied. The influence of ionic strength, buffer concentration, and temperature was evaluated using factorial analysis. Complex formation was not affected at low ionic strength, but increased considerably at higher values due to dehydration of the macromolecule. Complex formation was enhanced in phosphate solutions, particularly in the presence of dibasic phosphate ions. A linear relationship was found between the logarithm of the percentage of bound ligand and ionic strength and buffer capacity.

Increasing the temperature lowered complex formation. Although dehydration of the macromolecule also occurred, the decrease in complex formation could be attributed to the solubility increase of the ligand molecules. The influence of the degree of dissociation of the ligand molecules was investigated by factorial analysis. The compounds mainly interacted to a lesser extent in the dissociated than in the nondissociated state. In addition, a negative effect of a pyridine ring with respect to a phenyl ring was observed. The binding tendency was markedly increased by substituting the aromatic ring structure with hydroxyl functions and by esterification of the carboxyl function attached to the ring. The results suggested that lipophilicity and hydrogen bonding played a predominant role in povidone complexation.

**Keyphrases** □ Povidone—interaction with aromatic compounds, evaluation of complex formation by factorial analysis □ Complexation—evaluation of povidone–aromatic compound interaction by factorial analysis □ Factorial analysis—evaluation of complex formation, povidone–aromatic compound interaction □ Aromatic compounds—interaction with povidone, evaluation of complex formation by factorial analysis

The influence of parameters such as ionic strength, temperature, and buffer concentration and composition on the complex formation between small ligand molecules and macromolecules such as povidone has not yet been investigated systematically (1–9). However, the influence of these parameters is important for meaningful comparisons between the complexing tendencies of related ligand molecules (10) and for understanding the binding and thermodynamic characteristics involved (11–16).

The present report deals with a factorial analysis of these parameters.

## EXPERIMENTAL

**Reagents**—Povidone[1] with a molecular weight of 700,000 was used as the macromolecule and was oven dried at 50° until a constant weight was reached. The following ligand molecules were investigated: benzoic acid[2], nicotinic acid[3], isonicotinic acid[2], salicylic acid[4], nicotinamide[2], salicylamide[2], benzoic acid hydrazide[5], nicotinic acid hydrazide[6], isonicotinic acid hydrazide[4], iproniazide phosphate[7], salicylic acid hydrazide[6], 4-hydroxysalicylic acid[8], 5-hydroxysalicylic acid[4], 5-nitrosalicylic acid[8], methyl salicylate[4], and ethyl salicylate[2].

The following buffer solutions were used: hydrochloric acid–potassium chloride buffers (17) at pH 1.0 and 1.93, McIlvaine buffers (18) at pH 2.20–5.60, a phosphate buffer (17) at pH 7.00, a boric acid–disodium tetraborate buffer at pH 7.20 (19), and a boric acid–sodium hydroxide buffer (17) at pH 9.20. The solutions were brought to a determined ionic strength with sodium chloride. [Sodium chloride does not complex with povidone (6).] The pH of the solutions was controlled with a potentiometric pH measurement[9] and adjusted if necessary.

To control the influence of buffer ions two kinds of buffer solutions were used: the normal buffers are denoted by 1 and those with half the normal capacity are indicated as 0.5.

**Methods**—*Complex Formation Using Factorial Analysis*—Complex formation of the ligand molecules and povidone was investigated by ultrafiltration as previously described (10). The povidone concentration was 4.0%, and the ligand concentrations varied from $1.33 \times 10^{-3}$ to $1.00 \times 10^{-2}$ *M*, depending on their solubility at the pH values used. The complexing tendency expressed as percent of bound ligand (*B%*) was, in the ranges used, independent of the ligand concentration. The concentration of free ligand in the filtrate was determined, after appropriate dilution, with a double-beam spectrophotometer[10] at the respective $\lambda_{max}$ of the ligands. Corrections were made for possible membrane adsorption, and the percentage of bound ligand was calculated as a measure of the complexing tendency. For each sample, these values were obtained at two levels of the three parameters studied (*i.e.*, ionic strength, buffer composition, and temperature) and investigated by factorial analysis (10, 20–22).

For the binding of ligand molecules at pH 1.0, only ionic strength and buffer composition were investigated. At pH 7.00, for 4-hydroxysalicylic acid and 5-nitrosalicylic acid, only the temperature and buffer composition were investigated.

*Complex Formation at Varying Ionic Strengths*—The effect of ionic strength was determined in a series of solutions containing $1.00 \times 10^{-2}$ *M* salicylic acid and 4.0% povidone in McIlvaine buffer (18) (pH 2.20). Ionic strength varied from 0.15 to 6.00.

*Complex Formation at Varying Buffer Concentrations*—The effect of phosphate buffer (pH 7.00) was investigated for three ligand molecules by varying the buffer concentration from 0.0500 to 0.00834 *M*, expressed as dibasic phosphate ions.

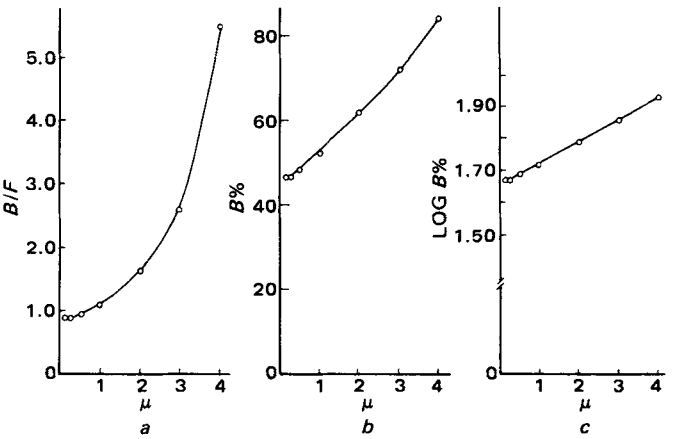


**Figure 1**—*Effect of ionic strength on the complexing tendency of salicylic acid ($1.00 \times 10^{-2}$ M) onto povidone (4.0%) at 25° and pH 2.20*

[1] Kollidon K90, BASF, Brussels, Belgium.
[2] U.C.B., Brussels, Belgium.
[3] B. D. H., Poole, England.
[4] Merck, Darmstadt, West Germany.
[5] Schuchardt, München, West Germany.
[6] Aldrich, Beerse, Belgium.
[7] Serva, Heidelberg, West Germany.
[8] Merck-Schuchardt, München, West Germany.
[9] Radiometer, Copenhagen, Denmark.
[10] Perkin-Elmer model 124.



*0022-3549/81/1100-1252$01.00/0*
*© 1981, American Pharmaceutical Association*

**Table I—Complex Formation of Various Cosolutes with Povidone (4.0%) as a Function of Ionic Strength at 25° and 0.5 Buffer**

| Cosolute | pH | Ionic Strength: Low Level μ | Low Level Bound Ligand, % | High Level μ | High Level Bound Ligand, % | Significant Difference |
|---|---|---|---|---|---|---|
| Benzoic acid | 1.0[a] | 0.15 | 34.3 | 0.30 | 34.7 | 0 |
| | 3.40[b] | 0.25 | 30.0 | 0.50 | 30.1 | 0 |
| | 5.00[b] | 0.25 | 11.9 | 0.50 | 11.8 | 0 |
| Nicotinic acid | 5.60[b] | 0.32 | 6.3 | 0.50 | 6.3 | 0 |
| Isonicotinic acid | 5.60[b] | 0.32 | 8.3 | 0.50 | 8.1 | 0 |
| Salicylic acid | 1.0[a] | 0.15 | 47.7 | 0.30 | 48.1 | 0 |
| | 2.20[b] | 0.15 | 46.8 | 1.00 | 52.9 | + |
| | 3.80[b] | 0.15 | 42.7 | 1.00 | 41.8 | 0 |
| | 7.00[c] | 0.25 | 44.0 | 0.50 | 44.1 | 0 |
| Salicylamide | 5.00[b] | 0.25 | 34.6 | 0.50 | 34.8 | 0 |
| | 7.20[d] | 0.15 | 32.7 | 0.30 | 32.7 | 0 |
| | 9.20[e] | 0.15 | 10.7 | 0.30 | 10.9 | 0 |
| Salicylic acid hydrazide | 7.00[c] | 0.25 | 33.1 | 0.50 | 33.9 | 0 |
| 4-Hydroxysalicylic acid | 1.0[a] | 0.15 | 72.2 | 0.30 | 72.4 | 0 |
| | 2.22[b] | 0.25 | 71.4 | 0.50 | 71.3 | 0 |
| | 4.22[b] | 0.25 | 61.9 | 0.50 | 62.0 | 0 |
| 5-Hydroxysalicylic acid | 1.0[a] | 0.15 | 59.0 | 0.30 | 59.0 | 0 |
| | 1.93[a] | 0.25 | 58.2 | 0.50 | 58.2 | 0 |
| | 3.93[b] | 0.25 | 51.3 | 0.50 | 51.3 | 0 |
| 5-Nitrosalicylic acid | 1.30[a] | 0.15 | 25.5 | 0.30 | 25.5 | 0 |
| | 3.30[b] | 0.25 | 38.1 | 0.50 | 38.1 | 0 |

[a] Hydrochloric acid–potassium chloride buffer. [b] MacIlvaine buffer. [c] Phosphate buffer. [d] Boric acid–disodium tetraborate buffer. [e] Boric acid–sodium hydroxide buffer.

*Desolvating Effect of Temperature on Macromolecule*—Solutions of povidone in different solvents were slowly heated, and the cloud point was determined.

## RESULTS AND DISCUSSION

**Factorial Analysis**—Factorial analysis was carried out as described previously (10). The three parameters were each investigated at a low and high level: temperature, 25 and 50°; buffer concentration, 0.5 and 1.0 and low or high ionic strength, depending on the buffers used.

With the data resulting from the ultrafiltration experiments, i.e., the percentage of bound ligand, analyses of variance were carried out and the significance of the individual parameters was evaluated with an *F* test (10). Results are summarized in Tables I–III.

Interaction between parameters were not observed except for salicylic acid at pH 2.20 where a significant relative positive interaction was observed between temperature and ionic strength.

In Tables I–III, the significance value for a 99% certainty level was indicated as 0, +, or −, corresponding with a zero, positive, or negative significant influence on complex formation when the respective factor was changed from a low to a high level.

Preliminary studies found that some derivatives showed no interaction with povidone. They are included in Table IV (the effects of the parameters were not investigated with them).

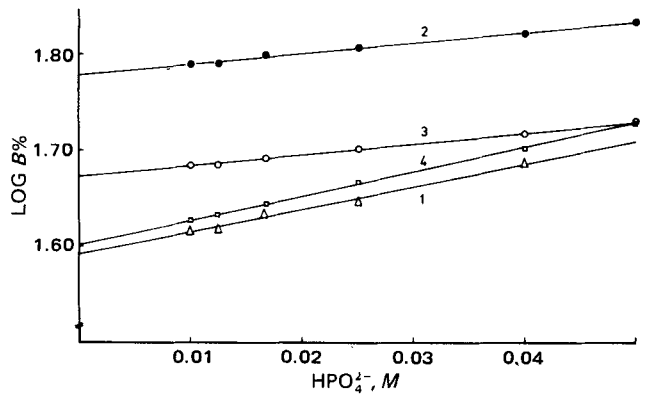


**Figure 2**—*Effect of phosphate ions (pH 7.00) on the complexing tendency of various cosolutes onto povidone (4.0%). Key: 1, salicylic acid (5.00 × 10⁻³ M), 25°, μ = 0.25; 2, 4-hydroxysalicylic acid (4.81 × 10⁻³ M), 25°, μ = 0.25; 3, 4-hydroxysalicylic acid (4.81 × 10⁻³ M), 50°, μ = 0.25; and 4, 5-nitrosalicylic acid (4.81 × 10⁻³ M), 25°, μ = 0.25.*

**Table II—Complex Formation of Various Cosolutes with Povidone (4.0%) as a Function of the Buffer Concentration Using Low Ionic Strength**

| Cosolute | Temperature | pH | Percent Bound Ligand, Buffer 0.5 | Percent Bound Ligand, Buffer 1.0 | Significant Difference | Percent Difference |
|---|---|---|---|---|---|---|
| Benzoic acid | 25° | 1.0[a] | 34.3 | 34.2 | 0 | |
| | 25° | 3.40[b] | 30.0 | 30.0 | 0 | |
| | 50° | 3.40[b] | 31.7 | 31.7 | 0 | |
| | 25° | 5.00[b] | 11.9 | 11.8 | 0 | |
| | 50° | 5.00[b] | 10.2 | 10.2 | 0 | |
| Nicotinic acid | 25° | 5.60[b] | 6.3 | 6.7 | 0 | |
| | 50° | 5.60[b] | 4.2 | 4.4 | 0 | |
| Isonicotinic acid | 25° | 5.60[b] | 8.3 | 8.0 | 0 | |
| | 50° | 5.60[b] | 6.3 | 6.3 | 0 | |
| Salicylic acid | 25° | 1.0[a] | 47.7 | 48.3 | 0 | |
| | 25° | 2.20[b] | 46.8 | 47.0 | 0 | |
| | 50° | 2.20[b] | 43.9 | 45.0 | 0 | |
| | 25° | 3.80[b] | 42.7 | 42.6 | 0 | |
| | 50° | 3.80[b] | 36.3 | 36.4 | 0 | |
| | 25° | 7.00[c] | 44.0 | 51.2 | + | 16.4 |
| | 50° | 7.00[c] | 36.9 | 42.1 | + | 14.1 |
| Salicylamide | 25° | 5.00[b] | 34.6 | 35.1 | 0 | |
| | 50° | 5.00[b] | 32.5 | 32.6 | 0 | |
| | 25° | 7.20[d] | 32.7 | 33.0 | 0 | |
| | 50° | 7.20[d] | 27.3 | 27.3 | 0 | |
| | 25° | 9.20[e] | 10.7 | 10.7 | 0 | |
| | 50° | 9.20[e] | 7.5 | 7.6 | 0 | |
| Salicylic acid hydrazide | 25° | 7.00[c] | 33.1 | 34.0 | + | 2.7 |
| | 50° | 7.00[c] | 30.6 | 31.5 | + | 2.9 |
| 4-Hydroxysalicylic acid | 25° | 1.0[a] | 72.2 | 72.6 | 0 | |
| | 25° | 2.22[b] | 71.4 | 71.4 | 0 | |
| | 50° | 2.22[b] | 61.6 | 61.9 | 0 | |
| | 25° | 4.22[b] | 61.9 | 62.0 | 0 | |
| | 50° | 4.22[b] | 51.4 | 51.5 | 0 | |
| | 25° | 7.00[c] | 64.5 | 68.6 | + | 6.4 |
| | 50° | 7.00[c] | 49.7 | 54.2 | + | 9.1 |
| 5-Hydroxysalicylic acid | 25° | 1.0[a] | 59.0 | 59.5 | 0 | |
| | 25° | 1.93[a] | 58.2 | 58.2 | 0 | |
| | 50° | 1.93[a] | 52.3 | 52.4 | 0 | |
| | 25° | 3.93[b] | 51.3 | 51.4 | 0 | |
| | 50° | 3.93[b] | 39.1 | 39.1 | 0 | |
| 5-Nitrosalicylic acid | 25° | 1.30[a] | 25.5 | 25.5 | 0 | |
| | 25° | 3.30[b] | 38.1 | 38.2 | 0 | |
| | 25° | 7.00[c] | 46 6 | 53.9 | + | 15.7 |
| | 50° | 7.00[c] | 41.9 | 49.3 | + | 17.7 |
| Methylsalicylate | 25° | | 88.1[f] | 87.3[c] | 0 | |
| Ethylsalicylate | 25° | | 95.5[f] | 91.1[c] | ?[g] | |

[a] Hydrochloric acid–potassium chloride buffer. [b] MacIlvaine buffer. [c] Phosphate buffer. [d] Boric acid–disodium tetraborate buffer. [e] Boric acid–sodium hydroxide buffer. [f] Water. [g] Since a little difference in free ligand concentration exerts a great influence on the percentage of bound ligand, the difference for the two levels is not significant.

**Theory of Multiple Equilibrium**—The principles and concepts of complex formation with macromolecules were delineated previously (11, 23–30).

**Ionic Strength**—Table I gives the results for the influence of ionic strength studied at two levels, at a temperature of 25° and a buffer concentration of half the normal buffer capacity.

With the experimental conditions used, ionic strength had no significant effect on complex formation of the cosolutes. However, for salicylic acid at pH 2.20, a significant positive effect was observed when the ionic strength was changed from 0.15 to 1.00 ($p > 0.001$). At this pH, a relative positive interaction was also noted between ionic strength and temperature ($0.01 < p < 0.001$), although this last factor exerted a negative effect when considered individually (see effect of temperature). This effect of ionic strength is represented in detail in Fig. 1.

Complex formation as a function of ionic strength is represented in three ways: the ratio of bound to free ligand concentration ($B/F$), the percentage of bound ligand ($B\%$), and the logarithm of bound ligand (log $B\%$).

Ionic strength has a great positive influence since the amount of bound ligand rose with a factor of 1.8 from $\mu = 0.15$ to 4.00. At higher ionic strength (>4.00) the macromolecule precipitated.

It was previously reported (31–38) that neutral salts enhance complex formation with nonionic macromolecules. This activity was attributed to the dehydrating effect of the salt making the water molecules less available for hydrogen bonding with the macromolecules, thereby de-

**Table III—Complex Formation of Various Cosolutes with Povidone (4.0%) as a Function of Temperature Using Low Ionic Strength and 0.5 Buffer**

| Cosolute | pH | Ionic Strength | Bound Ligand, % 25° | Bound Ligand, % 50° | Significant Difference |
|---|---|---|---|---|---|
| Benzoic acid | 3.40[a] | 0.25 | 30.0 | 31.7 | + |
| | 5.00[a] | 0.25 | 11.9 | 10.2 | − |
| Nicotinic acid | 5.60[a] | 0.32 | 6.3 | 4.2 | − |
| Isonicotinic acid | 5.60[a] | 0.32 | 8.3 | 6.3 | − |
| Salicylic acid | 2.20[a] | 0.15 | 46.8 | 43.9 | − |
| | 3.80[a] | 0.15 | 42.7 | 36.3 | − |
| | 7.00[b] | 0.25 | 44.0 | 36.9 | − |
| Salicylamide | 5.00[a] | 0.25 | 34.6 | 32.5 | − |
| | 7.20[c] | 0.15 | 32.7 | 27.3 | − |
| | 9.20[d] | 0.15 | 10.7 | 7.5 | − |
| Salicylic acid hydrazide | 7.00[b] | 0.25 | 33.1 | 30.6 | − |
| 4-Hydroxysalicylic acid | 2.22[a] | 0.25 | 71.4 | 61.6 | − |
| | 4.22[a] | 0.25 | 61.9 | 51.4 | − |
| | 7.00[b] | 0.25 | 64.5 | 49.7 | − |
| 5-Hydroxysalicylic acid | 1.93[a] | 0.25 | 58.2 | 52.3 | − |
| | 3.93[b] | 0.25 | 51.3 | 39.1 | − |
| 5-Nitrosalicylic acid | 7.00[c] | 0.25 | 46.6 | 41.9 | − |
| Methyl salicylate | Water | | 88.1 | 88.1 | 0 |
| Ethyl salicylate | Water | | 95.5 | 94.6 | 0 |

[a] MacIlvaine buffer. [b] Phosphate buffer. [c] Boric acid–disodium tetraborate buffer. [d] Boric acid–sodium hydroxide buffer.

creasing the aqueous solubility of the polymer and favoring the competing ligand polymer interaction. The precipitation of povidone observed at higher ionic strength (>4.00) indicated that this parameter effectively exerted a dehydrating effect on the macromolecule.

From the results represented in Fig. 1, the following relationships could be deduced:

$$\log B\% = a\mu + b \qquad \text{(Eq. 1)}$$

or:

$$B/F = \frac{10^{(a\mu + b)}}{100 - 10^{(a\mu + b)}} \qquad \text{(Eq. 2)}$$

The values $a$ and $b$, determined from the slope and intercept of Fig. 1*c* were 0.068 and 1.655, respectively.

Together with the macromolecule dehydration, which is a logarithmic function of the ionic strength (39), the percentage of bound ligand increased as an exponential function of ionic strength until precipitation. From the log $B\%$ graph as a function of the ionic strength, it was possible to eliminate the effect of this parameter by extrapolation to the ordinate. An increasing complexing tendency at higher ionic strength was observed with hydrophobic binding and Van der Waals forces.

**Buffer Concentration**—The influence of buffer concentration, studied at two levels, is reported in Table II.

No significant effect was noted with hydrochloric acid–potassium chloride buffer (pH 1.0), boric acid–disodium-tetraborate buffer (pH 7.20), boric acid–sodium hydroxide buffer (pH 9.20), or the MacIlvaine buffer (pH 2.20–5.60).

For the compounds investigated at pH 7.00 in phosphate buffer, a large positive effect of the buffer concentration was observed. Doubling the concentration of the buffer ions considerably enhanced complex formation: 16.4% for salicylic acid, 6.4% for 4-hydroxysalicylic acid, 15.7% for 5-nitrosalicylic acid, and 2.7% for salicylic acid hydrazide at 25°.

At the investigated pH values, the MacIlvaine buffer was composed mainly of monovalent phosphate and citrate ions. The phosphate buffer (pH 7.00) consisted of monobasic (61.9%), and dibasic ions (30.1%). Thus, the dibasic phosphate ions presumably affected the complexing tendency.

This enhancement in complex formation with bivalent ions can perhaps be explained in terms of macromolecule dehydration. This presumption is supported by the fact that the salting-out effect is a function of size and the hydration state of the ions (11). The pronounced dehydrating effect of bivalent phosphate ions was emphasized in an earlier experiment (see effect of temperature).

The effect of phosphate buffer was also investigated for three ligand molecules (Fig. 2). The logarithm of the percentage of bound ligand as a function of the buffer concentration showed a linear relationship. The intercept, obtained by extrapolation to the ordinate, represented the log percentage of bound ligand at infinite dilution, thereby eliminating the

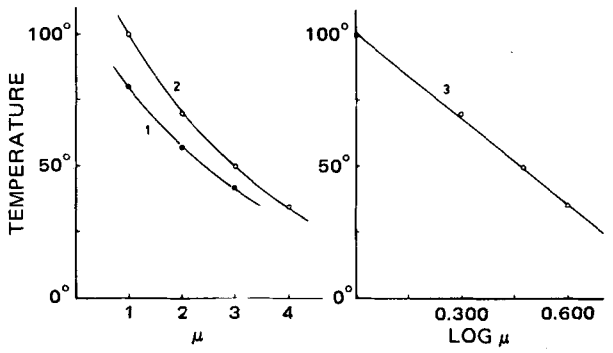


**Figure 3**—*Cloud point of the povidone (4.0%)–salicylic acid (1.00 × $10^{-2}$ M) complex as a function of temperature at pH 2.20. Key: 1, cloud point; 2, precipitation; and 3, cloud point.*

effect of the buffer. These values represented 38.8% of bound ligand for salicylic acid; 60.0 and 47.9%, respectively, at 25 and 50° for 4-hydroxysalicylic acid; and 40.6% for 5-nitrosalicylic acid. Comparison of these results with those of Table II shows that the complexing tendency of salicylic acid and 4-hydroxysalicylic acid was lowest at pH 7.00 where the two ligand molecules were fully dissociated. However, 5-nitrosalicylic acid seemed to have a higher complexing tendency onto povidone at higher pH values.

Ionic strength (Table I), had no effect on complex formation, and the effects of buffer concentration and ionic strength were compared. For both parameters, a linear relationship was found between the logarithm of the percentage of bound ligand and the ionic strength and buffer capacity.

**Temperature**—The effect of temperature was evaluated by factorial analysis carried out at 25 and 50°. Binding diminished significantly at the higher temperature (Table III). However, an exception was noted for benzoic acid at pH 3.40. The same effect was found for this compound in the nonionic state with povidone[11] (5). Methyl and ethyl salicylate also did not influence complexation.

Thermal energy would be expected to exert two antagonistic effects on complex formation. By thermal desolvation of the polymer chain, a more suitable environment for the interaction with the ligand molecules would be expected. However, thermal agitation might also decrease the association of the ligand molecules with the polymer by weakening the attractive forces between them (31, 40). It is the authors' opinion that another effect must be considered; temperature also enhances the solubility of the ligand molecules, probably decreasing the complexing tendency.

The results of the desolvating effect of temperature on povidone are given in Table V. No cloud point could be obtained with povidone solutions in water, ethanol, and 20% (v/v) ethanol when the solutions were heated to 100°. However, the solutions containing salts became clouded by temperature elevation, suggesting dehydration of povidone by salt. This effect, most pronounced with bivalent phosphate ions, could explain the positive effect of these ions on complex formation.

The same experiment was performed on the solutions represented in Fig. 1, and the results are shown in Fig. 3.

The cloud point and precipitation occurred at lower ionic strength as the temperature increased. This finding is in accordance with the relative positive interaction noted between ionic strength and temperature. When representing the logarithm of the ionic strength as a function of temperature where the solutions are clouded, a linear relationship is observed (Fig. 3). These results were also indicative of the dehydrating effect of temperature. When the clouded solutions were cooled, turbidity disappeared with the exception of the solution heated to 100° ($\mu = 1$).

**Effect of pH and Substituents**—The results obtained from factorial analysis (Tables I and II) indicated that ionic strength and buffer concentration had no influence on complex formation. Therefore, it is possible to discuss in a more meaningful way the influence of pH and dissociation of ligand molecules on complex formation. An exception was observed at pH 7.00, where the buffer effect was considerable (Table II). At this pH, the extrapolated values from Fig. 2 were used, representing the percentage of bound ligand at infinite buffer dilution and excluding the effect of the buffer.

The results for the different ligand molecules as a function of their pKa values and degree of dissociation are summarized in Table IV. The

[11] Kollidon K30, BASF, Brussels, Belgium.

**Table IV—Complex Formation of Various Cosolutes in Percentage of Bound Ligand with Povidone (4.0%) as a Function of pKa and pH at 25° Using Low Ionic Strength and 0.5 Buffer**

| Cosolute | pKa Cosolute | pH 1.0 | pKa Cosolute −1.00 | pKa Cosolute −0.80 | pKa Cosolute +0.80 | pKa Cosolute +1.00 | pH 7.00 |
|---|---|---|---|---|---|---|---|
| Benzoic acid | 4.2[a] | 34.3 | — | 30.0 | 11.9 | — | — |
| Nicotinic acid | 4.83[a] | 0.0 | — | 1.0 | 6.3 | — | — |
| Isonicotinic acid | 4.84[a] | 0.0 | — | 0.8 | 8.3 | — | — |
| Salicylic acid | 2.97[a] | 47.7 | — | 46.8 | 42.7 | — | 38.7[b] |
| 4-Hydroxysalicylic acid | 3.22[a] | 72.2 | 71.4 | — | — | 61.9 | 60.3[b] |
| 5-Hydroxysalicylic acid | 2.93[a] | 59.0 | 58.2 | — | — | 51.3 | — |
| 5-Nitrosalicylic acid | 2.30[a] | — | 25.5 | — | — | 38.1 | 40.2[b] |
| Methyl salicylate | — | — | — | — | — | — | 87.3 |
| Ethyl salicylate | — | — | — | — | — | — | 91.1 |
| Nicotinamide | 3.35[c] | — | 0.0 | — | 0.0 | — | 0.0 |
| Salicylamide | 8.20[d] | 34.6[e] | 32.7 | — | — | 10.7 | — |
| Benzoic acid hydrazide | 3.27[f] | — | — | 6.2 | — | — | 11.6 |
| Nicotinic acid hydrazide | 3.63[c] | 0.0 | 0.0 | — | — | — | 0.0 |
| Isonicotinic acid hydrazide | 3.81[c] | 0.0 | 0.0 | — | — | — | 0.0 |
| Iproniazid phosphate | — | 0.0 | — | — | — | — | 0.0 |
| Salicylic acid hydrazide | — | 0.0 | — | — | — | — | 33.1 |

[a] pKa = carboxyl function. [b] Extrapolated values for 4.0% povidone. [c] pKa = nitrogen of pyridine ring. [d] pKa = hydroxyl function. [e] pH 5.00. [f] pKa = hydrazide function.

**Table V—Cloud Point of Povidone Solutions as a Function of Temperature**

| Grams of Povidone + 25 ml of Solvent | Water | 20% (v/v) Ethanol | Ethanol | 3 *M* NaCl in Water | 3 *M* NaCl in 20% (v/v) Ethanol | 3 *M* NaCl + 0.12 *M* $H_2PO_4^-$ in Water | 3 *M* NaCl + 0.12 *M* $HPO_4^{2-}$ in Water |
|---|---|---|---|---|---|---|---|
| 1.0 | no | no | no | 83° | 90° | 78° | 73° |
| 2.0 | no | no | no | 83° | 90° | 79° | 74° |
| 3.0 | no | no | no | 83° | 90° | 79° | 75° |
| 5.0 | no | no | no | 84° | 94° | 80° | 76° |
| 6.0 | no | no | no | 85° | 98° | 83° | 76° |
| 7.5 | no | no | no | — | — | — | — |

compounds generally interacted to a lesser extent when dissociated than when undissociated. Exceptions were noted for nicotinic acid, isonicotinic acid, and 5-nitrosalicylic acid.

The low interaction tendency of the dissociated compounds could be attributed to their more hydrophilic nature. For the carboxylic acid derivatives, the complexing tendency followed the series: salicylic acid > benzoic acid > nicotinic acid ≃ isonicotinic acid. The same order was observed for the amide derivatives (salicylamide > nicotinamide) and the hydrazide derivatives (salicylic acid hydrazide > benzoic acid hydrazide > nicotinic acid hydrazide = isonicotinic acid hydrazide = iproniazide phosphate = no interaction).

A large negative influence of the pyridine ring with regard to the benzene ring was striking. Where benzoic acid, in the undissociated state (pH 1.0), showed complex formation of 34.3% and benzoic acid hydrazide (pH 7.00) showed complex formation of 11.6%, no interaction was noted for the pyridine derivatives. The introduction in the molecular structure of a hydroxyl function enhanced the complexing tendency; *e.g.*, compare salicylic acid with 47.7% of bound ligand against benzoic acid with 34.3%, and salicylic acid hydrazide with 33.1% of bound ligand against benzoic acid hydrazide with 11.6%. A second hydroxyl function enhanced complex formation considerably; *e.g.*, compare 4-hydroxysalicylic acid and 5-hydroxysalicylic acid with 72.2 and 59.0%, respectively, of bound ligand against salicylic acid with 47.7%. However, the introduction of a nitro function decreased the interaction (5-nitrosalicylic acid < 5-hydroxysalicylic acid).

The position of the substituents on the benzene ring also played an important role; *i.e.*, 4-hydroxysalicylic acid showed a higher complexing tendency than the 5-hydroxy derivative. Esterification of the carboxyl function with a methyl or ethyl function enhanced the interaction considerably. The alkyl chain length seemed to have a positive influence [ethyl salicylate (91.1 *B*%) > methylsalicylate (87.3 *B*%).] The negative effect of a nitro group as compared with a hydroxyl function was also observed by Jürgensen Eide and Speiser (5). In the case of the bulky nitro group, steric hindrance should play a role. The difference in interaction between 5-hydroxysalicylic acid and 4-hydroxysalicylic acid could be due to the higher solubility of the 5-hydroxy derivative in contrast to the 4-hydroxy derivative, accompanied by a decreased complexing tendency. However, a correlation between solubility and complex formation had exceptions. The solubility of 5-nitrosalicylic acid was much lower than that of the 5-hydroxy derivative. While the latter showed a higher complexing tendency, the same statement could be made for 5-hydroxysalicylic acid and salicylic acid, with the former showing a greater solubility and a more pronounced complexing tendency. The increasing complexing tendency of compounds in the dissociated state containing hydroxyl groups indicates that hydrogen bonding must play an important role in the interaction.

Moreover, the difference in complex formation between undissociated and respectively dissociated ligand molecules was not important; *e.g.*, for salicylic acid, the complexing tendency only decreased from 47.7 to 38.7 *B*%. Also, for 4-hydroxysalicylic acid and 5-hydroxysalicylic acid, the decrease in the percentage of ligand bound when going from the undissociated (pH 1.0) to the dissociated state (pH 7.00) was not very important. The correlation between degree of complexing tendency and pH and pKa of the drug and partition coefficients is being investigated.

## REFERENCES


(1) R. Voigt, H. H. Schultze, and R. Keipert, *Pharmazie*, **31**, 863 (1976).

(2) S. Keipert, I. Korner, and R. Voigt, *ibid.*, **31**, 790 (1976).

(3) H. P. Frank, S. Barkin, and F. R. Eirich, *J. Phys. Chem.*, **61**, 1375 (1957).

(4) W. Scholtan, *Makromol. Chem.*, **11**, 131 (1953).

(5) G. Jürgensen Eide and P. Speiser, *Acta Pharm. Suec.*, **4**, 185 (1967).

(6) E. Killmann, *Kolloid-Z. Z. Polym.*, **242**, 1103 (1970).

(7) *Ibid.*, **243**, 28 (1971).

(8) E. Ullmann, K. Thoma, and P. Mohrschulz, *Arch. Pharm.*, **302**, 756 (1969).

(9) G. Jürgensen Eide and P. Speiser, *Acta Pharm. Suec.*, **4**, 201 (1967).

(10) J. A. Plaizier and R. E. De Nève, *J. Pharm. Sci.*, **69**, 1403 (1980).

(11) J. T. Edsall and J. Wyman, "Biophysical Chemistry," vol. I, Academic, New York, N.Y., 1958.

(12) W. Kauzmann, *Adv. Protein Chem.*, **14**, 1 (1959).

(13) K. Münzel, *Dtsch. Apoth. Ztg.*, **107**, 1312 (1967)

(14) S. Keipert, J. Becker, and R. Voigt, *Pharmazie*, **32**, 280 (1977).

(15) I. M. Klotz, *Ann. N.Y. Acad. Sci.*, **226**, 18 (1973).

(16) E. J. Cohn and J. T. Edsall, "Proteins, Amino acids and Peptides

as Ions and Dipolar Ions," Reinhold, New York, N.Y., 1943.
(17) "Tables Scientifiques," 6th ed., J. R. Geigy, Ed., Documenta Geigy, Basel, Switzerland, 1962.
(18) P. J. Elving, J. M. Markovitz, and I. Rosenthal, *Anal. Chem.*, **28,** 1179 (1956).
(19) J. H. Block, E. B. Roche, T. O. Soine, and CH. O. Wilson, "Inorganic Medical and Pharmaceutical Chemistry," Lea & Febiger, Philadelphia, Pa., 1974.
(20) J. Philippe, "Les Méthodes Statistiques en Pharmacie et en Chimie," Masson, Paris, France, 1967.
(21) C. Chatfield, "Statistics of Technology," Chapman and Hall, London, England, 1975, p. 271.
(22) F. Yates "Design and Analysis of Factorial Experiments," Imperial Bureau of Soil Sciences, 1937 (cited in Ref. 20).
(23) G. Weber, in "Molecular Biophysics," A Pullman and M. Weissbluth, Eds., Academic, New York, N.Y., 1965.
(24) C. Tanford, "Physical Chemistry of Macromolecules," Wiley, New York, N.Y., 1966.
(25) J. Steinhardt and J. A. Reynolds, "Multiple Equilibria in Proteins," Academic, New York, N.Y., 1969.
(26) I. M. Klotz, in "The Proteins," vol. I, part B, H. Neurath and K. Bailey, Eds., Academic, New York, N.Y., 1953.
(27) I. M. Klotz, *Arch. Biochem.*, **9,** 109 (1946).
(28) I. M. Klotz and D. L. Hunston, *J. Biol. Chem.*, **250,** 3001 (1975).
(29) R. M. Rosenberg and I. M. Klotz, in "A Laboratory Manual of Analytical Methods of Protein Chemistry," vol. 2, P. Alexander and R. J. Block, Eds., Pergamon, New York, N.Y., 1960.
(30) G. Scatchard, *Ann. N.Y. Acad. Sci.*, **51,** 660 (1949).
(31) D. Guttman and T. Higuchi, *J. Am. Pharm. Assoc., Sci. Ed.*, **45,** 659 (1956).
(32) H. C. Ansel, *J. Pharm. Sci.*, **54,** 1159 (1965).
(33) A. E. M. El-Nimr, *Pharmazie*, **32,** 509 (1977).
(34) S. Keipert, J. Becker, and R. Voigt, *ibid.*, **32,** 228 (1977).
(35) S. Keipert, H. H. Schultze, and R. Voigt, *ibid.*, **32,** 339 (1977).
(36) R. Voigt, J. Becker, and S. Keipert, *ibid.*, **32,** 284 (1977).
(37) S. Keipert and R. Voigt, *ibid.*, **30,** 589 (1975).
(38) A. R. Hurwitz, P. P. Deluca, and H. B. Kostenbauder, *J. Pharm. Sci.*, **52,** 893 (1963).
(39) A. Green, *J. Biol. Chem.*, **93,** 495, 517 (1931).
(40) M. N. Khawan, R Tawashi, and H.-v. Czetsch-Lindenwald, *Sci. Pharm. (Wien)*, **32,** 271 (1964).

**ACKNOWLEDGMENTS**

Abstracted in part from a thesis submitted by J. A Plaizier-Vercammen to the Vrije Universiteit van Brussel in partial fulfillment of the Doctor of Philosophy degree requirements.

The authors thank Mr. G. R. Bultinck for technical assistance.

# Polymorphism of Spray-Dried Microencapsulated Sulfamethoxazole with Cellulose Acetate Phthalate and Colloidal Silica, Montmorillonite, or Talc

**H. TAKENAKA, Y. KAWASHIMA ˣ, and S. Y. LIN**

Received January 8, 1981, from the *Gifu College of Pharmacy, Mitahora, Gifu 502, Japan.* Accepted for publication March 27, 1981.

**Abstract** □ Sulfamethoxazole was microencapsulated with cellulose acetate phthalate and talc, colloidal silica, or montmorillonite clay by a spray-drying technique. The surface topography of the products varied with the type of excipient used and the pH of the suspending medium. The products without the excipient were coated with flake-like crusts, while the products containing the excipient tended to become well-rounded spheres. In addition, the crystalline form of sulfamethoxazole converted from Form I to an amorphism and Form II during the spray-drying process. This polymorphic transformation was attributed to the interaction of cellulose acetate phthalate with sulfamethoxazole. Increasing the concentration of cellulose acetate phthalate in the formulation increased the attainment of amorphism. Form II was also obtained by freeze and vacuum drying. Talc was the only excipient that contributed to polymorphism, which occurred in the alkaline suspension medium. Montmorillonite products prepared from the acidic medium exhibited an exothermic differential scanning calorimetry thermogram, which might be interpreted in terms of adsorption of the fused sulfamethoxazole with the internal surface of montmorillonite.

**Keyphrases** □ Microencapsulation—sulfamethoxazole, spray drying with cellulose acetate phthalate and colloidal silica, montmorillonite, or talc, polymorphism □ Polymorphism—microencapsulation of sulfamethoxazole, spray drying with cellulose acetate phthalate and colloidal silica, montmorillonite, or talc □ Sulfamethoxazole—microencapsulated, polymorphism, spray drying with cellulose acetate phthalate and colloidal silica, montmorillonite, or talc

The appropriate selection of the most suitable polymorphic form of medicaments with high thermodynamic activities frequently is the key to improving bioavailability or preventing caking in an aqueous vehicle.

The polymorphic form of a compound depends on the nature of crystallization, *i.e.*, the type of solvent used, the temperature of crystallization, *etc.* It has been documented that polymorphism occurs during spray drying. Fell and Newton (1) produced spray-dried lactose that was a mixture of $\alpha$-monohydrate, $\alpha$-anhydrous, and $\beta$-lactose forms. Kawashima *et al.* (2) reported that spray-dried sodium salicylate was polymorphic, composed of normal crystals and amorphisms. Another study (3) showed that the crystalline form of spray-dried sulfamethoxazole with cellulose acetate phthalate converted from Form I to Form II and an amorphism.

The present study examined the effects of cellulose acetate phthalate and excipients such as colloidal silica, talc, and montmorillonite clay on polymorphism. Tests were performed by freeze drying and vacuum drying at 70° using the same formulations as for spray drying. Another microcapsule of sulfamethoxazole with cellulose acetate phthalate was prepared by the coacervation method of Merkle and Speiser (4) as a reference to test polymorphism.

## EXPERIMENTAL

**Preparations of Microcapsules and Agglomerates**—Sulfamethoxazole[1] (50 g) and cellulose acetate phthalate[2] (10–50 g) were dis-

[1] Shionogi Pharmaceutical Co., Japan.
[2] Kishida Chemical Co., Japan.



*0022-3549/81/1100-1256$01.00/0*
*© 1981, American Pharmaceutical Association*

as Ions and Dipolar Ions," Reinhold, New York, N.Y., 1943.
(17) "Tables Scientifiques," 6th ed., J. R. Geigy, Ed., Documenta Geigy, Basel, Switzerland, 1962.
(18) P. J. Elving, J. M. Markovitz, and I. Rosenthal, *Anal. Chem.*, **28,** 1179 (1956).
(19) J. H. Block, E. B. Roche, T. O. Soine, and CH. O. Wilson, "Inorganic Medical and Pharmaceutical Chemistry," Lea & Febiger, Philadelphia, Pa., 1974.
(20) J. Philippe, "Les Méthodes Statistiques en Pharmacie et en Chimie," Masson, Paris, France, 1967.
(21) C. Chatfield, "Statistics of Technology," Chapman and Hall, London, England, 1975, p. 271.
(22) F. Yates "Design and Analysis of Factorial Experiments," Imperial Bureau of Soil Sciences, 1937 (cited in Ref. 20).
(23) G. Weber, in "Molecular Biophysics," A Pullman and M. Weissbluth, Eds., Academic, New York, N.Y., 1965.
(24) C. Tanford, "Physical Chemistry of Macromolecules," Wiley, New York, N.Y., 1966.
(25) J. Steinhardt and J. A. Reynolds, "Multiple Equilibria in Proteins," Academic, New York, N.Y., 1969.
(26) I. M. Klotz, in "The Proteins," vol. I, part B, H. Neurath and K. Bailey, Eds., Academic, New York, N.Y., 1953.
(27) I. M. Klotz, *Arch. Biochem.*, **9,** 109 (1946).
(28) I. M. Klotz and D. L. Hunston, *J. Biol. Chem.*, **250,** 3001 (1975).
(29) R. M. Rosenberg and I. M. Klotz, in "A Laboratory Manual of Analytical Methods of Protein Chemistry," vol. 2, P. Alexander and R. J. Block, Eds., Pergamon, New York, N.Y., 1960.
(30) G. Scatchard, *Ann. N.Y. Acad. Sci.*, **51,** 660 (1949).
(31) D. Guttman and T. Higuchi, *J. Am. Pharm. Assoc., Sci. Ed.*, **45,** 659 (1956).
(32) H. C. Ansel, *J. Pharm. Sci.*, **54,** 1159 (1965).
(33) A. E. M. El-Nimr, *Pharmazie*, **32,** 509 (1977).
(34) S. Keipert, J. Becker, and R. Voigt, *ibid.*, **32,** 228 (1977).
(35) S. Keipert, H. H. Schultze, and R. Voigt, *ibid.*, **32,** 339 (1977).
(36) R. Voigt, J. Becker, and S. Keipert, *ibid.*, **32,** 284 (1977).
(37) S. Keipert and R. Voigt, *ibid.*, **30,** 589 (1975).
(38) A. R. Hurwitz, P. P. Deluca, and H. B. Kostenbauder, *J. Pharm. Sci.*, **52,** 893 (1963).
(39) A. Green, *J. Biol. Chem.*, **93,** 495, 517 (1931).
(40) M. N. Khawan, R Tawashi, and H.-v. Czetsch-Lindenwald, *Sci. Pharm. (Wien)*, **32,** 271 (1964).

**ACKNOWLEDGMENTS**

Abstracted in part from a thesis submitted by J. A Plaizier-Vercammen to the Vrije Universiteit van Brussel in partial fulfillment of the Doctor of Philosophy degree requirements.

The authors thank Mr. G. R. Bultinck for technical assistance.

# Polymorphism of Spray-Dried Microencapsulated Sulfamethoxazole with Cellulose Acetate Phthalate and Colloidal Silica, Montmorillonite, or Talc

**H. TAKENAKA, Y. KAWASHIMA ˣ, and S. Y. LIN**

Received January 8, 1981, from the *Gifu College of Pharmacy, Mitahora, Gifu 502, Japan.* Accepted for publication March 27, 1981.

**Abstract** □ Sulfamethoxazole was microencapsulated with cellulose acetate phthalate and talc, colloidal silica, or montmorillonite clay by a spray-drying technique. The surface topography of the products varied with the type of excipient used and the pH of the suspending medium. The products without the excipient were coated with flake-like crusts, while the products containing the excipient tended to become well-rounded spheres. In addition, the crystalline form of sulfamethoxazole converted from Form I to an amorphism and Form II during the spray-drying process. This polymorphic transformation was attributed to the interaction of cellulose acetate phthalate with sulfamethoxazole. Increasing the concentration of cellulose acetate phthalate in the formulation increased the attainment of amorphism. Form II was also obtained by freeze and vacuum drying. Talc was the only excipient that contributed to polymorphism, which occurred in the alkaline suspension medium. Montmorillonite products prepared from the acidic medium exhibited an exothermic differential scanning calorimetry thermogram, which might be interpreted in terms of adsorption of the fused sulfamethoxazole with the internal surface of montmorillonite.

**Keyphrases** □ Microencapsulation—sulfamethoxazole, spray drying with cellulose acetate phthalate and colloidal silica, montmorillonite, or talc, polymorphism □ Polymorphism—microencapsulation of sulfamethoxazole, spray drying with cellulose acetate phthalate and colloidal silica, montmorillonite, or talc □ Sulfamethoxazole—microencapsulated, polymorphism, spray drying with cellulose acetate phthalate and colloidal silica, montmorillonite, or talc

The appropriate selection of the most suitable polymorphic form of medicaments with high thermodynamic activities frequently is the key to improving bioavailability or preventing caking in an aqueous vehicle.

The polymorphic form of a compound depends on the nature of crystallization, *i.e.*, the type of solvent used, the temperature of crystallization, *etc.* It has been documented that polymorphism occurs during spray drying. Fell and Newton (1) produced spray-dried lactose that was a mixture of $\alpha$-monohydrate, $\alpha$-anhydrous, and $\beta$-lactose forms. Kawashima *et al.* (2) reported that spray-dried sodium salicylate was polymorphic, composed of normal crystals and amorphisms. Another study (3) showed that the crystalline form of spray-dried sulfamethoxazole with cellulose acetate phthalate converted from Form I to Form II and an amorphism.

The present study examined the effects of cellulose acetate phthalate and excipients such as colloidal silica, talc, and montmorillonite clay on polymorphism. Tests were performed by freeze drying and vacuum drying at 70° using the same formulations as for spray drying. Another microcapsule of sulfamethoxazole with cellulose acetate phthalate was prepared by the coacervation method of Merkle and Speiser (4) as a reference to test polymorphism.

## EXPERIMENTAL

**Preparations of Microcapsules and Agglomerates**—Sulfamethoxazole[1] (50 g) and cellulose acetate phthalate[2] (10–50 g) were dis-

[1] Shionogi Pharmaceutical Co., Japan.
[2] Kishida Chemical Co., Japan.



*0022-3549/81/1100-1256$01.00/0*
*© 1981, American Pharmaceutical Association*

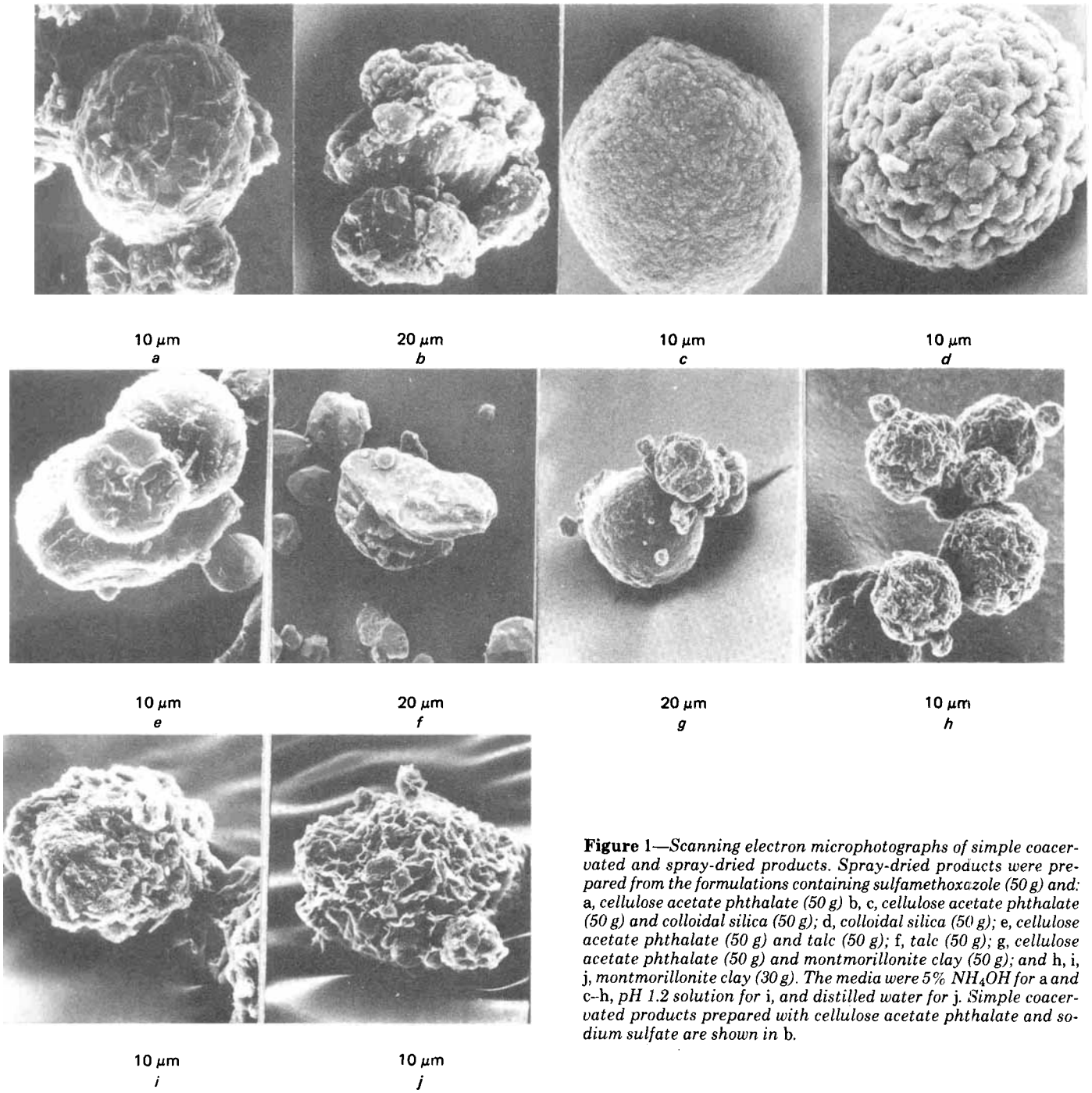


**Figure 1**—*Scanning electron microphotographs of simple coacervated and spray-dried products. Spray-dried products were prepared from the formulations containing sulfamethoxazole (50 g) and:* a, *cellulose acetate phthalate (50 g)* b, c, *cellulose acetate phthalate (50 g) and colloidal silica (50 g);* d, *colloidal silica (50 g);* e, *cellulose acetate phthalate (50 g) and talc (50 g);* f, *talc (50 g);* g, *cellulose acetate phthalate (50 g) and montmorillonite clay (50 g); and* h, i, j, *montmorillonite clay (30 g). The media were 5% $NH_4OH$ for* a *and* c–h, *pH 1.2 solution for* i, *and distilled water for* j. *Simple coacervated products prepared with cellulose acetate phthalate and sodium sulfate are shown in* b.

solved in 1 liter of 5% $NH_4OH$. To this solution was added 0, 30, or 50 g of colloidal silica[3], talc[4], or montmorillonite clay[5]. The resultant slurries were supplied for spray drying. Formulations without cellulose acetate phthalate were also prepared to test the influence of excipients alone on polymorphism. These slurries or solutions were atomized into a drying chamber by a centrifugal wheel atomizer at 40,000 rpm[6]. The drying chamber was maintained at 140 ± 10°, and the dried products were collected by a cyclone collector.

The detailed formulations for spray drying were as follows.

Spray drying for microencapsulation involved sulfamethoxazole (50 g) as the medicament, cellulose acetate phthalate (50 g) as the wall material, colloidal silica and montmorillonite clay (0, 30, and 50 g) as the excipients, and 1 liter of 5% $NH_4OH$ as the medium.

Spray drying for agglomeration involved sulfamethoxazole (50 g) as the medicament with colloidal silica, talc, and montmorillonite clay (30 and 50 g) in 1 liter of 5% $NH_4OH$; colloidal silica, talc, and montmorillonite clay (30 g) in 1 liter of pH 1.2 solution; and colloidal silica, talc and montmorillonite clay (30 g) in 1 liter of distilled water.

Evaporation at 70° in vacuum (20 mm Hg) or spray drying at 140 ± 5° involved sulfamethoxazole (50 g) as the medicament, cellulose acetate phthalate (10–50 g) as the additive, and 5% $NH_4OH$ as the medium.

Cellulose acetate phthalate microcapsules of sulfamethoxazole were prepared by the coacervation method of Merkle and Speiser (4). Sulfamethoxazole (10 g) was suspended in 100 ml of aqueous solution (pH 7.5) containing 2 g of cellulose acetate phthalate and 0.74 g of dibasic sodium phosphate. The system was maintained at 60° and agitated at 620 rpm. Then 25 ml of 20% (w/w) aqueous sodium sulfate solution preheated at 60° was added in small portions. The system was slowly cooled to 20°, and the coacervates were separated and washed with water to remove noncoacervated cellulose acetate phthalate. The coacervate wall was hardened by 2% aqueous acetic acid.

Five grams of sulfamethoxazole and cellulose acetate phthalate were dissolved in 100 ml of 5% $NH_4OH$. The solutions were vacuum freeze

[3] Japan Aerosil Co., Japan.
[4] Matsumura Sangyo Co., Japan.
[5] Veegum-K, R. T. Vanderbilt Co.
[6] Iwai Kikai Kogyo Co., Japan.

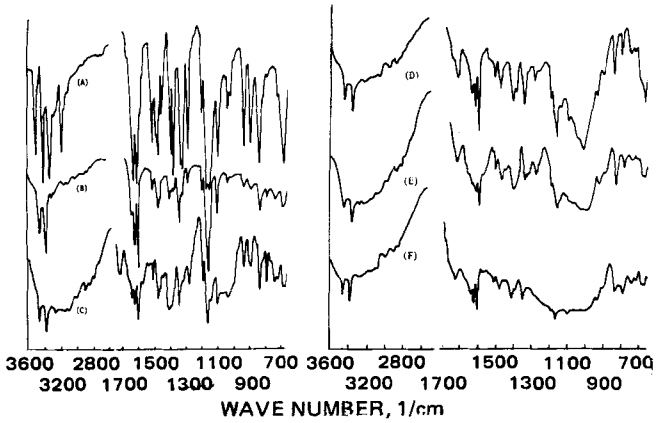


**Figure 2**—*IR spectra of original sulfamethoxazole and spray-dried products containing cellulose acetate phthalate. Key: A, Form I, original sulfamethoxazole, simple coacervated microcapsule; B, Form II; and C–F, spray-dried products prepared from the formulations containing 50 g of cellulose acetate phthalate (C), 50 g of cellulose acetate phthalate and 50 g of talc (D), 50 g of cellulose acetate phthalate and 50 g of montmorillonite clay (E), 50 g of cellulose acetate phthalate and 50 g of colloidal silica (F). The medium was 5% $NH_4OH$.*

dried at −20° ($10^{-3}$ mm Hg) in a freeze dryer[7].

One hundred milliliters of 5% $NH_4OH$ solution containing 5 g of sulfamethoxazole and cellulose acetate phthalate were evaporated at 70° in vacuum to remove ammonium hydroxide and water. The precipitated particles were supplied to test the crystalline form of sulfamethoxazole.

**Measurement of Physicochemical Properties**—The surface topography of the spray-dried particles coated with gold was investigated with a scanning electron microscope[8]. To determine the crystalline form of sulfamethoxazole, X-ray diffraction patterns, IR absorption spectra, and differential scanning calorimetry thermograms were obtained using an X-ray diffractometer[9], an IR spectrometer[10], and a differential scanning calorimetry calorimeter[11] run with a scanning rate of 5°/min, respectively.

## RESULTS AND DISCUSSION

**Surface Topography of Agglomerates and Microcapsules**—Surface topography of the agglomerates and microcapsules was investigated using scanning electron microscopy. The microcapsules with cellulose acetate phthalate prepared by spray drying and coacervation are shown in Figs. 1*a* and 1*b*, respectively. The surfaces of spray-dried microcapsules were composed of flake-like crusts. The simple coacervated microcapsules were aggregated to form an agglomerate.

When the additives were introduced to the formulations for spray drying, the resultant microcapsules became well-rounded spheres without flakes but varied in some degree, depending upon the type of additive used (Figs. 1*c*, 1*e* and 1*g*). The surface topography of agglomerates prepared by spray drying with the formulations containing only sulfamethoxazole and the excipient are seen in Figs. 1*d*, 1*f*, and 1*h*–1*j*. The agglomerates took various forms, depending on the type of excipient and the pH of the vehicle. The latter factor strongly affected the topography of agglomerates with montmorillonite clay (Figs. 1*g*–1*j*).

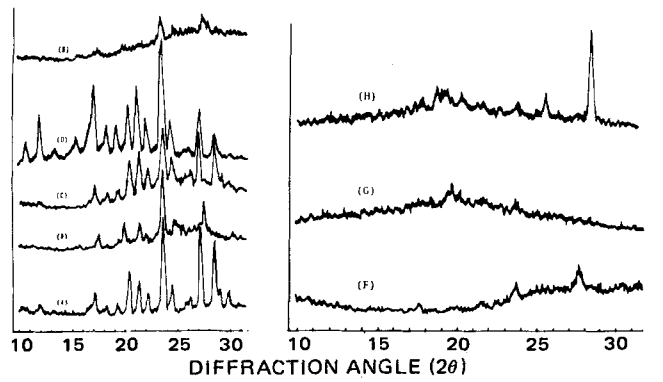


**Figure 3**—*X-ray diffraction patterns of original sulfamethoxazole, physical mixture, coacervated microcapsule, and spray-dried products with cellulose acetate phthalate. Key: A, Form I; B, Form II; C, physical mixture of sulfamethoxazole and cellulose acetate phthalate; D, simple coacervated microcapsule; and E–H, spray-dried products prepared from the formulations containing 50 g of cellulose acetate phthalate (E), 50 g of cellulose acetate phthalate and 50 g of colloidal silica (F), 50 g of cellulose acetate phthalate and 50 g of montmorillonite clay (G), and 50 g of cellulose acetate phthalate and 50 g of talc (H). The medium was 5% $NH_4OH$.*

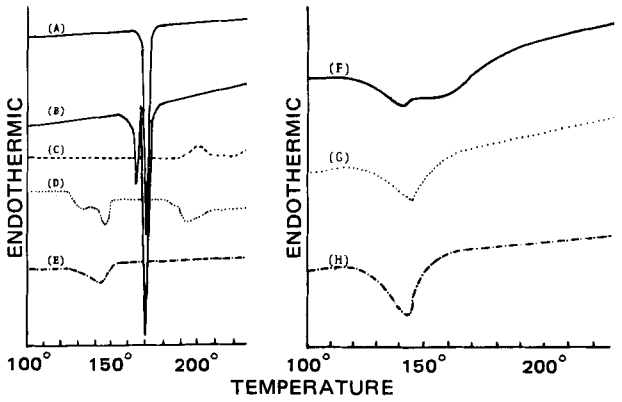


**Figure 4**—*Differential scanning calorimetric thermograms for original sulfamethoxazole, cellulose acetate phthalate, freeze-dried sulfamethoxazole, and spray-dried products containing cellulose acetate phthalate. Key: A, Form I; B, Form II; C, original cellulose acetate phthalate; E, freeze-dried sulfamethoxazole; and D and F–H, spray-dried products prepared from the formulations containing 50 g of cellulose acetate phthalate (D), 50 g of cellulose acetate phthalate and 50 g of colloidal silica (F), 50 g of cellulose acetate phthalate and 50 g of montmorillonite clay (G), and 50 g of cellulose acetate phthalate and 50 g of talc (H). The medium was 5% $NH_4OH$.*

**Effects of Cellulose Acetate Phthalate on Polymorphism**—The IR spectra of original sulfamethoxazole and spray-dried products with cellulose acetate phthalate are seen in Fig. 2. The crystalline form of original sulfamethoxazole was proved to be Form I by identification of its IR spectrum, characterized by intense bands at 3300 and 3150 $cm^{-1}$ attributed to the amide N–H stretching vibration (5). Regardless of whether the excipients were included in the formulations, all spray-dried products with cellulose acetate phthalate exhibited the characteristic absorption bands of Form II in their IR spectra, *i.e.*, weaker bands than those of Form I at 3300 and 3150 $cm^{-1}$ and additional bands at 1640, 1395, 1330, and 750 $cm^{-1}$.

Form II of sulfamethoxazole was prepared by recrystallizing its aqueous solution at dry ice–acetone temperature. It was also confirmed that the crystalline form of freeze- and vacuum-dried sulfamethoxazole always exhibited Form II when cellulose acetate phthalate was included. The sulfamethoxazole in the simple coacervated microcapsule proved to be Form I.

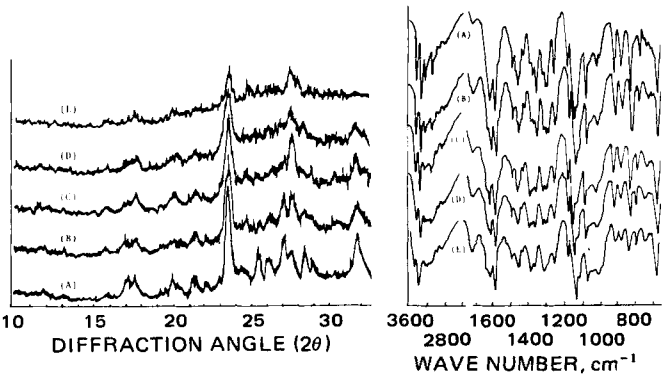


**Figure 5**—*IR spectra and X-ray diffraction patterns of spray-dried products with increasing amounts of cellulose acetate phthalate: A, 10 g; B, 20 g; C, 30 g; D, 40 g; and E, 50 g. The medium was 5% $NH_4OH$.*

[7] DC-35, Yamato Science Co., Japan.
[8] Nihon Denshi, JSM-S1.
[9] Nihon Denshi, JDX.
[10] Nihon Denshi, DS-403G.
[11] Rigaku, CN808521.

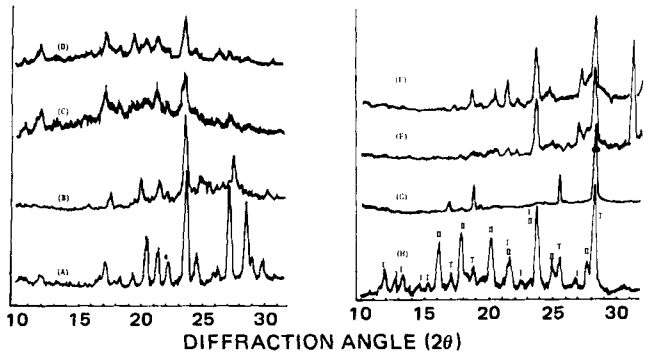


**Figure 6**—*X-ray diffraction patterns of original sulfamethoxazole and spray-dried products without cellulose acetate phthalate. Key: A, Form I; B, Form II; C–F and H, spray-dried products prepared from the formulations containing 30 g of colloidal silica (C), 30 g of montmorillonite clay (D), and 30 g of talc (E, F, and H); and G, original talc. Key for H: I, Form I; II, Form II; and T, talc. Media were 5% $NH_4OH$ (C, D, and H), distilled water (E), and pH 1.2 solution (F).*

The peaks in X-ray diffraction patterns of the excipients were less intense than those of the original crystals (Fig. 3). This finding suggests that some sulfamethoxazole crystals in the spray-dried products converted to a disordered form due to the rapid evaporation. The pattern for sulfamethoxazole in the simple coacervated microcapsule coincided with that of Form I.

In the differential scanning calorimetric thermogram of Form II, sharp endothermic peaks appeared at 166 and 171° (Fig. 4), attributed to the transition temperature from Form II to I and to the fusion temperature of Form I, respectively. Spray- and freeze-dried products containing cellulose acetate phthalate exhibited a broad peak at 140–150° in the thermogram. This characteristic discrepancy in the thermograms suggests that some sulfamethoxazole in the spray-dried products exists in amorphic form as already described.

To investigate the effect of cellulose acetate phthalate on the crystalline form, spray drying was performed with various amounts of cellulose acetate phthalate contained in the formulations. With increasing cellulose acetate phthalate concentration, the characteristic IR bands of Form II at 1640, 1395, and 1330 $cm^{-1}$ became more intense while the bands at 3300 and 3150 $cm^{-1}$ became weaker (Fig. 5). The reduced intensities of the X-ray diffraction patterns of the product with a high cellulose acetate phthalate concentration indicated increased amorphism. These findings suggested that cellulose acetate phthalate in the formulation caused polymorphism to occur. It was reported (5, 6) that sulfonamide polymorphism might be due to the formation of intermolecular hydrogen bonds. Hydrogen bonding may occur between the acetyl and hydroxyl groups of cellulose acetate phthalate and the *p*-amino and sulfonyl groups

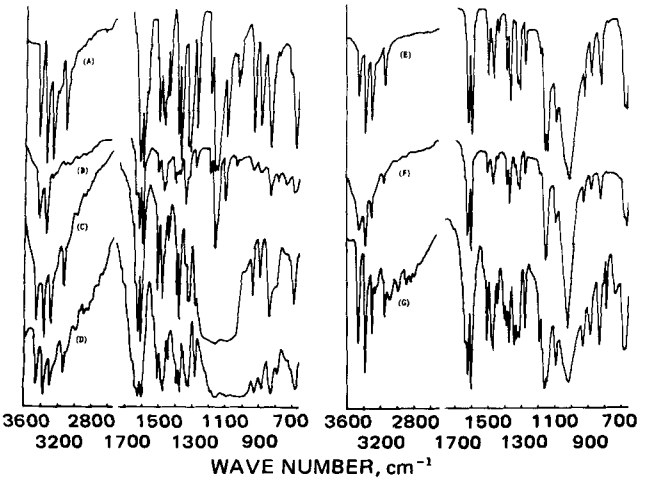


**Figure 7**—*IR spectra of original sulfamethoxazole and spray-dried products without cellulose acetate phthalate. Key: A, Form I; B, Form II; and C–G, spray-dried products prepared from the formulations containing 30 g of colloidal silica (C), 30 g of montmorillonite clay (D), and 30 g of talc (E–G). Media were 5% $NH_4OH$ (C, D, and G), pH 1.2 solution (E), and distilled water (F).*

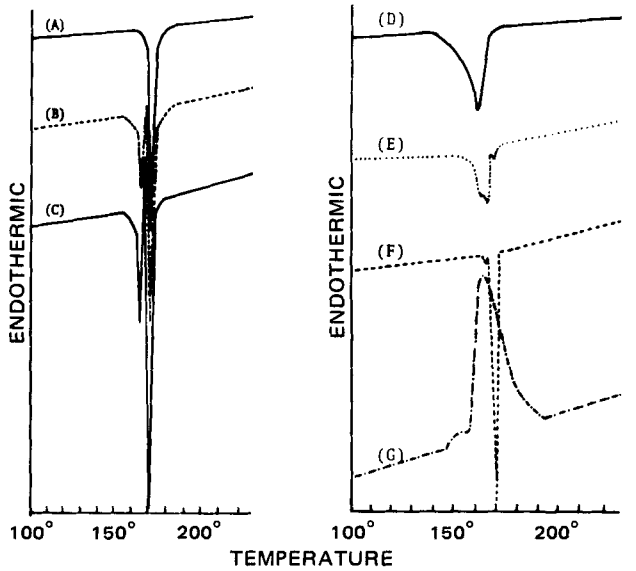


**Figure 8**—*Differential scanning calorimetric thermograms for original sulfamethoxazole and spray-dried products. Key: A, Form I; B, Form II; and C–G, spray-dried products prepared from the formulations containing 30 g of talc (C), 30 g of colloidal silica (D), and 30 g of montmorillonite clay (E–G). Media were 5% $NH_4OH$ (C–E), distilled water (F), and pH 1.2 solution (G).*

of sulfamethoxazole. This phenomenon, and the steric hindrance of cellulose acetate phthalate, may restrict the intermolecular hydrogen bonding of sulfamethoxazole.

**Effects of Excipients on Polymorphism**—To examine the effects of excipients on the polymorphism of spray-dried sulfamethoxazole, cellulose acetate phthalate was excluded from the formulations. The X-ray diffraction patterns (Fig. 6) and IR spectra (Fig. 7) of the products with montmorillonite clay and colloidal silica suggested that the products were the polymorphic mixture of Form I and amorphisms. The products with talc exhibited a sharp X-ray diffraction pattern, characteristic of the patterns of Form I and talc (Fig. 6). Furthermore, the pattern varied with the type of medium (Fig. 6). IR spectra proved the crystalline forms of the products prepared from the aqueous and acidic slurries to be Form I. Peaks in the IR spectra and X-ray diffraction patterns of products prepared from the ammonium slurries were characteristic of both Form I and II, indicating a polymorphic mixture.

The mechanism of polymorphic transformation that occurred in the alkaline medium was not resolved in the present study. However, previous investigators (7) reported that anionic dyes were selectively adsorbed with talc from aqueous solution. In alkaline medium, the anionic form of sulfamethoxazole could be strongly adsorbed with talc, causing reduced intermolecular hydrogen bonding of sulfamethoxazole, and possibly converting crystals from Form I to Form II. In the aqueous medium, the silanol group of colloidal silica and montmorillonite clay should be hydrated, preventing the formation of hydrogen bonds between sulfamethoxazole and the silanol groups. Thus, the drug molecule adsorbed only physically might be disordered when crystallized by spray drying, leading to amorphism.

Differential scanning calorimetric thermograms of the spray-dried products were characteristic of the type of excipient and medium used. The thermogram of the talc-containing product prepared from ammonium slurries was characteristic of that of Form II (Fig. 8), thus supporting the polymorphic transformation suggested previously by X-ray and IR analyses. The product with colloidal silica exhibited a broad endothermic peak at 150–160° in the thermogram, suggesting the coexistence of amorphism.

Thermograms of the product with montmorillonite clay varied with the type of medium used. The product from distilled water was Form I since most sulfamethoxazole crystals were not dissolved but only suspended in water. With the ammonium slurries, a broad peak resembling that of the product with colloidal silica appeared in the thermogram. When the acidic medium was used, the thermogram changed to an exothermic pattern having a peak at 164°. Porubcan *et al.* (8) reported that the distance between the interlayers of montmorillonite clay in an acidic medium is larger than in an alkaline medium. Thus, when the product prepared from the acidic medium was heated, sulfamethoxazole might

interact with the internal surface of montmorillonite clay since the distance between the interlayers is wide enough for holding the molecule. This interaction might produce some heat, leading to the exothermic thermogram in Fig. 8.

## REFERENCES


(1) J. T. Fell and J. M. Newton, *Pharm. Acta Helv.*, **45**, 520 (1970).

(2) Y. Kawashima, K. Matsuda, and H. Takenaka, *J. Pharm. Pharmacol.*, **24**, 505 (1972).

(3) H. Takenaka, Y. Kawashima, and S. Y. Lin, *J. Pharm. Sci.*, **69**, 1388 (1980).

(4) H. D. Merkle and P. Speiser, *ibid.*, **62**, 1444 (1973).

(5) S. S. Yang and J. K. Guillory, *ibid.*, **61**, 26 (1972).

(6) R. J. Mesley and E. E. Houghton, *J. Pharm. Pharmacol.*, **19**, 295 (1967).

(7) R. M. Hanson and C. W. Gould, *Anal. Chem.*, **23**, 670 (1951).

(8) L. S. Porubcan, C. J. Serna, J. L. White, and S. L. Hem, *J. Pharm. Sci.*, **67**, 1081 (1978).


## ACKNOWLEDGMENTS


The X-ray diffractometer and differential scanning calorimeter were used through the courtesy of Professor Otsuka at Meijyo University and Mr. Saito at Hokuriku Pharmaceutical Co., Japan.

This paper is Part X of studies on "Spray-Drying Agglomeration."


# Extended Hansen Solubility Approach: Naphthalene in Individual Solvents


**A. MARTIN *x, P. L. WU *, A. ADJEI ‡, A. BEERBOWER §, and J. M. PRAUSNITZ ¶**



Received January 30, 1981, from the **Drug Dynamics Institute, College of Pharmacy, University of Texas, Austin, TX 78712,* ‡*Abbott Laboratories, North Chicago, IL 60064,* §*Energy Center, University of California at San Diego, La Jolla, CA 92093,* and the ¶ *Department of Chemical Engineering, University of California, Berkeley, CA 94720.* Accepted for publication April 3, 1981.



**Abstract** □ A multiple regression method using Hansen partial solubility parameters, $\delta_D$, $\delta_P$, and $\delta_H$, was used to reproduce the solubilities of naphthalene in pure polar and nonpolar solvents and to predict its solubility in untested solvents. The method, called the extended Hansen approach, was compared with the extended Hildebrand solubility approach and the universal-functional-group-activity-coefficient (UNIFAC) method. The Hildebrand regular solution theory was also used to calculate naphthalene solubility. Naphthalene, an aromatic molecule having no side chains or functional groups, is "well-behaved"; *i.e.*, its solubility in active solvents known to interact with drug molecules is fairly regular. Because of its simplicity, naphthalene is a suitable solute with which to initiate the difficult study of solubility phenomena. The three methods tested (Hildebrand regular solution theory was introduced only for comparison of solubilities in regular solution) yielded similar results, reproducing naphthalene solubilities within ~30% of literature values. In some cases, however, the error was considerably greater. The UNIFAC calculation is superior in that it requires only the solute's heat of fusion, the melting point, and a knowledge of chemical structures of solute and solvent. The extended Hansen and extended Hildebrand methods need experimental solubility data on which to carry out regression analysis. The extended Hansen approach was the method of second choice because of its adaptability to solutes and solvents from various classes. Sample calculations are included to illustrate methods of predicting solubilities in untested solvents at various temperatures. The UNIFAC method was successful in this regard.



**Keyphrases** □ Naphthalene—solubility study, extended Hansen, extended Hildebrand, and UNIFAC approaches compared □ Solubility—of naphthalene in various solvents, extended Hansen, extended Hildebrand, and UNIFAC approaches compared □ Extended Hansen solubility approach—compared with extended Hildebrand and UNIFAC approaches, naphthalene solubility in various solvents


The solubility parameter concept (1) was originally designed to describe nonpolar solvent–solute systems, although it recently has been extended to the realm of commercial paints, inks, plastics, insecticides, and pharmaceuticals, which may include highly polar solvents and solutes.

The problem of estimating the solubility of crystalline solids in various solvents has been particularly intractable. This report uses partial solubility parameters together with multiple regression analysis to obtain equations that predict solubilities within an error of <30% relative to experiment. Results using a partial parameter–multiple regression method, referred to here as the extended Hansen solubility approach, were compared with those obtained by the extended Hildebrand solubility approach (2) and the universal-functional-group-activity-coefficient (UNIFAC) method (3, 4).

The interaction of a solute and solvent follows either from weak van der Waals forces or from strong forces of a "chemical" nature, such as hydrogen bonding and Lewis acid–base interactions (5). For solutions of interest in the pharmaceutical and biological sciences, both physical and chemical forces are likely to be important.

## THEORY

**Partial Solubility Parameters**—Burrell (6, 7) extended the original solubility parameter concept to estimate the solubility of coating materials (mainly polymers) in polar solvents of low, medium, and high hydrogen-bonding capacity. Hansen (8, 9) partitioned the cohesive energy density, $\Delta E/V$, for a species into contributions from dispersion forces, dipolar interactions, and hydrogen bonding:

$$\frac{\Delta E}{V} = \frac{\Delta E_D}{V} + \frac{\Delta E_P}{V} + \frac{\Delta E_H}{V} \qquad \text{(Eq. 1)}$$

or:

$$\delta^2 = \delta_D^2 + \delta_P^2 + \delta_H^2 \qquad \text{(Eq. 2)}$$

where:

$$\delta = (\Delta E^v/V)^{1/2} \cong \left(\frac{\Delta H^v - RT}{V}\right)^{1/2} \qquad \text{(Eq. 3)}$$

$\Delta E^v$ is the energy of vaporization of a liquid, $\Delta H^v$ is its enthalpy of vaporization, $R$ is the gas constant, $T$ is the absolute temperature, and $V$ is the liquid molar volume. The quantity $\delta$ is the total solubility parameter, and $\delta^2$ is the cohesive density for a solvent or solute. The term $\delta_D$ stands for the dispersion component of the total solvent or solute solubility parameter, $\delta_P$ is the polar component, and $\delta_H$ is the hydrogen-bonding component. These terms are the partial solubility parameters.




*0022-3549/81/1100-1260$01.00/0*



*© 1981, American Pharmaceutical Association*

interact with the internal surface of montmorillonite clay since the distance between the interlayers is wide enough for holding the molecule. This interaction might produce some heat, leading to the exothermic thermogram in Fig. 8.

## REFERENCES


(1) J. T. Fell and J. M. Newton, *Pharm. Acta Helv.*, **45**, 520 (1970).

(2) Y. Kawashima, K. Matsuda, and H. Takenaka, *J. Pharm. Pharmacol.*, **24**, 505 (1972).

(3) H. Takenaka, Y. Kawashima, and S. Y. Lin, *J. Pharm. Sci.*, **69**, 1388 (1980).

(4) H. D. Merkle and P. Speiser, *ibid.*, **62**, 1444 (1973).

(5) S. S. Yang and J. K. Guillory, *ibid.*, **61**, 26 (1972).

(6) R. J. Mesley and E. E. Houghton, *J. Pharm. Pharmacol.*, **19**, 295 (1967).

(7) R. M. Hanson and C. W. Gould, *Anal. Chem.*, **23**, 670 (1951).

(8) L. S. Porubcan, C. J. Serna, J. L. White, and S. L. Hem, *J. Pharm. Sci.*, **67**, 1081 (1978).


## ACKNOWLEDGMENTS


The X-ray diffractometer and differential scanning calorimeter were used through the courtesy of Professor Otsuka at Meijyo University and Mr. Saito at Hokuriku Pharmaceutical Co., Japan.

This paper is Part X of studies on "Spray-Drying Agglomeration."


# Extended Hansen Solubility Approach: Naphthalene in Individual Solvents


**A. MARTIN *x, P. L. WU *, A. ADJEI ‡, A. BEERBOWER §, and J. M. PRAUSNITZ ¶**



Received January 30, 1981, from the **Drug Dynamics Institute, College of Pharmacy, University of Texas, Austin, TX 78712,* ‡*Abbott Laboratories, North Chicago, IL 60064,* §*Energy Center, University of California at San Diego, La Jolla, CA 92093,* and the ¶ *Department of Chemical Engineering, University of California, Berkeley, CA 94720.* Accepted for publication April 3, 1981.



**Abstract** □ A multiple regression method using Hansen partial solubility parameters, $\delta_D$, $\delta_P$, and $\delta_H$, was used to reproduce the solubilities of naphthalene in pure polar and nonpolar solvents and to predict its solubility in untested solvents. The method, called the extended Hansen approach, was compared with the extended Hildebrand solubility approach and the universal-functional-group-activity-coefficient (UNIFAC) method. The Hildebrand regular solution theory was also used to calculate naphthalene solubility. Naphthalene, an aromatic molecule having no side chains or functional groups, is "well-behaved"; *i.e.*, its solubility in active solvents known to interact with drug molecules is fairly regular. Because of its simplicity, naphthalene is a suitable solute with which to initiate the difficult study of solubility phenomena. The three methods tested (Hildebrand regular solution theory was introduced only for comparison of solubilities in regular solution) yielded similar results, reproducing naphthalene solubilities within ~30% of literature values. In some cases, however, the error was considerably greater. The UNIFAC calculation is superior in that it requires only the solute's heat of fusion, the melting point, and a knowledge of chemical structures of solute and solvent. The extended Hansen and extended Hildebrand methods need experimental solubility data on which to carry out regression analysis. The extended Hansen approach was the method of second choice because of its adaptability to solutes and solvents from various classes. Sample calculations are included to illustrate methods of predicting solubilities in untested solvents at various temperatures. The UNIFAC method was successful in this regard.



**Keyphrases** □ Naphthalene—solubility study, extended Hansen, extended Hildebrand, and UNIFAC approaches compared □ Solubility—of naphthalene in various solvents, extended Hansen, extended Hildebrand, and UNIFAC approaches compared □ Extended Hansen solubility approach—compared with extended Hildebrand and UNIFAC approaches, naphthalene solubility in various solvents


The solubility parameter concept (1) was originally designed to describe nonpolar solvent–solute systems, although it recently has been extended to the realm of commercial paints, inks, plastics, insecticides, and pharmaceuticals, which may include highly polar solvents and solutes.

The problem of estimating the solubility of crystalline solids in various solvents has been particularly intractable. This report uses partial solubility parameters together with multiple regression analysis to obtain equations that predict solubilities within an error of <30% relative to experiment. Results using a partial parameter–multiple regression method, referred to here as the extended Hansen solubility approach, were compared with those obtained by the extended Hildebrand solubility approach (2) and the universal-functional-group-activity-coefficient (UNIFAC) method (3, 4).

The interaction of a solute and solvent follows either from weak van der Waals forces or from strong forces of a "chemical" nature, such as hydrogen bonding and Lewis acid–base interactions (5). For solutions of interest in the pharmaceutical and biological sciences, both physical and chemical forces are likely to be important.

## THEORY

**Partial Solubility Parameters**—Burrell (6, 7) extended the original solubility parameter concept to estimate the solubility of coating materials (mainly polymers) in polar solvents of low, medium, and high hydrogen-bonding capacity. Hansen (8, 9) partitioned the cohesive energy density, $\Delta E/V$, for a species into contributions from dispersion forces, dipolar interactions, and hydrogen bonding:

$$\frac{\Delta E}{V} = \frac{\Delta E_D}{V} + \frac{\Delta E_P}{V} + \frac{\Delta E_H}{V} \qquad \text{(Eq. 1)}$$

or:

$$\delta^2 = \delta_D^2 + \delta_P^2 + \delta_H^2 \qquad \text{(Eq. 2)}$$

where:

$$\delta = (\Delta E^v/V)^{1/2} \cong \left(\frac{\Delta H^v - RT}{V}\right)^{1/2} \qquad \text{(Eq. 3)}$$

$\Delta E^v$ is the energy of vaporization of a liquid, $\Delta H^v$ is its enthalpy of vaporization, $R$ is the gas constant, $T$ is the absolute temperature, and $V$ is the liquid molar volume. The quantity $\delta$ is the total solubility parameter, and $\delta^2$ is the cohesive density for a solvent or solute. The term $\delta_D$ stands for the dispersion component of the total solvent or solute solubility parameter, $\delta_P$ is the polar component, and $\delta_H$ is the hydrogen-bonding component. These terms are the partial solubility parameters.




*0022-3549/81/1100-1260$01.00/0*



*© 1981, American Pharmaceutical Association*

Table I—Naphthalene Parameters ($\delta_D$ = 9.4, $\delta_P$ = 1.0, $\delta_H$ = 1.9) and Solubility at 40° in Various Solvents, $V$ = 123 cm³/mole, $X_2^i(40°)$ = 0.46594

| Solvent | Molar Volume[a], $V_1$ | Total Solubility Parameter[a], $\delta_1$ | Dispersion Solubility Parameter, $\delta_D$ | Polar Solubility Parameter, $\delta_P$ | Hydrogen Bonding Solubility Parameter, $\delta_H$ | Mole Fraction Solubility, $X_2$ | Reference for Solubility Data |
|---|---|---|---|---|---|---|---|
| Hexane | 131.6 | 7.3 | 7.3 | 0.0 | 0.0 | 0.222 | 16 |
| Carbon tetrachloride | 97.1 | 8.7 | 8.7 | 0.0 | 0.3 | 0.395 | 16 |
| Toluene | 106.8 | 8.9 | 8.8 | 0.7 | 1.0 | 0.422 | 16 |
| Ethylidene chloride | 84.8 | 9.0 | 8.1 | 4.0 | 0.2 | 0.437 | 18 |
| Benzene | 89.4 | 9.1 | 9.0 | 0.0 | 1.0 | 0.428 | 16 |
| Chloroform | 80.7 | 9.3 | 8.7 | 1.5 | 2.8 | 0.467 | 19 |
| Chlorobenzene | 102.1 | 9.6 | 9.3 | 2.1 | 1.0 | 0.444 | 16 |
| Acetone | 74.0 | 9.8 | 7.6 | 5.1 | 3.4 | 0.378 | 16 |
| Carbon disulfide | 60.0 | 10.0 | 10.0 | 0.0 | 0.3 | 0.494 | 19 |
| 1,1-Dibromoethane | 92.9 | 10.1[b] | 8.4 | 3.7 | 4.1 | 0.456 | 18 |
| Ethylene dichloride | 79.4 | 10.2 | 9.3 | 3.6 | 2.0 | 0.452 | 18 |
| *sec*-Butanol | 92.5 | 10.8 | 7.7 | 2.8 | 7.1 | 0.1122 | 17 |
| Nitrobenzene | 102.7 | 10.8 | 9.8 | 4.2 | 2.0 | 0.432 | 16 |
| *tert*-Butanol | 94.3 | 10.9[b] | 7.8 | 2.8 | 7.1 | 0.1009 | 17 |
| Cyclohexanol | 106.0 | 10.9 | 8.5 | 2.0 | 6.6 | 0.232 | 19 |
| Aniline | 91.5 | 11.0 | 9.5 | 2.5 | 5.0 | 0.306 | 16 |
| Isobutanol | 92.8 | 11.1 | 7.4 | 2.8 | 7.8 | 0.0925 | 17 |
| Butanol | 91.5 | 11.3 | 7.8 | 2.8 | 7.7 | 0.116 | 16 |
| Isopropanol | 76.8 | 11.5 | 7.7 | 3.0 | 8.0 | 0.0764 | 17 |
| Ethylene dibromide | 87.0 | 11.7 | 9.6 | 3.3 | 5.9 | 0.439 | 18 |
| Propanol | 75.2 | 12.0 | 7.8 | 3.3 | 8.5 | 0.0944 | 17 |
| Acetic acid | 57.6 | 13.0 | 6.8 | 6.0 | 9.3 | 0.117 | 16 |
| Ethanol | 58.5 | 13.0 | 7.7 | 4.3 | 9.5 | 0.0726 | 17 |
| Methanol | 40.7 | 14.5 | 7.4 | 6.0 | 10.9 | 0.0437 | 16 |

[a] Molar volumes (cc/mole) and solubility parameters (cal/cm³)$^{1/2}$ are obtained at 25°. [b] The solubility parameters for *tert*-butanol and 1,1-dibromoethane are not found in the literature. The former was calculated by the group contribution method (9), and the latter was obtained by reference to the values for ethylene dichloride, ethylidene chloride, and ethylene dibromide.

As used here, hydrogen bonding is not restricted to hydrogen bonds in the classical sense but also refers to any type of highly polar, oriented interaction. Partial solubility parameters were originally calculated and adjusted to provide estimates of solubility and elastomer swelling (8, 9).

The dispersion parameter, $\delta_D$, was obtained from data for the compound's homomorph, defined as a saturated hydrocarbon having essentially the same chemical structure, size, and shape as those of the polar compound (8, 9). The polar parameter, $\delta_P$, was calculated using a modified equation from Böttcher (10, 11):

$$\delta_P^2 = \frac{12{,}108}{V^2}\frac{\epsilon - 1}{2\epsilon + n_D^2}(n_D^2 + 2)\mu^2 \qquad \text{(Eq. 4)}$$

where $V$ is the liquid molar volume, $\epsilon$ is the dielectric constant, $n_D$ is the refractive index for the D line of sodium, and $\mu$ is the dipole moment expressed in Debye units. The hydrogen bond parameter for a hydroxyl compound is obtained from an expression:

$$\delta_H = \left(\frac{\Delta H}{V}\right)^{1/2} \qquad \text{(Eq. 5)}$$

where $\Delta H$ is an average enthalpy of formation for hydrogen bonding, 4650 cal/mole, for each hydroxy group. Barton (5) reviewed various methods of calculating partial parameters.

The partial solubility parameters of Hansen are available for a large number of liquid solvents (9). Partial solubility parameters for only a few solids (represented as supercooled liquids), such as naphthalene and succinic anhydride, can be found in the literature. Hansen and Beerbower (9) presented a table of group contributions for calculating partial solubility parameters; from these data, $\delta_D$, $\delta_P$, and $\delta_H$ may be calculated for a liquid or solid (supercooled liquid).

The values can be adjusted to obtain suitable numbers that correspond well with experimental solubility results. Hoy *et al.* (12) developed an extensive compilation of partial and total solubility parameters.

One possible approach to reproducing experimental solubilities for a drug in pure solvents would be to write the solubility equation (1, 2) in terms of partial solubility parameters, followed by multiple regression analysis toward an expression for the desired solubilities. This extended Hansen solubility approach is discussed later. Since the partial solubility parameters of Hoy *et al.* (12) differ somewhat from those of Hansen and Beerbower (9), it is important to use either one system or the other rather than a combination of the two. Regression techniques employing the Hoy parameters result in different equations from those obtained with the Hansen parameters.

**Extended Hildebrand Approach**—A technique called the extended Hildebrand approach (2) was developed to reproduce the solubilities of drugs such as xanthine derivatives in mixed solvents, including dioxane and water, water and polyethylene glycol 400, glycerin and propylene glycol, and dioxane and formamide. The interaction energy, $W$, is regressed against the solvent solubility parameter, $\delta_1$, to obtain $W_{calc}$ which is then substituted into the extended solubility equation to reproduce the drug's solubility on the mole fraction scale. The derivation begins with a relation between the drug's mole fraction solubility, $X_2$, the ideal solubility, $X_2^i$, and the activity coefficient, $\alpha_2$:

$$-\log X_2 = -\log X_2^i + \log \alpha_2 \qquad \text{(Eq. 6)}$$

where $\log \alpha_2$ is expressed in terms of solute and solvent cohesive energy densities, $\delta^2$ and $\delta^1$, the solute–solvent interaction energy, $W$, and an "$A$ factor" from regular solution theory (1):

$$-\log X_2 = -\log X_2^i + A(\delta_1^2 + \delta_2^2 - 2W_{calc}) \qquad \text{(Eq. 7)}$$

$$A = V_2\phi_1^2/2.303RT \qquad \text{(Eq. 8)}$$

where $V_2$ is the molar liquid volume of the solute, $\phi_1$ is the volume fraction of the solvent, $R$ is the molar gas constant, and $T$ is the absolute temperature. A term, $[\ln(V_1/V_2) + 1 - (V_1/V_2)]$, from Flory–Higgins theory is sometimes added to solubility expressions such as Eq. 7 to account for the entropy of mixing of substances with considerably different molar volumes. The regression analyses discussed later showed that this term was statistically insignificant for the naphthalene solutions studied.

The extended solubility approach was tested with methylxanthines in binary solvent systems (2, 13, 14) and with naphthalene in some single solvents (15), but has not been explored in detail for individual solvent systems.

**UNIFAC**—A group contribution (UNIFAC) procedure was developed (3, 4) to investigate the solubilities of solids in pure and mixed liquid solvents. According to this method, the activity coefficient is separated into two parts: a combinatorial contribution, $\log \alpha^C$, which accounts for the molecular size and shape of the solute and solvent, and a residual contribution, $\log \alpha^R$, which accounts for intermolecular energies of attraction:

$$\log \alpha_2 = \log \alpha_2^C + \log \alpha_2^R \qquad \text{(Eq. 9)}$$

Details were given previously (4), and the method is briefly described in the *Appendix*.

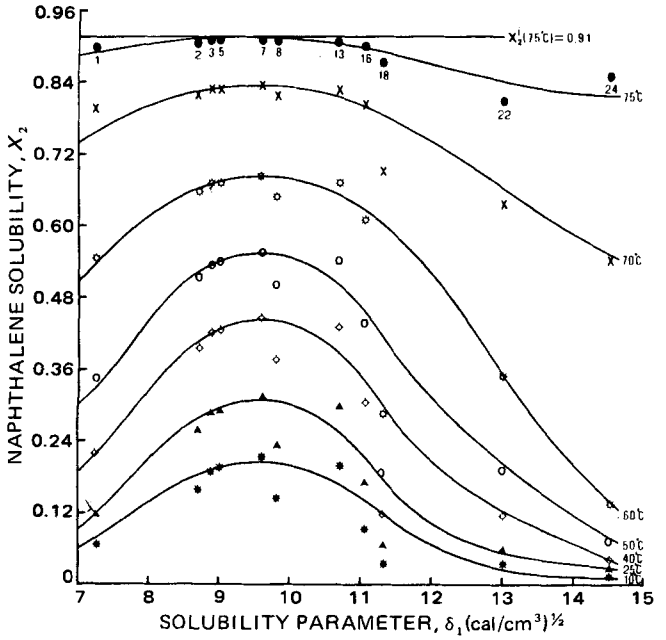


**Figure 1**—*Solubility of naphthalene in solvents from results of Ward (16) determined at 10–75°. Key:* ✱, *10°;* ▲, *25°;* ◇, *40°;* ○, *50°;* ✱, *60°;* x, *70°;* ●, *75°.*

## RESULTS AND DISCUSSION

The present study attempted to reproduce the solubility of naphthalene at 40° in solvents using three methods: (*a*) a partial solubility parameter method together with multiple regression, (*b*) the extended Hildebrand solubility approach (2, 13–15), and (*c*) the UNIFAC procedure (3, 4). Table I shows experimental solubilities reported previously (16–19), together with solvent solubility parameters (9) and molar volumes (9). Although the solubilities were obtained at 40°, $\delta_1$ and $V_1$ are customarily calculated at 25°.

Mole fraction solubilities of naphthalene, as determined (16) at 10–75°, are plotted in Fig. 1 against $\delta_1$, the solubility parameter of the pure solvent. The curves drawn through the points are more symmetrical than would be expected for an organic solid dissolved in polar and nonpolar solvents representing different solvent classes. Some polar solvents, such as acetone and butanol, yield points that are displaced from their proper temperature lines, but most points appear in an orderly arrangement on the bell-shaped curves. Figure 1 shows that the mole fraction solubilities of naphthalene, in a range of $\delta_1$ = 7.3–14.5, exhibit peaks in the curves; the peaks do not appear to shift with temperature. With increasing temperature, the naphthalene solubility curves become less peaked; at 75°, the curve is nearly horizontal, but $\delta_1 = \delta_2$ at the peak remains constant at ~9.6 over the 10–75° range. At 75°, naphthalene is only ~5° below its melting point (mp = 80.2°), and its ideal solubility $X_2^i$ (75°) is 0.9105. At this temperature, naphthalene forms nearly ideal solutions in the majority of solvents studied.

**Multiple Regression and Extended Hansen Approach**—Partial solubility parameters for naphthalene, $\delta_D$ = 9.4, $\delta_P$ = 1.0, and $\delta_H$ = 1.9 (total parameter = 9.64), were estimated from a table of group contributions currently under preparation[1]. An early version of the table is given in the literature (9). The regression subprogram[2] (20) allows a stepwise addition of independent variables, analysis of variance, and examination of the residuals by means of scatter plots. The multiple regression yielded Eq. 10 for naphthalene in 24 solvents at 40°:

$$\log \alpha_2 = 1.0488(\pm 0.1762)A(\delta_{1D} - \delta_{2D})^2 - 0.3148(\pm 0.0490)A(\delta_{1P} - \delta_{2P})^2 + 0.2252(\pm 0.0163)A(\delta_{1H} - \delta_{2H})^2 + 0.0451(\pm 0.0155) \quad \text{(Eq. 10)}$$

$$n = 24 \quad s = 0.0559 \quad R^2 = 0.9765 \quad F = 277 \quad F(3,20,0.01) = 4.94$$

Results obtained with Eq. 10 may be substituted into Eq. 6 for log $\alpha_2$ to calculate mole fraction solubility, $X_2$, as shown in Table II. When solubilities (Table II) are calculated with Eqs. 10 and 6, the procedure is referred to as the extended Hansen approach. The results compare favorably with observed solubilities: only one residual is >30% (*tert*-butanol, 53% error), and about half the results exhibit errors of <5%.

The extended Hansen approach may be used to estimate the solubility in solvents not included in the series under investigation. For example, the solubility of naphthalene in butyric acid at 40° is not found in Table II, but it may be calculated as follows. The partial parameters (9) for butyric acid are $\delta_D$ = 7.3, $\delta_P$ = 2.0, and $\delta_H$ = 5.2. Combining these terms with the values for naphthalene, one obtains $(7.3 - 9.4)^2 = 4.41$, $(2.0 - 1.0)^2 = 1.00$, and $(5.2 - 1.9)^2 = 10.89$. These values are introduced into Eq. 10: $\log \alpha^2 = 1.0488A(4.41) - 0.3148A(1.00) + 0.2252A(10.89) + 0.0451$. Value $A$ must be calculated first, using Eq. 8 with $V_2$ = 123.0, $V_1$ = 92.48, $R$ = 1.9872, and $T$ = 40° (313.15 °K). The volume fraction of the solvent, $\phi_1$, is unknown since it depends on the $X_2$ value, which is sought:

$$\phi_1 = V_1(1 - X_2)/[V_1(1 - X_2) + V_2X_2] \quad \text{(Eq. 11)}$$

Value $A$ is found by an iteration procedure (21), beginning with a value of 1.0 for $\phi_1$ and iterating until $X_2$ or $\phi_1$ no longer changes by more than some desired small value. The iteration yields $X_{2_{calc}} = 0.1959$. This result compares satisfactorily with $X_{2_{obs}} = 0.2487$, giving a calculated value within 21% of the observed mole fraction solubility.

Although calculation of the original regression equations requires an electronic computer, back-calculations (involving iteration) for estimating solubilities in various solvents can be done on a programmable hand calculator.

**Polynomial Regression and Extended Hildebrand Approach**—The term (log $\alpha_2$)/$A$ was regressed *versus* $\delta_1$ for naphthalene in the 24 solvents in a second- (quadratic) and third- (cubic) degree expression. To account for self-association of the alcohols, it was necessary to add an indicator variable, $I$, to the regression equations. In back-calculating solubilities, $I$ is given the value of 1 for alcohols and zero for all other solvents in the series. The quadratic expression did not reproduce the solubility data adequately and was omitted from further considerations.

The cubic equation, together with an indicator variable, resulted in a squared correlation, $R^2$, of 0.86:

$$\frac{\log \alpha_2}{A} = 6.1130(\pm 1.0859)I - 53.2569(\pm 19.6920)\delta_1 + 4.6506(\pm 1.8400)\delta_1^2 - 0.1290(\pm 0.0562)\delta_1^3 + 197.8011(\pm 69.0673) \quad \text{(Eq. 12)}$$

$$n = 24 \quad s = 2.0223 \quad R^2 = 0.8648 \quad F = 32 \quad F(4,19,0.01) = 4.50$$

Residuals expressed in percentages were reasonable for the solubilities of naphthalene in most solvents at 40°. However, some large errors re-

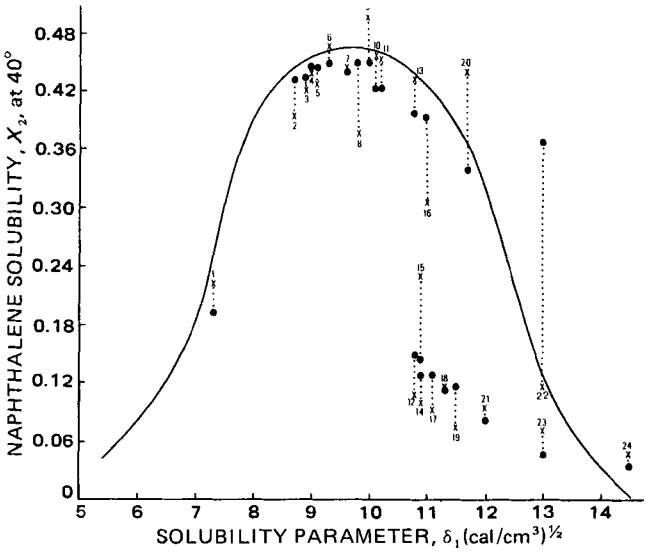


**Figure 2**—*Solubility of naphthalene in 24 individual solvents at 40°. The data is from Refs. 16–19. The curve, calculated using the Hildebrand expression, Eq. 13, rises to a maximum at $\delta_1 = \delta_2 = 9.6$, equal to naphthalene's ideal solubility, $X_2^i(40°) = 0.46594$. The experimental point (x) for each solvent is attached by a dotted line to the calculated solubility (●) obtained using Eqs. 6 and 12.*

[1] By A. Beerbower.
[2] Programmed on The University of Texas Cyber computer system.

**Table II—Four Methods of Solubility Analysis for Naphthalene in Pure Solvents at 40°**

| Solvent | Observed $X_2$ (40°) | Extended Hansen $X_2$ | Extended Hansen Residual | Extended Hildebrand $X_2$ | Extended Hildebrand Residual | UNIFAC $X_2$ | UNIFAC Residual | Regular Solution $X_2$ | Regular Solution Residual |
|---|---|---|---|---|---|---|---|---|---|
| Hexane | 0.222 | 0.2247 | −0.0027 | 0.1934 | 0.0286 | 0.2629 | −0.0409 | 0.2472 | −0.0252 |
| Carbon tetrachloride | 0.395 | 0.3956 | −0.0006 | 0.4311 | −0.0361 | 0.4071 | −0.0121 | 0.4464 | −0.0514 |
| Toluene | 0.422 | 0.4072 | 0.0156 | 0.4345 | −0.0125 | 0.4425 | −0.0205 | 0.4529 | −0.0309 |
| Ethylidene chloride | 0.437 | 0.4279 | 0.0091 | 0.4447 | −0.0077 | —[a] | —[a] | 0.4584 | −0.0214 |
| Benzene | 0.428 | 0.4192 | 0.0088 | 0.4437 | −0.0157 | 0.4499 | −0.0219 | 0.4603 | −0.0323 |
| Chloroform | 0.467 | 0.4080 | 0.0590 | 0.4483 | 0.0187 | 0.4695 | −0.0025 | 0.4640 | 0.0030 |
| Chlorobenzene | 0.444 | 0.4244 | 0.0196 | 0.4429 | 0.0011 | 0.3979 | 0.0461 | 0.4659 | −0.0219 |
| Acetone | 0.378 | 0.4421 | −0.0641 | 0.4484 | −0.0704 | 0.3628 | 0.0152 | 0.4655 | −0.0875 |
| Carbon disulfide | 0.494 | 0.4111 | 0.0829 | 0.4498 | 0.0442 | 0.4197 | 0.0743 | 0.4644 | 0.0296 |
| 1,1-Dibromoethane | 0.456 | 0.4234 | 0.0326 | 0.4370 | 0.0190 | 0.3837 | 0.0723 | 0.4617 | −0.0057 |
| Ethylene dichloride | 0.452 | 0.4547 | −0.0027 | 0.4390 | 0.0130 | —[a] | —[a] | 0.4606 | −0.0086 |
| *sec*-Butanol | 0.112 | 0.1446 | −0.0324 | 0.1498 | −0.0376 | 0.1132 | −0.0010 | 0.4369 | −0.3247 |
| Nitrobenzene | 0.432 | 0.4809 | −0.0489 | 0.3952 | 0.0368 | —[a] | —[a] | 0.4334 | −0.0014 |
| *tert*-Butanol | 0.1009 | 0.1549 | −0.0540 | 0.1416 | −0.0407 | 0.0819 | 0.0190 | 0.4303 | −0.3294 |
| Cyclohexanol | 0.232 | 0.2307 | 0.0013 | 0.1275 | 0.1045 | 0.2080 | 0.0240 | 0.4255 | −0.1935 |
| Aniline | 0.306 | 0.3856 | −0.0796 | 0.3926 | −0.0866 | 0.2689 | 0.0371 | 0.4250 | −0.1190 |
| Isobutanol | 0.0925 | 0.0693 | 0.0232 | 0.1276 | −0.0351 | 0.1474 | −0.0549 | 0.4170 | −0.3245 |
| Butanol | 0.116 | 0.1096 | 0.0064 | 0.1134 | 0.0026 | 0.1124 | 0.0036 | 0.4006 | −0.2846 |
| Isopropanol | 0.076 | 0.0981 | −0.0217 | 0.1165 | −0.0401 | 0.0948 | −0.0184 | 0.3959 | −0.3195 |
| Ethylene dibromide | 0.439 | 0.3744 | 0.0646 | 0.3390 | 0.1000 | 0.3832 | 0.0558 | 0.3587 | 0.0812 |
| Propanol | 0.094 | 0.0828 | 0.0116 | 0.0813 | 0.0131 | 0.0939 | 0.0005 | 0.3344 | −0.2400 |
| Acetic acid | 0.117 | 0.0871 | 0.0299 | 0.3090 | −0.1920 | 0.1267 | −0.0097 | 0.1273 | −0.0103 |
| Ethanol | 0.0726 | 0.0611 | 0.0115 | 0.0491 | 0.0235 | 0.0552 | 0.0174 | 0.1233 | −0.0507 |
| Methanol | 0.0437 | 0.0483 | −0.0046 | 0.0347 | 0.0090 | 0.0489 | −0.0052 | 0.0050 | −0.0387 |

[a] UNIFAC parameters not available for solvent functional groups.

sulted from this equation: cyclohexanol, 45%; *tert*-butanol, 40%; isobutanol, 38%; isopropanol, 53%; and acetic acid, 164%. The experimental points are shown in Fig. 2 attached by dotted lines to the solubilities predicted by use of the extended Hildebrand approach. The large error for acetic acid is unaccounted for but apparently results from the particular regression program and iteration procedure used. Alternative methods involving orthogonalization, root finding, and weighting functions are under investigation. The $X_2$ values and residuals are given in Table II, columns 5 and 6.

**UNIFAC Method**—Gmehling *et al.* (4) employed UNIFAC to estimate the solubilities of naphthalene, anthracene, and phenanthrene in several solvents. Their results were calculated, and new solvents were added in the current study; results shown in Table II, column 7, may be compared with the back-calculated mole fraction solubilities of the extended Hildebrand solubility method, column 5, and those obtained by the extended Hansen solubility approach, column 3. The extended Hansen and UNIFAC methods give remarkably similar results. As already indicated, a quantitative method for calculating solubilities in polar solvents is taken to be satisfactory if errors are no greater than ~30%. These two methods generally meet this standard. By contrast, the extended Hildebrand method gives errors of >30% for nine solvents. However, only one of these, acetic acid, produces a large error.

**Regular Solution Theory**—Column 9 of Table II shows solubilities of naphthalene in the 24 solvents at 40° calculated using the regular solution equation of Hildebrand and Scatchard for solids dissolved in liquid solvents (1). The expression is:

$$-\log X_2 = -\log X_2^i + A(\delta_1 - \delta_2)^2 \qquad \text{(Eq. 13)}$$

Equation 13 reproduces solubilities satisfactorily in nonpolar solvents (regular solutions) but fails for irregular systems with polar solvents showing self-association and solvation. The curve of Fig. 2 was plotted using the mole fractions calculated from the Hildebrand–Scatchard equation. Although the observed values are not well represented by Eq. 13 for polar solvents, the mole fraction solubility of naphthalene ($\delta_2$ = 9.64) in a range of solvents from hexane ($\delta_1$ = 7.3) to methanol ($\delta_1$ = 14.5) is at least in qualitative agreement with regular solution theory. For drug molecules having side chains and functional groups attached to the aromatic ring, the regular behavior of naphthalene solubilities is not expected to be found with single or binary solvents.

**Temperature Effects**—Several investigators (16–18, 22) plotted the mole fraction of naphthalene *versus* the reciprocal of absolute temperature; straight lines result for ideal and nearly ideal solutions. The slope of the ideal solution line provides a measure of the molar heat of fusion. For irregular solutions plotted in this manner, the lines ordinarily are curved. Chertkoff and Martin (23) evaluated solubility data employing a different plot, that of the solute mole fraction against the solubility parameter $\delta_1$ of pure or mixed solvents. In this approach, an approximately bell-shaped curve is obtained that reaches a maximum at $\delta_1 = \delta_2$ in regular systems; the mole fraction at this point corresponds to the ideal solubility. Figures 1 and 2 represent graphs plotted in this manner. They provide some information not readily evident from plots of log mole fraction *versus* $1/T$.

It would be useful to employ the solubility data of Fig. 2 at 40° to obtain solubilities at other temperatures, as shown in Fig. 1. Temperature appears in the ideal solubility term, which may be written[3] $\log X_2^i = (\Delta S^f/R) \log (T/T_m)$, and in $A = V_2\phi_1^2/2.303RT$. It might be reasoned that by use of the extended Hansen or extended Hildebrand regression equation (Eq. 10 or 12) and replacement of the temperature of 313°K by a value of 333°K, one could convert the solubility at 40° to an $X_2$ value at 60°.

The observed mole fraction solubility of naphthalene in hexane at 60° (333.15°K) is 0.547. The proper ideal solubility is used, and the temperature found in $A$ is changed from 40° (313.15°K) to 333.15°K; an iteration is then conducted (21) using the extended Hansen approach to arrive at a new $\phi_1$ value yielding $X_{2_{calc}} = 0.489$. This result represents a 10.6% error from the observed $X_2$ at 60°. The same procedure may be used to calculate the solubility of naphthalene in hexane at 20°. The error is 34%. Naphthalene forms an essentially regular solution in hexane, and the plot of log mole fraction *versus* $1/T$ for this solvent is straight, although it does not coincide with the ideal solubility line. For alcohols, plots of log $X_2$ *versus* $1/T$ are ordinarily curved, and extrapolation of naphthalene solubility in methanol at 40° to obtain $X_2$ at 60° by iteration results in an error of 313%. An attempt to extrapolate $X_2$ to 70 and 75°, however, produced errors of only 33 and 29.6%, respectively. At 20°, the result is 14.8% in error. The extended Hildebrand method yields similar results. Thus, the regression equations obtained at 40° give erratic solubility results for polar solvents at elevated temperatures. The errors are apparently due to the iteration procedure required in the extended Hansen and extended Hildebrand methods.

Hildebrand and Scott (1) discussed the influence of temperature on solubility parameters and provided $\delta$ values at various temperatures. Hansen and Beerbower (9) made estimates of the temperature coefficients of $\delta_D$, $\delta_P$, and $\delta_H$. However, as they pointed out, these estimates are needed only for the most polar or hydrogen bonded systems, since the function $V_2\phi_1^2(\delta_1 - \delta_2)^2$ is independent of temperature for near-regular solutions. The previous example of nonlinear behavior of methanol solutions could presumably be improved by using the type of temperature coefficients they suggested.

Another approach is to regress the solubility data of naphthalene from 10 through 60° (Fig. 1) using a single equation. This procedure provides a more reasonable prediction of solubilities at various temperatures and will be reported later.

[3] Ideal solubility is also calculated using the expression:

$$\log X^i = \frac{\Delta H_m^f}{2.303R}\left(\frac{T_m - T}{T_m T}\right)$$

Both forms are approximations, and it is not clear at this time which is more correct.

The UNIFAC method does not appear to suffer from the problems encountered with the regression approaches for calculating solubilities in polar solvents at elevated temperatures; it does not require an iteration procedure. In methanol at 40°, UNIFAC gives $X_{2_{calc}} = 0.0489$, a difference of 12% from $X_{2_{obs}}$; at 60°, $X_{2_{calc}}$ is 0.110, a difference of 17% from $X_{2_{obs}}$.

## SUMMARY

The work of Hildebrand and Scott (1), Scatchard (24), Hansen (8), and several other investigators has led to increased understanding of solubility phenomena. Yet, the formulation of a satisfactory approach to describe the solubility of crystalline solids in pure and mixed polar solvents has proved to be particularly difficult.

The present report applied three methods. The UNIFAC method requires only the solute's heat of fusion, the melting point, and a knowledge of the chemical structure of the solute and solvent. This method, yielding essentially the same accuracy as obtained by the extended Hansen regression method (one exception is the solubility in isobutanol) is judged far superior for predicting solubilities of naphthalene in untested solvents.

The extended Hansen method must be accepted as the second best method studied. Although it required solubility data in the initial regression step, the use of partial solubility parameters accounts for polar and hydrogen-bonding forces in the various solvents. For this reason, an indicator variable is not required in the regression equation of the extended Hansen approach. Furthermore, if new solvents are to be tested in the system under study, use of their partial solubility parameters should allow estimation of naphthalene solubility within reasonable accuracy. This expectation was found for butyric acid, where the solubility of naphthalene was predicted within 21%.

In earlier studies (2, 13, 14), the extended Hildebrand approach was successful in reproducing the solubility of solid drugs in binary solvents, both polar and nonpolar. Although it is satisfactory in the current work for most solvents studied, this method cannot be expected to apply where strong interactions exist. The predictive power of the extended Hildebrand approach is, therefore, less than that of the other two procedures.

By knowing $X_{2_{obs}}$ at a specified temperature for naphthalene in nonpolar solvents, it is possible to calculate the solubility at other temperatures using the extended Hansen or Hildebrand approach. However, for polar solvents such as methanol, this simple procedure is not successful. UNIFAC appears to be more suitable for calculating the solubility of naphthalene in polar and nonpolar solvents at various temperatures.

Naphthalene, a relatively simple molecule, is a good solute to begin a study of solubility in pure solvents; however, it is a poor model for drug solubility. Although this molecule provides $\pi$ electrons for solute–solvent interactions, its lack of functional groups and side chains renders it considerably less nonideal than those typically encountered in the pharmaceutical sciences.

Knowledge gained from these relatively simple and well-behaved systems must now be applied to real drug solutions in individual polar solvents before conclusions can be reached regarding the applicability of the extended Hansen, extended Hildebrand, and UNIFAC methods.

## APPENDIX

The UNIFAC method is based on the well-known group contribution method and was developed to estimate activity coefficients in mixtures of nonelectrolytes. As stated by Eq. 9, the logarithmic activity coefficient is divided into two parts, combinatorial ($\log \alpha_2^C$) and residual ($\log \alpha_2^R$). The combinatorial part results essentially from differences in sizes and shapes of the molecules in the mixture; the residual part is due mainly to interaction energies of species in solution.

The method involves extensive use of equations and definition of terms, but the user simply provides heats of fusion, melting points of solid solutes, and group numbers for the various atoms and chemical groups that make up the molecules. From the group numbers supplied, the computer program calculates volume, $R$, and area, $Q$, parameters as required for the combinatorial activity coefficient. Energies of interaction, $a_{mn}$ and $a_{nm}$, are calculated for the residual activity coefficient, where $m$ and $n$ are interacting groups and $a_{mn} \neq a_{nm}$. Tables of volume, area, and interaction energy parameters for some 300 groups are found in the literature (25).

## REFERENCES

(1) J. H. Hildebrand and R. L. Scott, "The Solubility of Nonelectrolytes," 3rd ed., Dover, New York, N.Y., 1964.

(2) A. Martin, J. Newburger, and A. Adjei, *J. Pharm Sci.*, **69,** 487 (1980).

(3) A. Fredenslund, J. G. Gmehling, J. Michelsen, M. L. Rasmussen, and J. M. Prausnitz, *Ind. Eng. Chem. Process Des. Dev.*, **16,** 450 (1977).

(4) J. G. Gmehling, T. F. Anderson, and J. M. Prausnitz, *Ind. Eng. Chem. Fundam.*, **17,** 269 (1978).

(5) A. F. M. Barton, *Chem. Rev.*, **75,** 731 (1975).

(6) H. Burrell, *Off. Dig.*, **27,** 726 (1955).

(7) *Ibid.*, *29*, 1159 (1957).

(8) C. M. Hansen, *J. Paint Technol.*, **39,** 505 (1967).

(9) C. M. Hansen and A. Beerbower, in "Encyclopedia of Chemical Technology," suppl. vol., 2nd ed., Wiley, New York, N.Y., 1971, pp 889–910.

(10) C. M. Hansen and K. Skaarup, *J. Paint Technol.*, **39,** 511 (1967).

(11) C. J. F. Böttcher, "Theory of Electric Polarization," Elsevier, New York, N.Y., 1952, chap. 5.

(12) K. Hoy, B. A. Price, and R. A. Martin, "Tables of Solubility Parameters," Union Carbide, Tarrytown, N.Y., 1975.

(13) A. Adjei, J. Newburger, and A. Martin, *J. Pharm. Sci.*, **69,** 659 (1980).

(14) A. Martin, A. N. Paruta, and A. Adjei, *ibid.*, in press.

(15) A. Martin, J. Newburger, and A. Adjei, *ibid.*, **68**(10), IV (1979).

(16) H. L. Ward, *J. Phys. Chem.*, **30,** 1316 (1926).

(17) A. A. Sunier, *ibid.*, **34,** 2582 (1930).

(18) A. A. Sunier and C. Rosenblum, *ibid.*, **32,** 1049 (1928).

(19) "Solubilities of Inorganic and Organic Compounds, vol. 1, Binary Systems," H. Stephen and T. Stephen, Eds., Pergamon, New York, N.Y., 1964.

(20) N. H. Nie, C. H. Hull, J. G. Jenkins, K. Steinbrenner, and D. H. Bent, "SPSS, Statistical Package for the Social Sciences," 2nd ed., McGraw-Hill, New York, N.Y., 1975, chap. 20.

(21) A. Martin, J. Swarbrick, and A. Cammarata, "Physical Pharmacy," 2nd ed., Lea & Febiger, Philadelphia, Pa., 1969, p. 303.

(22) J. H. Hildebrand and C. A. Jenks, *J. Am. Chem. Soc.* **42,** 2180 (1920).

(23) M. J. Chertkoff and A. Martin, *J. Am. Pharm. Assoc., Sci. Ed.*, **49,** 444 (1960).

(24) G. Scatchard, *Chem. Rev.*, **8,** 321 (1931).

(25) A. Fredenslund, J. Gmehling, and P. Rasmussen, "Vapor-Liquid Equilibria Using UNIFAC," Elsevier, New York, N.Y., 1977.

## ACKNOWLEDGMENTS

The authors appreciate the suggestions of Dr. Carl Metzler, The Upjohn Co., regarding the development of the statistical regression approaches. A. Martin is grateful to C. R. Sublett for the endowed professorship which supported part of the work.

# Thermodynamic Dependence of Interfacial Transfer Kinetics of Nonionized Barbituric Acid Derivatives in Two-Phase Transfer Cell

**PETER R. BYRON ˣ, ROGER T. GUEST *, and ROBERT E. NOTARI ***

Received November 28, 1980, from the *Pharmaceutics Research Group, Department of Pharmacy, University of Aston in Birmingham, Gosta Green, Birmingham, B4 7ET England.* Accepted for publication April 6, 1981. *Present address: College of Pharmacy, Ohio State University, Columbus, OH 43210.

**Abstract** □ A theory was developed to describe interfacial transport kinetics of a series of drug homologs in a two-phase transfer cell. When tested, the theory held true for 5,5-disubstituted barbituric acid derivatives in a preequilibrated octan-1-ol = (pH 5) aqueous buffer system maintained at 37° and stirred symmetrically at 50 and 100 rpm. Theoretical prediction of transfer kinetics was not possible in such a cell if the phases were stirred asymmetrically. For symmetric stirring, successful prediction of the transfer kinetics of any homolog in the series was possible from a knowledge of the partition coefficient and transfer kinetics of the parent compound, the partition coefficient of the homolog, and some easily determined system variables. The viscosity and density of the two phases and the phase-volume ratio were needed to define a system constant dependent on the solute diffusion coefficient, interfacial area, donor phase volume, and the boundary layer thickness for diffusion in the donor phase. A method is described to enable estimation of this constant from a knowledge of the transfer kinetics of the parent compound. The rank order of compounds in terms of their observed first-order transfer rate constants is shown to be dependent on the characteristics of the solvent system and stirring conditions employed, as well as on the physical chemistry of the solutes. The results are discussed in light of previously documented investigations.

**Keyphrases** □ Transfer kinetics—thermodynamics, nonionized barbituric acid derivatives in the two-phase transfer cell □ Barbituric acids—derivatives, thermodynamic dependence of interfacial transfer kinetics in the two-phase transfer cell □ Two-phase transfer cell—thermodynamic dependence of interfacial transfer kinetics of nonionized barbituric acid derivatives □ Thermodynamics—interfacial transfer kinetics of nonionized barbituric acid derivatives in the two-phase transfer cell

To exert a biological effect, a drug moiety must reach its receptor site by passing through a series of hydrophilic and hydrophobic regions. The ease with which this transfer is accomplished affects the duration and intensity of the resultant biological response.

## BACKGROUND

Two model systems used to investigate the transfer of solute from hydrophilic to hydrophobic regions are the two- and three-phase transfer cells (1, 2). Gordon and Sherwood (1) used a two-phase system of water and butanol to study the transfer of various solutes across the interface. Their studies provided data that supported the two-film theory of Lewis and Whitman (3). An aqueous *n*-octanol (pH 4.3) two-phase system was employed by Schumacher and Nagwekar (4) to study the transfer of sulfonamides. They (5) also varied the composition of the organic phase in the cell to determine the effect on the transport of the same drugs. The effect of varying the aqueous phase pH on salicylic acid transfer was also investigated (6). Since the transfer of ions through lipid membranes is fundamental to cell function, Ting *et al.* (7) used the two-phase transfer cell to investigate this transport for monovalent cations *in vitro*.

The three-phase transfer cell used (2) to study water diffusion and the transport of various salts through interfaces was modified by Perrin (8). It was used to study the transfer of solutes from an aqueous compartment of pH 2 through a lipid membrane to a second aqueous compartment at pH 7.4 to simulate gastric absorption of salicylic acid and aminopyrine. Doluisio and Swintosky (9) mimicked *in vivo* conditions using a three-phase rocking Y-tube apparatus in which the interfacial area available for drug transfer varied with respect to time. Correlations between *in vivo* drug absorption data and *in vitro* rate constants for three-phase transfer (where the pH of the aqueous compartments was varied) were also attempted for a series of sulfonamides (10).

Neither the solvent system nor the stirring arrangement associated with the respective phases of two- or three-phase transfer cells is standardized in the literature. This situation presents a problem when attempting to compare results among studies. Indeed, it was observed (11) that both the magnitude and rank order of the rate constants for drug transfer are significantly dependent on the design of the cell and the agitation conditions used.

This study demonstrates how the transport kinetics of a series of homologs may be successfully predicted from a knowledge of the transfer kinetics of the lead compound, its partition coefficient, the partition coefficients of the remaining homologs, and some simply determined system-dependent parameters in a symmetrically stirred two-phase transfer cell of known dimensions.

## THEORY

Byron *et al.* (12) used a two-phase transfer cell, containing equal volumes of a preequilibrated aqueous phase and light liquid petrolatum (Fig. 1), to study the kinetics of interfacial transport of a model solute (cyclohept-2-enone) in the presence and absence of competing degradation in the aqueous phase. Their results supported the validity of the two-film theory (3) with assumptions of no significant interfacial resistance, no thermal, electrical, and osmotic gradients, and steady-state diffusion in the two-phase transfer cell. Values for the ratio of the forward and reverse first-order rate constants for the partitioning process ($k_{12}/k_{21}$, Scheme I) from kinetic analysis agreed with equilibrium studies to determine the partition coefficient $K_D$. Thus, the cell (Fig. 1) was shown to conform kinetically to Scheme I when the stirring speed remained constant, provided that the partition coefficient of the compound was concentration independent over the concentration range studied and the compound was stable for the duration of the experiment.

The concentration $C_1$ of the solute in the donor aqueous phase was described by:

$$(C_1 - C_1^\infty) = (C_1^0 - C_1^\infty)\, e^{-(k_{12}+k_{21})t} \qquad \text{(Eq. 1)}$$

where $C_1 = C_1^0$ and $C_2 = 0$ at time $t = 0$, $C_1^\infty$ is the equilibrium concentration of the aqueous phase, and $k_{12}$ and $k_{21}$ are the first-order forward and reverse rate constants for the transfer process. Thus, a plot of $\ln(C_1 - C_1^\infty)$ *versus* time is linear with a negative slope $S$, defined by the sum of the forward and reverse rate constants ($k_{12} + k_{21}$) in Scheme I.

The partition coefficient ($K_D$) may be determined either by kinetic analysis (12) or equilibrium studies from:

$$K_D = k_{12}/k_{21} = C_2^\infty/C_1^\infty \qquad \text{(Eq. 2)}$$

where $C_2^\infty$ and $C_1^\infty$ are the equilibrium concentrations in the organic and aqueous phases, respectively. When a transfer experiment conforms to Scheme I, Eq. 1 may be rewritten in terms of $K_D$, $C_1^0$, and the observed first-order rate constant, $S$ ($= k_{12} + k_{21}$), by substituting for $C_2^\infty = (C_1^0 - C_1^\infty)$ in Eq. 2 and $C_1^\infty$ in Eq. 1 and rearranging to give:

$$C_1 = [C_1^0/(K_D + 1)][K_D e^{-St} + 1) \qquad \text{(Eq. 3)}$$

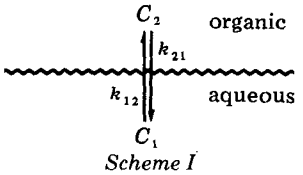


*Scheme I*

*0022-3549/81/1100-1265$01.00/0*
*© 1981, American Pharmaceutical Association*

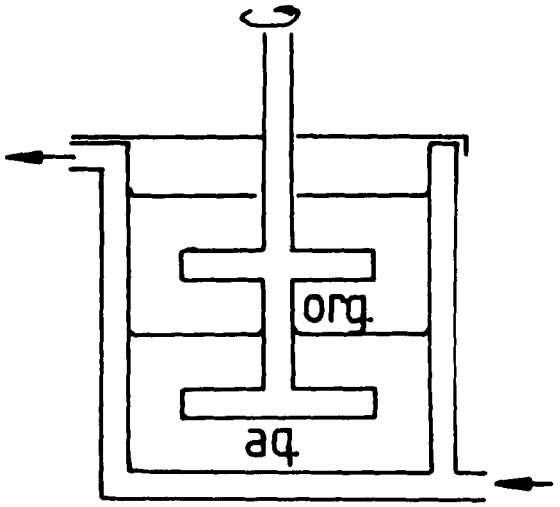


**Figure 1**—*Two-phase transfer cell with symmetric stirring.*

Equation 3 defines the $C_1$ *versus* time profile in the two-phase transfer cell given the aqueous donor phase concentration at $t = 0$, the partition coefficient, and the sum of the forward and reverse rate constants for the partitioning process.

Assuming the validity of the two-film theory (3) and Fick's first law of diffusion, Byron *et al.* (12) showed that the sum of the forward and reverse first-order rate constants in the two-phase transfer cell should be described by:

$$(k_{12} + k_{21}) = S = \frac{D_1 D_2 A(K_D V_2 + V_1)}{V_1 V_2 (D_2 K_D h_1 + D_1 h_2)} \quad \text{(Eq. 4)}$$

where subscripts 1 and 2 refer to the aqueous and organic phases, respectively, and $S$ is dependent on the solute diffusion coefficients ($D$), the phase volumes ($V$), the diffusion boundary layer thicknesses at the interface ($h$), and the solute partition coefficient ($K_D$). It follows from Eq. 4 that, if this theory and its assumptions hold true for the two-phase transfer cell given $D_1$, $D_2$, $V_1$, $V_2$, $h_1$, $h_2$, $A$, and $K_D$, the $C_1$ *versus* time profile could be predicted theoretically from Eq. 3 if an initial solute concentration $C_1^0$ were assumed.

The partition coefficients ($K_D$) of solutes in specified solvent systems at fixed temperature may be determined empirically. Alternatively, $K_D$ can be predicted for unsynthesized analogs (13, 14) from a knowledge of the partition coefficient of a lead compound and its substituents. In a transfer cell, the interfacial area and phase volumes may be kept constant throughout the experiment. The dependence of $S$ on $K_D$ (Eq. 4) for a given solvent system in the transfer cell at fixed stirring speed, however, still necessitates accurate theoretical prediction of $D_1$, $D_2$, $h_1$, and $h_2$. Theoretical predictions of absolute values for these parameters is problematic. Moreover, they will determine the nonlinear dependence of $S$ on $K_D$ and, thus, the changes in $C_1$ *versus* $t$ profiles (Eq. 3) that may be expected when an homologous series is ascended.

**Prediction of Diffusion Coefficients**—The Stokes–Einstein relationship (15) predicts the diffusion coefficient ($D_{AB}$) of a diffusing solute ($A$) in a specified solvent ($B$) as:

$$D_{AB} = \frac{RT}{6\pi\eta a N_A} \quad \text{(Eq. 5)}$$

where the coefficient is a function of the gas constant ($R$), the absolute temperature ($T$), Avogadro's number ($N_A$), the viscosity of $B$, $\eta$, and the radius ($a$) of the diffusing solute molecule. Whereas Eq. 5 has been shown to break down for solutes with molecular weights significantly less than 1000 (16), Wilke and Chang (17) developed Eq. 6 to predict $D_{AB}$ for solutes in dilute solution. The Wilke equation:

$$D_{AB} = (7.4 \times 10^{-10})\,(\psi_B M_B)^{1/2} T/(\eta \bar{V}_A^{0.6}) \quad \text{(Eq. 6)}$$

is empirical, although it is based on Eq. 5. Experimental determinations of $D_{AB}$ for numerous low molecular weight solutes ($A$) in various solvents ($B$) fall within 10% of the values predicted by Eq. 6 (17, 18). Equation 6 is written in the centimeter-gram-second system and takes into account the associating tendencies of the solvent molecules as an association parameter ($\psi_B$), their molecular weight ($M_B$), and replaces the molecular radius (Eq. 5) with $\bar{V}_A$, the molar volume of the solute (A) in cm$^3$/mole as a liquid at its normal boiling point. Typical solvent association parameters ($\psi_B$) were listed by Wilke and Chang (17).

**Prediction of Boundary Layer Thicknesses for Diffusion at Interface**—The boundary layer theory first introduced by Prandtl (19) and extended by Schlichting (20) assumes a condition of "no slip" at a solid–liquid or immiscible liquid–liquid interface due to molecular adhesion. This approach introduced the concept of a stagnant layer adjacent to an interface, where fluids are observed to behave in a nonideal fashion. If the velocity profile in one phase of the two-phase transfer cell is considered, then, provided a horizontal plane (Fig. 1) in the fluid adjacent to the stirring paddle approximates a rotating disk, Schlichting's boundary layer theory (21) predicts that the angular velocity of the fluid ($\omega$) is directly proportional to the kinematic viscosity of the fluid, $\nu(=\eta/\rho$, where $\rho$ is density), and inversely proportional to the square of the distance from the paddle ($x^2$) in the vertical direction (Fig. 1). Thus

$$\omega \propto \nu/x^2 \quad \text{(Eq. 8)}$$

such that $\omega$ will asymptotically approach zero as $x^2 \to \infty$. Moreover, it follows from Eq. 8 that in the case of symmetric stirring in a two-phase transfer cell:

$$\omega_1/\omega_2 = \nu_1/\nu_2 \quad \text{(Eq. 9)}$$

where subscripts 1 and 2 refer to the aqueous and organic phases, respectively. Equation 9 can be derived by writing Eq. 8 for each phase of the symmetrically stirred transfer cell and holding the distance $x$ from the stirring paddle constant, such that $0 < x_1 = x_2 < x_i$, where $x_i$ is the distance between the stirring paddle and the interface. It follows from Eq. 9 that for two immiscible solvents of different kinematic viscosities (Fig. 1), one solvent must move relative to the other under conditions of symmetric stirring where the angular velocities of both paddles are equal and constant.

Thus, when the condition of no slip is assumed at the interface, the bulk of the aqueous phase may be conceptualized as a disk with angular velocity ($\omega$) rotating relative to a stationary organic phase or as an organic phase with angular velocity ($-\omega$) rotating relative to a stationary aqueous phase. Schlichting's original work was based on the estimation of the boundary layer thickness as the distance from an interface required to enable the velocity of the fluid under consideration to approach that of the bulk. Marked differences occur in the types of equations used, dependent on whether velocity, thermal, or diffusive boundary layer thicknesses are to be calculated. Levich (22) introduced an equation, based on Schlichting's work, permitting the prediction of the boundary layer thickness for diffusion adjacent to a rotating-disk electrode in a stationary fluid. Levich's equation was shown to hold true for systems of the type depicted in Fig. 1 (23) and can be written for $h_1$ and $h_2$ (Eq. 4) such that:

$$h_1 = 1.62(D_1/\nu_1)^{1/3}(\nu_1/\omega)^{1/2} \quad \text{(Eq. 10)}$$

and

$$h_2 = 1.62(D_2/\nu_2)^{1/3}(\nu_2/\omega)^{1/2} \quad \text{(Eq. 11)}$$

where $\omega$ is the angular velocity of one phase relative to the other.

Prediction of absolute values for $D_1$ and $D_2$ and $h_1$ and $h_2$ remains problematic. The dimensionless ratios of the diffusion coefficients ($D_1/D_2$) and the diffusive boundary layer thicknesses ($h_1/h_2$) in the aqueous and organic phases, however, may be determined by writing Eq. 6 for $D_1$ and $D_2$ and solving for the quotient $D_1/D_2$, assuming $T$ is constant, such that:

$$D_1/D_2 = (\eta_2/\eta_1)[(\psi_1 M_1)/(\psi_2 M_2)]^{1/2} \quad \text{(Eq. 12)}$$

and dividing Eq. 10 by Eq. 11 to give

$$h_1/h_2 = (D_1/D_2)^{1/3}(\nu_1/\nu_2)^{1/6} \quad \text{(Eq. 13)}$$

Solving Eqs. 12 and 13 for $D_2$ and $h_2$ and substituting in Eq. 4 give:

$$S = [(D_1 A)/(V_1 h_1)]\{R_1(K_D + r)/[R_1 K_D + (R_1)^{1/3}(R_2)^{1/6}(\psi_1 M_1)^{1/3}(\psi_2 M_2)^{-1/3}]\} \quad \text{(Eq. 14)}$$

where $R_1 = \eta_1/\eta_2$, $R_2 = \nu_2/\nu_1$, and $r = V_1/V_2$. Equation 14 is now in a form that enables the prediction of the sum of the forward and reverse first-order rate constants ($k_{12} + k_{21}$) in Scheme I for any compound in an homologous series, provided that $S$ and $K_D$ are known for the parent compound. $K_D$ can be predicted for each compound under consideration, while the solvent system-dependent constants $R_1$, $R_2$, $r$, $\psi_1$, $\psi_2$, $M_1$, and $M_2$ may be determined easily.

The term $(D_1 A)/(V_1 h_1)$ must first be estimated experimentally for the system under consideration from a knowledge of the transfer kinetics

of the parent compound. This estimation can be made by rearranging Eq. 14 to give:

$$(D_1A)/(V_1h_1) = \{S[R_1K_D + (R_1)^{1/3}(R_2)^{1/6}(\psi_1M_1)^{1/3} (\psi_2M_2)^{-1/3}]\}/[R_1(K_D + r)] \quad \text{(Eq. 15)}$$

Viscometry and densitometry measurements on the mutually saturated binary solvent system under investigation (constant temperature) yields $R_1$ and $R_2$. The phase ratio ($r$) and molecular weights of the solvents ($M_1$ and $M_2$) are known. Wilke (17) quoted values for the association parameters $\psi_1$ and $\psi_2$, recommending values of 2.6 for water, 1.9 for methanol, 1.5 for ethanol, and 1.0 for benzene, ether, heptane, and other unassociated solvents.

The partition coefficient ($K_D$) may be determined experimentally from $C_2^\infty/C_1^\infty$ for the parent compound. The initiation of a transfer experiment by introduction of a bolus of the parent solute into the aqueous donor phase of the transfer cell and the study of its transfer kinetics at fixed temperature and stirring speed enable estimation of $S(=k_{12} + k_{21})$ according to Eq. 1. The term $(D_1A)/(V_1h_1)$ may then be determined from Eq. 15.

With fixed stirring conditions, constant temperature, and constant $V_1$, $A/(V_1h_1)$ should be independent of the solute under consideration. Moreover, it was shown (15) that the diffusion coefficients of nonassociated solutes change insignificantly within a homologous series because:

$$D \propto 1/\sqrt[3]{M_s} \quad \text{(Eq. 16)}$$

where $M_s$ is the molecular weight of the solute. The term $(D_1A)/(V_1h_1)$ can thus be considered constant within a homologous series once estimated under defined conditions for the parent compound in the two-phase transfer cell. Therefore, Eq. 14 can be used to calculate $S$ as a function of $K_D$ within a homologous series.

Given the theoretical estimation of $K_D$ for unsynthesized compounds the prediction of partitioning kinetics should be possible without exhaustive experiments. This theory was evaluated experimentally using a series of barbituric acid derivatives.

## EXPERIMENTAL

**Determination of $S$ for a Series of 5,5-Disubstituted Barbituric Acid Derivatives**—Transfer kinetics were studied for a series of 5,5-disubstituted barbituric acid derivatives (Table I) in the two-phase transfer cell shown in Fig. 1. The drugs in concentrations of $\sim 1.3 \times 10^{-4}$ $M$ were introduced as solutes into the donor aqueous phase. The cell used contained preequilibrated octan-1-ol[1] and 0.06 $M$ Sorensen's buffer (pH 5.0) (24). Preequilibration was effected by stirring for >6 hr prior to solute introduction. Phase volumes were kept constant such that $V_1 = V_2$, 90 ml ($r = 1$). During the transfer experiments, the phases were stirred[2] symmetrically (Fig. 1) with a 4-cm diameter stirring paddle positioned 1 cm from the interface in each phase, rotating at 50 or 100 (±0.5) rpm. The circular glass cell was 6.75 cm i.d.

The aqueous phase was pumped[3] through a flowcell in a spectrophotometer[4]. The concentration in the donor phase ($C_1$) was continuously monitored by automatically recording[5] the absorbance as a function of time at 222.5 nm (the isosbestic point for all the compounds) until equilibrium was attained. Control experiments monitoring 222.5 nm absorbance in the absence of the organic phase showed that Compounds I–VI were stable for the time course of a kinetic determination. Equilibrium partition coefficients determined at 37° were concentration independent in the range employed during the kinetic experiments. Plots based on Eq. 1 of $\ln(C_1 - C_1^\infty)$ *versus* $t$ were linear for >95% of the process. The terminal slope ($S$) was determined in each case by linear regression analysis.

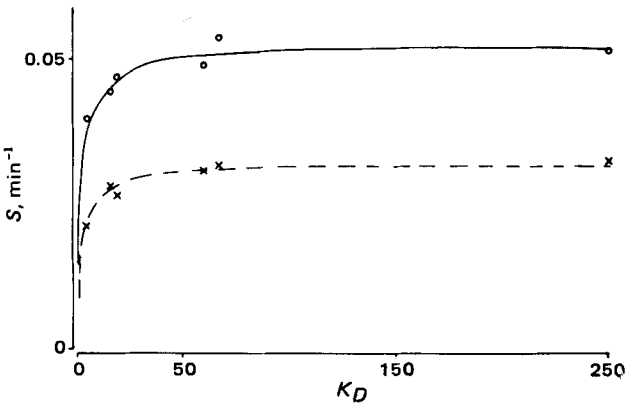


**Figure 2**—*Dependence of* S (=$k_{12}$ + $k_{21}$) *(Eq. 1; Scheme I), on* $K_D$ *for I–VI (Table I) at 50 (X) and 100 (O) rpm at 37°. The dashed (50 rpm) and solid (100 rpm) profiles are theoretical curves based on Eq. 14 after calculation of* ($D_1A$)/($V_1h_1$) *from Eq. 15.*

**Table I—Structures, Molecular Weight, pKa Values and Source of Barbituric Acid Derivatives Used in the Study**

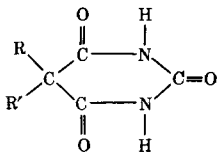

| Compound | R | R′ | Molecular Weight | pKa[a] (25°) | Source |
|---|---|---|---|---|---|
| I | $CH_3CH_2$– | $CH_3$—$CH_2$– | 184.20 | 7.91 | [b] |
| II | $CH_2$=$CHCH_2$– | $CH_3CH$(–$CH_3$) | 210.23 | 7.91 | [c] |
| III | $CH_2$=$CHCH_2$– | $CH_3CHCH_2$(–$CH_3$) | 224.25 | 7.68 | [c] |
| IV | $CH_2$=$CHCH_2$– | $CH_3CH_2CH$(–$CH_3$) | 224.25 | | [d] |
| V | $CH_2$=$CHCH_2$– | $CH_3(CH_2)_2CH$(–$CH_3$) | 238.27 | 8.08 | [c] |
| VI | $CH_2$=$CHCH_2$– | $CH_2$=$CHCH_2$– | 208.21 | 7.79 | [c] |

[a] Reference 25. [b] Hopkins and Williams, Essex, England. [c] Ganes Chemical Works, Carlstadt, N.J. [d] Sterling-Winthrop Research Institute, Rensselaer, N.Y.

**Partition Coefficients**—Values of $K_D$ were estimated in triplicate by equilibrating I–VI at 37° in the solvent system previously defined. The phase ratio ($r$) was adjusted such that concentrations in the aqueous phase gave $0.1 < (\text{Abs})_{222.5\text{ nm}} < 0.9$, and $K_D$ was calculated from:

$$K_D = [(C_1^0 - C_1^\infty)r]/C_1^\infty \quad \text{(Eq. 17)}$$

where $C_1^0$ and $C_1^\infty$ are the initial and final concentrations in the aqueous phase.

**Viscometry and Densitometry**—The viscosities and densities of mutually saturated octan-1-ol and 0.06 $M$ Sorenson's buffer (pH 5.0) were determined in replicate relative to water at 37° using an Ostwald U-tube viscometer and a 10-ml specific gravity bottle. Mean values for $\eta$ and $\rho$ enabled estimation of $R_1$ and $R_2$ (Eq. 14).

**Dependence of Transfer Kinetics on $K_D$**—Values for the ratios $R_1$ and $R_2$ were determined as previously described. Molecular weights $M_2$ and $M_1$ for preequilibrated octan-1-ol and 0.06 $M$ Sorenson's buffer (pH 5.0) were assumed to be 130.23 and 18.02, respectively, as if they were pure octanol and water. The association parameters $\psi_1$ and $\psi_2$ were assigned values of 2.6 and 1.0 (17). Values for $S$ were determined from experimental data for $C_1$ *versus* $t$ for each compound at both stirring speeds. Plots of $\ln(C_1 - C_1^\infty)$ *versus* $t$ were subjected to linear regression analysis to determine the value of the linear negative slope $S(=k_{12} + k_{21})$ according to the logarithmic form of Eq. 1. Values for the coefficient $(D_1A)/(V_1h_1)$ were calculated for I–VI based on $r = 1$ and their experimentally determined values for $S$ at 50 and 100 rpm using Eq. 15. Thus, two mean values for the coefficient were calculated at the different stirring speeds. The theoretical dependence of $S(=k_{12} + k_{21})$ on $K_D$ was determined for the octan-1-ol buffer system at 37° using Eq. 14. Calculated values for $S$ were compared to those determined experimentally for I–VI.

[1] Specgrade, Fisons Ltd., Loughborough, England.
[2] Model KQT59 stirrer, Citenco Ltd., Herts, England.
[3] Model RPD lab pump, Fluid Metering Inc., Oyster Bay, NY.
[4] Model SP500, Pye-Unicam, Cambridge, England.
[5] Model 26000 recorder, Bryans Southern Instruments, Mitcham, Surrey, England.

Table II—Theoretical and Experimental Estimates for $S$ ($=k_{12} + k_{21}$) at 50 and 100 rpm in Transfer Cell and Mean Octanol–pH 5.0 Buffer Partition Coefficients at 37° for I–VI

| Compound[a] | $K_D^b$ | 50 rpm $S_{th}^c$ | 50 rpm $S_{obs}^d$ | 50 rpm Percent Error[e] | 100 rpm $S_{th}^c$ | 100 rpm $S_{obs}^d$ | 100 rpm Percent Error[e] |
|---|---|---|---|---|---|---|---|
| I | 4.5 | 2.18 | 2.10 | 3.8 | 3.57 | 3.80 | −6.1 |
| II | 15.7 | 2.78 | 2.83 | −1.8 | 4.55 | 4.41 | 3.2 |
| III | 19.3 | 2.84 | 2.64 | 7.6 | 4.66 | 4.68 | −0.4 |
| IV | 60.0 | 3.08 | 3.06 | 0.7 | 5.04 | 4.89 | 3.1 |
| V | 67.0 | 3.09 | 3.17 | −2.5 | 5.07 | 5.36 | −5.4 |
| VI | 250.0 | 3.18 | 3.23 | −1.5 | 5.21 | 5.14 | 1.4 |

[a] Table I. [b] Observed, mean of three determinations. [c] Equation 14; expressed in $min^{-1} \times 10^2$. [d] ($k_{12} + k_{21}$) based on kinetic analysis (Eq. 1) ($min^{-1} \times 10^2$). [e] 100 ($S_{th} - S_{obs}$)/$S_{obs}$.

## RESULTS

**Determination of $S$ for a Series of 5,5-Disubstituted Barbituric Acid Derivatives**—Plots of $\ln(C_1 - C_1^\infty)$ *versus* $t$ based on Eq. 1 were linear for >95% of the partitioning process for each compound studied at either 50 or 100 rpm. Observed terminal slopes, $S_{obs}$ ($=k_{12} + k_{21}$), are documented in Table II after determination for each of the derivatives of I–VI by linear regression (correlation coefficient $r > 0.99$, $n > 10$).

**Partition Coefficients**—Partition coefficients as mean values from triplicate determinations for I–VI at 37° in the solvent system previously described are shown in Table I, these values are based on Eq. 17, with an experimental deviation from the mean of <8%.

**Viscometry and Densitometry**—Mean viscosity and density values of the aqueous and organic phases used in the study were determined as $0.7005 \times 10^{-2}$ and $4.806 \times 10^{-2}$ poise and 1.0017 and 0.8148 g/ml, respectively, at 37°.

**Dependence of Transfer Kinetics on Partition Coefficient**—Mean values for the coefficient $(D_1A)/(V_1h_1)$ were determined for I–VI as $3.21 \times 10^{-2}$ ($\pm 0.13 \times 10^{-2}$) and $5.26 \times 10^{-2}$ ($\pm 0.21 \times 10^{-2}$) $min^{-1}$ at 50 and 100 rpm, respectively (Eq. 15). The dashed and solid curves of $S$ *versus* $K_D$ in Fig. 2 were generated using Eq. 14 for the octanol buffer system with $(D_1A)/(V_1h_1)$ held constant at these mean values for 50 and 100 rpm. They show the theoretical dependence of the sum of the forward and reverse rate constants $k_{12}$ and $k_{21}$ (Scheme I) on the equilibrium partition coefficient $K_D$. Experimental determinations of $S$ ($=k_{12} + k_{21}$), determined by kinetic analysis of $C_1$ *versus* $t$ profiles for I–VI at the two stirring speeds (from data anlysis using Eq. 1), are shown. The percentage error involved when determining $S$ from Eq. 14 ($S_{th}$) as opposed to experimentally in the two-phase cell ($S_{obs}$) at either stirring speed is shown in Table II to be ≤8%. Table II summarizes these errors and the values of $S_{th}$, $S_{obs}$, and $K_D$ at 50 and 100 rpm for I–VI.

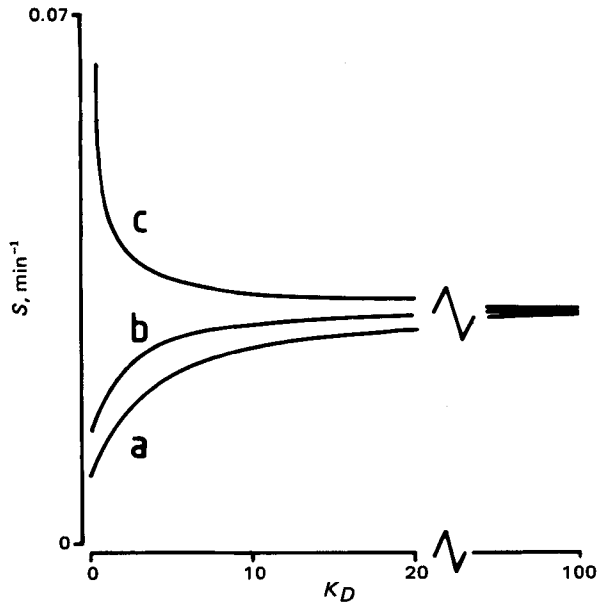


**Figure 3**—*Theoretical dependence of* S *on* $K_D$ *(Eq. 14) in the two-phase transfer cell at 50 rpm for (a) the octanol–aqueous system used in this study, (b) a butanol–aqueous system at 35°, and (c) a chloroform–aqueous system at 35°. The values of the coefficient* $(D_1A)/(V_1h_1)$ *and* r *were held constant at* $3.21 \times 10^{-2}$ $min^{-1}$ *and 1, respectively. Association parameters* ($\psi$) *were assigned values of 2.6, 1.0, 1.0, and 1.0 for water* (M = *18.02), octanol* (M = *130.23), butanol* (M = *74.12), and chloroform* (M = *119.38), respectively (17). The profile a was generated with* $R_1 = 0.149$ *and* $R_2 = 8.435$, *their experimentally determined values. For curves b and c, literature values (28, 29) were utilized for the pure solvents such that* $R_1 = 0.340$ *and 1.430 and* $R_2 = 3.522$ *and 0.480 for butanol–water and chloroform–water systems, respectively.*

## DISCUSSION

The theory describing the dependence of the sum of the forward and reverse first-order rate constants ($S$) in Scheme I on $K_D$ was derived in this study for solutes introduced into a donor phase of a stirred transfer cell (Eq. 14). For this theory to hold true, the solute must conform to Scheme I and neither dissociate nor associate in the organic or aqueous phases at experimental concentrations. An aqueous buffer (pH 5.0) was chosen to ensure that the barbituric acid derivatives were insignificantly ionized (<1%) in the aqueous phase of the cell, provided the pKa values quoted in Table I at 25° were ≥7 at 37°. These studies showed that the partition coefficients of I–VI varied insignificantly with concentration in the experimental ranges. This finding agrees with previous observations (26). Therefore, it was unlikely that these compounds existed significantly as other than unionized monomers in either phase.

The validity of the two-film theory in the two-phase transfer cell was established previously (1, 12). Experimental conditions were chosen such that both phases were mutually saturated, and the transfer cell was maintained at 37° to eliminate temperature gradients. Evaporation of water *via* diffusion through the upper organic layer was minimized by covering the cell and was negligible during 24 hr at 37°. The adequacy of Eqs. 1 and 3 in describing the experimental data, together with the absence of a visible lag time, implies rapid achievement of steady-state diffusion conditions in the transfer cell. The assumption of steady-state diffusion is involved in the derivation of Eq. 4. Similarly, the agreement between the continuous data for $C_1$ *versus* $t$ and Eqs. 1 and 3 supports the assumption of an effectively constant interfacial area, $A$, at both 50 and 100 rpm.

The remaining assumptions necessary to develop this theory and Eq. 14 require that solvent flow in each phase is essentially laminar (low Reynold's number) and that the bulk of the organic phase rotates in relation to the bulk of the aqueous phase. This approach enabled prediction of the dimensionless term $h_1/h_2$ by assuming the validity of the Levich equation (Eqs. 10 and 11) and the existence of symmetric stirring. Similarly, the validity of Wilke's equation (Eq. 6) and his solvent association parameters, $\psi_B$, were necessary for determination of $D_1/D_2$. Wilke's equation for low molecular weight nonassociating solute molecules in dilute solution enabled calculation of $(\psi_1 M_1)^{1/3}(\psi_2 M_2)^{-1/3}$ for use in Eqs. 14 and 15. The absence of significant interfacial resistance, osmotic gradients, effective constancy of diffusion coefficients within a series of drug derivatives, and the validity of these latter assumptions can only be verified by testing the dependence of $S$ on $K_D$ and by comparing the theory to empirical observations.

Figure 2 and Table II show the theoretical and experimental dependence of $S$ ($=k_{12} + k_{21}$) (Scheme I) on $K_D$ for I–VI in an octanol–aqueous system at 37°. The excellent agreement between experiment and theory (theoretical prediction of $S$ varies <8% from empirical determinations, Table II) demonstrated the validity of the assumptions for the two-phase transfer cell. Moreover, Fig. 2 and Eq. 14 demonstrate clearly how the transport kinetics of a series of drug analogs may be predicted from a knowledge of the transport kinetics of the parent compound and its partition coefficient. Given either experimental determination of the partition coefficient of subsequent analogs or its theoretical prediction for even unsynthesized compounds (13, 14), a single estimation

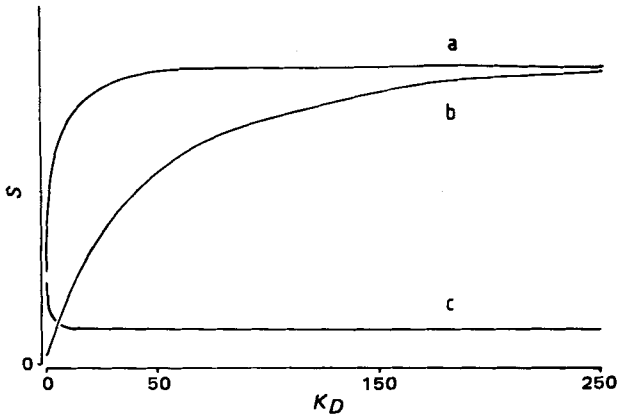


**Figure 4**—*Theoretical dependence of* S *on* $K_D$ *(Eq. 4) for conditions of symmetric (a) and asymmetric (b and c) stirring in an octanol–aqueous system at 37° in the two-phase transfer cell. The ratio of boundary layer thicknesses for diffusion,* $h_1/h_2$*, were varied such that* $h_1/h_2 = 1.12$ *(curve a; the present study with symmetric stirring), 0.1 (curve b), and 10 (curve c). Other variables were held constant (see text).*

of $(D_1A)/(V_1h_1)$ (Eq. 15), after determination of $R_1$, $R_2$, $r$, and $(\psi_1M_1)^{1/3}(\psi_2M_2)^{-1/3}$, is possible from kinetic analysis for $S$ $(=k_{12} + k_{21})$ (Eq. 1) for the parent compound in the transfer cell. The agreement between theory (Eq. 14) and experiment (Fig. 2) demonstrates that the $(D_1A)/(V_1h_1)$ estimate (Eq. 15) applies to the entire series at a fixed stirring rate. Therefore, once the system is defined, the dependence of $S$ on $K_D$ can be evaluated. Prediction of $C_1$ *versus* $t$ profiles for the remaining compounds in the series thus is possible for a given donor phase concentration at $t = 0$, $C_1^0$, using Eq. 3.

**Variation of Solvent Systems and Stirring Conditions**—Neither the solvent systems nor the stirring conditions associated with the two-phase transfer cells documented in the literature were standardized. Gordon and Sherwood (1) employed an aqueous–butanol system while Zecchi *et al.* (6) used benzene as the organic phase. Symmetric (27) and asymmetric (1) stirrers also were described. The dependence of transfer kinetics on $K_D$ in systems containing either various organic phases or asymmetric stirring methods will be different from that shown in Fig. 2 for the symmetrically stirred aqueous–octanol system.

Values for the solvent system dependent variables $R_1$, $R_2$, $\psi_1$, $\psi_2$, $M_1$, and $M_2$ were obtained for butanol–water and chloroform–water systems at 35° (17, 28, 29) and are documented (Fig. 3). The coefficient $(D_1A)/(V_1h_1)$ was held constant at $3.21 \times 10^{-2}$ min$^{-1}$. The theoretical dependence of $S$ on $K_D$ for these two systems with symmetric stirring and $r = 1$ is shown in Fig. 3 according to Eq. 14. The theoretical curve for the octanol–aqueous system used in the present study is shown for comparison. Although $K_D$ is itself a function of the solvent system employed, at a given $K_D$ value in Fig. 3 the gradient $dS/dK_D$ may be positive, negative, or zero, depending on the solvent system employed. This behavior disproves the often stated assumption that $S$ values are proportional to $K_D$ values.

To determine the effect of asymmetric stirring on the dependence of $S$ on $K_D$ for a given solvent system, it is necessary to solve Eq. 12 for $D_2$ and to substitute in Eq. 4. The value for the ratio $D_1/D_2$ was maintained at 4.032, its calculated value from Eq. 12 for the aqueous–octanol system at 37°. The phase volumes $V_1$ and $V_2$ were held constant and equal. Equation 4 was used to determine the dependence of $S$ on $K_D$ for $h_1/h_2 = 1.12$ (the ratio for symmetric stirring in the aqueous–octanol system at 37°), 0.1, and 10.0. Figure 4 illustrates the likely effect of asymmetric stirring where $h_1/h_2$ would be expected to change on the resultant dependence of $S$ on $K_D$ for a specified solvent system at fixed temperature. The gradient $dS/dK_D$ at a fixed $K_D$ value may be positive, negative, or zero, depending on the stirring conditions employed.

The results from extrapolation of the present theory are shown in Figs. 3 and 4. Studies are in progress to test these extrapolations experimentally in appropriate systems. These implications are fundamental to transport kinetic studies employing two- or three-phase transfer cells. Augustine and Swarbrick (10) used a three-phase transfer cell to rank a series of compounds dependent on a parameter proportional to $k_{12}$ (Scheme I). Other investigators (9) attempted to discriminate between compounds on the basis of their partitioning kinetics. However, it is clear from Figs. 3 and 4 that such a procedure in an unstandardized transfer cell is nothing more than a study of solvent systems and stirring paddles, provided that the present theory is correct. The observation (Figs. 3 and 4) that $dS/dK_D$ may be positive, negative, or zero at fixed $K_D$ means that $S$ $(=k_{12} + k_{21})$ and, therefore, $C_1$ *versus* $t$ profiles for a series of compounds may be ranked merely by the experimental solvent and stirring conditions.

The choice of solvent is a subject for debate in that the solvent system itself defines the partition coefficient of the compounds studied. The use of asymmetric stirring in two- and three-phase cells however, necessitates the absolute estimation of individual values for $h_1$ and $h_2$ (Eq. 4). Absolute boundary layer thicknesses can only be approximated (20). The dependence of $S$ on $K_D$ must be established empirically under asymmetric stirring conditions. The theoretical approach described in this paper, which is only applicable to symmetric stirring, utilizes the dimensionless ratio $h_1/h_2$ in the derivation of Eq. 14, which predicts the kinetics of transfer as a function of $K_D$.

## REFERENCES

(1) K. F. Gordon and T. K. Sherwood, *Chem. Eng. Progr., Symp. Ser.*, **50**, 15 (1954).

(2) H. L. Rosano, P. Duby, and J. H. Schulman, *J. Phys. Chem.*, **65**, 1704 (1961).

(3) W. K. Lewis and W. G. Whitman, *Ind. Eng. Chem.*, **16**, 1215 (1924).

(4) G. E. Schumacher and J. B. Nagwekar, *J. Pharm. Sci.*, **63**, 240 (1974).

(5) *Ibid.*, **63**, 245 (1974).

(6) V. Zecchi, L. Rodriguez, and M. Cini, *Farmaco Ed. Prat.*, **34**, 176 (1979).

(7) H. P. Ting, G. L. Bertrand, and D. F. Sears, *Biophys. J.*, **6**, 813 (1966).

(8) J. Perrin, *J. Pharm. Pharmacol.*, **19**, 25 (1966).

(9) J. T. Doluisio and J. V. Swintosky, *J. Pharm. Sci.*, **53**, 597 (1964).

(10) M. A. Augustine and J. Swarbrick, *ibid.*, **61**, 1656 (1972).

(11) *Ibid.*, **59**, 314 (1970).

(12) P. R. Byron, R. E. Notari, and E. Tomlinson, *J. Pharm. Sci.*, **69**, 527 (1980).

(13) A. Leo, C. Hansch, and D. Elkins, *Chem. Rev.*, **71**, 525 (1971).

(14) R. F. Rekker, "The Hydrophobic Fragmental Constant," Elsevier, Amsterdam, The Netherlands, 1977.

(15) O. Sten-Knudsen, "Membrane Transport in Biology I. Concepts and Models," G. Giebisch, D. C. Tosteson, and H. H. Ussing, Eds., Springer-Verlag, Berlin, Germany, 1978, p. 53.

(16) R. C. Reid and T. K. Sherwood, "The Properties of Gases and Liquids," McGraw-Hill, New York, N.Y., 1966, chap. 11.

(17) C. R. Wilke and P. Chang, *Am. Inst. Chem. Eng. J.*, **1**, 264 (1955).

(18) P. Chang and C. R. Wilke, *J. Phys. Chem.*, **59**, 592 (1955).

(19) L. Prandtl, "Essentials of Fluid Dynamics," Blackie and Son, London, England, 1952.

(20) H. Schlichting, "Boundary-Layer Theory," 7th ed., McGraw-Hill, New York, N.Y., 1979.

(21) *Ibid.*, pp. 102 *et seq.*

(22) B. Levich, *Discuss. Faraday Soc.*, **1**, 37 (1947).

(23) W. J. Albery, J. F. Burke, E. B. Leffler, and J. Hadgraft, *J. Chem. Soc. Faraday Trans. I*, **72**, 1618 (1976).

(24) "Documenta Geigy Scientific Tables," 7th ed., K. Diem and C. Lentner, Eds., Geigy Pharmaceuticals, Macclesfield, England, 1975, pp. 280 et seq.

(25) "Medicinal Chemistry, Vol. IV," F. F. Blicke and R. H. Cox, Eds., Wiley, New York, N.Y., 1959, p. 40.

(26) K. Kakemi, T. Arita, R. Hori, and R. Konishi, *Chem. Pharm. Bull.*, **15**, 1705 (1967).

(27) W. I. Higuchi, A. H. Ghanem, and A. B. Bikhazi, *Fed. Proc. Fed. Am. Soc. Exp. Biol.*, **29**, 1327 (1970).

(28) "C.R.C. Handbook of Chemistry and Physics," 59th ed., R. C. Weast, Ed., CRC Press, Boca Raton, Florida, 1978.

(29) R. N. Smith, C. Hansch, and M. M. Ames, *J. Pharm. Sci.*, **64**, 599 (1975).

# Pharmacokinetics of Isosorbide Dinitrate in Rhesus Monkey, Cynomolgus Monkey, and Baboon

**E. DOYLE ˣ and L. F. CHASSEAUD**

Received August 8, 1980, from the *Department of Metabolism and Pharmacokinetics, Huntingdon Research Centre, Huntingdon, PE18 6ES, England.* Accepted for publication May 18, 1981.

**Abstract** □ At 2 min after intravenous injection of isosorbide dinitrate (1 mg/kg), mean plasma drug concentrations were 565 ± 66 (*SD*), 586 ± 43, and 1572 ± 253 ng/ml in the rhesus monkey, cynomolgus monkey, and baboon, respectively. Following a relatively short distribution phase, mean plasma concentrations declined with half-lives of 62, 23, and 24 min in these three species, respectively. The time course of plasma concentrations could be described by a two-compartment open model, although a one-compartment open model was adequate for obtaining some pharmacokinetic parameters. Statistically significant differences among the species were observed in areas under the plasma concentration–time curves, plasma half-lives, and volumes of distribution. The pharmacokinetics of isosorbide dinitrate in baboons most closely resembled those in humans.

**Keyphrases** □ Isosorbide dinitrate—pharmacokinetics, intravenous administration compared in nonhuman primates □ Pharmacokinetics—isosorbide dinitrate, intravenous administration compared in nonhuman primates □ Vasodilators—isosorbide dinitrate, pharmacokinetics compared in nonhuman primates

Isosorbide dinitrate, an organic nitrate vasodilator, has been in clinical use for many years (1–3). This lipophilic drug is almost completely eliminated by biotransformation, being rapidly denitrated (4, 5) by the glutathione *S*-transferases (EC 2.5.1.18) (6). The urinary metabolites of isosorbide dinitrate in animals (7–10) and humans (11, 12) are the corresponding isomeric mononitrates and isosorbide, which are excreted free and probably partly conjugated with glucuronic acid. Sorbitol has also been shown to be a urinary metabolite of isosorbide dinitrate in humans (11).

Little has been reported of the pharmacokinetics of the drug in animals, probably because of the difficulty in measuring it in plasma; most early data were obtained using [$^{14}$C]isosorbide dinitrate. The recent development of adequately sensitive analytical methods now permits studies of the drug's pharmacokinetics in humans (13–15).

The present study evaluated the pharmacokinetics of isosorbide dinitrate in nonhuman primates.

## EXPERIMENTAL

**Materials**—Isosorbide dinitrate[1] solutions suitable for intravenous injection were prepared by dissolving the drug in aqueous 10% (v/v) ethanol. Solutions of nitroglycerin, 1% (w/v) in ethanol, were obtained commercially[2] and used as the internal standard.

**Animals**—Five female animals of each nonhuman primate species, ~1.5–3 years of age, were obtained commercially and maintained under conditions described previously (16). Animal body weights ranged as follows: rhesus monkey, 4–6 kg; cynomolgus monkey, 3–4 kg; and baboon, 4.5–7 kg.

**Dosage**—The animals were fasted for ~16 hr before and 7 hr after dosing, but water was provided at all times. Isosorbide dinitrate solution (1 mg/kg) was injected within 5 sec into a cephalic vein. This dose level was selected as one that might be used in chronic toxicity studies of the drug by this route. In humans, doses of 12.5 mg of isosorbide dinitrate have been infused during 2.5 hr (15).

Blood samples (2.5 ml) were withdrawn from a femoral vein before dosing and at 0.03, 0.08, 0.17, 0.33, 0.50, 0.75, 1.0, 1.5, 2.0, 3.0, and 4.0 hr (4.5 hr in the rhesus monkey) after dosing. The blood was taken into heparinized tubes, cooled in ice-cold water after mixing, and rapidly centrifuged to remove cells, which then were discarded. The plasma was stored at −20° until assayed. Isosorbide dinitrate is stable in plasma under these conditions.

**Drug Analysis**—Isosorbide dinitrate concentrations were measured in plasma by the electron-capture gas chromatographic procedure of Doyle *et al.* (17). Standard curves were prepared for three concentration ranges. Some analytical parameters are shown in Table I.

**Data Processing**—A two-compartment open model was fitted[3] to the plasma isosorbide dinitrate concentration–time data using a nonlinear least-squares curve fitting program (16). This program fits a curve to the observed data and selects a model by comparing the relative sizes of the initial and terminal phases, $\alpha$ and $\beta$, but does not allow user-defined selection of a model. A one-compartment model was fitted to the data as a possible alternative to a two-compartment model by normal regression techniques.

The criteria used to assess the data fit (obs = observed, exp = expected) from each species were: coefficient of determination, $r^2 = (G - R)/R$, where $G = \Sigma (\text{obs} - \overline{\text{obs}})^2$ and $R = \Sigma (\text{obs} - \text{exp})^2$; and residual mean square, $R/(n - 1 - p)$, where $n$ is the number of observations and $p$ is the number of parameters fitted (four parameters for a two-compartment model and two parameters for a one-compartment model). The average coefficients of determination ($r^2$) obtained were 0.9852, 0.9801, and 0.9925 in the two-compartment model and 0.9331, 0.9772, and 0.9885 in the

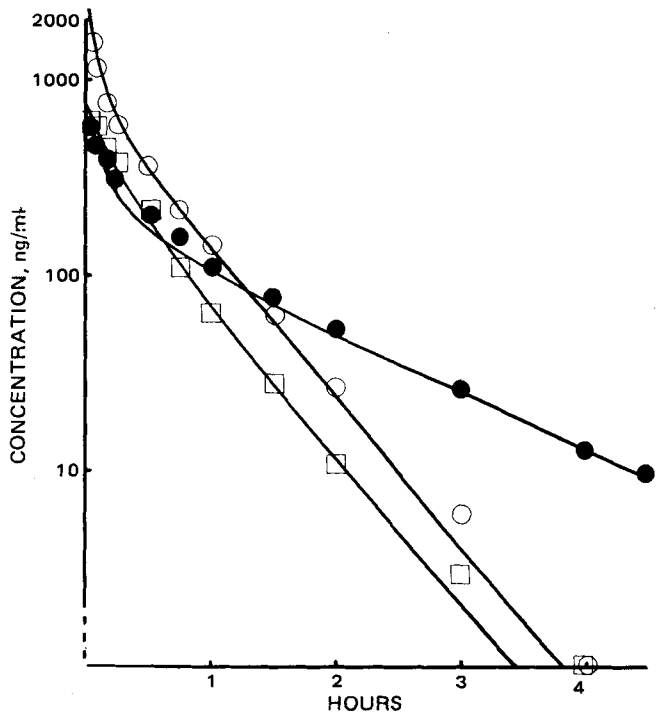


**Figure 1**—*Observed plasma concentrations of isosorbide dinitrate after a single 1.0-mg/kg iv dose to rhesus monkeys (●); cynomolgus monkeys (□); and baboons (○). Solid lines show computer-estimated concentrations.*

[1] Kindly provided by Pharma-Schwarz, Monheim, West Germany.
[2] Macarthys, Essex, England.
[3] ICL 2903 computer International Computers Ltd., Greenford, England.



*0022-3549/81/1100-1270$01.00/0*
*© 1981, American Pharmaceutical Association*

**Table I—Analytical Parameters for the Measurement of Isosorbide Dinitrate in the Plasma of Nonhuman Primates**

| Parameter | Concentration Range 0–10 ng/ml | 10–250 ng/ml | 100–1000 ng/ml |
|---|---|---|---|
| Regression line[a] (± *SD*) | $Y = (0.079 \pm 0.001)X$ | $Y = 0.003X - 0.028$ | $Y = 0.001X - 0.065$ |
| Accuracy[b] | ±100% at 1 ng/ml<br>±10% at 10 ng/ml | ±6% at 250 ng/ml | ±18% at 1000 ng/ml |
| Precision | ±8% at 10 ng/ml | ±5% at 250 ng/ml | ±2% at 1000 ng/ml |
| Limit of detection | 0.5 ng/ml | — | — |
| Recovery of internal standard (± *SD*) | 90 ± 4% at 5 ng/ml | 91 ± 3% at 125 ng/ml | 91 ± 3% at 500 ng/ml |
| Recovery of drug (± *SD*) | 90 ± 2% | 90 ± 4% | 83 ± 4% |

[a] $Y$ = peak height ratio; $X$ = drug concentration. [b] Defined as 95% confidence limits of the least-squares regression line.

one-compartment model for the rhesus monkey, cynomolgus monkey, and baboon, respectively. The residual mean squares obtained for the two-compartment model were 37, 87, and 73% of those obtained for a one-compartment model for the rhesus monkey, cynomolgus monkey, and baboon, respectively, indicating that the data were appreciably better fitted by a two-compartment model.

An analysis of variance was performed on each group of pharmacokinetic parameters. Group means were compared using the method of least significant differences in conjunction with the Newman–Keuls multiple comparison procedure (16). Significance testing was carried out at the 5 and 1% levels.

## RESULTS

**Plasma Concentrations**—After intravenous injection of isosorbide dinitrate (1 mg/kg), the mean plasma concentration at 2 min (the first time of blood sampling) was similar in the rhesus monkey (565 ng/ml ± 66 *SD*) and cynomolgus monkey (586 ng/ml ± 43 *SD*), whereas it was about threefold higher in the baboon (1572 ng/ml ± 253 *SD*) (Fig. 1). After a short distribution phase in the cynomolgus monkey and baboon, mean plasma concentrations declined with a half-life of ~25 min to the detection limit at ~4 hr after dosing. In the rhesus monkey, the initial and terminal phase ($t_{1/2\beta}$ ~60 min) were relatively longer than in the other two species.

**Pharmacokinetic Parameters**—The observed plasma concentrations of isosorbide dinitrate could be adequately described by a biexponential equation, $C_p = Ae^{-\alpha t} + Be^{-\beta t}$, where $C_p$ is the plasma drug concentration at time $t$; $A$ and $B$ are the zero-time intercepts of the initial and terminal phases of the concentration–time curve, respectively (Fig. 1); and $\alpha$ and $\beta$ are obtained from the slopes of these phases, respectively. Pharmacokinetic parameters were calculated using standard equations (18) for a two-compartment open model with elimination from the central compartment (Table II). Plasma concentrations predicted by this model were generally in good agreement with observed values (Fig. 1). However, since the distribution phase was short, pharmacokinetic parameters were also calculated using a one-compartment open model. There were no notable differences in parameters calculated with either of the two models, except perhaps in the elimination rate constant ($K_{el}$) (Table III). However, $K_{el}$ obtained for a one-compartment open model was almost identical to $\beta$ calculated for a two-compartment open model.

An analysis of variance of areas ($AUC$) under the plasma concentration–time curves showed that, in respect to this parameter, the cynomolgus monkey was significantly different from the other species and that the rhesus monkey was significantly different from the baboon (Table II).

**Table II—Mean Pharmacokinetic Parameters (± *SD*) for a Two-Compartment Open Model after a Single Dose of Isosorbide Dinitrate (1.0 mg/kg iv)**

| Parameter[a] | Rhesus Monkey[b] | Cynomolgus Monkey[b] | Baboon[b] |
|---|---|---|---|
| Body weight, kg | 4.8 ± 0.8 | 3.4 ± 0.4 | 5.8 ± 0.9 |
| $A$, ng/ml | 435 ± 113 | 384 ± 222 | 1139 ± 551 |
| $B$, ng/ml | 220 ± 74 | 427 ± 120 | 843 ± 183 |
| $\alpha$, $min^{-1}$ | 0.12 ± 0.13 | 0.17 ± 0.12 | 0.22 ± 0.08 |
| $\beta$, $min^{-1}$ | 0.01 ± 0 | 0.03 ± 0 | 0.03 ± 0.01 |
| $k_{12}$, $min^{-1}$ | 0.05 ± 0.07 | 0.04 ± 0.04 | 0.07 ± 0.03 |
| $k_{21}$, $min^{-1}$ | 0.05 ± 0.06 | 0.11 ± 0.08 | 0.12 ± 0.06 |
| $k_{el}$, $min^{-1}$ | 0.03 ± 0.01 | 0.05 ± 0.01 | 0.06 ± 0.01 |
| $Cl$, ml/min | 188 ± 29 | 200 ± 37 | 169 ± 30 |
| $t_{1/2\alpha}$, min | 10 ± 5 | 6 ± 3 | 3 ± 1 |
| $t_{1/2\beta}$, min | 62± 13[c] | 23 ± 2 | 24 ± 3 |
| $V_1$, liters | 7.1 ± 1.3 | 4.3 ± 0.8 | 3.0 ± 0.7 |
| $V_2$, liters | 6.0 ± 2.4 | 1.4 ± 0.7 | 1.9 ± 0.3 |
| $V_{D(ss)}$, liters | 13.2 ± 2.9[c] | 5.7 ± 0.8 | 4.9 ± 0.8 |
| $V_{D\beta}$, liters | 16.0 ± 2.5[c] | 6.7 ± 1.2 | 5.7 ± 1.0 |
| $AUC$, ng hr/ml | 409 ± 41[d] | 292 ± 47[e] | 575 ± 37 |
| $A/\alpha$, ng hr/ml | 61 ± 51 | 56 ± 40 | 101 ± 71 |
| $B/\beta$, ng hr/ml | 318 ± 39 | 237 ± 61 | 474 ± 74 |

[a] See text for details of abbreviations. [b] Data are the means of the results from individual animals. [c] Significance level (analysis of variance) for rhesus monkey compared to the other two species ($p < 0.01$). [d] Significance level (analysis of variance) for rhesus monkey compared to the baboon ($p < 0.05$). [e] Significance level (analysis of variance) for cynomolgus monkey compared to the other two species ($p < 0.01$).

## DISCUSSION

Relatively little data have been reported concerning the detailed pharmacokinetics of isosorbide dinitrate in animals. In dogs (9) and humans (13, 15), the plasma concentration–time course of isosorbide dinitrate appears to be adequately described by a one-compartment open model; in rats (5), a two-compartment open model appears to be more appropriate. Although a two-compartment open model seemed suitable in nonhuman primates (Table II), a one-compartment open model could be used without notable differences in calculated pharmacokinetic parameters (Table III). However, the distribution phase $A/\alpha$ contributed 14, 15, and 18% of the total area under the plasma concentration–time curve in the rhesus monkey, cynomolgus monkey, and baboon, respectively. This finding indicates that the distribution phase of isosorbide dinitrate, although short, should be considered in a pharmacokinetic analysis of the drug and that distribution of isosorbide dinitrate into a peripheral compartment is a feature of its pharmacokinetics in nonhuman primates.

The systemic clearance of isosorbide dinitrate can probably be regarded as reflecting hepatic clearance, although clearance in the intestinal mucosa also might take place after oral administration; in fact, only ~2% of an oral dose of isosorbide dinitrate appears to reach the peripheral circulation intact in the baboon[4]. Similar low absolute bioavailability of isosorbide dinitrate was reported to occur in humans (15).

In rhesus monkeys, the systemic clearance of isosorbide dinitrate was similar to the hepatic blood flow (50 ml/min/kg) reported for this species (19), as might be expected for a drug of high hepatic extraction ratio (5). By contrast, the systemic clearance of isosorbide dinitrate in humans appears to be ~10-fold lower than hepatic blood flow (15). Despite this species difference in clearance, the drug is subjected to an extensive first-pass effect in both these species, as in rats (5).

Volumes of distribution [$V_{D(ss)}$ and $V_{D(\beta)}$] and apparent half-lives of the terminal phase, $t_{1/2\beta}$, were significantly greater in the rhesus monkey than in the other species (Table II). However, clearance ($Cl$) and the apparent half-life of the initial phase, $t_{1/2\alpha}$, did not differ significantly among the species.

The mean volumes of distribution ($V_{Dss}$) represented 273, 168, and 84% of the body weight in the rhesus monkey, cynomolgus monkey, and baboon, respectively. These values presumably represent the relative extent of tissue uptake of isosorbide dinitrate in these species. In the baboon, the volume of distribution was not too dissimilar from the probable total body water volume.

Adopting the two-compartment model, the mean volume of the central compartment ($V_1$) was larger than that of the peripheral compartment ($V_2$) in all three species, the ratios being 1.2, 3.1, and 1.6 for the rhesus monkey, cynomolgus monkey, and baboon, respectively. These ratios indicate that distribution of isosorbide dinitrate into the peripheral compartment is of some importance in its disposition in the body. Indeed, simulation of the plasma concentration–time profile of isosorbide dinitrate in the central and peripheral compartments showed that equilibration between these two compartments was rapidly achieved. Peak mean isosorbide dinitrate concentrations in the peripheral compartment

[4] Huntingdon Research Centre, unpublished data.

**Table III—Mean Pharmacokinetic Parameters (± *SD*) for a One-Compartment Open Model Compared to a Two-Compartment Open Model following a Single Dose of Isosorbide Dinitrate (1 mg/kg)**

| Parameter[a] | One-Compartment Model[b] | | | Two-Compartment Model[b] | | |
|---|---|---|---|---|---|---|
| | Rhesus Monkey | Cynomolgus Monkey | Baboon | Rhesus Monkey | Cynomolgus Monkey | Baboon |
| *AUC*, ng hr/ml | 404[c] ± 51 | 281[d] ± 47 | 538 ± 21 | 409[c] ± 41 | 292[d] ± 47 | 575 ± 37 |
| *Cl*, ml/min | 189 ± 18 | 203 ± 22 | 173 ± 33 | 188 ± 29 | 200 ± 37 | 169 ± 30 |
| $t_{1/2}$, min[e] | 47[f] ± 4 | 29 ± 4 | 29 ± 2 | 62[f] ± 13 | 23 ± 2 | 24 ± 3 |
| $V_D$, liters[g] | 12.2[f] ± 2.0 | 8.5 ± 2.0 | 7.2 ± 1.5 | 13.2[f] ± 2.9 | 5.7 ± 0.8 | 4.9 ± 0.8 |
| $K_{el}$, min$^{-1}$ | 0.02 ± 0.01 | 0.02 ± 0.01 | 0.02 ± 0.01 | 0.03 ± 0.01 | 0.05 ± 0.01 | 0.06 ± 0.01 |

[a] For details of abbreviations, see text. [b] Data are the means of results from individual animals. [c] Significance level (analysis of variance) for rhesus monkey compared to the baboon ($p < 0.05$). [d] Significance level (analysis of variance) for cynomolgus monkey compared to the other two species ($p < 0.01$). [e] $t_{1/2} = t_{1/2\beta}$ for the two-compartment open model. [f] Significance level (analysis of variance) for rhesus monkey compared to the other two species ($p < 0.01$). [g] $V_D$ = total volume of distribution = $V_{D(ss)}$ for the two-compartment open model.

were 258, 394, and 727 ng/ml in the rhesus monkey, cynomolgus monkey, and baboon, respectively. Thereafter, concentrations in both compartments were similar.

Adopting a two-compartment open model, the mean ratios of $\beta/K_{el}$ of 0.43, 0.63, and 0.51 in the rhesus monkey, cynomolgus monkey, and baboon, respectively, indicated that these fractions of isosorbide dinitrate in the body were in the central compartment and were available for elimination at any time after completion of the drug distribution phase.

The plasma half-lives of isosorbide dinitrate in nonhuman primates (rhesus monkey, 62 min; cynomolgus monkey, 23 min; and baboon, 24 min) (Table II) were longer than those observed in humans [~9 min, (15)], dogs [~7 min, (9)], and rats [~1 min, (5)]. The latter value for rats was disputed by Reed *et al.* (20) who claimed that it only represented a tissue distribution phase. The activity of the enzyme system (glutathione *S*-transferases) responsible for the denitration of isosorbide dinitrate was shown to be sex dependent in rodents, but this has not been observed in humans and would not be expected in nonhuman primates (21). In none of these species, however, would isosorbide dinitrate be expected to accumulate under the once daily dosage regimen used in chronic toxicity studies. Comparison of the relatively straightforward biotransformation of isosorbide dinitrate in different species would probably not provide the best criteria for the selection of a suitable species for chronic toxicity studies; instead, a comparison of the drug's pharmacokinetics would be more appropriate. Therefore, using pharmacokinetic criteria, the fate of isosorbide dinitrate in humans (15) appears to be more closely reflected by baboons (Tables II and III) than by either of the other two nonhuman primate species studied.

## REFERENCES


(1) "Organic Nitrates," P. Needleman, Ed., Springer-Verlag, Berlin, West Germany, 1975.

(2) "Nitrate," W. Rudolph and W. Siegenthaler, Eds., Urban and Schwarzenberg, Munich, West Germany, 1976.

(3) "Nitrate II," W. Rudolph and A. Schrey, Eds., Urban and Schwarzenberg, Munich, West Germany, 1980.

(4) E. M. Johnson, A. B. Harkey, D. J. Blehm, and P. Needleman, *J. Pharmacol. Exp. Ther.*, **182,** 56 (1972).

(5) P. Needleman, S. Lang, and E. M. Johnson, *ibid.*, **181,** 489 (1972).

(6) J. H. Keen, W. H. Habig, and W. B. Jakoby, *J. Biol. Chem.*, **251,** 6183 (1976).

(7) A. J. Dietz, *Biochem. Pharmacol.*, **16,** 2447 (1967).

(8) D. E. Reed, J. F. May, L. G. Hart, and D. H. McCurdy, *Arch. Int. Pharmacodyn. Ther.*, **191,** 318 (1971).

(9) S. F. Sisenwine and H. W. Ruelius, *J. Pharmacol. Exp. Ther.*, **176,** 296 (1971).

(10) M. T. Rosseel and M. G. Bogaert, *Biochem. Pharmacol.*, **22,** 67 (1973).

(11) W. H. Down, L. F. Chasseaud, and R. K. Grundy, *J. Pharm. Sci.*, **63,** 1147 (1974).

(12) W. H. Down and L. F. Chasseaud, in "Nitrate II," W. Rudolph and A. Schrey, Eds., Urban and Schwarzenberg, Munich, West Germany, 1980, p. 29.

(13) D. F. Assinder, L. F. Chasseaud, and T. Taylor, *J. Pharm. Sci.*, **66,** 775 (1977).

(14) L. F. Chasseaud and T. Taylor, in "Nitrate II," W. Rudolph and A. Schrey, Eds., Urban and Schwarzenberg, Munich, West Germany, 1980, p. 22.

(15) T. Taylor, L. F. Chasseaud, and E. Doyle, *Biopharm. Drug. Dispos.*, **1,** 149 (1980).

(16) E. Doyle and L. F. Chasseaud, *Toxicology*, **19,** 159 (1981).

(17) E. Doyle, L. F. Chasseaud, and T. Taylor, *Biopharm. Drug Dispos.*, **1,** 141 (1980).

(18) M. Gibaldi and D. Perrier, in "Pharmacokinetics," vol. 1, J. Swarbrick, Ed., Dekker, New York, N.Y., 1975, p. 45.

(19) R. A. Branch, D. G. Shand, and A. S. Nies, *J. Pharmacol. Exp. Ther.*, **187,** 581 1973.

(20) D. E. Reed, J. M. Akester, J. F. Prather, J. R. Tuckosh, D. H. McCurdy, and C. Yeh, *ibid.*, **202,** 32 (1977).

(21) L. F. Chasseaud, *Adv. Cancer Res.*, **29,** 175 (1979).


## ACKNOWLEDGMENTS


The authors are grateful to their colleagues in the Department of Primate Toxicology for their care of the animals and to Dr. D. O. Chanter of the Department of Statistics for advice and computer facilities. They thank Dr. R. Bonn of Sanol-Schwarz Monheim, West Germany, for providing isosorbide dinitrate and Dr. J. N. Miller of Loughborough University for helpful discussions.

# Rapid and Specific High-Pressure Liquid Chromatographic Assay for Folic Acid in Multivitamin–Mineral Pharmaceutical Preparations

**W. H. TAFOLLA ˣ, A. C. SARAPU, and G. R. DUKES**

Received June 9, 1980, from the *Control Research and Development Laboratories, The Upjohn Company, Kalamazoo, MI 49001.* Accepted for publication April 1, 1981.

**Abstract** □ A high-pressure liquid chromatographic assay for folic acid in multivitamin–mineral pharmaceutical formulations was developed. The internal standard solution used for sample extraction contained a chelating agent, pentetic acid, for prevention of metal ion-catalyzed degradation of folic acid in the prepared samples. Samples were chromatographed using a paired-ion mobile phase (water–methanol, ~76:24; 0.015 *M* phosphate buffer, pH 7.0; and 0.3% tetrabutylammonium hydroxide) on a column packed with octadecylsilane bonded to microparticulate silica gel. Sample preparation was rapid, and total chromatographic time was ~20 min. The method was accurate, precise, and highly specific. Folic acid and the internal standard, methylparaben, were separated from other tablet components and a number of potential impurities and degradation products of folic acid.

**Keyphrases** □ Folic acid—high-pressure liquid chromatography, multivitamin–mineral pharmaceutical preparations □ High-pressure liquid chromatography—folic acid, multivitamin–mineral pharmaceutical preparations □ Multivitamin–mineral formulations—high-pressure liquid chromatography, folic acid

Previous work described the use of various organic ammonium salts as ion-pairing reagents for the separation of ascorbic acid and folic acid on columns packed with octadecylsilane bonded to 5–10-μm silica gel (1–4). A high-pressure liquid chromatographic (HPLC) method for the quantitation of folic acid bulk drug is now available for common use (5, 6). However, the successful separation and quantitation of folic acid in mineral-containing multivitamin pharmaceutical formulations have not been reported.

This report describes a stability-indicating and highly specific HPLC assay for folic acid, which was applied to mineral-containing multivitamin formulations and their mineral-free counterparts.

## EXPERIMENTAL

**Reagents and Materials**—Dihydrofolic acid[1], *dl*-L-tetrahydrofolic acid[1], *dl*-*N*-5-methyltetrahydrofolic acid[1] (sodium salt), *p*-aminobenzoic acid[1], pterine[1], pterin-6-carboxylic acid[1], *N*-(*p*-aminobenzoyl)-L-glutamic acid[1], and pteroic acid[2] were used as received. Reagents used were analytical reagent grade or better. The pharmaceutical preparations analyzed are commercially available, and their compositions are described in Table I.

**Instrumentation**—The liquid chromatograph consisted of a high-pressure pump[3], a valve injector[4] equipped with a 10-μl loop, heating tape[5] and associated temperature control unit[6], and a 280-nm fixed-wavelength UV detector[7] operated at a sensitivity of 0.01 aufs. Separations were performed on a 30-cm × 4-mm i.d. column containing 10-μm silica gel with bonded octadecylsilane[8]. Chromatograms were produced on a strip-chart recorder[9]. Peak responses were measured using an electronic integrator[10].

**Table I—Compositions of Representative Pharmaceutical Preparations**

| Coated Compressed Tablet with Minerals[a] | Compressed Tablet[b] and Soft Elastic Capsule[c] |
|---|---|
| Vitamin A, IU 5000 | 5000 |
| Vitamin D, IU 400 | 400 |
| Vitamin E, IU 15 | 15 |
| Vitamin C, mg 300 | 60 |
| Folic acid, mg 0.4 | 0.4 |
| Thiamine, mg 10 | 1.5 |
| Riboflavin, mg 10 | 1.7 |
| Niacin, mg 100 | 20 |
| Vitamin $B_6$, mg 6 | 2 |
| Vitamin $B_{12}$, μg 18 | 6 |
| Pantothenic acid, mg 10 | |
| Iodine, μg 150 | |
| Iron, mg 18 | |
| Copper, mg 2 | |
| Zinc, mg 15 | |
| Manganese, mg 1 | |
| Potassium, mg 5 | |

[a] Unicap T tablets, The Upjohn Co., Kalamazoo, Mich. [b] Unicap Chewable tablets, The Upjohn Co., Kalamazoo, Mich. [c] Unicap capsules, The Upjohn Co., Kalamazoo, Mich.

**Mobile Phase**—The mobile phase was prepared by adding 650 ml of water, 7.5 ml of a 40% aqueous solution of tetrabutylammonium hydroxide[11], 2.04 g of monobasic potassium phosphate, 7.0 ml of 3.0 *N* phosphoric acid, and 240 ml of methanol to a 1-liter volumetric flask. This mixture was diluted to volume with water, adjusted to pH 7.0 with phosphoric acid or ammonium hydroxide, membrane filtered[12], and degassed prior to use. (Column variations may require alterations in the methanol and phosphate concentrations.) A flow rate of 1.5 ml/min and a pressure of ~1300 psig were used. Column temperature was maintained at 35°.

**Internal Standard Solution**—The internal standard solution was prepared by mixing together 40 mg of methylparaben, 240 ml of methanol, 650 ml of water, 12 ml of a 40% aqueous solution of tetrabutylammonium hydroxide, 2.04 g of monobasic potassium phosphate, and 30 ml of a solution containing 100 mg/ml of pentetic acid (I) in 0.75 *N* ammonium hydroxide. This preparation was diluted to 1000 ml with water.

**Standard Preparation**—Approximately 32 mg of folic acid USP reference standard was accurately weighed into a 100-ml volumetric flask, diluted to volume with the internal standard solution, and mixed well until all of the folic acid reference standard was dissolved. Then 4.00 ml of this solution was pipetted into a second 100-ml volumetric flask, diluted to volume with the internal standard solution, and mixed well. This solution was subsequently protected from prolonged exposure to light.

**Sample Preparation**—*Folic Acid Bulk Drug*—Samples of folic acid bulk drug were prepared as described for the standard preparation.

*Tablets*—Ten tablets were accurately weighed and then finely powdered. A quantity of the powder equivalent to 0.3 mg of anhydrous folic acid was accurately weighed and transferred to a 35-ml centrifuge tube. The internal standard solution (25 ml) was pipetted into the centrifuge tube, and the headspace was immediately flushed with nitrogen and then stoppered tightly. This preparation was shaken vigorously for ~5 min,

[1] Sigma Chemical Co., St. Louis, Mo.
[2] Gillies International Inc., La Jolla, Calif.
[3] Mini-Pump model, Milton Roy Co., Riviera Beach, Fla.
[4] Model 70-10, Rheodyne Inc., Berkeley, Calif.
[5] Catalog No. BS-6 1/2, Briscoe Mfg. Co., Columbus, Ohio.
[6] Model ITC-J10, Valco Instruments Co., Houston, Tex.
[7] Model 1203, Milton Roy Co., Riviera Beach, Fla.
[8] μBondapak $C_{18}$, Waters Associates, Milford, Mass.
[9] Honeywell, Philadelphia, Pa.
[10] Model 23000-011, Spectra-Physics, Santa Clara, Calif.
[11] Catalog No. 17,878-0, Aldrich Chemical Co., Milwaukee, Wis.
[12] Type BD (0.6-μm), Millipore Corp., Bedford, Mass.

0022-3549/81/1100-1273$01.00/0
© 1981, American Pharmaceutical Association

**Table II—Folic Acid Bulk Drug Assay Results**

| Lot | This Work, % | USP HPLC Assay, % |
|---|---|---|
| A | 88.8 | 89.4 |
| B | 91.9 | 91.6 |
| C | 90.9 | 90.4 |
| D | 91.5 | 91.3 |
| E | 92.3 | 90.3 |
| F | 91.0 | 93.8 |
| Mean | 91.1 | 91.1 |

after which the resulting solution was membrane filtered[13]. The headspace of the sample container was again flushed with nitrogen and capped tightly until injected.

*Soft Elastic Capsules*—Ten capsules were accurately weighed and then cut in half. The capsule filling was transferred to a glass container, and the empty capsule shells were washed with two 25-ml portions of chloroform, which were discarded. The washed capsule shells were dried and weighed to determine the average capsule fill weight. A quantity of the capsule filling equivalent to 0.3 mg of anhydrous folic acid was accurately weighed and transferred to a 35-ml centrifuge tube, and ~30 ml of hexane then was added. The contents were shaken vigorously for ~5 min and then centrifuged at ~1070×*g* for 15 min.

The hexane was carefully aspirated, and the residue was dried at 60°. The internal standard solution (25 ml) was pipetted into the centrifuge tube containing the dried residue, and the headspace was immediately flushed with nitrogen and then stoppered tightly. This preparation was shaken vigorously for ~5 min, after which the resulting solution was membrane filtered. The headspace of the sample container was again flushed with nitrogen and capped tightly until injected.

**Calculations**—The folic acid content was calculated by the following equations.

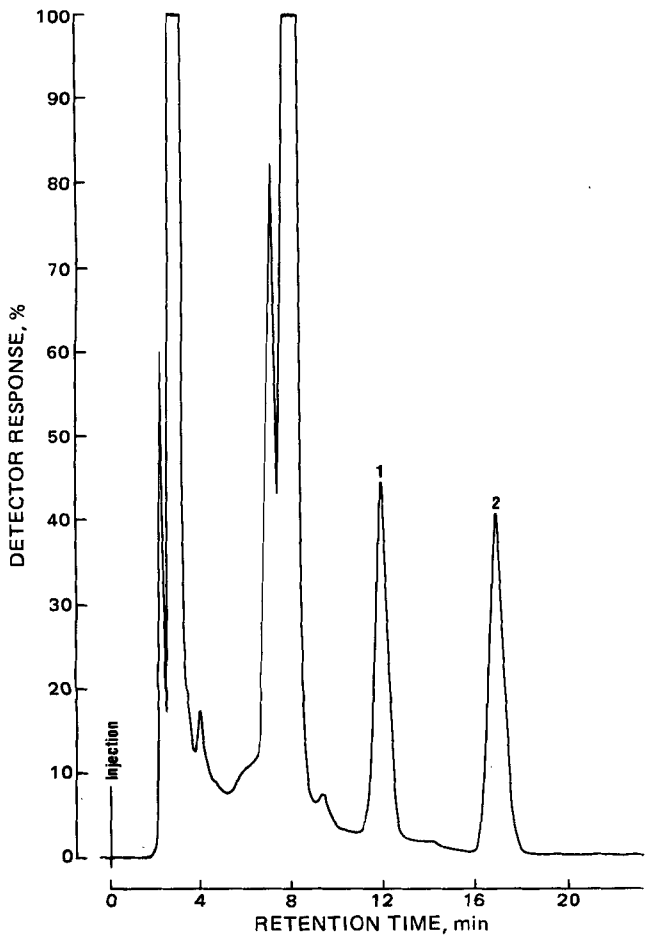


**Figure 1**—*Chromatogram of multivitamin–mineral pharmaceutical tablet preparation.*

[13] Type HA (0.45 mm), Millipore Corp., Bedford, Mass.

**Table III—Stability of Sample Preparation Solutions**

| Sample | Atmosphere | Folic Acid Remaining after 24 hrs in solution, % |
|---|---|---|
| Folic acid plus other vitamins and minerals[a] extracted in dilute sodium hydroxide without I and injected immediately | Air | 5–10[b] |
| Folic acid only in internal standard solution | Air | 100.8 |
| Folic acid plus minerals (copper, iron, potassium, manganese, and zinc) in internal standard solution | Air | 99.2 |
| Folic acid plus other vitamins and minerals[a] in internal standard solution | Air | 82.9 |
| | Oxygen enriched | 51.9 |
| | Nitrogen | 99.0 |

[a] See Table I. [b] Range of several trials. Results based on peak height approximations.

For bulk drug:

$$\frac{R_{sam}}{R_{std}} \times \frac{W_{std}}{W_{sam}} \times 100 = \% \text{ purity} \qquad \text{(Eq. 1)}$$

For tablets:

$$\frac{R_{sam}}{R_{std}} \times \frac{C_{std}}{W_{sam}} \times W_{tab} \times 25 = \text{mg/tablet} \qquad \text{(Eq. 2)}$$

For soft elastic capsules:

$$\frac{R_{sam}}{R_{std}} \times \frac{C_{std}}{W_{sam}} \times W_{sec} \times 25 = \text{mg/capsule} \qquad \text{(Eq. 3)}$$

where:

$R_{sam}$ = folic acid peak response divided by internal standard peak response of the sample preparation
$R_{std}$ = folic acid peak response divided by internal standard peak response of the reference standard preparation
$W_{std}$ = weight of folic acid (corrected for moisture) in milligrams in the reference standard preparation
$W_{sam}$ = weight of sample in milligrams
$C_{std}$ = folic acid concentration of the reference standard preparation in milligrams per milliliter (corrected for moisture)
$W_{tab}$ = average tablet weight in milligrams per tablet
$W_{sec}$ = average soft elastic capsule (sec) weight in milligram per capsule
25 = dilution volume in milliliters

## RESULTS AND DISCUSSION

**Selection of Ion-Pairing Reagent and Chromatographic Conditions**—Due to the known suitability of organic ammonium salts as ion-pairing reagents for acidic compounds, efforts were directed to the development of such a system for folic acid in multivitamin–mineral pharmaceutical formulations. Since the method was intended for routine use in a high-volume analytical laboratory, a readily available ion-pairing reagent was desirable. Possible choices included the series of organic ammonium hydroxide compounds, including tetramethylammonium hydroxide through tetrabutylammonium hydroxide.

**Table IV—Recovery of Folic Acid Added to Placebo Preparations**

| | Coated Compressed Tablet with Minerals | Compressed Tablet | Soft Elastic Capsule |
|---|---|---|---|
| Average recovery, % | 99.1 | 100.3 | 99.3 |
| Number of determinations | 8 | 5 | 7 |
| Range studied, mg/dosage unit | 0.3026–0.6972 | 0.3112–0.7130 | 0.2980–0.7178 |
| RSD, % | 1.5 | 0.9 | 1.7 |
| Correlation coefficient | 0.998 | 1.000 | 1.000 |

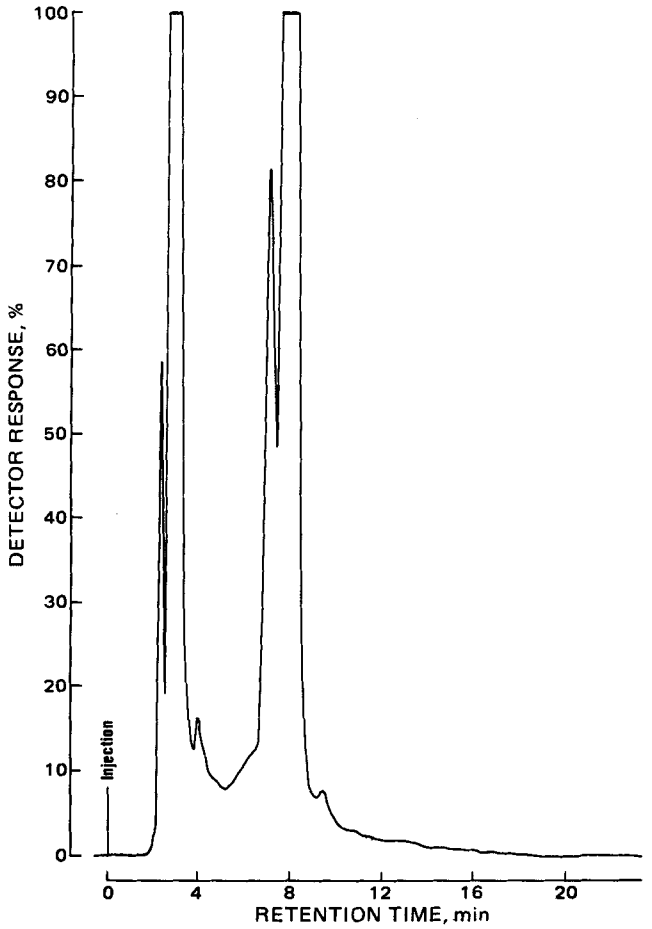


**Figure 2**—*Chromatogram of a placebo preparation containing all vitamins and minerals except folic acid.*

Tetramethylammonium hydroxide and tetraethylammonium hydroxide failed to separate folic acid from other vitamins and tablet excipients. Tetrapropylammonium hydroxide did produce adequate separation but resulted in unacceptably long chromatographic times due to retention of excipients.

The use of tetrabutylammonium hydroxide as a pairing ion provided a desirable separation and acceptable chromatographic times. Tablet excipients and other vitamins eluted rapidly, with folic acid being retained. The addition of a small quantity of monobasic potassium phosphate increased the separation of folic acid from the other vitamins and tablet excipients and provided improved efficiency. Optimum separations were usually achieved with a monobasic potassium phosphate concentration of ~0.015 *M*. The pH of the mobile phase also influenced the chromatography. Low pH values produced longer retention times for folic acid than the recommended pH 7.0, but broader peaks resulted.

Some variation of the potassium phosphate monobasic content or mobile phase pH may be required due to the chromatographic column being used. However, the chromatographic conditions described provided the best peak shapes for folic acid and the internal standard while adequate separation from other tablet constituents was maintained. The slightly elevated column temperature of 35° was employed to avoid varying the mobile phase composition to compensate for fluctuations in ambient temperature. Under these conditions, column life was comparable to that of other reversed-phase HPLC methods used for the analysis of pharmaceuticals.

**Bulk Drug Assays**—The method was tested for its comparability to the USP HPLC assay for folic acid bulk drug (4). The data presented in Table II indicate that the method yielded results for bulk drug lots that were equivalent to the official USP assay.

**Extraction of Folic Acid**—The extraction conditions used are extremely important for the successful quantitation of folic acid in mineral-containing multivitamin formulations. Under acidic conditions, folic acid has limited solubility and tends to be unstable (7). Other vitamins such as cyanocobalamin, pantothenate, riboflavin, thiamine, and ascorbic acid are unstable at high pH values (8). Furthermore, metal ion-catalyzed (particularly $Cu^{2+}$ and $Fe^{2+}$) oxidative degradation of ascorbic acid is known to occur in the presence of oxygen (9, 10). The oxidative degradation products of ascorbic acid (dehydroascorbic acid, diketogulonic acid, and oxalic acid) are powerful reducing agents. The use of ascorbic acid as a folic acid reductant is known (11).

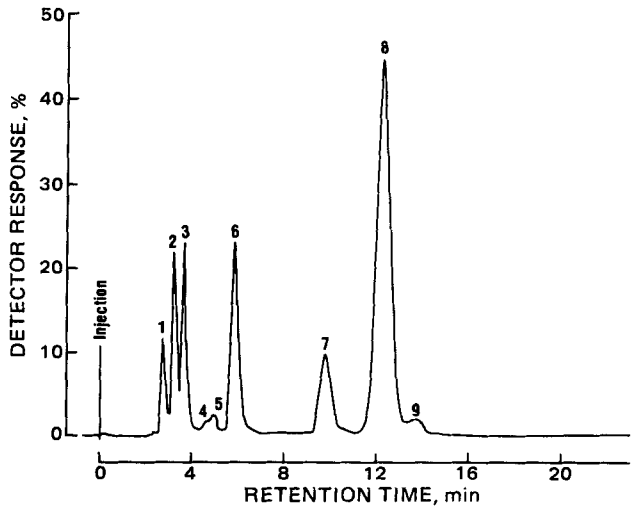


**Figure 3**—*Chromatogram of a mixture of folic acid and some known degradation products. Key: 1, pterine; 2,* p*-aminobenzoic acid; 3, pterin-6-carboxylic acid; 4 and 5, unknown; 6, pteroic acid and* N-(p*-amino-benzoyl)-*L*-glutamic acid; 7, dihydrofolic acid and tetrahydrofolic acid; 8, folic acid; and 9,* dl-N*-5-methyltetrahydrofolic acid.*

As shown in Table III, folic acid alone or in the presence of minerals did not degrade. However, when other vitamins were present and ascorbic acid was subject to metal ion-catalyzed oxidative degradation, folic acid degradation was observed. Attempts to extract folic acid from mineral-containing multivitamin formulations under high pH conditions using dilute sodium hydroxide or ammonium hydroxide resulted in only ~5–10% recovery of intact folic acid. The reversible enzymatic reduction of folic acid to dihydrofolic acid and tetrahydrofolic acid occurs in biological systems (12). However, it is believed that severely basic extraction conditions result in irreversible degradation of folic acid since these reduced folate species were not observed in chromatography of the above samples.

The internal standard solution used for extracting folic acid was designed to prevent degradation by the described pathways while still providing an efficient extraction. The internal standard solution had a pH of ~9.0–9.5, at which folic acid was readily solubilized. As folic acid and other vitamins and tablet components dissolved, the pH dropped to ~7.0–8.5, depending on the formulation. The lowered pH favors stability of other water-soluble vitamins and thus tends to limit interactions detrimental to folic acid. Metal ion-catalyzed degradation of the water-soluble vitamins was minimized by use of the chelating agent, I. Air oxidation was reduced by flushing the headspace of the extraction container with nitrogen. These extraction conditions produced excellent stability of sample solutions (Table III).

**Recovery of Folic Acid from Spiked Placebos**—The sample preparation procedure was rapid and simple. As shown in Table IV, average recoveries of 99.1–100.3% were obtained for placebo mixtures containing all of the other tablet vitamins, minerals, and excipients spiked with folic acid over a range of 0.2980–0.7178 mg/dosage unit. The relative standard deviations of the recoveries for these studies varied from 0.9 to 1.7%. Linear regression analysis of folic acid added *versus* peak area yielded correlation coefficients of 0.998–1.000.

**Specificity**—As shown in Figs. 1 and 2, folic acid and the internal standard, methylparaben, were well separated from the other ingredients contained in multivitamin–mineral formulations. The stability-indicating properties of the method were investigated by chromatographing authentic samples of known folic acid impurities and degradation products. As can be seen in Fig. 3, none of the compounds tested interfered with folic acid or the internal standard.

## REFERENCES

(1) S. P. Sood, L. E. Sartori, D. P. Wittmer, and W. G. Haney, *Anal. Chem.*, **48**, 796 (1976).

(2) R. B. H. Wills, C. G. Shaw, and W. R. Day, *J. Chromatogr. Sci.*, **15**, 262 (1977).

(3) V. D. Reif, J. T. Reamer, and L. T. Grady, *J. Pharm. Sci.*, **66**, 1112 (1977).
(4) "The United States Pharmacopeia," 19th rev., 5th suppl., Mack Publishing Co., Easton, Pa., Feb. 15, 1979, p. 94.
(5) S. K. Chapman, B. C. Greene, and R. R. Streiff, *J. Chromatogr.*, **145**, 302 (1978).
(6) A. R. Branfman and M. McComish, *ibid.*, **151**, 87 (1978).
(7) R. W. Stout, A. R. Cashmore, J. K. Coward, C. G. Horvath, and J. R. Bertino, *Anal. Biochem.*, **71**, 119 (1976).
(8) W. R. Driscoll, "Physical/Chemical Stabilization of Vitamins," Hoffmann-La Roche, Nutley, N.J., 1979, pp. 4–27.
(9) A. Sattar, J. M. deMan, and J. C. Alexander, *Can. Inst. Food Sci. Technol. J.*, **10**, 65 (1977).
(10) K. A. Conners, G. L. Amidon, and L. Kennon, "Chemical Stability of Pharmaceuticals," Wiley, New York, N.Y., 1979, pp. 138–150.
(11) C. K. Clifford and A. J. Clifford, *J. Assoc. Off. Anal. Chem.*, **60**, 1248 (1977).
(12) H. R. Mahler and E. H. Cordes, "Biological Chemistry," 2nd ed., Harper and Row, New York, N.Y., 1971, p. 406.

**ACKNOWLEDGMENTS**

Presented at the APhA Academy of Pharmaceutical Sciences, Kansas City Meeting, November 1979.

# Determination of Plasma Fentanyl by GC–Mass Spectrometry and Pharmacokinetic Analysis

**SHEN-NAN LIN *x, TSENG-PU F. WANG *, RICHARD M. CAPRIOLI*, and BENJAMIN P. N. MO ‡**

Received March 31, 1980, from the **Analytical Chemistry Center and the* ‡*Department of Anesthesiology, University of Texas Medical School, Houston, TX 77025.* Accepted for publication April 9, 1981.

**Abstract** □ GC–mass spectrometry was used to measure extremely low levels of fentanyl in dog plasma. Deuterated fentanyl was synthesized for use as an internal standard. Fentanyl was hydrolyzed to despropionyl fentanyl by 20% DCl in deuterium oxide. Mass spectrometric analysis of the product revealed that the molecular ion was three mass units higher than that of the authentic despropionyl fentanyl, indicating that the deuterium exchange reactions occurred at this stage. Deuterated despropionyl fentanyl was reesterified by propionyl chloride to fentanyl-$d_3$. The drug was assayed in biological fluids by extraction into ethyl acetate followed by analysis with GC–chemical-ionization mass spectrometry. The lowest measurable plasma fentanyl level is 500 pg/ml. The method is highly selective and is suitable for monitoring the time course of plasma drug levels. Evaluation of pharmacokinetic data from experiments using nine dogs revealed a triphasic phenomenon. No measurable amounts of the major metabolites, despropionyl fentanyl and norfentanyl, were detected.

**Keyphrases** □ Fentanyl—determination by GC–mass spectrometry and pharmacokinetic analysis in dog plasma □ GC–mass spectrometry—determination of plasma fentanyl, pharmacokinetic analysis □ Anesthetics—determination of plasma fentanyl by GC–mass spectrometry

Fentanyl[1], *N*-(1-phenethyl-4-piperidyl)propionanilide, is a potent narcotic analgesic widely used in clinical anesthesia. It has a rapid onset of effect and a short duration of action when compared with morphine and most other drugs of this group (1). Direct correlation between pharmacokinetic data and drug effect is difficult due to the lack of an analytical method suitable for measuring extremely small quantities of the drug in plasma (2–4). Only recently was fentanyl measurement in a subnanogram quantity made possible by radioimmunoassay (5). However, preparation of antiserum samples of fentanyl involves lengthy biological procedures. In addition, the possibility of cross interaction due to various biological components presents difficulties in using the radioimmunoassay method for specific analyses.

This report describes a sensitive and specific GC–mass spectrometric method using stable isotopically-labeled fentanyl-$d_3$ as an internal standard. The method is capable of quantitatively detecting subnanogram levels of fentanyl in plasma. After intravenous administration of 25, 50, or 100 μg of fentanyl/kg to dogs, the plasma level fell rapidly to 2.5 ng/ml within 30 min and then remained at 0.5–2 ng/ml for up to 3 hr.

[1] Sublimaze, McNeil Laboratories.

## EXPERIMENTAL

**Preparation of Fentanyl-$d_3$**—After 1.2 ml of 20% DCl in deuterium oxide[2] (99 atom % deuterium) was added to 25 μg of fentanyl[3], the solution was incubated overnight at 100°. The acidity of the reaction mixture was partially neutralized by 0.2 ml of 40% NaOD in deuterium oxide[2] (99 atom % deuterium), and the unreacted fentanyl was removed by extraction twice with 2 ml of ethyl acetate. The remaining aliquot of sample was again acidified by 1.2 ml of 20% DCl solution before evaporation to dryness *in vacuo*. To the residue, 20 μl of pyridine and 1 ml of propionyl chloride[2] were added, and the mixture was incubated at 60° for 1 hr. The final product, fentanyl-$d_3$, was then purified by extraction twice with 3 ml of ethyl acetate. After evaporation to dryness by a nitrogen stream, the residue was dissolved in 0.5 ml of ethyl acetate and stored in a refrigerator at 4°.

**Instrumentation**—Combined GC–chemical-ionization mass spectrometry[4] was employed with methane as the reagent gas and an electron energy of 150 ev. GC separation was carried out isothermally at 235° with a 0.91-m × 2-mm i.d. U-shaped glass column packed with 3% SE-30 on 80–100-mesh Gas Chrom Q[5]. The temperature of the GC injector and the separator was 250°.

**Biological Samples**—Two hours before fentanyl administration, the nonselective mongrel dogs, 12–14 kg, were anesthetized with 300 mg of pentobarbital sodium. Fentanyl (25, 50, or 100 μg/kg) was introduced intravenously by 1-min infusion, and blood samples were collected into heparinized vials at 1, 2, 4, 6, 8, 10, 15, 30, 45, 62, 90, 120, 150, and 180 min after infusion was completed. Plasma was separated from red blood cells by centrifugation at 2500 rpm in the cold and stored in a freezer at −40° when necessary.

**Extraction and Quantitation**—To 2 ml of plasma, a known amount of fentanyl-$d_3$ (25 ng in 25 μl of ethyl acetate) was added as an internal standard. After rigorous mixing with the aid of an agitator[6], the plasma

[2] Aldrich Chemical Co., Milwaukee, Wis.
[3] McNeil Laboratories, Fort Washington, Pa.
[4] Finnigan 3300 gas chromatograph-mass spectrometer equipped with a 6000 data acquisition.
[5] Applied Science Laboratories, State College, Pa.
[6] Vanlab, Scientific Industries, Bohemia, N.Y.



*0022-3549/81/1100-1276$01.00/0*
*© 1981, American Pharmaceutical Association*

(3) V. D. Reif, J. T. Reamer, and L. T. Grady, *J. Pharm. Sci.*, **66**, 1112 (1977).
(4) "The United States Pharmacopeia," 19th rev., 5th suppl., Mack Publishing Co., Easton, Pa., Feb. 15, 1979, p. 94.
(5) S. K. Chapman, B. C. Greene, and R. R. Streiff, *J. Chromatogr.*, **145**, 302 (1978).
(6) A. R. Branfman and M. McComish, *ibid.*, **151**, 87 (1978).
(7) R. W. Stout, A. R. Cashmore, J. K. Coward, C. G. Horvath, and J. R. Bertino, *Anal. Biochem.*, **71**, 119 (1976).
(8) W. R. Driscoll, "Physical/Chemical Stabilization of Vitamins," Hoffmann-La Roche, Nutley, N.J., 1979, pp. 4–27.
(9) A. Sattar, J. M. deMan, and J. C. Alexander, *Can. Inst. Food Sci. Technol. J.*, **10**, 65 (1977).
(10) K. A. Conners, G. L. Amidon, and L. Kennon, "Chemical Stability of Pharmaceuticals," Wiley, New York, N.Y., 1979, pp. 138–150.
(11) C. K. Clifford and A. J. Clifford, *J. Assoc. Off. Anal. Chem.*, **60**, 1248 (1977).
(12) H. R. Mahler and E. H. Cordes, "Biological Chemistry," 2nd ed., Harper and Row, New York, N.Y., 1971, p. 406.

**ACKNOWLEDGMENTS**

Presented at the APhA Academy of Pharmaceutical Sciences, Kansas City Meeting, November 1979.

# Determination of Plasma Fentanyl by GC–Mass Spectrometry and Pharmacokinetic Analysis

**SHEN-NAN LIN *x, TSENG-PU F. WANG *, RICHARD M. CAPRIOLI*, and BENJAMIN P. N. MO ‡**

Received March 31, 1980, from the **Analytical Chemistry Center and the* ‡*Department of Anesthesiology, University of Texas Medical School, Houston, TX 77025.* Accepted for publication April 9, 1981.

**Abstract** □ GC–mass spectrometry was used to measure extremely low levels of fentanyl in dog plasma. Deuterated fentanyl was synthesized for use as an internal standard. Fentanyl was hydrolyzed to despropionyl fentanyl by 20% DCl in deuterium oxide. Mass spectrometric analysis of the product revealed that the molecular ion was three mass units higher than that of the authentic despropionyl fentanyl, indicating that the deuterium exchange reactions occurred at this stage. Deuterated despropionyl fentanyl was reesterified by propionyl chloride to fentanyl-$d_3$. The drug was assayed in biological fluids by extraction into ethyl acetate followed by analysis with GC–chemical-ionization mass spectrometry. The lowest measurable plasma fentanyl level is 500 pg/ml. The method is highly selective and is suitable for monitoring the time course of plasma drug levels. Evaluation of pharmacokinetic data from experiments using nine dogs revealed a triphasic phenomenon. No measurable amounts of the major metabolites, despropionyl fentanyl and norfentanyl, were detected.

**Keyphrases** □ Fentanyl—determination by GC–mass spectrometry and pharmacokinetic analysis in dog plasma □ GC–mass spectrometry—determination of plasma fentanyl, pharmacokinetic analysis □ Anesthetics—determination of plasma fentanyl by GC–mass spectrometry

Fentanyl[1], *N*-(1-phenethyl-4-piperidyl)propionanilide, is a potent narcotic analgesic widely used in clinical anesthesia. It has a rapid onset of effect and a short duration of action when compared with morphine and most other drugs of this group (1). Direct correlation between pharmacokinetic data and drug effect is difficult due to the lack of an analytical method suitable for measuring extremely small quantities of the drug in plasma (2–4). Only recently was fentanyl measurement in a subnanogram quantity made possible by radioimmunoassay (5). However, preparation of antiserum samples of fentanyl involves lengthy biological procedures. In addition, the possibility of cross interaction due to various biological components presents difficulties in using the radioimmunoassay method for specific analyses.

This report describes a sensitive and specific GC–mass spectrometric method using stable isotopically-labeled fentanyl-$d_3$ as an internal standard. The method is capable of quantitatively detecting subnanogram levels of fentanyl in plasma. After intravenous administration of 25, 50, or 100 μg of fentanyl/kg to dogs, the plasma level fell rapidly to 2.5 ng/ml within 30 min and then remained at 0.5–2 ng/ml for up to 3 hr.

[1] Sublimaze, McNeil Laboratories.

## EXPERIMENTAL

**Preparation of Fentanyl-$d_3$**—After 1.2 ml of 20% DCl in deuterium oxide[2] (99 atom % deuterium) was added to 25 μg of fentanyl[3], the solution was incubated overnight at 100°. The acidity of the reaction mixture was partially neutralized by 0.2 ml of 40% NaOD in deuterium oxide[2] (99 atom % deuterium), and the unreacted fentanyl was removed by extraction twice with 2 ml of ethyl acetate. The remaining aliquot of sample was again acidified by 1.2 ml of 20% DCl solution before evaporation to dryness *in vacuo*. To the residue, 20 μl of pyridine and 1 ml of propionyl chloride[2] were added, and the mixture was incubated at 60° for 1 hr. The final product, fentanyl-$d_3$, was then purified by extraction twice with 3 ml of ethyl acetate. After evaporation to dryness by a nitrogen stream, the residue was dissolved in 0.5 ml of ethyl acetate and stored in a refrigerator at 4°.

**Instrumentation**—Combined GC–chemical-ionization mass spectrometry[4] was employed with methane as the reagent gas and an electron energy of 150 ev. GC separation was carried out isothermally at 235° with a 0.91-m × 2-mm i.d. U-shaped glass column packed with 3% SE-30 on 80–100-mesh Gas Chrom Q[5]. The temperature of the GC injector and the separator was 250°.

**Biological Samples**—Two hours before fentanyl administration, the nonselective mongrel dogs, 12–14 kg, were anesthetized with 300 mg of pentobarbital sodium. Fentanyl (25, 50, or 100 μg/kg) was introduced intravenously by 1-min infusion, and blood samples were collected into heparinized vials at 1, 2, 4, 6, 8, 10, 15, 30, 45, 62, 90, 120, 150, and 180 min after infusion was completed. Plasma was separated from red blood cells by centrifugation at 2500 rpm in the cold and stored in a freezer at −40° when necessary.

**Extraction and Quantitation**—To 2 ml of plasma, a known amount of fentanyl-$d_3$ (25 ng in 25 μl of ethyl acetate) was added as an internal standard. After rigorous mixing with the aid of an agitator[6], the plasma

[2] Aldrich Chemical Co., Milwaukee, Wis.
[3] McNeil Laboratories, Fort Washington, Pa.
[4] Finnigan 3300 gas chromatograph-mass spectrometer equipped with a 6000 data acquisition.
[5] Applied Science Laboratories, State College, Pa.
[6] Vanlab, Scientific Industries, Bohemia, N.Y.



*0022-3549/81/1100-1276$01.00/0*
*© 1981, American Pharmaceutical Association*

**Table I—Selective Ion Chemical-Ionization Mass Spectrometric Assessment of the Purity of Fentanyl-$d_3$**

| Compound | Relative Ion Intensities[a] | | | |
|---|---|---|---|---|
| | $MH^+ - 3$ | $MH^+ - 2$ | $MH^+ - 1$ | $MH^+$ |
| Fentanyl | 0.50 | 10.01 | 3.93 | 100 |
| Fentanyl-$d_3$ | 1.72 | 12.96 | 9.40 | 100 |
| Differences | 1.21 | 2.95 | 5.47 | |

[a] Relative ion intensities were calculated by taking the ion intensity of $MH^+$ as 100.

**Table II—Plasma Fentanyl Levels[a] (Nanograms per Milliliter) in Dogs after 50-μg/kg iv Dose**

| Minutes | Dog 1 | Dog 2 |
|---|---|---|
| 1 | 26.50 ± 0.62 (4) | 24.72 ± 0.52 (4) |
| 2 | 19.04 (2) | 15.14 ± 0.18 (4) |
| 4 | 13.74 (2) | 12.81 ± 0.38 (4) |
| 6 | 10.33 ± 0.41 (4) | 8.17 ± 0.06 (3) |
| 8 | 8.47 ± 0.29 (6) | 5.84 (2) |
| 10 | 6.78 ± 0.16 (4) | 4.13 ± 0.16 (3) |
| 15 | 4.83 (2) | 2.04 ± 0.04 (4) |
| 30 | 2.61 (2) | 1.25 (2) |
| 45 | 1.58 ± 0.04 (5) | 1.16 ± 0.07 (5) |
| 62 | 1.22 (2) | 0.66 ± 0.03 (3) |
| 90 | 1.11 (2) | 0.60 ± 0.07 (4) |
| 120 | 1.02 ± 0.03 (4) | 0.50 ± 0.05 (3) |
| 150 | 0.83 ± 0.02 (3) | 0.48 ± 0.03 (3) |
| 180 | 0.57 ± 0.06 (5) | |

[a] Mean ± *SD*; the number of determinations is shown in parentheses.

was allowed to stand for 5 min before saturation with ammonium carbonate. Extractions were performed twice with 3 ml of ethyl acetate. The organic layers were pooled and dried by a nitrogen stream. To this residue, 30 μl of ethyl acetate was added and 10 μl was used for analysis. Ions selectively monitored were *m/z* 340, 337, 281, and 233 corresponding to the pseudomolecular ions of fentanyl-$d_3$, fentanyl, despropionyl, and norfentanyl, respectively. Quantitation was performed by comparison of peak area with respect to that of the internal standard.

## RESULTS AND DISCUSSION

In addition to the pseudomolecular ion, $MH^+$, which appeared as the most abundant species, the chemical-ionization mass spectrum of fentanyl showed four fragment ions at mass units greater than 100, *i.e.*, *m/z* 245, 188, 186, and 150. The mass spectrum of fentanyl-$d_3$ showed that, in addition to the pseudomolecular ion, the ion species at 248 and 153 were isotopically labeled, with *m/z* 153 resulting from cleavage of the propionyl amide bond and *m/z* 248 resulting from cleavage of the benzyl bond. Both ion species contain the phenyl ring of the propionanilide moiety of the molecule.

To obtain deuterated fentanyl, fentanyl was first hydrolyzed by 20% DCl in deuterium oxide solution to produce despropionyl fentanyl and propionic acid. Deuteration appeared to occur at this stage. After extraction with ethyl acetate, analysis of an aliquot of the reaction mixture revealed that deuterated despropionyl fentanyl was the major component. The electron-impact mass spectrum of this compound revealed a weak but detectable *m/z* 283 ion, which corresponded to the molecular ion. Three major fragment ions were observed, at *m/z* 192, 149, and 96. The mass spectrum was similar to that of the nondeuterated despropionyl fentanyl recorded previously (6), except that *m/z* 283, 192, and 149 ions contained isotopic labels. The chemical-ionization mass spectrum of the component showed a pseudomolecular ion at *m/z* 284, which was also three mass units higher than that of the nondeuterated compound. Reesterization of deuterated despropionyl fentanyl was carried out by incubating the residue with propionyl chloride. Fentanyl-$d_3$ was then purified by extraction into ethyl acetate.

During the preparation of deuterated fentanyl, two extraction processes were performed to remove the unreacted intact drug from the product. The effectiveness of the extraction is demonstrated by the results of two experiments designed to assess the purity of fentanyl-$d_3$. Table I shows the relative ion intensities of $MH^+$, $MH^+ - 1$, $MH^+ - 2$, and $MH^+ - 3$ from 70 ng of fentanyl-$d_3$ and 100 ng of fentanyl by selective ion chemical-ionization mass spectrometry. Essentially, the differences in the relative ion intensities for $MH^+ - 3$, $MH^+ - 2$, and $MH^+ - 1$ between those of fentanyl and fentanyl-$d_3$ can be regarded as the relative ion intensities contributed by the molecular ions of fentanyl, fentanyl-$d_1$, and fentanyl-$d_2$, respectively. When taking the ion intensity of $MH^+$ of fentanyl-$d_3$ as 100, it appeared that the deuterated product was a composite of 1.1% fentanyl, 2.69% fentanyl-$d_1$, 4.99% fentanyl-$d_2$, and 91.2% fentanyl-$d_3$.

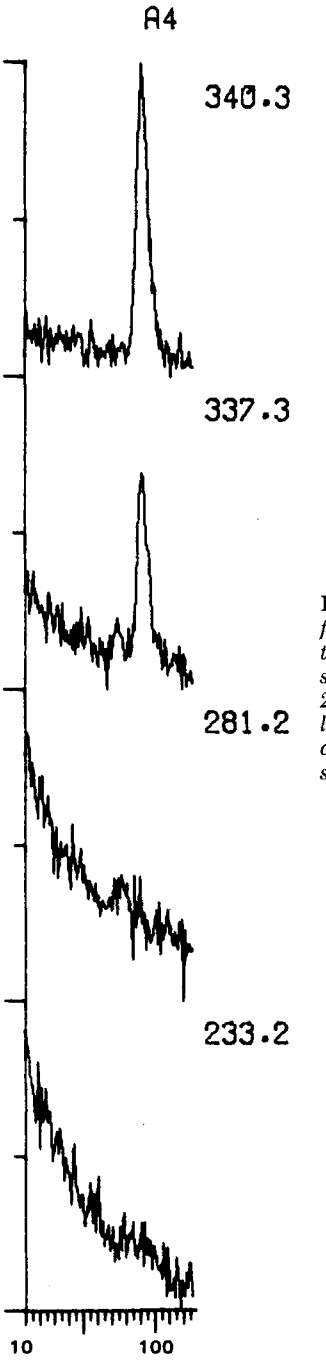


**Figure 1**—*Mass chromatogram of fentanyl in dog plasma using deuterated fentanyl-*$d_3$ *as an internal standard;* m/z *340.3, 337.3, 281.2, and 233.2 correspond to the pseudomolecular ions of fentanyl-* $d_3$*, fentanyl, despropionyl, and norfentanyl, respectively.*

To determine the percent yield of fentanyl-$d_3$ from the precursor, three separate ethyl acetate extracts corresponding to these reaction mixtures in which 25.0, 37.5, and 50.0 ng of fentanyl were used as the initial starting materials, were added with known amounts of fentanyl (5 ng/10 μl of ethyl acetate) as an internal standard. The unknown amounts of fentanyl-$d_3$ in the mixtures were then measured by chemical-ionization mass spectrometry, selectively monitoring $MH^+$ of fentanyl and fentanyl-$d_3$. The results showed that 23.2, 33.7, and 42.8 ng of the fentanyl were recovered as fentanyl-$d_3$; therefore, the percent yield of the chemical processes to obtain the deuterated compound was 89.4 ± 3.6%. The standard solution containing fentanyl-$d_3$ in ethyl acetate (1.75 μg/ml) was stored in a refrigerator at 4° and was stable after 3 months under these conditions. During this time, experiments to check the purity of fentanyl-$d_3$ were performed prior to each measurement of every batch of dog plasma.

Figure 1 shows the quantitative GC–mass spectrometric analysis of fentanyl in dog plasma, with pseudomolecular ions of fentanyl, *m/z* 337,

**Table III—Pharmacokinetic Parameters of Plasma Fentanyl [a]**

| Dose, μg/kg | Dog Number | $A$, ng/ml | $T_{1/2}\,\alpha$, min | $B$, ng/ml | $T_{1/2}\,\beta$, min | $C$, ng/ml | $T_{1/2}\,\gamma$, min |
|---|---|---|---|---|---|---|---|
| 25 | 005 | 57.41 | 1.61 | 6.33 | 25.68 | 2.51 | 57.54 |
| | 006 | 73.05 | 1.78 | 25.08 | 6.93 | 4.97 | 133.19 |
| 50 | 001 | 22.30 | 0.97 | 15.10 | 6.93 | 1.74 | 134.37 |
| | 002 | 19.90 | 3.73 | 1.22 | 6.97 | 1.14 | 110.75 |
| | 010 | 100.00 | 1.10 | 13.00 | 16.89 | 5.27 | 93.17 |
| 100 | 003 | 36.72 | 4.18 | 20.56 | 4.57 | 7.59 | 116.91 |
| | 004 | 99.99 | 1.29 | 24.29 | 9.11 | 9.87 | 95.23 |
| | 009 | 293.58 | 1.39 | 36.22 | 8.88 | 16.70 | 251.55 |
| Average ± SD | | | 2.01 ± 1.24 | | 10.75 ± 7.06 | | 124.09 ± 57.17 |

[a] Nonlinear estimation of triphasic pharmacokinetics of plasma fentanyl employed the NONLIN computer program from The Upjohn Co.

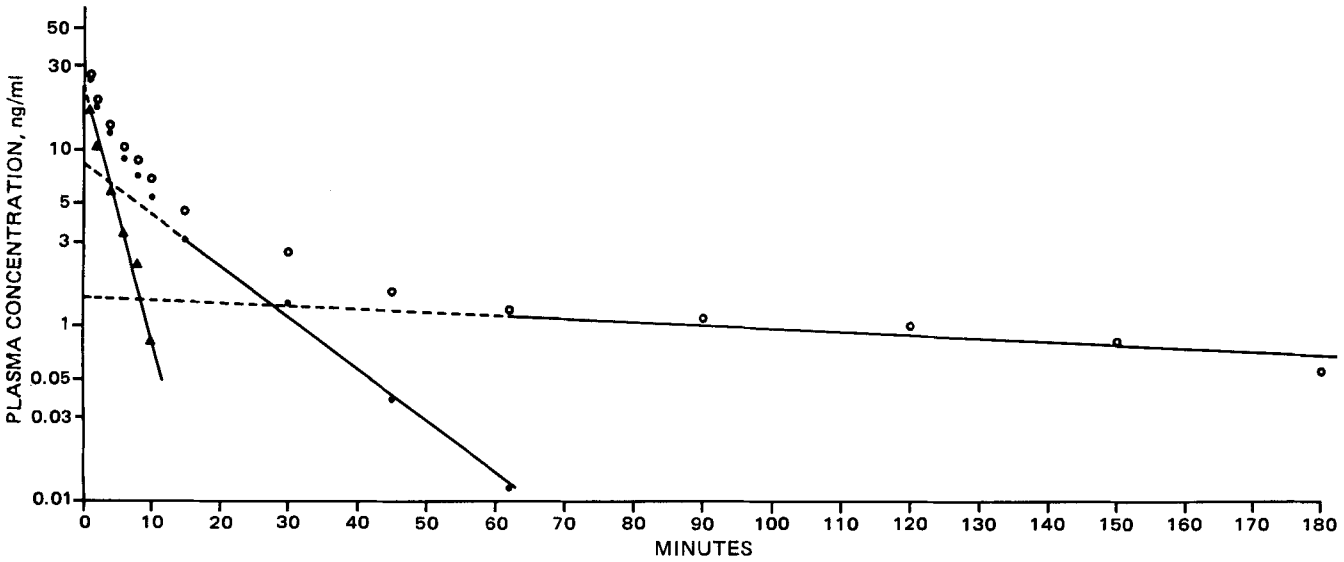


**Figure 2**—*Application of the method of residuals for nonlinear pharmacokinetic data (8) to the semilogarithmic plot of plasma fentanyl levels with respect to time. Three linear regions of first-order kinetics are shown. Key:* ○, *plasma fentanyl levels in a normal dog after 50 μg/kg iv dose; and* ▲ *and* ●, *data obtained by curve stripping.*

and fentanyl-$d_3$, $m/z$ 340, used for quantitative measurements. Since despropionyl fentanyl and norfentanyl are proposed major metabolites in the rat urine (6, 7), their $MH^+$ ions, $m/z$ 281 and 233, respectively, were also selectively monitored. In the first 28 plasma samples analyzed, these two metabolites were not found. The linear range of the calibration curve was determined by adding known amounts of fentanyl and fentanyl-$d_3$ to 2 ml of water. For standard solutions containing <5 ng of fentanyl/ml, 3.17 ng of internal standard was used; otherwise, 35.7 ng was used. Quantitative measurements were made by comparing the peak areas of fentanyl to that of the internal standard. The results from eight samples, ranging from 500 pg to 100 ng/ml of fentanyl, revealed a linear relationship between the actual and measured values determined by GC–mass spectrometry.

Table II shows plasma fentanyl levels in dogs after an intravenous bolus of 50 μg/kg. For plasma samples containing >1 ng of fentanyl/ml, the reproducibility of the analysis was within 6%; for those containing <1 ng/ml, it was ~12%. With its high sensitivity, the GC–mass spectrometric procedures allow the time course of the plasma fentanyl concentration to be followed for up to 3 hr. The lowest measured plasma concentration was 500 pg/ml. The lower limit of analysis by these methods using a signal to noise ratio of 2 was ~200 pg of fentanyl.

The plasma fentanyl concentration profile in a dog is illustrated in Fig. 2. Figure 2 also shows the results from application of the method of residuals to yield the second and third linear segments in addition to the easily recognizable terminal linear segment (8). The time course of the plasma fentanyl level appeared to follow a triphasic phenomenon. The first phase may have represented the uptake of [$^3$H]fentanyl by organs with extensive blood supplies, *e.g.*, lungs, kidneys, heart, and brain (2). The next phase was one of redistribution, especially from the lungs to the blood. Finally, the last phase represented that of metabolism and excretion. The three-compartmental pharmacokinetics of plasma fentanyl agreed with observations made by radioimmunoassay (4, 5) and radioisotope counting techniques (3).

Table III shows the pharmacokinetic parameters of plasma fentanyl of eight dogs by curve fitting with the NONLIN computer program (9). The plasma profile of fentanyl in dogs can be described by the equation $C(t) = Ae^{-\alpha t} + B^{-\beta t} + Ce^{-\gamma t}$, where $C(t)$ represents the fentanyl concentration at any time, $t$. The half-life, $T_{1/2}$, is calculated by using $0.693/\alpha$, $\beta$, or $\gamma$. The results shown in Table III indicate that the pharmacokinetic parameters vary widely among dogs. The same variability in the pharmacokinetic parameters of plasma fentanyl in humans was reported by Hull (10). Table III reveals that the half-lives of each compartment are more or less independent of the dose levels of fentanyl administered, despite the wide variation in the data. However, in contrast to other data (11), the intercepts ($A$, $B$, and $C$) are not dose dependent.

Finally, the average half-lives of the terminal linear phase (124.1 ± 57.2 min) and the middle phase (10.74 ± 7.05 min) shown in Table III are shorter than the values reported in the literature (3, 5, 10). These differences may be due to the different specificities of the techniques adapted for measuring the extremely low plasma levels of fentanyl in these two regions. The described GC–mass spectrometric technique is highly specific for several reasons. First, since selective ion monitoring measures only the pseudomolecular ions of fentanyl and fentanyl-$d_3$, the quantitative determination of plasma fentanyl was free from the interference of its own metabolites. Second, fentanyl in biological samples was repeatedly purified, first by extraction with ethyl acetate and then by GC separation. The sensitivity of measurements was extended from 500 pg/ml to 100 ng/ml, and the use of stable isotopically-labeled fentanyl as an internal standard greatly enhanced the accuracy and precision of the quantitative measurements.

## REFERENCES

(1) P. A. J. Janssen, C. J. E. Niemegeers, and J. G. H. Dory, *Drug Res.*, **13**, 502 (1963).

(2) R. Hess, A. Herz, and K. Friedel, *J. Pharmacol. Exp. Ther.*, **179**, 474 (1971).

(3) C. J. Hull and K. McLeod, *Br. J. Anaesth.*, **48**, 677 (1976).

(4) G. L. Henderson, J. Frinche, C. Y. Leung, M. Torten, and E. Benjamin, *J. Pharmacol. Exp. Ther.*, **192**, 489 (1975).

(5) M. Michiels, R. Hendriks, and J. Heykants, *Eur. J. Clin. Phar-*

*macol.*, **12**, 153 (1977).
(6) Y. Maruyama and E. Hosoya, *Keio J. Med.*, **18**, 59 (1969).
(7) I. Van Wijngaarden and W. Soudijn, *Life Sci.*, **7**, 1239 (1968).
(8) M. Gibaldi and D. Perrier, "Pharmacokinetics," Dekker, New York, N.Y., 1975, p. 281.
(9) C. M. Metzer, G. L. Elfring, and A. J. McEwen, *Biometrics*, **562**, Sept. (1974).
(10) C. J. Hull, *Br. J. Anaesth.*, **48**, 1121 (1976).
(11) D. A. McClain and C. C. Hug, Jr., *Anesthesiology*, **51**, 529 (1979).

**ACKNOWLEDGMENTS**

Supported in part by University of Texas Biomedical Research Grant 5-S07-RR05745 from the Division of Research Resources, National Institutes of Health.

## NOTES

# Plasma Protein Binding Interaction between Valproic and Salicylic Acids in Rhesus Monkeys

**C. T. VISWANATHAN** *§ **and R. H. LEVY** ‡x

Received March 12, 1981, from the *Department of Neurological Surgery, School of Medicine, and the ‡Department of Pharmaceutics, School of Pharmacy, University of Washington, Seattle, WA 98195. Accepted for publication April 7, 1981. §Present address: Biopharmaceutics Division, Food and Drug Administration, Rockville, MD 20857.

**Abstract** □ The effects of three levels of salicylic acid on the steady-state plasma concentrations of free and total valproic acid were examined in catheterized rhesus monkeys. Valproate was infused intravenously for a total of 41 hr, and salicylate was added after the first 8 hr. The three salicylate infusions were randomly assigned to each monkey. Valproate free fraction was determined by equilibrium dialysis. Statistically significant increases in valproate free fraction and total body clearance were observed after addition of salicylic acid. The increase in valproate clearance was positively correlated with the molar ratio of salicylate to valproate steady-state plasma concentrations. There was no significant change in valproate free concentration after salicylate treatment. The proposed mechanism of this *in vivo* interaction includes plasma protein binding displacement with no change in valproate intrinsic clearance.

**Keyphrases** □ Valproic acid—plasma protein binding interaction with salicylic acid, rhesus monkey □ Salicylic acid—plasma protein binding with valproic acid, rhesus monkey □ Plasma protein binding—interaction between valproic and salicylic acids, rhesus monkey

Valproic and salicylic acids are known to bind extensively to plasma proteins in humans (1–8) and rhesus monkeys (9–11). Three *in vitro* studies showed that salicylic acid decreases valproate binding to plasma or human serum albumin (12–14). However, there is no indication that such an interaction occurs *in vivo*. In addition, these two acids may interact at a metabolic level.

Epileptic patients on valproate treatment occasionally receive salicylates and, depending on its mechanism, this interaction may be of therapeutic significance. The present study was designed to investigate this interaction *in vivo* at the systemic level. Both drugs were administered by constant-rate intravenous infusion to achieve one steady-state concentration of valproic acid and three steady-state salicylic acid levels.

## EXPERIMENTAL

Four healthy male rhesus monkeys (*Macaca mulatta*) (mean weight 5.5 kg) were chair-adapted for 1 month prior to implantation of catheters. The jugular and femoral veins of each monkey were chronically catheterized to enable withdrawal of venous blood samples and drug infusion, respectively. The monkeys were maintained in three-level restraining chairs during the studies. Patency of catheters was assured by a slow, continuous saline infusion (1 ml/hr). Daily diet consisted of fresh fruit and monkey food.

Three studies were carried out in each monkey. In each study, valproic

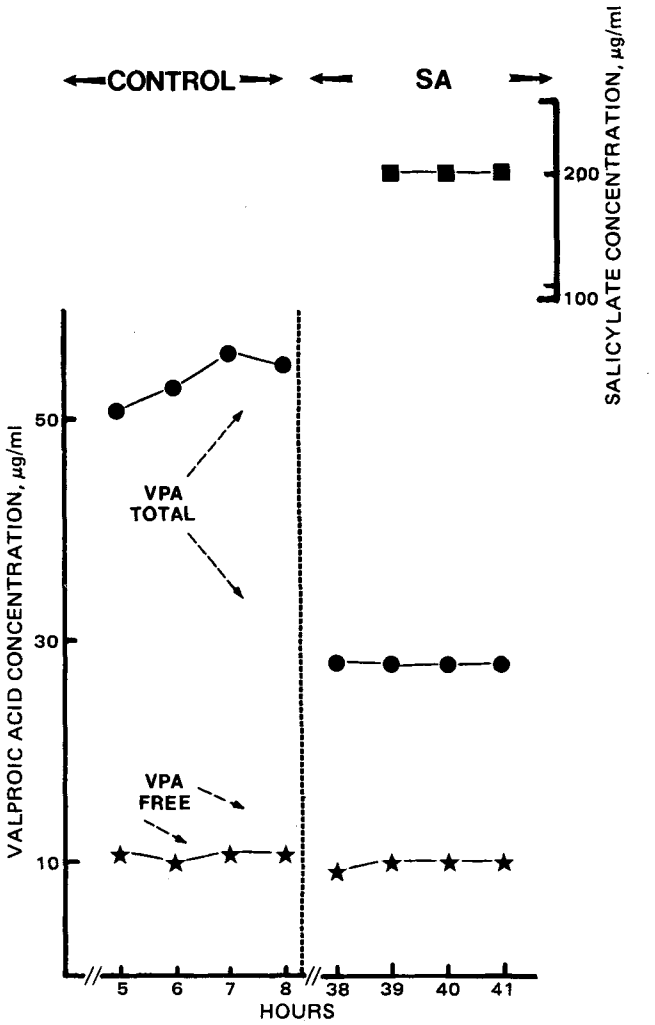


**Figure 1**—*Steady-state levels of total and free valproate (VPA) before and during salicylate (SA) infusion in Monkey 201.*

0022-3549/81/1100-1279$01.00/0
© 1981, American Pharmaceutical Association

*macol.*, **12**, 153 (1977).
(6) Y. Maruyama and E. Hosoya, *Keio J. Med.*, **18**, 59 (1969).
(7) I. Van Wijngaarden and W. Soudijn, *Life Sci.*, **7**, 1239 (1968).
(8) M. Gibaldi and D. Perrier, "Pharmacokinetics," Dekker, New York, N.Y., 1975, p. 281.
(9) C. M. Metzer, G. L. Elfring, and A. J. McEwen, *Biometrics*, **562**, Sept. (1974).
(10) C. J. Hull, *Br. J. Anaesth.*, **48**, 1121 (1976).
(11) D. A. McClain and C. C. Hug, Jr., *Anesthesiology*, **51**, 529 (1979).

**ACKNOWLEDGMENTS**

Supported in part by University of Texas Biomedical Research Grant 5-S07-RR05745 from the Division of Research Resources, National Institutes of Health.

## NOTES

# Plasma Protein Binding Interaction between Valproic and Salicylic Acids in Rhesus Monkeys

**C. T. VISWANATHAN** *§ **and R. H. LEVY** ‡x

Received March 12, 1981, from the *Department of Neurological Surgery, School of Medicine, and the ‡Department of Pharmaceutics, School of Pharmacy, University of Washington, Seattle, WA 98195. Accepted for publication April 7, 1981. §Present address: Biopharmaceutics Division, Food and Drug Administration, Rockville, MD 20857.

**Abstract** □ The effects of three levels of salicylic acid on the steady-state plasma concentrations of free and total valproic acid were examined in catheterized rhesus monkeys. Valproate was infused intravenously for a total of 41 hr, and salicylate was added after the first 8 hr. The three salicylate infusions were randomly assigned to each monkey. Valproate free fraction was determined by equilibrium dialysis. Statistically significant increases in valproate free fraction and total body clearance were observed after addition of salicylic acid. The increase in valproate clearance was positively correlated with the molar ratio of salicylate to valproate steady-state plasma concentrations. There was no significant change in valproate free concentration after salicylate treatment. The proposed mechanism of this *in vivo* interaction includes plasma protein binding displacement with no change in valproate intrinsic clearance.

**Keyphrases** □ Valproic acid—plasma protein binding interaction with salicylic acid, rhesus monkey □ Salicylic acid—plasma protein binding with valproic acid, rhesus monkey □ Plasma protein binding—interaction between valproic and salicylic acids, rhesus monkey

Valproic and salicylic acids are known to bind extensively to plasma proteins in humans (1–8) and rhesus monkeys (9–11). Three *in vitro* studies showed that salicylic acid decreases valproate binding to plasma or human serum albumin (12–14). However, there is no indication that such an interaction occurs *in vivo*. In addition, these two acids may interact at a metabolic level.

Epileptic patients on valproate treatment occasionally receive salicylates and, depending on its mechanism, this interaction may be of therapeutic significance. The present study was designed to investigate this interaction *in vivo* at the systemic level. Both drugs were administered by constant-rate intravenous infusion to achieve one steady-state concentration of valproic acid and three steady-state salicylic acid levels.

## EXPERIMENTAL

Four healthy male rhesus monkeys (*Macaca mulatta*) (mean weight 5.5 kg) were chair-adapted for 1 month prior to implantation of catheters. The jugular and femoral veins of each monkey were chronically catheterized to enable withdrawal of venous blood samples and drug infusion, respectively. The monkeys were maintained in three-level restraining chairs during the studies. Patency of catheters was assured by a slow, continuous saline infusion (1 ml/hr). Daily diet consisted of fresh fruit and monkey food.

Three studies were carried out in each monkey. In each study, valproic

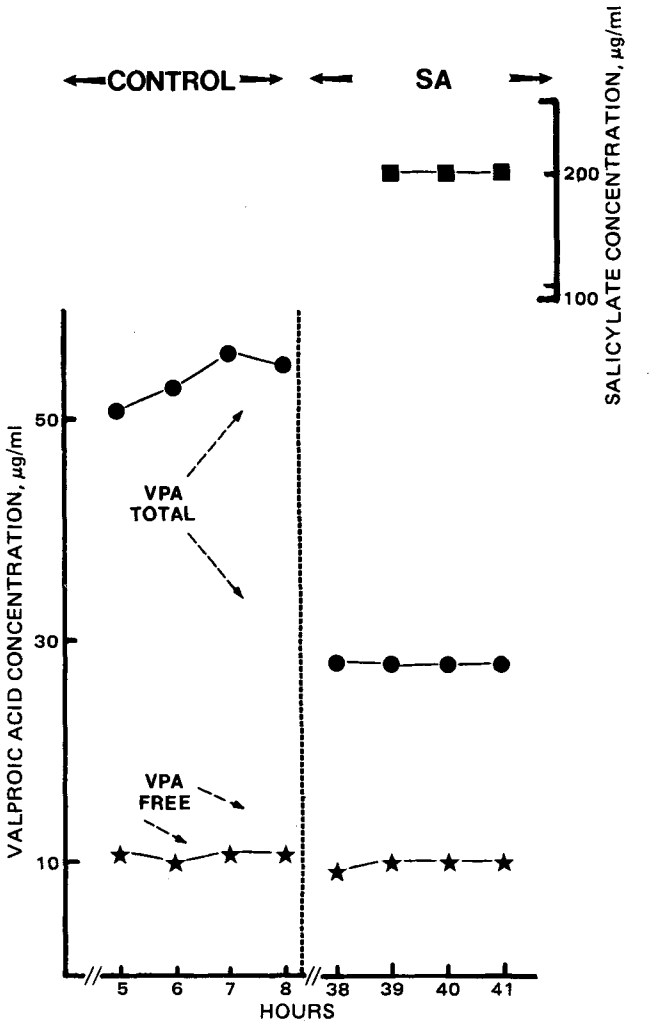


**Figure 1**—*Steady-state levels of total and free valproate (VPA) before and during salicylate (SA) infusion in Monkey 201.*

0022-3549/81/1100-1279$01.00/0
© 1981, American Pharmaceutical Association

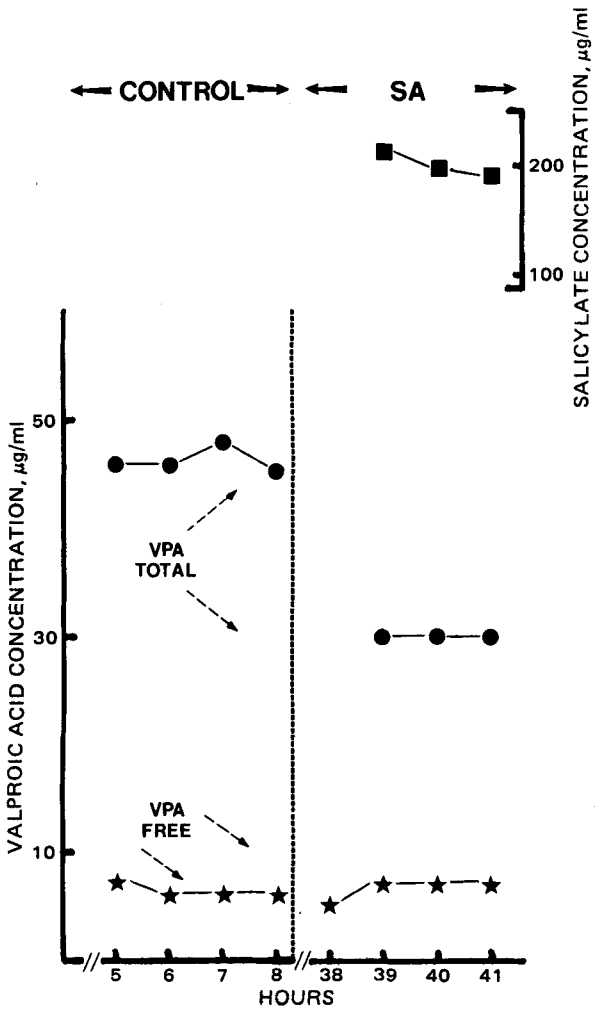


**Figure 2**—*Steady-state levels of total and free valproate (VPA) before and during salicylate (SA) infusion in Monkey 304.*

acid was infused for 41 hr (mean rate 74.4 mg/hr) and salicylic acid was added after the first 8 hr [valproic acid has a half-life of 1 hr in the monkey (15)]. The infusion rate of valproic acid was selected to yield levels in a clinically realistic range (30–80 μg/ml). The infusion rates of salicylic acid in the three studies were 55, 70, and 90 mg/hr. Study order was randomly assigned to each monkey, and a washout period of at least 2 weeks was allowed between studies.

Valproic and salicylic acids were administered as equivalents of sodium salts in sterile saline. All infusion equipment was covered with aluminum foil to protect salicylic acid from light.

Plasma samples were obtained at 5, 6, 7, and 8 hr following the start of infusion for control valproate steady-state levels and at 38, 39, 40, and 41 hr for steady-state levels of both drugs.

Valproate free fraction was determined by equilibrium dialysis. Each dialysis unit consisted of two 1-ml chambers separated by a dialysis membrane[1]. Plasma containing the drug (0.5 ml) was introduced into one chamber, and 0.5 ml of phosphate buffer (pH. 7.4) was added to the opposite chamber. The cells were kept immersed in a water bath at 37° for 24 hr. Valproate concentrations were measured from the buffer side (free drug) and plasma side (total drug) using a previously described GLC procedure (16). Plasma salicylate concentrations were determined as total salicylate by the spectrophotometric procedure of Wiseman *et al.* (17).

## RESULTS AND DISCUSSION

The effects of salicylate infusion on valproate steady-state levels are illustrated in Figs. 1 and 2 for Monkeys 201 and 304, respectively. Valproate free fraction and total body clearance before and after salicylate treatment are summarized in Table I; both increased significantly after salicylate treatment ($p < 0.05$). However, there was no significant change in the valproate free concentration ($p > 0.05$). As a result, total valproate levels decreased during valproate treatment. A significant correlation was obtained between the increase in valproate clearance and the molar ratio of salicylate to valproate ($y = 10.9x + 0.7$, $r = 0.93$, Fig. 3). Over 80% of the variability in the increase in valproate clearance can be explained by the salicylic acid concentration.

These findings indicate that salicylic acid is able to displace valproate acid from plasma protein binding sites *in vivo*. The results are consistent with the fact that valproic acid has a low extraction ratio in the rhesus monkey (15, 18). Pharmacokinetic theory predicts that the valproate free concentration should not be changed if salicylate affects valproate plasma binding without changing its intrinsic metabolic clearance (19). Several studies (12, 13) indicated that an *in vitro* plasma binding interaction exists between salicylic and valproic acids. If the interaction mechanism found in the rhesus monkey is also applicable in humans, this interaction should have little or no pharmacological consequence. However, since changes in total valproate levels would not reflect the changes in free levels, monitoring of the valproate free concentration would be indicated in patients receiving salicylates (20).

**Table I—Effect of Salicylic Acid on Valproic Acid Free Fraction and Systemic Clearance**

| Monkey | Free Fraction | | Systemic Clearance, liters/kg hr | |
|---|---|---|---|---|
| | Control | During Salicylate | Control | During Salicylate |
| 201 | 0.22 | 0.23[a] | 0.14 | 0.19 |
| | 0.33 | 0.75[b] | 0.15 | 0.21 |
| | 0.20 | 0.35[c] | 0.19 | 0.30 |
| 200 | 0.33 | 0.46 | 0.22 | 0.28 |
| | 0.15 | 0.25 | 0.30 | 0.57 |
| | 0.11 | 0.22 | 0.28 | 0.64 |
| 301 | 0.24 | 0.23 | 0.45 | 0.43 |
| | 0.29 | 0.74 | 0.30 | 0.45 |
| | 0.12 | 0.40 | 0.38 | 0.77 |
| 304 | 0.36 | 0.58 | 0.46 | 0.29 |
| | 0.19 | 0.23 | 0.24 | 0.30 |
| | 0.15 | 0.34 | 0.28 | 0.46 |
| | $p < 0.002$[d] | | $p < 0.0008$[d] | |

[a] Salicylate infusion rate of 55 mg/hr. [b] Salicylate infusion rate of 70 mg/hr. [c] Salicylate infusion rate of 90 mg/hr. [d] Comparisons were made by analysis of variance.

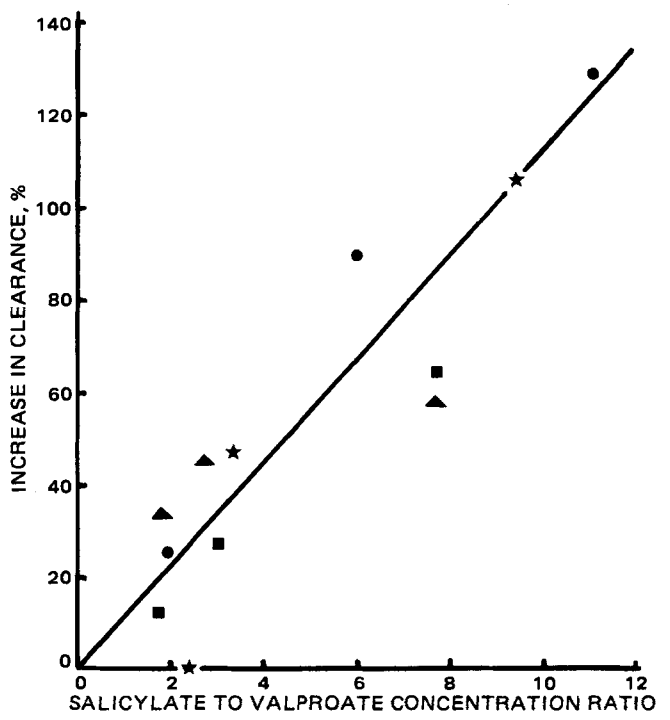


**Figure 3**—*Percent increase in valproate clearance correlated with the molar ratio of salicylate to valproate.*

[1] Dialyzer tubing, VWR Scientific, Seattle, WA 98124.

## REFERENCES

(1) J. A. Cramer and R. H. Mattson, *Ther. Drug Monitor.*, **1**, 105 (1979).

(2) R. Gugler and G. Mueller, *Br. J. Clin. Pharmacol.*, **5**, 441 (1978).

(3) R. Gugler, A. Schell, W. Eichelbaum, W. Frocher, and H-U. Schulz, *Eur. J. Clin. Pharmacol.*, **12**, 125 (1977).

(4) U. Klotz, *Arzneim-Forsch.*, **27**, 1085 (1977).

(5) U. Klotz and K. H. Antonin, *Clin. Pharmacol. Ther.*, **21**, 736 (1977).

(6) W. Löscher, *J. Pharmacol. Exp. Ther.*, **208**, 429 (1979).

(7) A. M. Taburet and E. Van der Kleijn, *Pharm. Weekbl.*, **112**, 356 (1977).

(8) T. N. Tozer, *Clin. Pharmacol. Ther.*, **26**, 380 (1979).

(9) R. H. Levy, in "Epilepsy: A Window to Brain Mechanisms," J. S. Lockard and A. A. Ward Jr., Eds., Raven, New York, N.Y., 1980, pp. 191–200.

(10) R. H. Levy, J. S. Lockard, and B. T. Ludwick, presented at the APhA Academy of Pharmaceutical Sciences, Washington, D.C. meeting, Apr. 1980.

(11) J. A. Sturman and M. J. H. Smith, *J. Pharm. Pharmacol.*, **19**, 621 (1967).

(12) J. S. Fleitman, J. Bruni, T. H. Perrin, and B. J. Wilder, *J. Clin. Pharmacol.*, **20**, 514 (1980).

(13) F. Schobben, T. B. Vree, and E. Van der Kleijn, in "Proceedings of the Congress and Symposium on Epilepsy, Amsterdam, September, 1977," Swets & Zeitlinger, B. V., Amsterdam, Netherlands, p. 271.

(14) S. Urien, Ph.D. thesis, University of Paris, Val-de-Marne, France, 1979.

(15) A. A. Lai, R. H. Levy, and L. Martis, *Therapie*, **35**, 221 (1980).

(16) R. H. Levy, L. Martis, and A. A. Lai, *Anal. Lett.*, **B11**, 257 (1978).

(17) E. H. Wiseman, Y. H. Chang, and D. L. Hobbs, *Clin. Pharmacol. Ther.*, **18**, 441 (1975).

(18) R. H. Levy, S. S. Lockard, I. H. Patel, and W. C. Congdon, *J. Pharm. Sci.*, **66**, 1154 (1977).

(19) G. Levy, *ibid.*, **65**, 1264 (1976).

(20) R. H. Levy, *Ther. Drug Monitor.*, **2**, 199 (1980).



## ACKNOWLEDGMENTS

Supported by National Institute of Neurological and Communicative Disorders and Stroke Research Grant NS-04053.


# Synthesis and Evaluation of Guanazole Prodrugs as Antineoplastic Agents


**CYNTHIA DIAS SELASSIE*, ERIC J. LIEN *x, and TASNEEM A. KHWAJA‡**



Received January 22, 1981, from the **Section of Biomedicinal Chemistry, School of Pharmacy, and the* ‡ *Department of Pathology, School of Medicine, University of Southern California, Los Angeles, CA 90033.* Accepted for publication April 16, 1981.



**Abstract** □ Nine amide derivatives of guanazole were synthesized, and eight of them were tested for antineoplastic activity *versus* L1210 cells *in vitro*. Several of these compounds exhibited activity comparable to or greater than that of guanazole.



**Keyphrases** □ Guanazole—synthesis and evaluation of prodrugs as antineoplastic agents □ Prodrugs—of guanazole, synthesis and evaluation as antineoplastic agents □ Antineoplastic agents—synthesis and evaluation of guanazole prodrugs


Guanazole (3,5-diamino-1,2,4-triazole, NSC 1895) was synthesized by Pellizzari (1) and discovered in a general screen by the National Cancer Institute. Subsequently, Brockman *et al.* (2) reported that guanazole inhibited DNA synthesis by inhibiting ribonucleotide reductase. Antitumor activity against various animal leukemias and tumors (3) and remissions in some patients with actute myelocytic leukemia (4) were reported. However, extensive clinical utilization of this drug has been limited by its high polarity and water solubility, low molecular weight, and relatively low potency, which warrants continuous intravenous infusion at frequent intervals (5).

Structure–activity relationship analysis of past and current work on guanazole derivatives established the importance of both amino groups for antineoplastic activity (2, 3). Thus, to circumvent the problem of the high elimination rate and to increase the efficacy of guanazole as an antieoplastic agent, amide derivatives with decreased polarity, water solubility, and increased molecular weight were synthesized (Scheme I). These compounds were then tested for anticancer activity *versus* L1210 cells *in vitro*.

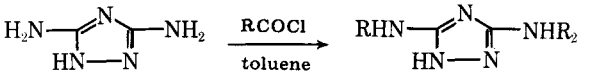


R = $CH_3$, $C_2H_5$, $C_3H_7$, $C_6H_5$, $CF_3$, $C_2F_5$, $C_3F_7$, $p$-$NO_2C_6H_4$

*Scheme I*

The compounds and their physical properties are outlined in Table I.

## EXPERIMENTAL

**Chemistry**—All solvents were analytical grade. All melting points were taken in open capillary tubes[1] and are corrected. Elemental analysis[2] was within ±0.4% of the theoretical values. All proton NMR spectra were recorded on a 60 MHz spectrometer[3] with tetramethylsilane as the internal standard and solvents such as deuterochloroform, dimethyl sulfoxide-$d_6$, and trifluoroacetic acid. IR spectra were recorded on a spectrophotometer[4] as potassium bromide pellets or Fluorolube mulls. UV spectra were recorded on a double-beam spectrophotometer[5]. TLC was performed using Eastman-type 6060 chromatogram sheets (silica gel), and the sheets were developed in an iodine chamber to check the purity of the amides.

Most of these derivatives were synthesized by a general procedure for the acylation of amines. The appropriate acid chloride or anhydride was condensed with guanazole, usually in the presence of a nonpolar solvent. Two typical reactions for preparing the amides are described using III and VI as examples.

One gram (0.01 *M*) of guanazole and 4.2 g (0.02 *M*) of trifluoroacetic anhydride were refluxed in dry toluene for 8 hr. The white precipitate

[1] Thomas Hoover melting-point apparatus.
[2] Performed by the Analytical Laboratory, California Institute of Technology, Pasadena, Calif.
[3] Hitachi Perkin-Elmer R-24.
[4] Beckman IR-4240.
[5] Perkin-Elmer Coleman 124.


0022-3549/81/1100-1281$01.00/0


© 1981, American Pharmaceutical Association

## REFERENCES

(1) J. A. Cramer and R. H. Mattson, *Ther. Drug Monitor.*, **1**, 105 (1979).

(2) R. Gugler and G. Mueller, *Br. J. Clin. Pharmacol.*, **5**, 441 (1978).

(3) R. Gugler, A. Schell, W. Eichelbaum, W. Frocher, and H-U. Schulz, *Eur. J. Clin. Pharmacol.*, **12**, 125 (1977).

(4) U. Klotz, *Arzneim-Forsch.*, **27**, 1085 (1977).

(5) U. Klotz and K. H. Antonin, *Clin. Pharmacol. Ther.*, **21**, 736 (1977).

(6) W. Löscher, *J. Pharmacol. Exp. Ther.*, **208**, 429 (1979).

(7) A. M. Taburet and E. Van der Kleijn, *Pharm. Weekbl.*, **112**, 356 (1977).

(8) T. N. Tozer, *Clin. Pharmacol. Ther.*, **26**, 380 (1979).

(9) R. H. Levy, in "Epilepsy: A Window to Brain Mechanisms," J. S. Lockard and A. A. Ward Jr., Eds., Raven, New York, N.Y., 1980, pp. 191–200.

(10) R. H. Levy, J. S. Lockard, and B. T. Ludwick, presented at the APhA Academy of Pharmaceutical Sciences, Washington, D.C. meeting, Apr. 1980.

(11) J. A. Sturman and M. J. H. Smith, *J. Pharm. Pharmacol.*, **19**, 621 (1967).

(12) J. S. Fleitman, J. Bruni, T. H. Perrin, and B. J. Wilder, *J. Clin. Pharmacol.*, **20**, 514 (1980).

(13) F. Schobben, T. B. Vree, and E. Van der Kleijn, in "Proceedings of the Congress and Symposium on Epilepsy, Amsterdam, September, 1977," Swets & Zeitlinger, B. V., Amsterdam, Netherlands, p. 271.

(14) S. Urien, Ph.D. thesis, University of Paris, Val-de-Marne, France, 1979.

(15) A. A. Lai, R. H. Levy, and L. Martis, *Therapie*, **35**, 221 (1980).

(16) R. H. Levy, L. Martis, and A. A. Lai, *Anal. Lett.*, **B11**, 257 (1978).

(17) E. H. Wiseman, Y. H. Chang, and D. L. Hobbs, *Clin. Pharmacol. Ther.*, **18**, 441 (1975).

(18) R. H. Levy, S. S. Lockard, I. H. Patel, and W. C. Congdon, *J. Pharm. Sci.*, **66**, 1154 (1977).

(19) G. Levy, *ibid.*, **65**, 1264 (1976).

(20) R. H. Levy, *Ther. Drug Monitor.*, **2**, 199 (1980).



## ACKNOWLEDGMENTS

Supported by National Institute of Neurological and Communicative Disorders and Stroke Research Grant NS-04053.


# Synthesis and Evaluation of Guanazole Prodrugs as Antineoplastic Agents


**CYNTHIA DIAS SELASSIE*, ERIC J. LIEN *x, and TASNEEM A. KHWAJA‡**



Received January 22, 1981, from the **Section of Biomedicinal Chemistry, School of Pharmacy, and the* ‡ *Department of Pathology, School of Medicine, University of Southern California, Los Angeles, CA 90033.* Accepted for publication April 16, 1981.



**Abstract** □ Nine amide derivatives of guanazole were synthesized, and eight of them were tested for antineoplastic activity *versus* L1210 cells *in vitro*. Several of these compounds exhibited activity comparable to or greater than that of guanazole.



**Keyphrases** □ Guanazole—synthesis and evaluation of prodrugs as antineoplastic agents □ Prodrugs—of guanazole, synthesis and evaluation as antineoplastic agents □ Antineoplastic agents—synthesis and evaluation of guanazole prodrugs


Guanazole (3,5-diamino-1,2,4-triazole, NSC 1895) was synthesized by Pellizzari (1) and discovered in a general screen by the National Cancer Institute. Subsequently, Brockman *et al.* (2) reported that guanazole inhibited DNA synthesis by inhibiting ribonucleotide reductase. Antitumor activity against various animal leukemias and tumors (3) and remissions in some patients with actute myelocytic leukemia (4) were reported. However, extensive clinical utilization of this drug has been limited by its high polarity and water solubility, low molecular weight, and relatively low potency, which warrants continuous intravenous infusion at frequent intervals (5).

Structure–activity relationship analysis of past and current work on guanazole derivatives established the importance of both amino groups for antineoplastic activity (2, 3). Thus, to circumvent the problem of the high elimination rate and to increase the efficacy of guanazole as an antieoplastic agent, amide derivatives with decreased polarity, water solubility, and increased molecular weight were synthesized (Scheme I). These compounds were then tested for anticancer activity *versus* L1210 cells *in vitro*.

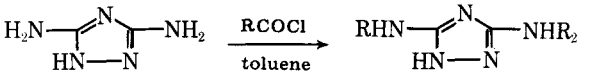


R = $CH_3$, $C_2H_5$, $C_3H_7$, $C_6H_5$, $CF_3$, $C_2F_5$, $C_3F_7$, $p$-$NO_2C_6H_4$

*Scheme I*

The compounds and their physical properties are outlined in Table I.

## EXPERIMENTAL

**Chemistry**—All solvents were analytical grade. All melting points were taken in open capillary tubes[1] and are corrected. Elemental analysis[2] was within ±0.4% of the theoretical values. All proton NMR spectra were recorded on a 60 MHz spectrometer[3] with tetramethylsilane as the internal standard and solvents such as deuterochloroform, dimethyl sulfoxide-$d_6$, and trifluoroacetic acid. IR spectra were recorded on a spectrophotometer[4] as potassium bromide pellets or Fluorolube mulls. UV spectra were recorded on a double-beam spectrophotometer[5]. TLC was performed using Eastman-type 6060 chromatogram sheets (silica gel), and the sheets were developed in an iodine chamber to check the purity of the amides.

Most of these derivatives were synthesized by a general procedure for the acylation of amines. The appropriate acid chloride or anhydride was condensed with guanazole, usually in the presence of a nonpolar solvent. Two typical reactions for preparing the amides are described using III and VI as examples.

One gram (0.01 *M*) of guanazole and 4.2 g (0.02 *M*) of trifluoroacetic anhydride were refluxed in dry toluene for 8 hr. The white precipitate

[1] Thomas Hoover melting-point apparatus.
[2] Performed by the Analytical Laboratory, California Institute of Technology, Pasadena, Calif.
[3] Hitachi Perkin-Elmer R-24.
[4] Beckman IR-4240.
[5] Perkin-Elmer Coleman 124.


0022-3549/81/1100-1281$01.00/0


© 1981, American Pharmaceutical Association

**Table I—Physical Properties of Guanazole Amides**

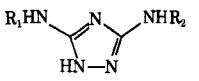

| Compound | $R_1$ | $R_2$ | Melting Point | Yield % | Formula | Analysis, % | Calc. | Found |
|---|---|---|---|---|---|---|---|---|
| I (3-amino-5-acetamido-1,2,4-triazole) | H | $COCH_3$ | 235–236° | 64 | $C_4H_7N_5O$ | C | 34.04 | 33.61 |
| | | | | | | H | 5.00 | 5.33 |
| | | | | | | N | 49.62 | 49.35 |
| II (3,5-diacetamido-1,2,4-triazole) | $COCH_3$ | $COCH_3$ | >250° | 81 | $C_6H_9N_5O_2$ | C | 39.36 | 39.30 |
| | | | | | | H | 4.92 | 4.99 |
| | | | | | | N | 38.25 | 38.20 |
| III (3,5-ditrifluoroacetamido-1,2,4-triazole) | $COCF_3$ | $COCF_3$ | >300° | 78 | $C_6H_3F_6N_5O_2$ | C | 24.74 | 25.11 |
| | | | | | | H | 1.03 | 1.17 |
| | | | | | | N | 24.05 | 24.18 |
| IV (3,5-dipropionamido-1,2,4-triazole) | $COCH_2CH_3$ | $COCH_2CH_3$ | >250° | 48 | $C_8H_{13}N_5O_2$ | C | 45.42 | 45.99 |
| | | | | | | H | 6.16 | 6.30 |
| | | | | | | N | 33.18 | 33.40 |
| V (3,5-dibutyramido-1,2,4-triazole) | $COC_3H_7$ | $COC_3H_7$ | >300° | 50 | $C_{10}H_{17}N_5O_2$ | C | 50.21 | 50.03 |
| | | | | | | H | 7.11 | 6.79 |
| | | | | | | N | 29.29 | 29.23 |
| VI (3-amino-5-heptafluorobutyramido-1,2,4-triazole) | H | $COC_3F_7$ | 300–301° | 91 | $C_6H_4F_7N_5O$ | C | 24.42 | 24.44 |
| | | | | | | H | 1.37 | 1.38 |
| | | | | | | N | 23.72 | (23.15) |
| VII (3,5-dipentafluoropropionamido-1,2,4-triazole) | $COC_2F_5$ | $COC_2F_5$ | 230–231° | 54 | $C_8H_3F_{10}N_5O_2$ | C | 24.56 | 25.01 |
| | | | | | | H | 0.76 | 0.76 |
| | | | | | | N | 17.90 | 18.28 |
| VIII (3,5-dibenzamido-1,2,4-triazole) | $COC_6H_5$ | $COC_6H_5$ | 314–315° | 71 | $C_{16}H_{13}N_5O_2$ | C | 62.54 | 62.26 |
| | | | | | | H | 4.23 | 4.08 |
| | | | | | | N | 22.80 | 22.92 |
| IX (3-amino-5-*p*-nitrobenzamido-1,2,4-triazole) | H | *p*-$NO_2C_6H_4CO$ | >300° | 20 | $C_9H_8N_6O_3$ | C | 43.54 | 43.48 |
| | | | | | | H | 3.22 | 3.44 |
| | | | | | | N | 33.87 | (32.62) |
| X (3,5-bis-*p*-nitrobenzamido-1,2,4-triazole) | *p*-$NO_2C_6H_4CO$ | *p*-$NO_2C_6H_4CO$ | >300° | 73 | $C_{16}H_{11}N_7O_6$ | C | 48.38 | 47.97 |
| | | | | | | H | 2.79 | 2.83 |
| | | | | | | N | 24.68 | 24.30 |

**Table II—Summary of IR Data for Guanazole Prodrugs**

| Compound | $\nu$N–H, $cm^{-1}$ | $\nu$C=O, $cm^{-1}$ | $\nu$C–N, $cm^{-1}$ | $\nu$C–H/C–F, $cm^{-1}$ |
|---|---|---|---|---|
| I | 3050–3400 | 1680 | 1610 | 2880, 2940 |
| II | 3100–3450 | 1680, 1720 | 1590 | 2860, 2960 |
| III | 3100–3300 | 1730, 1760 | 1630 | 1150–1230 |
| IV | 3200–3460 | 1690, 1710 | 1585 | 2860, 2880<br>2980, 2940 |
| V | 3100–3450 | 1680, 1720 | 1585 | 2840, 2880<br>2970, 2940 |
| VI | 3150–3450 | 1725 | 1635 | 1150–1220 |
| VIII | 3050–3400 | 1670, 1695 | 1590 | 3000, 710[a]<br>735[a] |
| IX | 3100–3460 | 1610 | 1610 | 3010, 708[a]<br>740[a] |
| X | 3100–3460 | 1695, 1720 | 1600 | 3010, 708[a]<br>740[a] |

[a] δC–H aromatic.

that formed was then washed with ether and dried *in vacuo* over phosphorus pentoxide. Drying afforded 2.26 g (78% yield) of the bis amide (III), mp 300°; IR (KBr): 1730 and 1760 ($\nu$C = 0) $cm^{-1}$.

One gram (0.01 *M*) of guanazole and 6.5 ml (1.58 g, 0.01 *M*) of heptafluorobutyric anhydride were refluxed in 10 ml of dry benzene for 4 hr. After standing overnight, the pale-yellow crystals were collected, washed with 5% ammonia, recrystallized from ethanol, and dried *in vacuo* over phosphorus pentoxide to yield 2.7 g (91% yield) of the product (VI), mp 300–301°; IR (KBr): 1725 ($\nu$C = 0) $cm^{-1}$.

**Biological Screening *versus* L1210 Cells *In Vitro***—For routine passage and during dose–response experiments, cells were maintained in asynchronous logarithmic growth at 37° in medium[6] supplemented with 10% fetal calf serum, 1% penicillin, and 1% streptomycin.

The cells were grown in a humidified incubator supplied with 95% air and 5% carbon dioxide at 37°. Stock cells were usually suspended at 6000–9000 cells/ml. The pH of the experimental flasks was adjusted to 7.4 with the addition of carbon dioxide. The drugs were solubilized with 1% dimethyl sulfoxide, diluted in phosphate-buffered saline, and added to the cell culture in 1:10 dilution to achieve the desired drug concentrations. Cell cultures were set up at 5000 cell/ml in duplicate for each drug concentration in 25-$cm^2$ flasks.

[6] Roswell Park Memorial Institute medium.

After 24, 48, and 72 hr of continuous drug exposure, the cells were harvested and counted using a Coulter counter. A control, 1% dimethyl sulfoxide-treated set of cultures, was included for each separate dose–response experiment. From the data obtained, a dose–response curve was drawn and the $ID_{50}$ value was calculated according to a reported method

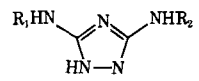

**Table III—NMR Chemical Shift of Prodrugs**

| Compound | $R_1$ | $R_2$ | Shift, (δ), ppm[a] |
|---|---|---|---|
| I[b] | H | $COCH_3$ | 1.83 (s) |
| II[c] | $COCH_3$ | $COCH_3$ | 2.37 (s) |
| IV[c] | $COC_2H_5$ | $COC_2H_5$ | 3.00 (q), 1.15 (t) |
| V[d] | $COC_3H_7$ | $COC_3H_7$ | 1.00 (t), 1.69 (m), 2.86 |
| VIII[b] | CO–$C_6H_5$ | $COC_6H_5$ | 7.40 (m), 7.80 (m) |
| IX[c] | H | CO–$C_6H_4$-*p*-$NO_2$ | 5.55 (s), 7.90, 8.10 (m) |
| X[c] | CO–$C_6H_4$-*p*-$NO_2$ | CO–$C_6H_4$-*p*-$NO_2$ | 8.20, 8.30 (m) |
| Guanazole[c] | H | H | 5.15 (s) |

[a] *S* = singlet, *t* = triplet, q = quartet, and m = multiplet. [b] In trifluoroacetic acid. [c] In dimethylsulfoxide-$d_6$. [d] In deuterochloroform.

Table IV—UV Absorption Spectra[a]

| Compound | $\lambda_{max}$, nm | $\epsilon$, $M^{-1}$ cm$^{-1}$ |
|---|---|---|
| I | 273 | 6,400 |
| II | 236 | 8,100 |
| III | 249 | 13,500 |
| IV | 236 | 9,200 |
| V | 236 | 2,200 |
| VI | 264 | 11,000 |
| VIII | 256 | 17,300 |
| IX | 260 | 16,000 |
| X | 264 | 43,000 |
| Guanazole | 200 | 500 |

[a] In Roswell Park Memorial Institute medium.

Table V—First-Order Rate Constants of Hydrolysis and Half-Lives of Guanazole Prodrugs

| Compound | $k$, hr$^{-1}$ | $t_{1/2}$, hr |
|---|---|---|
| I | 0.0128 | 54.0 |
| II | 0.0022 | 315.0 |
| III | 0.0087 | 79.0 |
| IV | 0.0030 | 231.0 |
| V | 0.0078 | 88.0 |
| VI | 0.0059 | 117.0 |
| VIII | 0.0050 | 138.0 |
| IX | 0.0113 | 61.0 |
| X | 0.0042 | 165.0 |

(6, 7). The $ID_{50}$ value represents the concentration of drug that halves the growth rate relative to untreated controls. Compound VII was not tested against L1210 cells *in vitro* due to insufficient quantity. The $ID_{50}$ value of VI could not be calculated due to negligible activity after 48 hr.

## RESULTS AND DISCUSSION

The amide derivatives were synthesized, and their structures were established by elemental analysis and IR, NMR, UV, and mass spectra (Tables II–IV). The hydrolysis rates of these amides are listed in Table V, and Table VI lists the calculated $ID_{50}$ values.

An assessment of the results *versus* L1210 cells revealed that, on the 1st day, VIII was substantially active. Solvolysis of this prodrug to an appreciable amount of guanazole by the medium was eliminated on the basis of the low hydrolysis rate ($t_{1/2}$ = 138 hr). Thus, VIII apparently shows activity *per se*, possibly due to its increased lipophilicity, which facilitates its transport into the cells where subsequent cytoplasmic hydrolysis may occur. However, increased interactions with the accessory binding site on the enzyme ribonucleotide reductase cannot be ruled out.

Compounds I and III showed activity comparable to that of guanazole against L1210 cells *in vitro*. Compound I, the most water soluble of the prodrugs, has a relatively short half-life ($t_{1/2}$ = 54 hr), which accounts for its activity after 48 hr. Compound III also has a short solvolytic half-life ($t_{1/2}$ = 79 hr), but its enhanced activity could be attributed to the release of trifluoroacetic acid, a well-known poison (8), as well as guanazole. The other prodrugs with extended half-lives may not have released guanazole in adequate amounts to exert the observed response. Some of the prodrugs such as VI, VIII, and IX might act as excellent depots of guanazole *in vivo*. *In vivo* testing of some of these compounds is in process.

Table VI—*In Vitro* Inhibition of L1210 by Guanazole Prodrugs

| Compound | $ID_{50}$, $M$ |
|---|---|
| Guanazole | $2.08 \times 10^{-4}$ |
| I | $2.40 \times 10^{-4}$ |
| II | $4.35 \times 10^{-3}$ |
| III | $1.90 \times 10^{-4}$ |
| IV | $4.67 \times 10^{-3}$ |
| V | $3.82 \times 10^{-2}$ |
| VIII | $9.26 \times 10^{-4}$ |
| IX | $2.32 \times 10^{-3}$ |
| X | $3.66 \times 10^{-3}$ |

## REFERENCES


(1) G. Pellizzari, *L'Orosi*, **17**, 143, 185 (1893).

(2) R. Brockman, S. Shaddix, W. Laster, and F. Schabel, Jr., *Cancer Res.*, **30**, 2358 (1970).

(3) M. Hahn and R. H. Adamson, *J. Natl. Cancer Inst.*, **48**, 783 (1972).

(4) D. Yakar, J. Holland, R. R. Ellison, and A. Freeman, *Cancer Res.*, **33**, 972 (1973).

(5) J. Hewlett, G. Bodey, C. Coltman, E. Freireich, A. Haut, and K. McCredie, *Clin. Pharmacol. Ther.*, **14**, 271 (1973).

(6) L. C. Miller and M. L. Tainter, *Proc. Soc. Exp. Biol. Med.*, **57**, 261 (1944).

(7) D. J. Finney, "Probit Analysis: A Statistical Treatment of the Sigmoid Response Curve," Cambridge University Press, 1947.

(8) W. Deichmann and H. Gerarde, "Toxicology of Drugs and Chemicals," Academic Press, New York, N.Y., 1969.


## ACKNOWLEDGMENTS


Presented in part at the APhA Academy of Pharmaceutical Sciences, Anaheim meeting, April 1979, and St. Louis Meeting, March 1981.

Abstracted in part from a thesis submitted by C. Dias Selassie to the University of Southern California in partial fulfillment of the Doctor of Philosophy degree requirements.

Supported in part by National Institutes of Health Biomedical Research Grant I S07 RR 05792-03, the Sigma Xi Grant-in-Aid of Research (C. D. Selassie), and the R.M. and J.L. Converse fund fellowship (C. D. Selassie).

The authors thank Ms. Stephanie Pentocost for technical assistance.

# Pharmacokinetics of Intravenous Chlorpheniramine in Children

JOHN A. THOMPSON *x, DUANE C. BLOEDOW *, and FRED H. LEFFERT ‡§

Received January 30, 1981, from the *School of Pharmacy, University of Colorado, Boulder, CO 80309, and the ‡Departments of Pediatrics, National Jewish Hospital and the University of Colorado School of Medicine, Denver, CO 80206. Accepted for publication March 20, 1981. §Present address: Professional Park-on-Cleveland, 3-B Cleveland Court, Greenville, SC 29607.

**Abstract** □ The disposition of chlorpheniramine was examined in seven children, 6–14 years of age, following a 0.1-mg/kg iv dose. Postinjection serum chlorpheniramine levels in each subject declined biexponentially, with the greatest intersubject variability occurring in the initial distribution of the drug. The volume of distribution at steady state ranged from 1.20 to 5.46 liters/kg. The chlorpheniramine serum clearance varied approximately twofold (234–470 ml/hr/kg) and generally decreased with age. The chlorpheniramine elimination half-life in children (mean of 9.6 hr) appeared shorter than that in adults, probably due to higher chlorpheniramine serum clearance in children.

**Keyphrases** □ Chlorpheniramine maleate—pharmacokinetics of intravenous drug in children □ Pharmacokinetics—intravenous chlorpheniramine maleate in children □ Antihistaminics—pharmacokinetics of intravenous chlorpheniramine maleate in children

Antihistamines represent a primary pharmacological approach to therapy for conditions such as allergic rhinitis and urticaria in patients of all ages. An appropriate antihistamine and its dose are often chosen by trial and error, sometimes with marginal success. Failure of an antihistamine to provide adequate relief could be due to intrinsic limitations in the drug's effectiveness or to suboptimal dosing due to a lack of pharmacokinetic information.

Although chlorpheniramine maleate has been a widely used antihistamine for many years, only limited pharmacokinetic information on it has been reported, and no information for children is available. Studies with adults reveal inconsistencies in biological half-life, with values ranging from 2 to 43 hr. (Table I) (1–7). Recently reported longer half-lives for chlorphreniramine have been attributed to longer blood sampling periods (6).

A highly sensitive assay procedure for chlorpheniramine was recently developed (8). The distribution and elimination of chlorpheniramine following intravenous administration of the drug to children were examined using this technique. This report presents the results of these studies.

## EXPERIMENTAL

**Methods**—Seven children, 6–14 years of age and 24–63 kg (Table II), were studied. The children were participating in a study of chronic rhinitis, and all had perennial rhinitis but no other significant medical problems. None had received antihistamines or any other medication for at least 1 month prior to the study. The children were studied for a 24-hr period[1].

Chlorpheniramine maleate[2], 0.10 mg/kg, was administered intravenously over 5 min by an infusion pump[3]. Serum was obtained from venous blood samples collected immediately prior to drug administration and at 0.25, 0.5, 1, 2, 4, 6, 8, 12, and 24 hr following completion of the 5-min infusion. Serum was stored at −70° until analyzed.

Chlorpheniramine analysis was performed by GLC–mass spectrometry. A tetradeuterated analog was prepared for use as the internal standard. Each serum sample (2.0 ml) was mixed with 85 ng of the internal standard, and extractions were carried out as previously described[4] (8). Final extracts were evaporated to dryness, redissolved in 5 μl of acetonitrile, and analyzed[5]. Ion current was monitored for $m/z$ 203 (chlorpheniramine) and 207 (tetradeuterated chlorpheniramine). Peak area ratios were converted to concentrations by using a calibration curve for the chlorpheniramine concentration range of 0–160 ng/ml.

**Table I—Summary of Available Information on Chlorpheniramine Half-Life in Adults**

| Half-Life, hr | Number of Subjects | Dose, mg | Route | Blood-Sampling Period, hr | Reference |
|---|---|---|---|---|---|
| 2[a] | 6 | 4 | Oral tablet | 5 | 1 |
| 12–15 | 6 | 12 | Oral tablets | 48 | 2 |
| 28 | 2 | 4 | Intravenous | 48 | 2 |
| 4 | 3 | 4 | Oral syrup | 12 | 3 |
| 24.5–36.3 | 4 | 8 | Oral capsule | 48 | 4 |
| 18 | 4 | 4,8,12 | Oral | 24 | 5 |
| 19–43 | 5 | 8 | Oral tablet | 60 | 6, 7 |
| 22, 23 | 2 | 5 | Intravenous | 60 | 6, 7 |

[a] Estimated from Ref.

The serum chlorpheniramine concentration ($C$) *versus* time curve for each subject was computer-fitted[6] (9) to the biexponential equation:

$$C = Ae^{-\alpha t} + Be^{-\beta t} \qquad \text{(Eq. 1)}$$

where $A$, $\alpha$, $B$, and $\beta$ are constants. Coefficients of determination ($r^2$) ranged from 0.991 to 1.000, and correlation coefficients ($r$) ranged from 0.989 to 0.997, indicating that the biexponential equation adequately describes the time course of serum chlorpheniramine concentrations after short-term intravenous infusion.

Following correction of $A$ and $B$ for the 5-min injection period, the intercepts ($A$ and $B$) and slopes ($\alpha$ and $\beta$) were used to calculate the distribution of half-life ($t_{1/2,\alpha}$), the biological half-life ($t_{1/2,\beta}$), the initial dilution volume ($V_1$), the volume of distribution at steady state ($V_{ss}$), the postdistribution volume ($V_\beta$), and the serum clearance ($Cl$) (10).

## RESULTS

The biexponential decline of serum chlorpheniramine in a representative child (Subject SW) is shown in Fig. 1. Pharmacokinetic parameters describing chlorpheniramine distribution and elimination in this group of children are summarized in Table II. In this small group, no significant correlations could be shown relating absolute (not weight-adjusted) distribution volumes or serum clearance to total body surface area (11) ($V_1$, $r = -0.399$; $V_{ss}$, $r = 0.467$; $V_\beta$, $r = 0.619$; and $Cl$, $r = 0.638$). Similarly, correlations relating absolute distribution volumes or clearance to total body weight were not significant($V_1$, $r = -0.394$; $V_{ss}$, $r = 0.511$; $V_\beta$, $r = 0.654$; and $Cl$, $r = 0.695$). The distribution volumes and clearance values in Table II have been weight adjusted to facilitate comparison to available literature data for chlorpheniramine disposition in adults.

The initial distribution of the drug was quite variable, as evidenced by a large intersubject variation in the initial dilution volume ($V_1$), $\alpha$, and $t_{1/2,\alpha}$. The intersubject variability of other pharmacokinetic parameters is in the range given for other drugs in children (12).

[1] Clinical Research Unit, National Jewish Hospital, Denver, Colo.
[2] Schering Corp., Kenilworth, N.J.
[3] Harvard Apparatus Co., Millis, Mass.

[4] *Erratum*—In Reference 8, the following corrections should be made. On page 708, column 1, the next to last line should read "a 0.10-mg/kg dose." On page 709, column 1, Table II, should read: Initial dilution volume ($V_c$), 2.982 liters/kg; Volume of distribution during postdistribution phase ($V_\beta$), 5.628 liters/kg; total body clearance 4.15 ml/min/kg. On page 709, column 2, line 6 should read "intravenous dose of 0.10 mg/kg."
[5] Model 5984A, Hewlett-Packard, Palo Alto, Calif.
[6] CDC 6400 computer.



0022-3549/81/1100-1284$01.00/0
© 1981, American Pharmaceutical Association

**Table II—Pharmacokinetic Parameters in Children following a 0.1-mg/kg iv Dose of Chlorpheniramine Maleate**

| Subject | Age, yr | Height, cm | Weight, kg | Surface Area,[a] $m^2$ | $\alpha$, $hr^{-1}$ | $t_{1/2,\alpha}$, hr | $\beta$, $hr^{-1}$ | $t_{1/2,\beta}$, hr | $V_1$, liters/kg | $V_{ss}$, liters/kg | $V_\beta$, liters/kg | $Cl$, ml/hr/kg |
|---|---|---|---|---|---|---|---|---|---|---|---|---|
| TM | 6 | 122 | 24 | 0.903 | 1.78 | 0.39 | 0.0796 | 8.7 | 1.93 | 4.79 | 5.19 | 413 |
| SB | 9 | 137 | 28 | 1.05 | 3.89 | 0.18 | 0.0794 | 8.7 | 1.35 | 3.80 | 3.96 | 314 |
| CG | 9 | 142 | 37 | 1.21 | 1.25 | 0.55 | 0.0857 | 8.1 | 1.87 | 4.76 | 5.49 | 470 |
| MP | 11 | 155 | 38 | 1.31 | 4.13 | 0.17 | 0.133 | 5.2 | 0.145 | 1.20 | 2.28 | 302 |
| TB | 12 | 147 | 33 | 1.18 | 1.31 | 0.53 | 0.0443 | 15.7 | 2.98 | 5.46 | 5.63 | 249 |
| SW | 14 | 165 | 57 | 1.62 | 4.38 | 0.16 | 0.0526 | 13.2 | 0.537 | 4.06 | 4.45 | 234 |
| MR | 14 | 165 | 63 | 1.69 | 4.41 | 0.16 | 0.0904 | 7.7 | 0.352 | 2.62 | 3.12 | 282 |
| Mean | | 148 | 40 | 1.28 | 3.02 | 0.31 | 0.0807 | 9.6 | 1.31 | 3.81 | 4.30 | 323 |
| ±*SD* | | 15 | 15 | 0.29 | 1.49 | 0.18 | 0.0288 | 3.6 | 1.03 | 1.46 | 1.26 | 87 |
| *CV*, % | | 10 | 38 | 23 | 49 | 58 | 36 | 38 | 79 | 38 | 29 | 27 |

[a] Estimated using the equation (11): surface area ($m^2$) = weight $(kg)^{0.425}$ × height $(cm)^{0.727}$ × 0.007184.

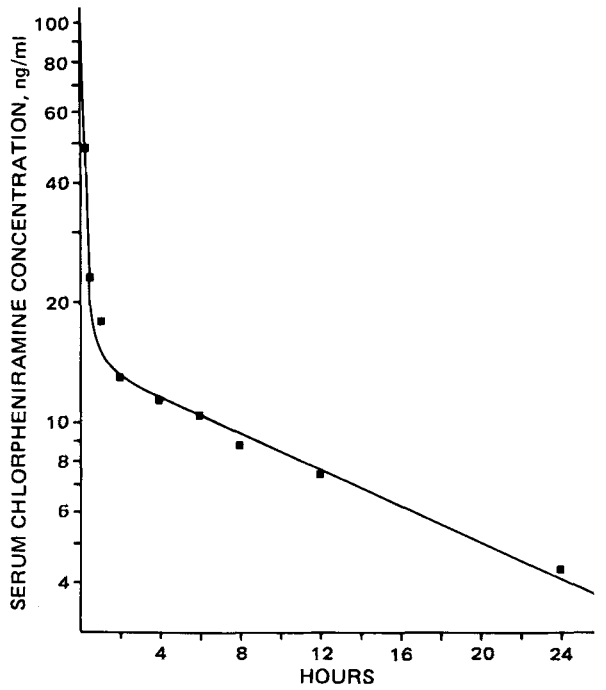


**Figure 1**—*Serum chlorpheniramine concentrations following the intravenous administration of a 0.1-mg/kg dose of chlorpheniramine maleate to Subject SW.*

## DISCUSSION

The biological half-life for chlorpheniramine in adults has been reported to be as short as 2 hr and as long as 43 hr (Table I). Recent adult studies used a sensitive liquid chromatographic method to show that the chlorpheniramine half-life was 22 and 23 hr following intravenous administration to two subjects and 19–43 hr following oral administration to five subjects (6, 7). The previously reported shorter half-lives for chlorpheniramine in adults could be attributed to shorter blood sampling periods (6) and assay differences. A comparison of the biological half-lives for chlorpheniramine in this group of children (5.2–15.7 hr, Table II) with biological half-lives reported recently for adults indicates that the drug is eliminated much more rapidly from children than from adults.

Biological half-life ($t_{1/2,\beta}$) is directly related to ($V_\beta$) and inversely related to $Cl$ according to:

$$t_{1/2,\beta} = \frac{0.693 \cdot V_\beta}{Cl} \qquad \text{(Eq. 2)}$$

Comparisons between recently reported adult data and the data from this study in children offer evidence that the shorter chlorpheniramine biological half-life in children is primarily due to a greater chlorpheniramine serum clearance in children rather than to a difference in distribution volumes. The chlorpheniramine postdistribution volume ($V_\beta$) in children averaged 4.30 liters/kg (range 2.28–5.63 liters/kg) and is similar to the postdistribution volume reported for adults (7) (3.2 and 3.6 liters/kg). The serum clearance for chlorpheniramine in children averaged 323 ml/hr/kg (range 234–470 ml/hr/kg), while plasma clearance in adults is ~100 ml/hr/kg (estimated from Ref. 7). The more rapid elimination of chlorpheniramine from children compared to adults is similar to that reported for other drugs (13). Interestingly, in this small sample of children the serum clearance of chlorpheniramine is negatively correlated with age ($r = -0.799$, $p < 0.05$) and, no correlation could be shown between serum clearance and weight ($r = -0.144$) or body surface area ($r = -0.551$).

Presently available information is insufficient for formulation of dosing recommendations for children; data on the relation between serum chlorpheniramine level and biological effect are needed. Little is known about the optimum chlorpheniramine serum concentration necessary for treatment of the clinical conditions for which the drug is used. In addition, since chlorpheniramine is commonly administered orally, an estimate of bioavailability would be necessary for formulating dosing recommendations. Studies in adults indicated that oral bioavailability is low (25 and 44% in two subjects following administration of tablets), possibly due to an extensive gut first-pass effect (7). Oral chlorpheniramine bioavailability estimates have not been reported for children.

Although optimum serum chlorpheniramine levels and bioavailability in children have not been reported, the apparent age-related differences in chlorpheniramine elimination indicate that adherence to a fixed milligram per kilogram maintenance dose may not be appropriate in all children. An oral dosage regimen of 0.35 mg/kg/day in four doses (or 0.0875 mg/kg every 6 hr) has been recommended for older infants and children (14). The desired average steady-state serum drug concentration ($\overline{C}_{ss}$) is directly related to the fraction of the oral dose absorbed ($F$) and the oral maintenance dose ($D$) and indirectly related to the serum clearance ($Cl$) and the dosing interval ($\tau$) according to:

$$\overline{C}_{ss} = \frac{F\,D}{Cl\,\tau} \qquad \text{(Eq. 3)}$$

With the assumption of no variation in bioavailability ($F$), the recommended oral dosage regimen could produce a twofold variation in average serum levels ($\overline{C}_{ss}$), based on the twofold variation in the chlorpheniramine serum clearance in the group of children studied (Table II). The data suggest that younger children may require a slightly larger milligram per kilogram dose than the older child to produce equivalent serum chlorpheniramine levels, barring age-related differences in bioavailability.

Based purely on pharmacokinetic considerations, frequent dosing of chlorpheniramine may not be necessary in adults because of the long elimination half-life (6, 7). The present study indicates that frequent dosing may be advisable in children to reduce possible widely fluctuating and perhaps excessive or subtherapeutic serum chlorpheniramine levels. Dosing frequency decisions are complicated, however, by the generally accepted statement that the therapeutic effect of chlorpheniramine is no longer than 4 hr (2). Whether this is true in children is unclear and deserving of additional study.

## REFERENCES

(1) W. E. Lange, J. M. Theodore, and F. J. Pruyn, *J. Pharm. Sci.*, **57**, 124 (1968).

(2) E. A. Peets, M. Jackson, and S. Symchowicz, *J. Pharmacol. Exp. Ther.*, **180**, 364 (1972).

(3) S. Hanna and A. Tang, *J. Pharm. Sci.*, **63**, 1954 (1974).

(4) P. Haefelfinger, *J. Chromatogr.*, **124**, 351 (1976).

(5) J. W. Barnhart and J. D. Johnson, *Anal. Chem.*, **49**, 1085

(1977).
(6) W. L. Chiou, N. K. Athanikar, and S. Huang, *N. Engl. J. Med.*, **300**, 501 (1979).
(7) S. M. Huang, N. K. Athanikar, K. Sridhar, Y. C. Huang, and W. L. Chiou, "Abstracts," vol. 8, no. 2, APhA Academy of Pharmaceutical Sciences, 1980, p. 82.
(8) J. A. Thompson and F. H. Leffert, *J. Pharm. Sci.*, **69**, 707 (1980).
(9) C. M. Metzler, G. L. Elfring, and A. J. McEwen, *Biometrics*, **30**, 562 (1974).
(10) M. Gibaldi and D. Perrier, "Pharmacokinetics," Dekker, New York, N.Y., 1975, pp. 48, 68, 177.
(11) D. DuBois and E. F. DuBois, *Arch. Intern. Med.*, **17**, 863 (1916).
(12) E. F. Ellis, R. Koysooko, and G. Levy, *Pediatrics*, **58**, 542 (1976).
(13) A. Rane and J. T. Wilson, *Clin. Pharmacokinet.*, **1**, 2 (1976).
(14) H. C. Shirkey, "Pediatric Clinical Pharmacology and Therapeutics in Drug Treatment," Adis Press, New York, N.Y., 1980, p. 126.

## ACKNOWLEDGMENTS

Partially supported by the Council for Research and Creative Work of the University of Colorado.

The authors thank Mr. John Ivy for assistance with the serum extractions.

# Application of One-Phase End-Point Change System in Two-Phase Titration to Amine Drug Analysis

**MASAHIRO TSUBOUCHI** *x, **HIROMI MITSUSHIO** ‡, **NAKAMICHI YAMASAKI** ‡, and **KIYOSHI MATSUOKA** ‡

Received December 2, 1980, from the *Laboratory of Chemistry, Kochi Medical School, Oko, Nankoku, Kochi 781-51, Japan, and the ‡ Department of Geology, Faculty of Science, Kochi University, Asakura, Japan. Accepted for publication March 30, 1981.

**Abstract** □ A titration method was developed for the determination of diphenhydramine, quinine, neostigmine, sparteine, strychnine, homatropine, atropine, physostigmine, and procaine in aqueous solution. Tetraphenylborate was used as a titrant with tetrabromophenolphthalein ethyl ester as an indicator in the presence of organic solvent. End-point detection was based on the color change of the indicator in the organic phase without movement of the indicator from one phase to the other.

**Keyphrases** □ Amine drugs—analysis, two-phase titration □ One-phase end-point change system—two-phase titration, amine drugs □ Two-phase titration—amine drugs, one-phase end-point change system

Titration methods permit the convenient determination of organic and inorganic ions without complex instrumentation. Solvent extraction techniques are also convenient in the titration field. Two-phase titration (ion-pair extraction–titration) using methylene blue was proposed by Weatherburn (1) in 1950. However, with this two-phase dye transfer titration method, it is generally difficult to detect the end-point because a dye color in an aqueous layer reflects to the organic layer (2). Subsequently, additional reports (2–5) described two-phase dye transfer procedures involving modifications of the methylene blue method and substitutions of various dyes for methylene blue.

Titration end-point detection, however, can be a problem with the two-phase titration method due to color reflectance between phases and differences in the color shade or hue in the two phases. These problems occur because the end-point detection in the two-phase titrations is based on the transfer of the indicator dye from one phase to the other, with end-points usually taken when color intensity is judged to be equal between the two phases. The two-phase titration has been applied only to the determination of surfactants. Mohammed and Cantwell (6) recently developed a two-phase photometric titration method for the determination of drugs and surfactants.

The present paper reports a new two-phase titration method based on the change of indicator in only one phase without movement of the indicator from one phase to the other. This one-phase end-point change system provided the two-phase titration method for the determination of amines in aqueous solution. Colorimetric and nonaqueous titrimetric methods were used for the determination of alkaloids or amines.

## EXPERIMENTAL[1]

**Reagents**—The potassium salt of tetrabromophenolphthalein ethyl ester, dissolved in ethanol to make a 0.1% solution, was used as the indicator.

**Buffer Solution**—A borate–phosphate buffer was prepared by adding 2 *N* $H_2SO_4$ to a 0.2 *M* dibasic sodium phosphate solution containing 0.1 *M* sodium borate.

**Titrant**—Sodium tetraphenylborate (3.422 g), dried at 80°, was dissolved in water and diluted to 1 liter to make a 0.01 *M* solution.

**Amine Solution**—Sample solutions of diphenhydramine, quinine, neostigmine, sparteine, strychnine, atropine, physostigmine, and procaine were prepared by dissolving their hydrochlorides, bromides, or sulfates in 0.002 *N* $H_2SO_4$. The solutions were standardized by the official method (7).

**Titration Procedure**—The proposed titration methods with a one-phase end-point change system are summarized in Table I. For example, the determination of diphenhydramine was as follows: 1–10 ml of diphenhydramine solution (0.01 or 0.005 *M*), 5 ml of borate–phosphate buffer (pH 5.5–7.5), 10 ml of ethylene dichloride, and 3–4 drops of indicator solution were placed in a 300-ml erlenmeyer flask. The mixture was titrated with 0.01 *M* tetraphenylborate solution with manual intermittent shaking to ensure equilibrium between the organic solvent and the aqueous phase.

The other amines or alkaloids in Table I were treated in the same manner as described for diphenhydramine.

## RESULTS AND DISCUSSION

**End-Point Color**—The one-phase end-point change system is based on the hydrophobic indicator, which is able to react with ions in the aqueous phase. The tetrabromophenolphthalein ethyl ester indicator is a monoprotic acid and can form ion associates or charge transfer complexes with amines or alkaloids (8). The initial mixture of the amines

[1] All chemicals were reagent grade; Wako Pure Chemical Industries, Tokyo, Japan.



0022-3549/81/1100-1286$01.00/0
© 1981, American Pharmaceutical Association

(1977).
(6) W. L. Chiou, N. K. Athanikar, and S. Huang, *N. Engl. J. Med.*, **300**, 501 (1979).
(7) S. M. Huang, N. K. Athanikar, K. Sridhar, Y. C. Huang, and W. L. Chiou, "Abstracts," vol. 8, no. 2, APhA Academy of Pharmaceutical Sciences, 1980, p. 82.
(8) J. A. Thompson and F. H. Leffert, *J. Pharm. Sci.*, **69**, 707 (1980).
(9) C. M. Metzler, G. L. Elfring, and A. J. McEwen, *Biometrics*, **30**, 562 (1974).
(10) M. Gibaldi and D. Perrier, "Pharmacokinetics," Dekker, New York, N.Y., 1975, pp. 48, 68, 177.
(11) D. DuBois and E. F. DuBois, *Arch. Intern. Med.*, **17**, 863 (1916).
(12) E. F. Ellis, R. Koysooko, and G. Levy, *Pediatrics*, **58**, 542 (1976).
(13) A. Rane and J. T. Wilson, *Clin. Pharmacokinet.*, **1**, 2 (1976).
(14) H. C. Shirkey, "Pediatric Clinical Pharmacology and Therapeutics in Drug Treatment," Adis Press, New York, N.Y., 1980, p. 126.

## ACKNOWLEDGMENTS

Partially supported by the Council for Research and Creative Work of the University of Colorado.

The authors thank Mr. John Ivy for assistance with the serum extractions.

# Application of One-Phase End-Point Change System in Two-Phase Titration to Amine Drug Analysis

**MASAHIRO TSUBOUCHI** *x, **HIROMI MITSUSHIO** ‡, **NAKAMICHI YAMASAKI** ‡, and **KIYOSHI MATSUOKA** ‡

Received December 2, 1980, from the *Laboratory of Chemistry, Kochi Medical School, Oko, Nankoku, Kochi 781-51, Japan, and the ‡ Department of Geology, Faculty of Science, Kochi University, Asakura, Japan. Accepted for publication March 30, 1981.

**Abstract** □ A titration method was developed for the determination of diphenhydramine, quinine, neostigmine, sparteine, strychnine, homatropine, atropine, physostigmine, and procaine in aqueous solution. Tetraphenylborate was used as a titrant with tetrabromophenolphthalein ethyl ester as an indicator in the presence of organic solvent. End-point detection was based on the color change of the indicator in the organic phase without movement of the indicator from one phase to the other.

**Keyphrases** □ Amine drugs—analysis, two-phase titration □ One-phase end-point change system—two-phase titration, amine drugs □ Two-phase titration—amine drugs, one-phase end-point change system

Titration methods permit the convenient determination of organic and inorganic ions without complex instrumentation. Solvent extraction techniques are also convenient in the titration field. Two-phase titration (ion-pair extraction–titration) using methylene blue was proposed by Weatherburn (1) in 1950. However, with this two-phase dye transfer titration method, it is generally difficult to detect the end-point because a dye color in an aqueous layer reflects to the organic layer (2). Subsequently, additional reports (2–5) described two-phase dye transfer procedures involving modifications of the methylene blue method and substitutions of various dyes for methylene blue.

Titration end-point detection, however, can be a problem with the two-phase titration method due to color reflectance between phases and differences in the color shade or hue in the two phases. These problems occur because the end-point detection in the two-phase titrations is based on the transfer of the indicator dye from one phase to the other, with end-points usually taken when color intensity is judged to be equal between the two phases. The two-phase titration has been applied only to the determination of surfactants. Mohammed and Cantwell (6) recently developed a two-phase photometric titration method for the determination of drugs and surfactants.

The present paper reports a new two-phase titration method based on the change of indicator in only one phase without movement of the indicator from one phase to the other. This one-phase end-point change system provided the two-phase titration method for the determination of amines in aqueous solution. Colorimetric and nonaqueous titrimetric methods were used for the determination of alkaloids or amines.

## EXPERIMENTAL[1]

**Reagents**—The potassium salt of tetrabromophenolphthalein ethyl ester, dissolved in ethanol to make a 0.1% solution, was used as the indicator.

**Buffer Solution**—A borate–phosphate buffer was prepared by adding 2 *N* $H_2SO_4$ to a 0.2 *M* dibasic sodium phosphate solution containing 0.1 *M* sodium borate.

**Titrant**—Sodium tetraphenylborate (3.422 g), dried at 80°, was dissolved in water and diluted to 1 liter to make a 0.01 *M* solution.

**Amine Solution**—Sample solutions of diphenhydramine, quinine, neostigmine, sparteine, strychnine, atropine, physostigmine, and procaine were prepared by dissolving their hydrochlorides, bromides, or sulfates in 0.002 *N* $H_2SO_4$. The solutions were standardized by the official method (7).

**Titration Procedure**—The proposed titration methods with a one-phase end-point change system are summarized in Table I. For example, the determination of diphenhydramine was as follows: 1–10 ml of diphenhydramine solution (0.01 or 0.005 *M*), 5 ml of borate–phosphate buffer (pH 5.5–7.5), 10 ml of ethylene dichloride, and 3–4 drops of indicator solution were placed in a 300-ml erlenmeyer flask. The mixture was titrated with 0.01 *M* tetraphenylborate solution with manual intermittent shaking to ensure equilibrium between the organic solvent and the aqueous phase.

The other amines or alkaloids in Table I were treated in the same manner as described for diphenhydramine.

## RESULTS AND DISCUSSION

**End-Point Color**—The one-phase end-point change system is based on the hydrophobic indicator, which is able to react with ions in the aqueous phase. The tetrabromophenolphthalein ethyl ester indicator is a monoprotic acid and can form ion associates or charge transfer complexes with amines or alkaloids (8). The initial mixture of the amines

[1] All chemicals were reagent grade; Wako Pure Chemical Industries, Tokyo, Japan.



0022-3549/81/1100-1286$01.00/0
© 1981, American Pharmaceutical Association

**Table I—Two-Phase Titration with One-Phase End-Point Change System for Determination of Amines [a]**

| Amine | pH in Aqueous Phase | Organic Solvent | Color Change in Organic Phase at End-Point |
|---|---|---|---|
| Diphenhydramine | 5.5–7.5 | Ethylene dichloride | Violet → yellow |
| Quinine | 4.5–6.0 | Nitroethane | Violet → yellow |
| Berberine | 5.0–9.5 | Chloroform | Blue → yellow |
| Neostigmine | 9.0–9.5 | Ethylene dichloride | Greenish blue → yellow |
| Sparteine | 5.0–9.0 | Ethylene dichloride | Blue → yellow |
| Alkaloids [b] | 5.5–6.5 | Ethylene dichloride | Reddish blue → greenish yellow |

[a] The indicator was tetrabromophenolphthalein ethyl ester, and the titrant was tetraphenylborate. [b] Strychnine, homatropine, atropine, physostigmine, and procaine.

or alkaloids in Table I, buffer solution, indicator, and organic solvent yields a solution with a colorless aqueous layer and a blue or violet organic phase. As the solution is titrated with tetraphenylborate, with thorough shaking after each addition of titrant, the organic solution turns green near the end-point. When 1 drop of excess is added, the organic phase turns yellow, indicating the titration end-point. The upper aqueous layer remains colorless throughout titration due to the water insolubility of the tetrabromophenolphthalein ethyl ester indicator. Amines or alkaloids cannot be determined by the two-phase dye transfer titration method with methylene blue as an indicator because the end-point is not clear.

**Effect of pH on Titration**—The effect of pH was studied by titrating a series of amines and alkaloids at various pH values. The titer was constant when the pH of the aqueous phase was within the range shown in Table I. When an amine (A) is titrated with a tetraphenylborate ion ($B^-$) solution, the $[A\text{-}H^+\cdot B^-]$ complex is formed in the organic layer. The end-point of the titration with the proposed indicator (Ind) is described by:

$$[A\text{-}H^+ \cdot Ind^-]_o + [B^-]_w + H^+ \rightarrow [A\text{-}H^+ \cdot B^-]_o + [H\text{-}Ind]_o$$

*violet or blue* — *yellow*

*Scheme I*

where $o$ is the organic phase and $w$ is the aqueous phase. The indicator in the $[A\text{-}H^+\cdot Ind^-]_o$ complex is substituted by the titrant ion to liberate the indicator in the nondissociated form.

The basic equilibria for the titration of diphenhydramine can be represented by:

$$D + B \rightleftharpoons [DB]$$

*Scheme IIa*

$$D + Ind \rightleftharpoons [DInd]$$

*Scheme IIb*

where D is the diphenhydramine. (For simplicity, charges are omitted.) The corresponding equilibrium constants are:

$$K_{DB} = [DB]/([D][B])$$

*Scheme IIIa*

$$K_{DInd} = [DInd]/([D][Ind])$$

*Scheme IIIb*

The effective stability constants ($K'$) at room temperature can be obtained by determining [DB] and [DInd] in the organic phase using spectroscopic absorption measurements at various pH values (9). A simple log $K'$–pH diagram is given in Fig. 1 for the titration. Line 1 represents pD or $-\log[D]$ at two equivalents of tetraphenylborate where $[B]_w = [BD]_o$. Line 2 corresponds to the pD or $-\log[D]$ values at which $[DInd]_o = [Ind]_o$. From the log $K'$–pH diagram, a theoretical titration curve is constructed for the 0.01 $M$ tetraphenylborate titration of 10 ml of 0.01 $M$ diphenhydramine at pH 6.5 (Fig. 2). The shaded areas indicate the region of the color change of tetrabromophenolphthalein ethyl ester indicator, with C corresponding to the point of 50% color change. A maximum color change is obtained by a minimum increment of titrant at this point. The fractional color change from 0.1 to 0.9 covers ~2 pD units. The theoretical titration curve at pH 6.5 was in good agreement with experimental values.

**Other Variables and Foreign Substances**—Larger amounts of buffer solution had no influence on titration, but amounts of <0.5 ml caused problems in phase separation. Initial volume fluctuations of the aqueous layer (5–25 ml) and the organic layer (7–15 ml) had no influence on the determination of the titration end-point. The effect of water-immiscible solvents on titration were tested: butyl acetate, benzene, carbon tetrachloride, chlorobenzene, chloroform, ethylene dichloride, $n$-hexane, isopentyl alcohol, methyl isobutyl ketone, nitrobenzene, nitroethane, and toluene. Of these solvents, the best ones for the titration are summarized in Table I.

The effect of several salts on the titration of 10 ml of 0.01 $M$ diphenhydramine solution indicated that the following ions did not interfere at the 0.01 $M$ level: $Na^+$, $Ca^{2+}$, $Mg^{2+}$, $NH_4^+$, $K^+$, $NO_3^-$, $SO_4^{2-}$, $CO_3^{2-}$, $Br^-$, $I^-$, $Cl^-$, acetate, citrate, and tannate. Amines such as thiamine and papaverine caused positive errors. Lauryl sulfate and mercury II interfered.

**Precision and Analysis of Practical Samples**—The reproducibility of the proposed method with 0.005 $M$ titrant solution was estimated from

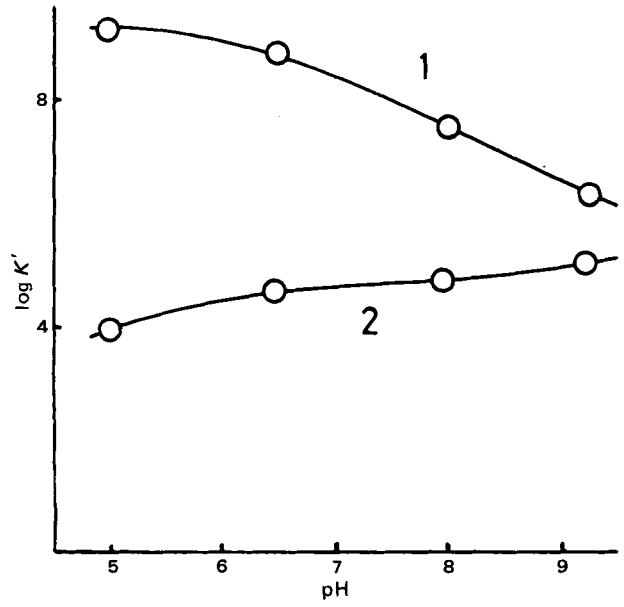


**Figure 1**—*Log K′–pH diagram. Key: 1, log $K'_{DB}$; and 2, log $K'_{DInd}$.*

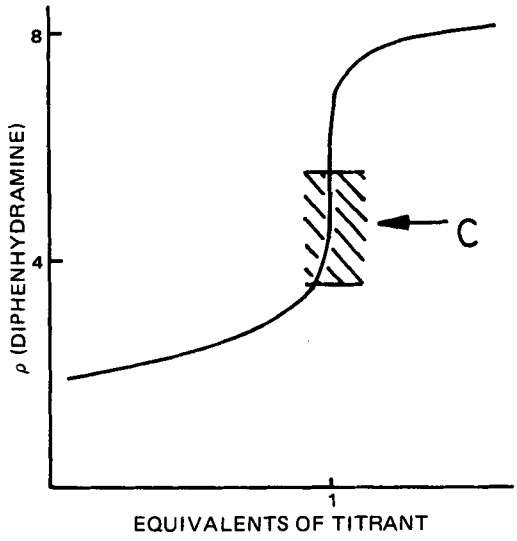


**Figure 2**—*Theoretical titration curve at pH 6.5; 10 ml of 0.01* M *diphenhydramine is titrated with 0.01* M *tetraphenylborate.*

the results of 10 sample solutions (5 ml), each with a sparteine concentration of 0.005 *M*. The mean titer was 5.02 ml, with a standard deviation of 0.05 ml. The relative error was ~2% when 5 ml of diphenhydramine solution was titrated according to the procedure.

Commercial products containing diphenhydramine (injection, 10 mg/ml; tablet, 90 mg/g; and ointment, 10 mg/g) were analyzed according to the proposed method and a spectrophotometric method (8). The results were 9.97, 91.0, and 9.90 mg of diphenhydramine/ml in the injection, tablet, and ointment, respectively, by the proposed method and 9.95, 90.7, and 9.87 mg/g, respectively, by the spectrophotometric method. Tablet samples were dissolved in dilute sulfuric acid. The solution was filtered with a glass filter. Ointment samples were dispersed with 15 ml of ether in a separator. The contents were extracted three times with 10-ml portions of 0.1 *N* $H_2SO_4$. The extracts were neutralized slightly with 0.1 *N* NaOH solution.

## REFERENCES


(1) A. S. Weatherburn, *J. Am. Oil Chem. Soc.*, **28**, 233 (1950).

(2) L. K. Wang and P. J. Panzardi, *Anal. Chem.*, **47**, 1472 (1975).

(3) M. E. Turney and D. W. Cannell, *J. Am. Oil Chem. Soc.*, **42**, 544 (1965).

(4) J. T. Gross, *Analyst*, **90**, 315 (1965).

(5) Y. Kasai, Y. Ueda, W. Yano, and W. Kimura, *Nippon Kagaku Kaishi*, **1972**, 2394.

(6) H. Y. Mohammed and F. F. Cantwell, *Anal. Chem.*, **52**, 553 (1980).

(7) "The Japanese Pharmacopoeia," 9th ed., Hirokawa Publishing, Tokyo, Japan, 1976.

(8) M. Tsubouchi, *J. Pharm. Sci.*, **60**, 943 (1971).

(9) M. Tsubouchi, *Bull. Chem. Soc. Jpn.*, **43**, 3164 (1970).


# Measurement of Pseudoephedrine Hydrochloride Dissolution Using Chloride-Ion Electrode


**S. T. CHEN, R. C. THOMPSON, and R. I. POUST** ˣ



Received October 24, 1980, from the *Pharmaceutical Research and Development Laboratories, Burroughs Wellcome Co., Greenville, NC 27834* Accepted for publication April 17, 1981.



**Abstract** □ Experiments were performed to determine the suitability of using a chloride-ion electrode for the measurement of pseudoephedrine hydrochloride dissolution from commercially available compressed tablets. Dissolution experiments were carried out in 500 ml of distilled water using the USP paddle method at 100 rpm. Both chloride ion and pseudoephedrine (UV spectrophotometry) were measured at six different sampling times. Percent dissolved *versus* time values were linearized on a log-normal probability basis. The slopes of individual lines obtained from the chloride and pseudoephedrine measurements were compared using a Student *t* test and did not differ significantly ($t = 0.415$, $df = 5$, $p > 0.05$). In addition to providing an efficient, inexpensive, and simple method for measuring pseudoephedrine hydrochloride dissolution rates, the chloride-ion electrode could be used in the measurement of dissolution rates for a wide variety of drugs available as hydrochloride salts.



**Keyphrases** □ Pseudoephedrine hydrochloride—measurement of dissolution using chloride-ion electrode □ Chloride-ion electrode—measurement of pseudoephedrine hydrochloride dissolution □ Dissolution—pseudoephedrine hydrochloride, measurement using chloride-ion electrode


There has been a significant increase in the use of dissolution rate testing for the development of new dosage forms as a quality assurance tool and as a predictor of bioavailability in instances where successful *in vivo–in vitro* correlations have been established. Recent activity has centered on the establishment of automated procedures and the optimization of existing methodology with emphasis on the USP rotating-basket and USP paddle methods (1). One interesting aspect has been the automation of analytical measurements, mainly through the use of flow-through cells in conjunction with various spectrophotometers (2–7). Another analytical procedure that lends itself to automation is the use of a specific ion electrode to measure directly the drug's counterion in the dissolution flask.

## BACKGROUND

A survey of the recent literature revealed limited use of selective ion electrodes for measurement of tablet or capsule dissolution rates. Mason *et al.* (8) described the use of a sodium-ion selective electrode for the measurement of dissolution rates of specially prepared sodium salicylate tablets. They found agreement between sodium-ion concentrations measured by the selective ion electrode and atomic absorption spectrophotometry. Sodium-ion concentrations agreed with salicylate concentrations measured spectrophotometrically. The method was later extended (9) to measure dissolution rates of commercial tablets containing warfarin sodium, butabarbital sodium, and sodium bicarbonate. Data obtained by selective ion electrode and spectrophotometric measurements were in agreement when both methods were utilized.

Thomas (10) used a potassium-ion specific electrode to study the release rate of potassium from several brands of slow-release potassium chloride tablets. Other investigators (11), using similar methodology, also studied the dissolution release pattern of sustained-release potassium chloride tablets. This report presents the results of similar studies using anion measurements; *i.e.*, a chloride-ion electrode was used to measure the dissolution rate of commercial pseudoephedrine hydrochloride tablets.

## EXPERIMENTAL

**Materials**—Pseudoephedrine hydrochloride tablets[1] (60 mg/tablet) and pseudoephedrine hydrochloride[2] were used as received. An ionic strength adjuster (5 *M* $NaNO_3$) was prepared by dissolving 42.5 g of sodium nitrate[3] in 100 ml of distilled water.

**Chloride-Ion Measurements**—Chloride ions were detected by a chloride-ion electrode[4] together with a double-junction electrode[5]. The electrodes were connected to an analyzer[6], which displayed direct millivolt readings of the measured potentials.

A calibration curve was constructed for pseudoephedrine hydrochloride. Standard solutions of 0.01–1.00 mg/ml were prepared. For each standard solution, 100 ml of solution and 2 ml of ionic strength adjuster were poured into a 150-ml glass beaker and thoroughly stirred. The millivolt reading was recorded once the reading stabilized. These values were then linearized by plotting them on a linear scale as a function of the logarithm of the chloride concentration.

**UV Spectrophotometric Measurements**—A Beer's law curve was constructed for pseudoephedrine hydrochloride in distilled water. The

[1] Sudafed tablets, batches 7L2089 and 7L2087, Burroughs Wellcome Co., Research Triangle Park, N.C.

[2] Batch P5705-4G, Burroughs Wellcome Co., Research Triangle Park, N.C.

[3] ACS reagent, Fisher Scientific, Pittsburgh, Pa.

[4] Model 94-17A, Orion Research, Cambridge, Mass.

[5] Model 90-02, Orion Research, Cambridge, Mass.

[6] Microprocessor Ionlyzer/901, Orion Research, Cambridge, Mass.




*0022-3549/81/1100-1288$01.00/0*



*© 1981, American Pharmaceutical Association*

the results of 10 sample solutions (5 ml), each with a sparteine concentration of 0.005 *M*. The mean titer was 5.02 ml, with a standard deviation of 0.05 ml. The relative error was ~2% when 5 ml of diphenhydramine solution was titrated according to the procedure.

Commercial products containing diphenhydramine (injection, 10 mg/ml; tablet, 90 mg/g; and ointment, 10 mg/g) were analyzed according to the proposed method and a spectrophotometric method (8). The results were 9.97, 91.0, and 9.90 mg of diphenhydramine/ml in the injection, tablet, and ointment, respectively, by the proposed method and 9.95, 90.7, and 9.87 mg/g, respectively, by the spectrophotometric method. Tablet samples were dissolved in dilute sulfuric acid. The solution was filtered with a glass filter. Ointment samples were dispersed with 15 ml of ether in a separator. The contents were extracted three times with 10-ml portions of 0.1 *N* $H_2SO_4$. The extracts were neutralized slightly with 0.1 *N* NaOH solution.

## REFERENCES


(1) A. S. Weatherburn, *J. Am. Oil Chem. Soc.*, **28**, 233 (1950).

(2) L. K. Wang and P. J. Panzardi, *Anal. Chem.*, **47**, 1472 (1975).

(3) M. E. Turney and D. W. Cannell, *J. Am. Oil Chem. Soc.*, **42**, 544 (1965).

(4) J. T. Gross, *Analyst*, **90**, 315 (1965).

(5) Y. Kasai, Y. Ueda, W. Yano, and W. Kimura, *Nippon Kagaku Kaishi*, **1972**, 2394.

(6) H. Y. Mohammed and F. F. Cantwell, *Anal. Chem.*, **52**, 553 (1980).

(7) "The Japanese Pharmacopoeia," 9th ed., Hirokawa Publishing, Tokyo, Japan, 1976.

(8) M. Tsubouchi, *J. Pharm. Sci.*, **60**, 943 (1971).

(9) M. Tsubouchi, *Bull. Chem. Soc. Jpn.*, **43**, 3164 (1970).


# Measurement of Pseudoephedrine Hydrochloride Dissolution Using Chloride-Ion Electrode


**S. T. CHEN, R. C. THOMPSON, and R. I. POUST** ˣ



Received October 24, 1980, from the *Pharmaceutical Research and Development Laboratories, Burroughs Wellcome Co., Greenville, NC 27834* Accepted for publication April 17, 1981.



**Abstract** □ Experiments were performed to determine the suitability of using a chloride-ion electrode for the measurement of pseudoephedrine hydrochloride dissolution from commercially available compressed tablets. Dissolution experiments were carried out in 500 ml of distilled water using the USP paddle method at 100 rpm. Both chloride ion and pseudoephedrine (UV spectrophotometry) were measured at six different sampling times. Percent dissolved *versus* time values were linearized on a log-normal probability basis. The slopes of individual lines obtained from the chloride and pseudoephedrine measurements were compared using a Student *t* test and did not differ significantly ($t = 0.415$, $df = 5$, $p > 0.05$). In addition to providing an efficient, inexpensive, and simple method for measuring pseudoephedrine hydrochloride dissolution rates, the chloride-ion electrode could be used in the measurement of dissolution rates for a wide variety of drugs available as hydrochloride salts.



**Keyphrases** □ Pseudoephedrine hydrochloride—measurement of dissolution using chloride-ion electrode □ Chloride-ion electrode—measurement of pseudoephedrine hydrochloride dissolution □ Dissolution—pseudoephedrine hydrochloride, measurement using chloride-ion electrode


There has been a significant increase in the use of dissolution rate testing for the development of new dosage forms as a quality assurance tool and as a predictor of bioavailability in instances where successful *in vivo–in vitro* correlations have been established. Recent activity has centered on the establishment of automated procedures and the optimization of existing methodology with emphasis on the USP rotating-basket and USP paddle methods (1). One interesting aspect has been the automation of analytical measurements, mainly through the use of flow-through cells in conjunction with various spectrophotometers (2–7). Another analytical procedure that lends itself to automation is the use of a specific ion electrode to measure directly the drug's counterion in the dissolution flask.

## BACKGROUND

A survey of the recent literature revealed limited use of selective ion electrodes for measurement of tablet or capsule dissolution rates. Mason *et al.* (8) described the use of a sodium-ion selective electrode for the measurement of dissolution rates of specially prepared sodium salicylate tablets. They found agreement between sodium-ion concentrations measured by the selective ion electrode and atomic absorption spectrophotometry. Sodium-ion concentrations agreed with salicylate concentrations measured spectrophotometrically. The method was later extended (9) to measure dissolution rates of commercial tablets containing warfarin sodium, butabarbital sodium, and sodium bicarbonate. Data obtained by selective ion electrode and spectrophotometric measurements were in agreement when both methods were utilized.

Thomas (10) used a potassium-ion specific electrode to study the release rate of potassium from several brands of slow-release potassium chloride tablets. Other investigators (11), using similar methodology, also studied the dissolution release pattern of sustained-release potassium chloride tablets. This report presents the results of similar studies using anion measurements; *i.e.*, a chloride-ion electrode was used to measure the dissolution rate of commercial pseudoephedrine hydrochloride tablets.

## EXPERIMENTAL

**Materials**—Pseudoephedrine hydrochloride tablets[1] (60 mg/tablet) and pseudoephedrine hydrochloride[2] were used as received. An ionic strength adjuster (5 *M* $NaNO_3$) was prepared by dissolving 42.5 g of sodium nitrate[3] in 100 ml of distilled water.

**Chloride-Ion Measurements**—Chloride ions were detected by a chloride-ion electrode[4] together with a double-junction electrode[5]. The electrodes were connected to an analyzer[6], which displayed direct millivolt readings of the measured potentials.

A calibration curve was constructed for pseudoephedrine hydrochloride. Standard solutions of 0.01–1.00 mg/ml were prepared. For each standard solution, 100 ml of solution and 2 ml of ionic strength adjuster were poured into a 150-ml glass beaker and thoroughly stirred. The millivolt reading was recorded once the reading stabilized. These values were then linearized by plotting them on a linear scale as a function of the logarithm of the chloride concentration.

**UV Spectrophotometric Measurements**—A Beer's law curve was constructed for pseudoephedrine hydrochloride in distilled water. The

[1] Sudafed tablets, batches 7L2089 and 7L2087, Burroughs Wellcome Co., Research Triangle Park, N.C.

[2] Batch P5705-4G, Burroughs Wellcome Co., Research Triangle Park, N.C.

[3] ACS reagent, Fisher Scientific, Pittsburgh, Pa.

[4] Model 94-17A, Orion Research, Cambridge, Mass.

[5] Model 90-02, Orion Research, Cambridge, Mass.

[6] Microprocessor Ionlyzer/901, Orion Research, Cambridge, Mass.




*0022-3549/81/1100-1288$01.00/0*



*© 1981, American Pharmaceutical Association*

Table I—Mean [a] (± *SEM*) Percent of Drug Dissolved from Two Separate Batches of 60-mg Pseudoephedrine Hydrochloride Tablets Analyzed by Chloride-Ion Measurement and UV Spectrophotometry

| Minutes | Batch 7L2089 | | Batch 7L2087 | |
|---|---|---|---|---|
| | Chloride Ion | UV Spectrophotometry | Chloride Ion | UV Spectrophotometry |
| 2 | 31.1 ± 1.2 | 31.3 ± 1.3 | 32.9 ± 3.8 | 29.5 ± 2.1 |
| 5 | 57.6 ± 1.8 | 60.9 ± 4.3 | 62.9 ± 6.3 | 49.2 ± 1.2 |
| 10 | 88.2 ± 1.7 | 81.8 ± 2.3 | 88.8 ± 4.6 | 76.2 ± 1.7 |
| 15 | 98.3 ± 0.5 | 93.8 ± 2.0 | 96.4 ± 1.4 | 92.1 ± 1.8 |
| 30 | 99.9 ± 0.1 | 99.0 ± 0.7 | 99.4 ± 0.2 | 99.3 ± 0.3 |
| 60 | 99.8 ± 0.2 | 98.2 ± 0.7 | 99.8 ± 0.2 | 99.3 ± 0.4 |

[a] $n = 6$.

absorbances of the standard and sample solutions were read at a wavelength of 257 nm[7].

**Dissolution Studies**—Dissolution studies were performed using the USP rotating-paddle method (1) at a stirring rate of 100 rpm. The dissolution medium consisted of 500 ml of distilled water and 10 ml of ionic strength adjuster for chloride-ion measurements. The ionic strength adjuster was omitted when UV measurements were made.

For measurements of chloride-ion concentrations, the electrodes were placed in the flask 5 cm from the bottom to permit direct measurement without sample withdrawal. Ten-milliliter samples were withdrawn with replacement and filtered through 0.65-$\mu$m membrane filters[8] for UV measurements. Direct readings and sample withdrawal were done at 2, 5, 10, 15, 30, and 60 min. These experiments were performed on two different batches of tablets. Six tablets from each batch were studied by each of the two analytical methods.

Measured concentrations were converted to amount dissolved, with correction for sample replacement where appropriate. The data was linearized using log-normal probability plots. The slopes of the resulting lines were statistically analyzed using a Student $t$ test.

## RESULTS AND DISCUSSION

The millivolt readings of the standard solutions were recorded on 3 consecutive days and indicated good reproducibility. A similar concentration range of standard solutions was prepared on 3 different days, and millivolt readings of each solution were recorded immediately after preparation with good reproducibility. A higher standard error of the mean (*SEM*) was observed at the 0.01-mg/ml concentration. Because the range of concentrations between 0.01 and 0.03 mg/ml was of minimal importance to the dissolution test, the calibration curve was established between 0.03 and 1.00 mg/ml and expressed as:

$$V = 125.62 - 53.55(\log D) \qquad \text{(Eq. 1)}$$

where $V$ is the potential (millivolts), $D$ is the drug concentration (milligrams per milliliter). Linear correlation coefficient ($r$) was 0.996.

Dissolution test results for both analytical methods are summarized in Table I for the two batches of 60-mg pseudoephedrine hydrochloride tablets. Although some differences existed at the 5-, 10-, and 15-min sampling times for both batches, no statistically significant differences were found between the dissolution rates as determined by the two methods at the 95% confidence level.

Initial attempts to use this method for the measurement of dissolution rates of sugar-coated 30-mg pseudoephedrine hydrochloride tablets resulted in large amounts (120–150% of label strength) of pseudoephedrine hydrochloride appearing in solution. Various experiments were conducted to determine the source of this considerable interference with the measurement of chloride ions. The results revealed that the major source was caused by certain unidentified ingredients in the coating material. These findings indicated that the chloride-ion electrode would be of limited use for obtaining dissolution rate profiles for such products. However, a standard could be established for the measurement of dissolution at a single time point as a quality assurance procedure.

The results of these studies demonstrate that use of a chloride-ion electrode is a rapid and effective way of generating dissolution data provided that interferences are minimal. Although this report is limited to a single drug, the method may have application for other drugs available as hydrochloride salts.

[7] Model 35 recording spectrophotometer, Beckman Instruments, Irvine, Calif.
[8] Millipore Corp., Bedford, Mass.

## REFERENCES


(1) "The United States Pharmacopeia," 20th rev., United States Pharmacopeial Convention, Rockville, Md., 1980, p. 959.

(2) L. C. Schroeter and J. G. Wagner, *J. Pharm. Sci.*, **51,** 957 (1962).

(3) J. M. Burger and R. A. Nash, *ibid.*, **60,** 300 (1971).

(4) W. F. Beyer and E. W. Smith, *ibid.*, **60,** 1556 (1971).

(5) J. B. Johnson, P. G. Kennedy, and S. H. Rubin, *ibid.*, **63,** 1931 (1974).

(6) C. Cakirijildiz, P. J. Mehta, W. Rahmen, and D. Schoenleber, *ibid.*, **64,** 1692 (1975).

(7) F. J. Cioffi, H. M. Abdou, and A. T. Warren, *ibid.*, **65,** 1234 (1976).

(8) W. D. Mason, T. E. Needham, and J. C. Price, *ibid.*, **60,** 1756 (1971).

(9) T. E. Needham, L. A. Luzzi, and W. D. Mason, *ibid.*, **62,** 1860 (1973).

(10) W. H. Thomas, *J. Pharm. Pharmacol*, **25,** 27 (1973).

(11) A. C. Cartwright and C. Shah, *ibid.*, **29,** 367 (1977).


## ACKNOWLEDGMENTS


Presented at the APhA Academy of Pharmaceutical Sciences, Kansas City meeting, November 1979.

# Binding of Drugs to Human Serum Albumin XVII: Irreversible Binding of Mercaptopurine to Human Serum Proteins

**INGVAR SJÖHOLM ˣ and BRITA STJERNA**

Received January 14, 1981, from the *Department of Pharmaceutical Biochemistry, Biomedical Center, University of Uppsala, S-751 23 Uppsala, Sweden.* Accepted for publication April 23, 1981.

**Abstract** □ Studies on the binding of mercaptopurine to human serum, human serum albumin, or orosomucoid gave varying results, with binding ranging from 20 to 90%. Binding has been shown to be affected by oxidizing agents, which increase binding at low concentrations, and by reducing agents, which decrease binding. Repeated equilibrium dialyses and gel filtration experiments indicated that mercaptopurine is partly irreversibly bound to serum proteins. This binding is oxidation dependent and probably involves the sulfhydryl group of the drug.

**Keyphrases** □ Mercaptopurine—irreversible binding to human serum proteins □ Binding—irreversible, of mercaptopurine to human serum proteins □ Antineoplastics—mercaptopurine, irreversible binding to human serum proteins

Loo *et al.* (1) reported that mercaptopurine is bound 19% in human plasma. However, preliminary studies in this laboratory using equilibrium dialysis to measure the binding of mercaptopurine to serum proteins *in vitro* gave varying results. Moreover, Scatchard analyses of data obtained from experiments with serum, purifed human serum albumin, and orosomucoid gave very low $n$ values, which were not compatible with reversible binding to a specific binding site. The variance obtained with different serum samples was even greater than that seen when identical samples were compared. However, aged serum samples generally gave higher binding (up to ~90%).

Further investigation indicated that binding was influenced by the presence of reducing or oxidizing agents, *e.g.*, mercaptoethanol and hydrogen peroxide. The present paper shows that the varying binding of mercaptopurine to serum proteins *in vitro* can be explained by irreversible binding phenomena involving the reactive mercapto group of the drug.

## EXPERIMENTAL

**Drugs**—6-Mercaptopurine was used in the unlabeled[1] or $^{14}$C-labeled[2] form. Radiochemical purity (>96%) was checked by TLC.

**Serum**—Two types of serum samples were used: (*a*) pooled normal serum obtained from healthy persons and stored frozen for a long time, and (*b*) freshly prepared normal serum from three healthy persons and used within several days. The blood was collected in untreated glass tubes without any additions.

**Equilibrium Dialysis**—Serum protein binding was determined by equilibrium dialysis at 20° against an isotonic phosphate buffer (2), pH 7.4, using standard membranes[3]. Duplicate determinations were performed, and the amount of serum and buffer was 500 μl on each side of the dialysis cell. The drug was dissolved in the buffer. The equilibration time was 17–19 hr. Control experiments indicated that equilibrium was reached within 15 hr. After equilibration, radioactivity was determined in duplicate with 200 μl of sample aliquots from both sides of the dialysis cells in 5 ml of Instagel.

**Gel Filtration**—Gel filtration was performed with Sephadex G-25[4] in a 25 × 1.5-cm column and a 0.005 $M$ phosphate buffer (pH 7.4) with 0.1 $M$ potassium chloride.

## RESULTS AND DISCUSSION

**Equilibrium Dialysis**—Quantitative studies on the binding of [$^{14}$C]mercaptopurine to serum proteins by equilibrium dialysis gave varying results. The variation was particularly large between fresh and aged serum samples, and addition of reducing or oxidating agents significantly affected binding. Table I summarizes some of the results obtained. Each group of results was obtained with identical serum samples at the same time but with different treatments. Thus, the binding to freshly drawn serum was ~20–30%, while serum stored frozen for ~3 years bound ~90% of the drug. If the freshly drawn serum was exposed to air, binding significantly increased with time. In contrast, addition of reducing substances (cysteine, dithiothreitol, or mercaptoethanol) profoundly impaired the binding of both aged and fresh serums.

The difference in the binding capacity of fresh and aged serums was probably due to serum oxidation since addition of small amounts of hydrogen peroxide increased binding (Table I). However, when hydrogen peroxide was increased to millimolar concentrations, the detected binding decreased. Later experiments with gel filtrations indicated that this effect was mainly due to the oxidation of mercaptopurine to the dimeric form, which has a lower affinity for albumin.

These results suggest that the binding of mercaptopurine to the serum proteins depends on the oxidation–reduction properties of the system. Thus, the sulfhydryl group of the mercaptopurine may be involved in the binding. Such binding involving a covalently bound S-group should not be easily reversible.

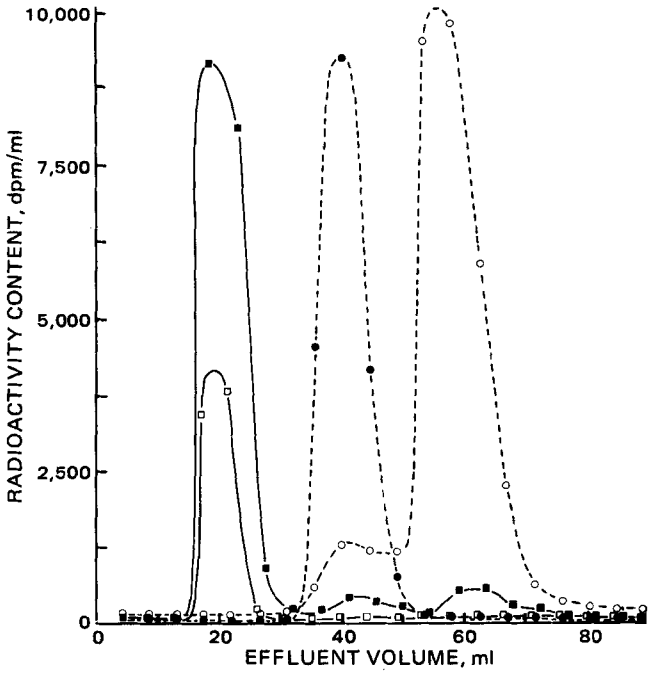


**Figure 1**—*Aged human serum with [$^{14}$C]mercaptopurine chromatographed in 0.1* M *potassium chloride with 0.005* M *phosphate, pH 7.4 (■). The protein peak fraction was rechromatographed under the same conditions (□). As controls, untreated [$^{14}$C]mercaptopurine was run alone (○) and after oxidation with hydrogen peroxide in excess (●) on the same column.*

[1] Wellcome Foundation, England.
[2] CEA (Commissariat á l'Energie Atomique), Gif-Sur-Yvette, France.
[3] Technicon.
[4] Pharmacia Fine Chemicals.



*0022-3549/81/1100-1290$01.00/0*
*© 1981, American Pharmaceutical Association*

**Table I—Binding [a] of 6-Mercaptopurine to Human Serum Proteins at Various Conditions**

| Sample | Mercaptopurine Concentration, $\mu M$ | Binding, Percent | Binding, Relative |
|---|---|---|---|
| Fresh serum | 2.5 | 30.8 | 100 |
| Fresh serum + mercaptoethanol (4.8 m$M$) | 2.5 | 6.5 | 21 |
| Fresh serum aged for 4 hr in air | 2.5 | 54.2 | 176 |
| Aged serum | 2.5 | 86.3 | 100 |
| Aged serum + mercaptoethanol (4.8 m$M$) | 2.5 | 26.0 | 30 |
| Fresh serum | 0.7 | 64.2 | 100 |
| Fresh serum + hydrogen peroxide (0.25 m$M$) | 0.7 | 95.1 | 148 |
| Fresh serum + hydrogen peroxide (2.5 m$M$) | 0.7 | 86.3 | 134 |
| Aged serum | 0.7 | 92.0 | |

[a] Binding was studied by equilibrium dialysis at 20° with an isotonic phosphate buffer (pH 7.4).

To test whether the binding is reversible or not, repeated equilibrium dialysis was performed. The buffer side of the dialysis cell was replaced with fresh buffer after equilibrium was attained. The cell was then equilibrated again. As shown in Table II, the free fraction on the buffer side reduced to about half of the original free fraction after the second equilibration. This result indicates an irreversible binding of mercaptopurine and an equal distribution of the initially unbound drug on the protein side between the two sides after buffer replacement. Nothing of the bound fraction was dissociated from the protein and redistributed to both sides of the dialysis cell. A repeated equilibrium dialysis was also performed with salicylic acid as a control. In this experiment, the original free fraction on the buffer side was recovered after the second equilibration, which indicates reversible binding as expected.

**Gel Filtration**—Another experiment was performed with gel filtration to test whether binding is reversible. A sample solution of [$^{14}$C]mercaptopurine in aged serum was run on a Sephadex G-25 column. The peak fraction containing the proteins and bound drug, *i.e.*, the first eluted peak, was run a second time. The chromatograms obtained are shown in Fig. 1. The second run gave only one peak, indicating that no free drug was present. These results support the hypothesis that binding is irreversible.

The same experiment was performed under identical conditions with salicylic acid, which is known to exhibit reversible binding to serum albumin. As expected, the second run showed that salicylic acid dissociated from the protein fraction.

When [$^{14}$C]mercaptopurine was run alone on the column, the chromatogram showed two peaks. Their relative size was directly correlated to the presence of any oxidizing agent, *e.g.*, hydrogen peroxide, which completely transferred the mercaptopurine into the dimeric form when added in excess. As shown in Fig. 1, the dimer was eluted between the protein and monomer peaks.

**Table II—Repeated Equilibrium Dialysis of [$^{14}$C]-Mercaptopurine (14,000 dpm/cell) and Human Serum**

| | Radioactivity, dpm: Protein Side | Radioactivity, dpm: Buffer Side | Fraction Bound, % |
|---|---|---|---|
| First equilibration | ND[a] | 1500 | 90.0 |
| | ND | 1317 | |
| Second equilibration after replacement of buffer | 11,727 | 817 | 93.5 |
| | 12,097 | 720 | |

[a] Not detected.

These results are compatible with the hypothesis that the sulfhydryl group of mercaptopurine is involved in an oxidation-dependent reaction with free sulfhydryl groups in proteins and/or in an oxidation-independent S–S interchange with the protein molecules. The mercaptopurine dimer does not bind or is only poorly bound to serum proteins.

Recently, similar results were found in a study on the binding of mercaptopurine to rat hepatic microsomal proteins (3). After oxidation of the labeled microsomal protein with performic acid, 75% of the radioactivity was released, suggesting that the drug was bound *via* a disulfide bond.

Binding studies *in vitro* with mercaptopurine and similar compounds should be performed with great care, excluding air and oxidizing agents. Biological samples with mercaptopurine, *e.g.* blood, plasma, or serum, should also be handled under well-controlled conditions, and results obtained under poorly defined conditions should be judged skeptically.

## REFERENCES

(1) T. L. Loo, J. K. Luce, M. P. Sullivan, and E. Frei, *Clin. Pharmacol. Ther.*, **9**, 180 (1968).

(2) M. Ehrnebo, S. Agurell, B. Jalling, and L. O. Boréus, *Eur. J. Clin. Pharmacol.*, **3**, 189 (1971).

(3) R. M. Hyslop and I. Jardine, in "Microsomes, Drug Oxidation, and Chemical Carcinogenesis," vol. 2, 4th ed., M. J. Coon, A. H. Conney, and R. W. Estabrook, Eds., Academic, New York, N.Y., 1980, p. 845.

## ACKNOWLEDGMENTS

Supported by the Swedish Medical Research Council (Project 13X-3162) and the I.F. Foundation for Pharmaceutical Research, Stockholm.

The authors thank Wellcome Foundation for the gift of 6-mercaptopurine.

# Synthesis of 4,4-Ditritio-(+)-nicotine: Comparative Binding and Distribution Studies with Natural Enantiomer

**WILLIAM C. VINCEK *, BILLY R. MARTIN, MARIO D. ACETO, HEM L. TRIPATHI, EVERETTE L. MAY ˣ, and LOUIS S. HARRIS**

Received December 1, 1980, from the *Department of Pharmacology, Medical College of Virginia, Virginia Commonwealth University, Richmond, VA 23298.* Accepted for publication April 9, 1981. * Present address: Merck Sharp and Dohme, West Point, PA 19486.

**Abstract** □ The preparation of 4,4-ditritio-(+)-nicotine (V*b*) (specific activity 10.3 Ci/mmole) from (+)-nicotine (I*b*) *via* (−)-4,4-dibromocotinine (III*b*) is described. Although I*b* is 10–30 times less potent than (−)-nicotine (I*a*) in the CNS, its binding affinity for the crude mitochondrial or nuclear fraction of whole rat brain is only three times less than that of I*a*. However, distribution studies showed that the maximum brain levels of (−)-[$^3$H]nicotine are nearly twice those of (+)-[$^3$H]-nicotine following administration of a 2-μg/kg dose. Binding affinity and disposition of the stereoisomers account for a portion of the pharmacological stereospecificity of nicotine.

**Keyphrases** □ 4,4-Ditritio-(+)-nicotine — synthesis, comparative binding and distribution with the natural enantiomer □ Stereoisomers—nicotine, binding affinity and disposition in rats □ Binding—nicotine stereoisomers, rats

The actions of nicotine on the central nervous system have been shown to be stereospecific (1–4). If nicotine's effects result from its interaction with receptors, then nicotine binding to brain tissue should reflect this selectivity. Recently (5), a synthesis and some preliminary binding data for 4,4-ditritio-(−)-nicotine (V*a*, specific activity 4.7 Ci/mmole) were presented. In those binding studies, excess (+)- and (−)-nicotine were equally effective in displacing (−)-[$^3$H]nicotine that was bound to rat brain, a finding that suggested nicotine binding lacked stereospecificity.

The stereospecificity of nicotine can be investigated further by comparing directly the binding and disposition of (+)- and (−)-[$^3$H]nicotine. The synthesis of radiolabeled (+)-nicotine, the enantiomer of V*a*, 4,4-ditritio-(−)-nicotine[1] (V*b*), prepared from (+)-nicotine according to Scheme I is reported here. An improved procedure for the hydrogenolysis of (+)-4,4- dibromocotinine (III*a*)[2], which was applied to the tritiolysis of III*b*, the enantiomer of III*a*, is also included. The resultant V*b* with a relatively high specific activity (10.3 Ci/mmole) has facilitated binding and disposition experiments with (−)- and (+)-nicotine (I*a* and I*b*, respectively).

## EXPERIMENTAL

**Chemistry**—*Conversion of (+)-4,4-Dibromocotinine (III*a*) to (−)-Nicotine (I*a*)*—Compound III*a*[2] (35 mg, 0.2 mmole), $[\alpha]_D^{25}$ +33.44°, $[\alpha]_{546}^{25}$ nm +39.48° (*c*, 2.234 in methanol)[3], prepared from I*a* (5, 6), in 0.5 ml of tetrahydrofuran was added to a suspension of 30 mg of 10% palladium-on charcoal, 0.03 ml (0.2 mmole) of triethylamine, and 1.0 ml of tetrahydrofuran under hydrogen. During 45–50 min of agitation, 4.4–4.6 ml (theory, 4.4 ml) of hydrogen was consumed. Filtration and evaporation of solvent *in vacuo* (without heating) gave (−)-cotinine (6) (essentially pure by TLC)[4], which was reduced to I*a* with aluminum lithium hydride (5).

*4,4-Ditritio-(+)-nicotine (V*b*)*—Conversion of I*b* (2) to (−)-4,4-dibromocotinine (III*b*), $[\alpha]_D^{25}$ −32.74, $[\alpha]_{546}^{25}$ nm −40.12 (*c*, 0.678 in methanol) (see corresponding values for III*a*), mp 121–122°, was effected in a 50% yield as described previously for the (−)-series (5), I*a* → III*a*. The resulting III*b* was tritiolyzed[5] as described for the hydrogenolysis of III*a*. This tritiated material, IV*b*, was reduced to V*b* with aluminum lithium hydride as described for IV*a* → V*a* (5). The purity of V*b* was determined by TLC[4]. Ninety-nine percent of the radioactivity corresponded to authentic (+)-nicotine (2) and none to cotinine.

*Determination of Specific Activity of V*b—As described previously for V*a* (5), V*b* was injected into a gas chromatograph–mass spectrometer[6] for single-ion monitoring of *m/z* 84, 86, and 88, the base peaks of [$^3H_0$]-V*b*, [$^3H_1$]-V*b*, and [$^3H_2$]-V*b*, respectively. From a [$^3H_0$]-V*b* calibration curve, it was determined that each microcurie of radiolabeled material contained 111, 41, and 5 ng of [$^3H_0$]-V*b*, [$^3H_1$]-V*b*, and [$^3H_2$]-V*b*, respectively. This translates into a specific activity of 10.3 Ci/mmole for V*b*.

**Binding Studies**—Brains from Sprague–Dawley rats were homogenized in isotonic sucrose, and crude nuclear pellets were obtained by centrifuging the homogenates at 1000×*g*. The supernates were spun at 10,000×*g* to provide crude mitochondrial pellets. The crude nuclear and crude mitochondrial pellets were resuspended in Krebs–Henseleit buffer (pH 8.4) to a final protein concentration of 3 mg/ml. The resuspended fractions were pipetted into microfuge tubes; then saline, unlabeled (+)-nicotine or unlabeled (−)-nicotine was added for a 5-min incubation period at 2°. Then radiolabeled nicotine was added for an additional 5-min incubation at 2°.

Bound and free nicotine were separated by centrifugation in a micro-

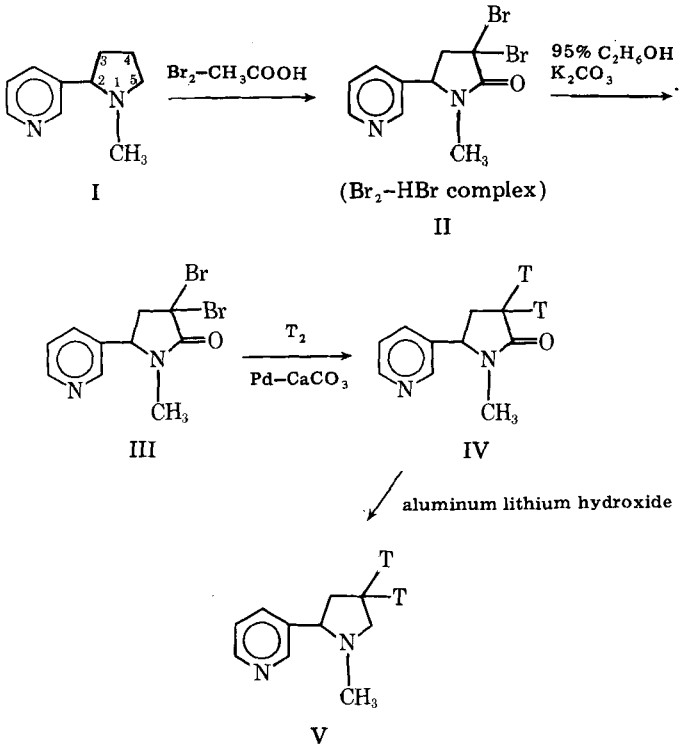


*Scheme I—a (−) and b (+) series*

[1] (+)-Nicotine has the *R* configuration.

[2] Erroneously recorded as (−)-4,4-dibromocotinine in Ref. 5.

[3] E. R. Bowman, Department of Pharmacology, Medical College of Virginia (personal communication) found $[\alpha]_{546}^{25}$ nm + 35.68° (*c*, 12.5 in ethanol) for III*a*.

[4] Silica gel plates GHLF from Analtech (Newark, Delaware) were developed in acetone–ether–concentrated ammonia (4:16:0.1). Nicotine $R_f$ was 0.55.

[5] Amersham-Searle, Arlington Heights, Ill.

[6] Finnigan 4000, Finnigan, Sunnyvale, Calif.



*0022-3549/81/1100-1292$01.00/0*
*© 1981, American Pharmaceutical Association*

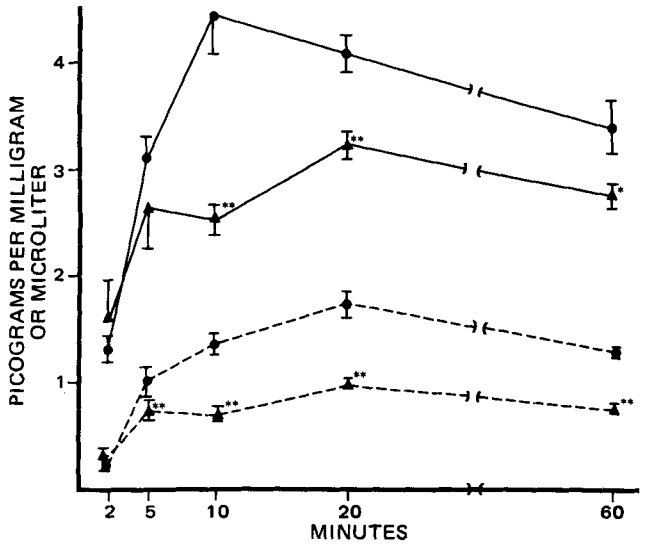


**Figure 1**—*Time course of (+)- and (−)-[$^3$H]nicotine (2 μg/kg) in rat brain and plasma. Results are expressed as mean ±SE (n = 5). Values are significantly different at p <0.005 (*) and p <0.001 (**) according to a Student t test. Key: (+)-[$^3$H]Nicotine, in brain (▲----▲) and plasma (▲—▲), and (−)-[$^3$H]nicotine, in brain (■----■) and plasma (●—●).*

fuge[7] for 3 min. The tips of the centrifuge tubes, which contained the pellets, were severed with a guillotine and vortexed with scintillation fluid (two parts of toluene containing 0.4% 2,5-diphenyloxazole and 0.01% 1,4-bis[2-(4-methyl-5-phenyloxazolyl)]benzene and one part of alkylphenoxypolyethoxyethanol[8]). Radioactivity was quantitated by liquid scintillation spectrometry, and quench was corrected by external standardization.

**Distribution Studies**—Sprague–Dawley rats were injected subcutanously with either (+)- or (−)-[$^3$H]nicotine ditartrate in saline (60 μCi/2 μg/kg, calculated as free base), and five rats were decapitated at each time point for each treatment. Blood from the cervical wound was collected in heparinized tubes, which was centrifuged at 1000×*g* to obtain plasma. Brains were homogenized[9] in five volumes of 0.5 *N* HCl. Total radioactivity was determined by counting 100 μl of plasma and tissue homogenates in aqueous counting scintillant[5]. An extraction technique that removed nicotine, but not metabolites, was used to quantitate [$^3$H]nicotine (7). Plasma (0.5 ml) and tissue homogenates (1.0 ml) were made basic with 3 drops of concentrated ammonia and 1 ml of 40% tribasic potassium phosphate. Nicotine ditartrate (1 mg/200 μl) was added as a carrier, and the samples were shaken with 10 ml of hexane. Hexane (8 ml) was removed and counted directly in 10 ml of scintillation fluid. Quench was corrected using external standardization. This extraction removed 90–95% of [$^3$H]nicotine, and no metabolites were detected in these extracts by TLC analysis[4].

## RESULTS AND DISCUSSION

**Binding Studies**—The high specific activity of (+)-[$^3$H]nicotine provided the opportunity to compare the binding characteristics and affinity of (+)-[$^3$H]nicotine to those of (−)-[$^3$H]nicotine. The physiochemical requirements for (+)-[$^3$H]nicotine binding to the crude nuclear and crude mitochondrial fractions of whole rat brain were similar to those described previously for (−)-[$^3$H]nicotine (5). Excess concentrations ($10^{-4}$ *M*) of the unlabeled stereoisomers were equally effective in displacing (+)-[$^3$H]nicotine. The quantity of saturable binding of (+)-[$^3$H]nicotine was less than that of (−)-[$^3$H]nicotine, while the amount of nonsaturable binding was similar for both. The ratio of saturable to nonsaturable binding was 1.06 and 0.64 for (−)-[$^3$H]nicotine and (+)-[$^3$H]nicotine, respectively. Scatchard plots of the saturable binding of (+)-[$^3$H]nicotine to the crude mitochondrial fraction revealed a $K_D$ value of $2.2 \times 10^{-7}$ *M*, which was approximately three times greater than that of (−)-[$^3$H]nicotine ($K_D = 6.3 \times 10^{-8}$ *M*). Binding to the crude nuclear fraction of whole rat brain was similar to that found for the crude mitochondrial fraction. The $K_D$ values for (+)-[$^3$H]nicotine and (−)-[$^3$H]nicotine were $2.6 \times 10^{-7}$ and $7 \times 10^{-8}$ *M*, respectively.

Previous reports indicated that (−)-nicotine was pharmacologically 10–30 times more potent than (+)-nicotine (2, 3). However, the *in vitro* binding of (−)-[$^3$H]nicotine to rat brain tissue appeared to lack stereospecificity in that (+)- and (−)-nicotine were equally effective in displacing (−)-[$^3$H]nicotine (5). These studies suggested that the isomers differed in efficacy rather than affinity. However, the direct comparison of (+)- and (−)-[$^3$H]nicotine binding data in the present study showed that (+)-[$^3$-H]nicotine has approximately one-third the affinity of (−)-[$^3$H]nicotine. Differences in both binding affinity and efficacy apparently account for pharmacological stereospecificity. Differences in brain levels of the stereoisomers could also contribute to potency differences that are based on dose.

**Distribution Studies**—The time course of (+)- and (−)-[$^3$H-]nicotine in rat brain and plasma is shown in Fig. 1. Maximum plasma levels of (+)- and (−)-[$^3$H]nicotine were observed at 10 and 20 min, respectively. Maximum brain levels of both stereoisomers occurred at 20 min. The brain and plasma concentrations of (−)-[$^3$H]nicotine were significantly greater than those of (+)-[$^3$H]nicotine for almost all time points. The differences in brain levels of the two stereoisomers are probably not due to binding affinity for brain or to penetration of the blood brain barrier but rather to differences in plasma levels. Levels of total radioactivity in plasma did not differ between the (+)- and (−)-[$^3$H]nicotine-treated animals at any time point.

These data suggest that both isomers are absorbed at a similar rate following subcutaneous injection. It would appear that (+)-[$^3$H]nicotine is metabolized at a faster rate than (−)-[$^3$H]nicotine, although this point needs investigation. The brain levels of total radioactivity in the (−)-[$^3$H]nicotine-treated animals were twice as high as those in the (+)-[$^3$H]nicotine treatment group, reflecting the poor penetrability of nicotine metabolites into brain. The differences in the brain levels of (+)- and (−)-[$^3$H]nicotine show that potency ratios of the stereoisomers of nicotine should be based on concentration at the target tissue rather than on dose.

## REFERENCES

(1) L. G. Abood, K. Lowry, A. Tometsko, and H. Booth, *J. Neurosci. Res.*, **3**, 327 (1978).

(2) M. D. Aceto, B. R. Martin, I. M. Uwaydah, E. L. May, L. S. Harris, C. Izazola-Conde, W. L. Dewey, T. J. Bradshaw, and W. V. Vincek, *J. Med. Chem.*, **22**, 174 (1979).

(3) M. D. Aceto, B. R. Martin, H. L. Tripathi, E. L. May, and A.E. Jacobson, *Pharmacologist*, **22**, 302 (1980).

(4) L. T. Meltzer, J. A. Rosecrans, M. D. Aceto, and L. S. Harris, *Psychopharmacology*, **68**, 283 (1980).

(5) W.C. Vincek, B. R. Martin, M. D. Aceto, and E. R. Bowman, *J. Med. Chem.*, **23**, 960 (1980).

(6) E. R. Bowman and H. McKennis, Jr., *Biochem. Prep.*, **10**, 36 (1963).

(7) A. Tsujimoto, T. Nakashima, S. Tanino, T. Dohi, and Y. Kurogochi, *Toxicol. Appl. Pharmacol.*, **32**, 32 (1975).

## ACKNOWLEDGMENTS

Supported by grants from the Council for Tobacco Research (1157) and the U.S. Public Health Service (DA-00490, DA-07027, and DA-02384).

[7] Model B, Beckman Instruments, Palo Alto, Calif.
[8] Triton X-100, New England Nuclear, Boston, Mass.
[9] Polytron, Brinkmann Instruments, Westbury, N.Y.

# Determination of Hematoporphyrin and Protoporphyrin by Ion-Pair Extraction with Chlorpromazine

**M. R. GASCO[x] and M. TROTTA**

Received April 8, 1980, from the *Istituto di Chimica Farmaceutica e Tossicologica dell'Università de Torino, Corso Raffaello 31, Torino, Italy.* Accepted for publication April 14, 1981.

**Abstract** □ A sensitive method based on ion-pair extraction is described for the quantification of hematoporphyrin and protoporphyrin using chlorpromazine as an ion-pair-forming agent. Extraction of the ion-pair in chloroform is obtained quickly at an optimum pH of 6.5 for hematoporphyrin and of 6.5–6.8 for protoporphyrin, giving an excellent recovery of the porphyrin. A stoichiometric relationship of 1:2 betweeen porphyrin and chlorpromazine is proved. Cyanocobalamin and liver extract do not interfere with the assay.

**Keyphrases** □ Hematoporphyrin—determination by ion-pair extraction with chlorpromazine □ Protoporphyrin—determination by ion-pair extraction with chlorpromazine □ Ion-pair extraction—determination of hematoporphyrin and protoporphyrin using chlorpromazine

Hematoporphyrin[1] (I) and protoporphyrin[1] (II) have been found in human bile and in urine of patients with various porphyrias (1, 2). Compound II is present in cirrhosis, hepatic tumors, cholestasis (3), and in lead intoxication (4).

Recently, the pharmacological actions of I were reviewed (5). Compound I is used in anemia with cyanocobalamin and liver extract; I and some of its charge transfer complexes show antidepressant activity (6–8).

Analysis by direct spectrophotometry is not suitable for porphyrins in urine or when colored substances, such as liver extract and cyanocobalamin, are present in I. Ion-pair formation of I with dialkylaminoalkylphenothiazines was noted (9), and a red precipitate formed at pH 6.0–6.5. In the present study, a method based on ion-pair extraction (10–12) was applied for assaying I and II using chlorpromazine hydrochloride[2] (III) as a reagent.

## EXPERIMENTAL

**Materials**—Hematoporphyrin dihydrochloride (I), protoporphyrin disodium salt (II), chlorpromazine hydrochloride (III), cyanocobalamin[1] (IV), liver extract (4 μg/ml of cyanocobalamin)[1] (V), and chloroform BP were used.

**Reagents**—The following solutions were used: $1 \times 10^{-4}$ *M* I, $1 \times 10^{-4}$ *M* II, and $1 \times 10^{-1}$ *M* III in the required buffer. The ionic strength was not adjusted, but the solutions were prepared in $1 \times 10^{-1}$ *M* phosphate buffer at various pH values.

**Preparation of Solid Complexes between Porphyrins and Chlorpromazine**—Compound I (60 mg) was dissolved in ~250 ml of pH 6.5 buffer and was precipitated by addition of 3 ml of III ($1 \times 10^{-1}$ *M*) with continuous stirring. The mixture was set aside for 30 min, filtered through a sintered-glass funnel (porosity 4), washed with 3-ml portions of ice-cold water, and dried under vacuum. The same procedure was followed for II but with a pH 6.8 buffer. A stoichiometric relationship was proved in both cases by NMR spectroscopy[3] and by spectrophotometry[4] according to the previously described methods (9).

**Effect of Chlorpromazine on Porphyrins Recovery**—Aliquots of I (6 ml, $1 \times 10^{-4}$ *M*) and III (0.1–1.6-ml, $1 \times 10^{-1}$ *M*) in pH 6.5 buffer were diluted in a 20-ml volumetric flask with the pH 6.5 buffer and then transferred to a separator. Extraction was accomplished by adding 20 ml of chloroform and then shaking thoroughly for 2 min. Absorbance was measured against chloroform from the blank experiment at 502 nm.

The same procedure was used for II with a pH 6.8 buffer and reading of the absorbance at 505 nm (Fig. 1).

**Effect of pH on Recovery**—Aliquots of I (6 ml, $1 \times 10^{-4}$ *M*) and III (1 ml, $1 \times 10^{-1}$ *M*) in buffered solutions of pH 5.8–7.0 were introduced into dry separators and diluted with 13-ml aliquots of the appropriate buffer. Each solution was shaken thoroughly for 2 min with 20 ml of chloroform. The absorbance of the separated organic phase was measured against chloroform from the blank experiment. The same procedure was used for II.

**Calibration Curve**—Stock solutions of I ($1 \times 10^{-4}$ *M*) and III ($1 \times 10^{-1}$ *M*) were used to prepare mixed standard solutions. The mixed standards were diluted to 20 ml with the buffer in a volumetric flask to yield a series of mixed working solutions containing 1–$2.5 \times 10^{-5}$ *M* I and $5 \times 10^{-3}$ *M* III. The working solutions in the separators were gently shaken for 2 min with 20 ml of chloroform. The absorbance of the chloroform extract was measured against the chloroform extract from the blank experiment.

The mean value of three experiments was taken in to obtain the calibration curve. The molar absorptivity ($\epsilon$) was 10,000 ± 100 at 502 nm. This value was confirmed by direct measurement of the absorbance of the solid complex in chloroform.

The same procedure was used for II; the molar absorptivity ($\epsilon$) was 11,000 ± 120 at 505 nm and was also confirmed by direct measurement of the absorbance of the solid complex in chloroform.

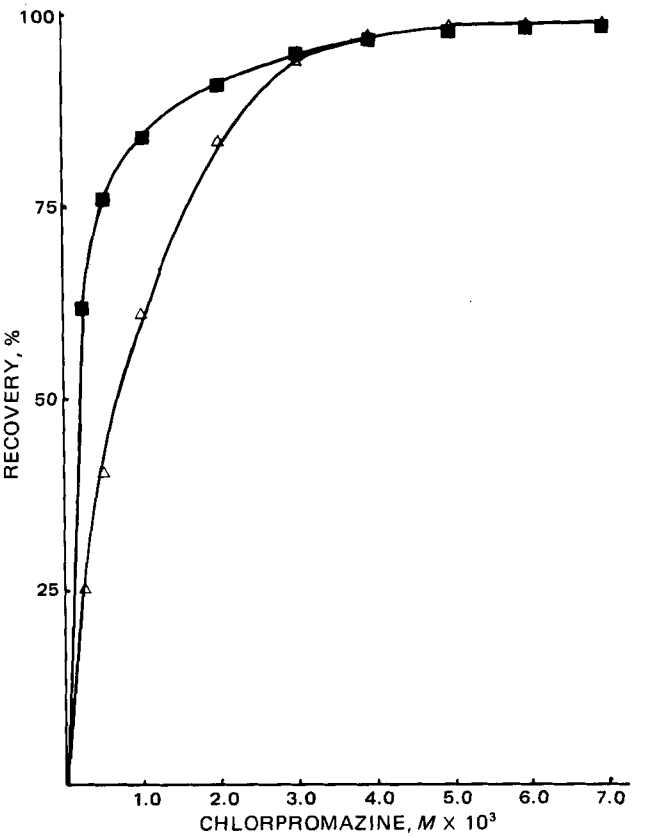


**Figure 1**—*Recovery of the chloroform extract as a function of chlorpromazine with concentrations of* $3 \times 10^{-5}$ M *hematoporphyrin* (△) *and* $3 \times 10^{-5}$ M *protoporphyrin* (●) *in the aqueous layer.*

[1] Fluka.
[2] Rhône-Poulenc.
[3] $^1$H-NMR (Varian A-60).
[4] Perkin-Elmer EPS-3T spectrophotometer.



*0022-3549/81/1100-1294$01.00/0*
*© 1981, American Pharmaceutical Association*

Table I—Recovery of 200 μg of Hematoporphyrin from 20-ml Solutions

| Buffer | In Presence of 20 μg of Cyanocobalamin | In presence of 25% Liver Extract |
|---|---|---|
| 197.5 | 199.0 | 201.0 |
| 197.0 | 197.3 | 196.5 |
| 198.2 | 200.0 | 197.5 |
| 199.8 | 197.5 | 197.2 |
| 200.0 | 196.5 | 199.2 |
| 199.0 | 197.5 | 198.0 |
| 198.5 ± 1.2[a] | 198.0 ± 1.4[a] | 198.2 ± 1.6[a] |

[a] Mean ± *SD*.

**Analysis of Porphyrins in Presence of Cyanocobalamin and Liver Extract**—A preliminary experiment performed using a chlorpromazine ion-pair method with a 5-ml aliquot of 4 μg/ml of cyanocobalamin or of liver extract showed no formation of colored complex in chloroform. Consequently, on assaying porphyrin (200 μg) in the presence of either of these solutions, no interference occurred and hematoporphyrin or protoporphyrin was easily and quantitatively extracted. Table I lists the replicate recovery results of 200 μg of I from 20-ml buffer solutions alone, in the presence of IV, and with 25% of V. The porphyrins were also completely extracted from urine according to the described ion-pair method with chlorpromazine.

## RESULTS AND DISCUSSION

The red complexes of hematoporphyrin and protoporphyrin assayed by the described method showed adherence to Beer's law. Figure 1 shows that a $5 \times 10^{-3}$ *M* concentration of chlorpromazine was necessary for a total recovery of the porphyrin at a concentration of $3 \times 10^{-5}$ *M*( ratio 3:500). Figure 2 shows the recovery profile of hematoporphyrin using a fixed ratio of 3:500 between porphyrin and chlorpromazine in chloroform from buffer solution as a function of pH. At pH 6.5, hematoporphyrin was completely extracted; protoporphyrin was completely extracted in a wider pH range.

The extracted species are well defined and the reported method can be considered sensitive and accurate. Table I shows that the mean recovery for hematoporphyrin was 99.0–99.2%.

The method can be applied for determining porphyrins in pathological urine.

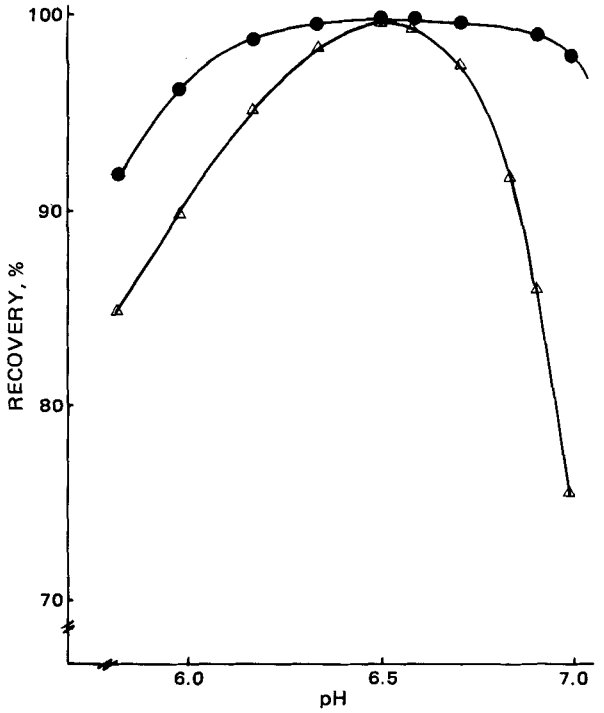


**Figure 2**—*Hematoporphyrin and protoporphyrin recovery–pH profile after 20-ml chloroform extraction of 20 ml of aqueous solution containing* $5 \times 10^{-3}$ M *hematoporphyrin (△) and* $3 \times 10^{-5}$ M *protoporphyrin (■).*

## REFERENCES


(1) A. A. Schotorst, J. Stevenick, L. N. Went, and D. Suurmond, *Clin. Chim. Acta*, **33**, 207 (1971).

(2) S. G. Smith, R. V. Belcher, R. Mahler, and J. Yudkin, *ibid.*, **23**, 241 (1969).

(3) E. De Salamanca, J. A. Herruzo, F. Arnalich, J. Pardo Rueda, *Rev. Esp. Enferm. Apar. Dig.*, **47**, 805 (1976); through *Chem. Abstr.*, **85**, 157559s (1976).

(4) A. Alvares, A. Fischbain, S. Sassa, K. Anderson, and A. Kappas *Clin. Pharmacol. Ther.*, **19**, 183 (1976).

(5) V. N. Luzgina, E. I. Filoppovich, and R. P. Eustigneeva, *Khim. Farm. Zh.*, **11**, 26 (1977); through *Chem. Abstr.*, **87** 47834m (1977).

(6) D. DeMaio and F. Belloni, *Clin. Ther.*, **47**, 591 (1968).

(7) G. Di Modica, French Demande 2,299,864 (Sept. 3 1976); through *Chem. Abstr.*, **86**, 165525p (1977).

(8) A. Brucato, G. Di Modica, F. Marletti, S. Mazzarese, D. Murgolo, and P. M. Provenzano, *Arzneim.-Forsch.*, **27**, 1015 (1977).

(9) M. R. Gasco, M. Trotta, and M. E. Carlotti, *Pharmazie*, **36**, 276 (1981).

(10) E. M. Girgis, Z. Gad, and M. Maram, *J. Pharm. Sci.*, **63**, 1764 (1974).

(11) F. S. Hom and W. R. Ebert, *ibid.*, **66**, 710 (1977).

(12) B. A. Persson and S. Eksborg, *Acta Pharm. Suec.*, **7**, 353 (1970).

# Area under the Plasma Concentration–Time Curve Resulting from Constant-Rate Drug Input

**Keyphrases** □ Drug infusion—relationship with area under the plasma concentration–time curve □ Equations—relationship between infusion equation and area under the plasma concentration–time curve

*To the Editor:*

Plasma concentration–time data obtained from constant-rate drug input (*i.e.*, intravenous infusion or constant-rate absorption) are frequently analyzed by dividing the resulting curve into two segments: concentrations achieved during and those obtained after stopping the infusion. However, equations are available for analyzing the entire curve, and computer programs are capable of fitting such data to the appropriate equation. Benet (1) encouraged use of the equation describing the entire concentration–time curve. This communication reports on the relationship between the parameters of an infusion equation and the total area under the plasma concentration–time curve ($AUC_0^\infty$).

## THEORY

Assuming, for simplicity, a one-compartment model, the equation describing the entire concentration–time curve is given by:

$$C = \left(\frac{FK_0}{KV}\right)(e^{KT} - 1)\,e^{-Kt} \qquad \text{(Eq. 1)}$$

where $F$ is the fraction of the dose absorbed ($F = 1$ for intravenous infusion), $K_0$ is the constant rate of drug input, $K$ is the elimination rate constant, $V$ is the apparent volume of distribution, $t$ is the time beginning from the start of infusion, and $T$ is the time of infusion (which equals $t$ during infusion). In fitting Eq. 1, it will generally appear in the form:

$$C = (A)(e^{KT} - 1)e^{-Kt} \qquad \text{(Eq. 2)}$$

where $A$ equals $FK_0/KV$. The terms $A$ and $K$ are treated as parameters and $T$ is fixed for intravenous infusion. In the case of constant-rate drug absorption (*e.g.*, sustained-release products), $T$ should also be treated as a parameter rather than holding it constant at some arbitrary value. The solid line shown in Fig. 1 represents plasma concentrations resulting from constant-rate drug input up to time $T$ and exponential decline in concentrations at later times.

The term $A$ in Eq. 2 may be recognized as the steady-state plasma concentration ($C_{ss}$) that would be achieved if infusion were to continue for a sufficiently long period of time. This value is denoted in Fig. 1 as the dashed line. The total area under the solid line in Fig. 1 may be shown to be equal to:

$$AUC_0^\infty = \frac{FK_0T}{KV} \qquad \text{(Eq. 3)}$$

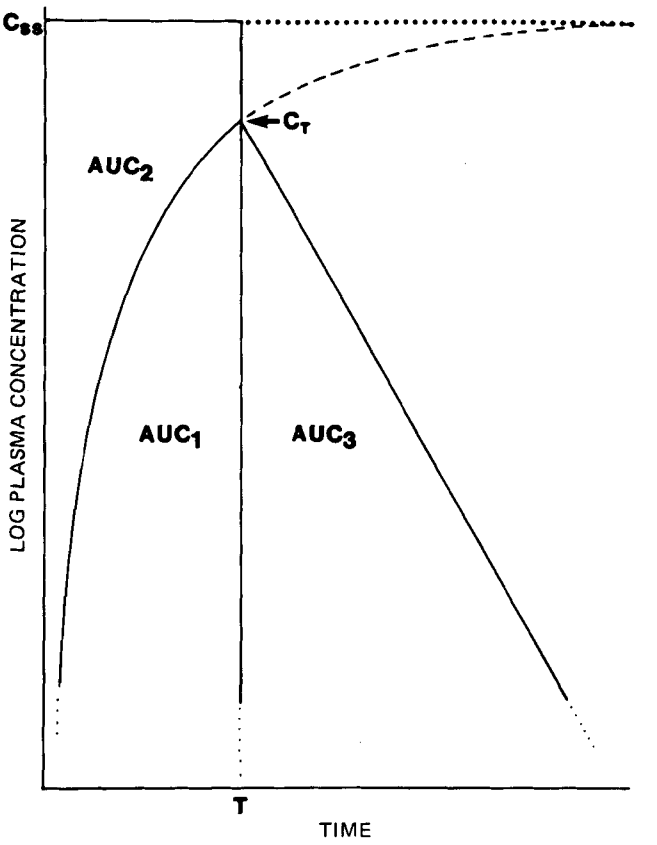


**Figure 1**—*Log-plasma concentration as a function of time during and after constant-rate drug infusion (solid line). Drug is infused for a time* T *and results in a maximum concentration,* $C_T$. *The dashed line represents the approach to a steady-state plasma concentration,* $C_{ss}$, *if infusion were to continue indefinitely. Also,* $AUC_1$ *is the area under the curve during infusion and up to time* T, $AUC_3$ *is the postinfusion area from time* T *to time* ∞, *and* $AUC_2$ *is the difference between,* $C_{ss}T$ *and* $AUC_1$.

where the product $FK_0T$ equals the dose absorbed.

Therefore, the product of the term $A$ (in Eq. 2) and $T$ will equal $AUC_0^\infty$:

$$AUC_0^\infty = \frac{FK_0T}{KV} = C_{ss}T = AT \qquad \text{(Eq. 4)}$$

Equation 4 may also be viewed by considering the geometric areas indicated in Fig. 1. The total area under the curve is equal to:

$$AUC_0^\infty = AUC_1 + AUC_3 \qquad \text{(Eq. 5)}$$

The calculated $AUC_0^\infty$ in Eq. 4, $AT$, is given by:

$$AUC_0^\infty = AUC_1 + AUC_2 = C_{ss}T = AT \qquad \text{(Eq. 6)}$$

Since $AUC_1$ is common to both Eqs. 5 and 6, $AUC_2$ must be equal to $AUC_3$.

$$AUC_2 = C_{ss}T - AUC_1 \qquad \text{(Eq. 7)}$$

$$AUC_2 = \frac{FK_0T}{KV} - \int_0^T \frac{FK_0}{KV}(1 - e^{-kt})\,dt \qquad \text{(Eq. 8)}$$

The integral in Eq. 8 may be shown to be equal to:



*0022-3549/81/1100-1296$01.00/0*
*© 1981, American Pharmaceutical Association*

$$\int_0^T \frac{FK_0}{KV}(1 - e^{-Kt})\,dt = -\frac{FK_0T}{KV} + \frac{FK_0}{KVK}(1 - e^{-KT}) \quad \text{(Eq. 9)}$$

Placing Eq. 9 into Eq. 8 gives:

$$AUC_2 = \frac{FK_0}{KVK}(1 - e^{-KT}) \quad \text{(Eq. 10)}$$

Equation 10 is equal to the plasma concentration at time $T$, divided by $K$:

$$AUC_2 = \frac{C_T}{K} \quad \text{(Eq. 11)}$$

This expression may be recognized as being equal to $AUC_3$ which is conventionally used to calculate the postinfusion area and, therefore, $AUC_2 = AUC_3$.

The relationship indicated in Eq. 4, that area is the product of $C_{ss}$ and $T$, appears not to have been previously reported. Furthermore, assuming linear kinetics, this relationship is model independent. The only difference in calculation for multicompartment models is that $AUC_0^\infty$ is the product of $T$ and the sum of all the appropriate coefficients (*e.g.*, $A + B$, in a two-compartment model).

(1) L. Z. Benet, *J. Pharm. Sci.*, **61**, 536 (1972).

*Michael Mayersohn*
Department of Pharmaceutical Sciences
College of Pharmacy
The University of Arizona
Tucson, AZ 85721

Received April 13, 1981.
Accepted for publication October 10, 1981.
Supported in part by Grant DA02680 from the National Institute on Drug Abuse.

## Kinetic Study on Rapid Reaction of Trinitrobenzenesulfonate with Human Serum Albumin

**Keyphrases** □ Trinitrobenzenesulfonate—kinetics of reaction with human serum albumin □ Kinetics—of reaction of trinitrobenezenesulfonate with human serum albumin □ Albumin, human serum—kinetics of reaction with trinitrobenzenesulfonate

*To the Editor:*

Trinitrobenzenesulfonate (I) has been used as a reagent for the chemical modification of amino groups in amino acids, peptides, and proteins (1–4). The basic mechanism for the reaction of I with amines (II) was proposed previously (5, 6) (Scheme I). The trinitrophenylated II (III) reacts further with sulfite ion (IV) to form the sulfite monoadduct (V). It was reported that III and V have UV absorption maxima at 340 and 420 nm, respectively, giving an isosbestic point at 367 nm during the reaction of III and IV (5, 6).

The distinction between, and identification of, the drug binding sites on human serum albumin were made previously by us on the basis of the inhibition of the reaction of *p*-nitrophenyl acetate with the albumin caused by several drugs (7). When the albumin was modified with I to characterize the drug binding sites, rapid reaction of I with the albumin was found. In this communication, we describe the localization of the reactive site on the albumin

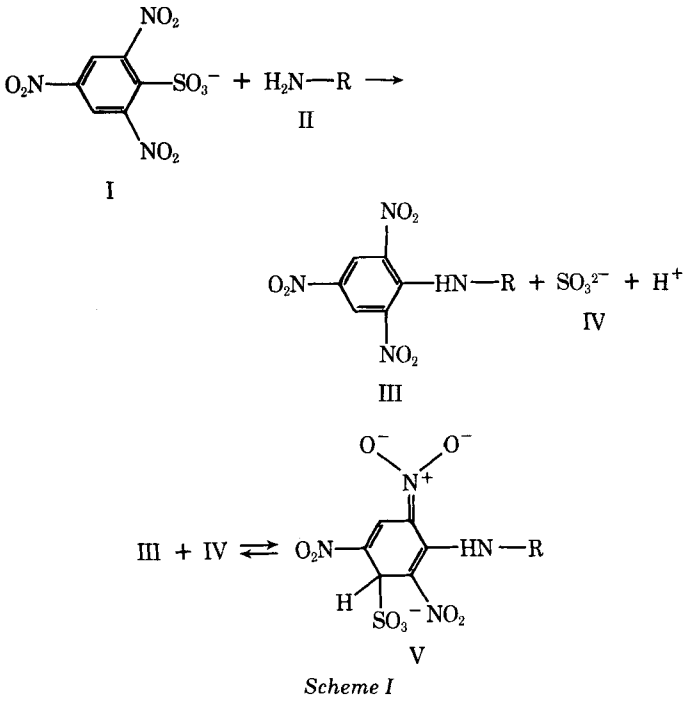


*Scheme I*

for I and the kinetics and mechanism for the reaction.

All reactions in this study were carried out in pH 7.4, 0.067 *M* phosphate buffer ($\mu = 0.2$, adjusted with sodium chloride) at 25°. To localize the reactive site on the albumin for I, the fluorescence spectra of the albumin excited at 300 nm were measured[1]. The intensity of the emission

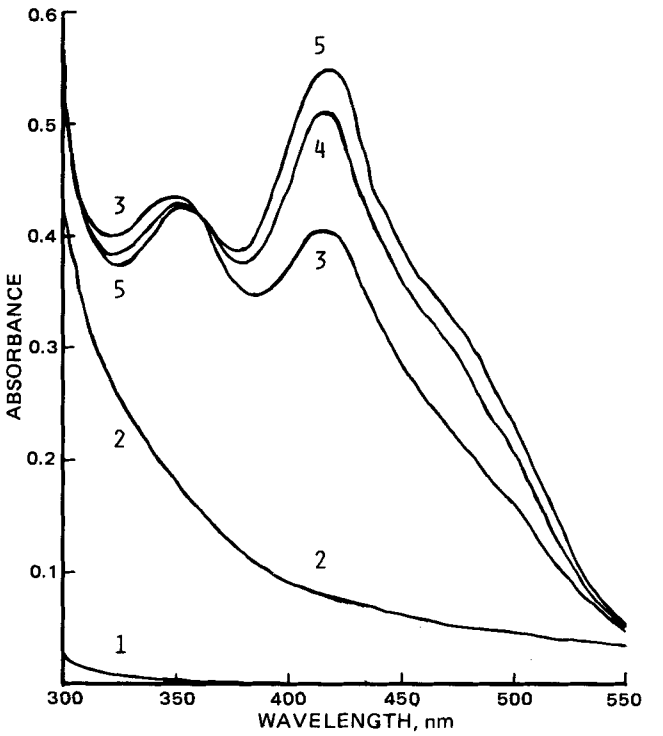


**Figure 1**—*UV absorption spectra. 1, 2.5 × 10⁻⁵ M I; 2, 1.0 × 10⁻⁴ M albumin; 3, 2.5 × 10⁻⁵ M I and 1.0 × 10⁻⁴ M albumin; 4, 2.5 × 10⁻⁵ M I, 1.0 × 10⁻⁴ M albumin, and 5.0 × 10⁻⁵ M NaHSO₃; and 5, 2.5 × 10⁻⁵ M I, 1.0 × 10⁻⁴ M albumin, and 1.0 × 10⁻⁴ M NaHSO₃.*

[1] RF-510 spectrofluorophotometer, Shimadzu, Kyoto, Japan.

0022-3549/81/1100-1297$01.00/0
© 1981, American Pharmaceutical Association

$$\int_0^T \frac{FK_0}{KV}(1 - e^{-Kt})\,dt = -\frac{FK_0T}{KV} + \frac{FK_0}{KVK}(1 - e^{-KT}) \quad \text{(Eq. 9)}$$

Placing Eq. 9 into Eq. 8 gives:

$$AUC_2 = \frac{FK_0}{KVK}(1 - e^{-KT}) \quad \text{(Eq. 10)}$$

Equation 10 is equal to the plasma concentration at time $T$, divided by $K$:

$$AUC_2 = \frac{C_T}{K} \quad \text{(Eq. 11)}$$

This expression may be recognized as being equal to $AUC_3$ which is conventionally used to calculate the postinfusion area and, therefore, $AUC_2 = AUC_3$.

The relationship indicated in Eq. 4, that area is the product of $C_{ss}$ and $T$, appears not to have been previously reported. Furthermore, assuming linear kinetics, this relationship is model independent. The only difference in calculation for multicompartment models is that $AUC_0^\infty$ is the product of $T$ and the sum of all the appropriate coefficients (*e.g.*, $A + B$, in a two-compartment model).

(1) L. Z. Benet, *J. Pharm. Sci.*, **61**, 536 (1972).

*Michael Mayersohn*
Department of Pharmaceutical Sciences
College of Pharmacy
The University of Arizona
Tucson, AZ 85721

Received April 13, 1981.
Accepted for publication October 10, 1981.
Supported in part by Grant DA02680 from the National Institute on Drug Abuse.

## Kinetic Study on Rapid Reaction of Trinitrobenzenesulfonate with Human Serum Albumin

**Keyphrases** □ Trinitrobenzenesulfonate—kinetics of reaction with human serum albumin □ Kinetics—of reaction of trinitrobenezenesulfonate with human serum albumin □ Albumin, human serum—kinetics of reaction with trinitrobenzenesulfonate

*To the Editor:*

Trinitrobenzenesulfonate (I) has been used as a reagent for the chemical modification of amino groups in amino acids, peptides, and proteins (1–4). The basic mechanism for the reaction of I with amines (II) was proposed previously (5, 6) (Scheme I). The trinitrophenylated II (III) reacts further with sulfite ion (IV) to form the sulfite monoadduct (V). It was reported that III and V have UV absorption maxima at 340 and 420 nm, respectively, giving an isosbestic point at 367 nm during the reaction of III and IV (5, 6).

The distinction between, and identification of, the drug binding sites on human serum albumin were made previously by us on the basis of the inhibition of the reaction of *p*-nitrophenyl acetate with the albumin caused by several drugs (7). When the albumin was modified with I to characterize the drug binding sites, rapid reaction of I with the albumin was found. In this communication, we describe the localization of the reactive site on the albumin

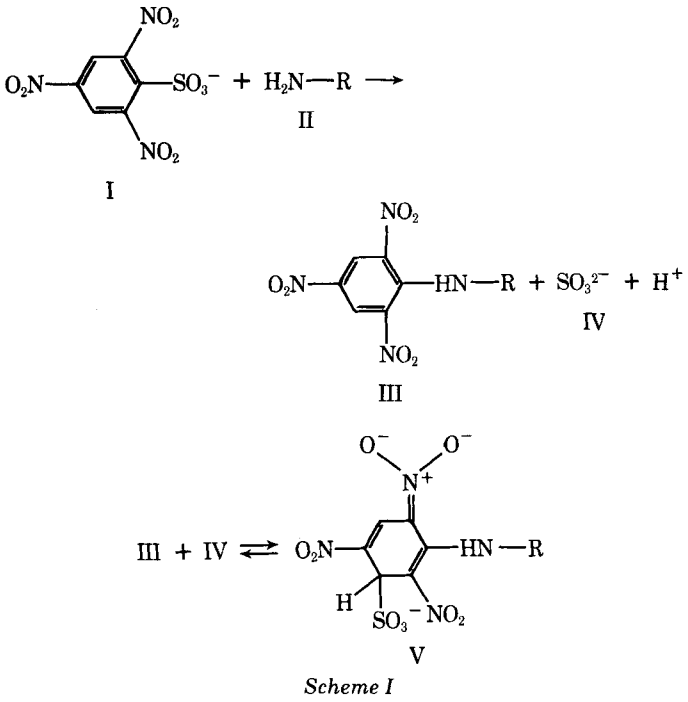


*Scheme I*

for I and the kinetics and mechanism for the reaction.

All reactions in this study were carried out in pH 7.4, 0.067 *M* phosphate buffer ($\mu = 0.2$, adjusted with sodium chloride) at 25°. To localize the reactive site on the albumin for I, the fluorescence spectra of the albumin excited at 300 nm were measured[1]. The intensity of the emission

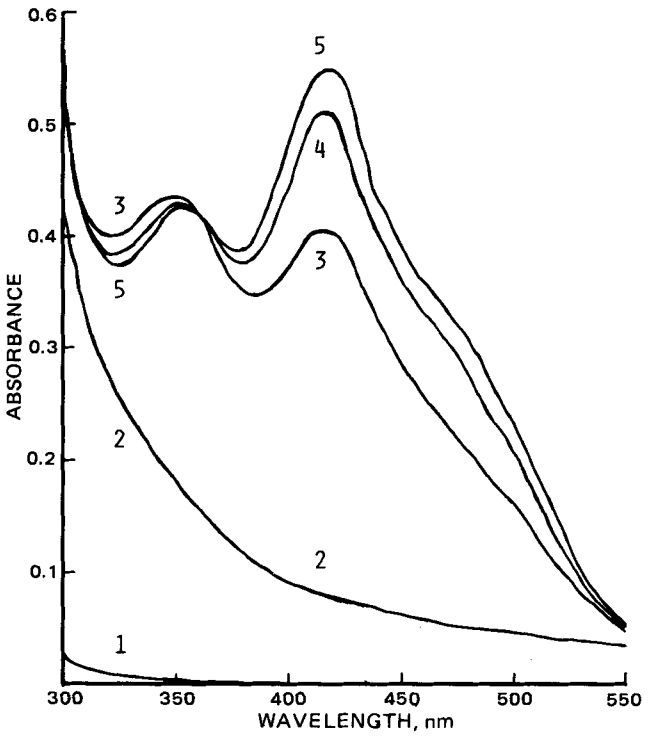


**Figure 1**—*UV absorption spectra. 1, 2.5 × 10⁻⁵ M I; 2, 1.0 × 10⁻⁴ M albumin; 3, 2.5 × 10⁻⁵ M I and 1.0 × 10⁻⁴ M albumin; 4, 2.5 × 10⁻⁵ M I, 1.0 × 10⁻⁴ M albumin, and 5.0 × 10⁻⁵ M NaHSO₃; and 5, 2.5 × 10⁻⁵ M I, 1.0 × 10⁻⁴ M albumin, and 1.0 × 10⁻⁴ M NaHSO₃.*

[1] RF-510 spectrofluorophotometer, Shimadzu, Kyoto, Japan.

0022-3549/81/1100-1297$01.00/0
© 1981, American Pharmaceutical Association

spectrum for the reaction mixture of I and the albumin was smaller than that for the albumin solution. This reduced emission spectrum indicates that the reactive site for I is located close to tryptophan residue 214, which is the lone tryptophan residue of the albumin (7–9). This important drug binding site on albumin was named Site I by Sudlow *et al.* (10) and U site by us (7).

When the reaction of I ($2.5 \times 10^{-5}$ *M*) with albumin ($1.0 \times 10^{-4}$ *M*) was followed spectrophotometrically at 340 nm, the reaction was completed rapidly. In contrast, when the reaction was monitored at 420 nm, the absorbance gradually increased (half-life ~30 sec) after the initial rapid increase in the absorbance up to ~0.25. Thus, the reaction proceeded *via* two steps. Figure 1 shows the UV absorption spectra of each reactant solution and the reaction mixtures after the spectral changes were complete. The spectra of 3, 4, and 5 show the isosbestic point at ~360 nm. These kinetic and spectroscopic results suggest that the reactions similar to Scheme I (trinitrophenylation and sulfite monoaddition) occur in the reaction of I with the albumin.

The rate of the trinitrophenylation of the albumin was followed at 360 nm (isosbestic point of III and V) with a stopped-flow spectrophotometer[2]. The pseudo-first-order analyses could be applied under the excess molar concentration of the albumin over that of I (2:8 concentration ratio). The pseudo-first-order rate constants ($\sim 2.5 \times 10^{-1}$ $sec^{-1}$) were almost independent of the albumin concentrations. This independence suggests that the trinitrophenylation occurs *via* Michaelis–Menten-type complex formation and that the dissociation constant of the complex is very small. Therefore, the overall reactions of I with the albumin may be represented as in Scheme II, where $k_2$ is the first-order rate constant of the I–albumin complex for the trinitrophenylation. The rate constants for the formation of V and the elimination of IV from V are expressed by $k_3$ and $k_{-3}$, respectively, and $K_S$ and $K_P$ represent the dissociation constants of the complex and V, respectively. Detailed studies on the kinetics and mechanism for the reactions shown in Scheme II are in progress.

$$\text{I} + \text{albumin} \overset{K_S}{\rightleftharpoons} \text{I–albumin} \xrightarrow{k_2} \text{III} + \text{IV} + \text{H}^+$$

$$\text{III} + \text{IV} \underset{k_{-3},\, K_P}{\overset{k_3}{\rightleftharpoons}} \text{V}$$

*Scheme II*


(1) G. E. Means and R. F. Feeney, "Chemical Modification of Proteins," Holden-Day, San Francisco, Calif., 1971.

(2) A. R. Goldfarb, *Biochemistry*, **5**, 2574 (1966).

(3) L.-O. Anderson, J. Brandt, and S. Johanson, *Arch. Biochem. Biophys.*, **146**, 428 (1971).

(4) C. Jacobson, *Int. J. Peptide Protein Res.*, **7**, 161 (1975).

(5) A. R. Goldfarb, *Biochemistry*, **5**, 2570 (1966).

(6) G. E. Means, W. I. Congdon, and M. L. Bender, *ibid.*, **11**, 3564 (1972).

(7) Y. Ozeki, Y. Kurono, T. Yotsuyanagi, and K. Ikeda, *Chem. Pharm. Bull.*, **28**, 535 (1980).

(8) J. Steinhardt, J. Krijin, and J. G. Leidy, *Biochemistry*, **10**, 4005 (1971).

(9) V. M. Rosenor, M. Oratz, and M. A. Rothchild, in "Albumin Structure, Function and Uses," J. R. Brown, Ed., Pergamon, Oxford, England, 1977, p. 27.

(10) G. Sudlow, D. J. Birkett, and D. N. Wade, *Mol. Pharmacol.*, **12**, 1052 (1976).



*Yukihisa Kurono*
*Kenichi Ichioka*
*Sawako Mori*
*Ken Ikeda* ˣ

Faculty of Pharmaceutical Sciences
Nagoya City University
Tanabe-dori, Mizuho-ku
Nagoya, 467, Japan



Received April 30, 1981.
Accepted for publication July 31, 1981.


[2] Model RA-401, Union Giken, Osaka, Japan.

A publication of the
American Pharmaceutical Association—
the National Professional Society
of Pharmacists

# JOURNAL OF PHARMACEUTICAL SCIENCES

## INDEX TO AUTHORS
## INDEX TO SUBJECTS

VOLUME 70
JANUARY TO DECEMBER, 1981

*Published monthly under the supervision of the Board of Trustees*

MARY H. FERGUSON
*Editor*

NANCY E. BROWN
*Production Editor*

JOHN PATRICK EVANS
*Copy Editor*

MICHAEL K. HAYES
*Copy Editor*

EDWARD G. FELDMANN
*Contributing Editor*

SAMUEL W. GOLDSTEIN
*Contributing Editor*

BELLE R. BECK
*Editorial Secretary*

EDWARD G. FELDMANN
*Acting Director of Publications*

EDITORIAL ADVISORY BOARD

John Autian
Norman R. Farnsworth
William J. Jusko
Herbert A. Lieberman
David E. Mann, Jr.
Ian W. Mathison
Gerald J. Papariello
Edward G. Rippie

JOURNAL OF PHARMACEUTICAL SCIENCES

DECEMBER 1981
VOLUME 70 NUMBER 12

RESEARCH ARTICLES

# Physicochemical Property Modification Strategies Based on Enzyme Substrate Specificities I: Rationale, Synthesis, and Pharmaceutical Properties of Aspirin Derivatives

**PRADIP K. BANERJEE * and GORDON L. AMIDON ***

Received November 3, 1980, from the *School of Pharmacy, University of Wisconsin, Madison, WI 53706.* Accepted for publication April 2, 1981. *Present address: Tablet Products Research and Development, Abbott Laboratories, North Chicago, IL 60064.

**Abstract** □ A rationale is developed for drug physicochemical property modification based on making derivatives that are substrates for known enzymes. The approach requires knowledge of the enzyme–substrate specificities to select the appropriate derivative. As a class, the digestive enzymes represent possible reconversion sites. It is shown that by using only known specificities of these enzymes, the physicochemical properties of a drug may be modified in almost any manner desired by appropriate derivative choice, with enzymatic regeneration remaining effective. The strategy is applied to making a stable aspirin derivative that is activated *in vivo*. Of the derivatives made, aspirin phenylalanine ethyl ester was shown to be stable in suspension form for over 4 years. It was also shown that aspirin is regenerated from the derivative in the presence of the enzymes α-chymotrypsin and carboxypeptidase *in vitro*. This biochemical approach to drug physicochemical property modification offers a new and powerful rationale for improving drug product efficacy.

**Keyphrases** □ Aspirin—derivatives, physicochemical property modification strategies based on enzyme specificities, synthesis, and pharmaceutical properties □ Derivatives—aspirin, physicochemical property modification strategies based on enzyme specificities, synthesis, and pharmaceutical properties □ Physicochemistry—aspirin derivatives, property modification strategies based on enzyme specificities, synthesis, and pharmaceutical properties

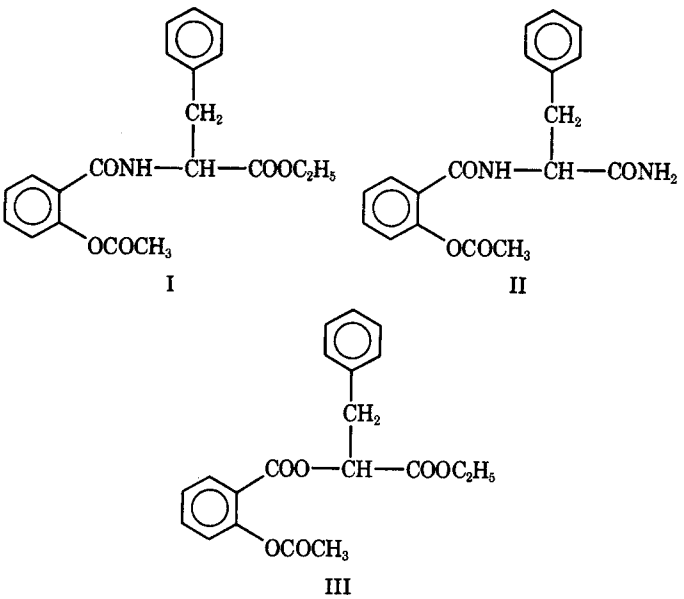


A number of inherent undesirable properties may preclude the use of a drug molecule in clinical practice, and drug derivatization has been long recognized as an important means of producing more efficacious pharmaceutical products. Central to the prodrug design is *in vivo* reconversion. The drug derivative must rapidly, or at a controlled rate, be reconverted to the active therapeutic agent *in vivo* while at the same time be sufficiently stable *in vitro* such that a stable pharmaceutical product can be developed. It was suggested (1) that hydrolytic enzymes could serve as an important class of reconversion sites. In the rational design of prodrugs, it is necessary to consider: (*a*) what structural modifications of the parent molecule are necessary to reduce or eliminate the particular undesirable effect, and (*b*) what conditions are available *in vivo* (enzymes, pH, *etc.*) to regenerate the parent molecule from the prodrug.

The objective of this report was to develop and test a rationale for prodrug design using current knowledge of the hydrolase enzyme specificities. By combining the current understanding of the enzyme specificities with the need for drugs with more desirable pharmaceutical properties, new and novel drug derivatives can be suggested.

0022-3549/81/1200-1299$01.00/0
© 1981, American Pharmaceutical Association

**Table I—Possible Changes in Physical Properties of Drugs with Free OH Groups**

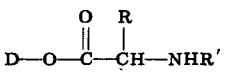

drug amino acid

| Drug | Amino Acid | R′ | Change in Physical Properties |
|---|---|---|---|
| Nonpolar | Polar–acidic–basic | H, $COCH_3$ | More polar–ionic |
| Polar | Nonpolar | $COCH_3$ | Less polar |
| Liquid at room temperature | Polar–nonpolar | H | To a salt |
| Low aqueous solubility | Acidic–basic | $HCOCH_3$ | To acid or base (salt) |

This study attempted to make aspirin derivatives such that a stable suspension formulation could be made. A secondary goal was to reduce the local gastric irritation and bleeding associated with aspirin therapy.

This report describes the synthesis and some pharmaceutical properties of aspirin phenylalanine ethyl ester (I), aspirin phenylalanine amide (II), and aspirin phenyllactic ethyl ester (III).

## THEORY

**Prodrug Considerations**—On the basis of the known specificities of the enzymes reviewed (1), a general rationale for modification of a drug's physical properties can be developed. Given that a drug has a free carboxyl, amino, or hydroxyl group, corresponding esters or amides of amino acids can be made so as to alter the physical properties in almost any desired direction from that of the parent drug, with one or more of the hydrolase enzymes serving as the *in vivo* reconversion site(s).

The diverse properties of the various amino acid residues, combined with the fact that they are usually nontoxic, gives this approach wide applicability. Classifying the amino acids as nonpolar, polar, acidic, and basic, a given drug molecule may be made more or less polar or more or less soluble in a given solvent. Its acid/base properties may be altered or completely changed (*i.e.*, converted from acidic to basic drug or vice versa), or it may be converted from a neutral compound to an ionic (acidic or basic) compound or from an ionic to a neutral compound. Thus, great flexibility is afforded the pharmaceutical scientist in modifying physical properties of drugs using this rationale.

Tables I–III briefly summarize some of these possibilities. In general, for compounds in Tables I and II, α-chymotrypsin, trypsin, elastase, or an aminopeptidase could serve as a reconversion site. For compounds in Table III, a carboxypeptidase or an initial cleavage of the ester group by α-chymotrypsin–trypsin–elastase followed by a carboxypeptidase would effect the reconversion.

A recent example of a prodrug approach utilizing lipases as target sites for reconversion is the study by Baugess *et al.* (2). The acetate and dodecanoate esters of acetaminophen were shown to be substrates for lipases. The acetate ester was completely hydrolyzed in 15 min *in vitro*, and its pharmacokinetics in dogs were indistinguishable from those of the parent drug. Since the proteolytic enzymes α-chymotrypsin and carboxypeptidase A are the target reconversion sites, their properties are briefly reviewed, followed by the aspirin derivatives selected.

**Table II—Possible Changes in Physical Properties of Drugs with Free $NH_2$ Groups**

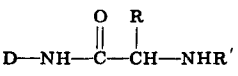

drug amino acid

| Drug | Amino Acid | R′ | Change in Physical Properties |
|---|---|---|---|
| Weak base | Nonpolar | $COCH_3$ | To a neutral compound |
| Weak base | Acidic | $COCH_3$ | To an acidic compound |
| Zwitterionic | Polar–nonpolar | $COCH_3$ | To an ionic (acidic) compound |
| Weak base | Polar–nonpolar | H | Change in pKa |

**α-Chymotrypsin**—α-Chymotrypsin, an endopeptidase involved in protein digestion, has a molecular weight of ~25,000 g/mole. α-Chymotrypsin catalyzes the hydrolysis of a broad spectrum of peptides, amides, and esters. An absolute requirement of the substrate candidate is that the amino acid residue be of L-configuration. Substrates having an aromatic residue (*e.g.*, phenylalanine, tryptophan, and tyrosine) are hydrolyzed at appreciable rates (3), but the hydrolysis of substrates having hydrophobic residues (*e.g.*, leucine and methionine) is also catalyzed (4).

Kinetic studies have revealed a bell-shaped relationship between the overall reaction rate and pH, with maximum activity occurring near pH 8. The kinetic scheme shown in Scheme I seems to apply to an α-chymotrypsin-catalyzed hydrolysis.

$$E + S \overset{K_S}{\rightleftharpoons} E\ S \overset{k_{+2}}{\underset{k_{-2}}{\rightleftharpoons}} E - P_2 \overset{k_{+3}}{\underset{k_{-3}}{\rightleftharpoons}} E + P_2$$
$$+$$
$$P_1$$

*Scheme I*

The three reaction steps represent the formation of the noncovalent (Michaelis) enzyme–substrate complex, the formation of an acyl enzyme with the loss of the leaving group, and the deacylation step. For nonspecific substrates with good leaving groups and for specific ester substrates, the deacylation step is rate limiting; for specific amides, the rate is determined by the acylation step.

**Carboxypeptidase A**—The primary action of carboxypeptidase A is that of a C-terminal exopeptidase. The enzyme is also a good esterase. Having a molecular weight of ~34,600 g/mole, the active enzyme consists of a single chain of 307 amino acid residues and one zinc ion. The amino acid sequence is known completely (5). The zinc ion has been shown to be essential for catalytic activity, even though its removal does not greatly affect the enzyme structure (6). There are two absolute requirements for potential carboxypeptidase A substrates (7, 8); the terminal carboxyl group must be free and the C-terminal residue must be of the L-configuration. The hydrolysis of substrates wherein R is a branched aliphatic or, optimally, an aromatic group is significantly favored.

**Aspirin Derivatives**—The chemical instability of aspirin was studied extensively (9–12). For present purposes, the pH of maximum stability is 2.5. The pH is below that usually observed for esters due to the presence of the carboxyl group, which functions as a general base catalyst and increases the reaction rate at pH 2.5–8. Aspirin, being a weak acid, also shows minimum solubility in acid. However, even suspensions of aspirin are not satisfactorily stable (12).

One approach to stabilizing aspirin is to esterify the carboxyl group. While this approach does improve stability, the esters (prodrugs) typically do not revert back to aspirin because the acetyl group is more labile than the ester group, with the resultant formation of salicylic acid esters (13). If the ester group were chemically more labile than the acetyl group, formulation instability would likely be a problem.

The aspirin derivatives in the present study (I–III) were chosen such that rapid biochemical reconversion in the intestinal tract would be affected. In each case, improved chemical stability is expected since the carboxyl group is masked. The esters and amides were chosen such that prodrug solubility would be somewhat less than that of the aspirin-free acid and further increase the stability of aspirin in suspension form. Other amino acid and ester groups could be chosen to obtain somewhat different physical properties if desired.

The biochemical reconversion of I–III is expected to be *via* an initial α-chymotrypsin hydrolysis of the ester or amide group followed by a

**Table III—Possible Changes in Physical Properties of Drugs with Free COOH Groups**

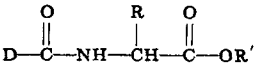

drug amino acid

| Drug | Amino Acid | R′ | Change in Physical Properties |
|---|---|---|---|
| Weak acid | Polar–nonpolar | H | change in pKa |
| Weak acid | Basic | H | Zwitterionic compound |
| Weak acid | Basic | $OC_2H_5$ | To a basic compound |
| Zwitterionic | Polar/nonpolar | $OC_2H_5$ | To a basic compound |

carboxypeptidase cleavage of the amide-releasing aspirin in the intestinal lumen or at the membrane wall (14). To the extent that the gastric irritation associated with oral dosing of aspirin is a local phenomenon (15–17), this approach may also reduce or eliminate the problem since aspirin would not be formed until the prodrug reached the intestine.

## EXPERIMENTAL

**Phenylalanine Ethyl Ester, Hydrochloride**—Thionyl chloride (10 ml) was added to ethanol (40 ml), portionwise, in cold. Phenylalanine (2.3 g) was added to the mixture and refluxed for 2 hr. The reaction mixture was cooled, and the solvent was evaporated under reduced pressure. The flaky solid residue was washed with cold anhydrous ether and was then purified by selective precipitation from the ethanol–ether mixture, mp 154–156°, yield 2.9 g.

**Aspirin Phenylalanine Ethyl Ester (I)**—Aspirin[1] (1.8 g) was dissolved in 35 ml of dry methylene chloride and dicyclohexylcarbodiimide[2] (1 g) was added to it at room temperature. The mixture was stirred for 2 hr, and the precipitated dicyclohexylurea was filtered off.

To the filtrate was added a mixture of phenylalanine ethyl ester hydrochloride (1.15 g, 5 mmoles) and triethylamine (0.5 g, 5 mmoles) dissolved in 10 ml of methylene chloride. The mixture was stirred overnight at room temperature and the solvent was removed under reduced pressure. Dry ethyl acetate (20 ml) was added to the residue. A white precipitate appeared, which was filtered and found to be dicyclohexylurea. The filtrate was washed three times with 10% sodium bicarbonate and three times with water to make it free from alkali and then dried over anhydrous magnesium sulfate. The dried extract was filtered, and the solvent was removed under reduced pressure.

The residue was dissolved in ethanol, and water was added until turbidity appeared. It was then kept in the freezer overnight. The oily precipitate solidified and was filtered and further purified by selective precipitation from ethanol–water mixtures, mp 72–74°, yield 1.6 g. The product gave a single spot on TLC. Structure was confirmed by NMR[3] and mass spectrum ($M^+$ = 356); NMR (90 MHz, $CDCl_3$): δ 1.35 (t, 3H, $CH_3$ of ethyl ester), 2.1 (S, 3H, $OCOCH_3$ of aspirin), 3.27 (d, 2H, aromatic $CH_2$ of phenylalanine), 4.2 (q, 2H, $COOCH_2$ of ethyl ester), 5.05 (m, 1H, CH of phenylalanine group), 7.1–7.65 (m, 7H, aromatic H), and 8.05 (d, 1H, aromatic H proton next to CONH group of aspirin nucleus).

**Phenylalanine Amide**—To a solution of L-phenylalanine (0.83 g) in water–dioxane (1:1, 8 ml) and triethylamine (1.05 ml, 7.5 m*M*) was added 2-*tert*-butoxycarbonyloxyamino-2-phenylacetonitrile[1] (1.36 g) at room temperature. The solution was stirred overnight at room temperature. After 15 ml of water was added to the reaction mixture, it was washed twice with 15-ml portions of ethyl acetate; the ethyl acetate washings were discarded. The aqueous layer was acidified to pH 2.0 by 5% citric acid solution and saturated with sodium chloride. It was then extracted with three 20-ml portions of ethyl acetate, and the combined ethyl acetate extracts were washed three times with saturated sodium chloride solution to make the organic extract acid free. The ethyl acetate extract was dried over anhydrous magnesium sulfate and filtered, and the solvent was removed under reduced pressure to obtain an oily residue of *tert*-butoxycarbonylphenylalanine, yield 1.2 g.

Ethyl chloroformate was added dropwise over 10 min at −10° to a well-stirred solution of *tert*-butoxycarbonylphenylalanine and triethylamine in dry tetrahydrofuran. The mixture was stirred for 30 min at −10° and then saturated with dry ammonia. The reaction mixture was stirred overnight at room temperature, the solvent was evaporated under reduced pressure, and the residue was stirred with 20 ml of ice-cold water, filtered, and dried at 40–60°. It was then treated with 4 *N* hydrochloric acid–dioxane for 30 min at room temperature. The solvent was removed to obtain a solid residue of L-phenylalanine amide hydrochloride.

**Aspirin Phenylalanine Amide (II)**—To a solution of 1.8 g of aspirin in 35 ml of dry methylene chloride was added 1.1 g of dicyclohexylcarbodiimide. The reaction mixture was stirred for 2 hr at room temperature, and a white precipitate of dicyclohexylurea was formed and removed by filtration. To the filtrate was added a mixture of 5 m*M* L-phenylalanine amide (1.1 g) and 5 m*M* triethylamine (0.7 ml) in 15 ml of methylene chloride. The reaction mixture was stirred overnight at room temperature, and the solvent was removed under reduced pressure. The residue was dissolved in chloroform and washed once with water, three times with 15-ml portions of 10% sodium bicarbonate, and three times with 10-ml portions of 2 *N* HCl, followed by a final washing with water to make it acid free.

The organic extract was evaporated to dryness under reduced pressure, and the residue was washed with ether, filtered, and recrystallized from chloroform, mp 176–178°, yield 1.4 g. The structure was identified by NMR and mass spectrum ($M^+$ = 327). The product gave a single spot on TLC; NMR (90 MHz, $CDCl_3$): δ 2.2 (s, 3H, $OCOCH_3$ of aspirin), 3.15 (d, 2H, aromatic $CH_2$ of phenylalanine), 4.92 (m, 1H, CH of phenylalanine group), 7.05–7.65 (m, 7H, aromatic H), and 7.85 (d, 1H, aromatic H proton next to CONH group of aspirin nucleus).

**Aspirin Phenyllactic Ethyl Ester (III)**—A solution of 0.4 g of aspirin chloride dissolved in 10 ml of tetrahydrofuran was chilled to 5°; to it was added a cooled solution of L-phenyllactic acid (0.33 g) in 4 ml of tetrahydrofuran. Aliquots of pyridine totaling 0.5 ml were added to the reaction mixture over 5 min, and the system was stirred at 5° for 1 hr. After an additional hour of stirring at room temperature, the solvent was removed on a rotary evaporator and the clear colorless oil was dissolved in chloroform. The chloroform solution was extracted with water, dried over anhydrous magnesium sulfate, and evaporated under reduced pressure to yield a colorless oil, which was purified by selective precipitation from chloroform by *n*-hexane. The oil did not solidify. Its purity was checked by TLC, and NMR and mass spectrometry were used to confirm its identity as L-phenyllactic acid ester of aspirin.

Aspirin phenyllactic acid (0.23 g) was dissolved in dry methylene chloride, and the solution was chilled to 0°. To it was added magnesium ethoxide-dried ethanol (0.35 ml) followed by dicyclohexylcarbodiimide (0.13 g, 0.7 mmole). After stirring at 0° for 1 hr, it was stirred for an additional 1 hr at room temperature. The solvent was removed under reduced pressure to obtain a clear colorless oil, which was further purified by selective precipitation from ethanol by water. The oil could not be solidified. TLC showed only one spot, the NMR and mass spectrometry ($M^+$ = 355) confirmed it to be III; NMR (90 MHz, $CDCl_3$): δ 1.3 (t, 3H, $CH_3$ of ethyl ester), 2.1 (s, 3H, $OCOCH_3$ of aspirin), 3.27 (d, 2H, aromatic $CH_2$ of phenylalanine), 4.2 (q, 2H, $COOCH_2$ of ethyl ester), 5.45 (m, 1H, CH of phenylalanine group), 7.05–7.65 (m, 7H, aromatic H), and 7.95 (d, 1H, aromatic H proton next to COO group of aspirin nucleus).

**Aspirin Phenylalanine**—Compound I (60 mg) was dissolved in 10 ml of ethanol and added to 100 ml of a pH 7.5 phosphate buffer solution containing α-chymotrypsin (100 mg). It was mixed well, allowed to stand for ~2 min, and then transferred to a 250-ml separator. It was then acidified with 2 *N* HCl to pH 1.0 and extracted with 100 ml of chloroform. A very thick emulsion resulted on shaking, and the layer had to be separated by centrifugation at 2000 rpm for 20 min.

The upper aqueous layer was aspirated out, the lower layer was dried over anhydrous magnesium sulfate, and the solvent was removed in a rotary evaporator to obtain a clear, colorless, oily residue, which was further purified by selective precipitation from ethanol with water. NMR and mass spectrometry ($M^+$ = 328) confirmed it to be aspirin phenylalanine; NMR (90 MHz, $CDCl_3$): δ 2.1 (s, 3H, $OCOCH_3$ of aspirin), 3.27 (d, 2H, aromatic $CH_2$ of phenylalanine), 5.05 (m, 1H, CH of phenylalanine group), 7.0–7.65 (m, 7H, aromatic H), and 7.85 (d, 1H, aromatic H proton next to CONH group of aspirin nucleus).

**TLC Systems**—To follow the hydrolysis of aspirin phenylalanine ethyl ester qualitatively and to identify the products, a TLC system was sought that would separate the reactants and products. Of several solvent systems tried, methanol–acetic acid–ether–benzene (1:18:60:20) was able to resolve aspirin and salicylic acid (which appears as a dense blue spot under short wavelength UV). The support was silica gel with $UV_{254}$ fluorescent background. This solvent system could not differentiate between aspirin and I. However, cyclohexane–chloroform acetic acid (4:5:1) was able to distinguish between aspirin and I but not between aspirin and salicylic acid.

TLC plates were run in both solvents simultaneously to allow identification of all the degradation products of I in simulated intestinal fluid. All chloroform extracts were spotted on silica gel plates, 0.25 mm thick, and developed for 15 cm in both solvents. The spots were detected under a short wavelength UV detector.

**Shelflife Studies of I**—Compound I (5 mg) was dissolved in 1 ml of ethanol and transferred quantitatively to a 100-ml volumetric flask, and the volume was made up with 0.066 *M* phosphate buffer of pH 7.5, 6.6, or 5.6. Aliquots (5 ml) were withdrawn at timed intervals, taken in 15-ml centrifuge tubes, and extracted with 5-ml portions of chloroform. The aqueous layer was removed by aspiration. Two 0.5-ml portions of the chloroform extracts were placed in 10-ml volumetric flasks, and the solvent was evaporated with a gentle nitrogen stream. To Flask A was added 0.5 ml of ethanol and 1 ml of 5 *N* NaOH. The mixture was heated in a

[1] Monsanto Co.
[2] Aldrich Chemical Co.
[3] Melting points were determined in capillaries and are uncorrected. NMR spectra were recorded with a Varian E-390 spectrometer with tetramethylsilane as the internal standard. All structures were confirmed by NMR and mass spectra.

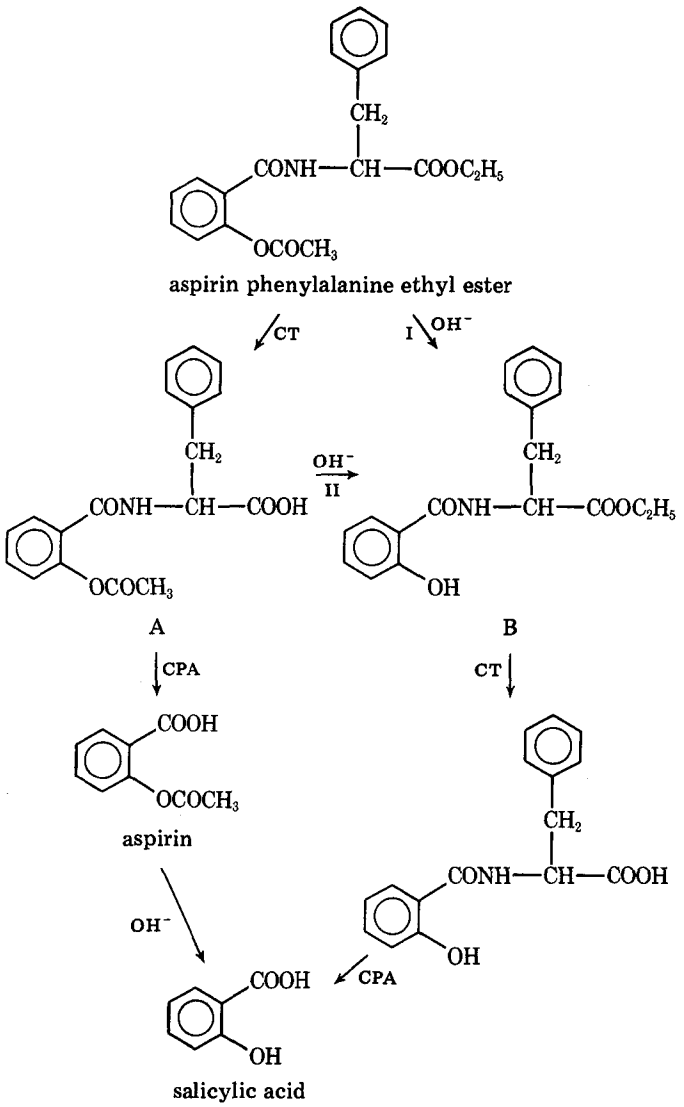


*Scheme II—Possible hydrolytic pathways of aspirin phenylalanine in presence of chymotrypsin (CT) and carboxypeptidase A (CPA) mixture.*

boiling water bath for 45 min and cooled to room temperature, and the volume was made up with distilled water. To Flask B was added 0.5 ml of ethanol, and the volume was made up with distilled water. Fluorescence of both the samples was determined at excitation/emission wavelengths of 328/400 nm.

Scheme II shows that of all possible degradation products, only I and salicylic acid phenylalanine ethyl ester (being nonionic) are extractable in chloroform. Salicylic acid phenylalanine ethyl ester has the same excitation and emission maxima as salicylic acid. Therefore, by subtracting the fluorescence of B from A, the fluorescence corresponding to salicylic acid generated by the alkali digestion of I was obtained. A standard solution of I carried through the described procedure served as the standard.

**Table IV—Enzyme Kinetic Parameters for Aspirin Derivatives** [a]

| | α-Chymotrypsin | | Carboxypeptidase | |
|---|---|---|---|---|
| | $K_m$, mole/liter | $K_{cat}$, $sec^{-1}$ | $K_m$, mole/liter | $K_{cat}$, $sec^{-1}$ |
| Aspirin phenylalanine ethyl ester (I) | $1 \times 10^{-6}$ | 2.91 | $1.3 \times 10^{-4}$ [b] | $8.5 \times 10^{-2}$ [b] |
| Aspirin phenyllactic ethyl ester (III) | $2.5 \times 10^{-5}$ | $3.7 \times 10^{-3}$ | $1 \times 10^{-4}$ | 25 |
| Aspirin phenylalanine amide (II) | $5.1 \times 10^{-4}$ | $5 \times 10^{-3}$ | $1.3 \times 10^{-4}$ | $8.5 \times 10^{-2}$ |

[a] References 18 and 19. [b] Done at pH 8.5.

**Table V—Estimated Range of *In Vivo* Reconversion Rates ($S_0 = 10^{-5}$ *M*)**

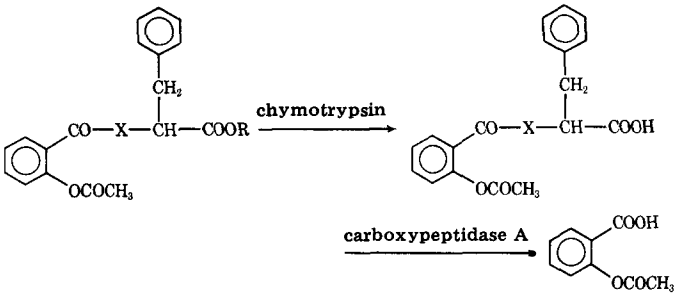


| Structure | $E_0$, *M* | pH | $t_{1/2}$ Maximal Rate (Zero Order), $v = k_{cat}E_0$ | $t_{1/2}$ Minimal Rate (First Order), $v = (k_{cat}/K_m)E_0S$ |
|---|---|---|---|---|
| X = NH R = $C_2H_5$ | $10^{-4}$ | 8.5 | 5.9 sec | 16.8 sec |
| X = O R = $C_2H_5$ | $10^{-4}$ | 7.5 | 13.5 sec | 61.9 sec |
| X = NH R = $C_2H_5$ | $10^{-6}$ | 8.5 | 10 min | 28 min |
| X = O R = $C_2H_5$ | $10^{-6}$ | 7.5 | 22.5 min | 103 min |

**Solubility Determination**—Compound I (~300 mg) was stirred with 100 ml of distilled water at 25.00 ± 0.02°. Aliquots of the solution were withdrawn until no change in concentration was observed. Equilibrium was reached in 20 hr. After the aliquots were diluted 10 times, 1 ml was placed in a 10-ml volumetric flask; 1 ml of 5 *N* NaOH was added, and the solution was heated in a boiling water bath for 45 min. After cooling, the solution was diluted to volume with distilled water, and fluorescence measurements were taken at excitation/emission wavelengths of 328/400 nm, using a $10^{-6}$ *M* solution of I, taken through all the described steps, as a standard. The solubility was determined to be $4.7 \times 10^{-4}$ *M*.

## RESULTS AND DISCUSSION

**Summary of Enzyme Kinetic Results**—The detailed enzyme kinetic studies were reported previously (15, 16), and only the most significant results are summarized here. Of the aspirin derivatives studied, I was the best substrate for α-chymotrypsin while aspirin phenyllactic acid was the best substrate for carboxypeptidase. The kinetic parameters are given in Table IV. The values for the kinetic parameters are consistent with values for other well-known substrates of these enzymes. Table V shows the aspirin reconversion process for the ethyl esters. Given the kinetic results in Table IV, the α-chymotrypsin hydrolysis step would be rate limiting for III while the carboxypeptidase hydrolysis step would be rate limiting for I. Both steps were slow for the amide derivative.

The very approximate estimates of the *in vitro* reconversion half-lives in Table V are based on the kinetic parameters for the appropriate rate-limiting step. Whether such estimates reflect the *in vivo* situation is not yet known. However, the results indicate that regeneration of aspirin *in vivo* is at least possible. Compound I was selected for further studies. This choice was based in part on the rapid first step of the reconversion. Since all derivatives had relatively low aqueous solubilities by design, the rapid hydrolysis of the ester, to produce an acid, would increase the dissolution rate of the ethyl ester and perhaps give better *in vivo* performance.

**Hydrolytic Pathway of I**—Scheme II shows the possible hydrolytic pathways for I. Figure 1 shows the TLC results on a solution containing the prodrug and α-chymotrypsin and carboxypeptidase. The results

**Table VI—Kinetic Rate Constants and Shelflife of I in Aqueous Solutions**

| pH | $k_{obs} \times 10^3$, $hr^{-1}$ | $t^{90}$, hr |
|---|---|---|
| 7.5 | 9.84 | 10.8 |
| 6.6 | 2.77 | 38.3 |
| 5.6 | 1.92 | 55.2 |

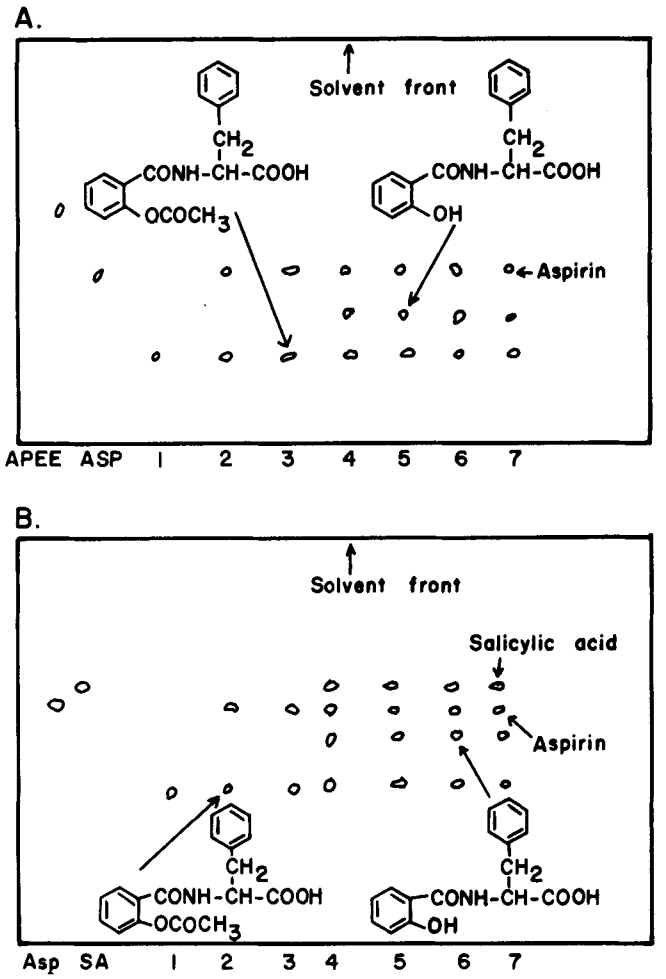


*Figure 1.—Thin-layer chromatogram of the chloroform extract of a mixture of I, α-chymotrypsin (50 mg/100 ml), and carboxypeptidase A (25 mg/100 ml) in pH 7.5 phosphate buffer. The support was silica gel with fluorescent indicator $UV_{254}$. The solvents were cyclohexane–benzene–acetic acid (4:5:1) (A) and methanol–acetic acid–ether–benzene (1:18:60:20) (B). Key: spot 1, 1 min; spot 2, 2 min; spot 3, 5 min; spot 4, 10 min; spot 5, 20 min; spot 6, 45 min; and spot 7, 2 hr. APEE = aspirin phenylalanine ethyl ester; ASP = aspirin; and SA = salicylic acid.*

indicate that the ethyl ester group is lost immediately and that aspirin phenylalanine appears. With time, aspirin appears, followed by salicylic acid and the phenylalanine derivative of salicylic acid. While more detailed kinetic studies are needed, these results demonstrate that aspirin is regenerated in solution in the presence of the enzymes.

**Shelflife Studies of I in Aqueous Solutions**—Logarithms of concentrations of I remaining in the aqueous solutions at various pH values were plotted against time. Reactions were followed up to 10% degradation. From the slopes of these plots, the pseudo-first-order rate constant, $k_{obs}$, was determined. The pseudo-first-order rate constants at several pH values and the corresponding shelflives are given in Table VI.

In case of suspension, the degradation rate is given by:

$$\frac{dc'}{dt} = k_1 s \qquad \text{(Eq. 1)}$$

where $c'$ is the concentration of the drug in solution (mass/volume), $k_1$ is the first-order rate constant, and $s$ is the solubility of the drug expressed in the same unit as $c'$. For $v$ milliliters of suspension:

$$v\frac{dc'}{dt} = \frac{dc}{dt}\,(\text{mass/time}) = -k_1 vs = -k_0 \qquad \text{(Eq. 2)}$$

where $k_0$ is the zero-order rate constant for the drug in suspension.

The solubility of I was $4.7 \times 10^{-4}$ $M$ (*i.e.*, 0.167 mg/ml) compared to that of $1.85 \times 10^{-2}$ $M$ (*i.e.*, 3.33 mg/ml) of aspirin. The calculated shelflife of a 600 mg/5 ml of suspension of I (*i.e.*, an equivalent of 300 mg/5 ml of aspirin) was found to be 4.27 years at pH 5.6 compared to 38 days for 300 mg/5 ml of aspirin suspension at its optimum pH (2.25) for stability.

## REFERENCES

(1) G. L. Amidon, R. S. Pearlman, and G. D. Leesman, in "Design of Biopharmaceutical Properties through Prodrugs and Analogs," E. B. Roche, Ed., American Pharmaceutical Association, Washington D.C., 1977.

(2) C. T. Baugess, J. H. Fincher, F. Sadik, and C. W. Hartman, *J. Pharm. Sci.*, **64,** 1489 (1975).

(3) L. Cunningham, *Comp. Biochem.*, **16,** 85 (1965).

(4) M. Rovery, M. Poilroux, A. Yoshida, and P. Desnuelle, *Biochim. Biophys. Acta*, **23,** 608 (1957).

(5) K. S. V. Sampath Kumar, J. B. Cleag, and K. A. Walsh, *Biochemistry*, **3,** 1728 (1964).

(6) J. H. Rupley and H. Neurath, *J. Biol. Chem.*, **235,** 609 (1960).

(7) H. Neurath, in "The Enzymes," 2nd ed., vol. IV, Academic, New York, N.Y., 1950, p. 11.

(8) H. Neurath and G. W. Schwert, *Chem. Rev.*, **46,** 69 (1950).

(9) L. J. Edwards, *Trans. Faraday Soc.*, **46,** 723 (1950).

(10) *Ibid.*, 696 (1952).

(11) E. R. Garrett, *J. Am. Chem. Soc.*, **79,** 3401 (1957).

(12) K. A. Connors, G. L. Amidon, and L. Kennon, "Chemical Stability of Pharmaceuticals," Wiley, New York, N.Y., 1979, p. 151.

(13) T. S. Pierre and W. P. Jencks, *J. Am. Chem. Soc.*, **90,** 3817 (1968).

(14) G. L. Amidon, G. D. Leesman, and R. L. Elliott, *J. Pharm. Sci.*, **69,** 1363 (1980).

(15) J. P. Leonards and G. Levy, *ibid.*, **59,** 1511 (1970).

(16) K. W. Anderson, *Arch. Int. Pharmacodyn. Ther.*, **152,** 379 (1964).

(17) C. Davison, D. H. Hertig, and R. DeVine, *Clin. Pharmacol. Ther.*, **7,** 329 (1966).

(18) P. K. Banerjee and G. L. Amidon, *J. Pharm. Sci.*, **70,** 1304 (1981).

(19) *Ibid.*, **70,** 1307 (1981).

## ACKNOWLEDGMENTS

Supported by grants from the University of Wisconsin Graduate School and The Upjohn Co.

# Physicochemical Property Modification Strategies Based on Enzyme Substrate Specificities II: α-Chymotrypsin Hydrolysis of Aspirin Derivatives

**PRADIP K. BANERJEE** * **and GORDON L. AMIDON** ˣ

Received November 3, 1980, from the *School of Pharmacy, University of Wisconsin, Madison, WI 53706.* Accepted for publication April 2, 1981. * Present address: Tablet Products Research and Development, Abbott Laboratories, North Chicago, IL 60064.

**Abstract** □ Three aspirin derivatives, aspirin phenylalanine ethyl ester, aspirin phenylalanine amide, and aspirin phenyllactic ethyl ester, were investigated with respect to their hydrolysis by α-chymotrypsin. Of the three compounds, aspirin phenylalanine ethyl ester was the best substrate, with $k_{cat} = 25\ sec^{-1}$ and $K_m = 1.3 \times 10^{-6}\ M$ at pH 8.0. The results for all substrates were in the range of expectation based on kinetic data for other substrates. The apparent latitude in the nature of the acylamide substituent of α-chymotrypsin substrates makes this enzyme a good potential reconversion site for many drug derivatives.

**Keyphrases** □ Aspirin—derivatives, hydrolysis by α-chymotrypsin □ Derivatives—aspirin, synthesis by α-chymotrypsin hydrolysis □ α-chymotrypsin—hydrolysis of aspirin derivatives □ Physicochemistry—modification strategies based on enzyme substrate specificities, α-Chymotrypsin hydrolysis of aspirin derivatives

Previously (1), a rationale for selecting amino acid derivatives of aspirin was described and the syntheses of aspirin phenylalanine ethyl ester (I), aspirin phenylalanine amide (II), and aspirin phenyllactic ethyl ester (III) were reported. These derivatives were so designed that after an initial cleavage of the terminal ethyl ester or amide linkage, carboxypeptidase A regenerates aspirin *in vivo*. This paper reports kinetic studies of these derivatives in the presence of α-chymotrypsin.

## EXPERIMENTAL

**Materials**—α-Chymotrypsin was obtained as a dialyzed, salt-free, lyophilized-powder[1]. The operational normality of α-chymotrypsin solutions was determined by a direct spectrophotometric titration as described previously (2).

**Kinetic Measurements**—The hydrolysis of the prodrugs was followed by automatic titration[2] at a constant pH.

All solvents and chemicals were reagent grade. Triple-distilled water was used in preparing solutions, and the reaction vessel was thermostated at 25.00 ± 0.02°. Dry nitrogen gas was gently blown into the reaction vessel to exclude atmospheric carbon dioxide from the system.

The titrating mechanism was set at the desired pH, and sufficient volume of the prodrug solution containing 0.1 *M* potassium chloride was pipetted into the reaction vessel and allowed to equilibrate for 10 min during magnet stirring. The solution was then brought to the desired pH; when a stable baseline was obtained, 10 μl of a suitable concentration of enzyme was added. The automatic titrating mechanism maintained the set pH during the hydrolytic reaction by adding increments of base as small as 0.1 μl and continuously recording the amount of base consumed *versus* time.

In runs with III, substrate stock solutions were made in acetonitrile. An aliquot of the stock solution was added to the reaction vessel containing a predetermined volume of 0.1 *M* potassium chloride solution, and then the titration was performed in the same manner as described.

The pH-stat results were fit by regression analysis to a polynomial of the form $y = a_0 + a_1 t + a_2 t^2$, where $y$ is the moles of alkali consumed, $t$ is time, and $a_1$ is the initial rate of hydrolysis.

[1] Aldrich Chemical Co.

[2] Radiometer TTI60 titrator, SBR3 titrigraph, ABU12 autoburet, and PHM61 pH meter.

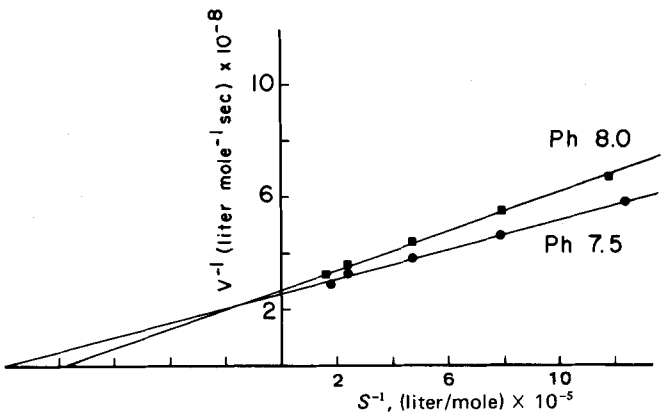


**Figure 1**—*Lineweaver–Burk plot for the hydrolysis of I by 1.79 × 10⁻⁹ M α-chymotrypsin at pH 7.5 and by 2 × 10⁻¹⁰ M α-chymotrypsin at pH 8.0.*

## RESULTS AND DISCUSSION

α-Chymotrypsin-catalyzed hydrolysis follows the general kinetic scheme shown in Scheme I.

$$E + S \underset{}{\overset{K_S}{\rightleftharpoons}} E \cdots S \underset{k_{-2}}{\overset{k_2}{\rightleftharpoons}} EP_2 \underset{k_{-3}}{\overset{k_3}{\rightleftharpoons}} E + P_2$$
$$\Big\downarrow +\ P_1$$

*Scheme I*

The initial rate is given by the Michaelis–Menten equation:

$$V_0 = \frac{k_{cat} E_0 S_0}{K_m + S_0} \qquad \text{(Eq. 1a)}$$

where $S_0$ and $E_0$ are the initial amounts of substrate and enzyme ($S_0 \gg E_0$), or by the Lineweaver–Burk equation:

$$\frac{1}{V_0} = \frac{1}{k_{cat} E_0} + \frac{K_m}{k_{cat} E_0} \frac{1}{S_0} \qquad \text{(Eq. 1b)}$$

Plots of $1/V_0$ *versus* $1/S_0$ for I and II at pH 7.5 and 8.0 are shown in Figs. 1 and 2. Straight lines were obtained in all cases, and $k_{cat}$ and $K_m$ were calculated from the slopes and intercepts. These results are summarized in Table I.

It was shown (3) that $k_{cat}/K_m$ is the most meaningful kinetic parameter for comparing different substrates. Good substrates will have a large $k_{cat}$ and low $K_m$ (tight binding) value and, hence, a large $k_{cat}/K_m$ value. At low substrate concentrations ($S \ll K_m$), the enzymatic reaction is first order (with $E_0$ constant), with the rate constant equal to $(k_{cat}/K_m)E_0$. Hence, at a given enzyme level, $E_0$, $k_{cat}/K_m$ determines the reaction rate at low substrate.

Table I shows that for I, $k_{cat}/K_m$ is smaller by a factor of six at pH 7.5 than at pH 8.0 but that $K_m$ does not change significantly. The $k_{cat}$ value was eight times smaller at pH 7.5 than at pH 8.0. For *N*-acetyl phenylalanine ethyl ester, $k_{cat}$ is three times smaller at pH 7 than at pH 7.8 (4). Both $K_m$ and $k_{cat}$ values for I were smaller than those for the *N*-acetyl derivatives. However, the ratio of $k_{cat}/K_m$ was of comparable magnitude to that for the *N*-acetyl derivative. A similar change in $k_{cat}/K_m$ was also noticed for I hydrolysis. The change in structure of the prodrug from ethyl ester to an amide caused a reduction in the hydrolysis rate by a factor of $10^5$. This finding was consistent with the results reported (4) for *N*-acetyl-L-phenylalanine derivatives.



*0022-3549/81/1200-1304$01.00/0*
*© 1981, American Pharmaceutical Association*

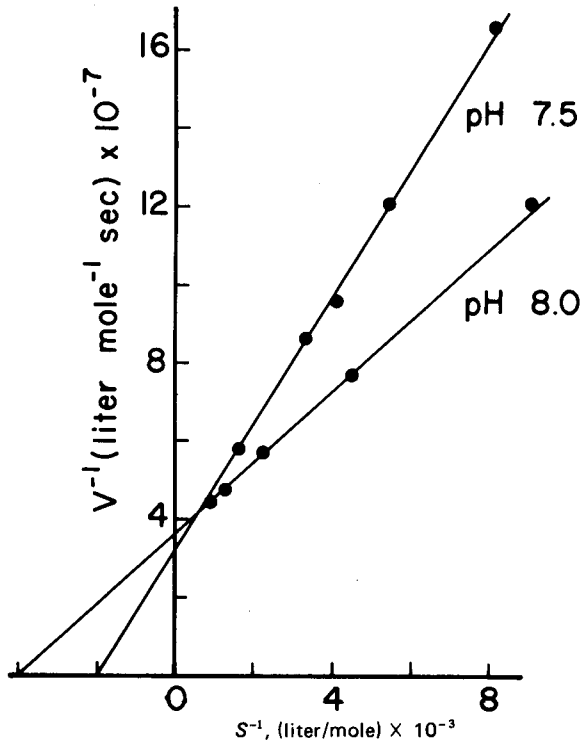


**Figure 2**—*Lineweaver–Burk plot for the hydrolysis of II by 6.26 × 10⁻⁶ M α-chymotrypsin at pH 7.5 and by 4.4 × 10⁻⁶ M α-chymotrypsin at pH 8.0.*

Correlation between hydroxide-ion-catalyzed hydrolysis rate constants and the first-order enzymatic hydrolysis rate constant, $k_{cat}/K_m$, was shown (3). For aspirin phenylalanine derivatives, the change in reactivity may be attributed to the electronic effect of the substituent rather than to any change in binding with the active site. Table I also shows that *N*-acetyl and *N*-aspirin derivatives have $k_{cat}/K_m$ values within an order of magnitude. Therefore, for these substrates, the chymotrypsin-catalyzed hydrolysis is reasonably independent of the drug molecule, a requirement for general application of this approach. The hydrolysis rates obtained were within the expected range.

Experiments with III had to be carried out under conditions of approximately equal substrate and enzyme concentrations. This approach violates one basic assumption of the derivation of the Michaelis–Menten equation ($S_0 \gg E_0$). Dixon (5) described an elegant and simple direct plot for determining $K_m$ when a substantial fraction of the substrate is bound.

**Table I—Kinetic Parameters for α-Chymotrypsin-Catalyzed Hydrolysis**

| Substrate | $K_m$, mole/liter | $k_{cat}$, $sec^{-1}$ | $\frac{k_{cat}}{K_m}$, moles sec/liter | pH |
|---|---|---|---|---|
| Aspirin phenylalanine ethyl ester (I) | $1 \times 10^{-6}$ | 2.91 | $2.91 \times 10^6$ | 7.5 |
| | $1.3 \times 10^{-6}$ | 25 | $1.92 \times 10^7$ | 8.0 |
| *N*-Acetyl phenylalanine[a] ethyl ester | $1.2 \times 10^{-3}$ [a] | 160[a] | $1.33 \times 10^5$ [a] | 7.8 |
| | $0.88 \times 10^{-3}$ [a] | 63[a] | $7.16 \times 10^4$ [a] | 6.99 |
| Aspirin phenyllactic ethyl ester (III) | $2.02 \times 10^{-5}$ | $7.93 \times 10^{-3}$ | $3.96 \times 10^2$ | 8.0 |
| | $2.5 \times 10^{-2}$ | $3.7 \times 10^{-3}$ | $1.48 \times 10^2$ | 7.5 |
| *O*-Acetyl phenyllactic[b] ethyl ester | $2.3 \times 10^{-2}$ | 0.6 | 26.1[b] | 8.0 |
| Aspirin phenylalanine amide (II) | $5.1 \times 10^{-4}$ | $5 \times 10^{-3}$ | 9.8 | 7.5 |
| | $2.4 \times 10^{-4}$ | $6.2 \times 10^{-3}$ | 24.7 | 8.0 |
| *N*-Acetyl phenylalanine[a] amide | $3 \times 10^{-2}$ [a] | $4.6 \times 10^{-2}$ [a] | 1.53[a] | 7.9 |

[a] Taken from Ref. 4. [b] Taken from Ref. 12.

The velocity at any $[S]$ is given by $v = k_{cat}[ES]$. At some given point on the velocity curve, one can write:

$$v = V_{max}\left(\frac{n-1}{n}\right) \quad \text{(Eq. 2)}$$

where $n$ is a whole number. Therefore, at the given point on the velocity curve:

$$k_{cat}[ES] = V_{max}\left(\frac{n-1}{n}\right) \quad \text{(Eq. 3)}$$

$$K_m = \frac{[E][S]}{[ES]} = \frac{([E]_0 - [ES])([S]_0 - [E])}{[ES]} \quad \text{(Eq. 4)}$$

After making appropriate substitutions, one obtains:

$$K_m = \frac{[S]_t}{n-1} - \frac{[E]_t}{n} \quad \text{(Eq. 5)}$$

A series of lines are drawn from the origin through points on the velocity curve where $v = V_{max}[(n-1)/n]$. Since $n$ is a whole number, the points correspond to $1/2V_{max}$, $2/3V_{max}$, $3/4V_{max}$, *etc.* Each line intersects a horizontal line of height $V_{max}$ at different $[S]_n$ values, called $[S]_2$ (for the line through $1/2V_{max}$), $[S]_3$ (for the line through $2/3V_{max}$), $[S]_3$ (for the line through $2/3V_{max}$), and so on. The value of each $[S]_n$ is given by:

$$[S]_n = \left(\frac{n}{n-1}\right)[S]_t \quad \text{(Eq. 6)}$$

where $[S]_t$ is the total substrate concentration required for a given $n$. Consequently:

$$[S]_t = \left(\frac{n-1}{n}\right)[S]_n \quad \text{(Eq. 7)}$$

and from Eq. 5:

$$K_m = \frac{[S]_n}{n} - \frac{[E]_t}{n} \quad \text{(Eq. 8)}$$

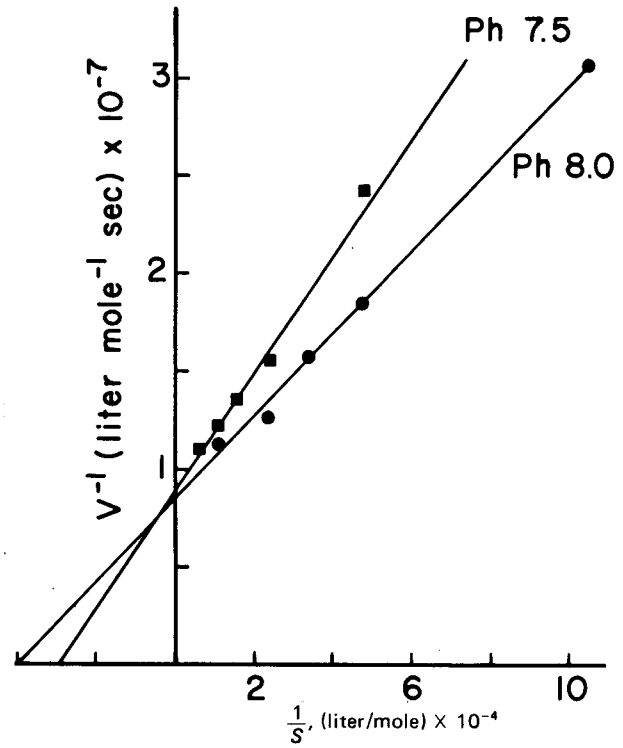


**Figure 3**—*Lineweaver–Burk plot for the hydrolysis of III by 3.02 × 10⁻⁵ M α-chymotrypsin at pH 7.5 and by 1.5 × 10⁻⁵ M α-chymotrypsin at pH 8.0.*

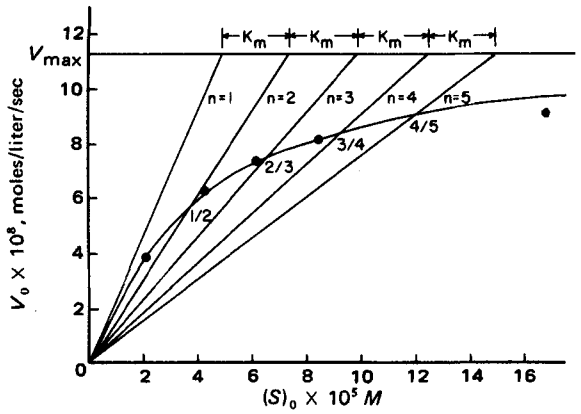


**Figure 4**—*Dixon plot for determining* $K_m$ *for the hydrolysis of III by* $3.02 \times 10^{-5}$ M *α-chymotrypsin at pH 7.5.*

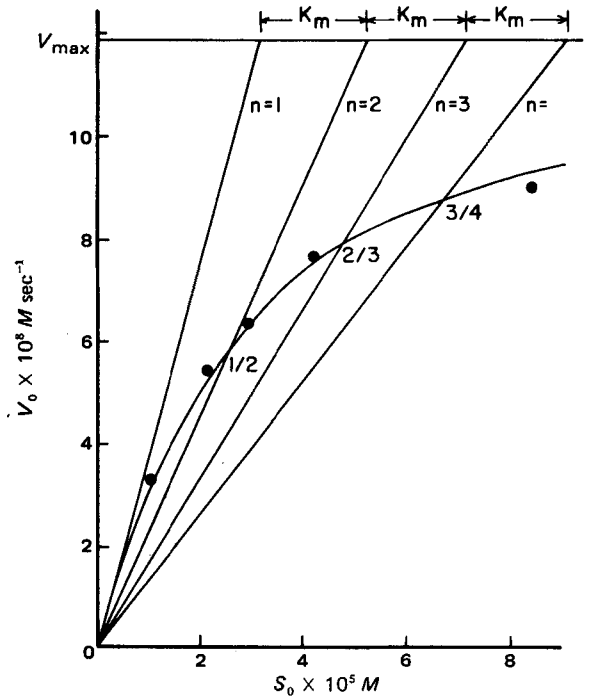


**Figure 5**—*Dixon plot for determining* $K_m$ *for the hydrolysis of III by* $1.5 \times 10^{-5}$ M *α-chymotrypsin at pH 8.0.*

or:

$$[S]_n = nK_m + [E]_t \qquad \text{(Eq. 9)}$$

The intercepts on the $V_{max}$ line occur at increments of $K_m$, *i.e.*:

$$[S]_n - [S]_{n-1} = K_m \qquad \text{(Eq. 10)}$$

This procedure requires a knowledge of $V_{max}$. It was shown (6) that if the $V_{max}$ value chosen is too low, the distances between the intercepts (*i.e.*, $K_m$) decrease toward the right. If the $V_{max}$ value chosen is too high, the intervals increase toward the right. Thus, the method gives a check on the assumed value of $V_{max}$.

The $V_{max}$ values used in the Dixon plots were obtained from the Lineweaver–Burk plots (Fig. 3) of the data. The Dixon plots are shown in Figs. 4 and 5; the intercepts were at constant intervals on the $V_{max}$ axis, indicating the validity of the $V_{max}$ values used. The $K_m$ values obtained by the Dixon method (Table I) were only slightly lower than those found by the Lineweaver–Burk method.

Table I shows that the $k_{cat}/K_m$ ratio was much lower for III than for its phenylalanine analog. This finding may be explained by the specificity of α-chymotrypsin in terms of sites on the enzyme complementary to the four groups oriented tetrahedrally about the α-carbon atom of the substrates (6–8). The substrate groups may fit into the corresponding sites or associate with them with varying effects. The α-acylamido group fits into its site and associates by hydrogen bonding (9, 10). For the phenyllactic acid derivative, the acylamido hydrogen capable of hydrogen bonding is lacking. This condition probably leads to less favorable orientation and a concomitant reduction in the reaction rate ($k_{cat}$).

It was shown (11) that all esters of the same acyl group give the same steady-state hydrolysis rate, indicating that deacylation is the rate-limiting step. For the amides, the rate depends on the amide group involved (*i.e.*, acylation is rate limiting). Therefore, for ester hydrolysis with α-chymotrypsin, $k_{cat} \approx k_3$; for amides, $k_{cat} \approx k_2$. It may be shown from the enzyme kinetic scheme (Scheme I) that $K_m$ and the equilibrium constant $K_s$ are related as follows:

$$K_m = \frac{k_3}{k_2 + k_3} K_s \qquad \text{(Eq. 11)}$$

If $k_2 \gg k_3$:

$$K_m \approx \frac{k_3}{k_2} K_s \qquad \text{(Eq. 12)}$$

If $k_3 \gg k_2$:

$$K_m \approx K_s \qquad \text{(Eq. 13)}$$

Bender and coworkers (4, 11) outlined some consequences of Scheme I for two types of substrates, esters and amides. They showed that the leaving groups (the ester or amide moieties) contribute very little, if anything, to the binding of substrates to α-chymotrypsin. Thus, $K_s$ values for amides and esters of the same acylamino acids should be similar. Because $K_s = K_m$ for the amide substrate, this experimentally determined value may be used as $K_s$ for the ester. In this way, all rate constants for various substrates can be evaluated. At pH 8.0, the values obtained for I are $K_s = 2.4 \times 10^{-4}$ *M*, $k_2 = 9.8 \times 10^3$ sec$^{-1}$, and $k_3 = 25$ sec$^{-1}$. The values for II are $K_s = 2.4 \times 10^{-4}$ *M*, $k_2 = 6.1 \times 10^{-3}$ sec$^{-1}$, and $k_3 = 25$ sec$^{-1}$.

Therefore, of the three synthesized prodrugs of aspirin, I showed the highest hydrolysis rate in the presence of α-chymotrypsin. The kinetic parameters obtained were within the range of expectation based on prior knowledge of the properties of α-chymotrypsin.

## REFERENCES

(1) P. K. Banerjee and G. L. Amidon, *J. Pharm. Sci.*, **70,** 1299 (1981).

(2) G. R. Schonbaum, B. Zerner, and M. L. Bender, *J. Biol Chem.*, **236,** 2930 (1960).

(3) M. L. Bender and F. J. Kezdy, *Ann. Rev. Biochem.*, **34,** 49 (1965).

(4) B. Zerner, R. P. M. Bond, and M. L. Bender, *J. Am. Chem. Soc.*, **86,** 3674 (1964).

(5) M. Dixon, *Biochem. J.*, **135,** 101 (1972).

(6) G. E. Hein and C. Niemann, *Proc. Natl. Acad. Sci. USA*, **47,** 1341 (1961).

(7) S. G. Cohen, J. Crossley, E. Khedouri, and R. Zand, *J. Am. Chem. Soc.*, **84,** 4163 (1962).

(8) H. R. Almond, D. T. Manning, and C. Niemann, *Biochemistry*, **1,** 243 (1962).

(9) S. G. Cohen, J. Crossby, E. Khedouri, R. Zand, and L. H. Klee, *J. Am. Chem. Soc.*, **85,** 1685 (1963).

(10) M. L. Bender and B. W. Turnquest, *ibid.*, **77,** 4271 (1955).

(11) M. L. Bender, G. E. Clement, C. R. Gunter, and F. J. Kezdy, *ibid.*, **86,** 3697 (1964).

(12) W. O. Maclure and H. Neurath, *Biochemistry*, **5,** 1425 (1966).

## ACKNOWLEDGMENTS

Supported by the University of Wisconsin Graduate School and The Upjohn Co.

# Physicochemical Property Modification Strategies Based on Enzyme Substrate Specificities III: Carboxypeptidase A Hydrolysis of Aspirin Derivatives

**PRADIP K. BANERJEE** * **and GORDON L. AMIDON** ˣ

Received November 3, 1980, from the *School of Pharmacy, University of Wisconsin, Madison, WI 53706.* Accepted for publication April 2, 1981. * Present address: Tablet Products Research and Development, Abbott Laboratories, North Chicago, IL 60064.

**Abstract** □ The aspirin derivatives aspirin phenylalanine and aspirin phenyllactic acid were studied as substrates for carboxypeptidase A. The phenyllactic acid derivative (an ester) was the best substrate but showed considerable product inhibition. The kinetic parameters for both substrates were in the range expected on the basis of other known substrates. The results indicate that the acylamide substituent (drug) has only a small effect on the enzyme kinetic parameters. Consequently, carboxypeptidase A may serve as a reconversion site for many drug derivatives.

**Keyphrases** □ Aspirin—derivatives, hydrolysis by carboxypeptidase A □ Derivatives—aspirin, hydrolysis by carboxypeptidase A □ Carboxypeptidase A—hydrolysis of aspirin derivatives □ Physicochemistry—modification strategies based on enzyme substrate specificities, carboxypeptidase A hydrolysis of aspirin derivatives

A rationale for making amino acid derivatives of aspirin and their synthesis was reported previously (1). The kinetics of hydrolysis of the derivatives were studied in the presence of $\alpha$-chymotrypsin, and aspirin phenylalanine ethyl ester was the most rapidly hydrolyzed substrate (2). The amino acid derivatives of aspirin were so designed that after the initial cleavage of the terminal ester or amide linkage by $\alpha$-chymotrypsin, carboxypeptidase A would hydrolyze the remaining ester or amide linkage to regenerate aspirin *in vivo*. This paper reports the results of the kinetic studies of aspirin phenylalanine (I) and aspirin phenyllactic acid (II) in the presence of carboxypeptidase A.

## EXPERIMENTAL

**Materials**—Compounds I and II were prepared by the methods already described (1). Carboxypeptidase A was obtained as a suspension of crystals in toluene–water[1]. Before use, enzyme crystals were washed twice with distilled water and dissolved in 3.0 *M* sodium chloride solution. The solutions were centrifuged and stored at 4° in concentrations of ~30 mg/ml. Such solutions were reported (3) to have exhibited no change in activity over several months. Working solutions were prepared daily by diluting the stock solutions to the desired concentrations with 1.0 *M* sodium chloride. Enzyme concentrations were measured by absorbance at 278 nm and using a molar absorptivity of $6.49 \times 10^4$ liters/mole cm (4).

For measuring enzyme activity, stock enzyme was diluted to a 10–25 $\mu$g/ml concentration in 10% lithium chloride immediately before use. The substrate solution was freshly prepared and contained 0.001 *M* hippuryl-L-phenylalanine, 0.025 *M* tromethamine, and 0.5 *M* sodium chloride. The spectrophotometer was set at 254 nm. In the control cell were placed 2.9 ml of substrate solution and 0.1 ml of 10% lithium chloride; in the test cell, 0.1 ml of enzyme solution was added at zero time to 2.9 ml of substrate solution. The increase in absorbance was recorded. Enzyme activity was calculated using the following:

$$\text{units/mg of protein} = \frac{\Delta A_{254}/\text{min}}{0.36 \times \dfrac{\text{mg of enzyme}}{\text{ml of reaction mixture}}} \quad \text{(Eq. 1)}$$

where a unit of activity is defined to be equal to 1 $\mu$mole of substrate hydrolyzed/min under the specified conditions and 0.36 is the molar absorbance index of hippuric acid that is formed stoichiometrically.

**Kinetic Measurements**—The hydrolyses of I and II were followed by automatic titration at constant pH.[2] The method was previously described (2).

## RESULTS AND DISCUSSION

**Aspirin Phenylalanine (I)**—The products of carboxypeptidase A-catalyzed hydrolysis of I are aspirin and phenylalanine. The pKa of the $\alpha$-amino group of phenylalanine is 9.24; at pH 7.5, it is present almost completely as $NH_3^+$. Thus, at pH 7.5, the dissociable proton is consumed by the product amino acid, thereby not requiring any external alkali to maintain the pH. However, at pH 8.5, 18.19% of the phenylalanine is present in the nonionized form. Experiments were performed at pH 8.5 rather than at pH 7.5, accounting for this factor.

In these studies, the Michaelis–Menten assumption of $S_0 \gg E_0$ was

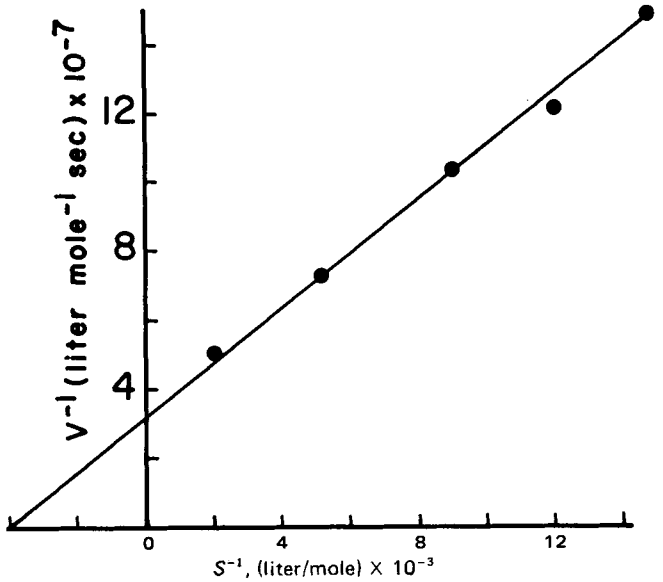


**Figure 1**—*Lineweaver–Burk plot for the hydrolysis of I catalyzed by $1.0 \times 10^{-5}$ M carboxypeptidase A at pH 8.5.*

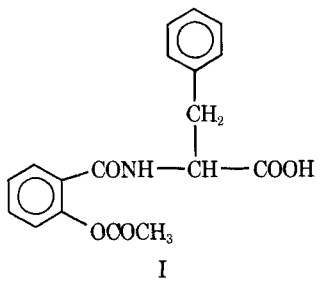


I

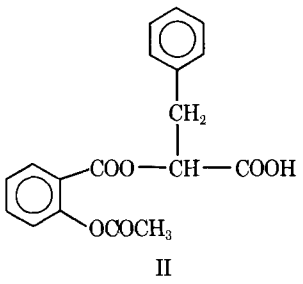


II

[1] Worthington Biochemicals Inc.

[2] Using a Radiometer TTI-60 titrator in conjunction with type SBR-3 titrigraph.

0022-3549/81/1200-1307$01.00/0
© 1981, American Pharmaceutical Association

**Table I—Kinetic Parameters for Carboxypeptidase Hydrolysis at pH 7.5**

| Substrate | $K_m$, mole/liter | $k_{cat}$, $sec^{-1}$ | $K_i$, mole/liter | $\frac{k_{cat}}{K_m}$, moles/sec/liter |
|---|---|---|---|---|
| Cinnamoyl phenylalanine[a] | $6 \times 10^{-4}$ | $2.1 \times 10^{-2}$ | — | 35 |
| Indoleacryloylphenylalanine[a] | $5.84 \times 10^{-4}$ | $1.4 \times 10^{-3}$ | — | 2.39 |
| Aspirin phenylalanine[b] (I) | $1.3 \times 10^{-4}$ | $8.47 \times 10^{-2}$ | — | 445 |
| Cinnamoyl phenyllactic acid | $1.87 \times 10^{-4}$ | 67 | $5.78 \times 10^{-5}$ | $3.58 \times 10^{5}$ |
| Furylacryloyl phenyllactic acid | $1.32 \times 10^{-4}$ | 47 | — | $3.56 \times 10^{5}$ |
| Aspirin phenyllactic acid (II) | $1 \times 10^{-4}$ | 25 | $4 \times 10^{-6}$ | $2.5 \times 10^{5}$ |

[a] Taken from Ref. 3. [b] Performed at pH 8.5.

not adhered to. A Lineweaver–Burk plot (Fig. 1) was used to obtain $V_{max}$, which was then used in the Dixon plot (Fig. 2) to obtain $K_m$. The $K_m$ value obtained from the Dixon plot was slightly lower than that obtained from the Lineweaver–Burk plot. The $K_m$ value for I shown in Table I was obtained from the Dixon plot.

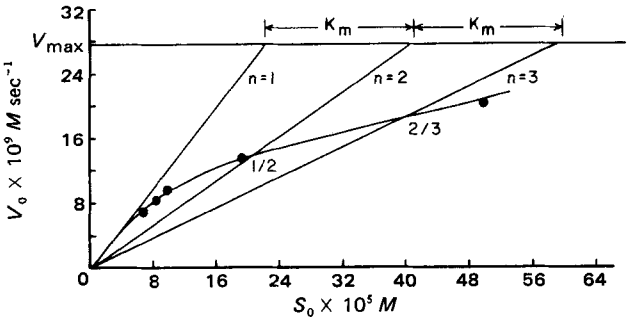


**Figure 2**—*Dixon plot for determining* $K_m$ *for the hydrolysis of I by 1.0* $\times 10^{-5}$ M *carboxypeptidase A at pH 8.5.*

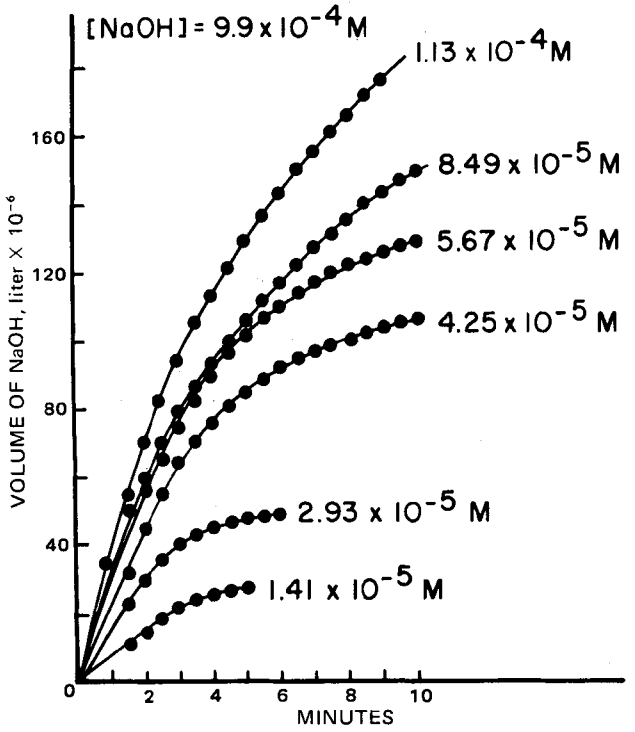


**Figure 3**—*Plot of volume of sodium hydroxide consumed* versus *time for the hydrolysis of II by 2.45* $\times 10^{-10}$ M *carboxypeptidase A at pH 7.5.*

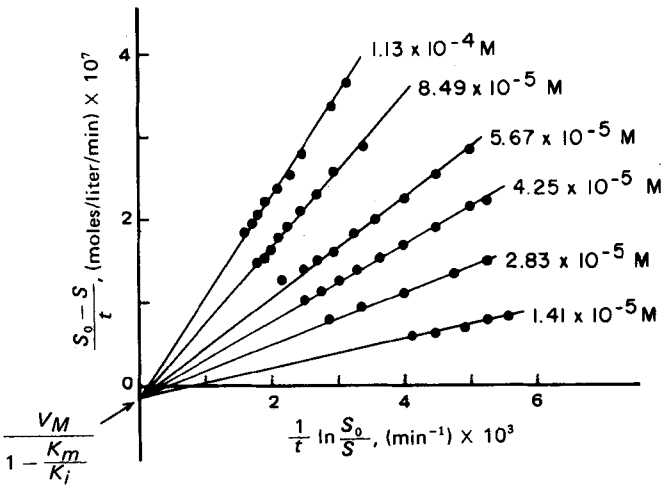


**Figure 4**—*Plot of integrated Michaelis–Menten equation for competitive product inhibition for the hydrolysis of II by 2.45* $\times 10^{-10}$ M *carboxypeptidase A at pH 7.5.*

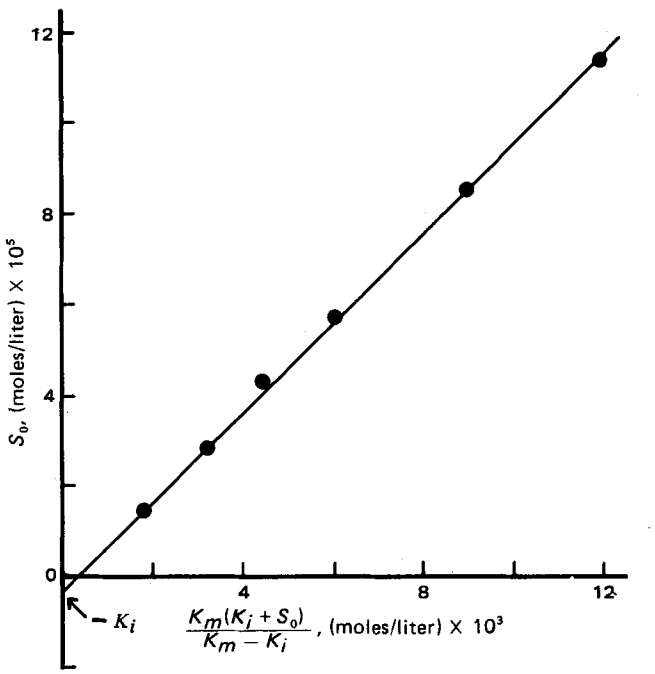


**Figure 5**—*Plot to obtain* $K_m$ *and* $K_i$ *from integrated Michaelis–Menten equation.*

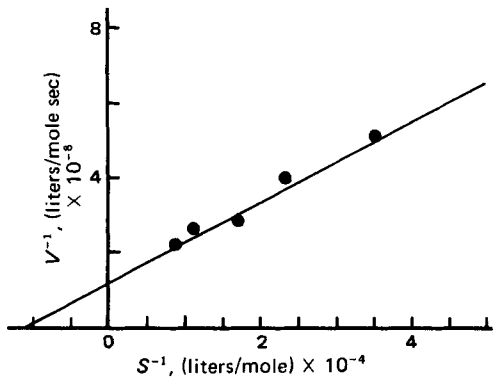


**Figure 6**—*Lineweaver–Burk plot for the hydrolysis of II by 2.45 × $10^{-10}$ M carboxypeptidase A at pH 7.5.*

**Aspirin Phenyllactic Acid (II)**—The results of six runs measuring the hydrolysis rates of II at six different concentrations catalyzed by carboxypeptidase A at pH 7.5 are illustrated in Fig. 3. The points shown were taken from the continuous record of the titrator for calculation purposes. The curves of this plot do not seem to follow a simple kinetic order, and the sharp decrease of hydrolysis rates with time suggests that product inhibition of the enzyme plays an important role. Significant product inhibition of carboxypeptidase A was reported (5, 6).

The scheme that fits the kinetics of the carboxypeptidase A-catalyzed hydrolysis of II is shown in Scheme I ($E$ is carboxypeptidase A, $S$ is II, $P_1$ is aspirin, and $P_2$ is L-phenyllactic acid). The L-phenyllactic acid ($P_2$) produced during hydrolysis acts as a competitive inhibitor.

$$E + S \underset{k_2}{\overset{k_1}{\rightleftarrows}} ES \overset{k_{cat}}{\rightleftarrows} E + P_1 + P_2$$

$$E + P_2 \underset{k_{-i}}{\overset{k_i}{\rightleftarrows}} EP_2$$

*Scheme I*

The corresponding integrated Michaelis–Menten equation is:

$$\frac{[S]_0 - [S]}{t} = \frac{K_m(K_i + [S]_0)}{(K_m - K_i)t} \ln([S]_0/[S]) + \frac{V_{max}}{1 - K_m/K_i} = \frac{a}{t} \ln \frac{[S]_0}{[S]} + \frac{V_{max}}{1 - K_m/K_i} \quad \text{(Eq. 2)}$$

where:

$$K_m = \frac{k_{-1} + k_2}{k_1}$$

$$K_i = \frac{k_{-i}}{k_i}$$

$$a = \frac{K_m(K_i + [S]_0)}{K_m - K_i}$$

**Table II—Kinetic Parameters for Carboxypeptidase A Hydrolysis of II**

| Kinetic Parameter | Calculated by Lineweaver–Burk Method | Calculated by Integrated Michaelis–Menten Equation |
|---|---|---|
| $K_m$, mole/liter | $8.74 \times 10^{-5}$ | $1 \times 10^{-4}$ |
| $K_i$, mole/liter | — | $4 \times 10^{-6}$ |
| $V_{max}$, mole/liter | $8.55 \times 10^{-9}$ | $6 \times 10^{-9}$ |
| $k_{cat}$, $sec^{-1}$ | 35 | 25 |

The integrated Michaelis–Menten equation for competitive product inhibition applies satisfactorily to the kinetic data obtained at pH 7.5 for II. This finding is illustrated by Fig. 4 in which $([S]_0 - [S])/t$ is plotted *versus* $1/t \ln([S]_0/[S])$. The linearity of the plots obtained is consistent with the proposed competitive product inhibition since the lines would curve for other types of product inhibition.

The intercept of the ordinate of Fig. 4 is a function of $V_{max}$, $K_m$, and $K_i$, and the slopes of the straight lines, $a$, are related to $K_m$, $K_i$, and $[S]_0$ by:

$$[S]_0 = a\left(1 - \frac{K_i}{K_m}\right) - K_i \quad \text{(Eq. 3)}$$

Thus, to separate the various kinetic parameters, Fig. 5 plots the values of $[S]_0$ *versus* the respective slopes, $a$, from Fig. 4. The intercept along the $[S]_0$ axis is $-K_i$; hence, $K_m$ and $V_{max}$ can be calculated. The $K_i$ value was considerably smaller than $K_m$, indicating strong competitive inhibition by the product, L-phenyllactic acid.

As a check on the applicability of the integrated Michaelis–Menten equation and the computed kinetic constants, $K_m$ and $V_{max}$ also were determined by the Lineweaver–Burk procedure. Figure 6 shows that the double reciprocal plot of the kinetic results is linear. The agreement between kinetic parameters calculated by the two procedures at pH 7.5 is good (Table II).

An overall summary of the carboxypeptidase A-catalyzed hydrolysis is given in Table I along with some results obtained from the literature for comparison purposes. Compound II was a better substrate than the corresponding phenylalanine derivative. The values of $k_{cat}/K_m$ obtained were comparable to those of the substrates reported previously, indicating that the reconversion rate was in the expected range and that the acylamide drug moiety had only a small effect on enzyme kinetics.

## REFERENCES

(1) P. K. Banerjee and G. L. Amidon, *J. Pharm. Sci.*, **70**, 1299 (1981).

(2) *Ibid.*, **70**, 1304 (1981).

(3) W. O. Maclure and H. Neuroth, *Biochemistry*, **5**, 1425 (1966).

(4) J. P. Bargetzi, K. S. V. Sampath Kumar, D. J. Cox, K. A. Walsh, and H. Neuroth, *ibid.*, **2**, 1468 (1963).

(5) E. T. Kaiser and F. W. Carson, *J. Am. Chem. Soc.*, **86**, 2922 (1964).

(6) P. L. Hall, B. L. Kaiser, and E. T. Kaiser, *ibid.*, **91**, 485 (1969).

# Pharmacokinetics of Indapamide in Dogs

**PETER E. GREBOW** ˣ **and JO A. TREITMAN**

Received November 10, 1980, from the *Biochemistry and Drug Disposition Department, Revlon Health Care Group, Tuckahoe, NY 10707.* Accepted for publication May 13, 1981.

**Abstract** □ Four beagle dogs received both an oral and intravenous dose (1 mg/kg) of indapamide in a crossover design. The blood levels and urinary excretion of intact indapamide were measured, and the pharmacokinetic parameters of the drug were defined. The results indicate that indapamide is completely bioavailable after an oral dose and does not undergo first-pass metabolism. Excretion of unchanged drug from the kidney accounted for only a small percentage of the drug's clearance. While the dog is very similar to the human in its handling of indapamide, the dog clears indapamide approximately twice as fast as humans.

**Keyphrases** □ Indapamide—pharmacokinetics in dogs □ Pharmacokinetics—indapamide, dogs □ Antihypertensive agents—indapamide, pharmacokinetics in dogs

Indapamide[1], 1-(3-sulfamyl-4-chlorobenzamido)-2-methylindoline, is a new antihypertensive agent which has been shown to be clinically effective at daily doses of 2.5 and 5.0 mg (1–5). A terminal elimination half-life of ~15 hr was observed in human volunteers who received 5.0-mg oral doses of indapamide (6). A study (7) in which humans received radiolabeled indapamide orally showed that the drug was extensively metabolized, with only ~5% of the administered drug excreted unchanged in the urine. Therefore, renal clearance was considered to account for only a small percentage of indapamide's total body clearance.

The present study in dogs was designed to define the pharmacokinetic parameters of indapamide. Dogs were given both oral and intravenous doses to determine the fraction of dose systemically available after the oral dose.

## EXPERIMENTAL

**Animals**—Four male beagle dogs, weighing an average of 12.1 kg, were administered ~1 mg/kg of indapamide as an oral solution or as an intravenous injection in a crossover design. Two dogs initially received the oral dose, while the other two received the intravenous dose. A 2-week wash-out period was used between doses. Prior to dosing, the dogs were fasted overnight. They were maintained in metabolism cages and provided with water *ad libitum* throughout the study. Four hours after dosing, the dogs were given 480 ml (16 oz) of dog food mixed with an equal volume of water.

**Treatment**—The oral solution was prepared by dissolving 100 mg of indapamide[2] in 50 ml of polyethylene glycol 400[3], followed by dilution with water to a final concentration of 0.2 mg/ml. Approximately 60 ml of this solution was administered to each dog *via* a gastric tube, followed by 25 ml of water to rinse the gastric tube. The intravenous solution was prepared by dissolving indapamide in absolute ethanol to a final concentration of 5 mg/ml. After administration of the intravenous dose as a bolus, the dogs received ~75 ml of water *via* a gastric tube.

Blood samples (6 ml) for the first 12 hr after dosing were collected by an indwelling catheter in the jugular vein of the dog. Thereafter, blood samples were collected by venipuncture from the cephalic vein. The samples were collected in plastic syringes and transferred to polypropylene tubes[4] for storage. Sodium oxalate was the anticoagulant. With the intravenous dose, blood samples were collected just prior to and at 0.25, 0.5, 1, 2, 4, 6, 8, 12, 24, 30, 48, and 72 hr after dosing. Blood samples were collected just prior to and at 0.5, 1, 2, 3, 4, 6, 8, 12, 24, 30, 48, and 72 hr after the oral dose.

Urine was collected by catheterization just prior to and at 4, 8, 12, 24, 48, and 72 hr after dosing. This urine was combined with the urine collected in the metabolism cages during the appropriate time intervals, and the total urine volume was measured. All samples were divided into aliquots, and the urine and blood samples were maintained at −20° until assayed.

**Assay of Indapamide in Blood and Urine**—Measurement of blood and urine concentrations of indapamide was performed using a semiautomated fluorescence assay (8). The procedure was shown to be sensitive (25 ng/ml) and specific for the intact drug.

**Data Treatment**—Pharmacokinetic parameters for the intravenous blood data were calculated by standard techniques (9, 10). A two-compartment open model (Scheme I) was used to describe the blood concentrations of indapamide following the intravenous dose. Blood concentrations ($C$) of indapamide for any time $t$ after an intravenous dose are given by the relationship:

$$C = Ae^{-\alpha t} + Be^{-\beta t} \quad \text{(Eq. 1)}$$

where $A$ and $B$ are the zero-time intercepts determined by extrapolation of the linear distribution ($\alpha$) and terminal elimination ($\beta$) phases, respectively. These rate constants were calculated by the methods of residuals using a least-squares best fit to calculate the slopes. The intercompartmental transfer rate constants were then calculated as follows:

$$k_{12} = \alpha + \beta - k_{21} - k_{10} \quad \text{(Eq. 2)}$$

$$k_{21} = \frac{A\beta + B\alpha}{A + B} \quad \text{(Eq. 3)}$$

$$k_{10} = \frac{\alpha\beta}{k_{21}} \quad \text{(Eq. 4)}$$

The volume of distribution of the central compartment ($V_c$) was calculated as follows:

$$V_c = \frac{\text{dose}}{A + B} \quad \text{(Eq. 5)}$$

The apparent volume of distribution, $V_\beta$, for indapamide was calculated using:

$$V_\beta = \frac{\text{dose}}{\beta AUC_{0-\infty}} \quad \text{(Eq. 6)}$$

where $AUC_{0-\infty}$ is as defined later.

The $V_\beta$ of indapamide after an oral dose was calculated using Eq. 6, which is model independent. However, the oral dose was considered to be only that fraction that was available. This fraction, $F$, was calculated as the ratio of the area under the blood *versus* time curve after an oral dose to that following an intravenous dose.

The following additional parameters were calculated for both the oral and intravenous administrations of indapamide: area under the blood concentration *versus* time curve for the first 48 hr ($AUC_{0-48}$), which was calculated by the trapezoidal rule; and total area under the blood concentration *versus* time curve ($AUC_{0-\infty}$), which was calculated using:

$$AUC_{0-\infty} = AUC_{0-48} + \frac{C_{48}}{\beta} \quad \text{(Eq. 7)}$$

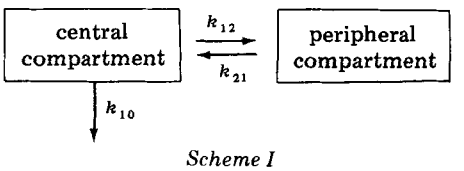


*Scheme I*

[1] RHC 2555.
[2] Revlon Health Care Group, Tuckahoe, N.Y.
[3] J. T. Baker Chemical Co., Phillipsburg, N.J.



*0022-3549/81/1200-1310$01.00/0*
© *1981, American Pharmaceutical Association*

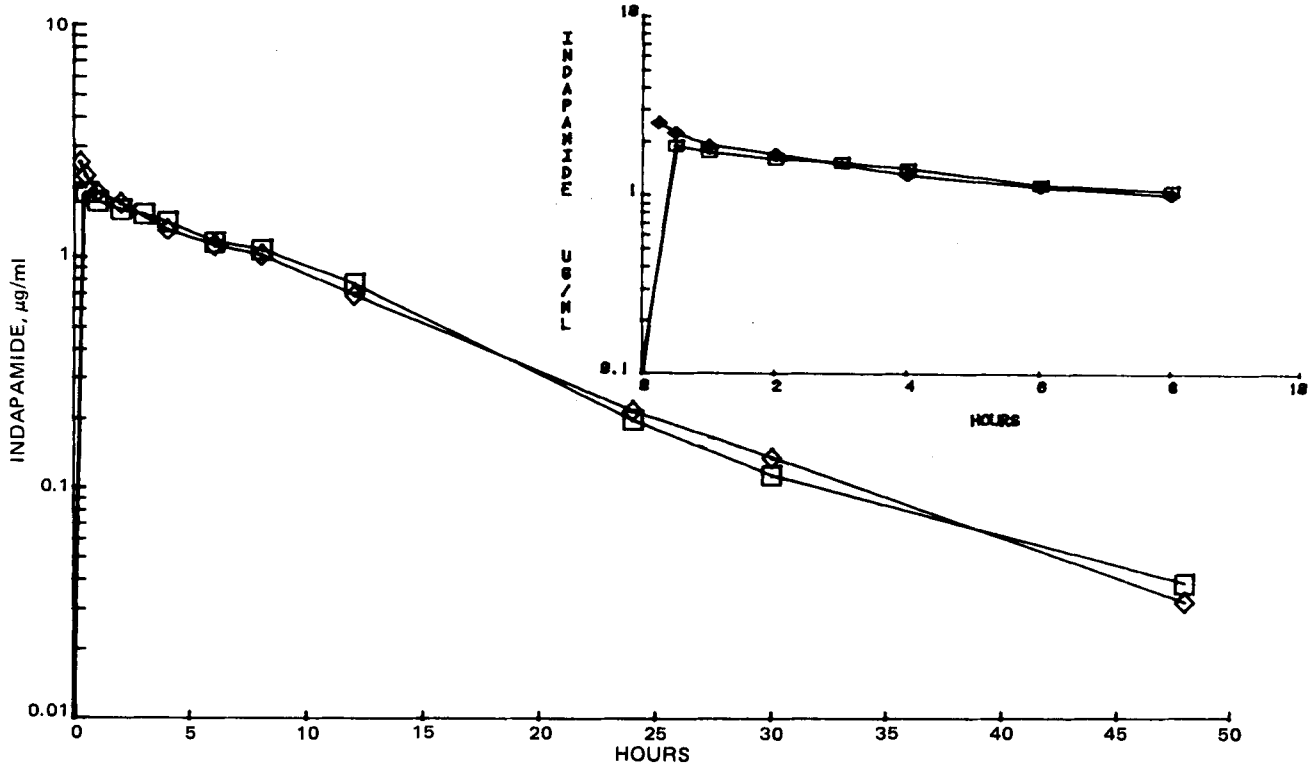


**Figure 1**—*Average indapamide blood concentrations after an oral (□) or intravenous (◇) dose of 1 mg/kg.*

where $\hat{C}_{48}$ was calculated from the slope of the terminal linear segment of the semilogarithmic plot of blood concentration *versus* time. The total body clearance ($Cl_T$) was calculated using:

$$Cl_T = V_\beta \beta \qquad \text{(Eq. 8)}$$

Average renal clearance ($Cl_R$) was determined by plotting the rate of excretion of unchanged indapamide in urine ($\Delta U/\Delta t$) as a function of the blood concentration of indapamide at the midpoint of the collection interval. The slope of this graph was calculated by linear regression and was equal to $Cl_R$. The total renal clearance was also estimated by dividing the total amount of indapamide recovered in the urine by $AUC_{0-\infty}$.

## RESULTS AND DISCUSSION

A two-compartment open model was chosen to describe the blood indapamide concentrations following the intravenous dose to dogs. This selection was made after visual inspection of the data. While these data possibly might be better described by an equation containing three or four exponential terms, the data at the latter time points were not sufficient to allow such analysis. The two-compartment model, however, appeared to be adequate since the fit of the theoretical to the experimental data was acceptable for all dogs, with correlation coefficients of at least 0.98. In addition, the $AUC_{0-48}$ values calculated from the parameters of the best fit were within 5% of the areas calculated by the trapezoidal rule.

Linear regression of the terminal elimination phase after an oral dose did not give evidence for a two-compartment model but for only a one-compartment one. This phenomenon occurs when the absorption rate constant of a drug is sufficiently close to the distribution rate constant that the distributive phase is not observed following absorption (9). The absorption rate of indapamide was not measured in this study since a sufficient number of points during the absorption phase was not obtained. Thus, only the analysis of the intravenous data was used to define the pharmacokinetic parameters of indapamide.

**Blood Concentrations**—Mean blood concentrations of indapamide in four dogs after an oral or intravenous dose of 1 mg/kg are shown in Fig. 1. After the oral dose, the average maximum blood concentration ($C_{max}$) obtained for indapamide was 1.95 μg/ml and the average time of peak blood concentrations ($T_{max}$) was 1.3 hr. Indapamide was rapidly absorbed after dosing with an oral solution.

Blood levels were significantly higher for the intravenous dose than the oral dose for only the 1st hr after dosing. At 4 hr after dosing, the average blood concentration of indapamide was higher after the oral dose than after the intravenous dose. The *AUC* values for the blood concentration *versus* time curves are shown in Table I. The average values for $AUC_{0-\infty}$ were 23.3 and 23.9 μg hr/ml for the oral and intravenous doses, respectively. It can be concluded from these data that the *AUC* values after the oral and intravenous doses were essentially the same and that the fraction of drug available was 1.0. Therefore, these results indicate that indapamide, although extensively metabolized (7), is completely bioavailable after an oral dose and does not undergo first-pass metabolism by the gut or liver.

A similar conclusion could be arrived at by using only the data obtained after the oral dose and calculating $F$ by the following (9):

$$F = \frac{Q}{Q + \dfrac{\text{dose}}{(AUC_{0-\infty})_{po}}} \qquad \text{(Eq. 9)}$$

**Table I—Pharmacokinetic Parameters for Intravenous and Oral Indapamide in Dogs**

| Parameter | Intravenous[a] | Oral |
|---|---|---|
| $AUC_{0-48}$, μg hr/ml | 23.5 ± 3.2 | 23.0 ± 1.4 |
| $AUC_{0-\infty}$, μg hr/ml | 23.9 ± 3.4 | 23.3 ± 1.4 |
| $C_{max}$, μg/ml | — | 1.95 ± 0.16 |
| $T_{max}$, hr | — | 1.3 ± 1.2 |
| $A$, μg/ml | 1.06 ± 0.54 | — |
| $\alpha$, $hr^{-1}$ | 2.48 ± 0.92 | — |
| $t_{1/2}\alpha$, hr | 0.32 ± 0.16 | — |
| $B$, μg/ml | 1.94 ± 0.28 | 1.95 ± 0.12 |
| $\beta$, $hr^{-1}$ | 0.087 ± 0.006 | 0.086 ± 0.002 |
| $t_{1/2}\beta$, hr | 8.04 ± 0.56 | 8.09 ± 0.20 |
| $k_{12}$, $hr^{-1}$ | 0.71 ± 0.36 | — |
| $k_{21}$, $hr^{-1}$ | 1.73 ± 0.82 | — |
| $k_{10}$, $hr^{-1}$ | 0.13 ± 0.02 | — |
| $V_c$, liters/kg | 0.34 ± 0.07 | — |
| $V_\beta$, liters/kg | 0.49 ± 0.06 | 0.50 ± 0.04 |
| $Cl_T$, ml/min/kg | 0.71 ± 0.09 | 0.72 ± 0.04 |
| $Cl_R$[b], ml/min/kg | 0.060 ± 0.008 | 0.059 ± 0.012 |

[a] Mean ± *SD*. [b] Amount of indapamide excreted in the urine (0–48 hr)/$AUC_{0-\infty}$.

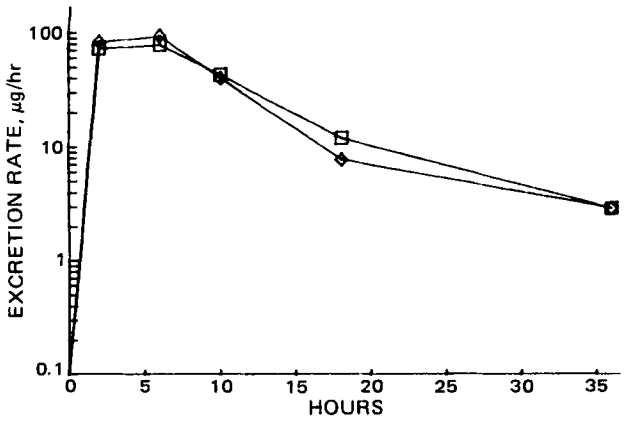


**Figure 2**—*Average indapamide urinary excretion rates after an oral (□) or intravenous (◇) dose of 1 mg/kg.*

where $Q$ is the liver blood flow in dogs [43 ml/min/hr (11)], the dose is 1 mg/kg, and the average $AUC_{0-\infty}$ is 1.95 μg hr/ml kg. A value of 0.98 was calculated for $F$ using these parameters.

The pharmacokinetic parameters were calculated for each dog after the intravenous and oral doses and are shown in Table I. The average terminal half-life for elimination of unchanged indapamide was 8 hr after both the oral and intravenous dose. The average $V_\beta$ was 0.50 for the oral dose and 0.49 liter/kg for the intravenous dose. Thus, there was no apparent difference in the way indapamide was handled after either an oral or intravenous dose. The average $V_c$ after the intravenous dose was calculated to be 0.34 liter/kg.

Plasma indapamide concentrations at 2 and 8 hr after dosing were measured, and the average ratio of whole blood to plasma concentrations for all samples was 5.4 ± 1.4.

**Urinary Excretion and Renal Clearance**—The average urinary excretion rate profiles after the intravenous and oral doses are shown in Fig. 2. Comparison of data after the oral and intravenous dose revealed no significant differences in the amount or rate of urinary excretion of unchanged indapamide. Within 48 hr after oral or intravenous dosing, averages of 8.2 and 8.1% of the dose were eliminated in the urine as unchanged indapamide, respectively. It was estimated that only ~0.2% of the dose was excreted in the urine as unchanged indapamide between 48 and 72 hr.

Renal clearance and average incremental renal clearance data for all dogs are presented in Table II. The renal clearance during the 4–8-hr interval was significantly higher than the values obtained for the other time intervals. This point caused considerable error in the calculation of renal clearance as evidenced by the increase in the correlation value when it was omitted. This temporal dependence of renal clearance was not related to the blood indapamide concentrations but instead may have been related to the administration of food and water to the dogs at 4 hr after dosing. This water intake may have increased the urine flow during the 4–8-hr period and thus decreased indapamide reabsorption.

However, while the renal clearance of indapamide appears to have been dramatically altered during this period, there was little change in total drug clearance because of the small involvement of the kidneys.

Renal clearance was also estimated by dividing the amount of unchanged indapamide excreted in the urine by 48 hr ($U_{0-48}$) after dosing by the $AUC_{0-\infty}$. This value should closely approximate the true value since a negligible amount of unchanged indapamide is excreted in the urine after 48 hr. The average values were 0.72 ml/min after the oral dose and 0.74 ml/min after the intravenous dose (Table I). These values compare favorably with those obtained graphically (0.79 and 0.87 ml/min, respectively).

**Table II—Average Renal Clearance of Indapamide in Four Dogs following Oral or Intravenous Dosing**

| Time Interval, hr | $C_B(\bar{T})$[a], μg/ml | $\Delta U/\Delta t$, μg/hr | $\Delta U/\Delta t/C_B(\bar{T})$, ml/min |
|---|---|---|---|
| | Oral Dosing | | |
| 0–4 | 1.633 | 73.1 | 0.746 |
| 4–8 | 1.168 | 79.8 | 1.139 |
| 8–12 | 0.826 | 43.6 | 0.880 |
| 12–24 | 0.416 | 12.2 | 0.489 |
| 24–48 | 0.088 | 3.0 | 0.568 |
| | $Cl_R$[b] = 0.89 ml/min; $r^2$ = 0.88 | | |
| | $Cl_R$[c] = 0.787 ml/min; $r^2$ = 0.97 | | |
| | Intravenous Dosing | | |
| 0–4 | 1.715 | 84.0 | 0.816 |
| 4–8 | 1.141 | 95.2 | 1.391 |
| 8–12 | 0.817 | 40.6 | 0.828 |
| 12–24 | 0.410 | 7.9 | 0.321 |
| 24–48 | 0.087 | 3.0 | 0.575 |
| | $Cl_R$[b] = 1.005 ml/min; $r^2$ = 0.81 | | |
| | $Cl_R$[c] = 0.873 ml/min; $r^2$ = 0.98 | | |

[a] Blood indapamide concentration at midpoint of time interval. Extrapolated values were used for those times when no blood sample was collected. [b] Renal clearance calculated by the graphical method using all points. [c] Renal clearance calculated by the graphical method excluding the 4–8-hr point.

Values of $C_{max}$ for blood concentrations of indapamide in humans (6) were ~0.3 μg/ml after a total dose of 5 mg (~0.07 mg/kg). These values, when corrected for dose, are approximately double the $C_{max}$ values obtained in the present study. This difference could be explained by the differences in the $V_\beta$ values of the two species. The values for dogs and humans are 0.5 and 0.3 liter/kg, respectively.

For humans, the elimination half-life has been reported as 15 hr (6); in the present study in dogs, a half-life of only 8 hr was observed. This difference may reflect a difference in the hepatic clearance rate in the two species since the renal clearance is ~10% or less of the total clearance for both species. Indeed, in both dogs and humans, indapamide clearance is considerably less than the liver blood flow, which may be a result of the drug's binding to the blood constituents and/or its intrinsic clearance.

## REFERENCES

(1) G. Onesti, D. Lowenthal, M. Affirme, C. Swartz, J. Shirk, R. Mann, and E. Schultz, *Clin. Pharmacol. Ther.* **21,** 113 (1977).

(2) P. Hatt and J. Lebrond, *Curr. Med. Res. Opin.* **3,** 138 (1975).

(3) P. Millier and P. Tcherdakoff, *ibid.*, **3,** 9 (1975).

(4) S. Witchitz, H. Elguedri, J. Giudicelli, A. Kamoun, and P. Chiche, *Therapie*, **29,** 109 (1974).

(5) R. Royer, *Curr. Med. Res. Opin, Suppl. 1*, **5,** 151 (1977).

(6) P. Grebow, C. Coutinho, M. Johnston, R. Pocelinko, J. Treitman, and E. Neiss, presented at the World Conference on Clinical Pharmacology and Therapeutics, London, England, 1980.

(7) D. Campbell, A. Taylor, Y. Hopkins, and J. Williams, *Curr. Med. Res. Opin., Suppl. 1*, **5,** 13 (1977).

(8) P. Grebow, J. Treitman, A. Yeung, and M. Johnston, *J. Pharm. Sci*, **70,** 306 (1981).

(9) M. Gibaldi and D. Perrier, "Pharmacokinetics," Dekker, New York, N.Y., 1975.

(10) J. Wagner, "Fundamentals of Clinical Pharmacokinetics," Drug Intelligence, Hamilton, Ill., 1975.

(11) G. Evans, A. Nies, and D. Shand, *J. Pharmacol. Exp. Ther.*, **186,** 114 (1973).

# Mass Transport Properties of Co(polyether)polyurethane Membranes II: Permeability and Sorption Characteristics

**WILLIAM A. HUNKE * and LLOYD E. MATHESON, Jr. ˣ**

Received September 4, 1979, from the *College of Pharmacy, University of Iowa, Iowa City, IA 52242.* Accepted for publication April 24, 1981. *Present address: Sterling-Winthrop Research Institute, Rensselaer, NY 12144.

**Abstract** □ A series of co(polyether)polyurethane polymers containing polyethylene glycol 600, 1000, or 1540 was synthesized, purified by reprecipitation, and cast into clear, tough, flexible membranes using the solution method. Hydration and membrane swelling increased with increasing polyethylene glycol molecular weight. Paroxypropione, 5-nitrosalicylic acid, sulfaguanidine, and phenylbutazone were used as penetrants at a 1 m*M* donor concentration. Transport rates through the 1540 and 1000 copolymer membranes were in decreasing order: paroxypropione > 5-nitrosalicylic acid > sulfaguanidine > phenylbutazone; however, through the 600 copolymer membrane the rates were paroxypropione ≫ 5-nitrosalicylic acid ~ sulfaguanidine. Phenylbutazone did not penetrate during the experiment. Good agreement was obtained between apparent diffusion coefficients calculated by both the time lag and nonsteady-state methods. Boundary layer effects were examined by variations in stirring speeds. Evidence that diffusion may occur primarily through the aqueous region of the hydrated membranes is presented.

**Keyphrases** □ Model membrane systems—polyurethane copolymers, permeability and sorption characteristics □ Copolymers, polyurethane—model membrane systems, permeability and sorption characteristics □ Permeability—polyurethane copolymers, model membrane systems, permeability and sorption characteristics

The systematic modification of a polymer structure to alter its diffusional characteristics is a promising approach for the development of new model membranes and drug delivery systems. It was suggested (1) that the hydrophilic–hydrophobic character of a membrane may be controlled by suitable structural modifications. Membranes, while combining the seemingly opposite properties of mechanical strength and the ability to swell in water, have been prepared by copolymerization of hydrophilic and hydrophobic reactants (2–4). The membranes formed from these copolymers allowed the transport of permeants at rates comparable to porous dialysis membranes, but with the apparent selectivity of partitioning-type membranes (5).

Therefore, a series of co(polyether)polyurethane polymers composed of hydrophilic polyethylene glycol 600, 1000, or 1540 blocks and hydrophobic urethan segments was synthesized and characterized as described previously (6). The purpose of this study was to determine the mechanism of diffusion for a group of ionizable permeants with a wide range of physical and chemical properties. Sorption of the permeants, paroxypropione, 5-nitrosalicylic acid, sulfaguanidine, and phenylbutazone, were examined. The system was also analyzed for boundary layer effects.

## EXPERIMENTAL

**Materials**—Paroxypropione[1], 5-nitrosalicylic acid[1], sulfaguanidine[2], and phenylbutazone[2] were used as received.

**Methods**—Beer's law plots were prepared for each permeant at 27, 37, and 47° in 0.05 *M* phosphate buffer. A thermostated UV-cell holder was used to control sample temperatures during spectrophotometric[3] analysis.

Permeability of the polymer membranes was studied at 27, 37, and 47° using the described permeants at constant donor concentrations. A diffusion cell similar to one designed by Flynn and Smith (7) was used (6). The donor side was connected *via* tubing[4] from its sampling ports to a two-channel tubing pump[5] and an open donor solution reservoir. The receiving side of the diffusion cell was similarly connected to a UV micro flowcell[6] and the other channel of the tubing pump. The tubing on the receiving side, between the UV micro flowcell and tubing pump, was cut to facilitate filling the receiving side of the diffusion cell. Pieces of tubing[7] were used in the tubing pump drive, for connections to the sampling ports and UV micro flowcell, and to reconnect the break in the receiving side tubing after filling. Internal stirring speeds were controlled by using a synchronous motor[8] attached through an external gear system.

A diffusion experiment was begun by mounting a hydrated membrane between the halves of the diffusion cell. The assembled diffusion cell was placed into its cell holder which, in turn, was immersed in a specially constructed water bath maintained at the desired temperature ±0.3°. The receiving side of the diffusion cell, tubing, and UV micro flowcell were filled with preheated buffer by turning on the pump. In all cases, the buffer was 0.05 *M* phosphate at pH 7.5. The tubing was connected under the surface of the buffer to exclude air from the system.

The spectrophotometer, with the UV micro flowcell in place, was zeroed against the blank buffer in a 1-cm quartz cell. The connecting tubing on the donor side was then pumped full of preheated 0.001 *M* permeant in buffer from the 200-ml donor reservoir. To initiate diffusion across the membrane, preheated permeant solution was injected into the donor side chamber through a sampling port using a glass syringe. The donor side tubing from the donor reservoir, which had been left unattached so that solution could be injected, was secured to the sampling port, and the absorbance was recorded continuously *versus* time. Sink conditions were maintained in all cases. The two-channel tubing pump was set to deliver ~18 ml/min. The exact flow rate was determined prior to a diffusion experiment by measuring the amount of solution delivered in 3 min.

The use of a donor solution reservoir ensured a constant donor solution concentration and thus eliminated the possibility that a significant portion of permeant would be sorbed by the membrane. Zentner *et al.* (8) discussed the treatment of diffusion data under these conditions.

Membranes were removed from the glass plates after hydration with buffer and were soaked for at least 20 min before use.

Permeability characteristics of the polymers were determined as a function of the drying time of the membranes, which were heated at 50° for up to 4 days. Normally, membranes were cast, dried at 50° overnight, and then stored in a desiccator at room temperature.

Permeability characteristics were also examined as a function of the length of time the membranes were stored in the desiccator after an initial drying time of 8–12 hr at 50°. Membranes cut from the same casting were stored for up to 10 days before hydrating and performing the diffusion experiments.

Distribution coefficients were determined in triplicate using a solution depletion method at 27, 37, and 47° for each permeant. The initial absorbate concentration was the same as the permeant donor solution

[1] Eastman Organic Chemicals, Rochester, NY 14650.
[2] Sigma Chemical Co., St. Louis, MO 63178.
[3] Model DB-G, Beckman Instruments, Fullerton, CA 92634.
[4] Teflon.
[5] Masterflex pump drive (5–100 rpm) with pump head No. 7016 and add-on pump head No. 7016, Cole-Parmer Instruments Co., Chicago, IL 60648.
[6] Model 8871, Beckman Instruments, Fullerton, CA 92634.
[7] Silastic, Tygon.
[8] Hurst Manufacturing Corp., Princeton, IN 47570.

0022-3549/81/1200-1313$01.00/0
© 1981, American Pharmaceutical Association

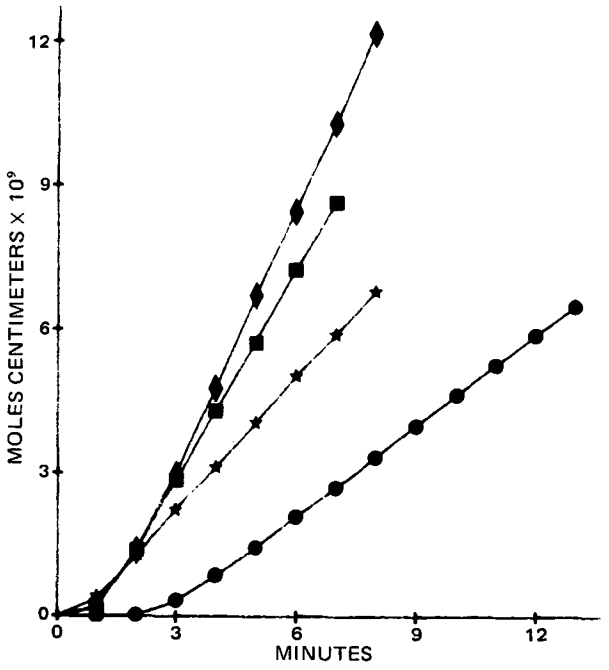


**Figure 1**—*Representative plot of diffusion through the 1540 copolymer membranes at 37° and 200 rpm for paroxypropione (◆), 5-nitrosalicylic acid (■), sulfaguanidine (★), and phenylbutazone (●) normalized for membrane thickness.*

concentration in the diffusion experiments. The time required to reach equilibrium for each polymer was estimated by preliminary absorption and diffusion experiments to be ~4 hr for the 1540 copolymer, 12 hr for the 1000 copolymer, and 24 hr for the 600 copolymer.

The permeant solution in each tube was assayed spectrophotometrically, and an experimental distribution coefficient was calculated by:

$$K = \frac{W_S/V_W}{C_S} \qquad \text{(Eq. 1)}$$

where $K$ is the distribution coefficient, $W_S$ is the equilibrium weight of permeant sorbed calculated from the concentration of the solution before and after sorption, $V_W$ is the membrane wet volume, and $C_S$ is the absorbate concentration in micrograms per milliliter remaining in solution after absorption completion.

To use this method, it was necessary to obtain a value for $V_W$. After absorption was complete, the membranes were removed from the solutions and dried overnight between two sheets of filter paper at 50°. Each membrane was then weighed to obtain the membrane dry weight, which was converted to wet volume, $V_w$, by:

$$V_w = \frac{V_R W_D}{\rho_D} \qquad \text{(Eq. 2)}$$

where $W_D$ is the dry weight of the membrane, $\rho_D$ is the dry density, and $V_R$ is the ratio of the wet membrane volume to the dry membrane volume. The $\rho_D$ and $V_R$ values were averages calculated from the wet and dry dimensions of three sample membranes of each type of polymer as described earlier (6).

## RESULTS AND DISCUSSION

Fabrication of the polymers into membranes results in the exposure of a large surface area of polymer to the potentially deleterious effects of light and moisture. No changes were observed in the diffusional characteristics of the membranes with increases in either drying or storage time.

Figure 1 is a representative plot showing the diffusion of all four permeants at 37° through the 1540 copolymer membrane. This plot was normalized for thickness of the membrane by multiplying the moles of permeant diffused by the thickness of the membrane. The rank order of transport was paroxypropione > 5-nitrosalicylic acid > sulfaguanidine > phenylbutazone in both the 1540 and 1000 copolymer membranes. The rank order of transport was paroxypropione ≫ sulfaguanidine ≥ 5-nitrosalicylic acid in the 600 copolymer. Phenylbutazone did not penetrate during the experiment.

Figure 2 is a composite plot representing the permeability of paroxypropione through the three different membranes at 37°. The rank order of permeability was 1540 copolymer > 1000 copolymer ≫ 600 copolymer.

The apparent permeability coefficient, $P'$, for each permeant was calculated from steady state using:

$$P' = \frac{(dm/dt)(h_m)}{(A)(C_d)} \qquad \text{(Eq. 3)}$$

where $dm/dt$ is the steady-state slope (mass per second), $h_m$ is the membrane thickness (centimeters), $A$ is the diffusional area of the membrane (square centimeters), and $C_d$ is the donor solution concentration (moles).

The apparent diffusion coefficient, $D'$, was calculated for each permeant in each polymer, except 5-nitrosalicylic acid and sulfaguanidine in the 600 copolymer, by:

$$D' = \frac{h_m^2}{(6)(t_L - t_c)} \qquad \text{(Eq. 4)}$$

where $t_L$ is the apparent lag time intercept and $t_c$ is the time required for the receiving side chamber contents to reach the UV micro flowcell. The term $t_c$ is given by:

$$t_c = \frac{3.7 \text{ ml}}{\text{pumping rate (ml/sec)}} \qquad \text{(Eq. 5)}$$

where 3.7 ml is the volume of the section of tubing leading from the diffusion cell to the UV micro flowcell. The results of the permeability experiments are shown in Table I for the 1540 copolymer.

Under certain circumstances, it may not be feasible to continue a diffusion experiment until steady-state diffusion is reached (9). An equation was derived to evaluate the diffusional parameters during the nonsteady-state period (10, 11):

$$\log \frac{M}{t^{1.5}} = \log \frac{8C_dK}{\sqrt{\pi h_m^2}} + \frac{3}{2}\log D' - \frac{h_m^2}{9.2D'}\frac{1}{t} \qquad \text{(Eq. 6)}$$

where $M$ is the amount permeated at $t$, the corrected time $(t - t_c)$ in seconds; $C_d$ is the concentration of the donor solution $(M)$; $K$ is the distribution coefficient; and $h_m$ is the thickness of the membrane. Use of the equation is restricted to early nonsteady-state diffusion across a single barrier. From the slope of a plot of $\log M/t^{1.5}$ *versus* $1/t$, the apparent diffusion coefficient of the permeant in the membrane can be calculated.

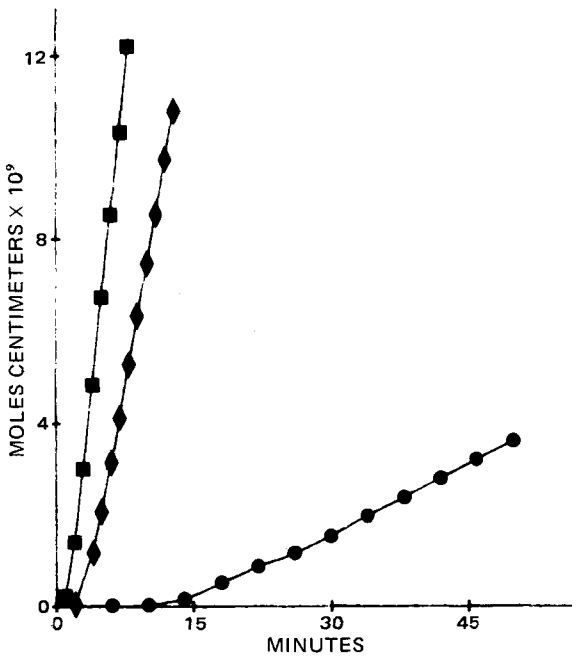


**Figure 2**—*Representative plot of diffusion of paroxypropione at 37° through 600 copolymer (●), 1000 copolymer (◆), and 1540 copolymer (■) membranes at 30, 200, and 200 rpm, respectively, normalized for membrane thickness.*

**Table I—Results of Diffusion Experiments [a] with the 1540 Copolymer**

| Permeant | Temperature | Apparent Permeability Coefficient × $10^6$, $cm^2$/sec | | Apparent Diffusion Coefficient × $10^8$, $cm^2$/sec | |
|---|---|---|---|---|---|
| | | 30 rpm | 200 rpm | 30 rpm | 200 rpm |
| Paroxypropione | 27° | 1.2 | 2.2 | 2.3 | 5.1 |
| | 37° | 1.8 | 3.0 | 3.6 | 7.5 |
| | 47° | 2.1 | 3.3 | 4.7 | 8.7 |
| 5-Nitrosalicylic acid | 27° | 1.3 | 1.8 | 3.4 | 6.3 |
| | 37° | 1.6 | 2.4 | 4.4 | 9.7 |
| | 47° | 1.8 | 2.9 | 5.6 | 13.0 |
| Sulfaguanidine | 27° | 1.0 | 1.4 | 5.9 | 12.0 |
| | 37° | 1.1 | 1.5 | 8.2 | 16.0 |
| | 47° | 1.2 | 1.8 | 8.2 | 22.0 |
| Phenylbutazone | 27° | 0.60 | 0.8 | 1.4 | 2.4 |
| | 37° | 0.73 | 1.1 | 1.9 | 3.2 |
| | 47° | 1.0 | 1.4 | 2.5 | 4.2 |

[a] Each value is the mean of three experiments.

This approach was used for the calculation of $D'$ for the diffusion of 5-nitrosalicylic acid and sulfaguanidine across the 600 copolymer since penetration was relatively slow. Boundary layer effects were negligible in this membrane. Permeability data are given in Table II.

Since paroxypropione penetrates the 600 copolymer rapidly enough to use the lag time steady-state method to calculate $D'$, the applicability of Eq. 6 was tested by calculating $D'$ utilizing both methods. The resulting apparent diffusion coefficient from the lag time was $1.5 \times 10^{-9}$ $cm^2$/sec, while the diffusion coefficient calculated using the nonsteady-state method was $1.2 \times 10^{-9}$ $cm^2$/sec.

Boundary layer effects can be seen in Table I. The apparent permeability coefficient for the permeants in the 1540 copolymer increased with an increasing stirring rate. In Fig. 3, the apparent permeability coefficients from a series of diffusion experiments for 5-nitrosalicylic acid through the 1540 copolymer at 37° are plotted *versus* stirring rates of 10–200 rpm. The apparent permeability coefficient increased with increasing stirring rate due to a reduction in thickness of the boundary layers on either side of the membrane. The boundary layer contribution was observed because of the relatively high diffusion coefficients of 5-nitrosalicylic acid in the 1540 copolymer.

This change is predicted for a series barrier where the boundary layers contribute a significant amount of resistance to the overall barrier resistance (8, 12–14). If diffusional processes are assumed to offer the most resistance to the overall permeation process, then under steady-state diffusion conditions and boundary layers of equal thickness:

$$F = \frac{C_d}{\frac{2h_l}{D_{aq}} + \frac{h_m}{KD}} \qquad \text{(Eq. 7)}$$

where $F$ is the flux, $C_d$ is the penetrant concentration in the bulk donor solution, $h_l$ is the boundary layer thickness, $h_m$ is the membrane thickness, $D_{aq}$ is the diffusion coefficient for the permeant in the aqueous phase, $D$ is the diffusion coefficient for the permeant in the membrane, and $K$ is the distribution coefficient. The terms in the denominator are defined as the aqueous boundary layer resistance and the membrane resistance to diffusion, respectively (15).

**Table II—Results of Diffusion Experiments with the 600 Copolymer at 30 rpm**

| Permeant | Temperature | Apparent[a] Permeability Coefficient × $10^8$, $cm^2$/sec | Apparent Diffusion Coefficient × $10^9$, $cm^2$/sec |
|---|---|---|---|
| Paroxypropione | 27° | 11.0 | 1.6 |
| | 37° | 17.0 | 2.6 |
| | 47° | 27.0 | 4.8 |
| 5-Nitrosalicylic acid | 27° | — | — |
| | 37° | 1.3 | 0.6 |
| | 47° | 2.6 | 1.4 |
| Sulfaguanidine | 27° | 0.5 | 0.5 |
| | 37° | 0.5 | 0.8 |
| | 47° | 0.9 | 1.9 |

[a] Apparent $P$ is the product of $D$ and the distribution coefficient.

Boundary layer effects were not significant in the 600 copolymer since an increase in $P'$ for paroxypropione in the 600 copolymer at 37° was not seen with increased stirring rates. Thus, $P'$ was calculated as $1.7 \times 10^{-7}$ $cm^2$/sec at both 30 and 200 rpm.

The apparent diffusion coefficient, $D'$, was also affected by changes in boundary layer contributions (Table I). This effect on $D'$ is due to the use of $t_L$, which is sensitive to the effects of the boundary layers.

The contribution of boundary layer resistance to the overall resistance of the barrier can be evaluated by plotting $1/P'$ *versus* $1/h_m$, as suggested by Hwang *et al.* (14), using

$$1/P' = \frac{1}{P} + \frac{2h_l}{D_{aq}}\frac{1}{h_m} \qquad \text{(Eq. 8)}$$

where $P$ is the permeability coefficient adjusted for the boundary layer contribution. The slope of such a plot is the resistance due to the boundary layer, $R_{2h_l}$, and the reciprocal of the intercept is $P$. Figure 4 shows such a plot for the diffusion of 5-nitrosalicylic acid at 37° through the 1540 copolymer at four stirring speeds. Table III contains the values of $P$ and $D$ for the four stirring speeds. These $P$ and $D$ values are essentially constant when compared to Fig. 3, which suggests that the boundary layer contribution was largely eliminated.

Figure 5 shows that the relative contribution of the membrane resistance to the overall barrier resistance increases with increasing stirring rate. The resistance of the membrane, $R_m$, is given by:

$$R_m = \frac{h_m}{P} \qquad \text{(Eq. 9)}$$

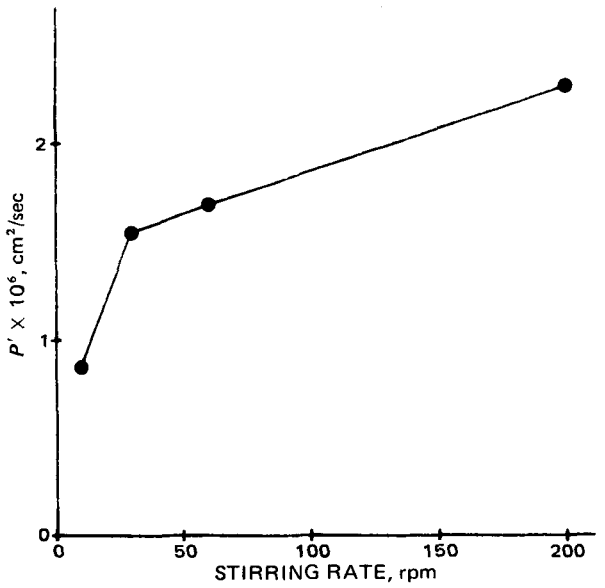


**Figure 3**—*Effect of stirring rate on the apparent permeability coefficient of 5-nitrosalicylic acid in the 1540 copolymer at 37°.*

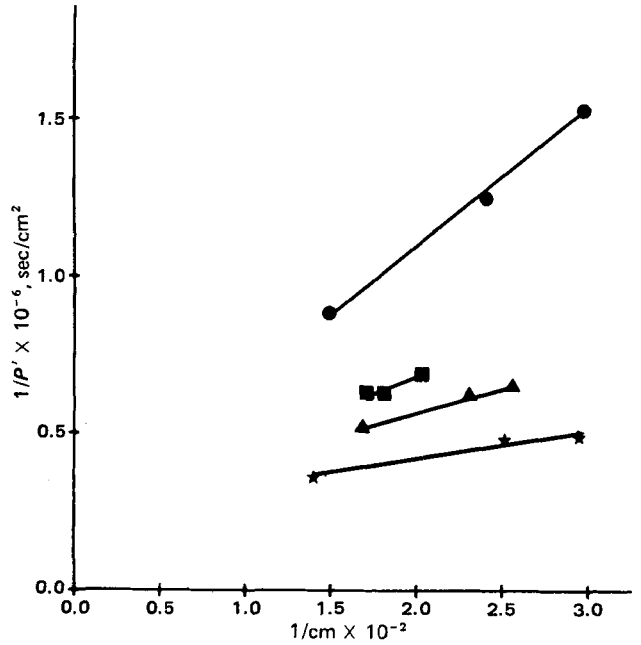


**Figure 4**—*Analysis of boundary layer effects of the diffusion of 5-nitrosalicylic acid in the 1540 copolymer at 37° and stirring speeds of 10 (●), 30 (■), 60 (▲), and 200 (★) rpm.*

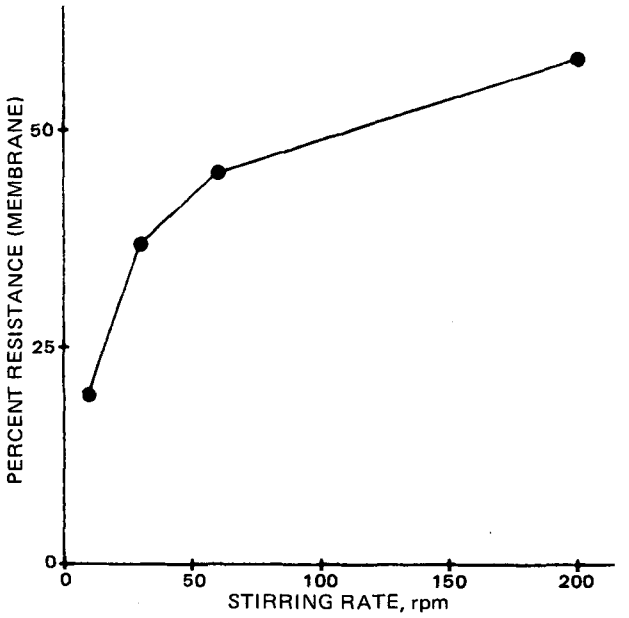


**Figure 5**—*Effect of stirring rate on the contribution of membrane resistance to the overall resistance of the barrier at 37° for 5-nitrosalicylic acid in the 1540 copolymer.*

**Table III—Dependence of Apparent Permeability Coefficient on Stirring Rate and Adjustment for Boundary Layer Effect of Diffusion of 5-Nitrosalicylic Acid in 1540 Copolymer Membrane at 37°**

| Revolutions per Minute | Membrane Thickness × $10^3$, cm | Apparent Permeability Coefficient × $10^6$, $cm^2$/sec | Permeability Coefficient × $10^6$, $cm^2$/sec | Diffusion[a] Coefficient × $10^8$, $cm^2$/sec |
|---|---|---|---|---|
| 10 | 3.4 | 0.66 | 4.7 | 2.3 |
| | 4.2 | 0.80 | | |
| | 6.7 | 1.14 | | |
| 30 | 5.5 | 1.60 | 4.0 | 1.9 |
| | 4.9 | 1.45 | | |
| | 5.8 | 1.61 | | |
| 60 | 5.9 | 1.9 | 3.9 | 1.9 |
| | 4.3 | 1.6 | | |
| | 3.9 | 1.5 | | |
| 200 | 3.4 | 2.0 | 4.1 | 2.0 |
| | 4.0 | 2.1 | | |
| | 7.1 | 2.8 | | |

[a] Calculated from $P/K$ where $K = 20.8$.

where $h_m$ is the membrane thickness (taken as $5.08 \times 10^{-3}$ cm) and $P$ is the reciprocal of the intercept of Eq. 8.

The diffusion data adjusted for boundary layer effects for the 1540 copolymer and the 1000 copolymer are given in Tables IV and V. The diffusion data for the 600 copolymer were not adjusted for boundary layer effects since no significant effects were observed. The adjusted $P$ and $D$ values are in the same rank order as the apparent permeability and apparent diffusion coefficients but are preferred since they represent the diffusional properties of the membrane alone and not the contribution of the boundary layers.

For each permeant, as the percent polyethylene glycol (or the percent water absorbed) increased, an increase in the magnitude of the diffusion coefficient was observed (Fig. 6). These results suggest that the extent of hydration of the membrane greatly influenced the diffusivity of a permeant in these membranes.

This dependence of $D$ on the hydration state of the membrane may be explained by the free volume theory (16, 17), which is given by:

$$\ln D = \ln D_{aq}\phi q_2 - V^*/V_{f,1}\left(\frac{1}{H} - 1\right) \qquad \text{(Eq. 10)}$$

where $D$ is the diffusion coefficient for the permeant in the swollen membrane, $D_{aq}$ is the aqueous diffusion coefficient for the permeant, $\phi q_2$ is the probability of finding a hole unobstructed by polymer large enough for the molecule to diffuse through, $V^*$ is a characteristic volume pa-

**Table IV—Results of Diffusion Experiments for the 1540 Copolymer at 200 rpm Adjusted for Boundary Layer Effects**

| Permeant | Temperature | Slope[a] × $10^2$, sec/cm | Intercept × $10^5$, sec/$cm^2$ | $r^2$ | Permeability Coefficient × $10^6$, $cm^2$/sec | Diffusion[b] Coefficient × $10^7$, $cm^2$/sec | Percent[c] Resistance due to Membrane |
|---|---|---|---|---|---|---|---|
| Paroxypropione | 27° | 5.4 | 3.4 | 0.961 | 2.9 | 0.7 | 77 |
| | 37° | 9.7 | 1.6 | 0.937 | 6.4 | 1.7 | 45 |
| | 47° | 7.4 | 1.3 | 0.954 | 7.9 | 2.5 | 46 |
| 5-Nitrosalicylic acid | 27° | 9.7 | 3.2 | 0.996 | 3.2 | 1.2 | 62 |
| | 37° | 12.0 | 1.9 | [d] | 5.2 | 2.5 | 45 |
| | 47° | 9.0 | 1.7 | 0.98 | 5.8 | 3.2 | 49 |
| Sulfaguanidine | 27° | 11.0 | 5.2 | 0.998 | 1.9 | 1.7 | 71 |
| | 37° | 12.0 | 3.9 | 0.963 | 2.5 | 2.6 | 62 |
| | 47° | 9.1 | 3.8 | 0.922 | 2.6 | 3.5 | 68 |
| Phenylbutazone | 27° | 20.0 | 9.2 | 0.998 | 1.1 | 0.4 | 70 |
| | 37° | 17.0 | 6.3 | 0.988 | 1.6 | 0.5 | 66 |
| | 47° | 11.0 | 5.0 | 0.944 | 2.0 | 0.7 | 69 |

[a] Slope of line constructed from the results of three diffusion experiments. [b] Calculated from $P/K$. [c] Percent of total barrier resistance provided by the membranes based on a membrane thickness of 0.00508 cm. [d] Estimated from only two data points.

**Table V—Results of Diffusion Experiments for the 1000 Copolymer at 200 rpm Adjusted for Boundary Layer Effects**

| Permeant | Temperature | Apparent Permeability Coefficient × $10^6$, $cm^2/sec$ | Permeability Coefficient × $10^6$, $cm^2/sec$ | Apparent Diffusion Coefficient × $10^8$, $cm^2/sec$ | Diffusion Coefficient × $10^7$, $cm^2/sec$ | Percent[a] Resistance due to Membrane |
|---|---|---|---|---|---|---|
| Paroxypropione | 27° | 1.3 | 1.5 | 2.3 | 0.25 | 90 |
| | 37° | 1.7 | 2.6 | 3.1 | 0.49 | 69 |
| | 47° | 2.2 | 5.1 | 4.6 | 1.10 | 47 |
| 5-Nitrosalicylic acid | 27° | 0.8 | 1.3 | 2.7 | 0.45 | 68 |
| | 37° | 1.0 | 1.3 | 4.1 | 0.58 | 76 |
| | 47° | 1.0 | 1.3 | 5.3 | 0.72 | 79 |
| Sulfaguanidine | 27° | 0.5 | 0.6 | 4.1 | 0.50 | 86 |
| | 37° | 0.6 | 0.9 | 6.0 | 0.86 | 76 |
| | 47° | 0.6 | 0.9 | 6.7 | 1.00 | 76 |
| Phenylbutazone | 27° | 0.2 | 0.2 | 0.7 | 0.07 | — |
| | 37° | 0.3 | 0.4 | 0.9 | 0.11 | 90 |
| | 47° | 0.5 | 0.7 | 1.2 | 0.19 | 68 |

[a] Percent of total barrier resistance provided by the membrane based on a membrane thickness of 0.00508 cm.

rameter for the permeant, $V_{f,1}$ is the free volume of water, and $H$ is the hydration of the membrane expressed as (wet volume − dry volume)/wet volume.

The hydration of the membrane calculated as a weight fraction was used here as an approximation for $H$ as discussed earlier (16). For a more rigorous treatment, the volume fraction may be used to calculate $H$.

Plots of the diffusion coefficient *versus* $(1/H - 1)$ for each permeant (except phenylbutazone) at 37° were made according to Eq. 10 and are shown in Fig. 7. The hydration of each polymer, $H$, was determined at room temperature and was used in all plots. While the water content of hydrogels are not necessarily temperature independent (18, 19), Refojo and Yasuda (20) showed changes in water content of only 3–4% for some hydrogels over 10–90°. Thus, changes in membrane hydration with temperature would be expected to be quite small and result in only slight differences in slope between the free volume plots at various temperatures.

Methods to correct the data for temperature-induced changes in swelling (hydration) were developed (18); but due to insufficient data, no correction for this effect was made here. The linearity of the free volume plots implies that the transport of the solutes through these membranes occurs primarily in water-filled pores or channels within the membranes.

The free volume theory of diffusion is most often applied to noninteractive systems in which the distribution coefficients range from 0 to 1. Therefore, further study may be required to confirm the applicability of the free volume theory of diffusion in these more interactive polymer–permeant systems.

Other evidence for the existence of small pores is given by the magnitude of the activation energy of diffusion for the permeants in the membrane (7–20 kcal/mole) compared to the activation energy of diffusion for a permeant in water (~4 kcal/mole) (9). This increase implies that the polymer chains form small pores that can impede the transport of the permeant through the aqueous regions in the membrane; thus, more energy is required for diffusion. It was suggested (17) that the hydrated polymer chains are relatively mobile, so that the size and shape of the water-filled pores or channels changes continuously.

The ability of the polymers to absorb the permeants was studied using a solution depletion method at three temperatures. The results are given in Table VI. The magnitude of the distribution coefficients indicates that a significant amount of permeant was sorbed. The rank order of the distribution coefficients was paroxypropione > phenylbutazone > 5-nitrosalicylic acid > sulfaguanidine. The distribution coefficients are not simply the result of permeant dissolved in water present inside the swollen membrane since, if this were the case, the $K$ values would range between zero and 1. Since the sorption experiments were done in buffer at pH 7.5, 5-nitrosalicylic acid (pKa 2.3) and phenylbutazone (pKa 4.4) were almost completely ionized and paroxypropione (pKa 7.8) was ~50% ionized. At pH 7.5, sulfaguanidine (pKa 2.8) was essentially unionized.

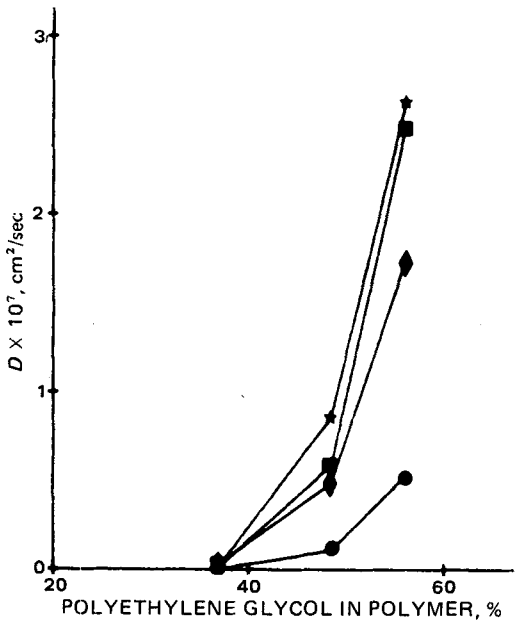


**Figure 6**—*Effect of polyethylene glycol content on the diffusion coefficients for paroxypropione (◆), 5-nitrosalicylic acid (■), sulfaguanidine (★), and phenylbutazone (●) at 37°.*

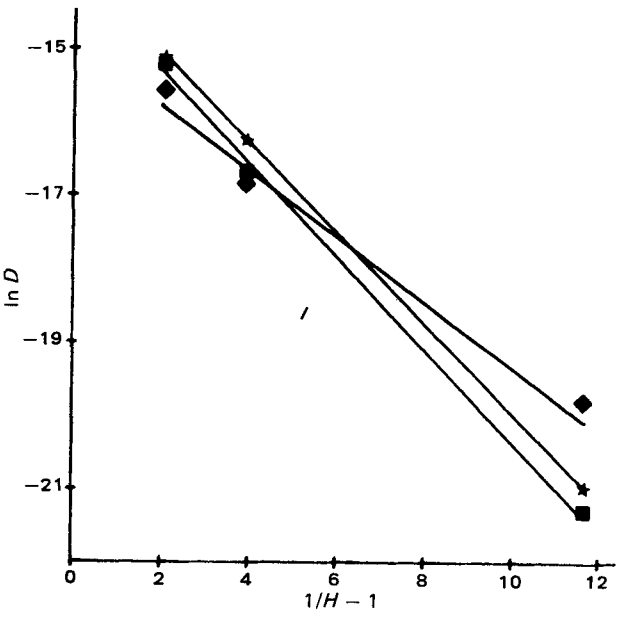


**Figure 7**—*Free volume plot for co(polyether)polyurethane membranes at 37° for paroxypropione (◆), 5-nitrosalicylic acid (■), sulfaguanidine (★), and phenylbutazone (●).*

**Table VI—Distribution Coefficients for Permeant–Polymer Systems**

| Permeant | Temperature | Distribution Coefficient[a] 600 Copolymer | 1000 Copolymer | 1540 Copolymer |
|---|---|---|---|---|
| Paroxypropione | 27° | 74.8 | 58.6 | 40.2 |
| | 37° | 63.3 | 53.2 | 37.0 |
| | 47° | 51.3 | 46.5 | 31.9 |
| 5-Nitrosalicylic acid | 27° | 26.7 | 28.3 | 25.4 |
| | 37° | 17.7 | 22.3 | 20.8 |
| | 47° | 13.2 | 18.5 | 17.7 |
| Sulfaguanidine | 27° | 9.8 | 12.7 | 11.5 |
| | 37° | 7.2 | 10.2 | 9.7 |
| | 47° | 4.7 | 8.2 | 7.6 |
| Phenylbutazone | 27° | 36.3 | 35.4 | 31.3 |
| | 37° | 33.3 | 34.3 | 30.0 |
| | 47° | 30.1 | 36.2 | 29.1 |

[a] Mean of three determinations.

This finding suggests that these polymers are capable of sorbing both the unionized and ionized forms of the molecules.

It can also be seen that, except for paroxypropione, the distribution coefficients are rather insensitive to polymer composition and the resulting hydration state of the membrane. For penetrants insensitive to polymer composition, it is difficult to deduce whether the hydrophilic or the hydrophobic portion is primarily responsible for sorption. In the case of paroxypropione, the increase in the distribution coefficient with decreasing polyethylene glycol content of the polymer suggests an affinity for a more hydrophobic environment. This finding lends support to other suggestions (3, 21) that the hydrophobic urethan block may provide a site for permeant interaction with these types of polymers.

It appears that the permeant loading of the membranes may be affected by the distribution coefficient of the drug, but the lack of correlation between the distribution coefficient and permeability indicates a lack of support for diffusion through the membrane material itself. Perhaps in polyethylene glycol copolymer membranes prepared with polyethylene glycols with molecular weights of <600, the distribution coefficient would be a better predictor of membrane permeability.

Highly ionic species are readily transported, and the apparent consistency of the data with the free volume theory for diffusion is consistent with the transport of some permeants through aqueous channels. That sorption of the various permeants by these membranes was demonstrated need not eliminate the aqueous channel mechanism of diffusion in favor of a partitioning mechanism. The sorption of permeants by the membrane may be, for example, a reversible binding of the permeant to the polymer chains. This would increase the membrane concentration of permeant but not necessarily require that the permeant dissolve in the polymer and diffuse through the polymer phase of the membrane. The permeant might alternatively desorb back into and subsequently diffuse through the aqueous phase. The path taken by the permeant through the swollen membrane depends on the relative permeability of the permeant in the aqueous and polymer phases (9). The ability of the polymer to absorb the penetrant had no predictive relationship with diffusion through the membranes.

## REFERENCES


(1) R. E. Kesting, "Synthetic Polymer Membranes," McGraw-Hill, New York, N.Y., 1971, p. 16.

(2) D. J. Lyman, B. H. Loo, and R. W. Crawford, *Biochemistry*, **3**, 985 (1964).

(3) D. J. Lyman and B. H. Loo, *J. Biomed. Mater. Res.*, 1, 17 (1967).

(4) W. M. Muir, R. A. Gray, J. M. Courtney, and P. D. Ritchie, *ibid.*, **7**, 3 (1973).

(5) D. J. Lyman and S. W. Kim, *Biomat. Med. Devices Artif. Organs*, **1**, 431 (1973).

(6) L. E. Matheson, Jr., and W. A. Hunke, *J. Pharm. Sci.*, **70**, 571 (1981).

(7) G. L. Flynn and E. W. Smith, *ibid.*, **60**, 1713 (1971).

(8) G. M. Zentner, J. R. Cardinal, J. Feijen, and Suk-Zu Song, *ibid.*, **68**, 970 (1979).

(9) G. L. Flynn, S. H. Yalkowsky, and T. J. Roseman, *ibid.*, **63**, 479 (1974).

(10) W. A. Rogers, R. S. Buritz, and D. Alpert, *J. Appl. Phys.*, **25**, 868 (1954).

(11) P.M. Short, E. T. Abbs, and C. T. Rhodes, *J. Pharm. Sci.*, **59**, 995 (1970).

(12) R. G. Stehle and W. I. Higuchi, *ibid.*, **61**, 1922 (1972).

(13) *Ibid.*, **61**, 1931 (1972).

(14) S. T. Hwang, T. E. S. Tang, and K. Kammermeyer, *J. Macromol. Sci.-Phys.*, **B5**, 1 (1971).

(15) G. L. Flynn and S. H. Yalkowsky, *J. Pharm. Sci.*, **61**, 838 (1972).

(16) H. Yasuda, C. E. Lamaze, and L. D. Ikenberry, *Makromol. Chem.*, **118**, 19 (1968).

(17) H. Yasuda and C. E. Lamaze, *J. Macromol. Sci.-Phys.*, **B5**, 111 (1971).

(18) S. Wisniewski and S. W. Kim, *J. Memb. Sci.*, **6**, 309 (1980).

(19) D. E. Gregonis, G. A. Russell, and J. D. Andrade, *Polymer*, **19**, 1279 (1978).

(20) M. F. Refojo and H. Yasuda, *J. Appl. Polym. Sci.*, **9**, 2425 (1965).

(21) D. J. Lyman, B. H. Loo, and W. M. Muir, *Trans. Am. Soc. Artif. Intern. Organs*, **11**, 91 (1965).


## ACKNOWLEDGMENTS


Abstracted in part from a dissertation submitted by W. A. Hunke to the University of Iowa in partial fulfillment of the Doctor of Philosophy degree requirements.

Supported in part by Initial Research Support for Junior Faculty, University of Iowa, and the National Institutes of Health.

The authors thank Dr. Douglas Flanagan for helpful discussions.

W. A. Hunke is a Fellow of the American Foundation for Pharmaceutical Education.

# Convenient Synthesis of 6-Nor-9,10-dihydrolysergic Acid Methyl Ester

**A. MICHAEL CRIDER *x, RICHARD GRUBB *, KENNETH A. BACHMANN *, and ARUN K. RAWAT ‡**

Received January 22, 1981, from the **College of Pharmacy, University of Toledo, Toledo, OH 43606*, and the ‡*Alcohol Research Center, C.S. 10002, Toledo, OH 43699.* Accepted for publication April 8, 1981.

**Abstract** □ 6-Nor-9,10-dihydrolysergic acid methyl ester (IV) was prepared by demethylation of 9,10-dihydrolysergic acid methyl ester (II) with 2,2,2-trichloroethyl chloroformate, followed by reduction of the intermediate carbamate (III) with zinc in acetic acid. The 6-ethyl-V and 6-*n*-propyl-VI derivatives were prepared by alkylation of IV with the appropriate halide. All of the ergoline derivatives were evaluated for stereotyped behavior in rats, with 6-nor-6-ethyl-9,10-dihydrolysergic acid methyl ester (V) being active but much less potent than apomorphine. Compound VI was evaluated for its effect on blood pressure; at a dose of 30 mg/kg ip, it significantly lowered diastolic pressure in normotensive rats.

**Keyphrases** □ Ergolines—demethylation of the *N*-6 methyl group by 2,2,2-trichloroethyl chloroformate □ Derivatives—6-alkyl, of 6-nor-9,10-dihydrolysergic acid methyl ester □ Stereotyped behavior—ergolines, synthesis of 6-alkyl derivatives of 6-nor-9,10-dihydrolysergic acid methyl esters and evaluation in rats

Various compounds containing the ergoline (I) ring system are potent inhibitors of prolactin release (1–8). Ergolines appear to inhibit prolactin release by a dopaminergic mechanism (9). Due to their prolactin inhibitory activity, ergolines such as bromocriptine and lergotrile have demonstrated potential therapeutic value in the control of postpartum lactation and amenorrhea–galactorrhea associated with hyperprolactinemia. Additionally, these ergoline derivatives have potential in the treatment of parkinsonism (10).

Replacement of the methyl group of I at position 6 by either ethyl or *n*-propyl groups increases prolactin inhibition (4, 6–7, 10). The most commonly employed method for demethylation of the *N*-6 methyl group of the ergoline system is a modification of the von Braun degradation (11), but an extremely poisonous cyanogen bromide is required in the reaction.

This paper reports a convenient synthesis of 6-nor-9,10-dihydrolysergic acid methyl ester (IV) utilizing 2,2,2-trichloroethyl chloroformate as the demethylating agent. The synthesis and pharmacological activity of the 6-ethyl-V and 6-*n*-propyl-VI derivatives of IV are also described.

## RESULTS AND DISCUSSION

**Chemistry**—The synthesis of 6-nor-9,10-dihydrolysergic acid methyl ester (IV) was described previously (11). In this investigation, demethylation at position 6 of 9,10-dihydrolysergic acid methyl ester (II) was accomplished by modification of the von Braun degradation. The intermediate 6-nor-6-cyanoergoline was reduced by hydrogenation in the presence of Raney nickel to yield IV. The 6-nor-6-cyanoergolines have also been reduced to yield 6-nor-ergolines with sodium borohydride (12) and with zinc in acetic acid (13).

Several recent reports described the use of 2,2,2-trichloroethyl chloroformate to demethylate tertiary methylamines (14–16). The corresponding demethylated trichloroethyl carbamate derivatives are easily cleaved by reduction with zinc in acetic acid. In view of our present research program to synthesize 6-nor-6-alkylergolines as potential

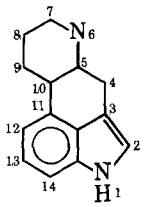

I

dopaminergic agonists, the use of 2,2,2-trichloroethyl chloroformate as a demethylating agent was of interest.

Treatment of II with 2,2,2-trichloroethyl chloroformate in refluxing methylene chloride with potassium bicarbonate as the base afforded 6-nor-6-(2,2,2-trichloroethoxycarbonyl)-9,10-dihydrolysergic acid methyl ester (III) in a 90% yield. Reduction of the carbamate (III) with zinc in acetic acid at room temperature readily gave IV.

The 6-nor-6-ethyl-V and 6-nor-6-*n*-propyl-VI derivatives were prepared by alkylation of IV with an appropriate alkyl iodide in dimethylformamide with potassium carbonate as the base. Although the preparation of 6-nor-6-ethyl-9,10-(V) (11) and 6-nor-6-*n*-propyl-9,10-dihydrolysergic acid methyl ester (VI) (17) has been described, the biological activity of these compounds has not yet been reported.

The use of 2,2,2-trichloroethyl chloroformate represents a novel method for demethylation of the *N*-6-methyl group. The carbamate III is a potentially useful intermediate for the synthesis of potent dopaminergic ergolines such as pergolide (8).

**Pharmacology**—Of those ergolines examined for inducibility of behavioral stereotypy, only V exhibited any activity in doses up to 30 mg/kg. Not only was V less potent than apomorphine when behavior was ranked according to Costall *et al.* (18) (Fig. 1), but qualitative differences in behavior were also observed. For example, V elicited less gnawing behavior than apomorphine but produced intense salivation. The highest dose of V tested for activity (25 mg/kg) approached the lowest dose for which lethality was observed (30 mg/kg). Death appeared due to respiratory arrest and was sometimes preceded by clonic seizures.

Table I lists the mean activity per rat. The activities for apomorphine and V are depicted in Figs. 1 and 2 and are expressed as a percentage of the maximum activity observed. The ratios of killed per treated rats are given in Table II.

During the tests for behavioral stereotypy, both II and VI were noted to elicit flushing of the tail, ears, and paws. This effect was especially pronounced and reproducible for VI and occasioned the analysis of VI on blood pressure. Compound VI did not significantly alter systolic pressure, but single intraperitoneal doses (30 mg/kg) significantly lowered

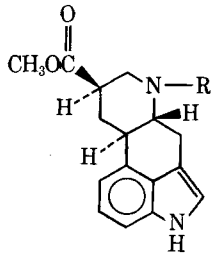

II: R = $CH_3$
III: R = $CO_2CH_2CCl_3$
IV: R = H
V: R = $CH_2CH_3$
VI: R = $CH_2CH_2CH_3$

0022-3549/81/1200-1319$01.00/0
© 1981, American Pharmaceutical Association

**Table I—Induction of Behavioral Stereotypes [a] in Rats**

| Compound | Dose[b], mg/kg | *n* | Mean Activity/Rat |
|---|---|---|---|
| Controls[c] | 1 | 6 | 0 |
| Apomorphine | 10 | 15 | 12.7 |
| II | 30 | 4 | 0.25 |
| III | 30 | 4 | 0 |
| V | 3 | 4 | 0.25 |
| | 6 | 4 | 1.0 |
| | 9 | 4 | 1.25 |
| | 15 | 4 | 2.25 |
| | 20 | 4 | 3.5 |
| | 25 | 4 | 5.25 |
| VI | 30 | 3 | 0.33 |

[a] Stereotypic behavior was scored according to the scale of Costall *et al.* (18). [b] All compounds were administered intraperitoneally in polyethylene glycol 400 (70%). [c] Controls received polyethylene glycol 400 (1 ml/kg).

diastolic pressure in normotensive rats (Fig. 3). The hypotensive effect of VI occurred at 2 hr and was sustained for 1 hr. The hypotensive effects of VI relative to polyethylene glycol 400 (PEG) may have been obscured by an apparently abrupt (although statistically insignificant) increase in diastolic pressure (Fig. 3).

Hypotensive activity with certain ergolinyl methyl esters was reported previously (19, 20).

## EXPERIMENTAL[1]

**6-Nor-6-(2,2,2 - trichloroethoxycarbonyl)-9,10-dihydrolysergic Acid Methyl Ester (III)**—A mixture of II (21) (0.425 g, 0.0015 mole), potassium bicarbonate (0.729 g, 0.0073 mole), and 2,2,2-trichloroethyl chloroformate (0.619 g, 0.0029 mole) in 60 ml of absolute methylene chloride was refluxed for 24 hr. 2,2,2-Trichloroethyl chloroformate (1.48 g, 0.0070 mole) was added, and refluxing was continued for an additional 24 hr. The reaction mixture was cooled, filtered, and evaporated under reduced pressure to yield a white solid. Recrystallization from absolute methanol gave 0.602 g (90%) of crystalline product, mp 208–210°; IR (KBr): 3485 (N–H, indole) and 1740 (C=O, ester and carbamate) $cm^{-1}$; NMR (dimethyl sulfoxide-$d_6$): $\delta$ 3.70 (s, 3H, $COOCH_3$), 4.90 (s, 2H, $OCH_2CCl_3$), 6.67–7.20 (m, 4H, aromatic), and 7.27 (s, 1H, NH).

*Anal.*—Calc. for $C_{19}H_{19}Cl_3N_2O_4$: C, 51.19; H, 4.30; Cl, 23.86; N, 6.29. Found: C, 51.14; H, 4.20; Cl, 24.21; N, 6.13.

**6-Nor-9,10-dihydrolysergic Acid Methyl Ester (IV)**—A solution of III (0.877 g, 0.0020 mole) in 100 ml of acetic acid was treated in one portion with powdered zinc dust (2.58 g, 0.039 g-atom), and the mixture was stirred for 60 hr at room temperature. Then the reaction mixture was filtered, and the inorganic residue was washed with acetic acid. The reaction mixture was diluted with water (100 ml) and extracted two times

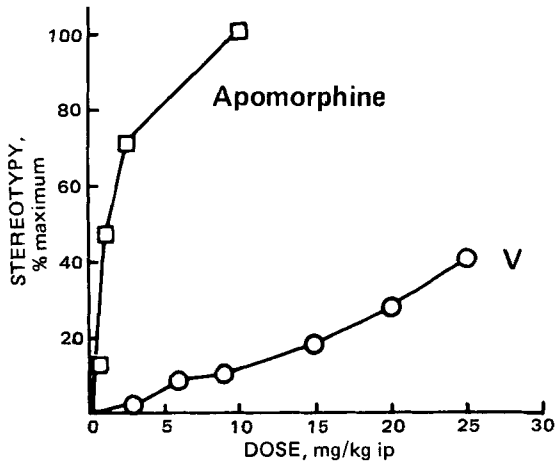


**Figure 1**—*Dose–response curves for stereotypic behavior induced by apomorphine (□) or V (○).*

[1] Melting points were determined on a Fisher-Johns melting-point apparatus and are uncorrected. IR spectra were recorded as potassium bromide pellets with a Perkin-Elmer 137 spectrophotometer. NMR spectra were recorded on a Varian EM 360A spectrometer. Chemical shifts are reported in parts per million ($\delta$) relative to tetramethylsilane (1%) as the internal standard. Analytical data were obtained from Micro-Analysis Inc., Wilmington, Del.

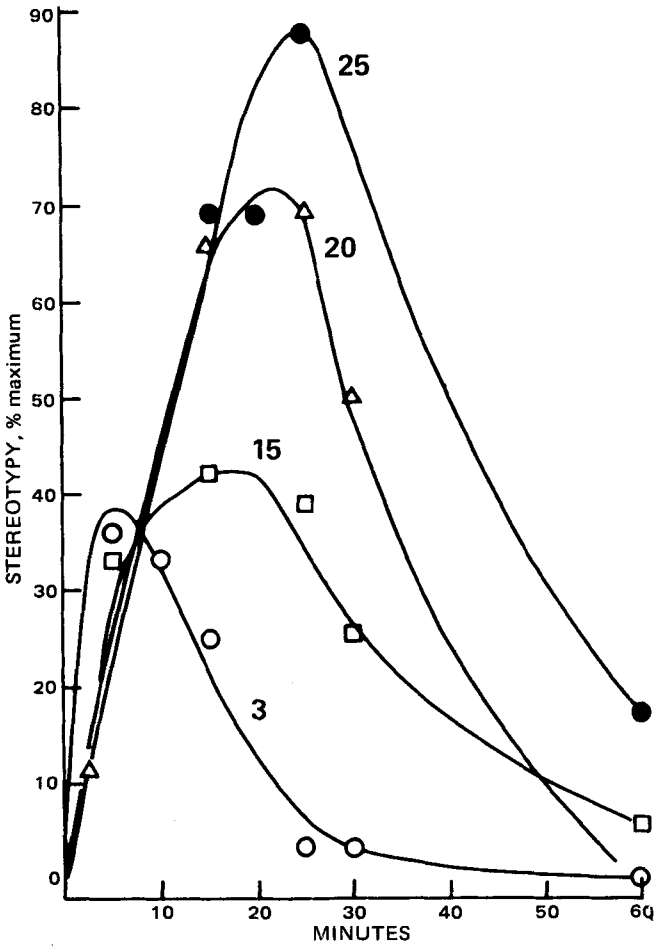


**Figure 2**—*Time course of stereotypic behavior induced by graded doses of V. Numbers denote doses of V (milligrams per kilogram).*

with 50-ml portions of chloroform. The aqueous acetic acid solution was cooled in an ice bath and carefully basified with 8 *N* $NH_4OH$ solution.

The basic solution was extracted three times with 75-ml portions of chloroform. The combined chloroform extracts were dried (sodium sulfate), filtered, and evaporated under reduced pressure to yield 0.384 g (72%) of a light-tan solid. The hydrogen maleate salt was prepared and recrystallized from methanol to yield analytically pure material, mp 211–213° [lit. (11) mp of the free base 172°]; IR (KBr): 3300 (N–H, indole) and 1700 (C=O, ester) $cm^{-1}$; NMR (dimethyl sulfoxide-$d_6$): $\delta$ 3.70 (s, 3H, $COOCH_3$), 7.10 (s, 1H, NH), and 6.50–7.17 (m, 4H, aromatic).

*Anal.*—Calc. for $C_{20}H_{22}N_2O_6$: C, 62.16; H, 5.75; N, 7.25. Found: C, 62.20; H, 5.88; N, 7.04.

**6-Nor-6-*n*-propyl-9,10-dihydrolysergic Acid Methyl Ester (VI)**—A mixture of IV (0.300 g, 0.0011 mole) and potassium carbonate (0.306 g, 0.0022 mole) in 25 ml of dimethylformamide was treated with *n*-propyl iodide (0.377 g, 0.0022 mole). After heating for 24 hr at 50°, the reaction mixture was cooled, filtered, and evaporated under reduced pressure to afford a light-brown oil. The oil was taken up into 200 ml of chloroform and washed with 200 ml of water. The chloroform phase was dried (sodium sulfate), filtered, and concentrated under reduced pressure to give a light-tan solid. Recrystallization from methanol afforded, in two crops, 0.162 g (47%) of analytically pure material, mp 215–216° [lit. (17) 212–214°]; IR (KBr): 3300 (N–H, indole) and 1730 (C=O, ester) $cm^{-1}$; NMR

**Table II—Lethality of V**

| Dose, mg/kg | Dead/Treated |
|---|---|
| 20 | 0/4 |
| 25 | 0/4 |
| 30 | 1/4 |
| 40 | 1/4 |
| 50 | 2/4 |

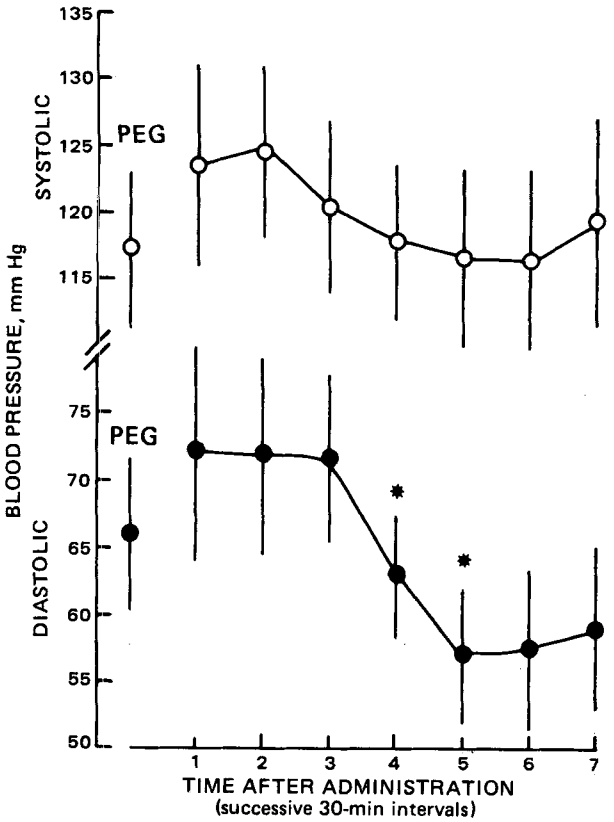


**Figure 3**—*Impact of VI on blood pressure. Vertical bars denote standard error of the mean (n = 4), and asterisk signifies* $p < 0.05$.

($CDCl_3$): δ 0.90 (t, 3H, $CH_2CH_2CH_3$), 1.07–3.53 (m, 13H), 3.70 (s, 3H, $COOCH_3$), 6.87–7.23 (m, 4H, aromatic), and 7.97 (s, 1H, NH).

*Anal.*—Calc. for $C_{19}H_{24}N_2O_2$: C, 73.02; H, 7.76; N, 8.97. Found: C, 73.04; H, 7.59; N, 8.94.

**6-Nor-6-ethyl-9,10-dihydrolysergic Acid Methyl Ester (V)**—This compound was synthesized from IV (0.202 g, 0.0008 mole), potassium carbonate (0.103 g, 0.0008 mole), and ethyl iodide (0.233 g, 0.0015 mole) in 25 ml of dimethylformamide in the same manner as described for VI. Column chromatography of the product with silica gel as the adsorbent and chloroform–methanol (95:5) as the solvent, gave, after evaporation of the solvents, 0.162 g (75%) of a light-brown solid, mp 168–169° [lit. (11) 170–174°]; IR (KBr): 3300 (N–H, indole) and 1730 (C=O, ester) $cm^{-1}$.

**Pharmacological Testing**—Ergolines II, III, V, and VI were evaluated for their ability to induce stereotypic behavior in rats. Stereotyped behavior was scored with the system of Costall *et al.* (18). Male Sprague–Dawley rats[2] were given intraperitoneal injections of test substances dissolved in polyethylene glycol 400 (70%). Dosages are listed in Table I. Apomorphine was used as a reference compound, and control animals received only polyethylene glycol 400 (1 ml/kg). Observations were made for 6 hr while animals were housed individually in clear, polycarbonate cages (25.4 × 46.4 × 20.3 cm).

The time course of V after single intraperitoneal doses was evaluated using a slightly different scoring system. Animals were accorded points graded for intensity as follows: no activity, 0; sniffing, 1, 2, or 3; licking, 4, 5, or 6; and gnawing, 7, 8, or 9. Figure 2 shows the time course for V following doses of 3, 9, 15, 20, and 25 mg/kg. Activity is expressed as a percentage of the maximum observed.

Blood pressure was recorded directly from the carotid artery. Heparinized rats were anesthetized with urethan (1.2 g/kg ip). Polyethylene cannula tubing[3] (0.58-mm i.d., 0.97-mm o.d.) was inserted into the carotid artery and connected *via* a three-way valve to a pressure transducer[4]. Recordings were made with a physiological recorder[5]. The system was calibrated prior to recording blood pressure for each animal. Both systolic and diastolic pressures were recorded continuously.

Each animal served as its own control, receiving polyethylene glycol 400 initially, followed by VI at a dose of 30 mg/kg. All injections were given intraperitoneally. Animals were allowed to stabilize for 60 min after injection of polyethylene glycol 400 and prior to the injection of VI dissolved in polyethylene glycol 400 (*vide supra*). Pressures for each animal for the control (polyethylene glycol 400) interval and for each successive 30-min interval after treatment with VI represent average pressures ($n = 7$) for the interval (Fig. 3). Pressure differences between polyethylene glycol 400 treatment and treatment with VI were evaluated for significance using the paired rank sum test of Wilcoxon (22).

The acute toxicity of V was determined by noting the number of animals surviving 24 hr after administration.

[2] Harland.
[3] Intramedic.
[4] Statham P23AA.
[5] Beckman Type R411 dynograph.

## REFERENCES

(1) H. G. Floss, J. M. Cassady, and J. E. Robbers, *J. Pharm. Sci.*, **62,** 699 (1973).

(2) J. M. Cassady, G. S. Li, E. B. Spitzner, H. G. Floss, and J. A. Clemens, *J. Med. Chem.*, **17,** 300 (1974).

(3) G. S. Li, J. M. Robinson, H. G. Floss, J. M. Cassady, and J. A. Clemens, *ibid.*, **18,** 892 (1975).

(4) A. M. Crider, J. M. Robinson, H. G. Floss, J. M. Cassady, and J. A. Clemens, *ibid.*, **20,** 1473 (1977).

(5) P. L. Stutz, P. A. Stadler, J. M. Vigouret, and A. Jaton, *ibid.*, **21,** 754 (1978).

(6) A. Cerny, J. Krepelka, and M. Semonsky, *Collect. Czech. Chem. Commun.*, **44,** 946 (1979).

(7) M. Beran, J. Krepelka, and M. Semonsky, *ibid.*, **44,** 3385 (1979).

(8) R. W. Fuller, J. A. Clemens, E. C. Kornfeld, H. D. Snoddy, E. B. Smalstig, and N. J. Bach, *Life Sci.*, **24,** 375 (1979).

(9) J. A. Clemens, E. B. Smalstig, and C. J. Shaar, *Acta Endocrinol.*, **79,** 230 (1975).

(10) N. J. Bach, E. C. Kornfeld, N. D. Jones, M. O. Chaney, D. E. Dorman, J. W. Paschal, J. A. Clemens, and E. B. Smalstig, *J. Med. Chem.*, **23,** 481 (1980), and references cited therein.

(11) T. Fehr, P. A. Stadler, and A. Hofmann, *Helv. Chim. Acta*, **53,** 2197 (1970).

(12) V. Prelog, B. C. Musick, J. R. Merchant, S. Julia, and M. Wilhelm, *ibid.*, **39,** 498 (1956).

(13) E. C. Kornfeld and N. J. Bach, U. S. pat. 4,166,182 (1979).

(14) T. A. Montzka, J. D. Matiskella, and R. A. Partyka, *Tetrahedron Lett.*, **1974,** 1325.

(15) R. F. Borne, J. A. Bedford, J. L. Buelke, C. B. Craig, T. C. Hardin, A. H. Kibbee, and M. C. Wilson, *J. Pharm. Sci.*, **66,** 119 (1977).

(16) J. R. Pfister, *J. Org. Chem.*, **43,** 4373 (1978).

(17) J. Krepelka, A. Cerny, R. Kotva, and M. Semonsky, *Collect. Czech. Chem. Commun.*, **42,** 1209 (1977).

(18) B. Costall, R. J. Naylor, and J. E. Olley, *Eur. J. Pharmacol.*, **18,** 83 (1972).

(19) M. Beran, J. Krepelka, K. Rezabek, M. Seda, and M. Semonsky, *Collect. Czech. Chem. Commun.*, **42,** 1407 (1977).

(20) J. Krepelka, M. Beran, K. Rezabek, V. Trcka, and M. Semonsky, Czechoslovakian pat. 171, 570 (1978); through *Chem. Abstr.*, **90,** 39102t (1979).

(21) W. A. Jacobs and L. C. Craig, *J. Biol. Chem.*, **106,** 393 (1934).

(22) R. G. Steele and J. H. Torrie, "Principles and Procedures of Statistics," McGraw-Hill, New York, N.Y., 1960, p. 402.

## ACKNOWLEDGMENTS

Supported by a faculty research award from the University of Toledo Faculty Research Awards and Fellowships Program.

The authors thank Dr. Fedrico Arcamone at Farmitalia Research Institute for a generous supply of dihydrolysergic acid.

# Preliminary Evaluation of Mesoionic 6-Substituted 1-Methylimidazo[2,1-*b*][1,3]thiazine-5,7-diones as Potential Novel Prodrugs of Methimazole

**ROBERT A. COBURN ˣ, MICHAEL D. TAYLOR, and WALTER L. WRIGHT**

Received February 20, 1981, from the *Department of Medicinal Chemistry, School of Pharmacy, State University of New York at Buffalo, Amherst, NY 14260.* Accepted for publication April 24, 1981.

**Abstract** □ A series of five 6-alkyl- and 6-aryl-mesoionic 1-methylimidazo[2,1-*b*][1,3]thiazine-5,7-diones was synthesized and found to produce 1-methyl-3*H*-imidazole-2-thione (methimazole) upon alkaline hydrolysis or treatment with amine or thiol reagents. The alkaline hydrolysis followed a second-order rate expression, being dependent on both substrate and hydroxide-ion concentrations. The rate constants for the five derivatives fell within 6–15 × $10^{-2}$ liter/mole min at 40°. These compounds were stable in aqueous acidic solutions and in human serum or rat liver homogenate under conditions producing rapid hydrolysis of the methimazole prodrug 1-carbethoxy-3-methylimidazole-2-thione (carbimazole).

**Keyphrases** □ Methimazole—potential new prodrugs, evaluation of mesoionic 6-substituted 1-methylimidazo[2,1-*b*][1,3]thiazine-5,7-diones □ Prodrugs—of methimazole, evaluation of mesoionic 6-substituted 1-methylimidazo[2,1-*b*][1,3]thiazine-5,7-thiones □ Thyroid inhibitors—methimazole evaluation of mesoionic 6-substituted 1-methylimidazo[2,1-*b*][1,3]thiazine-5,7-diones

Considerable interest has been directed toward the development of prodrugs to modify the pharmacodynamic properties of known therapeutic agents, and several labile functionalities have been employed to accomplish this goal (1, 2). During previous investigations (3–8) involving the syntheses and chemistry of bicyclic mesoionic heterocycles related to the purinones, several examples were found in which the novel structures of these heterocycles rendered them susceptible to nucleophilic attack, often leading to ring-opened products (5, 6).

The present study examined the feasibility of exploiting the nucleophilic susceptibility of mesoionic 6-substituted 1-methylimidazo[2,1-*b*][1,3]thiazine-5,7-diones[1] (I) in the development of a methimazole prodrug (II) in which both lipophilicity and lability might be controlled by substituents eliminated from the released drug.

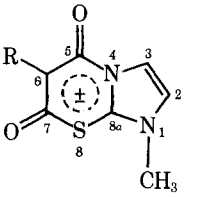

I

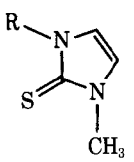

II: R = H
III: R = $CO_2C_2H_5$

## EXPERIMENTAL[2]

UV spectrophotometer[3] was employed for the collection of kinetic data wherein sample temperature was maintained with a circulating constant-temperature bath[4].

**Synthesis**—Five derivatives of I (Table I) were synthesized using a procedure generally useful in the synthesis of various similar mesoionic heterocycles (5, 8). Appropriately substituted malonic acids, obtained commercially or by ethoxycarbonation (9) of arylacetic acid esters, were converted in good yield by the use of phosphorus oxychloride to the corresponding bis-2,4,6-trichlorophenyl esters (10). Heating of a mixture of these esters and II neat at 120–140° produced I*a*–I*e* in moderate yields[5].

**Anhydro-5-hydroxy-1-methyl-7-oxo-6-phenyl-7*H*-imidazo[2,1-*b*][1,3]thiazinium Hydroxide (I*d*)**—The following procedure illustrates the preparation of the compounds in Table I. A mortar-ground mixture of II (3.0 g, 0.027 mole) and bis-2,4,6-trichlorophenyl phenylmalonate (14.4 g, 0.027 mole) was heated *via* an oil bath at 120° for 25 min while a slow nitrogen stream was introduced to carry off subliming trichlorophenol. The resulting melt was cooled and triturated with cold anhydrous ether (50 ml), filtered, and washed repeatedly with cold ether–acetone (2:1). The resulting pale-orange solid was recrystallized from acetone with carbon treatment to give I*d* as fine white needles (3.0 g, 44%, mp 287–289° dec. [lit. (11)mp 271–273° dec.]; IR (KBr): 3170 (w), 3140 (w), 1599 (s), 1581 (s), and 1572 (s) $cm^{-1}$; NMR (dimethyl sulfoxide-$d_6$): δ 8.10 (d, 1H, $J$ = 2 Hz, 3-H), 7.81 (d, 1H, $J$ = 2 Hz, 2-H), 7.50–7.15 (m, 5H, phenyl), and 3.77 (s, 3H, $CH_3$); UV (water): 234 (4.2 log ε), and 299 (3.9) nm.

**Reaction of I*d* with Benzylamine**—Benzylamine (170 mg, 1.6 mmoles) was added to a suspension of 20 mg (0.77 mmole) of I*d* in absolute ethanol (15 ml). The reaction mixture was stirred for 48 hr at room temperature, during which time the starting material dissolved. Reduction of the solution volume to ~5 ml by evaporation at reduced pressure and cooling gave 190 mg (72%) of *N,N'*-dibenzyl-2-phenylpropane-1,3-diamide as white crystals, mp 165–165.5°; IR (KBr): 3290 (m) and 1670 (s) $cm^{-1}$; NMR (dimethyl sulfoxide-$d_6$) δ 8.58 (t, 2H, $J$ = 6 Hz, NH, exchangeable with deuterium oxide), 7.37 (s, 5H, phenyl), 7.25 (s, 10H, phenyl), 4.58 (s, 1H, methine), and 4.35 (d, 4H, $J$ = 6 Hz, $CH_2$).

*Anal.*—Calc. for $C_{23}H_{22}N_2O_2$: C, 77.07; H, 6.19; N, 7.82. Found: C, 77.11; H, 6.22; N, 7.78.

The ethanolic filtrate obtained upon collection of this product was evaporated under reduced pressure, and the resulting solid residue was extracted with 10 ml of warm chloroform. The extract was filtered, and petroleum ether (10 ml) was added to give a precipitate. The precipitate was collected and recrystallized from chloroform–petroleum ether, yielding 70 mg of II (80%). This material was identical with an authentic sample of II as judged by TLC (silica gel, ethyl acetate, $R_f$ 0.38), mixed melting point (144–146°), and IR spectra.

**Reaction of I*d* with Thiobenzyl Alcohol**—A solution of thiobenzyl alcohol (140 mg, 1.2 mmoles) and I*d* (150 mg, 0.58 mmole) in 10 ml of absolute ethanol was refluxed for 1.25 hr. The oily residue, obtained upon evaporation of solvent under reduced pressure, was dissolved in ethyl acetate (2 ml) and placed on a silica gel column (30 g). Elution with ethyl acetate gave 52 mg of II (79%), mp 144–146°.

**1-Methyl-2(3*H*)-imidazolone (IV)**—The procedure employed was a modification of a reported method (12). Aminoacetaldehyde dimethyl acetal (3.65 g, 0.035 mole) was added dropwise over 10 min to a stirred solution of methyl isocyanate (1.85 g, 0.035 mole) in 15 ml of absolute

[1] Alternative nomenclature: 6-substituted anhydro-5-hydroxy-1-methyl-7-oxo-7*H*-imidazo[2,1-*b*][1,3]thiazinium hydroxides.

[2] Melting points were determined with a Fisher–Johns hot-stage apparatus and are uncorrected. Microanalyses were performed by Atlantic Microlab Inc., Atlanta, Ga. $^1$H-NMR spectra were recorded on a Varian T-60A spectrometer with tetramethylsilane as an internal standard. IR specrtra were recorded with a Perkin-Elmer 727B spectrophotometer and a Nicolet 7199 FT-IR interferometer. UV spectra were obtained with a Beckman model 25 spectrophotometer.

[3] Gilford model 2400.

[4] Tamson model TE-3.

[5] While this work was in progress, an alternative synthesis of I*d* was reported (11) using II and (chlorocarbonyl)phenylketene.



*0022-3549/81/1200-1322$01.00/0*
*© 1981, American Pharmaceutical Association*

**Table I—Mesoionic 6-Substituted 1-Methylimidazo[2,1-*b*][1,3]thiazine-5,7-diones**

| Compound | R | Melting Point[a] | Yield, % | Formula | Analysis, % Calc. | Found |
|---|---|---|---|---|---|---|
| Ia | $CH_3$ | 150–151° (A–E) | 31 | $C_8H_8N_2O_2S$ | C 48.97 | 48.54 |
| | | | | | H 4.11 | 4.07 |
| | | | | | N 14.28 | 13.96 |
| | | | | | S 16.34 | 16.15 |
| Ib | $C_2H_5$ | 194–195° (EA) | 29 | $C_9H_{10}N_2O_2S$ | C 48.47 | 48.40 |
| | | | | | H 5.09 | 4.95 |
| | | | | | N 14.13 | 14.19 |
| | | | | | S 16.17 | 16.15 |
| Ic | $CH_2C_6H_5$ | 185–186° (M) | 45 | $C_{14}H_{12}N_2O_2S$ | C 61.75 | 61.81 |
| | | | | | H 4.44 | 4.47 |
| | | | | | N 10.29 | 10.28 |
| Id | $C_6H_5$ | 287–289° dec. (A) | 44 | $C_{13}H_{10}N_2O_2S$ | C 60.45 | 60.18 |
| | | | | | H 3.90 | 3.93 |
| | | | | | N 10.85 | 10.79 |
| | | | | | S 12.41 | 12.34 |
| Ie | $4CH_3OC_6H_4$ | 294–296° dec. (A–M) | 25 | $C_{14}H_{12}N_2O_3S$ | C 58.32 | 58.37 |
| | | | | | H 4.20 | 4.24 |
| | | | | | N 9.72 | 9.69 |
| | | | | | S 11.12 | 11.14 |

[a] Crystallization solvents: A, acetone; E, diethyl ether; EA, ethyl acetate; and M, methanol.

**Table II—Rate Constants for Alkaline Hydrolysis of Ia–Ie**

| Compound | $k \pm SD \times 10^2$, liters/mole min[a] | Relative Rate |
|---|---|---|
| Ia | 8.92 ± 0.06 | 1.00 |
| Ib | 6.25 ± 0.27 | 0.70 |
| Ic | 7.32 ± 0.29 | 0.82 |
| Id | 14.7 ± 0.12 | 1.65 |
| Ie | 13.3 ± 0.44 | 1.49 |

[a] Second-order rate constants in aqueous sodium hydroxide (0.05–0.40 *N*) at 40° and constant ionic strength (2.00 *M*).

ethanol maintained at 0–5°. Following the addition, the solution was stirred for 1 hr at room temperature and then refluxed for 4 hr. Concentrated hydrochloric acid (0.03 ml) in water (10 ml) was added, and the solution was stirred overnight. Addition of 5 ml of 5% $NaHCO_3$ solution transformed the color from red to pale yellow. Filtration of the solution and evaporation under reduced pressure gave a viscous oil, which crystallized on standing. Recrystallization from chloroform–petroleum ether gave 1.97 g (57%) of IV as transparent plates, mp 140–142° [lit. (12) mp 139–140.5].

**Product Identification for Alkaline Hydrolysis of Ic**—A suspension of Ic (0.5 g, 1.8 mmoles) in 50 ml of 1 *N* NaOH was stirred for 48 hr, during which time all material dissolved. TLC analysis (silica gel, ethyl acetate) indicated the complete disappearance of starting material ($R_f$ 0.12) and the appearance of two new spots ($R_f$ 0.06 and 0.38) corresponding to those of an alkaline solution of benzylmalonic acid and II. The UV absorption spectrum of the reaction solution was identical to that of a 1 *N* NaOH solution containing 1.8 mmoles each of benzylmalonic acid and II.

The extract obtained by continuous extraction of the reaction solution with ethyl acetate for 24 hr was dried (magnesium sulfate) and evaporated to give II, as evidenced by mixed melting point and comparison of IR spectra. The reaction solution was acidified (pH 1) with concentrated hydrochloric acid and continuously extracted for 6 hr with ethyl acetate. The residue of the evaporated extract was identified as benzylmalonic acid by comparison of its IR spectrum with that of an authentic sample.

**Kinetics of Hydrolysis of Ia–Ie**—Stock solutions were prepared by dissolving Ia–Ie (50 μmoles) in 1 ml of dimethyl sulfoxide. Sodium hydroxide solutions were prepared (0.05, 0.15, 0.30, and 0.40 *N*) by dilution of 2.00 *N* NaOH with 2.00 *M* KCl. To cells containing the alkaline solutions (2 ml), equilibrated at 40.0 ± 0.1°, was added 10 μl of the stock solution. The loss of absorbance at 300 nm was monitered with the $OD_\infty$ value (optical density) observed to be 0 ± 2%. Pseudo-first-order rate constants were obtained from the slopes of the plots of $\ln[(OD_t - OD_\infty)/(OD_0 - OD_\infty)]$ *versus* time. Each compound was examined in triplicate. Second-order rate constants (Table II) were calculated from the linear regression of $k_{obs}$ with the hydroxide-ion concentration.

**Serum Hydrolysis of Ia, Ib, and III**—Substrate Ia (20 mg), Ib (20 mg), or III (30 mg) was dissolved in 5 ml of pH 7.4 phosphate buffer solution (0.05 *M*) at 37°. The substrate solution (1 ml) was added to 3 ml of human serum[6], and the resulting solution was shaken and incubated at 37°. Aliquots (75 μl) were taken at intervals and added to cells containing 3 ml of buffer solution. Absorbance of the resulting solution was recorded at 300 (Ia and Ib) or 290 (III) nm. A blank solution lacking substrate was similarly treated.

**Rat Liver Homogenate Treatment of Ia, Ib, and III**—A modification of a reported procedure (13) for the hydrolysis of acetanilide was employed. A 300-g male Sprague-Dawley rat was sacrificed, and the liver was removed, rinsed in cold 0.2 *M* buffer solution[7] (pH 8.1), blotted, and weighed (11 g). The liver was minced and homogenized in 20 ml of cold buffer in a chilled tissue grinder[8] maintained in an ice bath.

Buffer solutions of Ia, Ib, or III (1 mg/ml) and homogenate were separately equilibrated (37°) immediately prior to use. Substrate solution (3 ml), buffer (1 ml), and homogenate (2 ml) were mixed and incubated at 37° in a shaker bath. At intervals, a 0.5-ml aliquot was removed and added to 2 ml of ice-cold 10% trichloroacetic acid solution, which was then centrifuged (700 rpm, 3 min), and 1 ml of the supernate was added to a cell containing 3 ml of buffer. The absorbance of this solution was recorded at 300 (Ia and Ib) or 290 (III) nm. A blank solution employing buffer instead of substrate solution was similarly treated as well as a substrate solution of III in which buffer was substituted for homogenate.

## RESULTS

The mesoionic imidazothiazinediones (Ia–Ie) were white crystalline solids stable in light and air and showed no spectroscopic evidence of decomposition in 1 *N* HCl solution over 24 hr. In 1 *N* NaOH, Ic showed a gradual dissolution at room temperature as an apparent function of limited aqueous solubility and hydrolysis to benzylmalonate and II. No other products were detected by TLC or spectroscopic analyses. A potential alternative hydrolysis product, 1-methyl-2(3*H*)-imidazolone (IV), possibly resulting from hydroxide-ion attack at the bridgehead carbon position, was synthesized and found to be clearly distinguishable from II by the chromatographic and spectroscopic methods employed. Since the UV spectrum of the hydrolysis products showed no significant absorbance beyond 280 nm, the rate of alkaline hydrolysis was readily monitored by observing the loss of absorbance of the longest wavelength maxima of Ia–Ie at 300 nm.

The alkaline hydrolysis followed second-order kinetics, dependent on both substrate and hydroxide-ion concentration. The observed rate constants (Table II), showed only a twofold range of values for the five derivatives investigated. The second-order rate expression is consistent with either a rate-limiting attack by hydroxide ion or a rate-limiting decomposition of an adduct of I and hydroxide ion. No evidence was obtained concerning which pseudocarbonyl group is initially involved in the reaction.

[6] Grand Island Biological Co., Grand Island, N.Y.
[7] Trimethamine.
[8] Potter-Elvehjem, with Teflon resin pestle.

Compound II was produced in ethanolic solution from Ia or Id by reaction with two equivalents of benzylamine, with complete conversion within 48 hr at room temperature or 30 min at reflux. No other products except for the corresponding malondiamide were detected by chromatographic or spectral analyses. Compound II was also produced from Id by reaction for 75 min with thiobenzyl alcohol in refluxing ethanol.

Alkyl derivatives Ia and Ib were sufficiently water soluble to allow examination of their stability at pH 7.4 in the presence of human serum. Under conditions wherein III underwent rapid hydrolysis (complete conversion within 2 hr), Ia and Ib showed no evidence of decomposition in the presence of human serum for 10 hr at 37°. Similarly, Ia and Ib showed no evidence of decomposition in the presence of rat liver homogenate over 5 hr, while III was completely hydrolyzed within 5 min under the same conditions.

## DISCUSSION

Compound III, a derivative of II, is already in clinical use. Several studies in humans (14–17) have shown III to be absorbed and rapidly converted to II, an agent useful in the control of hyperthyroidism (18). Although III was designed as a potentially longer acting derivative of II (19), its conversion to II in serum is so rapid that there appears to be little therapeutic advantage over the use of II (17).

A number of bicyclic mesoionic pyrimidinedione derivatives have been reported to result from the condensation of bis-trichlorophenyl malonate esters and *sec*-amino azaheterocycles (5, 6, 20–23). These compounds, which may be viewed as 8-aza analogs of I, undergo ring opening in reaction with benzylamine by nucleophilic attack at the 5-position pseudocarbonyl group (5). However, there is some indication that anionic nucleophiles, such as hydroxide ion, attack the bridgehead carbon position of these 8-aza analogs (5). An analogous reaction of I with hydroxide ion could lead to the formation of IV. Alternatively, hydroxide-ion attack at the 5-position of I would produce a thiol ester, which would be susceptible to hydrolytic production of II. The general utility of mesoionic derivatization for prodrug modification would depend on the controllability of the hydrolytic and/or enzymic decomposition rates by use of various 6-position substituents. These substituents may also provide a means of influencing absorption and distribution by modifying the lipophilicity of the agent.

The conversion of I to II by alkaline hydrolysis and by amine and thiol reagents was demonstrated. However, the variety of substituents investigated showed only a limited influence on the rate of alkaline hydrolysis. The substituents employed exhibited a very limited range of electronic effects, being predominately electron-releasing groups. More strongly electron-withdrawing substituents would be expected to increase the electrophilicity of the pseudocarbonyl groups or to increase the concentration of the hydroxide-ion adduct, leading to an increased alkaline hydrolysis rate. Condensation of malonate esters containing *p*-nitrophenyl or acyl substituents with II was unsuccessful, probably because of the increased ease of malonate-carbanion formation. However, by analogy to the chemistry exhibited by the mesoionic pyrimidinediones (5), electrophilic substitution reactions on I should be facile at the 6-position.

In conclusion, although Ia–Ie produce II by alkaline hydrolysis or by reaction with amine or thiol reagents, their stability to human serum or rat liver homogenate indicate that their decomposition rate *in vivo* is likely to be insufficient. Other derivatives of I with electron-withdrawing 6-position substituents may overcome this deficiency.

## REFERENCES


(1) A. A. Sinkula and S. H. Yalkowsky, *J. Pharm. Sci.*, **64**, 181 (1975).

(2) V. Stella, in "Prodrugs as Novel Drug Delivery Systems," T. Higuchi and V. Stella, Eds., American Chemical Society, Washington, D.C., 1975, pp. 1–115.

(3) R. A. Coburn, *J. Heterocycl. Chem.*, **8**, 881 (1971).

(4) R. A. Coburn, R. A. Carapellotti, and R. A. Glennon, *ibid.*, **10**, 479 (1973).

(5) R. A. Coburn and R. A. Glennon, *ibid.*, **10**, 487 (1973).

(6) R. A. Coburn and B. Bhooshan, *J. Org. Chem.*, **38**, 3868 (1973).

(7) R. A. Coburn and R. A. Carapellotti, *Tetrahedron Lett.*, **1974**, 663.

(8) R. A. Coburn and R. A. Glennon, *J. Pharm. Sci.*, **62**, 1785 (1973).

(9) G. Zvilichovsky and U. Fotador, *Org. Proc. Prep. Int.*, **6**, 5 (1974).

(10) T. Kappe and W. Lube, *Monatsch. Chem.*, **102**, 781 (1971).

(11) K. T. Potts, R. Ehlinger, and S. Kanemasa, *J. Org. Chem.*, **45**, 2474 (1980).

(12) N. J. Leonard and D. F. Weimer, *J. Am. Chem. Soc.*, **98**, 8218 (1976).

(13) J. H. Weisburger and C. M. Goodall, *Life Sci.*, **7**, 263 (1968).

(14) G. G. Skellern, J. B. Stenlake, W. D. Williams, and D. G McLarty, *Br. J. Clin. Pharmacol.*, **1**, 265 (1974).

(15) G. H. Mortimer, D. C. Anderson, P. Liendo-ch, V. Chem, M. Self, and G. M. Besser, *Br. Med. J.*, **1**, 138 (1977).

(16) G. G. Skellern, B. I. Knight, F. M. Luman, J. B. Stenlake, D. G. McLarty, and M. J. Hooper, *Xenobiotica*, **7**, 247 (1977).

(17) T. Nakashima and A. Taurog, *Clin. Endocrinol.*, **10**, 637 (1979).

(18) W. D. Alexander, V. Evans, A. MacAnlay, T. F. Gallagher, Jr., and J. Londono, *Br. Med. J.*, **2**, 290 (1969).

(19) A. Lawson, *Lancet*, **2**, 619 (1951).

(20) R. A. Coburn, R. A Glennon, and Z. Chmielewicz, *J. Med. Chem.*, **17**, 1025 (1974).

(21) R. A. Glennon, M. E. Rogers, R. G. Bass, and S. B. Ryan, *J. Pharm. Sci.*, **67**, 1762 (1978).

(22) R. A. Glennon, R. G. Bass, and E. Schubert, *J. Heterocycl. Chem.*, **16**, 903 (1979).

(23) R. A. Glennon, M. E. Rogers, and M. K. El-Said, *ibid.*, **17**, 337 (1980).


## ACKNOWLEDGMENTS


Abstracted in part from dissertations presented by M. D. Taylor and W. L. Wright to the State University of New York at Buffalo in partial fulfillment of the Doctor of Philosophy degree requirements.

# Noninvasive Dissolution Measurement Using Perturbed Angular Correlation

**R. M. BEIHN * and G. A. DIGENIS ‡x**

Received June 12, 1980, from the **Veterans Administration Medical Center, Lexington, KY 40506*, and the ‡*Divisions of Medicinal Chemistry and Nuclear Medicine, Colleges of Pharmacy and Medicine, University of Kentucky, Lexington, KY 40506.* Accepted for publication April 6, 1981.

**Abstract** □ A novel noninvasive technique was developed to measure dissolution of the water-soluble component of a solid dosage form using indium 111 and perturbed angular correlation. The method involves time-delayed coincidence counting of two cascading γ-rays that exhibit angular correlation. This angular correlation can be perturbed if the intermediate excited state of the nucleus is reoriented due to an interaction with its environment. When such an interaction occurs, as in a phase change (solid to liquid), the perturbation changes can be shown by anisotropy. A highly perturbed condition in the solid state results in low values (0.02–0.04), while increasing values of anisotropy indicate dissolution. Anisotropy values reach 0.14–0.15 when the total unperturbed physical state (liquid) exists. The worth of this technique was demonstrated by both *in vitro* and *in vivo* determinations of dissolution rates.

**Keyphrases** □ Perturbed angular correlation—noninvasive dissolution measurement *in vivo* and *in vitro* □ Dissolution—noninvasive measurement *in vivo* and *in vitro* using perturbed angular correlation, solid dosage forms □ Noninvasive dissolution measurement—of solid dosage forms using perturbed angular correlation, *in vivo* and *in vitro*

Radionuclides with simple decay schemes have been widely utilized as labels for following drug absorption, metabolism, and excretion. External scintigraphy was used to follow labeled solid dosage forms while their behavior in the human stomach was monitored (1). Some radionuclides, following radioactive decay, emit two or more γ-rays in cascade; those γ-rays emitted following an initial one are released immediately or are delayed for some very predictable time unique to that nucleus.

## BACKGROUND

Indium 111 is a radionuclide with a delay during its γ-cascade (Scheme I). Occasionally, for some radionuclides the γ-rays may exhibit an angular correlation since the directional emission of a γ-ray depends on the orientation of the magnetic moment of the nucleus involved. For indium 111, this angular correlation can be perturbed if the intermediate excited state of the nucleus is reoriented due to an interaction with its environment. The major perturbing influence on the emission angular correlation is the interaction of external gradients of the quadrupole moment of the nucleus (2). The theory of perturbed angular correlation was thoroughly reviewed by Steffen and Frauenfelder (3, 4).

Some recent investigations used indium 111 and perturbed angular correlation measurements to monitor the structural and rotational behavior of biological macromolecules (5–7). It also was reported that inhibition of nuclear rotational properties of indium 111 by chemical binding, temperature reduction, and increased viscosity can be observed (8, 9).

The purposes of this work were to measure the conversion of one distinct state of nuclei to another, illustrating a phase change from solid indium chloride to liquid indium chloride, and to illustrate a noninvasive technique for measuring a phase change from solid to liquid in a solid dosage form using indium chloride (indium 111) and perturbed angular correlation.

## EXPERIMENTAL

**Dosage Form Preparation**—Three different formulations of solid dosage forms were prepared with commercially available excipients: Formulation 1, lactose (89%), microcrystalline cellulose (10%), and magnesium stearate (1%), (by weight); Formulation 2, dibasic calcium phosphate (89%), microcrystalline cellulose (10%), and magnesium stearate (1%); and Formulation 3, only sucrose. Each formulation was prepared in bulk for convenient storage. Several grams of each mixture was placed in separate round-bottom flasks, and 95% ethanol was added to allow a satisfactory suspension.

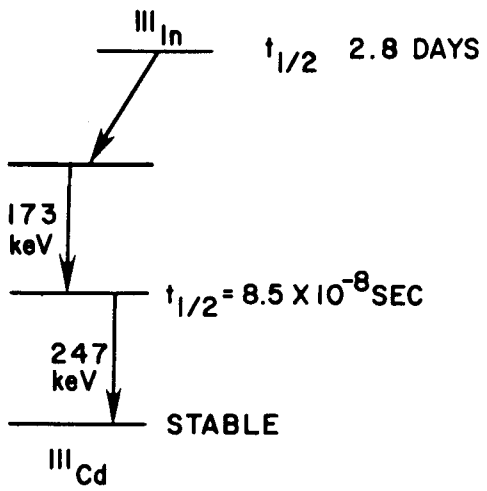


*Scheme I—Indium 111 decay scheme illustrating the γ-ray cascade with the delayed intermediate nuclear state following the first gamma emission.*

Indium 111 in the chloride[1] form was pipetted into each flask to an activity concentration of 20 μCi/200 mg of formulation powder. Indium 111 has a half-life of 2.8 days, and it decays by electron capture and γ-emission with energies of 173 and 247 kev (Scheme I). The ethanol was evaporated in a flask evaporator until dryness was achieved. The powder was removed by scraping, pulverized using a mortar and pestle, and then compressed into 200-mg tablets.

A representative number of tablets were counted for indium 111 activity using a γ-ray scintillation detector for homogeneity testing. Several tablets of each formulation were used for a disintegration time determination[2], and some were used to test for hardness[3].

**Instrumentation**—Three sodium iodide γ-ray detectors were positioned in a flat plane on three sides of a beaker in which the dosage form was tested (Fig. 1). The 12.7 × 7.62-cm detectors were positioned 20 cm from the geometric center of the beaker containing the tablet. For electronic clarity, the detectors were labeled 1, 2, and 3 such that Detector 2 was positioned 90° to Detector 1 and Detector 3 was positioned 180° to Detector 1 (Fig. 1).

The γ-ray spectrometry equipment[4] consisted of a single high voltage power supply for the three detectors, three preamplifiers, three linear amplifiers, and three pulse height analyzers designated 1, 2, and 3 (Fig. 1). There were two time-to-pulse height converters (TPC) for coincidence counting (designated A and B), two additional pulse height analyzers for selecting differential or integrated coincidence delay times, and two count scalers for recording the coincidence counts from Converters A and B (Fig. 1).

Pulse height Analyzer 1 was energy calibrated for counting the 173-kev

[1] Medi-physics, Emeryville, Calif.
[2] USP basket disintegration test.
[3] Erweka, 20 Broadway, New York, N.Y.
[4] ORTEC, Oak Ridge, Tenn.

0022-3549/81/1200-1325$01.00/0
© 1981, American Pharmaceutical Association

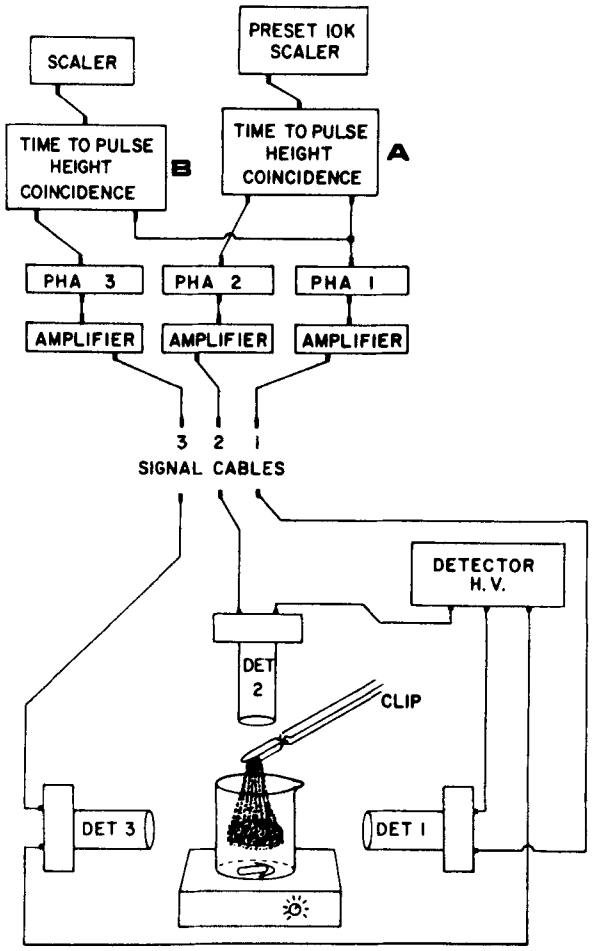


**Figure 1**—*Apparatus assembly illustrating the positioning of the radiation detectors in a flat plane around the tablet for an* in vitro *dissolution experiment using perturbed angular correlation. The schematic of electronic equipment required for coincidence counting between Detectors 1 and 2 (90°) and 1 and 3 (180°) is illustrated. A cotton gauze sheet containing the solid dosage form was suspended 6 cm from the bottom and in the center of a glass beaker containing the dissolution medium (see* Experimental*). Three pulse height analyzers (PHA) were utilized.*

γ-ray while Analyzers 2 and 3 were calibrated for the 247-kev emission. Converters A and B were calibrated to accept coincidence delay times between 70 and 100 nsec.

**Procedure**—The apparatus used for the experimental determination of dissolution consisted of a 10 × 10-cm single-layer cotton gauze sheet with a mesh size sufficiently small to prevent the tablet and larger particles from falling through. The gauze containing the solid dosage form was suspended 6 cm from the bottom and in the center of a 1000-ml glass beaker containing 700 ml of hydrochloric acid–water (Fig. 1). A hemostat clamped to the gauze and a ring stand held the dosage form in place. The aqueous dissolution medium was stirred with a magnetic stirring bar at ~100 rpm and remained at 25–26°.

Immediately after the tablet was immersed and positioned, serial coincident counting on the scalers was begun, which continued until the completion of the experiment. Throughout the experiment, 0.5-ml samples were removed using a 1-ml tuberculine syringe fitted with a 0.22-μm filter to prevent particles from being collected. These samples, removed at appropriate time intervals, were transferred to sample vials and counted in a well γ-counter.

## RESULTS AND DISCUSSION

Assessment of dosage form homogeneity was performed when tablets within a batch of each preparation were counted. Results indicate the tablets were prepared with a homogeneous distribution of indium 111 since they varied by only 2%.

The two γ-rays emitted during the indium 111 to cadmium 111 decay are illustrated in Scheme I. The 247 kev γ-ray is delayed by 85 nsec. The probability that it will be emitted at some time $t$ and at some angle $\theta$ to the direction of the 173-kev γ-ray is given by:

$$\omega(\theta, t) = \frac{1}{\tau} e - \frac{t}{\tau}\left[1 + A_2\left(\frac{3\cos^2\theta - 1}{2}\right)\right] \qquad \text{(Eq. 1)}$$

where $\tau$ is the mean life of the intermediate nuclear state ($1.21 \times 10^{-7}$ sec), $t$ is the interval of time between the two γ-rays, and $A_2$ is a coefficient −0.18. This numerical value of $A_2$ may vary with the solid angle subtended by the γ-ray detectors used. If $\tau$ is long enough and the magnitude of the electric field gradients at the nucleus from the environment are great enough, then the angular correlation of the two cascading γ-rays can be perturbed. When a perturbation factor $G_2(t)$ is inserted into the second term of Eq. 1, its approximate behavior can be shown by anisotropy to be:

$$A \simeq -\frac{3}{2} A_2 G_2(t) \qquad \text{(Eq. 2a)}$$

and:

$$A = 1 - \frac{\omega\,(180°, t)}{\omega\,(90°, t)} \qquad \text{(Eq. 2b)}$$

where $\omega(180°, t)$ and $\omega(90°, t)$ are coincident count rates in each of the two selected angles, 180 and 90°.

The coincidence counts from either the 180 or 90° detector are those counts of the 247-kev γ-ray that are detected within 70–100 nsec following the Detector 1 observation of the 173-kev γ-ray. The 173-kev γ-ray initiates a constant-rise time pulse in each A and B time-to-pulse height converter. When the 180 and 90° detectors count a 247-kev γ-ray, the rising pulse is stopped in Converter A or B, and its magnitude is analyzed with a differential window corresponding to 70–100-nsec delays. These coincidence counts were recorded on each of two scalers.

Since the perturbation factor $G_2(t)$ behavior can be shown by anisotropy ($A$), the coincidence counts $\omega\,(180°, t)$ from the 180° detector and those counts $[\omega\,(90°, t)]$ from the 90° detector were substituted into the relation $A = 1 - \omega\,(180°, t)/\omega\,(90°, t)$ for computation. For anisotropy ($A$) calibration, a maximum perturbed dry solid dosage form was counted. Then a sample of liquid [$^{111}$In]chloride was counted. The calculation of anisotropy ($A$) resulted in values of 0.02–0.04 for the perturbed state (dry) and of 0.14–0.15 for the unperturbed state (liquid), a mean increase of 4.8-fold.

To illustrate the changing of anisotropy values during a dissolution experiment, a sucrose tablet was prepared with [$^{111}$In]chloride as previously described. After it was placed in the apparatus, coincidence data were collected and calculated. The results from a typical experiment are shown in Fig. 2. The experiment ran for 26 min, with nine data points collected for the calculation of anisotropy. Initially, the anisotropy value was 0.02, representing the dry perturbed state; then, after ~24 min, the values of 0.14 for anisotropy were calculated, illustrating the unperturbed liquid state. Those intermediate anisotropy values represent varying numbers of indium 111 atoms in transition from the dry to the liquid state. By simply observing the graph in Fig. 2, the percent dissolution of the radionuclide from the solid form for any desired time can be found. After ~13 min, 50% of the indium 111 was in solution, which was verified by liquid sample removal and counting the indium 111 in a well scintil-

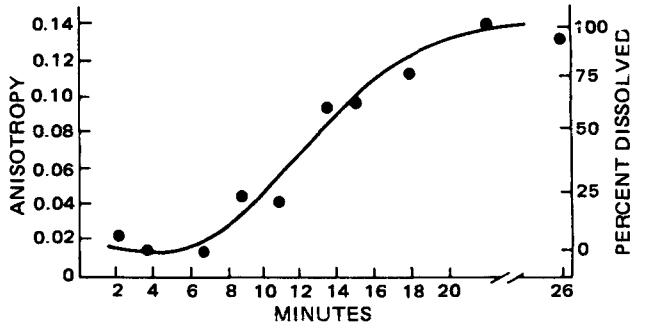


**Figure 2**—*Anisotropy* versus *time for a [$^{111}$In]chloride-labeled sucrose tablet measured* in vitro *using perturbed angular correlation, illustrating the progressive change of anisotropy corresponding to that quantity of the [$^{111}$In]chloride dissolved.*

**Table I—Summary of Perturbed Angular Correlation Dissolution Times [a] and Concomitant Sampling Verification *In Vitro* along with Physical Parameters of Each Dosage Form Tested**

| Tablet | Perturbed Angular Correlation Method Time[a], min[b] | Sampling Method Time[a], min[b] | Revolutions per Minute | Hardness | USP Disintegration Time, min[b] |
|---|---|---|---|---|---|
| Sucrose[c] | 10.8 ± 3.3 | 11.3 ± 3.4 | 100 | NA | NA |
| Lactose[d] | 5.8 ± 2.4 | 6.6 ± 2.6 | 100 | 9 | 6 |
| Dical[e] (Run 1) | 76 ± 9.0 | 80 ± 8.9 | 100 | 11 | 13 |
| Dical[e] (Run 2) | 60 ± 7.0 | 58 ± 7.6 | 400 | 11 | 13 |

[a] Time to achieve 50% dissolution. [b] Average of three determinations. [c] Sucrose (100%) and [$^{111}$In]chloride. [d] Lactose (89%), microcrystalline cellulose (10%), magnesium stearate (1%), and [$^{111}$In]chloride. [e] Dicalcium phosphate (89%), microcrystalline cellulose (10%), magnesium stearate (1%), and [$^{111}$In]chloride.

lation counter. All other experiments had samples removed for corroborative measurements.

Results for this and similar experiments indicate a time delay prior to the onset of tablet dissolution. The delay in the sucrose formulation was ~6 min (Fig. 2). Presumably, this observed delay was due to continued nuclear perturbation in the viscous stagnate layer from the highly structured aqueous conditions existing therein. As the [$^{111}$In]chloride escaped into the unstructured water of the media, the exhibition of free nuclear motion was evident in the notable change of the anisotropy values.

Two additional formulations were prepared, one (called "dical tablet") containing dibasic calcium phosphate (89%), microcrystalline cellulose (10%), and magnesium stearate (1%), and the other (called "lactose tablet") containing lactose (89%), microcrystalline cellulose (10%), and magnesium stearate (1%). Each formulation contained [$^{111}$In]chloride. Hardness and USP disintegration tests were conducted on these formulations. Perturbed angular correlation and sampling measurements were performed from the beginning of the dissolution experiment through completion (Table I). Table I shows that in all experiments there was good agreement between perturbed angular correlation measurements and the indium 111 sampling method for the determination of percent dissolution *in vitro* as a function of time.

Included in Table I are the results of perturbed angular correlation and sampling measurements for the dical tablet at two different stirring rates. Run 1 was stirred at 100 rpm, and Run 2 was stirred vigorously at ~400 rpm. When the stirring rate increased, the dissolution rate increased, indicated by both perturbed angular correlation and sampling measurements (Table I). The reduction in time was from 76 to 60 min using the perturbed angular correlation technique and from 80 to 58 min using the sampling method.

After the *in vitro* dissolution measurements using perturbed angular correlation were shown to be successful, an *in vivo* measurement on the lactose formulation was attempted on one subject to illustrate its *in vivo* applicability. Three detectors were positioned to view the anterior, posterior, and left lateral sides of the volunteer. It was estimated that they were equidistant from the stomach where the tablet would be located.

The calculated anisotropy values were not expected to be the same as those in the *in vitro* experiments, but their changing values would nevertheless reflect the physical state of the solid dosage form. The *in vivo* dissolution data are illustrated in Fig. 3. The anisotropy behavior is quite similar to that in the *in vitro* experiments, differing only in actual anisotropy values, including the delays of onset of dissolution.

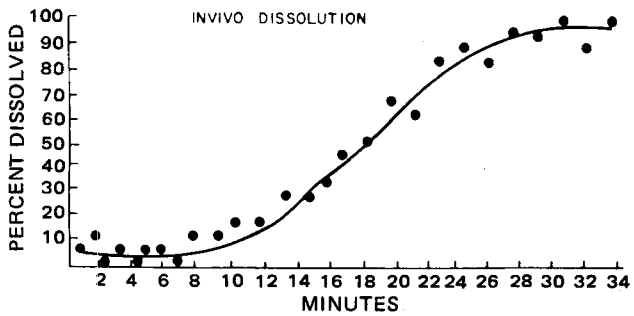


**Figure 3**—*Dissolution* versus *time for a lactose tablet measured in a human subject indium 111 and perturbed angular correlation. Graph shows an 8-min delay for onset of dissolution of the radionuclide, which was complete by 28 min.*

Figure 3 shows that 50% dissolution of [$^{111}$In]chloride from a lactose tablet was achieved in the stomach of the human subject in ~17 min, while the *in vitro* data on the identical dosage form (Table I) showed a dissolution in 5.8 min (perturbed angular correlation) and 6.6 min (sampling method). With a hardness value of 9, the USP disintegration test demonstrated a 6-min disintegration time for the lactose formulation. When the same volunteer with an identical lactose tablet was studied by a previously developed external scintigraphy technique (1), the tablet exhibited a disintegration time of 21 min. These results indicate that there is no good correlation between *in vitro* and *in vivo* measurements for the lactose formulation since they differ so widely in the times of disintegration and dissolution.

The dibasic calcium phosphate formulation was also tested with the same human volunteer. Table I shows that the dical formulation with a hardness of 11 disintegrated[2] in 13 min and that the times for 50% dissolution measured using perturbed angular correlation and sampling were 76 and 80 min, respectively. When the *in vivo* measurement using perturbed angular correlation was performed on this dibasic calcium phosphate formulation, there was evidence that ~40% dissolution had occurred over 30 min. No further dissolution was observed as illustrated by unchanging anisotropy values.

An identical dosage form was then examined *in vivo* by external scintigraphy (1) to gain insight into the dissolution of this dosage form by monitoring its disintegration behavior. The *in vivo* disintegration results showed the dosage form remained motionless in the lower stomach near the duodenal bulb for ~11 min and then began to disintegrate partially until 25 min. During this time, the loss of radioactivity from the original tablet was ~31%. The remaining core of the tablet was then expelled through the pyloric valve and proceeded to move through the small bowel, changing locations repeatedly. This main core of the tablet remained intact throughout the additional period of observation of 52 min.

The data obtained with the perturbed angular correlation method show that this technique, when coupled with external scintigraphy (1), may permit the *in vitro* and *in vivo* study of the disintegration behavior of a solid dosage form. This technique follows the dissolution pattern of the radionuclide and does not provide information on the dissolution of any particular component of the solid dosage form. The technique might prove useful in comparative studies in which various solid dosage formulations could be compared for their disintegration properties.

One further experiment was performed to assess the effects of the physical geometry of the source when acquiring perturbed angular correlation data. A drop of liquid [$^{111}$In]chloride was placed as a source in the bottom of a 150-ml glass beaker, yielding an anisotropy value of 0.13. When the bottom of the beaker was covered with a dilute solution of hydrochloric acid, the resulting anisotropy was 0.15. When the beaker was filled 25%, the anisotropy value was 0.17; when it was 50% filled, the anisotropy value was 0.15; and when it was 75% filled, the anisotropy value was 0.15. These results indicate no significant problem in detecting an unperturbed liquid state of indium 111 with varying geometric configurations.

## CONCLUSION

In the present study, a chemical phase change was observed in solid dosage forms using indium 111 and a perturbed angular correlation measurement. When this novel technique is performed in conjunction with a previously described external scintigraphy method (1), the study of the *in vivo* dissolution and disintegration behavior of a solid dosage form can be accomplished in a qualitative and quantitative manner. The technique monitors the extent of dissolution of the dosage form as a function of solubilization of the radionuclide from the solid dosage form.

The method does not measure dissolution of a pharmacologically active ingredient or any other ingredient in the solid dosage form.

With minor detector modifications, this method should contribute significantly in the evaluation of viscosity gradients and sedimentation rates in heterogeneous dosage forms.

## REFERENCES


(1) D. L. Casey, R. M. Beihn, G. A. Digenis, and M. B. Shambhu, *J. Pharm. Sci.*, **65**, 1412 (1976).

(2) "Table of Isotopes," C. M. Lederer, J. M. Hollander, and J. Perlman, Eds., Wiley, New York, N.Y., 1968, p. 252.

(3) R. M. Steffen and H. Frauenfelder, in "Perturbed Angular K. Correlations," E. Karlsson, E. Matthias, and R. Siegbahn, Eds., North-Holland, Amsterdam, The Netherlands, 1964.

(4) H. Frauenfelder and R. M. Steffen, in "Alpha, Beta, and Gamma-Ray Spectroscopy," K. Siegbahn, Ed., North-Holland, Amsterdam, The Netherlands, 1965.

(5) T. K. Leipeat, J. D. Baldeschwieler, and D. A. Shirley, *Nature*, **220**, 907 (1968).

(6) A. G. Marshall, L. G. Werbelow, and C. F. Meares, *J. Chem. Phys.*, **57**, 364 (1972).

(7) D. A. Goodwin, C. F. Mears, and C. H. Song, *Radiology*, **105**, 699 (1972).

(8) C. F. Mears, R. G. Bryant, J. D. Baldeschwieler, and D. A. Shirley, *Proc. Natl. Acad. Sci. USA*, **64**, 155 (1969).

(9) P. B. Hemmig and R. M. Steffen, *Phys. Rev.*, **92**, 832 (1953).


# Interaction of Tablet Disintegrants and Magnesium Stearate during Mixing I: Effect on Tablet Disintegration


**G. K. BOLHUIS, A. J. SMALLENBROEK, and C. F. LERK ×**



Received September 11, 1980, from the *Laboratory for Pharmaceutical Technology, State University Groningen, Antonius Deusinglaan 2, 9713 AW Groningen, The Netherlands.* Accepted for publication May 13, 1981.



**Abstract** □ The effect of magnesium stearate on the disintegration of tablets was studied. Three different preblends, containing a slightly or a strongly swelling disintegrant, were mixed before compression with magnesium stearate for different time periods. The results show that a strongly swelling disintegrant, such as sodium starch glycolate in contrast to potato starch, can reduce the deteriorating effect of hydrophobic lubricants on tablet disintegration. However, the interaction between magnesium stearate and potato starch or sodium starch glycolate and the resulting differences in disintegration characteristics can be masked by the use of disks in the USP disintegration apparatus.



**Keyphrases** □ Tablets—disintegration, effect of magnesium stearate during mixing □ Magnesium stearate—effect on tablet disintegration during mixing □ Disintegration—tablets, effect of magnesium stearate during mixing


Previous work (1, 2) showed that magnesium stearate can have a strong negative effect on binding properties of tablet excipients. The phenomenon of decreasing crushing strength with increasing mixing time is caused by the formation of a lubricant film interfering with particle binding. The lubricant film is a result of adhesion to the substrate of magnesium stearate molecules, which are sheared off mechanically from the magnesium crystals during mixing (1–4). The formation of such a hydrophobic film can dramatically decrease the wettability of a powder mix, as was shown for sodium chloride–magnesium stearate blends (4). Thus, the deteriorating effect of hydrophobic lubricants on tablet disintegration is not only dependent on the nature and concentration of the lubricant used (5–11) but also on the mixing intensity of the tablet ingredients with the lubricants (12, 13).

The present study concerned the effect of magnesium stearate on tablet disintegration. Three different preblends, containing a slightly or a strongly swelling disintegrant, were mixed before compression with magnesium stearate for different time periods. Particular attention was focused on the effect of disks in the USP disintegration apparatus.

## EXPERIMENTAL

**Materials**—The disintegrants used were dried potato starch[1] (moisture content ~8%) and sodium starch glycolate[2] NF XV. The other excipients were unmilled dibasic calcium phosphate dihydrate[3], extra-fine crystalline lactose[4], aspirin[5] (crystalline acetylsalicylic acid), and magnesium stearate[6].

**Methods**—*Mixing*—Preblends of filler and disintegrants were prepared by mixing[7] the excipients for 15 min, using glass vessels with a loading of ~20%. If not stated otherwise, the rotation speed was 90 rpm. After addition of 0.5% magnesium stearate, mixing was continued for a specified period.

*Tablet Compression*—Tablets were prepared by introducing manually 520.8 mg of the blend containing sodium starch glycolate or 625 mg of the blend containing potato starch into a prelubricated 13-mm die of a compression device mounted between the plattens of an instrumented hydraulic press[8]. The samples were compressed at a compression force of 20 kN with a loading rate of 2 kN/sec.

*Crushing Strength*—The crushing strength of the tablets was determined immediately after compression using a motorized instrument[9]. The data given are the means of at least five tablets.

*Disintegration time*—The disintegration time of the tablets was determined using the USP XIX apparatus. If not stated otherwise, the test was performed without disks. The data given are the means of the dis-

[1] Avebe G. A., Veendam, The Netherlands.
[2] Primojel, Avebe G. A., Veendam, The Netherlands.
[3] Emcompress, Edward Mendell Co., New York, N.Y.
[4] Lactose EFC, N. V. Hollandse Melksuikerfabriek, Uitgeest, The Netherlands.
[5] Feinkristallin (40-mesh USP), Bayer, Leverkusen, West Germany.
[6] Ph. Ned. grade, Lamers en Indemans's-Hertogenbosch, The Netherlands.
[7] Turbula mixer model 2P, W.A. Bachofen, Basel, Switzerland.
[8] Hydro Mooi, Appingedam, The Netherlands.
[9] Heberlein model WTP-3, Dr. K. Schleuniger, Zürich, Switzerland.




*0022-3549/81/1200-1328$01.00/0*


*© 1981, American Pharmaceutical Association*

The method does not measure dissolution of a pharmacologically active ingredient or any other ingredient in the solid dosage form.

With minor detector modifications, this method should contribute significantly in the evaluation of viscosity gradients and sedimentation rates in heterogeneous dosage forms.

## REFERENCES


(1) D. L. Casey, R. M. Beihn, G. A. Digenis, and M. B. Shambhu, *J. Pharm. Sci.*, **65**, 1412 (1976).

(2) "Table of Isotopes," C. M. Lederer, J. M. Hollander, and J. Perlman, Eds., Wiley, New York, N.Y., 1968, p. 252.

(3) R. M. Steffen and H. Frauenfelder, in "Perturbed Angular K. Correlations," E. Karlsson, E. Matthias, and R. Siegbahn, Eds., North-Holland, Amsterdam, The Netherlands, 1964.

(4) H. Frauenfelder and R. M. Steffen, in "Alpha, Beta, and Gamma-Ray Spectroscopy," K. Siegbahn, Ed., North-Holland, Amsterdam, The Netherlands, 1965.

(5) T. K. Leipeat, J. D. Baldeschwieler, and D. A. Shirley, *Nature*, **220**, 907 (1968).

(6) A. G. Marshall, L. G. Werbelow, and C. F. Meares, *J. Chem. Phys.*, **57**, 364 (1972).

(7) D. A. Goodwin, C. F. Mears, and C. H. Song, *Radiology*, **105**, 699 (1972).

(8) C. F. Mears, R. G. Bryant, J. D. Baldeschwieler, and D. A. Shirley, *Proc. Natl. Acad. Sci. USA*, **64**, 155 (1969).

(9) P. B. Hemmig and R. M. Steffen, *Phys. Rev.*, **92**, 832 (1953).


# Interaction of Tablet Disintegrants and Magnesium Stearate during Mixing I: Effect on Tablet Disintegration


**G. K. BOLHUIS, A. J. SMALLENBROEK, and C. F. LERK ×**



Received September 11, 1980, from the *Laboratory for Pharmaceutical Technology, State University Groningen, Antonius Deusinglaan 2, 9713 AW Groningen, The Netherlands.* Accepted for publication May 13, 1981.



**Abstract** □ The effect of magnesium stearate on the disintegration of tablets was studied. Three different preblends, containing a slightly or a strongly swelling disintegrant, were mixed before compression with magnesium stearate for different time periods. The results show that a strongly swelling disintegrant, such as sodium starch glycolate in contrast to potato starch, can reduce the deteriorating effect of hydrophobic lubricants on tablet disintegration. However, the interaction between magnesium stearate and potato starch or sodium starch glycolate and the resulting differences in disintegration characteristics can be masked by the use of disks in the USP disintegration apparatus.



**Keyphrases** □ Tablets—disintegration, effect of magnesium stearate during mixing □ Magnesium stearate—effect on tablet disintegration during mixing □ Disintegration—tablets, effect of magnesium stearate during mixing


Previous work (1, 2) showed that magnesium stearate can have a strong negative effect on binding properties of tablet excipients. The phenomenon of decreasing crushing strength with increasing mixing time is caused by the formation of a lubricant film interfering with particle binding. The lubricant film is a result of adhesion to the substrate of magnesium stearate molecules, which are sheared off mechanically from the magnesium crystals during mixing (1–4). The formation of such a hydrophobic film can dramatically decrease the wettability of a powder mix, as was shown for sodium chloride–magnesium stearate blends (4). Thus, the deteriorating effect of hydrophobic lubricants on tablet disintegration is not only dependent on the nature and concentration of the lubricant used (5–11) but also on the mixing intensity of the tablet ingredients with the lubricants (12, 13).

The present study concerned the effect of magnesium stearate on tablet disintegration. Three different preblends, containing a slightly or a strongly swelling disintegrant, were mixed before compression with magnesium stearate for different time periods. Particular attention was focused on the effect of disks in the USP disintegration apparatus.

## EXPERIMENTAL

**Materials**—The disintegrants used were dried potato starch[1] (moisture content ~8%) and sodium starch glycolate[2] NF XV. The other excipients were unmilled dibasic calcium phosphate dihydrate[3], extra-fine crystalline lactose[4], aspirin[5] (crystalline acetylsalicylic acid), and magnesium stearate[6].

**Methods**—*Mixing*—Preblends of filler and disintegrants were prepared by mixing[7] the excipients for 15 min, using glass vessels with a loading of ~20%. If not stated otherwise, the rotation speed was 90 rpm. After addition of 0.5% magnesium stearate, mixing was continued for a specified period.

*Tablet Compression*—Tablets were prepared by introducing manually 520.8 mg of the blend containing sodium starch glycolate or 625 mg of the blend containing potato starch into a prelubricated 13-mm die of a compression device mounted between the plattens of an instrumented hydraulic press[8]. The samples were compressed at a compression force of 20 kN with a loading rate of 2 kN/sec.

*Crushing Strength*—The crushing strength of the tablets was determined immediately after compression using a motorized instrument[9]. The data given are the means of at least five tablets.

*Disintegration time*—The disintegration time of the tablets was determined using the USP XIX apparatus. If not stated otherwise, the test was performed without disks. The data given are the means of the dis-

[1] Avebe G. A., Veendam, The Netherlands.
[2] Primojel, Avebe G. A., Veendam, The Netherlands.
[3] Emcompress, Edward Mendell Co., New York, N.Y.
[4] Lactose EFC, N. V. Hollandse Melksuikerfabriek, Uitgeest, The Netherlands.
[5] Feinkristallin (40-mesh USP), Bayer, Leverkusen, West Germany.
[6] Ph. Ned. grade, Lamers en Indemans's-Hertogenbosch, The Netherlands.
[7] Turbula mixer model 2P, W.A. Bachofen, Basel, Switzerland.
[8] Hydro Mooi, Appingedam, The Netherlands.
[9] Heberlein model WTP-3, Dr. K. Schleuniger, Zürich, Switzerland.




*0022-3549/81/1200-1328$01.00/0*


*© 1981, American Pharmaceutical Association*

**Table I—Effect of Mixing [a] with Magnesium Stearate on Properties of Tablets from Aspirin with Potato Starch or Sodium Starch Glycolate**

| Mixing Time with Magnesium Stearate, min | 20% Potato Starch | | 4% Sodium Starch Glycolate | |
|---|---|---|---|---|
| | Disintegration Time, sec | Crushing Strength, kg | Disintegration Time, sec | Crushing Strength, kg |
| 0 | 6 | 4.7 | 20 | 5.7 |
| 2 | 24 | <0.1 | 15 | 2.8 |
| 5 | 50 | <0.1 | 16 | 2.3 |
| 30 | 55 | <0.1 | 30 | 2.5 |

[a] A 0-min mixing time means no lubricant was added.

**Table II—Effect of Mixing [a] with Magnesium Stearate on Properties of Tablets from Dibasic Calcium Phosphate Dihydrate with Potato Starch or Sodium Starch Glycolate**

| Mixing Time with Magnesium Stearate, min | 20% Potato Starch | | 4% Sodium Starch Glycolate | |
|---|---|---|---|---|
| | Disintegration Time, sec | Crushing Strength, kg | Disintegration Time, sec | Crushing Strength, kg |
| 0 | 10 | 9.1 | 5 | 5.9 |
| 2 | 15 | 5.6 | 8 | 5.5 |
| 5 | 825 | 4.5 | 13 | 5.0 |
| 30 | >1800 | 4.2 | 56 | 5.2 |

[a] A 0-min mixing time means no lubricant was added.

**Table III—Effect of Mixing[a] with Magnesium Stearate on Properties of Tablets from Lactose with Potato Starch or Sodium Starch Glycolate**

| Mixing Time with Magnesium Stearate, min | 20% Potato Starch | | 4% Sodium Starch Glycolate | |
|---|---|---|---|---|
| | Disintegration Time, sec | Crushing Strength, kg | Disintegration Time, sec | Crushing Strength, kg |
| 0 | 22 | 5.5 | 16 | 4.5 |
| 2 | 40 | 0.1 | 18 | 1.0 |
| 5 | 125 | <0.1 | 21 | 0.9 |
| 30 | 375 | <0.1 | 26 | 0.4 |

[a] A 0-min mixing time means no lubricant was added.

integration time of six individual tablets.

## RESULTS AND DISCUSSION

Table I gives the effect of mixing time for mixing filler–disintegrant preblends with 0.5% magnesium stearate on both disintegration time and crushing strength of tablets compressed from aspirin with 20% potato starch or 4% sodium starch glycolate. The effect of mixing with magnesium stearate on the crushing strength of tablets without disintegrant is given in Fig. 1. Since the aspirin tablets showed only a slight decrease in crushing strength (from 4.5 to 3.2 kg) during 30 min of mixing with magnesium stearate (Fig. 1), the dramatic decrease (down to 0.1 kg with 2 min of mixing) in crushing strength of the tablets containing 20% potato starch must be attributed to a strong interaction between potato starch and magnesium stearate. This finding is consistent with previous results (3) showing that lubricants can exercise a strong negative effect on the binding properties of starch and starch derivatives.

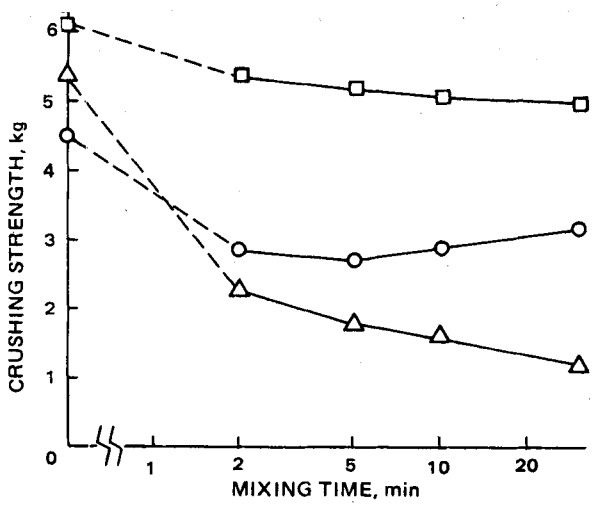


**Figure 1**—*Crushing strength* versus *mixing time (log scale) for tablets of fillers without disintegrants with 0.5% magnesium stearate. Key:* ○, *aspirin;* □, *dibasic calcium phosphate dihydrate; and* △, *lactose.*

In contrast to the decrease in crushing strength, the tablets showed a 10-fold increase in disintegration time after 5 min of mixing of the preblends with magnesium stearate. Since sodium starch glycolate is generally used in lower concentrations, the crushing strength of the aspirin tablets containing only 4% of this disintegrant exhibited a smaller decrease than the tablets containing 20% potato starch (Table I). The tablets initially showed a slight decrease in disintegration time with increasing mixing time with magnesium stearate, followed by a slight increase to values that are relatively low (especially when crushing strength is considered) compared with those of the tablets containing potato starch.

Table II shows the effect of mixing 0.5% magnesium stearate on tablets from dibasic calcium phosphate dihydrate with either 20% potato starch or 4% sodium starch glycolate. Since magnesium stearate hardly affected the binding properties of materials such as dibasic calcium phosphate dihydrate (Fig. 1), which undergo complete fragmentation under compression (3), the decrease in crushing strength of the tablets containing disintegrant must be caused by an interaction of the lubricant with the disintegrant.

Like the aspirin tablets, the dibasic calcium phosphate dihydrate tablets showed an increase in disintegration time with increasing mixing time with magnesium stearate. The most pronounced increase in disintegration time was exhibited by tablets containing 20% potato starch (Table II).

The lactose tablets showed an extremely strong decrease in crushing strength with an increase in mixing time of the blend with magnesium stearate (Table III). This result may be due to the effect of lubricant on the binding properties of both lactose (Fig. 1) and the disintegrants. A strong increase in disintegration time, which is consistent with the other results, was found for tablets with 20% potato starch; tablets with 4% sodium starch glycolate maintained fast disintegration, even when the

**Table IV—Effect of Mixing Velocity during Mixing[a] with Magnesium Stearate on Disintegration Time of Tablets from Dibasic Calcium Phosphate Dihydrate with 20% Potato Starch or 4% Sodium Starch Glycolate**

| Mixing Time with Magnesium Stearate, min | Disintegration Time, sec | | | |
|---|---|---|---|---|
| | 20% Potato Starch | | 4% Sodium Starch Glycolate | |
| | Mixing Velocity of 65 rpm | Mixing Velocity of 90 rpm | Mixing Velocity of 65 rpm | Mixing Velocity of 90 rpm |
| 0 | 10 | 10 | 5 | 5 |
| 2 | 13 | 15 | 7 | 8 |
| 5 | 21 | 825 | 9 | 13 |
| 10 | 325 | >1800 | 11 | 20 |
| 30 | >1800 | >1800 | 14 | 56 |

[a] A 0-min mixing time means no lubricant was added.

**Table V—Effect of Mixing[a] with Magnesium Stearate on Disintegration Time, Measured without and with Disks, of Tablets from Dibasic Calcium Phosphate Dihydrate with 20% Potato Starch or 4% Sodium Starch Glycolate**

| Mixing Time with Magnesium Stearate, min | Disintegration Time, sec | | | |
|---|---|---|---|---|
| | 20% Potato Starch | | 4% Sodium Starch Glycolate | |
| | Without disk | With disk | Without disk | With disk |
| 0 | 10 | 8 | 5 | 4 |
| 2 | 15 | 15 | 8 | 8 |
| 5 | 825 | 37 | 13 | 11 |
| 10 | >1800 | 65 | 20 | 11 |
| 30 | >1800 | 90 | 56 | 13 |

[a] A 0-min mixing time means no lubricant was added.

tablet blend had been mixed for 30 min with magnesium stearate.

These results indicate that all increases in tablet disintegration time must be caused by the formation of a lubricant film on substrate particles of magnesium stearate molecules during mixing. As expected from previous work (2), the deleterious effect of magnesium stearate on disintegration time was dependent on mixing intensity. Table IV shows that the disintegration time of the dibasic calcium phosphate dihydrate tablets with 20% potato starch after 5 min of mixing with lubricant decreased from 825 to 21 sec when the velocity of the mixer decreased from 90 to 65 rpm. Tablets with 4% sodium starch glycolate acquired a still shorter disintegration time when mixing intensity decreased.

The remarkable difference in effect of mixing the preblends containing potato starch or sodium starch glycolate with magnesium stearate on tablet disintegration must be attributed to the difference in disintegration behavior of these materials. The hydrophobic magnesium stearate film formed during mixing will have a negative effect on the wettability of the tablet ingredient particles and, therefore, retard water penetration into the tablets. Since a complete coating of lubricant is not formed during mixing (12), the lubricant film will not be perfect and water will enter the disintegrant particles. Since sodium starch glycolate particles, in contrast to potato starch particles, swell extensively when brought in contact with water (14), it may be assumed that a small amount of water can already destroy the hydrophobic lubricant film. Microscopic examination of lubricated sodium starch glycolate particles confirmed that the particles bulge when brought into water. However, the swelling of potato starch may be insufficient to collapse the lubricant film on the disintegrant particles.

The disintegration times given in Tables I–IV refer to the method described in USP XIX but without disks. Table V gives the effect of the disks on the disintegration times obtained. The results show that the deleterious effect of magnesium stearate on the disintegration time of dibasic calcium phosphate dihydrate tablets can largely be masked by the disks.

The differences in disintegration time obtained with and without disks are likely due to the mechanical damage of the lubricant film during the disintegration test by the disks used, so that water can penetrate even the lubricant-coated, slightly swelling, potato starch particles.

These results prove that the use of disks in the USP disintegration apparatus can mask differences in tablet formulation (15, 16) as well as differences in preparation conditions such as mixing intensity.

## REFERENCES


(1) G. K. Bolhuis, C. F. Lerk, H. T. Zijlstra, and A. H. de Boer, *Pharm. Weekbl.*, **110**, 317 (1975).

(2) C. F. Lerk, G. K. Bolhuis, and S. S. Smedema, *Pharm. Acta Helv.*, **52**, 33 (1977).

(3) A. H. de Boer, G. K. Bolhuis, and C. F. Lerk, *Powder Technol.*, **20**, 75 (1978).

(4) C. F. Lerk and G. K. Bolhuis, *Pharm. Acta Helv.*, **52**, 39 (1977).

(5) W. A. Strickland, Jr., E. Nelson, L. W. Busse, and T. Higuchi, *J. Am. Pharm. Assoc., Sci. Ed.*, **45**, 51 (1956).

(6) K. C. Kwan, F. O. Swart, and A. M. Mattocks, *ibid.*, **46**, 236 (1957).

(7) N. J. van Abbé and J. T. Rees, *ibid.*, **47**, 487 (1958).

(8) F. Jaminet, L. Delattre, and J. P. Delporte, *Pharm. Acta Helv.*, **44**, 418 (1969).

(9) E. Shotton, *Pharm. Ind.*, **34**, 256 (1972).

(10) N. O. Lindberg, *Acta Pharm. Suec.*, **9**, 207 (1972).

(11) L. Delattre, J. Gillard, F. Jaminet, and M. Roland, *J. Pharm. Belg.*, **31**, 497 (1976).

(12) A. C. Shah and A. R. Mlodozeniec, *J. Pharm. Sci.*, **66**, 1377 (1977).

(13) G. Ragnarsson, A. W. Hölzer, and J. Sjögren, *Int. J. Pharm.*, **3**, 127 (1979).

(14) E. Mendell, *Pharm. Acta Helv.*, **49**, 248 (1974).

(15) F. A. Campagna, G. Cureton, R. A. Mirigian, and E. Nelson, *J. Pharm. Sci.*, **52**, 605 (1963).

(16) L. Delattre and F. Jaminet, *Pharm. Acta Helv.*, **49**, 108 (1974).

# General Model for Dissolution Rates of $n$-Component, Nondisintegrating Spheres

**G. R. CARMICHAEL *, S. A. SHAH ‡§, and E. L. PARROTT ‡x**

Received January 9, 1981, from the *Chemical and Materials Engineering Program and the ‡Division of Pharmaceutics, College of Pharmacy, University of Iowa, Iowa City, IA 52242. Accepted for publication April 7, 1981. §Present address: Zenith Laboratories, Northvale, NJ 07646.

**Abstract** □ The dissolution rates of compressed spheres consisting of two and three components were measured. A general model for dissolution rates of $n$-component, nondisintegrating spheres is discussed. Experimental cases are presented to support the model for two- and three-component spheres, two-component interacting spheres, and three-component spheres containing two components that complex.

**Keyphrases** □ Dissolution—general model for $n$-component, nondisintegrating spheres ■ Spheres—$n$-component, nondisintegrating, general model for dissolution rates □ Models, dissolution—for $n$-component, nondisintegrating spheres

Few studies on dissolution rates have involved multicomponent solids. One early study (1) involving the dissolution of a two-component system examined the dissolution rates of several poorly soluble weak acids and tribasic sodium phosphate in various mole fractions. The dissolution rates of salicylic acid and povidone from compressed disks also were reported (2). Diffusion models also were suggested (3) for the dissolution of nondisintegrating multicomponent mixtures containing noninteracting components and complexing components. Shah and Parrott (4) applied the model to the dissolution of four two-component solids.

This study presents a general model for the dissolution rates of a nondisintegrating sphere containing any number of components. The model was developed from the viewpoint of mass transfer, and experimental cases are presented demonstrating its application to two- and three-component solids, two-component interacting solids, and three-component solids with two components interacting.

## THEORY

A model for the dissolution rate of a spherical solid particle may be described assuming that (*a*) the dissolution rate is diffusion controlled, (*b*) the diffusion layer thickness is always the same for all particles of the same size, (*c*) the concentration change of the dissolved solid in the dissolution medium is negligible, (*d*) the effective particle shape approximates a sphere, and (*e*) the initial solid composed of $n$ components is homogeneous.

From the viewpoint of mass transfer, if multicomponent diffusion effects are ignored, the change in mass with time, $dW_i/dt$, of a noninteracting component in the solid can be expressed as:

$$\frac{dW_i}{dt} = -k_i S_i (C_i^* - C_i) \qquad \text{(Eq. 1)}$$

where $k_i$ is the liquid phase mass transfer coefficient, $S_i$ is the surface area available for mass transfer, and $C_i^*$ and $C_i$ are the interfacial and bulk mass concentrations of species in the liquid phase, respectively, for components $i = 1$ to $n$. Since the surface area of a sphere is $4\pi r^2$, Eq. 1 may be written as:

$$\frac{dW_i}{dt} = -k_i 4\pi r_i^2 (C_i^* - C_i) \qquad \text{(Eq. 2)}$$

The mass of a given component in the solid is related to the volume of the particle, the mass fraction, $X_i$, and the bulk density, $\rho$. Since:

$$W_i = \frac{4}{3}\pi r_i^3 X_i \rho \qquad \text{(Eq. 3)}$$

and if $X_i$ is not a function of time, Eq. 2 may be written as:

$$-\frac{dr_i}{dt} = \frac{D_i (C_i^* - C_i)}{h X_i \rho} \qquad \text{(Eq. 4)}$$

where, for diffusion-controlled dissolution in which there is no chemical reaction, the liquid phase mass transfer coefficients are expressed in terms of diffusion coefficients, $D_i$, and the film thickness, $h$.

As dissolution proceeds, the more soluble components dissolve faster and are depleted near the solid–liquid interface, resulting in a surface layer composed of the least soluble component. At any time, the solid is conceptualized as consisting of a homogeneous core with the initial composition, an outer shell of the least soluble component, and, between them, $n - 2$ concentric layers comprised of components of intermediate solubilities. If the $n$th component is the least soluble component, Eq. 4 may be written as:

$$-\frac{dr_n}{dt} = \frac{D_n}{X_n h \rho}(C_n^* - C_n) \qquad \text{(Eq. 5)}$$

and:

$$-\frac{dr_i}{dt} = \frac{D_i (C_i^* - C_i)}{(h + r_n - r_i) X_i \rho} \qquad \text{(Eq. 6)}$$

where $h$ is the film thickness and $(h + r_n - r_i)$ includes an internal diffusion thickness (or resistance) of $r_n - r_i$.

Equations 2, 5, and 6 may be used to calculate the dissolution rates of $n$-component solids. The fluxes, $J_i$, may be found from the equations:

$$J_i = \frac{1}{S_n}\frac{dW_i}{dt} = -k_i \frac{S_i}{S_n}(C_i^* - C) \qquad \text{(Eq. 7)}$$

and:

$$J_n = \frac{1}{S_n}\frac{dW_n}{dt} = -k_n (C_n^* - C_n) \qquad \text{(Eq. 8)}$$

where the fluxes are normalized in terms of the external surface area, $S_n$, of the solid.

The weight of the solid at any time can be calculated from:

$$W = \sum_{i=1}^{n} W_i \qquad \text{(Eq. 9)}$$

These equations will be used to model the dissolution of two- and three-component solids. In addition, these equations can be modified to include cases with interaction between the components.

## EXPERIMENTAL

**Preparation of Compressed Spheres and Measurement of Densities**—Material that passed through an 80-mesh sieve but was retained on a 100-mesh sieve was compacted at 4540 kg of force, by means of a hydraulic press[1], into compressed spheres having a diameter of 1.270 ± 0.005 cm. The bulk density of the compressed spheres was determined by displacement (4). The true density of the material was determined by means of a pycnometer using $n$-heptane.

**Dissolution Rate**—The dissolution rate was determined in distilled water at 25 ± 0.1°, as described previously (5, 6), under conditions where the concentration of the solutes did not exceed 5% of solubility. The dissolution apparatus and procedure were described previously (4, 6), and the dissolution rates are given in Tables I and II.

**Analytical Procedures**—The simultaneous analysis of two-compo-

[1] Carver press, model C.


© 1981, American Pharmaceutical Association

**Table I—Composition and Experimental Dissolution Rates of Two-Component Solids Compressed at 4540 kg**

| Mole Fraction | | Dissolution Rate, g/hr/cm² | | |
|---|---|---|---|---|
| | | Aspirin–Salicylic Acid | | |
| $X_{ASA}$ | $X_{SAL}$ | ASA | SAL | Sphere |
| 1.0 | 0 | 0.0430 | — | 0.0430 |
| 0.9 | 0.1 | 0.0423 | 0.0036 | 0.0459 |
| 0.8 | 0.2 | 0.0415 | 0.0080 | 0.0495 |
| 0.7 | 0.3 | 0.0382 | 0.0125 | 0.0507 |
| 0.6 | 0.4 | 0.0336 | 0.0171 | 0.0507 |
| 0.5 | 0.5 | 0.0282 | 0.0216 | 0.0498 |
| 0.4 | 0.6 | 0.0215 | 0.0248 | 0.0463 |
| 0.3 | 0.7 | 0.0148 | 0.0264 | 0.0412 |
| 0.2 | 0.8 | 0.0088 | 0.0271 | 0.0359 |
| 0.1 | 0.9 | 0.0039 | 0.0272 | 0.0311 |
| 0 | 1.0 | — | 0.0272 | 0.0272 |
| | | Aspirin–Phenacetin | | |
| $X_{ASA}$ | $X_{PH}$ | ASA | PH | Sphere |
| 1.0 | 0 | 0.0430 | — | 0.0430 |
| 0.9 | 0.1 | 0.0370 | 0.0041 | 0.0411 |
| 0.8 | 0.2 | 0.0320 | 0.0079 | 0.0399 |
| 0.7 | 0.3 | 0.0269 | 0.0115 | 0.0384 |
| 0.6 | 0.4 | 0.0195 | 0.0129 | 0.0324 |
| 0.5 | 0.5 | 0.0130 | 0.0125 | 0.0255 |
| 0.4 | 0.6 | 0.0081 | 0.0120 | 0.0201 |
| 0.3 | 0.7 | 0.0051 | 0.0120 | 0.0171 |
| 0.2[a] | 0.8 | 0.0025 | 0.0098 | 0.0123 |
| 0.1[b] | 0.9 | 0.0010 | 0.0086 | 0.0096 |
| 0 | 1.0[b] | — | 0.0080 | 0.0080 |

[a] Compressed at 680 kg. [b] Melt method.

nent spheres of aspirin (ASA) and salicylic acid (SAL), and of aspirin and phenacetin (PH), and of three-component spheres of aspirin, caffeine (CAF), and phenacetin using simultaneous equations was discussed previously (4, 7).

## RESULTS AND DISCUSSIONS

**Two-Component, Noninteracting Solids**—Two systems (aspirin–salicylic acid and aspirin–phenacetin) were studied. The experimental dissolution rates for various compositions of both systems are given in Table I. The solubilities and diffusion coefficients used in the calculations are compiled in Table III. The weight of the spheres and the fluxes (dissolution rates) were calculated from Eqs. 1 and 5–9. These equations were solved simultaneously using a fourth-order Runge–Kutta procedure (8).

For example, at 2 hr, the theoretical predicted weights are compared to the experimentally determined weights for aspirin–salicylic acid spheres in Fig. 1 and for aspirin–phenacetin spheres in Fig. 2. The predicted weights are within 6% of the determined weights, and the calculated values indicate that the maximum loss of weight occurs at an intermediate value of $X_{ASA}$.

**Table III—Physical Parameters of Species in Water at 25°**

| Material | $D_i$, cm²/sec | $C_i^*$ g/ml |
|---|---|---|
| Aspirin | $8.01 \times 10^{-6}$ [a] | $4.44 \times 10^{-3}$ [a] |
| Salicylic acid | $10.12 \times 10^{-6}$ [b] | $2.24 \times 10^{-3}$ [c] |
| Caffeine | $6.79 \times 10^{-6}$ [d] | $23.2 \times 10^{-3}$ [e] |
| Phenacetin | $9.0 \times 10^{-6}$ [f] | $1.1 \times 10^{-3}$ [g] |
| Aspirin–caffeine complex | $6.79 \times 10^{-6}$ [h] | — |

[a] L. J. Edwards, *Trans. Faraday Soc.*, **47**, 1191 (1951). [b] J. W. Mullin and T. P. Cook, *J. Appl. Chem.*, **15**, 145 (1965). [c] N. A. Halla, *Am. J. Pharm.*, **132**, 406 (1960). [d] M. McCabe, *Biochem. J.*, **127**, 249 (1972). [e] A. N. Paruta, B. J. Sciarrone, and N. G. Lordi, *J. Pharm. Sci.*, **54**, 838 (1965). [f] C. D. Shively and D. O. Kildsig, *ibid.*, **61**, 1589 (1972). [g] A. Seidell, *J. Am. Chem. Soc.*, **92**, 1088 (1970). [h] Assumed to be the same as caffeine.

The general model predicts that maximum dissolution rates occur for composite solids in which there is no internal diffusion resistance (all the $r_i$ values are equal). This critical composition can be found by equating the right-hand sides of Eq. 6 with $r_n = r_i$ and $C_i = 0$; thus:

$$\frac{D_1 C_1^*}{hX_1\rho} = \frac{D_2 C_2^*}{hX_2\rho} \qquad \text{(Eq. 10)}$$

which can be rearranged to:

$$\frac{X_2}{X_1} = \frac{D_2 C_2^*}{D_1 C_1^*} \qquad \text{(Eq. 11)}$$

where $X_1 + X_2 = 1$.

In general, the $r_i$ values of the dissolving components are not equal and may vary with time. For example, in Fig. 3 the radius is plotted *versus* time for different initial compositions of aspirin and phenacetin. Where $X_{ASA} = 0.1$ and phenacetin comprises the outer shell, the external radius of the solid varies linearly with time while the radius of the homogeneous core varies nonlinearly. In Fig. 3, the internal diffusion thickness for aspirin is dependent on time. For the critical composition of the solid, the internal resistance is zero and $r_{ASA} = r_{PH}$.

Since the internal diffusion thickness is dependent on time, the fluxes are also time variant (Eqs. 7 and 8). Examples of this situation are shown in Fig. 4 for an aspirin–salicylic acid sphere with $X_{ASA} = 0.2$ and for aspirin–phenacetin spheres with $X_{ASA} = 0.2$ and 0.7. Since there is no internal resistance at $t = 0$, the fluxes have their maximum value; subsequently, the flux of the more soluble component decreases as the internal resistance is increased. The average flux, $\bar{J}$, may be calculated by:

$$\bar{J} = \frac{\int_0^t J(t)\,dt}{\int_0^t dt} \qquad \text{(Eq. 12)}$$

At 2 hr, the theoretical average fluxes of aspirin and salicylic acid were calculated and plotted in Fig. 5 for the aspirin–salicylic acid spheres of various composition. The symbols represent the experimental values. Similarly, the average fluxes of aspirin and of phenacetin are plotted *versus* composition in Fig. 6 for comparison to theoretical values.

**Table II—Composition and Experimental Dissolution Rates of Three-Component, Interacting System**

| Mole Fraction | | | Density, | Dissolution Rate[a], g/hr/cm² | | | |
|---|---|---|---|---|---|---|---|
| $X_{ASA}$ | $X_{PH}$ | $X_{CAF}$ | g/cm³ | ASA | PH | CAF | Sphere |
| 0.4 | 0.2 | 0.4 | 1.46 | 0.0650 | 0.0323 | 0.0701 | 0.1674 |
| | | | | 0.0679 | 0.0338 | 0.0733 | 0.1750 |
| 0.25 | 0.5 | 0.25 | 1.39 | 0.0077 | 0.0154 | 0.0083 | 0.0314 |
| | | | | 0.0079 | 0.0158 | 0.0085 | 0.0322 |
| 0.167 | 0.667 | 0.167 | 1.35 | 0.0026 | 0.0106 | 0.0029 | 0.0161 |
| | | | | 0.0026 | 0.0105 | 0.0028 | 0.0159 |
| 0.4 | 0.4 | 0.2 | 1.41 | 0.0167 | 0.0166 | 0.0090 | 0.0423 |
| | | | | 0.0165 | 0.0164 | 0.0089 | 0.0418 |
| 0.25 | 0.25 | 0.5 | 1.42 | 0.0452 | 0.0451 | 0.0975 | 0.1878 |
| | | | | 0.0446 | 0.0444 | 0.0961 | 0.1851 |
| 0.167 | 0.167 | 0.667 | 1.43 | 0.0495 | 0.0492 | 0.2127 | 0.3114 |
| | | | | 0.0454 | 0.0452 | 0.1952 | 0.2853 |
| 0.2 | 0.4 | 0.2 | 1.37 | 0.0160 | 0.0319 | 0.0345 | 0.0824 |
| | | | | 0.0169 | 0.0338 | 0.0365 | 0.0872 |
| 0.5 | 0.25 | 0.25 | 1.45 | 0.0368 | 0.0183 | 0.0198 | 0.0749 |
| | | | | 0.0362 | 0.0180 | 0.0196 | 0.0738 |
| 0.667 | 0.167 | 0.167 | 1.47 | 0.0417 | 0.0104 | 0.0113 | 0.0634 |
| | | | | 0.0409 | 0.0102 | 0.0111 | 0.0622 |
| 0.333 | 0.333 | 0.333 | 1.43 | 0.0290 | 0.0289 | 0.0313 | 0.0892 |

[a] Two determination for each composition.

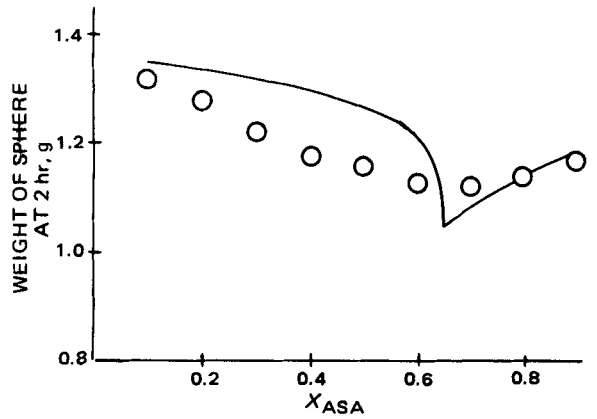


**Figure 1**—*Relation of composition to weight of a dissolving aspirin–salicylic acid sphere having a bulk density of 1.52 g/cm³. Smooth curve is theoretical, and points are experimental values.*

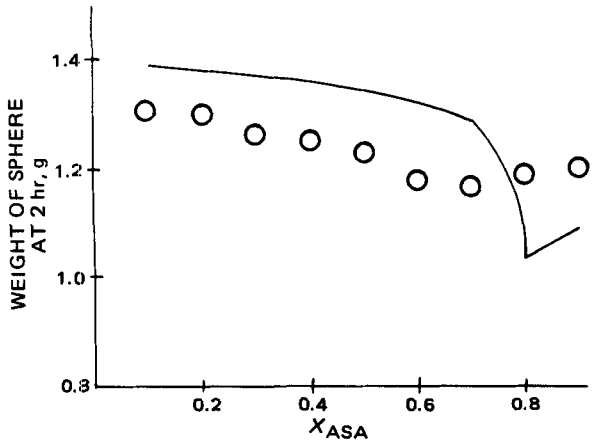


**Figure 2**—*Relation of composition to weight of a dissolving aspirin–phenacetin sphere having a bulk density of 1.42 g/cm³. Smooth curve is theoretical, and points are experimental values.*

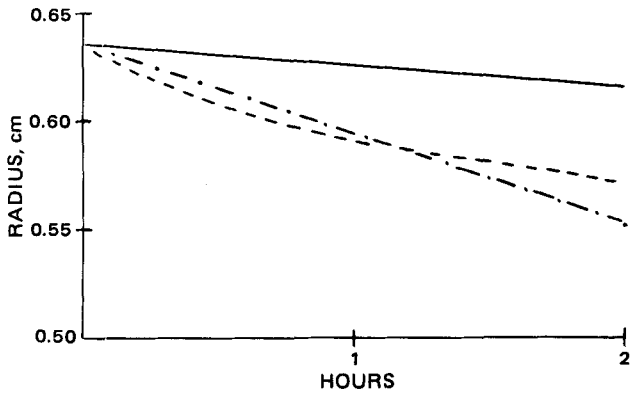


**Figure 3**—*Radius of layers of the components of a dissolving aspirin–phenacetin sphere with a bulk density of 1.42 g/cm³ as a function of time at the critical composition and at $X_{ASA}$ = 0.1. Key: —, $r_{PH}$ at $X_{ASA}$ = 0.1; ---, $r_{ASA}$ at $X_{ASA}$ = 0.1; and —·—, $r_{PH}$ = $r_{ASA}$ at $X_{ASA}$ = 0.8.*

**Three-Component, Noninteracting Solids**—For three-component, noninteracting solids, the critical composition is found from:

$$\frac{D_1C_1^*}{hX_1\rho} = \frac{D_2C_2^*}{hX_2\rho} = \frac{D_3C_3^*}{hX_3\rho} \qquad \text{(Eq. 13)}$$

or:

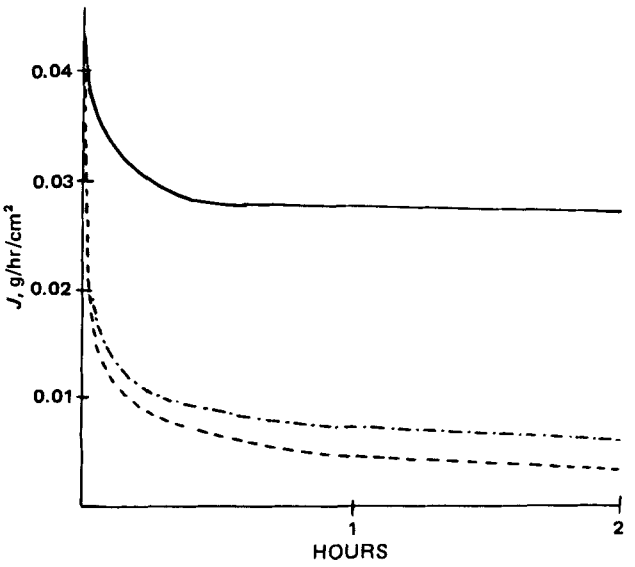


**Figure 4**—*Instantaneous flux from two-component spheres as a function of time. Key: —, $J_{PH}$ at $X_{ASA}$ = 0.7 and $X_{PH}$ = 0.3 with a bulk density of 1.42 g/cm³; ---, $J_{ASA}$ at $X_{ASA}$ = 0.2 and $X_{PH}$ = 0.8 with a bulk density of 1.42 g/cm³; and —·—, $J_{ASA}$ at $X_{ASA}$ = 0.2 and $X_{SAL}$ = 0.8 with a bulk density of 1.46 g/cm³.*

$$\frac{X_2}{X_1} = \frac{D_2C_2^*}{D_1C_1^*} \qquad \text{(Eq. 14)}$$

$$\frac{X_2}{X_3} = \frac{D_2C_2^*}{D_3C_3^*} \qquad \text{(Eq. 15)}$$

where $X_1 + X_2 + X_3 = 1$.

For the argument of model comparison, no interaction is assumed to occur in the dissolution of an aspirin–caffeine–phenacetin solid. With this assumption, the average fluxes for the components were calculated and plotted in Fig. 7 at $X_{PH}$ = 0.5. For $X_{PH}$ values greater than ~0.1, the phenacetin is the outer shell, and the flux of phenacetin is constant for all $X_{ASA}$ values. For $X_{PH}$ of < 0.1, either the caffeine or the aspirin can be the outer shell, depending on the composition. As shown in Fig. 8 at $X_{PH}$ = 0.05, if $X_{ASA} \geq 0.2$, aspirin is the outer shell, and if $X_{ASA} \leq 0.2$, phenacetin is the outer layer.

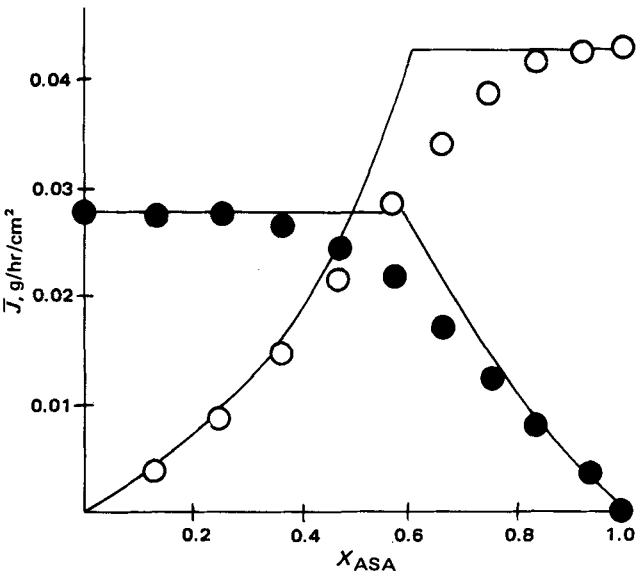


**Figure 5**—*Comparison of experimental fluxes of the components of aspirin–salicylic acid spheres with a bulk density of 1.4 g/cm³ of various compositions. Smooth curves are theoretical average fluxes. Key: ○, aspirin; and ●, salicylic acid.*

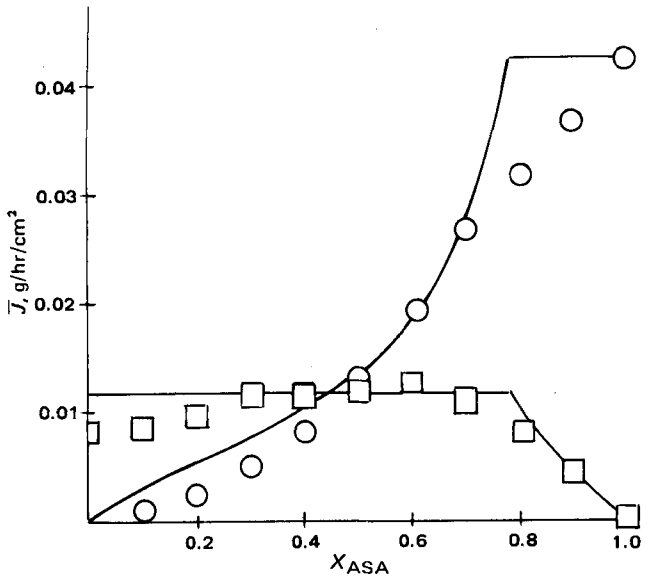


**Figure 6**—*Comparison of experimental fluxes of the components of aspirin–phenacetin spheres with a density of 1.4 g/cm³ of various compositions. Smooth curves are theoretical average fluxes. Key: ○, aspirin; and □, phenacetin.*

**Two-Component, Interacting Solids**—The general modeling discussed may be extended to include interacting solids. Consider the case in which components $A$ and $B$ react according to the reaction $A + B \rightleftarrows AB$ and the equilibrium constant, $K$, is expressed as:

$$K = \frac{\tilde{C}_{AB}}{\tilde{C}_A \tilde{C}_B} \qquad \text{(Eq. 16)}$$

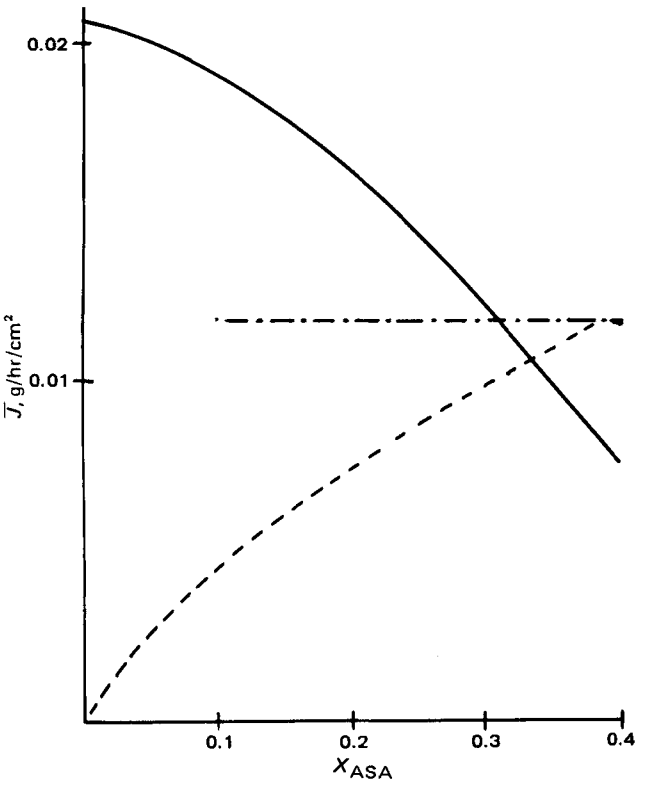


**Figure 7**—*Average fluxes of components of aspirin–caffeine–phenacetin spheres with a density of 1.5 g/cm³, $X_{PH}$ = 0.5, and various compositions of aspirin and caffeine. Key: ---, aspirin; —, caffeine; and -·-·-, phenacetin.*

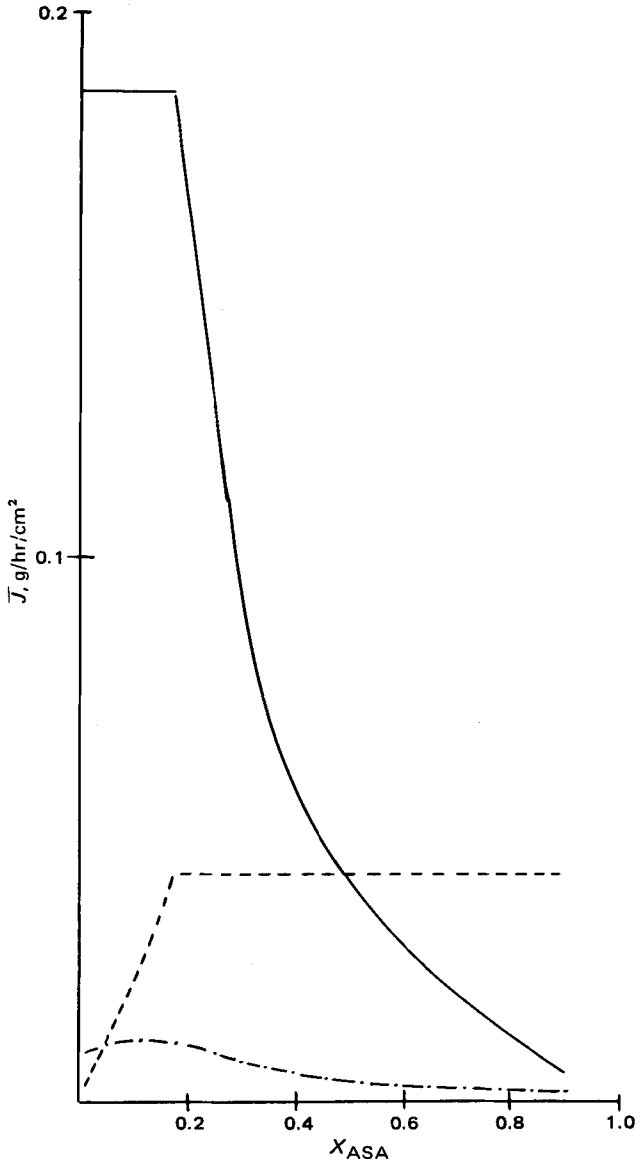


**Figure 8**—*Average fluxes of components of aspirin–caffeine–phenacetin spheres with a density of 1.5 g/cm³, $X_{PH}$ = 0.05, and various compositions of aspirin and caffeine. Key: ---, aspirin; —, caffeine; and -·-·-, phenacetin.*

with the concentrations being expressed in molar concentrations as indicated by tildes.

The mass transfer may be expressed for the two-component, interacting system by:

$$-\frac{dW_A}{dt} = k_A S_A C_A^* + k_{AB} S_B M_A \tilde{C}_{AB}^* \qquad \text{(Eq. 17)}$$

$$-\frac{dW_B}{dt} = k_B S_B C_B^* + k_{AB} S_A M_B \tilde{C}_{AB}^* \qquad \text{(Eq. 18)}$$

where $M_A$ and $M_B$ are the molecular weights of $A$ and $B$, respectively. Expressions for $r_A$ and $r_B$ may be found as discussed.

For the critical composition:

$$\frac{X_A}{X_B} = \frac{D_A C_A^* + M_A D_{AB} \tilde{C}_{AB}^*}{D_B C_B^* + M_B D_{AB} \tilde{C}_{AB}^*} \qquad \text{(Eq. 19)}$$

where $X_A + X_B = 1$.

Theoretically calculated values are drawn as solid lines in Fig. 9 in which the mass of a dissolving aspirin–caffeine sphere at 1 and 2 hr is plotted *versus* composition. The symbols represent experimental values. The model and experimental values are in good qualitative and quantitative agreement over the entire range of $X_{ASA}$.

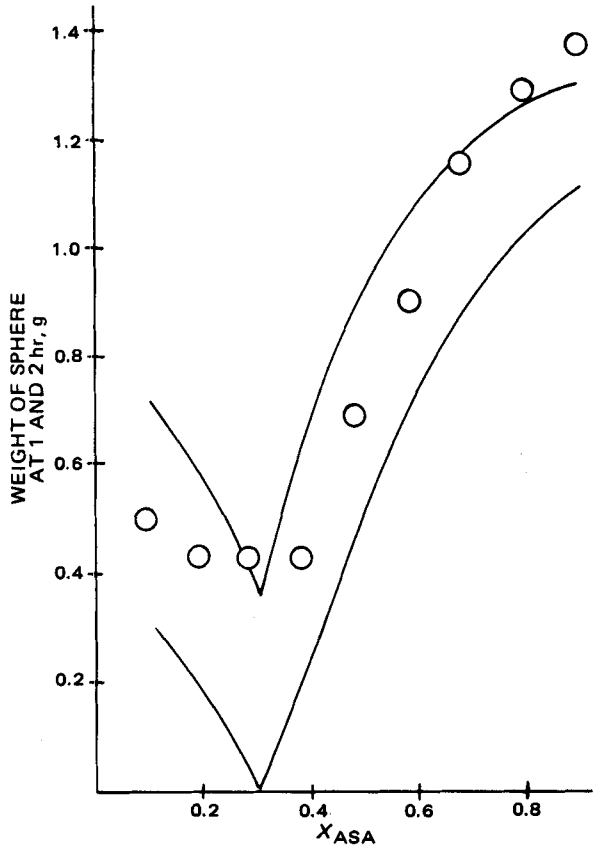


**Figure 9**—*Relation of composition to weight of a dissolving aspirin–caffeine sphere with a bulk density of 1.5 g/cm³. Smooth curves are theoretical, and points are experimental values. Key: upper curve, t = 1 hr; lower curve, t = 2 hr; and ○, experimental values at t = 1 hr.*

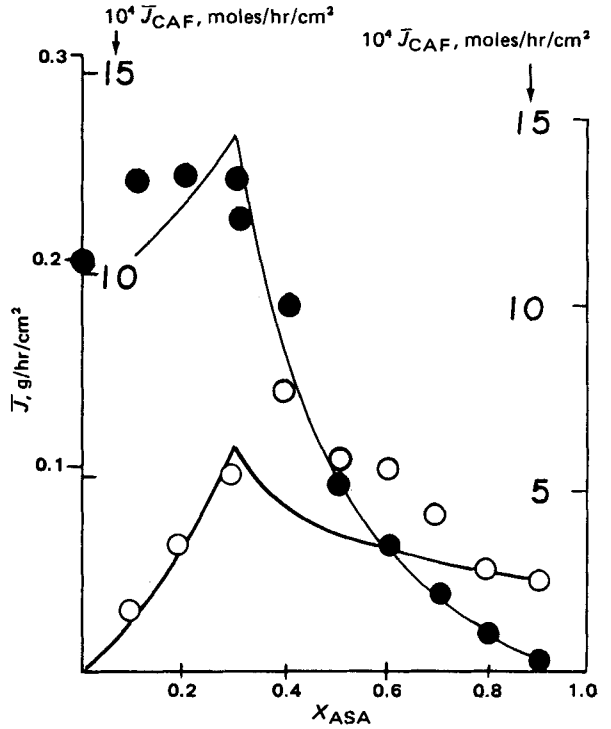


**Figure 10**—*Comparison of theoretical and experimental fluxes of the two components for an interacting two-component sphere with a bulk density of 1.5 g/cm³. Smooth curves are theoretical fluxes. Key: ○, aspirin; and ●, caffeine.*

The fluxes predicted by the model are compared to the experimentally determined fluxes in Fig. 10. The differences between interacting and noninteracting systems can be seen by comparing Fig. 10 with Figs. 5 and 6. There are no regions in a two-component, interacting system in which either flux is independent of the mass fraction. In addition, in a noninteracting system, the flux of aspirin can not exceed 0.043 g/hr/cm²; in interacting systems, the flux of aspirin can greatly exceed the noninteracting limit over a broad range of $X_{ASA}$ values.

**Three-Component Systems with Two Components Interacting**—If a third component, $I$, is added to the two-component, interacting system, then in addition to Eqs. 17 and 18, an equation for mass transfer of $I$ must be considered, *i.e.*:

$$-\frac{dW_I}{dt} = k_I S_I C_I^* \qquad \text{(Eq. 20)}$$

The expressions for the critical composition for this system are:

$$\frac{X_A}{X_B} = \frac{D_A C_a^* + M_A D_{AB} \tilde{C}_{AB}^*}{D_B C_B^* + M_B D_{AB} \tilde{C}_{AB}^*} \qquad \text{(Eq. 21)}$$

and:

$$\frac{X_I}{X_B} = \frac{D_I C_I^*}{D_B C_B^* + M_B D_{AB} \tilde{C}_{AB}^*} \qquad \text{(Eq. 22)}$$

where $X_I + X_A + X_B = 1$.

The equilibrium constant for the 1:1 aspirin–caffeine complex was reported to be 17.4 liters/mole (9). The hypothetical fluxes for each component of an aspirin–caffeine–phenacetin solid are shown in the remaining plots (see *Appendix*). The model for three components with two components interacting is plotted in Figs. 11 and 12, and it may be compared to Figs. 7 and 8 in which no interaction was hypothetically assumed between aspirin and caffeine. For $X_{PH} \geq 0.1$, the general shapes of the flux curves are similar (Fig. 11); however, for $X_{PH} \leq 0.1$, the effects of complexation are apparent (Fig. 12).

Due to caffeine–aspirin complexation, the flux of aspirin may be greater than in the hypothetical noninteracting case. In addition, for the inter-

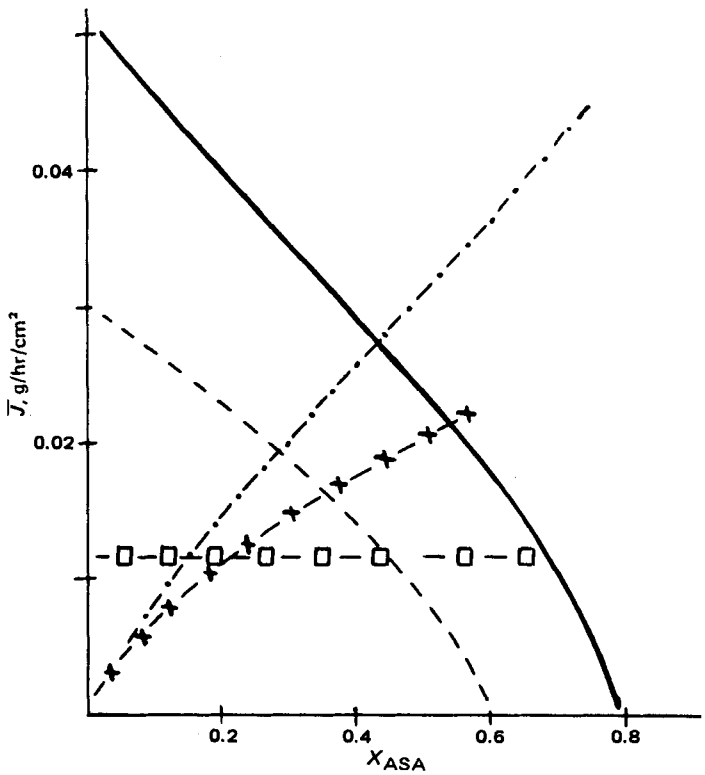


**Figure 11**—*Theoretical average fluxes of components of aspirin–caffeine–phenacetin spheres with a bulk density of 1.5 g/cm³, $X_{PH} \geq 0.1$, and various compositions of aspirin and caffeine. The hypothetical noninteracting case for this system is given in Fig. 7. Key: —, caffeine at $X_{PH} = 0.2$; - - -, caffeine at $X_{PH} = 0.4$; —·—, aspirin at $X_{PH} = 0.2$; ×–×–, aspirin at $X_{PH} = 0.4$; and □–□–, phenacetin at $X_{PH} = 0.2$ and $X_{PH} = 0.4$.*

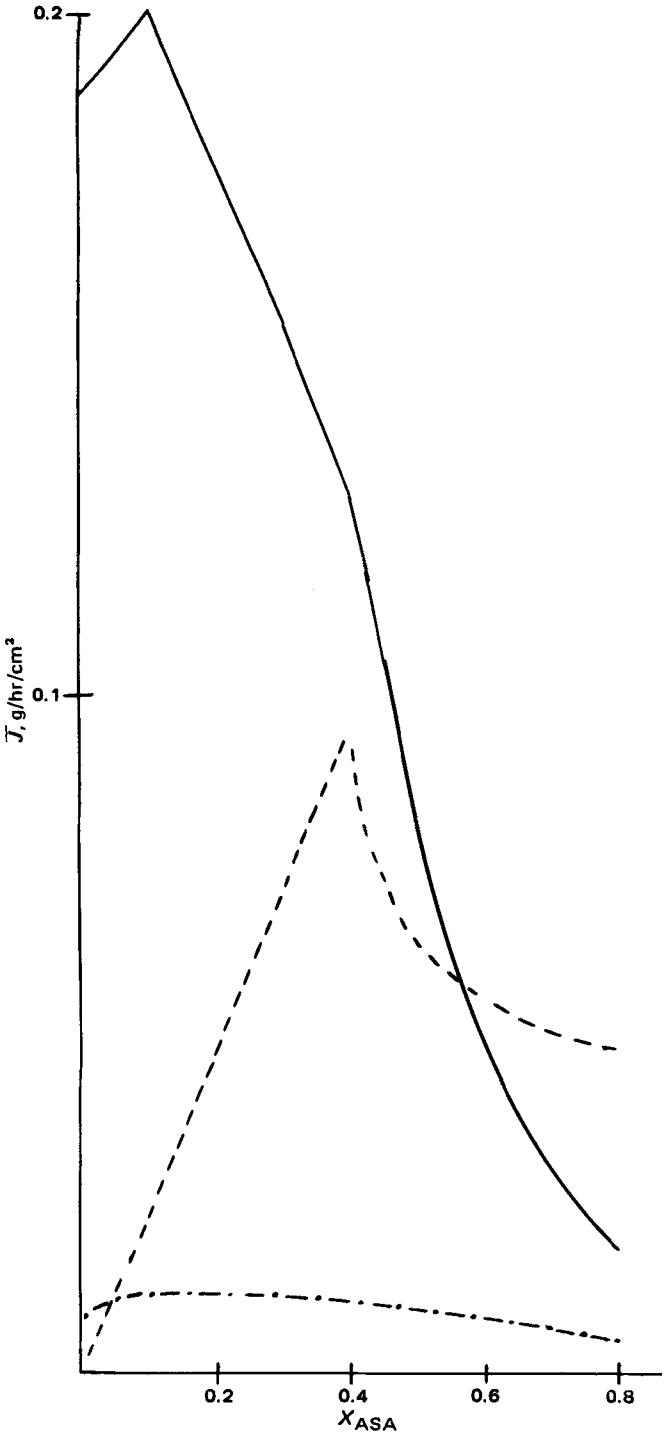


**Figure 12**—*Theoretical average fluxes of components of aspirin–caffeine–phenacetin spheres with a bulk density of 1.5 g/cm³, $X_{PH}$ = 0.05, and various compositions of aspirin and caffeine with complexation. Key: ---, aspirin; —, caffeine; and -·-·-, phenacetin.*

acting case, three distinct regions occur as shown in Fig. 12. For $X_{ASA} \geqq 0.4$, aspirin forms the outer shell, and the fluxes of all three components decrease with increases in $X_{ASA}$. For $0.1 \leqq X_{ASA} \leqq 0.4$, phenacetin comprises the outer shell, and the flux of phenacetin remains constant while the flux of aspirin increases and the flux of caffeine decreases as $X_{ASA}$ is greater. Caffeine forms the outer shell for $X_{ASA} \leqq 0.1$, and the fluxes of all three components increase as $X_{ASA}$ is greater.

The experimental data for the three-component, interacting system (Table II) are comparable with reasonable qualitative agreement to the theoretical values in the remaining figures. In Fig. 13 with equal mole fractions of aspirin and phenacetin, the flux of caffeine is shown to be an

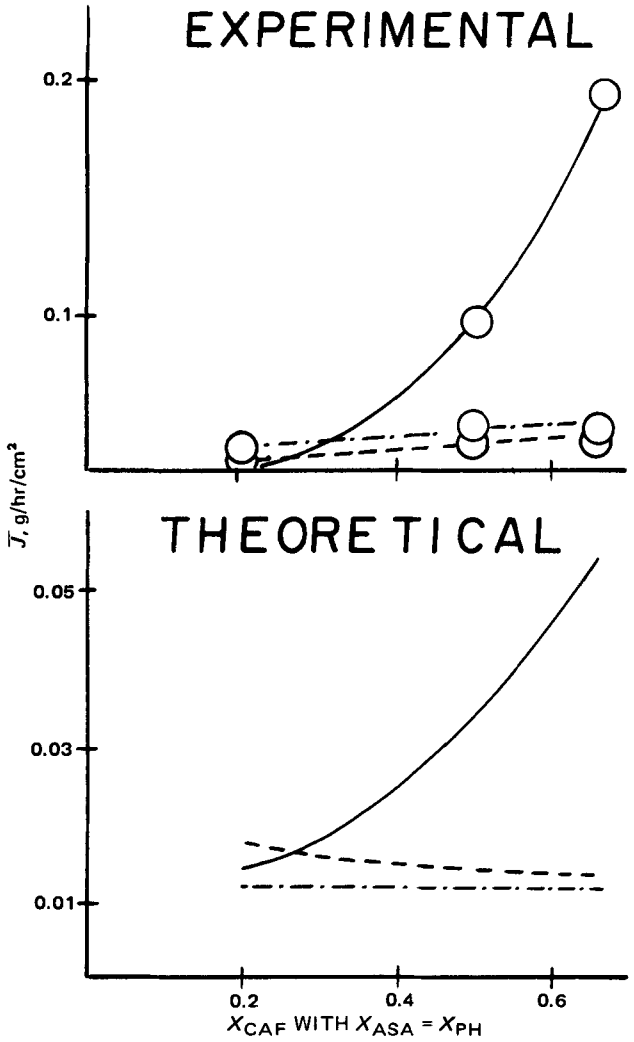


**Figure 13**—*Theoretical average and experimental fluxes of each component in a three-component, interacting system with equal mole fractions of aspirin and phenacetin. Densities are given in Table II. Key: ---, aspirin; —, caffeine; and -·-·-, phenacetin.*

increasing function of the mole fraction of caffeine; however, the fluxes of aspirin and phenacetin are relatively insensitive to the mole fraction of caffeine.

In Fig. 14 with equal mole fractions of aspirin and caffeine, the fluxes of aspirin and caffeine decrease exponentially as the mole fraction of phenacetin is increased, while the flux of phenacetin is less sensitive to change in the fraction of phenacetin. As shown in Fig. 15 with equal mole fractions of caffeine and phenacetin, the flux of aspirin increases as the mole fraction of aspirin increases, but the flux of caffeine decreases as the mole fraction of aspirin increases.

## APPENDIX

The mathematics of the calculation of the fluxes is illustrated for a three-component solid with two interacting components.

The equations for the flux of the dissolution of aspirin (ASA)–caffeine (CAF)–phenacetin (PH) solids with an interaction between the aspirin and caffeine are obtained from Eqs. 7 and 8 using Eqs. 17, 18, and 20 (see text for definitions):

$$J_{ASA}(t) = k_{ASA}\frac{S_{ASA}}{S_{PH}}C^{\cdot}_{ASA} + k_{ASA\text{-}CAF}\frac{S_{ASA}}{S_{PH}}M_{ASA}\bar{C}^{\cdot}_{ASA\text{-}CAF} \quad \text{(Eq. A1)}$$

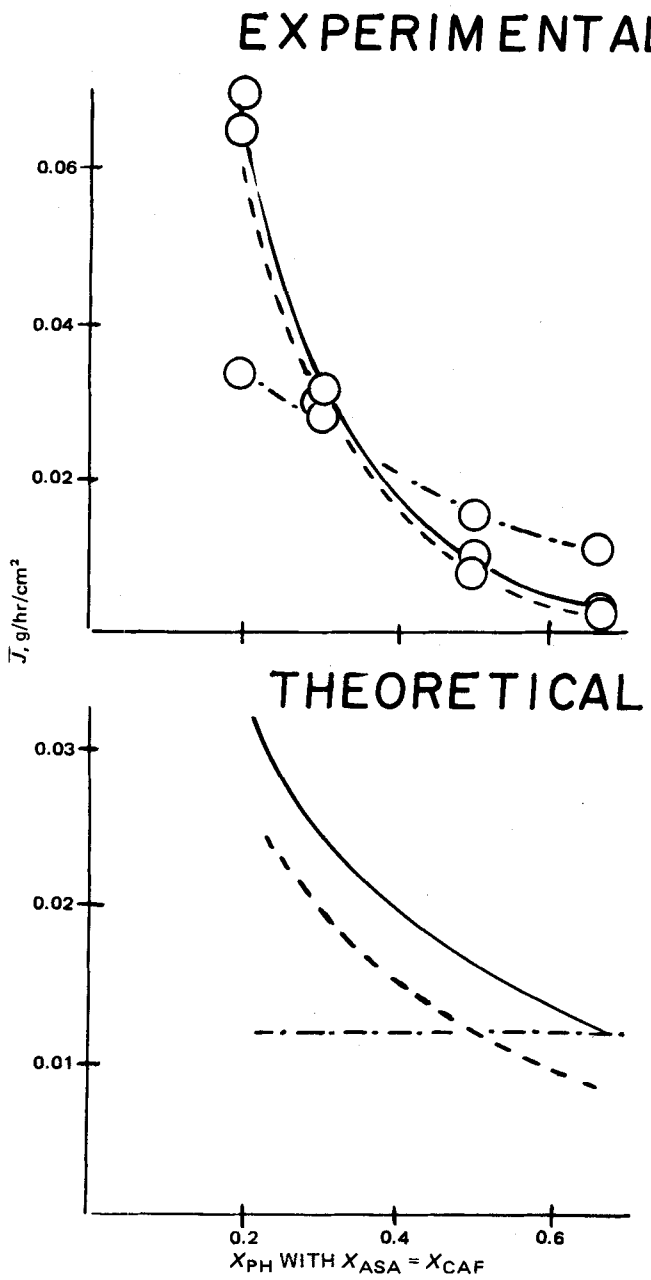


**Figure 14**—*Theoretical average and experimental fluxes of each component in a three-component, interacting system with equal mole fractions of aspirin and caffeine. Densities are given in Table II. Key: ---, aspirin; —, caffeine; and —·—, phenacetin.*

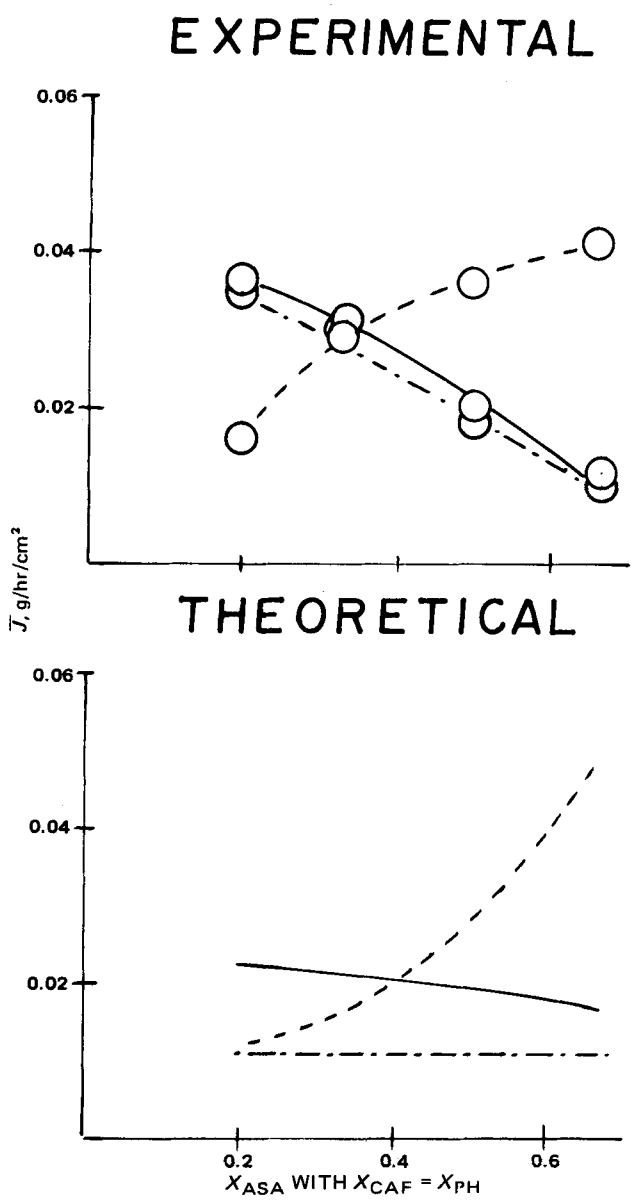


**Figure 15**—*Theoretical average and experimental fluxes of each component in a three-component, interacting system with equal mole fractions of caffeine and phenacetin. Densities are given in Table II. Key: ---, aspirin; —, caffeine; and —·—, phenacetin.*

$$J_{CAF}(t) = k_{CAF}\frac{S_{CAF}}{S_{PH}}C^{*}_{CAF} + k_{ASA\text{-}CAF}\frac{S_{CAF}}{S_{PH}}M_{CAF}\tilde{C}^{*}_{ASA\text{-}CAF} \quad \text{(Eq. A2)}$$

$$J_{PH}(t) = k_{PH}C^{*}_{PH} \quad \text{(Eq. A3)}$$

When phenacetin is the outer layer:

$$k_{ASA} = \frac{D_{ASA}}{h + r_{PH} - r_{ASA}} \quad \text{(Eq. A4)}$$

$$k_{CAF} = \frac{D_{CAF}}{h + r_{PH} - r_{CAF}} \quad \text{(Eq. A5)}$$

$$k_{PH} = \frac{D_{PH}}{h} \quad \text{(Eq. A6)}$$

and:

$$S_{ASA} = 4\pi r^2_{ASA} \quad \text{(Eq. A7)}$$

$$S_{CAF} = 4\pi r^2_{CAF} \quad \text{(Eq. A8)}$$

$$S_{PH} = 4\pi r^2_{PH} \quad \text{(Eq. A9)}$$

For the experimental conditions at 25°, the diffusivities and solubilities are given in Table III. The film thickness, $h$, was determined experimentally to be $30 \times 10^{-4}$ cm, and the equilibrium constant for a 1:1 aspirin–caffeine complex was taken as 17.4 liters/mole. With the use of these physical parameters and Eqs. A4–A9, Eqs. A1–A3 can be written as:

$$J_{ASA}(t) = \left(\frac{9.76 \times 10^{-8}}{30 \times 10^{-4} + r_{PH} - r_{ASA}}\right)\left(\frac{r_{ASA}}{r_{PH}}\right)^2 \text{g/cm}^2\text{/sec} \quad \text{(Eq. A10)}$$

$$J_{CAF}(t) = \left(\frac{2.22 \times 10^{-7}}{30 \times 10^{-4} + r_{PH} - r_{CAF}}\right)\left(\frac{r_{CAF}}{r_{PH}}\right)^2 \text{g/cm}^2\text{/sec} \quad \text{(Eq. A11)}$$

$$J_{PH}(t) = 3.3 \times 10^{-6}\ \text{g/cm}^2\text{/sec} \quad \text{(Eq. A12)}$$

As shown by these equations, the fluxes are dependent on the indi-

vidual radii. The equations describing the radii are obtained from Eq. 6:

$$-\frac{dr_{ASA}}{dt} = \frac{D_{ASA}C^*_{ASA} + D_{ASA\text{-}CAF}M_{ASA}\tilde{C}^*_{ASA\text{-}CAF}}{(h + r_{PH} - r_{ASA})X_{ASA}\rho} \quad \text{(Eq. A13)}$$

$$-\frac{dr_{CAF}}{dt} = \frac{D_{CAF}C^*_{CAF} + D_{ASA\text{-}CAF}M_{CAF}\tilde{C}^*_{ASA\text{-}CAF}}{(h + r_{PH} - r_{CAF})X_{CAF}\rho} \quad \text{(Eq. A14)}$$

$$-\frac{dr_{PH}}{dt} = \frac{D_{PH}C^*_{PH}}{hX_{PH}\rho} \quad \text{(Eq. A15)}$$

where:

$$X_{PH} + X_{ASA} + X_{CAF} = 1 \quad \text{(Eq. A16)}$$

At 25°, the equations can be written as:

$$-\frac{dr_{ASA}}{dt} = \frac{9.76 \times 10^{-8}}{(30 \times 10^{-4} + r_{PH} - r_{ASA})X_{ASA}\rho} \text{ cm/sec} \quad \text{(Eq. A17)}$$

$$-\frac{dr_{CAF}}{dt} = \frac{2.22 \times 10^{-7}}{(30 \times 10^{-4} + r_{PH} - r_{CAF})X_{CAF}\rho} \text{ cm/sec} \quad \text{(Eq. A18)}$$

$$-\frac{dr_{PH}}{dt} = \frac{3.33 \times 10^{-6}}{X_{PH}\rho} \text{ cm/sec} \quad \text{(Eq. A19)}$$

These equations are coupled ($r_{ASA}$ is a function of $r_{PH}$, *etc.*). For given values of $X_i$ and $\rho$, these equations can be solved simultaneously to yield $r_{ASA}$, $r_{CAF}$, and $r_{PH}$ as a function of time. A fourth-order Runge–Kutta procedure (8) was used in this study to solve these equations. When the radii are evaluated, the instantaneous fluxes may be calculated from Eqs. A10–A12. The average fluxes may be calculated using Eq. 12.

The equations describing the cases in which either aspirin or caffeine is the outer layer can be obtained similarly. The equations describing the hypothetical case in which aspirin and caffeine do not interact are obtained by setting $\tilde{C}^*_{ASA\text{-}CAF}$ to zero in these equations.

## REFERENCES


(1) E. Nelson, *J. Am. Pharm. Assoc., Sci., Ed.*, **46**, 607 (1957).

(2) M. Gibaldi and H. Weintraub, *J. Pharm. Sci.*, **57**, 832 (1968).

(3) W. I. Higuchi, N. A. Mir, and S. J. Desai, *ibid.*, **54**, 1405 (1965).

(4) S. A. Shah and E. L. Parrott, *ibid.*, **65**, 1784 (1976).

(5) E. L. Parrott, D. E. Wurster, and T. Higuchi, *J Am. Pharm. Assoc., Sci. Ed.*, **44**, 269 (1955).

(6) R. J. Braun and E. L. Parrott, *ibid.*, **61**, 175 (1972).

(7) S. A. Shah, Ph.D. thesis, University of Iowa, Iowa City, Iowa, 1975.

(8) B. Carnahan, H. A. Luther, and J. O. Wilkens, "Applied Numerical Methods," Wiley, New York, N.Y. 1969, pp. 361–365.

(9) T. Higuchi and D. A. Zuck, *J. Am. Pharm. Assoc., Sci. Ed.*, **42**, 138 (1953).


## ACKNOWLEDGMENTS


Abstracted in part from a dissertation submitted by S. A. Shah to the University of Iowa in partial fulfillment of the Doctor of Philosophy degree requirements.


# Reversed-Phase High-Pressure Liquid Chromatographic Analysis of Sulconazole in Plasma


**M. FASS ˣ, B. ZARO, M. CHAPLIN, and S. MATIN**



Received June 2, 1980, from *Syntex Research, Palo Alto, CA 94304.* Accepted for publication May 12, 1981.



**Abstract** □ A sensitive and specific analytical method for the measurement of sulconazole in plasma is described. The compound was extracted from plasma at pH 10 with hexane–methylene chloride. Samples were subjected to high-pressure liquid chromatography (HPLC) using an acetonitrile–phosphate buffer mixture as the mobile phase. The components of interest were measured using a variable-wavelength detector at 229 nm. Sulconazole concentrations of ≥0.5 μg/ml can be measured with confidence using this method. Linear calibration curves were constructed over the concentration range of 0.5–5 μg/ml for sulconazole from dog plasma. A dog was administered a single oral 1000-mg dose of tritiated sulconazole nitrate; total plasma radioactivity and sulconazole plasma levels determined by HPLC are reported.



**Keyphrases** □ Sulconazole—reversed-phase high-pressure liquid chromatographic analysis in plasma □ High-pressure liquid chromatography—analysis of sulconazole in plasma □ Antifungal agents—sulconazole, reversed-phase high-pressure liquid chromatographic analysis.


Sulconazole nitrate, 1-[β-(4″-chlorobenzylthio)-2′, 4′-dichlorophenethyl]imidazole mononitrate (I), is a potential new antimycotic agent[1] developed for human use. Since it is necessary to conduct animal toxicity studies supported by plasma level data for new drugs, a sensitive and specific analytical method was developed.

A high-pressure liquid chromatographic (HPLC) method for the determination of econazole, a structural analog of sulconazole, was described previously (1). Direct application of this extraction–injection method to sulconazole analysis provided unsatisfactory chromatography. Interfering peaks at the retention time of the compounds of interest were observed, and laborious distillation of ether prior to extraction to remove peroxides did not prevent random oxidative degradation of sulconazole.

This paper describes a reversed-phase HPLC method for the measurement of sulconazole in plasma using a structurally related analog as the internal standard. The method was applied to the measurement of sulconazole in the plasma of a dog given a single oral dose of 1000 mg of tritiated sulconazole nitrate.

## EXPERIMENTAL

**Reagents and Materials**—All solvents[2] were distilled-in-glass and liquid chromatography grade. All chemicals[1], available in-house, were analytical grade and were used without further purification. Inorganic reagents were prepared in purified water[3]. Standard solutions of sulconazole were prepared in methanol at the following concentrations: 40 μg/ml (stock solution) and 20, 16, and 4 μg/ml (spiking solutions). The internal standard solution was prepared in methanol at a concentration of 100 μg/ml. Solutions were stored at 4°. Standard solutions were prepared every 2 weeks.

[1] Syntex, Palo Alto, Calif.

[2] Burdick & Jackson Laboratories, Muskegon, Mich.

[3] Milli Q System, Millipore Corp., Bedford, Mass.




*0022-3549/81/1200-1338$01.00/0*



*© 1981, American Pharmaceutical Association*

vidual radii. The equations describing the radii are obtained from Eq. 6:

$$-\frac{dr_{ASA}}{dt} = \frac{D_{ASA}C^*_{ASA} + D_{ASA\text{-}CAF}M_{ASA}\tilde{C}^*_{ASA\text{-}CAF}}{(h + r_{PH} - r_{ASA})X_{ASA}\rho} \quad \text{(Eq. A13)}$$

$$-\frac{dr_{CAF}}{dt} = \frac{D_{CAF}C^*_{CAF} + D_{ASA\text{-}CAF}M_{CAF}\tilde{C}^*_{ASA\text{-}CAF}}{(h + r_{PH} - r_{CAF})X_{CAF}\rho} \quad \text{(Eq. A14)}$$

$$-\frac{dr_{PH}}{dt} = \frac{D_{PH}C^*_{PH}}{hX_{PH}\rho} \quad \text{(Eq. A15)}$$

where:

$$X_{PH} + X_{ASA} + X_{CAF} = 1 \quad \text{(Eq. A16)}$$

At 25°, the equations can be written as:

$$-\frac{dr_{ASA}}{dt} = \frac{9.76 \times 10^{-8}}{(30 \times 10^{-4} + r_{PH} - r_{ASA})X_{ASA}\rho} \text{ cm/sec} \quad \text{(Eq. A17)}$$

$$-\frac{dr_{CAF}}{dt} = \frac{2.22 \times 10^{-7}}{(30 \times 10^{-4} + r_{PH} - r_{CAF})X_{CAF}\rho} \text{ cm/sec} \quad \text{(Eq. A18)}$$

$$-\frac{dr_{PH}}{dt} = \frac{3.33 \times 10^{-6}}{X_{PH}\rho} \text{ cm/sec} \quad \text{(Eq. A19)}$$

These equations are coupled ($r_{ASA}$ is a function of $r_{PH}$, *etc.*). For given values of $X_i$ and $\rho$, these equations can be solved simultaneously to yield $r_{ASA}$, $r_{CAF}$, and $r_{PH}$ as a function of time. A fourth-order Runge–Kutta procedure (8) was used in this study to solve these equations. When the radii are evaluated, the instantaneous fluxes may be calculated from Eqs. A10–A12. The average fluxes may be calculated using Eq. 12.

The equations describing the cases in which either aspirin or caffeine is the outer layer can be obtained similarly. The equations describing the hypothetical case in which aspirin and caffeine do not interact are obtained by setting $\tilde{C}^*_{ASA\text{-}CAF}$ to zero in these equations.

## REFERENCES


(1) E. Nelson, *J. Am. Pharm. Assoc., Sci., Ed.*, **46**, 607 (1957).

(2) M. Gibaldi and H. Weintraub, *J. Pharm. Sci.*, **57**, 832 (1968).

(3) W. I. Higuchi, N. A. Mir, and S. J. Desai, *ibid.*, **54**, 1405 (1965).

(4) S. A. Shah and E. L. Parrott, *ibid.*, **65**, 1784 (1976).

(5) E. L. Parrott, D. E. Wurster, and T. Higuchi, *J Am. Pharm. Assoc., Sci. Ed.*, **44**, 269 (1955).

(6) R. J. Braun and E. L. Parrott, *ibid.*, **61**, 175 (1972).

(7) S. A. Shah, Ph.D. thesis, University of Iowa, Iowa City, Iowa, 1975.

(8) B. Carnahan, H. A. Luther, and J. O. Wilkens, "Applied Numerical Methods," Wiley, New York, N.Y. 1969, pp. 361–365.

(9) T. Higuchi and D. A. Zuck, *J. Am. Pharm. Assoc., Sci. Ed.*, **42**, 138 (1953).


## ACKNOWLEDGMENTS


Abstracted in part from a dissertation submitted by S. A. Shah to the University of Iowa in partial fulfillment of the Doctor of Philosophy degree requirements.


# Reversed-Phase High-Pressure Liquid Chromatographic Analysis of Sulconazole in Plasma


**M. FASS ˣ, B. ZARO, M. CHAPLIN, and S. MATIN**



Received June 2, 1980, from *Syntex Research, Palo Alto, CA 94304.* Accepted for publication May 12, 1981.



**Abstract** □ A sensitive and specific analytical method for the measurement of sulconazole in plasma is described. The compound was extracted from plasma at pH 10 with hexane–methylene chloride. Samples were subjected to high-pressure liquid chromatography (HPLC) using an acetonitrile–phosphate buffer mixture as the mobile phase. The components of interest were measured using a variable-wavelength detector at 229 nm. Sulconazole concentrations of ≥0.5 μg/ml can be measured with confidence using this method. Linear calibration curves were constructed over the concentration range of 0.5–5 μg/ml for sulconazole from dog plasma. A dog was administered a single oral 1000-mg dose of tritiated sulconazole nitrate; total plasma radioactivity and sulconazole plasma levels determined by HPLC are reported.



**Keyphrases** □ Sulconazole—reversed-phase high-pressure liquid chromatographic analysis in plasma □ High-pressure liquid chromatography—analysis of sulconazole in plasma □ Antifungal agents—sulconazole, reversed-phase high-pressure liquid chromatographic analysis.


Sulconazole nitrate, 1-[β-(4″-chlorobenzylthio)-2′, 4′-dichlorophenethyl]imidazole mononitrate (I), is a potential new antimycotic agent[1] developed for human use. Since it is necessary to conduct animal toxicity studies supported by plasma level data for new drugs, a sensitive and specific analytical method was developed.

A high-pressure liquid chromatographic (HPLC) method for the determination of econazole, a structural analog of sulconazole, was described previously (1). Direct application of this extraction–injection method to sulconazole analysis provided unsatisfactory chromatography. Interfering peaks at the retention time of the compounds of interest were observed, and laborious distillation of ether prior to extraction to remove peroxides did not prevent random oxidative degradation of sulconazole.

This paper describes a reversed-phase HPLC method for the measurement of sulconazole in plasma using a structurally related analog as the internal standard. The method was applied to the measurement of sulconazole in the plasma of a dog given a single oral dose of 1000 mg of tritiated sulconazole nitrate.

## EXPERIMENTAL

**Reagents and Materials**—All solvents[2] were distilled-in-glass and liquid chromatography grade. All chemicals[1], available in-house, were analytical grade and were used without further purification. Inorganic reagents were prepared in purified water[3]. Standard solutions of sulconazole were prepared in methanol at the following concentrations: 40 μg/ml (stock solution) and 20, 16, and 4 μg/ml (spiking solutions). The internal standard solution was prepared in methanol at a concentration of 100 μg/ml. Solutions were stored at 4°. Standard solutions were prepared every 2 weeks.

[1] Syntex, Palo Alto, Calif.

[2] Burdick & Jackson Laboratories, Muskegon, Mich.

[3] Milli Q System, Millipore Corp., Bedford, Mass.




*0022-3549/81/1200-1338$01.00/0*



*© 1981, American Pharmaceutical Association*

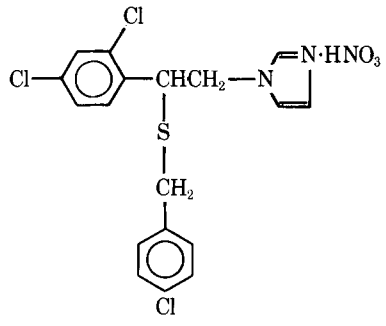

I

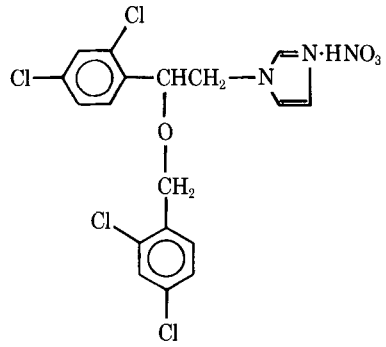

II

**Extraction**—Plasma (400 μl) was added to 400 μl of purified water in a 15-ml test tube. Samples were then fortified with the internal standard at the 12.5-μg/ml level (50 μl of 100 μg/ml of spiking solution) and made alkaline by the addition of 100 μl of 1 *N* potassium hydroxide. This mixture was extracted with 6 ml of hexane–methylene chloride (1:1). Tubes were shaken on a tilter for 3 min, and samples were then centrifuged[4] at 4000 rpm for 6 min. The upper organic layer was transferred to a 15-ml conical test tube and was blown to dryness under nitrogen. Samples were reconstituted in 100 μl of methanol, and 25 μl was injected onto the chromatograph.

**Preparation of Standard Curve**—Samples of control plasma were spiked with sulconazole at concentrations of 0.5, 1.0, 2.5, 4.0, and 5.0 μg/ml and with the internal standard at a fixed concentration of 12.5 μg/ml. Concentrations of sulconazole were calculated from calibration curves constructed by plotting the ratio of the peak height of sulconazole to the peak height of the internal standard *versus* the concentration of sulconazole spiked.

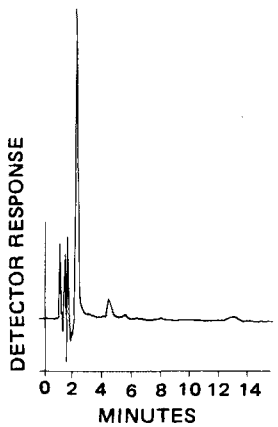


**Figure 1**—*Chromatogram of unfortified plasma. Conditions were a μBondapak $C_{18}$ column, acetonitrile–0.01 M $NaH_2PO_4$ buffer (pH 8.0) as the mobile phase, and a 2-ml/min flow rate.*

[4] Model HNS. IEC, Needham, Mass.

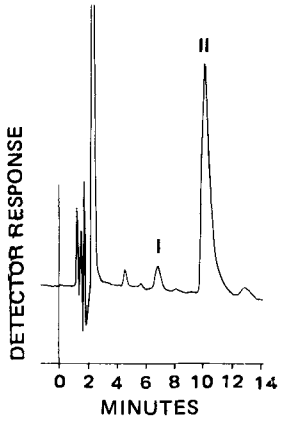


**Figure 2**—*Chromatogram of plasma fortified at the 0.5-μg/ml level with I and at the 12.5-μg/ml level with II.*

**HPLC and Chromatography Conditions**—A high-pressure liquid chromatograph[5] was equipped with a solvent programmer, an injector, and a spectrophotometric variable-wavelength detector[6] set at 229 nm. Samples were analyzed on a 4-mm × 30-cm reversed-phase column[7] fitted with a 4-mm × 8-cm precolumn[8]. The mobile phase was a solvent system of acetonitrile–0.01 *M* $NaH_2PO_4$ buffer (pH 8.0, 66:34), and the flow rate was 2 ml/min.

Each day, prior to sample injection, the column was equilibrated with mobile phase for ~20 min or until a level baseline was achieved. To check column suitability, a 25-μl aliquot of standard solution of sulconazole (20 μg/ml) and the internal standard (50 μg/ml) in methanol was injected onto the chromatograph under the described conditions. The suitability of the column was established by following three chromatographic parameters:

1. Resolution (R). The column was considered acceptable if the resolution of sulconazole and the internal standard was equal to or better than baseline separation or an *R* value of 1.5 as determined by the resolution equation (2).
2. Peak height ratio. A maximum variation of 5% for peak height ratio for injection on the same day was acceptable before major changes in the solvent system or column were implemented.
3. Retention time. The retention times for sulconazole and the internal standard were ~7 and 10 min, respectively. Retention times for replicate injections on a single day were not expected to vary by more than 5%.

**Figure 3**—*Chromatogram of plasma fortified at the 5-μg/ml level with I and at the 12.5-μg/ml level with II.*

**Figure 4**—*Chromatogram of plasma sample from a dog 6 hr after dosing with 1000 mg of tritiated sulconazole nitrate.*

[5] Model ALC/GPC-204 with U6K injector and model 660 solvent programmer, Waters Associates, Milford, Mass.
[6] Model 770, Schoeffel, Westwood, N.J.
[7] μBondapak $C_{18}$, Waters Associates, Milford, Mass.
[8] CoPell ODS, Whatman Inc., Clifton, N.J.

**Table I—Plasma Levels of Total Sulconazole Nitrate Radioequivalents and Concentration of Unchanged Drug in a Dog Given Tritium-Labeled Sulconazole Nitrate (1000 mg)**

| Hours after Dosing | Sulconazole Radioequivalents in Plasma, μg/ml | Unchanged Sulconazole, μg/ml |
|---|---|---|
| 0.5 | 1.150 | BDL[a] |
| 1.0 | 4.343 | 1.27 |
| 2.0 | 12.356 | 4.81 |
| 4.0 | 14.755 | 2.64 |
| 6.0 | 15.929 | 1.45 |
| 8.0 | 14.772 | 0.90 |
| 24.0 | 6.864 | BDL |
| 48.0 | 4.623 | BDL |
| 72.0 | 3.645 | BDL |
| 96.0 | 3.331 | BDL |
| 168.0 | 2.379 | BDL |

[a] Below detectable level.

**Dog Experiment**—A female beagle received 1000 mg (four capsules) of tritiated sulconazole nitrate after an overnight fast. A 20-ml water wash immediately followed the dose, and feeding was resumed 4 hr after dosing. Blood samples were drawn at 0.5, 1, 2, 4, 6, 8, 24, 48, 72, 96, and 168 hr following drug administration. Plasma levels of sulconazole nitrate radioequivalents and unchanged sulconazole were determined in these samples.

**Total Sulconazole Radioequivalent Determination**—Total sulconazole radioequivalents in dog plasma were determined by liquid scintillation spectrometry. Plasma samples of 0.1–0.2 ml were mixed with 10 ml of scintillation fluid[9]. Corrections were made for quenching and machine[10] efficiency by the automatic external standard method.

## RESULTS AND DISCUSSION

A sensitive and specific HPLC method was developed that utilized the natural 229-nm UV-absorbing property of sulconazole, measuring levels of ≥0.5 μg/ml.

A structurally similar compound miconazole nitrate 1-[2-(2,4-dichlorophenyl)-2-(2,4-dichlorobenzyloxy)ethyl]imidazole mononitrate (II), was used as the chromatographic internal standard. This compound possesses UV, extraction, and chemical properties similar to sulconazole and was chromatographically resolved under the described conditions.

Good chromatography was achieved by employing a relatively nonpolar extracting solvent containing no oxidants and a solvent system at a slightly basic pH. Reproducibility of this method was shown by construction of calibration curves over the concentration range of 0.5–5.0 μg/ml. The coefficients of variation obtained for the calibration curve points were 3.92, 2.05, 1.20, 2.5, and 1.09%, respectively (n = 5). A chromatogram of an unfortified plasma sample is shown in Fig. 1. Chromatograms of plasma samples fortified with 0.5 and 5 μg/ml of sulconazole are shown in Figs. 2 and 3, respectively. A chromatogram of a plasma sample taken from a dog 6 hr after oral dosing with a 1000-mg capsule of sulconazole nitrate is shown in Fig. 4.

A plasma sample from a dog dosed with sulconazole was extracted with methanol and subjected to TLC. An authentic sulconazole standard was run alongside on the same plate. The plate was developed with an ammonium hydroxide–chloroform–methanol system (1:99:1). After drying, 1-cm sections of the plate were scraped into liquid scintillation vials and counted for radioactivity. Based on $R_f$ values, it was determined that the percentage of radioactivity at the sulconazole $R_f$ value represented the same fraction of the total radioactivity as the level of sulconazole obtained by HPLC. These TLC data support the identity of the HPLC peak at the retention time of sulconazole.

[9] Oxifluor-$H_2O$, New England Nuclear, Boston, Mass.
[10] Scintillation counter, Packard Instrument Co., Chicago, Ill.

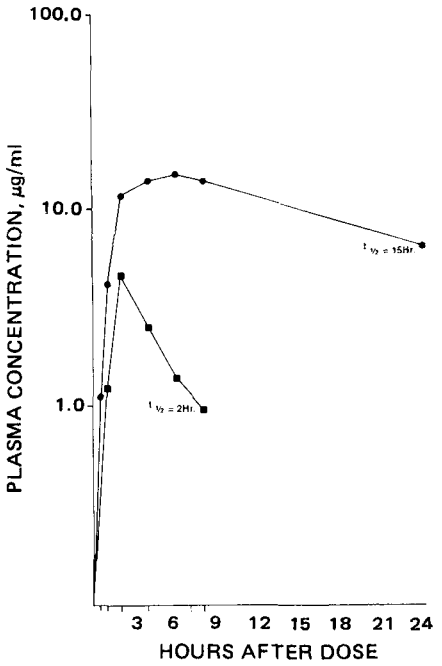


**Figure 5**—*Plasma levels of total sulconazole nitrate radioequivalents (●) and concentration of unchanged drug (■) in a dog given 1000 mg of tritium-labeled sulconazole nitrate.*

The overall recovery of sulconazole through the method was established by spiking plasma with tritiated sulconazole and processing the samples through the procedure. Radioactivity in the sample prior to injection onto the chromatograph was determined, and the recovery of sulconazole was 85%.

The developed method was applied to the analysis of plasma samples from a dog dosed with 1000 mg of tritiated sulconazole nitrate. Concentrations of total sulconazole radioequivalents and unchanged sulconazole in plasma are shown in Table 1 and Fig. 5. The peak unchanged sulconazole plasma level occurred at 2 hr following dose administration, and the peak total sulconazole radioequivalent level occurred at 6 hr after dosing. The half-life of unchanged sulconazole in this dog was 2 hr. The half-life observed for the total sulconazole radioequivalents was 15 hr. The data demonstrate that in the one animal studied, orally administered sulconazole is rapidly and extensively metabolized.

## REFERENCES

(1) R. Brodie, L. Chasseaud, and L. Walmsley, *J. Chromatogr.*, **155**, 209 (1978).

(2) "Basic Gas Chromatography," 5th ed., H. M. McNair and E. J. Bonelli, Eds., Consolidated Printers, Berkeley, Calif., 1967, p. 33.

## ACKNOWLEDGMENTS

The authors acknowledge Dr. Howard Parnes for synthesis of the tritiated sulconazole nitrate and Leigh Ann Wolfe for assistance with manuscript preparation.

# Relative Bioavailability of Aspirin Gum

**D. W. WOODFORD** * **and L. J. LESKO** ‡x

Received July 28, 1980, from the *College of Pharmacy, Rutgers University, New Brunswick, NJ 08854, and the ‡Drug Concentration Laboratory, University of Massachusetts Medical Center, Worcester, MA 01605. Accepted for publication April 8, 1981.

**Abstract** □ The bioavailability of aspirin gum relative to unbuffered aspirin tablets was determined in six normal volunteers. Twenty-four hours following the administration of two aspirin tablets, 91.2 ± 1.7 % (*SE*) of the 648-mg dose was recovered in the urine. The relative bioavailability of aspirin gum was 69.5 ± 3.4 % (*SE*), based on cumulative 24-hr urinary excretion of total salicylate after the chewing of three gum tablets for 15 min. The chewed gum was analyzed for total salicylate and contained an average of 37.8% of the administered dose. When added to the cumulative amount of total salicylate excreted in the urine at 24 hr after dosing, the salicylate contained in the chewed gum accounted for essentially 100% of the dose administered. Chewing aspirin gum for up to 30 min did not significantly ($p > 0.05$) reduce the amount of salicylate entrapped in the gum base when compared to chewing times of 5, 10, and 15 min. Based on the results of this study, four pieces of aspirin gum would be needed to provide the same amount of salicylate to the general circulation as two 324-mg aspirin tablets.

**Keyphrases** □ Aspirin gum—relative bioavailability compared to unbuffered aspirin tablets in six normal volunteers □ Bioavailability—aspirin gum compared to unbuffered aspirin tablets in six normal volunteers □ Dosage forms—comparison of salicylate availability from aspirin gum and unbuffered aspirin tablets

Aspirin is the most frequently used nonprescription analgesic, and selection of an aspirin product should be based on formulation preference and proven efficacy (1). Bioavailability studies have been conducted on many dosage forms of aspirin including aqueous solutions (2, 3), compressed tablets (4, 5), effervescent tablets (6, 7), controlled-release tablets (8), enteric-coated tablets (9–11), and rectal suppositories (12). These studies have shown that the bioavailability differences between products apparently are related to formulation factors. Recognizing the potential for therapeutic inequivalence, the American Pharmaceutical Association published a bioavailability monograph for aspirin (13).

One aspirin product omitted from this bioavailability monograph was aspirin chewing gum[1]. There have been no reported investigations in humans of the relative bioavailability of aspirin from gum formulations. Aspirin gum was introduced commercially in 1924; in 1976, the total sale of aspirin gum was nearly 80 million gum pieces[2]. The label claims for aspirin gum include "for the temporary relief of minor sore throat pain, headache, aches and pains of colds and flu and muscular aches and pains." The efficacy of aspirin gum as a systemic analgesic is dependent on the rate and extent of aspirin bioavailability.

This investigation evaluated the relative bioavailability of aspirin gum by comparing the urinary excretion of total salicylate after dosing with aspirin gum and regular aspirin tablets.

## EXPERIMENTAL

**Subjects**—Six male volunteers, 18–31 years of age (27.3 ± 1.5 years, mean ± *SE*) were selected. The study was approved by the institutional human studies review committee and valid, written, informed consent was obtained from each volunteer prior to his entering the study. The mean (±*SE*) body weight of the volunteers was 72.9 (±5.6) kg, and each volunteer was within 10% of his ideal body weight for his height and build (14). Each volunteer was determined to be in good physical health with no history of aspirin allergy, GI tract ulcers, or cardiac, hepatic, or renal disease.

The volunteers were instructed to refrain from taking any medication for at least 7 days prior to the study and to abstain from alcoholic beverages for 24 hr prior to dosing. All volunteers fasted, with the exception of water, for 12 hr prior to dosing, and fasting was continued for 4 hr after dosing. On the evening before each study day, the volunteers were instructed to empty their bladders and to drink 180 ml of water. Upon arising, the volunteers again emptied their bladders and drank 180 ml of water at 1 and 0.5 hr prior to dosing.

**Drug Administration**—On the 1st study day, the volunteers were assigned at random either the aspirin gum[3] or the aspirin tablets[4]; on the 2nd study day, the volunteers received the alternate formulation. The 2 study days were separated by a washout period of 7 days. At 8 am on each study day, the volunteers assigned the gum chewed three pieces (226.8 mg of aspirin/gum piece; total aspirin dose of 680.4 mg) for 15 min, swallowing saliva and any fragments of coating loosened by the chewing process. After chewing was completed, the gum was expectorated into a plastic vial and frozen at −20° for later salicylate analysis, and the volunteers were instructed to drink 120 ml of water. The volunteers assigned the aspirin tablets swallowed two tablets (324 mg of aspirin/tablet; total aspirin dose of 648 mg) with 120 ml of water. Previous replicate analysis for potency showed the gum and tablet to contain 98 and 105% of the label claim, respectively. To promote adequate urine flow, all volunteers were instructed to drink 180 ml of water 2 hr following the administration of each dosage form.

**Urine Collection**—Immediately before dosing, the volunteers emptied their bladders completely and an aliquot of the blank urine was collected and frozen at −20°. After dosing, urine was collected by complete voiding at 1, 2, 3, 4, 6, 8, 10, 12, and 24 hr. The volume and pH of voided urine were measured at each collection time, and an aliquot was frozen at −20° for salicylate analysis.

**Effect of Chewing Time**—Four of the six volunteers included in the bioavailability study were instructed to chew three aspirin gum pieces for 5, 10, 15, or 30 min, respectively, on 4 separate days. After chewing, the gum was expectorated into a plastic vial and the amount of salicylate remaining in the chewed gum was measured to determine if chewing time influenced salicylate release from the gum.

**Assay of Total Salicylate in Urine**—The total amount of salicylate in the urine samples was measured using the procedure of Chiou and Onyemelukwe (15). Briefly, 3.0 ml of urine and 2.0 ml of concentrated hydrochloric acid were added to a 50-ml culture tube, which was then incubated at 100° for 17 hr. After cooling to room temperature, 6.0 ml of chloroform was added to the tube and the mixture was shaken mechanically for 10 min. Following centrifugation, 3.0 ml of the chloroform was added to 6.0 ml of Trinders reagent (without mercuric chloride). After vortex mixing, the absorbance of the upper, aqueous phase was measured at 540 nm[5].

The concentration of salicylate in the urine sample was determined from a standard curve prepared by measuring the absorbance of sodium salicylate solutions of known concentrations after subjecting them to the described procedure. Each urine sample was analyzed in duplicate, and the average value was used to calculate the amount of total salicylate excreted during each collection interval. Urine blanks, urine standards spiked with known amounts of sodium salicylate, and aqueous sodium salicylate standard solutions were assayed with each batch of the vol-

[1] Aspergum, Plough, Memphis, TN 38151.
[2] Mr. McGee, personal communication, Plough, Memphis, TN 38151.
[3] Aspergum, lot 6060.
[4] Bayer aspirin tablets, lot 6L176, Glenbrook Laboratories, Division of Sterling Drug Inc., New York, NY 10016.
[5] DBGT spectrophotometer, Beckman Instruments, Irvine, Calif.

0022-3549/81/1200-1341$01.00/0
© 1981, American Pharmaceutical Association

**Table I—Mean ± *SE* Cumulative Amounts of Total Salicylate (Expressed as Milligrams of Aspirin Equivalents) Excreted in the Urine after Administration of Aspirin Gum or Tablets**

| Hours | Aspirin Excreted, mg: Gum (680.4-mg Dose) | Aspirin Excreted, mg: Tablet (648-mg Dose) |
|---|---|---|
| 1 | 30.7 ± 4.0 | 23.1 ± 3.9 |
| 2 | 66.3 ± 8.0 | 63.7 ± 6.2 |
| 3 | 114.0 ± 11.1 | 111.6 ± 7.2 |
| 4 | 166.0 ± 16.2 | 153.8 ± 11.6 |
| 6 | 244.0 ± 23.1 | 242.1 ± 17.9 |
| 8 | 296.8 ± 24.1 | 324.8 ± 25.1 |
| 10 | 347.0 ± 25.9 | 387.6 ± 28.1 |
| 12 | 385.3 ± 25.8 | 462.9 ± 28.0 |
| 24 | 433.6 ± 19.8 | 592.6 ± 11.1 |

unteer's urine samples as a quality control check. The total salicylate measured in the urine samples was converted to milligrams of aspirin by multiplying by 1.125.

**Assay of Total Salicylate in Chewed Gum**—The amount of salicylate contained in chewed gum was determined as follows. The chewed gum was placed in a flask containing 50 ml of 1 *N* HCl, heated to 100°, and stirred for 1 hr. After cooling to room temperature, the mixture was centrifuged and the hydrochloric acid was removed and diluted to 100 ml with 1 *N* HCl. This solution was diluted 1:100, and the absorbance of this diluted solution was measured spectrophotometrically at 240 nm. The concentration of salicylate in the solution was determined from a standard curve constructed by subjecting sodium salicylate solutions of known concentration to the same procedure previously described.

The absorbance spectrum of the salicylate solution obtained from the gum analysis was compared to the absorbance spectrum of a standard solution of sodium salicylate. There were no differences between the spectra in the general shape of the curves or the wavelengths where maxima and minima occurred, indicating that the observed absorbance was due to salicylate. The amount of salicylate recovered from the gum was converted to milligrams of aspirin by multiplying by 1.125.

**Bioavailability Calculations**—The relative bioavailability of aspirin gum ($F_{rel}$) was calculated as the percentage of aspirin equivalent eliminated in the urine in the 24 hr ($U_\infty$) following the administration of each dosage form after correcting for the dose ($D$) of aspirin administered:

$$F_{rel}(\%) = \left[\frac{U_\infty \text{ (gum)}}{U_\infty \text{ (tablet)}}\right]\left[\frac{D \text{ (tablet)}}{D \text{ (gum)}}\right] \times 100 \qquad \text{(Eq. 1)}$$

**Statistical Analysis**—A paired $t$ test was used to determine the significance of differences in the mean total aspirin bioavailability between the gum and the tablet, respectively. A one-way analysis of variance was used to determine the significance of the effect of chewing time on the amount of aspirin recovered from chewed gum.

## RESULTS AND DISCUSSION

Table I lists the mean ± *SE* amounts of total salicylate (in terms of equivalent aspirin) excreted in the urine at various intervals up to 24 hr following dosing. After tablet administration, a mean ± *SE* of 91.2 ± 1.7% of the aspirin dose was recovered in the urine. This percentage of dose recovered is consistent with the values reported by other investigators (16, 17) who recovered virtually 100% of the aspirin dose as metabolites in the urine. The analytical method used in this study to measure total salicylate in urine accounts for aspirin, salicylic acid, and all other metabolities. Collection of total urine for 24 hr also provides enough time for recovery of essentially all of the dose based on a plasma elimination half-life of salicylate of 3 hr after a single dose of ~650 mg (18). When aspirin gum was chewed, only 63.5 ± 2.9% (mean ± *SE*) of the dose was recovered.

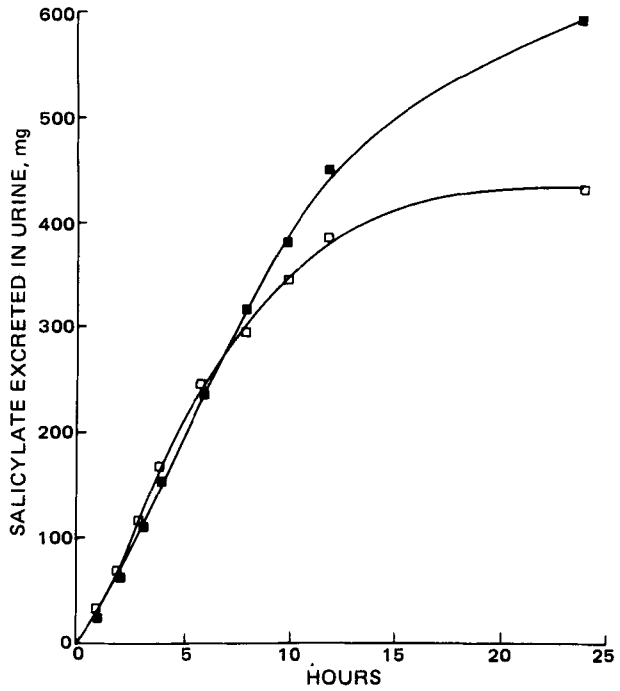


**Figure 1**—*Mean cumulative urinary salicylate (expressed as milligrams of aspirin) excretion curves for six subjects following administration of three aspirin gum pieces (680.4 mg) (□) or two aspirin tablets (648 mg) (■).*

Figure 1 shows the mean cumulative urinary excretion curves for six subjects following administration of gum and tablet dosage forms. Differences in the rate and extent of bioavailability are reflected in the shape of the curves. For up to 6 hr following dosing, the curves are practically superimposable, so it may be concluded that the dosage forms are bioequivalent in terms of bioavailability rate. However, beyond 6 hr, both curves begin to diverge and approach different asymptotic values. The total amounts (mean ± *SE*) of aspirin equivalent excreted in the urine 24 hr following the administration of the tablets and the gum were 592.6 ± 11.2 and 433.6 ±19.8 mg, respectively. The difference between dosage forms in the total amount of salicylate excreted shows that the extent of aspirin gum bioavailability was less than that of aspirin tablets.

The individual cumulative amount of total salicylate recovered in the urine at 24 hr following dosing and the relative bioavailability of aspirin gum are shown in Table II. The differences in total salicylate recovered in the urine were significant ($p < 0.05$), and the bioavailability of aspirin gum ranged from 61.0 to 81.0% (mean ± *SE* of 69.5 ± 3.4%). Since the renal clearance of free salicylate is pH dependent, urine pH possibly may influence the excretion pattern of aspirin metabolites and affect the evaluation of aspirin bioavailability. The pH of each urine sample col-

**Table II—Individual Cumulative Amounts of Total Salicylate (Expressed as Milligrams of Aspirin Equivalents) Excreted in the Urine 24 hr after Administration of Gum and Tablets and the Relative Bioavailability of Aspirin Gum**

| Subject | $U_\infty$, Gum[a], mg | $U_\infty$, Tablet[b], mg | $F_{rel}$, % |
|---|---|---|---|
| A | 410.8 | 587.7 | 67.6 |
| B | 497.2 | 586.7 | 81.0 |
| C | 460.1 | 565.1 | 77.1 |
| D | 369.0 | 572.2 | 61.0 |
| E | 466.1 | 634.7 | 69.5 |
| F | 398.4 | 618.2 | 61.0 |
| Mean | 433.6 | 592.6 | 69.5 |
| ±*SE* | 19.8 | 11.2 | 3.4 |

[a] Oral dose, 680.4 mg. [b] Oral dose, 648 mg.

**Table III—Total Amount of Salicylate (in Milligrams of Aspirin) Recovered in the Chewed Gum and Cumulative 24-hr Urine Collection after Administration of Three Aspirin Gum Pieces (680.4)**

| Subject | Gum, mg | Urine, mg | Total, mg |
|---|---|---|---|
| A | 263.3 | 410.8 | 674.1 |
| B | 249.8 | 497.2 | 747.0 |
| C | 222.4 | 460.1 | 682.5 |
| D | 345.2 | 369.0 | 714.2 |
| E | 204.5 | 466.1 | 670.6 |
| F | 259.5 | 398.4 | 657.9 |
| Mean | 257.5 | 433.6 | 691.1 |
| ±*SE* | ±19.8 | ±19.8 | ±13.6 |

**Table IV—Amount of Salicylate (in Milligrams of Aspirin) Remaining in Chewed Aspirin Gum after the Chewing of Three Gum Pieces (680.4 mg) by Four Volunteers**

| Chewing time, min | Volunteer | | | | Mean ± *SE* |
|---|---|---|---|---|---|
| | A | B | C | D | |
| 5 | 195.4 | 280.7 | 301.7 | 385.4 | 290.8 ± 39.0 |
| 10 | 250.0 | 177.1 | 279.7 | 216.8 | 230.9 ± 22.0 |
| 15 | 213.6 | 261.9 | 276.5 | 202.2 | 238.6 ± 18.2 |
| 30 | 170.4 | 209.5 | 217.0 | 242.1 | 209.8 ± 14.9 |

lected during the study was recorded, and average pH values of all urine samples collected following administration of the tablet and gum were 6.1 and 6.3, respectively. The differences in urine pH between the two sets of urine samples were not significant ($p > 0.05$) using a paired $t$ test, and it was concluded that urine pH did not influence the determination of relative bioavailability.

The amounts of salicylate remaining in the gum for each individual volunteer after chewing for 15 min are listed in Table III. The average amount of salicylate remaining in the gum represents 37.8% of the dose administered. When added to the 24-hr urinary recovery of salicylate, the amount of total salicylate in the chewed gum mass accounted for 101.6 ± 2.0% (mean ± *SE*) of the administered dose. Therefore, it may be concluded that the difference in the extent of bioavailability between aspirin gum and tablets is due to salicylate becoming entrapped or bound to the gum base during chewing.

Table IV shows the effect of chewing time on the amount of salicylate retained in the gum base. After 5 min, the average amount of salicylate in the chewed gum was equivalent to 42.7% of the administered dose. For chewing times of 10, 15, and 30 min, the average percentages of dose remaining in the gum between 5 min and the other chewing times were not significant ($p > 0.05$); therefore, the use of a 15-min chewing time in the bioavailability study did not influence the determination of relative bioavailability.

In aspirin bioavailability studies where single doses in excess of ~500 mg are used, consideration must be given to the possible effects of dose-dependent kinetics on the determination of relative bioavailability. This is particularly crucial in bioavailability studies based on the measurement of serum salicylate concentrations where dose-dependent kinetics may influence the shape of the serum concentration–time curve and possibly bias bioavailability calculations. In this study, total aspirin bioavailability for the gum and tablet was determined in terms of salicylate by analysis of total salicylate recovery in the urine for up to 24 hr. This type of bioavailability study design for aspirin eliminates any bias due to dose-dependent kinetics. In addition, measurement of total salicylate in the urine provides the most accurate estimation of total bioavailability because it masks intra- and interpatient variability in rates of salicylate absorption and metabolism which may affect the size and shape of a serum salicylate–time curve (19).

Since few studies have correlated relative bioavailability with relative therapeutic efficacy, the clinical significance of the inferior bioavailability of aspirin gum is unclear. However, many studies have shown aspirin to be superior to placebo in the treatment of pain, and it is generally thought that the onset and magnitude of pain relief are a function of the rate and extent of aspirin bioavailability from its dosage form. No published studies document the effectiveness of aspirin gum as a systemic analgesic, and, based on the data presented in this report, it may be concluded that two 324-mg aspirin tablets will provide as much salicylate to the general circulation as four 227-mg aspirin gums. Furthermore, the usual recommended adult dose of aspirin gum which is two pieces, is less than the minimum therapeutic dose of 324 mg.

## REFERENCES


(1) "Handbook of Nonprescription Drugs," 6th ed., American Pharmaceutical Association, Washington, D.C., 1979, p. 125.

(2) M. Rowland, S. Riegelman, P. A. Harris, S. D. Sholkoff, and E. J. Eyring, *Nature*, **215**, 413 (1976).

(3) M. Rowland, S. Riegelman, P. A. Harris, and S. D. Sholkoff, *J. Pharm. Sci.*, **61**, 379 (1972).

(4) W. L. Chiou and I. Onyemelukwe, *J. Clin. Pharmacol.*, **14**, 597 (1974).

(5) M. J. Rance, B. J. Jordan, and J. D. Nichols, *J. Pharm. Pharmacol.*, **27**, 425 (1975).

(6) J. R. Leonards, *Clin. Pharmacol. Ther.*, **4**, 476 (1963).

(7) G. Ekenved, R. Elofsson, and L. Solvell, *Acta Pharm. Suec.*, **12**, 323 (1975).

(8) L. E. Hollister and S. L. Kanter, *Clin. Pharmacol. Ther.*, **6**, 5 (1965).

(9) A. B. Morrison and J. A. Campbell, *J. Am. Pharm. Assoc., Sci Ed.*, **49**, 473 (1960).

(10) G. Levy and L. E. Hollister, *N.Y. State J. Med.*, **64**, 3002 (1964).

(11) R. L. Clark and L. Lasagna, *Clin. Pharmacol. Ther.*, **6**, 568 (1965).

(12) M. M. Nowak, B. Brundhofer, and M. Gibaldi, *Pediatrics*, **54**, 23 (1974).

(13) M. Mayersohn, *J. Am. Pharm. Assoc.*, **NS 17**, 107 (1977).

(14) "Metropolitan Life Insurance: Desirable Weights of Adults," Statistical Bulletin 40, New York, N.Y., 1959.

(15) W. L. Chiou and I. Onyemelukwe, *J. Pharm. Sci.*, **63**, 630 (1974).

(16) G. Levy, T. Tsuchiya, and L. P. Amsel, *Clin. Pharmacol. Ther.*, **13**, 285 (1972).

(17) G. Levy and T. Tamehiro, *Clin. Pharmacol. Ther.*, **13**, 317 (1972).

(18) G. Levy, *J. Pharm. Sci.*, **54**, 959 (1965).

(19) G. Levy and L. E. Hollister, *ibid.*, **53**, 1446 (1964).


## ACKNOWLEDGMENTS


Presented at the Basic Pharmaceutics Section, APhA Academy of Pharmaceutical Sciences, Kansas City Meeting, November 1979.

Abstracted in part from a thesis submitted by D. W. Woodford to the Massachusetts College of Pharmacy in partial fulfillment of the Master of Science degree requirements.

The assistance of the Word Processing Center in the preparation of the manuscript is gratefully acknowledged.

# Influence of Administration Route on Drug Delivery to a Target Organ

**SVEIN ØIE** ˣ **and JIN-DING HUANG**

Received November 3, 1980, from the *Department of Pharmacy, School of Pharmacy, University of California, San Francisco, CA 94143.* Accepted for publication April 16, 1981.

**Abstract** □ Mathematical relationships describing the delivery of drug to a target organ after intra-arterial, intravenous, and oral administration are presented. This discussion clearly demonstrates that administration into a blood vessel leading to the target organ often is superior to intravenous administration. However, this superiority is not clear from traditional plasma concentration monitoring data.

**Keyphrases** □ Drug delivery—to a target organ, influence of administration route, mathematical relationships □ Administration routes—influence on drug delivery to a target organ, mathematical relationships □ Mathematical models—influence of administration route on drug delivery to a target organ

When the rate and extent of drug absorption is of concern, the first choice for drug delivery is usually the intravenous route. Intravenous administration delivers drug directly into the bloodstream and virtually assures almost immediate delivery to the target organ(s). Because there is no drug loss at the administration site, a drug delivered intravenously is considered to be completely available to the body. However, if a drug were to precipitate during an intravenous injection due to poor solubility in plasma, distribution of the drug would be delayed. The precipitated drug would eventually redissolve and be distributed to the remainder of the body. Thus, the site of precipitation can be viewed as a site of retention rather than a site of loss.

Although no drug is lost at the administration site, there exists the possibility for drug loss in the body prior to its reaching the site of measurement or the target organ. For example, if a drug is administered intravenously, the drug must first traverse the lungs before it can be further distributed in the body. Thus, any drug eliminated in the lungs reduces the amount of drug available to the other organs (1). Furthermore, only a fraction of the drug not metabolized by the lungs leaves the left ventricle for the target organ. The remaining drug leaving the left ventricle circulates to other tissues and organs where elimination can occur before recirculation to the target organ is possible.

One way to circumvent the potential for drug loss is to administer the drug intra-arterially, *i.e.*, directly into an artery leading to the target organ (2, 3). Although intra-arterial injections are more difficult than venipuncture to perform, as well as being more uncomfortable for the patient, it is sometimes the preferred route (3–7). Intra-arterial drug administration ensures that the entire dose administered will reach the target organ.

Because little information exists in this area, no clearcut parameters have been established to determine the superiority of one administration route over another. Utilization of pharmacokinetic principles may prove to be useful.

The following report discusses mathematical relationships describing: (*a*) the amount of drug delivered to the target organ by both intra-arterial and intravenous administration routes, and (*b*) the amount of drug reaching the liver after an oral dose if the liver is the target organ. This latter situation parallels that of an intra-arterial injection into an artery leading to a target organ except that the drug must traverse the GI tract where loss can occur prior to its reaching the liver.

## KINETIC MODEL

A flow model for drug disposition, described in Scheme I, is used in this discussion. Compartment 1 is the lungs, receiving blood from the right ventricle; compartments 2 through $n$ represent the remainder of the body, compartmentalized and receiving blood from the left ventricle. Compartments 2 through $m$ are all capable of eliminating the drug and comprise the liver (Compartment 3), the mesenteric vascular bed (Compartment 2), the kidneys, *etc.*; compartment $m + 1$ to $n$ represents the organs and tissues incapable of eliminating the drug and are, therefore, considered to be storage compartments.

The blood clearance of any compartment ($Cl_i$) reflects the elimination rate with respect to the whole blood concentration entering the compartment ($C_{in}$) and not the concentration in the compartment itself (which would represent the intrinsic clearance of the compartments). From steady-state values, this is expressed as:

$$Cl_i = \left(\frac{dA_i/dt}{C_{in}}\right)_{ss} \qquad \text{(Eq. 1)}$$

where $dA_i/dt$ is the rate of elimination in compartment $i$, and $ss$ denotes steady-state conditions. More important, however, is the fact that clearance can be determined from the total amount eliminated from time zero to time infinity by the organ $[\int_0^\infty (dA_i/dt)\,dt]$ and the total area under the blood concentration *versus* time-curve from time zero to time infinity ($\int_0^\infty C_i\,dt$) entering the organ; *i.e.*:

$$Cl_i = \frac{\int_0^\infty (dA_i/dt)\,dt}{\int_0^\infty C_{in}\,dt} \qquad \text{(Eq. 2)}$$

Therefore, the arterial concentration (or left ventricle concentration) is used as a reference blood concentration for most organs. This procedure is identical to using the venous blood concentration from a storage compartment as the reference concentration. However, pulmonary clearance is defined with respect to the right ventricle concentration, although it is relatively easy to convert pulmonary clearance from its present definition ($Cl'_1$) to one with respect to left ventricle concentration ($Cl_1$) by using the following relationship:

$$Cl_1 = Cl'_1 \Big/ \left(1 - \frac{Cl'_1}{Q_1}\right) \qquad \text{(Eq. 3)}$$

where $Q_1$ is the pulmonary blood flow that is equal to the total cardiac output ($Q_C$). If the pulmonary clearance is low, the two clearances are essentially the same. Only if the pulmonary clearance is large is it necessary to make the conversion.

**Intra-Arterial Injection into Artery Leading to Target Organ**—If the target organ is $m$, the amount delivered to this organ ($A_{E,m}$) from time zero to time infinity is equal to:

$$A_{E,m} = D + \int_0^\infty C_L Q_m\,dt \qquad \text{(Eq. 4)}$$

where $D$ is the dose administered, $C_L$ is the left ventricle blood concentration, and $Q_m$ is the blood flow to the target organ. Blood flow is assumed to be time and concentration independent. The term $\int_0^\infty C_L\,dt$ can be obtained by the following development:



*0022-3549/81/1200-1344$01.00/0*
*© 1981, American Pharmaceutical Association*

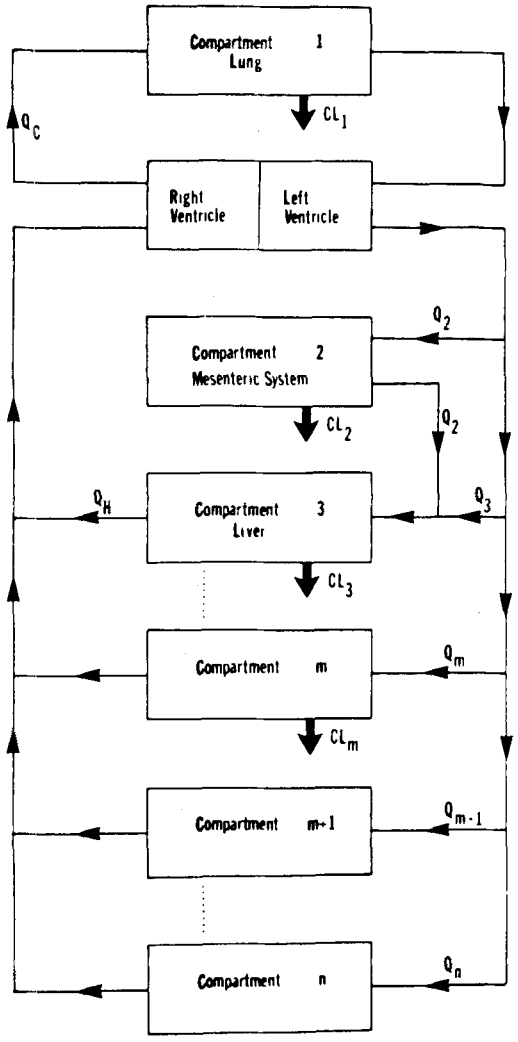


*Scheme I—Pharmacokinetic model of drug disposition.*

The fraction ($F_{L,i}$) of the drug delivered to an eliminating organ that leaves the same compartment is:

$$F_{L,i} = 1 - \text{fraction lost} = 1 - \frac{A_{\text{lost},i}}{A_{E,i}} = 1 - \frac{\int_0^\infty (dA_i/dt)\,dt}{\int_0^\infty Q_i C_{\text{in}}\,dt} \qquad \text{(Eq. 5)}$$

From Eqs. 2 and 5:

$$F_{L,i} = 1 - \frac{Cl_i}{Q_i} \qquad \text{(Eq. 6)}$$

The amount leaving the left ventricle ($A_{L,L}$) from time 0 to time infinity is equal to:

$$A_{L,L} = \sum_{i=2}^{m} \int_0^\infty C_L Q_i\,dt = Q_C \int_0^\infty C_L\,dt \qquad \text{(Eq. 7)}$$

where $Q_C$ is the cardiac output.

The total amount entering the left ventricle ($A_{E,L}$) is expressed by:

$$A_{E,L} = \int_0^\infty C_R Q_C \left(1 - \frac{Cl_1'}{Q_C}\right) dt = (Q_C - Cl_1') \int_0^\infty C_R\,dt \qquad \text{(Eq. 8)}$$

where $C_R$ is the blood concentration in the right ventricle. The amount leaving the right ventricle ($A_{L,R}$) can be expressed by:

$$A_{L,R} = \int_0^\infty C_R Q_C\,dt = Q_c \int_0^\infty C_R\,dt \qquad \text{(Eq. 9)}$$

By using the fraction lost in each eliminating compartment as expressed in Eq. 6, the total amount entering the right ventricle ($A_{E,R}$) can readily be obtained:

$$A_{E,R} = \int_0^\infty C_L \left[Q_2\left(1 - \frac{Cl_2}{Q_2}\right) + Q_3\right]\left(1 - \frac{Cl_3}{Q_2 + Q_3}\right) dt + \left[\sum_{i=4}^{m} C_L Q_i \left(1 - \frac{Cl_i}{Q_i}\right) dt\right] + \left(\sum_{i=m+1}^{n} \int_0^\infty C_L Q_i\,dt\right) + D\left(1 - \frac{Cl_m}{Q_m}\right) \qquad \text{(Eq. 10)}$$

The first part of the right-hand side of Eq. 10 takes into account that part of the hepatic blood flow which must pass through the GI tract *via* the mesenteric system before reaching the liver *via* the portal vein.

With the assumption that no elimination occurs in the ventricles, the amount leaving each ventricle from time zero to time infinity is equal to the amount entering. By combining Eqs 7–10 and defining $Q_2 + Q_3$ as the hepatic blood flow ($Q_H$), the following is obtained:

$$\int_0^\infty Cl\,dt = \frac{D\left(1 - \frac{Cl_m}{Q_m}\right)}{\frac{Cl_1' Q_C}{Q_C - Cl_1'} + \left(\sum_{i=2}^{m} Cl_i\right) - \frac{Cl_2 Cl_3}{Q_H}} \qquad \text{(Eq. 11)}$$

By combining Eqs. 4 and 11, the total amount entering the target organ after an intra-arterial injection into an artery leading to this organ is:

$$A_{E,m} = D\left(1 + \frac{Q_m - Cl_m}{\frac{Cl_1' Q_C}{Q_c - Cl_1'} + \left(\sum_{i=2}^{m} Cl_i\right) - \frac{Cl_2 Cl_3}{Q_H}}\right) \qquad \text{(Eq. 12)}$$

Furthermore, by combining Eqs. 3 and 12 to express all clearances with respect to the left ventricle concentration, the following is obtained:

$$A_{E,m} = D\left(1 + \frac{Q_m - Cl_m}{\left(\sum_{i=1}^{m} Cl_i\right) - \frac{Cl_2 Cl_3}{Q_H}}\right) \qquad \text{(Eq. 13)}$$

As can be seen from Eq. 13, the total amount reaching the target organ after an intra-arterial injection depends not only on the dose but also on the blood flow to this organ, its clearance, portal blood flow, and cardiac output, as well as the various clearances in the different parts of the body (see *Discussion*).

**Intra-Arterial Injection into Artery Not Leading to Target Organ**—In this case, the amount administered is assumed to be injected into Compartment $m - 1$ instead of the target organ, Compartment $m$. Thus, the amount delivered to Compartment $m$ is:

$$A_{E,m} = \int_0^\infty C_1 Q_m\,dt \qquad \text{(Eq. 14)}$$

Similarly to Eq. 13, $A_{E,m}$ can be expressed as:

$$A_{E,m} = D\frac{Q_m\left(1 - \frac{Cl_{m-1}}{Q_{m-1}}\right)}{\left(\sum_{i=1}^{m} Cl_i\right) - \frac{Cl_2 Cl_3}{Q_H}} \qquad \text{(Eq. 15)}$$

**Intravenous Bolus Dose Administration**—This situation is equivalent to delivering the drug directly into the right ventricle. In this case, by using similar development as in the two previous sections, the amount delivered to the target organ can be shown to be equal to:

$$A_{E,m} = \frac{DQ_m}{\left(\sum_{i=1}^{m} Cl_i\right) - \frac{Cl_2 Cl_3}{Q_H}} \qquad \text{(Eq. 16)}$$

**Oral Dose When Target Organ Is Liver**—The amount of an oral dose delivered to the liver ($A_{E,3}$) is equal to the amount leaving the GI tract [$D(1 - G)$] and escaping elimination in the GI wall. It is assumed that this amount is equal to the fraction that usually escapes elimination in the mesenteric system, $1 - (Cl_2/Q_2)$, plus the amount delivered *via* the vascular system through recirculation:

$$A_{E,3} = \int_0^\infty C_L \left[Q_2\left(1 - \frac{Cl_2}{Q_2}\right) + Q_3\right] + (1 - G)\left(1 - \frac{Cl_2}{Q_2}\right) \qquad \text{(Eq. 17)}$$

Using a similar development as for Eq. 10 and defining $(1 - G)$ [$1 - (Cl_2/Q_2)$] as $(1 - E)$, one obtains:

$$A_{E,3} = D\,(1-E)\left[1+\frac{(Q_H - Cl_2)\left(1-\frac{Cl_3}{Q_H}\right)}{\left(\sum_{i=1}^{m} Cl_i\right)-\frac{Cl_2Cl_3}{Q_H}}\right] \qquad \text{(Eq. 18)}$$

**Intravenous Dose When Target Organ is Liver**—The amount of drug delivered to the liver in this situation is equal to:

$$A_{E,3} = \int_0^\infty C_L\left[Q_2\left(1-\frac{Cl_2}{Q_2}\right)+Q_3\right] \qquad \text{(Eq. 19)}$$

By using a similar development as before, it can be demonstrated that:

$$A_{E,3} = \frac{D(Q_H - Cl_2)}{\left(\sum_{i=1}^{m} Cl_i\right)-\frac{Cl_2 - Cl_3}{Q_H}} \qquad \text{(Eq. 20)}$$

## DISCUSSION

**Intra-Arterial Injection Leading to Target Organ *versus* Intravenous Injection**—The ratio of the amount of drug entering the target organ from the intra-arterial to the intravenous injection ($Y_T$) can be obtained from Eqs. 13 and 16:

$$Y_T = 1+\frac{\left(\sum_{i=1}^{m-1} Cl_i\right)-\frac{Cl_2Cl_3}{Q_H}}{Q_m} \qquad \text{(Eq. 21)}$$

Because $Q_H$ always is larger than $Cl_2$ or $Cl_3$, this relationship is always greater than one as long as $\Sigma_{i=1}^{m-1} Cl_i$ is not zero. Therefore, Eq. 21 demonstrates that an intra-arterial injection of a drug into an artery leading to the target organ always delivers more drug to the target organ than an intravenous bolus dose. The single exception is when only the target organ eliminates the drug since then the two modes of administration are identical.

The advantage of intra-arterial administration increases under the following circumstances:

1. Lung clearance is high. In this case, the intravenously administered drug has to pass through the lungs and be partially metabolized before it can reach the target organ.
2. Elimination by other organs is high in comparison to target organ blood flow. In this case, a large amount of drug leaving the left ventricle per heart beat circulates to various organs where possibilities for elimination exist. Therefore, only a fraction of the drug is returned to the general circulation for recirculation to the target organ. This conclusion, however, is not readily determined from regular concentration monitoring data or from evaluation of bioavailability.

Bioavailability is practically determined as the amount delivered to the site of measurement from a test dose to that of a control dose. By considering the intra-arterial dose as the test dose, the intravenous dose as the control, and, for simplistic reasons, the sampling site as the venous side of storage compartment $n$, the bioavailability ($F$) can be expressed as:

$$F_T = \frac{\left(\int_0^\infty ClQ_n\,dt\right)\text{ intra-arterially}}{\left(\int_0^\infty ClQ_n\,dt\right)\text{ intravenously}} \qquad \text{(Eq. 22)}$$

Derivation yields:

$$F_T = 1-\frac{Cl_m}{Q_m} \qquad \text{(Eq. 23)}$$

This result indicates that an intravenous dose always delivers more drug to the sampling site than an intra-arterial injection. Therefore, use of this site to evaluate various drug administration routes may be inadequate and misleading.

A similar conclusion can be drawn from the theoretical evaluation of intra-arterial *versus* intravenous administration of chemotherapeutics by Chen and Gross (8). They evaluated a slightly different kinetic flow model, and their clearances were defined in terms of the intrinsic clearance values of the various organs at steady state. Again, however, an advantage of intra-arterial injections with respect to delivery to the target organ was observed ($Y_T$), in conjunction with a decreased systemic availability ($F_T$).

**Intra-Arterial Injection Not Leading to Target Organ *versus* Intravenous Injection**—In this case, the ratio of the amount delivered to the target organ from the various administration routes ($Y_N$) can be obtained from Eqs 14 and 15:

$$Y_N = 1-\frac{Cl_{m-1}}{Q_{m-1}} \qquad \text{(Eq. 24)}$$

and bioavailability is expressed by:

$$F_N = 1-\frac{Cl_{m-1}}{Q_{m-1}} \qquad \text{(Eq. 25)}$$

In this situation, it is clear that an intravenous dose delivers more drug to the target organ than an intra-arterial dose. The intra-arterial dose has to pass to a nontarget organ ($m-1$) where it can be partially eliminated before it reaches the venous circulation. However, the intravenous dose reaches the venous circulation directly; *i.e.*, if the decision is made to administer a drug intra-arterially, it is imperative to identify the target organ to ensure that the drug is administered into an artery leading to that target organ.

The use of venous drug concentration monitoring or traditional bioavailability determination accurately reflects the relative amounts reaching the target organ by these two administration routes only when intra-arterial administration is into an artery not leading to the target organ.

**Oral Dosing *versus* Intravenous Injection When Target Organ Is Liver**—From Eq. 18, it can be seen that the ratio of drug delivered to the liver by these two routes ($Y_0$) is equal to:

$$Y_0 = (1-E)\left[1+\frac{\left(\sum_{i=1}^{m} Cl_i\right)-Cl_3}{Q_H - Cl_2}\right] \qquad \text{(Eq. 26)}$$

Thus, it is possible to predict when oral administration is advantageous over intravenous injection if the target organ is the liver. However, extensive knowledge of the various clearances for a drug is required. In principle, the larger the fraction of the dose that reaches the liver in its first pass [$(1-E) \rightarrow 1$] and the larger the extrahepatic clearance is in comparison with hepatic blood flow, the greater is the likelihood for an oral dose to be superior to an intravenous injection.

Bioavailability ($F_0$) is equal to:

$$F_0 = (1-E)\left(1-\frac{Cl_3}{Q_H}\right) \qquad \text{(Eq. 27)}$$

This relationship always predicts that the intravenous route is superior to the oral route provided $E$ and $Cl_3$ are not zero.

Using traditional bioavailability determinations to decide on an optimal drug delivery route may sometimes be misleading. Based on this discussion, it appears that when blood (or plasma) concentration in a peripheral vein is used for determining the best administration route, the choice will invariably be the intravenous route. However, alternative routes are sometimes able to delivery more drug to the target organ than an intravenous dose. Therefore, care should be taken in drug plasma monitoring or the use of steady-state plasma concentrations or bioavailability data when different administration routes are considered for optimization of drug therapy.

On the other hand, if two dosage formulations given *via* the same route are compared, such reservation is not necessary. In this case, the drug traverses the same path before it reaches the measurement site or the target organ. Therefore, the ratio of the amount delivered to the measurement site accurately reflects the ratio reaching the target organ.

This discussion should not be considered as being limited to the two special examples provided. The same conclusions can be reached in other situations, such as intramuscular injection when the muscle is the target organ, inhalation when the lung is the target organ, and intrathecal injection when the spinal nerves are the target.

## REFERENCES


(1) W. L. Chiou, *J. Pharmacokinet. Biopharm.*, **3**, 193 (1975).

(2) L. Z. Benet, *ibid.*, **6**, 559 (1978).

(3) H. Buchwald, T. B. Grage, P. P. Vassilopoulos, R. D. Rohde, R. L. Varco, and P. J. Blackshear, *Cancer*, **45**, 866 (1980).

(4) K. Yamada, A. M. Bremer, C. R. West, J. Ghoorak, H. C. Park, and H. Takita, *ibid.*, **44**, 200 (1979).

(5) C. P. Karokousis, R. Lopez, R. Catane, U. Rao, R. Moore, and E. D. Holyoke, *J. Surg. Oncol.*, **13**, 21 (1980).

(6) K. Hollmann, W. Jesch, J. Kuehboeck, and J. Dimopoulos, *J. Maxillofac. Surg.*, **7**, 191 (1979).
(7) W. D. Ensminger, A. Rosowski, V. Raso, D. C. Levin, M. Glode, S. Come, G. Steele, and E. Frei, III, *Cancer Res.*, **38**, 3784 (1978).
(8) H.-S. G. Chen and J. F. Gross, *Cancer Treat. Rep.*, **64**, 31 (1980).

**ACKNOWLEDGMENTS**

Supported in part by Grant GM 28423 from the National Institutes of Health.

The authors thank Dr. Thomas N. Tozer for valuable discussions and suggestions.

# Determination of Flurbiprofen and Ibuprofen in Dog Serum with Automated Sample Preparation

**B. G. SNIDER ˣ, L. J. BEAUBIEN, D. J. SEARS, and P. D. RAHN**

Received December 1, 1980, from the *Control Research Laboratories, The Upjohn Company, Kalamazoo, MI 49001.* Accepted for publication April 23, 1981.

**Abstract** □ Methods for the determination of flurbiprofen and ibuprofen in dog serum were developed using high-performance liquid chromatography and automated serum extraction. Sample extraction was automated by use of cartridges packed with a styrene–divinylbenzene macroreticular resin in a microprocessor-controlled centrifugal system. The average recoveries were 98.9% for flurbiprofen and 94.5% for ibuprofen. The limits of detection were ~0.04 μg/ml for flurbiprofen at 254 nm and 0.5 μg/ml for ibuprofen at 230 nm. The relative standard deviations for the determination of a laboratory standard between days was 2.4% (20 μg/ml) for flurbiprofen and 1.7% (13 μg/ml) for ibuprofen. Peak height ratios were linear with concentrations of 0.04–100 μg/ml for flurbiprofen and 1.0–50 μg/ml for ibuprofen. These methods are simple, rapid, sensitive, and specific. The use of an automated sample preparation procedure improved the between-day precision by a factor of two when compared to a manual extraction procedure. These methods were applied to bioavailability studies in dogs.

**Keyphrases** □ Flurbiprofen—determination in dog serum with automated sample preparation □ Ibuprofen—determination in dog serum with automated sample preparation □ Bioavailability—determination of flurbiprofen and ibuprofen in dog serum with automated sample preparation

Flurbiprofen [*dl*-2-(2-fluoro-4-biphenylyl)propionic acid] and ibuprofen [*dl*-2-(*p*-isobutylphenyl)propionic acid] are nonsteroidal anti-inflammatory drugs. Several gas chromatographic (GC) procedures were previously developed for flurbiprofen (1) and ibuprofen (2–4). Methods using high-performance liquid chromatography (HPLC) were previously developed for ibuprofen (5, 6) and similar compounds: indoprofen (7), ketoprofen (8), and naproxen (8). To reduce the amount of labor and time involved in performing assays for flurbiprofen or ibuprofen in serum, an HPLC procedure using an automated sample processor[1] was developed. The previously developed GC procedures use manual liquid–liquid sample preparations and derivatization prior to analysis. Sample extraction with the automated sample processor uses a liquid–solid extraction with a cartridge packed with a styrene–divinylbenzene macroreticular resin in a microprocessor-controlled centrifugal system, resulting in reduced analysis effort and improved assay precision.

[1] Prep I, Dupont Co, Wilmington, Del.

## EXPERIMENTAL

**Reagents and Materials**—Reagents were of at least analytical reagent grade quality, and acetonitrile[2] was distilled-in-glass grade. Stock solutions of flurbiprofen[3] and ibuprofen[3] were prepared in pH 7.2 phosphate buffer (0.05 *M*).

**Instrumentation**—A variable-wavelength detector[4], a solvent pump[5], and an autoinjector[6] were used for the chromatographic analysis. Preparation of samples was performed with an automated sample processor.

**Chromatographic Conditions**—Chromatography took place on a 0.46-cm i.d. × 25-cm long column packed with octadecylsilane bonded to microparticulate silica[7] (10 μm). The precolumn, 4.2 cm × 0.3-cm i.d., was packed with octadecylsilane bonded to microparticulate silica[8] (30 μm). The mobile phase was acetonitrile–0.05 *M* acetic acid (40:60).

The flow rate was 2.0 ml/min, the column temperature was ambient, and the column back-pressure was ~1500 psi. The approximate retention times of flurbiprofen and ibuprofen were 14 and 19 min, respectively. Preliminary work was performed with the acetonitrile–water ratio at 50:50 and the flow rate at 1.2 ml/min. The mobile phase was filtered and deaerated by vacuum sonication prior to use.

**Automated Extraction**—The automated sample processor is designed to perform automatic extractions simultaneously of up to 12 liquid samples in 30 min or less. Centrifugal force is used to move solvents through an extraction resin bed. The system is composed of an inner rotor, which holds extraction columns, and a larger outer rotor, which holds the corresponding effluent and recovery cups. The extraction column is comprised of a sample reservoir and a resin bed. The rotor first spins clockwise to force the sample through the resin bed. A predetermined amount of wash solvent is forced through the resin bed and into an effluent cup. In this manner, unwanted components are removed from the column. The rotor direction is then reversed so that the extraction column is positioned over the recovery cup.

An aliquot of a second solvent elutes the component of interest and is collected in the recovery cup. If desired, the extract is then heated and blown to dryness. The dried extract is manually reconstituted and transferred to another instrument. Fifteen programs are currently available which vary timing, compartment temperature, and the option of sample evaporation.

**Assay Procedure**—Blank serum spiked with 100 μl of flurbiprofen or ibuprofen solutions in 0.05 *M* phosphate buffer (pH 7.2) was used to prepare standards to obtain a calibration curve for each chromatographic run. One milliliter of blank or sample serum was pipetted into the car-

[2] Burdick & Jackson, Muskegon, Mich.
[3] The Upjohn Co, Kalamazoo, Mich.
[4] Perkin-Elmer LC-55B, Norwalk, Conn.
[5] Model 100A, Altex Scientific, Berkeley, Calif.
[6] WISP model 710, Waters Associates, Milford, Mass.
[7] RP-8, Rheodyne, Berkeley, Calif.
[8] Permaphase ODS, Dupont, Wilmington, Del.

0022-3549/81/1200-1347$01.00/0
© 1981, American Pharmaceutical Association

(6) K. Hollmann, W. Jesch, J. Kuehboeck, and J. Dimopoulos, *J. Maxillofac. Surg.*, **7**, 191 (1979).
(7) W. D. Ensminger, A. Rosowski, V. Raso, D. C. Levin, M. Glode, S. Come, G. Steele, and E. Frei, III, *Cancer Res.*, **38**, 3784 (1978).
(8) H.-S. G. Chen and J. F. Gross, *Cancer Treat. Rep.*, **64**, 31 (1980).

**ACKNOWLEDGMENTS**

Supported in part by Grant GM 28423 from the National Institutes of Health.

The authors thank Dr. Thomas N. Tozer for valuable discussions and suggestions.

# Determination of Flurbiprofen and Ibuprofen in Dog Serum with Automated Sample Preparation

**B. G. SNIDER ˣ, L. J. BEAUBIEN, D. J. SEARS, and P. D. RAHN**

Received December 1, 1980, from the *Control Research Laboratories, The Upjohn Company, Kalamazoo, MI 49001.* Accepted for publication April 23, 1981.

**Abstract** □ Methods for the determination of flurbiprofen and ibuprofen in dog serum were developed using high-performance liquid chromatography and automated serum extraction. Sample extraction was automated by use of cartridges packed with a styrene–divinylbenzene macroreticular resin in a microprocessor-controlled centrifugal system. The average recoveries were 98.9% for flurbiprofen and 94.5% for ibuprofen. The limits of detection were ~0.04 μg/ml for flurbiprofen at 254 nm and 0.5 μg/ml for ibuprofen at 230 nm. The relative standard deviations for the determination of a laboratory standard between days was 2.4% (20 μg/ml) for flurbiprofen and 1.7% (13 μg/ml) for ibuprofen. Peak height ratios were linear with concentrations of 0.04–100 μg/ml for flurbiprofen and 1.0–50 μg/ml for ibuprofen. These methods are simple, rapid, sensitive, and specific. The use of an automated sample preparation procedure improved the between-day precision by a factor of two when compared to a manual extraction procedure. These methods were applied to bioavailability studies in dogs.

**Keyphrases** □ Flurbiprofen—determination in dog serum with automated sample preparation □ Ibuprofen—determination in dog serum with automated sample preparation □ Bioavailability—determination of flurbiprofen and ibuprofen in dog serum with automated sample preparation

Flurbiprofen [*dl*-2-(2-fluoro-4-biphenylyl)propionic acid] and ibuprofen [*dl*-2-(*p*-isobutylphenyl)propionic acid] are nonsteroidal anti-inflammatory drugs. Several gas chromatographic (GC) procedures were previously developed for flurbiprofen (1) and ibuprofen (2–4). Methods using high-performance liquid chromatography (HPLC) were previously developed for ibuprofen (5, 6) and similar compounds: indoprofen (7), ketoprofen (8), and naproxen (8). To reduce the amount of labor and time involved in performing assays for flurbiprofen or ibuprofen in serum, an HPLC procedure using an automated sample processor[1] was developed. The previously developed GC procedures use manual liquid–liquid sample preparations and derivatization prior to analysis. Sample extraction with the automated sample processor uses a liquid–solid extraction with a cartridge packed with a styrene–divinylbenzene macroreticular resin in a microprocessor-controlled centrifugal system, resulting in reduced analysis effort and improved assay precision.

[1] Prep I, Dupont Co, Wilmington, Del.

## EXPERIMENTAL

**Reagents and Materials**—Reagents were of at least analytical reagent grade quality, and acetonitrile[2] was distilled-in-glass grade. Stock solutions of flurbiprofen[3] and ibuprofen[3] were prepared in pH 7.2 phosphate buffer (0.05 *M*).

**Instrumentation**—A variable-wavelength detector[4], a solvent pump[5], and an autoinjector[6] were used for the chromatographic analysis. Preparation of samples was performed with an automated sample processor.

**Chromatographic Conditions**—Chromatography took place on a 0.46-cm i.d. × 25-cm long column packed with octadecylsilane bonded to microparticulate silica[7] (10 μm). The precolumn, 4.2 cm × 0.3-cm i.d., was packed with octadecylsilane bonded to microparticulate silica[8] (30 μm). The mobile phase was acetonitrile–0.05 *M* acetic acid (40:60).

The flow rate was 2.0 ml/min, the column temperature was ambient, and the column back-pressure was ~1500 psi. The approximate retention times of flurbiprofen and ibuprofen were 14 and 19 min, respectively. Preliminary work was performed with the acetonitrile–water ratio at 50:50 and the flow rate at 1.2 ml/min. The mobile phase was filtered and deaerated by vacuum sonication prior to use.

**Automated Extraction**—The automated sample processor is designed to perform automatic extractions simultaneously of up to 12 liquid samples in 30 min or less. Centrifugal force is used to move solvents through an extraction resin bed. The system is composed of an inner rotor, which holds extraction columns, and a larger outer rotor, which holds the corresponding effluent and recovery cups. The extraction column is comprised of a sample reservoir and a resin bed. The rotor first spins clockwise to force the sample through the resin bed. A predetermined amount of wash solvent is forced through the resin bed and into an effluent cup. In this manner, unwanted components are removed from the column. The rotor direction is then reversed so that the extraction column is positioned over the recovery cup.

An aliquot of a second solvent elutes the component of interest and is collected in the recovery cup. If desired, the extract is then heated and blown to dryness. The dried extract is manually reconstituted and transferred to another instrument. Fifteen programs are currently available which vary timing, compartment temperature, and the option of sample evaporation.

**Assay Procedure**—Blank serum spiked with 100 μl of flurbiprofen or ibuprofen solutions in 0.05 *M* phosphate buffer (pH 7.2) was used to prepare standards to obtain a calibration curve for each chromatographic run. One milliliter of blank or sample serum was pipetted into the car-

[2] Burdick & Jackson, Muskegon, Mich.
[3] The Upjohn Co, Kalamazoo, Mich.
[4] Perkin-Elmer LC-55B, Norwalk, Conn.
[5] Model 100A, Altex Scientific, Berkeley, Calif.
[6] WISP model 710, Waters Associates, Milford, Mass.
[7] RP-8, Rheodyne, Berkeley, Calif.
[8] Permaphase ODS, Dupont, Wilmington, Del.

0022-3549/81/1200-1347$01.00/0
© 1981, American Pharmaceutical Association

**Table I—Effect of Mobile Phase pH and Percent Acetonitrile on the Retention Times of Flurbiprofen and Ibuprofen (1.0 ml/min)**

| Acetonitrile, % | pH | Retention Time of Flurbiprofen, min | Retention Time of Ibuprofen, min |
|---|---|---|---|
| 60 | 3 | 6.3 | 7.8 |
| 55 | 3 | 6.9 | 8.7 |
| 50 | 3 | 9.6 | 12.6 |
| | 4 | 7.8 | 11.1 |
| | 5 | 5.4 | 8.7 |
| 40[a] | 3 | 17.0 | 22.0 |

[a] At 2.0 ml/min.

tridges. Standard cartridges were spiked with the appropriate stock solution and were rotated to promote mixing. A 0.2-ml aliquot of 0.5 *M* $H_2SO_4$ was added to each cartridge, which then was rotated to promote mixing. The cartridges were loaded into the automated sample processor. Water and methanol were added to the appropriate reservoirs in amounts sufficient to wash each cartridge with 1.0 ml of water and elute each cartridge with 2.0 ml of methanol. The addition of the washing and eluting solvents and the evaporation of the methanol by blowing air at 50° over the aluminum recovery cups were performed by the automated sample processor. The dried contents of the recovery cups were dissolved in the mobile phase. To determine ibuprofen at 10 μg/ml, the cups were reconstituted with 1 ml of mobile phase containing 6.0 μg of flurbiprofen/ml as the internal standard, and 0.2-ml aliquots of the reconstituted samples were chromatographed. In the determination of flurbiprofen, mobile phase containing ibuprofen was used to reconstitute the samples.

Peak heights were measured for flurbiprofen and ibuprofen, and the peak heights for the analyte were divided by that of the internal standard. Linear least-squares fit of the peak height ratios was used to calculate the serum drug concentration.

**Drug Administration**—Male beagle dogs were fasted for 16 hr prior to dosing and for 4 hr after administration. Flurbiprofen and ibuprofen were dosed as solutions of sodium salts (pH 7) in a hard gelatin capsule. For ibuprofen, 4 ml of a 20 mg/ml solution was administered to each dog; for flurbiprofen, 4 ml of a 12.5 mg/ml solution was administered. Blood was collected in 10-ml evacuation tubes and allowed to clot. Separated serum was stored at −18° prior to analysis.

## RESULTS AND DISCUSSION

**HPLC**—For the determination of flurbiprofen in the 0.04–2-μg/ml range, a mobile phase of acetonitrile–0.1 *M* acetic acid (50:50) was used with UV detection at 254 nm. The effect of the mobile phase pH and percent acetonitrile on the retention times of flurbiprofen and ibuprofen are shown in Table I. By using a low pH for the mobile phase, ion-pairing is not necessary for adequate retention of the two compounds. The relative retention times of some metabolites of flurbiprofen are shown in Table II, and all are well resolved from flurbiprofen as well as ibuprofen. The major metabolite in dogs is 4′-hydroxyflurbiprofen (9). At 254 nm, the molar absorbtivity of ibuprofen was only 1.2% that of flurbiprofen.

To determine flurbiprofen above 10 μg/ml, the ibuprofen concentration needed to provide equivalent responses became quite large, and problems occurred with low ibuprofen recovery with the manual extraction procedure. Therefore, UV absorbance was monitored at 230 nm to optimize ibuprofen sensitivity and still have adequate sensitivity for flurbiprofen. However, a peak that eluted at approximately the same retention time as ibuprofen was observed, and the mobile phase was changed to acetonitrile–0.05 *M* acetic acid in water (40:60) at 2.0 ml/min to separate this interfering peak from ibuprofen. A typical chromatogram of extracted blank serum and serum spiked with flurbiprofen and ibuprofen is shown in Fig. 1.

**Isolation of Flurbiprofen and Ibuprofen from Serum**—Various

**Table II—Relative Retention Times of Flurbiprofen, Ibuprofen, and Flurbiprofen Metabolites**

| Compound | Relative Retention Time, min |
|---|---|
| Flurbiprofen | 1.0 |
| Ibuprofen | 1.3 |
| 2′-Hydroxyflurbiprofen | 0.56 |
| 4′-Hydroxyflurbiprofen | 0.50 |
| 3′-Hydroxyflurbiprofen | 0.53 |

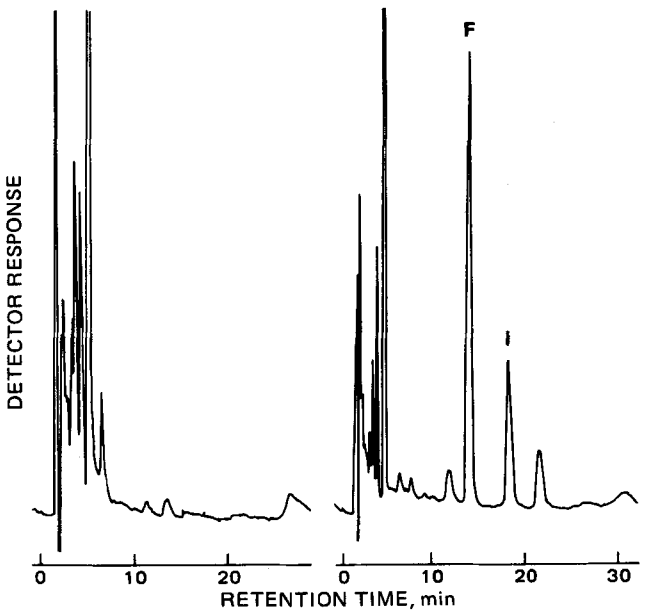


**Figure 1**—*HPLC chromatograms of drug serum extracts. Key: left, serum sample without administration of drug; and right, serum sample containing flurbiprofen (F) (6.0 μg/ml) and ibuprofen (I) (10 μg/ml).*

methods for the isolation of flurbiprofen and ibuprofen from serum were investigated. Precipitation of serum proteins with acetonitrile followed by analysis of the supernate was suggested as an alternative method for serum sample preparation (7). However, for flurbiprofen and ibuprofen, very low recoveries were obtained when this method was used, and the supernate contained a large amount of dissolved solids. Acidifying the serum before addition of acetonitrile improved recovery, but this approach was discontinued because of problems with injecting large amounts of acid. An extraction procedure developed previously (1) was used, except that toluene was substituted for benzene in the extraction, and the sample cleanup steps involving TLC were omitted. An automated sample extraction procedure was also developed and compared to the manual extraction procedure.

To optimize the automated extraction procedure, several different eluting solvents were investigated and the amounts of wash solvent, and eluting solvent, and the acid added were varied. These experiments attempted to reduce the amount of insoluble material acquired in extraction, to obtain quantitative recovery, and to minimize the number of extraneous peaks produced in the chromatogram. The more polar eluting solvents tended to yield cleaner reconstituted samples. The extent to which the serum was acidified influenced both flurbiprofen recovery and the number of extraneous peaks displayed in the chromatogram. Unacidified serum yielded 37% recovery. One late-eluting peak was eliminated by reducing the amount of acid used from 250 to 200 μl. For each extraction column, the use of 1.0 ml of water (wash solvent), 2.0 ml of methanol (eluting solvent), and 200 μl of 0.5 *M* $H_2SO_4$ produced the cleanest samples with the greatest recovery.

**Assay Linearity, Precision, and Accuracy**—Linearity of peak height ratios with the concentration of flurbiprofen and ibuprofen was investigated. Calibration curves prepared from serum spiked with the appropriate amounts of flurbiprofen or ibuprofen showed no significant deviation from linearity in the 0.04–100-μg/ml range for flurbiprofen and in the 1–200-μg/ml range for ibuprofen. Correlation coefficients for the fit of the experimental points to a line were between 0.998 and 1.000. The intercepts were not significantly different from zero in all cases, and no interferences from constituents in blank serum were found.

The extraction efficiency was determined over the same ranges as those for the linearity, and the average recoveries were 98.9 ± 3.3% and 94.5 ± 1.2% for flurbiprofen and ibuprofen, respectively.

To investigate the precision of the extraction process, six runs with six samples each of a pooled serum sample containing 20 μg of flurbiprofen/ml were prepared. The mean relative standard deviation of the extraction within the six samples was ~1.8%. The relative standard deviation for different runs of the automated sample processor was ~1.3%. Therefore, the extraction process was reproducible both within run and between run. This precision was obtained without adding the internal

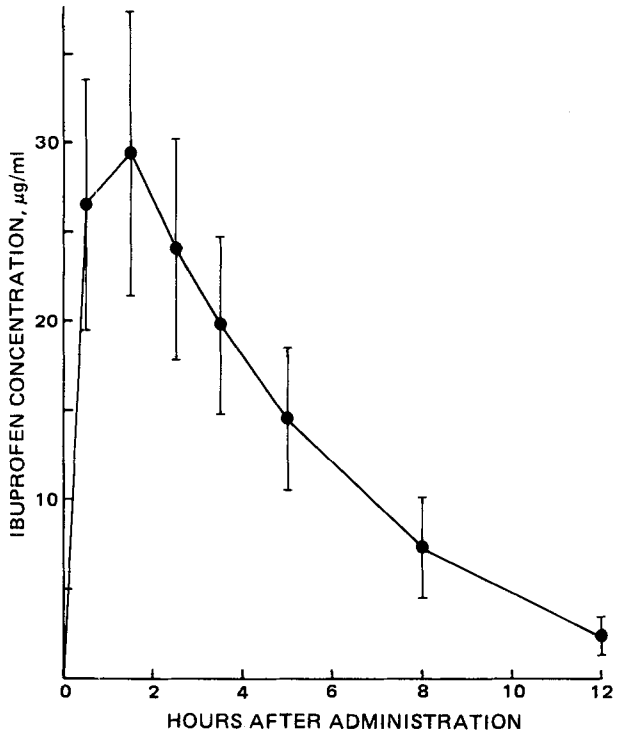


**Figure 2**—*Average (±SD) serum ibuprofen concentrations in male beagle dogs (n = 8, average weight 14.9 ± 2.2 kg) after single oral administration of 80 mg of ibuprofen as a solution of the sodium salt.*

standard prior to extraction, thus reducing the number of steps required for the assay.

The reproducibility of the entire assay was later demonstrated when a set of 300 samples was assayed in eight chromatographic runs of 16 hr each. The average of the laboratory standard (a pooled sample of serum) over the 8 days was 26.3 μg/ml, and the relative standard deviation was 2.4%. The relative standard deviation of standards in the 5–100 μg/ml concentration range was 3.2–0.8%. The relative standard deviation of the slope was 4%. The reproducibility of the extraction from day to day was a considerable improvement over the manual extraction procedure, which typically had a 6.0% *RSD* for the laboratory standard.

**Assay Sensitivity**—With a UV detector at 0.05 aufs, assay sensitivities based on a signal 2% of full scale were 1 and 2 μg/ml for flurbiprofen and ibuprofen, respectively, for a 0.06-ml injection from a reconstituted volume of 2 ml. When the dried extract was reconstituted in 1 ml and 0.2 ml was injected, the sensitivity was improved to 0.5 μg/ml for ibuprofen and to 0.2 μg/ml for flurbiprofen. Flurbiprofen can be determined at levels as low as 0.04 μg/ml if a 254-nm detector is used because absorbance is at a maximum at 248 nm and a single-wavelength detector at 254 nm has a higher signal to noise ratio than a variable-wavelength detector.

**Assay Problems**—Only a few problems occurred using the automated sample processor. Occasionally, the flow of samples through the cartridge was too slow, and water was left at the top of the cartridge at the end of analysis. This can result from insoluble material in the sample plugging the cartridge and from the cartridge drying out and flow becoming too slow. The first problem can be solved by filtering the sample, and placing an expiration date on the cartridge minimizes the second problem. The incidence of these problems was infrequent (~1%). The cartridges can be prescreened for suitability by placing 1.0 ml of water in them and checking to see if all of the water flowed through the cartridge in <1 min under the conditions typically used to force the serum–buffer mixture through the cartridge.

Another problem observed with ibuprofen was a change in recovery from 95 to 60% for one batch of cartridges when elution with 1 ml of methanol was used. The recovery between cartridges was still reproducible, with the assay variation being approximately the same for this lot as for other lots when 95% recovery was obtained. This finding is not surprising because of the reproducible manner in which the automated sample processor performs the extraction. For example, the relative standard deviation for the addition of eluting solvent to the cartridge was 1.5%. This situation is analogous to the use of a segmented flow system in which transfer of the sample through the various steps may not yield 100% recovery, but the recovery is reproducible from sample to sample. The reason for the dependence of recovery on the lot used involves the different elution properties of various lots of resin. If the standards are extracted with the same lot of cartridges as the samples, the change in recovery will not affect the quantitation unless the recovery becomes quite low. In this case, the detection limit and precision of the assay will be affected. The amount of methanol used for elution was changed to 2 ml/cartridge to minimize this problem, and recovery then increased from 60 to 86%.

**Serum Levels in Dogs**—The average serum concentration curve for the oral administration of 80 mg of ibuprofen is shown in Fig. 2. For ibuprofen, the average peak concentration was 29.4 μg/ml, the average time of individual peak occurrence was 1.5 hr, and the half-life calculated from the terminal slope was 2.8 hr. For flurbiprofen, the average peak concentration was 31.0 μg/ml, the average time of individual peak occurrence was 2.2 hr, and the half-life calculated from the terminal slope was 35 hr.

These methods are suitable for determining the pharmacokinetics of these two drugs and for evaluating drug availability from various dosage forms in dogs.

## REFERENCES

(1) D. G. Kaiser, S. R. Shaw, and G. J. Vangiessen, *J. Pharm. Sci.*, **63,** 567 (1974).

(2) D. G. Kaiser and G. J. Vangiessen, *ibid.*, **63,** 219 (1974).

(3) D. J. Hoffman, *ibid.*, **66,** 749 (1977).

(4) K. K. Midha, J. K. Cooper, J. W. Hubbard, and I. J. McGilveray, *Can. J. Pharm. Sci.*, **12,** 29 (1977).

(5) J. L. Shimek, N. G. S. Rao, and S. K. Wahba Khalid, *J. Pharm. Sci.*, **70,** 514 (1981).

(6) D. Pitre and M. Grandi, *J. Chromatogr.*, **170,** 278 (1979).

(7) D. B. Lakings, W. J. Haggerty, G. Rehagen, and H. Barth, *J. Pharm. Sci.*, **67,** 831 (1978).

(8) R. A. Upton, J. N. Buskin, T. W. Guentert, R. L. Williams, and S. Riegelman, *Clin. Pharmacol. Ther.*, **25,** 251 (1979).

(9) P. C. Risdall, S. S. Adams, E. L. Crampton, and B. Marchant, *Xenobiotica*, **8,** 691 (1978).

# Characterization of Albumin Microspheres by Sedimentation Field-Flow Fractionation

KARIN D. CALDWELL, GEORGE KARAISKAKIS *, MARCUS N. MYERS, and J. CALVIN GIDDINGS ×

Received January 19, 1981, from the *Department of Chemistry, University of Utah, Salt Lake City, UT 84112.* Accepted for publication May 12, 1981. *Present address: Department of Chemistry, University of Patras, Patras, Greece.

**Abstract** □ Sedimentation field-flow fractionation (FFF) is a new technique that separates and characterizes submicron particles. In the present work, two independent sedimentation FFF methods are presented to characterize bovine serum albumin microspheres in terms of particle size, polydispersity, and diffusion coefficient. Particle diameters and polydispersities determined by the two sedimentation FFF methods were in excellent agreement with each other and in good agreement with values calculated from transmission electron microscopy (TEM) measurements. The diameters calculated from the two FFF methods and TEM were 0.349, 0.346, and 0.354 μm, respectively.

**Keyphrases** □ Field-flow fractionation—characterization of albumin microspheres □ Microspheres—albumin, characterization by field-flow fractionation □ Particle characterization—by field-flow fractionation

Field-flow fractionation (FFF) is a high-resolution method capable of separating and characterizing a wide variety of macromolecules and particles of submicron and larger size (1, 2). Examples of materials previously studied include lattices (3), viruses (4), proteins (5), emulsions, liposomes, and blood cells.

In FFF, separation occurs in a thin-flow channel. A carrier solution transports components through the channel at different rates and then carries them to a collection device and/or a detector. The rate of migration is controlled by an external field (which retards migration) applied across the channel perpendicular to the flow. Different external fields lead to different "subtechniques" of FFF. Sedimentation FFF is a subtechnique utilizing a gravitational or centrifugal field.

The degree of retention (retardation relative to the carrier solution) in sedimentation FFF is determined by the particle mass and density, field strength, and carrier solution density. Field strength, flow rate, and carrier solution density can be varied to meet the requirements for resolution, analysis time, and maximum particle concentration. A recent review (2) presents details of the apparatus, applications, and a theory of retention.

## THEORY

In sedimentation FFF, particles migrate to one wall of the channel under the influence of centrifugal forces. This motion is counteracted by diffusion. After an appropriate relaxation time, these processes arrive at a steady-state balance, and particles of a given size form a diffuse layer of mean thickness $l$. The magnitude of $l$ is smallest for the largest particles, which interact most strongly with the field. When flow is started in the thin channel, a parabolic flow profile develops, with zero velocity at the walls. Because the speed of elution of a given particle type depends on the mean distance, small particles with large $l$ values elute ahead of large particles.

The degree of retention in FFF is measured by the retention ratio $R$:

$$R = V^0/V_r \qquad \text{(Eq. 1)}$$

where $V^0$ is the void volume of the channel and $V_r$ is the retention volume of the particle zone. For well-retained zones, $R$ is simply related to the dimensionless layer thickness retention parameter, $\lambda = l/w$:

$$R = 6\lambda \qquad \text{(Eq. 2)}$$

The value of $\lambda$ is determined by field strength, particle characteristics, and various experimental parameters. For spherical particles of diameter $d$:

$$\lambda = l/w = 6kT/\pi d^3 w \Delta\rho G \qquad \text{(Eq. 3)}$$

where $w$ is the channel thickness, $k$ is Boltzmann's constant, $T$ is the absolute temperature, $\Delta\rho$ is the difference between particle and carrier solution density, and $G$ is the field strength in units of acceleration. The combination of Eqs. 1–3 yields:

$$d = \left(\frac{36kT}{\pi w\, \Delta\rho G V^0}\right)^{1/3} V_r^{1/3} \qquad \text{(Eq. 4)}$$

From this equation, $d$ can be calculated directly from $V_r$ if the particle density is known.

In addition, the polydispersity and diffusion coefficient of a particulate sample can be calculated from the peak width of the eluted sample as measured by the plate height. The theory of plate height ($H$) in sedimentation FFF specifies that $H$ can be closely approximated by:

$$H = \chi w^2 \langle v \rangle / D + 9L(\sigma_d/d)^2 \qquad \text{(Eq. 5)}$$

where $D$ is the diffusion coefficient of the particles, $\langle v \rangle$ is the mean flow velocity of the carrier solution, $L$ is the channel length, and $\chi$ is the nonequilibrium coefficient, which, under normal conditions of high retention ($\lambda \to 0$), takes the form:

$$\chi = 24\lambda^3 \qquad \text{(Eq. 6)}$$

The $\chi$-containing term in Eq. 5 is for plate height due to nonequilibrium effects. The second term on the right of Eq. 5 represents the polydispersity contribution to $H$, expressed as a function of $\sigma_d$, the standard deviation of the particle diameter within the sample.

Diffusion coefficient $D$ can be expressed in terms of $d$ using the Stokes–Einstein equation:

$$D = kT/3\pi\eta d \qquad \text{(Eq. 7)}$$

where $\eta$ is the viscosity of the carrier solution.

There are two independent methods whereby polydispersity $\sigma_d$ can be calculated from the plate height. In Method A, the value of $d$ is obtained from retention measurements *via* Eq. 4; $D$ can then be calculated in terms of $d$ using Eq. 7. The only remaining unknown, $\sigma_d$, is calculated from Eq. 5 once experimental $H$ values are obtained (*Experimental*). In Method B, the flow rate is varied and a plot of $H$ *versus* $\langle v \rangle$ is prepared. From the slope, $24\lambda^3 w^2/D$, the value of $D$ is obtained. From the intercept, $9L(\sigma_d/d)^2$, the value of $\sigma_d$ can be calculated.

## EXPERIMENTAL

**Apparatus**—The apparatus described previously (2) for sedimentation FFF was used with one modification: the seal employed a polytef O-ring instead of the rubber ones used conventionally. This modification allowed 95% ethanol to be used as a carrier solution. The channel dimensions were length 47.5 × thickness 0.0254 × width 1.00 cm. The void volume of the column was measured as 0.90 ml by injection of a nonretained sample. A controller was used to set the motor speed of the centrifuge. The rotation rate was measured by a pulse counter connected to a slotted disk on the centrifuge shaft. Ancillary equipment included a metering pump, a UV monitor for detection at 254 nm, and a chart recorder.

Plate height $H$ was determined graphically from the elution diagrams displayed on the chart recorder in the following manner (6):

$$H = \frac{L}{5.54}\left(\frac{w_{1/2}}{s}\right)^2 \qquad \text{(Eq. 8)}$$



0022-3549/81/1200-1350$01.00/0
© 1981, American Pharmaceutical Association

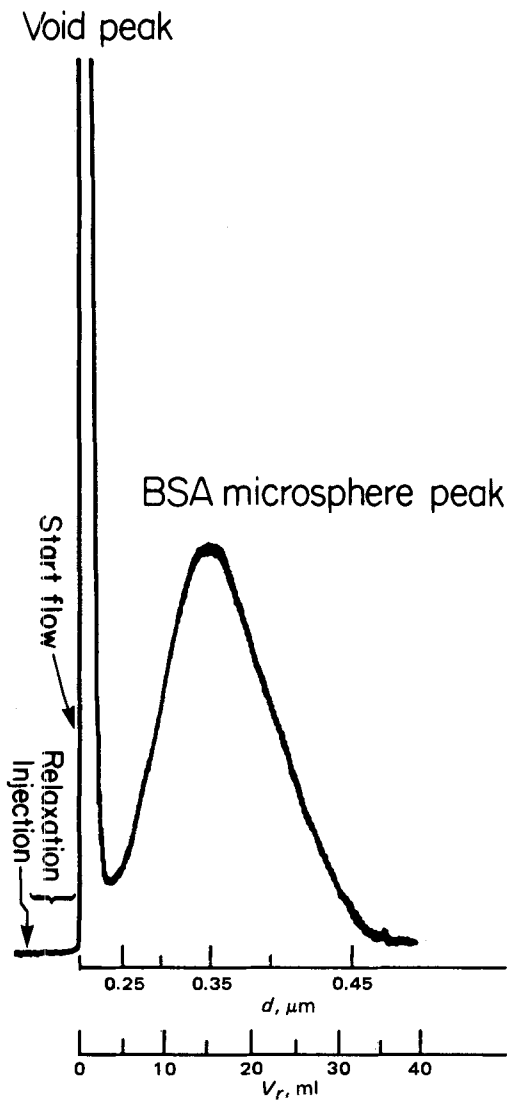


**Figure 1**—*Sedimentation FFF fractogram of bovine serum albumin (BSA) microspheres. Field strength was 13,510 cm sec$^{-2}$, and flow rate was 30 ml/hr. Retention volume and particle-size scale (from Eq. 3) are both shown on the horizontal axis.*

where $w_{1/2}$ equals the peak width on the chart measured at half the peak height and $s$ is the distance on the chart from the start of flow to the position of the peak maximum.

**Sample**—The bovine serum albumin microspheres were prepared using a procedure developed earlier (7) for preparation of human serum albumin for labeling with technetium 99m to visualize the reticuloendothelial system. Because the microspheres were not intended for medical use, the UV irradiation and autoclaving steps were omitted; instead, the microspheres were washed three times with ethanol and then suspended in ethanol. This preparation was injected into the sedimentation FFF column and fractionated by the conventional procedure (2).

The microspheres from this preparation were examined by transmission electron microscopy to compare the sedimentation FFF results to those obtained by an established procedure. The TEM results were calculated by measuring diameters of 300 particles from photomicrographs.

**Table I—Mean Particle Diameters for Albumin Microspheres Calculated at Various Field Strengths from FFF Retention Data** [a]

| Revolutions per Minute | $G$, cm sec$^{-2}$ | $d$, μm |
|---|---|---|
| 250 | 5277 | 0.353 |
| 300 | 7600 | 0.353 |
| 350 | 10,344 | 0.349 |
| 400 | 13,510 | 0.349 |
| 450 | 17,099 | 0.345 |
| 500 | 21,110 | 0.340 |
| Mean | | 0.348 |
| *SD* | | 0.005 |

[a] Flow rate was 30 ml/hr.

**Table II—Mean Particle Diameters for Albumin Microspheres Determined** [a] **at Various Flow Rates.**

| Flow Rate ml/hr | Flow Rate cm/sec | $V_r$, ml | $d$, μm |
|---|---|---|---|
| 23.5 | 0.257 | 15.7 | 0.349 |
| 26.0 | 0.284 | 15.5 | 0.346 |
| 30.0 | 0.328 | 15.8 | 0.349 |
| 34.0 | 0.372 | 15.5 | 0.346 |
| 39.0 | 0.426 | 15.4 | 0.346 |
| 44.0 | 0.481 | 14.8 | 0.341 |
| Mean | | | 0.346 |
| *SD* | | | 0.003 |

[a] Field strength was 400 rpm ($G$ = 13,510 cm sec$^{-2}$).

## RESULTS AND DISCUSSION

The first set of experiments consisted of sedimentation FFF runs at various field strengths (rotation rates). A typical fractogram is shown in Fig. 1. The purposes of these experiments were to verify that the theory provides self-consistent results under different experimental conditions and to provide redundant data for characterization of the albumin microspheres by Method A. The results of these experiments are given in Table I. The consistency in $d$ shows the application of theory to be valid

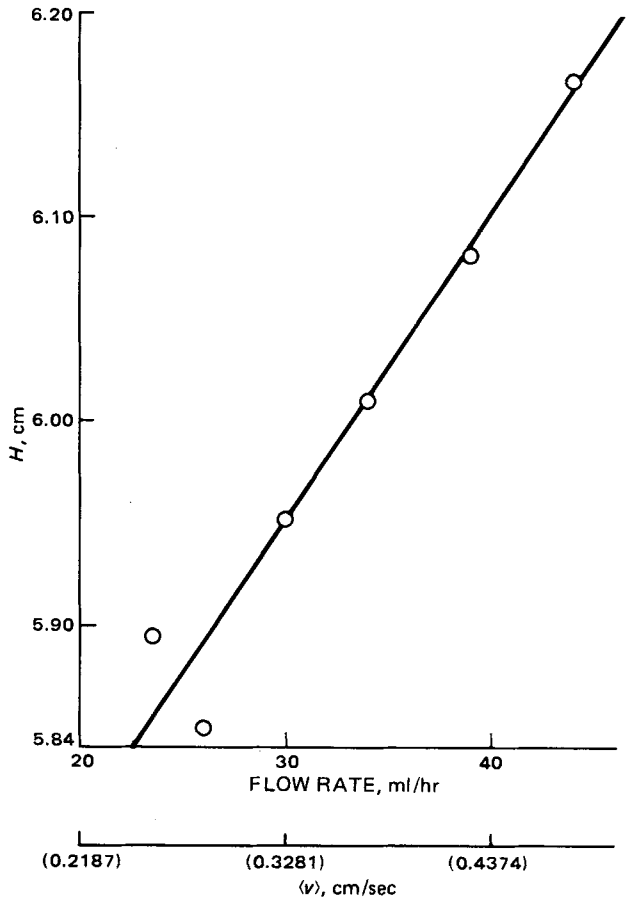


**Figure 2**—*Plot of plate height* versus *flow rate for albumin microspheres at a field strength of 13,510 cm/sec$^{-2}$.*

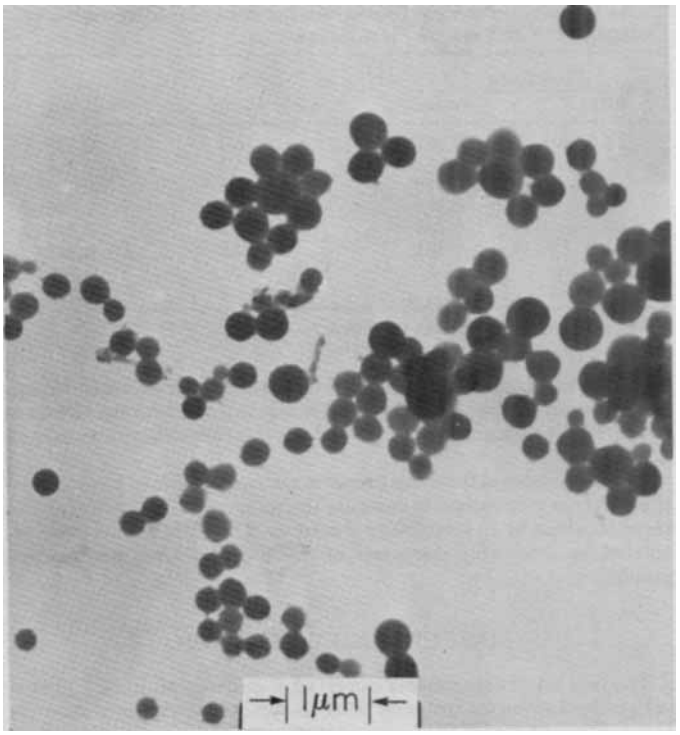


**Figure 3**—*TEM photomicrograph of albumin microspheres.*

over the range of rotation rates investigated (250–500 rpm). The density of the particles was assumed to be 1.36 g/ml based on literature values (8).

A second set of experiments was run at six different flow rates, maintaining a spin rate of 400 rpm. The results (Table II) demonstrate the consistency of mean particle diameter measured under different flow conditions. These results complement those of Table I in showing the FFF results to be independent of experimental conditions. The flow-dependent runs were also used to obtain the plate height data necessary for Method B. The plot of $H$ *versus* $\langle v \rangle$, necessary for Method B, is shown in Fig. 2.

Table III summarizes and compares the particle-size and polydispersity results obtained from the two FFF methods and the TEM observations. The first row of the table shows the results of Method A [called FFF(A)]. These results were obtained from the run (Fig. 1) at 400 rpm at a flow rate of 30 ml/hr. The ability to calculate valid data from just one run is based on unpublished results of separate experiments studying many monodisperse polystyrene latex samples on two different apparatus, which showed that plate height and thus polydispersity measurements were independent of field strength and the apparatus used. Because the instrument run time was only 1.5 hr, FFF(A) was the most rapid method of characterization.

**Table III—Characterization of Albumin Microspheres by Three Methods**

| Method | $d$, μm | $\sigma_d$, μm | $D$, cm²/sec |
|---|---|---|---|
| FFF(A) | 0.349 | 0.040 | $1.15 \times 10^{-8}$ |
| FFF(B) | 0.346 | 0.039 | $1.13 \times 10^{-8}$ |
| TEM | 0.354 | 0.062 | — |

The results of Method B [FFF(B)], requiring the calculation of $\sigma_d$ from the intercept of the $H$ *versus* $\langle v \rangle$ plot of Fig. 2, are also shown in Table III. This measurement of $\sigma_d$ requires more time than needed for FFF(A) because several separate runs are required to construct the plot of Fig. 2.

The third characterization was by the more conventional electron microscopy method. Table III lists the results of this characterization as well. Figure 3 is a typical photomicrograph from which measurements were made.

Table III shows that the two independent FFF methods yield results in excellent agreement. These results are further confirmed by reasonable agreement with those of electron microscopy. However, the FFF results, particularly from Method A, are much more conveniently obtained than those from TEM. FFF thus appears to be a rapid and accurate method for characterizing albumin microspheres and other submicron particles.

## REFERENCES

(1) J. C. Giddings, S. R. Fisher, and M. N. Myers, *Am. Lab.*, **10**, 15 (1978).

(2) J. C. Giddings, M. N. Myers, K. D. Caldwell, and S. R. Fisher, in "Methods of Biochemical Analysis," D. Glick, Ed., Wiley, New York, N.Y., 1980, p. 79.

(3) J. C. Giddings, M. N. Myers, and J. F. Moellmer, *J. Chromatogr.*, **149**, 501 (1978).

(4) K. D. Caldwell, T. T. Nguyen, J. C. Giddings, and H. M. Mazzone, *J. Virol. Methods*, **1**, 241 (1980).

(5) J. C. Giddings, F. J. Yang, and M. N. Myers, *Anal. Biochem.*, **81**, 395 (1977).

(6) L. R. Snyder and J. J. Kirkland, "Introduction to Modern Liquid Chromatography," 2nd ed., Wiley, New York, N.Y., 1979, chap. 2.

(7) U. Sheffel, B. A. Rhodes, T. K. Natarajan, and H. N. Wagner, *J. Nucl. Med.*, **13**, 498 (1972).

(8) J. T. Edsall, in "The Proteins," vol. II, 1st ed., N. Neurath and K. Bailey, Eds., Academic, New York, N.Y., 1953, p. 549.

## ACKNOWLEDGMENTS

Supported by National Institutes of Health Grant GM10851-23.

The authors are indebted to Mr. P. C. Briot and Dr. L. M. Okun of the Department of Biology, University of Utah, for preparing the albumin microspheres.

# Dissolution, Stability, and Absorption Characteristics of Dicumarol in Polyethylene Glycol 4000 Solid Dispersions

**WILLIAM R. RAVIS** ˣ **and CHIEN-YU CHEN**

Received January 21, 1981, from the *Department of Pharmacal Sciences, School of Pharmacy, Auburn University, Auburn, AL 36849.* Accepted for publication April 10, 1981.

**Abstract** □ The dissolution characteristics of dicumarol were markedly enhanced by preparing dispersions of drug in polyethylene glycol 4000. Solid dispersions of varying weight fractions were formed by a melt method without measurable drug degradation or evaporation. There were no significant differences in dissolution rates among weight fractions, with dynamic solubilities being ~2.5 times greater than dicumarol's equilibrium solubility. No indications of drug polymer complexation were noted from equilibrium or *in situ* absorption experiments. Incorporation of solid dispersions into direct compression tablets provided dosage forms with fast-release properties relative to test tablets of physical mixtures and a commercially available product. Percentages dissolved in 30 min were 370% greater for 1:3 and 1:5 (w/w) solid dispersion tablets compared to a commercial tablet at 37° with a pH 7.5 dissolution buffer. X-ray diffraction of test powder revealed that the crystalline nature of the drug had altered during fusion preparation. Dissolution traits and drug stability for solid dispersions were maintained over 1 year of storage.

**Keyphrases** □ Dicumarol—dissolution, stability, and absorption characteristics in polyethylene glycol 4000 solid dispersions □ Dissolution—dicumarol in polyethylene glycol 4000 solid dispersions □ Polyethylene glycol 4000—effect on dicumarol dissolution, stability, and absorption

The preparation of drug–polymer disperions by fusion and solvent techniques has successfully increased dissolution properties (1–8) and bioavailability (5, 6, 9–12) of poorly water-soluble drugs. Properties of water-soluble polymers such as large molecular size, high viscosity, and supercooling can provide a dispersed drug in a metastable or fast-release form (1, 2). Povidone has been a popular choice as an inert carrier for dispersions prepared by solvent or coprecipitation methods. Among several examples, griseofulvin (3), sulfathiazole (4), and reserpine (5, 6) demonstrate faster dissolution rates when they are dispersed in povidone by a solvent method. For the fusion or melt method, polyethylene glycols have been employed extensively. The dissolution of prednisolone, methyltestosterone, hydrocortisone, and digitoxin has been enhanced by polyethylene glycol fusion dispersions (7). Similarly, enhanced dissolution rates of griseofulvin (2, 8), nitrofurantoin, ethotoin, and coumarin (13) in polymer melt systems were reported.

The oral anticoagulant dicumarol, 3,3′-methylene-bis[4-hydroxycoumarin], is practically insoluble in water (14). It is reported to be poorly and erratically absorbed from both powder and tablet dosage forms (15–17). The bioavailability of dicumarol in tablets is influenced by the type and amount of excipients (18). This drug's classification as dissolution rate limited was supported in studies in dogs (19) where a strong relationship between dissolution data and bioavailability and prothrombin time was noted.

Reports of poor and erratic bioavailability serve as a stimulus for examining new dicumarol formulations that may provide more complete and consistent absorption. The present investigation reports the preparation of dicumarol and polyethylene glycol 4000 solid dispersions by a fusion method and discusses possible mechanisms for their fast-release properties.

## EXPERIMENTAL

**Preparation of Test Powders**—Solid dispersions of polyethylene 4000[1] and dicumarol[2] were prepared from physical mixtures by the fusion or melt method. Physical mixtures representing drug to polyethylene glycol 4000 ratios of 1:1, 1:3, and 1:5 (w/w) were heated over a thermostatic plate with constant stirring until a clear homogeneous melt was obtained. Melts were quickly poured on air-cooled aluminum pans or were glass-suspended in a vented hood. After 1 hr, solidified dispersions were stored in a desiccator for 2 days prior to pulverization.

Other physical mixtures containing heated drug and polymer were obtained by separately heating each component to 280° and then cooling and storing as described for dispersions. Particle-size reductions of physical mixtures were performed by a ball mill while reductions for solid dispersions and heated physical mixtures were accomplished by light tituration in a cooled mortar. Test powders were modified by sieving to provide particle sizes of 100–60 mesh for dispersions and physical mixtures and of <140 mesh for dicumarol.

**Stability Testing of Physical Mixtures and Solid Dispersions**—Assessments of dicumarol stability were conducted by UV spectroscopy, paper chromatography, and TLC. Alkaline solutions (0.1 *N* NaOH) prepared from powders and tablets were utilized in a paper separation with acetic acid–benzene–water (2:2:1) as a solvent (20) as well as for two thin-layer separations on silica gel plates[3] with fluorescent indicator[3]. Thin-layer solvent systems included 3 *M* ammonium hydroxide–ethyl acetate (1:1) and ether–chloroform–acetone (60:30:1). Additional separations were performed with solutions prepared by redissolving dicumarol precipitates obtained from acidified samples.

In chromatographic experiments in which [$^{14}$C]dicumarol[4] was incorporated into solid dispersions, silica gel plates were scraped in sections following development. The radioactivity of each scraping was determined by suspending each in cocktail[4] and counting with the aid of a liquid scintillation counter[5]. All samples were corrected for quenching by quench curves.

**Nonequilibrium Solubility Studies**—Powder dissolution testing was conducted with a 1000-ml, three-necked, round-bottom flask containing 700 ml of 0.05 *M* phosphate buffer (pH 7.5). The apparatus was maintained at 37.0 ± 0.5° by a water bath. To mix the medium, a sleeve stirrer positioned 4 cm from the flask bottom was connected to a constant-speed motor adjusted to 60 rpm. Test powders containing 100-mg equivalents of dicumarol were added to the medium at time zero followed by 4-ml sampling with replacement. Samples were immediately filtered with 0.05- or 0.22-$\mu$m filters[6], and absorbance values were obtained at 314 nm[7] for each sample before and following pH adjustment to 12 with 4 *N* NaOH. Amounts dissolved were calculated from standard curves in pH 7.5 and 12.0 media and corrected for sample dilution (21).

**Preparation of Test Tablets**—After storage of test powders for periods not exceeding 2 weeks, portions of physical mixtures and solid

[1] City Chemical Corp. New York, N.Y.
[2] Sigma Chemical Co., St. Louis, Mo.
[3] Eastman Kodak Co., Rochester, N.Y.
[4] Amersham-Searle, Arlington Heights, Ill.
[5] LS-150, Beckman Instruments, Fullerton, Calif.
[6] Millipore Corp., Bedford, Mass.
[7] Model 100-60, Hitachi Ltd. Tokyo, Japan.

0022-3549/81/1200-1353$01.00/0
© 1981, American Pharmaceutical Association

dispersions were combined and blended with anhydrous lactose[1]. The diluent was added to provide tablets of equal weight, 325 mg. To most formulations, 1% magnesium stearate[1] was added to minimize capping. Formulations were prepared as direct compression tablets with the aid of a single-punch tablet press[8]. Compression force was adjusted to give tablets of comparable hardness (4.4 ± 0.6 kg). Tablet lots were tested for hardness[9], content uniformity, thickness, dissolution, stability, and weight variation.

**Tablet Dissolution Studies**—The tablet dissolution apparatus, comprised of a beaker and basket arrangement, was maintained at 37.0 ± 0.5° by a water bath. The dissolution medium consisted of 1000 ml of deaerated, 0.05 *M* phosphate buffer (pH 7.5). Studies were conducted with test tablets and a selected commercial product. At frequent time intervals after immersion of the baskets, which were rotated at 50 rpm, 4.0-ml samples were withdrawn. Samples were filtered and treated as described for powder nonequilibrium studies.

**Absorption from *In Situ* Intestinal Loops**—Male Sprague-Dawley rats[10], 260–300 g, were fasted 24 hr prior to the procedure. After anesthetization with 40 mg of pentobarbital sodium[2]/kg ip, a midline incision was made. A 15-cm segment representing the upper jejunum was carefully cannulated and gently rinsed with warm saline to remove lumenal matter. Tubing was attached to each cannula and was then passed through a perfusion pump[11] leading to a reservoir. Perfusion was carried out in a recycling fashion with the 60 ml of drug containing buffer maintained at 37.0 ± 0.5° in the reservoir. The perfusion buffer was passed through the intestine in a proximal to distal direction at a calibrated rate of 4.8 ml/min. This rate provided rapid perfusion without overly distending the intestinal segment. Samples were taken from the reservoir, and amounts absorbed were corrected for fluid flux based on reservoir volume.

Dicumarol levels in perfusion samples were determined by a previously described method (17) as revised by Nagashima *et al.* (22).

**Data Analysis**—The amounts dissolved in powder and tablet dissolution studies were compared between preparations and sample times by one- or two-way analysis of variance and Tukey testing (23).

**X-Ray Diffraction Studies**—Test powders were firmly packed on a slide with glass windows. Diffraction spectra[12] were prepared by scanning at a rate of 2°/min in terms of a $2\theta$ angle.

## RESULTS AND DISCUSSION

**Preparation and Stability Studies**—The temperature required for obtaining melts of dicumarol with polyethylene glycol 4000 was below that of the pure drug, 290°, and measurably decreased as the weight fraction of polymer was increased. Lowering in melting points as a function of weight fraction for binary systems is not an unexpected or unique phenomenon (1, 24). For dicumarol–polyethylene glycol 4000 dispersions of 1:1, 1:3, and 1:5, melt temperatures necessary to obtain a visually clear, homogeneous liquid were 275, 263, and 255°, respectively. Dispersions of drug to polymer weight fractions of >1:1 (such as 2:1) could not be prepared at a temperature less than the drug's melting point. Smaller weight fractions were not considered appropriate based on results of powder dissolution studies.

Powdered and milled physical mixtures of 280° heated and unheated drug and polymer appeared white and crystalline, while melted dispersions were orange brown. Polarized light microscope examination indicated the presence of crystalline materials in dispersions and physical mixtures. The crystalline appearance of all physical mixtures, composed of heated and unheated components, resembled that of powdered dicumarol and polyethylene glycol while that of the melt dispersions was distinctly different. Fusion products contained smaller crystals of orange-like reflection dispersed in a clear polymer matrix.

The concern for possible drug degradation was emphasized by the coloration of fusion products and by other studies (7) demonstrating drug degradation in polyethylene glycol melts. Three chromatographic separations of $^{14}C$-labeled dicumarol dispersions failed to show any degradation materials. Similar chromatographic studies performed with solutions of dispersion powders and direct compression tablets that had been stored for 1 year revealed lack of degradation or drug loss.

It was concluded from the stability tests that, at the temperature required for drug–polymer melts, drug decomposition did not occur and, thus, was not responsible for the coloration of the fusion dispersions. The heating temperature necessary to discolor polymer or drug separately exceeded the melt temperatures for fusion. The orange-brown coloration apparently is unique to the solid dispersion. Differences in color between dispersions obtained by melting without measurable drug degradation and their physical mixtures were reported (2).

**Nonequilibrium Solubility Studies**—Solubility experiments for comparing powder dissolution rates demonstrated a dramatic enhancement in initial dicumarol solubility for the three dispersions (Fig. 1). Physical mixtures of heated materials gave similar release profiles to those of other physical mixtures and powdered drug. As summarized in Table I, the maximum observed solubility for dispersions over the 23-hr studies was approximately twofold greater than that of the physical mixtures, with maximum levels for dispersions noted at 60 min compared to >660 min for physical mixtures and pure drug.

Among the three weight fractions, significant differences in the amounts of dicumarol dissolved were not found at any sampling interval. Large variability in the initial amounts released by the dispersion appeared to mask any small differences that might exist between the prepared weight fractions. At the end of 23 hr, final dicumarol concentrations for all dispersions were 30% greater than dicumarol powder or dicumarol powder incorporated into physical mixtures. Comparisons of the percentage dissolved by time showed the drug levels to be constant for all dispersions for 8–23 hr. Whether dicumarol's solubility in the media of solid dispersion preparation approaches that of pure drug after 23 hr was not examined.

The supersaturated state of the media created by the solid dispersions represented a dissolution of <40% of the drug initially added to the system, thereby maintaining solid drug in excess throughout the experiments. Amounts dissolved in 10 min were eightfold greater for dispersions compared to powdered pure drug. Drug levels fell rapidly after 60 min for all dispersions, providing profiles that might be expected for a high energetic drug form (5, 25–28). The ratio of dynamic to equilibrium solubility for dicumarol dispersions was ~1.4 for all weight fractions, while the ratio of the dynamic solubility for dispersions relative to the equilibrium solubility for dicumarol powder was 2.5. Upon standing, drug crystallization and loss in UV absorbance were noted in withdrawn dissolution samples. To obtain solubility values accurately, it was necessary to filter and obtain absorbance measurements immediately.

UV spectra and calculations of amounts dissolved for alkalinized and nonalkalinized filtered samples from respective standard curves seemed to confirm the existence of a supersaturated state in the early time periods. Filtration of samples through 0.45–0.05-$\mu$m filters did not alter measured drug concentrations. A similar dissolution characteristic was described (28) for polymorphs of cortisone acetate. Another mechanism for describing the overshoot of equilibrium concentration during initial dissolution periods was proposed earlier (29). By this explanation, drug release from a polymer mixture continues after saturation as a result of further dissolution of drug in complex with polymer, which acts as a drug carrier.

The similarity of drug release for pure drug compared to physical mixtures demonstrates the relative noninteractive nature of drug and polymer such that wetting and complexation features of polyethylene glycol may be negligible in this dispersion system. Wetting effects may explain the slightly faster initial dissolution rates of physical mixtures compared to drug powder. Observations of higher equilibrium solubilities for the dispersion and the possible participation of the polymer as a

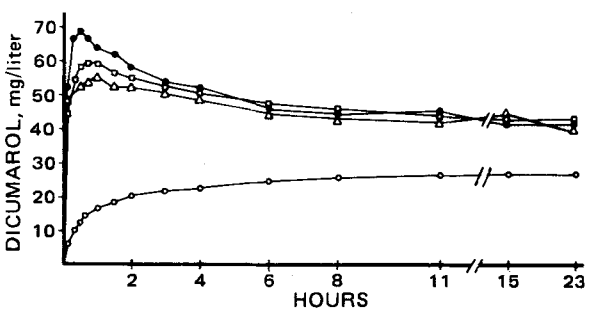


**Figure 1**—*Dissolution of dicumarol test preparations at 37°. Key:* ○, *dicumarol powder;* □, *1:1 (w/w) dicumarol–polyethylene glycol 4000 dispersion;* ●, *1:3 (w/w) dicumarol–polyethylene glycol 4000 dispersion; and* △, *1:5 (w/w) dicumarol–polyethylene glycol 4000 dispersion.*

[8] Stokes model F, Pennsalt Chemical Corp., Warminster, Pa.
[9] Stokes hardness testers, Pennsalt Chemical Corp., Warminster, Pa.
[10] Southern Animal Farms, Prattville, Ala.
[11] Harvard Apparatus Co., Millis, Mass.
[12] Philips X-ray diffraction unit type 12215/0.

**Table I—Summary of Dissolution and Equilibrium Solubility for Dicumarol Test Powders**

| Preparation | $t_{max}$, min | Dynamic Solubility, mg/liter | Concentration, mg/liter 10 min | 40 min | 1380 min |
|---|---|---|---|---|---|
| Dicumarol powder | >660 | 27.7 (0.6)[a] | 6.3 (2.1) | 14.9 (1.7) | 27.3 (0.6) |
| Physical mixtures | | | | | |
| 1:5 (w/w)[b] | >660 | 27.6 (1.4) | 14.9 (1.9) | 19.0 (2.9) | 27.6 (1.0) |
| 1:5 (w/w), heated[c] | >660 | 26.7 (2.7) | 10.1 (0.9) | 18.3 (3.9) | 24.9 (1.7) |
| Solid dispersions | | | | | |
| 1:1 (w/w) | 40 | 59.4 (4.3) | 44.6 (7.5) | 59.4 (4.3) | 41.6 (0.4) |
| 1:3 (w/w) | 30 | 69.3 (4.7) | 54.0 (5.4) | 67.4 (6.6) | 41.6 (6.6) |
| 1:5 (w/w) | 60 | 54.9 (10.0) | 49.0 (9.5) | 53.1 (8.7) | 41.4 (3.1) |
| Dicumarol powder with polyethylene glycol dissolution medium[d] | | | | | |
| 0.071% | >660 | 25.6 (1.1) | 5.9 (2.1) | 11.7 (1.6) | 26.7 (0.9) |
| 0.043% | >660 | 25.4 (1.4) | 7.5 (1.8) | 14.7 (3.0) | 25.0 (1.3) |
| 0.014% | >660 | 27.3 (1.6) | 9.1 (1.5) | 14.4 (1.3) | 26.3 (1.7) |

[a] Mean ±*SD*; $n = 6$. [b] Dicumarol–polyethylene glycol 4000 (w/w). [c] Drug and polymer heated separately to 280° and cooled prior to preparation of physical mixture. [d] Concentration of polyethylene glycol 4000 in dissolution medium.

**Table II—Summary of Tablet Dissolution Studies of Solid Dispersions, a Physical Mixture, and a Commercial Tablet of Dicumarol**

| Preparation | $t_{10\%}$ | Percent Dissolved 10 min | 30 min | 60 min | 90 min |
|---|---|---|---|---|---|
| Commercial | 13.5 | 4.1 (0.4)[a] | 15.0 (1.0) | 19.4 (2.4) | 22.2 (4.2) |
| Physical mixture, 1:5 | 31.0 | 4.7 (4.1) | 10.2 (8.1) | 12.5 (9.4) | 13.0 (8.5) |
| Solid dispersions | | | | | |
| 1:1[b] | 7.1 | 15.5 (2.3) | 46.6 (2.4) | 57.2 (1.8) | 73.8 (3.2) |
| 1:3[b] | 3.4 | 35.0 (5.1) | 67.1 (2.2) | 72.8 (1.7) | 74.3 (3.1) |
| 1:5[b] | 3.1 | 38.2 (2.0) | 72.8 (3.1) | 78.1 (3.6) | 79.0 (3.1) |
| 1:5 without magnesium stearate[b] | 2.2 | 48.4 (0.8) | 70.7 (2.1) | 76.0 (3.2) | 77.3 (2.8) |
| 1:1 polyethylene glycol 4000 medium[b] | 5.6 | 17.8 (2.6) | 52.0 (3.1) | 66.2 (5.2) | 73.0 (6.3) |
| 1:5, 1-year storage[b] | 3.0 | 39.6 (2.6) | 72.0 (2.6) | 79.6 (2.4) | 78.1 (2.8) |
| 1:1, 1-year storage[b] | 6.7 | 16.5 (1.6) | 47.6 (2.2) | 58.3 (1.5) | 75.2 (2.5) |

[a] Mean ± *SD*; $n = 6$. [b] Significantly ($p < 0.05$) greater amounts dissolved at all sampling periods compared to physical mixture or commercial product.

dissolution carrier presented a need to evaluate better any contributions that polymer and dicumarol complexation may have on the dispersion's performance. In addition, dicumarol was reported (30) to interact with povidone to form highly soluble complexes. With conditions identical to previous studies, polyethylene glycol was predissolved in the media at three concentrations corresponding to those expected for complete polymer dissolution in the dispersions. As summarized in Table I and Fig. 2, equilibrium solubilities after 6 hr were independent of polymer concentrations. Amounts released prior to 6 hr decreased slightly as the levels of polyethylene glycol increased, which may be the result of viscosity influences on release rate.

Neither milling, melting, nor separate heating of dicumarol or polyethylene glycol 4000 to a temperature exceeding that required for melts influences dissolution (Table I). Marked enhancement in dicumarol dissolution in prepared fusion dispersions apparently is unique to the fusion product and not secondary to the polymer effects or the results of applied temperature.

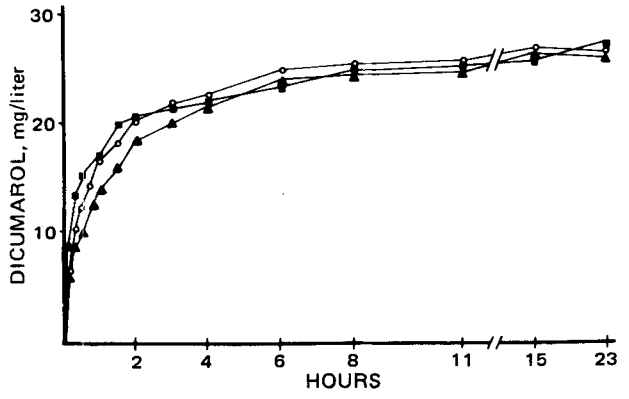


**Figure 2**—*Dissolution of dicumarol powder and physical mixture at 37°. Key: ○, dicumarol powder; ■, 1:5 (w/w) dicumarol–polyethylene glycol 4000 physical mixture; and ▲, dicumarol powder in 0.071% polyethylene glycol 4000 dissolution media.*

Since higher solubility of dicumarol in solid dispersions did not seem to be a consequence of polymer–drug complexation, the elevated drug levels during the latter portion of the equilibrium experiments may be the result of an inhibitory effect of the polymer on the drug's conversion to a stable, less soluble crystalline species. Prevention of nucleation and recrystallization to a stable crystalline form by solutions of high molecular weight polymers such as povidone was previously discussed (4, 5). In evaluating the influence of the drug–polymer dispersion ratio with respect to polymer medium concentration, retardation of stable crystal formation was independent of the polymer ratio. Therefore, the minimum inhibitory polymer levels appear to be <0.014% with 37° dissolution media.

**Tablet Dissolution Studies**—Solid dispersions and physical mixtures were incorporated into direct compression tablets to evaluate the effects of tableting on dicumarol release from solid dispersions and to provide a solid dosage form for future comparative bioavailability studies. Tablets were designed to be of equal weight by the addition of lactose and were nondisintegrating.

Results of tablet dissolution experiments expressed as percentage released are presented in Table II and Fig. 3. Calculation of dissolution rate constants through application of tablet dissolution models was considered inappropriate since previous nonequilibrium profiles revealed that observed release kinetics would be complex and reflective of both rapid release and crystallization. Comparisons of percentage dissolved at 5–90 min gave the rank order for the dissolution of test tablets containing 1% magnesium stearate as a lubricant: 1:5 = 1:3 >1:1 solid dispersions >1:5 physical mixture = commercial product.

Tablets containing the dispersions of 1:3 and 1:5 weight fractions showed marked increases in percentage released at 10, 30, 60, and 90 min compared to commercial and physical mixture forms with approximate increases of 290, 366, 290, and 245%, respectively. Dissolution profiles for tablets representing the three weight fractions stored for 1 year were identical to those for freshly prepared tablets. The markedly slower dissolution noted for the nondisintegrating tablet compared to previously examined powders indicates that this drug's dissolution may be further maximized by incorporating powdered dispersion into disintegrating tablets or capsules.

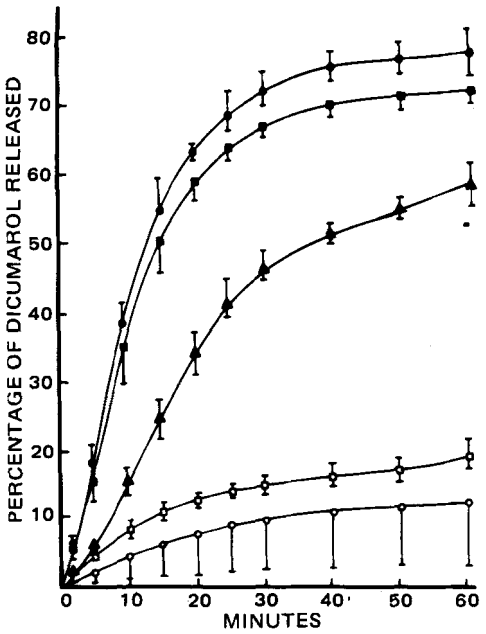


**Figure 3**—*Dissolution profiles of test tablets and a commercial product. Key: ●, 1:5 (w/w) dicumarol–polyethylene glycol 4000 dispersion; ■, 1:3 (w/w) dicumarol–polyethylene glycol 4000 dispersion; ▲, 1:1 (w/w) dicumarol–polyethylene glycol 4000 dispersion; ○, 1:5 (w/w) dicumarol–polyethylene glycol physical mixture; and □, commercial product.*

The inclusion of a lubricant, magnesium stearate, prevented tablet capping during direct compression. It was noted (18) that the incorporation of several magnesium compounds such as magnesium hydroxide and magnesium oxide into dicumarol formulations increased drug absorption. In that same study, magnesium stearate had no significant influence on the completeness of drug absorption, which is consistent with dissolution results in the present study showing equal or lower release rates for lubricant-containing tablets relative to those with no lubricant.

The apparent slower dissolution of dicumarol from the 1:1 dispersions compared to dispersions of higher percentages of polyethylene glycol 4000 could result from the greater portion of a slower dissolving diluent, lactose, in this formulation and/or to more extensive nucleation and conversion of a metastable to a less soluble stable form during the initial dissolution period. The latter explanation appears plausible considering the possible inhibitory effects of dissolved polymer on crystallization and recognizing that the low polymer to drug ratio tablet would supply the least polyethylene glycol concentration on dissolution. Substantial crystallization may occur initially if the levels of polymer in the bulk are below those necessary to inhibit renucleation. However, this explanation is probably inadequate since the 90-min percentages dissolved were not significantly different among the three ratios. In addition, predissolving the polymer did not alter the profiles for the 1:1 dispersion tablets. In experiments where the nondisintegrating tablets were removed from baskets after 20 min, 1:1 dispersion tablets appeared to dissolve slower. Thus, lactose dissolution may be rate limiting.

**X-Ray Diffraction Studies**—Spectra of unmilled dicumarol and milled polyethylene glycol 4000 appear in Fig. 4; spectra for the milled 1:1 dispersion and its physical mixture appear in Fig. 5. The major dicumarol diffraction peaks of 24.9, 26.9, and 11.8° could be identified in the solid dispersion sample as weak intensity peaks with ~18% of the intensity of drug alone in the physical mixture. All visible peaks for the physical mixture could be identified as those of polyethylene glycol 4000 or dicumarol. The intensities of major drug peaks were substantially greater in the physical mixture compared to the dispersion, which may indicate a loss in the drug's initial crystalline form during the fusion process. Peaks for the solid dispersions, appearing at ~23.4 and 20.8°, did not correspond to any of the major peaks noted for the polymer or drug. Other dicumarol peaks, such as measured at 10.4°, displayed increased intensity in the dispersion.

Observations of unidentifiable peaks accompanied by the disappearance of component peaks may be in accordance with spectral changes

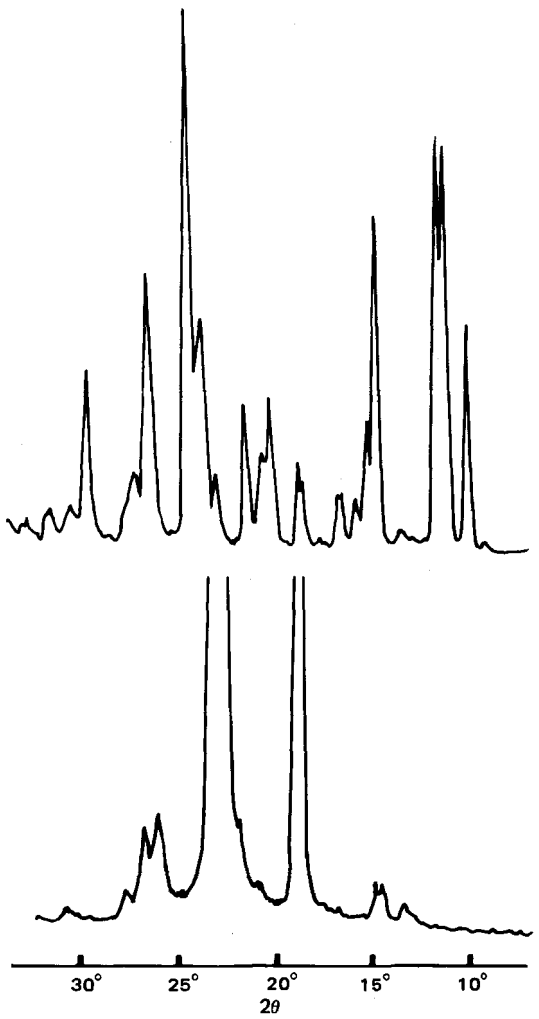


**Figure 4**—*X-ray diffraction spectra of dicumarol (top) and milled polyethylene glycol 4000 (bottom).*

expected for partial polymorphic conversion or solid solution. However, the presence of component peaks in the melts does not allow partial eutectic formation and particle-size reduction to be completely ruled out. The identification of well-defined peaks and the absence of a raising baseline seems to exclude amorphous drug formation as a major factor in the dispersion.

**Dicumarol *In Situ* Absorption**—*In situ* rat intestinal loops were utilized to examine dicumarol absorption from solutions prepared from drug alone, physical mixtures, and fusion dispersions. Solutions of high molecular weight polymer in the GI lumen may alter absorption by viscosity effects (31), solvent effects (32), and drug complexation (33). Table III shows the percentage of initial drug concentration remaining at 30 and 90 min for the recycling perfusion of jejunal segments. Dicumarol

**Table III—Absorption of Dicumarol by Infused [a] *In Situ* Intestinal Loops**

| | Percentage Remaining to be Absorbed [b] | | | |
|---|---|---|---|---|
| Minute | Dicumarol Powder | 1:5 Dicumarol–Polyethylene Glycol Physical Mixture | 1:5 Dicumarol–Polyethylene Glycol Dispersion | Statistical Analysis [c] |
| 0 | 100 | 100 | 100 | |
| 30 | 29.9 (4.9) [d] | 36.1 (9.0) | 34.7 (6.6) | NS [e] |
| 90 | 22.4 (3.4) | 22.7 (6.2) | 29.9 (3.4) | NS [e] |

[a] Recirculating infusion of a 15-cm segment at a rate of 4.8 ml/min. [b] Infusion buffer consisted of 60 ml of Krebs–Henseliet buffer with a dicumarol concentration of 10 μg/ml. [c] Analysis of variance with $p < 0.05$. [d] Mean ± *SD*; $n = 4$. [e] Not significant.

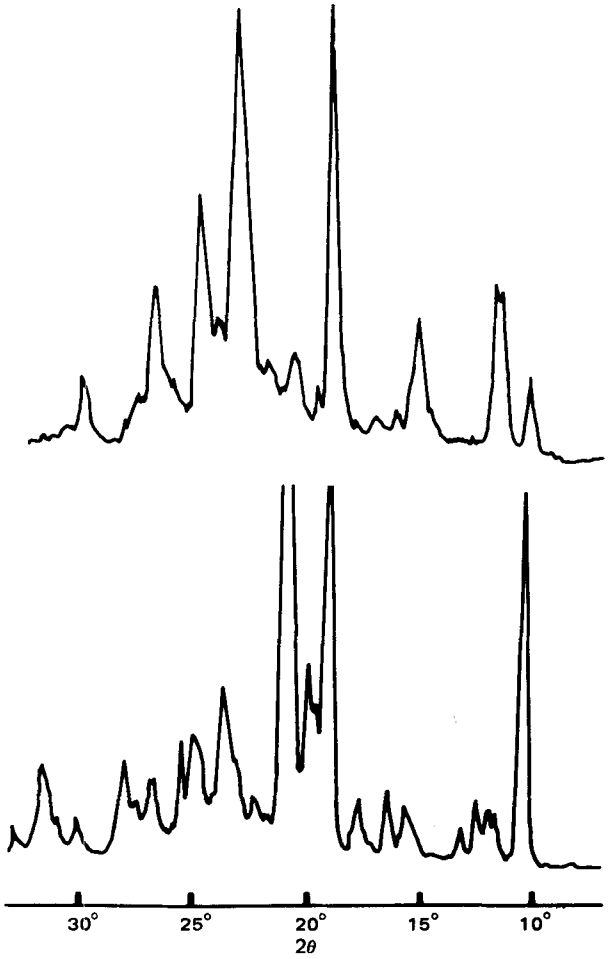


**Figure 5**—*X-ray diffraction spectra of 1:1 (w/w) dicumarol–polyethylene glycol 4000 physical mixture (top) and solid dispersion (bottom).*

rapidly disappeared from all perfusion buffers such that 68% was absorbed in the first 30 min. This initial rapid phase was possibly a result of tissue equilibrium since the absorption rates were substantially less during the 30–90-min interval. While initial *in situ* absorption was probably, in part, perfusion limited since the intestinal clearance rate of 2.3 ml/min was 48% of the perfusion rate, no significant effects of polyethylene glycol on this drug's absorption can be reported. These observations would confirm the absence of strong complexation as previously discussed as well as demonstrate that the polymer does not alter the membrane absorption of this drug *in situ*.

## CONCLUSIONS

Observations of rapid drug disappearance from *in situ* loops and low equilibrium solubility would support previous statements (16, 19) of dicumarol's dissolution rate-limited character and, thereby, formulation sensitivity. The present study showed that the dissolution characteristics of dicumarol can be enhanced through the preparation of melt fusion products with polyethylene glycol 4000 without detectable degradation. Unlike other polyethylene glycol–drug (8) dispersion systems, complexation between drug and polymer cannot be considered as a factor contributing to higher dissolution rates for powders and tablets. Preliminary studies of X-ray diffraction patterns demonstrated that fusion products contained crystalline materials that could not be identified as either pure drug or polymer.

Further investigations employing differential thermal analysis and X-ray diffraction need to be performed to characterize the apparent high energy form of dicumarol in fusion dispersions. Based on X-ray microscopy and dissolution results, partial polymorphic conversion or solid solution formation seems to be an attractive explanation. After 1 year of storage for powders and direct compressed tablets, stability was unaltered and enhanced dissolution traits appeared unaffected. Investigations are currently being conducted with the aid of the described tablet dosage form to evaluate dicumarol's dissolution–bioavailability relationship.

## REFERENCES

(1) W. L. Chiou and S. Riegelman, *J. Pharm. Sci.*, **60,** 1281 (1971).
(2) *Ibid.*, **58,** 1505 (1968).
(3) M. Mayersohn and M. Gibaldi, *ibid.*, **55,** 1323 (1966).
(4) A. P. Simonelli, S. C. Mehta, and W. I. Higuchi, *ibid.*, **58,** 538 (1969).
(5) E. I. Stupak, H. A. Rosenberg, and T. R. Bates, *J. Pharmacokinet. Biopharm.*, **2,** 511 (1974).
(6) E. I. Stupak and T. R. Bates, *J. Pharm. Sci.*, **61,** 400 (1972).
(7) W. L. Chiou and S. Riegelman, *ibid.*, **60,** 1569 (1971).
(8) W. L. Chiou, *ibid.*, **66,** 989 (1977).
(9) G. H. Svoboda, M. J. Sweeney, and W. D. Walkling, *ibid.*, **60,** 333 (1971).
(10) H. Sekikawa, T. Noganuma, J. Fujiwara, M. Nakono, and T. Arita, *Chem. Pharm. Bull.*, **27,** 31 (1979).
(11) W. L. Chiou and S. Riegelman, *J. Pharm. Sci.*, **60,** 1376 (1971).
(12) *Ibid.*, **59,** 937 (1970).
(13) A. S. Geneidi, F. A. Ali, and R. B. Salama, *ibid.*, **67,** 114 (1978).
(14) "The Merck Index," 9th ed., Merck & Co., Rahway, N.J., 1976, p. 3066.
(15) R. A. O'Reilly, P. M. Aggeler, and L. S. Leong, *Thromb. Diath. Haemorrhag.*, **11,** 1 (1964).
(16) E. Lozinski, *Can. Med. Assoc. J.*, **83,** 177 (1960).
(17) M. Weiner, S. Shapiro, J. Axelrod, J. R. Cooper, and B. B. Brodie, *J. Pharmacol. Exp. Ther.*, **99,** 409 (1950).
(18) M. J. Akers, J. L. Lach, and L. J. Fischer, *J. Pharm. Sci.*, **62,** 391 (1973).
(19) *Ibid.*, **62,** 1192 (1973).
(20) G. L. Clark and G. G. Hawley, "The Encyclopedia of Chemistry," Reinhold, New York, N.Y., 1966, p. 981.
(21) T. R. Bates, M. Gibaldi, and J. L. Kanig, *Nature*, **210,** 1331 (1966).
(22) R. Nagashima, G. Levy, and E. Nelson, *J. Pharm. Sci.*, **57,** 58 (1968).
(23) B. J. Winer, "Statistical Principles in Experimental Design," 2nd ed., McGraw-Hill, New York, N.Y., 1971, p. 198.
(24) A. Rindlay, "The Phase Rule," 9th ed., Dover, New York, N.Y., 1951, p. 477.
(25) J. Haleblian and W. McCrone, *J. Pharm. Sci.*, **58,** 911 (1969).
(26) M. L. Huang and S. Niazi, *ibid.*, **66,** 608 (1977).
(27) A. J. Aguiar and J. E. Zelmer, *ibid.*, **58,** 983 (1969).
(28) T. J. Macke, U. S. pat. 2,671,750 (1954).
(29) A. P. Simonelli, S. C. Mehta, and W. I. Higuchi, *J. Pharm. Sci.*, **65,** 355 (1976).
(30) M. J. Cho, A. G. Mitchell, and M. Pernarowski, *ibid.*, **60,** 720 (1971).
(31) G. Levy and W. J. Jusko, *ibid.*, **54,** 219 (1965).
(32) S. Stavchansky, A. Martin, and A. Loper, *Res. Commun. Chem. Pathol. Pharmacol.*, **24,** 77 (1979).
(33) P. Singh, J. K. Guillouz, T. D. Sokoloski, L. Z. Benet, and V. N. Bhatia, *J. Pharm. Sci.*, **55,** 63 (1966).

## ACKNOWLEDGMENTS

Presented in part at the Basic Pharmaceutics Section, APhA Academy of Pharmaceutical Sciences, Kansas City meeting, November 1979.

The authors thank Dr. B. Hajek of the School of Agriculture and Agricultural Experiment Station, Auburn University, for help in performing the X-ray diffraction investigations.

# Dissolution Kinetics of Phenylbutazone

K. G. MOONEY * §, M. RODRIGUEZ-GAXIOLA ‡, M. MINTUN ‡, K. J. HIMMELSTEIN ‡, and V. J. STELLA * ×

Received August 8, 1980, from the *Department of Pharmaceutical Chemistry and the ‡Department of Chemical Engineering, University of Kansas, Lawrence, KS 66045. Accepted for publication April 17, 1981. §Present address: Boehringer Ingelheim, Ridgefield, CT 06877.

**Abstract** □ This study investigated the possible effects of simultaneous, noninstantaneous, reversible chemical ionization of carbon acids on the dissolution of a typical pharmaceutical carbon acid, phenylbutazone, and its deutero analog. The dissolution rate *versus* pH profile for phenylbutazone was consistent with phenylbutazone acting as if it were an acid where the ionization can be considered instantaneous. In view of the dissolution behavior of phenylbutazone under various conditions, it is unlikely that the noninstantaneous ionization kinetics demonstrated for this compound play a major role in determining the dissolution rate, either *in vitro* or *in vivo*, since the average residence time in a typical aqueous diffusion layer for phenylbutazone dissolution is longer than the reaction time for its ionization. Slowing the reaction time with a primary isotope effect by deuterium substitution for the ionizable proton caused significant deviation from classical behavior for *d*-phenylbutazone.

**Keyphrases** □ Phenylbutazone—dissolution kinetics □ Kinetics—dissolution phenylbutazone □ Dissolution—kinetics of phenylbutazone □ Anti-inflammatory agents—phenylbutazone, dissolution kinetics

In modeling the dissolution of carboxylic acids into aqueous, alkaline media (1, 2), all reversible ionization reactions occurring in the diffusion layer are considered instantaneous[1]. Carbon acids, where the dissociating proton is bound to a carbon atom rather than to a heteroatom, have been shown to undergo noninstantaneous rates of ionization (3–5); *i.e.*, proton abstraction rate constants are considerably slower than $10^{10}$ $M^{-1}$/sec. The present study investigated the possible effects of simultaneous, noninstantaneous, reversible chemical ionization of carbon acids on the dissolution of phenylbutazone (I).

An anti-inflammatory agent, phenylbutazone was chosen because it has been demonstrated to have dissolution rate-limited absorption (6–9) and noninstantaneous ionization kinetics (3). Furthermore, studies on the mass transport of phenylbutazone have described behavior that seemed not entirely explicable by models with the assumption that this drug undergoes instantaneous ionization (10–12).

The pH-stat, rotating-disk system described previously (1) was particularly useful for the study of the phenylbutazone dissolution mechanism in aqueous media of variable bulk solution pH since buffers have been demonstrated to catalyze markedly the rate processes involved in its ionization (3). The inclusion of buffers in the dissolution medium complicates the theoretical considerations of any model and prevents any possible effects of noninstantaneous ionization on phenylbutazone dissolution rates from being observed.

## THEORETICAL

The ionization kinetics of phenylbutazone can be described by Schemes I and II and are adapted from the work of Stella and Pipkin (3). In these

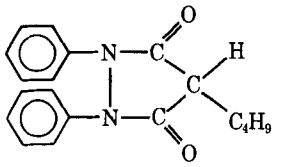

I

schemes, $K$ is the diketo form of phenylbutazone, $E^-$ is the enolate anion, and $OH^-$ and $H^+$ represent hydroxide and hydrogen ions, respectively. It was demonstrated (3) that in an aqueous solution of ionic strength ($\mu$) 0.1 and at 25°, an enol form comprises a minor portion of the total undissociated phenylbutazone (~2%). Therefore, it was assumed that solid phenylbutazone exists predominantly as the diketo form, and any ionization during dissolution due to reaction with water and hydroxide ion was regarded as occurring solely from this species.

It was assumed that a previously described (1) diffusion layer model generally applied; the only difference between the previous model and the present one was that chemical reactions involving the diketo or enolate forms of phenylbutazone were assumed to be noninstantaneous with respect to the diffusion process. Phenylbutazone species were not presumed to be in equilibrium with one another at any point within the diffusion layer.

When the bulk solution pH ($pH_{bulk}$) was maintained only by controlled addition of hydroxide ion from a pH-stat system (1), the various reactions occurring within the diffusion layer were given by Schemes I and II.

$$K \underset{k_2}{\overset{k_1}{\rightleftharpoons}} H^+ + E^-$$

*Scheme I*

$$K + OH^- \underset{k_4}{\overset{k_3}{\rightleftharpoons}} H_2O + E^-$$

*Scheme II*

Also occurring in the diffusion layer was the spontaneous ionization of water (Scheme III).

$$H^+ + OH^- \rightleftharpoons H_2O$$

*Scheme III*

At steady state during the dissolution of phenylbutazone, a mass balance for each diffusing species may be written accounting for both chemical ionization reactions and Fickian diffusion within the diffusion layer:

$$\frac{\partial[K]}{\partial t} = D_K \frac{\partial^2[K]}{\partial X^2} - \Big[[K](k_3[OH^-] + k_1) - [E^-](k_2[H^+] + k_4)\Big] = 0 \quad \text{(Eq. 1)}$$

$$\frac{\partial[E^-]}{\partial t} = D_E \frac{\partial^2[E^-]}{\partial X^2} - \Big[[E^-](k_2[H^+] + k_4) - [K](k_3[OH^-] + k_1)\Big] = 0 \quad \text{(Eq. 2)}$$

$$\frac{\partial[OH^-]}{\partial t} = D_{OH} \frac{\partial^2[OH^-]}{\partial X^2} - \Big[k_3[K][OH^-] - k_4[E^-]\Big] = 0 \quad \text{(Eq. 3)}$$

$$\frac{\partial[H^+]}{\partial t} = D_H \frac{\partial^2[H^+]}{\partial X^2} - \Big[k_2[E^-][H^+] - k_1[K]\Big] = 0 \quad \text{(Eq. 4)}$$

where $[K]$, $[E^-]$, $[OH^-]$, and $[H^+]$ represent the concentrations of the various species; $D_K$, $D_E$, $D_{OH}$, and $D_H$ are their diffusivities; $t$ is time; $k_{1-4}$ are the rate constants described in Schemes I and II; and where $x$ is the distance of any point from the solid-liquid interface.

The relationship between $[H^+]$ and $[OH^-]$ is defined in the diffusion layer by:

[1] Instantaneous is regarded here in the chemical kinetic sense, in which a reaction rate constant is at or approaches the diffusion-controlled limit of ~$2 \times 10^{10}$ $M^{-1}$/sec.



0022-3549/81/1200-1358$01.00/0
© 1981, American Pharmaceutical Association

$$K_w = [H^+][OH^-] \quad \text{(Eq. 5)}$$

but the relationships between $[K]$ and $[E^-]$ and $[H^+]$ and $[OH^-]$ cannot be given by a series of simple equilibria because of the noninstantaneous nature of the ionization reactions involved. Since the rates of interconversion between $K$ and $E^-$ at any point in the film depended on their respective concentrations and $[H^+]$ and $[OH^-]$ at that position, there was no simple analytical solution of Eqs. 1–4. Therefore, to predict whether the noninstantaneous nature of phenylbutazone ionization was likely to affect the dissolution rate of the acid, numerical integration methods were used with Eqs. 1–4 to provide approximate film concentration profiles for $[K]$ and interfacial pH values, $pH_0$, under various $pH_{bulk}$ conditions.

## EXPERIMENTAL

**Materials**—Phenylbutazone[2] and 2-naphthoic acid[3] were obtained in pure crystalline forms. Deuterium oxide[3] (99.9 mole % purity), deuterium chloride[3] solution (10 *M*), and sodium deuteroxide[3] (40% solution) were all used without further purification. Reagent grade hydrochloric acid[4] and sodium hydroxide[4] were obtained as prepared (1 *M*) solutions. All other chemicals were reagent grade.

**Preparation of Deuterated Phenylbutazone and 2-Naphthoic Acid**—Deuterated phenylbutazone was prepared by dissolving ~5 g of nondeuterated phenylbutazone in 50 ml of deuterium oxide and 1.0 ml of 40% sodium deuteroxide with vigorous agitation. Upon addition of 1–2 ml of 10 *M* deuterium chloride, a gel-like precipitate was formed; it was filtered and dried at 50–60° under vacuum for 1–2 hr. After recrystallization in 99.9% deuterated ethanol[3] (*d*-ethanol), TLC, using a solvent system of 7% (v/v) acetone in toluene, showed only one spot that corresponded to phenylbutazone.

The melting point of the pure phenylbutazone standard (starting material) was 105–106°, and that of the precipitate prior to recrystallization was 95–106° (transition observed in that range). The polymorphism of phenylbutazone has been well documented(13, 14), and it appeared that the highest melting and, therefore, most thermodynamically stable crystalline form of phenylbutazone, has a melting point of 105–106°. After recrystallization in *d*-ethanol and drying at 50–60° *in vacuo* for 2 hr, deuterated phenylbutazone (*d*-phenylbutazone) gave a sharp melting point of 105–106°. Therefore, it was assumed that the crystalline form of *d*-phenylbutazone was very similar to that of the pure nondeuterated material.

2-Naphthoic acid was deuterated in a similar manner, using approximately the same amounts of solid and reagents. On measuring the melting points of the starting protonated material and the deuterated precipitate, they were 184–185° (lit. mp 185–187°) and 179–181°, respectively. After recrystallization of the precipitated deuterated compound in *d*-ethanol, the melting point of the pure solid was only 180–181°, ~4° lower than the starting material.

IR and NMR spectra were obtained to confirm the deuteration sites in both compounds. Phenylbutazone was deuterated only at the 2-position, with the percentage deuteration being estimated at >90%. Naphthoic acid was similarly deuterated only on the exchangeable carboxy function, the percentage deuteration again being estimated at >90%. Both deuterated compounds were stored in a desiccator until required.

**Solubility and pKa Measurement of Phenylbutazone**—The aqueous solubility of phenylbutazone at $\mu = 0.5$ (potassium chloride) and 25° was determined as described earlier (1). Additionally, a spectrophotometric method was used to obtain the pKa of phenylbutazone independently. Phenylbutazone showed a strong bathochromic shift at 240–300 nm on addition of base to an aqueous solution of the compound. Thus, aliquots of an approximate $1.3 \times 10^{-5}$ *M* aqueous solution of phenylbutazone at $\mu = 0.5$ with potassium chloride were taken and, using 0.1–1.0 *M* NaOH or HCl, were adjusted to pH values of 2.0–10.0. The absorbance of each solution was measured at 262 nm with a UV–visible spectrometer[5].

The pKa and intrinsic solubility of 2-naphthoic acid were measured by the solubility method as described previously (1) at 25° and $\mu = 0.5$ (potassium chloride).

**Initial Dissolution Rate Measurement as Function of Rotation Speed and pH**—Phenylbutazone and 2-naphthoic acid in both their deuterated and protonated forms were compressed into solid disks of 1.3-cm diameter as described previously (1).

The adherence of the dissolution rate from a rotating disk of constant surface area at a given $pH_{bulk}$ to a diffusion layer-controlled model described by the Levich–Nernst relationship (1) was tested for in all four compounds. Phenylbutazone, 2-naphthoic acid, and deuterated 2-naphthoic acid (*d*-2-naphthoic acid) were tested in a medium of $pH_{bulk}$ 2.00 (0.49 *M* KCl–0.01 *M* HCl), $\mu = 0.5$, and 25°. Dissolution rates of phenylbutazone and *d*-phenylbutazone were also measured at $pH_{bulk}$ 6.50 as a function of disk rotation speed, using a pH-stat system to maintain the bulk solution pH constant. To compare phenylbutazone dissolution rates under acidic conditions, the dissolution rates of *d*-phenylbutazone were also measured at 600 rpm under acidic conditions. The method and apparatus used were exactly as described previously (1).

To measure dissolution rate as a function of $pH_{bulk}$, the solid acid disks were rotated at a constant speed in media of different pH values. For phenylbutazone and *d*-phenylbutazone, the disk rotation speed was 600 rpm; for *d*-2-naphthoic acid and 2-naphthoic acid, it was 450 rpm. The difference was due to the compound's relative solubilities and the period of time required to measure each dissolution rate.

**Dissolution Rate Simulations**—Where phenylbutazone and/or deuterated phenylbutazone dissolution was simulated, the boundary conditions were defined as follows:

1. At the rotating-disk surface, *i.e.*, $X = 0$, $[K]$ is given by the intrinsic solubility of phenylbutazone, $[HA]_0$.

2. To estimate the boundary condition for $[E^-]$ at the wall, the experimentally observed flux ($J_{obs}$) was used since it was equal to the sum of $K$ flux, $J_K$, and $E^-$ flux, $J_E$, and $[E^-]$ was changed successively until the value for $J_{obs}$ simulated was equal to $J_{obs}$ experimentally observed.

3. To set the boundary condition for $[OH^-]$, it was assumed that at any given point, the $[E^-]$ flux out of the diffusion layer should be equal to the influx of $[OH^-]$ plus the flux of $[H^+]$ out (1) since any change in the flux of $[OH^-]$ must also be reflected by corresponding changes in $[E^-]$ and $[H^+]$. This statement was expressed as:

$$\text{flux of } [E^-] \text{ out} = \text{flux of } [OH^-] \text{ in} + \text{flux of } [H^+] \text{ out} \quad \text{(Eq. 6)}$$

4. The value of $J_{OH}$, as well as of $J_E$ and $J_H$, can be calculated at any given point in the diffusion layer by using Fick's first law of diffusion (15). Then, when $[OH^-]$ flux calculated by this means was found to be equal to the value obtained using Eq. 6, the boundary condition for $[OH^-]$ was defined. Thus:

$$D_{OH}\frac{d[OH^-]}{dX} = \text{flux of } [E^-] - \text{flux of } [H^+] \quad \text{(Eq. 7)}$$

5. The boundary condition for $[H^+]$ at the wall was given by the equilibrium relationship between $[OH^-]$ and $[H^+]$ (Eq. 5).

6. Since the bulk concentrations for $E^-$ and $K$ were very low, they were considered to be zero (initial rates were assumed). The boundary conditions at $X = h$ for $[OH^-]$ and $[H^+]$ were given by the bulk pH. Thus, all boundary conditions required for the simulation of phenylbutazone dissolution were set. These conditions are summarized here.

At $X = 0$:

$$[K]_0 = \text{solubility of HA}$$

$$[E^-]_0;\ J_{obs} = J_K + J_E$$

$$[OH^-]_0;\ D_{OH}\frac{d[OH^-]}{dX} = J_E - J_h$$

$$[H^+]_0 = \frac{K_w}{[OH^-]_0}$$

At $X = h$:

$$[K]_h = 0$$

$$[E^-]_h = 0$$

$$[OH^-]_h = \text{from bulk pH}$$

$$[H^+]_h = \text{from bulk pH}$$

To solve the two-point value problem, conditions on each side of the boundary must be specified. This was not the case in these simulations. One alternative was to guess the initial slopes at one boundary and to solve the problem as an initial value problem "shooting" repeatedly at the other boundary until the known boundary conditions were satisfied (16, 17). Since this approach was costly and time consuming, a second

[2] Ciba-Geigy Pharmaceuticals, Summit, N.J.
[3] Aldrich Chemical Co., Milwaukee, Wis.
[4] Fisher Scientific Co., Fair Lawn, N.J.
[5] Model 219, Cary Instruments, Calif.

approach was taken where the dissolution of phenylbutazone was simulated assuming steady-state conditions. The nonsteady-state solution continued until steady state was achieved. It was necessary to establish four initial conditions besides the eight boundary conditions already described to solve the system as a nonsteady-state problem.

Thus, the initial conditions for phenylbutazone and all of the diffusing species were given by, at $t = 0$:

$$[K]_0 = \text{solubility of } [HA]_0$$

$$[OH^-]_0 = \text{from bulk pH}$$

$$[H^+]_0 = \text{from bulk pH}$$

$$[E^-]_0 = 0$$

The mathematical model representative of phenylbutazone dissolution was represented by a set of four nonlinear partial differential equations (Eqs. 1–4), which could be written in finite difference forms.

Let the diffusion layer be divided into $M$ grid points denoted by $X_i$, $i = 1,2,\ldots M$. The time index was given by the subscript $n$, where $n + 1$ is the new time and $n$ is the old time.

The left side of Eqs. 1–4 written in finite-difference approximation by:

$$\frac{\partial[N]}{\partial t} = \frac{[N]_{i,n+1} - [N]_{i,n}}{\Delta t} \qquad \text{(Eq. 8)}$$

where $N$ represents any of the species, $K$, $E^-$, $OH^-$, or $H^+$. The right side of Eqs. 1–4 can be written in terms of the Crank–Nicolson (15, 18) implicit finite-difference formulation, around the node $i$, as follows:

$$\frac{\partial^2[N]}{\partial X^2} = \frac{D_N}{2}\delta_X^2[N]_{i,n+1} + \frac{D_N}{2}\delta_X^2[N]_{i,n} - (\text{kinetic term})_{i,n+1} \qquad \text{(Eq. 9)}$$

where:

$$\delta_X^2[N]_{i,n+1} = \frac{[N]_{i-1,n+1} - 2[N]_{i,n+1} + [N]_{i+1,n+1}}{(\Delta X)^2} \qquad \text{(Eq. 10)}$$

$$\delta_X^2[N]_{i,n} = \frac{[N]_{i-1,n} - 2[N]_{i,n} + [N]_{i+1,n}}{(\Delta X)^2} \qquad \text{(Eq. 11)}$$

where $D_N$ is the diffusivity of the particular $N$ species being considered.

As shown by the preceding equations, the kinetic terms impose nonlinear characteristics to the system. If it is assumed that these kinetic terms are considered at time $n$ instead of time $n + 1$, the solution of these equations becomes available by using a Crank–Nicolson technique. This assumption causes no great deviation compared to the results obtained using the shooting method.

When Eqs. 1–4, expressed by finite-difference approximations, were applied to the various grid points in the diffusion layer, a set of $M - 1$ linear equations resulted at each time step. The coefficients formed a tridiagonal matrix, which could be solved by a Gaussian elimination technique (19) with a maximum of three variables per equation.

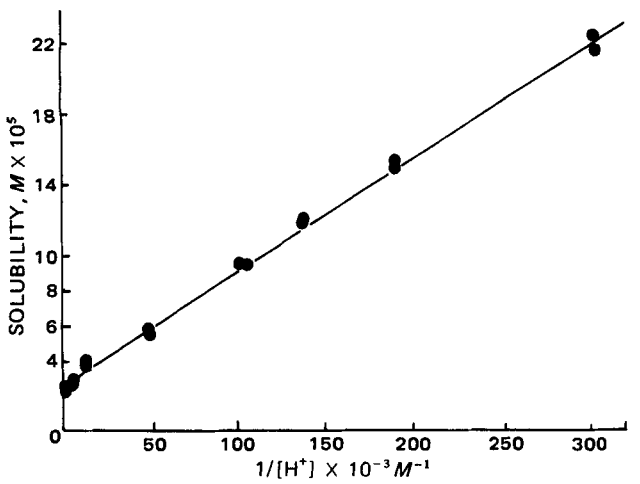


**Figure 1**—*Plot of the aqueous solubility of phenylbutazone* versus *1/[H⁺] (25° at μ = 0.5 with potassium chloride).*

After solving the system for $[N]_{i,n+1}$ at the next iteration, the process was tested for convergence at every grid node:

$$\frac{\text{abs}[\Delta[N]_{i,n+1} - \Delta[N]_{i,n}]}{\text{abs}\,\Delta[N]_{i,n+1}} < \text{convergence}$$

where $\Delta[N]_i$ was the difference of $[N]$ between two grid points, and the value of tolerance was specified.

The Crank–Nicolson method was stable for all values of the ratio $\lambda = \Delta t/(\Delta X)^2$ for linear equations. However, this system was not linear. When a small $\Delta t$ was used, the amount of computation was large. For the case of $\lambda < 4000$, the system was stable but convergence was reached over a longer period. When $\lambda > 20{,}000$, the system became unstable. Finally, when $\lambda = 4000$, the system converged rapidly, saving computation time.

## RESULTS AND DISCUSSION

The solubility of phenylbutazone was measured as a function of the reciprocal of the hydrogen-ion concentration ($1/[H^+]$) in 0.1 $M$ acetate buffers ($\mu = 0.5$ with potassium chloride). The results are plotted in Fig. 1. The intrinsic solubility of undissociated phenylbutazone species, $[HA]_0$, and the macroscopic dissociation constant, $K_a$, are related to the total solubility ($S$) of phenylbutazone by:

$$S = [HA]_0 + \frac{K_a[HA]_0}{[H^+]} \qquad \text{(Eq. 12)}$$

By plotting $S$ *versus* $1/[H^+]$, a straight-line relationship gives $[HA]_0$ as the intercept and $([HA]_0K_a)$ as the slope. Dividing the slope by the intercept gives $K_a$, which is the macroscopic dissociation constant for phenylbutazone (3).

The pKa of phenylbutazone determined by spectrophotometry may be given by:

$$\text{pKa} = \text{pH} + \log\frac{A_{\text{base}} - A_{\text{obs}}}{A_{\text{obs}} - A_{\text{acid}}} \qquad \text{(Eq. 13)}$$

where pKa is the macroscopic value measured at $\mu = 0.5$ with potassium chloride, $A_{\text{base}}$ is the absorbance of a given solution of phenylbutazone under basic conditions where the phenylbutazone is virtually 100% in its anion form, $A_{\text{acid}}$ is the absorbance of the same solution under acidic conditions where phenylbutazone exists essentially as 100% in the protonated form, and $A_{\text{obs}}$ is the absorbance of the same solution at a pH between the two extremes (denoted as pH in Eq.13). The pKa values of phenylbutazone under these experimental conditions were 4.61 (solubility technique) and 4.54 (spectrophotometric technique), and the intrinsic solubility was $2.61 \times 10^{-5}$ $M$.

**Deuteration of Phenylbutazone and 2-Naphthoic Acid**—IR and NMR studies of the deuterated and nondeuterated forms of phenylbutazone and 2-naphthoic acid showed conclusively that the acidic proton of the nondeuterated forms was exchanged for deuterium and that no other protons in the molecules were affected. NMR spectra of both pairs of compounds showed the disappearance of the acidic proton signal ($\delta$ 12.5 ppm for 2-naphthoic acid[6] and 3.2 ppm for phenylbutazone[7] with reference to a tetramethylsilane standard). On deuteration, no other differences in the NMR spectra were observed.

IR spectra of both forms of phenylbutazone were very similar except for a sharpening of a peak at 2860 $cm^{-1}$ and the presence of additional peaks at 2060 $cm^{-1}$ and 1100–1200-$cm^{-1}$ for the deuterated form. The IR spectra for both forms of 2-naphthoic acid showed a more noticeable difference between the compounds. The broad band, typically associated with intermolecular hydrogen bonding (2200–2100 $cm^{-1}$), was present in the spectrum of the protonated form but virtually absent in that of the deuterated form. This finding suggested that the lower melting point of the deuterated 2-naphthoic acid (180–181°) compared to that of the protonated form (184–185°) was due to a significantly lower degree of hydrogen (or deuterium) bonding in the deuterated 2-naphthoic acid.

**Initial Dissolution Rates as a Function of Disk Rotation Speed**—Table I shows the initial dissolution rates of phenylbutazone as a function of disk rotation speed in solutions of $pH_{bulk}$ 2.0 and 6.50 and of *d*-phenylbutazone as a function of the same disk rotation speeds at $pH_{bulk}$ 6.50. These data are plotted *versus* $\omega^{1/2}$ (a function of rotation speed) in Fig. 2. Table II shows the initial dissolution rates of 2-naphthoic acid and *d*-2-naphthoic acid in a solution of $pH_{bulk}$ 2.0 at varying disk

[6] Solvent used was deuterated chloroform–dimethyl sulfoxide-$d_6$, ~1:2.

[7] Solvent used was carbon tetrachloride with tetramethylsilane standard in deuterated chloroform.

**Table I—Initial Dissolution Rates ($J_{obs}$) of Phenylbutazone and *d*-Phenylbutazone at Varying Disk Rotation Speeds in Media of $\mu$ = 0.5 with Potassium Chloride and Varying $pH_{bulk}$ at 25°**

| Disk Rotation Speed, rpm | Phenylbutazone $\omega^{1/2}$[a] | Phenylbutazone $J_{obs}$ ($\pm SD$)[b] (at $pH_{bulk}$ 2.00[c]) × $10^5$ | Phenylbutazone $J_{obs}$[b] (at $pH_{bulk}$ 6.5[d]) × $10^5$ | *d*-Phenylbutazone, $J_{obs}$[b] (at $pH_{bulk}$ 6.5[d]) × $10^5$ |
|---|---|---|---|---|
| 100 | 3.24 | 1.23 (±0.26) | 3.68 | 3.04 |
| 200 | 4.58 | 1.66 (±0.04) | 4.74 | 3.66 |
| 300 | 5.61 | 1.80 (±0.17) | 5.88 | 4.32 |
| 450 | 6.87 | 2.04 (±0.12) | 6.64 | 4.94 |
| 600 | 7.93 | 2.58 (±0.34)[e] | 7.24 | 5.66 |
| 900 | 9.71 | — | 8.67 | 6.50 |

[a] The angular velocity of the disk in radians per second. [b] The standard deviation is from at least four measurements; where standard deviation values are not given, the mean was obtained from two or three similar values. (The $J$ units are mg $cm^{-2}$/sec and not moles $cm^{-2}$/sec). [c] In 0.01 *M* HCl/0.49 *M* KCl solution. [d] In 0.5 *M* KCl solution, pH-statted. [e] *d*-Phenylbutazone under these conditions gave an initial dissolution rate of $2.98 \times 10^{-5}$ ($\pm 0.23 \times 10^{-5}$) mg $cm^{-2}$/sec.

**Table II—Initial Dissolution Rates ($J_{obs}$) of 2-Naphthoic and *d*-2-Naphthoic Acids at Varying Disk Rotation Speeds in Media of $\mu$ = 0.5 with Potassium Chloride and $pH_{bulk}$ 2.00[a] at 25°**

| Rotation Speed, rpm | $\omega^{1/2}$[c] | $J_{obs}$ ($\pm SD$)[b] (at $pH_{bulk}$ 2.00 × $10^5$) 2-Naphthoic Acid | $J_{obs}$ ($\pm SD$)[b] (at $pH_{bulk}$ 2.00 × $10^5$) *d*-2-Naphthoic Acid |
|---|---|---|---|
| 100 | 3.24 | 3.63 (±0.09)[d] | 3.71 (±0.13) |
| 200 | 4.58 | 4.88 (±0.06) | 4.87 (±0.13) |
| 300 | 5.61 | 5.78 (±0.05) | 5.74 (±0.17) |
| 450 | 6.87 | 7.37 (±0.47) | 7.32 (±0.48) |
| 600 | 7.93 | 8.52 (±0.52) | 8.40 (±0.18) |
| 900 | 9.71 | 10.09 (±0.57) | 10.01 (±0.36) |

[a] Medium was 0.01 *M* HCl/0.49 *M* KCl with no pH-stat used during dissolution runs. [b] The standard deviation from three repeated runs. [c] The angular velocity of the disk in radians per second. [d] All units are in mg/$cm^2$/sec.

rotation speeds. These data were not plotted because they are essentially identical to those given previously (1). All the dissolution rate data as a function of rotation speed are summarized in Table III.

The Levich–Nernst model states that $J$, the dissolution rate from a rotating disk of solid material, is directly proprotional to $\omega^{1/2}$, a function of the disk's rotation speed, as seen by:

$$J = 0.62\, D^{2/3}\nu^{-1/6}C_S\omega^{1/2} \qquad \text{(Eq. 14)}$$

where $D$ is the diffusivity of the dissolving solute, $\nu$ is the kinematic viscosity of the dissolution medium, $C_S$ is the saturated solubility of the dissolving solute in the medium, and $\omega$ is the angular velocity of the rotating disk in radians per unit time. From Fig. 2, phenylbutazone under acidic conditions appeared to show a reasonable degree of linearity when $J$ was plotted against $\omega^{1/2}$. Therefore, phenylbutazone dissolves by a diffusion layer-controlled mechanism under acidic conditions since the correlation coefficient for this plot was reasonable and the calculated diffusivity from these data ($4.90 \times 10^{-6}$ $cm^2$/sec) was very close to that obtained from the square root relationship previously discussed (1) using the diffusivity of benzoic acid under identical conditions as a standard.

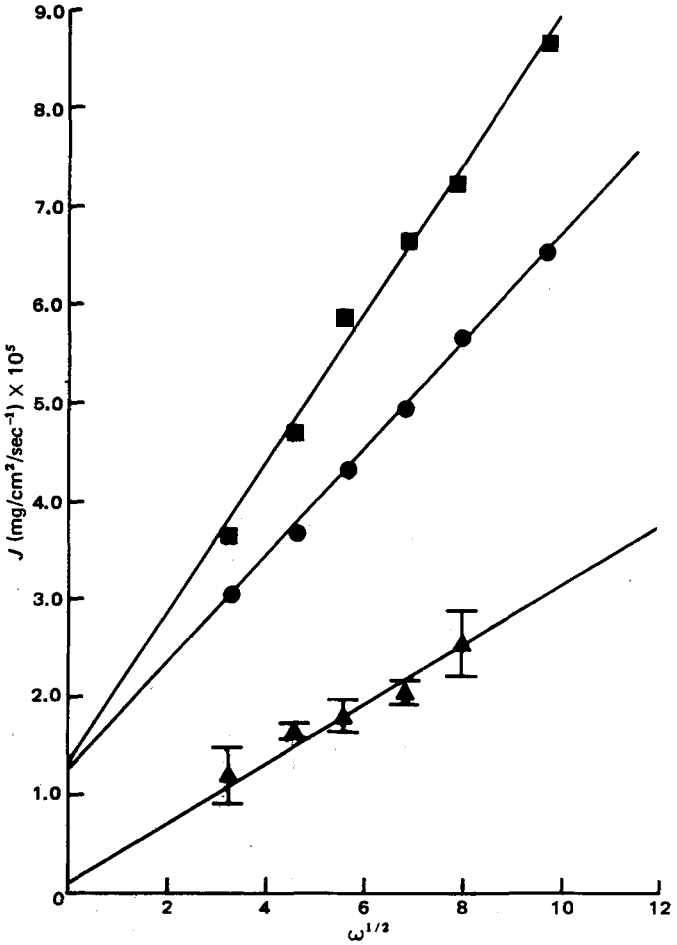


**Figure 2**—*Levich plot of the dissolution rate (J) as a function of the square root of the angular velocity ($\omega^{1/2}$) of a rotating disk of phenylbutazone (■) and d-phenylbutazone (●) at pH 6.5 (maintained by a pH-stat) and of phenylbutazone (▲) at pH 2.0 (25° at $\mu$ = 0.5 with potassium chloride).*

Initial dissolution rates of phenylbutazone and *d*-phenylbutazone with varying rotation speed at $pH_{bulk}$ 6.50 did not strictly obey the Levich model but showed the type of behavior that indomethacin displayed in earlier work under similar conditions (1). An additional mechanism appeared to be contributing to the dissolution rate of $pH_{bulk}$ 6.50, which was independent of the disk rotation speed as shown by a nonzero intercept.

It was assumed that a modified form of the Levich–Nernst relationship applies:

$$J = (0.62\, D^{2/3}\nu^{-1/6}C_S)\omega^{1/2} + \text{constant} \qquad \text{(Eq. 15)}$$

where the constant represents the nonzero intercept at zero rotation speed. The cause of this nonzero intercept is unknown but is being studied.

**Table III—Summary of Data Obtained for Protonated and Deuterated Forms of 2-Naphthoic Acid and Phenylbutazone from the $J_{obs}$ *versus* $\omega^{1/2}$ Regression Analysis (Data in Tables I and II) Performed at Varying $pH_{bulk}$ and 25°**

| Compound | $pH_{bulk}$ | Slope of $J_{obs}$ *versus* $\omega^{1/2}$ × $10^6$ | Intercept of $J_{obs}$ *versus* $\omega^{1/2}$ × $10^5$ | Correlation Coefficient for $r$ | Diffusivity from Slope, ($cm^2$/sec) × $10^6$ |
|---|---|---|---|---|---|
| 2-Naphthoic acid | 2.00 | 10.44 | 0.01 | 0.9991 | 6.52[a] |
| *d*-2-Naphthoic acid | 2.00 | 10.30 | 0.01 | 0.9989 | 6.39[a] |
| Phenylbutazone | 2.00 | 3.07 | 0.10 | 0.9792 | 4.80[b] |
| Phenylbutazone | 6.50 | 7.59 | 1.34 | 0.9961 | — |
| *d*-Phenylbutazone | 6.50 | 5.46 | 1.23 | 0.9975 | — |

[a] Calculated from Levich relationship (Eq. 14) and $[HA]_0$ = 2.23 mg/ml in $\mu$ = 0.5 with potassium chloride. [b] Calculated from Levich relationship (Eq. 14) and $[HA]_0$ = $8.1 \times 10^{-2}$ mg/ml.

**Table IV—Absolute Dissolution Rates from Rotating Disks of Phenylbutazone and *d*-Phenylbutazone (600 rpm) as a Function of Bulk Solution pH [a]**

| $pH_{bulk}$ | $pH_0$ (at $X = 0$) | $J^H_{obs}$ | $J^D_{obs}$ | $J^H_{theor}$ |
|---|---|---|---|---|
| 2.00 | 2.00 | 8.35 | 10.12 | 8.10 |
| 3.00 | 3.00 | 6.53 | — | 8.28 |
| 4.00 | 4.00 | 9.42 | 8.74 | 10.04 |
| 4.50 | 4.46 | — | 11.95 | 13.78 |
| 5.00 | 4.78 | 19.95 | 11.25 | 20.01 |
| 5.50 | 4.91 | — | 16.06 | 24.36 |
| 6.00 | 4.96 | — | 17.92 | 26.12 |
| 6.50 | 4.97 | — | 19.83 | 26.74 |
| 7.00 | 4.98 | 27.18 | 20.27 | 27.00 |
| 8.00 | 5.00 | 28.26 | 22.03 | 27.91 |
| 8.50 | 5.05 | 30.34 | 24.46 | 30.06 |
| 9.00 | 5.18 | 38.34 | 32.95 | 38.07 |
| 9.20 | 5.28 | 49.53 | — | 46.11 |
| 9.50 | 5.50 | 78.76 | 68.25 | 70.90 |
| 9.70 | 5.68 | 110.29 | — | 102.40 |
| 10.00 | 5.96 | 165.03 | 169.97 | 190.67 |
| 10.20 | 6.16 | 297.75 | — | 295.60 |

[a] $J^H_{theor}$ is the calculated flux, assuming phenylbutazone acts as a classical acid; $J^H_{obs}$ is the observed flux of phenylbutazone; and $J^D_{obs}$ is the observed flux of *d*-phenylbutazone. All values of $J$ are in units of moles $cm^{-2}/sec \times 10^{11}$.

The two forms of phenylbutazone did not dissolve at the same rate at a given disk rotation speed at $pH_{bulk}$ 6.5, with *d*-phenylbutazone dissolving more slowly than phenylbutazone. Although *d*-phenylbutazone dissolution rates were not extensively measured under acidic conditions, a value was determined at 600 rpm at $pH_{bulk}$ 2.00, and it did not differ significantly from that obtained for phenylbutazone under the same conditions. Hence, the difference in dissolution rates of these compounds at $pH_{bulk}$ 6.50 may be due to a difference in the ionization rates of the two species within the diffusion layer.

The dissolution rates of 2-naphthoic acid and *d*-2-naphthoic acids under acidic conditions as a function of disk rotation speed showed that there was no significant difference between the two compounds when ionization was suppressed during the dissolution process. Thus, it was assumed that the deuteration of 2-naphthoic acid did not affect the intrinsic solubility of the acid, despite differences in crystal lattice energies (assumed from the melting point data) being observed between the dissolving solids. In view of the lability of deuterium bonded to a carboxylic acid oxygen atom, the similarity between results obtained for the dissolution rates of the two forms of 2-naphthoic acid was probably due to rapid exchange of deuterium with hydrogen in water immediately at the solid–liquid interface during dissolution. Thus, the diffusion rate of the nondeuterated form away from the solid–liquid interface was observed in both cases.

**Initial Dissolution Rates as Function of $pH_{bulk}$**—Tables IV and V contain initial dissolution rate data for both deuterated and protonated forms of phenylbutazone and 2-naphthoic acid as a function of $pH_{bulk}$ (maintained by pH-stat) and at a constant rotation speed. Also included are the theoretical values expected if 2-naphthoic acid and phenylbutazone acted as classical acids, ionizing instantaneously as they diffused through the diffusion layer (1).

Adherence of the dissolution rates of 2-naphthoic acid to the model described earlier (1), assuming instantaneous chemical-ionization reactions within the diffusion layer, was already established. Since the values for 2-naphthoic acid and the *d*-2-naphthoic acid ($J^D_{obs}$) closely agreed at every $pH_{bulk}$ value tested and since these values approximated those predicted by theory ($J_{theor}$), it may be reasoned that the deuterated and nondeuterated forms of 2-naphthoic acid diffuse and simultaneously react with base in the same way and to the same extent. This reasoning also confirmed that the two compounds dissolved and instantaneously achieved equilibrium with the reacting base in the diffusion layer and, therefore, acted in a classical manner. This behavior was consistent with the more rapid exchange of deuterium for hydrogen relative to the time taken for the molecules to traverse the diffusion layer. If exchange occurred instantaneously for the *d*-2-naphthoic acid at the solid–liquid interface, then it should dissolve identically to 2-naphthoic acid.

The data for deuterated and nondeuterated phenylbutazone (Table IV and Fig. 3) may be compared in the same way as for 2-naphthoic acid. Comparison between the $J_{obs}$ values for the two phenylbutazone forms to the $J_{theor}$ values for the same $pH_{bulk}$ showed that the fluxes of *d*-phenylbutazone were significantly slower than those of phenylbutazone by ~10–45% over the neutral $pH_{bulk}$ range. Furthermore, phenylbutazone gave experimental dissolution rates very close in value to those predicted by the theory (1) that assumed instantaneous equilibrium. Therefore, at 25° and $\mu = 0.5$ with potassium chloride and over a wide range of bulk solution pH, phenylbutazone was an example of a compound dissolving into a reactive medium showing simultaneous noninstantaneous chemical reaction that could be treated as if its ionization was instantaneous; *i.e.*,

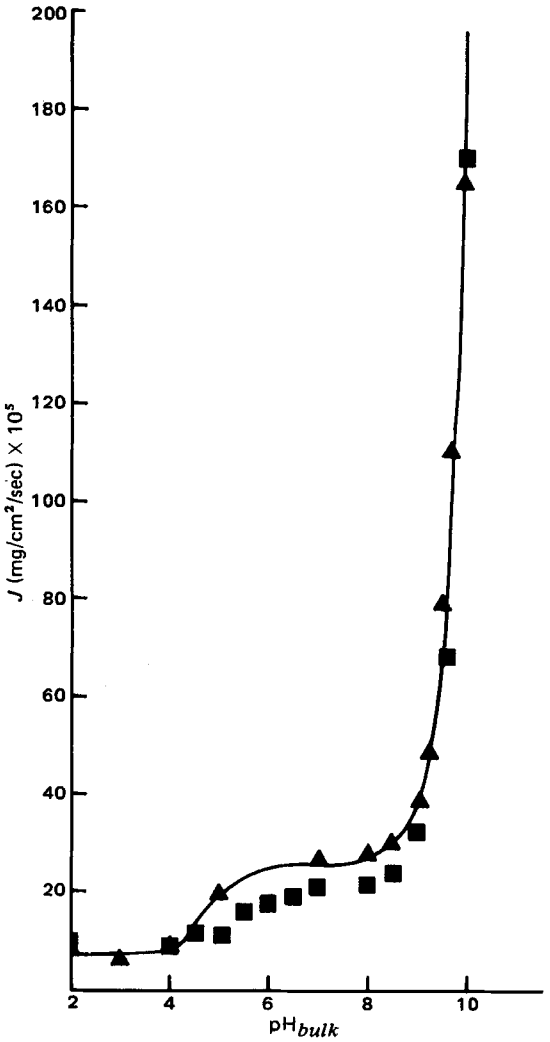


**Figure 3**—*Dissolution rate (J) versus $pH_{bulk}$ profile for phenylbutazone (▲) and d-phenylbutazone (■) from a rotating disk (600 rpm) dissolving in an aqueous medium (25° at $\mu = 0.5$ with potassium chloride). The $pH_{bulk}$ was maintained with a pH-stat. The continuous line represents the profile generated treating phenylbutazone as a carboxylic acid.*

**Table V—Absolute Dissolution Rates from Rotating Disks of 2-Naphthoic Acid (450 rpm) as a Function of Bulk pH [a]**

| $pH_{bulk}$ | $pH_0$ ($X = 0$ from theory) | $J^H_{theor}$, (moles $cm^{-2}/sec$) $\times 10^{10}$ | $J^H_{obs}$, (moles $cm^{-2}/sec$) $\times 10^{10}$ | $J^D_{obs}$, (moles $cm^{-2}/sec$) $\times 10^{10}$ |
|---|---|---|---|---|
| 2.00 | 2.00 | 3.950 | 4.280 | 4.249 |
| 6.00 | 4.28 | 11.130 | 13.300 | 13.547 |
| 7.00 | 4.29 | 11.200 | 13.820 | 13.853 |
| 8.00 | 4.29 | 11.270 | 13.590 | 13.754 |
| 8.50 | 4.30 | 11.430 | 14.170 | 14.056 |
| 9.00 | 4.33 | 11.940 | 14.990 | 15.305 |
| 9.20 | 4.35 | 12.400 | 16.150 | 16.561 |
| 9.50 | 4.42 | 13.760 | 18.240 | 18.683 |
| 10.00 | 4.49 | 22.560 | 27.360 | 26.520 |

[a] $J^H_{theor}$ is the calculated mass transport rate, $J^H_{obs}$ is the observed flux of the protonated acid, and $J^D_{obs}$ is the observed flux of the deuterated acid.

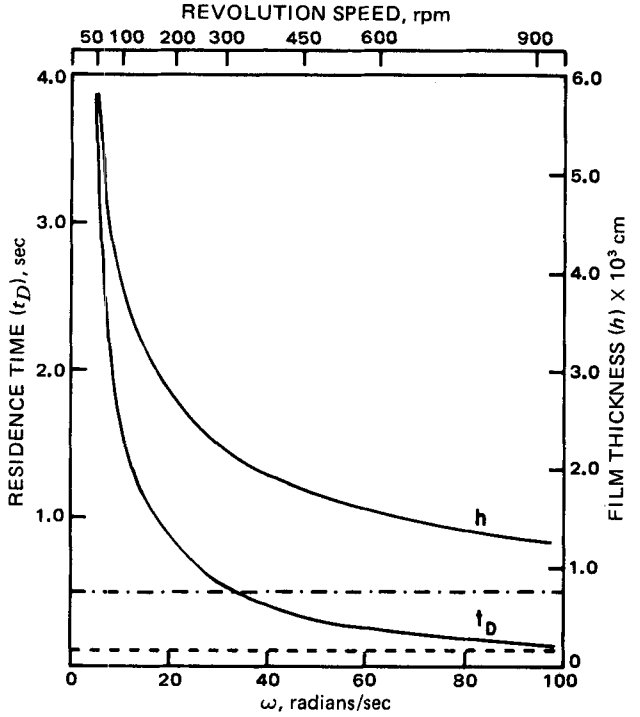


**Figure 4**—*Plot of residence time* ($t_D$) *and apparent diffusion layer thickness* (h) *for phenylbutazone as defined by Eqs. 18 and 19* versus *ω (angular velocity) for dissolution from a rotating disk. Times are shown for three half-lives for the deprotonation reaction (at* $pH_{bulk}$ *6.5). Key: ---, phenylbutazone, and -·-, d-phenylbutazone.*

the experimental results suggested that the ionization was still rapid enough that, relative to the diffusional processes, phenylbutazone still acted classically.

Contrary to the results shown for deuterated and nondeuterated 2-naphthoic acids, *d*-phenylbutazone dissolution between $pH_{bulk}$ 5.00 and 9.00 was markedly slower than that of phenylbutazone. It was thought that by studying *d*-phenylbutazone, where deuterium was exchanged for hydrogen at the ionizing center of the phenylbutazone molecule, any effects on its dissolution rate in reactive media due to the noninstantaneous ionization kinetics of phenylbutazone would be amplified. The rationale for this approach was explained earlier (12) and was based on the comparative strengths of a C–D and a C–H bond, a greater free energy of activation ($\Delta G^{\ddagger}$) being required to break the C–D bond for ionization than that required in the breaking of the C–H bond. Hence, the values of $k_1$ and $k_3$ in Schemes I and II should be smaller for *d*-phenylbutazone, whereas $k_2$ and $k_4$ should remain the same as in phenylbutazone if it is assumed that the reverse reaction, once the deuterium is removed, involves only protons.

**Residence Time and Ionization Reaction Time in Diffusion Layer**—When phenylbutazone diffuses across the aqueous diffusion layer during dissolution in an unreactive medium (*i.e.*, under acidic conditions) under steady-state conditions, the concentration profile for the acid will be linear as given by the Nernst model (1). Higuchi *et al.* (20) demonstrated that, under these conditions, the residence time ($t_D$), which was the average lifetime of a diffusing molecule in the diffusion layer of thickness $h$, was inversely proportional to the diffusivity of the molecule. The relationship between $t_D$, the diffusivity, and diffusion layer thickness is given by:

$$t_D = \frac{h^2}{2D_K} \qquad \text{(Eq. 16)}$$

where $D_K$ is as previously described. Since an expression for $h$ is given by the Levich rotating disk model shown by:

$$h = 1.612\, D_K^{1/3}\, \nu^{1/6}\, \omega^{-1/2} \qquad \text{(Eq. 17)}$$

substitution for $h$ may be performed in Eq. 16 to give:

$$t_D = \frac{1.3\, \nu^{1/3}}{D_k^{1/3}\, \omega} \qquad \text{(Eq. 18)}$$

Thus, for the specific case of steady-state initial dissolution conditions from a rotating disk, Eq. 18 states that $t_D$ is inversely proportional to $\omega$, the angular velocity of the disk in radians per unit time.

Figure 4 shows a plot of residence time and diffusion layer thickness *versus* $\omega$ for phenylbutazone, assuming that no chemical reaction occurs during the dissolution process (calculated from parameter values previously determined). For convenient representation of the relationship between $t_D$, $h$, and rotation speed, the abscissa is also marked in revolutions per minute (directly proportaional to $\omega$).

When phenylbutazone was dissolving into a medium of pH greater than its pKa, it would tend to dissociate according to the pH of the diffusion layer. With classical acids, this dissociation process was instantaneous, as described for 2-naphthoic acid. For a carbon acid such as phenylbutazone, however, the observed rate constant for the rate of approach to this equilibrium can be slow (3).

Astarita (21) defined a reaction time ($t_r$) that is similar to the half-life in a first-order or pseudo-first-order reaction and is given by:

$$t_r = \frac{1}{k} \qquad \text{(Eq. 19)}$$

where $k$ is a simple first-order or pseudo-first-order rate constant defining the reaction processs. Therefore, the $t_r$ value represents the time taken to complete 63% of the given reaction by a first-order mechanism.

If the given average reaction time was much longer than the average residence time of phenylbutazone in the diffusion layer under defined hydrodynamic conditions, the reaction would only effectively take place in the bulk solution. As the reaction time ($t_r$) decreased to where it became closer in value to $t_D$, the dissociation reaction would influence the flux as defined by Eqs. 1–4. Once $t_r$ becomes much smaller than $t_D$, phenylbutazone should behave classically, *i.e.*, as in the case of 2-naphthoic acid.

Phenylbutazone ionization kinetics cannot normally be represented by a simple overall first-order process (3). Stella and Pipkin (3) described an equation for calculating the observed buffer-independent rate constant for approach to the ionization equilibrium (Eq. 20) for phenylbutazone and specified conditions under which it may be simplified.

$$k_{obs} = k_1 + k_3[OH^-] + \frac{k_2[H^+]K_{a,enol}}{K_{a,enol} + [H^+]} + \frac{k_4 K_{a,enol}}{K_{a,enol} + [H^+]} \qquad \text{(Eq. 20)}$$

where $k_{obs}$ is the rate constant for the approach to equilibrium, $k_{1-4}$ are

**Table VI—Calculated $k_{obs}$ and ($t_r$) across the Diffusion Layer of Phenylbutazone Dissolving in $pH_{bulk}$ 6.50 Using a pH-stat at $\mu$ = 0.5 and 25°**

| Fractional Distance across Film ($x/h$)[a] | $pH_X$ | $[OH^-]_X$[b], $M$ | $[H^+]_X$[b], $M$ | $k_1$[c], $sec^{-1}$ | $\left(\frac{k_2[H^+]_X K_{a,enol}}{K_{a,enol} + [H^+]_X}\right)$[c] | $k_{obs}$[d], $sec^{-1}$ | $t_r = 1/k_{obs}$ × $10^2$ sec |
|---|---|---|---|---|---|---|---|
| 0 | 4.97 | $9.42 \times 10^{-10}$ | $1.06 \times 10^{-5}$ | 10.1 | 2.24 | 12.34 | 8.10 |
| 0.2 | 5.05 | $1.12 \times 10^{-9}$ | $8.96 \times 10^{-6}$ | 10.1 | 1.89 | 11.99 | 8.34 |
| 0.4 | 5.15 | $1.40 \times 10^{-9}$ | $7.16 \times 10^{-6}$ | 10.1 | 1.51 | 11.61 | 8.61 |
| 0.6 | 5.29 | $1.93 \times 10^{-9}$ | $5.18 \times 10^{-6}$ | 10.1 | 1.09 | 11.19 | 8.94 |
| 0.8 | 5.53 | $3.41 \times 10^{-9}$ | $2.93 \times 10^{-6}$ | 10.1 | 0.62 | 10.72 | 9.33 |
| 1.0 | 6.50 | $3.16 \times 10^{-8}$ | $3.16 \times 10^{-7}$ | 10.1 | 0.07 | 10.17 | 9.94 |

[a] Actual value of $h = 1.59 \times 10^{-3}$ cm. [b] Phenylbutazone is treated as a classical acid. [c] $k_1$, $k_2$, and $K_a$, enol from Ref. 3. [d] Defined by Eq. 21.

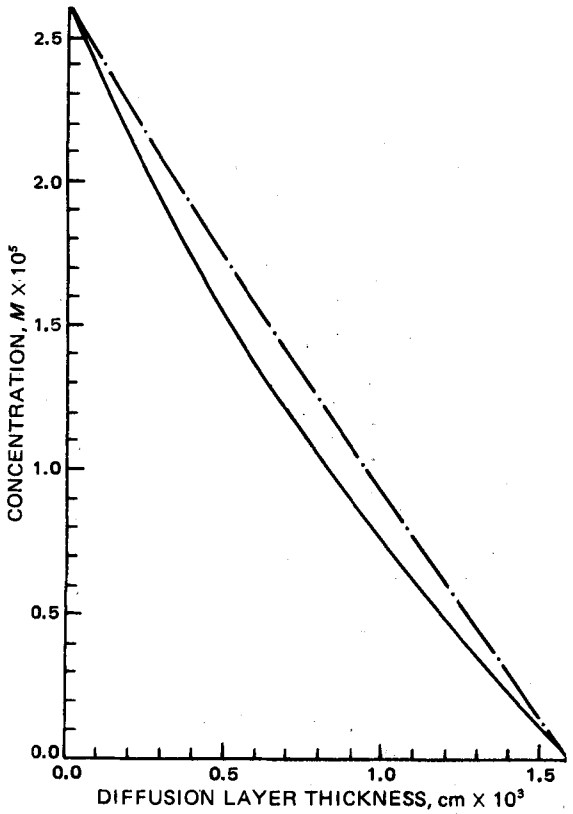


**Figure 5**—*Concentration profiles across an aqueous diffusion layer for phenylbutazone (– –) and* d*-phenylbutazone (–·–) at* $pH_{bulk}$ *5.*

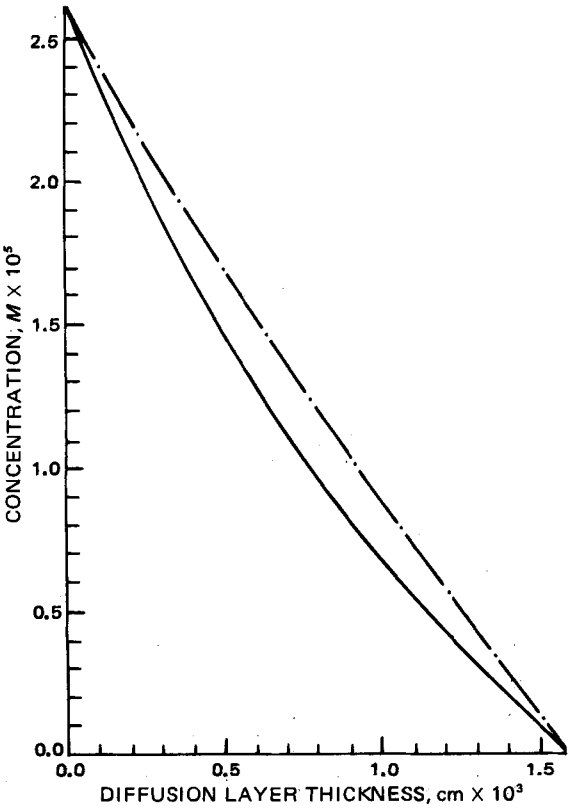


**Figure 6**—*Concentration profiles across an aqueous diffusion layer for phenylbutazone (– –) and* d*-phenylbutazone (–·–) at* $pH_{bulk}$ *7.*

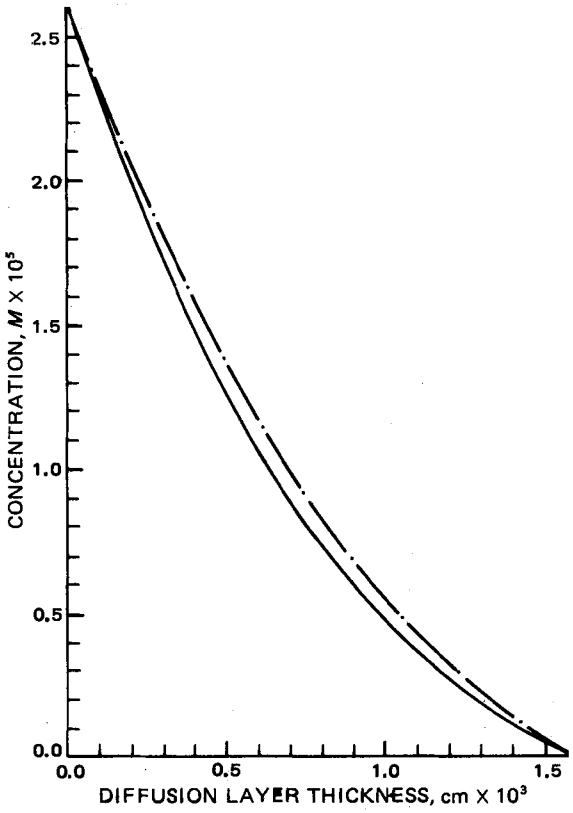


**Figure 7**—*Concentration profiles across an aqueous diffusion layer for phenylbutazone (– –) and* d*-phenylbutazone (–·–) at* $pH_{bulk}$ *9.*

as given previously, $[H^+]$ is the hydrogen-ion concentration, $[OH^-]$ is the hydroxide-ion concentration at which $k_{obs}$ is determined, and $K_{a,enol}$ is the dissociation constant of the enolic form of phenylbutazone (3). Although all of the data for these parameters were measured at $\mu = 0.1$ and 25° (3), it will be assumed that the values would remain reasonably unchanged in a medium of ionic strength 0.5.

From the phenylbutazone dissolution data measured in $pH_{bulk}$ 6.50 using varying rotation speeds and Eq. 20, it was possible to gain some insight into the approximate values of $k_{obs}$ within the diffusion layer during dissolution. Since the nondeuterated phenylbutazone dissolved in a classical manner in reactive media, the model used for instantaneous reaction (1) may be applied to phenylbutazone to estimate $[H^+]$ and $[OH^-]$ across the diffusion layer for any given bulk solution conditions.

Accordingly, $pH_{bulk}$ 6.50 at 600 rpm was chosen and the values of $[OH^-]$, $[H^+]$, and pH in the diffusion layer was calculated using the instantaneous reaction model (1). From these values, it was possible to use a simplified version of Eq. 20 to calculate the corresponding values for $k_{obs}$ at each point in the diffusion layer. The simplified form of Eq. 20 is given by:

$$k_{obs} = k_1 + \frac{k_2[H^+]K_{a,enol}}{K_{a,enol} + [H^+]} \qquad \text{(Eq. 21)}$$

which assumes from Eq. 20 that $k_3[OH^-]$ and $k_4$ are negligible relative to the other terms in the equation. Table VI shows the variation of $k_{obs}$ across the film if the equilibrium values of $[OH^-]_X$ and $[H^+]_X$ actually exist at a given position $X$ in the diffusion layer. Under these same conditions, $t_D$ is 0.27 sec at 600 rpm.

The $t_r$ values across the film do not differ by much and they approach the limiting value $t_r = 1/k_{obs} \simeq 0.1$ sec. This value is displayed in the plot given in Fig. 4; assuming that the deviation from Levich–Nernst behavior seen at $pH_{bulk}$ 6.50 in Fig. 2 is not significant, $t_D$ only approaches the limiting $t_r$ value when very rapid revolution speeds are used. Therefore, any effects that may be due to noninstantaneus ionization of phenylbutazone in the diffusion layer would only be significant when $t_D$ approaches the value of $t_r$. Note that the limiting pH at $X = 0$ was ~5. At this pH, the dissociation of phenylbutazone favors formation of its enolate anion. If $t_r$ for establishing this equilibrium was longer or about the same as $t_D$

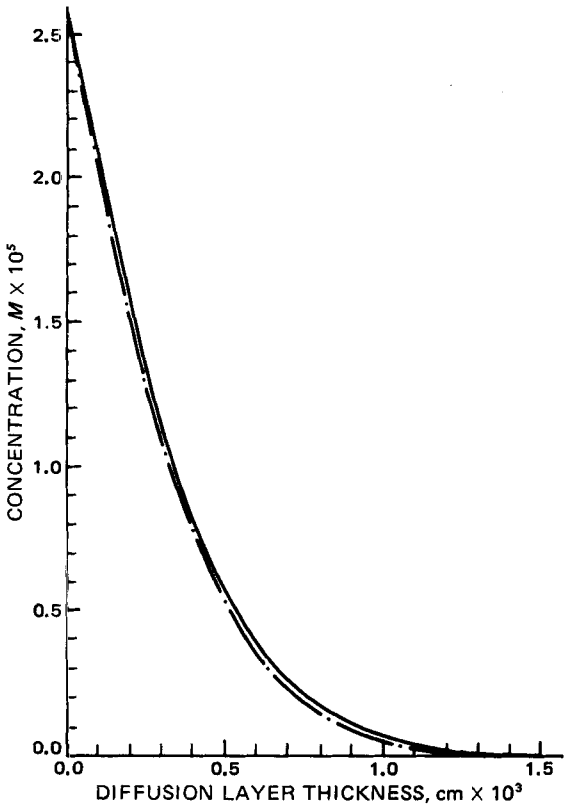


**Figure 8**—*Concentration profiles across an aqueous diffusion layer for phenylbutazone (– –) and* d*-phenylbutazone (-·-) at* $pH_{bulk}$ *10.*

in the diffusion layer, then deviation from classical behavior should have been observed under the described conditions.

To support these statements, the behavior of *d*-phenylbutazone under identical conditions was studied. Deuterated phenylbutazone should show a slower rate of approach to equilibrium in its ionization due to a primary isotope effect; *i.e.*, $k_1$ and $k_3$ for the initial dissociation of *d*-phenylbutazone will have a greater initial $t_r$ value than phenylbutazone under the same conditions. Therefore, the rotation speed at which $t_D$ becomes numerically similar to the limiting $t_r$ value was expected to be lower for *d*-phenylbutazone than for phenylbutazone, assuming again that the Levich–Nernst model applied and there were no differences in $D_{HA}$ and $[HA]_0$ between the two compounds.

The limiting $t_r$ value of *d*-phenylbutazone may be approximated by assuming a value for the primary isotope effect for the deprotonation of phenylbutazone. If a primary isotope effect of five was assumed (22) in $k_1$ (ignoring $k_3$), a limiting $t_r$ value of ~0.5 sec was calculated. This value was also displayed in Fig. 4 and indicated how $t_D$ approaches the limiting value of $t_r$ at much slower disk rotation speeds than in the case of phenylbutazone. Hence, any noninstantaneous reaction with base in the diffusion layer will affect the dissolution rates of *d*-phenylbutazone more than those of phenylbutazone under the same conditions. This finding was confirmed in Fig. 2 where the dissolution rates of *d*-phenylbutazone at $pH_{bulk}$ 6.50 were significantly slower than those of phenylbutazone under identical conditions.

The qualitative arguments expressed here were useful in interpreting the differences in dissolution rates between phenylbutazone and *d*-phenylbutazone. Figures 5–8, obtained by integrating numerically Eqs. 1–4, show the concentration gradients existing across the diffusion layer during dissolution of phenylbutazone and its deutero analog for pH 5, 7, 9, and 10. It was assumed in these simulations that *d*-phenylbutazone was dedeuterated by hydroxide ion and water five times slower than deprotonation of phenylbutazone. Calculated fluxes and pH at the interface are shown in Table VII.

The simulations appear to represent the flux data adequately. The observed dissolution rates for *d*-phenylbutazone were higher (pH 7 and 9) than the predicted theoretical values because deuterium was only abstracted once in practice but the model assumed that the rate of dissociation was that for deuterium for all abstractions. It can be seen from the figures that at pH 5 and 7, the concentration gradient between phenylbutazone and its deutero analog was more marked than when these two compounds dissolved under more basic conditions. At pH 9, the gradient difference was smaller; at pH 10, it was negligible. These results were consistent with the earlier argument that as the $pH_{bulk}$ is raised, the diffusion layer reaction time becomes faster and both phenylbutazone and *d*-phenylbutazone approach classical behavior ($t_r < t_D$). Thus, under neutral to slightly acidic conditions, deuterated phenylbutazone deviates from classical behavior. However, when basic conditions prevail, the dissolution of that compound was faster since the high concentration of hydroxide ion increased the rate of *d*-phenylbutazone ionization.

**Table VII—Simulated ($J_{theor}$) and Observed ($J_{obs}$) Initial Dissolution Rates for Phenylbutazone and *d*-Phenylbutazone at Various $pH_{bulk}$ Values** [a]

| $pH_{bulk}$ | $pH_0^{calc}$ [b] | Phenylbutazone | | *d*-Phenylbutazone | |
|---|---|---|---|---|---|
| | | $J_{theor}$ | $J_{obs}$ | $J_{theor}$ | $J_{obs}$ |
| 5 | 4.77 | 19.95 | 19.95 | 11.24 | 11.25 |
| 7 | 4.95 | 27.18 | 27.18 | 16.23 | 20.27 |
| 9 | 5.17 | 38.34 | 38.39 | 27.59 | 32.95 |
| 10 | 5.85 | 189.54 | 187.01 | 187.01 | 169.97 |

[a] All values of $J$ are in units of moles $cm^{-2}$/sec. [b] Calculated from the simulations.

In view of the dissolution behavior of phenylbutazone under various conditions, it is unlikely that noninstantaneous ionization kinetics, demonstrated so clearly for this compound (3), play a major role in determining the dissolution rate, either *in vitro* or *in vivo*. This is due to the fact that the average diffusion layer residency time for a typical aqueous diffusion layer is longer than the average reaction time for the ionization of this carbon acid.

## REFERENCES

(1) K. G. Mooney, M. Mintun, K. J. Himmelstein, and V. J. Stella, *J. Pharm. Sci.*, **70**, 13 (1981).

(2) *Ibid.*, **70**, 22 (1981).

(3) V. J. Stella and J. D. Pipkin, *J. Pharm. Sci.*, **65**, 1161 (1976).

(4) W. P. Jencks, "Catalysis in Chemistry and Enzymology," McGraw-Hill, New York, N.Y., 1969, pp. 175–178.

(5) J. R. Jones, *Prog. Phys. Org. Chem.*, **9**, 244 (1972).

(6) G. R. Van Petten, H. Feng, R. J. Whitney, and H. F. Lettau, *J. Clin. Pharmacol.*, **11**, 177 (1971).

(7) R. J. Whitney, H. Feng, D. Cook, G. R. Van Peteten, and H. F. Lettau, *ibid.*, **11**, 187 (1971).

(8) L. J. Lesson, "Proceedings of the Conference on Bioavailability of Drugs," B. B. Brodie and W. M. Heller, Eds., S. Karger, New York, N.Y., 1972, pp. 154–163.

(9) *J. Am. Pharm. Assoc.*, **NS16** p. 365 (1976).

(10) E. G. Lovering and D. B. Black, *J. Pharm. Sci.*, **63**, 671 (1974).

(11) *Ibid.*, **63**, 1399 (1974).

(12) V. J. Stella, *J. Pharm. Sci.*, **64**, 706 (1975).

(13) J. Matsunaga, N. Nambu, and T. Nagai, *Chem. Pharm. Bull.*, **24**, 1169 (1976).

(14) H. Ibrahim, F. Pisano, and A. Bruno, *J. Pharm. Sci.*, **66**, 669 (1977).

(15) J. Crank and P. Nicolson, *Proc. Cambridge Philos. Soc.*, **43**, 50 (1947).

(16) D. D. Morrison, J. D. Riley, and J. F. Zancanaro, *Commun. ACM*, **7**, 366 (1964).

(17) J. F. Holt, *ibid.*, **5**, 613 (1962).

(18) B. Carnahan, H. A. Luther, and J. O. Wilkes, "Applied Numerical Methods," Wiley, New York, N.Y., 1969, p. 451.

(19) *Ibid.*, pp. 269–281.

(20) T. Higuchi, H. K. Lee, and I. H. Pitman, *Farm. Aikak.*, **80**, 55 (1971).

(21) G. Astarita, "Mass Transfer with Chemical Reaction," Elsevier, New York, N.Y., 1967, p. 9.

(22) J. P. Klinman, in "Transition States of Biochemical Processes," R. D. Gandour and R. L. Schowen, Eds., Plenum, New York, N.Y. 1978, pp. 165–200.

## ACKNOWLEDGMENTS

Adapted in part from a dissertation submitted by K. G. Mooney to the University of Kansas in partial fulfillment of the Doctor of Philosophy degree requirements.

Supported by National Institutes of Health Grant GM 22357.

# High-Pressure Liquid Chromatography of Amiodarone in Biological Fluids

L. J. LESKO *x, A. MARION *, A. T. CANADA *, and C. HAFFAJEE ‡

Received January 5, 1981, from the * *Drug Concentration Laboratory, Department of Pharmacy and Clinical Pharmacy, and the* ‡ *Department of Medicine, University of Massachusetts Medical Center, Worcester, MA 01605.* Accepted for publication March 24, 1981.

**Abstract** □ A rapid, sensitive, and specific method of analysis for amiodarone in serum, urine, and tissue by high-pressure liquid chromatography is described. Sample preparation includes acidification with two volumes of 0.2 *M* acetate buffer followed by extraction into five volumes of hexane. The organic solvent is dried, and the residue is reconstituted in mobile phase and injected into the chromatograph. Separation is obtained using a silica column and a chloroform–methanol–ammonia mobile phase. Detection at 254 and 280 nm showed the assay to be specific in the presence of other commonly administered drugs. Levels of 0.05 μg/ml can be measured with a precision of ±15%; but with appropriate modification of the procedure, levels as low as 0.025 μg/ml can be measured with suitable precision. The inter- and intraday coefficient of variation for replicate analysis of spiked serum samples is <5%. This method is useful for single- and multiple-dose pharmacokinetic studies of amiodarone in animals and humans.

**Keyphrases** □ Amiodarone—high-pressure liquid chromatography in biological fluids □ High-pressure liquid chromatography—amiodarone in biological fluids □ Vasodilator—amiodarone, high-pressure liquid chromatography in biological fluids

Amiodarone[1] (I), a benzofuran derivative, is structurally similar to thyroxine. It is an effective antiarrhythmic agent for the treatment of supraventricular and ventricular tachyarrhythmias (1, 2). The pharmacokinetics of amiodarone have been studied in animals and humans following the administration of radiolabeled amiodarone and the measurement of total radioactivity in serum and urine (3). However, because of the nonspecificity of total radioactivity measurements, a sensitive and specific method of analysis for unlabeled amiodarone is needed. Flanagan *et al.* (4) described a high-pressure liquid chromatographic (HPLC) method for the measurement of amiodarone in plasma or serum with a sensitivity of 0.05 μg/ml, but they did not indicate if the assay was sensitive enough for single-dose pharmacokinetic studies. One disadvantage of their method is the use of a mobile phase containing 15 parts of ether. Its volatility may cause chromatographic variations.

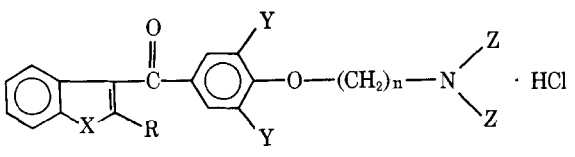

I: X = O, R = $C_4H_9$, Y = I, n = 2, Z = $C_2H_5$
II: X = S, R = $C_2H_5$, Y = Br, n = 3, Z = $C_3H_7$

[1] Cordarone, Labaz Laboratories, Ambares, France.

The present report describes a rapid, sensitive, and specific HPLC technique for amiodarone in serum, urine, or tissues. Because of a concentrating step during sample preparation, a sensitivity of 0.025 μg/ml with acceptable precision was obtained. This method was used to measure amiodarone in biological fluids of dogs and humans in single- and multidose pharmacokinetic studies and is acceptable for postmortem tissue analysis.

## EXPERIMENTAL

**Reagents and Chemicals**—Amiodarone hydrochloride[2] and the internal standard[2] (II), a benzothiophene derivative of amiodarone, were used as received. Chloroform[3], methanol[3], and hexane were HPLC grade. All other reagents and solvents were analytical grade quality and were used as received.

**Amiodarone Standard**—A stock solution of amiodarone (1.0 mg/ml) was prepared by dissolving 10.6 mg of amiodarone hydrochloride in 10.0 ml of methanol. Serum standards were prepared by spiking blank control serum with appropriate microliter volumes of the stock solution to obtain five serum standards with the following concentrations of amiodarone: 0.125, 0.25, 0.50, 1.0, and 2.0 μg/ml.

**Internal Standard**—A stock solution of the internal standard (1.0 mg/ml) was made by dissolving 10.0 mg in 10.0 ml of methanol. An internal standard working solution was prepared by dilution of an aliquot of the stock solution with acetate buffer to contain 0.5 μg/ml.

**Acetate Buffer**—A 0.2 *M* acetate buffer was prepared by mixing 10.9 parts of Solution A (27.2 g of hydrous sodium acetate/liter) with 89.1 parts of Solution B (11.5 ml of acetic acid/liter). The pH of the buffer was adjusted to 3.8 by dropwise addition of either acetic acid or 1 *N* NaOH.

**Instruments and Chromatographic Conditions**—A microparticulate, stainless steel, normal-phase column[4], 4.0 mm × 30 cm, at ambient temperature was used for separation. The column was used with a septumless injector[5], a solvent delivery system consisting of a dual-piston pump[6], and a dual fixed-wavelength UV absorbance detector[7] equipped with 254- and 280-nm filters. The eluting solvent was chloroform–methanol–ammonium hydroxide (98.95:1.0:0.05) at a flow rate of 0.8 ml/min. A dual-pen recorder[8] with a range of 0–10 mv was used with a chart speed of 0.5 cm/min. Peak heights were measured to the nearest half-millimeter with a metric ruler.

Prior to analysis, the chromatographic system was stabilized for 10–20 min and 20 μl of a standard test mixture of amiodarone (1 μg/ml) and the internal standard (1 μg/ml) in the mobile phase was injected into the chromatograph. A response factor was calculated from the resulting peak heights to confirm accurate operation.

**Sample Preparation**—To a disposable screw-capped glass culture tube (16 × 125 mm) were added 0.5 ml of serum or urine and 1.0 ml of the internal standard working solution. The sample was extracted with 5.0 ml of hexane by gentle shaking on a horizontal shaker[9] for 10 min. For tissue analysis, 1.0 ml of tissue homogenate, prepared by homogenizing 1.0 g of blotted tissue in 10.0 ml of distilled water, was mixed with 2.0 ml

[2] Labaz, Centre de Recherche, Brussels, Belgium.
[3] Burdick & Jackson Laboratories, Muskegon, Mich.
[4] μPorasil, Waters Associates, Milford, Mass.
[5] Model U6K, Waters Associates, Milford, Mass.
[6] Model 6000A, Waters Associates, Milford, Mass.
[7] Model 440, Waters Associates, Milford, Mass.
[8] Omniscribe, Houston Instruments, Austin, Tex.
[9] Eberbach Corp., Ann Arbor, Mich.



0022-3549/81/1200-1366$01.00/0
© 1981, American Pharmaceutical Association

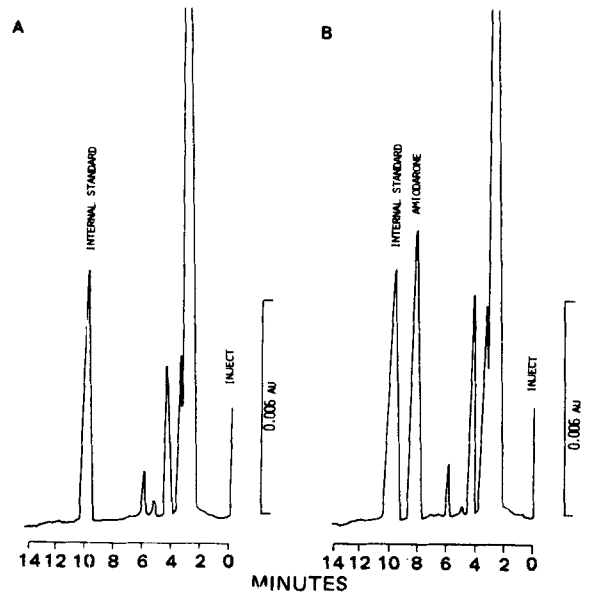


**Figure 1**—*Representative high-pressure liquid chromatogram of blank human serum (A) and human serum containing amiodarone, 1 μg/ml (B).*

of internal standard working solution and extracted with 10.0 ml of hexane. The organic phase (upper) was separated by centrifugation at 1600 × *g* for 5 min and transferred to a clean, disposable, glass test tube. The hexane was evaporated at 60° under a gentle nitrogen stream. The residue was reconstituted in 50 μl of mobile phase by vortex mixing[10], and 20 μl was injected into the liquid chromatograph. The concentration of amiodarone in the serum was determined from a calibration curve of peak height ratio (amiodarone to internal standard) *versus* amiodarone concentration in serum standards carried through this procedure.

## RESULTS AND DISCUSSION

Chromatograms obtained from blank human serum and serum spiked with amiodarone are shown in Fig. 1. The peaks representing amiodarone and the internal standard are symmetrical and well removed from the solvent front and extraneous serum peaks. The retention times of amiodarone and the internal standard are 8.2 and 10.0 min, respectively. Some control of retention times is possible by varying the proportion of ammonium hydroxide in the mobile phase. Increasing amounts of ammonium hydroxide decrease the retention times of both compounds. Reducing the amount of ammonium hydroxide increases retention times and results in notable peak tailing. Although the ratio of methanol in the mobile phase does not significantly alter retention times, a small quantity of methanol is useful in modifying the silica stationary phase and facilitating reproducible separation and peak symmetry.

Calibration curves of peak height ratio *versus* concentration were obtained by analyzing serum standards containing amiodarone in concentrations ranging from 0.05 to 2.0 μg/ml. Calibration curves were prepared using two different wavelengths for detection, 254 and 280 nm. (Detection at two wavelengths is a simple way to validate that there is only one solute under the peak of interest eluting from the column.) The calibration curves at both wavelengths were linear over the concentration range studied. The least-squares linear regression line representing the best fit of the amiodarone data at 254 nm had a slope of 1.69 and a *y* intercept (where *y* = peak height ratio) of −0.04 ($r$ = 0.999). The corresponding line at 280 nm had a slope of 1.01 and a *y* intercept of −0.03 ($r$ = 0.999). Although assay sensitivity is better at 254 nm, the assay is operated routinely at 280 nm. At this wavelength, detector noise is considerably less and solvent transparency to the detector is better, resulting in a more stable baseline and shorter equilibration time.

Assay precision was determined by repeated analysis of spiked serum samples containing low (0.25 μg/ml) and high (1.0 μg/ml) concentrations of amiodarone. The mean concentration, standard deviation, and coefficient of variation for intra- and interday analysis are shown in Table I. The within-day and day-to-day variation at each concentration was <5%.

[10]Vortex-genie, Scientific Industries, Springfield, Mass.

**Table I—Precision Data for the Determination of Amiodarone in Serum**

| Concentration, μg/ml | Intraday | | | Interday | | |
|---|---|---|---|---|---|---|
| | *n* | Mean ± *SD*, μg/ml | *CV*, % | *n* | Mean ± *SD*, μg/ml | *CV*, % |
| 1.0 | 5 | 0.993 ± 0.026 | 2.62 | 10 | 0.951 ± 0.040 | 4.21 |
| 0.25 | 5 | 0.230 ± 0.006 | 2.61 | 10 | 0.225 ± 0.011 | 4.89 |

The analytical recovery of amiodarone from serum was determined by comparing peak heights of amiodarone obtained by analyzing extracted, spiked serum specimens to the peak heights obtained by direct injection of methanolic solutions of amiodarone containing an amount of amiodarone equivalent to the amount in the spiked serum specimens. The mean ± *SD* recovery of amiodarone was 81.9 ± 5.0% ($n$ = 10) at a concentration of 1.0 μg/ml and 79.7 ± 2.5 ($n$ = 3) at a concentration of 0.25 μg/ml.

The sensitivity of this method is 0.05 μg/ml using 0.2 ml of serum samples and 0.01 aufs. The intraday coefficient of variation for spiked serum samples containing 0.05 μg/ml was ±13.0% ($n$ = 5). Lower concentrations of amiodarone may be detected with an analytical error of <±15% by increasing serum volume, detector attenuation, or injection volume. Detection at 254 nm would also increase sensitivity if necessary. Amiodarone concentrations of 0.025 μg/ml in serum were easily measurable by including such modifications in the procedure.

The described method for amiodarone analysis in serum has been used in single-dose pharmacokinetic studies and for monitoring serum amiodarone concentrations in patients receiving long-term amiodarone therapy. A typical serum amiodarone concentration–time profile obtained in two patients after administration of a single 800-mg oral loading dose is shown in Fig. 2. Amiodarone appears to be absorbed relatively slowly and disappears rapidly from the serum, at least following the first dose. Detailed studies of amiodarone pharmacokinetics in dogs and humans are being conducted.

The present assay uses a silica column and a nonaqueous mobile phase. Although bonded, reversed-phase systems using aqueous mobile phases are preferred by many chromatographers for the analysis of drugs in serum, a normal-phase, liquid–solid chromatographic system is useful for such drugs as amiodarone, cimetidine, trimethoprim, and tricyclic antidepressants. The mobile phase requirements are usually similar: a pure, organic solvent such as chloroform or methylene chloride of intermediate polarity similar to the solute; a small proportion of a miscible, more polar solvent, such as methanol or isopropanol, to modify the adsorbent activity of the stationary silica phase; and a small amount of base to adjust the ionization state of the solute and to minimize peak tailing. The amiodarone assay has been used for over 3 years and has proven to be simple, reliable, and accurate. Column life is often as long as 1 year or over 500 injections. The base in the mobile phase has not caused any apparent deterioration in column efficiency.

A single-step solvent extraction procedure is used to separate amiodarone from serum and to concentrate it. An acidic pH is optimal for the extraction. Organic solvents useful for extraction of amiodarone from serum include ether, methylene chloride, chloroform, and hexane. Hexane provides the cleanest extract and no back-extraction is required. Pretreatment of the serum before injection is rapid, and as many as 20–30 serum samples/day can be analyzed by one technician.

No endogenous substances or drugs have been found to interfere with

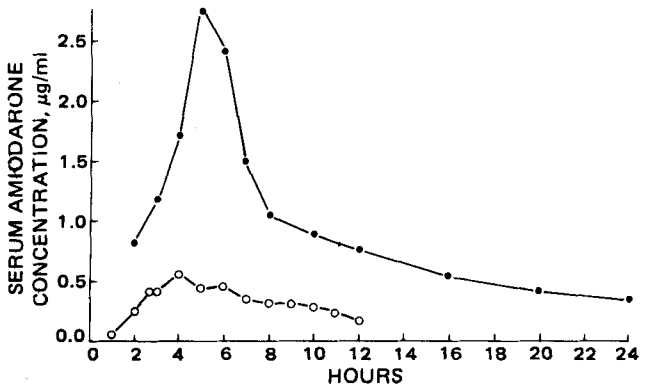


**Figure 2**—*Serum amiodarone concentrations in two patients after an 800-mg oral loading dose. Key:* ○, *Patient 1; and* ●, *Patient 2.*

amiodarone analysis using this procedure. The assay has been used for patients receiving amiodarone in combination with drugs such as procainamide, quinidine, lidocaine, disopyramide, digoxin, prednisone, furosemide, and other thiazide diuretics.

## REFERENCES


(1) M. B. Rosenbaum, P. A. Chiale, D. Ryba, and M. V. Elizari, *Am. J. Cardiol.*, **34**, 215 (1974).

(2) M. B. Rosenbaum, P. A. Chiale, M. S. Halpern, G. J. Nau, J. Przybylski, R. J. Levi, J. O. Latzari, and M. V. Elizari, *ibid.*, **38**, 935 (1976).

(3) J. Broekhuysen, R. Laruel, and R. Sion, *Arch. Int. Pharmacodyn.*, **177**, 340 (1969).

(4) R. J. Flanagan, G. C. A. Storey, and D. W. Holt, *J. Chromatogr.*, **187**, 391 (1980).


## ACKNOWLEDGMENTS


Presented at the Pharmaceutical Analysis and Control Section, APhA Academy of Pharmaceutical Sciences, San Antonio meeting, November 1980.

The authors gratefully acknowledge the assistance of J. Broekhuysen (Labaz) in the development of the assay and for supplying amiodarone and internal standard powders and thank P. Norkin (Labaz) for his helpful review of the manuscript. The technical assistance of A. Conlan, C. Oliver, J. Ericson, and M. Karcasinas in the preparation of the manuscript is appreciated.


# Influence of the Method of Application on Pharmacokinetics of Nitroglycerin from Ointment in Humans


**S. SVED *x, W. M. McLEAN ‡, and I. J. McGILVERAY ***



Received April 6, 1981, from the **Bureau of Drug Research, Health Protection Branch, Health and Welfare Canada, Ottawa, Ontario, Canada K1A 0L2*, and the ‡*Drug Consultation Services, Ottawa General Hospital, and Department of Pharmacology, University of Ottawa, Ottawa, Ontario, Canada K1H 8L6.* Accepted for publication June 2, 1981.



**Abstract** □ A study was designed to test the influence of surface area on the percutaneous absorption of nitroglycerin from a commercial ointment formulation, using a simple crossover design. On separate occasions, three volunteers were given 16 mg of nitroglycerin (2%) over a 25- and 100-cm$^2$ area. Plasma nitroglycerin concentration was measured at 30, 45, 60, and 90 min using a sensitive capillary GLC–electron-capture detection method capable of quantitating to 150 pg/ml. Plasma concentrations at all times increased at least twofold with the increased surface area; highest observed concentrations were 0.17 and 0.41 ng/ml, respectively. A fourth volunteer received 16 and 32 mg of nitroglycerin over 100 cm$^2$. Doubling the dose increased the 0–90-min *AUC* by only 76% but caused a 3.5-fold increase in the 90-min plasma concentration. These results suggest that the surface area of application significantly influences the pharmacokinetics of nitroglycerin ointment.



**Keyphrases** □ Nitroglycerin—ointments, effect of method of application on pharmacokinetics, humans □ Ointments—nitroglycerin, effect of method of application on pharmacokinetics, humans □ Pharmacokinetics—effect of method of application on nitroglycerin ointments, humans □ Vasodilators—nitroglycerin ointments, effect of method of application on pharmacokinetics, humans


Nitroglycerin (glyceryl trinitrate), a vasodilator, is used extensively in the treatment of angina, cardiac infarction, and other circulatory conditions (1). However, because of its rapid elimination (2, 3), sustained-release or percutaneous dosage forms were developed. It was recently shown (4) that the ointment dosage form is more bioavailable than a sustained-action oral capsule formulation, and evidence was presented (5) that blood concentrations obtained after ointment application were dose dependent. However, neither study examined the influence of surface area on percutaneous absorption. It was also demonstrated (6) that the amount of nitroglycerin absorbed through the skin of a rhesus monkey was dependent on the surface area (but not the anatomical area) of application; however, the importance of this finding may not be generally recognized in the everyday use of this dosage form.

The present study investigated the influence of the surface area of application of the ointment on nitroglycerin bioavailability.

## EXPERIMENTAL

Three healthy adult male volunteers were each given 650 mg of acetaminophen orally (to control possible side effects), followed by 16 mg of nitroglycerin as a 2% ointment[1]. In the first part of the experiment ("small area"), the ointment was spread on paper[2] cut to 25 cm$^2$, and the paper was applied over the chest near the sternum and covered with an adhesive bandage. In the second part ("large area"), performed 2 months later on the same volunteers, an identical amount of nitroglycerin ointment was spread over 100 cm$^2$ in the same region of the chest, outlined on the skin with the help of a template. The ointment was applied as uniformly as possible with a stainless steel spatula and immediately occluded with a sheet of aluminum foil attached with adhesive tape. A fourth volunteer received 16 and 32 mg of nitroglycerin ointment (2%) spread over 100 cm$^2$ as described for the large area experiment.

Blood (10 ml) was collected by venipuncture, using an all-glass syringe, at the times indicated in Tables I and II, and dispensed at once into a chilled glass tube containing 0.3 ml of heparin sodium (300 U/per tube) and 50 μl of 0.002 *M* $AgNO_3$ (7). The contents were mixed by inversion, centrifuged immediately in the cold (5 min, 2000 rpm, 4°), and the plasma was separated for the nitroglycerin assay.

The assay method[3] consisted of mixing 1 or 2 ml of plasma with 100 μl of 1 *M* $AgNO_3$ (8), extracting with 10 ml of redistilled pentane containing 3 ng of *o*-dinitrobenzene[4], and evaporating the solvent in an ice bath with a gentle nitrogen stream. The residue was redissolved in 25 μl of redistilled hexane, and 4 μl of this solution was chromatographed on a capillary GLC system[5] equipped with an electron-capture detector[6], using a 25-m methyl silicone gum-coated open tubular column[7]. The chromatographic conditions were carrier gas, helium (6-ml/min septum purge, 2-ml/min column flow); makeup gas, argon–methane (95:5, 30 ml/min); injection, splitless, at 200°, 30-sec delay; oven, programmed temperature from 80 to 130° at 30°/min; detector, 150°; and retention

[1] Nitrol, Kramer-Urban, Milwaukee, Wis.
[2] Appli-Ruler, provided by the manufacturer as package insert.
[3] To be described in detail elsewhere.
[4] RotoRack, Fisher Scientific, Ottawa, Canada. Extraction at 15 rpm, 20 min.
[5] Hewlett-Packard model 5730A with model 18740B capillary inlet system.
[6] Hewlett-Packard model 18713A linear electron-capture detector.
[7] Hewlett-Packard model SP 2100.




*0022-3549/81/1200-1368$01.00/0*


*© 1981, American Pharmaceutical Association*

amiodarone analysis using this procedure. The assay has been used for patients receiving amiodarone in combination with drugs such as procainamide, quinidine, lidocaine, disopyramide, digoxin, prednisone, furosemide, and other thiazide diuretics.

## REFERENCES


(1) M. B. Rosenbaum, P. A. Chiale, D. Ryba, and M. V. Elizari, *Am. J. Cardiol.*, **34**, 215 (1974).

(2) M. B. Rosenbaum, P. A. Chiale, M. S. Halpern, G. J. Nau, J. Przybylski, R. J. Levi, J. O. Latzari, and M. V. Elizari, *ibid.*, **38**, 935 (1976).

(3) J. Broekhuysen, R. Laruel, and R. Sion, *Arch. Int. Pharmacodyn.*, **177**, 340 (1969).

(4) R. J. Flanagan, G. C. A. Storey, and D. W. Holt, *J. Chromatogr.*, **187**, 391 (1980).


## ACKNOWLEDGMENTS


Presented at the Pharmaceutical Analysis and Control Section, APhA Academy of Pharmaceutical Sciences, San Antonio meeting, November 1980.

The authors gratefully acknowledge the assistance of J. Broekhuysen (Labaz) in the development of the assay and for supplying amiodarone and internal standard powders and thank P. Norkin (Labaz) for his helpful review of the manuscript. The technical assistance of A. Conlan, C. Oliver, J. Ericson, and M. Karcasinas in the preparation of the manuscript is appreciated.


# Influence of the Method of Application on Pharmacokinetics of Nitroglycerin from Ointment in Humans


**S. SVED *x, W. M. McLEAN ‡, and I. J. McGILVERAY ***



Received April 6, 1981, from the **Bureau of Drug Research, Health Protection Branch, Health and Welfare Canada, Ottawa, Ontario, Canada K1A 0L2*, and the ‡*Drug Consultation Services, Ottawa General Hospital, and Department of Pharmacology, University of Ottawa, Ottawa, Ontario, Canada K1H 8L6.* Accepted for publication June 2, 1981.



**Abstract** □ A study was designed to test the influence of surface area on the percutaneous absorption of nitroglycerin from a commercial ointment formulation, using a simple crossover design. On separate occasions, three volunteers were given 16 mg of nitroglycerin (2%) over a 25- and 100-cm$^2$ area. Plasma nitroglycerin concentration was measured at 30, 45, 60, and 90 min using a sensitive capillary GLC–electron-capture detection method capable of quantitating to 150 pg/ml. Plasma concentrations at all times increased at least twofold with the increased surface area; highest observed concentrations were 0.17 and 0.41 ng/ml, respectively. A fourth volunteer received 16 and 32 mg of nitroglycerin over 100 cm$^2$. Doubling the dose increased the 0–90-min *AUC* by only 76% but caused a 3.5-fold increase in the 90-min plasma concentration. These results suggest that the surface area of application significantly influences the pharmacokinetics of nitroglycerin ointment.



**Keyphrases** □ Nitroglycerin—ointments, effect of method of application on pharmacokinetics, humans □ Ointments—nitroglycerin, effect of method of application on pharmacokinetics, humans □ Pharmacokinetics—effect of method of application on nitroglycerin ointments, humans □ Vasodilators—nitroglycerin ointments, effect of method of application on pharmacokinetics, humans


Nitroglycerin (glyceryl trinitrate), a vasodilator, is used extensively in the treatment of angina, cardiac infarction, and other circulatory conditions (1). However, because of its rapid elimination (2, 3), sustained-release or percutaneous dosage forms were developed. It was recently shown (4) that the ointment dosage form is more bioavailable than a sustained-action oral capsule formulation, and evidence was presented (5) that blood concentrations obtained after ointment application were dose dependent. However, neither study examined the influence of surface area on percutaneous absorption. It was also demonstrated (6) that the amount of nitroglycerin absorbed through the skin of a rhesus monkey was dependent on the surface area (but not the anatomical area) of application; however, the importance of this finding may not be generally recognized in the everyday use of this dosage form.

The present study investigated the influence of the surface area of application of the ointment on nitroglycerin bioavailability.

## EXPERIMENTAL

Three healthy adult male volunteers were each given 650 mg of acetaminophen orally (to control possible side effects), followed by 16 mg of nitroglycerin as a 2% ointment[1]. In the first part of the experiment ("small area"), the ointment was spread on paper[2] cut to 25 cm$^2$, and the paper was applied over the chest near the sternum and covered with an adhesive bandage. In the second part ("large area"), performed 2 months later on the same volunteers, an identical amount of nitroglycerin ointment was spread over 100 cm$^2$ in the same region of the chest, outlined on the skin with the help of a template. The ointment was applied as uniformly as possible with a stainless steel spatula and immediately occluded with a sheet of aluminum foil attached with adhesive tape. A fourth volunteer received 16 and 32 mg of nitroglycerin ointment (2%) spread over 100 cm$^2$ as described for the large area experiment.

Blood (10 ml) was collected by venipuncture, using an all-glass syringe, at the times indicated in Tables I and II, and dispensed at once into a chilled glass tube containing 0.3 ml of heparin sodium (300 U/per tube) and 50 μl of 0.002 *M* $AgNO_3$ (7). The contents were mixed by inversion, centrifuged immediately in the cold (5 min, 2000 rpm, 4°), and the plasma was separated for the nitroglycerin assay.

The assay method[3] consisted of mixing 1 or 2 ml of plasma with 100 μl of 1 *M* $AgNO_3$ (8), extracting with 10 ml of redistilled pentane containing 3 ng of *o*-dinitrobenzene[4], and evaporating the solvent in an ice bath with a gentle nitrogen stream. The residue was redissolved in 25 μl of redistilled hexane, and 4 μl of this solution was chromatographed on a capillary GLC system[5] equipped with an electron-capture detector[6], using a 25-m methyl silicone gum-coated open tubular column[7]. The chromatographic conditions were carrier gas, helium (6-ml/min septum purge, 2-ml/min column flow); makeup gas, argon–methane (95:5, 30 ml/min); injection, splitless, at 200°, 30-sec delay; oven, programmed temperature from 80 to 130° at 30°/min; detector, 150°; and retention

[1] Nitrol, Kramer-Urban, Milwaukee, Wis.
[2] Appli-Ruler, provided by the manufacturer as package insert.
[3] To be described in detail elsewhere.
[4] RotoRack, Fisher Scientific, Ottawa, Canada. Extraction at 15 rpm, 20 min.
[5] Hewlett-Packard model 5730A with model 18740B capillary inlet system.
[6] Hewlett-Packard model 18713A linear electron-capture detector.
[7] Hewlett-Packard model SP 2100.




*0022-3549/81/1200-1368$01.00/0*


*© 1981, American Pharmaceutical Association*

**Table I—Effect of Surface Area on Nitroglycerin Absorption**

| Area, $cm^2$ | Minutes after Application | Blood Concentration, ng/ml (16-mg dose) Subject MT | Subject WN | Subject RL | Mean |
|---|---|---|---|---|---|
| 25 | 30 | 0.17 | 0.15 | 0.18 | 0.17 |
| | 60 | 0.13 | ND[a] | 0.16 | 0.14 |
| | 90 | ND[a] | ND[a] | ND[a] | — |
| 100 | 30 | [b] | 0.32 | 0.32 | 0.32 |
| | 45 | 0.47 | 0.36 | 0.39 | 0.41 |
| | 60 | 0.44 | 0.21 | 0.29 | 0.31 |
| | 90 | 0.32 | 0.16 | 0.26 | 0.25 |
| | *AUC* (0–90) | 0.48 | 0.33 | 0.39 | 0.40 |

[a] None detected (<0.05 ng/ml). [b] Sample unavailable.

**Table II—Effect of Dose on the Nitroglycerin Absorption**

| Area, $cm^2$ | Minutes after Application | Blood Concentration, ng/ml 16-mg Dose | 32-mg Dose |
|---|---|---|---|
| 100 | 30 | 0.31 | 0.20 |
| | 45 | 0.36 | 0.44 |
| | 60 | 0.37 | 0.88 |
| | 90 | 0.24 | 0.83 |
| | *AUC* (0–90) | 0.41 | 0.72 |

times, 3.8 min for nitroglycerin and 5.5 min for *o*-dinitrobenzene. Quantitation was by the peak height ratio method.

A two-compartment open model without lag time [$C_t = Ae^{-\alpha t} + Be^{-\beta t} - (A + B)e^{-k_a t}$] was used with an iterative computer program to fit a weighted ($1/y$) least-squares nonlinear regression curve to the experimental points. Goodness of fit was estimated as $r^2 = 1 - (\Sigma \text{ deviation}^2/\Sigma \text{ observation}^2)$.

## RESULTS AND DISCUSSION

The described method was specific for the unchanged drug and quantitative to ~0.15 ng/ml, and a detection limit of ~0.05 ng/ml. A standard curve, consisting of 20 determinations from 0.2 to 5.0 ng/ml, gave a mean relative standard deviation of 7.8% (range 2.5–12.3%) and a coefficient of determination ($r^2$) of 0.987. The regression of peak height ratio on concentration gave a slope of 0.483 ml/ng and an intercept of −0.004.

Table I shows the results obtained in three volunteers. After the application of 16 mg of nitroglycerin over 25 $cm^2$, the highest blood concentrations were observed at 30 min, with values of 0.15–0.18 ng/ml, close to the quantitation limit of the method, followed by a rapid decline to below the detection limits at 90 min. Because of these low concentrations, no meaningful area under the curve (*AUC*) values could be calculated. When the same amount of ointment was applied to the same volunteers but over a 100-$cm^2$ area, peak plasma concentrations occurred at 45 min and the decline was much slower. All concentrations were at least double the corresponding concentrations in the small area experiment.

For certain drugs, percutaneous absorption is known to be influenced by occluding the skin. However, this does not appear to be the case with nitroglycerin (9). In addition, it seems unlikely that the differences in the vapor barrier characteristics of the wax-impregnated paper used in the small area experiment and the aluminum foil used in all subsequent experiments would account for the differences obtained.

Table II shows the effect of dose on plasma nitroglycerin levels in one volunteer with the area held constant. The 16-mg dose over the 100-$cm^2$ area gave results very similar to those obtained for the three previous volunteers, although the relative absorption rate appeared to be marginally slower. With double the dose over the same surface area, absorption continued for a substantially longer time, as shown by the 3.5-fold increase in the 90-min blood concentration. However, the *AUC* (0–90 min) increased by only 76%, suggesting a nonlinear transfer process.

Preliminary pharmacokinetic studies for one experiment (Table II, 16 mg) prolonged for 6.5 hr (Fig. 1) suggest a two-compartment open model, with a distribution phase ($\alpha$) lasting for ~2 hr and a terminal

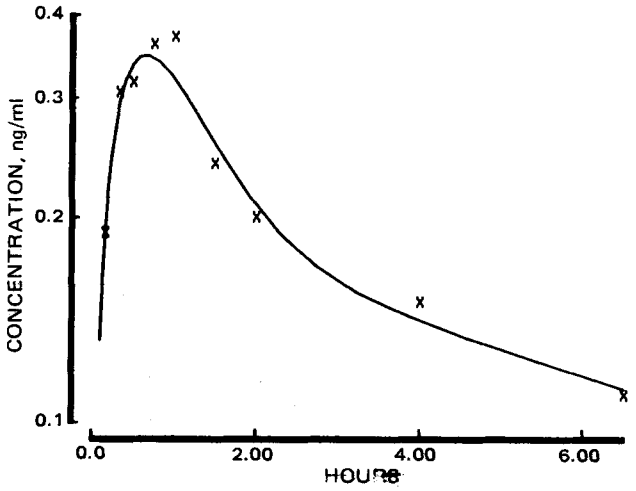


**Figure 1**—*Plasma profile of nitroglycerin following ointment application with a 16-mg dose in 2% ointment spread over 100 $cm^2$. The solid line indicates least-squares nonlinear regression to a two-compartment open model without lag time ($C_t = 28.1e^{-1.94t} + 0.197e^{-0.086t} - 28.3e^{-1.98t}$). Goodness of fit ($r^2$) = 0.994.*

decay ($\beta$) with a half-life of 3.5 hr. Nitroglycerin elimination from the blood is known to be rapid, with a half-life of 4–8 min after sublingual administration (4). Therefore, the apparent long terminal half-life in the present experiment must be due to other processes, *e.g.*, prolonged absorption.

These results agree well with those of Maier-Lenz *et al.* (4) who reported venous plasma concentrations between 0.4 and 0.7 ng/ml 60 min after the application of 30.6 mg of nitroglycerin in a 2% ointment, but they differ from those reported by Armstrong *et al.* (5), who obtained ~3 ng/ml after 0.27 mg of nitroglycerin/kg over 58 $cm^2$. The differences may be attributed largely to experimental design since the latter workers measured the concentration in arterial rather than venous blood and also examined percutaneus absorption in patients pretreated with intravenous nitroglycerin.

While the results reported here are only preliminary, they illustrate the cardinal importance of the application method, especially surface area, in the pharmacokinetics and, possibly, clinical efficacy of nitroglycerin ointments. These results indicate that the ointment should be carefully and consistently applied.

## REFERENCES

(1) Martindale, "The Extra Pharmacopoeia," 27th ed., A. Wade, Ed., Pharmaceutical Press, London, England, 1977, p. 1646.

(2) P. W. Armstrong, J. A. Armstrong, and G. S. Marks, *Circulation*, **59**, 585 (1979).

(3) *Ibid.*, **62**, 160 (1980).

(4) H. Maier-Lenz, L. Ringwelski, and A. Windorfer, *Arzneim.-Forsch.*, **30**, 320 (1980).

(5) P. W. Armstrong, J. A. Armstrong, and G. S. Marks, *Am. J. Cardiol.*, **46**, 670 (1980).

(6) P. K. Noonan and R. C. Wester, *J. Pharm. Sci.*, **69**, 365 (1980).

(7) H. Laufen, F. Scharpf, and G. Bartsch, *J. Chromatogr. Biomed. Appl.*, **146**, 457 (1978).

(8) R. A. Morrison and H.-L. Fung, "Abstracts," vol. 10, APhA Academy of Pharmaceutical Sciences, 1980, p. 126.

(9) S. T. Horhota and H.-L. Fung, *J. Pharm. Sci.*, **68**, 608 (1979).

## ACKNOWLEDGMENTS

The authors thank Dr. A. Balsys, Dr. R. Lalonde, Mr. M. Tierney, and Mrs. B. Hughes for expert advice and assistance and Mr. D. L. Wilson for the analyses.

# Effect of Pirprofen on Protein Binding of Warfarin and Tolbutamide in Human Plasma

**RICHARD C. LUDERS** ˣ **and DOLLY CHAO**

Received January 21, 1981, from the *Research Department, Pharmaceuticals Division, Ciba-Geigy Corporation, Ardsley, NY 10502.* Accepted for publication May 14, 1981.

**Abstract** □ The extent of warfarin and tolbutamide binding to plasma proteins was determined with and without pirprofen by an ultrafiltration procedure employing $^{14}C$-labeled drugs. Results from *in vitro* studies at 37° showed that the degree of binding amounted to 97.8% for warfarin and 95.6% for tolbutamide. The binding characteristics of these drugs were not altered when plasma containing either warfarin or tolbutamide at concentrations equivalent to those expected normally after therapeutic dosing were concomitantly spiked with therapeutic amounts of pirprofen. Consequently, potentiation resulting from drug displacement would not be anticipated in humans when pirprofen is administered along with warfarin or tolbutamide.

**Keyphrases** □ Pirprofen—effect on protein binding of warfarin and tolbutamide □ Tolbutamide—protein binding in presence of pirprofen □ Warfarin—protein binding in presence of pirprofen □ Binding, protein—tolbutamide and warfarin

Pirprofen, 3-chloro-4-(2,5-dihydro-1*H*-pyrol-1-yl)-α-methyl benzeneacetic acid, is a new nonsteroidal anti-inflammatory agent which is well tolerated and highly effective in the treatment of rheumatoid arthritis (1–3). Investigations in these laboratories showed that pirprofen is bound to plasma proteins to an extent greater than 99.8%[1]. Concurrent salicylate administration causes a reduction of plasma pirprofen concentrations of ~31% in rats (4) and ~38% in humans[1].

## BACKGROUND

It has been well established that concomitant administration of two highly protein-bound drugs can lead to a displacement of one drug by the other when the two drugs compete for the same binding sites (5, 6). Drug displacement results in the availability of more free or unbound drug, which, in turn, might lead to a change in the distribution and elimination of the affected drug (7, 8). Certain nonsteroidal anti-inflammatory drugs, such as phenylbutazone, when administered concomitantly with warfarin cause total plasma warfarin concentrations to decrease by 50% while free drug increases to 65% (9). A study in rats showed that ibuprofen increased total clearance and the anticoagulant effect of warfarin (10); however, human serum containing ibuprofen showed only a 10% increase in free warfarin (11). Naproxen caused a partial displacement (14–17%) of warfarin (12).

Since arthritics undergoing chronic pirprofen therapy also might receive other drugs concomitantly, it was important to study the relationship between pirprofen concentrations and protein binding of drugs likely to be administered with pirprofen. The results of *in vitro* binding studies with warfarin and tolbutamide are discussed in this paper.

## EXPERIMENTAL

Pooled heparinized human plasma was obtained from healthy volunteers and spiked with either [$^{14}C$]warfarin[2] (1 or 10 μg/ml) or [$^{14}C$]tolbutamide[3] (20, 40, 100, or 200 μg/ml) in the presence of pirprofen[4] (0, 25, 50, 100, or 200 μg/ml).

The spiked samples were allowed to equilibrate at room temperature for at least 1 hr. Plasma aliquots, 1 or 2 ml, of each sample were pipetted into membrane cones[5], which had been soaked previously in distilled water for a minimum of 1 hr. These membranes were contained in conical supports[6], which were placed inside centrifugation tubes[7]. To ensure a uniform filtration, the seam of the membrane cone was faced toward the rotating direction. A prerun centrifugation[8] of 12 minutes (~1000×*g*) was necessary to eliminate the water content of the membrane. The ultrafiltrate (~300 μl) was collected after a second centrifugation (7 min) at the same speed. Another group of samples was carried through the same procedure (equilibration and treatment of filter cones) at 37 ± 2°. The centrifugation at elevated temperature was accomplished by placing the centrifuge inside a large oven maintained at 37 ± 2°.

Aliquots of 10–150 μl of the spiked plasma samples and of the ultrafiltrate were mixed with 15 ml of scintillation cocktail[9] and assayed for carbon 14 by liquid scintillation spectrometry[10]. Unbound warfarin and tolbutamide were expressed in percent and were obtained from the ratio of radioactivity measurements in the ultrafiltrate (unbound drug) to those in whole plasma (total drug). Means and standard deviations were obtained from four analyses.

Recoveries of warfarin and tolbutamide from the filtration cones were determined prior to the binding studies. Two milliliters of a pH 7.4 buffer solution containing 199.8 ng of tolbutamide/ml or 10.5 ng of warfarin/ml was added to the filtration cones and carried through the described procedure. Aliquots of 400 μl of the filtrate were then taken for radioactivity measurements. The data obtained from four replicate analyses (Table I) gave average recoveries of 99 ± 0.4% for tolbutamide and 92 ± 0.5% for warfarin.

**Table I—Percent Recovery of [$^{14}C$]Tolbutamide and [$^{14}C$]-Warfarin from Filtration Cones**

| Drug | Concentration, ng/ml | Determinations[a] 1 | 2 | 3 | 4 | Average ±*SD* |
|---|---|---|---|---|---|---|
| Warfarin | 10.5[b] | 92 | 92 | 91 | 92 | 92 ± 0.5 |
| Tolbutamide | 199.8[c] | 98 | 99 | 99 | 99 | 99 ± 0.4 |

[a] Room temperature (22 ± 2°). [b] Equivalent to the amount of free drug in a plasma sample containing 1 μg of warfarin/ml. [c] Equivalent to the amount of free drug in a plasma sample containing 4 μg of tolbutamide/ml.

## RESULTS AND DISCUSSION

**Warfarin**—The results of binding studies at 37° (Fig. 1) indicate that the amount of free or unbound warfarin was 2.2 ± 0.15% (mean ± *SD*) for drug levels of 1–10 μg/ml. Conversely, 97.8% of the drug was bound to plasma protein. The data obtained at room temperature indicate about one-half as much unbound warfarin (1.1%). Yacobi and Levy (12) reported that 99.1% of the drug was bound to serum proteins for serum drug concentrations of 1.25 μg/ml.

When the warfarin samples (37°) were spiked with 50 μg/ml of pirprofen, a mean of 2.4 ± 0.24% (*SD*) was found; at 100 μg/ml, free warfarin averaged 2.3 ± 0.06% (*SD*). For these concentrations, pirprofen did not significantly ($p = 0.05$) alter warfarin binding. Since peak plasma concentrations of 23–44 μg/ml occur after chronic dosing with pirprofen (13) and since warfarin concentrations at steady state range from 1.6 to 4.1 μg/ml (9, 14), one would not expect warfarin to be displaced when therapeutic amounts of pirprofen are administered concomitantly with the anticoagulant. However, at pirprofen concentrations of 200 μg/ml or approximately four times the maximum levels found clinically, free

[1] To be published.
[2] Specific activity of 49 mCi/mmole, Amersham, Chicago, Ill.
[3] Specific activity of 47.6 mCi/mmole, New England Nuclear, Boston, Mass.
[4] Ciba-Geigy Corp., Ardsley, N.Y.
[5] CF-50, Amicon Corp., Lexington, Mass.
[6] CSIA, Amicon Corp., Lexington, Mass.
[7] CTI, Amicon Corp., Lexington, Mass.
[8] CT 1300, Adams Dynac, Raycomm Industries, Inc., Freehold, N.J.
[9] Scintisol, Isolab, Inc., Akron, Ohio.
[10] SL 4000, Intertechnique, Fairfield, N.J.



0022-3549/81/1200-1370$01.00/0
© 1981, American Pharmaceutical Association

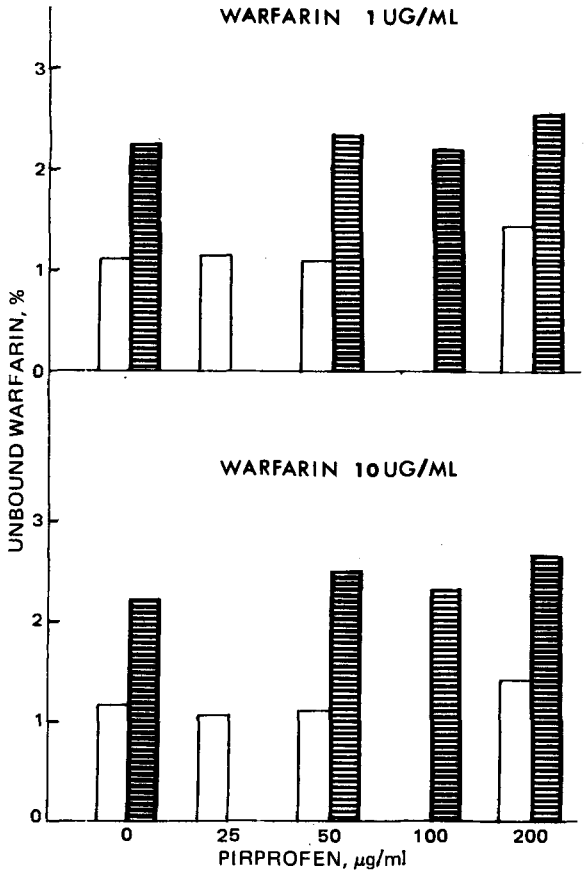


**Figure 1**—*Effect of pirprofen on the* in vitro *plasma binding of warfarin. Key:* □, *room temperature; and* ▤, *37°.*

warfarin increased by 27 (room temperature) and 20% (37°).

**Tolbutamide**—The extent of binding to plasma proteins was 95.6 ± 0.15% (mean ± *SD*) at 37° for plasma tolbutamide levels between 40 and 100 µg/ml (Fig. 2). Similar results were obtained at room temperature for tolbutamide concentrations between 20 and 100 µg/ml. These values are comparable to those of Miller *et al.* (15), who reported 96.8 and 96.0% binding in young and old subjects, respectively, for plasma drug concentrations of 100 µg/ml, and to those of Zilly *et al.* (16), who found 95% binding following a 20-min intravenous infusion of 1600 mg of tolbutamide.

At 37°, no change in tolbutamide binding (95.6 ± 0.17%; $p = 0.05$) was observed when plasma samples containing 40–100 µg of tolbutamide/ml were spiked with pirprofen at levels up to 50 µg/ml. An increase in free tolbutamide was noted, however, for higher tolbutamide concentrations. As observed in Fig. 2, free tolbutamide increased to 8.0 (room temperature) and 9.9% (37°) for tolbutamide levels of 200 µg/ml. Although levels of this magnitude are not normally maintained after dosing with tolbutamide (17–19), the *in vitro* binding data suggest that binding sites were nearing saturation, resulting in greater availability of unbound drug. At these high concentrations, there is a suggestion that pirprofen can partially displace tolbutamide. The results (room temperature and 37°) show that the addition of 50 µg of pirprofen/ml increased free tolbutamide to ~11% of the total drug fraction.

In conclusion, pirprofen did not alter the binding characteristics of tolbutamide or warfarin when these compounds were added to plasma (*in vitro*) at levels expected normally after therapeutic dosing. Consequently, a change in pharmacological response from warfarin or tolbutamide resulting from drug displacement would not be anticipated in humans when either of these compounds is administered concomitantly with pirprofen.

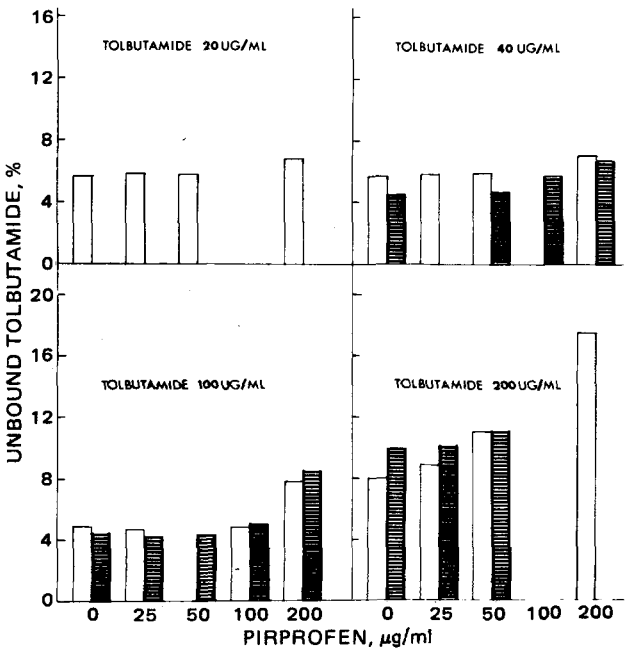


**Figure 2**—*Effect of pirprofen on the* in vitro *plasma binding of tolbutamide. Key:* □, *room temperature; and* ▤, *37°.*

## REFERENCES

(1) R. T. Reid, *J. Clin. Pharmacol.*, **20,** 145 (1980).

(2) M. B. Maggio-Cavaliere, L. Bonus, and O. B. Gum, *ibid.*, **16,** 8 (1976).

(3) J. D. Proctor, E. F. Evans, V. Campos, J. Velandia, D. Pollack, W. Wingfield, and A. Wasserman, *Clin. Pharmacol. Ther.*, **16,** 69 (1974).

(4) T. A. Thompson, C. H. Borman, R. S. Goodblatt, and W. J. Roth, III, *J. Pharm. Sci.*, **68,** 996 (1979).

(5) K. F. Brown and M. J. Crooks, *Biochem. Pharmacol.*, **25,** 1175 (1976).

(6) R. A. Henry and W. D. Wosilait, *Toxicol. Appl. Pharmacol.*, **33,** 367 (1975).

(7) A. Hasselblatt, *Toxic Probl. Drug Comb.*, **13,** 89 (1972).

(8) S. Garten and W. D. Wosilait, *Comp. Gen. Pharmacol.*, **3,** 83 (1972).

(9) W. L. Schary, R. J. Lewis, and M. Rowland, *Res. Commun. Chem. Pathol. Pharmacol.*, **10,** 663 (1975).

(10) J. T. Slattery, A. Yacobi, and G. Levy, *J. Pharm. Sci.*, **66,** 943 (1977).

(11) J. T. Slattery and G. Levy, *ibid.*, **66,** 1060 (1977).

(12) A. Yacobi and G. Levy, *Res. Commun. Chem. Pathol. Pharmacol.*, **15,** 369 (1976).

(13) R. C. Luders, M. B. Maggio-Cavaliere, H. P. Egger, O. B. Gum, O. Resnick, M. F. Bartlett, M. J. Gaito, A. Soo, and C. Li, *Clin. Pharmacol. Ther.*, **21,** 721 (1977).

(14) A. Breckenridge, M. Orme, H. Wesseling, R. J. Lewis, and R. Gibbons, *ibid.*, **15,** 424 (1973).

(15) A. K. Miller, J. Adir, and R. Vestol, *J. Pharm. Sci.*, **67,** 1192 (1978).

(16) W. Zilly, D. D. Breimer, and E. Richter, *Eur. J. Clin. Pharmacol.*, **9,** 219 (1975).

(17) P. Anderson and E. S. Vesell, *Clin. Pharmacol. Ther.*, **16,** 1059 (1974).

(18) W. E. Braselton, E. D. Bransome, and T. A. Huff, *Diabetes*, **26,** 50(1976).

(19) J. Sheldon, J. Anderson, and L. Stoner, *ibid.*, **14,** 362 (1965).

# Importance of Radiochemical Purity of Radiolabeled Drugs Used for Determining Plasma Protein Binding of Drugs

**Keyphrases** □ Binding, plasma protein—effect of radiochemical impurity of radiolabeled drugs □ Drugs, radiolabeled—effect of radiochemical impurity on determination of plasma protein binding of drugs □ Impurity, radiochemical—of radiolabeled drugs, effect on determination of plasma protein binding of drugs

*To the Editor:*

Plasma protein binding of drugs has been the subject of intensive study for many years. It is an important pharmacological parameter, since it frequently affects drug distribution and elimination (1–3) and duration and intensity of pharmacological effects of drugs (4–6). A number of factors are known to affect the determination of drug protein binding, including the use of vacuum container[1] blood collection tubes (7, 8), some polyvinyl intravenous tubing (7, 9), and the administration of heparin (used therapeutically or as heparin lock) (9, 10). All of these factors result in diminished drug binding. An additional factor that has not received sufficient attention, although it has been stressed (11), is the importance of radiochemical purity of the radiolabeled drugs used in the determination of drug protein binding.

Equilibrium dialysis has become the most commonly used method for determining drug protein binding in clinical pharmacokinetic studies. Tracer amounts of radiolabeled drugs are added on either side of the dialysis membrane, usually on the buffer side. After dialysis has reached equilibrium, the unbound or free fraction of the drug ($f_f$) is usually calculated as the ratio of the radioactivity determined in the buffer phase to that determined in the plasma phase, correcting for volume differences, if any, between the two phases subjected to liquid scintillation counting, as follows:

$$f_f = \frac{R_B \times V_P}{R_P \times V_B} \qquad \text{(Eq. 1)}$$

where $R_B$ and $R_P$ represent the radioactivities determined in the buffer and plasma phases, respectively, and $V_P$ and $V_B$ represent the volumes of the plasma and buffer phases counted, respectively.

These calculations assume that the radiolabeled drug used is absolutely void of any radiochemical impurities. However, this is usually not the case unless the radiolabel is purified before use, since most commercially available radiolabeled drugs contain unknown, although small, amounts of radiochemical impurities. These radiochemical impurities containing the radioactive isotope (usually carbon 14 or tritium) may be a starting material or intermediary compounds in the chemical synthesis of the radiolabeled drug, or breakdown products of the drug.

[1] Vacutainer.

To evaluate the effects of varying degrees of radiochemical impurities present in the dialysis on the determination of plasma protein binding of drugs, Eq. 1 has to be modified. The observed free fraction ($f_f'$) can be calculated for varying combinations of the true or actual free fraction ($f_f$) and the fraction of impurities in the radiolabel used ($f_i$) assuming that $V_P$ equals $V_B$, using the expression:

$$f_f' = \frac{[R_T - (R_T \times f_i)]\, f_f + \left(\frac{R_T \times f_i}{2}\right)}{[R_T - (R_T \times f_i)] + \left(\frac{R_T \times f_i}{2}\right)} \qquad \text{(Eq. 2)}$$

where the numerator represents $R_B$ and the denominator represents $R_P$ in Eq. 1 and $R_T$ represents the total radioactivity added (consisting of both the drug of interest and the impurities); it is assumed that the radiochemical impurities are not bound to plasma proteins and distribute evenly in the plasma and buffer phases. The former terms in the numerator and denominator in Eq. 2 represent the actual free fraction, while the sum of the latter terms in the numerator and denominator represents the radioactivity due to radiochemical impurities.

Simulations were carried out using Eq. 2 to illustrate the effects of varying degrees of radiochemical impurities in the radiolabel used on the determination of plasma protein binding of drugs. Figure 1 shows simulations of the observed free fraction *versus* the actual free fraction, when the impurities in the radiolabel vary from 2.5–10% of the total radioactivity added. It can be seen that increasing the percentage of impurities in the radiolabel results in an

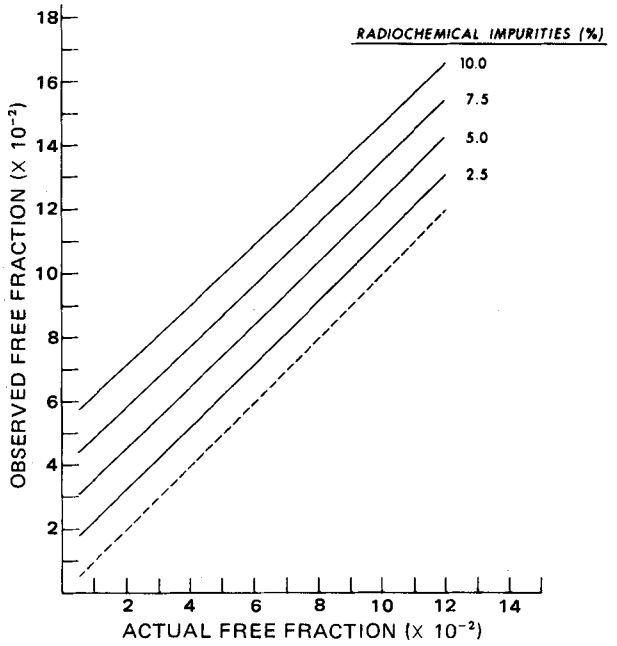


**Figure 1**—*Effects of varying degrees of radiochemical impurities present in dialysis on the determination of plasma protein binding of drugs.*



0022-3549/81/1200-1372$01.00/0
© 1981, American Pharmaceutical Association

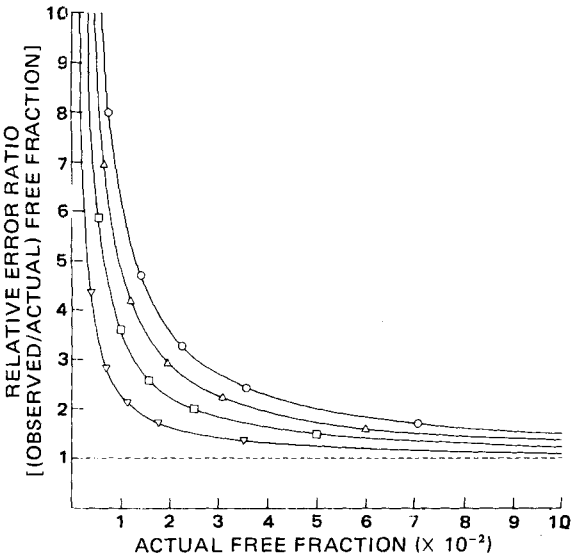


**Figure 2**—*Effects of varying degrees of radiochemical impurities present in dialysis on the relative error involved in the determination of plasma protein binding of drugs. Key:* ○, *10.0;* △, *7.5;* □, *5.0; and* ▽, *2.5% radiochemical impurities.*

upward shift of the linear relationship between the observed *versus* the actual free fraction.

However, the relative error on the determination of drug protein binding caused by the radiochemical impurities varies markedly depending on the actual free fraction; the lower the actual free fraction the greater the relative error and vice versa. This relative error can be expressed as the ratio of the observed to actual free fraction, which indicates how many times higher the observed free fraction is than the actual free fraction.

Figure 2 shows a plot of this relative error ratio *versus* the actual free fraction. It has an expected hyperbolic form for any given degree of radiochemical impurities present because the independent variable is in the denominator of the dependent variable. It can be seen from Fig. 2 that the observed free fraction will be ~2.3–6.3 times higher than an actual free fraction of 0.01 when radiochemical impurities vary from 2.5–10%, while the observed free fraction is only ~1.1–1.5 times higher than an actual free fraction of 0.1 with the same range of radiochemical impurities present.

The use of a radiolabel containing radiochemical impurities in dialysis for the determination of protein binding in clinical pharmacokinetic studies will not only result in a wrong value, but it will make all comparisons of binding data difficult. Such comparisons are frequently of interest, *e.g.*, when evaluating the effects of other drugs or disease states on the protein binding of drugs or when comparing drug binding in different groups of age or sex. This effect can be illustrated by two groups of drug binding data with average actual free fractions of 0.01 and 0.02. When a radiolabel with 5% radiochemical impurities is used, this 100% difference in the actual free fractions will reduce to a 28% difference in the free fractions, *i.e.*, the observed free fractions will be 0.035 and 0.045. It is likely that a true statistically significant difference among various groups of binding data may therefore become obscured. Because of the significance of drug protein binding in clinical pharmacology, it is suggested that radiolabels used for the determinations of plasma protein binding of drugs be purified prior to dialysis, *e.g.*, by high-pressure liquid chromatography, and that the stability of the radiolabel be verified postdialysis in both buffer and plasma phases.

(1) G. R. Wilkinson and D. G. Shand, *Clin. Pharmacol. Ther.*, **18**, 377 (1975).

(2) G. Levy, in "The Effect of Disease States on Pharmacokinetics," L. Z. Benet, Ed., American Pharmaceutical Association, Washington, D.C., 1976, p. 137.

(3) T. D. Bjornsson, P. J. Meffin, S. Swezey, and T. F. Blaschke, *J. Pharmacol. Exp. Ther.*, **210**, 316 (1979).

(4) A. H. Anton, *ibid.*, **129**, 282 (1960).

(5) D. G. McDevitt, M. Frisk-Holmberg, J. W. Hollifield, and D. G. Shand, *Clin. Pharmacol. Ther.*, **20**, 152 (1976).

(6) G. Levy, *J. Pharm. Sci.*, **65**, 1264 (1976).

(7) R. H. Cotham and D. G. Shand, *Clin. Pharmacol. Ther.*, **18**, 535 (1974).

(8) O. Borgå, K. M. Piafsky, and O. G. Nilsen, *ibid.*, **22**, 539 (1977).

(9) M. Wood, D. G. Shand, and A. J. J. Wood, *ibid.*, **25**, 103 (1979).

(10) K. M. Giacomini, S. E. Swezey, J. C. Giacomini, and T. F. Blaschke, *Life Sci.*, **27**, 771 (1980).

(11) A. Yacobi and G. Levy, *J. Pharmacokinet. Biopharm.* **3**, 439 (1975).

*Thorir D. Bjornsson*[x]
*James E. Brown*
*Christian Tschanz*
Division of Clinical
Pharmacology, Departments of Pharmacology and Medicine, Duke University Medical Center
Durham, NC 27710

Supported in part by Grants HL 24343 and NS 06233 from the National Institutes of Health.

Thorir D. Bjornsson is a recipient of a Pharmaceutical Manufacturers Association Foundation Faculty Development Award in Clinical Pharmacology. James E. Brown is a recipient of a fellowship from the Canadian Heart Association.

## Determination of Renal Clearances Using Arterial and Venous Plasma: Procainamide in Rabbits

**Keyphrases** □ Procainamide—renal clearance, determination using timed-interval method, rabbits □ Renal clearance—determination of procainamide using arterial and venous plasma, rabbits □ Pharmacokinetics—determination of renal clearance of procainamide using arterial and venous plasma, rabbits

*To the Editor:*

The timed-interval method is commonly employed in pharmacokinetic studies to determine the renal clearance ($Cl_r$) of a drug compound:

$$Cl_r = \frac{X_{t_1-t_2}}{AUC_{t_1-t_2}} \qquad \text{(Eq. 1)}$$

where $X_{t_1-t_2}$ and $AUC_{t_1-t_2}$ are the amount of the intact drug excreted and the area under the plasma concentration curve between times $t_1$ and $t_2$, respectively. To date, the potential effect of the source of plasma data, either arterial or venous, on the estimation of clearance using Eq. 1 has rarely been evaluated. The arterial and venous differences of six compounds were recently reported (1). The present

0022-3549/81/1200-1373$01.00/0
© 1981, American Pharmaceutical Association

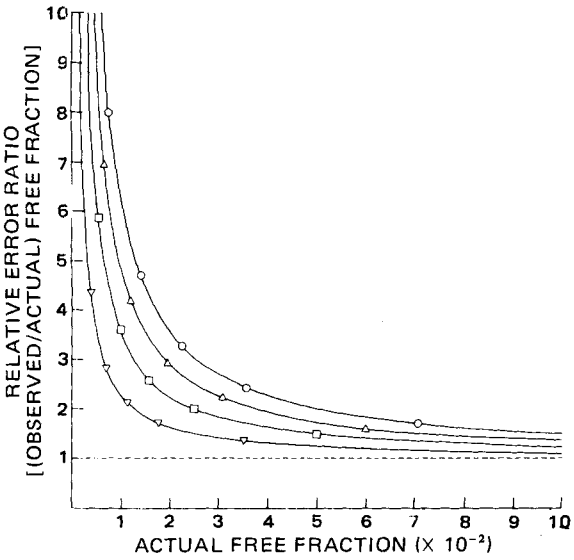


**Figure 2**—*Effects of varying degrees of radiochemical impurities present in dialysis on the relative error involved in the determination of plasma protein binding of drugs. Key:* ○, *10.0;* △, *7.5;* □, *5.0; and* ▽, *2.5% radiochemical impurities.*

upward shift of the linear relationship between the observed *versus* the actual free fraction.

However, the relative error on the determination of drug protein binding caused by the radiochemical impurities varies markedly depending on the actual free fraction; the lower the actual free fraction the greater the relative error and vice versa. This relative error can be expressed as the ratio of the observed to actual free fraction, which indicates how many times higher the observed free fraction is than the actual free fraction.

Figure 2 shows a plot of this relative error ratio *versus* the actual free fraction. It has an expected hyperbolic form for any given degree of radiochemical impurities present because the independent variable is in the denominator of the dependent variable. It can be seen from Fig. 2 that the observed free fraction will be ~2.3–6.3 times higher than an actual free fraction of 0.01 when radiochemical impurities vary from 2.5–10%, while the observed free fraction is only ~1.1–1.5 times higher than an actual free fraction of 0.1 with the same range of radiochemical impurities present.

The use of a radiolabel containing radiochemical impurities in dialysis for the determination of protein binding in clinical pharmacokinetic studies will not only result in a wrong value, but it will make all comparisons of binding data difficult. Such comparisons are frequently of interest, *e.g.*, when evaluating the effects of other drugs or disease states on the protein binding of drugs or when comparing drug binding in different groups of age or sex. This effect can be illustrated by two groups of drug binding data with average actual free fractions of 0.01 and 0.02. When a radiolabel with 5% radiochemical impurities is used, this 100% difference in the actual free fractions will reduce to a 28% difference in the free fractions, *i.e.*, the observed free fractions will be 0.035 and 0.045. It is likely that a true statistically significant difference among various groups of binding data may therefore become obscured. Because of the significance of drug protein binding in clinical pharmacology, it is suggested that radiolabels used for the determinations of plasma protein binding of drugs be purified prior to dialysis, *e.g.*, by high-pressure liquid chromatography, and that the stability of the radiolabel be verified postdialysis in both buffer and plasma phases.

(1) G. R. Wilkinson and D. G. Shand, *Clin. Pharmacol. Ther.*, **18**, 377 (1975).

(2) G. Levy, in "The Effect of Disease States on Pharmacokinetics," L. Z. Benet, Ed., American Pharmaceutical Association, Washington, D.C., 1976, p. 137.

(3) T. D. Bjornsson, P. J. Meffin, S. Swezey, and T. F. Blaschke, *J. Pharmacol. Exp. Ther.*, **210**, 316 (1979).

(4) A. H. Anton, *ibid.*, **129**, 282 (1960).

(5) D. G. McDevitt, M. Frisk-Holmberg, J. W. Hollifield, and D. G. Shand, *Clin. Pharmacol. Ther.*, **20**, 152 (1976).

(6) G. Levy, *J. Pharm. Sci.*, **65**, 1264 (1976).

(7) R. H. Cotham and D. G. Shand, *Clin. Pharmacol. Ther.*, **18**, 535 (1974).

(8) O. Borgå, K. M. Piafsky, and O. G. Nilsen, *ibid.*, **22**, 539 (1977).

(9) M. Wood, D. G. Shand, and A. J. J. Wood, *ibid.*, **25**, 103 (1979).

(10) K. M. Giacomini, S. E. Swezey, J. C. Giacomini, and T. F. Blaschke, *Life Sci.*, **27**, 771 (1980).

(11) A. Yacobi and G. Levy, *J. Pharmacokinet. Biopharm.* **3**, 439 (1975).

*Thorir D. Bjornsson*[x]
*James E. Brown*
*Christian Tschanz*
Division of Clinical
Pharmacology, Departments of Pharmacology and Medicine, Duke University Medical Center
Durham, NC 27710

Supported in part by Grants HL 24343 and NS 06233 from the National Institutes of Health.

Thorir D. Bjornsson is a recipient of a Pharmaceutical Manufacturers Association Foundation Faculty Development Award in Clinical Pharmacology. James E. Brown is a recipient of a fellowship from the Canadian Heart Association.

## Determination of Renal Clearances Using Arterial and Venous Plasma: Procainamide in Rabbits

**Keyphrases** □ Procainamide—renal clearance, determination using timed-interval method, rabbits □ Renal clearance—determination of procainamide using arterial and venous plasma, rabbits □ Pharmacokinetics—determination of renal clearance of procainamide using arterial and venous plasma, rabbits

*To the Editor:*

The timed-interval method is commonly employed in pharmacokinetic studies to determine the renal clearance ($Cl_r$) of a drug compound:

$$Cl_r = \frac{X_{t_1-t_2}}{AUC_{t_1-t_2}} \qquad \text{(Eq. 1)}$$

where $X_{t_1-t_2}$ and $AUC_{t_1-t_2}$ are the amount of the intact drug excreted and the area under the plasma concentration curve between times $t_1$ and $t_2$, respectively. To date, the potential effect of the source of plasma data, either arterial or venous, on the estimation of clearance using Eq. 1 has rarely been evaluated. The arterial and venous differences of six compounds were recently reported (1). The present

0022-3549/81/1200-1373$01.00/0
© 1981, American Pharmaceutical Association

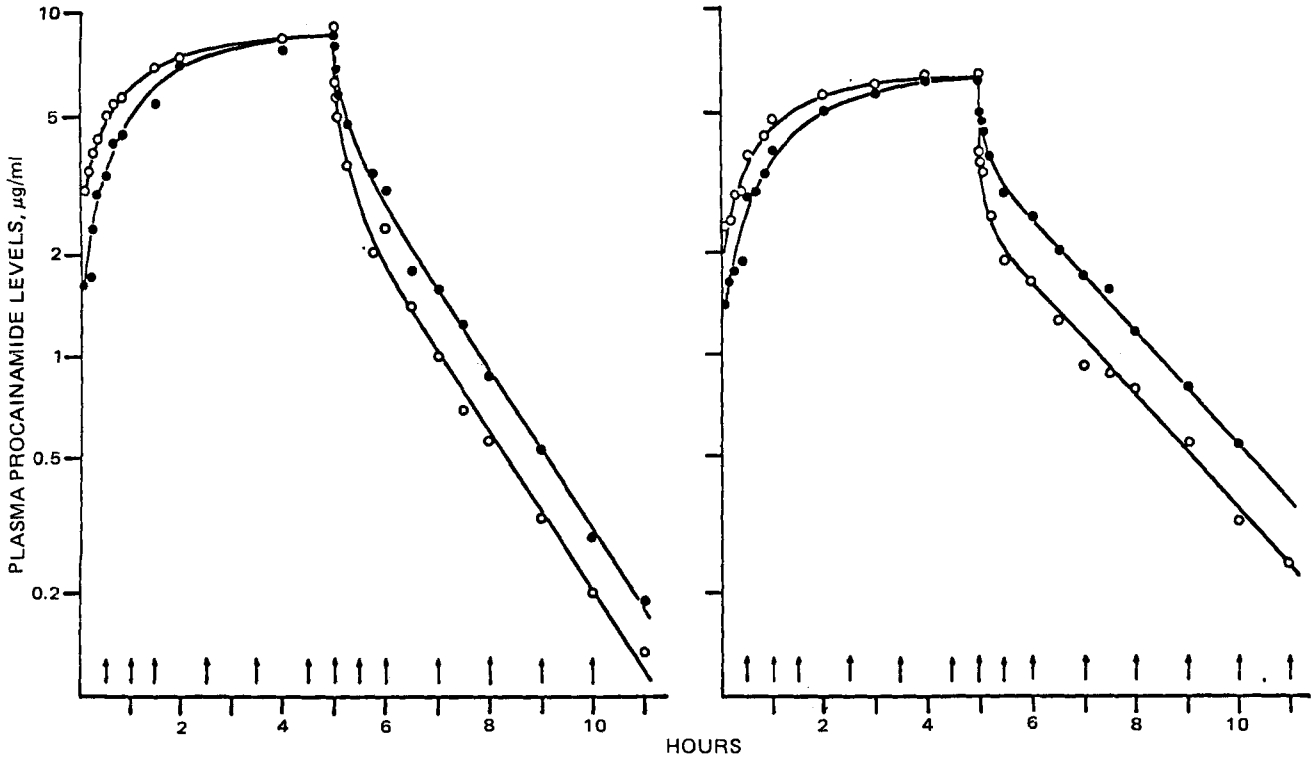


**Figure 1**—*Arterial (○) and venous (●) plasma procainamide concentration following constant intravenous infusion of procainamide hydrochloride, 52.4 and 92.4 mg/hr for 5 hr into rabbit 1 (left) and rabbit 2 (right), respectively. The arrows indicate the end of each renal clearance determination period.*

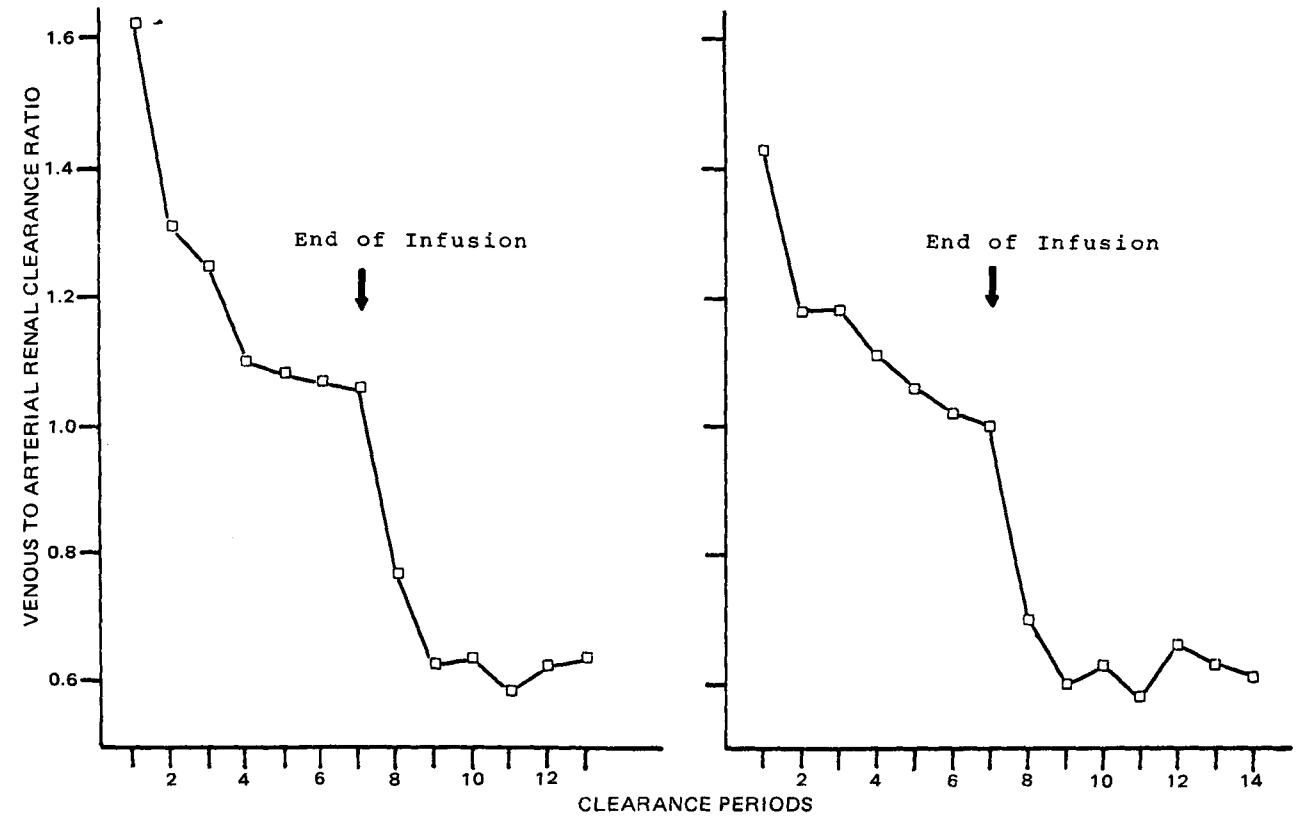


**Figure 2**—*Venous to arterial renal clearance ratios during and after constant intravenous infusion of procainamide hydrochloride in rabbit 1 (left) and rabbit 2 (right). The abscissa represents the number of renal clearance determination periods.*

communication reports the preliminary results of the influence of arterial–venous (A–V) differences on the determination of renal clearance of procainamide in rabbits using the described method during and after intravenous infusion.

The right carotid artery and the jugular vein of two pigmented male rabbits were catheterized with polyethylene tubings after anesthetization with 1.0 g of urethan/kg[1]. A third catheter was placed into the sacral part of the vena cava *via* the right femoral vein. The tip of the cannula was positioned at the junction of the femoral branch and was confirmed after termination of the experiment. The animals were allowed to recover overnight. Infusion solutions were prepared by dissolving varied amounts of procainamide hydrochloride[2] in normal saline before the study and were administered to the rabbits by a constant-infusion syringe pump[3] into the jugular vein for 5 hr. Arterial and venous blood were collected simultaneously from the carotid artery and femoral vein together with urine samples at predetermined times during and after infusion. A pediatric Forley catheter was introduced into the urinary bladder for collection of urine. Distilled water (3 × 20 ml) was flushed into the bladder shortly before each collection time. An aliquot from the pooled urine and washings was collected. Plasma and urine procainamide concentrations were determined by a modified HPLC assay (2).

The plasma profiles of the two rabbits are shown in Fig. 1. During the infusion arterial plasma levels rose rapidly and appeared to reach steady state at 5 hr. Venous plasma levels, however, were lower than the arterial levels at all times but approached them asymptotically toward the end of the infusion. Both curves began to drop with the venous curve being higher than the arterial curve shortly after the infusion. During the terminal phase, both curves decayed virtually parallel to each other with mean venous to arterial (V/A) ratios of ~1.6 for both rabbits.

Renal clearances were determined by Eq. 1 and the resultant V/A clearance ratios are shown in Fig. 2. Renal clearance measurements using venous data resulted in persistently higher values during infusion and lower values postinfusion than arterial data.

By definition, renal clearance is defined as the virtual volume of arterial plasma flowing into the kidney completely cleared of drug per unit of time. The drug concentrations in the systemic arterial plasma can be considered practically identical at any time. Therefore, it seems only appropriate that Eq. 1 is used with arterial plasma data, unless there is no significant A–V difference. Our results suggest that venous data gave rise to overestimation of renal clearance during infusion and underestimation postinfusion. At steady state, both arterial and venous plasma levels appeared to be identical (Fig. 1); hence, no difference in renal clearance estimate is to be expected from using either data.

The problem of venous sampling in clearance measurements was pointed out earlier (3) and was the subject of a recent review (4). Since relatively little effort has been directed toward the differentiation of arterial and venous blood data in pharmacokinetic analysis, our data provided evidence of the existence of significant A–V differences (Fig. 1) and its consequences (Fig. 2) in renal clearance estimations. It is our opinion that sampling arterial plasma is preferred in renal clearance studies in animals using the described timed-interval method. Nevertheless, venous sampling could be useful when employing steady-state infusion or multiple dosing (area during a dosing interval at steady state) methods. The latter methods should be of special value in human studies where the risk of arterial sampling can be avoided.

(1) W. L. Chiou, G. Lam, M. L. Chen, and M. G. Lee, *Res. Commun. Chem. Pathol. Pharmacol.*, **32**, 27 (1981).

(2) M. A. F. Gadalla, G. W. Peng, and W. L. Chiou, *J. Pharm. Sci.*, **67**, 869 (1978).

(3) C. Brun, T. Hilden, and R. Raaschou, *J. Clin. Invest.*, **28**, 144 (1949).

(4) W. L. Chiou and G. Lam, *Int. J. Clin. Pharmacol. Ther. Toxicol.*, in press.

*Gilbert Lam*
*Win L. Chiou*[x]
Department of Pharmacy
College of Pharmacy
University of Illinois at the Medical Center
Chicago, IL 60612

[1] Sigma Chemical Co., St. Louis, Mo.
[2] Courtesy of American Critical Care, McGaw Park, Ill.
[3] Model 341, Sage Instruments, Cambridge, Mass.

In the article titled "Radioimmunoassay Procedure for Terfenadine in Human Plasma" (1), the following correction should be made:

On page 1419, the structure should appear as shown here:

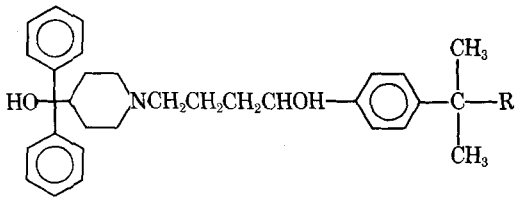

*Ia*: R = $CH_3$
*Ib*: R = $CH_2OH$
Ic: R = COOH

(1) C. E. Cook, D. L. Williams, M. Myers, C. R. Tallent, G. A. Leeson, R. A. Okerholm, and G. J. Wright, *J. Pharm. Sci.*, **69**, 1419 (1980).

---

In the article titled "Thermal Hardness Coefficient of Tablets" (1), the following corrections should be made:

On page 329, column 1, Table I title should read: Average (±*SD*) Hardness of Tablets in Kiloponds at Various Temperatures (±1°).

On page 329, column 2, line 11 should read as follows: temperature was increased (~ − 0.02 kilopond/degree) for Products A–E.

(1) E. L. Parrott, *J. Pharm. Sci.*, **70**, 328 (1981).

---

In the article titled "Nitroglycerin Pharmacokinetics after Intravenous Infusion in Normal Subjects" (1), the following correction should be made:

On page 1055, column 1, line 5 under Assay, Caprylene should read Octalene (aldrin).

(1) E. F. McNiff, A. Yacobi, F. M. Young-Chang, L. H. Golden, A. Goldfarb, and Ho-Leung Fung, *J. Pharm Sci.*, **70**, 1054 (1981).

In the article titled "Antitumor Agents XLII: Comparison of Antileukemic Activity of Helenalin, Brusatol, and Bruceantin and Their Esters on Different Strains of P-388 Lymphocytic Leukemic Cells" (1), the following correction should be made:

On page 1148, the structure should appear as shown here:

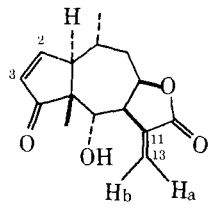

I

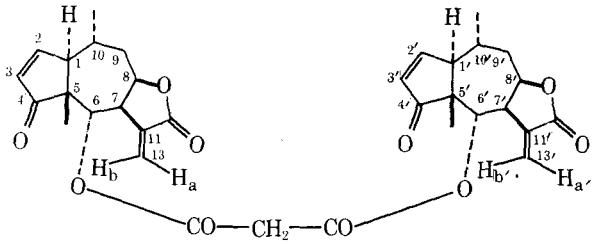

II

(1) I. H. Hall, K. H. Lee, M. Okano, D. Sims, T. Ibuka, Y. E. Liou, and Y. Imakura, *J. Pharm. Sci.*, **70**, 1147 (1981).